ANGEWANDTE CHEMIE

International Edition in English

Volume 25 · Number 1
January 1986
Pages 1–114

[3+2] Cycloaddition Approaches to Five-Membered Rings via Trimethylenemethane and Its Equivalents

New Synthetic Methods (55)

By Barry M. Trost*

The power of cycloadditions for ring formation derives from the potential for chemo-, regio-, diastereo-, and enantioselectivity. Trimethylenemethane (TMM) and its equivalents offer the possibility of extending such benefits to the synthesis of five-membered rings. Three types of conjunctive reagents appear to be promising candidates: 1) selected 4-alkylidene-4,5-dihydro-3*H*-pyrazoles, 2) 2-[(trimethylsilyl)methyl]allyl esters and halides, and 3) alkylidenecyclopropanes. Thermal reactions, especially intramolecular ones, effect the cycloaddition of the pyrazoles to olefins—especially electron-poor olefins. The latter two precursors require a catalyst, notably a palladium complex, to unlock the synthetic potential. With the 2-[(trimethylsilyl)methyl]allyl esters, a general chemo-, regio-, and diastereoselective cycloaddition with typical Diels-Alder dienophiles forms methylenecyclopentanes in both inter- and intramolecular fashion. A tin analogue allows extension of this cycloaddition to aldehydes, and, in a related sequence, to ketones and imines to form 3-methylenetetrahydrofurans and 3-methylenepyrrolidines with excellent diastereoselectivity. The 2-[(trimethylsilyl)methyl]allyl esters also serve to effect net methylenecyclopentane annulation to cyclic enols. Such adducts can further undergo three-carbon intercalation or combined ring contraction-spiroannulation simply by the use of either a nucleophilic or electrophilic trigger. Alkylidenecyclopropanes undergo cycloadditions to both electron-rich and electron-poor olefins when stimulated by metal catalysts, especially palladium. A complementary regiochemistry to the approach based upon silicon conjunctive reagents is observed. The availability of these cycloadditions provides new strategies for the synthesis of natural products.

1. Introduction

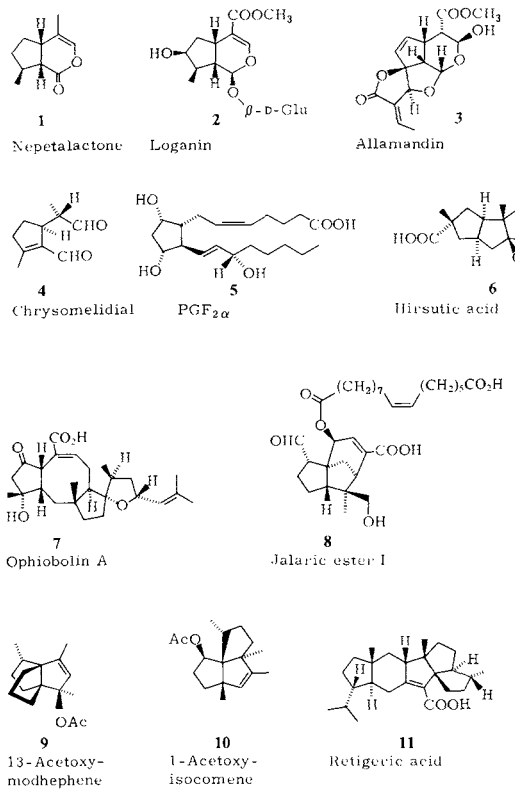
Cyclopentanoids, also termed quinanes, constitute an exploding area of natural and non-natural products.[1] While the presence of a five-membered ring in the steroid nucleus generated some interest in methods for its synthesis, problems associated with stereocontrolled formation of such rings frequently turned the formation of the steroid D ring into a synthesis of a six-membered ring followed by ring contraction. The iridoids[2] represent an early recognized, important class of cyclopentanoid monoterpenes. They are exemplified in Table 1 by nepetalactone **1**,[3] the active principle of catnip, loganin **2**,[4] a key biosynthetic intermediate of alkaloids, and allamandin **3**,[5] an antibiotic and antitumor agent, as well as close relatives like chrysomelidial **4**,[6] a constituent of the defense secretion of the beetles *Gastrophysa cyanea* and *Plagiodera versicolora*. The emergence of such a ring system as a major structural feature in natural products came with the structure elucidation of the prostanoids, represented by $PGF_{2\alpha}$ **5**,[7]

[*] Prof. B. M. Trost
S. M. McElvain Laboratories of Organic Chemistry
Department of Chemistry, University of Wisconsin-Madison
Madison, WI 53706 (USA)

 © VCH Verlagsgesellschaft mbH, D-6940 Weinheim, 1986 0570-0833/86/0101-0001 $ 02.50/0

and of hirsutic acid C **6**,[8] a triquinane antibiotic whose unusual structure eluded assignment, owing in part to the occurrence of a rather unusual structural rearrangement in the X-ray diffractometer. A plethora of natural products, some bearing one or more five-membered rings as appendages as in ophiobolin A **7**,[9] some being derivatives of well-known substances such as jalaric ester I **8**,[10] a derivative of the cedrenes, and some being rather unusual structures such as 13-acetoxymodhephene **9**,[11] 1-acetoxyisocomene **10**,[12] and retigeranic acid **11**,[13] have recently been isolated and identified (Table 1).

Table 1. Representative cyclopentanoid (quinane) natural products.

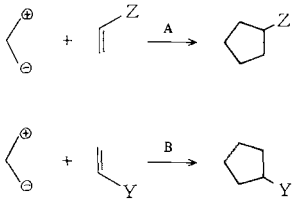


In addition to the natural products, some theoretically intriguing systems also are based upon five-membered rings. For example, the pentalenes are potentially antiaromatic molecules with interesting electronic properties. Dodecahedrane exemplifies a class of molecules whose unusual geometries are often reflected in interesting properties.

The ability to explore the cyclopentanoids ultimately depends upon their accessibility. In considering synthetic strategies, the concept of cycloaddition becomes very attractive. The chemo-, regio-, and diastereoselectivity associated with the Diels-Alder reaction has profoundly influenced the strategy for the synthesis of six-membered rings. The virtues of the Diels-Alder reaction encourage the manipulation of the adducts for formation of other rings.

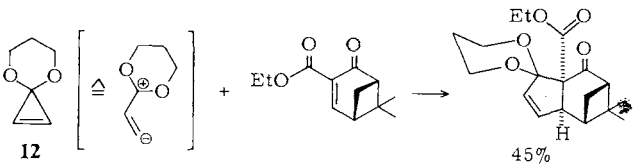
To reap the benefits of cycloadditions, however, direct formation of five-membered rings would be more practical. Indeed, 1,3-dipolar cycloaddition is an established methodology for the formation of heterocycles, which, by further reactions, may be transformed into many other structural units.[14] Until recently, however, the use of cycloadditions to make five-membered carbocyclic rings was a missing link.

In close analogy to the Diels-Alder reactions, a [3+2] strategy (as depicted in Scheme 1) for formation of five-membered rings is conceivable.



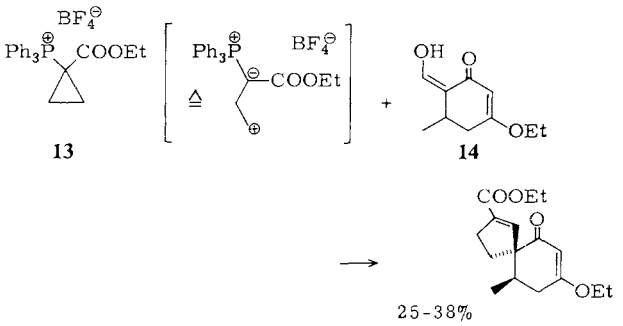
Scheme 1. Formation of cyclopentanes by 1,3-dipolar cycloaddition. Z = electron acceptor, Y = electron donor.

The use of polarized cyclopropanes as synthons for the 1,3-dipoles has brought some progress.[15] For example, cyclopropenone ketal **12** thermally adds to strongly electron-deficient double bonds (Scheme 2), an addition of type A according to Scheme 1.



Scheme 2. Reaction conditions: 75 °C, 13 h, C_6H_6, N_2.

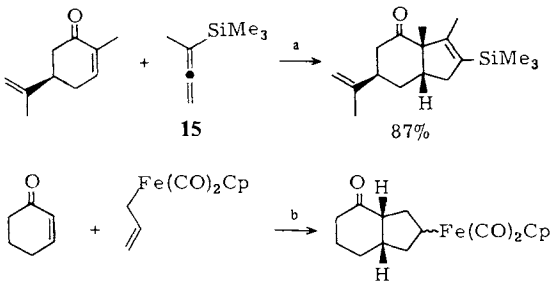
On the other hand, the cyclopropylphosphonium salt **13** adds to enols such as the hydroxymethylene derivative **14** (Scheme 3). This reaction formally represents an addition of type B (Scheme 1) to an electron-rich double bond.[16]



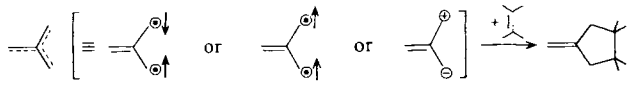
Scheme 3. Reaction conditions: RT, 1-2 d, NaH/hexamethylphosphoric triamide (HMPA).

Metals may play an important role in such reactions. In main-group chemistry, the addition of allenylsilanes (e.g., **15**) to enones, catalyzed by Lewis acids, represents a most unusual cyclopentene annulation (Scheme 4).[17] A transition-metal version using the iron compound **16** proceeds in moderate to low yields.[18] Both reactions exemplify reactions of type A (Scheme 1), where the acceptor is an electron-deficient olefin. All of these cases most likely involve stepwise processes.

An alternative approach makes use of the theoretically interesting trimethylenemethane **17** (Scheme 5).



Scheme 4. Reaction conditions: a) $TiCl_4$, −78°C, 1 h, CH_2Cl_2; b) $AlBr_3$, −78°C, 10 min, CH_2Cl_2, 0°C, 1 h. Cp = η^5-cyclopentadienyl.



Scheme 5. The trimethylenemethane synthon (TMM) **17** and its [3+2] cycloaddition to olefins.

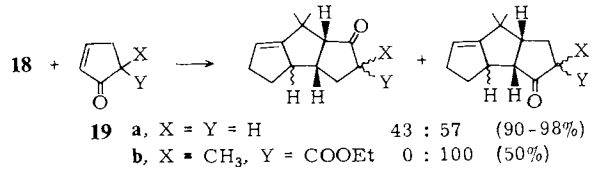
The products from such a cycloaddition also possess a quite useful functionality for further structural elaboration. Attempts to exploit such a route synthetically in the parent system have been frustrated by the lack of suitable methods to generate this reactive intermediate and/or its uncontrolled reactivity.[19] Taming the behavior of trimethylenemethane by forming its iron tricarbonyl complex went overboard in the opposite direction.[20,21] This species is almost devoid of reactivity. The attractiveness of this route continues, however, to lead to studies aimed at defining synthetically viable approaches to the use of trimethylenemethane or its equivalents. This review summarizes these synthetic ventures.

2. Trimethylenemethanes (2-Methylene-1,3-propanediyls)

Whereas capture of trimethylenemethane itself by olefins proceeds in poor yields, the constrained analogue **18** leads to cycloaddition products in good yields (Scheme 6).[22]

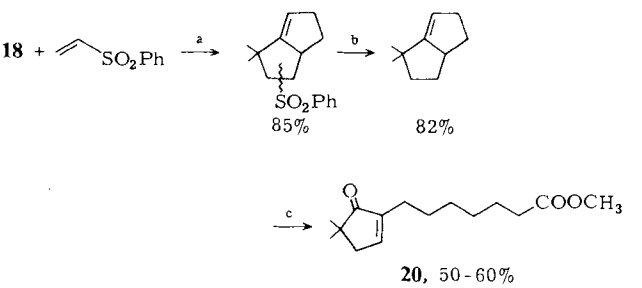
Reaction of **18** with dimethyl acetylenedicarboxylate produces the corresponding cycloadduct in 76% yield. These fused-ring products arise mainly from trapping of the singlet trimethylenemethane since a quite different spectrum of products arises from the triplet.

The diylophilicity of a series of olefins toward the singlet diradical derived from **18** roughly parallels their dienophilicity.[23] It is noteworthy that cyclopentenones **19a** and **19b** react well,[24] even though such acceptors are normally poor dienophiles. Whereas **19a** reacts with poor regioselectivity, the substituted acceptor **19b** reacts with excellent regioselectivity although the yield is lower. Steric factors may account for this selectivity (Scheme 7).



Scheme 7. Reaction conditions: 65–70°C, 1 h.

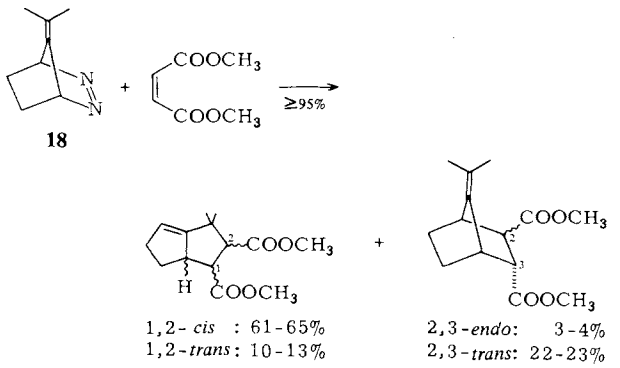
The first step in a synthesis of the dimethylprostaglandin precursor **20** is the intermolecular trapping of **18** with phenyl vinyl sulfone (Scheme 8).[25] Regio- and diastereoselectivity problems, however, limit the usefulness of this intermolecular reaction.



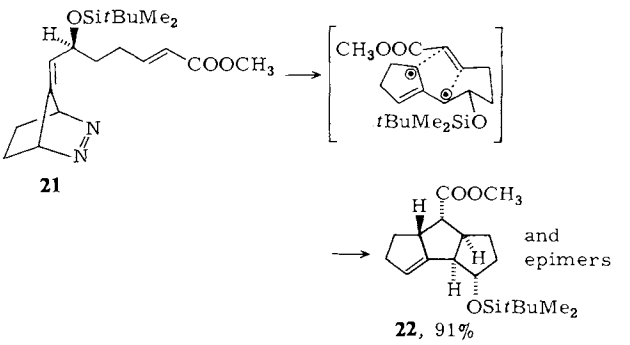
Scheme 8. Reaction conditions: a) Δ, CH_3CN; b) 6% sodium amalgam, Na_2HPO_4, RT, 2.5 h, CH_3OH; c) roughly ten steps.

Intramolecular trapping of such species, on the other hand, proves very useful. For example, thermal (CH_3CN, reflux) or photochemical decomposition of the azo compound **21** leads preferentially (11 : 1 to 26 : 1) to the triquinane **22**,[26] presumably invoking the bias of the siloxy substituent for an equatorial-like orientation in the intermediate diyl (Scheme 9).

Acceptors without an electron-withdrawing group normally afford much lower yields. In a synthesis of (±)-

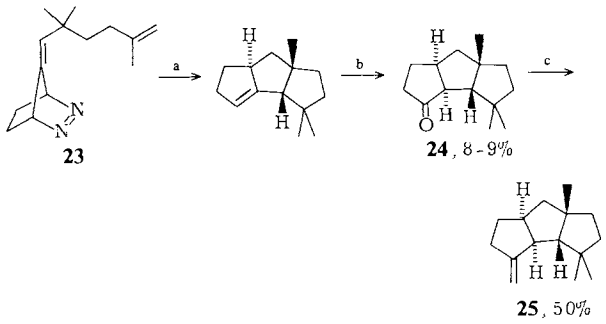


Scheme 6. Reaction conditions: 60°C, 2–8 h, CH_3CN.



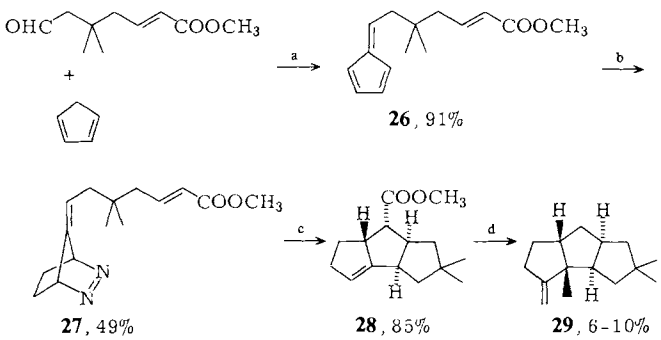
Scheme 9. Reaction conditions: Δ, 2.5 h, CH_3CN.

$\Delta^{9(12)}$-capnellene **25**, the ketone **24** is obtained in only 8–9% overall yield from the diyl precursor **23** (Scheme 10).[24b,27]

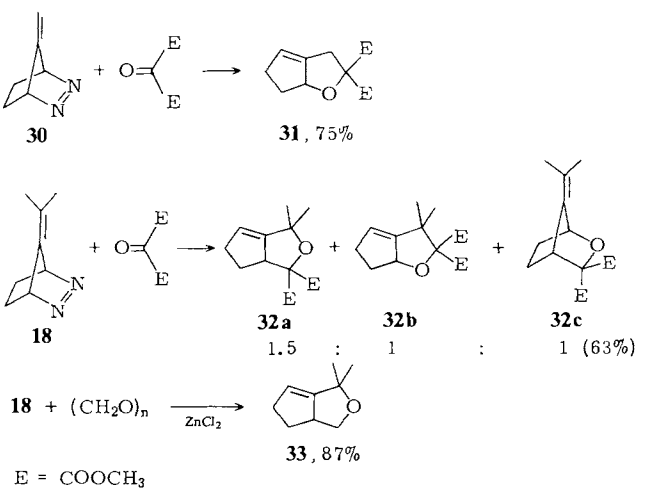


Scheme 10. Synthesis of (±)-$\Delta^{9(12)}$-capnellene **25**. Reaction conditions: a) Δ, 66 h, tetrahydrofuran (THF); b) 1. BH_3·THF, 2. $H_2O_2/OH^{\ominus}$, 3. pyridinium chlorochromate (PCC), diatomaceous earth, c) $Ph_3P{=}CH_2$.

A synthesis of (±)-hirsutene **29** is based upon this synthetic strategy.[28] The requisite diyl precursor **27** arises from the fulvene **26** by a straightforward series of three reactions (Scheme 11). The diyl is trapped by the acrylate group in excellent yield to give the triquinane skeleton **28**, which requires only minor structural adjustments to complete the synthesis.



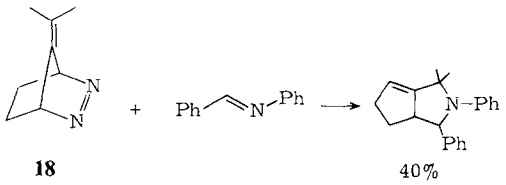
Scheme 11. Synthesis of (±)-hirsutene **29**. Reaction conditions: a) 5–10°C→RT, Et_2NH; b) 1. bis(2,2,2-trichloroethyl) diazodicarboxylate, 0°C; 2. potassium diazodicarboxylate/AcOH; 3. electrolytic deprotection, 4. $K_3Fe(CN)_6$, 0°C; c) Δ, 6 h, CH_3CN; d) eleven steps.



Scheme 12. Addition of 2-alkylidene-1,3-cyclopentanediyls to carbonyl groups.

Multiple bonds involving heteroatoms can also be suitable diylophiles.[29] Reactive carbonyl groups such as that in dimethyl mesoxalate trap the diyl from either **18** or its unsubstituted analogue **30**. The formation of **31** from **30** is in agreement with frontier orbital considerations; however, steric effects apparently outweigh this electronic bias such that **32a** is predominantly formed from the precursor **18**. With a less reactive carbonyl partner, addition of a Lewis acid promotes cycloaddition; for example, in the presence of zinc dichloride, formaldehyde gives an excellent yield of **33**(Scheme 12).

Even an unsubstituted imine may serve as a diylophile, although the yield is only modest (Scheme 13).

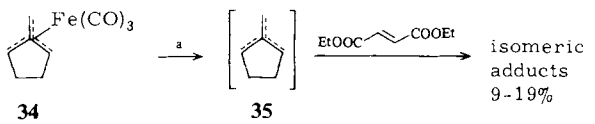


Scheme 13. Addition of a 2-alkylidene-1,3-cyclopentanediyl to benzylideneaniline.

The possible expansion of the use of selective trimethylenemethane (TMM) systems appears promising. The seed for adaptations of strategies based upon such species is planted in the form of intramolecular variants. The structural requirements for good yields of trapping products with high regio- and stereocontrol and the synthetic routes to appropriate precursors appear to be current limitations.[30]

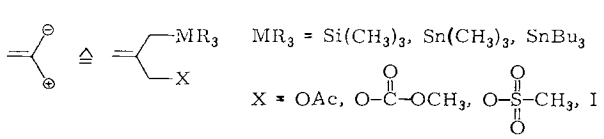
3. Transition-Metal-Substituted Intermediates: Use of 1,3-Bifunctional Conjunctive Reagents

The excitement of isolating stable TMM–metal complexes subsequently vanished as a result of their poor reactivity in cycloadditions. For example, whereas generation of the diyl **35** from the azo precursor **30** led to excellent trapping yields, the liberation of **35** from **34** led to cycloaddition yields of only 9–19% (Scheme 14).[20]



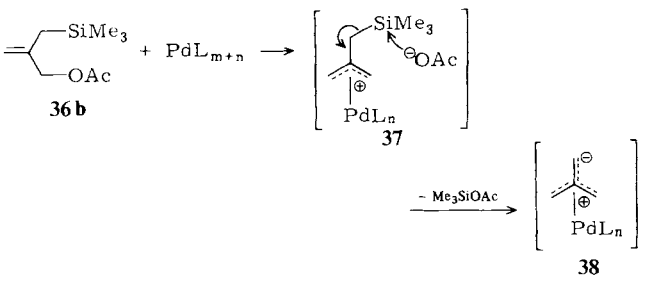
Scheme 14. Reaction conditions: a) $Me_3N^{\ominus}$–O°, 60°C, C_6H_6.

In considering a zwitterion equivalent of TMM, synthons for a carbanion and carbocation that do not self-annihilate are required. Silyl and stannyl groups serve as carbanion equivalents; carboxylate as well as more reactive leaving groups such as methanesulfonate and halide may serve as carbocation equivalents (Scheme 15).



Scheme 15. TMM equivalents.

The mutual compatibility of such synthons translates into a lack of reactivity and establishes the need for an activator. Palladium(0) complexes serve as such activators because they can readily effect the ionization of even poor leaving groups.[31] In the resulting π-allylpalladium intermediate **37**, the C-Si bond is weakened by the proximal positive charge, resulting in formation of the palladium complex of TMM **38** as a fleeting reactive intermediate.

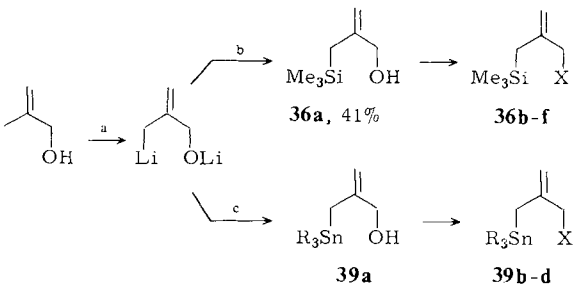


36b **37** **38**

Scheme 16. Activation of the TMM equivalent **36b** by complex formation with palladium(0).

3.1. Preparation of Conjunctive Reagents

The synthesis of species such as those shown in Scheme 15 proceeds most directly by lithiation and subsequent silylation or stannylation of methallyl alcohol according to Scheme 17.[32]

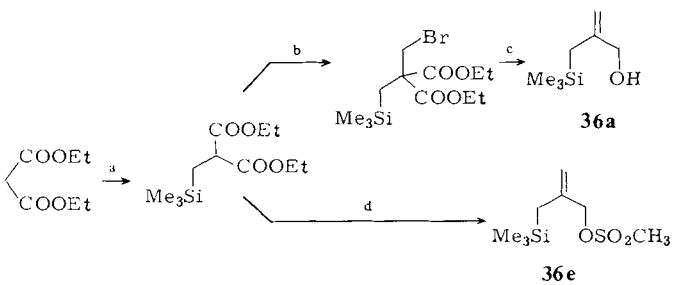


36: **b**, X = OAc; **c**, X = $OCOOCH_3$; **d**, X = OCOPh; **e**, X = OSO_2CH_3; **f**, X = I

39: **b**, R = Me, X = OAc; **c**, R = Bu, X = OAc; **d**, R = Bu, X = OSO_2CH_3

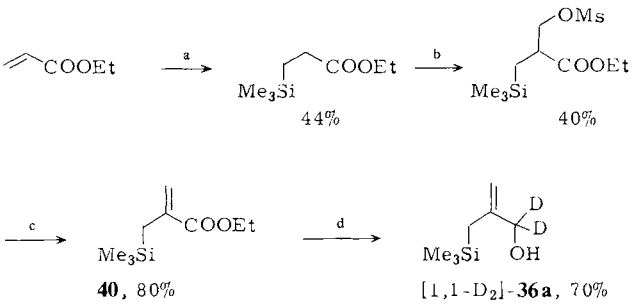
Scheme 17. Reaction conditions: a) 2 BuLi/tetramethylethylenediamine (TMEDA), 0°C, 4 h; RT, 40 h, hexane/Et_2O/THF; b) Me_3SiCl, $H_3O^{\oplus}$; c) R_3SnCl, $H_3O^{\oplus}$.

Alternatively, two routes from diethyl malonate using the expensive (chloromethyl)- or (iodomethyl)trimethylsilane also provide reagents of type **36** (Scheme 18).[33,34]



Scheme 18. Reaction conditions: a) 1. NaOEt/EtOH, Δ; 2. Me_3SiCH_2I or Me_3SiCH_2Cl, Δ; b) 1. NaH, C_6H_6; 2. CH_2Br_2, Δ; c) 1. KOH/H_2O, Δ, EtOH; 2. $LiAlH_4$; d) 1. NaH/$LiAlH_4$, Δ, THF; 2. CH_3SO_2Cl/collidine, 0°C, dimethylformamide (DMF).

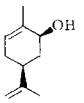
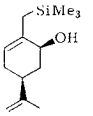
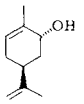
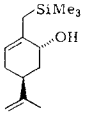
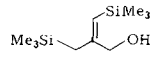
Ethyl acrylate also serves as a readily available starting material in a route where the silicon source is again the inexpensive chlorotrimethylsilane. Scheme 19 outlines this route to a 1,1-dideutero analogue of **36a**, although it can also be used to prepare **36a** itself.[35]



Scheme 19. Reaction conditions: a) Me_3SiCl/Li; b) 1. $LiN(iPr)_2$, THF; 2. $(CH_2O)_n$, 3. CH_3SO_2Cl/Et_3N; c) 1,8-diazabicyclo[5.4.0]undec-7-ene (DBU), RT, Et_2O; d) $LiAlD_4$, −25°C, Et_2O.

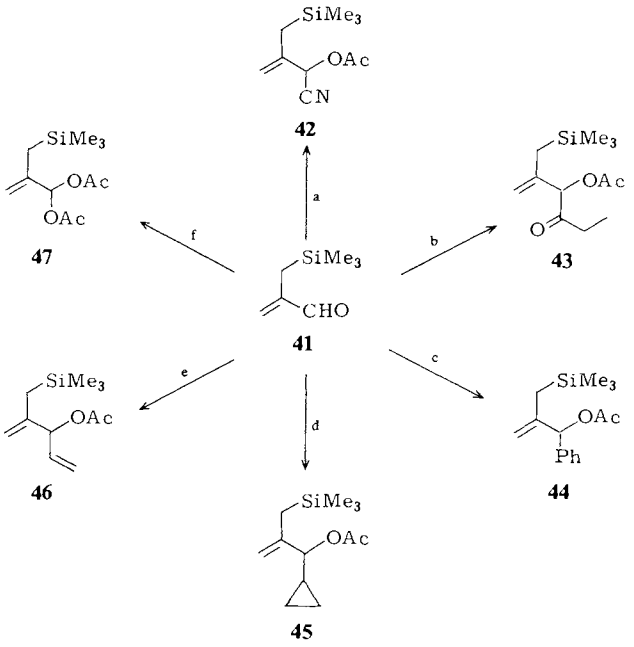
The direct metalation approach (cf. Scheme 17) serves as a general route from readily available alcohols. As shown in Table 2, a number of alcohols can be silylated at the methyl group under these conditions. Although this direct approach is very effective, the presence of functionality is limited by the use of *n*-butyllithium.

Table 2. *C*-Silylation of dilithiated methallyl alcohols.

No.	Alcohol	Silylated product	Yield [%]	Ref.
1			67	[36]
2			75	[37]
3			37	[38]
4			>51	[39]
5			98	[39]

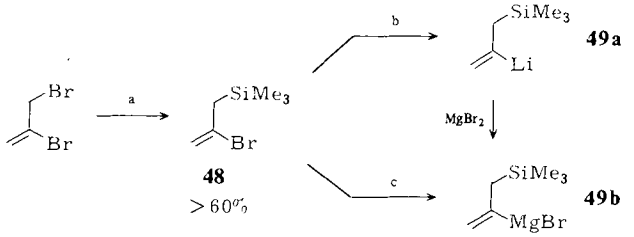
The ready availability of the aldehyde **41** by Swern oxidation (dimethylsulfoxide (DMSO)/oxalyl chloride) of the alcohol **36a** opens a very general approach to substituted TMM precursors (**42**–**47**) as illustrated in Scheme 20.[38,40] The acceptor conjunctive reagent **41** opens the entire arena of organometallics as possible reaction partners.

A donor conjunctive reagent permits the expansion of the reaction partners to carbonyl compounds. The isopropenyl bromide **48**,[41] easily derived from commercially available 2,3-dibromopropene, undergoes smooth halogen-



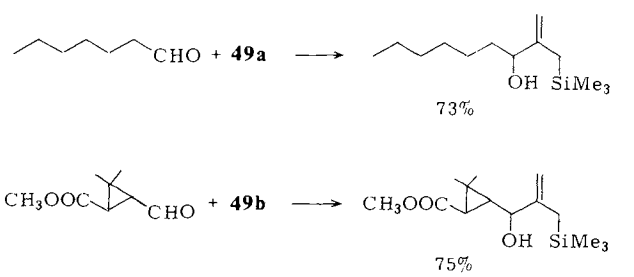
Scheme 20. Preparation of substituted 1,3-bifunctional conjunctive reagents from the aldehyde **41**. a) 1. Me_3SiCN, ZnI_2, neat, 83%; 2. Ac_2O, 9 mol-% $FeCl_3$, neat, 0°C, 81%. b) 1. $EtCH(SCH_3)_2/nBuLi$, THF, −78→0°C, 65%; 2. Ac_2O/pyridine, 4-dimethylaminopyridine (DMAP), RT, 95%; 3. $AgNO_3$, 95% $EtOH/H_2O$, 50°C, 83%. c) 1. PhLi, Et_2O, −78→20°C, 82%; 2. AcCl/pyridine, DMAP, CH_2Cl_2, 90%. d) 1. (*cyclo*-C_3H_5)MgBr, THF, 89%; 2. AcCl/pyridine, DMAP, CH_2Cl_2, 72%. e) 1. $LiCHCH_2$, Et_2O, −60→20°C; 2. AcCl, DMAP, CH_2Cl_2, 73% overall. f) Ac_2O, 5 mol-% $FeCl_3$, neat, 0°C, 71%.

metal exchange with *tert*-butyllithium to give **49a**. Addition of anhydrous magnesium bromide produces the Grignard reagent **49b** (Scheme 21).



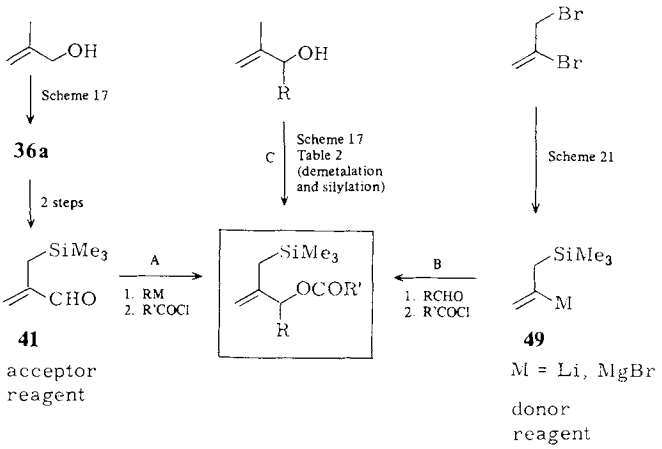
Scheme 21. Reaction conditions: a) (2 Me_3SiLi + 3 CuCN), 0°C, THF/HMPA or 1. $HSiCl_3/Et_3N$, CuCl, 2. 3 CH_3MgBr, Et_2O; b) *t*BuLi, −78°C, Et_2O; c) Mg turnings.

The vinyllithium reagent **49a** adds easily to aldehydes or ketones, e.g. to heptanal (Scheme 22).[38] The Grignard reagent **49b** shows good chemoselectivity in its additions to aldehydes and ketones (Scheme 22).[42]



Scheme 22. Examples of the use of **49a** and **49b**.

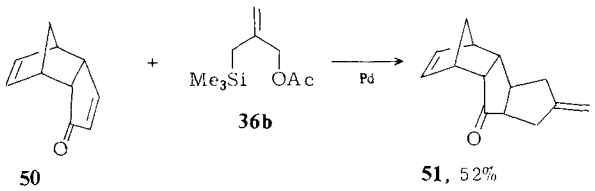
A number of approaches exist to create the 1,3-bifunctional units required for cycloaddition. These are summarized in Scheme 23. Besides the direct metalation (pathway C), the most useful general approaches involve the employment of 2-[(trimethylsilyl)methyl]propenal **41** (pathway A) or of 1-[(trimethylsilyl)methyl]ethenyllithium **49a** or 1-[(trimethylsilyl)methyl]ethenylmagnesium bromide **49b** (pathway B).



Scheme 23. Main synthetic pathways (A, B, and C) to 1,3-bifunctional conjunctive reagents of type **42**–**47**.

3.2. Cycloadditions with the Unsubstituted TMM System

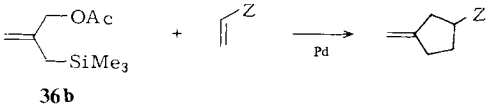
The lack of any information regarding the feasibility or type of reaction to be expected from a palladium complex of TMM led to the use of the bifunctional trapping agent **50**, which possesses both an electron-rich and an electron-poor olefinic bond. Heating a mixture of this dienone and the silyl-acetate **36b** in the presence of a catalytic amount of a palladium(0) complex leads to clean cycloaddition to the electron-deficient double bond to give adduct **51** (Scheme 24).[43] Products derived from attack at the electron-rich double bond are not observed.



Scheme 24. Reaction conditions: ≈5 mol-% $[(Ph_3P)_4Pd]$, ≈2.5 mol-% $Ph_2PCH_2CH_2PPh_2$ (DPPE), Δ, THF.

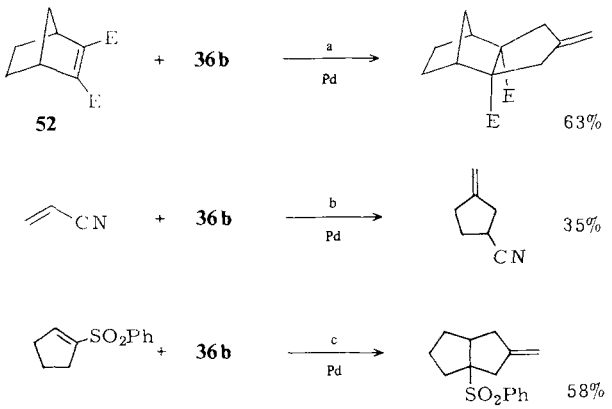
The reaction is generalized in Scheme 25. The acceptor requires an electron-withdrawing group—similarly to a dienophile in a Diels-Alder reaction.

Suitable activators on the olefinic bond that have been tested to date include an ester,[43] a cyano,[43,44] and a sul-



Scheme 25. Z = electron-withdrawing group.

fone group (Scheme 26)[43,44] in addition to a ketone carbonyl group (Scheme 24). Any electron-withdrawing group that activates an olefin in terms of a Michael reaction should function similarly here. As in the case of the Diels-Alder reaction, the use of 2-cycloalkenones leads to poor yields. However, 2-cyclopentenones (e.g., **50** in Scheme 24) are an exception.



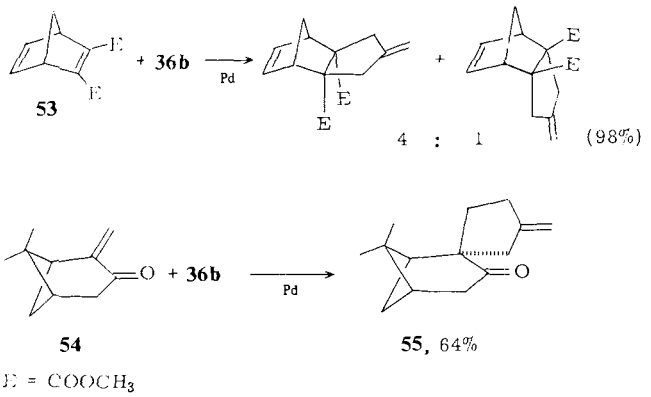
E = $COOCH_3$

Scheme 26. Reaction conditions: a) $(iPrO)_3P/Pd(OAc)_2$ (6 : 1), Δ, 3.5 h, THF; b) 6 mol-% $[(Ph_3P)_4Pd]$, 60 °C, 6 d, toluene; c) ≈5 mol-% $[(Ph_3P)_4Pd]$, ≈1.5 mol-% DPPE, Δ, 40 h, THF.

The choice of catalyst can substantially affect the yield of this process. An excellent catalyst arises by simply mixing palladium acetate with 6–8 molar equivalents of triisopropyl phosphite, the latter serving to both reduce the palladium(II) and ligate the formed palladium(0); the catalyst may be formulated as $[\{(iPrO)_3P\}_nPd]$ where n is probably 3 or 4.[39,45] This catalyst increases the yield of the cycloaddition of **36b** to the diester **53** from 78 to 98%[46] and promotes formation of the cycloadduct **55** in 64% yield from enone **54**[47] (Scheme 27). While the turnover numbers have not been determined, they are probably high. For a typical laboratory-scale reaction, 0.1–10 mol-% of catalyst, depending on the scale of the reaction (the larger the scale, the smaller the amount of catalyst), has been employed. For larger-scale reactions, even smaller amounts of catalyst will probably be satisfactory.

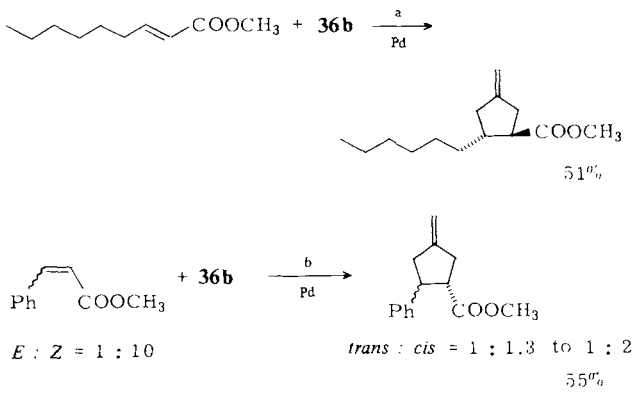
The tin analogues of **36b**, the esters **39b** and **39c**, also participate in these cycloadditions.[48,49] In contrast to the normal observation that the tin derivative improves the reaction, the higher reactivity of the C–Sn bond leads to lower yields due to decomposition of the conjunctive reagent **39** competing with the cycloaddition.

The stereoselectivity of the cycloaddition normally is very good. The geometry of (*E*)-olefins is retained in the product; however, that of (*Z*)-olefins is partly lost (Scheme 28).[43,44]



E = $COOCH_3$

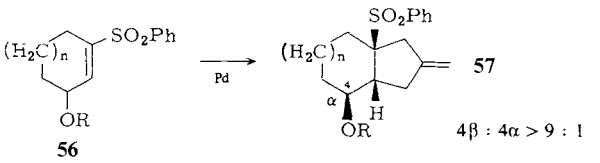
Scheme 27. Catalyst: $[\{(iPrO)_3P\}_nPd]$.



Scheme 28. Reaction conditions: a) $[(Ph_3P)_4Pd]$/DPPE, Δ, 12 h, THF; b) as in a), but only 3 h.

Diastereoselectivity also tends to be high. For example, acceptors **50** (Scheme 24), **52** (Scheme 26), and **54** (Scheme 27) form only one diastereomer, the TMM unit adding to the less-hindered face. Some loss of selectivity occurs in the case at the norbornadiene **53** (Scheme 27), which may arise from coordination of palladium to the second double bond, although simple steric arguments cannot be ruled out.[43,50]

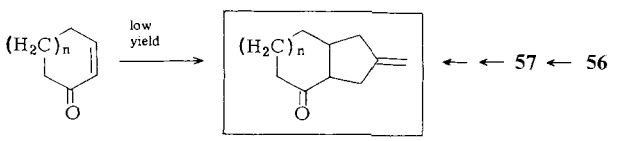
Diastereoselectivity with sulfone acceptors has particular importance because of the versatility offered by the adducts. Simple substituents bonded through oxygen effect good selectivity in both six- and seven-membered rings (Scheme 29).[51]



n = 1, R = $SitBuMe_2$: 87%
n = 2, R = CH_2OCH_3 : 93%

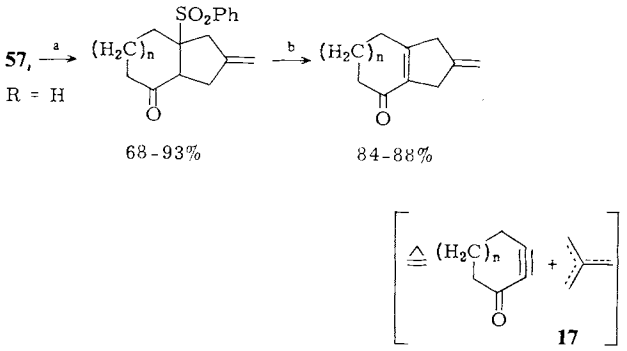
Scheme 29. Reaction conditions: $[\{(iPrO)_3P\}_nPd]$, toluene.

These adducts serve as the equivalents of stereocontrolled addition to 2-cyclohexenone and 2-cycloheptenone (two acceptors that react poorly or not at all) because of the ease of desulfonylation (Scheme 30).



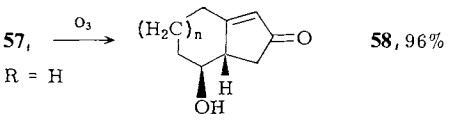
Scheme 30. n = 1, 2.

Alternatively, the leaving group ability of the sulfone transforms this reaction into an equivalent of addition to the hypothetical 2-cycloalkynones (Scheme 31).



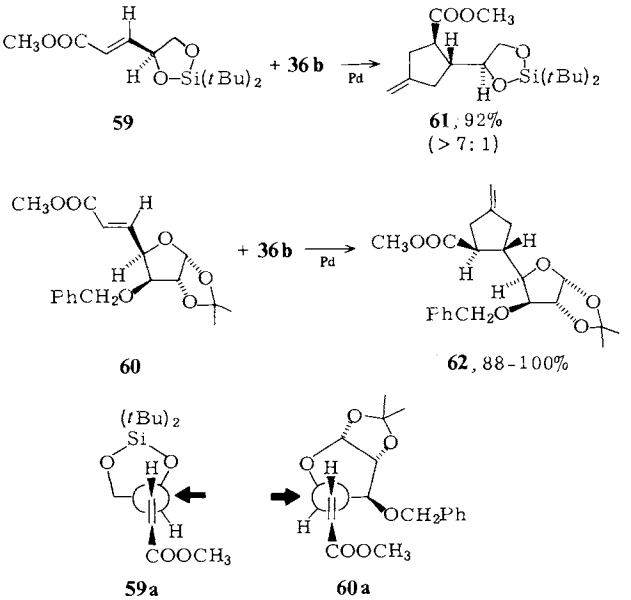
Scheme 31. Reaction conditions: a) DMSO/$(COCl)_2$; b) Al_2O_3.

A most useful variant of this sequence arises by ozonolysis of these adducts to form the cyclopentenones **58** (Scheme 32), which corresponds to a useful cyclopentenone annulation.



Scheme 32. Cyclopentenone annulation.

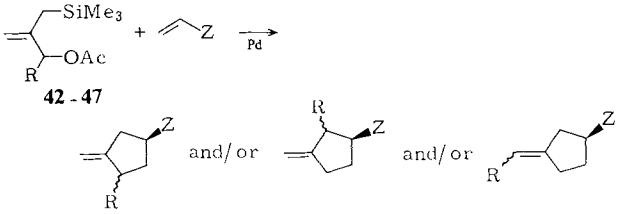
Acyclic systems also show excellent diastereoselectivity. Reaction of the acrylate **59** occurs with >7:1 diastereoselectivity, and the more elaborate acrylate **60** gave only one detectable diastereomer (Scheme 33).[47] Minimization of dipole-dipole and steric interactions suggests conformers **59a** and **60a** should be favored. Independent verification of the stereochemistry in the case of **61** supports this contention.



Scheme 33. Catalyst: $[\{(iPrO)_3P\}_nPd]$.

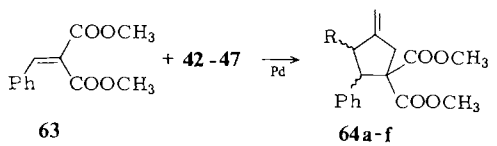
3.3. Cycloadditions with Substituted TMM Systems

The generality of this cycloaddition approach depends upon the range of donors (i.e., substituted TMM precursors) as well as acceptors. Questions of regiochemistry immediately arise since the symmetry of the parent system is destroyed. Combining the three possible regioisomers with the two diastereomers that are possible in each case leads to a total of six possible products (Scheme 34).



Scheme 34. Z = electron-withdrawing group.

Dimethyl benzylidenemalonate **63** serves as a standard acceptor to test the compatibility of various substituents as well as the regioselectivity of the reaction. Conjunctive reagents **42–47** all condense with this acceptor if $[(Ph_3P)_4Pd]$ or, more commonly, $[\{(iPrO)_3P\}_{3-4}Pd]$ is used as catalyst, preferably in hot dioxane (Scheme 35).[40] The compatibility of reactive functional groups, such as cyano, keto, and ester groups, and the lack of isomerization of the double bond into the thermodynamically more stable endocyclic conjugated position confirms the mildness of the reaction conditions. The case of the *gem*-diacetate precursor **47** is particularly striking since the product **64f**, an allylic acetate, is potentially very labile toward Pd^0 catalysts.

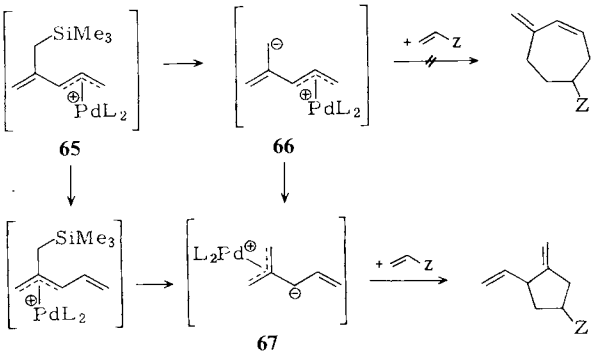


Scheme 35. Synthesis of **64a–f**.

Reagent	Product	R	Yield [%]	
42	**64a**	CN	54	*trans*
43	**64b**	COEt	59	*trans*
44	**64c**	Ph		*cis + trans*
45	**64d**	cyclopropyl	61	*cis + trans*
46	**64e**	$CH{=}CH_2$	89	*cis + trans*
47	**64f**	OAc	86	*cis + trans*

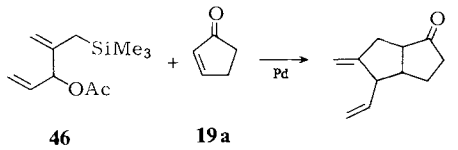
The surprising formation of only five-membered-ring products with the vinyl derivative **46** suggests that the kinetically favored π-allylpalladium cation **65**, which should produce seven-membered-ring products via the zwitterion **66**, is not a product-determining intermediate (Scheme 36).[38,40] Eventually, all intermediates funnel through **67**, which is presumably the product-determining intermediate.

As in the parent cases, the choice of catalyst can improve the reactions. The yield from the cycloaddition of **46** with 2-cyclopentenone **19a** increases from 50% to 60%



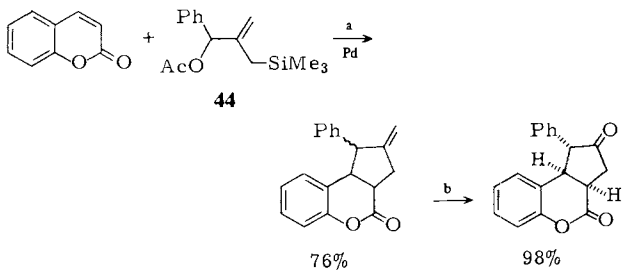
Scheme 36. Z = electron-withdrawing group.

upon switching from $[(Ph_3P)_4Pd]$ to $[\{(iPrO)_3P\}_{3-4}Pd]$ as catalyst (Scheme 37).[38,40]



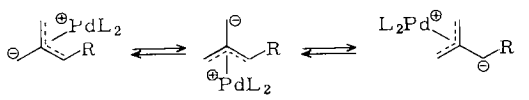
Scheme 37. For catalysts and yields see text.

In all cases (Schemes 35 and 37), a single regioisomer results. The TMM precursors bearing an electron-withdrawing group (**42** and **43**) also give only single stereoisomers (**64a** and **64b**, respectively), which are assigned the *trans* geometry. All the remaining cases produce mixtures. Since, synthetically, the exocyclic methylene group will frequently be oxidatively cleaved to give the ketone, which can be readily epimerized, the stereoselectivity problem is not severe. For example, the adduct of **44** and coumarin, which is a 70 : 30 stereoisomeric mixture, undergoes ozonolysis to afford a single cyclopentanone (Scheme 38).[39,40]



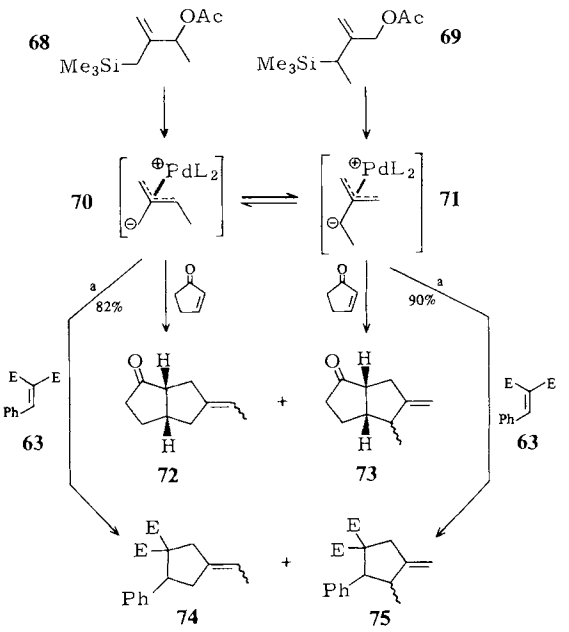
Scheme 38. Reaction conditions: a) $[(Ph_3P)_4Pd]$, Δ, toluene; b) 1. ozone, 2. thin layer chromatography.

Does the regioselectivity derive from the regioselective reaction of the TMM precursor? Assuming an η^3 structure for the TMM-palladium complex (Scheme 39), the question may be restated as follows. Do the unsymmetrical TMM complexes equilibrate faster than they undergo cycloaddition?



Scheme 39. η^3-Structure of the TMM-palladium complex.

The isomeric methyl-TMM precursors **68** and **69** allow such a concept to be tested since **68** should kinetically generate the complex **70** and **69** the complex **71** (Scheme 40).[52] With a less reactive trap, such as 2-cyclopentenone, both precursors give identical product mixtures, in which adduct **73** greatly predominates over adduct **72** (> 20 : 1).[36] On the other hand, a much more reactive trap, such as dimethyl benzylidenemalonate **63**, leads to some trapping before complete equilibration. Thus, a slightly larger amount of adduct **74** is formed from **68** (**74** : **75** = 1 : 3.3) than from **69** (**74** : **75** = 1 : 6.7),[52] although in both cases, adducts derived from **71** are favored (cf. Section 5). Thus, the methyl analogue **68** follows the same trend as all the other derivatives in terms of regioselectivity. The results indicate that the regioselectivity of the cycloaddition is largely independent of the regiochemistry of the precursors. In choosing the TMM precursor, therefore, the selection need only be determined by synthetic availability.

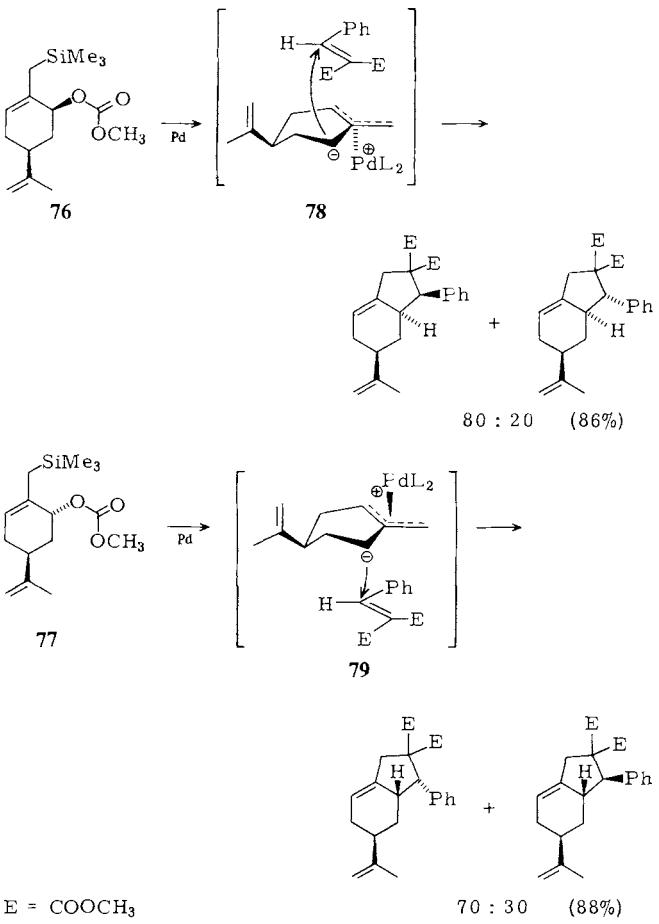


Scheme 40. Test of the regioselectivity of Pd^0-catalyzed cycloadditions using **68** and **69**. In **73**, the ratio α : β is 1 : 1, in **75**, 1 : 1.4. Reaction conditions: a) $[(Ph_3P)_4Pd]$, Δ, THF.

Reactants	Products	Yield [%]	Product ratios
68 + cyclopentenone	**72** + **73**		< 5 : > 95
69 + cyclopentenone	**72** + **73**		< 5 : > 95
68 + **63**	**74** + **75**	82	23 : 77
69 + **63**	**74** + **75**	90	13 : 87

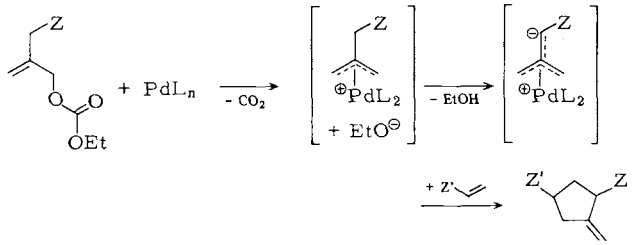
The substituted TMM systems allow examination of the stereochemistry with respect to the TMM unit. As shown in Scheme 41, the reactions are regioselective and *cis/trans* stereoselective, but, as expected, complete racemization occurs.[53] Surprisingly, the reaction proceeds with overall net retention of the *cis* and *trans* configurations of **76** and **77**, respectively—an observation that suggests that the olefin approaches distal to the metal as depicted in **78** and **79**, in contrast to almost all metal-catalyzed olefin oligomerizations. Furthermore, the reaction shows an "endo-type" selectivity—a further analogy to the Diels-Alder

reaction. Unlike the Diels-Alder reaction, minimization of steric interactions in an end-on approach (as depicted in **78** and **79**) accounts for this observation. The excellent regioselectivity combined with the diastereocontrol makes this annulation approach very useful.



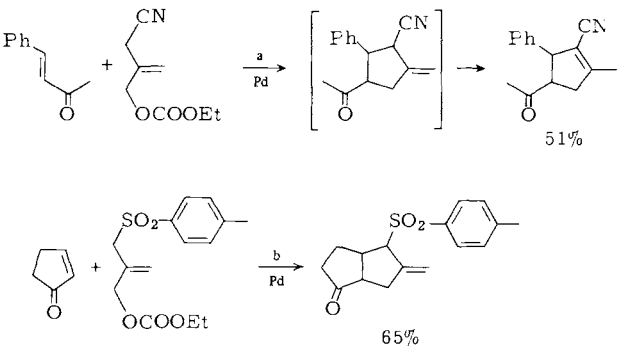
Scheme 41. Reaction conditions: [$(Ph_3P)_4Pd$], Δ, THF. Racemates are formed.

In the special case of substituents Z that are good anion-stabilizing groups, a non-silyl TMM derivative also serves as a suitable substrate (Scheme 42).



Scheme 42. Z, Z' = electron-withdrawing groups.

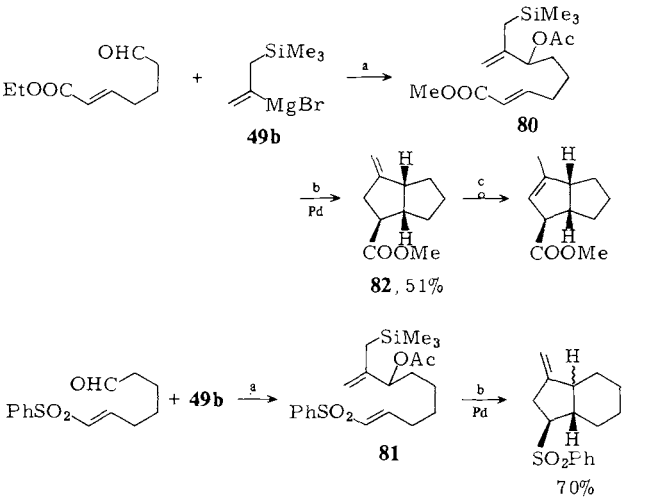
A leaving group that can generate a sufficiently strong base effects proton abstraction to create the TMM analogue in the special case when the anion-stabilizing group is on the carbon from which the proton must be removed. Two groups have met this requirement so far, cyano and sulfonyl (Scheme 43).[54]



Scheme 43. Reaction conditions: a) [$Pd_2(dba)_3(CHCl_3)$], DPPE, Δ, 1 h, THF; b) as in a) but 10 h. dba = dibenzylideneacetone [31c].

3.4. Intramolecular Cycloadditions

The extraordinary usefulness of the intramolecular Diels-Alder reaction encourages exploration of its [3+2] counterpart. The donor conjunctive reagent **49** (cf. Scheme 21) provides ready access to the requisite substrates as shown in Scheme 44.[41] For the intramolecular cycloaddition, a sterically less-encumbered catalyst, $(dppe)_2Pd$, is preferred. Heating **80** and **81** in the presence of this catalyst in refluxing THF or 1,2-dimethoxyethane (DME) results in elimination of trimethylsilyl acetate to give the bicyclo[3.3.0]octane and bicyclo[4.3.0]nonane skeletons, respectively. The acid-catalyzed isomerization of the diastereomerically pure bicyclic compound **82** illustrates one possible reaction of the exocyclic methylene group.



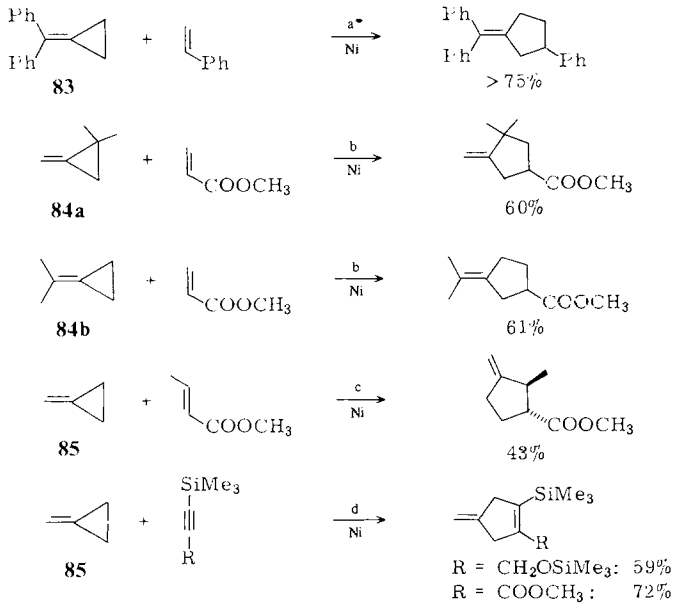
Scheme 44. Reaction conditions: a) 1. Grignard reaction, 2. AcCl/pyridine, DMAP; b) [$(Ph_3P)_4Pd$], DPPE, Δ, THF or DME; c) TosOH, 55°C, $CHCl_3$.

4. The Methylenecyclopropane Strategy

In spite of the thermal isomerizations of methylene cyclopropanes, which proceed through trimethylenemethane,[19,55] this reactive intermediate has seldom been trapped from such precursors. In the special case of 5-alkylidenebicyclo[2.1.0]pentane, trapping does occur at low temperatures; nevertheless, such methods appear unpromising for synthetic purposes. The possibility that tran-

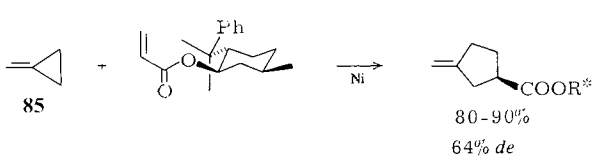
sition metals may facilitate cycloadditions of methylenecyclopropane arises from the observation that disrotatory opening of these reactive strained rings occurs smoothly under the influence of diiron nonacarbonyl to give isolable trimethylenemethane iron tricarbonyl complexes.[56–58] A molybdenum complex forms in like fashion.[59] As in the earlier work on such complexes, further reactions of such TMM derivatives have not been reported.

On the other hand, low-valent nickel catalyzes the codimerization of methylenecyclopropanes with both electron-rich[60] and electron-poor olefins (Scheme 45).[60–64] In addition, electron-rich and electron-poor alkynes codimerize in the presence of such catalysts to form 4-methylenecyclopentenes.[64b] For the parent system, the yields are acceptable only for electron-poor acceptors. Methylenecyclopropanes with two substituents on the methylene group give satisfactory yields with both types of olefins. High regioselectivity accompanies these reactions and indicates that TMM species are not likely intermediates.



Scheme 45. Reaction conditions: a) $Ni(cod)_2$, 40–60 °C, toluene; b) $Ni(acrylonitrile)_2$, 60 °C, 48 h, reaction bomb tube; c) $Ni(cod)_2$, 35 °C, 20 h; d) $Ni(cod)_2$/TOPP 1:1, 80 °C, 5–8 h, autoclave. cod = 1,5-cyclooctadiene; TOPP = tris(*o*-biphenylyl)phosphite.

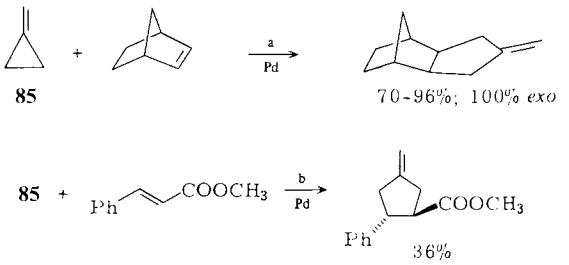
The possibility for asymmetric induction in such a codimerization where both acceptor and donor are simultaneously bonded to the metal appears high as reflected in a 64% diastereomeric excess in the simple reaction of 8-phenylmenthyl acrylate (Scheme 46).[65a] The absolute configuration has not been established but is assigned by analogy to the Diels-Alder reaction with the same acrylate as well as to organocuprate additions.[65b] Unfortunately, only very



Scheme 46. R* = (1*R*,3*R*,4*S*)-8-phenylmenthyl. Reaction conditions: $Ni(cod)_2$, RT, 4 h, toluene.

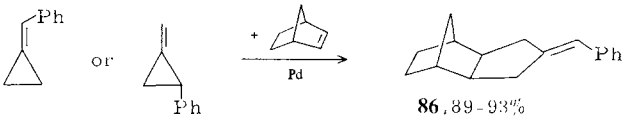
simple acceptors have been used to date. The difficulty in preparing and handling the catalysts constitutes a drawback to this approach.

Palladium catalyzes similar reactions, as is shown in Scheme 47 by the codimerization of **85** with both norbornene[66,67] and methyl cinnamate.[67,68] The best catalysts are trialkylphosphane-palladium(0) complexes such as $[(iPr_3P)_nPd]$ generated from palladium bis(acetylacetonate), bis(dibenzylideneacetone)palladium, or (η^3-allyl)(η^5-cyclopentadienyl)palladium.



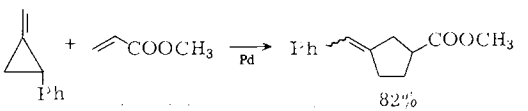
Scheme 47. Reaction conditions: a) $Pd(acac)_2/iPr_3P/Et_2AlOEt$ (1:1:2), 100 °C, 1 h, C_6H_6, reaction bomb tube; b) [(allyl)CpPd]/iPr_3P (1:1), 100–140 °C, toluene, reaction bomb tube. acac = acetylacetonato.

Unlike the nickel-catalyzed reactions, the regioselectivity appears to be independent of the structure of the starting methylenecyclopropane.[69] In the codimerization of norbornene with either of the phenyl-substituted compounds in Scheme 48, the same product mixture, with **86** as the predominant product, resulted.



Scheme 48. Reaction conditions: $(dba)_2Pd/iPr_3P$ (1:1), 70–90 °C.

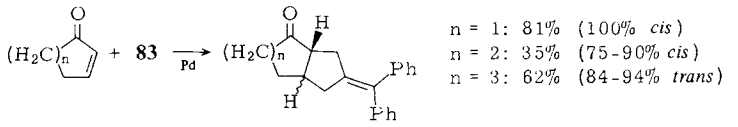
1-Methylene-2-phenylcyclopropane reacts with methyl acrylate to give a single regioisomer bearing the phenyl group only on the exocyclic methylene carbon (Scheme 49).[70] It should be noted at this point that the regiochemistry of Pd-catalyzed additions of the 1,3-bifunctional silylacetate conjunctive reagents is totally different from that of the methylenecyclopropanes.



Scheme 49. Reaction conditions: $(dba)_2Pd/iPr_3P$ (1:1).

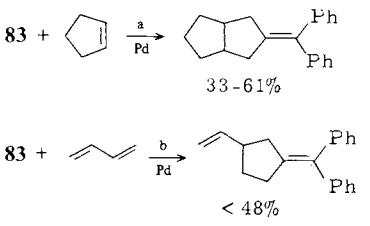
The efficiency of these cycloadditions appears highly dependent upon the nature of the substituents in the methylenecyclopropane with the order being approximately vinyl > alkyl > H > aryl. Methylenecyclopropane adds to simple acrylates but very few other acceptors have been reported. Thus, 2-cycloalkenones are particularly poor acceptors. For example, the use of 2-cyclohexenone leads to alkylation rather than cycloaddition.[71] On the other hand, diphenylmethylenecyclopropane **83** reacts with 2-cycloal-

kenones to give regioisomerically pure products (Scheme 50).[72]



Scheme 50. Reaction conditions: [(allyl)CpPd]/iPr$_3$P (1:1), 80–130°C, toluene.

The diphenyl derivative **83** also reacts with a variety of simple electron-rich olefins including 1-butene and cyclopentene, as well as with conjugated olefins like styrene and 1,3-butadiene. Examples are shown in Scheme 51.

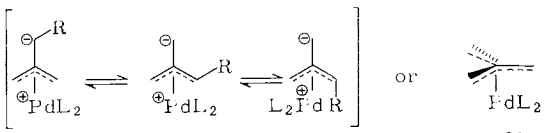


Scheme 51. Reaction conditions: a) [(allyl)CpPd]/iPr$_3$P (1:1), 130°C, 6 h, toluene; b) as in a) but 120°C, 8 h.

The location of the substituents also appears to be important. Of the *gem*-dimethyl analogues **84a** and **84b** (Scheme 45), the isopropylidene derivative **84b** undergoes codimerization with norbornene, whereas the methylene derivative **84a** merely isomerizes. In general, 2-alkyl- and 2,3-dialkyl-1-methylenecyclopropanes undergo codimerization either poorly or not at all, whereas the alkylidenecyclopropanes react smoothly. The exception is the series of phenyl-substituted derivatives, which undergo cycloaddition regardless of where the substituent is located.

5. Mechanisms

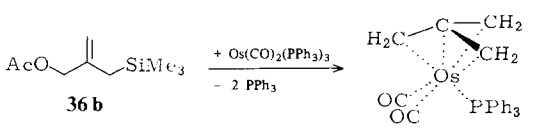
The cycloadditions of 2-[(trimethylsilyl)methyl]allyl esters catalyzed by palladium(0) appear to be in accord with polar (η^3-TMM)PdL_2 species such as **87a–c** as intermediates (Scheme 52).[35,73] The alternative η^4-coordinated form **88** must also be considered (cf. Scheme 39).



87a **87b** **87c** **88**

Scheme 52. Possible structures of TMM-Pd complexes.

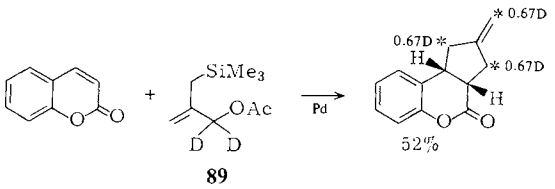
Support for the formation of an η^3- or η^4-TMM complex, is provided by the isolation of a TMM–metal complex from the silyl-acetate 1,3-bifunctional reagents in the case of osmium (Scheme 53) and iridium.[74]



36b

Scheme 53. An (η^4-TMM)-Os complex.

Deuterium labeling studies using **89** reveal complete scrambling of the label in the cycloaddition with coumarin (Scheme 54).[35,50]

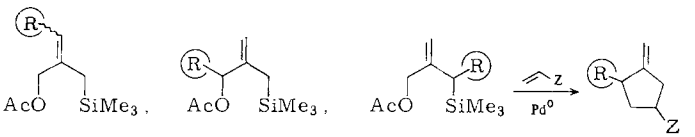


89

Scheme 54. Reaction conditions: 5 mol-% [(Ph$_3$P)$_4$Pd], 2 mol-% DPPE, Δ, THF.

The symmetry of the intermediate demanded by this result would be in accord with either rapid equilibration among **87a–c** or the η^4 structure **88**. A decision in favor of the η^3 structure **87** derives from the lack of any deuterium scrambling in reactions of **89** with carbon acids in the presence of palladium catalysts—clearly indicating the kinetic generation of an η^3 species. Furthermore, the degree of isomerization of substituted TMM-Pd conjunctive reagents in the cycloaddition reaction depends upon the nature of the acceptor. Whereas the two methyl-substituted TMM precursors **68** and **69** give the same product mixture with 2-cyclopentenone (see Section 3.3),[36,52] the more reactive trapping agent dimethyl benzylidenemalonate **63** leads to only partial isomerization (Scheme 40). That a larger amount of **74** is formed from **68** than from **69** is consistent with trapping of **70** being competitive with its isomerization.

The regioselectivity of the reactions is remarkable. All substituents tested to date, be they electron donating or electron withdrawing, end up preferentially at the carbon in the product that becomes bonded to the β carbon of the acceptor (Scheme 55). **87a** (cf. Scheme 52) thus represents the reactive form regardless of the electronic character of the R group.

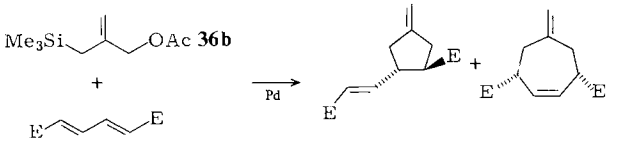


Scheme 55. Regioselectivity of [3+2] cycloadditions.

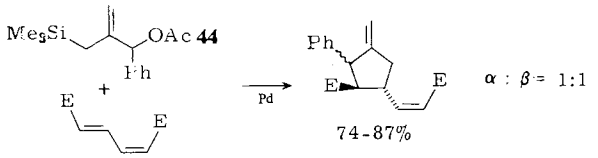
Calculations support these conclusions.[75,76] The η^3 structures **87a–c** are calculated to be more stable than the η^4 structure **88**. Surprisingly, **87a** is calculated to be more stable than **87b** or **87c** regardless of the substituent. It is obvious that electron-withdrawing groups such as cyano and carbonyl prefer to be on the most electron-rich carbon of the TMM unit; it is understandable that conjugating groups like vinyl and phenyl prefer this carbon; it is heresy, however, that an electron-donating group like methyl or acetoxy (+M, −I) prefers this carbon. The metal is responsible for this violation of the normal rules of stability. The electron repulsion experienced by the electron-donating substituent in **87a** is apparently offset, energetically, by the increased bonding energy to the metal.

Is the reaction concerted or stepwise? The partial loss of olefin geometry (cf. Scheme 28)[43] and the observation of

seven-membered-ring formation in the reaction of dimethyl *trans,trans*-muconate **90** with **36b** support the notion of a stepwise process.[77] On the other hand, dimethyl *cis,trans*-muconate **91** undergoes addition of **44** preferentially to the *trans* double bond (Scheme 56).



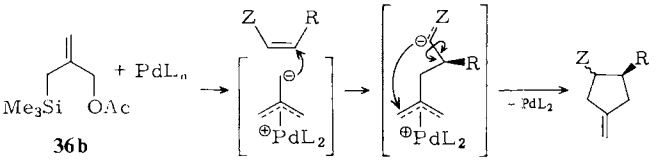
90 $[(Ph_3P)_4Pd]$, DPPE, THF, Δ: 62 : 38 (47%)
$[(Ph_3P)_4Pd]$, DPPE, dioxane, Δ: 79 : 21 (98%)
$[\{(iPrO)_3P\}_nPd]$, THF, Δ: 52 : 48 (89%)



91 E = $COOCH_3$

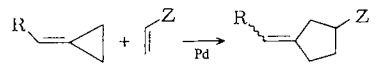
Scheme 56. Cycloaddition to *cis/trans* isomers.

Huisgen has stated that "the ratio of the *trans/cis* rates offers an elegant and theoretically clear criterion for concerted additions leading to five- and six-membered rings."[14c] This criterion suggests a concerted reaction. At present, the best interpretation appears to be a stepwise reaction initiated by nucleophilic attack, in which the ring closure occurs competitively with bond rotations (Scheme 57).



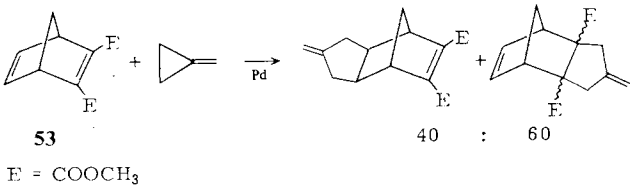
Scheme 57. Stepwise mechanism of [3 + 2] cycloaddition.

These results are strikingly different from those observed in the Pd-catalyzed codimerization of methylenecyclopropanes. In these cases, Scheme 58 best summarizes the regioselectivity.



Scheme 58. Regioselectivity in the codimerization of alkylidenecyclopropanes.

The observed regioselectivity differs from that theoretically predicted for $(\eta^3$-TMM)PdL_2. The fact that the experimental observations of the silyl-acetate reactions agree fully with theory lends credence to the theoretical description of $(\eta^3$-TMM)PdL_2. Furthermore, the lack of chemoselectivity in catalyzed additions of methylenecyclopropane **85** to norbornadiene **53**, which results in cycloaddition to both double bonds (Scheme 59), differs dramatically from the reactions of the silyl-acetate species, which result exclusively in addition to the electron-deficient double bond (Scheme 27).

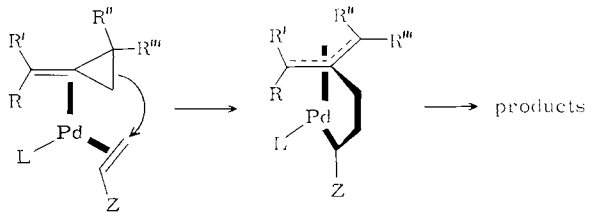


E = $COOCH_3$

Scheme 59. Reaction conditions: [(allyl)CpPd], iPr_3P.

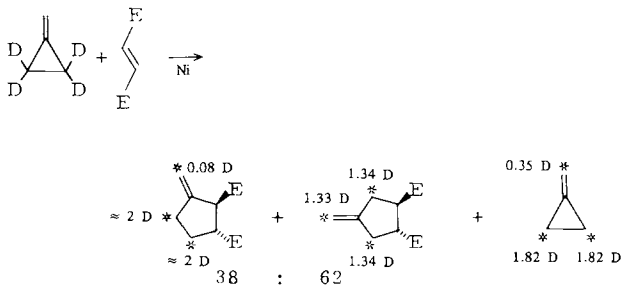
What, then, is the explanation for the reactions of alkylidenecyclopropanes? The picture becomes even murkier in that their reactions with carbon acids such as dimethyl malonate[69] parallel the reactions of the silyl-acetate species.[35]

A clue may reside in the ligand effects on the reaction. In the codimerization of the methylenecyclopropanes, a P : Pd ratio of 1 : 1 and the use of trialkylphosphanes such as triisopropylphosphane are optimal. In the silyl-acetate reactions, P : Pd ratios of ≥ 2 : 1 are preferred and triisopropylphosphane fails to serve as a ligand. It is possible that with alkylidenecyclopropanes direct dimerization on the metal occurs (Scheme 60) rather than prior opening to the TMM-Pd complex.



Scheme 60. Direct codimerization of alkylidenecyclopropanes.

Such an interpretation is in accord with the nickel-catalyzed codimerizations of methylenecyclopropane. In these cases, opening of the 1,2 as well as the 2,3 bond of **85** is observed.[62,79,80] Furthermore, Ni(0) complexes of methylenecyclopropane can be isolated.[62,81] Nevertheless, a TMM-Ni intermediate appears to be involved, in part, in the codimerization of methylenecyclopropane with dimethyl fumarate based upon deuterium labeling results (Scheme 61).[80]

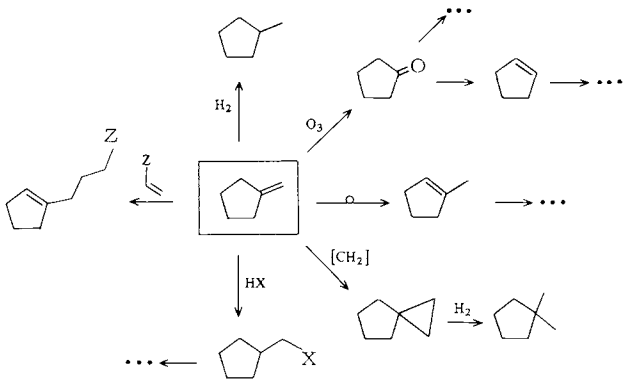


E = $COOCH_3$

Scheme 61. Reaction conditions: Ni(acrylonitrile)$_2$, 60 °C, 2.5 h, C_6H_6, ≈ 1% conversion.

6. Applications of Metal-Catalyzed TMM Additions

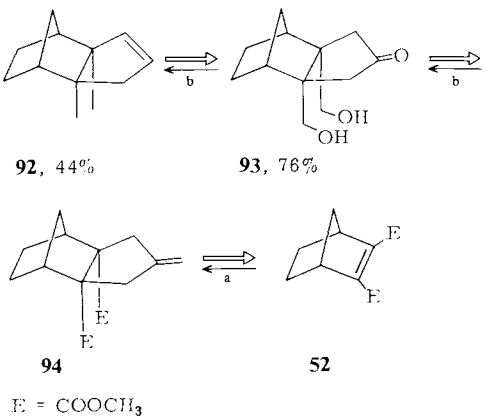
The direct cycloaddition approach to five-membered rings creates synthetic strategies not heretofore available. The exocyclic methylene group that arises in syntheses with TMM serves as a very versatile functionality for further elaboration (Scheme 62). Its easy oxidative cleavage to a ketone carbonyl group establishes its most important structural equivalent. The formation of a methyl or *gem*-dimethyl grouping is self-evident. Ene reactions, furthermore, allow chain elongations.



Scheme 62. Elaboration of the exocyclic double bond.

6.1. (±)-Albene

Albene **92** illustrates the types of problems that can be resolved using such cycloadditions, since a five-membered ring is fused *exo* to a norbornene system. Attack from the less-hindered face of the norbornene **52** directly creates the requisite stereochemistry (Scheme 63). Indeed, either the silyl-acetate species **36b** or methylenecyclopropane **85** add to give the requisite adduct, which was converted into albene. The simple five-step sequence starts from the readily available dimethyl 2,3-norbornenedicarboxylate (**52**).[45]



92, 44% **93**, 76%

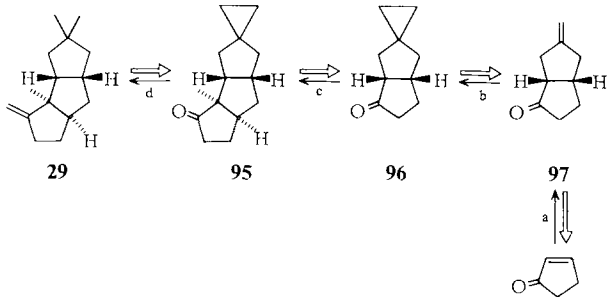
94 **52**

E = $COOCH_3$

Scheme 63. (±)-Albene **92**. a) Reaction with **36b** according to Scheme 26 (yield: 63%) or reaction with **85**, [(allyl)CpPd]/iPr_3P (yield: 80%); b) two steps.

6.2. (±)-Hirsutene

The easy creation of a *gem*-dimethyl group provides an entry into hirsutene **29**.[82] A key step involves the use of alkylative cyclopentanone annulation with diphenylsulfoniocyclopropanide,[83] which simplifies **95** to **96** in the retrosynthetic analysis (Scheme 64). The easy cyclopropanation of **97** to form **96** reveals the presence of a trimethylenemethane unit and the obvious formation of **97** by cycloaddition to 2-cyclopentenone. Indeed, both the silyl-acetate species **36b**[43] and methylenecyclopropane **85**[82] undergo cycloaddition with 2-cyclopentenone, a reaction that allows transformation of this strategy into a synthesis of hirsutene, as outlined in Scheme 64.[82]

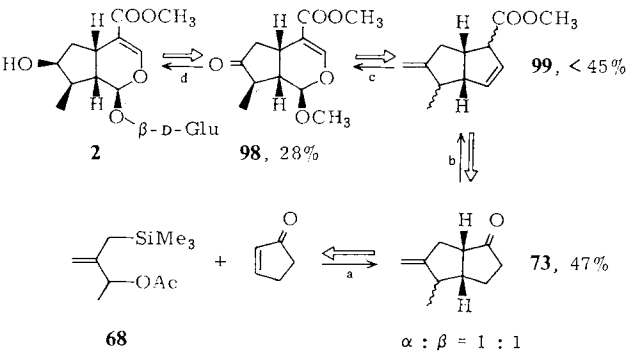


29 **95** **96** **97**

Scheme 64. (±)-Hirsutene **29**. a) Cycloaddition with **36b** or **85**; b) Et_2Zn, CH_2I_2; c) four steps; d) two steps.

6.3. (±)-Loganin

The iridoids constitute a more complex family of cyclopentanoids. Loganin **2**, a key intermediate in the biosynthesis of alkaloids, is derived from the ketone **98** in four steps. The presence of a hidden 1,5-dialdehyde in **98**, the ready accessibility of such a functionality by oxidative cleavage of a cyclopentene ring, and the synthon relationship between an exocyclic methylene group and a ketone simplify the problem to the diene **99**, which should be convertible in a single oxidation step into **98** (Scheme 65). Furthermore, by proceeding through the ketone, the stereochemistry of the methyl group in the early stages of synthesis becomes irrelevant since it can be easily epimerized to the thermodynamically favored, required configuration in **98**. The accessibility of the β,γ-unsaturated ester **99** from the cyclopentanone system **73** by standard methods reveals the presence of a methyl-substituted TMM unit. The cycloaddition of the requisite methyl-substituted silyl-acetate species **68** with 2-cyclopentenone to give **73** (see Scheme 40) allows this analysis to be transformed into a loganin synthesis as outlined in Scheme 65.[36]



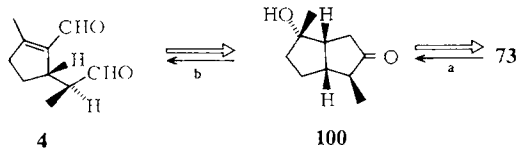
2 **98**, 28% **99**, < 45%

68 **73**, 47% α : β = 1 : 1

Scheme 65. (±)-Loganin **2**. Reaction conditions: a) $Pd(OAc)_2/(iPrO)_3P$; b) three steps; c) 1. ozonolysis; 2. $CH_3OH/H^{\oplus}$; 3. $NaOCH_3$; d) four steps.

6.4. (±)-Chrysomelidial

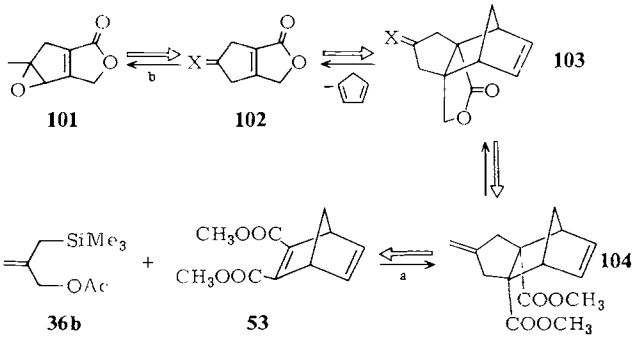
A structure related to loganin is the *seco*-iridoid chrysomelidial **4**, a constituent of the larval defense secretion of a chrysomelide beetle. The problem of side-chain stereochemistry is resolved by converting it into a problem of ring stereochemistry as in **100**. Since thermodynamic epimerization at the methyl-bearing carbon can be relied upon to produce the correct stereochemistry, this aspect need not concern us in the earlier stages. Once again, the recognition of the synthon relationship between a ketone and an exocyclic methylene group combined with the obvious ability to create the tertiary alcohol by methyllithium addition simplifies the task to the synthesis of **73** (see Schemes 40 and 65). The cycloaddition approach provides the key bicycle **100** in only four steps in contrast with a fourteen-step synthesis using conventional approaches.[84] In this case, the annulated five-membered ring is ultimately cleaved to create the side chains of **4** (Scheme 66).



Scheme 66. (±)-Chrysomelidial **4**. a) Three steps, b) seven steps.

6.5. (±)-2β-Hydroxyjatrophone Precursor

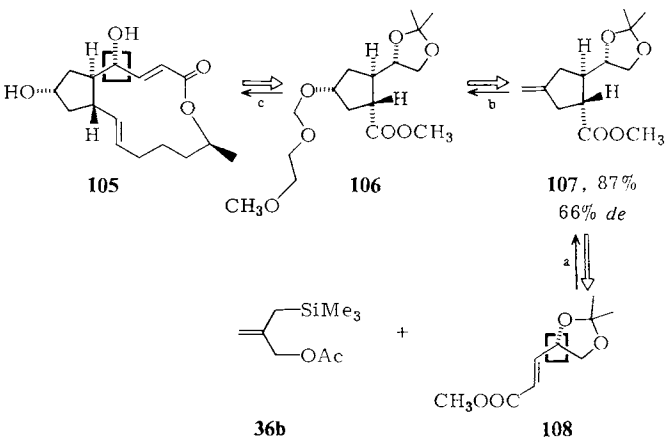
A projected synthesis of 2β-hydroxyjatrophone envisions the use of the highly functionalized cyclopentene **101** as a key intermediate. The accessibility of such an epoxide by simple methods from **102** immediately discloses the elements of TMM. The inability to use acetylenes as substrates for cycloaddition led to the use of the cyclopentadiene adduct **103** as a synthetic equivalent of the double bond in **102**. By so doing, the simple transformation of a diester to a lactone suggests **104** as the logical precursor (see Scheme 27). The efficiency of this route (Scheme 67) is highlighted by the approximately 60% overall yield of **101** from the norbornadiene diester **53**.[46]



Scheme 67. X = methylene or (protected) keto group. a) cf. Scheme 27; b) two steps.

6.6. (+)-Brefeldin A

Brefeldin A **105** represents a significant challenge in terms of the functionality, the macrocyclic ring, and absolute stereochemistry. Four of the five chiral centers are retained in the cyclopentane **106** (Scheme 68). The readily recognized relationship between a ketone and an exocyclic methylene group converts **106** into **107** in the retrosynthetic direction. The features of trimethylenemethane embodied in **107** once again demonstrate the widespread utility of the TMM approach. In this case, the critical question of the diastereoselectivity of addition to **108** arises. The availability of **108** from D-mannose translates this approach into an enantioselective one in which the one epimeric center of **108** increases to four epimeric centers in **106**. The final center in **105** arises from an independent synthesis of the lower side chain. Using our standard cycloaddition conditions, a good diastereoselective (4 : 1) cycloaddition occurs to give the methylenecyclopentane **107**. Sixteen subsequent steps complete the synthesis of optically pure (+)-brefeldin A **105** (Scheme 68).[85]



Scheme 68. (+)-Brefeldin A **105**. Reaction conditions: a) $Pd(OAc)_2$/$(iPrO)_3P$; b) three steps: c) thirteen steps. C-4 in the starting material **108** and the corresponding C atom in the product **105** are enclosed in boxes.

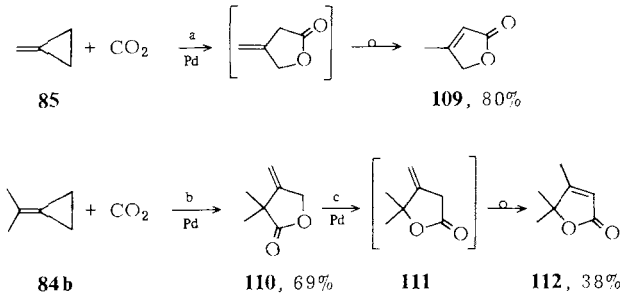
Although the [3+2] cycloaddition strategy to form five-membered rings is still in its infancy, the syntheses accomplished to date begin to show the effective solutions to problems of selectivity that such an approach offers. The exocyclic methylene group is an exceedingly important part of this strategy since it provides a handle for structural elaboration. Clearly, the opportunities have barely been probed yet.

7. Additions to C=O and C=N Bonds

The possibilities for stereocontrolled heterocyclic synthesis arising from Diels-Alder type additions to carbonyl groups raises the question whether five-membered heterocycles may also be approached using this chemistry. The presence of tetrahydrofuran and γ-butyrolactone structures in so many biologically important natural products highlights the relevance of such a question.

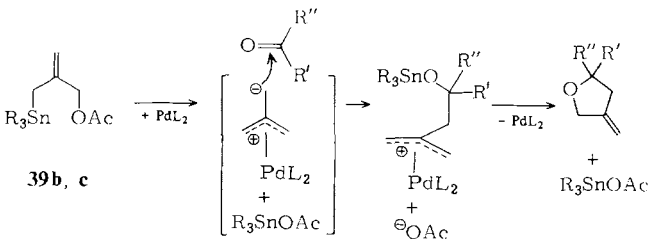
The codimerization of methylenecyclopropanes with carbon dioxide leads to γ-lactones (Scheme 69).[86,87] If an easily enolizable hydrogen exists in the initial adduct, isomerization to the γ-butenolide occurs under the reaction conditions. This addition appears to be reversible with the proper catalyst. The γ-butyrolactone **110** undergoes a

reversal of the elements of CO_2 using a catalyst bearing DPPE ligands (but not Ph_3P) to give initially **111**, which, as expected, isomerizes to the γ-butenolide **112**.[88]



Scheme 69. Reaction conditions: a) 40 bar CO_2 at RT, [(allyl)CpPd]/Ph_3P (1:4), DMF, 165–170°C, 2 h; b) 40 bar CO_2 at RT, $(dba)_2Pd/Ph_3P$ (1:4), C_6H_6, 130°C, 20 h; c) 60 bar CO_2, $(dppe)_2Pd$, C_6H_6, 110°C, 1.5 h.

Considering the nucleophilic characteristics of the $(TMM)PdL_2$ species, addition to carbonyl groups of aldehydes and ketones would appear feasible as outlined in Scheme 70. Because of the generally poor nucleophilic properties of oxygen toward π-allylpalladium intermediates and because the tin ethers have been reported[89] to react more smoothly, the tin analogues **39b,c** of the 1,3-bifunctional conjunctive reagents would appear to be more promising.

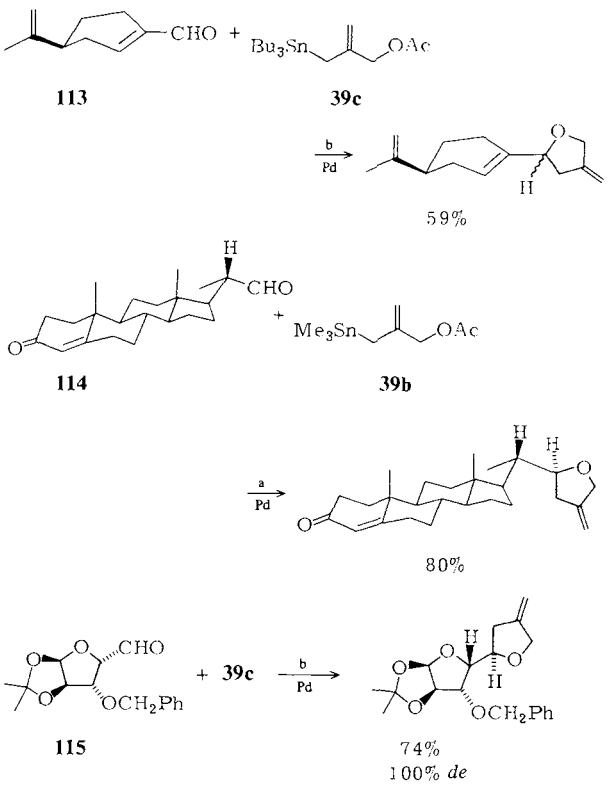


Scheme 70. Addition of $(TMM)PdL_2$ to carbonyl groups (cf. Scheme 57).

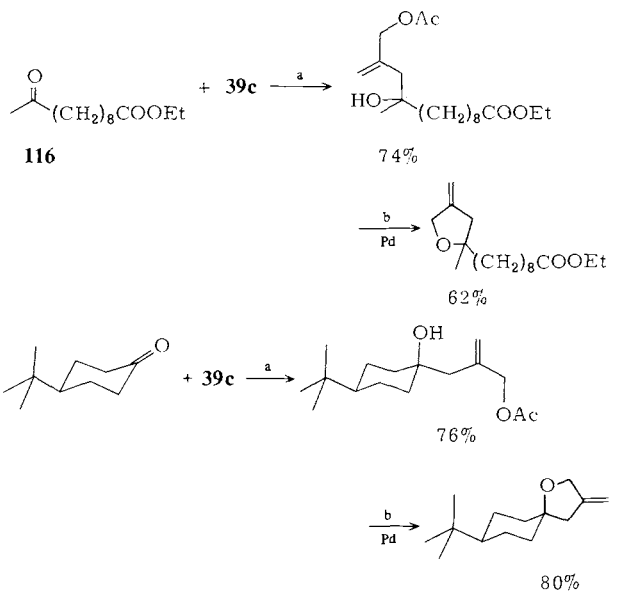
Initial studies with the silyl reagent **36b** did not lead to cycloaddition.[43] On the other hand, an excellent chemoselective addition occurs upon mixing the trimethyltin reagent **39b** with aldehydes even at room temperature (Scheme 71).[49] Remarkably, even α,β-unsaturated aldehydes such as **113** undergo cycloaddition to the carbonyl group in preference to cycloaddition to the double bond! Excellent diastereoselectivity accompanies this reaction.

Not only 3-oxo-23,24-bisnor-4-cholen-22-al **114** but also the *xylo* aldehyde **115**, a model for an ionophore synthesis, forms only a single diastereomer.

Ketones do not undergo this cycloaddition in satisfactory yields. On the other hand, Lewis-acid-initiated additions of allylstannanes to ketones suggested that a two-stage sequence might enhance the scope of this cycloaddition. Indeed, chemoselective addition of **39c** to the ketoester **116** occurs smoothly in the presence of boron trifluoride at −78°C (Scheme 72).[48] The initial adduct smoothly cyclizes using a palladium catalyst prepared in situ. With 4-*tert*-butylcyclohexanone, equatorial attack is strongly preferred.

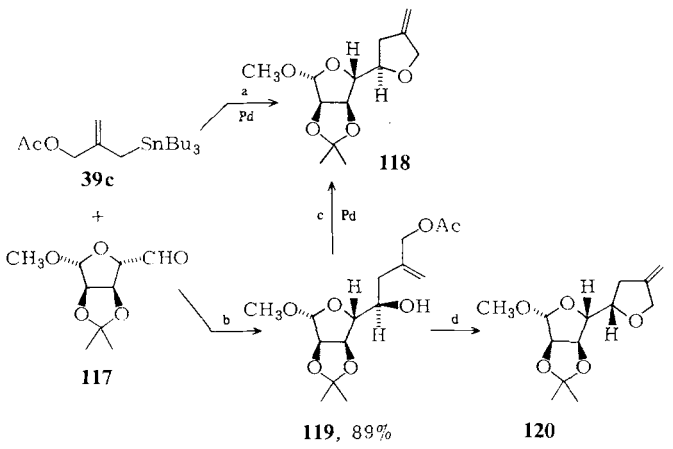


Scheme 71. Reaction conditions: a) 3 mol-% $Pd(OAc)_2/Ph_3P$, 40°C, dioxane; b) as in a), but Δ.



Scheme 72. Reaction conditions: a) $BF_3 \cdot Et_2O$, −78°C, 1 h, CH_2Cl_2; b) $Pd(OAc)_2/Ph_3P/BuLi$ (1:6:2), in situ; DBU, Δ, 16–36 h, dioxane.

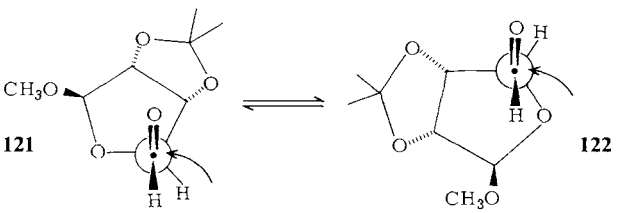
Performing this sequence in such a two-stage fashion has an advantage in the ability to manipulate the overall stereochemistry. Thus, *ribo* aldehyde **117** produces only the annulation product **118** in the one-step cycloaddition. The same compound also arises from the palladium-catalyzed cyclization of the initial adduct **119** in the two-step sequence.[48] Alternatively, mesylation converts the OH group at the α-C atom in the initial adduct **119** into a leaving group, so that cyclization upon treatment with base re-



Scheme 73. Reaction conditions: a) 3 mol-% $Pd(OAc)_2/Ph_3P$, dioxane; b) $BF_3 \cdot Et_2O$, $-78°C$, CH_2Cl_2; c) $[(Ph_3P)_4Pd]$, DBU, Δ, dioxane; d) 1. CH_3SO_2Cl, Et_3N; 2. KOH, H_2O, CH_3OH. Yields of **118** via a: 81%; via c: 60%.

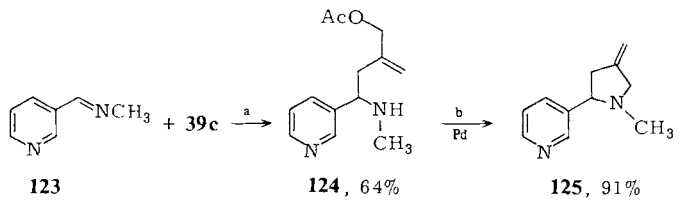
sults in inversion of this stereocenter in the final product **120**.[49] Thus, from aldehyde **117**, either diastereomeric annulated product, **118** or **120**, is available.

The stereochemistry observed follows the normal Felkin-Anh rules invoking reaction via rotamer **121**, although the rotamer **122**, which better minimizes nonbonded interactions, also rationalizes these results (Scheme 74).



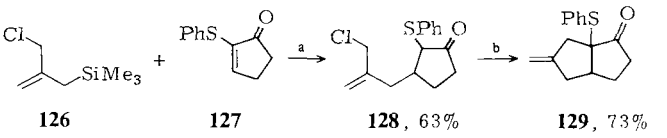
Scheme 74. Two rotamers of the reactant **117**.

The Lewis-acid-catalyzed reaction extends this strategy for heterocycle synthesis to pyrrolidines. Thus, the nicotine aldehyde imine **123** reacts with allylstannanes in the presence of a Lewis acid. Amines are excellent nucleophiles in palladium-catalyzed alkylations and thus these adducts smoothly cyclize to form 3-methylenepyrrolidines as exemplified in the synthesis of the nicotine analogue **125** (Scheme 75).[48]



Scheme 75. Reaction conditions: a) $BF_3 \cdot Et_2O$, $-78°C$, CH_2Cl_2; b) $[(Ph_3P)_4Pd]$, DBU, Δ, dioxane.

Such a strategy has also been used with enones as acceptors, preferably with those that are particularly good Michael acceptors. [2-(Chloromethyl)allyl]trimethylsilane **126** does not undergo addition to 2-cyclopentenone in the presence of Lewis acids in satisfactory yield (8%) but does add to 2-(phenylthio)-2-cyclopentenone **127** in good yields (Scheme 76).[34]

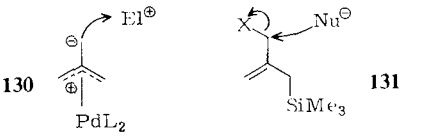


Scheme 76. Reaction conditions: a) $EtAlCl_2$, $-78 \rightarrow 0°C$, CH_2Cl_2; b) KO*t*Bu, *t*BuOH, RT, 3 h.

This approach may complement the direct metal-catalyzed cycloaddition in cases such as 2-cycloalkenones, which fail to satisfactorily cyclize in the transition-metal-catalyzed reaction.

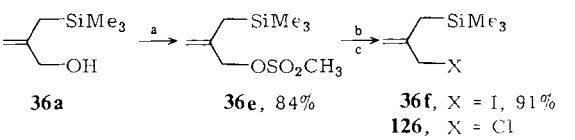
8. Ancillary Strategies for Incorporating a TMM Structural Unit

The use of $(TMM)PdL_2$ as a reactive intermediate for incorporating a TMM unit depends upon reactions initiated by its nucleophilicity, as shown by **130**. An approach that inverts the electronic sense of this TMM unit such that it reacts with nucleophiles, as shown by **131**, would greatly enhance the utility of these 1,3-bifunctional reagents (Scheme 77).



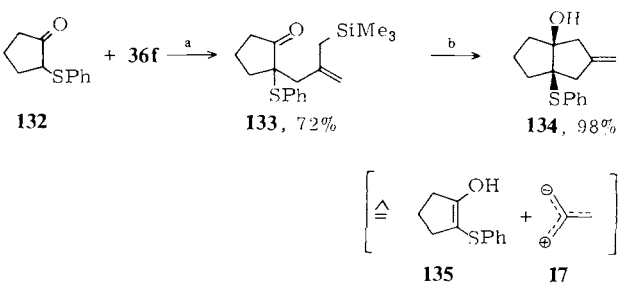
Scheme 77. Nucleophilic (**130**) and electrophilic (**131**) TMM species.

The halides **36f** and **126** and the mesylate **36e**, which are derived from the alcohol **36a**, serve as such electrophilic synthons (Scheme 78).[90,91]



Scheme 78. Reaction conditions: a) CH_3SO_2Cl/Et_3N, 0°C, CH_2Cl_2; b) NaI, Δ, acetone (→ **36f**); c) LiCl, 0°C, DMF (→ **126**).

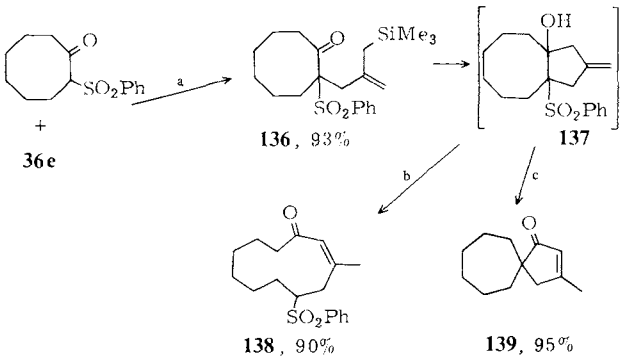
The trimethylsilyl group, even though it is remote from the carbon undergoing substitution, retards alkylation.[91] Nevertheless, stabilized anions react smoothly to give the products of simple alkylation (Scheme 79). Fluoride ion promotes efficient cyclization of the resulting allylsilane,



Scheme 79. Reaction conditions: a) KH, DME; b) Bu_4NF, Δ, 1 h, THF.

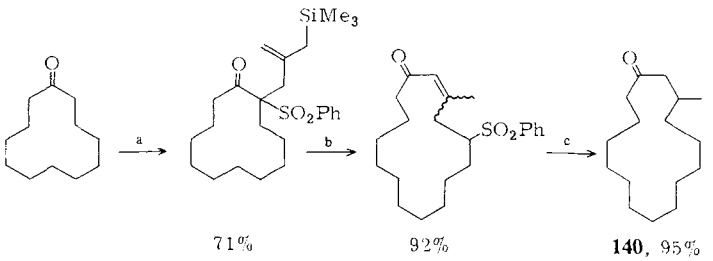
e.g., **133**, to effect a formal methylenecyclopentane annulation onto an electron-rich double bond (enol **135**).

If 2-(phenylsulfonyl)cyclooctanone is used, the alkylated intermediate product **136** cyclizes to the reactive methylenecyclopentane **137**. In the presence of fluoride ion, the β-hydroxysulfone fragments to the ring-enlarged product, which isomerizes to the more stable conjugated enone **138**.[90,92] On the other hand, if Lewis acids are employed to promote the cyclization, intermediate **137** undergoes a pinacol-type rearrangement with expulsion of the phenylsulfonyl group to give, after isomerization of the double bond into a conjugated position, the spiro cyclopentenone **139**.[93] The intermediate methylenecyclopentane **137** can be isolated in 70% yield using ethylaluminum dichloride at −78 °C. Thus, from intermediate **136**, a nucleophilic trigger effects a net three-carbon intercalation (**136** → **138**) and an electrophilic trigger effects a combined ring contraction-spiroannulation (**139** → **139**) (Scheme 80).



Scheme 80. Reaction conditions: a) KOH/KI/$(Bu_4N)_2SO_4$, CH_2Cl_2/H_2O; b) Bu_4NF, 55 °C, 0.5 h, THF; c) $EtAlCl_2$, CH_2Cl_2, RT → Δ, 3 h.

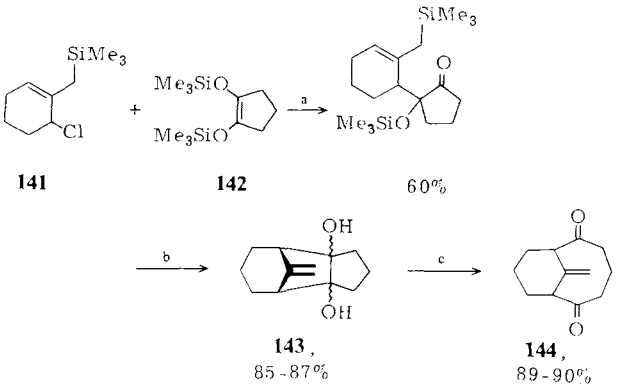
The three-carbon intercalation provides a very efficient strategy for the synthesis of muscone **140** from cyclododecanone (62% overall yield; Scheme 81).[90]



Scheme 81. (±)-Muscone **140**. Reaction conditions: a) 1. $Br_2/CHCl_3$; 2. $PhSO_2Na$; 3. NaH/**36e**; b) Bu_4NF, 55 °C, 0.5 h, THF; c) 1. H_2/Pd; 2. Na/Hg.

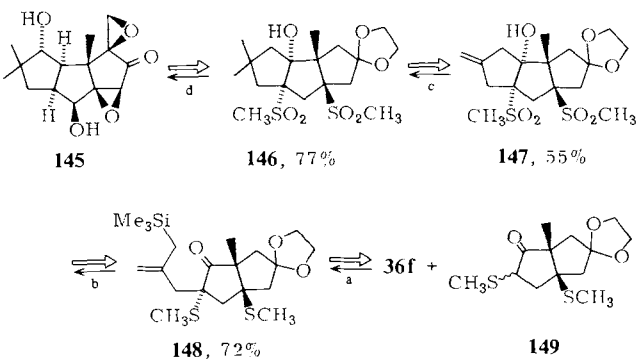
A slight variant of this sequence serves as an approach to the bicyclo[5.3.1]undecane system of the taxanes, which are antitumor agents (Scheme 82).[37] Careful treatment with a Lewis acid effects alkylation of the enediol bis(silyl) ether **142** by the cyclic TMM system **141**.[94] Cyclization as in Schemes 79–81 creates the "methylenecyclopentane" **143**, which is oxidatively cleaved to give **144**.

The synthetic equivalent of the cycloaddition to an enol (see **135**) forms the basis for a synthesis of coriolin **145**, an

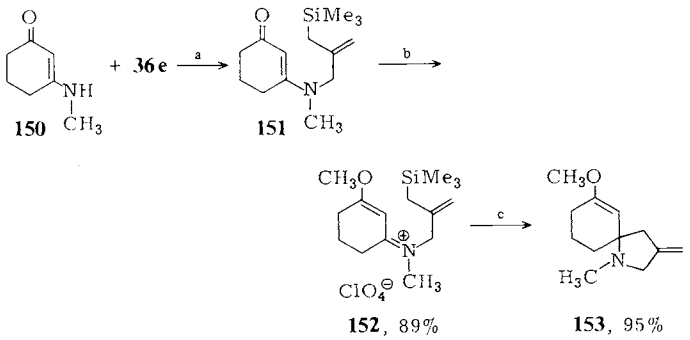


Scheme 82. Reaction conditions: a) $ZnCl_2$, 0 °C, 2 h, CH_2Cl_2; b) 1. $EtAlCl_2$, −78 °C, toluene; 2. $H_3O^{\oplus}$; c) $NaIO_4$, RT, 1–3 d, CH_3OH/H_2O.

antitumor agent and antibiotic that is the most complicated member of the hirsutene family (Scheme 83).[95] Manipulating functionality conceptually suggests **146** as a viable intermediate. The possibility of creating a *gem*-dimethyl group from an exocyclic methylene group simplifies the target further to **147**. At this point, the presence of the elements of methylenecyclopentane is quite obvious and can arise by annulation of an enol with the electrophilic versions of the 1,3-bifunctional conjunctive reagents. The sluggishness of alkylation of a β-ketosulfone led to the use of the β-ketosulfide **149** as the nucleophile that reacts with the iodide **36f**. Although cyclization to complete the annulation proceeds quantitatively upon exposing the β-ketosulfide **148** to fluoride ion, the ultimate need for the sulfone led to oxidation of **148** followed by cyclization to **147**. Cyclopropanation and catalytic hydrogenolysis simply converts the exocyclic methylene group into the *gem*-dimethyl unit of **146**. With this effective annulation protocol for the enol of the β-ketosulfide **149**, the stage was set for the completion of the synthesis, which mainly required adjustment of the oxidation pattern. The inverse polarity conjunctive reagents also are used for construction of heterocycles. In a novel sequence, the vinylogous amide **150** is alkylated with **36e** (Scheme 84).[96] *O*-Alkylation of **151** creates the iminium salt **152** for final ring closure. Photostimulation effectively achieves the nucleophilic addition of the allylsilane and consequently completes the annulation.

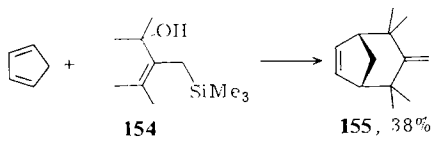


Scheme 83. (±)-Coriolin **145**. Reaction conditions: a) KH, DME, RT; b) 1. *m*-chloroperbenzoic acid (63% yield); 2. Bu_4NF, THF (87% yield); c) 1. CH_2I_2/Et_2Zn; 2. H_2/PtO_2; d) twelve steps.



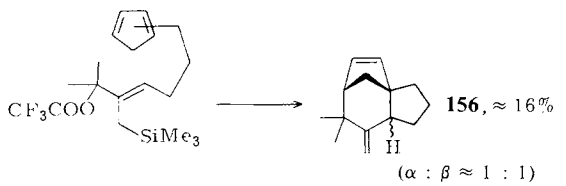
Scheme 84. Reaction conditions: a) NaH/THF; b) CH_3I, $AgClO_4$; c) $h\nu$, $\lambda > 280$ nm, CH_3CN.

These electrophilic versions of TMM participate in a [4+3] type of cycloaddition that can be envisioned as a cycloaddition of an allyl cation to the diene, which is symmetry allowed in a suprafacial sense.[97] For example, the highly substituted 1,3-bifunctional silyl alcohol **154** requires only exposure to a Lewis acid to generate a reactive electrophile and participate in a cycloaddition (Scheme 85).[98] Although the yields are modest, alternative approaches failed.



Scheme 85. Reaction conditions: $TiCl_4$, $PhNHCH_3$, $-20°C$, 3 h, CH_2Cl_2.

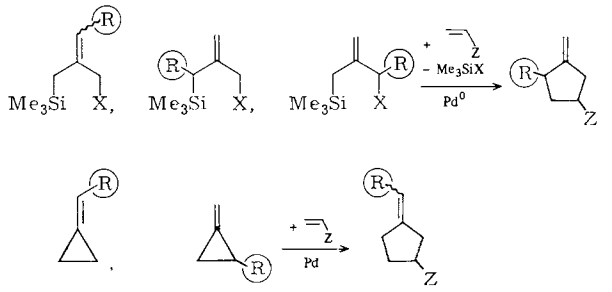
An intramolecular version of this reaction creates the basic ring system of the zizaenes (Scheme 86), albeit only in 16% yield.[99]



Scheme 86. Reaction conditions: $ZnCl_2/SiO_2$, $-30°C$, CH_2Cl_2/pentane.

9. Conclusion

Transforming trimethylenemethanes from intellectual curiosities into synthetic tools continues to be an exciting challenge. One key appears to be the discovery of a transition metal, palladium, that achieves a proper balance between stability and reactivity and that unlocks the synthetic potential of this type of reactive intermediate. The applicability of this principle of using transition-metal templates as carriers for reactive intermediates, which had previously only been applied in the realm of physical studies in the case of TMM, has proven to be extremely powerful. The bonus of complementary regioselectivity depending upon the choice of precursors, as outlined in Scheme 87, is synthetically very useful even though it is not yet satisfactorily explicable.



Scheme 87. The dependence of regioselectivity on the choice of precursor.

The functionality available and the selectivity of this cycloaddition provide unusual opportunities for efficiency in the synthesis of cyclopentanoids.

I wish to thank my collaborators who are all identified in the references and who have played such a critical role in developing the chemistry coming from our laboratories. Support of our work from the National Science Foundation and the National Institutes of Health is gratefully acknowledged. I also thank Professors Daniel Little and Paul Binger for making available unpublished work from their laboratories.

Received: June 4, 1985 [A 560 IE]
German version: *Angew. Chem. 98* (1986) 1

[1] Reviews: L. A. Paquette, *Top. Curr. Chem. 119* (1984) 1; B. M. Trost, *Chem. Soc. Rev. 11* (1982) 141; W. I. Taylor, A. R. Battersby (Eds.): *Cyclopentanoid Terpene Derivatives (Organic Substances of Natural Origin. Vol. 2)*, M. Dekker, New York 1969.
[2] L. J. El-Naggar, J. L. Beal, *J. Nat. Prod. 43* (1980) 649.
[3] E. J. Eisenbraun, C. E. Browne, R. L. Irvin-Willis, D. J. McGurk, E. L. Eliel, D. L. Harris, *J. Org. Chem. 45* (1980) 3811, and references cited therein.
[4] A. R. Battersby in J. E. Saxton (Ed.): *Alkaloids (London)* [Specialist Periodical Reports] *1* (1971) 31.
[5] Structure: S. M. Kupchan, A. L. Dessertine, B. T. Blaylock, R. F. Bryan, *J. Org. Chem. 39* (1974) 2477; synthesis: B. M. Trost, J. M. Balkovec, M. K.-T. Mao, *J. Am. Chem. Soc. 105* (1983) 6755; B. M. Trost, J. M. Balkovec, *Tetrahedron Lett. 26* (1985) 1807.
[6] Structure: J. Meinwald, T. H. Jones, T. Eisner, K. L. Hicks, *Proc. Natl. Acad. Sci. USA 74* (1977) 2189; synthesis: J. Meinwald, T. H. Jones, *J. Am. Chem. Soc. 100* (1978) 1883.
[7] Reviews: B. Samuelsson, *Recent Prog. Horm. Res. 34* (1978) 239; K. C. Nicolaou, G. P. Gasic, W. E. Barnette, *Angew. Chem. 90* (1978) 360; *Angew. Chem. Int. Ed. Engl. 17* (1978) 293.
[8] F. W. Comer, F. McCapra, I. H. Qureshi, J. Trotter, A. I. Scott, *Chem. Commun. 1965*, 310; F. W. Comer, F. McCapra, I. H. Qureshi, A. I. Scott, *Tetrahedron 23* (1967) 4761; synthesis: H. Hashimoto, K. Tsuzuki, F. Sakan, H. Shirahama, T. Matsumoto, *Tetrahedron Lett. 1974*, 3745; B. M. Trost, C. D. Shuey, F. DiNinno, Jr., *J. Am. Chem. Soc. 101* (1979) 1284; M. Shibasaki, M. Yamazaki, K. Iseki, S. Ikegami, *Tetrahedron Lett. 23* (1982) 5311; A. E. Greene, M.-J. Luche, J.-P. Deprès, *J. Am. Chem. Soc. 105* (1983) 2435.
[9] S. Nozoe, M. Morisaki, K. Tsuda, Y. Iitaka, N. Takahashi, S. Tamura, K. Ishibashi, M. Shirasaka, *J. Am. Chem. Soc. 87* (1965) 4968.
[10] A. N. Singh, V. V. Mhaskar, S. Dev, *Tetrahedron 34* (1978) 595; G. B. V. Subramanian, U. Majumdar, R. Nuzhat, V. K. Mahajan, K. N. Ganesh, *J. Chem. Soc. Perkin Trans. 1 1979*, 2167.
[11] F. Bohlmann, C. Zdero, R. Bohlmann, R. M. King, H. Robinson, *Phytochemistry 19* (1980) 579.
[12] F. Bohlmann, C. Zdero, *Phytochemistry 20* (1981) 2529.
[13] M. Kaneda, R. Takahashi, Y. Iitaka, S. Shibata, *Tetrahedron Lett. 1972*, 4609.
[14] Reviews: a) A. P. Kozikowski, *Acc. Chem. Res. 17* (1984) 410; b) J. J. Tufariello, *ibid. 12* (1979) 396; W. Oppolzer, *Angew. Chem. 89* (1977) 10; *Angew. Chem. Int. Ed. Engl. 16* (1977) 10; c) R. Huisgen, *ibid. 75* (1963) 604, 742 and *2* (1963) 565, 633; d) V. Jäger, H. Grund, V. Buss, W. Schwab, I. Müller, R. Schohe, R. Franz, R. Ehrler, *Bull. Soc. Chim. Belg. 92* (1983) 1039; e) for 1,3-cycloaddition type of reactions of allyl and heteroallyl organolithium reagents, see T. Kauffmann, *Angew. Chem. 86* (1974) 715; *Angew. Chem. Int. Ed. Engl. 13* (1974) 627.
[15] D. L. Boger, C. E. Brotherton, *J. Am. Chem. Soc. 106* (1984) 805.

[16] P. L. Fuchs, *J. Am. Chem. Soc. 96* (1974) 1607; W. G. Dauben, D. J. Hart, *ibid. 99* (1977) 7307.
[17] R. L. Danheiser, D. J. Carini, A. Basak, *J. Am. Chem. Soc. 103* (1981) 1604.
[18] A. Bucheister, P. Klemarczyk, M. Rosenblum, *Organometallics 1* (1982) 1679; see also: R. Baker, R. B. Keen, M. D. Morris, R. W. Turner, *J. Chem. Soc. Chem. Commun. 1984,* 987.
[19] Reviews: P. Welzel, *Nachr. Chem. Tech. Lab. 31* (1983) 638; J. A. Berson, *Acc. Chem. Res. 11* (1978) 446; P. Dowd, *ibid. 5* (1972) 242; F. Weiss, *Q. Rev. Chem. Soc. 24* (1970) 278.
[20] J. A. Mondo, J. A. Berson, *J. Am. Chem. Soc. 105* (1983) 3340.
[21] a) K. Ehrlich, G. F. Emerson, *J. Am. Chem. Soc. 94* (1972) 2464; b) R. Pettit, J. S. Ward, *Chem. Commun. 1970,* 1419.
[22] L. R. Corwin, D. M. McDaniel, R. J. Bushby, J. A. Berson, *J. Am. Chem. Soc. 102* (1980) 276.
[23] C. D. Duncan, L. R. Corwin, J. H. Davis, J. A. Berson, *J. Am. Chem. Soc. 102* (1980) 2350.
[24] a) R. D. Little, A. Bukhhari, M. G. Venegas, *Tetrahedron Lett. 1979,* 305; b) R. D. Little, G. W. Muller, M. G. Venegas, G. L. Carroll, A. Bukhari, L. Patton, K. Stone, *Tetrahedron 37* (1981) 4371.
[25] R. D. Little, L. Brown, *Tetrahedron Lett. 21* (1980) 2203.
[26] K. J. Stone, R. D. Little, *J. Am. Chem. Soc. 107* (1985) 2495.
[27] R. D. Little, G. L. Carroll, *Tetrahedron Lett. 22* (1981) 4389.
[28] R. D. Little, G. W. Muller, *J. Am. Chem. Soc. 103* (1981) 2744.
[29] R. D. Little, H. Bode, K. J. Stone, O. Wallquist, R. Dannecker, *J. Org. Chem. 50* (1985), in press.
[30] See, however, K. J. Stone, R. D. Little, *J. Org. Chem. 49* (1984) 1849.
[31] Reviews: a) B. M. Trost, *Tetrahedron 33* (1977) 2615; b) B. M. Trost, *Acc. Chem. Res. 13* (1980) 385; c) B. M. Trost, T. R. Verhoeven in G. Wilkinson, F. G. A. Stone, E. W. Abel (Eds.): *Comprehensive Organometallic Chemistry, Vol. 8,* Pergamon Press, Oxford 1982, p. 799; d) J. Tsuji: *Organic Synthesis with Palladium Compounds,* Springer, Berlin 1980.
[32] B. M. Trost, D. M. T. Chan, T. N. Nanninga, *Org. Synth. 62* (1984) 58.
[33] A. Hosomi, H. Hashimoto, H. Sakurai, *Tetrahedron Lett. 21* (1980) 951.
[34] S. Knapp, U. O'Connor, D. Mobilio, *Tetrahedron Lett. 21* (1980) 4557.
[35] B. M. Trost, D. M. T. Chan, *J. Am. Chem. Soc. 105* (1983) 2326.
[36] B. M. Trost, T. N. Nanninga, *J. Am. Chem. Soc. 107* (1985) 1293.
[37] B. M. Trost, H. Hiemstra, *J. Am. Chem. Soc. 104* (1982) 886.
[38] D. M. T. Chan, *Ph. D. Thesis,* University of Wisconsin, Madison, WI 1982.
[39] T. N. Nanninga, *Ph. D. Thesis,* University of Wisconsin, Madison, WI 1985.
[40] B. M. Trost, T. N. Nanninga, T. Satoh, *J. Am. Chem. Soc. 107* (1985) 721.
[41] B. M. Trost, D. M. T. Chan, *J. Am. Chem. Soc. 104* (1982) 3733; B. M. Trost, B. P. Coppola, *ibid. 104* (1982) 6879; H. Nishiyama, H. Yokoyama, S. Narimatsu, K. Itoh, *Tetrahedron Lett. 23* (1982) 1267.
[42] B. M. Trost, H. Morton, unpublished.
[43] B. M. Trost, D. M. T. Chan, *J. Am. Chem. Soc. 105* (1983) 2315.
[44] B. M. Trost, D. M. T. Chan, *J. Am. Chem. Soc. 101* (1979) 6429.
[45] B. M. Trost, P. Renaut, *J. Am. Chem. Soc. 104* (1982) 6668.
[46] B. M. Trost, J. Balkovec, S. R. Angle, unpublished.
[47] B. M. Trost, J. Lynch, P. Renaut, *Tetrahedron Lett.*, in press.
[48] B. M. Trost, P. J. Bonk, *J. Am. Chem. Soc. 107* (1985) 1778.
[49] B. M. Trost, P. J. Bonk, unpublished.
[50] B. M. Trost, D. M. T. Chan, *J. Am. Chem. Soc. 102* (1980) 6359.
[51] B. M. Trost, P. R. Seoane, unpublished.
[52] B. M. Trost, D. M. T. Chan, *J. Am. Chem. Soc. 103* (1981) 5972.
[53] B. M. Trost, T. N. Nanninga, *J. Am. Chem. Soc. 107* (1985) 1075.
[54] I. Shimizu, Y. Ohashi, J. Tsuji, *Tetrahedron Lett. 25* (1984) 5183.
[55] J. J. Gajewski, *Mech. Mol. Migr. 4* (1971) 1; see also M. Rule, J. A. Mondo, J. A. Berson, *J. Am. Chem. Soc. 104* (1982) 2209; M. Rule, R. F. Salinaro, D. R. Pratt, J. A. Berson, *ibid. 104* (1982) 2223.
[56] R. Noyori, T. Nishimura, H. Takaya, *Chem. Commun. 1969,* 89.
[57] A. R. Pinhas, B. K. Carpenter, *J. Chem. Soc. Chem. Commun. 1980,* 17.
[58] See also W. E. Billups, L. P. Lin, B. A. Baker, *J. Organomet. Chem. 61* (1973) C 55; W. E. Billups, L.-P. Lin, O. A. Gansow, *Angew. Chem. 84* (1972) 684; *Angew. Chem. Int. Ed. Engl. 11* (1972) 637.
[59] S. G. Barnes, M. Green, *J. Chem. Soc. Chem. Commun. 1980,* 267.
[60] P. Binger, P. Bentz, *J. Organomet. Chem. 221* (1981) C 33.
[61] R. Noyori, T. Odagi, H. Takaya, *J. Am. Chem. Soc. 92* (1970) 5780.
[62] See also P. Binger, M. Cetinkaya, M. J. Doyle, A. Germer, U. Schuchardt, *Fundam. Res. Homogeneous Catal. 3* (1979) 271.
[63] P. Binger, A. Brinkmann, P. Wedemann, *Chem. Ber. 116* (1983) 2920.
[64] a) P. Binger, P. Wedemann, *Tetrahedron Lett. 24* (1983) 5847; b) P. Binger, Q.-H. Lü, P. Wedemann, *Angew. Chem. 97* (1985) 333; *Angew. Chem. Int. Ed. Engl. 24* (1985) 316.
[65] a) P. Binger, A. Brinkmann, W. J. Richter, *Tetrahedron Lett. 24* (1983) 3599; b) W. Oppolzer in W. Bartmann, B. M. Trost (Eds.): *Selectivity - a Goal for Synthetic Efficiency,* Verlag Chemie, Weinheim 1984, p. 137.
[66] P. Binger, U. Schuchardt, *Chem. Ber. 113* (1980) 3334.
[67] P. Binger, U. Schuchardt, *Angew. Chem. 89* (1977) 254; *Angew. Chem. Int. Ed. Engl. 16* (1977) 249.
[68] P. Binger, U. Schuchardt, *Chem. Ber. 114* (1981) 3313.
[69] P. Bentz, *Dissertation,* Universität Kaiserslautern 1982.
[70] A. Germer, *Dissertation,* Universität Bochum 1978.
[71] G. Balavoine, C. Eskenazi, M. Guillemot, *J. Chem. Soc. Chem. Commun. 1979,* 1109.
[72] P. Binger, P. Bentz, *Angew. Chem. 94* (1982) 636; *Angew. Chem. Int. Ed. Engl. 21* (1982) 622; *Angew. Chem. Suppl. 1982,* 1385.
[73] B. M. Trost, D. M. T. Chan, *J. Am. Chem. Soc. 101* (1979) 6432.
[74] M. D. Jones, R. D. W. Kemmitt, A. W. G. Platt, D. R. Russell, L. J. S. Sherry, *J. Chem. Soc. Chem. Commun. 1984,* 673.
[75] D. J. Gordon, R. F. Fenske, T. N. Nanninga, B. M. Trost, *J. Am. Chem. Soc. 103* (1981) 5974.
[76] T. A. Albright, *J. Organomet. Chem. 198* (1980) 159.
[77] B. M. Trost, T. N. Nanninga, D. M. T. Chan, *Organometallics 1* (1982) 1543.
[78] P. Binger, private communication.
[79] R. Noyori, Y. Kumagai, I. Umeda, H. Takaya, *J. Am. Chem. Soc. 94* (1972) 4018.
[80] R. Noyori, M. Yamakawa, H. Takaya, *Tetrahedron Lett. 1978,* 4823.
[81] L. S. Isaeva, T. A. Peganova, P. V. Petrovskii, D. B. Furman, S. V. Zotova, A. V. Kudryashev, O. V. Bragin, *J. Organomet. Chem. 258* (1983) 367; P. Binger, M. J. Doyle, R. Benn, *Chem. Ber. 116* (1983) 1.
[82] P. Binger, lecture delivered at the University of Wisconsin, Madison, WI, on 10 June 1983.
[83] B. M. Trost, M. J. Bogdanowicz, *J. Am. Chem. Soc. 95* (1973) 5311; B. M. Trost, S. Kurozumi, *Tetrahedron Lett. 1974,* 1929.
[84] K. Kon, S. Isoe, *Tetrahedron Lett. 21* (1980) 3399.
[85] B. M. Trost, J. Lynch, P. Renaut, D. J. Steinman, *J. Am. Chem. Soc.*, in press.
[86] a) Y. Inoue, T. Hibi, M. Satake, H. Hashimoto, *J. Chem. Soc. Chem. Commun. 1979,* 982; b) cf. formation of α-methylene-γ-butyrolactones with 2-bromomethylacrylate esters: E. Öhler, K. Reininger, U. Schmidt, *Angew. Chem. 82* (1970) 480; *Angew. Chem. Int. Ed. Engl. 9* (1970) 457.
[87] P. Binger, H.-J. Weintz, *Chem. Ber. 117* (1984) 654.
[88] Y. Inoue, T. Hibi, Y. Kawashima, H. Hashimoto, *Chem. Lett. 1980,* 1521.
[89] E. Keinan, M. Sahai, *J. Chem. Soc. Chem. Commun. 1984,* 648.
[90] B. M. Trost, J. E. Vincent, *J. Am. Chem. Soc. 102* (1980) 5680.
[91] B. M. Trost, D. P. Curran, *Tetrahedron Lett. 22* (1981) 5023.
[92] B. R. Adams, *Ph. D. Thesis,* University of Wisconsin, Madison, WI, 1984.
[93] B. M. Trost, B. R. Adams, *J. Am. Chem. Soc. 105* (1983) 4849.
[94] B. M. Trost, M. J. Fray, *Tetrahedron Lett. 25* (1984) 4605.
[95] B. M. Trost, D. P. Curran, *J. Am. Chem. Soc. 102* (1980) 5699; *103* (1981) 7380.
[96] T. Tiner-Harding, J. W. Ullrich, F.-T. Chiu, S.-F. Chen, P. S. Mariano, *J. Org. Chem. 47* (1982) 3360.
[97] Review: H. M. R. Hoffmann, *Angew. Chem. 96* (1984) 29; *Angew. Chem. Int. Ed. Engl. 23* (1984) 1.
[98] H. M. R. Hoffmann, A. Weber, R. J. Giguere, *Chem. Ber. 117* (1984) 3325.
[99] H. M. R. Hoffmann, R. Henning, O. R. Lalko, *Angew. Chem. 94* (1982) 464; *Angew. Chem. Int. Ed. Engl. 21* (1982) 442.

The $\sigma^2\pi^4$ Triple Bond between Molybdenum and Tungsten Atoms: Developing the Chemistry of an Inorganic Functional Group

By Malcolm H. Chisholm*

Numerous analogies between organic and inorganic chemistry have emerged in recent years. The most prominent example is the isolobal relationship. Many reactions have shown that metal-metal double and triple bonds exhibit a pattern of reactivity similar to that of alkenes and alkynes. In compounds containing a $\sigma^2\pi^4$ triple bond between molybdenum and tungsten atoms, the M-M bond order can be increased from three to four by reductive elimination or decreased from three to two or one by oxidative addition. Complexes with M≡M bonds can be used to prepare clusters or can serve as catalysts. In this review relationships between structure (electronic and stereochemical) and reactivity that are characteristic for modern inorganic chemistry are discussed.

1. Introduction

It is interesting, at least from a historical perspective, that unsaturation between carbon atoms in simple hydrocarbons was recognized on the basis of chemical reactivity long before the concept of σ and π bonds was understood or even advanced. By contrast, the "discovery" of multiple bonds between the transition elements was laid carefully on a physical and theoretical groundwork based on an understanding of the molecular and electronic structure of such compounds.[1] Once the extent of the field of multiple bonds had been surveyed, interest naturally turned toward chemical reactivity. Are there simple chemical tests available to distinguish between M-M quadruple, triple, and double bonds based on reactivity? Some 20 years after the discovery of the M-M quadruple bond,[2] the answer is still no! In part this should not be surprising since it is not unreasonable that a triple bond between say rhenium atoms should react in any way like a triple bond between osmium or tungsten atoms, just as the triple bonds in ethyne, dinitrogen, and carbon monoxide are quite different in their chemical reactivity. However, this is only a part of the problem. Two other factors enter in and are certainly equally important.

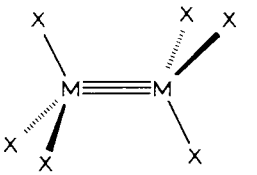
First, the simple molecular orbital (MO) description of the double or triple bonds between carbon atoms is, respectively, $\sigma^2\pi^2$ and $\sigma^2\pi^4$, whereas triple bonds between tungsten atoms, for example, may have a variety of MO configurations: $\sigma^2\pi^4$, $\sigma^2\pi^2\delta^2$, $\pi^4\delta^2$, and even $\sigma^2\pi^4\delta^2\delta^{*2}$. In the latter case, even though the population of both δ and δ* orbitals leads to a cancellation of the δ contribution, the reactivity of this type of triple bond is, as might be expected, quite different from that of triple bonds having the $\sigma^2\pi^4$ configuration. There is an obvious analogy here to the double bonds in say ethylene and dioxygen, which show vastly different chemistry.

The second factor is that the M-M bonding configuration $\sigma^2\pi^4$ for a triple bond, or any of the others listed above, is an oversimplification. In reality a mixing of metal-ligand and metal-metal bonding may occur, and always does occur in the presence of bridging ligands. The highest-energy orbitals (HOMO/LUMO) may be ligand centered, thereby greatly modifying or even obscuring completely the reactivity of the M-M multiple bond. To some extent the latter phenomenon has a parallel in the substituent effects in simple organic alkenes and alkynes, although the effects in transition-metal chemistry are even greater than in organic chemistry.

With this background in mind, my group has been trying over the past 10 years to develop systematically the chemistry of triple bonds between molybdenum and tungsten atoms, keeping the M-M configuration constant, namely, $\sigma^2\pi^4$. This review deals with our present understanding of the bonding and reactivity of this class of compounds. Wherever possible, analogies with the chemistry of the C≡C bond will be presented, since all chemists are familiar with the chemistry of alkynes.

2. The $\sigma^2\pi^4$ M≡M Bond

The simplest complexes having a $\sigma^2\pi^4$ M≡M bond are the unbridged d^3-d^3 dinuclear compounds of molybdenum and tungsten.[3] These include the ethane-like dimers M_2X_6, **1**, X = R (e.g., CH_2SiMe_3), NMe_2, OR, and SAryl,[4]



1

together with a wide variety of mixed-ligand-containing compounds of formula $M_2X_{6-n}Y_n$, where X and Y can be any combination of the above groups and Y may be a halide for n = 2 and X = NMe_2. The structure of $Mo_2(NMe_2)_6$ is shown in Figure 1.

For **1**, X = OR, there is a clear separation in energy between the $\sigma^2\pi^4$ M≡M bonding orbitals and the orbitals of the metal-oxygen σ bonds and oxygen lone pairs. This shows up very nicely in the He(I) and He(II) photoelectron

[*] Prof. M. H. Chisholm
Department of Chemistry, Indiana University
Bloomington, IN 47405 (USA)

 © VCH Verlagsgesellschaft mbH, D-6940 Weinheim, 1986 0570-0833/86/0101-0021 $ 02.50/0

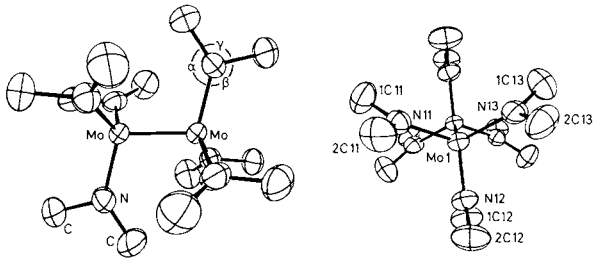
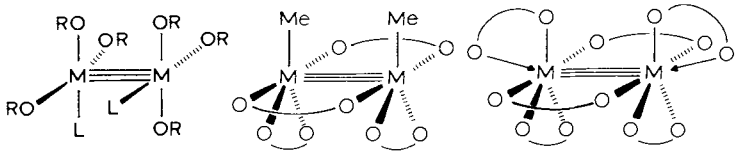


Fig. 1. Two views of the $Mo_2(NC_2)_6$ skeleton of $Mo_2(NMe_2)_6$ showing the unbridged Mo≡Mo bond (Mo-Mo distance: 2.214(3) Å) and the staggered ethane-like Mo_2N_6 moiety (Mo-N: 1.98 Å, Mo-Mo-N: 104°). Left: View perpendicular to Mo-Mo axis. Right: View along Mo-Mo axis. The NC_2 planes are aligned along the Mo-Mo axis, creating six proximal and six distal methyl groups.

spectra, where the ionization energies of the M-M π orbitals and σ orbital are ca. 6-7 and 7-7.5 eV, respectively, whereas those of the M-O σ bonds and the oxygen lone pairs are in the range 8-10 eV. There are some interesting differences in the ionization energies as a function of the metal and the alkoxide ligands, the ease of electron removal being in the order tBuO > iPrO > tBuCH$_2$O and W > Mo.[5,6] These differences are important in determining subtle differences in the chemistry of the $M_2(OR)_6$ compounds (see Section 3). In the compounds $M_2(NMe_2)_6$, there are Me_2N-M π bonds and Me_2N non-bonding electron pairs, the latter being close in energy to the M-M π bonds. In the M_2R_6 compounds, there is extensive mixing of the M-C and M-M bonding orbitals, which all transform as either a or e in a symmetry group with a threefold axis.

In general there is a problem with σ bonds even in the simple diatomics like CO, which, in fact, has several σ components, namely, bonding, non-bonding, and antibonding.[7] In ethyne there is extensive mixing of C-C and C-H σ bonding orbitals such that the C≡C configuration $\sigma^2\pi^4$ is also only an approximation. So too in compounds of type **1** is the M-M configuration $\sigma^2\pi^4$ only a good approximation. Similar arguments can be extended to the d^3-d^3 dimers **2**-**4** with four-, five-, and even six-coordinate metal atoms.



2 **3** **4**

Examples of compounds of type **2** include $[Mo_2(OR)_6L_2]$ compounds, where L is a neutral donor ligand such as an amine, pyridine, or a tertiary phosphane.[8] Other examples arise from the presence of four monodentate and two bidentate ligands at the dinuclear center, e.g., $[M_2(NMe_2)_4(ArylN_3Aryl)_2]$[9] and $[M_2(OR)_4(acac)_2]$.[10] Examples of type **3** and **4** are less common but again the employment of bidentate ligands is helpful, particularly those with small "bite" angles. For instance, in the two compounds of type **3** $[W_2Me_2(O_2CNEt_2)_4]$[11] and $[W_2(CH_2tBu)_2(O_2CMe)_2(S_2CNEt_2)_2]$[12], there are two O_2CX ligands spanning the W≡W bond; two bidentate ligands (O_2CNEt_2 or S_2CNEt_2) and two monodentate ligands (Me or CH_2tBu) complete the coordination such that each tungsten atom forms five bonds to ligand atoms that lie roughly in the same plane. The only structurally characterized compounds of type **4** are $W_2(O_2CNMe_2)_6$[11] and $W_2(O_2Ct$Bu$)_6$.[13] The six bidentate ligands at the $(W{\equiv}W)^{6+}$ center allow the formation of five W-O bonds in a plane perpendicular to the W-W axis supplemented by weak W→O bonds along the W-W axis. The latter vary in length from 2.4 to 2.7 Å and thus the formation of the sixth W-O bond has little perturbation on the structure of compounds of type **3**.

In compounds of types **1**-**4**, the M≡M bond may be considered to be formed from interactions of metal d_{z^2} atomic orbitals to give the σ bond and d_{xz} and d_{yz} atomic orbitals to give π_x and π_y components, respectively. This simple picture is supported by calculations.[14-16] Whenever the molecules contain a threefold axis of symmetry, the π_x and π_y orbitals will be degenerate. For symmetries lower than those found for compounds of type **1**, the degeneracy of the π_x and π_y orbitals will be formally removed, but the two π components will be of similar energy. As a result, facile rotation about the $\sigma^2\pi^4$ M≡M bond is commonly observed and, at least to a first-order approximation, restricted rotations correspond to steric constraints of the ligands spanning the M≡M bond.[17]

The other metal atomic orbitals, s, p_x, p_y, $d_{x^2-y^2}$, and d_{xy}, are used to form M-L bonds in the xy plane: three M-L σ and two M-L π bonds in **1**, four M-L σ and one M-L π bond in **2**, and five M-L σ bonds in **3**. The M-M distances span the range 2.2 to 2.4 Å with W-W distances being ca. 0.08 Å longer than Mo-Mo distances in otherwise identical compounds.

3. Chemical Reactions

3.1. Interconversion of M-M Multiple Bonds

It seemed that redox reactions should, by elimination and addition, allow the interconversion of bond orders between metal atoms in a manner akin to that well established for the interconversion of carbon-carbon bonds of order 3, 2, and 1. Moreover, many of the principles already established for oxidative additions and reductive eliminations in mononuclear chemistry[18-22] should be transferable to dinuclear chemistry. *Cotton* and *Walton* were the first to show that simple electrochemical oxidations and reductions could interconvert M-M bonds of order 4, 3.5, and 3 by feeding electrons into and removing them from δ and δ* orbitals.[1] Our work has focused attention on chemical reactions wherein the ligands are intimately involved in the redox reaction.

3.1.1. Formation of $\sigma^2\pi^4\delta^2$ Quadruple Bonds by Reductive Eliminations from Compounds Containing $\sigma^2\pi^4$ Triple Bonds

Our initial strategy was to devise routes to thermodynamically stable quadruply bonded compounds via elimi-

nation of kinetically labile organic molecules or fragments. Suitable precursor compounds were the 1,2-diorgano dimetal tetraamides, which can readily be prepared from $M_2(NMe_2)_6$ according to the reaction sequence outlined in Reactions (a) and (b).

$$M_2(NMe_2)_6 \xrightarrow[-2\,Me_3SiNMe_2]{+2\,Me_3SiCl} 1,2\text{-}[M_2Cl_2(NMe_2)_4] \quad (a)$$

$$1,2\text{-}[M_2Cl_2(NMe_2)_4] \xrightarrow[-2\,LiCl]{+2\,LiR} 1,2\text{-}[M_2R_2(NMe_2)_4] \quad (b)$$

A wide variety of R groups have been attached to the dinuclear metal center, including R = Me, Et, Pr (*n* and *i*), Bu (*n*, *i*, *s*, and *t*), Ph, *o*- and *p*-tolyl, CH_2Ph, CH_2CMe_3, and CH_2SiMe_3.[23,24] The dimetallacycles ($R=(CH_2)_4$) have also been prepared.[25]

These compounds contain a central ethane-like $M_2N_4C_2$ core with M≡M distances in the range of 2.2 Å (M = Mo) to 2.3 Å (M = W). In the solid state either *anti* or *gauche* rotamers may be found; in solution there is generally a mixture of the two with the equilibrium favoring the *gauche* form. These compounds are thermally stable at room temperature and may be sublimed in vacuo (10^{-4} torr) at ca. 80–120 °C with little decomposition. The reluctance of these compounds to undergo facile β-hydrogen elimination can be understood in terms of the existence of (1) the M≡M bond and (2) the strong Me_2N–M π bond. Metal d orbitals are not available for M–H–C interactions.[23] Also, on thermodynamic grounds, we would not expect the formation of a M–M quadruply bonded compound to be favored by either C–C or C–N coupling reactions since the inorganic residue formed by such an elimination, $Mo_2(NMe_2)_4$ or $Mo_2R(NMe_2)_3$, has no known analogue and is expected to be a relatively high-energy species.

Since CO_2 is known[26] to react with M–NMe_2 bonds to generate, by a formal insertion process, carbamate ligands, O_2CNMe_2, a reaction between $[M_2R_2(NMe_2)_4]$ compounds and CO_2 was expected to open up a route to $M_2(O_2CNMe_2)_4$ compounds, analogues of the well-known carboxylates of formula $Mo_2(O_2CR)_4$ (*Mo*≡*Mo*),[11] providing that the organo ligands R could be eliminated by a kinetically labile pathway.

This expectation was realized in the chemistry of 1,2-$[Mo_2R_2(NMe_2)_4]$ compounds, where R is an alkyl group containing a β-hydrogen atom. These react with CO_2 to give the desired tetracarbamate [Reaction (c)].[27]

$$[Mo_2R_2(NMe_2)_4] + 4\,CO_2 \longrightarrow Mo_2(O_2CNMe_2)_4 + \text{alkene} + \text{alkane} \quad (c)$$

Similarly, reactions involving 1,3-diaryltriazines led to elimination from the dimolybdenum center and formation of quadruply bonded compounds of formula $Mo_2(ArylN_3Aryl)_4$ (*Mo*≡*Mo*) [Reaction (d)].[27]

$$1,2\text{-}[Mo_2R_2(NMe_2)_4] + 4\,ArylNNNHAryl \longrightarrow Mo_2(ArylN_3Aryl)_4 + 4\,HNMe_2 + \text{alkene} + \text{alkane} \quad (d)$$

Rather interestingly, the tungsten analogues $[W_2R_2(NMe_2)_4]$ (R = an alkyl ligand containing β-hydrogen atoms) do not react according to (c) and (d).[28] However, a general procedure for the formation of W–W quadruple bonds has been devised, involving the addition of carboxylic anhydrides to $[M_2R_2(NMe_2)_4]$ [Reaction (e)] (R′ = Me, Et, *t*Bu, Ph).[29]

$$1,2\text{-}[M_2R_2(NMe_2)_4] + 4\,R'COOCR' \longrightarrow M_2(O_2CR')_4 + 4\,R'CONMe_2 + \text{alkene} + \text{alkane} \quad (e)$$

By labeling the alkyl ligands of $[M_2R_2(NMe_2)_4]$, we have found that the β-hydrogen atom of one alkyl ligand is transferred to the α-carbon atom of the other in the elimination step, as shown in Reaction (f).[27]

$$CD_3CH_2\text{–}M{\equiv}M\text{–}CH_2CD_3 \longrightarrow M{\equiv}M + CD_3CH_2D + CD_2{=}CH_2 \quad (f)$$

In reactions involving the metallacyclic compound $[Mo_2(CH_2)_4(NMe_2)_4]$, the formation of the Mo–Mo quadruple bond is accompanied by the liberation of two equivalents of ethylene.[28]

Reactions employing $[M_2R_2(NMe_2)_4]$ compounds where R is an alkyl ligand lacking β-hydrogen atoms, e.g., Me, $PhCH_2$, or $tBuCH_2$, cannot undergo this type of reductive elimination (alkyl group disproportionation). Upon reaction of these compounds with CO_2, compounds of the type $[M_2R_2(O_2CX)_4]$, where $X = NMe_2$[11] or R′,[30] have been isolated. Reductive elimination is still possible, however, and may occur by a radical pathway, which may be promoted either thermally or photochemically. The ease of reductive elimination follows the order Mo > W and $R = PhCH_2 > tBuCH_2$.[31,32] An extension of this type of reductive elimination involves reactions of $[(L_nM')(Me_2N)_2M{\equiv}M(NMe_2)_2(M'L_n)]$, where $L_nM' = CpFe(CO)_2$ or $(Me_3Sn)_3Sn$ [Reaction (g)].[28,33,34]

$$[(L_nM')(Me_2N)_2Mo{\equiv}Mo(NMe_2)_2(M'L_n)] + 4\,CO_2 \longrightarrow Mo_2(O_2CNMe_2)_4 + 2\,L_nM'^{\odot} \quad (g)$$

The fate of $L_nM'^{\odot}$, like that of $R^{\odot}$, depends on its relative reactivity. $[CpFe(CO)_2]^{\odot}$ and $PhCH_2^{\odot}$ undergo dimerization in aromatic solvents. $[(Me_3Sn)_3Sn]^{\odot}$ undergoes decomposition to Me_4Sn and Sn(metal), while $tBuCH_2^{\odot}$ abstracts hydrogen or deuterium from the solvent.

In some instances, reductive elimination was found to occur in what might have been considered the least likely of conditions. For example, during the reaction of $[Mo_2(iBu)_2(NMe_2)_4]$ with *i*PrOH [Reaction (h)], $[Mo_2(OiPr)_4(HOiPr)_4]$, which contains a Mo–Mo quadruple bond, is formed as purple crystals.[35]

$$[Mo_2(iBu)_2(NMe_2)_4] + i\text{PrOH(excess)} \xrightarrow{\text{hexane}} [Mo_2(OiPr)_4(HOiPr)_4] + 4\,HNMe_2 + i\text{BuH} + Me_2C{=}CH_2 \quad (h)$$

3.1.2. Oxidative Additions to Compounds Containing $\sigma^2\pi^4$ Triple Bonds with Formation of $(M{=}M)^{8+}$ and $(M\text{–}M)^{10+}$ Compounds

Following a similar strategy, we attempted to convert a $(M{\equiv}M)^{6+}$ compound into known $(M{=}M)^{8+}$ or $(M\text{–}M)^{10+}$

compounds. The dinuclear alkoxide $Mo_2(OiPr)_6$ was converted into $Mo_2(OiPr)_8$ by reaction with diisopropyl peroxide [Reaction (i)].[36] Steric considerations are apparently important since reactions employing analogous complexes containing *t*BuO ligands and/or *t*BuOO*t*Bu failed to yield oxidative-addition products.[36]

$$Mo_2(OiPr)_6 + iPrOOiPr \longrightarrow Mo_2(OiPr)_8 \quad (i)$$

Halogens, X_2, add to $Mo_2(OiPr)_6$ in solution to give directly $[Mo_2X_4(OiPr)_6]$ (X = Cl, Br, I); only in the case of I_2 is there any evidence for the formation of an intermediate.[26] Similarly, reactions of a variety of substituted (H, alkyl, and Cl) *ortho*-quinones with $M_2(OR)_6$ yield 2:1 adducts,[8,37] as do α-diketones [Reaction (j)].[38] In these reactions, each ligand is reduced by two electrons upon complexation to the M_2 center.

$$M_2(OR)_6 + 2 \;\text{O=C–C=O} \longrightarrow [M_2(OR)_6(O\text{–}C\text{=}C\text{–}O)_2] \quad (j)$$

In the reaction between $Mo_2(OiPr)_6$ and 1,4-diisopropyl-1,4-diaza-1,3-butadiene, the 1:1 adduct $[Mo_2(OiPr)_6(iPrNCH{=}CHNiPr)]$ ($M{=}M$) is formed. Formally, this reaction may be viewed as a Diels-Alder type of addition to the Mo≡Mo bond, although the X-ray structure analysis reveals that the bisamide ligand is chelated to only one metal atom.[39]

The $M_2(OR)_6$ compounds also react with π-acceptor ligands such as CO and acetylenes to form 1:1 adducts, which may be viewed as a redox reaction between the π-acceptor ligand and the M≡M bond as donor.[40] From studies of these reactions it is clear that the reducing power of the W≡W bond is greater than that of the Mo≡Mo bond. In this context, the remarkable metathesis reactions involving $W_2(OtBu)_6$ and alkynes or nitriles [Reactions (k) and (l)] may be viewed as oxidative cleavages, which are favored for W but not Mo.[41,42]

$$W_2(OtBu)_6 + RC{\equiv}CR \longrightarrow 2(tBuO)_3W{\equiv}CR \quad (k)$$
$$W_2(OtBu)_6 + RC{\equiv}N \longrightarrow (tBuO)_3W{\equiv}CR + (tBuO)_3W{\equiv}N \quad (l)$$

The reactions between the M≡M bonds in $M_2(OR)_6$ compounds and the triple bonds in alkynes, nitriles, and carbon monoxide, which are quite fascinating, have been the subject of a recent review[40] and consequently are not discussed further in this article.

3.1.3. Mechanistic Considerations Concerning Oxidative Additions and Reductive Eliminations from Dinuclear Centers

Although in the first few years our efforts were aimed at establishing these types of reactions, the intimate pathway by which they proceed provides a fascinating area for continued research. In the reductive elimination of alkane and alkene from the dinuclear metal center, does β-hydrogen activation occur across the M≡M bond or does alkyl migration occur first, so that the essential features of the elimination parallel reductive elimination from mononuclear metal complexes? The answers to questions like these are currently uncertain but a case can be made for redox chemistry occurring at *one* metal center followed by rapid ligand redistribution reactions. For example, it has been shown that addition of PMe_3 to 1,2-$[Mo_2(CH_2Ph)_2(OiPr)_4]$ produces a facile 1,2 benzyl migration with formation of $[(iPrO)_3Mo{\equiv}Mo(CH_2Ph)_2(OiPr)(PMe_3)]$.[43] The oxidative addition of *i*PrOH to $W_2(OiPr)_6$ to give $[W_2(\mu\text{-}H)(OiPr)_7]_2$, on the other hand, does not proceed in the absence of added base ($HNMe_2$, NMe_3, etc.).[44] Here, a case can be made for initial base promoted formation of a bridged d^3-d^3 dimer followed by oxidative addition of *i*PrOH to one tungsten center. Clearly, detailed mechanistic studies represent an important area for future research.

3.2. Cluster Syntheses

Metal-carbon and metal-metal multiple bonds have been found to be good reagents for metal-cluster building reactions. *Stone*[45] has emphasized the synthetic strategy that has at its root isolobal relationships[46] involving the coordination of C-C double and triple bonds to coordinatively unsaturated metal centers. Many of the ideas advanced by *Stone* and co-workers can be carried over to the chemistry of the M-M triple bonds of configuration $\sigma^2\pi^4$. In addition, many cluster-building reactions of d^0 metal complexes with M≡M compounds can be viewed in terms of redox reactions wherein the electrons of the M-M triple bond are used to form new metal-metal bonds. Alternatively, the M≡M bond may act as a reducing agent toward other metal-ligand bonds, again leading to new M-M and M-L bonding in cluster assembly reactions. Finally, since the M≡M bonds are generally shielded by bulky ligands around the metal center, oligomerization reactions are not favored. Controlled substitution of bulky groups by less bulky groups will thus favor oligomerization. These principles are exemplified in the following cluster building reactions.

3.2.1. $M{\equiv}M(\sigma^2\pi^4) + M'{\equiv}X(d^0)$

The comproportionation of d^0 oxomolybdenum alkoxides with $Mo_2(OR)_6$ compounds provided the first example of this type of reaction [Reaction (m)].[47,49]

$$Mo_2(OR)_6 + MoO(OR)_4 \longrightarrow [Mo_3(\mu_3\text{-}O)(\mu_3\text{-}OR)(\mu_2\text{-}OR)_3(OR)_6] \quad (m)$$

Such reactions are limited by the steric properties of the R group. The oxo-capped triangular Mo_3 compounds are formed when R = *i*Pr and CH_2tBu. When R = *t*Bu, stable (isolable) $M_3O(OR)_{10}$ compounds are not formed. Reaction (m) is directly extendable to the syntheses of $W_3O(OR)_{10}$ compounds by related reactions involving $WO(OR)_4$ and $W_2(OR)_6$ compounds. It is also possible to make the mixed-metal compounds $[Mo_2WO(OR)_{10}]$ (R = *i*Pr, CH_2tBu) [Reaction (n)].[50]

$$Mo_2(OR)_6 + WO(OR)_4 \longrightarrow [Mo_2WO(OR)_{10}] \quad (n)$$

Attempts to prepare the related compounds $[W_2MoO(OR)_{10}]$ failed, probably because the oxo group transfer from d^0-Mo to d^0-W is thermodynamically favorable and the triangular complex breaks apart to give $WO(OR)_4$ compounds. In the case of the bulky *t*BuO ligands, this provides a route to the mixed-metal d^3-d^3 dimers [Reaction (o)], although their isolation free from the homonuclear compounds $M_2(OtBu)_6$ has not been possible.

$$W_2(OtBu)_6 + MoO(OtBu)_4 \longrightarrow WO(OtBu)_4 + MoW(OtBu)_6 \quad (o)$$

Similar reactions employing the carbyne complex $(tBuO)_3W{\equiv}CR'$ and $M_2(OR)_6$ compounds have led to the isolation of W_3 and Mo_2W alkylidyne-capped clusters [Reactions (p) and (q)].[51,53] Steric factors are again important (R = *i*Pr, CH_2tBu, R' = Me, Et, Ph).[53]

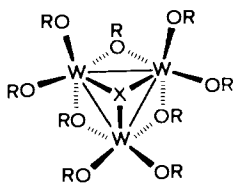
$$(tBuO)_3W{\equiv}CR' + W_2(OR)_6 \xrightarrow[\text{hexane/ROH}]{25\,^\circ C} [W_3(\mu_3\text{-}CR')(\mu_2OR)_3(OR)_6] \quad (p)$$

$$(tBuO)_3W{\equiv}CR' + Mo_2(OR)_6 \xrightarrow[\text{hexane/ROH}]{25\,^\circ C} [Mo_2W(\mu_3\text{-}CR')(\mu_2\text{-}OR)_3(OR)_6] \quad (q)$$

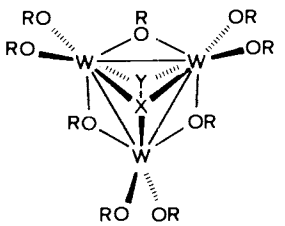
Attempts to prepare the analogous nitrido complexes $[M_2M'(\mu_3\text{-}N)(\mu_2\text{-}OR)_3(OR)_6]$ failed, but, in the presence of alcohols, ROH, imido-capped compounds have been isolated for both molybdenum and tungsten [Reaction (r)].[54,55]

$$(tBuO)_3M{\equiv}N + M_2(OR)_6 \xrightarrow[\text{hexane/ROH}]{25\,^\circ C} [M_3(\mu_3\text{-}NH)(\mu_3\text{-}OR)(\mu_2\text{-}OR)_3(OR)_6] \quad (r)$$

The structure of the alkylidyne-capped M_3 clusters is depicted by **5**, while that common to the oxo- and imido-capped complexes is depicted by **6**. In each case the six electrons of the M≡M bond are used to form three localized M–M single bonds (a^2e^4) in the symmetry group C_3.



5, R = *i*Pr, CH_2tBu; X = Me, Et, Ph



6, R = *i*Pr, CH_2tBu; X = NH, O; Y = OR

By changing the stoichiometry of these reactions, other products may sometimes be obtained. For example, we have prepared a fascinating tetranuclear nitrido molybdenum complex as shown in Reaction (s). We have reason to believe that related alkylidyne complexes may be similarily accessible.[55,56] The molecular structure of the complex $[Mo_4(\mu_3\text{-}N)_2(OiPr)_{12}]$ is shown in Figure 2.

$$Mo_2(OiPr)_6 + 2(iPrO)_3Mo{\equiv}N \xrightarrow[\text{hexane}]{25\,^\circ C} [Mo_4(\mu_3\text{-}N)_2(OiPr)_{12}] \quad (s)$$

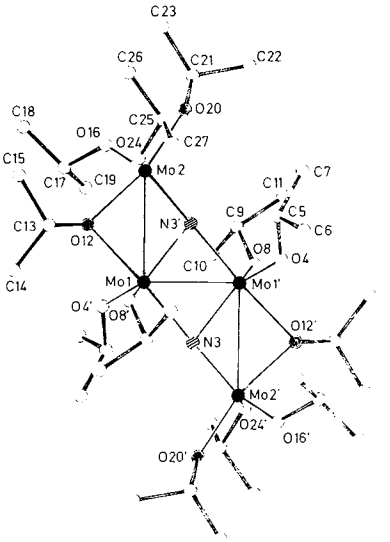


Fig. 2. The centrosymmetric structure of $[Mo_4(\mu_3\text{-}N)_2(OiPr)_{12}]$ in the crystal (ball-and-stick drawing) showing the T-shaped coordination about the nitrogen atoms and the trigonal bipyramidal coordination at each molybdenum atom. The atoms O20, O12, N3, Mo2, and Mo1, together with their symmetry-related atoms, lie in a plane. Important distances [Å]: Mo1-Mo1' 2.552(1), Mo1-Mo2 2.918(1), Mo2-N3' 1.841(2), Mo1-N3 2.034(2), Mo1-N3 1.996(2).

It seems quite likely that similar reactions of $M_2(OR)_6$ compounds with d^0-Nb^V, d^0-Ta^V, or d^1-Re^{VI} oxo, nitrido, or alkylidyne complexes could lead to similar clusters.

3.2.2. 2 M≡M → M_4

The only homonuclear triple bond that is stable with respect to oligomerization is found in N_2. For phosphorus, the dimerization of P_2 to P_4 is rapid, and subsequent oligomerization to polymeric P_x (red or black) is kinetically slow but thermodynamically favorable. In an attempt to oligomerize the M≡M bonds in $M_2(OR)_6$ compounds, we have studied the replacement of the OR group by halides. We believed that substitution of a more electronegative and smaller halide would increase the Lewis acidity of the metal and also make association sterically possible.

Several synthetic routes have been devised for this task, which so far has only been undertaken for molybdenum. We have thereby obtained a fascinating group of $[M_4X_4(OR)_8]$ compounds whose structures are dependent on both the nature of X and R.

The reaction between PF_3 and $Mo_2(OtBu)_6$ (molar ratio 2:1) proceeds smoothly in hexane at temperatures between −78 and 0 °C to give $[Mo_4F_4(OtBu)_8]$ [Reaction (t)].[57,58]

$$2\,Mo_2(OtBu)_6 + 4\,PF_3 \xrightarrow{\text{hexane}} Mo_4F_4(OtBu)_8 + 4\,tBuOPF_2 \quad (t)$$

The molecular structure of $[Mo_4F_4(OtBu)_8]$ is shown in Figure 3. Each molybdenum atom is coordinated by four ligands that lie roughly in a plane and joined to one other molybdenum atom by a Mo≡Mo bond (2.26 Å). The molecule can be viewed as a dimer, $[Mo_2(\mu\text{-}F)_2(OtBu)_4]_2$, which is consistent with the electronic absorption spectrum.[58]

Moreover, the mere addition of PMe_3 leads to cleavage and formation of $[Mo_2F_2(O\mathit{t}Bu)_4(PMe_3)_2]$,[58] which is a compound of type **2**.

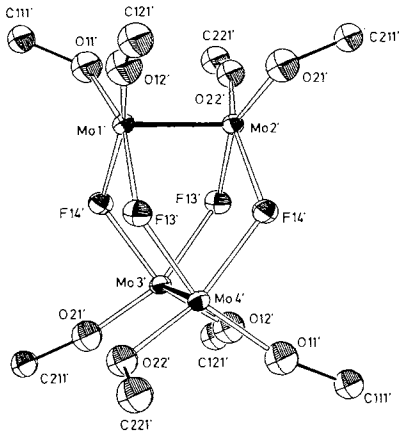


Fig. 3. An ORTEP view of the central skeleton of $[Mo_4(\mu\text{-}F)_4(O\mathit{t}Bu)_8]$. Important distances [Å] and angles [°]: Mo1'-Mo2' 2.262(2), Mo3'-Mo4' 2.263(2), Mo1'-Mo3' 3.743(2), Mo1'-Mo4' 3.730(2), Mo2'-Mo3' 3.713(2), Mo2'-Mo4' 3.700(2), Mo-(μ-F) 2.10(2) (averaged), Mo-O 1.94(2) (averaged), Mo-F-Mo 125° (averaged).

$[Mo_4Cl_4(O\mathit{i}Pr)_8]$ can be prepared from the reaction between $Mo_2(O\mathit{i}Pr)_6$ and MeCOCl (molar ratio 1:2) in toluene, and related reactions employing Me_3SiBr and Me_3SiI allow syntheses of bromo and iodo analogues [Reaction (u)].[59,60]

$$2\,Mo_2(O\mathit{i}Pr)_6 + 4\,Y{-}X \xrightarrow[\text{toluene}]{25\,^\circ C} [Mo_4X_4(O\mathit{i}Pr)_8] + 4\,YO\mathit{i}Pr \qquad (u)$$

$Y = MeCO, Me_3Si;\ X = Cl, Br, I$

The molecular structure of the chloro compound in the solid state (Fig. 4) consists of a square of molybdenum atoms with Mo-Mo distances of 2.37(1) Å, eight μ_2-O*i*Pr ligands, four lying above the Mo_4 plane and four below, and Mo-Cl bonds radiating from the center of the Mo_4-square.[59]

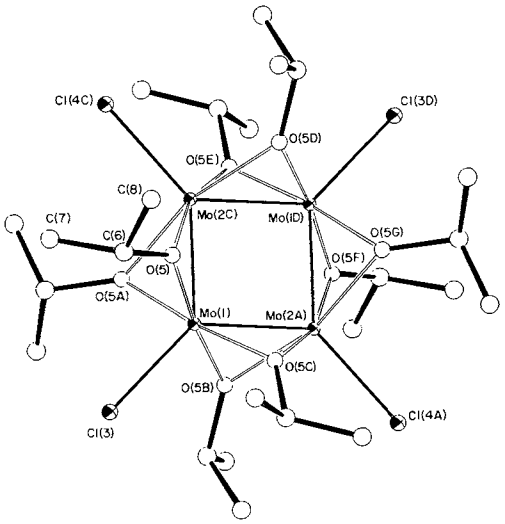


Fig. 4. An ORTEP view of the skeleton of $[Mo_4Cl_4(O\mathit{i}Pr)_8]$. The $Mo_4Cl_4O_8$ unit has virtual, but not crystallographically imposed D_{4h} symmetry. Each molybdenum atom is in a square-pyramidal environment ($ClMoO_4$) with the Cl atom occupying the axial position. Important distances [Å]: Mo-Mo 2.37, Mo-O 1.98, Mo-Cl 2.44.

The molecular structure of the bromo compound in the solid state (Fig. 5) consists of an Mo_4-butterfly with five short Mo-Mo distances, (average: 2.51(2) Å) and one long (non-bonding) Mo-Mo distance (3.1 Å). Two O*i*Pr ligands cap the two Mo_3 triangles, four symmetry-related μ_2-O*i*Pr ligands bridge the edges, and two O*i*Pr ligands, as well as the four bromo ligands, are terminal.[59]

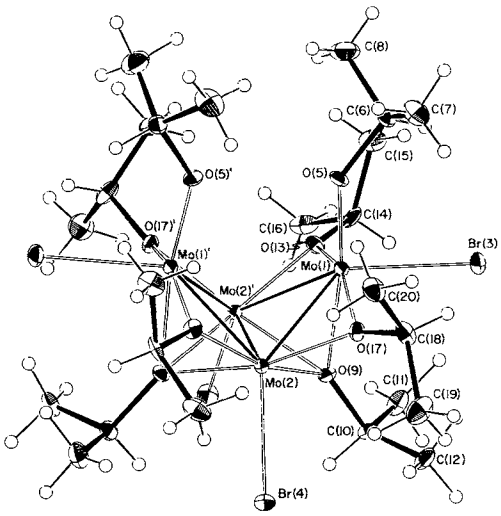


Fig. 5. An ORTEP view of the structure of $[Mo_4Br_4(O\mathit{i}Pr)_8]$. The molecule has C_{2v} symmetry with two equivalent μ_3-O*i*Pr ligands (Mo-(μ_3-O) 2.19 Å), four equivalent μ_2-O*i*Pr ligands (Mo-(μ_2-O) 2.02 Å), two terminal O*i*Pr ligands (Mo-O 1.84 Å), and four terminal bromo ligands (Mo-Br 2.59 Å). Each molybdenum atom is in a square-pyramidal environment ($BrMoO_4$) with the Br atom in the axial position. The Mo_4 butterfly has five Mo-Mo distances of 2.51 Å (averaged) and one long, formally non-bonding, Mo-Mo distance of 3.1 Å between the wing-tip Mo atoms Mo(1) and Mo(1)'.

The molecular structure of the iodo compound has not been determined by a single-crystal X-ray study, but from infrared and ^{1}H-NMR data it can be seen to be directly analogous to the bromo compound.[60]

Rather interestingly, all three $[Mo_4X_4(O\mathit{i}Pr)_8]$ compounds (X = Cl, Br, I) adopt a butterfly Mo_4 geometry with C_{2v} symmetry in toluene solutions at low temperatures but are fluxional at room temperature, showing O*i*Pr ligand exchange on the NMR time scale.[60] Furthermore, it is possible to isolate an intermediate compound in the synthesis of $[Mo_4X_4(O\mathit{i}Pr)_8]$ (X = Cl, Br), namely, $[Mo_4X_3(O\mathit{i}Pr)_9]$. On the basis of an X-ray study, the bromo compound is found to have a butterfly Mo_4 unit (Fig. 6).[60] The ^{1}H-NMR spectrum (Fig. 7) of the chloro compound supports an analogous structure.

Why does $[Mo_4Cl_4(O\mathit{i}Pr)_8]$ adopt a square Mo_4 structure whereas the related bromo and iodo compounds, and even the immediate precursor, have butterfly Mo_4 structures? The only logical answer to this question is that packing forces are sufficient to cause a geometry change in the solid-state structure of $[Mo_4Cl_4(O\mathit{i}Pr)_8]$ and that the total energies of the square and butterfly molecules are very similar. At first this might seem surprising, but both can be considered as fragments of the well-known $[Mo_6(\mu_3\text{-}X)_8]^{4+}$ structure (see Fig. 8).[61-63] The fluxional process interconverting the O*i*Pr ligands in solution is intramolecular and

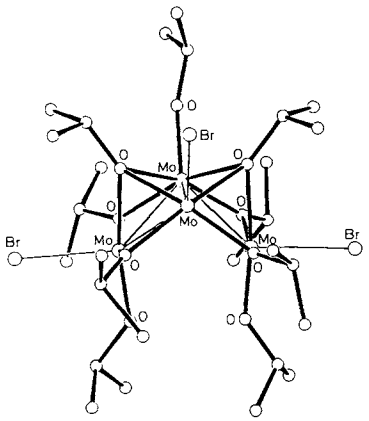


Fig. 6. The structure of $[Mo_4Br_3(OiPr)_9]$ (ball-and-stick drawing). The Cl and I analogues have the same type of structure, which differs from that of the $[Mo_4Br_4(OiPr)_8]$ molecule (Fig. 5) by the replacement of one Br atom by O*i*Pr on one of the central molybdenum atoms. The Mo–Mo, Mo–O, and Mo–Br distances are essentially identical to those in $[Mo_4Br_4(OiPr)_8]$ (see caption to Fig. 5) except that the Mo–O bond of the additional O*i*Pr ligand is longer (1.94 Å).

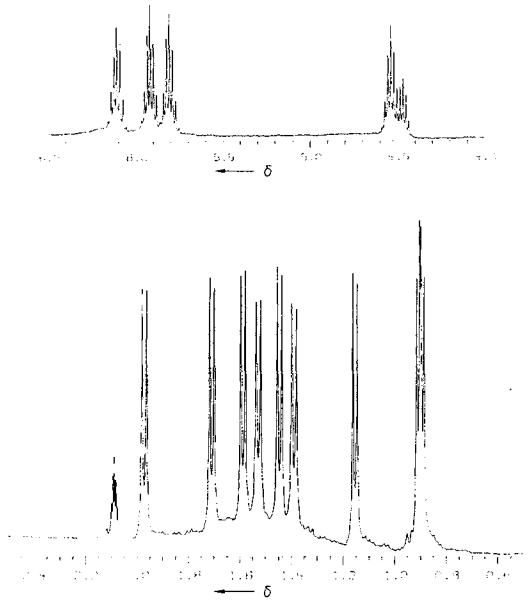


Fig. 7. ^{1}H-NMR spectrum of $[Mo_4Cl_3(OiPr)_9]$ ([D_8]toluene, 22°C, 360 MHz). Top: five methine septets in the integral ratio 2:2:2:2:1; bottom: the nine partially overlapping sets of methyl doublets. The molecule has only a mirror plane of symmetry containing the backbone Mo atoms, the Br atom, and the unique Mo–O bond between the O*i*Pr ligand and one of the backbone Mo atoms (see Fig. 6).

could well involve the interchange Mo_4-butterfly ⇌ Mo_4-square.

Thus far we have not been able to prepare and characterize the fluoro compound $[Mo_4F_4(OiPr)_8]$, which may have yet another geometry or be unstable with respect to further oligomerization. However, by reaction of $Mo_2(OiPr)_6$ with MeCOF (molar ratio 1:1) or PF_3 [Reaction (v)], we have been able to isolate a crystalline sub-

$$2\,Mo_2(OiPr)_6 + 2\,MeCOF/PF_3 \xrightarrow[\text{toluene}]{-80^\circ C} [Mo_4(\mu\text{-}F)_2(\mu\text{-}OiPr)_2(OiPr)_8] + 2\,MeCOOiPr/iPrOPF_2 \quad (v)$$

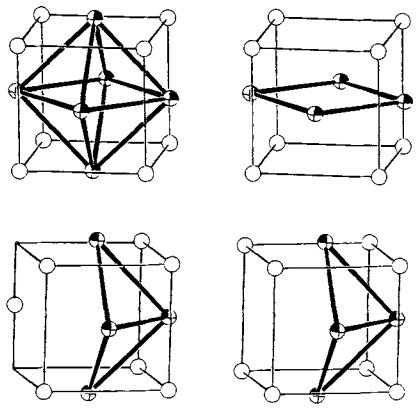


Fig. 8. Cube-octahedral structure of $[Mo_6(\mu_3\text{-}X)_8]^{4+}$ compounds (top left); Mo_4O_8 moiety in $[Mo_4Cl_4(OiPr)_8]$ (top right); Mo_4O_8 moiety in $[Mo_4Br_4(OiPr)_8]$ (bottom right); $Mo_4I_7^{2+}$ moiety in $Mo_4I_{11}^{2-}$ (bottom left): S. Stensrad, B. J. Helland, M. W. Babich, R. A. Jacabson, R. E. McCarley, *J. Am. Chem. Soc. 100* (1978) 6257.

stance of formula $[Mo_4F_2(OiPr)_{10}]$, which has a rectangular Mo_4 unit in the solid state with two Mo≡Mo bonds (2.23 Å) and two Mo–Mo non-bonding distances of 3.7 Å (Fig. 9).[60]

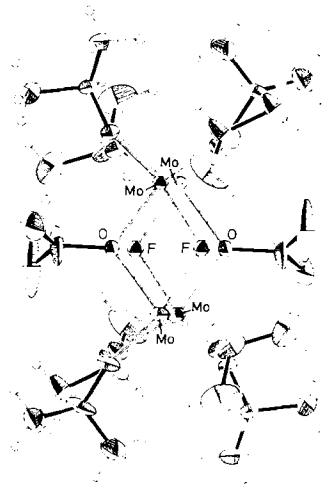


Fig. 9. An ORTEP view of the centrosymmetric structure of $[Mo_4F_2(OiPr)_{10}]$ (Mo-Mo distance: 2.23 Å). The dimer $[Mo_2(\mu\text{-}F)(\mu\text{-}OiPr)(OiPr)_4]_2$ is formed by fluoride and alkoxide bridges. The non-bonding Mo–Mo distances are 3.41 Å and the Mo–F–Mo and Mo–O–Mo angles 109° and 108°, respectively.

It should be noted that the rectangular Mo_4 unit found for $[Mo_4F_2(OiPr)_{10}]$ provides a way of preserving the Mo≡Mo bonds—namely, by the formation of bridging fluoride groups—that is an alternative to the bisphenoid Mo_4 unit in $[Mo_4F_4(OtBu)_8]$ (Fig. 3).

It is tempting to suggest that all reactions involving replacement of halide by OR proceed in a similar manner for $Mo_2(OR)_6$ compounds, differing only in the dimerization of the two dinuclear centers. This is controlled by both the steric properties of R and the nature of the halide. The initial dimerization occurs via Mo–X–Mo bridges as seen for X = F in the characterized products. However, for X = Cl, Br, or I, the halide is capable of forming relatively acute Mo–X–Mo angles, which allow, with OR bridge forma-

tion, the assembly of Mo_4 cluster units. Of course, more work still needs to be done to characterize compounds of empirical formula $MoF(OiPr)_2$, which could turn out to be higher oligomers than the $[Mo_4X_4(OR)_8]$ compounds thus far characterized.

Although the thrust of this article is placed on syntheses involving compounds with M≡M bonds, it is worth noting, at least in passing, that these 12e Mo_4 clusters are fascinating with respect to geometry and electronic structure. The structure of $[Mo_4Cl_4(OiPr_8]$ provides the first example of a 12e square M_4 unit and is well suited for modern calculational techniques.

Fenske-Hall calculations reveal that the Mo_4^{12+} unit is indeed an inorganic analogue of square cyclobutadiene, although the introduction of the ligands removes the strict analogy with the C_4H_4 molecule.[64] The twelve electrons are accommodated in M-M bonding molecular orbitals; ten electrons occupy M-M σ orbitals and two electrons an M-M π orbital. An orbital energy-level diagram that follows the mainly Mo-Mo bonding MOs of the Mo_4^{12+} core through the various stages of ligand addition for the model compound $[Mo_4Cl_4(OH)_8]$ is shown in Figure 10.

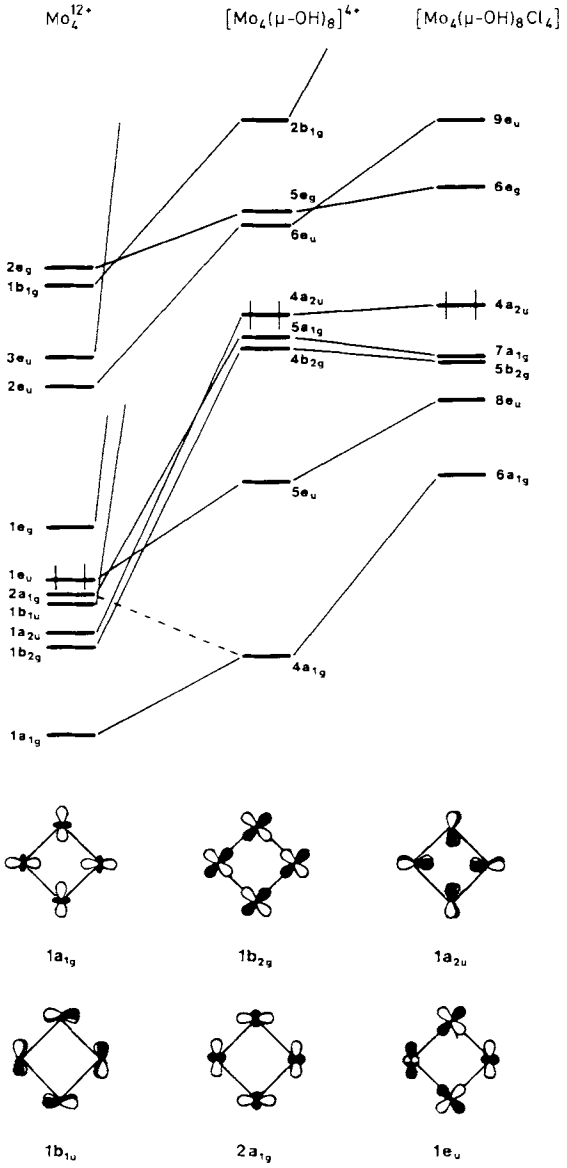


Fig. 10. MO correlation diagram for a square Mo_4^{12+} unit (left), following the mainly M-M bonding orbitals as ligation occurs through (1) introduction of the eight μ-OH ligands (center) and (2) introduction of the four terminal Cl ligands (right). The twelve electrons of the Mo_4^{12+} cluster occupy MOs belonging to the irreducible representations a_{1g} (two), b_{2g}, a_{2u}, b_{1u}, and e_u, which arise from the interactions of Mo d atomic orbitals (bottom). Note: only one of the e_u set is shown pictorially, and in Mo_4^{12+} the HOMO, $1e_u^2$, represents a diradical. There are eight electrons in M-M σ MOs and four in M-M π MOs (a_{2u} and b_{1u}); Mo_4^{12+} is thus the formal inorganic analogue of C_4H_4. Introduction of the eight μ-OH ligands increases the energy of the $1b_{1u}$ orbital. The introduction of the four Cl ligands principally affects the energies of the a_{1g} and e_u orbitals. In the resulting hypothetical $[Mo_4(\mu\text{-}OH)_8Cl_4]$, ten electrons occupy M-M σ MOs (a_{1g}, e_u, b_{2g}, and a_{1g}) and two electrons a π MO, a_{2u}, which is the HOMO.

3.2.3. $M{\equiv}M + M'L \rightarrow M_2(L')M'$

The reducing power of the M≡M bond can be used in reactions with metal complexes that contain redox-active ligands. In the heteronuclear metal complexes formed, the ligand L, originally bonded to one metal center, is now bonded to the M_2 center (M = Mo, W) and changed in character (L→L'); both the formal oxidation state and, of course, the mode of bonding are different since the newly created ligand, L', is now shared between M' and the M_2 group. The general applicability of this concept should be far reaching and is well illustrated in the following two reactions.

1. Alkynes react with $M_2(OR)_6$ compounds to give a wide variety of compounds: alkylidyne η^1 and μ complexes via C≡C scission, alkyne adducts, and a variety of products derived from C-C coupling reactions.[40] The reactions between alkynylmetal complexes (M'L) and $M_2(OR)_6$ might be expected to lead to heteronuclear C_1 or C_2 carbido-containing compounds. The reaction between $W_2(OtBu)_6$ and *trans*-$[Pt(C{\equiv}CH)_2(PMe_2Ph)_2]$ (molar ratio 2:1) leads by successive elimination of *t*BuOH to *trans*-$[Pt\{C_2W_2(OtBu)_5\}_2(PMe_2Ph)_2]$ [Reaction (w)].[65]

$$\textit{trans}\text{-}[Pt(C{\equiv}CH)_2(PMe_2Ph)_2] + W_2(OtBu)_6 \xrightarrow[-t\text{BuOH}]{25\,^\circ C,\ \text{hexane}}$$

$$\textit{trans}\text{-}[Pt(C{\equiv}CH)\{C_2W_2(OtBu)_5\}(PMe_2Ph)_2] \xrightarrow[-t\text{BuOH}]{+W_2(OtBu)_6} \quad \text{(w)}$$

$$\textit{trans}\text{-}[Pt\{C_2W_2(OtBu)_5\}_2(PMe_2Ph)_2]$$

trans-$[Pt\{C_2W_2(OtBu)_5\}_2(PMe_2Ph)_2]$ adopts a centrosymmetric structure in the solid state (Fig. 11). The square-planar geometry about the platinum atom together with the observed Pt-P and Pt-C distances and coupling constants ($^1J_{^{195}Pt-^{31}P} = 2776$ Hz and $^1J_{^{195}Pt-^{13}C} = 801$ Hz) are consistent with the view that this compound may be considered a derivative of Pt^{II}. However, the $C_2W_2(OtBu)_5$ moiety shows that redox chemistry has occurred between the $(W{\equiv}W)^{6+}$ center and the C≡C moiety. Indeed, based on C-C, W-C, and W-W distances, the C_2 ligand is best viewed as a dicarbido ligand, C_2^{4-}, with charge being partitioned as −1 to Pt, −1 to W3 and −2 to W2.

2. In that no new metal-metal bonds are formed, the above reaction does not truly conform to the description of a cluster-building reaction. An example of a reaction in which both ligand reduction and M-M' bond formation

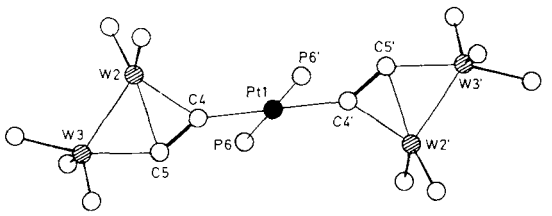


Fig. 11. The structure of the central skeleton of *trans*-$[Pt\{C_2W_2(O/Bu)_5\}_2(PMe_2Ph)_2]$ (ball-and-stick drawing). The PtC_2W_2 unit is planar. Selected distances [Å] and angles [°]: Pt-C4 2.06(1), Pt-P 2.29(1), W-W 2.44(1), W2-C4 2.05(1), W2-C5 2.12(1), W3-C5 2.06(1), W-O 1.91(2) (averaged), C4-C5 1.33(1), Pt1-C4-C5 144.0(1), Pt-C4-W2 140.5(1), W2-C4-C5 74.4(1), W3-C5-C4 140.2(1), W2-C5-C4 68.6(1), W2-C5-W3 71.7(1).

occur is the reaction between $[W_2(OiPr)_6(py)_2]$ ($M{\equiv}M$) and $[Fe_2(CO)_6(\mu\text{-}S_2)]$ ($M{-}M$) [Reaction (x)].[66]

$$[W_2(OiPr)_6(py)_2] + [Fe_2(CO)_6(\mu\text{-}S_2)] \xrightarrow[\text{hexane}]{25\,^\circ C} [W_2Fe_2(\mu_3\text{-}S)_2(OiPr)_6(CO)_5(py)] + py + CO \quad (x)$$

Given the formula $[W_2Fe_2S_2(OiPr)_6(CO)_5(py)]$ one would be hard pressed to predict the molecular structure, which is shown in Figure 12. The ^{1}H-NMR and infrared data of the compound *in solution* are consistent with expectations based on this structure. Furthermore, the molecule is not fluxional on the NMR time scale.

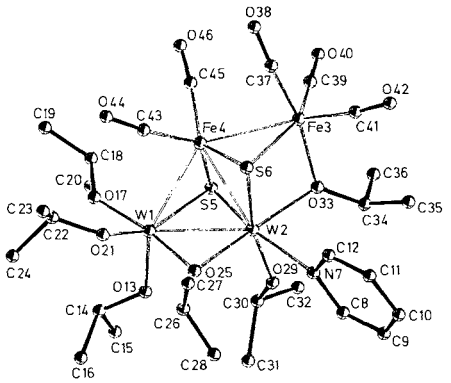


Fig. 12. Structure of $[W_2Fe_2S_2(OiPr)_6(CO)_5(py)]$ in the crystal (ball-and-stick drawing), showing the μ_3-S ligands capping triangular W_2Fe and Fe_2W units below and above the W_2Fe_2 plane. Important M-M distances [Å]: W1-W2 2.714(1), W1-Fe4 2.699(3), W2-Fe3 3.148(3), W2-Fe4 2.632(3).

There are several points worthy of note. 1) The S_2^{2-} ligand in $[Fe_2(CO)_6(S_2)]$ has been reduced to two S^{2-} ligands, which cap the two M_2M' triangles above and below the planar W_2Fe_2 unit. 2) The loss of one CO ligand, formally from Fe4, leaves one Fe atom electron-deficient with respect to the 18-electron rule. The carbene-like Fe center, Fe4, thus adds across the $(W{=}W)^{8+}$ moiety resulting from the S_2^{2-} reduction noted above. 3) The W_2 center has thus been formally oxidized to $(W\text{-}W)^{10+}$, consistent with its W-W distance of 2.714(1) Å and the pseudo-octahedral coordination about each W atom.[8] 4) The electron count at Fe3 satisfies the 18-electron rule in the absence of a W-Fe bond (W2-Fe3 3.148(3) Å) but with a dative bond formed by the μ-O*i*Pr ligand.

4. Concluding Remarks

1. There is an extensive coordination chemistry involving $\sigma^2\pi^4$ triple bonds between molybdenum and tungsten atoms. Not all tungsten and molybdenum d^3-d^3 dimers have this type of M-M bond and the systematic interconversion of various types of d^3-d^3 dimers having the M-M bonding configurations $\sigma^2\pi^4$, $\pi^4\delta^2$, $\sigma^2\pi^2\delta^2$, or $\sigma^2\pi^2\delta^2\delta^{*2}$ remains to be achieved.

2. It is possible to increase M-M bond orders from three to four and to decrease them from three to two or one in a manner somewhat akin to that well documented in organic chemistry. The reactions described here involve oxidative addition or reductive elimination from the dinuclear metal center. The detailed reaction pathway of such reactions remains a topic for active research. The coupling of oxidative addition and reductive elimination opens up the possibility of using these dinuclear centers in catalytic reactions. At least two such processes have already been observed: a) the oligomerization of alkynes in their reactions with $Mo_2(OR)_6$ compounds[67] and b) the isomerization of terminal alkenes to *cis*-2-alkenes by $[W_2(H)(OiPr)_7]_2$.[68]

3. The M≡M moiety provides a building block for the synthesis of heteronuclear compounds. This may be by direct attachment to the M≡M moiety as in the synthesis of compounds of the type $[M_2\{Sn(SnMe_3)_3\}_2(NMe_2)_4]$, which retain the central ethane-like $Sn(N)_2M{\equiv}M(N)_2Sn$ skeleton (M = Mo or W) or by the use of redox reactions involving either ligands or electron-deficient metal centers. The latter often, but not necessarily, afford cluster-building reactions. It is also possible to devise oligomerization reactions involving the M≡M bonds. Thus far, a fascinating array of 12e Mo_4-containing compounds have been characterized. We do not envisage that the reactions should stop here but rather expect that further oligomerization reactions should be possible giving M_6- or M_8-containing compounds.

4. The M_2 center can serve both as a reducing agent and a template for C-C bond coupling reactions involving RC≡CR, RC≡N, and C≡O ligands. These have not been described in this article since a recent review dealt specifically with this aspect of the chemistry of M≡M bonds.[40] It should be noted, however, that the reducing power of the dimetal center, particularly the W≡W bond in $W_2(OtBu)_6$, far exceeds that displayed by mononuclear metal centers. The reactions between alkynes and nitriles, which lead to cleavage of the W≡W bond with formation of W≡CR and W≡N groups, respectively, represent a formal 6e reduction of the RC≡CR or RC≡N ligands. In some instances it takes more than one dinuclear center to effect cleavage of a C-X multiple bond, as is the case in the reaction between acetone and $[W_2(OiPr)_6(py)_2]$ [Reaction (y)], which provides a molecular model for the McMurray reaction.[69,70]

$$2[W_2(OiPr)_6(py)_2] + 2\,Me_2C{=}O \xrightarrow[\text{hexane}]{25\,^\circ C} [W_4O_2(OiPr)_{12}] + Me_2C{=}CMe_2 \quad (y)$$

Clearly, the opportunities for organic and inorganic syntheses using metal-metal multiple bonds are just beginning to be realized.

I thank my co-workers for their various and talented contributions and the National Science Foundation for financial support over the past several years for work in this area.

Received: September 16, 1985 [A 561 IE]
German version: *Angew. Chem. 98* (1986) 21

[1] F. A. Cotton, R. A. Walton: *Multiple Bonds Between Metal Atoms*, Wiley, New York 1982.
[2] F. A. Cotton, N. F. Curtis, C. B. Harris, B. F. G. Johnson, S. J. Lippard, J. T. Mague, W. R. Robinson, J. S. Wood, *Science 145* (1964) 1305.
[3] M. H. Chisholm, F. A. Cotton, *Acc. Chem. Res. 11* (1978) 356.
[4] M. H. Chisholm, J. F. Corning, K. Folting, J. C. Huffman, *Polyhedron 4* (1985) 383.
[5] F. A. Cotton, G. G. Stanley, B. Kalbacher, J. C. Green, E. Seddon, M. H. Chisholm, *Proc. Natl. Acad. Sci. USA 74* (1977) 3109.
[6] E. M. Kober, D. L. Lichtenberger, unpublished results.
[7] H. B. Gray, R. L. DeKock: *Chemical Structure and Bonding*, Benjamin/Cummings, Menlo Park, CA, USA 1980.
[8] M. H. Chisholm, *Polyhedron 2* (1983) 681.
[9] M. H. Chisholm, K. Folting, D. A. Haitko, J. C. Huffman, *Inorg. Chem. 20* (1981) 171.
[10] M. H. Chisholm, K. Folting, J. C. Huffman, A. L. Ratermann, *Inorg. Chem. 23* (1984) 613.
[11] M. H. Chisholm, F. A. Cotton, M. W. Extine, B. R. Stults, *Inorg. Chem. 16* (1977) 603.
[12] M. H. Chisholm, W. G. Van Der Sluys, J. C. Huffman, unpublished results.
[13] M. H. Chisholm, J. A. Heppert, D. A. Hoffman, J. C. Huffman, *Inorg. Chem. 24* (1985) 3214.
[14] B. E. Bursten, F. A. Cotton, J. C. Green, E. A. Seddon, G. G. Stanley, *J. Am. Chem. Soc. 102* (1980) 4579.
[15] M. B. Hall, R. A. Koh, *Inorg. Chem. 22* (1983) 728; *J. Am. Chem. Soc. 102* (1980) 2104.
[16] T. Ziegler, *J. Am. Chem. Soc. 105* (1983) 7543.
[17] M. H. Chisholm, K. Folting, J. C. Huffman, I. P. Rothwell, *Organometallics 1* (1982) 251.
[18] J. Halpern, *Acc. Chem. Res. 3* (1970) 386.
[19] L. Vaska, *Acc. Chem. Res. 1* (1968) 335.
[20] J. P. Collman, *Acc. Chem. Res. 1* (1968) 136.
[21] J. K. Kochi: *Organometallic Mechanisms and Catalysis*, Academic Press, New York 1978.
[22] C. A. Tolman, *Chem. Soc. Rev. 1* (1972) 337.
[23] M. H. Chisholm, D. A. Haitko, J. C. Huffman, *J. Am. Chem. Soc. 103* (1981) 4046.
[24] M. J. Chetcuti, M. H. Chisholm, K. Folting, D. A. Haitko, J. C. Huffman, J. Janos, *J. Am. Chem. Soc. 105* (1983) 1163.
[25] M. J. Chetcuti, M. H. Chisholm, H. T. Chiu, J. C. Huffman, *Polyhedron 4* (1985) 1213.
[26] M. H. Chisholm, M. W. Extine, *J. Am. Chem. Soc. 99* (1977) 782, 792.
[27] M. J. Chetcuti, M. H. Chisholm, K. Folting, D. A. Haitko, J. C. Huffman, *J. Am. Chem. Soc. 104* (1982) 2138.
[28] M. H. Chisholm, H. T. Chiu, unpublished results.
[29] M. H. Chisholm, H. T. Chiu, J. C. Huffman, *Polyhedron 3* (1984) 759.
[30] M. H. Chisholm, D. M. Hoffman, J. C. Huffman, W. G. Van Der Sluys, S. Russo, *J. Am. Chem. Soc. 106* (1984) 5386.
[31] M. J. Chetcuti, M. H. Chisholm, K. Folting, J. C. Huffman, J. Janos, *J. Am. Chem. Soc. 104* (1982) 4684.
[32] M. H. Chisholm, W. G. Van Der Sluys, unpublished results.
[33] M. J. Chetcuti, M. H. Chisholm, H. T. Chiu, J. C. Huffman, *J. Am. Chem. Soc. 105* (1983) 1060.
[34] M. H. Chisholm, H. T. Chiu, K. Folting, J. C. Huffman, *Inorg. Chem. 23* (1984) 4097.
[35] M. H. Chisholm, K. Folting, J. C. Huffman, R. J. Tatz, *J. Am. Chem. Soc. 106* (1984) 1153.
[36] M. H. Chisholm, C. C. Krikpatrick, J. C. Huffman, *Inorg. Chem. 20* (1981) 871.
[37] T. P. Blatchford, M. H. Chisholm, J. C. Huffman, unpublished results.
[38] M. H. Chisholm, J. C. Huffman, A. L. Ratermann, *Inorg. Chem. 22* (1983) 4100.
[39] M. H. Chisholm, J. C. Huffman, J. J. Koh, unpublished results.
[40] M. H. Chisholm, D. M. Hoffman, J. C. Huffman, *Chem. Soc. Rev. 14* (1985) 69.
[41] R. R. Schrock, M. L. Listemann, L. G. Sturgeoff, *J. Am. Chem. Soc. 104* (1982) 4291.
[42] M. L. Listemann, R. R. Schrock, *Organometallics 4* (1985) 74.
[43] M. H. Chisholm, J. C. Huffman, R. J. Tatz, *J. Am. Chem. Soc. 106* (1984) 5385.
[44] M. H. Chisholm, J. C. Huffman, C. A. Smith, *J. Am. Chem. Soc.*, in press.
[45] F. G. A. Stone, *Angew. Chem. 96* (1984) 85; *Angew. Chem. Int. Ed. Engl. 23* (1984) 89.
[46] R. Hoffmann, *Angew. Chem. 94* (1982) 725; *Angew. Chem. Int. Ed. Engl. 21* (1982) 711.
[47] M. H. Chisholm, K. Folting, J. C. Huffman, C. C. Kirkpatrick, *J. Am. Chem. Soc. 103* (1981) 5967.
[48] M. H. Chisholm, K. Folting, J. C. Huffman, C. C. Kirkpatrick, *Inorg. Chem. 23* (1984) 1021.
[49] M. H. Chisholm, F. A. Cotton, A. Fang, E. M. Kober, *Inorg. Chem. 23* (1984) 749.
[50] M. H. Chisholm, K. Folting, J. C. Huffman, E. M. Kober, *Inorg. Chem. 24* (1985) 241.
[51] M. H. Chisholm, D. M. Hoffman, J. C. Huffman, *Inorg. Chem. 23* (1984) 3683.
[52] M. H. Chisholm, K. Folting, J. A. Heppert, D. M. Hoffman, J. C. Huffman, *J. Am. Chem. Soc. 107* (1985) 1234.
[53] M. H. Chisholm, B. K. Conroy, D. M. Hoffman, J. C. Huffman, *J. Am. Chem. Soc.*, in press.
[54] M. H. Chisholm, D. M. Hoffman, J. C. Huffman, *Inorg. Chem. 24* (1985) 796.
[55] M. H. Chisholm, N. S. Marchant, unpublished results.
[56] M. H. Chisholm, K. Folting, J. C. Huffman, J. Leonelli, N. S. Marchant, C. A. Smith, L. C. E. Taylor, *J. Am. Chem. Soc. 107* (1985) 3722.
[57] M. H. Chisholm, J. C. Huffman, R. L. Kelly, *J. Am. Chem. Soc. 101* (1979) 7100.
[58] M. H. Chisholm, D. L. Clark, J. C. Huffman, *Polyhedron 4* (1985) 1203.
[59] M. H. Chisholm, R. J. Errington, K. Folting, J. C. Huffman, *J. Am. Chem. Soc. 104* (1982) 2025.
[60] M. H. Chisholm, D. L. Clark, J. C. Huffman, unpublished results.
[61] H. Schäfer, H. G. Schnering, *Angew. Chem. 76* (1964) 833.
[62] L. J. Guggenberger, A. W. Sleight, *Inorg. Chem. 8* (1969) 2041.
[63] P. C. Healy, D. L. Keppert, D. Taylor, A. H. White, *J. Chem. Soc. Dalton Trans. 1973*, 646.
[64] B. E. Bursten, M. H. Chisholm, D. L. Clark, unpublished results.
[65] R. J. Blau, M. H. Chisholm, K. Folting, R. J. Wang, *J. Chem. Soc. Chem. Commun. 1985*, 1582.
[66] M. H. Chisholm, J. C. Huffman, J. J. Koh, unpublished results.
[67] M. H. Chisholm, K. Folting, J. C. Huffman, I. P. Rothwell, *J. Am. Chem. Soc. 104* (1982) 4389.
[68] M. Akiyama, M. H. Chisholm, F. A. Cotton, D. A. Haitko, D. Little, J. Leonelli, *J. Am. Chem. Soc. 103* (1981) 779.
[69] T. P. Blatchford, M. H. Chisholm, K. Folting, J. C. Huffman, *J. Chem. Soc. Chem. Commun. 1984*, 1295.
[70] J. E. McMurry, *Acc. Chem. Res. 16* (1983) 405.

The Chemistry of the Noncrystalline State

By Stephen R. Elliott, C. N. R. Rao, and John M. Thomas*

This article sets out to describe and account for the chemical and physical consequences of the presence of gross disorder in solids. Knowledge of the structure of such disordered materials is an obvious prerequisite to a further understanding of other properties and behavior, and our current knowledge of the structure of various noncrystalline systems is discussed together with the experimental techniques which need to be employed in order to obtain such information. The so-called glass transition, which takes place as a liquid is supercooled below the crystallization temperature, is discussed in terms of the various models which have been proposed to account for this phenomenon. The effect of noncrystallinity on electronic properties is also discussed, and we highlight new developments in the understanding of electron localization and transport processes. Finally, two applications of amorphous solids are considered in some detail: optical fibers for use in communication networks and "superionic" glasses for possible use in solid-state batteries.

1. Introduction

Many catalysts and catalyst supports, most optical fibers and numerous other optical components, several xerographic photoreceptors and thin-film transistors, large-area solar cells, a substantial proportion of biominerals—these and some other materials of considerable technological and biological importance have one feature in common: they are noncrystalline. Chemists are so innured to the pictures portrayed in textbooks of elemental structural chemistry that they are apt to assume that all solids are devoid of structural irregularity. There is a subconscious tendency to believe that solid materials are composed of unit cells which are regularly stacked or properly packed in a three-dimensionally repeated fashion. But even crystalline solids contain defects ranging in character from those of a point nature (where there are vacancies or interstitial species), to line defects (dislocations) through to sub-grain boundaries (i.e. intersecting or aligned dislocations) which separate microcrystallites of one orientation from adjacent ones of another. Chemists have known for a long time, however, how to produce solids which are noncrystalline even though they may have been ignorant of the structural niceties of such solids—silica glass is an obvious example, but even liquids such as isopentane when cooled to 65 K and ethanol cooled to 90 K form a glass (as anyone who has looked into ways of establishing the validity of the third law of thermodynamics knows), and so do very many other materials. Even metals and alloys, if quenched sufficiently rapidly to low temperatures, can form noncrystalline, isotropic solids.

Noncrystalline solids possess no long-range order (i.e. no translational periodicity—see Fig. 1). Their structure can be viewed as being similar to that of a frozen liquid, but with the thermal fluctuations present in a liquid frozen out leaving only "static" structural disorder. As a result, X-ray diffraction patterns consisting of sharp Bragg spots or rings, characteristic of the periodicity (long-range order) in single crystals or polycrystalline aggregates, respectively, become broadened into diffuse haloes. The same effect is observed of course also for very small microcrystallites (having diameters less than $\simeq 50$ Å), and as such sometimes it is difficult, by diffraction means alone, to determine whether an "X-ray amorphous" material is truly amorphous or just grossly disordered. In certain cases, however, e.g. in the case of Si or Ge, a Bragg peak characteristic of a particular interatomic spacing in the crystal is completely absent in the amorphous phase,[1] and so in such cases there is little or no ambiguity. The atoms in a glass, however, are seldom distributed completely at random, as the simple picture might imply, but rather there is often present a considerable degree of *local* structural or chemical order. The extent of the structural "order" within an amorphous or noncrystalline solid (we use the terms

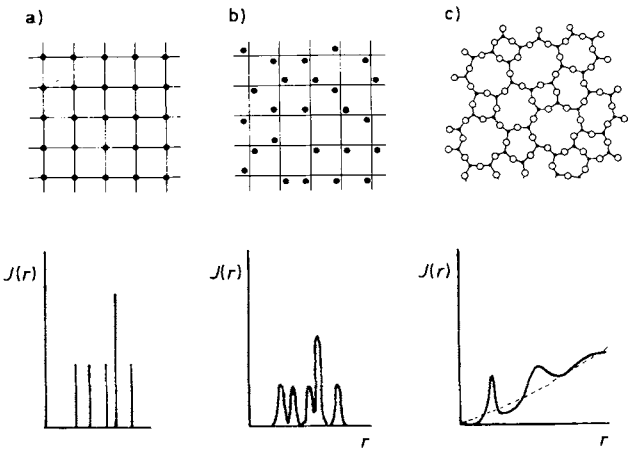


Fig. 1. Types of disorder. (a) Ordered lattice; (b) vibrational disorder; (c) topological disorder. The radial distribution functions (RDFs), $J(r)$, describing such two-dimensional structures are shown below each figure. Note that the widths of all peaks are equal in the RDF of a lattice with just vibrational disorder, whereas the peaks become progressively wider with increasing distance for a topologically disordered structure as a result of static disorder (bond angle fluctuations etc.).

[*] Prof. J. M. Thomas, Dr. S. R. Elliott
Department of Physical Chemistry, University of Cambridge
Lensfield Road, Cambridge CB2 1EP (UK)
Prof. C. N. R. Rao
Solid-State and Structural Chemistry Unit
Indian Institute of Science
Bangalore 560012 (India)

 © VCH Verlagsgesellschaft mbH, D-6940 Weinheim, 1986 0570-0833/86/0101-0031 $ 02.50/0

synonymously) is the subject of much current debate and we return to it later in Sections 4 and 5.

A recent exciting development has been the discovery[2] of long-range *orientational* order accompanied by fivefold point-group symmetry in small regions of rapidly quenched specimens of the alloy $Al_{86}Mn_{14}$; tenfold symmetry axes were observed in the patterns of sharp Bragg spots produced by electron diffraction for certain orientations of the specimens. The importance of such observations lies in the fact that classical crystallography precludes the presence of fivefold or tenfold symmetry axes for truly periodic crystals, i.e. those having long-range translational order. Spurious tenfold symmetry in diffraction patterns can be produced by twinning of ordinary crystals, but lattice-imaging micrographs of the Al-Mn alloys clearly reveal the existence of five coexisting sets of atomic planes with normals pointing to the vertices of a regular decagon. Thus, the fivefold symmetry appears to be an intrinsic property, and the structures containing such symmetry elements have been termed "quasi-crystals".[3] Although several theories have been proposed to account for quasi-crystals (see ref. [4] for a review), none at present are entirely satisfactory. Two different approaches have been used: one which focuses on the geometric arrangement of atoms in space, and the other which describes the structure in terms of a density function $\rho(r)$ (or more conveniently in terms of the Fourier transform of the density in reciprocal space, ρ_q) using the Landau theory for crystallization. The former approach was first used by *Levine* and *Steinhardt*,[3] who considered the structure to be constructed from a "Penrose tiling" in three dimensions, a 3D analogue of the 2D aggregates of two types of rhombuses, found to have fivefold symmetry,[5] and which produced optical Fourier transform patterns having tenfold symmetry.[6] The quasi-crystal is distinguished by the existence of two characteristic length scales in the structure, whose ratio is an irrational number; for the case of the Penrose tiling, this ratio is the golden mean, $\tau=(\sqrt{5}+1)/2$. Calculations of the diffraction patterns for such quasi-crystals yield a series of sharp diffraction spots having icosahedral symmetry, in agreement with experiment, even though there is no long-range translational periodicity in the structure. The discovery of fivefold symmetry in diffraction patterns of otherwise apparently perfectly crystalline materials has not just revolutionized the science of crystallography; the theoretical advances required to understand the nature of such quasi-crystalline structures should in turn shed much light on the structure of amorphous materials themselves.

The layman's conception of a "glass" is simply that of an optically transparent, silica-based material; and whilst many amorphous materials produced are indeed of this variety and used in a range of applications, both traditional (window materials, utensils) and advanced technological (glass fibers for optical communications), very many other materials can also be rendered amorphous (see Table 1).[1,7] Some of these non-siliceous amorphous materials have important technical applications. Amorphous selenium films, for instance, form the photoreceptors at the heart of the Xerox process; certain organic glasses are used in an analogous fashion. Some halide glasses have promise as optical fiber materials for use at long wavelengths; amorphous metallic films and ribbons have a variety of prospective applications, including transformer cores and magnetic shielding, superconducting magnetic windings, and high-strength ribbons in fiber-reinforced composites; amorphous films containing a high proportion of chalcogens offer a wide variety of opto-electronic applications, including optical storage media and resists for photo- or electron-beam lithography. Semiconducting amorphous silicon films (containing about 5 percent hydrogen) are currently used as large-area solar cells, for xerography, and as thin-film transistors. In addition many supported catalysts[8] (e.g. 'V_2O_5' on titania[9] used extensively for selective oxidation of hydrocarbons—cf. Section 8) are unquestionably amorphous in the sense conveyed in this article.

Table 1. Some representative non crystalline solids, their principal bonding type and the temperature T_c at which they form when cooled from the vapor, or the glass-transition temperature T_g if cooled from the melt, at an appropriate rate for each material.

Material	Type of bond	T_c [K]	T_g [K]
Tetracene ($C_{18}H_{12}$)	van der Waals	—	< 180
Isopentane	van der Waals	—	65
H_2O	Hydrogen bridges	—	140
Se	covalent	—	320
SiO_2	covalent/ionic	—	1450
BeF_2	ionic	—	600
Bi	metallic	< 4	—
$Au_{0.8}Si_{0.1}Ge_{0.1}$	metallic	—	300

An amorphous solid may be regarded as differing from its crystalline counterpart in containing excess free energy and entropy. These are incorporated during the process of preparation, and this must be sufficiently rapid to preclude the formation of crystalline material by not allowing time for the atoms to reach the lowest energy state, viz. the crystal. Thus, vapor can be rapidly quenched[10,11] to form amorphous thin films using the techniques of evaporation or sputtering, or the glow-discharge or thermal decomposition of unstable molecular species.[1] Crystalline solids can also be rendered amorphous directly by radiation damage by using high-energy neutrons, or electrons or other radiations as in "metamict" minerals such as uranium-containing zircon ($ZrSiO_4$). They may be amorphized even by the simple expedient[11] of allowing solvent molecules of crystallization to evaporate at modest temperatures (see below). Solid-state reactions may also produce amorphous solids from starting crystalline materials. An interesting recent development in this area has been the demonstration[12] that the absorption of hydrogen by a *crystalline* Zr_3Rh alloy produces a hydrided *amorphous* material. The reason for this rather remarkable behavior appears to be that the diffusion coefficients of the metal atoms are less than that of the hydrogen. The most energetically stable *crystalline* products of the hydriding reaction are the hydride ZrH_2 and Rh metal: in order to form these products, there must be an appreciable degree of metal diffusion, which cannot take place at low temperatures, and so an (X-ray) amorphous product is formed instead. But, perhaps the most common technique for preparing noncrystalline materials is by the rapid quenching of a liquid to form a glass—a method discovered accidentally by the

Phoenicians to generate glass from a melt of lime, sand, and soda.

2. The Glass Transition

Glasses are distinct from other amorphous materials by virtue of a characteristic transition, the so-called glass transition, that they exhibit.[13] At the glass transition temperature, T_g, the super-cooled liquid departs from the equilibrium behavior (Fig. 2), the actual value of T_g itself depending on the cooling rate. T_g is generally around $0.67\,T_f$, where T_f is the fusion temperature. The glass transition also has features apparently similar to those found in second-order phase transitions. For example, C_p and other second derivatives of Gibbs' free energy increase sharply at T_g. As seen in Figure 2, the entropy of a liquid would become equal to that of a crystal well above 0K, provided that there is no intervening transition. This problem is circumvented by postulating the existence of a transition at a temperature T_0, (thermodynamic transition temperature) which limits the decrease in entropy. In order to avoid the paradoxical situation as to what happens when $T < T_0$, in the absence of a transition, one assumes that the glass crystallizes at $T > T_0$. What is interesting is that T_0 values estimated from calorimetry (C_p vs lg T plots) are close to those obtained from Equation (1), which describes the temperature variation of viscosity and other dynamic properties:

$$\psi = \psi_0 \exp[A/(T - T_0)] \tag{1}$$

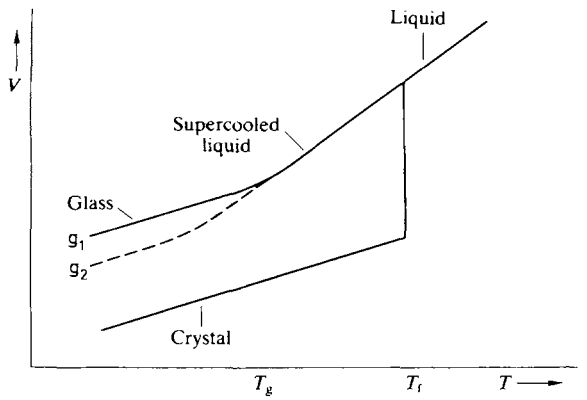


Fig. 2. Schematic illustration of the changes in volume which can occur on cooling a liquid. Crystallization may occur (at T_f), or if the liquid is supercooled below this temperature, glass formation can occur. The temperature marking the break in the slopes of V vs T is termed the glass-transition temperature, T_g. Note that the actual value of T_g varies with cooling rate q ($q_1 > q_2$; the T_g value in the figure holds for q_1).

An "ideal" glass has been defined as one in which T_g approaches T_0. Nonideality of a glass would then be a measure of the entropy frozen in at T_g (this becoming zero when $T_g = T_0$). The existence of a thermodynamic transition at T_0 has not been observed so far, since relaxation times are too long below T_g. The experimental T_g itself occurs when the relaxation time attains a constant value on the time scale of the experiment.

A variety of relaxation, spectroscopic and other techniques have been employed to investigate the behavior of various properties of glass around T_g, but the nature of the glass transition is still not completely understood.[13, 14] Noteworthy among the various models proposed for the transition are the free volume model[15] and the configurational entropy model,[16] and these have been reviewed in the literature.[13]

The entropy frozen-in below the glass transition has a fairly large non-configurational component. The role of communal entropy has been considered and it is suggested that the communal entropy vanishes at T_g, when the liquid-like properties cease to exist.[17] This would require the glass transition to be insensitive to cooling history, but this is contrary to experience. Recent computer experiments[18] as well as electron microscopic studies[19] have indicated the existence of ordered regions or clusters (with noncrystalline motifs) distributed in a tissue material of lower density. When clusters grow in number and size, a congelation to a glass occurs resulting in the elimination of configurational entropy; the tissue material in the intercluster regions could continue to undergo configurational changes, thereby accounting for significant values of the configurational entropy. A cluster model of the glass transition has been developed with the relative size of the cluster as the order parameter.[20]

The term glass transition is generally used in connection with positionally disordered materials, but the transition is also found in solids that are characterized by other degrees of freedom. For example, orientational disorder in plastic crystals may be quenched to yield "glassy crystals" which exhibit glass-like transitions.[21] Disorder in dipole interactions may be frozen-in to yield dipole glasses (similar to spin glasses), typical examples[22] being KBr doped with CN^- ions or $KTaO_3$ doped with Li^+. Frozen liquid crystals are also found to exhibit glass-like transitions.[23] Thus, the glassy state includes long-range disorder of many types while the glass transition manifests itself when relaxational and experimental time scales intersect.

Simulation of the local structures of liquids has its origins in the classic work of *Bernal* who used mechanical assemblies for this purpose. The importance of non space-filling symmetries (such as the icosahedral and the pentagonal) to "ordered" aggregates in the amorphous state has been indicated by some of the studies. The role of such aggregates or clusters in understanding the glass transition was pointed out earlier. Computer simulation studies[24] have yielded useful information on the prototype glass transition in simple liquids, although the use of high quenching rates limits the applicability of the results. The high fictive temperatures of the simulated glasses suggest high diffusion rates. Both hard and soft spheres can be compacted into amorphous assemblies, but the characteristic C_p discontinuity is absent in these cases. The hard sphere ensemble shows that the diffusivity D does not vary linearly with free volume at low temperatures and V_0^D in Equation (2),

$$D = A \exp[-B/(V - V_0^D)] \tag{2}$$

seems to represent the *Bernal*'s limiting dense random packing of hard spheres. Computer simulation studies have yet to demonstrate clearly the existence of the C_p

overshoot, which is the hallmark of the experimental glass transition. Molecular dynamics simulation studies do, however, provide valuable insights into ion movements in glasses.[25]

3. Vitreous Water or Amorphous Solid Water

Water is by far the most common substance that one can think of and yet its extraordinary properties and behavior continue to confound us. While the various models and predictions have helped in understanding the nature of liquid water, they have always met with failure of one kind or another. Amorphous solid water can be produced by vapor deposition of dilute gas molecules on a cold substrate.[26] The resulting material appears glassy and is amorphous to X-rays. A glass transition has been noticed in such deposits[27] and the T_g predicted by the extrapolation of data for binary salt solutions (139 K) was until recently considered to be consistent with the T_g obtained by thermal measurements.[28] The heat capacity of amorphous solid water measured by adiabatic calorimetry does indeed show an increase, as expected of a glass transition.[29] The extrapolated T_g was however not considered to be compatible with the heat capacity of liquid water.[28]

The structure of amorphous solid water prepared by vapor deposition is not different from what is expected for the low-temperature ground state for liquid water. Ultrafast quenching of samples of liquid water has been found to produce amorphous material similar to that prepared by vapor deposition; furthermore, crystallization does not occur during such cooling.[30,31] Crystallization of amorphous solid water occurs around 162 K. What is rather puzzling about amorphous solid water is the very recent observation[32] that no thermal manifestation of the glass transition occurs anywhere in the temperature region predicted by the extrapolation of the data on binary salt solutions.[32] It appears that water in the amorphous state is not any easier to understand than in the liquid state.

4. The Structure of Amorphous Materials

The determination of the structure of amorphous materials has remained a challenge ever since X-ray diffraction was first used as a structural tool for such solids in the 1930's. The problem lies in the fact that in the absence of periodicity (i.e. regularly spaced planes of atoms), the scattering of X-rays (or neutrons or electrons) produces diffuse haloes of scattered intensity, rather than the sharp Bragg spots or lines characteristic of single crystals (see Fig. 3 and 4). Expressed in terms of the scattering vector, $k = 4\pi \sin\theta/\lambda$, in reciprocal space, the intensity is a damped series of broad oscillations superimposed on the square of the atomic form factor, $f_x^2(k)$. Real-space information can be obtained from the scattered intensity data by Fourier transformation after suitable normalizations have been carried out. The resulting curve, the radial distribution function (RDF), $J(r)$, exhibits peaks (Fig. 3b) at distances corresponding to the *average* interatomic separation for the first shell, second shell, etc., superimposed on a background curve, the average density parabola, $4\pi r^2\rho^0$. Although there is a severe problem for higher-lying peaks in that *different* shells can contribute to the *same* peak in the RDF, nevertheless, for the first (and second) peak, the *area* under the peak in the RDF gives the coordination number directly.

The difficulty with a structural interpretation of the RDF of an amorphous material lies in the fact that the RDF is an average quantity; it describes the spatially averaged structural arrangement about a given origin atom, and is a chemical average over all types of atom in the sample. Just as in endeavoring to describe the structure of a liquid via RDF's, we proceed likewise with amorphous solids. The very same obstacles encountered in specifying the structure of liquids are also encountered here: the RDF itself is not sufficiently sensitive to variations in the model, partly because it is a spatially-averaged property.

Since very many amorphous materials contain several

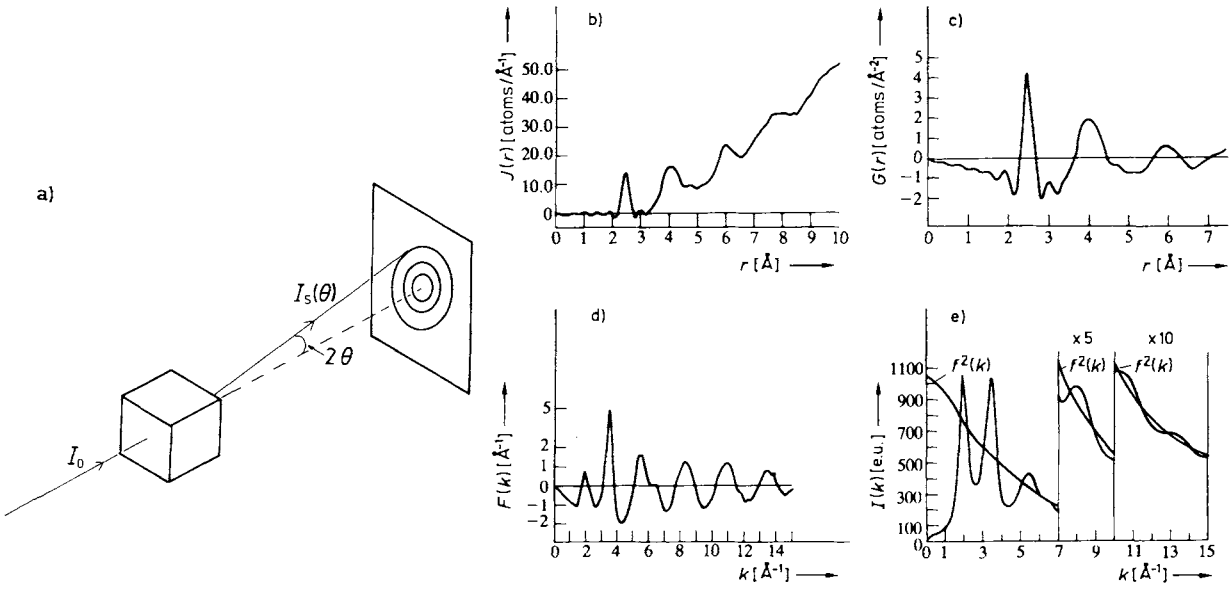


Fig. 3. (a) Schematic illustration of the experimental arrangement used in a diffraction measurement; (b)-(e) X-ray scattering data for a-Ge (after *Temkin* et al. [33]). (b) the RDF (cf. Fig. 1c); (c) the reduced RDF; (d) the reduced scattering intensity; (e) the total (corrected) measured scattering intensity.

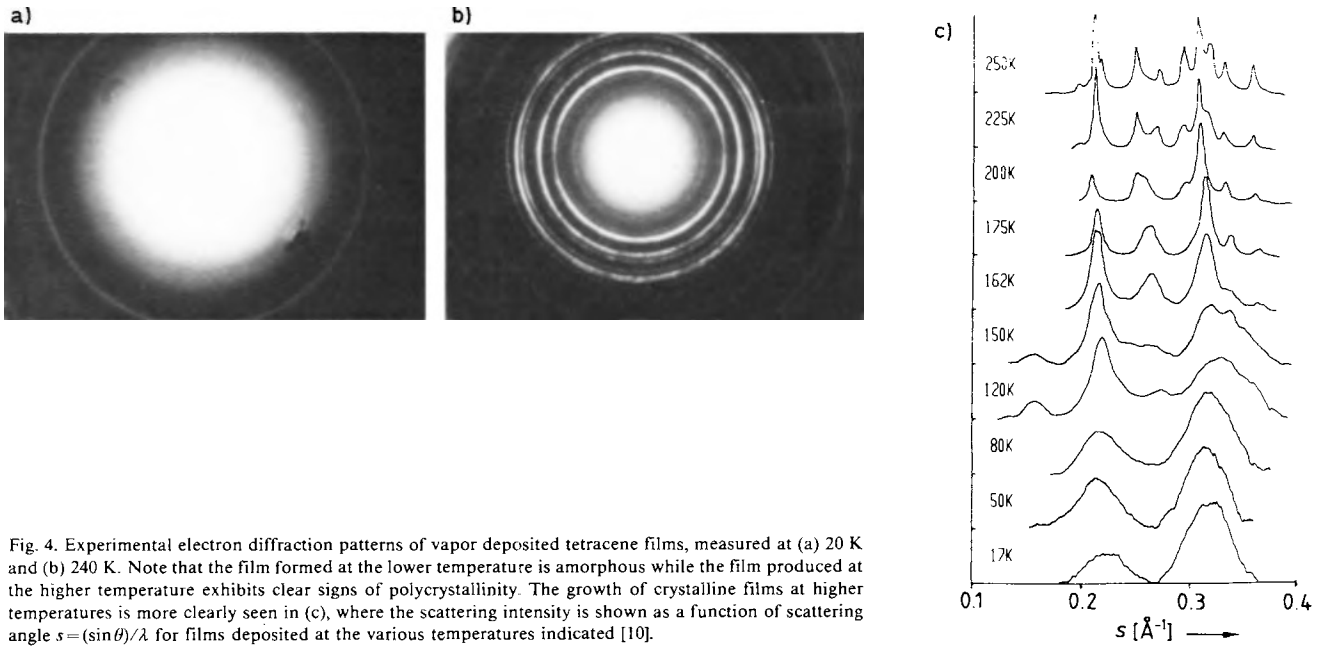


Fig. 4. Experimental electron diffraction patterns of vapor deposited tetracene films, measured at (a) 20 K and (b) 240 K. Note that the film formed at the lower temperature is amorphous while the film produced at the higher temperature exhibits clear signs of polycrystallinity. The growth of crystalline films at higher temperatures is more clearly seen in (c), where the scattering intensity is shown as a function of scattering angle $s=(\sin\theta)/\lambda$ for films deposited at the various temperatures indicated [10].

components, this lack of chemical specificity of conventional diffraction techniques is a severe handicap. One technique which is chemically specific and of considerable promise is the method of extended X-ray absorption fine structure (EXAFS).[34–36] In this, X-rays from a broad-band source (e.g. synchrotron radiation or Bremsstrahlung from a conventional X-ray generator) eject photoelectrons from an atom if the X-ray photon energy is greater than the binding energy of a core electron (say from the K-shell). The photoelectron will be backscattered from any surrounding atoms and interference can occur between outgoing and backscattered states, depending on the energy of the initial X-ray (and hence the kinetic energy of the photoelectron); in this way the X-ray absorption coefficient is modulated, leading to "fine structure" on the high energy side of the (K) edge (see Fig. 5). The method is chemically specific because the X-ray absorption edges of different atoms fall at different energies, and hence the EXAFS for different elements can be well separated in energy (Fig. 5b). Real-space structural information can be obtained from the experimental EXAFS data by Fourier transformation after suitable background subtractions and normalizations. The method is particularly sensitive to the nearest-neighbor environment, but does not probe interatomic correlations beyond about the third nearest neighbor. It is a technique particularly suited for the structural study of disordered materials since it does not depend for success upon the presence of long-range order.

Another technique which is capable of elucidating the structural characteristics of simple (elemental or binary) amorphous materials is electron Compton scattering.[38,39] Compton scattering generally, whether it involves scattering of γ (or X-ray) photons or high energy electrons, can yield[39] the ground state wave-functions of the material under investigation. Even when there is no long-range order, the local electronic environment surrounding a central atom can be probed via the so-called reciprocal form factor. As the form factors for the corresponding crystalline materials are well known by separate determinations, the experimentally derived Compton profile yields the reciprocal form factor, $B(z)$, as defined in Equation (3).

$$B(z)=\int_{-\infty}^{+\infty}\exp(ip_z\cdot z)J(p_z)\,\mathrm{d}p_z=\iiint_{-\infty}^{+\infty}\psi(r-z)\psi(r)\,\mathrm{d}r \qquad (3)$$

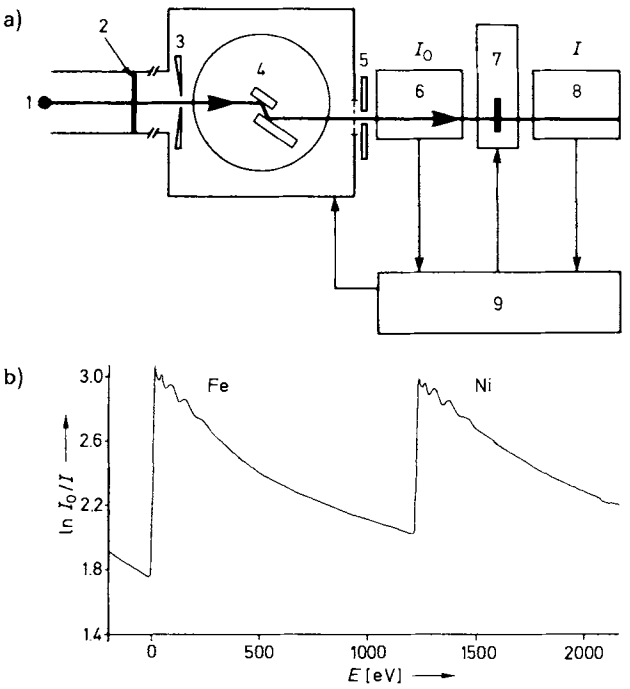


Fig. 5. (a) Schematic illustration of the experimental arrangement employed for transmission EXAFS measurements. 1: Source point of synchroton radiation; 2: Be window; 3: slit; 4: monochromator channel-cut crystal; 5: mask; 6, 8: ionization chambers 1 and 2 in which intensities of the incident and transmitted X-rays, respectively, are measured; 7: sample; 9: computer. (b) K-edge EXAFS spectra of Fe and Ni in $Fe_{40}Ni_{40}B_{20}$ glass at 77 K (after [37]). E signifies energy above Fe K edge.

In other words, the Compton profile $J(p_z)$ [Equation (4)], defined as the projection of the momentum density $\rho(p)$ onto the scattering vector p_z, where

$$J(p_z) = \int_{-\infty}^{+\infty} \rho(p)\,dp_x \cdot dp_y \qquad (4)$$

can be determined directly from experimental Compton profiles. The reciprocal form factor is[38] the overlap of the ground-state wave-function with itself as a function of the distance r. For the amorphous material, this gives us a means of ascertaining the local bonding. In this way it was recently established[40] that noncrystalline elemental carbon involved predominantly sp^2 not sp^3 bonding (i.e. was essentially graphitic).

Another chemically specific structural probe which has great potential for the study of amorphous solids is nuclear magnetic resonance (NMR),[41] which is capable of giving high-resolution (liquid-like) spectra if special ancillary techniques such as magic-angle spinning or multiple-pulse sequencing are employed with modern pulse (Fourier transform) spectrometers;[42] the method is again sensitive mainly to the nearest-neighbor environment. Earlier broad-line NMR studies[43] yielded important, but somewhat limited, structural information, particularly concerning borate glasses. ^{29}Si magic-angle-spinning NMR (MAS-NMR) is proving to be particularly useful in both crystalline and noncrystalline siliceous solids.[44] There is a well-established correlation[45] between the anisotropic ^{29}Si chemical shift (δ values; standard: tetramethylsilane) and the T-O-T angle (T≡Si or Al) given by

$$\delta = -25.44 - 0.5793\ (\theta/\text{deg})$$

so that quantitative deductions about local structure can be made from the observed ^{29}Si chemical shifts. When zeolite A, an aluminosilicate (having the empirical formula $Na_{12}Al_{12}O_{48} \cdot 27\,H_2O$) crystallizes out from an amorphous gel precursor the change in T-O-T bond angles in going from $Si(O\text{-}Al)_4$ (gel) to $Si(O\text{-}Al)_4$ (zeolite A) results in a readily detectable change (from -85.1 to -90.8 ppm with respect to tetramethylsilane TMS) in the ^{29}Si isotropic shift characteristic of the $Si(OAl)_4$ environment. Conversely, when zeolite-A is rendered amorphous by high-temperature (hydrothermal) treatment typical of that employed in procedures for burying radioactive waste, the chemical shifts (and line widths) change as shown in Figure 6.

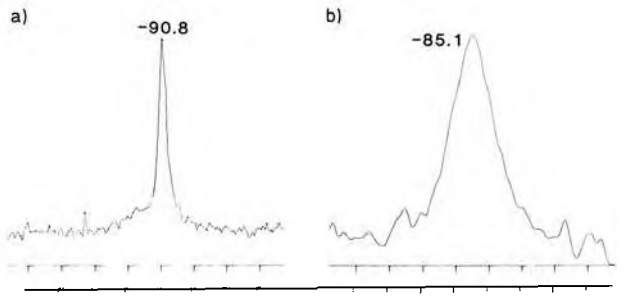


Fig. 6. Section of the ^{29}Si MAS-NMR spectrum of zeolite A (a) before and (b) after amorphization (e.g., as in the sealing of radioactive waste for disposal) [8]. δ values, standard TMS.

Dupree and *Pettifer*[46] have recently shown how line shapes in ^{29}Si-MAS-NMR spectra can be used to set limits to the T–O–T angles present within a glass.

MAS-NMR is ideally suited to probe local site environments and to determine changes in site occupancies during solid-state transformations. So far, most work has been done on systems containing ^{27}Al, which, being a quadrupolar nucleus, relaxes rapidly, thereby yielding good-quality spectra in relatively short-duration experiments.[44] But there is clearly abundant scope for the exploration of organic glasses (via the ^{13}C, ^{1}H, ^{2}H and ^{3}H nuclei) and for a variety of inorganic systems with the *sixty* or so nuclei that exhibit magnetic resonance of acceptable intensity.

5. Models of the Amorphous State

One of the first models to describe the amorphous state was proposed by *Zachariasen* in 1932 for the case of *covalently bonded solids*.[47] The structure was supposed to be formed from polyhedra (e.g. SiO_4 tetrahedra in the case of SiO_2), connected together to form a "*continuous random network*" (CRN), in which long-range order is destroyed by allowing freedom of rotation of neighboring polyhedra about the connecting atom, i.e. the T-O-T angle is allowed to take up a variety of values. Note that the term "random network" is somewhat of a misnomer here, for the structure is not truly random in the statistical sense; well-defined local order exists in the glass by virtue of the existence of the polyhedra, and if the polyhedra connect together to form say rings, then the distribution of torsion ("dihedral") angles for neighboring units is not uniform (i.e. random), but instead certain dihedral angles are preferred.

In 1971, *Polk*[48] demonstrated that it was possible to build an extended continuous random network (consisting of 440 atoms), based on an invariant coordination number of four, for tetrahedrally bonded amorphous semiconductors such as silicon and germanium. The key point about *Polk*'s work was that even when all bond lengths were kept close to their equilibrium value (for the crystalline state) no intolerable bond-length strain was produced, provided a modest spread in angles was permitted. Significantly, five-, six-, and seven-membered rings were present in such a continuous network—there are only six-membered rings in the crystalline semiconductors but, even more important, the density of the resulting noncrystalline structure differed from that of the corresponding (diamond-like) structure by about one percent. The message here is that, for covalently bonded, relatively simple amorphous solids (Si, Ge, SiO_2, GeO_2, etc.) the short-range order is very similar to that which prevails in the corresponding crystals. (Even in the ionic noncrystalline solid formed by BeF_2, 4:2 coordination is still retained in view of the magnitude of the respective ionic radii, $r_{Be^{2+}} = 0.27$ Å, $r_{F^-} = 1.31$ Å, thereby favoring 'tetrahedral' coordination of fluoride ions around the central cations.)

The question of "intermediate-range" order, beyond the short-range local structure characterized by the polyhedral units in covalent glasses, is also of much current interest. In particular, there is a growing body of evidence for the

existence of rather well-defined clusters of atoms, containing 10 or more atoms, in the structure of certain covalent glasses (e.g. Ge–Se alloys); vibrational spectroscopy as well as diffraction experiments indicate their presence, and, as we have seen, certain aspects of glass-transition behavior can be understood in terms of the existence of clusters (see Section 2).

Polymeric solids, typified by polystyrene, poly(vinyl chloride) and poly(vinylidene chloride) more often than not are noncrystalline—some chemical ingenuity is required to produce crystalline polymers—and here the "*random coil model*" is the most appropriate description (see Fig. 7). Like the continuous random network model, the random coil model implies a homogeneous, single-phase solid. It is superior to an earlier, contending theory proposed to account for the behavior of polymeric organic glasses, namely the microcrystalline model, in which microcrystallites of crystalline polymer are embedded in a surrounding noncrystalline matrix. This is incompatible with all the experimental facts for organic glasses, as it is also for most other kinds of glasses. There are, however, partially crystalline polymers (e.g. poly(4-methyl-1-pentene) and poly(ethylene glycol)) in which well-defined coiled regions *are* embedded within the randomly coiled analogue. Likewise, in polyethylene it is well-known that there are amorphous regions connecting the ordered, folded-chain elements in the so-called crystalline material.

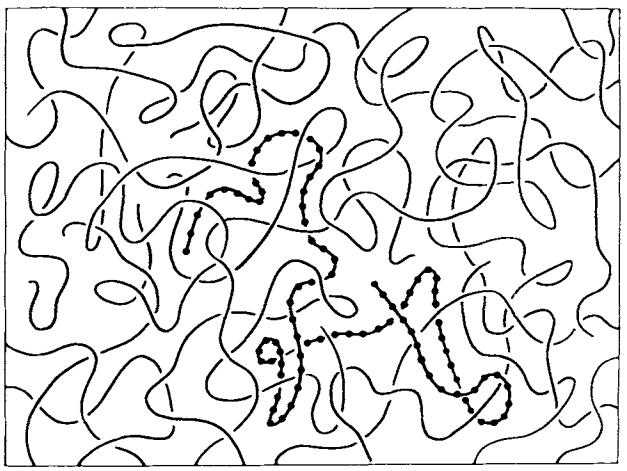


Fig. 7. Schematic diagram of the random-coil model for the structure of polymeric glasses. One chain is clearly marked for ease of visualization (after [7]).

Ionic-covalent, noncrystalline solids are typified by amorphous zeolites (general formula $M_{x/n}(AlO_2)_x(SiO_2)_y \cdot m\,H_2O$). Here, there are several levels of structural order in the parent crystalline form: local order, such as tetrahedrally coordinated Si^{4+} and Al^{3+} ions forming TO_4 tetrahedra, and variously connected tetrahedra which produce a range of possible polyhedral units (Fig. 8a) that can, in turn, be joined to form a three-dimensional solid (Fig. 8b). In partially amorphized zeolitic structures the scale of residual local ordering is such as to be quite amenable to high-resolution electron microscopy (Fig. 9a). Islands of crystalline structure, as well as more or less isolated patches consisting of a few (or a single) polyhedral units, can be directly identified[49–51] in such micrographs. Moreover, if strongly scattering ions (e.g. UO_2^{2+}) are introduced, by ion exchange, into the microcrystalline region of a zeolitic glass, the locally ordered parts of the solid are readily seen[51] (Fig. 9b). For comparison Figure 9c shows an HREM image of dehydrated silica gel which is thought to be a *bona fide* example of the continuous random network model.[49]

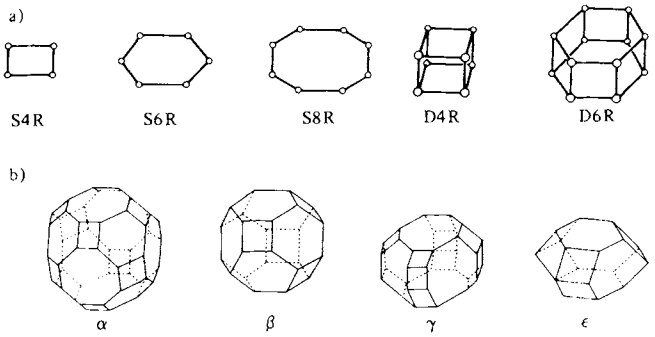


Fig. 8. (a) Simple building blocks and (b) various kinds of polyhedra formed when TO_4 tetrahedra are corner-linked. S, D and R denote single, double and ring respectively. Thus a hexagonal prism, being a double six ring, is designated D6R. The β cage is made up of eight S6R and six S4R.

Glassy metals and metallic *alloys* are best thought of, structurally, as being made up of a *dense random packing of hard spheres*. The notion of dense random packing (DRP) figured eminently in the classic work of *Bernal*[52] on the structure of monoatomic liquids. *Bernal*'s work on liquids involved ball bearings packed into rubber bladders, kneaded, set in black paint with the positions analyzed by hand and eye. Later variants of this approach entailed computer simulations. All these approaches showed that it is possible to generate a randomly-packed model which is sufficiently dense (64 per cent occupancy of available space compared with 74 per cent in cubic or hexagonal close packing of spheres) to reproduce experiment. Such a DRP model involves no crystalline regions provided the spheres are not bounded by a regular surface. (Spheres poured into a cylinder can be densely, randomly packed: this is not the case if poured into a cubic or rectangular box!)

Whereas it is well known that, in the closest packing of spheres (as in crystalline metals such as Ag, Au and Pt), there are 'holes' which are tetrahedral and octahedral in shape (as indeed there are in close-packed anions, e.g., in the structures of Fe_2O_3 and Fe_3O_4), *Bernal* observed that, in the DRP model, holes were of five distinct types. In addition to the tetrahedral and octahedral holes (see Fig. 10) there are three others. All these are polyhedra with equal triangular facets (i.e. deltahedral objects) which are small enough not to admit another sphere of the same size. These are known as Bernal's 'canonical holes'. It transpires that an almost indefinite number of structures, each with almost identical nearest-neighbor distances, can be formed by packing the five deltahedra together. *Finney* constructed a dense randomly packed structure, composed of 7994 'atoms' with a packing efficiency of 44 percent. The (total) radial distribution function (see Fig. 11a) for this structure compares well with that determined experimentally for amorphous $Ni_{76}P_{24}$, although the agreement

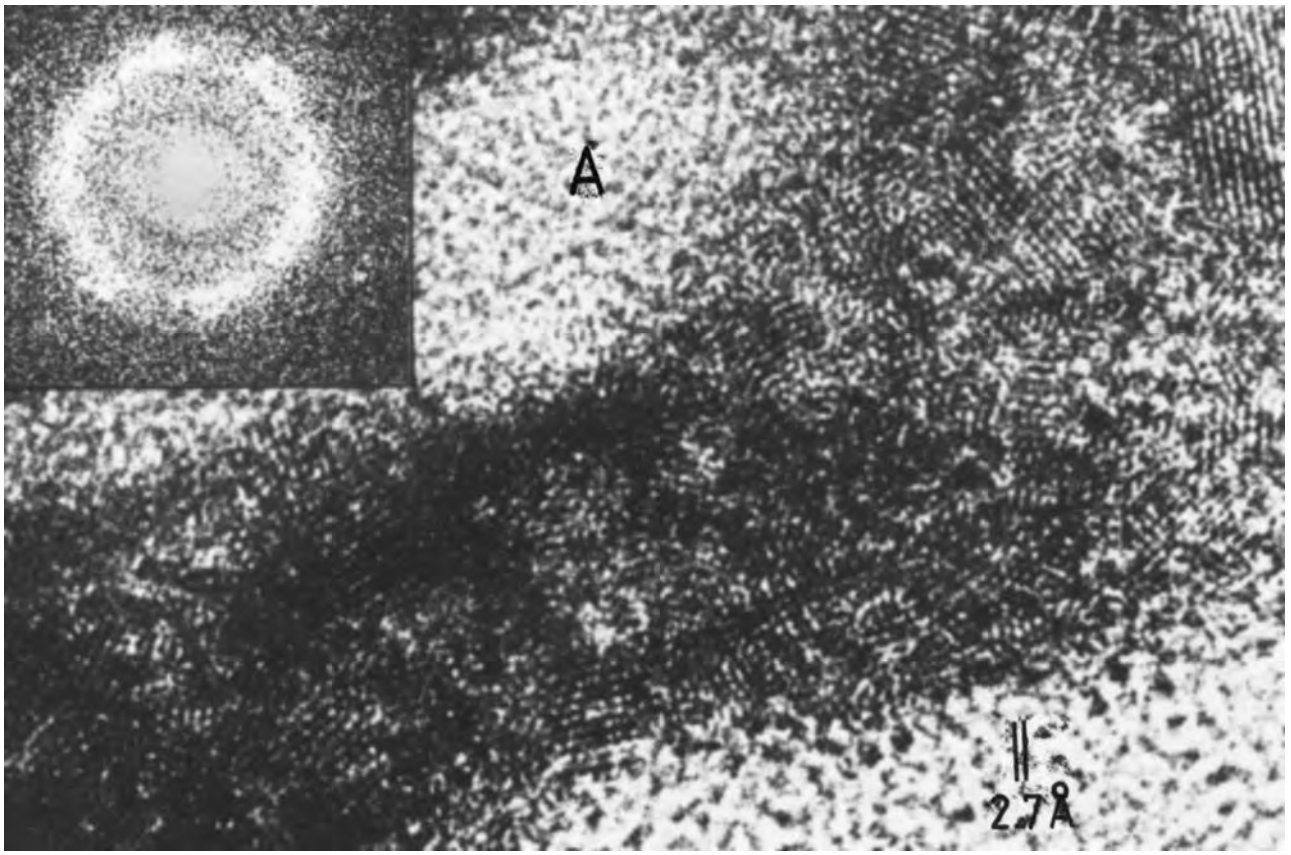


Fig. 9a. High resolution electron micrograph (HREM) of amorphous zeolite A.

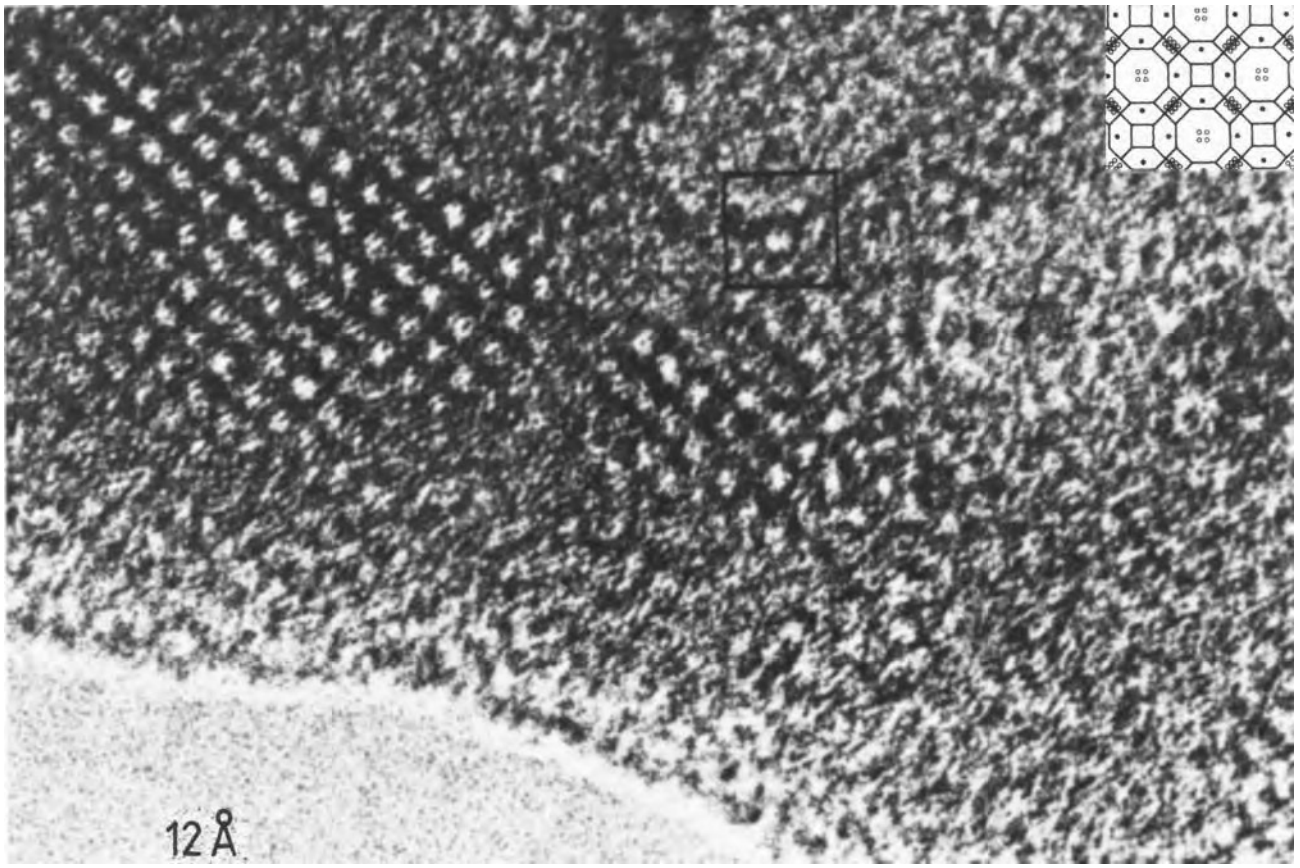


Fig. 9b. High resolution electron micrograph of microcrystalline zeolite Y. A "supercage" is framed.

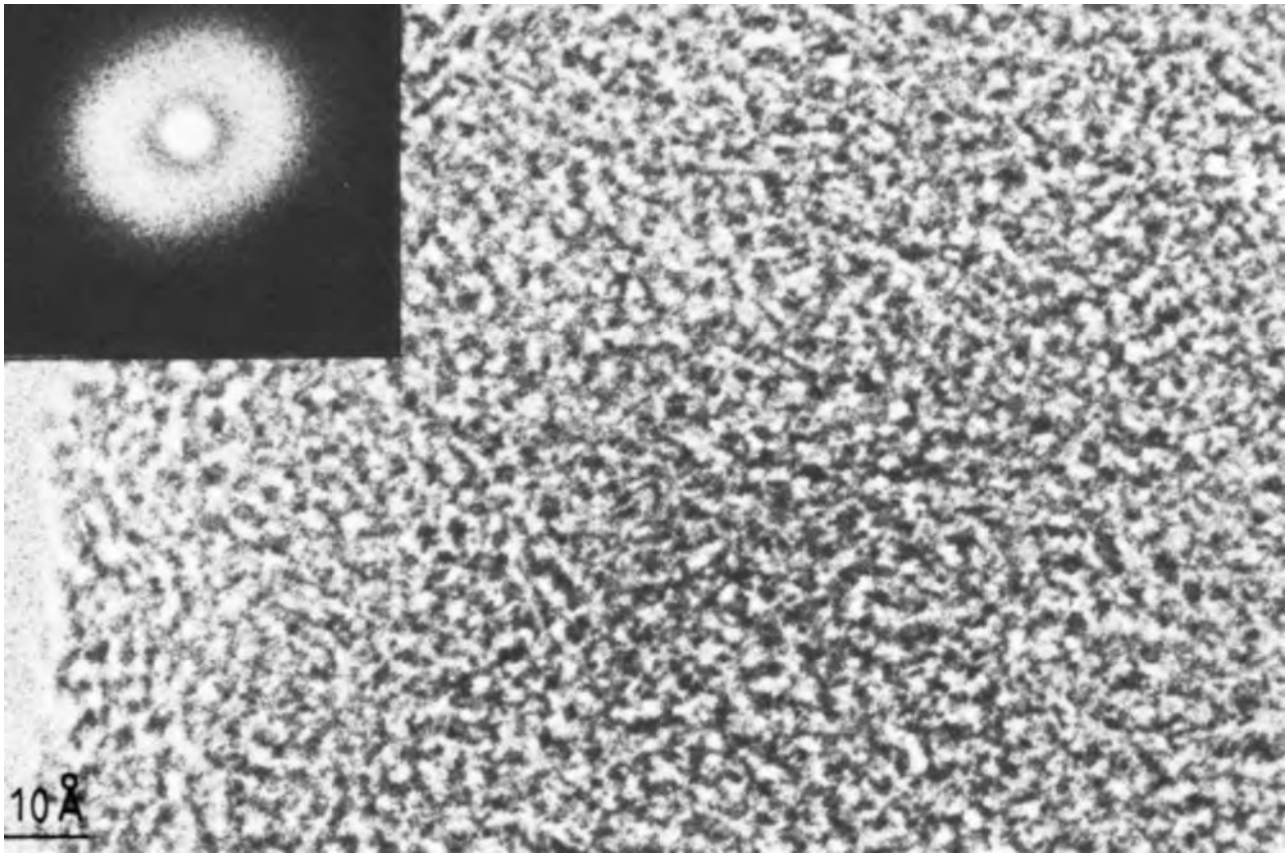


Fig. 9c. High resolution electron micrograph of random network amorphous region of dehydrated silica gel.

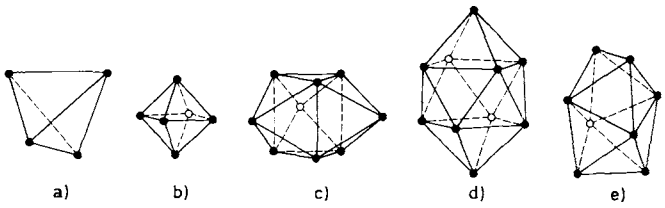


Fig. 10. The five "canonical" holes described by *Bernal*. They are a) tetrahedron; b) octahedron; c) trigonal prism (capped with three half-octahedra); d) Archimedian anti-prism (capped with two half-octahedra); e) tetragonal dodecahedron.

for the individual partial pair correlation functions is less good (Fig. 11b and c).

The DRP model does, however, certainly seem to account well for the structure of amorphous metal-metal alloys, say Zr-Cu. However, there is an important class of amorphous metallic alloys which do not appear to be described by this model—these are the so-called "metglas" alloys formed from approximately 80% transition metal and 20% semimetal (e.g. B, Si, P), this being approximately the eutectic composition. In these materials, chemical or-

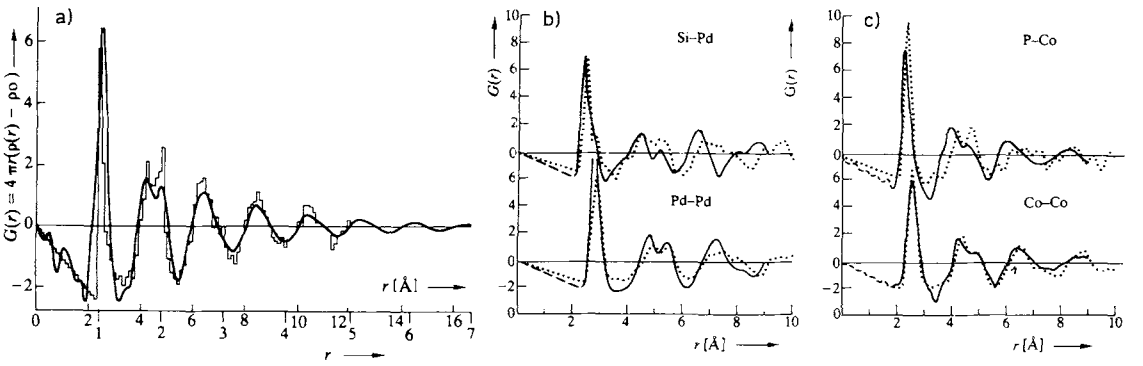


Fig. 11. Reduced radial distribution curves $G(r)$ (cf. Fig. 3c). (a) Calculated for the Finney DRP model compared with the experimental curve for a Ni-P glass; (r is given in units of the diameter of the sphere); (b) and (c) reduced RDFs calculated for the Gaskell trigonal prismatic model compared with experimental curves for Pd-Si and Co-P glasses.

dering beyond that expected for the DRP model appears to exist, and a detailed understanding of the structure is lacking, although it has been suggested that crystalline motifs such as trigonal prismatic units might exist in the glass. It is well known[53] that the structure of *crystalline* transition metal-semimetal alloys, such as cementite (Fe_3C) or Fe_3P (not quite the same composition, note, as that of the glasses, which is approximately Fe_4P, for example) comprise trigonal prismatic structural units consisting of MT_6 arrangements, in which M is the semimetal and T the transition metal (see Fig. 10c). It has been suggested by *Gaskell*[53] that the structure of the glassy alloys also consists primarily of such well-ordered local units (see Fig. 11b). In this way, semimetal-semimetal nearest-neighbor avoidance is achieved (consistent with diffraction evidence), which is not the case for the DRP model, in which it is supposed that the small semimetal atoms, such as P, reside in the canonical polyhedral holes in the structure, and as such, there is nothing to stop them being nearest neighbors. It is of interest to note in passing that the trigonal prismatic model for the structure of metallic glasses can be thought of as a bridge between the CRN and DRP approaches; it can be regarded as a random network of trigonal prismatic structural polyhedra (somewhat distorted to allow complete connectivity), or alternatively, since the trigonal prism is one of the Bernal canonical holes, it can be regarded as a special case of a DRP, in which only one type of polyhedron is allowed to exist. The precise structure of metal glasses is, however, still the subject of some dispute.

The general question of the extent of chemical ordering in amorphous materials is of considerable interest. In crystalline solids, nonstoichiometry can be achieved by several distinct means.[54] Certain crystalline solids can be progressively denuded of one of their constituents leaving the structure more open but in broad architectural terms quite intact. Some perovskites (ABO_3), e.g. $CaMnO_3$, behave[55,56] in this fashion when reduced by H_2 or hydrocarbons to yield ABO_{3-x} ($0 < x < 0.5$), the residual oxygen vacancy sites adopting ordered structures. Another way in which gross nonstoichiometry can be accommodated is for local, but well-defined collapsed regions, such as crystallographic shear planes, to be introduced at intervals through the bulk solid whilst, at the same time, preserving the local coordination, e.g. $MO_3 \rightarrow MO_{3n-1}$, MO_{3n-2}, MO_{3n-3}, etc. ($n = 3 \ldots 20$). In amorphous materials however, gross nonstoichiometry, which can be more or less continuously varied, can be achieved in a different manner, there being no translationally repeated sharply-defined architectural unit in the structure to begin with. This continuous variation can be realized, for the case of a covalent solid, by the local environment changing, so that, say, more like-atom bonds of the elements in excess of that corresponding to stoichiometry are produced.

6. Structural and Chemical Changes in Noncrystalline Solids

It should not be thought that the structure of an amorphous solid is immutable. For instance, a glass quenched rapidly from the melt is in a metastable state, in several senses. If it is held at a temperature near T_g for a sufficient length of time, the structure "stabilizes", and the glass evolves to a state characteristic of a material produced using a slower quench rate. Apart from being able to explore such local, shallow potential minima, the glass is of course energetically metastable with respect to the crystalline state, and will tend to crystallize if held at or above T_g for a sufficiently long period of time. An as-deposited amorphous thin film can also have its structure altered in this manner by thermal means.

There are indications[57] that considerable motion, including transport and agglomeration of ions may occur rather freely within noncrystalline structures. Some polyethylene oxide and organic polycarbonate glasses, for example, permit facile migration of ions such as Li^+ at low temperatures (ca. 60–80 °C) and this fact is harnessed[58] in certain types of solid-state batteries (e.g. those utilizing metallic lithium and TiS_2 into which Li^+ species are readily incorporated).

Another phenomenon, worthy of further investigation, is the precipitation from glassy materials at relatively very low temperatures, of phases which are normally prepared at much higher temperatures. Thus, FeS crystallizes[59] out of a Fe-containing As_2S_3 noncrystalline solvent. Certain glasses, based on alloys containing S or Se, suffer[60] structural changes when irradiated by light. The nature of such photostructural changes, which can be removed by annealing at T_g is, at present, uncertain, although the photoinduced changes are not confined to the structure alone since changes in the optical properties and even in chemical properties (e.g. photo-enhanced dissolution of metals) are also observed. These effects have many potential technological applications, including optical storage media and resists for photo- or electron-beam lithography.

7. Electronic Properties

The effect of structural disorder on the electronic properties of solids may at first sight be thought to be small: glasses can be variously metals, semiconductors or insulators, like crystals, and indeed even the overall shape of the bands of electron states in an amorphous solid (e.g. Si) can be broadly similar to that observed in the corresponding crystal (see Fig. 12). However, the presence of disorder does have[61–63] at least two very important ramifications: electrons can be spatially *localized* by the existence of spatial (topological) disorder, and the absence of periodicity means that the reciprocal lattice vector, k, is no longer a good quantum number. (It should be noted in passing that disorder can produce exactly the same effects for vibrational excitations, i.e. phonons.)

There obviously cannot exist a *reciprocal* lattice if a periodic *spatial* lattice is absent, as is the case for a disordered material, and thus the reciprocal lattice vector k becomes redundant as a description of the solid and of the excitations (electronic or vibrational) which occur within it. The unimportance of k for disordered solids leads to an immediate paradox, namely, why theoretically should a forbidden energy gap appear between bands of states for an

amorphous material? It is common experience that this is the case: for instance, common silicate glass is transparent to photons in the visible spectrum (and indeed has a band gap of almost 10 eV). The paradox arises because electrons in *crystalline* solids are conventionally described within the Bloch formalism, i.e. the electron wave function has the form of a plane wave, modulated according to Equation (5) by the function $\mu_k(r)$, which has the periodicity of the underlying lattice:

$$\psi_k(r)=\mu_k(r)\exp(ik\cdot r) \tag{5}$$

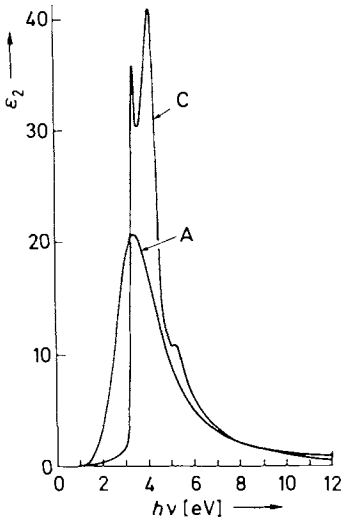


Fig. 12. Optical absorption spectra for crystalline (C) and amorphous (A) silicon. The shape of the absorption bands is related to the joint density of states. Note the sharp features in the spectrum of the crystal (a result of the constraint of k-conservation and the existence of singularities in the joint density of states) are absent in the spectrum of the amorphous material as a result of the loss of k-conservation (ε_2 is the imaginary part of the dielectric constant).

Interference between Bloch waves results in standing waves being set up and an energy difference (band gap) arises for the cases where the electron density is concentrated near the ion cores and where it is concentrated between the cores. Such an explanation is manifestly inapplicable for noncrystalline materials, and instead of invoking long-range order and its effect on the electrons, the answer must be sought in the *local* order in a glass. We have already seen that indeed the local order of (covalent) materials is very similar for both the amorphous and crystalline forms; for example Ge and Si in both forms consist of atoms in tetrahedral coordination. If just two (short-range) interactions are considered between the sp^3-hybrid orbitals emanating from each atom, one an intersite interaction (V_2) responsible for the separation of bonding and antibonding orbitals and the other (V_1) an intrasite interaction responsible for the width of the bands (see Fig. 13), then according to *Weaire* and *Thorpe* a gap between valence and conduction band is predicted as long as the following condition is satisfied:[63]

$$V_2 > 2V_1 \tag{6}$$

Thus, the existence of a band gap for a noncrystalline solid can be understood in terms of *chemical* concepts.

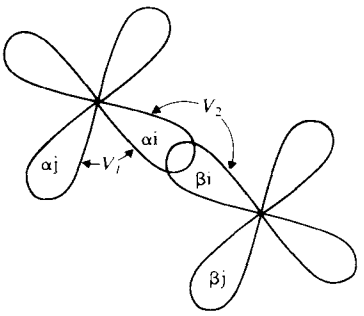


Fig. 13. Weaire-Thorpe model: Intersite (V_2) and intrasite (V_1) interactions.

There are two further consequences of the unimportance of k in disordered materials which are worth mentioning here. The first is that electron (or phonon) states cannot be described in terms of a "band structure", i.e. E vs k (or equivalently a dispersion curve, ω vs q), but instead the "density of states" is the only parameter which equally well applies to an amorphous material as to a crystalline solid. (See Figure 14 for a schematic representation of the form of the density of electron states for an amorphous semiconductor.) The second ramification of the fact that k is no longer a good quantum number is that optical spectra are affected. In crystals, periodicity dictates that the wave vector of the initial and final states involved in the transition is conserved; no such restriction applies for the amorphous case and as a result the spectra of amorphous materials do not exhibit the sharp features characteristic of crystals and which are due to critical points in the joint density of states (i.e. when $\nabla_k E=0$) dominating the matrix element for the transition (see Fig. 12).

The other important effect of disorder on electron states is the possibility of *localization*. Whilst this behavior is not unusual as viewed by a chemist, for whom the concept of localization of electrons in molecular orbitals is commonplace, it is most unusual for those versed in conventional *crystalline* solid-state theory, such as physicists, for whom the electron states in solids are viewed in terms of essentially free electrons only weakly scattered by the ion cores. One approach proposed by *Mott* et al.[61] is that in an amorphous material there exists a critical energy below which (for electrons in the conduction band) the electrons are spatially localized in the region of a single atomic site, and above which they are spatially extended throughout the material, as in a crystal, although the phases of the wave function may be random from site to site. This picture is indicated in Figure 14, and the critical energies E_c in the conduction band and E_v in the valence band are often termed "mobility edges". This is because electrons in extended states, say just above E_c, do not require thermal energy for transport in the bands (their motion being diffusive) and consequently they have relatively high mobilities ($\mu \simeq 10\ cm^2\ V^{-1}\ s^{-1}$), whereas localized electrons can only move from site to site via interactions with phonons and consequently their mobility is activated and much smaller ($\mu \simeq 10^{-2}\ cm^2\ V^{-1}\ s^{-1}$); the thousandfold change in mobility (and hence conductivity) at E_c and E_v means that ($E_c - E_v$) marks a "mobility gap" even though the density of (localized) electron states may well extend considerably

into this region and be continuous through E_c and E_v (see Fig. 14).

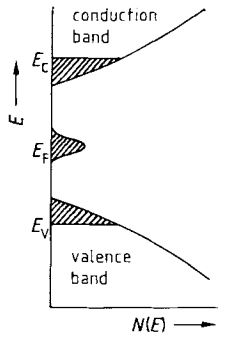


Fig. 14. Schematic density of states, $N(E)$, for an amorphous semiconductor. The mobility edges at E_c and E_v are shown, and all states lying in energy between these levels are localized (and shown shaded). A band of states near the Fermi level, E_F, due to defects, is also shown.

It should be mentioned in passing that structural effects such as dangling bonds have electron states which lie approximately in the middle of the gap, near the Fermi energy, E_F. Electrical conduction by means of transport amongst these levels can only proceed by a process of phonon-assisted tunneling, in which the probability of transfer between two sites separated in distance by R and in energy by W (see Fig. 15) is given by

$$p = \nu_{ph} \exp(-2\alpha R) \exp(-W/kT) \tag{7}$$

where ν_{ph} is a typical phonon frequency. The first exponential factor represents the tunneling probability between the two sites having localized electron wave functions associated with them of the form $\psi \propto \exp(-\alpha r)$, and the second factor represents the probability of a phonon existing having an energy W. At very low temperatures, the proba-

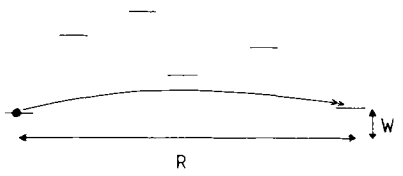


Fig. 15. Schematic diagram of the variable-range hopping process for electron transport among defect electron energy levels near the Fermi level at low temperatures.

bility of electron transfer can be optimized by tunneling, *not* to the nearest site but to a more distant site which has a smaller energy difference, W. Optimization of this sort led *Mott* to derive his famous law for "variable-range hopping" [Eq. (8)] where the factor A is defined by Equation (9)

$$\sigma = \sigma_0 \exp(-AT^{-1/4}) \tag{8}$$

$$A = 2.1[\alpha^3/kN(E_F)]^{1/4} \tag{9}$$

and where $N(E_F)$ is the density of states at the Fermi level. Such behavior has been observed many times in various amorphous semiconductors, and an example[64] for the case of a-silicon is shown in Figure 16. An interesting effect is observed when the conductivity is measured in gap geometry and the thickness of a film is progressively reduced: when the thickness of the film, d, becomes comparable to the hopping distance, the transport process be-

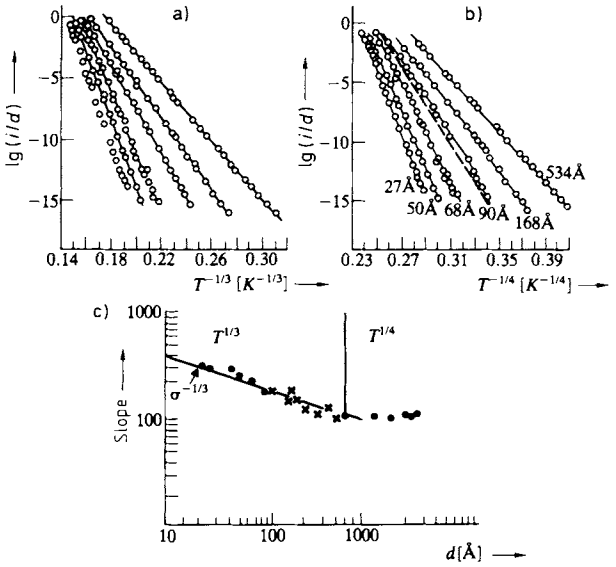


Fig. 16. Variable-range hopping conduction in a-Si; a) two-dimensional transport exhibiting $T^{-1/3}$ behavior; b) three-dimensional transport exhibiting $T^{-1/4}$ behavior; i/d is the quotient of the current strength and thickness of the conducting layer (in Å); c) dependence of the exponents on the thickness d.

comes essentially *two*-dimensional and a different temperature dependence of the conductivity is predicted in accordance with Equation (10), where the constant B becomes thickness dependent [Eq. (11)]:

$$\sigma_{2D} = \sigma_0' \exp(-BT^{-1/3}) \tag{10}$$

$$B = [3\alpha^2/dkN(E_F)]^{1/3} \tag{11}$$

This picture of a well-defined mobility edge, with electrical conduction at high temperatures taking place by means of electron transport in the bands of extended states beyond the mobility edges, has not gone unchallenged however. A rival theory for electrical conduction has been proposed[62], particularly for the case of chalcogenide glasses (alloys of Ge, As etc. containing S and Se), in terms of "polaron" transport. A polaron is a charge carrier which causes a considerable amount of lattice distortion when it occupies a site. As a result the charge carrier digs itself a potential well; it must carry the lattice distortion along with it when it moves, and hence the mobility is thermally activated. Polarons can be of several types (see Fig. 17): "electrostatic" polarons can exist in ionic solids, where the lattice distortion occurs because of the electrostatic interaction between the ions of the lattice and the charge carrier; "molecular" polarons exist when the interaction is of a covalent type involving some change in the bonding between atoms when a charge carrier is inserted between them, and such polarons are found in solid rare gases and perhaps in chalcogenide glasses, where a hole formed in a chalcogen p-π orbital (forming the top of the valence band) can result in a local distortion. The essential differences between the polaron model and the band model for electronic conduction in amorphous semiconductors can be illustrated by reference to the defining equation for the conductivity, σ [Eq. (12)]

$$\sigma = ne\mu \tag{12}$$

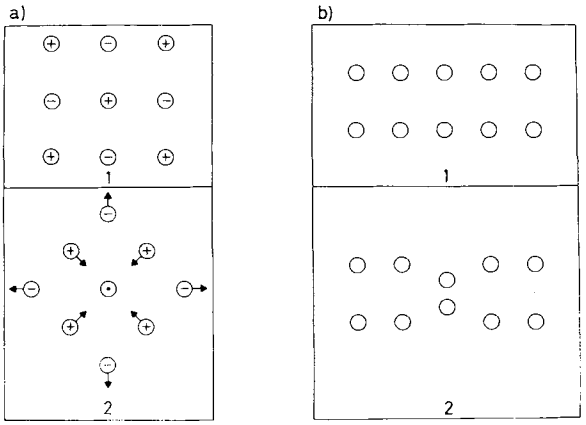


Fig. 17. Schematic representation: (a) electrostatic and (b) molecular polarons. 1: Undisturbed lattice; 2: effects of the polarons.

where n is the charge-carrier density, e the electronic charge, and μ the mobility. The band model assumes that μ is high and temperature independent (transport in extended states) and that n is small and thermally activated (carriers must be thermally excited across the band gap), whereas the polaron model assumes that μ is small and thermally activated (because transport involves interaction with phonons) and that n is large and temperature independent (because every atomic site can form a polaron center). It is still not clear which model is the more appropriate.

The other challenge to *Mott*'s picture of the electronic structure of noncrystalline solids has been to the concept of the mobility edge. Recent studies[65] of localization using so-called scaling methods (similar to those employed in studies of phase-transition phenomena) have indicated that the mobility and conductivity change in a continuous, rather than a discontinuous, manner through the localization transition. Experimental support[66] for this picture has come from studies of *crystalline* phosphorus-doped silicon (Si : P), where the randomly distributed P atoms act as donors, and the electrons experience a disorder potential due to the random positions of the P^+ ions; Figure 18 shows the behavior observed. It is interesting to note from this figure that values of the conductivity are measured *below* the value of the "minimum metallic conductivity", $\sigma_{min} \approx 500\,\Omega^{-1}\,cm^{-1}$, proposed by *Mott* as the limiting conductivity of a disordered material on approaching the localization transition (i.e. $E = E_c$; cf. Fig. 14) from the metallic side.

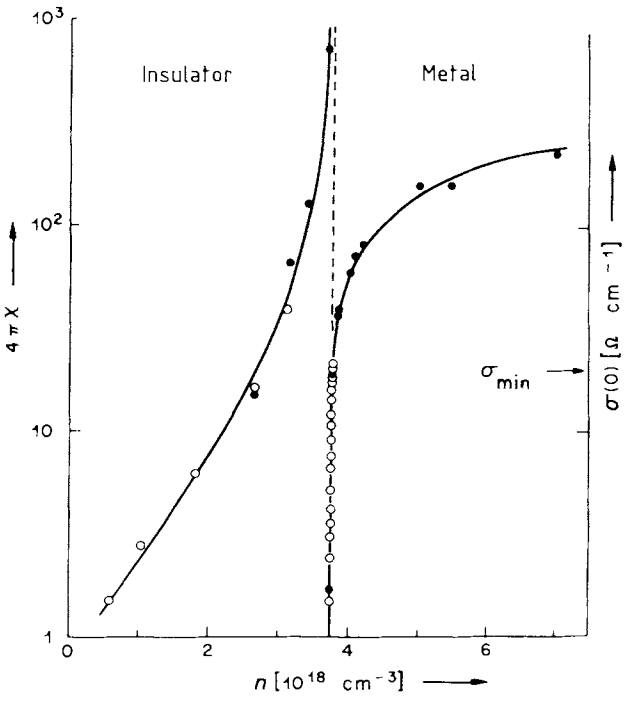


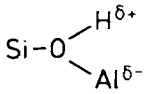
Fig. 18. Crystalline phosphorus-doped silicon; behavior of the conductivity, σ, and the susceptibility, χ, as a function of the charge carrier density n near the localization edge for electrons.

8. Heterogeneous Catalysis and the Noncrystalline State

It has long been recognized that periodicity in a crystallographic sense, though often a vital and generally desirable attribute of most heterogeneous catalysts, is by no means essential. Indeed there are well-known molten salt catalysts which, by definition, lack long-range order. One of these, molten $ZnCl_2$, was used over a century ago by *La Bel* et al.[67] to synthesize hexamethylbenzene in a 'one-step' conversion of methanol.

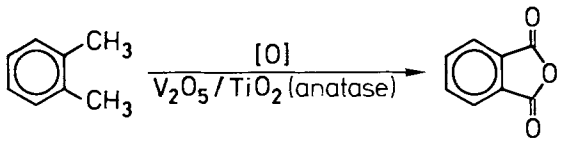
$$CH_3OH \longrightarrow C_6(CH_3)_6 + H_2O.$$

Perhaps the most widely known and arguably the most widely used catalysts until the advent of zeolitic catalysts in the petrochemicals industry in the mid sixties, are the silica-alumina 'gels', consisting usually of about 10 to 25 per cent Al_2O_3 in solid-solution in 'X-ray amorphous' silica (SiO_2). This composition range has advantageous Brønsted acidity attributable to the presence of accessible groups of the type,



from which the proton is rather readily detached by a conjugate base, such as an olefin. Such Brønsted acidity, coupled with the very large surface areas (typically 200–800 $m^2\,g^{-1}$) is the root cause of the catalytic activity of amorphous SiO_2–Al_2O_3 materials and gives rise to their widespread use in isomerization, hydration, and cracking of hydrocarbons.

There has been much speculation as to whether supported catalysts are amorphous or whether they possess crystallographic order, and indeed persuasive arguments have recently been formulated suggesting that a close epitactic match between a crystalline support (the substratum) and an oriented monolayer (supported) active catalyst phase is a prerequisite for the performance of oxide catalysts for the selective oxidation of hydrocarbons. To be specific, supported V_2O_5 catalysts on the anatase polymorph of TiO_2 are of considerable commercial importance,[9] since they exhibit high activity and selectivity in the oxidative conversions of *o*-xylene to phthalic anhydride, a valuable precursor in the production of anthraquinone and polyesters.



(V_2O_5—alone or when supported on other substrates—is a rather indifferent catalyst for this reaction.)

EXAFS and XANES (X-ray absorption near edge structure) investigations on typical V_2O_5/TiO_2 catalysts and a range of related compounds leave us in little doubt that the catalytically active (monolayer) phase of V_2O_5 supported on anatase is *not* in epitactic registry with the substratum but is in a state of structural disorder. The experimental facts and their interpretation are briefly as follows. In Figure 19 we show the EXAFS spectra, beyond the K-edge of

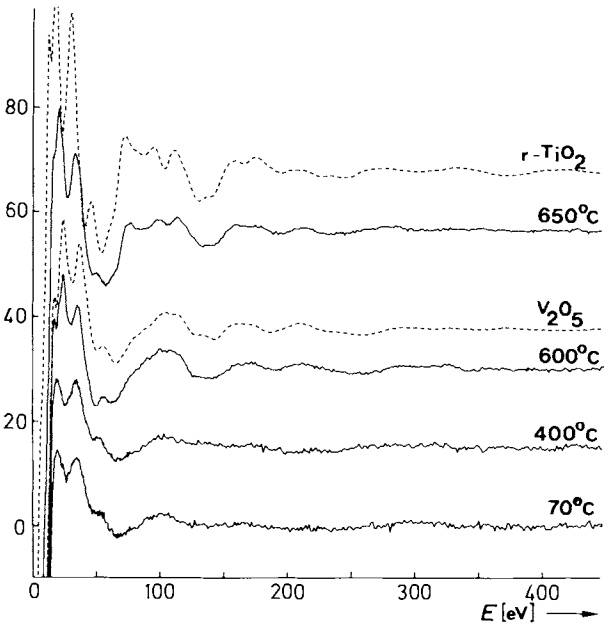


Fig. 19. EXAFS spectra for the vanadium edge of the V_2O_5 monolayer on TiO_2 (anatase) after 5 h heat treatments at various temperatures: EXAFS spectra of crystalline V_2O_5 and TiO_2 (rutile) shown as dashed curve. E denotes the energy above the absorption edge of vanadium. The numbers on the ordinates denote the EXAFS amplitude.

vanadium ($Z=23$), for a typical V_2O_5/TiO_2 (anatase) catalyst after heat treatment at various temperatures; also shown are the EXAFS spectra of crystalline V_2O_5 and of TiO_2 rutile (beyond the K-edge of titanium ($Z=22$)). It is clear that the bottom two EXAFS curves in Figure 19 are essentially the same and possess poor structure, characteristic of a poorly crystalline or amorphous phase. Few or no structural changes occur upon heating the system to 350 °C, which is not far removed from the optimal temperature for catalytic conversion. On heating beyond 600 °C, we know, from X-ray diffraction and microcalorimetry, that the finely dispersed anatase sinters and the vanadium oxide is liberated. Clearly the jettisoned oxide is, from its EXAFS spectrum, indistinguishable from *crystalline* V_2O_5. Upon yet further heating (to 650 °C) some oxygen is expelled and a solid-solution, $Ti_{1-x}V_xO_4$, forms, possessing a rutile structure (as indicated by the top two curves in Figure 19). XANES studies fully confirm this picture. Moreover, a quantitative treatment of the EXAFS data yields further insight into the basic structural unit of the catalytically active, disordered phase: it has two terminal V-O bonds of length 1.65 Å and two bridging V-O-Ti bonds in which the V-O distance is 1.90 Å.

It would be premature to draw too many conclusions from the V_2O_5/TiO_2 (anatase) system. Until such time as EXAFS data for a range of temperatures (under *in situ* conditions) become available it is difficult to decide whether the intrinsic disorder in the active catalyst is of a static or dynamic kind. Moreover, we do not yet know how generally valid is the picture of noncrystallinity for supported monolayers of catalytically active materials anchored to crystalline substrate.

9. Materials Applications and Design

A variety of materials of vital technological importance are amorphous or quasi-crystalline. For instance, a promising photovoltaic material for conversion of solar energy into electricity is amorphous hydrogenated silicon. Magnetic, electric, and other properties of materials rendered amorphous promise several applications as well. The ease of fabrication of glassy or amorphous materials makes them attractive for use in a variety of situations. Thus, there are available glasses which are transparent in most regions of the electromagnetic spectrum, glasses which are semiconducting, glasses which behave like ferroelectrics, and glasses with controlled magnetic behavior. Ferroelectric glasses (such as $LiNbO_3$) and glasses with controlled anisotropy of properties are materials worthy of further exploration. We shall deal here, however, with fast-ion conducting glasses and fibers for optical communication in some detail.

One of the most exciting current applications of a glass is the replacement of copper telephone cables by optical fiber light-guides. Light, in either a single mode or a multimode, propagates down the fiber by a process of total internal reflection, a process which occurs whenever light from a high refractive index medium strikes the interface between it and a low index medium with greater than a critical angle of incidence.

Obviously for long-distance applications, the glass fiber must be extremely transparent, i.e. have a very low light loss. There are two possible sources of light loss, scattering and absorption. Scattering (from density fluctuations) follows the Rayleigh law, i.e. the scattered intensity is proportional to λ^{-4}, where λ is the wavelength of the propagating light. There are two possible absorption mechanisms, depending on the wavelength of the light. At short wavelengths, the light can cause electronic excitation across the forbidden energy gap of the insulating glass: the spectral dependence of this absorption process follows the so-called Urbach law, viz. $\alpha = A\exp(B/\lambda)$, i.e. the absorption band has an exponential edge tailing into the gap, and for silica glass, this edge lies in the hard UV region. At the other end of the wavelength scale, i.e. in the IR region, the absorption of light arises from excitation of phonon (vibrational) modes in the glass, and this too has an exponential spectral dependence, viz. $\alpha = C\exp(-D/\lambda)$. The resulting

wavelength dependence of the overall optical loss in a glass thus has a characteristic V-shaped profile, as shown in Figure 20. Light losses due to Rayleigh scattering are obviously minimized for light of long wavelengths. The low-loss "window" is then given by the intersection of the Rayleigh curve with the multiphonon absorption edge, which for SiO_2 occurs at about 1.6 μm, with a theoretical loss of only ~0.2 dB/km, although actual fibers are found to have losses near 10 dB/km, resulting principally from absorption by OH groups, a ubiquitous impurity.

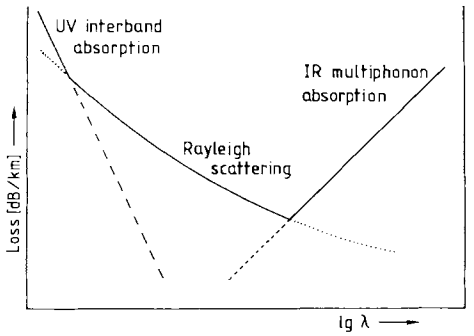


Fig. 20. Mechanisms of light loss in optical fibers as a function of the wavelength λ.

Since Rayleigh scattering decreases with increasing wavelength, losses can be further reduced by making fibers out of materials for which the multiphonon edge lies at a longer wavelength than for SiO_2, and hence intersects the Rayleigh curve at a longer wavelength and a lower value of loss (see Fig. 20). The frequency of phonon modes in a glass can be "tailored" either by choosing a material with a weaker force constant or containing heavier atoms than SiO_2. An example of the former strategy is to use *fluoride* glasses based on ZrF_4 (containing other fluorides such as LaF_3 and BaF_2 as well), where the fluorine atoms are for the most part twofold coordinated in the structure (like the oxygen atoms in SiO_2), but the bonding between cation and anion is weaker. Whilst these glass materials have extremely low theoretical losses ($\simeq 10^{-3}$ db/km), they are difficult to make and to form fibers from without crystallization taking place. The other alternative, namely substituting light (Si) atoms by heavier ones (e.g. Ge or Sb) has also been tried and losses of about 5 db/km have been achieved for GeO_2–Sb_2O_3 alloy glasses.

There is a large and growing number of solids in which certain ions exhibit unusually rapid transport. Such materials associated with high ionic conductivity and small activation energies for ion migration are called fast ion conductors.[68] Typical materials exhibiting fast ion conduction (FIC) are iodides related to AgI and oxides of the type $Zr_{1-x}Ca_xO_{2-x}$ and $Na_{1-x}Al_{11}O_{17+x/2}$ (β-alumina). Much of the early work on fast ion conduction was related to crystalline materials, but many fast ion conducting glasses have been discovered in recent years. Both Li^+ and Ag^+ conducting glasses are known. AgI is almost always a component of the Ag^+-containing FIC's; Li^+ FIC's are generally formed in systems with network structures. The ionic conductivity of these fast ion conducting glasses[69] is comparable to those of crystalline FIC's (Fig. 21). The glass

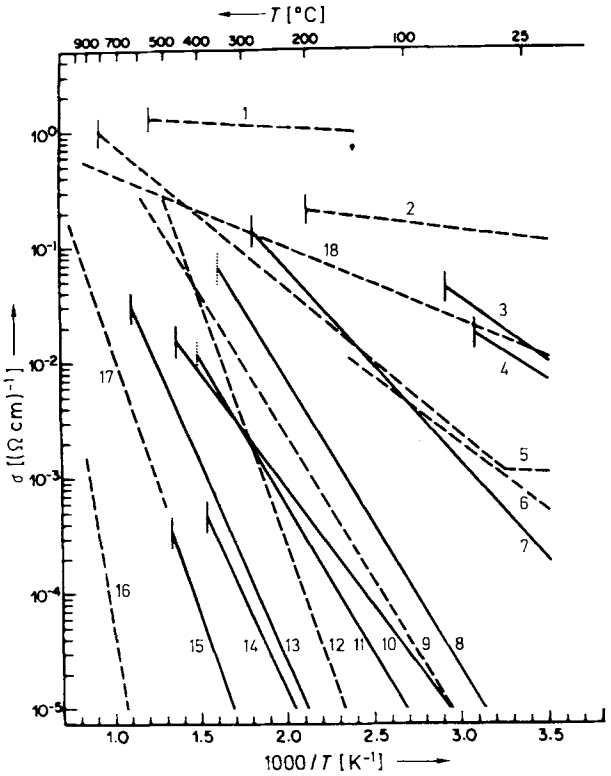


Fig. 21. Ionic conductivities of a variety of amorphous ( ) and crystalline (---) superionic conductors as a function of the temperature [69]. Vertical lines: T_g and T_f, respectively (see Fig. 2); vertical dotted lines: T_g, estimated. 1: α-AgI; 2: $RbAg_4I_5$; 3: $29.8\,Ag_2O$-$40.4\,(AgI)_2$-$29.8\,P_2O_5$; 4: $28.6\,Ag_2O$-$42.8\,(AgI)_2$-$28.6\,MoO_3$; 5: Li_3N; 6: β-PbF_2-2% KF; 7: $60\,Ag_2S$-$5\,GeS$-$45\,GeS_2$; 8: $35\,Li_2O$-$30\,Li_2SO_4$-$10\,(LiCl)_2$-$12.5\,SiO_2$-$12.5\,B_2O_3$; 9: $Li_4B_7O_{12}Cl$; 10: Li_2O-$Nb_2O_5(LiNbO_3)$; 11: $26.9\,Li_2O$-$9.0\,(LiCl)_2$-$64.1\,B_2O_3(Li_4B_7O_{12}Cl)$; 12: $LiAlSiO_4$; 13: $25\,Li_2O$-$25\,Al_2O_3$-$50\,SiO_2(LiAlSiO_4)$; 14: $Zr_{0.6}Ba_{0.33}Y_{0.07}F_{3.27}$; 15: $25\,Li_2O$-$75\,B_2O_3$; 16: $LiNbO_3$; 17: ZrO_2-9% Y_2O_3; 18: $NaAl_{11}O_{17}$ (β-alumina).

FIC's offer several advantages for their use in power devices and related systems, besides the ease of fabrication. Properties of glassy materials can be manipulated through composition control. The isotropic behavior of glasses can also be of considerable advantage.

Received: September 20, 1985 [A 562 IE]
German version: *Angew. Chem. 98* (1986) 31

[1] S. R. Elliott: *Physics of Amorphous Materials*. Longman, London 1984.
[2] D. Shechtman, I. Bleck, D. Gratias, J. W. Cahn, *Phys. Rev. Lett. 53* (1984) 1951.
[3] D. Levine, P. J. Steinhardt, *Phys. Rev. Lett. 53* (1984) 2477.
[4] D. R. Nelson, B. I. Halperin, *Science 229* (1985) 233; cf. also L. Pauling, *Nature (London) 317* (1985) 512.
[5] R. Penrose, *Bull. Inst. Math. Appl. 10* (1974) 266.
[6] A. L. Mackay, *Physica 114A* (1982) 609; *Sov. Phys. Crystallogr. 26* (1981) 517.
[7] R. Zallen: *The Physics of Amorphous Solids*, Wiley, New York 1983.
[8] J. M. Thomas, *Proc. 8th Int. Congress on Catalysts, Berlin 1984, Vol. 1*, Verlag Chemie, Weinheim 1984, p. 31; *Pure Appl. Chem.*, in press.
[9] R. Kozlowski, R. F. Pettifer, *J. Chem. Soc. Chem. Commun. 1983*, 438; *J. Phys. Chem. 87* (1983) 5178.
[10] R. Elermann, G. M. Parkinson, H. Bässler, J. M. Thomas, *J. Phys. Chem. 86* (1982) 313; *87* (1983) 544.
[11] J. M. Thomas, *Ultramicroscopy 8* (1982) 13.
[12] X. L. Yeh, K. Samwer, W. L. Johnson, *Appl. Phys. Lett. 42* (1983) 242.
[13] R. Parthasarathy, K. J. Rao, C. N. R. Rao, *Chem. Soc. Rev. 12* (1983) 361.
[14] J. Wong, C. A. Angell: *Glass Structure by Spectroscopy*, Marcel Dekker, New York 1976.
[15] M. H. Cohen, G. S. Grest, *Adv. Chem. Phys. 48* (1981) 455.

[16] J. H. Gibbs in J. D. Mackenzie (Ed.): *Modern Aspects of the Vitreous State*. Butterworths, London 1963.
[17] H. Kanno, *J. Non-Cryst. Solids 37* (1983) 203.
[18] M. R. Hoare, J. A. Barker in P. H. Gaskell (Ed.): *The Structure of Non-Crystalline Materials*. Taylor and Francis, London 1977.
[19] P. H. Gaskell, D. J. Smith, C. J. D. Catto, J. R. O. Cleaver, *Nature (London) 281* (1979) 465; L. A. Bursill, J. M. Thomas, K. J. Rao, *ibid. 289* (1981) 159.
[20] K. J. Rao, C. N. R. Rao, *Mater. Res. Bull. 13* (1982) 1337.
[21] H. Suga, S. Seki, *Faraday Discuss. Chem. Soc. 69* (1980) 221; R. Parthasarathy, K. J. Rao, C. N. R. Rao, *J. Phys. Chem. 88* (1984) 49.
[22] S. Bhattachanya, S. R. Nagel, L. Fleishman, S. Susman, *Phys. Rev. Lett. 46* (1984) 1266; U. T. Höchli, H. E. Weibel, L. A. Botner, *J. Phys. C 12* (1979) L563.
[23] G. P. Johari, J. W. Goodby, *J. Chem. Phys. 77* (1982) 565; G. P. Johari, *ibid. 77* (1982) 4619.
[24] C. A. Angell, J. H. R. Clarke, L. V. Woodcock, *Adv. Chem. Phys. 48* (1981) 397; L. Woodcock, C. A. Angell, *Phys. Rev. Lett. 47* (1980) 1129.
[25] C. A. Angell in J. M. Honig, C. N. R. Rao (Eds.): *Preparation and Characterization of Materials*. Academic Press, New York 1981.
[26] M. S. Sceats, S. A. Rice in F. Franks (Eds.): *Water. A Comprehensive Treatise, Vol. 7*, 1982.
[27] J. A. McMillan, S. C. Los, *J. Chem. Phys. 42* (1965) 529.
[28] C. A. Angell, E. J. Sare, *J. Chem. Phys. 52* (1970) 1055.
[29] M. Sugisaki, H. Sugan, S. Seki, *J. Chem. Soc. Jpn. 41* (1968) 2591.
[30] P. Brugellen, E. Mayer, *Nature (London) 288* (1980) 569, 579.
[31] J. Dubochet, J. Lepault, R. Freeman, *J. Microsc. (Oxford) 128* (1982) 219.
[32] D. R. MacFarlane, C. A. Angell, *J. Phys. Chem. 88* (1984) 759.
[33] R. J. Temkin, G. A. N. Connell, W. Paul, *Adv. Phys. 22* (1973) 581.
[34] E. A. Stern, *Phys. Rev. B 11* (1974) 4836; B. K. Teo, *Acc. Chem. Res. 13* (1980) 412.
[35] D. R. Sandstrom, F. W. Lytle, *Annu. Rev. Phys. Chem. 30* (1979) 215.
[36] R. Parthasarathy, P. R. Sarode, K. J. Rao, C. N. R. Rao, *Proc. Indian Nat. Sci. Acad., Part A 48* (1982) 119.
[37] J. Wong, *Top. Appl. Phys. 46* (1981).
[38] B. G. Williams, G. M. Parkinson, T. G. Sparrow, C. J. Eckhardt, J. M. Thomas, *Chem. Phys. Lett. 78* (1981) 434.
[39] B. G. Williams, J. M. Thomas, *Int. Rev. Phys. Chem. 3* (1983) 39.
[40] B. G. Williams, T. G. Sparrow, J. M. Thomas, *J. Chem. Soc. Chem. Commun. 1983*, 1434.
[41] E. R. Andrew, *Int. Rev. Phys. Chem. 1* (1981) 195.
[42] E. Lippmaa, M. Alla, T. Juherm, *Proc. 19th Ampere Congress Heidelberg 1976*, p. 113.
[43] P. J. Bray in L. D. Pye, V. D. Frechette, N. J. Kreidl (Eds.): *Borate Glasses: Structure, Properties, Applications*. Plenum, New York 1978.
[44] C. A. Fyfe, J. M. Thomas, J. Klinowski, G. C. Gobbi, *Angew. Chem. 95* (1983) 257; *Angew. Chem. Int. Ed. Engl. 22* (1983) 259; J. M. Thomas, J. Klinowski, P. A. Wright, R. Roy, *ibid. 95* (1983) 643 and *22* (1983) 614.
[45] J. M. Thomas, J. Klinowski, S. Ramdas, B. K. Hunter, D. T. B. Tennakoon, *Chem. Phys. Lett. 102* (1983) 148; S. Ramdas, J. Klinowski, *Natu4e (London) 308* (1984) 521.
[46] R. Dupree, R. F. Pettifer, *Nature (London) 308* (1984) 523.
[47] W. H. Zachariasen, *J. Am. Chem. Soc. 54* (1932) 3841.
[48] D. E. Polk, *J. Non-Cryst. Solids 5* (1971) 365.
[49] L. A. Bursill, J. M. Thomas, *J. Phys. Chem. 85* (1981) 3007.
[50] J. M. Thomas, L. A. Bursill, *Angew. Chem. 92* (1980) 755; *Angew. Chem. Int. Ed. Engl. 19* (1980) 745.
[51] L. A. Bursill, J. M. Thomas, K. J. Rao, *Nature (London) 289* (1981) 157.
[52] J. D. Bernal, *Proc. R. Soc. London Ser. A 280* (1964) 299.
[53] P. H. Gaskell, *J. Non-Cryst. Solids 32* (1979) 207.
[54] C. N. R. Rao, *Chem. Scr. 19* (1982) 124.
[55] A. Reller, D. A. Jefferson, J. M. Thomas, M. K. Uppal, *J. Phys. Chem. 87* (1983) 913.
[56] A. Reller, J. M. Thomas, D. A. Jefferson, M. K. Uppal, *Proc. R. Soc. London*, in press.
[57] T. G. Fowler, S. R. Elliott, *J. Non-Cryst. Solids 59-60* (1983) 957.
[58] B. G. Silhernagel, M. S. Whittingham, *J. Chem. Phys. 64* (1976) 3670.
[59] T. G. Fowler, *Ph. D. Thesis*, University of Cambridge 1984.
[60] S. R. Elliott, *J. Non-Cryst. Solids 59-60* (1983) 899.
[61] N. F. Mott, E. A. Davis: *Electronic Processes in Non-Crystalline Materials*, 1979.
[62] D. Emin in P. G. Le Comber, J. Mort (Eds.): *Electronic and Structural Properties of Amorphous Semiconductors*, Academic Press, New York 1973.
[63] D. Weaire, M. F. Thorpe, *Phys. Rev. B 4* (1971) 2508, 3518.
[64] M. L. Knotek in M. G. Brodsky, S. Kirkpatrick, D. Weaire (Eds.): *Proc. Int. Conf. on Tetrahedrally Bonded Amorphous Semiconductors, Vol. 20*, 1974, p. 297.
[65] E. Abrahams, P. W. Anderson, D. C. Liccardello, T. V. Ramakrishnan, *Phys. Rev. Lett. 42* (1979) 673.
[66] H. F. Hess, K. De Londe, T. F. Rosenbaum, G. A. Thomas, *Phys. Rev. B 25* (1982) 5578.
[67] J. A. Le Bel, W. H. Greene, *Am. Chem. J. 2* (1880) 20.
[68] P. Hagenmuller, W. Van Gool (Eds.): *Solid Electrolytes*. Academic Press, New York 1978.
[69] H. L. Tuller, D. P. Button, D. R. Uhlmann, *J. Non-Cryst. Solids 40* (1980) 93.

Molecular Biological Background of the Species and Organ Specificity of Influenza A Viruses

By Christoph Scholtissek*

Influenza is one of the great plagues which is not yet under control. The reason for this is the immense variability of the infecting agent, the influenza A viruses. These viruses behave like a chameleon: they adapt very rapidly to varying environments. New strains are "synthesized," which can escape the immune response of the host, cross species barriers, and become highly pathogenic. We are beginning to understand the molecular background of this extraordinarily high variability. The genome of influenza A viruses consists of eight single-stranded RNA segments, each of which constitutes a gene. The total base sequence of the eight RNA segments of several strains is known. If a suitable organism becomes doubly infected with two different influenza A strains, each of the RNA segments behaves like a chromosome. This means that by reassortment of the 16 RNA segments, $2^8 - 2 = 254$ new combinations (= reassortants) are theoretically possible, each having different properties. Furthermore, mutations in the various RNA segments are relatively easily tolerated. Another great problem resides in the enormous reservoir of different influenza A viruses in the animal kingdom, especially in feral waterbirds. In these birds the avian influenza A viruses normally cause at most mild symptoms, and therefore these viruses are distributed over and between continents. Bearing this in mind it appears to be necessary to develop new ideas as to how to overcome this great plague.

1. Introduction

Influenza A viruses are the causative agents of the great pandemics, e.g., the Spanish influenza in 1918/19 and the Hong Kong pandemic in 1968. Furthermore, under natural conditions, influenza A viruses—in contrast to type B and C viruses—infect other species in addition to humans, including birds, horses, pigs, seals, mink, and whales, in which they cause various symptoms. Therefore, only influenza A viruses will be treated in this article.

1.1. Structure

Influenza A viruses have a relatively complex structure (Fig. 1, right).[1] They have a lipid bilayer, which is derived from the host cell during maturation and contains two different glycoproteins on the exterior surface. One is the hemagglutinin (HA), which, as a trimer, binds to the neuraminic acid-containing receptors of the host cell. The HA is the most important immunogenic component, since the infected organism produces neutralizing antibodies against this glycoprotein. The second surface component is the receptor-destroying enzyme, the neuraminidase (NA), which is less important with respect to the immune defense of the organism. Although this enzyme has been studied extensively,[2,3] many questions remain concerning its role during natural infection.

The lipid bilayer is covered on the inside by the matrix or membrane (M) protein. The nucleocapsid exhibits a thread-like helical structure as revealed by the electron microscope. Its main component is the basic nucleoprotein (NP). Only ten molecules of each of the three so-called P proteins (PB1, PB2, and PA) are present in the nucleocapsid. Embedded in this structure is the genetic material of the influenza A virus, which consists of single-stranded RNA (vRNA). In contrast to most other viruses, the RNA of the influenza A virus does not exist as a single molecule per viral particle, but as eight segments. Each segment constitutes one gene (Fig. 1, left).[4,5] The nucleocapsid has RNA-polymerase activity—i.e., the complementary RNA (cRNA) is synthesized on the internal vRNA templates.

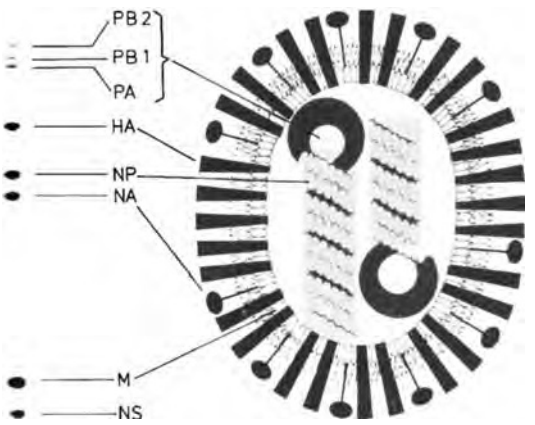


Fig. 1. Structure and structural elements of an influenza A virus (right) and assignment of the gene products (middle) to the viral RNA segments (genes) separated by polyacrylamide gel electrophoresis (left). The polymerase complex is located in the interior of the particle. It consists of the three P proteins PB2, PB1, and PA and the nucleoprotein NP. The lipid bilayer is covered on the inside by the membrane or M protein. The two glycoproteins hemagglutinin (HA) and neuraminidase (NA) are located on the exterior surface. The smallest RNA segment contains the information for two nonstructural proteins (NS).

[*] Prof. Dr. C. Scholtissek
Institut für Virologie des Fachbereichs Veterinärmedizin und Tierzucht der Universität
Frankfurter Strasse 107, D-6300 Giessen (FRG)

 © VCH Verlagsgesellschaft mbH, D-6940 Weinheim, 1986 0570-0833/86/0101-0047 $ 02.50/0

1.2. Nomenclature

The proteins inside the virus, such as the NP or M proteins, are group-specific antigens, according to which the influenza viruses are categorized as types A, B, or C. Since these viral components cannot be reached in the intact particle by monospecific antibodies, they are not under the selection pressure of the immune system of the host and are therefore genetically conserved in contrast to the surface components HA and NA.

The influenza A viruses are divided into subtypes according to significant serological differences in their HAs and NAs. At present thirteen HA and nine NA subtypes are known. They have been found in nature in almost all possible combinations,[6] but only three different HA and two different NA subtypes have been found among virus isolates obtained from humans. In naming influenza viruses, one adds to the name the type (A, B or C) and the species from which the virus was isolated, except for human viruses. The site of isolation, the isolate number, and the year of isolation are also noted. In most cases, a simplified version of the serotypes for the HA (H) and NA (N) is added to the end of the name. The following isolate, which was obtained in 1976 from a duck in Alberta (Canada), will be used as an example: A/duck/Alberta/35/76 (H1N1).

1.3. The Multiplication Cycle

The influenza viruses belong to the negative-strand viruses. This means that the RNA isolated from virus particles (vRNA) is not infectious, since it has no messenger RNA (mRNA) function. Since a noninfected cell does not contain an RNA-dependent RNA polymerase, all negative-strand viruses must provide their own enzyme. After adsorption onto the host cell and fusion of the viral membrane with cellular membranes, the nucleocapsid is set free and migrates into the cell nucleus. There, the very complicated synthesis of the viral messenger RNA begins. In the first step, the viral polymerase complex binds to the fully

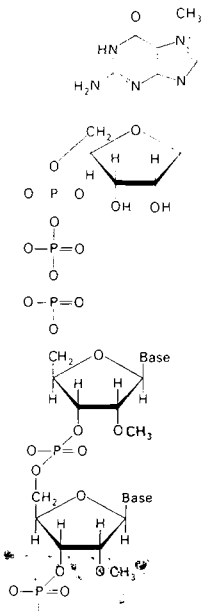


Fig. 2. Fully methylated cap structure at the 5′ end of an eukaryotic messenger RNA.

methylated cap structure (see Fig. 2) at the 5′ end of a newly synthesized precursor mRNA (high-molecular-weight, heterogeneous nuclear RNA: hnRNA) of the host cell and cleaves this hnRNA at a point 10–13 nucleotides from the 5′ end, following a purine (Fig. 3). This 5′ end of

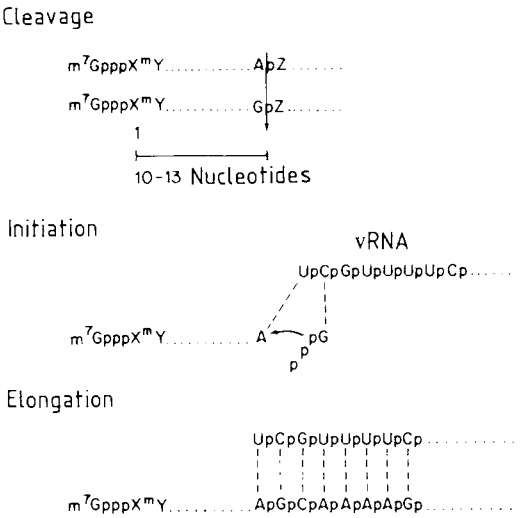


Fig. 3. Three steps that are necessary for the start of influenza-virus-specific messenger RNA synthesis. 1. Binding of the viral polymerase complex to the fully methylated cap structure of the newly synthesized cellular hnRNA and cleavage 10 to 13 nucleotides from the 5′ end, following a purine nucleotide. 2. Initiation of viral messenger RNA by base-pairing of the last uridine monophosphate at the 3′ end of the vRNA with the purine at the 3′ end of the cellular starter molecule, and incorporation of the first guanosine triphosphate (base-pairing with the penultimate cytidine monophosphate of the vRNA). 3. Elongation of the viral messenger RNA according to the Watson-Crick rules (according to *Krug* [7]).

the cellular hnRNA functions as a primer molecule for the viral mRNA synthesis (base-pairing according to the Watson-Crick rules), so that after this last purine nucleotide the RNA sequence is complementary to the 3′ end of the vRNA.[7] Close to the 5′ end of the vRNA is a signal for the unspecific addition of a polyadenylic acid tail of 50–200 AMPs. Thus, the residual 16 nucleotides at the 5′ end of the vRNA are not transcribed. This means that the eight influenza-virus-specific mRNA segments synthesized in vivo are heterogeneous at the 5′ end, because almost any cellular hnRNA can function as a primer molecule. Moreover, since some information is missing at the 3′ end, this cRNA cannot function as a template for the synthesis of vRNA segments that are later incorporated into mature viral particles. Therefore, a second type of viral cRNA is synthesized in virus-infected cells, which contains neither the cap structure and cellular RNA sequences at the 5′ end nor the polyadenylic acid tail at the 3′ end, but consists of the total, unmodified complementary sequence.[8] Both types of viral cRNA—for all eight segments—are found in the infected cell. The mechanisms by which their synthesis is regulated are completely unknown. For each of the six largest vRNA segments, only one mRNA is transcribed, while for each of the two smallest vRNA segments two different mRNAs are synthesized. One of these mRNAs is created by splicing so that for RNA segment 7, besides the unspliced mRNA coding for the M protein, a second spliced mRNA coding for the nonstructural M2 protein is

transcribed. Correspondingly, the RNA segment 8 contains the information for the two nonstructural proteins NS1 and NS2.[9] The mechanism by which the correct eight vRNA segments are selected and assembled during virus maturation is not yet known.

The nonglycosylated viral proteins (presumably with the exception of the M2 protein) are synthesized on free polysomes in the cytoplasm of the infected cell, while the glycoproteins (and presumably also the M2 protein) are produced on membrane-bound polysomes. During migration via the Golgi apparatus to the cytoplasmic membrane of the host cell, certain modifications of the viral glycoproteins occur such as the trimming and maturation of the carbohydrate side chains, the incorporation of fatty acids, and the cleavage of the HA into the cleavage products HA_1 and HA_2, which are held together by disulfide bridges.[10] By assembly of the various structural elements and budding, new infectious virus particles are formed.

1.4. Assignment of the RNA Segments to the Gene Products

In order to assign the RNA segments to the corresponding gene products, we isolated a large number of temperature-sensitive (ts) mutants of fowl plague virus (A/FPV/Rostock/34; H7N1) after mutagenesis with fluorouracil and selection using the plaque enlargement technique.[11] Primary chick embryo cells (CEC) in culture were doubly infected pairwise with all ts mutants. A plaque test was performed with the culture fluid at the so-called nonpermissive temperature (40°C). If the ts defects of the two isolates used for double infection are in different RNA segments (i.e., genes) reassortment to wild-type virus should be possible (see Fig. 4) by complementation of the genes without a defect. If, however, the two defects are located in exactly the same RNA segments, reassortment to wild-type virus is not possible. In this way it is possible to place all ts mutants into eight recombination groups in accordance with the number of RNA segments. Correspondingly, a rough assignment of the various groups of ts mutants to specific biological defects can be made.[12] If CEC at 40°C are doubly infected with a ts mutant of FPV and another influenza A subtype that cannot form plaques on these host cells (see Section 4), all plaque-formers obtained at 40°C are necessarily reassortants in which at least the defective gene of FPV is replaced by the allelic gene of the superinfecting influenza A strain. The derivation of the various RNA segments in the reassortants, whether they are supplied by the one or the other parent strain, has been determined by the hybridization technique.[13] Another possibility to determine the derivation of the various genes in reassortants is to compare the migration rates of both the RNA segments and the viral proteins of the parent viruses. The tryptic fingerprints of the parents and reassortants can also be compared.[14] The results obtained with FPV are shown in Figure 1.

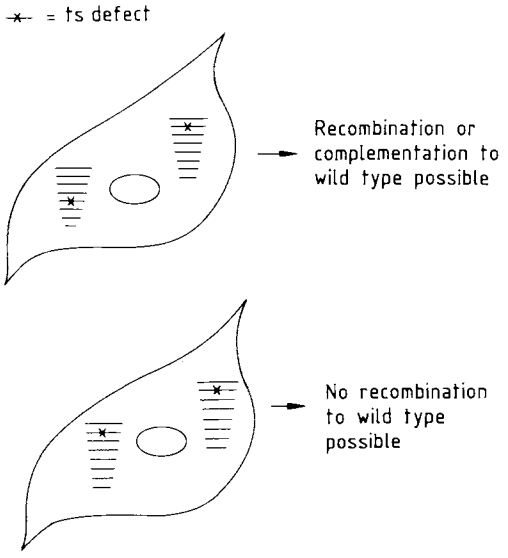


Fig. 4. Scheme to explain reassortment (recombination) to wild type after double infection of a cell by two different temperature-sensitive (ts) mutants of an influenza A virus. The ts defects are located either in two different or in the same segments. Selection for the wild-type virus is carried out at the nonpermissive temperature of 40°C.

2. Molecular Background of the Influenza Pandemics and Epidemics

2.1. Antigenic Shift

Every 10 to 20 years a human influenza A virus suddenly appears with new surface glycoproteins, against which no neutralizing antibodies are present in the human population. Such a new strain can start a pandemic (antigenic shift). When the A/Hong Kong/1/68 (H3N2) virus was analyzed by the hybridization technique, it was found that all genes except the HA gene were almost identical with those of the earlier H2N2 virus (A/Singapore/1/57). The HA gene of the Hong Kong strain, however, was highly related to the allelic gene of an influenza A virus isolated earlier in 1963 from a duck in the Ukraine.[15] Therefore, we envisage the creation of the Hong Kong virus according to Figure 5. All genes involved in species specificity, i.e., necessary for multiplication and causing symptoms in humans, were derived from the foregoing H2N2 strain during reassortment in a doubly infected host—possibly in pigs (see Section 6.2.). Only the HA gene is contributed by the animal virus. That means that in nature "a wolf in sheep's clothing" was produced in order to overcome the immune defense of the organism. With regard to the Singapore strain, which caused the pandemic in 1957, it was found that only the RNA segments 1, 5, 7, and 8 were de-

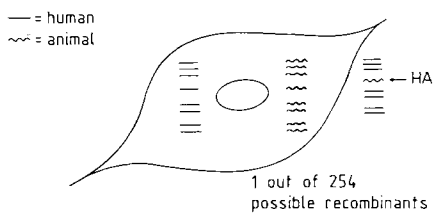


Fig. 5. Scheme to explain the creation of a new pandemic influenza A strain (antigenic shift). A cell becomes doubly infected by an animal virus and by the prevailing human influenza A strain. One of the 254 possible new reassortants has the gene constellation shown on the right. Only the HA gene is derived from the animal strain, while all the other genes are derived from the human virus.

rived from a foregoing human H1N1 strain. Segments 2, 3, 4, and 6, i.e., both genes coding for surface glycoproteins, were replaced.[15]

There is another possible explanation for the appearance of an influenza pandemic: a virus strain disappears for many years from the human population, but when a new generation has grown up it suddenly reappears. This happened in 1977 when an H1N1 virus caused a pandemic. This strain was almost indistinguishable from an H1N1 virus already isolated in 1950.[16,17] Mainly young people born after 1950 were infected by this virus since the older population still had protecting antibodies against it. Possibly, in 1950, this virus had changed its species specificity by replacing genes (see Section 3), had survived in the new host for 27 years and, by replacement of the same genes, went back to the original host. In a corresponding model experiment in the laboratory, we have been able to change the host range of fowl plague virus twice by replacing the necessary genes.[18]

2.2. Antigenic drift

The sudden appearance of new influenza A strains caused by replacements of genes coding for the surface glycoproteins is rendered possible by the segmented genome. Besides this antigenic shift there exists also the relatively slow process of mutation of the surface glycoproteins and selection of corresponding variants by the immune system. This is called antigenic drift. A quite strong antigenic drift is found with influenza A viruses because within the HA and NA molecules there are domains in which mutations are seldom lethal—i.e., these domains are not really necessary for the function of HA or NA. However, the antigenic determinants are located in these areas. In contrast to the other genes, which are highly conserved, the HA and NA genes contain regions of high genetic variability[19] and exactly these domains are identical with the antigenic sites[20,21] (see Fig. 6). In spite of the antigenic drift there are still serological cross reactions to a certain extent between the original virus and its variant—i.e., the variants are partly recognized by the antibodies already present. Therefore, such drift viruses usually start epidemics, which are not so severe and are often confined to certain areas.

3. The Influence of Reassortment on Pathogenicity, Host Specificity, and Organ Tropism

3.1. Construction of Nonpathogenic Reassortants

In nature, "wolves in sheep's clothing" are produced by the antigenic shift. Therefore, we[22] and others[23,24] have tried to obtain live vaccine strains by constructing "a sheep in wolf's clothing." The genes coding for the surface glycoproteins are kept, while the genes responsible for the pathogenicity are replaced. By the method described in Section 1.4, using our ts mutants, we obtained a large number of reassortants of fowl plague virus. When these reassortants were tested for their pathogenicity in chicken, it became apparent that replacement of RNA segment 1 (PB2 gene) by the allelic gene of the human A/PR/8/34 (H1N1) strain led to a virus completely nonpathogenic for chicken



Fig. 6. Schematic tertiary structure of the hemagglutinin monomer of the A/Aichi/2/68 (H3N2) strain. The four symbols ▲, ●, ■, and ◆ indicate mutations in the four antigenic sites, which lead to immunological changes. The broad lines represent α-helix, the flat arrows β-sheet (taken from the cover of *Nature (London) 289* (1981) No. 5796 with permission of Macmillan Journals Ltd.) [21].

but containing the surface antigens of the pathogenic strain. Chickens inoculated with this reassortant withstood a superinfection with the wild-type FPV. When the swine influenza virus A/sw/1976/31 was used for the same purpose, the corresponding reassortant was as pathogenic as the wild type. In this case a ts mutant with a defect in the PB1 gene (RNA segment 2) had to be used. The reassortant of FPV that contains the RNA segment 2 of the swine virus was also completely nonpathogenic for chicken and can therefore be regarded as a potential live vaccine strain.[22] During these studies we were not able to predict which gene of the dangerous virus had to be replaced by the gene of the other prototype virus in order to lose pathogenic properties. However, we recognized that the gene constellation coding for the polymerase complex, or better the correct cooperation of its gene products, is important in this context (see Section 1.1).[25] In further studies it was found that the nonpathogenic reassortants of FPV multiplied only slowly at the body temperature of the chicken (41 °C) so that in the infected organism the immune defense is fast enough to prevent the disease. This observation enabled us to rapidly isolate potential vaccine strains by double infection (even starting with two highly pathogenic parent strains) and selection using the plaque enlargement technique of reassortants that grow only slowly at 41 °C. All these reassortants were nonpathogenic for chickens and had replaced genes belonging to the polymerase complex.[26]

3.2. Neurotropic Reassortants

If it is possible to lose, by reassortment, pathogenic properties of influenza A viruses, it should also be possible

to start with two harmless parent strains and create reassortants highly pathogenic for a certain host. Mice are especially suitable to study an increase in pathogenicity, since these animals are free of influenza under natural conditions. As long as influenza strains are not adapted by passaging (i.e., by several cycles of infection and isolation) to grow in these animals, mice artificially infected with these viruses normally do not become sick. When reassortants between fowl plague virus and other human or avian influenza strains were tested in young mice, it turned out that certain reassortants were able to kill the animals. In contrast to the parent strains, these highly pathogenic reassortants grew in mouse brains to high titers. The same reassortants also multiplied in mouse brain cells cultured in vitro, in contrast to the parent viruses. Here again, the replacement of certain polymerase genes was important.[27,28] A correlation between the gene constellation and neurotropism for reassortants between the avian parents FPV and virus N is shown in Table 1.[29] This is an especially clear

Table 1. Multiplication of reassortants obtained from fowl plague virus (F) and A/chicken/Germany "N"/49 (N) in lungs and brains after intranasal inoculation of two-day-old mice. With exception of the first virus (virus N), the genes PB2, HA, NA, and M of the reassortants are derived from fowl plague virus. If the PB1 and/or PA genes are derived from virus N, the reassortants are neurotropic for mice. If, in addition, the NS gene is derived from virus N, the virus titer found in the brain increases even further. On the other hand, replacement of the NP gene causes loss or decrease of neurotropic properties. All animals with detectable virus in their brains die. However, the mean time required for death correlates inversely with the virus titer in the brains [29].

Origin of the genes				Virus titer four days after infection [plaque-forming units/mL suspension]	
PB1	PA	NP	NS	Lung	Brain
N	N	N	N	10^4	$<10^1$
F	F	F	F	10^1	$<10^1$
N	F	F	F	10^6	10^3
N	F	F	N	10^6	10^5
F	N	F	F	10^6	10^4
N	N	F	F	10^7	10^5
N	N	F	N	10^7	10^6
F	F	N	F	$<10^1$	$<10^1$
F	N	N	F	$<10^1$	$<10^1$
N	N	N	F	10^6	10^4

example of a change of organ tropism by reassortment paralleled by an increase in pathogenicity. Most importantly, immunized mice are not protected against an intranasal infection—which is the natural route of infection—by these neurotropic reassortants, since the virus is taken up by the nerve endings in the nasal mucosa and spreads via the olfactory bulb over the entire brain. Immunization only prevents viremia and a generalized infection[30] but has no influence on virus multiplication in the brain, and the animals die.[31]

In nature this kind of increase of pathogenicity seems indeed to happen. In 1979 many dead seals were found on the New England coast of the USA. From the lungs and brains of these dead animals an influenza A virus could be isolated.[32] When this virus was analyzed genetically, it appeared to be a reassortant between avian influenza A viruses.[33]

4. The Influence of Mutation on Pathogenicity and Host Range

In general, loss of pathogenic properties by mutation and selection of nonpathogenic variants can be achieved by passaging a highly pathogenic virus in another host. Several years ago the possible use of temperature-sensitive (ts) mutants of influenza viruses as potential candidates for a live vaccine was proposed. The idea is that such viruses can multiply at the relatively low temperature in the respiratory tract and induce there the production of antibodies of mainly the IgA class. The body temperature in the lower respiratory tract, however, would prevent further multiplication of the ts mutants.[34,35] Viruses that are adapted to growth at low temperature by many passages at 25 °C and thus have a large number of mutations seem to be especially suitable for this purpose, since the probability of reversion to the wild-type virus is very low.[36,37] However, the following facts have to be taken into consideration: Due to the segmented genome, suppressor mutations[38,39] and suppressor recombinations[40] (i.e. the suppression of the ts property by mutation in a different gene or replacement of a different gene by one from a prototype strain, without loss of the ts mutation) with influenza viruses are quite frequent, so that reversion to the ts^+ phenotype (i.e., the ability to multiply at the nonpermissive temperature) is measurable even with viruses with multiple ts defects. An exact analysis of such ts mutants has revealed that the reversion rate to the ts^+ phenotype depends on the RNA segment in which the ts defect is located. The reversion rate is highest in those genes whose gene products cooperate with other viral proteins. Thus reversion, in this case, is mainly due to suppressor mutation. When double mutants are passaged in tissue cultures at intermediate temperatures, ts^+ revertants are found after a few passages. At high temperature the mutant is lost (no replication). At low temperature there is no selection pressure and therefore revertants have no chance to develop. Correspondingly, chickens infected intratracheally by such double mutants of FPV (relatively low temperature in the upper respiratory tract) died or became sick. When they were infected intramuscularly (immediately 41 °C), no symptoms were recognized.[41] Therefore, the respiratory tract does not appear to be promising as a route of application for ts mutants.

Furthermore, it was found that during passage of the nonpathogenic reassortants described in Section 3.1 at the elevated temperature highly pathogenic variants rapidly appeared.[42] This demonstrates that even the replacement of a whole RNA segment does not lead to a safe live vaccine.

In infected cells the cleavability of the hemagglutinin (HA) into the cleavage products HA_1 and HA_2 by trypsin-like enzymes is a presupposition for numerous cycles of multiplication of influenza A viruses.[43,44] Therefore, the cleavability of the HA is an important factor for pathogenicity.[45] Unless small amounts of trypsin are added to the culture medium, noninfectious virus particles are released from cells in which a corresponding protease is not present or is unable to cleave the HA of a given influenza virus.[43,44,46] The cleavability of the HA depends, on the one hand, on the virus strains under investigation and, on the

other hand, on the host cell. For example, all influenza viruses so far tested multiply in the chorioallantoic membrane of embryonated chicken eggs. The released virus particles contain a cleaved HA and can therefore be used to infect primary chick embryo cells (CEC) in culture. However, only a few strains of the H5 and H7 subtypes are released from these cells with a cleaved HA and are able to form plaques on CEC. The other virus strains undergo only a single cycle of multiplication in CEC and do not form plaques on these cells.[43,44,45] Therefore, one would expect that the HA gene of a virus whose HA cannot be cleaved in a certain cell can be changed by mutation in such a way that the gene product can be cleaved. Exactly this has been achieved during adaptation of an influenza virus by passaging it in a normally (almost) nonpermissive cell line. The variants obtained in this way produced virus particles with cleaved HA and multiplied in this host cell to high titers. A comparison of the sequence of the HA of the original virus with that of the variant revealed that the cleavability in this host correlated with the replacement of a single amino acid.[47] This example demonstrates that after a single point mutation a virus can be released from a previously nonpermissive cell in an infectious form.

Nature takes advantage of this possibility in order to increase the pathogenicity of an influenza virus for its natural host. In the spring of 1983 in a chicken farm in Pennsylvania, an influenza virus was isolated that caused only mild symptoms in chickens such as decreased egg production. However, in October of the same year many chickens died in the surrounding farms. From these chickens an influenza virus was isolated, which, except for a few point mutations, was identical to the earlier isolate. The virus with low pathogenicity was released from primary chick embryo fibroblasts with an almost uncleaved HA, and the virus titer in these cells in culture was very low. In contrast, the highly pathogenic variant was released from the same tissue culture cells with a cleaved HA, and the titer was very high. Here also the sequencing of the HA genes revealed that this change in pathogenicity was due to the replacement of a single amino acid, which led to the loss of a carbohydrate side chain.[48]

5. Possible Organ Tropism by Stability of the Virus in an Acidic Environment

The cleaved hemagglutinin of influenza A viruses undergoes an irreversible conformational change at a pH between 5 and 6. This conformational change is correlated with the fusion of the viral membrane with the membrane of endosomes (intracellular vesicles) and, in this way, with the entrance of the nucleocapsid into the infected cell.[49] In viruses with a noncleaved HA this conformational change does not occur. Such viruses cannot start an infection, since they do not undergo the conformational change of the HA and, therefore, are not taken up into endosomes.[50] If viruses with a cleaved HA in free solution are exposed to low pH, a conformational change occurs which leads to an irreversible loss of infectivity. Many viruses with noncleaved HA, however, withstand a long treatment at a pH far below 5. These viruses need, for their further replication, a short treatment with an enzyme with a trypsin-like cleavage specificity (see Section 4). The highly pathogenic avian influenza viruses are, in contrast to nonpathogenic strains, released from most cells with a cleaved HA[45] and are therefore extremely sensitive to low pH.[51] Water birds are the greatest reservoir for the various influenza A viruses, which are more or less nonpathogenic for their natural host and are transported and distributed by these birds over great distances.[52] They multiply in these animals in a well-defined part of the gut.[53] The natural route by which water birds are infected is not yet known. In the laboratory, however, they can be infected easily via the cloaca. If this is also the natural route of infection, then the viruses surviving in lake water[54] with uncleaved HA might penetrate to a region within the intestine where enough trypsin is still present for their activation, and multiplication could begin. In lower regions of the intestine, where trypsin is absent, the virus would be produced with a noncleaved HA and would be released via the feces into the lake water. This behavior of avian influenza A viruses would explain, on the one hand, why they have such a defined organ tropism and are nonpathogenic in water birds, and on the other hand, why they spread in nature so easily. Furthermore, this would also explain why the highly pathogenic avian viruses, owing to their high sensitivity toward low pH (uric acid, which predominates in avian feces, has a pK value of 5.5), do not spread very well and, therefore, do not eradicate their natural host.[51] The above-mentioned property of the HA of viruses of water birds is surely not the only factor determining the organ tropism, since in the laboratory reassortants between duck and human viruses can have a different organ tropism.[55]

6. The Role of the Nucleoprotein in Organ and Species Specificity

6.1. The Nucleoprotein as Phosphoprotein

Viruses can only infect a cell if it carries corresponding receptors for the virus. Receptors for influenza A viruses are neuraminic acid-containing glycoproteins or glycolipids, such as gangliosides. Although there are clear receptor specificities for influenza viruses, depending on the linkage of the neuraminic acid,[56] all vertebrate cells have almost all kinds of neuraminic acid-containing receptors. Therefore, all warm-blooded vertebrate cells so far tested can be, at least abortively, infected by influenza A viruses. This means that there must exist other factors that forbid or allow these viruses to multiply in such cells. Important is the presence within the cell, or in its immediate neighborhood, of an enzyme with a trypsin-like cleavage specificity (cleavage after Arg and Lys) to cleave the hemagglutinin into the cleavage products HA_1 and HA_2. Since reassortants exist, however, in which the HA is cleavable in certain cells but which nevertheless do not multiply in these cells,[18] there must be further restrictions.

The question is whether or not the host cell modifies one or several viral components in such a way that the virus can multiply. In nature a commonly used method to modify proteins is phosphorylation.[57] There are at least three

virus-specific proteins in influenza viruses which could be phosphorylated. These are the NP,[58-62] the M protein,[63] and the NS1 protein.[64] Since in all influenza A virus strains studied so far the NP is phosphorylated, but not in all virus-infected cells the NS_1 or M protein, we have concentrated our studies first on the phosphorylation of the NPs.[65]

If, indeed, cellular protein phosphokinases with different specificities determine whether the phosphorylated NP can exert its function during virus replication, the following predictions can be made: 1) If the same host cells are infected with different influenza A viruses, the phosphopeptide fingerprints of the NPs after labeling with [^{32}P]-orthophosphate in vivo and digestion of the isolated NPs with trypsin should be different. 2) The phosphopeptide fingerprints of the NP of a given influenza A virus should be different if different cells were used for propagation of that virus. 3) If the function, i.e., the phenotype, of the NP is changed by mutation, the phosphopeptide fingerprints of the NP should also be influenced. As shown in Figure 7, the phosphopeptide fingerprints of the NPs are indeed specific for the virus used for infection of one and the same cell type. Furthermore, the pattern depends on the host cell used for virus propagation and it has been shown that the fingerprints co-vary with the ts mutation in the NP gene and with reversion to the wild type. These observations do not strictly prove but are nonetheless compatible with the idea that the infected organism controls the replication of viral proteins via phosphorylation. At present we are attempting to influence virus replication by compounds that specifically interfere with cellular protein phosphokinases. Hormones, which may influence the disease at this level, are of special interest. The first results of investigations along this line have shown that insulin, at close to physiological concentrations, can retard virus replication. This effect is potentiated by compounds that interfere with the phosphorylation of the insulin receptor.[66]

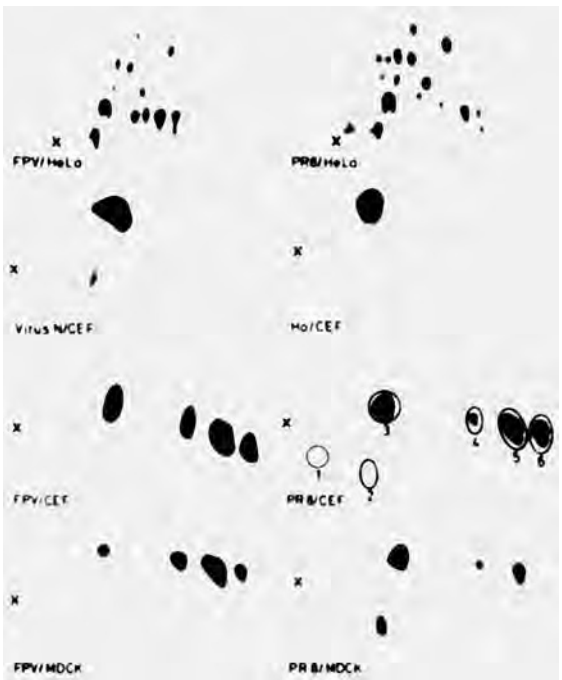


Fig. 7. Phosphopeptide fingerprints of the nucleoproteins of different influenza A strains, which were labeled with [^{32}P]-orthophosphate in different cells. The following viruses were investigated: fowl plague virus (A/FPV/Rostock/34), virus N (A/chicken/Germany "N"/49), HO (A/Hong Kong/1/68), and PR8 (A/PR/8/34). The following host cells where investigated: CEF = primary chick embryo fibroblasts; MDCK = immortal canine kidney cells; HeLa = immortal human carcinoma cells. The virus yield in MDCK cells is on average about 10% of that in CEF; the yield in HeLa cells is about 0.1% of that in CEF. During growth in HeLa cells, the nucleoprotein (NP) is overphosphorylated. During growth in MDCK cells, the PR8 NP is missing phosphopeptide 6. In FPV-infected MDCK cells, the major phosphopeptide 3 is only weakly labeled [65].

6.2. The Nucleoprotein as a Possible Determinant of Species Specificity

According to our experience, avian influenza viruses under natural conditions do not infect humans, and human viruses do not infect birds. The same holds true for horses and the equine influenza viruses. However, pigs are apparently an exception. Human influenza A strains have been isolated from pigs,[67] and farmers have been infected with porcine influenza viruses present in their pig herds.[68,69] Furthermore, there is circumstantial evidence that porcine influenza viruses have infected turkeys under natural conditions.[70] These observations raise the question which viral components are responsible for the species barrier.

The first hint for the role of the nucleoprotein in determining the species specificity came from experiments in which the defective genes of ts mutants of fowl plague virus were to be replaced by the allelic genes of the A/Hong Kong/1/68 (H3N2) virus after double infection of primary chick embryo cells at the nonpermissive temperature (see Section 1.4). This replacement was possible with all ts mutants except those carrying a defect in the HA or NP genes. The replacement was not possible in the case of the HA gene because the HA of the Hong Kong strain is not cleavable in chick embryo cells.[13] The failure to replace the defective NP gene of FPV was not understandable at first, since replacement was possible after double infection with equine, porcine, or avian influenza viruses. When for the double infection another host cell was used, namely, an immortal canine kidney cell line (MDCK), the replacement of the defective NP gene of FPV by the gene of the Hong Kong virus was possible. These reassortants carrying the HA of FPV, which grew excellently on MDCK cells, were unable to multiply on chick embryo cells and were nonpathogenic for chicken.[18] Thus, the fowl plague virus was forced by replacement of its NP gene to change its host.

Within the last decade *Shortridge* et al. have isolated a large number of H3N2 viruses from humans, birds, and pigs in the area of South China. As a consequence of the age-old agricultural techniques practiced in that region, humans, ducks, and pigs always live in close contact.[71] Therefore, these isolates are especially suitable to study the question how far influenza viruses are able to cross the species barrier. We have investigated eight human, ten porcine, and fifteen avian H3N2 isolates using the above-mentioned double-infection or so-called rescue test with mutants having a ts defect in the NP gene of FPV in order to determine whether we could isolate reassortants capable of multiplying in chick embryo cells. As shown in Table 2, we

were unable to replace the NP of the ts mutants of FPV with that of any of the human isolates (i.e., to rescue the ts mutants), whereas all avian strains were able to rescue these mutants. For the porcine strains, rescue was possible with two isolates (Sw126 and Sw127), but not with the other eight strains. According to the hybridization data, the NP gene of the Sw126 and Sw127 isolates exhibited the same low genetic relatedness to the NP gene of the human A/WSN/33 (H1N1) strain as did the avian H3N2 strains. The other porcine isolates, which behaved in the rescue test like the human viruses, were genetically more closely related to the NP gene of the WSN virus (Table 2). The NPs were also tested serologically using five different monoclonal antibodies directed against the NP of the WSN strain. In this test the isolates Sw126 and Sw127 showed intermediate behavior (Table 2). Our results are compatible with the idea that the human H3N2 viruses cannot be transmitted directly to birds and presumably also not the other way around without prior reassortment in pigs. The pigs seem to be more tolerant toward the multiplication of human and avian influenza viruses. In the example studied here, the species specificity apparently is determined by the NP gene or its gene product. The genes coding for the surface glycoproteins H3 and N2 can presumably cross the species barrier quite easily, since they were found on all isolates studied, independent of the species. The experiments on double infection with mutants with ts defects in other genes of FPV demonstrate that these genes also do not play an important role in determining the species specificity.[72]

Table 2. Summary of properties of H3N2 influenza A viruses isolated from humans, pigs, or birds. WSN is a test strain originally isolated from man; 3/1, 5/1 etc. are individual monoclones that produce the monoclonal antibodies used in these studies.

Property under study	Virus isolated from: Human all isolates	Pigs all, except Sw126 and Sw127	Poultry all isolates	Pigs only Sw126 and Sw127
Ability to replace the NP gene of FPV (rescue)	–	–	+	+
Hyhridization with RNA segment 5 of WSN, RNase resistance [%]	28–31	28	17	17–18
Binding of monoclonal antibodies against the NP of WSN; monoclones bound	3/1, 5/1, 7/3	3/1, 5/1, 7/3	3/1, 5/1, 7/3, 150/4, 469/4	3/1, 5/1, 150/4

The isolates Sw126 and Sw127 are intermediate in behavior with respect to the NP genes compared with human and avian H3N2 strains (Table 2). This could mean that these NPs are of avian origin and are now on the way to becoming adapted to the new host. The phosphopeptide fingerprints of the NPs of these two viruses are identical with those of the other porcine H3N2 strains but different from the avian and human H3N2 isolates.[72]

The particular position of the pigs as hosts for influenza A viruses of different origin is of special interest for understanding the sudden appearance of new pandemic strains by reassortment. The special living conditions in China would specifically explain why most of the pandemics start from the area of South China.[71] Changing these conditions might help to avoid or at least to lower the probability of the antigenic shift.

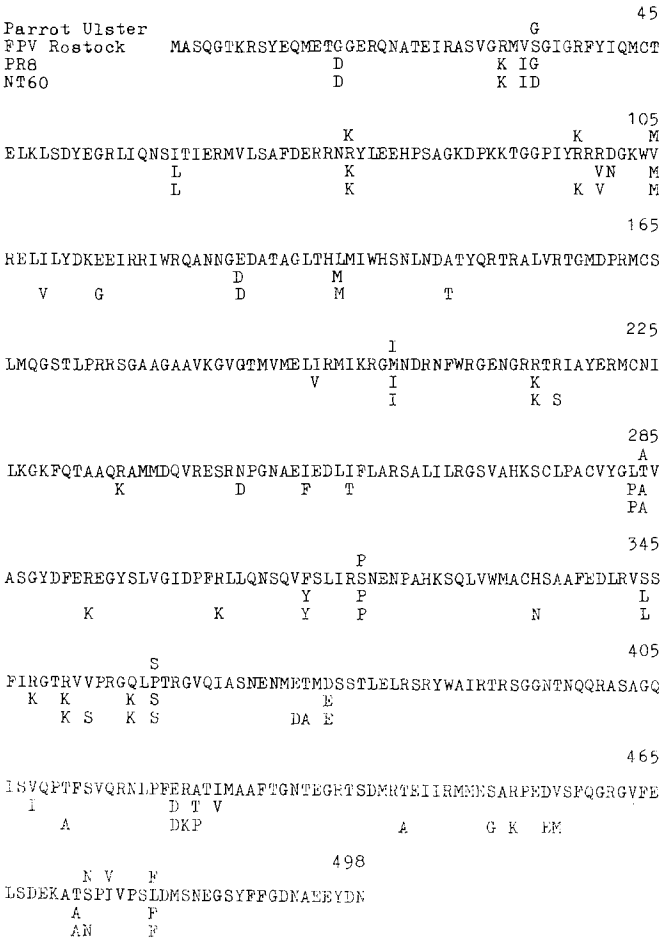


Fig. 8. Comparison of the amino acid sequences of the nucleoprotein of the four influenza A viruses A/parrot/Ulster/73 (H7N1), A/FPV/Rostock/34 (H7N1), A/PR/8/34 (H1N1), and A/NT/60/68 (H3N2). The sequence of the nucleoprotein of the FPV is presented in the one-letter code. For the other three viruses only the amino acid replacements are shown. The four NPs each contain 498 amino acids [73].

A comparison of the amino acid sequences of the NPs of human and avian isolates are also in agreement with the idea that NPs can adapt to the new host. As shown in Figure 8, the amino acid sequence of the NP of an influnza A virus isolated from a parrot in 1973 (A/parrot/Ulster/73) is highly related to the sequence of fowl plague virus. However, of the eleven amino acid replacements in the NP of the parrot virus, eight are identical with those of the human A/PR/8/34 virus and nine are identical with those of the human A/NT/60/68 virus. This clearly demonstrates that the NP of the parrot strain is located genetically between that of FPV and the human viruses.[73] However, further comparisons of sequences are necessary to strengthen the point that NPs can adapt to the new host. In the case of the Parrot/Ulster strain, the question arises again whether an intermediary host was also necessary for the adaptation.

7. Outlook

Because of the specific structure of the segmented genome, influenza A viruses are extremely variable. This variability is due, on the one hand, to the possibility of constructing new viruses by reassortment, which is not possible with viruses whose genome is not segmented. On the other hand, mutations in one gene do not have direct polar effects (e.g., changes of the secondary structure of the RNA or of the polyprotein) on another gene, which is normally the case for viruses with a nonsegmented genome. Therefore, influenza A viruses can adapt very rapidly to new conditions; and variants appear which can easily escape certain selection pressures such as the immune defense system of the infected organism. For this reason it is extremely difficult to develop a safe live vaccine. Even the application of a killed or split vaccine, as it is used today, is not without problems, since it is unpredictable which variant will show up next. And we are always somehow behind schedule.

Another problem is caused by the large reservoir of influenza A viruses in the animal kingdom, especially in water birds. Feral ducks and other water birds travel thousands of kilometers each year—also from continent to continent—and distribute the various influenza viruses all over the world. This is possible because these strains do not cause clinical symptoms in their hosts. Surely, it is not a selection advantage for a virus to be especially pathogenic for its host, since such a virus would be eradicated by eradication of its host. However, influenza viruses can afford to produce such highly pathogenic strains, since from the large reservoir new reassortants with different properties can always be "synthesized." An example is the sudden appearance of the H7N7 strain that was responsible for killing so many seals on the New England coast of the USA during the winter of 1979/80. This virus never reappeared in this population, although another influenza A virus belonging to a different subtype was isolated later. It is not unlikely that the highly pathogenic fowl plague viruses, which sporadically appear and have been isolated in different parts of the world, are indeed unique creations, since in most instances the subtype combinations are different.

Taking into consideration the properties of influenza A viruses described here, it is unlikely that in the near future we will be able to eradicate the causative agent of human influenza—in contrast to smallpox or polio, where we either have succeeded already or will succeed soon.

The experiments performed in the author's laboratory were supported by the Deutsche Forschungsgemeinschaft (Sonderforschungsbereich 47) and by the Fonds der Chemischen Industrie. I thank these institutions for their generous help. Furthermore, I thank Dr. R. Rott for helpful discussions, Dr. B. Simpson for help with the manuscript, and Mrs. M. Seitz for typing.

Received: October 21, 1985 [A 564 IE]
German version: *Angew. Chem. 98* (1986) 47

[1] P. W. Choppin, R. W. Compans in E. D. Kilbourne (Ed.): *The Influenza Virus and Influenza*, Academic Press, New York 1975, p. 15.
[2] J. Blok, G. M. Air, W. G. Laver, C. W. Ward, G. G. Lilley, E. F. Woods, C. M. Roxburgh, A. S. Inglis, *Virology 119* (1982) 109.
[3] P. M. Colman, C. W. Ward, *Curr. Top. Microbiol. Immunol. 114* (1985) 177.
[4] P. Palese, *Cell 10* (1977) 1.
[5] C. Scholtissek, *Curr. Top. Microbiol. Immunol. 80* (1978) 139.
[6] V. S. Hinshaw, R. G. Webster, R. J. Rodriguez, *Arch. Virol. 67* (1981) 191.
[7] R. M. Krug in P. Palese, D. W. Kingsbury (Eds.): *Genetics of Influenza Viruses*, Springer, Vienna 1983, p. 70.
[8] J. J. Skehel, A. J. Hay, *J. Gen. Virol. 39* (1978) 1.
[9] R. A. Lamb in P. Palese, D. W. Kingsbury (Eds.): *Genetics of Influenza Viruses*, Springer, Vienna 1983, p. 21.
[10] H.-D. Klenk, R. Rott, *Curr. Top. Microbiol. Immunol. 90* (1980) 19.
[11] R. W. Simpson, G. K. Hirst, *Virology 35* (1968) 41.
[12] C. Scholtissek, A. L. Bowles, *Virology 67* (1975) 576.
[13] C. Scholtissek, E. Harms, W. Rohde, M. Orlich, R. Rott, *Virology 74* (1976) 332.
[14] E. Harms, W. Rohde, F. Bosch, C. Scholtissek, *Virology 86* (1978) 413.
[15] C. Scholtissek, W. Rohde, V. von Hoyningen, R. Rott, *Virology 87* (1978) 13.
[16] C. Scholtissek, V. von Hoyningen, R. Rott, *Virology 89* (1978) 613.
[17] K. Nakajima, U. Desselberger, P. Palese, *Nature (London) 274* (1978) 334.
[18] C. Scholtissek, I. Koennecke, R. Rott, *Virology 91* (1978) 79.
[19] C. Scholtissek, *Virology 93* (1979) 594.
[20] I. A. Wilson, J. J. Skehel, D. C. Wiley, *Nature (London) 289* (1981) 366.
[21] D. C. Wiley, I. A. Wilson, J. J. Skehel, *Nature (London) 289* (1981) 373.
[22] C. Scholtissek, R. Rott, M. Orlich, E. Harms, W. Rohde, *Virology 81* (1977) 74.
[23] A. S. Beare: *Basic and Applied Influenza Research*, CRC Press, Boca Raton, FL, USA 1982, p. 211.
[24] B. R. Murphy, M. L. Clements, H. F. Maassab, A. J. Buckler-White, S.-F. Tian, W. T. London, R. M. Chanock in C. H. Stuart-Harris (Ed.): *The Molecular Virology and Epidemiology of Influenza*, Academic Press, New York 1984, p. 211.
[25] C. Scholtissek, *Behring Inst. Mitt. 69* (1981) 30.
[26] R. Rott, M. Orlich, C. Scholtissek, *Virology 120* (1982) 215.
[27] A. Vallbracht, B. Flehmig, H.-J. Gerth, *Intervirology 11* (1979) 16.
[28] C. Scholtissek, A. Vallbracht, B. Flehmig, R. Rott, *Virology 95* (1979) 492.
[29] J. Bonin, C. Scholtissek, *Arch. Virol. 75* (1983) 255.
[30] A. Vallbracht, C. Scholtissek, B. Flehmig, H.-J. Gerth, *Virology 107* (1980) 452.
[31] M. Reinacher, J. Bonin, O. Narayan, C. Scholtissek, *Lab. Invest. 49* (1983) 686.
[32] R. Geraci, D. J. St. Aubin, I. K. Barker, R. G. Webster, V. S. Hinshaw, W. J. Bean, H. L. Ruhnke, J. H. Prescott, G. Early, A. S. Baker, S. Madoff, R. T. Schooly, *Science 215* (1982) 1129.
[33] V. S. Hinshaw, W. J. Bean, R. G. Webster in D. P. Nayak (Ed.): *Genetic Variation among Influenza Viruses*, Academic Press, New York 1981, p. 515.
[34] H. W. Kim, J. O. Arrobio, C. D. Brandt, R. H. Parrott, B. R. Murphy, D. D. Richman, R. M. Chanock, *Pediatr. Res. 10* (1976) 238.
[35] B. R. Murphy, R. M. Chanock in D. P. Nayak (Ed.): *Genetic Variation among Influenza Viruses*, Academic Press, New York 1981, p. 601.
[36] H. F. Maassab, *Nature (London) 213* (1967) 612.
[37] N. J. Cox, A. P. Kendal, A. A. Shilov, G. I. Alexandrova, Y. Z. Ghendon, A. I. Klimov, *J. Gen. Virol. 66* (1985) 1697.
[38] B. R. Murphy, M. D. Tolpin, J. G. Massicot, H. Y. Kim, R. H. Parrott, R. M. Chanock, *Ann. N. Y. Acad. Sci. 354* (1980) 172.
[39] C. Scholtissek, S. B. Spring in D. P. Nayak (Ed.): *Genetic Variation among Influenza Viruses*, Academic Press, New York 1981, p. 399.
[40] C. Scholtissek, S. B. Spring, *Virology 118* (1982) 28.
[41] C. Scholtissek, R. Rott, *Virus Res. 1* (1984) 117.
[42] R. Rott, M. Orlich, C. Scholtissek, *Virology 126* (1983) 459.
[43] H.-D. Klenk, R. Rott, M. Orlich, J. Blödorn, *Virology 68* (1975) 426.
[44] S. G. Lazarowitz, P. W. Choppin, *Virology 68* (1975) 440.
[45] F. X. Bosch, M. Orlich, H.-D. Klenk, R. Rott, *Virology 95* (1979) 191.
[46] G. Appleyard, H. B. Maber, *J. Gen. Virol. 25* (1974) 351.
[47] R. Rott, M. Orlich, H.-D. Klenk, M. L. Wang, J. J. Skehel, D. C. Wiley, *EMBO J. 3* (1984) 3329.
[48] Y. Kawaoko, C. Naeve, R. G. Webster, *Virology 139* (1984) 303.
[49] J. J. Skehel, P. M. Bayley, E. B. Brown, S. R. Martin, M. D. Waterfield, J. M. White, I. A. Wilson, D. C. Wiley, *Proc. Natl. Acad. Sci. USA 79* (1982) 968.
[50] C. Scholtissek, *Arch. Virol.*, in press.
[51] C. Scholtissek, *Arch. Virol. 85* (1985) 1.
[52] R. G. Webster, W. G. Laver in E. D. Kilbourne (Ed.): *The Influenza Viruses and Influenza*, Academic Press, New York 1975, p. 269.
[53] R. G. Webster, M. Yakhno, V. S. Hinshaw, W. J. Bean, G. Murti, *Virology 84* (1978) 268.
[54] V. S. Hinshaw, R. G. Webster, B. Turner, *Intervirology 11* (1979) 66.

[55] V. S. Hinshaw, R. G. Webster, C. W. Naeve, B. R. Murphy, *Virology 128* (1983) 260.
[56] H. H. Higa, G. N. Rogers, J. C. Paulson, *Virology 143*, in press.
[57] P. Cohen, *Eur. J. Biochem. 151* (1985) 439.
[58] M. L. Privalsky, E. E. Penhoet, *J. Virol. 24* (1977) 401.
[59] M. L. Privalsky, E. E. Penhoet, *Proc. Natl. Acad. Sci. USA 75* (1978) 3625.
[60] M. L. Privalsky, E. E. Penhoet, *J. Biol. Chem. 256* (1981) 5368.
[61] T. Petri, N. J. Dimmock, *J. Gen. Virol. 57* (1981) 185.
[62] J. W. Almond, V. Felsenreich, *J. Gen. Virol. 60* (1982) 295.
[63] A. Gregoriades, T. Christie, K. Markarian, *J. Virol. 49* (1984) 229.
[64] T. Petri, S. Patterson, N. J. Dimmock, *J. Gen. Virol. 61* (1982) 217.
[65] O. Kistner, H. Müller, H. Becht, C. Scholtissek, *J. Gen. Virol. 66* (1985) 465.
[66] C. Scholtissek et al., unpublished.
[67] W. D. Kundin, *Nature (London) 288* (1970) 587.
[68] W. R. Dowdle, M. A. W. Mattwick, *J. Infect. Dis. 136* (1977) 386.
[69] V. S. Hinshaw, W. J. Bean, R. G. Webster, B. C. Easterday, *Virology 84* (1978) 51.
[70] V. S. Hinshaw, R. G. Webster, W. J. Bean, J. Downie, D. A. Senne, *Science 220* (1983) 206.
[71] K. F. Shortridge, C. H. Stuart-Harris, *Lancet ii* (1982) 812.
[72] C. Scholtissek, H. Bürger, O. Kistner, K. F. Shortridge, *Virology*, in press.
[73] H. Steuler, B. Schröder, H. Bürger, C. Scholtissek, *Virus Res. 3* (1985) 35.

Multiple Bonds between Transition Metals and "Bare" Main Group Elements: Links between Inorganic Solid State Chemistry and Organometallic Chemistry

By Wolfgang A. Herrmann*

In memoriam Professor Wilhelm Klemm

The last two decades have seen a dramatic development in the study of metal-metal multiple bonds, particular successes being recorded in the field of organometallic chemistry. Syntheses designed to produce novel transition metal complexes with single, double, triple and quadruple metal-metal bonds occupy a most important place in such research, as also do reactivity studies. A striving to establish general principles has provided much of the motivation for such work, but one less obvious goal—the commercial application of the catalytic properties of metal-metal multiple bonding systems, in the medium and long term—should not be overlooked. All aspects of the investigations of metal-metal multiple bonds also apply to a particular class of compound that has, however, enjoyed little limelight and thus deserves the present review: complexes with multiple bonds between transition metals and substituent-free ("bare") main group elements. Although based mostly on accidental discoveries, the few noteworthy examples are now beginning to unfold general concepts of synthesis that are capable of being extended and thus are deserving of exploitation in preparative chemistry. The availability of further structural patterns exhibiting multiple bonds between transition metals and ligand-free main group elements might enable preparative organometallic chemistry to expand in a completely new direction (for instance by the stabilizing or activation of small molecules at the metal complex). This essay discusses the chemistry of complexes of bare carbon, nitrogen, and oxygen ligands (carbido-, nitrido-, and oxo-complexes) and their relationships to higher homologues from both a synthetic and a structural point of view.

1. Introduction

The topic "organometallic chemistry", after 40 years of research, is a monumental one. The basic structures have often become so embellished as to be scarcely recognizable.[1,2] The rich variety of structures is far from being exhausted, since new structural principles, provided by consideration of novel materials, in turn allow the recognition of relationships to other areas of chemistry and of new concepts capable of extension.[3,4] Although the great diversity of carbon-containing ligands underlines the smooth transition to organic chemistry, the core structures of polynuclear complexes are clearly closely related to the structures of inorganic materials and, like those, more or less determined by conditions of synthesis, atomic radius ratios and electron configurations of the combining atoms. Similarly to inorganic solid state chemistry, organometallic chemistry comprises materials ranging from small ensembles of metals via medium-sized clusters to giant multiatomic frameworks such as are seen in gold and palladium chemistry (e.g. the cubic close-packed "giant sphere" $Au_{55}[P(C_6H_5)_3]_{12}Cl_6$—precursor of a new gold modifica-

[*] Prof. Dr. W. A. Herrmann
Anorganisch-chemisches Institut der Technischen Universität München
Lichtenbergstrasse 4, D-8046 Garching (FRG)

tion based on Au_{13} cuboctahedra—and the water-soluble $Pd_{570\pm30}$-giant with 240 ± 13 ligands[5-8]).

The structures of polyatomic clusters should not be forgotten, even if the current article stresses the topic of multiple bonds between transition metals and "bare" main group elements. The author has not striven to provide a catalog, but rather to demonstrate the connection between preparation and structure of such complexes and also that between "bare" main group atoms with low or high coordination numbers. The restriction of the scope of this article to the carbon, nitrogen, and oxygen groups was necessary to prevent its becoming too unwieldy. Although it may be too early to generalize, it is hoped that typical reactivity patterns of multiple bonds between transition metals and substituent-free main group elements will gradually emerge.

2. Bare Carbon Group Elements as Bridging Ligands

2.1. Cage Structures

Several years ago, complexes containing bare carbon ligands were regarded as laboratory curiosities. These days, however, clusters of this type can be routinely prepared, even if the reactivity of the carbon atom in its metal "cage" is difficult to characterize or to classify.[9-15] Aliphatic hydrocarbons and a wide range of carbon-containing ligand precursors are appropriate for the synthesis of interstitial carbide cluster compounds. The famous textbook examples **1–4** deserve special mention here (Fig. 1), not least for their aesthetic attractiveness.

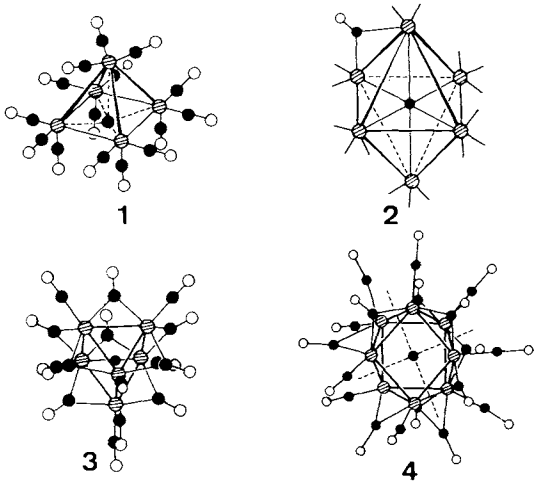
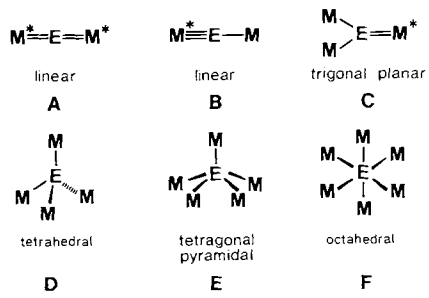


Fig. 1. Atomic carbon in isolable, discrete transition metal cage structures with five, six, and eight metal vertices (atom key: C black, metal atoms hatched, O as circles). Except for the Fe_5C cluster **1**, which displays a sterically exposed carbon atom, these complexes all involve interstitial (encapsulated) carbon ligands.—$Fe_5C(CO)_{15}$ **1**: the five-coordinated carbon atom lies 15 pm out of the basal plane of the Fe_5 pyramid, with FeC bond lengths 189 pm (basal) and 196 pm (axial).—$Ru_6C(CO)_{17}$ **2**, an octahedral 86e complex, isoelectronic with the structurally analogous $[Fe_6C(CO)_{16}]^{2-}$ anion.—$[Rh_6C(CO)_{15}]^{2-}$ **3**: the carbon atom is at the center of an Rh_6 trigonal prism (six terminal, nine edge-bridging CO ligands; 90e cluster).—$[Co_8C(CO)_{18}]^{2-}$ **4**, an interstitial carbide complex with a square antiprismatic metal framework (Co–C 195–220 pm).

The Fe_5C- and Ru_6C-cage structures **1** and **2** are representatives of the basic structural types **E** (square pyramidal) and **F** (octahedral), respectively (see Scheme 1). Multiple bonding between the central atom E (here carbon) and the transition metals M cannot be seriously considered here. Despite the differing frameworks, the C_1 ligands in both these and all other known cases contribute four electrons to the cluster cores.



Scheme 1. Possible types of coordination for bare carbon group elements.

It is striking that the structural types **A** and **B** (linear) and **C** (trigonal planar) do not occur for carbon,[*] although these geometries in particular have shown themselves to be stable for the higher homologues (see Sections 2.2–2.4). The organomercury compounds of general composition $C(HgR)_4$ [R = alkyl, aryl] may be considered as examples of the tetrahedral class **D**.[16]

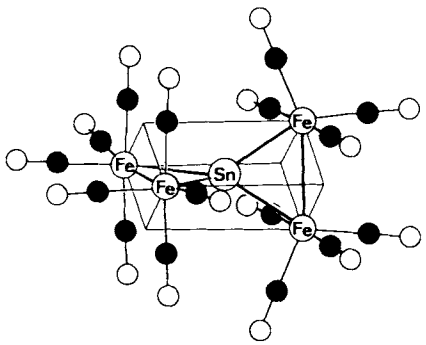


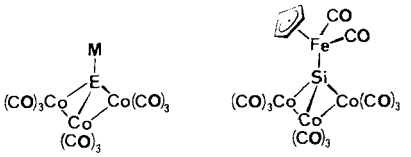
Fig. 2. Scale drawing of the approximately D_{2d}-symmetrical $SnFe_4$ cluster compound **5**, the first cluster example of unsubstituted tin. **5** is isolobal with spiropentane. The tin–iron bond lengths are ca. 254 pm, with FeSnFe angles of 69° and 133°. Weak interactions between the $5d_{z^2}$ and $5d_{xy}$ orbitals of tin and the $3d_{x^2-y^2}$ orbitals of the iron atoms are assumed to occur in this unique molecule.

F. G. A. Stone et al. discovered the first coordination compound of a substituent-free tin atom in 1966; the Fe_4Sn cluster compound

$[(\mu_4\text{-Sn})\{Fe_2(CO)_8\}_2]$ **5**[17]

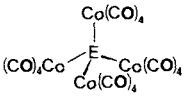
which according to *R. Hoffmann* is an "inorganic spiropentane" fitting well into the nowadays powerful concept of the isolobal analogy,[3] shows a tin atom with distorted tetrahedral environment (Fig. 2; Scheme 1, type **D**). The structurally characterized complexes **6a** and **9** (Fig. 3, Scheme 1, type **D**) contain carbonylcobalt fragments

[*] A possible exception is represented by the structurally not yet unambiguously characterized porphyrin complex of composition $[(\mu\text{-C})\{Fe(TPP)\}_2]$ (TPP = tetraphenylporphyrin), cf. D. Mansuy, J.-P. Lecomte, J.-C. Chottard, J. F. Bartoli, *Inorg. Chem. 20* (1981) 3119.

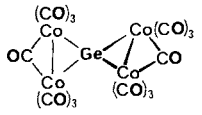


6a. E = Si, M = $Co(CO)_4$
6b. E = Ge, M = $Co(CO)_4$
6c. E = Ge, M = $Mn(CO)_5$

7



8a. E = Sn
8b. E = Pb



9

grouped around four-coordinate silicon and germanium.[18–22] Similar structures may be assumed for the interesting $FeCo_3Si$ compound **7**, prepared by *Malisch* et al. by metalation of the silyl ligand of $[(\eta^5\text{-}C_5H_5)Fe(CO)_2(SiH_3)]$ with octacarbonyldicobalt,[20] and for the complexes **8a** and **8b**, obtained by *Schmid* et al. by treatment of elemental tin and lead, respectively, with octacarbonyldicobalt.[18, 19]

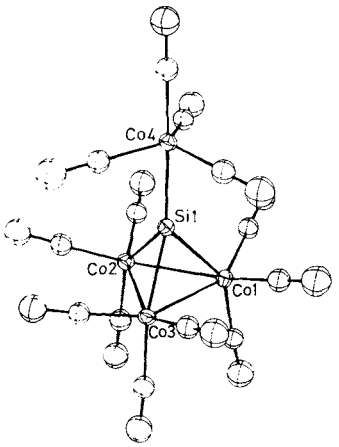
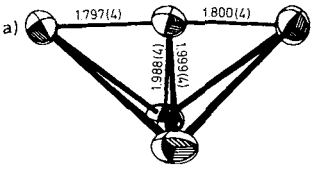


Fig. 3. The C_{3v}-symmetrical structure of the silicon complex **6a**, obtained in 5% yield from $Na[Co(CO)_4]$ and SiI_4 (*n*-hexane, 50°C, UV irradiation, 14 d). The pseudotetrahedrally coordinated silicon atom caps symmetrically to a Co_3 triangular face (Co-Si 221.8 pm, Co-Si-Co 71.9°) and also bears a $Co(CO)_4$ group (Co-Si 228.8 pm, Co-Si-Co 137.3° (av.)).

To these isolated examples can be added the long list of carbido clusters, which demonstrate the substituent-free carbon atom in a wide variety of coordination modes. Although the pentanuclear iron complex **1** (Fig. 1) was for a long time the only representative of this class, nowadays the chemistry of complexes of the bare carbon atom ranks among the most favored themes of organometallic laboratories. The elementary steps in the coordination of carbon monoxide to transition metals have become an important area of research in the quest to elucidate the mechanism of the Fischer-Tropsch synthesis and other industrially important syn-gas reactions.[23]

Notwithstanding the current variety of carbido clusters, there is as yet no structurally reliably characterized example of substituent-free carbon multiply bonded to two metal centers in structures of type **A** and thus available for further reactions on the simple grounds of steric accessibility. The closest approach to M*=C=M* structures is provided by *Bradley*'s Fe_4C butterfly **10**, the fascinating framework of which species is shown in Figure 4a.[12] One of the two FeCFe units is almost linear (175°) with very short Fe-C bonds (ca. 180 pm) to which double bonding character may be attributed. Substitution at the exposed carbon atom, as in **11**,

$[Fe_4C(CO)_{13}]$ **10**



$[Fe_4(CCO_2CH_3)(CO)_{12}]^-$ **11**

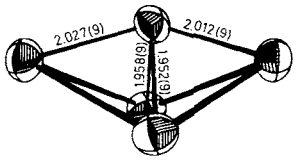


Fig. 4. Butterfly structures of the cores of a) the carbido cluster **10** and b) of the anion **11** present in $[NEt_4][Fe_4(CCO_2CH_3)(CO)_{12}]$. In both cases the Fe_4 polyhedra are folded into a "roof" form (dihedral angles 101 and 130°, respectively) with a μ_4-C_1 ligand.

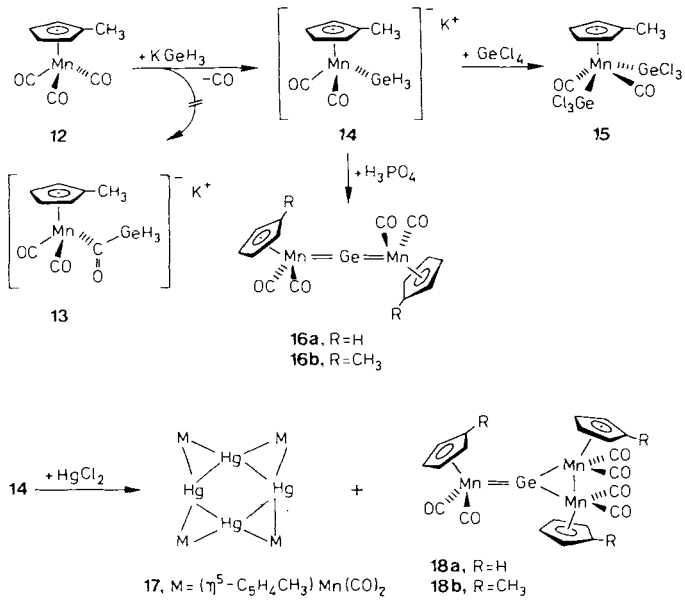
lowers the FeCFe angle by 28° while increasing the bond lengths by approximately 22 pm (Fig. 4b). The structure of **10** offers a plausible model for the chemical environment of carbidic carbon at catalytically active transition metal surfaces.[24]

2.2. Substituent-Free Germanium as Bridging Ligand

2.2.1. Syntheses

A serendipitous discovery of particular significance happened in 1981 when *E. Weiss* et al. obtained type **A** and type **C** compounds containing unsubstituted germanium (e.g. E = Ge; Scheme 1) attached to organometallic fragments through formal double bonds.[25] Reaction of $KGeH_3$ with the carbonylmanganese complex **12** did not lead to the germylcarbonyl derivative **13**, the expected product of a so-called Hieber base reaction, but, with CO elimination, to the pseudotetrahedral, pyrophoric complex anion **14**, the GeH_3 ligand of which proved to be a useful precursor for other germanium-containing materials.[26] Upon reaction of **14** with germanium(IV) chloride the neutral complex **15** is formed in 45% yield; X-ray structure analysis shows the presence of two *trans*-oriented trichlorogermyl groups. With non-oxidizing mineral acids, however, the Mn_2Ge complex **16b** is formed in 40% yield. **16b** is an orange-red, diamagnetic, crystalline, air-stable compound that demonstrates for the first time the structural type **A** (Scheme 1), characterized by a cumulated multiple bonding system between transition metals and a two-coordinate, substituent-free element of the fourth main group. In contrast, reaction of mercury(II) chloride with the complex anion **14** yields the planar (!) star-shaped Mn_4Hg_4 complex **17** in 55% yield and, albeit only in a yield of 1%, the Mn_3Ge complex **18a** (type **C**, Scheme 1), which may be considered as a distant oxidation product of

the germyl precursor **14**. The mechanism of formation of the spectacular germanium complexes **16b** and **18b** is still unclear. It is however accepted that the germanium-hydrogen bond in the precursor **14** is extremely labile to sub-



stitution. This suggested the use of monogermane, GeH_4, as a productive source of bare germanium ligands, particularly since oxidative addition reactions of organogermanium compounds R_nGeH_{4-n} (n = 0-3) are well-documented in transition metal chemistry.[28] Along this line we succeeded in preparing the Mn_3Ge compound **18a** by treatment of the solvent-stabilized organometallic fragment

$[(\eta^5\text{-}C_5H_5)Mn(CO)_2(thf)]$ **19**

with monogermane in tetrahydrofuran (THF) at room temperature.[29] This method gives appreciably better yields (40-60%, cf. 1% above) and, furthermore, avoids the need to prepare $KGeH_3$ (from the binary hydride GeH_4 and potassium metal). It should be noted at this point that the use of the binary hydrides EH_x has convincingly proved to be a general method of introducing a bare main group element E into transition metal complexes.

The French group of *Corriu* has shown in numerous publications that organosilanes add smoothly and readily to coordinatively unsaturated organometallic fragments to give hydrido(silyl) complexes.[30] The parent compound monosilane, SiH_4, behaves in an essentially similar manner upon reaction with the 16e-fragment of the compound

$[(\eta^5\text{-}C_5Me_5)Mn(CO)_2(thf)]$ **20**

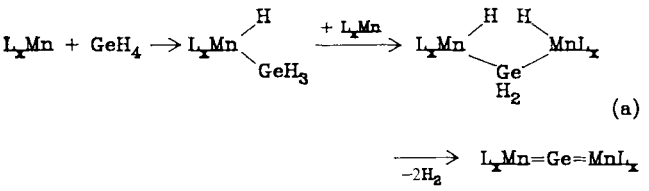
to give the Mn_2-complex

$[(\mu\text{-}SiH_2)\{(\eta^5\text{-}C_5Me_5)Mn(CO)_2H\}_2]$ **21**,

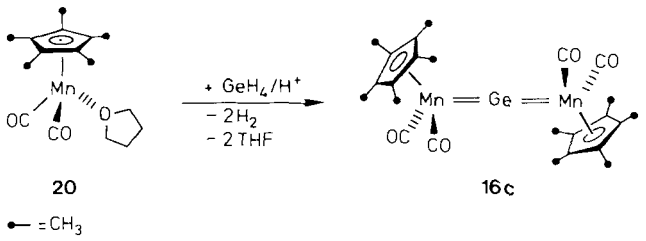
the X-ray structure of which shows the expected bent MnSiMn skeleton with two terminal hydrido ligands at manganese.[31] Attempts to split off H_2 thermolytically, with the intention of preparing the still unknown silicon complex

$[(\mu\text{-}Si)\{(\eta^5\text{-}C_5Me_5)Mn(CO)_2\}_2]$ **22**

have been unsuccessful; these failures may be attributed to the comparatively high stability of the SiH bonds in the complex **21**. As long as there are no indications to the contrary, the sequence (a) may be assumed, at least as a tentative working hypothesis, to represent the formation of unsubstituted germanium atoms at transition metal centers.



X-ray structure analyses have shown that the Mn_3Ge compounds **18a** and **18b** (type **C**), in contrast to the more simply constituted Mn_2Ge derivatives **16a** and **16b** (type **A**), are sterically rather crowded (see Fig. 7 and 8).[25,32] It was therefore to be expected that bulky ligands in the precursor species **19** would tend selectively to form complexes with *linear* MnGeMn backbones. Proof of this is seen in the straightforward synthesis of the compound **16c** by reaction of the solvent complex $[(\eta^5\text{-}C_5Me_5)Mn(CO)_2(thf)]$ **20** with monogermane in the presence of sulfuric acid.[29,33] While the coordination of a further 16e-fragment (e.g. $[(\eta^5\text{-}C_5H_5)Mn(CO)_2]$) to one of the two MnGe multiple bonds of the cyclopentadienyl compound **16a** is possible, and indeed leads smoothly to the Mn_3Ge system **18a**,[32] this addition reaction fails to occur in the case of the pentamethylcyclopentadienyl derivative **16c**.



Simply because of their size, germanium atoms call for an increase of their coordination sphere and preferentially give up their multiple bonds in favor of incorporation in cluster structures. The New Zealand group of *Mackay* and *Nicholson* was recently able, by the action of monogermane or digermane on octacarbonyldicobalt,[21,22] to prepare the structurally fascinating cobalt-germanium clusters **23** (Fig. 5) and **24** (Fig. 6), both striking and excellent examples of tetrahedral M_4Ge and square-pyramidal M_5Ge systems, respectively (types **D** and **E**, Scheme 1).

23 $[(\mu_4\text{-}Ge)\{Co_2(CO)_7\}_2]$ $[(\mu_5\text{-}Ge)_2\{[Co(CO)_4]_2[Co(CO)_3]_4\}]$ **24**

Schmid et al. had in 1977 reported the Co_4Ge complex **6b**, accessible by thermolytic CO abstraction from **23**.[18a] In-

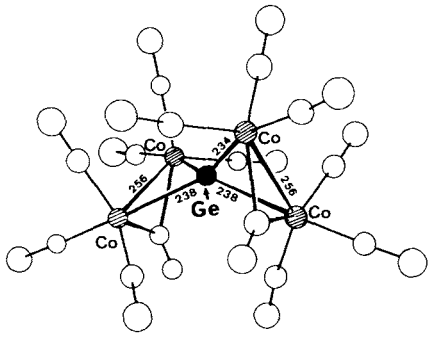


Fig. 5. A germanium atom as spirocenter: crystal structure of **23**, which compound is isovalent with $[(\mu_4\text{-Sn})\{Fe_2(CO)_8\}_2]$ **5** (Fig. 2). The two closed Co_2Ge moieties lie almost at right angles to each other (dihedral angle 96°). The angles at the spirocenter are 66° and 135°; the molecule possesses C_2 symmetry. The same core geometry is seen in the complex cation $[(\mu_4\text{-As})\{(\eta^5\text{-}C_5H_5)_2Co_2(CO)_2\}_2]^+$ **53** (Fig. 24).

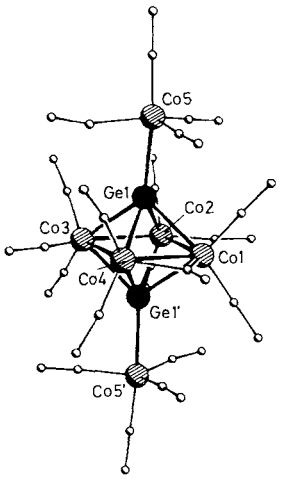


Fig. 6. Structure of the Co_6Ge_2 cluster **24** in the crystal. The octahedral, *closo* Co_4Ge_2 framework bears eleven CO ligands at the four cobalt atoms. All CoGe bond lengths lie in the range 239–243 pm. This complex is formed by the effect of heat on the isolable precursor compound $[Ge_2Co_6(CO)_{20}]$ of unknown structure (possibly a Ge-spirocycle).

terestingly, even alkylgermanes such as CH_3GeH_3 can transfer germanium atoms onto suitable carbonylmetal complexes. If polygermane mixtures are used, the reaction with organometallic fragments never preserves the GeGe bonds.[21,22] Germanium has not yet been incorporated into the center of an octahedral M_6 group, presumably because of its size (cf. carbon, Section 2.1).

2.2.2. *Structural Chemistry*

It is no surprise that the germanium ligands in the polynuclear Co_xGe_y complexes **23** and **24** are not associated with multiple bonding; in general, cluster compounds arise from the aggregation of smaller, reactive fragments. The only realistic hope of obtaining an authentic multiply bonded system, such as the manganese complexes **16a–c** and **18a,b** (Fig. 7 and 8), is that the atom ensemble will be kinetically stable. The extremely short MnGe bonds in **16c** (Fig. 7) are proof enough of multiple bonding in a cumulated (type **A**) system; the Mn=Ge bond lengths of ca. 218 pm (Table 1) are comparable with those of the bridged MnMn triple bond (217.0(1) pm) in the related complex

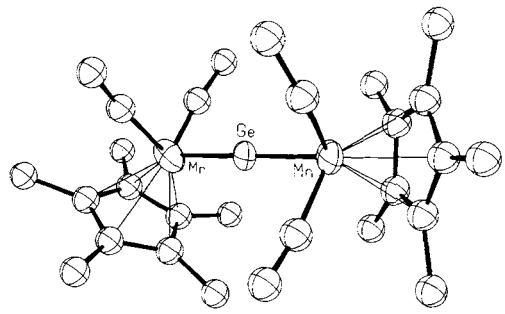


Fig. 7. Molecular structure of the Mn_2Ge compound **16c** (type **A**, Scheme 1), with its linear Mn=Ge=Mn system (Mn-Ge 218(2) pm, Mn-Ge-Mn 179(1)°) and anticlinal conformation (cf. Fig. 10).

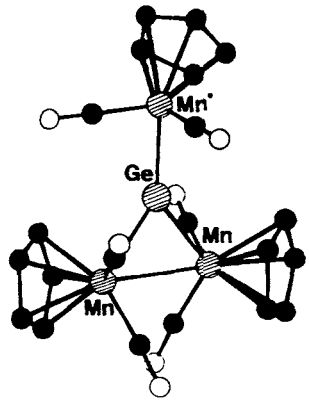


Fig. 8. Molecular structure of the Mn_3Ge compound **18b** with its trigonal-planar core geometry (type **C**, Scheme 1). The exocyclic Mn*-Ge bond (225.0(1) pm) is a formal double bond, whereas the endocyclic Mn-Ge bonds (236.0(1), 236.4(1) pm) should be considered as single bonds according to the EAN rule and the principle of isolobal analogy. CH_3 groups are omitted.

$[(\eta^5\text{-}C_5Me_5)_2Mn_2(\mu\text{-}CO)_3]$.[34,35] This similarity may be attributed to the almost exactly equal covalent radii of germanium and manganese,[35] which statement is at least true for $[(\eta^5\text{-}C_5H_5)Mn(CO)_2]$ derivatives. Genuine single bonds between germanium and low oxidation state manganese are at least 25 pm longer: $[(CO)_5Mn(GeH_3)]$ (249 pm, gas phase electron diffraction), $[(CO)_5Mn(GePh_3)]$ (260 pm), and $[(\mu\text{-}GeMe_2)\{Mn_2(CO)_9\}]$ (248–252 pm)[36–38] may be cited as reference compounds. The formal double bonds in the trigonal-planar Mn_3Ge complexes **18** (type **C**) (structure of **18b**, see Fig. 8) occur in the intermediate range around 225 pm; the reactivity of these systems will be discussed in Section 2.2.4.

2.2.3. *Bonding in Cumulated M*-E-M* Complexes*

The bonding scheme in the linear Mn_2Ge complex **16b** was, in the original publication, described on the basis of simple electron bookkeeping (noble gas rule, EAN rule) as an "organometallic allene system" with sp-hybridized germanium.[25] This view has since been extensively revised on the basis of Fenske-Hall calculations as well as evidence from vibrational spectroscopy and structural chemistry; triple bonding contributions are now being discussed.[39] An allene-type system would be associated with a rotational barrier of ca. 70 kcal/mol, whereas the infrared spectrum indicates the presence of a mixture of rotamers.

Table 1. Structure types and bond lengths in complexes with bonds between transition metals and "bare" main group elements [a].

Bonding	Compound	Structure-type	Bond lengths [pm] Single bonding	Double bonding	Triple bonding
4th Main group					
Silicon					
Si-Co	$[(\mu_4\text{-Si})\{[Co(CO)_4][Co(CO)_3]_3\}]$ **6a**	**D**	221.9 228.8		
Germanium					
Ge-W	$[(\mu_3\text{-Ge})\{W(CO)_5\}_3]$	**C**	257.9(2) 258.9(2)	250.5(2)	
Ge-Mn	$[(\mu\text{-Ge})\{(\eta^5\text{-}C_5H_4Me)Mn(CO)_2\}_2]$ **16b**	**A**	—	220.4(1)	
	$[(\mu\text{-Ge})\{(\eta^5\text{-}C_5Me_5)Mn(CO)_2\}_2]$ **16c**	**A**	—	218(2)	
	$[(\mu_3\text{-Ge})\{(\eta^5\text{-}C_5H_5)Mn(CO)_2\}_3]$ **18a**	**C**	236.0(1) 236.4(1)	225.0(1)	
	$[(\mu_3\text{-Ge})\{(\eta^5\text{-}C_5H_4Me)Mn(CO)_2\}_3]$ **18b**	**C**	235.9(2) 238.0(1)	226.0(2)	
Ge-Mn/Fe	$[(\mu_4\text{-Ge})\{[(\eta^5\text{-}C_5H_4Me)Mn(CO)_2][Fe(CO)_4]_3\}]$ **27**	**D**	243.1(1) (*Ge-Mn*) 239.4(1) 241.6(1) } (*Ge-Fe*) 242.7(1)		
Ge-Fe	$[(\mu_4\text{-Ge})\{Fe_2(CO)_8\}_2]$ **26**	**D**	237.8–243.8		
Ge-Co	$[(\mu_4\text{-Ge})\{Co_2(CO)_7\}_2]$ **23**	**D**	234–238		
	$[(\mu_5\text{-Ge})_2[Co(CO)_4]_2[Co(CO)_3]_4]$ **24**	**E**	239.0–243.4		
Tin					
Sn-W	$[(\mu_3\text{-Sn})\{W(CO)_5\}_3]$ **28**	**C**	277.6(2) 278.9(2)	270(2)	
Sn-Mn	$[(\mu_3\text{-Sn})\{(\eta^5\text{-}C_5H_4Me)Mn(CO)_2\}_3]$ **29**	**C**	254.8(8) 253.4(8)	242.4(8)	
Sn-Fe	$[(\mu_4\text{-Sn})\{Fe_2(CO)_8\}_2]$ **5**	**D**	254		
Lead					
Pb-Mn	$[(\mu\text{-Pb})\{(\eta^5\text{-}C_5H_5)Mn(CO)_2\}_2]$ **30**	**A**		245.9(1)	
5th Main group					
Nitrogen					
N-Mo	$[Mo(\equiv N)Cl_4]^{\ominus}$	**G**			166
N-Re	$\{(\mu\text{-N})ReCl_4\}_\infty$ **32a**	**I**	248		158
N-Ta	$[(\mu\text{-N})\{TaBr_5\}_2]^{3-}$ **32b**	**H**		186	
N-Ir	$[NH_4]_2[(\mu_3\text{-N})\{Ir(SO_4)_2(H_2O)\}_3]$ **33**	**J**		192	
Phosphorus					
P-Mn/Fe	$[(\mu_3\text{-P})_2\{[(\eta^5\text{-}C_5H_5)Mn(CO)_2]_2[Fe(CO)_3]_2\}]$ **40**	**K**		210 (*P-Mn*) 218 (*P-Fe*)	
P-Cr/W	$[(\mu_3\text{-P})\{[Cr(CO)_5]_2[(\eta^5\text{-}C_5H_5)W(CO)_2]\}]$ **41**	**K**	230.5(5) } (*P-Cr*) 242.8(5) } 226.8(4) (*P-W*)		
Arsenic					
As-Cr/Mn	$[(\mu_3\text{-As})\{[Cr_2(CO)_9][Mn(CO)_5]\}]$ **44**	**J**		234.5 } (*As-Cr*) 235.3 } 234.7 (*As-Mn*)	
6th Main group					
Sulfur					
S-Cr	$[(\mu\text{-S})\{(\eta^5\text{-}C_5H_5)Cr(CO)_2\}_2]$ **57a**	**R**			207.1(1) 207.6(1)
S-V	$[(\mu\text{-S})\{(dppe)V(CO)_3\}_2]$ **59a**	**R**			217.2(1)
S-Ni	$[(\mu\text{-S})\{(p_3)Ni\}_2][B(C_6H_5)_4]_2$ **58b**	**R**			203.4(2)
S-Co	$[(\mu\text{-S})\{(np_3)Co\}_2]$ **58a**	**R**			212.8(1)
S-Mo	$[(\mu\text{-S})\{[HB(pz)_3]Mo(CO)_2\}_2]$	**R**			218.1(1)
Selenium					
Se-Cr	$[(\mu\text{-Se})\{(\eta^5\text{-}C_5H_5)Cr(CO)_2\}_2]$ **60**	**R**			220.6(1) 221.1(1)
Se-V	$[(\mu\text{-Se})\{(dppe)V(CO)_3\}_2]$ **59b**	**R**			229.8(2)
Se-Mo	$[(\mu\text{-Se})\{[HB(pz)_3]Mo(CO)_2\}_2]$	**R**			232.3(1)
Tellurium					
Te-Cr	$[(\mu\text{-Te})\{(\eta^5\text{-}C_5H_5)Cr(CO)_3\}_2]$ **62**	**P**	279.9(1) 281.4(1)		
Te-Mn	$[(\mu\text{-Te})\{(\eta^5\text{-}C_5Me_5)Mn(CO)_2\}_2]$ **64**	**Q**		245.9(2)	
Te-Mn	$[(\mu_3\text{-Te})\{(\eta^5\text{-}C_5H_5)Mn(CO)_2\}_3]$ **65**	T		246–251	
Te-V	$[(\mu\text{-Te})\{(dppe)V(CO)_3\}_2]$ **59c**	**Q**		251.4(3) 252.2(3)	

[a] All complex compounds have been referenced in the text. The designated structural types refer to the Schemes 1, 3, and 4. The (formal) bond orders are classified according to the noble gas rule. - Abbreviations: dppe = bis(diphenylphosphino)ethane, np_3 = tris(2-diphenylphosphinoethyl)amine, p_3 = 1,1,1-tris(diphenylphosphinomethyl)ethane, $HB(pz)_3$ = hydridotris(3,5-dimethylpyrazolyl)borate.

A detailed molecular orbital discussion of this problem is thoroughly treated in the original literature,[39] but as a summary (see orbital scheme of Fig. 9) it should be stated

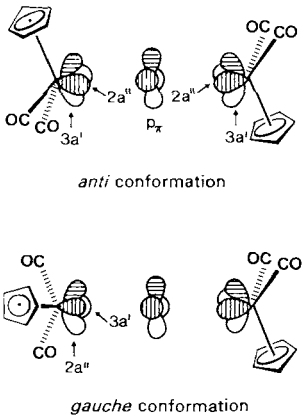


Fig. 9. Schematic representation of the most important π orbital interactions in linear type **A** complexes (Scheme 1) of composition $[(\mu\text{-E})\{(\eta^5\text{-}C_5R_5)M(CO)_2\}_2]$ (here: E = Ge, M = Mn) in the conformations *anti* (above) and *gauche* (below). The p_π orbitals of the monatomic bridging ligand are shown. The same scheme can be applied to the isovalent complexes of type **R** (Scheme 4), e.g. compounds **57a**, **b** (Section 4.1).

here that the metal-centered orbitals 2a″ and 3a′ are of very similar energy and that the π-electron system of the three atoms possesses an approximate cylindrical symmetry. Similar bonding systems can be seen in the isovalent sulfur and selenium complexes of general formula $[(\mu\text{-E})\{(\eta^5\text{-}C_5R_5)Cr(CO)_2\}_2]$ (E = S, Se; R = H, Me) (Section 4). The Mn_2Ge complex **16c** displays both anticlinal conformers **16A** and **16B** in the crystal, the feasible antiperiplanar form **16C** not being observed; for **16b**, however, the antiperiplanar conformation is the only rotameric form observed (Fig. 10).

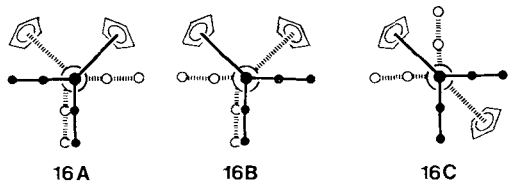
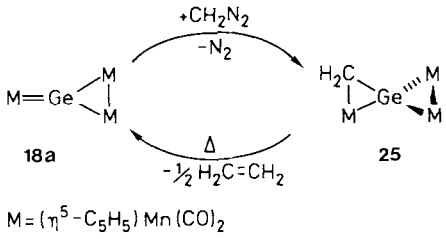


Fig. 10. Anticlinal (**16A** and **16B**) and antiperiplanar (**16C**) conformations of the M=E=M complexes of type **A** (Scheme 1), seen as Newman projections.

2.2.4. *Reactivity*

Multiple bonding systems can only display reasonable reactivity when they are sterically exposed and thus accessible to substrate molecules. In organometallic complexes with their numerous, often quite bulky ligands this is not always the case, but the Mn_xGe compounds discussed here do indeed show the hoped-for reactivity. Diazomethane transfers its methylene group to the obviously very reactive Mn=Ge double bond of **18a**, with evolution of N_2, at temperatures from −20 to 0°C. The metallaspirane **25** is formed in 85-95% yield. The MnGe single bonds, as expected, do not react.[29] ^{1}H-NMR spectroscopy shows **25** to have a fluctional geometry: below −50°C three well-resolved C_5H_5 signals can be seen, two of which become broader as the temperature is raised and finally merge to a single line at 20°C, with the simultaneous appearance of a broad CH_2 signal. These results can be interpreted in terms of a mutual rotation of both three-membered rings at the spirocenter (Ge) or, alternatively, of a *cis/trans* isomerization within the binuclear fragment $[(\eta^5\text{-}C_5H_5)_2Mn_2(CO)_4]$.



It is interesting that **25** decomposes slowly in solution above 50°C and immediately upon melting (112°C) with quantitative evolution of ethylene, whereupon the precursor **18a** is regenerated intact. In the presence of hydrogen this simple thermolysis also evolves methane. The reversible elimination of methylene allows **25** to be classified, in agreement with the NMR data and in contrast to the related tellurium compound $[(\mu\text{-}TeCH_2)\{(\eta^5\text{-}C_5Me_5)Mn(CO)_2\}_2]$ (see Section 4.3.1), as a thermolabile metallaspirane, in which the methylene bridging of a substituent-free main group element and a transition metal is realized for the first time. The $Fe(CO)_4$ group is isolobal with the methylene fragment,[3] and does indeed add to the double bond of **16b**; in this case, consecutive metathesis reactions lead to the spirocyclic products **26** (8%) and **27** (21%). Single-crystal X-ray structure analysis shows that the germanium atom (formerly in the cumulated multiple bonding system of **16b**) is now at a spiro center (Fig. 11), forming single bonds to iron and manganese (Table 1). We have already referred to the addition of the $(\eta^5\text{-}C_5H_5)Mn(CO)_2$ system (isolobal with both methylene and $Fe(CO)_4$) to the linear Mn_2Ge complex **16a**, leading to formation of the trigonal planar Mn_3Ge derivative **18a**.[32]

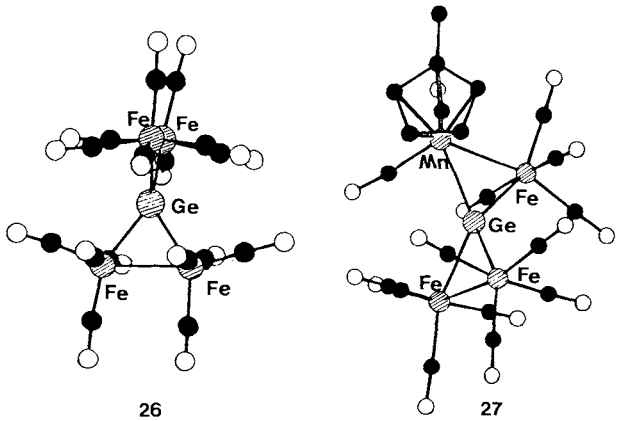
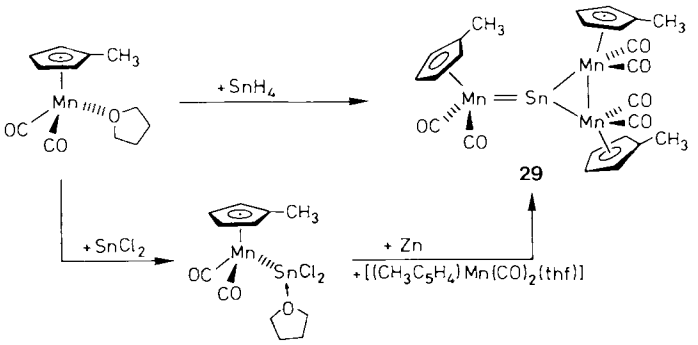


Fig. 11. Structure of the addition metathesis products of the reaction of $Fe_2(CO)_9$ with the Mn_2Ge complex **16b**: left, $[(\mu_4\text{-}Ge)\{Fe_2(CO)_8\}_2]$ **26**; right, $[(\mu_4\text{-}Ge)\{Fe_2(CO)_8\}\{Fe(CO)_4\}\{(\eta^5\text{-}C_5H_4Me)Mn(CO)_2\}]$ **27**. For bond lengths, see Table 1.

2.3. Substituent-Free Tin as Bridging Ligand

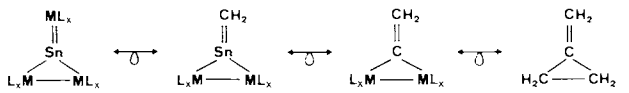
Tin forms not only the prototypal M_4Sn spirocycle **5** with distorted tetrahedral geometry of the M_4 framework and tin–metal single bonds (see Section 2.1). Substituent-free tin has recently proved to be not inferior to its germanium homologue (see above) in forming trigonal planar systems (type **C**, Scheme 1). The two isovalent M_3Sn complexes **28** and **29** (M = W or Mn) are synthesized according to different strategies.[40,41] The tungsten compound **28** is formed in 8–37% yield upon reaction of the ionic com-



28 $[(\mu_3\text{-Sn})\{W(CO)_5\}_3]$ $[(\mu_3\text{-Sn})\{(\eta^5\text{-}C_5H_4CH_3)Mn(CO)_2\}_3]$ **29**

plex $Na_2[W_2(CO)_{10}]$ with tin(IV) chloride while the isolobal manganese derivative **29** $[W(CO)_5 \leftrightarrow (\eta^5\text{-}C_5R_5)Mn(CO)_2]$ is obtained from the neutral precursor $[(\eta^5\text{-}C_5H_4Me)Mn(CO)_2(thf)]$, either in one step with stannane, SnH_4, (55% yield) or in two steps from tin(II) chloride, leading first to the isolable dichlorostannanediyl complex $[(\eta^5\text{-}C_5H_4Me)Mn(CO)_2(SnCl_2)(thf)]$, which is then dehalogenated with zinc dust in the presence of the solvent complex $[(\eta^5\text{-}C_5H_4Me)Mn(CO)_2(thf)]$. The final product **29** is air-stable (yield 60%).

The structures of **28** and **29** are very similar (cf. Figure 12). The M_3Sn groups are planar and are reminiscent of the structures of μ-vinylidene complexes[42,43] and their (as yet unknown) stanna derivatives, with which they are (like with methylenecyclopropane) connected via the isolobal chain of Scheme 2. The M_2Sn moieties form isosceles



Scheme 2.

triangles with relatively long metal–metal and metal–tin distances, which, considering the metallic covalent radii, are best interpreted as single bonds.[40,41] Like the MCM units in μ-methylene and μ-vinylidene complexes, the MSnM units in **28** and **29** enclose acute angles (74.1°, 75.5° respectively). The exocyclic organometallic fragments $W(CO)_5$ and $(\eta^5\text{-}C_5R_5)Mn(CO)_2$, isolobal with methylene,[3] are bound to the tin atom via markedly shortened bonds; the extent of this shortening is, as in the analogous germanium compounds **18**, 7–11 pm with respect to the normal MSn single bond length.

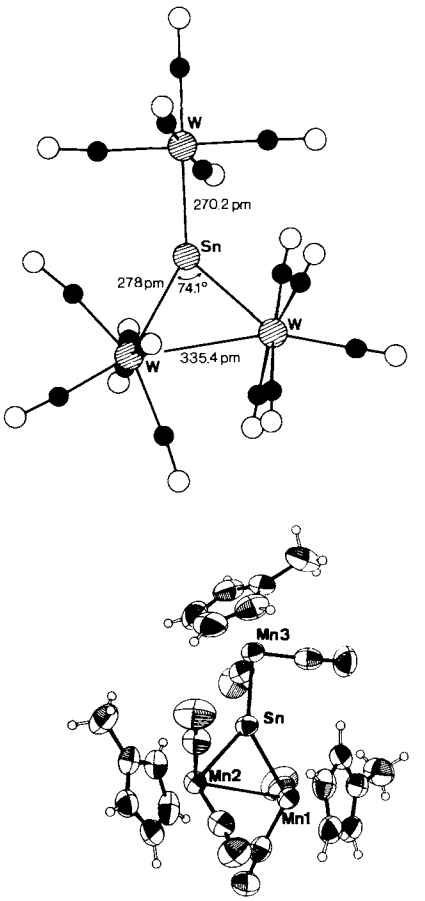


Fig. 12. Crystal structures of the complexes **28** (top) and **29** (bottom). In both complexes the substituent-free tin atom is trigonal planar coordinated (type **C**, Scheme 1).

We have just recently been able to synthesize the complex $[(\mu\text{-Sn})\{(\eta^5\text{-}C_5Me_5)Mn(CO)_2\}_2]$, the first organometallic compound with two-coordinate tin, by reaction of $[(\eta^5\text{-}C_5Me_5)Mn(CO)_2(thf)]$ **20** with either SnH_4 (one step) or $SnCl_2$ (two steps).[44]

2.4. Substituent-Free Lead as Bridging Ligand—The First Example

Although the coupling of a substituent-free germanium or tin atom to an organometallic fragment is often achieved via the hydride route, this method fails with lead, the heaviest member of the group, because of the instability of monoplumbane. Notwithstanding the danger that the potentially more promising low-valent halides might not be completely converted into substituent-free main group ligands on reaction with organometallic complexes, we allowed the substitution-labile solvent complex **19** to react with lead(II) chloride. In this manner we obtained the Mn_2Pb complex **30**, a deep red-brown compound that is relatively sensitive to light and oxygen in solution but is air-stable for a short time up to 130°C in the crystalline state.[45] It is too early to make reliable statements as to

$$2\,[(\eta^5\text{-}C_5H_5)Mn(CO)_2(thf)] + PbCl_2 \longrightarrow \underset{\mathbf{19}}{} \qquad (b)$$

$$[(\mu\text{-Pb})\{(\eta^5\text{-}C_5H_5)Mn(CO)_2\}_2] + \ldots$$
$$\mathbf{30}$$

the mechanism of the formation of **30**, particularly because considerable quantities of finely-divided lead are precipitated during the reaction; however, it is relevant that **30** is not formed from the precursor **20** with elemental lead, even when the latter is converted into a reactive form by high-power sonication. It is possible that the first step involves formation of a dichloroplumbanediyl complex; upon reaction of germanium(II) chloride with **19**, the mono- and binuclear dichlorogermanediyl complexes $[(\eta^5\text{-}C_5H_5)Mn(CO)_2(GeCl_2)]$ (as solvent adduct) and $[(\mu\text{-}GeCl_2)\{(\eta^5\text{-}C_5H_5)Mn(CO)_2\}_2]$ (solvent-free), respectively, are present in solution.[46,47] **30** is likely to be formed from a labile intermediate of this type by consecutive halogen abstraction.

A single crystal X-ray study proved that **30** is the first example of a substituent-free lead atom bonded to transition metals by multiple bonds. The triatomic MnPbMn-backbone is linear (177.2(1)°), and there are thus no direct Mn···Mn contacts (Fig. 13).

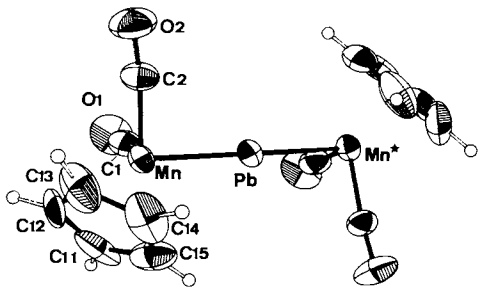


Fig. 13. ORTEP picture of the crystal structure of **30**. Selected bond lengths [pm] and angles [°]: Mn-Pb 245.9(1), Mn-C1 185(2), Mn-C2 181(1), C1-O1 111(2), C2-O2 113(2) pm; Mn-Pb-Mn* 177.2(1), Mn-C1-O1 174(1), Mn-C2-O2 174(1)°; torsion angle C2-Mn-Mn*-C1 −115.2(5)°.

According to the bonding models evolved for the analogous germanium complexes **16a** and **16c** (Mn-Ge 218–220 pm), the bridging lead atom should also be involved in cumulated double bonds with triple bonding components. The Mn-Pb bond lengths (245.9(1) pm) justify this view; Mn-Pb single bond lengths can be more or less reliably estimated as 265–270 pm by extrapolation from known structural data;[48] Mn=Pb double bonds should be at least 20 pm shorter, and at the same time ca. 20 pm longer than the analogous Mn=Ge double bonds. The trends that we and *Huttner* et al. have discovered for germanium and tin complexes is thus continued to the heavier elements (see Table 1).

2.5. Do Carbyne Complexes M*≡C–M and Their "Big Brothers" M*≡E–M Exist?

Since we have discussed triple bonding components for the extended structural type **A**, the question arises as to whether the asymmetric bridging mode between (different) transition metals, also giving a linear structural type (**B**), can be demonstrated. Although this is a mere paper speculation, experiences with the carbyne chemistry of *Fischer*[49] justify a certain degree of optimism. If M* is a 15e- and M is a 17e-organometallic fragment, the following isolobal relationships may be drawn up:

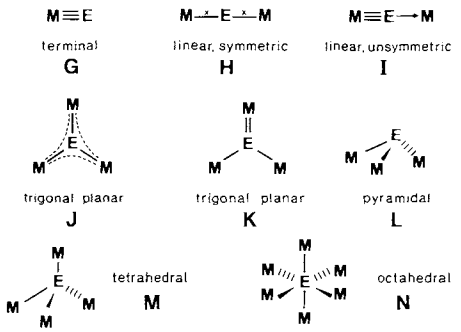
$$HC{\equiv}C{-}H \xrightarrow{-e^-} M^*{\equiv}C{-}H \xrightarrow{-e^-} M^*{\equiv}C{-}M \xrightarrow{-e^-} \underset{\mathbf{B}}{M^*{\equiv}E{-}M} \quad (c)$$

It is not clear whether the "Big brothers" of carbon—silicon, germanium, tin, and lead—are compatible with the carbyne-analogous complexes of structure type **B** with colinear single and triple bonds, but we see a genuine chance of realizing the carbon complexes M*≡C–M; should it not be possible to combine Fischer carbynes $L_xM^*{\equiv}C{-}X$ with metal-containing 1e-ligands, either by "salt metathesis" (e.g. with $Na[Mn(CO)_5]$; X = halogen, SiR_3, etc.) or by oxidative addition (X = H; e.g. to $[(\eta^5\text{-}C_5R_5)Ir(CO)]$ fragments; CH activation)? Imagination and skill of the organometallic chemist are called upon to close this remaining gap in the already wide range of structural types.

3. Bare Nitrogen Group Elements as Bridging Ligands

3.1. Nitrido Ligands

Scheme 3 shows the most prominent of the many structural varieties in which the members of the nitrogen group function as unsubstituted ligands to transition metals. In



Scheme 3. Possible types of coordination of substituent-free elements of the fifth main group.

contrast to the bare carbon ligand, which is most often encountered encapsulated in metal polyhedra, nitrogen frequently forms mono-, bi- and trinuclear structures characterized by multiple bonds between the nitrido ligand and the adjacent transition metal atoms.[50,51] As *Strähle* and *Dehnicke* have shown in their highly informative essay,[52] inorganic azides (e.g. chloro- and iodoazide, XN_3) and nitrogen trichloride, NCl_3, are excellent reagents for the introduction of bare nitrogen into transition metal complexes; hydrazine, ammonia, and potassium amide can also be used.

Archetypal examples of mono- and binuclear nitride complexes with terminal (type **G**), symmetric bridging (**H**) or asymmetric bridging (**I**) nitrogen are shown in Figure 14. A typical, extremely short metal-nitrogen triple bond (161.4(13) pm) is seen in the pseudo-octahedral complex anion $[OsNCl_5]^{2-}$ **31**,[53] which at the same time represents an excellent example of the *trans* influence of terminal nitrido ligands (Fig. 14a); the bond between the metal atom and the ligand *trans* to the M≡N bond can be up to 30 pm longer than that between the metal atom and the identical *cis* ligand! This *trans* influence is quite often so strong that

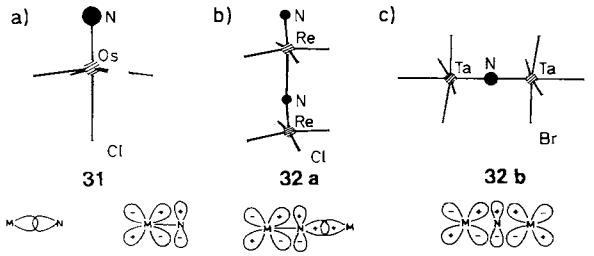


Fig. 14. Bare N_1 ligands in mono- and binuclear complexes (top), with simplified MO bonding schemes (bottom).—a) Structure of $[OsNCl_5]^{2-}$ **31** (Os-N 161.4(13) pm, Os-Cl_{ax} 260.5(4) pm (av.), Os-Cl_{eq} 236.4(4) pm (av.)); b) Part of the column structure of $[ReNCl_4]_\infty$ **32a** (Re-N 158(4) and 248(4) pm, Re-Cl 227 pm (av.)); c) structure of $[Ta_2NBr_{10}]^{3-}$ **32b** (Ta-N 185.9, Ta-Br_{ax} 273.8(6), Ta Br_{eq} 251.4(3) (av.) pm).

the effected *trans* ligand site even remains unoccupied; a similar effect is the dissociation equilibrium (d) of $[MoNCl_5]^{2-}$, which can be demonstrated in dichloromethane solution.[54]

$$[MoNCl_5]^{2-} \rightleftharpoons [MoNCl_4]^- + Cl^- \qquad (d)$$

Other well-documented examples of structures containing metal-nitrogen triple bonds are the tetragonal pyramidal complex anions $[MNCl_4]^-$ (M = Mo, W, Re, Ru, Os); the metal-nitrogen bond lengths range between 166 pm (Mo) and 157 pm (Ru);[52] triply bonded nitrido ligands and the isoelectronic carbyne groups (CR) are the strongest known π-donors in coordination chemistry. As can be seen from the schematic representation in Figure 14a (bottom), the M≡N bond is interpreted in terms of a combination of a σ-bond and two degenerate π-bonds, the lone pair conferring only weak basic properties on the nitrido ligand.

Under certain conditions the lone pair of the nitrido ligand can coordinate a further metal complex fragment; a linear N-bridged arrangement (such as in the columnar structure of tetrachloro(nitrido)rhenium **32a**) is thereby formed (Fig. 14b).[55] The bridge is markedly asymmetric, with quite different bond lengths of 158 and 248 pm; the short bond can be interpreted as a triple bond (cf. terminal M≡N), whereas the long bond corresponds to a σ-type single bond in which the occupied sp orbital of the nitrogen atom overlaps with a vacant d^2sp^3 hybrid metal orbital (Fig. 14b, bottom). If the requirements for the formation of two degenerate d_π-p_π-d_π three-center molecular orbitals are met, each being occupied by an electron pair (Fig. 14c, bottom), then symmetric nitrido bridges are formed, with colinear double bonds to both metal atoms. A good example is the complex anion $[Ta_2NBr_{10}]^{3-}$ **32b**, with the Ta-N distances amounting to 186 pm.[56]

The trigonal planar type **J**, more often encountered for the heavier group V homologues, is represented in nitrogen chemistry by one single example only, the iridium complex **33** investigated by *Griffith* et al.; the Ir_3N moiety displays three identical Ir-N bond lengths of 192 pm[57] and is presumably held together by the bonding situation schematically drawn in Figure 15, with (for each metal atom) a σ-bond and a p_π-d_π overlap between the occupied N(p_z) orbital and a metal d_{xz} orbital.

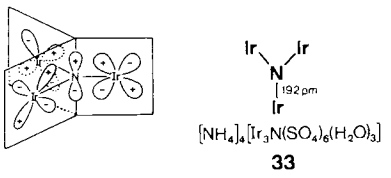


Fig. 15. Bonding behavior of the Ir_3N complex **33** as the only known example of a trigonal-planar nitrogen bridge (**J** in Scheme 3).—A T-shaped M_3N moiety has been found in the complex $[Mo_3N(O)(CO)_4(\eta^5\text{-}C_5H_5)_3]$: N. D. Feasey, S. A. R. Knox, A. G. Orpen, *J. Chem. Soc. Chem. Commun. 1982*, 75.

3.2. Clusters with Interstitial Atoms of the Nitrogen Group

To demonstrate the relationship to the structurally fascinating class of carbido clusters (Section 2.1), we must remind one here of the cluster compounds with interstitial nitrogen atoms, the first example of which was prepared by the Milan group of *Martinengo* by the reaction of $K_2[Co_6(CO)_{15}]$ with nitrosyl tetrafluoroborate.[58] Figure 17a shows that the complex anion $[Co_6N(CO)_{15}]^-$ **34** (and also the Rh analogue) has a trigonal prismatic metal atom architecture with approximate D_{3h} symmetry. The bare nitrogen ligand resides in the cavity of the Co_6 polyhedron, and hence the structural analogy to the isoelectronic carbido clusters $[M_6C(CO)_{15}]^{2-}$ (M = Co, Rh; see **3** in Fig. 1) is obvious. The nearly equal cobalt-nitrogen bond lengths of ca. 194 pm imply a covalent radius of 67 pm for the interstitial nitrogen atom. The Fe_4N-cluster

$[N(PPh_3)_2][Fe_4N(CO)_{12}]$ **35**

was prepared by *Gladfelter* et al. by a similar deoxygenation of the nitrosyl group, using as starting materials $[N(PPh_3)_2][Fe(CO)_3NO]$ and $Fe_3(CO)_{12}$.[59]

35 shows a tetranuclear Fe_4-butterfly geometry (approximate C_{2v} symmetry) with a sterically exposed low-valent nitrogen ligand that, because of the observed ready protonation reaction, is clearly electron-rich (Fig. 16). As in the isosteric Fe_4C cluster **10**, one almost linear atom sequence (Fe3-N-Fe4 179.0°) with strikingly short bonds

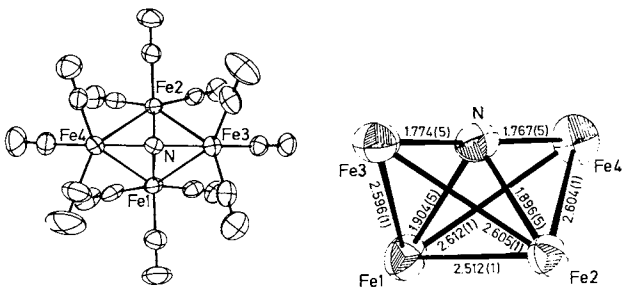


Fig. 16. Left: Structure of the anion of $[N(PPh_3)_2][Fe_4N(CO)_{12}]$ **35** in the crystal. Right: Core structure with bond lengths. The N_1 ligand is sterically exposed and thus reactive; the anion can, e.g., be protonated with H_3PO_4, giving the neutral complexes $[HFe_4N(CO)_{12}]$ and $[Fe_3(\mu_3\text{-}NH)(CO)_{10}]$.

(ca. 177 pm) is supported by a bent Fe1-N-Fe2 moiety with considerably longer FeN bonds (ca. 190 pm).

Let us now proceed to the organometallic chemistry of bare phosphorus and, in particular, to the spectacular Rh_9P ion **36**.

$[Rh_9P(CO)_{21}]^{2-}$ **36**

Surprisingly, triphenylphosphane served as the source of the phosphorus atom, which is finally encapsulated in a capped square antiprism of nine rhodium atoms (Fig. 17b). To construct the cluster ion **36**, triphenylphosphane was heated in an autoclave with $[Rh(CO)_2(acac)]$ under carbon monoxide (300 bar CO; acac = acetylacetonate).[60] It is instructive to consider the spatial requirements of a bare atom of the nitrogen group. Figure 17 compares the smallest possible *closo* clusters with interstitial N, P, As or Sb atoms. The nitrogen atom is accommodated in a closed M_6 framework (here a trigonal prism, Fig. 17a), while phosphorus requires an M_9 cage (Fig. 17b), or at least an opening up of the M_6 structure to a basket-type framework as can be seen in the case of the cluster compound

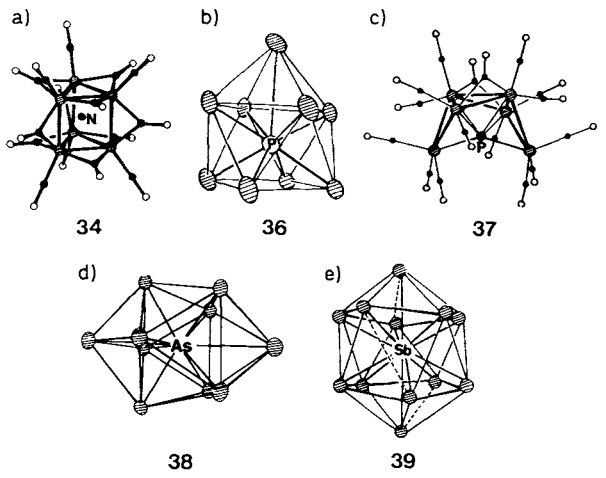


Fig. 17. Clusters with interstitial elements of the nitrogen group. – a) The ion $[Co_6N(CO)_{15}]^-$ **34** possesses a trigonal prismatic framework; in the structurally analogous rhodium complex, six chemically and magnetically equivalent metal atoms are detectable by ^{15}N-NMR spectroscopy. The N atom has the coordination number (CN) 6. – b) The P_1 ligand of the *closo* complex anion $[Rh_9P(CO)_{21}]^{2-}$ **36** is encapsulated in a monocapped cubic antiprism (CN 9 for phosphorus). – c) A smaller M_x cage has to be open on at least one side because of the size of the P atom, as in the ion $[Co_6P(CO)_{16}]^-$ **37** (CN 6 for phosphorus). – d) and e) Increasing spatial demands of the heavier homologues arsenic and antimony lead to the even larger cavities in the M_{10} and M_{12} cages of the ions $[Rh_{10}As(CO)_{22}]^{3-}$ **38** (CN 10 for arsenic) and $[Rh_{12}Sb(CO)_{27}]^{3-}$ **39** (CN 12 for antimony).

$[Co_6P(CO)_{16}]^-$ **37**

in Figure 17c.[61] Impressive evidence for the increasing spatial requirements of the higher homologues is provided by the doubly capped square antiprismatic μ_{10}-arsenic cluster **38** and the icosahedral μ_{12}-antimony cage **39**, both from the fine series of rhodium complexes[62,63] (Fig. 17d and 17e, respectively).

38 $[Rh_{16}As(CO)_{22}]^{3-}$ $[Rh_{12}Sb(CO)_{27}]^{3-}$ **39**

The covalent radius of antimony is twice as large as that of nitrogen (N 70, P 110, As 120, Sb 140, Bi 150 pm). Encapsulated bismuth is not yet known, but the element is quite capable of homonuclear cluster formation in ions such as Bi_5^{3+} (trigonal bipyramid, D_{3h}), Bi_8^{2+} (square antiprism, D_{4d}) and Bi_9^{5+} (triply capped trigonal prism, $C_{3h} \approx D_{3h}$). For the related elements antimony, arsenic, phosphorus, lead, tin, and germanium, mainly the groups of *von Schnering* and *Corbett* have prepared and structurally characterized a fascinating array of homopolyions in Zintl phases (e.g. P_{11}^{3-}, Ge_9^{2-}/Ge_9^{4-}, Sn_9^{4-}, Pb_5^{2-} and As_{11}^{3-}).[64-69] Such main group clusters can in turn encapsulate smaller atoms; good examples of this are basic lead(II) perchlorate $[Pb_6O(OH)_6(ClO_4)_4 \cdot H_2O]$[70] which shows an encapsulated oxygen atom in a Pb_4-tetrahedron and the long-known basic beryllium(II) acetate $[Be_4O(O_2CCH_3)_6]$.[71]

3.3. Substituent-Free Mono- and Biatomic Bridging Ligands Containing Phosphorus, Arsenic, and Antimony

The trigonal planar coordination type **K** (Scheme 3) with triply metalated phosphorus as central component was first verified by *Huttner* et al. in the unprecedented complexes **40** and **41**.[72,73]

$[\{(\eta^5\text{-}C_5H_5)Mn(CO)_2\}_2P_2\{Fe(CO)_3\}_2]$ **40**

$[(\mu_3\text{-}P)\{[Cr(CO)_5]_2[(\eta^5\text{-}C_5H_5)W(CO)_2]\}]$ **41**

The general strategy of synthesis is based on the dehalogenation of halogenophosphanediyl ligands (=PX) or phosphorus trihalide ligands (PX_3). The heteronuclear Mn_2Fe_2-compound **40** is obtained on reaction of $[(\eta^5\text{-}C_5H_5)Mn(CO)_2(PBr_3)]$ with the well-known halogen trapper $Fe_2(CO)_9$.[72] Each of the two phosphorus atoms and its three nearest neighbor atoms lie in a plane (maximum deviation 5 pm), the interplanar angle being almost orthogonal (94.1°) (Fig. 18, top). The empty p orbital of the bare phosphorus ligand is filled by back bonding from manganese donor orbitals; the manganese-phosphorus bond length (210 pm) is even shorter than in conventional phosphanediyl (phosphinidene) complexes, where the bonds are also shortened by manganese-d_π-phosphorus-p_π interactions.

The Cr_2-complex $[(\mu\text{-}PBr)\{Cr(CO)_5\}_2]$ reacts with the complex anion $[(\eta^5\text{-}C_5H_5)W(CO)_3]^-$ with salt metathesis to give the μ_3-phosphorus complex **41**, a fine example of the structure type **K** in Scheme 3. The structural details of this complex are consistent with a bonding interpretation according to which the exocyclic phosphorus-chromium bonds incorporate more π-bonding than the endocyclic bonds (Fig. 18, bottom).

A much marveled-at curiosity in the organometallic chemistry of phosphorus is the P_2 complex

$[\{Cr(CO)_5\}_2P_2\{Co(CO)_3\}_2]$ **42**

(see Fig. 19); its preparation is not essentially different from that of the P_1 complexes **40** and **41** described above, but leads to coupling of two phosphorus atoms—a conse-

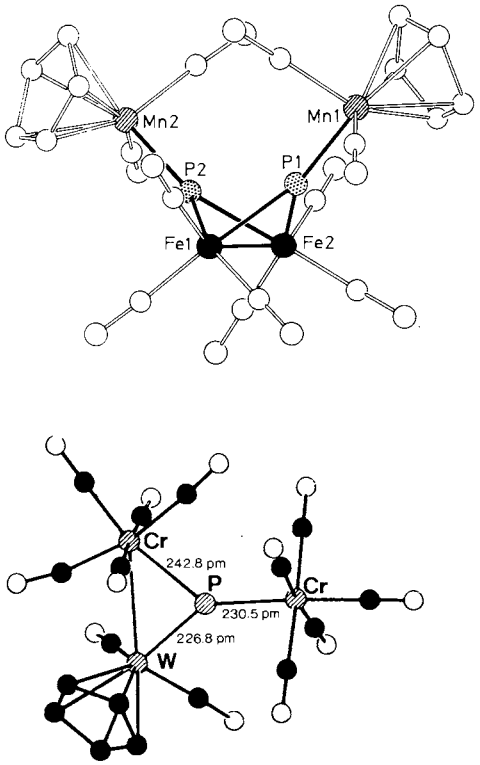


Fig. 18. Bare phosphorus ligands with trigonal planar coordination (type **K**, Scheme 3). Top: Structure of the $Mn_2Fe_2P_2$ complex **40** in the crystal (approximate C_2 symmetry). Structural data of **40**: Fe-P 218.1 (av.), Mn-P 210.0 (av.), Fe-Fe 267.5(3) pm.—Bottom: Structure of the Cr_2WP complex **41**.

quence of the differing electron balance in the organometallic fragments concerned.[74]

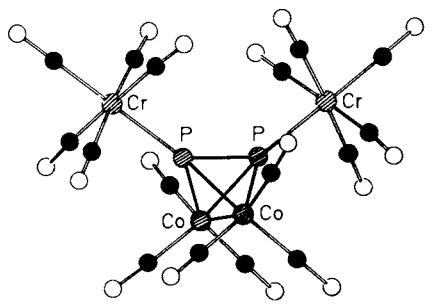


Fig. 19. P_2 fragments as 8e ligands. Crystal structure of the $Cr_2Co_2P_2$ complex **42**. The Co_2P_2-tetrahedron bears two $Cr(CO)_5$ groups at phosphorus. The compound is isolobal with dimethyltetrahedrane $C_4H_2(CH_3)_2$ (because of $Cr(CO)_5 \leftarrow\sigma\rightarrow CH_3^+$; $P \leftarrow\sigma\rightarrow C^-$; $Co(CO)_3 \leftarrow\sigma\rightarrow CH$). Structural data: P-P 206.0(5), Co-P 224.7 (av.), Cr-P 227.7 (av.) pm.

Such coupling reactions are the rule in the organometallic chemistry of arsenic, but the structural type **J**/**K** can also be attained; the method used for the isovalent P_1 complexes can, with minor variations, be used for arsenic. The complexes **43** and **44** can be cited as examples; their structures (Fig. 20) have been confirmed by X-ray structure analyses.[40]

$[(\mu_3\text{-As})\{[Cr(CO)_5]_2[Mn(CO)_5]\}]$ **43**

$[(\mu_3\text{-As})\{[Cr_2(CO)_9][Mn(CO)_5]\}]$ **44**

Starting from the complex $[(\mu\text{-AsCl})\{Cr(CO)_5\}_2]$, the expected primary substitution product **43** can be obtained by reaction with the nucleophilic $[Mn(CO)_5]^-$ anion; a comparison of the UV spectrum of **43** with that of $[(\mu\text{-}AsCH_3)\{(\eta^5\text{-}C_5H_5)Mn(CO)_2\}_2]$ underlines the isolobal relationship $CH_3 \leftarrow\sigma\rightarrow [Mn(CO)_5]^-$.[3] The spectrum is also consistent with the X-ray crystallographically determined structure (Fig. 20, left);[74] there are two short arsenic-chromium bonds (242–244 pm) and an appreciably longer arsenic-manganese bond (251 pm), although chromium and manganese, because of their immediate neighborhood in the periodic table, are not otherwise distinguishable here with X-ray methods. The complex decarbonylates rapidly in solution at 80 °C, forming the Cr_2AsMn structure **44** (Fig. 20, right), in which the arsenic-manganese bond is shortened to 235 pm and thereby is indistinguishable from the arsenic-chromium bonds.

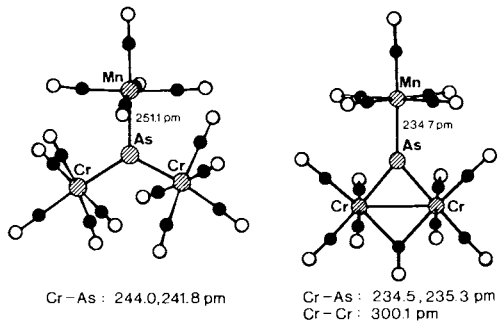


Fig. 20. Structure of the complexes **43** (left) and **44** (right) in the crystal. In both complexes the substituent-free arsenic is trigonal planar coordinated (**J** in Scheme 3).

The coupling of bare arsenic atoms can be achieved by a modified synthetic strategy, which involves the use of arsenic-containing precursors with easily removable substituents. The synthesis of the μ_2-AsH- and μ_2-As_2-complexes **45** and **46**, respectively, is an excellent example.[76,77] The AsH complex **45** (Fig. 21, top) is formed on reaction of

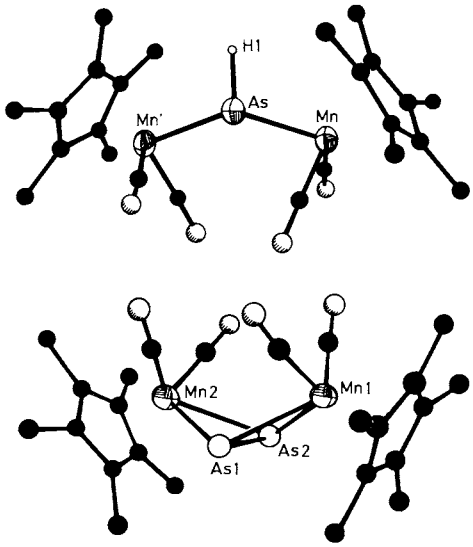
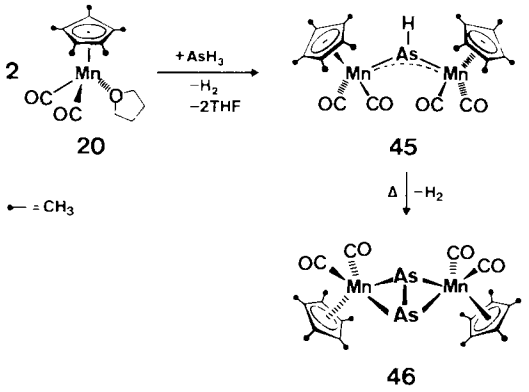
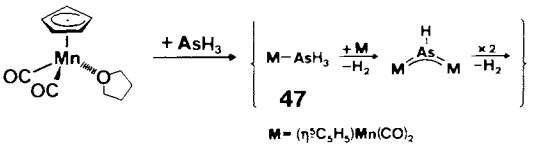


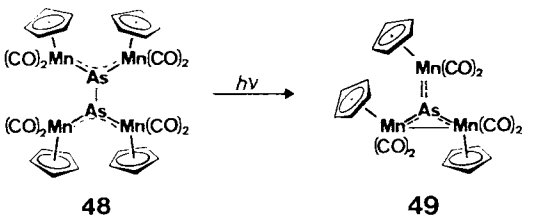
Fig. 21. Top: Structure of the AsH complex **45** in the crystal (Mn-As 224.7(1) pm, Mn-As-Mn' 139.3(1)°).—Bottom: Structure of the As_2 complex **46** in the crystal (As1-As2 222.5(2), Mn-As 255.6 pm (av.)).

$[(\eta^5\text{-}C_5Me_5)Mn(CO)_2(thf)]$ **20** with arsane; it is converted in >85% yield into the As_2 complex **46** (Fig. 21, bottom) upon solid state thermolysis (high vacuum, 120–140 °C); **46** displays a butterfly framework rather than the expected tetrahedrane.



Attempts to prepare the arsane complex $[(\eta^5\text{-}C_5H_5)Mn(CO)_2(AsH_3)]$ **47** led instead in >80% yield to the Mn_4As_2 complex **48**, for which spectroscopic data allowed an unambiguous structural assignment; the structure can be understood as a combination of two AsH precursors of the type **45**, via elimination of H_2, and provides further evidence for the weakness of the AsH bond.[76] A similar coupling reaction is no longer feasible if the much more bulky pentamethylcyclopentadienyl ligands are used (cf. Fig. 21, top). The As_2 complex **48**, also obtainable by reductive dehalogenation of $[(\mu\text{-AsCl})\{(\eta^5\text{-}C_5H_5)Mn(CO)_2\}_2]$ with zinc dust, is in turn a suitable precursor of the trigonal planar As_1-complex **49**,[77] which is formed on irradiation.





Unsubstituted As_2-ligands—As_2 itself is the main component of arsenic vapors at high temperature—are formed under mild reaction conditions also from arsenic(III) chloride, or thermolytically from cycloarsanes (e.g. *cyclo*-As_5R_5; $R=CH_3$, C_6H_5). The As_2 moieties function, depending upon the type and number of the coordinated organometallic fragments, as 4e-, 6e-, or 8e-ligand. The D_{3h}-symmetrical tungsten complex

$[(\mu_3,\eta^2\text{-}As_2)\{W(CO)_5\}_3]$ **50**

should be mentioned as an outstanding example of a series of interesting compounds; it possesses a considerable aesthetic appeal. **50** is obtained by the reaction of $AsCl_3$ with either $[W(CO)_5(thf)]$ or $Na_2[W_2(CO)_{10}]$, and has been structurally characterized (Fig. 22).[79a] The AsAs bond length is

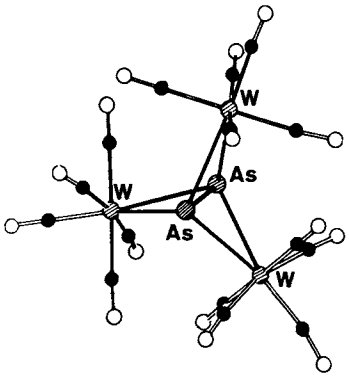


Fig. 22. Structure of the W_3As_2 complex **50** in the crystal, with As_2 being present as a μ_3,η^2-ligand. **50** is isolobal with bicyclo[1.1.1]pentane, C_5H_8, according to the connectivity modes As $-\sigma-$ CH and $W(CO)_5$ $-\sigma-$ CH_2.

227.9(4) pm, markedly shorter than expected for an AsAs single bond. The triple bond of the free As_2 molecule is lengthened by interaction with the organometallic fragment in a similar manner to that for CC or NN bonds in acetylene or dinitrogen complexes, respectively. A theoretical study of such systems shows that the strong π-acceptor capability of the As_2 molecule makes an important contribution to the stability of the organometallic fragment. A weak π bond between the arsenic atoms is associated with low-lying π* energy levels, which can combine favorably with the d orbitals of the transition metal. When As_2 fragments are bonded to two metal centers in the manner of acetylenes, as in $[(\mu_2,\eta^2\text{-}As_2)\{(\eta^5\text{-}C_5H_5)W(CO)_2\}_2]$,[80] they behave as bases and thus readily add 16e fragments such as, e.g., $Cr(CO)_5$. The antimony compound

$[(\mu_3,\eta^2\text{-}Sb_2)\{W(CO)_5\}_3]$ **51**

analogous to **50**, is obtainable by the analogous reaction and it also possesses a star-shaped structure.[79b] Arsenic attains a higher degree of aggregation in the triple-decker sandwich complex

$[\{(\eta^5\text{-}C_5H_5)Mo\}_2(\mu,\eta^4\text{-}As_5)]$ **52**

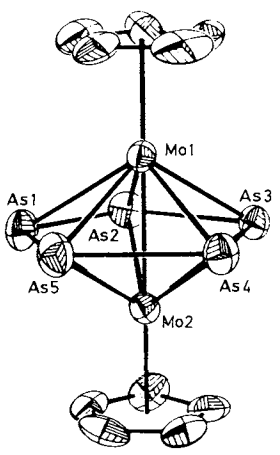


Fig. 23. Structure of the triple-decker sandwich complex **52** containing a planar As_5 ring. The As-As bond lengths lie in the range 238.9–276.2 pm.

with its planar As_5 ring enclosed by two molybdenum atoms (Fig. 23).[81] Just recently, *Scherer* et al. have been able to synthesize an analogous complex with *cyclo*-P_5.[81b]

An example of the structural type **M** of Scheme 3 (organometallic arsonium ion) is furnished by the half-open tetrahedron of the Co_4As complex cation **53** (Fig. 24).[82]

$[(\mu_4\text{-As})\{(\eta^5\text{-}C_5H_5)Co(CO)\}_3]^+$ **53**

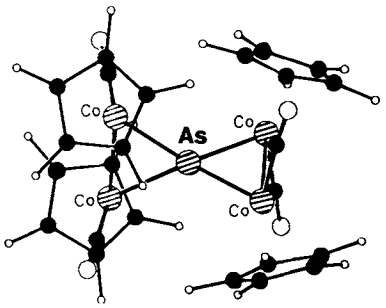


Fig. 24. Structure of the Co_4As complex ion **53** in the crystal (Co-As 227 (av.), Co-Co 260, Co···Co 414 pm).

3.4. Bare Bismuth Ligands

Bismuth, the largest and heaviest element of the fifth main group, can also occur as a substituent-free ligand bound to transition metals. There is no authentic example of a metal-bismuth multiple bond (i.e. the structural types **G**–**K** in Scheme 3 are unknown for bismuth), but M_3Bi moieties (type **L**) have demonstrated their stability in several representatives. The cobalt and iron complexes **54** and **55** respectively, obtainable from metallic bismuth, bismuth(III) chloride or sodium bismuthate(V), contain pyramidal bismuth bridges (Fig. 25).[18a,75]

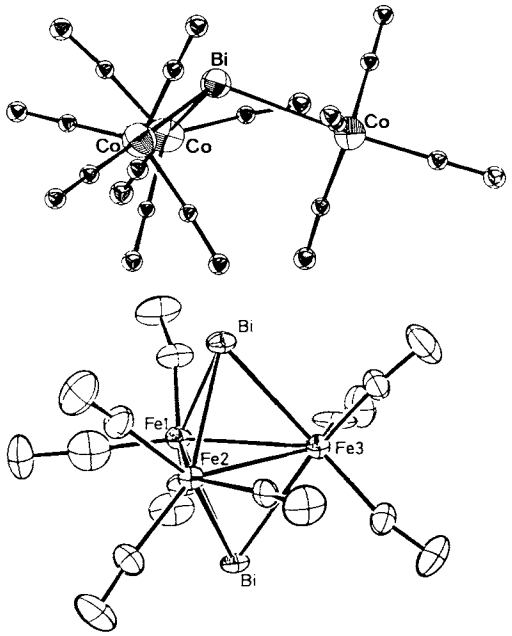


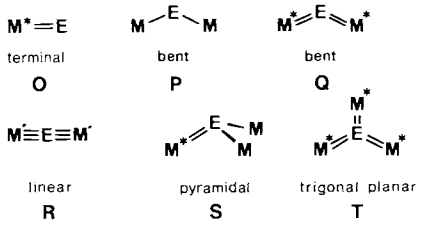
Fig. 25. Molecular structures of the pyramidal μ_3-Bi complexes **54** (top) and **55** (bottom). **54** has no Co-Co bond; **55** has three Fe-Fe bonds. The M_3Bi geometry of **55** tends more towards the pyramidal than that of **54** (Fe-Bi-Fe 62.6° av., Co-Bi-Co 107° av.) because of the shorter MM bonds. The iridium complex $[(\mu_3\text{-Bi})\{Ir_3(CO)_9\}]$ similar to **55** has been described by *Schmid* et al. [19b].

$[(\mu_3\text{-Bi})\{Co(CO)_4\}_3]$ **54** $[(\mu_3\text{-Bi})_2\{Fe_3(CO)_9\}]$ **55** $[(\mu_3,\eta^2\text{-}Bi_2)\{W(CO)_5\}_3]$ **56**

The only known Bi_2 complex **56** contains, like its arsenic and antimony analogues **50** and **51** respectively,[79a,b] no metal–main group element multiple bonds, but displays considerable multiple bonding character in the BiBi interaction (bond length 281.8(3) pm).[79c] Soluble bismuth cluster molecules could be important for the explanation of the mechanism of the industrially important ammonoxidation of propene ("SOHIO process"), which relies on highly active bismuth/tungsten oxide catalysts.

4. Bare Oxygen Group Elements as Bridging Ligands

The complex chemistry of oxygen and its homologues is extensive. Bonding to transition metal centers leads to structural types **O**–**T** (Scheme 4), if higher nuclearity clusters are not considered. Substituent-free oxygen shows preference for forming terminal bonds (type **O**) or symmetric, bent bridges (**P**). The availability of d orbitals at the metal centers leads preferentially with the higher homologues to incorporation in multiple bonding systems (d_π-p_π interactions) with frameworks **Q**–**T**, but oxygen too is known in linear and trigonal planar structures as in the ions $[Ru_2OCl_{10}]^{4-}$,[83] $[Si_2O_7]^{6-}$ (and coesite),[50] $[O(HgCl)_3]^+$, and in metal dioxides of the rutile type. The highest coordination number (CN 10) of a chalcogen atom is seen in the doubly capped square antiprism of the cluster ion $[Rh_{10}S(CO)_{22}]^{2-}$.[84]



Scheme 4. Possible types of coordination for substituent-free elements of the 6th main group.

4.1. Bent and Linear Coordination

We shall begin with the surprises which have arisen in the chemistry of bare sulfur, selenium, and tellurium in the last few years. Although bent S_1 bridges (type **P**) are so common that their mention here would depart from the scope of this review, the discovery and correct interpretation of the Cr_2S compound **57a** (type **R**; Fig. 26) by *Legzdins* et al. in 1979 proved to be another landmark in organometallic chemistry.[85] They obtained **57a** by reaction of trithiazyl trichloride, $N_3S_3Cl_3$, with the complex ion $[(\eta^5\text{-}C_5H_5)Cr(CO)_3]^-$.

$[(\mu\text{-S})\{(\eta^5\text{-}C_5H_5)Cr(CO)_2\}_2]$ **57a**

Cumulated triple bond systems of this type have since been obtained from the most varied strategies of synthesis

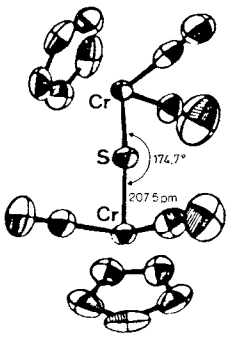
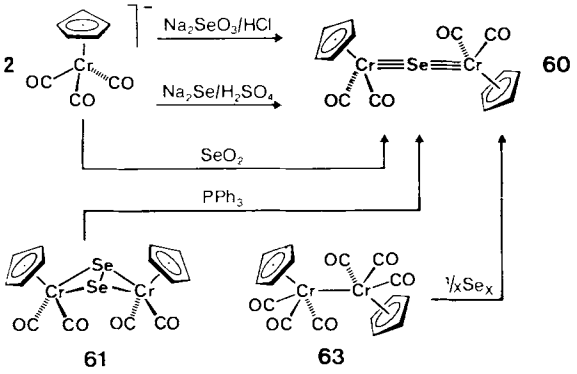


Fig. 26. Structure of the Cr_2S complex **57a** in the crystal. **57a** is a prototypal example of cumulated M'≡E≡M' complexes (E = chalcogen; type **R**, Scheme 4). The metal-sulfur bond is the shortest known (CrS 207.4 pm (av.)).

as summarized in Scheme 5. A necessary condition for the existence of linear M'≡E≡M' complexes is that the organometallic fragments M' must be 15e systems, capable of taking up all the valence electrons of the bare bridging ligand.



Scheme 5.

Other established precursors of unsubstituted sulfur ligands are elemental sulfur, hydrogen sulfide and sodium sulfite/hydrochloric acid; for the construction of analogous selenium systems, favored reagents are red or black selenium, sodium selenite/hydrochloric acid, and selenium(I) chloride.[86-90,94-98,106] Possibly the first examples of extended M_2S molecules, although their full significance was not realized at the time, were the d^8 configurated cobalt and nickel compounds **58a** and **58b**, respectively,

58a $[(np_3)Co{=}S{=}Co(np_3)]$ $[(p_3)Ni{=}S{=}Ni(p_3)][BPh_4]_2$ **58b**
$np_3 = N(CH_2CH_2PPh_2)_3$ $p_3 = H_3CC(CH_2PPh_2)_3$

isolated by *Sacconi* et al. back in 1978. The M_2S backbones are strictly linear and display strikingly short bonds (Fig. 27). To quote the authors from their original publication:[90] "Noteworthy is the Ni-S bond distance (2.034(2) Å), which is the shortest ever found for such a linkage in transition metal complexes ... Since the two individual d^8 entities would be paramagnetic, it seems probable that a superexchange mechanism through the sulfur atom, utilizing p_π orbitals of the sulfur and orbitals of higher energy of the metal (symmetry D_{3d} or D_{3h}) is involved. This interaction (which must be introduced to account for the diamagnetism of the complexes) will be favored by the linearity of the sulfur bridge and by the relatively low electronegativity of the sulfur atom".

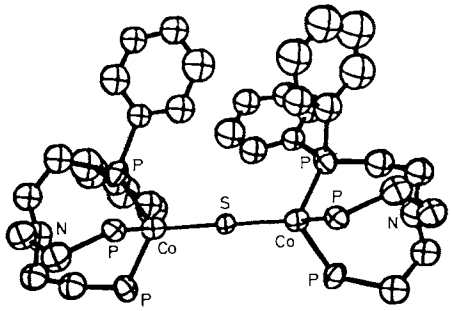


Fig. 27. Molecular structure of the Co_2S complex **58a** in the crystal.

Related complexes with linear $[MoSMo]^{2+}$, $[MoSMo]^{6+}$ and $[MoSeMo]^{2+}$ units (Mo-S 218.1(1) and 217.1(1) pm; Mo-Se 232.3(1) pm, see Table 1) are now known,[91-93] as are the low-valent vanadium compounds **59**.[94,95]

$[(\mu\text{-E})\{(dppe)V(CO)_3\}_2]$ dppe = $Ph_2PCH_2CH_2PPh_2$
59a, E = S; **59b**, E = Se; **59c**, E = Te

If one accepts packing effects as the origin of the crystallographically significant deviation from linearity, the μ-tellurium complex **59c**, with V-Te-V 165.9°, may be considered the first example of "linear", two-coordinate tellurium (type **R**) in organometallic chemistry, particularly since the V-Te bond lengths are quite short (251.4 and 252.2 pm); the fully analogous μ-S and μ-Se complexes **59a,b** display strictly linear bridges (as does the sulfur derivative **57a**) with short VSe bond lengths at 229.8(2) pm. The structure of the V_2S complex **59a** is shown in Figure 28.

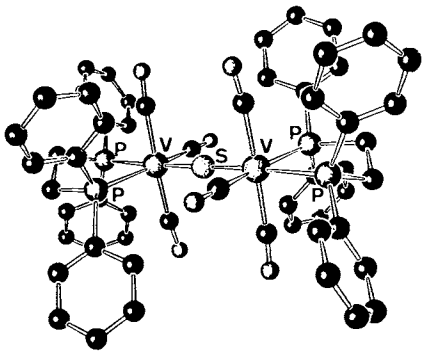


Fig. 28. Structure of the V_2S complex **59a** in the crystal. The V≡S triple bonds in the complex can be postulated on the basis of the V-S bond length (217.2(1) pm).

4.2. Chromium-Selenium, Chromium-Tellurium, and Manganese-Tellurium Bonds

Despite their cumulated multiple bonding systems (type **R**), the Cr_2S complexes **57a**, **b**

$[(\mu\text{-S})\{(\eta^5\text{-}C_5R_5)Cr(CO)_2\}_2]$
57a, R = H; **57b**, R = CH_3

are chemically remarkably inert. In order to induce some reactivity (by exploiting longer bonds with essentially the same bonding systems), *Rohrmann* (in our Munich laboratories) and, later, *Goh* and *Weiss* et al. opened up the chemistry of complex **60** (Scheme 5).[94–98] The partial extrusion of selenium from the diselenido complex **61** (Fig. 29, top) by means of triphenylphosphane is a particularly fascinating route to **60**, which, like its sulfur analogue (Fig. 26), contains a linear backbone (Fig. 29, bottom). The very short Cr-Se bonds (220–221 pm) support the presence of cumulated triple bonds (see Section 2.2.3).[39]

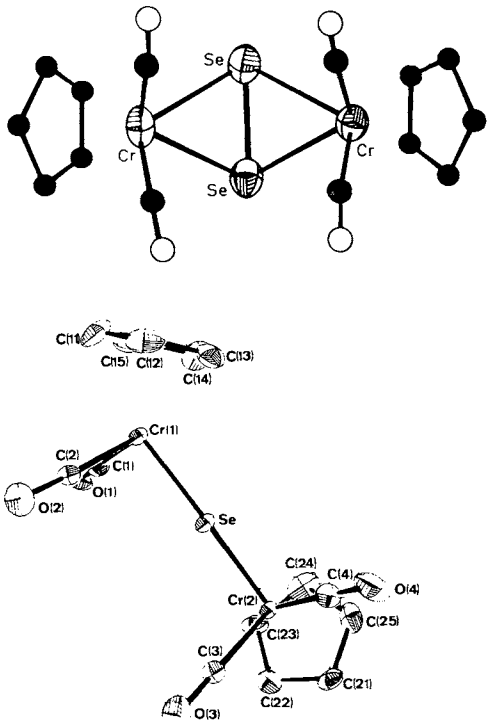


Fig. 29. Molecular structures of the folded Cr_2Se_2 complex **61** (top) and of the linear Cr_2Se complex **60** (bottom) in the crystal. The CrSe bonds in **61** are, as expected, appreciably longer (253–254 pm) than in **60** (220–221 pm). The total length of ca. 440 pm renders the CrSeCr backbone of **60** sterically accessible and therefore reactive.

On fractional crystallization, **60** is obtained in two crystal modifications with different solid-state infrared spectra; this phenomenon is probably to be ascribed to the existence of rotational isomers. The immediate equilibration of the isomers in solution and the occurrence of only one proton NMR signal for both C_5H_5 groups (down to the lowest attainable temperatures) point to a free rotation of the halves of the molecule about the Cr-Se-Cr axis. Such a rotation of the L_xM moieties about M≡E≡M bonds for compounds of this type is also consistent with MO calculations;[39] rotational isomers have been shown by X-ray structure analysis to coexist in analogous complexes but have hitherto eluded separation.[85]

Attempts to prepare tellurium compounds analogous to the sulfur and selenium complexes **57** and **60** have so far failed, despite the use of a wide range of synthetic methods. The reaction sequences end at the stage of the bent μ-Te complex **62** (structural type **P**) which has very long

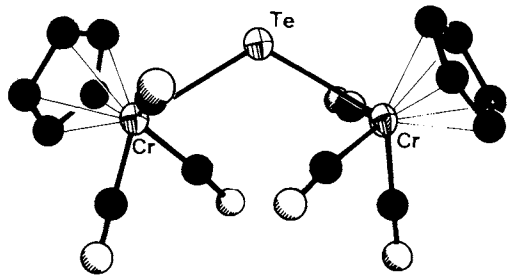
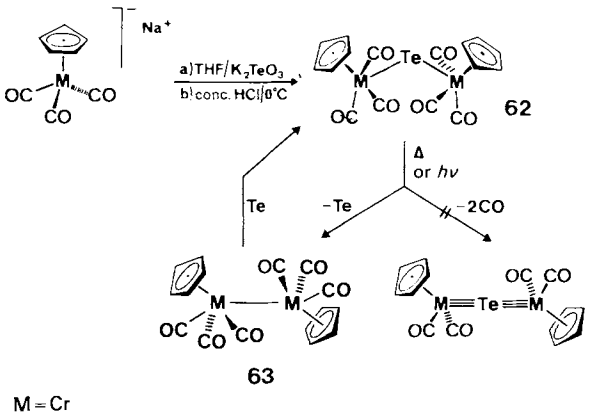


Fig. 30. In contrast to the Cr_2Se complex **60** (Fig. 29, bottom), the Cr_2Te complex **62** (type **P**, Scheme 4), with two more CO groups, displays a bent core geometry and is isolobal with $(CH_3)_2Te$. The CrTe bonds are very long (280–281 pm) and correspond to simple single bond character; the compound is basic and can be protonated at the μ-Te atom.

CrTe single bonds (280–281 pm; Cr-Te-Cr 117.2°) (Fig. 30). Contrary to expectation, **62** cannot be decarbonylated to the target compound $[(\mu\text{-Te})\{(\eta^5\text{-}C_5H_5)Cr(CO)_2\}_2]$; when it is heated or exposed to light, extrusion of the tellurium bridge takes place, with formation of the CrCr compound **63**, which in turn is a suitable starting material for the preparation of **62** (reaction with elemental tellurium, 97% yield).[99] If the 17e-fragments M of the structural type **P**



(Scheme 4) are replaced by 16e-fragments M*, compounds of type **Q** are obtained; these are again bent at E, but display M*=E double bonds. They are isolobal with sulfur dioxide. The only confirmed example, **64**, originates from manganese chemistry and was prepared by *Hecht* in our group when he treated the solvent complex **20** with Al_2Te_3/HCl, a reaction that was surprisingly successful.[100] The angle at tellurium in the Mn_2Te unit, 123.8(1)°, is as expected for an sp^2-hybridized chalcogen group element. The MnTe bond lengths, 245.9(2) pm, clearly prove the presence of multiple bonds, since MnTe single bonds would be expected to be 270 pm on the basis of the covalent radii (Mn ca. 133, Te 137 pm) (Fig. 31, top).

$[(\mu\text{-Te})\{(\eta^5\text{-}C_5Me_5)Mn(CO)_2\}_2]$ **64**

$[(\mu_3\text{-Te})\{(\eta^5\text{-}C_5H_5)Mn(CO)_2\}_3]$ **65**

Correspondingly short bonds are observed in the trigonal planar μ_3-tellurium complex **65** (type **T**, av. MnTe 248.5 pm; see Fig. 31, bottom), prepared by *Herberhold* et al. using the same method but also obtainable from elemental tellurium.[101,102] A comparison of both compounds (Fig. 31) emphasizes the structural analogy between the

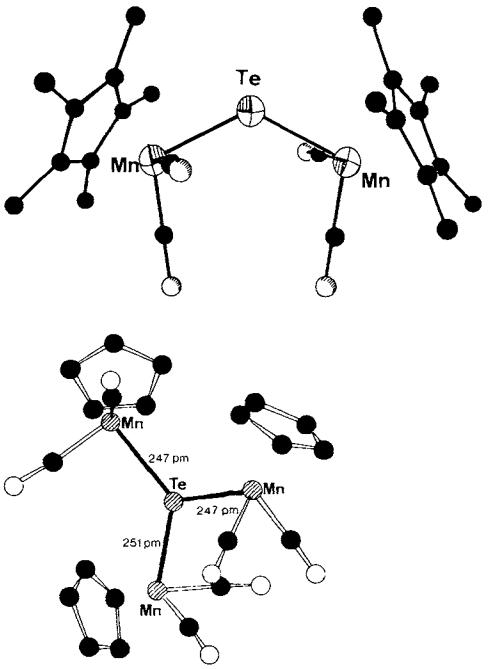


Fig. 31. Organometallic analogues of TeO_2 and TeO_3 with bent and trigonal planar skeletal geometries, respectively. Top: Structure of the μ-Te complex **64** in the crystal; bottom: structure of the μ_3-Te complex **65** in the crystal. The short MnTe bonds are best interpreted as double bonds.

above complexes **64** and **65** and the chalcogen oxides XO_2 (bent) and XO_3 (planar), respectively, because of the isolobal relationship[3,4]

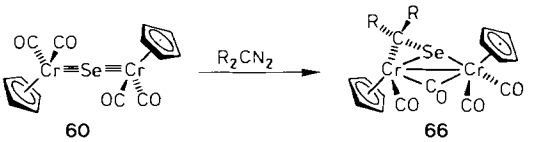
$$O \leftarrow\!\!\circ\!\!\rightarrow S \leftarrow\!\!\circ\!\!\rightarrow Se \leftarrow\!\!\circ\!\!\rightarrow Te \leftarrow\!\!\circ\!\!\rightarrow [(\eta^5\text{-}C_5R_5)Mn(CO)_2] \quad (e)$$

4.3. Multiple Bond Reactivity of π-Bonded Selenium and Tellurium Bridges

Although the μ-S complexes $[(\mu\text{-}S)\{(\eta^5\text{-}C_5R_5)Cr(CO)_2\}_2]$ (**57a**, **b**) are chemically remarkably inert despite their cumulated triple bonds at the bridge atom, complexes with multiple bonded selenium and tellurium bridges do undergo reactions.

4.3.1. Alkylidene Additions

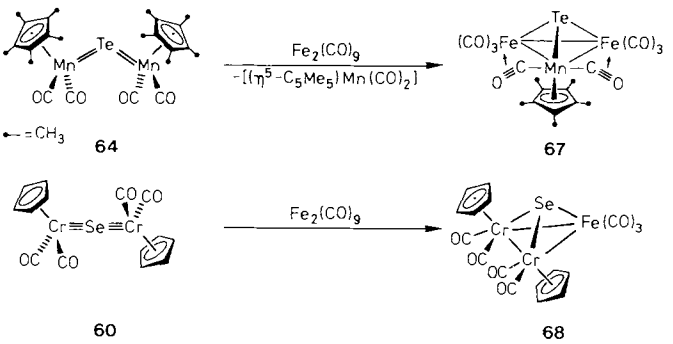
The μ-Se complex **60** smoothly adds methylene and small alkylidene groups to one of the Cr≡Se bonds to give **66**.[96,97] The tellurium complex **64**, an example of structural type **Q**, reacts analogously—a reaction that should be generalizable for M′≡E and M*=E structural elements. The reader is reminded here of the successful diazoalkane route to μ-alkylidene complexes of transition metals.[103] Complex **65**, with its planar Mn_3Te central unit, is accessible to methylene groups too, as is the related Mn_3Ge complex **18a** (Section 2.2.4), but loses one of the M* groups on reaction with diazomethane.[29]



60 R = H, CH_3 66

4.3.2. Formation of Cluster Structures

Organometallic fragments are also capable of adding to Mn=Te and Cr≡Se groups. In this way, the $MnFe_2Te$-



tetrahedrane cluster compound **67** (Fig. 32) is obtained from **64** and $Fe_2(CO)_9$.[104] Reaction of the μ-Se complex

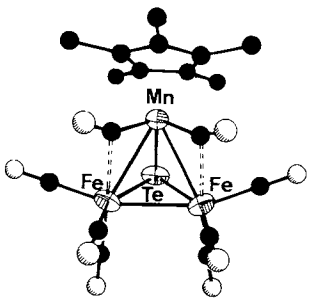


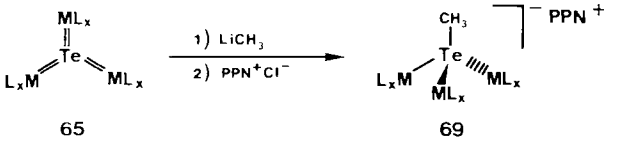
Fig. 32. Structure of the $MnFe_2Te$ tetrahedrane cluster **67** in the crystal; the M-Te bond lengths (247-251 pm) indicate single bonding.

60 with $Fe_2(CO)_9$ furnishes a product (**68**) which is structurally closely related to the $MnFe_2Te$ compound **67**.[105]

4.3.3. Nucleophilic and Electrophilic Reactions with Extension of Bridge Coordination

We were able to show in comparative studies that bridging tellurium atoms in structural type **P** display pronounced nucleophilicity, but are electrophilic in type **T**. Two typical examples can be noted here: The complex **62** (type **P**) undergoes reversible protonation with Brønsted acids and electrophilic methylation with $CF_3SO_3CH_3$,[106] but is resistant to nucleophilic methylating agents (e.g. MeLi). The opposite is the case for complex **65** (type **T**), in which, because of its extensive participation in π-bonding, the bridge atom is particularly electron-deficient and is thus attacked by alkyllithium reagents, but not by elec-

trophilic protonating and methylating agents. Methylation of **65** with methyllithium gives a salt **69** whose anion is ex-



65 69

$L_xM = (\eta^5\text{-}C_5H_5)Mn(CO)_2$

$PPN^+ = (C_6H_5)_3P{=}N{=}P(C_6H_5)_3$

tremely air-sensitive. The Mn_3TeCH_3 anion of **69** adopts a slightly pyramidalized structure and is hence far away from the expected tetrahedral geometry (Fig. 33).[106, 107]

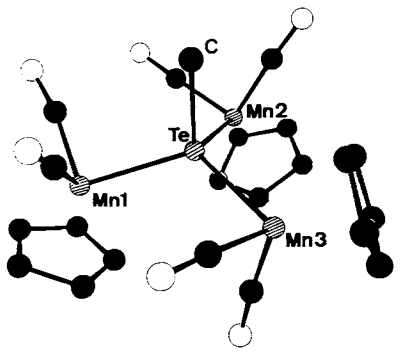


Fig. 33. Structure of the anion of **69** in the crystal. Selected dimensions: Mn-Te 257.4 (av.), Te-C 215(1) pm; Mn-Te-Mn 115.4 (av.), Mn-Te-C 102.5 (av.)°, sum of angles at Te 346°.

According to the isolobal relationship $[(\eta^5\text{-}C_5H_5)Mn(CO)_2] \leftarrow\!\!\!\!\!\!\bigcirc\!\!\!\!\!\!\rightarrow CH_2 \leftarrow\!\!\!\!\!\!\bigcirc\!\!\!\!\!\!\rightarrow CH_3^+$,[3,4] electron-rich bridging atoms of structural type **P** should be prone to coordinate to unsaturated organometallic fragments. Thus, the μ-Se compound **70**,[106] isovalent with the tellurium complex **62**, reacts with the solvent complex $[(\eta^5\text{-}C_5H_5)Mn(CO)_2(thf)]$ (**19**), with smooth formation of the adducts **71** and **72** (Fig. 34).[108]

$$[(\mu\text{-Se})\{(\eta^5\text{-}C_5H_5)Fe(CO)_2\}_2] + [(\eta^5\text{-}C_5H_5)Mn(CO)_2(thf)] \longrightarrow$$

70 **19**

(f)

$$[(\eta^5\text{-}C_5H_5)_3MnFe_2Se(CO)_6] + [(\eta^5\text{-}C_5H_5)_3MnFe_2Se(CO)_5]$$

71 **72**

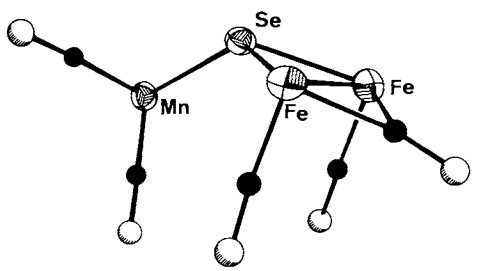


Fig. 34. Structure of the Fe_2MnSe complex **72** in the crystal. **72** is a representative of structural type **S** (Scheme 4). The π-bonded C_5H_5 ligands of iron and manganese are omitted for clarity. The sum of angles at Se is 314.9°.

4.3.4. Redox Chemistry

The delocalized π-electron systems of the Cr_2S, Cr_2Se, Mn_3Te and Mn_2Te complexes manifest themselves also in the electrochemical behavior of the complexes: Cyclovoltammograms of all the complexes display two reversible (or at least quasi-reversible) one-electron reduction steps (Table 2).[109] Figure 35 shows the voltammogram of the Cr_2Se

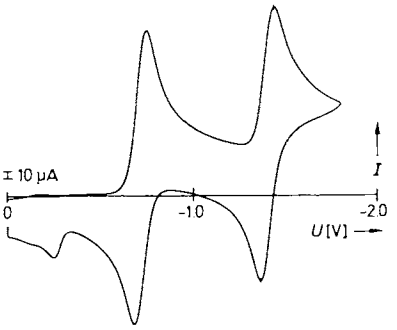


Fig. 35. Cyclovoltammogram of the Cr_2Se complex **60**, recorded in *N,N*-dimethylformamide/0.1 M TBAP vs SCE (100 mV/s; 28°C). The two reduction steps $\mathbf{60} \rightarrow [\mathbf{60}]^- \rightarrow [\mathbf{60}]^{2-}$ are reversible ($E^1_{1/2} = -0.72$ V, $E^2_{1/2} = -1.40$ V).

Table 2. First and second reduction steps ($E^1_{1/2}$ and $E^2_{1/2}$) of some μ-S-, μ-Se- and μ-Te-complexes [a].

Complex	$E^1_{1/2}$ [V]	ΔE [mV] [b]	$E^2_{1/2}$ [V]	ΔE [mV] [b]
$[(\mu\text{-S})\{(\eta^5\text{-}C_5H_5)Cr(CO)_2\}_2]$ **57a**	−0.92 (qr)	70	−1.48 (qr)	90
$[(\mu\text{-S})\{(\eta^5\text{-}C_5Me_5)Cr(CO)_2\}_2]$ **57b**	−1.15 (qr)	70	−1.80 (qr)	110
$[(\mu\text{-Se})\{(\eta^5\text{-}C_5H_5)Cr(CO)_2\}_2]$ **60**	−0.72 (r)	65	−1.40 (qr)	70
$[(\mu_3\text{-Te})\{(\eta^5\text{-}C_5H_4CH_3)Mn(CO)_2\}_3]$	−0.55 (r)	70	−1.18 (r)	70
$[(\mu\text{-Te})\{(\eta^5\text{-}C_5Me_5)Mn(CO)_2\}_2]$ **64**	−0.82 (r)	60	−1.72 (qr)	80

[a] r = reversible, qr = quasi-reversible. [b] ΔE is the difference between the half-wave potentials of the forward and backward reactions.

compound **60** as one example. According to the electrochemical series of Figure 36, the complexes illustrated

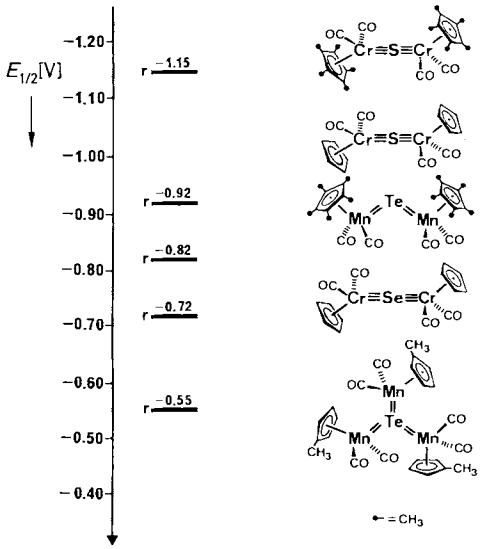


Fig. 36. Electrochemical series for selected complexes that contain multiple bonds between transition metals and bare main group elements. The first reduction potentials are given (measured in *N,N*-dimethylformamide/0.1 M TBAP solution); r = reversible. For further data see Table 2.

should also undergo reduction reactions on a preparative scale, provided suitable reducing agents can be found. (The observable oxidation steps in the region +0.46 to −0.87 V are irreversible). The selenium complex **60** will again serve as an example here. The potentials −0.72 V (radical anion)/−1.40 V (dianion) would suggest that reducing agents with potentials between these values might make the radical anion accessible. The reaction with cobaltocene ($E_{1/2}[Cp_2Co^+/Cp_2Co] = -0.77$ V, *N,N*-dimethylformamide[110]) in tetrahydrofuran/diethyl ether at −30 °C slowly gives the black, crystalline, ionic complex

$[(\eta^5\text{-}C_5H_5)_2Co]^+[(\eta^5\text{-}C_5H_5)_3Cr_3(CO)_6Se]^-$ **73**[111]

The complex anion of this compound has a planar (!) Cr_3Se backbone containing a Cr_2Se three-membered ring (Fig. 37). The exo- and endocyclic CrSe bonds (227.9(2) and 233.2(2)/234.3(2) pm, respectively) have different bond multiplicities; the CrCr bond, with a length of 308.3(2) pm, compares with a single bond. The linear Cr_2Se complex **60** is isoelectronic with the Mn_2Ge compound **16a** and both systems are considered as having

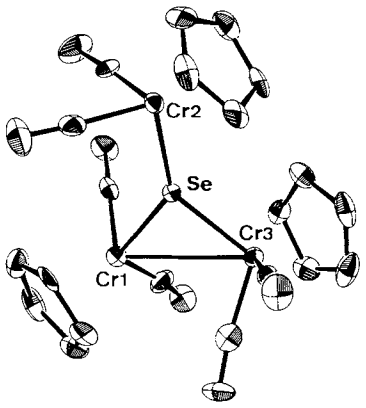
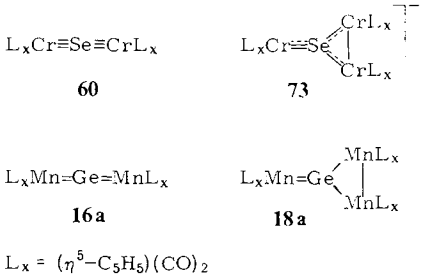


Fig. 37. Structure of the complex anion of **73** in the crystal (−60 °C). The planar (!) Cr_3Se backbone represents a novel type of coordination, which is not shown in Scheme 4. The salt-like compound crystallizes from tetrahydrofuran/diethyl ether (−30 °C) with one equivalent of THF.

identical bonding systems (cf. Section 2.2.3), whereas the Cr_3Se complex anion of **73** is isoelectronic with the neutral Mn_3Ge compound **18a** (Scheme 6). The central bare selenium atom contributes all valence electrons for bonding to the three $[(\eta^5\text{-}C_5H_5)Cr(CO)_2]$ fragments, which are isolobal with CH and CH_2^+ fragments. Hence, for the singly charged complex anion of **73**, as for **18**, there is an isolobal relationship to methylenecyclopropane because of $Se \leftarrow\!\!\!\!\!\!\rightarrow C^{2-} \leftarrow\!\!\!\!\!\!\rightarrow CH^-$, $Ge \leftarrow\!\!\!\!\!\!\rightarrow C$, and $(\eta^5\text{-}C_6H_5)Mn(CO)_2 \leftarrow\!\!\!\!\!\!\rightarrow CH_2$.[3,4]

As can be seen from the ^{1}H-NMR spectra ([D$_6$]acetone) **73** has a fluctional structure: At −80 °C, three well resolved C_5H_5 signals are observed, two of which become broader on increasing the temperature, and at ca. −50 °C finally merge to a single line. This finding can be explained in terms of a *cis/trans* isomerization in the dinuclear fragment $[(\eta^2\text{-}C_5H_5)Cr(CO)_2]_2$. The appearance of a sharp signal for the exocyclic $[(\eta^5\text{-}C_5H_5)Cr(CO)_2]$ unit between −80 and 25 °C is indicative of a free rotation of this



Scheme 6.

structural unit about the CrSe bond. **73** is extremely oxygen-sensitive and on contact with air immediately reverts to the starting material **60**, although not quantitatively. It is stable in solution only at low temperature and decomposes quickly at room temperature, giving the selenium-free salt $[(\eta^5\text{-}C_5H_5)_2Co]^+[(\eta^5\text{-}C_5H_5)Cr(CO)_3]^-$ (X-ray structure analysis[112]) and a carbonyl-free $[(\eta^5\text{-}C_5H_5)CrSe]_x$-cluster molecule of unknown structure. The composition of the diamagnetic (!) complex **73** shows that the one-electron reduction of **60** can lead to secondary reactions, which in the present case form polynuclear molecules. The CrSe complex **60** also reacts, immediately, with potassium superoxide, KO_2, as a reducing agent in the presence of [2.2.2]-cryptand, under fragmentation, forming the structurally characterized novel complex anion $[(\eta^5\text{-}C_5H_5)Cr(CO)_2(\eta^2\text{-}Se_2)]^-$ **74**.[113]

5. Prospects

In this essay we have encountered unsubstituted ("bare") elements of the carbon, nitrogen and oxygen groups as distinctive structural subunits, both in multiple bonding systems of limited extent and also encapsulated in transition metal clusters. Although there is still not the rich variety of compounds that we might have expected on the basis of our two decades' experience of metal-metal multiple bonds, it is to be hoped that preparative methods will prove capable of development. For the heavier, more metallic main group elements, the high reactivity of the elemental modifications themselves and of the binary hydrides on reaction with organometallic complexes is striking. The relationship to the chemistry of the transition metals is very close, since the atomic radii and the electronic structures are broadly comparable. Structural similarities with classical inorganic solid state chemistry have become quite obvious by now, and it is to be expected that iso- and heteropolyanions such as Se_4^{2+}, Te_4^{2+}, Te_5^{2-}, Te_6^{4+}, $[Au_2Te_4]^{2-}$, and $[As_{10}Te_4]^{2-}$[50,64c,115] will soon form part of the organometallic chemist's arsenal. The chemistry of multiple bond systems consisting of transition metals and bare main group elements promises, on the basis of current knowledge, to be a rich one; probably, it will basically not differ too much from the reactivity of metal-metal multiple bonds, and is likely to find applications in catalysis.

This essay arose from a lecture that I gave at the Technical University of Munich. My thanks are due to my students for their intelligent questions and comments, which caused me to think more deeply about several topics. I am also

thankful for the skill and resourcefulness of my coworkers, who have carried out their contributions to the work described here with diligence and perseverance: Basile Koumbouris (chemistry of arsenic), Heinz-Josef Kneuper (germanium, tin, and lead), Jürgen Rohrmann (sulfur, selenium, and tellurium), Christian Hecht (selenium and tellurium), Erdmuthe Voss (silicon), Rolf Hörlein and Dr. Josef Weichmann (germanium) deserve special mention. The structure determinations were performed by Dr. Eberhardt Herdtweck of our Munich laboratory and the groups of my colleagues Manfred L. Ziegler (Heidelberg University), Ivan Bernal (University of Houston) and Heinrich Nöth (Munich University), who are all to be thanked for their contributions. My colleague Hans Bock (Frankfurt University) provided intellectual stimulation and also contributed practically to the useful electrochemical studies mentioned at the end of this review. The whole research area described here owes much to the impulse it received from the work of the following groups of Herberhold (Bayreuth University), Huttner (Konstanz University), and Weiss (Hamburg University), to whom I am indebted for frank discussions. Finally, I would like to express my gratitude to Freya and our children for their continuous patience.

Received: October 14, 1985 [A 563 IE]
German version: *Angew. Chem. 98* (1986) 57
Translated by Dr. *Peter G. Jones*, Göttingen

[1] G. Wilkinson, F. G. A. Stone, E. W. Abel (Ed.): *Comprehensive Organometallic Chemistry*, Pergamon Press, Oxford 1982. This monumental work, which consists of nine volumes comprising 8750 pages, is today a standard work of reference on organoelement chemistry.

[2] J. Buckingham (Ed.): *Dictionary of Organometallic Compounds*, Chapman and Hall, London 1984. This three-volume work references 14000 organometallic compounds.

[3] The isolobal analogy has proven to be one of the most successful concepts in the designing of synthetic strategies: R. Hoffmann, *Angew. Chem. 94* (1982) 725; *Angew. Chem. Int. Ed. Engl. 21* (1982) 711.

[4] Review of the applications of the isolobal analogy concept in organometallic chemistry: F. G. A. Stone, *Angew. Chem. 96* (1984) 85; *Angew. Chem. Int. Ed. Engl. 23* (1984) 85.

[5] Review: G. Schmid, *Struct. Bonding (Berlin) 62* (1985) 51.

[6] Original works: a) G. Schmid, R. Pfeil, R. Boese, F. Bandermann, S. Meyer. G. H. M. Calis, J. W. A. van der Velden, *Chem. Ber. 114* (1981) 3634; b) L. R. Wallenberg, J.-O. Bovin, G. Schmid, *Surf. Sci. 156* (1985) 256; c) cf. also the Rh_{55} Cluster $[Rh_{55}(PrBu_3)_{12}Cl_{20}]$: G. Schmid, U. Giebel, W. Huster, *Inorg. Chim. Acta 85* (1984) 97.

[7] Gold modification $(Au_{13})_n$: G. Schmid et al., unpublished.—The present highlight of straightforward cluster syntheses is marked by the compound $[Ni_{34}Se_{22}\{P(C_6H_5)_3\}_{10}]$: D. Fenske, J. Ohmer, J. Hachgenei, *Angew. Chem. 97* (1985) 993; *Angew. Chem. Int. Ed. Engl. 24* (1985) 993.

[8] M. N. Vargaftik, V. P. Zagorodnikov, P. Stolyarov, I. I. Moiseev, V. A. Likholobov, D. I. Kochubey, L. Chuvilin, I. Zaikovsky, K. I. Zamaraev, G. I. Timofeeva, *J. Chem. Soc. Chem. Commun. 1985*, 937.

[9] Reviews (Clusters): a) P. Chini, *J. Organomet. Chem. 200* (1980) 37; b) E. L. Muetterties, *ibid. 200* (1980) 177; c) W. L. Gladfelter, G. L. Geoffroy, *Adv. Organomet. Chem. 18* (1980) 207; d) H. Vahrenkamp, *ibid. 22* (1983) 169.

[10] Reviews (Carbidoclusters): P. Chini, G. Longoni, V. G. Albano, *Adv. Organomet. Chem. 14* (1976) 285.

[11] E. H. Braye, L. F. Dahl, W. Hübel, D. L. Wampler, *J. Am. Chem. Soc. 84* (1962) 4633.

[12] J. S. Bradley, G. B. Ansell, M. E. Leonowicz, E. W. Hill, *J. Am. Chem. Soc. 103* (1981) 4968.

[13] a) J. S. Bradley, E. W. Hill, G. B. Ansell, M. A. Modrick, *Organometallics 1* (1982) 1634; b) J. S. Bradley, G. B. Ansell, E. W. Hill, *J. Am. Chem. Soc. 101* (1979) 7417; c) M. R. Churchill, J. Wormald, J. Knight, M. J. Mays, *ibid. 93* (1971) 3073.

[14] a) V. G. Albano, P. Chini, G. Chini, M. Sansoni, D. Strumbolo, B. T. Heaton, S. Martinengo, *J. Am. Chem. Soc. 98* (1976) 5027 ($[Co_8C(CO)_{18}]^{2-}$ and $[Co_6C(CO)_{14}]^{-}$); b) G. Ciani, G. D'Alfonso, M. Freni, P. Remiti, A. Sironi, *J. Chem. Soc. Chem. Commun. 1982*, 339 ($[Re_7C(CO)_{21}]^{2-}$); c) D. H. Farrar, P. F. Jackson, B. F. G. Johnson, J. Lewis, J. N. Nicholls, *ibid. 1981*, 415 ($[Ru_6C(CO)_{17}]$); d) D. F. Shriver, E. Holt, *J. Organomet. Chem.*, in press; e) J. H. Davis, M. A. Beno, J. M. Williams, J. Zimmie, M. Tachikawa, E. L. Muetterties, *Proc. Natl. Acad. Sci. USA 78* (1981) 668.

[15] Recent reviews: a) M. Tachikawa, E. L. Muetterties, *Progr. Inorg. Chem. 28* (1981) 203; b) J. S. Bradley, *Adv. Organomet. Chem. 22* (1983) 1.

[16] Examples: a) D. K. Breitinger, K. Geibel, W. Kress, R. Sendelbeck, *J. Organomet. Chem. 191* (1980) 7; b) D. K. Breitinger, W. Kress, R. Sendelbeck, K. Ishiwada, *ibid. 243* (1983) 245.

[17] a) J. D. Cotton, J. Duckworth, S. A. R. Knox, P. F. Lindley, I. Paul, F. G. A. Stone, P. Woodward, *Chem. Commun. 1966*, 253; b) P. F. Lindley, P. Woodward, *J. Chem. Soc. A 1967*, 382; c) J. D. Cotton, S. A. R. Knox, I. Paul, F. G. A. Stone, *J. Chem. Soc. A 1967*, 264.

[18] a) G. Schmid, G. Etzrodt, *J. Organomet. Chem. 137* (1977) 367; b) G. Schmid, V. Bätzel, G. Etzrodt, *ibid. 112* (1976) 345.

[19] a) G. Etzrodt, R. Boese, G. Schmid, *Chem. Ber. 112* (1979) 2574; b) W. Kruppa, D. Bläser, R. Boese, G. Schmid, *Z. Naturforsch. B 37* (1982) 209.

[20] W. Malisch, H.-U. Wekel, I. Grob, F.-H. Köhler, *Z. Naturforsch. B 37* (1982) 601.

[21] R. F. Gerlach, K. M. Mackay, B. K. Nicholson, W. T. Robinson, *J. Chem. Soc. Dalton Trans. 1981*, 80.

[22] S. P. Foster, K. M. Mackay, B. K. Nicholson, *Inorg. Chem. 24* (1985) 909.

[23] Organometallic aspects of the Fischer-Tropsch synthesis: W. A. Herrmann, *Angew. Chem. 94* (1982) 118; *Angew. Chem. Int. Ed. Engl. 21* (1982) 117, and references cited therein.

[24] a) V. Ponec, *Catal. Rev. Sci. Eng. 18* (1978) 1517; b) P. Bileon, J. N. Helle, W. M. H. Sachtler, *J. Catal. 58* (1978) 95.

[25] W. Gäde, E. Weiss, *J. Organomet. Chem. 213* (1981) 451.

[26] W. Gäde, E. Weiss, *Chem. Ber. 114* (1981) 2399; cf. D. Melzer, E. Weiss, *ibid. 117* (1984) 2464.

[27] W. Gäde, E. Weiss, *Angew. Chem. 93* (1981) 796; *Angew. Chem. Int. Ed. Engl. 20* (1981) 803.

[28] P. Rievière, M. Rivière-Baudet, J. Satgé in [1], *Vol. 2*, p. 399ff.

[29] W. A. Herrmann, J. Weichmann, U. Küsthardt, A. Schäfer, R. Hörlein, C. Hecht, E. Voss, R. Serrano, *Angew. Chem. 95* (1983) 1019; *Angew. Chem. Int. Ed. Engl. 22* (1983) 979; *Angew. Chem. Suppl. 1983*, 1543.

[30] Reviews: a) E. Colomer, R. J. P. Corriu, *Top. Curr. Chem. 96* (1981) 79; b) B. J. Aylett, *Adv. Inorg. Radiochem. 25* (1982) 1.

[31] W. A. Herrmann, E. Voss, E. Guggolz, M. L. Ziegler, *J. Organomet. Chem. 284* (1985) 47.

[32] a) D. Melzer, E. Weiss, *J. Organomet. Chem. 255* (1983) 335; h) *ibid. 263* (1984) 67.

[33] J. D. Korp, I. Bernal, R. Hörlein, R. Serrano, W. A. Herrmann, *Chem. Ber. 118* (1985) 340.

[34] W. A. Herrmann, R. Serrano, J. Weichmann, *J. Organomet. Chem. 246* (1983) C57.

[35] I. Bernal, J. D. Korp, W. A. Herrmann, R. Serrano, *Chem. Ber. 117* (1984) 434.

[36] D. W. H. Rankin, A. Robertson, *J. Organomet. Chem. 85* (1975) 225.

[37] Yu. T. Struchkov, K. N. Anisimov, O. P. Osipova, N. E. Kolobova, A. N. Nesmeyanov, *Dokl. Akad. Nauk. SSSR 172* (1967) 15.

[38] K. Triplett, M. D. Curtis, *J. Am. Chem. Soc. 97* (1975) 5747.

[39] N. M. Kostic, R. F. Fenske, *J. Organomet. Chem. 233* (1982) 337.

[40] G. Huttner, U. Weber, B. Sigwarth, O. Scheidsteger, H. Lang, L. Zsolnai, *J. Organomet. Chem. 282* (1985) 331, and references cited therein.

[41] W. A. Herrmann, H.-J. Kneuper, E. Herdtweck, unpublished.

[42] Review: M. I. Bruce, A. G. Swincer, *Adv. Organomet. Chem. 22* (1983) 60.

[43] Recent work: W. A. Herrmann, C. Weber, M. L. Ziegler, O. Serhadli, *J. Organomet. Chem.*, in press, and references cited therein.

[44] W. A. Herrmann, H.-J. Kneuper, unpublished.

[45] W. A. Herrmann, H.-J. Kneuper, E. Herdtweck, *Angew. Chem. 97* (1985) 1060; *Angew. Chem. Int. Ed. Engl. 24* (1985) 1062.

[46] P. Jutzi, W. Steiner, *Chem. Ber. 109* (1976) 3473.

[47] W. A. Herrmann, H.-J. Kneuper, E. Herdtweck, unpublished (synthesis and X-ray structure analysis of $[(\mu\text{-}GeCl_2)\{(\eta^5\text{-}C_5H_5)Mn(CO)_2\}_2]$: Mn-Ge 233.7(1), 236.7(1) pm; triclinic).

[48] Cf., for example the discussion in Ref. [99] on the covalent radii of metal atoms and bond orders, together with the relative literature: a) L. Pauling: *The Nature of the Chemical Bond*, 3th edition; b) A. F. Wells: *Structural Inorganic Chemistry*, 5th edition, Clarendon Press, Oxford 1985; see also W. A. Herrmann, J. Weichmann, R. Serrano, K. Blechschmitt, H. Pfisterer, M. L. Ziegler, *Angew. Chem. Suppl. 1983*, 363, footnote 32.

[49] a) Original publication: E. O. Fischer, G. Kreis, C. G. Kreiter, J. Müller, G. Huttner, H. Lorenz, *Angew. Chem. 85* (1973) 618; *Angew. Chem. Int. Ed. Engl. 12* (1973) 564; b) Reviews: E. O. Fischer, U. Schubert, *J. Organomet. Chem. 100* (1975) 59; E. O. Fischer, *Angew. Chem. 86* (1974) 651 (Nobel-Vortrag); *Adv. Organomet. Chem. 14* (1976) 1.

[50] N. N. Greenwood, A. Earnshaw: *Chemistry of the Elements*, Pergamon Press, Oxford 1984.

[51] F. A. Cotton, G. Wilkinson: *Advanced Inorganic Chemistry – A Comprehensive Text*, 4th Edition, John Wiley & Sons, New York 1980.

[52] K. Dehnicke, J. Strähle, *Angew. Chem. 93* (1981) 451; *Angew. Chem. Int. Ed. Engl. 20* (1981) 413.
[53] D. Bright, J. A. Ibers, *Inorg. Chem. 8* (1969) 709.
[54] a) K. Dehnicke, W. Kolitsch, *Z. Naturforsch. B 32* (1977) 1485; b) W. Kolitsch, K. Dehnicke, *ibid. B 25* (1970) 1080.
[55] W. Liese, K. Dehnicke, I. Walker, J. Strähle, *Z. Naturforsch. B 34* (1979) 693.
[56] K.-P. Frank, J. Strähle, J. Weidlein, *Z. Naturforsch. B 35* (1980) 300.
[57] M. Ciechanowicz, W. P. Griffith, D. Pawson, A. C. Skapski, *Chem. Commun. 1971*, 876.
[58] S. Martinengo, G. Ciani, A. Sironi, B. T. Heaton, J. Mason, *J. Am. Chem. Soc. 101* (1979) 7095.
[59] D. E. Fjare, W. L. Gladfelter, *J. Am. Chem. Soc. 103* (1981) 1572; see also: M. A. Collins, B. F. G. Johnson, J. Lewis, J. M. Mace, J. Morris, M. McPartlin, W. J. H. Nelson, J. Puga, P. R. Raithby, *J. Chem. Soc. Chem. Commun. 1983*, 689 (Ru_4N- and Os_4N-cluster compounds).
[60] J. L. Vidal, W. E. Walker, R. L. Pruett, R. C. Schoening, *Inorg. Chem. 18* (1979) 129.
[61] P. Chini, G. Ciani, S. Martinengo, A. Sironi, L. Longhetti, B. T. Heaton, *J. Chem. Soc. Chem. Commun. 1979*, 188.
[62] J. Vidal, *Inorg. Chem. 20* (1981) 243.
[63] J. Vidal, J. M. Troup, *J. Organomet. Chem. 213* (1981) 351.
[64] a) W. Schmettow, H. G. von Schnering, *Angew. Chem. 89* (1977) 895; *Angew. Chem. Int. Ed. Engl. 16* (1977) 857; b) H. G. von Schnering, D. Fenske, W. Hönle, M. Binnewies, K. Peters, *Angew. Chem. 91* (1979) 755; *Angew. Chem. Int. Ed. Engl. 18* (1979) 679; c) Cf., especially the review on "Homonuclear Bonding of Main Group Elements" by H. G. von Schnering, *Angew. Chem. 93* (1981) 44; *Angew. Chem. Int. Ed. Engl. 20* (1981) 33.
[65] Review: H. Schäfer, B. Eisenmann, W. Müller, *Angew. Chem. 85* (1973) 742; *Angew. Chem. Int. Ed. Engl. 12* (1973) 694 and references cited therein as well as in [50].
[66] a) P. A. Edwards, J. D. Corbett, *Inorg. Chem. 16* (1977) 903; b) J. D. Corbett, P. A. Edwards, *J. Am. Chem. Soc. 99* (1977) 3313; c) C. H. E. Belin, J. D. Corbett, A. Cisar, *ibid. 99* (1977) 7163; d) S. C. Critchlow, J. D. Corbett, *J. Chem. Soc. Chem. Commun. 1981*, 236; e) R. C. Burns, J. D. Corbett, *J. Am. Chem. Soc. 104* (1982) 2804; f) J. D. Corbett, D. G. Adolphson, D. J. Merriman, P. A. Edwards, F. J. Armatis, *ibid. 97* (1975) 6267.
[67] Review: J. D. Corbett, *Progr. Inorg. Chem. 21* (1976) 129.
[68] R. W. Rudolph, W. L. Wilson, *J. Am. Chem. Soc. 103* (1981) 2480, and references cited therein; F. Teixidor, M. L. Luetkens, R. W. Rudolph, *ibid. 105* (1983) 149.
[69] a) L. L. Lohr, *Inorg. Chem. 20* (1981) 4229; b) R. C. Burns, R. J. Gillespie, J. A. Barnes, M. J. McGlinchey, *ibid. 21* (1982) 799 (MO calculations); c) R. J. Gillespie, J. Passmore, *Adv. Inorg. Chem. Radiochem. 17* (1975) 49.
[70] T. G. Spiro, D. H. Templeton, A. Zalkin, *Inorg. Chem. 8* (1969) 856; cf. also the structure of $[Pb_4O\{Si(C_6H_5)_3\}_6]$: C. Gaffney, P. G. Harrison, T. J. King, *J. Chem. Soc. Chem. Commun. 1980*, 1251.
[71] See [50], p. 136.
[72] H. Lang, L. Zsolnai, G. Huttner, *Angew. Chem. 95* (1983) 1016; *Angew. Chem. Int. Ed. Engl. 22* (1983) 976; *Angew. Chem. Suppl. 1983*, 1451.
[73] See [40]; cf. also [72].
[74] H. Lang, L. Zsolnai, G. Huttner, *Angew. Chem. 95* (1983) 1017; *Angew. Chem. Int. Ed. Engl. 22* (1983) 976; *Angew. Chem. Suppl. 1983*, 1463; cf. also: A. Vizi-Orosz, G. Palyi, L. Marko, R. Boese, G. Schmid, *J. Organomet. Chem. 288* (1985) 179; C. F. Campana, A. Vizi-Orosz, G. Palyi, L. Marko, L. F. Dahl, *Inorg. Chem. 18* (1979) 3054.
[75] a) K. H. Whitmire, C. B. Lagrone, M. R. Churchill, J. C. Fettinger, L. V. Biondi, *Inorg. Chem. 23* (1984) 4227; b) M. R. Churchill, J. C. Fettinger, K. H. Whitmire, *J. Organomet. Chem. 284* (1985) 13.
[76] W. A. Herrmann, B. Koumbouris, T. Zahn, M. L. Ziegler, *Angew. Chem. 96* (1984) 802; *Angew. Chem. Int. Ed. Engl. 23* (1984) 812.
[77] W. A. Herrmann, B. Koumbouris, A. Schäfer, T. Zahn, M. L. Ziegler, *Chem. Ber. 118* (1985) 2472.
[78] Original works on this topic: a) G. Huttner, J. Borm, L. Zsolnai, *J. Organomet. Chem. 263* (1984) C 33, and references cited therein; b) G. Huttner, H.-D. Müller, A. Frank, H. Lorenz, *Angew. Chem. 87* (1975) 714; *Angew. Chem. Int. Ed. Engl. 14* (1975) 705; c) B. Sigwarth, L. Zsolnai, O. Scheidsteger, G. Huttner, *J. Organomet. Chem. 235* (1982) 43, and references cited therein.
[79] a) B. Sigwarth, L. Zsolnai, H. Berke, G. Huttner, *J. Organomet. Chem. 226* (1982) C 5; b) G. Huttner, U. Weber, B. Sigwarth, O. Scheidsteger, *Angew. Chem. 94* (1982) 210; *Angew. Chem. Int. Ed. Engl. 21* (1982) 411; c) G. Huttner, U. Weber, L. Zsolnai, *Z. Naturforsch. B 37* (1982) 707.
[80] G. Huttner, B. Sigwarth, O. Scheidsteger, L. Zsolnai, O. Orama, *Organometallics 4* (1985) 326; cf. P. J. Sullivan, A. L. Rheingold, *ibid. 1* (1982) 1547.
[81] a) A. L. Rheingold, M. J. Foley, P. J. Sullivan, *J. Am. Chem. Soc. 104* (1982) 4727; b) O. J. Scherer, J. Schwalb, G. Wolmershäuser, W. Kaim, R. Gross, *Angew. Chem.*, in press.
[82] C. F. Campana, L. F. Dahl, *J. Organomet. Chem. 127* (1977) 209.
[83] A. F. Wells: *Structural Inorganic Chemistry*, 4th Edition, Clarendon Press, Oxford 1975, p. 416 f. and p. 664.
[84] G. Ciani, L. Garlaschelli, A. Sironi, S. Martinengo, *J. Chem. Soc. Chem. Commun. 1981*, 563.
[85] T. J. Greenhough, B. W. S. Kolthammer, P. Legzdins, J. Trotter, *Inorg. Chem. 18* (1979) 3543.
[86] L. Y. Goh, T. W. Hambley, G. B. Robertson, *J. Chem. Soc. Chem. Commun. 1983*, 1458.
[87] M. Herberhold, D. Reiner, B. Zimmer-Gasser, U. Schubert, *Z. Naturforsch. B 35* (1980) 1281.
[88] W. Hieber, J. Gruber, *Z. Anorg. Allg. Chem. 296* (1958) 91.
[89] M. Höfler, A. Baitz, *Chem. Ber. 109* (1976) 3147.
[90] C. Mealli, S. Midollini, L. Sacconi, *Inorg. Chem. 17* (1978) 632.
[91] D. L. Lichtenberger, J. L. Hubbard, *Inorg. Chem. 23* (1984) 2718.
[92] C. Potvin, J.-M. Manoli, J. M. Brégeault, *Inorg. Chim. Acta 72* (1983) 103.
[93] S. Lincoln, S.-L. Soong, S. A. Koch, M. Sato, J. H. Enemark, *Inorg. Chem. 24* (1985) 1355.
[94] J. Schiemann, P. Hübener, E. Weiss, *Angew. Chem. 95* (1983) 1021; *Angew. Chem. Int. Ed. Engl. 22* (1983) 980.
[95] N. Albrecht, P. Hübener, U. Behrens, E. Weiss, *Chem. Ber. 118* (1985) 4059.
[96] W. A. Herrmann, J. Rohrmann, A. Schäfer, *J. Organomet. Chem. 265* (1984) C 1.
[97] W. A. Herrmann, J. Rohrmann, H. Nöth, C. K. Narula, I. Bernal, M. Draux, *J. Organomet. Chem. 284* (1985) 189; ibid. *289* (1985) C26.
[98] L. Y. Goh, Ch. Wei, E. Sinn, *J. Chem. Soc. Chem. Commun. 1985*, 462.
[99] W. A. Herrmann, J. Rohrmann, M. L. Ziegler, T. Zahn, *J. Organomet. Chem. 273* (1984) 221.
[100] W. A. Herrmann, C. Hecht, M. L. Ziegler, B. Balbach, *J. Chem. Soc. Chem. Commun. 1984*, 686.
[101] M. Herberhold, D. Reiner, D. Neugebauer, *Angew. Chem. 95* (1983) 46; *Angew. Chem. Int. Ed. Engl. 22* (1983) 59; *Angew. Chem. Suppl. 1983*, 20.
[102] W. A. Herrmann, C. Bauer, J. Weichmann, *J. Organomet. Chem. 243* (1983) C 21.
[103] Reviews: a) W. A. Herrmann, *Angew. Chem. 90* (1978) 855; *Angew. Chem. Int. Ed. Engl. 17* (1978) 800; b) *J. Organomet. Chem. 250* (1983) 319; c) *Adv. Organomet. Chem. 20* (1982) 159; d) *Pure Appl. Chem. 54* (1982) 65; e) W. A. Herrmann in B. L. Shapiro (Ed.): *Organometallic Compounds - Synthesis, Structure, and Theory*, Texas A & M University Press, College Station, TX, USA 1983, p. 383 ff.; f) J. E. Hahn, *Progr. Inorg. Chem. 31* (1984) 205.
[104] W. A. Herrmann, C. Hecht, M. L. Ziegler, T. Zahn, *J. Organomet. Chem. 273* (1984) 323.
[105] W. A. Herrmann, J. Rohrmann, unpublished results.
[106] W. A. Herrmann, J. Rohrmann, C. Hecht, *J. Organomet. Chem. 290* (1985) 53.
[107] W. A. Herrmann, C. Hecht, E. Herdtweck, unpublished results.
[108] W. A. Herrmann, J. Rohrmann, M. L. Ziegler, T. Zahn, *J. Organomet. Chem. 295* (1985) 175.
[109] H. Bock, A. Veltmann, unpublished results; A. Veltmann, *Diplomarbeit*, Universität Frankfurt 1984.
[110] N. E. Murr, E. Laviron, *Tetrahedron Lett. 1975*, 875.
[111] W. A. Herrmann, J. Rohrmann, unpublished.—The radical anion of **60** has been characterized ESR spectroscopically (H. Bock et al., unpublished).
[112] W. A. Herrmann, J. Rohrmann, M. L. Ziegler, G. Sergeson, unpublished.
[113] W. A. Herrmann, J. Rohrmann, unpublished.
[114] Monograph: F. A. Cotton, R. A. Walton: *Multiple Bonds Between Metal Atoms*, Wiley, New York 1982; see also the review by *M. H. Chisholm* in this issue: M. H. Chisholm, *Angew. Chem. 98* (1986) 21; *Angew. Chem. Int. Ed. Engl. 25* (1986) 21.
[115] a) R. C. Haushalter, C. M. O'Connor, J. P. Haushalter, A. M. Umarji, G. K. Shenoy, *Angew. Chem. 96* (1984) 147; *Angew. Chem. Int. Ed. Engl. 23* (1984) 169; R. C. Haushalter, *ibid. 97* (1985) 414 and *24* (1985) 433; b) B. Eisenmann, H. Jordan, H. Schäfer, *ibid. 93* (1981) 211 and *20* (1981) 197.

When submitting manuscripts, authors of articles intended for publication as "Communications" are requested to read the "Notice to Authors" reproduced in the January issue of the journal following the list of contents; upon request, a copy can be obtained from the editorial office.

Ag_3O_4, the First Silver(II,III) Oxide**

By *Burkhard Standke* and *Martin Jansen**

In memory of Wilhelm Klemm

Divalent silver in a square-planar oxygen environment was unknown up to now. In accordance with the formulation $Ag^+Ag^{3+}O_2$, AgO is described as mixed valent,[1] a contention that has been disputed. During the decomposition of Ag_2O_3, which we had prepared earlier and characterized by an X-ray structure analysis,[2] we obtained evidence for the existence of a new phase between Ag_2O_3 and AgO. In both thermal investigations (differential thermogravimetry) and electrochemical methods (discharge curve), the stage at which silver(III) oxide decomposes into "silver(II) oxide" and oxygen exhibited an apparent critical point. A binary oxide with a composition between Ag_2O_3 and AgO contains (insofar as a peroxidic or hyperoxidic nature can be excluded) silver in different oxidation states. Its detection and the characterization of its structure could contribute to the clarification of the vague and often contradictory statements made concerning higher silver oxides ($AgO_{\geq 1}$).[3]

We obtained the expected mixed-valent oxide, Ag_3O_4, by anodic oxidation of solutions of silver salts (e.g., AgF or $AgClO_4$) at potentials that were lower than those used in the preparation of Ag_2O_3.[4]

Ag_3O_4 separates out as plate-like, metallic, black crystals. According to thermal investigations (simultaneous differential thermal analysis and thermogravimetric analysis, Netzsch STA 429, extrapolation to a heating rate of 0°C/s), the decomposition to AgO begins at 63°C in a strongly exothermic reaction. Accordingly, Ag_3O_4 is more stable than Ag_2O_3. Ag_3O_4 decomposed already at room temperature upon irradiation with X-rays. Therefore, the X-ray studies[6] were carried out at −50°C. Under these conditions, the reference reflections exhibit no decrease in intensity during the course of measurement.

According to the X-ray structure analysis, silver in Ag_3O_4 is exclusively present in a square-planar oxygen environment (Fig. 1). This coordination is preferred for d^9- and d^8-configurated transition-metal ions and characterizes the new compound as silver(II,III) oxide. A formulation with mono- and divalent silver—roughly in analogy with the suggestion for AgO[1]—is thus ruled out. The composition of the unit cell, corresponding to $Ag_2^{2+}Ag_4^{3+}O_8$, and the occupation of two point sites in $P2_1/c$ of appropriate multiplicity (Ag1 on 2a, and Ag2 on 4e) suggest the assignment of Ag1 and Ag2 to oxidation states +2 and +3, respectively. This conflicts, however, with the Ag–O bond lengths, which are slightly, but significantly, shorter for Ag1 (average value: 203 pm) compared with Ag2 (average value: 207 pm). Thus, it is necessary to assume extensive charge equalization over the silver positions with a slightly higher effective positive charge on Ag1. The larger Ag–O distances compared with those of Ag_2O_3 are in agreement with this assumption. The deviations of the AgO_4 polyhedrons from the ideal geometry are of the same order as the experimental error for Ag1 (point symmetry $\bar{1}$); for Ag2, they are larger, especially with regard to the angles (cf. Fig. 1). Ag2 lies about 13 pm from the "best plane" through the four neighboring O atoms. The AgO_4 structural units are linked together via common corners and edges to form a three-dimensional spatial network in which oxygen always joins three silver ions to one another, corresponding to the simplest possible formal representation $AgO_{4/3}$. Two polyhedrons around each Ag2 share a common edge; this structural unit with point symmetry $\bar{1}$ is shown in Figure 1, bottom. We hope to obtain further details of the bonding situation, in particular, the possible lo-

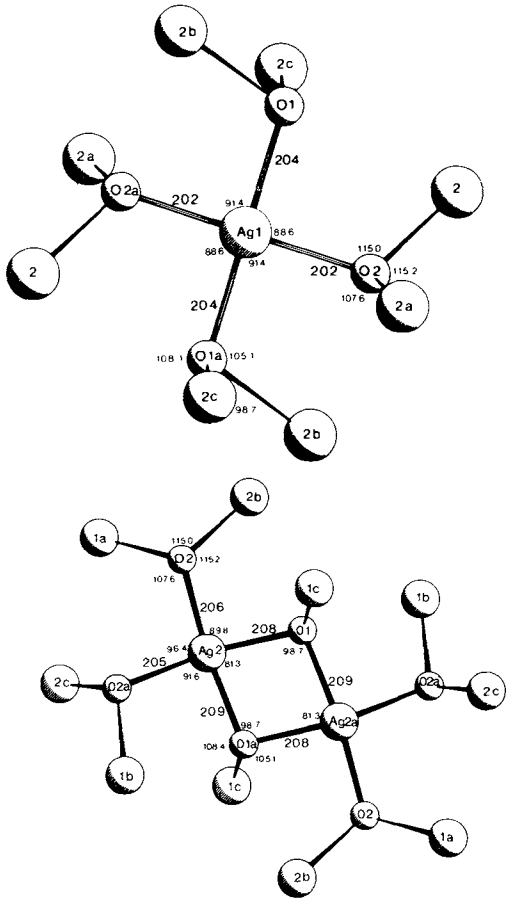


Fig. 1. Perspective view of the coordination polyhedron around Ag1 (above) and Ag2 (below) and the second nearest neighbors in each case. The smaller spheres represent Ag, distances [pm], angles [°]. The maximum standard deviations for the bond lengths and angles are 0.8 pm and 0.4°.

[*] Prof. Dr. M. Jansen, Dipl.-Chem. B. Standke
Institut für Anorganische Chemie der Universität
Callinstrasse 9, D-3000 Hannover 1 (FRG)

[**] This work was supported by the Fonds der Chemischen Industrie.

calization of charge at low temperatures, by measuring the magnetic susceptibility.

Received: May 8, 1985 [Z 1297 IE]
Publication delayed at authors' request
German version: *Angew. Chem. 98* (1986) 78

[1] J. A. McMillan, *J. Inorg. Nucl. Chem. 13* (1960) 28.
[2] B. Standke, M. Jansen, *Angew. Chem. 97* (1985) 114; *Angew. Chem. Int. Ed. Engl. 24* (1985) 118.
[3] *Gmelin Handbuch der anorganischen Chemie, Silber B1*, Verlag Chemie, Weinheim 1971, p. 102.
[4] The electrolysis was carried out in a platinum dish (as cathode) with a ca. 12-cm long, 0.4-mm thick spirally wound platinum wire as anode. AgF was preferentially used as electrolyte. In the electrolytes used, the kind of oxidation product formed is clearly dependent on the concentration of silver: in a concentration range of 0.45–1.2 mol/L, the clathrate $Ag_7O_8HF_2$ [5] is formed along with Ag_3O_4. Pure $Ag_7O_8HF_2$ is formed above a concentration of 1.3 mol/L, whereas pure Ag_3O_4 is formed only when the concentration is below 0.35 mol/L. In order to increase the conductivity, the aqueous solution of silver salt was saturated, in each case, with sodium fluoride. The optimal conditions for the synthesis of pure Ag_3O_4 are as follows: $c_{Ag^+}=0.2$ mol/L, $c_{F^-}=2$ mol/L, $U=0.8$ V, $I=12$ mA, $T=0°C$, anodes as described in text. The crystals that grew on the anode were washed with distilled water (0°C) and methanol (0°C) and dried for a short period of time in vacuum.
[5] A. C. Gossard, D. K. Hindermann, M. B. Robin, N. A. Kuebler, T. H. Geballe, *J. Am. Chem. Soc. 89* (1967) 7121.
[6] $P2_1/c$; $a=358.2(4)$, $b=921.1(9)$, $c=568.6(5)$ pm; $\beta=106.1(8)°$; $Z=2$; four-circle diffractometer AED2, Siemens; $Mo_{K\alpha}$; data collection at $-50°C$; 391 unique structure factors, 372 with $F>3\sigma(F)$; $R=0.041$, $R_w=0.034$.

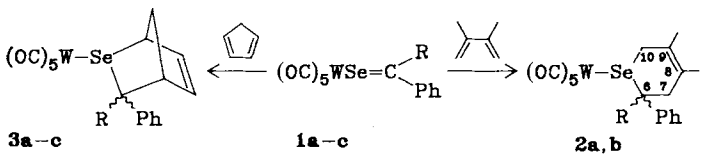
[4+2] Cycloadditions with Transition-Metal-Coordinated Selenoaldehydes and Selenoketones as Heterodienophiles**

By *Helmut Fischer,* Ulrike Gerbing, Jürgen Riede,* and *Reinhard Benn*

Monomeric selenobenzaldehydes and diarylselenoketones are not stable as free species. In the coordination sphere of transition metals, however, they can be formed from molecular fragments and stabilized by bonding to the metal.[1,2] The extremely high reactivity of the free selenoaldehydes and -ketones is thereby only reduced, so that the complexes should be useful as easily handled synthetic building blocks for those selenacycles that are only accessible with difficulty via other routes. This is demonstrated by their reactions with 1,3-dienes.

Deep blue pentacarbonyl(selenobenzaldehyde)tungsten **1a**[1] reacts with dimethylbutadiene and cyclopentadiene at $-30°C$ in a small amount of pentane or dichloromethane within a few seconds, undergoing [4+2] cycloaddition to give the yellow selenacyclohexene and selenanorbornene complexes **2a** and **3a**, respectively.[3] The corresponding reactions of the selenoketone complexes **1b** and **1c** proceed analogously, albeit more slowly.[3] The rate of reaction decreases with increasing electron density in the Se=C bond of the metal-coordinated dienophile—i.e., in the series **1a**, **1c**, **1b**.

The structures of the yellow complexes **2** and **3**, which are stable at room temperature, were confirmed by elemental analyses and IR, NMR, and mass spectra.[4] In addition, an X-ray structure analysis was carried out for **2b** (Fig. 1).[5] The coordination geometry around the selenium atom is a distorted pyramid. The C_5Se ring is nonplanar:



3a–c **1a–c** **2a,b**

a, R = H; **b**, R = Ph; **c**, R = p-$C_6H_4CF_3$

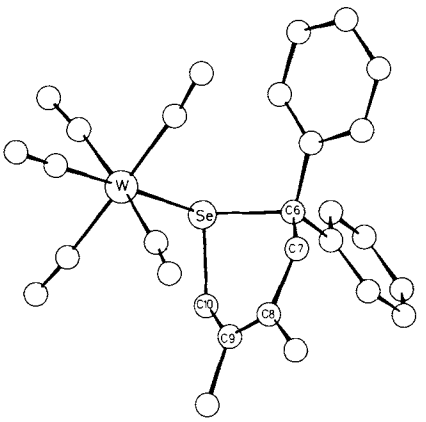


Fig. 1. Crystal structure of **2b**. Selected distances [pm] and angles [°]: W-Se 267.4(1), Se-C6 201.2(10), C6-C7 152.4(13), C7-C8 153.5(14), C8-C9 134.3(17), C9-C10 147.0(14), Se-C10 194.8(9); W-Se-C6 113.6(3), W-Se-C10 107.3(3), C6-Se-C10 91.9(4); angle between the planes C7-C8-C9-C10 and Se-C6-C7: 134.6°.

the C7-C8-C9-C10 plane is bent toward the $(CO)_5W$ fragment and is nearly coplanar with the plane of the CO groups in *cis* positions to Se. The W-Se distance in **2b** (267.4(1) pm) is longer than that in **1a** (263.5(2) and 263.7(2) pm in the two crystallographically independent molecules[1]). On the basis of the $^3J(H,H)$ coupling in the ^{1}H-NMR spectrum of **2a** at $-80°C$, the conformer with the phenyl group in quasi-equatorial position is presumably favored. At higher temperatures, an exchange of the geminal protons takes place for **2b**, probably owing to the pyramidal inversion of selenium. At room temperature, the signals of **3** are strongly broadened; upon cooling to $-80°C$, however, neither further broadening nor splitting of the resonances is observed for **3c**. Since the barrier for the pyramidal inversion of selenium is 58.5 kJ mol^{-1} for $[(CO)_5W\{Se(CH_2SiMe_3)_2\}]$,[6] **3c** is probably present as only one conformer in solution.

The reactions of the chromium complex $[(CO)_5Cr\{Se=C(H)Ph\}]$ and the corresponding thiobenzaldehyde complexes of chromium and tungsten, $[(CO)_5M\{S=C(H)Ph\}]$ (M = Cr, W),[7] with dimethylbutadiene and cyclopentadiene are analogous to the reaction of **1a**. In principle, the heterocycles may be released from the metal by oxidation of the central atom with $(NH_4)_2Ce(NO_3)_6$ as shown, for example, by the Diels-Alder adduct from $[(CO)_5Cr\{S=C(H)Ph\}]$ and dimethylbutadiene.[8] Other molecules of the type X=Y that are not stable as free species should also be employable in an indirect fashion, via their metal complexes, for the formation of heterocycles.

Received: August 1, 1985;
revised: October 12, 1985 [Z 1410 IE]
German version: *Angew. Chem. 98* (1986) 80

[*] Priv.-Doz. Dr. H. Fischer, U. Gerbing, J. Riede
Anorganisch-chemisches Institut der Technischen Universität München
Lichtenbergstrasse 4, D-8046 Garching (FRG)
Dr. R. Benn
Max-Planck-Institut für Kohlenforschung
Kaiser-Wilhelm-Platz 1, D-4330 Mülheim a. d. Ruhr (FRG)

[**] This work was supported by the Deutsche Forschungsgemeinschaft and the Fonds der Chemischen Industrie.

[1] H. Fischer, S. Zeuner, J. Riede, *Angew. Chem. 96* (1984) 707; *Angew. Chem. Int. Ed. Engl. 23* (1984) 726.
[2] H. Fischer, S. Zeuner, *Z. Naturforsch. B38* (1983) 1365.
[3] Experimental procedure: Solutions of **1** (0.2 mmol) and 2 mL of dimethylbutadiene or cyclopentadiene in dichloromethane or pentane were stirred at −30°C (**1a**) or room temperature (**1b**, **1c**) for a few seconds (**1a**), 5 min (**1c**), or 10 h (**1b**). The solutions turned from dark blue to reddish orange. After removal of the solvent in vacuum, the residue was chromatographed at −25°C with pentane/CH_2Cl_2 (10:1) on silica gel and the yellow band was eluted. The solvent was removed in vacuum and the residue was recrystallized from pentane. Yield: 53–85%. m.p. = 72°C (**2a**), 145°C (decomp.) (**2b**), 73°C (**3a**), 107°C (**3b**), 86°C (decomp.) (**3c**).
[4] IR (ν(CO), hexane): **2a**: 2071 (m), 1979 (w), 1941 (s), 1935 (vs), 1930 (s, sh); **2b**: 2071 (m), 1978 (w), 1940 (vs), 1929 (s); **3a**: 2070 (m), 1977 (w), 1941 (vs), 1933 (m, sh); **3b**: 2071 (m), 1979 (vw), 1946 (s), 1938 (vs), 1929 (m); **3c**: 2071 (m), 1980 (w), 1947 (s), 1939 (vs), 1933 (sh) cm^{-1}. — ^1H-NMR (**2a**, **2b**, and **3b** in CD_2Cl_2, **3a** and **3c** in CD_3COCD_3): **2a** (400 MHz, −80°C): δ = 1.73 (s, CH_3 on C8), 1.84 (s, CH_3 on C9), 2.44 and 2.65 (m, ^2J = 17.2 Hz, H_e and H_a on C7), 3.54 and 3.64 (m, ^2J = 14.6 Hz, H_a and H_e on C10), 4.07 (dd, ^3J = 11.7 and 4.0 Hz, H_a on C6), 7.3 (m, Ph); **2b** (400 MHz, −80°C): δ = 1.72 (s, CH_3 on C8), 1.88 (s, CH_3 on C9), 2.78 and 3.03 (d, ^2J = 15.2 Hz, H_a and H_e on C10), 2.85 and 3.23 (d, ^2J = 18.9 Hz, H_e and H_a on C7), 7.1–7.5 (m, 10 H, Ph); **2b** (400 MHz, 27°C): δ = 1.78 (s, CH_3 on C8), 1.93 (s, CH_3 on C9), 3.1 (m, 4 H, CH_2 of C7 and C10), 7.1–7.5 (m, 10 H, Ph); **3a** (60 MHz, 27°C): δ = 2.24 (m, *anti*-CH), 2.37 (m, *syn*-CH), 3.42 (m, CH), 4.46 (m, HCSe), 5.04 (m, =CH), 6.55 (m, =CH), 6.65 (m, CPh*H*), 7.2–7.6 (m, Ph); **3b** (60 MHz, 27°C): δ = 2.46 (s, *anti*-CH), 2.52 (s, *syn*-CH), 3.83 (m, CH), 4.80 (m, HCSe), 5.62 (m, =CH), 6.45 (dd, ^3J = 5.6 and 2.8 Hz, =CH), 7.2–7.8 (m, 10 H, Ph); **3c** (60 MHz, 27°C): δ = 2.67 (m, CH_2), 4.28 (m, CH), 5.13 (m, HCSe), 5.83 (m, =CH), 6.67 (m, =CH), 7.4 (m, Ph), 7.7 (m, C_6H_4).
[5] **2b**: $P2_1/c$, a = 1345.5(3), b = 1485.2(3), c = 1329.6(3) pm, β = 118.84(1)°, $V = 2327 \times 10^6$ pm^3, $\rho_{calcd} = 1.86\ g \cdot cm^{-3}$, Z = 4, 2857 reflections ($I > 1.96\sigma(I)$), R_1 = 0.035 (Syntex $P2_1$, $Mo_{K\alpha}$). Further details of the crystal structure investigation are available on request from the Fachinformationszentrum Energie, Physik, Mathematik GmbH, D-7514 Eggenstein-Leopoldshafen 2, on quoting the depository number CSD-51586, the names of the authors, and the journal citation.
[6] E. W. Abel, S. K. Bhargava, K. G. Orwell, *Progr. Inorg. Chem. 32* (1984) 1.
[7] H. Fischer, S. Zeuner, *Z. Naturforsch. B40* (1985) 954.
[8] For the preparation of the resulting heterocycle, 3,6-dihydro-4,5-dimethyl-2-phenyl-2*H*-thiopyran, by trapping of thermally generated thiobenzaldehyde with 2,3-dimethylbutadiene, see the recent article by J. E. Baldwin, R. C. G. Lopez, *Tetrahedron 39* (1983) 1487.

Hexa-*tert*-butyldisilane—the Molecule with the Longest Si–Si Bond**

By *Nils Wiberg,** *Harald Schuster, Arndt Simon,** and *Karl Peters*

Recently, a silicon compound with an unusually long Si–Si bond, hexa-*tert*-butylcyclotrisilane (251.1 pm; normal Si–Si single bond: 234 pm), was described.[1] We now report hexa-*tert*-butyldisilane **1**, a compound with a considerably longer Si–Si bond.

1 is not accessible from tri-*tert*-butylsilylsodium or -potassium **2** (M = Na, K) and tri-*tert*-butylhalosilane **3** (X = Cl, Br).

$$t\mathrm{Bu_3SiM} + \mathrm{XSi}t\mathrm{Bu_3} \not\longrightarrow t\mathrm{Bu_3Si{-}Si}t\mathrm{Bu_3} + \mathrm{MX}$$
2 **3** **1**

1 is formed, however, by reaction of nitrosyl cations (in the form of nitrosyl tetrafluoroborate) with **2**.[2] Apparently, NO^+ acts as an oxidizing agent, which transforms $t\mathrm{Bu_3Si^-}$ into—dimerizing—tri-*tert*-butylsilyl radicals.

$$\mathbf{2}\ \mathbf{2} \xrightarrow[-2\mathrm{NO},\ -2\mathrm{M^+}]{+2\mathrm{NO^+}} 2\ \{t\mathrm{Bu_3Si^{\odot}}\} \longrightarrow \mathbf{1}$$

The colorless, crystalline compound **1**, which is readily soluble in organic media and melts at 162°C, is stable toward air and moisture. In mesitylene, it decomposes at 100°C—possibly via the free radicals $t\mathrm{Bu_3Si^{\odot}}$—with formation of tri-*tert*-butylsilane (half-life of decomposition at 100°C: 6.8 h).

$$\mathbf{1} \xrightarrow[\text{Mesitylene}]{100^{\circ}\mathrm{C},\ (+2\mathrm{H})} 2\,t\mathrm{Bu_3SiH}$$

The NMR spectra of **1** are very simple, in accordance with its symmetrical structure.[3] In the mass spectrum of **1**, no molecular ion peak is observed, as is the case for many other tri-*tert*-butylsilyl compounds.[3] The Si–Si stretching vibration in the Raman spectrum lies at comparatively small wave number ($\nu_{Si-Si} = 271\ cm^{-1}$).[3] In the UV spectrum of **3**, no absorption band appears above 200 nm.[3]

The X-ray structure determination[5] of **1** shows an unusually long Si–Si bond (269.7 pm). This distance apparently results (despite a staggered conformation) from mutual repulsion of the *tert*-butyl groups (Fig. 1). This inter-

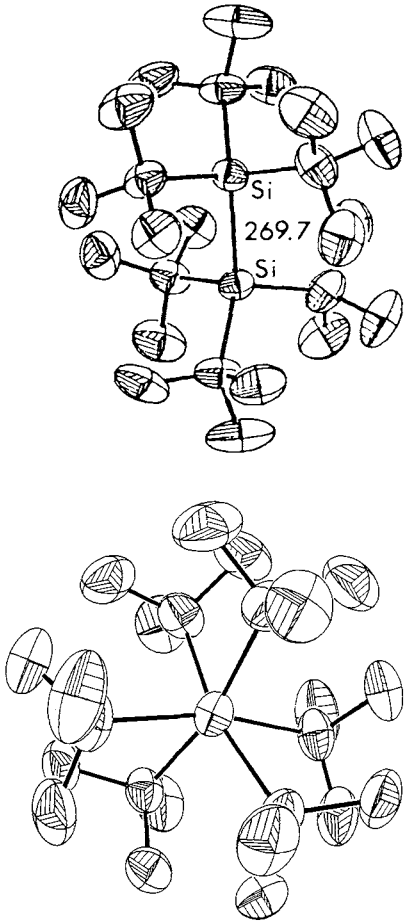


Fig. 1. Above: Stereoprojection of the crystal structure of **1**. Si–Si bond lengths [pm]. Below: Newman projection of the crystal structure of **1** along the Si–Si axis.

[*] Prof. Dr. N. Wiberg, H. Schuster
Institut für Anorganische Chemie der Universität
Meiserstrasse 1, D-8000 München 2 (FRG)
Prof. Dr. A. Simon, Dr. K. Peters
Max-Planck-Institut für Festkörperforschung
Heisenbergstrasse 1, D-7000 Stuttgart 80 (FRG)

[**] Compounds of Silicon, Part 62.—Part 61: N. Wiberg, K. Schurz, G. Fischer, *Angew. Chem. 97* (1985) 1058; *Angew. Chem. Int. Ed. Engl. 24* (1985) 1053.

pretation is supported by the significantly lengthened Si-C bonds (199 pm compared with 187 pm for the single bond) and the expanded angle at the tertiary C atoms (C-C-C between 104.2 and 106.5°, Si-C-C between 110.9 and 114.8°). The Si-Si distance in **1** corresponds to a Pauling bond order of 0.45 and, as in the case of hexa-*tert*-butylcyclotrisilane,[1] the sum of the bond orders for the Si atom in **1** (2.55) is considerably less than the expected value of four.

The variability in the distance between Si atoms is remarkable. The distance for a bonding interaction found in **1** is larger than that in fibrous SiO_2 (258 pm[6]), although the interaction in the latter case is repulsive. The extreme case of the approach of Si atoms toward one another as a consequence of their surrounding was recently found in cyclosiloxanes $(-R_2Si-O-)_2$.[7] In that case, the Si-Si distance is shorter (231 pm) than that of a Si-Si single bond.

Received: September 12, 1985;
supplemented: October 16, 1985 [Z 1461 IE]
German version: *Angew. Chem. 98* (1986) 100

[1] A. Schäfer, M. Weidenbruch, K. Peters, H. G. von Schnering, *Angew. Chem. 96* (1984) 311; *Angew. Chem. Int. Ed. Engl. 23* (1984) 302.

[2] *Experimental procedure:* Potassium (0.782 g, 20.0 mmol) and tri-*tert*-butyliodosilane (3.263 g, 10.0 mmol) [4] were allowed to react in refluxing heptane for 6 h. Nitrosyl tetrafluoroborate (0.771 g, 6.60 mmol) in 20 mL of heptane was added to the tBu_3SiK-containing reaction solution so formed after it had been cooled to −100°C. The reaction mixture was warmed to room temperature and filtered to separate the colorless precipitate (KBF_4). All volatiles were removed from the solvent at room temperature in high vacuum and the residue was dissolved in 30 mL of pentane. Colorless, crystalline **1** (0.58 g, 1.46 mmol, 44%) was obtained at −30°C.

[3] **1**: ^{1}H-NMR (C_6D_6): $\delta = 1.379$. tBu_3SiX (X = H, halogen): ^{1}H-NMR (C_6D_6): $\delta = 1.12$-1.16. **1**: ^{13}C-NMR (C_6D_6): $\delta = 27.28$ ($C(CH_3)_3$), 34.63 ($C(CH_3)_3$); ^{29}Si-NMR (C_6D_6): $\delta = 28.7$; MS (15 eV) m/z 341 ($M^+ - t$Bu, 11%), 199 (tBu_3Si^+, 15%), 115 ($tBu_3Si^+ - 2C_3H_6$, 100%). Me_3Si-$SiMe_3$: Raman: ν(Si-Si) = 404 cm^{-1}; longest wavelength UV absorption: $\lambda_{max} = 198$ nm, ε ca. 8000 (cf. E. Hengge, *Top. Curr. Chem. 51* (1974) 52).

[4] M. Weidenbruch, H. Pesel, W. Peter, R. Steichen, *J. Organomet. Chem. 141* (1977) 9.

[5] *Structure data:* Four-circle diffractometer $P2_1$, room temperature, $Mo_{K\alpha}$, graphite monochromator; 3061 observed reflections, 1742 with $F > 3\sigma(F)$; Ibca, $a = 1135.5(7)$, $b = 2944.8(13)$, $c = 1594.8(7)$ pm, $Z = 8$, $\rho_{calcd} = 0.994$ g cm^{-3}; $R = 0.063$ for anisotropic refinement of the Si and C atoms (H atoms isotropic). Further details of the structure investigation are available on request from the Fachinformationszentrum Energie, Physik, Mathematik GmbH, D-7514 Eggenstein-Leopoldshafen 2, on quoting the depository number CSD-51574, the names of the authors, and the journal citation.

[6] A. Weiss, A. Weiss, *Z. Anorg. Allg. Chem. 276* (1954) 93.

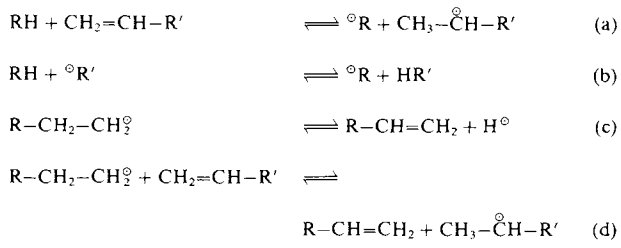
[7] M. J. Fink, K. J. Haller, R. West, J. Michl, *J. Am. Chem. Soc. 106* (1984) 822.

Metathesis of Alkyl Radicals and Alkenes—a Novel Elementary Reaction of Alkyl Radicals

By *Jürgen O. Metzger**

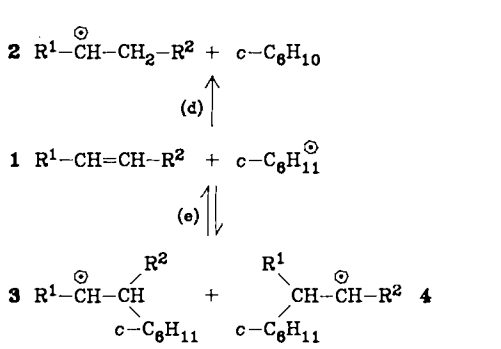
A notable gap exists in the series of known elementary reactions (a)-(c) of alkyl radicals in which a hydrogen atom is transferred: the thermochemically possible transfer (d) of a β-hydrogen atom of an alkyl radical to an alkene with the formation of a new alkyl radical and a new alkene.

The search for an example of the frequently postulated[1] reaction (d) appeared promising since corresponding reactions in analogous oxygen-containing systems are



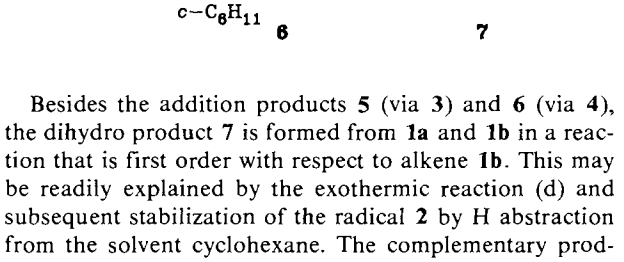
known.[2] The first experimental example of reaction (d) is reported here.

Reaction (d) should be possible to observe as a reaction competing with the addition (e) of an alkyl radical to the CC double bond of an alkene.



a, $R^1 = R^2 =$ COOMe; **b**, $R^1 =$ Ph; $R^2 =$ COOMe

As an example, the addition of cyclohexane to dimethyl fumarate **1a** and to methyl cinnamate **1b** was studied. This radical chain reaction (f) can be carried out above 250°C under mainly thermodynamic control with respect to the addition (e).[3]



(f)

Besides the addition products **5** (via **3**) and **6** (via **4**), the dihydro product **7** is formed from **1a** and **1b** in a reaction that is first order with respect to alkene **1b**. This may be readily explained by the exothermic reaction (d) and subsequent stabilization of the radical **2** by H abstraction from the solvent cyclohexane. The complementary product, cyclohexene, was identified in the reaction mixture (**7a** : cyclohexene, ca. 1.2 : 1) as the dibromo adduct.

The experimental results (Table 1) are easily understandable. The metathesis (d), as a "closed-shell" reaction, has a higher activation energy than the "open-shell" reaction (b). Accordingly, the amount of the dihydro product **7** increases relative to the amounts of addition products **5** and **6** with increasing temperature (experiments 1-5). The reaction rate of (d) is independent of the concentration of H donor in contrast to that of (b). Therefore, the relative amount of **7** increases with lower concentrations of cyclohexane; **7** can even become the main product (experiments 5-9). The addition of radical formers such as 2,3-diphenylbutane[4] increases the rate of formation of both competitive products equally (experiment 4). Activated

[*] Priv.-Doz. Dr. J. O. Metzger
Fachbereich Chemie der Universität
Postfach 2503, D-2900 Oldenburg (FRG)

Table 1. Reactions of cyclohexane with dimethyl fumarate **1a** and methyl cinnamate **1b** [a]. **5a**≡**6a**.

No.	T [°C]	[c-C_6H_{12}] [b]	Conversion **1a** [c]	[**5a**] [c]	[**7a**] [c]	**5a**/**7a**	Conversion **1b** [c]	[**5b**] [c]	[**6b**] [c]	[**7b**] [c]	Σ**5b**, **6b**/**7b**
1 [d]	250	5.76	>99	71	3.1	22.9	11	4.2	1.3	0.4	13.7
2	360	5.56	>99	78	5.3	14.7	46	22.7	8.8	8.0	3.9
3	390	5.13	>99	75.6	6.4	11.8	25 [e]	9.5	3.8	4.7	2.8
4	390	5.13	—	—	—	—	56 [e, f]	18.9	7.7	9.5	2.8
5	400	5.00	>99	70.1	6.2	11.3	55	20.7	8.3	11.4	2.5
6	400	3.65	>99	65.5	7.1	9.2	44	14.6	5.9	9.5	2.2
7	400	2.44	97	62.9	7.6	8.3	30	8.2	3.4	6.8	1.7
8	400	0.90	79	40.7	9.1	4.5	10	1.7	0.7	2.3	1.0
9	400	0.40	49	14.1	7.7	1.8	4	0.4	0.2	0.9	0.7

[a] With the exception of No. 1, the reactions were carried out in a high-pressure, high-temperature flow reactor [3,7] in a stainless steel capillary; reaction time 2–3 min; molar ratio cyclohexane : **1** = 1000 : 1. The concentration of cyclohexane was adjusted by variation of the pressure. The addition products are stable under the reaction conditions. Under the same conditions at 400°C, less than 1% of **5b** decomposes to **7b**. [b] mol/L. [c] Yields and conversion in mol-% based on unreacted **1**. [d] Reaction in duran glass ampules; reaction time 10 min. Upon addition of activated charcoal (1 mg/mL reaction solution) as radical trap, only traces of the products were formed. [e] Reaction time 1 min. [f] Addition of 10 mol-% 2,3-diphenylbutane based on **1b**.

charcoal as a radical trap inhibits the formation of both products (experiment 1). The kinetic chain length is estimated to be 100 from the amount of chain-terminating product cyclohexylcyclohexane (ca. 1 mol-% based on reacted starting material **1a**).

Alternative explanations for the formation of the dihydro product **7**, such as the frequently postulated pericyclic H transfer[5] or the symproportionation of alkene and alkane to give two alkyl radicals (a),[3,6] are clearly ruled out on the basis of the experimentally confirmed radical chain reaction. A conceivable β-cleavage of the cyclohexyl radical (c) and addition of the H atom to the alkene **1** would be a reaction of zero order with respect to **1** and thus is also ruled out.

The unequivocal experimental proof of the metathesis of alkyl radicals and alkenes (d) and the reaction conditions required for it to occur show that chain transfer during polymerization[1a] via this reaction, which has been frequently postulated, is unlikely. A thermal pericyclic hydrogenation of alkenes with alkanes[5] is also kinetically unlikely.

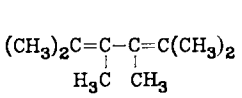
Received: July 18, 1985;
revised: October 7, 1985 [Z 1395 IE]
German version: *Angew. Chem. 98* (1986) 79

[1] a) P. Ehrlich, G. A. Mortimer, *Adv. Polym. Sci. 7* (1970) 386; b) H. F. Kauffmann, H. Harms, O. F. Olaj, *J. Polym. Sci. Polym. Chem. Ed. 20* (1982) 2943.
[2] H. D. Becker in S. Patai (Ed.): *The Chemistry of the Hydroxyl Group*, Interscience, London 1971, p. 835.
[3] J. O. Metzger, *Angew. Chem. 95* (1983) 914; *Angew. Chem. Int. Ed. Engl. 22* (1983) 889; *Angew. Chem. Suppl. 1983*, 1256.
[4] C. Rüchardt, H.-D. Beckhaus, *Angew. Chem. 92* (1980) 417; *Angew. Chem. Int. Ed. Engl. 19* (1980) 429.
[5] D. F. Feller, M. W. Schmidt, K. Ruedenberg, *J. Am. Chem. Soc. 104* (1982) 960.
[6] A. Heesing, W. Müllers, *Chem. Ber. 113* (1980) 24.
[7] P. Köll, J. Metzger, *Angew. Chem. 90* (1978) 802; *Angew. Chem. Int. Ed. Engl. 17* (1978) 754.

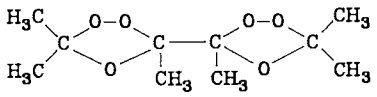
A Stable Diozonide of a Conjugated Diene by Ozonolysis of 2,3,4,5-Tetramethyl-2,4-hexadiene on Polyethylene

By *Karl Griesbaum** and *Willi Volpp*

Stable diozonides of conjugated dienes were hitherto unknown. Admittedly, the diozonides of 2,3-dimethyl-1,3-butadiene and of isoprene could be obtained by ozonolysis of the respective dienes in pentane, but they exploded violently upon attempted isolation.[1] Since ozonides are known to be stabilized by methyl substituents, ozonolysis of **1** in pentane was also attempted, but no ozonide was obtained.[2] This is concordant with the experience that tetrasubstituted olefins do not furnish the corresponding ozonides.[3] We have recently found, however, that ozonolysis of olefins adsorbed on polyethylene may provide ozonides from olefins for which other methods of ozonation fail.[4]



1



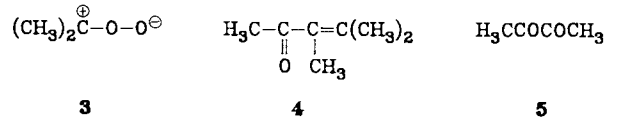
2

Ozonolysis of **1** on powdered polyethylene at −75°C and subsequent chromatographic separation of the crude product (water-cooled column 3 × 62 cm, 200 g of silica gel; *n*-pentane/diethyl ether 20 : 1, ca. 14 mL/min) afforded a mixture of two ozonides of structure **2**, probably the *meso*- and *rac*-isomers, in ca. 43% yield. They could be isolated by HPLC separation (column 3.2 × 12 cm, Lichrosorb Si 60, particle size 5 μm; *n*-pentane/diethyl ether 20 : 1, ca. 7.5 mL/min), albeit not yet assigned stereochemically. Each of the isomers gave a positive peroxide test, correct values for the elemental analysis, a $(M+1)^{\oplus}$ ion at *m/z* 235 in the CI/MS analysis, two quartets ($\delta = 1.30$, 1.43, $J = 0.64$ Hz, and $\delta = 1.30$, 1.40, $J = 0.61$ Hz, respectively) and a singlet ($\delta = 1.52$, each) with relative intensities of 1 : 1 : 1 in the ^{1}H-NMR spectrum (C_6D_6, TMS), three quartets ($\delta = 20.16$, 23.12, 24.94 and $\delta = 20.13$, 23.41, 24.93, respectively) and two singlets ($\delta = 108.98$, 109.60 and $\delta = 108.88$, 109.76, respectively) in the ^{13}C-NMR spectrum ($CDCl_3$, TMS), and no carbonyl absorption in the IR spectrum. The two isomers show significant differences in their melting points (51°C and < −60°C, respectively). At −20°C each ozonide was stable for months, whereas at room temperature decomposition was observed to take place after a few hours. Reduction of a mixture of the isomers of structure **2** with $LiAlH_4$ gave a mixture of *meso*- and *rac*-2,3-butanediol as well as 2-propanol; **2** reacts with triphenylphosphane to give a mixture of acetone, biacetyl **5**, and acetic anhydride.

It is known that **1** is cleaved by ozone to give **3**, **4**, and **5**.[2,5] Consistent with the finding that carbonyl oxides do not undergo cycloadditions with non-activated ketones,[3]

[*] Prof. Dr. K. Griesbaum, Dipl.-Chem. W. Volpp
Engler-Bunte-Institut, Bereich Petrochemie der Universität
Kaiserstrasse 12, D-7500 Karlsruhe (FRG)

 © VCH Verlagsgesellschaft mbH, D-6940 Weinheim, 1986 0570-0833/86/0101-0081 $ 02.50/0



3 **4** **5**

carbonyl oxide **3** reacted with itself in pentane to give dimers, trimers, and oligomers.[2] By contrast, in the ozonolysis of **1** on polyethylene, the primary fragments **3**, **4**, and **5** apparently remained fixed at their places of origin, so that **3** could not react with itself and thus was indirectly forced to undergo cycloadditions with the keto groups in **4** and/or **5**.

Received: September 25, 1985 [Z 1469 IE]
German version: *Angew. Chem. 98* (1986) 108

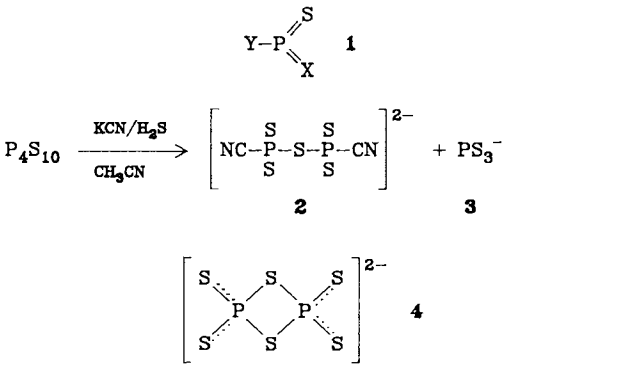
[1] K. Griesbaum, H. Keul, G. Zwick, unpublished results.
[2] K. Griesbaum, G. Zwick, *Chem. Ber. 118* (1985) 3041.
[3] P. S. Bailey: *Ozonation in Organic Chemistry, Vol. 1*, Academic Press, New York 1978, p. 25 ff.
[4] K. Griesbaum, W. Volpp, R. Greinert, *J. Am. Chem. Soc. 107* (1985) 5309.
[5] K. Griesbaum, G. Zwick, *Chem. Ber.*, in press.

Trithiometaphosphate PS_3^-—an Anion with Phosphorus of Coordination Number 3**

By *Herbert W. Roesky,* Reinhart Ahlrichs,** and *Stefan Brode*

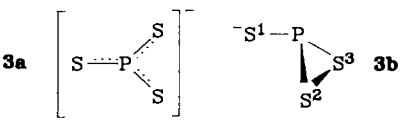
Dedicated to Professor Fritz Seel on the occasion of his 70th birthday

A number of sulfur-containing phosphoranes **1** in which phosphorus has coordination number 3 have been reported in recent years.[1-3] X can be O, S, NR, or CR_2 and Y either NR_2 or aryl. We report here the reaction of P_4S_{10} with KCN and H_2S, which affords the trithiometaphosphate anion PS_3^- **3** in addition to the known $[(CNPS_2)_2S]^{2-}$ **2**.[4] **3** was isolated as the tetraphenylarsonium salt.[5] The reaction, the mechanistic details of which are not yet known, is very surprising since alkali metals react with sulfur and phosphorus at 750 °C to give only the dimeric anion **4**.[6] We assume that the large cation kinetically inhibits the formation of the dimer. Monomeric metaphosphate PO_3^- has only been identified in the gas phase or in solution.[7] Recently, a tris(methylene)phosphate ion of type $[P(=C<)_3]^-$ was reported.[8]



The tetraphenylarsonium salt of **3** was obtained from methanol as yellow crystals (m.p. = 183 °C) and its composition confirmed by elemental analysis and field-desorption mass spectroscopy. Thus, the peak for the Ph_4S^+ ion is observed at *m/z* 383 (+FD) and that for the PS_3^- ion at *m/z* 127 (−FD). Ions with larger or smaller mass numbers were not detected. This result rules out the presence of a dimeric or polymeric anion. In the ^{31}P-NMR spectrum (acetone/C_6D_6) a signal is observed at $\delta = 52.3$ (85% H_3PO_4 ext.), in the region where signals for diiminophosphoranes (phosphorus with coordination number 3) are normally found ($\delta = 45$–55).[9]

As shown by X-ray structure analysis, $[Ph_4As][PS_3]$ forms monoclinic crystals in the space group C2 with the cell parameters $a = 18.944(4)$, $b = 7.101(1)$, $c = 13.393(2)$, and $\beta = 134.67(1)$. The thermal motion of the anion prevented a refinement of the structure. Nevertheless, these results indicate a pyramidal structure and, therefore, the dimeric $[P_2S_6]^{2-}$ as well as the linear structure $[SPSS]^-$ can be ruled out.[9, 10] Thus, only structures **3a** and **3b** need be considered.



3a **3b**

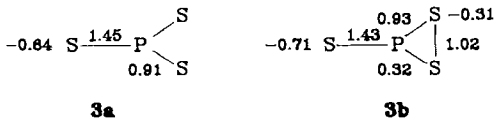
Since $[AsPh_4]^+$ is a relatively large cation and, therefore, electrostatic interactions should not have a large effect on PS_3^-, it appeared reasonable to carry out ab initio calculations for the free PS_3^- ion in order to determine the structures and relative energies of **3a** and **3b**. Molecular orbital (MO) calculations using the self-consistent field (SCF) method[11] gave the following structural parameters: **3a**: symmetry D_{3h}, P-S 196 pm; **3b**: symmetry C_s, $P\text{-}S^1$ 199 pm, $P\text{-}S^2$ 221 pm, $S^2\text{-}S^3$ 212 pm, $S^1\text{-}P\text{-}S^2 = 112°$. Experience has shown[12] that the interatomic distances are generally underestimated by only a few pm at this level of calculation. Furthermore, the $[SPSS]^-$ chain and the planar ring with C_{2v} symmetry were included in the calculations. Upon optimization of geometry, the chain gives the structure **3b**, and the ring has a very high energy for reasonable distances (dissociation into $[SPS]^-$ and S).

In order to determine the relative energies of **3a** and **3b**, configuration interaction calculations (CI) were carried out using the CPF method,[13] a more flexible basis set[14] being used. **3a** was found to be more stable than **3b**: SCF: $\Delta E = E(\mathbf{3a}) - E(\mathbf{3b}) = 141$ kJ/mol; CPF: $\Delta E = 122$ kJ/mol. The CPF result is probably more accurate and should have an error of 20–30 kJ/mol.

In order to visualize the electronic structure, a population analysis of the SCF wave functions was carried out. The method used[15, 16] characterizes the bonding relationships by net atomic charges for the atoms (Q_A) and by "shared electron numbers" (SEN) assigned to the bonds. The SEN gives the number of electrons that can be equally assigned to the two atoms involved in bonding; it is a reliable indication of the strength of a covalent bond.[15] The results are shown in Scheme 1. In order to better understand the SEN, it should be noted that for strongly covalent single bonds (C-H, C-C, H-H) SEN is about 1.4 and for polar single bonds 1.0 (for HF).

[*] Prof. Dr. H. W. Roesky
Institut für Anorganische Chemie der Universität
Tammannstrasse 4, D-3400 Göttingen (FRG)
Prof. Dr. R. Ahlrichs, Dipl.-Chem. S. Brode
Institut für Physikalische Chemie und Elektrochemie
(Lehrstuhl für Theoretische Chemie) der Universität
Kaiserstrasse 12, D-7500 Karlsruhe (FRG)

[**] This work was supported by the Deutsche Forschungsgemeinschaft and the Fonds der Chemischen Industrie. We thank the Rechenzentrum der Universität Karlsruhe for excellent service. We thank Dr. *M. Noltemeyer* and Prof. *G. M. Sheldrick* for the structure investigation.



Scheme 1.

In Figure 1 the SCF orbital energies ε of the high-energy MOs of **3a** are given (the relationships for **3b** are simple and are discussed in the text) and the corresponding MOs are characterized.

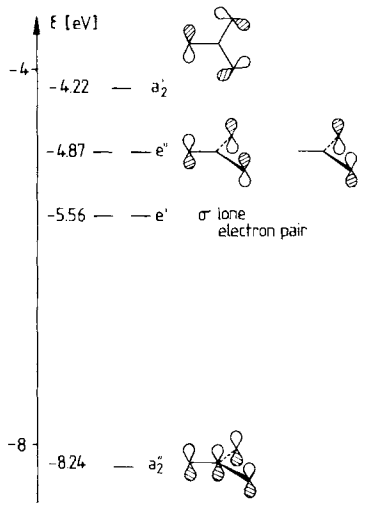


Fig. 1. Schematic representation of the energetically high-lying MOs for PS_3^- (structure **3a** with D_{3h} symmetry).

In addition to the three PS σ bonds present in both **3a** and **3b**, a 6-electron 4-center π system (MOs a_2'' and e'') is present in **3a** and an SS bond in **3b**. The sums of the covalent bond strengths are similar for the two structures. The sum of the SEN is 4.35 for **3a** and 4.31 for **3b**. The π system in **3a** is most stable for the planar structure. The energy required to achieve planarity is difficult to estimate but should not be large. In PCl_3, the ClPCl angle is already 100.3°; the larger coulombic repulsion of the ligands in PS_3^- should lead to an even larger angle.

Decisive for the relative stability of **3a** and **3b** are the charge distributions, which, in each case, are a consequence of the electronic structure. In **3b**, the negative charge, as expected, is localized primarily on S^1. A weak charge delocalization is achieved by $3p_\pi(S^1)$-$3d_\pi(P)$ back-bonding, which strengthens the PS^1 bond. This is reflected in the SEN of 1.43 (compared with $SEN(PS^2)=0.93$) and in the relatively short PS^1 distance of 199 pm. The SS bond in **3b** is relatively weak (SEN = 1.02) owing to the charge on the S atoms ($Q_S=-0.31$). The localization of the charge on S^1, which is not stabilized by the proximity of a highly positively charged P atom, as in **3a**, is reflected above all in the orbital energies of the highest MOs in **3b**, which correspond to the lone electron pairs on S^1: $\varepsilon(a')=-3.6$ eV, $\varepsilon(a'')=-3.7$ eV. These orbitals are considerably higher in energy than the MOs in **3a** (Fig. 1), which is crucial for the instability of **3b**.

The charge distribution in **3a** is determined by the π system. Only the bonding a_2'' MO has $3p_\pi(P)$ contributions; in contrast, the e'' MOs do not have such contributions (Fig. 1). Consequently, the net result is a transfer of ca. one π-electron from P to the ligands S—in agreement with the population analysis ($Q(P)=+0.91$). The positive charge on the P atom favors stabilizing $3d_\pi(P)$ contributions to e'' so that those MOs are weakly bonding. A simple Hückel MO calculation gives the bonding a_2'' π MO a π bond order of $3^{-1/2}=0.58$. The partial double bond character of the PS bond in **3a** is clearly reflected in the $SEN(PS)=1.45$ (compared with $SEN(PS^2)=0.93$ in **3b**) and in the short PS distance (196 pm).

The calculations show that PS_3^- has a planar structure with D_{3h} symmetry in the gas phase. However, the molecule is not very rigid; shifting the P atom 16 pm out of the plane increases the energy only 10 kJ/mol. Therefore, a pyramidal structure cannot be ruled out in the solid state.

Received: July 1, 1985;
supplemented: October 25, 1985 [Z 1371 IE]
German version: *Angew. Chem. 98* (1986) 91

[1] E. Niecke, D.-A. Wildbredt, *J. Chem. Soc. Chem. Commun. 1981*, 72; E. Niecke, A. Seyer, D.-A. Wildbredt, *Angew. Chem. 93* (1981) 687; *Angew. Chem. Int. Ed. Engl. 20* (1981) 675.

[2] R. Appel, F. Knoch, H. Kunze, *Angew. Chem. 95* (1983) 1008; *Angew. Chem. Int. Ed. Engl. 22* (1983) 1004.

[3] L. N. Markovski, V. D. Romanenko, A. V. Ruban, A. B. Drapilo, *J. Chem. Soc. Chem. Commun. 1984*, 1692.

[4] H. W. Roesky, F. N. Tebbe, E. L. Muetterties, *Inorg. Chem. 9* (1970) 832.

[5] *Experimental procedure:* P_4S_{10} (22.2 g, 0.05 mol) and KCN (32.5 g, 0.5 mol) were stirred in 250 mL of CH_3CN at room temperature. The solution warmed up to ca. 50°C. As soon as it had cooled down to room temperature, H_2S (excess) was admitted over 3 h. The reaction mixture was then filtered and the volatile products were removed from the filtrate in vacuum. The solid residue was dissolved in 100 mL of H_2O, which did not result in warming of the solution. A solution containing 30 g of nPr_4NBr in 150 mL of H_2O was added to this solution. A yellow precipitate forms (30 g), 15 g of which redissolves in 150 mL of CH_3OH upon suspension. The remaining solid, which can be recrystallized from CH_3CN/CH_3OH (5:1) is $[nPr_4N]_2[(NCPS_2)_2S]$. The methanol solution was concentrated in a hood, affording a viscous oil. This was dissolved in 50 mL of CH_3OH by warming and then treated with a solution of Ph_4AsCl (excess) in CH_3OH. Careful concentration at room temperature afforded yellow crystals of $[Ph_4As][PS_3]$ (yield: 3 g).

[6] W. Brockner, R. Becker, B. Eisenmann, H. Schäfer, *Z. Anorg. Allg. Chem. 520* (1985) 51.

[7] M. Henchman, A. A. Viggiano, J. F. Paulsen, A. Freedman, J. Wormhoudt, *J. Am. Chem. Soc. 107* (1985) 1453; Review: F. H. Westheimer, *Chem. Rev. 81* (1981) 313.

[8] R. Appel, F. Gaitzsch, F. Knoch, *Angew. Chem. 97* (1985) 574; *Angew. Chem. Int. Ed. Engl. 24* (1985) 589.

[9] E. Niecke, D.-A. Wildbredt, *Chem. Ber. 113* (1980) 1549.

[10] IR (nujol): $\nu=1565$ s, 1180 m, 1160 m, 1068 s, 1030 m, 1016 m, 988 s, 730 vs, 687 vs, 680 vs, 615 s, 604 s, 464 vs, 445 vs, 345 vs, 335 vs cm^{-1}.—Raman: $\nu=242$ s, 486 s, 614 w, 670 s, 884 s, 1000 vs, 1028 m, 1088 m, 1182 m, 1502 m, 1582 s, 1634 m, 1756 w. Assigned with the assumption of D_{3h} symmetry: 242 ν_4 (E'), 486 ν_1 (A_1'), 614 ν_2 (A_2''), 670 ν_3 (E') [see: J. Weidlein, U. Müller, K. Dehnicke: *Schwingungsspektroskopie*, Thieme, Stuttgart 1982]; *R. Becker* und *W. Brockner* (*Z. Naturforsch. A 39* (1984) 1120) assume the presence of a PS_3^- ion in the melt at 550°C on the basis of vibrational spectroscopy.

[11] Double zeta basis set, extended to include 3d functions (for P and S): 11s, 7p, 1d contracted to (6s, 4p, 1d).

[12] P. Pulay, A. Fogarasi, F. Rang, J. E. Boggs, *J. Am. Chem. Soc. 101* (1979) 2550.

[13] The Coupled Pair Functional (CPF) method accounts exactly for single and double excitations with respect to the SCF wave function and approximates effects of higher excitations: R. Ahlrichs, P. Scharf, C. Ehrhardt, *J. Chem. Phys. 82* (1985) 890.

[14] As [11] but two sets of 3d functions were used in each case. Furthermore, a diffuse p set was included for sulfur.

[15] R. Ahlrichs, C. Ehrhardt, *Chem. Unserer Zeit 19* (1985) 120; C. Ehrhardt, R. Ahlrichs, *Theor. Chim. Acta 68* (1985) 231, and literature cited therein.

[16] The calculations were carried out with the KARLSRUHE program system; R. Ahlrichs, H.-J. Böhm, C. Ehrhardt, P. Scharf, H. Schiffer, H. Lischka, M. Schindler, *J. Comput. Chem. 6* (1985) 200. The calculations of CI type include up to 262000 configurations exactly; a further 10^9 were approximately considered in the CPF method.

The Polymeric Silver Complexes $[Ag\{S_n(CN)_2\}_2][AsF_6]$ (n = 3, 4): Stable Coordination Compounds of Dicyanotri- and Dicyanotetrasulfanes

By *Herbert W. Roesky,* Thomas Gries, Jürgen Schimkowiak,* and *Peter G. Jones*

Dedicated to Professor Max Schmidt on the occasion of his 60th birthday

The behavior of cyanosulfanes toward metals and metal ions is unknown. However, reactions such as the synthesis of a 1,2,4-thiadiazole from cyanogen and sulfur, which takes place only in the presence of copper metal, demonstrate the influence of metal centers.[1] Dicyanotrisulfane **1**, first prepared in 1885 by *Schneider*,[2] and dicyanotetrasulfane **2**[3] are unstable compounds, which tend to undergo polymerization in air; **2**, in particular, decomposes at room temperature within a few minutes, forming orange triazines.[4] We recently found that in the reaction of **1** with hexafluoroacetone the S–S bonds remain intact.[5] Although metal complexes of the cyanosulfanes were unknown up to now, both cyanogen and organic disulfanes form stable compounds with silver hexafluoroarsenate **3**.[6, 7]

The reactions of **1** and **2** with $AgAsF_6$ in liquid sulfur dioxide lead, without decomposition, to the silver complexes **4**[8] and **5**,[9] which we have been able to isolate as light yellow and orange-yellow crystals, respectively.

$$2\,S_n(CN)_2 + Ag[AsF_6] \xrightarrow{SO_2} [Ag\{S_n(CN)_2\}_2][AsF_6]$$

1, n = 3 **3** **4**, n = 3
2, n = 4 **5**, n = 4

According to single-crystal X-ray analyses and vibrational spectra,[10] **4** and **5** contain intact polysulfane chains. The dicyanosulfanes **1** and **2** serve in these complexes as bridging ligands and undergo coordination through their terminal nitrogen atoms. **4** is a chain polymer (Fig. 1), **5** a layer polymer (Fig. 2).

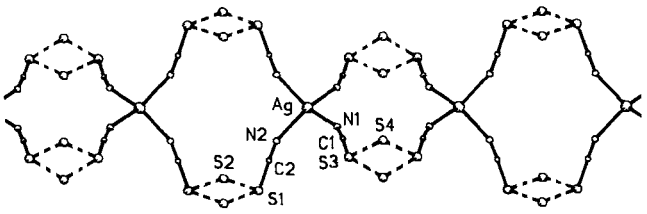


Fig. 1. Crystal structure of the polymeric cation (chain polymer) of **4**. Space group $P4_2/mnm$, $a = b = 1051.0(5)$, $c = 1527.0(2)$ pm, $Z = 4$. $R = 0.049$ for 691 absorption-corrected reflections with $F > 4\sigma(F)$ and $2\theta_{max} = 50°$ ($Mo_{K\alpha}$). Ag lies on the special position x, $1-x$, 0 (symmetry mm 2, As on 1/2, 0, 3/4 ($\bar{4}$), S1, S4, N2, and C2 on x, x, z (m), S2 on x, $1-x$, z (m), N1 and C1 on x, y, 1/2 (m). The S2 and S4 positions are half-occupied, indicating twofold disorder of these atoms (broken bonds indicate the alternative positions). S3 also is disordered (alternative half-occupied positions on both sides of the mirror plane x, y, 0). For clarity, only the idealized position of S3 is shown. The ligands **1** each bridge two silver atoms, the coordination geometry of which is a slightly compressed tetrahedron; the silver atom are "end-on" coordinated to nitrogen atoms of four ligands **1**. Bond lengths [pm] and angles [°]: Ag-N1 227.4(11), Ag-N2 230.1(10), S1-S2 199.7(6), S3-S4 207.4(5), C1-N1 113.6(14), C1-S3 170.8(11), C2-S1 169.6(11), C2-N2 112.4(14); N1-Ag-N1′ 105.1(5), N1-Ag-N2 112.4(3), N2-Ag-N2′ 102.5(5), C1-N1-Ag 156.7(9), C2-N2-Ag 159.2(9), S3-S4-S3′ 101.0(4), S1-S2-S1′ 109.7(2), S4-S3-C1 96.4, C2-S1-S2 104.3(4), N1-C1-S3 168.9(5), S1-C2-N2 178.5(10) [14].

[*] Prof. Dr. H. W. Roesky, Dipl.-Chem. T. Gries, J. Schimkowiak, Priv.-Doz. Dr. P. G. Jones
Institut für Anorganische Chemie der Universität
Tammannstrasse 4, D-3400 Göttingen (FRG)

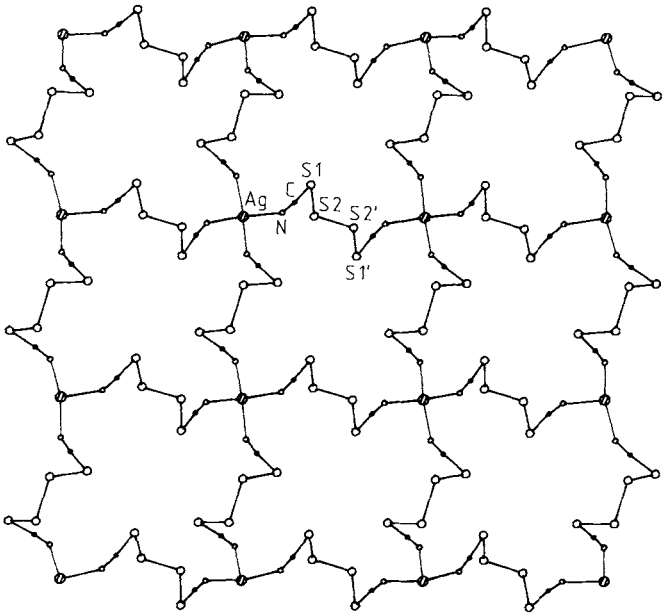


Fig. 2. Crystal structure of the polymeric cation (layer polymer) of **5** (projection along z; Ag atoms hatched). Space group $P\bar{4}$, $a = b = 838.1(2)$, $c = 666.1(2)$ pm, $Z = 1$. $R = 0.037$ for 822 absorption-corrected reflections with $2\theta_{max} = 55°$ ($Mo_{K\alpha}$). Absolute structure [12] by η refinement [13]; $\eta = +1.06(6)$. The silver atoms lie on the special positions 0, 0, 0, the arsenic atoms on 1/2, 1/2, 0 (symmetry $\bar{4}$). The silver atoms are coordinated to one terminal nitrogen atom of each of four molecules of **2**, resulting in a slightly compressed tetrahedral geometry. By linking of the second ligand nitrogen atom with a further silver atom, an undulating, two-dimensional layer polymer is formed. Bond lengths [pm] and angles [°]: Ag-N 228.8(7), S1-S2 206.1(4), S2-S2′ 200.3(4), C-S1 169.5(8), C-N 113.2(10), C-S1-S2 98.5(3), S1-S2-S2′ 105.6(2), S1-C-N 175.2(7), Ag-N-C 152.5(6). Torsion angles of the ligands: C-S1-S2-S2′ 104°, S1-S2-S2′-S1′ −85° [14].

Since the S_3 structural units are disordered in **4**, their structure can be discussed only with some reservations. In complex **4**, dicyanotrisulfane is in the *cis* conformation, as in the free species.[11] The C–N distances are strikingly short in **4** and **5**: 113.0 pm in **4** and 113.2 pm in **5**, compared with 121 pm in **1** (average values). The same is true for the S–S distances (206.1 and 200.3 pm in **5**, compared with 212 pm in **1**). The similar Ag–N distances in **4** and **5** (average value: 228 pm) are 10 pm shorter than in the dicyano complex.[6]

Complexes **4** and **5** are stable up to 25 °C, but decompose upon exposure to moisture or light. Upon melting, they afford clear liquids, which polymerize at 125 (**4**) and 110 °C (**5**) with evolution of gas.

Received: September 10, 1985;
revised: October 21, 1985 [Z 1458 IE]
German version: *Angew. Chem. 98* (1986) 93

[1] H. W. Roesky, K. Keller, J. W. Bats, *Angew. Chem. 95* (1983) 904; *Angew. Chem. Int. Ed. Engl. 22* (1983) 1029; *Angew. Chem. Suppl. 1983*, 1323.
[2] R. Schneider, *J. Prakt. Chem. 32* (1885) 187.
[3] H. Lecher, A. Goebel, *Ber. Dtsch. Chem. Ges. 55* (1922) 1483. It was possible to stabilize **2** by complex formation for the first time and to determine its crystal structure by X-ray analysis.
[4] *Gmelin Handbuch der anorganischen Chemie, Kohlenstoff, Teil D 5*, Springer, Berlin 1977, p. 233.
[5] H. W. Roesky, N. K. Homsy, H. G. Schmidt, *Z. Anorg. Allg. Chem.*, in press.
[6] H. W. Roesky, H. Hofmann, J. Schimkowiak, P. G. Jones, K. Meyer-Bäse, G. M. Sheldrick, *Angew. Chem. 97* (1985) 403; *Angew. Chem. Int. Ed. Engl. 24* (1985) 417.
[7] H. W. Roesky, T. Gries, P. G. Jones, K. L. Weber, G. M. Sheldrick, *J. Chem. Soc. Dalton Trans. 1984*, 1781.

[8] SO_2 (20 mL) was condensed at −190°C into a pressure flask containing 1.0 g (6.8 mmol) of **1** and 1.0 g (3.4 mmol) of **3**. The colorless solution was allowed to warm up in the dark to room temperature and stirred for 18 h. The moderately soluble precipitate that formed was filtered off and the solvent was removed from the filtrate in vacuum. The residue was recrystallized from SO_2, affording 1.6 g (79%) of **4** as pale yellow crystals, m.p. = 115°C (decomposition at 125°C).—IR (nujol): ν = 2175, 700, 575, 498, 464, and 395 cm^{-1}.—Raman: ν = 2175, 683, 658, 498, 460, 430, and 206 cm^{-1}.

[9] Freshly prepared **2** (1.56 g, 8.7 mmol), which had been dried in a vacuum at −30°C, was heated rapidly to the melting point (−3°C) and then added under a stream of nitrogen to **3** (1.29 g, 4.3 mmol) in a pressure flask at −190°C. In the evacuated flask, 20 mL of SO_2 was condensed and the stirred solution was then slowly warmed in a cold bath (−50°C) in the dark over 4 h to room temperature. After two hours of stirring, the sparingly soluble solid was filtered off and the solvent removed from the filtrate. Orange crystals of **5** were obtained by recrystallizing the residue from SO_2. Yield: 1.9 g (67%), m.p. = 92°C (decomposition at 110°C).—IR (nujol): ν = 2165, 705, 692, 685, 465, and 395 cm^{-1}.—Raman: ν = 2165, 678, 506, 438, 420, 401, 223, 189, 180, 127, 93, and 78 cm^{-1}.

[10] The Raman- and IR-active ν(C≡N) vibrations are shifted by 19 (**4**) and 13 (**5**) cm^{-1}, respectively, to shorter wavelengths by complexation. ν(C-S), ν(S-S), δ(C-S-S), and δ(S-S-S) frequencies are also shifted; the number of bands, however, remains the same, thereby confirming that no sulfur-sulfur bonds are broken.

[11] The crystal structure of **1** could only be imprecisely determined by X-ray diffraction at −20°C (R = 0.25), while that of **2** is unknown. Cf. F. Fehér, K. H. Linke, *Z. Anorg. Allg. Chem. 327* (1964) 151; O. Foss, *Acta Chem. Scand. 10* (1956) 136.

[12] P. G. Jones, *Acta Crystallogr. A 40* (1984) 660.

[13] D. Rogers, *Acta Crystallogr. A 37* (1981) 734.

[14] Further details of the crystal structure investigations are available on request from the Fachinformationszentrum Energie, Physik, Mathematik GmbH, D-7514 Eggenstein-Leopoldshafen 2, on quoting the depository number CSD-51607, the names of the authors, and the journal citation.

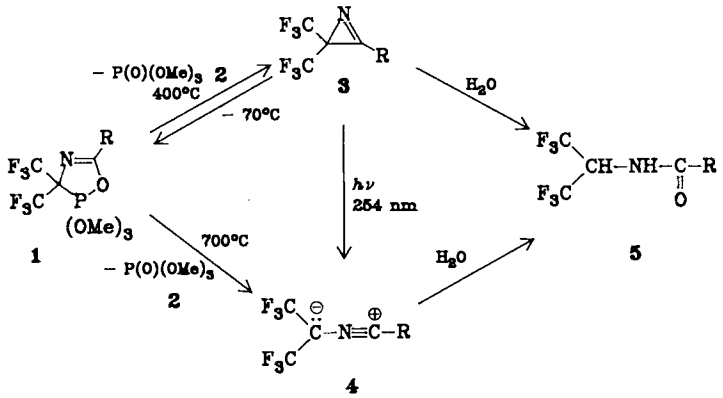
Nitrile Ylides and Azirines: Gas-Phase Generation from 2,3-Dihydro-1,4,2λ⁵-oxazaphospholes and Matrix Isolation**

By *Curt Wentrup,* Stephan Fischer, Hans-Michael Berstermann, Martin Kuzaj, Holger Lüerssen,* and *Klaus Burger*

Nitrile ylides are among the most important nitrilium betaines.[1,2] Although nitrile ylides have been directly observed, mostly by UV spectroscopy following photochemical generation from 2*H*-azirines,[2] and a single example of a stable nitrile ylide has been reported,[3] there has been no direct observation of thermally generated nitrile ylides. We now wish to report the first such example.

Flash vacuum pyrolysis of 5-*tert*-butyl-3,3-bis(trifluoromethyl)-2,3-dihydro-1,4,2λ⁵-oxazaphosphole **1a**[4] at 400°C/10^{-3} torr with isolation of the products on a KBr window at −196°C for IR spectroscopy resulted in the quantitative formation of trimethyl phosphate **2** and a new species characterized by a triplet at ν = 1740 (m), 1715 (s), and 1695 (m) cm^{-1}. On warming the window to −70°C, this species reacted with the phosphate **2** to regenerate the starting material, as seen by the simultaneous disappearance of the triplet and the appearance of a new band at 1620 cm^{-1} (characteristic of **1a**). After warming to room temperature and opening the apparatus, the sample remaining on the window was identified as pure **1a**.

In similar experiments, in which the pyrolysis products were isolated in a cold trap at −196°C, it was possible to distill the new compound into a second cold trap in high vacuum, thus freeing it from **2** and preventing the regeneration of **1a**. The sample thus obtained showed a ^{19}F-NMR signal at δ = 73.07 as expected for a bis(trifluoromethyl)azirine;[5] it was extremely sensitive to moisture and hydrolyzed to the amide **5a** simply on exposing the apparatus to the atmosphere. On the basis of the spectroscopic and chemical properties, the new compound is identified as the azirine **3a**. Hydrolysis with cleavage of the C-C bond (**3a** → **5a**) is normal for bis(trifluoromethyl)azirines.[5a]



a, R = $C(CH_3)_3$; **b**, R = C_6H_5

When the pyrolysis of **1a** was carried out at 700-860°C and the products examined by IR spectroscopy at −196°C, the azirine **3a** was no longer observed; instead, a species absorbing strongly at ν = 2250 cm^{-1} had appeared. This species, too, was sensitive to moisture and hydrolyzed on warming up (−90 to −50°C) to give the same product (**5a**), as seen by the disappearance of the band at ν = 2250 cm^{-1} simultaneous with the appearance of a band at ν = 1680 cm^{-1} (characteristic of **5a**). The ^{1}H-NMR spectrum of the isolated product established its identity as **5a**, formed in virtually quantitative yield.[6]

On the basis of the IR spectrum and the reactivity we identify the high temperature species as the nitrile ylide **4a**. The asymmetric stretching vibration at ν = 2250 cm^{-1} is similar to that reported for the only nitrile ylide isolated so far.[3] Further bands belonging to **4a** appear at ν = 1460 (m), 1365 (m), 1345 (m), 1280 (s), 1250 (m), 1225 (m), 1215 (m), 1180 (vs), 1095 (s), 995 (vs), 890 (m), 770 (m) cm^{-1}. Trapping reactions of thermally generated **4a** in solution have been described previously.[4]

Further proof for the identity of the nitrile ylide **4a** is given by its photochemical formation from the matrix-isolated azirine **3a**. The azirine was generated at 400°C and isolated in argon on a BaF_2 window at 11 K. Subsequent irradiation with a low-pressure Hg lamp (λ = 254 nm) resulted in the slow disappearance of the azirine triplet concomitant with the appearance of the bands due to the nitrile ylide **4a**.[6]

The corresponding 5-phenyloxazaphosphole **1b** reacted similarly to give the azirine **3b** (IR: ν = 1730, 1690 cm^{-1}; ^{19}F-NMR: δ = 72.88), which reverted quantitatively to **1b** on warming up and reacted with water to give **5b**. In this

[*] Prof. Dr. C. Wentrup [+], Dipl.-Chem. S. Fischer, Dipl.-Chem. H.-M. Berstermann, Dipl.-Chem. M. Kuzaj, Dipl.-Chem. H. Lüerssen
Fachbereich Chemie der Universität
Hans-Meerwein-Strasse, D-3550 Marburg (FRG)
Prof. Dr. K. Burger
Institut für Organische Chemie der Technischen Universität München
D-8046 Garching (FRG)

[+] New address: Department of Chemistry, University of Queensland St. Lucia, Brisbane, Qld. (Australia) 4067

[**] This work was supported by the Deutsche Forschungsgemeinschaft, the Fonds der Chemischen Industrie, and the University of Queensland.

case, however, high-temperature pyrolysis (870°C) did not lead to the clean formation of the ylide **4b**.

In continuation of our studies of thermally generated nitrilium betaines[7] we have also prepared nitrile sulfides.[8]

Received: August 19, 1985 [Z 1435 IE]
German version: *Angew. Chem. 98* (1986) 99

[1] R. Huisgen, *Angew. Chem. 75* (1963) 604; *Angew. Chem. Int. Ed. Engl. 2* (1963) 565.
[2] H.-J. Hansen, H. Heimgartner in A. Padwa (Ed.): *1,3-Dipolar Cycloaddition Chemistry, Vol. 1*, Wiley, New York 1984, p. 177ff.
[3] E. P. Janulis, Jr., S. R. Wilson, A. J. Arduengo III, *Tetrahedron Lett. 25* (1984) 405.
[4] K. Burger, J. Fehn, *Chem. Ber. 105* (1972) 3814. K. Burger, J. Albanbauer, F. Manz, *ibid. 107* (1974) 1823.
[5] a) C. G. Krespan, *J. Org. Chem. 34* (1969) 1278; b) C. S. Cleaver, C. G. Krespan, *J. Am. Chem. Soc. 87* (1965) 3716.
[6] **3** reacts faster with **2** than does **4**. It is not at present possible to determine whether **4** also reacts with **2** to regenerate **1**, or whether this occurs via the reversion **4**→**3**→**1**.
[7] C. Wentrup, S. Fischer, A. Maquestiau, R. Flammang, *Angew. Chem. 97* (1985) 74; *Angew. Chem. Int. Ed. Engl. 24* (1985) 56.
[8] C. Wentrup et al., unpublished.

$[Et_4N][M(SCH_2CH_2S)_3]$ (M = Nb, Ta), Homoleptic 1,2-Ethanedithiolate Complexes of Niobium and Tantalum**

By *Kazuyuki Tatsumi, Yoitsu Sekiguchi, Akira Nakamura,* Roger E. Cramer,** and *John J. Rupp*

Very few niobium and tantalum complexes with thiolate ligands have so far been reported.[1-3] During investigations of dithiolates of metals of the vanadium group we were able to synthesize **1**–**3**, the first homoleptic 1,2-ethanedithiolate complexes of niobium and tantalum, by reaction of $NbCl_5$ (or $TaCl_5$) with $LiSCH_2CH_2SLi$.[4a]

$[Li(thf)_3][Nb(SCH_2CH_2S)_3]$ **1** $[Et_4N][M(SCH_2CH_2S)_3]$ **2**, M = Nb; **3**, M = Ta

When $NbCl_5$ was allowed to react with $Li_2S_2C_2H_4$ in benzene and then in THF, the air-sensitive compound **1** was obtained.[4b] Cation exchange of **1** with Et_4NCl in acetonitrile yielded the tetraethylammonium salt **2**,[4c] which is relatively air-stable (several hours). With the stoichiometry established, it was found that **2** could be synthesized more readily from a 1:3:1 mixture of $NbCl_5$, $Li_2S_2C_2H_4$, and Et_4NCl in acetonitrile. A similar procedure with $TaCl_5$ instead of $NbCl_5$ afforded the Ta complex **3**.[4d]

$$NbCl_5 + LiSCH_2CH_2SLi \xrightarrow{C_6H_6} \text{brown powder} \xrightarrow{THF} \mathbf{1}$$

$$MCl_5 + LiSCH_2CH_2SLi \xrightarrow[CH_3CN]{Et_4NCl} [Et_4N][M(SCH_2CH_2S)_3]$$

(Et_4NCl ↓ CH_3CN)

2, M = Nb; **3**, M = Ta

[*] Prof. Dr. A. Nakamura, Dr. K. Tatsumi, Y. Sekiguchi
Department of Macromolecular Science, Faculty of Science, Osaka University
Toyonaka, Osaka 560 (Japan)
Prof. Dr. R. E. Cramer, Dr. J. J. Rupp
Department of Chemistry, University of Hawaii
Honolulu, HI 96822 (USA)

[**] This work was supported by the Japanese Society for the Promotion of Science and the National Science Foundation (NSF) of the USA in connection with the Japan-United States Cooperative Science Program (joint research between *K. Tatsumi* and *A. Nakamura* in Osaka and *J. W. Gilje* and *R. E. Cramer* in Honolulu). *R. E. C.* acknowledges partial support from an NSF grant (CHE 8210244).

The anion of the complex has—according to an X-ray structure analysis of **2**—an approximate C_3 symmetry (Fig. 1). This is evident from the well-ordered propeller-type arrangement of the three SCH_2CH_2S ligands: S-Nb-S, 81.58(4)-82.14(4)°; S-Nb-S (*trans*), 156.29(4)-157.55(4)°. The torsional angles (ϕ) of the three chelate ligands are 31.4, 30.6, and 29.41° indicating that the coordination sphere defined by the six sulfur atoms is midway between trigonal-prismatic ($\phi = 0°$) and octahedral ($\phi = 60°$). For the very recently described Ti complex **4**,[5] the torsional angles are similar, ranging from $\phi = 35°$ to 42°. However, this stereochemistry contrasts with the trigonal-prismatic geometry found for the niobium complex **5**,[3b] $\phi = 0.7°$ (av.).

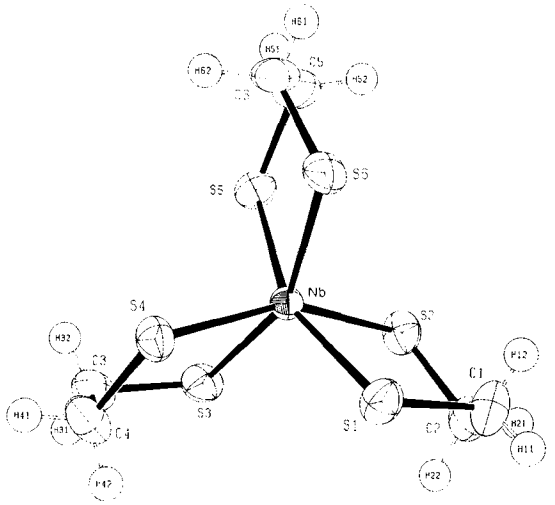


Fig. 1. An ORTEP representation of the structure of the complex anion in **2** with 50% probability ellipsoids. Monoclinic, space group $C2$, $a = 19.920(3)$, $b = 8.0424(9)$, $c = 14.070(2)$ Å, $\beta = 101.55(5)°$, $\rho_{calc.} = 1.503$ g cm^{-3}, $Z = 4$, $\mu(Mo_{K\alpha}) = 10.06$ cm^{-1}. The structure was solved by MULTAN 80 and refined to $R_w = 0.0292$ and $R_G = 0.0294$ using the SHELX program system with all atoms anisotropically refined except for hydrogen atoms. In this figure, the thermal parameters of the H atoms are arbitrarily fixed at 0.05 (3702 observed reflections $I > 3\sigma(I)$, 4228 measured reflections, 328 refined parameters). Selected bond lengths [Å]: Nb-S 2.425(1)-2.4422(9); C-S, 1.811(5)-1.823(5); C-C, 1.493(8)-1.499(7); C-H, 0.87(5)-1.04(5). The locations of hydrogen atoms are normal. The absolute configuration of the complex anion was determined to be Λ by refinement of both configurations using the complete data set which spanned Friedel pairs. Further details of the crystal structure investigation are available on request from the Director of the Cambridge Crystallographic Data Centre, Lensfield Road, Cambridge CB21EW (England) on quoting the full citation of this journal.

$[Et_4N]_2[Ti(SCH_2CH_2S)_3]$ **4** $[Ph_4As][Nb(1,2\text{-}S_2C_6H_4)_3]$ **5**

Apart from the complexes $[Ta(1,2\text{-}S_2C_5H_4)_3]^-$[3a] and $[Zr(1,2\text{-}S_2C_6H_4)_3]^{2-}$,[10] dithiolate chelates having π-conjugated bridges prefer to form trigonal-prismatic complexes,[6] while those without π-systems, e.g. **1**–**3**, distort from trigonal-prismatic. The C–S bond distances in **2** (av. 1.816(5) Å) are substantially longer than those in **5** (av. 1.745(9) Å), since the S atoms in SCH_2CH_2S have a different π donor ability than the S atoms in $1,2\text{-}S_2C_6H_4$. However, the observed Nb–S distances in **2** (av. 2.434(7)) are surprisingly close to those of **5** (av. 2.44(1) Å). Nevertheless, because of the decreased steric bulk of SCH_2CH_2S compared to that of $1,2\text{-}S_2C_6H_4$, and the longer C–S distance in the former compound, we anticipate that the anions of **2** (and **3**) are more reactive than $[Nb(S_2C_6H_4)_3]^-$, the anion of **5**.[11]

It follows from the ^{1}H-NMR spectrum that **1** contains three THF molecules, presumably surrounding the Li cation. The SCH_2CH_2S ligands of **1** ($(CD_3)_2SO$ solution) give a sharp singlet at $\delta = 3.69$ in the ^{1}H-NMR spectrum at room temperature, which is slightly shifted to $\delta = 3.67$ for **2** and to $\delta = 3.87$ for **3**. The FIR spectrum of **2** shows bonds arising from Nb–S stretching vibrations in $D_3(O_h)$ symmetry: 354 (s) [$E(T_{1u})$], 388 (s) [$A_2(T_{1u})$], 240 cm^{-1} (w) [$E(E_g)$].[7] The corresponding bands of the Ta complex **3** appear at 335 (s), 318 (s), and 225 cm^{-1} (w). These shifts agree quite well with what one would expect from the difference in the relative atomic masses of Nb and Ta;[8] thus, the Nb–S and the Ta–S bonds are essentially equal in strength. The similarity of the IR absorption patterns, especially those of the $E(T_{1u})$–$A_2(T_{1u})$ splitting, indicates that the structures of **2** and **3** are isotypic. The cyclovoltammograms exhibit a quasi-reversible one-electron reduction ($[M(SCH_2CH_2S)_3]^-/[M(SCH_2CH_2S)_3]^{2-}$): $E_{1/2}(Nb) = 1.20$ V; $E_{1/2}(Ta) = -1.56$ V (vs. SCE). The additional electron is transferred to the lowest nonbonding metal d level of a_1 symmetry (LUMO);[9] thus, the observed first reduction potentials verify that the d-level of **2** lies energetically lower than that of **3**. The higher positioning of Ta d levels also manifests itself in the systematic blue shift of all the four UV-visible absorption bands on going from **2** to **3**. The role of the d energy levels has occasionally been noted in the conformational choice (trigonal-prismatic or octahedral) for $[M(1,2\text{-}S_2C_6H_4)_3]$ complexes.[3, 10] No such effect, however, is visible in the case of $S_2C_2H_4$ complexes, for **2**, **3**, and the Ti complex are similar in structure.

Received: July 9, 1985;
supplemented: October 17, 1985 [Z 1380 IE]
German version: *Angew. Chem.* 98 (1986) 95

[1] M. J. Bunker, A. de Cian, M. L. H. Green, J. J. E. Moreau, N. Siganporia, *J. Chem. Soc. Dalton Trans. 1980*, 2155.

[2] K. Tatsumi, J. Takeda, Y. Sekiguchi, M. Kohsaka, A. Nakamura, *Angew. Chem. 97* (1985) 355; *Angew. Chem. Int. Ed. Engl. 24* (1985) 332.

[3] Tris(benzenedithiolato) complexes: a) J. L. Martin, J. Takats, *Inorg. Chem. 14* (1975) 73, 1358; b) M. Cowie, M. J. Bennett, *ibid. 14* (1975) 1589.

[4] a) *Procedure:* **1**: Careful addition of $Li_2S_2C_2H_4$ (7.53 g, 71 mmol) to a vigorously stirred benzene solution (200 mL) of $NbCl_5$ (6.21 g, 23 mmol) at 0°C immediately afforded a brown precipitate. After filtration the precipitate was dissolved in THF to give a deep red solution from which, after filtering off the insoluble dark brown residue, the compound **1** was isolated as a deep red crystalline powder (50%).—**2**: An acetonitrile solution of **1** was treated slowly with one equivalent of Et_4NCl in acetonitrile; **2** was formed as analytically pure, deep-red crystals (80%). Crystalline **2** was also formed upon addition of one equivalent of Et_4NCl to a 1:3 mixture of $NbCl_5$ and $Li_2S_2C_2H_4$ in acetonitrile (50%). X-ray quality crystals of **2** were obtained upon recrystallization from acetonitrile or DMF. The Ta analogue **3** was synthesized in a similar way by reaction of $TaCl_5$, $Li_2S_2C_2H_4$ (3 eq.), and Et_4NCl in acetonitrile; orange crystals, yield 66%. All operations were carried out under an argon atmosphere, using dry solvents. **2** and **3** gave satisfactory elemental analyses. The cyclovoltammogram was recorded at a platinum-wire auxiliary electrode in $(CH_3)_2SO$ solution (ca. 4×10^{-3} M) with 0.1 M n-Bu_4NClO_4 electrolyte.—b) **1**: deep red crystalline powder; ^{1}H-NMR (100 MHz, $(CD_3)_2SO$, room temperature): $\delta = 3.69$ (s, 12H, SCH_2CH_2S), $\delta = 3.64$ (m, 12H, THF), $\delta = 1.78$ (m, 12H, THF); UV/VIS (λ_{max} ($\varepsilon \times 10^4$), CH_3CN: 268 (1.2), 325 (1.5), 388 (1.3), 526 nm (0.7).—c) **2**: deep red crystals; ^{1}H-NMR: $\delta = 3.67$ (s, 12H, SCH_2CH_2S), $\delta = 3.22$ (q, $J_{HH} = 7$ Hz, 8H, NCH_2CH_3), $\delta = 1.10$ (t, $J_{HH} = 7$ Hz, 12H, NCH_2CH_3); UV/VIS (CH_3CN): 264 (1.2), 323 (1.6), 384 (1.3), 520 nm (0.6).—d) **3**: orange crystals; ^{1}H-NMR: $\delta = 3.87$ (s, 12H, SCH_2CH_2S), the signals arising from $[Et_4N]^+$ are the same as those observed for **2**; UV/VIS (CH_3CN): 246 (0.9), 292 (1.4), 332 (1.1), 443 nm (0.5).

[5] J. R. Dorfman, C. P. Rao, R. H. Holm, *Inorg. Chem. 24* (1985) 453.

[6] All dithiolene complexes except $[Mo(S_2C_2(CN)_2)_3]^{2-}$ are trigonal-prismatic: see for example; M. Draganjac, D. Coucouvanis, *J. Am. Chem. Soc. 105* (1983) 139, and references cited therein.

[7] The notation $E(T_{1u})$ means that the vibration is of E symmetry in the D_3 point group, which arises from the T_{1u} vibration of the parent O_h point group. Note that the $A_1[A_{1g}]$ vibrational mode is IR silent.

[8] The square root of the reduced-mass ratio, $[\mu(Ta\text{-}S)/\mu(Nb\text{-}S)]^{1/2}$, is 1.07.

[9] a) Extended Hückel calculations on $[Nb(SCH_2CH_2S)_3]^-$ were carried out for various torsional angles ϕ. For $\phi = 30°$, the a_1 (LUMO) level was calculated to be ca. 0.5 eV lower than the next lowest e level. b) R. Hoffmann, J. M. Howell, A. R. Rossi, *J. Am. Chem. Soc. 98* (1976) 2484.

[10] M. J. Bennett, M. Cowie, J. L. Martin, J. Takats, *J. Am. Chem. Soc. 95* (1973) 7504.

[11] *Note added in proof* (December 16, 1985): The complex anions $[M(SCH_2CH_2S)_3]^-$ (M = Nb, Ta) were found to undergo an unusual rearrangement via cleavage of a C–S bond in the presence of water, resulting in formation of $[MS(SCH_2CH_2S)(SCH_2CH_2SCH_2CH_2S)]^-$.

Synthesis of *erythro*-D- and -L-4-Pentenetriols. Selective Epoxy Allyl Alcohol Hydrolysis with Retention or Twofold Inversion (Enantiomerization)**

By *Brigitte Häfele, Detlef Schröter,* and *Volker Jäger**

For studies on stereoselection in cycloadditions,[1] we required 5-substituted 4-vinyldioxolanes with *erythro (cis)* configuration (cf. **4**–**6**). We report here two approaches, starting from either D-ribonolactone D-**1** (a) or 1,4-pentadien-3-ol (divinylcarbinol) **7**, which make accessible D- and L-**6** with high diastereomer and enantiomer ratios (Scheme 1).

The D-*erythro* compounds **4**–**6** were prepared from D-ribonolactone D-**1** in a straightforward manner.[2] The tosylate D-**6**—which was known to be crystalline from parallel studies[3]—was obtained as a single diastereomer; $[\alpha]_D^{20} = -44.5$ ($c = 1.87$, $CHCl_3$).

In order to synthesize the L-*erythro* compounds, a route based on the asymmetric epoxidation of *Sharpless* et al.[4] was devised. Results with chiral, secondary allylic alcohols[4b-d, 5] suggested **7** as a promising starting material. **7**, an achiral compound with four stereoheterotopic faces, should undergo addition from the *Re,Re* face with high stereoselectivity when the (+)-diethyl tartrate (DET) version of the above reaction is used.[6]

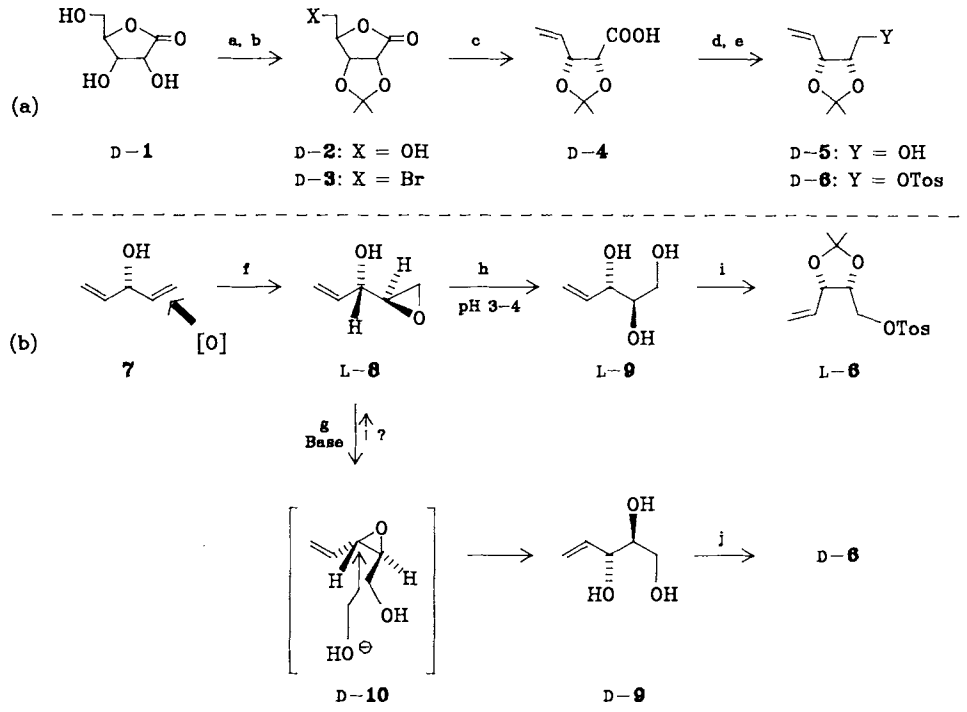
Indeed, epoxidation of **7** gave, after distillative workup,[5] the epoxy allyl alcohol **8** (55–65%), along with *tert*-butyl hydroperoxide/*tert*-butyl alcohol. Since attempts to isolate pure **8**, which is present as a single diastereomer (^{13}C-NMR), failed,[7] the mixture was treated with potassium hydroxide in aqueous dioxane at 100°C to afford the crude triol **9** (viscous oil with positive optical rotation[7b]). Tosylation and acetonation of **9** afforded the crystalline tosylate **6**, again as a single diastereomer; $[\alpha]_D^{20} = -27.6$ ($c = 0.54$, $CHCl_3$).

Comparison of this optical rotation with the value for D-**6** (obtained from D-**1**) indicates a ca. 80:20 ratio of D-**6**/L-**6**, which is at variance with the established steric course of this reaction. First, the sequence had proceeded with very high diastereo- but rather low enantioselectivity. Second, the *wrong major enantiomer* had been formed!

The analysis of these results made clear that this D-**6**/L-**6** mixture could *not* reflect the actual stereofacial differentiation of the (+)-DET epoxidation, since D-**8** (and

[*] Prof. Dr. V. Jäger, Dipl.-Chem. B. Häfele, Dipl.-Chem. D. Schröter
Institut für Organische Chemie der Universität
Am Hubland, D-8700 Würzburg (FRG)

[**] This work was supported by the Deutsche Forschungsgemeinschaft, the Fonds der Chemischen Industrie, and Bayer AG, Wuppertal-Elberfeld. These results were presented in August, 1985, in Waterloo (Canada) at the Xth International Congress of Heterocyclic Chemistry, cf. [1b]. We are grateful to Ms. *B. Kuhn* and Ms. *D. Michel* for experimental assistance.



Scheme 1. Routes to protected D- and L-4-pentenetriols from (a) ribonolactone D-**1** and (b) 1,4-pentadien-3-ol **7**. The diastereomer ratios are given in brackets. a) Ref. [2a]. b) *N*-Bromosuccinimide, PPh_3 [2b]; D-**3**: 80%, m.p. = 88.5–89.5 °C, $[\alpha]_D^{25}$ −44.7 (c = 1.01, $CHCl_3$); cf. ref. [2c]. c) Zn-Cu, acetone, reflux [2d]; D-**4**: 85%, [> 97 : 3 by ^{1}H- and ^{13}C-NMR] [2e, f]. d) $LiAlH_4$; D-**5**: 93%, $[\alpha]_D^{20}$ −44.0 (c = 4.89, $CHCl_3$ [> 99 : 1 by ^{13}C-NMR]. e) TosCl, pyridine, CH_2Cl_2, 50 °C, 7 d; D-**6**: 57%, m.p. = 56–57 °C (from petroleum ether/Et_2O), $[\alpha]_D^{20}$ −44.5 (c = 1.87, $CHCl_3$); [> 98 : 2 by HPLC and NMR]. f) *t*BuOOH, Ti(O*i*Pr)$_4$, *R,R*-(+)-diethyl tartrate (2 : 1 : 1), CH_2Cl_2, −24 °C, 26 h (cf. [4a, e]); boiling range 70–100 °C/15 torr (Kugelrohr); composition: L-**8** 40–60%, rest *t*BuOH/*t*BuOOH; overall yield 55–65% (estimated by ^{1}H-NMR), [> 95 : 5 by ^{13}C-NMR]. g) KOH (6 equiv.), H_2O-dioxane (1 : 1.2), 100 °C, 16 h; boiling range 150–170 °C/0.1 torr (Kugelrohr); D-**9**: 68%; [> 95 : 5 by ^{13}C-NMR], $[\alpha]_D^{18}$ = +21.7 (c = 0.567, CH_3OH) [7b]. h) H_2O, pH 3–4, 60 °C, 18 h; boiling range 150–170 °C/0.1 torr (Kugelrohr); L-**9**: 61%, $[\alpha]_D^{18}$ = −25.5 (c = 1.336, CH_3OH). In other runs, rotations of 24.2 to 28.4 were obtained. D-**9**, obtained from D-**5** (starting from D-**1**), showed $[\alpha]_D^{18}$ = +27.6 (c = 0.89, CH_3OH). i) TosCl (1.1 equiv.), pyridine (3 equiv.), 0 °C → room temperature, 16 h; L-**9** monotosylate: 60–70% after flash chromatography on silica (Et_2O/ethyl acetate/NEt_3 8 : 2 : 0.1); $Me_2C(OMe)_2$ (1.5 equiv.)/$SnCl_2$ (cat.)/1,2-dimethoxyethane, 60 °C, 75 min; L-**6**: 59%, m.p. = 55–56 °C (from petroleum ether/ether), $[\alpha]_D^{20}$ = +42.0 (c = 1.005, $CHCl_3$). j) Analogous to i).

hence D-**6**) would have been produced by attack mainly at the *Si,Si* face of **8**, i.e., the *least* reactive one.[4b,c]

Indeed, epoxide hydrolysis by the strong base employed turned out to be the stereo-diverting step: hydrolysis at pH 3–4 gave the triol **9** in ca. 60% yield with higher and opposite rotation[7b] (see Scheme 1). As described above, this triol was converted into the tosylate **6**, which, after crystallization, showed a specific rotation of $[\alpha]_D^{20}$ +42.0 (c = 1.005, $CHCl_3$). This corresponds to a D-**6**/L-**6** ratio of ca. 3 : 97, in accordance with expectation.

The reaction of L-**8** with strong base to yield D-**9** as the major enantiomer is thus rationalized as a net *enantiomerization by a two-step double inversion* (see Scheme 1). This unusual course of an epoxy alcohol Payne rearrangement/opening[4d,8] is attributed to the fact that the allylic position in D-**10** is more strongly activated than the (usually favored) terminal position in L-**8**.

The optically active C_5 building blocks described here have many potential uses.[9] In addition, the reaction sequence in Scheme 1 (b) may allow for stereocontrol at two levels: L- and D-**8** are both accessible from **7** by employing either (+)- or (−)-DET, respectively, in the epoxidation step; both enantiomers of **9** may be obtained from the single epoxy allyl alcohol L-**8** if conditions for complete double inversion can be elaborated.

Received: July 18, 1985;
revised: October 25, 1985 [Z 1393 IE]
German version: *Angew. Chem. 98* (1986) 89

[1] a) V. Jäger, R. Schohe, E. F. Paulus, *Tetrahedron Lett. 24* (1983) 5501; K. N. Houk, S. R. Moses, Y.-D. Wu, N. G. Rondan, V. Jäger, R. Schohe, F. R. Fronczek, *J. Am. Chem. Soc. 106* (1984) 3880; b) review: V. Jäger, I. Müller, R. Schohe, M. Frey, R. Ehrler, B. Häfele, D. Schröter, *Lect. Heterocycl. Chem.*, in press.

[2] a) L. Hough, J. K. N. Jones, D. L. Mitchell, *Can. J. Chem. 36* (1958) 1720; b) S. Hanessian, M. M. Ponpipom, P. Lavalee, *Carbohydr. Res. 24* (1982) 45; c) C. S. Wilcox, L. M. Thomasco, *J. Org. Chem. 50* (1985) 546; d) cf. V. Jäger, H. Grund, W. Schwab, *Angew. Chem. 91* (1979) 91; *Angew. Chem. Int. Ed. Engl. 18* (1979) 78; e) for related syntheses of unsaturated sugars see B. Bernet, A. Vasella, *Helv. Chim. Acta 67* (1984) 1328, and references cited therein; f) alternative synthesis of the methyl ester of **4**: R. W. Hoffmann, W. Ladner, *Chem. Ber. 116* (1983) 1631.

[3] Vinylmagnesiumbromide additions to 2,3-*O*-isopropylidene-D-glyceraldehyde gave at best a 75 : 25 mixture of *erythro/threo* adducts ($ZnCl_2$ added) with substantial racemization, as found after separation and transformation into *erythro*-**6**: D. Schröter, V. Jäger, unpublished results 1984/1985. For related studies see K. Mead, T. L. McDonald, *J. Org. Chem. 50* (1985) 422; review: J. Mulzer, *Nachr. Chem. Tech. Lab. 32* (1984) 16, 146.

[4] a) T. Katsuki, K. B. Sharpless, *J. Am. Chem. Soc. 102* (1980) 5974; J. G. Hill, K. B. Sharpless, *Org. Synth. 63* (1984) 66; b) V. S. Martin, S. S. Woodard, T. Katsuki, Y. Yamada, M. Ikeda, K. B. Sharpless, *J. Am. Chem. Soc. 103* (1981) 6237; c) K. B. Sharpless, C. H. Behrens, T. Katsuki, A. W. M. Lee, V. S. Martin, M. Takatani, S. M. Viti, F. J. Walker, S. S. Woodard, *Pure Appl. Chem. 55* (1983) 589; d) for reviews see [4c] and C. H. Behrens, K. B. Sharpless, *Aldrichim. Acta 16* (1983) 67; S. Masamune, W. Choy, J. S. Petersen, L. R. Sita, *Angew. Chem. 97* (1985) 1; *Angew. Chem. Int. Ed. Engl. 24* (1985) 1; e) shortened workup: B. D. Johnston, A. C. Oehlschlager, *Can. J. Chem. 62* (1984) 2148.

[5] For related cases of stereodifferentiation see J. J. Partridge, N. K. Chadha, M. R. Uskoković, *J. Am. Chem. Soc. 95* (1973) 532, 7171.

[6] Nonstereoselective peroxy-acid epoxidation of **7**: D. Holland, J. Fraser Stoddart, *Carbohydr. Res. 100* (1982) 207.

[7] a) Satisfactory elemental analyses were obtained for D-3 to D-6 [Route (a)] and D-/L-6 [Route (b)]; b) due to difficulties in purification of such compounds and uncertainties in the polarometric determinations of their enantiomer ratios, the specific rotations of the triols (viscous oils) must be taken as approximate values; cf. discussion by V. Schurig, *Kontakte* (Darmstadt) *1985* (1) 54.

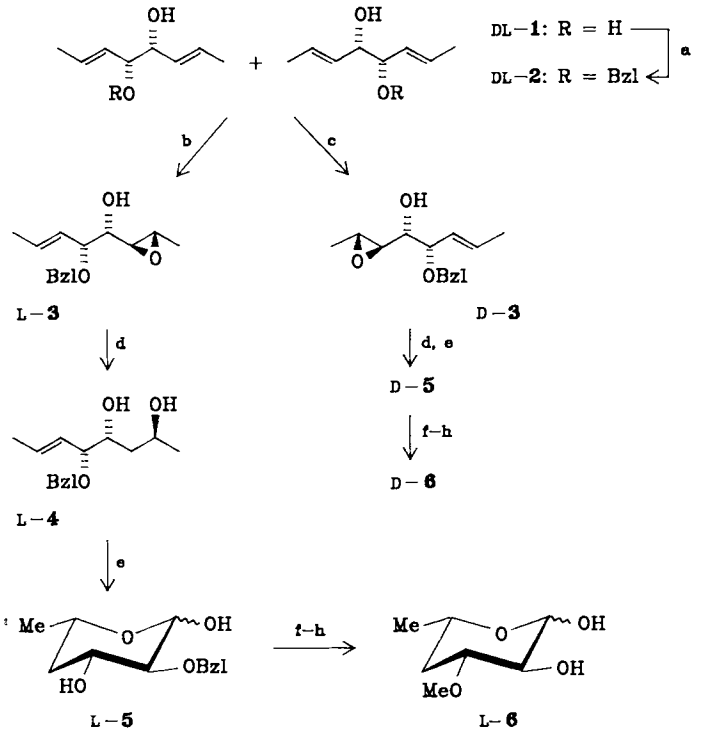
[8] G. B. Payne, *J. Org. Chem. 27* (1962) 3819.

[9] A related approach based on divinylglycol was devised by Prof. Dr. *R. R. Schmidt* (see U. Küfner, R. R. Schmidt, Angew. Chem. 98 (1986) 90, Angew. Chem. Int. Ed. Engl. 25 (1986) 89. We thank Prof. *Schmidt* for informing us about their results prior to publication and for discussions.

Synthesis of Deoxyhexoses from Divinylglycols—The Synthesis of D- and L-Chalcose

By *Ulrike Küfner* and *Richard R. Schmidt**

Deoxyhexoses and especially 2,6- and 4,6-dideoxyhexoses are components of numerous natural products.[1] We have developed a variable concept for the synthesis of enantiomerically pure dideoxy sugars starting from racemic or *meso*-divinylglycols,[2,3] which requires only a few steps and is exemplified by the synthesis of D- and L-chalcose (D-**6** and L-**6**) (Scheme 1).[4,5]



Scheme 1. Synthesis of D- and L-chalcose, D-**6** and L-**6**. a) $PhCH_2Br$, dimethylformamide (DMF), $BaO/Ba(OH)_2$ (46%), b) $Ti(OiPr)_4$, *t*BuOOH, CH_2Cl_2, (+)-diethyl tartrate (35%), c) $Ti(OiPr)_4$, *t*BuOOH, CH_2Cl_2, (−)-diethyl tartrate (35%), d) Red-Al, tetrahydrofuran (86%), e) 1. O_3, $MeOH/CH_2Cl_2$; 2. Me_2S (81%), f) $PhCH_2OH$, HCl (70%), g) MeI, NaH, DMF (83%), h) Pd/C, H_2, ethyl acetate (89%).

[*] Prof. Dr. R. R. Schmidt, Dipl.-Chem. U. Küfner
Fakultät für Chemie der Universität
Postfach 5560, D-7750 Konstanz (FRG)

[**] De Novo Synthesis of Carbohydrates and Related Natural Products, Part 20. This work was supported by the Deutsche Forschungsgemeinschaft and the Fonds der Chemischen Industrie.—Part 19: [3].

The *threo*-dipropenylglycol DL-**1**, which is obtained by reductive dimerization of crotonaldehyde[6] and simple separation of the diastereomers,[2] reacts with benzyl bromide to give the monobenzyl derivative DL-**2**. Sharpless oxidation[7] leads to kinetic resolution of the racemate with formation of the enantiomerically pure epoxides D-**3** and L-**3**, respectively. In order to obtain the other isomer in each case, the unreacted starting materials, enriched in L-**2** and D-**2**, respectively, are allowed to react further, thereby affording correspondingly higher yields (ca. 70%) of L-**3** and D-**3**. The epoxide ring in L-**3** is opened regioselectively with Red-Al (sodium hydridobis(2-methoxyethoxy)aluminate) to give the triol derivative L-**4**; analogous opening of hydroxyalkyl-substituted epoxides has already been observed.[8] Ozonolysis of L-**4** affords the 2-*O*-benzyl-protected 4,6-dideoxy-L-*xylo*-hexose L-**5** in only four steps. Conversion into the benzyl glycoside, 3-*O*-methylation, and hydrogenolytic debenzylation give L-chalcose L-**6**[9] in good yield. Similarly, the 4,6-dideoxyhexose D-**5** and D-chalcose D-**6**[9] are obtained from D-**3**.

Received: October 7, 1985 [Z 1487 IE]
German version: *Angew. Chem. 98* (1986) 90

[1] S. Hanessian, *Adv. Carbohydr. Chem. 21* (1966) 143; N. R. Williams, J. D. Wander in W. Pigman, D. Horton (Eds.): *The Carbohydrates. Chemistry and Biochemistry, Vol. 1B*, Academic Press, New York 1980, p. 761 ff.

[2] In addition, 4,6-dideoxy-*lyxo*-hexoses were prepared from *erythro*-dipropenylglycol and the 2,6-dideoxyhexose D-digitoxose from *erythro*-divinylglycol. U. Küfner, planned *Dissertation*, Universität Konstanz.

[3] The pheromone *exo*-brevicomin was synthesized from *threo*-divinylglycol: U. Küfner, R. R. Schmidt, *Synthesis 1985*, 1060

[4] Chalcose syntheses starting from carbohydrates: a) N. K. Kochetkov, A. J. Usov, *Tetrahedron Lett. 1963*, 519; b) S. McNally, W. G. Overend, *Chem. Ind. (London) 1964*, 2021; c) A. B. Foster, M. Stacey, J. M. Webber, J. H. Westwood, *J. Chem. Soc. 1965*, 2319; d) B. T. Lawton, D. J. Ward, W. A. Szarek, J. K. N. Jones, *Can. J. Chem. 47* (1969) 2899; e) K. Kefurt, Z. Kefurtová, J. Jarý, *Collect. Czech. Chem. Commun. 38* (1972) 2627; f) H. Redlich, W. Roy, *Carbohydr. Res. 68* (1979) 275.

[5] De novo chalcose synthesis: a) R. M. Srivastava, R. K. Brown, *Can. J. Chem. 48* (1970) 830; b) K. Torsell, M. P. Tyagi, *Acta Chem. Scand. B 31* (1977) 7; c) A. Banaszek, A. Zamojski, *Rocz. Chem. 45* (1971) 391; d) S. Danishefsky, J. F. Kerwin, *J. Org. Chem. 47* (1982) 1597.

[6] W. G. Young, L. Levanas, Z. Jesaitis, *J. Am. Chem. Soc. 58* (1936) 2274.

[7] T. Katsuki, K. B. Sharpless, *J. Am. Chem. Soc. 102* (1980) 5974; V. S. Martin, S. S. Woodard, T. Katsuki, Y. Yamada, M. Ikeda, K. B. Sharpless, *ibid. 103* (1981) 6237.

[8] J. M. Finan, Y. Kishi, *Tetrahedron Lett. 23* (1982) 2719; S. M. Viti, *ibid. 23* (1982) 4541.

[9] L-**6**: $[\alpha]_D^{25} = -78$ ($c = 0.66$, H_2O after 3–24 h) [4b]; m.p. = 89–90 °C [4b]; D-**6**: $[\alpha]_D = +77$ ($c = 0.6$, H_2O after 3–18 h); m.p. = 90.5–91 °C.

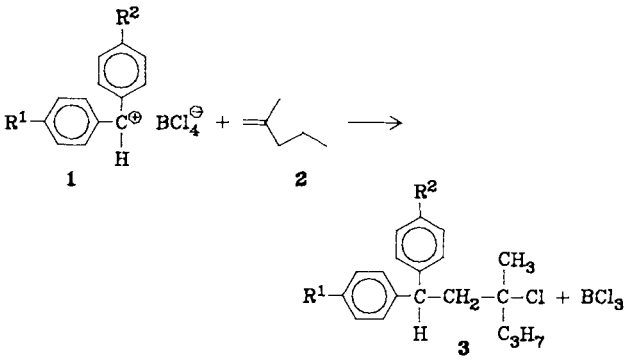
Direct Determination of Rate Constants for the Addition of Carbenium Ions to Alkenes**

By *Reinhard Schneider, Ute Grabis,* and *Herbert Mayr**

The rates of the addition of carbenium ions to alkenes are important for the understanding of carbocationic polymerizations and with regard to reactivity-selectivity relationships. Probably because such reactions are difficult to control, kinetic investigations have only been carried out under special conditions, e.g., with radiolytically generated carbenium ions.[1] Based on our previous work on the selective formation of 1:1 products from carbenium ions

[*] Prof. Dr. H. Mayr, Dipl.-Chem. R. Schneider, U. Grabis
Institut für Chemie der Medizinischen Universität
Ratzeburger Allee 160, D-2400 Lübeck 1 (FRG)

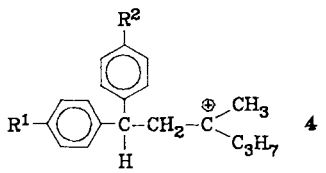
[**] This work was supported by the Deutsche Forschungsgemeinschaft and the Fonds der Chemischen Industrie. We thank Prof. Dr. *O. Nuyken*, Mainz, and *R. Bederke*, Lübeck, for their help in constructing the apparatus.



and alkenes, we have now developed a method for the determination of the corresponding reaction rates.

The diarylcarbenium tetrachloroborates **1a–1e** can quantitatively be generated from the corresponding diarylmethyl chlorides and boron trichloride in dichloromethane at -20 to -90°C. When 2-methyl-1-pentene **2** is added to these solutions, the addition products **3a–3e**, which are practically un-ionized under these conditions, are formed (>90% yield). The course of these reactions can easily be followed conductometrically and photometrically (fiber optics) since the electrical conductivity and the absorption of visible light decrease to less than 3% of the initial values.

The reactions were found to be first order with respect to both alkene and carbenium ion over the entire concentration range examined (**2**: 1.1×10^{-2} to 8.6×10^{-5} mol/L; **1d**: 4.1×10^{-3} to 4.1×10^{-5} mol/L). One to two equivalents of BCl_3 are sufficient to achieve complete ionization of **1a–1d**, whereas complete ionization of the di-*p*-tolyl compound **1e** requires approximately 500 equivalents of BCl_3 in the concentration range studied. The reaction rate of **1d** (2.1×10^{-4} mol/L) is not influenced by variation of the BCl_3 concentration from 10^{-1} to 3.6×10^{-3} mol/L.



The addition of **1** to **2** initially yields the carbenium ion **4**, and it is conceivable that **4** either reacts with $BCl_4^{\ominus}$ to give **3** and BCl_3 or undergoes retroaddition to give **1** and **2**. The latter possibility, i.e., the reversible formation of **4**, was excluded since the addition of 10^{-2} mol/L of benzyltriethylammonium tetrachloroborate to a 10^{-4} M solution of **1d**-$BCl_4^{\ominus}$ did not affect the reaction rate. The same conclusion can be derived from the observation that the systems **1a**-$BCl_4^{\ominus}$ ($k_2=2.9\times10^{-2}$ L mol^{-1} s^{-1}), **1a**-$BBr_3Cl^{\ominus}$ (2.7×10^{-2} L mol^{-1} s^{-1}), and **1a**-$SnCl_5^{\ominus}$ (2.5×10^{-2} L mol^{-1} s^{-1}) show similar reactivity toward **2**, although the rate of the reaction **4** → **3** is altered when the anion is varied.[3] The observation that the reaction rate of **1d** is not affected when the $BCl_4^{\ominus}$ concentration is increased 100 fold indicates that either specific ion pairs do not exist or that ion pairs and free ions do not differ in their reactivity toward **2**.

The decreasing electron-releasing ability of R^1 and R^2 in going from **1a** to **1e** is accompanied by an increase in reactivity of 5 orders of magnitude (Table 1). In accordance with the solvolysis rates of methoxy-substituted diphenylmethyl derivatives,[4] we do not find a linear correlation between $\lg k_2$ and σ^+. A uniform reaction mechanism and the absence of ion-pair effects is also indicated by the linear correlation between $\ln k_2/T$ and $1/T$ in the temperature ranges investigated (mostly -30 to -70°C). These plots allow the determination of the activation parameters $\Delta H^{\neq}$ and $\Delta S^{\neq}$. Especially in the additions of the less-stabilized carbenium ions, the entropy term $T\Delta S^{\neq}$ is the main contribution to the free energy of activation. Whereas the activation entropy is almost unaffected by the variation of R^1 and R^2, $\Delta H^{\neq}$ decreases considerably with decreasing stabilization of the carbenium ions **1a–1e**. If $\Delta S^{\neq}$ of the corresponding addition of the diphenylmethyl cation **1** (R^1, $R^2=H$) is assumed to be of the same order of magnitude, $\Delta H^{\neq}$ is estimated to be zero or negative.

Table 1. Rate constants (CH_2Cl_2, -70°C) and activation parameters for the addition of diarylcarbenium tetrachloroborates **1** to 2-methyl-1-pentene **2**.

	R^1	R^2	k_2 [a] [L mol^{-1} s^{-1}]	k_{rel}	$\Delta H^{\neq}$ [kJ/mol]	$\Delta S^{\neq}$ [J mol^{-1} K^{-1}]	$\Delta G^{\neq}$ (-70°C) [kJ/mol]
1a	OCH_3	OCH_3	2.9×10^{-2}	1	29.8	−125	55.1
1b	OCH_3	OPh	1.7×10^{-1}	5.9			51.9
1c	OCH_3	CH_3	3.4	117	22.7	−120	47.1
1d	OCH_3	H	2.4×10^{1}	828	18.8	−122	43.6
1e	CH_3	CH_3	3.6×10^{3}	124000	11.6	−117	35.4

[a] Reproducibility for **1a–1d** better than ±5%; for **1e**, better than ±10%.

In accord with these conclusions, a negative activation enthalpy (-25 kJ/mol) was reported for the carbocationic polymerization of *p*-methoxystyrene,[5] in which attacking and resulting carbenium ion correspond to the same structural type. The small (positive or negative) activation enthalpies and large negative activation entropies for the additions of reactive carbenium ions to alkenes are in accordance with previously reported data for the corresponding reactions of carbenes and radicals.[6]

Received: August 21, 1985;
revised: September 16, 1985 [Z 1437 IE]
German version: *Angew. Chem. 98* (1986) 94

[1] a) Y. Wang, L. M. Dorfman, *Macromolecules 13* (1980) 63; b) O. Brede, J. Bös, W. Helmstreit, R. Mehnert, *Radiat. Phys. Chem. 19* (1982) 1, and references cited therein.
[2] a) H. Mayr, *Angew. Chem. 93* (1981) 202; *Angew. Chem. Int. Ed. Engl. 20* (1981) 184; b) H. Mayr, W. Striepe, *J. Org. Chem. 48* (1983) 1159; c) H. Mayr, R. Schneider, *Makromol. Chem., Rapid Commun. 5* (1984) 43.
[3] G. Heublein, S. Spange, P. Hallpap, *Makromol. Chem. 180* (1979) 1935.
[4] S. Nishida, *J. Org. Chem. 32* (1967) 2692, 2695, 2697.
[5] R. Cotrel, G. Sauvet, J. P. Vairon, P. Sigwalt, *Macromolecules 9* (1976) 931.
[6] a) Carbenes: K. N. Houk, N. G. Rondan, J. Mareda, *Tetrahedron 41* (1985) 1555; b) radicals: J. M. Tedder, J. C. Walton, *Adv. Phys. Org. Chem. 16* (1978) 51.

Amino Acid Derivatives from *N*-(Arylmethylene)dehydroalanine Methyl Esters**

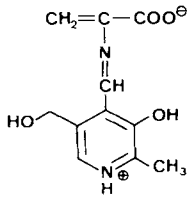
By *Günter Wulff** and *Helmut Böhnke*

N-Pyridoxylidenedehydroalanine **1** has been postulated to be a reactive intermediate in the pyridoxal-phosphate-catalyzed biosynthesis of some amino acids;[2] for example,

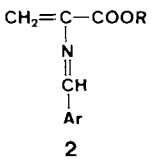
[*] Prof. Dr. G. Wulff, Dr. H. Böhnke
Institut für Organische Chemie II der Universität
Universitätsstrasse 1, D-4000 Düsseldorf (FRG)

[**] Activated Dehydroamino Acids, Part 2. This work was supported by the Fonds der Chemischen Industrie and the Deutsche Forschungsgemeinschaft.—Part 1: [1].

tryptophan is formed in vivo by Michael addition of the enamine indole to **1**. It had not been possible to isolate or synthesize pure **1** up to now owing to its extreme lability.[3]



1

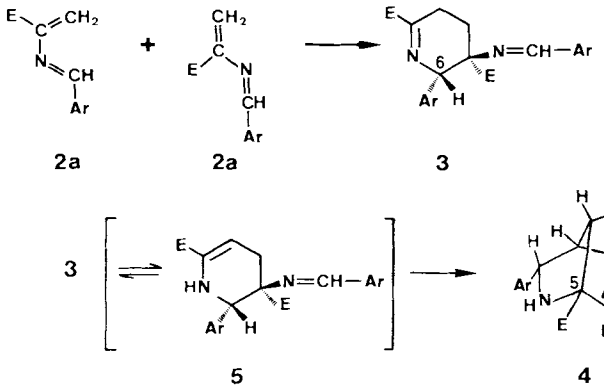


2

2a, Ar = 4-(C_6H_5)C_6H_4 ; R = CH_3
2b, Ar = C_6H_5 ; R = CH_3

We recently synthesized and characterized the esters **2a** and **2b**, the first compounds having the general structure **2**, from which **1** is also derived.[1] We report here their interesting properties.

2a can be obtained at −90 °C in pure, crystalline form in high yields.[1] However, when it is left in solution for a short time at room temperature, a dimer crystallizes out in yields of up to 56%, which was shown to be the tetrahydropyridine derivative **3**.[4] **3** is obtained as a pure racemic diastereomer. It is formed by [4+2] cycloaddition. The 2-azabutadiene structure of **2a** functions as the 4π component, while the doubly activated CC double bond of **2a** acts as the dienophile.



2a **2a** **3**

5 **4**

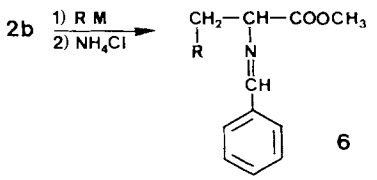
E = $COOCH_3$; Ar = 4-(C_6H_5)C_6H_4

Since **3** is also very reactive, its subsequent reactions can only be prevented by the appropriate choice of solvent so as to promote rapid crystallization. In solution at room temperature, **3** reacts within a few hours to give, with high selectivity in 92% yield, the diastereomerically pure 3,6-diazabicyclo[3.2.1]oct-2-ene derivative **4**.[4] Its formation from **3** probably proceeds via the enamine **5**.[5] In this reaction, the nucleophilic β-C atom of the endocyclic enamine moiety attacks intramolecularly the electrophilic carbon atom of the exocyclic azomethine group.

The relative configuration of C1 with respect to C5 of **4** results from the *cis* geometry of this cyclization. The *endo* position of the *p*-biphenylyl group on C7 is established unequivocally by the $^3J(^1H(C1)\text{-}^1H(C7))$ coupling constant of 4.2 Hz.

4 is the final product of a sequence of reactions beginning with the unstable **2** and proceeding via **3**. Compounds **3** and **4** are readily accessible, novel, cyclic amino acid derivatives.

In order to investigate the suitability of **2b** as a Michael acceptor in the synthesis of amino acids,[6] it was allowed to react with organometallic compounds directly after its preparation (see Table 1).



6

a, R = Me ; **b**, R = Bu ; **c**, R = *s*Bu ; **d**, R = *t*Bu ; **e**, R = Ph

Table 1. Addition of organometallic compounds RM to **2b** in diethyl ether (n.d. = not determined).

RM	*t* [h]	*T* [°C]	Product	Yield of **6** [%] [7] [a]	[b]
MeMgBr	3.0	−78→0	**6a**	< 10	n.d.
BuLi	2.0	−78→0	**6b**	< 10	n.d.
$Me_2CuLi\cdot(LiI)$	1.5	−15	**6a**	95	61
$Bu_2CuLi\cdot(LiI)$	1.0	−15	**6b**	57	48
$sBu_2(CN)CuLi_2$	2.0	−15	**6c**	85	45
$tBu_2(CN)CuLi_2$	2.0	−15	**6d**	77	49
$Ph_2CuLi\cdot(LiI)$	5.0	−78	**6e**	n.d.	31
$Me_2CuMgBr\cdot(LiI)$	1.5	−15	**6a**	30	n.d.
$Me_2CuMgBr\cdot(LiI)$	1.5	−15	**6a**	78 [c]	n.d.

[a] Determined by ^{1}H-NMR spectroscopy. [b] Isolated (see [7]). [c] In tetrahydrofuran (THF) as solvent.

As expected,[8] MeMgBr and BuLi hardly underwent reaction with **2b** to give **6a** and **6b**, respectively. When diorganocopper(I) reagents R_2CuLi[9] were used, the desired Michael addition was strongly preferred (see Table 1). The amount of side reaction (addition to the C=O and/or C=N bond) was significantly smaller.[10]

The cuprates of the type $R_2(CN)CuLi_2$ studied by *Lipshutz* et al.[11] have proved useful for the addition of the groups R = *s*Bu and *t*Bu. The addition of $sBu_2(CN)CuLi_2$ gave, after distillation, the two racemic diastereomers of **6c** in a ratio of 7:3 as estimated by ^{13}C-NMR spectroscopy. In the reaction of **2b** with $Me_2CuMgBr\cdot(LiI)$, a change of the solvent (THF instead of ether) resulted in a significant increase in yield.

Overall, the cross-conjugated system **2b** shows the expected behavior of a Michael acceptor and can, despite its low stability, be used advantageously for the synthesis of complicated amino acid derivatives. **2b** thus corresponds to a reactive a^3 synthon in the synthesis of amino acids.

Received: August 22, 1985;
revised: October 25, 1985 [Z 1438/1439 IE]
German version: *Angew. Chem.* 98 (1986) 101

[1] G. Wulff, H. Böhnke, *Angew. Chem.* 96 (1984) 362; *Angew. Chem. Int. Ed. Engl.* 23 (1984) 380.
[2] See, e.g., H. G. Floss, J. C. Vederas in C. Tamm (Ed.): *New Comprehensive Biochemistry, Vol. 3: Stereochemistry*, Elsevier, Amsterdam 1982, p. 161.
[3] See also, e.g., W. Weiner, J. Winkler, S. C. Zimmerman, A. W. Czamik, R. Breslow, *J. Am. Chem. Soc.* 107 (1985) 4093.
[4] The structures of **3** and **4** were established by spectroscopic means (IR, MS, ^{1}H- and ^{13}C-NMR) and by elemental analysis. Determination of the relative configuration at C4 of **4** was not possible on the basis of the spectroscopic data. Examination of models indicates that the *p*-biphenylyl group is *exo*. The resulting configuration for C4 relative to C5 was thus taken as a basis for the corresponding atom in the formula of **3**, namely, C6. The unequivocal determination of this configuration remains to be established by X-ray crystallography.
[5] The amount of **5** in the reaction mixture was too small for direct spectroscopic detection.
[6] Michael additions for C-C bond formation had already been carried out on the less reactive *N*-acyl derivatives of open-chain dehydroalanines, merely by addition of carbon acids. In the recently described addition of

cuprates, a mixture of **7–9** was obtained in which the Michael addition product was present in only minor amounts: J. A. Bajgrowicz, A. El Hallaoui, R. Jacquier, C. Pigiere, P. Viallefont, *Tetrahedron 41* (1985) 1833.
R–CH_2–CH(NHBz)–COR **7**, R–CH_2–CH(NHBz)–$COOCH_3$ **8**, R–CH_2–C($COCH_3$)–(NHBz)–CH_2–CH(NHBz)–$COOCH_3$ **9**

[7] The products **6a–6e** were identified on the basis of their mass, ^{1}H-, and ^{13}C-NMR spectra. All new compounds afforded correct elemental analyses. Yields are based on the amount of *N*-benzylidene serine methyl esters employed.

[8] T. L. Ho, *Tetrahedron 41* (1985) 1.

[9] General experimental procedure: An imidazole-free solution of **2b** (4 mmol) [1] was added to an ether solution containing 20 mmol of R_2CuLi [C. R. Johnson, C. A. Dutra, *J. Am. Chem. Soc. 95* (1973) 7777] over 10 min at −15°C. After 1–5 h of reaction time (see Table 1), followed by hydrolysis (saturated NH_4Cl solution), and subsequent work-up, the products were distilled with a Kugelrohr apparatus in an oil-pump vacuum.

[10] An attack on the β-carbon atom of **2b** leads to a stabilized dihetero pentadienyl anion, an attack on the C=N bond to an energetically less favorable 1-azaallyl anion.

[11] B. H. Lipshutz, R. S. Wilhelm, J. A. Kozlowski, *Tetrahedron 40* (1984) 5005.

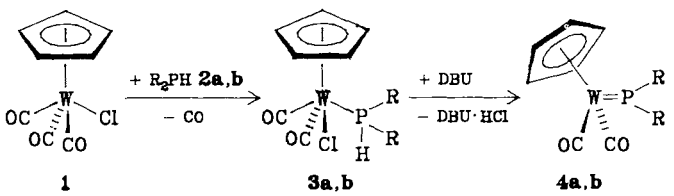
Synthesis, Structure, and Addition Reactions of $[Cp(CO)_2W{=}PR_2]$, R = *i*Pr, *t*Bu**

By *Klaus Jörg, Wolfgang Malisch,* Wolfgang Reich, Angelika Meyer,* and *Ulrich Schubert*

Dedicated to Professor Max Schmidt on the occasion of his 60th birthday

We recently reported a novel method for introducing phosphorus–metal double bonds into complexes of the type $[Cp(CO)_2M{=}PR_2]$ by 1,2-elimination of hydrogen chloride or dimethylamine from the complexes $[Cp(CO)_2M(H)PR_2X]$ (M = Mo, W; X = Cl, Me_2N).[1] Following the synthesis of *P*-alkoxy- and *P*-dimethylamino-substituted species we have now succeeded in preparing the previously unknown *P*-alkyl derivatives. Such derivatives are of special interest for studying double bond reactivity, which in this case is unaffected by hetero substituents.[1–3]

Since the corresponding chlorophosphane-metal hydride is not available,[4] complexes **3a, b** with phosphorus-hydrogen and metal-chlorine groups must be used as starting substances. The complexes **3a, b** are obtainable from the chloro complex **1** and the secondary phosphanes **2a, b** in boiling benzene,[5] and, according to the IR and NMR data, separate as pure *cis* isomers (diastereotopism of the alkyl groups, intensity ratio $\nu(CO)_s : \nu(CO)_{as} > 1$).[6] Their dehydrohalogenation to the double-bond complexes **4a, b** with 1,8-diazabicyclo[5.4.0]undec-7-ene (DBU) in methylcyclohexane at room temperature proceeds smoothly and cleanly. Upon cooling, **4a, b** precipitate from pentane as violet microcrystalline powders that are readily soluble in benzene and very sensitive to air. They melt with decomposition to give $(tBu_2P)_2$ and the dinuclear complex $[Cp(CO)_2W]_2$ via cleavage of the W=P bond.



The composition of **4a, b**, which, on account of a kinetic stabilization, are highly stable towards aggregation,[7] is confirmed by elemental analysis and by mass spectrometric data. The large *J*(PW) coupling constants of 591 and 552 Hz, respectively, for **4a** and **4b** (which are characteristic for phosphorus-metal double-bond complexes) and the respective $\delta(^{31}P)$ values of 401 and 373,[5] may be regarded as proof of the structure. The non-equivalence of the *tert*-butyl groups observed in the ^{1}H-NMR spectrum below −50°C reveals that the conformation with the doubly bonded P_2P ligand oriented "perpendicular" to the cyclopentadienyl unit is the energetically most favorable in solution.[8] The $\Delta G^{\neq}$ value for rotation about the metal-phosphorus double bond is, according to the temperature-dependent ^{1}H-NMR spectra, 10.3 kcal/mol. The X-ray structure analysis of **4b** is consistent with the molecular structure with "vertical" conformation and an exactly planar phosphorus atom (Fig. 1).[9] The W–P bond length (2.28 Å) lies in the range typical for a phosphorus-tungsten double bond (2.26 Å).[10]

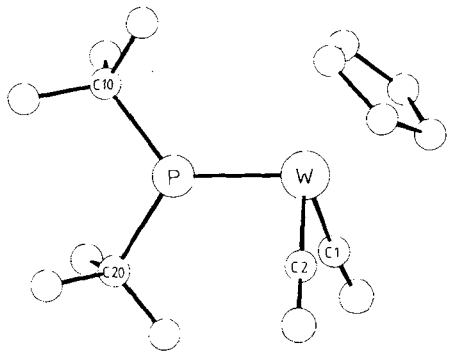
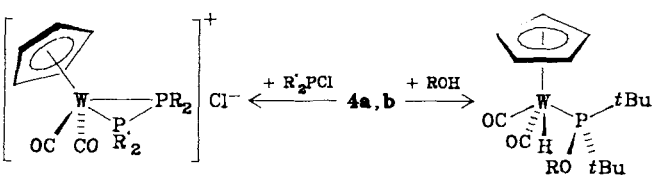


Fig. 1. Crystal structure of **4b**. The hydrogen atoms have been omitted for clarity. Selected bond lengths [Å] and angles [°]: W-P 2.284(4), P-C10 1.90(2), P-C20 1.91(2), W-C1 1.87(1), W-C2 1.94(2); M-W-P 134.4, W-P-C10 126.1(6), W-P-C20 124.4(6), C10-P-C20 109.4(8), P exactly planar, C1-W-C2 79.8(8), C1-W-P 93.6(6), C2-W-P 92.4(5). Further details of the crystal structure investigation are available on request from the Fachinformationszentrum Energie, Physik, Mathematik GmbH, D-7514 Eggenstein-Leopoldshafen 2, on quoting the depository number CSD 51700, the names of the authors, and the full citation of the journal.

Despite the shielding by bulky alkyl groups, the W=P bonds of **4a, b** are very reactive. Water, methanol or ethanol add spontaneously with formation of the *cis*-configurated complexes **5a–c**. Upon reaction with the chlorophos-



6a: R = R' = *i*Pr
6b: R = *t*Bu, R' = Me

5a: R = H
5b: R = Me
5c: R = Et

[*] Prof. Dr. W. Malisch, K. Jörg, W. Reich, Dr. A. Meyer, Prof. Dr. U. Schubert [†]
Institut für Anorganische Chemie der Universität
Am Hubland, D-8700 Würzburg (FRG)

[†] X-ray structure analysis.

[**] Main Group Element-Transition Metal Multiple Bonds, Part 7. This work was supported by the Deutsche Forschungsgemeinschaft and the Fonds der Chemischen Industrie. We thank Dr. *G. Lange* and Dr. *W. Buchner* for recording the mass spectra and NMR spectra, respectively.—Part 6: W. Malisch, K. Jörg, E. Gross, M. Schmeusser, A. Meyer, *Phosphorus Sulfur*, in press.

phanes R_2PCl (R = *i*Pr, *t*Bu), heterocyclic cleavage of the P-Cl bond takes place, followed by addition of R_2P^+ to the W=P double bond. This results in formation of the acetonitrile-soluble complexes **6a,b**, in which the diphosphane is coordinated side-on to the metal.

This type of coordination, shown for the first time for diphosphanes, follows from the appearance of only one *J*(PP) coupling in the case of **6b** and from the simple ^{183}W satellite pattern in the case of **6a** [*J*(WP) = 143 Hz] and **6b** [*J*(WP) = 112 Hz (Me_2P), 160 Hz (tBu_2P)].[11] The rapid olefin-like rotation of the $(R_2P)_2$ ligand attached to the metal of **6a**, **b** [$\Delta G^{\neq} = 13.5$ kcal/mol (**6a**)] and its unusually large *J*(PP) coupling of 400 Hz[12] in **6b** suggest a composition of the diphosphenium cation $[R_2P{=}PR_2]^{2+}$, hitherto unknown in the free state, and the metal fragment $Cp(CO)_2W^{\circ}$ for **6a**, **b**.

Experimental

3b: A solution of **1** (615 mg, 1.67 mmol) and **2c** (244 mg, 1.67 mmol) in benzene (60 mL) yielded, after boiling for 28 h under reflux, filtration, evaporation to dryness in vacuo, dissolution in methylcyclohexane (12 mL) and freezing (−78 °C), 642 mg (80%) of orange-red crystalline powder **3b**.—M.p. 128 °C (decomp.).

4b: A solution of **3b** (620 mg, 1.27 mmol) in methylcyclohexane (60 mL) was combined within 30 min at −78 °C with a suspension of DBU (192 mg, 1.16 mmol) in methylcyclohexane (10 mL) and the mixture stirred for 2 h. Subsequent filtration, evaporation to dryness in vacuo, and low-temperature crystallization from 15 mL of pentane/methylcyclohexane (3 : 2) gave 456 mg (80%) of **4b**, m.p. 109 °C (decomp.). **4a** was obtained analogously. Yield 398 mg (88%).—Violet crystalline powder, m.p. 69 °C (decomp.).

5a/b/c: Degassed H_2O/anhydrous MeOH/EtOH 3003 mg (166.7 mmol)/1030 mg (32.1 mmol)/2368 mg (51.4 mmol), respectively, were treated dropwise with solutions of **4b** in 10/5/10 mL of benzene. After removal of the solvent in vacuo the residue was washed with pentane and dried in vacuo. Yields 78/72/74%, respectively, of ocher colored/brown/light-brown solids.—M.p. 121/124/130 °C.

6a/6b: A solution of **4a** (386 mg, 0.89 mmol)/**4b** (172 mg, 0.38 mmol) in 50/20 mL of benzene was treated dropwise with iPr_2PCl/Me_2PCl (196 mg, 0.89 mmol) (84 mg, 0.38 mmol). **6a/6b** precipitated immediately. In each case the separated solid was washed with pentane and dried in vacuo.—Yield 76/84%.—Bright yellow solids.—M.p. 190—193/202 °C.

Received: September 9, 1985;
revised: October 12, 1985 [Z 1457 IE]
German version: *Angew. Chem. 98* (1986) 103

[1] E. Gross, K. Jörg, K. Fiederling, A. Göttlein, W. Malisch, R. Boese, *Angew. Chem. 96* (1984) 705; *Angew. Chem. Int. Ed. Engl. 23* (1984) 738.

[2] A. H. Cowley, *Chem. Rev.*, in press; L. D. Hutchins, E. N. Duesler, R. T. Paine, *Organometallics 3* (1984) 399.

[3] W. Malisch, E. Gross, A. Göttlein, unpublished.

[4] Reaction of $[Cp(CO)_3W{-}H]$ and tBu_2PCl does not afford the expected precursor $[Cp(CO)_2(tBu_2PCl)W{-}H]$ but only the decomposition products $[Cp(CO)_3W]_2$ and $(tBu_2P)_2$.

[5] Spectroscopic data: **3b**: $^{31}P\{^1H\}$-NMR (C_6D_6, 40.5 MHz, 35 °C): $\delta = 50.8$ ($^1J(WP) = 240$ Hz); IR (C_6H_6): $\nu(PH) = 2268$ cm^{-1} (w); $\nu(CO) = 1949$ (vs), 1863 (s) cm^{-1}.—**4a**: $^{31}P\{^1H\}$-NMR (C_6D_6, 40.5 MHz, 35 °C): $\delta = 401.9$ ($^1J(WP) = 591$ Hz); IR (C_6H_6): $\nu(CO) = 1941$ (vs), 1863 (vs) cm^{-1}.—**4b**: ^1H-NMR (C_6H_6, 60 MHz, 30 °C): $\delta = 5.37$ (s, 5H, H_5C_5), 1.40 (d, $^3J(PCCH) = 12.2$ Hz, 18H, H_3CCP). $^{31}P\{^1H\}$-NMR (C_6D_6, 40.5 MHz, 35 °C): $\delta = 373.4$ ($^1J(WP) = 552$ Hz); IR (C_6H_6): $\nu(CO) = 1932$ (vs), 1849 (s) cm^{-1}.—**5a**: ^1H-NMR (C_6H_6, 60 MHz, 30 °C): $\delta = 5.0$ (s, 5H, H_5C_5), 1.2 (d, $^2J(PCH) = 13$ Hz, 18H, H_3CCP), −7.45 (d, $^2J(PWH) = 65$ Hz, 1H, WH); $^{31}P\{^1H\}$-NMR (C_6D_6, 40.5 MHz, 35 °C): $\delta = 165.1$ ($^1J(WP) = 285.78$ Hz); IR (C_6H_6): $\nu(OH) = 3233$ cm^{-1} (w); $\nu(CO) = 1931$ (vs), 1845 (s) cm^{-1}.—**6a/b**: ^1H-NMR (CD_3NO_2/CH_3CN, 60 MHz, 30 °C): $\delta = 5.75$ (s, 5H, H_5C_5), 2.81–2.06 (m, $^3J(HCCH) = 7.0$ Hz, 4H, HCC), 1.75 (vdt $|^3J(HCCP') = 17.8$ Hz, $^3J(HCCH) = 7.0$ Hz, 6H, H_3C), 1.53 (vdt $|^3J(HCCP) + {}^4J(HCCP')| = 22.3$, $^3J(HCCH) = 7.0$ Hz, 6H, H_3C)/$\delta = 5.75$ (s, 5H, H_5C_5), 2.12 (d, $^2J(HCP) = 9.2$ Hz, 6H, H_3CP), 1.43 (d, $^3J(HCCP) = 15.2$ Hz, H_3CCP); $^{31}P\{^1H\}$-NMR (CD_3CN, H_3PO_4 ext.): $\delta = -73.0$ ($^1J(WP) = 143$ Hz)/(PMe_2): $\delta = -62.2$ ($^2J(PWP) = 400$, $^1J(WP) = 112$ Hz); ($PtBu_2$): $\delta = -109.6$ ($^2J(PWP) = 400$, $^1J(WP) = 160$ Hz); IR (CH_3CN): $\nu(CO) = 1977$ (vs), 1900 (s)/1975 (vs), 1903 (s) cm^{-1}.

[6] The structure of **3b** has been confirmed by X-ray structure analysis. W-P 2.518(1), W-Cl 2.491(1), P-H 1.52(3) Å; CO-W-CO 76.2(2), P-W-C_1 79.5(1), P-W-C2 111.2(1), C_{11}-P-C_{21} 110.8(2)°; W. S. Sheldrick, private communication.

[7] The methyl and ethyl compounds, which can be prepared analogously, are only detectable via trapping reactions at −20 °C. M. Schmeusser, K. Jörg, E. Gross, W. Malisch, unpublished.

[8] B. E. R. Schilling, R. Hoffmann, J. W. Faller, *J. Am. Chem. Soc. 101* (1979) 592.

[9] X-ray structure analysis of **4b**: C2/c ($Z = 8$), $a = 28.067(10)$, $b = 8.547(3)$, $c = 16.978(7)$ Å, $\beta = 124.67(3)°$, $\rho_{calcd.} = 1.79$ g/cm^3. 2088 independent reflections ($2° \leq 2\Theta \leq 48°$, $Mo_{K\alpha}$ radiation). $R = 0.059$, $R_w = 0.057$ using all reflections.

[10] M. Yoshifuji, I. Sima, N. Inamoto, K. Hirotsu, T. Higuchi, *J. Am. Chem. Soc. 103* (1981) 4587.—R. J. Klingler, W. M. Butler, M. D. Curtis, *ibid. 100* (1978) 5034.—R. D. Adams, D. M. Collins, F. A. Cotton, *Inorg. Chem. 13* (1975) 1086.

[11] In the case of a dimeric structure with six-membered ring arrangement, phosphorus-phosphorus couplings should appear in the ^{183}W-satellite spectrum of **6a**. Cf. Y. Koie, L. Shinoda, Y. Saito, *Inorg. Chem. 20* (1981) 4408. In the case of **6b** the two couplings $^1J(PP)$ and $^2J(PWP)$ would be expected. We thank Dr. *W. Buchner* for valuable discussions.

[12] A. H. Cowley, *Polyhedron 3* (1984) 389.

Wittig Reaction with Carbon Suboxide: Synthesis of Dimethyl 1,5-Diphenyl-1,2,3,4-pentatetraenedicarboxylate**

By *Franz W. Nader** and *Angelika Brecht*

Despite their interesting stereochemical properties very few derivatives of 1,2,3,4-pentatetraene are known,[1] and none of those so far reported contain functional groups. The only instance of a stereoisomeric resolution of a chiral pentatetraene derivative was described in 1979 by *Jochims* et al.[2]

The Wittig reaction should in principle provide a synthetic entry to this class of compounds, since it allows, inter alia, the conversion of heterocumulenes into C-cumulenes by carbonyl olefination. Thus, reactions of ketenes with ylides lead to allenes,[3] while reactions of propadiene ylides with ketones[4] and of propadienone derivatives with simple ylides[5] lead to butatrienes. Following this concept, symmetrically substituted pentatetraenes **4** ought to be accessible by double Wittig reaction of the heterocumulene carbon suboxide **1** and simple ylides **2**, with the butatrienone derivative **3** being formed as intermediate.

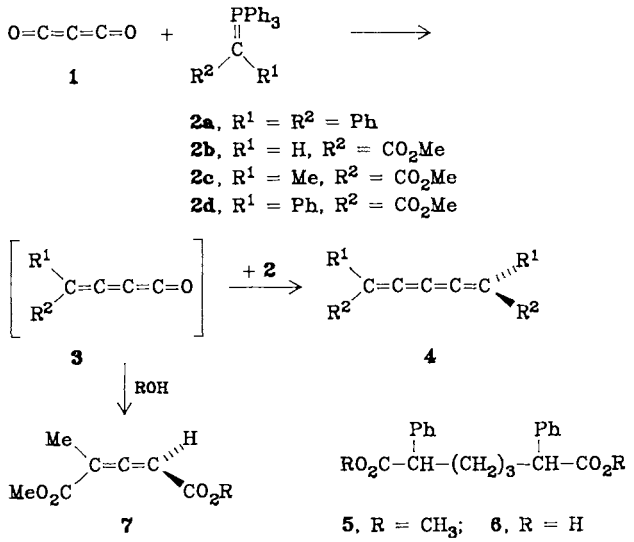
Although the reactivity of carbon suboxide has been studied in detail,[6a] Wittig reactions of this compound have hitherto been overlooked.[6b]

Of the various methods available for the synthesis of C_3O_2[7] we initially employed the procedure described by *Hopff* et al.[9] and based on the method due to *Staudinger* et al.,[8] which furnishes C_3O_2 in ethereal solution. It emerged, however, that the course of the reaction is strongly dependent upon the nature of the solvent. We therefore resorted to the thermolysis of bis(trimethylsilyl) malonate, the method of *Birkofer* and *Sommer*,[10] in which C_3O_2 is distilled into petroleum ether.

The Wittig reactions with carbon suboxide are best carried out in benzene at high dilution ($c < 0.01$ M). Reaction with **2a** does indeed lead to formation of the respective tetraene **4a** (detection by IR and ^1H-NMR spectroscopy) but nevertheless always accompanied by substantial amounts of benzophenone and diphenylmethane, the latter preventing a chromatographic purification. In the reaction of the ylide **2b**, the C_3O_2 was rapidly consumed, but

[*] Priv.-Doz. Dr. F. W. Nader, A. Brecht
Organisch-chemisches Institut der Universität
Im Neuenheimer Feld 270, D-6900 Heidelberg (FRG)

[**] Chemistry of the Cumulenes, Part 5.—Part 4: F. W. Nader, C.-D. Wacker, *Angew. Chem. 97* (1985) 877; *Angew. Chem. Int. Ed. Engl. 24* (1985) 852.



neither desired product nor triphenylphosphane oxide could be detected. The ylide **2c** reacts rapidly at room temperature with formation of $Ph_3P{=}O$ and large amounts of polymeric material; by thin-lay chromatography a substance was detected, which, upon column chromatographic separation of the dark brown reaction solution, could be isolated as a colorless oil. This, however, rapidly decomposed to a red tar—even at low temperatures. The IR spectrum showed a medium strong band at 2050 cm^{-1}, which was interpreted as an indicator of the substance being the tetraene **4c**.

The best results were afforded by the ylide **2d**: It reacts with C_3O_2 to give the lemon-yellow, crystalline pentatetraene dicarboxylate **4d** in yields of up to 46%.[11] The structure of **4d** was unequivocally characterized by the IR cumulene band at 2040 cm^{-1}, by the ^{1}H-NMR spectrum, and by its hydrogenation (4 equivalents of H_2) to the α,α'-diphenylpimelic acid dimethyl ester **5**, which was hydrolyzed to the crystalline dicarboxylic acid **6**.[12]

In the absence of air, the crystalline tetraene **4d** is storable over long periods at room temperature, and almost indefinitely at −20°C. In dilute solution, **4d** is storable for short periods; in higher concentrations ($c > 0.01$ M), and especially in the oily form, rapid decomposition occurs, ultimately leading to polymers and presumably initiated by dimerization reactions. It was therefore impossible to obtain a definite ^{13}C-NMR spectrum of **4d**. The instability in concentrated solutions is also the reason for not having been able to isolate the oily di-(−)-menthyl ester analogous to **4d**, thus preventing a study of the asymmetric induction in this reaction.

As expected, the tetraene diester **4d** readily reacts with nucleophiles such as, e.g., alcohol/alkoxide (catalytically), amines, and triphenylphosphane, whereupon well-defined but unusual Michael adducts are formed.[13] For this reason, all attempts to prepare the dicarboxylic acid by basic ester cleavage failed—even under the mild conditions of the two-phase system [18]crown-6/tetrahydrofuran/KOH/H_2O), which proved successful in the case of the analogous butatrienecarboxylates.[14]

The butatrienone intermediate **3** could be detected in the 1:1 reactions of C_2O_3 with **2c** by trapping with alcohols such as, e.g., methanol and benzyl alcohol. In each case the allenedicarboxylate **7** was formed in 10–15% yield as the only well-defined product; the colorless oils gave characteristic ^{1}H-NMR spectra (coupling between allene-H and CH_3-group).

In order to synthesize unsymmetrically substituted pentatetraenes, butatrienones such as **3** must be used. Possible starting materials for their preparation are alkyl esters of 4-chloroformyl-2,3-butadienoic acids unsubstituted in the 4-position.[15] In our first investigations, pentatetraene diesters were obtained in yields of up to 75%.

Received: August 26, 1985;
supplemented: October 9, 1985 [Z 1443 IE]
German version: *Angew. Chem. 98* (1986) 105

[1] R. Kuhn, H. Fischer, H. Fischer, *Chem. Ber. 97* (1964) 1760; L. Skattebøl, *Tetrahedron Lett. 1965*, 2175; G. Karich, J. C. Jochims, *Chem. Ber. 110* (1977) 2680; M. von Herrath, D. Rewicki, *Justus Liebigs Ann. Chem. 1977*, 582; A. Oostveen, C. J. Elsevier, J. Meijer, P. Vermeer, *J. Org. Chem. 47* (1982) 371.

[2] K. Bertsch, M. A. Rahman, J. C. Jochims, *Chem. Ber. 112* (1979) 567.

[3] G. Wittig, A. Haag, *Chem. Ber. 96* (1963) 1535; H. J. Bestmann, H. Hartung, *ibid. 99* (1966) 1198; G. Kresze, G. Runge, E. Ruch, *Justus Liebigs Ann. Chem. 756* (1972) 112; R. W. Lang, H.-J. Hansen, *Helv. Chim. Acta 63* (1980) 438.

[4] H. J. Bestmann, G. Schmid, *Tetrahedron Lett. 1975*, 4025.

[5] S. Fernandez, *Diplomarbeit*, Universität Heidelberg 1985.

[6] a) Recent review: T. Kappe, E. Ziegler, *Angew. Chem. 86* (1974) 529; *Angew. Chem. Int. Ed. Engl. 13* (1974) 491. b) An article on the reactions of carbon suboxide with phosphonium ylides, including **2a**, has already appeared in the literature. Although the authors could identify triphenylphosphane oxide among the reaction products, an indication of the respective carbonyl olefination reaction is lacking. 1,3-Cyclobutanedione derivatives, as well as diphenylmethane and benzophenone in the case of **2a**, could be isolated and characterized: H. F. van Woerden, H. Clairfontain, C. F. van Valkenburg, *Recl. Trav. Chim. Pays-Bas 88* (1969) 158. We thank a referee for having brought this to our attention.

[7] D. Borrmann in Houben-Weyl-Müller (Ed.): *Methoden der Organischen Chemie, Bd. 7/4*, Thieme, Stuttgart 1968, p. 286.

[8] H. Staudinger, S. Bereza, *Ber. Dtsch. Chem. Ges. 41* (1908) 4461.

[9] H. Hopff, G. Hegar, *Helv. Chim. Acta 44* (1961) 2016.

[10] L. Birkofer, P. Sommer, *Chem. Ber. 109* (1976) 1701.

[11] The ylide **2d** (23 g, 56 mmol) was dissolved in anhydrous benzene (800 mL) under N_2 in a 1 L single-necked flask. The stirred solution was treated with 28 mmol of C_3O_2 (petroleum ether solution, $c = 0.2$–0.6 M) and three drops of triethylamine. After 6 d, the dark red-brown solution was transferred portionwise onto three columns (2.5 cm (ID) × 35 cm) packed with silica-gel and eluted with benzene. The combined deep-yellow eluates (1.1 L) proved to be pure (TLC). The benzene was now removed by evaporation under oil-pump vacuum (maximum bath-temperature 30°C) and simultaneously replaced by petroleum ether (b.p. 110–120°C) via a dropping funnel. Yellow crystals of the tetraene ester finally began to separate out. The mixture was then concentrated to about 50 mL and the resulting crystalline mass recovered by filtration. Lemon-yellow crystals (recrystallization: 1 mL of ice-cold CH_2Cl_2 and 10 mL of petroleum ether per 100 mg of **4d**; −20°C) m.p. 120°C (decomp.). Yield: 4.3 g (46%).—IR (KBr): $\nu = 2040$ cm^{-1} (ms, cumulene band); ^{1}H-NMR (90 MHz, $CDCl_3$): $\delta = 3.87$ (s, 6H, $2OCH_3$), 7.30 (m, 6H, *m-/p*-arene-H), 7.70 (m, 4H, *o*-arene-H); correct elemental analysis.

[12] 300 mg of **4d** was added to a prehydrogenated suspension of Raney nickel in ethyl acetate (50 mL) and the mixture hydrogenated. Uptake of H_2 was complete within 30 min (90 mL $H_2 = 4$ equiv. H_2). After filtration and removal of solvent there remained 250 mg of **5** as a colorless oil [^{1}H-NMR (60 MHz, $CDCl_3$): $\delta = 1.27$ (m, 2H, $-CH_2-$), 1.95 (quint. 4H, $-CH_2-CH$), 3.53 (t, 2H, α/α'-CH-Ph), 3.59 (s, 6H, $2OCH_3$), 7.33 (m, 10H, arene-H)]. Since the ester **5** did not crystallize, it was hydrolyzed with 10% NaOH in methanol/water at room temperature. After the usual work-up, **6** was obtained as a colorless oil which crystallized on standing. Colorless crystals (benzene/petroleum ether), m.p. 100–103°C (not diastereomerically pure).—^{1}H-NMR (60 MHz, $CDCl_3$): $\delta = 0.73$–2.37 (two m, 6H, $(CH_2)_3$), 3.30–3.67 (m, 2H, α/α'-CH-Ph), 7.22 (s, 10H, arene-H), 9.77 (broad s, 2H, CO_2H); correct elemental analysis. M.p. (Lit.) 147–149°C (diastereomerically pure, presumably *meso*): C. G. Screttas, M. Micha-Screttas, *J. Org. Chem. 44* (1979) 713.

[13] Michael additions to butatriene and pentatetraene dicarboxylic acid esters: F. W. Nader, C.-D. Wacker, unpublished.

[14] F. W. Nader, C.-D. Wacker, *Angew. Chem. 97* (1985) 876; *Angew. Chem. Int. Ed. Engl. 24* (1985) 851.

[15] F. W. Nader, A. Brecht, S. Kreisz, *Chem. Ber.*, in press.

Synthesis and Structure of 1,3-Diphenyltriazenidogold(I), a Tetrameric Molecule with Short Gold-Gold Distances**

By *Johannes Beck* and *Joachim Strähle**

Polynuclear complexes whose metal atoms have d^{10} configuration are currently attracting a great deal of attention, primarily because of the much debated subject of metal-metal bonding between d^{10} centers. Hückel MO calculations[1-3] show that a bonding interaction results by incorporation of vacant s- and p-orbitals. Cu^I forms a series of such polynuclear complexes with Cu-Cu distances of not more than 235 pm.[1,4] In the case of complexes with monovalent gold, Au-Au distances of down to as short as 260 pm are not uncommon.[3,5,6] In clusters containing Au^I along with another metal, still shorter distances have been observed.[7]

In most cases the short metal-metal distances are favored by bridging ligands. A remarkable exception is the cluster **1**,[8] in which a Pt^0-Pt^0 bond of 276 pm without bridging ligand has been found.

$[Pt(t\mathrm{Bu})_2P(CH_2)_3P(t\mathrm{Bu})_2]_2$ **1**

Bridging ligands can also stabilize d^{10}-d^{10} interactions by accomodating antibonding charge density from the metals via their π-system.[9] As also shown by trimeric 1,5-ditolyl-1,4-pentaazadien-3-idocopper(I), with its extremely short Cu-Cu distances,[4] polyazenido ligands are especially capable of effecting such a stabilization. We have therefore prepared the complex 1,3-diphenyltriazenidogold(I) **2**. In metal complexes the 1,3-diphenyltriazenide functions either as a bidentate chelate ligand to a metal atom or as a bridging ligand for two metal atoms. The short distance between the two outer nitrogen atoms (223 pm) gives rise thereby to short metal-metal distances.

The structures of several complexes with divalent metals are already known.[10] The Cu^I complex **3** is dimeric with a Cu-Cu distance of 245 pm,[11] the corresponding complex of dimethyltriazenide **4** is tetrameric. The four Cu atoms form a rhombus with a mean Cu-Cu distance of 266 pm.[12]

$[Au(PhNNNPh)]_4$ **2** $[Cu(PhNNNPh)]_2$ **3**

$[Cu(H_3CNNNCH_3)]_4$ **4** $[Au(CH_3CSS)]_4$ **5**

Au^I can form both types of complex with single negatively charged bidentate ligands. For example, dipropyldithiocarbamatogold(I) is dimeric with a Au-Au distance of 276 pm,[13] whereas the tetramer **5** containing a rhombic Au_4 ring is formed with the dithioacetato ligand.[9] The mean Au-Au distance of 301 pm in this complex is, however, markedly longer than in the metal (288.4 pm[14]).

We obtained tetrameric **2** from AuI and $Na(PhN_3Ph)$ in liquid ammonia.[15] The yellow, air-stable compound crystallizes from tetrahydrofuran (THF)/hexane as rectangular crystals of the composition **2**·THF which decompose without melting above 180°C. A molecular weight determination revealed that **2** is also tetrameric in $CHCl_3$ solution. In the IR spectrum, the asymmetric N-N stretching vibration appears at 1380 cm^{-1}.

The structure determination[16] (Fig. 1) shows that four atoms are located at the corners of a rhombus and the four ligands form bridges alternately above and below the plane of the Au_4 ring.

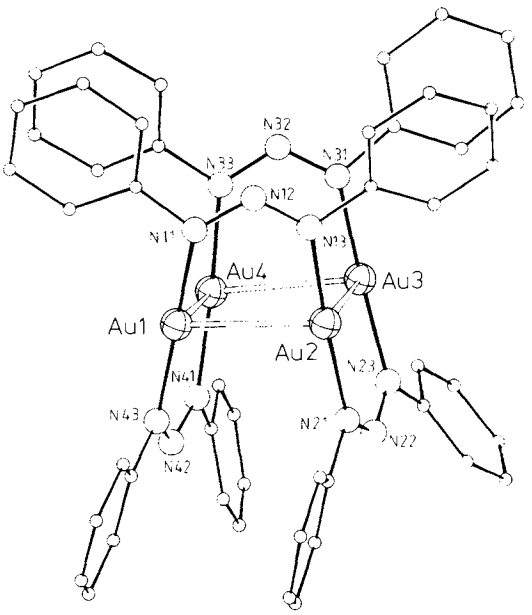


Fig. 1. Structure of **2** in the crystal of **2**·THF. Important bond lengths [pm] and angles [°]: Au1-Au2 284.8(1), Au2-Au3 285.6(1), Au3-Au4 285.5(1), Au4-Au1 284.2(1), Au2-Au4 331.9(1), Au-N 201.8(5) to 206.6(5), N-N 127.7(7) to 130.6(6); Au2-Au1-Au4 71.38(1), Au1-Au2-Au3 108.51(1), Au2-Au3-Au4 71.07(1), Au1-Au4-Au3 108.72(1), N-Au-N 175.2(2) to 178.0(2), N-N-N 118.3(6) to 118.9(5).

The mean gold-gold distance of 285 pm is somewhat shorter than in the metal; so a bonding interaction may therefore be assumed. The Au_4 ring is folded at an angle of 7° along the Au1-Au3 axis, with Au2, for example, protruding about 21 pm from the plane of the other three gold atoms. The gold-nitrogen distances (204 pm) lie in the range typical for gold-nitrogen single bonds. The gold atoms are linearly coordinated, and the N-Au-N angles are on average 176°. The bridging N_3-unit and the two associated gold atoms always lie in a plane (N23 shows the largest deviation (9 pm) from the Au2/Au3/N21/N22/N23 plane). Opposite planes each form a dihedral angle of about 22°. The N-N distances are almost equivalent. They lie between 127.7 and 130.6 pm and thus correspond to slightly stretched double bonds, as are also found in other triazenido complexes[10-12] and in the essentially ionic 1,5-ditolyl-1,4-pentaazadien-3-idothallium(I) complex.[17]

Received: September 4, 1985;
supplemented: October 16, 1985 [Z 1451 IE]
German version: *Angew. Chem. 98* (1986) 106

[*] Prof. Dr. J. Strähle, Dipl.-Chem. J. Beck
Institut für Anorganische Chemie der Universität
Auf der Morgenstelle 18, D-7400 Tübingen 1 (FRG)

[**] This work was supported by the Deutsche Forschungsgemeinschaft and the Fonds der Chemischen Industrie.

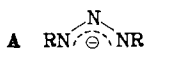
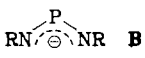
[1] P. K. Mehrotra, R. Hoffmann, *Inorg. Chem. 17* (1978) 2178.
[2] A. Dedieu, R. Hoffmann, *J. Am. Chem. Soc. 100* (1978) 2074.
[3] Y. Jiang, S. Alvarez, R. Hoffmann, *Inorg. Chem. 24* (1985) 749.
[4] J. Beck, J. Strähle, *Angew. Chem. 97* (1985) 419; *Angew. Chem. Int. Ed. Engl. 24* (1985) 409.
[5] S. Gambarotta, C. Floriani, A. Chiesi-Villa, C. Guastini, *J. Chem. Soc. Chem. Commun. 1983*, 1304.
[6] P. G. Jones, *Gold Bull. 14* (1981) 102; *ibid. 14* (1981) 159; *ibid. 16* (1983) 114.
[7] P. Braunstein, J. Rose, *Gold Bull. 18* (1985) 17.
[8] T. Yoshida, T. Yamagata, T. H. Tulip, J. A. Ibers, S. Otsuka, *J. Am. Chem. Soc. 100* (1978) 2063.

[9] O. Piovesana, P. F. Zanazzi, *Angew. Chem. 92* (1980) 579; *Angew. Chem. Int. Ed. Engl. 19* (1980) 561; B. Chiari, O. Piovesana, T. Tarantelli, P. F. Zanazzi, *Inorg. Chem. 24* (1985) 366.
[10] M. Corbett, B. F. Hoskins, M. J. McLeod, B. P. O'Day, *Aust. J. Chem. 28* (1975) 2377.
[11] I. D. Brown, J. D. Dunitz, *Acta Crystallogr. 14* (1961) 480.
[12] J. E. O'Connor, G. A. Janusonis, E. R. Corey, *J. Chem. Soc. Chem. Commun. 1968*, 445.
[13] R. Hesse, P. Jennische, *Acta Chem. Scand. 26* (1972) 3855.
[14] L. Pauling: *The Nature of the Chemical Bond*, Cornell University Press, Ithaca, New York 1960.
[15] Procedure: 1 g of AuI and 0.68 g of $Na(PhN_3Ph)$ [18] were each separately dissolved in 50 mL of liquid ammonia. After combining the two solutions, the ammonia was allowed to "boil" off. The red residue was extracted twice with 20 mL of toluene. There remained 0.3 g (25%) of **2**, which was recrystallized from THF/*n*-hexane.
[16] **2**·THF: $P\bar{1}$, $a = 1350.1(5)$, $b = 1600.9(3)$, $c = 1241.6(2)$ pm, $\alpha = 91.69(1)$, $\beta = 108.93(2)$, $\gamma = 80.71(2)°$, $Z = 2$, $R = 0.026$ for 4836 independent reflections with $I \geq 3\sigma(I)$ and 622 refined parameters (Enraf-Nonius CAD4, $Mo_{K\alpha}$). Further details of the crystal structure investigation are available on request from the Fachinformationszentrum Energie, Physik, Mathematik GmbH, D-7514 Eggenstein-Leopoldshafen 2, on quoting the depository number CSD-51609, the names of the authors, and the full citation of the journal.
[17] J. Beck, *Dissertation*, Universität Tübingen 1986.
[18] W. Beckh, J. Tafel, *Ber. Dtsch. Chem. Ges. 27* (1894) 2315.

$Me_3SiNPNSiMe_3^{\ominus}$, the Monophosphorus Analogue of a Triazenido Ligand**

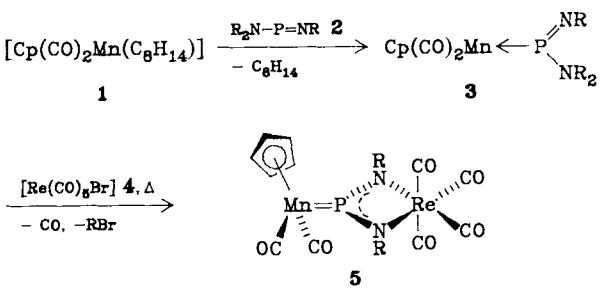
By *Otto J. Scherer,* Ekkehard Franke,* and *Jürgen Kaub*

If the central N atom in the triazenido ligand **A** is replaced by a P atom, the monophosphorus analogue **B** is obtained (cf. the complex-stabilized RPCHPR, R = 2,4,6-$(t\text{Bu})_3C_6H_2$[1]). Whereas only the two terminal N atoms of **A** are used in coordination (monodentate, chelating, or μ-bridging),[2] the η^1 type of P coordination, in addition to the chelate type, is observed for **B** (**B** as a tridentate 6e donor ligand).

A   **B**

The *cis*-cyclooctene complex **1** undergoes ligand exchange reaction with the amino(imino)phosphane **2** to give the complex **3**, which reacts in turn with the rhenium complex **4** to give the species **5** in which **B** is present as a 6e donor.

5[3] forms yellow, extremely air-sensitive (brown coloration) crystals, which are sparingly soluble in hexane but readily soluble in benzene, toluene, and dichloromethane. Its $^{31}P\{^1H\}$-NMR signal ($\delta = 394.6$) is significantly shifted to lower field in comparison with the precursor **3** ($\delta = 312.5$).[4]



Cp = η^5–C_5H_5; R = $SiMe_3$; C_8H_{14} = *cis*–cyclooctene

The X-ray structure analysis[5] confirms the tridentate coordination of the $RNPNR^{\ominus}$ ligand (Fig. 1). **5** exhibits approximate C_S symmetry. The geometry around the P (360°) and the N atoms (359, 360°) is trigonal planar. The atoms Mn, P, N1, Si1, N2, Si2, Re, C15, and C17 lie in a plane. The dihedral angle between the planes $C_5H_{5(centr.)}$, Mn, P and N1, P, N2 is 91°.

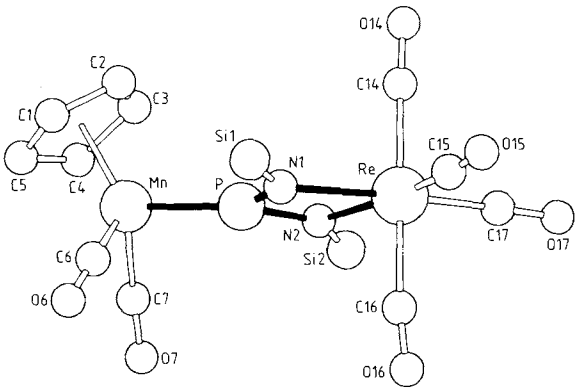


Fig. 1. Crystal structure of **5** (methyl groups and hydrogen atoms have been omitted for clarity). Selected bond lengths [Å] and angles [°] (see also text): Mn-P 2.122(8), P-N1 1.60(3), P-N2 1.62(2), N1-Si1 1.78(3), N2-Si2 1.78(2), Re-N1 2.19(2), Re-N2 2.19(2), Re-C15 1.94(3), Re-C17 1.89(3); N1-P-N2 97(1), P-N1-Re 98(1), P-N2-Re 98(1), N1-Re-N2 66.7(8), P-Mn-C6 93.4(8), P-Mn-C7 95.0(8), P-Mn-$C_5H_{5(centr.)}$ 123.

In the cluster **6a**,[6a] which is also planar at the P atoms and which has a P_2Fe_2 butterfly skeleton, the corresponding planes nearly coincide. This orientation (conformation), which is preferred on the basis of theoretical calculations,[7] is energetically unfavorable for **5**, possibly as a result of steric and electronic effects. The stepwise-formed exocyclic Mn-P bond is remarkably short (2.122(8) Å); it is only slightly longer than that of **6a**[6a] (mean value: 2.10 Å) but shorter than that in the phosphanediyl complex **6b**[6b] (mean value: 2.184 Å). As discussed already in the case of **6**,[6] this bond has multiple bond character.

$[\{Cp(CO)_2Mn{=}P\}_2Fe_2(CO)_6]$ **6a** $[\{Cp(CO)_2Mn\}_2PC_6H_5]$ **6b**

$[(OC)_5Cr\{P(=NR')(NR_2)\}]$ $[Pt\{P(=NR')(NRR')\}_3]$
7 R = $SiMe_3$, R' = *t*Bu **8**

trans-$[(Ph_3P)_2(OC)_2\overline{ReN(R)NNR}]$
9, R = *p*-MeC_6H_4

As a result of its charge and its bonding to the $Re(CO)_4$ fragment, the $Me_3SiNPNSiMe_3^{\ominus}$ ligand apparently exhibits more pronounced π-acceptor behavior than the amino(imino)phosphane ligand in complexes of type **7**[8a] and **8**[8b]. The lengths of the Re-N bonds (2.19(2) Å) and the Re-C bonds (C15, C17) *trans* to them are nearly identical to those of the comparable triazenido complex **9**[9] (mean values: Re-N 2.19, Re-C 1.92 Å). The mean value of the P-N distances (1.61 Å) in **5** is that expected based on the values of the free ligand **2** (P=N 1.545(2), P–N 1.674(1) Å).[10]

[*] Prof. Dr. O. J. Scherer, Dipl.-Chem. E. Franke, Dipl.-Chem. J. Kaub [+]
Fachbereich Chemie der Universität
Erwin-Schrödinger-Strasse, D-6750 Kaiserslautern (FRG)
[+] X-ray analysis.
[**] This work was supported by the Fonds der Chemischen Industrie.

Received: September 6, 1985;
revised: October 10, 1985 [Z 1453 IE]
German version: *Angew. Chem. 98* (1986) 83

[1] R. Appel, W. Schuhn, F. Knoch, *Angew. Chem. 97* (1985) 421; *Angew. Chem. Int. Ed. Engl. 24* (1985) 420.
[2] For example, F. A. Cotton, G. Wilkinson: *Anorganische Chemie*, 4th ed., Verlag Chemie, Weinheim 1982, p. 133; *Advanced Inorganic Chemistry*, 4th ed., Wiley-Interscience, New York 1980, p. 131.
[3] Experimental procedure: **3**: **1** (1.197 g, 4.18 mmol) [11] and **2** (1.165 g, 4.18 mmol) [12] in 20 mL of toluene were stirred at 90°C for ca. 3.5 h. After removal of all volatiles, the product was dried for several hours in an oil-pump vacuum. **3** separated out quantitatively as a pure (NMR) red oil, which could not be induced to crystallize (NMR and IR data [4]). **5**: **3** (1.901 g, 4.18 mmol) and **4** (1.698 g, 4.18 mmol) were refluxed in 30 mL of xylene for ca. 15 h (end of reaction determined by ^{1}H-NMR). After removal of all volatiles, the product was dried for several hours in an oil-pump vacuum. The yellow, partially viscous residue was dissolved in ca. 30 mL of toluene, filtered through filter flocks and cooled for 1 d at 0°C and again at −35°C. After the toluene had been decanted, the yellow crystals were washed with ca. 3 mL of cold toluene and dried in vacuum (10 torr). Yield: 1.28 g (46%).
[4] ^{31}P{^{1}H}-NMR (81.0 MHz, 20°C, C_6D_6, 85% H_3PO_4 ext.). During the conversion of **3** into **5**, a transient singlet appears at $\delta = 234.9$, which we assign to the intermediate $[Cp(CO)_2Mn{-}P(NR_2)(=NR){\rightarrow}Re(CO)_4Br]$. ^{13}C{^{1}H}-NMR (50.28 MHz, [D$_6$]acetone, TMS int.) **3** (−60°C): $\delta = 231.7$ (d, CO, $^2J(PC) = 34.2$ Hz), 85.8 (s, C_5H_5), 4.10, 3.63 (s, $SiCH_3$). **5** (−40°C): $\delta = 232.9$ (d, CO, Mn, $^2J(PC) = 19.8$ Hz), 197.7, 191.7 (s, CO, Re), 83.4 (s, C_5H_5), 1.6 (s, $SiCH_3$). ^{1}H-NMR (200 MHz, C_7D_8, TMS int.) **3** (80°C): $\delta = 4.19$ (d, 5 H, $^3J(PH) = 1.8$ Hz), 0.32 (s, 18 H), 0.21 (s, 9 H). **5** (20°C): $\delta = 4.08$ (d, 5 H, $^3J(PH) = 1.5$ Hz), 0.41 (s, 18 H). IR: **3** (*n*-hexane) $\nu(CO) = 1970$ (s), 1912 cm^{-1} (s). **5** (C_6H_6): $\nu(CO) = 2020$ (s), 1940 (sh), 1910 (vs, br), 1890 (s, br), 1840 cm^{-1} (m, br).
[5] **5**: $P2_12_12_1$, $a = 18.070(6)$, $b = 11.361(3)$, $c = 12.325(4)$ Å, $Z = 4$, $\rho_{calcd} = 1.87$ g·cm^{-3}, 1417 observed of 1893 unique reflections ($Mo_{K\alpha}$, $F_0^2 \geq 2.0\sigma(F_0^2)$, $2\theta \leq 45°$); $R = 0.059$, $R_w = 0.053$. Further details of the crystal structure investigation are available on request from the Fachinformationszentrum Energie, Physik, Mathematik GmbH, D-7514 Eggenstein-Leopoldshafen 2, on quoting the depository number CSD 51579, the names of the authors, and the journal citation.
[6] a) H. Lang, L. Zsolnai, G. Huttner, *Angew. Chem. 95* (1983) 1016; *Angew. Chem. Int. Ed. Engl. 22* (1983) 976; *Angew. Chem. Suppl. 1983*, 1451; b) G. Huttner, H.-D. Müller, A. Frank, H. Lorenz, *ibid. 87* (1975) 714 bzw. *14* (1975) 705.
[7] B. E. R. Schilling, R. Hoffmann, D. L. Lichtenberger, *J. Am. Chem. Soc. 101* (1979) 585.
[8] a) S. Pohl, *J. Organomet. Chem. 142* (1977) 185, 195; b) O. J. Scherer, R. Konrad, C. Krüger, Y.-H. Tsay, *Chem. Ber. 115* (1982) 414.
[9] R. Graziani, L. Toniolo, U. Casellato, R. Rossi, L. Magon, *Inorg. Chim. Acta 52* (1981) 119.
[10] S. Pohl, *Chem. Ber. 112* (1979) 3159.
[11] G. Brauer: *Handbuch der Präparativen Anorganischen Chemie, Bd. 3*, Enke, Stuttgart 1981, p. 1887.
[12] O. J. Scherer, N. Kuhn, *Chem. Ber. 107* (1974) 2123.

Facile Synthesis of Pentaphenylnickelocene and Other Pentaphenylcyclopentadienylnickel and -cobalt Complexes**

By *Wolfgang Kläui** and *Ludwig Ramacher*

Pentamethylcyclopentadienyl complexes have been extensively studied in recent years.[1] They can be obtained from halogeno-transition-metal complexes $[ML_mX_n]$ and alkali-metal-, Grignard- or thallium-cyclopentadienides. Several reports show that the synthesis of transition-metal-pentaphenylcyclopentadienyl complexes via this route is possible.[2-4] The preparation of alkali-metal-pentaphenylcyclopentadienides is, however, not unproblematical. When pentaphenylcyclopentadiene is allowed to react with alkali metals, formation of the remarkably stable pentaphenylcyclopentadienyl radical is frequently observed as a side reaction. Furthermore, the secondary products of this radical are often difficult to separate. We have therefore searched for an alternative entry to perphenylated cyclopentadienyl-metal complexes.

Using the reaction of pentacarbonyliron with bromopentaphenylcyclopentadiene to give bromodicarbonyl(pentaphenylcyclopentadienyl)iron[5] as starting point, we found that the oxidative addition of bromopentaphenylcyclopentadiene is an elegant method for the preparation of pentaphenylcyclopentadienyl-nickel and -cobalt complexes. C_5Ph_5Br is easier to obtain than C_5Ph_5H and is smoothly accessible in large amounts in analytically pure form.[6] Reaction of stoichiometric amounts of C_5Ph_5Br and tetracarbonylnickel in tetrahydrofuran (THF) leads to the formation of di-μ-bromobis(pentaphenylcyclopentadienylnickel) **1** in almost quantitative yield.

$$C_5Ph_5Br + Ni(CO)_4 \longrightarrow [(C_5Ph_5)Ni(\mu\text{-}Br)_2Ni(C_5Ph_5)]\ \mathbf{1}$$

The chloro compound can be prepared in the same way. **1** is remarkably stable towards heat (no decomposition below 200°C), but is sensitive to air in solution. It is the second halogeno-bridged cyclopentadienylnickel compound of this type so far reported. The corresponding pentamethylcyclopentadienyl compound, first synthesized by *Kölle* et al., is storable only below −10°C.[7] The analogous unsubstituted cyclopentadienyl complex is not known. Depending upon the temperature, varying amounts of the carbonyl complex **2** are also found to be formed in addition to the dimeric compound **1**. The complex **2**, which is probably the primary product of the reaction, can be synthesized by reaction of **1** with CO at room temperature and normal pressure in THF.[8] The method used for the synthesis of **2** can also be used for the synthesis of **3**[8] starting from C_5Ph_5Cl.[6] It is surprising that **2** and **3** are the first stable compounds of type **A** that have become accessible. We have been able to prepare the iodo complex **4** for the first time by halide-exchange from **2** in acetone.[8] The carbonyl complexes **2**, **3**, and **4** are, like **1**, deep-red crystalline compounds that are storable in presence of air for weeks at room temperature but air-sensitive in solution. They are of interest as starting substances for the synthesis of sandwich complexes of the type **B** and **C**.[9] **1** reacts with thallium cyclopentadienide in THF to give the previously unknown pentaphenylnickelocene **5**.[10]

The air-sensitive, olive-green compound is, as expected, paramagnetic in solution and in the solid state. The magnetic moment (dichloromethane, Evans method) is $\mu_{eff} = 2.9$ B.M. The magnetic moment of the solid was found to be $\mu_{eff} = 3.2$ B.M. at 25°C.

$[(C_5Ph_5)Ni(CO)Br]$ **2** $\quad$ $[(C_5Ph_5)Ni(CO)Cl]$ **3**

$[(C_5Ph_5)Ni(CO)I]$ **4** $\quad$ $[(C_5Ph_5)Ni(C_5H_5)]$ **5** $\quad$ $[(C_5Ph_5)Co(CO)_2]$ **6**

$[(C_5R_5)Ni(CO)X]$ **A**, X = Cl, Br $\quad$ $[(C_5Ph_5)NiLX]$ **B** $\quad$ $[(C_5Ph_5)NiL_2]^{\oplus}$ **C**

Pentaphenylnickelocene **5** can be reversibly oxidized at +0.085 V and +0.98 V (SCE) in dichloromethane to the mono- and dication, respectively (Fig. 1). The oxidation potentials are shifted slightly compared to those of the unsubstituted nickelocene (−0.02 V, + ~0.9 V under identical conditions). The markedly greater stability of the pen-

[*] Prof. Dr. W. Kläui, Dipl.-Chem. L. Ramacher
Institut für Anorganische Chemie der Technischen Hochschule
Templergraben 55, D-5100 Aachen (FRG)

[**] This work was supported by the Fonds der Chemischen Industrie. We thank Prof. Dr. *H. Lueken* for measuring the magnetic susceptibilities and Mrs. *S. Paul* and Priv.-Doz. Dr. *U. Kölle* for recording the cyclovoltammograms.

taphenylnickelocinium dication compared to that of $[Ni(C_5H_5)_2]^{2+}$ is probably due to the sterically very bulky pentaphenylcyclopentadienyl ring. By way of contrast electronic effects are responsible for the stability of the corresponding permethylated dication.[11]

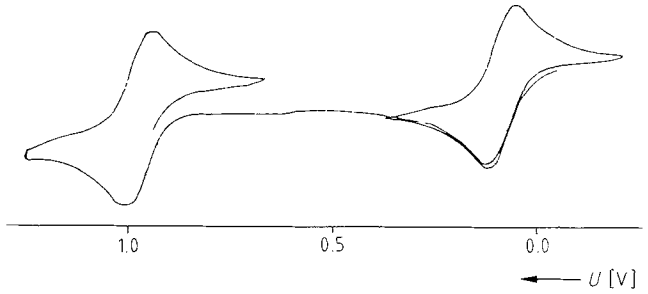


Fig. 1. Cyclovoltammogram of **5** in $CH_2Cl_2/[Bu_4N]PF_6$; Pt electrodes, 100 m V s^{-1}.

Reaction of C_5Ph_5Br with octacarbonyldicobalt in THF led to a product mixture from which we were unable to isolate any pentaphenylcyclopentadienyl complexes. However, we were able to synthesize dicarbonylpentaphenylcyclopentadienyl cobalt **6** in good yields by reaction of C_5Ph_5Br with $K[Co(CO)_4]$.[12] This compound too is distinguished by its exceptional thermal stability compared to that of the corresponding C_5H_5- and C_5Me_5-compounds. It is, e.g., sublimable in vacuo at 180°C. However, in the solid state it is rather sensitive to oxidation. Preliminary investigations have shown that **6** is suitable as starting compound for the photochemical synthesis of cyclooctadiene(pentaphenylcyclopentadienyl)cobalt and probably also for a series of analogous bis(olefin) complexes.

Five phenyl groups appear to stabilize cyclopentadienyl complexes even more strongly than do five methyl groups. We have now found that the oxidative addition of halogenopentaphenylcyclopentadienes also constitutes a simple strategy for the synthesis of C_5Ph_5 complexes of 4d and 5d metals.

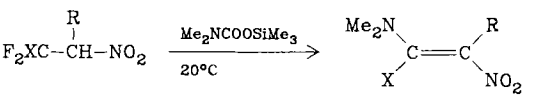
Received: September 6, 1985 [Z 1454 IE]
German version: *Angew. Chem. 98* (1986) 107

[1] See, e.g., P. T. Wolczanski, J. E. Bercaw, *Acc. Chem. Res. 13* (1980) 121; P. M. Maitlis, *ibid. 11* (1978) 301; R. B. King, *Coord. Chem. Rev. 20* (1976) 155.
[2] J. Powell, N. I. Dowling, *Organometallics 2* (1983) 1742.
[3] R. Zhang, M. Tsutsui, *Youji Huaxue 1982*, 435; *Chem. Abstr. 98* (1983) 198374q.
[4] M. J. Heeg, C. Janiak, J. J. Zuckerman, *J. Am. Chem. Soc. 106* (1984) 4259.
[5] S. McVey, P. L. Pauson, *J. Chem. Soc. 1965*, 4312.
[6] We have prepared C_5Ph_5Br and C_5Ph_5Cl from tetracyclone on a 50 g scale (see, e.g., A. K. Youssef, M. A. Ogliaruso, *J. Org. Chem. 37* (1972) 2601; W. Broser, P. Siegle, H. Kurreck, *Chem. Ber. 101* (1968) 69; K. Ziegler, B. Schnell, *Justus Liebigs Ann. Chem. 445* (1925) 266).
[7] U. Kölle, B. Fuss, F. Khouzami, J. Gersdorf, *J. Organomet. Chem. 290* (1985) 77.
[8] *Procedure.* **1**: A solution of C_5Ph_5Br (5.0 g, 9.5 mmol) in anhydrous THF (30 mL) was treated with 1.25 mL (9.6 mmol) of $Ni(CO)_4$, and the mixture stirred for 24 h. The resulting reddish brown precipitate was filtered off, washed with a small amount of THF, and then dried in a high vacuum. Yield 5.2 g (90%). The product contained a small amount of **2** and was suitable in this form for further reactions.—**2**: Upon passage of CO through a suspension of **1** in THF at 25°C a dark-red, clear solution was obtained. The solvent was removed by bubbling with CO, and the reddish brown product that separated was briefly dried in vacuo. IR (KBr): 2047 cm^{-1} (ν(CO)).—**1**, Cl instead of Br: C_5Ph_5Cl (1.0 g, 2.1 mmol) and $Ni(CO)_4$ (0.27 mL, 2.1 mmol) in THF (10 mL), 50°C, analogously to the preparation of **1**. Yield 0.99 g (88%), correct C,H analysis.—**3**: By gassing a suspension of **1**, Cl instead of Br, with CO as described for **2**. IR (KBr): 2052 cm^{-1} (ν(CO)).—**4**: A suspension of **2** (200 mg, 0.33 mmol) in acetone was treated with excess NaI. After 5 h the solvent was removed by distillation and the residue was taken up in dichloromethane; undissolved NaI and NaBr were removed by filtration, and the filtrate evaporated to dryness. Yield: 180 mg (83%). IR (KBr): 2039 cm^{-1} (ν(CO)). The mass spectrometrically controlled bromide/iodide exchange went to completion.
[9] Complexes of type **B** are formed upon reaction of **1** with stoichiometric amounts of L, e.g. tertiary phosphites, at room temperature in dichloromethane. Purification by column chromatography on silica gel; yield ca. 70%. Cationic complexes C are formed upon reaction of **1** with an excess of L in the presence of $TlBF_4$ in dichloromethane. Purification on a silica gel column with acetone. Yield ca. 80%.
[10] *Procedure.* **5**: A suspension of **1** (300 mg, 0.26 mmol) in freshly distilled THF (10 mL) was treated with 140 mg (0.52 mmol) of thallium cyclopentadienide. After 2 h the green solution was filtered and evaporated to dryness. Subsequent purification by chromatography on silica gel with THF (2 ×) under nitrogen followed by removal of the eluent by distillation afforded 260 mg (88%) of **5** as an olive-green microcrystalline powder. Correct C,H analysis. MS (EI, 70 eV, 160°C) *m/z* 568 ($M^{\oplus}$, ^{58}Ni).
[11] U. Kölle, F. Khouzami, *Angew. Chem. 92* (1980) 658; *Angew. Chem. Int. Ed. Engl. 19* (1980) 640.
[12] *Procedure.* **60**: A solution of $K[Co(CO)_4]$ (0.69 g, 3.3 mmol) in THF (50 mL) was treated with 1.72 g (3.3 mmol) of C_5Ph_5Br and the mixture stirred for 3 d at room temperature. The solvent was then removed by distillation and the reddish-brown residue chromatographed at +10°C on a silica gel column (eluent: first hexane, then ether/dichloromethane 1 : 1). The dicarbonyl complex **6** was eluted as a purple solution, which, after evaporation to dryness, furnished 1.50 g (81%) of **6** as a reddish brown, microcrystalline powder. The product is air-sensitive and can be purified by sublimation at 180°C in vacuo. Correct C,H analysis. IR (CH_2Cl_2): 2010, 1952 cm^{-1} (ν(CO)). MS (EI, 70 eV, 25°C) *m/z* 560 ($M^{\oplus}$).

Di- and Trifluoro-Substituted Dilithium Compounds for Organic Syntheses**

By *Dieter Seebach,* Albert K. Beck,* and *Philippe Renaud*

Fluoroorganic compounds are of increasing interest, mainly for the synthesis of biologically active products.[1] Fluoro substitution can cause problems in synthetic transformations, since fluoride can act as a leaving group.[2] Thus, the β-fluoro-substituted nitroalkanes **1**[3] do not undergo base-catalyzed nitroaldol additions to carbonyl compounds:[4] β-elimination is so strongly favored that reaction of **1** with *N,N*-dimethyl(trimethylsilyl)carbamate affords fluorine-free nitroenamines **2**. To our great surprise, the dilithio derivatives **3** and **4** of the fluoronitroalkanes **1a**,



1a: R = H, X = F
1b: R = X = H
1c: R = Me, X = F

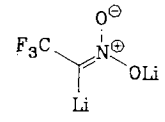
2a: R = H, X = NMe_2 (75%)
2b: R = X = H (62%)
2c: R = Me, X = NMe_2 (67%)

1b could be generated with butyllithium, were of comparable stability (up to −70°C) to the nonfluorinated analogues,[5] and reacted with aldehydes and ketones to give the adducts **6–9** (Table 1; for experimental procedure see ref. [5]). The adducts were formed in 50–60% yield but

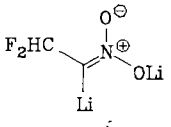
[*] Prof. Dr. D. Seebach, A. K. Beck, Dipl.-Chem. P. Renaud
Laboratorium für Organische Chemie der
Eidgenössischen Technischen Hochschule
ETH-Zentrum, Universitätstrasse 16, CH-8092 Zürich (Switzerland)

[**] Partially from the projected Ph. D. thesis of *P. R.*—The fluoronitroethanes were supplied by Bayer AG, Leverkusen.

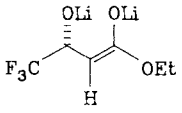
readily decomposed during purification (chromatography or distillation), so that they were often hydrogenated directly to the corresponding amino alcohols.



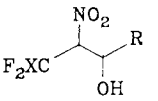
3



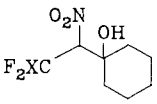
4



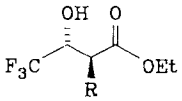
5



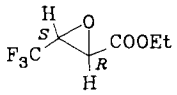
6, X = F; **7**, X = H



8, X = F; **9**, X = H



10



11

Table 1. Products **6**–**9** from the dilithio derivatives **3** and **4** of fluorinated nitroethanes [3] and carbonyl compounds (yields of pure products from distillation; ratios of diastereomers from ^{13}C-NMR spectra; NMR data of major isomers: enrichment of diastereomers is possible as described for the nonfluorinated analogues [6]).

Product	Yield [%] crude (pure) [ratio of diast.]	^{13}C-NMR, δ J(C,F) [Hz]
		$\delta(CNO_2)/^2J$
6a, R = *t*Bu	90 (60) [1 : 1]	84.6/29.8
6b, R = C_6H_5	60 (40) [2 : 1]	91.1/29.1
6c, R = 4-NO_2–C_6H_4	55 (35) [3 : 1]	90.5/29.1
6d, R = 3,4-(OCH_2O)C_6H_3	50 (25) [2.5 : 1]	91.0/28.4
8	60 (30)	92.9/28.4
		$\delta(CHF_2)/^1J$
7a, R = *t*Bu	40 (15) [a]	112.9/246.6
7b, R = C_6H_5	30 (12) [2 : 1]	111.5/247.8
9	60 (4)	112.8/245.6

[a] Determination of the ratio of diastereomers not possible by ^{13}C-NMR.

A double deprotonation is also possible with the (*R*)-trifluorohydroxybutanoate **10a**. This compound is readily available in >90% enantiomeric excess (*ee*) through yeast reduction of the corresponding β-ketoester.[7] At low temperatures (≤ -25 °C), the enolate-alkoxide **5** does not undergo γ-elimination (to an epoxide or a cyclopropane), and, like the nonfluorinated analogue,[8] can be alkylated (→ **10b**–**10d**) or cyclized (→ **11**) diastereoselectively (Table 2; for experimental procedure see ref. [8]).

Table 2. Products **10** and **11** from the dilithio derivative **5** of ethyl (*R*)-4,4,4-trifluoro-3-hydroxybutanoate **10a** (92% *ee*) [7] and CH_3I, CH_2=CH–CH_2Br, $C_6H_5CH_2Br$, I_2 (yields of >95% configurationally pure samples from flash chromatography; % *ds* = [(A/A + B) × 100] from ^{13}C-NMR spectra of crude products; NMR signal of C(3) of major isomer; $[\alpha]_D$ at c = 1.2 in $CHCl_3$).

Product	Yield [%] (% *ds*)	$[\alpha]_D^{RT}$	^{13}C-NMR, δ values ^2J (C,F) [Hz]
10a, R = H		+20.1	67.4/32
10b, R = Me	45 (86)	+10.0	72.7/31
10c, R = CH_2–CH=CH_2	52 (93)	− 0.8	70.8/31
10d, R = CH_2–C_6H_5	47 (80)	−31.6	70.5/31
11	18 (83)	−18.6	52.6/42

Although *mono*lithiated fluoro compounds capable of undergoing α-, β-, and/or γ-elimination have been known for a long time,[2,9] the reagents **3**–**5** are the first *poly*lithiated derivatives of this type.[10] They offer accessibility to a variety of new fluorinated organic compounds with additional functional groups.

Received: September 16, 1985 [Z 1463 IE]
German version: *Angew. Chem. 98* (1986) 96

[1] Recent reviews: A. Haas, M. Lieb, *Chimia 39* (1985) 134; H. Millauer, W. Schwertfeger, G. Siegemund, *Angew. Chem. 97* (1985) 164; *Angew. Chem. Int. Ed. Engl. 24* (1985) 161; *J. Synth. Org. Chem. Jpn. 42* (1984) 770–849.
[2] J. C. Tatlow, *J. Fluorine Chem. 25* (1984) 99.
[3] B. Baasner, H. Hagemann, E. Klauke, DOS 3305201, 3305202 (1983), Bayer AG; *Chem. Abstr. 102* (1984) 5684k, 5685m.
[4] An exception is formaldehyde: I. L. Knunyants, L. S. German, I. N. Rozhkov, *Izv. Akad. Nauk. SSSR Ser. Khim. 1964*, 1630.
[5] D. Seebach, F. Lehr, *Angew. Chem. 88* (1976) 540; *Angew. Chem. Int. Ed. Engl. 15* (1976) 505; T. Mukhopadhyay, D. Seebach, *Helv. Chim. Acta 65* (1982) 385; M. Eyer, D. Seebach, *J. Am. Chem. Soc. 107* (1985) 3601.
[6] D. Seebach, A. K. Beck, T. Mukhopadhyay, E. Thomas, *Helv. Chim. Acta 65* (1982) 1101.
[7] D. Seebach, P. Renaud, W. B. Schweizer, M. F. Züger, M.-J. Brienne, *Helv. Chim. Acta 67* (1984) 1843; D. Seebach, P. Renaud, *ibid. 68* (1985) 2342.
[8] D. Seebach, J. Aebi, D. Wasmuth, *Org. Synth. 63* (1985) 109, and references cited therein.
[9] D. Seyferth, T. Wada, G. Raab, *Tetrahedron Lett. 1960*, No. 22, 20; J. L. Adcock, E. B. Renk, *J. Org. Chem. 44* (1979) 3431.
[10] A special case is the Li_2 derivative of a CF_3-substituted β-lactam: P. F. Bevilacqua, D. D. Keith, J. L. Robert, *J. Org. Chem. 49* (1984) 1430.

Selenium-rich Chalcogen Rings Se_5S, Se_5S_2, and Se_7 from Titanocene Pentaselenide**

By *Ralf Steudel,* Maria Papavassiliou, Eva-Maria Strauss,* and *Risto Laitinen*

While the synthesis of sulfur-containing homocycles and heterocycles by reaction of titanocene pentasulfide with non-metal chlorides has been studied in detail, nothing has hitherto been reported about analogous reactions of titanocene pentaselenide.[1] We report here on the synthesis and properties of the six- and seven-membered ring molecules Se_5S and Se_5S_2 and Se_7, respectively, which can be prepared according to Equations (a) to (c).

$$[(C_5H_5)_2TiSe_5] + SCl_2 \longrightarrow Se_5S + [(C_5H_5)_2TiCl_2] \quad (a)$$
$$[(C_5H_5)_2TiSe_5] + S_2Cl_2 \longrightarrow Se_5S_2 + [(C_5H_5)_2TiCl_2] \quad (b)$$
$$[(C_5H_5)_2TiSe_5] + Se_2Cl_2 \longrightarrow Se_7 + [(C_5H_5)_2TiCl_2] \quad (c)$$

Se_5S was obtained from CS_2 in the form of deep-red, shiny, hexagonal needles,[2] whose composition,[3] Raman spectrum,[4a] and crystal structure[5] proved the presence of thiapentaselenacyclohexane. The HPLC retention time[6] lies, as expected, between that of Se_4S_2 and Se_6 (Se_4S_2 2.94, Se_5S 3.07, Se_6 3.40 min; dead time 1.40 min; eluent: methanol).

[*] Prof. Dr. R. Steudel, Dipl.-Chem. M. Papavassiliou, Dipl.-Chem. E.-M. Strauss, Dr. R. Laitinen
Institut für Anorganische und Analytische Chemie der Technischen Universität
Strasse des 17. Juni 135, D-1000 Berlin 12

[**] Sulfur compounds, Part 95. This work was supported by the Deutsche Forschungsgemeinschaft, the Alexander-von-Humboldt Stiftung, the Fonds der Chemischen Industrie, and the TU Berlin (MIT-Sondermittel). – Part 94: [10a].

Crystalline Se_5S is stable for days at 20°C; upon heating, however, a change of the crystal shape is observed at 100°C, indicated in the DSC diagram[7] by a (endothermic) peak at 105°C and a (exothermic) peak at 110°C. Further peaks at 160°C (endothermic) and 165°C (exothermic) indicate melting and polymerization. In CS_2 solution, Se_5S decomposes at 20°C within 5 h, mainly to the heterocycles Se_7S, Se_6S, and Se_5S_3, which were identified by their HPLC retention times.[6] Upon prolonged stirring of the solution, Se_8 and Se_6S_2 are also formed.

The crystal and molecular structures of Se_5S correspond entirely to those of S_6[8] and Se_6[9] both of which form chair-like rings. The atomic positions are occupied statistically by S and Se. The reduction in symmetry from D_{3d} for S_6 and Se_6 to C_s for Se_5S manifests itself in the Raman spectrum by removal of all degenerations and of the rule of mutual exclusion. The observed[4a] and calculated[10a] vibrational spectra are in good agreement.

Seven-membered chalcogen rings claim special interest because of their unusual structures[11] and because of their resulting high reactivity.[12] We have therefore synthesized Se_5S_2 and Se_7 [Equations (b) and (c), respectively].

Se_5S_2 crystallizes from CS_2 at −50°C in the form of dark-red, rod-like crystals, which, in contrast to S_7[12] and Se_2S_5,[13] are stable for months at 20°C.[14] Se_5S_2 apparently decomposes with polymerization at 90–100°C (color change from red to silver), and the substance melts only at 146°C. A DSC investigation showed an endothermic transformation at 70–85°C, followed by an exothermic reaction (polymerization) at 85–95°C and a melting peak at 135–150°C (heating rate 5°C/min).[7]

The chromatogram (HPLC)[6] of a freshly prepared CS_2 solution of pure Se_5S_2 shows a large Se_5S_2 peak and two small peaks, which, on the basis of their retention times (2.94 and 4.94 min; Se_5S_2: 3.49 min; dead time: 1.4 min), can be assigned to the compounds 1,2-Se_4S_2 and 1,2-Se_6S_2 by comparison with reference substances.[6, 13] Se_5S_2 decomposes in CS_2 at 20°C within 60 min, essentially according to Equation (d); this can be interpreted in terms of a mechanism previously proposed by us and involving a hypervalent intermediate.[13] On prolonged reaction, further eight-membered selenium-sulfur rings are formed.

$$2\,Se_5S_2 \longrightarrow Se_4S_2 + Se_6S_2 \qquad (d)$$

Se_6S_2 has been isolated together with residual Se_5S_2 by cooling the CS_2 solution to −78°C; it crystallizes in the form of orange-colored bar-shaped crystals and must be manually separated from the accompanying Se_5S_2 by sorting according to crystal shape and color under the microscope. The Raman spectrum of Se_6S_2[4b] agrees well with the spectrum calculated[10b] for a crown-shaped cyclic molecule 1,2-Se_6S_2 with the Se atoms in neighboring positions.

The Raman spectrum of Se_5S_2 (Fig. 1) cannot be interpreted in terms of a single conformation. This follows from a comparison of the spectra of numerous crystallizations. Rather, it can be shown by argument along the same lines as for the assignment of the Raman spectrum of Se_2S_5[13] and by comparison with calculated wave numbers,[10a] that the isomers **A** and **C** (Fig. 2) are formed alongside each other in the form of mixed crystals. The isomers **B** and/or **D**, which probably give rise to the very weak lines at 425 and 380 cm^{-1},[10a] can only be present in traces. The concentration ratio **[A]:[C]** is all the smaller the lower the temperature of crystallization, and at −78°C is roughly estimated (from the peak areas of the SeS stretching vibrations) to be 1:1. At higher temperatures (up to −20°C) more **A** than **C** is formed; above −10°C, **C** is partially transformed in the crystalline state into **A**, such that an estimated ratio of 4:1 is reached at 20°C.

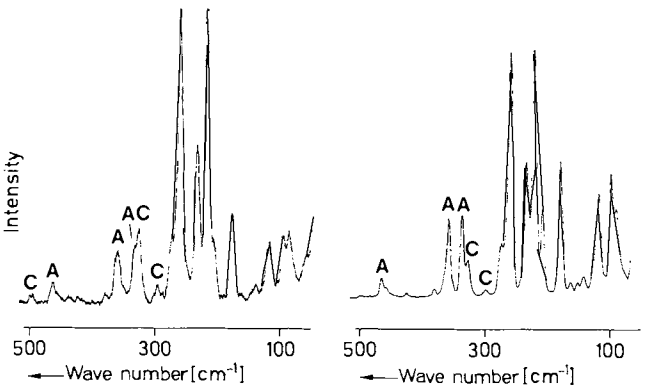


Fig. 1. Left: Raman spectrum of Se_5S_2, which was recrystallized at −50°C from CS_2. Right: Spectrum of the same sample after warming to −10°C; warming to higher temperatures (up to 45°C) did not lead to any change in the spectrum. Measuring temperature −100°C; for wave numbers see [4c].

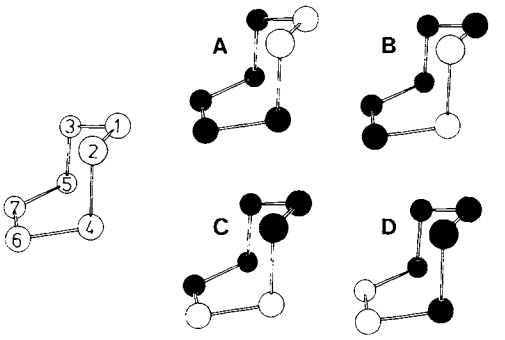


Fig. 2. Numbering of the atoms in Se_5S_2 (left) and molecular structure of four isomers of Se_5S_2.

An X-ray crystal structure analysis carried out on such a crystal at 20°C[15] confirmed this analysis: Accordingly, the atomic sites 1 and 2 (see Fig. 2) are occupied with sulfur to ca. 75% (±5%), the sites 3 and 4 to ca. 15%, the site 6 to ca. 10%, and the sites 5 and 7 to 0%. Due to this disorder, the bond lengths and angles cannot be determined, but there is no doubt about the molecular conformation: Comparison of the torsional angles (Table 1) shows that the conformation of Se_5S_2 corresponds very closely to that of the S_7 molecule[11], so that a chair conformation can be assumed also for Se_7 and other seven-membered chalcogen rings.

Table 1. Equivalent torsional angles of Se_5S_2 and γ-S_7. The atomic numbers given correspond to those in Figure 2. Standard deviations in parenthesis.

	Se_5S_2	γ-S_7
3-1-2-4	80.1(4)	78
2-1-3-5	78.0(4)	76
1-2-4-6	109.4(3)	109
1-3-5-7	109.0(3)	107
2-4-6-7	81.3(2)	82
3-5-7-6	85.3	84
4-6-7-5	1.5(2)	0.4

cyclo-Se_7 was obtained according to Equation (c) as a dark-red powder[16] consisting of microscopically small

needles, and was identified by HPLC.[17] The Raman spectrum[4d] agrees exactly with that of "orthorhombic selenium",[18a] which is formed on recrystallization of glassy selenium from CS_2 and for which the molecular size Se_7 has been derived from the unit cell, which contains 28 atoms.[18b] An X-ray structure analysis of Se_7 has not been reported yet. In contrast to S_7, solid Se_7 is also stable for days at 20°C; at 96°C the crystals turn shiny silver, due to transformation into gray selenium, and melt at 221°C.

Selenium-sulfur rings containing all Se atoms in neighboring positions are, as we have found, the main components of selenium-rich Se–S melts (HPLC analysis after quenching to 0°C and extraction with CS_2 at 20°). These include the compounds Se_5S, Se_5S_2 and Se_6S_2, which have now been obtained in pure form for the first time. Their investigation can contribute to an understanding of the complex composition of liquid selenium and the amorphous (glassy) selenium prepared therefrom on quenching.

Received: August 13, 1985;
supplemented: October 9, 1985 [Z 1428 IE]
German version: *Angew. Chem. 98* (1986) 81

[1] H. Köpf, B. Block, M. Schmidt, *Chem. Ber. 101* (1968) 272.

[2] *Procedure:* A solution of $[Cp_2TiSe_5]$ (1.15 g, 2 mmol) in anhydrous CS_2 (215 mL) was treated at 20°C with a solution of SCl_2 (0.13 mL, 2 mmol) in CS_2 (13 mL). A mixture of Se_5S and $[Cp_2TiCl_2]$ precipitated out. The reaction mixture was allowed to stand for 24 h at −78°C and the precipitate filtered off and washed portionwise at 20°C with 300 mL of trichloromethane and 100 mL of pentane. Yield: 0.6 g of Se_5S (sometimes still containing small amounts of Se_8).

[3] This compound gave correct analytical data; we thank Prof. Dr. *P. Brätter* and Dipl.-Chem. *W. Gatschke* (Hahn-Meitner-Institut, Berlin) for the selenium determinations by neutron activation analysis.

[4] Cary 82 spectrometer, krypton laser (647.1 nm); wave numbers [cm^{-1}], relative intensities vs = very strong, s = strong, m = medium, w = weak, vw = very weak, sh = shoulder, sample temperature −100°C. a) Se_5S: 351 s, 253 vs, 237 m, 188 w, 154 m, 130 w, 111 m, 108 m, 76/71 m. b) Se_6S_2: 462 w, 451 vw, 378 w, 360 sh, 354 m, 259 vs, 253 sh, 200 w, 175 w, 164 m, 129 m, 112 s, 92 m, 86 m, 79 m, 55 m, 47 m, 40 w, 30 m, 19 m. c) Se_5S_2: 499 (**C**), 468 (**A**), 460, 361 (**A**), 340 (**A**), 330 (**C**), 302 (**C**), 279, 263, 238, 224, 212, 182, 165, 147, 126, 121, 102, 95. d) Se_7: 277 m, 260 sh, 256 vs, 232 m, 222 s, 127 s, 88 m.

[5] Crystallographic data of Se_5S: $R\bar{3}$, $a = 1124.3(3)$, $c = 437.4(1)$ pm, $V = 0.4789(2)$ nm^3, $Z = 18$, $\rho_{calc} = 4.44$ g cm^{-3}, $\mu(Mo_{K\alpha}) = 310.0$ cm^{-1}. Syntex $P2_1$ diffractometer, 1314 reflections, 342 with $I \geq 2\sigma(I)$, $R = 0.069$, empirical absorption corrections. Further details of the crystal structure investigations are available on request from the Fachinformationszentrum Energie, Physik, Mathematik GmbH, D-7514 Eggenstein-Leopoldshafen 2, on quoting the depository number CSD 51601, the names of the authors, and the full citation of the journal.

[6] For the HPLC analysis of selenium-sulfur rings see R. Steudel, E.-M. Strauss, *Z. Naturforsch. B38* (1983) 719; R. Laitinen, N. Rautenberg, J. Steidel, R. Steudel, *Z. Anorg. Allg. Chem. 486* (1982) 116.

[7] Differential Scanning Calorimetry; instrument: Perkin-Elmer DSC 2.

[8] J. Steidel, J. Pickardt, R. Steudel, *Z. Naturforsch. B33* (1978) 1554.

[9] Y. Miyamoto, *Jpn. J. Appl. Phys. 19* (1980) 1813.

[10] a) R. Laitinen, R. Steudel, E.-M. Strauss, *J. Chem. Soc. Dalton Trans. 1985*, 1869; b) R. Laitinen, R. Steudel, *J. Mol. Struct. 68* (1980) 19.

[11] R. Steudel, J. Steidel, J. Pickardt, F. Schuster, R. Reinhardt, *Z. Naturforsch. B35* (1980) 1378.

[12] M. Schmidt, B. Block, H. D. Block, H. Köpf, E. Wilhelm, *Angew. Chem. 80* (1968) 660; *Angew. Chem. Int. Ed. Engl. 7* (1968) 632; F. Fehér, D. Kurz, *Z. Naturforsch. B24* (1969) 1089; R. Steudel, S. Passlack-Stephan, G. Holdt, *Z. Anorg. Allg. Chem. 517* (1984) 7.

[13] R. Steudel, E.-M. Strauss, *Angew. Chem. 96* (1984) 356; *Angew. Chem. Int. Ed. Engl. 23* (1984) 362.

[14] Procedure: A solution of $[Cp_2TiSe_5]$ (1.60 g, 3 mmol) in anhydrous CS_2 (300 mL) was treated at 20°C within 1 min with a solution of S_2Cl_2 (0.24 mL, 3 mmol) in CS_2 (23 mL). The originally deep-violet solution turned paler in color and $[Cp_2TiCl_2]$ precipitated out. The mixture was filtered within 2 min (glass frit) and the filtrate collected at −78°C. After 24 h the crystallized crude product was isolated and then washed with trichloromethane and pentane at 20°C to remove $[Cp_2TiCl_2]$ (yield of Se_5S_2 1.1 g) and then recrystallized three times from CS_2 by dissolution at 20°C and cooling to −78°C.

[15] X-ray structure analysis of Se_5S_2: $P2_12_12_1$, $a = 1357.4(5)$, $b = 1292.4(8)$, $c = 435.2(1)$ pm, $V = 0.7636(6)$ nm^3, $Z = 4$, $\rho_{calc} = 3.99$ g cm^{-3}, $\mu(Mo_{K\alpha}) = 261.9$ cm^{-1}. Syntex $P2_1$ diffractometer: 1079 reflections, 670 with $I \geq 2\sigma(I)$, $R = 0.058$, $R_w = 0.054$, empirical absorption correction [5].

[16] *Procedure:* Cp_2TiSe_5 (575 mg, 1 mmol) in anhydrous CS_2 (500 mL) was treated with stirring at 20°C with a solution of Se_2Cl_2 (222 mg, 0.97 mmol) in CS_2 (8 mL). The initially deep-violet solution turned bright-red in color due to formation of $[Cp_2TiCl_2]$, which remained in solution. After 5 min, the dark-red percipitate was filtered off under suction and air-dried: yield 400 mg Se_7 (75%).

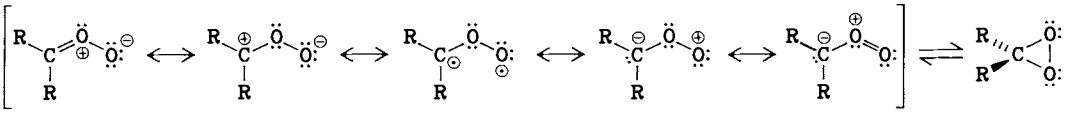
[17] For the HPLC analysis of selenium homocycles see R. Steudel, E.-M. Strauss, *Adv. Inorg. Chem. Radiochem. 28* (1984) 135; *Z. Naturforsch. B36* (1981) 1085.

[18] a) K. Nagata, Y. Miyamoto, *Jpn. J. Appl. Phys. 23* (1984) 704; b) K. Nagata, H. Tashiro, Y. Miyamoto, *ibid. 20* (1981) 2265.

Thianthrene 5-Oxide as Mechanistic Probe in Oxygen Transfer Reactions: The Nucleophilic Character of Carbonyl Oxides**

By *Waldemar Adam,* Heinz Dürr, Wolfgang Haas,* and *Bhushan Lohray*

The mechanistic aspects of short-lived intermediates such as the carbonyl oxides (Criegee Zwitterions) are currently the subject of intensive study.[1] Particularly interesting is the question on which of the hypothetical resonance structures **1a–e** best reflects the chemical behavior of the



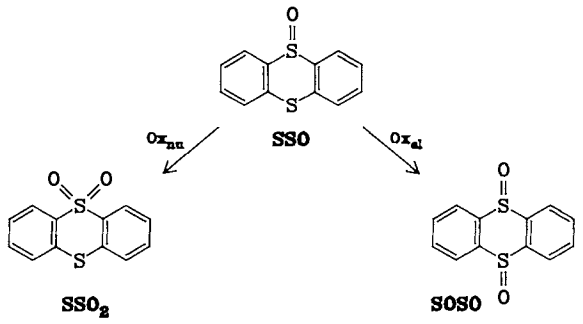
1a **1b** **1c** **1d** **1e** **2**

carbonyl oxides or whether even the cyclic valence structure of the dioxirane **2** applies. For example, in oxygen transfer to π-bonds (alkenes, arenes) and heteroatoms (amines, sulfides, sulfoxides, phosphanes) the negatively charged terminal oxygen in **1a**, **b** should be more nucleophilic than the radical type oxygen in **1c** or the positively charged or uncharged oxygen in **1d** or **1e**, respectively. Recently,[2] it could be demonstrated by intramolecular competition with thianthrene 5-oxide (**SSO**), that carbonyl oxides **1** transfer oxygen more nucleophilically than dioxiranes **2**. Thus, nucleophilic oxidants (Ox_{nu}) preferably oxidize at the sulfoxide sulfur to give mainly thianthrene 5,5-dioxide (**SSO_2**), while electrophilic oxidants (Ox_{el}) react predominantly at the sulfide sulfur to afford thianthrene 5,10-dioxide (**SOSO**).

[*] Prof. Dr. W. Adam, Dr. B. Lohray [+], Dr. W. Haas
Institut für Organische Chemie der Universität
Am Hubland, D-8700 Würzburg (FRG)
Prof. Dr. H. Dürr
Institut für Organische Chemie der Universität
D-6600 Saarbrücken (FRG)

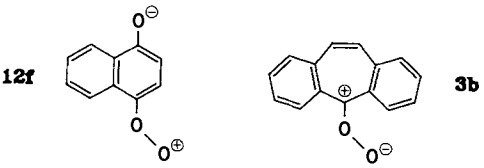
[+] Alexander-von-Humboldt fellow (1984/1985)

[**] This work was supported by the Deutsche Forschungsgemeinschaft and the Fonds der Chemischen Industrie.



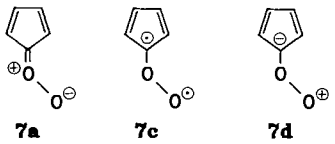
This mechanistic probe further revealed (Table 1) that the R substituent of the carbonyl oxide **1** influences the nucleophilic character of the terminal oxygen: alkyl-substituted derivatives such as **4** and **5** lead expectedly to the most nucleophilic transfer of oxygen, whereas phenyl-substitution (**8**) and benzoyl-substitution (**10**) give rise to less nucleophilic oxygen transfer. This tendency can hardly be explained in terms of steric effects. The question arises as to whether one of the resonance structures **1a–e** of the carbonyl oxides could be intentionally favored by appropriate substitution, that is can the electronic character of the terminal oxygen be changed at will? Should this be possible, then differentiation between carbonyl oxides **1** and dioxiranes **2** ought to be possible using thianthrene 5-oxide as mechanistic probe. Our experimental results are presented in Table 1.

The X_{SO} scale (X_{SO} = molar fraction of nucleophilic attack at the sulfoxide group of thianthrene 5-oxide) extends from $X_{SO} = 1.00$ for dibenzotropone oxide **3** to $X_{SO} = 0.61$ for 1,4-naphthoquinone oxide **12**. Consequently, it follows that appropriate substitution can increase the X_{SO} value of the carbonyl oxides (typically 0.80–0.96[2]) even up to the maximum value $X_{SO} = 1.00$ or can decrease X_{SO} to the value for dioxiranes (typically 0.57–0.67[2]). Control experiments rule out photooxidation of thianthrene 5-oxide by electron transfer, since the latter could explain the lower value $X_{SO} = 0.61$. On the basis of these facts we presume that the resonance structure **12f** of 1,4-naphthoquinone oxide is favored through aromatization. In contrast, the



complete nucleophilic oxygen transfer of dibenzotropone oxide **3**, in which aromatization stabilizes the positive charge, can be explained in terms of the resonance structure **3b**. If this aromatization is suppressed as in dibenzodihydrotropone oxide **9**, then less nucleophilic oxygen transfer is observed.

In the cases discussed so far, the electron density of the terminal oxygen in the carbonyl oxide correlates very well with the nucleophilic character of the oxygen transfer to thianthrene 5-oxide. Quite contrary to expectation, however, was the behavior of fluorene oxide **6** and cyclopentadienone oxide **7**, for which on the basis of the resonance structure **7d** we would have expected that oxygen transfer should have proceeded at least as electrophilically as in the case of **12**. The observed pronounced nucleophilic oxygen transfer is best explained in terms of **7a**. The same applies also for **6**.



Unfortunately, IR spectroscopic investigations on matrix-isolated cyclopentadienone oxide **7** led to controversial data for its electronic structure.[3] *Chapman* et al.[3a] prefer, on the basis of $\nu_{CO} \approx 1390\ cm^{-1}$, the resonance structure **7a**, whereas *Dunkin* et al.[3b,c] argue in favor of the resonance structures **7c**, **d**. However, the resonance structure **7d** is in no way compatible with the observed pronounced nucleophilic oxygen transfer. Less nucleophilic oxygen transfer was also expected for the diradical-type resonance structure **7c**, since the *tert*-butylperoxy radical transfers oxygen strongly electrophilically to the thianthrene 5-oxide ($X_{SO} = 0.03$).[4]

Until further spectroscopic investigations clarify this dispute on the electronic character of carbonyl oxide **7**, we favor **7a** as the most plausible resonance structure. The recent direct IR spectroscopic demonstration that cyclopentadienone corresponds to a "normal" α,β-unsaturated ketone,[5] suggests that its carbonyl oxide should transfer oxygen, predominantly nucleophilically.

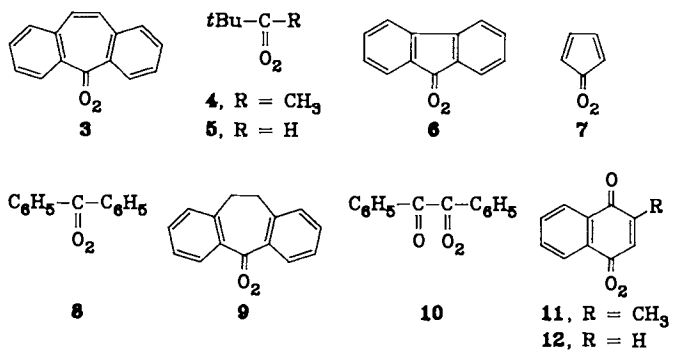


Table 1. Oxygen transfer to thianthrene 5-oxide with carbonyl oxides **3–12**, generated by photooxygenation of diazoalkenes [a].

Carbonyl oxide	Yield [mmol/L] [b] SSO_2 (n_{SO})	SOSO (n_S)	X_{SO} [c]
3	0.974	–	1.00
4	2.06	0.131	0.94
5	4.43	0.408	0.92
6	21.7	1.62	0.93
7	0.795	0.115	0.87
8	3.72	0.747	0.83
9	6.25	1.30	0.83
10	3.00	0.774	0.80
11	0.989	0.464	0.68
12	0.961	0.607	0.61

[a] Singlet oxygen was generated photochemically by sensitization with tetraphenylporphine. The reaction was carried out in anhydrous dichloromethane at −20 to 0°C. Control experiments showed that neither singlet oxygen nor diazoalkane alone caused oxygen transfer. [b] Quantitative determination by HPLC on LiChrosorb Si60, 5 μm, using a petroleum ether (50–70°C)/ethyl acetate/methanol mixture (960 : 40 : 4) as eluent, 3.0 mL/min, bis(*p*-nitrophenyl)sulfone as internal standard. [c] Mole fraction of oxygen transfer at the sulfoxide sulfur $X_{SO} = n_{SO}/[n_{SO} + n_S]$), error ±0.03.

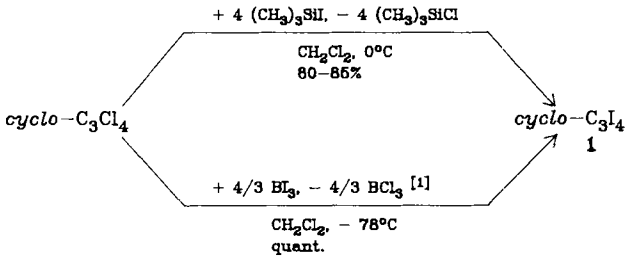
Received: August 14, 1985;
supplemented: October 1, 1985 [Z 1430 IE]
German version: *Angew. Chem.* 98 (1986) 85

[1] R. L. Kuczkowski in A. Padwa (Ed.): *1,3-Dipolar Cycloaddition Chemistry. Vol. 2*, Wiley, New York 1984, p. 197-276.
[2] W. Adam, W. Haas, G. Sieker, *J. Am. Chem. Soc. 106* (1984) 5020.
[3] a) O. L. Chapman, T. C. Hess, *J. Am. Chem. Soc. 106* (1984) 1842; b) G. A. Bell, I. R. Dunkin, *J. Chem. Soc. Chem. Commun. 1983*, 1213; c) G. A. Bell, I. R. Dunkin, *Tetrahedron 41* (1985) 339.
[4] W. Haas, *Dissertation*, Universität Würzburg 1985.
[5] G. Maier, L. H. Franz, H.-G. Hartan, K. Lanz, H. P. Reisenauer, *Chem. Ber. 118* (1985) 3196.

cyclo-C_3I_4—The First Saltlike Halocarbon**

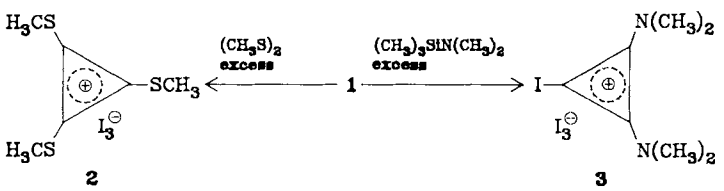
By *Robert Weiss,* Georg-E. Miess, Alfons Haller,* and *Werner Reinhardt*

The energy-rich perhalogenocyclopropenes *cyclo*-C_3X_4 (X = F, Cl, Br), which are widely used synthetic building blocks, are volatile, thermally relatively stable, covalent compounds.[1] During our investigations of iodocarbenium ions[2,3] we have now been able to synthesize the last missing member of this class of substances, namely *cyclo*-C_3I_4 **1**; compound **1** differs dramatically in its structure and reactivity from its lighter homologues.



Scheme 1.

1 can be conveniently obtained from *cyclo*-C_3Cl_4 in two different ways (Scheme 1); in these halogen-exchange reactions it separates from CH_2Cl_2 as an analytically pure, yellow-brown crystalline powder (m.p. 80°C, *violent decomposition;* vide infra). The insolubility of **1** is indicative of an ionic structure, proof for which is provided by the IR spectrum. The dearth of bands in the spectrum, which is dominated by an intense absorption at 1200 cm^{-1}, points to a high degree of symmetry of **1**. A comparison of the IR spectrum with the IR spectra of known *cyclo*-$C_3X_3^{\oplus}$ systems (X is a ligand which is bound via an element of main group 6 or 7) shows that this band arises from the characteristic E′-ring deformation vibration of the cyclopropenium ion (SCH_3 1241,[5] $SeCH_3$ 1220,[5] $TeCH_3$ 1169,[5] Cl 1313,[4] Br 1276[4]). The position of this band reflects the expected red shift in going from the lighter to the heavier halogen substituents, as is also observed in the series of organochalcogeno-substituted cyclopropenium systems. No band appears in the range 1600–2000 cm^{-1}, which rules out a covalent cyclopropene or isomeric allene structure.[6]

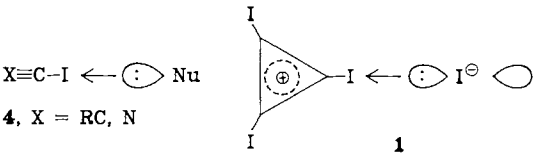


Derivatizations of **1** using previously established strategies led in high yields to the known cyclopropenium systems **2** and **3**,[7] thus lending further support to the presence of an intact three-membered ring in **1**. All our findings indicate that **1** is best formulated as triiodocyclopropenium iodide, $C_3I_3^{\oplus}I^{\ominus}$, *thus making this compound the first saltlike halocarbon.*

When **1** is synthesized in the presence of one equivalent of I_2, a blackish violet salt of the composition C_3I_6 is formed whose IR spectrum is identical in the region down to 600 cm^{-1} with that of **1**. The compound must therefore be *cyclo*-$C_3I_3^{\oplus}I_3^{\ominus}$. This is all the more remarkable, as all previously known *cyclo*-C_3X_6 systems (X = F, Cl, Br) have a *cyclopropane structure.*[1]

Iodine obviously claims a special position as ligand within the series of homologous tetrahalogeno-*cyclo*-C_3 compounds.

The following structural and electronic aspects are of importance for an understanding of this phenomenon: According to recent calculations[8] the electronegativity (2.46) of the iodine bound via a 5 p orbital corresponds to that of sp^3-hybridized carbon. This implies considerable +I donor properties of the iodine ligand for **1**, since it is bound to an sp-hybridized C-atom.[9] Since the ring C-atoms in **1** also carry positive partial charges, the electropositivity of the iodine ligands in *cyclo*-$C_3I_3^{\oplus}$ should be more pronounced than in electronically comparable neutral systems such as I–C≡C–I and I–C≡N.[10] It is known that these two systems tend to form linear n→σ* complexes of the type **4** with 3c/4e configuration.[11] For *cyclo*-$C_3I_3^{\oplus}$, the iodide counterion is, in principle, an ideal partner for the realization of such a hypervalent contact.[2,3] Since cation and anion are, in principle, trifunctional, there is the additional possibility that the structure of **1** in the solid state is characterized by three-dimensional n→σ* association similarly to that of $CI_5^{\oplus}$.[12] This possibility of stabilization provides a further argument in favor of an ionic structure for **1** and is consistent with the observed insolubility of this compound.



The iodine-iodine contacts should have a tendency to promote facile α-elimination of I_2 from **1**; this does in fact take place, but *explosively,* upon rapidly heating the salt. Besides I_2, exclusively a homogeneous, satiny black powder of composition $C_{13}I$ is formed. This confirms that **1**—rather like NI_3—tends to decompose to the elements. It still remains to be clarified whether **1** can be converted at low temperatures into other C_3-derivatives—either thermally, photochemically, or in the presence of iodine acceptors.

Danger! On several occasions **1** *exploded violently,* not only when handled in the dry state at room temperature, but also upon dissolution in polar solvents (e.g. CH_3OH, CH_3CN). *As a cautionary measure it is therefore strictly advised that not more than 1 mmol of the salt be prepared in a*

[*] Prof. Dr. R. Weiss, Dipl.-Chem. G.-E. Miess, cand. chem. A. Haller, Dipl.-Chem. W. Reinhardt
Institut für Organische Chemie der Universität Erlangen-Nürnberg
Henkestrasse 42, D-8520 Erlangen (FRG)

[**] Iodocarbenium Ions, Part 3. This work was supported by the Deutsche Forschungsgemeinschaft and the Fonds der Chemischen Industrie. *G.-E. M.* thanks the Konrad-Adenauer-Stiftung for a scholarship.—Part 2: [3].

single experiment, and, equally important, that no work-up operation or manipulation of the substance be attempted with other than moist (CH_2Cl_2) samples.

Received: August 23, 1985 [Z 1441 IE]
German version: *Angew. Chem. 98* (1986) 102

[1] a) S. W. Tobey, R. West, *J. Am. Chem. Soc. 88* (1966) 2481; b) P. B. Sargeant, C. G. Krespan, *ibid. 91* (1969) 415; c) W. Weber, A. de Meijere, *Angew. Chem. 92* (1980) 135; *Angew. Chem. Int. Ed. Engl. 19* (1980) 138; d) D. Wendisch in Houben-Weyl: *Methoden der Organischen Chemie, 4th Edit., vol. IV/3*, Thieme, Stuttgart 1971, p. 15 ff.
[2] R. Weiss, H. Wolf, U. Schubert, T. Clark, *J. Am. Chem. Soc. 103* (1981) 6142.
[3] A. E. Reed, F. Weinhold, R. Weiss, J. Macheleid, *J. Phys. Chem. 89* (1985) 2688.
[4] R. West, A. Sado, S. Tobey, *J. Am. Chem. Soc. 88* (1966) 2488.
[5] R. Weiss, C. Schlierf, K. Schloter, *J. Am. Chem. Soc. 98* (1976) 4668.
[6] IR analysis of tetraiodoallene: A. M. Snider, Jr., P. F. Krause, F. A. Miller, *J. Phys. Chem. 80* (1976) 1262.
[7] For the synthesis of salts of type **2** cf. [5]. For the synthesis of salts of type **3** cf.: Z. Yoshida, H. Konishi, Y. Miura, H. Ogoshi, *Tetrahedron Lett. 1977*, 4319. The $I_3^{\oplus}$ ion in **2** and **3** originated from I_2-generating redox processes accompanying the substitution process at the three-membered ring.
[8] J. Mullay, *J. Am. Chem. Soc. 106* (1984) 5842.
[9] R. Weiss, K. G. Wagner, C. Priesner, J. Macheleid, *J. Am. Chem. Soc. 107* (1985) 4491, and references cited therein.
[10] According to MNDO calculations (R. Weiss, R. Roth, unpublished) the positive partial charge on the iodine in *cyclo*-$C_3I_3^{\oplus}$ is 0.42, in C_2I_2 0.28, in ICN 0.31.
[11] C. Laurence, M. Queignec-Cabanetos, B. Wojtkowiak, *J. Chem. Soc. Perkin Trans. 2 1982*, 1605.
[12] J. A. Creighton, K. M. Thomas, *J. Mol. Struct. 7* (1971) 173.

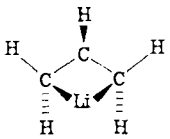
Crystal Structure of the η^3-Allyllithium Compound [1,3-Diphenylallyllithium · Diethyl Ether]$_n$**

By *Gernot Boche,* Heinz Etzrodt, Michael Marsch, Werner Massa, Gerhard Baum, Hans Dietrich,* and *Waruno Mahdi*

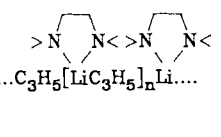
Allyl-transition metal complexes count among the most studied species in organometallic chemistry.[1] In the case of allyllithium, however, no evidence has hitherto been put forward of an η^3-structure in the solid state, as found in the transition metal complexes. According to calculations, monomeric allyllithium has such an η^3-structure in which the H atoms, as in some transition metal complexes,[11] are bent out from the plane of the C atoms (cf. **1**).[2-4]

According to a crystal structure determination of allyllithium · tetramethylenediamine (TMEDA), polymer chains are present in which the Li atoms coordinated to TMEDA each couple two terminal allylic-C atoms (Cf. **2**).[5] In tetrahydrofuran, allyllithium is present as a monomeric[6b] η^3-compound.[6]

In 1,3-diphenylallyllithium · diethyl ether **3** we found for the first time η^3-allyllithium moieties also in the solid state. They aggregate to form polymeric chains[7] (Fig. 1). The lithium atoms lie almost symmetrically above and below the allyl group. The Li-C2 distance being shorter than the Li-C1 and Li-C3 distances, corresponds to the situation found in most allyl-transition metal complexes.[1d,g] The angle C1-C2-C3 (131(1)°) is quite large. This is consistent with the comparably small $^1J(^{13}CH^2)$ coupling constants of allyl-alkali metal compounds in solution and with quantum mechanical calculations.[1h,4] The expected bending of the substituents in monomeric allyllithium compounds (see **1**) does not occur in **3**, apparently because of stacking. The 1,3-diphenylallyl moieties are approximately planar (maximum deviation from the best plane: 8 pm) and are inclined at 120° to each other in the direction of the chain. Compound **3** crystallizes from a diethyl ether/hexane/benzene mixture.[8] In diethyl ether, allyllithium has a degree of aggregation of at least 10.[9] Since this should be greater in diethyl ether/hexane/benzene and should similarly hold for 1,3-diphenylallyllithium, the crystal structure of **3** probably largely corresponds to its structure in solution.



1[2]



2[5]

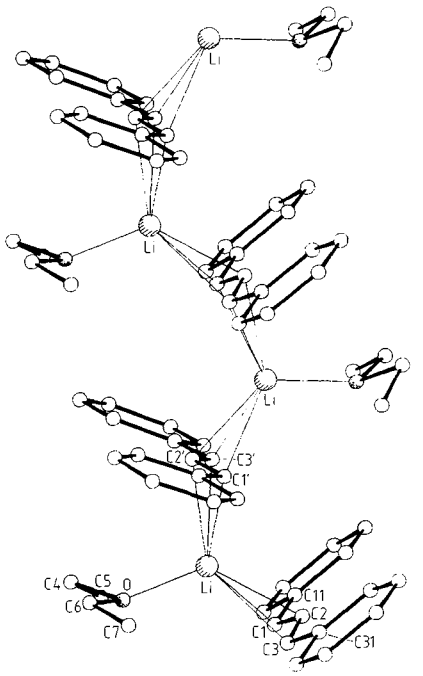


Fig. 1. Section of the polymeric chain structure of **3**. The atoms are represented by spheres with arbitrary radii. Selected bond lengths [pm] and bond angles [°]: Li-C1 248(3), Li-C2 230(3), Li-C3 250(3), Li-O 192(3), Li-C1' 240(3), Li-C2' 232(3), Li-C3' 252(3), C1-C11 147(1), C1-C2 139(1), C2-C3 138(2), C3-C31 145(1); C11-C1-C2 127(1), C1-C2-C3 131(1), C2-C3-C31 127(1).

Structures of the "η^3-allyl type" have been known since *Stucky* et al. elucidated the crystal structure of benzyllithium · triethylenediamine.[10a] Interestingly, the frequently occurring benzyllithium type structure, likewise possible in **3**,[2,10b] is not found. The energy difference between such structures should, however, be small, as has been shown by

[*] Prof. Dr. G. Boche, Dr. H. Etzrodt, M. Marsch, Priv.-Doz. Dr. W. Massa, G. Baum
Fachbereich Chemie der Universität
Hans-Meerwein-Strasse, D-3550 Marburg (FRG)
Prof. Dr. H. Dietrich, W. Mahdi
Fritz-Haber-Institut der Max-Planck-Gesellschaft
Faradayweg 4-6, D-1000 Berlin 33

[**] This work was supported by the Fonds der Chemischen Industrie and the Deutsche Forschungsgemeinschaft. We thank Prof. Dr. *R. Allmann*, Fachbereich Geowissenschaften der Universität Marburg, for helpful discussions and the NATO for a traveling scholarship.

the polymorphism in the case of dilithium 1,2-diphenylbenzocyclobutadienediide.[11, 12]

Received: September 2, 1985;
supplemented: October 7, 1985 [Z 1445 IE]
German version: *Angew. Chem. 98* (1986) 84

[1] Some relevant publications: a) G. Wilke, B. Bogdanović, P. Hardt, P. Heimbach, W. Kaim, M. Kröner, W. Oberkirch, K. Tanaka, E. Steinrücke, D. Walter, H. Zimmermann, *Angew. Chem. 78* (1966) 157; *Angew. Chem. Int. Ed. Engl. 5* (1966) 151; b) R. Uttech, H. Dietrich, *Z. Kristallogr. 122* (1965) 60; c) U. Franke, E. Weiss, *J. Organomet. Chem. 139* (1977) 305; d) J. A. Kaduk, A. T. Poulos, J. A. Ibers, *ibid. 127* (1977) 245 (in this work the structures of several allyl-transition metal complexes are discussed); e) T. H. Tulip, J. A. Ibers, *J. Am. Chem. Soc. 101* (1979) 4201; f) D. M. P. Mingos in G. Wilkinson, F. G. A. Stone, E. W. Abel (Eds.): *Comprehensive Organometallic Chemistry, Vol. III*, Pergamon, Oxford 1982; g) T. H. Cymbaluk, R. D. Ernst, V. W. Day, *Organometallics 2* (1983) 963; h) R. Benn, A. Rufińska, *ibid. 4* (1985) 209, and references cited therein; i) R. Goddard, C. Krüger, F. Mark, R. Stansfield, X. Zhang, *ibid. 4* (1985) 285, and references cited therein; j) P. W. Jolly, *Angew. Chem. 97* (1985) 279; *Angew. Chem. Int. Ed. Engl. 24* (1985) 283.

[2] a) T. Clark, E. D. Jemmis, P. von R. Schleyer, J. S. Binkley, J. A. Pople, *J. Organomet. Chem. 150* (1980) 1; b) T. Clark, C. Rhode, P. von R. Schleyer, *Organometallics 2* (1983) 1344; c) G. Decher, G. Boche, *J. Organomet. Chem. 259* (1983) 31.

[3] Other bending modes of the H atoms were deduced on the basis of ^1J(C,H) and ^3J(H,H) coupling constants: M. Schlosser, M. Stähle, *Angew. Chem. 94* (1982) 142; *Angew. Chem. Int. Ed. Engl. 21* (1982) 145; *Angew. Chem. Suppl. 1982*, 198; see also [2b, 4].

[4] H. Albrecht, K. Zimmermann, G. Boche, G. Decher, *J. Organomet. Chem. 262* (1984) 1. Further calculations on the structure of allyl "anions" are cited in this work, and $^1J(^{13}CH^2)$ coupling constants of these compounds are also discussed. Most recent calculations on allyllithium, which are in very good agreement with comparable data on **3**, are given in a paper by P. von R. Schleyer, *J. Am. Chem. Soc. 107* (1985) 4793. Structural data on the allyl anion in the gas phase, on the other hand, deviate considerably, see J. M. Oakes, G. B. Ellison, *J. Am. Chem. Soc. 106* (1984) 7734.

[5] H. Köster, E. Weiss, *Chem. Ber. 115* (1982) 3422.

[6] Unsymmetrically bridged: a) M. Schlosser, M. Stähle, *Angew. Chem. 92* (1980) 497; *Angew. Chem. Int. Ed. Engl. 19* (1980) 487; b) M. Stähle, M. Schlosser, *J. Organomet. Chem. 220* (1981) 277; symmetrically bridged: c) W. Neugebauer, P. von R. Schleyer, *ibid. 198* (1980) C 1.

[7] X-ray structure analysis: 154 K, red needle, ca. $0.6\times0.09\times0.07$ mm^3; $P2_12_12_1$, $a=1770.2(8)$, $b=746.5(6)$, $c=1231.0(7)$ pm, $Z=4$, $\rho_{calc}=1.120$ g cm^{-3}; due to the crystal being very small, only 570 independent reflections with $F_0>3\sigma(F_0)$ (from a total of 905 reflections with $\theta\leq20°$) could be measured (four-circle diffractometer CAD4, Enraf-Nonius, graphite monochromator, $Mo_{K\alpha}$ radiation). Direct methods; because of the small number of reflections, refinement with phenyl residues as rigid groups with idealized geometry (C–C 139.5 pm), H atoms at calculated positions (C–H 95 pm) and with isotropic temperature factors for the diphenylallyl moiety and anisotropic factors for the stronger vibrating or somewhat disordered ether group. $R_g=0.068$, $R_w=0.074$ with $w=1.8/\sigma^2(F_0)$, 86 parameters. Further details of crystal structure investigation are available on request from the Fachinformationszentrum Energie, Physik, Mathematik GmbH, D-7514 Eggenstein-Leopoldshafen 2, on quoting the depository number CSD 51693, the names of the authors, and the full citation of the journal. Similar polymeric structures are found, e.g., in $[C_5H_5In]$ and $[C_5H_5Tl]$ (E. Frasson, F. Menegus, C. Panattoni, *Nature (London) 1963*, 1087), $[(C_5H_5)_2Pb]$ (C. Panattoni, G. Bombieri, U. Croatto, *Acta Crystallogr. 21* (1966) 823), $[C_5H_4C(CN(C(CN)_2]^-Tl^+$ (M. B. Freeman, L. G. Sneddon, J. C. Huffman, *J. Am. Chem. Soc. 99* (1977) 5194), $[(C_5H_5)Na\cdot tmeda]$ (T. Aoyagi, H. M. M. Shearer, K. Wade, G. Whitehead, *J. Organomet. Chem. 175* (1979) 21), see also: E. Canadell, O. Eisenstein, *Organometallics 3* (1984) 759. E. R. Tidwell, B. R. Russell, *J. Organomet. Chem. 80* (1974) 175, calculated (with the aid of CNDO/2) structures of allyllithium dimers, and speculated thereby on a polymeric structure having certain similarities to **3**. The calculated structure of an allyllithium-lithium hydride complex can also be considered as model for the structure of **3** (P. von R. Schleyer, A. J. Kos, E. Kaufmann, *J. Am. Chem. Soc. 105* (1983) 7617).

[8] Preparation of **3**: A solution of 1,3-diphenylpropene (100 mg, 0.51 mmol) in benzene (1 mL) and *n*-hexane (1 mL) was treated at room temperature with diethyl ether (1.2 molar equivalents) and then with *n*-butyllithium in hexane (1.2 molar equivalents). After 16 h the solvent was removed from the red, very thin needle-like crystals with the aid of a fine pipette. The crystals were then washed with *n*-hexane and dried at 10^{-4} torr.

[9] P. West, J. I. Purmont, S. V. McKinley, *J. Am. Chem. Soc. 90* (1968) 797.

[10] a) S. P. Patterman, I. L. Karle, G. D. Stucky, *J. Am. Chem. Soc. 92* (1970) 1150; b) review: W. Setzer, P. von R. Schleyer, *Adv. Organomet. Chem. 24* (1985) 353.

[11] G. Boche, H. Etzrodt, W. Massa, G. Baum, *Angew. Chem. 97* (1985) 858; *Angew. Chem. Int. Ed. Engl. 24* (1985) 863.

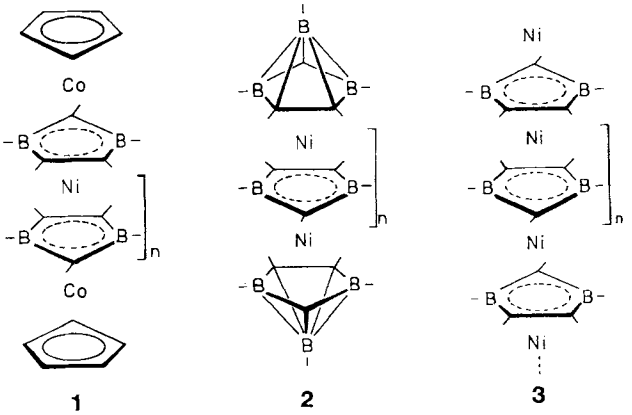
[12] A structure of the "η^3-azaallyl type" has recently been described: a) D. Colgan, R. I. Papasergio, C. L. Raston, A. H. White, *J. Chem. Soc. Chem. Commun. 1984*, 1708; b) see also P. von R. Schleyer, R. Hacker, H. Dietrich, W. Mahdi, *ibid. 1985*, 622.

Polymeric (η^5,μ-2,3-Dihydro-1,3-diborolyl)nickel—the First Polydecker Sandwich Compound**

By *Thomas Kuhlmann, Siegmar Roth, Jacques Rozière,* and *Walter Siebert**

Dedicated to Professor Max Schmidt on the occasion of his 60th birthday

Polydecker sandwich compounds are one-dimensional transition-metal complex systems which should exhibit electrical conductivity. INDO-MO calculations[1] on eleven model compounds have yielded different band structures, which are a function of the metals (Mn-Zn) and the bridge ligands coupling them: Polymeric $[(Mn(C_5H_5)]_n$ is an insulator, $[Zn(B_5H_5)]_n$ an electrical conductor. The syntheses of oligodecker sandwich compounds with carbacycles have hitherto only led to triple-decker compounds,[2] whereas with the electron-deficient 2,3-dihydro-1,3-diborolyl ligand it has been possible to synthesize tetra-, penta-, and hexadecker-complexes of type **1** (n = 1–3).[3] These results and the unusual conversion of bis(2,3-dihydro-1,3-diborole)nickel sandwich complexes into the oligodeckers[4] **2** (n = 1–8) at room temperature demonstrate that the 13e fragment $[Ni(R_5C_3B_2)]$ is an electronically favorable stacking unit. We report here on the synthesis and properties of the first polydecker sandwich compound **3**.

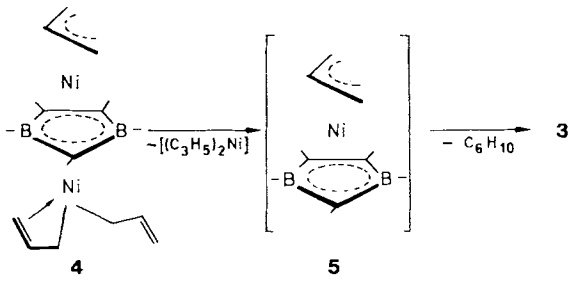


1 **2** **3**

[*] Prof. Dr. W. Siebert, Dr. T. Kuhlmann
Anorganisch-chemisches Institut der Universität
Im Neuenheimer Feld 270, D-6900 Heidelberg 1 (FRG)
Dr. S. Roth
Max-Planck-Institut für Festkörperforschung
Heisenbergstrasse 1, D-7000 Stuttgart 80 (FRG)
Prof. Dr. J. Rozière
Laboratoire des Acides Minéraux
Université des Sciences et Techniques du Languedoc
F-34060 Montpellier Cedex (France)

[**] This work was supported by the Deutsche Forschungsgemeinschaft, the Land Baden-Württemberg (Schwerpunkt Nr. 31—Komplexchemie), the Fonds der Chemischen Industrie, and BASF AG.

Reaction of 1,3,4,5-tetramethyl-2,3-dihydro-1,3-diborole[5] with an excess of bis(allyl)nickel leads at low temperature to the dinuclear complex **4**.[6] In solution it reacts slowly to give the tetradecker $[\{(C_3H_5)Ni(Me_4HC_3B_2)\}_2Ni]$, whereupon nickel, hexadiene, and small amounts of polymeric products separate out. When thin layers of **4** are heated in vacuo, the condensation product $[(\eta^3\text{-}C_3H_5)_2Ni]$ and hexadiene are removed from the reaction mixture. A black film forms on the wall of the flask, which upon cooling splinters into shiny metallic platelets. The almost quantitative formation of polymeric **3** presumably proceeds via the complex **5** initially formed from **4**.



3 is remarkably stable towards heat and is insoluble in organic solvents. Upon measurement of the capacity[7] in propylene carbonate/$LiClO_4$ a partial dissolution of the polydecker electrode took place. Analysis of the very oxygen-sensitive polymer[8] yielded the empirical formula $C_7H_{13}B_2Ni$ calculated for the stacking unit. Compound **3** ignites in a stream of O_2, while suspensions in mesitylene take up two molecules of oxygen per stacking unit.[9]

The allyl group (m/z 41) is the only fragment that can be observed in low intensity in the mass spectrum up to 620 K. Solid-state NMR investigations show broad ^{11}B- and ^{13}C-signals in the diamagnetic range;[10] a recording of ^1H-decoupled spectra is not possible on account of discharging in the sample. In the X-band ESR spectrum the polymer shows a very broad signal (864 G, $g=2.25$) at 280 K; below 50 K a new signal appears at $g=2.10$ whose intensity increases on further cooling, while the original signal disappears. At 2 K a relatively sharp signal (165 G) is present which is assigned to Ni^{2+}.[11]

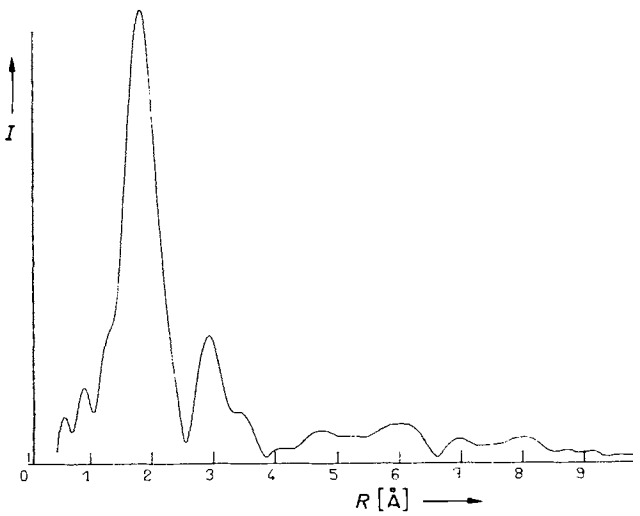


Fig. 1. Fourier transformed EXAFS spectrum (77 K) of the nickel polymer **3**; phase shift not corrected.

EXAFS investigations on **3** (Fig. 1) confirm the polydecker structure with the expected nickel : ligand ratio of 1 : 1. The EXAFS data yield two nickel-ring atom distances (Ni-C or Ni-B) of 2.17(2) and 2.56(2) Å in the ratio 1 : 1 and one Ni-Ni distance of 3.35(2) Å. Each Ni atom has, however, only *one* nickel atom as a neighbor at a distance of 3.35(2) Å. This and the short Ni-C(B) distance of 2.17 Å are consistent with a $Ni(C_3B_2)Ni$ group, which has also been found in a pentadecker[3b,12]. A coupling of this seven-atom cluster with other C_3B_2 rings over the longer distances Ni-C(B) (2.56 Å) leads to polymeric **3**. For such an arrangement, there must be a longer Ni-Ni distance, which can scarcely be observed in the EXAFS measurement; we have evidence of a further Ni-Ni distance in the 3.8-3.9 Å range.

The two-contact powder conductivity[13] of **3** at 2500 bar is 0.25 S cm^{-1}. Four-contact measurements give 10^{-2} S cm^{-1}. The temperature dependence of the conductivity was measured in the range from 380 to 30 K. The conductivity decreases upon cooling over the entire range. At 300 K a jump by a factor of about 2 occurs, thus indicating a structural phase transition. Near room temperature the temperature coefficient of the conductivity corresponds to an activation energy of 0.08 eV. The conductivity data are better described in terms of the equation

$$\sigma=\sigma_0\exp[-(T/T_0)^{1/4}]$$

which is characteristic for variable range hopping in strongly perturbed semiconductors and in conducting polymers.[14]

A numerical fit furnishes the parameters $\sigma_0=1.2\times10^{-3}$ S cm^{-1} and $T_0=5\times10^5$ K. These values lie in the range that is also found for strongly "doped" polyacetylenes. The resistance of **3** increases rapidly in the presence of oxygen or iodine.

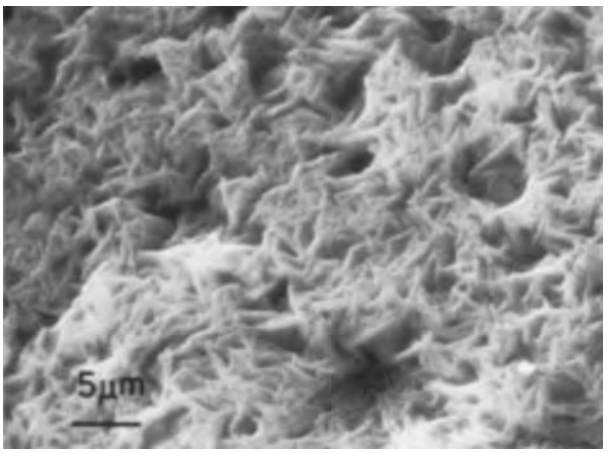


Fig. 2. Electron photomicrograph (magnification 2000×) of **3**.

Figure 2 shows an electronmicrograph of the polymer, present in isotropic distribution. A definite statement cannot be made about the average chain length of the stacking molecule. As MS investigations up to 620 K have shown, allyl groups are eliminated in low intensity from the polymer.

Received: September 2, 1985;
supplemented: October 28, 1985 [Z 1446 IE]
German version: *Angew. Chem.* 98 (1986) 87

[1] M. C. Böhm, *Z. Naturforsch. A 39* (1984) 223.
[2] a) H. Werner, *Angew. Chem. 89* (1977) 1; *Angew. Chem. Int. Ed. Engl. 16* (1977) 1; b) J. Moraczewski, W. E. Geiger, *J. Am. Chem. Soc. 100* (1978) 7429; c) S. P. Kolesnikov, J. E. Dobsen, P. S. Skell, *ibid. 100* (1978) 999; d) A. W. Duff, K. Jonas, R. Goddard, H.-J. Kraus, C. Krüger, *ibid. 105* (1983) 5479.
[3] a) W. Siebert, J. Edwin, H. Wadepohl, H. Pritzkow, *Angew. Chem. 94* (1982) 148; *Angew. Chem. Int. Ed. Engl. 21* (1982) 149; b) M. W. Whiteley, H. Pritzkow, U. Zenneck, W. Siebert, *ibid. 94* (1982) 464 and *21* (1982) 453; c) T. Kuhlmann, W. Siebert, *Z. Naturforsch. B 40* (1985) 167; d) W. Siebert, *Angew. Chem. 97* (1985) 924, *Angew. Chem. Int. Ed. Engl. 24* (1985) 943.
[4] a) T. Kuhlmann, H. Pritzkow, U. Zenneck, W. Siebert, *Angew. Chem. 96* (1984) 994; *Angew. Chem. Int. Ed. Engl. 23* (1984) 965; b) T. Kuhlmann, *Dissertation*, Universität Heidelberg 1985.
[5] W. Siebert, U. Ender, W. Herter, *Z. Naturforsch. B 40* (1985) 326.
[6] Procedure for **4**: 0.55 g (4.6 mmol) of 1,3,4,5-tetramethyl-2,3-dihydro-1,3-diborole [5] was added to a solution of 2 g (14.3 mmol) of bis(allyl)nickel in 50 mL of petroleum ether (40/60) at −180 °C under nitrogen and the resulting mixture was stirred for 2 h at −15 °C. Petroleum ether and excess $[Ni(C_3H_5)_2]$ were then removed from the mixture at −15 °C and the product chromatographed on a low-temperature column (−20 °C, Al_2O_3, deactivated with 5% H_2O). **4** was isolated as a deep orange-yellow, thermolabile and oxygen-sensitive oil (1.16 g, 70%) [4b]; ^1H NMR (300 MHz; [D$_8$]toluene, −10 °C): $\delta = 4.84$ (sept, 1H), 4.32 (m, 2H), 3.52 (d, 2H, $J(HH) = 8.1$ Hz), 2.86 (s, 1H), 2.82 (d, 2H, $J(HH) = 14.7$ Hz), 2.66 (d, 2H, $J(HH) = 6.6$ Hz), 1.76 (m, 2H), 1.47 (s, 6H), 1.43 (d, 2H, $J(HH) = 13.2$ Hz), 1.32 (m, 2H), 0.45 (s, 6H); ^{11}B NMR (C_6D_6): $\delta = 21.6$; EI-MS: m/z 358 (M^+, 71%). Procedure for **3**: A horizontally fixed cylindrical flask containing a solution of **4** (0.5 g, 1.45 mmol) in petroleum ether (5 mL) was rotated during evacuation so that a uniform film was formed on the wall of the flask (approx. 40 cm^2 surface area). The cylinder was slowly heated in an oil bath to 160 °C, whereupon $[Ni(C_3H_5)_2]$ and hexadiene were released and trapped in a cool trap. Small amounts of the reddish orange tetradecker $[\{(\eta^3\text{-}C_3H_5)Ni(Me_4HC_3B_2)\}_2Ni]$ also distilled over. Upon cooling, the black film splintered into irregular platelets (0.1 to 1.0 cm in length), which were washed three times with petroleum ether and dried in a vacuum. Yield 330 mg (89%) of **3**, which is stable up to 500 °C.
[7] ≈ 15 Ah/kg; H. Möhlwald, BASF AG.
[8] Mikroanalytisches Laboratorium Dornis und Kolbe, Mülheim a. d. Ruhr (FRG).
[9] R. Köster, Max-Planck-Institut für Kohlenforschung, Mülheim a. d. Ruhr (FRG).
[10] D. Förster, Bruker AG, Karlsruhe (FRG).
[11] B. Kanellakopulos, Kernforschungszentrum Karlsruhe (FRG).
[12] EXAFS investigations of the tetradecker sandwich compound **1** (n = 1) were in good agreement with the X-ray structure data [3a]. The EXAFS studies were carried out by *J. R.* in the Laboratoire pour l'Utilisation du Rayonment Electromagnetique, Orsay (France).
[13] a) H. Münstedt, BASF AG; b) D. Schweitzer, Max-Planck-Institut für Medizinische Forschung, Heidelberg (FRG).
[14] K. Ehinger, S. Roth, *Philos. Mag.*, in press.

The Structure of Chlorosilyl-*N,N*-dimethylamine in the Gaseous and Solid Phases

By *David G. Anderson, Alexander J. Blake, Stephen Cradock,* E. A. V. Ebsworth, David W. H. Rankin,* and *Alan J. Welch*

Silylamines exhibit some striking structural features that are related to the ability of four-covalent silicon to accept additional electrons, using its vacant 3d orbitals. Thus, trisilylamine[1] and disilylamines[2] have planar coordination at nitrogen, while *N,N*-dimethyl(silyl)amine (which appears to have a non-planar nitrogen in the gas phase[3]) forms a cyclic pentamer in the crystal[4] with five-coordinate silicon linked by four-coordinate nitrogen, all the Si-N bonds being equivalent.

[*] Dr. S. Cradock, D. G. Anderson, Dr. A. J. Blake, Prof. E. A. V. Ebsworth, Dr. D. W. H. Rankin, Dr. A. J. Welch
Department of Chemistry, University of Edinburgh
West Mains Road, Edinburgh EH9 3JJ (Scotland)

As part of systematic a study of silylamines and their structures we have prepared chlorosilyl-*N,N*-dimethylamine **1**. This compound has been briefly reported by *Emsley*.[5] We have synthesized it by reaction of dichlorosilane with two molar equivalents of dimethylamine in the gas phase, and characterized it by its IR and Raman spectra in the gas, liquid, and solid phase, and by its NMR spectra in solution.

$ClH_2Si-N(CH_3)_2$ **1**

The vibrational spectra of **1** are strikingly different in the gas and the annealed solid phases, particularly in the region associated with Si-N stretching modes (600–900 cm^{-1}). A prominent band at 688 cm^{-1} (IR, gas)/694 cm^{-1} (Raman, liquid) is absent in the annealed solid, being apparently replaced by two bands in each spectrum, with frequencies of 796 and 619 cm^{-1} in the IR spectrum, and of 802 and 610 cm^{-1} in the Raman spectrum. These observations suggested that the species present in the annealed solid was not monomeric, as in the gas and the liquid; they would be consistent with a centrosymmetric dimer unit with a Si_2N_2 ring, but do not suffice as proof that such a ring is present. Accordingly, we used electron diffraction in the gas phase and X-ray diffraction in the annealed solid phase in order to determine the molecular structures unequivocally in each case. The results confirmed our initial conjectures from the vibrational spectra, revealing that **1** forms a novel centrosymmetric dimer in the crystal.

According to the electron diffraction pattern gaseous **1** is monomeric, with the expected four-coordinate silicon (Fig. 1a). The Si-N and Si-Cl bond lengths are similar to those found in related compounds, 168.9(4) pm and

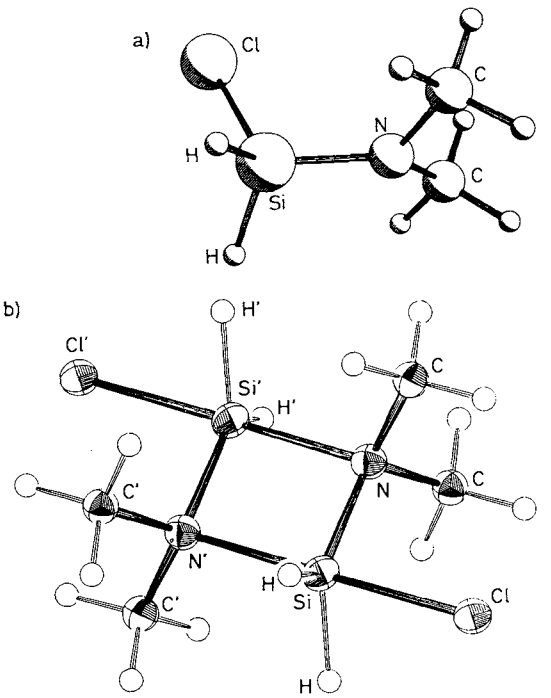


Fig. 1. a) Structure of gaseous monomeric chlorosilyl-*N,N*-dimethylamine **1** at 298 K. Bond lengths [pm] and angles [°]: Si-Cl 207.0(2), Si-N 168.9(4), Si-H 147(2), N-C 146.4(4), C-H 110.2(5); Cl-Si-N 113.0(6), Si-N-C 121(1), C-N-C 115(1). b) Structure of **1** in the crystal at 116 K. The Si_2N_2Cl group is almost planar; the dimer contains a center of inversion. Bond lengths [pm] and angles [°]: Si-Cl 223.1(6), Si-N 181.4(13), Si-H 149(1), N-C 149.8(18), Si'-N 205.4(13); Cl-Si-N 96.1(5), Si-N-C 112.8(9), C-N-C 108.8(14), N-Si-N' 83.0(5), Si-N-Si' 97.0(6).

207.0(2) pm respectively. The Si–N bond is slightly shorter than those in other *N,N*-dimethyl(silyl)amines (171–172 pm), which are themselves shorter than those in other silylamines,[6] whereas the Si–Cl bond is somewhat longer than that found in SiH_3Cl (205 pm). The nitrogen appears very slightly non-planar, though this may well be a shrinkage effect, and the ClSiN and CNC planes are almost perpendicular to each other.

The crystal structure[7] consists of well-separated dimers (Fig. 1b), packed in sheets parallel to *ac*, about 500 pm apart, with dimers in one plane above interstices in the plane below. The dimer has crystallographically-required C_{2h} symmetry. The central Si_2N_2 unit is not equilateral; two opposite Si–N distances are 181.4(13) pm, whilst the other two are much longer, 205.4(13) pm. The dimers can therefore be described in terms of two strongly-interacting monomers. The strength of the interaction is shown by the extent to which the normal tetrahedral coordination at Si is distorted in the dimer; the N–Si–Cl angle 96.1(5)° is much smaller than in the gas-phase monomer (113.0(6)°), allowing the additional bond to N′ to develop. The N′···Si–Cl angle is 179.0(4)°, very close to linear, so that Si is adopting trigonal bipyramidal coordination, though the "axis" ClSiN is not strictly perpendicular to the "equatorial plane" containing N′ and the two H atoms attached to Si. The fact that the Cl atom adopts the axial position rather than an equatorial position is in accord with its position in the "apicophilicity series", which has been proposed[12] to account for some observed structures of pentacoordinate phosphorus compounds.

The effect of the additional Si···N′ interaction on the Si–Cl and Si–N bond lengths is striking; these are, respectively, 16 and 12 pm longer in the crystal than in the gas-phase monomer, even though the Si–Cl bond is *trans* to the additional Si···N′ bond and the Si–N bond is almost orthogonal to it. The lengthened Si–Cl bond may be compared with other Si–Cl bonds *trans* to nitrogen at five- or six-coordinated silicon, with lengths such as 227.4 pm and 239.3 pm.[13] The Si–N···Si′ angle (97.0(6)°) probably represents a compromise between 90° (as would be needed for a square Si_2N_2 unit, and as is appropriate to trigonal bipyramidal coordination at Si) and the tetrahedral angle of 109.47°. We may regard the dimer as a "frozen" intermediate in an S_N2 reaction involving attack at Si by N′; the leaving group is Cl, and the putative "product" would be an ionic form of the dimer, with all Si–N bonds equal in length.

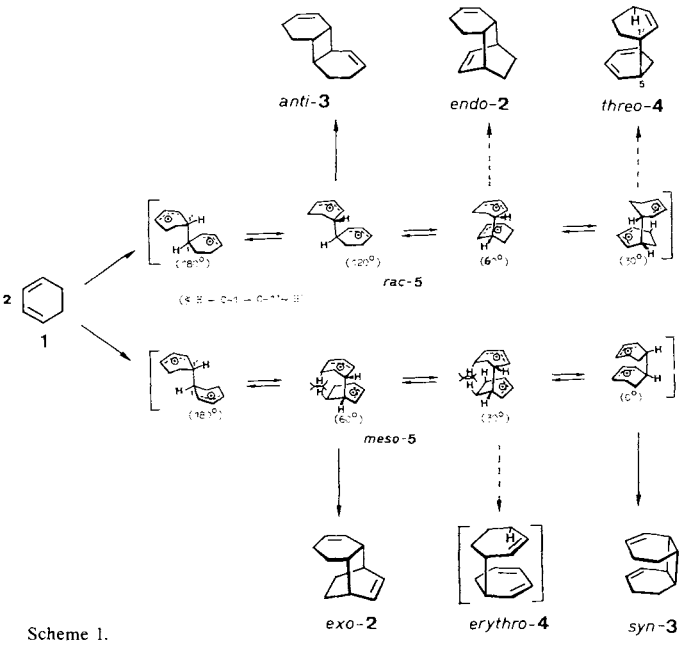
Received: September 16, 1985;
supplemented: October 21, 1985 [Z 1464 IE]
German version: *Angew. Chem. 98* (1986) 97

[1] K. Hedberg, *J. Am. Chem. Soc. 77* (1955) 6491.
[2] G. Gundersen, D. W. H. Rankin, H. E. Robertson, *J. Chem. Soc. Dalton Trans. 1985*, 191.
[3] C. Glidewell, D. W. H. Rankin, A. G. Robiette, G. M. Sheldrick, *J. Mol. Struct. 6* (1970) 231.
[4] a) R. Rudmann, W. C. Hamilton, S. Novick, T. D. Goldfarb, *J. Am. Chem. Soc. 89* (1967) 5157; b) A. J. Blake, E. A. V. Ebsworth, A. J. Welch, *Acta Crystallogr. C40* (1984) 895.
[5] J. Emsley, *J. Chem. Soc. A 1968*, 1009.
[6] G. Gundersen, R. Mayo, D. W. H. Rankin, *Acta Chem. Scand. Ser. A 38* (1984) 579.
[7] Monoclinic, space group $C2/m$, $a=676.59(22)$, $b=995.0(3)$, $c=849.40(27)$ pm, $\beta=114.70(4)°$, $V=0.5195$ nm^3, $Z=4$, $\varrho_{calc.}=1.402$ g cm^{-3}, $T=116$ K, $\mu(Mo_{K\alpha})=0.79$ mm^{-1}. A conical crystal (0.27 × 0.20 mm) was grown in a tapered capillary tube in situ on a Weissenberg goniometer and transferred as described previously [8] to an Enraf-Nonius CAD4 diffractometer. From 427 unique data ($1° \leq \Theta \leq 22.5°$), corrected for absorption [9], 282 with $F \geq 4\sigma(F)$ were used to solve (Patterson [10]) and refine (difference Fourier, full-matrix least-squares [11]) the structure. Non-hydrogen atoms were refined anisotropically and, after location, methyl hydrogens were refined as parts of rigid groups; r(Si–H) was constrained to 150 ± 5 pm. Final residuals $R=0.0970$, $R_w=0.1097$. The atomic coordinates for this work are available on request from The Director of the Cambridge Crystallographic Data Centre, University Chemical Laboratory, Lensfield Road, Cambridge CB21EW. Any request should be accompanied by the full literature citation for this communication.
[8] A. J. Blake, S. Cradock, E. A. V. Ebsworth, D. W. H. Rankin, A. J. Welch, *J. Chem. Soc. Dalton Trans. 1984*, 2029.
[9] DIFABS. Program to apply empirical absorption corrections. N. Walker, D. Stuart, *Acta Crystallogr. A 39* (1983) 158.
[10] SHELX84. Program for crystal structure solution. G. M. Sheldrick, Universität Göttingen 1983.
[11] SHELX76. Program for crystal structure refinement. G. M. Sheldrick, University of Cambridge, 1976.
[12] R. G. Cavell, D. D. Poulin, K. I. The, A. J. Tomlinson, *J. Chem. Soc. Chem. Commun. 1974*, 19.
[13] G. Sawitzki, H. G. von Schnering, *Chem. Ber. 109* (1976) 3728.

Mechanism of the Thermal 1,3-Cyclohexadiene Dimerization: A Non-Concerted Diels-Alder Reaction Leading to the *exo*-[4 + 2] Adduct and a Novel [6 + 4]-Ene Reaction**

By *Frank-Gerrit Klärner,* Barbara M. J. Dogan, Otto Ermer, William von E. Doering,* and *Martin P. Cohen*

In the thermal dimerization of 1,3-cyclohexadiene **1** a novel stereospecific [6 + 4]-ene reaction was observed which competed with [2 + 2]- and the already known [4 + 2]-cycloadditions.[1] A study of the pressure dependence (up to 7 kbar) gave relatively large differences in the activation volumes, which are explainable, inter alia, in terms of a non-concerted Diels-Alder dimerization to the *exo*-adduct.

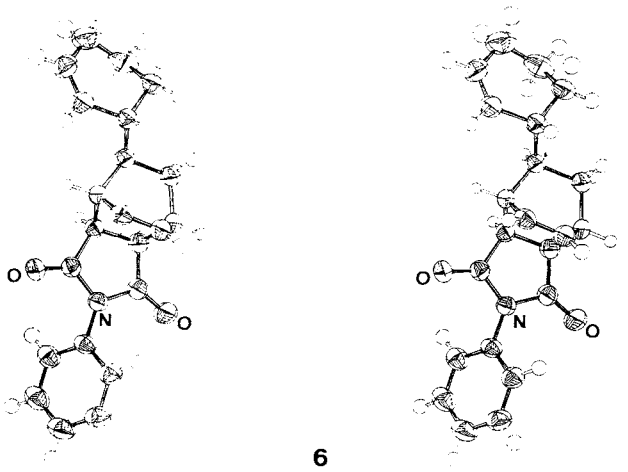


Scheme 1.

[*] Prof. Dr. F.-G. Klärner, Dr. B. M. J. Dogan, Priv.-Doz. Dr. O. Ermer
Fakultät für Chemie der Universität
Postfach 102148, D-4630 Bochum 1 (FRG)
Prof. Dr. W. von E. Doering, Dr. M. P. Cohen
Department of Chemistry, Harvard University
Cambridge, MA 02138 (USA)

[**] This work was sponsored by the Minister für Wissenschaft und Forschung des Landes Nordrhein-Westfalen and the Fonds der Chemischen Industrie (FRG) and by the National Science Foundation (USA).

At temperatures above 150°C, **1** dimerizes to the [4+2] Diels-Alder adducts *endo*-**2** and *exo*-**2**.[1] Below 150°C, not only *endo*-**2** and *exo*-**2** but also the [2+2]-cycloadducts *syn*-**3** and *anti*-**3** and a further unknown dimer are formed (at 110°C in the ratio 74.3 : 11.4 : 4.1 : 2.5 : 7.7). The product mixture can be separated gas chromatographically and *endo*-**2** and *exo*-**2** as well as *syn*-**3** and *anti*-**3** can be individually identified by comparison with authentic samples[2] prepared via an alternative route. The previously unknown dimer is—according to its spectra and its degradation to 3-vinylcyclohexene (via Diels-Alder addition with methyl acetylenedicarboxylate and subsequent Alder-Rickert cleavage)—an isomer of 5-(2-cyclohexenyl)-1,3-cyclohexadiene **4**.[3] An elucidation of the stereochemistry at C-5 and C-1′ is provided by the crystal structure analysis of the Diels-Alder adduct **6** (Fig. 1), which was prepared from the liquid dimer **4** by reaction with *N*-phenylmaleimide.[4] According to the X-ray diffraction pattern, **4** has the *threo* configuration and is formally the result of a [6+4]-ene reaction vinylogous to the conventional [4+2]-ene reaction.



6

Fig. 1. Stereoview of the structure of **6** in the crystal (with vibration ellipsoids (50%) for the heavy atoms); isotropic temperature factors of the H atoms reduced by a common factor.

We have investigated the pressure- and temperature-dependence of the 1,3-cyclohexadiene dimerization at 70.5°C in the range from 1 to 7000 bar and at 70–150°C under normal pressure. A strategy analogous to that described by *Stewart*[5] for the dimerization of chloroprene was used in an attempt to obtain an insight into complex processes with several reaction paths. Our results are listed in Table 1. All the dimers are stable at 70°C up to 3000 bar as well as at 110°C and normal pressure. This stability is also reflected in the product ratios being independent of the reaction times. At 70°C and 7000 bar *threo*-**4** reacts slowly to give gas-chromatographically undetectable, high molecular weight compounds (conversion: 33% after 74 h). Under normal pressure *threo*-**4** first starts to disproportionate at higher temperatures in benzene and cyclohexene (5% after 22 h at 161°C)—presumably as a result of a retro-[4+2]-ene reaction. At 118.8 and 151.5°C the known[2] rearrangements of *syn*- and *anti*-**3** into *exo*- and *endo*-**2**, respectively, slowly take place. In each case product ratios are extrapolated to zero reaction time.

The five products of the cyclohexadiene dimerization can be divided into two stereochemical classes (Scheme 1): The *endo*-**2**, *anti*-**3**, and *threo*-**4** dimers are formally derived from the diradical *rac*-**5**, whereas *exo*-**2**, and *syn*-**3** are derived from *meso*-**5** (formation of *erythro*-**4** is not observed).

The [2+2]-cycloadducts *anti*-**3** and *syn*-**3** are doubtlessly formed in two steps via the diradicals *rac*-**5** and *meso*-**5**. Besides the two-step routes indicated in Scheme 1, also concerted [4+2]-cycloadditions and [6+4]-ene processes must be considered for the formation of the remaining dimers. Differentiation between the various mechanisms is possible by comparison of the activation volumes of formation of those dimers which can be formed from one and the same diradical. The activation volumes of the reaction leading to *exo*-**2** and *syn*-**3** are, within the limits of error, equal. This finding suggests a similar mechanism of formation for both products. Assuming that formation of *syn*-**3** involves a two-step process, *exo*-**2** is accordingly the product of a non-concerted Diels-Alder reaction.[6] The activation volumes of the reactions leading to *endo*-**2** and *threo*-**4** are, respectively, 10 and 14 cm^3/mol more negative than the activation volume of the reaction leading to *anti*-**3**.

Table 1. Pressure- and temperature-dependence of the dimerization of **1** and [5,5,6,6-D_4]-**1**.

T [°C]	p [bar]		Rate constants $k_{1,i} \times 10^9$ [L mol^{-1} s^{-1}] [a]			
		i: *endo*-**2**	*exo*-**2**	*syn*-**3**	*anti*-**3**	*threo*-**4**
70.5 [b]	1	1.19	0.141	0.0472	0.0261	0.151
	3000	15.0	1.02	0.327	0.134	2.71
	7000	129.	5.35	1.34	0.502	31.5
118.8	1	71.8 [c]	11.2	4.06	2.32	7.25
		75.1 [d]	10.9	3.92	2.30	3.54
151.5 [b]	1	658.	120.	40.1	31.9	62.0
70.5	ΔV_0^* [cm^3/mol] [e]	−28	−22	−22	−18	−32
	$\Delta\Delta V_0^*$ [cm^3/mol]	−10	−4	−4	(0)	−14
118.8	k_H/k_D [d]	0.95	1.03	1.04	1.01	2.42
	E_A [kcal/mol] [f]	22.6	24.2	24.3	25.3	21.5
	lg$A$	5.46	5.51	5.10	5.52	3.87

[a] The specific rate constants were calculated from the time dependence (at least four times) of the gas-chromatographically determined product concentrations (70-cm glass capillary column (silicone oil OV101), 120°C, dodecane as internal standard) by the least squares method. Standard deviations < 2.5%. [b] $[1]_0 = 1.73$ mol/L. [c] $[1]_0 = 1.33$ mol/L. [d] $[[5,5,6,6\text{-}D_4]\text{-}1]_0 = 1.33$ mol/L; the kinetic isotope effects k_H/k_D are corrected for the deuterium distribution determined from the MS and ^{2}H-NMR spectra [3] of 5,5,6,6-D_4-**1**: $k_H = k_{H(exp)}/4$; $k_D = k_{D(exp)} - 0.513\,k_H)/3.487$. [e] ΔV_0^* and $\Delta\Delta V_0^*$ were calculated from the pressure dependence of the rate constants ($k_{p,i} \equiv k_{1,i}$) or the product ratios (referred to *anti*-3: $k_{p,i} \equiv p_i/p_{anti\text{-}3}$) directly obtainable from the GC analyses, using $k_{p,i} = a_i + b_{i,p} + c_i p^2$; $\Delta V_{0,i}^*$ and $\Delta\Delta V_{0,i}^* = -b_i RT$ at 70.5°C; error of $\Delta\Delta V_{0,i}^* < 1$ cm^3/mol. [f] The Arrhenius parameters were calculated from the temperature dependence of $k_{1,i}$ at 1 bar by the least squares method (standard deviations of $E_A < 0.5$ kcal/mol).

This indicates that their transition states are significantly more compact. Consequently, these three adducts have no common intermediate, so that *endo*-**2** (always the main product of the Diels-Alder reaction) and *threo*-**4** are most likely formed by concerted mechanisms.

To our knowledge there is no precedent for the [6+4]-ene reaction.[7] To confirm the proposed mechanism we have therefore measured the kinetic isotope effect of the dimerization of 5,5,6,6-tetradeuterio-1,3-cyclohexadiene, which was prepared according to a procedure given in the literature for the synthesis of **1**[8] from tetradeuterioethylene and 1,2,3,4-tetrachloro-5,5-dimethoxy-1,3-cyclopentadiene. The primary isotope effect k_H/k_D, with a value of 2.42 (Table 1), is of the same order of magnitude as in the normal [4+2]-ene reaction.[9]

The conclusions drawn from the pressure-dependence for the cyclohexadiene dimerizations are consistent with the activation energies obtained from the temperature-dependence. For the formation of *exo*-**2** and *syn*-**3** these are practically of equal magnitude, whereas those for the formation of *endo*-**2** and *threo*-**4** are smaller than for the formation of *anti*-**3** (Table 1). The smaller activation barriers can be regarded as an indicator of a certain degree of resonance stabilization ($\leq$2.7 and 3.8 kcal/mol, respectively) of the transition state of the concerted processes. The small differences in the activation energies clearly show, however, that these transition states are only slightly more favorable than that of the diradical process. The steric and secondary electronic effects occurring in a concerted approach to *exo*- and *endo*-**2**, indicated in Scheme 1 only for the diradical intermediates, could give rise to the change in mechanism from the *endo*- to the *exo*-Diels-Alder reaction.

The structures of the transition states of the [6+4]-ene reactions leading to the *threo*- and *erythro*-products are comparable with those of the chair- and boat-Cope rearrangements, respectively, of 1,5-hexadiene.[10] Similar factors as in the boat Cope rearrangement could therefore be responsible for *erythro*-**4** not being formed.

Received: September 26, 1985 [Z 1473 IE]
German version: *Angew. Chem. 98* (1986) 109

[1] F. Hofmann, P. Damm, *Mitt. Schlesischen Kohlenforschungsinst. Kaiser-Wilhelm-Ges. 2* (1925) 97 (*Chem. Zentralbl. 1926 I*, 2342); K. Alder, G. Stein, *Justus Liebigs Ann. Chem. 496* (1932) 197; G. R. de Maré, G. Huybrechts, M. Toth, P. Goldfinger, *Trans. Farad. Soc. 67* (1971) 1397.

[2] A gas-chromatographically separable mixture of *exo*-**2**, *syn*-**3**, and *anti*-**3** was prepared by sensitized photolysis of **1**. D. Valentine, N. J. Turro, Jr., G. S. Hammond, *J. Am. Chem. Soc. 86* (1964) 5202; G. O. Schenck, S.-P. Mannsfeld, G. Schomburg, C. H. Krauch, *Z. Naturforsch. B 19* (1964) 18; Y. L. Bahyrel, D. J. MacGregor, T. L. Penner, G. S. Hammond, *J. Am. Chem. Soc. 94* (1972) 637.

[3] Experimental details are given in dissertations by *M. P. Cohen* ("The Crossed Diels-Alder Reaction: A Mechanistic Inquiry"), Harvard University 1982, and by *B. M. J. Dogan* ("Organische Reaktionen unter hohem Druck; der Druckeffekt auf Konkurrenzreaktionen"), Universität Bochum 1984.

[4] Monoclinic crystals (from toluene); m.p. 162–165 °C; space group $P2_1/c$, $Z=4$, $a=6.222(5)$, $b=14.878(22)$, $c=18.555(23)$ Å, $\beta=96.51(8)°$; intensity measurements at room temperature on a four-circle diffractometer; solution of structure by direct methods; refinement using 2461 reflections with $|F_0|>3\sigma(F_0)$; $R=0.051$, $R_w=0.044$; all crystallographic calculations with the SHELX 76 program system. We thank Dr. *W. Gebert*, Bochum, for the intensity measurements. The observed molecular structure shows no unusual features. The cyclohexene ring has the usual half-chair conformation with approximate C_2 symmetry; its corresponding torsional angles of 2.6, 13.1, −44.7, and 62.7° (sequence beginning with the double bond; standard deviations ca. 0.3°) compare very well with experimental and calculated values for gaseous cyclohexene (electron diffraction, force field calculations). Further details of the crystal structure investigation are available on request from the Fachinformationszentrum Energie, Physik, Mathematik GmbH, D-7514 Eggenstein-Leopoldshafen 2, on quoting the depository number CSD-51710, the names of the authors, and the full citation of the journal.

[5] C. A. Stewart, Jr., *J. Am. Chem. Soc. 93* (1971) 4815; *94* (1972) 635.

[6] Examples of other non-concerted Diels-Alder reactions: V. Mark, *J. Org. Chem. 39* (1974) 3179, 3181; G. Huybrechts, B. van Mele, *Int. J. Chem. Kinet. 10* (1978) 1183. Review: J. Sauer, R. Sustmann, *Angew. Chem. 92* (1980) 773; *Angew. Chem. Int. Ed. Engl. 19* (1980) 779.

[7] In the thermolysis of *anti*-[4+4]-dicyclopentadiene, a dimer analogous to *threo*-**4** is observed, which, in this case, is the product of a diradical process. W. Grimme, L. Schumachers, W. R. Roth, R. Breuckmann, *Chem. Ber. 114* (1981) 3197.

[8] P. G. Gassman, J. L. Marshall, *Org. Synth. Coll. Vol. V* (1973) 91, 424.

[9] Review: W. R. Dolbier, Jr. in E. Buncel, C. C. Lee (Eds.): *Isotopes in Organic Chemistry. Vol. 1* ("Isotopes in Molecular Rearrangements"), Elsevier, Amsterdam 1975, p. 51 ff.

[10] M. J. Goldstein, M. S. Benzon, *J. Am. Chem. Soc. 94* (1972) 7147, and references cited therein.

Periodic Potential Surfaces in Crystal Structures

By *Reinhard Nesper* and *Hans-Georg von Schnering**

Wilhelm Klemm In Memorium

We first started calculating periodic equipotential surfaces (PEPS) at the beginning of 1984;[1] in the meantime we have developed a computer program which now allows, for the first time, a combined representation of crystal structures or structural features and calculated PEPS.[2] Over the past two years, *Andersson* et al. have reported on several occasions on the relationships between periodic minimal surfaces (PMS) and crystal structures.[3–5] Such minimal surfaces, which are most simply defined as surfaces of zero mean curvature, are figures of exceptional harmony, familiar to all who have played with soap bubbles. They can be disjunct or periodically continuous, that is exhibit translational symmetry; they can be free or not free of intersections. The periodic minimal surfaces so far reported in the literature,[6] however, do not allow simple and complete assignment to the symmetry of the 230 space groups characterizing 3D translational space, and, moreover they are difficult to derive via the relationships described by *Weierstrass*[7] or other numerical approximations.[8] Furthermore, it can be shown that no PMSs exist for certain space groups.[2] Despite all the fascination in the idea of spatial division by PMSs and in their curvilinear properties, an immediate reference to physical properties has so far been lacking. In our opinion PEPS should close this gap.

We have investigated PEPS of Coulomb fields of simple point charges in the various space group symmetries and thereby established that the zero potential surfaces (POPS), in particular, are topologically very similar to the respective PMS of the same symmetry (Fig. 1a, top left: POPS for "CsCl" (symmetry $Im\bar{3}m$; corresponds to the P-surface of *Schwarz*)). When the two partial structures are commutative, the POPS divide the space into two equal halves and are invariant to interchange of the partial structures. They are then also topologically closely related with interpenetrating sphere packings of the corresponding symmetry.[9, 10] But contrary to what was previously presumed,[11] not the PEPS are in general similar to the well-known PMS but the POPS, since only they are subject to any comparable topological invariants. It also does not

[*] Prof. Dr. H. G. von Schnering, Dr. R. Nesper
Max-Planck-Institut für Festkörperforschung
Heisenbergstrasse 1, D-7000 Stuttgart 80 (FRG)

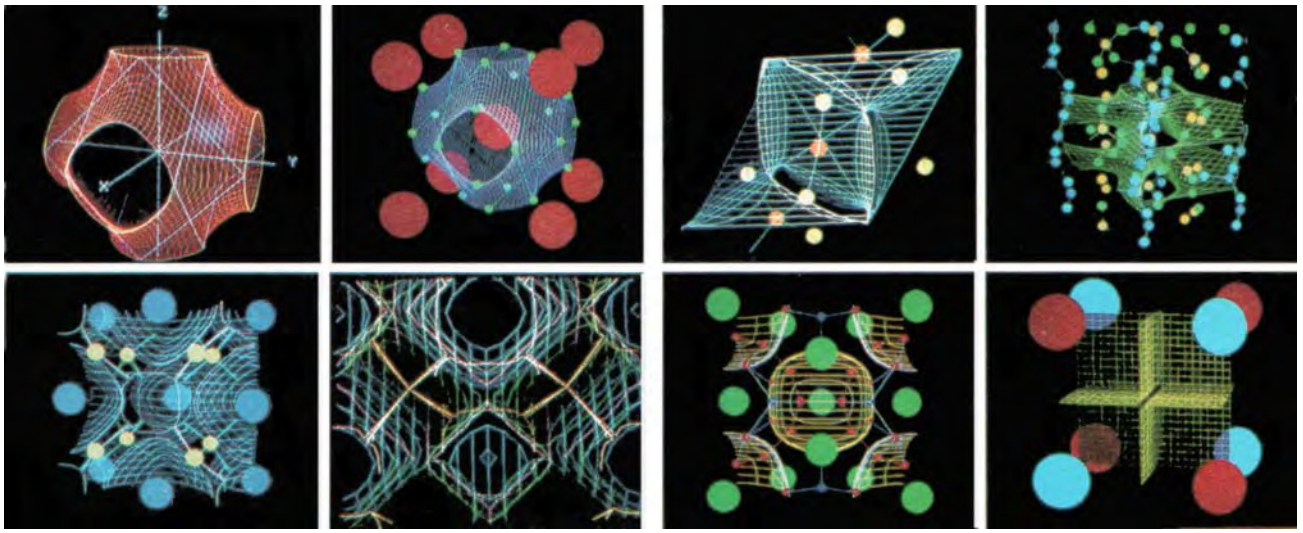


Fig. 1. Top left: POPS of the $Im\bar{3}m$ symmetry, generated in the space group $Pm\bar{3}m$ with (+) in 1a and (−) in 1b. Top right: The same POPS with the experimentally determined distribution of Ag^+ (green) and I^- (red) in the superionic conductor AgI.—Bottom left: POPS for "CaF_2" ($Fm\bar{3}m$), and the atomic distribution of Pb^{2+} (blue) and F^- (yellow); the experimentally determined paths of the F^- ions (green and white lines) follow the topology of the POPS.—Bottom right: Section with POPS (blue), a neighboring PEPS of negative potential (green) and the F^- paths (yellow and white).

Fig. 2. Top left: Q* surface with the structure of β-quartz (Si = orange).—Top right: Q* surfaces with the structure of $CaSO_4(H_2O)_{0.8}$ with Ca (dark yellow), S (light yellow) and O (green and blue). Bottom left: POPS of the A15 structure ($Pm\bar{3}m$) with the clathrate structure of $Xe_8(H_2O)_{46}$: Xe (green), O (red and blue).—Bottom right: POPS of the $Pm\bar{3}m$ symmetry, typical for the NaCl structure.

hold in the case of POPS that the mean curvature necessarily disappears ($H=0$); it follows, however, from the interchange ability of (+) and (−) for commutative partial structures that the *overall* mean curvature disappears ($\overline{H}=0$).

The astonishing consequence with which nature quite obviously exploits the topology of POPS and PMS will be demonstrated with a few examples:

1) In the superionic conductor AgI the experimentally determined preferred positions and paths of Ag^+[12] lie exactly on the corresponding POPS with $Im\bar{3}m$ symmetry (Fig. 1, top left). The positions with low field gradients perpendicular to the POPS are preferred. In contrast, the free spaces in the center of the cubes surfaces are not used (Fig. 1, top right). Migration of the Ag^+ ions through this space would have to be along higher field gradients.

2) The experimentally determined, curved paths of the F^- ions in the ionic conductor PbF_2[13] follow the course of the corresponding POPS ($Fm\bar{3}m$ symmetry; Fig. 1, bottom left). The PEPS of negative potential adjacent to the POPS (Fig. 1, bottom right) clearly shows the anharmonicity of the potential in the direction of the fluorine paths. The free space in the region of the unoccupied position $\frac{1}{2}\,\frac{1}{2}\,\frac{1}{2}$ is apparently not used.[13] A movement in this direction would have to follow higher field gradients, i.e. less parallel to PEPS.

3) The POPS Q* was calculated for $P6_222$ symmetry, without using the structure of quartz. It divides the space into two topologically equal four-branched tunnel systems, almost tailor made for a tetravalent framework. This POPS has helical fragments along $\frac{1}{3}\,\frac{2}{3}z$ and $\frac{2}{3}\,\frac{1}{3}z$, but also intersections of 120° along $00z$ (Fig. 2, top left). The structures of α-quartz (low-quartz) ($P3_121$) and β-quartz (high quartz) ($P6_422$) follow exactly this topology, whereby one tunnel system is occupied and the other remains vacant. The hydrate $CaSO_4(H_2O)_{0.8}$ crystallizes in the subgroup $P3_121$ of Q*.[14] Here, all the Ca atoms are located in the center of the one labyrinth, the S atoms in the center of the other, while the O atoms of the sulfate groups lie very close to the POPS Q* (Fig. 2, top right). The symmetry of the POPS Q* is distinguished by two 3_1 screw axes, and by one 6_2 screw axis which produces the intersections. No significant changes occur for moderate distortional variants of Q*. If, however, the point charges generating the Coulomb field[1] are shifted from $x=\frac{1}{2}$ to $x=\frac{1}{3}$, then the POPS continually changes to an intersection-free surface of the cubic-P type (CsCl). Topological relationships between space groups and various crystal systems are clearly in evidence in this instance. Furthermore, such correlations could be of importance for phase transformations.

4) Figure 2 (bottom left) shows the POPS for the A15-type structure and the reported structures of Cr_3Si (large circles) as well as of clathrate-I = $Xe_8(H_2O)_{46}$ (large and small circles). These POPS, like those of PbF_2, do not form any interconnecting surface but bubbles of $m\bar{3}$ symmetry about the Si positions. In the clathrate the Xe atoms occupy the positions of the Cr and Si atoms in the A15 structure, while the O atoms of the H_2O molecules are practically all on the POPS. Only one O position is lying in space, and this is exclusively the partly occupied site in defect chlathrate structures (e.g. $K_8Ge_{44}\square_2$[15]).

5) The NaCl structure contains an equally simple and unusual POPS: Three sets of orthogonal planes form closed cubes around the charge centers! This is the only case known so far in which the two generating charged centers are completely shielded. In this instance the POPS obviously shows the ideal conditions for an ionic compound AB (Fig. 2, bottom right).

Periodic potential surfaces are especially important for the elucidation of problems regarding diffusion, electron density, and phase transformations as well as topological problems in general.

Procedure

The potential spaces are determined after occupation of selected point configurations [16] in the appropriate space groups with (+)- and (−)-charges using the Ewald procedure applied to prescribed 3D meshes. The PEPS for CsCl is obtained for the charge distribution (+) on the Wyckoff positions 1a and (−) on 1b in $Pm\bar{3}m$, respectively. Both positions fix primitive point configurations P. That is the pertinent POPS is characterized by $P^{\{+\}}_{(1a)} \wedge P^{\{-\}}_{(1b)}$ and is given the symbol P* ($Im\bar{3}m$). In the same way the Schwarz D surface is obtained from the combination $D^{\{+\}}_{(8a)} \wedge D^{\{-\}}_{(8b)}$ in $Fd\bar{3}m$. Other than hitherto reported,[6] it belongs to the Cheshire group $Pn\bar{3}m$, since the generating point configurations already have $Fd\bar{3}m$ symmetry. Color pictures: Using DI-3000 graphic software, own programs, and an AED-767 colorgraphic screen.

Received: November 7, 1985 [Z 1524 IE]
German version: *Angew. Chem. 98* (1986) 111

[1] R. Nesper, H. G. von Schnering, *Z. Kristallogr. 170* (1985) 138.
[2] R. Nesper, H. G. von Schnering, unveröffentlicht.
[3] S. Andersson, T. S. Hyde, H. G. von Schnering, *Z. Kristallogr. 168* (1984) 1.
[4] S. T. Hyde, S. Andersson, *Z. Kristallogr. 168* (1984) 221.
[5] S. T. Hyde, S. Andersson, *Z. Kristallogr. 170* (1985) 225.
[6] A. H. Schoen, *NASA Technical Note* D-5541 (1970).
[7] K. Weierstrass: *Mathematische Werke I, Bd. 3.* Mayer & Müller, Berlin 1903.
[8] H. J. Wagner, *Computing 19* (1977) 35.
[9] W. Fischer, *Z. Kristallogr. 133* (1971) 18; *ibid. 138* (1983) 129; *ibid. 140* (1984) 50.
[10] W. Fischer, E. Koch, *Acta Crystallogr. A 32* (1976) 225.
[11] A. L. Mackay, *Physica B + C (Amsterdam) 131* (1985) 300.
[12] R. J. Cava, F. Reidinger, B. J. Wünsch, *Solid State Commun. 24* (1977) 411.
[13] R. Bachmann, H. Schulz, *Solid State Ionics 9* (1983) 521.
[14] W. Abriel, *Acta Crystallogr. C39* (1983) 956.
[15] L. Llanos, *Dissertation*, Universität Stuttgart 1982.
[16] T. Hahn (Ed.): *International Tables for Crystallography, Vol. A*, Reidel, Dordrecht, Holland 1983, p. 819ff.

BOOK REVIEWS

Kristallstruktur und chemische Bindung. By *A. Weiss* and *H. Witte*. Verlag Chemie, Weinheim 1983, xi, 396 pp., bound, DM 98.00.—ISBN 3-527-25612-1

In the typical classical German tradition of dividing chemistry into basic fields, this monograph treats that part of the "physical chemistry of solids" (i.e. with a minimum of compounds) which is concerned with the relationships between physical properties, structures, and chemical bonding. This vitally necessary and until now missing contribution is intended for students in the second half of their courses, but is also quite suitable for experienced colleagues in university and industry who require basic information concerning this area of chemistry. It would be desirable for this book, which is written by leading experts in the field, to become a part of the miniaturized "library" of young chemists, since basic knowledge of this particular field is going to be necessary in the future. The treatment is deliberately kept simple and the most important areas are discussed in about 200 pages divided into seven sections, namely: lattice energy and its importance for the stability of solids; the band model for metals and semiconductors; the importance of the typical cooperative properties for solids and their connection with structure and bonding; the importance of anisotropy in solids; lattice dynamics; defects in solids; high polymers and amorphous materials. These are preceded by two chapters on the fundamentals of crystallography and chemical bonding. An important section amounting to 90 pages then follows describing experimental methods such as diffraction, angular momentum methods, Mössbauer spectroscopy, optical methods, X-ray and photoelectron spectroscopy, and Compton scattering. Essential data and relationships are included in an appendix, as well as a structural discussion using the mineral olivine as an example.

As terse an introduction as that in this monograph is unlikely to escape the wishes of colleagues of the main field for supplementation and change. A few of these are: (1) the difference between lattice and structure must be defined and employed without compromise; (2) the fundamental importance of symmetry, not just for crystalline materials, is not nearly enough emphasized; (3) specific heats, magnetism, magnetic fields, conductivity, low temperatures, high pressures do not find a place under the important experimental methods; (4) with respect to the topic of this book, the selection of substances is very limited and the choice of structures conveys a dangerous impression to the reader that only a dozen examples are required for an understanding of the relevant relationships. This book has been well produced by the publisher, but was it really necessary that each fraction, each root sign etc. should inevitably lead to a doubling of the line spacing?

Hans-Georg von Schnering [NB 681 IE]
Max-Planck-Institut für Festkörperforschung Stuttgart (FRG)

1,3-Dipolar Cycloaddition Chemistry. Edited by *A. Padwa*. Wiley Interscience, New York 1984. Volume I: xiii, 817 pp.; Volume II: xiii, 704 pp., hardback, together $ 392, ($ 292 in USA).—ISBN 0-471-00354-X

1,3-Dipolar cycloadditions were first carried out by *Buchner* in 1888 with esters of diazoacetic acid. Many other examples followed; however, the fundamental principle of this reaction was not recognized until the pioneering formulation of the general concept by *Huisgen*, also at Munich. 1,3-dipolar additions play an important rôle in the synthesis of heterocycles and also, increasingly, in the regio- and stereoselective construction of carbo- and acyclic compounds. The great advances with regard to the theory and mechanism of these reactions are due to the work of the Munich school, the formulation of the Woodward-Hoffmann rules, and the application of *Fukui*'s frontier orbital concept, in particular by *Sustmann*, *Bastide*, and *Houk*. The reactivity and the regioselectivity of the concerted-asynchronous 1,3-dipolar cycloadditions can thus be satisfactorily interpreted or predicted in many cases. Yet, until now a comprehensive account of this area was not available, in spite of many monographs or chapters dealing with separate aspects (this is equally true for the even more famous sister reaction, the Diels-Alder addition).

A. Padwa, together with a further 18 authors from six countries, has now succeeded in producing a collective

volume of ca. 1500 pages that will fill this gap for many years, albeit in a not entirely satisfying way.

R. Huisgen's introductory chapter (*Introduction, Survey, Mechanism*, 176 pp. with 522 references) consists of a highly readable excursion through the history of this chemistry. It covers all aspects of 1,3-dipole reactions, presented concisely, clearly and with exemplary formula schemes. Although stress is laid on the essential Munich contributions, the (self)critical commentaries on the entire arsenal of methods available for mechanistic studies are a delight, with terse general introductions in each case, pointing out the relationships to other reaction types, with practical directions and topical observations. This is informative reading for anyone interested in reaction mechanisms in particular, or in the formulation, development, and consolidation of one of the great general concepts of organic chemistry!

The subsequent chapters are concerned with the most important classes of 1,3-dipoles, above all those involving C, N and O [chapters 2–11; oxyallyl is dealt with, carbonyl ylides are not (?)] as well as with the unifying principles (chapters 12–15). In detail: nitrile ylides (2; *Hansen, Heimgartner*, 114 pages/231 references); nitrile oxides and imines (3; *Caramella, Grünanger*, 102/552), diazoalkanes (4; *Regitz, Heydt*, 166/714); azides and N_2O (5; *Lwowski*, 94/253), azomethine ylides (6; *Lown*, 80/182); azomethine imines (7; *Grashey*, 84/394), mesoionic ring systems (8; *Potts*, 82/203); nitrones (9; *Tufariello*, 86/384); azimines, azoxy and nitro compounds (10, *Storr*, 32/65); ozone and carbonyl oxides (11; *Kuczkowski*, 80/194); intramolecular 1,3-dipolar cycloadditions (12; *Padwa*, 130/388); theory of 1,3-dipolar cycloadditions (13; *Houk, Yamaguchi*, 44/89); 1,3-dipolar cycloreversions (14; *Bianchi, Gandolfi*, 92/419); higher order dipolar cycloadditions (15; *Crabb, Storr*, 52/98). Both volumes are carefully edited; printing mistakes and errors of fact are rare in the text and in the numerous formula diagrams, as well as in the author and subject indices (65 and 40 pages, respectively).

Each author is known for his research in the area he deals with, and together they present competent and, for the greater part, systematic surveys organized according to their own interests. I should like to single out chapters 1, 2, 4, 7, 9, 12 and 14 as being "reader friendly" (systematic arrangement; up-dated literature coverage; experimental details/yields; interesting cross-references and suggestions). It should be noted that the entire project has, in my opinion, been concluded rather carelessly. Points at issue: "coordination of the chapters", "formula diagrams", "cut-off date/up-dating of literature references", "current developments and outlook", "price". As is often the case with multi-author projects (cf. the Patai series), the individual chapters are not coordinated. Thus, for example, about half of the contents of chapters 12 and 15 can be found elsewhere. Chapter 11 presents an extensive discussion of the individual steps of alkene ozonolysis and *only* this (80 pages, with one reference from 1982); later a more precise and up to date synopsis appears (chapter 14, 8 pp., 20 references from 1982/3). Discussions on mechanisms, reactivity, and regioselectivity occur in many sections on the individual dipoles, although these subjects comprise the general theme of chapters 1 and 13!

Two of the 15 chapters contain clearly laid out formula schemes, probably executed by the authors. The rest seems to have been produced by the press: sprawling, badly set out, with bond angles and spatial formulas that are out of question (by contrast, those of the ApSimon series of the same press are excellent).

The cut-off date of the literature references, very important to the user, is dealt with pitifully. The foreword dates from March 1984; no indications appear in the individual chapters, which were obviously concluded in 1980/1 (a praiseworthy exception is chapter 7). Gratefully, a few authors (chapters 2, 4, 7, 9, 12, 14) make use of addenda to bring their contributions up to date, i.e. to the end of 1982/1983, as can be learnt by examining the lists of references. Thus, recent developments in this field are sometimes not covered (cf. *Nachr. Chem. Tech. Lab. 32* (1984) Vol. 10 and 11): a) the Vedejs method (1979) for the generation of synthetically useful 1,3-dipoles *without* aryl substituents; b) stereoelectronic effects in the use of chiral dipoles or dipolarophiles.

The present volumes appear at the end of a long era in which, thanks to *Huisgen*, these reactions have developed from being mechanistically puzzling curiosities to being theoretically attractive and rationalizable ones, and further, have advanced to the point of being useful, because of being "predictable" tools in organic synthesis. Adding 3 + 2 the right way is going to become routine (it is in part already) and will have fruitful repercussions on the recognition and solution of new theoretical problems. These surveys will play their part in that.

Summary: A few deficiencies notwithstanding, the Padwa books are a rich mine of information for any chemist involved in reaction mechanisms, cycloadditions, heterocycles or stereoselective synthesis. For the newcomer they offer a stimulating starting point. Without doubt, this enterprise will be a commercially successful one; however, the horrific cost of these volumes will probably make them library-shelf copies only, against the intention and to the alarm of many of the authors involved.

Volker Jäger [NB 686]
Institut für Organische Chemie
der Universität Würzburg (FRG)

Total Synthesis of Natural Products: The "Chiron" Approach. By *S. Hanessian*. Pergamon Press, Oxford 1983. xvii, 291 pp., Paperback, £ 11.25.—ISBN 0-08-030715-9

The utilization of carbohydrates as chiral building blocks for the synthesis of enantiomerically pure target molecules has, in recent times, become one of the most powerful and versatile synthetic strategies. Due to some unique advantages, such as low cost, flexibility and efficiency, this approach has been used extensively for the synthesis of complex natural products. The vast amount of synthetic work done in this area, in conjunction with the high potential for widespread applications, dictated the need for an authoritative monograph on the subject. Stephen Hanessian, who has been a long time leader in the conceptual development and exploitation of this technology, was able to produce an excellent "how-to" monograph, filled with a plethora of well-analyzed examples.

The book is divided into sixteen chapters, arranged in seven parts (Basic concepts, Design, Discovery and Execution). Chapters 1–4 give a general introduction to the subject and illustrate the basis of this methodology, by giving some guidelines on how to analyze a target molecule in terms of carbohydrate-derived precursors. The author suggests here the use of the term "*chiron*" to describe these enantiomerically pure synthons. Chapters 5–10 deal with the synthesis of natural products with "apparent carbohydrate-type symmetry", such as those having a tetrahydrofuran or a tetrahydropyran ring. Justifiably, this section of

the book is the largest one, covering more than 1/3 of the total pages. Chapters 11 and 12 describe the application of this methodology to molecules with "partially-hidden carbohydrate-type symmetry", such as the leukotrienes and various other acyclic and cyclic natural products. Chapters 13–15 demonstrate the power of this approach to the synthesis of natural products with "hidden carbohydrate-type symmetry", such as the prostaglandins, the macrolides and other complex antibiotics. Finally, Chapter 16 gives a brief outline of a computer program, designed to assist the chemist in identifying optically active chiral precursors.

Numerous natural products of all types are represented in the examples given in the book. Each synthesis is illustrated with two flow charts, one for the retrosynthetic analysis and one for the actual synthesis. Although these charts are quite clearly presented, they would have been more readable if the various reagents and conditions were placed on the arrows, rather than the bottom of the chart.

In general, this is a well-written authoritative monograph on a very important topic in organic synthesis, and should find a broad spectrum of readers in academia and industry. It will definitely be a useful addition to any library, private or communal.

K. C. Nicolaou [NB 696 IE]
Department of Chemistry
University of Pennsylvania
Philadelphia, PA 19104 (USA)

New Books

The following books have been received by the editor. All the publications listed are available through W & P Buchversand für Wissenschaft und Praxis, Boschstrasse 12, D-6940 Weinheim (Federal Republic of Germany). Tel. (06201) 606-0, Telex 465516 vchwh d, Telefax (06201) 602328.

Advances in Polymer Science. Series Editors: *H.-J. Cantow, G. Dall'Asta, K. Dušek, J. D. Ferry, H. Fujita, M. Gordon, G. Henrici-Olivé, G. Heublein, H. Höcker, J. P. Kennedy, W. Kern, S. Okamura, S. Olivé, C. G. Overberger, T. Saegusa, G. V. Schulz, W. P. Slichter,* and *J. K. Stille.* Springer-Verlag, Heidelberg 1985. **Vol. 64: Polymer Membranes.** Edited by *M. Gordon.* ix, 155 pp., bound, DM 82.00.—ISBN 3-540-13483-2; **Vol. 65: Analysis/Networks/Peptides.** ix, 230 pp., bound, DM 118.00.—ISBN 3-540-13656-8; **Vol. 66: Characterization of Polymers in the Solid State I: Part A: NMR and Other Spectroscopic Methods, Part B: Mechanical Methods.** Edited by *H. H. Kausch* and *H. G. Zachmann.* xi, 222 pp., bound, DM 128.00.—ISBN 3-540-13779-3; **Vol. 67: Characterization of Polymers in the Solid State II: Synchrotron Radiation, X-Ray Scattering and Electron Microscopy.** Edited by *H. H. Kausch* and *H. G. Zachmann.* xi, 233 pp., bound, DM 128.00.—ISBN 3-540-13780-7

Glass Capillary Chromatography in Clinical Medicine and Pharmacology. Edited by *H. Jaeger.* Marcel Dekker, Basel 1985. 656 pp., bound, SFr. 299.00.—ISBN 0-8247-7103-6

The Chemistry of Natural Products. Edited by *R. H. Thomson.* The Blackie Publishing Group, Glasgow 1985. xii, 467 pp., bound, £ 46.00.—ISBN 0-412-00551-4

The Chemistry of Heterocyclic Compounds. Series Editors: *A. Weissberger* and *E. C. Taylor.* **Pyridine and its Derivatives. Part Five.** Edited by *G. R. Newkome.* John Wiley, Chichester 1985. xi, 714 pp., bound, £ 202.40.—ISBN 0-471-05072-5

Specialist Periodical Reports. Mass Spectrometry. Vol. 7. Edited by *R. A. W. Johnstone.* The Royal Society of Chemistry, London 1985. xii, 427 pp., bound, £ 51.50.—ISBN 0-85186-318-3

Progress in Pesticide Biochemistry and Toxicology. Vol. 4. Edited by *D. H. Jutson* and *T. R. Roberts.* John Wiley, Chichester 1985. x, 368 pp., bound, £ 42.00.—ISBN 0-471-90460-0

Polymer Colloids. Edited by *R. Buscall, T. Corner,* and *J. F. Stageman.* Elsevier Applied Science Publishers, London 1985. xii, 324 pp., bound, £ 38.00.—ISBN 0-85334-312-8

Soda, Teer und Schwefelsäure. Der Weg zur Grosschemie. By *D. Osteroth.* rororo reference book in the series Kulturgeschichte der Naturwissenschaften und der Technik. Issued by the Deutsches Museum München. Rowohlt Taschenbuch Verlag, Reinbek bei Hamburg 1985. 254 pp., paperback, DM 14.80.—ISBN 3-499-17720-X

Registered names, trademarks, etc. used in this journal, even without specific indication thereof, are not to be considered unprotected by law.

© VCH Verlagsgesellschaft mbH, D-6940 Weinheim, 1986. - Printed in the Federal Republic of Germany by Zechnersche Buchdruckerei, Speyer/Rhein.

All rights reserved (including those of translation into foreign languages). No part of this issue may be be reproduced in any form – by photoprint, microfilm, or any other means – nor transmitted or translated into a machine language without written permission from the publishers. Only single copies of contributions, or parts thereof, may be reproduced for personal use.

Valid for users in the USA: The appearance of the code at the bottom of the first page of an article in this journal (serial) indicates the copyright owner's consent that copies of the article may be made for personal or internal use, or for the personal or internal use of specific clients. This consent is given on the condition, however, that the copier pay the stated per-copy fee through the Copyright Clearance Center, Inc., for copying beyond that permitted by Sections 107 or 108 of the U.S. Copyright Law. This consent does not extend to other kinds of copying, such as copying for general distribution, for advertising or promotional purposes, for creating new collective works, or for resale. For copying from back volumes of this journal see 'Permissions to Photo-Copy: Publisher's Fee List' of the CCC.

Editorial office: Pappelallee 3, D-6940 Weinheim, Federal Republic of Germany, Telephone (06201) 602315, Telex 465516 vchwh d, Telefax (06201) 602328.

Editor: *P. Gölitz.*

Associate editors: *D. I. Loewus, A. Stimson.* **Editorial assistant:** *E. Scheuermann.*

Publishers: VCH Verlagsgesellschaft mbH. (Managing Directors: *Prof. Dr. Helmut Grünewald* and *Hans Dirk Köhler*), Pappelallee 3, D-6940 Weinheim, Federal Republic of Germany. Correspondence concerning advertisements should be addressed to VCH Verlagsgesellschaft mbH. (Advertising Manager *R. J. Roth*), Boschstr. 12, P.O. Box 1260/1280, D-6940 Weinheim, Federal Republic of Germany, Telephone Weinheim (06201) 602-0, Telex 465516 vchwh d, Telefax (06201) 602328.

ANGEWANDTE CHEMIE
International Edition in English
Volume 25 · Number 2
February 1986
Pages 115–196

Physicochemical and Cytochemical Investigations on the Binding of Ethidium and Acridine Dyes to DNA and to Organelles in Living Cells

By Herbert W. Zimmermann

Ethidium and acridine dyes are classical model substances for studying the binding of small, pharmacologically active molecules to DNA. Intercalation between the DNA base pairs is nearly always proposed as the most important type of binding. According to our investigations, however, there is a second type of binding, which also occurs when the concentration of the bound molecules is low and will be referred to here as external or preintercalative binding. The experimental binding isotherms show that the binding constant for intercalation K_{S1} is considerably smaller than that for external binding K_{S2} ($K_{S1} \ll K_{S2}$). This surprising result is not due to the binding enthalpy ($\Delta H^0_{S1} \approx \Delta H^0_{S2}$) but to the binding entropy ($\Delta S^0_{S1} \ll \Delta S^0_{S2}$). Electrostatic interactions between the dye and the DNA represent the most important contribution to both types of binding; they are supplemented by hydrogen bonds and hydrophobic interactions. The behavior of a substance in living cells, however, cannot be reliably predicted from its in vitro binding to DNA. Very few substances are bound to the DNA of the nuclear chromatin in cell culture; for example, dyes often accumulate instead in the lysosomes. In some cases the dye binds specifically and very efficiently to the mitochondria of the living cell, especially to the mitochondrial membranes, the sites of oxidative phosphorylation.

1. Introduction

In 1961 *Lerman*[1] published his fundamental studies on the binding of proflavine to DNA in which he first proposed the intercalation model. However, intercalation is by no means limited to proflavine—it is observed in many more or less planar cationic molecules with conjugated π-electron systems, the classical examples being ethidium and the aminoacridines. These substances can be classified as pharmacologically active dyes in the sense defined by *Paul Ehrlich*, which include not only trypanocides as well as antimalarial and antibacterial drugs but also mutagens and carcinogens. Many antibiotics are assumed to bind similarly. The pharmacological activity of all these substances is most likely related to their intercalation, which is currently under much discussion as a model for interpreting biological and pharmacological phenomena. The extraordinary interest shown in this type of binding has resulted in a flood of publications that is almost impossible to survey. Accordingly, a review of this highly branched and wide-ranging subject will not be given in this article—the reader is instead referred to the literature, e.g., the competent articles by *Peacocke*[2] and *Waring*,[3] which provide the newcomer to this field with access to both earlier and more recent studies.

[*] Prof. Dr. H. W. Zimmermann
Institut für Physikalische Chemie der Universität
Albertstrasse 21, D-7800 Freiburg (FRG)

 © VCH Verlagsgesellschaft mbH, D-6940 Weinheim, 1986 0570-0833/86/0202-0115 $ 02.50/0

Intercalation is an unusual type of binding between the DNA polyanion and dye cations, in which the cation undergoes insertion between the DNA base pairs. The double helix must therefore unwind to create sufficient space for the intercalated molecule. An objective observer would scarcely dare to predict this unusual binding geometry, since simpler possibilities can be conceived to account for the binding of a molecular cation to the DNA polyanion. Why do they not occur? Or if they do, why are they not of biological importance?

A great deal of effort was required to establish the intercalation model, which is supported by several indirect and direct lines of evidence.[3] The model is now generally accepted, even though some problems still remain to be solved in detail. The X-ray structure studies of *Sobell* et al.[4-6] on low-molecular-weight, crystalline ethidium-DNA complexes are generally regarded as being the most convincing proof of intercalation. Other authors extended these investigations to complexes between low-molecular-weight DNA and aminoacridines;[3] intercalation was found in all cases, the binding geometry being adapted to the different molecular conditions. Despite the magnificent achievements of these authors, it must be pointed out that the DNA used in these studies was only two base pairs long. It is therefore justifiable to ask whether the results obtained in these studies can be applied without any reservations to high-molecular-weight DNA, particularly in view of the fact that the binding geometry in the crystal is determined by the condition of electroneutrality and minimization of the lattice energy.

A few earlier X-ray structure studies were also performed on high-molecular-weight dye-DNA fibers.[1,7] The fiber diagrams of these complexes only provide a limited amount of information, however, and do not allow any detailed conclusions to be drawn about the binding geometry. In another X-ray structure study, carried out on a high-molecular-weight, crystalline ethidium-tRNA complex, *Liebman* et al.[8] found that the ethidium cations are bound externally to the biopolymer although intercalation in the double-helical regions of the tRNA employed was, in principle, possible and indeed expected. This finding is of importance because it was made on a complex between a dye and natural tRNA. Unfortunately, however, this study has not been followed up.

The conclusion to be drawn from these X-ray studies is that both intercalation and external binding are possible. The type of binding and the geometry that are adopted in each particular case, however, cannot be easily predicted. This complicates our problem because we are now confronted with not only one but at least two types of binding.

Chemical binding can be characterized by thermodynamic parameters, e.g., the equilibrium constant (binding constant) between the bound and free species, the binding enthalpy, and the binding entropy. These parameters do not depend on the binding mechanism. The thermodynamics of intercalation has been dealt with in a number of investigations[2,3] but in most cases only a few selected molecules were studied. Very few authors have gone to the trouble of performing comparative binding studies to determine which structural features a molecule must possess in order to bind to DNA.[2,3,9,10] Supplementary studies of a series of simple, systematically modified molecules under identical experimental conditions are required.

The interest shown in binding enthalpies and entropies has also been surprisingly small so far.[2,3,11-13] These parameters are the thermodynamic key for understanding chemical binding and should provide valuable information for the discussion of intercalation. This lack of information is due to the considerable amount of experimental work that is needed to obtain these data with sufficient reliability. Furthermore, thermodynamic studies are regarded as being dull and unattractive. However, intercalation is such an unusual type of binding that it should be better understood if only because of its importance in biology and pharmacology. We have therefore carried out further studies on this subject, which will be discussed and summarized below.[14-19] We endeavored not only to fill in the gaps mentioned above but also tried to study another problem: it has long been known and many authors have confirmed[2,3] that the binding constants of dye cations to DNA depend strongly on the concentration of salts in the dye-DNA solution and decrease with increasing salt concentrations. This finding has always been interpreted as an indication of the involvement of electrostatic interactions in dye binding. According to the theory of the condensation of counterions onto polyelectrolytes,[20,21] which is now generally accepted, DNA is almost saturated with counterions even at low salt concentrations.[21] Strong dependence of the binding constant on the salt concentration is therefore not easy to understand and requires further studies.

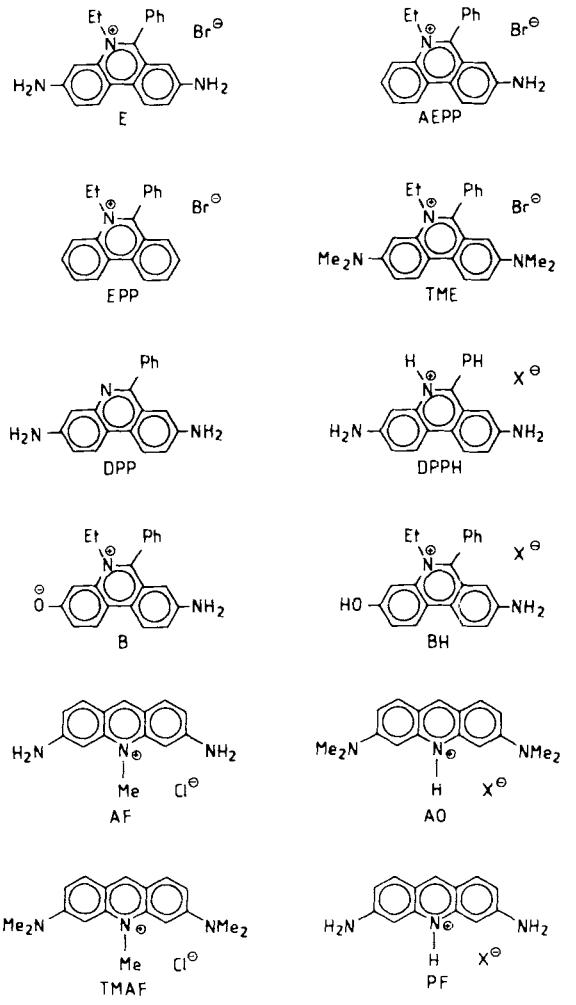
Binding constants can be determined experimentally from binding isotherms, the simplest type being that of *Scatchard*.[22] The Scatchard isotherm is a linear representation of the Langmuir adsorption isotherm and is based on the law of mass action. It applies—and surprisingly well—when relatively few molecules are bound to the biopolymer and when the interactions between these molecules can be neglected. Deviations from linearity are found when the dye occupies more of the DNA. Several explanations have been proposed to account for this phenomenon: different types of bound molecules, which vary in their affinities for the substrate; interactions between the bound molecules, which result in cooperative effects; the binding of molecules that simultaneously occupy several binding sites. A variety of models have been developed which take into consideration these aspects.[2,3,23-33] The large number of models demonstrates in itself that it is difficult to interpret curved Scatchard isotherms unambiguously. Furthermore, experimental errors can result in the simulation of slightly curved binding isotherms. We have therefore restricted the following studies to the linear portion of the Scatchard isotherm and thus to low concentrations of bound molecules. This was done for two main reasons:

1. In vivo the binding of a pharmacon to DNA is limited because the quantity administered is necessarily restricted. The linear portion of the Scatchard isotherm is consequently of primary interest for the discussion of the biological and pharmacological significance of binding. It will be shown below or at least made highly plausible that the linear region of the Scatchard isotherm is accounted for by two different types of binding—namely, intercala-

tion and external or pre-intercalative binding. Although external binding is thermodynamically more favorable than intercalation, the latter may dominate under the conditions found in the cell. The question still has to be answered as to whether the pharmacon really does bind to the DNA in living cells.

2. The linear region of the Scatchard isotherm approximately obeys the law of mass action. Binding can therefore be discussed in terms the chemist is familiar with—i.e., binding constants (equilibrium constants), binding enthalpies, and entropies.

We have measured the binding isotherms of several, selected ethidium and acridine dyes with calf thymus DNA in aqueous medium under identical experimental conditions. The measured binding constants, enthalpies, and entropies can therefore be compared directly with one another. The substances are summarized in Scheme 1. Comparison of the binding properties of the molecules reveals the importance of electrostatic interactions, hydrogen bonds, and hydrophobic interactions in binding.



Scheme 1. E, ethidium bromide; AEPP, 8-amino-5-ethyl-6-phenylphenanthridinium bromide; EPP, 5-ethyl-6-phenylphenanthridinium bromide; TME, tetramethylethidium bromide; DPP, 3,8-diamino-6-phenylphenanthridine; DPPH, protonated DPP; B, 8-amino-5-ethyl-6-phenylphenanthridinium-3-olate; BH, protonated *B*; AF, acriflavine; AO, protonated acridine orange; TMAF, tetramethylacriflavine; PF, protonated proflavine.

2. Experimental Remarks

The binding isotherms between a dye molecule D and a nucleic acid N can be determined experimentally in many ways.[2,3] The aim of all of these methods is to measure the concentrations C of the bound (b) and free (f) dye (C_{Db} and C_{Df}, respectively) for different concentrations of the dye, $C_D = C_{Df} + C_{Db}$, and nucleic acid, C_N. This problem seems to be simple and almost trivial, but in practice there are, unfortunately, many traps which falsify the results or even render them unusable. Experimental methodology must therefore be discussed.

We have determined our binding isotherms by means of absorption spectrophotometry. The longest wavelength absorption band of D is usually shifted to a longer wavelength when a dye molecule is bound to DNA; moreover, the intensity of the band decreases. At long wavelengths the absorption spectra for different C_D and C_N values generally intersect at one or more isosbestic points: the free and bound dye are in equilibrium with each other. We have limited our studies to those systems and experimental conditions in which the thermodynamic equilibrium is substantiated by isosbestic points. Isosbestic points are not observed at short wavelengths because not only the free and bound dye but also the nucleic acid absorb in this region.

The concentrations C_{Df} and C_{Db} can be obtained from the measured extinction coefficient ε.

$$\varepsilon C_D = \varepsilon_f C_{Df} + \varepsilon_b C_{Db}$$

In addition to C_D and C_N, the molar extinction coefficients of the free and bound dye (ε_f and ε_b, respectively) must also be known exactly. Even small errors in these parameters can produce systematic differences which simulate curved Scatchard binding isotherms. Some critical problems must therefore be pointed out.

ε_f can be obtained from the absorption spectra of dye solutions that obey the Beer-Lambert law. In the case of associating substances (e.g., aminoacridines) complications arise, which necessitate extrapolation to $C_D = 0$.[18]

ε_b is the limiting value of the absorption spectrum at a high excess of nucleic acid, $C_N \rightarrow \infty$. This limit can only be reached approximately under the usual experimental conditions. It is therefore advisable to use an extrapolation method originally proposed by *Benesi* and *Hildebrand*,[34] which we have adapted for this problem.[14]

Determination of C_D is trivial provided that an analytically pure sample of the dye is available. Unfortunately, this criterion is often disregarded; many researchers who employ their dyes without testing them would be amazed at the magnificent ranges of colors which appear on a simple thin layer chromatogram. Even chromatographically pure substances can obstinately retain solvent residues (water, alcohol, etc.), which resist drying under a high vacuum and result in incorrect sample weights.

The concentration of mononucleotide units present, C_N, is best determined by phosphate analysis. Several reliable methods are available.[35,36]

Small statistical errors are unavoidable despite careful work and observance of all the usual precautionary meas-

ures; under unfavorable conditions they can lead to considerable problems. This applies especially to the Scatchard plots of binding isotherms that involve differences between large numbers; small errors are then greatly amplified. The points obtained are not in a line as expected but scattered. This can be overcome to some extent by averaging a large number of independent, individual measurements, which naturally involves a great deal of effort.

Another possibility is to smooth the experimentally measured values. If, for example, the extinction ε is determined at different nucleic acid concentrations C_N for a given C_D and then plotted against C_N, a group of points is generally obtained that only deviates slightly from an ideal curve. Nevertheless, these small differences can cause larger deviations in the Scatchard plot. In order to minimize errors, an empirically smoothed curve can be drawn through the points in the plot of ε versus C_N and new, improved values can then be determined. Statistical errors are thereby suppressed while systematic differences are retained. We empirically smooth the measured values with a computer program originally developed by *Weidner*[37] for analogous problems in the X-ray structure study of liquids. This automated procedure is preferable to smoothing "by hand."

The expectations placed on the accuracy of the determined binding constants, binding enthalpies, and especially the binding entropies should not be too high, owing to the experimental difficulties already described. The data provide, however, a useful basis for the following discussion.

3. Langmuir and Scatchard Binding Isotherms

In the simplest case the binding of a dye molecule D to the biopolymer DNA [Reaction (a)] can be characterized by two parameters: the binding constant K and the fraction n of the mononucleotide that is capable of binding. Both parameters can be determined with the aid of the Scatchard binding isotherm.

$$D + DNA \overset{K}{\rightleftharpoons} D\text{-}DNA \qquad (a)$$

If the concentration of the bound molecules, C_{Db}, is sufficiently small, cooperative binding phenomena can be neglected. The law of mass action (LMA) applies to the equilibrium concentrations of the free and bound dye molecules (C_{Df} and C_{Db}, respectively) and the available free binding sites of the nucleic acid (C_{Nf}) [Eq. (1)].

$$K = C_{Db}/C_{Nf}\,C_{Df} \qquad (1)$$

The concentration of the mononucleotide present is C_N and that of the available binding sites $n\,C_N$. The factor n ($0 < n < 1$) takes into consideration that on average only a fraction of the binding sites are capable of binding D. If C_{Db} molecules are bound at equilibrium, the concentration of free binding sites still available is given by

$$C_{Nf} = n\,C_N - C_{Db}$$

Combination of this equation with Equation (1) yields Equation (2).

$$K_S = C_{Db}/[(n\,C_N - C_{Db})\,C_{Df}] \qquad (2)$$

As discussed in Section 4, the equilibrium constant $K = K_S$ is adapted to the method of counting the binding sites according to *Scatchard*. Substituting $r = C_{Db}/C_N$, the number of bound molecules per mononucleotide unit, gives the Langmuir adsorption isotherm [Eq. (3)].

$$r = n\,K_S\,C_{Df}/(1 + K_S\,C_{Df}) \qquad (3)$$

Simple rearrangement yields the Scatchard form of the binding isotherm [Eq. (4)]:[22]

$$r/C_{Df} = K_S(n - r) \qquad (4)$$

If r/C_{Df} is plotted against r and Equation (4) applies, a straight line with a negative slope is obtained which intersects the abscissa at $r = n$. The slope of the line provides K_S. Thus, n and K_S can be determined. In this simplest plot the extrapolated value $r = n$ characterizes the maximum number of bound dye molecules per mononucleotide. However, this interpretation can lead to contradictions (see Section 4). It is better to regard $r = n$ as the upper limit of the range in which the LMA is at least approximately obeyed and in which the dye molecules are bound to the nucleic acid independently of one another.

Scatchard binding isotherms for the ethidium bromide–DNA system (E/DNA) at low dye concentrations are given in Figure 1.[14] In addition to E and DNA, the aqueous solutions also contain NaCl as a neutral salt. The isotherms shown in Figure 1 correspond to different salt concentrations C_S. When r is small, all the isotherms can be approximated as straight lines; the LMA is thus formally obeyed. When r is larger, positive deviations from linearity are found. This region of curved Scatchard isotherms will not be discussed here for the reasons given above.

The slopes of the straight lines for different C_S values differ (Fig. 1). All the extrapolated lines intersect the ab-

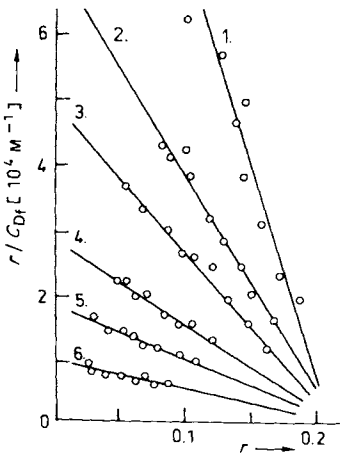


Fig. 1. Scatchard binding isotherms for the E/DNA system at various concentrations C_S of the competitor salt S = NaCl. 1. $C_S = 2 \times 10^{-3}$ M, 2. 0.05 M, 3. 0.1 M, 4. 0.25 M, 5. 0.5 M, 6. 1.0 M. pH = 7.7, T = 298 K [14].

scissa, however, at $n = 0.21$ within the limits of error. Thus, n is virtually independent of the salt concentration C_S (Fig. 2). The same behavior is also observed with the salts KCl and $MgCl_2$.[14] Therefore, n is also independent of the type of salt (Fig. 2). In the low r region, linear Scatchard isotherms are also obtained at different temperatures; these isotherms once again intersect the abscissa at $n = 0.21$ and are independent of S and C_S.[14] Thus, n is a parameter that characterizes the binding of the dye to the biopolymer.

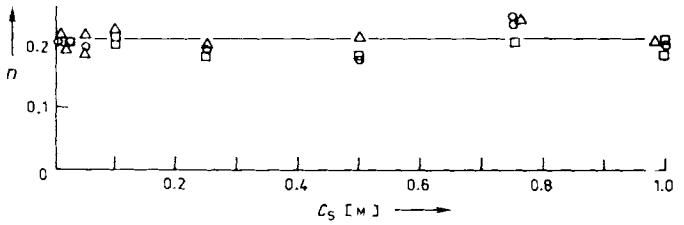


Fig. 2. Binding parameter n for the E/DNA system at various concentrations C_S of the competitor salt S = NaCl (○), KCl (□), $MgCl_2$ (△). pH = 7.7, T = 298 K [14].

Determination of n from the point of intersection of the extrapolated Scatchard plot with the abscissa is—like all extrapolations—subject to error. It should therefore be pointed out that, in the case of the E/DNA/NaCl system, n can also be obtained by a second, independent method, which consists of directly titrating the dye present with a DNA solution of known concentration, the end point being determined spectroscopically.[14] The titration is not subject to any special conditions such as the validity of the LMA or the extinction coefficients of the free and bound species. The value determined by titration, $n = 0.21$, is independent of C_S over a wide range of concentrations and is identical to the extrapolated value.

The slopes of the binding isotherms and thus the binding constant K_S depend not only on the temperature T but also on the type of salt S and its concentration C_S.[14] Consequently, $K_S = K_S(T, C_S)$ has the character of an apparent equilibrium constant. Figure 3 shows K_S as a function of the concentration C_S of the salts NaCl, KCl, and $MgCl_2$ at the standard temperature $T = 298$ K. K_S decreases as C_S increases—very rapidly in the case of $MgCl_2$ and more slowly for NaCl and KCl. When C_S is sufficiently large, K_S apparently approaches a limiting value, K_{S1}, which is small but differs from zero. The curves in Figure 3 can be approximated as hyperbolas that intersect the ordinate when $C_S = 0$ and reach an asymptotic value K_{S1} as $C_S \to \infty$ (Fig. 3).

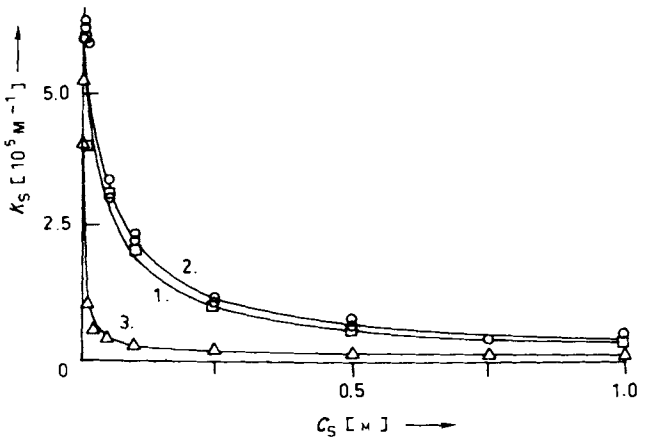


Fig. 3. Dependence of the apparent Scatchard binding constant K_S of the E/DNA system on the concentration C_S of the competitor salt S = NaCl (○), KCl (□), $MgCl_2$ (△). pH = 7.7, T = 298 K. 1.–3. calculated curves [Eq. (21), data taken from Table 1] [14].

In the same way as the binding constant K_S, the number of dye molecules bound per mononucleotide unit, r, also falls as the salt concentration increases (Fig. 4).[14] The bound dye is apparently displaced from the polymer. The decrease in r is once again much more pronounced for $MgCl_2$ than for NaCl. The bound dye E cannot, however, be completely displaced from the DNA even at high salt concentrations ($C_S = 2$ M). The curves shown in Figure 4 indicate that r, like K_S, approaches a limiting value at high salt concentrations C_S, which is attained more quickly in the presence of $MgCl_2$ than NaCl. Studies at very high C_S values can only be interpreted to a limited extent because the competitive salt effect is masked by phenomena that are difficult to assess, such as salting out effects and denaturation of the polymer. We have therefore generally restricted our measurements on competitive effects to concentrations $C_S \leq 1$ M.

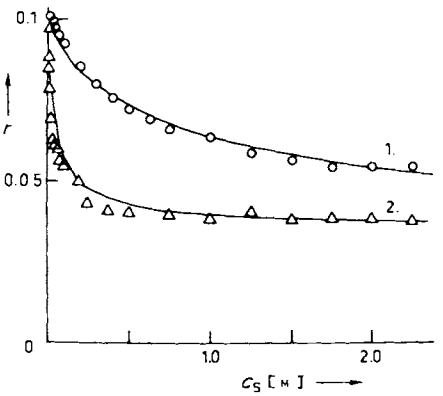


Fig. 4. Number $r = C_{Db}/C_N$ of bound dye molecules per DNA mononucleotide unit of the E/DNA system as a function of the concentration C_S of the competitor salt S = NaCl (○), $MgCl_2$ (△). Dye concentration $C_D = 2.5 \times 10^{-5}$ M, DNA concentration $C_N = 2.5 \times 10^{-4}$ M. pH = 7.7, T = 298 K. 1. and 2. calculated curves [Eq. (18), data taken from Table 1] [14].

The standard binding enthalpy ΔH_S^0 and entropy ΔS_S^0 can be determined from the temperature dependence of the Scatchard binding constants K_S with the aid of the van't Hoff equation [Eq. (5)].

$$\ln K_S = -\Delta H_S^0/RT + \Delta S_S^0/R \qquad (5)$$

The temperature range available for determining ΔH_S^0 and ΔS_S^0 is only very small because the DNA denatures at high temperatures and the solution solidifies at low temperatures. A large number of single measurements are therefore required to minimize experimental errors. Figure 5 shows the temperature dependence of K_S for the E/DNA system by means of van't Hoff plots at various concentrations, C_S, of the competitive salts NaCl, KCl, and $MgCl_2$.[14] The plots are groups of approximately parallel straight lines. The apparent binding enthalpy ΔH_S^0 is thus

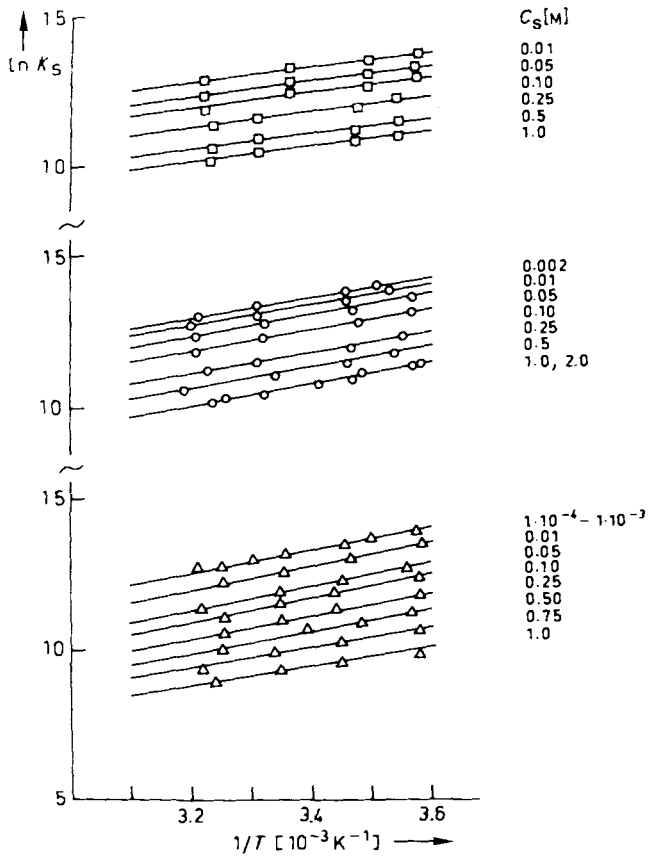


Fig. 5. Temperature dependence of the apparent Scatchard binding constant K_S of the E/DNA system at various concentrations C_S of the competitor salt S = NaCl (○), KCl (□), $MgCl_2$ (△). pH = 7.7 [14].

largely independent of S and C_S (Fig. 6), whereas the dependence of the binding constant K_S on S and C_S is reflected in the behavior of the apparent binding entropy ΔS_S^0 (Fig. 7).

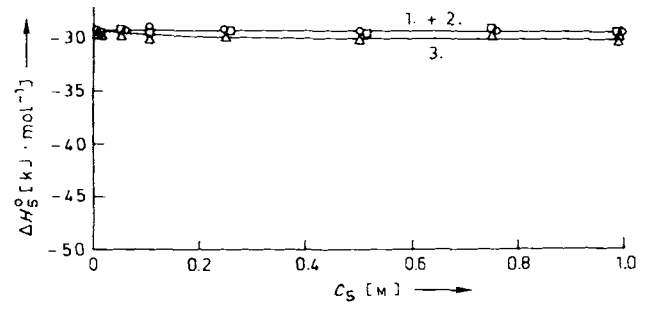


Fig. 6. Dependence of the apparent Scatchard binding enthalpy ΔH_S^0 of the E/DNA system on the concentration C_S of the competitor salt S = NaCl (○), KCl (□), $MgCl_2$ (△). pH = 7.7. 1.-3. calculated curves [Eq. (21) and (5), data taken from Tables 1 and 2] [14].

Finally, I would like to refer to the pioneering work of *Waring*[38] and of *LePecq* and *Paoletti*,[12] who, in 1965 and 1967, respectively, investigated the binding of ethidium bromide to DNA in wide-ranging studies. They described linear Scatchard isotherms with $n = 0.2$ that were independent of the DNA base composition. Accordingly, binding of E to DNA does not display pronounced base specificity. These authors also found that the binding constant K_S de-

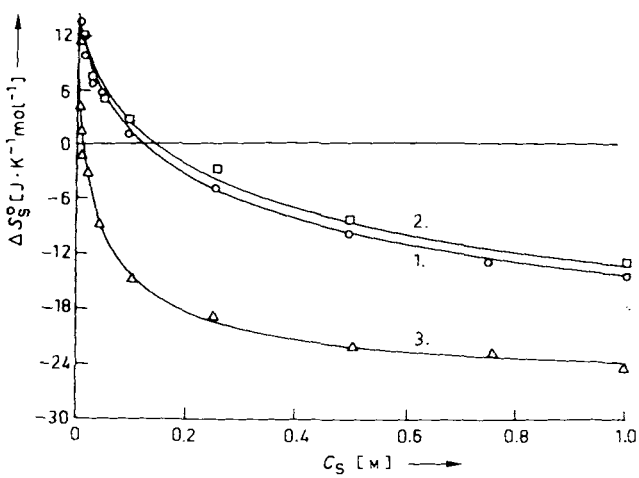


Fig. 7. Dependence of the apparent Scatchard binding entropy ΔS_S^0 of the E/DNA system on the concentration C_S of the competitor salt S = NaCl (○), KCl (□), $MgCl_2$ (△). pH = 7.7. 1.-3. calculated curves [Eq. (21) and (5), data taken from Tables 1 and 2] [14].

creases as the salt concentration increases and approaches a plateau at high C_S values. The quantity of dye bound then remained constant and was virtually independent of the salt concentration C_S. *LePecq* and *Paoletti* were the first to describe the temperature dependence of K_S and attempted to determine ΔH_S^0 and ΔS_S^0 from measurements made at two temperatures (23 and 37 °C) for different NaCl concentrations. There are many qualitative parallels between the findings of these authors and our measurements. In quantitative terms, however, they differ considerably, especially as regards the dependence of the thermodynamic parameters K_S, ΔH_S^0, and ΔS_S^0 on the salt concentration C_S. We believe that these differences are due to experimental difficulties, which we have endeavored to overcome in our investigations.

4. Crothers Binding Isotherm, the Law of Mass Action, and the Counting of Binding Sites

In deriving the Scatchard binding isotherm it is formally assumed that only nC_N of the C_N mononucleotides employed are capable of binding a dye molecule D. A free molecule in the solution "sees" $C_{Nf} = nC_N - C_{Db}$ free binding sites and chooses one to which it then binds. The number of free DNA sites is then reduced by one. The equilibrium constant K_S is adapted to this method of counting the binding sites.

According to the studies of *Waring*[30] and *LePecq* and *Paoletti*,[12] binding of E to DNA does not exhibit base-specific preferences. Intercalation between all neighboring DNA base pairs should therefore be equally possible. The experimental value for the binding parameter $n \cong 0.2$ is too small, however, and is not consistent with this expectation. In order to take the equivalence of the binding sites into account, *Armstrong* et al.[39] and *Crothers* et al.[27,40] proposed another method for counting the binding sites, which is referred to in the literature as the nearest neighbor exclusion principle. According to this method, intercalation is, in principle, possible between all neighboring DNA

base pairs and all the binding sites are equivalent. If one of the sites is occupied, however, binding to the neighboring sites is hindered. *Crothers* et al.[40] used this exclusion principle as the basis for deriving the following binding isotherm using the matrix method [Eq. (6)]:

$$r'/C_{Df} = K_C \cdot (1-2r')^2/(1-r') \tag{6}$$

r' refers to the concentration of base pairs $C'_N = C_N/2$, and $r' = C_{Db}/C'_N = 2r$. The binding constant describes the binding of D to the unperturbed DNA binding sites; i.e., when r' is small, Equation (7) applies.

$$\lim_{r' \to 0} K_C = C_{Db}/C'_N C_{Df} \tag{7}$$

Equation (6) no longer contains the binding parameter n since it is fixed by the formalism. The limiting behavior of Equation (6) when $r' < 1$ is of sole interest in the following discussion. Substitution of the infinite geometrical series

$$1/(1-r') = 1 + r' + r'^2 + \cdots$$

into Equation (6) yields Equation (8).

$$r'/C_{Df} = K_C(1 - 3r' + r'^2 + \text{higher terms}) \tag{8}$$

If r' is sufficiently small, the progression in Equation (8) can be approximated by ignoring the terms following the linear r' term. If the concentration of the mononucleotides C_N is reintroduced, Equation (8) gives Equation (9).[14]

$$r/C_{Df} = 3K_C[(1/6) - r] = K_S(n - r) \tag{9}$$

When r is small, the Crothers binding isotherm is therefore also of the Scatchard type. Comparison of the coefficients gives $K_S = 3K_C$ and $n = 1/6 = 0.17$. A binding parameter of $n = 0.17$, which is in agreement with the theory, was indeed found for the aminoacridines we studied; in the case of ethidium bromide and its derivatives the experimental value of $n = 0.21$ is somewhat higher. If only the linear portion of the binding isotherm is considered, the law of mass action also formally applies to the nearest neighbor exclusion model. The Crothers isotherm differs from the Scatchard isotherm in the way the binding sites are counted.

The exclusion principle of binding sites proposed by *Armstrong* et al. and *Crothers* et al. makes physical sense. The law of mass action can be applied to this method of counting binding sites. The mononucleotide concentration used is again C_N, and the possible binding sites are given by a fraction pC_N. When a molecule of D is bound, an average of q neighboring DNA sites are assumed to be blocked. The concentration of free binding sites is then $C_{Nf} = pC_N - qC_{Db}$ and, from Equation (1), Equations (10) and (11) are obtained.

$$K_Z = C_{Db}/[(pC_N - qC_{Db})C_{Df}] \tag{10}$$

$$r/C_{Df} = qK_Z[(p/q) - r] = K_S(n - r) \tag{11}$$

Comparison of the coefficients with the Scatchard isotherm yields $K_S = qK_Z$ and $n = p/q$. In the case of the nearest neighbor exclusion model, for example, $C'_N = pC_N = C_N/2$, $p = 1/2$. Comparison of Equations (11) and (9) reveals that binding of one molecule of D to a DNA binding site blocks $q = 3$ base pairs in the linear region of the Crothers binding isotherm when r is small. This means that—in contradiction to the name of the model—not only the neighboring sites but also the next nearest sites are excluded from binding. At this point it should be recalled that in favorable cases this value, $q = 3$, can be determined directly by titration and not only by extrapolation of the linear region of the binding isotherm. On titration the properties of the system change "discontinuously" in the vicinity of the end point. Therefore, n is a physically relevant parameter and characterizes the range that obeys the LMA.

The Crothers isotherm approaches the limiting value $(1-2r') = 0$ when $C_{Df} \to \infty$ and then reaches the maximum value of bound molecules $r' = C_{Db}/C'_N = 1/2$ or $C_{Db} = C'_N/2$. In agreement with the nearest neighbor exclusion principle, an average of one dye molecule is bound to every second base pair when the DNA is saturated with D ($q = 2$).

In practice, Equation (11) is more versatile then Equation (9) because p/q is not fixed by a model and q—as a mean value—is not only an integer but can also be a fraction. Only the two constants $K_S = qK_Z$ and $n = p/q$ can be determined directly by experiment. The three unknowns K_Z, p, and q cannot be obtained from these equations without making further assumptions about p or q. This leads to fundamental difficulties in the discussion of the binding constants. The equilibrium constants K_S and K_Z are based on different methods of counting the binding sites. This difference is reflected in the binding entropy but not in the binding enthalpy. If $K_S = qK_Z$ is substituted into Equation (5), Equations (12) and (13) are obtained.

$$\Delta H^0_S = \Delta H^0_Z \tag{12}$$

$$\Delta S^0_S = \Delta S^0_Z + R \ln q \tag{13}$$

It is not our intention to develop a theory to account for the binding between the dye and DNA but rather to describe and interpret our experimental findings. It is initially advisable to rely solely on experimentally accessible data. We therefore have to make do with the Scatchard isotherm, bearing in mind the fact that it is based on an incorrect way of counting the binding sites. Since ΔS^0_S and ΔS^0_Z only differ by an additive constant, a comparative qualitative discussion is possible even at this level. The isotherms described above can easily be interconverted by means of calculation. The Scatchard isotherm can then always be changed into another binding isotherm with the aid of special assumptions about p and q.

5. A Simple Equilibrium Model for Describing the Competitive Effect, $K_S = K_S(T, C_S)$

According to Figures 3 and 4, K_S and r at first fall rapidly as C_S increases but then approach a limit at high C_S values. A competitive salt effect occurs. The metal cations M of the salt S displace the dye cations D bound to the

DNA. A residue of bound dye cations is, however, generally observed even at very high competitor concentrations.[3, 14] In contrast, the binding parameter n is practically independent of S and C_S (Fig. 2).[3, 14] Two models will be compared to describe these findings.

1. D undergoes two types of binding to DNA, 1 and 2, which can be distinguished by means of the competitive effect. Type 1 binding is resistant to competitive salts and still occurs at high salt concentrations (noncompetitive binding). In type 2 binding, on the other hand, D may be displaced by competitors M (competitive binding). Using the theory of counterion condensation, *Record* et al.[21] have demonstrated that approximately 88% of the negative charge of the DNA polyanion in aqueous solution is compensated by the "binding" of metal cations M such as $Na^{\oplus}$ or $K^{\oplus}$. The charge compensation is independent of the concentration of the cations M in the solution within a wide range of concentrations. According to the theoretical studies of *Manning*,[20] this charge compensation is essential for stabilization of the polyanion. Presumably, the dye cations also contribute to compensating the charge of the DNA and are thus bound. The competitive effect exerted by metal cations M on dye cations D can thus be interpreted as an exchange of these ions at the DNA.

2. There is only one type of binding but two contributions to the binding energy—an electrostatic component resulting from the interactions between the dye cation D and the DNA polyanion and a second contribution that is composed of the interactions of the π-electrons with the DNA base pairs, hydrogen bonds, etc. According to this model, advocated by *Fromherz*,[41] the competitive salt effect is a result of the compensation of the electrostatic component by the binding of the competitor cations M; the second component remains unaffected. This model undoubtedly displays some interesting features but it is difficult to reconcile with the theory of counterion condensation. Since the quantity of counterions M bound to the DNA polyanion is not only very high but also independent of the concentration of M in solution, the electrostatic binding component should always be largely compensated and, moreover, should not be affected by varying C_S. In the following discussion, preference will be given to the first model on account of this inconsistency.

When r is sufficiently small, the Scatchard isotherms are virtually straight lines for all competitor concentrations C_S (Fig. 1). The LMA then applies—at least approximately. The noncompetitive type 1 binding

$$D + DNA_1 \overset{K_{S1}}{\rightleftharpoons} D\text{-}DNA_1$$

is described by the binding constant K_{S1} and the binding parameter n_1 [Eq. (14)].

$$K_{S1} = C_{Db1}/[(n_1 C_N - C_{Db1}) C_{Df}] \tag{14}$$

In the case of competitive type 2 binding, it must be taken into account that about 88% of the negative charge of the DNA is compensated by the counterions M but that at most only 20% of the mononucleotide can bind the dye. The competitive effect can then be described by a simplified reaction originally proposed by *Record* et al. [Reaction (b)].[21]

$$M + D\text{-}DNA_2 \overset{1/K_{S4}}{\rightleftharpoons} D + M\text{-}DNA_2 \tag{b}$$

Reaction (b) can be divided into two steps [Reactions (c) and (d)].

$$D\text{-}DNA_2 \overset{1/K_{S2}}{\rightleftharpoons} D + DNA_2 \tag{c}$$

$$M + DNA_2 \overset{K_{S3}}{\rightleftharpoons} M\text{-}DNA_2 \tag{d}$$

These are formally assigned the binding constants K_{S2} and K_{S3} for the binding of D and M, respectively, to the DNA; the binding parameter is n_2. Equations (15) and (16) are thereby obtained.

$$K_{S2} = C_{Db2}/[(n_2 C_N - C_{Db2} - C_{Mb}) C_{Df}] \tag{15}$$

$$K_{S3} = C_{Mb}/[(n_2 C_N - C_{Db2} - C_{Mb}) C_{Mf}] \tag{16}$$

It must be emphasized that the separation of Reaction (b) into steps (c) and (d) only involves the exchange of the cations D and M at the DNA. This exchange process may approximately obey the LMA, but the condensation of the counterions M to the DNA polyanion does not. Equation (17) is then obtained for the ion exchange according to Reaction (b).

$$K_{S4} = K_{S2}/K_{S3} = C_{Db2} C_{Mf}/(C_{Df} C_{Mb}) \tag{17}$$

K_{S4} is the binding constant of D to DNA in the presence of M.

Elementary calculations using the terms

$$C_D = C_{Db} + C_{Df}$$

$$C_{Db} = C_{Db1} + C_{Db2}$$

$$C_M = C_{Mf} + C_{Mb}$$

$$r = r_1 + r_2 = (C_{Db1} + C_{Db2})/C_N$$

yield Equation (18).[14]

$$r = n_1 K_{S1} C_{Df}/(1 + K_{S1} C_{Df}) + n_2 K_{S2} C_{Df}/(1 + K_{S2} C_{Df} + K_{S3} C_{Mf}) \tag{18}$$

This is an extension of the Langmuir isotherm to two types of binding, as has already been proposed, in principle, by *Peacocke* et al.,[23] and has been extended here to apply to the competitive effect. Conversion of Equation (18) into the Scatchard form gives Equation (19).[14]

$$r/C_{Df} = K_{S1}(n_1 - r) + K_{S2}(n_2 - r)/(1 + K_{S3} C_{Mf}) + K_{S1} K_{S2}(n_1 + n_2 - r) C_{Df}/(1 + K_{S3} C_{Mf}) \tag{19}$$

In the limiting case where $C_D \ll C_N$, the following apply: $C_D/C_N \to 0$, $C_{Df} \to 0$, and $r \to 0$. The third term on the right-hand side of Equation (19) can then be neglected. The Scatchard isotherm then consists of two additive, independent, linear components, which describe noncompetitive and competitive binding. Linear Scatchard isotherms can still be expected even at somewhat higher C_D/C_N concen-

tration ratios. According to our experiments, the binding parameter n is independent of S, C_S, and C_M within the limits of error when r is small. Apparently, $n=n_1=n_2$. In order to produce the competitive salt effect, relatively high competitor concentrations must also be used; in this case, $C_N \ll C_M$ and $C_{Mb} \ll C_{Mf} \approx C_M$. Under these conditions, Equation (19) can be rearranged to give Equation (20).[14]

$$r/C_{Df} = \{K_{S1} + K^*_{S2}/(1+K_{S3}C_M)\}(n-r) \quad (20)$$

Under our experimental conditions, the experimentally accessible effective binding constant $K^*_{S2}=K_{S2}(1+G)$ differs only slightly from K_{S2}. If C_{Df} and r are sufficiently small, the function

$$G = K_{S1}C_{Df}[1+1/(1-u)] = K_{S1}C_{Df}[2+u+u^2+\cdots]$$
$$u = r/n < 1$$

can either be neglected when compared with 1 or replaced by its mean value $\overline{G}$. Equation (20) then approximately describes Scatchard isotherms which—in agreement with the experimental findings—intersect the abscissa at $r=n$ independently of S, C_S, and T. Comparison of Equation (20) with Equation (4) gives the apparent Scatchard equilibrium constant $K_S=K_S(T, C_S)$ in the form of Equation (21).[14]

$$K_S = K_{S1} + K^*_{S2}/(1+K_{S3}C_M) \quad (21)$$

In the case of molecules that are only bound competitively ($K_{S1}=0$), Equation (22) applies.

$$K_S = K_{S2}/(1+K_{S3}C_M) \quad (22)$$

In the case of the competitor salts NaCl, KCl, and $MgCl_2$, $C_M=C_S$. Equations analogous to Equation (22) are known.[12,42,43]

Equations (21) and (22) are hyperbolic equations. They describe the dependence of the Scatchard binding constant K_S on the competitor concentration $C_M=C_S$. In the E/DNA system the curves shown in Figure 3 were calculated using Equation (21) and the binding constants K_{S1}, K^*_{S2} or K_{S2}, and K_{S3} were determined by means of linear regression (Table 1). The binding isotherms in Figure 4 were then finally determined with the aid of these constants and Equation (18).[14] The agreement between the calculated curves and the experimental values is surprisingly good. It must be borne in mind that some radical simplifications have been made in the course of the derivation.

The binding constants K_{S1} and K^*_{S2} or K_{S2} are, as is to be expected, independent of the type of competitor within the range of error. The competitor specificity is reflected in the binding constant K_{S3}. Accordingly, $Mg^{2\oplus}$ is a much stronger competitor than $Na^{\oplus}$ or $K^{\oplus}$.

Unlike K_S, the independent constants K_{Si}, i = 1-3, depend solely on T. The standard binding enthalpies ΔH^0_{Si} and entropies ΔS^0_{Si} can be determined from the temperature dependence of K_{Si} in the customary way by using the van't Hoff equation. As an example, the temperature dependence of K_{Si} for the E/DNA system is given in the form of a van't Hoff plot in Figure 8. The ΔH^0_{Si} and ΔS^0_{Si} values thus obtained are listed in Table 2. The binding enthalpies and entropies of the noncompetitive and competitive types of binding (types 1 and 2, respectively) are once again independent of the type of competitor within the relatively large range of error. The individual properties of the competitor are described by the thermodynamic parameters of binding of M.[14]

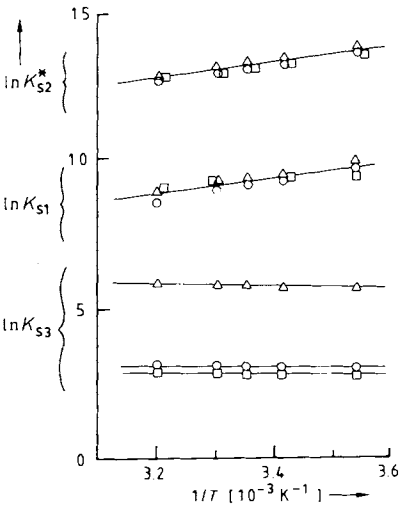


Fig. 8. Temperature dependence of the actual binding constants K_{S1}, K^*_{S2}, and K_{S3} of the E/DNA system, competitor salt S = NaCl (○), KCl (□), $MgCl_2$ (△). pH = 7.7 [14].

Table 2. Binding enthalpies ΔH^0_{Si} [kJ mol^{-1}] and binding entropies ΔS^0_{Si} [J K^{-1} mol^{-1}] of noncompetitive and competitive binding i = 1-3. E/DNA system, competitor salts NaCl, KCl, and $MgCl_2$ [14].

Competitor		K_{S1}	K^*_{S2}	K_{S2}	K_{S3}
NaCl	ΔH^0_{Si}	−28	−29	—	+ 1.7
	ΔS^0_{Si}	−21	+13	—	+28
KCl	ΔH^0_{Si}	−27	−29	—	+ 0.4
	ΔS^0_{Si}	−17	+17	—	+21
$MgCl_2$	ΔH^0_{Si}	−29	−30	—	+ 2.1
	ΔS^0_{Si}	−21	+17	—	+42
mean	ΔH^0_{Si}	−28	−29	−27	—
	ΔS^0_{Si}	−20	+16	+18	—

The data given in Table 2 were employed in conjunction with Equation (21) and the van't Hoff equation [Eq. (5)] to calculate the dependence of the apparent binding enthalpies ΔH^0_S and entropies ΔS^0_S on the competitor concentration C_S.[14] The calculated curves for the E/DNA system are shown in Figures 6 and 7. There is good agreement between the experimental values and the theoretical curves over the whole range of concentrations; this once again confirms the usefulness of the described equilibrium model.

Table 1. Binding constants K_{S1}, K^*_{S2}, K_{S2} and K_{S3} [M^{-1}] for the E/DNA system and the competitor salts NaCl, KCl, $MgCl_2$; $T=298$ K [14].

Competitor	K_{S1}	K^*_{S2}	K_{S2}	K_{S3}
NaCl	1.0×10^4	6.2×10^5	—	22
KCl	1.1×10^4	6.5×10^5	—	19
$MgCl_2$	1.2×10^4	7.0×10^5	—	350
mean	1.1×10^4	6.6×10^5	5.6×10^5	—

6. The Noncompetitively Bound Dye Cations Intercalate

The binding constants K_{S1} and K_{S2} for the noncompetitive and competitive binding of ethidium cations to DNA differ by more than one order of magnitude (Table 1, $K_{S1} \ll K_{S2}$). This is also found to be the case for other dyes (Table 3). The intercalated molecules are largely screened off from their surroundings by the neighboring DNA base pairs and the anionic phosphodiester residues together with their bound counterions. Accordingly, changes in the competitor concentration should only have a slight effect on their binding. It therefore seems reasonable to assign the noncompetitive binding with its smaller binding constant K_{S1} to the intercalated dye cations. However, the intercalated molecules would then be much more weakly bound than is customarily assumed to be the case. In order to clarify this discrepancy we used optical polarization to study the geometry of the noncompetitive binding of ethidium cations to DNA.

Many authors have described experiments in which they determined the orientation of intercalated dye molecules in mechanically aligned dye-DNA preparations by using the absorption of linearly polarized light (see ref. [17]). Different methods are available for mechanically aligning high-molecular-weight dye-DNA preparations, such as drawing and spinning fibers and films, drawing polyvinyl alcohol foils containing nucleic acid, and flow orientation of solutions. In all of these methods it is presumed that the longitudinal axis of the double helix is orientated in the mechanically preferred direction $\vec{k}$.

The dichroic ratio of light absorption serves as a measure of the quality of orientation [Eq. (23)].

$$R = A_{\parallel}/A_{\perp} \tag{23}$$

$A_{\parallel}$ and $A_{\perp}$ are the absorbances of the dye band of the preparation when the polarizer $\vec{e}_p$ is set parallel and perpendicular to $\vec{k}$, respectively. If the dye molecules are statistically equally distributed, then $A_{\parallel} = A_{\perp}$ and $R = 1$. If alignment is complete, the dichroic ratio of a band that is polarized in or perpendicularly to the preferred direction $\vec{k}$ ($A_{\perp}$ or $A_{\parallel} = 0$, respectively) assumes a limiting value of $R = \infty$ or $R = 0$, respectively. Dyes with a planar chromophore are usually used for intercalation experiments. The transition moment $\vec{m}$ of the long-wavelength dye band then lies in the molecular plane. According to *Lerman*, however, the molecular plane of intercalated dyes is perpendicular to the longitudinal DNA axis. This means that for ideally orientated dye-DNA preparations $\vec{m} \perp \vec{k}$, $A_{\parallel} = 0$, and $R = 0$. Dichroic ratios ranging from 0.25 to 0.50 have been measured for various mechanically orientated dye-DNA preparations (see ref. [17]). These ratios are significantly less than 1, the value for statistical distribution; the dichroic ratio $0 < R < 1$ also indicates intercalation. These figures are not, however, convincing. The experimental dichroic ratio should differ very little from $R = 0$ if the dye molecules are intercalated; the value $0 < R < 1$, on the other hand, is compatible with other molecular arrangements.

In order to obtain unequivocal results we improved the experimental methodology in three respects.[17]

1. In the dye-DNA preparations investigated in earlier studies, the dye was bound both noncompetitively and competitively. Since only the geometry of the noncompetitively bound dye is of interest here, we ensured that the preparations were free of competitively bound molecules by adding a competitor salt. If a suitable preparative procedure is adopted, highly viscous dye-DNA gels can be synthesized from which very fine, excellently orientated fibers can be drawn. These fibers are birefringent—the more so, the better the mechanical orientation. The sites of best orientation for optical polarization measurements can then be selected under the polarization microscope.

2. So far, macroscopically orientated samples have always been employed for investigating linear dichroism. Since it is almost impossible to prevent the microscopic arrangement of these preparations from being nonuniform, all the microscopic states are averaged during measurement. The results obtained are thus poor and R is shifted in the direction of an equal statistical distribution. We therefore performed our measurements on microscopic samples using a microspectrophotometer equipped with a polarizer and an analyzer. The sites of best orientation in the preparation were located with the aid of the birefringence of the dye-DNA fibers and then measured by means of optical polarization.

3. The dye-DNA fibers are dichroic and birefringent. We have developed a formalism that takes the dichroism and birefringence of the sample into consideration and permits the determination of the dichroic ratio R_0, corrected for the birefringence, from the experimental material.

We studied a highly orientated E-DNA fiber as an example.[17] R_0 varies considerably within the preparation, ranging from 0.03 to 0.5. In order to prove intercalation the smallest value, $R_0 = 0.03$, is usually preferred but this is problematic. It is better to characterize the quality of the orientation at the site under investigation using an independent criterion. We used an indirect criterion for selection. It can be assumed that the mechanical orientation of the fiber will be better the finer the preparation. The layer thickness d is directly proportional to an experimentally accessible factor $K = K(d)$.[17] If R_0 is plotted versus $K(d)$, a correlation should be obtained which can be used to determine the limiting value of R_0 in an ideally orientated sample for $K(d) \rightarrow 0$ and thus $d \rightarrow 0$. The demands made on the correlation should naturally not be too high; it depends on the relationship between the layer thickness and the quality of the orientation (i.e., the experimental skill of the preparer), and this is difficult to assess. The correlation for the E-DNA fiber studied is shown in Figure 9 and is better than originally expected. If a straight line is drawn through the points by means of linear regression, extrapolation to $K(d) = 0$ gives the dichroic ratio of an ideal sample as being $R_0 = 0.00$. This is precisely the value that is expected from *Lerman*'s intercalation model. Consequently, we presume that the noncompetitively bound ethidium cations—which are the only ones present according to the preparative method used—do indeed intercalate. The smaller binding constant K_{S1} can then be assigned to the intercalated molecules. It can be assumed that the same applies to other intercalated dyes.

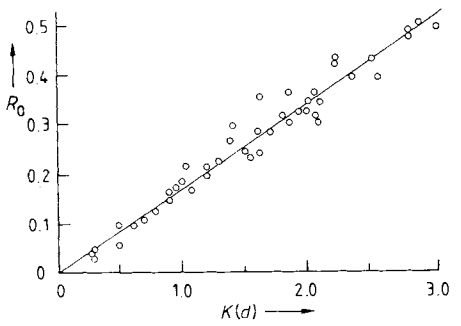


Fig. 9. Correlation between the corrected dichroic ratio R_0 and the layer thickness parameter $K(d)$ for the E/DNA/$MgCl_2$ system [17].

The extrapolation $K(d)\rightarrow 0$ only covers a very small range, namely from the smallest measured value $R_0=0.03$ to $R_0=0.00$. In earlier studies extrapolations were made from $R=0.25$–0.5 to $R=0.0$; the improvement made to the method is obvious.

7. Structural Features of Intercalated and Externally Bound Dye Cations

Intercalated dye cations inside the double helix are largely protected against the action of competitors. The competitively bound molecules can, in contrast, be displaced by competitor cations. These molecules are apparently bound further outward on the DNA. This external binding should not, however, be regarded as consisting of electrostatic 1 : 1 complexes between the dye cations and the anionic DNA phosphodiester groups. Such complexes are indeed known and have already been described by *Feulgen*[44] but they are found at high concentration ratios C_D/C_N and are usually poorly soluble, $n=1$ and $r\approx 1$. Our experiments, however, were performed at $C_D/C_N \ll 1$ ($r \ll 1$). According to our investigations, the binding parameters for noncompetitive and competitive binding are approximately the same ($n_1=n_2=n$). For the ethidium derivatives studied $n=0.21$, and for the acridine derivatives $n=0.17$. External binding in which $n\approx 0.2$ is thus a separate type of binding which can be experimentally distinguished from the 1 : 1 complex where $n=1$.

External binding in which $n_1=n_2$ also displays one of the features of intercalation. Competitive binding is perhaps a precursor of intercalation in which, for example, the bound molecules are only partially inserted between the DNA base pairs. It is noteworthy in this context that *Gursky*[45] and *Peacocke* et al.[24,46] have already proposed other binding geometries for DNA-bound dye cations that differ from the classical intercalation model.[3] The hypothesis that several types of binding with different geometries may occur when r is small is therefore by no means unreasonable. Studies still have to be performed on the geometries of external or pre-intercalative binding.

Intercalation and external binding take place independently of one another and only interfere slightly with one another in the region of sufficiently small r values, which we have limited ourselves to. The Scatchard isotherm [Eq. (20)] can thus be formally divided into two additive components when $n_1=n_2=n$, namely, $K_{S1}(n-r)$ and $K^*_{S2}(n-r)/(1+K_{S3}C_M)$, which are related to intercalation and external binding, respectively. The binding parameter n will not be discussed in more detail on account of the difficulties described in Section 4. The relationship $n_1=n_2=n$ should be regarded here as an experimental finding.

Comparative study of the binding constants K_{S1}, K_{S2}, and K_{S3} of a series of systematically modified dyes provides further insight into intercalation and external binding (cf. Scheme 1). The molecules were investigated under comparable experimental conditions and the binding constants were determined with the aid of the model already described (cf. Table 3).[14–16, 18, 19]

Table 3. Binding constants K_{S1}, K_{S2}, and K_{S3} [M^{-1}] and equilibrium constants K_{S4} for systems consisting of a dye D, DNA, and a competitor salt S; $T=298$ K.

D	K_{S1}	K_{S2}	S	K_{S3}	K_{S4}
E [14]	1.1×10^4	5.6×10^5	NaCl	22	2.5×10^4
			$MgCl_2$	350	1.6×10^3
DPPH [15]	0.9×10^4	7.5×10^5	NaCl	25	3.0×10^4
			$MgCl_2$	380	2.0×10^3
AEPP [15]	0.8×10^4	3×10^5	NaCl	30	1×10^4
BH [19]	0.9×10^4	1.0×10^6	NaCl	33	3.0×10^4
AF [18]	4.2×10^4	1.0×10^6	NaCl	30	3.3×10^4
AO [18]	3.0×10^4	7.0×10^5	NaCl	24	2.9×10^4
EPP [15]	≈ 0	5×10^4	NaCl	30	2×10^3
TME [16]	≈ 0	1.6×10^5	NaCl	30	5.3×10^3
TMAF [18]	≈ 0	3.0×10^5	NaCl	25	1.2×10^4
DPP [15]	≈ 0	≈ 0			
B [19]	≈ 0	≈ 0			

The significance of electrostatic interactions, hydrogen bonds, and hydrophobic interactions in the binding of dye molecules to DNA was noted very early.[2, 3, 10, 12] On the basis of our studies, dye molecules can be divided into three groups (see Scheme 1 on p. 117).

1. Dyes that both intercalate and are bound externally (E, AEPP, DPPH, BH, AF, AO). These dyes are cations and contain NH_2, NH, and OH groups that can act as proton donors for hydrogen bonds formed between the dye and the DNA. The electron donor for the hydrogen bond is very likely the DNA phosphodiester residue. $K_{S1} \ll K_{S2}$ is valid for all molecules. The intercalation binding constant is much smaller than the external binding constant. The binding constants K_{S1} and K_{S2} of the various molecules only differ slightly from one another: $K_{S1}=1\times10^4$–4×10^4 M^{-1}, $K_{S2}=4\times10^5$–1×10^6 M^{-1}.

2. Dyes that are bound externally but do not intercalate (EPP, TME, TMAF). These dyes are cations and do not contain any functional groups that can act as proton donors for hydrogen bonds formed between the dye and the DNA. The bound molecules are displaced from the DNA by competitor salts. Intercalated molecules cannot be detected within the experimental range of error ($K_{S1}\approx 0$). The binding constant for external binding varies between the limits $K_{S2}=5\times10^4$ and 3×10^5 M^{-1}, and is less than the values found for the parent compounds E and AF. The dyes belonging to group 2 show that external binding is a separate type of binding from intercalation.

3. Dyes that neither intercalate nor undergo external binding (DPP, B). These molecules are electrically neutral

and contain functional groups that can form hydrogen bonds with DNA. Binding to DNA has not, however, so far been demonstrated experimentally ($K_{S1} \approx 0$, $K_{S2} \approx 0$). This cannot be due to steric hindrance because protonation produces the dye cations DPPH and BH, which are capable of intercalation and external binding.

The binding constant K_{S3} for the binding of competitor cations to DNA only varies within a narrow range for the various dyes, which is determined by the experimental accuracy and the approximations made in the formalism. $K_{S3} = 2 \times 10^1$–$3 \times 10^1\ M^{-1}$ is found for the competitor salt NaCl and $4 \times 10^2\ M^{-1}$ for $MgCl_2$. As expected, divalent magnesium is a stronger competitor than monovalent sodium.

The equilibrium constants K_{S4} [Eq. (17)] for the exchange between the dye and competitor (cations D and M, respectively) at the DNA are also listed in Table 3. K_{S4} for the commonly used competitor salt NaCl is of the same order of magnitude as the binding constant K_{S1} of intercalation. This could be one of the reasons why it has not so far been possible to clearly distinguish between intercalation and external binding in the region of small r values.

Comparison of the binding constants K_{S1} and K_{S2} given in Table 3 shows that the most important binding component for intercalation and external binding is electrostatic interaction that is supplemented by hydrogen bonds (group 1). If hydrogen bonds cannot be formed, only weak external binding is observed (group 2). If electrostatic interaction is impossible, binding does not take place even if the molecule is capable of forming hydrogen bonds (group 3). When compared with electrostatic interactions, both hydrophobic interactions and hydrogen bond formation appear to be of minor significance. If hydrophobic interactions were predominant, they would force DPP and B to bind to DNA. Both molecules should be more strongly hydrophobic than the DPPH or BH cations, which are formed on protonation of DPP and B and readily bind to DNA. Nevertheless, hydrophobic interactions and hydrogen bonds are involved in the binding process (Section 8).

Discussion of the binding constant gives an overall, uniform impression of the interaction contributions that result in intercalation and external binding. It must not be forgotten, however, that we have studied simple molecules whose binding can be approximately described by a simple model. In the case of more complicated molecules, resort must be made to more complicated theories. Complications can be expected even for proflavine (PF), a classical, intercalating acridine dye. PF exhibits structural features that are similar to those of acriflavine (AF) and acridine orange (AO), namely, two NH_2 groups in positions 3 and 6 and a NH group in position 10 (Scheme 1). The latter is formed by protonation of the strongly basic molecule at the aza nitrogen atom. In AF and AO, hydrogen bonds are involved in intercalation and external binding. The related molecule tetramethylacriflavine (TMAF) can be derived from AF or AO by replacing the NH_2 or NH groups by $N(CH_3)_2$ or NCH_3 groups, respectively, and is incapable of forming hydrogen bonds; it does not intercalate and only undergoes weak external binding. On account of the different positions of the NH_2 and NH groups in AF and AO, it can be assumed that the binding geometries of these molecules to DNA differ. PF combines the structural features of AF and AO. It is therefore conceivable that different intercalated and externally bound molecular species are formed when PF is bound to long-chain DNA; these differ with respect to their geometries and thermodynamic parameters. Further investigations are still required.[47]

8. The Thermodynamic Disadvantage of Intercalation compared with External Binding

The binding constants given in Table 3 show that in the region of small r values intercalation is less favorable than external binding ($K_{S1} \ll K_{S2}$). This finding is surprising and contradicts normal expectations. In order to obtain a more accurate picture of the binding conditions we determined the binding enthalpies ΔH^0_{Si} and entropies ΔS^0_{Si} ($i = 1$–3) of E, AF, AO, and TMAF (Table 4).[14, 18] The experimental difficulties encountered in these measurements and the consequent errors, especially in the case of the binding entropies, have already been referred to in Section 2. The values are, however, sufficiently accurate for the purposes of the following qualitative discussion.

Table 4. Binding enthalpies ΔH^0_{Si} [kJ mol^{-1}] and binding entropies ΔS^0_{Si} [J K^{-1} mol^{-1}] of binding types $i = 1$–3 for systems consisting of a dye D, DNA, and a competitor salt S.

D	ΔH^0_{S1}	ΔH^0_{S2}	ΔS^0_{S1}	ΔS^0_{S2}	S	ΔH^0_{S3}	ΔS^0_{S3}
E [14]	−28	−27	−20	+18	KCl	+0.4	+21
					NaCl	+1.7	+28
					$MgCl_2$	+2.1	+42
AF [18]	−26	−26	− 2	+28	NaCl	≈0	+29
AO [18]	−30	−28	−15	+20	NaCl	≈0	+23
TMAF [18]	—	−15	—	+54	—	[a]	[a]

[a] Not determined experimentally [18].

The binding enthalpies ΔH^0_{S1} and ΔH^0_{S2} for the intercalation and external binding of E, AF, and AO to DNA are negative and are the same within the limits of error ($\Delta H^0_{S1} = \Delta H^0_{S2} < 1$). They scarcely differ for the different dyes. The differences between the binding constants K_{S1} and K_{S2} can thus be attributed to the binding entropy. There is an increase in entropy when external binding occurs ($\Delta S^0_{S2} > 0$), but in the case of intercalation the entropy change is either negative (E, AO) or almost zero (AF). In all cases, $\Delta S^0_{S1} \ll \Delta S^0_{S2}$. Since a gain in entropy is thermodynamically favorable, external binding dominates over intercalation ($K_{S2} \gg K_{S1}$).

A negative binding enthalpy ΔH^0_{S2} and a positive binding entropy ΔS^0_{S2} are also observed in the external binding of TMAF to DNA; both of these conditions are thermodynamically favorable. The enthalpy change is, however, considerably smaller and the entropy change considerably larger than the corresponding values found for the external binding of E, AF, or AO to DNA.

The binding enthalpies of all competitor cations are virtually zero ($\Delta H^0_{S3} \approx 0$). Binding is possible as a result of the thermodynamically favorable increase in entropy ($\Delta S^0_{S3} > 0$); it is thus an entropic effect. The binding entropy depends within the limits of error on the competitor cation but not on the dye.

The values for the binding enthalpies and entropies of the competitor cations, ΔH^0_{S3} and ΔS^0_{S3}, respectively, are typical of hydrophobic interactions. Magnesium, sodium, and potassium ions are so-called structure-forming ions; $Mg^{2\oplus}$ is stronger than $Na^{\oplus}$, which in turn is stronger than $K^{\oplus}$.[48,49] The water molecules in the hydration shells of structure-forming ions are more tightly and rigidly bound than those in the surrounding bulk water. This structure formation produces a thermodynamically unfavorable fall in entropy. When competitor cations are bound to DNA, water molecules must be transferred from the hydration shell to the bulk water for steric reasons. The necessary energy can be supplied from the electrostatic interaction energy. The binding enthalpy of the competitor cations is therefore not negative but virtually zero ($\Delta H^0_{S3} \approx 0$). The transferred water molecules, on the other hand, gain degrees of freedom of motion; the gain is the larger, the more rigidly and tightly the molecules were originally bound. The water molecules remaining in the hydration shell also gain degrees of freedom of motion as partial charge compensation occurs during formation of ion pairs between the competitor cation and the anionic binding site of the DNA. The net gain in degrees of freedom of motion is responsible for a thermodynamically more favorable increase in entropy, which more than compensates for the entropy decrease due to the immobilization of the bound ions. This gain in entropy ($\Delta S^0_{S3} > 0$) is the driving force for binding cations as a result of hydrophobic interactions and, as is to be expected, increases in the direction of increasing structure formation ($K^{\oplus} < Na^{\oplus} < Mg^{2\oplus}$, Table 4).

Dye cations are also structure-forming ions.[14] Unlike the small metal cations, water molecules are more loosely bound to the large organic molecules. In the case of TMAF, less energy is therefore required to transfer a water molecule from the hydration shell of the dye cation to the bulk water; the overall energy balance remains negative ($\Delta H^0_{S2} < 0$). The gain in entropy ($\Delta S^0_{S2} > 0$) is once again characteristic of a hydrophobic interaction. It is especially large for the external binding of TMAF on account of the five methyl groups of the molecule.

The energy balance for the external binding of E, AF, and AO is more negative than for TMAF because additional hydrogen bonds are formed between the dye and the DNA ($\Delta H^0_{S2} < 0$). Hydrophobic interactions again result in an increase of entropy ($\Delta S^0_{S2} > 0$).

The binding enthalpies for intercalation and external binding are practically the same ($\Delta H^0_{S1} \approx \Delta H^0_{S2}$). In both types of binding the molecules apparently endeavor to saturate the valences at their disposal in the same way. It is thus understandable that the absorption spectra of the intercalated and externally bound dye cations scarcely differ. The spectral changes are virtually identical for both types of binding.

The finding that $\Delta S^0_{S1} \ll \Delta S^0_{S2}$ is surprising. It must, however, be appreciated that the double helix stiffens on intercalation[3] and that the loss of degrees of freedom of motion of both the DNA and the intercalated dye is responsible for a decrease in entropy when compared with external binding. In intercalation this thermodynamically unfavorable loss of entropy must be offset by a correspondingly large enthalpy decrease.

The binding entropy plays a critical role in the binding of dye and competitor cations (D and M, respectively) to DNA. According to Equation (13), the method used to count the binding sites affects the binding entropy but not the binding enthalpy [Eq. (12)]. The magnitude of this effect can be estimated as follows. Application of Equation (13) with $n_1 = n_2 = n = p_i/q_i$ (i = 1-3) gives Equation (24).

$$\Delta S^0_{Zi} = \Delta S^0_{Si} - R \ln q_i \tag{24}$$

In the case of intercalation it can be assumed that on an average each base pair provides one potential binding site; therefore, $p_1 = 1/2$ and $q_1 = 1/2n$. If we presume that each DNA phosphodiester group represents a potential binding site for the external binding of D or M, then $p_{2,3} = 1$ and $q_{2,3} = 1/n$. In the case of the ethidium and acridine dyes studied, $n = 0.21$ (0.17), $R \ln q_1 = 7$ (9), and $R \ln q_{2,3} = 13$ (15) $JK^{-1}\,mol^{-1}$ (the values for the acridine dyes are given in parentheses). The ΔS^0_{Zi} values are on the whole less than the ΔS^0_{Si} values. Although the binding entropies change, our comparative qualitative discussion is still valid. The binding constants, enthalpies, and entropies can thus be understandably interpreted within a uniform framework.

9. Biological and Pharmacological Aspects of Dye Binding

According to our studies, the binding constant for intercalation is much smaller than that for external binding ($K_{S1} \ll K_{S2}$). Intercalation is therefore less thermodynamically favorable in vitro than external binding. This difference between the binding constants is a result of the binding entropies ($\Delta S^0_{S1} \ll \Delta S^0_{S2}$) since the enthalpies of the two types of binding are almost equal ($\Delta H^0_{S1} \approx \Delta H^0_{S2}$). The living cell contains a complex mixture of inorganic salts. Physiological saline is a simple equivalent for these salts; its NaCl concentration is $C_S \approx 0.15$ M. According to Equation (21) (Fig. 3), the apparent binding constant K_S drops markedly in the region of small C_S values as the salt concentration increases. The competitively bound molecules (type 2) are already largely displaced at $C_S = 0.15$ M, whereas the noncompetitively bound, intercalated molecules (type 1) are not affected by the action of the competitor. It can therefore be estimated that, in vivo, either intercalation dominates over external binding ($r_1 > r_2$) or the contributions of the two types of binding are comparable ($r_1 \approx r_2$).

Acridine and ethidium derivatives are mutagenic;[2,3,50] they must therefore enter the cell and interact with DNA. The uptake and transport of substances in living cells are, however, very complex, selective processes. The question therefore arises as to whether the biological and pharmacological actions of these substances can solely be attributed to their binding to DNA or whether binding to DNA is a side reaction, the bulk of the dye molecule perhaps acting in a different way. Some experiments will therefore finally be described in which the sites of preferred dye accumulation in the living cell are visualized directly.

The acridine and ethidium derivatives discussed in this article are highly fluorescent dyes (fluorochromes) and can

be detected very sensitively inside the cell with the fluorescence microscope. The low dye concentrations that can be detected by fluorescence microscopy are generally not toxic or are only of limited toxicity for the cell. This provides a way of following the route taken by the fluorochrome in the living cell and of identifying the site of dye accumulation.

The cell materials used in our model experiments are tissue cultures of HeLa cells and LM cells (mouse fibroblasts) which are relatively easy to obtain experimentally and are of a consistent quality. Tissue cultures have the advantage that the cells grow in a monolayer on a support (coverslips) where they can easily be observed with a microscope. The cells are incubated together with the support in a dye solution of concentration C_D at 37 °C; after incubating for a period τ_I, the cells are rinsed in Hank's solution to remove excess dye and then examined under the fluorescence microscope.

Fixed cells behave totally differently from living cells after treatment with fluorochromes. We will first consider a tissue culture of ethanol-fixed HeLa cells that were stained with the fluorochrome AO under appropriate conditions. The cell nucleus fluoresces intense green-yellow, while the cytoplasm and nucleoli are an intense orange. It is known from spectroscopic studies that AO undergoes association in aqueous solution as its concentration increases;[51,52] this is accompanied by changes in the absorption and fluorescence spectra. The monomers likewise fluoresce green-yellow, whereas the dimers fluoresce orange. Accordingly, AO is present in the nucleus in its monomeric form but occurs as a dimer in the cytoplasm and nucleoli. The substrates to which the dye binds in the cell are also known from enzymatic digestion experiments—they are the nucleic acids DNA and RNA. If the nuclear DNA or the RNA in the cytoplasm and nucleoli is degraded, the associated staining disappears. The dye can thus be employed as an analytical reagent for detecting DNA and RNA. *Von Bertalanffy* et al.[53] have developed the fluorochrome staining of cytological material with AO for the diagnosis of malignant tumors. The same fluorescence microscopy pictures, however, are also shown by other cells that divide rapidly.

Green fluorescent nuclei are also observed after vital staining of HeLa cells with the fluorochrome AO. The fluorescence is, however, relatively weak. The chromosomes of cells undergoing mitosis are stained by the fluorochrome. It therefore seems reasonable to assume that the dye is bound to the DNA localized in the nucleus and the chromosomes. It can be demonstrated that the cell functions are not significantly affected by vital staining.[54] The vital staining of chromosomes with the basic acridine dye 3-amino-6-methoxy-9(2-hydroxyethylamino)acridine, which we have recently investigated, is especially impressive (Fig. 10).[55] The cells can tolerate high fluorochrome concentrations and long incubation periods without a detectable fall in their respiratory activity.

Vital fluorochrome staining of the nuclear chromatin, however, is a rare exception. The nuclei of living cells usually exhibit virtually no fluorescence, a property that is regarded as a criterion for assessing tissue cultures as being healthy. Under suitable conditions, however, numerous

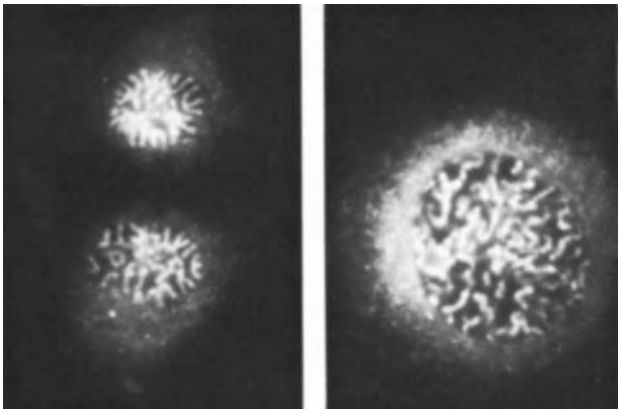


Fig. 10. Fluorescent chromosomes in mitotic LM cells after vital staining with 3-amino-6-methoxy-9(2-hydroxyethylamino)acridine. Dye concentration $C_D = 1 \times 10^{-3}$ M, incubation period $\tau_I = 45$ min, magnification $\times 1000$ [55]. Left: Telophase. Right: Prophase.

small, intensely fluorescent organelles can be observed in the cytoplasm which may accumulate near the nucleus. The organelles that accumulate the dye are the lysosomes.[56,57] When AO is used for vital staining, the cytoplasm is studded with orange-fluorescing lysosomes. Many other dyes are also accumulated in the lysosomes of living cells, such as the basic fluorochrome 3-dimethylamino-6-methoxyacridine, which is closely related to AO (Fig. 11). In fixed cells the same dye produces Bertalanffy-like fluorochrome staining of DNA in the nucleus and of RNA in the nucleolus and cytoplasm.[58]

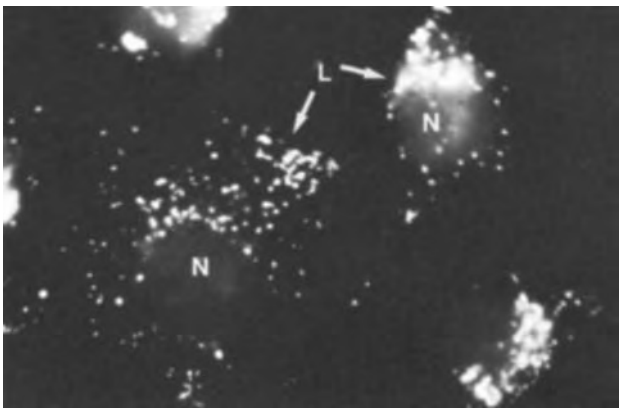


Fig. 11. Fluorescent lysosomes L in the cytoplasm of LM cells after vital staining with 3-dimethylamino-6-methoxyacridine. Dye concentration $C_D = 1 \times 10^{-5}$ M, incubation period $\tau_I = 4.5$ h, magnification $\times 1000$. The intensely fluorescing lysosomes are either distributed in the cytoplasm or accumulated near the nucleus. The cell nucleus N fluoresces very weakly and the cytoplasm scarcely fluoresces at all. The cytoplasm is therefore not observed in fluorescence microscopy [55].

Lysosomes do not contain nucleic acids; they are the digestive organelles of the cell. Their task is to enzymatically cleave substances inside the cell and then direct the cleaved products so that they can be metabolized. Dyes are difficult to digest; indeed, they can be enriched in the lysosomes by an unknown mechanism in such high concentrations that they associate. If the lysosomes cannot store any more dye, the fluorochrome reaches the nucleus, resulting generally in cell death. Cell death can be recognized by

intense fluorescence of the cell nucleus. The dye is very probably bound to the DNA of the nuclear chromatin. Dye accumulation in the lysosomes apparently has a protective function, namely to prevent the dye from interacting with the vitally important nucleic acids.

Small modifications of the molecular structure suffice to produce a completely different response of the cell to the action of a fluorochrome. AO, for example, is a strong base whose nitrogen atom in position 10 is almost completely protonated at pH = 7; the dye is accumulated in the lysosomes as a cation. Alkylation of AO results in the formation of the related 10-alkylacridinium orange cations. Alkyl-AOs—like the parent compound—fluoresce intensely and associate at higher concentrations in an aqueous medium.[59] We studied n-C_mH_{2m+1}-AOs ($m = 1$–9). When $m > 9$, the substances dissolve poorly in water. Methyl-AO behaves similarly to AO when it is used for the vital staining of HeLa or LM cells; dye accumulation in the lysosomes is observed along with a weak fluorescence of the mitochondria. In the case of ethyl-AO, however, the microscopic picture changes drastically; the dye is now preferentially bound to the cell mitochondria.[60] The vital staining of the mitochondria becomes more pronounced as the chain length of the alkyl residue increases (Fig. 12).[61] In the case of nonyl-AO, for example, only fluorescent mitochondria can be recognized under the fluorescence microscope; neither the lysosomes, the nuclear chromatin, nor the cytoplasm are stained by the fluorochrome. Bertalanffy-like staining can be produced with the same dye in fixed cells; the fluorochrome is then bound to the DNA and RNA in the nucleus and cytoplasm.

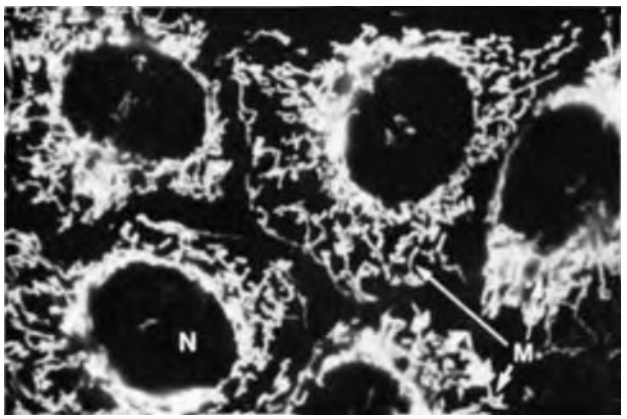


Fig. 12. Fluorescent filamentous mitochondria M in the cytoplasm of HeLa cells after vital staining with 10-n-nonylacridinium orange chloride. Dye concentration $C_D = 5 \times 10^{-7}$ M, incubation period $\tau_I = 10$ min, magnification $\times 1000$. Neither the cell nucleus nor the cytoplasm is observed in fluorescence microscopy [61, 63].

Vital staining of the mitochondria with nonyl-AO is very specific and efficient;[61] it even occurs when the dye concentration of the incubation medium is $C_D = 1 \times 10^{-8}$ M. This concentration is one order of magnitude smaller than the hydrogen ion concentration of pure water. At 5×10^{-7} M the fluorescent mitochondria can already be observed after an incubation period of $\tau_I < 1$ min. When $C_D \geq 1 \times 10^{-7}$ M and $\tau_I = 10$ min, the dye is bound to the mitochondria in such high concentrations that it dimerizes. The mitochondria of cells that are cultured in a dye-free medium after vital staining retain the dye for more than one week.

The entire energy metabolism of the cell takes place in the mitochondria: respiration, the electron transport processes, and the vitally important synthesis of ATP. The majority of the enzymes responsible for oxidative phosphorylation are localized on the internal mitochondrial membranes and the membranes of the cristae. Our investigations indicate that nonyl-AO is bound to these membranes by hydrophobic interactions.[61] The respiratory activity is a measure of the functional capability of the mitochondria. In HeLa cells neither the oxygen consumption nor the mitochondrial ultrastructure is affected up to $C_D \leq 5 \times 10^{-7}$ M and $\tau_I = 10$ min. With higher dye concentrations and longer incubation periods, inhibition of respiration is observed, which is accompanied by ultrastructural changes, especially in the internal mitochondrial membranes and the membranes of the cristae.[61,62] In the terminal stage (5×10^{-6} M and 30–60 min) the hydrophobic dye cations transform the mitochondria into multilamellar liposomes and bizarre myelin bodies. It is remarkable that these dramatic ultrastructural changes can only be seen in the mitochondria under the electron microscope. The other cell membranes (e.g., the nuclear membrane) appear to be resistant to the action of the dye. Binding of the dye to the nuclear membrane has not yet been demonstrated by fluorescence microscopy. Hydrophobic interactions between the dye and the mitochondrial membranes represent one contribution to binding,[61,63] which is, however, apparently supplemented by another mitochondrial-specific component.[61]

Not only alkyl-AOs but also other dyes that are bound to DNA in vitro, such as E, TME, and BH, produce drastic changes in the ultrastructure of the mitochondria.[64–66] TME has the strongest effect and is the most strongly hydrophobic of the ethidium derivatives mentioned. We therefore presume that the ultrastructural changes may be due to the hydrophobic interactions between the dye and the mitochondrial membranes.

These few examples should suffice to demonstrate that the in vitro binding of acridine and ethidium derivatives to DNA does not allow unequivocal conclusions to be made about the binding and sites of accumulation of the same substance in living cells. The accumulation of dyes in the lysosomes evidently provides the living cell with a mechanism for protecting the nuclear chromatin and prevents the toxic substances from being bound to the DNA. It is still not exactly known under which conditions this mechanism is modified so that the dye is instead bound to the mitochondria. The specific binding of substances to the mitochondrial membranes, where oxidative phosphorylation takes place, is of general interest as it provides a way of directly or indirectly interfering with energy metabolism. Exploitation of this principle for pharmacological purposes should prove to be rewarding.

I am indebted to the Bundesministerium für Forschung und Technologie and the Deutsche Forschungsgemeinschaft for supporting these studies. I am especially grateful to my

co-workers—who are all cited in the list of references—for their enthusiastic efforts and productive discussions.

Received: April 30, 1985 [A 565 IE]
German version: *Angew. Chem. 98* (1986) 115
Translated by Dr. *Gail Schulz*, Seeheim-Jugenheim

[1] L. S. Lerman, *J. Mol. Biol. 3* (1961) 18.
[2] A. R. Peacocke in R. M. Acheson (Ed.): *Acridines*, 2nd ed., Wiley, New York 1973, p. 723 ff.
[3] M. J. Waring in E. F. Gale, E. Cundliffe, P. E. Reynolds, M. H. Richmond, M. J. Waring (Eds.): *The Molecular Basis of Antibiotic Action*, 2nd ed., Wiley, New York 1981, p. 273 ff.
[4] H. M. Sobell, C. C. Tsai, S. G. Gilbert, S. C. Jain, T. D. Sacore, *Proc. Natl. Acad. Sci. USA 73* (1976) 3068.
[5] C. C. Tsai, S. C. Jain, H. M. Sobell, *J. Mol. Biol. 114* (1977) 301.
[6] S. C. Jain, C. C. Tsai, H. M. Sobell, *J. Mol. Biol. 114* (1977) 317.
[7] W. Fuller, M. J. Waring, *Ber. Bunsenges. Phys. Chem. 68* (1964) 805.
[8] M. Liebman, J. Rubin, M. Sundaralingam, *Proc. Natl. Acad. Sci. USA 74* (1977) 4821.
[9] G. Löhr, G. Achterer, *Biopolymers 8* (1969) 595.
[10] L. P. G. Wakelin, M. J. Waring, *Mol. Pharmacol. 10* (1974) 544.
[11] J. Chambron, M. Daune, C. Sadron, *Biochim. Biophys. Acta 123* (1966) 306.
[12] J. B. LePecq, C. Paoletti, *J. Mol. Biol. 27* (1967) 87.
[13] S. Ichimura, M. Zama, H. Fujita, T. Ito, *Biochim. Biophys. Acta 190* (1969) 116.
[14] J. Pauluhn, H. W. Zimmermann, *Ber. Bunsenges. Phys. Chem. 82* (1978) 1265.
[15] J. Pauluhn, H. W. Zimmermann, *Ber. Bunsenges. Phys. Chem. 83* (1979) 76.
[16] J. Pauluhn, R. Grezes, H. W. Zimmermann, *Ber. Bunsenges. Phys. Chem. 83* (1979) 708.
[17] E. Ohmes, J. Pauluhn, J.-U. Weidner, H. W. Zimmermann, *Ber. Bunsenges. Phys. Chem. 84* (1980) 23.
[18] H. Wille, J. Pauluhn, H. W. Zimmermann, *Z. Naturforsch. C37* (1982) 413.
[19] J. Röding, H. W. Zimmermann, *Ber. Bunsenges. Phys. Chem. 86* (1982) 729.
[20] G. S. Manning, *Q. Rev. Biophys. II, 2* (1978) 179.
[21] M. T. Record, T. M. Lohman, P. de Haseth, *J. Mol. Biol. 107* (1976) 107.
[22] G. Scatchard, *Ann. N. Y. Acad. Sci. 51* (1949) 660.
[23] A. R. Peacocke, J. N. H. Skerrett, *Trans. Faraday Soc. 52* (1956) 261.
[24] A. Blake, A. R. Peacocke, *Biopolymers 6* (1968) 1225.
[25] A. V. Hill, *J. Physiol. (London) 40* (1910) 4.
[26] J. Wylman, Jr., *Adv. Protein Chem. 19* (1964) 223.
[27] D. M. Crothers, *Biopolymers 6* (1968) 575.
[28] G. Schwarz, *Biophys. Struct. Mech. 2* (1976) 1.
[29] G. Schwarz, *Biophys. Chem. 6* (1977) 65.
[30] J. D. McGhee, P. H. von Hippel, *J. Mol. Biol. 86* (1974) 469.
[31] A. S. Zasedatelev, G. V. Gurskii, M. V. Volkenshtein, *Mol. Biol. 5* (1971) 245; *Chem. Abstr. 75* (1971) 15042 n.
[32] J. Ramstein, M. Leng, N. R. Kallenbach, *Biophys. Chem. 5* (1976) 319.
[33] W. D. Wilson, I. G. Lopp, *Biopolymers 18* (1979) 3035.
[34] H. A. Benesi, J. H. Hildebrand, *J. Am. Chem. Soc. 71* (1949) 2703.
[35] C. H. Fiske, Y. Subbarow, *J. Biol. Chem. 66* (1925) 375.
[36] H. Eibl, W. E. M. Lands, *Anal. Biochem. 30* (1969) 51.
[37] J.-U. Weidner, private communication.
[38] M. J. Waring, *J. Mol. Biol. 13* (1965) 269.
[39] R. W. Armstrong, T. Kurucsev, U. P. Strauss, *J. Am. Chem. Soc. 92* (1970) 3174.
[40] J. L. Bresloff, D. M. Crothers, *J. Mol. Biol. 95* (1975) 103.
[41] P. Fromherz, *Chem. Phys. Lett. 109* (1984) 407.
[42] G. Schwarz, *Eur. J. Biochem. 12* (1970) 442.
[43] G. Schwarz, W. Balthasar, *Eur. J. Biochem. 12* (1970) 461.
[44] R. Feulgen, *Hoppe Seylers Z. Physiol. Chem. 84* (1913) 309.
[45] G. V. Gursky, *Biofizika 11* (1966) 737.
[46] N. J. Pritchard, A. Blake, A. R. Peacocke, *Nature (London) 212* (1966) 1360.
[47] B. Marcandalli, C. Winzek, J. K. Holzwarth, *Ber. Bunsenges. Phys. Chem. 88* (1984) 368.
[48] H. G. Hertz, M. D. Zeidler, *Ber. Bunsenges. Phys. Chem. 68* (1964) 821.
[49] E. Wicke, *Angew. Chem. 78* (1966) 1; *Angew. Chem. Int. Ed. Engl. 5* (1966) 106.
[50] A. Albert: *The Acridines*, 2nd ed., Edward Arnold, London 1966.
[51] V. Zanker, *Z. Phys. Chem. 199* (1952) 225.
[52] V. Zanker, *Z. Phys. Chem. 200* (1952) 250.
[53] L. von Bertalanffy, F. D. von Bertalanffy, *Ann. N. Y. Acad. Sci. 84* (1960) 225.
[54] R. B. Hill, K. B. Bensch, D. W. King, *Nature (London) 184* (1959) 1429.
[55] K. Petschel, A. Naujok, H. W. Zimmermann, *Histochemistry 76* (1982) 219.
[56] H. Koenig, *J. Cell Biol. 19* (1963) 87.
[57] D. Wittekind, *Acta Histochim. (Suppl.) 1* (1958) 247.
[58] K. Petschel, A. Naujok, P. Kempter, W. Seiffert, H. W. Zimmermann, *Histochemistry 80* (1984) 311.
[59] M. Septinus, W. Seiffert, H. W. Zimmermann, *Histochemistry 79* (1983) 443.
[60] U. Erbrich, A. Naujok, K. Petschel, H. W. Zimmermann, *Histochemistry 74* (1982) 1.
[61] M. Septinus, T. Berthold, A. Naujok, H. W. Zimmermann, *Histochemistry 82* (1985) 51.
[62] U. Erbrich, T. Berthold, H. W. Zimmermann, *Histochemistry 76* (1982) 211.
[63] U. Erbrich, M. Septinus, A. Naujok, H. W. Zimmermann, *Histochemistry 80* (1984) 385.
[64] E. Heinen, A. Lepoint, R. Bassleer, G. Goessens, *Beitr. Pathol. 153* (1974) 353.
[65] G. Soslau, M. M. K. Nass, *J. Cell Biol. 51* (1971) 514.
[66] J. H. Röding, A. Naujok, H. W. Zimmermann, *Histochemistry*, in press.

Resonance Raman Spectroscopy, and Its Application to Inorganic Chemistry

New Analytical Methods (27)

By Robin J. H. Clark* and Trevor J. Dines

Resonance Raman spectra are obtained when the wave number of the exciting radiation is close to, or coincident with, that of an electronic transition of the scattering species. Such spectra are usually characterized by a very large enhancement of the intensities of particular Raman bands, sometimes with the appearance of intense overtone and combination tone progressions. The technique provides detailed information about excited electronic states because it is only the vibrational modes associated with the chromophore that are resonance-Raman active. Additionally, the high sensitivity is such that compounds at concentrations as low as 10^{-6} mol/L may be detected, enabling resonance Raman spectroscopy to be used as an analytical tool and for the study of chromophores in molecules of biological interest.

1. Introduction

The theory and practice of resonance Raman (RR) spectroscopy have both been developed substantially over the past decade to the extent that it is now possible to present a coherent picture of the subject within the confines of a single article. The object of the present review is to do this in a readily comprehendable manner and also to review the applications of the subject within the broad bounds of inorganic chemistry. To this end, Section 2 relates to the theoretical development of the subject, as it now stands. In particular, the relation between normal and RR scattering is developed, as is the nature of A-, B-, C- and D-term scattering, and scattering by both totally symmetric and non-totally symmetric modes. The significance of the depolarization ratio of a Raman band is also outlined, both with respect to vibrational as well as electronic band assignments.

Following a discussion of experimental techniques in Section 3, the results of many studies of inorganic compounds are then reviewed beginning with diatomic species and progressing through increasingly complicated species to metalloporphyrins and related species. In order to achieve conciseness this section has been restricted to RR studies reported since 1977, a comprehensive compilation of the earlier work being available already.[1] The investigations of small molecules (Section 4) have been considered in detail because these have contributed most to the understanding of the RR effect. The discussion of larger molecules (Section 5) has been restricted to a few illustrative examples and the reader is referred to reviews dealing specifically with metal-metal bonded species,[2] mixed-valence molecules,[3,4] and metalloporphyrins.[5] The attention of the reader is also directed elsewhere for reviews of RR studies on semiconductors,[6] electronic Raman scattering,[7] and time-resolved resonance Raman (TR^3) experiments.[8]

Many people have contributed to the development of experimental and theoretical aspects of the subject, notably *Albrecht*,[9-12], *Shorygin*,[13,14] *Behringer*,[15,16] *Peticolas*,[17,18] *Koningstein*,[19-21] *Rousseau* et al.,[22], *Clark*,[1,23,24] *Stewart*,[1,24] *Spiro*,[25-27] *Kiefer*,[28] *Tsuboi*,[29,30] *Mortensen*,[31] *Siebrand* and *Zgierski*,[32] *Barron*,[33,34] *Hong*,[35] and *Heller*.[36,37] Although a variety of different systems of nomenclature have been used to present the subject, that adopted in this review is essentially due to *Clark* and *Dines*.[7,38]

The central feature of interest in RR spectroscopy is the fact that, when the wave number of the exciting line is made to coincide with that of an allowed electronic transition in a molecule, the intensities of certain Raman bands of the scattering molecule are greatly enhanced relative to their off-resonance values. Thus the technique is a much more sensitive one than is normal Raman spectroscopy. Moreover, it proves to be a much more specific technique in the sense that it is solely modes to do with the chromophore in the scattering molecule which can be enhanced at resonance. Thus, information relating to the chemically significant parts of molecules is obtainable by this form of Raman spectroscopy. RR spectroscopy can also be applied to the determination of the displacements of the potential surfaces of excited states relative to that of the ground state, a matter of considerable importance in spectroscopy, photophysics, and photochemistry. The manner in which this may be done is outlined in the following pages.

2. Theory of Resonance Raman Scattering

In this section the theoretical approach that is most commonly used in the interpretation of RR data is outlined, based on the earlier developments of *Albrecht* et al.[9,10] and *Shorygin* et al.[13,14] RR scattering is described, in the energy-frame, in terms of the Kramers-Heisenberg dispersion formula,[39] obtained by second-order perturbation theory. Other approaches that have been described recently include the time correlator theory[36,37] and the optical transform theory.[11,12] These are claimed to be able to

[*] Prof. Dr. R. J. H. Clark and Dr. T. J. Dines
Christopher Ingold Laboratories
University College London
20 Gordon Street, London WC1H 0AJ (UK)

 © VCH Verlagsgesellschaft mbH, D-6940 Weinheim, 1986 0570-0833/86/0202-0131 $ 02.50/0

deal more easily with polyatomic molecules in which several modes are RR-active, but this view is not yet generally accepted.

For a Raman transition between two states $|i\rangle$ and $|f\rangle$ of a scattering system, the intensity of light scattered at 90° to the direction of irradiation is given by Equation (1).

$$I_{fi}(\pi/2) = \frac{\pi^2}{\varepsilon_0^2}(\tilde{\nu}_0 \pm \tilde{\nu}_{fi})^4 \mathscr{I}_0 \sum_{\rho,\sigma} [\alpha_{\rho\sigma}]_{fi}[\alpha_{\rho\sigma}]^*_{fi} \quad (1)$$

$\mathscr{I}_0$ is the irradiance of the incident radiation, $\tilde{\nu}_0$ and $\tilde{\nu}_{fi}$ are the wave numbers of the exciting line and of the Raman transition $|f\rangle \leftarrow |i\rangle$, respectively, ε_0 is the permittivity of free space, and $[\alpha_{\rho\sigma}]_{fi}$ is the $\rho\sigma$th element of the transition polarizability tensor [Eqn. (2)].

$$[\alpha_{\rho\sigma}]_{fi} = \frac{1}{hc}\sum_r \left[\frac{[\mu_\rho]_{fr}[\mu_\sigma]_{ri}}{\tilde{\nu}_{ri} - \tilde{\nu}_0 + i\Gamma_r} + \frac{[\mu_\sigma]_{fr}[\mu_\rho]_{ri}}{\tilde{\nu}_{rf} + \tilde{\nu}_0 + i\Gamma_r}\right] \quad (2)$$

In this equation $[\mu_\rho]_{fr}$ is the ρth component of the transition dipole moment associated with the transition $|f\rangle \leftarrow |r\rangle$ and $i\Gamma_r$ is a damping factor, which is related to the lifetime of the state $|r\rangle$. Strictly, the summation is over all states $|r\rangle$ of the system, including $|i\rangle$ and $|f\rangle$, but it has been shown that, for Raman scattering, $|i\rangle$ and $|f\rangle$ may be excluded from the sum.[40] (In the SI system, I is in W, $\mathscr{I}_0$ in W m^{-2}, ε_0 in F m^{-1}, $[\alpha_{\rho\sigma}]_{fi}$ in C V^{-1} m^2 and $[\mu_\rho]_{fr}$ in C m. The use of the unit cm^{-1} for wave number requires that the right-hand side of Equation (2) be multiplied by 10^8.) For vibrational Raman scattering excited far from resonance, the tensor is symmetric, i.e. $\alpha_{\rho\sigma} = \alpha_{\sigma\rho}$, but it may become asymmetric for electronic Raman (ER) and RR scattering.

The nature of the Raman effect is determined by the initial and final eigenstates $|i\rangle$ and $|f\rangle$, and by the proximity of the wave number of the exciting radiation to that of any electronic transition of the system. Clearly, the RR effect occurs when $\tilde{\nu}_0 \approx \tilde{\nu}_{ri}$, resulting in an increase of $[\alpha_{\rho\sigma}]_{fi}$ and consequently an enhancement of the Raman intensity. In order to answer such questions as which Raman bands may undergo enhancement and why overtone progressions are observed in RR spectra it is necessary to probe the dependence of $[\alpha_{\rho\sigma}]_{fi}$ on the properties of excited states by looking closely at Equation (2). As a prelude to such an analysis it is instructive to consider first the case of normal, i.e. non-RR scattering.

2.1. Normal Raman Scattering

The adiabatic Born-Oppenheimer approximation is invoked, in which the vibronic states $|i\rangle$, $|f\rangle$, and $|r\rangle$ are formed by products of the pure vibrational and the pure electronic states. The latter are referred to some fixed positions of the nuclei and are parametrically dependent on the normal coordinates, Q_k, of the molecule.

Assuming that the system is initially and finally in the ground electronic state $|g\rangle$ (i.e. a vibrational Raman transition, for instance, is under consideration), we may write:

$$\begin{aligned} |i\rangle &= |gm\rangle = |g\rangle|m\rangle \\ |f\rangle &= |gn\rangle = |g\rangle|n\rangle \\ |r\rangle &= |ev\rangle = |e\rangle|v\rangle \end{aligned} \quad (3)$$

where $|e\rangle$ represents an excited electronic state and $|m\rangle$, $|n\rangle$, and $|v\rangle$ represent vibrational states of the scattering species. This enables the transition polarizability to be rewritten in the form

$$[\alpha_{\rho\sigma}]_{gn,gm} = \frac{1}{hc}\sum_{ev}\left(\frac{\langle n|[\mu_\rho]_{ge}|v\rangle\langle v|[\mu_\sigma]_{eg}|m\rangle}{\tilde{\nu}_{ev,gm} - \tilde{\nu}_0 + i\Gamma_{ev}} + \frac{\langle n|[\mu_\sigma]_{ge}|v\rangle\langle v|[\mu_\rho]_{eg}|m\rangle}{\tilde{\nu}_{ev,gn} + \tilde{\nu}_0 + i\Gamma_{ev}}\right) \quad (4)$$

where $[\mu_\rho]_{ge}$ is the pure electronic transition moment associated with the transition $|g\rangle \leftarrow |e\rangle$. Under the conditions for which the Born-Oppenheimer condition is valid, the dependence of such an electronic transition moment on the k normal coordinates of the system, Q_k, is small. Thus, $[\mu_\rho]_{ge}$ may be expressed as a rapidly converging Taylor series expanded around the equilibrium position:

$$[\mu_\rho]_{ge} = [\mu_\rho]^0_{ge} + \sum_k [\mu_\rho]'_{ge} Q_k + \cdots \quad (5)$$

where $[\mu_\rho]'_{ge} = \partial[\mu_\rho]_{ge}/\partial Q_k$. Higher order terms in this series are, in most cases, negligibly small. A second simplification arises from the Born-Oppenheimer approximation in that the electronic and vibrational parts of the integrals in Equation (4) may be separated, such that, for example

$$\langle n|[\mu_\rho]_{ge}|v\rangle = [\mu_\rho]^0_{ge}\langle n|v\rangle + \sum_k [\mu_\rho]'_{ge}\langle n|Q_k|v\rangle \quad (6)$$

The following approximations may also be made in the ideal limit of excitation far from any region of electronic absorption:

(1) The denominators in the transition polarizability are large and insensitive to the vibrational quantum numbers m, n, and v, such that differences between the various $\tilde{\nu}_{ev,gm}$ and $\tilde{\nu}_{ev,gn}$ may be neglected;
(2) The states $|v\rangle$ represent a complete orthonormal set and the sums over them may be evaluated by invoking the closure theorem, which states that $\sum_v |v\rangle\langle v| = 1$, and arises from the matrix product rule $\sum_j A_{ij} B_{jk} = (AB)_{ik}$;
(3) Since $(\tilde{\nu}_{ev,gm} - \tilde{\nu}_0)$ and $(\tilde{\nu}_{eg,gn} + \tilde{\nu}_0)$ are much larger than the damping factors, $i\Gamma_{ev}$, the latter may be neglected.

With these approximations, and noting that

$$(\tilde{\nu}_e - \tilde{\nu}_0)^{-1} + (\tilde{\nu}_e + \tilde{\nu}_0)^{-1} = 2\tilde{\nu}_e(\tilde{\nu}_e^2 - \tilde{\nu}_0^2)^{-1}$$

the transition polarizability may be recast in the following form:

$$\begin{aligned} [\alpha_{\rho\sigma}]_{gn,gm} = {} & \frac{1}{hc}\sum_e \frac{2\tilde{\nu}_e}{(\tilde{\nu}_e^2 - \tilde{\nu}_0^2)}[\mu_\rho]^0_{ge}[\mu_\sigma]^0_{eg}\langle n|m\rangle \\ & + \frac{1}{hc}\sum_e\sum_k \frac{2\tilde{\nu}_e}{(\tilde{\nu}_e^2 - \tilde{\nu}_0^2)}\{[\mu_\rho]'_{ge}[\mu_\sigma]^0_{eg} + [\mu_\rho]^0_{ge}[\mu_\sigma]'_{eg}\}\langle n|Q_k|m\rangle \\ & + \frac{1}{hc}\sum_e\sum_{k,k'} \frac{2\tilde{\nu}_e}{(\tilde{\nu}_e^2 - \tilde{\nu}_0^2)}[\mu_\rho]'_{ge}[\mu_\sigma]'_{eg}\langle n|Q_k Q_{k'}|m\rangle \end{aligned} \quad (7)$$

Because n and m are both vibrational quantum numbers of the ground electronic state, the overlap integral

$\langle n|m\rangle = \delta_{nm}$. Thus, the first term in Equation (7) contributes only to Rayleigh scattering. The integral $\langle n|Q_k|m\rangle$ is non-zero if $n = m \pm 1$ and has the value $[h(m+1)/8\pi^2 c\tilde{\nu}_k]^{1/2}$ for $n = m+1$ and $[hm/8\pi^2 c\tilde{\nu}_k]^{1/2}$ for $n = m-1$. It follows that the second term in Equation (7) is responsible for both the Stokes and the anti-Stokes Raman scattering for vibrational fundamentals. The third term gives rise to first overtones ($k = k'$) and binary combination tones ($k \neq k'$), but is usually so small that bands so attributed are very weak in normal Raman scattering. It is obvious that the magnitude of $[\alpha_{\rho\sigma}]_{gn,gm}$ is unaffected by transposition of the coordinate suffixes ρ and σ. Hence the transition polarizability tensor is symmetric about the leading diagonal and has only six independent components. It may be regarded essentially as a ground state property of the system.

2.2. Resonance Raman Scattering

In the usual treatment of RR scattering the adiabatic Born-Oppenheimer approximation is assumed to be valid, but the other assumptions associated with normal Raman scattering are assumed no longer to apply. That is to say:

(1) The v-dependence of the denominators in Equation (4) cannot be neglected, so that the closure theorem may not be invoked;
(2) the wave-number difference $(\tilde{\nu}_{ev,gm} - \tilde{\nu}_0)$ is comparable with the damping factor, $i\Gamma_{ev}$, so that the latter may not be neglected;
(3) the first-order term $\partial[\mu_\rho]_{ge}/\partial Q_k = [\mu_\rho]'_{ge}$ in the Taylor expansion of Equation (5) needs to be defined explicitly.

In the Herzberg-Teller[41] perturbation description of vibronic coupling the derivative of the transition moment arises because the variation in the Hamiltonian with respect to the normal coordinate Q_k can mix the state $|e\rangle$ with other states $|s\rangle$ of the appropriate symmetry, viz.

$$[\mu_\rho]_{ge} = [\mu_\rho]^0_{ge} + \sum_s \sum_k [\mu_\rho]^0_{gs} \frac{h^k_{es}}{\Delta\tilde{\nu}_{es}} Q_k + \cdots \tag{8}$$

$$h^k_{es} = \langle e|\partial H/\partial Q_k|s\rangle_{Q_k=0}$$

where $|s\rangle$ represents another excited state. As before, higher order terms are generally negligible.

The term $h^k_{es}/\Delta\tilde{\nu}_{es}$ is a measure of the strength of vibronic coupling of the states $|e\rangle$ and $|s\rangle$ via the normal coordinate Q_k. The Herzberg-Teller expansion is only valid for weak vibronic coupling, i.e. within the framework of the adiabatic Born-Oppenheimer approximation. It is not applicable to cases in which there is strong vibronic coupling, i.e. when $\Delta\tilde{\nu}_{es}$ is of the order of vibrational wave numbers (in which case non-adiabatic coupling is important) or zero (such as for a degenerate state, in which Jahn-Teller (JT) coupling occurs).

Some considerable simplification of the transition polarizability is made possible for excitation under resonance conditions. This is because, as $\tilde{\nu}_0$ approaches some particular transition wave number $\tilde{\nu}_{ev,gm}$, the relevant excited state will dominate the sum over states. It is therefore generally sufficient to consider only one, or at most, two electronic manifolds. Also, the non-resonant part of the transition polarizability may be neglected at resonance. Applying these considerations to Equation (4) it is evident that there are now four contributions (the so-called A, B, C, and D-terms) to the transition polarizability, viz.

$$[\alpha_{\rho\sigma}]_{gn,gm} = A + B + C + D \tag{9}$$

where

$$A = \frac{1}{hc}[\mu_\rho]^0_{ge}[\mu_\sigma]^0_{eg} \sum_v \frac{\langle n_g|v_e\rangle\langle v_e|m_g\rangle}{\tilde{\nu}_{ev,gm} - \tilde{\nu}_0 + i\Gamma_{ev}} \tag{10}$$

$$B = \frac{1}{h^2c^2} \sum_{s\neq e} [\mu_\rho]^0_{gs}[\mu_\sigma]^0_{eg} \frac{h^k_{se}}{\Delta\tilde{\nu}_{se}} \sum_v \frac{\langle n_g|Q_k|v_e\rangle\langle v_e|m_g\rangle}{\tilde{\nu}_{ev,gm} - \tilde{\nu}_0 + i\Gamma_{ev}} + \frac{1}{h^2c^2} \sum_{s\neq e} [\mu_\rho]^0_{ge}[\mu_\sigma]^0_{sg} \frac{h^k_{es}}{\Delta\tilde{\nu}_{es}} \sum_v \frac{\langle n_g|v_e\rangle\langle v_e|Q_k|m_g\rangle}{\tilde{\nu}_{eg,gm} - \tilde{\nu}_0 + i\Gamma_{ev}} \tag{11}$$

$$C = \frac{1}{h^2c^2} \sum_{s\neq g} [\mu_\rho]^0_{se}[\mu_\sigma]^0_{eg} \frac{h^k_{gs}}{\Delta\tilde{\nu}_{gs}} \sum_v \frac{\langle n_g|Q_k|v_e\rangle\langle v_e|m_g\rangle}{\tilde{\nu}_{ev,gm} - \tilde{\nu}_0 + i\Gamma_{ev}} + \frac{1}{h^2c^2} \sum_{s\neq g} [\mu_\rho]^0_{ge}[\mu_\sigma]^0_{es} \frac{h^k_{sg}}{\Delta\tilde{\nu}_{sg}} \sum_v \frac{\langle n_g|v_e\rangle\langle v_e|Q_k|m_g\rangle}{\tilde{\nu}_{ev,gm} - \tilde{\nu}_0 + i\Gamma_{ev}} \tag{12}$$

$$D = \frac{1}{h^3c^3} \sum_{s,s'\neq e} [\mu_\rho]^0_{gs}[\mu_\sigma]^0_{s'g} \frac{h^k_{es}h^{k'}_{es'}}{\Delta\tilde{\nu}_{es}\Delta\tilde{\nu}_{es'}} \sum_v \frac{\langle n_g|Q_k|v_e\rangle\langle v_e|Q_{k'}|m_g\rangle}{\tilde{\nu}_{ev,gm} - \tilde{\nu}_0 + i\Gamma_{ev}} \tag{13}$$

In these equations the vibrational quantum numbers n, v and m have been subscripted to indicate the electronic state to which they refer, all other terms having been defined previously. We now look closely at each of these four contributions.

2.2.1. *A-term Resonance Raman Scattering*

For the A-term contribution to the transition polarizability to be non-zero it is necessary that the following two conditions are fulfilled:

(1) The transition dipole moments $[\mu_\rho]^0_{ge}$ and $[\mu_\sigma]^0_{eg}$ must be non-zero;
(2) The products of vibrational overlap integrals (Franck-Condon factors), $\langle n_g|v_e\rangle\langle v_e|m_g\rangle$, must be non-zero for at least some values of v.

The first of these two conditions dictates that the resonant electronic transition should be electric-dipole-allowed. Thus the technique requires excitation within the contour of an intense absorption band, such as one of charge transfer (CT) or π-π^* type. Excitation within the contour of a weak band, e.g. one resulting from a ligand-field or spin-forbidden transition, would not be expected to produce a significant A-term. The restrictions imposed by the second condition are less obvious and therefore warrant a more detailed discussion.

Vibrational overlap integrals of the type $\langle n_g|v_e\rangle$ are zero (except for the case $n = v$) unless the vibrational wave functions χ_n and χ_v are non-orthogonal. For any one vibrational mode ν_k of a molecule non-orthogonality of these wave functions will subsist if, between the ground state and excited states, there is either (a) a difference of vibrational wave number ($\tilde{\nu}^e_k \neq \tilde{\nu}^g_k$), i.e. a change in shape of the

potential energy surface, or (b) a displacement of the potential energy minimum along the normal coordinate, ΔQ_k. Symmetry arguments dictate that such a displacement may only occur for totally symmetric modes unless the molecular symmetry is altered in the excited state. If the molecular symmetry is the same in the ground and excited states, then geometric changes are confined to combinations of alterations in bond lengths and bond angles that, overall, do not change the molecular symmetry. Thus, the geometric changes are confined to those along totally symmetric symmetry coordinates which, of course, relate only to displacements along totally symmetric normal coordinates. However, if a change of molecular symmetry accompanies the electronic transition, this restriction no longer applies. The term totally symmetric then applies not to the ground state point group but to the subgroup formed by the operations that are common to both the ground- and excited-state point groups (the common group).

As shown in Figure 1, four cases (a)—(d) may be distinguished: It is obvious that in case (a) the orthogonality of the wave functions would not be removed and in such a situation there would be no A-term for any vibrational mode. Case (b) produces non-zero overlap integrals for both totally and non-totally symmetric modes, whereas cases (c) and (d) only apply to totally symmetric modes. In practice it is found that a significant change of vibrational wave number usually occurs only where there is a displacement of the potential energy minimum, hence case (d) is the most important. Dependent on the magnitude of ΔQ, the Franck-Condon factors, $\langle n_g|v_e\rangle\langle v_e|m_g\rangle$, may have appreciable size for up to several quanta of n. Thus the A-term can give rise to overtones of intensity comparable to that of the fundamental.

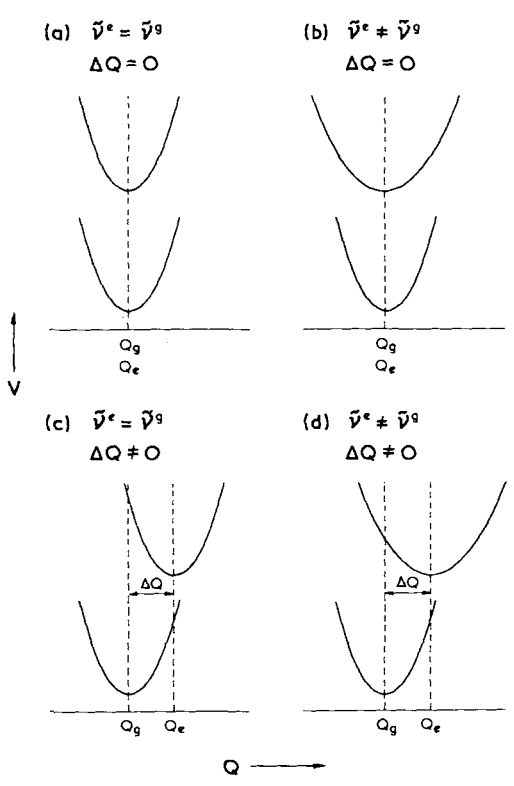


Fig. 1. Potential energy diagrams for the ground and resonant excited states, showing the four cases (a)—(d) (see text).

2.2.2. B-Term Resonance Raman Scattering

The B-term contribution to the transition polarizability arises from the vibronic coupling of the resonant state to other excited states. Its magnitude is dependent on the vibronic coupling integral h^k_{es}, on the products of vibrational transition integrals and overlap integrals, e.g. $\langle n_g|Q_k|v_e\rangle\langle v_e|m_g\rangle$, on the transition dipole moments $[\mu_\rho]^0_{ge}$ and $[\mu_\sigma]^0_{sg}$, and on the energy difference between the coupled states, $hc(\tilde{\nu}_s - \tilde{\nu}_e)$. For the B-term to be non-zero it is a requirement that both the resonant transition and the transition $|s\rangle \leftarrow |g\rangle$ should be electric-dipole-allowed. Because of the additional factor $h^k_{es}(\nu_s - \nu_e)^{-1}$ in the equation, the B-term is usually very much smaller than the A-term. However, if the resonant transition gives rise to zero or very small displacements ΔQ_k, then only the diagonal overlap integrals (i.e. $n = v$, $v = m$) are non-vanishing and the A-term becomes zero. In the harmonic oscillator approximation $\langle n_g|Q_k|v_e\rangle$ and $\langle v_e|Q_k|m_g\rangle$ are non-zero for $n = v \pm 1$ and $v = m \pm 1$. Thus, under the conditions for which the B-term is of importance (diagonal overlap integrals) the products $\langle n_g|Q_k|v_e\rangle\langle v_e|m_g\rangle$ and $\langle n_g|v_e\rangle\langle v_e|Q_k|m_g\rangle$ are restricted to the cases where $n = m \pm 1$ and, in the low temperature limit ($m = 0$), only two such products would contribute, viz. $\langle 1_g|Q_k|0_e\rangle\langle 0_e|0_g\rangle$ and $\langle 1_g|1_e\rangle\langle 1_e|Q_k|0_g\rangle$. It is usually the case that coupling to only one other state $|s\rangle$ needs to be considered and the summation may be dropped, giving the following expression for the B-term:

$$B = \frac{1}{h^2c^2}[\mu_\rho]^0_{gs}[\mu_\sigma]^0_{eg}\frac{h^k_{se}}{\Delta\tilde{\nu}_{se}}\left(\frac{\langle 1_g|Q_k|0_e\rangle\langle 0_e|0_g\rangle}{\tilde{\nu}_{e0,g0} - \tilde{\nu}_0 + i\Gamma_{e0}}\right) + \frac{1}{h^2c^2}[\mu_\rho]^0_{ge}[\mu_\sigma]^0_{sg}\frac{h^k_{es}}{\Delta\tilde{\nu}_{es}}\left(\frac{\langle 1_g|1_e\rangle\langle 1_e|Q_k|0_g\rangle}{\tilde{\nu}_{e1,g0} - \tilde{\nu}_0 + i\Gamma_{e1}}\right) \quad (14)$$

Clearly, B-term scattering occurs only for fundamentals ($n = 1$) and the symmetry selection rules are constrained by the symmetries of the states $|e\rangle$ and $|s\rangle$. The vibronic coupling integral h^k_{es} is non-zero if the irreducible representation of Q_k (i.e. Γ_k) is contained in the direct product $\Gamma_e \otimes \Gamma_s$. It follows that B-term activity may be expected for both totally symmetric and non-totally symmetric vibrations, but for the former to be realized it is necessary that $|e\rangle$ and $|s\rangle$ have the same symmetry.

2.2.3. C- and D-Term Resonance Raman Scattering

The C-term differs from the B-term in that the ground state, rather than the resonant excited state, is vibronically coupled to other excited states. It is normally assumed that the C-term is negligibly small, due to the large energy separation between the ground state and excited states. To our knowledge no experimental evidence for C-term scattering has yet been presented.

The D-term is also very much smaller than the B-term. It may give rise to first overtones ($k = k'$) and binary combination tones ($k \neq k'$) of both totally symmetric and non-totally symmetric modes. The observation of weak overtones and binary combination tones in the RR spectra of some metalloporphyrin species has been ascribed to D-term scattering (see Sections 2.4 and 5.4).

2.3. Resonance Raman Scattering Involving Totally Symmetric Modes

Raman bands attributed to totally symmetric fundamentals may acquire intensity under resonance conditions from either the A- or B-terms of the transition polarizability. It is generally the case, however, that only the A-term contribution is important, for the reasons mentioned in Section 2.2. In this section we discuss in detail the properties of A- and B-term RR scattering for totally symmetric fundamentals and their overtones. To begin with we consider the simplest case of a species possessing only one totally symmetric mode (such as diatomic, tetrahedral or square planar (MX_4), or octahedral (MX_6) molecules), in which case only diagonal components of the transition polarizability, $[\alpha_{\rho\rho}]_{gn,gm}$, are non-zero. If it is further assumed that (a) only a single resonant excited state $|e\rangle$ makes a significant contribution, and (b) all molecules are initially in the $m=0$ vibrational level of the ground electronic state (low temperature limit) then

$$[\alpha_{\rho\rho}]_{gn,g0} = \frac{1}{hc}\,|[\mu_\rho]^0_{ge}|^2 \sum_v \frac{\langle n_g|v_e\rangle\langle v_e|0_g\rangle}{\tilde{\nu}_{ev,g0}-\tilde{\nu}_0+i\Gamma_{ev}} \tag{15}$$

For a system with only one totally symmetric normal coordinate, Q_1, the vibrational overlap integrals are one-dimensional. Assuming harmonic potentials for the states $|g\rangle$ and $|e\rangle$, the overlap integrals may be calculated using the recurrence formulas derived by *Manneback*:[42]

$$\langle 0_e|0_g\rangle = \left(\frac{2(\tilde{\nu}^e_1\tilde{\nu}^g_1)^{1/2}}{\tilde{\nu}^e_1+\tilde{\nu}^g_1}\right)^{1/2} \exp\left(\frac{-\Delta^2}{2}\right) \tag{16a}$$

$$\begin{aligned}\langle n_g|v_e+1\rangle = &-\left(\frac{v}{v+1}\right)^{1/2}\left(\frac{\tilde{\nu}^g_1-\tilde{\nu}^e_1}{\tilde{\nu}^g_1+\tilde{\nu}^e_1}\right)\langle n_g|v_e-1\rangle\\ &+\left(\frac{n}{v+1}\right)^{1/2}\frac{2(\tilde{\nu}^e_1\tilde{\nu}^g_1)^{1/2}}{\tilde{\nu}^e_1+\tilde{\nu}^g_1}\langle n_g-1|v_e\rangle\\ &-\left(\frac{1}{v+1}\right)^{1/2}\Delta\left(\frac{2\nu^g_1}{\tilde{\nu}^g_1+\tilde{\nu}^e_1}\right)^{1/2}\langle n_g|v_e\rangle\end{aligned} \tag{16b}$$

$$\begin{aligned}\langle n_g+1|v_e\rangle = &\left(\frac{n}{n+1}\right)^{1/2}\left(\frac{\tilde{\nu}^g_1-\tilde{\nu}^e_1}{\tilde{\nu}^g_1+\tilde{\nu}^e_1}\right)\langle n_g-1|v_e\rangle\\ &+\left(\frac{v}{n+1}\right)^{1/2}\frac{2(\tilde{\nu}^e_1\tilde{\nu}^g_1)^{1/2}}{\tilde{\nu}^e_1+\tilde{\nu}^g_1}\langle n_g|v_e-1\rangle\\ &+\left(\frac{1}{n+1}\right)^{1/2}\Delta\left(\frac{2\tilde{\nu}^g_1}{\tilde{\nu}^g_1+\tilde{\nu}^e_1}\right)^{1/2}\langle n_g|v_e\rangle\end{aligned} \tag{16c}$$

where the dimensionless shift parameter Δ is given by

$$\Delta = \left(\frac{4\pi^2 c}{h}\right)^{1/2}\Delta Q_1\left(\frac{\tilde{\nu}^e_1\tilde{\nu}^g_1}{\tilde{\nu}^e_1+\tilde{\nu}^g_1}\right)^{1/2} \tag{16d}$$

The displacement, ΔQ_1, of the excited-state potential minimum is related to the displacement along the symmetry coordinate ΔS_1 by the equation

$$\Delta Q_1 = \mu^{1/2}\Delta S_1 \tag{17}$$

where μ is the reduced mass associated with the vibration. Expressions for ΔQ_1 in terms of Δr for a number of common molecular geometries are summarized in Table 1.

Table 1. Relationship between ΔQ_1 and Δr for various molecular geometries.

$\Delta Q_1 = \mu^{1/2}\Delta S_1$

Molecular type	Point group	μ	ΔS_1	ΔQ_1
XY	$C_{\infty v}$	$\frac{m_x m_y}{m_x+m_y}$	Δr	$\left[\frac{m_x m_y}{m_x+m_y}\right]^{1/2}\Delta r$
X_2	$D_{\infty h}$	$m_x/2$	Δr	$(m_x/2)^{1/2}\Delta r$
MX_2, X_3	$D_{\infty h}$	m_x	$\frac{1}{\sqrt{2}}(\Delta r_1+\Delta r_2)$	$(2m_x)^{1/2}\Delta r$
MX_3, X_3, X_4	D_{3h}	m_x	$\frac{1}{\sqrt{3}}(\Delta r_1+\Delta r_2+\Delta r_3)$	$(3m_x)^{1/2}\Delta r$
MX_4, X_4	D_{4h}, T_d	m_x	$\frac{1}{2}(\Delta r_1+\Delta r_2+\Delta r_3+\Delta r_4)$	$2(m_x)^{1/2}\Delta r$
MX_6, X_6	O_h	m_x	$\frac{1}{\sqrt{6}}(\Delta r_1+\Delta r_2+\Delta r_3+\Delta r_4+\Delta r_5+\Delta r_6)$	$(6m_x)^{1/2}\Delta r$

The Franck-Condon overlap integrals may possess appreciable magnitudes for up to several quanta of n if ΔQ_1 is sufficiently large, in which case several overtones of ν_1 may appear in the RR spectrum. The intensity distribution within such an overtone progression depends on the magnitude of ΔQ (and hence on the bond length change Δr) and, in general, the larger the displacement the greater is the extent of the progression. Thus, excitation resonant with charge-transfer or π-π^* transitions of small molecules typically produces RR spectra that are characterized by an intense overtone progression $v_1 \nu_1$.

Substitution of Equation (15) into Equation (1) and expansion of the square modulus of $[\alpha_{\rho\rho}]_{gn,g0}$ gives the following expression for Stokes A-term RR intensities:

$$\begin{aligned}I_{gn,g0}(\pi/2) = &K(\tilde{\nu}_0-\tilde{\nu}_{gn,g0})^4\,|[\mu_\rho]^0_{ge}|^4\\ &\times\sum_v\sum_{v'}\frac{\langle n_g|v_e\rangle\langle v_e|0_g\rangle\langle n_g|v'_e\rangle\langle v'_e|0_g\rangle[\varepsilon_v\varepsilon_{v'}+\Gamma_v\Gamma_{v'}]}{(\varepsilon_v^2+\Gamma_v^2)(\varepsilon_{v'}^2+\Gamma_{v'}^2)}\end{aligned} \tag{18}$$

where $\varepsilon_v = \tilde{\nu}_{ev,g0}-\tilde{\nu}_0$ and K incorporates all of the constants appearing in Equations (1) and (15). From this expression it is possible to calculate the variation of the intensities of the fundamental and overtone bands throughout the region of the resonant absorption band. Such a plot, which is called an excitation profile (EP), differs markedly from the absorption spectrum if the vibrational fine structure of the latter is resolved (small Γ). Whereas absorption profiles are simply given by the superposition (i.e. sum) of the individual vibronic bands, the double summation in Equation (18) involves cross-terms ($v \neq v'$) which produce interference between the contributions from different vibronic states. These interference effects may result in an increase or decrease in scattered intensity compared with that arising solely from the sum of the individual resonances ($v=v'$). However, when Γ is large these interferences are not apparent and both the excitation profiles and the absorption spectrum are smooth and devoid of fine structure. The maxima of the excitation profiles are then blue-shifted for successive overtones, the differ-

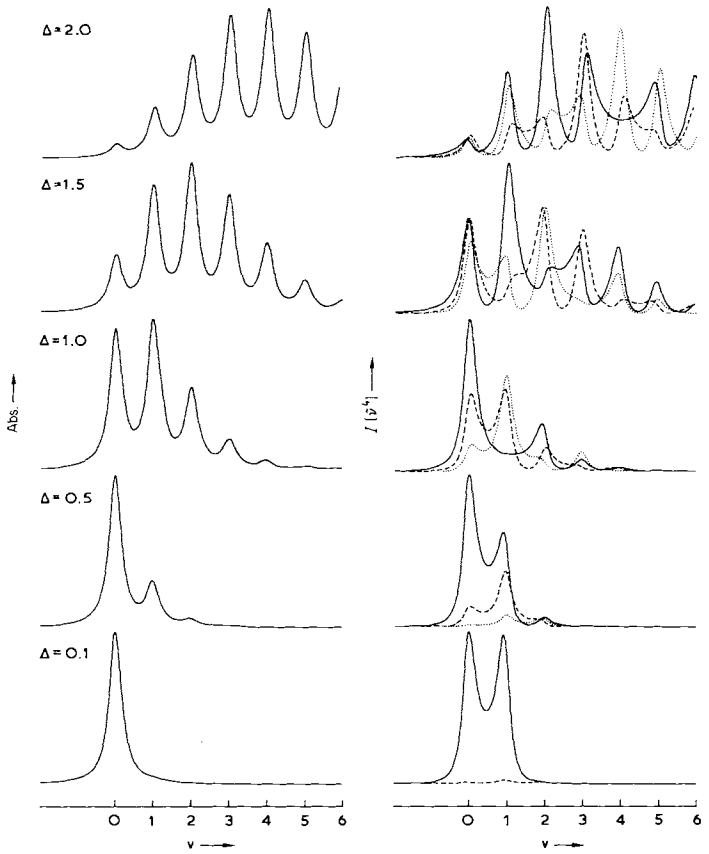


Fig. 2. Left, Absorption spectra, and right, resonance Raman excitation profiles (ν_1 (——), $2\nu_1$ (---) and $3\nu_1$ (····) bands) for different values of the shift parameter Δ; $\tilde{\nu}^e = \tilde{\nu}^g$ and $\Gamma = 0.2\,\tilde{\nu}^e$ (abscissa is expressed in terms of excited-state vibrational quanta v). Abs = Absorption, I = Raman intensity.

ence in peak position being approximately equal to the vibrational wave number of the excited state.

In Figure 2 is shown the effect of the displacement parameter Δ on Raman intensities. For simplicity a model system has been chosen in which $\tilde{\nu}^e = \tilde{\nu}^g$ and $\Gamma = 0.2\,\tilde{\nu}^e$ and the EPs are displayed for ν_1, $2\nu_1$ and $3\nu_1$ for several values of Δ. These profiles clearly demonstrate the above-mentioned interference effects and it is evident that EPs are more sensitive to variation in Δ than are absorption bands. It is readily seen that, as Δ increases, the EP maximum is shifted to higher wave number and that the intensities of overtones increase with respect to that of the fundamental, becoming the more intense in some regions.

By fitting calculated excitation profiles to experimental data the parameters Δ and Γ may be extracted. Thus, the technique provides a sensitive method for the determination of excited state geometries and lifetimes and several results of such calculations are discussed in later sections. It is, however, important to appreciate that lifetime, i.e. homogeneous, broadening is not the only contribution to bandwidths and that the influence of inhomogeneous broadening must also be taken into account. Inhomogeneous broadening is due to the variation of molecular environment (i.e. molecules occupying different sites) and the "spread" of electronic energies resulting from it is described by a Gaussian or Lorentzian distribution about the mean value. Although a Gaussian distribution would normally be the correct description of inhomogeneous broadening, the influence of the band shape is not very great and a Lorentzian function is usually chosen for simplicity.[43,44] The inhomogeneous band shape is then given by

$$\mathscr{S}(\tilde{\nu}) = \frac{\gamma}{[\langle\tilde{\nu}_{e0}\rangle - \tilde{\nu}_{e0}]^2 + \gamma^2} \tag{19}$$

where γ is the inhomogeneous bandwidth (half width at half maximum) and $\langle\tilde{\nu}_{e0}\rangle$ is the average value of the electronic transition wave number. The effect of inhomogeneous broadening on the transition polarizability is taken into account by convolution with the above band-shape function, integrating over all possible values of $\tilde{\nu}_{e0}$:

$$[\alpha_{\rho\rho}]_{gn,g0} = \frac{1}{hc}\,|[\mu_\rho]^0_{ge}|^2 \int_{-\infty}^{\infty} \left(\sum_v \frac{\langle n_g|v_e\rangle\langle v_e|0_g\rangle}{\tilde{\nu}_{ev,g0} - \tilde{\nu}_0 + i\Gamma_{ev}}\right) \mathscr{S}(\tilde{\nu})\cdot d\tilde{\nu}_{e0} \tag{20}$$

Such integrals have been evaluated by *Siebrand* et al.,[43,44] and the following expression is obtained for the Raman intensity:

$$I_{gn,g0}(\pi/2) = K(\tilde{\nu}_0 - \tilde{\nu}_{gn,g0})^4 |[\mu_\rho]^0_{ge}|^4 \sum_v \sum_{v'} \langle n_g|v_e\rangle\langle v_e|0_g\rangle\langle n_g|v'_e\rangle\langle v'_e|0_g\rangle \times \left(\frac{[(\varepsilon_v - \varepsilon_{v'})^2 + 4\Gamma\Sigma][\varepsilon_v\varepsilon_{v'} + \Sigma^2] - 2(\varepsilon_v - \varepsilon_{v'})\gamma\Sigma}{[\varepsilon_v^2 + \Sigma^2][\varepsilon_{v'}^2 + \Sigma^2][(\varepsilon_v - \varepsilon_{v'})^2 + 4\Gamma^2]}\right) \tag{21}$$

where $\Sigma = \Gamma + \gamma$.

In most cases Γ is small, rarely exceeding about $0.5\,\tilde{\nu}^e_1$, but γ may range from zero (putting $\gamma = 0$ in Equation (21) yields Equation (18)) to a few thousand cm^{-1}. Where excitation profiles are broad and unresolved, γ is the dominant bandwidth contribution. Homogeneous broadening and inhomogeneous broadening have markedly different effects on the excitation profiles, as illustrated in Figure 3.

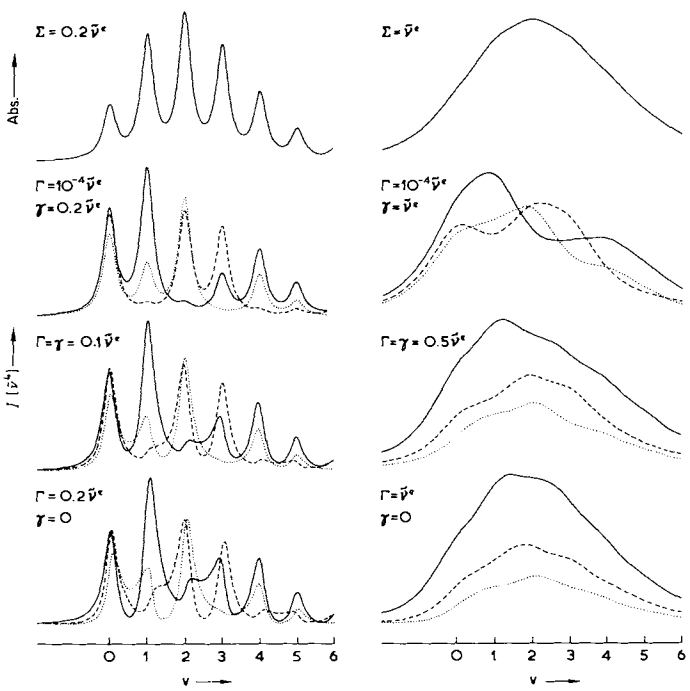


Fig. 3. Top, Absorption spectra, and bottom, resonance Raman excitation profiles (ν_1 (——), $2\nu_1$ (---) and $3\nu_1$ (····) bands) for $\tilde{\nu}^e = \tilde{\nu}^g$, $\Delta = 1.5$ and $\Sigma = 0.2\,\tilde{\nu}^e$ or $\tilde{\nu}^e$ (abscissa expressed in terms of excited-state vibrational quanta, v). The excitation profiles are given for $\Gamma/\gamma = \infty$, 1 and ca. 0 (Γ may not be equated to zero because the excitation profile is then indeterminate). Abs = Absorption, I = Raman intensity.

The principal differences are that (a) γ plays no part in the aforementioned interference phenomena, and (b) increasing the Γ contribution (maintaining constant Σ) decreases the intensity of overtones relative to that of the fundamental. By measuring EPs of molecules in different environments (i.e. different solvents or host lattices) it is possible to determine Γ, and hence the excited-state lifetime, since this is largely independent of molecular environment. This information cannot be obtained from absorption spectra because these are insensitive to variation in the relative contributions of Γ and γ, the bandwidths being given by the sum Σ.

So far the treatment has been restricted to molecules with only one totally symmetric mode and for which only one excited state contributes to the transition polarizability. This latter assumption is not justified when two or more (N) excited states are in close proximity to one another, and the transition polarizability must then include the sum of contributions from each state, viz.

$$[\alpha_{\rho\rho}]_{gn,g0} = \frac{1}{hc}\sum_{i=1}^{N}|[\mu_\rho]^0_{ge_i}|^2\sum_{v_i}\frac{\langle n_g|v_{e_i}\rangle\langle v_{e_i}|0_g\rangle}{\tilde{\nu}_{e_iv}-\tilde{\nu}_0+i\Gamma_{e_iv}} \tag{22}$$

The Raman intensity is given by

$$I_{gn,g0}(\pi/2) = K(\tilde{\nu}_0-\tilde{\nu}_{gn,g0})^4\sum_{i=1}^{N}\sum_{i'=1}^{N}|[\mu_\rho]^0_{ge_i}|^2|[\mu_\rho]^0_{ge_{i'}}|^2 \times \sum_{v}\sum_{v'}\langle n_g|v_{e_i}\rangle\langle v_{e_i}|0_g\rangle\langle n_g|v'_{e_{i'}}\rangle\langle v'_{e_{i'}}|0_g\rangle$$
$$\times\left(\frac{[(\varepsilon^i_v-\varepsilon^{i'}_{v'})^2+(\Gamma_i+\Gamma_{i'})(\Sigma_i+\Sigma_{i'})][\varepsilon^i_v\varepsilon^{i'}_{v'}+\Sigma_i\Sigma_{i'}]-\frac{1}{2}(\varepsilon^i_v-\varepsilon^{i'}_{v'})(\gamma_i+\gamma_{i'})(\Sigma_i+\Sigma_{i'})}{[(\varepsilon^i_v)^2+\Sigma_i^2][(\varepsilon^{i'}_{v'})^2+\Sigma_{i'}^2][(\varepsilon^i_v-\varepsilon^{i'}_{v'})^2+(\Gamma_i+\Gamma_{i'})^2]}\right) \tag{23}$$

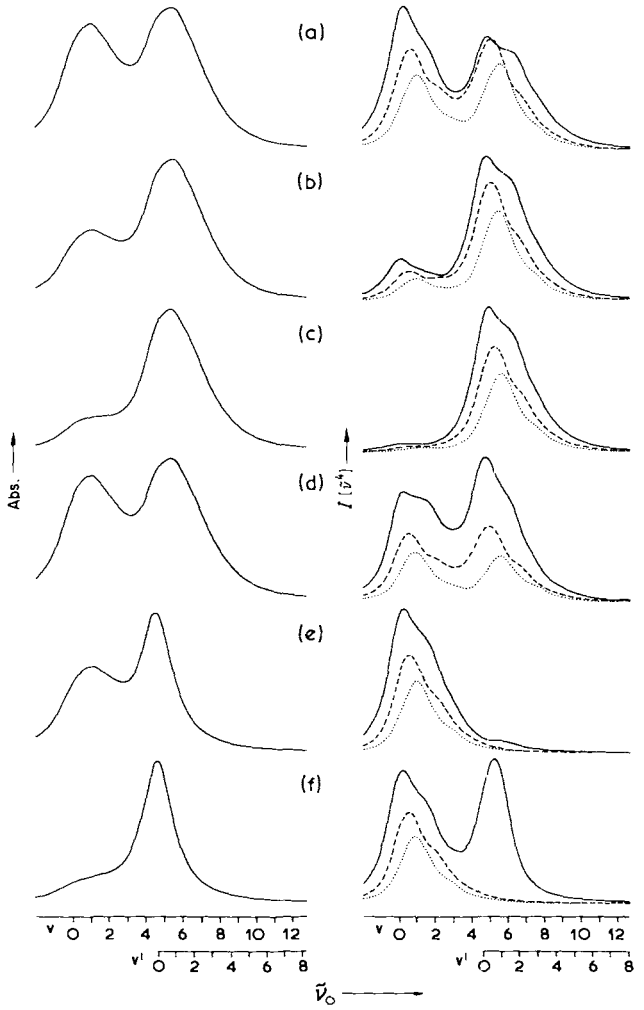


Fig. 4. Absorption spectra and resonance Raman excitation profiles (ν_1 (——), $2\nu_1$ (– – –), and $3\nu_1$ (· · · ·) bands) for a selection of different examples in which two electronic transitions, $|e_1\rangle\leftarrow|g\rangle$ and $|e_2\rangle\leftarrow|g\rangle$, contribute. (a) $R_{12}=1$, $\Delta_1=\Delta_2=1.5$; (b) $R_{12}=2$, $\Delta_1=\Delta_2=1.5$; (c) $R_{12}=5$, $\Delta_1=\Delta_2=1.5$; (d) $R_{12}=1$, $\Delta_1=1.5$, $\Delta_2=-1.5$; (e) $R_{12}=1$, $\Delta_1=1.5$, $\Delta_2=0.1$; (f) $R_{12}=5$, $\Delta_1=1.5$, $\Delta_2=0.1$. $R_{12}=|[\mu_\rho]^0_{ge_2}/[\mu_\rho]^0_{ge_1}|^2$; Δ_1 and Δ_2 are the displacement parameters for the two transitions. The abscissa is expressed in terms of vibrational quanta of the excited states $|e_1\rangle$ (v) and $|e_2\rangle$ (v'), where $\tilde{\nu}^{e_1}=\tilde{\nu}^{e_2}$. Other parameters used in the calculation are $\Delta\nu_{e_2e_1}=4.3\,\tilde{\nu}^{e_1}$ and $\Gamma=\gamma=0.5\,\tilde{\nu}^{e_1}$. The observed interference effects are diminished when Γ and γ are made smaller.

In addition to the interferences between vibronic contributions of the same state there are also interferences between the contributions from different states; these arise from the sign differences of ε^i_v values at certain positions and will also occur if Δ is positive for one state but negative for a second. Some examples of interference effects are shown in Figure 4.

The extension of the theory to molecules with several totally symmetric modes is straightforward if it may be assumed that the normal coordinates of the excited state are identical to those of the ground state. The multi-dimensional overlap integrals $\langle\bar{n}_g|\bar{v}_e\rangle$ may then be expressed as products of one-dimensional ones:

$$\langle\bar{n}_g|\bar{v}_e\rangle = \langle(n_1\,n_2\,n_3\ldots n_N)_g|(v_1\,v_2\,v_3\ldots v_N)_e\rangle = \prod_{i=1}^{N}\langle n_{ig}|v_{ie}\rangle \tag{24}$$

Substitution of these products into either Equation (18) (one-state) or Equation (23) (multi-state) enables excitation profiles to be calculated. By fitting these to experimental data, values for ΔQ_1, ΔQ_2, etc., can be deduced, i.e. the displacement of the excited-state potential minimum along each of the totally symmetric normal coordinates. The relationship between these displacements and the geometric changes attendant upon electronic excitation (bond-length and bond-angle changes) is less straightforward than in the single-mode case. Internal coordinates are related to normal coordinates by the matrix equation

$$\mathbf{R} = \mathbf{L}\mathbf{Q} \tag{25}$$

where $\mathbf{R}$ is a column matrix comprising the $3N-6$ internal coordinates, $\mathbf{Q}$ is a column matrix of the $3N-6$ normal coordinates, and $\mathbf{L}$ is a square matrix effecting the transformation from normal to internal coordinates; it is obtained by solution of the vibrational secular equation. For the states $|g\rangle$ and $|e\rangle$ we may write

$$\mathbf{R}_g = \mathbf{L}_g\mathbf{Q}_g \qquad \mathbf{R}_e = \mathbf{L}_e\mathbf{Q}_e \tag{26}$$

$$\mathbf{R}_e - \mathbf{R}_g = \mathbf{L}_e\mathbf{Q}_e - \mathbf{L}_g\mathbf{Q}_g \tag{27}$$

By making the assumption that the **L** matrix is unchanged in the excited state (which is necessary in the absence of a detailed knowledge of the excited-state vibrations), it follows that

$$\mathbf{R}_e - \mathbf{R}_g = \mathbf{L}(\mathbf{Q}_e - \mathbf{Q}_g)$$
$$\text{or } \Delta\mathbf{R} = \mathbf{L}\Delta\mathbf{Q} \tag{28}$$

where $\Delta\mathbf{R}$ is a column matrix of the internal coordinate changes and $\Delta\mathbf{Q}$ is a column matrix of the normal coordinate displacements. We may take advantage of molecular symmetry by recasting this equation in the form

$$\Delta\mathbf{R} = \tilde{\mathbf{U}}\,\mathscr{L}\,\Delta\mathbf{Q} \tag{29}$$

where $\tilde{\mathbf{U}}$ is the transpose of the matrix relating internal coordinates to symmetry coordinates and $\mathscr{L}$ is the symmetrized version of the **L** matrix. The $\mathscr{L}$ matrix factorizes into a block diagonal form and only the block involving totally symmetric coordinates needs to be considered.

RR spectra of molecules possessing more than one totally symmetric mode may display overtone progressions for each of the active vibrations, i.e. those for which there are normal coordinate displacements. Additionally there may also be combination band progressions involving quanta of more than one mode. In general it is true that the most displaced coordinate will give rise to the greatest intensity enhancement and the longest overtone progression. On this basis it is still possible to make a qualitative assessment of the excited-state geometry from RR data when detailed calculations cannot be performed.

A special case of the A-term scattering regime exists when each of the displacements, ΔQ, is very small but non-zero.[38] In this situation it can be seen from Equations (16) that, assuming $\tilde{\nu}_i^e = \tilde{\nu}_i^g$, the overlap integrals have the values

$$\langle 1_g|1_e\rangle = \langle 0_g|0_e\rangle = 1$$
$$\langle 1_g|0_e\rangle = -\langle 0_g|1_e\rangle = -\Delta$$

Integrals in which either n or v has a value of 2 or more and $n \neq v$ may be approximated to zero because they involve higher powers of Δ ($\Delta \ll 1$ and so $\Delta^2 \ll \Delta$). The summation over the levels v is therefore restricted to the $v=0$ and $v=1$ contributions, and Franck-Condon factors will be non-zero only for $n=0$ (Rayleigh scattering) and $n=1$ (fundamental Raman scattering). Thus, in the small displacement approximation, overtones are forbidden.

The multi-dimensional Franck-Condon factors may be expressed in the following form:

$$\langle \bar{n}_g|\bar{v}_e\rangle\langle \bar{v}_e|\bar{0}_g\rangle = \langle 1_{ag}|0_{ae}\rangle\langle 0_{ae}|0_{ag}\rangle \prod_{i=1}^{m-1} \langle 0_{ig}|v_{ie}\rangle^2$$
$$\text{or } \langle 1_{ag}|1_{ae}\rangle\langle 1_{ae}|0_{ag}\rangle \prod_{i=1}^{m-1} \langle 0_{ig}|v_{ie}\rangle^2 \tag{30}$$

Within the framework of the small-displacement approximation the product has the value unity, allowing each vibrational mode to be treated as an independent oscillator.

The excitation profile for the ath fundamental is then given by

$$I_{g1_a,g0} = K(\tilde{\nu}_0 - \tilde{\nu}_{g1_a,g0})^4 |[\mu_\rho]^0_{ge}|^4 \times \Delta_a^2 \frac{\left\{\frac{\Sigma}{\Gamma}[\varepsilon_0^2+\varepsilon_1^2+2\Sigma^2][(\varepsilon_1-\varepsilon_0)^2+4\Gamma^2]-2[\varepsilon_0\varepsilon_1+\Sigma^2][(\varepsilon_0-\varepsilon_1)^2+4\Gamma\Sigma]\right\}}{(\varepsilon_0^2+\Sigma^2)(\varepsilon_1^2+\Sigma^2)[(\varepsilon_0-\varepsilon_1)^2+4\Gamma^2]} \tag{31}$$

where Δ_a is the displacement parameter for the ath totally symmetric mode, the wave number of which is $\tilde{\nu}_a$. Although it is not possible to determine absolute values for the displacement parameters in this approximation, the relative magnitudes (but not signs) may be deduced from the relative intensities of the RR bands. Taking account of molecules initially in $m>0$ vibrational levels, the relative displacements can be calculated from

$$\frac{|\Delta_a|}{|\Delta_b|} = \left\{\frac{I_{g1_a,g0}}{I_{g1_b,g0}}\left(\frac{\tilde{\nu}_0-\tilde{\nu}_b}{\tilde{\nu}_0-\tilde{\nu}_a}\right)^4\left(\frac{1-\exp(-hc\tilde{\nu}_a/kT)}{1-\exp(-hc\tilde{\nu}_b/kT)}\right)\frac{\tilde{\nu}_b^2}{\tilde{\nu}_a^2}\right\}^{1/2} \tag{32}$$

As pointed out earlier, B-term scattering may occur for totally symmetric modes if the excited states $|e\rangle$ and $|s\rangle$ are of the same symmetry. B-term excitation profiles for totally symmetric modes are given by

$$I_{g1_a,g0} = K|[\mu_\rho]^0_{ge}|^2 |[\mu_\rho]^0_{gs}|^2 \left(\frac{h^a_{es}}{\Delta\tilde{\nu}_{es}}\right)^2 (\tilde{\nu}_0-\tilde{\nu}_{g1_a,g0})^4 \times \frac{\left\{\frac{\Sigma}{\Gamma}[\varepsilon_0^2+\varepsilon_1^2+2\Sigma^2][(\varepsilon_1-\varepsilon_0)^2+4\Gamma^2]+2[\varepsilon_0\varepsilon_1+\Sigma^2][(\varepsilon_0-\varepsilon_1)^2+4\Gamma\Sigma]\right\}}{(\varepsilon_0^2+\Sigma^2)(\varepsilon_1^2+\Sigma^2)[(\varepsilon_0-\varepsilon_1)^2+4\Gamma^2]} \tag{33}$$

The wave-number-dependent part of this expression differs from that of Equation (31) in that the second term in the numerator is positive rather than negative. This may result in destructive interference between the 0-0 and 0-1 maxima and constructive interference elsewhere, the opposite being true for the A-term. Figure 5 shows examples of B-term and small-displacement A-term excitation profiles, while Figure 6 shows the effect of A-term/B-term interference; this occurs when the two terms have similar magnitudes.[45] The interference is constructive for the 0-0 resonance and destructive for the 0-1 resonance, but this behavior is reversed if the transition moments $[\mu_\rho]^0_{ge}$ and $[\mu_\rho]^0_{gs}$ have opposite signs. Similar excitation profiles may result if there is non-adiabatic coupling of the states $|e\rangle$ and $|s\rangle$ (vide infra).

2.4. Resonance Raman Scattering Involving Non-Totally Symmetric Modes

RR bands attributed to non-totally symmetric fundamental vibrations may acquire intensity via one of three scattering mechanisms:

(1) A-term activity due to a change of molecular symmetry in the resonant excited-state;
(2) A-term activity due to excited-state JT coupling;
(3) B-term scattering, involving the vibronic coupling of the resonant state to a second electronic excited state.

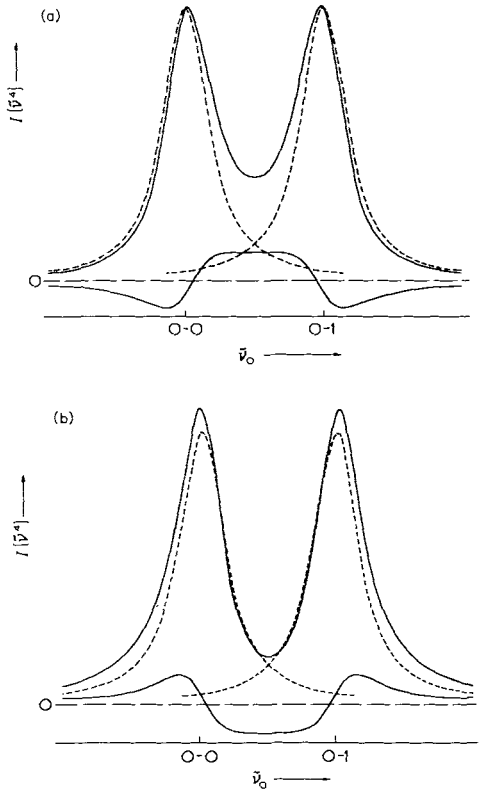


Fig. 5. Excitation profiles for (a) small displacement A-term scattering, and (b) B-term scattering, showing the 0-0 and 0-1 contributions (---) and the interference contribution (——) to the Raman intensity I, calculated with $\Gamma=\gamma=0.1\,\tilde{\nu}^e$.

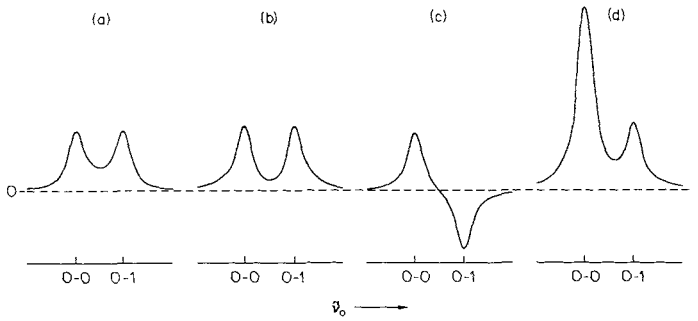


Fig. 6. Excitation profile (d) for A-term/B-term interference showing (a) the A-term, (b) B-term, and (c) interference contributions to the Raman intensity for the case where the A-term and B-term are equal. The calculations were obtained with $\Gamma=\gamma=0.1\,\tilde{\nu}^e$, and only small changes occur when Γ/γ is varied.

If a molecule undergoes a change of symmetry upon excitation then the A-term active modes are those that are totally symmetric in the subgroup formed by the symmetry operations common to the ground- and excited-state point groups (common group). A good example is provided by the molecule ethylene which has a planar D_{2h} geometry in the ground state and a twisted D_{2d} geometry in the first $^1B_{1u}$ excited state. The common group is D_2 and, by correlation of D_2 to D_{2h}, it is seen that the A-term active modes are those of a_g and a_u symmetry. Of course the a_u fundamental (ν_7, the twist about the C=C bond) is Raman inactive but even quanta thereof, i.e. $2\nu_7$, $4\nu_7$, etc., have A_g symmetry and are accordingly Raman active. Excitation within the contour of the π-π^* transition of ethylene using 193.4 nm irradiation[46] yields RR spectra displaying progressions in the ν(C=C) mode and even harmonics of $\nu_7(a_u)$. This recent study thus provided the first unambiguous evidence for a twisted excited state for ethylene. It is a general empirical rule that the vibrational coordinates responsible for converting a molecule from its ground- to excited-state geometry will give rise to resonance-enhanced Raman bands (*Tsuboi*'s rule[47]).

In cases where the resonant excited state is degenerate, A-term activity may arise for some non-totally symmetric modes. The non-totally symmetric vibrations belonging to the irreducible representations contained in the symmetric direct product $\{\Gamma_e \otimes \Gamma_e\}$ may be responsible for JT coupling in the excited state. Some common examples of excited states so influenced are $T_2(T_d)$, $T_{1u}(O_h)$ and $E_u(D_{4h})$, for which the direct products are as follows:

$$T_2 \otimes T_2 = \{A_1 + E + T_2\} + [T_1]$$
$$T_{1u} \otimes T_{1u} = \{A_{1g} + E_g + T_{2g}\} + [T_{1g}]$$
$$E_u \otimes E_u = \{A_{1g} + B_{1g} + B_{2g}\} + [A_{2g}]$$

Vibrations transforming as the antisymmetric part of the direct product (given in square brackets) are not JT active because they do not lift the degeneracy of the excited state. This point is best illustrated by reference to an ion belonging to the D_{4h} point group, e.g. in Figure 7 is shown the effect of vibrations of b_{1g}, b_{2g} and a_{2g} symmetry for the square planar $[Pt(CN)_4]^{2-}$ ion. It is evident that, whereas b_{1g} and b_{2g} vibrations remove the C_4-axis (which is responsible for the double degeneracy), an a_{2g} vibration does not; thus the b_{1g} and b_{2g} modes, but not the a_{2g} mode, are JT active.

The effect of excited-state JT effects on RR spectra may be summarized as follows:

(1) The appearance of combination band progressions involving quanta of totally symmetric modes plus one quantum of a JT-active vibration (small JT effect);

(2) the appearance of combination band progressions involving quanta of totally symmetric modes plus multiple quanta of JT-active vibrations, as well as overtone progressions of the latter (strong JT effect).

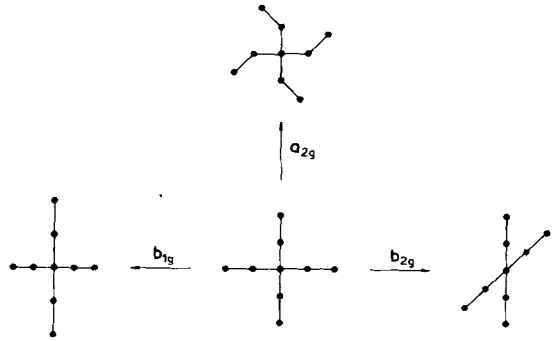


Fig. 7. Diagram showing the effect of a_{2g}, b_{1g} and b_{2g} distortions on a D_{4h} species, e.g. $[Pt(CN)_4]^{2-}$.

It is to be expected that the excited-state JT effect is a dynamic one and that no permanent distortion of the molecule occurs. Thus the major geometric changes accompanying excitation to a degenerate excited state are those involving totally symmetric modes and case (2) is something of a rarity.

For many polyatomic molecules B-term scattering is the major source of RR activity for non-totally symmetric modes. As pointed out earlier, its magnitude is dependent on the vibronic coupling integral h^k_{es}. It is therefore necessary that, for a non-totally symmetric coordinate Q_k to be B-term active, it must be effective in coupling the resonant state $|e\rangle$ to a second excited state $|s\rangle$. Expressed group theoretically, Γ_k must be contained in the product $\Gamma_e \otimes \Gamma_s$. From Equation (14) the transition polarizability is given by

$$[\alpha_{\rho\sigma}]_{g1,g0} = \frac{1}{h^2c^2}[\mu_\rho]^0_{gs}[\mu_\sigma]^0_{eg}\frac{h^k_{se}}{\Delta\tilde{\nu}_{es}}\langle 1|Q_k|0\rangle(\varepsilon_0 + i\Gamma)^{-1} + \frac{1}{h^2c^2}[\mu_\rho]^0_{ge}[\mu_\sigma]^0_{sg}\frac{h^k_{es}}{\Delta\tilde{\nu}_{es}}\langle 1|Q_k|0\rangle(\varepsilon_1 + i\Gamma)^{-1} \quad (34)$$

where $\langle 1|Q_k|0\rangle = \langle 1_e|Q_k|0_g\rangle = \langle 1_g|Q_k|0_e\rangle$

Close examination of this expression reveals that $\alpha_{\rho\sigma} \neq \alpha_{\sigma\rho}$, i.e. that the polarizability tensor is asymmetric. The latter may be expressed as the sum of symmetric and antisymmetric tensors, viz.

$$\alpha_{\rho\sigma} = \left(\frac{\alpha_{\rho\sigma} + \alpha_{\sigma\rho}}{2}\right) + \left(\frac{\alpha_{\rho\sigma} - \alpha_{\sigma\rho}}{2}\right) \quad (35)$$

where the matrix elements are given by

$$[\alpha_{\rho\sigma}]_{g1,g0} \pm [\alpha_{\sigma\rho}]_{g1,g0} = \frac{1}{h^2c^2}\frac{h^k_{es}}{\Delta\tilde{\nu}_{es}}\langle 1|Q_k|0\rangle \times \{[\mu_\rho]^0_{gs}[\mu_\sigma]^0_{eg} + [\mu_\rho]^0_{ge}[\mu_\sigma]^0_{sg}\}\left(\frac{1}{\varepsilon_0 + i\Gamma} \pm \frac{1}{\varepsilon_1 + i\Gamma}\right) \quad (36)$$

Excitation profiles for Raman bands involving symmetric (+) and antisymmetric (−) tensor contributions are given by

$$I^{(\pm)}_{g1,g0} = K\frac{\left\{\frac{\Sigma}{\Gamma}[\varepsilon_0^2 + \varepsilon_1^2 + 2\Sigma^2][(\varepsilon_1 - \varepsilon_0)^2 + 4\Gamma^2] \pm 2[\varepsilon_0\varepsilon_1 + \Sigma^2][(\varepsilon_0 - \varepsilon_1)^2 + 4\Gamma\Sigma]\right\}}{(\varepsilon_0^2 + \Sigma^2)(\varepsilon_1^2 + \Sigma^2)[(\varepsilon_0 - \varepsilon_1)^2 + 4\Gamma^2]} \quad (37)$$

The antisymmetric tensor EP resembles that arising from the small displacement A-term, i.e. there is constructive interference between the 0-0 and 0-1 resonances and destructive interference elsewhere. Thus, the antisymmetric tensor contribution becomes zero outside of the resonance region and normal, i.e. off-resonance, vibrational Raman scattering is controlled exclusively by a symmetric polarizability tensor. By contrast, electronic Raman transitions can involve antisymmetric scattering even in the off-resonance case. The most notable observations of antisymmetric scattering by non-totally symmetric modes have been for metalloporphyrin systems. Resonance Raman spectra obtained by excitation within the Q-band (E_u symmetry) are dominated by B-term scattering by vibrations which couple the Q-state to the higher energy Soret state (also of E_u symmetry). The B-term active vibrations are given by

$$E_u \otimes E_u = A_{1g} + A_{2g} + B_{1g} + B_{2g}$$

and the antisymmetric part of the product, A_{2g}, gives rise to antisymmetric scattering. Weak overtones of a_{1g}, a_{2g}, b_{1g}, and b_{2g} modes are sometimes observed in metalloporphyrin RR spectra and represent the only known examples of D-term scattering.

In concluding this section it should be pointed out that two complications may arise:

(1) Interference between contributions to the transition polarizability from JT-activity (intramanifold coupling) and B-term activity (intermanifold coupling);
(2) Non-adiabatic coupling, which may arise when the states $|e\rangle$ and $|s\rangle$ are close together, i.e. when $\Delta\tilde{\nu}_{es}$ is comparable with vibrational band wave numbers.[48]

The effect of either of these two processes is that the 0-0 and 0-1 peaks in the excitation profiles display unequal intensities. Modes of a_{2g} symmetry are JT inactive and show only the non-adiabatic effect, which favors the 0-1 resonance. This contrasts with the behavior of the other modes which tend to produce stronger 0-0 scattering, arising from interference between the inter- and intramanifold contributions.

2.5. Depolarization Ratios

The depolarization ratio for 90° Raman scattering excited by linearly polarized incident radiation (see Fig. 8) is given by

$$\rho(\pi/2) = \frac{{}^{\perp}I_{\parallel}(\pi/2)}{{}^{\perp}I_{\perp}(\pi/2)} \quad (38)$$

where $\perp$ and $\parallel$ are defined by reference to the scatter plane (the plane containing the directions of propagation of the incident and scattered radiation) and the superscripts and subscripts refer to incident and scattered polarizations, respectively. For an assembly of randomly orien-

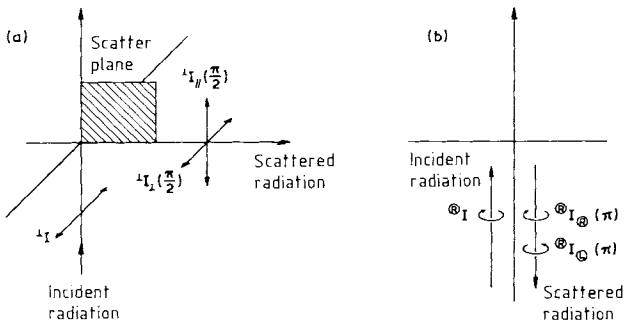


Fig. 8. The geometry for scattering at (a) 90° using linearly polarized incident radiation, and (b) 180° using circularly polarized incident radiation.

tated molecules $\rho(\pi/2)$ may be expressed in terms of the tensor invariants $\bar{\alpha}$, γ_s, and γ_{as} thus:

$$\rho(\pi/2) = \frac{3\gamma_s^2 + 5\gamma_{as}^2}{45\bar{\alpha}^2 + 4\gamma_s^2} \tag{39}$$

where

$$\gamma_s^2 = \tfrac{1}{2}[(\alpha_{xx}-\alpha_{yy})^2 + (\alpha_{yy}-\alpha_{zz})^2 + (\alpha_{zz}-\alpha_{xx})^2 + \tfrac{3}{2}[(\alpha_{xy}+\alpha_{yx})^2 + (\alpha_{yz}+\alpha_{zy})^2 + (\alpha_{zx}+\alpha_{xz})^2]]$$

$$\gamma_{as}^2 = \tfrac{3}{4}[(\alpha_{xy}-\alpha_{yx})^2 + (\alpha_{yz}-\alpha_{zy})^2 + (\alpha_{zx}-\alpha_{xz})^2]$$

For vibrational non-RR scattering γ_{as}^2 is zero, because, as stated previously, the antisymmetric polarizability tensor vanishes under these conditions. The following behavior is then observed:[49]

(1) For non-totally symmetric modes only off-diagonal polarizability tensor elements, $\alpha_{\rho\sigma}$, and the combination $(\alpha_{xx}-\alpha_{yy})$ are non-zero. Therefore $\bar{\alpha}=0$ for all non-totally symmetric modes and $\rho(\pi/2)=3/4$;
(2) for cubic molecules $\alpha_{xx}=\alpha_{yy}=\alpha_{zz}$, hence $\gamma_s^2=0$ for totally symmetric modes and $\rho(\pi/2)=0$. Both $\bar{\alpha}$ and γ_s^2 may be non-zero for the totally symmetric modes of non-cubic molecules and $0 \leqslant \rho(\pi/2) \leqslant 3/4$.

Depolarization ratios for RR scattering are determined by the symmetry of the resonant transition and can provide a valuable tool for the determination of electronic band assignments. For totally symmetric modes of molecules not belonging to the point groups C_1, C_i, C_s, C_2 or C_{2h}, only the diagonal polarizability components, $\alpha_{\rho\rho}$, are non-zero. If the resonant transition is non-degenerate then only one of these will be non-zero (say α_{xx} if the transition is x-polarized) and, from Equations (39), $\rho(\pi/2)=1/3$. Similarly, it can be shown that a doubly-degenerate resonant transition (x,y-polarization) gives rise to $\rho(\pi/2)=1/8$, and that a cubic molecule for which only triply-degenerate transitions are electric-dipole-allowed (x,y,z-polarization), $\rho(\pi/2)=0$. Two further cases may arise when either two non-degenerate transitions lie close together or when a non-degenerate transition is in close proximity to a doubly-degenerate one. In the former case the $\rho(\pi/2)$ value will depend on the relative magnitudes of, say α_{xx} and α_{yy}, illustrated in Figure 9, and will vary as functions of the excitation wave number $\tilde{\nu}_0$ (polarization dispersion). Likewise, in the second case the $\rho(\pi/2)$ value will depend on the relative magnitudes of say $\alpha_{xx}=\alpha_{yy}$ and α_{zz}; this situation is shown in Figure 10.

If the molecular point group is either C_1, C_i, C_s, C_2 or C_{2h} then off-diagonal components, $\alpha_{\rho\sigma}$, may also be non-zero if B-term scattering occurs. Thus, the $\rho(\pi/2)$ is most likely to be within the range 0 to 3/4.

Departure from the above-mentioned behavior is expected if the electronic ground state is degenerate, for then the Raman transition is not a purely vibrational one. The Raman transition is $|g\rangle|n\rangle \leftarrow |g\rangle|0\rangle$, in the low temperature limit, and the irreducible representation for this process is given by $\Gamma_g \otimes \Gamma_n \otimes \Gamma_g \otimes \Gamma_1$ (the v=0 level is necessarily totally symmetric). It is clear that, for a non-degenerate ground state, the product is simply Γ_n because $\Gamma_g \otimes \Gamma_g = \Gamma_1$. However, it is equally clear that if the ground state is degenerate then this will affect the symmetry of the transition. As an example, consider a doubly degenerate E_g'' ground state of an octahedral molecule (O_h point group). The product $E_g'' \otimes E_g'' = A_{1g} + T_{1g}$, and thus the Raman bands attributed to $\nu_1(a_{1g})$ and its overtones will transform as $A_{1g}+T_{1g}$. Both $\bar{\alpha}$ and γ_{as}^2 will be non-zero and $\rho(\pi/2)$ may take any value between zero and infinity, depending on the relative magnitudes of $\bar{\alpha}$ and γ_{as}^2, and will show dispersion throughout the resonance region. Such behavior has been observed for $[IrBr_6]^{2-}$ and $[IrCl_6]^{2-}$,[50] where the ground state is the E_g'' spin-orbit component of the $^2T_{2g}$ term.

If the ground state is orbitally non-degenerate but possesses spin degeneracy then strong spin-orbit coupling may cause mixing of the ground state with degenerate excited states of the same spin degeneracy. Thus, the ground state acquires some degenerate character and the depolarization ratios of totally symmetric modes may become anomalously large. The only reported observation of this is for $[FeBr_4]^-$ where spin-orbit coupling causes the $^6A_1$ ground state to be mixed with sextet excited states, and $\rho(\pi/2)=0.15$ is observed for the ν_1 band in the RR spectrum.[51,52]

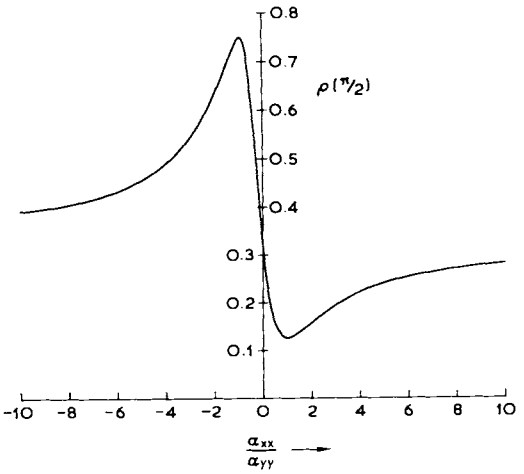


Fig. 9. Plot of $\rho(\pi/2)$ versus α_{xx}/α_{yy} for the case in which two non-degenerate transitions contribute to the transition polarizability.

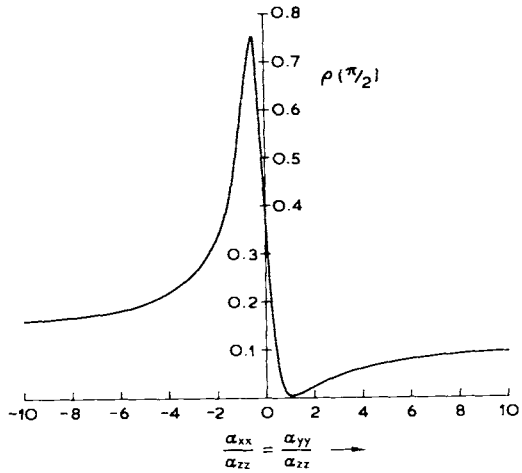


Fig. 10. Plot of $\rho(\pi/2)$ versus $\alpha_{xx}/\alpha_{zz}=\alpha_{yy}/\alpha_{zz}$ for the case in which one degenerate and one non-degenerate transition contribute to the transition polarizability.

$$\rho(\pi/2)=\frac{3}{4}+\frac{5}{4}\frac{\gamma_{as}^2}{\gamma_s^2}=\frac{3}{4}+\frac{5}{4}\left|\frac{[\alpha_{p\sigma}]_{gn,g0}-[\alpha_{\sigma p}]_{gn,g0}}{[\alpha_{p\sigma}]_{gn,g0}+[\alpha_{\sigma p}]_{gn,g0}}\right|^2=\frac{3}{4}+\frac{5}{4}\frac{\left\{\frac{\Sigma}{\Gamma}[\varepsilon_0^2+\varepsilon_1^2+2\Sigma^2][(\varepsilon_1-\varepsilon_0)^2+4\Gamma^2]-2[(\varepsilon_1-\varepsilon_0)^2+4\Gamma\Sigma][\varepsilon_1\varepsilon_0+\Sigma^2]\right\}}{\left\{\frac{\Sigma}{\Gamma}[\varepsilon_0^2+\varepsilon_1^2+2\Sigma^2][(\varepsilon_1-\varepsilon_0)^2+4\Gamma^2]+2[(\varepsilon_1-\varepsilon_0)^2+4\Gamma\Sigma][\varepsilon_1\varepsilon_0+\Sigma^2]\right\}} \tag{40}$$

For non-totally symmetric modes $\bar{\alpha}$ is zero and the $\rho(\pi/2)$ value is dependent on the relative sizes of γ_s^2 and γ_{as}^2. If, for a given symmetry class, there are only symmetric or antisymmetric tensor components, then $\rho(\pi/2)=3/4$ or ∞, respectively, and does not display dispersion. Examples of such vibrational modes are the b_{1g} and b_{2g} modes (symmetric tensor) and a_{2g} modes (antisymmetric tensor) of metalloporphyrins. By contrast, for cases in which both symmetric and antisymmetric tensor components transform as the same irreducible representation (e.g. B_{1g}, B_{2g} or B_{3g} in the D_{2h} point group), $\rho(\pi/2)$ lies between 3/4 and ∞ and displays dispersion throughout the resonance region. The variation of $\rho(\pi/2)$ with excitation wave number [Equation (40)] is readily obtained from Equations (37) and (39).
The depolarization ratio $\rho(\pi/2)$ maximizes at the midpoint between the 0-0 and 0-1 resonances and decreases asymptotically towards 3/4 on either side. Its maximum value is a function of Γ and γ, as shown in Figure 11.

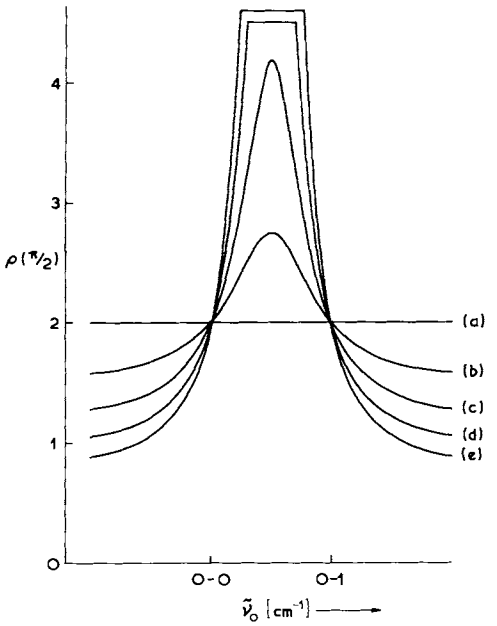


Fig. 11. Polarization dispersion for mixed symmetric/antisymmetric B-term scattering. (a) $\Gamma=10^{-4}\bar{\nu}^e$, $\gamma=0.1\bar{\nu}^e$; (b) $\Gamma=0.025\bar{\nu}^e$, $\gamma=0.075\bar{\nu}^e$; (c) $\Gamma=\gamma=0.05\bar{\nu}^e$; (d) $\Gamma=0.075\bar{\nu}^e$, $\gamma=0.025\bar{\nu}^e$; (e) $\Gamma=0.1\bar{\nu}^e$, $\gamma=0$.

The overtones of non-degenerate non-totally symmetric modes all transform as the totally symmetric representation and their $\rho(\pi/2)$ values will be the same as for totally symmetric fundamentals. Overtones of degenerate fundamentals transform as the symmetric part of the direct product (e.g. in the O_h point group $\{E_g\otimes E_g\}=A_{1g}+E_g$ and $\{T_{2g}\otimes T_{2g}\}=A_{1g}+E_g+T_{2g}$). $\rho(\pi/2)$ values for the overtones of degenerate vibrations have been determined by *Pawlikowski* and *Zgierski*.[53]

An alternative method of investigating the polarization properties of RR scattering involves the use of circularly polarized incident radiation and a 180° scattering geometry, as shown in Figure 8. The quantities that are determined are the reversal ratio, $\mathscr{P}(\pi)$, which is the ratio of the intensity of contra-rotating to that of co-rotating scattered light, and the degree of circularity, $\mathscr{C}(\pi)$, of the scattered light:

$$\mathscr{P}(\pi)=\frac{{}^{\circledR}I_{\textcircled{L}}(\pi)}{{}^{\circledR}I_{\circledR}(\pi)}=\frac{{}^{\textcircled{L}}I_{\circledR}(\pi)}{{}^{\textcircled{L}}I_{\textcircled{L}}(\pi)}=\frac{45\bar{\alpha}^2+\gamma_s^2+5\gamma_{as}^2}{6\gamma_s^2} \tag{41}$$

$$\mathscr{C}(\pi)=\frac{{}^{\circledR}I_{\circledR}(\pi)-{}^{\circledR}I_{\textcircled{L}}(\pi)}{{}^{\circledR}I_{\circledR}(\pi)+{}^{\circledR}I_{\textcircled{L}}(\pi)}=-{}^{\textcircled{L}}\mathscr{C}(\pi)=\frac{45\bar{\alpha}^2-5\gamma_s^2+5\gamma_{as}^2}{45\bar{\alpha}^2+7\gamma_s^2+5\gamma_{as}^2} \tag{42}$$

The measurement of Raman spectra excited with both circularly and linearly polarized radiation permits the determination of all three tensor invariants, and so-called "complete" polarization measurements have been carried out for a number of molecules.[54–58] Furthermore, it has recently been shown that meaningful circular polarization measurements can be obtained from samples dispersed in alkali halide disks.[59]

Using the information presented in this section in conjunction with point group tables it is possible for the reader to determine the depolarization ratio, under resonance conditions, for a vibration of any type in any point group. A tabulation of $\rho(\pi/2)$ values for the symmetry classes of all the common point groups is given in Ref. [1].

3. Experimental Techniques

The apparatus required for the excitation, dispersion and detection of RR scattering is precisely the same as that used for normal Raman spectroscopy, although sample illumination procedures are more critical. In order that RR spectroscopy may be applied to a wide range of molecules it is necessary that laser excitation throughout the visible and near UV spectral regions be available. Most RR studies to date have involved excitation provided by CW argon-ion and krypton-ion lasers and CW dye lasers, the latter providing continuously tunable radiation from 395 to 800 nm with seven different dyes (stilbene 1, stilbene 3, coumarin 30, sodium fluorescein, rhodamine 6G, rhodamine 101, and LD 700). Unfortunately, ion lasers provide only a small number of lines in the near-UV (330–370 nm), so it has been necessary to use different laser sources in order to obtain tunable radiation down to 250 nm. At the time of writing, three systems are in current use:

(1) Frequency-doubled output of a mode-locked ion or dye laser. With a repetition rate of ca. 40 MHz the radiation is quasi-CW, but only modest average power can be obtained (ca. 10–20 mW);

(2) Frequency-narrowed excimer lasers and excimer-pumped dye lasers. These have a repetition rate of ca. 10 Hz and average power of the order of 1–10 W; they are, however, very expensive;
(3) Frequency-tripled and -quadrupled pulsed Nd:YAG lasers which may be used to pump a dye laser. Such systems have found considerable application in time-resolved resonance Raman (TR^3) studies.

For most RR studies the scattered light is detected by photomultiplier tubes using photon-counting methods, in many cases employing dedicated computers which also control the spectrometer. In recent years many experiments have been performed using multichannel detection involving either a TV camera (intensifier-vidicon) or diode array. Multichannel detection reduces the time required to obtain a spectrum by several orders of magnitude, thus permitting RR studies of photochemically labile species. In combination with picosecond pulsed lasers, multichannel detection facilitates TR^3 experiments in which transient species and molecules in optically (or radiolytically) pumped excited states may be investigated.[8]

Sample illumination procedures present certain problems associated with strong absorption of the laser beam. These are:

(1) The need for optimization of the concentration of the scattering species in order to achieve a compromise between absorption and scattering processes. Experience has shown that the optimum concentration is best determined experimentally by trial-and-error, but several attempts have been made to calculate optimum sample concentrations for a wide variety of different scattering geometries;

(2) the avoidance of overheating the sample at the laser focus. Various rotating cells for solids, liquids, and gases have been employed and some workers have used devices which enable the focused laser beam to be swept over the sample in a linear or circular fashion. Recently, the use of flowing samples for TR^3 studies has been described;[8]

(3) The elimination of photolysis and luminescence. These can now be discriminated against by the TR^3 techniques mentioned above. Luminescence rejection can be achieved by using single-channel spectrometers in conjunction with pulsed lasers by time-adjusted gating of the photon-counting electronics.

Profound advantages accrue from measuring RR spectra of samples maintained at low temperature, viz. that of minimizing hot-band contribution to intensities and of alleviating thermolysis. This procedure results in a sharpening of the spectral features, thereby improving resolution and signal-to-noise ratios. Several cryostats are available for Raman studies, the most popular being those in which liquid nitrogen (77 K) or liquid helium (4 K) are used as coolants, and also closed-cycle helium gas cryostats (10–12 K). The latter are widely used for matrix-isolation studies.

4. Resonance Raman Studies of Small Molecules

4.1. Diatomic Molecules

Diatomic species (both neutral and ionic) have been subjected to some of the most detailed RR investigations during the last two decades. While many of the earlier studies were concerned with stable species, such as halogen and interhalogen molecules and ions, more recent work has centered on studies of matrix-isolated diatomic metal species. Data on the latter are summarized in Table 2, that on the former being included in earlier tabulations.[1,23]

Recent investigations of the halogens have been concerned with the theoretical interpretation of the spectra of Br_2[77–79] and Cl_2.[80–82] Whereas RR scattering from I_2 can be accounted for by assuming that the transition polarizability is dominated by a single electronic state, $^3\Pi_{0u}^+$ (see Ref. [1] and references therein), scattering from Br_2 contains a contribution from the repulsive $^1\Pi_{1u}$ state. A theoretical study of the EPs[79] has clearly demonstrated the involvement of both states in the scattering process. The theoretical model took account of interference between these contributions but assumed negligible coupling between the two states; this might be an unjustified assumption because the agreement between theory and experiment is poor in the 19500–21000 cm^{-1} region. The RR behavior of Cl_2 is quite different in that there seems to be no contribution from the $^3\Pi_{0u}$ state. A RR spectrum displaying an eight-membered progression is observed for 363.8-nm excitation within the contour of the $^1\Pi_{1u} \leftarrow {}^1\Sigma_g^+$ absorption band. However, the intensity enhancement factor of the fundamental for UV excitation with respect to visible, i.e. non-resonant, excitation is only 1.3, and the intensity of the first overtone is only 1/3 of that of the fundamental. These observations have been explained in terms of non-resonant contributions to the polarizability from higher energy states, especially a $^1\Sigma_u^+$ state at 78500 cm^{-1}. The reason for the absence of a $^3\Pi_{0u}^+$ contribution for Cl_2 is that the transition to this state is spin-forbidden. Its contribution to the RR scattering of Br_2 and, to a greater extent, to that of I_2, obtains from the induction of allowed character into the $^3\Pi_{0u}^+ \leftarrow {}^1\Sigma_g^+$ transition via spin-orbit coupling (this increases in the order Cl < Br < I).

Recent developments in the RR spectroscopy of matrix-isolated metal dimers are of special interest because they provide valuable experimental data upon which to test quantum-chemical calculations. An example of RR scattering by a metal dimer is shown in Figure 12 and Table 1 lists the results obtained so far on diatomic species, although many other metal dimers have been characterized by luminescence spectroscopy.[65] The occurrence of luminescence for some regions of excitation has precluded the more extensive application of RR spectroscopy and renders difficult the measurement of excitation profiles. It is to be hoped that these problems may be overcome in the near future in order that the theoretical interpretation of the spectra may proceed. In particular, it is noted that no unambiguous electronic band assignments have yet been proposed for metal dimers.

Table 2. Resonance Raman data on diatomic species. λ_{max} = wavelength of the electronic band, λ_0 = wavelength of the excitation radiation, ω_e = harmonic wave number, x_e = anharmonicity constant.

Species	State	Electronic band assignment	λ_{max} [nm]	λ_0 [nm]	ω_e [cm^{-1}]	$\omega_e x_e$ [cm^{-1}]	Comments	Ref.
Bi_2	Kr matrix, 8 K	$A \leftarrow X$	560	568.2	172.7	0.35		[60, 61]
	Ar matrix, 10 K			555	174.3	0.39	Molecular constants obtained from luminescence spectrum superimposed on Raman spectrum	
Br_2^-	aq. soln. 295 K	$^2\Sigma_g^+ \leftarrow {}^2\Sigma_u^+$	360	355	187.2	−5.17		[62]
Ca_2	Kr matrix, 12 K	$^1\Sigma_u^+ \leftarrow {}^1\Sigma_g^+$	664	647.1	80	0.35	Ca_2 is a van der Waals dimer in the ground state. The excited state is more strongly bound ($\omega_e = 117$ cm^{-1})	[63, 64]
Cl_2^-	aq. soln. 295 K	$^2\Sigma_g^+ \leftarrow {}^2\Sigma_u^+$	345	355	286.4	−3.83		[62]
Cr_2	Ar matrix, 12–15 K			514.5	427.5	15.75		[65]
$^{56}Fe_2$	Ar, Kr matrices, 11 K			457.9	299.6	1.4	The observation of a four-membered anti-Stokes progression is ascribed to radiative population due to long vibrational lifetimes	[66]
FeNi	Ar, Kr matrices, 11 K			457.9	320.0	1.32		[67]
Mn_2	Ar matrix, 12–15 K		650	676.4	124.69	0.24	Two electronic Raman bands observed at 135.7 and 196.7 cm^{-1}	[67]
Pb_2	Kr, Xe matrices, 8–10 K	$FO_u^+ \leftarrow XO_g^+$	515	476.2, 647.1	110	0.75		[68]
	Xe matrix, 12 K			496.5	108	0.4		[69]
	Ar, Ne matrices, 8–10 K			514.5	110 (Ne), 112.2 (Ar)	0.35	In Ar matrices a second strong progression is observed ($\omega_e = 123$, $\omega_e x_e = 0.26$ cm^{-1}) assigned to Raman scattering from the electronic excited A state at ca. 5500 cm^{-1}	[70]
S_2^-	Ultramarine green lattice	$^2\Pi_g \leftarrow {}^2\Pi_u$	393	406.7	597.0	2.5 ± 0.15	$\rho\left(\frac{\pi}{2}\right) = 0.14 \pm 0.03$ for fundamental of species in solution (Na_2S_4/DMF) confirms that transition is x,y-polarized. $\Delta r = 0.30 \pm 0.01$ Å, $\Gamma = 300 \pm 50$ cm^{-1} and $\gamma = 400 \pm 50$ cm^{-1} [a, b]	[71, 72]
Sc_2	Ar matrix, 12–15 K			676.4	238.91	0.93		[67]
Se_2^-	Ultramarine selenium, 80 K	$^2\Pi_g \leftarrow {}^2\Pi_u$	490	488.0	329.6 ± 0.3	0.70 ± 0.03	$\Delta r = 0.32 \pm 0.02$ Å, $\Gamma = 150 \pm 50$ cm^{-1} and $\gamma = 400 \pm 100$ cm^{-1} [b]	[72]
Sn_2	Ar matrix, 12 K		490	488.0	188	0.53		[73, 74]
Ti_2	Ar matrix, 11 K			632.8	407.9	1.08	Anti-Stokes progression also observed, implying long vibrational lifetimes	[75]
V_2	Ar matrix, 11 K			488.0	537.5	4.2	Anti-Stokes progression. Three other Stokes progressions observed, assigned to electronic Raman and scattering from an excited state	[75]
Xe_2^+	$[SbF_6]^-$ salt in SbF_5 solution	$^2\Pi_{1/2g} \leftarrow {}^2\Sigma_u^+$	710	676.4	123	0 ± 1	Isoelectronic with I_2^-	[76]

[a] DMF = dimethylformamide. [b] Obtained from calculations of excitation profiles.

One aspect of these studies that deserves mention concerns the observation of anti-Stokes overtone progressions in Ca_2, Fe_2, Ti_2, and V_2. These cannot arise from thermal population of vibrational levels of the ground state because, at ca. 10 K, all molecules must be in the $v = 0$ level. The effect has been attributed to population of the $v > 0$ levels by the RR process, implying that these levels have long, but as yet undetermined, lifetimes. Such a phenomenon could form the basis of an infrared laser.

Finally, in this section, attention is drawn to recent work on the radical anions S_2^- and Se_2^- in ultramarines.[72] The ultramarine host lattice has a structure in which the radicals are trapped and stabilized in octahedral holes in the aluminosilicate lattice. Detailed measurements of the exci-

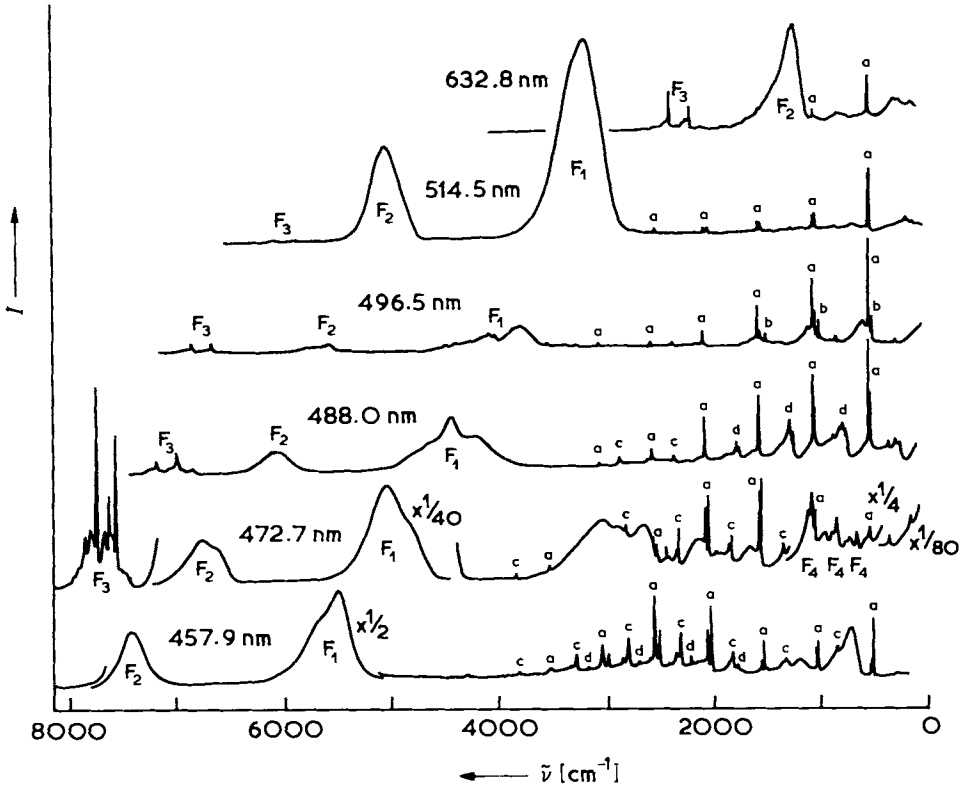


Fig. 12. Resonance Raman spectra of vanadium isolated in a solid argon matrix at 15 K, obtained using various excitation lines. The progressions consist of (a) ground state Raman bands, (b) excited state Raman bands, and (c) and (d) electronic Raman bands. The bands designated F1, F2, F3, and F4 are assigned to fluorescence (after Ref. [75]).

tation profiles of the ν, 2ν, and 3ν RR bands of the radicals were fitted to Equation (21), thus enabling the determination of the bond length changes attendant upon excitation. These are substantial (0.30 and 0.32 Å for S_2^- and Se_2^- respectively), reflecting the decrease in bond order from 1.5 in the $^2\Pi_u$ ground state to 0.5 in the $^2\Pi_g$ excited state. The potential use of ultramarine host lattices for trapping other small species (both stable and unstable) offers an attractive possibility for their detailed investigation by RR spectroscopy.

4.2. Triatomic and Tetratomic Molecules

A summary of the recent investigation on the RR spectra of triatomic molecules is given in Table 3. Several of these have been concerned with the characterization of metal trimers in noble gas matrices. The properties of metal trimers are less well established than for dimers but structural information on the former is of importance since it is only with these that a proper comparison between cluster and bulk metal properties can be made. However, at this early stage there is still considerable controversy over electronic band assignments. Most of the spectra obtained can be interpreted in terms of a C_{2v} or distorted D_{3h} ground state for the scattering species but, in the case of Cu_3, evidence has been obtained to show that it is a Jahn-Teller fluxional molecule, pseudorotating even at 15 K.

RR data pertaining to tetratomic molecules are summarized in Table 4. Although there have been fewer studies of tetratomic molecules than of diatomic and triatomic species, a number of important features of these studies are worthy of comment. The recently reported investigation of gaseous NH_3 heralds a new era of RR studies involving the use of far-UV excitation. By using the fifth harmonic of a pulsed Nd:YAG laser (212.8 nm), *Ziegler* and *Hudson*[96] were able to excite the singlet electronic transition of lowest energy (ca. 190 nm) assigned to the transfer of an electron from the nitrogen lone pair to a 3s Rydberg-type orbital. This excitation results in a change of molecular geometry from C_{3v} to D_{3h}, as evidenced by a long overtone progression in the deformation mode ν_2 in the absorption spectrum. The RR spectrum displays a progression $\nu_2\nu_2$ extending to $\nu_2=4$ and also a combination band progression $\nu_1+\nu_2\nu_2$ extending to $\nu_2=4$. This latter observation constitutes the first direct evidence from which it may be concluded that the N–H bond length changes upon excitation to the 190-nm state. Measurements of excitation profiles should enable the N–H bond-length change to be calculated.

The square planar molecules S_4^{2+}, Se_4^{2+}, and Te_4^{2+} are 6π-electron systems and they are thus examples of inorganic aromatic molecules. In each case the allowed electronic transition of lowest energy is $\pi^*\leftarrow\pi$ ($^1E_u\leftarrow{}^1A_{1g}$), corresponding to the transfer of a electron from the nonbonding e_g orbital to the antibonding b_{2u} orbital. Excitation within the contour of the relevant absorption bands gives rise to RR spectra that are characterized by an intense progression $\nu_1\nu_1$ and weaker subsidiary progressions

Table 3. Resonance Raman data on triatomic species.

Species	State	Electronic band assignment	λ_{max} [nm]	λ_0 [nm]	ω_1 [cm^{-1}]	x_{11} [cm^{-1}]	Comments	Ref.
ClO_2	$CFCl_3$ soln., 295 K	$^2A_2 \leftarrow {}^2B_1$	362	457.9	951.2	− 4.8	$\omega_2 = 451.4$ cm^{-1}, $x_{12} = -8.1$ cm^{-1}; $\Delta Q_1 = 0.81$ Å amu$^{1/2}$ and $\Gamma = 240$ cm^{-1} [a]	[83, 84]
Cr_3	Ar matrix, 12-15 K			514.5	313	− 2	$\nu_2 = 123$ cm^{-1}, $\nu_3 = 226$ cm^{-1}	[65]
Cu_3	Ar matrix, 12-15 K			595.9	[b]	[b]	Pseudorotating JT molecule	[85]
I_3^-	Cs^+ salt in Ar matrix, 12-16 K	$\sigma_u^* \leftarrow \pi_g$	355	476.5	113.4 ± 0.2	− 0.32 ± 0.04		[86]
Ni_3	Ar matrix, 10 K			488.0	232.3	− 1.0	Bond angle 90-100° [c]	[87]
NO_2	Ar, Kr and Xe matrices, 15 K	$^2B_2 \leftarrow {}^2A_1$	≈ 500	488.0, 514.5	(Ar) 1326.5 ± 0.5	− 6.0 ± 0.5	$x_{22} = -0.6 \pm 0.3$, $x_{13} = -29 \pm 3$, $x_{33} = -25 \pm 3$ cm^{-1}	[88]
					(Kr) 1329.1 ± 0.5	− 7.5 ± 0.5	$x_{22} = -0.7 \pm 0.3$, $x_{13} = -31 \pm 3$, $x_{23} = -10 \pm 1$, $x_{33} = -25 \pm 2$ cm^{-1}	
					(Xe) 1321.9 ± 0.5	− 6.1 ± 0.5	$x_{22} = -0.8 \pm 0.1$, $x_{13} = -31 \pm 3$, $x_{23} = -12 \pm 1$, $x_{33} = -30 \pm 3$ cm^{-1}	
O_3^-	γ-irradiated $NaClO_3$, 11 K	$^2A_2 \leftarrow {}^2B_1$	≈ 440	457.9	(a) 1031.6 (b) 1034.5	− 4.4 − 3.25	$\Delta Q_1 = 0.63$ Å amu$^{1/2}$, $\Gamma = 514$ cm^{-1} [a, d]. (a), (b): non-equivalent sites of the O_3^- ions	[89]
	γ-irradiated $Ba(ClO_3)_2 \cdot 2H_2O$			457.9	(a) 1050 (b) 1060	− 11.2 − 12.6		[90]
	γ-irradiated $AgClO_3$			514.5	(a) 1009 (b) 1023	− 5.4 − 8.4		[91]
	γ-irradiated $Cd(ClO_3)_2$, 15-300 K			457.9	1022	− 3		[92]
Pb_3	Xe matrix, 12 K		455	488.0	117	− 0.2	D_{3h} geometry. $\nu_2(e') = 96$ cm^{-1}	[68, 69]
S_3^-	DMF soln. HMPA soln. [f]	$^2A_2 \leftarrow {}^2B_1$	600	647.1	537.5 536.1	− 1.3 − 1.3		[71]
Sb_3	Ar matrix, 13 K			476.5	~ 218	~ 0.3		[93]
Sc_3	Ar matrix, 12-15 K			676.4	247	− 0.5	Geometry close to D_{3h}, $\nu_2 = 145$ cm^{-1}, $\nu_3 = 151$ cm^{-1}. Electronic Raman transition at 395 cm^{-1}	[67]
$^{80}Se_3$	Ar and N_2 matrices, 15 K			514.5	312.15 ± 0.2	− 0.53 ± 0.02		[94]
Te_3	N_2 matrix, 15 K			647.1	($^{126}Te_3$) 206.33 ± 0.15 ($^{130}Te_3$) 203.1 ± 0.1	0.24 ± 0.03 0.22 ± 0.05	C_{2v} geometry, $\theta = 120 \pm 10°$ (from calculations). Multiple bonding inferred from $f_r + f_{rr} = 2.1 \pm 0.1$ mdyn Å^{-1}	[95]

[a] From calculations of excitation profiles. [b] Irregular overtone progression precludes calculation. [c] Deduced from isotopic fine structure. [d] From calculations of the absorption spectrum. [e] Estimated from observation of overtone at 192 cm^{-1}. [f] HMPA = hexamethylphosphoric acid triamide.

Table 4. Resonance Raman data on tetratomic species.

Species	State	Electronic band assignment	λ_{max} [nm]	λ_0 [nm]	ω_1 [cm^{-1}]	x_{11} [cm^{-1}]	Comments	Ref.
Bi_4	Ar and Kr matrix, 8-10 K		670	676.4	152.5	− 0.3		[60, 61]
NH_3	45 torr, 295 K	$^1A_2'' \leftarrow {}^1A_1'$	192	212.8	[a]	[a]	Molecular geometry changes to D_{3h} in the excited state as evidenced by RR activity of ν_2	[96]
S_4^{2+}	Soln. in 65% oleum	$^1E_u \leftarrow {}^1A_{1g}$	330	350.7	584.7 ± 0.5	− 0.35 ± 0.05	$x_{12} = -0.5 \pm 1$ cm^{-1}	[97]
Se_4^{2+}	Soln. in 25% oleum	$^1E_u \leftarrow {}^1A_{1g}$	410	406.7	321.8 ± 0.5	− 0.55 ± 0.05	$x_{12} = -1.3 \pm 1.0$ cm^{-1}	[97]
Te_4^{2+}	Soln. in conc. H_2SO_4	$^1E_u \leftarrow {}^1A_{1g}$	510	514.5	219.5 ± 0.5	− 0.30 ± 0.05		[97]
	$Te_4[Al_2Cl_7]_2$ solid, 80 K				214.1 ± 0.5	− 0.16 ± 0.05	$x_{12} = -0.8 \pm 0.5$ cm^{-1}	
$[S_3N]^-$	$[Ph_3P{=}N{=}PPh_3]^+$-salt, 295 K	$^1A' \leftarrow {}^1A'$	468	488.0			Progressions observed involving all three stretching fundamentals, indicating that the electronic transition is delocalized over all four atoms	[92]

[a] Irregular overtone progressions precluded the calculation of molecular constants.

$\nu_1\nu_1+\nu_2$ and $\nu_1\nu_1+\nu_3$, the latter being evidence for excited-state JT effects involving $Q_2(b_{1g})$ and $Q_3(b_{2g})$. However, for Se_4^{2+} and Te_4^{2+}, ν_3 is overlapped by ν_1, as evidenced by $\rho(\pi/2)=0.33$. For excitation resonant with an E_u state (x,y-polarization) the theoretical requirement is that $\rho(\pi/2)=1/8$ for ν_1 and 3/4 for ν_3; thus the measured ρ value for the overlapping bands results from an intensity ratio $I(\nu_1)/I(\nu_3)$of 1.3. An analysis of the vibrational data showed that the coalescence of ν_1 and ν_3 arises because the interaction force constant associated with two adjacent bonds (f_{rr}) is near zero.

4.3. Tetrahedral Molecules

RR investigations of tetrahedral species (Table 5) have been centered on (a) transition metal oxo- and thio-anions, and (b) main group and transition metal tetrahalides. In each case excitation was into the contour of the charge-transfer absorption band of lowest energy in the visible/near UV region. The resonant electronic transition involves the promotion of an electron from the t_1 orbital localized on the ligands to the e metal-ligand antibonding orbital (Fig. 13). Such an electronic transition results in a significant lengthening of the bonds; thus the RR spectra are characterized by intense overtone progressions in the $\nu_1(a_1)$ mode. Additionally, subsidiary progressions are observed which involve single quanta of one or more of the non-totally symmetric modes $\nu_2(e)$, $\nu_3(t_2)$ and $\nu_4(t_2)$, i.e. progressions of the type $\nu_1\nu_1+\nu_2$, etc. These are attributed to JT coupling in the triply degenerate excited state, all three non-totally symmetric modes being potentially JT active.

In cases where the absorption spectra and excitation profiles display vibrational fine structure, serious attempts have been made to calculate the bond-length changes attendant upon excitation by fitting the experimental data to Equation (21). These bond-length changes, which range from 0.029 Å for $[WS_4]^{2-}$ to 0.046 Å for $[MnO_4]^-$, are given in Table 4, together with the other parameters involved in the calculations. However, all of the bond-length changes determined for tetrahedral molecules have been miscalculated due to use of an erroneous relation between Δr and ΔQ. The values in the literature[24, 99, 102, 112, 115] are a factor of two greater than the correct ones, which are given in this review. The absorption spectrum and experimental and calculated EPs for $[MnO_4]^-:K[ClO_4]$ are shown in Figure 14. By comparison with the bond-length changes determined for the diatomic species (e.g. 0.30 Å for S_2^-), these values are small. This is because the change of bond order upon excitation is also much smaller, from 2.25 to 2.125, as compared to 1.5 to 0.5 for S_2^-.

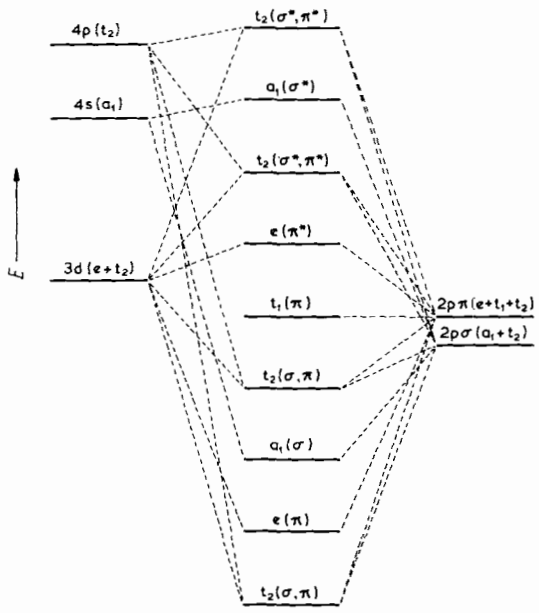


Fig. 13. Schematic molecular orbital diagram for tetrahedral transition-metal complexes.

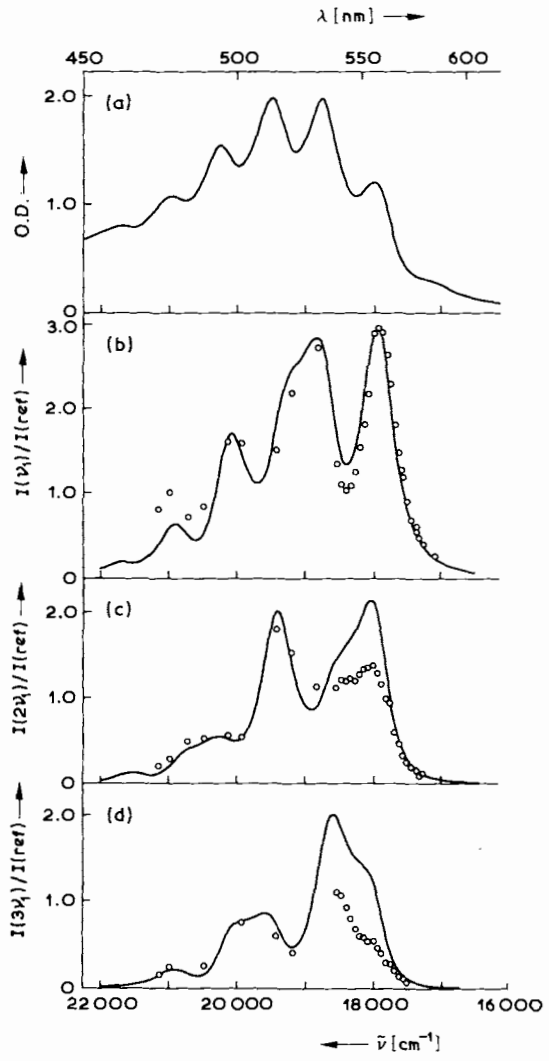


Fig. 14. (a) Absorption spectrum of $[MnO_4]^-:K[ClO_4]$ in a $K[ClO_4]$-disk at room temperature. O.D. = optical density. (b)–(d) Experimental (○) excitation profiles for the ν_1, $2\nu_1$, and $3\nu_1$ bands of $[MnO_4]^-$, respectively. The full lines represent the (best fit) calculated profiles for $\Gamma=300\ cm^{-1}$, $\gamma=0$, and $\Delta r=0.46$ Å (after [24]).

The electronic spectrum of $[WS_4]^{2-}$ in the 400–450 nm region consists of a strong band at ca. 400 nm and a weak shoulder at ca. 430 nm. The strong band has been assigned to the fully-allowed $^1T_2\leftarrow{}^1A_1$ transition arising from the $e\leftarrow t_1$ electronic transition. However, the excited $(t_1)^5(e)^1$ configuration gives rise to three other terms, $^1T_1$, $^3T_1$ and

Table 5. Resonance Raman data on tetrahedral XY_4 species.

Species	State	Electronic band assignment	λ_{max} [nm]	λ_0 [nm]	ω_i [cm^{-1}]	x_{11} [cm^{-1}]	Comments	Ref.
$[CrO_4]^{2-}$	Ag^+ salt, Na_2SO_4 disk, 15 K	$^1T_2 \leftarrow {}^1A_1$		647.1			EP red-shifted from absorption maximum; no overtone progression observed	[98]
	aq. soln. 295 K			360–410			Measurement of ν_1-EP; Calculations yielded $\Gamma = 730$ cm^{-1}, $\Delta r = 0.039$ Å, $\tilde{\nu}_{00} = 24987$ cm^{-1}	[99]
$[FeBr_4]^-$	$[Bu_4N]^+$ salt, KBr disk, 80 K	$^6T_2 \leftarrow {}^6A_1$	472	476.5	203.8 ± 0.2	-0.35 ± 0.05	$x_{13} \approx 1$ cm^{-1}	[52, 56, 100]
$[FeCl_4]^-$	$[Et_4N]^+$ salt, $MeNO_2$ soln., 295 K	$^6T_2 \leftarrow {}^6A_1$	365	363.8	335.2 ± 0.2	-0.54 ± 0.07		[52]
GeI_4	C_6H_{12} soln., 295 K	$^1T_2 \leftarrow {}^1A_1$	360.4	363.8	158.9 ± 0.1	-0.09 ± 0.02		[101]
$[MnO_4]^-$	$[MnO_4]^-$: K[ClO$_4$], KBr disk, 295 K	$^1T_2 \leftarrow {}^1A_1$	545	514.5	848.6 ± 0.3	-0.88 ± 0.07	$x_{13} \approx -2.3$ cm^{-1}; $\Gamma = 300$ cm^{-1} [a], $\Delta r = 0.046 \pm 0.003$ Å [a]	[24, 102, 103]
	$[Ph_4P]^+$ salt, KBr disk, 295 K			514.5	837.9 ± 0.4	-1.3 ± 0.2	$x_{13} \approx -2.6$ cm^{-1}; $\Gamma = 240$ cm^{-1} [a], $\Delta r = 0.045$ Å [a]	[24, 103]
	^{18}O-enriched K[MnO$_4$], RbBr disk, 295 K			514.5	846.8 ± 0.1	-1.22 ± 0.09	$[Mn^{16}O_4]^-$	[104, 105]
					829.4 ± 0.1	-1.24 ± 0.09	$[Mn^{16}O_3{}^{18}O]^-$	
					817.8 ± 0.1	-1.18 ± 0.09	$[Mn^{16}O_2{}^{18}O_2]^-$	
					807.7 ± 0.1	-1.11 ± 0.09	$[Mn^{16}O^{18}O_3]^-$	
					798.4 ± 0.1	-0.99 ± 0.06	$[Mn^{18}O_4]^-$	
	$[Ph_4As]^+$ salt, 295 K			514.5	837.1 ± 0.5	-1.19 ± 0.1		[106]
	$[Ph_4P]^+$ salt, 295 K			514.5	836.4 ± 0.5	-1.04 ± 0.1		[106]
	$[Et_4N]^+$ salt, KBr disk, 80 K			514.5	838.9	-1.7		[107]
	Ag^+ salt, 295 K			514.5	797.0 ± 0.3	$+1.4 \pm 0.3$	positive x_{11} value ascribed to polarizing effect of Ag^+ cation	[108]
$[MnO_4]^{2-}$	$[MnO_4]^{2-}$: CsI, 80 K	$^2T_2 \leftarrow {}^2E$	580	514.5	806.3 ± 0.4	-1.7 ± 0.1		[109]
	$K_2[MnO_4]$, 295 K			514.5	818.3	-2.3		[104]
	$Ba[MnO_4]$, 295 K			514.5	828.0	-3.3		[104]
	$[MnO_4]^{2-}$: $K_2[CrO_4]$, 80 K			568.2	817.7 ± 0.5	-1.7 ± 0.2	$x_{13} = -2.0 \pm 0.5$ cm^{-1}; $\Gamma = 250 \pm 10$ cm^{-1} [a], $\Delta r = 0.035 \pm 0.001$ Å [a], $\tilde{\nu}_{00} = 15900$ cm^{-1} [a]	[110]
$[MoS_4]^{2-}$	aq. soln., 295 K	$^1T_2 \leftarrow {}^1A_1$	472	488.0	454	0 ± 0.5		[111]
	$[Bu_4N]^+$ salt, KBr disk, 80 K			476.5	452.0 ± 0.3	-0.47 ± 0.05	$x_{13} = -2.5 \pm 1.0$ cm^{-1}; $\Gamma = 265 \pm 10$ cm^{-1} [a], $\Delta r = 0.035 \pm 0.003$ Å [a], $\tilde{\nu}_{00} = 20233$ cm^{-1} [a]	[112]
$[MoSe_4]^{2-}$	aq. soln., 295 K	$^1T_2 \leftarrow {}^1A_1$	563	568.2	265	0 ± 0.5		[111]
$[PS_4]^{3-}$	Cu^+ salt, 80 K	$^1T_2 \leftarrow {}^1A_1$	480	476.5	393.3 ± 0.2	-0.46 ± 0.03		[113]
SnI_4	C_6H_{12} soln., 295 K	$^1T_2 \leftarrow {}^1A_1$	364.5	363.8	151.2 ± 0.2	-0.02 ± 0.02		[101]
$TiBr_4$	C_6H_{12} soln., 295 K	$^1T_2 \leftarrow {}^1A_1$	348.7	363.8	232.8 ± 0.1	-0.07 ± 0.01	$x_{12} = -0.8$, $x_{13} = -2.7$, $x_{14} \approx 0.7$ cm^{-1}	[114]
$[WS_4]^{2-}$	$[NH_4]^+$ salt, 80 K	$^1T_2 \leftarrow {}^1A_1$	395	406.7	490.5 ± 0.5	-1.1 ± 0.1		[115]
	$[Bu_4N]^+$ salt, 80 K				478.4 ± 0.5	-0.44 ± 0.05	$\Gamma = 100 \pm 10$ cm^{-1} [a], $\gamma = 150 \pm 20$ cm^{-1} [a], $\Delta r = 0.029 \pm 0.001$ [a], $\tilde{\nu}_{00} = 24650 \pm 10$ cm^{-1} [a]	
$[WSe_4]^{2-}$	aq. soln., 295 K	$^1T_2 \leftarrow {}^1A_1$		488.0	279.5	0 ± 0.5		[111]

$^3T_2$, and the 430-nm shoulder has been assigned to the $^1T_1 \leftarrow {}^1A_1$ transition. The two other possible assignments are ruled out on the grounds that (a) the $^3T_2 \leftarrow {}^1A_1$ transition would be expected to be of much lower energy than $^1T_2 \leftarrow {}^1A_1$,[159] and (b) $^3T_1 \leftarrow {}^1A_1$ is both spin- and orbitally-forbidden. Excitation profiles measured throughout the $^1T_2 \leftarrow {}^1A_1$ and $^1T_1 \leftarrow {}^1A_1$ bands display minima in the region of the latter (Fig. 15). This behavior can be accounted for by interference between the $^1T_2$ and $^1T_1$ contributions to the transition polarizability. Calculations were performed on the assumption that Δr is the same for both states (Fig. 16). This seems reasonable as these two terms arise from

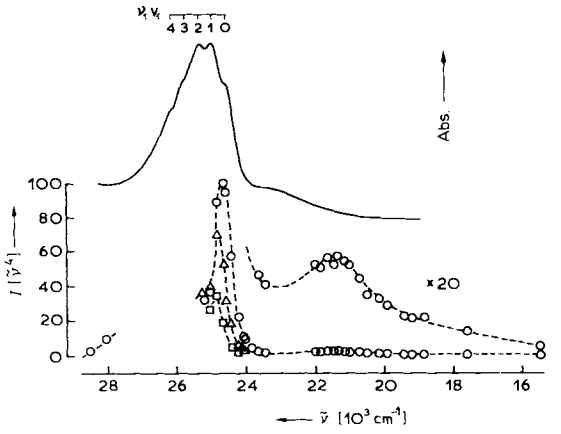


Fig. 15. Electronic absorption spectrum of $[Bu_4N]_2[WS_4]$ at 14 K (solid line) and the excitation profiles for ν_1 (o), $2\nu_1$ (△) and $3\nu_1$ (□) at 80 K (after Ref. [115]).

the same excited configuration. Corroborative evidence for the $^1T_1 \leftarrow {}^1A_1$ assignment is provided by the observation of, and analogous assignment for, similar bands in the absorption spectra of $[CrO_4]^{2-}$ [116] and $[MnO_4]^-$.[117] Unfortunately, these occur in less accessible regions (385 and 850 nm, respectively) and thus have not yet been subjected to RR investigation.

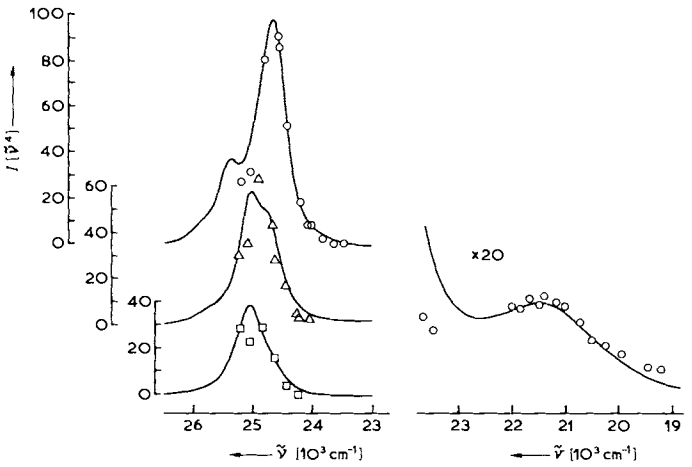


Fig. 16. Calculated (solid lines) and experimental excitation profiles for the ν_1 (o), $2\nu_1$ (△), and $3\nu_1$ (□) bands of $[Bu_4N]_2[WS_4]$ at 80 K (after Ref. [115]).

Attention is drawn to the observation of $\rho(\pi/2)=0.15$ for the ν_1 band of $[FeBr_4]^-$, where a value of zero might, at first sight, be expected. The non-zero value has been shown to be due to an antisymmetric contribution to the transition polarizability tensor,[56, 100] resulting from spin-orbit coupling of the $^6A_1$ ground state with various excited states of the same spin multiplicity. The magnitude of the antisymmetric tensor contribution is likely to be governed by the spin-orbit coupling constant for both the metal and ligand atoms, and the reciprocal of the energy separation between the ground state and those excited states to which it is coupled. On this basis it would be expected that ν_1 $\rho(\pi/2)$ values for the series of molecules $[FeX_4]^-$ would increase in the order X = Cl < Br < I. Partial support for this hypothesis is provided by the observation that $\rho(\pi/2)=0$ for the ν_1 band of $[FeCl_4]^-$. Studies on the $[FeI_4]^-$ molecule were precluded by its rapid decomposition in solution.

4.4. Planar Four-Coordinate Molecules

There have been no new reported RR studies on square planar MX_4-type molecules during the last few years, and the reader is referred to earlier reviews[1, 23] for examples of these. However, there have been a number of RR investigations of bis(dithio) complexes of nickel(II)[118–123] and copper(II),[120, 121] which have assisted in the electronic band assignments for these molecules. The copper complexes are of particular interest as they are model compounds for the study of copper(II)-sulfur interactions in blue copper proteins. In all of the systems studied, absorption bands in the visible region were assigned to metal-ligand charge transfer (MLCT) transitions on the basis that excitation within the contours of these bands yields intense RR spectra dominated by several totally symmetric modes. Due to the lack of bands attributable to either overtones or non-totally symmetric modes in most of these spectra, it may be concluded that any changes of geometry in the MLCT excited states are confined to minor alterations of some bond lengths and angles. One notable exception is the "red" form of bis(dithiooxalato)nickel(II)[123] for which the following progressions were observed: $\nu_1\nu_1$ extending to $\nu_1=6$, and $\nu_1\nu_1+\nu_2$ extending to $\nu_1=4$, where ν_1 is a combination of CC and CS stretching coordinates and ν_2 is a combination of CO and CC stretching coordinates. Clearly, there is a significant change in the size of the C_2S_2Ni ring upon electronic excitation.

4.5. Five-Coordinate Molecules

The only five-coordinate molecules to have been studied recently are the tetrahalooxotechnetate(V) ions, $[TcOX_4]^-$, where X = Br[124] or I.[125] For the bromide a progression reaching to $4\nu_4$ was observed, where ν_4 is the b_1 class $\nu(TeBr_4)$ mode. This is clear evidence for a strong excited-state JT effect involving Q_4. Additionally, weak bands assigned to $2\nu_1$ and $2\nu_1 \pm \nu_4$ were observed, where ν_1 is the $\nu(TcO)$ mode. The RR spectrum of the iodide displays a progression in $\nu_1\nu_1$ extending to $5\nu_1$ ($\omega_1 = 1005.3 \pm 0.2$, $x_{11} = -4.7 \pm 0.1$ cm^{-1}) and several weaker progressions of the sort $\nu_1\nu_1+\nu_i$, where ν_i is ν_2, ν_3, ν_4, ν_6 or an unidentified lattice mode. Weak first overtones of $\nu_2(a_1)$, $\nu_3(a_1)$, $\nu_4(b_1)$, and $\nu_8(e)$ are also observed and it may be concluded that excited-state JT effects are weaker for the iodide than for the bromide.

4.6. Octahedral Molecules

The results of RR studies of hexahalometalate ions are summarized in Table 6. The ions concerned are derivatives of d^3, d^4, and d^5 transition metals and the $d^{10}s^2$ complexes $[TeX_6]^{2-}$, X = Br or Cl. The low spin d^4 and d^5 species are of special interest in that the $^3T_{1g}$ and $^2T_{2g}$ ground terms are split by spin-orbit interaction to give, respectively, four

Table 6. Resonance Raman data on hexahalometalate ions. ER Bands = Electronic Raman bands. MROA-experiment = Magnetic Raman Optical activity experiment.

Species	State	Electronic band assignment	λ_{max} [nm]	λ_0 [nm]	ω_1 [cm^{-1}]	x_{11} [cm^{-1}]	Comments	Ref.
$[IrBr_6]^{2-}$	K^+ salt, aq. soln.	$U'_u(^2T_{2u}) \leftarrow E''_g(^2T_{2g})$	604	510–680			[a]	[50]
	$[Bu_4N]^+$ salt, KBr disk, 80 K and 15 K			600	210.3	0 ± 0.5	ER-band $\Gamma_8 \leftarrow \Gamma'_7(^2T_{2g})$ origin at 4990 cm^{-1}, progressions involving ν_1 and ν_5	[126, 127]
	K^+ salt, aq. soln.			514.5, 577.5			MROA-experiment; negative g-value for ground state	[128]
$[IrCl_6]^{2-}$	$[Bu_4N]^+$ salt, 15, 80 K	$U'_u(^2T_{2u}) \leftarrow E''_g(^2T_{2g})$	495	488.0	341.4	0 ± 0.3	ER-band $\Gamma_8 \leftarrow \Gamma'_7(^2T_{2g})$ with origin at 5500 cm^{-1}, progressions involving ν_1, ν_2 and ν_5	[126, 127, 129, 130]
	$[Bu_4N]^+$ salt, MeCN-soln., K^+ salt, HCl soln., 295 K						MROA-experiments have established a negative value for $E''(^2T_{2g})$ and positive one for $U'(^2T_{2g})$ [a]	[50, 131, 132]
$[OsBr_6]^{2-}$	$[Bu_4N]^+$ salt, 80 K	$2T_{1u} \leftarrow A_{1g}$	450	457.9	211.4	0 ± 0.4	$x_{12} = -2 \pm 1$, $x_{15} = -0.5 \pm 1$ cm^{-1}; ER-bands at 2810, 4850, 5000 cm^{-1} assigned to $\Gamma_4 \leftarrow \Gamma_1$, $\Gamma_5 \leftarrow \Gamma_1$, $\Gamma_3 \leftarrow \Gamma_1$	[126, 133, 134]
	K^+ salt, HBr soln., 295 K			488.0			Assigments confirmed by ρ measurements, positive g factor for $\Gamma_4(^3T_{1g})$	[132, 134]
$[OsCl_6]^-$	$[Et_4N]^+$ salt, 80 K	$^4T_{2u} \leftarrow {}^4A_{2g}$	500	488.0	376.6 ± 0.6	-0.8 ± 0.2	Band origin at 5800 cm^{-1} assigned to $\Gamma_8(^2T_{2g}) \leftarrow \Gamma_8(^4A_{2g})$. $\rho(\pi/2) = 0.2$	[135]
$[OsCl_6]^{2-}$	K^+ salt, HCl soln., 295 K	$T_{1u} \leftarrow A_{1g}$	324, 375	325, 454.5			ER-Bands at 2780, 5060 and 5190 cm^{-1} assigned to $\Gamma_4 \leftarrow \Gamma_1$, $\Gamma_5 \leftarrow \Gamma_1$ and $\Gamma_3 \leftarrow \Gamma_1$ on the basis of ρ measurements	[50, 134]
	$[Bu_4N]^+$ salt, 80 K			514.5			Electronic origins at 2800, 4880 and 5090 cm^{-1}	[127]
$[OsI_6]^{2-}$	K^+ salt, $H[ClO_4]$ soln., 295 K	$T_{1u} \leftarrow A_{1g}$	387, 556, 565, 576	514.5			ER-bands at 2640, 4600 cm^{-1} (assigned to $\Gamma_4 \leftarrow \Gamma_1$ and $\Gamma_{3,5} \leftarrow \Gamma_1$ on the basis of ρ measurements)	[134]
	$[Bu_4N]^+$ salt, 80 K			647.1	156.9 ± 1	-0.8 ± 0.5	Band origins at 2580 ($\Gamma_4 \leftarrow \Gamma_1$), 4440 ($\Gamma_3 \leftarrow \Gamma_1$), 4710 cm^{-1} ($\Gamma_5 \leftarrow \Gamma_1$)	[127]
$[RuBr_6]^{2-}$	$[Bu_4N]^+$ salt, KBr disk, 80 K	$T_{1u} \leftarrow A_{1g}$ ($t_{2u}(\pi) \rightarrow t_{2g}$)	580	568.2	200.8	-0.15	Band origins at 752 ($\Gamma_4 \leftarrow \Gamma_1$), 1850 cm^{-1} ($\Gamma_{3,5} \leftarrow \Gamma_1$)	[136]
$[RuCl_6]^{2-}$	$[Ph_4P]^+$ salt, KCl disk, 80 K	$T_{1u} \leftarrow A_{1g}$ ($t_{1u}(\pi,\sigma) \rightarrow t_{2g}$)	520	501.7	326.5	-0.11	Band origins at 1529 cm^{-1} assigned to $\Gamma_{3,5} \leftarrow \Gamma_1$. Progression in $\nu_1 \nu_1$ based on this origin observed for $\lambda_0 = 457.9$ nm	[136]
$[TeX_6]^{2-}$ X = Br or Cl	$[Bu_4N]^+$ salts, MeCN soln., 295 K	$^{1,3}T_{1u} \leftarrow {}^1A_{1g}$	320–470 (Br) 260–405 (Cl)	356.4 337.5			$\rho(\pi/2) = 0.18 \pm 0.02$ for $2\nu_2$ of $[TeBr_6]^{2-}$ in good agreeement with theoretical prediction (3/14)	[137]

[a] Anomalous depolarization ratios for ν_1, ν_2 and ν_5 ascribed to antisymmetric tensor contributions resulting from ground-state degeneracy.

and two states (Fig. 17). These states all lie within ca. 5000 cm^{-1} of each other and in each case Raman bands have been observed which may be assigned to transitions from the ground to these states. The most recently reported study is of the vibrational and electronic RR spectra of the $[RuCl_6]^{2-}$ and $[RuBr_6]^{2-}$ ions. The RR spectra and EPs for $[RuCl_6]^{2-}$ are shown in Figure 18. The electronic and vibrational Raman bands display maximum intensity for resonance with different excited states, although it is not understood why this should be so.

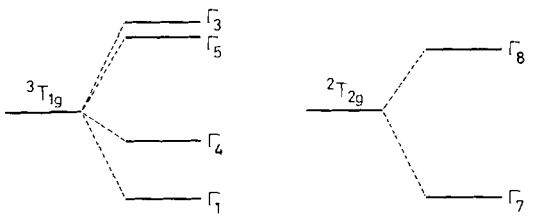


Fig. 17. Qualitative energy level diagrams for the spin-orbit splitting of the $^3T_{1g}$ and $^2T_{2g}$ ground terms.

The $5d^5$ species $[IrCl_6]^{2-}$ and $[IrBr_6]^{2-}$ possess Kramers degenerate $\Gamma_6(^2T_{2g})$ ground states. As a consequence of the ground-state degeneracy, the three Raman-active fundamentals (ν_1, ν_2 and ν_5) all give rise to anomalously polarized bands.[50] Some of the hexahalometalates have been investigated by the relatively new technique of magnetic Raman optical activity, which enables the sign of the

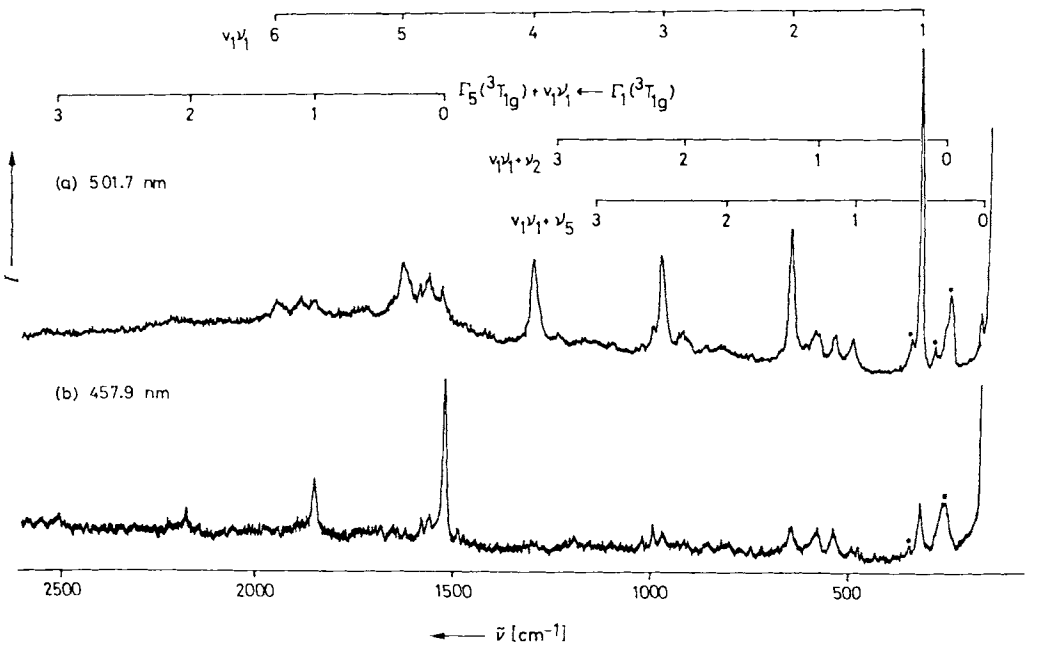


Fig. 18. Resonance Raman spectra of $[Ph_4P]_2[RuCl_6]$ in a CsCl disk at ca. 80 K excited by (a) 501.7 nm and (b) 457.9 nm radiation. Bands marked by an asterisk are due to impurities (after Ref. [136]).

ground-state g-factor to be determined from circular intensity differential measurements.[131]

4.7. Species with No Discrete Vibrating Unit

In this section we discuss some recent RR studies on the two-dimensional layer compounds ZrS_3[138] and HfS_3.[139] Although these are strictly semiconductor species we have chosen to include them because their RR behavior is in many ways similar to that of small molecular species. ZrS_3 has a band gap energy of about 2.5 eV (20000 cm^{-1}) and excitation in this region produces RR spectra that are dominated by progressions involving three fundamentals, at 152, 285, and 326 cm^{-1}. These are assigned to the vibrational R_y' motion, the totally symmetric stretching mode of Zr-S_I interchain bonds, and the $\nu_s(ZrS_2^{2-})$ vibration, respectively. Off-resonance polarized Raman spectra indicate that the intensities of all three of these bands are dominated by α_{yy} components. Since the excitation profiles of these bands were found to maximize close to the absorption maximum at 492 nm, it was concluded that the transition must be y-polarized ($A_u \leftarrow A_g$ in the C_{2h} factor group). Neglecting any changes of vibrational wave number in the excited state, the best fit to the excitation profiles was calculated with the parameters $\tilde{\nu}_{00} = 20325$ cm^{-1}, $\Gamma = 450$ cm^{-1}, and $A = 0.894$ (285 and 326 cm^{-1} bands) or 1.0 (152 cm^{-1} band).

For HfS_3 the first absorption maximum is at ca. 22700 cm^{-1} and excitation in this region produces RR spectra and excitation profiles that are similar to those of ZrS_3. The most enhanced bands are the four totally symmetric modes at 128, 261, 275, and 322 cm^{-1}, which were shown by off-resonance Raman orientation measurements to be dominated by their α_{yy} components. It was postulated that at least two allowed y-polarized transitions contribute to the RR scattering process for both HfS_3 and ZrS_3.

5. Resonance Raman Studies of Larger Polyatomic Molecules

5.1. Six-Coordinate Transition Metal Complexes

There have been a number of RR studies of tris(α-diimine) and related complexes of iron(II),[140-145] ruthenium(II),[146-152] and, to a lesser extent, osmium(II).[141,148] A great deal of interest has been focused on $[Ru(bpy)_3]^{2+}$, bpy = 2,2'-bipyridyl, because of its importance as a photocatalyst for the photodecomposition of water. RR investigations of $[Ru(bpy)_3]^{2+}$ have involved (a) excitation resonant with the first singlet MLCT excited state at 22000 cm^{-1}, and (b) optical pumping of the first triplet MLCT state (via the singlet), designated $[^*Ru(bpy)_3]^{2+}$, followed by resonant excitation from the populated triplet state to a higher triplet state. The latter enables the measurement of the RR spectrum of the ion in the first triplet excited state. This is characterized by a number of new vibrational bands which are ca. 60 cm^{-1} lower than for the ion in its ground state. The similarity between these bands and those of the bipyridyl radical anion have led to the conclusion that the electron transfer from the metal is to one bpy ligand only (rather than to a molecular orbital encompassing all three), such that the excited state may be formulated as $[Ru^{III}(bpy)_2(bpy^{\bullet -})]^{2+}$. Additional evidence for the localized model is provided by (a) the observation of additional bands which are unshifted with respect to the ground state, indicating the presence of neutral bipyridyl ligands in the excited state, (b) similar behavior for $[Os(bpy)_3]^{2+}$, substituted bis(bipyridyl)ruthenium(II) complexes, and *fac*-$[XRe(CO)_3(bpy)]$, X = Br or Cl.[148,152]

Tris(α-diimine)iron(II) complexes exhibit a strong absorption band in the visible region ($\lambda_{max} = 524$ nm for $[Fe(bpy)_3]^{2+}$) which has been assigned to a MLCT $^1E \leftarrow {}^1A_1$ transition on the basis of single-crystal polarized absorp-

tion studies. In each case there is an unresolved shoulder ca. 1500 cm^{-1} above the absorption maximum, which could be assigned to a vibronic side-band or to a second electronic transition. RR spectra and excitation profiles of these complexes have been measured using excitation throughout the absorption region and the results interpreted in terms of a single transition giving rise to a 0-0 and a conglomerate of 0-1 bands.[140] This conclusion was reached on the bases that (a) the most enhanced Raman bands are those in the 1400–1600 cm^{-1} region (ligand ring vibrations involving C–C and C–N bonds) and (b) these modes are responsible for the vibronic sideband in the absorption spectra. However, the RR band depolarization ratios vary between 0.10 and 0.71,[140] an observation which is inconsistent with RR scattering involving only a $^1E \leftarrow {}^1A_1$ resonant transition ($\rho(\pi/2) = 1/8$ for totally symmetric modes), but which could be accounted for by contributions from both ^1E and $^1A_2$ resonant excited states. New absorption and CD spectroscopic data obtained for $[Fe(bpy)_3]^{2+}$ indicate that there may be a number of transitions within this spectral region.[153] A reassessment of the RR spectrum of the ion is in progress in our laboratory.

A number of carbonyl-imine and -diimine complexes of Cr, Mo, W, Re and Fe have been investigated by *Stufkens* et al.[154–157] The RR spectra of these complexes were obtained by excitation within the MLCT band of lowest energy, i.e. in the 400–600 nm region. In common with the diimine complexes discussed previously, the spectra display only polarized Raman bands. Thus the scattering mechanism is undoubtedly of A-term origin and the small displacement approximation is probably valid because any bands attributable to overtones are very weak. The MLCT bands have been shown to consist of the overlap of three or four bands on the basis of RR EPs and magnetic circular dichroism spectra. These bands are assigned to charge transfer resulting from the promotion of an electron from one of the metal d-orbitals to a π^* orbital localized on the diimine ligand. The RR data are consistent with this assignment in that the most enhanced Raman bands are those associated with the diimine ligand, i.e. bands in the 1400–1600 cm^{-1} region which are attributed to ν(CC) and ν(CN) stretching modes. Surprisingly, it is found that the ν_s(*cis*-CO) bands are also enhanced, which implies that the CO bond lengths are affected by transitions to an MLCT state. That the ν_s(*trans*-CO) bands do not display RR activity suggests that the effect is not due either to the oxidation of the metal atom or to a change of π-backbonding accompanying the transition. Instead, it is believed that the RR activity of ν_s(*cis*-CO) is due to an excited state interaction between the diimine and the *cis*-carbonyl ligands. Such an interaction is expected to increase as the central atom becomes smaller, this inference being supported by the observation that, for the series [M(CO)$_4$(diazabutadiene)], where M = Cr, Mo, or W, the intensity of ν_s(*cis*-CO) increases with respect to ν_s(CN) in the order W < Mo < Cr. It was also found that these compounds are photoreactive when irradiated in the presence of a phosphane ligand within the MLCT band. This process results in the substitution of a *cis*-carbonyl group by the phosphane with a quantum yield varying from 10^{-2} to 10^{-4}. The quantum yield is found experimentally to be directly related to the Raman intensity of the ν(*cis*-CO) band, and complexes which do not display a RR effect for this vibration are photochemically stable. These results clearly show that RR spectroscopy is a powerful tool for the interpretation of the photochemistry of inorganic molecules.

RR studies of $K_3[Cr(CN)_5NO]$[158] at resonance with the $^2B_2 \leftarrow {}^2B_1$ chromium-to-NO transition have shown that the most enhanced Raman band, and the one which forms the longest (to three members) progression, is ν(CrN). Intensity ratio calculations have led to the conclusion that the CrN bond length increases by ca. 0.10 Å on excitation to this MLCT state, but that the CrC bond length also increases, though by a lesser amount (ca. 0.07 Å).

5.2. Metal–Metal Bonded and Bridged Species

Of the very large number of metal-metal bonded species known,[160] those for which RR studies have proved to be particularly valuable are the quadruply bonded ones $[Mo_2Cl_8]^{4-}$, $[Mo_2Br_8]^{4-}$, and $[Re_2X_8]^{2-}$, X = F, Cl, Br, or I.[161–166] In each case the eight halogen atoms are situated virtually at the corners of a cube, thereby encapsulating the M_2 unit, the MMX angle being ca. 105° in each case. The molybdenum and rhenium species are effectively isoelectronic, the molybdenum species possessing a single moderately intense and highly structured band in the visible region. The principal progression-forming mode giving rise to this structure has, in each case, been identified as the MM stretch. For the rhenium species there are a number of bands throughout the visible/near UV region (Fig. 19). The lowest energy band in each case, as for the molybdenum

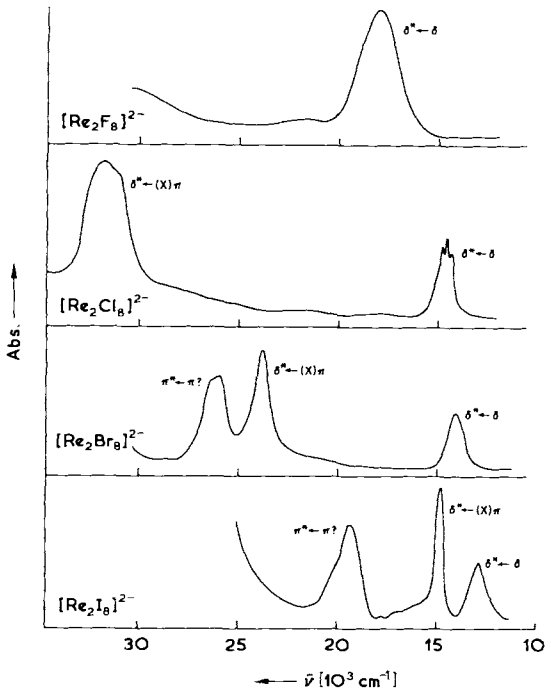


Fig. 19. Electronic absorption spectra of the complexes $[Bu_4N]_2[Re_2X_8]$ at ca. 14 K in the region of their $\delta^* \leftarrow \delta$, $\delta^* \leftarrow \pi(X)$ and $\pi^* \leftarrow \pi$ (?) transitions. ($Cs[BF_4]$, KCl, KBr, and CsI disks for X = F, Cl, Br, or I, respectively) (after Ref. [167]).

species, has been assigned to the $^1A_{2u} \leftarrow {}^1A_{1g}$ ($\delta^*(b_{1u}) \leftarrow \delta(b_{2g})$) transition. Excitation of such an ion from the ground to the $^1A_{2u}$ state in effect changes the MM bond order from four to three, with consequential increase in bond length (hence the observed progression in ν(MM)).

Irradiation within the contour of the $\delta^* \leftarrow \delta$ band leads, in each case, to the generation of an RR spectrum characterized by (a) substantial enhancement to the intensity of ν(MM) and (b) the development of a long (at most to eleven members) progression in ν(MM). These results confirm the conclusion drawn from the electronic spectra, namely that the equilibrium MM bond length in the δ^* state is significantly longer than that in the ground state. The set of four dirhenium anions are particularly interesting (Fig. 20). Raman spectra of these ions, in each case obtained at resonance with the $\delta^* \leftarrow \delta$ transition, give rise to long progressions in ν(ReRe) (318, 275, 276, and 257 cm^{-1} for X = F, Cl, Br, or I, respectively); these observations clearly indicate the similar nature of the lowest electronic transition in each case. This conclusion is substantiated by measurements of the depolarization ratio of the ν(ReRe) Raman band at resonance with the $\delta^* \leftarrow \delta$ transition. This has been found to take the value 1/3 for $[Re_2F_8]^{2-}$, $[Re_2Cl_8]^{2-}$ and $[Re_2Br_8]^{2-}$, a result which is only possible if the resonant electronic transition is z-polarized (Section 2.5). This is precisely the polarization of the $\delta^* \leftarrow \delta$ transition (transition moment A_{2u} in the D_{4h} symmetry point group to which the ions belong).[167, 168]

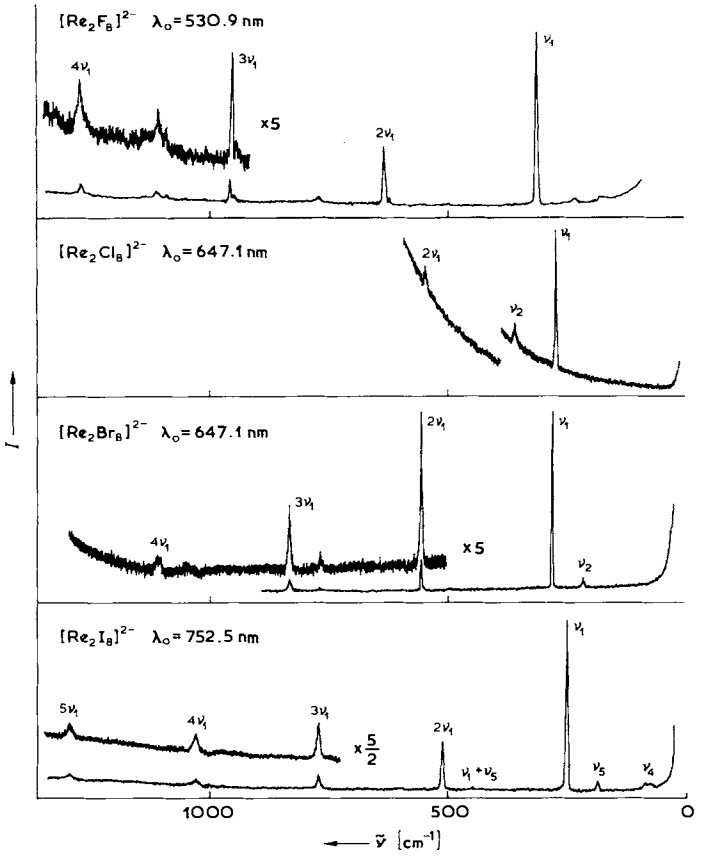


Fig. 20. Resonance Raman spectra of the complexes $[Bu_4N]_2[Re_2X_8]$ at ca. 80 K in the region of their $\delta^* \leftarrow \delta$ transitions (after Refs. [167], [168]).

Irradiation within the contour of the second electronic transition of each ion produces substantially different spectra in each case (Fig. 21). Such RR spectra are characterized by resonance enhancement to the bands attributed to ν(ReX) and its overtones. (ν(ReX) occurs at 624, 362,

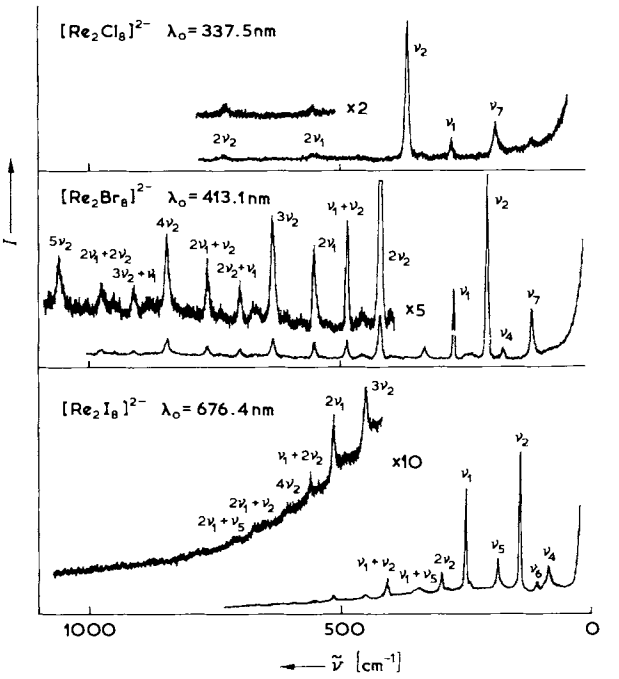


Fig. 21. Resonance Raman spectra of the complexes $[Bu_4N]_2[Re_2X_8]$ at ca. 80 K in the region of their $\delta^* \leftarrow \pi(X)$ transitions (after Refs. [167], [168]).

211 and 152 cm^{-1} for X = F, Cl, Br or I, respectively). Thus, the principal structural change undergone by each ion on excitation to its second excited state is along the ReX coordinate. This result clearly implies that the second electronic transition is in each case of the halogen-to-metal charge-transfer type. The assignment of the second strong band in the electronic spectra of the $[Re_2X_8]^{2-}$ ions is thus clearly $b_{1u}(\delta^*) \leftarrow X, e_g(\pi)$, $^1E_u \leftarrow {}^1A_{1g}$. This result is confirmed by the fact that the measured depolarization ratio of the ν(ReX) band of $[Re_2Cl_8]^{2-}$ and $[Re_2Br_8]^{2-}$ at resonance with the second electronic band is 0.15, i.e. close to the value of 1/8, as required for a $^1E_u \leftarrow {}^1A_{1g}$ transition.

Many other metal-metal multiply bonded species yield richly detailed RR spectra at resonance with their lowest electronic transition. The most notable of the recent studies along these lines have been those on $[Ru_2(O_2CR)_4Cl]$, R = H, CH_3, C_2H_5, or C_3H_7,[169] and related studies on diosmium and dirhodium carboxylates.[170, 171] In addition to the bond between them the metal atoms are bridged by the carboxylate ligands.

Another type of bridged species is that in which the metal atoms are separated by one or more atoms. Of these, $[Ru_2OCl_{10}]^{4-}$ (Fig. 22) and related ions have been subjected to the most intensive RR investigations.[172, 173] The spectra of these ions are characterized by intense progressions involving the M–O–M stretching coordinate (ν_1), the axial and equatorial metal–halogen stretches (ν_2 and ν_3), the $\delta(OMX_{eq})$ coordinate (ν_4), and even quanta of the infrared-active modes $\nu_5(\nu_{as}(MOM))$ and $\nu_9(\delta(MOM))$. It is

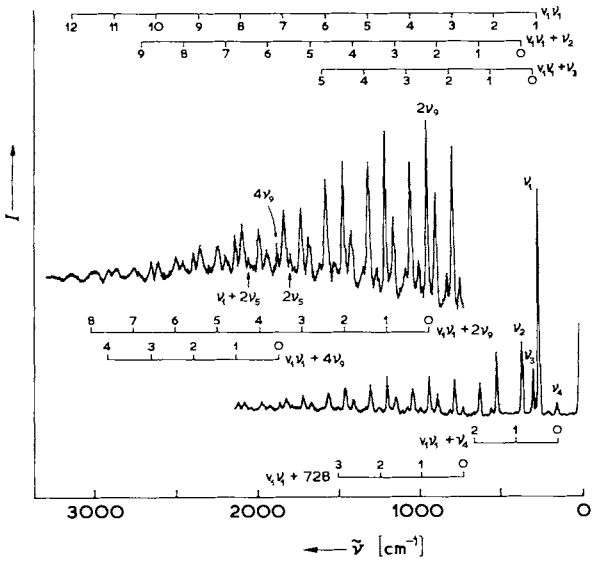


Fig. 22. Resonance Raman spectrum of $K_4[Ru_2OCl_{10}]$ at ca. 80 K, obtained with 488.0 nm excitation (after Ref. [173]).

clear, then, that there must be a substantial alteration of molecular geometry accompanying the resonant, $^1A_{2u} \leftarrow {}^1A_{1g}$, electronic transition. The observation of progressions involving even quanta of $\nu_5(a_{2u})$ and $\nu_9(e_u)$ is strong evidence for a reduction in symmetry in the excited state, although it is not obvious what that symmetry might be.

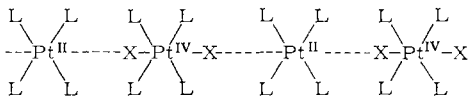
Other bridged species that have been studied recently include ones in which the bridging moiety is N,[174] N_2,[175], or O_2 (both peroxo and superoxo).[176] In all cases the RR spectra are characterized by a number of bands attributable to totally symmetric fundamentals. Together with the absence of any overtones for most of these species this observation indicates that the geometric changes attendant upon excitation are small and spread over many atoms.[38] There have been several studies of μ_2- and μ_3-sulfur-bridged species in which there are $[MS_4]^{2-}$ sub-units, where M = Mo or W.[177-179] Considerable interest has developed in the molybdenum complexes, some of which are model compounds for the MoFe cofactor of nitrogenase.

5.3. Mixed-Valence Complexes

Complexes in which the metal atom is present in more than one oxidation state are of considerable importance, not only in inorganic chemistry, but also in bioinorganic chemistry and geology. Thus, at least 40 elements in the periodic table form mixed-valence complexes, many of which have very striking properties. Mixed-valency is central to the role of Fe_4S_4 clusters for promoting redox processes in enzymes such as ferredoxin and rubredoxin, and many minerals (particularly iron minerals) contain the metal in at least two oxidation states.

The two most significant properties of mixed-valence complexes are their colors and their electrical conductivities. Each of these properties differs substantially, in many cases, from those of the constituent single-valence species. In the first place, the colors of certain mixed-valence species are so intense that they have been used as dyestuffs (e.g. Prussian blue, ruthenium red), while in the second place, certain mixed-valence complexes are best described as one-dimensional conductors (e.g. $[K_2Pt(CN)_4 \cdot Br_{0.30} \cdot 3H_2O]$ (KCP)). The reader is referred elsewhere to recent reviews of the classification and properties of mixed-valence complexes.[3,4]

The colors of mixed-valence complexes are dominated by intervalence transitions which, being electric-dipole allowed, are in general intense. Raman studies of such complexes at resonance with the intervalence bands prove to be very sensitive probes of the geometric changes undergone on excitation from the ground to the intervalence state. Particularly detailed studies of certain types of linear-chain complexes have now been made, viz. that of Wolffram's red and its analogues, which are examples of Pt^{II}/Pt^{IV} mixed-valence complexes of the type **1**, where



1

L = amine, X = Cl, Br, or I. Irradiation within the contour of the intervalence band of such complexes leads to enormous intensification of the band attributed to the symmetric chain-stretching mode, $\nu_1(X\text{-}Pt^{IV}\text{-}X)$, together with the development of a long, intense, overtone progression $\nu_1 \nu_1$ (reaching to, at most, 18 members) (Fig. 23). These results

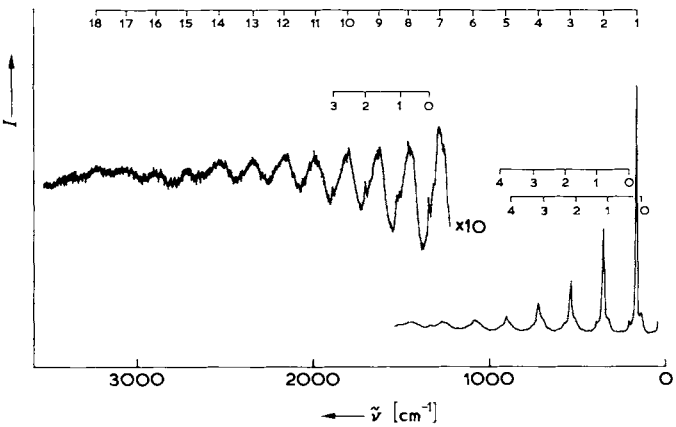
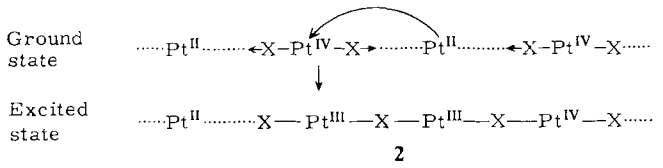


Fig. 23. Resonance Raman spectrum of $[Pt(tn)_2][Pt(tn)_2Br_2][ClO_4]_4$ in a KBr disk at ca. 80 K, obtained with 488.0 nm excitation (after Ref. [180]), tn = 1,3-diaminopropane.

indicate that the Pt^{IV}-X bond lengths increase substantially (probably by at least 0.1 Å)[180] on excitation of the complex from the ground to the intervalence state. This structural change is precisely that expected (on conductance grounds) on excitation to the Pt^{III}/Pt^{III} intervalence state since, in its relaxed geometry in this state (as in **2**), the axial halogen atoms would be expected to be midway between the Pt^{III} ions.

The assignment of the progression-forming mode to the symmetric chain-stretching vibration has been confirmed



2

by single crystal orientation measurements, an example of which is shown in Figure 24.

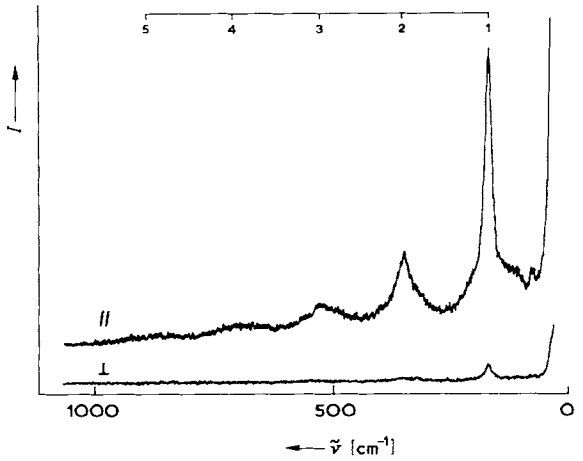


Fig. 24. Resonance Raman spectra of a single crystal of $[Pt(tn)_2][Pt(tn)_2Br_2][ClO_4]_4$ at ca. 298 K with the incident radiation polarized along the crystal Z axis and the scattered radiation ($\lambda_0 = 568.2$ nm) measured for polarization parallel and perpendicular to the Z axis (after Ref. [180]).

Related studies have been carried out on analogous mixed-valence Pd^{II}/Pd^{IV} chain complexes, and also on certain mixed-metal, mixed-valence complexes (e.g. Ni^{II}/Pt^{IV} and Pd^{II}/Pt^{IV} chain complexes), with similar results.[181-183] In all cases, harmonic wave numbers and anharmonicity constants have been calculated from the observed band wave numbers, and tabulated.[3] It has recently been discovered that, for certain linear-chain mixed-valence platinum complexes, the wave number, ν_1, of the symmetric chain-stretching mode increases as the excitation wave number (ν_0) increases.[184] For any set of complexes the wave-number change

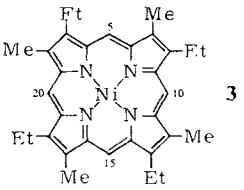
$\nu_1(\nu_0 = \text{high wave number}) - \nu_1(\nu_0 = \text{low wave number})$

increases in the order Cl < Br < I and is largest for those complexes in which the $Pt^{II} \cdots Pt^{IV}$ separation is least and for which the bond length ratio $r(Pt^{IV}\text{-}X)/r(Pt^{II}\text{-}X)$ is nearest to unity. This behavior, which is not observed for any of the equatorial modes, is believed to be due to solid state effects rather than an intrinsically mixed-valence property.

One other type of mixed-valence complex that is worthy of note is the so-called Creutz-Taube ion, $[(NH_3)_5Ru(pyrazine)Ru(NH_3)_5]^{5+}$, in which the ruthenium oxidation states are formally +2 and +3 or both +2.5. Various spectroscopic techniques have led to conflicting conclusions concerning the electronic structure of this ion, especially on the extent of valence-delocalization.[185] RR spectra display several broad bands assigned to totally symmetric modes which are probably associated with the pyrazine ring. However, the spectroscopic evidence obtained to date has not unequivocally established whether the odd electron is delocalized or trapped on one Ru atom, and further investigations are in progress. Another mixed-valence Ru^{II},Ru^{III} complex that has been investigated recently is $[(NH_3)_3Ru(\mu_3\text{-}X_3)Ru(NH_3)_3]^{2+}$ (X = Cl, Br, or I). Whereas the A_1' ground state of this complex is localized (non-equivalent Ru centers), RR spectroscopy has indicated that, in the A_2'' excited state (14000-17000 cm^{-1}), the odd electron is delocalized.[186]

5.4. Metalloporphyrins

The study of metalloporphyrins and heme proteins by RR spectroscopy has developed into a major field of research since the pioneering work, over a decade ago, of *Spiro*.[25] Several comprehensive reviews of this subject have been written[5, 11, 26, 27] and it is our intention here to present only the essential features of metalloporphyrin RR spectra.



3

Absorption spectra of metalloporphyrins consist of an intense near UV band ($\varepsilon \approx 10^5$ M^{-1} cm^{-1}), called the Soret band, and a weaker ($\varepsilon \approx 10^4$ M^{-1} cm^{-1}) Q band in the visible region which displays a 0-0 and conglomerate 0-1 maxima. The positions of these bands vary considerably according to the central metal atom, its spin- and oxidation-state, and substituents on the metalloporphyrin ring (shown in Fig. 25) but typically the Soret band is at around 400-450 nm and the Q-band around 550-600 nm. Both bands are assigned to $\pi\text{-}\pi^*$ $^1E_u \leftarrow {}^1A_{1g}$ transitions (in the idealized D_{4h} geometry) associated with the porphyrin ring. The electronic structures of metalloporphyrins have been investigated in some considerable detail by *Gouterman*,[187] and it has been shown that these two transitions arise from the promotion of electrons from filled, nearly degenerate, $1a_{1u}$ and $3a_{2u}$ orbitals to unfilled $4e_g$ orbitals. As a consequence of configuration interaction the transition to the higher energy Soret state is dipole-allowed while that to the Q state is nearly forbidden. Thus the latter transition acquires intensity by (Herzberg-Teller) vibronic coupling of the Soret and Q states, via a_{1g}, a_{2g}, b_{1g}, and b_{2g} vibrations, which give rise to the 0-1 conglomerate band.

RR spectra excited within the contour of the Q-band consist of the vibronically (B-term) active fundamentals of the porphyrin ring, which are distinguishable by their depolarization ratios: $\rho = 1/8$ (a_{1g}), $\rho = \infty$ (a_{2g}) and $\rho = 3/4$ (b_{1g} and b_{2g}). Deviations from these values bear witness to the lowering of the symmetry, especially to the loss of the fourfold axis, due to substituents on the porphyrin ring or to interaction with the environment within which the molecule is accommodated. Then, mixed symmetric/antisymmetric scattering may occur (see Section 2.5) giving

$3/4 < \rho < \infty$ for non-totally symmetric modes, and deviation from $\rho = 1/8$ might be observed for the totally symmetric modes. However, the latter are usually quite weak for Q-band excitation, and it may be impossible to obtain sufficiently accurate polarization data. Weak overtones of some of the non-totally symmetric fundamentals are sometimes observed, and have been ascribed to D-term scattering.

By contrast, RR spectra obtained by excitation within the contour of the Soret band are dominated by bands attributed to totally symmetric fundamentals. These owe their activity to an A-term scattering regime in which the displacement parameters are quite small. There have been far fewer studies of Soret-excited RR spectra, mainly because excitation in this region is not so widely available in most laboratories; however, it is expected that this situation will change, and that a wealth of experimental data will soon build up. In particular, Soret excitation offers the opportunity of monitoring the lowering of the symmetry (from D_{4h}) by measuring deviations of ρ from 1/8.

There have been several measurements of excitation profiles (mostly confined to the Q-band region). These have been analyzed in terms of contemporary RR theory. Typically, EPs display two maxima within the Q-band (0-0 and 0-1) which are of unequal intensity. For B-term scattering it is predicted that the 0-0 and 0-1 resonances are of equal intensity. As pointed out in Section 2.4, deviations from equal scattering intensity arise from (a) non-adiabatic coupling between the Q and Soret states, and (b) JT distortion in the Q state. The a_{2g} modes (those for which $\rho = \infty$) are not JT-active and therefore show only the non-adiabatic effect which favors the 0-1 resonance. Polarized ($\rho = 1/8$) and depolarized ($\rho = 3/4$) bands tend to show stronger 0-0 scattering, believed to arise from additional A-term contributions. Enhanced scattering in the 0-1 region can also arise from A-term/B-term interference.[45] Examples of all of these effects can be seen in the Q-band EPs of nickel aetioporphyrin I (see **3**) (Fig. 25),[188] which represent the most complete Q-band profiles obtained for a symmetric metalloporphyrin.

The most detailed excitation profiles in the Soret region have been obtained for ferrocytochrome c (1362 cm^{-1} band) and ferricytochrome c (1374 cm^{-1} band) by *Champion* and *Albrecht*.[189] The EP of the former is asymmetric and has higher intensity in the 0-1 region, whereas the latter shows a broad structureless peak slightly blue-shifted from the 0-0 position. These observations were accounted for by a theoretical model encompassing both homogeneous and inhomogeneous broadening and a multidimensional subspace of vibrational and librational modes in the excited state. The latter was calculated analytically by approximating the product of Franck-Condon factors with the density of states to a truncated Lorentzian distribution. However, *Shelnutt*[190] has convincingly demonstrated that the enhanced scattering in the 0-1 region can be accounted for by a single-mode calculation including interference between inter- and intramanifold coupling (i.e. A-term/B-term interference).

In this short section we have attempted to present the essential features of metalloporphyrin RR scattering. As already pointed out a vast literature on this subject exists,

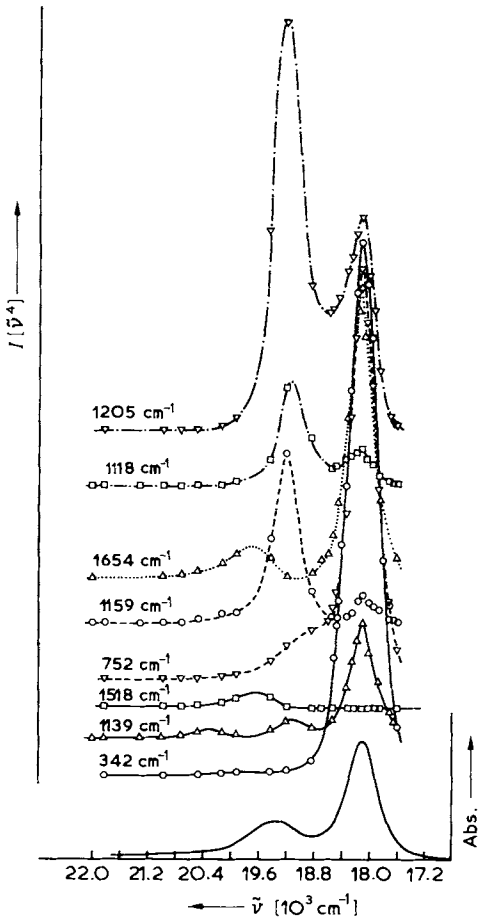


Fig. 25. Q-band resonance Raman excitation profiles of nickel(II) aetioporphyrin I in $CDCl_3$. Bands at 1118 and 1205 cm^{-1} are inversely polarized, those at 752, 1159 and 1654 cm^{-1} are depolarized, and those at 342, 1139 and 1518 cm^{-1} are polarized. The uppermost excitation profile relates to the [5,10,15,20-D_4]-derivative (after Ref. [188]).

the major interest being concerned with biological aspects, such as electron transfer, respiratory function, catalysis, and metal transport or storage. Furthermore, the intricacies of the theoretical analysis of the spectra have become rather complicated due to the large number of phenomena involved. A recent paper by *Shelnutt*[19] is commended, in which is developed a simple model of vibronic states that brings out the essential features of metalloporphyrin RR spectra, excitation profiles, and polarization dispersion.

6. Conclusion and Future Outlook

The sensitivity of RR spectroscopy has transformed the technique of Raman spectroscopy from being one of greatly restricted use in inorganic and analytical chemistry to one of great value. Not only can species frequently be detected at very low concentrations by RR spectroscopy, but information is obtained specifically about the chromophoric center in the species. Since this part of a molecule is usually the one of greatest chemical interest—particularly in molecules of biochemical importance—increasing attention is being paid to RR studies of such species. Increasing attention is also being paid to the spectroscopy of molecules in excited electronic states, to the nature and spectroscopy of species generated at electrode surfaces, to ther-

mally sensitive species isolable only in matrices, and to the spectroscopy of transients in chemical reactions.

It is to be expected that, during the next few years, new developments of RR theory will considerably increase the amount of information obtainable from experimental data. In particular it is envisaged that more attention will be paid to the theoretical analysis of excitation profiles and to the polarization dispersion of Raman bands of molecules for which the absorption spectra are devoid of vibrational structure. In conjunction with the availability of a wider range of excitation lines, this will enable the RR technique for the determination of excited-state molecular geometries to be applied to a considerably larger number of inorganic molecules.

Received: March 5, 1985 [A 566 IE]
German version: *Angew. Chem. 98* (1986) 131

[1] R. J. H. Clark, B. Stewart, *Struct. Bonding (Berlin) 36* (1979) 1.
[2] D. F. Shriver, C. B. Cooper, *Adv. Infrared Raman Spectrosc. 6* (1980) 127.
[3] R. J. H. Clark, *Adv. Infrared Raman Spectrosc. 11* (1984) 95.
[4] R. J. H. Clark, *Chem. Soc. Rev. 13* (1984) 219.
[5] R. H. Felton, N.-T. Yu in D. Dolphin (ed.): *The Porphyrins, Vol. 3*, Academic Press, New York 1978, p. 347.
[6] P. Y. Yu, *Top. Curr. Phys. 14* (1979) 211.
[7] R. J. H. Clark, T. J. Dines, *Adv. Infrared Raman Spectrosc. 9* (1982) 282.
[8] G. H. Atkinson, *Adv. Infrared Raman Spectrosc. 9* (1982) 1.
[9] A. C. Albrecht, *J. Chem. Phys. 34* (1961) 1476.
[10] J. Tang, A. C. Albrecht, *Raman Spectrosc. 2* (1970) 33.
[11] P. M. Champion, A. C. Albrecht, *Annu. Rev. Phys. Chem. 33* (1982) 353.
[12] B. R. Stallard, P. M. Champion, P. R. Cullis, A. C. Albrecht, *J. Chem. Phys. 78* (1983) 712.
[13] P. P. Shorygin, *Pure Appl. Chem. 4* (1962) 87.
[14] L. L. Krushinskii, P. P. Shorygin, *Opt. Spectrosc. 11* (1961) 12, 80.
[15] J. Behringer, *Raman Spectrosc. 1* (1967) 168.
[16] J. Behringer, *Mol. Spectrosc. Chem. Soc., London [Specialist Periodical Reports] 2* (1974) 100; *3* (1976) 163.
[17] W. L. Peticolas, L. Nafie, P. Stein, B. Fanconi, *J. Chem. Phys. 52* (1970) 1576.
[18] B. B. Johnson, W. L. Peticolas, *Annu. Rev. Phys. Chem. 27* (1976) 465.
[19] J. A. Koningstein: *Introduction to the Theory of the Raman Effect*, D. Reidel, Dordrecht 1972.
[20] J. A. Koningstein, *Mol. Spectrosc. Chem. Soc., London [Specialist Periodical Reports] 4* (1977) 196.
[21] J. A. Koningstein, *Vib. Spectra Struct. 9* (1981) 115.
[22] D. L. Rousseau, J. M. Friedman, P. F. Williams, *Top. Curr. Phys. 11* (1979) 203.
[23] R. J. H. Clark, *Adv. Infrared Raman Spectrosc. 1* (1975) 143.
[24] R. J. H. Clark, B. Stewart, *J. Am. Chem. Soc. 103* (1981) 6593.
[25] T. G. Spiro, T. M. Loehr, *Adv. Infrared Raman Spectrosc. 1* (1975) 98.
[26] T. G. Spiro, P. Stein, *Annu. Rev. Phys. Chem. 28* (1977) 501.
[27] T. G. Spiro, *Phys. Bioinorg. Chem. Ser. 2* (1983) 89.
[28] W. Kiefer, *Adv. Infrared Raman Spectrosc. 3* (1977) 1.
[29] Y. Nishimura, A. Y. Hirakawa, M. Tsuboi, *Adv. Infrared Raman Spectrosc. 5* (1978) 217.
[30] A. Y. Hirakawa, M. Tsuboi, *Vib. Spectra Struct. 12* (1981) 145.
[31] O. S. Mortensen, S. Hassing, *Adv. Infrared Raman Spectrosc. 6* (1980) 1.
[32] W. Siebrand, M. Z. Zgierski, *Excited States 4* (1979) 1.
[33] L. D. Barron, E. N. Svendsen, *Adv. Infrared Raman Spectrosc. 8* (1981) 322.
[34] L. D. Barron, J. Vrbancich, *Adv. Infrared Raman Spectrosc. 12* (1985) 215.
[35] H.-K. Hong, *J. Chem. Phys. 67* (1977) 801, 813; *68* (1978) 1253.
[36] S.-Y. Lee, E. J. Heller, *J. Chem. Phys. 71* (1979) 4777.
[37] D. J. Tannor, E. J. Heller, *J. Chem. Phys. 77* (1982) 202.
[38] R. J. H. Clark, T. J. Dines, *Mol. Phys. 42* (1981) 193; *45* (1982) 1153.
[39] H. A. Kramers, W. Heisenberg, *Z. Phys. 31* (1925) 681.
[40] O. S. Mortensen, E. N. Svendsen, *J. Chem. Phys. 74* (1981) 3185.
[41] G. Herzberg, E. Teller, *Z. Phys. Chem. 21* (1933) 410.
[42] C. Manneback, *Physica 17* (1951) 1001.
[43] A. P. Penner, W. Siebrand, *Chem. Phys. Lett. 39* (1976) 11.
[44] W. Siebrand, M. Z. Zgierski, *J. Phys. Chem. 86* (1982) 4718.
[45] R. J. H. Clark, T. J. Dines, *Chem. Phys. Lett. 79* (1981) 321.
[46] L. D. Ziegler, B. S. Hudson, *J. Chem. Phys. 79* (1983) 1197.
[47] A. Y. Hirakawa, M. Tsuboi, *Science 188* (1975) 359.
[48] G. J. Small, E. S. Yeung, *Chem. Phys. 9* (1975) 379.
[49] D. A. Long: *Raman Spectroscopy*, McGraw-Hill, New York 1977.
[50] H. Hamaguchi, *J. Chem. Phys. 66* (1977) 5757; *69* (1978) 569.
[51] R. J. H. Clark, P. C. Turtle, *J. Chem. Soc. Faraday Trans. 2 72* (1976) 1885.
[52] R. J. H. Clark, T. J. Dines, *Chem. Phys. 70* (1982) 269.
[53] M. Pawlikowski, M. Z. Zgierski, *Chem. Phys. Lett. 48* (1977) 201; *J. Raman Spectrosc. 7* (1978) 106.
[54] M. Pézolet, L. A. Nafie, W. L. Peticolas, *J. Raman Spectrosc. 1* (1973) 455.
[55] J. Nestor, T. G. Spiro, *J. Raman Spectrosc. 1* (1973) 539.
[56] P. Stein, J. M. Brown, T. G. Spiro, *Chem. Phys. 25* (1977) 237.
[57] P. W. Jensen, *Chem. Phys. Lett. 77* (1981) 267.
[58] P. Stein, P. W. Jensen, T. G. Spiro, *Chem. Phys. Lett. 80* (1981) 451.
[59] R. D. Peacock, B. Stewart, *J. Raman Spectrosc. 15* (1984) 396.
[60] K. Manzel, V. Engelhardt, H. Abe, W. Schulze, F. W. Froben, *Chem. Phys. Lett. 77* (1981) 514.
[61] F. Ahmed, E. R. Nixon, *J. Chem. Phys. 74* (1981) 2156; *75* (1981) 110.
[62] R. Willbrandt, N.-H. Jensen, A. H. Sillesen, K. B. Hansen, *Chem. Phys. Lett. 106* (1984) 503.
[63] V. E. Bondybey, J. H. English, *Chem. Phys. Lett. 60* (1978) 69.
[64] J. C. Miller, L. Andrews, *J. Chem. Phys. 68* (1978) 1701.
[65] D. P. DiLella, W. Limm, R. H. Lipson, M. Moskovits, K. V. Taylor, *J. Chem. Phys. 77* (1982) 5263.
[66] M. Moskovits, D. P. DiLella, *J. Chem. Phys. 73* (1980) 4917.
[67] M. Moskovits, D. P. DiLella, W. Limm, *J. Chem. Phys. 80* (1984) 626.
[68] K. Manzel, W. Schulze, F. W. Froben, *Chem. Phys. Lett. 82* (1981) 557.
[69] D. D. Stranz, R. K. Khanna, *J. Chem. Phys. 74* (1981) 2116.
[70] H. Sontag, B. Eberle, R. Weber, *Chem. Phys. 80* (1983) 279.
[71] R. J. H. Clark, D. G. Cobbold, *Inorg. Chem. 17* (1978) 3169.
[72] R. J. H. Clark, T. J. Dines, M. Kurmoo, *Inorg. Chem. 22* (1983) 2766.
[73] R. A. Teichman, M. Epting, E. R. Nixon, *J. Chem. Phys. 68* (1978) 336.
[74] M. A. Epting, M. T. McKenzie, E. R. Nixon, *J. Chem. Phys. 73* (1980) 134.
[75] C. Cossé, M. Fonassier, T. Mejean, M. Tranquille, D. P. DiLella, M. Moskovits, *J. Chem. Phys. 73* (1980) 6076.
[76] L. Stein, J. R. Norris, A. J. Downs, A. R. Minihan, *J. Chem. Soc. Chem. Commun. 1978*, 502.
[77] H. Chang, D.-M. Hwang, *J. Chem. Phys. 67* (1977) 3624.
[78] J. A. Coxon, N. Gramari, M. Jacon, *J. Raman Spectrosc. 8* (1979) 63.
[79] O. Atabek, R. Lefebvre, M. Jacon, *J. Chem. Phys. 72* (1980) 2683.
[80] H. Chang, D.-M. Hwang, *J. Chem. Phys. 67* (1977) 4777.
[81] H. Chang, D.-M. Hwang, *J. Raman Spectrosc. 7* (1978) 254.
[82] F. Ghandow, M. Jacon, E. N. Svendsen, J. Oddershede, *J. Chem. Phys. 79* (1983) 2150.
[83] H. H. Eysel, H. J. Bernstein, *J. Raman Spectrosc. 6* (1977) 140.
[84] M. T. Bourgeois, M. Jacon, D. Van Labeke, H. H. Eysel, *J. Raman Spectrosc. 6* (1977) 146.
[85] D. P. DiLella, K. V. Taylor, M. Moskovits, *J. Phys. Chem. 87* (1983) 524.
[86] L. Andrews, E. S. Prochaska, A. Loewenschuss, *Inorg. Chem. 19* (1980) 463.
[87] M. Moskovits, D. P. DiLella, *J. Chem. Phys. 72* (1980) 2267.
[88] F. Bolduan, H. J. Jodl, *J. Mol. Spectrosc. 91* (1982) 404.
[89] J. B. Bates, *J. Chem. Phys. 69* (1978) 1934.
[90] G. M. Gualberto, M. A. Tenan, H. Vegers, L. C. M. Miranda, J. Peizl, *Phys. Rev. B 17* (1978) 919.
[91] L. C. Campelo, F. E. A. Melo, J. M. Filho, R. S. Katiyar, H. Vargas, *J. Raman Spectrosc. 10* (1981) 33.
[92] J. Bojes, T. Chivers, W. G. Laidlaw, M. Trsic, *J. Am. Chem. Soc. 104* (1982) 4837.
[93] H. Sontag, R. Weber, *Chem. Phys. 70* (1982) 23.
[94] H. Schnöckel, H.-J. Goecke, R. Elsper, *Z. Anorg. Allg. Chem. 494* (1982) 78.
[95] H. Schnöckel, *Z. Anorg. Allg. Chem. 510* (1984) 72.
[96] L. D. Ziegler, B. Hudson, *J. Phys. Chem. 88* (1984) 1110.
[97] R. J. H. Clark, T. J. Dines, L. T. H. Ferris, *J. Chem. Soc. Dalton Trans. 1982*, 2237.
[98] R. J. H. Clark, T. J. Dines, *Inorg. Chem. 21* (1982) 3585.
[99] E. Campani, F. Ferri, G. Gorini, E. Polacco, G. Masetti, *Chem. Phys. Lett. 107* (1984) 91.
[100] L. D. Barron, C. Meehan, *Chem. Phys. Lett. 66* (1979) 444.
[101] R. J. H. Clark, T. J. Dines, *Inorg. Chem. 19* (1980) 1681.
[102] R. J. H. Clark, D. G. Cobbold, B. Stewart, *Chem. Phys. Lett. 69* (1980) 488.
[103] R. J. H. Clark, T. J. Dines, *J. Chem. Soc. Faraday Trans. 2 78* (1982) 723.
[104] A. H. Jubert, E. L. Varetti, *J. Mol. Struct. 79* (1982) 285.
[105] A. H. Jubert, E. L. Varetti, *J. Raman Spectrosc. 13* (1982) 83.

[106] A. H. Jubert, S. G. Manca, E. J. Baran, E. L. Varetti, *Z. Anorg. Allg. Chem. 492* (1982) 197.
[107] H. Homborg, *Z. Anorg. Allg. Chem. 498* (1983) 25.
[108] A. H. Jubert, E. L. Varetti, E. J. Baran, *J. Raman Spectrosc. 15* (1984) 139.
[109] T. P. Martin, S. Onari, *Phys. Rev. B 15* (1977) 1093.
[110] R. J. H. Clark, T. J. Dines, J. M. Doherty, *Inorg. Chem. 24* (1985) 2088.
[111] E. Königer-Ahlborn, A. Müller, *Spectrochim. Acta A 33* (1977) 273.
[112] R. J. H. Clark, T. J. Dines, M. L. Wolf, *J. Chem. Soc. Faraday Trans. 2 78* (1982) 679.
[113] M. L. A. Temperini, O. Sala, H. J. Bernstein, *Chem. Phys. Lett. 59* (1978) 10.
[114] R. J. H. Clark, T. J. Dines, *Chem. Phys. Lett. 64* (1979) 499.
[115] R. J. H. Clark, T. J. Dines, G. P. Proud, *J. Chem. Soc. Dalton Trans. 1983,* 2019.
[116] L. W. Johnson, S. P. McGlynn, *Chem. Phys. Lett. 7* (1970) 618.
[117] C. J. Ballhausen, I. B. Trabjerg, *Mol. Phys. 24* (1972) 689.
[118] R. J. H. Clark, P. C. Turtle, *J. Chem. Soc. Dalton Trans. 1977,* 2142.
[119] L. Tosi, A. Garnier, *J. Chem. Soc. Dalton Trans. 1978,* 53.
[120] O. Siiman, *Inorg. Chem. 19* (1980) 2889.
[121] R. Czernuszewicz, E. Maslowsky, K. Nakamoto, *Inorg. Chim. Acta 40* (1980) 199.
[122] R. Czernuszewicz, G. Y. Lim, D. T. Haworth, K. Nakamoto, *Inorg. Chim. Acta 44* (1980) L 167.
[123] R. S. Czernuszewicz, K. Nakamoto, D. P. Strommen, *J. Am. Chem. Soc. 104* (1982) 1515.
[124] W. Preetz, G. Peters, *Z. Naturforsch. B 35* (1980) 1355.
[125] G. Peters, W. Preetz, *Z. Naturforsch. B 36* (1981) 138.
[126] R. J. H. Clark, P. C. Turtle, *J. Chem. Soc. Faraday Trans. 2 74* (1978) 2063.
[127] H. Homborg, *Z. Anorg. Allg. Chem. 493* (1982) 104, 121.
[128] L. D. Barron, J. Vrbancich, R. S. Watts, *Chem. Phys. Lett. 89* (1982) 71.
[129] R. J. H. Clark, P. C. Turtle, *Chem. Phys. Lett. 51* (1977) 265.
[130] H. Hamaguchi, M. Tasumi, *J. Chem. Phys. 78* (1983) 131.
[131] L. D. Barron, C. Meehan, J. Vrbancich, *Mol. Phys. 41* (1980) 945.
[132] L. D. Barron, J. Vrbancich, *J. Raman Spectrosc. 14* (1983) 118.
[133] H. Homborg, *Z. Anorg. Allg. Chem. 460* (1980) 17, 27.
[134] K.-I. Ikeda, S. Maeda, *Inorg. Chem. 17* (1978) 2698.
[135] W. Preetz, M. Bruns, *Z. Naturforsch. B 38* (1983) 680.
[136] R. J. H. Clark, T. J. Dines, *Mol. Phys. 52* (1984) 859.
[137] R. J. H. Clark, M. J. Stead, *Chem. Phys. 91* (1984) 113.
[138] C. Sourisseau, Y. Mathey, *Chem. Phys. Lett. 74* (1980) 128; *Chem. Phys. 63* (1981) 143.
[139] S. P. Gwet, Y. Mathey, C. Sourisseau, *Phys. Status Solidi B 123* (1984) 503.
[140] R. J. H. Clark, P. C. Turtle, D. P. Strommen, B. Streusand, J. Kincaid, K. Nakamoto, *Inorg. Chem. 16* (1977) 84.
[141] B. Streusand, A. T. Kowal, D. P. Strommen, K. Nakamoto, *J. Inorg. Nucl. Chem. 39* (1977) 1767.
[142] P. J. Miller, R. S.-L. Chao, *J. Raman Spectrosc. 8* (1979) 17.
[143] R. S. Czernuszewicz, K. Nakamoto, D. P. Strommen, *Inorg. Chem. 19* (1980) 793.
[144] P. W. Jensen, *Chem. Phys. Lett. 77* (1981) 267.
[145] L. Griffiths, B. P. Straughan, D. J. Gardiner, *J. Chem. Soc. Dalton Trans. 1983,* 305.
[146] R. F. Dallinger, W. H. Woodruff, *J. Am. Chem. Soc. 101* (1979) 4391.
[147] M. Forster, R. E. Hester, *Chem. Phys. Lett. 81* (1981) 42.
[148] P. G. Bradley, N. Kress, B. A. Homberger, R. F. Dallinger, W. H. Woodruff, *J. Am. Chem. Soc. 103* (1981) 7441.
[149] M. Basu, H. D. Gafney, T. C. Strekas, *Inorg. Chem. 21* (1982) 2231.
[150] R. W. Balk, D. J. Stufkens, R. J. Crutchley, A. B. P. Lever, *Inorg. Chim. Acta 64* (1982) L49.
[151] W. K. Smothers, M. S. Wrighton, *J. Am. Chem. Soc. 105* (1983) 1067.
[152] S. McClanahan, T. Hayes, J. Kincaid, *J. Am. Chem. Soc. 105* (1983) 4486.
[153] J. Ferguson, F. Herren, *Chem. Phys. Lett. 89* (1982) 371; J. Ferguson, F. Herren, G. M. McLaughlin, *ibid. 89* (1982) 376; J. Ferguson, F. Herren, *Chem. Phys. 76* (1983) 45.
[154] D. J. Stufkens, *J. Mol. Struct. 79* (1982) 67, and references cited therein.
[155] R. W. Balk, D. J. Stufkens, A. Oskam, *J. Chem. Soc. Dalton Trans. 1982,* 275.
[156] M. W. Kokkes, D. J. Stufkens, A. Oskam, *J. Chem. Soc. Dalton Trans. 1983,* 439.
[157] D. J. Stufkens, M. W. Kokkes, A. Oskam, *J. Mol. Struct. 114* (1984) 61.
[158] Y.-Y. Yang, J. I. Zink, *J. Am. Chem. Soc. 106* (1984) 1500.
[159] T. Ziegler, A. Rauk, E. J. Baerends, *Chem. Phys. 16* (1976) 209.
[160] F. A. Cotton, R. A. Walton: Metal Atoms, Wiley-Interscience, New York 1982.
[161] R. J. H. Clark, M. L. Franks, *J. Am. Chem. Soc. 97* (1975) 2691.
[162] R. J. H. Clark, M. L. Franks, *J. Am. Chem. Soc. 98* (1976) 2763.
[163] R. J. H. Clark, N. R. D'Urso, *J. Am. Chem. Soc. 100* (1978) 3088.
[164] W. Preetz, L. Rudzik, *Angew. Chem. 91* (1979) 159; *Angew. Chem. Int. Ed. Engl. 18* (1979) 150.
[165] W. Preetz, G. Peters, L. Rudzik, *Z. Naturforsch. B 34* (1979) 1240.
[166] H. D. Glicksman, R. A. Walton, *Inorg. Chem. 17* (1978) 3197.
[167] R. J. H. Clark, M. J. Stead in M. H. Chisholm (ed.): *Inorganic Chemistry: Toward the 21st Century,* ACS Symp. Ser. No. 211, 1983, p. 235.
[168] R. J. H. Clark, M. J. Stead, *Inorg. Chem. 22* (1983) 1214.
[169] R. J. H. Clark, L. T. H. Ferris, *Inorg. Chem. 20* (1981) 2759.
[170] R. J. H. Clark, A. J. Hempleman, H. M. Dawes, M. B. Hursthouse, C. D. Flint, *J. Chem. Soc. Dalton Trans. 1985,* 1775.
[171] R. J. H. Clark, A. J. Hempleman, C. D. Flint, *J. Am. Chem. Soc.*, in press.
[172] R. J. H. Clark, M. L. Franks, P. C. Turtle, *J. Am. Chem. Soc. 99* (1977) 2473.
[173] J. R. Campbell, R. J. H. Clark, *Mol. Phys. 36* (1978) 1133; *J. Chem. Soc. Faraday Trans. 2 76* (1980) 1103.
[174] J. R. Campbell, R. J. H. Clark, *J. Chem. Soc. Dalton Trans. 1981,* 1239.
[175] J. R. Campbell, R. J. H. Clark, M. J. Stead, *J. Chem. Soc. Dalton Trans. 1983,* 2005.
[176] R. E. Hester, E. M. Nour, *J. Raman Spectrosc. 11* (1981) 43, 49, 59, 64.
[177] A. Müller, A.-M. Dommröse, W. Jaegermann, E. Krickemeyer, S. Sarkar, *Angew. Chem. 93* (1981) 1119; *Angew. Chem. Int. Ed. Engl. 20* (1981) 1061.
[178] A. Müller, R. R. Filgueira, W. Jaegermann, S. Che, *Naturwissenschaften 68* (1981) 93.
[179] R. J. H. Clark, T. J. Dines, G. P. Proud, *J. Chem. Soc. Dalton Trans. 1983,* 2299.
[180] R. J. H. Clark, M. Kurmoo, *Inorg. Chem. 19* (1980) 3522.
[181] R. J. H. Clark, V. B. Croud, M. Kurmoo, *Inorg. Chem. 23* (1984) 2499.
[182] S. D. Allen, R. J. H. Clark, V. B. Croud, M. Kurmoo, *Phil. Trans. Roy. Soc. A 314* (1985) 131.
[183] R. J. H. Clark, V. B. Croud, *Inorg. Chem. 24* (1985) 588.
[184] R. J. H. Clark, M. Kurmoo, *J. Chem. Soc. Faraday Trans. 2 79* (1983) 519.
[185] U. Fürholz, H.-B. Bürgi, F. E. Wagner, A. Stebler, J. H. Ammeter, E. Krausz, R. J. H. Clark, M. J. Stead, A. Ludi, *J. Am. Chem. Soc. 106* (1984) 121.
[186] R. S. Armstrong, J. K. Beattie, P. del Favero, V. M. Ellis, N. S. Hush, *Inorg. Chim. Acta 89* (1984) L33.
[187] M. Gouterman in D. Dolphin (ed.): *The Porphyrins, Vol. 3,* Academic Press, New York 1978, p. 1.
[188] J. A. Shelnutt, L. D. Cheung, R. C. C. Chang, N.-T. Yu, R. H. Felton, *J. Chem. Phys. 66* (1977) 3387.
[189] P. M. Champion, A. C. Albrecht, *J. Chem. Phys. 71* (1979) 1110; *72* (1980) 6498.
[190] J. A. Shelnutt, *J. Chem. Phys. 72* (1980) 3948.
[191] J. A. Shelnutt, *J. Chem. Phys. 74* (1981) 6644.

When submitting manuscripts, authors of articles intended for publication as "Communications" are requested to read the "Notice to Authors" reproduced in the January issue of the journal following the list of contents; upon request, a copy can be obtained from the editorial office.

The Ferrocenylmethyl(Fem) Group as a Highly Lipophilic and Chromophoric Group for the Masking of Peptide Bonds**

By *Heiner Eckert** and *Christoph Seidel*

In the course of exploring a new strategy for the chemical synthesis of peptides,[1] which is characterized by the use of strongly lipophilic and chromophoric groups, we have developed a method for the masking of peptide bonds. The treatment of the chemically reactive functional groups is largely covered by the conventional protecting group methodology.[2] Peptide bonds, on the other hand, are particularly "physically reactive"—i.e., they exert a great effect on the secondary structure and solubility of a peptide. Such conformational effects often make the synthesis of peptides difficult. *Weygand* et al. have attempted to prevent[3] these effects by using the 2,4-dimethoxybenzyl group.[3a] *Ugi* et al. recognized the preparative value of the lipophilic and chromophoric ferrocenylalkyl group in stereospecific reagents.[3b] The *tert*-butoxycarbonylation of the peptide bond in a prolyl-glycine derivative was recently described by *Ragnarsson* et al.[3c]

The chromophoric (yellow) ferrocenylmethyl(Fem) group[4] makes possible an economically practical, regenerative masking of peptide bonds in order to suppress or manipulate the secondary structures of peptide derivatives and in order to solubilize them lipophilically. The Fem group can be introduced by facile catalytic reductive alkylation of amino acids or amino acid esters with commercially available ferrocenecarbaldehyde **1** and hydrogen. The highly selective palladium(II) phthalocyanine[5] may be used as hydrogenation catalyst. Whereas **1** is only reduced extremely slowly, the azomethine **2** obtained from **1** and the amino acid or the amino acid ester undergoes hydrogenation within a few hours. The Fem-amino acids, or their esters, are thereby formed in high yields without racemization (Table 1) and without undergoing further reduction. The racemization-free course of the reaction is exemplified by reaction of the amino acid phenylalanine, which is highly susceptible to racemization. After isolation and subsequent hydrogenation of ferrocenylmethylene-Phe-O*t*Bu, the ester Fem-Phe-O*t*Bu is deblocked using trifluoroacetic acid and the specific optical rotation of the free phenylalanine is measured to be $[\alpha]_D^{25}$ −32.7. This value is identical with that of the starting phenylalanine. Fem-amino acids are very stable; for example, Fem-Gly-OMe can be distilled (b.p. = 235 °C/0.1 torr) quantitatively

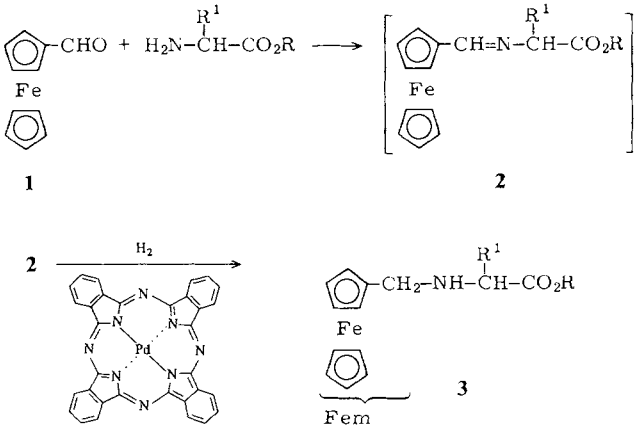


Table 1. Synthesis of Fem-amino acids and derivatives (**3**, R = H, Me, *t*Bu or Na).

	Fem–NH–CHR¹–CO₂R **3**	Yield [%]	M.p. [°C]	$[\alpha]^{25}$ (λ [nm])
3a	Fem–Gly–OH	73	198	—
3b	Fem–Gly–OMe	60	oil	—
3c	Fem–Ala–ONa	83	232	−38.3 (546)
3d	Fem–Ala–OMe	71	oil	−73.3(546); −53.4 (589)
3e	Fem–Phe–ONa	82	305	− 9.5(546)
3f	Fem–Phe–O*t*Bu	81	oil	−13.8 (589)
3g	Fem–Leu–O*t*Bu	85	oil	−26.7 (546)
3h	Fem–Val–O*t*Bu	89	oil	−34.0 (546); −23.5 (589)

without undergoing decomposition. In contrast, the corresponding "free" H-Gly-OMe ester undergoes quantitative decomposition within a few hours at room temperature to give 2,5-diketopiperazine.

The coupling of *N*-protected amino acids with Fem-amino acid derivatives **3** to give peptides **4**, which have Fem-masked peptide bonds, can be carried out conveniently according to the DCCI method[2a,6] within a few hours (Table 2). The yields are generally high. Even the coupling of Tcboc-Val-OH[6] with Fem-Val-O*t*Bu **3h**, which is a sterically highly hindered reaction, affords **4f** in 50% yield. The investigation of the racemization[2a] during the coupling of Boc-Gly-Fem-Ala-OH with H-Leu-O*t*Bu using DCCI showed that the Izumiya test peptide derivative Boc-Gly-Fem-Ala-Leu-O*t*Bu (92% yield) contained 27% D-alanine and 73% L-alanine. The comparable reaction without the Fem group under the same conditions afforded the test peptide derivative (84% yield) with 12% D-alanine and 88% L-alanine. This observation must be taken into consideration in fragment condensations, which are subject to racemization. In contrast, the coupling of Tcboc-Fem-Ala-OH with H-Leu-O*t*Bu (85% yield) gives a product with < 0.02% D-alanine. This means that no racemization occurs in the coupling of *N*-urethaneprotected Fem-amino acids, which makes a stepwise peptide synthesis relatively easy.

Intermediates that contain the Fem group can be purified by column chromatography on inexpensive silica gel with hexane-containing solvent systems (high resolution). This is due to their extremely high lipophilicity[7] and their strong yellow color. The Fem group may be cleaved with trifluoroacetic acid/β-thionaphthalene in dichloromethane

[*] Dr. H. Eckert, C. Seidel
Organisch-chemisches Institut der Technischen Universität München
Lichtenbergstrasse 4, D-8046 Garching (FRG)

[**] This work was supported by the Deutsche Forschungsgemeinschaft.

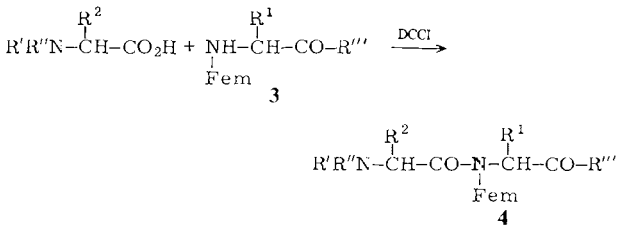


Table 2. Coupling reactions with Fem-amino acid derivatives **3** to give peptides **4** containing Fem-protected peptide bonds [6].

Starting materials	Products	Yield [%]
Z–Ala–OH + Fem–Phe–O*t*Bu **3f**	Z–Ala–Phe–O*t*Bu (Fem) **4a**	83
Boc–Gly–OH + Fem–Ala–OMe **3d**	Boc–Gly–Ala–OMe (Fem) **4b**	91
Boc–Gly–OH + Fem–Ala–Leu–O*t*Bu	Boc–Gly–Ala–Leu–O*t*Bu (Fem) **4c**	75
Tcboc–Phe–OH + Fem–Leu–O*t*Bu **3g**	Tcboc–Phe–Leu–O*t*Bu (Fem) **4d**	93
Tcboc–Fem–Gly–OH + Fem–Gly–OMe **3b**	Tcboc–Fem–Gly–Gly–OMe (Fem) **4e**	80
Tcboc–Val–OH + Fem–Val–O*t*Bu **3h**	Tcboc–Val–Val–O*t*Bu (Fem) **4f**	50

within 2–4 h at the same rate as that observed for cleavage of the Boc or O*t*Bu groups.

Experimental Procedure

Fem-amino acid esters 3 (R = alkyl): A mixture consisting to the amino acid amino acid (10 mmol), **1** (2.14 g, 10 mmol), anhydrous Na_2CO_3 (2.12 g, 20 mmol), and palladium(II) phthalocyanine (0.06 g, 0.1 mmol)/[5] in 40 mL of methanol was saturated with H_2 and then vigorously stirred under H_2 (from a gas burette) for several hours, until gas absorption stopped. The suspension was filtered through a 4-cm thick layer of Na_2SO_4, which is then washed with methanol, and the filtrate is concentrated to 10–20 mL. Addition of ether results in precipitation of the sodium salt of the Fem-amino acid. This is recrystallized from water or methanol/water, affording yellow crystals.

Fem-amino acid esters 3, (R = alkyl): A mixture consisting of the amino acid ester or its hydrochloride (10 mmol), **1** (2.14 g, 10 mmol), and palladium(II) phthalocyanine (0.06 g, 0.1 mmol) [5] in 10 mL of methanol and 20 mL of ethyl acetate (triethylamine (0.8 mL, 11 mmol) added in the case of the amino acid ester hydrochlorides) was saturated with H_2 and vigorously stirred under H_2 (from a gas burette) for several hours, until gas absorption stopped. The reaction mixture was then filtered through a 4-cm thick layer of Na_2SO_4, which was washed with ethyl acetate, and the filtrate was concentrated. The residue was chromatographed on silica gel with hexane/ethyl acetate (ca. 3 : 1). A deep orange oil was obtained.

Coupling reaction to give 4: The *N*-urethane-protected amino acid (10 mmol) and the Fem-amino acid ester **3** (10 mmol), R = alkyl, were cooled to −20 °C in 40 mL of dichloromethane. A solution of DCCI (2.27 g, 11 mmol) in 10 mL of dichloromethane was added over 5 min and the cold bath was then removed. After 12 h, the dicyclohexylurea was filtered off and the filtrate was concentrated. The residue was chromatographed on silica gel with hexane/ethyl acetate (ca. 3 : 1) [7]. A yellow solid was obtained.

Received: August 13, 1985;
supplemented: November 15, 1985 [Z 1427 IE]
German version: *Angew. Chem. 98* (1986) 168

[1] a) H. Eckert, Y. Kiesel, C. Seidel, C. Kaulberg, H. Brinkmann, 5th USSR-FRG Symposium on Chemistry of Peptides and Proteins, Odessa (USSR), May 16–21, 1985; b) H. Eckert, C. Seidel, 1st German-Japanese Symposium on Peptide Chemistry (Akabori Conference). Grainau (FRG), June 12–13, 1985.

[2] a) E. Wünsch in Houben-Weyl: *Methoden der Organischen Chemie, 4. Aufl., Bd. 15*, Thieme, Stuttgart 1974; b) A. Hubbuch, *Kontakte 1979*, No. 3, p. 14; c) E. E. Büllesbach, *ibid. 1980*, No. 1, p. 23.

[3] a) F. Weygand, W. Steglich, J. Bjarnason, R. Akhtar, N. Chytil, *Chem. Ber. 101* (1968) 3623; b) D. Marquarding, P. Hoffmann, H. Heitzer, I. Ugi, *J. Am. Chem. Soc. 92* (1970) 1969; c) L. Grehn, U. Ragnarsson, *Angew. Chem. 97* (1985) 519; *Angew. Chem. Int. Ed. Engl. 24* (1985) 510.

[4] We propose Fem as an abbreviation for ferrocenylmethyl.

[5] H. Eckert, G. Fabry, Y. Kiesel, G. Raudaschl, C. Seidel, *Angew. Chem. 95* (1983) 894; *Angew. Chem. Int. Ed. Engl. 22* (1983) 881; *Angew. Chem. Suppl. 1983*, 1291.

[6] Boc = *tert*-butoxycarbonyl, DCCI = dicyclohexylcarbodiimide, Tcboc = 2,2,2-trichloro-*tert*-butoxycarbonyl [2b], Z = benzyloxycarbonyl.

[7] The peptide derivatives **4** in Table 2 have R_F values in hexane/ethyl acetate (3 : 1) of 0.35 to 0.7 (Kieselgel 60 TLC plates).

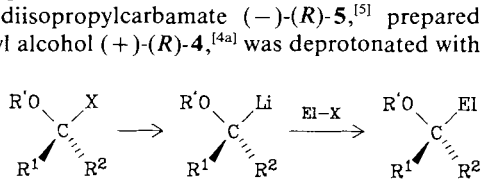
α-Deprotonation of an α-Chiral 2-Alkenylcarbamate with Retention and Lithium-Titanium Exchange with Inversion—the Homoaldol Reaction with 1,3-Chirality Transfer**

By *Dieter Hoppe** and *Thomas Krämer*

Dedicated to Professor Hans Musso on the occasion of his 60th birthday

Chiral 1-oxy alkyllithium compounds **2** (R^1, R^2 = alkyl, H) are configurationally stable,[1] and their substitution reactions with electrophiles to give **3** proceed with retention. The tin-lithium exchange[1] of stannanes **1a** has proved useful for the synthesis of **2**. In contrast, the reductive cleavage of monothioketals or monothioacetals[2] **1b** to give **2** is accompanied by racemization or epimerization, since radicals having low barriers to inversion are formed as intermediates. The simplest conceivable route—the stereospecific deprotonation of **1c** (R^1, R^2 = alkyl)—is not promising owing to the insufficient kinetic acidity of **1c**. Although resonance-stabilizing groups (e.g., R^1 = phenyl or vinyl) increase the carbon acidity of **1c**, they also increase the danger of racemization of **2** since they favor planarity and dissociation into ion pairs. We have now investigated the α-deprotonation of the optically active, α-chiral 2-alkenylcarbamate **5**[3] as well as the subsequent lithium-titanium exchange and the carbonyl addition, and report here our surprising results.

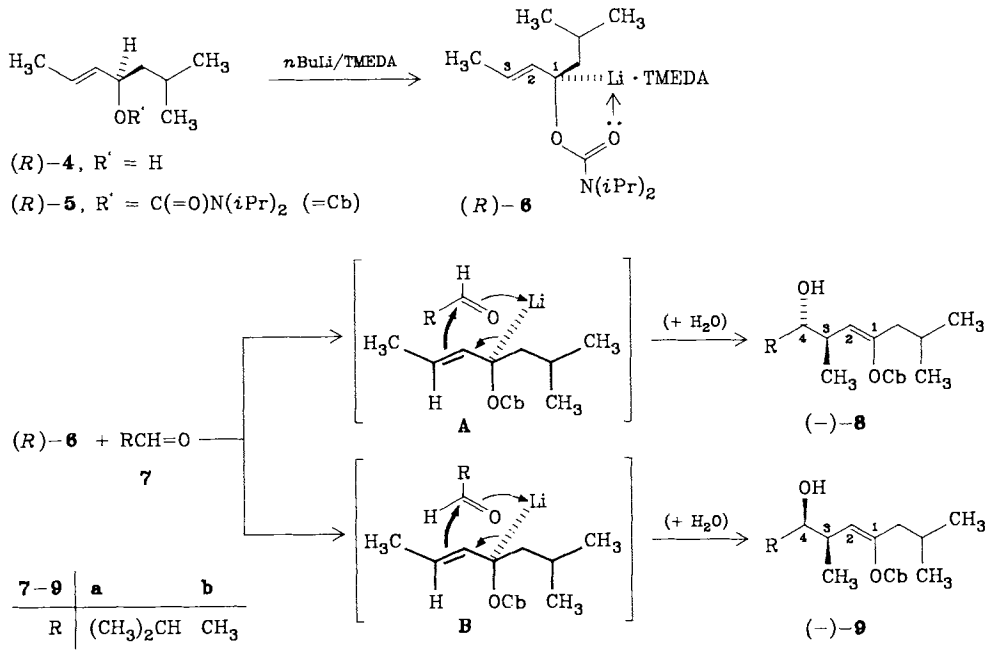
The *N*,*N*-diisopropylcarbamate (−)-(*R*)-**5**,[5] prepared from the allyl alcohol (+)-(*R*)-**4**,[4a] was deprotonated with



1a, X = $SnBu_3$
1b, X = SPh
1c, X = H

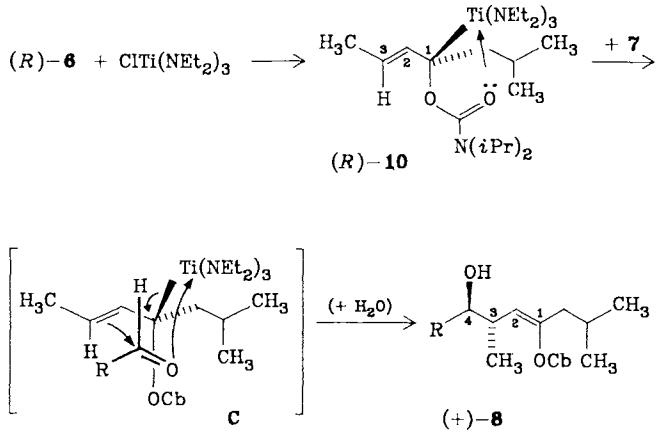
[*] Prof. Dr. D. Hoppe
Institut für Organische Chemie der Universität
Olshausenstrasse 40, D-2300 Kiel 1 (FRG)
T. Krämer
Institut für Organische Chemie der Universität
Tammannstrasse 2, D-3400 Göttingen (FRG)

[**] Metalated Nitrogen Derivatives of Carbon Dioxide in Organic Synthesis, Part 31. This work was supported by the Deutsche Forschungsgemeinschaft and the Fonds der Chemischen Industrie.—Part 30: D. Hoppe, C. Gonschorrek, E. Egert, D. Schmidt, *Angew. Chem. 97* (1985) 706; *Angew. Chem. Int. Ed. Engl. 24* (1985) 700.

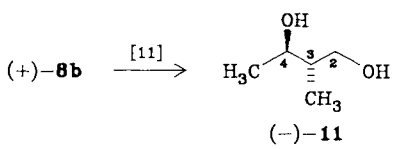


n-butyllithium (ether/hexane, 0.95 equiv. *N,N,N',N'*-tetramethylethylenediamine (TMEDA), 7 h at −78 °C),[3b] and the intermediary lithium compound **6** was trapped with 2-methylpropanal **7a**. Along with 25% of the starting material (68% *ee*[7]), the optically active (*Z*)-*anti* adduct[3a] (−)-**8a** (yield 24%, 52% *ee*[7,8]) and the (*Z*)-*syn* isomer (−)-**9a** (yield 29%, ≥25% *ee*[7,8]) were obtained.[6]

In a further experiment—under otherwise identical conditions—the "cation" Li was exchanged for Ti, before the addition of the aldehyde, by treatment with 1.1 equivalents of chlorotris(diethylamino)titanium[9,10] (2 h at −78 to −70 °C). Addition of **7a** to the titanium compound **10** afforded only one adduct, the (*Z*)-*anti* diastereomer (+)-**8a** (yield 36%, 35% *ee*[7,8]). Similarly, after metalation and metal exchange, (*R*)-**5** afforded the adduct (+)-**8b** (yield 58%, 41% *ee*[7,8]) upon addition of aldehyde **7b**. The absolute configuration of (+)-**8b** was determined to be (3*S*,4*R*) by degradation[11] to the known diol[12] (−)-(2*S*,3*R*)-**11**.



7/8: **a**, R = $(CH_3)_2CH$; **b**, R = CH_3



Since, for the carbonyl addition reactions of α-chiral allylmetal compounds[1c,13] (corresponding to the transition states **A**–**C**), the asymmetric induction at C-3 (1,3-chirality transfer) is determined by the configuration at C-1—and not by the aldehyde **7**—the (3*S*,4*R*) configuration for (+)-**8a** and the (3*R*,4*S*) configuration for (−)-**8a** are also established. (−)-**9a** can be converted into (−)-**8a** by oxidation/reduction[14] with inversion at C-4 and, therefore, has the (3*R*,4*R*) configuration. The lithium and titanium compounds (*R*)-**6** and (*R*)-**10** that afford the excess enantiomer in each case thus have opposite configurations at C-1.[15]

The following important conclusions can be drawn from these results: (1) The deprotonation of (*R*)-**5** to give (*R*)-**6** occurs with *retention*. Lithium compounds of type **6** racemize only slowly ($t_{rac\,1/2} \geq 7$ h) under the reaction conditions at temperatures below −70 °C. Accordingly, the lithium in **6** must—despite the possibility of resonance in the anion[16,17]—be tightly bonded (covalently?) to the nonplanar-coordinated C-1. (2) Titanium compounds[10] of type **10** are also largely configurationally stable at temperatures below −70 °C. The lithium-titanium exchange of (*R*)-**6** to give (*R*)-**10** takes place with *inversion*.[18] Since inversion has never been observed for intermolecular electrophilic substitution at an sp^3-hybridized C atom,[19] it remains to be shown whether our exceptional results are due to the transition-metal "cation," to the allyl system, or to the interplay of both. (3) If it is possible to further suppress the racemization, these findings would provide a very flexible procedure for the enantioselective homoaldol reaction,[1c,20] which is very attractive with respect to both the constitution and configuration of the target molecule.

Received: September 23, 1985 [Z 1465 IE]
German version: *Angew. Chem. 88* (1986) 171

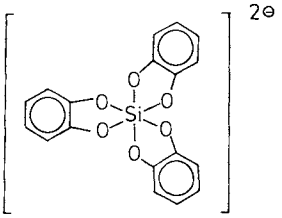
[1] a) W. C. Still, C. Sreekumar, *J. Am. Chem. Soc. 102* (1980) 1201; b) J. S. Sawyer, T. L. Macdonald, G. J. McGarvey, *ibid. 106* (1984) 3376, and

references cited therein; c) V. J. Jephcote, A. J. Pratt, E. J. Thomas, *J. Chem. Soc. Chem. Commun. 1984*, 800; d) P. Lesimple, J.-M. Beau, P. Sinaÿ, *ibid. 1985*, 894.
[2] For example, see: T. Cohen, M.-T. Lin, *J. Am. Chem. Soc. 106* (1984) 1130; J.-M. Lancelin, L. Morin-Allory, P. Sinaÿ, *J. Chem. Soc. Chem. Commun. 1984*, 355.
[3] a) Review: D. Hoppe, *Angew. Chem. 96* (1984) 930; *Angew. Chem. Int. Ed. Engl. 23* (1984) 932; see also b) D. Hoppe, R. Hanko, A. Brönneke, F. Lichtenberg, E. van Hülsen, *Chem. Ber. 118* (1985) 2822.
[4] a) (*R*)-**4** [4b]: Prepared from *rac*-**4** by kinetic resolution of enantiomers (according to *Sharpless* [4c]) using (*R,R*)-diisopropyl tartrate, $[\alpha]_D^{25}$ +7.18 (c = 1.2, $CHCl_3$), 67% *ee*. Determined for the (*S*)-1-methoxy-1-phenyl-1-(trifluoromethyl)acetate by ^{19}F-NMR spectroscopy [4d].—b) K. Chan, N. Cohen, J. P. DeNoble, A. C. Specian, Jr., G. Saucy, *J. Org. Chem. 41* (1976) 3497; c) V. S. Martin, S. S. Woodard, T. Katsuki, Y. Yamada, M. Ikeda, K. B. Sharpless, *J. Am. Chem. Soc. 103* (1981) 6237; d) J. A. Dale, D. L. Dull, H. S. Mosher, *J. Org. Chem. 34* (1969) 2543.
[5] 67% *ee*, $[\alpha]_D^{25}$ −11.6 (c = 1.1, $CHCl_3$).
[6] **8a** and **9a** were separated by medium pressure chromatography on silica gel: **8a** (**9a**): R_F = 0.48 (0.40), ether/petroleum ether (1 : 1).
[7] Corrected values, based on enantiomerically pure (−)-**5**.
[8] Averaged values from comparison of optical rotations and determination of the enantiomeric ratio using tris[3-heptafluoropropylhydroxymethylene)-(+)-camphorato]europium(III). Specific optical rotation, extrapolated to 100% *ee*: (+)-**8a**: $[\alpha]_D^{25}$ 8.0; (+)-**8b**: +1.8, (−)-**9a**: −5.2 (c = 1.0–2.0, CH_3OH).
[9] R. Hanko, D. Hoppe, *Angew. Chem. 94* (1982) 378; *Angew. Chem. Int. Ed. Engl. 21* (1982) 372.
[10] Reviews: M. T. Reetz, *Top. Curr. Chem. 106* (1982) 1; B. Weidmann, D. Seebach, *Angew. Chem. 95* (1983) 12; *Angew. Chem. Int. Ed. Engl. 22* (1983) 31.
[11] Reaction conditions: 1) (+)-**8b** (30% *ee*), acetic anhydride, triethylamine, 10 mol-% 4-(dimethylamino)pyridine; 2) O_3, 1.0 equiv. methanesulfonic acid in methanol/dichloromethane, −70 to −20°C; dimethyl sulfide; 3) $LiAlH_4$/tetrahydrofuran, 0°C.—(−)-**11**: $[\alpha]_D^{24}$ −1.05 (c = 2.4, ethanol), 17% *ee* [12].
[12] C. Nájera, M. Yus, D. Seebach, *Helv. Chim. Acta 67* (1984) 289.
[13] R. W. Hoffmann, B. Landmann, *Angew. Chem. 96* (1984) 427; *Angew. Chem. Int. Ed. Engl. 23* (1984) 437.
[14] Swern oxidation of (−)-**9a** ($[\alpha]_D^{24}$ −0.92), followed by reduction of the ketone with $NaBH_4$ (isopropanol, 20°C), gave (−)-**8a** ($[\alpha]_D^{24}$ −1.55), 19% *ee* (corrected [7] 25% *ee*), along with (−)-**9a** (59 : 41). Therefore, (−)-**9a** must have at least the same enantiomeric purity.
[15] The asymmetric induction cannot be due to chiral associates (e.g., *rac*-**6**·(*R*)-**5** or *rac*-**10**·(*R*)-**5**) since similar results are obtained with completely deprotonated carbamates (e.g., starting from (*R*)-**5**, ethyl instead of isobutyl).
[16] Structure of allyllithium compounds (review): P. von R. Schleyer, *Pure Appl. Chem. 56* (1984) 151; see also: M. Schlosser, M. Stähle, *Angew. Chem. 94* (1982) 142; *Angew. Chem. Int. Ed. Engl. 21* (1982) 145; *Angew. Chem. Suppl. 1982*, 198, and references cited therein.
[17] Chiral, phenyl-substituted cyclic α-(aminoalkyl)lithium derivatives: a) D. Seebach, J. Hansen, P. Seiler, J. M. Gromek, *J. Organomet. Chem. 285* (1985) 1; b) M. F. Loewe, M. Boes, A. I. Meyers, *Tetrahedron Lett. 26* (1985) 3295, and references cited therein.
[18] Note the change of CIP priorities.
[19] I. Fleming, M. Rowley, *Tetrahedron Lett. 26* (1985) 3857, and references cited therein. Theory: E. D. Jemmis, J. Chandrasekhar, P. v. R. Schleyer, *J. Am. Chem. Soc. 101* (1979) 527.
[20] H. Roder, G. Helmchen, E.-M. Peters, K. Peters, H.-G. von Schnering, *Angew. Chem. 96* (1984) 895; *Angew. Chem. Int. Ed. Engl. 23* (1984) 898.

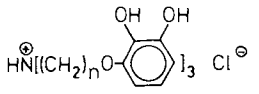
Novel Octahedral Si and Ge Complexes with a Hexadentate Diphenol Ligand

By *Bernardo Wolff* and *Armin Weiss**

Catechol forms the very stable complex anions **1** with silicon[1,2] in which silicon has sixfold coordination, which is unusual for an oxygen environment at normal pressure. The structure of **1** has been elucidated by X-ray structure analysis.[3] Even quartz can be transformed into such complexes in aqueous suspension at pH values between 8 and 10.[4] The question arises whether further stabilization of the complex can be achieved by intramolecular bridging of the catechol ligands. Therefore, we have synthesized the new hexadentate ligands **2**.



1



2a, n=2 ; **2b**, n=3

When tris[3-(2,3-dihydroxyphenoxy)propyl]ammonium chloride **2b** is allowed to react with tetraethoxysilane in refluxing methanol in the presence of triethylamine, the colorless salt **3** separates out within a few hours.

$[HNEt_3][MC_{27}H_{28}NO_9]$ **3**, M = Si; **4**, M = Ge

The ^{29}Si-NMR spectrum of **3** exhibits a singlet at δ = −138.55. This value agrees well with known ^{29}Si-NMR data for other hexacoordinated complex anions of Si with catechol.[5] The protons of the propanediyl chain give broad multiplets with unresolved fine structure in the ^{1}H-NMR spectrum. The propanediyl chains in the complex are probably present in a fixed conformation, the protons of the three methylene groups giving rise to a multiline ABMNCD spin system.

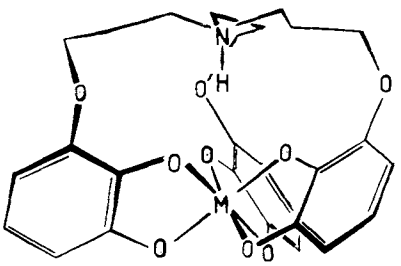


Fig. 1. Structural model of the complex anions of **3** and **4**.

Several bands are observed in the IR spectrum of **3** between 600 and 700 cm^{-1} (Fig. 2); these have been assigned

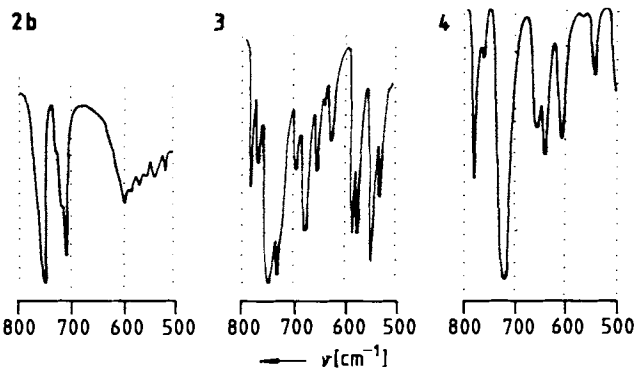


Fig. 2. Section of the IR spectra of the free ligand **2b** as well as the complex compounds **3** and **4**.

[*] Prof. Dr. A. Weiss, Dipl.-Chem. B. Wolff
Institut für Anorganische Chemie der Universität
Meiserstrasse 1, D-8000 München 2 (FRG)

to the Si-O stretching vibrations in the SiO_6 octahedron. With ligand **2b**, no absorptions are observed in this region (Fig. 2). A value of $\nu = 692\ cm^{-1}$ has been reported for the Si-O stretching vibration in $(NH_4)_2[Si(o\text{-}O_2C_6H_4)_3]$.[6]

When a saturated solution of **3** is evaporated, **3** slowly crystallizes as small cubes. It is moderately soluble in dimethylsulfoxide (DMSO), sparingly soluble in CH_3CN, and insoluble in water. The striking stability of the complex anion of **3** is demonstrated by two observations. If a suspension of fine-grained **3** in aqueous 2 N acetic acid is stirred at room temperature, no major changes are observed in the IR spectrum and in the X-ray powder diagram after 24 h; however, after about 3 weeks, the compound has undergone quantitative decomposition under these conditions. The simple catechol complexes **1** undergo immediate cleavage to catechol and silicic acid in dilute acetic acid. On the other hand, a suspension of finely divided amorphous SiO_2 ("Aerosil 380") in a refluxing methanolic solution of **2b** (ca. 0.04 M) and excess sodium acetate is completely transformed in one week into the sodium salt analogous to **3**. NaF is required as a catalyst in this reaction. The product was characterized by both spectroscopy and X-ray diffraction.

2b reacts with $GeCl_4$ to form the salt **4**, which, like **3**, is moderately soluble in DMSO and sparingly soluble in acetonitrile. Upon slow evaporation of acetonitrile solutions, **4** forms small, birefringent cubes. The IR spectra of **3** and **4** are virtually identical, apart from small shifts of the bands. Between 600 and 670 cm^{-1}, **4** exhibits absorptions that are assigned to Ge-O vibrations. They are characteristically shifted to smaller wave numbers compared with the analogous bands of **3** (Fig. 2).

Weissenberg photographs confirm that the germanium and silicon compounds are isotypic.[7] The lattice constant of **4** is only 6.0 pm larger ($a = 1841.5(22)$ pm) than that of **3**. This is in accord with the replacement of the Si by the somewhat larger Ge atom. In addition, the structure of **4** (Fig. 3) corresponds to the model of Figure 1, as established by a crystal structure analysis.[7] The Ge-O bond lengths are 187.2(6) and 188.0(6) pm. The bond angles in the central GeO_6 octahedron deviate somewhat from the values for a regular octahedron. The isotypism of the structures of **3** and **4** shows that the anions have the same structure.[8]

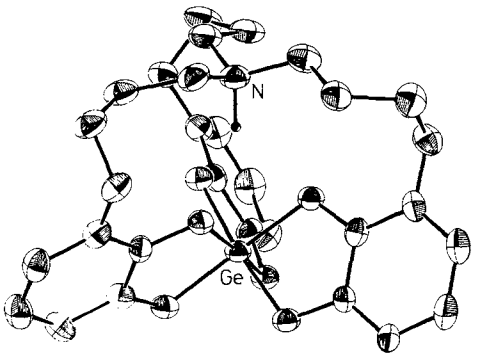


Fig. 3. ORTEP plot of the structure of the anion of **4**.

For larger central atoms (e.g., Sn) the ligand **2b** tends to form amorphous (X-ray diffraction) oligomers or polymers. Such compounds are also formed with Si or Ge as the central atom when **2a** is used in place of **2b** as ligand. Owing to the short bridges, the intramolecular complex formation apparently results in unfavorable conformations and, therefore, ring strains.

Experimental Procedure

Preparation of **3**: **2b** (2 g, 3.6 mmol), tetraethoxysilane (0.81 mL, 3.6 mmol), and triethylamine (1.5 mL, 10.9 mmol) were dissolved under nitrogen in 50 mL of refluxing methanol. After the solution had been refluxed for 12 h, the precipitate was filtered off, washed with methanol, and dried in high vacuum. Yield: 2.17 g (93%) colorless powder. The product was recrystallized by dissolving it in ca. 200 mL of refluxing acetonitrile (1 h), filtering off the insoluble matter, and allowing the clear solution to evaporate slowly in the air. Small cubic crystals formed. The undissolved residue may be treated similarly. Correct elemental analysis. The crystals turn dark above ca. 230°C and decompose at 300°C. IR (KBr): ν [cm^{-1}]: 3055 (m-s), 2940 (m), 1592 (vs), 1481 (vs), 1465 (vs), 1272 (vs), 1257 (vs), 1230 (s), 1219 (s), 1060 (vs), 847 (s), 740 (s), 670 (m), 573 (m), 562 (m), 533 (m-s). ^{1}H-NMR ([D$_6$]DMSO): $\delta = 1.17$ (t, $^3J = 7.20$ Hz, 9H, NCH_2CH_3), 1.78 (m, br., unresolved, 6H, $OCH_2CH_2CH_2N$), 3.08 (q, $^3J = 7.20$ Hz, 6H, NCH_2CH_3), 2.97 (m, br., unresolved, covered by the preceding signal, 6H, $OCH_2CH_2CH_2N$), 3.74 (m, br., unresolved, 6H, $OCH_2CH_2CH_2N$), 6.01-6.34 (m, ArylH, 9H), 8.14 (s, br., 1H, NH), 8.90 (s, br., 1H, NH). ^{13}C-NMR ([D$_6$]DMSO): $\delta = 8.48$ (NCH_2CH_3), 22.53 ($NCH_2CH_2CH_2O$), 45.76 (NCH_2CH_3), 49.38 ($NCH_2CH_2CH_2O$), 70.57 ($NCH_2CH_2CH_2O$), 105.99, 110.24, 115.46, 141.00, 144.82, 152.88 (C_{Aryl}). The ^{29}Si-NMR spectrum was recorded in [D$_6$]DMSO.—Preparation of **4**: **2b** (1 g, 1.8 mmol) was dissolved in 25 mL of anhydrous methanol. A solution containing 0.19 mL (1.6 mmol) of $GeCl_4$ and 3 mL (21.7 mmol) of dry triethylamine in 25 mL of anhydrous methanol was added to the refluxing solution of **2b** under nitrogen. A colorless precipitate forms immediately. The solution was refluxed for ca. 30 min following the addition and then filtered. The product was washed with warm methanol and dried in high vacuum. Yield: 0.94 g (94%) colorless powder. Crystals were obtained as described for **3**. Correct elemental analysis. The crystals slowly turn dark above ca. 230°C and decompose at 325°C. IR (KBr): ν [cm^{-1}]: 3085 (s), 2935 (m), 1583 (s), 1460 (vs), 1272 (vs), 1256 (vs), 1230 (s), 1218 (s), 1055 (vs), 839 (s), 719 (vs), 653 (m), 639 (m), 606 (m), 412 (m), 344 (s). ^{1}H-NMR ([D$_6$]DMSO): $\delta = 1.14$ (t, $^3J = 7.25$ Hz, 9H, NCH_2CH_3), 1.79 (m, br., unresolved, 6H, $NCH_2CH_2CH_2O$), 3.08 (q, $^3J = 7.26$ Hz, 6H, NCH_2CH_3), ca. 3.0 (m, br., unresolved, covered by the preceding signal, 6H, $NCH_2CH_2CH_2O$), 3.72 (t, br., unresolved, 6H, $NCH_2CH_2CH_2O$), 6.07-6.37 (m, 9H, ArylH), 7.68 (s, br., 1H, NH), 8.86 (s, br., 1H, NH). ^{13}C-NMR [D$_6$]DMSO): $\delta = 8.58$ (NCH_2CH_3), 22.85 ($NCH_2CH_2CH_2O$), 45.74 (NCH_2CH_3), 49.61 (NCH_2CH_2O), 70.88 ($NCH_2CH_2CH_2O$), 107.13, 110.38, 115.16, 142.38, 144.69, 152.33 (C_{Aryl}).

Received: May 7, 1985;
revised: November 20, 1985 [Z 1294 IE]
German version: *Angew. Chem. 98* (1986) 173

[1] A. Rosenheim, O. Sorge, *Ber. Dtsch. Chem. Ges. 53* (1920) 132.
[2] Armin Weiss, G. Reiff, Alarich Weiss, *Z. Anorg. Allg. Chem. 311* (1961) 312.
[3] J. J. Flynn, F. P. Boer, *J. Am. Chem. Soc. 91* (1969) 5756.
[4] Armin Weiss, G. Hofmann, G. Reiff, *Beitr. Silikose-Forsch., Sonderband 3* (1960) 21.
[5] J. A. Cella, J. D. Cargioli, E. A. Williams, *J. Organomet. Chem. 186* (1980) 13.
[6] E. Funck in H. Volkmann (Ed.): *Handbuch der Infrarotspektroskopie*, Verlag Chemie, Weinheim 1972, p. 240.
[7] **3**: *Pa* 3, $a = 1835.5(2)$ pm, $Z = 8$, $\rho_{exp.} = 1.37$ g/cm^3, $\rho_{calcd} = 1.38$ g/cm^3.—**4**: *Pa* 3, $a = 1841.5(22)$ pm, $Z = 8$, $\rho_{exp} = 1.44$ g/cm^3, $\rho_{calcd} = 1.46$ g/cm^3. Single-crystal diffractometer Nicolet R3M, $Cu_{K\alpha}$ radiation, graphite monochromator. 1134 reflections with $|F| \geq 3\sigma|F|$ from 1245 symmetry-independent reflections. Numerical absorption correction ($\mu = 17.28\ cm^{-1}$). $R = R_w = 0.084$. We thank Dr. *H. Lotter*, Institut für Pharmazeutische Biologie der Universität München, for measurements. Further details of the crystal structure investigation are available on request from the Fachinformationszentrum Energie, Physik, Mathematik GmbH, D-7514 Eggenstein-Leopoldshafen 2, by quoting the depository number CSD-51641, the names of the authors, and the journal citation.
[8] This was also confirmed by an X-ray diffraction study of Dr. *U. Nagel*, München, whom we warmly thank.

Decamethylsilicocene—Synthesis and Structure**

By *Peter Jutzi,* Dieter Kanne,* and *Carl Krüger*

Dedicated to Professor Max Schmidt on the occasion of his 60th birthday

We recently reported the syntheses of the decamethylmetallocenes of germanium and tin starting from the bis(pentamethylcyclopentadienyl) dihalides of these elements.[1] We have now been able to synthesize the analogous silicon compound using this procedure. Reaction of dichloro[bis(pentamethylcyclopentadienyl)]silane **1**[2] with naphthalenelithium, naphthalenesodium, or naphthalenepotassium in tetrahydrofuran (THF) affords bis(pentamethylcyclopentadienyl)silanediyl (decamethylsilicocene) **2**.[3]

$$(Me_5C_5)_2SiCl_2 \xrightarrow[THF]{MC_{10}H_8} (Me_5C_5)_2Si \quad (M = Li, Na, K)$$

1 **2**

The colorless,[4] crystalline compound **2** undergoes ready sublimation in an oil-pump vacuum and is thermally stable (m.p. = 171 °C), but it is extremely air-sensitive (presumably undergoing oxidation). The silicocene **2** is readily soluble in aprotic solvents such as hexane, benzene, and chlorinated hydrocarbons. According to cryoscopic molecular weight determinations, it is a monomer in benzene.

In the $^{13}C\{^1H\}$-NMR spectrum the ring and the methyl carbon atoms each exhibit only one sharp signal, and in the ^1H-NMR spectrum the protons of the methyl groups also exhibit only one sharp signal. On the basis of the chemical shifts,[5] this is more indicative of the presence of a π-complex than of a rapidly fluctuating σ-structure in solution. One resonance at very high field strength is observed in the ^{29}Si-NMR spectrum ($\delta = -577$).[6] If the ^{29}Si and ^{119}Sn chemical shifts are correlated, the value for **2** is in the expected range. Chemical and electron-impact ionization mass spectroscopy yield almost exclusively the ion fragment m/z 163 ($C_5Me_5Si^+$).

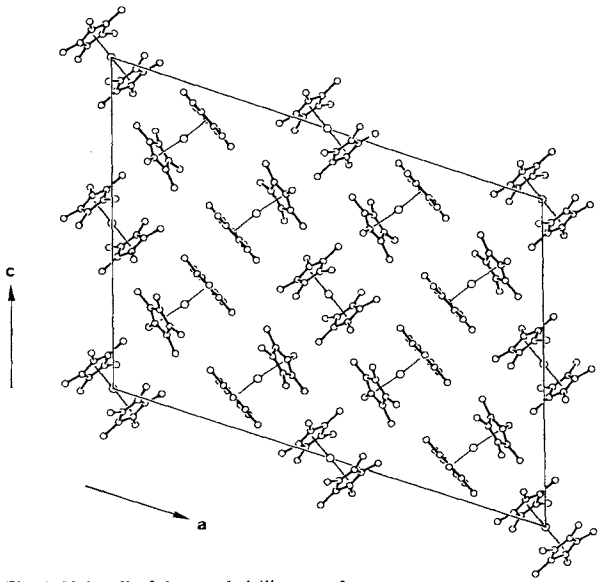


Fig. 1. Unit cell of decamethylsilicocene **2**.

[*] Prof. Dr. P. Jutzi, Dipl.-Chem. D. Kanne
Fakultät für Chemie der Universität, Anorganische Chemie
Universitätsstrasse, D-4800 Bielefeld 1 (FRG)
Prof. Dr. C. Krüger
Max-Planck-Institut für Kohlenforschung
Kaiser-Wilhelm-Platz 1, D-4330 Mülheim a. d. Ruhr (FRG)

[**] This work was supported by the Deutsche Forschungsgemeinschaft.

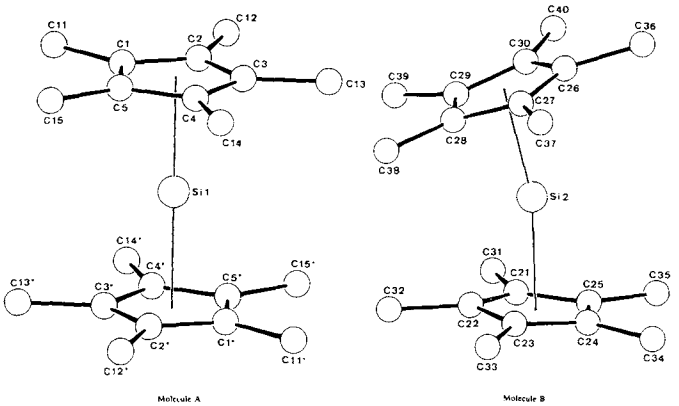


Fig. 2. Crystal structure of decamethylsilicocene **2**.

The single-crystal structure analysis[7] affords a surprising result. Two conformers are present in the unit cell in the ratio 1 : 2 (Fig. 1). Whereas in the molecule A, in which Si1 occupies a center of inversion, the two pentamethylcyclopentadienyl rings are staggered and their planes strictly parallel (Fig. 2, left), they are staggered and form an interplanar angle of 25.3° in molecule B (Fig. 2, right). Whereas the Si-C separations are equidistant in molecule A (mean value 2.42(1) Å), they lie between 2.324(8) Å (Si2-C22, Si2-C28) and 2.526(7) Å (Si2-C25) or 2.541(7) Å (Si2-C26) in B. The distance between the Si atoms and the center of gravity of the Cp rings is 2.11 Å in A and 2.12 Å in B. All methyl groups lie in the planes of the Cp rings within the given error limits (±0.006 Å). The C-C distance, averaged over 15 bonds, is 1.394(15) Å, the likewise averaged C-CH_3 distance 1.501(9) Å. The arrangement of the molecules in the crystal (Fig. 1) suggests that the interplanar angle of molecule B is caused by intermolecular interactions and packing effects.

Decamethylsilicocene **2** is the first silanediyl that is stable under normal conditions and the first π-complex with silicon as the central atom.

Received: October 1, 1985 [Z 1478 IE]
German version: *Angew. Chem. 98* (1986) 163

[1] P. Jutzi, B. Hielscher, *J. Organomet. Chem. C25* (1985) 291.

[2] P. Jutzi, D. Kanne, unpublished.

[3] *Experimental procedure:* A solution containing 33 mmol of naphthalenesodium in 100 mL of THF was added at −70 °C to 3.1 g (8.4 mmol) of **1** in 70 mL of THF over 5 h. The reaction mixture was allowed to warm up to room temperature and the solvent was then removed in vacuum. After fractional sublimation, the product was recrystallized from *n*-pentane. Yield: 376 mg (15%), colorless crystals (m.p. = 171 °C). — ^1H-NMR (300 MHz, $CDCl_3$): $\delta = 1.89$ (s, C_5Me_5). ^{13}C-NMR (75.5 MHz, $CDCl_3$): $\delta = 119.1$ (s, C_5), 10.0 (s, Me_5). ^{29}Si-NMR (59.6 MHz, C_6D_6): $\delta = -577$. Correct elemental analysis.

[4] Of interest are the colors of the decamethylmetallocenes of the 4th main group: colorless (Si), light yellow (Ge), dark yellow (Sn), orange red (Pb).

[5] $(C_5Me_5)_2M$: $\delta(^{13}C)$ (75.5 MHz, $CDCl_3$): M = Si: 119.1, 10.0; M = Ge: 118.1, 9.8; M = Sn (in C_6D_6): 117.0, 10.1; M = Pb: 117.6, 9.7. — $\delta(^1H)$ (60 MHz, C_6H_6): M = Si: 1.99; M = Ge: 2.04; M = Sn: 2.07; M = Pb: 2.24.

[6] This is the highest value for a silicon compound.

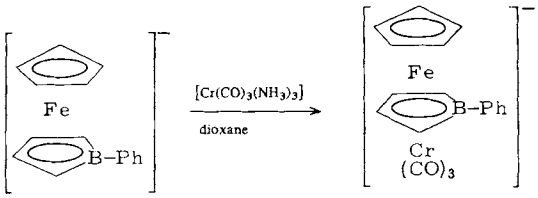
[7] Cell parameters: $a = 31.969(5)$, $b = 8.525(1)$, $c = 23.212(3)$ Å, $\beta = 108.75(1)°$, $V = 5990.8$ Å^3, $\rho_{calcd} = 0.99$, space group $C2/c$, $Z = 12$, 6746 reflections; 2611 reflections with $I \geq 2\sigma(I)$; 286 refined parameters; hydrogen atoms on calculated sites were not considered in the refinement; $R = 0.088$, $R_w = 0.096$, Refinement in the space group Cc leads to the same results. Further details of the crystal structure investigation are available on request from the Fachinformationszentrum Energie, Physik, Mathematik GmbH, D-7514 Eggenstein-Leopoldshafen 2, by quoting the depository number CSD 51619, the names of the authors, and the journal citation.

Synthesis of Anionic Triple-Decker Complexes Having Closed 30e Valence Shells by Stacking of Sandwich Anions with $Cr(CO)_3$ Fragments**

By *Gerhard E. Herberich,** *Bernd Hessner, Judith A. K. Howard, Dieter P. J. Köffer,* and *Roland Saive*

The 30 valence electron rule[2] plays the same role for triple-decker complexes as the 18-electron rule for mononuclear organometallic complexes. Indeed, of the numerous triple-decker complexes with boron-containing heterocycles as central ligands, those having closed 30e valence shells are particularly common and especially stable.[3] It is surprising, therefore, that no anionic 30e triple-decker complexes have been reported so far. This is primarily due to the fact that no reactions are known that would allow introduction of 12e fragments into a sandwich complex.

We now have found that (borole)metal sandwich anions, like the isolobal systems benzene, cyclopentadienide, 1-methylboratabenzene ion,[4a] and 7,8-carbollide ion $[7,8\text{-}C_2B_9H_{11}]^{2-}$,[4b] react with the 12e building block $Cr(CO)_3$.



1 2

Thus, **1**[5] reacts regiospecifically with $[Cr(CO)_3(NH_3)_3]$ to give the triple-decker anion **2**;[6] the phenyl group is not attacked. In contrast to **1**, complex **2** is stable in aqueous solution and was isolated in the form of a purple-red, light-sensitive $[NMe_3Ph]^+$ salt.[6]

The anion **2** has a typical triple-decker structure (Fig. 1).[7] The ring ligands are nearly planar (deviation <0.5 pm) and lie in nearly parallel planes (deviation 1.9°).[7] One CO group almost eclipses the B atom (deviation 11.1°); the same conformation was also found for $[(\mu\text{-}2\text{-}EtC_4H_3BPh)\{Mn(CO)_3\}_2]$.[1]

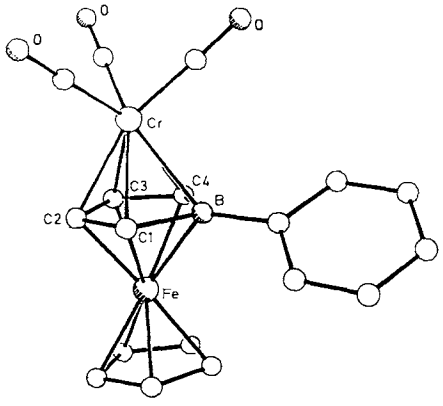


Fig. 1. Structure of the anion **2** in the crystal of the $[NMe_3Ph]^+$ salt. Selected distances [pm]: Cp-Fe 165.4, C_4B-Fe 163.9, C_4B-Cr 186.5; Fe-B 215.3(3), Fe-C(C_4B) 205.6 (average), Cr-B 232.0(3), Cr-C(C_4B) 224.3 (average), B-C1 156.5(4), B-C4 156.5(4), C1-C2 144.7(4), C3-C4 144.3(4), C2-C3 146.2 (4).

The Cr–CO distances (average 180.8 pm) are not significantly longer than in $[NMe_4][CpCr(CO)_3]$ (average 180 pm[8]); the charge distribution in the $Cr(CO)_3$ group of **2** is accordingly very similar to that of $[CpCr(CO)_3]^-$. In accordance with this, the $\tilde{\nu}$(CO) data of the $[NMe_3Ph]^+$ salt of **2** [(CH_2Cl_2) 1895 (s), 1779 (s), 1764 (s) cm^{-1}] and of $[NMe_3Ph][CpCr(CO)_3]$ [(CH_2Cl_2) 1888 (s), 1773 (s), 1756 (s, sh) cm^{-1}] show that the donor ability of **1** is only slightly weaker than that of Cp^-.

Other 18e anions with borole ligands, e.g., $[CoL_2]^-$, $[RhL_2]^-$, and $[LMn(CO)_3]^-$ (L = C_4H_4BMe and C_4H_4BPh), also react with $[Cr(CO)_3(NH_3)_3]$ to afford the corresponding anionic 30e triple-decker complexes.[9]

Received: October 4, 1985 [Z 1483 IE]
German version: *Angew. Chem. 88* (1986) 177

[1] G. E. Herberich, J. Hengesbach, G. Huttner, A. Frank, U. Schubert, *J. Organomet. Chem. 246* (1983) 141.
[2] J. W. Lauher, M. Elian, R. H. Summerville, R. Hoffmann, *J. Am. Chem. Soc. 98* (1976) 3219.
[3] J. Edwin, M. Bochmann, M. C. Böhm, D. E. Brennan, W. E. Geiger, C. Krüger, J. Pebler, H. Pritzkow, W. Siebert, W. Swiridoff, H. Wadepohl, J. Weiss, U. Zenneck, *J. Am. Chem. Soc. 105* (1983) 2582; G. E. Herberich in G. Wilkinson, F. G. A. Stone, E. W. Abel: *Comprehensive Organometallic Chemistry, Vol. 1*, Pergamon, Oxford 1982, p. 381; W. Siebert, *Adv. Organomet. Chem. 18* (1980) 301.
[4] a) G. E. Herberich, D. Söhnen, *J. Organomet. Chem. 254* (1983) 143; b) M. F. Hawthorne, H. W. Ruhle, *Inorg. Chem. 8* (1969) 176.
[5] G. E. Herberich, W. Boveleth, B. Hessner, D. P. J. Köffer, M. Negele, R. Saive, *J. Organomet. Chem.*, in press; cf. G. E. Herberich, B. Hessner, W. Boveleth, H. Lüthe, R. Saive, L. Zelenka, *Angew. Chem. 95* (1983) 1024; *Angew. Chem. Int. Ed. Engl. 22* (1983) 996; *Angew. Chem. Suppl. 1983*, 1503.
[6] *Experimental procedure:* $[CpFeH(C_4H_4BPh)]$ (230 mg, 0.88 mmol), prepared photochemically from $[Fe(CO)_3(C_4H_4BPh)]$ [5] and C_5H_6, was treated with NaH in 20 mL of dioxane. After gas evolution had ceased, the orange solution was decanted, treated with $[Cr(CO)_3(NH_3)_3]$ (165 mg, 0.88 mmol), and heated at 100°C for 4 h. Removal of the solvent, precipitation of the product from 20 mL of H_2O with 232 mg (0.88 mmol) of $[NMe_3Ph]I$ in 10 mL of H_2O, and crystallization from CH_2Cl_2/Et_2O afforded 220 mg (0.41 mmol, 47%) of the $[NMe_3Ph]^+$ salt of **2** as analytically pure, deep red, air-sensitive needles, m.p. = 138°C (decomp.). — ^{1}H-NMR (270 MHz, [D$_6$]acetone): δ = 8.04, 7.70, 7.19, 7.04 (4 m, 2 H, 5 H, 2 H, 1 H; 2 Ph), 4.11 (m, 3-/4-H), 3.86 (s, Cp), 3.85 (s, 3 Me), 2.53 (m, 2-/5-H). — ^{11}B-NMR ([D$_6$]acetone, $BF_3 \cdot OEt_2$ ext.): δ = 9.4.
[7] Nicolet P3m, $Mo_{K\alpha}$ radiation, 220 K. $[NMe_3Ph]^+$ salt of **2**: $P2_1/c$, a = 1334.6(10), b = 635.1(2), c = 2940(2) pm; β = 97.05(6)°; V = 2.473(3) nm^3; Z = 4; ρ_{calcd} = 1.432 g cm^{-3}; 3727 unique reflections with $I > 3.5\sigma(I)$, R = 0.0340, R_w = 0.0355, $W^{-1} = \sigma^2(F_0) + 0.00035|F_0|^2$. Further details of the crystal structure investigation are available on request from the Fachinformationszentrum Energie, Physik, Mathematik GmbH, D-7514 Eggenstein-Leopoldshafen 2, by quoting the depository number CSD-51654, the names of the authors, and the journal citation.
[8] R. Feld, E. Hellner, A. Klopsch, K. Dehnicke, *Z. Anorg. Allg. Chem. 442* (1978) 173.
[9] G. E. Herberich, B. Hessner, D. P. J. Köffer, R. Saive, unpublished results.

[*] Prof. Dr. G. E. Herberich, Dr. B. Hessner, Dipl.-Chem. D. P. J. Köffer, Dipl.-Chem. R. Saive
Institut für Anorganische Chemie der Technischen Hochschule
Professor-Pirlet-Strasse 1, D-5100 Aachen (FRG)
Dr. J. A. K. Howard
Department of Inorganic Chemistry, The University of Bristol
Cantock's Close, Bristol BS8 1TS (England)

[**] Triple-Decker Complexes, Part 4. This work was supported by the Deutsche Forschungsgemeinschaft and the Fonds der Chemischen Industrie. — Part 3: [1].

The Three-Dimensionally Non-Molecular Polyadamantanoid Structure of $Cd(SPh)_2$**

By *Don Craig, Ian G. Dance,** and *Robert Garbutt*

A characteristic property of the long-known compounds $M(SPh)_2$ is their sparing solubility in inert solvents, presumed but not proven to be a consequence of non-molecu-

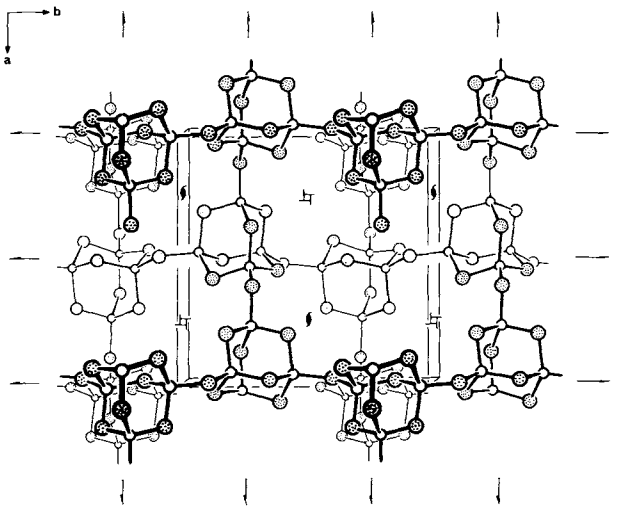
[*] Prof. Dr. I. G. Dance, D. Craig, R. Garbutt
School of Chemistry, University of New South Wales
PO Box 1, Kensington, NSW 2033 (Australia)

[**] This research was supported by the Australian Research Grants Scheme.

lar crystal structures. When M is tetrahedrally coordinated, possible non-molecular structures include tetrahedra edge-linked in one dimension $^{1}_{\infty}\{M(\mu\text{-}SPh)_{4/2}\}$, or vertex-linked in two dimensions $^{2}_{\infty}\{M(\mu\text{-}SPh)_{4/2}\}$. The confirmed structure of $Zn_4(SPh)_8(MeOH)$[1] prompted the suggestion[2] of a two-dimensionally non-molecular structure for $M(SPh)_2$ comprised of linked adamantanoid cages $^{2}_{\infty}\{(\mu\text{-}SPh)_6M_4(\mu\text{-}SPh)_{4/2}\}$. Until now no *three*-dimensionally non-molecular crystal structure of any type has been reported or proposed for a homoleptic metal thiolate.

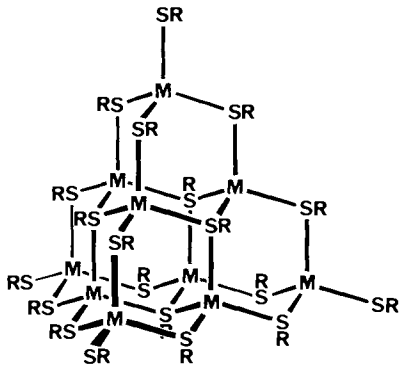
Bis(benzenethiolato)cadmium(II), **1**, prepared by standard methods from benzenethiol, triethylamine, and cadmium nitrate in ethanol, and crystallized from dimethylformamide (DMF) by addition of alcohols, acetone, or acetonitrile, has the three-dimensionally non-molecular polyadamantanoid structure $^{3}_{\infty}\{(\mu\text{-}SPh)_6Cd_4(\mu\text{-}SPh)_{4/2}\}$ (Fig. 1).[3] Each adamantanoid cage is linked through its four outer (terminal) PhS^- ligands to four surrounding cages. Linked cages occur in zig-zag chains (along 2_1 axes) parallel to *a* and *b*, but in the third orthogonal direction the cage linkages occur in fourfold helical sequences about pseudo 4_1 (exact 2_1) axes (marked on Fig. 1).[4] These helical connections, and the consequent interweaving of the chains parallel to *a* and *b* are the source of the three-dimensional non-molecularity. An alternative presentation of the structure of **1** derives from the conception of the Cd_4S_{10} adamantanoid cage as a large tetrahedron (edge-centered and comprised of four vertex-sharing coordination tetrahedra). The vertex linkage pattern of these large tetrahedra is very similar to that in α-cristobalite and many related compounds.[5] However the structure of **1** is unprecedented for complexes with organic substituents: the phenyl groups that are accommodated between the adamantanoid cages of **1** are responsible for the openness of the structure and the 20 Å translation along *c*. Two-dimensionally non-molecular polyadamantanoid structures also occur in the metal chalcogenides $KInSe_2$, $TlGaSe_2$ and $Ag_3B_5S_9$.[6]

Even though **1** is high melting (340 °C) it is very soluble in DMF (ca. 1.3 g/mL at ambient temperature). The ^{113}Cd-NMR spectrum (66.6 MHz, natural isotopic abundance, standard 0.1 M $Cd(NO_3)_2$) of **1** in DMF shows one temperature dependent signal; at $T = 220$, 240, 260 K, $\delta(^{113}Cd) = 593$, 588, 578 and $\nu_{1/2} = 150$, 275, 1350 Hz. The signal broadens with increasing temperature up to 300 K. The chemical shift of this species, which predominates in a slowly exchanging equilibrium at low temperature, is very close to that of the adamantanoid cage $[Cd_4(SPh)_{10}]^{2-}$ ($\delta = 586$ at 260 K),[7,8] and is consistent with the Cd^{2+} in **1** being coordinated only by PhS^-.[9] We propose that the principal species generated when **1** dissolves in DMF is molecular $Cd_{10}(SPh)_{20}$, with the tetra-adamantanoid cage structure (Fig. 2).



$^{3}_{\infty}\{(\mu\text{-}SPh)_6Cd_4(\mu\text{-}SPh)_{4/2}\}$ **1**

Fig. 1. The polyadamantanoid framework in crystalline $Cd(SPh)_2$ **1** (drawn with all phenyl groups omitted). The larger dotted circles are the sulfur atoms. The view direction is tilted 3° from the *c* axis. Average bond distances [Å] and angles [°] are (intra-cage bridges are S^b, inter-cage bridges are S^v): Cd-S^b 2.543, Cd-S^v 2.530 Å; S^b-Cd-S^b 109.2, S^b-Cd-S^v 109.6, Cd-S^b-Cd 108.8, Cd-S^v-Cd 136.0.



tetrahedro-$(\mu_3\text{-}SPh)_4$-*octahedro*-Cd_6-*truncated-tetrahedro*-$(\mu\text{-}SPh)_{12}$-*tetrahedro*-$(CdSPh)_4$ **2**

Fig. 2. Proposed structure for $Cd_{10}(SPh)_{20}$ **2**, which is formed upon dissolution of **1** in DMF.

The structure of **2** has already been postulated by extension from $[S_4Cd_{10}(SPh)_{16}]^{4-}$,[10] and should not incur intramolecular interference of ligand substituents. The ^{113}Cd-NMR line widths at 220 K are too large to permit resolution of the two Cd sites in **2**, with $(\mu_3\text{-}SPh)_2(\mu\text{-}SPh)_2Cd$ and $(\mu\text{-}SPh)_3CdSPh$ coordination, or resolution of any Cd-Cd scalar coupling.[7,8] Straightforward aggregation of the adamantanoid cages of **1** to form **2** cannot be sufficient for general dissolution of **1** in inert solvents, and other species in equilibrium with that giving the observed line presumably contain some coordinated DMF and give ^{113}Cd-NMR signals at much higher field.

Received: October 9, 1985;
revised: November 22, 1985 [Z 1490 IE]
German version: *Angew. Chem. 98* (1986) 178

[1] I. G. Dance, *J. Am. Chem. Soc. 102* (1980) 3445.
[2] I. G. Dance, *Polyhedron*, in press.
[3] Colorless crystals, orthorhombic, $a = 15.490(2)$, $b = 15.626(2)$, $c = 20.803(3)$ Å, $Mo_{K\alpha}$ radiation, $\mu = 20.13$ cm^{-1}, $\rho_{obs.} = 1.77$, $\rho_{calc.} = 1.74$ g cm^{-3}, $Z = 4$, 3475 observed reflections out of 4884 measured, $R = 0.03$, $R_w = 0.035$. Further details of this crystal structure can be obtained from the Director of the Cambridge Crystallographic Data Centre, University Chemical Laboratory, Lensfield Road, Cambridge CB2 1EW (UK). Any request should be accompanied by the full literature citation of this journal.
[4] Disregarding the phenyl substituents, the crystal structure is pseudo-tetragonal, space group $P4_12_12$.
[5] M. O'Keefe, B. G. Hyde, *Acta Crystallogr. B 32* (1976) 2923.
[6] B. Krebs, *Angew. Chem. 95* (1983) 113; *Angew. Chem. Int. Ed. Engl. 22* (1983) 113.
[7] P. A. W. Dean, J. J. Vittal, *J. Am. Chem. Soc. 106* (1984) 6436.
[8] I. G. Dance, J. K. Saunders, *Inorg. Chim. Acta 96* (1985) L71.
[9] The only hetero ligands known to maintain $\delta(^{113}Cd) > 580$ are S^{2-} [8] and alkylthiolate: G. K. Carson, P. A. W. Dean, M. J. Stillman, *Inorg. Chim. Acta 56* (1981) 59. Addition of Cl^- in small amounts to **1** gives species with $(\mu\text{-}SPh)_3CdCl$-coordination, and signals at $\delta = 563$ (260 K).
[10] I. G. Dance, A. Choy, M. L. Scudder, *J. Am. Chem. Soc. 106* (1984) 6285.

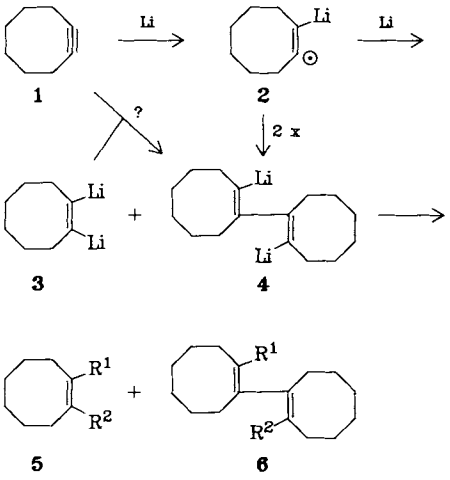
Vicinal Dilithioalkenes by Addition of Lithium to Simple Cyclic and Acyclic Alkynes**

By *Adalbert Maercker,* Thomas Graule,* and *Ulrich Girreser*

Dedicated to Professor Hans Jürgen Bestmann on the occasion of his 60th birthday

Addition of lithium to diphenylacetylene affords, depending on the conditions, either the unstable *cis*-dilithiostilbene[2] or the dimeric 1,4-dilithio-1,2,3,4-tetraphenyl-1,3-butadiene.[3] Only the latter has found applications as a difunctional organolithium compound in synthetic chemistry.[4] We have now attempted to extend this reaction to dialkylacetylenes in order to develop, ultimately, an approach to the synthesis of aliphatic, vicinal dilithioalkenes, which have not yet been prepared.[5]

In order to exclude the possibility of lithium hydride elimination, the most important competing reaction in the synthesis of polylithium organic compounds,[6] we initially selected di-*tert*-butylacetylene as a starting material—however, without success. No reaction was observed, even after heating the compound with lithium powder for eight hours in diethyl ether, tetrahydrofuran (THF), or cyclopentane.



a: $R^1 = R^2 = H$; **b**: $R^1 = R^2 = D$
c: $R^1 = H$; $R^2 = CH_3$; **d**: $R^1 = R^2 = CH_3$

The reaction with cyclooctyne **1**,[7] however, proceeded successfully. This strained cycloalkyne reacts with excess lithium powder in diethyl ether at −35°C under argon over the course of 2 h to give a yellow solution of *cis*-1,2-dilithiocyclooctene **3**, which is stable for several hours at −40°C but undergoes decomposition with a half-life of 1 h at room temperature. After the excess lithium had been filtered off, the reaction mixture was treated with CH_3OD. GC/MS analysis (internal standard: decalin) established the presence of 64% *cis*-1,2-dideuteriocyclooctene **5b** (96% D_2, 4% D_1)[8] and 19% 2,2'-dideuterio-1,1'-bicyclooctenyl **6b** (85% D_2, 10% D_1),[9] which is formed by deuterolysis of the dilithio compound **4**, the product of dimerization. In addition, traces of unidentified compounds (total < 1%) were detected by gas chromatography; the remainder (16%) consisted of nonvolatile reaction products.

In a second experiment, the reaction mixture was treated with dimethyl sulfate. The corresponding *cis*-1,2-dimethylcyclooctene **5d** (65%)[10] and 2,2'-dimethyl-1,1'-bicyclooctenyl **6d**[11] (9%) were obtained along with the monomethylated compounds **5c**[12] and **6c**[13] and the hydrolysis products **5a**[14] and **6a**[15] (Table 1).

Table 1. Solvent-dependent yields of monomeric and dimeric products in the addition of lithium to cyclooctyne followed by subsequent reaction with dimethyl sulfate. See also [7].

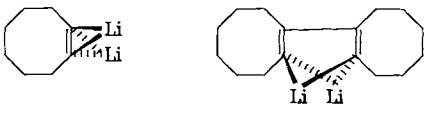
	Et_2O (−35°C) [%]	THF (−30°C) [%]	cyclopentane (−10°C) [%]
1	–	–	5
5a	2	12	2
5c	3	10	–
5d	65	15	13
6a	4	15	4
6c	4	6	7
6d	9	30	50
? [a]	13	12	19

[a] Higher-molecular-weight products not detectable by gas chromatography.

The yield of **3** is poorer in THF at the same reaction temperature. However, not only is more of the dimer **4** formed, but also the dilithio compounds partly undergo decomposition by reaction with the solvent. Thus, even at −30°C, considerable amounts of the monomethyl compounds **5c** and **6c** as well as the hydrolysis products **5a** and **6a** are formed (Table 1). No reaction takes place at lower temperatures.

In cyclopentane the reaction of cyclooctyne **1** with lithium only begins to take place at −10°C. The large proportion of dimeric and higher-molecular-weight products is possibly due to the higher reaction temperature (Table 1).

The structures of the dilithio compounds **3** and **4** are still unknown. Experimental results for *cis*-dilithiostilbene[2] and ab initio calculations on *cis*-1,2-dilithioethylene[16] and 1,4-dilithio-1,3-butadiene[17] suggest doubly bridged structures such as **3A** and **4A**, respectively. ^{13}C- and ^6Li-NMR spectroscopic studies of the ^6Li-labeled compounds did not afford definitive results.[18]



3A **4A**

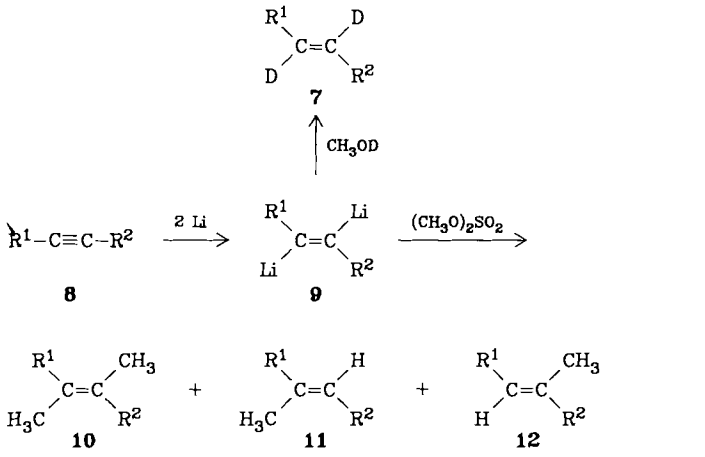
Since, contrary to our fears, no elimination of lithium hydride from 1,2-dilithiocyclooctene **3** occurred at low temperatures, we have also studied the reaction of sterically less-hindered, open-chain alkynes with lithium.

Indeed, treatment of 3-octyne **8a** with freshly prepared lithium powder (2% sodium) results in addition—which, however, proceeds slowly—to the triple bond. Interestingly, solely *trans* addition is observed, giving **9a**. The reaction is complete after 48 h in diethyl ether at room temperature. The insoluble product, a silvery, pale green sediment, still contains excess lithium. The deuterolysis was

[*] Prof. Dr. A. Maercker, Dipl.-Chem. T. Graule, U. Girreser
Institut für Organische Chemie der Universität
Adolf-Reichwein-Strasse, D-5900 Siegen (FRG)

[**] Polylithium Organic Compounds, Part 5. This work was supported by the Fonds der Chemischen Industrie.—Part 4: [1].

carried out by very slow addition of a 10% solution of CH_3OD in diethyl ether at $-30°C$ (**danger of explosion**) and afforded pure *trans*-3-octene **7a** (77% D_2, 18% D_1, 5% D_0) in 96% yield according to GC/MS analysis. In addition, traces of unidentified compounds (total < 1%) were detected by gas chromatography; the remaining products (3%) were nonvolatile substances. Dimeric products were only formed, this time, in trace amounts (< 1%).



a: $R^1 = C_2H_5$, $R^2 = C_4H_9$; **b**: $R^1 = R^2 = C_3H_7$; **c**: $R^1 = R^2 = C_4H_9$

Derivatization was also carried out with a 10% solution of dimethyl sulfate in diethyl ether at 0°C (very slowly, **danger of explosion**); (*E*)-3,4-dimethyl-3-octene **10a** (62%) was obtained along with the monomethylated compounds (*E*)-3-methyl-3-octene **11a** and (*E*)-4-methyl-3-octene **12a** (together 6%) as well as 15% of the hydrolysis product **7a** (D_0). Furthermore, several unidentified products (total ca. 9%) were detected by gas chromatography; the remaining substances (8%) were nonvolatile.

Table 2. Addition of lithium to open-chain alkynes in diethyl ether at room temperature and trapping of the organolithium intermediates.

Starting material	*t* [h]	Trapping reagent	Yield [%] [a] 7 (degree of deuteration)	10	11 (+ 12)
8a	48	CH_3OD	96 (77% D_2; 18% D_1; 5% D_0)	—	—
	48	$(CH_3O)_2SO_2$	15 (D_0)	62	6
8b	24	CH_3OD	90 (67% D_2; 20% D_2; 13% D_0)	—	—
	16	$(CH_3O)_2SO_2$	2 (D_0)	73	11
8c	48	CH_3OD	85 (64% D_2; 30% D_1; 6% D_0)	—	—

[a] Not optimized.

As expected, the symmetrically substituted acetylenes 4-octyne **8b** and 5-decyne **8c** also underwent reaction with lithium. Derivatization with dimethyl sulfate resulted, this time, in the formation of only one side product, since for $R^1 = R^2$ the monomethyl compounds **11** and **12** are identical (Table 2). Only *trans* addition is observed; the *cis* addition of lithium to cyclooctyne **1** and diphenylacetylene,[2] however, suggests a subsequent *cis-trans* isomerization, as we have found to be the case for unsubstituted 1,2-dilithioethylene.[19]

Received: August 19, 1985;
supplemented: November 26, 1985 [Z 1433 IE]
German version: *Angew. Chem. 98* (1986) 174

[1] A. Maercker, R. Dujardin, *Angew. Chem. 97* (1985) 612; *Angew. Chem. Int. Ed. Engl. 24* (1985) 571.

[2] G. Levin, J. Jagur-Grodzinski, M. Szwarc, *J. Am. Chem. Soc. 92* (1970) 2268.

[3] W. Schlenk, E. Bergmann, *Justus Liebigs Ann. Chem. 463* (1928) 71; L. I. Smith, H. H. Hoehn, *J. Am. Chem. Soc. 63* (1941) 1184.

[4] Cf. J. J. Eisch, *Organomet. Synth. 2* (1981) 98, 176; F. C. Leavitt, T. A. Manuel, F. Johnson, *J. Am. Chem. Soc. 81* (1959) 3163; F. C. Leavitt, T. A. Manuel, F. Johnson, L. U. Matternas, D. S. Lehmann, *ibid. 82* (1960) 5099; E. H. Braye, W. Hübel, I. Caplier, *ibid. 83* (1961) 4406.

[5] After reaction of *trans*-2-butene with lithium vapor at 850°C and subsequent deuterolysis, $CH_3CD{=}CHCH_3$ and $CH_3CD{=}CDCH_3$ in a ratio of 3:2 were detected in 10% yield along with traces of perdeuterated 2-butene: J. A. Morrison, C. Chung, R. J. Lagow, *J. Am. Chem. Soc. 97* (1975) 5015; the probable intermediacy of 1,2-dilithiocyclopropene was established in the reaction of phenyllithium with allyl chloride: D. E. Applequist, E. G. Saurborn, *J. Org. Chem. 37* (1972) 1676.

[6] A. Maercker, M. Theis, A. J. Kos, P. von R. Schleyer, *Angew. Chem. 95* (1983) 755; *Angew. Chem. Int. Ed. Engl. 22* (1983) 733.

[7] *Experimental procedure:* Approximately 2% of a solution of **1** (1.08 g, 10 mmol) in 30 mL of diethyl ether was added to 0.3 g (43 mmol) of lithium powder (2% sodium) suspended in 5 mL of anhydrous diethyl ether under argon at −5°C. After start of the reaction (yellow coloration of the reaction mixture), the suspension was cooled to −35°C and the remainder of the solution of **1** was added over 2 h. The excess lithium was then filtered off under inert gas. In order to carry out the derivatization, the filtrate was cooled to −70°C and a 10% solution of CH_3OD or dimethyl sulfate in diethyl ether was added with stirring.

[8] U. H. Andrews, J. E. Baldwin, M. W. Grayston, *J. Org. Chem. 47* (1982) 287. **5b**: MS (70 eV): *m/z* 112 ($M^{\oplus}$, 51.6%), 97 ($M^{\oplus}-CH_3$, 16.1), 84 ($M^{\oplus}-C_2H_4$, 64.5), 69 ($C_5H_5D_2^{\oplus}$, 100), 56 ($C_4H_4D_2^{\oplus}$, 74.2), 41 ($C_3H_5^{\oplus}$, 67.7); ^{13}C-NMR (20.1 MHz, $CDCl_3$): $\delta = 129.8$ ($^1J(^{13}C,D) = 23.5$ Hz, C-1, C-2), 29.2 (C-5, C-6), 26.1 (C-4, C-7), 25.3 (C-3, C-8); ^{1}H-NMR (80 MHz, $CDCl_3$): $\delta = 2.13$ (s, br, H-3, H-8; 4H), 1.50 (s, br, H-4–H-7; 8H).

[9] **6b**: MS (70 eV): *m/z* 220 ($M^{\oplus}$, 50.0%), 205 ($M^{\oplus}-CH_3$, 5.9), 192 ($M^{\oplus}-C_2H_4$, 35.3), 177 ($C_{13}H_{17}D_2^{\oplus}$, 17.6), 164 ($C_{12}H_{16}D_2^{\oplus}$, 55.9), 149 ($C_{11}H_{13}D_2^{\oplus}$, 32.4), 136 ($C_{10}H_{12}D_2^{\oplus}$, 38.2), 122 ($C_9H_{10}D_2^{\oplus}$, 44.1), 109 ($C_8H_9D_2^{\oplus}$, 61.8), 95 ($C_7H_7D_2^{\oplus}$, 100), 81 ($C_6H_5D_2^{\oplus}$, 91.2), 68 ($C_5H_6D^{\oplus}$, 73.5), 55 ($C_4H_7^{\oplus}$, 55.9), 41 ($C_3H_5^{\oplus}$, 91.2).

[10] A. C. Cope, H. C. Campbell, *J. Am. Chem. Soc. 74* (1952) 179. **5d**: MS (70 eV): *m/z* 138 ($M^{\oplus}$, 53.8%), 123 ($M^{\oplus}-CH_3$, 15.4), 110 ($M^{\oplus}-C_2H_4$, 34.6), 95 ($C_7H_{11}^{\oplus}$, 69.2), 81 ($C_6H_9^{\oplus}$, 92.3), 67 ($C_5H_7^{\oplus}$, 100), 55 ($C_4H_7^{\oplus}$, 65.4), 41 ($C_3H_5^{\oplus}$, 69.2); ^{13}C-NMR (20.1 MHz, $CDCl_3$): $\delta = 129.0$ (C-1, C-2), 33.9, 29.6, 27.5 (C-3–C-8), 19.3 (CH_3); ^{1}H-NMR (80 MHz, $CDCl_3$): $\delta = 1.7$ (s, br, H-3, H-8; 4H), 1.2 (s, CH_3; 6H), 1.0 (s, br, H-4–H-7; 8H).

[11] **6d**: MS (70 eV): *m/z* 246 ($M^{\oplus}$, 81.0%), 231 ($M^{\oplus}-CH_3$, 26.5), 218 ($M^{\oplus}-C_2H_4$, 11.0), 203 ($C_{15}H_{23}^{\oplus}$, 11.5), 189 ($C_{14}H_{21}^{\oplus}$, 26.0), 175 ($C_{13}H_{19}^{\oplus}$, 39.5), 161 ($C_{12}H_{17}^{\oplus}$, 46.5), 147 ($C_{11}H_{15}^{\oplus}$, 38.0), 133 ($C_{10}H_{13}^{\oplus}$, 50.0), 119 ($C_9H_{11}^{\oplus}$, 65.0), 107 ($C_8H_{11}^{\oplus}$, 90.0), 90.0), 93 ($C_7H_9^{\oplus}$, 85.5), 81 ($C_6H_9^{\oplus}$, 90.0), 67 ($C_5H_7^{\oplus}$, 72.0), 55 ($C_4H_7^{\oplus}$, 100), 41 ($C_3H_5^{\oplus}$, 39.0); ^{13}C-NMR (20.1 MHz, $CDCl_3$): $\delta = 136.0$ (C-2, C-2'), 129.0 (C-1, C-1'), 32.5, 31.5, 30.0, 28.5, 27.5, 26.5 (C-3–C-8, C-3'–C-8'), 20.0 (CH_3).

[12] **5c**: MS (70 eV): *m/z* 124 ($M^{\oplus}$, 27.5%), 109 ($M^{\oplus}-CH_3$, 12.5), 96 ($M^{\oplus}-C_2H_4$, 77.5), 81 ($C_6H_9^{\oplus}$, 65.0), 67.0 ($C_5H_7^{\oplus}$, 100), 55 ($C_4H_7^{\oplus}$, 52.5), 41 ($C_3H_5^{\oplus}$, 70.0).

[13] **6c**: MS (70 eV): *m/z* 232 ($M^{\oplus}$, 54.3%), 217 ($M^{\oplus}-CH_3$, 14.3), 204 ($M^{\oplus}-C_2H_4$, 28.6), 189 ($C_{14}H_{21}^{\oplus}$, 17.1), 175 ($C_{13}H_{19}^{\oplus}$, 28.6), 161 ($C_{12}H_{17}^{\oplus}$, 40.0), 147 ($C_{11}H_{15}^{\oplus}$, 42.9), 135 ($C_{10}H_{15}^{\oplus}$, 34.3), 121 ($C_9H_{13}^{\oplus}$, 54.3), 105 ($C_8H_9^{\oplus}$, 74.3), 93 ($C_7H_9^{\oplus}$, 94.3), 81 ($C_6H_9^{\oplus}$, 100), 67 ($C_5H_7^{\oplus}$, 91.4), 55 ($C_4H_7^{\oplus}$, 91.4), 41 ($C_3H_5^{\oplus}$, 97.1).

[14] A. Cornu, R. Massot: *Compilation of Mass Spectral Data, Vol. 1*, Heyden, London 1975, p. 90 B.

[15] D. S. Greidinger, D. Ginsburg, *J. Org. Chem. 22* (1957) 1406. **6a**: MS (70 eV): *m/z* 218 ($M^{\oplus}$, 23.6%), 203 ($M^{\oplus}-CH_3$, 4.5), 190 ($M^{\oplus}-C_2H_4$, 24.7), 175 ($C_{13}H_{19}^{\oplus}$, 14.6), 162 ($C_{12}H_{18}^{\oplus}$, 38.2), 148 ($C_{11}H_{16}^{\oplus}$, 22.5), 135 ($C_{10}H_{15}^{\oplus}$, 34.8), 121 ($C_9H_{13}^{\oplus}$, 28.1), 107 ($C_8H_{11}^{\oplus}$, 40.4), 91 ($C_7H_7^{\oplus}$, 84.3), 79 ($C_6H_7^{\oplus}$, 100), 67 ($C_5H_7^{\oplus}$, 75.3), 55 ($C_4H_7^{\oplus}$, 53.9), 41 ($C_3H_5^{\oplus}$, 75.3).

[16] Y. Apeloig, T. Clark, A. J. Kos, E. D. Jemmis, P. von R. Schleyer, *Israel J. Chem. 20* (1980) 43 (cf. addendum p. 49). See also: P. von R. Schleyer, E. Kaufmann, A. J. Kos, T. Clark, J. A. Pople, *Angew. Chem. 98* (1986) 164; *Angew. Chem. Int. Ed. Engl. 25* (1986) 169.

[17] A. J. Kos, P. von R. Schleyer, *J. Am. Chem. Soc. 102* (1980) 7928.

[18] We thank Dipl.-Chem. *D. Moskau* and Prof. *H. Günther* for the measurements.

[19] A. Maercker, T. Graule, W. Demuth, unpublished results.

1,2-Dilithioethylene Isomers and Their Mechanisms of Interconversion: an Ab Initio Study**

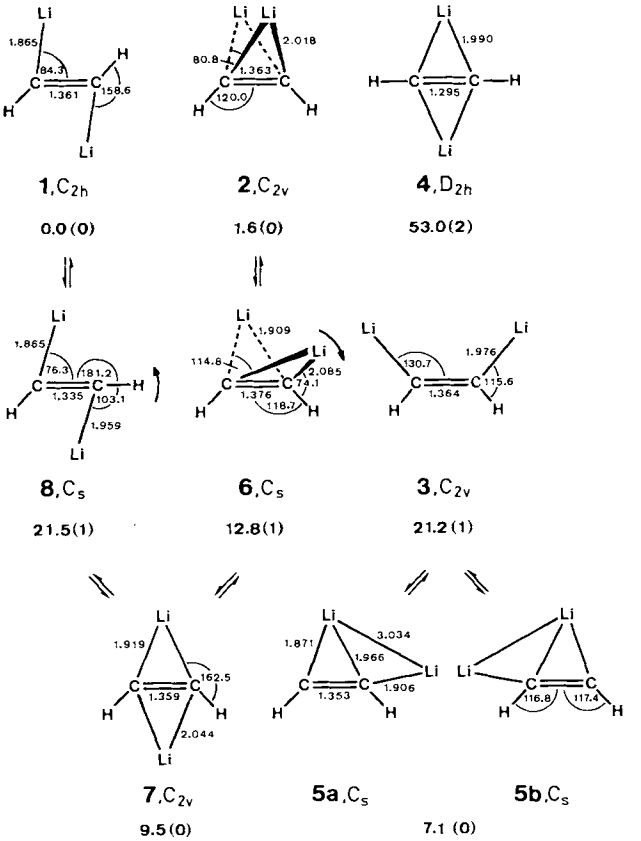
By *Paul von Ragué Schleyer,* Elmar Kaufmann, Alexander J. Kos, Timothy Clark,* and *John A. Pople*

Polylithium compounds favor unusual geometries, quite unlike those of typical organic compounds.[1] Our earlier theoretical study of 1,2-dilithioethylene structures[2] is illustrative. The *trans* isomer **1** was found to prefer a distorted planar, partially bridged geometry. At the levels of theory employed in 1979, the nonplanar doubly bridged *cis* isomer **2** was found to be slightly more stable than **1**, and substantially lower in energy than the "classical" *cis* structure **3**. The more symmetrical (D_{2h} point group) bridged structure **4** was much higher in energy. At that time, experimental attempts to prepare 1,2-dilithioethylene had been unsuccessful.[3] The recent achievement of this goal by *Maercker* et al.[4] prompts us to report our further studies in this area. *Maercker*'s results indicate that *cis*-1,2-dilithioethylene rearranges readily into the more stable *trans* isomer. We now propose a mechanism for this isomerization.

Recent developments in theoretical methods[5,6] facilitate the characterization of stationary points on potential energy surfaces. Thus, both **1** and **2** are now confirmed to be minima (no imaginary frequencies[7]), but **3** is a transition-state structure (one imaginary frequency[7]) and **4**, with two imaginary frequencies,[7] has little chemical significance. All $C_2H_2Li_2$ structures have now been reoptimized with the polarized split valence 6-31G* basis set and the relative energies have been calculated at the correlated MP2/6-31G*//6-31G* level with zero-point energy corrections at 3-21G//3-21G (Scheme 1, Table 1). While these new relative energies for **1**–**4** differ only modestly from our earlier values,[2] the *trans* isomer **1** is now found to be somewhat more stable than any *cis* isomer, in agreement with the experimental findings.[4]

Four new stationary points, **5**–**8**, have been located on the potential energy surface. The unsymmetrical planar *cis* isomer **5** was found to be 14 kcal/mol more stable than **3**, which is the transition-state structure for the degenerate interconversion of the equivalent minima **5a** and **5b**. However, doubly bridged **2** is still the most stable *cis* isomer.

The most favorable pathway we have found for the transformation of **2** (*cis*) into **1** (*trans*) does not involve rotation around the carbon-carbon double bond, but rather in-plane inversion of one of the CH groups. The first step of this process is the rearrangement of **2** into another doubly bridged *cis* isomer, **7**, in which both lithiums are in the molecular plane. The rearrangement **2**→**7** involves movement of the lithiums apart, as indicated by the arrow in the transition state **6**. The much greater stability of **7** over **4** is noteworthy, and is due to the strong preference for bent vinyl anion centers.[8] Indeed, **8**, the transition-state structure for the overall *cis-trans* interconversion



Scheme 1. Stationary points on the potential energy surface of 1,2-dilithioethylene. Relative energies, given below each structure in kcal/mol, were calculated at the MP2/6-31G*//6-31G* level and include zero-point energy corrections. The number of imaginary frequencies [7] (at the 3-21G level) is enclosed in parentheses: 0 = minima, 1 = transition-state structures, 2 = higher order saddle points. Some geometrical parameters are given (in Å and degrees).

(i.e., the highest energy point through which the process occurs), has only one nearly linear H–C=C geometrical arrangement. The energy required for the linear distortion in **8** is roughly half that required for linearization of both H–C=C moieties simultaneously, as in **4**.

Table 1. Total energies (−a.u.) of 1,2-dilithioethylene isomers.

Structure	Point group	3-21G//3-21G	6-31G*//6-31G*	MP2/6-31G*//6-31G*	ZPE [a]	IFs [b]
1	C_{2h}	91.17162	91.69609	91.97728	19.7	—
2	C_{2v}	91.17528	91.69333	91.97585	20.4	—
3	C_{2v}	91.14501	91.66420	91.94233	18.9	−149
4	D_{2h}	91.09371	91.60975		18.3	−1234, −1059
5	C_s	91.16672	91.68629	91.96578	19.5	—
6	C_s	91.14701	91.67378	91.95483	18.2	−207
7	C_{2v}	91.15029	91.67776	91.96123	19.0	—
8	C_s	91.13301	91.65365	91.94110	18.3	−942

[a] Zero-point energies in kcal/mol; these are multiplied by 0.9 to give the final relative energies in Scheme 1. [b] Imaginary frequencies in cm^{-1} [7].

We thus predict the barrier for the isomerization of **2** into **1** to be about 20 kcal/mol for a hypothetical gas-phase process. This relatively low value is consistent with *Maercker*'s findings in solution,[4] where, however, solvation and aggregation effects will further influence the rela-

[*] Prof. Dr. P. von R. Schleyer, Dipl.-Chem. E. Kaufmann, Dr. A. J. Kos, Dr. T. Clark
Institut für Organische Chemie der Universität Erlangen-Nürnberg
Henkestrasse 42, D-8520 Erlangen (FRG)
Prof. Dr. J. A. Pople
Department of Chemistry, Carnegie-Mellon University
Pittsburgh, PA 15235 (USA)

[**] This work was supported by the Deutsche Forschungsgemeinschaft, the Fonds der Chemischen Industrie, and the Alexander von Humboldt Foundation (a special award to *J. A. Pople*). We thank Prof. *A. Maercker*, Siegen, for informing us of his work prior to publication and Prof. *K. N. Houk*, Los Angeles, for his interest.

tive energies. Nevertheless, it seems likely that vinyl inversion will be the preferred *cis-trans* isomerization mechanism in solution as well. In an increasing number of cases, our predicted structures of organolithium compounds, although calculated for isolated monomers, have proven to be remarkably accurate when compared with subsequently determined X-ray structures, especially with regard to the carbanion moieties.[1,9]

Received: October 2, 1985;
revised: December 9, 1985 [Z 1479 IE]
German version: *Angew. Chem. 98* (1986) 164

[1] P. von R. Schleyer, *Pure Appl. Chem. 56* (1984) 151; *55* (1983) 355, and literature cited therein.
[2] Y. Apeloig, T. Clark, A. J. Kos, E. D. Jemmis, P. von R. Schleyer, *Israel J. Chem. 20* (1980) 43.
[3] See, e.g., D. Seyferth, S. C. Vick, *J. Organomet. Chem. 144* (1978) 1. However, 1,2-dilithiocyclopropenes and vicinally polylithio-substituted benzenes are among known molecules of this type. See [2] and E. D. Jemmis, J. Chandrasekhar, P. von R. Schleyer, *J. Am. Chem. Soc. 101* (1979) 2848.
[4] A. Maercker, private communication. See also A. Maercker, T. Graule, U. Girreser, *Angew. Chem. 98* (1986) 174; *Angew. Chem. Int. Ed. Engl. 25* (1986) 167.
[5] Gaussian 82 (J. S. Binkley, M. J. Frisch, K. Raghavachari, R. A. Whiteside, H. B. Schlegel, E. M. Fluder, J. A. Pople, Carnegie-Mellon University, as adapted for CYBER computers by A. Sawaryn and T. Kovář, along with the standard basis sets and other routines incorporated into this program, was employed.
[6] See W. J. Hehre, L. Radom, P. von R. Schleyer, J. A. Pople: *Ab Initio Molecular Orbital Theory, A Handbook of Computational Chemistry*, Wiley, New York 1985.
[7] "Imaginary frequencies" correspond to negative eigenvalues of the force constant (Hessian) matrix and characterize stationary points on potential energy surfaces.
[8] The vinyl anion inversion barrier was calculated to be 27.5 kcal/mol at MP2/4-31+G//4-31+G: J. Chandrasekhar, J. G. Andrade, P. von R. Schleyer, *J. Am. Chem. Soc. 103* (1981) 5609.
[9] See: W. Setzer, P. von R. Schleyer, *Adv. Organomet. Chem. 24* (1985) 353; J. J. Stezowski, H. Hoier, D. Wilhelm, T. Clark, P. von R. Schleyer, *J. Chem. Soc. Chem. Commun. 1985*, 1263.

Synthesis of the all-L-Configurated Cyclotetradepsipeptide *cyclo*[-L-Val-L-Lac-]$_2$ by the Combined Protection/Activation Method with the 2,4-Bis(methylthio)phenoxycarbonyl Group

By *Horst Kunz** and *Hans-Jürgen Lasowski*

Dedicated to Professor Rolf C. Schulz on the occasion of his 65th birthday

The natural cyclic depsipeptides are characterized by selective complexing ability and antibiotic activity.[1] Since their biosynthesis[2] differs from that of other peptides, they are not accessible by means of gene technology. The most difficult step of chemical depsipeptide synthesis is the cyclization. Especially in the case of ring closure to give the smaller cyclodepsipeptides, the success of the synthesis depends strongly on the configuration of the building blocks, as *Shemyakin* et al.[3] have shown for several tetradepsipeptides, **1**, prepared from *N*-methylvaline and α-hydroxyisovaleric acid. The yields were 40–75% as long as at least one of the four building blocks had a different configuration from the others. In contrast, the all-D-configurated diastereomer of **1** could be cyclized in only 8% yield.

H-MeVal-Hyiv-MeVal-Hyiv-OH **1**

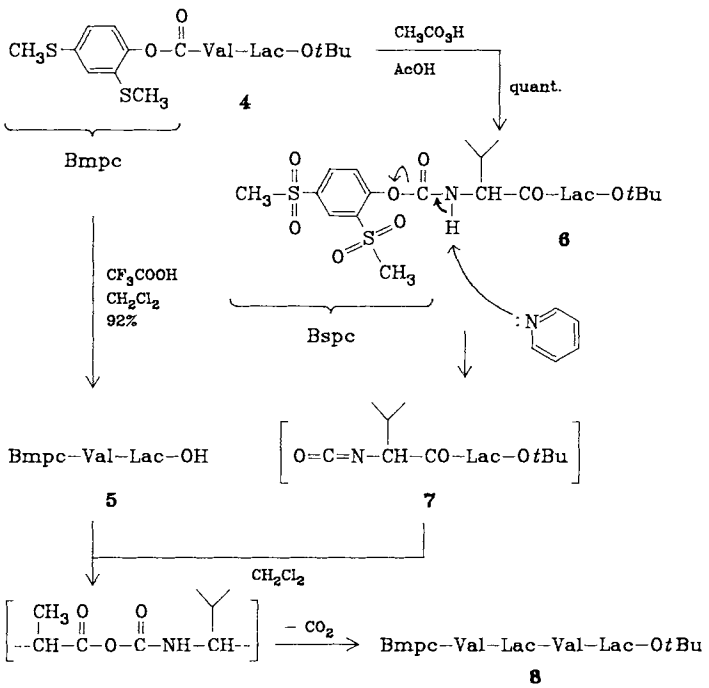
When the amino acid building blocks in **1** have no *N*-methyl groups, the tendency to cyclize is even smaller despite the opposite configurations of the building blocks. The corresponding cyclodepsipeptide was formed in only 6% yield.[3] Nonetheless, cyclotetradepsipeptides without *N*-methyl groups are formed in nature, e.g., *cyclo*[-L-Hyiv-L-Ile-Hyiv-D-*allo*-Ile-], whose precursors, moreover, are all-L-configurated.[4]

In investigations concerning new methods of depsipeptide synthesis,[5] we have now developed a concept for the chemical cyclization of peptides, even such tetradepsipeptides as **2**, whose building blocks all have the same configuration and no *N*-methyl groups.

H[-L-Val-L-Lac-]$_2$OH ⟶ *cyclo*[-L-Val-L-Lac-]$_2$
2 **3**

This ring closure, which is difficult on account of both of the factors discussed above, we carried out using the 2,4-bis(methylthio)phenoxycarbonyl(Bmpc) amino protecting group, which is capable of undergoing activation. It is added to the amino acids by means of 2,4-bis(methylthio)phenyl chloroformate, as has already been described for the 4-methylthiophenoxycarbonyl(Mtpc) group.[6] The coupling of the Bmpc-amino acids with L-lactic acid is also carried out analogously to the procedure already described[6] with benzenesulfonyl chloride.[7]

The Bmpc group of the protected depsipeptide **4** is stable toward trifluoroacetic acid in dichloromethane, so that the *tert*-butyl ester groups can be selectively cleaved with formation of **5**. The Bmpc group in **4** can be activated to



Scheme 1. Reaction conditions: **5** (20 mmol) and **6** (20 mmol) in 160 mL of dry dichloromethane and 32 mL of dry pyridine, 4 Å molecular sieves, room temperature, preparative HPLC in petroleum ether/ethyl acetate (4:1). **8** is formed in 57% yield (based on **5**).

[*] Prof. Dr. H. Kunz, Dr. H.-J. Lasowski
Institut für Organische Chemie der Universität
Johann-Joachim-Becher-Weg 18–20, D-6500 Mainz (FRG)

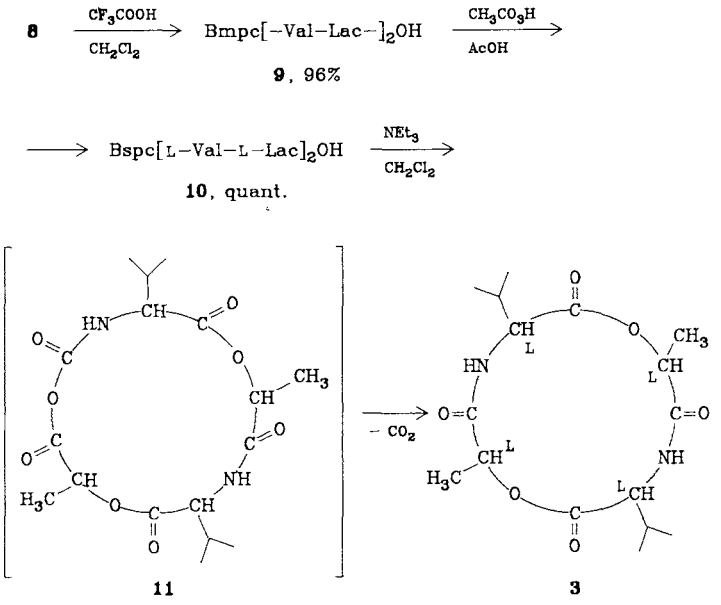
[**] This work was supported by the Deutsche Forschungsgemeinschaft and the Fonds der Chemischen Industrie.

the 2,4-bis(methylsulfonyl)phenoxycarbonyl (Bspc) group in **6** with anhydrous peracetic acid (10%)[8] (Scheme 1).

Even pyridine causes the elimination of 2,4-bis(methylsulfonyl)phenol from the Bspc group, resulting in the formation of the isocyanate **7** from **6**. If **7** is released in the presence of the carboxyl component **5** that is to be coupled, direct reaction occurs, via the mixed carboxylic acid–carbamic acid anhydride, leading to the desired protected tetradepsipeptide **8**.

In this case, the Mtpc group used earlier by us[6] has the disadvantage that for the elimination from the sulfonyl (Mspc) form triethylamine is required, which partly attacks the nonactivated Mtpc group. The depsipeptides obtained in this way contain lower homologues (detectable by analytical HPLC) that cannot be separated. Therefore, no cyclization was achieved with this group.

In order to carry out the cyclization, **8** is deblocked at the *C*-terminal end with trifluoroacetic acid to give **9**, which then reacts with anhydrous peracetic acid at the *N*-terminal protecting group to afford activated **10** (Scheme 2).



Scheme 2. Reaction conditions: **10** (0.25 mmol) in 200 mL of dry CH_2Cl_2 and 50 mL of dry NEt_3, 4 Å molecular sieves, 20 d, room temperature, chromatography in petroleum ether/ethyl acetate (2 : 1). **3** is formed in 33% crude and 11% pure yield.

In dilute dichloromethane solution in the presence of triethylamine, **10** undergoes elimination of disulfonylphenol. The isocyanate formed undergoes intramolecular reaction to give the cyclic mixed anhydride **11** (not isolated). Compound **11** eliminates CO_2 to form the desired cyclotetradepsipeptide **3**, the first synthetically obtained cyclotetradepsipeptide that consists only of identically configurated building blocks having no *N*-methyl groups. That compound **3** (which according to the results of *Shemyakin* et al.[3] should hardly be accessible) could be prepared according to Scheme 2 is due in part to the fact that **11**, with a less strained fourteen-membered ring, is formed initially. In **11** the two ends that are to be coupled are arranged favorably, so that spontaneous elimination of CO_2 leads to formation of the twelve-membered ring. **3** is obtained from chloroform/petroleum ether as a colorless compound which is pure according to HPLC (heptane/ethyl acetate 85 : 15) ($[\alpha]_D^{22}$ −32.4 (c = 0.08, CH_2Cl_2); FD-MS: m/z 342 (M^+)). In the 400-MHz ^{1}H-NMR spectrum[9] each kind of proton gives only one signal (with the exception of the diastereotopic valine methyl protons). Accordingly, epimerization of the activated L-lactic acid building block in the cyclic mixed anhydride **11** is unlikely, since this would otherwise be observed in the NMR spectrum of **3**.

Received: September 3, 1985;
supplemented: October 8, 1985 [Z 1450 IE]
German version: *Angew. Chem. 98* (1986) 170

[1] Review: Y. A. Ovchinnikov, V. T. Ivanov, *Int. Rev. Sci. Org. Chem. Ser. Two 6* (1976) 219.
[2] J. E. Walker, S. Otani, D. Perlman, *FEBS Lett. 20* (1972) 162.
[3] M. M. Shemyakin, Y. A. Ovchinnikov, V. T. Ivanov, A. V. Evstratov, J. J. Michaleva, G. D. Ryabova, *Zh. Obshch. Khim. 42* (1972) 2320.
[4] R. O. Okotore, D. W. Russell, *Experientia 27* (1971) 380.
[5] H. Kunz, H.-G. Lerchen, *Angew. Chem. 96* (1984) 798; *Angew. Chem. Int. Ed. Engl. 23* (1984) 808.
[6] H. Kunz, K. Lorenz, *Angew. Chem. 92* (1980) 953; *Angew. Chem. Int. Ed. Engl. 19* (1980) 932.
[7] M. M. Shemyakin, *Angew. Chem. 71* (1959) 741.
[8] R. Criegee in Houben-Weyl-Müller: *Methoden der Organischen Chemie, 4. Aufl., Bd. 8*, Thieme, Stuttgart 1952, p. 41.
[9] **3**: 400 MHz-^{1}H-NMR ([D$_6$]acetone): δ = 7.88 (d, J = 9 Hz, 2H, NH), 5.23 (q, J = 7 Hz, 2H, α-CH(Lac)), 4.19 (t, J = 9 Hz, 2H, α-CH (Val)), 2.05 (m, 2H, under [D$_6$]acetone signals, β-CH (Val)), 1.50 (d, J = 7 Hz, 6H, CH_3 (Lac)), 0.94 (2 × d, J = 7 Hz, 12H, CH_3 (Val)).

A Simple Route to the Intramolecular Quinhydrone of [2.2]Paracyclophanediene**

By *Michael Stöbbe, Stephan Kirchmeyer, Gunadi Adiwidjaja,* and *Armin de Meijere**

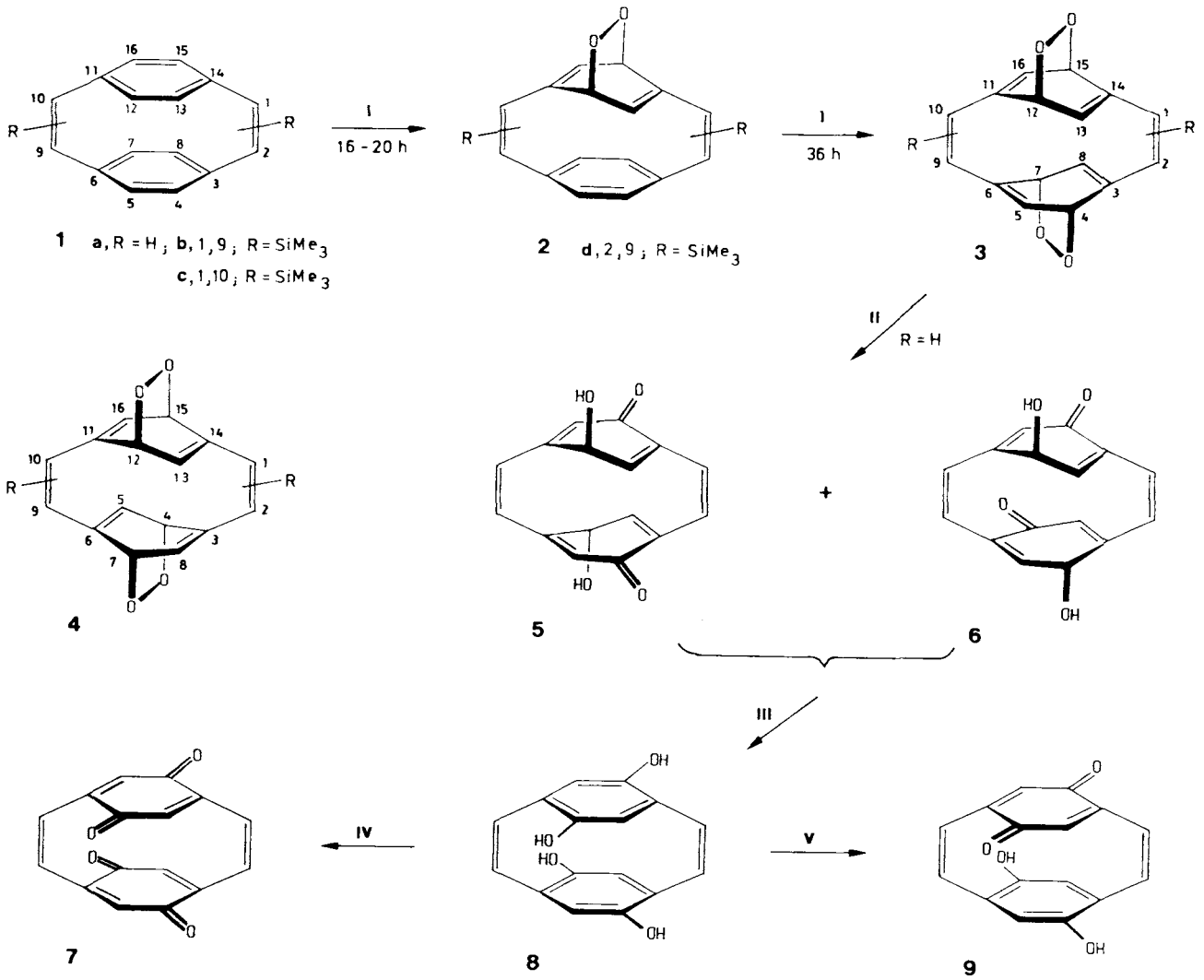
Dedicated to Professor Rolf Huisgen on the occasion of his 65th birthday

Molecules exhibiting intramolecular charge transfer are useful, among other things, as rigid models to test experimentally charge transfer as a function of distance.[1,2] All previously reported systems of this kind containing the [2.2]- or [3.3]paracyclophane skeleton have been constructed in multistep sequences by the combination of suitably substituted molecular halves. The twofold addition of singlet oxygen ($^1O_2$) to [2.2]paracyclophane-1,9-diene **1a** provides a short route to a further system of this kind.

The photooxidation of **1a** yields the endoperoxide **2a**[3] and a by-product (2–3%), which is formed in a slow secondary reaction and has an appreciably higher R_F value. This product was purified by column chromatography using polar eluents and identified by NMR spectroscopy as a *single* bisendoperoxide, either **3a** or **4a**. Reaction of pure **2a** with $^1O_2$ gave **3a** or **4a**[4] in better yield (28%). **3a** or **4a** could be recrystallized (colorless, monoclinic, explosive dec. > 115 °C). X-ray analysis, however, did not result in a definitive structural assignment: the data indicate that the O-atoms lie at a position intermediate between those expected for diastereomers **3a** and **4a**. This evidently results from a statistical distribution of the enantiomers of **3a** in

* Prof. A. de Meijere, Dipl.-Chem. M. Stöbbe, Dipl.-Chem. S. Kirchmeyer, Dr. G. Adiwidjaja
Institut für Organische Chemie der Universität
Martin-Luther-King-Platz 6, D-2000 Hamburg 13 (FRG)

[**] This work was supported by the Stiftung Volkswagenwerk, the Fonds der Chemischen Industrie, E. Merck AG, and Chemische Werke Hüls AG. *M. S.* thanks the Studienstiftung des deutschen Volkes for a Promotionsstipendium.



Scheme 1. I: $^3O_2$, *hv*, tetraphenylporphyrin, $CHCl_3$, 20°C; II: NEt_3, CH_2Cl_2, 0-20°C, 14-18 h; III: MeOH/AcOH/CF_3CO_2H (1:1:0.16), 6 h reflux; IV: $Ce(NH_4)_2(NO_3)_6$, CH_2Cl_2/THF/H_2O, 20°C, 2 min; V: O_2/SiO_2, 24 h.

the crystal array. The clarification of the stereochemical question and the unambiguous assignment of the structure to diastereomer **3a** was finally achieved by the reaction sequence leading to the single quinhydrone **9** (Scheme 1).

Treatment of **3a** with triethylamine gave a mixture of the diastereomeric bisquinols **5** and **6**[4] (60%), which could be separated by column chromatography and purified by fractional recrystallization. The rearrangement of **5** and **6** to the bishydroquinone **8**[4] (40%) required treatment with trifluoroacetic acid. **8** was readily oxidized to the bisquinone **7**[4] (yellow crystals, dec. >200°C) with cerium(IV) ammonium nitrate.

A single quinhydrone, **9**, was obtained by air oxidation of **8**, which was adsorbed on silica gel. Subsequent column chromatography (SiO_2) yielded **9**[4] as brown-black crystals (73%, dec. > 180°C). The configuration of **9** was unambiguously established by its UV/VIS spectrum, which shows absorption bands at $\lambda_{max}(\lg\varepsilon)=330$ (3.43) and 517 nm (2.14) (ethanol), since the charge-transfer band corresponds in both position and extinction coefficient to that of pseudo-*ortho*-[2.2]paracyclophanequinhydrone,[1] [$\lambda_{max}(\lg\varepsilon)=317$ (3.46) and 515 (2.23) (methanol)]. The pseudo-*gem* quinhydrone of [2.2]paracyclophane, has a charge-transfer band that is distinctly more intense and at shorter wavelength [$\lambda_{max}(\lg\varepsilon)=495$ nm (3.20) (methanol)].[1]

The observed diastereoselectivity in the addition of $^1O_2$ to the monoadduct **2** is probably based on both steric and electronic factors. The transition state leading to the unobserved **4a** would be less favorable sterically because of the very close contact between H atoms on C8/C13 and on C5/C16. **3a** would be electronically favored since, according to MNDO calculations,[5] the coefficients in the HOMO of **2a** are larger on C4/C7 than on C5/C8, resulting in a better transition-state interaction with the LUMO of $^1O_2$.

The addition of $^1O_2$ to 1,9-bis(trimethylsilyl)[2.2]paracyclophanediene **1b**,[4,6] which is much more soluble in hydrocarbon solvents than **1a**, led by way of **2b** to the 1,9-bis(trimethylsilyl) derivative **3b**[4] (8%), which is readily soluble in dichloromethane. Analogously, a ca. 1:1 mixture of 1,9-**1b** and 1,10-bissilyldiene **1c**[4,6] gave a mixture of the three endoperoxides **2b**, **2c**, and **2d** (22, 32, and 8%) and the bisendoperoxide **3c**[4] (9.4%), formed by the preferential further reaction of 1,10-**2c** and/or the 2,9-bissilyl derivative **2d**. Products **3b** and **3c** open the way to the cor-

responding silyl derivatives of **7**, **8**, and **9**, which, because of their expected better solubility, will facilitate further physical and chemical investigations of this class of compounds.

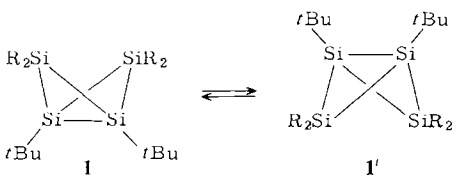
Received: September 24, 1985 [Z 1467 IE]
German version: *Angew. Chem. 98* (1986) 162

[1] H. A. Staab, W. Rebafka, *Chem. Ber. 110* (1977) 3333, and references cited therein.
[2] H. A. Staab, C. P. Herz, C. Krieger, M. Rentea, *Chem. Ber. 116* (1983) 3813.
[3] I. Erden, P. Gölitz, R. Näder, A. de Meijere, *Angew. Chem. 93* (1981) 605; *Angew. Chem. Int. Ed. Engl. 20* (1981) 583.
[4] All new compounds were characterized spectroscopically (IR, ^{1}H- and ^{13}C-NMR) and gave satisfactory elemental analyses. ^{1}H-NMR (270 MHz): **3a** ($CDCl_3$): $\delta = 4.90$ (dd, $^3J = 6.0$, $^4J = 1.8$; 4,7,12,15-H), 6.40 (s; 1,2,9,10-H), 6.41 (m; 5,8,13,16-H). **7**: ($CDCl_3$): 6.26 (s; 4H), 6.71 (s; 4H). **8** ([D$_6$]acetone): 6.18 (s; 4H), 6.71 (s; 4H), 7.14 (s; 4H, O*H*). **9** ([D$_6$]acetone): 6.03 (d, $^4J = 0.6$; 13,16-H), 6.17 (d, $^4J = 1.9$; 5,8-H), 6.57 (dd, $^3J = 10.0$, $^4J = 1.9$; 2,9-H), 6.86 (d, $^3J = 10.0$; 1,10-H), 7.93 (s; 2H, O*H*).
[5] M. J. S. Dewar, W. Thiel, *J. Am. Chem. Soc. 99* (1977) 4899.
[6] A ca. 1:1 mixture of **1b** and **1c** was obtained by the reductive silylation (Mg/Me$_3$SiCl) in THF (ultrasonication) of 1,9- and 1,10-dibromo[2.2]paracyclophanediene **1** (R = Br), which in turn were obtained by double dehydrobromination of the crude tetrabromides of [2.2]paracyclophane [7]. Pure **1b** was analogously prepared from purified 1,1,9,9-tetrabromo[2.2]paracyclophane [7]. M. Stöbbe, A. de Meijere, unpublished results.
[7] K. C. Dewhirst, D. J. Cram, *J. Am. Chem. Soc. 80* (1958) 3115.

The Tetrasilabicyclo[1.1.0]butane System: Structure of 1,3-Di-*tert*-butyl-2,2,4,4-tetrakis-(2,6-diethylphenyl)tetrasilabicyclo[1.1.0]butane**

By *Ray Jones, David J. Williams, Yoshio Kabe,* and *Satoru Masamune**

Our efforts directed toward the construction of strained cyclic silicon systems[1] have recently culminated in the synthesis of the title compound **1**,[2] the first uncharged[3] tetrasilabicyclo[1.1.0]butane derivative.[4] The weakness and high reactivity of the critical Si1–Si3 bond of **1** were anticipated and, indeed, are shown by the chemical reactivity of this compound. The puckered ring system undergoes rapid inversion (**1** ⇄ **1'**) and the central bond is readily cleaved by oxygen and chlorine as well as water.[2] We report here the crystal structure of compound **1**.[5]



R = 2,6-$Et_2C_6H_3$

The molecule (Fig. 1) has approximate, noncrystallographic, twofold symmetry about an axis perpendicular to the Si1–Si3 bond.[6] The Si1–Si3 distance (2.373(3) Å) is typical for a cyclic Si–Si bond.[7] However, the peripheral Si–Si bonds are all significantly shorter than in other cyclotetrasilane systems.[7] There is also, interestingly, a small alternation in the bond lengths around the ring. The dihedral angle between the two three-membered rings is 121° and the nonbonding Si2–Si4 distance is 3.475 Å. The Si–C bond lengths are normal and range between 1.921(7) and 1.959(7) Å.

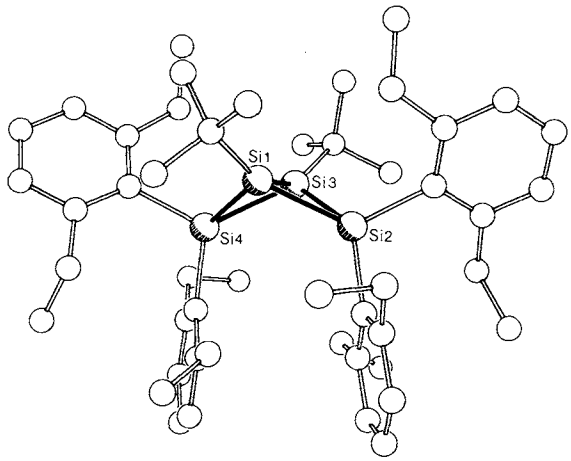


Fig. 1. Crystal structure of **1** [5]. Bond lengths [Å] and bond angles [°]: Si1–Si2 2.311(3), Si1–Si4 2.336(3), Si2–Si3 2.334(4), Si3–Si4 2.308(3), Si1–Si3 2.373(3); Si1–Si2–Si3 61.4(1), Si1–Si3–Si2 58.8(1), Si1–Si3–Si4 59.8(1), Si1–Si4–Si3 61.4(1), Si2–Si1–Si3 59.8(1), Si3–Si1–Si4 58.7(1), Si2–Si1–Si4 96.8(1), Si2–Si3–Si4 96.9(1).

In view of the extremely facile ring inversion, the relatively short Si1–Si3 distance is somewhat unexpected. It is shorter than the Si–Si bonds in hexa-*tert*-butylcyclotrisilane (ca. 251 pm)[1h] and hexa-*tert*-butyldisilane (ca. 270 pm),[8] the latter of which exhibits the longest Si–Si bond observed so far. While, due to the bulky substituents, the observed geometry of the silicon framework may be slightly distorted from that of the unknown parent tetrasilabicyclo[1.1.0]butane, the Si1–Si3 bond is undoubtedly bent and rich in p-character. The (carbon) bicyclobutane system has been extensively investigated;[9] comparative studies of sila-analogues should therefore be interesting and important from both theoretical and experimental viewpoints.[10]

Received: September 25, 1985;
supplemented: November 13, 1985 [Z 1468 IE]
German version: *Angew. Chem. 98* (1986) 176

[*] Prof. S. Masamune, Dr. Y. Kabe
Department of Chemistry, Massachusetts Institute of Technology
Cambridge, Massachusetts 02139 (USA)
Dr. D. J. Williams, R. Jones
Chemical Crystallography Laboratory
Department of Chemistry, Imperial College
London SW2 2AY (UK)

[**] This work was supported by the National Science Foundation (USA).

[1] (a) S. Masamune, Y. Hanzawa, S. Murakami, T. Bally, J. F. Blount, *J. Am. Chem. Soc. 104* (1982) 1150; (b) S. Masamune, H. Tobita, S. Murakami, *ibid. 105* (1983) 6524; (c) S. Murakami, S. Collins, S. Masamune, *Tetrahedron Lett. 25* (1984) 2131; (d) S. Masamune, S. Murakami, J. T. Snow, H. Tobita, D. J. Williams, *Organometallics 3* (1984) 333; (e) J. C. Dewan, S. Murakami, J. T. Snow, S. Collins, S. Masamune, *J. Chem. Soc. Chem. Commun. 1985*, 892; (f) H. Watanabe, T. Okawa, M. Kato, Y. Nagai, *ibid. 1983*, 781; (g) H. Watanabe, Y. Kougo, Y. Nagai, *ibid. 1984*, 66; (h) A. Schafer, M. Weidenbruch, K. Peters, H. G. v. Schnering, *Angew. Chem. 96* (1984) 311; *Angew. Chem. Int. Ed. Engl. 23* (1984) 302.
[2] S. Masamune, Y. Kabe, S. Collins, D. J. Williams, R. Jones, *J. Am. Chem. Soc. 107* (1985) 5552. Compound **1** represents the first bicyclobutane derivative whose bicyclic ring consists solely of an element of the 4th main group other than carbon. See [4] for bicyclobutane derivatives containing elements of the 5th main group.
[3] For the Si_4^{2-} cluster anion in Ba_3Si_4, see B. Eisenmann, K. H. Janzen, H. Schäfer, A. Weiss, *Z. Naturforsch. B 24* (1969) 457. Also see H. G. von Schnering, *Angew. Chem. 93* (1981) 44; *Angew. Chem. Int. Ed. Engl. 20* (1981) 33.

[4] Tetraphosphabicyclobutane derivatives: R. Riedel, H.-D. Hausen, E. Fluck, *Angew. Chem. 97* (1985) 1050; *Angew. Chem. Int. Ed. Engl. 24* (1985) 1056; E. Niecke, R. Rüger, B. Krebs, *ibid. 94* (1982) 553 and *21* (1982) 544. 2,4-Di-*tert*-butyltetraarsabicyclobutane: M. Baudler, S. Wietfeldt-Haltenhoff, *ibid. 96* (1984) 361 and *23* (1984) 379.

[5] Orthorhombic, $a=11.244(3)$, $b=18.521(5)$, $c=21.985(6)$ Å, $V=4578$ Å^3, space group $P2_12_12_1$, $Z=4$, $\rho_{calcd}=1.11$ gcm^{-3}, $\mu(Cu_{K\alpha})=14$ cm^{-1}. The crystals are extremely air and moisture sensitive and subject to serious twinning. Data for a small slightly twinned crystal [6] sealed under argon in a Lindemann glass capillary tube were measured on a Nicolet R3m diffractometer with graphite monochromated $Cu_{K\alpha}$ radiation using the ω-scan routine. The structure was solved by direct methods and refined anisotropically, with the aromatic rings being treated as idealized rigid bodies. $R=0.0734$, $R_w=0.071$, for 2546 independent observed reflections [$\theta \leq 58°$, $|F_0| > 3\sigma(xF_0)$]. The slightly high final value of R is probably a consequence of the high thermal vibration of the ethyl groups and the small amount of twinning in the only suitable crystal available [6]. Further details of the crystal structure investigation are available on request from the director of the Cambridge Crystallographic Centre University Chemical Laboratory, Lensfield Road, Cambridge CB2 1EW (England) by quoting the full literature citation.

[6] The conformation adopted by the molecule is chiral and the space group, which is non-centrosymmetric, contains molecules of one chirality only.

[7] For instance, in *trans,trans,trans*-(*t*BuMeSi)$_4$ the Si-Si bond is 2.377 Å long: C. J. Hurt, J. C. Calabrese, R. West, *J. Organomet. Chem. 91* (1975) 273. For other examples, see footnote [14] in [1a].

[8] N. Wiberg, H. Schuster, A. Simon, K. Peters, *Angew. Chem. 98* (1986) 100; *Angew. Chem. Int. Ed. Engl. 25* (1986) 79.

[9] For recent literature, see, e.g.: H. Irngartinger, A. Goldmann, R. Schappert, P. Garner, C. L. Go, P. Dowd, *J. Chem. Soc. Chem. Commun. 1985*, 113; M. Eisenstein, F. L. Hirshfeld, *Acta Crystallogr. Sect. B 39* (1983) 61; P. G. Gassman, M. L. Greenlee, D. A. Dixon, S. Richtsmeier, J. Z. Gougontas, *J. Am. Chem. Soc. 105* (1983) 5865.

[10] For the 2,4-disilabicyclobutane system see G. Fritz, S. Wartanessian, E. Matern, W. Höule, H. G. von Schnering, *Z. Anorg. Allg. Chem. 475* (1981) 87.

[2.2]Indenophane Dianion: A Novel Double-Layered Dianion

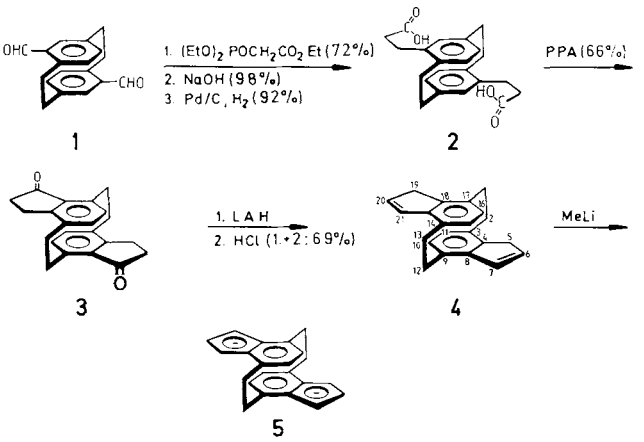
By *Ron Frim, Friedrich-Wilhelm Raulfs, Henning Hopf,** and *Mordecai Rabinovitz**

[2.2]Paracyclophanes are aromatic hydrocarbons with unique steric and electronic properties. The two π-systems interpenetrate, so that they behave as one π-system.[1-3] Paracyclophane anions are of interest in view of the proximity of the two anionic moieties and their mutual interaction. Anionic paracyclophanes have been previously studied.[4] *Haenel*[5] has described the preparation and ^{1}H-NMR spectra of anions derived from *syn*- and *anti*-[2.2](2,7)fluorenophanes, but no ^{13}C-NMR spectra of these species have been reported.[6] We report here the preparation and the ^{1}H- and ^{13}C-NMR spectroscopic data of the dianion of [2.2]indenophane **5** and the monoanion of [2.2]benzoindenophane **7**. This is the first comprehensive study of the properties and through-space interactions of double-layered mono- and dianions.

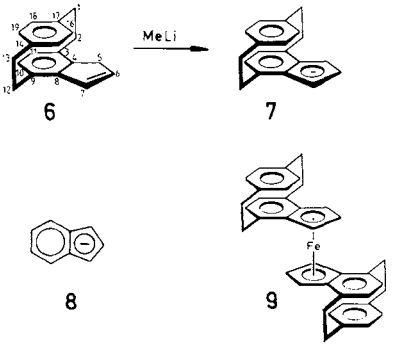
The starting material in the preparation of [2.2]indenophane **4** is the dialdehyde **1**,[7c] which underwent a chain elongation by the Wittig-Horner reaction followed by reduction of the double bond and cyclization of the diacid **2** to give the "[2.2]indanonophane" **3**. The diketone **3** was reduced to the corresponding diol, which was then dehydrated to the [2.2]indenophane **4**.[7] A similar route starting from 4-formyl[2.2]paracyclophane afforded the benzoindenophane **6**.[7]

[*] Prof. M. Rabinovitz, R. Frim
Department of Organic Chemistry
The Hebrew University of Jerusalem
Jerusalem 91904 (Israel)
Prof. Dr. H. Hopf, Dipl.-Chem. F.-W. Raulfs
Institut für Organische Chemie der Universität
Hagenring 30, D-3300 Braunschweig (FRG)

Reaction of **4** and **6** with methyllithium in [D$_8$]tetrahydrofuran ([D$_8$]THF) at -78°C led to the corresponding anions **5** and **7**. When **4** was allowed to react with a colorless solution of MeLi in [D$_8$]THF (prepared from a commercial solution of MeLi in ether) in the NMR tube, the solution turned orange. After several minutes, clean ^{1}H- and ^{13}C-NMR spectra, entirely different from those of **4**, were recorded (Table 1). The ^{1}H-NMR spectrum is very simple and shows a triplet and a doublet for the five-membered-ring protons at $\delta=6.35$ (H-6, H-20) and 5.80 (H-5, H-7, H-19, H-21), respectively, a singlet at $\delta=5.23$ for the aromatic protons, and an AA'BB' multiplet for the ethano bridge protons at $\delta=3.27$–2.87.



When a double-layered dianion such as **5** is formed from a neutral precursor, the following NMR spectral phenomena may be expected: (a) shielding due to the negative charges, (b) deshielding resulting from the formation of conjugated 10π-electron systems, and (c) a through-space interaction between the two halves of the double-layered structure. The center of gravity of the ^{1}H-NMR spectrum of **5** is at $\delta=4.53$, while that of the hydrocarbon **4** is at $\delta=4.65$. This shows that the shielding effect due to the charge is overcome by the diatropicity of the two indenylide aromatic components (even when the change of hybridization of C-5 and C-19 is taken into account). According to well-known correlations,[8] the net effect of the charge alone would have shifted the center of gravity of the spectrum of this three-dimensional dianion to $\delta=3.45$. The comparison with the ^{1}H-NMR spectrum of the indenylide monoanion **8**[9] is revealing. The six-membered-ring protons of **5** show a very significant high-field shift compared to those of **8** (ca. 2 ppm), while the five-membered-ring protons of **5** and **8** show similar chemical shifts. This phenomenon cannot be attributed to a charge delocaliza-



tion effect since such a charge delocalization should also prevail in **8**. It should therefore be attributed to the through-space interaction of the two fully aromatic halves of the dianion.

The chemical shifts of the five-membered-ring protons of the monoanion **7** are similar to those of corresponding protons of **5** and **8** (see Table 1). The six-membered-ring protons are again shifted to higher field but to a lesser degree than in **5**. This phenomenon can be rationalized in terms of a lesser degree of through-space interaction, since only one indenyl moiety interacts with only one benzene moiety. In the ferrocenophane **9**[7b] derived from **6**, the five-membered-ring protons are shifted strongly to high field, but the six-membered-ring protons show only a slight high-field shift of ca. 0.3 ppm (Table 1).

Only six lines appear in the ^{1}H-decoupled, ^{13}C-NMR spectrum of the dianion **5** due to its high degree of symmetry. The ^{13}C chemical shifts (Table 1) also point to a higher degree of charge density residing at the five-membered ring as compared to the six-membered ring. Nonetheless, the formation of a dianion can be deduced from the shift of all signals to high field (relative to those of **4**). As expected, monoanion **7** shows ten lines in the ^{1}H-decoupled ^{13}C-NMR spectrum (Table 1), all of which are shifted to high field.

Table 1. ^{1}H- and ^{13}C-NMR spectroscopic data for **4**–**9** [a].

Compd.	^{1}H-NMR	^{13}C-NMR
4 [b]	6.91 (2H, dt, J_1 = 5.6, J_2 = 1.9, vinylic) 6.53 (2H, dt, J_1 = 5.6, J_2 = 1.9, vinylic) 6.20 (center, 4H, AA'BB', δ_A = 6.22, δ_B = 6.17, J = 7.8, six-membered ring, H-10, H-11, H-15, H-16) 3.14 (center, 8H, m, bridge protons) 3.20–2.86 (4H, m, five-membered ring, H-5, H-5, H-19, H-19)	146.32, 144.11, 134.26 132.60, 132.04, 131.89 126.76, 125.58, 39.13 31.97, 30.91
5 [b]	6.35 (2H, t, J = 3.4, five-membered ring, H-6, H-20) 5.80 (4H, t, J = 3.4, five-membered ring, H-5, H-7, H-19, H-21) 5.23 (4H, s, six-membered ring, H-10, H-11, H-15, H-16) 3.27–2.87 (8H, m, bridge protons, H-1, H-2, H-12, H-13)	130.77, 127.92, 118.88 111.48, 92.24, 33.21
6 [b]	6.76 (1H, dt, J_1 = 5.5, J_2 = 2.0, vinylic) 6.48 (1H, dt, J_1 = 5.5, J_2 = 2.0, vinylic) 6.65–6.30 (6H, m, six-membered ring) 3.40–2.70 (8H, m, bridge protons, H-1, H-2, H-12, H-13) 3.12–2.86 (2H, m, five-membered ring, H-5, H-5')	146.53, 146.96, 138.69 138.38, 134.81, 132.92 132.69, 132.60, 132.58 132.11, 132.01, 130.28 127.83, 125.24, 38.76 34.57, 34.00, 32.30, 32.28
7 [b]	6.39 (1H, t, J = 3.1, five-membered ring, H-6) 6.27 (2H, s, six-membered ring) 5.93 (2H, s, six-membered ring) 5.83 (2H, s, six-membered ring) 5.82 (2H, d, J = 3.1, five-membered ring, H-5, H-7) 2.88–2.71 (8H, m, bridge protons, H-1, H-2, H-12, H-13)	136.85, 131.72, 130.97 130.00, 121.78, 121.12 113.55, 96.12, 35.56 34.57
8 [b]	5.93 (2H, d, J = 3.3, H-1, H-3) 6.59 (1H, t, J = 3.3) 7.31 (2H, m, six-membered ring) 7.40 (t, 2H, m, six-membered ring)	91.7, 115.6, 119.3, 113.6, 129.7 [d]
9 [c]	6.32 (4H, s, six-membered ring) 6.12 (4H, s, six-membered ring) 5.63 (4H, s, six-membered ring) 3.75 (2H, t, J = 2.3, five-membered ring) 3.67 (4H, d, J = 2.3, five-membered ring) 2.82–2.52 (16H, m, bridge protons)	

[a] Chemical shifts (δ values) relative to TMS, coupling constants in Hz. The ^{13}C-NMR spectra are ^{1}H-decoupled. [b] In [D$_8$]THF at room temperature. The solution of the anions contains residual diethyl ether. [c] In $CDCl_3$ at room temperature. [d] See [9].

As *Edlund* et al. have demonstrated for indenyllithium and related systems, the NMR spectra are influenced by solvation of both the cation *and* the anion.[10] The same is probably true for **5** and **7**.

Anions **5** and **7** react with D_2O to give mixtures of products. Dianion **5** gives dideuterated derivatives, as shown by mass spectroscopy (*m/z* 286). Monoanion **7** affords a monodeuterated derivative (*m/z* 247).

The surprisingly stable anions **5** and **7** represent a new class of stacked anionic structures. The interaction of the two components of which this system is composed seems to be very significant, especially in **5**. The high-field shift of 0.97 ppm for the signals of the six-membered-ring protons of **5** (compared with those of **4**) indicates an even stronger interaction than the one prevailing in the [2.2]paracyclophanes. Furthermore, the comparison between the two ionic structures **5** and **7** shows the greater importance of the interaction between two negatively charged moieties in **5** relative to that in **7**.

Received: September 30, 1985;
supplemented: November 27, 1985 [Z 1475 IE]
German version: *Angew. Chem. 98* (1986) 160

[1] For recent reviews on the chemistry of [2$_n$]cyclophanes see: V. Boekelheide, *Acc. Chem. Res. 13* (1980) 65; H. Hopf, J. Kleinschroth, *Angew. Chem. 94* (1982) 485; *Angew. Chem. Int. Ed. Engl. 21* (1982) 469.

[2] V. Boekelheide, *Top. Curr. Chem. 113* (1983) 87; H. Hopf in P. M. Keehn, S. M. Rosenfeld (Eds.): *Cyclophanes*, Academic Press, New York 1983, p. 521 ff.

[3] H. Hopf, *Naturwissenschaften 70* (1983) 349.

[4] W. Huber, K. Müllen, O. Wennerström, *Angew. Chem. 92* (1980) 636; *Angew. Chem. Int. Ed. Engl. 19* (1980) 624.

[5] M. W. Haenel, *Tetrahedron Lett. 1977*, 1273.

[6] Two *s*-indacenophane dianions have been prepared by *Hafner* et al. The ^{1}H-NMR spectrum of 12,16(12,18)-dihydro[2]paracyclo[2](4,8)-*s*-indacenophane dianion is similar to that of **7** (δ = 5.54 (Aryl-H), 2.68 (bridge CH_2), 6.49 and 6.84 (indacene moiety)); P. Bickert, *Dissertation*, Technische Hochschule Darmstadt 1983.

[7] a) H. Hopf, S. El-Tamany, F.-W. Raulfs, *Angew. Chem. 95* (1983) 631; *Angew. Chem. Int. Ed. Engl. 22* (1983) 633; b) a detailed preparation is reported in H. Hopf, F.-W. Raulfs, *Israel J. Chem. 25* (1985) 210; c) H. Hopf, F.-W. Raulfs, D. Schomburg, *Tetrahedron*, in press.

[8] a) G. Fraenkel, R. E. Carter, A. McLachlan, J. H. Richards, *J. Am. Chem. Soc. 82* (1960) 5846; b) R. Schaefer, W. F. Schneider, *Can. J. Chem. 41* (1963) 966; c) H. Spiesecke, W. F. Schneider, *Tetrahedron Lett. 1961*, 468.

[9] a) J. B. Grutzner, J. M. Lawlor, L. M. Jackman, *J. Am. Chem. Soc. 94* (1972) 2306; b) G. Fraenkel, J. G. Russel, Y.-M. Chen, *ibid. 95* (1973) 3208; c) H. Günther, A. Shyoukh, D. Cremer, K. H. Frisch, *Justus Liebigs Ann. Chem. 1978*, 150; d) U. Edlund, *Org. Magn. Reson. 12* (1979) 661; *ibid. 10* (1977) 593.

[10] B. Eliasson, D. Johnels, S. Wold, U. Edlund, *Acta Chem. Scand. B 36* (1982) 155; U. Edlund, B. Eliasson, J. Kowalewski, L. Trogen, *J. Chem. Soc. Perkin Trans. 2 1981*, 1260.

$[Co_4(\mu_3\text{-}As)_3(\mu_3,\eta^3\text{-}As_3)(PPh_3)_4]$, a Product of the Reaction of $[CoCl_2(PPh_3)_2]$ with $PhAs(SiMe_3)_2$**

By *Dieter Fenske** and *Johannes Hachgenei*

Recently, we described the reaction of $[MCl_2(PPh_3)_2]$ (M = Co, Ni) with $PhP(SiMe_3)_2$, which results in the formation of the complexes $[Co_4(\mu_3\text{-}PPh)_4(PPh_3)_4]$ and $[Ni_8(\mu_4\text{-}PPh)_6(PPh_3)_4]$,[1] respectively, along with Me_3SiCl. More-

[*] Prof. Dr. D. Fenske, Dipl.-Chem. J. Hachgenei
Institut für Anorganische Chemie der Universität
Engesserstrasse, Geb. Nr. 30.45, D-7500 Karlsruhe (FRG)

[**] This work was supported by the Deutsche Forschungsgemeinschaft and the Fonds der Chemischen Industrie. We thank the staff of the Institut für Kristallographie der Universität Karlsruhe for their help in obtaining the crystal data.

over, the reaction of $[MCl_2(PPh_3)_2]$ with $E(SiMe_3)_2$ (E = S, Se) affords in high yields clusters such as $[Co_7S_6Cl_2(PPh_3)_5]$, $[Co_6E_8(PPh_3)_6]^n$ (E = S, n = +1, E = Se, n = 0), $[Ni_8S_6Cl_2(PPh_3)_6]$, $[Ni_8S_5(PPh_3)_7]$, $[Co_9Se_{11}(PPh_3)_6]$, and $[Ni_{34}Se_{22}(PPh_3)_{10}]$.[2,3] We have now studied the application of this principle to the synthesis of complexes containing AsPh ligands.

When $[FeCl_2(PPh_3)_2]$ is allowed to react with $PhAs(SiMe_3)_2$ a redox reaction is observed, which gives Fe, $(AsPh)_n$, and Me_3SiCl. In contrast, reaction of $[CoCl_2(PPh_3)_2]$ **1** with $PhAs(SiMe_3)_2$ results in the formation of an intense green solution (with the formation of a small amount of Co). Dark green crystals of **2** are obtained from the filtrate in a yield of 95% (based on As).[4]

$$\underset{\mathbf{1}}{[CoCl_2(PPh_3)_2]} \xrightarrow{PhAs(SiMe_3)_2} \underset{\mathbf{2}}{[Co_4(\mu_3\text{-}As)_3(\mu_3,\eta^3\text{-}As_3)(PPh_3)_4]}$$

In the ^{1}H-NMR spectrum of the paramagnetic Co_4As_6 cluster, the signals of the phenyl protons appear at $\delta = 6.80$–8.40. No ^{31}P-NMR signal can be observed. According to the X-ray structure analysis, the structure of **2** consists of a Co_4 tetrahedron, three Co_3 faces of which are each capped by a μ_3-As ligand (As2, As2a, As2b) and one face of which (Co1, Co1a, Co1b) is linked to an As_3 ring (As1, As1a, As1b) (Fig. 1).[5] Cluster **2** may be regarded as a heterocubane cluster having the formula $[Co_4(\mu_3\text{-}As)_4(PPh_3)_4]$ in which one μ_3-As is replaced by an η^3-As_3 ligand. In addition, each Co atom is coordinated by PPh_3 (P1, P2). Cluster **2** can alternatively be regarded as having been derived from a Co_3As_3 octahedron (As1, As1a, As1b, Co1, Co1a, Co1b) that is connected by a Co_3 face to a $Co_4(\mu_3\text{-}As)_3$ unit. The η^3-E_3 complexes (E = P, As) reported so far, on the other hand, are regarded as derivatives of the tetrahedral $As_4(P_4)$ in which As or P is replaced by an isolobal transition-metal fragment.[6,8]

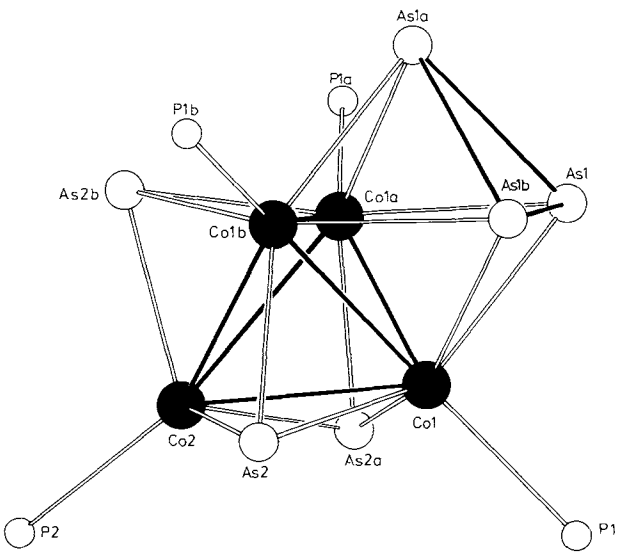


Fig. 1. Crystal structure of the cluster **2** (without phenyl groups). P1, P1a, P1b, and P2 represent the P atoms of the PPh_3 ligands. Most important bond lengths [pm] (±0.1 pm) and bond angles [°] (±0.1°): Co1-Co1a(Co1b) 243.8, Co1-As1 248.8, Co1-As1b 243.3, Co1-Co2 261.6, Co1-P1 220.1, Co1-As2 229.4, Co2-As2 227.4, Co2-P2 217.5, As-As (in η^3-As_3) 246.3; As-As-As (in η^3-As_3) 60.0, Co-Co-Co 55.4–62.2, Co2-(μ_3-As)-Co 64.2–69.8, P1-Co1-As1 99.8, P1-Co1-As2 101.7–105.1, P2-Co-As2 112.2, (μ_3-As)-Co1-As2 91.5–93.0, Co1b-Co1-As1b 61.4, As1b-Co1-As1 60.1, Co1b-Co1a-As1 90.4, Co1a-As1-As1b 90.3, Co1a-As1-As1a 61.1, As1a-As1-Co1 89.0.

Cluster **2** has a threefold axis. Co2 and P2 occupy the 6c sites and Co1, As1, As2, and P1 the 18f sites (in the space group $R\bar{3}$). The As1–As1a distance of 246.3(2) pm is in accord with the As–As distances in As_4, $(AsPh)_6$,[7] and the Co_2As_3 cluster **3**; however, it is 10 pm longer than the As–As distance in the As_3 complexes **4** and **5**.[8] Co1 is bonded to four As ligands and one PPh_3 ligand (P1) in a square-pyramidal fashion. In contrast, Co2 is coordinated by three μ_3-As ligands and one PPh_3 ligand (P2) in a distorted tetrahedral fashion.

$$\underset{\mathbf{3}}{[(triphos)Co\text{-}\mu(\eta^3\text{-}As_3)Co(triphos)]^{2+}} \qquad \underset{\mathbf{4}}{[As_3Co(CO)_3]}$$

$$\underset{\mathbf{5}}{[(C_5H_5)Mo(CO)_2As_3]}$$

The shortening of the As–As bonds in **4** and **5** (compared with those in As_4) is explained by an increase in bonding and a decrease in antibonding interactions within the As_3 ring. The bonding situation in **2** is obviously different since each As atom of the η^3-As_3 ligand is bonded to two Co atoms. The Co1–As1 a distance (243.3–248.8(2) pm) is about as large as that in **4** (244 pm) and longer than that in **3** (241 pm). The bonds between the Co atoms and the μ_3-As (Co1-As2: 229.3(2), Co2-As2: 227.4(2) pm) are significantly shorter.

If η^3-As_3 and μ_3-As are considered to be 3e donors and PPh_3 a 2e donor, **2** contains 56 valence electrons (eight electrons for six Co–Co bonds) and thus four electrons fewer than expected for an M_4 cluster having a tetrahedral structure. In agreement with this observation, the Co–Co bonds have differing lengths (Co1-Co2: 261.6(2), Co1-Co1a: 243.8(1) pm).[1,9]

The formation of **2** is surprising since it occurs at room temperature with cleavage of the As–C(Ph) bond. Evidence for the instability of As–C bonds has already been reported.[8,10] Cluster **2** reacts with $Co_2(CO)_8$, $Ni(CO)_4$, $[M(CO)_5(thf)]$ (M = Cr, Mo), and $[CpMo(CO)_3]_2$ to give cluster compounds that have not yet been identified.

Received: October 7, 1985 [Z 1488 IE]
German version: *Angew. Chem. 98* (1986) 165

[1] D. Fenske, R. Basoglu, J. Hachgenei, F. Rogel, *Angew. Chem. 96* (1984) 160; *Angew. Chem. Int. Ed. Engl. 23* (1984) 160; D. Fenske, J. Hachgenei, F. Rogel, *ibid. 96* (1984) 959 and *23* (1984) 982.

[2] D. Fenske, J. Hachgenei, J. Ohmer, *Angew. Chem. 97* (1985) 684; *Angew. Chem. Int. Ed. Engl. 24* (1985) 706.

[3] D. Fenske, J. Ohmer, J. Hachgenei, *Angew. Chem. 97* (1985) 993; *Angew. Chem. Int. Ed. Engl. 24* (1985) 993.

[4] *Experimental procedure:* **1** (12 g, 18.3 mmol) in 100 mL of tetrahydrofuran was treated at room temperature with $PhAs(SiMe_3)_2$ (5.50 g, 18.4 mmol). The solution immediately turns intense green. After 3 d, the precipitated cobalt (0.35 g) was removed by filtration. The solvent was evaporated and the residue was recrystallized from hot toluene.

[5] **2** crystallizes from toluene with three molecules of toluene per molecule of **2**. Space group $R\bar{3}$, $Z = 6$, lattice parameters (180 K): $a = b = 1432.2(4)$, $c = 7354.0(22)$ pm, $\alpha = \beta = 90°$, $\gamma = 120°$, $\mu(Mo_{K\alpha}) = 23.7$ cm^{-1}. Syntex R3, $2\theta < 52°$, 6447 reflections, 4370 with $I > 2\sigma(I)$. Patterson methods; Co, P, As, C refined anisotropically (H positions calculated). Further details of the crystal structure investigation are available on request from the Fachinformationszentrum Energie, Physik, Mathematik GmbH, D-7514 Eggenstein-Leopoldshafen 2, by quoting the depository number CSD 51645, the names of the authors, and the journal citation.

[6] C. A. Ghilardi, S. Midollini, A. Orlandini, L. Sacconi, *Inorg. Chem. 19* (1980) 301; A. Vizi-Orosz, V. Galamb, G. Palyi, L. Marko, G. Bor, G. Natile, *J. Organomet. Chem. 107* (1976) 235; M. DiVaira, L. Sacconi, *Angew. Chem. 94* (1982) 338; *Angew. Chem. Int. Ed. Engl. 21* (1982) 330.

[7] K. Hedberg, E. W. Hughes, J. Wieser, *Acta Crystallogr. 14* (1961) 369.

[8] A. S. Foust, M. S. Foster, L. F. Dahl, *J. Am. Chem. Soc. 91* (1969) 5631; J. Bernal, H. Brunner, W. Meier, H. Pfisterer, J. Wachter, M. Ziegler, *Angew. Chem. 96* (1984) 428; *Angew. Chem. Int. Ed. Engl. 23* (1984) 438; O. J. Scherer, H. Sitzmann, G. Wolmershäuser, *ibid. 96* (1984) 979 and *23* (1984) 968.

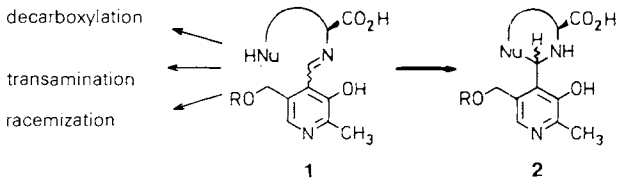
[9] Trinh-Toan, W. P. Fehlhammer, L. F. Dahl, *J. Am. Chem. Soc. 94* (1972) 2289; M. A. Neumann, Trinh-Toan, L. F. Dahl, *ibid. 94* (1972) 2283; R. S. Gall, C. Ting-Wah Chu, L. F. Dahl, *ibid. 96* (1974) 4019.

[10] A. Rheingold, P. Sullivan, *Organometallics 1* (1982) 1574; R. Jones, B. Whittlesey, *J. Am. Chem. Soc. 107* (1985) 1078.

The First Evidence of Endogenous Pyridoxyl Isoquinoline Alkaloids in Mammalian Organisms**

By *Gerhard Bringmann** and *Stephan Schneider*

The ease with which the biosynthesis of isoquinoline alkaloids from arylethylamines and aldehydes or α-keto acids can be imitated in vitro[1] led very early to the assumption[2] that such condensation reactions could also take place in mammalian organisms, e.g., after alcohol consumption.[3] In particular, the aldehyde pyridoxal **5**, the key coenzyme in amino acid metabolism, might react with endogenous dinucleophilic amines to give the alkaloid-like metabolites **2** via the biochemically familiar Schiff base intermediates **1** (Scheme 1). We now report the first evidence for the in vivo formation of novel alkaloids



Scheme 1.

in mammalian organisms from vitamin B_6 **3** and L-Dopa **4**, which are administered in unphysiologically high doses, often gram amounts, in the treatment of certain metabolic disorders, such as Parkinson's disease[4] and homocystinuria.[5] Such alkaloids are also unknown in plants.

Using in vitro model reactions, we first synthesized the isoquinoline alkaloids **8**–**11** (which are derived from vitamin B_6) from pyridoxal **5** or pyridoxal phosphate **6** and L-Dopa **4** or dopamine under physiological conditions[6] (water, pH 6–8, 35 °C), compound **7** probably being an intermediate (Scheme 2). After their constitution and configuration[7] had been established (^{1}H-NMR data in Table 1), an analytical method was elaborated for these extremely polar, in part multi-zwitterionic substances. Using ion-pair-assisted reverse phase HPLC (RP 18; 0.01 M H_3PO_4 in H_2O + 0.3% sodium dodecyl sulfate / 0.01 M H_3PO_4 in CH_3OH), we found conditions that permitted the efficient chromatographic separation and detection of these substances in nanogram quantities, even in complex biological systems.

After intravenous administration of therapeutically common doses (20 mg/kg) of pyridoxine **3** and L-Dopa **4** to Wistar rats, however, the expected isoquinoline **11** could not be detected in the blood, even if, instead of **3**, the aldehyde pyridoxal **5**, which is able to undergo condensation, was injected. Instead, we found even more polar metabolites in both cases, which are chromatographically (HPLC, see above) identical with the *O*-phosphorylated heterocycles **8** and **10**.

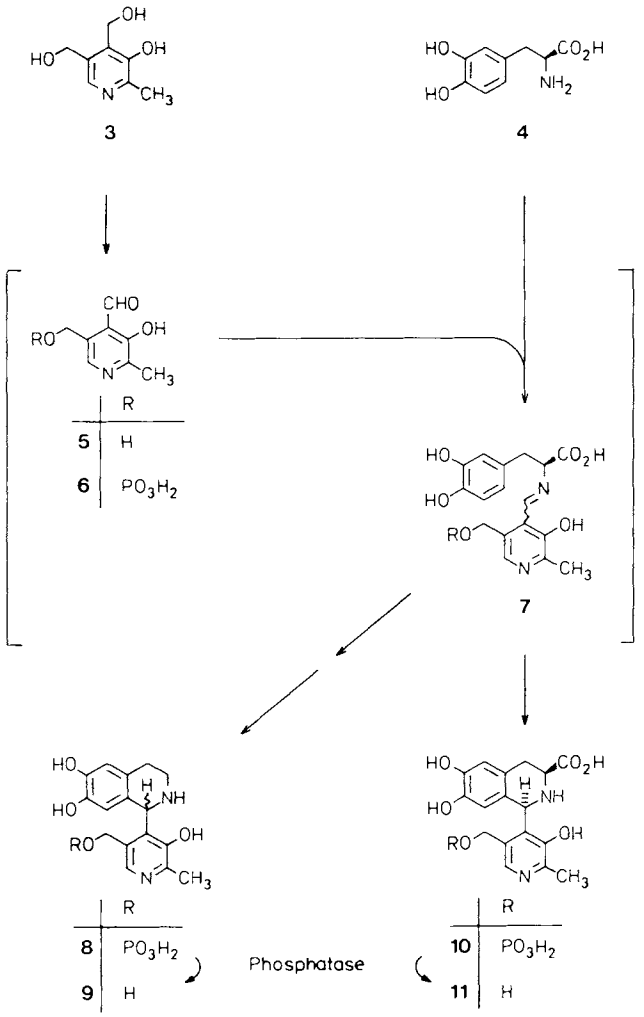
In order to confirm the identification of **8** and **10** and to quantify their formation, we carried out animal experiments with [4,5-^{14}C]pyridoxine **3***. For a reverse isotope dilution analysis, blood plasma, obtained from venous blood after incubation (2–6 h), was treated with unlabeled **8** or **10** and with the unlabeled educt **3**. After addition of 5% trifluoroacetic acid, the proteins were centrifuged off, and the supernatant was freeze dried. Preparative HPLC (for conditions see above) and subsequent separation of the ion-pair reagent afforded **8*** and **10***, which were purified to constant radioactivity by crystallization. In order to obtain preliminary information regarding the distribution of these novel metabolites in the body and their possible biotransformation, we also analyzed the liver. The results of the animal experiments are summarized in Table

Table 1. ^{1}H-NMR data for the condensation products **8**, **9**, **10**, and **11** (300 MHz, tetramethylsilane or sodium[2,3-D_4]-3-trimethylsilylpropionate int., δ values).

	8 (DCl/D_2O)	**9** (CD_3SOCD_3)	**10** (CD_3SOCD_3)	**11** (CD_3SOCD_3)
1-H	4.85 (mc)	5.26 (mc)	5.40 (mc)	5.35 (mc)
3-H_e	1.91 (dddd, J = 17.0, 4.5, 1.9 Hz)		—	—
3-H_a	2.13 (ddd, J = 17.0, 12.0, 5.5 Hz)	2.58 (mc)	3.60 (dd, J = 10.4, 3.9 Hz)	3.67 (dd, J = 10.9, 4.3 Hz)
4-H_e	2.69 (ddd, J = 13.1, 5.5, 1.9 Hz)	2.86 (mc)	2.98 (dd, J = 16.2, 3.9 Hz)	2.95 (dd, J = 15.6, 4.3 Hz)
4-H_a	2.43 (ddd, J = 13.1, 12.0, 4.5 Hz)	2.89 (mc) 3.26 (mc)	2.90 (ddd, J = 16.2, 10.4, 0.7 Hz)	2.85 (ddd, J = 15.6, 10.9, 0.8 Hz)
5-H	not observed	6.48 (s)	6.55 (s)	6.54 (s)
8-H	not observed	6.04 (s)	6.00 (s)	6.05 (s)
6′-H	7.33 (s)	7.94 (s)	7.99 (s)	7.96 (s)
5′-CH_2	4.15 (dd, J = 12.9, 7.0 Hz) 4.26 (dd, J = 12.9, 7.8 Hz)	4.56, 4.64 (2d, J = 12.8 Hz)	4.98 (mc)	4.55, 4.62 (2d, J = 12.7 Hz)
CH_3	1.55 (s)	2.22 (s)	2.27 (s)	2.24 (s)

[*] Priv.-Doz. Dr. G. Bringmann, Dr. S. Schneider
Organisch-chemisches Institut der Universität
Orléansring 23, D-4400 Münster (FRG)

[**] Endogenous Alkaloids in Humans, Part 2. This work was supported by the Minister für Wissenschaft und Forschung des Landes Nordrhein-Westfalen and by the Fonds der Chemischen Industrie (a grant and a fellowship for *S. S.*). We thank Priv.-Doz. Dr. *K. D. Richter*, Zentrale Tierexperimentelle Einrichtung der Universitätskliniken Münster, for valuable suggestions and Dipl.-Chem. *M. Zsiška* for experimental assistance in the animal experiments. Part 1: G. Bringmann, *Naturwissenschaften 66* (1979) 22.



Scheme 2. In vitro and in vivo formation of pyridoxyl isoquinoline alkaloids.

2.[8] For a further structural proof, the alkaloids **8*** and **10*** could be dephosphorylated in vitro to the radioactive alcohols **9*** and **11*** using an acid phosphatase (E.C. 3.1.3.2).

Table 2. Results of the reverse isotope dilution analysis after administration of pyridoxine **3*** (10 μCi, 20 mg/kg) and L-Dopa **4** (20 mg/kg) to rats.

Isolated alkaloid (sample)	Incubation time [h]	Total radio-activity [nCi]	Absolute rate of incorporation [%] × 10^2	Alkaloid content [ng/mL or ng/g]
8 (blood)	4	1.9	1.9	133
8 (blood)	6	3.0	3.0	206
8 (liver)	6	0.2	0.2	28
10 (blood)	2	0.7	0.7	53
10 (blood)	4	0.8	0.8	57
10 (liver)	6	<0.007	<0.007	<1

The identification of pyridoxyl isoquinoline alkaloids in living mammalian organisms expands the range of specific, enzymatically catalyzed reactions of vitamin B_6 to include the probably nonenzymatic Pictet-Spengler condensation to heterocyclic metabolites.

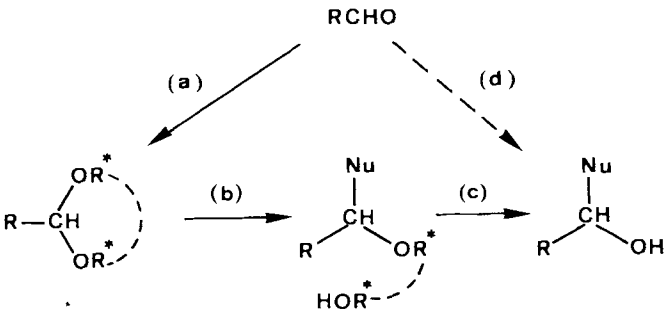
Received: October 2, 1985;
supplemented: November 11, 1985 [Z 1481 IE]
German version: *Angew. Chem. 88* (1986) 167

[1] W. Whaley, T. Govindachari, *Org. React. 6* (1951) 151.
[2] P. Holtz, K. Stock, F. Westermann, *Nature (London) 203* (1964) 656.
[3] See, e.g., M. Sandler, S. Carter, K. Hunter, G. Stern, *Nature (London) 241* (1973) 439; J. L. Cashaw, K. McMurtrey, H. Brown, V. E. Davis, *J. Chromatogr. 99* (1974) 567; M. A. Collins, W. Nijm, G. Borge, G. Teas, C. Goldfarb, *Science 206* (1979) 1184. Review: M. A. Collins in A. Brossi: *The Alkaloids, Vol. XXI*, p. 329, Academic Press, New York 1983.
[4] H. Bader: *Lehrbuch der Pharmakologie und Toxikologie*, Edition Medizin, Verlag Chemie, Weinheim 1983.
[5] H. Groebe, *Dtsch. Med. Wochenschr. 98* (1973) 1313.
[6] C. Schöpf, H. Bayerle, *Justus Liebigs Ann. Chem. 513* (1934) 190.
[7] The configuration of the pyridoxyl substituents on C-1 in **10** and **11** was determined from the ^{1}H-NMR ^5J coupling between 1-H_a and 4-H_a to be equatorial, and therefore *cis* with respect to the equatorial carboxyl group and (1*R*). In order to carry out the mass spectrometric analysis, **8** and **10** were enzymatically dephosphorylated to **9** and **11** (acid phosphatase, H_2O, pH 5), since they could not be detected as phosphoric esters, even when mild ionization techniques (field desorption or fast atom bombardment) were used.—The synthesis of these condensation products has already been described. However, their spectroscopic characterization was incomplete since, in particular, the configuration of possible epimeric products was not taken into consideration: E. A. Rudd, W. C. Cunningham, J. W. Thanassi, *J. Med. Chem. 22* (1979) 233; C. Borri Voltattorni, A. Orlacchio, A. Giartosio, F. Conti, C. Turano, *Eur. J. Biochem. 53* (1975) 151; T. Kametani, M. Koizumi, K. Okui, Y. Nishii, M. Ono, *J. Med. Chem. 15* (1972) 203; J. H. Fellman, E. S. Roth, *Biochemistry 10* (1971) 408; H. F. Schott, W. G. Clark, *J. Biol. Chem. 196* (1952) 449.
[8] In interpreting the absolute rates of incorporation of radioactivity (total radioactivity of the isolated alkaloids divided by that of the labeled precursor **3** × 100), it is necessary to take into consideration the fact that the precursors, which are familiar to the body, also undergo competing metabolic reactions after their distribution in the living organism and that, moreover, the alkaloids seem to undergo rapid further transformations.

Preparation of Optically Active Alcohols from 1,3-Dioxan-4-ones. A Practical Version of the Asymmetric Synthesis with Nucleophilic Substitution at Acetal Centers**

By *Dieter Seebach,** *René Imwinkelried*, and *Gerhard Stucky*

Several groups have recently investigated the preparation of optically active secondary alcohols via chiral, nonracemic acetals, as shown in Scheme 1.[1–8] Since the chiral "auxiliary" is sacrificed, the usefulness of this method crucially depends upon the price of the auxiliary. The compounds employed thus far, 2,3-butanediol (A)[1,2,8] 2,4-pentanediol (B),[2,3,5,8] *N,N,N',N'*-tetramethyltartaramide (C),[4] mandelic acid (D),[6] and 1-phenylethanol (E),[7] have

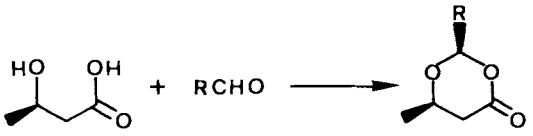


Scheme 1. For (a) to (d) see text.

[*] Prof. Dr. D. Seebach, Dipl.-Chem. R. Imwinkelried, Dipl.-Chem. G. Stucky
Laboratorium für Organische Chemie
der Eidgenössischen Technischen Hochschule
ETH-Zentrum, Universitätstrasse 16, CH-8092 Zürich (Switzerland)
[**] Part of the projected Dissertation of *R. I.* and of the Master's Thesis (1985) of *G. St.*, ETH Zürich.

the following disadvantages: expensive auxiliary (A, B, E); poor yields of the acetals in step (a) (D); insufficient stereoselectivity in step (b) (A, D, E); removal of auxiliary in step (c) requires oxidation (all but E); constitutionally identical, diastereotopic leaving groups in the asymmetric substitution (b) (all but D); very delicate reaction conditions must be followed (see, for instance, ref. [3]).

Owing to our experiences,[7,9] it occurred to us that the 1,3-dioxan-4-ones **1**–**7** should be ideal intermediates for the realization of the conversion (d): (1) the two acetal oxygens in **1**–**7** are constitutionally heterotopic and of vastly different nucleofugicity; (2) (*R*)-3-hydroxybutanoic acid is available from inexpensive[10] poly(hydroxybutanoate), the (*S*) enantiomer by yeast reduction of acetoacetate;[11] (3) the dioxanones **1**–**7** may be prepared in good yields from *aliphatic* aldehydes[12] and 3-hydroxybutanoic acid in benzene[13] (5–10 mol-% pyridinium 4-toluenesulfonate) with azeotropic removal of water. A 70–90% yield of a *cis/trans* mixture (9 : 1) is formed, from which the pure *cis* isomer may be obtained by recrystallization from ether/pentane[14] (Table 1); (4) removal of the chiral "auxiliary" after nucleophilic ring opening of the acetal requires simple β-elimination from a 3-alkoxy acid.



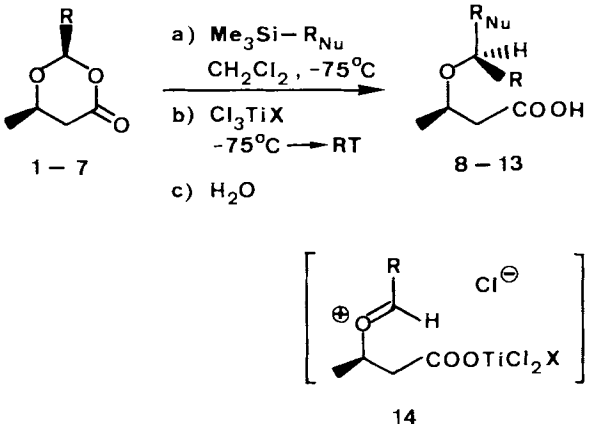
1 – 7

Table 1. *cis*-1,3-Dioxan-4-ones **1**–**7** from (*R*)-3-hydroxybutanoic acid and aliphatic aldehydes; yields of recrystallized, pure *cis* isomers (except **1** and **5**).

Product	R	Yield [%]	M.p. [°C]
1	CH_3	60	—
2	$CH(CH_3)_2$	61	ca. −25
3	$C(CH_3)_3$	40	82.2–82.8
4	n-C_7H_{15}	71	ca. −20
5	n-C_8H_{17}	66	ca. −25
6	$CH_2CH_2C_6H_5$	66	49.7–50.9
7	CCl_3	50	113.6–114.4

Indeed, when the dioxanones **1**–**7** are treated at −75 °C with a silyl nucleophile, Me_3SiR_{Nu}, and titanium tetrachloride or isopropoxytitanium trichloride, the β-alkoxy acids **8**–**13** are produced in high yields and with high diastereoselectivities[15] (Table 2). The reactions are performed with normal concentrations (ca. 0.3–0.4 M in CH_2Cl_2) and mixing periods of the reactants—even at higher temperatures (see Experimental Procedure and No. 2 in Table 2). The products are purified through base extraction and are isolated without chromatography. Moreover, even the *cis/trans* mixtures (9 : 1) of the dioxanones furnish products of the same configurational purity as those obtained from the pure *cis* isomers (see No. 4, 6, 9 in Table 2; we do not know whether this is due to *cis–trans* equilibration under the reaction conditions, or else due to a common intermediate oxonium ion **14**[6]).

The "chiral auxiliary" is removed from the alkoxy acids by treatment with excess lithium diisopropyl amide (LDA) in tetrahydrofuran (THF) to give the alcohols **15**–**18** with >90% *ee*[16] (Table 3). The byproduct, crotonic acid, is removed by extraction with aqueous alkali. The optically active alcohols are purified and isolated by distillation. To avoid epimerization by base, the nitrile **12** was hydrolyzed to the amide (H_2O_2, K_2CO_3, MeOH, 1-hexene)[17] prior to treatment with 3.0 molar equivalents of LDA (−78 °C → RT) to give **18**. No racemization was observed.

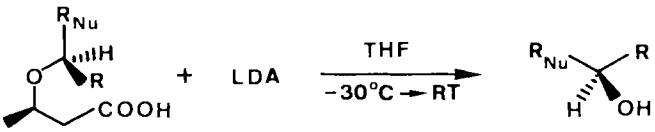


1 – 7 **8 – 13** **14**

Table 2. Preparation of the β-alkoxy acids **8**–**13** [15] with substitution at the acetal carbon atom.

No.	Starting material	*ds* [%]	X in Cl_3TiX	Product	R_{Nu}	Yield [%]	*ds* [%]
1	**6**	>98	Cl	**8**	$CH_2CH{=}CH_2$	95	87
2	**6**	>98	$OCHMe_2$	**8**	$CH_2CH{=}CH_2$	95	97 [a]
3	*ent*-**6**	>98 [b]	$OCHMe_2$	*ent*-**8**	$CH_2CH{=}CH_2$	87	97
4	**5**	90	$OCHMe_2$	**9**	$CH_2CH{=}CH_2$	99	96
5	**6**	>98	Cl	**10**	C≡C–H[c]	87	98.5
6	**6**	90	Cl	**10**	C≡C–H[c]	77	98
7	**6**	>98	Cl	**11**	C≡C–CH_3	50	98
8	**6**	>98	Cl	**12**	CN	99	98
9	**1**	90	Cl	**13**	CN	65	98.5

[a] Reaction at 0 °C affords 95% *ds* [b] 92% *ee*. [c] Reaction with $Me_3Si-C{\equiv}C-SiMe_3$.



8 – 13 **15 – 18**

Table 3. Cleavage of the β-alkoxy carboxylic acids **8**–**12** with formation of the alcohols **15**–**18** [16].

Starting material	LDA [equiv.]	Prod. (config.)	Yield [%]	*ee* [%]	$[\alpha]_D$
8	2.2	**15** (*R*)	80	94	+22.5 [a]
ent-**8** [b]	2.2	*ent*-**15** (*S*)	75	84	−20.5 [a]
9	2.2	**16** (*R*)	78	92	+10.2 [c]
10	3.2	**17**	67	97	−19.2 [b]
12 [d]	3.0	**18** (*R*)	68	96	+33.8 [e]

[a] In $CHCl_3$, $c = 2$. [b] 92% *ee*. [c] In CCl_4, $c = 3.5$. [d] **12**, $R_{Nu} = CONH_2$. [e] In EtOH, $c = 1.8$.

Conversions with nucleophiles other than those described here are possible. We are convinced that the procedure proposed here will eventually become a method of choice for asymmetric syntheses with substitution at acetal centers.

Experimental Procedure

A solution of $TiCl_4$ (11 mmol) in CH_2Cl_2 (5 mL, 2 M) [for $R_{Nu} = CH_3CH{=}CH_2$, $Cl_3Ti(OCHMe_2)$ [18] (1 M in CH_2Cl_2) was used] was added within 7–10 min to a solution of the 1,3-dioxan-4-one **1**–**7** (10 mmol) and Me_3SiR_{Nu} (13 mmol) in 20 mL of the same solvent with stirring at −75 °C. The reaction mixture was warmed to room temperature over ca. 12 h followed by addition of 15 mL H_2O and extraction with ether. The β-alkoxy acids **8**–**13** were extracted into 2 N aqueous NaOH, freed with conc. HCl, extracted with ether, and isolated, after drying over $MgSO_4$, by evaporative removal of the solvent.

Received: October 17, 1985 [Z 1501 IE]
German version: *Angew. Chem. 98* (1986) 182

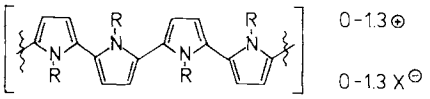
[1] J. M. McNamara, Y. Kishi, *J. Am. Chem. Soc. 104* (1982) 7371.
[2] A. Ghribi, A. Alexakis, J. F. Normant, *Tetrahedron Lett. 25* (1984) 3083.
[3] J. D. Elliott, J. Steele, W. S. Johnson, *Tetrahedron Lett. 25* (1985) 2535, and references cited therein.
[4] J. Fujiwara, Y. Fukutami, M. Hasegawa, K. Maruoka, H. Yamamoto, *J. Am. Chem. Soc. 106* (1984) 5004.
[5] A. Mori, J. Fujiwara, K. Maruoka, H. Yamamoto, *J. Organomet. Chem. 285* (1985) 83.
[6] S. H. Mashraqui, R. M. Kellogg, *J. Org. Chem. 49* (1984) 2513.
[7] R. Imwinkelried, D. Seebach, *Angew. Chem. 97* (1985) 781; *Angew. Chem. Int. Ed. Engl. 24* (1985) 765.
[8] P. A. Bartlett, W. S. Johnson, J. D. Elliott, *J. Am. Chem. Soc. 105* (1983) 2088.
[9] D. Seebach, H.-O. Kalinowski, *Nachr. Chem. Techn. Lab. 24* (1976) 415; D. Seebach, H.-F. Chow, R. F. W. Jackson, K. Lawson, M. A. Sutter, S. Thaisrivongs, J. Zimmermann, *J. Am. Chem. Soc. 107* (1985) 5292.
[10] Poly(hydroxybutanoate) can be purchased from Marlborough Biopolymers Ltd. MBL, Elta House, Yarm Road, Stockton-on-Tees, Cleveland TS18 3RX, England. The constantly falling price is currently ca. $50/kg. Procedures for the depolymerization: D. Seebach, M. F. Züger, *Helv. Chim. Acta 65* (1982) 495; *Tetrahedron Lett. 25* (1984) 2747. Monomeric enantiomeric 3-hydroxybutanoic acid derivatives are also—expensive—commercial products.
[11] Procedures and review: D. Seebach, M. A. Sutter, R. H. Weber, M. F. Züger, *Org. Synth. 63* (1984) 1.
[12] P. Aeräs, K. Pihlaja, *Tetrahedron Lett. 1970*, 4095.
[13] Aldehydes without α-branching can also be converted into dioxanones in CH_2Cl_2.
[14] Dioxanones, which are liquid at room temperature, are recrystallized at −75 °C.
[15] The *ds* values of **8**–**13** were determined by ^{13}C-NMR spectroscopy of the free acids and by GC analysis (OV-1701, 18-m capillary) of the corresponding methyl esters prepared from the crude products.
[16] The *ee* values of **15**–**18** were determined by GC (OV-1701, 18-m capillary) and/or by ^{19}F-NMR analysis of the corresponding Mosher ester (ester of 3,3,3-trifluoro-2-methoxy-2-phenylpropionic acid, MTPA ester). The absolute configuration follows from comparison of the sign of rotation (α_D) with literature data: **15** [7]; **16** [8]; **17** not correlated; **18**: V. Prelog, M. Wilhelm, *Helv. Chim. Acta 37* (1954) 1634.
[17] E. J. Corey, D. N. Crouse, J. E. Anderson, *J. Org. Chem. 40* (1975) 2140.
[18] D. Seebach, B. Weidmann, L. Widler in R. Scheffold (Ed.): *Modern Synthetic Methods 1983, Vol. 3*, Salle + Sauerländer, Frankfurt am Main/Aarau 1983.

Ferrocene-Modified Polypyrrole Films by Electrochemical Copolymerization**

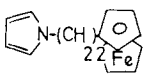
By *Alfred Haimerl* and *Andreas Merz**

Polypyrrole can be readily prepared in the form of films on suitable electrodes by anodic oxidation.[1] Its properties—it can be reversibly charged with ca. one elementary charge per 3–4 monomeric units and it is electrically conducting in the potential range of ca. −0.2 to +1.0 V[2]—make it a technologically interesting material, like polyacetylene.[3] We are presently investigating its potential use in the modification of electrodes for organic electrochemistry.

The structure of the polymer has not yet been satisfactorily elucidated. However, since pyrroles substituted at nitrogen[4] or in the 3,4-positions[5] can be polymerized as well, it must be assumed that the pyrrole moieties are linked via the 2,2′-positions and that the polymer contains at least partial structures as shown in formula **1a**.[6]



1a, R = H; **1b**, R = H/(CH$_2$)$_2$Fc



2

The structure **1a** suggests that the properties of the polypyrrole film should be influenced by substitution at the N-atom. In order to modify the electrochemical characteristics of polypyrrole films it is best to incorporate redox active substituents with redox potentials within the conductivity region of the polymer. We have prepared *N*-(2-ferrocenylethyl)pyrrole **2**[7] and investigated its electrochemical behavior. The cyclovoltammogram of **2** (Fig. 1a) shows a reversible oxidation of the ferrocene redox system at +0.38 V[8] and an irreversible oxidation of the pyrrole moiety at +1.40 V; this peak is shifted about +250 mV compared to unsubstituted pyrrole. On repeated scanning of the potential range no changes in the voltammogram occur like those observed for pyrrole on film formation (Fig. 1b). Likewise, electrochemical polymerization of **2** is not achieved by controlled current or potential electrolysis.

Ferrocene-containing polypyrrole layers **1b** can, however, be prepared by *copolymerization* of **2** with pyrrole.[9] Figure 1c shows the development of the electrode coating during the continuous cyclovoltammetry of a 1 : 1 solution of **2** and pyrrole. The successive curves demonstrate the growth of the polypyrrole film, recognizable as in Figure 1b by the broadening of the voltammogram similar to a

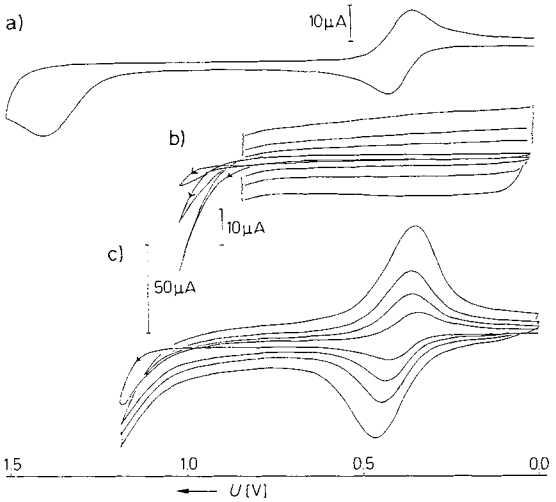


Fig. 1. Cyclovoltammograms of **2**, pyrrole, and a mixture of both. 0.1 M $[Bu_4N][ClO_4]/CH_3CN$; scan rate 50 mV s^{-1}; 0.03-cm^2 Pt disk. a) 7×10^{-4} M **2**; b) 7×10^{-4} M pyrrole (1st, 2nd, 3rd, 8th, 14th, and 24th scan); c) 7×10^{-4} M **2** + 7×10^{-4} M pyrrole (1st, 5th, 10th, and 20th scan).

[*] Prof. Dr. A. Merz, Dipl.-Chem. A. Haimerl
Institut für Organische Chemie der Universität
Universitätsstr. 31, D-8400 Regensburg (FRG)

[**] This work was supported by the Fonds der Chemischen Industrie and the Deutsche Forschungsgemeinschaft.

capacitive current, and the increase of the ferrocene content. The curve of the first run shows the irreversible oxidation peak of pyrrole. The pyrrole radical cation that is formed here apparently serves as polymerization initiator; the polymerization is promoted by its addition to pyrrole or **2**.[5, 10] Apparently the radical cation of **2** *cannot* function as initiator.[11] The final curve in Figure 1c is approximately reproduced in pure solvent after withdrawal of the electrode from the polymerization solution. Better layers are obtained by copolymerization with controlled current density with $[Bu_3NH][PhSO_3]$ as supporting electrolyte.[12] The cyclovoltammogram in Figure 2 also demonstrates the reversible complete discharge of the polypyrrole film.[13]

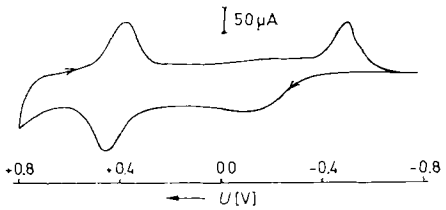


Fig. 2. Steady-state cyclovoltammogram of a layer of **1b** on a Pt-disk electrode; for conditions see caption to Figure 1. Coating solution: each 0.05 M pyrrole and **2** in 0.1 M $[Bu_3NH][PhSO_3]/CH_3CN$ + 1% H_2O; galvanostatic (40 mA cm^{-2} for 5 s).

The ferrocene-containing polypyrrole layers **1b** can serve as model substance for modified polypyrroles on the basis of *N*-substituted pyrrole monomers. An application as a reference electrode for non-aqueous solvents free of salt-bridges[14] already emerges: by application of a potential of +0.38 V the polymer layer of a **1b**-coated platinum wire is brought to a 1 : 1 ratio of ferrocene and ferrocinium ion. As a "zero-current" reference electrode in a three electrode device the wire maintains this potential for several hours in acetonitrile. During storage in air, however, a considerable negative potential drift takes place, corresponding to a decrease in the content of ferrocenium ions.[15] By improvement of the coating technique and elucidation of optimum storage conditions the development of a practical reference electrode seems possible.

Received: October 11, 1985 [Z 1493 IE]
German version: *Angew. Chem. 98* (1986) 179

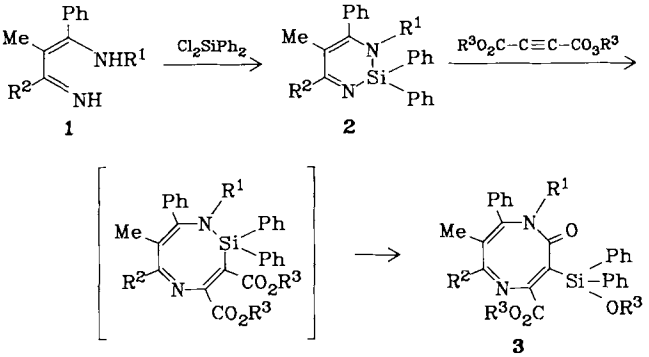
[1] A. F. Diaz, K. K. Kanazawa, G. P. Gardini, *J. Chem. Soc. Chem. Commun. 1979*, 635; R. A. Bull, F. Fan, A. J. Bard, *J. Electrochem. Soc. 129* (1982) 1009; E. M. Gennies, G. Bidan, A. F. Diaz, *J. Electroanal. Chem. 149* (1982) 33.
[2] All potentials are referred to a saturated calomel electrode (SCE).
[3] H. Naarmann, *Angew. Makromol. Chem. 109/110* (1982) 29; A. Merz, *Nachr. Chem. Tech. Lab. 30* (1982) 16; R. Noufi, *Appl. Phys. Commun. 3* (1983) 33.
[4] A. F. Diaz, A. Martinez, K. K. Kanazawa, *J. Electroanal. Chem. 130* (1981) 181.
[5] T. Lee, US-Pat. 4487667; see also *Chem. Abstr. 102* (1985) 174999.
[6] A. Asavapiriyanont, G. K. Chandler, G. A. Gunawardena, D. Pletcher, *J. Electroanal. Chem. 177* (1984) 229.
[7] **2**: golden yellow platelets, m.p. 101–102 °C, prepared from the tosylate of 2-ferrocenylethanol and pyrrolepotassium.
[8] E_0' for methylferrocene in the same system is +0.36 V: C. P. Andrieux, A. Merz, J.-M. Saveant, R. Tomahogh, *J. Am. Chem. Soc. 106* (1984) 1957.
[9] M. V. Rosenthal, T. A. Skotheim, A. Melo, M. I. Floris, *J. Electroanal. Chem. 185* (1985) 297. In this work the authors report on a pyrrole/*N*-(*p*-nitrophenylpyrrole) copolymer, which naturally shows no additional redox activity in the conductivity region.
[10] *Heinze* et al. postulate the coupling of radical cations as polymerization-initiating step. If **2** is incorporated according to this mechanism then this must take place via a homogeneous redox disproportionation. J. Heinze, M. Dietrich, J. Mortensen, *Ber. Bunsenges. Phys. Chem.*, in press.
[11] In contrast to this finding, the direct anodic polymerization of two *N*-substituted pyrrole derivatives with still more bulky substituents has been reported: G. Bidan, A. Deronzier, J. C. Moutet, *J. Chem. Soc. Chem. Commun. 1984*, 1185; G. Bidan, A. Deronzier, J. C. Moutet, *Nouv. J. Chim. 8* (1984) 501.
[12] H. Naarmann, G. Koehler, J. Schlag, DOS 3226278 (BASF); see also *Chem. Abstr. 100* (1984) 93546d.
[13] The black, modified polypyrrole films thus prepared, thin layers of which are violet-colored, adhere firmly and are readily reproducible.
[14] The ferrocene/ferrocenium redox pair has been recommended by the IUPAC as a solvent-independent reference system: G. Gritzner, J. Kuta, *Pure Appl. Chem. 54* (1982) 127; *Bard* et al. suggested a similar electrode based on polyvinylferrocene: P. J. Peerce, A. J. Bard, *J. Electroanal. Chem. 108* (1980) 221.
[15] M. Sato, T. Yamada, A. Nishikama, *Chem. Lett. 1980*, 925.

A Facile Synthesis of a New Class of Eight-Membered Heterocycles from 1-Azabutadienes**

By *José Barluenga,* Miguel Tomás, Alfredo Ballesteros, Vicente Gotor, Carl Krüger,** and *Yi-Hung Tsay*

1-Azabutadienes are useful building blocks in organic synthesis.[1] The more stable, easily available 4-amino-1-azabutadienes **1**[2] have proved to be valuable starting materials for the preparation of five- and six-membered nitrogen-containing heterocycles, some of them with other heteroatoms (O, S, P) incorporated in the ring.[3] Furthermore, organosilicon compounds have found wide application in synthetic chemistry[4] and the use of species with silicon–nitrogen bonds in the synthesis of nitrogen-containing functional groups[5] and heterocycles[6] has been reported.

We report here an easy, regioselective preparation of a new class of eight-membered nitrogen-containing heterocycles. Reaction of **1** with dichlorodiphenylsilane at room temperature gave high yields of substituted 1,2-dihydro-1,3,2-diazasilines **2**.[7] Interestingly, when esters of acetylenedicarboxylic acid were added to a solution of **2** in benzene and the mixture heated at 60 °C, 1,5-diazocine-2(1*H*)-ones **3** were formed in good yields;[7, 8] examples are given in Table 1.



[*] Prof. Dr. J. Barluenga, Dr. M. Tomás, A. Ballesteros, Prof. Dr. V. Gotor
Departamento de Química Orgánica, Facultad de Química
Universidad de Oviedo, SP-33071-Oviedo (Spain)
Prof. Dr. C. Krüger, Y.-H. Tsay
Max-Planck-Institut für Kohlenforschung
D-4330 Mülheim an der Ruhr (FRG)

[**] This work was supported in part by the Comisión Asesora de Investigación Científica y Técnica (CAICYT).

Table 1. 1,2-Dihydro-1,3,2-diazasilines **2** and 1,5-diazocin-2(1*H*)-ones **3** from 4-amino-1-azabutadienes **1**. Tol = 4-tolyl, *c*Hex = cyclohexyl.

	R^1	R^2	Products **2** Yield [%]	Products **2** M.p. [°C] [a, b]	R^3	Products **3** Yield [%] [c]	Products **3** M.p. [°C] [a]
a	Ph	Ph	95	260–262	Me	71	172–174
b	Ph	Ph			Et	69	185–186
c	Ph	Tol	93	169–171	Et	67	186–187
d	Ph	Tol			Me	61	164–166
e	Tol	Ph	91	237–239	Me	63	170–172
f	Tol	Tol	89	160–162	Me	60	167–169
g	Ph	*c*Hex	90	133–135	Me	62	148–149

[a] Recrystallized from hexane/chloroform; melting points are uncorrected. [b] Decomposition. [c] Based on **1**.

The formation of compounds **3** can be explained by addition of the imine nitrogen–silicon bond to the activated carbon–carbon triple bond of the ester[9] followed by silicon-assisted intramolecular rearrangement.

Compounds **3** were characterized on the basis of their elemental analyses and spectroscopic (IR, ^{1}H-, and ^{13}C-NMR) and mass spectrometric data;[10] an X-ray structure of **3c** confirmed the assignments[11] (Fig. 1).

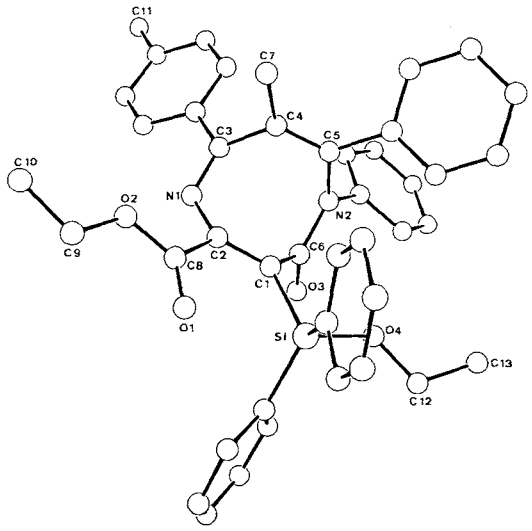
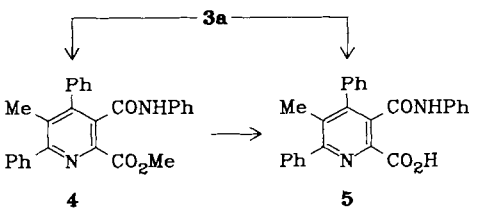


Fig. 1. Crystal structure of **3c** [11].

Heterocycles **3** rearrange in acidic or basic solution, undergoing desilylation to give the corresponding pyridines. Thus, treatment of **3a** with two molar equivalents of either trifluoroacetic acid in chloroform (48 h) or constant boiling hydriodic acid in benzene (6 h), reagents known to induce protodesilylation in vinyl silanes,[12] afforded quantitatively the heterocycle **4** (m.p. = 196–198 °C). Ring contraction of **3a** also took place under normal ester hydrolysis conditions (KOH, refluxing EtOH, 5 h) giving the acid **5** (m.p. = 180–182 °C); compound **5** was alternatively formed by hydrolysis of **4**.



The strategy described here provides a facile entry to 1,5-diazocine-2(1*H*)-ones **3**, which, to the best of our knowledge, have not been described previously.[13] Analogous perhydro derivatives are encountered in the homaline alkaloid skeletons;[14] substituted 3,4-dihydro-1,5-benzodiazocine-2(1*H*)-ones have been reported to exhibit biological activity.[15]

Received: September 9, 1985;
revised: November 15, 1985 [Z 1455 IE]
German version: *Angew. Chem. 98* (1986) 190

[1] a) S. Cheng, A. T. Lupo Jr., F. W. Fowler, *J. Am. Chem. Soc. 105* (1983) 7696; b) M. Komatsu, H. Ohgishi, S. Takamatsu, Y. Oshiro, T. Agawa, *Angew. Chem. 94* (1982) 214; *Angew. Chem. Int. Ed. Engl. 21* (1982) 213; *Angew. Chem. Suppl. 1982*, 483; c) M. Komatsu, S. Takamatsu, M. Uesaka, S. Yamamoto, Y. Oshiro, *J. Org. Chem. 49* (1984) 2691; d) D. L. Boger, *Tetrahedron 39* (1983) 2869.

[2] H. Hoberg, J. Barluenga, *Synthesis 1970*, 142.

[3] a) J. Barluenga, M. Tomás, V. Rubio, V. Gotor, *J. Chem. Soc. Chem. Commun. 1979*, 675; b) J. Barluenga, J. Jardón, V. Rubio, V. Gotor, *J. Org. Chem. 48* (1983) 1379; c) J. Barluenga, J. F. López-Ortiz, M. Tomás, V. Gotor, *J. Chem. Soc. Perkin Trans. 1 1981*, 1891; d) J. Barluenga, J. Jardón, F. Palacios, V. Gotor, *Synthesis 1985*, 309.

[4] a) E. C. Colvin: *Silicon in Organic Synthesis*, Butterworths, London 1981; b) W. P. Weber: *Silicon Reagents for Organic Synthesis*, Springer, New York 1983; c) Z. N. Parnes, G. I. Bolostova, *Synthesis 1984*, 991.

[5] a) I. Fleming in D. Barton, W. P. Ollis (Eds.): *Comprehensive Organic Chemistry, Vol. 3*, Pergamon Press, Oxford 1979, p. 592; b) R. J. P. Corriu, V. Huynh, J. J. E. Moreau, *Tetrahedron Lett. 25* (1984) 1887; c) R. J. P. Corriu, J. J. E. Moreau, M. Pataud-Sat, *Organometallics 4* (1985) 623.

[6] a) F. Z. Basha, J. F. De Bernardis, *Tetrahedron Lett. 25* (1984) 5271; b) A. Shanzer, *Angew. Chem. 92* (1980) 325; *Angew. Chem. Int. Ed. Engl. 19* (1980) 327; c) C. H. Yoder, J. J. Zuckerman, *Chem. Commun. 1966*, 694.

[7] *Experimental procedure:* To a solution of **1** (5 mmol) and Et_3N (12 mmol) in benzene (40 ml) was slowly added under argon a solution of Cl_2SiPh_2 (6 mmol) in benzene (20 mL). The mixture was stirred overnight at room temperature and then filtered (Et_3NHCl). The filtrate was heated with the acetylenedicarboxylic acid ester (6 mmol) at 60 °C for 24 h and the resulting mixture hydrolyzed (2 N H_2SO_4, 80 mL), extracted with ether, and concentrated; column chromatography (silica gel, hexane/ether 2:1) and recrystallization (hexane/chloroform) gave the pure diazozines **3**. The diazasilines **2** could be isolated and purified from their benzene solutions, before addition of the esters, by solvent evaporation in vacuum and recrystallization (hexane/chloroform).

[8] Azabutadienes **1** react with esters of acetylenedicarboxylic acid, J. Barluenga, S. Fustero, V. Gotor, *Synthesis 1975*, 191.

[9] For addition of simple silylamines to esters of acetylenedicarboxylic acid, see T. A. George, M. F. Lappert, *J. Organometallic Chem. 14* (1968) 327.

[10] Spectral data of compounds **2** are in agreement with the proposed structure, but their mass spectra do not show the corresponding molecular peak. Structure **2** is supported by the fact that its reaction with 3 N KOH or thionyl chloride led to the azabutadienes **1** and to the known 1,2,6-thiadiazine-*S*-oxides [3c], respectively.

[11] **3c**, Pbca, $a = 11.3282(5)$, $b = 19.536(1)$, $c = 34.015(1)$ Å, $Z = 8$, $\rho_{calcd} = 1.19$ g cm^{-3}, $\mu(Cu_{K\alpha}) = 8.71$ cm^{-1}, Enraf-Nonius CAD4 diffractometer; 8684 measured reflections, of which 5298 were observed ($I \geq 2\sigma(I)$): $R = 0.056$, $R_w = 0.072$ for 451 parameters. Further details of the crystal structure investigation may be obtained from the Fachinformationszentrum Energie, Physik, Mathematik GmbH, D-7514 Eggenstein-Leopoldshafen 2 (FRG), on quoting the depository number CSD 51567, the names of the authors, and the journal citation.

[12] a) T. H. Chan, W. Mychajlowskij, B. S. Ong, D. N. Harpp, *J. Org. Chem. 43* (1978) 1526; b) T. H. Chan, I. Fleming, *Synthesis 1979*, 761.

[13] For syntheses of 1,5-diazocines, see F. A. L. Anet, J. A. Moore in A. R. Katritzky, C. W. Rees (Eds.): *Comprehensive Heterocyclic Chemistry, Vol. 7*, Pergamon Press, Oxford 1984, p. 681.

[14] a) L. Crombie, R. C. F. Jones, A. R. Mat-Zin, S. Osborne, *J. Chem. Soc. Chem. Commun. 1983*, 960; b) H. H. Wasserman, G. D. Berger, *Tetrahedron 39* (1983) 2459.

[15] a) A. V. Bogatskii, S. A. Andronati, T. A. Voronina, V. V. Danilin, L. N. Nerobkova, *Khim.-Farm. Zh. 14* (1981) 45; b) H. Ott, US Pat. 3577557 (Dec. 9, 1966); *Chem. Abstr. 75* (1971) 49158v.

Stable Selenocarbonyl Ylides**

By *Rudolf Allmann, Franz-Josef Kaiser, Magda Krestel,* and *Gunther Seitz**

Suitably "push-pull"-substituted carbonyl ylides[1,2] or thiocarbonyl ylides[3] have sufficient stability for isolation and have been the subject of several detailed investigations during the last ten years. Isolable selenocarbonyl ylides, on the other hand, were hitherto unknown.[4] We report here on the synthesis and characteristic properties of the first stable compounds of this type with cyclopropenylium and bis(methylene) or bis(imino)cyclopropanide functions as stabilizing termini.

As we have found, the selone function in the diaminocyclopropeneselones **1**, which are readily accessible from the cyclopropenylium salts **6** and sodium hydrogen selenide,[5] is sufficiently nucleophilic to displace triethylamine from the zwitterions **2**[6] or **3**.[7] For the synthesis of **4a** [yield 84%, m.p. 178°C (dec.)], one hours' heating in anhydrous dichloromethane until complete removal of triethylamine suffices; the synthesis of **5c** (yield 85%, m.p. 230°C (dec.) was achieved by one hours' reaction in boiling ethanol. On cooling the reaction solution the desired selenocarbonyl ylides **4** and **5** precipitate as colorless to pale-beige, air-stable crystals and can be recrystallized from nitromethane. **4c** [m.p. 207°C (dec.)] could be obtained in 52% yield via another route. **2** was converted with freshly prepared sodium hydrogen selenide into the salt **7**,[8] which reacts smoothly with the salt **6c**[9] to yield the selenocarbonyl ylide **4c**.

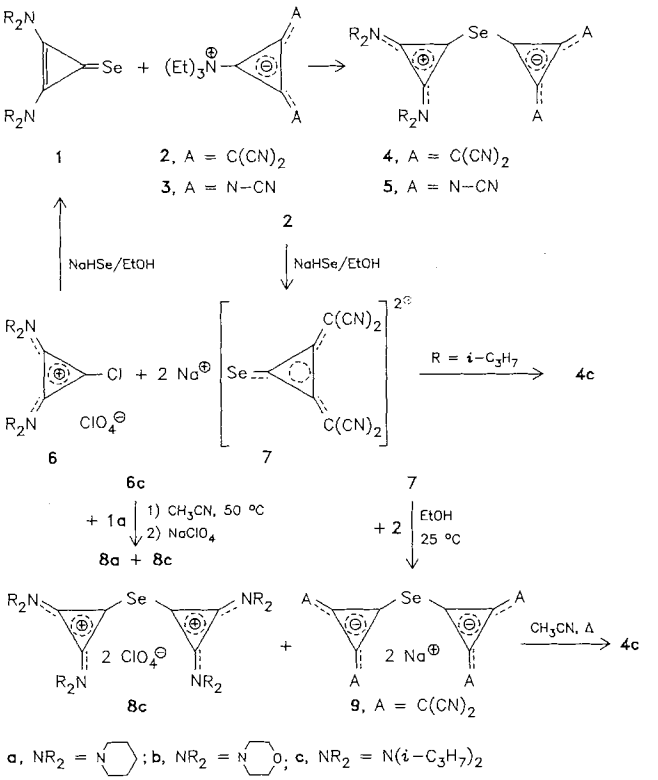
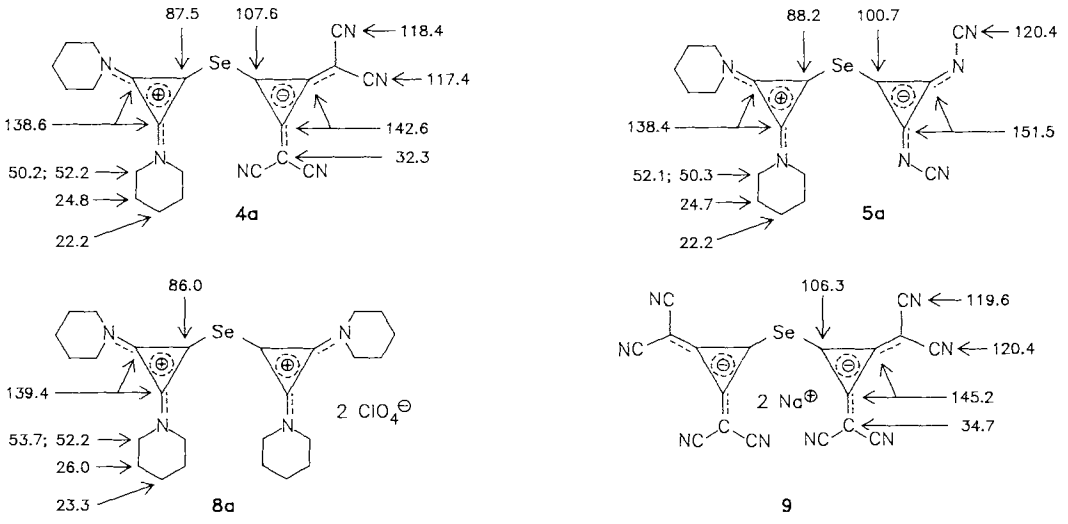


Table 1. Selected spectroscopic data of **4a**, **5a**, **8a**, and **9**. IR (KBr): $\tilde{\nu}$ [cm^{-1}] (C_3 = three-membered rings); UV: λ_{max} [nm] (lgε); ^{13}C-NMR (25 MHz, **4a** and **5a** in [D$_6$]DMSO, **8a** in CD_3CN, standard: ^{13}C-signals of the solvent, **9** in D_2O, dioxane external): δ values.

Cpd.	IR	UV
4a	2205, 2190 (CN), 1905, 1830, 1605, 1455 (C_3)	332 sh (3.93), 287 (4.54)
5a	2160 (CN), 1910, 1840, 1610, 1440 (C_3)	237 (4.49), 312 (3.67)
8a	1900, 1595 (C_3)	272 (4.18)
9	2215, 2200 (CN), 1835, 1440 (C_3)	287 (4.78), 343 (4.10)



[*] Prof. Dr. G. Seitz, Apotheker F.-J. Kaiser
Pharmazeutisch-chemisches Institut der Universität
Marbacher Weg 6, D-3550 Marburg (FRG)
Prof. Dr. R. Allmann, M. Krestel
Fachbereich Geowissenschaften der Universität
Hans-Meerwein-Strasse, D-3550 Marburg (FRG)

[**] This work was supported by the Deutsche Forschungsgemeinschaft and the Fonds der Chemischen Industrie.

The constitutions of **4** and **5** were verified by elemental analyses and spectra (Table 1). The assignment of the signals in the particularly informative ^{13}C-NMR spectra was accomplished by comparison with the data of the likewise novel selenium-bridged three-membered ring compounds **8** and **9**. The dication perchlorate **8a** can be obtained

(along with **8c**) from **6c** and **1a** as the product of a symmetrization reaction[10] [yield 22%, m.p. 233 °C (dec.), from CH_3CN/ether]. The sparingly soluble sodium dianion **9** is formed upon reaction of **7** with **2** [yield 50%, m.p. >300 °C, from $CH_3CN/CHCl_3$]. **8c** and **9** are thermodynamically unstable compared to **4c**, the zwitterionic combination of both three-membered ring derivatives: Upon heating the salts **8c** and **9** in acetonitrile, **4c** was obtained (yield 42%) together with an hitherto unidentified yellow substance. Remarkably, the (^{13}C)-δ values for the cationic terminus and the anionic terminus of **4a** are almost identical to those in the dication of **8a** and in the dianion of **9**, respectively (Table 1). The occurrence of two signals each for the nitrile C atoms and the C atoms in the α-position to the piperidine-N in **4a** points to hindrance to rotation and thus to a high bond order for the corresponding bonds to *both* three-membered rings.

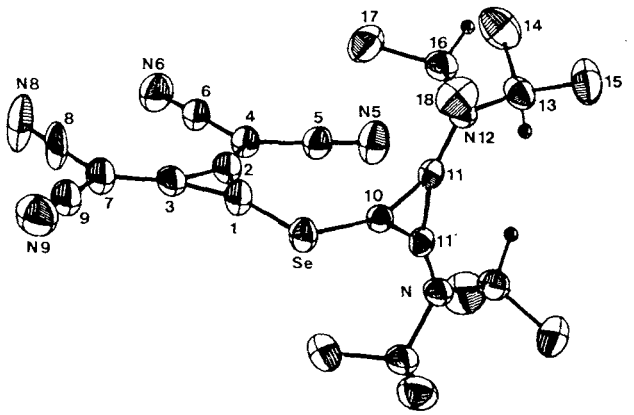


Fig. 1. Molecular structure of **4c** in the crystal. Pnma, $a = 15.919(3)$, $b = 13.050(3)$, $c = 11.927(3)$ Å, $Z = 4$, $\rho_{calc} = 1.334$ g cm^{-3} (with $4H_2O$ in the unit cell), 2014 reflections, $R = 0.067$, $R_w = 0.075$. The methyl hydrogen atoms (all in staggered form) are not shown. The mirror plane passes through the Se, C1–10 and N5,6,8,9 atoms and between C11–C11′ etc. The vibration ellipsoids (except for H) are drawn at the 50% probability level. Further details of the crystal structure investigations are available on request from the Fachinformationszentrum Energie, Physik, Mathematik GmbH, D-7514 Eggenstein-Leopoldshafen 2, on quoting the depository number CSD-51666, the names of the authors, and the full citation of the journal.

The structure of **4c** was determined X-ray crystallographically (Fig. 1). The planar anionic terminus lies in a mirror plane. The almost planar cationic terminus is perpendicular thereto and is bisected by the mirror plane. Both three-membered rings contain one long bond and two short bonds;[11] the bonds to the ring substituents show a high proportion of double bond character ($n \approx 1.5$). The CSeC bond angle is 92.8°, while the two C–Se bond lengths differ only slightly, being 1.88 and 1.90 Å. This corresponds to a C_{sp}–Se bond order of $n \approx 1.0$.

Received: September 25, 1985 [Z 1470 IE]
German version: *Angew. Chem. 98* (1986) 191

[1] E. P. Janulis, Jr., A. J. Arduengo, III, *J. Am. Chem. Soc. 105* (1983) 5929, and references cited therein.
[2] Reviews: R. Huisgen, *Angew. Chem. 89* (1977) 589; *Angew. Chem. Int. Ed. Engl. 16* (1977) 572; K. N. Houk, N. G. Rondan, C. Santiago, C. J. Gallo, R. W. Gandour, G. W. Griffin, *J. Am. Chem. Soc. 102* (1980) 1504.
[3] Review: F. Duus in N. Jones (Ed.): *Comprehensive Organic Chemistry, Vol. 3*, Pergamon Press, Oxford 1979, p. 406.
[4] A. G. Schultz, *J. Org. Chem. 40* (1975) 3466, discusses a selenocarbonyl ylide as intermediate of an organoselenium photoreaction; M. P. Cava, L. E. Saris, *J. Chem. Soc. Chem. Commun. 1979*, 617, formulate a selenazolone with a selenocarbonyl ylide resonance formula.
[5] Z. Yoshida, H. Konishi, H. Ogoshi, *J. Chem. Soc. Chem. Commun. 1975*, 359.
[6] T. Fukunaga, *J. Am. Chem. Soc. 98* (1976) 610.
[7] B. Gerecht, G. Offermann, G. Seitz, *Synthesis 1982*, 726.
[8] G. Seitz, F.-J. Kaiser, unpublished.
[9] Z. Yoshida, Y. Tawara, *J. Am. Chem. Soc. 93* (1971) 2573; cf. also R. Weiss, *Tetrahedron Lett. 1979*, 3295.
[10] Selenium-bridged dications, cf. G. Maas, B. Singer, *Chem. Ber. 116* (1983) 3659.
[11] Cf. G. Maas, P. J. Stang, *J. Org. Chem. 48* (1983) 3038.

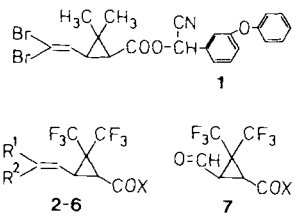
Synthesis of Bis(trifluoromethyl)-Analogues of the Pyrethroids**

By *Helmut Mack* and *Michael Hanack**

Dedicated to Professor Hans Jürgen Bestmann on the occasion of his 60th birthday

By systematic variation of the structure of the active substances of natural pyrethrums,[1] it has been possible over the past 15 years to develop highly active and, in particular, photostable pyrethroids, e.g. decamethrin **1**.[2] The structural modifications were primarily carried out in the ester components and in the side chain of the cyclopropanecarboxylate.[3] Almost all synthetic pyrethroids contain two geminal methyl groups on the cyclopropane ring, since these have a decisive influence on the insecticidal activity.[4]

We have now synthesized for the first time the pyrethroids **2–6** containing two trifluoromethyl groups, the corresponding caronaldehyde **7**, and the fenvalerate analogue **8d**.[5,6]



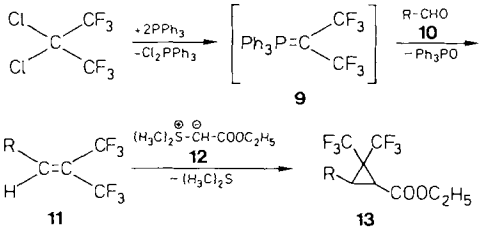
	R^1	R^2	2-8	X
2	Cl	Cl	**a**	OH
3	CH_3	CH_3	**b**	OC_2H_5
4	Br	Br	**c**	Cl
5	CF_3	CF_3	**d**	O–CH(CN)-3-C_6H_4–O–C_6H_5
6	Cl, CF_3			

Using our new method[5] for the synthesis of the Wittig reagent **9**,[7] the geminal 1,1-bis(trifluoromethyl)olefins **11a–c** employed as intermediates can be synthesized in a simple way in 61–83% yield. Reaction of the readily accessible 2,2-dichlorohexafluoropropane[8] with triphenylphosphane directly affords the thermally unstable phosphorus ylide **9**. This is generated in situ and immediately allowed to react with the aldehydes **10a**,[9] **10b**,[10] and **10c**[11] to give the new olefins **11a–c**.[5] In analogy to the Michael reaction, the sulfur ylide **12**[12] is added to **11a–c** in the β-position.

[*] Prof. Dr. M. Hanack, Dr. H. Mack
Institut für Organische Chemie der Universität
Lehrstuhl für Organische Chemie II
Auf der Morgenstelle 18, D-7400 Tübingen (FRG)

[**] *H. M.* thanks the Studienstiftung des Deutschen Volkes for a postgraduate scholarship.

Finally, γ-elimination of dimethyl sulfide leads to the compounds **13a–c** in 42–84% yield.[5] In all cases the *trans*-configuration predominates, to the extent of ca. 90–95%.



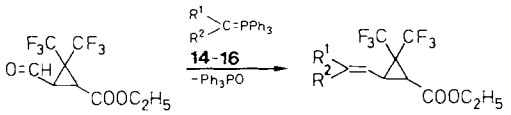
9

11 **13**

10, 11, 13	R	
a	$Cl_2C{=}CH$	**13a** ≡ **2b** → **2a**
b	$(CH_3)_2CH{-}CHCl$	**13b** → **3a**
c	$(C_2H_5O)_2CH$	**13c** → **7b**

Alkaline hydrolysis of the ester **13a** (≡ **2b**) leads to formation of **2a** (yield 94%); in the same way, the ester **13b** furnishes the carboxylic acid **3a** (yield 91%) in a one pot reaction under alkaline conditions. Cleavage of acetal from **13c** with acid furnishes the hexafluorocaronaldehyde **7b** in 93% yield.

7b is the central intermediate in the synthesis of substituted ethyl 3-(1-alkenyl)-2,2-bis(trifluoromethyl)cyclopropanecarboxylates. Reaction of **7b** with the phosphoranes **14**,[13] **15**,[5] and **16**[14] affords the pyrethroid esters **4b**, **5b**, and **6b**, respectively, in 43–95% yield;[5] these can be converted by acid hydrolysis into the pyrethroid acids **4a**, **5a**, and **6a**, respectively.

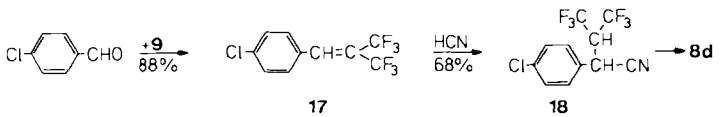


7b **4b,5b,6b**

	R^1	R^2
4, 14	Br	Br
5, 15	CF_3	CF_3
6, 16	{Cl, CF_3}	

The acid chlorides **2a** and **3c**, generated by reaction of sulfinyl chloride with **2a** and **3a**, respectively, are allowed to react with 2-hydroxy-2-(3-phenoxyphenyl)acetonitrile[15] to give the pyrethroids **2d** and **3d**.

A simple route was also found for the synthesis of the hexafluorofenvalerate **8d**. 4-Chlorobenzaldehyde reacts with the phosphorane **9**[5] to give the bis(trifluoromethyl)olefin **17**. Addition of hydrocyanic acid under basic conditions then leads to formation of the nitrile **18** (68% yield referred to overall conversion). 2-Hydroxyisobutyronitrile is a suitable reagent for supplying the HCN. Subsequent acid hydrolysis of **18** leads, via the carboxylic acid **8a** (94%) and in analogy to **2d**, to the fenvalerate analogue **8d**. All the new compounds were unequivocally characterized by ^{1}H-, ^{13}C-NMR, IR, and MS spectroscopy.[16]



17 **18**

Received: October 4, 1985;
revised: November 25, 1985 [Z 1485 IE]
German version: *Angew. Chem. 98* (1986) 181

CAS Registry numbers:
trans-**2a**, 99903-45-4; **2d**, 82224-37-1; *trans*-**3a**, 99903-46-5; **3d**, 99903-55-6; *trans*-**4a**, 99903-52-3; *trans*-**4b**, 99903-49-8; *trans*-**5a**, 99903-53-4; *trans*-**5b**, 99903-50-1; *trans*-**6a**, 99903-54-5; *trans*-**6b**, 99903-51-2; *trans*-**7c**, 99903-47-6; **8a**, 99903-58-9; **8b**, 82224-38-2; **10a**, 2648-51-3; **10b**, 53394-32-4; **10c**, 5344-23-0; **11a**, 99903-40-9; **11b**, 99903-41-0; **11c**, 99903-42-1; *trans*-**13a**, 99903-43-2; **13b**, 99923-35-0; *trans*-**13c**, 99903-44-3; **14a**, 42867-45-8; **14b**, 73607-10-0; **14c**, 99903-48-7; **17**, 99903-56-7; **18**, 99903-57-8; $(F_3C)_2CCl_2$, 1652-80-8; PPh_3, 603-35-0; $Me_2\overset{+}{S}CHCO_2Et$, 7380-81-6; PhO-3-$C_6H_4$CH(CN)OH, 39515-47-4; 4-$ClC_6H_4CHO$, 104-88-1.

[1] J. E. Casida (Ed.): *Pyrethrum, The Natural Insecticide*, Academic Press, New York 1973.
[2] M. Elliott: *Synthetic Pyrethroids*, Am. Chem. Soc., Washington 1977.
[3] R. Wegler (Ed.): *Chemie der Pflanzenschutz- und Schädlingsbekämpfungsmittel, Vol. 7*, Springer, Berlin 1981; D. Arlt, M. Jautelat, R. Lantzsch, *Angew. Chem. 93* (1981) 719; *Angew. Chem. Int. Ed. Engl. 20* (1981) 703.
[4] M. Elliott, N. F. Janes, *Chem. Soc. Rev. 7* (1978) 473.
[5] H. Mack, *Dissertation*, Universität Tübingen 1985.
[6] The derivatives **2–4** and **8** are in fact mentioned in a Japanese patent, but without any description of the synthesis and without any physical data. See Y. Katsuda, J. P. 8240440, Japan Kokai, Tokyo Koho; *Chem. Abstr. 97* (1982) 38559.
[7] D. J. Burton, Y. Inouye, *Tetrahedron Lett. 1979*, 3397.
[8] J. T. Maynard, *J. Org. Chem. 28* (1963) 112; B. S. Farah, E. E. Gilbert, *ibid. 30* (1965) 1241.
[9] M. Levas, E. Levas, *Bull. Soc. Chim. Fr. 26* (1959) 1800.
[10] A. Reinink, J. Grendelman, DOS 2641356; Shell Internationale Research Maatschappij B.V.; *Chem. Abstr. 87* (1977) 5398; C. L. Stevens, B. T. Gillis, *J. Am. Chem. Soc. 79* (1957) 3448; analogous procedure for the preparation of 2-chloro-2-methylpropanal.
[11] H. Stetter, K. H. Mohrmann, *Synthesis 1981*, 129.
[12] G. B. Payne, *J. Org. Chem. 32* (1967) 3351.
[13] E. J. Corey, P. L. Fuchs, *Tetrahedron Lett. 1972*, 3769.
[14] H. Havant, *Res. Discl. 219* (1982) 239, No. 21903.
[15] D. A. Pulman, *Pestic. Sci. 14* (1983) 182.
[16] Note added in proof (January 21, 1986): After completion of this work, Y. Kobayashi et al. (*Chem. Pharm. Bull. 33* (1985) 4085) reported the preparation of bis(trifluoromethyl)cyclopropane derivatives from hexafluorosenecioic acid ethyl ester.

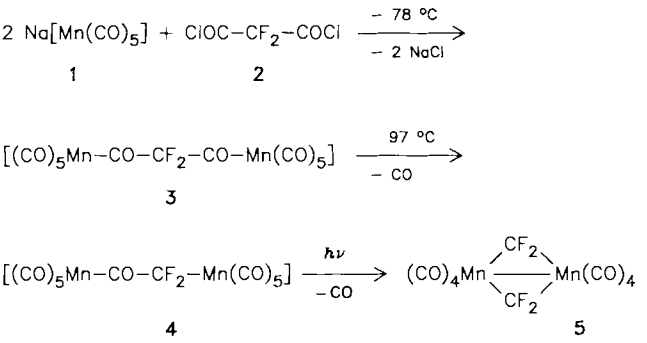
CF_2-Bridged Metal Complexes**

By *Wolfgang Schulze, Hans Hartl,* and *Konrad Seppelt**

CH_2-bridged metal complexes have been investigated extensively; they are of interest with regard to the mechanism of catalytic processes such as the Fischer-Tropsch synthesis.[1] In spite of the well-known analogy between CH- and CF-compounds very little is known about CF_2-bridged metal complexes, since the methods currently in use for the preparation of their CH_2-bridged counterparts are not suitable for CF_2-bridged complexes. *Seel* et al. have already described the complexes $[Co_2(CF_2)(CO)_7]$, $[Co_2(CF_2)_2(CO)_6]$, and $[Fe_2(CF_2)_2(CO)_7]$,[2,3] but without giving structural data. We report here, with two examples, a synthetic route which affords direct access to CF_2-bridged complexes, and the structural properties of such complexes.

[*] Prof. Dr. K. Seppelt, Dr. W. Schulze, Prof. Dr. H. Hartl
Institut für Anorganische und Analytische Chemie der
Freien Universität
Fabeckstr. 34–36, D-1000 Berlin 33

[**] This work was sponsored by the Fonds der Chemischen Industrie. We thank Dr. *D. Lentz* for kindly supplying a sample of trifluoromethyl isocyanide.



Sodium pentacarbonylmanganate **1** reacts with difluoromalonyl dichloride **2** to give the malonyl compound **3**, which decomposes almost completely upon heating, undergoing extrusion of one molecule of CO to give the difluoroacetyl complex **4**. Further heating leads only to the known complex $[(CO)_5MnCF_3]$. UV irradiation, however, gives $Mn_2(CO)_{10}$ and the doubly CF_2-bridged complex **5**. According to an X-ray structure analysis, **5** is highly symmetric (Fig. 1). The CO ligands *trans* to the CF_2 bridges are more tightly bound than the *cis* ligands.

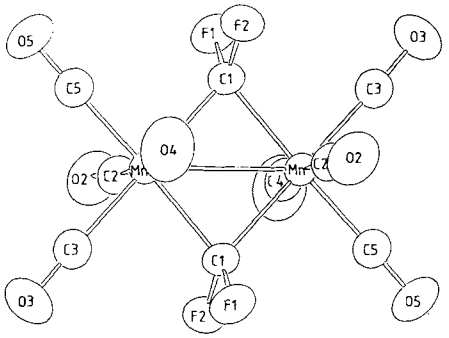
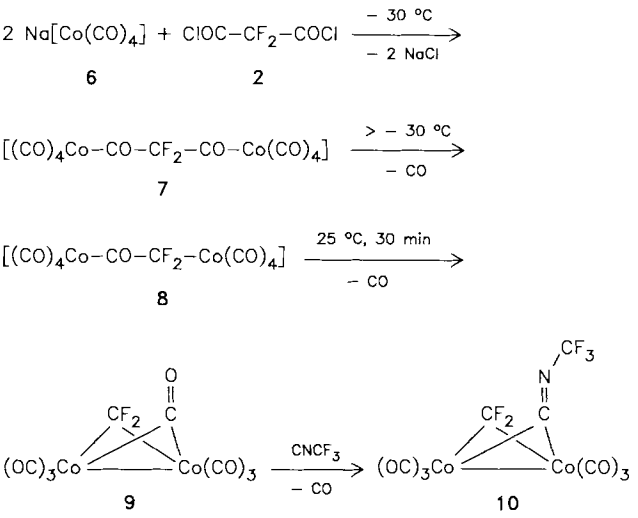


Fig. 1. Structure of $[(CO)_4Mn(\mu\text{-}CF_2)_2Mn(CO)_4]$ **5** in the crystal. Crystallographic data: $P2_1/n$, $a=8.367(2)$, $b=10.613(3)$, $c=7.996(2)$ Å, $\beta=90.01(2)$, $V=710.04$ Å^3, $Z=2$, $\rho_{calc}=2.03$ g·cm^{-3}, $\mu=8.9$ cm^{-3}, $R=0.020$, $R_t=0.033$; 3024 measured reflections, 1248 crystallographically independent observations with $I>2.0\sigma(I)$, 110 refined parameters. The manganese atoms essentially remain in an octahedral environment. Selected distances [Å] and angles [°]: Mn-Mn 2.664(3), Mn-C1 2.026(4), Mn-C2 1.880(6), Mn-C3 1.846(4), C1-Mn-C1 98.2(1), F1-C1-F2 102.7(2). Further details of the crystal structure investigation are available on request from the Fachinformationszentrum Energie, Physik, Mathematik GmbH, D-7514 Eggenstein-Leopoldshafen 2, on quoting the depository number CSD-51697, the names of the authors, and the full citation of the journal.

If sodium tetracarbonylcobaltate **6** is allowed to react with difluoromalonyl dichloride **2**, multiple elimination of CO already takes place at room temperature. The complexes **7** and **8** were only detected as intermediates by ^{19}F-NMR spectroscopy (**7**: $\delta(F)=-92.3$, **8**: $\delta(F)=-32.2$). The Co_2-complex **9** is formed as end product in high yields; the orange-yellow liquid is probably identical to the compound $[Co_2(CF_2)(CO)_7]$ described by *Seel* et al.[2] The ^{13}C-NMR spectrum of **9** (up to -40 °C) shows a singlet for the time-averaged equivalent CO groups as well as a triplet for the CF_2 group. In the ^{19}F-NMR spectrum the singlet line of the CF_2 group ($\delta=44.7$) does not change on lowering the temperature to -100 °C. The intramolecular CO exchange of all CO ligands must therefore be still rapid even at -100 °C.

The CO bridge, which obviously participates in the intramolecular exchange, can be replaced by the $CNCF_3$ ligand, which strongly prefers the bridge positions[4] (**9** → **10**). The two fluorine atoms of the CF_2 group of **10** are not equivalent; the coupling constant of the geminal fluorine atoms is quite small (12.2 Hz).



The method described here should, in principle, be of general utility for the introduction of CF_2 bridges.

Experimental

3: **2** (2.2 mmol) was added to a stirred solution of **1** [5] (4 mmol) in anhydrous oxygen-free tetrahydrofuran (THF) at -78 °C. After 2 hours' stirring, slow warming to room temperature, and removal of the solvent in a high vacuum, there remained a yellowish-orange greasy solid. The fraction soluble in CH_2Cl_2 was chromatographed on silica gel (4 × 60 cm column) with CH_2Cl_2/petroleum ether 40-60 (1 : 3) at 0 °C. **3** was eluted as an almost colorless zone. After crystallization from CH_2Cl_2/pentane at -40 °C, **3** was obtained as air-stable, pale yellow needles. Yield 445 mg (55%). M.p. 97 °C (dec.).—MS: *m/z* 496 ($M^{\oplus}$) and fragments. IR (pentane) ν(CO) = 2122 (m), 2067 (w), 2039 (vs), 2013 (s), 1641 (m, br) cm^{-1}. ^{19}F-NMR (CH_2Cl_2, $CFCl_3$ ext.): $\delta=-96.5$.

4: 1 mmol of **3** was melted in an argon atmosphere for 15 min at 97 °C, and evolution of gas was observed. After cooling down, the yellow-brown melt was dissolved in $CHCl_2$ and chromatographed at 0 °C on silica gel (4 × 60 cm column) with CH_2Cl_2/petroleum ether 40-60 (1 : 3). **4** was eluted as a yellow zone; air-stable, yellow crystals were obtained upon crystallization from CH_2Cl_2/pentane. Yield 398 mg (85%). M.p. 99 °C (dec.).—MS: *m/z* 468 ($M^{\oplus}$) and fragments. IR (pentane) ν(CO) = 2113 (s), 2038 (vs, sh), 2022 (s), 2007 (vs), 1967 (w), 1641 (m, sh) cm^{-1}. ^{19}F-NMR (CH_2Cl_2, $CFCl_3$ ext.): $\delta=-41.7$.

5: A solution of **4** (0.1 mmol) in pentane (250 mL) was irradiated with a Phillips immersion lamp (HPK 125 W) for 30 mins at 0 °C under inert gas in a circulated photolyzer. After removal of the solvent in a high vacuum, the yellowish orange residue was taken up in a few mL of CH_2Cl_2. The solution was chromatographed on silica gel in a medium-pressure column with pentane (column: 2.5 × 60 cm, Merck silica gel 0.015-0.040 mm). The second orange zone contained **5**. The pentane solution was evaporated down to ca. 10 mL; upon slow cooling of the solution to -50 °C, **5** was obtained as air-stable yellow crystals. Yield 5 mg (12%). M.p. 118 °C.—MS: *m/z* 434 ($M^{\oplus}$) and fragments. IR (pentane): ν(CO) = 2084 (s), 2035 (vs), 2028 (vs), 1985 (w) cm^{-1}. Raman (solid) ν(CO): 2121 (s), 2038 (vs), 2020 (vs), 2004 (m) cm^{-1}. ^{19}F-NMR (pentane, $CFCl_3$ ext.): $\delta=71.6$.

9: **2** (1.1 mmol) was added to a stirred solution of **6** [5] (2 mmol) in anhydrous oxygen-free diethyl ether (60 mL) at -30 °C. The solution turned yellowish-orange in color. After warming and 30 minutes' stirring, the solution was fractionally distilled under high vacuum. **9** was collected at -30 °C as a yellow, air-stable solid, m.p. -2 °C. **9** is thermally stable (up to 80 °C) and photochemically stable. Yield 325 mg (90%). The spectroscopic data (^{19}F-NMR, IR, and MS) were identical with the values given in the literature [2]. ^{13}C-NMR (CD_2Cl_2, TMS ext.): $\delta=200.5$ (CO), 194.1 (CF_2, $J(CF)=390$ Hz). ^{19}F-NMR (CD_2Cl_2, $CFCl_3$ ext.): $\delta=44.7$.

10: $CNCF_3$ (2 mmol) was condensed under high vacuum into a solution of **9** (2 mmol) in pentane (10 mL). The stirred solution was warmed to room temperature. Fractional distillation under high vacuum afforded **10** in the collector cooled at -60 °C; air-stable yellow crystals, m.p. -18 °C. Yield quantitative.—MS: *m/z* 431 ($M^{\oplus}$) and fragments. IR (pentane) ν(CO) = 2140 (s), 2110 (vs), 1990 (vs), 2038 (m), ν(CN) = 1720 (s, br) cm^{-1}. ^{19}F-NMR (pentane, $CFCl_3$ ext.): $\delta=43.3$, 26.1 (CF_2, $J=12.2$ Hz), -58.8 (CF_3). ^{13}C-NMR

(CD_2Cl_2, TMS ext., −25°C): δ = 196.0 (CO), 192.3 (CF_2, $^1J(CF)$ = 395 Hz), 236 (CN), 116.5 (CF_3, $^1J(CF)$ = 263 Hz.

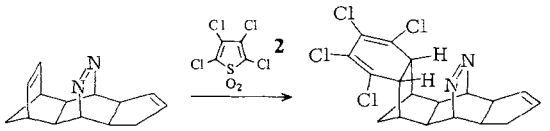
Received: October 9, 1985;
revised: December 2, 1985 [Z 1491 IE]
German version: *Angew. Chem. 98* (1986) 189

[1] W. A. Herrmann, *Adv. Organomet. Chem. 20* (1982) 159; *Angew. Chem. 94* (1982) 118; *Angew. Chem. Int. Ed. Engl. 21* (1982) 117.
[2] F. Seel, R. D. Flaccus, *J. Fluorine Chem. 12* (1978) 81.
[3] F. Seel, G. V. Röschenthaler, *Z. Anorg. Allg. Chem. 386* (1971) 297.
[4] J. Brüdgam, H. Hartl, D. Lentz, *Z. Naturforsch. B39* (1984) 721.
[5] R. B. King, *Adv. Organomet. Chem. 2* (1964) 158ff.

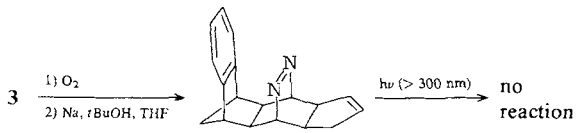
Laticyclic 1,5-Conjugation between Parallel, Neighboring Azo-Groups and Phenyl Groups**

By *Karin Beck* and *Siegfried Hünig**

Since the discovery of the first system **1**, with parallel oriented C=C/N=N bonds[1] with analyzed[2] laticyclic 1,5-conjugation,[3] general methods have been developed for the synthesis of related systems by [4+2]-Cycloadditions with cyclic azines as electron-deficient dienes.[4] It emerged thereby that the size of the ring (five-membered ring (5), six-membered ring (6)), which the π-bridges span, has no influence on the smooth [2+2]-photocyclization to diazetidines with a cage structure.[1a,5] This is valid in the case of C=C(5)/N=N(6) (e.g. **1**), C=C(6)/N=N(6), C=C(5)/N=N(5), and, as shown by **7**, also in the case of C=C(6)/N=N(5) (for further examples see ref. [6]). We have now checked whether a hitherto unknown [6+2]-photocyclization takes place upon replacement of the etheno-bridge by an *o*-phenylene bridge in these systems.



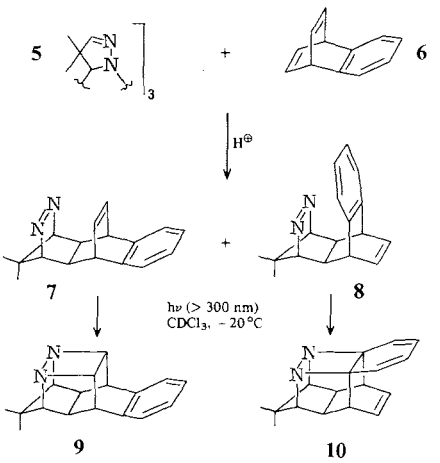
1 **3**



4

We report here on the first positive result.[7] The desired *o*-phenylene bridge can be incorporated with one of the cycloaddends (here benzobarrelene **6**) or by subsequent conversion of the double bond in a benzene ring.

The trimeric 4,4-dimethyl-4*H*-pyrazole **5** reacts under proton catalysis conditions[4] with **6** to give a 4:1 mixture of the adducts **7** and **8** (phenylene (6)/N=N(5)), which can be separated chromatographically.[8] The expected cycloadducts **9** and **10** are formed almost quantitatively (no by-products recognizable in the ^{1}H-NMR spectrum of the reaction solution) upon unsensitized irradiation ($\lambda > 300$ nm, $CDCl_3$, −20°C). As expected, **9** and **10** do

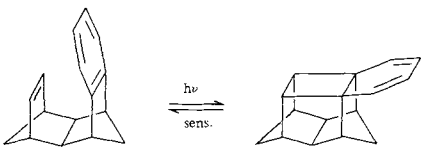


not show any absorptions UV for the azo group. In the ^{1}H-NMR spectrum ($CDCl_3$, δ values) the signals of the etheno bridge (5.93 (dd)) migrate into the region typical for diazetidines (4.08 (mc)) during the transition **7**→**9**, whilst those of the arene remain virtually stationary (7.06→7.25). Conversely, in the reaction **8**→**10** the signals of the olefinic protons of **10** (5.64, 5.88) appear in place of those of the arene (7.08), whereas those of the additional double bond remain virtually stationary (6.65 (dd)→6.23 (dd)). In addition, the signals of the protons on the bridgeheads of the azo bridges experience a typical upfield shift of ≈1.2 pm upon closure of the diazetidine ring: **7** (4.64 (bs))→**9** (3.42 (bs)); **8** (4.45 (bs))→**10** (3.19 (bs)). That is, both the interaction with the etheno bridge (cf. [2]) as well as that with the phenylene residue is so strong upon n-π*- and/or π-π*-excitation of the azo group that the extraordinarily efficient photoextrusion from the 2,3-diazabicyclo[2.2.1]heptene (Φ_{N_2} = 1.00[9]) present in **7** and **8** is completely overshadowed.[10] Interestingly, compound **4**, in which the bridges are, as it were, interchanged (phenylene(5)/N=N(6)), is not cyclized under the same irradiation conditions.[10] It remains unchanged, since it contains the photostable 2,3-diazabicyclo[2.2.2]octene skeleton.[2,9] The different interaction between the parallel π systems observable in the UV spectrum (in each case in hexane) corresponds to the difference in photochemical behavior. The bathochromic shift in **1** (λ_{max} = 396 nm (ε = 155))[1] of 15 nm compared to that in the same system with an ethano bridge **1** [2H] (λ_{max} = 381 nm (ε = 155))[4b] is only 6 nm in the case of the benzo derivative **4** (λ_{max} = 387 nm (ε = 185)). In contrast, the bathochromic shift of 9 nm in the transition from **7** [2H] (hydrogenated etheno bridge (λ_{max} = 354 (ε = 366)) to **7** (λ_{max} = 363 nm (ε = 370)) stays the same in the case of the benzo derivative **8** (λ_{max} = 364 nm (ε = 641)), while the intensity almost doubles.—**4**[11] is formed by addition of tetrachlorothiophene dioxide **2**[12] to **1** via the readily interceptable intermediate **3**, which, after smooth dehydrogenation,[13] is dehalogenated[15] in the conventional way[14] to **4**.

Of the systems with laticyclic 1,5-conjugation still to be examined, namely *o*-phenylene(6)/N=N(6) (which in the meantime has also attracted interest from another point of view[16]) and *o*-phenylene(5)/N=N(5), at least the latter is expected to photocyclize upon direct excitation. A photo-

[*] Prof. Dr. S. Hünig, Dipl.-Chem. K. Beck
Institut für Organische Chemie der Universität
Am Hubland, D-8700 Würzburg (FRG)

[**] This work was supported by the Deutsche Forschungsgemeinschaft, the Fonds der Chemischen Industrie, and BASF AG, Ludwigshafen (FRG).



11 **12**

equilibrium of the *o*-phenylene(5)/C=C(5) analogue **11** with the [6+2]cycloadduct **12** has already been observed, but only upon sensitized excitation.[17]

Received: October 17, 1985 [Z 1500 IE]
German version: *Angew. Chem. 98* (1986) 193

[1] a) Preliminary communication: W. Berning, S. Hünig, *Angew. Chem. 89* (1977) 825; *Angew. Chem. Int. Ed. Engl. 16* (1977) 777; b) W. Berning, S. Hünig, F. Prokschy, *Chem. Ber. 117* (1984) 1455.

[2] B. Albert, W. Berning, C. Burschka, S. Hünig, H.-D. Martin, F. Prokschy, *Chem. Ber. 114* (1981) 423.

[3] Cf. review: H.-D. Martin, B. Mayer, *Angew. Chem. 95* (1983) 281; *Angew. Chem. Int. Ed. Engl. 22* (1983) 283.

[4] a) K. Beck, A. Höhn, S. Hünig, F. Prokschy, *Chem. Ber. 117* (1984) 517; b) S. Hünig, F. Prokschy, *ibid. 117* (1984) 534.

[5] B. Albert, W. Berning, C. Burschka, S. Hünig, F. Prokschy, *Chem. Ber. 117* (1984) 1465.

[6] K. Beck, Dissertation, Universität Würzburg 1986.

[7] The structures of all the new compounds are consistent with their elemental analyses and UV, IR, ^{1}H-NMR, and ^{13}C-NMR spectra. The latter compare very well with those of the related systems already discussed in detail in the literature [1b, 4, 5].

[8] A mixture of **5** (500 mg, 1.74 mmol), trifluoroacetic acid (1.20 mL, 15.5 mmol) and **6** (802 mg, 5.20 mmol) was stirred for 1 d at RT. The crude product isolated with water/$CHCl_3$/K_2CO_3 was, after Kugelrohr distillation (25 °C/0.01 torr), separated several times (with heavy losses) by medium-pressure chromatography (petroleum ether/ethyl acetate (9 : 1); the products were sublimed at 60 °C/0.01 torr. Yield: 63 mg (5%) **7**, m.p. 147–148 °C, and 16 mg (1%) **8**, m.p. 158–159 °C.

[9] Cf. also P. S. Engel, D. W. Horsey, D. E. Keys, C. J. Nalepa, L. R. Soltero, *J. Am. Chem. Soc. 105* (1983) 7108, and references cited therein.

[10] An NMR tube containing **4**, **7** or **8** in $CDCl_3$ was secured to an immersion cylinder cooled to −20 °C and irradiated with a 150-W Hg-high-pressure lamp (Pyrex filter). On completion of reaction (^{1}H-NMR monitoring), the solvent was removed. The crude product, after purification on a silica gel column, was sublimed in vacuo. 30 mg of **7** (0.12 mmol) furnished 20 mg (67%) of **9**, m.p. 177–178 °C. 15 mg (0.06 mmol) of **8** yielded 8.6 mg (57%) of **10**, m.p. 130 °C (dec.).

[11] **4** was discussed in a lecture delivered at a conference convened by the Arbeitsgemeinschaft Organische Chemie at Bad Nauheim (FRG), October 4–6, 1984.

[12] M. S. Raasch, *J. Org. Chem. 45* (1980) 856.

[13] Since the dehydrogenation even takes place with atmospheric oxygen in boiling benzene, a dyotropic terminal-group transfer of hydrogen to the azo group could be at issue. This transfer has already been demonstrated in the case of a related system at 200 °C with an ethano group as neighbor (D. Ginsburg, M. Koral, *Tetrahedron 29* (1973) 2373.

[14] N. J. Hales, H. Heaney, J. H. Hollinshead, *Synthesis 1975*, 707.

[15] A mixture of **1** (1.01 g, 3.96 mmol) and **2** (841 mg, 3.96 mmol) in chloroform (10 mL), which was allowed to stand for 7 d at room temperature, afforded 1.61 g (101%) of **3** (^{1}H-NMR spectroscopically pure). Extraction of the solid yielded 1.40 g (88%) of **3**, m.p. 166–168 °C. A weak stream of air was passed through a solution of **3** (1.40 g, 3.48 mmol) in boiling benzene (50 mL) for 2 d. The product obtained upon evaporating the solution to dryness was purified by extraction with acetic acid; there remained 1.10 g (79%) of **4**[CI_4], m.p. 274–276 °C. The crude product obtained from **4**[CI_4] (0.250 mmol), Na (100 mg), and *t*BuOH (0.30 mL) in THF (4.00 mL) afforded, by the procedure given in ref. [14], 43 mg (66%) of **4** (m.p. 197–199 °C) after chromatography on silica gel and subsequent sublimation.

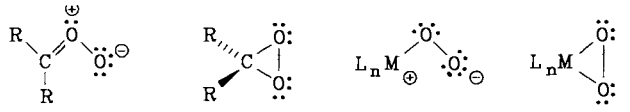
[16] The ^{13}C,^{13}C-coupling constants of the C atoms on the nitrogen bridges of the homologues of **4** and its azoxy derivative, which are accessible by means of our method, have recently been reported: H. Fritz, G. Fischer, W. Marterer, H. Prinzbach, *Tetrahedron Lett. 26* (1985) 4427.

[17] H. Prinzbach, G. Sedelmeier, C. Krüger, R. Goddard, H.-D. Martin, R. Gleiter, *Angew. Chem. 90* (1978) 297; *Angew. Chem. Int. Ed. Engl. 17* (1978) 271.

Thianthrene 5-Oxide as Mechanistic Probe in Oxygen Transfer Reactions: Substrate Complexation in Oxidations with Transition Metal Peroxides**

By *Waldemar Adam** and *B. Bhushan Lohray*

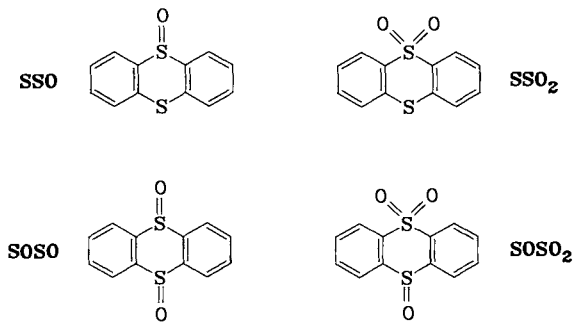
Recently, we succeeded in determining quantitatively the electronic character of oxidizing agents by employing oxygen transfer to thianthrene 5-oxide (**SSO**).[1] Thus, we showed that carbonyl oxides **1** and dioxiranes **2** are chemically different species.[2] Peroxo complexes of transition



1 **2** **3** **4**

metals can be represented, analogously to **1** and **2**, in terms of their dipolar structure **3** and the cyclic valence structure **4**, respectively.[3] Expectedly the terminal oxygen of **3** should be transferred more nucleophilically to thianthrene 5-oxide than by **4**. Prior complexation of the substrate at the metal center would, however, mask the electronic character of the oxygen transfer. A necessary condition for the use of thianthrene 5-oxide as mechanistic probe for the electronic character of a species is that the oxygen transfer takes place directly at the peripheral oxygen without prior complexation of the oxidizing agent. However, the question whether complexation of the substrate takes place in oxidations with transition-metal peroxides is presently being actively debated.[4] Consequently, the determination of the product pattern in the oxygen transfer by these peroxo complexes to thianthrene 5-oxide offers the unique opportunity of either gaining insight into the electronic character of these oxidizing agents or demonstrating prior complexation of the substrate at the transition metal center. Our present results (see a–d) suggest that thianthrene 5-oxide is first complexed by the metal at the sulfide sulfur and that the oxygen is transferred subsequently.

a) The diperoxo complexes (HMPT)CrO_5, (HMPT)MoO_5, (HMPT)$_2$$MoO_5$, (HMPT)($H_2O$)$MoO_5$, (HMPT)$WO_5$, and (HMPT)($H_2O$)$WO_5$ (HMPT = hexamethylphosphoric triamide) were allowed to react with thianthrene 5-oxide (**SSO**) in CH_2Cl_2 in the ratio 1 : 10, respectively. Independent of the transition metal and ligands, the amount of oxygen transfer to the sulfoxide sulfur to



[*] Prof. Dr. W. Adam, Dr. B. B. Lohray [+]
Institut für Organische Chemie der Universität
Am Hubland, D-8700 Würzburg (FRG)

[+] Alexander-von-Humboldt Fellow (1984/1985)

[**] This work was supported by the Deutsche Forschungsgemeinschaft, the Fonds der Chemischen Industrie, and the Stiftung Volkswagenwerk.

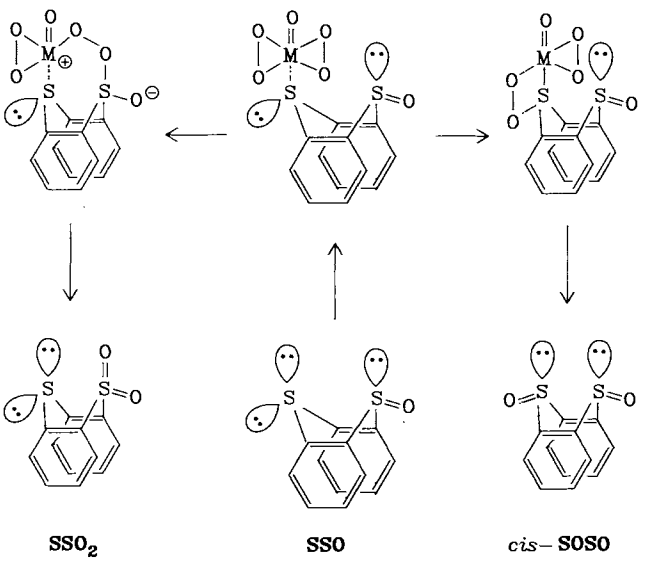
give the thianthrene 5,5-dioxide (**SSO_2**) and to the sulfide sulfur to give the thianthrene 5,10-dioxide (**SOSO**) was about equal (0.50 ± 0.05).

b) A competition experiment with an equimolar mixture of **SSO_2** and **SOSO** showed that **SOSO** was oxidized about three times more rapidly than **SSO_2** by (HMPT)MoO_5.

c) A ^{31}P-NMR spectrum, recorded immediately after mixing **SSO** and (HMPT)$_2MoO_5$ in $CDCl_3$, showed the presence of bound HMPT ($(\delta^{31}P) = 37.8$) and free HMPT ($(\delta^{31}P) = 28.2$) at ca. 37 °C. Precipitation of the metal peroxide by dilution with ether and immediate filtration afforded ca. 4% of oxidized thianthrene 5-oxide as a 1 : 1 mixture of **SSO_2** and **SOSO** in the filtrate.

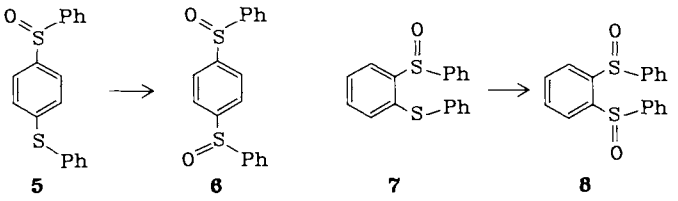
d) Only the *cis*-isomer of thianthrene 5,10-dioxide (*cis*-**SOSO**) was formed when **SSO** was oxidized with (HMPT)MoO_5 in CH_2Cl_2. As shown by control experiments, authentic *trans*-**SOSO** was stable under the conditions of the oxygen transfer and the HPLC analysis.

A plausible mechanism for these observations is outlined in Scheme 1. The metal center is first complexed at the nucleophilic sulfide sulfur of **SSO** by ligand exchange. Subsequently, the oxygen is transferred transannularly to the sulfoxide sulfur with formation of **SSO_2**. Oxidation at the complexed sulfide sulfur leads to *cis*-**SOSO**.



Scheme 1. Mechanism of complexation for oxygen transfer to thianthrene 5-oxide **SSO**.

Unexpected is the finding that the products **SSO_2** and *cis*-**SOSO** are formed in equal amounts. According to molecular models, in the well-known folded conformation of **SSO** the transannular oxygen transfer can take place comfortably. The steric shielding of the equatorial lone pair favors the required axial complexation at the sulfide sulfur by the *peri*-hydrogen atoms. This very special arrangement of the oxygen donor and oxygen acceptor also promotes formation of *cis*-**SOSO**. Peripheral attack without complexation would lead to *cis*- and *trans*-**SOSO**. A further prerequisite is presumably the necessary distance between the sulfoxide sulfur and the complexed molybdenum oxidizing agent. The following reactions support this concept: oxygen transfer with (HMPT)MoO_5 in CH_2Cl_2 to 1-(phenylsulfinyl)-4-(phenylthio)benzene **5** and to the *ortho* isomer **7** gave, besides traces of the trioxides (double oxygen transfer), exclusively the disulfoxides **6** and **8**, respectively. "Transannular" oxygen transfer in the case of the derivative **7** would lead to the sulfone. Hence, for transannular oxygen transfer to take place, the conformational arrangement of the sulfide lone pair to be complexed and its steric accessibility are also important, as well as the proper distance between the sulfur centers.



These conditions are apparently optimally fulfilled in the case of the rigid and folded thianthrene 5-oxide. This concept is further supported by the fact that a 1 : 1 mixture of *cis*- and *trans*-disulfoxide **8** was obtained in the oxidation of **7** with (HMPT)MoO_5,[5] whereas only *cis*-**SOSO** was formed from **SSO**, alongside **SSO_2**. We presume that both sulfide lone pairs can be complexed in the case of **7**, but only the axial lone pair in the case of **SSO** (Scheme 1). Furthermore, the almost exclusive oxidation of the substrates **5** and **7** at the sulfide sulfur reflects the electrophilic character[6] of the transition metal peroxides.

We postulate that for the transannular oxygen transfer (only *cis*-**SOSO**; 1 : 1 ratio of **SOSO** : **SSO_2**) to occur between thianthrene 5-oxide **SSO** and (HMPT)MoO_5 one can presume that the sulfide sulfur of the oxygen acceptor **SSO** must be complexed at the metal center of the oxygen donor (HMPT)MoO_5 during the oxygen transfer. Whether this complexation also takes place with other substrates (olefins, amines, phosphanes etc.) cannot be generalized.[4] The concept does, however, provide interesting possibilities for stereoselectively controlled oxygen transfer in synthesis.

Received: October 24, 1985;
revised: December 6, 1985 [Z 1508 IE]
German version: *Angew. Chem. 98* (1986) 185

[1] W. Adam, W. Haas, G. Sieker, *J. Am. Chem. Soc. 106* (1984) 5020.
[2] W. Adam, H. Dürr, W. Haas, B. B. Lohray, *Angew. Chem. 98* (1986) 85; *Angew. Chem. Int. Ed. Engl. 25* (1986) 101.
[3] H. Mimoun, *Angew. Chem. 94* (1982) 750; *Angew. Chem. Int. Ed. Engl. 21* (1982) 734.
[4] a) R. C. Michalson, R. E. Palermo, K. B. Sharpless, *J. Am. Chem. Soc. 99* (1977) 1990; b) P. Chaumette, H. Mimoun, L. Saussine, J. Fischer, A. Mitschler, *J. Organomet. Chem. 250* (1983) 291; c) R. Curci, S. Giannattasio, O. Sciacovelli, L. Troisi, *Tetrahedron 40* (1984) 2763; d) F. Di Furia, G. Modena, *Pure Appl. Chem. 54* (1982) 1852.
[5] G. Leandri, M. Pallati, *Bull. Sci. Fac. Chim. Ind. (Bologna) 14* (1956) 54.
[6] F. Di Furia, G. Modena, R. Seraglia, *Synthesis 1984*, 325.

Optically Active α-Chloro-(*E*)-crotylboronate Esters by Allyl Rearrangement

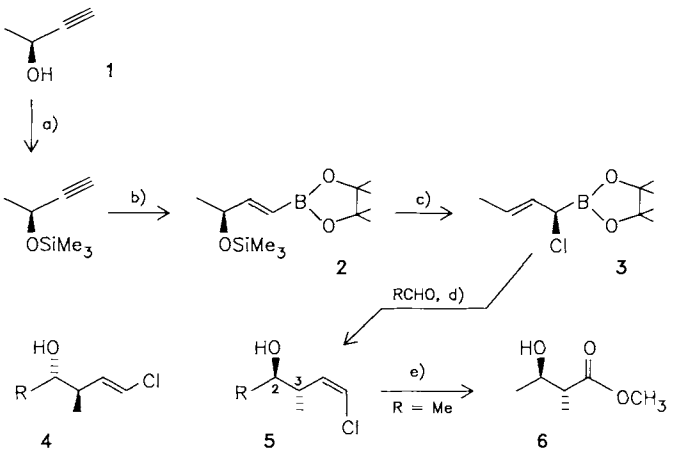
By *Reinhard W. Hoffmann** and *Stefan Dresely*

Esters of α-chloroallylboronic acid[1] belong to the α-chiral allylmetal compounds, whose addition to aldehydes proceeds with high or complete transfer of chirality.[2] Un-

[*] Prof. Dr. R. W. Hoffmann, Dipl.-Chem. S. Dresely
Fachbereich Chemie der Universität
Mans-Meerwein-Str., D-3550 Marburg (FRG)

fortunately, we were unable to synthesize the homologous α-chlorocrotylboronate **3** according to the method of *Matteson* et al.[3] We therefore developed an alternative route to **3** using an allyl rearrangement (Scheme 1). Racemic or optically active 3-butyn-2-ol **1** was silylated and hydroborated with dicyclohexylborane. The resulting alkenyldicyclohexylborane could be selectively oxidized[4] at the two alkyl-boron bonds with trimethylamine oxide to give the vinylboronate, which was transesterified with pinacol to give **2**. Subsequent reaction with sulfinyl chloride and attendant allyl rearrangement afforded the α-chloro-(*E*)-crotylboronate **3**, which was allowed to react without purification with a series of representative aldehydes.

Cleavage of the initially formed borates with nitrilotriethanol followed by chromatography on silica gel with petroleum ether/ethyl acetate furnished the homoallyl alcohols **5** (Table 1).



Scheme 1. a) Hexamethyldisilazane, quantitative; b) dicyclohexylborane/dimethoxyethane 0–25 °C, then 2 equiv. Me_3NO 25 °C, then 1 equiv. pinacol 25 °C, 80–85% yield; c) $SOCl_2$, petroleum ether 25 °C, ca. 75% yield; d) 12 h 20 °C, petroleum ether, work-up with nitrilotriethanol; e) O_3, CH_3OH.

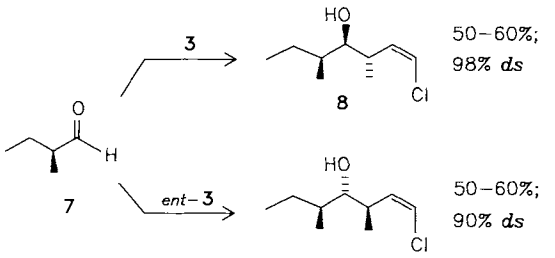
Table 1. Synthesis of homoallyl alcohols **5** according to Scheme 1. Yields based on **2**.

	R	Yield [%]	*ee* [%]
5a	C_6H_5	53–68	96 [a]
5b	CH_3	53–60	92 [b]
5c	C_2H_5	47–65	96 [b]
5d	$(CH_3)_2CH$	55–84	95 [b]
5e	n-C_5H_{11}	60–67	92 [c]

[a] Determined gas-chromatographically after conversion into the isopropylurethane [6]. [b] Determined gas-chromatographically as urethane after derivatization with (*S*)-(−)-1-phenylethyl isocyanate. [c] Determined as in [a] after hydrogenation of the double bond and hydrogenolytic cleavage of the C–Cl bond [1].

The double bond in **5** is *Z*-configurated, $^3J = 7$ Hz. The anti-configuration of the hydroxyl and methyl groups follows from the conversion of **5b** into the known[7] ester (−)-**6**. The absolute configuration of **5b** can thereby also be confirmed as being (2*R*,3*S*), which presumably arises from (*S*)-**1** via (*R*)-**3**.[1] The diastereomeric purity of the isolated products was, according to the ^{13}C-NMR spectra, 95%. However, the crude product was found to contain up to 5% of **4**, which was apparently removed during chromatography.

Thus, on starting from **1**, with 97% *ee*, the homoallyl alcohols **5a** or **5c** are formed with practically the same enantiomeric purity. Hence all steps proceed with a high level of chirality transfer. The slight racemization in the other cases could occur at the stage of **3**. Since both enantiomers of the butynol **1** can readily be obtained by simple resolution,[5] both enantiomers of the reagents **3** and the homoallyl alcohols **5** are accessible as well.



The quality of a chiral reagent is assessed on its ability to override a 1,2-asymmetric induction originating from a chiral aldehyde.[8] The extent of asymmetric induction originating from aldehyde **7**[9] revealed itself in the addition of the achiral (unsubstituted) (*E*)-crotylboronate ester, whereby the product with the same configuration as **8** is formed with a selectivity of 83%.[7] Here, the reaction of **7** with the chiral reagent **3** resulted in an increased diastereoselectivity of 98%. With *ent*-**3**, a reversal of stereocontrol could in fact be achieved to a considerable extent. In this case the selectivity is presumably limited by partial racemization (of either **3** or **7**).

Received: November 4, 1985;
supplemented: November 28, 1985 [Z 1519 IE]
German version: *Angew. Chem. 98* (1986) 186

[1] R. W. Hoffmann, B. Landmann, *Angew. Chem. 96* (1984) 427; *Angew. Chem. Int. Ed. Engl. 23* (1984) 437.
[2] M. M. Midland, S. B. Preston, *J. Am. Chem. Soc. 104* (1982) 2330; D. J. S. Tsai, D. S. Matteson, *Organometallics 2* (1983) 236; V. J. Jephcote, A. J. Pratt, E. J. Thomas, *J. Chem. Soc. Chem. Commun. 1984*, 800; T. Hayashi, *Chem. Scr. 25* (1985) 61; H. C. Brown, P. K. Jadhav, K. S. Bhat, *J. Am. Chem. Soc. 107* (1985) 2564.
[3] K. M. Sadhu, D. S. Matteson, G. D. Hurst, J. M. Kurosky, *Organometallics 3* (1984) 804.
[4] R. Köster, Y. Morita, *Justus Liebigs Ann. Chem. 704* (1967) 70.
[5] R. Weidmann, A. Schoofs, A. Horeau, *Bull. Soc. Chim. Fr. 1976*, 645.
[6] W. A. König, W. Francke, I. Benecke, *J. Chromatogr. 239* (1982) 227.
[7] R. W. Hoffmann, U. Weidmann, *Chem. Ber. 118* (1985) 3966.
[8] S. Masamune, W. Choy, J. S. Petersen, L. R. Sita, *Angew. Chem. 97* (1985) 1; *Angew. Chem. Int. Ed. Engl. 24* (1985) 1.
[9] Prepared by Swern oxidation of the alcohol with tri-*n*-butylamine as auxiliary base. For the rotation value see R. W. Hoffmann, H. J. Zeiss, W. Ladner, S. Tabche, *Chem. Ber. 115* (1982) 2357; and references cited therein.

Heteronuclear 'Star Clusters': $[Ni_2Pt_2W_4(\mu_3\text{-}CPh)_4(CO)_8(\eta\text{-}C_5H_5)_4]$ and $[Ni_2Pt_2W_4(\mu_2\text{-}CR)(\mu_3\text{-}CR)_3(CO)_8(\eta\text{-}C_5H_5)_4]$ (R = Ph or *p*-C_6H_4Me)**

By *Gregory P. Elliott, Judith A. K. Howard, Takaya Mise, Christine M. Nunn,* and *F. Gordon A. Stone**

Metal cluster compounds in which the metal atoms are ligated by CO, η-C_5H_5, tertiary phosphanes, and other π-

[*] Prof. Dr. F. G. A. Stone, G. P. Elliott, Dr. J. A. K. Howard, Dr. T. Mise, C. M. Nunn
Department of Inorganic Chemistry, University of Bristol
Bristol BS8 1TS (UK)

[**] This work was supported by the U.S.A.F. Office of Scientific Research (Grant 82-0070) and by the U.K. Science and Engineering Research Council.

acceptor groups have been the subject of intensive study for many years. The great majority of such species have structures in which the metal cores are based on polyhedra with triangular faces.[1] Less common are cluster compounds comprising chains of metal atoms, although the isolobal model[2,3] has been successfully applied to the systematic synthesis of species containing chains of platinum and tungsten atoms bridged by carbyne ligands.[4] During the course of studies in this area, we have discovered a new type of metal cluster species possessing a ring of eight metal atoms and involving three different transition elements.

Treatment of the trinuclear complexes **1a** and **1b**[4,5] in tetrahydrofuran at room temperature with $[Ni(cod)_2]$ affords the $Ni_2Pt_2W_4$-clusters **2** and **3**, or **4**, respectively.[6]

tion study. A band at 1838 cm^{-1} (CH_2Cl_2) in the infrared spectrum is assigned to the semi-bridging CO ligands.

The black isomeric species **3a** and **3b** are formed in equal amounts, and have closely related structures. This is clearly shown by the NMR data.[6] Thus, the $^{13}C\{^1H\}$-NMR spectrum of the isomeric mixture reveals that **3a** and **3b** each contain one edge-bridging and three triply-bridging CPh ligands. Moreover, the NMR data for the black isomers **4a** and **4b**[6,9] show that these species are structurally similar to **3a** and **3b**. An X-ray structure analysis, which was carried out on a crystal obtained from a solution of the mixture of **4a** and **4b**, showed that both isomers were present in the crystal.[10] The core structures of these asymmetric isomers are shown in Figure 2, together with the core of **2** for comparison. It will be seen that the difference between the asymmetric isomers lies in the disposition of the μ_2-CR ligand: in one isomer it bridges a Ni–W bond and in the other a Pt–W bond.

$$[PtW_2(\mu_2\text{-}CR)_2(CO)_4(\eta\text{-}C_5H_5)_2] \xrightarrow{[Ni(cod)_2]} [Ni_2Pt_2W_4(\mu_3\text{-}CPh)_4(CO)_8(\eta\text{-}C_5H_5)_4] + [Ni_2Pt_2W_4(\mu_2\text{-}CR)(\mu_3\text{-}CR)_3(CO)_8(\eta\text{-}C_5H_5)_4]$$

1a, R = Ph; **1b**, R = *p*-$C_6H_4CH_3$ — **2** — **3a**, **b**, R = Ph; **4a**, **b**, R = *p*-$C_6H_4CH_3$

According to an X-ray structural analysis, the core of the green cluster **2**[7] consists of a ring of eight metal atoms (Fig. 1). The four tungsten atoms form the points of a 'star', with the two nickel atoms *trans* to each other and the two platinum atoms *trans* to each other. The Ni···Pt separations (mean 2.763(3) Å) suggest little or no direct bonding between these metal atoms. Such distances are probably the consequence of the stereochemical demands of the μ_3-CPh groups.[8] The four carbyne groups occupy triply bridging sites with respect to the metal atoms, two being above and two being below the slightly puckered $Ni_2Pt_2W_4$ ring. The $^{13}C\{^1H\}$- and $^{195}Pt\{^1H\}$-NMR spectra of **2**[6] show, respectively, one resonance for the ligated μ_3-C nuclei and one signal for the platinum atoms. This is in accord with the symmetrical structure established by the X-ray diffrac-

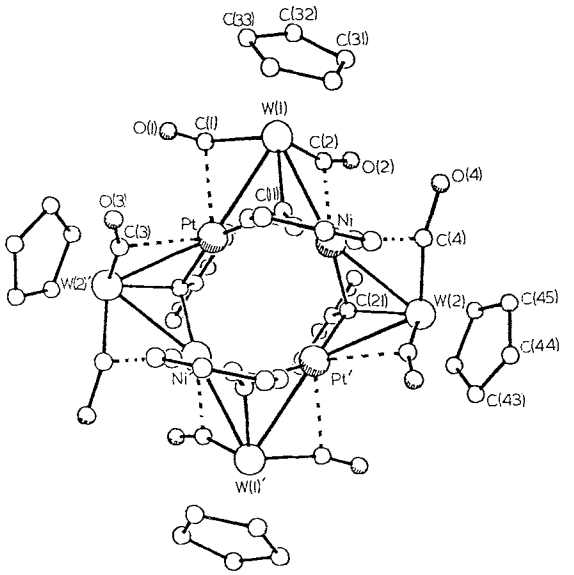


Fig. 1. Crystal structure of **2**. Selected bond lengths [Å] and angles [°] (mean values): Ni–W 2.646(3), Pt–W 2.741(2), Ni···Pt 2.763(3), μ_3-C–Ni 2.00(3), μ_3-C–Pt 2.09(3), μ_3-C–W 1.96(3); W–C–O 163.6.

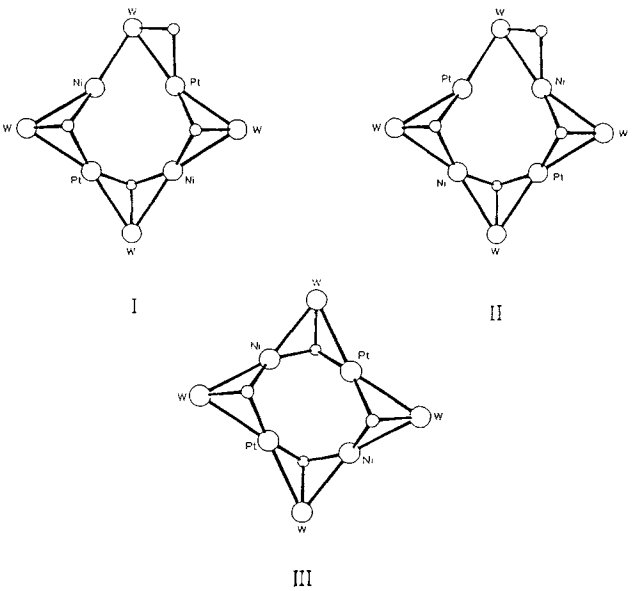


Fig. 2. The core structures of the cluster compounds **3** and **4** (I and II) and of **2** (III), showing the metal atoms and the ligated carbon atoms of the carbyne groups.

Several trimetal complexes have been described with two carbyne ligands occupying either edge or triply bridging sites,[11] and monotungstentriosmium compounds are known having two CR groups bicapping a WOs_3 tetrahedron.[12] Compounds **2**–**4** are the first reported examples of species having four bridging carbyne groups. Their preparation should lead to the discovery of new reactivity patterns for these ligands in a multinuclear metal environment. Moreover, the presence in these clusters of open rings of metal atoms and carbyne groups raises the interesting possibility of introduction of other molecules within

the cavities. In **2** the transannular Ni···Ni and Pt···Pt separations are 4.137 and 3.614 Å, respectively.

Received: November 19, 1985 [Z 1542 IE]
German version: *Angew. Chem. 98* (1986) 183

[1] B. F. G. Johnson (Ed.): *Transition Metal Clusters*, Wiley-Interscience, Chichester 1980; P. Chini, G. Longoni, V. G. Albano, *Adv. Organomet. Chem. 14* (1976) 285; B. F. G. Johnson, J. Lewis, *Adv. Inorg. Chem. Radiochem. 24* (1981) 255; B. F. G. Johnson, R. E. Benfield, *Top. Stereochem. 12* (1981) 253; E. L. Muetterties, *J. Organomet. Chem. 200* (1980) 177.

[2] R. Hoffmann, *Angew. Chem. 94* (1982) 725; *Angew. Chem. Int. Ed. Engl. 21* (1982) 711.

[3] F. G. A. Stone, *Angew. Chem. 96* (1984) 85; *Angew. Chem. Int. Ed. Engl. 23* (1984) 89.

[4] M. R. Awang, G. A. Carriedo, J. A. K. Howard, K. A. Mead, I. Moore, C. M. Nunn, F. G. A. Stone, *J. Chem. Soc. Chem. Commun. 1983*, 964; G. P. Elliott, J. A. K. Howard, T. Mise, I. Moore, C. M. Nunn, F. G. A. Stone, *J. Chem. Soc. Dalton Trans.*, in press.

[5] T. V. Ashworth, M. J. Chetcuti, J. A. K. Howard, F. G. A. Stone, S. J. Wisbey, P. Woodward, *J. Chem. Soc. Dalton Trans. 1981*, 763.

[6] The compounds were obtained in yields of ca. 60–80% after chromatography on alumina and crystallization. Although it was possible to separate **2** from **3a** and **3b**, it was not possible to separate **3a** from **3b**, nor **4a** from **4b**. Isomers **3a** and **3b**, and **4a** and **4b**, are formed in approximately equal amounts as deduced from peak intensities in the ^{13}C-NMR spectra.—Selected NMR data: **2** ($CDCl_3$): ^1H-NMR: $\delta = 5.05$ (C_5H_5); $^{13}C\{^1H\}$-NMR: $\delta = 299.4$ (μ_3-C); $^{195}Pt\{^1H\}$-NMR (to high frequency of $\Xi(^{195}Pt)$ 21.4 MHz): $\delta = 1246$.—**3a** and **3b**: ^1H-NMR ($CDCl_3$): $\delta = 4.58$, 4.81, 5.09, 5.13, 5.14, 5.15, 5.35, and 5.38 (C_5H_5); $^{13}C\{^1H\}$-NMR (CD_2Cl_2): $\delta = 325.6$, 313.6 (μ_2-C), 297.6, 297.3, 290.7, 287.7, 287.0, and 284.5 (μ_3-C); $^{195}Pt\{^1H\}$-NMR: $\delta = 1737$ ($J_{PtPt} = 410$ Hz), 1649 ($J_{PtPt} = 245$ Hz), 1138 ($J_{PtPt} = 410$ Hz), and 1005 ($J_{PtPt} = 245$ Hz). **4a** and **4b** (CD_2Cl_2), ^1H-NMR: $\delta = 4.61$, 4.84, 5.05, 5.09, 5.10, 5.12, 5.34 and 5.37 (C_5H_5); $^{13}C\{^1H\}$-NMR: $\delta = 326.4$, 314.0, (μ_2-C); 297.6, 297.2, 290.8, 288.2, 288.0, and 284.8 (μ_3-C); $^{195}Pt\{^1H\}$-NMR: $\delta = 1726$ ($J_{PtPt} = 410$, $J_{WPt} = 132$ Hz), 1641 ($J_{PtPt} = 234$ Hz), 1139 ($J_{PtPt} = 410$, $J_{WPt} = 117$ Hz), and 1002 ($J_{PtPt} = 234$ Hz).

[7] a) Monoclinic, space group $C2/c$ (No. 15), $Z = 4$, $a = 12.98(1)$, $b = 22.14(1)$, $c = 19.31(1)$ Å, $\beta = 93.77(6)°$, $V = 5533(7)$ Å^3; $\rho_{calc.} = 2.50$ g cm^{-3}, $F(000) = 3791$, $\mu(Mo_{K\alpha}) = 142.70$ cm^{-1}; $2\theta \leq 40°$ ($Mo_{K\alpha}$, $\lambda = 0.71069$ Å, $\theta - 2\theta$ scan, 293 K); 2356 absorption corrected reflections. Patterson method (Nicolet XTL), $R_1 = 0.068$, $R_2 = 0.072$ ($I \geq 1.0\sigma(I)$); b) further details for the crystal structure analysis are available on request from the Cambridge Crystallographic Data Centre, University Chemical Laboratory, Lensfield Road, Cambridge CB2 1EW (UK). Any request should be accompanied by the full literature citation for this communication.

[8] The clusters described herein are structurally different from a growing number of compounds with a 'raft' arrangement of metal atoms, e.g. $[Hg_3Os_9(CO)_{33}]$: M. Fajardo, H. D. Holden, B. F. G. Johnson, J. Lewis, P. R. Raithby, *J. Chem. Soc. Chem. Commun. 1984*, 24; $[Ir_3Pt_3(\mu\text{-}CO)_3(CO)_3(\eta\text{-}C_5Me_5)_3]$:M. J. Freeman, A. D. Miles, M. Murray, A. G. Orpen, F. G. A. Stone, *Polyhedron 3* (1984) 1093; $[Fe_3Pt_3(CO)_{15}]^{n-}$ (n = 1 or 2): G. Longoni, M. Manassero, M. Sansoni, *J. Am. Chem. Soc. 102* (1980) 7973. In these species the core consists of closed triangles of metal atoms with shared edges.

[9] In the synthesis of **4a** and **4b** there was evidence for the formation (ca. 10%) of a symmetrical cluster akin to **2**. However, it was not possible to isolate it; as expected it showed only a single resonance ($\delta = 1236$) in its $^{195}Pt\{^1H\}$-NMR spectrum.

[10] In the $Ni_2Pt_2W_4$ ring the tungsten sites are not disordered, but the nickel and platinum positions show 40:60% disorder with the platinum present in the μ_2-carbyne ring site 60% of the time. Triclinic, space group $P(\bar{1})$ (No. 2), $Z = 2$, $a = 11.853(4)$, $b = 12.796(5)$, $c = 21.76(1)$ Å, $\alpha = 105.85(5)$, $\beta = 89.80(4)$, $\gamma = 114.06(3)°$, $V = 2877(3)$ Å^3; $\rho_{calc.} = 2.62$ g cm^{-3}, $F(000) = 2027$, $\mu(Mo_{K\alpha}) = 138.21$ cm^{-1}; $2\theta \leq 50°$ ($\theta - 2\theta$ scan, 200 K); 5077 absorption corrected intensities. Current $R_1 = 0.100$, $R_2 = 0.106$ ($I \geq 5\sigma(I)$). See also [7b]. Selected bond lengths [Å] (mean values): W-Pt(Ni) 2.691(4), Ni···Pt 2.783(5), μ_3-C-W 1.96(5), μ_3-C-Pt(Ni) 2.02(5), μ_2-C-W 1.84(9), μ_2-C-Pt(Ni) 1.96(9).

[11] See, for example: K. P. C. Vollhardt, E. C. Walborsky, *J. Am. Chem. Soc. 105* (1983) 5507; J. R. Fritch, K. P. C. Vollhardt, *Angew. Chem. 92* (1980) 570; *Angew. Chem. Int. Ed. Engl. 19* (1980) 559; A. D. Clauss, J. R. Shapley, C. N. Wilker, R. Hoffmann, *Organometallics 3* (1984) 619; D. Nuel, F. Dahan, R. Mathieu, *ibid. 4* (1985) 1436; M. Lourdichi, R. Mathieu, *Nouv. J. Chim. 6* (1982) 231; G. A. Carriedo, J. C. Jeffery, F. G. A. Stone, *J. Chem. Soc. Dalton Trans. 1984*, 1597.

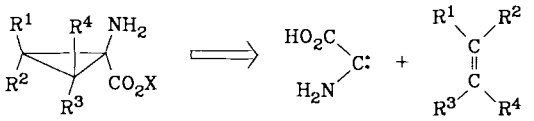
[12] J. T. Park, J. R. Shapley, M. R. Churchill, C. Bueno, *J. Am. Chem. Soc. 105* (1983) 6182.

Synthetic Equivalent for Aminocarboxycarbene; Synthesis of 1-Amino-1-cyclopropanecarboxylic Acid Methyl Esters

By *Ulrich Schöllkopf,* Manfred Hauptreif, Joachim Dippel, Martin Nieger,* and *Ernst Egert**

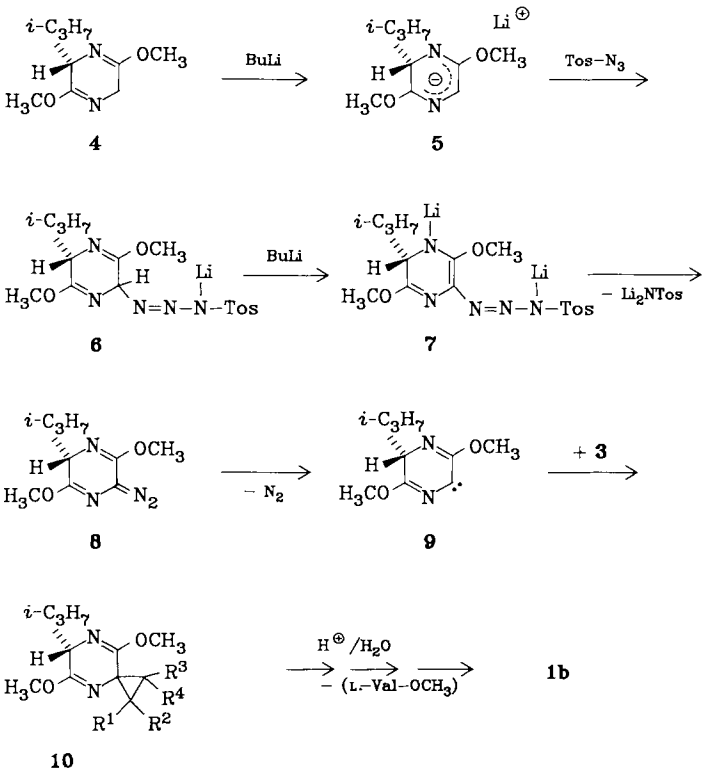
Dedicated to Professor Heinz A. Staab on the occasion of his 60th birthday

1-Amino-1-cyclopropanecarboxylic acids of type **1a** attract special interest because of their proven or potential biological activity.[1] Although conventional methods for the synthesis of this class of amino acids are already well known,[2–4] an entry to such compounds on a carbene basis in accordance with the reaction **2** + **3** → **1** is still lacking since there has so far been no synthetic equivalent available for aminocarboxycarbene **2**.



1a, X = H; **1b**, X = CH_3 **2** **3**

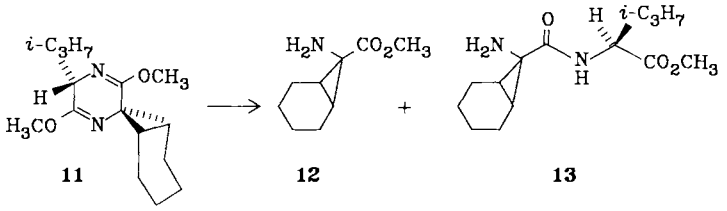
During studies on asymmetric amino acid syntheses with bislactim ethers of diketopiperazines[5] we have observed that a diazo-group transfer[6] can be carried out with tosyl azide in the case of lithiated bislactim ethers **5** of *cyclo*(L-Val-Gyl-), whereby the diazo compound **8**, the precursor of the carbene **9**, is formed. To achieve good yields of **8** it



4 **5** **6** **7** **8** **9** **10**

[*] Prof. Dr. U. Schöllkopf, Dipl.-Chem. M. Hauptreif, Dr. J. Dippel
Institut für Organische Chemie der Universität
Tammannstrasse 2, D-3400 Göttingen (FRG)
Dr. E. Egert, M. Nieger
Institut für Organische Chemie der Universität
Tammannstrasse 4, D-3400 Göttingen (FRG)

is essential to add a second equivalent of butyllithium after the addition of tosyl azide. Presumably, the dilithium compound **7**, which is stable at ca. −70°C, is formed as intermediate but loses dilithium tosylamide with formation of **8** upon warming to room temperature. If **8** is generated in the presence of an olefin, spiro compounds of type **10** are obtained, which can be hydrolyzed to methyl valinate and 1-amino-1-cyclopropanecarboxylic acid methyl esters of type **1b**. We postulate the carbene **9** as intermediate; this adds to the double bond of the olefin.[7] **9** contains a latent carboxy group and a latent amino group and is thus a synthetic equivalent for the synthon **2**.



11 **12** **13**

As typical example we describe the synthesis of the 7-aminobicyclo[4.1.0]heptane-7-carboxylic acid methyl ester **12** with *endo* amino group via the adduct **11** of the carbene **9** and cyclohexene.[8] The carbene addition takes place with high diastereoselectivity (ca. 49:1 in favor of **11**).[11] We were able to elucidate the configuration of **12** by X-ray structure analysis of the dipeptide ester **13** (cf. Fig. 1),[9] which precipitates as byproduct upon hydrolysis of **11**. If it is assumed that **9** is a singlet carbene with a

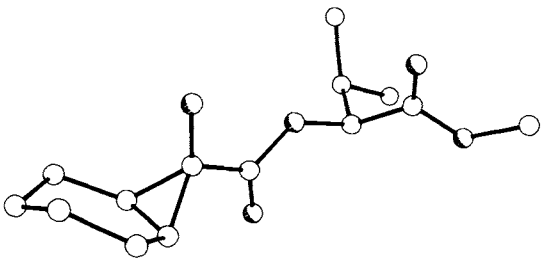


Fig. 1. Structure of the dipeptide ester **13** in the crystal [9]. Remarkably, the "envelope" conformation of the cyclohexane ring is apparently induced by the three-membered ring: One C atom is displaced 54 pm from the plane by the remaining ring atoms ($\sigma = 3$ pm). This is accompanied by a considerable widening of the bond angles in the cyclohexane ring ($113° < \alpha < 120°$).

vacant p-orbital perpendicular to the heterocycle plane, the olefins **3** should preferably enter from the *Re* side. In the case of olefins without a symmetry plane perpendicular to the double bond, optically active aminocyclopropanecarboxylic acids of type **1a** should be formed.

Experimental

11: *n*-Butyllithium (3.2 mmol; 2 mL of a 1.6 N solution in hexane) was added dropwise at −70°C to a solution of **4** (0.55 g, 3 mmol) [10] in tetrahydrofuran (5 mL). The mixture was stirred for 15 min and then transferred at −70°C via a Telefon tube into a solution of tosyl azide (0.59 g, 3 mmol) in THF (5 mL). After 2.5 hours' stirring at −70°C the reaction mixture was treated with *n*-butyllithium (3.2 mmol; 2 mL of a 1.6 N solution in hexane) such that the temperature did not rise above −70°C. After 30 minutes' stirring at −70°C the deep-red solution was transferred within 60 min through a Telefon tube (cooled with dry ice) into 30 mL of cyclohexene at room temperature. After 18 h the mixture was filtered, and the filter-cake washed twice with 50 mL of diethyl ether. The filtrate was washed twice with 30 mL of 5% aqueous sodium hydroxide and once with 30 mL of water. After drying over magnesium sulfate and removal of the solvent in a vacuum, 0.56 g (71%) of **11** was obtained; b.p. 80°C/0.005 torr (Kugelrohr distillation), diastereomeric ratio 49:1 [11]. IR (film): 1685 (C=N) cm^{-1}. ^{1}H-NMR ($CDCl_3$): $\delta = 0.75$ and 1.02 [2d, $J = 7.2$ Hz; 6H, $C(CH_3)_2$], 1.1-1.9 (m; 10H, CH_2 and CH), 1.95-2.40 [m; 1H, $CH(CH_3)_2$], 3.62 and 3.68 (2s; 6H, OCH_3), 4.14 (d, $J = 4$ Hz; 1H, 2-H). ^{13}C-NMR ($CDCl_3$): $\delta = 16.88$ and 18.79 (CH), 17.94, 18.53, 21.79 and 22.91 (CH_2), 22.25 and 23.31 (CH_3), 32.35 (CH), 43.03 (C_{quart}, C-2), 52.35 and 52.52 (CH_3), 61.46 (CH), 163.42 and 164.74 (C=N).

12: A mixture of **11** (0.264 g, 1 mmol), 0.25 N hydrochloric acid (8 mL), and THF (4 mL) was stirred for 7 d at room temperature. After washing with diethyl ether (2 × 10 mL), the aqueous phase was first treated with 20 mL of diethyl ether and then, with stirring, with concentrated ammonia solution until pH 9. The ether phase was separated off and the alkaline aqueous phase washed once again with ether (2 × 20 mL). After drying the combined ether phases over magnesium sulfate, the ether was removed in a vacuum. The residue was chromatographed on silica gel (low-pressure chromatography, silica gel 60, 500 × 15 mm column, eluted with ether/petroleum ether = 2:1); yield 72 mg (43%) of **12** as oil ($R_F = 0.5$) and 99 mg (38%) of the dipeptide ester **13** ($R_F = 0.4$) of m.p. 90-91°C. **12**, IR (film): 3375 and 3320 (N−H), 1720 cm^{-1} (C=O). ^{1}H-NMR ($CDCl_3$): $\delta = 1.0$-2.1 (m; 12H, NH_2, and alkyl-*H*), 3.63 (s; 3H, OCH_3). *N*-(3,5-dinitrobenzoyl) derivative: m.p. 177-178°C.

Received: November 8, 1985 [Z 1525 IE]
German version: *Angew. Chem. 98* (1986) 187

[1] a) K. Shiraishi, K. Konoma, H. Sato, A. Ichihara, S. Sakamura, K. Nishiyama, R. Sakai, *Agric. Biol. Chem. 43* (1979) 1753; b) D. H. Rich, J. P. Tam, *Synthesis 1978*, 46; c) I. Arenal, M. Bernabé, E. Fernández-Alvarez, A. M. Gibello, An. Quim. 79c (1983) 65; d) C. Walsh, R. A. Pascal, M. Johnston, R. Raines, D. Dikskit, A. Krantz, M. Honma, *Biochemistry 20* (1981) 7509; e) M. C. Pirrung, *J. Am. Chem. Soc. 105* (1983) 7207; M. C. Pirrung, G. M. McGeehan, *Angew. Chem. 97* (1985) 1074; *Angew. Chem. Int. Ed. Engl. 24* (1985) 1044.

[2] Cyclopropanation of derivatives of α,β-dehydroamino acids: a) U. Schöllkopf, R. Harms, D. Hoppe, *Justus Liebigs Ann. Chem. 1973*, 611; b) I. Arenal, M. Bernabé, E. Fernandez-Alvarez, M. L. Izqzierdo, S. Penades, *J. Heterocycl. Chem. 20* (1983) 607; c) S. W. King, J. M. Riordan, E. M. Holt, C. H. Stammer, *J. Org. Chem. 47* (1982) 3270; H. Kimura, C. H. Stammer, *ibid. 48* (1983) 2440.

[3] Cycloalkylation of glycine anion equivalents: B. Gallenkamp, R. Schröder, K. Luerssen, Eur. Pat. Anm. 30287 (1979); *Chem. Abstr. 95* (1981) 150043s [1b, c, e, 2a].

[4] Curtius rearrangement of cyclopropane-1,1-dicarboxylic acids: E. J. Baldwin, R. M. Adlington, B. J. Rawlings, *Tetrahedron Lett. 26* (1985) 481; M. L. Izquierdo, I. Arenal, M. Bernabé, E. Fernandes-Alvarez, *Tetrahedron 40* (1985) 215.

[5] U. Schöllkopf, *Pure Appl. Chem. 55* (1983) 1799; *Chem. Scr. 25* (1985) 105; in K. Streith, H. Prinzbach, G. Schill (Eds.): *Organic Synthesis: An Interdisciplinary Challenge*, Blackwell Scientific Publications, Oxford 1985, p. 101ff.

[6] M. Regitz, *Synthesis 1972*, 351.

[7] We consider the alternative route for formation of **10**, namely the addition of **8** to **3** followed by nitrogen elimination, as unlikely, since diazoalkanes tend not to add to isolated, unstrained or non-activated double bonds.

[8] Cyclopentene and cycloheptene react analogously. Other olefins were not investigated.

[9] **13**: colorless needles from *n*-hexane/acetone. Crystal dimensions: 0.6 × 0.2 × 0.1 mm^3, $P2_12_12_1$, $a = 965.7(1)$, $b = 1190.0(1)$, $c = 1304.2(1)$ pm, $V = 1.499$ nm^3, $Z = 4$, $\mu = 0.08$ mm^{-1} ($Mo_{K\alpha}$); 3524 measured reflections $2\theta_{max} = 50°$, 1104 symmetry independent reflections with $|F| > 3\sigma_F$ used for the solution of the structure (direct methods) and the structure refinement; C, N, and O atoms refined anisotropically, H atoms located by electron density difference determination and refined with a "riding" model (only the coordination of the H atoms of the amino group and the cyclopropane ring refined free). Further details of the crystal structure investigation are available on request from the Fachinformationszentrum Energie, Physik, Mathematik GmbH, D-7514 Eggenstein-Leopoldshafen 2, on quoting the depository number CSD-51698, the names of the authors, and the full citation of the journal.

[10] U. Schöllkopf, U. Groth, C. Deng, *Angew. Chem. 93* (1981) 793; *Angew. Chem. Int. Ed. Engl. 20* (1981) 798. The bislactim ether is commercially available from Merck-Schuchardt.

[11] Determined by capillary GC.

Kirk-Othmer Concise Encyclopedia of Chemical Technology. Edited by *M. Grayson* and *D. Eckroth*. John Wiley and Sons, New York 1985. xxxii, 1318 pp., bound, $ 172.85.—ISBN 0-471-86977-5.

The condensation of twenty-six volumes of information into a single reference volume is a formidable task, especially when not only text but also a large number of tables, figures, graphs, charts, formulas, and even pictures are involved. The editors of the renowned *Kirk-Othmer Encyclopedia of Chemical Technology* have achieved this goal in such a way that the abridgment, the *Concise Encyclopedia of Chemical Technology,* should find wide use, both by professionals as a single source of key information and as a guide to further literature and by students as a lucid introduction to the multifarious aspects of the chemical industry.

Each subject in the twenty-four main volumes and supplementary volume of the parent work has been condensed and, in some cases, updated. The entries include important chemical substances (acetaldehyde to zirconium), chemical processes (absorption to zone refining), and the many facets of chemical technology itself (from the manufacture of dyes and the processing of milk to the large-scale production of antibiotics and chemotherapeutic agents and the recent applications of genetic engineering). The curious reader will find discussions of the design of experiments, fine art examination and conservation, information retrieval, nomenclature, patents, recycling, regulatory agencies, trademarks and copyrights, and much more.

Only a small fraction of the original tables and figures remain, but those selected are the most important. Likewise, the number of references has been drastically reduced, but those given are fairly up-to-date and enable the reader to locate efficiently further sources of information. Moreover, the numerous formulas, subheadings, and cross-references, as well as the index, facilitate the search for specific facts. Lists of conversion factors, abbreviations, and unit symbols at the front and of nomenclature under some entries (for example, "Mass Transfer" and "Thermodynamics") further assist the reader.

The entry "Phosphorus Compounds" illustrates the amount of condensation involved. In the third edition of *Kirk-Othmer,* the subject is treated in fifty pages, which include eighteen tables and nine figures and conclude with sixty-seven references. The *Concise Encyclopedia* handles the subject in a little over two pages, three tables, and five general references (although the smaller print size and the larger pages roughly double the informational content per page). Nonetheless, the entry presents key information, including the physical properties of the phosphorus sulfides, halides, and oxides, the phosphorous acids, the phosphazenes and other phosphorus-nitrogen compounds, and phosphine and its derivatives as well as descriptions of their industrial preparation and main applications. Illustrated are the structures of the phosphorus oxo acids and the phosphorus sulfides along with a diagram of a plant for the production of phosphorus trichloride and phosphorus pentachloride.

Of course, any reference work that attempts to distill the essentials of so huge a body of information as that presented in *Kirk-Othmer*'s third edition is bound to disappoint at times. The individual reader will no doubt find the treatment of some topics too cursory and that of others too drawn out. Moreover, the explosive growth in the number of new chemical substances and the continual introduction of new technologies will outdate some entries. These limitations are inherent in any such work, however, and are more than outweighed by the sheer wealth of useful information that is presented here in a well-organized, clearly written manner. My only qualm is that the price may deter some, especially students, from purchasing the book, which, in order to be most useful, should be readily at hand.

David I. Loewus [NB 730 IE]
Angewandte Chemie, Weinheim

Chemistry of the Elements. By *N. N. Greenwood* and *A. Earnshaw*. Pergamon Press, Oxford 1984, 1542 pp., hardback, $ 95.00.—ISBN 0-08-022056-8

The appearance of a new textbook on a fundamental scientific discipline is an important literary occurrence. If the new work can establish itself, it will influence the knowledge and way of thinking of generations of students for years to come. The existing works have certainly done this, and the traces are generally easy to identify. The author's selection of material and his distribution of emphasis amongst the theoretical concepts can direct a mass of young talents towards certain areas while others remain apparently unattractive—at least they were to the author. Furthermore, it is the case that if standard works do not accomodate new material early enough, then the rising generation is educated in a certain language with inadequate teaching and learning aids while those learning in other languages are already getting to grips with new perspectives.

Such disadvantageous developments can only be avoided if genuine alternatives appear on the market and lead to fruitful competition. In this sense the appearance of the German translation of *Cotton* and *Wilkinson* was, in its day, the extraordinarily beneficial compensation for the failings of *Holleman-Wiberg* that was then unmistakably showing its age. This is not to imply that from then on everyone would be happy with the new style of textbook—it quickly becomes evident from edition to edition that many outmoded ideas may have been opposed too forcefully.

Greenwood and Earnshaw, which has been available from mid 1984 is a very remarkable book, quite aside from its natural rôle as a complement to the assortment of traditional texts. In a "test drive" over several months, this reviewer got so used to the new vehicle that he rarely wanted to bring the other models out of the garage. The book rarely disappointed, neither when complete chapters were used to refresh knowledge nor when "spot checks" were made to recall individual facts. Incidentally, it should be emphasized at the outset that, in spite of the title, this is a textbook of *inorganic chemistry*. This is true at any rate to the extent that no organic chemistry is included. Fortunately, fringe areas in all directions are considered so that practically no stone is left unturned in respect of the definition of inorganic chemistry, surprisingly dismissed in the foreword as an outmoded concept.

The greatest advantage of the book is that it has already taken into account the most up to date developments. The

extensive bibliography is spread through the text; its entries, both in the biographical/historical part and, not least, in the scientific/technical sections really do extend into 1983. Naturally, it would have been astounding if this success had been uniform and it must be said that, for example, more than 2 sentences (on p. 110) could have been wished on the natride ion, Na^-, and on the corresponding oxidation state of gold, Au^-, (on p. 1367); nor is the most recent technology in iron and steel production included. Yet such points are exceptions which require practically microscopic examination of the text.

Optically the text is well produced with pleasing formula depictions and clearly laid out tables and diagrams. Annoyingly, the latter are not free of mistakes: on p. 58 the caption is twiceover puzzling (H_2!). Blocks of text printed on a grey background emphasize special sections; for some people this will seem overdone since it breaks up the continuity of the text or at least renders it clumsy. The theoretical chapters and the selection of material show a distinct preference for the s and p block elements, to which 1000 of the total 1500 pages are given over. d and f block elements are banished to the last third of the book so that little space remains for their coordination and organometallic chemistry. However, this does not amount to being "anti Cotton and Wilkinson", since it is precisely in the chapters on the transition elements that the authors have striven to pick out the essential points from a superabundance of facts.

Ultimately the question must be posed whether the book leans toward molecular or solid state chemistry and whether it can be recommended to protagonists of either case. The answer must be that the former prevails. Here the book is best able to satisfy high expectations. However, in all the other passages too it makes fascinating reading material, especially for students in first or middle semesters, as well as for the practising chemist and the chemistry teacher.

The presentation of the book is pleasing and convenient; the English is pleasantly relaxed but still precise. The book could well be taken from the writing desk, if not straight into bed, at least as far as the sofa. For around DM 100 (in paperback) it is edifying entertainment, well worth the money.

Is a German translation desirable? For reasons already given in the introduction this would be an enrichment, assuming that the German version was immediately brought back up to date and that the language was kept as fluent as in the original so that nothing was lost in this respect. The book would then easily be in a position to compete with (the new) Holleman-Wiberg and Cotton and Wilkinson could only stay in contention so long as it too was modernized and reorganized.

In the introduction (by *R. J. Gillespie*) and in the authors' foreword referred to above, it transpires that "Chemistry of the Elements" breaks with the tradition of British and American textbooks insofar that it is concerned more with timeless facts and phenomena, which theoretical concepts can be measured against and directed towards. This is supposed to stimulate the curiosity without which future research cannot thrive. As is well known, this approach is not so novel in German textbooks and so this newcomer fits well into our landscape.

Professor *Greenwood* was distinguished in 1983 with one of the major awards of the German Chemical Society. He would have deserved it for this textbook alone, even if many of the modern results about boron compounds were not based on his scientific work. In the circumstances no one would begrudge the fact that the chapter on boron hydride compounds has turned out too long.

Hubert Schmidbaur [NB 688 IE]
Anorganisch-chemisches Institut
der Technischen Universität München (FRG)

The Chemistry of the Catalyzed Hydrogenation of Carbon Monoxide. By *G. Henrici-Olivé* and *S. Olivé*. Springer Verlag, Berlin 1984. x, 231 pp., hardback, DM 146.00.— ISBN 3-540-13292-9

The oil crisis and a looming oil shortage have brought about strong growth in the interest in carbon monoxide derived from coal. In recent years various monographs concerned with the hydrogenation of carbon monoxide have already appeared. Thus, duplications in the description of CO hydrogenation reactions were inevitable. The book at hand, which deals with the literature up to the beginning of 1984, gives a good survey of the present state, and of the problems encountered in homogeneous and heterogeneous catalytic hydrogenation of CO. Mechanistic considerations assume a central position, and the chemistry of organometallic complexes stands, to a certain degree, at the center of attention. The attempt to build a bridge between molecular chemistry and possible surface species is successful. The authors have been able to choose the essential aspects of the relevant coordination chemistry from the extensive literature and have illustrated clearly the "metal-organic zoo" of possible surface compounds by model reactions. Here the book is of great value.

In 11 chapters the following areas are covered: *Transition metal-hydrogen/carbon monoxide interactions:* those reactions that are seen as significant in the hydrogenation of CO, e.g. hydride formation, CO coordination and CO bond cleavage are introduced in two opening chapters. *Non-catalytic interactions of CO with H_2:* apart from mechanistic aspects of the interaction of CO and H_2, the formation of formyl-, formaldehyde-, methoxy-, and carbide complexes is dealt with. *Key reactions in catalysis:* this chapter is devoted to certain key reactions, e.g. insertion of CO, formaldehyde and olefins, as well as elimination of hydrogen and the influence of ligands. *Catalysts and supports:* here the interactions of molecular complexes with carriers is presented. *Methanation:* after the first part of this book has mainly been concerned with model reactions, the consideration of catalytic processes begins with methanation. Again, mechanistic aspects such as carbide mechanism and CO insertion mechanism are the central themes. *Methanol from CO and H_2:* the homogeneous and heterogeneous catalysis of methanol formation is described in this very short chapter. *Fischer-Tropsch synthesis:* this is the longest chapter. Alongside model reactions stand such technical parameters as the influence of pressure and temperature. *Homogeneous CO hydrogenation:* in the first section hydroformylation is introduced, in the second, the formation of polyalcohols. *Methanol as raw material:* this chapter, which is concerned with the homologation and conversion of methanol on zeolites, does not entirely fit in the supposed context of CO-hydrogenation. *Attempt of unified view:* In this chapter an attempt is made to simplify the general problem of CO hydrogenation from a mechanistic standpoint.

For those interested in the chemistry of organometallic complexes, the book contains many well known reactions. Nevertheless, the purchase of this book can be recommended on account of its comprehensive approach. It of-

fers an abundance of information about model reactions of organometallic compounds to the chemist or physicist working in the field of heterogeneous hydrogenation of CO.

Willi Keim [NB 691 IE]
Institut für Technische Chemie und Petrolchemie
der Technischen Hochschule Aachen (FRG)

New Books

The following books have been received by the editor. All the publications listed are available through W & P Buchversand für Wissenschaft und Praxis, Boschstrasse 12, D-6940 Weinheim (Federal Republic of Germany). Tel. (06201) 606-0, Telex 465516 vchwh d, Telefax (06201) 602328.

Recent Developments in the History of Chemistry. Edited by *C. A. Russell*. The Royal Society of Chemistry, London 1985. x, 333 pp., bound, £ 27.50.—ISBN 0-85186-917-3

Organic Photochemistry, Vol. 7. Edited by *A. Padwa*. Marcel Dekker, New York 1985. xi, 498 pp., bound, $ 89.75 (USA and Canada), $ 107.50 (all other countries).—ISBN 0-8247-7421-3

Symmetry in Bonding and Spectra. An Introduction. By *B. E. Douglas* and *C. A. Hollingsworth*. Academic Press, Orlando, Florida 1985. xii, 456 pp., bound, $ 39.00.—ISBN 0-12-221340-8

The Biology of Crustacea. Series Editor: *D. E. Bliss*. **Vol. 9: Integument, Pigments, and Hormonal Processes.** Volume Editors: *D. E. Bliss* and *L. H. Mantel*. Academic Press, Orlando, Florida 1985. xxix, 550 pp., bound, $ 79.00.—ISBN 0-12-106409-3

Methods in Enzymology. Series Editors: *S. P. Colowick* and *N. O. Kaplan*. Academic Press, Orlando, FL 1985. **Vol. 109: Hormone Action, Part I: Peptide Hormones.** Edited by *L. Birnbaumer* and *B. W. O'Malley*. xxviii, 891 pp., bound, $ 85.00.—ISBN 0-12-182009-2; **Vol. 110: Steroids and Isoprenoids. Part A.** Edited by *J. H. Law* and *H. C. Rilling*. xxv, 460 pp., bound, $ 55.00.—ISBN 0-12-182010-6

Advances in Chemical Physics. Series Editors: *I. Prigogine* and *S. A. Rice*. **Vol. LVIII: Tagged-Particle Motion in Dense Media: Dynamics Beyond the Boltzmann Equation.** By *T. Keyes* and *A. J. Masters*. ix, 381 pp., bound, £ 87.25.—ISBN 0-471-81349-4; **Vol. LIX: Index Volumes I-LV.** Edited by *P. L. Radloff*. 376 pp., bound, £ 92.50.—ISBN 0-471-80427-4; **Vol. LX: Photodissociation and Photoionization.** By *K. P. Lawley*. John Wiley, Chichester 1985. ix, 474 pp., bound, £ 47.50.—ISBN 0-471-90211-X

Specialist Periodical Reports. Organometallic Chemistry. Vol. 13. A Review of the Literature Published During 1983. By *E. W. Abel* and *F. G. A. Stone*. The Royal Society of Chemistry, London 1985. xv, 491 pp., bound, £ 82.00.—ISBN 85186-611-5

Chemistry of Hydrocarbon Combustion. By *D. J. Hucknall*. Chapman and Hall, London 1985. viii, 415 pp., bound, £ 39.50.—ISBN 0-412-26110-3

The Hirn System. Nomenclature of Organic Chemistry. Principles. By *K. Hirayama*. Springer-Verlag, Berlin 1985. ix, 149 pp., bound, DM 138.00.—ISBN 3-540-15031-5

Ecological Studies. Analysis and Synthesis. Series Editors: *W. D. Billings, F. Golley, O. L. Lange, J. S. Olson, H. Remmert*. **Vol. 52: Air Pollution by Photochemical Oxidants. Formation, Transport, Control, and Effects on Plants.** Edited by *R. Guderian*. Springer-Verlag, Berlin 1985. xi, 346 pp., bound, 158.00.—ISBN 3-540-13966-4

Chemical Analysis. Series Editors: *P. J. Elving, J. D. Winefordner*, and *I. M. Kolthoff*. John Wiley, Chichester 1985. **Vol. 76: Receptor Modeling in Environmental Chemistry.** By *P. K. Hopke*. vii, 319 pp., bound, £ 86.75.—ISBN 0-471-89106-1; **Vol. 77: Molecular Luminescence Spectroscopy. Methods and Applications: Part 1.** Edited by *S. G. Schulman*. x, 826 pp., bound, £ 98.25.—ISBN 0-471-86848-5; **Vol. 78: Inorganic Chromatographic Analysis.** Edited by *J. C. Macdonald*. xiii, 450 pp., bound, £ 75.20.—ISBN 0-471-86263-0; **Vol. 79: Analytical Solution Calorimetry.** Edited by *J. K. Grime*. xvi, 401 pp., bound, £ 69.40.—ISBN 0-471-86942-2

Practical Approach Series. Series Editors: *D. Rickwood* and *B. D. Hames*. **Affinity Chromatography: A Practical Approach.** Edited by *P. D. G. Dean, W. S. Johnson*, and *F. A. Middle*. IRL Press, Oxford 1985. xv, 215 pp., paperback, £ 11.00.—ISBN 0-904147-71-1

Registered names, trademarks, etc. used in this journal, even without specific indication thereof, are not to be considered unprotected by law.

© VCH Verlagsgesellschaft mbH, D-6940 Weinheim, 1986. – Printed in the Federal Republic of Germany by Zechnersche Buchdruckerei, Speyer/Rhein.

All rights reserved (including those of translation into foreign languages). No part of this issue may be be reproduced in any form – by photoprint, microfilm, or any other means – nor transmitted or translated into a machine language without written permission from the publishers. Only single copies of contributions, or parts thereof, may be reproduced for personal use.

Valid for users in the USA: The appearance of the code at the bottom of the first page of an article in this journal (serial) indicates the copyright owner's consent that copies of the article may be made for personal or internal use, or for the personal or internal use of specific clients. This consent is given on the condition, however, that the copier pay the stated per-copy fee through the Copyright Clearance Center, Inc., for copying beyond that permitted by Sections 107 or 108 of the U.S. Copyright Law. This consent does not extend to other kinds of copying, such as copying for general distribution, for advertising or promotional purposes, for creating new collective works, or for resale. For copying from back volumes of this journal see 'Permissions to Photo-Copy: Publisher's Fee List' of the CCC.

Editorial office: Pappelallee 3, D-6940 Weinheim, Federal Republic of Germany, Telephone (06201) 602315, Telex 465516 vchwh d, Telefax (06201) 602328.

Editor: *P. Gölitz*.

Associate editors: *D. I. Loewus, A. Stimson*. **Editorial assistant:** *E. Scheuermann*.

Publishers: VCH Verlagsgesellschaft mbH. (Managing Directors: *Prof. Dr. Helmut Grünewald* and *Hans Dirk Köhler*), Pappelallee 3, D-6940 Weinheim, Federal Republic of Germany. Correspondence concerning advertisements should be addressed to VCH Verlagsgesellschaft mbH. (Advertising Manager *R. J. Roth*), Boschstr. 12, P.O. Box 1260/1280, D-6940 Weinheim, Federal Republic of Germany, Telephone Weinheim (06201) 602-0, Telex 465516 vchwh d, Telefax (06201) 602328.

ANGEWANDTE CHEMIE
International Edition in English
Volume 25 · Number 3
March 1986
Pages 197–296

Cluster Beam Chemistry—from Atoms to Solids

By T. Patrick Martin*

How do the properties of a solid gradually evolve as atoms are brought together to form increasingly larger units? In order to answer this question one must study aggregates of atoms too large to be called molecules but still too small to have even the structure of a crystal. Recent advances in both theory and experiment have made possible some first explorations in this long neglected but fascinating field of study. This review will emphasize the generation, growth, and properties of homo- and heteronuclear clusters in the vapor phase, particular attention being paid to mass spectrometric investigations.

1. Introduction

Recently it has become possible to produce and detect aggregates of atoms varying continuously in size from two to several hundred atoms. Because these aggregates have attracted wide-ranging attention, a colorful but confusing array of terms has been used to describe them, including small particles, microclusters, grains, oligomers, specks, and microcrystals. Considering this state of affairs it is best to define several terms as they will be used in this article. A ring of eight sulfur atoms or a tetrahedron of phosphorus atoms cannot with good conscience be called a cluster. Such stable units exist in the vapor, liquid, and solid phases and have long been called *molecules*. Because molecules are readily available, their proerties are usually well investigated. The term *cluster* will be reserved for atom aggregates that are not found in appreciable numbers in an equilibrium vapor. Clusters therefore represent new objects for investigation (Fig. 1).[1–4]

Clearly this use of the word cluster differs from that employed for many years to describe several classes of new crystalline cluster compounds.[5–8] However, one of the objectives of cluster beam research is to determine whether these units, already identified in solids, can also exist as isolated clusters or even as clusters of clusters in the vapor phase.

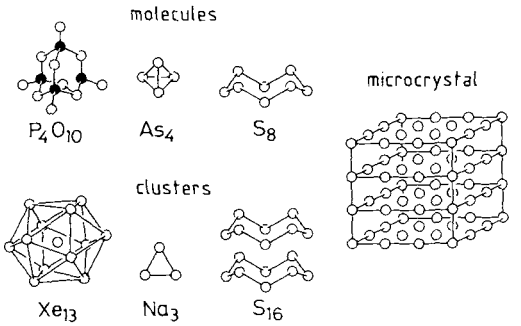


Fig. 1. Molecules, clusters, and a microcrystal. Clusters do not exist in equilibrium vapors. Microcrystals have the symmetry of the crystalline bulk substance.

After a cluster reaches a critical size, it is no longer free to rearrange its structure each time a new atom is added. A final lattice structure becomes frozen into the cluster. This crystallization may occur for aggregates containing less than 100 atoms. Still it is convenient and meaningful to give these aggregates a new name, *microcrystals*, because deviations from the bulk structure can be described as a surface relaxation.

Why are the properties of clusters of interest? We would like to understand the crystal growth process on a microscopic level. Everytime a new atom or molecule condenses

[*] Dr. T. P. Martin
Max-Planck-Institut für Festkörperforschung
Heisenbergstrasse 1, D-7000 Stuttgart 80 (FRG)

 © VCH Verlagsgesellschaft mbH, D-6940 Weinheim, 1986 0570-0833/86/0303-0197 $ 02.50/0

onto a cluster, the atoms in the cluster completely rearrange themselves; the cluster "reconstructs." We would like to know the sequence of structures a cluster assumes as it grows from a molecule into a crystal.

Another reason for studying clusters is to learn how the electronic band structure of a solid develops. This is represented in Figure 2 by a simple Hückel calculation of the electronic energy levels of silicon clusters with increasing size. It is of interest to observe how the discrete levels coalesce to form bands and at what stage a distinct gap appears between filled and unfilled states.

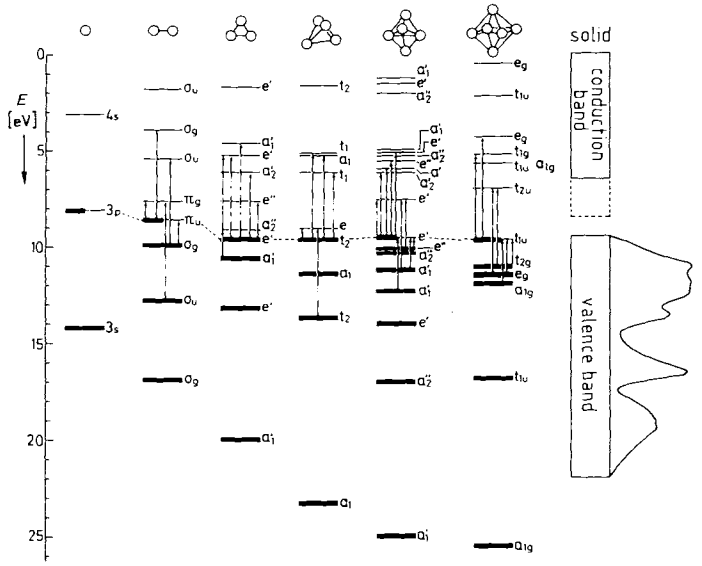


Fig. 2. Calculated electronic energy levels of Si atoms and clusters.

A question often asked is, how many metal atoms are required to form a cluster that has metallic properties? One characteristic property of a metal is its optical response, i.e., its interaction with light. A single Li atom has a very simple absorption spectrum, consisting of essentially one line in the visible (Fig. 3). This absorption can be well described as a one-electron transition from a 2s to a 2p state. A lithium crystal, on the other hand, has a completely different absorption spectrum. The absorption is strong in the far-infrared, goes through a minimum in the visible, and rises again in the ultraviolet (Fig. 3). The reason for the strong far-infrared absorption is that very low energy photons can excite electrons from the continuum of states just below the Fermi energy to states just above the Fermi energy. The strong UV absorption is caused by interband transitions. Suppose we chip off a small corner of the crystal, producing a microcrystal that contains only 50 atoms. The absorption spectrum changes completely. A relatively broad absorption maximum appears in the visible (Fig. 3). This absorption is due to a plasmon excitation, i.e., a collective excitation of outer electrons. The Li crystal also exhibits plasmon excitations, but these excitations have a longitudinal character and do not couple to transverse light waves. In the microcrystal one can consider a plasmon as a collective sloshing motion of the electrons from one side of the microcrystal to the other. Obviously, such a motion has a strong dipole moment, thus giving rise to the strong absorption band in the visible. The absorption of light by a Li atom is well described within the one-electron picture. However, this picture cannot describe even qualitatively the plasmon excitations that dominate the optical response of a 50-atom cluster. Between a few atoms and 50 atoms, we must completely change our way of looking at optical response. Clusters offer us the opportunity of studying this transition.

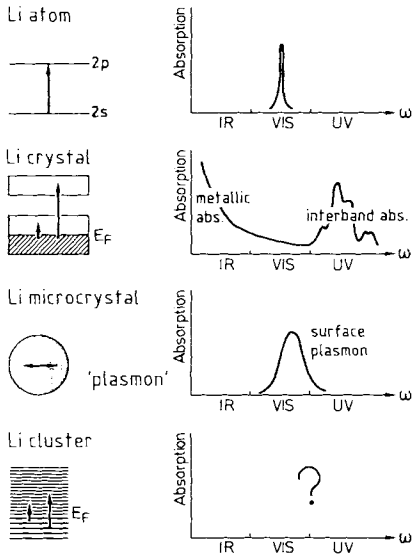


Fig. 3. Absorption of light by lithium in various stages of aggregation.

Another reason for studying clusters is that the technique of cluster-beam mass spectrometry offers a new and convenient method of allowing elements to react in a controlled manner and of determining the stability of the reaction products.[9] This topic will be the main theme of this article, which will begin with a very brief review of work in the field of cluster preparation.

2. Four Case Studies

Four case studies will first be presented, each representing a different method of cluster preparation, a different substance, and a different level of interpretation.

2.1. Water Clusters Produced by Gas Expansion

It has been known for several decades[10,11] that when a gas under relatively high pressure (1 bar) expands into a vacuum through a small (0.1-mm) nozzle, clusters condense out of the cooled gas. The size distribution of the clusters can be controlled by varying the expansion parameters. This technique has been used to study a large variety of gas-phase and vapor-phase clusters, including those of hydrogen,[12] water,[13-21] sodium,[22-27] inert gases,[28-33] and tetracene.[34,35] Figure 4 shows the mass spectrum of water clusters formed by expanding a mixture of H_2O (4.6 torr) in argon through a 0.22-mm nozzle. The average cluster size increases with increasing total pressure and the mass peak corresponding to the cluster $[H(H_2O)_{21}]^+$ stands out particularly strongly. This finding is usually interpreted to indicate an enhanced stability for the 21-molecule water cluster. What does this cluster look like? Ice has a wurtzite

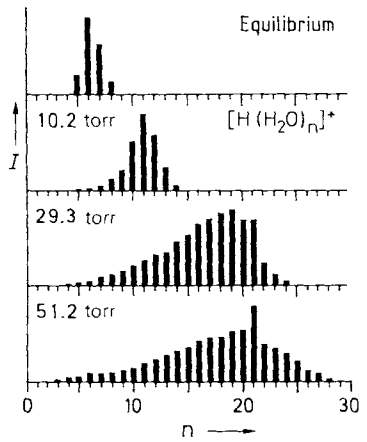


Fig. 4. Dependence of the size of water clusters on total pressure (determined by mass spectrometry). The water clusters were produced by expanding a mixture of H_2O vapor and argon at the indicated pressure through a 0.22-mm orifice into a vacuum [14]. n = number of water molecules per cluster; I = relative amount of cluster.

structure in which each oxygen atom is surrounded tetrahedrally by four other oxygen atoms. One hydrogen atom is found between each pair of oxygen atoms. It is not possible to find a highly symmetric arrangement of 21 H_2O molecules within the wurtzite structure. However, the tetrahedral bonding scheme may be used to construct a dodecahedral cage consisting of 20 H_2O molecules. In fact, such a cage has been identified in many clathrate compounds. The stability of the dodecahedron could explain the strength of the n = 21 peak in the mass spectrum (i.e., the 20 molecules comprising the dodecahedron surround a central, charged molecule).

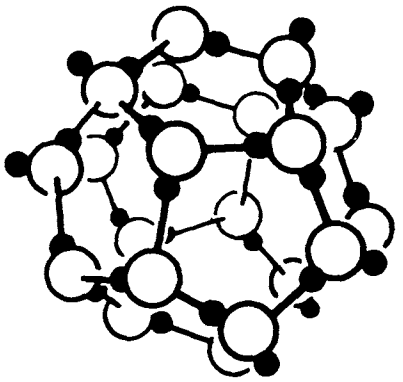


Fig. 5. Clathrate cage composed of twenty water molecules.

2.2. Alkali Halide Clusters Produced by Ion Bombardment

If an intense beam of high-energy (5-keV) xenon ions (Xe^+) is directed against a solid surface (e.g., CsI), secondary ions are ejected from the surface and can be detected in mass spectrometer. These secondary ions include not only simple, ionized molecules but also large clusters containing hundreds of atoms.[36-41] A mass spectrum of $[Cs(CsI)_n]^+$ clusters produced in this way is shown in Figure 6. The peak corresponding to the cluster $[Cs_{14}I_{13}]^+$ is particularly strong. Analogous clusters produced from NaCl[41-43] and CuBr[44] have also been shown to have an enhanced stability. Since this cluster is too small to be observed directly, theoretical considerations are required in order to determine its structure. Stable cluster configurations can be calculated at widely varying levels of sophistication. The simplest method uses a model involving the packing of hard spheres. At the other end of the scale, stable structures can be determined by elaborate configuration interaction calculations of the total energy. Such calculations are appropriate for all types of clusters but are limited in practice to very small clusters of light atoms. The total energy of clusters with either purely ionic[45,47] or purely van der Waals[48] bonding can be determined much more simply. It is possible to define a size-independent,

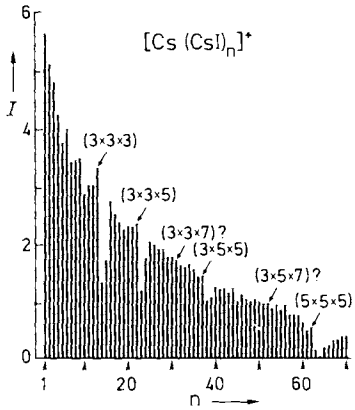


Fig. 6. Size distribution of $[Cs(CsI)_n]^+$ clusters determined by secondary mass spectrometry (SIMS). The numbers in parentheses indicate the sizes of perfect, rectangular clusters. I is a measure of the intensity of the mass peak (lg counts per second) [37].

two-body interatomic potential. By summing this potential over all atom pairs, a multidimensional total energy surface is obtained. Each minimum on this surface corresponds to a stable cluster configuration. The main computational difficulty is not to define the surface but to find all true minima without getting trapped at a saddle point with a low curvature.

Such total energy calculations indicate that $[Na_{14}Cl_{13}]^+$ has more than the usual binding energy. The reason for this is quickly seen by looking at the structure of this cluster (Fig. 7). $[Na_{14}Cl_{13}]^+$ is highly symmetric, resembling a

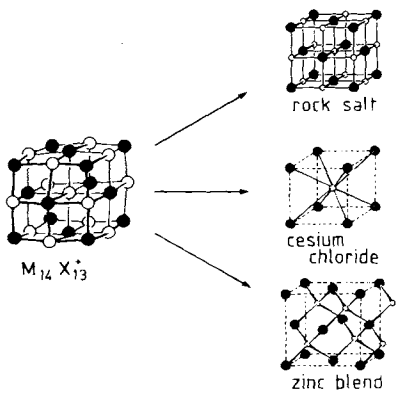


Fig. 7. The most stable form of the metal halide cluster $[M_{14}X_{13}]^+$ (left) and the crystal structures of NaCl, CsI, and CuBr (right, top to bottom).

portion of the rock salt structure. Calculations with parameters appropriate for the compounds CuBr and CsI indicate that the cubic cluster $[M_{14}X_{13}]^+$ is responsible for the strong peaks in the mass spectra of these substances also. This is quite surprising because CuBr and CsI condense to form crystals of the zinc blende (coordination number (CN) 4) and cesium chloride type (CN 8), respectively. Thus, the rock salt form (CN 6) appears to be energetically favored in the early stages of growth of not only NaCl but also CsI and CuBr.

2.3. Quenching of Ge and Sn Vapors in Helium Gas

Most substances when heated to a sufficiently high temperature in an inert-gas atmosphere produce a dense smoke composed of microcrystals.[49-52] The linear dimension of the microcrystals varies from 10 to 1000 Å depending on experimental conditions. Recently, a time-of-flight mass spectrometric study showed that the technique of inert-gas evaporation produces not only microcrystals but also clusters containing fewer than 100 atoms.[53,54]

Not all elemental vapors produce a detectable number of clusters when quenched in helium gas. Germanium and tin, however, form clusters readily and are particularly interesting because a transition from covalent to metallic bonding occurs in the solid forms. Perhaps this transition is reflected in the cluster mass spectra. Mass peaks of the Ge_x^+ clusters (Fig. 8) are strong for x = 6, 10, 14, 15, and 18

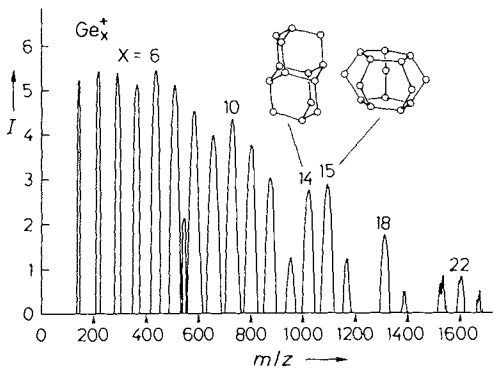


Fig. 8. Mass spectrum of clusters formed by quenching Ge vapor in He gas. Peaks corresponding to clusters with x = 6, 10, 14, 15, and 18 Ge atoms are particularly strong. Two structures having bond angles of nearly 109° are indicated.

and particularly weak for x = 13, 17, 20, and 24. A discussion of the structures of these stable clusters should be based on total energy calculations. However, such calculations have only been made for very small Ge clusters.[55] Therefore, we will limit the discussion to pointing out several atomic arrangements within a Ge crystal. The basic structure in such a crystal is a six-membered ring in the chair conformation; this structure can form the basis of an adamantane system, which can in turn be enlarged still further. In this way a sequence of closed polycyclic Ge_x structures is formed corresponding to x = 6 + 4a where a is an integer. A plausible structure may also be formulated for the Ge_{15}^+ cluster ion (Figure 8).

The dominant feature of the mass spectrum of the Sn_x^+ clusters is the weakness, or in this case the absence, of the peak for x = 14 (Fig. 9). In this respect tin resembles lead.[53] That tin should more resemble lead than germanium can be seen already in the solid state. Although tin does have a low-temperature semiconducting crystalline modification with the diamond structure (α-Sn), at room

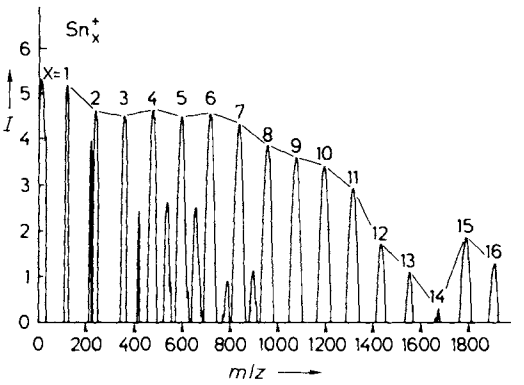


Fig. 9. Mass spectrum of clusters formed by quenching Sn vapor in He gas.

temperature it is a metal with the β-Sn structure (CN 6). Once again we can only speculate as to the cause of the instability of the cluster ion Sn_{14}^+. There are several close-packed structures corresponding to Sn_{13}^+ consisting of a central atom surrounded by a complete shell of twelve outer atoms.[4] An additional atom, which lies on the surface of such a highly symmetric, compact core, could be expected to be weakly bonded.

2.4. Carbon Clusters by Laser Evaporation

A pulsed cluster source has been developed which uses a focused laser beam for vaporization.[56-59] The vaporization is timed to occur at the peak of a high-pressure He pulse. Such a source is particularly appropriate for time-of-flight mass spectrometry. It has the advantage that essentially any material can be vaporized, even carbon.[56] The mass spectrum of C_x^+ clusters has a bimodal size distribution. For x < 30, clusters containing both even and odd numbers of atoms have been observed. The peaks corresponding to x = 3, 11, 15, and 19 are particularly strong. For x > 30, however, only clusters containing even numbers of atoms have been observed. Recently, a C_{60} cluster was generated and found to be particularly stable.[56b] This cluster, named "Buckminsterfullerene," is assumed to owe its stability to its highly symmetric, spherical structure.[56c]

3. Heteronuclear Clusters

Heteronuclear clusters, i.e., clusters composed of more than one element, can be produced by allowing the elements to react in the vapor phase.[9] The composition of the clusters can be determined by mass spectrometry. By varying the partial pressures of the two elements, the stability of clusters having all conceivable compositions can be tested in just one experiment. Various combinations of elemental vapors (Ge, Sn, Pb, Ga, In, Cs, Rb, Sr, Tm, Eu, Cl, O, S, and P) have been allowed to react in the vapor

phase and then thermally quenched in cold He gas. Heteronuclear clusters condensed out of the vapor and were identified using a quadrupole mass spectrometer. The average cluster composition could be changed by varying the partial pressure of the two elements. Of particular interest are mass peaks having unusually strong or weak intensities, because such peaks allow clusters of unusually high or low stability to be identified.[4] Also significant in such experiments is the observation of a sequence of strong mass peaks corresponding to clusters with the composition $(A_xB_y)_n$. This identifies the unit A_xB_y as a building block for cluster construction and for possible use in the synthesis of new solids.

3.1. Experimental Procedures

Elemental vapors are produced in ovens of various design and allowed to react in a chamber containing from 0.7- to 5-mbar He gas. The outer mantel of the reaction chamber is cooled with liquid nitrogen. The kind of oven used depends on the element to be evaporated. For S, Rb, Cs, and P, the oven consists of a resistively heated quartz crucible (1 cm in diameter and 8 cm long) with a pocket at the bottom to hold a thermocouple. The crucible fits snugly into an Al_2O_3 cylinder grooved and wrapped with a Ta coil. This unit is inserted into a closely fitting second cylinder (also made of Al_2O_3). This is followed by several layers of radiation shielding. The outermost cylinder is a stainless steel jacket having good thermal contact with a water-cooled electrode. The same unit can be used for evaporation of Pb, In, and Ga, except that in these cases a graphite rather than a quartz crucible is required. A stainless steel crucible is used for Tm and Eu. The high temperatures necessary for the evaporation of Sn require that the oven length be scaled down by a factor of almost 2. Ge is evaporated from a resistively heated graphite tube.

The reaction chamber contains two of these ovens. The vapors from the ovens are mixed and cooled. Heteronuclear clusters condense out of the supersaturated vapor and pass through a 3-mm diameter hole into an intermediate chamber where the excess He gas is pumped off with a turbopump (150 L/s). The cluster beam then passes through a 1-mm diameter hole into a high-vacuum chamber containing a quadrupole mass spectrometer (pumped with a 360-L/s turbopump). The cluster beam intersects the axis of the spectrometer, where the clusters are ionized with 80-eV electrons. The spectrometer can be operated in the range from 1 to 2000 amu. A quartz-film thickness monitor, located on the farside of this chamber, allows the total mass flux in the cluster beam to be measured. A schematic drawing of the apparatus is shown in Figure 10.

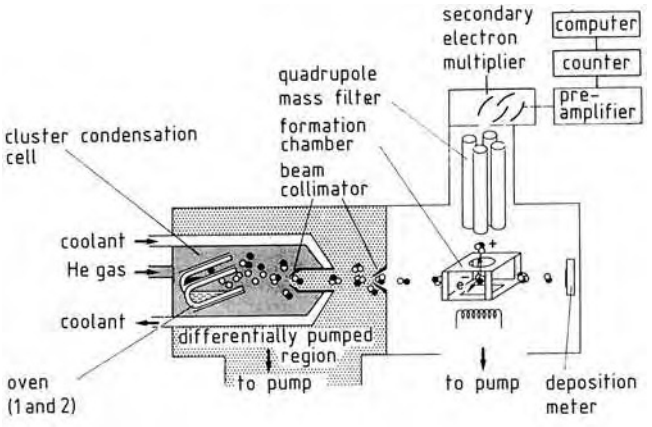


Fig. 10. Experimental apparatus (schematic) for the formation, reaction, and mass spectrometric analysis of clusters.

3.2. The Cesium–Sulfur System

3.2.1. Sulfur Clusters

The cesium–sulfur system is of particular interest since it permits the investigation of an entire range of cluster compositions from pure sulfur to pure cesium. The mass spectrum of a mixture of clusters formed by quenching pure sulfur vapor in He gas is shown in Figure 11, top. Clusters containing from 2 to 56 sulfur atoms are easily identified.

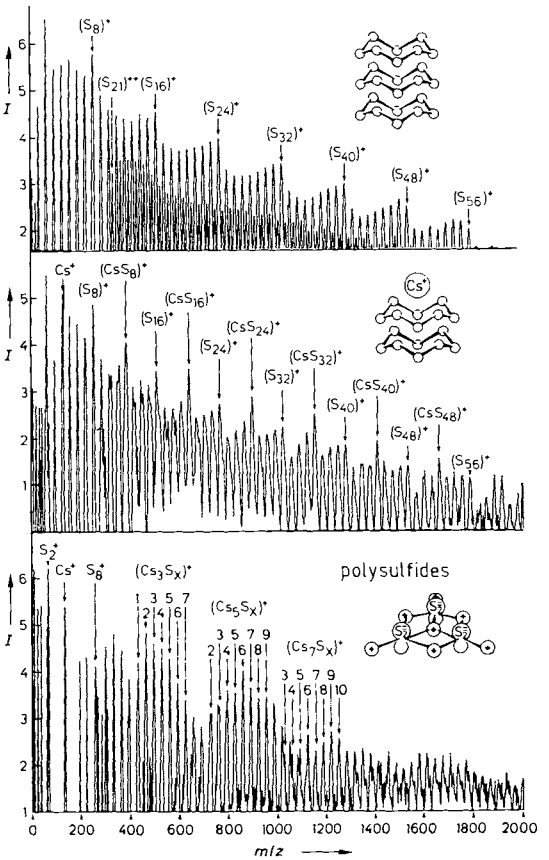


Fig. 11. Mass spectra of a mixture of clusters formed by quenching various mixtures of sulfur vapor and cesium vapor in He gas. Pure sulfur clusters are constructed out of S_8 rings (top). Clusters with composition $[CsS_{8n}]^+$ seem to be stable against fragmentation (middle). At increased partial pressure of Cs, polysulfide clusters composed of Cs^+ ions and S_2^{2-} and S_3^{2-} ions (bottom) appear.

The mass peaks corresponding to clusters containing 8, 16, 24, 32, and 40 sulfur atoms are particularly strong. Apparently sulfur clusters have a tendency to be constructed out of eight-atom building blocks, presumably ring molecules. In large clusters the molecules are bonded together by means of weak van der Waals forces. Orthorhombic sulfur is constructed in exactly the same way (i.e., S_8 rings are

stacked one on top of another). Thus, the cluster mass spectrum appears to reflect the initial growth of a sulfur crystal. This is somewhat surprising since the clusters are all positively charged. In fact, the removal of a lone pair electron from one of the sulfur rings does appear to affect the overall stability of the cluster. Although the clusters S_{8n}^+ are represented by strong peaks (Fig. 11, top), neighboring peaks corresponding to the loss of one to seven atoms are almost as strong. This gives the spectrum a step-like appearance.

Doubly positively charged sulfur clusters S_n^{2+} appear for $n=20$ or 21. The uncertainty in this value arises from the fact that S_{20}^{2+} is superimposed on S_{10}^+. The existence of a critical size for the appearance of doubly ionized clusters has been substantiated in a number of systems[60] and is thought to reflect the instability of small clusters in which two positive charges are forced to exist in close proximity.

3.2.2 *Cesium Polysulfide Clusters*

A mass spectrum of clusters produced by mixing a small amount of cesium vapor with sulfur vapor is shown in Figure 11, middle. The spectra of the Cs-S system must be analyzed carefully since four sulfur atoms (128 amu) are distinguishable from one Cs atom (133 amu) only in high resolution mass spectra. Fortunately, the required resolution lies just within the specifications of our quadrupole analyzer. The series of peaks in Figure 11, middle, due to pure sulfur clusters is very strong. The unusual strength of peaks corresponding to S_{8n}^+ is once again noteworthy. However, the strongest peaks in the spectrum belong to the series $[CsS_{8n}]^+$. Apparently, only one Cs atom is bonded to each sulfur cluster. Presumably, the positive charge on each cluster tends to be localized on the Cs atom. Removal of even a lone pair electron from a sulfur ring apparently leads to considerable fragmentation (see Section 3.2.1). A sulfur cluster containing one Cs atom, on the other hand, can be ionized with only a small amount of fragmentation. This is reflected in the mass spectra by the presence of a clear maximum in the series of peaks at $[CsS_{8n}]^+$ rather than a step. Presumably, Cs^+ is located on the central axis of a stack of S_8 rings and is bound to the rings through a point charge-induced dipole electrostatic interaction.

One might expect that by increasing the partial pressure of Cs vapor, additional metal atoms would be incorporated into the S_{8n} clusters. But this is not what happens (Fig. 11, bottom). An entirely new type of cluster appears, in which the S_8 rings are broken up into smaller chains (S_2^{2-} and S_3^{2-} ions). We can gain insight into the structure and bonding of polysulfide clusters by considering the results of investigations on BaS_2 and BaS_3 crystals, which contain the same polyatomic anions.[61,62] BaS_2 crystals are made up of Ba^{2+} and S_2^{2-} dianions. The exact structure of this crystal is rather complicated, the lattice being monoclinic with four BaS_2 formula units per unit cell. However, if one considers an idealized crystal constructed by replacing the S_2^{2-} ions by single anions located at the centers of the dianions, the picture simplifies considerably. The idealized crystal has a slightly distorted rock salt structure: each Ba^{2+} ion is surrounded by six S_2^{2-} units and vice versa. Apparently, the bonding between Ba^{2+} and S_2^{2-} is essentially ionic. The same conclusion can be drawn from the results of investigations on BaS_3.[61] This crystal is tetragonal, each unit cell containing two formula units. The sulfur is solely in the form of trisulfide units with an angle of 114.9° and an S-S bond length of 2.076 Å. However, the essentially ionic nature of the bonding between Ba^{2+} and S_3^{2-} is revealed by the observation that the two units are arranged in a slightly distorted CsCl type structure.

3.2.3. *Cesium Sulfide and Subsulfide Clusters*

Increasing the Cs partial pressure still further results in the formation of cesium sulfide clusters $[Cs(Cs_2S)_n]^+$ (see Fig. 12, top). These clusters are built out of Cs^+ and S^{2-} ions. No strong intensity anomalies were observed for clusters with $n=1$–6. The possible structure of these sulfides will be discussed below in connection with cesium oxide clusters for which explicit calculations have been made (see Section 3.4).

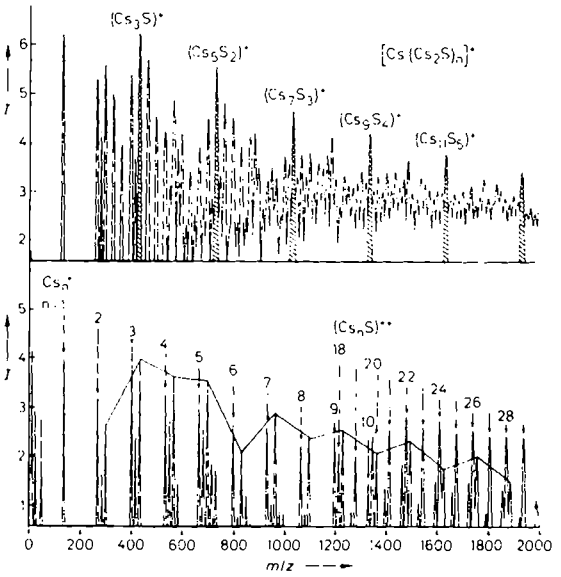


Fig. 12. Mass spectrum of cesium/cesium sulfide clusters (composed of Cs^+ and S^{2-} ions) (top) and of cesium/cesium subsulfide clusters (below). The mass peaks due to $[Cs_nS]^+$ clusters (connected) alternate in intensity (bottom).

If sulfur is evaporated at a very low oven temperature (53 °C), it is possible to produce cesium-rich subsulfide clusters (see Fig. 12, bottom). In the mass spectrum the peaks of the pure Cs clusters are each followed by an intense cesium sulfide peak (which are joined by lines for clarity). Exactly halfway between each Cs_n^+ and $[Cs_nS]^+$ peak, additional weaker peaks appear which are due partly to cesium oxide clusters and partly to doubly ionized cesium sulfide clusters. The intensities of the Cs peaks alternate and that of $[Cs_6S]^+$ is particularly weak.

3.3. The Cesium Chloride and Rubidium Chloride Systems

Alkali clusters have been intensively studied both experimentally and theoretically.[45] In the experiments car-

ried out until now a solid salt was used as the source for the production of clusters.[38-43,63] By using cesium metal and gaseous chlorine we are able to study Cs–Cl clusters deviating strongly from the normal stoichiometry.

3.3.1. Cesium Subchloride Clusters

The relative yields of clusters formed when only a small amount of chlorine gas is introduced into the system is shown in Figure 13. The top curve indicates that if only one Cl atom is incorporated into the cluster, mass peaks corresponding to $[Cs_2Cl]^+$, $[Cs_4Cl]^+$, $[Cs_6Cl]^+$, $[Cs_8Cl]^+$, etc., are particularly strong. However, if two Cl atoms are incorporated into the cluster, an odd number of Cs atoms are preferred, i.e., the peaks $[Cs_3Cl_2]^+$, $[Cs_5Cl_2]^+$, $[Cs_7Cl_2]^+$, etc., are strong. Inspection of the entire series of curves in Figure 13 reveals that, if the number of Cs atoms

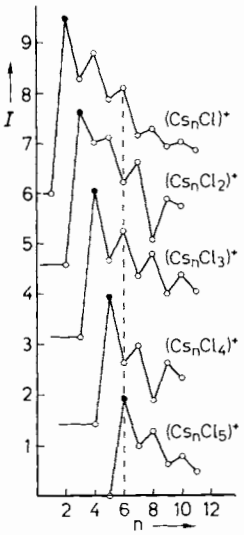


Fig. 13. The yield of cesium subchloride clusters formed by quenching Cs vapor in a mixture of He and Cl_2. Noteworthy is the vertical and horizontal alternation in the amount of cluster formed. The filled circles correspond to clusters containing ions with rare gas electronic configurations.

plus the number of Cl atoms is odd, the peak in the mass spectrum is strong. This result can be understood if all electrons are required to occur in pairs. Each Cs atom and each Cl atom has one unpaired electron. Therefore, the total number of atoms must be odd, since one electron is removed upon ionization. This effect has already been observed for pure alkali metal clusters.[22,64] The rule can be stated more generally; *a highly stable cluster, either charged or neutral, must contain only paired electrons.* The same rule will be seen to apply also to oxide, sulfide, and phosphide clusters.

3.3.2. Rubidium Chloride Clusters

As the partial pressure of chlorine is increased, the cluster mass spectrum simplifies considerably. A series of very strong peaks emerges corresponding to clusters with the composition $[M(MX)_n]^+$. Because of this simplification in the spectrum, a lighter alkali metal can be used without causing confusion due to overlapping peaks. Figure 14 shows the results for the Rb–Cl system for which mass

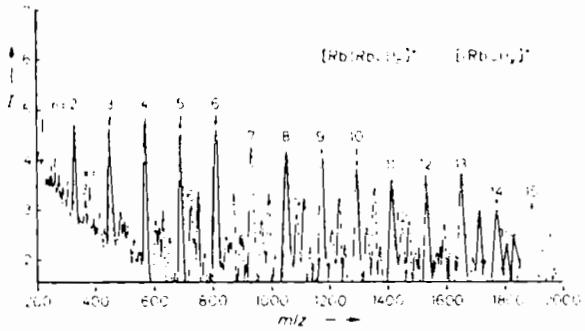


Fig. 14. Mass spectrum of rubidium chloride clusters formed by quenching Rb vapor in a mixture of He and Cl_2. Noteworthy is the intense peak $[Rb(RbCl)_{13}]^+$ and the relatively high intensities in the $[(RbCl)_x]^+$ series (x = 3, 6, 9, 12, and 15).

peaks can be observed for clusters containing up to 30 atoms.

The peaks for the clusters $[Rb(RbCl)_n]^+$ with n equal to 6, 9, and 13 are particularly strong. A second series of peaks, each peak occurring exactly halfway between peaks of the principal series, is due to doubly ionized clusters $[Rb_2(RbCl)_n]^{2+}$. A third series corresponds to clusters with composition $[(RbCl)_x]^+$. Peaks in this series stand out strongly for x = 3, 6, 9, 12, and 15.

Clusters in the principal series do not contain equal numbers of rubidium and chloride atoms. This fact reflects the strongly ionic character of the clusters and can be explained as follows: Mass selection is possible only if a cluster is charged. If all electrons in the cluster are localized and paired, the electrons most easily removed belong to the chloride ions. After ionization, the neutral chlorine atom is bonded to the remaining ions in the cluster only through a monopole-induced dipole interaction. This interaction is weak compared with the large amount of energy that is converted into vibrational motion during the ionization. Therefore, the neutral chlorine atom is lost, resulting in the formation of a cluster with composition $[Rb(RbCl)_n]^+$.

The intensity of a given line in a mass spectrum is influenced by many factors; the stability of the neutral clusters entering the ionization chamber, the cross section for ionization, the probability of fragmentation, and finally the stability of the ionized products. The relative stability of clusters can be determined by minimizing the total energy, which is given by the sum of all two-body interactions.[46,47]

$$V_{ij} = \frac{Z_i Z_j}{r_{ij}} + A \exp(-r_{ij}/\rho) \qquad \text{(a)}$$

The symmetries of the most stable configurations depend on the form of the two-body interaction.[63] Nonetheless, Figure 15 gives a fairly good representation of the stable forms of alkali halide clusters $[M_nX_{n-1}]^+$.

The calculated energy per MX unit for the most stable form of RbCl clusters with rock salt structure, ranging in size from 6 to 32 atoms, is shown in Figure 16. The binding energy for neutral clusters is particularly large for n = 6, 9, 12, and 15, because stacked six-membered rings and six-atom rectangles are the favored structures. The curve for

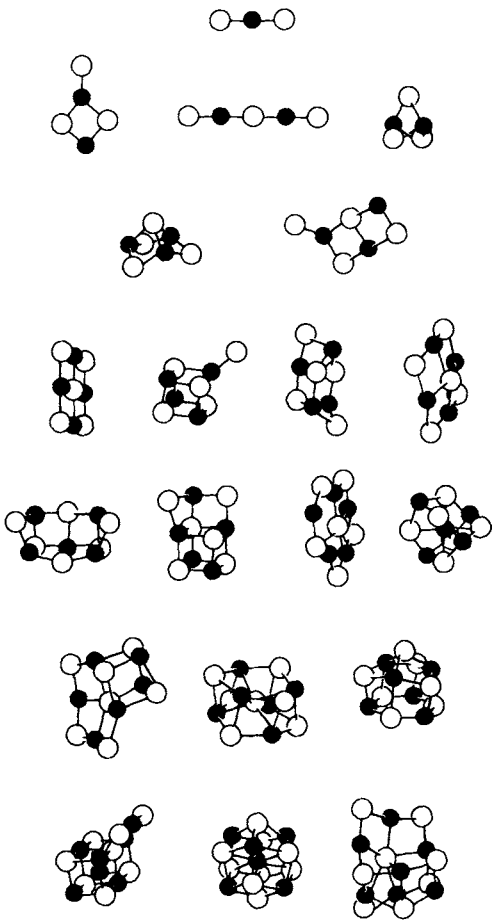


Fig. 15. Calculated stable configurations of alkali halide clusters.

charged clusters with composition $[Rb_nCl_{n-1}]^+$ is rather smooth except for $[Rb_{14}Cl_{13}]^+$, which appears to have more than the usual binding energy. The reason for this is quickly seen by looking at the structure of this cluster (Fig. 16). $[Rb_{14}Cl_{13}]^+$ is highly symmetric, resembling a portion of the rock salt structure.

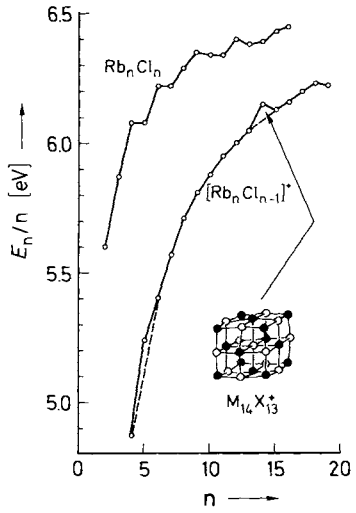


Fig. 16. Binding energy per MX unit for the most stable forms of positively charged and neutral clusters.

3.4. The Cesium–Oxygen System

The elements cesium and oxygen combine to form a bewildering array of crystalline compounds (Cs_7O, Cs_4O, $Cs_{11}O_3$, Cs_2O_2, Cs_2O_3, CsO_2, and CsO_3). The structures of the suboxides Cs_7O, Cs_4O, and $Cs_{11}O_3$ are particularly intersting and unusual.[29] Crystallographic investigations indicate that these compounds are composed of $Cs_{11}O_3$ clusters having strongly ionic character.[65–68] However, the bonding between the clusters is metallic. This bonding model is supported by comparison of the interatomic distances in the suboxides with the corresponding distances in normal oxides and pure metals. The metal–oxygen distances in the suboxide clusters are nearly the sum of the ionic radii, whereas the metal–metal distances between clusters are nearly those found in the pure alkali metal.

The superoxides owe their formation to the ability of oxygen to appear as O_2^{2-}, O_2^-, or O_3^- ions.[68] Cesium oxide clusters of all possible compositions were produced by evaporating cesium metal into a $He-O_2$ gas mixture containing an increasing amount of oxygen.

3.4.1. Cesium Clusters

Almost no clusters could be detected in the mass spectrometer if oxygen-free helium was used as the quenching gas. Upon addition of 0.01% oxygen (10^{-4} mbar), the cluster signal rose three orders of magnitude (Fig. 17). The intensity of the peaks of the pure Cs clusters also increased

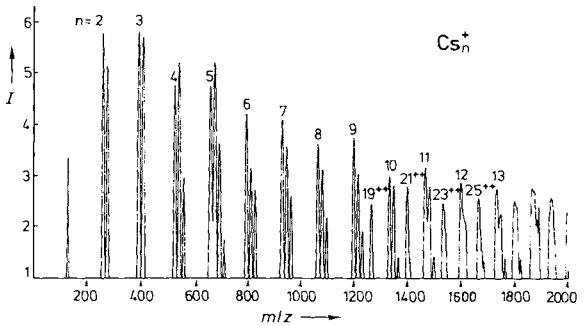


Fig. 17. Mass spectrum of a mixture of lightly oxidized Cs clusters. The mass peaks of the pure cesium clusters Cs_n^+ and Cs_n^{2+} have been labeled explicitly. Each subsequent peak indicates the addition of one or more oxygen atoms.

dramatically, indicating that these clusters may be fragments created during the ionization process. The first peak in every group corresponds to a pure Cs cluster containing the indicated number of atoms. The following, closely spaced peaks correspond to clusters containing one or two additional oxygen atoms. The intensities of the peaks of the pure metal clusters alternate. Peaks corresponding to clusters containing an odd number of Cs atoms are stronger. Since the clusters are positively charged, an odd number of atoms means an even number of valence electrons. Apparently, Cs clusters containing paired electrons have an enhanced stability.

After the group marked n = 9, new peaks appear exactly halfway between the pure Cs peaks. This new series corre-

sponds to doubly ionized cesium and cesium oxide clusters. For large clusters the individual peaks in each group have merged together. This is not due to a worsening of the mass resolution at high masses but to the newly emerging doubly ionized oxides, which are now separated by only 8 amu.

The intensity of the doubly ionized, pure metal clusters rises sharply at $n = 19$. Configuration interaction[70-72] and density functional[73-75] calculations have shown that small metal clusters do not necessarily have closed-packed structures. Still it is worth pointing out that there exist two highly symmetric arrangements of 19 spheres,[48] a large octahedral structure and a double icosahedron.

3.4.2. Cesium Suboxide Clusters

Increasing the amount of oxygen in the He buffer gas to 0.1% results in the formation of metal-rich suboxide clusters (Fig. 18). In order to observe irregularities in the intensities more easily, it is convenient to make comparisons between clusters containing the same number of oxygen atoms. The peak corresponding to the cluster $[Cs_6O]^+$ is particularly weak.

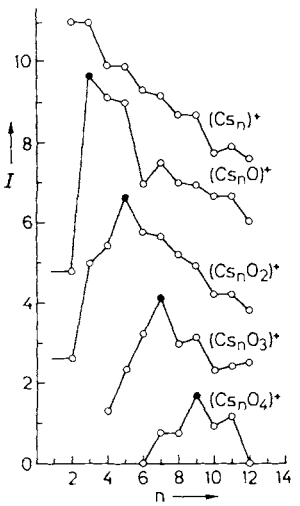


Fig. 18. Composition of a mixture of cesium-rich suboxide clusters (see text).

The strongest peak in each series corresponds to the normal oxide $[Cs(Cs_2O)_n]^+$ (solid circles in Fig. 18). As more cesium atoms are added to the normal oxide cluster, the peak intensities tend to alternate. However, the alternation is in the horizontal direction (Cs) only and not in the vertical direction (anions) as was the case for the halides (Fig. 13). The different behavior of the oxides and halides supports, nonetheless, the same rule (Section 3.3.1): stable clusters prefer to have paired electrons. Strong peaks are found not only for $[Cs_3O]^+$, $[Cs_5O]^+$, $[Cs_7O]^+$, etc., but also for $[Cs_3O_2]^+$, $[Cs_5O_2]^+$, $[Cs_7O_2]^+$, etc.

Electron correlation calculations for Li_4O offer some insight into the bonding of suboxide clusters.[76,77] The most stable form, even for the positive ion, seems to have tetrahedral geometry. Although the central oxygen atom acquires a negative charge of 0.87, Li–Li bonding makes a large contribution to the total energy.

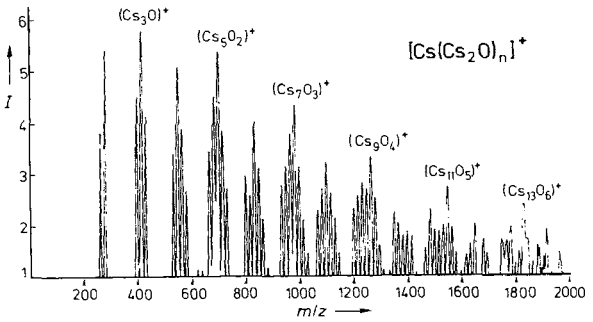


Fig. 19. Mass spectrum of a mixture of cesium oxide clusters formed by quenching Cs vapor in a mixture of He and O_2 gas.

3.4.3. Cesium Oxide Clusters

If the concentration of O_2 in helium is raised to 0.6%, a mixture of clusters is obtained, the mass spectrum of which is shown in Figure 19. Certain clusters containing an odd number of cesium atoms are represented particularly strongly. These clusters have the composition $[Cs(Cs_2O)_n]^+$, two Cs atoms for each oxygen and one extra Cs atom for the positive charge. Each of the ions in these clusters has a rare gas electronic configuration. In this respect they might be regarded as normal oxides. The distribution of charge between the ions is therefore unambiguous, namely, Cs^+ and O^{2-}. Therefore, Equation (a) may be used to calculate the structures of the stable configurations. The parameters, $A = 4000$ eV and $1/\rho = 3.03$ Å^{-1}, were chosen so that the Cs–O distance in $[Cs_5O_2]^+$ is that observed for crystalline Cs_2O.

$[Cs_3O]^+$ has only one stable configuration, a planar structure with a binding energy of 119.46 eV with respect to dissociation into ions. The dimer has two stable configurations. The symmetric dimer with a threefold symmetry axis (Fig. 20, top right) has 0.6 eV more binding energy than the unsymmetric dimer. Larger clusters with a threefold axis are also energetically favored over less symmetric structures. The cluster $[Cs_7O_3]^+$ consists of a Cs_3O_3 ring

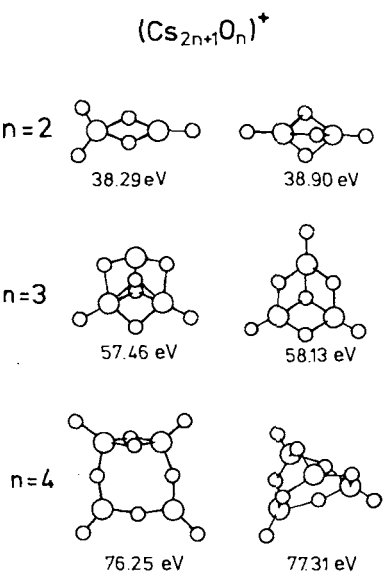


Fig. 20. The most stable configurations of $[Cs_{2n+1}O_n]^+$ clusters containing ions with rare gas electronic configurations. The total binding energy is given below each structure.

along with one central and three terminal Cs atoms. The most stable form of $[Cs_9O_4]^+$ has 77.31 eV of binding energy, 1 eV more than its closest competitor.

3.4.4. *Cesium Superoxide Clusters*

The character of the mass spectrum changes again as the oxygen concentration is increased to about 40% (Fig. 21).

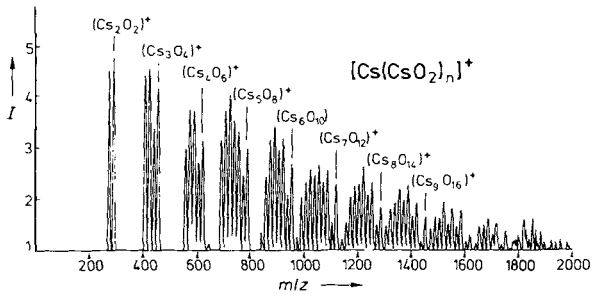


Fig. 21. Mass spectrum of a mixture of cesium oxide and cesium hyperoxide clusters. Each group of peaks begins with clusters containing O^{2-} ions, goes through a maximum for clusters containing O_2^{2-} ions, and ceases abruptly at clusters containing O_2^- ions.

In addition to clusters containing O^{2-} and O_2^{2-} ions, the oxygen-rich clusters $[Cs(CsO_2)_n]^+$, which contain O_2^- ions, are formed. Thus, as expected, clusters containing an even number of oxygen atoms show up more strongly in the mass spectrum. Although no calculations are available for the structure of large superoxide clusters, LCAO-MO SCF calculations indicate that Li_2O_2 is planar with D_{2h} symmetry.[78]

3.5. Lead-Indium Clusters

If the elements in a heteronuclear cluster are chemically equivalent and the vapors of the two elements are mixed together in a ratio of about 1:1, then clusters having all possible compositions should appear in the mass spectrum. The probability of finding a cluster with a given size and composition should follow a binomial distribution.

Lead and indium have nearly the same electronegativity and mix very well; the mass spectrum of a mixture of clusters is correspondingly complicated (Fig. 22). Rather than trying to label all peaks in this spectrum, we have connected the peaks corresponding to clusters containing eight atoms, starting with In_8 and ending with Pb_8. Clusters containing an odd number of In atoms, i.e., containing an even number of electrons (in the ion), appear to be particularly stable. $[Pb_2In_6]^+$ is an exception.

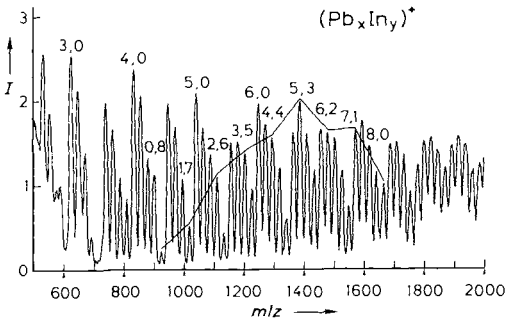


Fig. 22. Mass spectrum of a mixture of Pb-In clusters. The peaks of the pure Pb clusters have been labeled (3,0; 4,0; 5,0; etc.). Each immediately following peak corresponds to the removal of one Pb atom and the addition of two In atoms. The peaks corresponding to eight atom clusters (0,8; 1,7; 2,6; etc.) have been connected.

3.6. Cesium-Lead Clusters

When two metals are mixed together, the properties of the mixture usually do not change continuously with concentration.[5] In the solid state the discontinuities are due to the formation of well-defined intermetallic compounds.[6] Strong evidence exists that such compounds form even in the liquid state.[79,80] Here we present evidence for the existence of analogous heteronuclear clusters in the vapor phase.

Intermetallic compounds are particularly stable if the two metals are characterized by a large electronegativity difference. A classic example is CsAu.[80,81] When Cs and Au are mixed in the ratio 1:1, a compound is formed with an ionic character similar to that of CsCl. In fact, CsAu crystallizes in the CsCl structure. Even though Cs and Au, separately, are excellent electrical conductors, the 1:1 mixture is nonmetallic in both the liquid and solid phases.

The Cs-Pb system is particularly interesting because of the large electronegativity difference between its two components. In an early study of a solution of this alloy in liquid NH_3, *Zintl* and co-workers[5] came to the conclusion that there was polar bonding between the Pb_9^{4-} anions and the alkali metal ions. The obvious question is therefore whether evidence can be found in cluster mass spectra for the existence of Pb_9 groups and for charge transfer between Cs and Pb. A mass spectrum of a mixture of Cs-Pb clusters is shown in Figure 23. Pb_9 is just light enough to

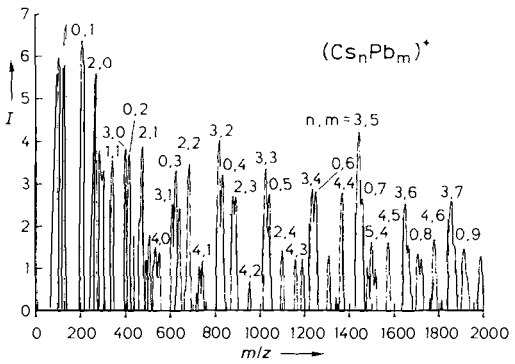


Fig. 23. Mass spectrum of a mixture of Cs-Pb clusters. Peaks corresponding to $[Cs_3Pb_2]^+$ and $[Cs_3Pb_5]^+$ are particularly strong.

fall within the mass region (1-2000 amu) accessible with our mass spectrometer. However, the cluster we are looking for is $[Cs(Cs_4Pb_9)]^+$, since, in addition to nine Pb atoms, four Cs^+ ions are needed to compensate the charge on Pb_9^{4-}, and one additional Cs^+ is required to provide the overall positive charge on the cluster. This cluster has a mass of 2529 amu, well above the mass limit. We solved this problem by investigating a system with lighter elements (see Section 3.7). First, however, there are several features of the Cs-Pb mass spectra that must be pointed

out. Two of the strongest peaks in the spectrum correspond to the clusters $[Cs_3Pb_2]^+$ and $[Cs_3Pb_5]^+$. As discussed below, evidence exists[82] that Pb_5 is a very stable polyanion and has the exact charge required to explain the mass peak, i.e., Pb_5^{2-}.

Although *Zintl* was able to identify many polyanions in solution, these ions did not prove to be sufficiently stable to act as building blocks for the construction of crystals when the solvent was evaporated. This problem was solved by *Corbett* and co-workers[83] who stabilized the sodium salts of the polyanions in crystals by complexation with 4,7,13,16,21,24-hexaoxa-1,10-diazatricyclo[8.8.8]hexacosane (2,2,2-crypt). In this way they were not only able to grow the salt $[2,2,2\text{-crypt } Na]_2^+[Pb_5]^{2-}$ but also to determine the structure of the P_5^{2-} polyanion (trigonal bipyramidal).

Thus, the strongest peak in the mass spectrum (for a cluster containing more than two atoms) corresponds to $[Cs_3Pb_5]^+$. The structure can probably be described as a cluster within a cluster; that is, a covalently bonded, trigonal bipyramid of five Pb atoms ionically bonded to three, symmetrically placed, outer Cs ions.

3.7. Cesium-Tin Clusters

The Cs-Pb system has the advantage that the small number of isotopes present results in sharp mass peaks. However, Pb is so heavy that the stability of two important clusters, the Zintl cluster $[Cs_5Pb_9]^+$ and the cluster $[Cs_5Pb_{10}]^+$, cannot be checked with our spectrometer. What is the significance of this second cluster? We stated in the introduction that two types of information concerning stability can be obtained from the mass spectra of clusters. A single, intense, isolated mass peak indicates a highly stable cluster; a periodicity in the mass spectrum means that this cluster can be used as a building block to construct larger clusters. Since $[Cs(Cs_2Pb_5)]^+$ is stable, the question arises whether the next cluster in the series $[Cs(Cs_2Pb_5)_2]^+$ is also stable. In order to determine the stability of such clusters we turn to the analogous system containing the lighter element Sn. This change has the disadvantage, however, that, because Sn has many more isotopes, the mass peaks are broader. A mass spectrum of a mixture of Cs-Sn clusters is shown in Figure 24. Although the mass peaks are broad, pure Sn clusters containing as many as ten atoms can be identified. Among the heteronuclear clusters, $[Cs_3Sn_5]^+$, $[Cs_3Sn_9]^+$, and $[Cs_5Sn_9]^+$ appear to be particularly stable (intense mass peaks). The first cluster type was already observed in the Cs-Pb system; the last cluster was expected from earlier work.[5,83]

The cluster $[Cs_3Sn_9]^+$ supports the existence of the polyanion Sn_9^{2-}. Although this polyanion has never been observed for Sn, a Ge analogue has been stabilized[83] as part of a complicated solid, [(2,2,2-crypt $K)_6$ $Ge_{18}\cdot 2.5$ en], which contains Ge_9^{4-} and Ge_9^{2-} anions. The structure of Ge_9^{2-} is probably similar to that of Sn_9^{2-} (Fig. 25).

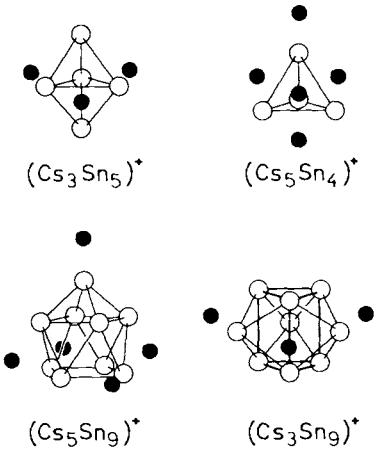


Fig. 25. The structure of several polyanions (empty circles) [24-28] and the probable distribution of alkali metal ions (filled circles) in the corresponding Cs-Sn clusters.

Not found in the mass spectrum of Cs-Sn clusters (Fig. 24) is a strong peak corresponding to $[Cs(Cs_2Sn_5)_2]^+$. That is, the Sn_5^{2-} polyanion does not act as a building block for larger clusters and is therefore less likely to be found as a unit in pure crystals.

Increasing the Cs partial pressure results in the cluster mass spectrum shown in Figure 26. All peaks due to pure Sn clusters are absent. Two series of peaks emerge—one for clusters containing three Cs atoms and the other for clusters containing five Cs atoms. This selectivity reflects the strong tendency to form clusters with paired electrons only. Sn atoms contain an even number of valence electrons, Cs atoms an odd number. However, one Cs electron is ejected on cluster ionization. Therefore, an odd number of Cs atoms leads to an even number of electrons in the cluster ion.

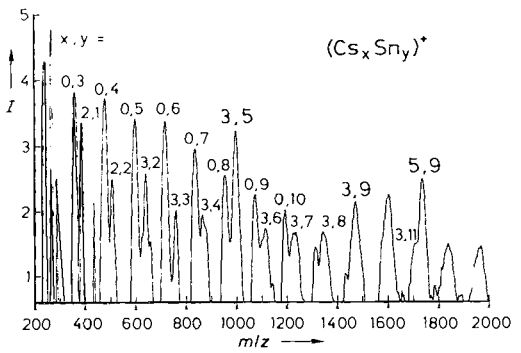


Fig. 24. Mass spectrum of a mixture of Cs-Sn clusters. The peaks are broad due to the large number of Sn isotopes. The clusters $[Cs_3Sn_5]^+$ and $[Cs_5Sn_9]^+$ are particularly stable.

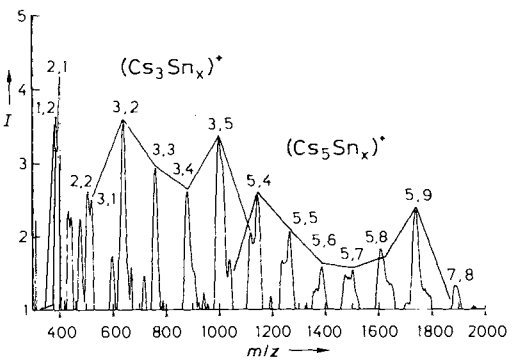


Fig. 26. Mass spectrum of a mixture of Cs-Sn clusters.

Among clusters having a higher Cs content, $[Cs_5Sn_4]^+$ is unusually stable. This may indicate the presence of the polyanion Sn_4^{4-}. Since this anion is isoelectronic with P_4, it would be expected to have a tetrahedral structure. In fact, tetrahedral Ge_4^{4-} units have been observed in lithium and sodium germanide crystals.[84-86] $[Cs_5Sn_4]^+$ could also be described as $[Cs(Cs_2Sn_2)_2]^+$. The mass peak corresponding to the first member of this sequence, $[Cs(Cs_2Sn_2)]^+$, is also strong.

3.8. Indium–Phosphorus Clusters

InP is a good semiconductor. However, the InP molecule is not found in the vapor phase. On evaporation, InP dissociates into In atoms and P_4 and P_2 molecules. Therefore, we would not have been surprised to find that In and P do not react in the vapor phase—but they do. A mass spectrum of the mixture of clusters is shown in Figure 27. The shaded peaks correspond to pure In clusters. The peaks immediately following each shaded peak correspond to clusters containing one or two P atoms. Clusters containing three P atoms are also present but they are one order of magnitude weaker. In Figure 27 we have joined with a short vertical bar the peaks of clusters containing one or two P atoms but the same number of In atoms. The peak corresponding to $[In_6P]^+$ is stronger than that of $[In_6P_2]^+$, whereas the peak identified as $[In_7P]^+$ is weaker than that of $[In_7P_2]^+$. In general, $[In_xP]^+$ clusters are more stable for even values of x and $[In_xP_2]^+$ clusters are more stable for odd values of x. This is another manifestation of the rule that stable clusters prefer to have an even number of electrons. $[In_5P]^+$ is an exception to this rule. Two other clusters that stand out from the rest are $[In_9P_2]^+$ and $[In_8P_3]^+$.

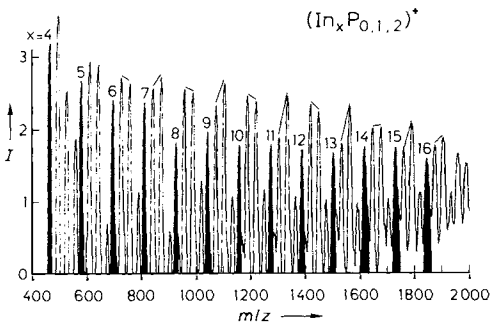


Fig. 27. Mass spectrum of a mixture of In–P clusters formed by combining red phosphorus vapor (390 °C) with indium vapor (970 °C). Black peaks correspond to pure In clusters. Each subsequent peak corresponds to the addition of one more P atom. Clusters containing an odd number of atoms tend to be more stable.

3.9. Potassium–Phosphorus Clusters

A mass spectrum of clusters formed by quenching the mixed vapors of red phosphorus and potassium is shown in Figure 28. Analysis of this spectrum reveals a double periodicity; that is, two highly stable building blocks exist. One series corresponds to the clusters $[K(K_3P_7)_n]^+$. P_7^{3-} is a well-known[8] polyanion of phosphorus occurring in several compounds, including K_3P_7. The other series indicates the existence of a new polyanion, P_4^{2-}. The clusters observed in this case are $[K(K_2P_4)_n]^+$. Also easily identified are the mixed clusters $[K(K_2P_4)_n(K_3P_7)_m]^+$. The polyanion P_4^{2-} may have the butterfly configuration (Fig. 28), already observed[87] in R_2P_4 ($R=(Me_3Si)_2N$, 2,4,6-tBu$_3$C$_6$H$_2$).

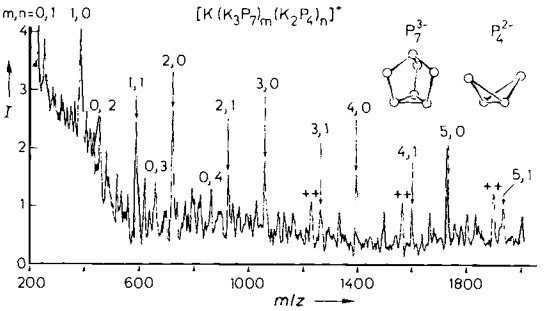


Fig. 28. Mass spectrum of a mixture of K–P clusters formed by combining potassium vapor (230 °C) with red phosphorus vapor (390 °C) in cold He gas. The clusters contain the phosphorus polyanions P_7^{3-} and P_4^{2-}.

3.10. Clusters Prepared from Elements of the 5th and 6th Main Groups

Arsenic and sulfur combine to form a rich variety of compounds. As_4S_4 (realgar) is composed of eight-atom molecules weakly bonded to one another by van der Waals forces. As_2S_3 has a polymeric layer structure (orpiment). Finally, molten As–S can be quenched to form a glass. One motivation for studying the relative stability of As–S clusters is the identification of other highly stable building blocks, which could lead to the synthesis of new compounds. Moreover, information concerning the stability of cluster ions in the vapor phase could shed light on the structure of glasses.

Before examining the results of experiment, it is useful to first consider qualitatively what types of clusters might be expected in quenched vapors containing various As:S ratios. Pure arsenic vapor is known to contain As_4 molecules. On quenching the vapor, these molecules would presumably condense into As_{4n} clusters composed of tetrahedral units weakly bonded to one another. The first sulfur atoms to be incorporated into the As_4 tetrahedral unit can be expected to bridge As atoms. This will be possible until all six edges of the tetrahedron are occupied by S atoms. High stability is expected for the symmetric molecules As_4S_3, As_4S_4, and As_4S_6 (Fig. 29). Pure sulfur has two crystalline forms, which consist of ordered arrays of S_8 rings. These rings can persist even into the melt. Therefore, clusters composed of S_8 rings weakly bonded together would not be unexpected. On the other hand, sulfur also forms polymer chains. Addition of a small amount of As to the vapor could result in the linking of rings and chains together. Two of the bonds to arsenic are required in order to incorporate the As atom into the ring. The remaining valence is available for branching (Fig. 29, top right), or it can form an As–As bond with a second arsenic atom in the same ring or in another sulfur ring.

Before analyzing the relatively complex mass spectra of As–S clusters, it is instructive to first consider the spectra of two seemingly closely related materials, phosphorus sul-

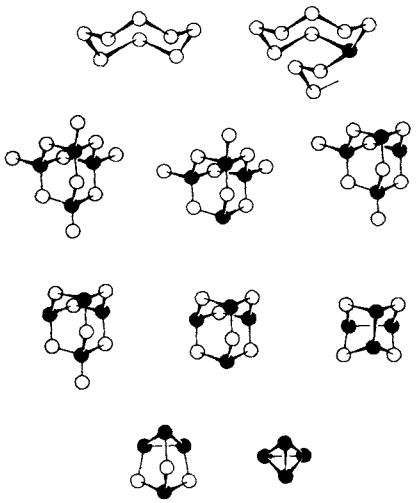


Fig. 29. Some probable structures of As_nS_m molecules and clusters. Filled circles are As atoms, empty circles are S atoms.

fides and arsenic oxides. The mass spectrum of a mixture of clusters formed by quenching the vapor of P_4S_3 in helium gas is shown in Figure 30. The analysis of this spectrum is made difficult by the similarity of the atomic masses of the two component atoms, ^{31}P and ^{32}S. In principle, we can determine from a low-resolution mass spectrum only the total number of atoms in a cluster. Each

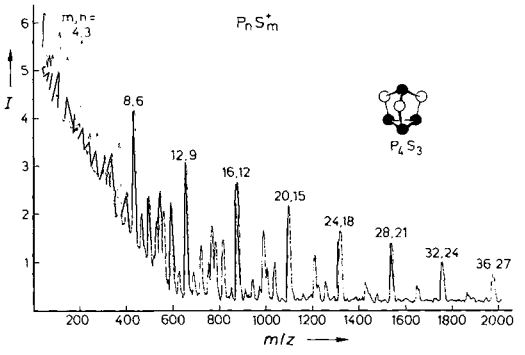


Fig. 30. Mass spectrum of clusters formed by quenching of P_4S_3 vapor.

strong line in the spectrum is separated from the other strong lines by a distance corresponding to seven atoms. Since P_4S_3 is a stable molecule,[88] the strong lines most likely correspond to the clusters $[P_4S_3]_n^+$ (n = 1–9). The next strongest lines occur exactly halfway between the strongest lines and are, therefore, probably due to the doubly ionized clusters $[P_4S_3]_n^{2+}$. Double ionization without fragmentation appears to be more probable in large clusters, where the excess positive charge can occupy a greater volume, thus reducing the energy of the species. The weaker lines correspond to fragments. The most important feature of the mass spectrum of the P–S clusters can be seen at first glance: it is extremely simple. Singly and doubly charged clusters of only one type are observed. These clusters are constructed from P_4S_3 building blocks. Presumably, these units are only weakly bonded to one another, as is the case in the molecular crystal. This simplicity is in sharp contrast to the mass spectrum of As–S clusters (see below).

The mass spectrum of clusters formed by quenching the vapor of As_2O_3 in helium is also easy to interpret (Fig. 31).[89] The mass peaks of the clusters $[As_4O_6]_n^+$ (n = 1, 2, 3, ...) are strongest. As_4O_6 is a building block in two mod-

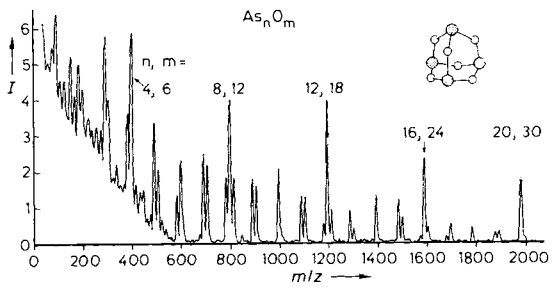


Fig. 31. Mass spectrum of clusters formed by quenching of As_2O_3 vapor.

ifications of arsenic oxide, arsenolite and claudetite. The As_4O_6 units are weakly bonded to one another to form cubic and monoclinic structures in the crystal. Since the most intense lines in the cluster mass spectrum belong to As_4O_6, As_8O_{12}, $As_{12}O_{18}$, $As_{16}O_{24}$, and $As_{20}O_{30}$, it is clear that stable As_4O_6 units are also building blocks in the formation of clusters. The next strongest peaks occur exactly halfway between the strongest peaks and are therefore probably due to either $[As_4O_6]_n^{2+}$ or $[As_2O_3]_n^+$. This ambiguity did not exist for the corresponding peaks of the P–S clusters. In that case they were identified as doubly ionized clusters.

Figure 32 shows the mass spectrum of clusters formed by the evaporation of As_2S_3 glass.[89] The spectrum contains many lines, but all can be assigned to $[As_nS_x]^+$ clusters. The peaks corresponding to n = 4, 6, 8, and 10 have been labeled explicitly. The remaining peaks are due to clusters with odd values of n. Particularly strong lines are observed, for example for $[As_4S_3]^+$, $[As_4S_4]^+$, $[As_4S_8]^+$, $[As_6S_9]^+$, $[As_8S_{13}]^+$, and $[As_{10}S_{17}]^+$. It would not be proper to conclude that these clusters necessarily occur in the beam of neutral clusters, because relatively high energy (70-eV) electrons have been used for ionization. This results in high sensitivity but also in a high degree of fragmentation. It is valid to assume, however, that a strong line in the mass spectrum indicates the existence of a highly stable cluster of the same mass, be it neutral cluster or ionized fragment. The fragmentation, far from being a hindrance, allows us to examine the stability of a larger variety of clusters than is found in the beam of neutral clusters.

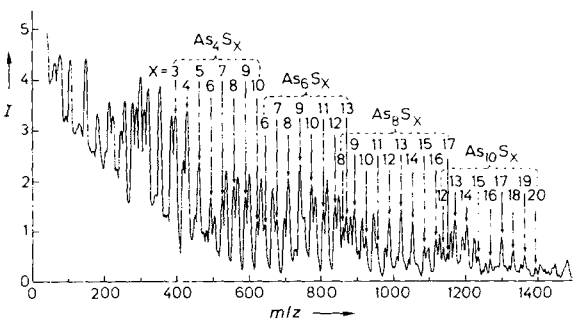


Fig. 32. Mass spectrum of clusters formed by quenching As_2S_3 vapor.

Although many As–S clusters can be identified as being highly stable, only As_4S_4 is observed to act as a building block in the formation of larger van der Waals clusters. Many of the other clusters, such as $[As_7S_{13}]^+$ are probably stable only in the ionic form and are therefore not suitable as building units in the absence of charge compensating anions. On the other hand, these stable ions could be of interest in the synthesis of ionic cluster compounds.

As_2S_3 condenses into a glassy state. As_2S_3 glass prepared from the melt is thought to contain almost exclusively As–S bonds.[90] As_2S_3 condensed from the vapor phase, on the other hand, seems to contain a large fraction of homonuclear bonds. Assuming that As_2S_3 glass has the same local composition as these clusters, we can draw the following conclusions: The molecule As_4S_6 plays no important role in the structure of As_2S_3 glass. Our mass spectra suggest that the first stable building block with composition $As_{2n}S_{3n}$ is the molecule As_6S_9. In addition, excess sulfur does not result in the formation of S–S bonds but rather in fourfold-coordination of As atoms by terminal sulfur atoms.

4. Concluding Remarks

Not all elements are equally suited for the type of investigation reported in this article. The ideal element has the following properties: a high vapor pressure at low temperature; only one isotope; high reactivity; not too large but not too small atomic mass. If an element is too heavy, large clusters cannot be observed in the mass range available to us (0–2000 amu). If the element is too light, the masses of the reaction products overlap one another, making it difficult to assign mass peaks.

It would appear from these findings that a strong peak in a mass spectrum usually reflects a high stability of the corresponding charged cluster. This is true not only for cluster ions, for example $[Rb_{14}Cl_{13}]^+$, but also for the more covalently bonded suboxides and subhalides for which the total electron spin seems to play a decisive role. The question arises to what extent the stability of the neutral parent cluster influences the mass spectra. The results for the pure sulfur clusters and for As–O, As–S, P–O, and P–S clusters indicate that very stable neutral clusters (S_8, As_4O_6, P_4S_3) can indeed be observed as positive ions by mass spectroscopy even though the removal of an electron decreases their stability. However, these "neutral clusters' are so strongly bonded that they appear in the solid, liquid, and vapor phases and are therefore more appropriately called molecules. In summary, neutral clusters composed of exceptionally highly stable units (molecules) can appear as strong peaks in mass spectra. However, in general, the character of a mass spectrum is determined by the stability of charged fragments.

Although the stable clusters M_9O_2 and $M_{11}O_3$ found in cesium and rubidium suboxide crystals can be thought of as being constructed from face-sharing M_6O octahedra, our mass spectrometric study shows that the clusters $[M_6O]^+$ and $[M_6S]^+$ are particularly unstable. Therefore, this cluster probably does not act as a building block for the growth of larger clusters.

An important finding of our investigations is the rule that stable clusters contain an even number of electrons. This rule is particularly valid for subhalide and suboxide clusters and indicates that a strong covalent contribution is made to the bonding of metal-rich clusters. The normal halides, for which each ion has a rare gas electronic configuration, can be well described by a purely ionic model of the bonding.

Mass spectrometry of clusters formed by the reaction and quenching of elementary vapors should prove to be of value in the search for new compounds. The composition of the clusters can be changed quickly and continuously by adusting the oven temperature of each of the elements. The relative stability of each cluster can be immediately determined from the mass spectrum. However, it is important to remember that it is usually the stability of a charged fragment that is being measured.

Mass spectra are capable of indicating two different degrees of cluster stability. An isolated, intense mass peak indicates a high stability for a particular cluster. A periodic appearance of intense peaks indicates that a cluster is stable not only as an isolated unit but can be used as a building block in the construction of larger clusters. It should be possible to synthesize solids from the same unit. The two kinds of stability are illustrated by clusters containing the two polyanions Sn_5^{2-} and P_4^{2-}. Although $[Cs(Cs_2Sn_5)]^+$ is stable as an isolated cluster, it does not appear to have a strong tendency to build larger units $[Cs(Cs_2Sn_5)_n]^+$. The tetraphosphorus dianion does occur in the sequence of mass peaks $[K(K_2P_4)_n]^+$ and is therefore a candidate for a new solid compound.

Many stimulating discussions with H. G. von Schnering and A. Simon are gratefully acknowledged.

Received: April 23, 1985 [A 568 IE]
Geman version: *Angew. Chem. 98* (1986) 197

[1] See articles in Proc. Int. Meet. Small Particles and Inorg. Clusters in *J. Phys. (Paris), Suppl. C2* (1977) and *Surf. Sci. 106* (1981); *156* (1985).
[2] See articles in J. Bourdon (Ed.): *Growth and Properties of Metal Clusters, Applications to Catalysis and the Photographic Process*, Elsevier, Amsterdam 1980.
[3] See articles in: *Ber. Bunsenges. Phys. Chem. 88* (1984) 188–314.
[4] Recent review: a) T. D. Märk, A. W. Castleman, Jr., *Adv. At. Mol. Phys. 20* (1985) 65–172; b) T. P. Martin, *Festkörperprobleme 24* (1984) 1–24.
[5] E. Zintl, *Angew. Chem. 52* (1939) 1.
[6] H. Schäfer, B. Eisenmann, W. Müller, *Angew. Chem. 85* (1973) 742; *Angew. Chem. Int. Ed. Engl. 12* (1973) 694.
[7] A. Simon, *Angew. Chem. 93* (1981) 23; *Angew. Chem. Int. Ed. Engl. 20* (1981) 1.
[8] H. G. von Schnering, *Angew. Chem. 93* (1981) 44; *Angew. Chem. Int. Ed. Engl. 20* (1981) 33.
[9] T. P. Martin, *J. Chem. Phys. 81* (1984) 4426.
[10] E. W. Becker, K. Bier, W. Henkes, *Z. Phys. 146* (1956) 333.
[11] O. F. Hagena, W. Obert, *J. Chem. Phys. 56* (1972) 1793.
[12] J. Gspann, K. Körting, *J. Chem. Phys. 59* (1973) 4726.
[13] S.-S. Lin, *Rev. Sci. Instrum. 44* (1973) 576.
[14] J. O. Searcy, J. B. Fenn, *J. Chem. Phys. 61* (1974) 5292.
[15] G. D. Stein, J. A. Armstrong, *J. Chem. Phys. 58* (1973) 1999.
[16] D. Dreyfuss, H. Y. Wachmann, *J. Chem. Phys. 76* (1982) 2031.
[17] R. J. Beuhler, L. Friedmann, *J. Chem. Phys. 77* (1982) 2549.
[18] A. J. Stace, C. Moore, *Chem. Phys. Lett. 96* (1983) 80.
[19] G. Torchet, P. Schwartz, J. Farges, M. F. de Feraudy, B. Raoult, *J. Chem. Phys. 79* (1983) 6196.
[20] H. Haberland, H.-G. Schindler, D. R. Worshop, *Ber. Bunsenges. Phys. Chem. 88* (1984) 270.
[21] O. Echt, D. Kreisle, M. Knapp, E. Recknagel, *Chem. Phys. Lett. 108* (1984) 401.

[22] A. Herrmann, S. Leutwyler, E. Schumacher, L. Wöste, *Helv. Chim. Acta 61* (1978) 453.
[23] M. M. Kappes, R. W. Kunz, E. Schumacher, *Chem. Phys. Lett. 91* (1982) 413.
[24] J. L. Gole, G. J. Green, S. A. Pace, D. R. Preuss, *J. Chem. Phys. 76* (1982) 2247.
[25] K. I. Peterson, P. D. Dav, R. W. Farley, A. W. Castleman, Jr., *J. Chem. Phys. 80* (1984) 1780.
[26] W. D. Knight, K. Clemenger, W. A. de Heer, W. A. Saunders, M. Y. Chou, M. L. Cohen, *Phys. Rev. Lett. 52* (1984) 2141.
[27] G. Delacretaz, L. Wöste, *Surf. Sci. 156* (1985) 770.
[28] T. A. Milne, A. E. Vandegrift, F. T. Greene, *J. Chem. Phys. 52* (1970) 1552.
[29] J. Farges, B. Raoult, G. Torchet, *J. Chem. Phys. 59* (1973) 3454.
[30] O. Echt, K. Sattler, E. Recknagel, *Phys. Rev. Lett. 47* (1981) 1121.
[31] A. Ding, J. Hesslich, *Chem. Phys. Lett. 94* (1983) 54.
[32] L. Friedman, R. J. Beuher, *J. Chem. Phys. 78* (1983) 4669.
[33] A. J. Stace, *Chem. Phys. Lett. 113* (1985) 355.
[34] A. Amirav, U. Even, J. Jortner, *J. Chem. Phys. 75* (1981) 2489; *86* (1982) 3345.
[35] U. Even, J. Jortner, *J. Chem. Phys. 87* (1983) 28.
[36] F. Honda, G. M. Lancaster, Y. Fukuda, S. W. Rabelais, *J. Chem. Phys. 69* (1978) 4931.
[37] J. Campana, T. M. Barlak, R. J. Colton, J. J. De Corpo, J. R. Wyatt, B. I. Dunlap, *Phys. Rev. Lett. 47* (1981) 1046.
[38] T. M. Barlak, J. E. Campana, R. J. Colton, J. J. De Corpo, J. R. Wyatt, *J. Chem. Phys. 85* (1981) 3840.
[39] T. M. Barlak, J. R. Wyatt, R. J. Colton, J. J. De Corpo, J. E. Campana, *J. Am. Chem. Soc. 104* (1982) 1212.
[40] T. M. Barlak, J. E. Campana, J. R. Wyatt, R. J. Colton, *J. Chem. Phys. 87* (1983) 3441.
[41] W. Ens, R. Beavis, K. G. Standing, *Phys. Rev. Lett. 50* (1983) 27.
[42] R. Pflaum, P. Pfau, K. Sattler, E. Recknagel, *Surf. Sci. 156* (1985) 165.
[43] T. P. Martin, *Ber. Bunsenges. Phys. Chem. 88* (1984) 300.
[44] T. P. Martin, A. Kakizaki, *J. Chem. Phys. 80* (1984) 3956.
[45] T. P. Martin, *Phys. Rep. 95* (1983) 167.
[46] T. P. Martin, *J. Chem. Phys. 67* (1977) 5207; *69* (1980) 2036; *72* (1980) 3506.
[47] D. O. Welch, O. W. Lazareth, G. J. Dienes, R. D. Hatcher, *J. Chem. Phys. 64* (1976) 835; *68* (1978) 2159.
[48] M. R. Hoare, *Adv. Chem. Phys. 40* (1979) 49.
[49] K. Kimoto, Y. Kamiya, M. Nonoyama, R. Uyeda, *Jpn. J. Appl. Phys. 2* (1963) 702.
[50] N. Wada, *Jpn. J. Appl. Phys. 7* (1968) 1287.
[51] C. G. Granqvist, R. A. Buhrman, *J. Appl. Phys. 47* (1976) 2200.
[52] H. Abe, W. Schulze, B. Tesche, *Chem. Phys. 47* (1980) 95.
[53] K. Sattler, J. Mühlbach, E. Recknagel, *Phys. Rev. Lett. 45* (1980) 821.
[54] P. Pfau, K. Sattler, J. Mühlbach, R. Pflaum, E. E. Recknagel, *J. Phys. F12* (1982) 2131.
[55] G. Pacchioni, D. Plavsic, J. Koutecky, *Ber. Bunsenges. Phys. Chem. 87* (1983) 503.
[56] a) E. A. Rohlfing, D. M. Cox, A. Kaldor, *J. Chem. Phys. 8* (1984) 3322; b) H. W. Kroto, J. R. Heath, S. C. O'Brien, R. F. Curl, R. E. Smalley, *Nature (London) 318* (1985) 162.
[57] D. W. Powers, S. G. Hansen, M. E. Gensic, A. C. Pulu, J. B. Hopkins, T. G. Dietz, M. A. Duncan, P. R. R. Langridge-Schmith, R. E. Smalley, *J. Phys. Chem. 86* (1982) 2556.
[58] V. E. Bondybey, J. H. Englisch, *J. Chem. Phys. 76* (1982) 2165.
[59] S. J. Riley, E. K. Parks, G. C. Nieman, L. G. Pogo, S. Wexler, *J. Chem. Phys. 80* (1984) 1360.
[60] K. Sattler, J. Mühlbach, O. Echt, P. Pfau, E. Recknagel, *Phys. Rev. Lett. 47* (1981) 160.
[61] H. G. von Schnering, N. K. Goh, *Naturwissenschaften 61* (1974) 272.
[62] G. J. Janz, E. Roduner, J. W. Coutts, J. R. Downey, Jr., *Inorg. Chem. 15* (1976) 1751.
[63] J. Diefenbach, T. P. Martin, *Surf. Sci. 156* (1985) 234.
[64] M. Leleyter, P. Joyes, *J. Phys. (Paris) 36* (1975) 343; *J. Phys. (Paris) Suppl. C2* (1977) 11.
[65] A. Simon, *Struct. Bonding (Berlin) 36* (1979) 81–127.
[66] A. Simon, *Z. Anorg. Allg. Chem. 431* (1977) 5; *422* (1976) 208; *395* (1973) 301.
[67] A. Simon, W. Brämer, H.-J. Deiseroth, *Inorg. Chem. 17* (1978) 875.
[68] T. P. Martin, H.-J. Stolz, G. Ebbinghaus, A. Simon, *J. Chem. Phys. 70* (1979) 1096.
[69] H. Föppl, *Z. Anorg. Allg. Chem. 297* (1957) 12.
[70] J. Koutecky, G. Pacchioni, *Ber. Bunsenges. Phys. Chem. 88* (1984) 233.
[71] G. Pacchioni, J. Koutecky, *Chem. Phys. 71* (1982) 181; *J. Chem. Phys. 77* (1982) 5850.
[72] D. Plavsic, J. Koutecky, G. Pacchioni, V. Bonacic-Koutecky, *J. Phys. Chem. 87* (1983) 1096.
[73] J. Flad, H. Stoll, H. Preuss, *J. Chem. Phys. 71* (1979) 3042.
[74] J. Flad, G. Igel, M. Dolg, H. Stoll, H. Preuss, *J. Chem. Phys. 75* (1983) 331; M. P. Iniguez, C. Baladron, J. A. Alonso, *Surf. Sci. 127* (1983) 367.
[75] R. Car, J. L. Martins, *Surf. Sci. 106* (1981) 280.
[76] P. von R. Schleyer, E.-U. Würthwein, J. A. Pople, *J. Am. Chem. Soc. 104* (1982) 5839.
[77] E.-U. Würthwein, P. von R. Schleyer, J. A. Pople, *J. Am. Chem. Soc. 106* (1984) 6973.
[78] M. Allavena, E. Blaisten-Barojas, B. Silva, *J. Chem. Phys. 75* (1981) 787; G. Bravo, E. Blaisten-Barojas, *Chem. Phys. Lett. 108* (1984) 237.
[79] W. van der Lugt, W. Geertsma, *J. Non-Cryst. Solids 61* (1984) 187.
[80] H. Hoshino, R. W. Schmutzler, F. Hensel, *Phys. Lett. 51A* (1975) 7.
[81] N. E. Christensen, S. Kollar, *Solid State Commun. 46* (1983) 727.
[82] a) T. P. Martin, *J. Chem. Phys. 83* (1985) 78; b) T. Scheuring, K. G. Weil, *Surf. Sci. 156* (1985) 457.
[83] a) P. A. Edwards, J. D. Corbett, *Inorg. Chem. 16* (1977) 903; b) C. H. E. Belin, J. D. Corbett, A. Cisar, *J. Am. Chem. Soc. 99* (1977) 7163.
[84] E. Busman, *Z. Anorg. Allg. Chem. 313* (1961) 90.
[85] J. Witte, H. G. von Schnering, *Z. Anorg. Allg. Chem. 327* (1964) 260.
[86] J. Llanos, R. Nesper, H. G. von Schnering, *Angew. Chem. 95* (1983) 1026; *Angew. Chem. Int. Ed. Engl. 22* (1983) 998.
[87] a) E. Niecke, R. Rüger, B. Krebs, *Angew. Chem. 94* (1982) 553; *Angew. Chem. Int. Ed. Engl. 21* (1982) 544; b) R. Riedel, H.-D. Hausen, E. Fluck, *ibid. 97* (1985) 1050 and *24* (1985) 1056.
[88] H. G. von Schnering in A. L. Rheingold (Ed.): *Homoatomic Rings and Chains*, Elsevier, Amsterdam 1977, p. 317.
[89] T. P. Martin, *Solid State Commun. 47* (1983) 111; *J. Chem. Phys. 80* (1984) 170.
[90] A. J. Apling, A. J. Leadbetter, A. C. Wright, *J. Non-Cryst. Solids 23* (1977) 369.

New Methods for the Synthesis of Glycosides and Oligosaccharides—Are There Alternatives to the Koenigs-Knorr Method?

New Synthetic Methods (56)

By Richard R. Schmidt*

Dedicated to Professor Rudolf Gompper on the occasion of his 60th birthday

Glycoproteins, glycolipids, and glycophospholipids (glycoconjugates) are components of membranes. The oligosaccharide residue is responsible for intercellular recognition and interaction; it acts as a receptor for proteins, hormones, and viruses and governs immune reactions. These significant activities have stimulated interest in oligosaccharides and glycoconjugates. With their help it should be possible to clarify the molecular basis of these phenomena and to derive new principles of physiological activity. Major advances in the synthesis of oligosaccharides have been made by the use of the Koenigs-Knorr method, in which glycosyl halides in the presence of heavy-metal salts are employed to transfer the glycosyl group to nucleophiles. The disadvantages of this procedure have led to an intensive search for new methods. Such methods will be discussed in this article. Emphasis is placed on glycoside and saccharide formation by 1-*O*-alkylation, on the trichloroacetimidate method, and on activation through the formation of glycosylsulfonium salts and glycosyl fluorides.

1. Introduction

Carbohydrates and proteins were long viewed quite differently. Proteins were considered particularly important because of enzymatic activity (i.e., as carriers of specific biological information). Corresponding properties were not established for the carbohydrates; they were assumed to have only structural, protective, and energy-storing functions. The large number of biological polymers in which carbohydrates and proteins are chemically linked to each other by a covalent bond (glycoproteins) were not recognized until the beginning of the 1950s. Thus, much effort was often expended in attempts to remove "sugar impurities" from proteins or "protein impurities" from sugars. Only in the last twenty years has it been shown that covalently linked glycoconjugates of carbohydrates and proteins are ubiquitous and occur, for example, as components of cell membranes (Fig. 1).[1-3] In addition, glycoconjugates of carbohydrates and lipids (glycolipids) or phospholipids (glycophospholipids) are encountered in membranes.[4] The biological information in these substances is carried mainly by the carbohydrate part.[5,6]

The membranes of different cells differ from one another in their composition and in the arrangement and mobility of their components. A central role of the immune system of mammalian organisms is the recognition and discrimination of endogenous and exogenous structures.[7] The immune system monitors the constancy of the cellular surfaces in the organism. It responds when the tolerance limits of the endogenous surface structure are exceeded.

Membrane glycoproteins and lipids, specifically their oligosaccharide components, govern these tolerance limits;[2,5,8] they are therefore decisive for specific immune reactions. Moreover, they fulfill important functions in intercellular recognition and interaction, in the control of cell growth and thus tumor formation, and in the interaction with biologically active factors such as enzymes, hormones, bacteriotoxins, and viruses. As an example, glycosphingolipids undergo significant changes when malignant cell growth starts. In particular, the structure of the hydrophilic carbohydrate residue becomes simplified.[8]

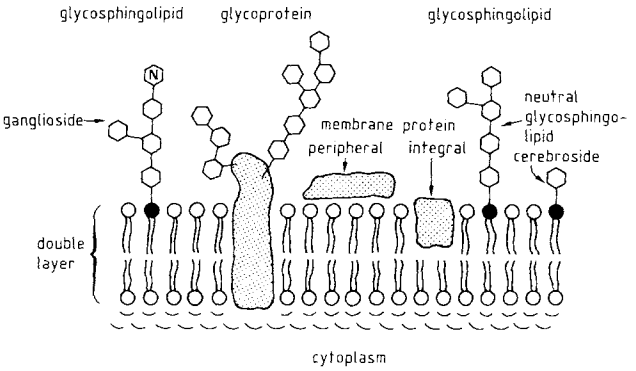


Fig. 1. Cell membranes of erythrocytes with carbohydrate and protein components, schematic. The hexagons represent hexopyranose units, the hexagon marked with N indicates an *N*-acetylneuraminic acid unit. ○= in the double layer represents a phosphoglycerolipid or phosphosphingolipid, ●= represents a ceramide.

The biological significance of glycoconjugates should be viewed by the synthetic chemist as a major challenge. The synthesis and modification of oligosaccharide units and their coupling with appropriate lipids, phospholipids, and proteins is essential to extend our knowledge on the molecular mode of action of glycoconjugates and, furthermore, to derive new principles of physiological activity, since homogeneous compounds are often only very difficultly accessible from biological material.

[*] Prof. Dr. R. R. Schmidt
Fakultät Chemie der Universität
Postfach 5560, D-7750 Konstanz (FRG)

2. Synthesis of Complex Oligosaccharides—General Aspects

2.1. General Remarks

The synthesis of oligosaccharides is characterized by a much larger number of possibilities for coupling than that of other natural biopolymers, such as peptides or proteins and ribo- or deoxyribonucleotides. The comparison of the number of possible isomers of di-, tri-, tetra-, and pentasaccharides with those of the corresponding peptides and nucleotides given in Table 1 impressively illustrates this point.[9] The wide structural variety renders sugars and, in particular, oligosaccharides ideal as carriers of biological information. In contrast to peptides and nucleotides, in which the informational content is determined solely by the number and sequence of different monomer units, the informational content of oligosaccharides is fixed additionally by the site of the coupling, by the configuration of the glycosidic linkage (α or β), and by the occurrence of branching. Thus, polymers made up of carbohydrates can carry considerably more information per building block than proteins and nucleic acids.

The structural variety, however, complicates the specific biosynthesis of complex *oligo*saccharides. "Zipper" processes are not known. In general, the formation of each saccharide linkage requires a specific enzyme; thus, in comparison with the synthesis of proteins and nucleic acids, much more effort is required. Therefore it is not surprising that complex *poly*saccharides with corresponding functions are unknown.

The chemical synthesis of oligosaccharides is also more complicated than that of other biopolymers. Up to a few years ago, the unambiguous synthesis of a di- or trisaccharide was an outstanding achievement.[10–12] We have only learned how to synthesize more complex oligosaccharides in the last few years.[13,14] The construction of each individual oligosaccharide poses a new challenge, requiring a knowledge of methods, experience, and experimental dexterity. There are no universal methods either for chemical in vitro or for biological in vivo syntheses.

Table 1. Isomeric possibilities for biopolymers [9]. D- and L-forms not included.

Product	Composition	Number of isomers	
		Peptide, nucleic acid [a]	Saccharide [b]
monomer	Z	1	1
dimer	Z_2	1	11
trimer	Z_3	1	120
tetramer	Z_4	1	1424
pentamer	Z_5	1	17872
monomer	Z	1	1
dimer	YZ	2	20
trimer	XYZ	6	720
tetramer	WXYZ	24	34560
pentamer	VWXYZ	120	2144640

[a] 3′→5′ deoxyribo- or ribonucleic acid. [b] Referred to hexopyranoses (Glc, Gal, Man, ...).

In a disaccharide synthesis, two polyfunctional sugar components must be linked. Regioselectivity is generally achieved when the glycosylating component (glycosyl donor) possesses selectively protected hydroxyl groups and an activating group at the anomeric C atom and when the sugar component with the free hydroxyl group (glycosyl acceptor) possesses protecting groups at all other hydroxyl functions (Fig. 2). Thus, complicated protecting strategies and suitable procedures for activation at the anomeric C atom are required. In addition, the coupling step must oc-

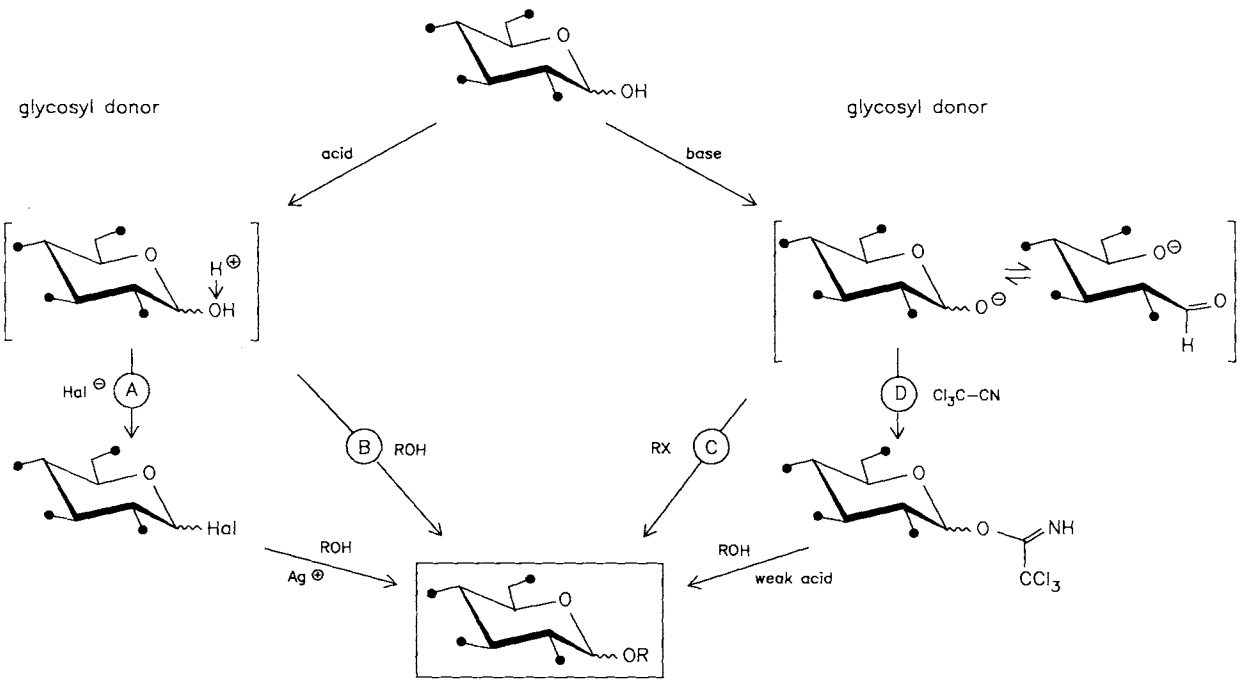


Fig. 2. Syntheses of glycosides and saccharides, schematic. R = alkyl, aryl, (mono)saccharide moiety. Ⓐ Koenigs-Knorr method (glycosyl halide activation). Ⓑ Fischer-Helferich method (acid activation). Ⓒ 1-*O*-Alkylation (base activation). Ⓓ Trichloroacetimidate method (base-acid activation); instead of trichloroacetonitrile, other reagents of the type A≡B or A=B=C can be employed (e.g., ketene imines $R_2C{=}C{=}NR$).

cur diastereoselectively with respect to formation of an α- or β-linkage.

2.2. Oligosaccharides by the Koenigs-Knorr Method

In the classical Koenigs-Knorr method, dating from 1901, and the subsequently developed, efficient variants, the activation is achieved through the formation of glycosyl halides (halogen = bromine, chlorine) and their reaction in the presence of heavy-metal salts (preferentially silver salts).[13-16] Recent reviews[13,14] give the following general picture.

(1) The reactivity of the glycosyl donor (i.e., the glycosyl halide) can be varied over relatively wide ranges by the choice of the halogen, the catalyst (promotor), and the protecting group pattern.
(2) Diastereoselectivity in the coupling is attained by
   (a) participation of neighboring groups for β-glycosides of D-glucose, D-glucosamine, D-galactose, and D-galactosamine and for α-glycosides of D-mannose, L-fucose, and L-rhamnose,
   (b) in situ anomerization of the α-glycosyl halide to the more reactive β-glycosyl halide,[17] which reacts preferentially to give the more stable α-glycosides of D-glucose, D-glucosamine, D-galactose, and D-galactosamine (exploitation of the anomeric effect), and
   (c) heterogeneous catalysis,[18] which gives good results in the difficult formation of the β-D-mannose linkage.
(3) The reactivity of the glycosyl acceptor, which, for D-glucopyranose, gives the approximate order water > methanol > ethanol > 6-OH ≫ 3-OH > 2-OH > 4-OH groups of D-glucose, is controlled by the choice of the protecting groups (steric and electronic effects) and by modification of the structure (e.g., formation of 1,6-anhydro structures).[13]

The application of these generalizations has led to excellent results.[13,14]

In spite of the development of efficient variants, however, severe, partly inherent disadvantages of the Koenigs-Knorr method for the synthesis of oligosaccharides could not be overcome. These disadvantages include the following:

(1) Relatively harsh conditions are needed for the generation of the glycosyl halide;
(2) The glycosyl halides exhibit low thermal stability and can often be generated only in situ and at lower temperatures, thus necessitating the use of compounds that are frequently sterically nonhomogeneous and sometimes even impure;
(3) the glycosyl halides are highly sensitive to hydrolysis;
(4) the heavy-metal salts are expensive;
(5) the use of heavy-metal salts, especially in large scale reactions, is often dangerous (toxicity of mercury salts, explosions with silver perchlorate; these risks can be reduced sometimes by using catalytic amounts).

Many attempts have been made to develop competitive methods, which do not require the use of heavy-metal salts, to synthesize glycosides or saccharides.[19] However, until recently, their general significance was described as being modest.[13]

2.3. Derivation of New Principles for Glycoside Synthesis

The Koenigs-Knorr method for glycoside synthesis consists of a two-step reaction (Fig. 2, Path Ⓐ): introduction of a leaving group at the anomeric center and catalytic nucleophilic substitution of this leaving group. In general, for a sterically uniform α- or β-coupling, both steps must proceed under steric control. This is achieved mainly by exploitation of stereoelectronic effects (anomeric and inverse anomeric effects) and neighboring group participation and by the choice of catalyst (see Section 2.2). The acid-catalyzed glycosylation according to the Fischer-Helferich method (Fig. 2, Path Ⓑ), which proceeds via normal acetal formation, does not involve an isolable intermediate and, partly as a result of its reversibility, has attained hardly any significance for the synthesis of complex saccharides. A new saccharide synthesis must meet the following requirements:[19]

(1) The first step must involve a sterically uniform activation of the anomeric center with formation of a stable glycosyl donor having either an α- or β-structure,
(2) the second step should involve a catalyzed, sterically uniform, irreversible glycosyl transfer to the acceptor, proceeding with either retention or inversion at the anomeric center and in high chemical yield; the configuration of other glycosidic bonds must not be affected in the process.

Apart from the acid activation (Fig. 2, Paths Ⓐ and Ⓑ), the simplest form of activation is base activation with formation of the 1-alkoxide of a pyranose or furanose (Fig. 2, Paths Ⓒ and Ⓓ). Direct 1-*O*-alkylation (Section 3; Fig. 2, Path Ⓒ) is unlikely to fulfill both of the requirements given above for a glycoside synthesis. Ring-chain tautomerism and anomerization, instability of aldehydic intermediates in basic media, and insufficient or undifferentiated reactivities of the α- and β-alkoxides lower the expectations for a stereocontrolled glycoside or oligosaccharide synthesis; or, are there other, unrecognized controlling factors?

The stereocontrolled trapping of the base-generated 1-alkoxide by addition to a triple bond system A≡B (or to a compound containing cumulative double bonds A=B=C) to give a stable intermediate (Fig. 2, Path Ⓓ), would seem to be more promising than the direct 1-*O*-alkylation. The formation of stable intermediates is promoted by independent catalysis of the activation and glycosylation steps. Thus, after basic activation and trapping (first step), mild acid treatment, which leads to irreversible acetal formation, remains as the simplest form of catalysis for the glycosylation (second step). The multiple bond system A≡B (or A=B=C) must be selected accordingly. The trichloroacetimidate method makes use of this apparently simple

concept (Section 4). In addition, other imidate methods and other base-catalyzed 1-*O*-activation methods will be discussed.

The exchange of the anomeric hydroxyl group of carbohydrates for chlorine or bromine according to the Koenigs-Knorr method has been extended in recent years to include, in particular, the electronegative elements nitrogen, sulfur, and fluorine. Therefore, recent results with other elements as leaving groups will also be mentioned (Section 5).

The examples given in this review have been chosen so as to illustrate typical reaction conditions and results in oligosaccharide synthesis.

3. Direct 1-*O*-Alkylation

3.1. General Considerations

The direct 1-*O*-alkylation of furanoses and pyranoses with simple alkylating agents, particularly methyl iodide and dimethyl sulfate, has long been known.[20-27] Depending on the reaction conditions, either α- or β-glycosides are formed. Furthermore, *Bredereck* and *Hambsch*[28] obtained trehalose mixtures in moderate yields from tetra-*O*-methylglucose and the corresponding glycosyl halide in a basic medium.

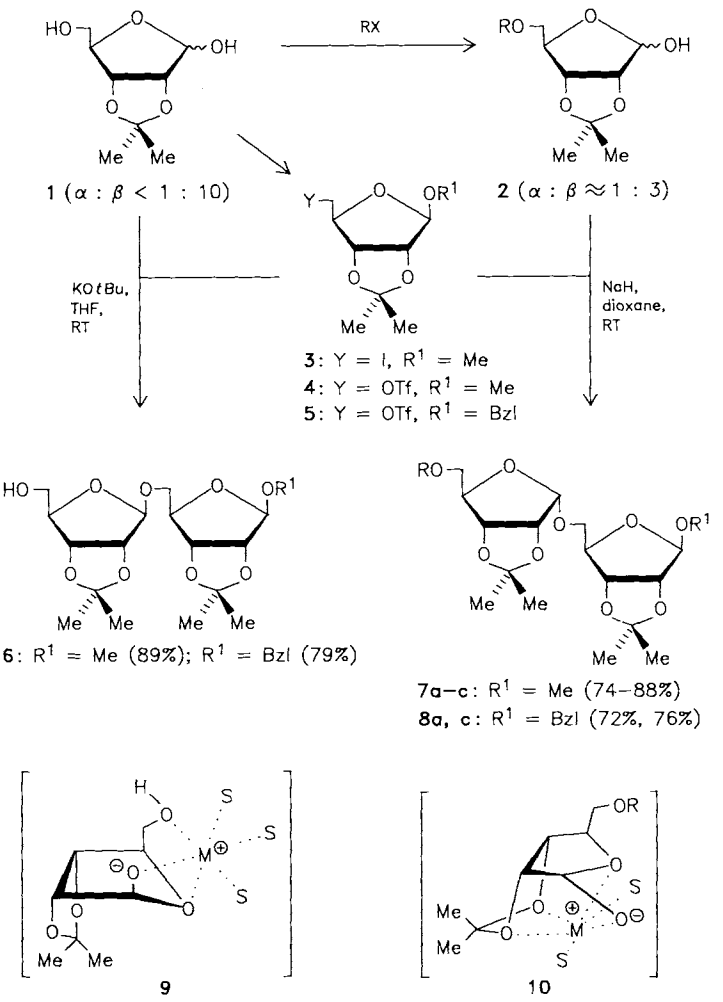
When all remaining hydroxyl groups are blocked by protecting groups, the ring-chain tautomerism between the two anomeric forms and the open-chain form (Fig. 2, Path ©) alone gives three possible sites of attack for the alkylating agent. Thus, the yield, regioselectivity, and stereoselectivity of the direct 1-*O*-alkylation are governed by at least the following factors:

(1) the stability of the generated, deprotonated species,
(2) the ring–chain tautomeric equilibrium and its dynamics,
(3) the relative reactivities of the three *O*-deprotonated species.

3.2. Direct 1-*O*-Alkylation of D-Ribofuranose and D-Mannofuranose

In our first experiments, we used the iodine derivative **3** (Y = I) as the alkylating agent, the 2,3,5-protected D-ribose **2a**, and various bases for the 1-*O*-deprotonation. However, this system was not sufficiently reactive.[29] The introduction of the trifluoromethanesulfonate (triflate) leaving group fundamentally changed the situation: Treatment of the 5-*O*-unprotected D-ribose **1** with one equivalent of base and the triflates **4** and **5** afforded exclusively (i.e., regio- and stereoselectively) the β-linked disaccharides **6** in excellent yield (Scheme 1).[30] This result was attributed initially to the preference of substrate **1** for adopting the β-furanose form and to the higher acidity of the anomeric hydroxyl group in comparison with the primary 5-hydroxyl group.

This interpretation was shown to be incorrect by the introduction of bulky protecting groups at the 5-*O* atom of **1** to give the derivatives **2a–c**: 1-*O*-alkylation with the triflates **4** and **5** led almost exclusively to the corresponding α-linked disaccharides **7a–c** and **8a**, **c**, respectively, even though the β-anomer predominates in the 1-*O*-protonated substrates. Therefore, in addition to steric effects of the 5-*O*-substituents, the formation of differing intramolecular complexes (**9** and **10**) of the metal ions with the 1-oxides was suggested.[30]

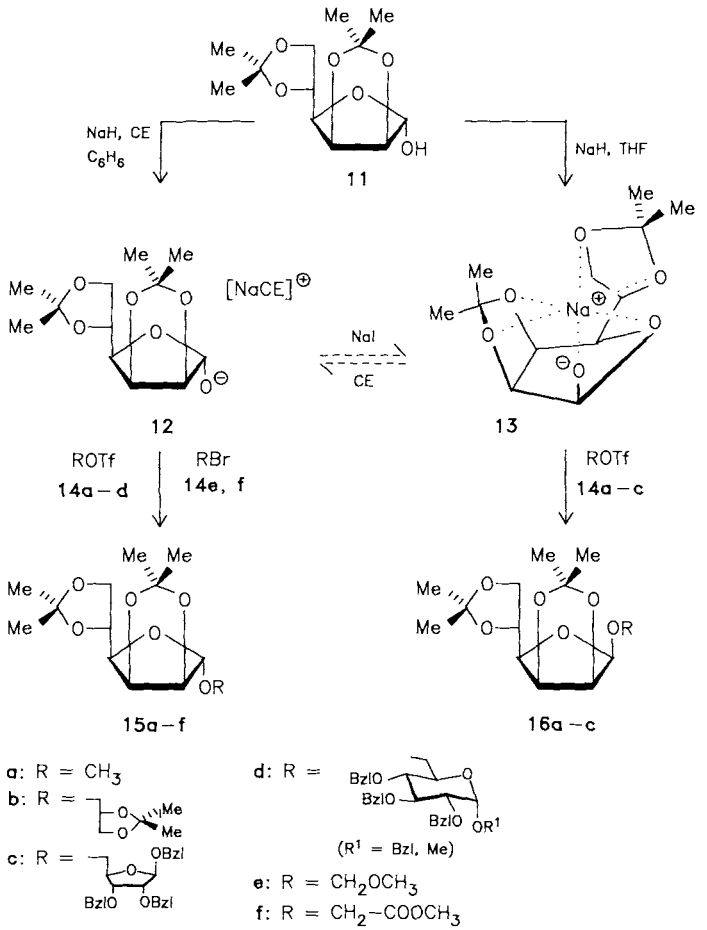


Scheme 1. **a**: R = trityl, **b**: R = methoxytrityl, **c**: R = *tert*-butyldimethylsilyl. — THF = tetrahydrofuran, Tf = trifluoromethanesulfonyl, Bzl = benzyl, S (in **9** and **10**) = solvent molecule.

The effect of the intramolecular metal-ion complexation was further substantiated by investigations on the D-mannofuranose **11**.[31,32] In contrast to the synthesis of the α-D-mannofuranosides **15**, the stereoselective synthesis of the β-D-mannofuranosides **16** by the usual glycosidation methods is difficult.[10,12] The 1,2-*cis* arrangement of the functional groups in **11** is opposed by an unfavorable steric and electronic interaction and the anomeric effect as stereoelectronic effect. Thus, as expected, the α-anomer **15** is obtained from the reaction of **11** with methyl iodide and silver oxide in dimethylformamide (DMF) (Kuhn methylation).[33] However, reaction of the sodium salt of **11** with methyl iodide in benzene gives the β-anomer **16** as the main product.[33] Formula **13** shows that the β-oxide has practically ideal crown ether geometry, which probably stabilizes the β-configuration in less solvating media but

decreases the reactivity.[31,32] Good β-selectivity with especially reactive electrophiles is thus to be expected under kinetic control.

Following this hypothesis, we alkylated **11** with the triflates **14a–c** and obtained almost exclusively the β-D-mannofuranosides **16a–c**. Furthermore, the expected influence of the reactivity of the electrophile on the anomeric ratio could be confirmed by reactions with the α-halo ether **14e** and the α-halo ester **14f** (Scheme 2).[32]

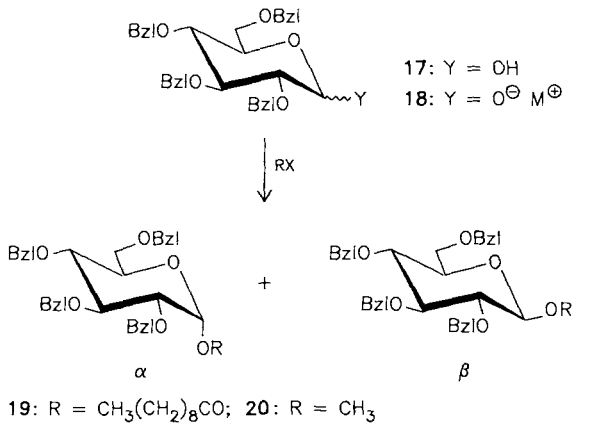


Scheme 2. CE = dibenzo[18]crown-6.

If the intramolecular complexation is responsible for the high β-selectivity, more strongly solvating conditions should promote the α-selectivity. This was confirmed by the addition of an equimolar amount of the crown ether dibenzo[18]crown-6.[31,32] The alkylating agents **14a–f** then gave exclusively the α-D-mannofuranosides **15a–f**. Addition of sodium iodide leads to competition of the sodium ions for the crown ether so that the anion **12** can revert partly to the anion **13**.

3.3. Direct 1-*O*-Alkylation of Glycopyranoses with Primary Triflates

Can the excellent results with respect to both yield and regio- and stereoselectivity obtained by the direct 1-*O*-alkylation of protected and partially unprotected D-ribofuranoses and D-mannofuranoses also be achieved with glycopyranoses? This question was initially examined for reactions with the 2,3,4,6-tetra-*O*-benzyl-D-glucose **17** (Scheme 3).[34,35]



Scheme 3. Reaction of **17** via **18**, Y = O⊖Li⊕, with RX = $CH_3(CH_2)_8COCl$ gives **19**; reaction of **17** via **18**, Y = O⊖Na⊕ with RX = CH_3OTf **14a** gives **20**.

According to *Pfeffer* et al.,[36] **17** exists at room temperature in benzene or THF in an anomeric ratio of α : β ≈ 3 : 2. More recent studies give a value of 4 : 1,[37] which is in better agreement with our results. This ratio is not changed significantly by 1-*O*-lithiation to give **18**, Y = O⊖Li⊕.[36] However, when the acylation of this lithiated species with decanoyl chloride is studied as a function of solvent and temperature, other relations are obtained (Fig. 3). Higher temperatures, especially in benzene, favor the β-product **19β**.[36]

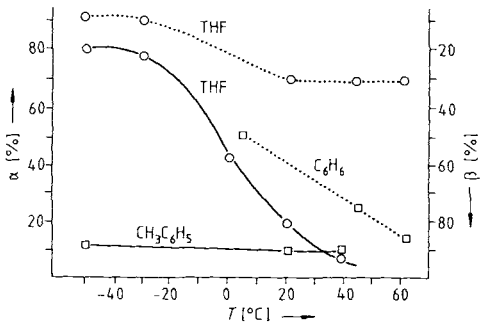


Fig. 3. Reaction of tetrabenzylglucose **17** via **18**, Y = O⊖Li⊕, with decanoyl chloride to give **19α, β** (···) and of **17** via **18**, Y = O⊖Na⊕, with methyl triflate **14a** to give **20α, β** [35] (—) as a function of temperature and solvent.

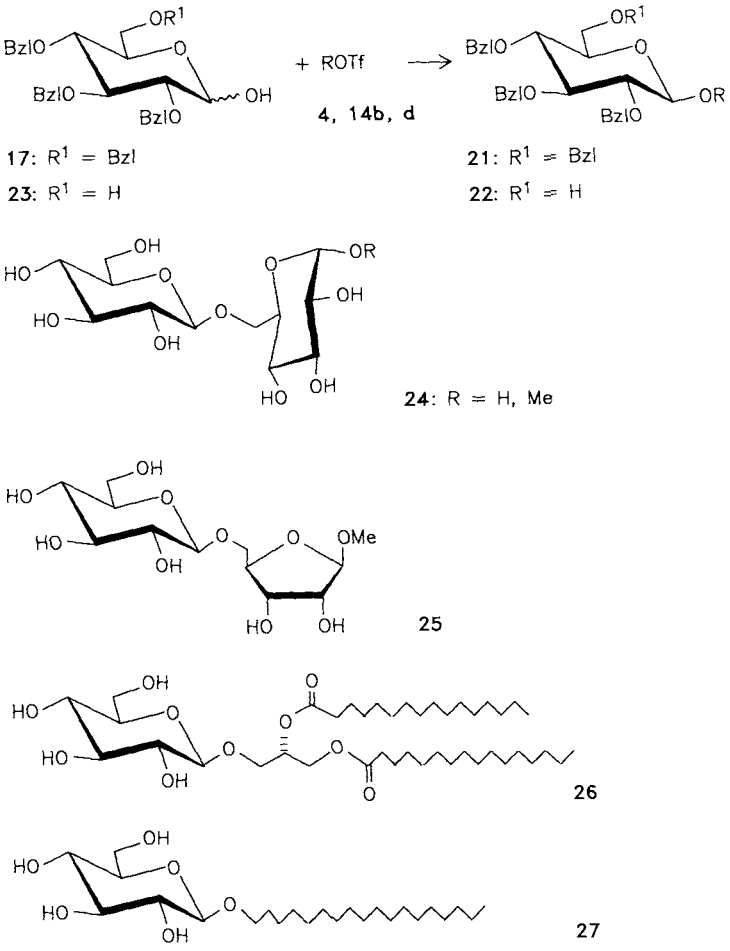
The same result, in principle, is obtained with the sodium salt **18**, Y = O⊖Na⊕, and methyl triflate **14a** (Fig. 3);[35] higher temperatures favor the β-product **20β** even more markedly. The rate of the α/β anomerization and the increased nucleophilicity of the β-oxide salt **18β** were assumed to explain this finding.[34,35] In contrast to the results obtained with the mannofuranose **11**, the addition of crown ether had no significant influence. Thus, intramolecular complexation probably does not play a major role.[29,35]

The 1-*O*-methylation of tetrabenzylglucose **17** demonstrates a method for stereocontrol of this reaction, which

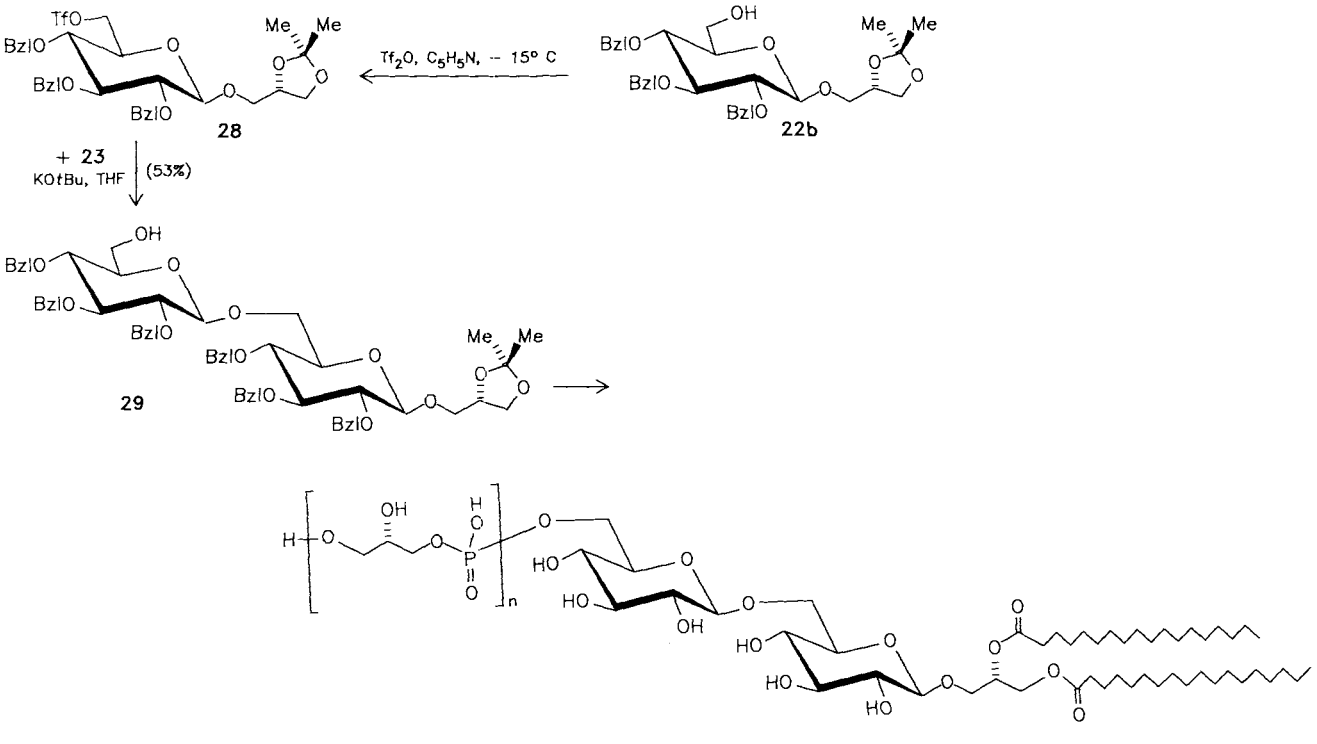
was also successful for reactions with the triflates **4** and **14b,d**. When sodium hydride in dioxane at room temperature was used, the β-glycosides **21** were obtained practically exclusively. The partially protected glucose derivative **23** also underwent regioselective reaction when one equivalent of base was added. Only the β-anomer **22** was formed. Cleavage of the protecting groups afforded the disaccharides **24** and **25** and the glycolipid analogues **26** and **27** in a simple manner and in excellent yields (Scheme 4). Recently, the complex lipoteichoic acid carrier fragments **30** were prepared in this way (Scheme 5).[38,39] Compound **22b** was first converted into the triflate **28**, which underwent direct reaction with **23** to give the 6′-*O*-unprotected disaccharide-glycerol derivative **29**. Compound **29** was transformed in a few steps into product **30**. Similarly, 6-*O*-unprotected 2,3,4-tri-*O*-benzylgalactoses and 2,3,4-tri-*O*-benzylxyloses were combined to give β-pyranosides.[34,40]

The effect of sterically demanding protecting groups on the stereochemistry of glycoside formation was studied with the help of the 6-*O*-methoxytrityl group in compound **32**.[34,35] At lower temperatures, i.e., when the rate of anomerization is slow, reaction with the triflate **14d** gave, indeed, the isomaltose derivative **33**, which was subsequently deprotected to give **31**. Reaction with the triflate **14b** under identical conditions, however, gave the β-glycoside **34** exclusively. Cleavage of the acid-labile protecting groups of **34** gave the β-glucopyranosylglycerol **35** (Scheme 6). According to the concepts developed above, steric and reactivity differences in the triflates should be responsible for these findings.

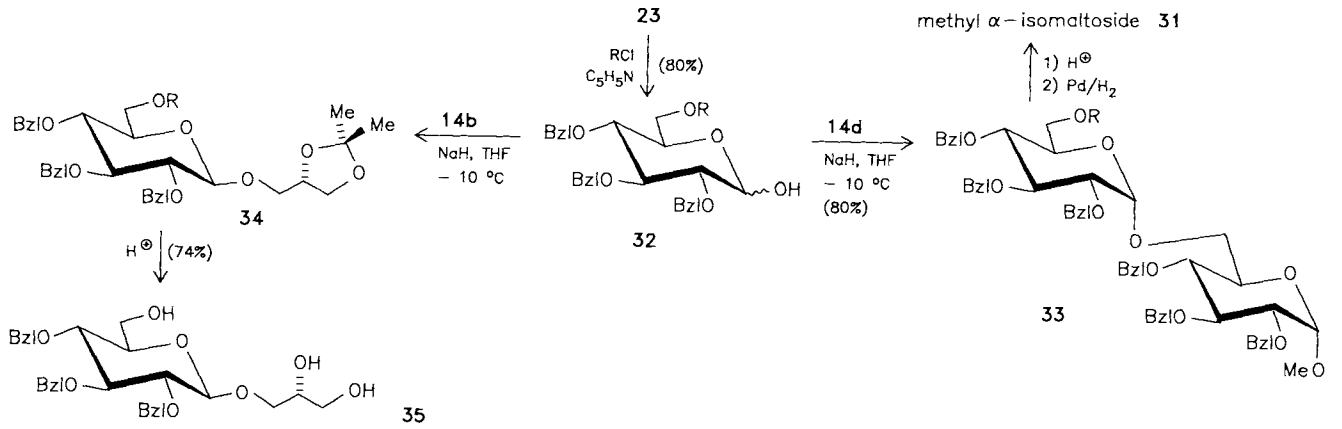
The syntheses of β-D-mannopyranosides, like those of β-D-mannofuranosides, are also accompanied by particular difficulties[13] (see Section 2.2). However, the observation



Scheme 4. Conversion of **17** into **21**: NaH, dioxane, RT; of **23** into **22**: KO*t*Bu, THF, RT. **24** is formed from **17** or **23** and **14d** via **21** or **22**, respectively, and **25** is formed from **17** or **23** and **4** via **21** or **22**, respectively.



Scheme 5. **22b** is the product formed from **23** and **14b**.

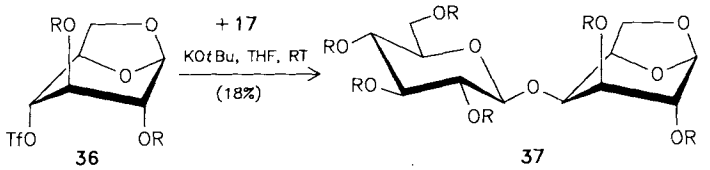


Scheme 6. R = methoxytrityl.

that the thermodynamically less stable anomer is preferentially formed at higher temperatures (cf. Fig. 3) made their direct synthesis also possible.[32]

3.4. Direct 1-*O*-Alkylation with Secondary Triflates

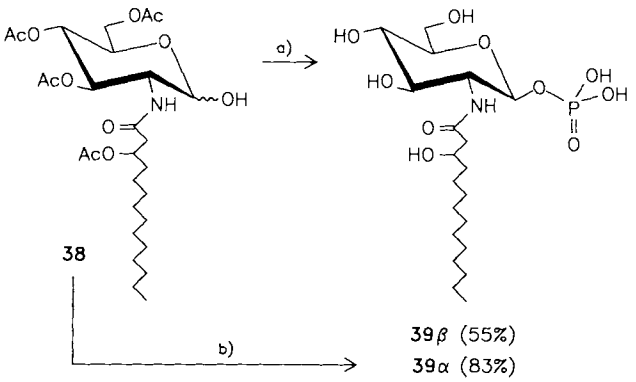
The direct 1-*O*-alkylation of carbohydrates by primary triflates has become a simple method for the synthesis of glycosides and saccharides because of its facility and the yields and stereoselectivities obtained. The question was whether similar results could be obtained with secondary triflates, which are less stable and undergo nucleophilic substitution less readily. Earlier studies had shown that decomposition reactions of the triflates predominate.[40] A modest success, however, was achieved in the reaction of the 1,6-anhydroglucose triflate **36** with the tetrabenzylglucose **17** to give the disaccharide **37**.[40] This example also illustrates the unusual aspect of this method of disaccharide synthesis: as a result of the inversion of configuration of the triflate center, the starting material and the product no longer belong to the same series of sugars (Scheme 7).



Scheme 7. R = Bzl.

3.5. 1-*O*-Acylation and 1-*O*-Phosphorylation

The possibilities for regio- and stereocontrol of 1-*O*-alkylations should also be exploited to a greater extent for directing 1-*O*-acylations and 1-*O*-phosphorylations.[41] The selective 1-*O*-acylation of unprotected lactoses[42] and the 1-*O*-phosphorylation of glucosamine,[43] in particular, should be mentioned. Thus, in analogy to the work of *Granata* and *Perlin*,[44] the β-phosphate **39β** was obtained from the 3,4,6-tri-*O*-acetylglucosamine derivative **38** and dibenzyl phosphorochloridate in the presence of thallium(I) ethoxide as base in benzene/acetonitrile after cleavage of the protecting groups (Scheme 8).[43] The corresponding α-phosphate **39α** was prepared similarly in high yield by the use of butyllithium as base in THF at −60 °C.[43]



Scheme 8. a) 1) TlOEt, benzene/acetonitrile, 2) dibenzyl phosphorochloridate, 3) H_2/Pd, 4) NaOMe; b) 1) BuLi, THF, 2) to 4) as in a).

3.6. Steric Effects, Chelate Effects, and Stereoelectronic Effects on 1-*O*-Alkylation

Primary triflates are excellent reagents for regio- and stereoselective 1-*O*-alkylation, whereby protection of all the other hydroxyl groups of the nucleophile is not necessary. For the furanoses studied, the stereocontrol results primarily from steric and chelate effects, according to present knowledge, whereas for the pyranoses, the rate of anomerization and the different nucleophilicities of the α- and β-oxide atoms are the governing factors. In particular, the increased nucleophilicities of the β-oxide atoms of the gluco-, galacto-, and mannopyranoses studied are worthy of note, because they enable the thermodynamically less stable anomers to be obtained preferentially.

On the assumption that the pyranoses in question have predominantly or exclusively the $^4C_1$ conformation, the higher nucleophilicity of the β-oxide can be attributed to a steric effect in combination with a stereoelectronic effect, resulting from repulsions of the lone electron pairs or from dipole effects (Fig. 4).[19,35,45] This effect[46] should be more pronounced in pyranosyl β-oxides, with three lone electron pairs on the oxide atom, than in pyranosides. Recently, such an effect in pyranosides was discussed briefly in con-

nection with the differing reactivities of the α- and β-anomers.[47,48]

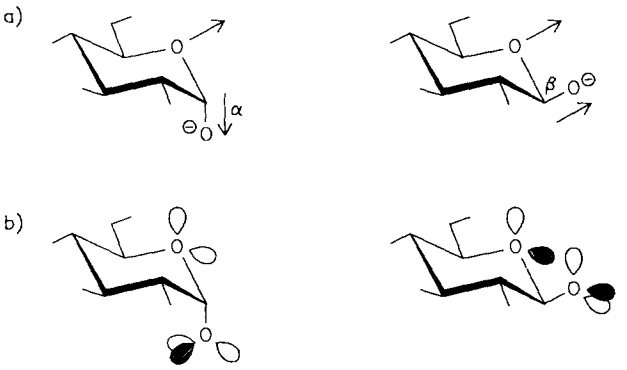


Fig. 4. Increased nucleophilicity of the β-oxide: explanation a) by unfavorable dipole-dipole interaction, b) by repulsion of lone electron pairs.

For the same reasons as with the thermodynamically efficient anomeric effect in the α-mannopyranoses, this kinetically efficient stereoelectronic effect[45] should be particularly pronounced in mannopyranosyl β-oxide. Thus, β-mannopyranosides can be obtained in spite of steric hindrance. The stereoelectronic effects in α- and β-furanosyl oxides should differ less for conformational reasons. The significance of this stereoelectronic effect for kinetically controlled, reversible reactions will become apparent from the results on the formation of *O*-glycosyl trichloroacetimidates (see Section 4.1).

4. Synthesis and Reactions of *O*-Glycosyl Trichloroacetimidates and Other 1-*O*-Activated Carbohydrates

4.1. The Trichloroacetimidate Method—Synthesis of *O*-Glycosyl Trichloroacetimidates

The direct 1-*O*-alkylation of carbohydrates demonstrates that pyranoses and furanoses deprotonated at the 1-*O* atom react analogously to alkoxides. Although the higher acidity of the 1-OH group of the hemiacetal might be expected to result in a lower nucleophilicity of the 1-oxide, the stereoelectronic effect apparently partially compensates for this influence.

These results and the observed stereocontrol suggest that pyranoses and furanoses should undergo base-catalyzed addition directly and in a stereocontrolled manner to suitable triple bond systems A≡B or compounds containing cumulative double bonds A=B=C (see Fig. 2). The stable intermediates thus obtained should, by appropriate choice of the centers A and B or A, B, and C, respectively, have good glycosyl donor properties in the presence of acid. The water liberated in the glycoside formation is transferred, in two separate steps, to the activating agent, which, by taking up water, provides the driving force for the whole process. This simple concept should fulfill the requirements given above for a good glycoside or saccharide synthesis (see Section 2.3).

From these points of view, *O*-glycosyl imidates are suitable intermediates provided that they can be obtained as stable compounds directly from nitriles or ketene imines under base catalysis and that they exhibit a high glycosyl transfer potential upon treatment with acid (cf. Fig. 2). *O*-β-Glycosyl *N*-methylacetimidates, first prepared by *Sinaÿ* et al.,[49] do not fulfill this requirement. They must be synthesized laboriously from α-glycosyl halides in the presence of three molar equivalents of silver oxide. Furthermore, only the β-imidates are known and these have proved to be relatively unreactive in acid-catalyzed glycosidation[13] (see Section 4.3).

Electron-deficient nitriles such as trichloroacetonitrile are known to undergo direct and irreversible, base-catalyzed addition of alcohols to give *O*-alkyl trichloroacetimidates (Fig. 5, X = Cl).[50] This imidate synthesis has the advantages that the free imidates can be isolated as stable adducts, which are less sensitive than their salts to hydrolysis. The pioneering work on this reaction was carried out by *Nef*;[51] in the meantime the reaction has found interesting applications.[52]

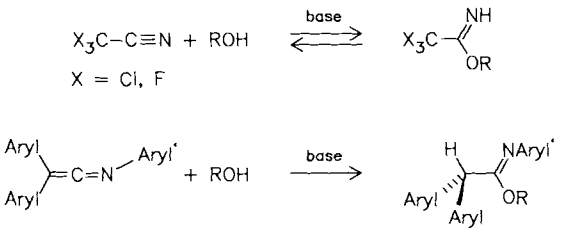
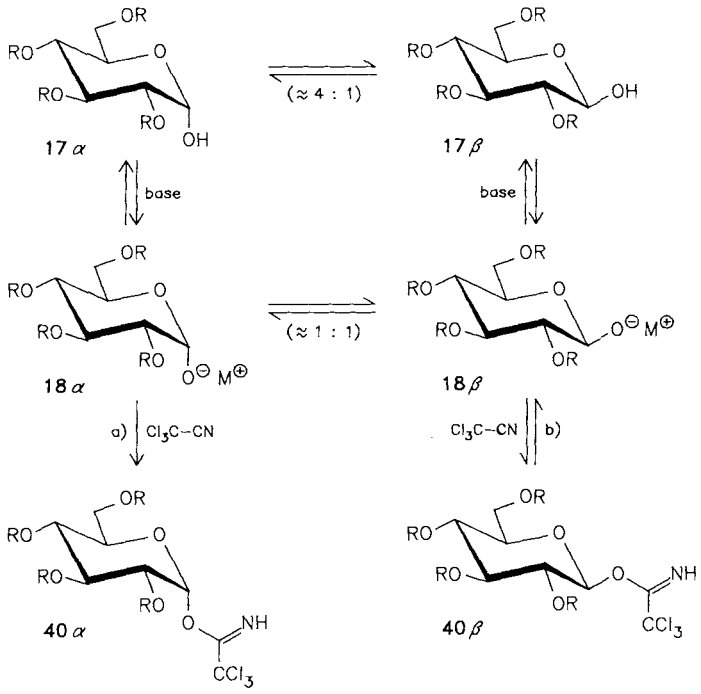


Fig. 5. Base-catalyzed addition of alcohols to activated nitriles and ketene imines.

Can the mild, base-catalyzed formation of *O*-alkyl trichloroacetimidates be extended to the preparation of *O*-glycosyl trichloroacetimidates? The results of our initial experiments with tetrabenzylglucose **17** in which sodium hydride was used as base were at first surprising but, on consideration of the results obtained for direct 1-*O*-alkylation (Section 3), understandable. The *O*-α-glucopyranosyl trichloroacetimidate **40α** was isolated in almost quantitative yield (Scheme 9).[53] Simple filtration through silica gel was sufficient to purify **40α**.[54,55] Compound **40α** is crystalline and can be stored at +5 °C without any special precautions, whereas the corresponding α-glycosyl bromide, for instance, is stable at −80 °C for only a short time.[17] Product **40α** is also surprisingly stable at higher temperatures (e.g., in dry toluene at +110 °C).

A detailed study showed that, following the formation of the oxide, the β-trichloroacetimidate **40β** is formed preferentially or even exclusively in a very rapid and reversible addition reaction (Fig. 6a). However, this product anomerizes in a slow, base-catalyzed reaction (via retro-reaction, oxide anomerization, and renewed addition) practically completely to the α-trichloroacetimidate **40α** with the electron-attracting 1-substituent in an axial position.[19,45] The markedly higher reactivity of the 1-oxide atom in **18β** as compared with that in **18α** can be demonstrated by the use of potassium carbonate as base (Fig. 6b). Potassium car-



Scheme 9. a) Thermodynamically controlled product formation; b) kinetically controlled product formation. R = Bzl, M = Na, K.

bonate catalyzes the addition relatively rapidly and practically quantitatively, whereas it has only a small effect on the retro-reaction. Thus, the β-anomer **40β** also can be isolated as a pure product in 78% yield. The stabilities of the two anomers are comparable. The corresponding β-glycosyl halides were generated as intermediates.[13]

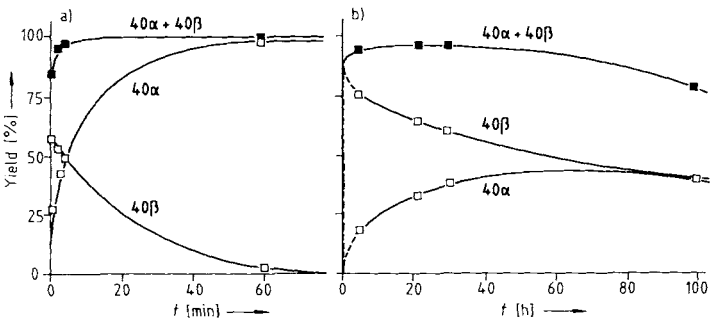


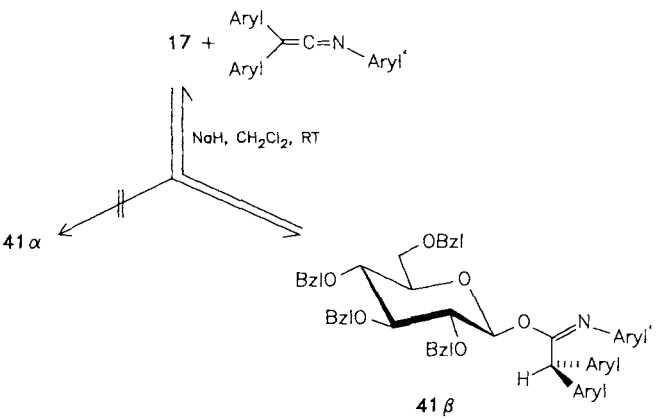
Fig. 6. Course of the base-catalyzed formation of *O*-(tetrabenzylglucopyranosyl)trichloroacetimidate **40α** and **40β** from tetrabenzylglucose **17** and trichloroacetonitrile a) with NaH, b) with K_2CO_3 as base.

The kinetically controlled, rapid formation of the β-trichloroacetimidate **40β** and the slower, thermodynamically controlled formation of the α-trichloroacetimidate **40α** support the theory that the higher nucleophilicity of **18β** results mainly from a stereoelectronic effect.

Comparable results have since been obtained with other carbohydrates, with carbohydrates having other protecting groups, and with 2-azido-2-deoxy and 2-deoxy-2-phthalimido sugars.[19,45,53-74] The stereoselective anomeric activation of carbohydrates and their derivatives through the formation of *O*-glycosyl trichloroacetimidates is applicable to all important *O*-protected hexopyranoses (glucose, galactose, mannose, glucosamine, and galactosamine), hexofuranoses, pentopyranoses, and pentofuranoses, as well as to glucuronic acid and muramic acid. Thus, the first requirement for a new glycoside or saccharide synthesis (see Section 2.3) is fulfilled. Other nitriles (e.g., trifluoroacetonitrile) have not proved to be so successful as trichloroacetonitrile.[19]

The difference in the rates of formation of the α- and β-*O*-glycosyl trichloroacetimidates, the reversibility of the reaction, and the differing kinetic stabilities of the anomers have been used to govern the type of product formed. Restriction of the reversibility should lead exclusively to the product of the kinetically controlled reaction. This result is expected for reactions with *N*-substituted ketene imines because the proton in the addition product is bonded to a C atom (Fig. 5), which, under the conditions of direct imidate formation, is not easily deprotonated. Therefore, this product is protected from retro-cleavage.

As expected, the corresponding *O*-β-glucosyl imidate **41β** is obtained exclusively from the reaction between tetrabenzylglucose **17** and *N*,2,2-triarylketene imines with sodium hydride as base (Scheme 10).[19,53,54] The strong



Scheme 10. Aryl, Aryl' = phenyl, *p*-chlorphenyl, etc.

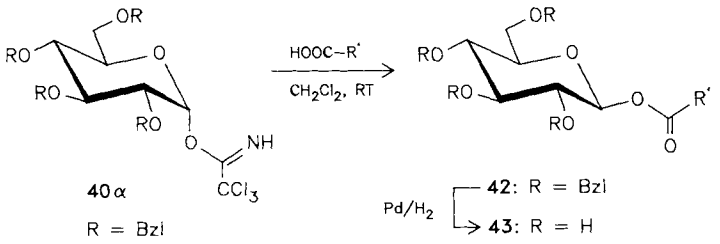
anomeric effect in the *O*-benzyl-protected mannopyranose is manifested both kinetically and thermodynamically in this reaction:[19] with trichloroacetonitrile and sodium hydride as base only the α-imidate is isolated; with *N*,2,2-triarylketene imines only the β-imidate is formed in spite of the steric hindrance on the β-side. This is a further indication of the significance of stereoelectronic effects.

4.2. Reactions of *O*-Glycosyl Trichloroacetimidates

Ultimately, the significance of the *O*-glycosyl trichloroacetimidates is derived solely from their glycosylation potential under acidic catalysis. This potential has indeed been confirmed in many investigations.

4.2.1. Carboxylic Acids and Phosphoric Acids as O-Nucleophiles

The direct glycosylation of Brønsted acids is a particularly advantageous property of these new glycosyl do-

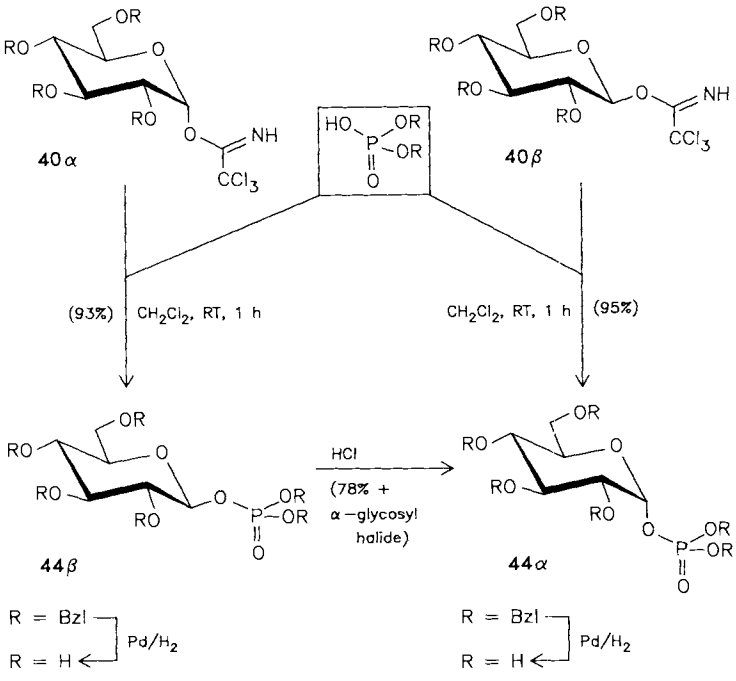


Scheme 11. Examples for acids HOOC-R: formic acid (70% yield of **42**), acetic acid (84%), benzoic acid (82%), *o*-chlorobenzoic acid (80%), acetylsalicylic acid (87%), methyl 2,3-*O*-isopropylidene-β-D-ribofuranoside uronic acid (66%), 3-indoleacetic acid (78%).

nors.[53,74] Carboxylic acids react with the *O*-α-glucosyl trichloroacetimidates **40α**, with inversion of configuration at the anomeric center to give the β-*O*-acyl compounds **42** (Scheme 11).[53,69] The reactions are performed at room temperature using equimolar amounts of acid and without the addition of a further catalyst. The examples given illustrate the versatility of this simple and mild method for 1-*O*-glycosylation of carboxylic acids, which also may be of interest for the modification of pharmaceuticals.[75] This method differs fundamentally from the conventional 1-*O*-acylation of pyranoses and furanoses (see Section 3.5) and from the esterification of trichloroacetonitrile-activated carboxylic acids.[76] In addition, it is less tedious than the corresponding reactions with the Sinaÿ imidates, which are derived from glycosyl halides (see Section 4.3).[77] Reactions of carboxylic acids can also be employed for racemate resolution.[69]

Glycosyl phosphates and glycophospholipids are intermediates in biological glycosyl transfer and are constituents of cell membranes (see Section 1). Syntheses of these compounds starting from 1-*O*-unprotected or 1-*O*-acylated carbohydrates mostly gave products with low α/β-selectivities. Improvements in this respect have been reported, especially in the last few years[64] (see also Section 3.5[43,44]).

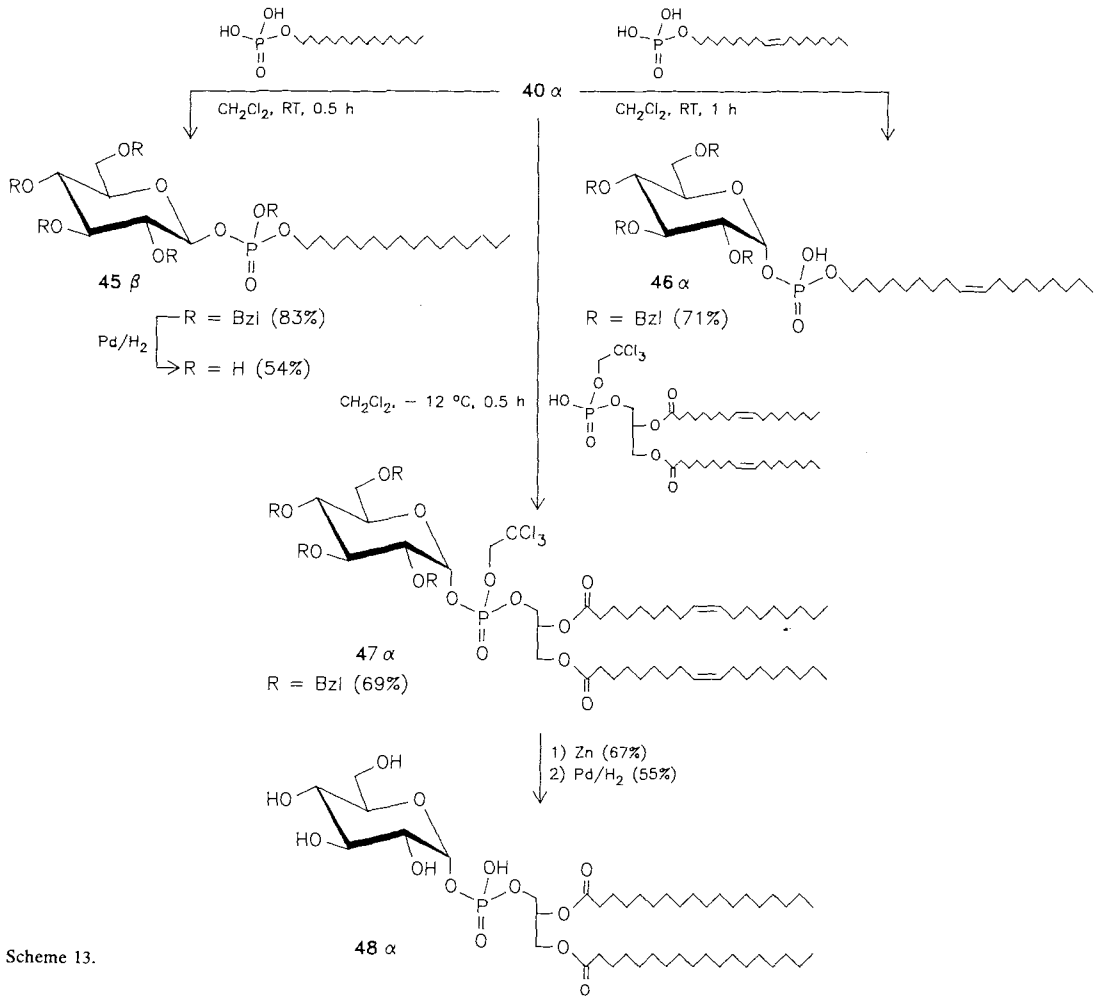
The uncatalyzed glycosyl transfer from *O*-glycosyl trichloroacetimidates to phosphoric acid mono- and diesters opens up a simple route to the above compounds. Reaction of **40α** with highly pure dibenzyl phosphate gives, with inversion, the expected β-phosphate **44β**; the α-phosphate **44α** is obtained analogously from the β-trichloroacetimidate **40β** (Scheme 12).[54,58,64] Even in the presence of traces of strong acid, the β-phosphate **44β** undergoes anomerization to the thermodynamically more stable α-phosphate **44α**. Thus, the stereochemical result of this glycosyl phosphate synthesis depends on the purity and acidity of the phosphoric acid ester (autocatalysis of the anomerization). This is confirmed by further reactions of **40α**, especially with phosphoric acid monoesters to give glycophospholipids.[64] The β-glycosyl hexadecyl phosphate **45β** is obtained by the use of highly pure hexadecyl phosphate. This reaction is markedly accelerated by the addition of boron trifluoride etherate, which results in exclusive formation of the α-anomer **45α**. Analogous observations were made for the reactions of **40α** to give the compounds **46α** and **47α** and for the conversions of galactopyranosyl,[64] mannopyranosyl,[64] talopyranosyl,[78] and 2-azido-2-deoxyglucopyranosyl[79] trichloroacetimidates into the corresponding glycosyl phosphates. In general, the α-product, which is favored by the anomeric effect and which is usually encountered in nature, is obtained more easily or, under acidic catalysis, exclusively. The unprotected glucophosphoglycerolipid **48α** is prepared by reduction and hydrogenation of **47α** (Scheme 13).



Scheme 12.

4.2.2. Alcohol Components as O-Nucleophiles—Synthesis of Glycosides, Oligosaccharides, and Glycoconjugates

For reaction as *O*-nucleophiles with *O*-glycosyl trichloroacetimidates, alcohol components generally require the presence of an acid catalyst.[53,74] Boron trifluoride etherate at −40°C to room temperature in dichloromethane as solvent has proved to be eminently suitable.[54,69] This is exemplified by the reactions of α-trichloroacetimidate **40α** with cholesterol **49a** and with glucose derivatives **49b-e** to give the glycosides or disaccharides **50α** and **50β** (Table 2). Under these conditions with the non-neighboring-group-active 2-*O*-benzyl protecting group, preferred inversion to give the β-product (1,2-*trans*) is observed. This inversion is favored by lower temperatures. *p*-Toluenesulfonic acid and other Brønsted acids are not suitable as catalysts for the formation of the thermodynamically less stable β-product. Analogous observations were made in the syntheses of (1→6)-branched and linear cellotetraoses **52** and **53**, respectively, starting from disaccharide **50c-β** via the trisaccharide **51**, and in the syntheses of the glucuronate disaccharides and glycoside **55a-c** and **56**, respectively, starting from the α-glucuronate trichloroacetimidate **54α** (Scheme 14).[56] *O*-Benzyl-protected α-galactopyranosyl trichloroacetimidate behaves in principle in a similar manner.[54] Studies on the synthesis of digitoxin glucopyranosides



Scheme 13.

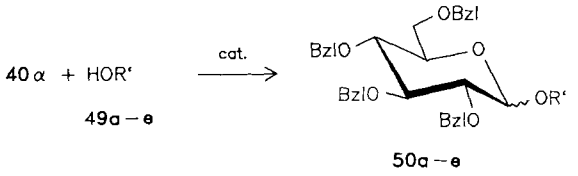


Table 2. Reaction of the trichloroacetimidate **40α** with the acceptors **49a–e** to give the corresponding glycosides **50α** and **50β**. R = Bzl. Catalyst A: toluenesulfonic acid; B: boron trifluoride etherate.

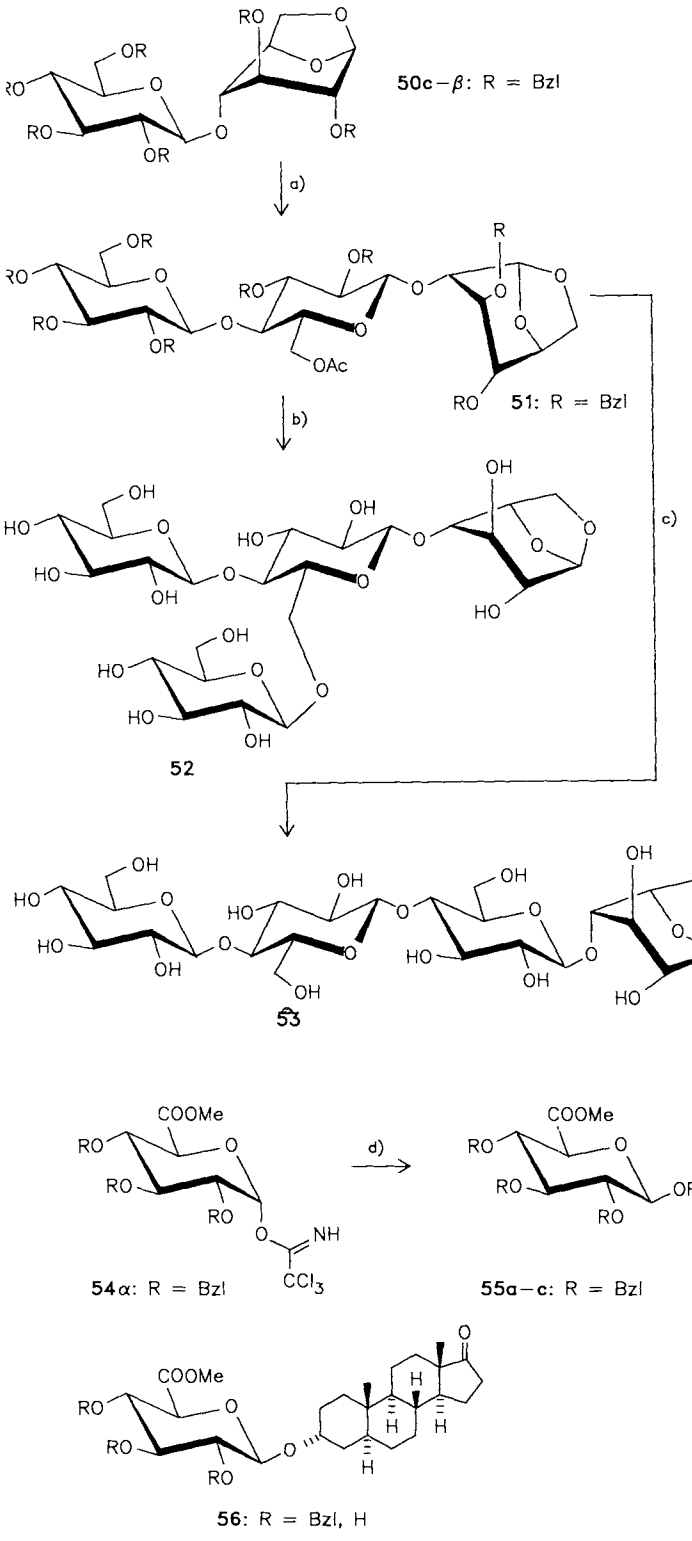
49 HOR'	Cat.	T [°C]	t [h]	Yield [%]	50α : 50β
	A	+20	2	70	2 : 1
	A	−10	48	80	1 : 1
a	A	−40	36	61	1 : 5
	B	20	20	70	2 : 3
	B	−18	2.5	78	1 : 13
b	B	−18	2.5	90	1 : 16
	B	−40	2	85	1 : 19
c	B	−38	1.5	90	1 : 10
d	B	−30	2.5	81	1 : 4
e	B	−35	3.5	32	only β

showed that markedly better results were obtained with the trichloroacetimidate method than with the Koenigs-Knorr method.[80] In addition, *O*-glycosylserine building blocks for the synthesis of glycopeptides were prepared in this way.[65,81]

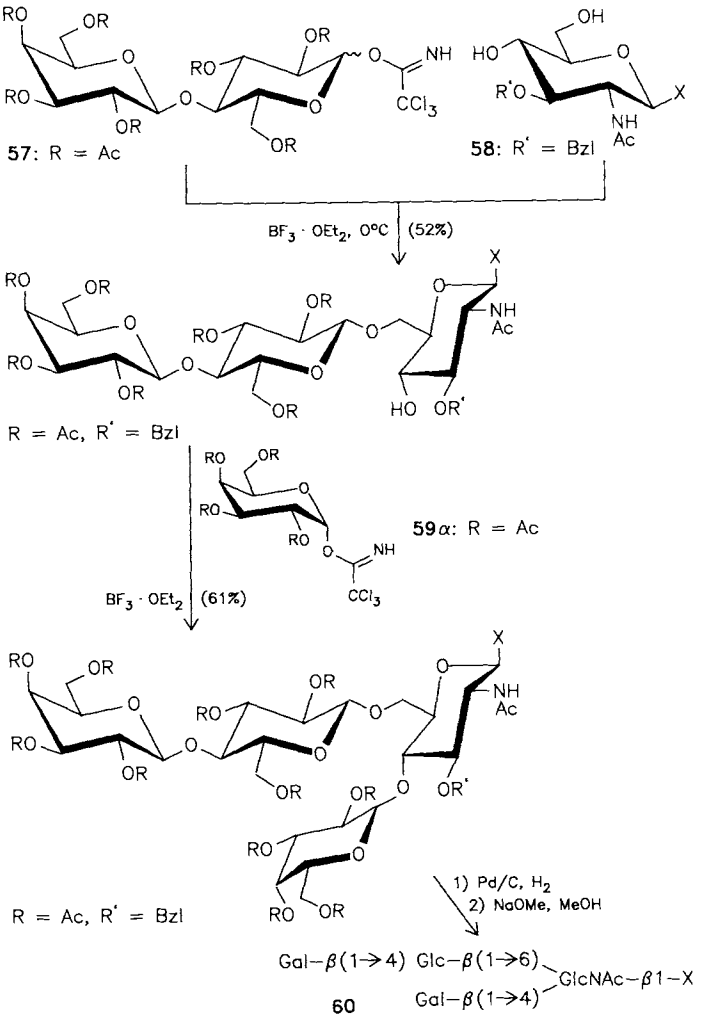
Peracetylated α- and β-trichloroacetimidates of glucose and galactose react to give, as expected from the neighboring-group participation of the 2-*O*-acetyl group, exclusively the β-glycosides or β-saccharides (1,2-*trans*). This was confirmed, for example, by *Sinaÿ* and *Amvam-Zollo*[82] with the synthesis of the tetrasaccharide antigen **60** starting from the α-lactosyl and α-galactopyranosyl trichloroacetimidates **57** and **59α**, respectively, as donors and 4,6-*O*-unprotected *N*-acetylglucosamine **58** as acceptor, which additionally contains a spacer (Scheme 15). Corresponding studies in which the Koenigs-Knorr method was used were considerably less successful.[82] These authors also performed comparative studies on the synthesis of *N*-acetyllactosamine by the trichloroacetimidate method, different variants of the Koenigs-Knorr method, and the ortho ester method (see Section 5). For this example, the trichloroacetimidate method was shown to be at least competitive.[82] The per-*O*-acetylated α-glucosyl trichloroacetimidate **61α** is also suitable for glycosylating the anomeric hydroxyl group of tetraacetylglucose **62** (Scheme 16). The β,β-linked trehalose **63** was isolated in good yield, whereas it could only be obtained in low yield by the Koenigs-Knorr method.[83]

Reactions with per-*O*-benzylated α-mannopyranosyl trichloroacetimidate[54,84] and *O*-glycosylated derivatives[85] at lower temperatures in the presence of boron trifluoride etherate as catalyst gave preferentially or exclusively α-glycosides and α-saccharides; these results reflect the stronger anomeric effect.[54,84,85] Corresponding results were obtained also with the *O*-benzyl-protected α-rhamnopyranosyl trichloroacetamidate.[84] *O*-Acetyl-protected α-mannopyranosyl trichloroacetimidate also gave exclusively α-glycosides and α-saccharides (1,2-*trans*)[54] as a result of neighboring-group participation.

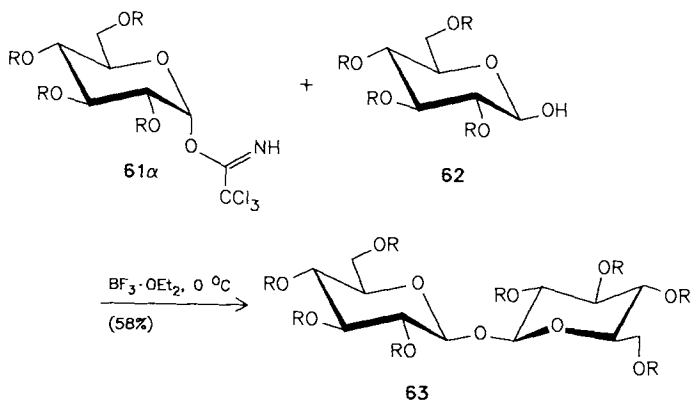
Because of the great importance of 2-amino sugars, especially *N*-acetylglucosamine and *N*-acetylgalactosamine, in complex oligosaccharides and glycoconjugates (see Section 1), their stereoselective coupling in glycoside and sac-



Scheme 14. a–e see Table 2. a) 1) CF_3COOH, $HOAc/Ac_2O$, 2) $Bzl-NH_2$, 3) Cl_3CCN, NaH, 4) **49c**, $BF_3 \cdot OEt_2$; b) 1) NaOMe, MeOH, 2) **40α**, $BF_3 \cdot OEt_2$, 3) Pd/C, H_2; c) 1)-4) as in a), 5) Pd/C, H_2; d) **49a–c**, $BF_3 \cdot OEt_2$, −25°C.



Scheme 15. X = O-CH_2CH_2-O-CH_2CH_2-O-CH_2COOMe (spacer).

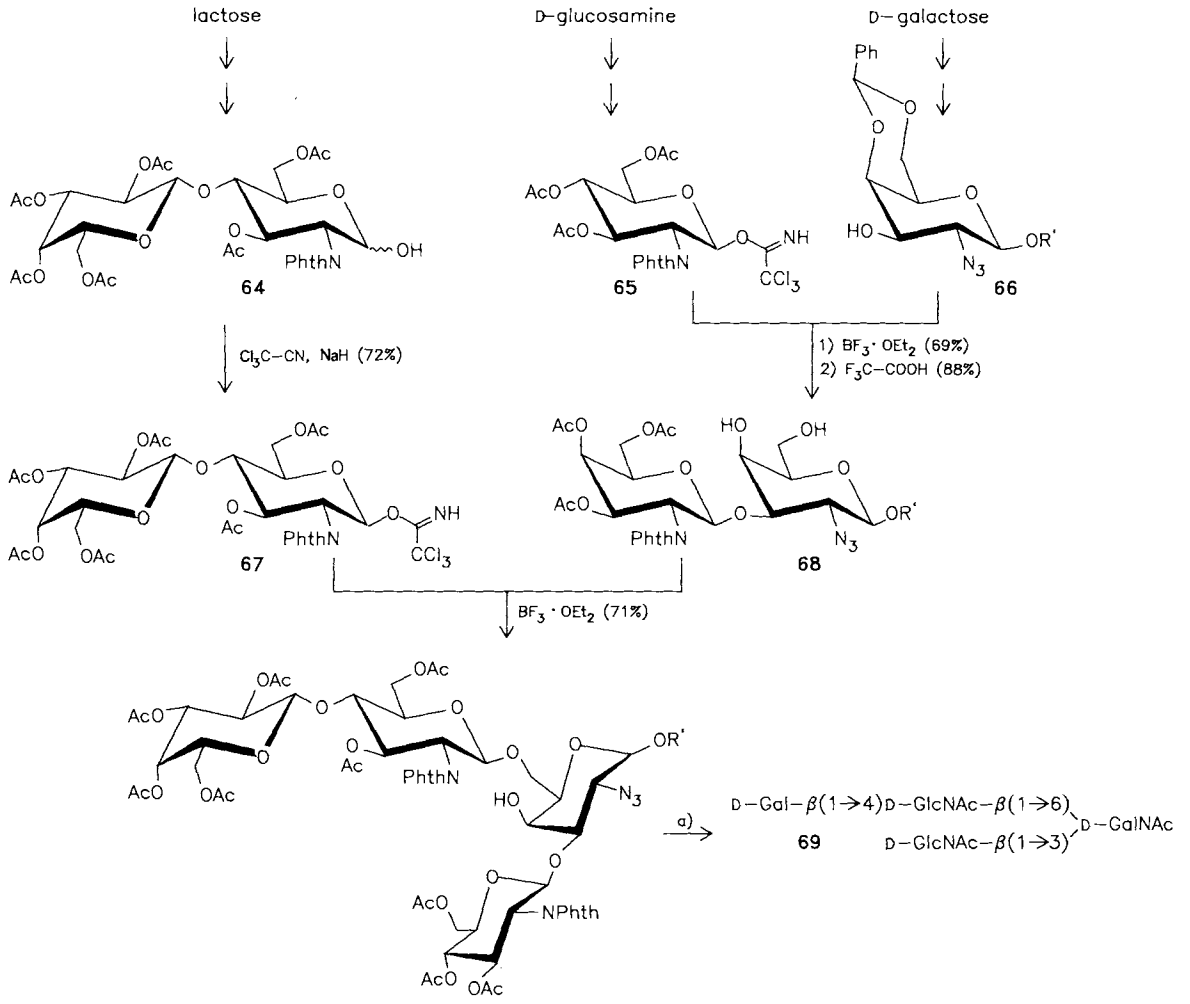


Scheme 16. R = Ac.

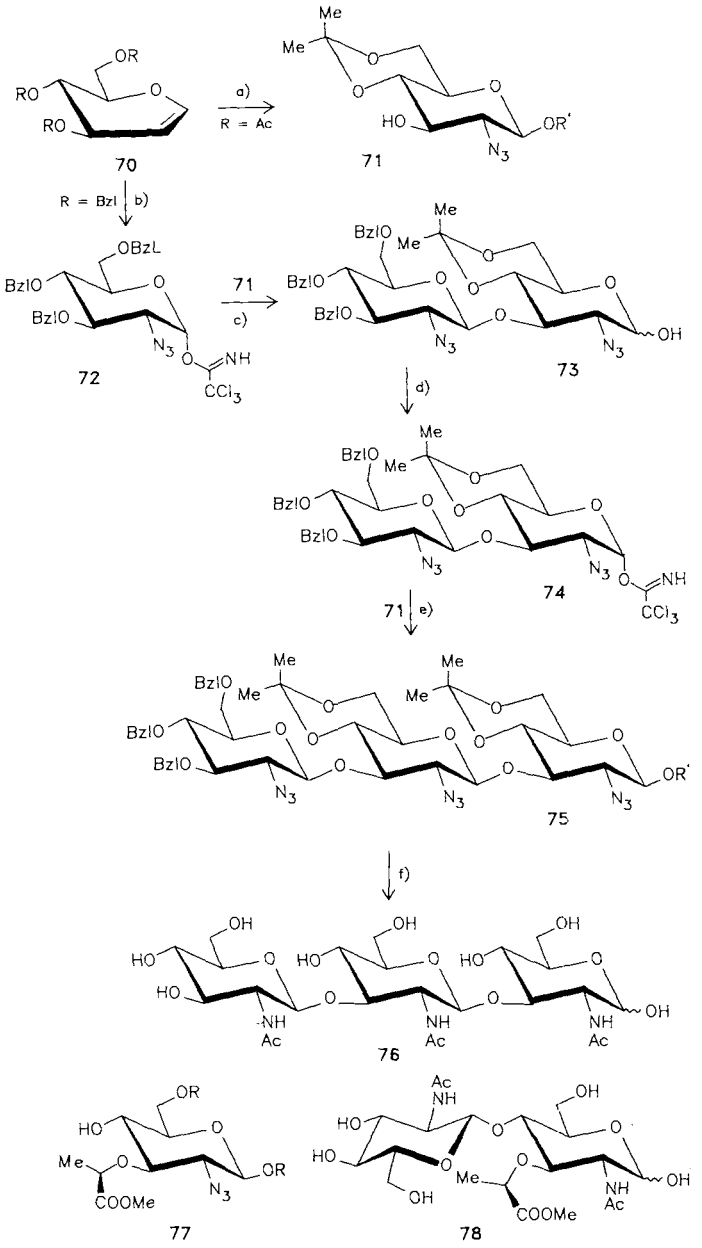
charide syntheses is of particular interest. A new glycosidation process must also prove itself in this field in order to satisfy the requirement of having wide scope. Therefore, we turned to the synthesis of oligosaccharides of the "core region" of *O*-glycoproteins of the mucin type.

Epithelial mucous secretions consist mainly of glycoproteins in which the oligosaccharide part is *O*-glycosidically linked to the amino acids L-serine or L-threonine through 2-acetylamino-2-deoxy-D-galactose.[2a,3] Galactose is frequently linked to the galactosamine to give a Gal-β(1→3)GalNAc disaccharide unit. However, a new structural type, which contains the GlcNAc-β(1→3)GalNAc disaccharide unit, has also been isolated from mucous secretions.[86] Compounds with this structure are of interest with respect to dysfunctions of the respiratory tract. For instance, the tetrasaccharide **69** was identified as the "core region" of glycoproteins isolated from bronchial mucous secretions of patients suffering from chronic bronchitis or cystic fibrosis.[86] This tetrasaccharide was obtained by a convergent synthesis based on the trichloroacetimidate method.[65,66] Lactose was first converted into the *N*-phthaloyllactosamine **64**, from which the stable trichloroacetimidate **67** was prepared as lactosaminyl donor. The disaccharide acceptor **68** was synthesized correspondingly from glucosamine (via its trichloroacetimidate **65**) and galactose (via the azide derivative **66**). The boron trifluoride etherate catalyzed coupling of **67** with **68** proceeded with β-specificity, as did the synthesis of **68**, owing to the *N*-phthaloyl group. Cleavage of the protecting groups led to the tetrasaccharide **69** (Scheme 17).

The occurrence of glucosamine in a variety of β-glycosidic linkages necessitates differing protecting group strategies. Accordingly, studies on the glycosidic coupling of 2-azido-2-deoxy-D-glucose containing *O*-benzyl and *O*-isopropylidene protecting groups were performed using the trichloroacetimidate method.[68] Here, the high diastereoselectivity of the reaction was expected to be achieved only as a result of the strict inversion of configuration in the trichloroacetimidate and not as a result of neighboring-group participation. The trisaccharide **75** of the capsule polysaccharide of *Neisseria meningitidis* (serum group L)[87] serves as an example. The *O*-benzyl-protected 2-azidoglucosyl trichloroacetimidate **72** (as donor) was synthesized from D-glucal **70** (R = Bzl). Compound **72** was coupled, under boron trifluoride etherate catalysis, with the 3-*O*-unprotected 2-azidoglucose derivative **71** (as acceptor), obtained from D-glucal **70** (R = Ac), to give exclusively the β(1→3)-linked disaccharide **73**. Conversion of **73** into the α-trichloroacetimidate **74**, as disaccharide donor, and reaction of **74** with the glycosyl acceptor **71** gave the tri-



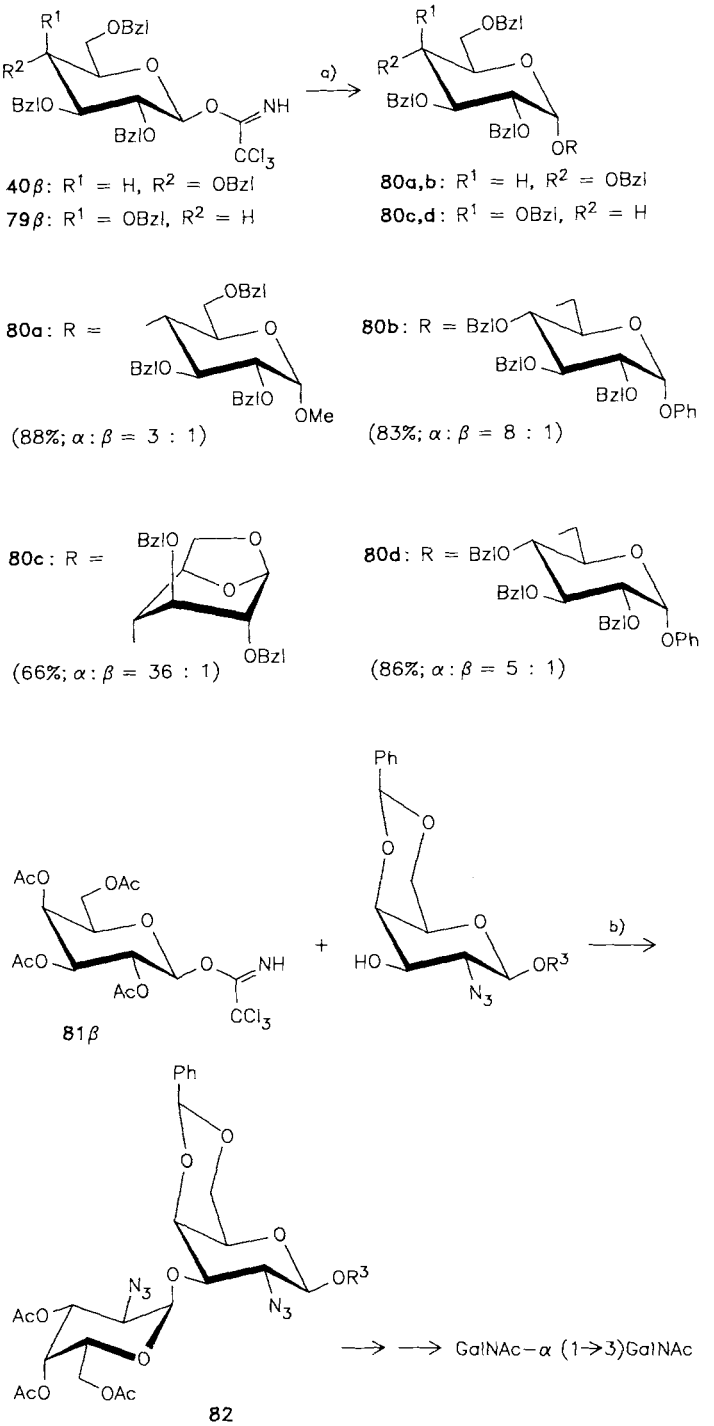
Scheme 17. Phth = phthaloyl, R' = *tert*-butyldimethylsilyl. a) 1) N_2H_4, 2) pyridine, Ac_2O, 3) Bu_4NF, 4) $NiCl_2$, $NaBH_4$, 5) K_2CO_3, MeOH.



Scheme 18. R′ = *tert*-butyldimethylsilyl. a) 1) Azidonitration with $(NH_4)_2Ce(NO_3)_6$, 2) *tert*-butyldimethylsilyl chloride, imidazole (overall yield 52%); b) 1) azidonitration (53%), 2) Cl_3C-CN, NaH (98%); c) 1) $BF_3 \cdot OEt_2$ (92%), 2) Bu_4NF (68%); d) Cl_3CCN, NaH (62%); e) $BF_3 \cdot OEt_2$, $-10\,^{\circ}C$ (70%); f) 1) Bu_4NF, Ac_2O (70%), 2) CF_3COOH (100%), 3) Ac_2O, pyridine (75%), 4) Pd/C, H_2, Ac_2O (100%), 5) NaOMe, MeOH (100%).

saccharide **75** with β-specificity. Cleavage of the protecting groups then gave the expected trisaccharide **76** (Scheme 18). In the same way, the disaccharide unit **78** of the cell-wall peptidoglycan of bacteria was built up from the imidate **72** and the muramic acid derivative **77**.[79]

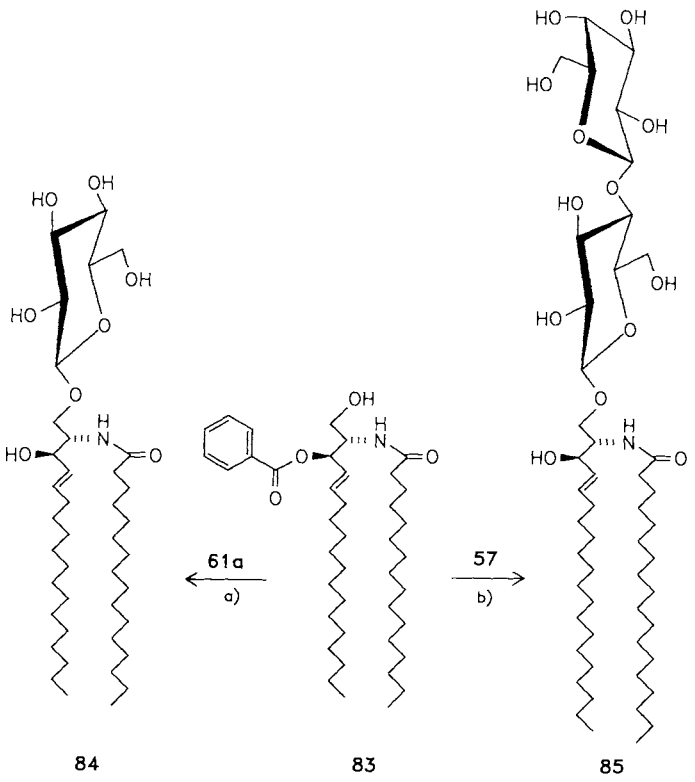
The syntheses of α-glucopyranosides **80a,b** (1,2-*cis*) and, especially, of α-galactopyranosides **80c,d** (1,2-*cis*) were achieved starting from the *O*-benzyl-protected β-trichloroacetimidates **40β** and **79β**, respectively (Scheme 19).[88] In these reactions good results were obtained with diethyl ether as the solvent and trimethylsilyl triflate as the catalyst. The latter catalyst has also proved suitable for the synthesis of α-glycosides of glucosamine and galactosamine (both 1,2-*cis*).[65] For instance, the α-linked disaccharide **82** was prepared in a diastereoselective manner from the β-trichloroacetimidate of 2-azido-2-deoxygalactose **81β**.



Scheme 19. R^3 = *tert*-butyldimethylsilyl. a) Et_2O, HOR, RT, 1 h, $TfOSiMe_3$; b) CH_2Cl_2, $-20\,^{\circ}C$, $TfOSiMe_3$ (70%).

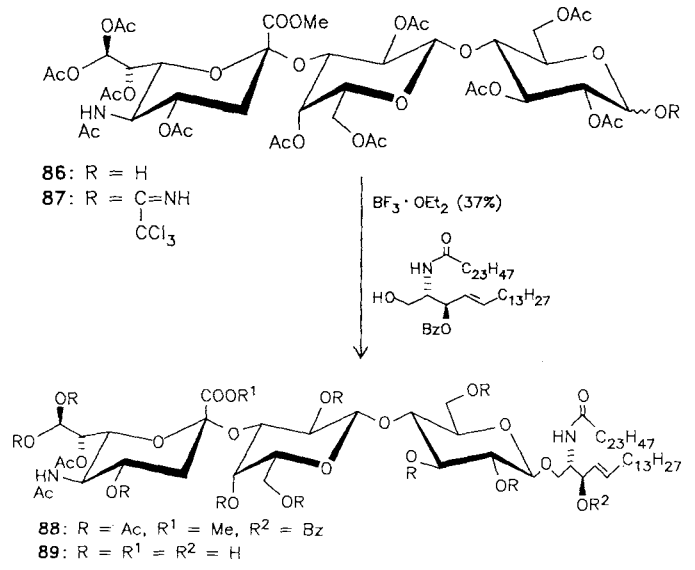
The significance of membrane constituents discussed in Section 1 demonstrates the necessity for developing glycosphingolipid syntheses. The required D-*erythro*-ceramide acceptor was prepared in the form of its 3-*O*-benzoylated derivative **83** by the use of a method developed by us.[89] The trichloroacetimidate method for glycosylating this compound[67] gave better results than the Koenigs-Knorr

or Helferich-Weis methods.[90] Thus, the glucosyl cerebroside **84** was obtained from the *O*-acylated α-glycosyl trichloroacetimidate **61α** and the lactosyl cerebroside **85** from the *O*-acylated α-lactosyl trichloroacetimidate **57** (Scheme 20).[91] Such compounds have proved to be active



Scheme 20. a) 1) $BF_3 \cdot OEt_2$ (55%), 2) NaOMe, MeOH (100%); b) 1) $BF_3 \cdot OEt_2$ (36% from added **83**, 72% from reacted **83**), 2) NaOMe, MeOH (87%).

in the healing of wounds.[71] Recently, *Ogawa* et al. synthesized the G_{M3} ganglioside **89**[92] and the asialo-G_{M1} and asialo-G_{M2} gangliosides[93] using the trichloroacetimidate method. The trisaccharide **86**, prepared by classical methods, was converted into the α-trichloroacetimidate **87** in



Scheme 21. Bz = benzoyl.

good yield and allowed to react with a ceramide in the presence of boron trifluoride etherate. The protected G_{M3} ganglioside **88** thus obtained was deprotected to give **89** (Scheme 21).[93]

The results obtained hitherto for *O*-glycoside formation with the trichloroacetimidate method give the following general picture. With acid catalysis, glycosides and saccharides generally are obtained under mild conditions in good yields and often in a sterically homogeneous form. Depending on the catalysts and protecting groups, reactivities are achieved that are comparable to those obtained for the glycosyl halide/silver triflate system. With very unreactive glycosyl acceptors, imidate rearrangements and/or glycosyl fluoride formation are sometimes observed.[70,72] According to our present experience, a sterically homogeneous reaction course with hexopyranoses is favored by the following factors:

(1) Neighboring-group participation gives rise to 1,2-*trans*-glycosides, i.e., β-glycosides with D-glucose, D-glucosamine, D-galactose, and D-galactosamine and α-glycosides with D-mannose and L-rhamnose.
(2) At low temperatures with boron trifluoride etherate catalysis, non-neighboring-group-active protecting groups lead preferentially to inversion products. In this way 1,2-*trans*-glycosides (i.e., β-glycosides) of D-glucose, D-glucosamine, D-muramic acid, D-glucuronic acid, D-galactose, and D-galactosamine can be prepared from the α-trichloroacetimidates.
(3) With the stronger catalyst trimethylsilyl triflate, non-neighboring-group-active protecting groups lead preferentially to the thermodynamically more stable product. In this way 1,2-*cis*-glycosides (i.e., α-glycosides) of D-glucose, D-glucosamine, D-galactose, and D-galactosamine have been prepared.

Only a few of the important types of linkage occurring in natural products (such as α-L-fucoside, β-D-mannoside, and β-L-rhamnoside) remain to be studied in detail. With the present state of methodological development, only β-D-mannose and β-L-rhamnose might present problems. Thus, the second requirement for a new saccharide synthesis (see Section 2.3) may be considered to be fulfilled "almost completely" after only a few years of research.

The successes with the *O*-glycosyl trichloroacetimidates up to now have forced studies on *O*-glycosyl *N*,2,2-triarylacetimidates **41** into the background.[53,54] Variations of the substituents on the imidate part could make "tailor-made glycosyl donors" available. However, the steric requirements of the triaryl-substituted imidate group may be disadvantageous for reactions at the anomeric center and for the required separation of the large triarylacetamide molecule from the reaction products.

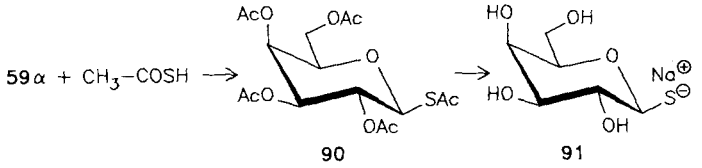
4.2.3. N-, S-, and C-Nucleophiles

Up to now, only a few studies with *N*-nucleophiles have been performed. Hydrazoic acid, as a strong acid, reacts with **40α** to give the expected α-azide without any additional catalyst.[69] Nitrogen heterocycles, however, require an acid catalyst; thus, bis-trimethylsilylated uracil and thy-

mine gave exclusively the β-linked nucleosides at room temperature with boron trifluoride etherate as catalyst.[69,94,95] Reactions of **40α** in acetonitrile as solvent with a carboxylic acid as activator gave *N*-bisacylated *N*-glucosides via nitrilium salts.[69] Corresponding reactions with *O*-glycosyl *N*-methylacetimidates[49] demonstrated the markedly higher reactivity of the *O*-glycosyl trichloroacetimidates.

The strong interest in 1-thioaldoses and 1-thioglycosides,[41,55,96,97] including their recent use as protecting groups and for glycosyl transfer (see Sections 5.1 and 5.2), was a motivation for studying the high reactivity of *O*-glycosyl trichloroacetimidates in the glycosylation of *S*-nucleophiles.[55] Hitherto, 1-thioglycosides were prepared mainly by direct nucleophilic substitution of glycosyl halides with thiolates or by *S*-alkylation of metal salts of 1-thioaldoses (see Section 3).[41,96,98,99]

The acetyl-protected α-glucosyl and α-galactosyl trichloroacetimidates **61α** and **59α**, respectively, react with thiols in the presence of boron trifluoride etherate as catalyst to give β-configurated 1-thioglycosides in high yields. Surprisingly, with the benzyl-protected α-trichloroacetimidate **40α** under identical conditions, α-configurated 1-thioglycosides are obtained exclusively. Because the anomeric effect in alkyl 1-thioglycosides approximately corresponds to that in alkyl glycosides,[100] both anomers should be formed, even under thermodynamic control.[10] Obviously, the glycosyl transfer to the *S*-nucleophile in these cases occurs by a different mechanism. It was assumed that, as in S_Ni reactions, the configuration is retained by intramolecular reaction in a close ion pair.[55]



90 91

Scheme 22.

Like carboxylic acids, thioacetic acid reacts, for example, with the acetyl-protected α-galactosyl trichloroacetimidate **59α** without a further catalyst to give the 1-acetylthio compound **90** directly. By cleavage of the acetyl groups, the sodium salt **91** of the known 1-thio-β-D-galactopyranose can be obtained conveniently (Scheme 22).[101]

Structurally very different *C*-glycosides with interesting biological properties are found in nature.[102] In addition, *C*-glycosides have been recognized as partial structures of many natural products and, thus, they are of interest as chiral building blocks in natural products synthesis.[103] This large biological and preparative interest is reflected in the extensive research in this field.[104] Here, only successful studies with *O*-glycosyl trichloroacetimidates as glycosyl donors and phenol ethers,[59,105] silyl enol ethers,[72] trimethylsilyl cyanide,[72] or allyltrimethylsilane[72] as *C*-acceptors will be mentioned. These results are suitable to confirm the wide scope of application of *O*-glycosyl trichloroacetimidates as glycosyl donors. Comparable reactions of glycosyl halides are unknown.

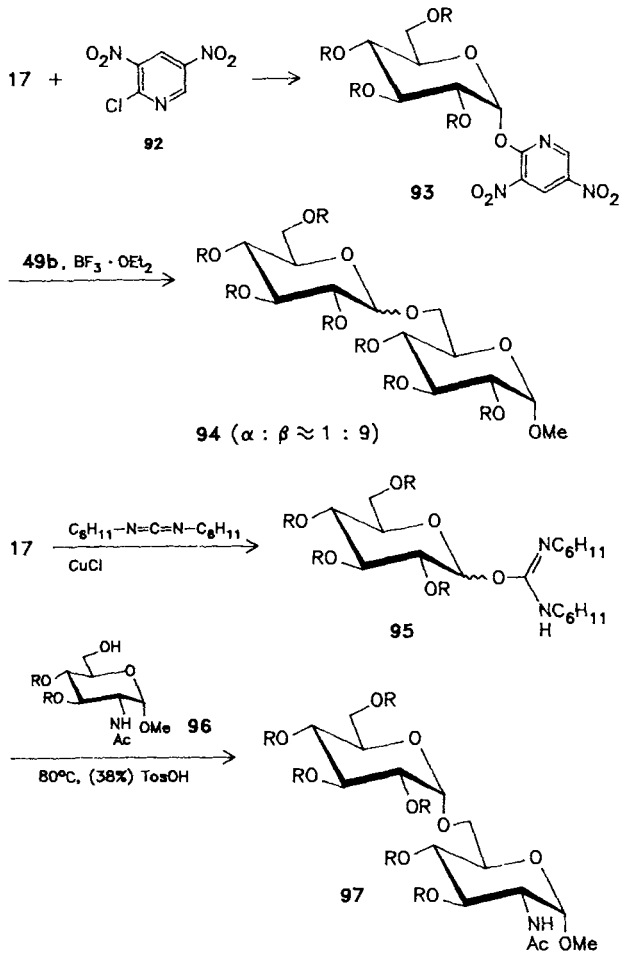
4.3. Other Methods Involving Imidates or Imidate-Like Intermediates

The β-*O*-glycosyl imidates prepared by *Sinaÿ* et al.[49] from α-glycosyl halides and *N*-substituted amides (particularly *N*-methylacetamide) using three equivalents of silver oxide have been discussed above (see ref. [13] and Section 4.1). These compounds require acid catalysis (usually *p*-toluenesulfonic acid, see also ref. [69]) for the transfer of especially reactive hexopyranosyl groups (mainly tetrabenzylgalactose, tribenzylfucose, and tetrabenzylglucose); the reactions proceed with inversion to form α-glycosidic linkages.[49,77,82,106] Neighboring-group-active protecting groups such as 2-*O*-acetyl groups lead to ortho ester formation and not directly to the glycoside or saccharide.[77] As a result of their laborious syntheses and comparatively low reactivities, these imidates have only been employed in special cases to date.[106]

Some of the necessary glycosyl halides were prepared from the 1-*O*-unsubstituted sugars using the Vilsmeier-Haack reagent $Me_2\overset{\oplus}{N}=CHCl\ Cl^{\ominus}$.[106] *Gross* et al.[107] have shown spectroscopically that the *O*-glycosyl iminium esters are stable at low temperatures and can undergo reaction with glycosyl acceptors to give disaccharides. However, two equivalents of silver toluenesulfonate are required to remove the chloride and liberate the *p*-toluenesulfonic acid. The chemical yields are good but, as expected, low α/β-selectivities are observed. In principle, the same problem arises on activation of the anomeric center with 2-fluoro-1-methylpyridinium toluenesulfonate.[108,109]

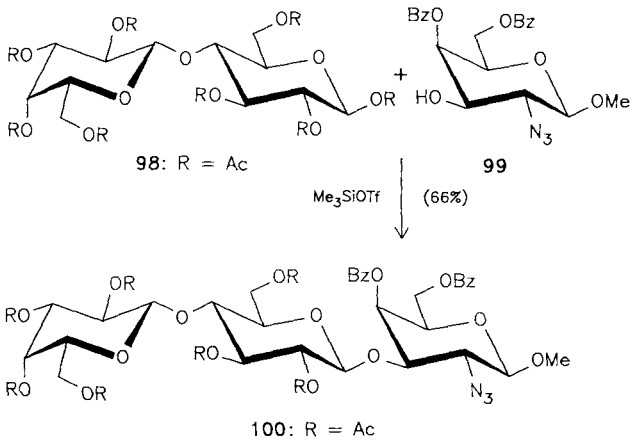
Mukaiyama et al.[110] have also suggested the use of the 3,5-dinitro-2-pyridyl group for activating carbohydrates. This group can be introduced easily by reaction of the corresponding chloro compound **92** in the presence of base, potassium fluoride, and crown ether. Not unexpectedly, the α-product **93** is formed preferentially with tetrabenzylglucose **17**. In the presence of boron trifluoride etherate, primary and simple secondary alcohols can be converted into β-glucosides (e.g., **94**) in good chemical yields and with good stereoselectivities. This glycosyl transfer method is that most closely related to the trichloroacetimidate method. Routes for the specific preparation of the corresponding β-configurated intermediates have not been developed, and hydroxyl groups that are difficult to glycosidate have not been studied to date.

Other groups analogous to the imidates are the isourea groups introduced by *Ishido* et al.[111] These are generated in situ from carbodiimides in the presence of copper(I) chloride and react with nucleophiles at about 80°C. Phenols,[111,112] thiophenol,[111,112] carboxylic acids,[111,113,117] and carbohydrates[111,114] have been used as nucleophiles. The corresponding glycosides are obtained, but sometimes in only modest yields and with low diastereoselectivities. On reaction of **17** with *N,N'*-dicyclohexylcarbodiimide, the *O*-glycosylisourea derivative **95** is formed as an intermediate and reacts, under drastic conditions, with the glucosamine derivative **96** to give the α-disaccharide **97** (Scheme 23).



Scheme 23. R = Bzl.

hydrooxazoles are presumed to be intermediates in these reactions. Similarly, boron trifluoride etherate is used to prepare simple *O*-glycosides from 1-*O*-acetylated *N*-phthaloylglucosamine and -lactosamine derivatives.[121] In the last few years, especially the use of trimethylsilyl triflate as catalyst has afforded good results for *N*-[122] and *O*-glycoside[13,123] syntheses. For example, *Ogawa* et al.[123] reported the successful reaction of primary hydroxyl groups of sugars. *Paulsen* and *Paal*[13,124] achieved reaction of the corresponding secondary hydroxyl groups. For example, the peracetylated lactose **98** and the 3-*O*-unprotected azidogalactose **99** were coupled to give the β-linked trisaccharide **100** (Scheme 24). In all of the examples studied, the glycosyl donor had neighboring-group-active protecting groups so that stereoselectivity was ensured. Ortho esters have been suggested as intermediates. These simple procedures are valuable additions to oligosaccharide synthesis.



Scheme 24.

4.4. 1-*O*-Acyl Compounds and Ortho Ester Formation

The disadvantage of a low activation of the glycosyl moiety for glycosyl transfer, which is obvious in the case of isourea formation, is even more pronounced in the case of carbonate activation.[115] Disaccharides can be prepared only by condensations of melts at about 160–180°C.

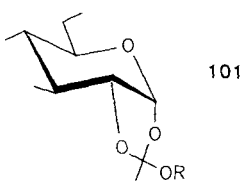
When the glycosyl donor properties of the 1-*O*-unsubstituted sugar are reduced, glycosylation can still be achieved by the use of correspondingly stronger acid catalysts; however, the process is not applicable to acid-labile sugars. Such reactions are especially successful with simple alcohols as acceptors. This approach, ultimately leads to the conditions of the Fischer-Helferich method (Fig. 2), which does without a 1-*O*-activated intermediate and builds up the glycosyl donor potential solely by the action of strong acids.

Helferich and *Schmitz-Hillebrecht*[116] were able to convert 1-*O*-acylated sugars into simple *O*-glycosides using Lewis acids (especially $ZnCl_2$).[10,117,118] *Hanessian* and *Banoub*[119] prepared disaccharides using tin tetrachloride. Using iron(III) chloride and tetramethylurea as acid scavenger, *Kiso* and *Anderson*[120] achieved disaccharide coupling between 1-*O*-acetylated *N*-acetylglucosamines and the primary and secondary hydroxyl groups of sugars. Di-

An interesting variant of the glycoside synthesis, reported by *Hanessian* and *Banoub*,[125] is the reaction of 1-*O*-acyl sugars, possessing neighboring-group-active protecting groups, with amide acetals as acceptors and tin tetrachloride as catalyst.

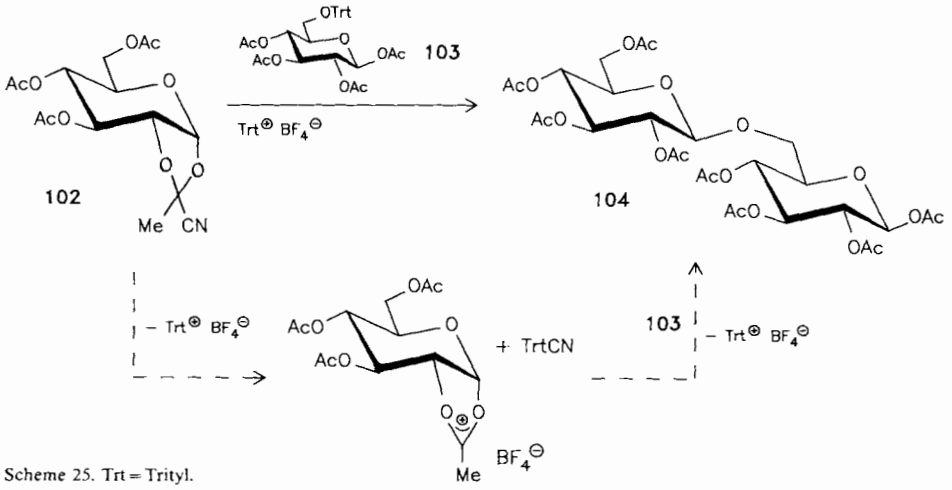
1-*O*-Acyl sugars with *O*-benzyl protecting groups were activated using trityl perchlorate by *Mukaiyama* et al.[126] For example, the bromoacetate of tetra-*O*-benzyl-β-D-glucose afforded preferentially α-glycosides. Our investigations[127] on the direct reduction of the carboxyl groups of 1-*O*-acyl sugars led to the successful synthesis of simple glycosides.

The synthesis of ortho esters from glycosyl halides and their mercury-salt-catalyzed rearrangement to glycosides and saccharides have been known for a long time.[10,13] Activation of the C–O glycoside bond for glycosyl transfer results from the alkylating character of ortho esters (see **101**); thus, as expected, treatment of the ortho esters with carboxylic acids results in the formation of 1-*O*-acyl com-



101

pounds.[128] *Kochetkov* et al.,[129] in particular, have developed the ortho ester method. One disadvantage of this method is the formation of the 2-*O*-unsubstituted sugar by a competing protonation at the 2-*O* atom.[130] This side reaction can be avoided by formation of the acyloxonium intermediate and trapping it with cyanide.[129] For example, the ketal **102**, derived from pentaacetylglucose, is converted into peracetylgentiobiose **104** in good yield by reaction with the 6-*O*-tritylglucose derivative **103** in the presence of trityl tetrafluoroborate according to the method of *Bredereck* et al.[131] Compound **102** reacts with trityl tetrafluoroborate to form initially triphenylacetonitrile and an acyloxonium intermediate, which, in turn, reacts irreversibly with the trityl ether **103** to give the disaccharide **104** (Scheme 25). In this way, the presence of strong acids (e.g., HBF_4) is avoided. This method has also been used for the synthesis of polysaccharides such as α(1→3)-L-rhamnan.[132] The same advantage is attained by the introduction of an alkylthio group.[133] *O*-Trityl sugars as acceptors with trityl perchlorate as coactivator result in good yields of 1,2-*trans*-linked disaccharides of glucose, galactose, mannose, and rhamnose.[133,134]

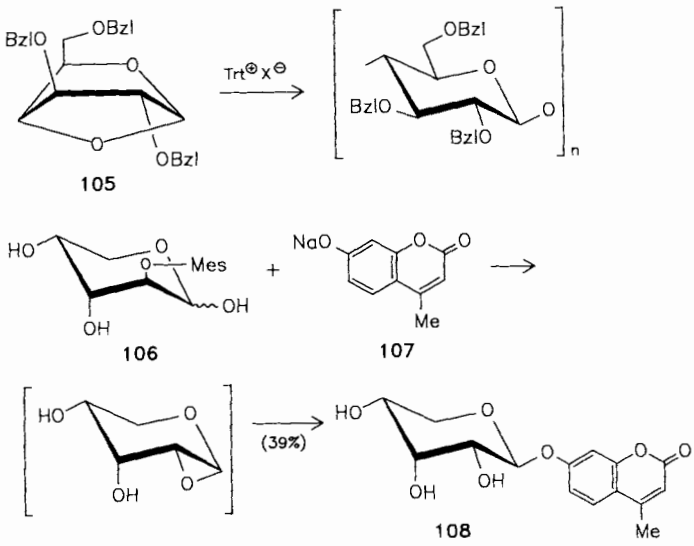


Scheme 25. Trt = Trityl.

4.5. Anhydro Sugars as Intermediates

Similar to the ortho ester method is the formation of anhydro compounds as activated intermediates. For example, *Micheel* et al.[135] employed the 1,4-anhydro-α-D-glucopyranose **105** in a synthesis of polymeric sugars (Scheme 26). The use of trityl hexafluorophosphate and hexafluoroantimonate resulted exclusively in β(1→4) coupling.

More obvious is the use of the strongly activated 1,2-anhydro sugars for glycoside synthesis. *Brigl*'s anhydride was thus used for the syntheses of the disaccharides maltose,[136] maniocose,[137] sucrose,[138] and trehalose.[139] However, only modest yields of the disaccharides were obtained by reactions of the 4-*O*-unprotected glucose derivatives in dry toluene at 130°C. Attempts to prepare iridoid glycosides gave similar results.[141] Since the thermodynamically more stable α-saccharides are formed preferentially in these reactions, the possibilities with reactive 1,2-anhydrides probably are not exhausted. This is illustrated by the synthesis of the ribopyranoside **108**, starting from the 2-*O*-mesyl compound **106** and the sodium salt of 7-hydroxy-4-methylcoumarin **107**, via the anhydro compound; controlled ring opening to give exclusively 1,2-*trans* coupling was observed (Scheme 26).[142] Acyclic enol ether epoxides were also suggested for glycoside synthesis.[143]

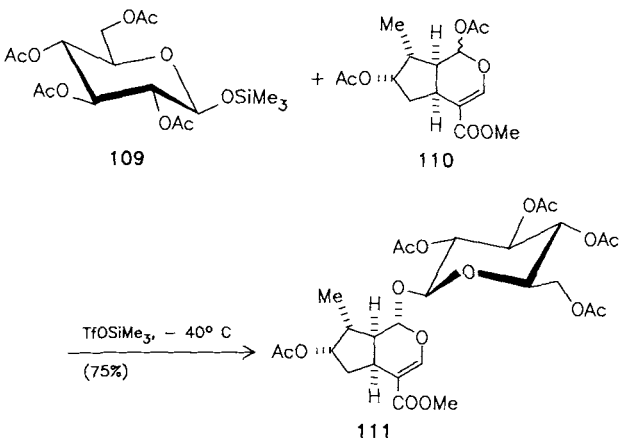


Scheme 26.

4.6. 1-*O*-Silylated Sugars as Intermediates

1-*O*-Trimethylsilylglycosides, obtainable in anomerically pure form from 1-*O*-unprotected sugars,[144] have been shown by *Tietze* et al.[144,145] to be useful in the synthesis of phenylglycosides. With *O*-silylated phenols as acceptors and trimethylsilyl triflate as catalyst, practically exclusively β-glucopyranosides are obtained from compounds with neighboring-group-active acyl protecting groups and practically exclusively the corresponding α-glucopyranosides from compounds with inactive benzyl protecting groups.

In this way, α- and β-glycosides with 1,1'-diacetal structures have been prepared at lower temperatures with retention of configuration.[146] Iridoid glycosides could also be synthesized in this manner.[147] For example, the loganin pentaacetate **111** was prepared from the 1-*O*-silylated glucose derivative **109** with loganol diacetate **110** as the acceptor (Scheme 27).



Scheme 27.

The glycosylation potential of the *O*-silylated glycosides probably does not exceed that of normal glycosides, so that the catalyst and the formation of hexamethyldisiloxane are responsible for the course of the reaction. The stereocontrol results from neighboring-group participation or from the anomeric effect. The retention of configuration of the 1-*O*-silylated intermediate in the 1,1'-diacetal formation probably results from intermediary 1-*O*-alkoxyalkylation. Corresponding results obtained for 1-*O*-alkylations can be interpreted similarly.[29,32] This interpretation is supported further by the trifluoromethanesulfonic anhydride activated formation of trehalose.[148] In all these reactions, the conditions of the transglycosidation[149] or the Fischer-Helferich method are employed, which are not suitable for the synthesis of more complex oligosaccharides.

4.7. 1-*O*-Sulfonylated Sugars as Intermediates

The generation of a better leaving group by 1-*O*-toluenesulfonyl formation has been known for a long time.[150,151] These compounds were prepared by reaction of the corresponding α-glycosyl halides with silver toluenesulfonate, predominantly α-toluenesulfonates being obtained. According to *Schuerch* et al.,[151] the introduction of an electron-attracting acyl or carbonyl group at the 6-*O* atom leads to stabilization of the 1-*O*-toluenesulfonate group. In this way, especially in ether as solvent, α-glycopyranosides could be obtained preferentially from glucose and galactose when 2-*O*-benzyl protecting groups were employed. The stereochemistry of this reaction is explainable by the intermediacy of an onium species with ether as a reaction partner.[16,152] The corresponding *p*-nitrobenzenesulfonyl derivative of 2,3,4,6-tetrabenzylglucose, generated as an intermediate from silver triflate, *p*-nitrobenzenesulfonyl chloride, and triethylamine, gives β-glucopyranosides in dichloroethane as solvent.[153] Under identical conditions but in the presence of dimethylacetamide, α-saccharides are formed,[154] presumably via an iminium ester intermediate (see Section 4.3). In this reaction, the glycosyl donor is used in a fourfold excess.

By introducing a strongly electron-attracting group at the 2-*O* atom (mesyl, *p*-nitrobenzoyl, or benzoyl group), it was possible to strengthen the S_N2 character of the substitution at the anomeric carbon atom to such a degree that β-glycopyranosides of glucose,[155] galactose,[156] and even mannose[157] and rhamnose[157] could be obtained. The amounts of reagent and the difficult stereocontrol of both intermediate and end product prevent a broader application of this straightforward method. Apparently, the route via glycosyl halides and their activation with silver triflate, as reported by *Hanessian* and *Banoub*,[158] which is, in effect, a variant of the Koenigs-Knorr method, is considerably more efficient.

Studies on 1-*O*-activation with the Mitsunobu reagent have not attained general significance.[159,160]

5. Leaving Groups with Elements other than Oxygen at the Anomeric Center: O/Element Exchange for 1-*O*-Activation

The exchange of the anomeric hydroxyl group for a better leaving group, e.g., chlorine or bromine, is realized in the Koenigs-Knorr method, which makes use of coactivation by halophilic metal salts.[13] Due to their relative instability, the more reactive iodine compounds[151a,161] have not gained importance. Silver and mercury salts, above all, have proved successful as metal salts. The introduction of silver triflate as a homogeneous catalyst by *Hanessian* and *Banoub*[158] and of silver silicate as a heterogeneous catalyst by *Paulsen* et al.[13,18] have considerably improved the efficiency and scope of this method. Other metal salts also have been examined.[162,163]

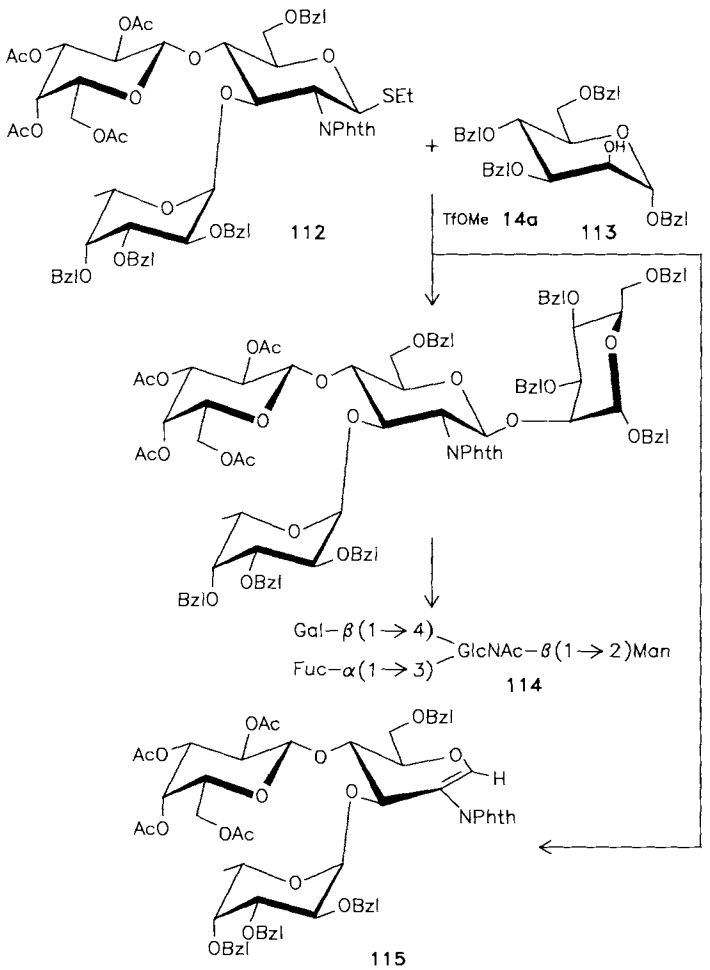
Because of the extensive literature on the Koenigs-Knorr method, the question whether other elements can be introduced as leaving groups at the anomeric center and be exchanged in a stereocontrolled manner by *O*-nucleophiles should be discussed. Of the electronegative elements that are particularly suitable for nucleophilic substitution, there remain, apart from oxygen (Section 4), chlorine, bromine, and iodine (see above), the elements nitrogen, sulfur, phosphorus, and fluorine. Of these, the first two can be envisaged in various bonding forms.

5.1. Ammonium, Sulfonium, Phosphonium, and Nitrilium Intermediates

Ammonium, sulfonium, and phosphonium groups are suitable as leaving groups for the formation of stabilized carbonium ions, although they have different leaving-group tendencies. *Schuerch* et al.[151b,164–166] have studied these groups at the anomeric centers of carbohydrates. Starting from α-bromo-2,3,4,6-tetrabenzylglucose and -galactose, the corresponding onium compounds were generated by reaction with amines, dialkyl sulfides, or tertiary

phosphanes. NMR data confirm the β-configuration, which would be expected from the inverse anomeric effect.[167] Methanolysis studies showed the expected order of reactivity: sulfonium > ammonium > phosphonium compounds.[165] In view of their low reactivity, further studies on phosphonium compounds were unnecessary. Predominantly α-glycosides were obtained as products. Studies on disaccharide synthesis with a reactive 6-*O*-unprotected glucopyranoside and various ammonium leaving groups gave modest results with regard to yield and stereoselectivity. The best results were obtained when diethyl ether or triethylamine/acetone was used as solvent.[166]

Recently, *Lönn* reported good glycosidation results for sulfonium leaving groups.[168-170] β-Alkylthio derivatives of *N*-phthaloylglucosamine were *S*-methylated with methyl triflate, and the β-glycosides were obtained in good yields owing to phthaloylamido group control. For example, the tetrasaccharide **114** was constructed from the trisaccharide **112** as donor and the mannose derivative **113** as acceptor.[170] This tetrasaccharide has been found as a structural element of glycoproteins in the urine of patients suffering from fucosidosis.[171] The 1,2-elimination, previously observed by *Kronzer* and *Schuerch*,[165] was observed as a competing reaction to give, in this case, the glycal derivative **115** (Scheme 28). A nonasaccharide was built up in the same way. Glycosidation with non-neighboring-group-active protecting groups at the 2-*O* atom gave α/β mixtures

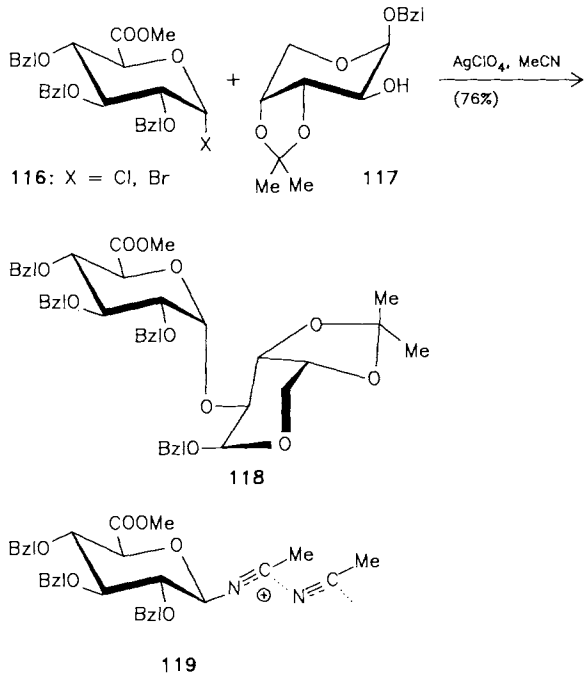


Scheme 28.

in high yields; with diethyl ether as solvent, the best α-selectivity was observed.[168] New methods for the preparation of thioglycosides have been described recently by *Hanessian* et al.[172] and *Nicolaou* et al.[173]

Glycosyl disulfides, sulfonates, and sulfones are not practical as glycosyl donors.[174]

The nitrile group in nitrilium compounds acts as a leaving group, especially when formally stable carbonium ions are formed. The leaving properties are favored when a nitrile is used as the solvent since the nucleophilic attack at the nitrilium *C* atom is then hindered by the formation of a nitrilium-nitrile conjugate.[16,175] Therefore, we have converted α-halo derivatives of glucuronic acid **116** into the *N*-glucosylnitrilium-acetonitrile conjugates **119** by treatment with silver perchlorate in acetonitrile as solvent; as a result of the inverse anomeric effect, the β-product is formed.[16,176] Disaccharides (e.g., **118**) were obtained in very good yields and with high α-selectivities with glycosyl donors such as the arabinose derivative **117** (Scheme 29).



Scheme 29.

Correspondingly, riburonic acids were coupled in a β-glycosidic manner.[176] An analogous process using cladinose was employed for the synthesis of erythromycin.[177]

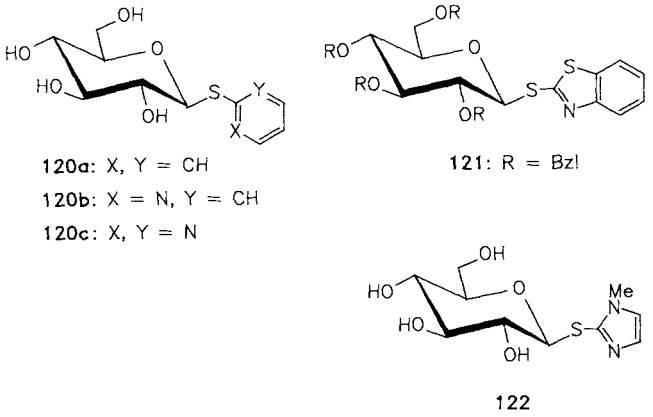
Nitrilium salts react to give *N*-acylglycosylamines and glycosylamines.[49,69,178] Their conversion into diazonium compounds also affords glycosyl donors.[179]

5.2. Activation of Thioglycosides by Thiophilic Metal Salts and *N*-Bromosuccinimide

The anomeric thioalkyl group in glycosides and saccharides opens up possibilities for selective activation owing to its good stability as a protecting function and as a result of sulfur-specific reactions (see Section 5.1). Particularly obvious is the selective activation of thioglycosides by thiophilic metal salts. *Ferrier* et al.[180,181] and *VanCleve*[182] car-

ried out the first systematic studies with mercury(II) salts. By using phenylmercury triflate, *Garegg* et al.[183] were able to convert phenyl-β-thioglycosides of tetrabenzylglucose and tetrabenzylgalactose to disaccharides in good yields and with high α-selectivities. Phenyl-β-thioglycosides of tetraacylglucose and tetraacylgalactose gave inconsistent results for as yet unknown reasons.

Comparative studies by *Hanessian* et al.[184] on the proton activation of phenylthio- and pyridin-2-ylthioglucopyranosides **120a** and **120b**, respectively, demonstrated the dramatic effect of the heteroatom (remote activation) as a basic anchor for the proton and as a better leaving group, resulting from the negative inductive effect. *Mukaiyama* et al.[185] previously exploited this effect for glycosylation with the benzothiazolylthioglucoside **121** in the presence of copper(II) triflate as catalyst. *Hanessian* et al.[184] studied the reaction of the *O*-unprotected glucosylthioheterocycles **120b,c** and **122** with reactive glycosyl acceptors using mercury(II) nitrate as catalyst and acetonitrile as solvent (Scheme 30). They obtained glycosides and the disaccharide Glc(1→6)Gal in good yields but with only modest α/β-selectivities. Benzothiazolylthio activation was also employed successfully in a synthesis of erythromycin.[177]

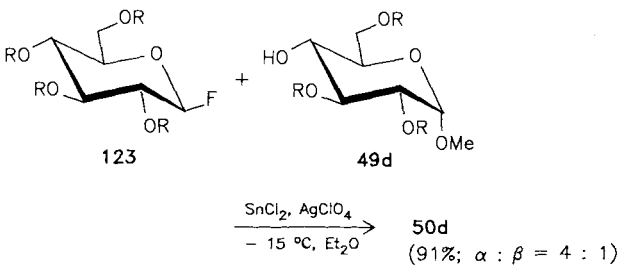


Scheme 30.

In addition to protons and metal salts, bromonium ions are also thiophilic. Thus, thioglycosides can serve as convenient substrates for the synthesis of glycosyl bromides through introduction of bromine.[186] If the counterion of the bromonium ion is a poor nucleophile, as is the case with *N*-bromosuccinimide (NBS), then the introduction of alcohols as nucleophiles, for example, should be possible in competition. This has been confirmed already by *Hanessian* et al.[184] Recently, *Nicolaou* et al.[173] reported on the wide scope of this method starting from phenylthioglycosides; however, low α/β-selectivities were frequently obtained. The described "intramolecular glycosidation," in which 1,6-anhydro derivatives were obtained, should be of particular value.

5.3. Activation by Fluoride

The use of fluoride at the anomeric center as leaving group has aroused interest in the last few years.[187] This brings us full circle back to the Koenigs-Knorr method. Being a poorer leaving group, fluoride leads to intermediates more stable than glycosyl chlorides and bromides. In addition, fluorophilic properties are found not only in heavy-metal salts. These facts show that reactive promoters are necessary for activation. In the first studies by *Mukaiyama* et al.,[187] tin(II) chloride/silver perchlorate was employed for activation. Syntheses of glycosides and disaccharides starting from the glycosyl fluoride **123** afforded good α-selectivities; with the 4-*O*-unprotected glucoside **49d**, the α-form of the maltoside **50d** was formed preferentially (Scheme 31). This method was used by *Nicolaou* et al.[188,189] for the synthesis of complex glycosides and oligosaccharides such as the rhynchosporides.[189] Glycosyl transfer was effected by activation with 1.8 equivalents each of tin(II) chloride and silver perchlorate in ether at −15°C. With neighboring-group-active acyl protecting groups, β-coupling was achieved. Analogously, *Mukaiyama* et al.[109] obtained α-ribofuranosides preferentially from β-ribofuranosyl fluoride with tin(II) chloride/silver perchlorate as promotor and β-arabinofuranosides from α-arabinofuranosyl fluoride with tin(II) chloride alone. *Noyori* et al.[190] were able to activate glycosyl fluorides with tetrafluorosilane and trimethylsilyl triflate when the acceptors were used in the form of their trimethylsilyl ethers. Good yields but frequently only modest α/β-selectivities were observed.



Scheme 31. R = Bzl.

Mukaiyama et al.[108,185,187] prepared isolable glycosyl fluorides by reaction of the 1-*O*-unprotected compounds with 2-fluoro-1-methylpyridinium toluenesulfonate in the presence of triethylamine. Generally, anomeric mixtures were obtained. Anomerization to the thermodynamically more stable fluoride could be effected.[109,191] The interest in glycosyl fluorides has led to further new syntheses,[192] whereby diethylaminosulfur trifluoride (DAST) in tetrahydrofuran has proved to be particularly valuable.[37,193] *Nicolaou* et al.[188] converted phenylthioglycosides into glycosyl fluorides by reaction with NBS/DAST and HF-pyridine/NBS.

Because of the methodological analogies, the results with glycosyl fluorides have to be compared with those obtained with the classical Koenigs-Knorr method (i.e., results with glycosyl chlorides and bromides). However, with the results presently available, a conclusive evaluation with regard to the requirements listed in Section 2.3 for a new glycoside synthesis is not possible. Glycosyl fluorides, like the trichloroacetimidates, have also proved useful in the syntheses of, for example, *C*-glycosides,[104a,194,195] so that a

broad application is guaranteed for these glycosyl donors.

6. Summary and Prospects

In spite of the complexity of oligosaccharide syntheses, enormous progress has been achieved by new methods and by modifications of the Koenigs-Knorr method. The controlled, efficient synthesis of an oligosaccharide or a glycoconjugate—a dream just a decade ago—can be planned and performed today.

Particularly worthy of note are two new methods: the stereocontrolled, direct 1-*O*-alkylation of sugars, which makes saccharides accessible by a particularly simple method; and the trichloroacetimidate method, which leads to stable *O*-glycosyl trichloroacetimidates with high glycosylation potentials in a stereocontrolled manner by utilization of kinetic and thermodynamic stereoelectronic effects. Neither method requires heavy-metal salts and both are suitable for large-scale preparations. The selective activation of alkyl- or arylthioglycosides with thiophilic reagents or of glycosyl fluorides with fluorophilic reagents present interesting perspectives.

In spite of these advances, chemical oligosaccharide syntheses are still not quantitative, diastereospecific reactions. Thus, further development of the available methods is desirable. In addition, the regioselective reactivity of partially protected glycosyl acceptors must be studied and exploited; initial investigations have already been performed.[66, 70, 82, 196]

As mentioned at the beginning of this article, each chemical oligosaccharide synthesis is a special problem requiring both knowledge of methods and experimental dexterity. The differing reactivities and stereoselectivities of donors and acceptors, which depend in part on the effect of protecting groups, neighboring groups, through-space steric interactions, and amphiphilic properties, make the development of generalizable reaction conditions for oligosaccharide synthesis difficult, in contrast to the presently available possibilities for peptide and oligonucleotide synthesis. The diversity of the combinations of sugars with themselves and with other sugars (see Table 1) has also forced nature to adopt special solutions. The imitation of these specific enzymatic processes in the laboratory would require an arsenal of enzymes that are not available today, although interesting initial successes have been reported.[197]

I thank my colleagues who developed the direct 1-O-alkylation and trichloroacetimidate methods during the course of master and doctoral theses at the University of Konstanz. These are G. Effenberger, A. Eßwein, M. C. Faas, G. Grundler, P. Hermentin, M. G. Hoffmann, K.-H. Jung, W. Kinzy, R. Kläger, A. Köhn, K. Laesecke, J. Lutz, J. Michel, U. Moering, M. Reichrath, M. Roos, E. Rücker, M. Stumpp, B. Wegmann, and P. Zimmermann.—Thanks are also due to the Deutsche Forschungsgemeinschaft and the Fonds der Chemischen Industrie for financial support of this work.

Received: October 21, 1985 [A 569 IE]
German version: *Angew. Chem. 98* (1986) 213
Translated by Dr. *R. E. Dunmur*, Stuttgart

[1] a) N. Sharon, *Sci. Am. 230* (1974) (No. 5) 78; b) N. Sharon: *Complex Carbohydrates, Their Biochemistry, Biosynthesis and Functions*, Addison Wesley, Reading, MA, USA 1975.
[2] a) N. S. Sharon, H. Lis, *Chem. Eng. News 59* (1981) No. 13, p. 21; b) N. Sharon, *Trends Biochem. Sci. 9* (1984) 198.
[3] J. Montreuil, *Adv. Carbohydr. Chem. Biochem. 37* (1980) 157.
[4] S. J. Singer, *Annu. Rev. Biochem. 43* (1974) 805.
[5] S. Hakamori, *Annu. Rev. Biochem. 50* (1981) 733, and references cited therein.
[6] Y.-T. Li, S.-C. Li, *Adv. Carbohydr. Chem. Biochem. 40* (1982) 235.
[7] F. M. Burnet: *Self and not-self. Cellular Immunology Book one*, Melbourne University Press, Victoria/Cambridge University Press, London 1969.
[8] T. Feizi, R. A. Childs, *Trends Biochem. Sci. 10* (1985) 24; T. Feizi, *Nature (London) 314* (1985) 53.
[9] I thank Mr. *A. Enhsen* for the calculation of these numbers. See also [2a].
[10] G. Wulff, G. Röhle, *Angew. Chem. 86* (1974) 173; *Angew. Chem. Int. Ed. Engl. 13* (1974) 157.
[11] K. Igarashi, *Adv. Carbohydr. Chem. Biochem. 34* (1977) 243.
[12] A. F. Bochkov, G. E. Zaikov: *Chemistry of the O-Glycosidic Bond; Formation and Cleavage*, Pergamon Press, Oxford 1979.
[13] H. Paulsen, *Angew. Chem. 94* (1982) 184; *Angew. Chem. Int. Ed. Engl. 21* (1982) 155, and references cited therein.
[14] H. Paulsen, *Chem. Soc. Rev. 13* (1984) 15.
[15] R. R. Schmidt, P. Hermentin, *Chem. Ber. 112* (1979) 2659.
[16] R. R. Schmidt, E. Rücker, *Tetrahedron Lett. 21* (1980) 1421.
[17] R. U. Lemieux, K. B. Hendriks, R. V. Stick, K. James, *J. Am. Chem. Soc. 97* (1975) 4056.
[18] H. Paulsen, O. Lockhoff, *Chem. Ber. 114* (1981) 3102.
[19] R. R. Schmidt, J. Michel, M. Roos, *Liebigs Ann. Chem. 1984*, 1343.
[20] T. Purdie, J. C. Irvine, *J. Chem. Soc. 83* (1903) 1021.
[21] W. N. Haworth, *J. Chem. Soc. 107* (1919) 8.
[22] H. Bredereck, G. Hagellock, E. Hambsch, *Chem. Ber. 87* (1954) 35.
[23] R. Kuhn, H. Trischmann, J. Löw, *Angew. Chem. 67* (1955) 32.
[24] D. Roth, W. Pigman, *J. Am. Chem. Soc. 82* (1960) 4608.
[25] D. M. Hall, O. A. Stanem, *Carbohydr. Res. 12* (1970) 421.
[26] A. H. Haines, K. C. Symes, *J. Chem. Soc. C 1971*, 2331; A. H. Haines, *Adv. Carbohydr. Chem. Biochem. 33* (1976) 55.
[27] A. Zamojski, H. Bazymska, *Rocz. Chem. 49* (1975) 2113, and references cited therein..
[28] H. Bredereck, E. Hambsch, *Chem. Ber. 87* (1954) 38.
[29] R. R. Schmidt, M. Reichrath, unpublished results.
[30] R. R. Schmidt, M. Reichrath, *Angew. Chem. 91* (1979) 497; *Angew. Chem. Int. Ed. Engl. 18* (1979) 466.
[31] R. R. Schmidt, M. Reichrath, U. Moering, *Tetrahedron Lett. 21* (1980) 3561.
[32] R. R. Schmidt, U. Moering, M. Reichrath, *Chem. Ber. 115* (1982) 39.
[33] M. H. Randall, *Carbohydr. Res. 11* (1969) 173.
[34] R. R. Schmidt, U. Moering, M. Reichrath, *Tetrahedron Lett. 21* (1980) 3565.
[35] R. R. Schmidt, M. Reichrath, U. Moering, *J. Carbohydr. Chem. 3* (1984) 67.
[36] P. E. Pfeffer, G. G. Moore, P. D. Hoagland, E. S. Rothman, *ACS Symp. Ser. 39* (1976) 155.
[37] W. Rosenbrook, Jr., D. A. Riley, P. A. Lartey, *Tetrahedron Lett. 26* (1985) 1.
[38] J. J. Oltvort, C. A. A. van Boeckel, J. H. de Koning, J. H. van Boom, *Recl. Trav. Chim. Pays-Bas 101* (1982) 87.
[39] J. J. Oltvort, M. Kloosterman, C. A. A. van Boeckel, H. van Boom, *Carbohydr. Res. 130* (1984) 147.
[40] R. R. Schmidt, U. Moering, unpublished results.
[41] The 1-*S*-alkylation for the synthesis of thioglycosides, which is easier to perform, has been known for a long time: D. Horton, D. Hutson, *Adv. Carbohydr. Chem. Biochem. 18* (1963) 123.
[42] F. Roulleau, D. Plusquellec, E. Brown, *Tetrahedron Lett. 24* (1983) 719; D. Plusquellec, F. Roulleau, E. Brown, *ibid. 25* (1984) 1901.
[43] M. Inage, H. Chaki, S. Kusumoto, T. Shiba, *Chem. Lett. 1982*, 1281.
[44] A. Granata, A. S. Perlin, *Carbohydr. Res. 94* (1981) 165.
[45] R. R. Schmidt, J. Michel, *Tetrahedron Lett. 25* (1984) 821.
[46] As this effect has same origin as the thermodynamically effective anomeric effect, the term "kinetic anomeric effect" was suggested [45].
[47] V. G. S. Box, *Heterocycles 19* (1982) 1939.
[48] P. Deslongchamps: *Stereoelectronic Effects in Organic Chemistry*, Pergamon Press, Oxford 1983, p. 29 ff.
[49] a) J. R. Pougny, P. Sinaÿ, *Tetrahedron Lett. 1976*, 4073; b) J. R. Pougny, J. C. Jacquinet, M. Nassr, M. L. Milat, P. Sinaÿ, *J. Am. Chem. Soc. 99* (1977) 6762.
[50] D. C. Neilson in S. Patai (Ed.): *The Chemistry of Amidines and Imidates*, Wiley, New York 1975, p. 349 ff.
[51] J. U. Nef, *Justus Liebigs Ann. Chem. 287* (1895) 274.

[52] a) F. Cramer, K. Pawelzik, H. Baldauf, *Chem. Ber. 91* (1958) 1049; b) F. Cramer, H. Baldauf, *ibid. 94* (1961) 976; c) F. C. Schäfer, G. A. Peters, *J. Org. Chem. 26* (1961) 412; d) L. E. Overman, *Acc. Chem. Res. 13* (1980) 218; e) T. Iversen, D. R. Bundle, *J. Chem. Soc. Chem. Commun. 1981*, 1240.

[53] R. R. Schmidt, J. Michel, *Angew. Chem. 92* (1980) 763; *Angew. Chem. Int. Ed. Engl. 19* (1980) 731.

[54] J. Michel, *Dissertation*, Universität Konstanz 1982.

[55] R. R. Schmidt, M. Stumpp, *Liebigs Ann. Chem. 1983*, 1249.

[56] R. R. Schmidt, J. Michel, *Angew. Chem. 94* (1982) 77; *Angew. Chem. Int. Ed. Engl. 21* (1982) 72; *Angew. Chem. Suppl. 1982*, 78.

[57] R. R. Schmidt, G. Grundler, *Synthesis 1981*, 885.

[58] R. R. Schmidt, M. Stumpp, J. Michel, *Tetrahedron Lett. 23* (1982) 405.

[59] R. R. Schmidt, M. Hoffmann, *Tetrahedron Lett. 23* (1982) 409.

[60] R. R. Schmidt, G. Grundler, *Angew. Chem. 94* (1982) 790; *Angew. Chem. Int. Ed. Engl. 21* (1982) 775; *Angew. Chem. Suppl. 1982*, 1707.

[61] R. R. Schmidt, M. Hoffmann, *Angew. Chem. 95* (1983) 417; *Angew. Chem. Int. Ed. Engl. 22* (1983) 406; *Angew. Chem. Suppl. 1983*, 543.

[62] R. R. Schmidt, G. Grundler, *Angew. Chem. 95* (1983) 805; *Angew. Chem. Int. Ed. Engl. 22* (1983) 776.

[63] K. Laesecke, R. R. Schmidt, *Liebigs Ann. Chem. 1983*, 1910.

[64] R. R. Schmidt, M. Stumpp, *Liebigs Ann. Chem. 1984*, 680.

[65] G. Grundler, R. R. Schmidt, *Liebigs Ann. Chem. 1984*, 1826.

[66] G. Grundler, R. R. Schmidt, *Carbohydr. Res. 135* (1985) 203.

[67] R. R. Schmidt, R. Kläger, *Angew. Chem. 97* (1985) 60; *Angew. Chem. Int. Ed. Engl. 24* (1985) 65.

[68] W. Kinzy, R. R. Schmidt, *Liebigs Ann. Chem. 1985*, 1537.

[69] R. R. Schmidt, J. Michel, *J. Carbohydr. Chem. 4* (1985) 141.

[70] R. R. Schmidt, M. Faas, K. H. Jung, *Liebigs Ann. Chem. 1985*, 1546.

[71] R. R. Schmidt in P. Böger (Ed.): *Wirkstoffe im Zellgeschehen, Konstanzer Bibliothek Bd. 1*, Universitätsverlag Konstanz 1985, p. 55.

[72] M. G. Hoffmann, R. R. Schmidt, *Liebigs Ann. Chem.*, in press.

[73] R. R. Schmidt, unpublished.

[74] R. R. Schmidt, Lecture 1st Eur. Symp. Carbohydr. Glycoconjugates, Vienna 1981.

[75] J. E. Truelove, A. A. Hussain, H. B. Kostenbander, *J. Pharm. Sci. 69* (1980) 231.

[76] F. Cramer, K. Pawelzik, F. W. Lichtenthaler, *Chem. Ber. 91* (1958) 1555.

[77] P. Sinaÿ, *Pure Appl. Chem. 50* (1978) 1437.

[78] A. Eßwein, *Diplomarbeit*, Universität Konstanz 1984.—Analogous results were also obtained with phosphonic and phosphinic acids.

[79] W. Kinzy, R. R. Schmidt, unpublished.

[80] H. Rathore, T. Hashimoto, K. Igarashi, H. Nukaya, D. S. Fullerton, private communication.

[81] H. Kunz, H. Waldmann, *Angew. Chem. 96* (1984) 49; *Angew. Chem. Int. Ed. Engl. 23* (1984) 71.

[82] P. H. Amvam Zollo, *Dissertation*, Université Orléans 1983.

[83] S. J. Cook, R. Khan, J. M. Brown, *J. Carbohydr. Chem. 3* (1984) 343.

[84] P. Fügedi, A. Liptak, P. Nanasi, *Carbohydr. Res. 107* (1982) C5.

[85] T. Ogawa, Lecture, Euchem Conference on Synthesis of Low-Molecular Weight Carbohydrates of Biological Significance, Stockholm, June 1982.

[86] a) A. Slouiany, B. L. Slouiany, *J. Biol. Chem. 253* (1978) 7301; b) G. Lamblin, M. Lhermitte, A. Boersma, P. Roussel, *ibid. 255* (1980) 4595; c) E. F. Hounsell, M. Fukuda, M. E. Powell, T. Feizi, S. Hakamori, *Biochem. Biophys. Res. Commun. 92* (1980) 1143; d) H. van Halbeek, L. Dorland, J. F. G. Vliegenthart, W. E. Hull, G. Lamblin, M. Lhermitte, A. Boersma, P. Russel, *Eur. J. Biochem. 127* (1982) 7.

[87] H. J. Jennings, C. W. Lugowski, F. E. Ashton, R. A. Ryan, *Carbohydr. Res. 112* (1983) 105.

[88] B. Wegmann, *Diplomarbeit*, Universität Konstanz 1985.

[89] a) R. R. Schmidt, R. Kläger, *Angew. Chem. 94* (1982) 215; *Angew. Chem. Int. Ed. Engl. 21* (1982) 210; *Angew. Chem. Suppl. 1982*, 393; b) P. Zimmermann, *Diplomarbeit*, Universität Konstanz 1984.

[90] a) P. Tkaczuk, E. R. Thornton, *J. Org. Chem. 46* (1981) 4393; b) D. Shapiro, H. M. Flowers, *J. Am. Chem. Soc. 83* (1961) 3327; c) D. Shapiro: *Chemistry of Sphingolipids*, Hermann, Paris 1969; d) D. Shapiro, A. J. Achter, *Chem. Phys. Lipids 22* (1978) 197; e) R. Gigg, *ibid. 26* (1980) 287.

[91] R. Kläger, *Dissertation*, Universität Konstanz 1985.

[92] M. Sugimoto, T. Ogawa, *Glycoconjugate J. 2* (1985) 5.

[93] M. Sugimoto, T. Horisaki, T. Ogawa, *Glycoconjugate J. 2* (1985) 11.

[94] M. Hoffmann, *Diplomarbeit*, Universität Konstanz 1981.

[95] U. Niedballa, H. Vorbrüggen, *Angew. Chem. 82* (1970) 449; *Angew. Chem. Int. Ed. Engl. 9* (1970) 461.

[96] D. Horton, J. D. Wander in W. Pigman, D. Horton, J. D. Wander (Eds.): *The Carbohydrates, Chemistry and Biochemistry, 2nd ed., Vol. 1B*, Academic Press, New York 1980, p. 799–842.

[97] See [55], ref. [5–11].

[98] D. Horton, *Methods Carbohydr. Chem. 2* (1963) 368, 433.

[99] S. Hanessian, Y. Grimdon, *Carbohydr. Res. 86* (1980) C4.

[100] a) E. L. Eliel, E. Juaristi, *ACS Symp. Ser. 87* (1979) 95; b) A. J. Kirby: *The Anomeric Effect and Related Stereoelectronic Effects at Oxygen*, Springer, Berlin 1983, p. 10.

[101] a) D. Horton, M. J. Miller, *Carbohydr. Res. 1* (1969) 335; b) V. Paces, J. Frgala, *J. Chromatogr. 79* (1979) 373; c) I. Goodman, L. Salce, G. H. Hitchings, *J. Med. Chem. 11* (1968) 516.

[102] a) S. Hanessian, A. G. Pernet, *Adv. Carbohydr. Chem. Biochem. 33* (1976) 111; b) J. G. Buchanan in W. Herz, H. Grisebach, G. W. Kirby (Eds.): *Progress in the Chemistry of Organic Natural Products, Vol. 9*, Springer, New York 1983, p. 284.

[103] a) S. Hanessian: *Total Synthesis of Natural Products. The Chiron Approach*, Pergamon Press, Oxford 1983; b) T. D. Inch, *Tetrahedron 40* (1984) 3161.

[104] a) G. H. Posner, S. R. Haines, *Tetrahedron Lett. 26* (1985) 1823; b) A. Giannis, K. Sandhoff, *ibid. 26* (1985) 1479, and references cited therein.

[105] G. Effenberger, *Dissertation*, Universität Konstanz 1986.

[106] a) J. R. Pougny, M. A. M. Nassr, N. Naulet, P. Sinaÿ, *Nouv. J. Chim. 2* (1978) 389; b) J.-C. Jacquinet, P. Sinaÿ, *J. Org. Chem. 42* (1977) 720; c) J.-C. Jacquinet, *Tetrahedron 35* (1979) 365; d) M.-L. Milat, P. Sinaÿ, *Angew. Chem. 91* (1979) 501; *Angew. Chem. Int. Ed. Engl. 18* (1979) 464; e) J.-C. Jacquinet, P. Sinaÿ, *J. Chem. Soc. Perkin Trans. 1 1979*, 319; f) J.-C. Jacquinet, D. Duchet, M.-L. Milat, P. Sinaÿ, *ibid. 1981*, 326; g) M.-L. Milat, P. Sinaÿ, *Carbohydr. Res. 92* (1981) 183; h) M.-L. Milat, P. Amvam Zollo, P. Sinaÿ, *ibid. 100* (1982) 263; i) P. H. Amvam Zollo, J.-C. Jacquinet, P. Sinaÿ, *ibid. 122* (1983) 201; j) P. J. Garegg, T. Koarnström, *ibid. 90* (1981) 61.

[107] a) V. Dourtoglou, J.-C. Ziegler, B. Gross, *Tetrahedron Lett. 1979*, 4371; b) V. Dourtoglou, B. Gross, *J. Carbohydr. Chem. 2* (1983) 57.

[108] T. Mukaiyama, Y. Hashimoto, Y. Hayashi, S. Shoda, *Chem. Lett. 1984*, 557.

[109] T. Mukaiyama, Y. Hashimoto, S. Shoda, *Chem. Lett. 1983*, 935.

[110] S. Shoda, T. Mukaiyama, *Chem. Lett. 1979*, 847.

[111] H. Tsutsumi, Y. Kawai, Y. Ishido, *Chem. Lett. 1978*, 629.

[112] H. Tsutsumi, Y. Ishido, *Carbohydr. Res. 88* (1981) 61.

[113] H. Tsutsumi, Y. Ishido, *Carbohydr. Res. 111* (1982) 75.

[114] S. Horvat, L. Varga, J. Horvat, *Synthesis 1986*, 209.

[115] Y. Ishido, S. Inaba, A. Matsuno, T. Yoshino, H. Umezawa, *J. Chem. Soc. Perkin Trans. 1 1977*, 1382.

[116] B. Helferich, E. Schmitz-Hillebrecht, *Ber. Dtsch. Chem. Ges. 66* (1933) 378.

[117] R. U. Lemieux, *Adv. Carbohydr. Chem. Biochem. 9* (1954) 1.

[118] R. I. Sarybaeva, V. A. Afanas'ev, G. E. Zaikov, L. S. Shchelokova, *Russ. Chem. Rev. 46* (1977) 722.

[119] S. Hanessian, J. Banoub, *Carbohydr. Res. 59* (1977) 261.

[120] M. Kiso, L. Anderson, *Carbohydr. Res. 72* (1979) C12.

[121] J. Dahmén, T. Frejd, G. Magnusson, G. Noori, *Carbohydr. Res. 114* (1983) 328.

[122] a) H. Vorbrüggen, K. Krolikiewicz, B. Blunuf, *Chem. Ber. 114* (1981) 1234; b) H. Vorbrüggen, K. Krolikiewicz, *Angew. Chem. 87* (1975) 417; *Angew. Chem. Int. Ed. Engl. 14* (1975) 421.

[123] T. Ogawa, K. Beppu, S. Nakabayashi, *Carbohydr. Res. 93* (1981) C6.

[124] H. Paulsen, M. Paal, *Carbohydr. Res. 135* (1984) 53.

[125] S. Hanessian, J. Banoub, *Tetrahedron Lett. 1976*, 657, 661.

[126] T. Mukaiyama, S. Kobayashi, S. Shoda, *Chem. Lett. 1984*, 907.

[127] R. R. Schmidt, J. Michel, *J. Org. Chem. 46* (1981) 4787.

[128] J. Leroux, A. S. Perlin, *Carbohydr. Res. 94* (1981) 108.

[129] A. F. Bochkov, N. K. Kochetkov, *Carbohydr. Res. 39* (1975) 355.

[130] A. F. Bochkov, V. I. Betanely, N. K. Kochetkov, *Carbohydr. Res. 30* (1973) 418.

[131] H. Bredereck, A. Wagner, D. Geissel, P. Gross, U. Hutten, H. Ott, *Chem. Ber. 95* (1962) 3056.

[132] N. K. Kochetkov, N. N. Malysheva, *Tetrahedron Lett. 21* (1980) 3093, and references cited therein.

[133] N. K. Kochetkov, L. V. Backinowsky, Y. E. Tsvetkov, *Tetrahedron Lett. 1977*, 3681.

[134] L. V. Backinowsky, Y. E. Tsvetkov, N. F. Balan, N. E. Byramova, N. K. Kochetkov, *Carbohydr. Res. 85* (1980) 209.

[135] F. Micheel, O. E. Brodde, *Liebigs Ann. Chem. 1975*, 1107, and references cited therein.

[136] R. U. Lemieux, *Can. J. Chem. 31* (1953) 949.

[137] G. Maghim, *Bull. Soc. Chim. Belg. 77* (1968) 575.

[138] R. U. Lemieux, G. Huber, *J. Am. Chem. Soc. 78* (1956) 4117.

[139] R. U. Lemieux, H. F. Bauer, *Can. J. Chem. 32* (1954) 340.

[140] P. C. Wyss, J. Kiss, W. Arnold, *Helv. Chim. Acta 58* (1975) 1847.

[141] L.-F. Tietze, P. Marx, *Chem. Ber. 111* (1978) 2441.

[142] M. Claeyssens, E. Saman, C. K. DeBruyne, *J. Carbohydr. Nucleosides Nucleotides 5* (1978) 33.

[143] F. Nicotra, L. Panza, F. Ronchetti, G. Russo, L. Toma, *Tetrahedron Lett. 26* (1985) 807.

[144] L.-F. Tietze, R. Fischer, H. J. Guder, *Synthesis 1982*, 946.

[145] L.-F. Tietze, R. Fischer, H. J. Guder, *Tetrahedron Lett. 23* (1982) 4661.

[146] a) L.-F. Tietze, U. Niemeyer, P. Marx, K. H. Glüsenkamp, L. Schwenen, *Tetrahedron 36* (1980) 735; b) L.-F. Tietze, R. Fischer, *Tetrahedron Lett. 22* (1981) 3239; c) *Angew. Chem. 93* (1981) 1002; *Angew. Chem. Int. Ed. Engl. 20* (1981) 969.
[147] L.-F. Tietze, R. Fischer, *Angew. Chem. 95* (1983) 902; *Angew. Chem. Int. Ed. Engl. 22* (1983) 902.
[148] A. A. Pavia, J. M. Rocheville, S. N. Ung, *Carbohydr. Res. 79* (1980) 79.
[149] T. G. Bonner, E. J. Bourne, S. McNally, *J. Chem. Soc. 1962*, 761.
[150] B. Helferich, R. Gootz, *Ber. Dtsch. chem. Ges. 62* (1929) 2788.
[151] a) R. Eby, C. Schuerch, *Carbohydr. Res. 34* (1974) 79; b) T. J. Lucas, C. Schuerch, *ibid. 39* (1975) 39; c) V. Maronsek, T. J. Lucas, P. J. Wheat, C. Schuerch, *ibid. 60* (1978) 85; d) R. Eby, C. Schuerch, *ibid. 50* (1976) 203; e) R. Eby, *ibid. 70* (1979) 75; f) R. Eby, C. Schuerch, *ibid. 77* (1979) 61.
[152] G. Wulff, U. Schröder, J. Wichelhaus, *Carbohydr. Res. 72* (1979) 280.
[153] S. Koto, Y. Hamada, S. Zen, *Chem. Lett. 1975*, 587.
[154] a) N. Morishima, S. Koto, S. Zen, *Chem. Lett. 1982*, 1039; b) S. Koto, N. Morishima, M. Owa, S. Zen, *Carbohydr. Res. 130* (1984) 73.
[155] R. Eby, C. Schuerch, *Carbohydr. Res. 102* (1982) 131.
[156] V. K. Srivastava, S. J. Sondheimer, C. Schuerch, *Carbohydr. Res. 86* (1980) 203.
[157] V. K. Srivastava, C. Schuerch, *Carbohydr. Res. 79* (1980) C 13; *J. Org. Chem. 46* (1981) 1121.
[158] S. Hanessian, J. Banoub, *Carbohydr. Res. 53* (1977) C 13.
[159] a) G. Grynkiewicz, *Carbohydr. Res. 53* (1977) C 11; b) H. Achenbach, J. Witzke, *Liebigs Ann. Chem. 1981*, 2384.
[160] a) W. A. Szarek, H. C. Jarell, J. K. Jones, *Carbohydr. Res. 57* (1977) C 13; b) O. Mitsumobu, *Synthesis 1981*, 1.
[161] J. F. Kronzer, C. Schuerch, *Carbohydr. Res. 34* (1974) 71.
[162] P. J. Garegg, P. Ossowski, *Acta Chem. Scand. 37* (1983) 249.
[163] A. Lubineau, A. Malleron, *Tetrahedron Lett. 26* (1985) 1713.
[164] A. C. West, C. Schuerch, *J. Am. Chem. Soc. 95* (1973) 1333.
[165] F. J. Kronzer, C. Schuerch, *Carbohydr. Res. 33* (1974) 273.
[166] R. Eby, C. Schuerch, *Carbohydr. Res. 39* (1975) 33.
[167] R. U. Lemieux, A. R. Morgan, *Can. J. Chem. 43* (1965) 2205.
[168] H. Lönn, *Chem. Commun. Univ. Stockholm 1984*, No. 2.
[169] H. Lönn, *Carbohydr. Res. 139* (1985) 105.
[170] H. Lönn, *Carbohydr. Res. 139* (1985) 115.
[171] K. Yamashita, Y. Tachibana, S. Takada, I. Matsuda, S. Arashima, A. Kobata, *J. Biol. Chem. 254* (1979) 4820.
[172] S. Hanessian, Y. Guindon, *Carbohydr. Res. 86* (1980) C 3.
[173] K. C. Nicolaou, S. P. Seitz, D. P. Papahatjis, *J. Am. Chem. Soc. 105* (1983) 2430.
[174] R. J. Ferrier, R. H. Furneaux, P. C. Tyler, *Carbohydr. Res. 58* (1977) 397.
[175] Y. Pocker, D. N. Kevill, *J. Am. Chem. Soc. 87* (1969) 4771, and references cited therein.
[176] E. Rücker, *Dissertation*, Universität Konstanz 1980.
[177] R. B. Woodward, E. Logusch, K. P. Nambiar, K. Sakan, D. E. Ward, B.-W. Au-Yeung, P. Balaram, L. J. Browne, P. J. Card, C. H. Chen, R. B. Chênevert, A. Fliri, K. Frobel, H.-J. Gais, D. G. Garratt, K. Hayakawa, W. Heggie, D. P. Hesson, D. Hoppe, I. Hoppe, J. A. Hyatt, D. Ikeda, P. A. Jacobi, K. S. Kim, Y. Kobuke, K. Kojima, K. Krowicki, V. J. Lee, T. Leutert, S. Malchenko, J. Martens, R. S. Mathews, B. S. Ong, J. B. Press, T. V. Rajan Babu, G. Rousseau, H. M. Sauter, M. Suzuki, K. Tatsuta, L. M. Tolbert, E. A. Truesdale, I. Uchida, Y. Ueda, T. Uyehara, A. T. Vasella, W. C. Vladuchick, P. A. Wade, R. M. Williams, H. N.-C. Wong, *J. Am. Chem. Soc. 103* (1981) 3215.
[178] A. A. Pavia, S. N. Ung-Chhun, J. L. Durand, *J. Org. Chem. 46* (1981) 3158.
[179] O. Larm, K. Larsson, M. Wannong, *Acta Chem. Scand. B31* (1977) 475.
[180] R. J. Ferrier, R. W. Hay, N. Vethaviyasar, *Carbohydr. Res. 27* (1973) 55.
[181] R. J. Ferrier, S. R. Haines, *Carbohydr. Res. 127* (1984) 157.
[182] J. W. VanCleve, *Carbohydr. Res. 70* (1970) 161.
[183] P. J. Garegg, C. Henrichson, T. Norberg, *Carbohydr. Res. 116* (1983) 162.
[184] S. Hanessian, C. Bacquet, N. Lehong, *Carbohydr. Res. 80* (1980) C 17.
[185] T. Mukaiyama, T. Nakatsuka, S. Shoda, *Chem. Lett. 1979*, 487.
[186] S. Koto, T. Uchida, S. Zen, *Chem. Lett. 1972*, 1049.
[187] T. Mukaiyama, Y. Murai, S. Shoda, *Chem. Lett. 1981*, 431.
[188] K. C. Nicolaou, R. E. Dolle, D. P. Papahatjis, J. L. Randall, *J. Am. Chem. Soc. 106* (1984) 4189.
[189] K. C. Nicolaou, J. L. Randall, G. T. Furst, *J. Am. Chem. Soc. 107* (1985) 5556.
[190] S. Hashimoto, M. Hayashi, R. Noyori, *Tetrahedron Lett. 25* (1984) 1379.
[191] Y. V. Voznij, L. N. Koikov, A. A. Galoyan, *Carbohydr. Res. 132* (1984) 339.
[192] G. H. Klemm, R. J. Kaufman, R. S. Sishu, *Tetrahedron Lett. 23* (1982) 2927.
[193] G. H. Posner, S. R. Haines, *Tetrahedron Lett. 26* (1985) 3.
[194] Y. Araki, K. Watanabe, F.-H. Kuan, K. Itoh, N. Kobayashi, Y. Ishido, *Carbohydr. Res. 127* (1984) C 3.
[195] K. C. Nicolaou, R. E. Dolle, A. Chucholowski, J. L. Randall, *J. Chem. Soc. Chem. Commun. 1984*, 1153.
[196] H. Paulsen, M. Paal, D. Hadamczyk, K.-M. Steiger, *Carbohydr. Res. 131* (1984) C 1.
[197] G. M. Whitesides, C.-H. Wong, *Angew. Chem. 97* (1985) 617; *Angew. Chem. Int. Ed. Engl. 24* (1985) 617.

3-Chloropropyltrialkoxysilanes—Key Intermediates for the Commercial Production of Organofunctionalized Silanes and Polysiloxanes

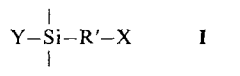
By Ulrich Deschler,* Peter Kleinschmit, and Peter Panster

Dedicated to Dr. Konrad Henkel on the occasion of his 70th birthday

Silicon and carbon may be looked upon as the two fundamental antipodes with respect to the naturally occurring forms of matter and life on earth: Silicon plays the key role in the "petrification" of inanimate matter, while carbon is the representative element for the "incarnation" of living organisms. If a scientist were to search for a highly efficient method of uniting inorganic and organic matter, he would, at a very early stage of attempting to solve this problem, combine these two natural principles of matter and think of "bireactive" molecules containing a silicon functionality for bonding to inorganic material on the one hand and a carbon functionality for anchoring to an organic counterpart on the other. The title compounds and their derivatives epitomize such molecules: they are wanderers between both (chemical) worlds. Owing to their bifunctionality they are capable of binding to inorganic (especially siliceous) systems as well as to organic polymers. Whether their commercial application concerns the strengthening of polyester resins with glass fibers for use in boatbuilding or the incorporation of silica as a filler in rubber mixtures for the manufacture of wear-resistant tires or even the immobilization of enzymes on glass spheres for carrying out reactions in enzyme reactors—in all cases organofunctionalized silanes guarantee a reliable and permanent union between two otherwise "incompatible" material systems.

1. Introduction

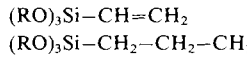
Hydrolyzable organofunctionalized silanes, as represented by the general formula **I**, have two reactive centers:



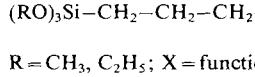
I

They are bifunctional in nature, bearing one reactive center X attached to a tetracoordinated silicon atom via a carbon-to-silicon bond and at least one group Y that is subject to hydrolysis under the influence of water (e.g. Y = Hal, OR, NR_2).

With regard to their industrial application, the bifunctional silanes of composition **II** and **III** are the most important:



II



III

R = CH_3, C_2H_5; X = functional group

In this review we shall limit our discussion to silanes of type **III** containing a *functional group X* attached to silicon via a trimethylene spacer group on one side and a *hydrolyzable trimethoxy* or *triethoxy silyl group* on the other.

[*] Dr. U. Deschler, Dr. P. Kleinschmit, Dr. P. Panster
Degussa, Forschung Chemie Anorganisch
Postfach 1345, D-6450 Hanau 1 (FRG)

Organofunctionalized silanes are a relatively new class of compounds. They were first prepared in the early 1940s, after the discovery of the *Mueller-Rochow-process*[1] and the *hydrosilylation reaction*.[2]

The potential of such compounds was soon realized, and, by 1949, the first industrial applications for these silanes had already evolved: *Silane-treated glass fibers* showed superior performance as reinforcement materials for organic resins.[3] In 1962, more than 100 organofunctionalized silanes—many of them derivatives of 3-chloropropyltrichlorosilane **1**—had been evaluated in glass-fiber reinforced polyester and epoxy laminates, and the term *coupling agent*, describing their function in these composites, was well established.[4] Later on, the use of silane couplers was extended to other *polymer systems reinforced by particulate inorganic fillers*, since silanes could almost be tailor-made to fit a certain polymer-filler combination.[5]

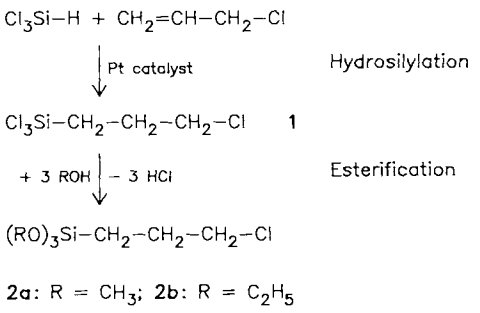
A major breakthrough in this field was achieved in the early 1970s when certain derivatives of the title compounds proved to be effective coupling agents in *silica-reinforced* rubber articles, especially *tires*.[6] Since then, other applications for silanes **III** in the fields of *surface modification*, *active substrate immobilization* and *silane polycondensation* have been published.

As a result of this development, organofunctionalized silanes are produced today on a commercial scale in the United States of America, in Japan, and in Europe. They have become the fourth important class of commercially used organosilicon compounds, the others being silicones,[7] organosilicates,[8] and silylating agents.[9]

2. Syntheses

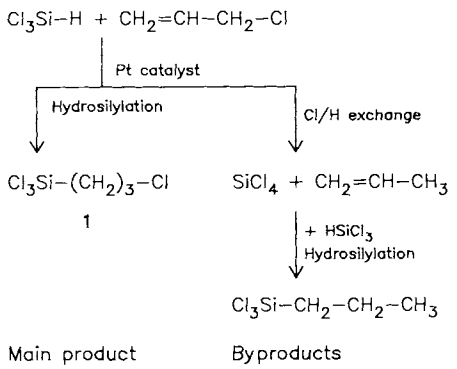
2.1. Synthesis of 3-Chloropropyltrialkoxysilanes

The industrial production of the title compounds **2** involves a two-step process as shown in Scheme 1.



Scheme 1. Industrial synthesis of the title compounds **2** via trichloro-3-chloropropylsilane **1**, b.p. 182°C/750 torr [10]. **2a**: b.p. 195°C/750 torr [10]; **2b**: b.p. 124°C/30 torr [10].

The catalytic addition of trichlorosilane to allyl chloride using various catalysts has already been reviewed.[2a] Most effective are homogeneous or heterogeneous platinum catalysts, which lead to almost quantitative conversion of allyl chloride, although a partial reduction of allyl chloride as side reaction cannot be avoided (Scheme 2).



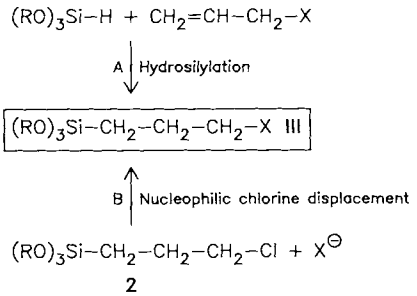
Scheme 2. Products of the addition of trichlorosilane to allyl chloride.

As a result of this side reaction, propene, silicon tetrachloride, and trichloropropylsilane are formed. Under favorable reaction conditions, yields of 66% to 83% of **1** have been claimed.[10,11] **1** is a colorless liquid and can be purified by rectification.

The trichlorosilyl group in **1** readily reacts with alcohols to give a trialkoxysilyl function. Only methanol and ethanol proved to be of industrial significance in reaction step 2 of Scheme 1 yielding the title compounds **2** as colorless liquids. Difficulties in conducting these esterification reactions arise from evolution of hydrogen chloride, which, under these reaction conditions, leads to formation of alkyl chlorides, water, and even ethers. The most undesired byproduct is water, since it causes oligomerization of **2**. Methods for fast HCl-removal have been published,[12] thus allowing high yields of **2**.

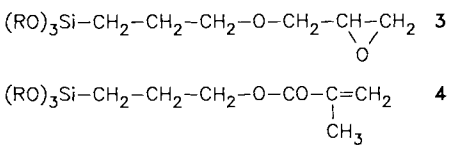
2.2. Synthesis of Organofunctionalized Derivatives of 3-Chloropropyltrialkoxysilanes

Silanes of type **III** are generally produced by the two synthetic routes depicted in Scheme 3.



Scheme 3. Methods for the synthesis of organofunctionalized silanes of type **III**. A, B see text.

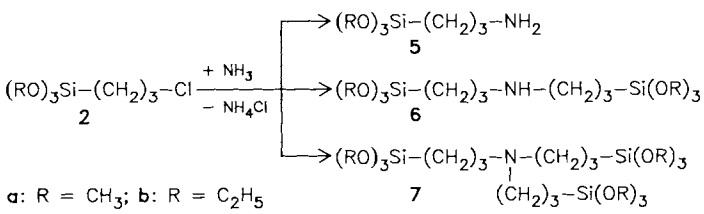
The *hydrosilylation of 3-functionalized 1-propenes* with trialkoxysilanes (Route A) necessitates the implementation of comparatively strict industrial safety measures because of the hazardous and toxic nature of trialkoxysilanes.[13] Technically important examples of this reaction involve the utilization of allyl glycidyl ether[14] and allyl methacrylate[15] for the production of epoxy- and methacryl-functionalized silanes **3** and **4**, respectively.



In this review we mainly deal with the production of silanes according to the second reaction path in Scheme 3 (Route B), namely the one involving *nucleophilic chlorine displacement* in **2**.

2.2.1. *Ammonia as Nucleophile*

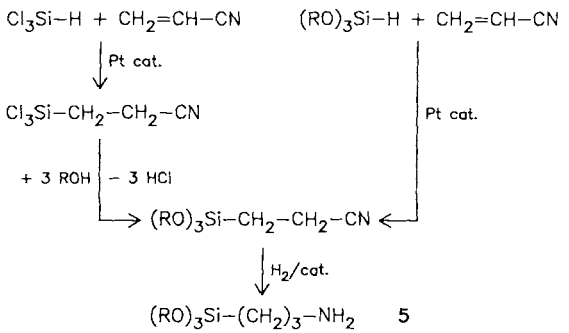
Numerous publications[16,17] have been concerned with the reaction of anhydrous ammonia with **2** as shown in Scheme 4. For complete conversion of the starting materials **2**, which cannot be separated from the products **5** by distillation, the reaction of **2** with ammonia must be conducted at elevated temperatures and under pressure using



Scheme 4. Amino-functionalized silanes by reaction of **2** with ammonia. **5a**: b.p. 104°C/30 torr [16]; **5b**: b.p. 115°C/19 torr [16]; **6a**: b.p. 115°C/0.1 torr (distillation in a thin-film evaporator); **6b**: b.p. 145°C/1 torr [17a]; **7a**: b.p. 155°C/0.05 torr (distillation in a thin-film evaporator); **7b**: b.p. 200°C/1 torr [17a].

a large excess of ammonia. Under these conditions formation of the secondary amines **6** and tertiary amines **7** cannot be avoided. Since until now only the primary amines **5a**, **b** (in particular **5b**) have been of commercial interest, many efforts have been made to raise the yields above 50%, the value reported in the original publication.[17a] In one approach sodium methoxide was used as an HCl-acceptor, resulting in a 74% yield of the desired silane **5a**.[17b] A yield of 81% of **5b** was claimed under special reaction conditions.[17c]

In order to avoid formation of the undesired by-products **6** and **7**, another synthetic concept has been developed for the commercial production of **5** as shown in Scheme 5. The hydrosilylation of acrylonitrile with trichlorosilane[18] followed by the esterification of the trichlorosilyl function[19] yields 2-cyanoethyltrialkoxysilanes, which can also be obtained by addition of trialkoxysilanes to



Scheme 5. Industrial method for the production of byproduct-free **5**.

acrylonitrile.[20] Catalytic reduction of the nitrile function leads exclusively to the primary amines **5**.[21]

The direct hydrosilylation of allylamine with trialkoxysilanes has been described as a third preparative entry to **5**,[22] but it does not seem to be competitive, for economic reasons.

2.2.2. *Ethylenediamine as Nucleophile*

The ethylenediamine derivative of **2** has also claimed importance for numerous technical applications. In its preparation according to Equation (a) at least a 2.5-fold excess of amine has to be employed in order to remove the by-product hydrogen chloride effectively and to avoid the formation of doubly silylpropyl-substituted ethylenediamine.[16,23]

$$\underset{\mathbf{2}}{(RO)_3Si-(CH_2)_3-Cl} + H_2N-(CH_2)_2-NH_2 \longrightarrow \underset{\mathbf{8}}{(RO)_3Si-(CH_2)_3-NH-(CH_2)_2-NH_2} + HCl \qquad (a)$$

8a: R = CH_3, b.p. 146 °C/15 torr[16]
8b: R = C_2H_5, b.p. 156 °C/15 torr[16]

In the absence of a solvent the reaction mixture separates into two phases. Distillation of the upper layer furnishes the desired products **8** in yields of up to 88%.[23]

The hydrosilylation of allylethylenediamine with trialkoxysilanes[22b] as an alternative access to **8** does not seem to be competitive because of high costs for raw materials and comparatively low yields of desired silanes.

2.2.3. *Disodium Tetrasulfide as Nucleophile*

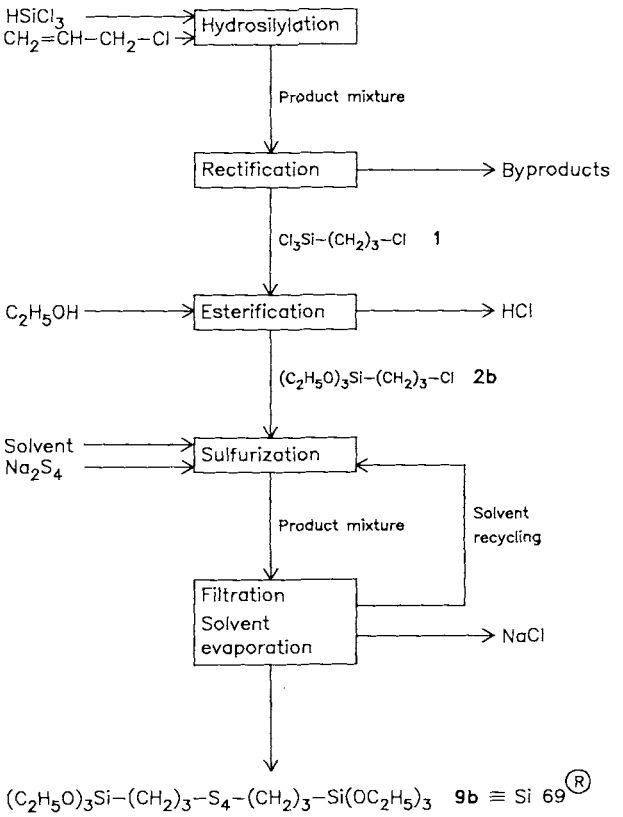
The chlorine displacement in **2** according to Equation (b) using disodium tetrasulfide as nucleophile, which can be prepared separately[24] or generated in situ,[25] is also of commercial importance.

$$2\underset{\mathbf{2}}{(RO)_3Si-(CH_2)_3-Cl} + Na_2S_4 \longrightarrow \underset{\mathbf{9}}{(RO)_3Si-(CH_2)_3-S_4-(CH_2)_3-Si(OR)_3} + 2\,NaCl \qquad (b)$$

a: R = CH_3; **b**: R = C_2H_5

When the reaction is carried out in boiling alcohol as solvent (methanol for the reaction of **2a**, ethanol for that of **2b**), the yellow tetrasulfanes **9** are obtained in almost quantitative yield.[25]

The ethyl derivative **9b** (trade name "Reinforcing agent Si 69®", Degussa) has become one of the most important organofunctionalized silanes known today and is used mainly as a coupling agent in silica-filled rubber systems. It has been produced on a technical scale at Degussa's plant in Antwerp since 1976, using a three-step process as shown in Scheme 6. The characteristic properties of the commercially available product are listed in Table 1.



Scheme 6. Simplified flow diagram for the industrial synthesis of **9b**.

Table 1. Typical properties of **9b**.

Color and appearance:	Yellowish liquid
Boiling point at 1013 mbar:	Decomposition above 250°C
Pour point:	ca. −80°C
Flash point (DIN 51758):	>100°C
Density at 20°C:	1.095 g/cm³
Viscosity at 20°C:	ca. 11.4 cP
Total sulfur:	>22.0%
Polysulfidic sulfur:	> 9.5%
Toxicology:	Nontoxic according to tests on acute toxicity, *local skin toleration, local mucous membrane* toleration and sensitization

As is known for other dialkyltetrasulfanes,[26] in an equilibrium reaction the tetrasulfanes **9** can disproportionate to a mixture of polysulfanes having different sulfur chain-lengths. The proportions of the individual polysulfanes in such mixtures is dependent, inter alia, upon the pH value and the temperature,[27] and can be determined quantitatively by HPLC[28] and ^{1}H-NMR spectroscopy.[29] The short-chain members of the series of bis(silylpropyl)polysulfanes can be individually prepared by special synthetic methods up to and including the tetrasulfane;[29a,30] this is outlined in Equation (c) for the case of **9a**.

$$\underset{\textbf{10a}}{2(CH_3O)_3Si-(CH_2)_3-SH} + S_2Cl_2 \longrightarrow (CH_3O)_3Si-(CH_2)_3-S_4-(CH_2)_3-Si(OCH_3)_3 + 2HCl \quad (c)$$

9a

In addition, further methods for the synthesis of the silanes **9** have been proposed.[31]

2.2.4. *Hydrogensulfide as Nucleophile*

Mercapto-functionalized silanes **10** can be obtained from **2** and anhydrous solutions of alkali-metal or ammonium salts of hydrogen sulfide according to Equation (d).[32]

$$\underset{\textbf{2}}{(RO)_3Si-(CH_2)_3-Cl} + MHS \longrightarrow (RO)_3Si-(CH_2)_3-SH + MCl \quad (d)$$

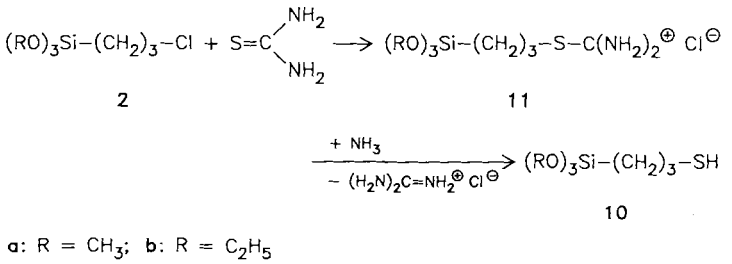
10

10a: R = CH_3, b.p. 53°C/0.8 torr[23a]
10b: R = C_2H_5, b.p. 112°C/14 torr[24a]

Alkali-metal hydrogensulfides (M = Na, K) seem to be less suitable (long reaction times, moderate yields[32a]) than the corresponding amine/H_2S combinations (M = NH_3,[32b] $N(CH_3)_3$,[32b] $H_2N-(CH_2)_2-NH_2$[32c]), where yields of up to 90% at reaction times of, at best, several hours and at temperatures of about 100°C are reported.

Another route to **10** is the reaction of halosilanes **2** with thiourea leading to the corresponding isothiuronium salts **11** and subsequent cleavage of the latter by means of ammonia (or other alkaline materials) as shown in Scheme 7.[33]

This synthesis can also be carried out as a "one-pot-process".[33] According to the patent literature substantial

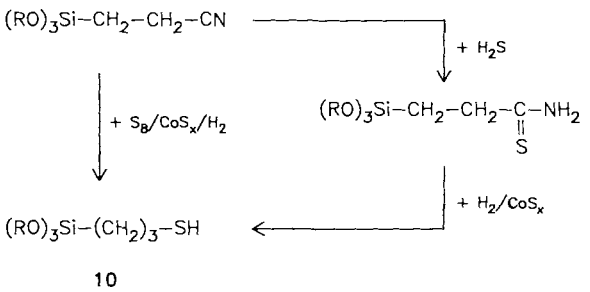


a: R = CH_3; b: R = C_2H_5

Scheme 7. Production of **10** via the isothiuronium salt **11**.

improvements with respect to yield, purity, and reaction conditions are achieved when dimethylformamide is used as solvent.[33c]

A third method for the preparation of the silanes **10** is based on the catalytic addition of H_2S to 2-cyanoethyltrialkoxysilanes as outlined in Scheme 8.[34]



Scheme 8. Production of **10** from cyanoethyltrialkoxysilanes.

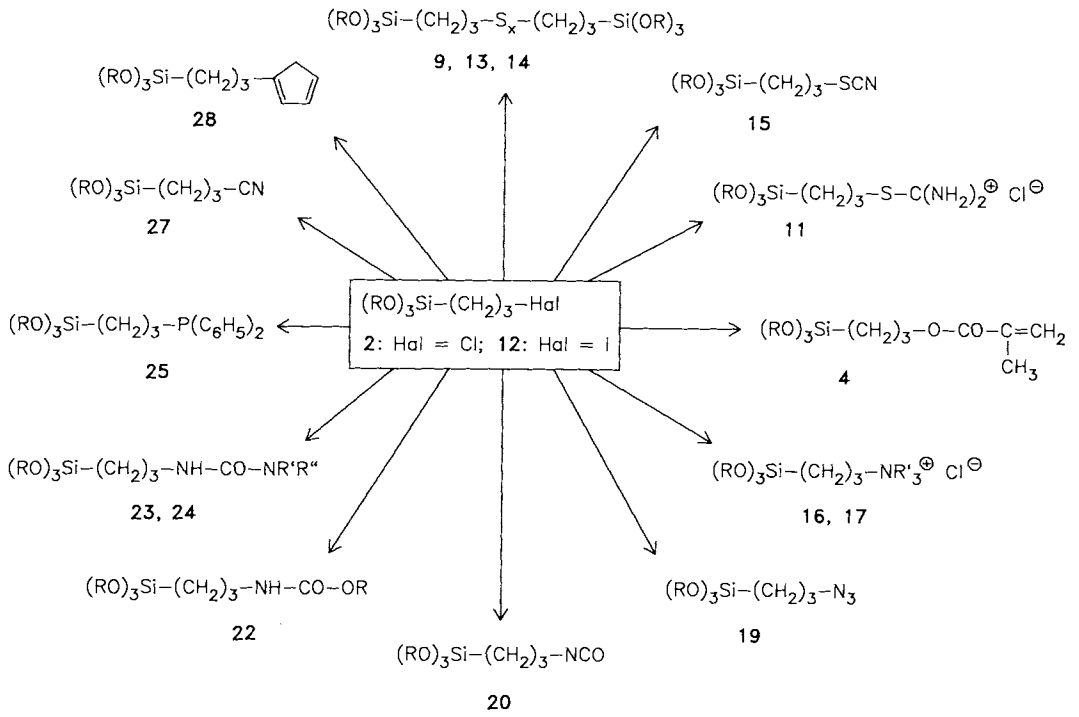
2.2.5. *Other Nucleophiles*

Numerous other organofunctionalized silanes are known that are derived from **2** by nucleophilic chlorine displacement. With exception of the methacryl-functionalized silanes **4**, which, however, are not produced technically from **2** (cf. Scheme 3), these silanes still play a subordinate role, at least quantitatively, so that details of the production conditions will not be dealt with here. Rather, the multitude of silanes accessible via **2** and the iodide **12** will be outlined in general with Scheme 9 and Table 2.

3. Industrial Applications of Bifunctional Silanes

The applicability of a certain organofunctionalized silane is determined by the *reactivities* of its *functional groups*.

All the silanes under discussion have a *trialkoxysilyl group* in common; hence their chemical reactivity towards hydroxy-functional substrates are quite similar. As a result of this reactivity a bonding interaction between silane molecules and substrate surface is observed. The nature of this bonding, and the structure of the resulting silane film, depends upon the reaction conditions applied during silanization and has been investigated and reinterpreted several times. The monomolecular layer repeatedly given in the literature (Scheme 10) in which the silicon atoms are covalently bonded via oxygen bridges to one another and to the solid surface is only observed in certain individual cases[55] after silanization.



Scheme 9. Bifunctional silanes obtainable by nucleophilic displacement of halogen from **2** and **12**.

Table 2. Organofunctionalized silanes $(RO)_3Si-(CH_2)_3-X$, obtained from **2** by nucleophilic substitution. **a**: $R=CH_3$; **b**: $R=C_2H_5$.

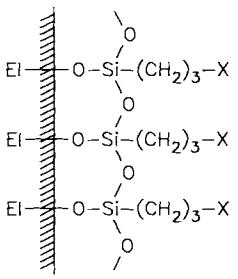
Nucleophile	X		B.p. [°C/torr]	Ref. [a]
Iodide	I	**12a** **12b**	79/2 100/5	[35]
Monosulfide	$S-(CH_2)_3-Si(OR)_3$	**13a** **13b**	180/8 193/8	[25e] ([29a, 36])
Disulfide	$S_2-(CH_2)_3-Si(OR)_3$	**14a** **14b**	139/0.04 154/0.04	[25c,e] ([37])
Thiocyanate	SCN	**15a** **15b**	118/0.8 97/0.1	[38]
Thiourea	$S-C(NH_2)_2^{\oplus}Cl^{\ominus}$	**11**	highly viscous liquid	[39]
Methacrylate	$O-CO-C(CH_3)=CH_2$	**4a** **4b**	105/5 112/5	[40] ([15, 22a])
Trimethylamine	$N(CH_3)_3^{\oplus}Cl^{\ominus}$	**16**	solid	[41]
Triethylamine	$N(C_2H_5)_3^{\oplus}Cl^{\ominus}$	**17**	solid	[41, 42]
N,N-Dimethyloctadecylamine	$N(CH_3)_2-C_{18}H_{37}^{\oplus}Cl^{\ominus}$	**18**	highly viscous liquid	[41a, 43]
Azide	N_3	**19a** **19b**	49/0.8 76/0.7	[44]
Isocyanate	NCO	**20a** **20b**	84/1 75/0.05	[45] ([46])
Isocyanate	$1/3(NC=O)_3$ (isocyanurate)	**21a** **21b**	236/0.2 255/0.2 [b]	[45]
Isocyanate/Alcohol	NH–CO–OR	**22a** **22b**	90/1.4 110/0.1	[45, 47]
Isocyanate/Diallylamine	$NH-CO-N(CH_2-CH=CH_2)_2$	**23**	highly viscous liquid	[48]
Isocyanate/Caprolactam	$NH-CO-N-(CH_2)_5-CO$	**24**	[c]	[49]
Diphenyl phosphide	$P(C_6H_5)_2$	**25a** **25b**	157/0.5 180/0.7	[50]

Table 2. (continued).

Nucleophile	X		B.p. [°C/torr]	Ref. [a]
Phenyl phosphide	$P(C_6H_5)-(CH_2)_3-Si(OR)_3$	**26a** **26b**	$140/10^{-3}$ [d] $180/5\times10^{-3}$ [d]	[e]
Cyanide	CN	**27a** **27b**	67/0.4 79/0.6	[51] ([32c, 52])
Cyclopentadienide	C_5H_5	**28a** **28b**	85/0.5 88/0.05	[53]

[a] References to alternative routes to the same product without use of **2** are given in parenthesis. [b] Decomposition. [c] Liberation of **20** above 140°C/12 torr. [d] Distillation in a thin-film evaporator. [e] P. Panster, unpublished results.

Depending upon the method of silanization chosen, much "thicker" silane layers are also formed at the phase interface,[56] the exact nature of which has been interpreted differently.[57] In any case a key role might be played by the catalytic amounts of water present at the phase interface, which enables a reversible opening and reformation of the oxygen bridges via intermediacy of hydrogen bonds:[58] It is by this reversible bond formation in the presence of water that stress along the filler-to-silane interface can be released.



Scheme 10. Monomolecular layer of silane as idealized concept of a bonding interaction between trialkoxysilanes and hydroxyfunctional surfaces. El = Si, Al, Ti, Zr, Fe, Zn, Cr, C, etc. [54].

The reactivity of the trialkoxysilyl group as discussed above is one of the two factors determining the usefulness of a certain silane. The other is the specific nature of the *functional group X*. Since X can be varied extensively (see Scheme 9 and Table 2) there is a wide scope of applications for these ccompounds today.[5,59]

In this paper the term industrial applications is used for those applications where silane quantities ranging from about 100 tons to more than 1000 tons per year are involved worldwide. This does not imply, however, that other applications to be discussed in Section 4 are of no commercial importance.

3.1. Glass-Fiber Reinforced Thermosetting and Thermoplastic Resins

It is not only for historic reasons that this field of silane coupling application is discussed first[3]: The silane treatment of glass fibers before their incorporation into various polymer systems is one of the "big volume" silane applications today, even though the quantities of silane used generally only amount to 0.1–0.5% of the weight of glass.[60]

Depending on the polymer system to be reinforced, an appropriate choice of functional group X must be made: Amino-, epoxy-, methacryl- or chloro-functionalized silanes such as **5**, **3**, **4**, and **2**, respectively, play a major role in this respect.[60]

The most important polymer systems in use (e.g., for the production of glass fiber reinforced laminates for construction of boat and car bodies) are unsaturated polyester, epoxy, and phenolic resins.[5] Suitable silane/polymer combinations have already been reviewed several times.[4,60,61]

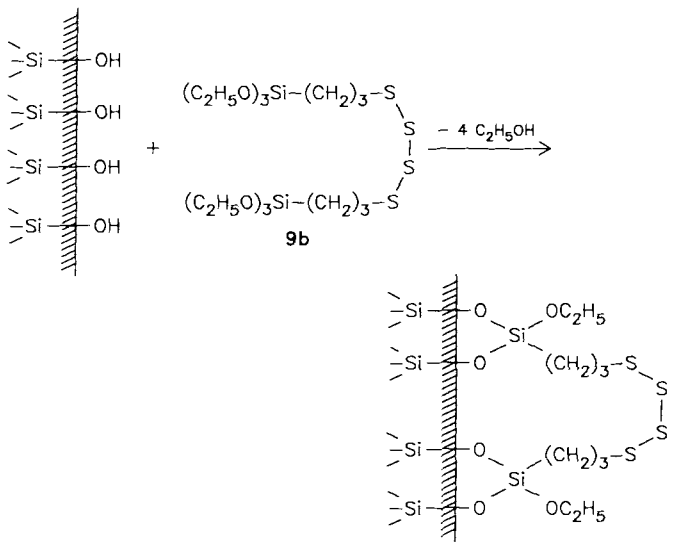
3.2. Mineral-Filled Rubbers (Elastomers)

Highly dispersed carbon blacks are the classical reinforcement fillers for almost all types of natural and synthetic rubbers.[62] Although precipitated silicas with similar particle sizes and surface areas were developed some forty years ago and have been produced since then on a technical scale,[63] their use in the rubber industry has, until recently, been restricted to special applications (e.g., shoe soles, certain mechanical rubber goods[63b]). The main disadvantages of silicas in this area, compared to the corresponding carbon blacks, are a considerably higher compound viscosity and a prolonged scorch time, both causing difficulties in the processing steps;[63b,64] furthermore, the attainable cross-linking density in sulfur-curing systems is reduced, resulting in a lower rubber reinforcement.[6,63b,64c]

It could be shown that these technical shortcomings in fact arise from the incompatibility of the two phases involved: The silica particles, with their hydrophilic surface,[65] very poorly interact with the hydrophobic rubber matrix. This problem can be overcome by installing chemical bonds between the two differing matrices with the aid of suitable bifunctional silanes.[66,67] This concept will be described in some detail choosing **9b** as an example, because this silane has developed into today's most successful and widely used *coupling agent for silica-filled rubbers* (especially natural rubber (NR) and styrene-butadiene rubber (SBR)).[6,63b,64c,67,68]

In the course of the manufacturing process for rubber goods **9b** *reacts* with silica or silica/carbon black reinforced rubber compounds *in a twofold manner*: In the first step, during the mixing process at temperatures below the curing temperature, the triethoxysilyl groups of **9b** become bonded to the filler surface. Formation of siloxane bonds takes place with elimination of ethanol (Scheme 11).

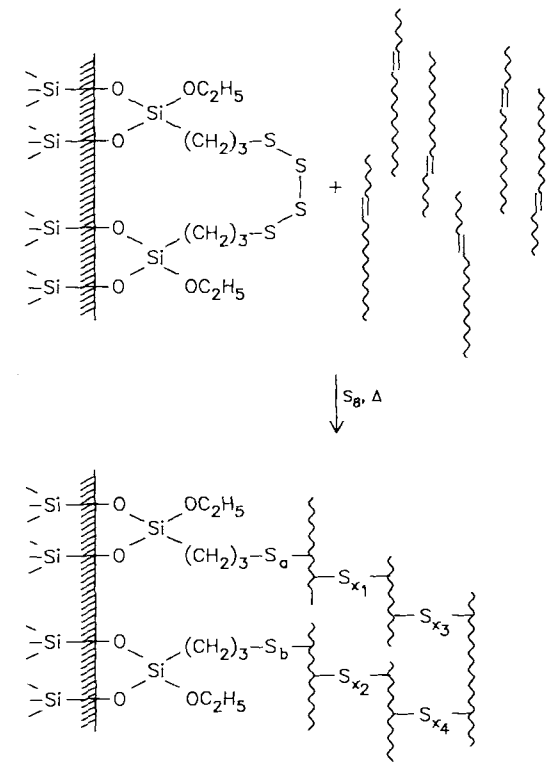
As a result of this *hydrophobation of the silica surface*, the high Mooney viscosity of silica-filled rubber com-



Scheme 11. Filler hydrophobation with **9b**.

pounds is reduced to values normally observed with carbon blacks. In order to achieve total hydrophobation of commercial rubber grade silicas (BET surface area $\sim 175\ m^2/g$; silanol group density $\sim 5\text{-}6/nm^2$) about 13 parts of **9b** per 100 parts of silica are required, taking into account that, because of steric reasons, only up to four of the six ethoxy groups of **9b** can react with silanol groups of the silica.[67a] However, in practice, far smaller amounts of silane already lead to a remarkable reduction in the compound viscosity.[67a]

In the second step (cf. Scheme 12), which starts at higher temperatures under curing conditions (e.g. 150–170 °C, in



Scheme 12. Coupling of the filler hydrophobated by **9b** with elastomers during vulcanization (in the presence of sulfur), idealized ($a+b=4$, $1 \leq x_i \leq 8$).

the presence of accelerators and in the presence or absence of sulfur), the sulfur chain of **9b** is split and the fragments are added to double bonds of the elastomer, thus forming *covalent sulfur-to-carbon bonds* which chemically link together the filler particles and the rubber network.[6, 63b, 67a–c]

The combined use of silica and **9b** in rubber materials, especially NR and SBR (for the use of **9b** in ethylene-propylene-diene rubber cf. [69]), leads to products with mechanical properties equal to or even superior to those of rubbers filled with carbon blacks.[67a, e] Hence, for the first time, substitution of semi-active and active carbon blacks in carcass and tread mixtures of car tires has become technically feasible without any loss of performance.[64c] From an economic viewpoint, however, the combination SiO_2/**9b** cannot, at least under present conditions, compete with carbon blacks as a reinforcement system for automobile tires.

The reason for today's increasing industrial use of various SiO_2/**9b** formulations in the rubber industry is to be seen in the technical superiority of durable rubber products that can be manufactured on this basis: Besides its role as coupling agent, the silane **9b** can—independently of the kind of filler— also act as *new type of reversion-free cross-linking agent*.

A "normal" sulfur vulcanization process proceeds in two phases with respect to the S–C cross-linking density (cf. Fig. 1). At the beginning ($t < t_e$), the number of S–C bonds formed per unit of time with increasing temperature is far greater than that of the thermally ruptured bonds, so that the overall number of S–C cross-linking sites increases. Reversion occurs at long curing times ($t > t_e$) and causes more S–C bonds to be split than newly formed, which results in unsatisfactory mechanical properties of the cured rubber article. Reversion is a problem, for example, in the manufacture of certain mechanical rubber goods and massive speciality tires such as the so-called off-the-road or heavy duty truck tires, where long curing times have to be applied in order to complete vulcanization through the thick rubber walls. Hitherto, attempts have been made to solve this problem by using the lowest possible curing temperature.[67d] A new concept by which reversion can be eliminated involves using a three-component cure system containing sulfur, accelerator and **9b** (*equili-*

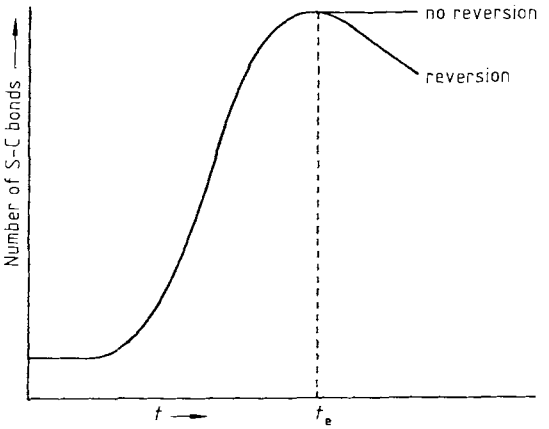


Fig. 1. Idealized vulcanization curves for normal and reversion-free sulfur cross-linking.

brium cure system), allowing higher vulcanization temperatures and shorter vulcanization periods for thick-walled rubber goods without loss of performance.[67d, 68e]

A few other silane derivatives of **2** are used to a limited extent in the rubber industry in combination with naturally occurring silicate fillers (silane applications in the automobile industry, e.g. in tires, bumpers, hoses, gaskets and windscreen sealants have been reviewed[70]). Table 3 lists some known examples of silane/rubber/filler combinations from the patent literature.

Table 3. Use of bifunctional silanes in filler-reinforced rubber.

Silane	Type of rubber [a]	Filler [b]	Ref.
2	halogenated	SiO_2	[71, 72]
	NR, SBR	SiO_2, clay	[66d]
5	NR, SBR	SiO_2, clay	[66]
	EPDM	clay	[73e]
8	EPDM	clay	[73b, c]
9b	NR, SBR	clay	[74]
10	NR, SBR	SiO_2, clay	[66, 75]
	EPDM	clay	[73, 75]
11	halogenated	SiO_2	[76]
	NR, SBR	SiO_2, clay	[66d]
15	NR, SBR	SiO_2	[38]
28	EPDM	SiO_2, clay	[53]

[a] NR = natural rubber, SBR = styrene-butadiene rubber, EPDM = ethylene-propylene-diene rubber. [b] Clay: collective term, for naturally occurring fillers, mainly consisting of aluminum silicates (kaolinites) containing additional cations (Fe, Mg, etc.).

3.3. Sealants

Sealants basically consist of highly viscous organic prepolymers and inorganic fillers besides plasticizers, solvents or curing agents. The sealants are cured after application to yield a semielastic material. In order to provide good adhesion to inorganic surfaces, sealants usually contain adhesion promoters. Organofunctional silanes if used as integral blend additives can serve this purpose.[77] Thus, silanes such as **3**, **5**, **8** and **10** are extensively used in polysulfide, polyurethane, polyvinyl chloride and silicone based sealants.[77, 78] Silanes may also be present in primer formulations to improve the adhesion of the sealant to an inorganic surface. However, the use of silane-containing primers[79] is losing importance because of the additional working step involved compared with sealants already containing silane.

3.4. Foundry Sand Molds

Several techniques for the preparation of foundry sand molds are available in the metal casting industry. Usually quartz sand is employed as principle refractory material for preparing molds, and normally small amounts of organic resins such as phenol or furan resins are used to function as binding material during mold production. However, since these organic components decompose with formation of volatiles at the temperatures used for casting, the quality of the castings deteriorates; therefore, any method permitting a reduction in the quantity of binder is most welcome. This can be achieved by incorporation of about 0.1% of aminosilane **5b** into the molding sand, which allows the amount of organic binder to be reduced from 3% to 1.5%.[80] Other useful silanes known from the patent literature include **3**, **4**, **8** and **10**[81] and urea derivatives of **5**.[82]

4. Other Applications of Bifunctional Silanes

Besides the "big volume" applications discussed above, numerous other areas are known where bifunctional silanes have proven useful. Literally thousands of patent publications deal with these various applications of silanes, thus making it impossible to mention all of them here. Therefore, in this review we shall only consider a selection of those uses which are already of some commercial importance (see, e.g., Sections 4.1.1, 4.1.2, 4.2.5, and 4.2.10) although the silane quantities involved may be small or which in our opinion bear a reasonable potential for further development.

For the purpose of an easy comprehensive survey these applications will roughly be classified into the fields of *coupling*, *substrate modification*, and *silane polycondensation*.

4.1. Coupling Applications

In principle, bifunctional silanes can provide a bonding interface between organic and inorganic matrices, as discussed in Section 3 for filler reinforced elastomers. It is essential for all coupling applications that the silane accumulates at the interface. Depending upon the nature of the organic and inorganic phases, this can either be achieved by addition of a silane (as an *integral blend additive*) to a prepolymer provided there is sufficient silane mobility in the organic polymeric material or, when mobility is poor, by *pretreatment of the inorganic surface* with pure (dry blending) or diluted silanes, either by immersion, painting or spraying.[59] Since the second mode of silane application involves an additional treatment step, the first method is used whenever possible. Pretreatment of the inorganic surface on the other hand allows a better control of the interface and is especially useful in coupling applications on massive structures (sealants, coatings, adhesives), where *primers* containing silanes[83] are used for surface pretreatment.

4.1.1. Particulate Mineral-Filled Thermosetting and Thermoplastic Resins

Numerous particulate mineral fillers have been found to improve the mechanial properties of filled polymer pieces after treatment with an appropriate silane coupler (silica, alumina, glass, aluminum and iron particles, clay, titanium oxide, and zinc oxide[59]).

Suitable methods for applying silanes to inorganic particulate fillers are filler treatment by organic or aqueous so-

lutions or by dry blending resulting in changes of physical properties (improved wettability by organic resins, reduced particle agglomeration) and of the processibility (improved dispersibility, reduced viscosity) of the silanized material.

Before curing, most thermosetting resins contain reactive centers suitable for chemical bonding to silanized fillers, as for instance unsaturated polyester, phenolic or epoxy resins. Certain thermoplasts (polydienes, polyvinyl chloride, polystyrene) also enable regular silane-to-polymer bonding by formation of covalent bonds.[5] In thermoplasts of relatively low molecular weight use can be made of end-group reactivity, as for instance in the case of polybutylene terephthalate.[5] Most thermoplasts, however, do not provide reactive centers for chemical bonding to silane couplers, so that the observed coupling interaction must be physical in nature: Aminosilanes **5**, for instance, play a major role in coupling inorganic fillers to polyesters, polyamides or polycarbonates via *hydrogen bonds*.[5] Silanes **4** containing a methacryl function may bind to unreactive thermoplasts (e.g. to polyethylene) by formation of *interpenetrating polymer networks* at the interface.[84] The *solution compatibility* of the organic part of a silane with a certain thermoplast may serve as a measure of the physical coupling interaction.[59] Several reviews have appeared concerning suitable filler/silane/resin combinations.[5,59,85]

A promising strategy for covalently coupling "unreactive" thermoplastic resins with silanized fillers involves the use of azide-functionalized silanes, e.g. **19**, which, at molding temperatures liberate reactive nitrene[86] and imine intermediates[87] that are expected to insert into C–H bonds of polyolefins.[5,88]

4.1.2. Dental Materials

Dental varnish and filling materials based on filler reinforced peroxide-curable acrylic polymers containing methacryl-functionalized silanes **4** have been described in numerous publications[89,90] and are used extensively. Thereby, the silane provides adhesion of the organic polymer to the natural tooth material.

4.1.3. Rock/Asphalt Mixtures

The rock/asphalt mixtures used in road building contain up to 95% of mineral aggregates, which may either be siliceous (e.g. granite) or calcareous (e.g. limestone) in nature. These mineral contents are held together by a bituminous binder. It was already established at a very early stage of organosilane chemistry that certain alkylsilanes may very well serve as adhesion promoters in rock/asphalt mixtures, though the technique proposed for silane processing (treatment of the mineral components with silane vapors) was prohibitive for realization on a large scale.[91] Many years later, the use of organofunctionalized silanes, such as **4**, **5**, **8**, **10**, and, in particular **9b**, for this purpose was published in connection with a very favorable method of silane addition:[92] The silane is first treated with carbon black or silica and can then be admixed in a quasi-powdered form with the solid mineral components.[92b]

4.1.4. Coatings for Siliceous and Metallic Surfaces

Adhesion of organic coatings (paints or inks) to inorganic surfaces (glass, steel, aluminum) is improved, if the uncured coating material contains a silane like **2**, **3**, **4**, **5**, **8**, or **10** as additive.[93] For optimum performance the silane must accumulate at the interface, which is quite easily achieved in the case of latex coatings.[83a] In other cases the same effect can be realized with an undercoat of silane-containing primer.[83,93]

4.1.5. Coatings for Organic "Glasses"

Transparent organic polymers such as polycarbonates or polyacrylates are superior to silicate glass from the point of view of handling and processibility, but cannot compete with inorganic glasses as far as resistance to abrasion and scratching is concerned.[94] This disadvantage can be overcome by applying a thin layer of siliceous material onto the polymer surface. Here again bifunctional silanes such as **3** and **4** can decisively improve the coupling between inorganic coating and organic surface.[95]

4.1.6. Adhesives

Silanes find another application which is closely related to those discussed in Sections 3.3 and 4.1.4, namely as additives to or primers for adhesives that are used to improve the adhesion between inorganic materials (ceramics, glasses, metals).[96] The adhesive strength of thermosetting and thermoplastic polymers can be increased markedly by addition of small amounts (ca. 1%) of silane to the adhesive.[96a] The choice of silane coupler largely depends upon the curing mechanism of the adhesive: The silanes **3**, **4**, **5**, and **10** are claimed to be of particular value in the more important adhesive systems currently on the market.[96]

4.2. Fixation of Functional Groups and Active Compounds to Inorganic Substrates

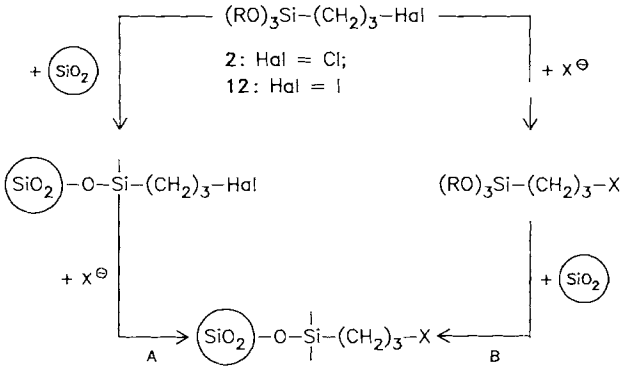
The immobilization of functional groups or (macro-)molecules showing a certain reactivity in the homogeneous phase on solid supports has attracted increasing interest during the last two decades, especially in the fields of transition metal-[97] and enzyme-catalysis,[98] organic synthesis,[99] chromatography,[100] and ion exchange.[101]

The advantages of these immobilized systems are the ease of separation and inexpensive recycling on the one hand, and the high stability and long lifetime on the other.[97,98]

Organic polymers were the first carriers to be used commercially.[99d] Inorganic supports such as silica, silica gel, alumina and other mineral oxides proved to be superior with respect to structural stability, swelling behavior, thermal properties and aging, accessibility of reactive centers, and insolubility in organic media.[97]

One concept developed for the immobilization of functional groups or active molecules on inorganic substrates involves their attachment via bifunctional silanes (e.g., **2** and its derivatives).[97e,98e]

Two synthetic routes have proven useful for the preparation of functionalized surfaces with the title compounds, namely those shown in Scheme 13.[102]



Scheme 13. Preparation of silanized silica with the silanes **2** and **12**. SiO_2 in a circle denotes silica carrier (without surface groups). A, B see text.

According to route A, the silanes **2** or **12** are first attached to the carrier; the resulting silanized silica is then modified by nucleophilic substitution with the functional group X. Route B involves the reverse procedure, i.e., substitution of **2**/**12** with X followed by attachment of the resulting silane derivative to the carrier. Route A is preferred in those cases only, when the nucleophile also reacts with the trialkoxysilyl group. Alkoxypropylsilylated surfaces, for instance, can only be prepared via route A (X = OR).[103]

4.2.1. Textile Fiber Treatment

The silanization of textile fibers (including cotton as well as synthetic fibers) was one of the very early applications of hydrolyzable organosilanes; this enabled the manufacture of water-repellent textiles.[104] Today, silicones are the only organosilicon compounds of commercial importance in this field of application.[105]

In the early 1970s, it was found that ammonium-functionalized silanes, especially **18**, exhibit bactericidic and algaecidic activity after attachment to glass or other siliceous carriers[106] and textile fibers;[107] this immediately suggested the utilization of these silanes for the manufacture of surgical drapes.[107b]

4.2.2. Liquid Crystals

After fixation to glass, some bifunctional silanes, e.g. the long-chain ammoniopropylsilane **18**, impose a certain steric orientation upon an organic substrate, since all alkyl chains in **18** tend to orientate parallel to each other.[108] This effect can be utilized for the manufacture of liquid crystal displays.[108] Silanized liquid crystal phases have been prepared starting from the isocyanate **20**.[109]

4.2.3. Metal (Oxide) Electrodes

Elements such as Si[55a] or Ag[110] and metal oxides such as Al_2O_3,[110] SnO_2,[111] TiO_2,[112] or PbO[55b] have been covered with monolayers of the silanes **2**,[111a] **4**,[55b] **5**,[55a,111a,c] **8**,[111a,e] **10**,[110,111b] and **27**.[111d] Redox active molecules can be attached to these silanized surfaces by chemical reaction, thereby changing the electron-transfer properties of the underlying electrode.[111,112] Attachment of light absorbing redox dye molecules to silanized electrodes was proposed as a concept for construction of photoelectrochemical devices.[113]

4.2.4. Electrostatographic Developing Materials (Toners)

Numerous photocopying printers are based on electrostatographic processes: Under the influence of light, latent electrostatic images are formed as negative charge patterns on an electroreceptor surface. In the indirect process this latent image is developed by a toner powder of reversed polarity and transferred to plain paper. Basically, toners consist of an organic resin and a dye pigment. Their performance is highly improved by a uniform and stable distribution of positive charges within the powder. This uniform distribution can be achieved by addition of fumed silica particles pretreated with aminosilanes such as **5**, **6** or **8**.[114]

4.2.5. Chromatography

Hydrolyzable organosilanes have become an important tool for the preparation of modified silica gels[100a] that are used as stationary phases in *gas-*[115] and *liquid-chromatography*[115c,116] (especially *HPLC*[117]) as well as in *thin layer chromatography*.[118] Long-chain alkylsilanes play a major role in *reversed phase chromatography*,[119] but will not be discussed here further. Besides hydrophobicity, other physicochemical properties useful for chromatographic separations can be conferred on silica gel by modification with organofunctionalized silanes.

A selection of silanized phases that are useful for liquid chromatography is listed in Table 4.

4.2.6. Metal (Ion) Extraction

In principle, all silanes containing electron donating or chelating groups, for instance **5**, **8**, **10** and **13**, exhibit metal-ion complexing properties after attachment to an inorganic support.[128] Another access to such metal adsorbing materials is provided by the silanization of inorganic substrates with the silanes **2**, **5** or **12** and subsequent incorporation of the complexing group according to Route B in Scheme 13.[129] Practical utilizations published for these materials include the removal of metal-ions (especially uranyl ions[128a,129b]) from aqueous media and organic media (e.g. from kerosene[129b]) as well as the preconcentration of metal ions (e.g., for analytical detection[130]).

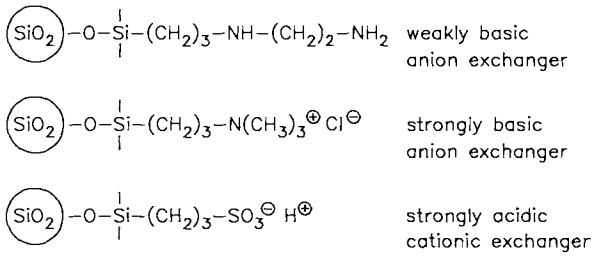
4.2.7. Ion Exchangers

The silanization of inorganic carriers with **8**,[124c] **16**[124d] or a sulfonate-functionalized silane derived from **10**[123a] or **11**[39a] yields materials showing ion exchange properties

Table 4. Preparation of special column materials for liquid chromatography by silanization.

Silane	Treatment	Property	Chromatography	Ref.
3	Opening of the epoxide ring	Polar "diol" phase	Absorption and	[120]
5	None	Polar "amine" phase	partition	[120a, d, 121]
27	None	Polar "nitrile" phase	chromatography	[120a, 121a, 122]
10, **11**	Oxidation to the sulfonate group	Cation exchanging phase	Ion-exchange chromatography	[39a, 123]
16, **17**	None	Anion exchanging phase		[120a, 124]
5	Reaction with tetra-nitrofluorenone	Interaction with π-electron systems	Charge-transfer chromatography	[125]
8	Loading with metal ions	Interaction with complexing agents	Ligand-exchange chromatography	[126]
5	Binding of biomolecules (amino acids, proteins, enzymes)	Interaction with bio-substrates	Bioaffinity chromatography	[98b,e, 127]

(Scheme 14). Alternatively, these ion exchangers can be prepared by silanization of inorganic substrates with halo-functionalized silanes **2** or **12** followed by nucleophilic substitution with tertiary amines[131] or sulfite ion.[123b]

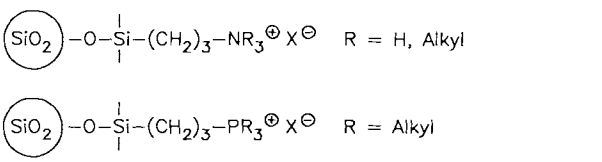


Scheme 14. Silanized siliceous materials as ion exchangers.

A principal disadvantage of these ion exchangers is their relatively low capacity as compared to that of conventional organic exchangers.[101a, 124d] New inorganic ion exchangers with hydrolytically stable bonding of the functional groups to the carrier, which can be obtained by polycondensation of bifunctional silanes, have higher capacities (cf. Section 4.3).

4.2.8. *Phase Transfer Catalysts*

Only ten years after first being described in the literature, phase transfer catalysts are already being used on an industrial scale for heterogeneous catalysis.[132] A group of such catalysts[133] (cf. Scheme 15) is accessible by modification of silica[133a,b] or alumina[133c] with ammonium[133a,c] and phosphonium[133b,c] active groups, once again via the two routes in Scheme 13.[133a]



Scheme 15. Examples of phase-transfer catalysts for heterogeneous catalysis.

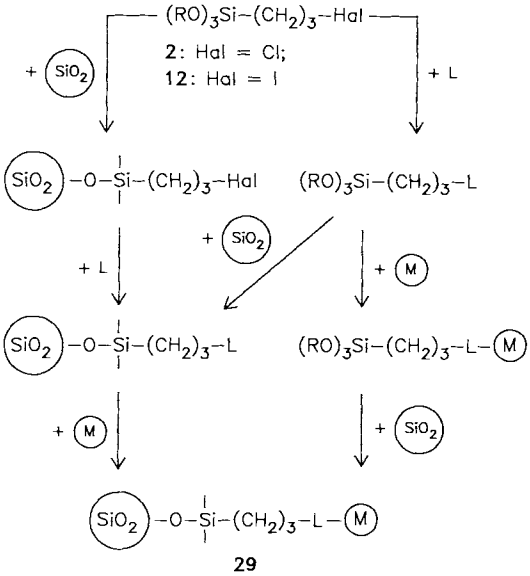
The influence of various alkyl substituents attached to the onium center on activity and selectivity was studied[133a], as also was the influence of the bridge length (3–27 atoms) between the silyl group and the onium function.[133b,c]

4.2.9. *Transition-Metal Catalysts*

The immobilization of catalytically active transition-metal centers on oxidic carriers (SiO_2, Al_2O_3, TiO_2, SnO_2, ZnO_2, MgO)[134] is also possible with certain silanes;[97e] thereby, the advantages of homogeneous (well defined active sites, availability of all metal centers, flexible steric and electronic environment) and heterogeneous (easy recovery and recycling) catalysis[97b] should be combined.

The preparation of these transition-metal catalysts can be carried out by several routes, since silanization, introduction of the ligand-group, and attachment of the metal center can be achieved in various orders of succession, as indicated in Scheme 16.[102, 135]

Selected examples of siliceous carriers silanized with derivatives of **2** are listed in Table 5.



Scheme 16. Preparation of immobilized transition-metal complexes **29** from **2** or **12** (see also Tables 5).

Table 5. Transition-metal complexes of type **29** as heterogeneous catalysts, prepared with bifunctional silanes.

Silane	Metal	Catalyzed reaction	Ref.
5	Rh	Hydroformylation	[136a]
	Pd	Hydrogenation	[136b-d]
8	Rh	Hydrogenation	[137, 138]
10	Rh	Hydrogenation	[139a]
		Hydrosilylation	[139b]
13	Rh	Hydrogenation	[135b]
		Hydroformylation	[135b]
25	Rh	Hydrogenation	[50c, 138, 140a-c]
	Rh	Hydroformylation	[136a]
	Rh	Hydrosilylation	[140d, e]
27	Pd	Hydrogenation	[136d]
	Pt	Hydrosilylation	[141]

4.2.10. Enzymes and Polypeptides

After immobilization on solid carrier materials, enzymes can easily be utilized in industrial processes. Once again, inorganic supports, such as glass beads or silica gel, exhibit greater structural and operational stability as well as a higher resistance to microbial attack as compared to carriers based on organic polymers.[98]

Numerous methods have been described for the coupling of enzymes to silanized supports.[5, 142, 143] A few of them, starting with silanes **5**,[142] **10**,[142a] and **12**,[143] are summarized in Scheme 17 to demonstrate exemplary bonding environments of fixed enzymes.

Porous glass beads treated with **5b** are commercially available for enzyme immobilization[144] and are used in packed-bed reactors for the degradation of yeast and for the isomerization of fructose.[98c, e]

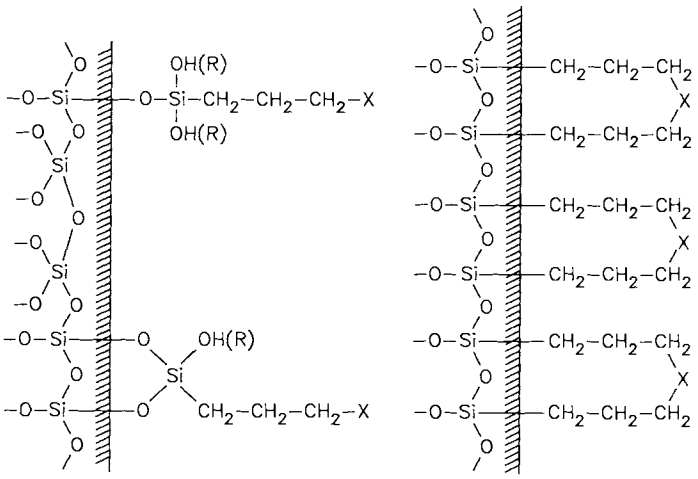
Of the numerous *analytical applications* of immobilized enzymes,[145] only those are mentioned here, in which silanized supports are involved, namely *bioaffinity chromatography* (cf. Table 4) and *enzyme flow analysis*.[98c, 146] Silanized glass beads have also been proposed for substrate immobilization for the sequence analysis of peptides and proteins by *Edman degradation*.[147]

4.3. A New Class of Functionalized Organopolysiloxanes by Polycondensation of 6, 7, 13, 14, and 26

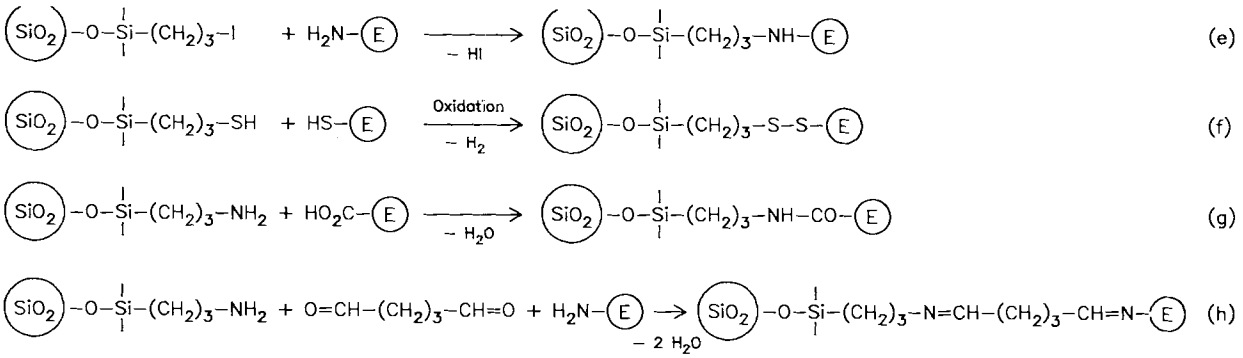
Silanized inorganic materials have a number of advantages compared to organic polymers; nevertheless, their properties as supports for immobilized functional groups and active compounds are not optimal. Because of the relatively low concentration of surface hydroxy groups, on average only 1-1.5 of three possible bonds are formed between the organofunctionalized silane and the support. As a consequence, the concentration of functional groups is quite low and the silane-to-surface bond is labile, especially in alkaline aqueous media.

In view of this, a newly developed concept may provide an interesting alternative: Polycondensation of suitable bifunctional silane monomers leads to solids with a *siliceous core* and a *high concentration of functional groups*, which, moreover, are bound to the matrix via carbon-silicon bonds that are stable towards hydrolysis.

Scheme 18 shows the qualitative difference between silicic acid that has been treated with bifunctional silanes and polycondensed silanes.



Scheme 18. Silanized siliceous surface (left) obtained from a monomer $(RO)_3Si-(CH_2)_3-X$, and polycondensed functionalized silanes (right), obtained from a monomer $(RO)_3Si-(CH_2)_3-X-(CH_2)_3-Si(OR)_3$.

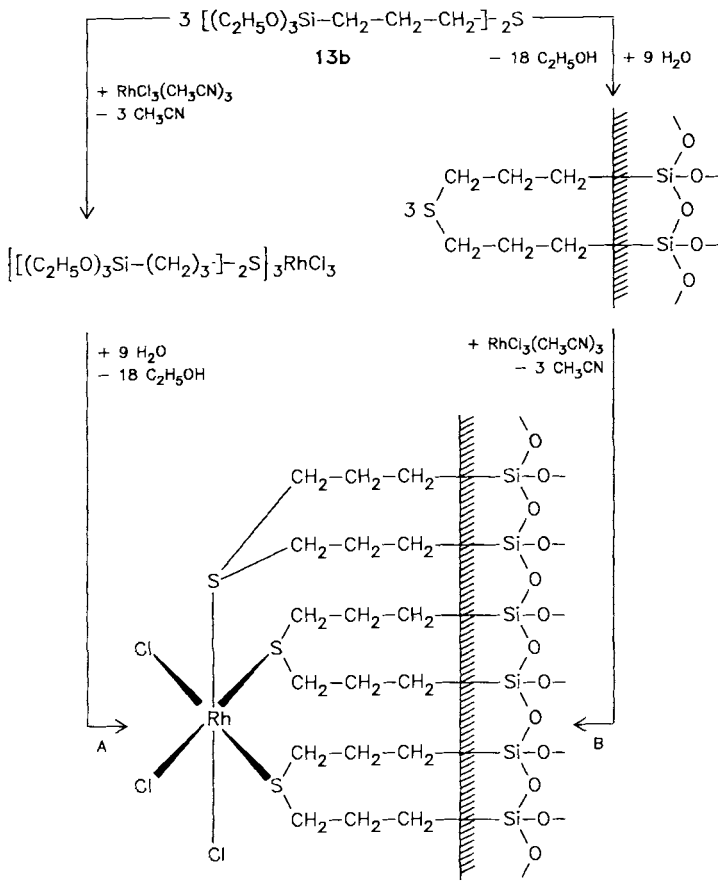


Scheme 17. Selected reactions for the coupling of enzymes (E) to siliceous carriers silanized with **12**, **10**, and **5**. (f): cysteine coupling; (g): carbodiimide coupling; (h) Schiffs-base coupling.

The physical and chemical properties of the solid silane polycondensates can be tailor-made during or after the polycondensation for particular purposes; examples are, as *heterogeneous metal complex catalysts* and *ion exchangers*.

4.3.1. Immobilized Metal Complex Catalysts with Organopolysiloxane Structure

Following this concept we have prepared rhodium complexes as heterogeneous catalysts, starting from sulfide-functionalized silane precursors **13b**.[135] Two synthetic routes met with success (Scheme 19): Either **13b** is first allowed to react with a rhodium compound, e.g. tris(acetonitrile)trichlororhodium to give a monomeric complex,[135] which is subsequently polycondensed (Route A), or **13b** is first polycondensed and then converted into the rhodium complex (Route B).[148] In both cases the spontaneous polycondensation furnishes an insoluble solid. It was found that the polymeric rhodium complex does not necessarily need to be stoichiometrical, with a ligand/metal ratio of 3:1. If desired, more sulfide ligands can be present in the polymer complex. By means of so-called cross-linking agents or cocatalysts, which are incorporated into the matrix, control of the sulfide density is possible. For example, tetraalkyl silicates and tetraalkyl titanates can be used for this purpose. The carriers for these polymeric complexes can in this way be tailor-made for certain catalytic requirements.



Scheme 19. Synthesis of organopolysiloxane-based thiorhodium complexes as heterogeneous catalysts. A, B see text.

Rhodium complexes prepared from other silane precursors appear to be even more promising as heterogeneous catalysts: Thus, polymeric phosphanerhodium complexes with siliceous frameworks are obtained from the phosphane-functionalized silane **26b** according to the procedure outlined in Scheme 19. Again the phosphane/metal ratio can be adjusted to meet certain catalytic requirements.[149] Finally, aminorhodium complexes of this type can also be prepared in the same manner, starting from the amino-functionalized silanes **6b** or **7b**.[150]

Rhodium is just one typical example as catalytic center: Naturally, analogous immobilized complexes with other transition metals can also be synthesized.[149a, 150b, 151]

Table 6. Typical fields of application for some organopolysiloxane-based transition-metal complexes as heterogeneous catalysts.

Catalyst composition [a]	Catalyzed reaction
"$RhH(CO)\{S[(CH_2)_3-SiO_{3/2}]_2\}_3$"	Hydrogenation
$RhCl_3\{N[(CH_2)_3-SiO_{3/2}]_3\}_3 \cdot 2PPh_3$	Hydrogenation
$RhCl_3\{S[(CH_2)_3-SiO_{3/2}]_2\}_3$	Hydroformylation
$RhCl_3\{N[(CH_2)_3-SiO_{3/2}]_3\}_3$	Hydroformylation
$RhCl_3\{C_6H_5-P[(CH_2)_3-SiO_{3/2}]_2\}_3$	Carbonylation
$IrCl_3\{C_6H_5-P[(CH_2)_3-SiO_{3/2}]_2\}_3$	Carbonylation
$\{H_3C-N[(CH_2)_3-SiO_{3/2}]_3\}_2^{2+}[PtCl_4]^{2-}$	Hydrosilylation
$PtCl_2\{N[(CH_2)_3-SiO_{3/2}]_3\}_2$	Hydrosilylation

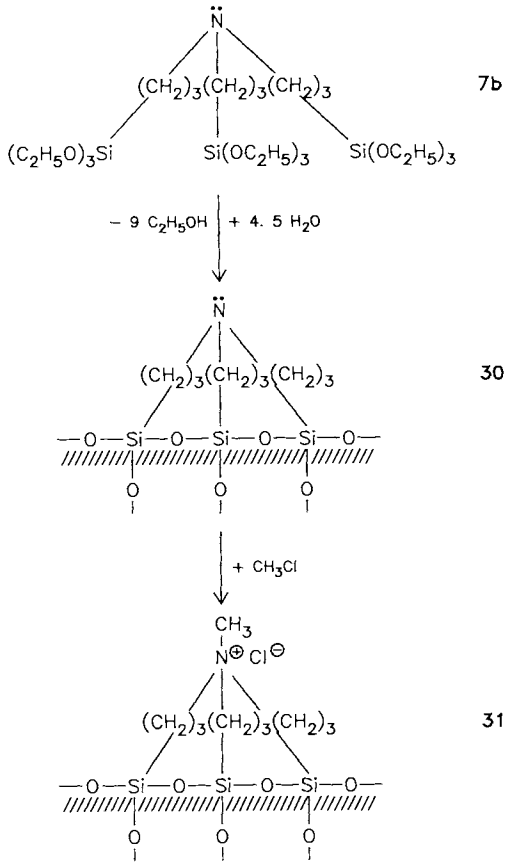
[a] The notation $X[(CH_2)_3-SiO_{3/2}]_n$ signifies that the complex is a complete polycondensate of a trialkoxysilane precursor of the composition $X[(CH_2)_3-Si(OR)_3]_n$ with n = 2, 3.

The catalytic properties of a few selected examples listed in Table 6 are very promising; however, the systems will have to be optimized prior to their employment on an industrial scale.

4.3.2. New Ion Exchangers with Organopolysiloxane Structure

For the synthesis of anion exchangers on the basis of polycondensed amino-functionalized silane precursors[150a, 152] the reaction of the title compounds with ammonia had to be optimized in a new direction: under well-defined reaction conditions and stoichiometries, the reaction already presented in Scheme 4 leads almost quantitatively to the tertiary amine **7b**,[150a] which, upon addition of water readily undergoes condensation to give an amino-functionalized solid **30** containing a polysiloxane framework (Scheme 20). This substance, which itself is a weakly basic ion exchanger can be quaternized, e.g. with methyl chloride, to give **31**, which can function as a strongly basic anion exchanger.

After the usual condensation process, both types of exchanger are obtained in the form of unsymmetrical particles, which can be milled and classified according to size. Their surface areas in this form are in a range of about 0 to 700 m^2/g, depending upon the conditions of preparation. Recently, a process was developed by us which also allows the preparation of *spherical particles* with grain sizes of about 0.1–1.5 mm and surface areas from only a few m^2/g up to about 700 m^2/g (Fig. 2). The exchange capacities, which can be controlled, inter alia, by insertion of different quantities of cross-linking agents (e.g. tetraalkyl silicates)



Scheme 20. Production of organopolysiloxane-based weakly basic and strongly basic anion exchangers **30** and **31**, respectively.

into the polysiloxane matrix, are, in the case of the strongly basic type exchanger **31**, partly in excess of 1.6 meq $Cl^{\ominus}$/mL, and thus reach the upper values of conventional organic exchanger systems.[101] The main advantage of the new exchangers lies in their high temperature stability, up to 200°C. This is primarily a consequence of the threefold matrix-bound ion-exchanging groups.

Strongly acidic cation exchangers can also be obtained on the basis of this concept[153] (Scheme 21).

Their synthesis starts from the silane **14b**, which is polycondensated in the usual manner.[153a] The cation-exchang-

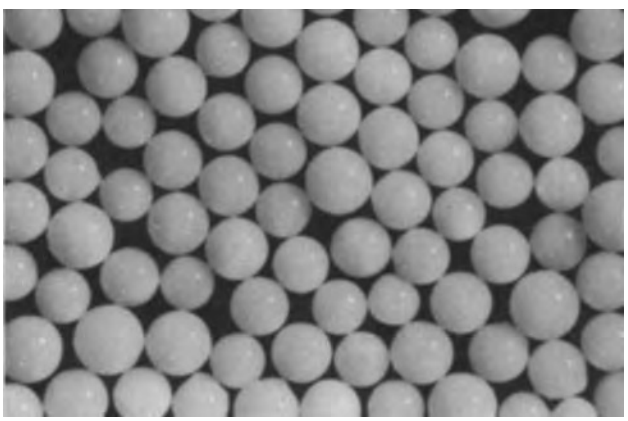
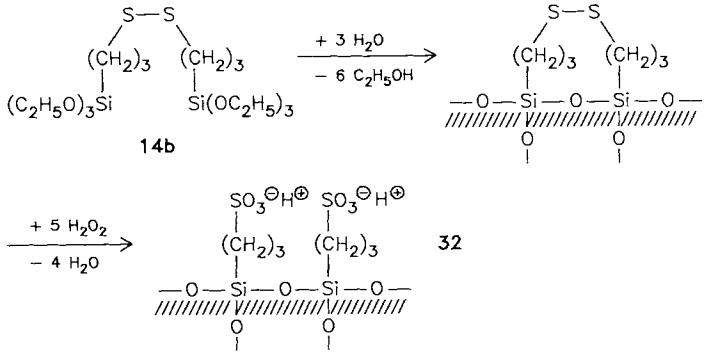


Fig. 2. Organopolysiloxane-based anion exchangers of type **31** in the form of spherical particles (magnified about eleven times).



Scheme 21. Production of organopolysiloxane-based strongly acidic cation exchanger **32**.

ing sulfonate groups are generated in the resulting solid material by subsequent oxidative cleavage of the disulfide bridges, e.g. with hydrogen peroxide; exchange capacities of 1–2 meq/g can be achieved.[153b]

Materials of type **32** show similarly good properties as the anion exchangers discussed above, especially a high temperature stability of up to 300°C. Therefore they can also be used as solid catalysts in acid-catalyzed reactions at elevated temperatures.

5. Conclusion

3-Chloropropyltrialkoxysilanes, and some derivatives obtainable therefrom by nucleophilic displacement of chlorine, have been produced on a commercial scale for about 20 years. They were originally used as *coupling agents*, mainly in *glass fiber-reinforced thermoplasts*, in organic *sealants* containing inorganic fillers, and in *casting molds* prepared from foundry sand and organic binders. Within the last decade the benefit of silanes for the rubber industry has been established, since sulfur derivatives of the title compounds have been found to be useful as coupling agents in *silica-reinforced rubber articles* (e.g., *special tires*) or as essential ingredients of *equilibrium cure systems* for sulfur-curable elastomers. Less important with respect to the silane quantities involved are coupling applications in the fields of particulate filler-reinforced thermoplasts, dental materials, rock/asphalt mixtures, coatings and adhesives, though foreseeable future developments are likely to result in higher silane consumptions in these areas, too.

A second group of applications for these compounds with a high potential in future developments exists in the *modification of hydroxy-functional surfaces* in a very general sense: Until now promising practical realizations have been achieved by silanization of glass (e.g. for the preparation of liquid crystal display systems), of silica (e.g. for the manufacture of toners), and of textile fibers or metal oxide electrodes. The *fixation of functional groups and active compounds* to inorganic carriers with the help of bifunctional silanes as a special type of surface modification has shown promise in the fields of chromatography, metal extraction, and catalysis, and is used commercially in certain *enzyme reactors*.

Finally, certain derivatives of 3-chloropropyltrialkoxysilanes, after *polycondensation*, yield *solid functional polysi-*

loxanes. Possible utilizations of these materials include the manufacture of ion exchangers and the preparation of transition-metal complexes as heterogeneous catalysts.

Future demands on silanes in all the areas listed above will most likely be met with the help of known silanes (e.g., by *optimization of the silane-to-substrate interface*) rather than by the development of new classes of silanes. Parallel to the discovery of yet unknown or to the expanded use of known composite materials new or extended markets for bifunctional silanes can be expected in the future.

Received: July 16, 1985 [A 567 IE]
German version: *Angew. Chem. 98* (1986) 237

[1] a) Review: V. Bazant, J. Joklik, J. Rathousky, *Angew. Chem. 80* (1968) 133; *Angew. Chem. Int. Ed. Engl. 7* (1968) 112; b) D. T. Hurd, *J. Am. Chem. Soc. 67* (1945) 1813.

[2] a) Review: E. Lukevics, Z. V. Belyakova, M. G. Pomerantseva, M. G. Voronkov, *J. Organomet. Chem. Libr. 5* (1977) 1; b) E. W. Pietrusza, L. H. Sommer, F. C. Whitmore, *J. Am. Chem. Soc. 70* (1948) 484.

[3] a) J. Bjorksten, L. L. Yaeger, J. E. Henning, *Ind. Eng. Chem. 46* (1954) 1632; b) D. J. Vaughan, *Tech. Pap. Soc. Plast. Eng. 23* (1977) 330.

[4] E. P. Plueddemann, H. A. Clark, L. E. Nelson, K. R. Hoffman, *Mod. Plast. 1962 (8)*, 135.

[5] B. Arkles, *CHEMTECH 1977*, 766.

[6] F. Thurn, S. Wolff, *Kautsch. Gummi Kunstst. 28* (1975) 733.

[7] W. Noll: *Chemie und Technologie der Silicone*, Verlag Chemie, Weinheim 1968, 2nd edition.

[8] B. Arkles in *Kirk-Othmer: Encyclopedia of Chemical Technology, Vol. 20*, Wiley, New York 1982, 3rd edit., p. 912.

[9] a) C. A. Roth, *Ind. Eng. Chem. Prod. Res. Dev. 11* (1972) 134; b) B. E. Cooper, *Process Biochem. 1980*, 9; c) L. Birkhofer, A. Ritter, *Angew. Chem. 77* (1965) 414; *Angew. Chem. Int. Ed. Engl. 4* (1965) 417.

[10] J. W. Ryan, G. K. Menzie, J. L. Speier, *J. Am. Chem. Soc. 82* (1960) 3601.

[11] a) C.-D. Seiler, H.-J. Vahlensieck, DBP 2815316 (April 8, 1978), Dynamit Nobel; b) T. Lindner, N. Zeller, V. Frey, G. Engelsberger, P. John, R. Riedle, DBP 2851456 (November 28, 1976), Wacker.

[12] a) S. Nitzsche, I. Bauer, W. Graf, N. Zeller, DBP 2061189 (December 11, 1970), Wacker; b) H.-J. Kötzsch, C.-D. Seiler, H.-J. Vahlensieck, DBP 2800017 (January 2, 1978), Dynamit Nobel; c) P. Fischer, R. Groh, H.-J. Vahlensieck, DOS 3236628 (October 4, 1982), Dynamit Nobel.

[13] M. G. Voronkov, G. I. Zelchan, E. Lukevitz: *Silizium und Leben*, Akademie-Verlag, Berlin 1975, p. 228.

[14] E. P. Plueddemann, G. Fanger, *J. Am. Chem. Soc. 81* (1959) 2632.

[15] a) E. P. Plueddemann, H. A. Clark, US-Pat. 3258477 (July 19, 1963), Dow Corning; b) T. Lindner, N. Zeller, G. Engelsberger, R. Riedle, DAS 3000768 (January 10, 1980), Wacker.

[16] J. L. Speier, C. A. Roth, J. W. Ryan, *J. Org. Chem. 36* (1971) 3120.

[17] a) V. B. Jex, D. L. Bailay, US-Pat. 2832754 (January 21, 1955), Union Carbide; b) R. Kleinstück, DOS 2521399 (May 14, 1975), Bayer; c) F.-R. Kappler, C.-D. Seiler, H.-J. Vahlensieck, DBP 2749316 (November 4, 1977), Dynamit Nobel.

[18] a) J. C. Saam, US-Pat. 2860153 (April 25, 1957), Dow Corning; b) V. B. Jex, US-Pat. 3257440 (December 23, 1955), Union Carbide.

[19] C. F. Schubert, US-Pat. 3008975 (June 24, 1958), Union Carbide.

[20] I. Ojima, M. Kumagai, Y. Nagai, *J. Organomet. Chem. 111* (1976) 43; Jap. Pat. 7632528 (September 6, 1974); *Chem. Abstr. 85* (1976) 192872k.

[21] V. B. Jex, D. L. Bailey, US-Pat. 2930809 (October 12, 1956), Union Carbide.

[22] a) H. Knorre, W. Rothe, DAS 1271712 (December 16, 1966), Degussa; b) P. Gerhardt, C.-D. Seiler, H.-J. Vahlensieck, DBP 2161716 (December 13, 1971), Dynamit Nobel; c) N. Holtschmidt, K. Friedrich, M. Leupold, DOS 2408480 (February 22, 1974), Bayer; d) J. Schlapa, P. Loetzsch, B. Fischer, S. Dathe, W. Pieschnik, DDR-Pat. 151944 (September 4, 1980); e) N. S. Chu, B. Kanner, C. L. Schilling, US-Pat. 4481364 (September 26, 1983), Union Carbide.

[23] a) J. L. Speier, US-Pat. 2971864 (March 26, 1958), Dow Corning; b) R. J. Lisanke, R. A. Pike, DAS 1152695 (August 18, 1961), Union Carbide; c) Jap. Pat. 81104891 (January 28, 1980), Toray; *Chem. Abstr. 96* (1982) 52495s.

[24] a) F. Fehér, H. J. Berthold, *Z. Anorg. Allg. Chem. 273* (1953) 144; b) F. Bittner, W. Hinrichs, H. Hovestadt, L. Lange, E. Splett, DOS 3436698 (October 6, 1984), Degussa.

[25] a) E. Meyer-Simon, F. Thurn, R. Michel, DBP 2141159 (August 17, 1971), Degussa; b) F. Thurn, E. Meyer-Simon, R. Michel, DBP 2212239 (March 14, 1972), Degussa; c) H.-D. Pletka, R. Michel, DBP 2542534 (September 24, 1975), Degussa; d) W. Buder, H.-D. Pletka, R. Michel, R. Schwarz, G. Düsing, DBP 2712866 (March 24, 1977), Degussa; e) P. Panster, R. Michel, P. Kleinschmit, U. Deschler, DOS 3311340 (March 29, 1983), Degussa.

[26] a) T. L. Pickering, K. J. Saunders, A. V. Tobolsky in A. V. Tobolsky (Ed.): *The Chemistry of Sulfides*, Wiley, New York 1968, p. 61; *J. Am. Chem. Soc. 89* (1967) 2364; b) M. B. Berenbaum in A. V. Tobolsky (Ed.): *The Chemistry of Sulfides*, Wiley, New York 1968, p. 221.

[27] a) M. Schmidt, G. Talsky, *Chem. Ber. 90* (1957) 1673; b) G. Schwarzenbach, A. Fischer, *Helv. Chim. Acta 43* (1960) 1365; c) A. Teder, *Ark. Kemi 30* (1968) 379; *31* (1969) 173; *Acta Chem. Scand. 25* (1971) 1722.

[28] K. O. Hiller, B. Masloch, H. J. Möckel, *Z. Anal. Chem. 280* (1976) 293.

[29] a) W. Buder, *Z. Naturforsch. B34* (1979) 790; b) D. Grant, J. R. van Wazer, *J. Am. Chem. Soc. 86* (1964) 3012.

[30] E. Meyer-Simon, W. Schwarze, F. Thurn, R. Michel, DBP 2141160 (August 17, 1971), Degussa.

[31] a) P. Janssen, K.-D. Steffen, DOS 2360471 (December 5, 1973), Dynamit Nobel; b) J. E. Bittell, J. L. Speier, *J. Org. Chem. 43* (1978) 1687.

[32] a) A. N. Pines, J. G. Marsden, S. Stermann, Brit. Pat. 1102251 (February 3, 1965), Union Carbide; b) J. L. Speier, US-Pat. 4082790 (March 10, 1975), Dow Corning; c) G. M. Omietanski, H. E. Petty, US-Pat. 3849471 (December 14, 1972), Union Carbide.

[33] a) G. Koerner, G. Rossmy, DBP 1163818 (May 5, 1962), Goldschmidt; b) J. A. Rakus, J. G. Sharpe, US-Pat. 3590065 (July 18, 1969), Dow Corning; c) T. G. Selin, US-Pat. 4401826 (September 10, 1982), General Electric.

[34] a) One-step synthesis: J. Y. Pui Mui, US-Pat. 4012403 (March 18, 1976), Union Carbide; b) Two-step synthesis: H. E. Petty, Eur. Pat. 18094 (March 21, 1980), Union Carbide.

[35] a) M. G. Voronkov, V. M. Dyakov, Y. A. Lukina, G. A. Samsonova, N. M. Kudyakov, *Zh. Obshch. Khim. 45* (1975) 2010; b) F. G. Young, L. R. Pennington, US-Pat. 3780127 (October 2, 1972), Union Carbide; c) P. Panster, A. Karl, W. Buder, P. Kleinschmit, DBP 3047995 (December 19, 1980), Degussa.

[36] M. G. Voronkov, F. P. Kletsko, N. N. Vlasova, L. N. Gont, V. I. Kaigorodova, *Izv. Akad. Nauk SSSR Ser. Khim. 1977*, 1849.

[37] P. Janssen, K.-D. Steffen, DOS 2360470 (December 5, 1973), Dynamit Nobel.

[38] G. Rocktäschel, F. Thurn, H. Fleischhauer, W. Schwarze, H. Westlinning, US-Pat. 3798196 (July 16, 1971), Degussa.

[39] a) J. W. Ryan, US-Pat. 3215718 (November 24, 1961), Dow Corning; b) A. Karl, W. Buder, P. Kleinschmit, DOS 3220712 (June 2, 1982), Degussa.

[40] a) K. Ariga, M. Takamizawa, T. Mayuzumi, S. Imai, Jap. Pat. 6723332 (August 23, 1965), Shin-Etsu; *Chem. Abstr. 68* (1968) 95935z; b) H. Sakurai, K. Ogi, Jap. Pat. 7773826 (December 15, 1975), Mitsubishi Metal; *Chem. Abstr. 87* (1977) 168191h; c) Jap. Pat. 81104890 (January 28, 1980), Toray; *Chem. Abstr. 96* (1982) 52496t.

[41] a) A. Karl, W. Buder, P. Kleinschmit, DOS 3047994 (December 19, 1980), Degussa; b) Jap. Pat. 82114594 (January 5, 1981), Mitsubishi Metal; *Chem. Abstr. 98* (1983) 107537f.

[42] R. H. Krahnke, L. F. Stebleton, DBP 1621849 (February 17, 1967), Dow Corning.

[43] C. A. Roth, US-Pat. 3560385 (November 1, 1968), Dow Corning.

[44] a) A. W. Borel, Eur. Pat.-Anm. 18503 (March 27, 1980), Phillips Petroleum; b) A. Karl, W. Buder, DOS 3040382 (October 25, 1980), Degussa.

[45] A. Berger, US-Pat. 3494951 (September 20, 1967), General Electric.

[46] a) Hydrosilylation $CH_2{=}CH{-}CH_2{-}NCO + HSi(OR)_3$: J. Iyoda, A. Nagata, Jap. Pat. 7765225 (November 25, 1975); *Chem. Abstr. 87* (1977) 135906s; b) from silyl carbamates: E. Hedaya, T. Spyros, US-Pat. 4130576 (December 19, 1977), Union Carbide; c) gas-phase reaction $Cl_3Si{-}(CH_2)_3{-}NCO + 3\,ROH$: E. W. Bennett, US-Pat. 3651117 (September 8, 1970), Union Carbide; d) review: V. P. Kozyukov, V. D. Sheludyakov, V. F. Mironov, *Russ. Chem. Rev. 42* (1973) 662.

[47] B. B. Hardman, W. T. Madigan, US-Pat. 4036813 (November 26, 1975), General Electric.

[48] a) E. J. Pepe, J. G. Marsden, US-Pat. 4046794 (June 18, 1973), Union Carbide; b) U. Deschler, W. Buder, P. Kleinschmit, R. Michel, DAS 3424534 (July 4, 1984), Degussa.

[49] U. Deschler, P. Kleinschmit, R. Michel, DOS 3524215 (July 6, 1985), Degussa.

[50] a) F. G. Young, US-Pat. 3987009 (December 12, 1974), Union Carbide; b) M. Capka, *Synth. React. Inorg. Met.-Org. Chem. 7* (1977) 347; c) T. Okano, T. Kobayashi, H. Konishi, J. Kiji, *Bull. Chem. Soc. Jpn. 55* (1982) 2675.

[51] V. B. Jex, R. Y. Mixer, US-Pat. 3177236 (April 30, 1962), Union Carbide.

[52] a) Hydrosilylation of allyl nitrile with $HSiCl_3$ followed by alcoholysis: V. B. Jex, US-Pat. 3168544 (August 23, 1961), Union Carbide; b) hydrosilylation of allyl nitrile with $HSi(OR)_3$: V. Bazant, M. Capka, I. Dietzmann, H. Fuhrmann, J. Hetflejs, H. Pracejus, DDR-Pat. 103902 (September 15, 1972); c) Addition of HCN to allylsilanes: E. S. Brown, E. A. Rick, F. D. Mendicino, US-Pat. 3595897 (November 12, 1968), Union Carbide.

[53] U. Deschler, P. Panster, P. Kleinschmit, S. Wolff, E. H. Tan, DOS 3427922 (July 28, 1984), Degussa.

[54] a) H. Schmidbaur, *Angew. Chem. 77* (1965) 206; *Angew. Chem. Int. Ed. Engl. 4* (1965) 201; b) F. Schindler, H. Schmidbaur, *ibid. 79* (1967) 697 and *6* (1967) 683.

[55] a) I. Haller, *J. Am. Chem. Soc. 100* (1978) 8050; b) J. D. Miller, H. Ishida, *Surf. Sci. 148* (1984) 601.

[56] a) W. A. Zisman, *Ind. Eng. Chem. Prod. Res. Dev. 8* (1969) 98; b) K. W. Allen, M. G. Stevens, *J. Adhes. 14* (1982) 137.

[57] a) M. R. Rosen, *J. Coat. Technol. 50* (1978) 70; b) H. Ishida, *Polym. Compos. 5* (1984) 101; *Polym. Sci. Technol. 27* (1985) 25; c) S. R. Culler, H. Ishida, J. L. Koenig, *J. Colloid Interface Sci. 106* (1985) 334.

[58] E. P. Plueddemann, *Mod. Plast. 1970* (3), 92.

[59] E. P. Plueddemann: *Silane Coupling Agents*, Plenum Press, New York 1982.

[60] E. P. Plueddemann in *Kirk-Othmer: Encyclopedia of Chemical Technology, Vol. 20*, Wiley, New York 1982, 3rd edit., p. 967.

[61] a) R. C. Hartlein, *Ind. Eng. Chem. Prod. Res. Dev. 10* (1971) 92; b) P. E. Cassidy, B. J. Yager, *J. Macromol. Sci. Rev. Polym. Technol. D1* (1971) 1; c) A. Harnier, *Plastverarbeiter 26* (1975) 299.

[62] a) H. Westlinning, *Kautsch. Gummi Kunstst. 15* (1962) WT 475; b) S. Wolff, *ibid. 27* (1974) 511.

[63] a) E. Heitz, *Gummi Asbest Kunstst. 28* (1975) 286; b) S. Wolff, *Kautsch. Gummi Kunstst. 32* (1979) 312; c) E. M. Dannenberg, *Elastomerics 1981* (12) 30; d) M. P. Wagner: *Additives for Plastics. Vol. 1*, Academic Press, New York 1978, p. 9.

[64] a) E. M. Dannenberg, *Rubber Age 85* (1959) 431; b) J. Shah, E. F. Seeberger, *Gummi Asbest Kunstst. 27* (1974) 592; c) S. Wolff, K. Burmester, E. H. Tan, *Kautsch. Gummi Kunstst. 29* (1976) 691, 766.

[65] H. P. Boehm, *Chem.-Ing.-Tech. 46* (1974) 716.

[66] a) L. P. Ziemianski, C. A. Pagano, M. W. Ranney, *Rubber World 1970* (10) 53; b) M. P. Wagner, *ibid. 1971* (8) 46; c) M. W. Ranney, G. M. Cameron, B. W. Lipinski, *Kautsch. Gummi Kunstst. 26* (1973) 409; d) E. P. Plueddemann, *Dev. Rubber Technol. 1979*, 183.

[67] a) S. Wolff, *Kautsch. Gummi Kunstst. 34* (1981) 280; b) *Rubber Chem. Technol. 55* (1982) 967; c) *Kautsch. Gummi Kunstst. 30* (1977) 516; d) *ibid. 32* (1979) 760; e) *ibid. 36* (1983) 969.

[68] a) F. Thurn, K. Burmester, J. Pochert, S. Wolff, DBP 2255577 (November 13, 1972), Degussa; b) S. Wolff, J. Pochert, F. Thurn, K. Burmester, DBP 2401056 (January 10, 1974), Degussa; c) K. Burmester, S. Wolff, E. Klötzer, F. Thurn, DBP 2447614 (October 5, 1974), Degussa; d) S. Wolff, E. H. Tan, DBP 2536674 (August 18, 1975), Degussa; e) S. Wolff, E. H. Tan, DBP 2848559 (November 9, 1978), Degussa.

[69] a) P. K. Pal, S. K. De, *Rubber Chem. Technol. 56* (1983) 737; b) P. K. Pal, S. N. Chakravarty, S. K. De, *J. Appl. Polym. Sci. 28* (1983) 659.

[70] M. W. Ranney, K. J. Sollman, G. M. Cameron, *Kautsch. Gummi Kunstst. 28* (1975) 597.

[71] S. Wolff, *Kautsch. Gummi Kunstst. 33* (1980) 1000.

[72] a) S. Wolff, E. H. Tan, DOS 2819638 (May 5, 1978); DBP 2933345 (August 17, 1979), both Degussa; b) S. Wolff, L. Rothbühr, H. Grewatta, DBP 2933346 (August 17, 1979), Degussa.

[73] a) D. M. Schwaber, F. Rodriguez, *Rubber Plast. Age 1967* (10) 1081; b) G. W. MacDonald, *Rubber Age 1970* (4) 66; c) T. A. Grillo, *ibid. 1971* (8) 37; d) A. L. Barbour, *ibid. 1972* (11) 44; e) M. W. Ranney, C. A. Pagano, *Rubber Chem. Technol. 44* (1971) 1080.

[74] D. Kerner, P. Kleinschmit, A. Parkhouse, S. Wolff, DOS 3314742 (April 23, 1983), Degussa.

[75] a) G. M. Cameron, M. W. Ranney, K. J. Sollman, *Eur. Rubber J. 1974* (3) 37; b) M. W. Ranney, G. M. Cameron, B. W. Lipinski, *Gummi Asbest Kunstst. 27* (1974) 600; c) C. Hepburn, *Plast. Rubber Int. 9* (1984) (3) 12.

[76] S. Wolff, W. Buder, H. Grewatta, DBP 3319251 (May 27, 1983), Degussa.

[77] H. Lucke in *Ullmann: Encyklopädie der technischen Chemie, Vol. 14*, Verlag Chemie, Weinheim 1977, 4th edit., p. 260.

[78] a) E. G. Millen, US-Pat. 3476826 (May 23, 1966), Thiokol; b) J. L. Speier, J. W. Keil, W. G. Gowdy, US-Pat. 3440302 (March 22, 1965), Dow Corning; c) D. J. Smith, E. H. Sorg, E. V. O'Grady, F. Walters, US-Pat. 3659896 (March 17, 1970), Thiokol; d) M. W. Ranney, R. J. Pickwell, US-Pat. 4000347 (March 27, 1975), Union Carbide; e) R. M. Myers, E. F. Kutch, M. M. Sitter, Fr. Pat. 2321582 (August 18, 1975), Novogard; *Chem. Abstr. 88* (1978) 8672h.

[79] H. Lucke, *Adhäsion 1971* (11) 376.

[80] G. Horn, *Plaste Kautsch. 26* (1979) 634.

[81] a) R. H. Cooper, US-Pat. 3234159 (May 15, 1961), Dow Chemical; b) J. Robins, R. J. Schafer, US-Pat. 3403721 (June 13, 1966), Ashland Oil; c) D. Epstein, J. Bugg, DOS 2236192 (July 24, 1972); d) H. C. Anderson, R. B. Lembke, US-Pat. 4108826 (June 20, 1977); e) R. J. Schafer, R. H. Toeniskoetter, US-Pat. 4124556 (March 16, 1977), Ashland Oil.

[82] a) J. G. Marsden, E. J. Pepe, Eur. Pat.-Anm. 77036 (October 7, 1982), Union Carbide; b) J. G. Marsden, H. E. Petty, A. C. Vecere, P. Morabito, Eur. Pat.-Anm. 114400 (December 27, 1983), Union Carbide.

[83] a) E. P. Plueddemann, *Prog. Org. Coat. 11* (1983) 297; b) F. Liang, P. Dreyfuss, *J. Appl. Polym. Sci. 29* (1984) 3147.

[84] J. Gähde, *Plaste Kautsch. 22* (1975) 626.

[85] a) S. Sterman, J. G. Marsden, *Ind. Eng. Chem. 58* (1966) 33; b) S. Reichel, *Plaste Kautsch. 15* (1968) 501; c) B. W. Lipinski, *Seifen Öle Fette Wachse 98* (1972) 230; d) J. G. Marsden, L. P. Ziemianski, *Br. Polym. J. 1979* (12) 199; e) V. Chvalovsky in V. Chvalovsky, J. M. Baflama (Ed.): *Carbon-Functional Organosilicon Compounds*, Plenum Press, New York 1984, p. 1.

[86] a) L. Horner, A. Christmann, *Angew. Chem. 75* (1963) 707; *Angew. Chem. Int. Ed. Engl. 2* (1963) 599; b) R. A. Abramovitch, B. A. Davis, *Chem. Rev. 64* (1964) 149; c) W. Pritzkow, D. Timm, *J. Prakt. Chem. 32* (1966) 178.

[87] R. W. Layer, *Chem. Rev. 63* (1963) 489.

[88] a) P. J. Orenski, J. G. Marsden, *Tech. Pap. Soc. Plast. Eng. 22* (1976) 68; b) G. A. McFarren, T. F. Sanderson, F. G. Schappell, *Polym. Eng. Sci. 17* (1977) 46.

[89] a) A. Breustedt, K. Felgentreff, *Dtsch. Stomatol. 22* (1972) 676; b) A. Breustedt, K. Felgentreff, D. Wandelt, *ibid. 22* (1972) 825; c) A. Gross, *Chem. Unserer Zeit 13* (1979) 142; d) K.-J. M. Söderholm, *J. Dent. Res. 63* (1984) 1321.

[90] a) J. A. Orlowski, D. V. Butler, Eur. Pat.-Anm. 60911 (March 24, 1981), Blendax; b) T. Fusayama, J. Yamauchi, Eur. Pat.-Anm. 89187 (March 10, 1983), Kuraray; c) W. Podszun, F. Bley, M. Walkowiak, DOS 3316851 (May 7, 1983), Bayer.

[91] a) L. Havestadt, H. Arens, DBP 800685 (March 30, 1949), Goldschmidt; b) J. C. Roediger, US-Pat. 2609305 (July 24, 1947), Standard Oil.

[92] a) R. J. Schmidt, P. E. Graf, US-Pat. 4036661 (February 12, 1973); US-Pat. 4038096 (February 12, 1973), both Chevron; b) K.-H. Müller, W. Barthel, DOS 3028365 (July 26, 1980); DOS 3236381 (October 1, 1982), both Degussa.

[93] a) E. P. Plueddemann, *J. Paint Technol. 40* (1968) 1; *42* (1970) 600; b) P. Walker, *J. Coat. Technol. 52* (1980) 49; *J. Oil Colour Chem. Assoc. 65* (1982) 415, 436; *66* (1983) 188; *67* (1984) 108, 126.

[94] J. Hennig, *Kunststoffe 71* (1981) 103.

[95] a) S. Taniyama, G. Shimaoka, DBP 3003651 (February 1, 1980), Mitsubishi Gas Chemical; b) R. H. Baney, J. R. January, DBP 3014411 (April 15, 1980), Dow Corning; c) K.-P. Jäckel, DOS 3115198 (April 15, 1981), BASF; d) R. Osterloh, K.-P. Jäckel, DOS 3140522 (October 13, 1981), BASF; e) K. L. Benjamin, US-Pat. 4486565 (February 18, 1983), Dow Corning.

[96] a) C. Kirchner, *Adhäsion 1969*, 257; b) D. Gerbet, *Plaste Kautsch. 17* (1970) 813; c) P. E. Cassidy, J. M. Johnson, G. C. Rolls, *Ind. Eng. Chem. Prod. Res. Dev. 11* (1972) 170; d) F. D. Swanson, S. J. Price, *Adhes. Age 1972* (3) 26; *1973* (6) 23; e) K. Kornett, *ZIS Mitt. 26* (1984) 1067.

[97] a) C. U. Pittmann, G. O. Evans, *CHEMTECH 1973*, 560; b) Z. M. Michalska, D. E. Webster, *ibid. 1975*, 117; c) R. H. Grubbs, *ibid. 1977*, 512; d) D. D. Whitehurst, *ibid. 1980*, 44; e) D. C. Bailey, S. H. Langer, *Chem. Rev. 81* (1981) 110.

[98] a) H. Lang, N. Hennrich, H. D. Orth, W. Brümmer, M. Klockow, *Chem.-Ztg. 96* (1972) 595; b) G. P. Royer, *CHEMTECH 1974*, 694; c) K. J. Skinner, *Chem. Eng. News 1975* (August 18), 22; d) R. Keller, E. Fischer, M. Schlingmann, *Chem. Ind. (Düsseldorf) 34* (1982) 524; e) J. F. Kennedy, J. M. S. Cabral in W. H. Scouten (Ed.): *Solid Phase Biochemistry*, Wiley, New York 1983, p. 254.

[99] R. B. Merrifield, *J. Am. Chem. Soc. 85* (1963) 2149; b) K. Hermann, *Chem. Unserer Zeit 11* (1977) 54; c) D. C. Neckers, *J. Chem. Ed. 52* (1975) 695; *CHEMTECH 1978*, 108; d) A. Akelah, D. C. Sherrington, *Chem. Rev. 81* (1981) 557.

[100] a) K. Unger, *Kontakte (Darmstadt) 1979* (2), 32; b) G. Schwedt, *Umschau 79* (1979) 183.

[101] a) K. Unger, K. Berg, D. Nymah, T. Lothe, *Colloid Polym. Sci. 252* (1974) 317; b) F. Martinola, *Chem.-Ing.-Tech. 51* (1979) 728.

[102] K. G. Allum, R. D. Hancock, I. V. Howell, S. McKenzie, R. C. Pitkethly, P. J. Robinson, *J. Organomet. Chem. 87* (1975) 203.

[103] S. P. Hopper, M. J. Tremelling, E. W. Goldman, *J. Organomet. Chem. 191* (1980) 363.

[104] a) J. R. Elliot, R. H. Krieble, US-Pat. 2507200 (February 10, 1945), General Electric; b) H. Arens, DBP 958465 (January 20, 1951), Goldschmidt.

[105] P. Hardt, *Textilveredlung 19* (1984) 143.

[106] a) P. A. Walters, E. A. Abbott, A. J. Isquith, *Appl. Microbiol. 24* (1972) 859; *25* (1973) 253; US-Pat. 3817739 (November 12, 1971); US-Pat. 3865728 (November 12, 1971); US-Pat. 3730701 (May 14, 1971), all

Dow Corning; b) C. A. Roth, DBP 2408192 (February 20, 1974), Dow Corning.
[107] a) W. W. Eudy, US-Pat. 4282366 (November 6, 1979); US-Pat. 4406892 (April 2, 1981), both International Paper Company; b) A. F. Baldwin, US-Pat. 4408996 (October 9, 1981); US-Pat. 4395454 (July 20, 1982); US-Pat. 4411928 (February 24, 1982); US-Pat. 4414268 (October 9, 1981); US-Pat. 4425372 (July 20, 1982); US-Pat. 4467013 (July 20, 1982); all Burlington Industries; c) P. M. Burril, S. Westall, US-Pat. 4421796 (September 24, 1982), Dow Corning.
[108] a) F. J. Kahn, *Appl. Phys. Lett. 22* (1973) 386; b) F. J. Kahn, G. N. Taylor, H. Schonhorn, *Proc. IEEE 61* (1973) 823; c) J. A. Castellano, *Liq. Cryst. Ordered Fluids 1984*, 763; d) M. Kaufmann, H. Schad, US-Pat. 4492432 (July 14, 1981), Brown Boveri.
[109] G. E. Totten, T. C. Williams, US-Pat. 4316041 (February 19, 1980), Union Carbide.
[110] P. N. T. van Velzen, *Surf. Sci. 140* (1984) 437.
[111] a) P. R. Moses, L. Wier, R. W. Murray, *Anal. Chem. 47* (1975) 1882; b) R. J. Burt, G. J. Leigh, C. J. Pickett, *J. Chem. Soc. Chem. Commun. 1976*, 940; c) B. E. Firth, L. L. Miller, *J. Am. Chem. Soc. 98* (1976) 8272; d) G. J. Leigh, C. J. Pickett, *J. Chem. Soc. Dalton Trans. 1977*, 1797; e) A. Diaz, *J. Am. Chem. Soc. 99* (1977) 5838.
[112] P. R. Moses, R. W. Murray, *J. Am. Chem. Soc. 98* (1976) 7435.
[113] N. R. Armstrong, V. R. Shepard, *J. Electroanal. Chem. Interfacial Electrochem. 115* (1980) 253; *131* (1982) 113.
[114] a) A. K. Chatterji, M. Custozzo, D. K. Kiriazides, J. J. Russel, J. P. Serio, US-Pat. 3720617 (May 20, 1970), Xerox; b) H. Oguchi, K. Saito, T. Kubo, Jap. Pat. 77135739 (May 10, 1976), Toshiba; *Chem. Abstr. 88* (1978) 161450d; c) N. Furuya, T. Morii, Jap. Pat. 8299350 (June 11 1982), Nippon Aerosil; d) M. Takenouchi, S. Urawa, DOS 3330380 (August 23, 1983), Canon.
[115] a) A. H. Al-Taiar, J. R. Lindsay Smith, D. J. Waddington, *Anal. Chem. 42* (1970) 935; b) J. J. De Stefano, J. J. Kirkland, *J. Chromatogr. Sci. 12* (1974) 337; c) I. Sebestian, I. Halasz, *Adv. Chromatogr. 1976*, 75; d) J. K. Haken, *J. Chromatogr. 300* (1984) 1.
[116] a) R. E. Leitch, J. J. De Stefano, *J. Chromatogr. Sci. 11* (1973) 105; b) D. C. Locke, *ibid. 11* (1973) 120; c) E. Grushka, E. J. Kikta, *Anal. Chem. 49* (1977) 1004A; d) G. B. Cox, *J. Chromatogr. Sci. 15* (1977) 385.
[117] a) R. E. Majors, *J. Chromatogr. Sci. 15* (1977) 334; *18* (1980) 488; b) R. E. Majors, H. G. Barth, C. H. Lochmueller, *Anal. Chem. 54* (1982) 323R; *56* (1984) 300R.
[118] a) U. A. T. Brinkmann, G. De Vries, *J. High Resolut. Chromatogr. Chromatogr. Commun. 5* (1982) 476; b) T. Omori, M. Okamoto, F. Yamada, *Chromatographia 1982*, 152; *J. High Resolut. Chromatogr. Chromatogr. Commun. 6* (1983) 47; c) H. E. Hauck, W. Jost, *GIT Suppl. 3: Chromatogr. 1983*, 3; *Anal. Biochem. 135* (1983) 120; d) L. W. Doner, C. L. Fogel, L. M. Biller, *Carbohydr. Res. 125* (1984) 1.
[119] a) K. Karch, I. Sebestian, I. Halasz, *J. Chromatogr. 122* (1976) 3; b) H. Colin, G. Guiochon, *ibid. 141* (1977) 289; c) P. Roumeliotis, K. K. Unger, *ibid. 149* (1978) 211; d) N. H. C. Cooke, K. Olsen, *Am. Lab. (Fairfield, Conn.) 11* (1979) 45; *J. Chromatogr. Sci. 18* (1980) 512; e) W. R. Melander, C. Horvath, *ibid. 15* (1977) 393; *High-Perform. Liq. Chromatogr. 1980*, 113.
[120] a) A. Pryde, *J. Chromatogr. Sci. 12* (1974) 486; b) K. K. Unger, N. Becker, P. Roumeliotis, *J. Chromatogr. 125* (1976) 115; c) P. Roumeliotis, K. K. Unger, *ibid. 185* (1979) 445; d) N. Becker, K. Unger, *Fresenius Z. Anal. Chem. 304* (1980) 374.
[121] a) R. E. Majors, M. J. Hopper, *J. Chromatogr. Sci. 12* (1974) 767; b) S. A. Wise, S. N. Chesler, H. S. Hertz, L. R. Hilpert, W. E. May, *Anal. Chem. 49* (1977) 2306.
[122] a) R. K. Gilpin, W. R. Sisco, *Anal. Chem. 50* (1978) 1337; b) E. L. Weiser, A. W. Salotto, S. M. Flach, L. R. Snyder, *J. Chromatogr. 303* (1984) 1.
[123] a) I. Sebestian, Brit. Pat. 1506226 (May 29, 1975); b) R. D. Hancock, J. M. Kirk, Eur. Pat. 8902 (August 20, 1979), BP; c) N. Weigand, I. Sebestian, I. Halasz, *J. Chromatogr. 102* (1979) 325; d) A. K. Roy, A. Burgum, S. Roy, *J. Chromatogr. Sci. 22* (1984) 84.
[124] a) F. Meiller, DOS 2433409 (July 11, 1974), Rhone-Progil; b) M. Caude, R. Rosset, *J. Chromatogr. Sci. 15* (1977) 405; c) S. R. Abbott, US-Pat. 4290892 (March 2, 1979); d) S. R. Abbott, US-Pat. 4322542 (January 17, 1980); US-Pat. 4430496 (March 16, 1982), all Varian.
[125] a) C. H. Lochmüller, C. W. Amoss, *J. Chromatogr. 108* (1975) 85; b) C. H. Lochmüller, R. R. Ryall, C. W. Amoss, *ibid. 178* (1979) 298.
[126] a) N. H. C. Cooke, R. L. Viavattene, R. Eksteen, W. S. Wong, G. Davies, B. L. Karger, *J. Chromatogr. 149* (1978) 391; b) F. K. Chow, E. Grushka, *ibid. 185* (1979) 361.
[127] a) G. R. Gray, *Anal. Chem. 52* (1980) 9R; b) W. H. Scouten in W. H. Scouten (Ed.): *Solid Phase Biochemistry*, Wiley, New York 1983, p. 1.
[128] a) R. D. Hancock, I. V. Howell, Brit. Pat. 1503315 (May 28, 1974); US-Pat. 4203952 (September 8, 1977), both BP; b) L. J. Crane, R. Ganapathy, Eur. Pat.-Anm. 106327 (October 13, 1983), Baker Chemical; c) E. P. Plueddemann, US-Pat. 4448694 (September 4, 1981), Dow Corning.
[129] a) G. D. Schucker, K. F. Sugarvara, H. H. Weetoll, US-Pat. 3886080 (September 4, 1973), Corning Glass; *Anal. Chem. 46* (1974) 489; b) R. D. Hancock, I. V. Howell, Brit. Pat. 1530039 (July 9, 1976); Brit. Pat. 1532295 (July 29, 1976), both BP; c) E. P. Plueddemann, US-Pat. 4071546 (August 30, 1976), Dow Corning; d) R. D. Hancock, J. M. Kirk, Eur. Pat.-Anm. 11484 (November 14, 1979), BP.
[130] a) D. E. Leyden, G. H. Luttrell, *Anal. Chem. 47* (1975) 1612; b) D. E. Leyden, G. H. Luttrell, W. K. Nonidez, D. B. Werho, *ibid. 48* (1976) 67; c) F. K. Chow, E. Grushka, *ibid. 50* (1978) 1346; *J. Chromatogr. 199* (1980) 283; d) T. Seshadri, A. Kettrup, *Fresenius Z. Anal. Chem. 296* (1979) 247; e) D. E. Leyden, D. S. Kendall, L. W. Burggraf, F. J. Pern, M. De Bello, *Anal. Chem. 54* (1982) 101.
[131] a) G. B. Cox, C. R. Loscombe, M. J. Slucutt, K. Sugden, J. A. Upfield, *J. Chromatogr. 117* (1976) 269; b) P. Tundo, P. Venturello, E. Angeletti, *J. Am. Chem. Soc. 104* (1982) 6547.
[132] W. T. Ford, *CHEMTECH 1984*, 436.
[133] a) F. Rolla, W. Roth, L. Horner, *Naturwissenschaften 64* (1977) 337; b) P. Tundo, P. Venturello, *J. Am. Chem. Soc. 101* (1979) 6606; *103* (1981) 856; c) P. Tundo, P. Venturello, E. Angeletti, *ibid. 104* (1982) 6551.
[134] J. Evans, B. P. Gracey, *J. Chem. Soc. Chem. Commun. 1980*, 852.
[135] a) P. Panster, W. Buder, P. Kleinschmit, DBP 2834691 (August 8, 1978), Degussa; b) P. Panster, W. Buder, P. Kleinschmit, DBP 2858038 (August 8, 1978), Degussa.
[136] a) K. G. Allum, R. D. Hancock, I. V. Howell, R. C. Pitkethly, P. J. Robinson, *J. Catal. 43* (1976) 322; b) L. Horner, H. Ziegler, *Justus Liebigs Ann. Chem. 1976*, 628; c) L. Horner, F. Schumacher, *ibid. 1976*, 633; d) Y-Z. Zhou, Y.-Y. Jiang, *J. Organomet. Chem. 251* (1983) 31.
[137] T. O. Mitchell, D. D. Whitehurst, US-Pat. 3980583 (February 19, 1974); US-Pat. 4400561 (December 10, 1981), both Mobil Oil.
[138] a) H. Knözinger, E. Rumpf, *Inorg. Chim. Acta 30* (1978) 51; b) E. W. Thornton, H. Knözinger, B. Tesche, J. J. Rafalko, B. C. Gates, *J. Catal. 62* (1980) 117.
[139] a) H. Schumann, G. Cielusek, S. Jurgis, E. Hahn, J. Pickardt, J. Blum, Y. Sasson, A. Zoran, *Chem. Ber. 117* (1984) 2825; b) R. E. Williams, US-Pat. 4503160 (August 29, 1983), General Electric.
[140] a) I. V. Howell, P. J. Robinson, Brit. Pat. 1418786 (April 4, 1973); b) Z. Kozak, M. Capka, *Collect. Czech. Chem. Commun. 44* (1979) 2624; c) M. Czakova, M. Capka, *J. Mol. Catal. 11* (1981) 313; d) Z. M. Michalska, M. Capka, J. Stoch, *ibid. 11* (1981) 323; e) B. Marciniec, W. Urbaniak, P. Pawlak, *ibid. 14* (1982) 323.
[141] M. Capka, J. Hetflejs, *Collect. Czech. Chem. Commun. 39* (1974) 154.
[142] a) H. W. Weetall, *Methods Enzymol. 44* (1966) 134; *Res. Dev. 1971* (12) 18; b) J. J. Hansen, J. C. Thygesen, M. Winther-Nielsen, Eur. Pat.-Anm. 131251 (July 4, 1984).
[143] H. Mazarguil, F. Meiller, P. Monsan, US-Pat. 4034139 (April 16, 1975), Rhone Poulenc.
[144] W. Haller in W. H. Scouten (Ed.): *Solid Phase Biochemistry*, Wiley, New York 1983, p. 535.
[145] a) H. H. Weetall, *Anal. Chem. 46* (1974) 602A; b) L. D. Bowers, P. W. Carr, *ibid. 48* (1976) 544A; c) H. Nishikawa in W. H. Scouten (Ed.): *Solid Phase Biochemistry*, Wiley, New York 1983, 17.
[146] a) J. F. Rusling, G. H. Luttrell, L. F. Cullen, G. J. Papariello, *Anal. Chem. 48* (1976) 1211; b) R. S. Schifreen, D. A. Hanna, L. D. Bowers, P. W. Carr, *ibid. 49* (1977) 1929.
[147] a) E. Wachter, H. Hofner, W. Machleidt, *Solid-Phase Methods Protein Sequence Anal., Proc. Int. Conf., 1st* 1975, 31; b) W. Machleidt, E. Wachter, *Methods Enzymol. 47* (1977) 263.
[148] P. Panster, W. Buder, P. Kleinschmit, DBP 2858037 (August 8, 1978), Degussa.
[149] a) P. Panster, P. Kleinschmit, DOS 3029599 (August 5, 1980), Degussa; b) P. Panster, P. Kleinschmit, DBP 3050815 (August 5, 1980), Degussa.
[150] a) P. Panster, W. Buder, P. Kleinschmit, DBP 3120214 (May 21, 1981), Degussa; b) P. Panster, P. Kleinschmit, DBP 3131954 (August 13, 1981), Degussa.
[151] a) P. Panster, M. Englisch, P. Kleinschmit, DOS 3404702 (February 10, 1984), Degussa; b) P. Panster, R. Michel, W. Buder, P. Kleinschmit, DOS 3404703 (February 10, 1984), Degussa.
[152] P. Panster, P. Kleinschmit, US-Pat. 4410669 (May 10, 1982), Degussa.
[153] a) P. Panster, W. Buder, R. Gradl, P. Kleinschmit, DOS 3226091 (July 10, 1982), Degussa; b) P. Panster, H. Grethe, P. Kleinschmit, DOS 3226093 (July 13, 1982), Degussa.

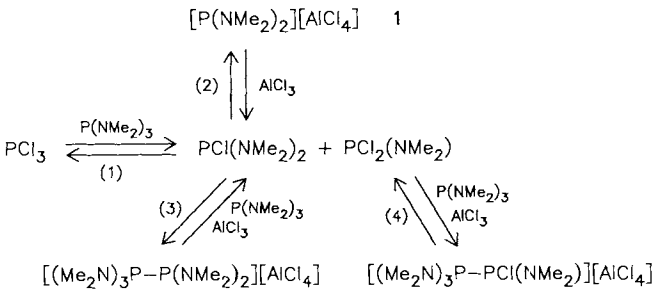
When submitting manuscripts, authors of articles intended for publication as "Communications" are requested to read the "Notice to Authors" reproduced in the January issue of the journal following the list of contents; upon request, a copy can be obtained from the editorial office.

New Products from PCl_3, $P(NMe_2)_3$, and $AlCl_3$**

By *Alfred Schmidpeter** and *Siegfried Lochschmidt*

Dedicated to Professor Rolf Appel on the occasion of his 65th birthday

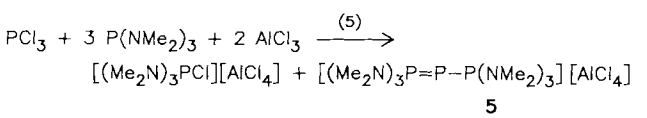
PCl_3 reacts with $P(NMe_2)_3$, resulting in substituent exchange [reaction (1)].[1] When $AlCl_3$ is present as a third component, the phosphenium tetrachloroaluminate **1** and phosphonium tetrachloroaluminates **2** and **3** are formed according to reactions (2) to (4).[2]



Because PCl_3, Ph_3P, and $AlCl_3$ undergo a redox reaction to give the triphosphenium salt **4**,[3]

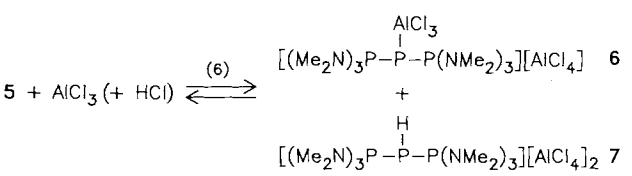
$[Ph_3P{=}P{-}PPh_3][AlCl_4]$ **4**

it was of interest to find out whether the system PCl_3/$P(NMe_2)_3$/$AlCl_3$ could undergo the corresponding reaction (5) to form **5**. The theoretically required molar ratio of the reactants $PCl_3 : P(NMe_2)_3 : AlCl_3$ (1 : 3 : 2) for the formation of **5** lies just between that for the formation of **3** (1 : 2 : 1.5) and that for the formation of **2** (1 : 5 : 3). Compound **5** had been synthesized earlier from **4** by means of $Ph_3P/P(NMe_2)_3$ exchange and proved to be stable,[3] so that we undertook a new investigation of the system PCl_3/$P(NMe_2)_3$/$AlCl_3$.

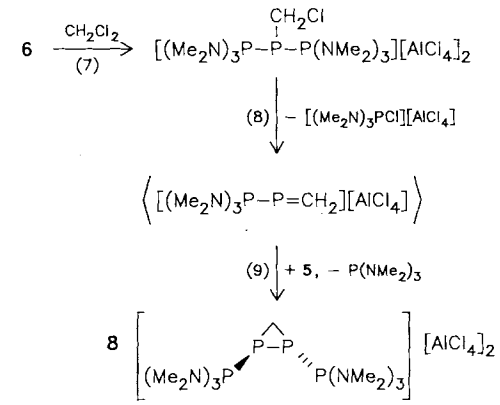


We found that the sequence in which the reactants are added determines the products of the reaction: If a 1 : 3 mixture of PCl_3 and $P(NMe_2)_3$ in CH_2Cl_2 is initially prepared, so that the substituent-exchange reaction (1) can occur, then the subsequently added $AlCl_3$ reacts according to reactions (2) to (4). The reactions are reversible and, as expected from the stoichiometry, reaction (2) becomes predominant with increasing amounts of $AlCl_3$; when $AlCl_3 : PCl_3$ is 4 : 1, it is virtually the only reaction. On the other hand, if $P(NMe_2)_3$ and $AlCl_3$ in a molar ratio of 3 : 2 are dissolved in CH_2Cl_2 at 0 °C (cf. ref. [2]) and subsequently treated with PCl_3, then reductive formation of **5** takes place according to reaction (5).

Products **1** and **5**, formed via these two pathways, cannot be interconverted. Although different ratios of the reactants (1 : 2 : 3 and 1 : 3 : 2, respectively) are involved in their formation, subsequent compensation (i.e., addition of $P(NMe_2)_3$ or $P(NMe_2)_3/PCl_3$ mixtures to **1** or of $AlCl_3$ to **5**/$[(Me_2N)_3PCl][AlCl_4]$ does not effect the desired change.



With an equimolar amount of $AlCl_3$, **5**, in a fast reaction, gives the adduct **6** [reaction (6)].[4] A small amount of the product **7**[5] is also formed by addition of HCl (presumably from the solvent) (cf. ref. [3, 6]). Over approximately a week at room temperature, compound **6** reacts completely with CH_2Cl_2 to give the diphosphoniodiphosphirane tetrachloroaluminate **8**.[7] Although no intermediates can be observed, comparable reactions suggest that initial chloromethylation occurs [reaction (7)][3,6] followed by cleavage of the resulting intermediate [reaction (8)] and formation of the three-membered-ring compound **8** by [2 + 1] addition of a phosphoniophosphanediyl (formed by dissociation of **5**; cf. ref. [8]) to the P=C system [reaction (9)]. Like di-*tert*-butyldiphosphirane,[9] **8** is formed as the *trans* isomer and is characterized by a ^{31}P-NMR spectrum[7] of the $[AB]_2$ type.

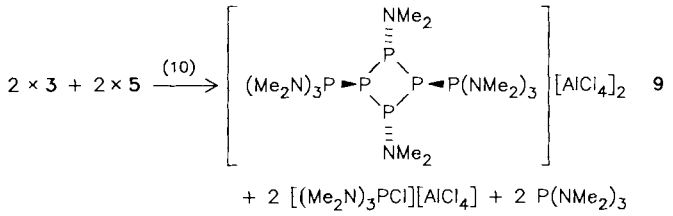


If PCl_3 is added, as described above, at 0 °C to a $P(NMe_2)_3/AlCl_3$ mixture, which, however, contains less $AlCl_3$ (molar ratio 1 : 3 : 1), then $AlCl_3$ is consumed only

[*] Prof. Dr. A. Schmidpeter, Dr. S. Lochschmidt
Institut für Anorganische Chemie der Universität
Meiserstrasse 1, D-8000 München 2 (FRG)

[**] This work was supported by the Deutsche Forschungsgemeinschaft and the Fonds der Chemischen Industrie.

according to reaction (5). The remaining half of the $P(NMe_2)_3$ and PCl_3 undergoes substituent exchange (1) and reacts with subsequently added $AlCl_3$ to give **3** according to reaction (4). If more $AlCl_3$ is added, reaction (10) occurs, resulting in an equal decrease in the amounts of **3** and **5** and in the formation of a new product. On the basis of the ^{31}P-NMR spectrum ($[AB]_2C_2$ spin system),[10] this product was identified as the 1,3-diphosphoniocyclotetraphosphane **9** (all-*trans* isomer, cf. ref. [9]).



Depending on the sequence of addition, therefore, the three-component system $PCl_3/P(NMe_2)_3/AlCl_3$ may be used to prepare either the salt **1**, **5**, or **9**, whereby the oxidation state n/3 of phosphorus steadily decreases: n = 9, 7, 5. Consequently, the amount of $[(Me_2N)_3PCl][AlCl_4]$ formed also steadily increases. The reaction to give the product with n = 3 (reduction of Me_2NPCl_2 to $(Me_2NP)_x$) has not yet been possible.[11]

Owing to the competing and subsequent reactions, reaction (5) is not well suited for the preparative formation of **5**. On the other hand, the tetraphenylborate[8] of the same cation

$[(Me_2N)_3P{=}P{-}P(NMe_2)_3][BPh_4]$ **10**

may be synthesized analogously and in a facile manner by addition of PCl_3 to $P(NMe_2)_3/NaBPh_4$.[12]

Received: August 14, 1985;
revised: October 21, 1985 [Z 1429 IE]
Publication delayed at the authors' request
German version: *Angew. Chem. 98* (1986) 271

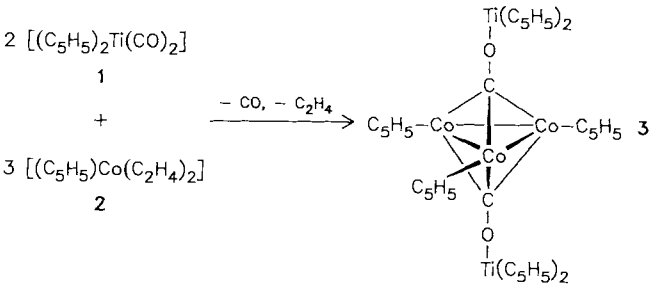
[1] J. R. Van Wazer, L. Maier, *J. Am. Chem. Soc. 86* (1964) 811.
[2] C. W. Schultz, R. W. Parry, *Inorg. Chem. 15* (1976) 3046.
[3] A. Schmidpeter, S. Lochschmidt, W. S. Sheldrick, *Angew. Chem. 97* (1985) 214; *Angew. Chem. Int. Ed. Engl. 24* (1985) 226.
[4] ^{31}P-NMR of **6** (AB_2): $\delta_A = -142$, $\delta_B = +70$; $J_{AB} = 290$ Hz.
[5] ^{31}P-NMR of **7** (AB_2): $\delta_A = -131$, $\delta_B = +63$; $J_{AB} = 270$ Hz, $^1J_{PH} = 241$ Hz.
[6] A. Schmidpeter, S. Lochschmidt, K. Karaghiosoff, W. S. Sheldrick, *J. Chem. Soc. Chem. Commun. 1985*, 1447.
[7] ^{31}P-NMR of **8** ($AA'BB'$): $\delta_A = -198$ (ring phosphorus), $\delta_B = +67$ (phosphonio group); $J_{AA'} = \mp 120$ Hz, $J_{AB} = \mp 312$ Hz, $J_{AB'} = \pm 47$ Hz, $J_{BB'} = \mp 48$ Hz. An X-ray structure investigation has been carried out on a differently substituted diphosphoniodiphosphirane. S. Lochschmidt, G. Müller, B. Huber, A. Schmidpeter, *Z. Naturforsch. B41* (1986), in press.
[8] A. Schmidpeter, S. Lochschmidt, A. Willhalm, *Angew. Chem. 95* (1983) 561; *Angew. Chem. Int. Ed. Engl. 22* (1983) 545; *Angew. Chem. Suppl. 1983*, 710.
[9] M. Baudler, F. Saykowski, *Z. Naturforsch. B33* (1978) 1208; M. Baudler, G. Reuschenbach, *Z. Anorg. Allg. Chem. 464* (1980) 9.
[10] ^{31}P-NMR of **9** ($AA'BB'C_2$): $\delta_A = -24$ (phosphonio-substituted ring phosphorus), $\delta_C = +18$ (amino-substituted ring phosphorus, cf. [11]), $\delta_B = +69$ (phosphonio groups).
[11] R. B. King, N. D. Sadanani, P. M. Sundaram, *Phosphorus Sulfur 18* (1983) 125.
[12] *Experimental procedure:* **10**: PCl_3 (0.78 mL, 8.4 mmol) was added with vigorous stirring to $P(NMe_2)_3$ (4.74 mL, 26.1 mmol) and $NaBPh_4$ (6.00 g, 17.4 mmol) in 120 mL of dimethoxyethane. After 2 h, the colorless precipitate was separated and extracted with 100 mL of CH_2Cl_2. After concentration of the extracts by a factor of ten, crystallization occurred to give 3.92 g (69%) of **10**: m.p. = 161 °C; ^1H-NMR: $\delta = 2.76$, $J_{PNCH} = 10.7$ Hz.—^{31}P-NMR (AB_2): $\delta_A = -194$, $\delta_B = +85$; $J_{AB} = 513$ Hz (cf. [3]).

Synthesis and Structure of the Co_3Ti_2 Complex $[\{\mu_3\text{-}[(C_5H_5)_2TiOC]\}_2\{(C_5H_5)_3Co_3\}]$: CO Reduction by Two Different Metal Centers

By *Sandro Gambarotta, Sergio Stella, Carlo Floriani,* Angiola Chiesi-Villa,* and *Carlo Guastini*

Metal-oxygen bond formation is the driving force for the reduction of carbon monoxide by early transition metals. For example, CO is reduced by ZrH complexes to methanol, formaldehyde, and C_2 compounds.[1] The reductive coupling of CO is achieved by reaction of $[(C_5H_5)_2Fe_2(\mu\text{-}CO)_2(CO)_2]$ with $[(C_5H_5)_2ZrN_2]_2N_2$.[2] Other metal carbonyls react with oxophilic metal complexes in low oxidation states, electron transfer occurring from the oxophilic metal center to the metal atom of the carbonyl complex; this provides a strong acidic site for the carbonyl's oxygen.[3] In this way, $[(C_5Me_5)_2Yb\text{-}OC\text{-}Co(CO)_3]$[4] and $[(C_5H_5)_2(thf)Ti\text{-}OC\text{-}Mo(CO)_2(C_5H_5)]$[5] were obtained. These reactions are not real reductions of CO, because the fragment $\geqslant C{-}O{-}M$ (M = early transition metal) is not formed. A few examples of such reductions are provided by the reactions of $[(C_5Me_5)_2V]$[6] and $[C_5H_5)Ti(CO)_2]$[7] with $Co_2(CO)_8$ to form the complex $[(CO)_9Co_3CO\text{-}M]$. Indeed, this type of complex is very well documented when M = Ti, Zr, and Hf in the form of cyclopentadienyl derivatives.[8] These compounds were synthesized, however, by the metathesis reaction between $[(CO)_9Co_3COLiS_n]$ and $[(C_5H_5)_2MCl_2]$ derivatives or by the reaction between $[(C_5H_5)_2MCl_2]$ and $Co_2(CO)_8$.[8]

We report here the reduction of CO to a $\geqslant C{-}O{-}$ ligand promoted by a Ti^{II} complex acting as a one-electron reducing agent. This result was achieved by reaction of the titanium complex **1** with an equimolar amount of the cobalt complex **2** in toluene.[9] The solution was gently heated to 50 °C for a few minutes, then allowed to stand at room temperature for one day. Crystals of the air-sensitive Co_3Ti_2 complex **3** formed (yield: ca. 55%).



The Ti atoms in **3** have an oxidation number of +3 [$\mu_{eff} = 1.85$ BM at 293 K per titanium]. The IR spectrum shows a broad, strong CO band centered at $\tilde{\nu} = 1300\ cm^{-1}$. The structure of **3** (Fig. 1)[10] consists of an equilateral triangle of Co atoms, each of which is bonded to an η^5-

[*] Prof. Dr. C. Floriani [+], Dr. S. Gambarotta, S. Stella
Dipartimento di Chimica e Chimica Industriale,
Università di Pisa
I-56100 Pisa (Italy)
Dr. A. Chiesi-Villa, Dr. C. Guastini
Istituto di Strutturistica Chimica,
Centro di Studio per la Strutturistica Diffrattometrica del CNR,
Università di Parma
I-43100 Parma (Italy)
[+] Present address:
Chemistry Department, Columbia University
Havemeyer Hall, Box 307, New York, NY 10027 (USA)

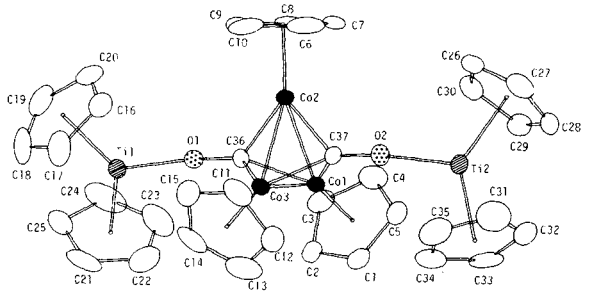


Fig. 1. Crystal structure of **3** [10]. Important bond lengths [Å] and bond angles [°]: Co1-Co2 2.404(2), Co1-Co3 2.385(2), Co2-Co3 2.401(2), Co1-C36 1.88(1), Co1-C37 1.87(1), Co2-C36 1.91(1), Co2-C37 1.89(1), Co3-C36 1.87(1), Co3-C37 1.88(1), Ti1-O1 1.89(1), Ti2-O2 1.91(1), O1-C36 1.30(2), O2-C37 1.29(2); Co2-Co1-Co3 60.2(1), Co1-Co2-Co3 59.5(1), Co1-Co3-Co2 60.3(1), Ti1-O1-C36 164.6(8), Ti2-O2-C37 160.2(8).

cyclopentadienyl ligand that is nearly perpendicular to the plane defined by the three Co atoms; the dihedral angles range from 87.9(3) to 89.5(4)°. A $(C_5H_5)_2TiOC$ group caps each of the two faces of the Co_3 triangle; the C–O bonds are nearly perpendicular to the Co_3 plane (89.1(1)°). Co–C and Ti–O bond distances are very close to those found in $[Co_3(CO)_9(\mu_3\text{-}C{-}O{-}MX(C_5H_5)_2)]$.[8] The C–O bond distances (ca. 1.30 Å) indicate, as expected, a reduced form of carbon monoxide. The large C–O–Ti angles (164.6(8) and 160.2(8)°) are probably due to a partial double bond between titanium and oxygen. A strong band centered at $\tilde{\nu} = 795\ cm^{-1}$ can be assigned to the Ti–O vibration. Bond distances within the $[(C_5H_5)_3Co_3]$ fragment are very close to those found in $[(C_5H_5)_3Co_3(CO)_3]$,[11] $[(C_5H_5)_3Co_3(\mu_3\text{-}CMe)(\mu_3\text{-}CCO_2Me)]$,[12] and $[(C_5H_5)_4Co_4(CO)_2]$[13] complexes. Complex **3** may be regarded as the two-electron reduction product of the $[(C_5H_5)_3Co_3(CO)_3]$ cluster.[11,14]

Received: October 15, 1985 [Z 1498 IE]
German version: *Angew. Chem. 98* (1986) 283

[1] P. T. Wolczanski, J. E. Bercaw, *Acc. Chem. Res. 13* (1980) 121; S. Gambarotta, C. Floriani, A. Chiesi-Villa, C. Guastini, *J. Am. Chem. Soc. 105* (1983) 1690; G. Erker, *Acc. Chem. Res. 17* (1984) 103.

[2] D. H. Berry, E. J. Bercaw, A. J. Jircitano, K. B. Mertes, *J. Am. Chem. Soc. 104* (1982) 4712; C. P. Casey, R. F. Jordan, A. L. Rheingold, *Organometallics 3* (1984) 504.

[3] C. P. Horwitz, D. F. Shriver, *Adv. Organomet. Chem. 23* (1984) 219; W. A. Herrmann, *Angew. Chem. 94* (1982) 118; *Angew. Chem. Int. Ed. Engl. 21* (1982) 117.

[4] T. D. Tilley, R. A. Andersen, *J. Chem. Soc. Chem. Commun. 1981*, 985; *J. Am. Chem. Soc. 104* (1982) 1772; J. M. Boncella, R. A. Andersen, *Inorg. Chem. 23* (1984) 432.

[5] J. S. Merola, R. A. Gentile, G. B. Ansell, M. A. Modrick, S. Zentz, *Organometallics 1* (1982) 1731.

[6] J. Martin, C. Moise, *J. Organomet. Chem. 232* (1982) C 55; C. Moise, J. F. Reynoud, J. C. Leblanc, R. Broussier, *ibid. 240* (1982) C 15.

[7] G. Fochi, C. Floriani, unpublished results.

[8] G. Schmid, V. Batzel, B. Stutte, *J. Organomet. Chem. 113* (1976) 67; B. Stutte, G. Schmid, *ibid. 155* (1978) 203; G. Schmid, B. Stutte, R. Boese, *Chem. Ber. 111* (1978) 1239, 1603.

[9] K. Jonas, E. Deffense, D. Habermann, *Angew. Chem. 95* (1983) 729; *Angew. Chem. Int. Ed. Engl. 22* (1983) 716; *Angew. Chem. Suppl. 1983*, 1005.

[10] Space group $P\bar{1}$, $a = 13.783(3)$, $b = 12.871(3)$, $c = 12.355(3)$ Å, $\alpha = 102.05(2)$, $\beta = 108.55(2)$, $\gamma = 69.50(2)°$; $V = 1934.6(8)$ Å^3, $Z = 2$, $\rho_{calcd} = 1.50$ g cm^{-3}; $F(000) = 896$, $\lambda(Mo_{K\alpha}) = 0.71069$ Å, $\mu(Mo_{K\alpha}) = 16.85$ cm^{-1}. The structure was solved by MULTAN and refined anisotropically for all nonhydrogen atoms except for the carbon atoms of the toluene solvent molecule, which was found to be disordered over two positions. The hydrogen atoms were introduced in calculated positions for the final refinement ($U_{iso} = 0.100$ Å^2). 3683 unique observed reflections [$I > 3\sigma(I)$] collected at room temperature ($6° < 2\theta < 47°$), $R = 0.068$. Intensities were corrected for absorption. Further details of the crystal structure investigation are available on request from the director of the Cambridge Crystallographic Data Centre, University Chemical Laboratory, Lensfield Road, Cambridge CB2 1EW (England) on quoting the full journal citation.

[11] F. A. Cotton, J. D. Jamerson, *J. Am. Chem. Soc. 98* (1976) 1273; W. I. Bailey, F. A. Cotton, J. D. Jamerson, B. W. S. Kolthammer, *Inorg. Chem. 21* (1982) 3131.

[12] H. Yamazaki, Y. Wakatsuki, K. Aoki, *Chem. Lett. 1979*, 1041.

[13] S. Gambarotta, C. Floriani, A. Chiesi-Villa, C. Guastini, *J. Organomet. Chem. 296* (1985) C 6.

[14] R. B. King, *Inorg. Chem. 5* (1966) 2227; K. P. C. Vollhardt, J. E. Bercaw, R. G. Bergman, *J. Organomet. Chem. 97* (1975) 283; W. S. Lee, H. H. Brintzinger, *ibid. 127* (1977) 87.

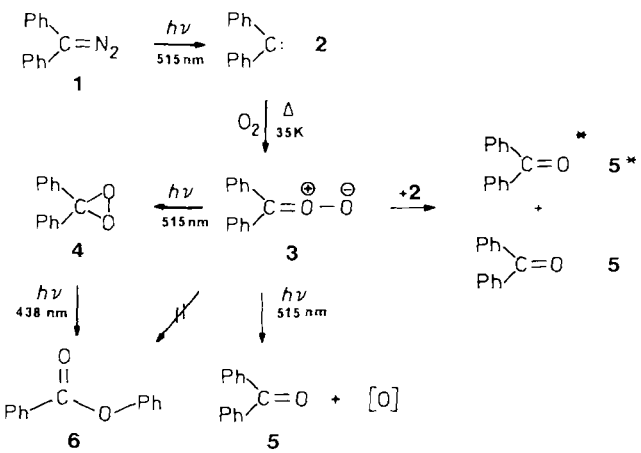
Benzophenone *O*-Oxide**

By *Wolfram Sander**

Carbonyl oxides are important intermediates in the ozonolysis of olefins, in the oxidation of carbenes with molecular oxygen,[1-5] and presumably also in enzymatic oxygenations.[6] Despite this importance, only the resonance-stabilized cyclopentadienone *O*-oxide[2,3a] and its benzannulated derivatives[3c] have been characterized spectroscopically following matrix isolation in argon or nitrogen. For benzophenone *O*-oxide **3**, which has been extensively studied by trapping experiments in solution, the only spectroscopic evidence available is a UV/VIS spectrum from a laser photolysis experiment.[1] The structure, whether open-chain or cyclic (dioxirane), could not be determined.[1a] Attempts to isolate **3** in a matrix failed on account of the instability of this compound.[2]

The IR and UV/VIS spectroscopic characterization of matrix-isolated benzophenone *O*-oxide **3** is reported here. This technique also made possible the elucidation of the photochemistry of **3** as well as of the mechanism of chemiluminescence in the oxidation of **2**.

Diphenylcarbene **2** was generated by photolysis ($\lambda > 515$ nm, 8 K) of matrix-isolated diphenyldiazomethane **1**[2] and characterized by comparison of the IR and UV spectra (cf. Fig. 1 and 2) with literature data.[2,4] By doping the argon matrix with 0.5–15% O_2, we found increasing amounts of oxidation products with increasing oxygen content. Because the diffusion of O_2 in solid argon at 8 K is very slow,[7,8] **2** is only oxidized, under these conditions, by O_2 molecules in the immediate proximity of the carbene



[*] Dr. W. Sander
Organisch-chemisches Institut der Universität
Im Neuenheimer Feld 270, D-6900 Heidelberg (FRG)

[**] This work was supported by the Deutsche Forschungsgemeinschaft. I thank Prof. Dr. *R. Gleiter* for his support.

center. When the O_2 content was 1%, free carbene **2** was still present in addition to the oxidation products. Therefore, the experiments described here were carried out at this O_2 concentration.

The reaction between **2** and O_2 was controlled by varying the temperature of the matrix. If the matrix was warmed slowly (1 K/min) from 8 K to 45 K (softening of the matrix) and then cooled again to 8 K, **2** underwent almost complete conversion, and an intense yellow color indicated the formation of a new species. The UV/VIS maximum of this new compound at 422 nm (Fig. 2) agrees well with that of **3** found by *Scaiano* et al. in a laser photolysis experiment (acetonitrile, room temperature).[1a,b]

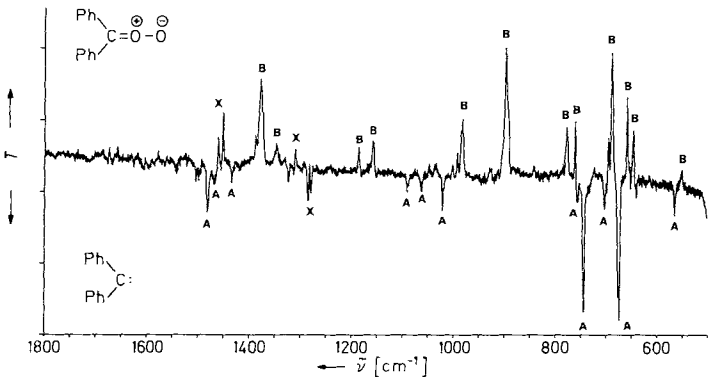


Fig. 1. Difference IR spectrum of the reaction $2 + O_2 \rightarrow 3$. The spectrum shows the changes that occur after warming the matrix from 8 K to 40 K over 20 min. Bottom part: before reaction; top part: after reaction. A, diphenylcarbene **2**; B, benzophenone *O*-oxide **3**; X, unknown side products and bands that were not completely subtracted.

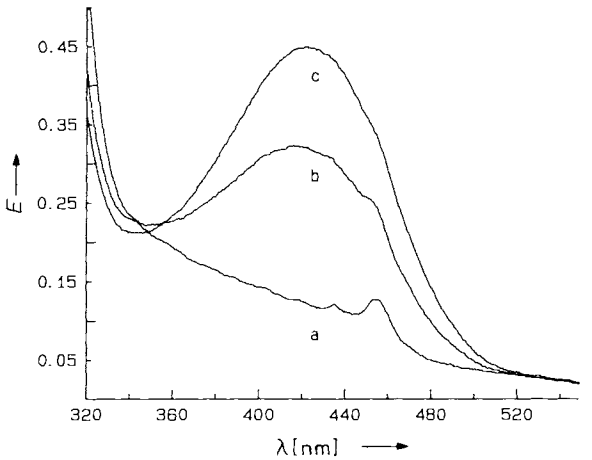


Fig. 2. UV spectra of the reaction $2 + O_2 \rightarrow 3$. a) Diphenylcarbene in Ar/O_2 at 8 K; b) after warming the matrix over 10 min to 35 K, **2** has undergone partial reaction; c) after warming the matrix over 10 min to 40 K, **2** has undergone complete conversion to **3** ($\lambda_{max} = 422$ nm).

The assignment of IR bands to **3** was achieved by observing the changes in the IR spectrum during an analogous annealing experiment (Fig. 1).[9] Noteworthy is the good agreement of the bands at 1377 (m), 1185 (w), 1158 (w), 983 (m), and 897 (s) cm^{-1} with corresponding bands of cyclopentadienone *O*-oxide.[10] This is presumably due to the large contribution of O-O and C-O vibrations to these bands. In order to allow more exact assignments, the experiments were repeated with $^{18}O_2$-containing matrices. The bands listed above exhibited the strongest isotopic shifts in the IR spectrum.[9] On the basis of the band position and the isotopic shift (35 cm^{-1}) and in agreement with studies on alkyl peroxides,[11] we assign the band at 897 cm^{-1} to the O-O vibration.[12] On account of its relatively large intensity, the band at 1377 cm^{-1} is presumably a fundamental vibration. The isotopic shift of 8 cm^{-1} suggests a large contribution of the C-O vibration to this band.

The carbonyl oxide **3** is more sensitive than diphenyldiazomethane **1** to irradiation with visible light. It was therefore found only after thermal reaction of **2** with O_2 and not after direct irradiation of **1**. When **3** was irradiated for a few minutes ($\lambda > 515$ nm), all the IR bands assigned to this compound disappeared. A new compound, **4**,[13] was formed along with small amounts of benzophenone **5** (Scheme 1). **5** was not formed upon thermal reaction of **2** with O_2.

The identification of **4** as diphenyldioxirane is based on the following evidence:

- Upon irradiation with short-wavelength light ($\lambda > 438 \pm 10$ nm), **4** undergoes rearrangement to give phenyl benzoate **6**. This demonstrates that **4** contains two oxygen atoms. Because both the precursor **3** and the final product **6** contain two phenyl groups, it is plausible that **4** also contains two intact phenyl groups.
- The IR spectrum of **4**[13] shows no bands in the carbonyl or carboxyl region.
- Labeling with ^{18}O results in a shift of the weak band at 590 cm^{-1} by 14 cm^{-1} to lower wave numbers. This strong shift can only be explained by assuming a large contribution of O-O vibrations to this absorption.

When the matrix was warmed from 10 to 50 K, a strong luminescence was observed, depending on the concentration of oxygen, at $T > 35$ K. A similar luminescence had been observed earlier upon oxidation of **2** in organic glasses[4] or in Freon[5] at 77 K and identified as the phosphorescence of benzophenone. In order to study the luminescence in more detail, the total emission from the matrix was measured as a function of temperature (glow curve) with a photomultiplier. At several points along the curve, spectra were recorded with an optical multichannel analyzer. Under all experimental conditions, the phosphorescence spectrum of benzophenone was found.

Comparison of the glow curve with the conversion curve (conversion of **2** as a function of temperature for a constant rate of warming) showed that the chemiluminescence is not directly related to the reaction $2 + O_2 \rightarrow 3$. The luminescence was almost completely suppressed by high O_2 concentrations (> 1%), although the formation of **3** was demonstrated unequivocally. The strongest luminescence was observed when the matrix contained no O_2 and the carbene **2** reacted with the unavoidable surface contaminants (air layer due to small leaks in the vacuum system) upon rapid evaporation of the matrix ($T > 45$ K). These findings indicate that, in order to generate the chemiluminescence, both free carbene **2** and carbonyl oxide **3** (as oxygen transfer agent) must be present.

The chemiluminescence mechanism found in the oxidation of phenylcarbene—reaction of the free carbene with oxygen atoms[8]—plays a minor role in the oxidation of **2**, because the formation of oxygen atoms and **5** proceeds in low yield compared with the formation of **3**, **4**, and **6**.

Received: October 24, 1985;
revised: December 18, 1985 [Z 1507 IE]
German version: *Angew. Chem. 98* (1986) 255

CAS Registry numbers:
1, 86508-70-5; **3**, 15409-32-2; **5**, 119-61-9; **6**, 93-99-2.

[1] a) N. H. Werstiuk, H. L. Casal, J. C. Scaiano, *Can. J. Chem. 62* (1984) 2391; b) H. L. Casal, S. E. Sugamori, J. C. Scaiano, *J. Am. Chem. Soc. 106* (1984) 7623; c) H. L. Casal, M. Tanner, N. H. Werstiuk, J. C. Scaiano, *ibid. 107* (1985) 4616.

[2] a) O. L. Chapman, T. C. Hess, *J. Am. Chem. Soc. 106* (1984) 1842; b) T. C. Hess, *PhD Thesis*, University of California, Los Angeles 1978.

[3] a) G. A. Bell, I. R. Dunkin, *J. Chem. Soc. Chem. Commun. 1983*, 1213; b) I. R. Dunkin, C. J. Shields, G. A. Bell, 5th International Meeting on Spectroscopy of Matrix-Isolated Species Abstracts, Fontevraud 1985; c) I. R. Dunkin, G. A. Bell, *Tetrahedron 41* (1985) 339.

[4] a) A. M. Trozzolo, R. W. Murray, E. Wasserman, *J. Am. Chem. Soc. 84* (1962) 4990; b) A. M. Trozzolo, W. A. Gibbons, *ibid. 89* (1967) 239.

[5] N. J. Turro, J. A. Butcher, Jr., G. J. Hefferon, *Photochem. Photobiol. 34* (1981) 517.

[6] G. A. Hamilton in O. Hayaishi (Ed.): *Molecular Mechanism of Oxygen Activation*, Academic Press, New York 1974, p. 405.

[7] G. C. Pimentel in A. M. Bass, H. P. Broida (Eds.): *Formation and Trapping of Free Radicals*, Academic Press, New York 1960, p. 69.

[8] W. Sander, *Angew. Chem. 97* (1985) 964; *Angew. Chem. Int. Ed. Engl. 24* (1985) 988.

[9] **3**: IR (Ar, 10 K): 1377 (m), 1346 (w), 1185 (w), 1158 (w), 1047 (w), 983 (m), 897 (s), 777 (m), 689 (s), 659 (m), 647 (m) cm^{-1}.—^{18}O-**3**: IR (Ar, 10 K): 1369 (m), 1179 (w), 1151 (w), 977 (m), 862 (s), 777 (m), 689 (s), 654 (m), 646 (m) cm^{-1}.

[10] Our data are in good agreement with those in [2] but in poorer agreement with those in [3a]. The discrepancy between the IR data for cyclopentadienone *O*-oxide in [2] and [3a] is due, according to *Dunkin* et al. [3b], to a photoisomerization in *Chapman*'s experiment [12]. Because **3** is formed almost exclusively by a thermal route, a photoisomer is ruled out.

[11] P. A. Budinger, J. R. Mooney, J. G. Grasselli, P. S. Fay, A. T. Guttman, *Anal. Chem. 53* (1981) 884.

[12] The maximum isotopic shifts calculated for diatomic C-O oscillators are 33 cm^{-1} for the band at 1377 cm^{-1} and 21 cm^{-1} for the band at 897 cm^{-1}. See S. Pinchas, I. Laulicht: *Infrared Spectra of Labelled Compounds*, Academic Press, New York 1971, p. 238ff.

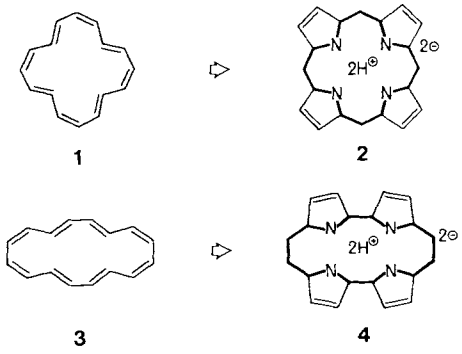
[13] **4**: IR (Ar, 10 K): 760 (m), 698 (m), 629 (w), 590 (w) cm^{-1}.—^{18}O-**4**: IR (Ar, 10 K): 756 (m), 695 (m), 628 (w), 576 (w) cm^{-1}.

Porphycene—a Novel Porphin Isomer**

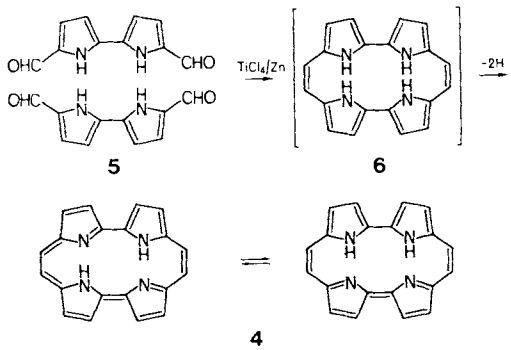
By *Emanuel Vogel,* Matthias Köcher, Hans Schmickler,* and *Johann Lex*

Porphin **2**, the parent compound of the porphyrins, contains a central 16-membered ring that corresponds to the dianion of [16]-85-annulene **1**[***] in configuration and conformation (planar).[1] In addition, **2** and $\mathbf{1}^{2\ominus}$ bear a distinct relationship in their π-electron structure, since **2** may be regarded alternatively as a diaza[18]annulene (outer pathway of conjugation) or as a tetraaza[16]annulene dianion (inner pathway of conjugation; drawn boldface in the formula).[2,3] The [16]annulene dianion model appears to be especially suited for the understanding of the spectroscopic properties of metalloporphyrins.[4]

These observations in conjunction with a study of 1,6:9,14-bismethano[16]annulene (CH_2-bridged **3**)[5] made us become aware of the analogy existing between the dianion of the hypothetical [16]-51-annulene **3**[***] and the porphin structural isomer **4**. Compared with $\mathbf{3}^{2\ominus}$, however, compound **4** has the geometrical advantage that it is nearly planar, because the nonbonding H,H interactions that force $\mathbf{3}^{2\ominus}$ to adopt a nonplanar conformation are absent. To our great surprise, there was no evidence in the literature for either **4** or derivatives of **4**, even though the synthesis of structural variants of **2** has long been pursued intensively in porphyrin research.[6]



We report here on the synthesis and properties of "porphycene" **4**, which, in accordance with our supposition, is porphyrin-like and aromatic.[7] Compound **4** is formed in 2–3% yield as the only nonpolymeric product by the reductive coupling of 5,5′-diformyl-2,2′-bipyrrole **5**[6c] with low-valent titanium.[8] The reaction, which presumably involves



6 as a readily oxidized intermediate, was carried out as follows: **5** (940 mg, 5 mmol) was added to a slurry of the titanium reagent, prepared from 9.49 g (50 mmol) of titanium tetrachloride and 6.55 g (100 mg-atom) of activated zinc in the presence of 2.5 mL of pyridine in 400 mL of tetrahydrofuran (THF), and the reaction mixture was then refluxed for 4 h. After conventional workup, a product was obtained from which **4** could easily be separated by chromatography on silica gel (column: 3 cm × 10 cm) with ether/pentane (1 : 1). Compound **4**, which is stable toward air, dissolves in organic solvents to give blue solutions showing beautiful red-violet fluorescence, and crystallizes from benzene in the form of violet needles (the compound undergoes sublimation above 250 °C with virtually no decomposition); yield: 20 mg.

Convincing evidence as to the structure and aromaticity of **4** is provided by the spectra of the compound. The ^{1}H-NMR spectrum (Fig. 1) exhibits only a singlet at $\delta = 9.83$ (H_C), an AB system at $\delta = 9.67$ (H_A) and 9.23 (H_B) ($J_{AB} = 4.36$ Hz, $J_{AN} = 0.85$ Hz, $J_{BN} = 0.72$ Hz) and a relatively broad signal at $\delta = 3.15$ (H_N)[9] (relative intensities 2 : 2 : 2 : 1); in the ^{13}C-NMR spectrum (75.5 MHz, $CDCl_3$), five signals appear, occurring at $\delta = 130.50$ (C_B), 125.85 (C_A), 114.98 (C_C), 144.84, and 135.87 (quaternary carbon atoms). The equivalence of the four pyrrole rings, as indicated by the simplicity of the ^{1}H- and ^{13}C-NMR spectra, is readily explained by assuming that **4**, like many porphyrins, is subject to an NH tautomerism that is rapid on the NMR time-scale. In view of the far-reaching analogies in the NMR spectra of porphycene **4** and porphin **2**, it is striking that the NH signal of **4** is significantly less shifted

[*] Prof. Dr. E. Vogel, M. Köcher, Dr. H. Schmickler, Dr. J. Lex
Institut für Organische Chemie der Universität
Greinstrasse 4, D-5000 Köln 41 (FRG)

[**] This work was supported by the Stiftung Volkswagenwerk and the Fonds der Chemischen Industrie.

[***] For nomenclature see [1].

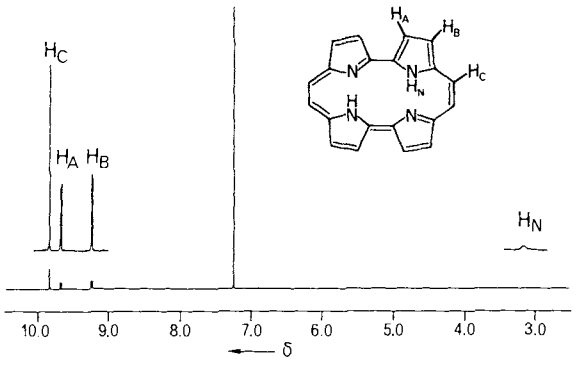


Fig. 1. ^{1}H-NMR spectrum of porphycene **4** (300 MHz, $CDCl_3$).

to high field, relative to that of pyrrole ($\delta = 7.70$), than that of **2** ($\Delta\delta = 4.55$ and 11.46 ppm, respectively[2]). This finding is suggestive of strong intramolecular N-H···N hydrogen bonding in **4**, which is expected if the molecule is planar. The UV/VIS spectrum (benzene) of **4** also reveals the porphyrin-like nature of the compound since it consists of a double band at $\lambda = 358/370$ nm ($\varepsilon = 139200$ and 106900), which may be interpreted as a Soret band, along with three longer wavelength bands at $\lambda = 558$ (34200), 596 (30400), and 630 nm (51900). In addition, the mass spectrum (electron-impact ionization, 75 eV) of **4** is reminiscent of that of porphyrins in that the molecular ion (m/z 310) gives rise to the base peak and the doubly charged molecular ion (m/z 155, intensity 10%) causes a further prominent peak.[10, 11] The IR spectrum of **4** is noteworthy insofar as it exhibits no typical N-H stretching vibration.[12]

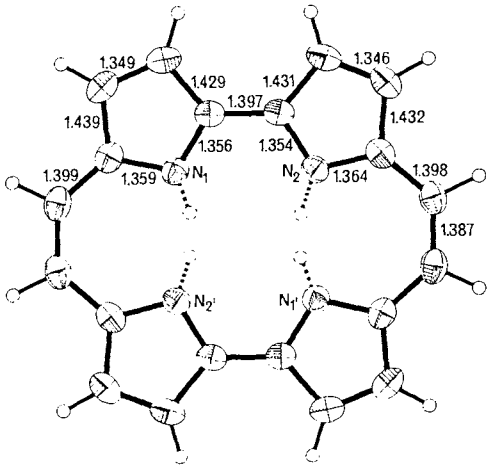


Fig. 2. Structure of porphycene **4** in the—partly disordered—crystal (bond lengths in Å) [13].

According to an X-ray structure analysis (Fig. 2),[13] **4** is partly disordered in the crystal. The molecules are (on the average) centrosymmetric and, like porphin **2**,[3] virtually planar (maximum distance of the C and N atoms from the mean plane: ±0.04 Å; for **2**: ±0.02 Å). **4** is slightly strained since, as a consequence of the planarity, the CCC angles in the 16-membered ring are expanded to 131 and 132°, respectively.[14] In contrast to **2**, it was not possible in the case of **4** (at least at room temperature) to assign the two imino hydrogen atoms unequivocally to specific nitrogen atoms. This difficulty is most likely due to a statistical distribution of NH tautomers in the crystal or to rapid interconversion of the tautomers during the time required for measurement. Therefore, the bond lengths given in Figure 2 apply to a spatially and/or time averaged structure. As already revealed by molecular models, the cavity between the four pyrrole rings, which is significant for the properties of **4**, is smaller than that in **2**: The four nitrogen atoms form a rectangle, the sides of which are 2.83 Å (N_1N_2) and 2.63 Å ($N_1N_{2'}$)[15] long (NN distance in **2**: 2.89 Å). In view of the very short $N_1N_{2'}$ and $N_2N_{1'}$ distances, **4** must be distinguished by strong hydrogen bonding (as already evidenced by the NMR spectrum); this conclusion becomes even more compelling if one takes into account that the N-H···N hydrogen bonds are in a nearly linear arrangement.[16]

Despite the smaller cavity, porphycene **4** is capable of forming stable metalloporphyrin-type complexes. It appears, however, that the tendencies of formation of these "metalloporphycenes" are, in general, somewhat lower than those of the corresponding metalloporphyrins (conditions for the synthesis of nickel porphycene: $NiCl_2$/dimethylformamide, 8 h, reflux).[17]

Received: October 25, 1985 [Z 1509 IE]
Publication delayed at the authors' request
German version: *Angew. Chem. 98* (1986) 262

CAS Registry numbers:
4, 100572-96-1; **4** (Ni complex), 100655-28-5; **5**, 86568-92-5.

[1] J. F. M. Oth, H. Baumann, J.-M. Gilles, G. Schröder, *J. Am. Chem. Soc. 94* (1972) 3498.

[2] a) H. H. Inhoffen, J. W. Buchler, P. Jäger, *Fortschr. Chem. Org. Naturst. 26* (1968) 284; b) H. Scheer, J. J. Katz in K. M. Smith: *Porphyrins and Metalloporphyrins*, Elsevier, Amsterdam 1975, p. 405; c) T. R. Janson, J. J. Katz in D. Dolphin: *The Porphyrins, Vol. IV*, Academic Press, New York 1979, p. 1.

[3] The structural analysis of porphin **2**, according to which the NH hydrogen atoms are localized on two pyrrole rings that are situated diagonally to each other, indicates that the outer 18π-electron pathway of conjugation is preferred. B. M. L. Chen, A. Tulinsky, *J. Am. Chem. Soc. 94* (1972) 4144.

[4] The UV/VIS spectra of octaethylporphinatomagnesium and $\mathbf{1}^{2\oplus}$ are almost identical: J.-H. Fuhrhop, *Angew. Chem. 86* (1974) 363; *Angew. Chem. Int. Ed. Engl. 13* (1974) 321.

[5] a) D. Tanner, O. Wennerström, E. Vogel, *Tetrahedron Lett. 23* (1982) 1221; b) E. Vogel, U. Kürschner, H. Schmickler, J. Lex, O. Wennerström, D. Tanner, U. Norinder, C. Krüger, *ibid. 26* (1985) 3087; c) K. Müllen, T. Meul, E. Vogel, U. Kürschner, H. Schmickler, O. Wennerström, *ibid. 26* (1985) 3091.

[6] a) Porphyrins with various heteroatoms: A. W. Johnson in K. M. Smith (Ed.): *Porphyrins and Metalloporphyrins*, Elsevier, Amsterdam 1975, p. 729; b) homoporphyrins: H. J. Callot, E. Schaeffer, *J. Org. Chem. 42* (1977) 1567; c) sapphyrins: V. J. Bauer, D. L. J. Clive, D. Dolphin, J. B. Paine III, F. L. Harris, M. M. King, J. Loder, S.-W. Chien Wang, R. B. Woodward, *J. Am. Chem. Soc. 105* (1983) 6429; d) pentaphyrin: H. Rexhausen, A. Gossauer, *J. Chem. Soc. Chem. Commun. 1983*, 275; e) platyrins: E. LeGoff, R. A. Berger, O. G. Weaver, *Abstr. 10th Int. Congr. Heterocycl. Chem.*, Waterloo, Canada 1985.

[7] The name porphycene is suggested for **4**, because this compound possesses structural features of both porphyrins and acenes. The solubility and chromatographic behavior indicates that **4** is less polar than **2** and thus more similar to hydrocarbons.

[8] a) T. Mukaiyama, T. Sato, J. Hanna, *Chem. Lett. 1973*, 1041; b) J. E. McMurry, M. P. Fleming, *J. Am. Chem. Soc. 96* (1974) 4708; J. E. McMurry, *Acc. Chem. Res. 16* (1983) 405; c) D. Lenoir, *Synthesis 1977*, 553; d) an example for the use of the McMurry reaction in porphyrin chemistry was recently reported: G. Holze, H. H. Inhoffen, *Angew. Chem. 97* (1985) 887; *Angew. Chem. Int. Ed. Engl. 24* (1985) 867.

[9] The signal of the NH protons remain unchanged too −110°C (CD_2Cl_2/CF_2Br_2, 1:1), the lowest temperature achieved so far. **4** undergoes H/D exchange only very slowly in THF/D_2O. For this reason, the *N*-deuterated compound may be prepared most practically by successive treatment of **4** with butyllithium (in ether) and D_2O.

[10] H. Budzikiewicz in D. Dolphin: *The Porphyrins, Vol. III*, Academic Press, New York 1978, p. 395. A detailed mass spectrometric study of **4** and its derivatives is being carried out with Prof. *H. Budzikiewicz* (Universität Köln).

[11] High-resolution mass spectra and elemental analysis are correct.

[12] IR spectrum (KBr) of **4**. ν = 3099, 1562, 1469, 1410, 1224, 1167, 1054, 932, 813, 745, and 651 cm^{-1}. An evaluation of the IR spectrum by means of *N*-deuterated **4** is in progress.

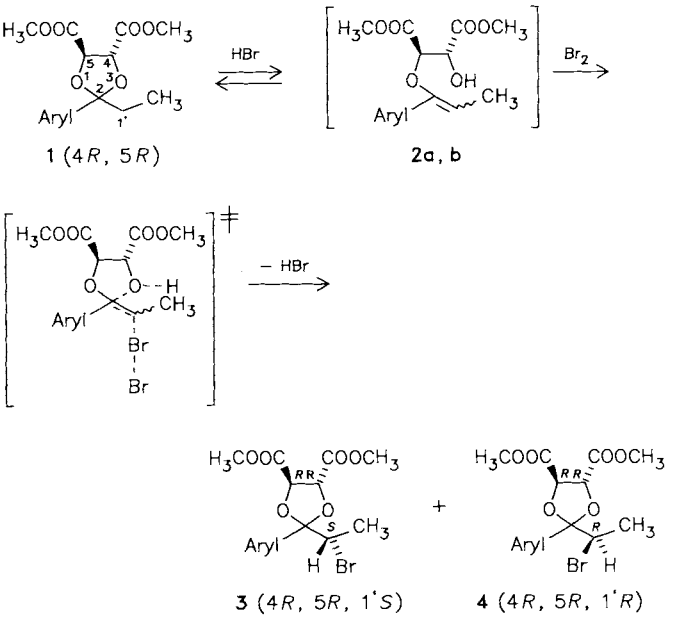
[13] **4** forms monoclinic crystals, space group $P2_1/c$, $a = 10.088(3)$, $b = 4.987(1)$, $c = 15.464(4)$ Å, $\beta = 108.36(2)°$, $Z = 2$; 710 reflections, $R = 0.030$. Further details of the crystal structure investigation may be obtained from the Fachinformationszentrum Energie, Physik, Mathematik GmbH, D-7514 Eggenstein-Leopoldshafen 2 (FRG), on quoting the depository number CSD-51701, the names of the authors, and the journal citation.

[14] Remarkably, expansion of CCC angles on this order of magnitude is observed even for maleic acid. M. N. G. James, G. J. B. Williams, *Acta Crystallogr. B30* (1974) 1249.

[15] A similarly short NN distance (2.626 Å) has also been found for the hydroperchlorate salt of the "proton sponge" 4,5-bis(dimethylamino)fluorene. H. A. Staab, T. Saupe, C. Krieger, *Angew. Chem. 95* (1983) 748; *Angew. Chem. Int. Ed. Engl. 22* (1983) 731.

[16] We thank Prof. *O. Ermer* (Universität Köln) for helpful discussions in the interpretation of the X-ray structure data of **4**.

[17] According to investigations of Dr. *K. Pramod* (note added in proof, January 22, 1986): **4** has also been converted into the zinc, copper, and cobalt complexes.



Asymmetric Bromination of Enantiomerically Pure Acetals of Alkyl Aryl Ketones

By *Graziano Castaldi,* Silvia Cavicchioli, Claudio Giordano,** and *Fulvio Uggeri*

In the course of our studies on the synthesis of 2-arylalkanoic acids, we required acetals of optically active α-functionalized alkyl aryl ketones as intermediates.[1] To this end, we investigated the α-bromination of the enantiomerically pure alkyl aryl acetals **1** and *ent*-**1**, which are readily prepared from alkyl aryl ketones and the dimethyl ester of (2*R*,3*R*)- and (2*S*,3*S*)-tartaric acid in high yields.[2,3]

Thus, by adding bromine (10 mmol) to a solution of the (4*R*,5*R*) acetal **1** (10 mmol) in CCl_4 (20 mL) at 15 °C in the presence of a catalytic amount of HBr, a mixture of the diastereomeric α-bromo acetals **3** and **4** is obtained in high yield with **3** in high diastereomeric excess (^{1}H-NMR, HPLC, see Table 1). As expected, the absolute configuration at C-1 is reversed when *ent*-**1** is used as starting material.[4] The absolute configuration at C-1 of **3** and **4** was assigned by means of their rearrangement (1,2-aryl shift with 100% inversion of configuration) into the corresponding 2-arylalkanoic acids of *S* and *R* configuration, respectively.[2,5]

The reaction appears to be very general as it can be applied to acetals derived from many alkyl aryl ketones as well as from other tartaric acid derivatives.[5] The main feature of the reaction is the high diastereoselectivity observed even at room temperature; in contrast, most asymmetric syntheses require lower temperatures.[6] A catalytic amount of HBr is required to promote the reaction, the role of HBr being to set up the equilibrium between the acetal **1** and its enol forms **2a**, **b** (*E*/*Z* isomers).

The observed asymmetric induction is presumably the result of diastereofacial selection in the kinetically controlled attack of electrophilic bromine on the double bond of the enol ether intermediates **2a**, **b** with anchimeric assistance by the hydroxyl group.

The asymmetric α-bromination of acetals has been employed as the key step of a new synthesis of enantiomerically pure 2-arylalkanoic acids.[5] The method has also been successfully applied to the industrial manufacturing of optically pure (2*S*)-(+)-2-(6-methoxy-2-naphthyl)propanoic acid (Naproxen),[5] which is the most important of the optically active 2-arylalkanoic acids.[7]

Moreover, α-bromo acetals **3** and **4** have been hydrolyzed to the corresponding optically active α-bromo ketones,[8] thus extending the synthetic scope of the reaction. Thus, the mixture of **3a** and **4a** (Table 1) was hydrolyzed, without racemization, by treatment with methanesulfonic acid in methanol.[9]

Table 1. Yields and diastereomeric ratios for the bromination of **1a**–**1d** to **3a/4a**–**3d/4d**.

1–4	Aryl	Yield 3 + 4 [%]	Ratio 3 : 4
a	5-bromo-6-methoxy-2-naphthyl	98	90 : 10 [a]
b	*p*-methoxyphenyl	95	92 : 8
c	phenyl	94	93 : 7
d	*p*-chlorophenyl	93	94 : 6

[a] The bromination of **1a** requires two moles of bromine per mole of **1a**.

Received: November 5, 1985;
supplemented: December 18, 1985 [Z 1521 IE]
German version: *Angew. Chem. 98* (1986) 273

[*] Dr. G. Castaldi, Dr. S. Cavicchioli, Dr. C. Giordano, Dr. F. Uggeri
Zambon Chimica S.p.A., Organic Chemistry Department
Via Cimabue 26/28, I-20032 Cormano-Milano (Italy)

[1] C. Giordano, G. Castaldi, F. Uggeri, *Angew. Chem. 96* (1984) 413; *Angew. Chem. Int. Ed. Engl. 23* (1984) 413.

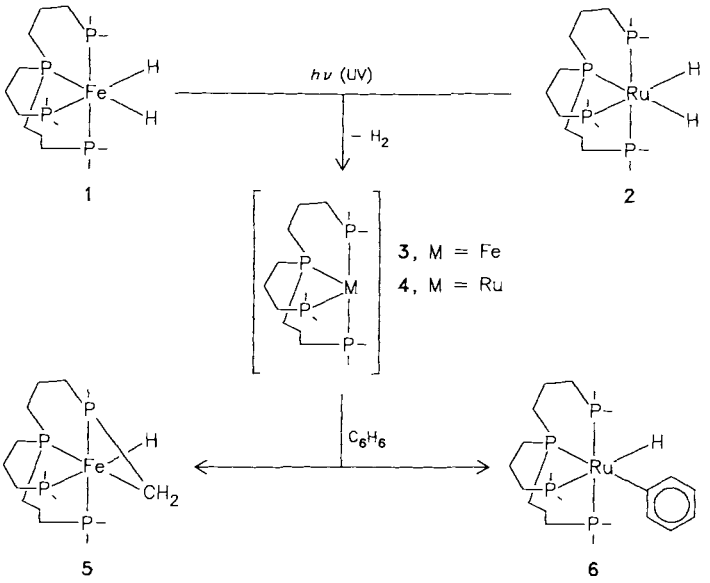
[2] The alkyl aryl acetals **1** were prepared by reacting the corresponding alkyl aryl ketones with the dimethyl ester of tartaric acid in the presence of trimethyl orthoformate and an acid catalyst.

[3] For a review article on the use of tartaric acid in asymmetric syntheses, see D. Seebach, E. Hungerbühler in R. Scheffold (Ed.): *Modern Synthetic Methods, Vol. 2*, Salle/Sauerländer, Aarau 1980, p. 91–171; for the use of chiral acetals in other asymmetric syntheses, see: J. Fujiwara, Y. Fukutani, M. Hasegawa, K. Maruoka, H. Yamamoto, *J. Am. Chem. Soc. 106* (1984) 5004; I. Arai, A. Mori, H. Yamamoto, *ibid. 107* (1985) 8254; E. A. Mash, K. A. Nelson, *ibid. 107* (1985) 8256; M. Suzuki, K. Kimura, S. Terashima, *Tetrahedron Lett. 52* (1985) 6481.

[4] All products were fully characterized by ^{1}H-NMR, IR, and mass spectroscopy as well as by HPLC and elemental analyses.

[5] G. Castaldi, S. Cavicchioli, C. Giordano, F. Uggeri, Eur. Pat. 158913 (1985), Zambon Chimica; G. Castaldi, S. Cavicchioli, C. Giordano, F. Uggeri, unpublished.

[6] J. D. Morrison, H. S. Mosher (Eds.): *Asymmetric Organic Reactions*. American Chemical Society, Washington D.C. 1976; J. D. Morrison (Ed.): *Asymmetric Synthesis, Vols. 1-5*, Academic Press, New York 1983-1985.
[7] T. Y. Shen, *Angew. Chem. 84* (1972) 512; *Angew. Chem. Int. Ed. Engl. 11* (1972) 460; S. H. Ferreira, J. R. Vane: *Antiinflammatory Drugs*, Springer, Berlin 1979, p. 321.
[8] G. Castaldi, C. Giordano, S. Cavicchioli, unpublished.
[9] *Experimental procedure:* A 90:10 mixture of **3a** and **4a** (10 mmol) was added to a solution of methanol (5 mL) in methanesulfonic acid (20 mL). The reaction mixture was stirred at 20°C for 18 h and then poured onto crushed ice and extracted with dichloromethane. The organic phase was washed with water and a 2% $NaHCO_3$ solution and dried over sodium sulfate. Evaporation of the solvent in vacuo gave 2.8 g (75%) of 2-(*S*)-(+)-2-bromo-1-(5-bromo-6-methoxy-2-naphthyl)propan-1-one. $[\alpha]_D^{20} = +130°$ ($c = 0.5$, $CHCl_3$). The enantiomeric excess was 80% as determined by ^{1}H-NMR analysis with the optically active shift reagent Eu(hfc)$_3$.



Metal Dependence of Cyclometalation and Arene C–H Activation in the Photolysis of *cis*-$H_2M[P(CH_2CH_2CH_2PMe_2)_3]$ (M = Fe, Ru) in Benzene**

By *Martin Antberg* and *Lutz Dahlenburg**

The cleavage of hydrocarbon C–H bonds at metal centers is currently the subject of much research in organometallic chemistry. Besides a few derivatives of "hard" metal ions,[1] the Ir^I and Rh^I complex fragments $(C_5R_5)(L)M$ (R = H, Me; L = CO, PMe_3)[2] have proved particularly potent as arene and alkane activators. Also promising are the Ru^0 and Os^0 species $(C_6R_6)(L)M$ (L = alkylphosphane)[3] and the tetrakis (P ligand) systems L_4M of iron, ruthenium, and osmium. The latter often undergo *intra*molecular isomerization, however, to give cyclometalated hydridometal(II) complexes,[4] so that only the 16e fragment $(Me_2PCH_2CH_2PMe_2)_2M$ (M = Fe, Ru, Os)[5a-c] and $[(MeO)_3P]_2(Me_3P)_2M$ (M = Ru, Os)[5d] have proved suitable so far for the *inter*molecular C–H cleavage.

We have now found that the photolytic dehydrogenation of the *cis*-dihydrides $(pp_3)FeH_2$ **1**[6b] and $(pp_3)RuH_2$ **2**[6d] (both of which are stabilized by our "pp_3" ligand $P(CH_2CH_2CH_2PMe_2)_3$[6a]) in C_6H_6 leads, depending on the central metal atom, to either *intra*- or *inter*molecular C–H activation. In the iron system, internal addition to $H-CH_2P$ results in formation of the three-membered-ring derivative **5**. In the ruthenium system, on the other hand, $H-C_6H_5$ cleavage results in formation of the phenyl hydride **6**.[7a]

The structures of **5** and **6** were established by elemental analysis and spectroscopy.[7b-f] The dt splitting of the ^{1}H-coupled Fe*C* resonance of **5** ($J(PC) = 13$, $J(CH_2) = 148$ Hz) rules out a CH_2 cleavage product formed by metalation of the trimethylene chains, as has been discussed, for example, for (dmpp)($\overline{C_7H_{17}P_2}$)FeH (dmpp = $Me_2P(CH_2)_3PMe_2$, $C_7H_{18}P_2$).[4c]

For both reactions, we postulate intermediate 16e d^8 fragments $(pp_3)M$, **3** and **4**, respectively, because these incorporate particularly advantageous structural features for the oxidative C–H addition owing to their bent, *cis*-unsaturated configuration.[8] The *metal*-dependent transition between intra- and intermolecular C–H addition, the first example of its kind, might be due to the different crowding of the groups and the different chelate ring strain in the required intermediates **3** and **4**: The M–Cl distances in the dichloro complexes $[FeCl_2(pp_3)]$, ca. 239 and 241 ppm,[6c] and $[RuCl_2(pp_3)]$, ca. 251 and 252 ppm,[6d] demonstrate that the covalent radius of the ruthenium atom stabilized by the pp_3 ligand is at least 10 pm larger than that of the iron atom in the same coodination environment. The 16e Ru^0 system should therefore be more strained and more open at the central metal atom, which, on the one hand, suppresses the cyclometalation and, on the other hand, facilitates the approach of a solvent molecule. Increased ring strain and reduced crowding of the groups are also responsible, according to *Karsch*,[4c] for the *ligand*-dependent change in reactivity from intramolecular addition in the case of $[Me_2P(CH_2)_3PMe_2]_2Fe$ to intermolecular reaction in the case of $[Me_2P(CH_2)_2PMe_2]_2Fe$. The transition from intramolecular C–H addition by the Ru and Os species $(Me_3P)_4M$ to intermolecular C–H cleavage by the phosphite-substituted 16e fragment $[(MeO)_3P]_2(Me_3P)_2M$, described by *Werner* and *Gotzig*,[4f,5d] likewise represents a favoring of the intermolecular reaction in the case of less-filled coordination spheres.

Received: November 6, 1985;
revised: December 30, 1985 [Z 1523 IE]
German version: *Angew. Chem. 98* (1986) 274

[*] Prof. Dr. L. Dahlenburg, Dipl.-Chem. M. Antberg
Institut für Anorganische und Angewandte Chemie der Universität
Martin-Luther-King-Platz 6, D-2000 Hamburg 13 (FRG)

[**] Oligophosphane Ligands, Part 16. This work was supported by the Deutsche Forschungsgemeinschaft, the Fonds der Chemischen Industrie, and Degussa AG.—Part 15: M. Antberg, L. Dahlenburg, N. Höck, C. Prengel, *Phosphorus Sulfur*, in press.

[1] J. P. Rothwell, *Polyhedron 4* (1985) 177, and references cited therein.
[2] a) A. H. Janowicz, R. G. Bergman, *J. Am. Chem. Soc. 104* (1982) 352; *105* (1983) 3929; b) M. J. Wax, J. M. Stryker, J. M. Buchanan, C. A. Kovac, R. G. Bergman, *ibid. 106* (1984) 1121; c) R. A. Periana, R. G. Bergman, *Organometallics 3* (1984) 508; d) j. K. Hoyano, W. A. G. Graham, *J. Am. Chem. Soc. 104* (1982) 3723; e) J. K. Hoyano, A. D. McMaster, W. A. G. Graham, *ibid. 105* (1983) 7190; f) A. J. Rest, I. Whitell, W. A. G. Graham, J. K. Hoyano, A. D. McMaster, *J. Chem. Soc. Chem. Commun. 1984*, 624; g) W. D. Jones, F. J. Feher, *J. Am. Chem. Soc. 104* (1982) 4240; *Organometallics 2* (1983) 562; *J. Am. Chem. Soc. 106* (1984) 1650.
[3] a) H. Kletzin, H. Werner, *Angew. Chem. 95* (1983) 916; *Angew. Chem. Int. Ed. Engl. 22* (1983) 873; b) H. Werner, K. Roder, *J. Organomet. Chem. 281* (1985) C 38; c) R. H. Morris, M. Shiralian, *ibid. 260* (1984) C 47.
[4] a) H. H. Karsch, H.-F. Klein, H. Schmidbaur, *Angew. Chem. 87* (1975) 630; *Angew. Chem. Int. Ed. Engl. 14* (1975) 637; *Chem. Ber. 110* (1977) 2200; b) H. H. Karsch, D. Neugebauer, *Angew. Chem. 94* (1982) 322; *Angew. Chem. Int. Ed. Engl. 21* (1982) 312; c) H. H. Karsch, *Chem. Ber. 117* (1984) 3123; d) J. W. Rathke, E. L. Muetterties, *J. Am. Chem. Soc. 97* (1975) 3272; d) H. Werner, R. Werner, *J. Organomet. Chem. 209* (1981)

C 60; f) H. Werner, J. Gotzig, *Organometallics 2* (1983) 547; g) J. Gotzig, R. Werner, H. Werner, *J. Organomet. Chem. 285* (1985) 99.

[5] a) J. Chatt, J. M. Davidson, *J. Chem. Soc. 1965*, 843; b) F. A. Cotton, D. L. Hunter, B. A. Frenz, *Inorg. Chim. Acta 15* (1975) 155; c) C. A. Tolman, S. D. Ittel, A. D. English, J. P. Jesson, *J. Am. Chem. Soc. 100* (1978) 4080, 7577; *101* (1979) 1742; d) H. Werner, J. Gotzig, *J. Organomet. Chem. 284* (1985) 73.

[6] a) M. Antberg, C. Prengel, L. Dahlenburg, *Inorg. Chem. 23* (1984) 4170; b) synthesis from $[(pp_3)FeCl_2]$ [6c] and $LiAlH_4$/tetrahydrofuran in analogy to $[(pp_3)RuH_2]$ [6d]; c) M. Antberg, L. Dahlenburg, *Inorg. Chim. Acta 104* (1985) 51; d) *ibid. 111* (1986) 73.

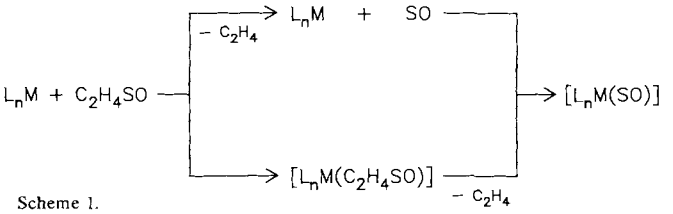
[7] a) Experimental conditions: 10^{-1}–10^{-2} M solution of the complex, 4 h irradiation (Philips HPK 125 W, Solidex filter) at ca. 293 K, gas-volumetric monitoring of H_2 evolution; b) **5** (yellow solid); IR (KBr): $\tilde{\nu}$=1747 (FeH), 879 (FeCP) [4a] cm^{-1}. ^{1}H-NMR (360.13 MHz, C_7D_8, 297 K): δ=−0.3, −0.5 (br, each 1 H; $FeCH_2$), −12.2 (broad ABCDX spectrum; $J(P_AH)\approx 16$, $J(P_BH)\approx 48$, $J(P_CH)\approx 51$, $J(P_DH)\approx 66$ Hz; 1 H; FeH) [7d]. ^{31}P-NMR (145.79 MHz, C_6D_6/C_6H_6, 297 K): ABCD spectrum with $\delta(P_A)$=39.3, $\delta(P_B)$=38.0, $\delta(P_C)$=22.9, $\delta(P_D)$=−6.9, $J(P_AP_B)\approx 0$ and $J(P_AP_C)\approx J(P_AP_D)\approx J(P_BP_C)\approx J(P_BP_D)\approx J(P_CP_D)\approx 44$ Hz [7d]. ^{13}C-NMR (90.56 MHz, C_6D_6, 297 K): δ=−25.4 (dt, J(PC)=13, J(CH)=148 Hz; $FePCH_2$); c) **6** (colorless solid); IR (KBr): $\tilde{\nu}$=1808 (RuH), 3037, 1012, 733 (C_6H_5) cm^{-1}. ^{1}H-NMR (360.13 MHz, C_6D_6, 280 K): δ=7.95 (m, 2 H; *ortho*), 7.18–7.10 (m, 3 H; *meta*+*para*) [2g, 3c], −9.01 (ddt; *trans*-J(PH)=84.5, *cis*-J(PH)=20.7, *cis*-$J(P_2H)$=28.4 Hz; 1 H; RuH). ^{31}P-NMR (145.79 MHz, C_6D_6/C_6H_6, 297 K): δ=3.3 (dt; *cis*-J(PP)=24, *cis*-$J(PP_2)\approx 34$ Hz; *trans*-PRuC), −0.6 (dd; *cis*-J(PP)=24 and 34 Hz; *trans*-PRuP), −9.7 (q; *cis*-$J(PP_3)$=24 Hz; *trans*-PRuH). ^{13}C-NMR (20.15 MHz, C_6D_6, 297 K): δ=150.4 (dd; J(PC)=3 and 10 Hz; *ipso*), 131.9, 130.6 (each s; *ortho*), 125.5, 124.5 (each s; *meta*), 119.9 (s; *para*) [7e]; d) ABCD assignment arbitrary; e) B. E. Mann, B. F. Taylor: *^{13}C NMR Data for Organometallic Compounds*, Academic Press, London 1981; f) the spectroscopic data do not allow a differentiation to be made between the coordination models represented in the formulas and isomeric structures with exchanged MH and MC building bocks.

[8] J.-Y. Saillard, R. Hoffmann, *J. Am. Chem. Soc. 106* (1984) 2006.

Complex Stabilization of Disulfur Dioxide in the Fragmentation of Thiirane *S*-Oxide on Bis(triphenylphosphane)platinum(0)**

By *Ingo-Peter Lorenz** and *Jürgen Kull*

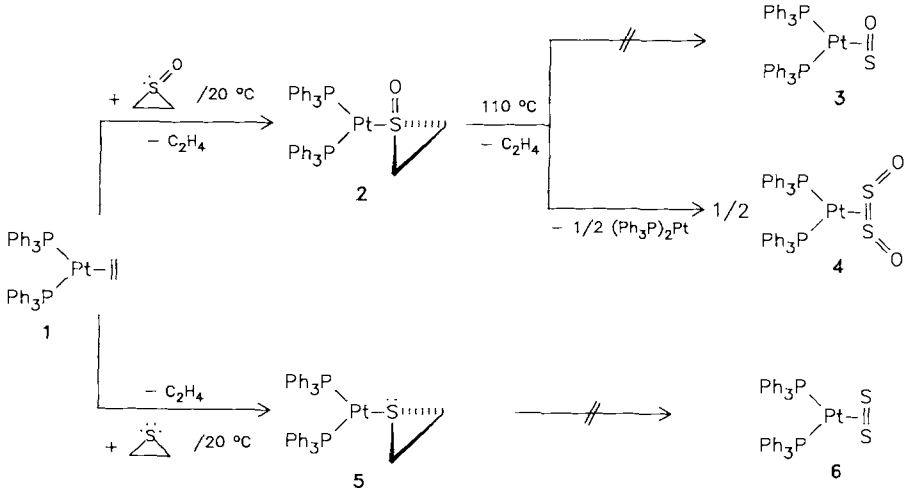
Complex stabilization of sulfur monoxide has been achieved by several methods. Particularly favorable is the fragmentation of thiirane *S*-oxide in the presence of coordinatively unsaturated or substitutionally labile transition-metal complexes.[1–3] Two reaction mechanisms are conceivable: (1) initial fragmentation of C_2H_4SO with in situ complex stabilization of SO; (2) initial coordination of C_2H_4SO with subsequent elimination of ethylene (Scheme 1). It was suggested that the second mechanism of reaction is operative in the synthesis of $[\{(C_5H_5)(CO)_2Mn\}_2SO]$;[3] this is further supported by ^{31}P-NMR data.[2b] We have now succeeded in isolating the first thiirane *S*-oxide complex **2** as an intermediate in the synthesis of the disulfur dioxide complex **4** from the ethylene complex **1**. This is strong support for the second reaction mechanism discussed above.



Scheme 1.

Reaction of equimolar amounts of $[(Ph_3P)_2Pt(C_2H_4)]$ **1** and C_2H_4SO affords the yellow complex **2** in nearly quantitative yield; complex **2** is stable in air up to 70 °C. In toluene at 110 °C, **2** undergoes fragmentation to form not the η^2-SO complex **3** but rather the S_2O_2 complex **4** (Scheme 2).[4] S_2O_2 has been suggested as the unstable, initial product of SO decomposition in the gas phase[5] (cf. Scheme 3); S_2O_2 has only been prepared as a ligand via an oxidative pathway starting from the η^2-S_2 ligand.[6,7]

The compositions and structures of the new compounds **2** and **4** were determined by elemental analysis and by mass, IR, ^{1}H-NMR, and ^{31}P-NMR spectroscopy. For comparison, the spectroscopic data for the thiirane complex **5**, which is accessible by a reaction analogous to that used to prepare **2**, is also given in Table 1. However, **5** cannot be converted into the S_2 complex **6**.



Scheme 2.

The FD mass spectra of **2**, **4**, and **5** exhibit peaks for the respective molecular ions. In the IR spectra of **2** and **4**, the ν(SO) bands lie at surprisingly long wavelength compared with those of *S*-coordinated dimethylsulfoxide (DMSO)

[*] Prof. Dr. I.-P. Lorenz, cand. chem. J. Kull
Institut für Anorganische Chemie der Universität
Auf der Morgenstelle 18, D-7400 Tübingen (FRG)

[**] This work was supported by the Deutsche Forschungsgemeinschaft, NATO (R.G. 116/81), and the Fonds der Chemischen Industrie. We thank Prof. Dr. *G. van Koten*, Amsterdam, for valuable discussions.

complexes of platinum(II)[8] and the only known S_2O_2 complex.[6,7] This is presumably due to the better π-donor ability of the $[(Ph_3P)_2Pt^0]$ fragment. The PtS stretching vibrations of **2**, **4**, and **5** give bands between 300 and 400 cm^{-1}. ν(SS) of **4** is unequivocally assigned to the band at 657 cm^{-1}.

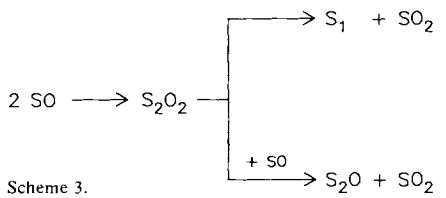
Table 1. Selected spectroscopic data for the complexes **2**, **4**, and **5**.

Complex	FD-MS [a] m/z (M^+)	IR [cm^{-1}] [b] ν(SO)	ν(SS)	ν(PtS)	^{1}H-NMR (δ values) [c]	^{31}P-NMR [d] δ values	J [Hz]
2	795	953	–	329	4.4–5.7	18.75;	2518 (PtP)
						20.25;	1960 (PtP)
							10 (PP)
4	815	882	657	398	–	5.66;	4009 (PtP)
		870					
5	779	–	–	315	4.1–5.2	14.30;	4042 (PtP)

[a] Relative to ^{195}Pt. [b] KBr. [c] C_6D_6, 20°C. [d] Toluene, −40°C.

In the ^{1}H-NMR spectrum of the adduct **2**, the AA'BB' multiplet, which is unresolved owing to complicated coupling relationships, appears at $\delta = 4.4$–5.7. Such a multiplet is also found for the thiirane complex **5** at $\delta = 4.1$–5.2. Such a large low-field shift in comparison to those of the free ligands ($\delta = 2.02$ (m) and 2.29 (s) in $CDCl_3$) is not observed for the complexation of DMSO and dimethyl sulfide and rules out the formation of the thiaplatinacyclobutane $[(Ph_3P)_2\overline{PtS(O)_nCH_2CH_2}$ (n = 0, 1).

The unequivocal structural confirmation was provided by the ^{31}P{^{1}H}-NMR spectra, which exhibit only one signal for **4** and **5** but an AB quartet with the expected ^{195}Pt satellites and the usual Pt–P coupling constants[9] for **2**. For **5**, no evidence of a hindering of rotation around the Pt–S bond or of an inversion of the pyramidal sulfur is observed. In **2**, on account of the nonequivalence of the P atoms and the equivalence of the CH_2 units, the SO group must lie in the P_2PtS plane. The driving force for formation of this structure could be the favorable orbital overlap in the π-system Pt=S=O. The spectroscopic findings could also be interpreted, on the other hand, in terms of η^2-SO coordination. The ^{31}P-NMR data of the S_2O_2 complex **4** are comparable with those of the η^2-O_2 complex $[(Ph_3P)_2PtO_2]$ ($\delta = 16.4$, $J_{PtP} = 4059$ Hz[10]); S_2O_2 is presumably, therefore, η^2-coordinated in **4** as in the complex cation $[(diphos)_2IrS_2O_2]^+$[6,7] (diphos = $Ph_2P-CH_2CH_2-PPh_2$) and—for steric and electronic (π-donor) reasons—twisted. According to microwave spectroscopic investigations, free S_2O_2 is planar and *cis*-configurated.[11]



Scheme 3.

It has thus been possible to expand the role of thiirane *S*-oxide as a source of SO in organometallic chemistry. Starting from C_2H_4SO, we and *Rauchfuss* et al. have identified, in addition to the SO complexes,[1–3] C_2H_4SO (**2**), S_2O_2 (**4**), S_2O,[7] and $C_2H_4S_2$ complexes.[12] The course of SO decomposition shown in Scheme 3 has, therefore, an analogy in the complex chemistry in solution.

Received: November 11, 1985 [Z 1529 IE]
German version: *Angew. Chem. 98* (1986) 276

[1] K. S. Arulsamy, K. K. Pandey, U. C. Agarwala, *Inorg. Chim. Acta 54* (1981) L51.
[2] a) W. A. Schenk, J. Leißner, C. Burschka, *Angew. Chem. 96* (1984) 787; *Angew. Chem. Int. Ed. Engl. 23* (1984) 806; b) *Z. Naturforsch. B40* (1985) 1264.
[3] I.-P. Lorenz, J. Messelhäuser, W. Hiller, K. Haug, *Angew. Chem. 97* (1985) 234; *Angew. Chem. Int. Ed. Engl. 24* (1985) 228.
[4] *Experimental procedure:* **2**: Upon addition of C_2H_4SO (91 mg, 1.2 mmol) to 897 mg (1.2 mmol) of **1** in 50 mL of toluene, the solution turned from yellow to orange; it was then stirred for 2 h at room temperature, concentrated in vacuum, and treated with 100 mL of petroleum ether (30/50°C), resulting in the precipitation of light yellow, finely crystalline **2**. Compound **2** was filtered off, washed with diethyl ether and petroleum ether, and dried in vacuum. M.p. = 91°C (dec.); yield: 868 mg (91%).—**4**: **2** (868 mg, 1.1 mmol) was dissolved in 40 mL of toluene and the solution was stirred for 5 h at 110°C, resulting in the gradual formation of a deep color and precipitation. After cooling of the finally red solution to room temperature, the reaction was worked up as described above, resulting in the precipitation of orange, air stable **4**. M.p. = 171°C (dec.); yield: 290 mg (65%).
[5] P. W. Schenk, R. Steudel, *Angew. Chem. 77* (1965) 437; *Angew. Chem. Int. Ed. Engl. 4* (1965) 402; *Inorg. Sulfur Chem. 1968*, 367; J. T. Herron, R. E. Huie, *Chem. Phys. Lett. 76* (1968) 322.
[6] G. Schmid, G. Ritter, T. Debaerdemaeker, *Chem. Ber. 103* (1975) 3008.
[7] J. E. Hoots, D. A. Lesch, T. B. Rauchfuss, *Inorg. Chem. 23* (1984) 3130.
[8] C. Eaborn, K. Kundu, A. Pidcock, *J. Chem. Soc. Dalton Trans. 1981*, 933.
[9] P. S. Pergosin, R. W. Kunz: *Phosphorus-31 and Carbon-13 NMR of Transition Metal Phosphine Complexes*, Springer, Berlin 1979.
[10] A. Sen, J. Halpern, *Inorg. Chem. 19* (1980) 1073.
[11] F. J. Lovas, E. Tiemann, D. R. Johnson, *J. Chem. Phys. 60* (1974) 5005.
[12] J. Messelhäuser, I.-P. Lorenz, K. Haug, W. Hiller, *Z. Naturforsch. B40* (1985) 1064.

Synthesis of $[Cu_3Os_3H_9(PMe_2Ph)_9]$, a Bimetallic Raft, by Reductive Elimination of Alcohol or H_2**

By *Timothy H. Lemmen, John C. Huffman,* and *Kenneth G. Caulton**

Among heteronuclear clusters, polyhydrides are particularly important because they bear transferable hydrogen reducing equivalents and because they permit determination of hydrogen migrational preferences on model alloy phases. We report here the synthesis and structural characterization of a neutral complex with a Cu_3Os_3 framework; the raftlike geometry leaves the metals open on two sides. Equally important, the synthesis employs two unprecedented[1] methods for the formation of metal–metal bonds, alcohol elimination and H_2 elimination.

Reaction of $[CuO\mathit{t}Bu]_4$ with $[H_4Os(PMe_2Ph)_3]$ proceeds without hydrogen evolution to yield a product that bears a stoichiometric resemblance to the alkali metal analogue $[KOsH_3(PM_2Ph)_3]$ [(Eq. (a)].[2]

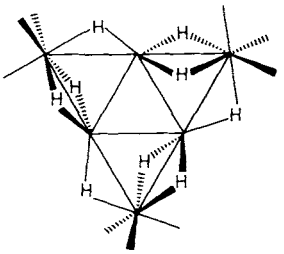
$$1/4[CuO\mathit{t}Bu]_4 + [H_4Os(PMe_2Ph)_3] \longrightarrow 1/x[CuOsH_3(PMe_2Ph)_3]_x + \mathit{t}BuOH \quad \text{(a)}$$

1

[*] Prof. Dr. K. G. Caulton, Dr. J. C. Huffman, T. H. Lemmen
Department of Chemistry and Molecular Structure Center,
Indiana University
Bloomington, IN 47405 (USA)

[**] This work was supported by U.S. National Science Foundation (CHE 83-05281), by award of a Lubrizol Fellowship to *T. H. L.*, and by gifts of chemicals from Johnson Matthey Co. We thank *Scott Horn* for skilled technical assistance.

The phosphane ligands in compound **1** are equivalent according to the ^{1}H- and ^{31}P-NMR data at +30° and −75°.[3] The hydride ligands show an AA'A''XX'X'' pattern, which is indicative of a *facial* $[H_3Os(PMe_2Ph)_3]$ unit. An X-ray diffraction study[4] of crystals of **1** grown from toluene/pentane shows it to be a trimer with the empirical formula $[Cu_3Os_3H_9(PMe_2Ph)_9]$. The molecular core is a planar raft of the six metal atoms (Fig. 1). The three copper atoms form an equilateral triangle with each Cu–Cu edge asymmetrically bridged by an $[H_3Os(PMe_2Ph)_3]$ unit. Each pyramidal $[Os(PMe_2Ph)_3]$ moiety is oriented such that one phosphorus lies in the Os_3Cu_3 plane, and the three $[Os(PMe_2Ph)_3]$ groups are oriented in phase such that the molecule has an idealized C_3 axis. The ^{1}H-NMR data permit the conclusion that one hydride is *trans* to every Os–P bond (see Scheme 1).



Scheme 1. Idealized structure of **1**.

The inequivalent Cu–Os distances support this placement of hydride ligands since all three singly hydride-bridged Cu–Os distances are longer (2.636(2) Å) than those that are doubly hydride-bridged (2.595(2) Å). Cryoscopic measurements prove that **1** dissolves without dissociation in benzene at 5 °C. With the structure established, it is possible to deduce from the NMR data that the molecule executes a facile local rearrangement in solution: rigid body rotation of the intact octahedral $[(PMe_2Ph)_3OsH_3]$ unit about its internal threefold axis. However, rapid migration of hydrogen between osmium centers is excluded by the ^{1}H-NMR data, implying a substantial activation energy for hydrogen migration via a hydride *terminally* bound to copper.

The same Cu_3Os_3 cluster **1** is formed by elimination of H_2 [Eq. (b)].

$$1/2[HCuPPh_3]_6 + 3[H_4Os(PMe_2Ph)_3] \longrightarrow \underset{\mathbf{1}}{[CuOsH_3(PMe_2Ph)_3]_3} + 3\,PPh_3 + 3\,H_2 \qquad (b)$$

The success of this reaction is noteworthy since no phosphane scrambling is observed and since coordinated PPh_3 is released. PPh_3 thus cannot disrupt the $[Cu_3Os_3(\mu\text{-}H)_9]$ bonding network. R_3PAu is frequently a structural "ersatz" hydrogen.[5] It is therefore remarkable that the product of Equation (b) is not the predicted complex $[(Ph_3PCu)H_3Os(PMe_2Ph)_3]$, an isolobal substitution product of pentagonal bipyramidal $[H_4Os(PMe_2Ph)_3]$. Presumably, the Cu_3 triangles in **1** are particularly stable on account of Cu–Cu bonding (2.626(3) Å) and/or because of the trigonal and quasi-planar CuH_3 unit.

The two synthetic routes to **1**, alcohol elimination and H_2 elimination, are of great conceptual simplicity and are unprecedented[1] and rare,[6] respectively, in heterobimetallic chemistry. The observed mild conditions, high yield, and product selectivity suggest that this will become a synthetic procedure of broad utility for coupling metals at

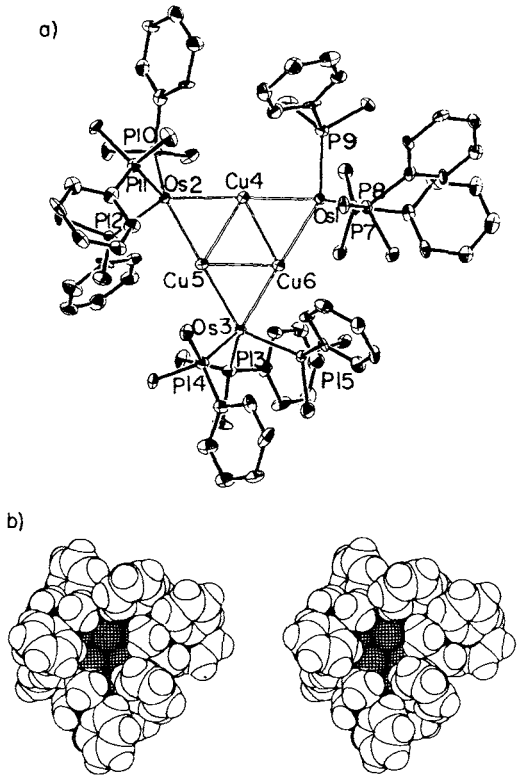


Fig. 1. a) ORTEP drawing of the crystal structure of **1** (without hydrogen atoms) viewed down the idealized C_3 axis. b) Stereoscopic space-filling drawing from the same perspective, with metal atoms hatched. The accessibility of the copper centers through the tunnel of phenyl and methyl groups is evident.

will. At the same time, this work, taken together with other recent results,[7–10] shows that, whereas gold leads to *closo* polyhedral bimetallic clusters, copper (often as a Cu_3 unit) frequently forms flat arrays more amenable to the approach and modification of substrate molecules.[11]

Equation (a) is significant in demonstrating that a transition metal hydride has the ability to liberate alcohol from a copper alkoxide.[12] Methanol synthesis from $CO + H_2$ over a copper/zinc oxide catalyst[13] may therefore occur by reductive elimination from ZnH and $CuOCH_3$ moieties.

Received: November 14, 1985;
revised: January 21, 1986 [Z 1538 IE]
German version: *Angew. Chem. 98* (1986) 267

[1] D. A. Roberts, G. L. Geoffroy in G. Wilkinson, F. G. A. Stone, E. W. Abel (Eds.): *Comprehensive Organometallic Chemistry, Vol. 6*, p. 763. Pergamon, London 1982.

[2] J. C. Huffman, M. A. Green, S. L. Kaiser, K. G. Caulton, *J. Am. Chem. Soc. 107* (1985) 5111.

[3] Reaction of $[OsH_4(PMe_2Ph)_3]$ with $[CuO\mathit{t}Bu]_4$ (Os : Cu 1 : 1) or $[H_6Cu_6(PPh_3)_6]$ (Os : Cu 1 : 1) on a 0.02-mmol scale in a minimum of benzene at 25 °C is complete (^{1}H-NMR) within 2 h to give **1** in 70 or 75% yield, respectively. ^{1}H-NMR (360 MHz, 21 °C, C_6D_6): $\delta = -9.51$ (m, OsH_3Cu), 1.66 (d, PMe, $J = 6$ Hz), as well as phenyl resonances. ^{31}P-NMR (40.5 MHz, 30 °C, C_6D_6): $\delta = -29.6$. Cryoscopic molecular weight determination: 2210 ± 240 (calcd.: 2014).

[4] Crystallographic data (−161 °C): $a = 20.759(7)$, $b = 29.553(15)$, $c = 13.143(4)$ Å, $\beta = 107.76(2)°$, $V = 7678.9$ Å^3, $Z = 4$, space group $P2_1/n$; $R(F) = 0.049$, $R_w(F) = 0.049$ using carbon-bound hydrogens in idealized locations. A search for metal-bound hydrogens revealed only five of the nine; therefore, these were omitted entirely. Selected structural parameters: Os–P = 2.295(4) Å to 2.313(4) Å, P-Os-P = 93.75(14)° to 106.37(14)°. All Cu-Os-Cu and Cu-Cu-Cu angles are within 1.6° of 60°. All Os-Cu-Os angles are within 3.6° of 180°. Further details of the crystal structure determination can be obtained from the director of the Cambridge Crystallographic Data Centre, Lensfield Road, Cambridge CB2

IEW (UK), by quoting the names of the authors and the journal citation.
[5] K. Wald, J. W. Lauher, *J. Am. Chem. Soc. 103* (1981) 7648.
[6] For a synthesis of Pt-Si and Pt-Ge complexes via H_2 elimination, see J. Chatt, C. Eaborn, S. Ibekwe and P. N. Kapoor, *Chem. Commun. 1967*, 869.
[7] A. L. Casalnuovo, J. A. Casalnuovo, P. V. Nilsson, L. H. Pignolet, *Inorg. Chem. 24* (1985) 2554.
[8] G. Doyle, B. T. Heaton, E. Occhiello, *Organometallics 4* (1985) 1224.
[9] L. F. Rhodes, J. C. Huffman, K. G. Caulton, *J. Am. Chem. Soc. 107* (1985) 1759.
[10] L. F. Rhodes, J. C. Huffman, K. G. Caulton, *J. Am. Chem. Soc. 105* (1983) 5137.
[11] The comparative situation for Ag_3 triangles is reported in F. Bachechi, J. Ott, L. M. Venanzi, *J. Am. Chem. Soc. 107* (1985) 1760.
[12] Compare the hydrogenolysis of $[R_3PCuO\mathit{t}Bu]_2$: G. V. Goeden, K. G. Caulton, *J. Am. Chem. Soc. 103* (1981) 7354.
[13] H. L. Kung, *Catal. Rev. 22* (1980) 235.

2-(2,4,6-Tri-*tert*-butylphenyl)-1-arsaethyne—the First Compound Containing an Arsenic-Carbon Triple Bond

By *Gottfried Märkl** and *Hans Sejpka*

Since the synthesis of 2,2-dimethylpropylidinephosphane **1a**, the first phosphaethyne that was found to be stable at room temperature, by *G. Becker* et al.,[1] several stable phosphaethynes, **1b–1d**,[2–4] have been reported. In contrast, stable arsaethynes **2** were unknown until now.

R–C≡P **1**

a, R = *tert*-butyl[1]
b, R = 9-triptycyl[2]
c, R = adamantyl[3]
d, R = 2,4,6-tri-*tert*-butylphenyl[4]

R–C≡As **2**

a, R = 2,4,6-tri-*tert*-butylphenyl

This is not very surprising, because the arsinines[5] (arsabenzene) and the arsaalkenes,[6] which contain the –As=C bond are also less stable than the corresponding phosphorus compounds and can undergo decomposition with formation of brown, arsenic-containing products. Synthesis of **2** by KOH- or $[(n\mathrm{Bu})_4\mathrm{N}]$F-catalyzed elimination of hexamethyldisiloxane from the arsaalkenes $Me_3Si \sim As{=}C(OSiMe_3)R$, in analogy to the synthesis of **1**, has not, therefore, been possible so far.

Recently, we showed[4] that 2,4,6-tri-*tert*-butylbenzoyl chloride **5** undergoes reaction with tris(trimethylsilyl)phosphane only at elevated temperatures, e.g., in refluxing dimethoxyethane to give the phosphaethyne **1d** along with 1,4-bis(trimethylsiloxy)-1,4-bis(2,4,6-tri-*tert*-butylphenyl)-2,3-diphosphabutadiene and traces of the phosphaalkene precursor of **1d**. The corresponding reaction of **5** with tris(trimethylsilyl)arsane **3**[7] results primarily in the formation of the brown, arsenic-containing decomposition products.

We have now found that, upon addition of the acid chloride **5** to a solution of lithium bis(trimethylsilyl)phosphide·2THF in tetrahydrofuran (THF) [prepared from tris(trimethylsilyl)phosphane and *n*BuLi in THF[8]], exclusively the phosphaethyne **1d** (yield 12–20%) is formed after 48 h at room temperature, in contrast to the reaction with $P(SiMe_3)_3$.

Lithium bis(trimethylsilyl)arsenide·2THF **4** (see ref. [7a]), prepared from tris(trimethylsilyl)arsane **3** and methyllithium, also undergoes reaction at room temperature with the acid chloride **5** in anhydrous THF. After reaction for 20 h under nitrogen in the dark, chromatographic workup (oven-dried silica gel 60) of the portion of the reaction mixture that is soluble in *n*-pentane affords a pale yellow, crystalline compound, m.p. = 114–116 °C, which, according to spectroscopic and analytical data, is 2-(2,4,6-tri-*tert*-butylphenyl)-1-arsaethyne **2a**, the first stable compound containing an arsenic-carbon triple bond.

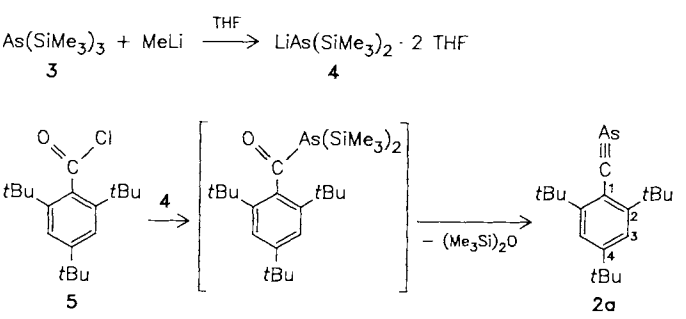


Table 1. Spectroscopic data for the arsaethyne **2a** and comparison with the ^{13}C-NMR data for phosphaethyne **1d**.

MS (70 eV, *m/z* (rel. int.)): $[M+H]^{\oplus}$, 333 (5%); $M^{\oplus\ominus}$, 332 (26%); $[M-{}^{\ominus}CH_3]^{\oplus}$, 317 (4%); $[M-{}^{\ominus}C_4H_9]^{\oplus}$, 256 (16%); $[M-{}^{\ominus}AsH_2]^{\oplus}$, 255 (28%); $[M-{}^{\ominus}AsH-{}^{\ominus}CH_3]^{\oplus\ominus}$, 241 (25%); $[256-C_4H_8]^{\oplus}$, 200 (30%); $[255-C_4H_8]^{\oplus}$, 144 (33%); $[199-C_4H_8]^{\oplus\ominus}$, 143 (22%); $[144-{}^{\ominus}CH_3]^{\oplus}$, 129 (14%); $C_4H_9^{\oplus}$, 57 (100%)

High resolution (MS): $M^{\oplus\ominus}$, found 332.14795, calcd. 332.14853, ΔmM 0.58, 1.70 ppm, $C_{19}H_{29}As$; $[M-{}^{\ominus}AsH-{}^{\ominus}CH_3]^{\oplus\ominus}$, found 241.19573, calcd. 241.19563, ΔmM 0.10, 0.40 ppm, $C_{18}H_{25}$; $[M-{}^{\ominus}AsH_2]^{\oplus}$, found 255.21156, calcd. 255.21128, ΔmM 0.28; 1.00 ppm, $C_{19}H_{27}$

^{1}H-NMR (250 MHz, $CDCl_3$, δ values): $C(CH_3)_3$: 1.29 (s, 9H); $C(CH_3)_3$: 1.70 (s, 18H); phenyl-H: 7.28 (s, 2H)

$^{13}C\{^1H\}$-NMR (62.89 MHz, $CDCl_3$):

	2a	**1d** [a]	*J*(PC) [Hz]
C1	131.70 (s)	124.78 (d)	22.0
C2	157.01 (s)	156.89 (d)	5.79
C3	121.10 (s)	121.07 (d)	1.48
C4	150.96 (s)	151.40 (d)	6.33
C5	37.10 (s)	37.03 (s)	1.77
C6	31.20 (s)	30.92 (s)	
C7	35.49 (s)	35.45 (s)	
C8	31.07 (s)	31.14 (s)	
C≡As	191.86 (s)		
C≡P [b]		168.87 (d)	53.22

[a] For direct comparison. [b] **1a**, δ = 184.8 (d, *J*(PC) = 38.5 Hz); **1b**, δ = 163.3–165.1 (d, *J*(PC) = 46.4–46.7 Hz); **1c**, δ = 184.7 (d, *J*(PC) = 39.0 Hz).

In the high-resolution *mass spectrum* of **2a** (Table 1), the peak for the molecular ion confirms the elemental composition; the pattern of fragmentation is largely in agreement with that of the phosphaethyne **1d**. The 250-MHz *^{1}H-NMR spectrum* (Table 1) is in accord with the structure. In the *$^{13}C\{^1H\}$-NMR spectrum*, the signal of the sp C atom appears at δ = 191.86. Table 1 permits a comparison with the spectral data of phosphaethynes **1**.

Received: December 2, 1985 [Z 1563 IE]
German version: *Angew. Chem. 98* (1986) 286

[*] Prof. Dr. G. Märkl, Dipl.-Chem. H. Sejpka
Institut für Organische Chemie der Universität
Universitätsstrasse 31, D-8400 Regensburg (FRG)

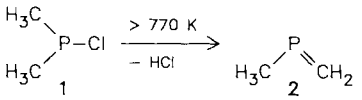
[1] G. Becker, G. Gresser, W. Uhl, *Z. Naturforsch. B36* (1981) 16.
[2] G. Märkl, H. Sejpka, *Tetrahedron Lett. 26* (1985) 5507.
[3] T. Allspach, M. Regitz, G. Becker, W. Becker, *Synthesis 1986*, 31.
[4] G. Märkl, H. Sejpka, *Tetrahedron Lett. 27* (1986) 171.
[5] See, e.g., G. Märkl, R. Liebl, H. Baier, *Liebigs Ann. Chem. 1981*, 1610; R. Liebl, *Dissertation*, Universität Regensburg 1980.
[6] G. Becker, G. Gutekunst, *Z. Anorg. Allg. Chem. 470* (1980) 144.
[7] a) G. Becker, G. Gutekunst, H. J. Wessely, *Z. Anorg. Allg. Chem. 462* (1980) 113; b) see also G. Märkl, F. Lieb, *Tetrahedron Lett. 1967*, 3489.
[8] G. Fritz, W. Hölderich, *Z. Anorg. Allg. Chem. 422* (1976) 104.

$H_3C-P=PCH_2$: An Ylide with Two-Coordinate Phosphorus?

By *Hans Bock** and *Martin Bankmann*

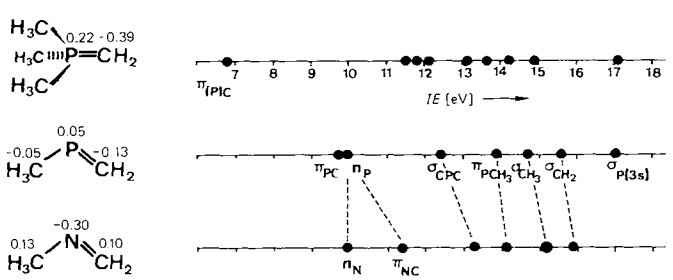
Dedicated to Professor Rolf Appel on the occasion of his 65th birthday

An large number of X–P=Y compounds containing 18 valence electrons and phosphorus of coordination number 2 have been synthesized: Examples are Cl–P=O,[1] Cl–P=S,[1] $H_3C-P=S$,[2] and $Cl-P=CH_2$.[3] All are bent, as predicted by the Walsh rules,[4] and may be regarded as propene analogues within the "united atom" approximation.[5] We report here on 2-phosphapropene **2**, which can be prepared from chlorodimethylphosphane **1** by gas-phase pyrolysis and identified by its photoelectron (PE) and mass spectra (Fig. 1).



According to the useful rule of thumb $(\Sigma np_{El}+\Sigma 1s_H)/2=n\,IE_n^v$,[7] six intense ionization bands are expected in the He(I) PES measurement region for molecules having the composition C_2H_5P and containing seven $np_{Element}$ and five $1s_H$ valence electrons. All of them are indeed observed for both 2-phosphapropene **2** (Fig. 1) and the isomeric phosphirane $(H_2C)_2PH$.[8] The first band in the PE spectrum of **2** is due to two ionizations, which, according to MNDO calculations, involve the removal of electrons from the $\pi_{P=C}$ bond with formation of the radical cation ground state $\tilde{X}(^2A'')$ and from the lone pair at the P atom with formation of the radical cation in its first excited state $\tilde{A}(^2A')$. Between 12 eV and 16 eV, four ionizations from the molecular skeleton follow, which can be characterized as $\sigma_{HCPCH}(a')$, $\pi_{CH_3}(a'')$, $\sigma_{CH_3}(a')$, and $\sigma_{CH_2}(a')$. According to the MNDO calculation, the weak-intensity band at 17.0 eV may be assigned to a radical cation state with a large phosphorus 3s contribution.[9]

Of particular interest is the electron distribution in $H_3C-P=CH_2$ **2** as calculated by MNDO, which is supported experimentally by comparison of the PE spectroscopic data of **2** with those of trimethyl(methylene)phosphorane $(H_3C)_3P=CH_2$,[10] the simplest known phosphorus ylide, and the isosteric methyl(methylene)amine $H_3C-N=CH_2$[11] (see Scheme 1).



Scheme 1. MNDO charge distribution (left) and PE spectroscopic ionization energies (right) of $(H_3C)_3P=CH_2$, $H_3CP=CH_2$, and $H_3CN=CH_2$.

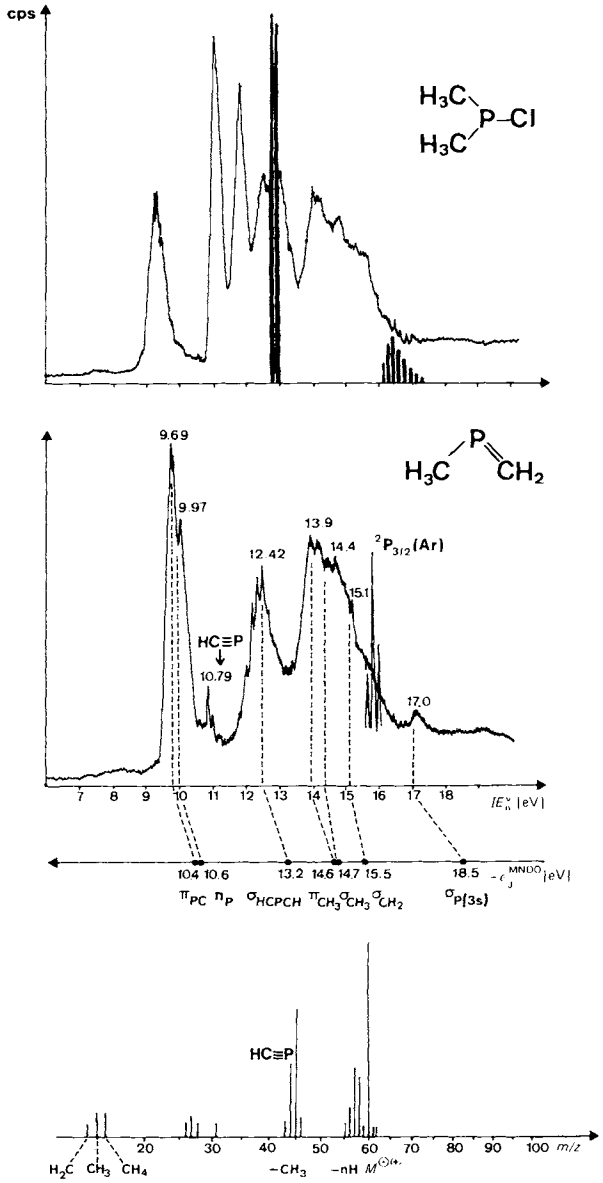


Fig. 1. He(I) PE spectra of the starting material $(H_3C)_2PCl$ **1** (above), which contains traces of HCl (black), and the pyrolysis product at 820 K, $H_3C-P=CH_2$ **2** (middle). Excess starting material and the cleavage product HCl are removed by condensation in a cold trap, which is introduced between the oven (quartz tube: 2 cm × 30 cm) and the spectrometer and which is cooled with ethanol/N_2 to 170 K. The PE spectrum of **2** can be assigned, e.g. (cf. text), by means of Koopman's correlation, $IE_n^v=-\varepsilon_j^{MNDO}$, on the basis of MNDO eigenvalues. Under the pyrolysis conditions that were optimized by PE spectroscopy, it is also possible to record the mass spectrum (below). Both the PE and the mass spectra confirm the formation of HC≡P, which is presumably formed at higher temperature according to $H_3C-P=CH_2\rightarrow CH_4+HC\equiv P$ [6].

The PE spectra of all P ylides exhibit a band at low ionization energies (5.95 to 6.85 eV[10]), which is assigned to electron removal from the polar $P^{\delta\oplus}=C^{\delta\ominus}$ bond exhibiting a high negative charge density at the C atom. In contrast, the first ionization of $H_3C-P=CH_2$ **2** is observed only at 9.69 eV and its PE spectrum is very similar to that of $H_3C-N=CH_2$,[11] the change of sequence $\pi_{PC}<n_P\Rightarrow n_N<\pi_{NC}$ being a consequence of the high effective charge at the nitrogen and the wider CNC angle (compared with CPC in **2**). The calculated charge densities

[*] Prof. Dr. H. Bock, Dipl.-Chem. M. Bankmann
Institut für Anorganische Chemie der Universität
Niederurseler Hang, D-6000 Frankfurt am Main 50 (FRG)

[**] Gas-Phase Reactions, Part 54. This work was supported by the Land Hessen, the Deutsche Forschungsgemeinschaft, the Fonds der Chemischen Industrie, and Hoechst AG.—Part 53: H. Bock, R. Dammel, *Inorg. Chem. 24* (1985) 4427.

(Scheme 1) illustrate that the four-coordinate ylide phosphorus contributes much less to the π delocalization than the two-coordinate phosphorus in **2**.[12] The new molecule $H_3C-P=CH_2$ **2**, therefore, is best characterized as being a 2-phosphapropene and not an ylide.

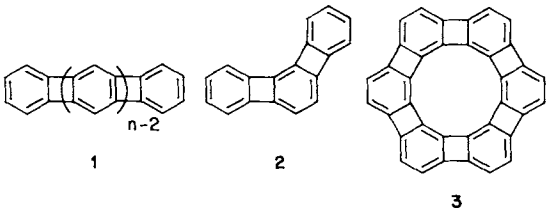
Received: December 3, 1985 [Z 1564 IE]
German version: *Angew. Chem. 98* (1986) 287

[1] M. Binnewies, B. Solouki, H. Bock, R. Becherer, R. Ahlrichs, *Angew. Chem. 96* (1984) 704; *Angew. Chem. Int. Ed. Engl. 23* (1984) 731. For F–P=O and Br–P=O see references cited therein.
[2] Cf. the review of *O. J. Scherer* on "Phosphorus, Arsenic, Antimony, and Bismuth Multiply Bonded Systems with Low Coordination Number—Their Role as Complex Ligands" (*Angew. Chem. 97* (1985) 905; *Angew. Chem. Int. Ed. Engl. 24* (1985) 924) and references cited therein.
[3] M. J. Hopkinson, H. W. Kroto, J. F. Nixon, N. P. C. Simmons, *J. Chem. Soc. Chem. Commun. 1976*, 513. Gas-phase structure: B. Bak, N. S. Kristiansen, H. Svanholt, *Acta Chem. Scand. Ser. A 36* (1982) 1. In the mean time, the synthesis has also been achieved by reaction of gaseous H_3PCl with solid KOR, and the isolated compound could be characterized by NMR spectroscopy at 260 K: R. Carrie (Universität Rennes), *Abstr. CNRS Colloquium la Tour de Carol*, May 1985. A comprehensive review has appeared on alkylidenephosphanes that are kinetically stabilized by bulky substituents: G. Becker, W. Becker, O. Mundt, *Phosphorus Sulfur 14* (1983) 267.
[4] A. D. Walsh, *J. Chem. Soc. 1953*, 2266. Cf. also: R. J. Buenker, S. D. Peyerimhoff, *Chem. Rev. 74* (1974) 127, and references cited therein.
[5] See, for example, E. Heilbronner, H. Bock: *Das HMO-Modell und seine Anwendung, Bd. 1*, 2nd ed., Verlag Chemie, Weinheim 1978, p. 60f.
[6] During the methyl azide pyrolysis, first methanimine $H_2C=NH$ and, at higher temperatures, hydrogen cyanide HC≡N are formed: H. Bock, R. Dammel, L. Horner, *Chem. Ber. 114* (1981) 220.
[7] Cf. the review by H. Bock, B. G. Ramsey, *Angew. Chem. 85* (1973) 773; *Angew. Chem. Int. Ed. Engl. 12* (1973) 734.
[8] D. H. Aue, H. M. Webb, W. R. Davidson, M. Vidal, M. T. Bowers, H. Goldwhite, L. E. Vertal, J. E. Douglas, P. A. Kollmann, G. L. Kenyon, *J. Am. Chem. Soc. 102* (1980) 5151.
[9] Cf. the review by H. Bock on "Photoelectron Spectra and Bonding in Phosphorus Compounds" (*Pure Appl. Chem. 44* (1975) 343).
[10] K. A. Ostoja-Starzewski, H. Bock, *J. Am. Chem. Soc. 98* (1976) 8486.
[11] R. Dammel, *Dissertation*, Universität Frankfurt 1985. Cf. also: D. C. Frost, B. MacDonald, C. A. McDowell, N. P. C. Westwood, *J. Electron Spectrosc. Relat. Phenom. 14* (1978) 379; K. V. L. N. Sustri, R. F. Curl, Jr., *J. Chem. Phys. 41* (1964) 77.
[12] The PE spectrum of $H_3C-P=CH_2$ can be satisfactorily assigned by MNDO calculations without including phosphorus d orbitals in the basis set (Fig. 1). Therefore, the answer to the "Hamlet" question for phosphorus bonds, "to d or not to d," is no, except when a highly correlated eigenfunction containing polarization components is desired.

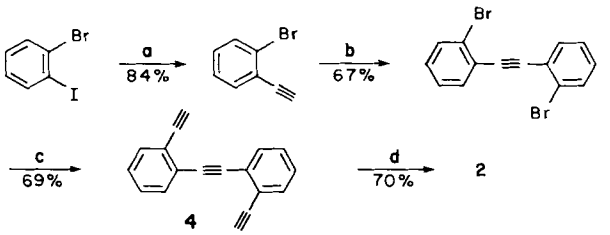
Novel Synthesis of the Angular [3]Phenylene (Terphenylene) by Cobalt-Catalyzed Cyclization of Bis(2-ethynylphenyl)ethyne: a Molecule with an Internal Cyclohexatriene Ring**

By *Rainer Diercks* and *K. Peter C. Vollhardt**

We recently reported[1] an iterative approach by linear cyclobutabenzoannulation to the [n]phenylenes **1**, a novel class of theoretically interesting molecules in which (formally) aromatic benzene rings alternate with antiaromatic cyclobutadienes. There is a topologically alternative series in which the rings are fused in an angular manner as in **2**; this series culminates in the "anti-kelulene" **3**. In **3** both the inside and outside π circuits are 4n, unlike in kekulene.[2] In an effort to approach **3** by application of cobalt-catalyzed alkyne cyclizations,[3] we chose as a test system **2**, prepared earlier by a high-temperature pyrolysis route in low yield.[4] This molecule and its isomer **1** have been the target of several conflicting theoretical treatments.[1d, 5] By making available larger quantities of **2** and investigating its chemistry and structure, we hope to resolve some of the controversy surrounding these compounds.



A retrosynthetic analysis of **2** suggests bis(2-ethynylphenyl)ethyne **4** as the most straightforward precursor. However, considering the four-membered-ring strain in biphenylene, estimated to lie between 64.3 and 75.4 kcal mol^{-1},[6] and assuming that in **2** such strain is cumulative, there was the possibility that the conversion of **4** into **2** was contrathermodynamic, since the cyclotrimerization of ethyne to benzene releases only 143 kcal mol^{-1}[3] (or, for **4** → **2**, $4\,C_t(C_B)+2\,C_t(H)-4\,C_b(C_B)-2\,C_B(H)=-144.2$ kcal mol^{-1}).[7] Moreover, an intramolecular cyclization of the type required had never been reported[3] and in fact failed for the related 1,5,9-decatriyne.[8]



Scheme 1. **a**: 1) Trimethylsilylacetylene, $[PdCl_2(PPh_3)_2]$, CuI, Et_3N, 25°C; 2) CH_3OH, potassium hydroxide; **b**: *o*-bromoiodobenzene, $[PdCl_2(PPh_3)_2]$, CuI, Et_3N, 25°C; **c**: 1) trimethylsilylacetylene, $[PdCl_2(PPh_3)_2]$, CuI, Et_3N, 110°C; 2) CH_3OH, potassium hydroxide; **d**: 1) $[(C_5H_5)Co(CH_2=CH_2)_2]$, tetrahydrofuran, −30°C; 2) CO (8 atm), 100°C.

An efficient and convergent synthesis of **4** is depicted in Scheme 1. It begins with *o*-bromoiodobenzene,[9] which undergoes iterative sequences of palladium-catalyzed couplings with trimethylsilylacetylene and deprotections.[10] Gratifyingly, cyclization of **4** (m.p. = 74°C) with $[(C_5H_5)Co(CO)_2]$[3] as catalyst (30%) or, better, stepwise with $[(C_5H_5)Co(CH_2=CH_2)_2]$[11] gave **2** as yellow crystals in 70% yield (m.p. = 185°C, lit. [4] 175–177°C). The spectral data agree with those reported. The four quaternary carbons (not previously located) resonate (C_6D_6, 125 MHz, 25°C) at $\delta = 136.16$, 149.44, 149.49, and 150.88 (2C each), which, except for the relatively high-field position of the first peak, are similar to the values for related compounds.[1d, 12] The coupling constant between the two hydrogens on the central ring ($J = 6.42$ Hz, not previously determined) was obtained from ^{13}C satellite ^1H-NMR mea-

[*] Professor Dr. K. P. C. Vollhardt, Dr. R. Diercks
Department of Chemistry, University of California,
and the Materials and Molecular Research Division,
Lawrence Berkeley Laboratory
Berkeley, CA 94720 (USA)

[**] This work was supported by the National Institutes of Health (CA 20173). *K. P. C. V.* is a Miller Research Professor in Residence (1985–1986). *R. D.* was the recipient of a NATO Science Fellowship (1984–1985). The X-ray structural analysis was carried out by Dr. *F. J. Hollander*, staff crystallographer.

surements. It is less than J_{H1-H2} (6.6 Hz) in **1**, n = 3,[1d] suggesting strong bond localization. Consistent with this notion, catalytic hydrogenation of **2** (Pd-C, 10-atm H_2) proceeded cleanly (99%) to give a hexahydro derivative, assigned the all-*cis* configuration.[13] Its conformational mobility is restricted at −60 °C.[13] Interestingly, in a competitive hydrogenation experiment, **1** reacted 2–3 times faster than **2**.

Preliminary cyclic voltammetry on **2** (Pt electrode vs. $Ag/Ag^{\oplus}$, CH_3CN, 0.1 M $Bu_4N^{\oplus}PF_6^{\ominus}$) reveals a reversible one-electron ($E_{1/2} = -2.34$ V) and, in contrast to **1**, n = 3, an irreversible two-electron reduction wave ($E = -2.73$ V) in addition to an irreversible oxidation wave ($E = 0.96$ V). Exposure to a potassium mirror changed the color of a solution of **2** in [D_8]tetrahydrofuran instantly from yellow to green (presumably the color of its radical anion); however, unlike **1**, n = 3, no dianion $\mathbf{2}^{2\ominus}$ was observed upon prolonged reaction.

The ^{1}H-NMR spectrum of **2** exhibits an unusually strongly shielded singlet for the central aromatic hydrogens ($CDCl_3$, $\delta = 6.13$;[4] C_6D_6, $\delta = 5.96$), which initially[4] seemed to be indicative of the presence of two strongly paratropic cyclobutadienoid rings. Recently, an alternative explanation involving reduced diatropism of the central benzene ring was suggested.[1d, 14] In light of this uncertainty and in order to compare the structural features of **2** with those of a tetrasilyl derivative of **1**, n = 3,[1b,d] an X-ray structural study was carried out (Fig. 1).[15]

Finally, the structural data and the successful catalytic conversion of **4** into **2** allow us to estimate an upper limit for the combined ring strain in **2**: ΔH^0 of **4** → **2** (cyclohexatriene) = $4\,C_t(C_B) + 2\,C_t(H) - 4\,C_D(C_B,C) - 2\,C_D(C_D,H) = -122.54$ kcal mol^{-1}. This value also suggests that the second cyclobutadiene moiety in **2** adds considerably less strain than the first[6] to the system.

Received: November 18, 1985 [Z 1539 IE]
German version: *Angew. Chem. 98* (1986) 268

CAS Registry numbers:
2, 65513-20-4; **4**, 27499-64-5; *o*-BrC_6H_4I, 583-55-1; *o*-$BrC_6H_4C{\equiv}CH$, 766-46-1; $TMSC{\equiv}CH$, 1066-54-2; $(o\text{-}BrC_6H_4)_2C_2$, 38399-13-2; $(C_5H_5)Co(C_2H_4)_2$, 69393-67-5.

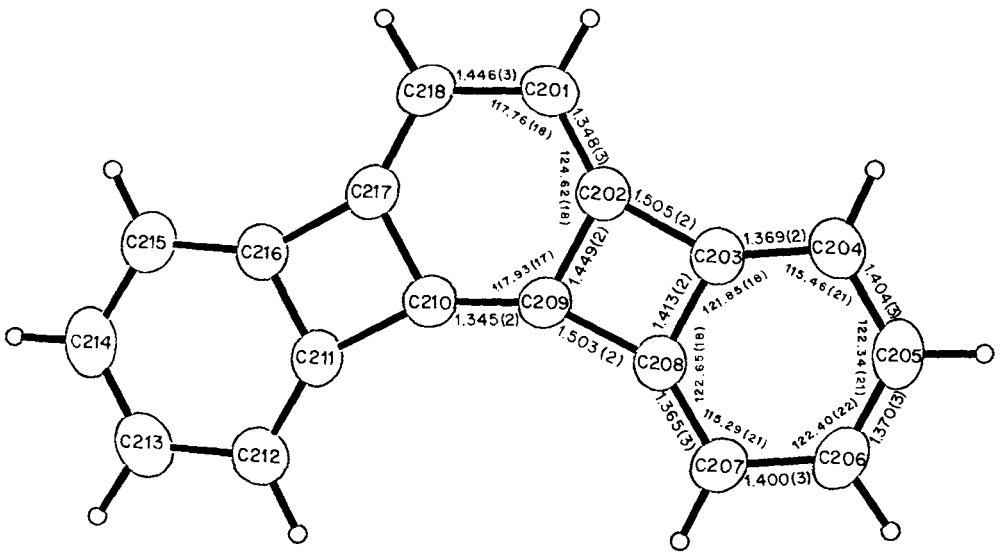


Fig. 1. ORTEP drawing of the crystal structure of **2** (IUPAC name: benzo[3,4]cyclobuta[1,2-*a*]biphenylene). Ellipsoids are scaled to represent the 50% probability surface. Selected bond lengths [Å] and angles [°] are taken from the center one of three closely similar and quite symmetrical molecules stacked in the unit cell. The bond angles in the four-membered rings deviate from 90° by less than 1°.

The molecule is completely flat. In contrast to the framework of **1**, n = 3, the outside benzene rings show very little bond alternation. This bond alternation is comparable to that in strained cycloalkabenzenes[16a] and consistent with the more recent ^{1}H-NMR analysis.[1d, 14] The bonds in the central ring, however, are *considerably more localized than in all related structures* synthesized in order to detect the elusive cyclohexatriene unit[1, 16] and are comparable to the bonds in 1,3-buta-,[17] 1,3-cyclohexa-,[18] and 1,3-cyclopentadiene[19]! We conclude that **2** contains the first such unit verified by X-ray analysis.

[1] a) B. C. Berris, G. H. Hovakeemian, K. P. C. Vollhardt, *J. Chem. Soc. Chem. Commun. 1983*, 502; b) H. G. Hovakeemian, K. P. C. Vollhardt, *Angew. Chem. 95* (1983) 1001; *Angew. Chem. Int. Ed. Engl. 22* (1983) 994; c) H. E. Helson, K. P. C. Vollhardt, Z.-Y. Yang, *ibid. 97* (1985) 120 and *24* (1985) 114; d) B. C. Berris, G. H. Hovakeemian, Y.-H. Lai, H. Mestdagh, K. P. C. Vollhardt, *J. Am. Chem. Soc. 107* (1985) 5670.
[2] a) H. A. Staab, F. Diederich, *Chem. Ber. 116* (1983) 3487; b) H. A. Staab, F. Diederich, C. Krieger, D. Schweitzer, *ibid. 116* (1983) 3504.
[3] K. P. C. Vollhardt, *Angew. Chem. 96* (1984) 525; *Angew. Chem. Int. Ed. Engl. 23* (1984) 539.
[4] J. W. Barton, R. B. Walker, *Tetrahedron Lett. 1978*, 1005.
[5] a) M. Randic, *Tetrahedron 33* (1977) 1905; *J. Am. Chem. Soc. 99* (1977) 444; *Pure Appl. Chem. 52* (1980) 1587; b) T. H. K. Barron, J. W. Barton, J. D. Johnson, *Tetrahedron 22* (1966) 2609; c) C. Glidewell, D. Lloyd, *ibid. 40* (1984) 4455.
[6] a) A. F. Bedford, J. G. Carey, I. T. Millar, C. T. Mortimer, H. D. Springall, *J. Chem. Soc. 1962*, 3895; b) W. D. Good, *J. Chem. Thermodynamics 10* (1978) 553.
[7] S. W. Benson: *Thermochemical Kinetics*, 2nd ed., Wiley-Interscience, New York 1976.
[8] W. V. Dower, K. P. C. Vollhardt, unpublished results, and *Angew. Chem. 94* (1982) 712; *Angew. Chem. Int. Ed. Engl. 21* (1982) 685; *Angew. Chem. Suppl. 1982*, 1545.
[9] H. Heaney, I. T. Millar, *Org. Synth. Coll. Vol. 5* (1973) 1120.
[10] Three of the intermediates have been prepared previously by other routes: H. A. Staab, H. Mack, A. Nissen, *Chem. Ber. 105* (1972) 2310; H. Hommes, H. D. Verkruijsse, L. Brandsma, *Tetrahedron Lett. 22* (1981) 2495; R. L. Letsinger, J. R. Nazy, *J. Am. Chem. Soc. 81* (1959) 3013.
[11] K. Jonas, E. Deffense, D. Habermann, *Angew. Chem. 95* (1983) 729; *Angew. Chem. Int. Ed. Engl. 22* (1983) 716; *Angew. Chem. Suppl. 1983*, 1005.
[12] A. J. Jones, P. J. Garratt, K. P. C. Vollhardt, *Angew. Chem. 85* (1973) 260; *Angew. Chem. Int. Ed. Engl. 12* (1973) 241.

[13] all-*cis*-4b,5,6,6a,10b,10c-Hexahydro-**2**: MS: *m/z* 232 ($M^{\oplus}$); ^{1}H-NMR ($CDCl_3$, 300 MHz, 25°C): $\delta = 1.6$ (bs, 2H), 1.80 (m, 2H), 3.66 (bs, 2H), 3.95 (bs, 2H), 6.93 (m, 4H), 7.07 (m, 4H); ^{13}C-NMR ($CDCl_3$, 50 MHz, 25°C): $\delta = 41.36$, 42.07 (2C), 121.67, 122.83, 126.61, 126.90, 148.058, 148.061; ^{1}H-NMR ($CDCl_3$, 300 MHz, −60°C): $\delta = 1.07$ (ddd, $J = 18$, 18, 17 Hz, 1H), 1.83 (ddd, $J = 23$, 13, 2.6 Hz, 1H), 1.87 (dd, $J = 11$, 11 Hz, 1H), 2.09 (b d, $J = 7.5$ Hz, 1H), 3.52 (ddd, $J = 23$, 12, 6 Hz, 1H), 3.86 (m, 2H), 4.11 (dd, $J = 10$, 5 Hz, 1H), 6.70 (d, $J = 7.1$ Hz, 1H), 7.00 (m, 3H), 7.12 (t, $J = 7.5$ Hz, 1H), 7.18 (t, $J = 7.4$ Hz, 1H), 7.27 (t, $J = 7.3$ Hz, 1H), 7.35 (d, $J = 7.1$ Hz, 1H).

[14] J. W. Barton, D. J. Rowe, *Tetrahedron 41* (1985) 1323.

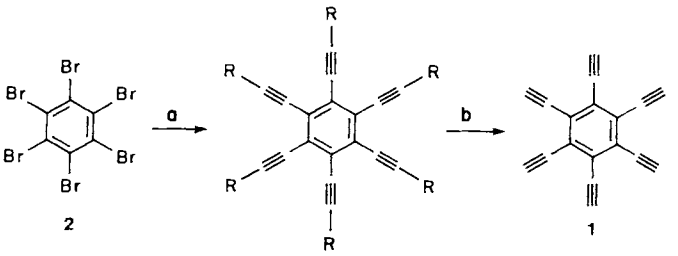
[15] Monoclinic, $C2/c$, $a = 28.1885(22)$, $b = 14.8313(15)$, $c = 18.7964(18)$ Å, $\beta = 119.747(7)°$, $V = 6822.8(24)$ Å^3 at 25°C, $Z = 24$, $\rho_{calcd} = 1.32$ g cm^{-3}, $\mu_{calcd} = 0.70$ cm^{-1}; $Mo_{K\alpha}$ radiation (graphite monochromator); $3° \leq 2\theta \leq 50°$; reflections collected 6647, 5994 unique with $F^2 > 1.5\sigma(F^2)$; $R = 0.036$, $R_w = 0.044$. Further details of the crystal structure investigation may be obtained from the Fachinformationszentrum Energie, Physik, Mathematik GmbH, D-7514 Eggenstein-Leopoldshafen 2 (FRG), on quoting the depository number CSD 51749, the names of the authors, and the journal citation.

[16] a) A. Greenberg, J. F. Liebman: *Strained Organic Molecules*. Academic Press, New York 1978; b) F. H. Allen, *Acta Crystallogr. B37* (1981) 900; c) J. D. Korp, R. P. Thummel, I. Bernal, *Tetrahedron 33* (1977) 3069; R. P. Thummel, J. D. Korp, I. Bernal, R. L. Harlow, R. L. Soulen, *J. Am. Chem. Soc. 99* (1977) 6916; R. E. Cobbledick, F. W. B. Einstein, *Acta Crystallogr. B32* (1976) 1908; E. R. Boyko, P. A. Vaughan, *ibid. 17* (1964) 152.

[17] W. Haugen, M. Traetteberg, *Acta Chem. Scand. 20* (1966) 1726; K. Kuchitsu, T. Fukuyama, Y. Morino, *J. Mol. Struct. 1* (1967–68) 463; C. W. Bock, P. George, G. J. Mains, M. Trachtman, *ibid. 49* (1978) 211.

[18] S. Saebo, J. E. Boggs, *J. Mol. Struct. 73* (1981) 137.

[19] J. Kao, N. L. Allinger, *J. Am. Chem. Soc. 99* (1977) 975.



Scheme 1. a) $[PdCl_2(PPh_3)_2]$, CuI, PPh_3 (for **3a** only), Et_3N, RC≡CH; (**3a**: 34%; **3b**: 28%); b) from **3a**: KO*t*Bu, *t*BuOH (undetermined yield); from **3b**: KF·2 H_2O, [18]crown-6, DME, 10 min (99%).

Hexaethynylbenzene**

By *Rainer Diercks, James C. Armstrong, Roland Boese,* and *K. Peter C. Vollhardt**

Hexaethynylbenzene **1** is exceedingly interesting for a variety of reasons: (1) It is aesthetically pleasing because of its symmetry. (2) It is the only other known $C_{18}H_6$ isomer,[1,2] the first being 1,7,13-cyclooctadecatriene-3,5,9,11,15,17-hexayne.[1] The two compounds are potentially interconvertible by a series of Cope-like rearrangements.[3] (3) Its π-framework may be stabilized by double aromaticity[4] involving the two orthogonal sets of ethynyl π-orbitals, which should exhibit strong through-bond and/or through-space interactions.[5] (4) It should function as a highly electron-rich species on which to anchor transition-metal clusters with potentially novel catalytic activity.[6] (5) It may be a unique starting material for cobalt-catalyzed cyclizations leading ultimately to triangular multiphenylenes.[7] (6) Finally, it should be an exceptional monomer in (co)polymerizations to furnish novel conducting materials.[8]

The most straightforward preparation of **1** can be envisaged to proceed through a palladium-catalyzed hexaethynylation of a hexahalobenzene with a protected alkyne, followed by deprotection.[9] Although such a strategy proved futile with hexaiodobenzene,[10] we have found that hexabromobenzene **2** undergoes this remarkable sixfold carbon-carbon bond formation not only to give **3a** but also **3b**, either employing 2-methyl-3-butyn-2-ol or trimethylsilylacetylene[11] (Scheme 1), and that **3** can be deprotected to give **1** (Table 1). Whereas deprotection of **3a** always resulted in the formation of **1** contaminated with partially protected material, deprotection of **3b** proved to be much more convenient and proceeded essentially quantitatively.[12]

Table 1. Physical data for **3a**, **b**, and **1**.

3a [10]: m.p. > 300°C (dec.); UV (CH_3OH): $\lambda = 273$ (sh, $\lg\varepsilon = 4.88$), 289 (5.13), 297 (sh, 4.83), 309 (4.85) nm; IR (KBr): $\tilde{\nu} = 3340$, 2991, 2939, 2233, 1420, 1378, 1366, 1220, 1156, 958 cm^{-1}; ^{1}H-NMR (CD_3COCD_3): $\delta = 4.56$ (s, 6H), 1.58 (s, 36H); ^{13}C-NMR (CD_3OD-CD_3COCD_3, 1:1): $\delta = 128.1$, 105.2, 65.9, 31.7; MS (70 eV): *m/z* 570 (53), 552 (10), 465 (100), 425 (19), 300 (18).

3b: m.p. = 320°C (dec.); UV (hexane): $\lambda = 286$ (sh, $\lg\varepsilon = 4.76$), 291 (4.86), 302 (5.18), 315 (sh, 4.87), 321 (4.95) nm; IR (KBr): $\tilde{\nu} = 2970$, 2910, 2160, 1400, 1250, 940, 850, 760, 705, 640 cm^{-1}; ^{1}H-NMR ($CDCl_3$): $\delta = 0.26$ (s); ^{13}C-NMR ($CDCl_3$): $\delta = 128.0$, 105.2, 101.0, 0.016; MS (70 eV): *m/z* 654.2828 (calculated: 654.2841).

1: UV (DME): $\lambda = 267$ (sh, $\lg\varepsilon$ (based on quantitative conversion of **3b**) = 4.77), 279 (5.02), 289 (sh, 4.69), 298 (4.76) nm; IR (DME): $\tilde{\nu} = 3240$, 2100 cm^{-1}. Further bands obscured by solvent; ^{1}H-NMR (C_6D_6): $\delta = 3.17$ (s); ^{13}C-NMR (CD_3SOCD_3): $\delta = 128.0$, 91.54, 79.38; MS (70 eV): *m/z* 222 (100), 221 (22), 220 (14), 152 (19).

Hexaethynylbenzene **1** can be precipitated as a white powder, which turns brown slowly in the absence of air but rapidly in its presence. **1** is only soluble in the more polar solvents, such as THF, dimethoxyethane (DME), or dimethylsulfoxide (DMSO), in which it can be stored in dilute form. Preliminary results show that **1** and **3b** form complexes with transition metals.

The spectral data for **1** and **3** are similar to those for other ethynylbenzenes.[9,13] Thus, there are no readily detectable spectral indications of peripheral conjugation. The UV spectra exhibit considerable bathochromic shifts and relatively larger extinction coefficients compared with those found for phenylacetylene and phenyl(trimethylsilyl)acetylene.[14] Curiously, whereas the mass spectrum of phenyl(trimethylsilyl)acetylene shows a base peak corresponding to $M^{\oplus} - CH_3$ (*m/z* 159) and no significant signal for $Me_3Si^{\oplus}$,[15] the latter signal forms the base peak and the only dominant fragmentation signal for **3b**. Because of the

[*] Prof. Dr. K. P. C. Vollhardt, Dr. R. Diercks, J. C. Armstrong
Department of Chemistry, University of California,
and the Center for Advanced Materials,
Lawrence Berkeley Laboratory
Berkeley, CA 94720 (USA)
Dr. R. Boese
Institut für Anorganische Chemie der Universität-Gesamthochschule
Postfach 103764, D-4300 Essen 1 (FRG)

[**] This work was supported by the U.S. Department of Energy (Materials Sciences Division, Office of Basic Energy Sciences, Office of Energy Research, Contract No. DE-AC03-67SF00098). *J. C. A.* was an IBM Polymer Fellow (1984–1985). *R. D.* was the recipient of a NATO Science Fellowship (1984–1985). *K. P. C. V.* is a Miller Research Professor in Residence (1985–1986).

novelty of the structures of these molecules, an X-ray structural analysis was carried out on **3b** (Fig. 1).[16]

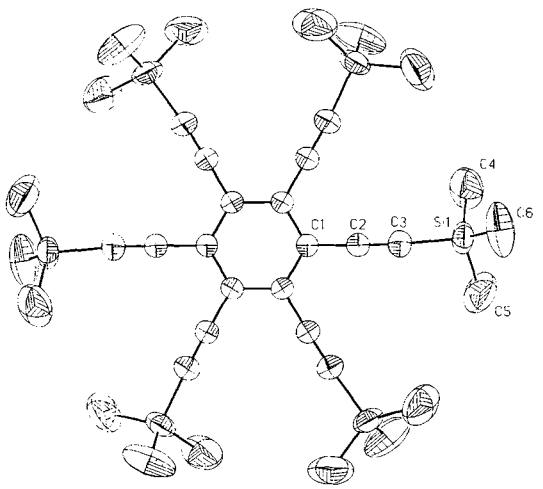


Fig. 1. Crystal structure of **3b** [16]. Important bond lengths [Å] and angles [°]: C1-C2 1.432(3), C1-C1a 1.406(3), C1-C1b 1.406(1), C2-C3 1.195(3), Si1-C3 1.836(2), C2-C1-C1a 120.3(2), C2-C1-C1b 119.7(2), C1-C2-C3 176.5(2), Si1-C3-C2 175.0, C1-C2-C3-Si1 17.5, C2-C1-C1a-C2a 4.4. C1a and C1b indicate the C atoms adjacent to C1 in the benzene ring.

Surprisingly, the molecule (at least in the crystalline state) distorts from perfect symmetry and the alkyne units are not completely linear. All trimethylsilyl groups are "twisted" from a symmetrical radialene structure in alternating directions above and below the molecular plane and in the same direction along the C1-C2-C3 axis (Fig. 2). The closest intramolecular "nonbonded" H-H distance from one trimethylsilyl group to another is 2.72 Å.

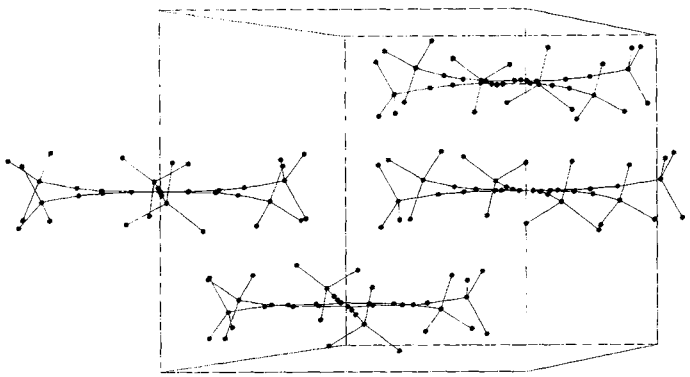


Fig. 2. Side view of the unit cell of the crystal structure of **3b** [16].

A calculated ideal symmetry (planar system, torsional angle C1-C2-C3-Si1 0°, same bond lengths) results in a "nonbonded" H-H separation of 2.30 Å, which is less than the sum of the van der Waals radii of two hydrogens. It must be assumed that the distortions in the molecule are (at least to a major part) due to intramolecular repulsions of the bulky silyl substituents. The aromatic double bonds are longer (by almost 0.02 Å) than those in phenylacetylene,[17] whereas the bond to the alkynyl group and the triple bond are slightly shorter.

Received: December 2, 1985 [Z 1560 IE]
German version: *Angew. Chem. 98* (1986) 270

CAS Registry numbers:
1, 100516-61-8; **2**, 87-82-1; **3a**, 70603-27-9; **3b**, 100516-62-9; HC≡CTMS, 1066-54-2; HC≡CCMe$_2$OH, 115-19-5; CuI, 7681-65-4; PdCl$_2$(PPh$_3$)$_2$, 13965-03-2.

[1] W. H. Okamura, F. Sondheimer, *J. Am. Chem. Soc. 89* (1967) 5991.
[2] I. Agranat, B. A. Hess, Jr., L. J. Schaad, *Pure Appl. Chem. 52* (1980) 1399; M. Randic, N. Trinajstic, *J. Am. Chem. Soc. 106* (1984) 4428.
[3] R. Jones, R. G. Bergman, *J. Am. Chem. Soc. 94* (1972) 660.
[4] J. Chandrasekhar, E. D. Jemmis, P. von R. Schleyer, *Tetrahedron Lett. 1979*, 3707.
[5] H. D. Martin, B. Mayer, *Angew. Chem. 95* (1983) 281; *Angew. Chem. Int. Ed. Engl. 22* (1983) 283.
[6] E. Sappa, A. Tiripicchio, P. Braunstein, *Coord. Chem. Rev. 65* (1985) 219.
[7] K. P. C. Vollhardt, *Angew. Chem. 96* (1984) 525; *Angew. Chem. Int. Ed. Engl. 23* (1984) 539.
[8] G. Wegner, *Angew. Chem. 93* (1981) 352; *Angew. Chem. Int. Ed. Engl. 20* (1981) 361; W. Wiedemann, *Chem. Ztg. 106* (1982) 275, 313; R. H. Baughman, J. L. Bredas, R. R. Chance, R. L. Elsenbaumer, L. W. Shacklette, *Chem. Rev. 82* (1982) 209; G. A. Pagani, G. Gardini, *Chim. Ind. (Milan) 66* (1984) 244; R. W. Munn, *Chem. Brit. 20* (1984) 709; T. Masuda, T. Higashimura, *Acc. Chem. Res. 17* (1984) 51.
[9] B. C. Berris, G. H. Hovakeemian, Y.-H. Lai, H. Mestdagh, K. P. C. Vollhardt, *J. Am. Chem. Soc. 107* (1985) 5670.
[10] a) C. H. Cloutour, U. Groth, K. P. C. Vollhardt, unpublished results; b) the synthesis of **3a** has been claimed but the product was ill-characterized and could not be deprotected: A. A. Moroz, M. S. Shvartsberg, I. L. Kotlyarevskii, *Izv. Akad. Nauk SSSR, Ser. Khim. 1979*, 851.
[11] S. J. Havens, P. M. Hergenrother, *J. Org. Chem. 50* (1985) 1763.
[12] *Experimental procedure:* **3b**: Hexabromobenzene (1.104 g, 2.00 mmol), [PdCl$_2$(PPh$_3$)$_2$] (140 mg, 0.199 mmol), CuI (20 mg, 0.105 mmol), and trimethylsilylacetylene (1.2 g, 12.22 mmol) were heated to 100°C in a Fischer-Porter bottle. More alkyne was added twice in portions of 0.6 g (6.1 mmol) every 24 h. Aqueous workup, followed by chromatography on silica (hexane-CH$_2$Cl$_2$, 85:15) gave **3b** (367 mg, 28%).— **1**: Deprotection was achieved by treatment of **3b** (643 mg, 0.981 mmol) in DME (140 mL, degassed) under N$_2$ with KF·2H$_2$O (7.5 g, 79.68 mmol) and [18]crown-6 (296 mg, 1.233 mmol) for 2.5 h at 0°C. The progress of the reaction can be clearly monitored by thin-layer chromatography. Addition of benzene (100 mL) gave the product as a white precipitate.
[13] a) R. Nast, H.-P. Müller, *Chem. Ber. 111* (1978) 415; b) T. B. Grindley, K. F. Johnson, A. R. Katritzky, H. J. Keogh, C. Thirkettle, R. D. Topsom, *J. Chem. Soc. Perkin Trans. 2 1974*, 282.
[14] H. Bock, H. Alt, *Chem. Ber. 103* (1970) 1784.
[15] W. P. Weber, A. K. Willard, H. G. Boettger, *J. Org. Chem. 36* (1971) 1620.
[16] Rhombohedral, $R\bar{3}$, $a=b=15.729(5)$, $c=15.809(9)$ Å, $\alpha=\beta=90°$, $\gamma=120°$, $V=3387(3)$ Å^3, $Z=3$, $\rho_{calcd}=0.97$ g cm^{-3}, $\mu=1.99$ cm^{-1}; Mo$_{K\alpha}$ radiation: (graphite monochromator); scan range: $3°\leq 2\theta\leq 60°$; reflections collected 2562; 1529 treated as observed ($F_0\geq 4.5\delta(F)$), $R=0.059$, $R_w=0.060$. Further details of the crystal structure investigation may be obtained from the Fachinformationszentrum Energie, Physik, Mathematik GmbH, D-7514 Eggenstein-Leopoldshafen 2 (FRG), on quoting the depository number CSD-51695, the names of the authors, and the journal citation.
[17] A. P. Cox, I. C. Ewart, W. M. Stigliani, *J. Chem. Soc. Faraday Trans. 2 71* (1975) 504.

A Simple Access to 2-Epoxy Alcohols: Titanium(IV)-Catalyzed Oxygen Transfer from Allylic Hydroperoxides**

By *Waldemar Adam,* Axel Griesbeck*, and *Eugen Staab*

Whereas the chemistry of saturated hydroperoxides in the presence of metals has been the subject of numerous studies,[1] little is as yet known about the behavior of the corresponding unsaturated hydroperoxides.[2] Reactions with titanium(IV) isopropoxide have, to our knowledge, so far not been described.

In the presence of stoichiometric or catalytic amounts (1-5 mol-%) of Ti(O*i*Pr)$_4$, the allylic hydroperoxides **1a-d**[3] are converted into the corresponding 2-epoxy alcohols **2a-d** under mild conditions.

[*] Prof. Dr. W. Adam, Dr. A. Griesbeck, Dipl.-Chem. E. Staab
Institut für Organische Chemie der Universität
Am Hubland, D-8700 Würzburg (FRG)

[**] This work was supported by the Deutsche Forschungsgemeinschaft (Sonderforschungsbereich 172: Molekulare Mechanismen kanzerogener Primärveränderungen), the Stiftung Volkswagenwerk, and the Fonds der Chemischen Industrie.

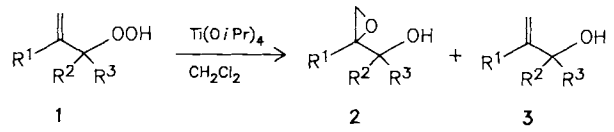


Table 1. Synthesis of 2-epoxy alcohols **2** [a].

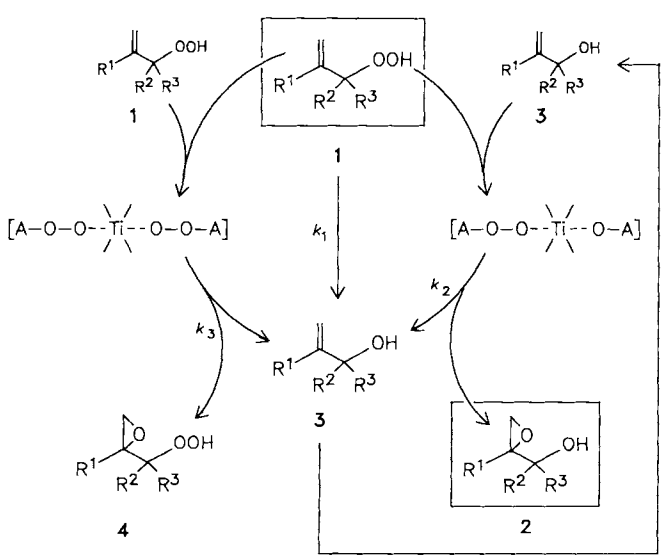
	R^1	R^2	R^3	Epoxy alcohol **2**	
				Yield [%] [b]	d. r. [c]
a	*t*Bu	H	H	87	
b	Me	*t*Bu	H	84	95:5
c	Me	Me	Me	91	
d	CO_2Et	Me	H	68 [d]	90:10

[a] Ca. 0.1 M hydroperoxide solution, 0 °C, 1–5% $Ti(OiPr)_4$ in the case of **1a–c**, equimolar amounts in the case of **1d**; addition of 1 mL of H_2O per mmole $Ti(OiPr)_4$ on completion of the reaction (monitored by TLC and NMR); filtration over celite. [b] Yields after Kugelrohr distillation. [c] Diastereomeric ratios (d. r.) determined by 400-MHz ^{1}H-NMR. [d] In addition, **3d** is formed in 25% yield. **2d** and **3d** were not separated; assignment by comparison of ^{1}H- and ^{13}C-NMR spectra with authenic samples.

Table 1 shows that, independent of the degree of substitution (primary, secondary or tertiary) of the hydroperoxide **1**, the corresponding epoxy alcohols **2** can be isolated in good yields. In the case of the epoxy alcohols **2b** and **2d** the two possible diastereomers are formed in 95:5 and 90:10 ratios, respectively. In the reaction of **1d**, the allylic alcohol **3d** is a by-product; moreover, larger quantities of $Ti(OiPr)_4$ than usual must be used. This finding prompted us to carry out a mechanistic study of this novel oxygen transfer reaction.

For the model study we chose the reaction of **1c** with $Ti(OiPr)_4$. The results are summarized as follows:

- the oxygen transfer does not take place (or only to a small extent) intramolecularly:[4] **1c** is stable for long periods in the presence of catalytic amounts of $Ti(OiPr)_4$ (5%).
- the chain carrier in the step **1c**→**2c** is the allylic alcohol **3c**; addition of small amounts of **3c** to a 20:1 mixture of **1c** and $Ti(OiPr)_4$ accelerates the reaction considerably.
- the epoxy hydroperoxide **4c** could not be detected at any time during the course of the reaction. Independently prepared **4c**[5] transfers oxygen considerably slower than the allylic hydroperoxide **1c** and should accumulate in the reaction **1c**→**2c**.



Scheme 1. A=R^1-C(=CH_2)-CR^2R^3-.

Therefore, we propose the mechanism outlined in Scheme 1. In the case of the allylic hydroperoxide **1c**, k_2 must be substantially greater than k_1; consequently, **3c** lies below the NMR detection limit. Furthermore, k_3 is negligibly small and **4c** does not participate. In the reaction of **1d** with $Ti(OiPr)_4$ the rate constants k_1 and k_2 are of about the same order of magnitude; hence, **3d** accumulates. This also explains why larger amounts (30–40 mol%) of $Ti(OiPr)_4$ are necessary for completion of the reaction **1d**→**2d**.

The reaction outlined here enables the conversion of allylic hydroperoxides, readily accessible by ene reaction with singlet oxygen,[6] into synthetically valuable 2-epoxy alcohols.

Received: November 25, 1985;
supplemented: December 19, 1985 [Z 1549 IE]
German version: *Angew. Chem. 98* (1986) 279

[1] a) G. Sosnovsky, D. J. Rawlinson in D. Swern (ed.): *Organic Peroxides, Vol. 2*, Wiley, New York 1971; b) K. B. Sharpiess, T. R. Verhoeven, *Aldrichim. Acta 12* (1979) 63.

[2] a) R. A. Sheldon, J. K. Kochi: *Metal-catalyzed Oxidations of Organic Compounds*, Academic Press, New York 1981, p. 33; b) K. Allison, P. Johnson, G. Foster, M. B. Sparke, *Ind. Eng. Chem. 5* (1966) 166; c) J. E. Lyons, *Adv. Chem. Ser. 132* (1974) 64.

[3] **1a–c** were prepared by photooxygenation (dichloromethane, tetraphenylporphin, 150 W Na-lamp, 0 °C) of the corresponding olefins. **1d** is formed as sole product in the photooxygenation (tetrachloromethane, tetraphenylporphin, 150 W Na-lamp, 0 °C) of ethyl (*E*)-2-methyl-2-butenoate (88% yield); W. Adam, A. Griesbeck, unpublished results.

[4] *Allison* et al. [2b] report an intramolecular and *Lyons* [2c] an intermolecular reaction of allylic hydroperoxides with organovanadium compounds.

[5] D. Leclerq, J.-P. Bats, P. Picard, J. Moulines, *Synthesis 1982*, 778.

[6] a) K. Gollnick, H. J.Kuhn in H. H. Wasserman, R. W. Murray (Eds.): *Singlet Oxygen*, Academic Press, New York 1979, p. 287–429; b) M. Matsumoto in A. A. Frimer (Ed.): *Singlet Oxygen, Vol. 2, Part 1*, CRC Press, Boca Raton, FL, USA 1985.

Tris(pentacarbonylrhenium)-sulfonium, -selenonium, and -telluronium Ions: Synthesis and Structure of $[\{(OC)_5Re\}_3E]^{\oplus}BF_4^{\ominus}$ (E = S, Se, Te)**

By *Wolfgang Beck,* Wolfgang Sacher,* and *Ulrich Nagel*

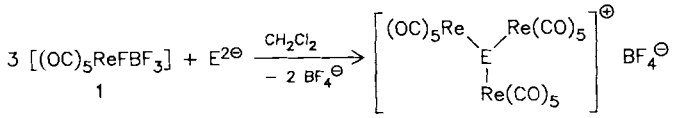
Dedicated to Professor Rudolf Gompper on the occasion of his 60th birthday

Pentacarbonyl(tetrafluoroborato)rhenium(I) **1** behaves like the coordinatively and electronically unsaturated cation $(OC)_5Re^{\oplus}$ and adds numerous nucleophiles.[1] $(OC)_5Re^{\ominus}$ (16e) is isolobal[2] with the carbenium ion $R_3C^{\oplus}$ (6e). We have now found a further analogy between inorganic and organic chemistry in the reaction of **1** with alkali metal chalcogenides, which leads to the tris-metalated sulfonium, selenonium, and telluronium salts **2–4**, respectively. This reaction corresponds to the alkylation of chalcogenides (e.g. with alkyl halides). **1** was allowed to react heterogeneously with Na_2S, Na_2Se, and Li_2Te at 20 °C in

[*] Prof. Dr. W. Beck, W. Sacher, Dr. U. Nagel
Institut für Anorganische Chemie der Universität München
Meiserstr. 1, D-8000 München 2 (FRG)

[**] Organometallic Lewis Acids, Part 22. This work was supported by the Deutsche Forschungsgemeinschaft and the Fonds der Chemischen Industrie.—Part 21: K. Raab, M. Appel, W. Beck, *J. Organomet. Chem. 291* (1985) C28.

dichloromethane with careful exclusion of moisture. The IR spectra (Table 1) of **2–4** are very similar to one another in the $\tilde{\nu}$(CO) region.



[(OC)$_5$Re(OH)BF$_3$] **5**

2: E = S
3: E = Se
4: E = Te

Table 1. IR data [cm^{-1}] of **2–5**.

	$\tilde{\nu}$(CO) [a]	$\tilde{\nu}$(OH) [b]	$\tilde{\nu}$(BF) [b]
2	2145 s, 2060 vs, 2045 s, 2006 s		1060 m
3	2142 s, 2056 vs, 2045 s, 2011 s		1060 *m*
4	2137 s, 2054 vs, 2045 s, 2016 s		1060 m
5		3365 m	1092 m, 963 m 772 w

[a] In nitromethane. [b] In Nujol.

Star shaped complexes of the type EM_3 with metal-chalcogen single bonds and no metal–metal bonds are rare, e.g. **6–9**,[3–6] whereas numerous carbonylchalcogen clusters

[{(Ph$_3$P)Au}$_3$S]$^{\oplus}$Cl$^{\ominus}$ **6**[3]
[{(η^5-C$_5$H$_5$)(CO)$_2$Fe}$_2$SeMn(CO)$_2$(η^5-C$_5$H$_5$)] **7**[4]
[H$_3$CTe{Mn(CO)$_2$(η^5-C$_5$H$_5$)}$_3$]$^{\ominus}$ **8**[5]
[Re$_3$S$_2$(CO)$_{13}$SnMe$_3$] **9**[6]

with μ_3-chalcogen bridges have been described in the literature.[7] The X-ray structure analysis of **4** (Fig. 1) shows a Te–Re distance of 284 pm, corresponding to Re–Te single bonding; a comparable Te–W distance (274 pm) was found in the case of [W(CO)$_5$]$_3$Te$_2$.[9] In contrast, in [{(η^5-C$_5$H$_5$)(CO)$_2$Mn}$_3$Te][8] the Mn=Te double-bond length is 249 pm. As in the case of the (Fe_2Mn)Se moiety in **7**,[4] a

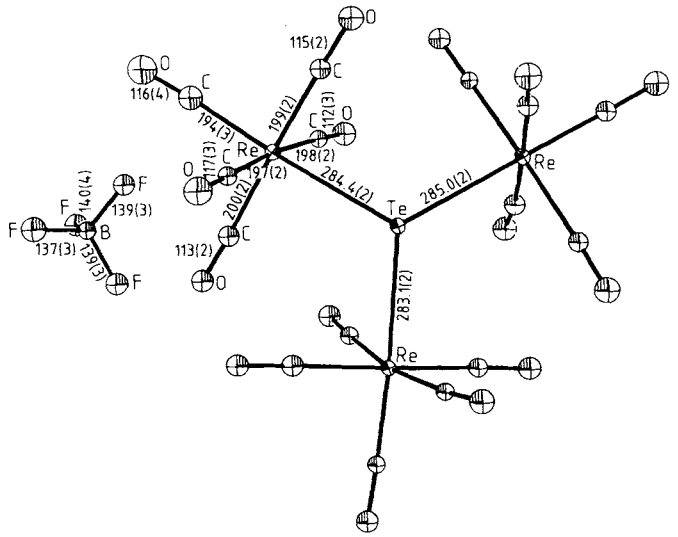


Fig. 1. Low-temperature molecular structure (−50 °C) of **4** in the crystal, 20% probability level. Bond lengths [pm]. Space group *C2/c*, a = 3169(1), b = 697.8(2), c = 2665.6(8) pm, β = 103.56(3)°, V = 5.730(3) nm^3, Z = 8. Crystal size = 0.1 × 0.1 × 0.1 mm^3, μ(Mo$_{K\alpha}$) = 138.8 cm^{-1} (absorption corrected), 5341 collected, 4817 independent, 3644 observed ($I > 2\sigma(I)$) reflections. Number of refined parameters 193; heavy atoms Re and Te anisotropic. R = 0.061, R_w = 0.060, $w = 1/(\sigma^2(F) + g \cdot F^2)$, g = 0.0005. Maximum residual electron density 3.26 (in heavy atoms), 1.74 (external) e·pm^{-3} × 10^6. H-atoms (nitromethane) placed at calculated positions [13].

sum angle of 338° is found for the Re_3Te moiety in **4** (cf. Table 2).

Table 2. Important bond lengths [pm] and angles [°] of [{(OC)$_5$Re}$_3$E]$^{\oplus}$NF$_4^{\ominus}$ **2**, **4**.

	2, E = S	**4**, E = Te
Average E–Re distance	254.8(5)	284.2(1)
Angle Re–E–Re	119.4(4), 120.8(3), 118.3(3)	114.5(1), 111.3(1), 112.0(1)
Sum of angles in the Re$_3$E moiety	358.5(6)	337.8(2)
Distance of Re$_3$-plane from E	18(1)	79(1)

On preparing a single crystal of **2** in nitromethane/ether, partial hydrolysis took place with formation of **5**. This compound crystallizes together with **2** in one crystal (cf. Figures 2 and 3) and could thus be analyzed at the same

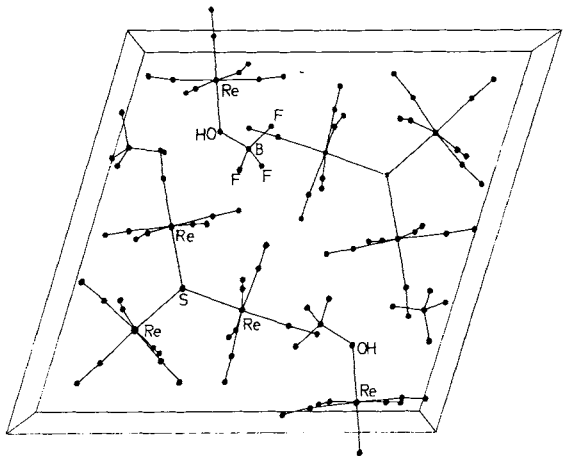


Fig. 2. Unit cell of the crystal of **2** and **5** (measurement at room temperature). Space group P$\bar{1}$, a = 734.7(3), b = 1584.4(5), c = 1608.7(6) pm, α = 106.96(3), β = 91.34(3), γ = 92.24(3)°, V = 1.789(1) nm^3, Z = 2. Crystal size 0.2 × 0.1 × 0.1 mm^3, μ(Mo$_{K\alpha}$) = 138.5 cm^{-1} (absorption corrected), 18288 collected, 6180 independent, 3981 observed ($I > 2\sigma(I)$) reflections. Number of refined parameters 247, heavy atoms Re and S anisotropic. R = 0.077, R_w = 0.072, $w = 1/(\sigma^2(F) + g \cdot F^2)$, g = 0.0008. Maximum residual electron density 2.16 e·pm^{-3} × 10^6 [13].

time. A remarkable feature of **2** is the almost planar arrangement of the $Re_3S^{\oplus}$ moiety (cf. Table 2). This is due more to the spatial requirement of the three Re(CO)$_5$ moie-

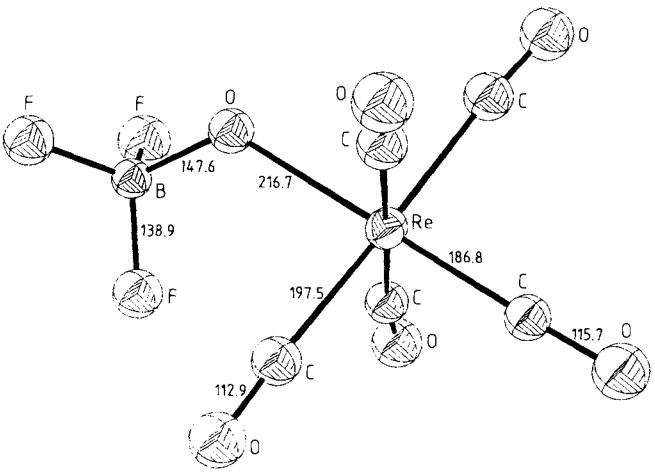


Fig. 3. Molecular structure (at room temperature) of **5** in the crystal. Bond lengths [pm] [13].

ties and less to a significant metal-chalcogen π-bonding in **2**. Because of the greater Re-chalcogen distance, a pyramidal structure is possible in **4**. The Re-S distance of 254 pm in **2** is identical with that in $[Re_3S_2(CO)_{13}SnMe_3]$ containing a μ_3-SRe_3 unit (254 pm).[6] In complexes with metal-sulfur multiple bonds, the metal-S distances are considerably shorter.[10] As proposed earlier,[11] the trifluorohydroxoborate ligand in the crystal of **2** and **5** is bound to the rhenium via the oxygen atom; $F_3B\text{-}F\cdots H\text{-}OBF_3$ hydrogen bridges (F-O 267 pm) are observed between the OH-group and the "free" $BF_4^{\ominus}$ ion.

Experimental

All reactions were carried out in anhydrous solvents under argon. **1** was prepared immediately before the reaction from $[Re(CO)_5CH_3]$ and HBF_4 (54% solution in diethyl ether) [12]. The alkali-metal chalcogenides were dried for several hours in a high vacuum at about 40–50°C.—**2**: A suspension of **1** (0.29 mmol, 120 mg) and Na_2S (0.15 mmol, 12 mg) in CH_2Cl_2 (3 mL) was stirred for 18 h at room temperature. The residue was centrifuged off, washed with 2 mL of CH_2Cl_2, and dried in a high vacuum. When the bands of the coordinated $BF_4^{\ominus}$ ion no longer appeared in the IR spectrum of the product mixture, the residue was extracted twice with 3 mL of nitromethane. **2** was precipitated by dropwise addition of the intensely red-violet solution into 20 mL of Et_2O; yield after drying for 4–5 h in a high vacuum at 30–40°C: 60 mg (55%).—**3** and **4** were prepared analogously. *Properties of* **2**–**4**: stable in air, decomposition above 120°C with brown coloration; **2** red-violet; **3** blue-violet; **4** red.

Received: December 2, 1985;
supplemented: January 15, 1986 [Z 1562 IE]
German version: *Angew. Chem. 98* (1986) 280

[1] K. Raab, W. Beck, *Chem. Ber. 118* (1985) 3830, and references cited therein.
[2] R. Hoffmann, *Angew. Chem. 94* (1982) 725; *Angew. Chem. Int. Ed. Engl. 21* (1982) 711.
[3] C. Kowala, J. M. Swan, *Aust. J. Chem. 19* (1966) 547.
[4] W. A. Herrmann, J. Rohrmann, M. L. Ziegler, T. Zahn, *J. Organomet. Chem. 295* (1985) 175.
[5] W. A. Herrmann, J. Rohrmann, C. Hecht, *J. Organomet. Chem. 290* (1985) 53.
[6] E. Röttinger, V. Küllmer, H. Vahrenkamp, *Chem. Ber. 110* (1977) 1216.
[7] Cf. e.g. H. Vahrenkamp, *Angew. Chem. 87* (1975) 363; *Angew. Chem. Int. Ed. Engl. 14* (1975) 322; M. D. Curtis, W. M. Butler, *J. Chem. Soc. Chem. Commun. 1980*, 998.
[8] M. Herberhold, D. Reiner, D. Neugebauer, *Angew. Chem. 95* (1983) 46; *Angew. Chem. Int. Ed. Engl. 22* (1983) 59; *Angew. Chem. Suppl. 1983*, 10.
[9] O. Scheidsteger, G. Huttner, K. Dehnicke, J. Pebler, *Angew. Chem. 97* (1985) 434; *Angew. Chem. Int. Ed. Engl. 24* (1985) 428.
[10] T. J. Greenhough, B. W. S. Kolthammer, P. Legzdins, J. Trotter, *Inorg. Chem. 18* (1979) 3543; A. Müller, E. Diemann, R. Jostes, H. Bögge, *Angew. Chem. 93* (1981) 957; *Angew. Chem. Int. Ed. Engl. 20* (1981) 934.
[11] K. Raab, B. Olgemöller, K. Schloter, W. Beck, *J. Organomet. Chem. 214* (1981) 81.
[12] K. Raab, W. Beck, *Chem. Ber. 117* (1984) 3169.
[13] Further details of the crystal structure investigation are available on request from the Fachinformationszentrum Energie, Physik, Mathematik GmbH, D-7514 Eggenstein-Leopoldshafen 2, on quoting the depository number CSD-51755, the names of the authors, and the full citation of the journal.

$[Re_4^{IV}S_{22}]^{4-}$, a Highly Symmetrical Metal-Sulfur Cluster with Six S_3^{2-} Ligands

By *Achim Müller,* Erich Krickemeyer,* and *Hartmut Bögge*

Dedicated to Professor Rolf Appel on the occasion of his 65th birthday

Homo- and heteronuclear metal-sulfur clusters of the early transition metals are of special interest in connection with heterogeneous catalysis.[1] Thus, e.g., $[Mo_3^{IV}S_{13}]^{2-}$ is a model for the catalyst MoS_2 and the products of the thermal decomposition of its NH_4^+ salt are excellent catalysts for various processes, such as, e.g., the desulfurization of crude oil.[1] The corresponding rhenium compounds should, in view of their modified electronic structure, be even better catalysts. We have now succeeded in isolating $[Re_4S_{22}]^{4-}$, the first discrete *rhenium*-sulfur cluster, in the form of the NH_4^+ salt **1**.[2] The cluster anion $[Re_4S_{22}]^{4-}$ contains hitherto unknown M_2S_3 rings.

$[NH_4]_4[Re_4S_{22}]\cdot 0.3\,NH_4Cl\cdot 0.7\,H_2O$ **1**

The reddish-brown, diamagnetic salt **1**, which crystallizes in the cubic system, is soluble in H_2O; it is formed upon heating a perrhenate solution with an aqueous polysulfide solution, using $NH_2OH\cdot HCl$ as reducing agent.[9] It was characterized by elemental analysis, magnetic measurements, UV/VIS, IR and Raman spectroscopy,[3] as well as by thermogravimetry, powder diffraction,[4] and a single-crystal X-ray structure analysis.[5] Four Re and four S atoms form a cube (Fig. 1, left). The coordination number 6 of the metal atom is achieved by six S_3^{2-} ligands bridging the faces of the cube; this type of cluster stabilization was hitherto unknown. With this type of coordination the cluster anion (despite its relatively large size) has almost T_d symmetry[6] (fulfilled exactly for the fragment without central S3 atoms). The six Re_2S_3 rings have envelope conformation (see Figure 1 on the right with torsional angles).

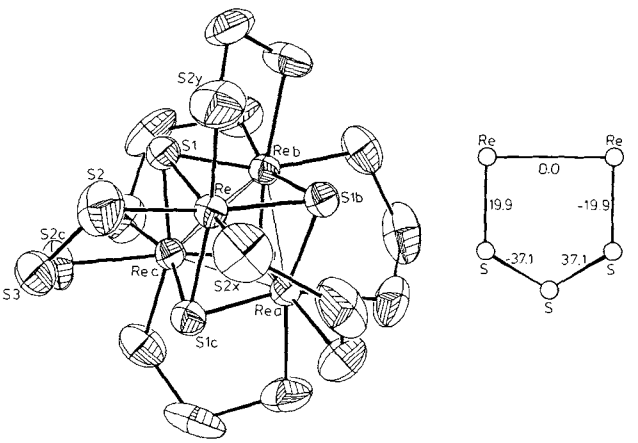


Fig. 1. Left: Structure (thermal ellipsoids at the 40% probability level) of the $[Re_4S_{22}]^{4-}$ anion in crystals of **1**. Important bond lengths [pm] and angles [°]: Re-Rec 276.4(3), Re-S1 231.9(7), Re-S2 246.3(12), S2-S3 214.0(30), S1-S1c 366.9(19); S1-Re-S1c 104.6(4), S1-Re-S2 87.7(4), S1-Re-S2x 159.5(6), S2-Re-S2x 76.3(7), Re-S1-Rec 73.2(2), Re-S2-S3 108.4(9), S2-S3-S2c 112.3(10)). Right: Re_2S_3 ring system with torsional angles [°].

The Re atoms are linked by metal-metal bonds, which is inferred from the diamagnetism of **1** and the short Re-Re distances (ca. 276 pm). The presence of the Re_4 tetrahedron is consistent with our counting rule for clusters.[7] According to Extended-Hückel SCCC-MO calculations the cluster anion of **1** has six bonding MOs (a_1, e, t_2, occupied in the cluster) and six antibonding MOs (t_1, t_2 unoccupied), which have predominant Re-5d character. The stabilization of the Re_4S_4 cluster, however, is essentially due to the Re-S bonding system (MOs: a_1, e, t_1, $2t_2$). Owing to the high symmetry of $[Re_4S_{22}]^{4-}$, there are only a few bands in the vibrational spectra of **1**.[3]

According to preliminary studies, **1** thermally decomposes in a vacuum in several steps to ReS_2, and, finally,

[*] Prof. Dr. A. Müller, E. Krickemeyer, Dr. H. Bögge
Fakultät für Chemie der Universität
Postfach 8640, D-4800 Bielefeld (FRG)

above 1000 °C to rhenium and sulfur.[8] The intermediates could be potentially useful hydrodesulfurization catalysts.

Received: October 31, 1985;
supplemented: December 12, 1985 [Z 1514 IE]
German version: *Angew. Chem. 98* (1986) 258

[1] A. Müller, *Polyhedron*, in press; S. Harris, R. R. Chianelli, *J. Catal. 86* (1984) 400; H. Topsøe, B. S. Clausen, *Catal. Rev. Sci. Eng. 26* (1984) 395.

[2] For interesting cross-linked octahedral clusters cf. W. Bronger, *Angew. Chem. 93* (1981) 12; *Angew. Chem. Int. Ed. Engl. 20* (1981) 52.

[3] IR (solid: CsI disk): ca. 3500 (m) ($\nu(H_2O)$), ca. 3150 (m) ($\nu_{as}(NH_4^+)$), 1600 (m) ($\delta(H_2O)$), 1400 (s) ($\delta_{as}(NH_4^+)$), ca. 500 (m, br) (H_2O-libration), 465 (m) (ν_{as}(S-S), F_2), 339 (m) ($\nu_{as}(Re_4S_4)$, F_2), 230 (m); Raman (solid; $\lambda_e = 647.1$ nm): 460 (br) (ν_s(S-S), A_1), 185 (s) ($\nu_s(Re_4S_4)$, A_1); UV/VIS (solid, reflectance/cellulose standard): $\lambda \approx 600$ (sh), ≈ 440 (sh), ≈ 350 nm.

[4] Strong reflections at $d = 880$, 763, 538, 459, 400, 349, 311, 293, 257, 253, 240, 232, 229, 219, 213, 198 pm. The measured diagram is in very good agreement with that calculated from the data of the single crystal X-ray structure analysis regarding positions of reflections and their intensities.

[5] **1** crystallizes in the space group $F\bar{4}3m$; $a = 1518.1(3)$ pm, $V = 3498.7 \times 10^6$ pm^3, $Z = 4$, $\rho_{calc} = 2.94$ g cm^{-3}. Empirical absorption correction; solution of structure by heavy atom methods; $R = 0.047$ for 191 independent reflections ($F_0 > 3.92\sigma(F_0)$); Syntex $P2_1$ diffractometer, $Mo_{K\alpha}$ radiation, graphite monochromator. Further details of the crystal structure investigations of **1** and **2** [9] are available on request from the Fachinformationszentrum Energie, Physik, Mathematik GmbH, D-7514 Eggenstein-Leopoldshafen 2, on quoting the depository number CSD-51671, the names of the authors, and the full citation of the journal.

[6] In the crystal, $[Re_4S_{22}]^{4-}$ has the site symmetry $\bar{4}3m$ (T_d). S3 is disordered at two positions, 69.1 pm above and below the Re-S2-S2c-Rec plane.

[7] A. Müller, R. Jostes, F. A. Cotton, *Angew. Chem. 92* (1980) 921; *Angew. Chem. Int. Ed. Engl. 19* (1980) 875; A. Müller, R. Jostes, W. Eltzner, Chong-Shi Nie, E. Diemann, H. Bögge, M. Zimmermann, M. Dartmann, U. Reinsch-Vogell, Shun-Che, S. J. Cyvin, B. N. Cyvin, *Inorg. Chem. 24* (1985) 2872.

[8] A. Müller, E. Diemann, E. Krickemeyer, unpublished.

[9] Note added in proof (Februar 14, 1986): The chloride-free compound $(NH_4)_4[Re_4S_{22}] \cdot 2H_2O$ (**2**) has now been obtained by reaction of ammonium perrhenate with an aqueous polysulfide solution at ca. 60 °C. In this case, S_7^{2-} acts as a reducing agent. The bond lengths and angles determined for **2** by X-ray structure analysis resemble those of **1**.

$[Bi_2^{III}S_{34}]^{4-}$, the Hitherto Sulfur-Richest Complex

By *Achim Müller**, *Marion Zimmermann*, and *Hartmut Bögge*

The chemistry of polysulfido complexes is always full of surprises—especially for the structural chemist.[1,2] We have now been able to synthesize the sulfur-rich compound

$[AsPh_4]_4[Bi_2S_{34}]$ **1**,

the complex anion of which has a remarkable structure (Fig. 1). Small, brownish-red crystals of **1** are obtained in good yield upon reaction of a CH_3CN polysulfide solution with $BiCl_3$ in the presence of Ph_4AsCl.[3] The salt was characterized by elemental analysis, IR and Raman spectroscopy,[4] and a complete X-ray structure analysis.[5]

In the anion $[Bi_2S_{34}]^{4-}$ the two Bi atoms, which are linked via a S_6^{2-} chain, are each coordinated to two bidentate S_7^{2-} ligands (Fig. 1). The coordination polyhedron of each Bi atom is a strongly distorted square pyramid (influence of the lone pair!), whose apex is formed by the coordinating atom of the S_6^{2-} chain. As expected, the axial Bi-S bonds, with a mean length of 268.3 pm, are shorter than the equatorial ones (281.7 pm). The torsional angles

[*] Prof. Dr. A. Müller, Dipl.-Chem. M. Zimmermann, Dr. H. Bögge
Fakultär für Chemie der Universität
Postfach 8640, D-4800 Bielefeld 1 (FRG)

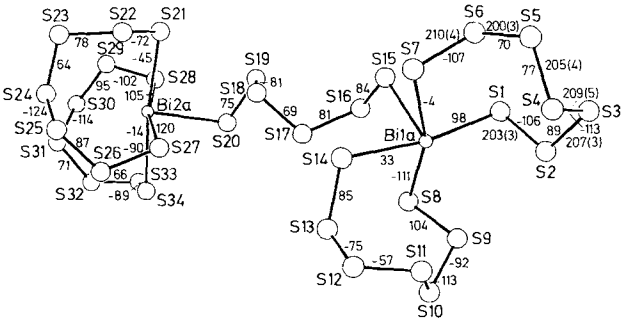


Fig. 1. Structure of the $[Bi_2S_{34}]^{4-}$ ion [5] in crystals of **1** with torsional angles [°], bond lengths [pm] for one S_7^{2-} ligand; other bond lengths [pm] (mean values): Bi-S_{eq} 281.7; Bi-S_{ax} 268.3; selected bond angles [°]: S-Bi-S 72.3(7)-103.8(7) and 161.3(7)-171.7(10); S-S-S (S1-S7-ring) 102.8(16)-110.3(14); S-S-S (S_6 chain) 105.7(14)-113.0(18).

(Fig. 1) show that the S_6^{2-} chain has an all-*trans* conformation and that the BiS_7 eight-membered ring roughly approximates a "boat-chair" conformation[6] (with the Bi atoms causing strong distortion). The four mirror planes to be expected for such a conformation run approximately through the S2 and S6, S9 and S13, S22 and S26, and S29 and S33 atoms.

Neither a complex with a bridging S_6^{2-} ligand nor one with a bidentate S_7^{2-} ligand has hitherto been reported in the literature. The latter fact is surprising, as this type of coordination is most frequently observed in the case of polysulfide ligands; so far, only one structural type with a tridentate S_7^{2-} ligand has been reported.[7] Since the successful isolation of **1** there are now examples for n = 3-7 and 9 that are known for the monocyclic MS_n systems.[1,2]

Received: October 31, 1985 [Z 1515 IE]
German version: *Angew. Chem. 98* (1986) 259

CAS Registry number:
1, 100681-55-8.

[1] M. Draganjac, T. B. Rauchfuss, *Angew. Chem. 97* (1985) 745; *Angew. Chem. Int. Ed. Engl. 24* (1985) 742.

[2] A. Müller, E. Diemann, *Adv. Inorg. Chem. Radiochem. 30*, in press.

[3] Procedure: CH_3CN (100 mL, AR) was first treated with a stream of NH_3 for 10 min and then, after addition of Ph_4AsCl (1 g) and S_8 (1 g), with a stream of H_2S for 45 s (flow rate: 10 L/h). The mixture was stirred for a further 30 s and then treated with a solution of $BiCl_3$ (1 g) in dimethylformamide (30 mL); after ca. 1 min the dark precipitate was filtered off. On storing the dark reddish-brown filtrate in a sealed vessel at 20-25 °C, dark brown crystals (brownish-red streak) of **1** precipitated within 1-2 d; these were filtered off and washed several times with H_2O, isopropyl alcohol, toluene, and diethyl ether. (The PPh_4^+ salt can be prepared analogously.) Yield: 0.56 g (ca. 60%).

[4] IR (solid, CsI pellet; weak bands of the PPh_4^+ salt, since the bands of the $AsPh_4^+$ ion partly mask the relevant region for the anion of **1**): 500, 465, 456, 448 cm^{-1} (ν(S-S)); Raman (solid; $\lambda_e = 647.1$ nm; bands below 500 cm^{-1} with medium to strong intensity): 449, 450 (ν(S-S)), 277, 264, 234, 186 cm^{-1}.

[5] **1** crystallizes in the triclinic system; $P\bar{1}$, $a = 1423.1(7)$, $b = 1816.3(8)$, $c = 2393.5(11)$ pm, $\alpha = 72.45(3)$, $\beta = 80.71(4)$, $\gamma = 86.15(4)°$, $V = 5820.2 \times 10^6$ pm^3, $Z = 2$, $\rho_{calc} = 1.74$ g cm^{-3}. Empirical absorption correction. Solution of structure by heavy atom methods; $R_w = (\sum w(|F_0| - |F_c|)^2 / \sum w|F_0|^2)^{1/2} = 0.108$ ($w = \sigma^{-2}(F_0)$), $R = 0.149$ for 4300 independent reflections ($F_0 > 3.92\sigma(F_0)$); Syntex $P2_1$ diffractometer; $Mo_{K\alpha}$ radiation. The anion of **1** is statistically distributed over two sites in the ratio 0.9:0.1 (structure of the main component in Fig. 1). This disorder could be resolved quite well for the Bi atoms, but not for the S atoms (limited data set due to small size of crystal). Further details of the crystal structure investigation are available on request from the Fachinformationszentrum Energie, Physik, Mathematik GmbH, 7514-Eggenstein-Leopoldshafen 2, on quoting the depository number CSD-51670, the names of the authors, and the full citation of the journal.

[6] R. Bucourt, *Top. Stereochem. 8* (1974) 159.

[7] J. Gotzig, A. L. Rheingold, W. Werner, *Angew. Chem. 95* (1984) 813; *Angew. Chem. Int. Ed. Engl. 23* (1984) 814.

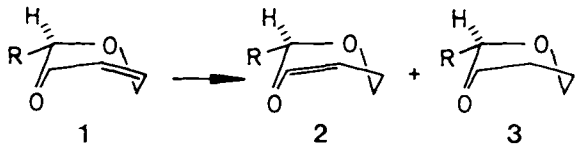
Asymmetric Double-Bond Isomerization of 4,7-Dihydro- to 4,5-Dihydro-1,3-dioxepins

By *Herbert Frauenrath** and *Thomas Philipps*

Allyl alcohols and allyl ethers can be converted by transition metal-catalyzed double-bond isomerization into aldehydes and enol ethers, respectively.[1] Recently, the isomerization of prochiral substrates with chiral catalysts has also been investigated in connection with studies on asymmetric syntheses,[2] but so far only the isomerization of allylamines to enamines has been successfully achieved.[3]

We report here on the hitherto uninvestigated asymmetric double-bond isomerizations of prochiral 4,7-dihydro-1,3-dioxepins **1**, which, in contrast to the above mentioned educts, do not contain a center of prochirality at the double bond, but have a prochiral acetal C-atom at the 2-position of the seven-membered heterocycle. Such isomerizations of **1** lead to optically active 4,5-dihydro-1,3-dioxepins **2**, which are suitable precursors, e. g., for the synthesis of 2,3-substituted tetrahydrofurans or 3,4-substituted 4-butanolides.[4]

For the asymmetric isomerization of **1**, we used $Ru_2Cl_4(diop)_3$[5] and $[Rh(cod)Cl]_2$/diop,[6] which we converted with $NaBH_4$ in CH_3OH/THF in situ into the catalytically active hydridic species (Table 1).



1 **2** **3**

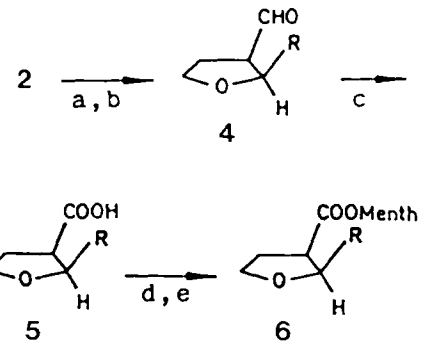
Table 1. Asymmetric isomerization of the dioxepins **1** [a]. **a**, R = *n*-C_4H_9; **b**, R = CH_2-CH_2-Cl; **c**, R = CH_2CH_2-CN. diop = *P,P'*-(2,2-dimethyl-1,3-dioxolanediyldimethylene)bis(diphenylphosphane); cod = 1,5-cyclooctadiene; THF = tetrahydrofuran.

Catalyst	1	2			3
		Conversion [%] [b]	Yield [%] [c]	*ee* [%] [d]	Yield [%] [c]
$Ru_2Cl_4(diop)_3$	**a**	97	91	13	4
	b	95	83	9	5
	c	93	84	25	5
$[Rh(cod)Cl]_2$/diop (1:2)	**a**	100	61	3	32
$[Rh(cod)Cl]_2$/diop (1:4)	**a**	95	91	12	2
	b	99	88	12	7
	c	92	80	23	6

[a] 0.5 mmol of catalyst in 40 mL THF/20 ml CH_3OH, then 0.5 g of $NaBH_4$, 0.1 mol of **1**, 24 h, room temperature, N_2. Catalyst deactivation by bubbling with air. Work-up by distillation. Catalysts were used with (+)- or (−)-diop. [b] Determined gas-chromatographically. [c] After distillation. [d] Reproducibility ±2%.

Almost complete conversions were achieved at room temperature with catalyst concentrations of 0.5 mol-%. Hydrogenation to the 1,3-dioxepanes **3** was generally only of a secondary nature. The highest enantiomeric excess (*ee* 25%) was observed with $Ru_2Cl_4(diop)_3$ as catalyst for **1c**.[7] The *ee* values depend on the substituents R (Table 1).

For the determination of the enantiomeric excess, the products **2** were first transformed into the 2-substituted *cis*-tetrahydrofuran-3-carbaldehydes **4**[8] and then converted via **5** into the menthyl esters **6**[9] (see Scheme 1), whose diastereomeric excesses were determined gas-chromatographically.[10]



Scheme 1. a) $BF_3 \cdot Et_2O$, −30 °C, in CH_2Cl_2, $HC(OCH_3)_3$. b) $H_2O/H^{\oplus}$ in THF. c) CrO_3/H_2SO_4 in acetone/water. d) $SOCl_2$. e) Menthol/pyridine in ether.

Received: December 11, 1985;
revised: December 17, 1985 [Z 1492 IE]
German version: *Angew. Chem. 98* (1986) 261

[1] S. G. Davies: *Organotransition Metal Chemistry: Applications to Organic Synthesis*, Pergamon Press, Oxford 1982, p. 266.
[2] H. B. Kagan in G. Wilkinson, F. G. A. Stone, E. W. Abel (Ed.): *Comprehensive Organometallic Chemistry, Vol. 8*, Pergamon Press, Oxford 1982, p. 463.
[3] H. Kumobayashi, S. Akutagawa, S. Otsuka, *J. Am. Chem. Soc. 100* (1978) 3949; K. Tani, T. Yamagata, S. Otsuka, S. Akutagawa, H. Kumobayashi, T. Taketomi, H. Takaya, A. Miyashita, R. Noyori, *ACS Symp. Ser. 185* (1982) 187; K. Tani, T. Yamagata, T. Tatsuno, Y. Yamagata, T. Tomita, S. Akutagawa, H. Kumobayashi, S. Otsuka, *Angew. Chem. 97* (1985) 232; *Angew. Chem. Int. Ed. Engl. 24* (1985) 217.
[4] H. Frauenrath, T. Philipps, *Liebigs Ann. Chem. 1985*, 1951.
[5] B. R. James, R. S. McMillan, R. H. Morris, D. K. W. Wang, *Adv. Chem. Ser. 167* (1978) 122.
[6] J. Chatt, L. M. Venanzi, *J. Chem. Soc. 1957*, 4735; H. B. Kagan, T. P. Dang, *J. Am. Chem. Soc. 94* (1972) 6429.
[7] The absolute configurations of **2** are so far unknown. For simplicity, only one arbitrarily chosen enantiomer has been illustrated.
[8] H. Frauenrath, J. Runsink, H.-D. Scharf, *Chem. Ber. 115* (1982) 2728.
[9] For a more accurate determination, the chiral acid chlorides were in each case esterified with (+)- and (−)-menthol.
[10] 5 m OV 101 on Gaschrom 80–100 mesh, 200 °C, pressure of carrier gas 2.6 bar. Retention times of the diasteromers: **6a**: 50.4 and 52.6 min; **6b**: 64.2 and 66.9 min; **6c**: 52.4 and 55.0 min.

[*] Dr. H. Frauenrath, T. Philipps
Institut für Organische Chemie der Technischen Hochschule
Prof.-Pirlet-Strasse 1, D-5100 Aachen (FRG)

Palladium(II) and Platinum(II) Complexes of 1,4,7,10,13,16-Hexathiacyclooctadecane**

By *Alexander J. Blake, Robert O. Gould, Aidan J. Lavery,* and *Martin Schröder**

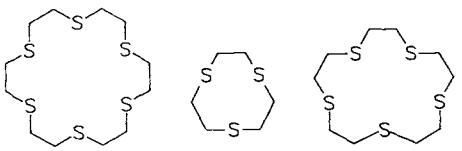
Although the coordination chemistry of first row transition metal ions with macrocyclic ligands has been an area

[*] Dr. A. J. Blake, Dr. R. O. Gould, Dr. A. J. Lavery, Dr. M. Schröder
Department of Chemistry, University of Edinburgh
West Mains Road, Edinburgh EH9 3JJ (Scotland)

[**] This work was supported by the Science and Engineering Research Council (UK) (to *A. J. L.*). Generous loans of platinum from Johnson-Matthey PLC are gratefully acknowledged.

of extensive research over the past twenty years,[1] by comparison the corresponding complexation of second and third row metals to non-porphyrinoid macrocycles remains an area to be fully developed. As part of a general study on the synthesis of platinum group metal complexes of macrocyclic ligands, we have investigated the complexation of d^8 metal ions with the polythia ligands **1** and **2**.

Whereas oxygen donor polyether crown ligands and related ionophores are known to bind, sometimes highly selectively, Group I and II metal ions, the corresponding polythia ligands appear to bind transition metal ions more effectively. Homoleptic octahedral complexes of the type $[M(\mathbf{1})]^{2\oplus}$ ($M=Co^{II}$, Ni^{II}),[2] $[M(\mathbf{2})_2]^{2\oplus}$ ($M=Co^{II}$, Ni^{II}, Cu^{II}),[3] and the tetrahedral and trigonal bipyramidal species $[Cu(\mathbf{3})]^{\oplus}$ and $[Cu(\mathbf{3})]^{2\oplus}$[4] have been described. More recently, we have synthesized the binuclear dicopper(I) adduct $[Cu_2(\mathbf{1})(NCCH_3)_2]^{2\oplus}$[5] in which **1** is coordinated fa-



1 2 3

cially via three sulfur donor atoms to each tetrahedral copper(I) unit. In connection with our studies aimed at further developing new coordination modes for the potentially hexadentate ligand **1**, we report here the synthesis and single crystal X-ray structures of the square planar complexes $[M(\mathbf{1})]^{2\oplus}$ ($M=Pd^{II}$, Pt^{II}), the first examples of platinum group metal complexation to **1**, and one of the few thiaether macrocyclic coordinations to Pd^{II} or Pt^{II}.[1,6,7]

1,4,7,10,13,16-Hexathiacyclooctadecane **1** (hexathia[18]-crown-6), isolated from the preparation of **2**,[3,8] was refluxed with one molar equivalent of $PdCl_2$ or $PtCl_2$ in $CH_2Cl_2:CH_3CN$ (1:3 v/v) for 4 h to give a yellow solution. The reaction mixture was filtered, and on addition of $NaBPh_4$ yellow-brown crystals of $[M(\mathbf{1})][BPh_4]_2$ were deposited in up to 70% yield. The single crystal X-ray structures of these complexes were undertaken[9] to confirm their connectivities and stereochemistries.

The conformation of the macrocycle in the isomorphous $[Pd(\mathbf{1})]^{2\oplus}$ and $[Pt(\mathbf{1})]^{2\oplus}$ cations (Fig. 1) is an S-shaped dou-

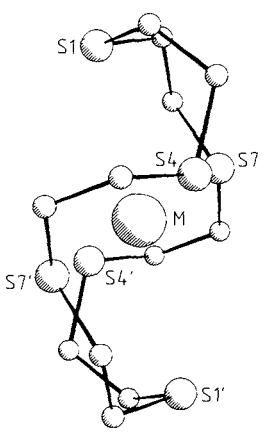


Fig. 1. Structure of the cation $[M(\mathbf{1})]^{2\oplus}$ in the $[M(\mathbf{1})][BPh_4]_2$ crystal, M = Pd or Pt. Most important angles [°]: M = Pd: S1-Pd-S4 75.06(5), S1-Pd-S7 103.88(5), S4-Pd-S7 86.24(5); M = Pt: S1-Pt-S4 74.16(8), S1-Pt-S7 104.78(8), S4-Pt-S7 86.76(9).

ble boat wherein the M^{II} ion at the molecular inversion center is coordinated to the four sulfur donor atoms S4, S7, S4′, and S7′ in a square planar arrangement with Pd-S = 2.3114(14), 2.3067(15) Å and Pt-S = 2.2980(25), 2.2948(24) Å reflecting the difference in ionic radii between Pd^{II} and Pt^{II}.[7,10] The two remaining sulfur donors, S1 and S1′, participate in weak interactions with the central M^{II} ion, characterized by particularly long Pd-S [3.2730(17) Å] and Pt-S [3.380(3) Å] distances. Interestingly, the S-M-S angles in these complexes deviate substantially from 90°; this contrasts with the values observed for the essentially octahedral Ni^{II} and Co^{II} complexes of **1**, which show angles of close to 90° around the metal center.[2]

These results confirm the possibility of square planar stereochemistry being adopted by the coordinatively ambivalent hexathia macrocycle **1** on binding to a large, stereochemically constrained d^8 metal ion and suggest that binding of **2** to such metal ions might yield complexes of the type $[M(\mathbf{2})_2]^{2\oplus}$ ($M=Pd^{II}$, Pt^{II}) and $[M(\mathbf{2})_2]^{\oplus}$ ($M=Rh^{I}$, Ir^{I}) with square planar stereochemistries and weak M-S axial interactions.[11]

Received: October 28, 1985;
revised: December 1985 [Z 1510 IE]
German version: *Angew. Chem. 98* (1986) 282

[1] G. A. Melson (Ed.): *Coordination Chemistry of Macrocyclic Compounds*, Plenum Press, New York 1979.

[2] a) D. St. C. Black, I. A. McLean, *Tetrahedron Lett. 1969*, 3961; b) *Aust. J. Chem. 24* (1971) 1401; E. J. Hintsa, J. R. Hartman, S. R. Cooper, *J. Am. Chem. Soc. 105* (1983) 3739; J. R. Hartman, E. J. Hintsa, *J. Chem. Soc. Chem. Commun. 1984*, 386.

[3] W. N. Setzer, C. A. Ogle, G. S. Wilson, R. S. Glass, *Inorg. Chem. 22* (1983) 266.

[4] P. W. R. Corfield, C. Ceccarelli, M. D. Glick, I. W.-Y. Moy, L. A. Ochrymowycz, D. B. Rorabacher, *J. Am. Chem. Soc. 107* (1985) 2399.

[5] R. O. Gould, A. J. Lavery, M. Schröder, *J. Chem. Soc. Chem. Commun. 1985*, 1492.

[6] For example of S_2P_2 coordination to Pt^{II}: E. P. Kyba, C. N. Clubb, S. B. Larson, V. J. Schueler, R. E. Davis, *J. Am. Chem. Soc. 107* (1985) 2141.

[7] S. G. Murray, F. R. Hartley, *Chem. Rev. 81* (1981) 365.

[8] Syntheses of **2** [3] and **1**: A solution of *bis*-(2-mercaptoethyl) sulfide (17.5 g, 0.114 mol), benzyltrimethylammonium methoxide (40% solution in methanol, 200 mL) (from Aldrich Chemical Co.) in methanol (250 mL), and a solution of 1,2-dichloroethane (11.3 g, 0.114 mol) in methanol (450 mL) were added simultaneously from two dropping funnels over a period of 4 h to stirred refluxing methanol (300 mL) under N_2. After addition of the reactants, the reaction mixture was refluxed for a further 1 h, allowed to cool, and the precipitated benzyltrimethylammonium chloride was filtered off and washed with methanol. The methanol filtrate and methanol washings were combined and the solvent removed in a vacuum. The residue was extracted with diethyl ether (3 × 100 mL) and the ether solution of **2** reduced to dryness. The crude product was purified by column chromatography on silica gel (60-120 mesh) eluting with hexane:ethyl acetate (9:1 v/v) and **2** recrystallized from dichloromethane:ethanol (4:1 v/v). Typical yield: 1.0 g (2.4%); m.p. 84°C.—The 2 + 2 condensation product **1** was isolated by extracting the residue left after extraction with diethyl ether as described above with hot dichloromethane (3 × 200 mL). The dichloromethane was removed in a vacuum and the product recrystallized from dichloromethane:diethyl ether (4:1 v/v) to give **1**. Yield: 6.5 g (32%); MS: *m/z* 360 ($M^{\oplus}$), ^{1}H-NMR ($CDCl_3$, 80 MHz): $\delta = 2.81$ (s, CH_2); IR (KBr): $\tilde{\nu} = 2900$, 1415, 1298, 1192, 1145, 840, 712, 681, 659, 660 cm^{-1}.

[9] $[Pd(\mathbf{1})][BPh_4]_2$, monoclinic, $P2_1/c$: $a = 12.913(4)$, $b = 12.092(4)$, $c = 17.436(7)$ Å, $\beta = 108.496(22)°$; $V = 2582$ Å^3, $\rho_{calcd} = 1.422$ g·cm^{-3}, $Z = 2$; 4598 data measured to $\theta = 25°$, refinement based on 3602 data with $F \geq 3.0\sigma(F)$. At convergence R, $R_w = 0.0541$, 0.0567 respectively for 158 parameters; $[Pt(\mathbf{1})][BPh_4]_2$, monoclinic, $P2_1/c$, $a = 12.982(9)$, $b = 12.063(8)$, $c = 17.487(15)$, $\beta = 108.46(5)°$; $V = 2598$ Å^3, $\rho_{calcd} = 1.527$ g·cm^{-3}, $Z = 2$; 3306 data measured to $\theta = 22°$, refinement based on 2340 data with $F \geq 2.5\sigma(F)$. At convergence, R, $R_w = 0.0395$, 0.0429 respectively for 158 parameters.—In the case of $[Pt(\mathbf{1})][BPh_4]_2$, intensity statistics showed that reflections with $k + l = 2n$ were strong relative to those

with $k+l=2n+1$, giving the location of the metal atom on a special position. The structure solution was completed using the DIRDIF system [12]. By virtue of the isostructuralism of the two complexes it was possible to take the final coordinates from the converged Pt structure as starting values for the refinement of the Pd structure. For refinement [13] hydrogen atoms were included in fixed, calculated positions; at convergence, the difference electron density map showed no feature above 1.25 and 1.07 eÅ^{-3} for M = Pd[II], Pt[II] respectively. Further details of the crystal structure investigation are available on request from the Director of the Cambridge Crystallographic Data Centre, University Chemical Laboratory, Lensfield Road, Cambridge CB2 1EW. Any request should be accompanied by the full literature citation for this communication.

[10] N. N. Greenwood, A. Earnshaw: *Chemistry of the Elements*, Pergamon Press 1984, p. 1497; R. D. Shannon, *Acta Crystallogr. A 32* (1976) 751.

[11] For analogous N-donor tridentate macrocyclic complexes of Pt[II] see K. Wieghardt, M. Köppen, W. Swiridoff, J. Weiss, *J. Chem. Soc. Dalton Trans. 1983*, 1869.

[12] P. T. Beurskens, W. P. Bosman, H. M. Doesbury, Th. E. M. van den Hark, P. A. J. Prick, J. H. Noordik, G. Beurskens, R. O. Gould, V. Parthasarathai, *D. I. R. D. I. F., Applications of Direct Methods to Difference Structure Factors*, University of Nijmegen, Netherlands 1983.

[13] G. M. Sheldrick: SHELX76, *Program for Crystal Structure Refinement*, University of Cambridge, 1976.

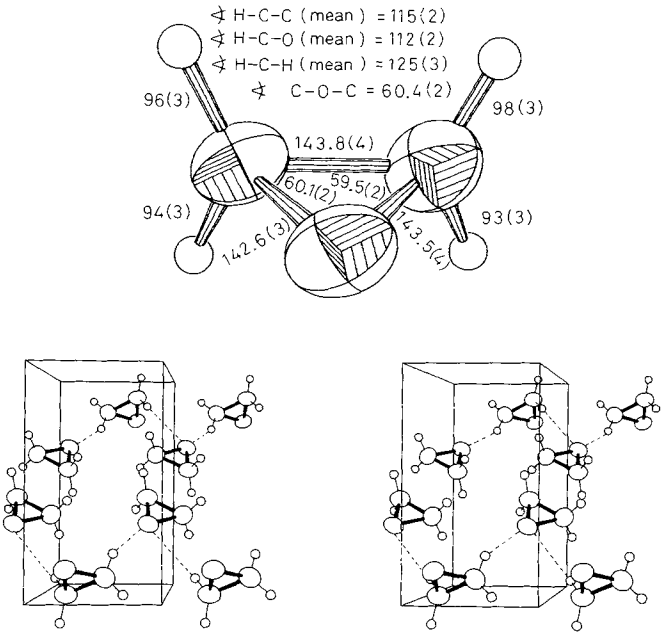


Fig. 1. Top: Molecular structure of ethylene oxide in the crystal at 150 K, with bond lengths [pm] and angles [°]. Bottom: Stereoview of the crystal structure of ethylene oxide in an x,y projection. C-H···O contacts close to or shorter than the van-der-Waals distances are shown as broken lines (ORTEP [17]).

Ethylene Oxide—X-Ray Structure Analysis (at 150 K) and ab initio Calculations**

By *Peter Luger,* Chakib Zaki, Jürgen Buschmann,* and *Rainer Rudert*

Dedicated to Professor George A. Jeffrey on the occasion of his 70th birthday

In a series of studies on the structure of small, unsubstituted cyclic ethers we have so far determined the crystal structures of tetrahydrofuran,[1] oxetane,[2] and dioxane.[3] We have now been able to prepare crystals of ethylene oxide (oxirane). Its crystal structure and accompanying ab initio calculations are reported herein. Apart from in a conference report on the structure of cyclopropane,[4] no results of an X-ray structure analysis of a nonsubstituted three-membered ring have so far been published. In the works of *Jeffrey* et al.[5,6] on ethylene oxide hydrate the three-membered ring was treated with rigid geometry.

The ethylene oxide, which is gaseous at room temperature (m.p. 161 K, b.p. 284 K), was crystallized in situ on a Stoe four-circle diffractometer by a method described in Refs. [1,2], and the intensity measurements were carried out at 150 K.[7] After convergence of the refinement, a difference Fourier synthesis showed a residual electron-density maximum in the ring plane outside of the ring and equidistant from the two C atoms (distance to the C-C bond 70 pm), pointing to the existence of bent bonds in the three-membered ring.

In the crystal, the ethylene oxide molecule is, within the estimated standard deviations, practically an equilateral triangle (Fig. 1, top). The C-O bond (mean value 143.1 pm) has about the same length as in the other cyclic ethers; only in oxetane is it longer (146.0 pm). The C-C bond length is shorter than that found for ethylene oxide by other methods. It is also shorter than that found for a number of derivatives by other methods[11] (Table 1).

Table 1. Bond lengths [pm] in ethylene oxide determined by various methods.

C-O	C-C	C-H	Method	Ref.
Experimental				
145(5)	156(5)	105(7)	Electron diffraction	[8]
143.5(1)	147.0(1)	108.3(2)	Microwave	[9]
143.4(2)	147.0(3)	108.5(4)	spectroscopy	[10]
143.1(4)	143.8(4)	95(3)	X-ray structure	this work
144.1	144.9	96 [a]	analysis	this work
144.3(13)	147.0(18)	—	Mean value [b]	—
ab-initio calculations				
143.3	148.3	108.8	(STO-3G)	[18]
147.0	147.4	107.1	(HF/3-21G)	[19]
146.9	147.4	107.1	(HF/3-21G*)	this work
145.9	146.1	106.9	(HF/4-31G)	[20]
145.9	146.4	107.1	(HF/6-31G)	[20]
140.1	145.3	107.7	(HF/6-31G*)	[19]
139.9	145.2	107.8	(HF/6-31G**)	[20]
143.7	146.3	108.7	(MP2/6-31G*)	this work

[a] "Rigid body" correction [14–16] with the temperature parameters of all atoms. The results of this correction should be regarded with some care, since only isotropic temperature factors are available for the hydrogen atoms. [b] Average values from twelve X-ray and neutron diffraction studies on ethylene oxide derivatives carried out after 1975 (source: Cambridge Data File [11]).

A complete optimization of the geometry by ab initio calculations[12] was carried out at the MP2/6-31G* level, and the results were compared with those of earlier calculations (Table 1). Compared to the results of the X-ray structure analysis, which indicated that all bonds in the ring are almost of the same length, the MP2/6-31G* calculations gave the same C-O bond lengths, but a longer C-C bond length.

In the crystal lattice of ethylene oxide (Fig. 1), two intermolecular C-H···O contacts fall within the van-der-Waals distance (van-der-Waals radii of 152 pm for O and

[*] Prof. Dr. P. Luger, Dipl.-Phys. C. Zaki, Dr. J. Buschmann, Dipl.-Phys. R. Rudert
Institut für Kristallographie der Freien Universität
Takustr. 6, D-1000 Berlin 33

[**] This work was supported by the Deutsche Forschungsgemeinschaft and the Fonds der Chemischen Industrie.

120 pm for H are assumed[13]). Contacts of this sort were also observed in the crystal structure of oxetane.[2]

Received: October 21, 1985;
revised: December 13, 1985 [Z 1503 IE]
German version: *Angew. Chem. 98* (1986) 254

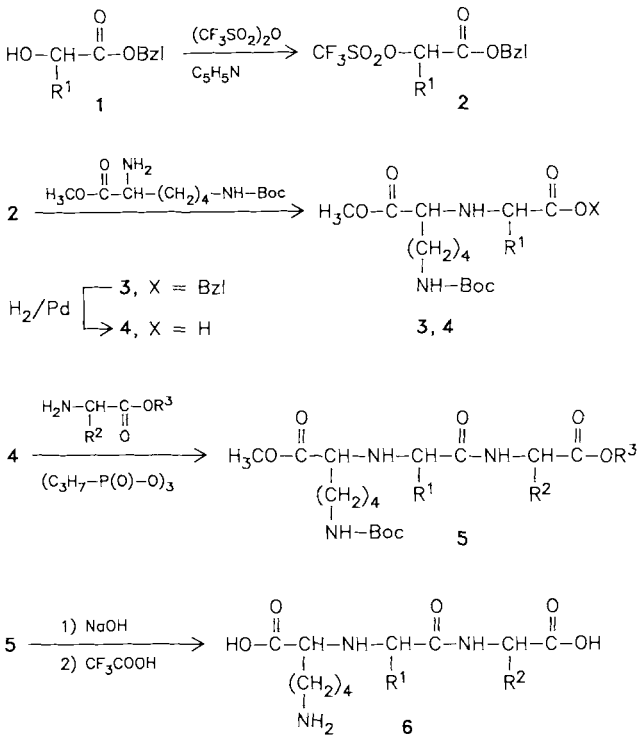
CAS Registry number:
Oxirane, 75-21-8.

[1] P. Luger, J. Buschmann, *Angew. Chem. 95* (1983) 423; *Angew. Chem. Int. Ed. Engl. 22* (1983) 410; *Angew. Chem. Suppl. 1983*, 537.
[2] P. Luger, J. Buschmann, *J. Am. Chem. Soc. 102* (1984) 7118.
[3] J. Buschmann, P. Luger, E. Müller, *Abstr. 8th Eur. Crystallogr. Meet.*, Liège 1983, p. 133.
[4] D. Nijveldt, A. Vos, A. F. Cameron, *Abstr. 7th Eur. Crystallogr. Meet.*, Jerusalem 1982, p. 153.
[5] R. K. McMullan, G. A. Jeffrey, *J. Chem. Phys. 42* (1965) 2725.
[6] F. Hollander, G. A. Jeffrey, *J. Chem. Phys. 66* (1977) 4699.
[7] Crystallographic data for ethylene oxide at 150 K: $a=464.5(4)$, $b=840.7(6)$, $c=666.4(7)$ pm, $\beta=100.00(8)°$, space group $P2_1/n$, $Z=4$, $R=0.048$ for 339 observed reflections (Stoe four-circle diffractometer, Ni-filtered $Cu_{K\alpha}$ radiation, $\omega-2\theta$ scan, $2\theta<113°$). Further details of the crystal structure investigation are available on request from the Fachinformationszentrum Energie, Physik, Mathematik GmbH, D-7514 Eggenstein-Leopoldshafen 2, on quoting the depository number CSD 51792, the names of the authors, and the full citation of the journal.
[8] P. G. Ackermann, J. E. Mayer, *J. Chem. Phys. 4* (1936) 377.
[9] T. E. Turner, J. A. Howe, *J. Chem. Phys. 27* (1957) 974.
[10] Ch. Hirose, *Bull. Chem. Soc. Jpn. 47* (1974) 1311.
[11] O. Kennard, D. G. Watson, W. G. Town, *J. Chem. Soc. 12* (1972) 14.
[12] J. S. Binkley, M. J. Frisch, D. J. DeFrees, K. Raghavachari, R. A. Whiteside, H. B. Schelgel, E. M. Fluder, J. A. Pople: *Gaussian 82, Users Manual*. Department of Chemistry, Carnegie-Mellon University, Pittsburgh, PA, USA 1983.
[13] A. Bondi, *J. Chem. Phys. 68* (1964) 441.
[14] V. Schomaker, K. N. Trueblood, *Acta Crystallogr. B 24* (1968) 63.
[15] C. Scheringer, *Acta Crystallogr. A 28* (1972) 616.
[16] C. Scheringer, *Acta Crystallogr. A 34* (1978) 428.
[17] C. K. Johnson: *ORTEP, Report ORNL-5138*, Oak Ridge National Laboratory, TN, USA 1976.
[18] W. A. Lathan, L. Radom, P. C. Hariharan, W. J. Hehre, J. A. Pople, *Top. Curr. Chem. 40* (1973) 1.
[19] R. A. Whiteside, M. J. Frisch, J. A. Pople (Eds.): *Carnegie-Mellon Quantum Chemistry Archive*, 3rd edit., Carnegie-Mellon University, Pittsburgh, PA, USA 1983.
[20] B. A. Hess, Jr., L. J. Schaad, P. L. Polavarapu, *J. Am. Chem. Soc. 106* (1984) 4348.

Synthesis of *N*-(1-Carboxy-5-aminopentyl)dipeptides as Inhibitors of Angiotensin Converting Enzyme**

By *Rüdiger Escher* and *Peter Bünning**

N-Carboxymethyldipeptides have gained great importance in recent years as inhibitors of angiotensin converting enzyme (ACE) in the treatment of hypertension and conjestive heart failure.[1] In the form of *N*-(1-carboxy-5-aminopentyl)dipeptides, these inhibitors are, moreover, valuable tools for biochemical studies on ACE; owing to their functional ε-amino group they are suitable, after coupling to a gel matrix, as ligands for an affinity chromatography of the enzyme. The following synthetic routes provide access to these *N*-substituted dipeptides: reductive amination of α-keto acids or reaction of primary amines with α-bromo-, α-methanesulfonyloxy-, or α-trifluoromethanesulfonyloxy-carboxylic esters **2**. However, only the reaction of esters **2** with amino acid derivatives furnish *N*-substituted α-aminocarboxylates **3** in high yield via Walden inversion.[2] In this way, a series of *N*-(1-carboxy-5-aminopentyl)glycyl- and *N*-(1-carboxy-5-aminopentyl)alanyl-amino acids, **6a** and **6b** respectively, were synthesized.



Scheme 1. Synthesis of *N*-(1-carboxy-5-aminopentyl)dipeptides **6**. Bzl = benzyl, Boc = butoxycarbonyl. **a**, $R^1=H$; **b**, $R^1=CH_3$.

The synthesis of the *N*-(1-carboxy-5-aminopentyl)dipeptides **6** is outlined in Scheme 1. For the synthesis of the glycyl derivatives **6a** and the L-alanyl derivatives **6b**, benzyl glycolate **1a** and benzyl D-lactate **1b** were allowed to react with trifluoromethanesulfonic acid anhydride/pyridine to give **2a** and **2b**, respectively. The low stability of the ester **2a** necessitated careful reaction with two equivalents of N^{ε}-Boc-L-lysine methyl ester, whereupon one equivalent served as base for buffering of the liberated trifluoromethanesulfonic acid. In contrast, for the reaction of the ester **2b**, equimolar amounts of N^{ε}-Boc-L-lysine methyl ester could be employed, with triethylamine as base. The benzyl group was removed from the products **3** by catalytic hydrogenation; subsequent condensation of **4** with amino acid esters by the propylphosphonic anhydride method[3] furnished the protected dipeptide derivatives **5**. Hydrolysis of the esters with sodium hydroxide and cleavage of the Boc group with trifluoroacetic acid then afforded the active ACE inhibitors **6** (Table 1).

Investigation of the inhibition of ACE by the compounds **6** showed that the IC_{50} values vary over a range from 5500 nmol/L for the weakest inhibitor, $\mathbf{6a_1}$, to 10 nmol/l for the strongest inhibitor, *N*-(1-carboxy-5-aminopentyl)-L-alanyl-L-alanine, $\mathbf{6b_2}$ (Table 1).

The inhibitors were coupled to a Sepharose 6B matrix (Pharmacia, Freiburg) according to the carbodiimide method[5] via a spacer, which was synthesized from 1,4-bis

[*] Priv.-Doz. Dr. P. Bünning, Lebensmittelchem. R. Escher
Biochemisches Institut der Universität
Hermann-Herder-Str. 7, D-7800 Freiburg (FRG)

[**] This work was supported by the Deutsche Forschungsgemeinschaft and the Fonds der Chemischen Industrie. We wish to thank Dr. *H. Urbach*, *Dr. R. Henning*, Dr. *F. Effenberger*, and Mrs. *U. Burkard* for their valuable help with this work.

Table 1. Synthesis of *N*-(1-carboxy-5-aminopentyl)dipeptides **6** and inhibition of angiotensin converting enzyme (ACE) by these compounds.

$H_3CO-CO-CH[(CH_2)_4-NHBoc]-NH-CHR^1-CO-NH-CHR^2-COOR^3$ **5**
$HOOC-CH[(CH_2)_4-NH_2]-NH-CHR^1-CO-NH-CHR^2-COOH$ **6**

R^1	R^2	R^3 in **5**	Product	**5**, Yield [%] [a]	IC_{50} [b] [nmol/L]
H	H	C_2H_5	**6a**$_1$	49	5500
H	CH_3	CH_3	**6a**$_2$	49	130
H	*i*-C_3H_7	CH_3	**6a**$_3$	42	790
H	Bzl	C_2H_5	**6a**$_4$	52	170
CH_3	H	C_2H_5	**6b**$_1$	57	160
CH_3	CH_3	CH_3	**6b**$_2$	57	10
CH_3	*i*-C_3H_7	CH_3	**6b**$_3$	56	15
CH_3	Bzl	C_2H_5	**6b**$_4$	57	12

[a] Yield of **5** referred to **1**: The step **5**→**6** proceeds with ca. 70% yield. [b] Concentration of **6** at which half maximal inhibition of ACE from rabbit lungs occurs under standard assay conditions [4] (enzyme concentration: 2 nmol/L).

(2,3-epoxypropoxy)butane and 6-(4-aminobenzamido)hexanoic acid.[6] The compounds **6a**$_2$, **6a**$_3$, **6a**$_4$, and **6b**$_1$ are suitable as ligands for affinity chromatography of ACE. The highest yields of enzyme are achieved with **6a**$_2$ and **6b**$_1$; in contrast **6a**$_1$ gives only a very slight binding of the enzyme to the affinity resin, whereas the enzyme is tightly but almost irreversibly bound by the ligands **6b**$_2$ to **6b**$_4$.

The synthesis described here affords *N*-(1-carboxy-5-aminopentyl)dipeptides **6** in high yields. They exhibit a broad spectrum of inhibition towards ACE, and are valuable tools for biochemical studies of this enzyme.

Experimental

1a: A mixture of glycolic acid (7.60 g, 100 mmol) and triethylamine (10.10 g, 100 mmol) in ethyl acetate (50 mL) was treated with 11.50 g (90 mmol) of benzyl chloride.[7] After 6 hours' boiling, the mixture was filtered and the filtrate worked up by distillation. Yield: 6.72 g (45%) **1a**, b.p. 136 °C/14 torr.

2a: A stirred mixture of **1a** (1.66 g, 10 mmol) and pyridine (0.89 mL, 11 mmol) in CH_2Cl_2 (40 mL) was treated dropwise for 20 min at −12 °C with 1.84 mL (11 mmol) of trifluoromethanesulfonic acid anhydride. Column chromatography on silica gel at 4 °C with CH_2Cl_2 and subsequent evaporation of the eluate to dryness afforded 2.24 g of **2a** (75%).

3a: A stirred solution of **2a** (2.24 g, 7.5 mmol) in CH_2Cl_2 (30 mL) was treated with 3.90 g (15 mmol) of H-Lys(Boc)-OMe at −15 °C. After one hours' stirring, the reaction solution was washed with water, dried over $MgSO_4$, evaporated down, and chromatographed on a silica gel column with ethyl actate/cyclohexane (1:1, v/v). Yield of **3a**: 2.75 g (90%).

4a: A solution of **3a** (2.45 g, 6 mmol) in 250 mL of methanol was hydrogenated with Pd/C (10%) for 4 h. After filtration and evaporation, **4a** crystallized at 4 °C. Yield: 1.62 g (85%).

5a$_2$: A mixture of **4a** (0.64 g, 2 mmol), Ala-OMe-HCl (0.84 g, 6 mmol), and triethylamine (2.51 mL, 18 mmol) in CH_2Cl_2 (60 mL) was treated dropwise at −12 °C with 1.4 mL of a dichloromethane solution containing 50 wt-% propylphosphonic anhydride. After 4 hours' stirring at room temperature, the mixture was washed with ice-water, then with saturated KH_2PO_4 solution (pH 4.5), and finally with saturated NaCl solution; after drying over $MgSO_4$, 0.7 g (86%) of oily **5a**$_2$ was obtained.

6a$_2$: A solution of **5a**$_2$ (0.40 g, 1 mmol) in acetone (3 mL) was treated with 2.0 mL of 0.5 M NaOH and the mixture shaken for 8 h; after addition of a further 2.0 mL of 0.5 M NaOH, the mixture was shaken for a further 24 h. After neutralization with trifluoroacetic acid, the organic phase was evaporated in vacuo and then chromatographed on a silica gel column with ethyl acetate. Subsequent elution with methanol and renewed evaporation afforded the Boc-protected compound. This was suspended in 80 µL of water, treated dropwise at 0 °C with 770 µL (10 mmol) of trifluoroacetic acid, and stirred for 3 h at 23 °C. Evaporation to dryness and subsequent exchange of the trifluoroacetate by acetate on Amberlite IRA 93 (Serva, Heidelberg) followed by lyophilization afforded **6a**$_2$ as the hydroacetate.

Received: November 6, 1985;
revised: January 2, 1986 [Z 1522 IE]
German version: *Angew Chem. 98* (1986) 264

CAS Registry numbers:
1a, 30379-58-9; **1b**, 74094-05-6; **2a**, 77902-89-7; **2b**, 93836-43-2; **3a**, 100573-69-1; **3b**, 100603-66-5; **4a**, 100573-70-4; **4b**, 100573-71-5; **5a**$_1$, 100573-72-6; **5a**$_2$, 100573-73-7; **5a**$_3$, 100573-74-8; **5a**$_4$, 100573-75-9; **5b**$_1$, 100573-76-0; **5b**$_2$, 100573-77-1; **5b**$_3$, 100573-78-2; **5b**$_4$, 100573-79-3; **6a**$_1$, 100573-80-6; **6a**$_2$, 100573-81-7; **6a**$_3$, 100573-82-8; **6a**$_4$, 100573-83-9; **6b**$_1$, 100573-84-0; **6b**$_2$, 100573-85-1; **6b**$_3$, 100573-86-2; **6b**$_4$, 100573-87-3; ACE, 9015-82-1; $(CF_3SO_2)O$, 358-23-6; H-Phe-OEt, 3081-24-1; H-Val-OMe, 4070-48-8; H-Gly-OEt, 459-73-4; H-Lys(Boc)-OMe, 3017-32-1; H-Ala-OMe·HCl, 2491-20-5.

[1] C. S. Sweet, E. H. Ulm in A. Scriabine (Ed.): *New Drugs Annual: Cardiovascular Drugs*. Raven Press, New York 1984, p. 1.
[2] a) C. D. Beard, K. Baum, V. Grakausus, *J. Org. Chem. 38* (1973) 3673; b) F. Effenberger, U. Burkard, D. Willfahrt, *Angew. Chem. 95* (1983) 50; *Angew. Chem. Int. Ed. Engl. 22* (1983) 65.
[3] H. Wissmann, H.-J. Kleiner, *Angew. Chem. 92* (1980) 129; *Angew. Chem. Int. Ed. Engl. 19* (1980) 133.
[4] B. Holmquist, P. Bünning, J. F. Riordan, *Anal. Biochem. 95* (1979) 540.
[5] P. Cuatrecasas, *J. Biol. Chem. 245* (1970) 3059.
[6] L. Sundberg, J. Porath, *J. Chromatogr. 90* (1974) 87.
[7] J.-C. Micheau, A. Lattes, *Bull. Soc. Chim. Fr. 11 (1970)*, 4018.

Thin Layer Chromatographic Separation of Stereoisomeric Dipeptides

By *Kurt Günther*,* *Jürgen Martens*, and *Maren Schickedanz*

We have recently developed a method for the *direct* enantiomeric resolution of D,L-amino acids by ligand exchange on thin-layer chromatographic plates.[1-4] Our strategy not only constitutes a simple and rapid analytical method[5] but also enables the determination of trace amounts of each of the enantiomers.[3,4] The requisite chromatographic plates are now commercially available.[6]

The thin-layer chromatographic separation of diastereomeric dipeptides has already been well documented,[7,8] but the separation of enantiomeric dipeptides by thin-layer chromatography has, to our knowledge, never been reported.

As long ago as 1979, *Lindner* et al.[9] reported the HPLC separation of enantiomeric dipeptides after dansylation. For the gas-chromatographic determination of amino-acid enantiomers in proteins and peptides these must be previously cleaved under acid conditions.[10] Stereoisomeric dipeptides can also be separated by gas-chromatography, but this requires previous esterification and perfluoroacylation of the sample.[11] A direct separation of the enantiomers by gas chromatography is of course impossible in the case of dipeptides. Experience has shown that there is always the danger of racemization taking place, both during the derivatization as well as upon hydrolysis. Consequently, a *direct* analytical method as described in this communication is much to be preferred over these methods.

It has now been possible for the first time to accomplish the *direct* separation of enantiomeric and diastereomeric dipeptides. In this new approach a derivatization is unnecessary. Figure 1 shows a typical example of a separation of enantiomeric dipeptides on Chiralplate®.[6]

In the enantiomeric separations (Table 1, top) it emerges that the antipodes with *C*-terminal L-configuration always

[*] Dr. K. Günther, M. Schickedanz
Forschung Chemie, Degussa AG
Postfach 1345, D-6450 Hanau 1 (FRG)
Dr. J. Martens
Koordination Pharma, Degussa AG
Postfach 110533, D-6000 Frankfurt am Main 11 (FRG)

give a smaller R_f value than the corresponding enantiomeric dipeptide with *C*-terminal D-configuration.

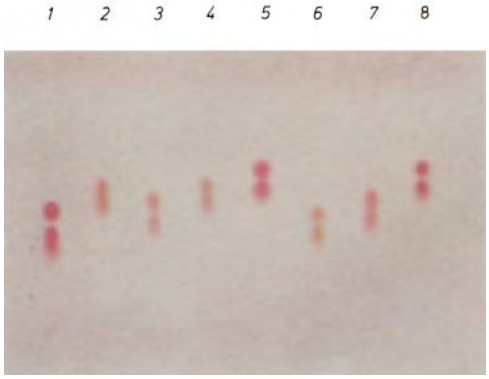


Fig. 1. Photograph of a thin-layer chromatogram of enantiomeric dipeptides on Chiralplate®. Eluent: methanol/water/acetonitrile = 5/5/3 (v/v/v). Racemic dipeptides: 1) D-Leu-L-Leu and L-Leu-D-Leu; 2) Gly-D,L-Val; 3) Gly-D,L-Leu; 4) Gly-D,L-Phe; 5) D-Ala-L-Phe and L-Ala-D-Phe; 6) Gly-D,L-Trp; 7) Gly-D,L-Ile; 8) D-Met-L-Met, and L-Met-D-Met.

Table 1. Thin-layer chromatographic separation of the enantiomers and diastereomers of dipeptides on Chiralplate® [a].

Enantiomeric dipeptides	R_f value (configuration)	Eluent [b]
Gly-L-Phe	0.57 (L)	B
Gly-D-Phe	0.63 (D)	
Gly-L-Leu	0.53 (L)	B
Gly-D-Leu	0.60 (D)	
Gly-L-Ile	0.54 (L)	B
Gly-D-Ile	0.61 (D)	
Gly-L-Val	0.58 (L)	B
Gly-D-Val	0.62 (D)	
Gly-L-Trp	0.48 (L)	B
Gly-D-Trp	0.55 (D)	
D-Leu-L-Leu	0.48	B
L-Leu-D-Leu	0.57	
D-Leu-L-Leu	0.19	A
L-Leu-D-Leu	0.26	
D-Ala-L-Phe	0.59	B
L-Ala-D-Phe	0.65	
D-Ala-L-Phe	0.21	A
L-Ala-D-Phe	0.26	
D-Met-L-Met	0.64	B
L-Met-D-Met	0.71	
D-Met-L-Met	0.29	A
L-Met-D-Met	0.33	
Diastereomeric dipeptides	**R_f value**	**Eluent [b]**
L-Leu-L-Leu	0.45	B
L-Leu-D-Leu	0.53	
L-Ala-L-Ala	0.64	B
L-Ala-D-Ala	0.70	
L-Ala-L-Phe	0.59	B
L-Ala-D-Phe	0.65	
L-Met-L-Met	0.62	B
L-Met-D-Met	0.71	

[a] Length of run 13 cm. [b] A: methanol/water/acetonitrile = 5/5/20 (v/v/v); B: methanol/water/acetonitrile = 5/5/3 (v/v/v).

Diastereomeric dipeptides can of course also be separated by the method described here. A few selected examples from a host of such separations that have already been accomplished are listed in Table 1 (bottom).

Procedure

In each run a 1% solution of the mixture of stereoisomeric dipeptides (2 μL) to be separated was applied to a commercially available Chiralplate®[6] and then developed (30–90 min) with the eluents mentioned in Table 1. After drying, the spots were made visible by spraying with 0.1% ninhydrin reagent. As can be seen in Figure 1 it should also be possible to determine trace amounts of the antipodes.

Received: October 28, 1985;
supplemented: December 10, 1985 [Z 1511 IE]
German version: *Angew. Chem. 98* (1986) 284

[1] K. Günther, J. Martens, M. Schickedanz, *Angew. Chem. 96* (1984) 514; *Angew. Chem. Int. Ed. Engl. 23* (1984) 506.
[2] K. Günther, J. Martens, M. Schickedanz, *Naturwissenschaften 72* (1985) 149.
[3] K. Günther, J. Martens, M. Schickedanz, *Fresenius Z. Anal. Chem. 322* (1985) 513.
[4] K. Günther, J. Martens, M. Schickedanz, *Arch. Pharm. (Weinheim) 319* (1986), in press.
[5] U. A. T. Brinkman, D. Kamminga, *J. Chromatogr.*, in press.
[6] Chiralplate®. Manufacturer: Macherey & Nagel, D-5160 Düren. The chiral selector is (2*S*,4*R*,2′*RS*)-4-Hydroxy-1-(2-hydroxydodecyl)proline (cf. [1]).
[7] A. Arendt, A. Kotodziejczyk, T. Solotowska, *Chromatographia 9* (1976) 123.
[8] L. Lepri, P. G. Desideri, D. Heimler, S. Giannessi, *J. Chromatogr. 265* (1983) 328.
[9] W. Lindner, J. N. Le Page, G. Davies, D. E. Seitz, B. L. Karger, *J. Chromatogr. 185* (1979) 323.
[10] H. Frank, W. Woiwode, G. Nicholson, E. Bayer, *Liebigs Ann. Chem. 1981*, 354.
[11] N. Ôi, M. Horiba, H. Kitahara, H. Shimada, *J. Chromatogr. 202* (1980) 302, and references cited therein.

Reversible Interconversion of C–C and C–N Multiple Bond Systems on Clusters**

By *Wolfgang Bernhardt, Christine von Schnering,* and *Heinrich Vahrenkamp**

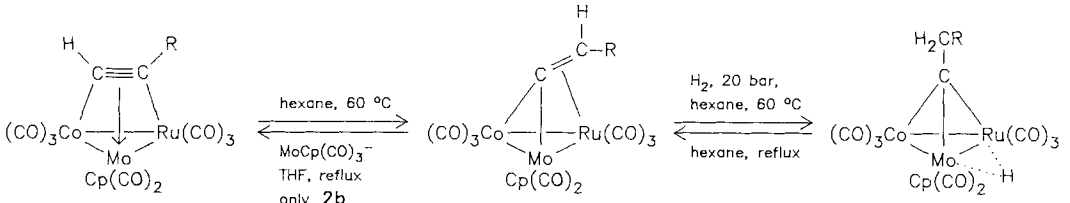
Redox transformations of unsaturated organic systems as well as C–C bond forming reactions in the coordination sphere of clusters are appropriate objectives in order to investigate the cluster-surface analogy.[1] Accordingly, hydrogenation and dehydrogenation reactions of cluster-bound C–C and C–N multiple bond systems have been well studied,[2] and examples are known for each step of the reaction sequence $C{\equiv}C \rightleftarrows C{=}C \rightleftarrows C{-}C$ or $C{\equiv}N \rightleftarrows C{=}N \rightleftarrows C{-}N$. In special cases, it has been possible to realize the entire sequence in one direction for a compound or to demonstrate the reversibility of specific steps.[2,3] However, compounds have not yet been found for which the entire sequence can be realized in both directions. We have now been able to carry out reversible transformations of cluster-bound multiple bond systems for both the C–C and the C–N systems.

The reversible acetylene–vinylidene–alkylidyne transformation was achieved on a RuCoMo framework. The acetylene-bridged clusters **1** are formed from the clusters $[RuCo_2(CO)_9(HC{=}CR)]$ (R = H, *t*Bu)[4] by metal exchange with $Na[MoCp(CO)_3]$ (Cp = cyclopentadienyl) in tetrahydrofuran (THF). When the clusters **1** are heated in hexane to 60 °C, they are transformed, as expected, into the vinylidene-bridged clusters **2**. Complex **2a** can then be con-

[*] Prof. Dr. H. Vahrenkamp, Dipl.-Chem. W. Bernhardt, Dipl.-Chem. C. von Schnering
Institut für Anorganische und Analytische Chemie der Universität Albertstrasse 21, D-7800 Freiburg (FRG)

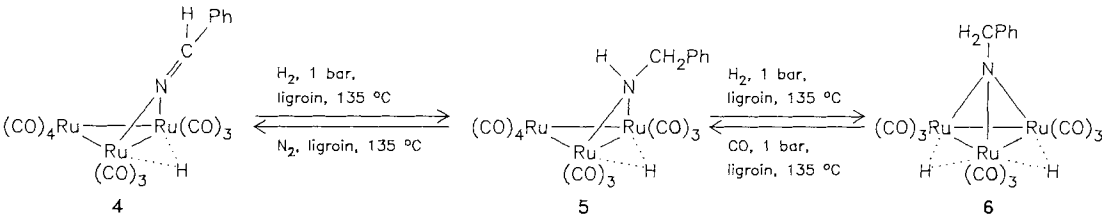
[**] This work was supported by the Fonds der Chemischen Industrie and by Heraeus.

verted into **3a** by treatment with hydrogen (20 bar) in hexane at 60 °C.[5] The reverse reaction, **3a** → **2a**, takes place in refluxing hexane in the absence of hydrogen; no example was known for such a spontaneous alkylidyne-vinylidene transformation. All these reactions proceed nearly quantitatively. Completion of the reverse sequence was achieved by metal exchange of $[RuCo_2(CO)_9(C{=}CHtBu)]$[4] with $Na[MoCp(CO)_3]$, which afforded in low yield the expected **2b** along with the isomerized product **1b**.



a, R = H; b, R = *t*Bu

The reversible imide-amide-nitrene transformation was achieved with the previously described compounds **4**, **5**, and **6**.[6] While the transformation **4** → **5** → **6** occurs upon heating under hydrogen at normal pressure,[6a] **6** is converted back into **5** in 77% yield upon refluxing in ligroin (135 °C) under CO at normal pressure. The thermal dehydrogenation of **5** to give **4** likewise occurs in boiling ligroin, albeit only as a side reaction, the main reaction being



the decarbonylation to give **6**; both decarbonylation and dehydrogenation are inhibited by CO. As in the analogous Fe_3 system,[3] the further dehydrogenation of **4** to the unknown $[Ru_3(CO)_9(\mu_3\text{-}\eta^2\text{-}PhC{\equiv}N)]$ was not observed.

The reaction sequences **1** ⇄ **2** ⇄ **3** and **4** ⇄ **5** ⇄ **6** confirm that the interconversion of organic ligands on M_3 clusters may be controlled by the composition of the clusters (cf. the C-C system on the Os_3 or $RuCo_2$ unit[2,4] and the C-N system on the Fe_3 or Os_3 unit[3]). The present state of knowledge of preparative organometallic chemistry allows a wide range of directed cluster syntheses. The next challenge is to formulate and to systematize the relationship between M_3 unit and the direction of ligand transformation. A further goal is to find methods to release the transformed C-C or C-N substrate and to recover the starting cluster, which has so far been achieved only under special conditions.[7]

Received: November 11, 1985 [Z 1527 IE]
German version: *Angew. Chem. 98* (1986) 285

[1] Cf. E. L. Muetterties, M. J. Krause, *Angew. Chem. 95* (1983) 135; *Angew. Chem. Int. Ed. Engl. 22* (1983) 135.
[2] Cf. A. J. Deeming in B. F. G. Johnson (Ed.): *Transition Metal Clusters*, Wiley, New York 1980, p. 391.
[3] M. A. Andrews, H. D. Kaesz, *J. Am. Chem. Soc. 101* (1979) 7238, 7255; Z. Dawoodi, M. J. Mays, K. Henrich, *J. Chem. Soc. Dalton Trans. 1984*, 433.
[4] E. Roland, W. Bernhardt, H. Vahrenkamp, *Chem. Ber. 118* (1985) 2858.
[5] The composition of the new complexes was confirmed by elemental analysis and mass spectroscopy. Typical IR (C_6H_{12}) and ^{1}H-NMR spectra ($CDCl_3$, int. TMS): **1a**: IR $\tilde{\nu}$ = 2083 (s), 2051 (vs), 2036 (m), 2025 (vs), 1995 (m), 1982 (s), 1910 (m), 1880 (m) cm^{-1}; ^{1}H-NMR: δ = 8.45, 7.60 (each 1 H, d, J = 3.6 Hz), 5.43 (5 H). **2a**: IR $\tilde{\nu}$ = 2088 (s), 2075 (sh), 2047 (vs), 2040 (sh), 2029 (vs), 2017 (s), 1994 (s), 1986 (s), 1947 (m), 1865 (m) cm^{-1}; ^{1}H-NMR: δ = 5.42 (5 H), 4.81, 4.36 (each 1 H, d, J = 3.0 Hz). **3a**: IR $\tilde{\nu}$ = 2090 (sh), 2080 (w), 2045 (m), 2032 (s), 2019 (vs), 1995 (w), 1979 (w), 1970 (w), 1965 (w), 1915 (vw, br) cm^{-1}. ^{1}H-NMR: δ = 5.45 (5 H), 3.88 (3 H), −14.62 (1 H).
[6] a) W. Bernhardt, H. Vahrenkamp, *Angew. Chem. 96* (1984) 362; *Angew. Chem. Int. Ed. Engl. 23* (1984) 381; b) P. Michelin Lausarot, M. Turini, G. A. Vaglio, M. Valle, A. Tiripicchio, M. Tiripicchio Camellini, P. Garibaldi, *J. Organomet. Chem. 273* (1984) 239.
[7] J. B. Keister, M. W. Pagne, M. J. Muscatella, *Organometallics 2* (1983) 219; G. L. Geoffroy, R. A. Epstein, *Inorg. Chem. 16* (1977) 2795.

2-Dewar Phosphinines—a New Class of Compounds Containing Two-Coordinate Phosphorus**

By *Jürgen Fink, Wolfgang Rösch, Uwe-Josef Vogelbacher,* and *Manfred Regitz**

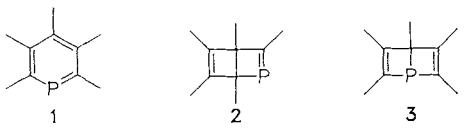
Dedicated to Professor Rolf Appel on the occasion of his 65th birthday

Phosphinines **1** have long been known and their reactivity has been studied in great detail.[1] However, their bicyclic isomers, the 2- and 1-phosphabicyclo[2.2.0]hexadienes (2- and 1-Dewar phosphinines) **2** and **3**, respectively, were, to the best of our knowledge, unknown.

We obtained **6** and **7**, the first compounds of type **2**, by reaction of the kinetically stabilized cyclobutadienes **4a**[2]

[*] Prof. Dr. M. Regitz, Dipl.-Chem. J. Fink, Dipl.-Chem. W. Rösch, Dipl.-Chem. U.-J. Vogelbacher
Fachbereich Chemie der Universität
Erwin-Schrödinger-Strasse, D-6750 Kaiserslautern

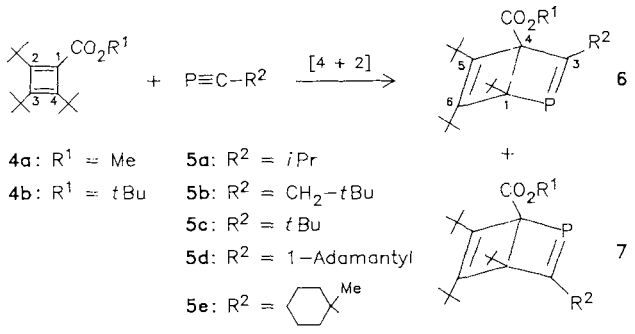
[**] Phosphorus Compounds with Unusual Coordination, Part 9. This work was supported by the Fonds der Chemischen Industrie, the Deutsche Forschungsgemeinschaft, and the Landesregierung von Rheinland-Pfalz.—Part 8: W. Rösch, U.-J. Vogelbacher, T. Allspach, M. Regitz, *J. Organomet. Chem.*, in press.



1 2 3

and **4b**[3] with the phosphaalkynes **5a–e**.[4] For steric reasons, the cycloaddition takes place at C-1 and C-4 and occurs in such a way that, in the product, the ester substituent and the substituent R^2 of the phosphaalkyne are preferentially or exclusively in neighboring positions (quantitative yields; **6** ≥ 85%, **7** ≤ 15%). It is understandable that the reactions with **4a** proceed more selectively than those with **4b**. Compounds **6a–d** are obtained from the mixture of Dewar phosphinines **6/7** by crystallization from pentane or petroleum ether (30–75°C) in isomerically pure form (Table 1). Surprising is the stability of the phosphabicycles toward atmospheric oxygen (a single crystal of **6d** is still intact after several weeks) as well as their thermal stability (the mixture **6g/7g** can be distilled at 220°C without decomposition). The aromatization observed in the case of the nitrogen analogues (**6**, N instead of P)[5] can therefore not be achieved by heating.

Decisive for the determination of the constitution of the Dewar phosphinines **6a–h** are the ^{31}P-NMR signals (δ = 312–317) and the ^{13}C-NMR signals of C-3 (δ = 223.6–242.1; $^1J_{P,C}$ = 31.7–36.5 Hz), the low-field position being typical for the phosphaalkene moiety.[6] The existence of regioisomers **7a–c** and **7e–h** is indicated by their phosphorus signals, which are shifted to high field relative to those



of **6** (δ = 285–300); these signals were used for quantitative analysis of the products. The small difference in the chemical shifts of C-5 and C-6 (Table 1) reveals—as mentioned above—the reaction centers of the cycloaddition.[7]

The X-ray structure analysis of **6d**[8] confirms the conclusions made on the basis of NMR spectroscopy (Fig. 1). The two four-membered-ring moieties are planar within threefold standard deviation and the dihedral angle is 113°.

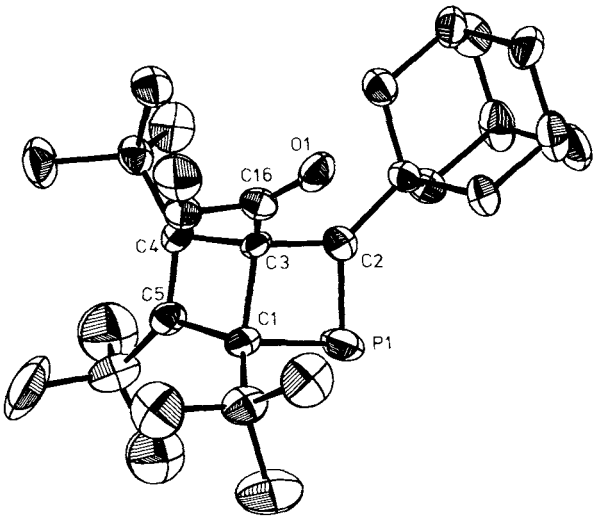


Fig. 1. ORTEP plot of one of the two independent molecules of **6d** [9]; the hydrogen atoms are omitted for clarity. Selected bond lengths [Å] and bond angles [°]: P1-C1 1.89(1), P1-C2 1.68(1), C1-C3 1.59(1), C1-C5 1.53(1), C2-C3 1.54(1), C3-C4 1.54(1), C4-C5 1.35(1); C1-P1-C2 79.5(4), P1-C1-C3 88.2(5), C3-C1-C5 85.3(6), P1-C2-C3 98.3(6), C1-C3-C2 93.9(6), C1-C3-C4 85.8(6), C3-C4-C5 93.9(6), C1-C5-C4 95.0(7).

Experimental Procedure

6c: A solution of **5c** (400 mg, 4 mmol) [4] in 1 mL of pentane (dry) was added to a solution of **4a** (835 mg, 3 mmol) [2] in 10 mL of pentane (dry) under argon at −78°C. The mixture was allowed to thaw after 1 h (decolorization). Evaporation afforded 1.14 g (100%) of a pale yellow, oily mixture of the isomers **6c** and **7c** (96 : 4 by ^{31}P-NMR spectroscopy), which, after kugelrohr

Table 1. Characteristic data for the 2-Dewar phosphinines **6** (δ values, J in Hz). Preparation of **6a, b** at 20°C, of **6c–h** of −78°C, followed by thawing to 20°C, both in pentane.

	R^1	R^2 [a]	**6** : **7**	M.p. [°C]	^{31}P-NMR [b]	^{13}C-NMR [c] C-1 ($^1J_{P,C}$)	C-3 ($^1J_{P,C}$)	C-4 ($^2J_{P,C}$)	C-5 ($^3J_{P,C}$)	C-6 ($^2J_{P,C}$)
6a	Me	*i*Pr	97 : 3	79	312	69.9 (19.6)	237.9 (33.4)	73.7 (3.8)	158.0 (6.1)	153.2 (20.2)
6b	Me	CH_2–*t*Bu	93 : 7	84	314	71.8 (19.5)	223.6 (36.5)	75.3 (–)	157.6 (6.2)	153.4 (19.6)
6c	Me	*t*Bu	96 : 4	90	315	67.1 (17.7)	239.8 (33.5)	73.2 (5.9)	157.7 (5.9)	153.9 (17.9)
6d	Me	1-Ad	100 : 0	119	314	67.8 (17.6)	241.5 (33.7)	73.4 (6.1)	158.2 (6.1)	154.6 (19.0)
6e	Me	C_7H_{13}	98 : 2	[d]	315	67.4 (17.9)	242.1 (33.4)	73.6 (5.5)	158.0 (6.1)	154.2 (18.9)
6f	*t*Bu	*t*Bu	85 : 15	[d]	316	68.0 (17.0)	240.5 (31.7)	75.9 (5.2)	157.5 (6.6)	155.0 (19.4)
6g	*t*Bu	1-Ad	85 : 15	[d]	317	68.6 (17.1)	241.7 (32.0)	75.8 (6.3)	158.0 (6.0)	155.2 (20.0)
6h	*t*Bu	C_7H_{13}	85 : 15	[d]	316	68.1 (17.3)	242.1 (34.5)	75.9 (6.0)	157.7 (5.1)	154.8 (19.0)

[a] 1-Ad = 1-adamantyl; C_7H_{13} = 1-methylcyclohexyl. [b] C_6D_6, 85% H_3PO_4 (ext.). [c] $CDCl_3$ or C_6D_6, TMS (int.). [d] Oil, distillative separation of regioisomer **7** was not possible.

distillation at 120°C (oven temperature) and 10^{-3} mbar, formed a glassy solid. Recrystallization from pentane at −78°C afforded 980 mg (87%) of colorless crystals (isomerically pure): m.p. = 90°C. A 63:37 mixture of the isomers **6c**:**7c** is present in the mother liquor.

Received: November 12, 1985 [Z 1533 IE]
German version: *Angew. Chem. 98* (1986) 265

[1] Review: G. Märkl in *Houben-Weyl: Methoden der Organischen Chemie, 4. Aufl., Bd. E1*, Thieme, Stuttgart 1982, p. 72ff.
[2] S. Masamune, N. Nakamura, M. Suda, H. Ona, *J. Am. Chem. Soc. 95* (1973) 8481.
[3] P. Eisenbarth, M. Regitz, *Chem. Ber. 115* (1982) 3796.
[4] **5a**, **b**, **e**: W. Rösch, U.-J. Vogelbacher, T. Allspach, M. Regitz, *J. Organomet. Chem.*, in press; **5c**: G. Becker, G. Gresser, W. Uhl, *Z. Naturforsch. B36* (1981) 16; **5d**: T. Allspach, M. Regitz, G. Becker, W. Becker, *Synthesis*, in press.
[5] J. Fink, M. Reigtz, *Bull. Soc. Chim. Fr.*, in press.
[6] R. Appel, F. Knoll, J. Ruppert, *Angew. Chem. 93* (1981) 771; *Angew. Chem. Int. Ed. Engl. 20* (1981) 731.
[7] The differently substituted olefinic C atoms of the product formed by the cycloaddition of **5** to C-2 and C-3 of **4** should exhibit a $\Delta\delta$ value of about 20 ppm; cf. [3].
[8] Monoclinic, $P2_1/c$; $a = 15.594(3)$, $b = 31.177(3)$, $c = 11.025(3)$ Å, $\beta = 90.59(2)°$; $Z = 8$ (2 independent molecules), $\rho_{calcd} = 1.13$ g cm^{-3}. 6563 independent reflections (Enraf-Nonius CAD4, $Mo_{K\alpha}$, $2\theta \leq 44°$), of which 3951 were observed for $I \geq 2\sigma(I)$; direct methods (MULTAN); $R = 0.096$, $R_w = 0.095$. Further details of the crystal structure investigation may be obtained from the Fachinformationszentrum Energie, Physik, Mathematik GmbH, D-7514 Eggenstein-Leopoldshafen 2 (FRG), on quoting the depository number CSD-51793, the names of the authors, and the journal citation.
[9] The values correspond to averaged values from the two independent molecules.

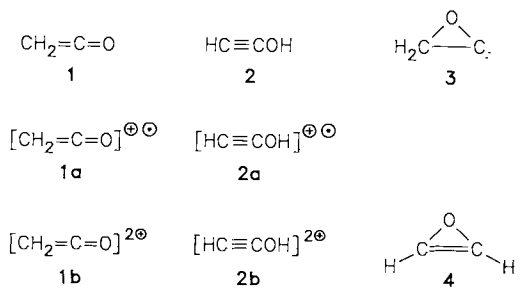
Hydroxyacetylene: Generation and Characterization of the Neutral Molecule, Radical Cation and Dication in the Gas Phase**

By *Ben van Baar, Thomas Weiske, Johan K. Terlouw,* and *Helmut Schwarz**

Dedicated to Professor David Ginsburg on the occasion of his 65th birthday

Neutral C_2H_2O isomers[1a] as well as their singly[1b] and doubly charged[1c] analogues have recently been examined by "state of the art" ab initio MO calculations. Apart from the well known ketene, **1**, these calculations also predict the isomers hydroxyacetylene (ethynol) **2**, the carbene oxiranylidene **3**, and oxirene **4** to be potentially observable stable species in the gas phase. However, because of the very low barrier predicted for the isomerization **4** → **1** it is highly improbable that **4** will ever be generated as a stable species.[2] For the systems $C_2H_2O^{\oplus\odot}$ and $C_2H_2O^{2\oplus}$ it is predicted[1b,c] that, apart from **1a** and **1b**, **2a** and **2b** should also be stable. We report here the generation and characterization of **2**, **2a**, and **2b** as stable species in the gas phase.

The use of tandem mass spectrometers[3] enables not only monocations to be structurally characterized under solvent-free conditions,[4] but also dications to be prepared



from monocations by the technique of "charge stripping mass spectrometry"[5]

$$m^{\oplus} + N \longrightarrow m^{2\oplus} + N + e^{\ominus}$$

and monocations to be neutralized by reaction with metal vapors or inert gases such as xenon.[6]

$$m^{\ominus} + Xe \longrightarrow m + Xe^{\oplus\odot}$$

Re-ionization of these neutral species by collision with helium (Neutralization Re-ionization Mass Spectrometry, NRMS[6]) allows them to be characterized on the basis of their ionic dissociation products.[7]

The radical cation $[HC{\equiv}COH]^{\oplus\odot}$ **2a** of hydroxyacetylene can be generated by decarbonylation of $[HC{\equiv}C{-}COOH]^{\oplus\odot}$ (70 eV electron impact ionization). The collisional activation (CA) spectrum of **2a** (Fig. 1B) is completely different from that of **1a** (Fig. 1A); thus, **2a** and **1a** do not isomerize within the mass spectrometric time scale ($t < 10^{-5}$ s). Further, the two spectra also show several peaks of structurally diagnostic value. In the case of **2a**, loss of HC (*m/z* 29) is much more pronounced than the formation of *m/z* 28 (loss of H_2C or HC + H), whereas in the case of **1a** the reverse holds true. Analogously, the CA spectrum of **1a** displays a peak for the loss of oxygen (*m/z* 26) which is almost absent in **2a**. The weak but readily recognizable peak at *m/z* 17 ($OH^{\oplus}$) in the spectrum of **2a** has its counterpart at *m/z* 16 in **1a**. Examination of $[HC{\equiv}C{-}OD]^{\oplus\odot}$, obtained by decarbonylation of $[HC{\equiv}C{-}CO_2D]^{\oplus\odot}$, confirms our analysis (Fig. 1C). The corresponding mass shifts (*m/z* 29 → *m/z* 30; *m/z* 17 → *m/z* 18; *m/z* 25 → *m/z* 25) are in agreement with the analysis of the spectrum of **2a**.

The heat of formation of **2a**, $\Delta H_f^0 \leq 247$ kcal/mol, was derived from the appearance energy (AE) for the loss of CO from metastable $[HC{\equiv}C{-}CO_2H]^{\oplus\odot}$ (using AE = 11.4 ± 0.2 eV, determined by the Burgers/Holmes method,[8] $\Delta H_f^0(CO) = -26.4$ kcal/mol[9], and $\Delta H_f^0(HC{\equiv}CCO_2H) = -42$ kcal/mol).[10] The ion **2a** is less stable than its isomer **1a** by 36 kcal/mol; theoretical calculations[1b] predict an energy difference of 45 kcal/mol.[11]

Further insight into the gas phase chemistry of **1a** and **2a** is provided by their unimolecular dissociations. Excited **1a** dissociates unimolecularly into $CH_2^{\oplus\odot}$ and CO with a release of translation energy (T_k) of $T_{0.5} = 2.0$ meV.[12,13] Assuming that the loss of $H^{\odot}$ from **2a** by direct cleavage

$$[HC{\equiv}C{-}OH]^{\oplus\odot} \longrightarrow H{-}\overset{\oplus}{C}{=}C{=}O + H^{\odot}$$
2a

has no barrier for the reverse reaction, this process is estimated to have an activation energy of 68 kcal/mol (from ΔH_f^0(**2a**) = 247 kcal/mol and ΔH_f^0 products: $H\overset{\oplus}{C}{=}C{=}O$

[*] Prof. Dr. H. Schwarz, Dr. T. Weiske
Institut für Organische Chemie der Technischen Universität
Strasse des 17. Juni 135, D-1000 Berlin 12
Dr. J. K. Terlouw, B. van Baar
Analytical Chemistry Laboratory
University of Utrecht
Croesestraat 77, NL-3522 AD Utrecht (Netherlands)

[**] This work was supported by the Fonds der Chemischen Industrie and the Deutsche Forschungsgemeinschaft. *J. K. T.* thanks the Deutscher Akademischer Austauschdienst (DAAD) for a Science Exchange Award.

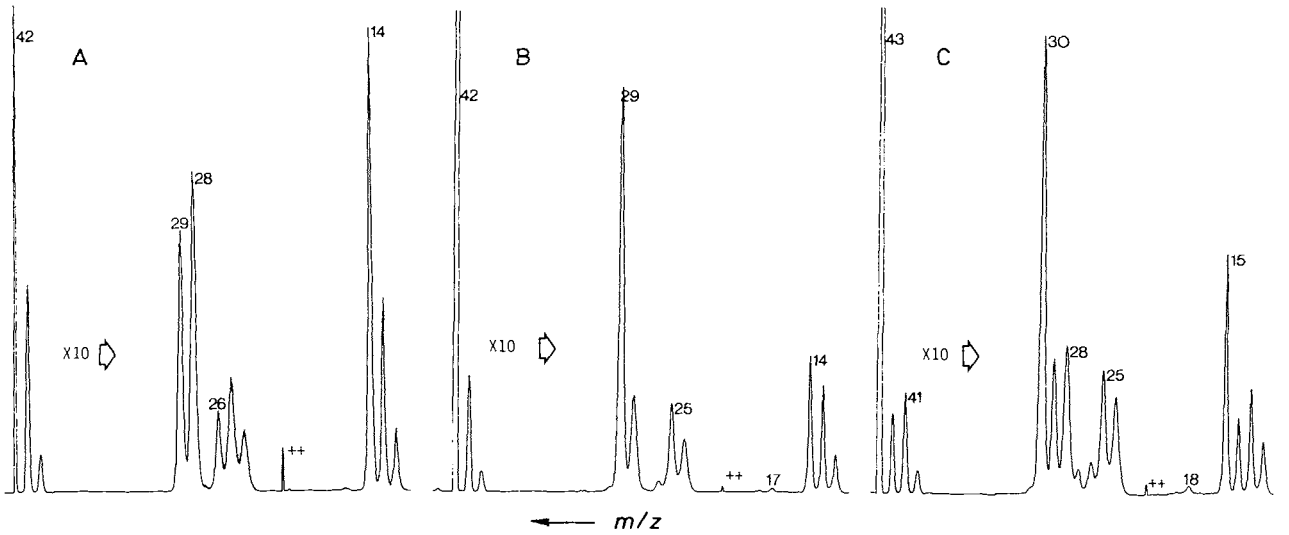


Fig. 1. Collision activation (CA) spectra of A) $[CH_2{=}C{=}O]^{\oplus\odot}$ **1a**, B) $[HC{\equiv}COH]^{\oplus\odot}$ **2a**, and C) $[HC{\equiv}COD]^{\oplus\odot}$.

$=263$ kcal/mol[6d] and $H^{\odot}=52$ kcal/mol[9]). Since theoretical calculations predict the isomerization **2a** → **1a** to require 79 kcal/mol, **2a** and its analogue $[HC{\equiv}C{-}OD]^{\oplus\odot}$ are expected to dissociate unimolecularly by loss of $H^{\odot}$ and $D^{\odot}$, respectively. The experimental finding that **2a** exclusively produces $CH_2^{\oplus\odot}$ by loss of CO, and the fact that the kinetic energy release in this reaction is much larger ($T_{0.5}=26$ meV) than that for the direct cleavage in **1a**, implies the following: 1) The dissociation **2a** → $CH_2^{\oplus\odot}$ only occurs from ions having internal energies in excess of that at the thermochemical threshold. 2) Prior to this reaction, **2a** isomerizes into energy-rich **1a**; this step seems to be rate-determining in the sequence **2a** → **1a** → $CH_2^{\oplus\odot}$, and from the thermochemical data for **2a**, $CH_2^{\oplus\odot}$, and CO a *minimum* value of 60 kcal/mol is readily derived for the isomerization barrier, E^0. 3) Isomerization of **2a**, via a barrier of $60<E^0<79$ kcal/mol, suppresses the direct loss of $H^{\odot}$ (or $D^{\odot}$ from $HC{\equiv}COD^{\oplus\odot}$) and thus this cleavage must involve a significant barrier.

Hydroxyacetylene H–C≡C–OH **2** is less stable than ketene **1** by 36 kcal/mol; the high barrier of 73 kcal/mol for the isomerization **2** → **1** indicates that once generated **2** should at least be stable in the gas phase. We have utilized a NRMS experiment to generate neutral **2** from the corresponding ion **2a** by neutralizing it with an electron donor. Thus, mass selected $HC{\equiv}COH^{\oplus\odot}$ ions were neutralized with xenon in a tandem collision cell[6d]; the ions not neutralized in the first cell were diverted by a deflector electrode and only the remaining beam of highly accelerated neutral molecules **2** was allowed to enter the second collision cell. Here, the neutral molecules were re-ionized by impact excitation with He to **2a** and the CA spectrum was recorded.

Figure 2 shows the NRMS spectra of **1a**, **2a**, and $[HC{\equiv}COD]^{\oplus\odot}$. Comparison of the structurally diagnostic features of the spectra leads to the conclusion that neutralization of $[HC{\equiv}COH]^{\oplus\odot}$ **2a** yields stable hydroxyacetylene **2**, which, under the conditions of the experiment, does not isomerize to the thermodynamically more stable ketene **1**.[14]

The dication [HC≡COH]$^{2\oplus}$ **2b** of hydroxyacetylene is, according to MP2/6-31G*//4-31G computations, ca. 59 kcal/mol less stable than **1b**.[1c] Dications **1b** are accessible by charge stripping from **1a**; the ionization energy (IE)

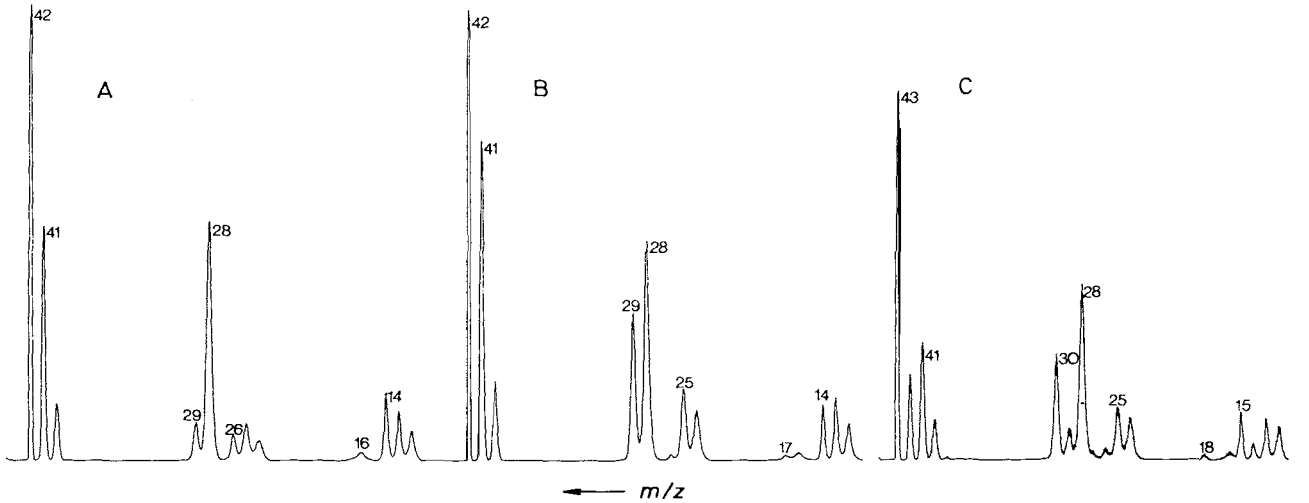


Fig. 2. NRMS of A) $[CH_2{=}C{=}O]^{\oplus\odot}$ **1a**. B) $[HC{\equiv}COH]^{\oplus\odot}$ **2a**, and C) $[HC{\equiv}COD]^{\oplus\odot}$.

for **1a** → **1b** + e$^{\ominus}$ is 18.6 eV.[1c] It already follows from the presence of the narrow signal at *m/z* 21 in Figure 1B that charge stripping of **2a** also yields a stable dication and preliminary measurements of the ionization energies for **2a** → **2b** + e$^{\ominus}$ give IE = 18–19 eV. Ab initio MO calculations (MP2/6-31G*//4-31G) yield a value of 18.6 eV for the adiabatic ionization of **2a**;[1c] the recently computed (MP3/6-31G*//6-31G*)[15] value for the vertical transition to the triplet ground state of **2b** is 18.5 eV.

Conclusion: The existence of keto/enol tautomeric pairs of neutral and singly or doubly charged species is now well established. The present work provides the first experimental evidence that the ynol of the most simple ketene/ynol tautomeric pair, hydroxyacetylene, exists as a stable neutral molecule **2**, radical cation **2a**, and dication **2b**, as predicted by theory.

Received: November 8, 1985;
revised: December 19, 1985 [Z 1526 IE]
German version: *Angew. Chem. 98* (1986) 275

[1] a) W. J. Bouma, R. H. Nobes, L. Radom, C. E. Woodward, *J. Org. Chem. 47* (1982) 1869; b) W. J. Bouma, P. M. W. Gill, L. Radom, *Org. Mass Spectrom. 19* (1984) 610; c) W. Koch, F. Maquin, D. Stahl, H. Schwarz, *J. Chem. Soc. Chem. Commun. 1984*, 1679.
[2] G. Maier, H. P. Reisenauer, T. Sayrac, *Chem. Ber. 115* (1982) 2192.
[3] F. W. McLafferty (Ed.): *Tandem Mass Spectrometry*, Wiley-Interscience, New York 1983.
[4] J. L. Holmes, *Org. Mass Spectrom. 20* (1985) 169.
[5] Review: W. Koch, F. Maquin, D. Stahl, H. Schwarz, *Chimia 39* (1985) 376.
[6] Selected references: a) P. O. Danis, C. Wesdemiotis, F. W. McLafferty, *J. Am. Chem. Soc. 105* (1983) 7454; b) P. C. Burgers, J. L. Holmes, A. A. Mommers, J. K. Terlouw, *Chem. Phys. Lett. 102* (1983) 1; c) P. C. Burgers, J. L. Holmes, A. A. Mommers, J. E. Szulejko, J. K. Terlouw, *Org. Mass Spectrom. 19* (1984) 442; d) J. L. Holmes, A. A. Mommers, J. K. Terlouw, C. E. A. A. Hop, *Int. J. Mass Spectrom. Ion Proc.*, in press.
[7] Review: K. Levsen, H. Schwarz, *Mass Spectrom. Rev. 2* (1983) 77.
[8] P. C. Burgers, J. L. Holmes, *Org. Mass Spectrom. 17* (1982) 123.
[9] H. M. Rosenstock, K. Draxl, B. W. Steiner, J. T. Herron, *J. Phys. Chem. Ref. Data Suppl. 1, 6* (1977).
[10] J. L. Holmes, private communication.
[11] Note that the relative stability of hydroxyacetylene versus ketene decreases in going from the neutral molecules **2**/**1** to the radical cations **2a**/**1a**, whereas the reverse invariably obtains with enol/keto tautomeric pairs, where the order of stability may even change. Review: H. Schwarz, *Proc. 10. Intern. Mass Spectrom. Conf.* Swansea (1985), in press.
[12] R. Stockbauer, *Int. J. Mass Spectrom. Ion Phys. 25* (1977) 401; N. J. Hijazi, J. L. Holmes, J. K. Terlouw, *Org. Mass Spectrom. 14* (1979) 119.
[13] J. C. Lorquet, *Int. J. Mass Spectrom. Ion Phys. 38* (1981) 343.
[14] The relatively intense peak at *m/z* 28 in the NRMS of **1a** relates to the large cross section [6d] for collisional re-ionization of CO generated by dissociation of **1a** in the first CA cell.
[15] W. Koch, unpublished results.

Influence of External Negative Charges on the Absorption Maxima of Symmetrical Cyanines. A Study with Model Compounds and Artificial Bacteriorhodopsin Pigments**

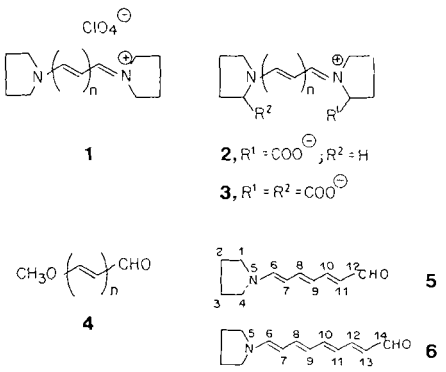
By *Mordechai Sheves** and *Noga Friedman*

Symmetrical cyanine dyes show narrow, red-shifted absorption maxima (relative to the corresponding protonated Schiff base) as a result of their highly delocalized π electrons. Perturbation that reduces the symmetry of a symmetrical cyanine should result in blue shifts and broadening of the electronic spectrum.

Bacteriorhodopsin (bR) is the protein pigment of the purple membrane of the halophilic microorganism *Halobacterium halobium*.[1] Its role is to convert light energy into a proton gradient across the membrane, which is subsequently used to synthesize ATP via a chemiosmotic mechanism. bR consists of all-*trans*-retinal linked to the ε-amino group of a lysine residue to form a protonated Schiff base.[2]

The absorption maximum of bR (λ_{max} = 570 nm) is red-shifted relative to that of the protonated retinal Schiff base in methanol solution (λ_{max} = 440 nm). At present, it is assumed that this red shift is a consequence of several factors: (1) weak hydrogen bonding to the positively charged Schiff base nitrogen;[3] (2) a planar *s-trans* ring–chain conformation of the retinal chromophore in the binding site;[4] (3) an interaction between an ion-pair in the protein near the cyclohexene moiety and the retinal chromophore.[3d,e,4] Recently, an artificial bR pigment containing a cyanine dye chromophore, which exhibited a narrow, red-shifted absorption maximum (relative to bacteriorhodopsin), was prepared.[5] Calculations[6] predicted that this characteristic absorption should originate from interaction of the polyene with negative charges symmetrically distributed along the chromophore.

In this study, we have examined the effect of a nonsymmetrical distribution of negative charges along the polyene on the absorption maximum of symmetrical cyanines, using compounds **1**–**3**, which bear symmetrically (**1** and **3**) or nonsymmetrically (**2**) distributed negative charges.



Cyanines **1** were prepared as described earlier.[7] Compounds **2** (mixtures of *syn–anti* isomers) were prepared by condensation of the corresponding merocyanines (obtained by basic hydrolysis of **1**, cf. **5** and **6**) with proline. Compounds **3** (likewise mixtures of *syn–anti* isomers) were synthesized by condensation of **4** with proline followed by addition of Et_3N. Compounds **1**, **2**, and **3** exhibited very similar absorption maxima in both ethanol and methylene chloride. The introduction of the second negative charge (see **3**) only slightly changed the absorption maxima and the bandwidth (as measured at the half-height) (Table 1). None of the recorded absorption maxima was shifted following dilution up to 10^{-5} M, which was necessary to minimize the possibility of aggregation. Thus, the absorption maxima of symmetrical cyanines are not affected significantly by the location of their counterion in organic solvents.

[*] Dr. M. Sheves, Dr. N. Friedman
Department of Organic Chemistry, The Weizmann Institute of Science
Rehovot 76100 (Israel)

[**] *M. S.* is an incumbent of the Morris and Ida Wolf Career Development Chair. This work was supported by the Frances and Lillian Schermer Trust. We thank Prof. *K. Nakanishi* for stimulating discussions.

Table 1. Absorption maxima, λ_{max}, and bandwidths at half-height, $\tilde{\nu}_{1/2}$, of symmetrical cyanines **1–3**.

Cyanine	EtOH		CH_2Cl_2	
	λ_{max} [nm]	$\tilde{\nu}_{1/2}$ [cm^{-1}]	λ_{max} [nm]	$\tilde{\nu}_{1/2}$ [cm^{-1}]
1a	320	3750	323	3790
2a	324	3480	325	3500
3a	324	3500	327	3760
1b	422	1700	427	1670
2b	424	1920	429	2100
3b	429	1880	431	2470
1c	521	1380	530	1240
2c	526	1460	530	1230
3c	528	1330	534	1400
1d	625	1040	635	1020
2d	631	1190	639	1160
3d	633	1200	642	1100

The symmetry of chromophores **1a–d** and high degree of charge delocalization in the ground state are reflected in their ^1H- and ^{13}C-NMR spectra (Table 2).

Table 2. ^1H- and ^{13}C-NMR data of **1a–d** and **1a**, **b**, **2a**, **b**. For numbering of the atoms see **5** and **6**. J in Hz.

^1H-NMR (CD_3OD): **1a**: $\delta = 5.52$ (t, 1, $J = 12$, 7-H), 7.92 (d, 2, $J = 12$, 6(8)-H); **1b**: $\delta = 5.67$ (t, 2, $J = 11.8$, 7(9)-H), 7.48 (t, 1, $J = 11.8$, 8-H), 7.72 (d, 2, $J = 11.7$, 6(10)-H); **1c**: $\delta = 5.74$ (t, 2, $J = 11.8$, 7(11)-H), 6.26 (t, 1, $J = 12.6$, 9-H), 7.30 (t, $J = 11.8$, 2, 8(10)-H), 7.70 (d, 2, $J = 11.8$, 6(12)-H); **1d**: $\delta = 5.95$ (t, 2, $J = 12$, 7(13)-H), 6.21 (t, 2, $J = 12$, 9(11)-H), 7.17 (t, 1, $J = 12$, 10-H), 7.25 (t, 2, $J = 12$, 8(12)-H), 7.45 (d, 2, $J = 12$, 6(14)-H)

^{13}C-NMR (CD_3OD): **1a**: $\delta = 92.90$ (C-7), 159.66 (C-6/8); **2a** [a]: $\delta = 93.49$, 93.12 (C-7), 159.65, 159.74, 159.83, 160.88 (C-6/8); **1b**: $\delta = 105.16$ (C-7/9), 158.76 (C-6/10), 163.57 (C-8); **2b** [a]: $\delta = 105.44$, 105.55, 105.59, 106.31 (C-7/9), 158.50, 159.09, 160.12 (C-6/10), 163.45, 163.72 (C-8)

[a] *syn-anti* mixture.

The ^{13}C-NMR spectra indicate that **2a**, **b** do not differ significantly from **1a**, **b** with respect to charge delocalization and the high degree of symmetry. The corresponding carbon atoms in **1a** and **2a** have virtually identical chemical shifts. This is also true for **1b** and **2b**. This insensitivity to location of the counterion (symmetrical in **1** and unsymmetrically fixed in **2**) is reflected in the absorption maxima of these cyanines (Table 1).

To gain further information on the influence of external charges on the electronic spectra of symmetrical cyanines, we incubated merocyanine **5** (obtained by basic hydrolysis of **1c**) with bacterioopsin[8] for 48 h (pH = 6.5, 20 mM HEPES buffer). This resulted in formation of the artificial pigment **V**, which has an absorption maximum at $\lambda = 530$ nm (Fig. 1) with a narrow bandwidth (1350 cm^{-1}). Competition experiments with all-*trans*-retinal showed that the chromophore occupied the binding site. Similarly, incubation of merocyanine **6** with bacterioopsin (1 h) afforded pigment **VI**, which absorbed at $\lambda = 640$ nm with a bandwidth of 1100 cm^{-1}. Both artificial pigments exhibit similar absorption maxima and bandwidths to those of the corresponding cyanines **1c** and **2c** or **1d** and **2d**, respectively, in EtOH and CH_2Cl_2 (Table 1).

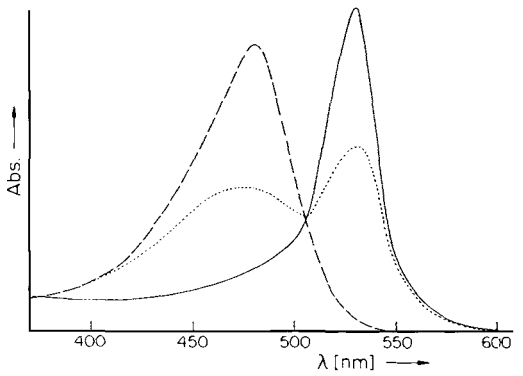


Fig. 1. Incubation of merocyanine **5** with bleached purple membrane at 25°C, pH = 6.5; formation of the artificial bacteriorhodopsin pigment **V** (---) Absorption after 1 min; (· · · ·) after 12 h; (——) after 48 h.

Artificial bR pigments based on dihydroretinals exhibit opsin shifts that vary, depending on the length of the chromophore. (The opsin shift is defined as the difference between the absorption of the pigment and that of a protonated Schiff base of the corresponding retinal chromophore in MeOH.)[9] For example, it was suggested that the pigments derived from 5,6- and 7,8-dihydroretinals differ quite significantly from each other on account of different charge distribution introduced by the protein around these two chromophores.[3d,9] Pigments **V** and **VI** are comparable to 7,8- and 5,6-dihydro pigments, respectively, in their chromophore length. However, the absence of significant opsin shifts points to the insensitivity of symmetrical aliphatic cyanines to charge distribution around their polyene skeleton. This result is consistent with our experimental observation in organic solvents that the absorption maxima of symmetrical cyanines are not affected significantly by interaction with external negative charges.

The red-shifted absorption maxima and the narrow bandwidth of symmetrical cyanines reflect the high degree of charge delocalization in both the ground and excited states; the charge in these cyanines is distributed similarly, in each case, along the polyene chain.[10] This phenomenon is not perturbed by interaction with nonsymmetrically distributed negative charges in the vicinity of the nitrogen atoms. Similar arguments hold for the insensitivity of the absorption maxima to solvent polarity. This behavior is completely different from that found in protonated retinal Schiff bases, which are markedly influenced by nonconjugated charges,[3e] because the positive charge is distributed differently in the ground and excited states.

Received: August 30, 1985;
revised: December 30, 1986 [Z 1444 IE]
German version: *Angew. Chem. 98* (1986) 260

CAS Registry numbers:
1a, 56337-40-7; **1b**, 100683-37-2; **1c**, 100683-39-4; **1d**, 21044-72-4; **2a**, 100683-40-7; **2b**, 100683-41-8; **2c**, 100683-42-9; **2d**, 100683-43-0; **3a**, 100701-08-4; **3b**, 100683-45-2; **3c**, 100683-47-4; **3d**, 100683-49-6; **5**, 100683-50-9.

[1] D. Oesterhelt, W. Stoeckenius, *Nature (London) New Biol. 233* (1971) 149.
[2] Reviews: a) W. Stoeckenius, R. Lozier, R. Bogomolni, *Biochim. Biophys. Acta 505* (1979) 215; b) M. Ottolenghi, *Adv. Photochem. 12* (1980) 97; c) R. Birge, *Annu. Rev. Biophys. Bioeng. 10* (1981) 315.
[3] a) P. Blatz, J. Mohler, *Biochemistry 14* (1975) 2304; b) M. Sheves, N. Friedman, A. Albeck, M. Ottolenghi, *ibid. 24* (1985) 1260; c) M. Muradin-Szweykowska, J. A. Pardoen, D. Dobbelstein, L. J. P. Van Amsterdam, J. Lugtenburg, *Eur. J. Biochem. 140* (1984) 173; d) J. L. Spudich, D. A. McCain, K. Nakanishi, M. Okabe, N. Shimizu, H. Rodman, B. Honig, *Biophys. J.*, in press; e) T. Baasov, M. Sheves, *J. Am. Chem. Soc. 107* (1985) 7524; f) G. Harbison, J. Herzfeld, R. Griffin, *Biochemistry 22* (1983) 1.
[4] a) G. Harbison, J. Herzfeld, S. O. Smith, R. A. Mathies, J. Pardoen, J. Lugtenburg, R. G. Griffin, *Biophys. J. 47* (1985) 92a; b) G. Harbison, S. O. Smith, J. Pardoen, J. M. L. Courtin, J. Lugtenburg, J. Herzfeld, R. A. Mathies, R. G. Griffin, *Biochemistry 24* (1985) 6955; c) T. Schreckenbach, B. Walckhoff, D. Oesterhelt, *ibid. 17* (1978) 5353.
[5] F. Derguini, C. G. Caldwell, M. G. Motto, V. Balogh-Nair, K. Nakanishi, *J. Am. Chem. Soc. 105* (1983) 646.

[6] T. Kakitani, H. Kakitani, B. Honig, K. Nakanishi, *J. Am. Chem. Soc. 105* (1983) 648.
[7] S. S. Malhotra, M. C. Whiting, *J. Chem. Soc. 1960*, 3812.
[8] F. Tokunaga, T. Ebrey, *Biochemistry 17* (1978) 1915.
[9] K. Nakanishi, V. Balogh-Nair, M. Arnaboldi, K. Tsujimoto, B. Honig, *J. Am. Chem. Soc. 102* (1980) 7945.
[10] M. Klessinger, *Theor. Chim. Acta 5* (1966) 251.

Remarkable Ease of Ring Oxidation in Cerium(IV) Bisporphyrinates with Double-Decker Structure**

By *Johann W. Buchler,* Kyra Elsässer, Martina Kihn-Botulinski,* and *Bernd Scharbert*

Dedicated to Professor Hans Herloff Inhoffen on the occasion of his 80th birthday

The structure of the reaction center of bacterial photosynthesis in *Rhodopseudomonas viridis* was recently elucidated by *Huber* et al.[1] This extensive membrane protein complex proves to contain the long postulated "special pair", a bacteriochlorophyll b dimer $(BChl)_2$, in which the tetrapyrrole ligands cohere about 3 Å apart from each other via π-π interactions of the two pyrrole rings I. According to present knowledge,[1] this "special pair" donates an electron to a neighboring bacteriopheophytin monomer (BPhe) according to Eqn. (a) under the action of light quanta.

$$(BChl)_2 + BPhe + h\nu \longrightarrow (BChl)_2^{\oplus} + BPhe^{\ominus} \quad (a)$$

The ionized "special pair", $(BChl)_2^{\oplus}$, is recognized by a characteristic absorption band at about 1300 nm in the near infrared (NIR).[2]

We recently described sandwich-like lanthanoid bisporphyrinates, e.g., the cerium(IV) derivative of 5,10,15,20-tetra(*p*-tolyl)porphyrin, $Ce(TTP)_2$,[3] and the derivatives of 2,3,7,8,12,13,17,18-octaethylporphyrin, $Ce(OEP)_2$,[4,5] $Pr(OEP)_2$,[4] and $Eu(OEP)_2$,[4] which contain Ce^{IV}, Pr^{III}, and Eu^{III}, respectively, as central ions; in the case of the trivalent lanthanoid ions, the formula $Ln(OEP)_2$ can only be explained in terms of one porphyrin ligand being present in the complexes as dianion $(OEP)^{2\ominus}$ and the other as radical monoanion $OEP^{\odot\ominus}$. The combination of two porphyrin systems in different oxidation states is recognized in $Pr(OEP)_2$ and $Eu(OEP)_2$, inter alia, by characteristic absorption bands in the NIR at 1400 and 1280 nm, respectively, which can be tentatively assigned to an internal charge transfer (CTI).[6]

The finding that the cation $(BChl)_2^{\oplus}$ in Eqn. (a) likewise absorbs in the NIR at 1300 nm, suggests that these absorptions could be a common characteristic of such mixed valence tetrapyrrole dimers. In the meantime, the double-deckers $Ln(OEP)_2$ with all lanthanoids excepting Pm have been prepared. With exception of the Ce^{IV} derivative all complexes show a NIR band whose wave number monotonously decreases with increasing ionic radius of the rare-earth metal.[6] These observations finally prompted attempts to convert the neutral Ce^{IV} double-deckers likewise into mixed valence cations by oxidation according to Eqn. (b); formulated for octaethylporphyrin, Eqn. (b) then describes a redox system analogous to the "special pair".

$$Ce(OEP)_2 \rightleftharpoons Ce(OEP)_2^{\oplus} + e^{\ominus} \quad (b)$$

Indeed, the oxidation is realized on a preparative scale by reaction of the Ce^{IV} double-decker $Ce(TTP)_2$ with the hexachloroantimonate of the phenoxathiin radical cation[7] in 1,2-dichloroethane (DCE) according to Eqn. (c).

$$Ce(TTP)_2 + [phenoxathiin]^{\odot\oplus}SbCl_6^{\ominus} \longrightarrow Ce(TTP)_2SbCl_6 + phenoxathiin \quad (c)$$

1a

$Ce(TTP)_2PF_6$ **1b** $Ce(OEP)_2SbCl_6$ **2** $Ce(TPP)_2SbCl_6$ **3**

After evaporation to dryness and redissolution in DCE/toluene, blue-violet crystals of **1a** · 2 DCE separate. **2** and **3**, the derivative of 5,10,15,20-tetraphenylporphyrin, are obtained likewise. The salts are characterized by elemental analyses and conductivity measurements, and by their UV/VIS, IR, and NMR spectra.[8] As expected, NIR bands are observed at 1340 nm (**1a**), 1270 nm (**2**), and 1350 nm (**3**) showing halfwidths of about 300 nm.

The redox potentials for the reversible first ring oxidation to **1a** or **2** are taken from the cyclic voltammograms (Fig. 1). The waves appearing in the more positive potential region correspond to an oxidation to the dication; the quasi-reversible waves lying in the negative region presumably indicate the reduction to Ce^{III}. Electrolysis of $Ce(TTP)_2$ in CH_2Cl_2/NBu_4PF_6 at a controlled potential of about +0.7 V affords **1b**[8] after removal of the solvent and recrystallization from acetone.

Very informative is a comparison of the redox potentials (calomel electrode, CH_2Cl_2/NBu_4PF_6) for the first ring oxidation. On comparison with the documented monoporphyrins the following series emerges: TTP complexes: Zn(TTP): 0.81 V, $Ce(TTP)_2$: 0.62 V; TPP complexes: Zn(TPP): 0.71 V,[10] $Ce(TTP)_2$: 0.68 V, Mg(TPP): 0.54 V;[10] OEP complexes: Zn(OEP): 0.69 V, Mg(OEP): 0.53 V, $Ce(OEP)_2$: 0.17 V. In general, these potentials decrease in going from the zinc to the magnesium complexes;[10,11] Mg(OEP) belongs to the metal porphyrins that are particularly readily oxidized at the ring. In the case of the tetraarylporphyrins the value for the cerium double-decker lies between those of the magnesium complex and the zinc

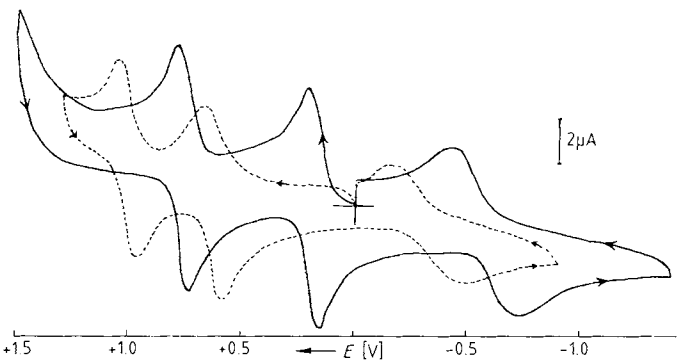


Fig. 1. Cyclic voltammograms of the cerium(IV) bisporphyrinates $Ce(TTP)_2$ (----), 1.0×10^{-4} mol/L, and $Ce(OEP)_2$ (—), 1.2×10^{-4} mol/L; scan rate 100 mV/s, solvent CH_2Cl_2, supporting electrolyte NBu_4PF_6, Pt-disk electrode, calomel reference electrode.

[*] Prof. Dr. J. W. Buchler, Dipl.-Ing. K. Elsässer, Dipl.-Ing. M. Kihn-Botulinski, Dipl.-Chem. B. Scharbert
Institut für Anorganische Chemie der Technischen Hochschule
Hochschulstrasse 4, D-6100 Darmstadt (FRG)

[**] Metal Complexes with Tetrapyrrole Ligands, Part 41. This work was supported by the Deutsche Forschungsgemeinschaft, the Fonds der Chemischen Industrie, and the Vereinigung von Freunden der Technischen Hochschule Darmstadt.—Part 40: [5].

complex; however, in going from the mono- to the bisporphyrin there is a further substantial drop in the value. If the electron-attracting aryl groups in the *meso* positions are replaced by the electron-donating, peripheral ethyl groups the ring oxidation to the radical cation is noticeably enhanced: the oxidation potential of the cerium double-decker is about 0.36 V lower than that of the magnesium complex.

$(BChl)_2$ exists likewise as a pair of highly alkylated yet hydrogenated tetrapyrrole systems. In the case of bacteriochlorophyll a, the association of the "special pair" effects a further enhancement in the ring oxidation in addition to that due to the presence of the magnesium: The oxidation potential of the dimer is about 0.2 V smaller than that of the monomer.[12] A corresponding, but clearly smaller effect by about 0.07 V was recently established in the case of the dimers of 5,10,15,20-tetrakis(benzo[15]crown-5)porphyrinatomagnesium, which are formed from this complex by reaction with potassium salts.[13]

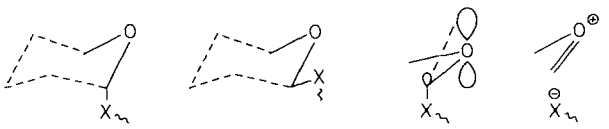
Received: November 11, 1985;
revised: January 2, 1986 [Z 1528 IE]
German version: *Angew. Chem. 98* (1986) 257

[1] J. Deisenhofer, O. Epp, K. Miki, R. Huber, H. Michel, *J. Mol. Biol. 180* (1984) 385, and references cited therein.
[2] M. S. Davis, A. Forman, L. K. Hanson, J. P. Thornber, J. Fajer, *J. Phys. Chem. 83* (1979) 3325.
[3] J. W. Buchler, H.-G. Kapellmann, M. Knoff, K.-L. Lay, S. Pfeifer, *Z. Naturforsch. B38* (1983) 1339.
[4] J. W. Buchler, M. Knoff in G. Blauer, H. Sund (Eds.): *Optical Properties and Structure of Tetrapyrroles*, de Gruyter, Berlin 1985, p. 91.
[5] J. W. Buchler, A. De Cian, J. Fischer, M. Kihn-Botulinski, H. Paulus, R. Weiss, *J. Am. Chem. Soc.*, in press.
[6] a) J. W. Buchler, K. Elsässer, M. Kihn-Botulinski, B. Scharbert, S. Tansil, *ACS Symp. Ser.*, in press; b) M. Kihn-Botulinski, Dissertation, Technische Hochschule Darmstadt 1986.
[7] P. Gans, J.-C. Marchon, C. A. Reed, J.-R. Regnard, *Nouv. J. Chim. 5* (1981) 203.
[8] Some data for the Cer(IV) bisporphyrinate salts **1a**, **1b**, **2**, and **3**: UV/VIS, λ_{max} [nm] (lgε): **1a**: 390 (4.96), 1340 (3.67); **1b**: 396 (5.27), 542 (4.08), 1350 (3.42); **2**: 354 (4.94), 515 (3.87), 808 (4.50), 1270 (3.75), 1762 (3.14); **3**: 384 (5.04), 662 (3.53), 1350 (3.93).—IR (KBr), $\tilde{\nu}$ [cm^{-1}]: **1a** and **1b**: 1290; **2**: 1525; **3**: 1270 ("oxidation state marker" after [9]).—^{1}H-NMR (300 MHz, CD_2Cl_2, TMS int.): δ values (lines and fine structure in part strongly broadened by paramagnetism): **1a**: 3.78 (*p*-CH_3), 7.81, 8.00 (*m*- or *o*-H); **1b**: 3.20 (*p*-CH_3), 7.04, 7.99 (*o*-H, *endo* or *exo*), 7.52, 7.85 (*m*-H, *endo* or *exo*); **2**: 2.25 (very broad and strong; only signal); **3**: 7.07, 7.65, 8.81 (Aryl-H); signals of peripheral protons in **1a**, **1b**, and **3** not discernible.—Specific conductivities κ [S·cm^{-1}] in DCE: **1a**: 2.0×10^{-6}; **2**: 2.7×10^{-6}; **3**: 2.2×10^{-6}.
[9] E. T. Shimomura, M. A. Philippi, H. M. Goff, W. F. Scholz, C. A. Reed, *J. Am. Chem. Soc. 103* (1981) 6778.
[10] A. Stanienda, G. Biebl, *Z. Phys. Chem. (N.F.) 52* (1967) 254.—These authors have investigated Zn(TPP) and Mg(TPP) in butyronitrile/$LiClO_4$.
[11] J. H. Fuhrhop, K. M. Kadish, D. G. Davis, *J. Am. Chem. Soc. 95* (1973) 5140.
[12] R. R. Prince, P. L. Dulton in R. C. Clayton, W. R. Sistrom (Eds.): *The Photosynthetic Bacteria*, Plenum Press, New York 1978, p. 439.
[13] G. Bhaskar Maiya, V. Krishnan, *Inorg. Chem. 24* (1985) 3253.

Solvent Polarity and the Anomeric Effect**

By *Benzion Fuchs,* Aviyakar Ellencweig, Evgeny Tartakovsky,* and *Pinchas Aped*

The anomeric effect is one of the most studied and reviewed phenomena in modern organic chemistry.[2,3] It was first discovered in carbohydrates[4] and interpreted in terms of electrostatic interactions between the C–X and C–O–C dipoles, for example, in **1** and **2**. The lesser stability of **2** was attributed to repulsive interactions between parallel dipoles or lone pairs. A subsequently postulated[3c] and then theoretically supported[5–7] interpretation invoked delocalization of a lone pair of electrons (n_p) on oxygen into the σ^* orbital (see **3**) of the adjacent C–X bond in **1** and hence its stabilization relative to **2**. While the second (MO) approach, with its valence bond counterpart (double bond–no bond resonance, **3**↔**4**) has been increasingly accepted, the extent to which each of the above phenomena may contribute to the origin of the anomeric effect has not yet been systematically investigated, let alone solved.



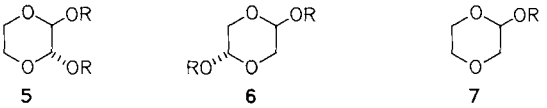
1 **2** **3** **4**

The strongest argument in favor of the initial, electrostatic rationalization of the anomeric effect was its apparent suppression by polar solvents since these were found to stabilize the equatorial forms of carbohydrates[3a,b,h,j] or other, simpler systems.[8] We now report data that are in apparent contradiction to this trend, suggesting that, in reality, polar solvents may *enhance* the anomeric effect.

We recently reported[10] that *trans*-2,3- and *trans*-2,5-dimethoxy-1,4-dioxanes **5a** and **6a**, respectively, as well as the analogous diphenoxy and diacetoxy derivatives (R = Ph, Ac) overwhelmingly prefer the diaxial conformation, mainly because of the anomeric effect but also because of *gauche* effects. This conformational preference is so strong that no significant changes could be experimentally detected by variation of temperature or solvent polarity. The corresponding bis(trimethylsiloxy) derivatives **5b** and **6b** and di(*tert*-butoxy) derivatives **5c** and **6c**[11] exist as conformational mixtures of diaxial and diequatorial forms. We have now carried out a detailed ^{1}H-NMR spectroscopic analysis of the CH_2–CH_2 (AA'BB') system in **5b** and **5c** and of the CH_2–CHOR system in **6b**, **6c**, and **7a** in various solvents and evaluated the conformational composition using the following relation:[10b]

$$J_{exp} = X J_{aa} + (1 - X) J_{ee}$$

Representative data for solutions in $CDCl_3$ are given in Table 1 and the evaluated conformational compositions in five solvents are listed in Table 2. (The literature values for 2-methoxy-1,4-dioxane **7a**[3f], in fact, promoted the present study.)



5 **6** **7**

a, R = Me; b, R = $SiMe_3$; c, R = *t*Bu

Tables 1 and 2 reveal a striking picture: increased solvent polarity stabilizes diequatorial conformations in the *trans*-2,3-disubstituted derivatives, whereas the opposite is true in the monosubstituted and 2,5-disubstituted analogues. This can be understood only in conjunction with the dipole moments that we have calculated for the 2-methoxy-1,4-dioxanes **7a** and the *trans*-2,3- and *trans*-2,5-

[*] Prof. Dr. B. Fuchs, Dr. A. Ellencweig, E. Tartakovsky, P. Aped
School of Chemistry, Tel-Aviv University
Ramat-Aviv, 69978 Tel-Aviv (Israel)

[**] Structure and Conformation of Heterocycles, Part 15.—Part 14: [1].

Table 1. Selected ^{1}H-NMR data for substituted 1,4-dioxanes of types **5**, **6**, and **7** [a].

Pattern [b]		**5a** [c]	**5b**	**5c**	**6a** [c]	**6b**	**6c**	**7b**
C^5H_2	$^2J(gem)$	−11.52	−11.78	−11.85	−11.50	−12.15	−11.62	−12.10
|	$^3J(trans)$	11.30	6.63	6.51	1.45	5.66	6.35	5.65
C^6H_2	$^3J(trans')$	1.47	5.92	6.08				
or	$^3J(cis)$	2.99	2.86	2.89	1.85	2.25	2.50	2.30
	δ(A(A'))	3.41	3.34	3.55	3.46	3.94	3.85	3.88
C^2HOR								
|	δ(B(B'))	4.06	3.79	3.96	4.02	3.39	3.40	3.41
C^3H_2	δ(X)				4.51	4.88	4.79	4.73

[a] Measured at 90 MHz in ca. 10% $CDCl_3$/TMS; J in Hz. [b] AA'BB' spectra in **5** (evaluated by simulation techniques); ABX spectra in **6** and **7** (evaluated by direct analysis). [c] Taken from ref. [10] for the sake of ready comparison.

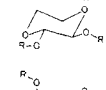
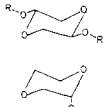
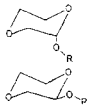
Table 2. Proportion (%) of diaxial or axial conformers in flexible 1,4-dioxanes of types **5**, **6**, and **7** in selected solvents [a].

Solvent (E_T) [b]	**5b**	**5c**	**6b**	**6c**	**7b**	**7a** [d]
CCl_4 (32.5)	63	64 [e]	25	26	28	60 [f]
$CDCl_3$ (39.1) [c]	53	51	32	23	32	70
$(CD_3)_2CO$ (42.2)	60	62	41	31	29	
CD_3CN (46.0)	60		46	32	36	67 [g]
CD_3OD (55.5) [c]	50	50		31		

[a] Evaluated from ^{1}H-NMR data (±5%); cf. Table 1 [10b]. [b] E_T values taken from C. Reichardt, *Angew. Chem. 77* (1965) 30; *Angew. Chem. Int. Ed. Engl. 4* (1965) 29. [c] Similarly peculiar behavior of chloroform among hydrogen bonding solvents in systems with anomeric effects has been noted by *Lemieux* [3f]. [d] Taken from Fig. 14 in [3f]. [e] In [D_8]toluene (33.9). [f] In carbon disulfide (32.6). [g] In dimethylsulfoxide (45.0).

dimethoxy-1,4-dioxanes **5a** and **6a**, respectively, using simple vector addition techniques[13, 14] as well as molecular mechanics (e.g. MM2 as recently parametrized to include the anomeric effect) (Table 3).[11, 12]

Table 3. Dipole moments μ of the two lowest energy conformations ((di)axial and (di)equatorial) of **5a**, **6a**, and **7a**, as calculated by vector addition (VA) and molecular mechanics (MM2—parametrized for the anomeric effect). R = Me.

		μ [D]		$\Delta\mu$ [D]	
		VA	MM2	VA	MM2
5a		0.2	0.5	1.5	0.8
		1.7	1.3		
6a		0.0	0.0	0.0	0.0
		0.0	0.0		
7a		1.5	1.3	0.0	−0.2
		1.5	1.1		

The conclusion to be drawn from Tables 2 and 3 is compelling: The stabilization of diequatorial forms by polar solvents occurs only in the *trans*-2,3-dialkoxy- or *trans*-2,3-disiloxy-1,4-dioxanes for which μ(diequatorial) > μ(diaxial). This is found, e.g., for the 2-alkoxy- or 2-siloxytetrahydropyrans.[8, 15] When the μ values are similar, however, as in the 2,5-dialkoxy- and 2,5-disiloxy-1,4-dioxanes, the proportion of diaxial (or axial) conformer increases. Since this occurs in all cases with $\mu_{ax} = \mu_{eq}$, both when $\mu = 0$ and when $\mu \neq 0$, as well as with a number of different substituents (R = Me, *t*Bu, $SiMe_3$) and until solvation energy data become available,[16] we can think of only one explanation: the well-known stabilization of equatorial forms by polar media in compounds exhibiting anomeric effects is due to a fortuitous codirectionality of *molecular* dipole moments ($\mu_{eq} > \mu_{ax}$) with the *local* group moment (in R–X–C–Y–R'). However, when $\mu_{eq} \approx \mu_{ax}$ (in spite of the local group moments), the opposite is true: the (di)axial contribution increases, i.e., *polar solvents actually enhance the anomeric effect*, as one could expect from the resonance **3** ↔ **4**. This suggests that hyperconjugative[3k] electron delocalization ($n_p - \sigma^*$)[3c, 5] is the main origin of the so-called anomeric effect.

Received: September 12, 1985 [Z 1459 IE]
German version: *Angew. Chem. 98* (1986) 289

CAS Registry numbers:
5b, 53226-11-2; **5c**, 68470-79-1; **6b**, 6891-61-8; **6c**, 100604-28-2; **7a**, 20732-36-9; **7b**, 100604-29-3.

[1] B. Fuchs, L. Schleifer, E. Tartakovsky, *Nouv. J. Chim. 8* (1984) 275.
[2] a) W. A. Szarek, D. Horton (Eds.): *ACS Symp. Ser. 87* (1979); b) A. J. Kirby: *The Anomeric Effect and Related Stereoelectronic Effects at Oxygen*, Springer, Berlin 1983; c) P. Deslongchamps: *Stereoelectronic Effects in Organic Chemistry*, Wiley, New York 1983.
[3] a) R. U. Lemieux in P. de Mayo (Ed.): *Molecular Rearrangements, Vol. 2*, Interscience, New York 1964, p. 709; b) S. J. Angyal, *Angew. Chem. 81* (1969) 172; *Angew. Chem. Int. Ed. Engl. 8* (1969) 157; c) C. Romers, C. Altona, H. R. Buys, E. Havinga, *Top. Stereochem. 4* (1969) 39; see also C. Altona, *Ph. D. Thesis*, University of Leiden 1964; d) E. L. Eliel, *Acc. Chem. Res. 3* (1970) 1; *Angew. Chem. 84* (1972) 779; *Angew. Chem. Int. Ed. Engl. 11* (1972) 739; *Kem. Tidskr. 81* (1969) 22; e) J. C. Martin, *Ann. Chim. 6* (1971) 205; f) R. U. Lemieux, *Pure Appl. Chem. 25* (1971) 527; g) N. S. Zefirov, N. M. Schechtman, *Usp. Khim. 40* (1971) 593; h) J. F. Stoddart: *Stereochemistry of Carbohydrates*, Wiley, New York 1971, p. 172; i) S. Wolfe, *Acc. Chem. Res. 5* (1972) 102; j) H. Paulsen, *Starch 27* (1975) 397; k) L. Radom in I. D. Csizmadia (Ed.): *Molecular Structure and Conformation*, Elsevier, Amsterdam 1982, chapter 1.
[4] a) J. T. Edward, *Chem. Ind. (London) 1955*, 102; b) R. U. Lemieux, N. J. Chü, *Abstr. Am. Chem. Soc. Meeting 133* (1958) 31 N.
[5] a) S. David, O. Eisenstein, W. J. Hehre, L. Salem, R. Hoffmann, *J. Am. Chem. Soc. 95* (1973) 3806; b) O. Eisenstein, N. T. Anh, Y. Jean, A. Devaquet, J. Cantacuzene, L. Salem, *Tetrahedron 30* (1974) 1717.
[6] a) G. A. Jeffrey, J. A. Pople, L. Radom, *Carbohydr. Res. 38* (1974) 81; b) G. A. Jeffrey, J. A. Pople, S. Brinkley, S. Vishweshara, *J. Am. Chem. Soc. 100* (1978) 373.
[7] S. Wolfe, M.-H. Whangbo, D. J. Mitchell, *Carbohydr. Res. 69* (1979) 1.
[8] Cf. Table in [2b], p. 9, and references cited therein.
[9] B. Fuchs, A. Ellencweig, U. Burkert, *Tetrahedron 40* (2011).
[10] a) B. Fuchs, A. Ellencweig, *Nouv. J. Chim. 3* (1979) 145; b) The J_{aa} and J_{ee} values were taken from conformationally homogeneous systems [10a]. For the 2,3-disubstituted 1,4-dioxanes **5** (AA'BB' spectra $J_{aa} = 11.3$ and $J_{ee} = 1.47$ Hz; for the 2,5-disubstituted derivatives **6** (ABX spectra) $J_{aa} = 7.7$ and $J_{ee} = 1.2$ Hz.
[11] a) P. Aped, Y. Apeloig, A. Ellencweig, I. Goldberg, M. Karni, B. Fuchs, E. Tartakovsky, submitted for publication; b) L. Norskov-Lauritsen, N. L. Allinger, *J. Comput. Chem. 5* (1984) 326.
[12] Since the force field we use is parametrized neither for $SiMe_3$ nor for *t*Bu, their derivatives can not be reliably calculated by this method [11a]. It appears, however, that they show the same trends and the data in Tables 2 and 3 can be combined and rationalized as described.
[13] F. Borremans, M. Anteunis, *J. Chem. Ed. 53* (1976) 23.
[14] A. L. McLellan: *Tables of Experimental Dipole Moments*, Freeman, London 1963, p. 95, 125, 156.
[15] a) A. J. de Hoog, H. R. Buys, C. Altona, E. Havinga, *Tetrahedron 25* (1969) 3365; b) A. J. de Hoog, H. R. Buys, *Tetrahedron Lett. 1969*, 4175.
[16] We are aware, of course, of the complexity of the problem concerning solvation energies [17a–c], where quadrupolar and even octupolar terms

may have to be considered [17d]. However, we think that the described phenomenon and its significance are too striking to be ignored until calculated solvation energies are available.

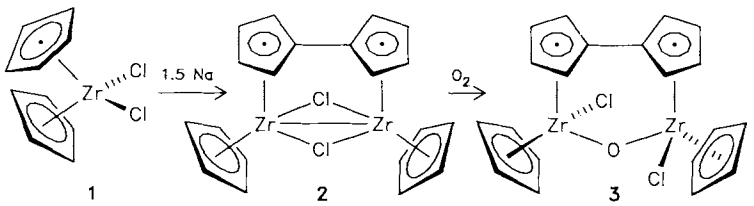
[17] a) R. J. Abraham, T. M. Siverns, *J. Chem. Soc. Perkin Trans. 2 1972*, 1587; b) R. J. Abraham, Z. L. Rosetti, *ibid. 1973*, 582; c) R. J. Abraham in B. Pullman (Ed.): *Environmental Effects on Molecular Structure and Properties*, D. Reidel, Dordrecht 1976, p. 1; d) M. L. Stien, M. Claessens, A. Lopez, J. Reisse, *J. Am. Chem. Soc. 104* (1982) 5902 and other papers in this series.

Novel Fulvalene Derivatives of Zirconium: A Facile Entry into Organozirconium(III) Chemistry**

By *Terence V. Ashworth, Tomas Cuenca Agreda, Eberhardt Herdtweck,* and *Wolfgang A. Herrmann**

Despite numerous investigations in recent years,[1,2] the chemistry of low-valent zirconium remains relatively undeveloped in comparison to that of titanium. Whereas the organometallic chemistry of trivalent titanium is fairly extensive,[3] including, in particular, a number of dimeric titanium derivatives containing the $\eta^5:\eta^5$-fulvalene ligand,[4] the corresponding chemistry of Zr(III) is rather scanty,[1,2,5] and in only one single instance has the presence of a fulvalene ligand been postulated.[6] During our investigations of synthetic routes to low-valent organozirconium derivatives we have discovered a simple, high-yield synthesis of the key compound **2**. This compound represents the first undisputed example of a dimeric compound of Zr(III) containing a fulvalene ligand, and it offers a unique opportunity to develop the chemistry of dinuclear complexes of low-valent zirconium.

Reduction of the cyclopentadienyl complex **1** in toluene with sodium amalgam (1% Na) containing exactly 1.5 molar equivalents of sodium afforded a dark red solid in high yield (75%) which could be characterized as the fulvalene complex **2**.[7] The mass spectrum of this complex confirmed its dinuclear structure, while the ^{1}H- and ^{13}C-NMR



1 2 3

spectra revealed the presence of a $\eta^5:\eta^5$-fulvalene ligand in a molecule possessing an averaged plane of symmetry through the central carbon–carbon bond of the fulvalene ligand and the metal atoms. This requires that the chloride ligands occupy coordination sites bridging the two zirconium centers.

So far, all attempts at obtaining crystals for an X-ray diffraction study of **2** have met without success. Compound **2** reacts quantitatively, however, with oxygen to give the pale-yellow derivative **3**, which has been characterized by

[*] Prof. Dr. W. A. Herrmann, Dr. T. V. Ashworth, Dr. T. Cuenca Agreda, Dr. E. Herdtweck
Anorganisch-chemisches Institut der Technischen Universität München
Lichtenbergstrasse 4, D-8046 Garching (FRG)

[**] This work was supported by the Deutsche Forschungsgemeinschaft, the Bundesministerium für Forschung und Technologie, the Alexander-von-Humboldt Foundation (Fellowships to *T. V. A.* and *T. C. A.*), and Hoechst Aktiengesellschaft.

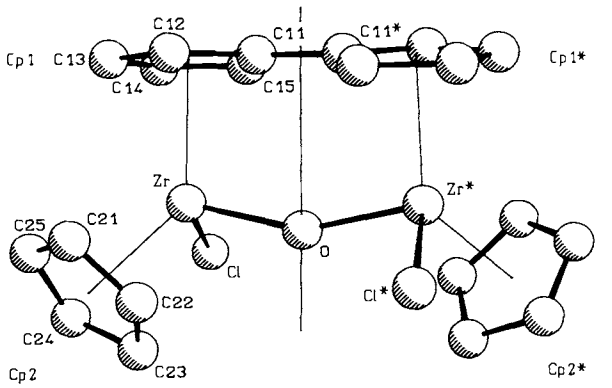


Fig. 1. PLUTO drawing [9] of the structure of **3** in the crystal. **3** crystallizes with 0.5 mol toluene disordered around a center of symmetry. Selected bond lengths [pm] and angles [°]: Zr-Cl 247.1(1), Zr-O 194.3(1), Zr-Cp1 223.0(4), Zr-Cp2 222.7(5), Cl-Zr-O 98.1(1), Zr-O-Zr* 156.0(2), Cp = centroids of the Cp-ligands.

X-ray structural analysis[8] (Fig. 1). The two zirconium atoms in **3** are linked by the fulvalene and an oxygen atom. The remaining coordination positions about each metal atom are taken up by a $C_5H_5^-$ and a Cl-ligand. The coordination geometry is similar to that of the related complexes **4**[10] and **5**,[11] but the presence of the fulvalene ligand leads to interesting conformational distinctions. Whereas the ligands attached to the ZrOZr unit of the latter compounds adopt a staggered conformation, in the novel complex **3** the ligands are eclipsed (Fig. 2). Furthermore the torsional angle a is confined to 13.5° and reduces the non-bonded distance (3.801(1) Å) between the zirconium atoms. This gives rise to a ZrOZr angle of 156.0(4)° in **3** (cf. 168.9° in **4**) which is the largest deviation from linearity yet observed in oxo-bridged cyclopentadienyl transition metal dimers.[11]

$[\{ZrCl(\eta^5\text{-}C_5H_5)_2\}_2(\mu\text{-}O)]$ **4** $[\{Zr(SC_6H_5)(\eta^5\text{-}C_5H_5)_2\}(\mu\text{-}O)]$ **5**

The spectroscopic data[7] for **3**, obtained in solution, are consistent with the above structure (Fig. 1). The mirror symmetry observed in the NMR spectra of **2** is lost in **3** (*ABCD*-spin system in the ^{1}H-NMR spectrum).

$[\{ZrCl(\eta^5\text{-}C_5H_5)_2\}_2O]$ **4** $[\{ZrCl(\eta^5\text{-}C_5H_5)\}_2(\eta^5:\eta^5\text{-}C_5H_4\text{-}C_5H_4)O]$ **3**

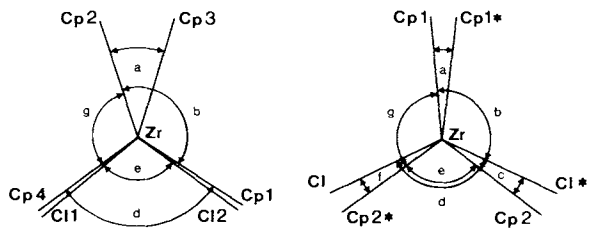


Fig. 2. Molecular conformation of μ-oxo complexes **4** (left) and **3** (right) along the Zr–Zr* vector.

	a	b	c	d	e	f	g
4	34.7	143.5	1.9	109.2	105.4	1.8	109.2
3	13.5	121.4	13.8	130.7	103.0	13.8	121.7

In **4** the angles c and f, respectively, are taken between Cp1 and Cl2, Cl1 and Cp4. The atoms Cl2, Cp3, Cp4 are coordinated to Zr*.

That the rigid fulvalene bridging ligand can bind two metal atoms in close proximity is well known.[12] As demonstrated by the synthesis of **2**, this has now also been accomplished with the rarely investigated Zr^{III} complexes. The potential of universally modifying such complexes by replacement of the chloro ligands by other functionalities is now receiving our active attention.

Received: November 12, 1985;
supplemented: December 18, 1985 [Z 1534 IE]
German version: *Angew. Chem. 98* (1986) 278

[1] K. I. Gell, T. V. Harris, J. Schwartz, *Inorg. Chem. 20* (1981) 481.

[2] K. I. Gell, J. Schwartz, *J. Am. Chem. Soc. 103* (1981) 2687; G. Fochi, G. Guidi, C. Floriani, *J. Chem. Soc. Dalton Trans. 1984*, 1253; T. Cuenca, P. Royo, *J. Organomet. Chem. 293* (1985) 61; S. R. Wade, M. G. H. Wallbridge, G. R. Willey, *J. Chem. Soc. Dalton Trans. 1983*, 2555.

[3] G. P. Pez, J. N. Armor, *Adv. Organomet. Chem. 19* (1981) 1; M. Bottrill, P. D. Gavens, J. McMeeking in G. Wilkinson, F. G. A. Stone, E. W. Abel (Eds.): *Comprehensive Organometallic Chemistry, Vol. 3*, Pergamon, Oxford 1982, p. 281.

[4] Titanium complexes of fulvalenes: a) H. H. Brintzinger, J. E. Bercaw, *J. Am. Chem. Soc. 92* (1970) 6182; b) A. Davison, S. S. Wreford, *ibid. 96* (1974) 3017; c) L. J. Guggenberger, F. N. Tebbe, *ibid. 95* (1973) 7870; d) *ibid. 98* (1976) 4137; e) J. J. Salzmann, P. Mosiman, *Helv. Chim. Acta 50* (1976) 1831; f) G. J. Olthof, *J. Organomet. Chem. 128* (1977) 367; g) E. G. Perevalova, I. F. Urazowski, D. A. Lemenovskii, Y. L. Slovokhotov, Y. T. Struchkov, *ibid. 289* (1985) 319.

[5] D. J. Cardin, M. F. Lappert, C. L. Raston, P. I. Riley in G. Wilkinson, F. G. A. Stone, E. W. Abel (Eds.): *Comprehensive Organometallic Chemistry, Vol. 3*, Pergamon, Oxford 1982, p. 606.

[6] A structure analogous to **2** has been proposed for $[\{ZrI(C_5H_4)(\eta^5\text{-}C_5H_5)\}_n]$ $(n>2)$,[11] although no mass spectrum could be obtained, and cryoscopic molecular weight studies suggested a concentration-dependent oligomerization.

[7] *Experimental:* A solution of **1** (1.17 g, 4 mmol) in toluene (50 mL) was treated with 1% Na/Hg (0.138 g Na, 6 mmol) and stirred for 12 h under nitrogen. The resultant dark red reaction mixture was then heated under reflux for 8 h. After filtration, evaporation, and recrystallization from toluene/*n*-hexane, the product was obtained as a dark red air-sensitive powder. Yield: 0.76 g (75%). An analytically pure sample was obtained by vacuum sublimation (10^{-5} torr). At ca. 120°C the oxo derivative **3** sublimed and pure **2** was obtained at 190°C.—*Spectra: EI-MS:* **2**, $M^{\oplus}$ 508; **3**, $M^{\oplus}$ 524; both molecular ions exhibit an isotopic pattern typical of an ion containing a Zr_2Cl_2 moiety.—*IR* of **3** (KBr, $\tilde{\nu}$(ZrOZr), cm^{-1}): 735 s and 702 s.—*NMR* (270 MHz, C_6D_6, 34°C): **2**: ^1H: $\delta = 5.57$ (s, 10 H, C_5H_5), 4.93 (pseudotriplet, 4 H), and 3.97 (pseudotriplet, 4 H). The pseudotriplets arise from an AA'BB' spin system with $J_{exp} \approx J_{AB'} \approx 2.7$ Hz.—^{13}C: $\delta = 104.7$ (C_5H_5), 104.6 and 101.1 (C2, C3), 106.2 (C1).—**3**: ^1H (270 MHz, $CDCl_3$, +28°C): $\delta = 6.27$ (s, 10 H, C_5H_5), 6.75 (m*, 2 H), 6.56 (M*, 2 H), 6.32 (m*, 2 H), 5.97 (m*, 2 H); m* = multiplets of an ABCD system.—^{13}C: $\delta = 114.2$ (C_5H_5), 104.2, 111.8, 113.7, 114.6 (C2-5), C1 not observed.

[8] B. A. Frenz et al.: *SDP, Structure Determination Package*, College Station, TX 77840 (USA). **3**, pale yellow crystals (from toluene); $V = 2583.9 \times 10^6$ pm^3, $C2/c$, $Z = 4$, $F_{000} = 794$, $\rho = 1.59$ g cm^{-3}, $\mu = 10.2$ cm^{-1}; CAD-4 (Enraf Nonius), $Mo_{K\alpha}$, graphite monochromator, ω-scan ($\Delta\omega = 0.80° + 0.30 \tan\theta$, $2° \leq \theta \leq 22°$), $t_{max} = 60$ s, h(−16/16), k(0/13), l(−15/15), 1471 reflections ($I > 1\sigma(I)$).—Solution of structure: Patterson and difference Fourier methods; all non-hydrogen atoms refined anisotropically; H-atoms calculated from ideal geometry, included in structure factor calculations, but not refined; $R = 0.046$, $R_w = 0.055$.—Further details of the crystal structure determination are available on request from the Fachinformationszentrum Energie, Physik, Mathematik GmbH, D-7514 Eggenstein-Leopoldshafen 2, on quoting the depository number CSD-51661, the names of the authors, and the full citation of the journal.

[9] S. Motherwell, *PLUTO, Program for Plotting Molecules and Crystal Structures*, Cambridge (UK).

[10] J. F. Clarke, M. G. B. Drew, *Acta Crystallogr. B30* (1974) 2267.

[11] J. L. Peterson, *J. Organomet. Chem. 166* (1979) 179, and references therein.

[12] K. P. C. Vollhardt, T. W. Weidman, *Organometallics 3* (1984) 82; J. C. Smart, C. J. Curtis, *Inorg. Chem. 16* (1977) 1788, and references therein.

BOOK REVIEWS

Principles of Nucleic Acid Structure. By *W. Saenger*. Springer Verlag, Berlin 1984. xx, 556 pp., bound, DM 79.00.—ISBN 3-540-90761-0

Wolfram Saenger has done a considerable service for the community of scientists interested in nucleic acids with the publication of his monograph "Principles of Nucleic Acid Structure". The book is a rich compendium of information about the three dimensional properties of DNA, RNA, and related compounds, with particular emphasis on structure at the level of nucleosides and nucleotides. The magnitude of the task can be appreciated by examination of the size of the reference list, which includes over 1400 items.

Particularly commendable features include the careful definition of terms provided in Chapter 2, much needed in a field beleaguered for years by competing systems of nomenclature. The book states clearly the standard definitions recommended in 1983 by the IUPAC-IUB subcommission, and adheres to their use with high fidelity. The same chapter includes a detailed description of the nomenclature of pseudorotation, which provides a systematic scheme for describing the conformation of the ribose ring. This is followed in Chapter 4 with an authoritative account of the principles which underlie the preference for particular sugar ring puckers. The distinction between *syn* and *anti* conformations of the base relative to the sugar ring is also examined in detail, as are the principles which govern the rotational orientations about P-O bonds.

Chapters 5 and 6 consider physical properties of the nucleic bases, such as charge densities, protonation and tautomerization equilibria, spectroscopic properties, and the tendency to hydrogen-bond in solution. Stacking forces and the thermodynamics of double helix formation are also treated. These subjects are followed by a chapter detailing the properties of modified nucleotides, including those of general biochemical interest such as the cyclic nucleotides and pyrophosphate-containing compounds.

The book devotes considerable space to several nicely illustrated chapters describing the many possible helical structures of nucleic acids, including the extensive polymorphism of DNA. Both crystallographic results and models built from fiber diffraction studies are presented in some detail. Even some of the generally discredited models are dredged up from the past, presumably to give a flavor of the nature of debate in the field.

Later chapters in the book will be found widely useful for their structural account of subjects such as tRNA, drug-DNA complexes, and the rapidly developing field of protein-nucleic acid interactions. Included among the latter are some general principles of amino acid-nucleotide interactions and the structural features underlying the interaction of ordered protein segments with nucleic acid

helices. Specific structures examined in detail include tobacco mosaic virus, specific DNA-binding proteins such as CAP and *cro*, and nucleosomes.

The early chapters of the book are rather intensively technical, and unfortunately lacking in general signposts, so that the non-specialist reader will find the going rather tortuous; the later chapters are significantly better in this regard, and should be quite useful as reference material for students and professionals alike in the fields of molecular biology and biochemistry.

All research-level monographs contain errors, and this one is no exception, although I did not find many. The proofreading was generally very good, but a too-generous sprinkling of double bonds around the purine and pyrimidine ring systems was allowed to sneak through in Chapter 2, which may confuse beginning students. The only error of principle which I feel obliged to mention is the incorrect treatment of the dissection of linking number into twist and writhe. Both the text and the figures make it seem that one can determine the writhe of a superhelical structure simply by counting the number of superhelical turns. This error (the writhe of a superhelix depends on its pitch) sets back understanding of DNA topology substantially.

This is a valuable reference book, which should be on the shelves of all who are interested in the structure and function of nucleic acids.

Donald M. Crothers [NB 722 IE]
Department of Chemistry,
Yale University, New Haven (USA)

Bio-inorganic Chemistry. By *R. W. Hay*. Ellis Horwood, Chichester 1984. 191 pp., stitched, $ 24.95.—ISBN 0-470-20066-9

Inorganic biochemistry is in a turbulent state of development. An up-to-date introduction to this field which is not only aimed at specialists is years overdue. Thus, *Hay*'s book will encounter an eagerly expectant public—and, to come straight to the point, it is therefore particularly disappointing.

The introductory chapter, short and informative, is concerned with biologically essential metal ions, with their ligands in physiological media and with some of their chemical characteristics that are relevant in this context. Subsequently, the important physical methods of inorganic biochemistry are described, necessarily by means of examples. Only the section on EXFAS, the most important of the new sources of information for the investigation of metal binding in proteins, is more extensive.

Apart from a short (and adequate) chapter on the biochemistry of the alkali metals and alkaline earths, the book is devoted to the rôle of the transition metals in biology. Here, the reader is confronted with a lamentably disorganized collection of partly out-of-date information with very arbitrary emphases and exclusions. To begin with the positive: the chapter on substrate-activating metalloenzymes (carboxypepsidase, carboanhydrase and alcohol dehydrogenase) amounts to an up-to-date, well thought out introduction. It is clear that the author's own research interests lie in this area. Unfortunately, in the case of carboanhydrase, of the many model systems examined, the most convincing one by *Groves* (1981) is missing. Equally well handled are oxygen fixation and iron-sulfur proteins—a considerable achievement in light of the abundance of proteins with Fe-S clusters known today.

Set against this, the presentation of the theme "oxygen transport" suffers from *Hay*'s after all very "inorganic" viewpoint. The willful impression is conveyed that iron-porphyrin can accomplish the transport perfectly well on its own and that the protein is only a sort of packing. Hemoglobin itself is pushed into the background by the depth and extent of the treatment of model systems and of the (biochemically irrelevant) cobalt-oxygen complexes.

It becomes really annoying in the section on the fascinating catalytic properties of cytochromes of type P450. These heme proteins "can" hydroxylate alkanes under physiological conditions. In 1982 (for which year the book claims to present the state of knowledge) much was already known about the mechanism responsible for this. We are offered a random selection from the state of discussion around 1980; the rôles of the axially coordinated sulfur and of the active Fe-O species are either quite wrongly represented or simply not referred to. Cytochrome P450, catalase and hemoglobin are three heme proteins whose remarkably different interactions with oxygen are decisively determined by axial ligands of the heme iron: the opportunity of a comparative discussion of these three is let slip. This is particularly regrettable because in this case "inorganic" and "biochemical" interests really have coalesced in ideal fashion to a genuine "bioinorganic" research area.

The biochemistry of iron in aerobic media offers the chance of a sheer "exciting" account of how the insolubility of iron(III) hydroxide has been come to terms with. On uptake, transport and storage, before and during its inclusion in functional proteins, the iron is kept in solution through a seamless sequence of strong complexing agents. Unfortunately, the few particulars on this are dotted right through the whole book so that the connection is lost in exotic detail and is not made very comprehensible. The biochemistry of copper is equally unsystematically handled: a direct comparison of the three types of copper binding centers in proteins is sought in vain; this certainly does not facilitate the understanding of the not-yet-expert (and the book is aimed at students!).

It only remains to be pointed out that one of the functionally most important and "bio-inorganically" interesting metallo-proteins—cytochrome-c-oxidase, currently the subject of much research, receives no more than a passing reference from the author. The purchase of this book can be recommended to no-one—least of all its intended readership of advanced students.

Michael Weller [NB 700 IE]
VCH Verlagsgesellschaft, Weinheim (FRG)

Methods of Enzymatic Analysis. Vol. 6. Metabolites 1: Carbohydrates. Edited by *H. U. Bergmeyer, J. Bergmeyer,* and *M. Grassl*. 3rd Edition. Verlag Chemie, Weinheim 1984. xxix, 701 pp., bound, DM 295.00.—ISBN 3-527-26046-3

This volume describes analyses for carbohydrates and related compounds. The coverage is broad: from poly-, oligo-, and disaccharides through monosaccharides to three-, two-, and one-carbon compounds. The four chapters of this volume are subdivided into sections. Each section normally covers the analysis of a single metabolite, although, several metabolites which can be co-analyzed are occasionally grouped together. Certain important com-

pounds are covered by several sections, each employing a different analytical technique. These sections, which have been prepared by a number of different authors, have been brought together by the editors into a very even and high-quality volume.

The coverage of the third edition is essentially the same as that of the second edition. The chapter on poly-, oligo-, and disaccharides covers the important energy storage materials (starch, glycogen and inulin), plant structural materials (cellulose, pectin and polygalacturonic acid), other, clinically important polysaccharides (hyaluronate, chondroitin and sialic acid etc.) and several disaccharides of interest in food chemistry (raffinose, sucrose, lactose and maltose).

The monosaccharide chapter, the bulk of the book, mainly covers hexoses and pentoses. Glucose, its oxidized and amino derivatives and some of their phosphate derivatives account for 25% of the chapter. Also well covered are galactose, mannose, fructose and derivatives. Ascorbate, dehydroascorbate, sorbose and two derivatives, *myo*-inositol and its 1-phosphate round out the hexose coverage. The pentoses are represented by 6 ribo-sugars, arabinose and 3 xylo-sugars. Octulose 1,8-bisphosphate sedoheptulose 7-phosphate and 1,7-bisphosphate, and two erythrose derivatives are also covered.

The chapter on 3-carbon compounds, which contains assays for PEP, pyruvate, hydroxypyruvate, lactate and methylglyoxalate, concentrates on assays for glyceraldehyde, glycerol and glycerate and their derivatives.

The final chapter covers formate, formaldehyde, acetyl phosphate and 7 of the 9 common oxygenated C-2 compounds (only glycolic acid and oxaldialdehyde are omitted).

Most of the analytical procedures are the same as those in the second edition. Some obsolete procedures have been replaced or omitted and some of those that have been retained have been revised and modified to incorporate new developments.

Each section is highly detailed and contains more, valuable explanatory text and background than the second edition. Each section begins with the structure of the analyte, a new addition since the second edition. Some information about the substance (history, physical and biological properties, biogenesis, occurrence, properties relevant in analysis, references and standards, etc.) is provided, and is followed by a brief, critical review of other available analytical methods for the substance.

The core of each section—the assay—is extensive. The principle of the assay is first explained with text and equations. Sections listing optimum measurement conditions, necessary equipment, and reagents then follow. Specific information about reagent and solution purity, preparation, storage and stability and about specimen collection, processing and stability help the analyst consistently to obtain valid data. The assay procedure itself takes a "cookbook" approach which allows even unfamiliar workers to execute the analysis successfully the first time. The detailed, step-by-step procedure covers all aspects of data collection and processing including the calculations and formulae needed to work-up the raw data. Finally, a discussion of precision, accuracy, sensitivity, limit of detection, error and specificity aids in evaluating the method.

Each section is well-referenced. The references are up-to-date as a cursory inspection reveals many from 1982 and 1983. Several appendices listing commonly encountered constants, abbreviations and formulae are provided. Unfortunately, the index is little more than an alphabetization of the table of contents. Although the lack of cross-indexing may be inconvenient to some, the book's format makes finding information straightforward.

This volume is not, nor was intended to be, a comprehensive handbook. However, its more than one hundred individual assays cover all of the most commonly analyzed materials and many which are less common. This volume is a valuable work of reference and guide and is strongly recommended to those doing analyses of biological materials.

George M. Whitesides [NB 704 IE]
Harvard University,
Cambridge (USA)

Strategies and Tactics in Organic Synthesis. Edited by *T. Lindberg*. Academic Press, New York 1984. xiv, 370 pp., hardback, $ 57.00.—ISBN 0-12-450280-6

In our peace-loving time everbody talks about "strategies" not only in the army but also in industrial concerns, on football grounds and, not least, in organic synthesis. In the title of the book under consideration "strategies" are even combined with "tactics". Is organic synthesis a war game? The analogy cannot be rejected out of hand. After all, anyone who has struggled through a multi-step synthesis knows the feeling of standing against an insidious foe who does not play by the rules and can only be overcome by heroic effort. Thus, this book sets out to report not only the successes but also the setbacks and dead ends which even brilliant synthetic chemists cannot avoid. It aims to show how the "strategy" of a plan conceived in broad terms must finally be helped along by manifold "tactical" variations. Precisely this fascinating struggle with matter is concealed by the conventional form of publication, which aims at a concise account of positive results.

Thirteen celebrated american synthetic chemists report in individual chapters on spectacular projects that were successfully concluded. The round is opened by *V. Boekelheide*'s "superphane" (19 pages); then *R. Danheiser* reports on *Corey*'s gibberellin acid synthesis (50 pages), *J. Fried* on the epoxide route to the prostaglandin system (12 pages), *P. Magnus* on his new indole-alkaloid synthesis (39 pages), *S. Masamune* on the macrolide aglycon tylonolide (30 pages) *K. C. Nicolaou* on the endiandric acid cascade (18 pages), *L. A. Paquette* on dodecahedrane (25 pages), *M. F. Semmelhack* on the methylenecyclobutenes fommanosin and illudol (21 pages), *A. B. Smith III* on iatrophone (51 pages), *R. V. Stevens* on tricyclic pyridine alkaloids (23 pages), *K. P. C. Vollhardt* on cobalt induced alkyne cyclization (25 pages), *S. M. Weinreb* on the hetero-Diels-Alder route to the alkaloid streptonigrin (20 pages), and, finally, *J. D. White* on the synthesis of methynolide via [3+4] additions to furan derivatives (19 pages).

This variegated programme conveys a gripping picture of the aims and ability of modern organic synthesis. Achievements are described here which, not all that long ago, would have been banished to the realm of fantasy. Just consider the intricate stereo- and protecting group problems in the macrolide synthesis or the exotic bond linkages in superphane or dodecahedrane. The difficulties were enormous yet again and again the strategies, mostly based on systematic retro-synthetic analysis, led to the target, thanks, not least to "tactical" dexterity, determination, and to the co-workers. To this extent the comparison with

chess, which has often been used and is here cited by *Magnus*, is wide of the mark. Chess is a purely intellectual pursuit, involving none of the physical labor of benchwork, which makes the experience of defeat that much more bitter and painful.

The reader obtains much more inside information about the development of the project as a whole from the personal style of the chapters. The initial motivation, which mostly lay in the magnitude of the synthetic challenge, the first model experiments up to the actual laborious realization, calling on all the cunning and ability of the chemist, and finally the relief at the successful conclusion, all this can be followed and reiterated without difficulty. The length of each chapter reflects the engagement of its author; thus *Danheiser*'s contribution is certainly the most fascinating, especially since it is written from the standpoint of a graduate student and not that of the group leader.

Each chapter is accompanied by a wealth of formula schemes and literature references which contribute information to the whole, as do the numerous practical directions; better still would have been experimental sections with descriptions of the key experiments.

Summary: The book in question shows the way to a stimulating new approach to the documentation of organic synthesis. It inspires both enthusiasm and the wish to match the author's achievements. However, there are two flies in the ointment: the material is not easy to follow, even for those in the field, and the price of around DM 180. practically rules out the private acquisition of the book.

Johann Mulzer [NB 689 IE]
Institut für Organische Chemie
der Freien Universität Berlin

Bacterial Endotoxin. Chemical, Biological, and Clinical Aspects. Edited by *J. Y. Homma, S. Kanegasaki, O. Lüderitz, T. Shiba,* and *O. Westphal.* Verlag Chemie, Weinheim 1984. ix, 420 pp., bound, DM 118.00.—ISBN 3-527-26164-8

The recent progress in endotoxin research is summarized in 33 contributions by leading groups from Japan, West Germany, and the United States of America. The book has been published at a time when the decisive breakthrough in the chemical analysis and synthesis of the toxic component of endotoxin, the lipid A moiety, had been achieved. Structure elucidation and chemical synthesis has now confirmed that the important biological actions of endotoxins from gram-negative bacteria reside in the lipid A moiety, as proposed 3 decades ago by *O. Westphal* and *O. Lüderitz.*

Several chapters deal with the endotoxic activities of synthetic lipid A analogs and modified lipopolysaccharides and contribute thereby to an improved understanding of the structural requirements for certain biological activities; some of these are desirable, such as induction of the tumor necrosis factor by endotoxin. Most of the toxic actions of bacterial endotoxins in humans and animals result from the production of endogenous mediators. This mediator theory of *V. Menkin* has now gained strong support and one contribution focuses on the role of arachidonic acid metabolites, particularly prostanoids and leukotrienes, generated by macrophages under the influence of endotoxin.

Remarkable progress in the analysis of endotoxins, including the ones detectable in blood under pathophysiological conditions, is reflected in the chapters on the Limulus test and the Limulus coagulation cascade. However, the specificity of this test for endotoxins is still unsatisfactory when applied for the clinical diagnosis of endotoxemia.

The book provides an excellent and highly competent survey of recent developments in endotoxin research. In selecting certain aspects, the reader should follow the Table of Contents since an Index with key words is lacking. But this is a minor obstacle in view of the wealth of information offered to those working and interested in the exciting area of endotoxin research.

Dietrich Keppler [NB 703 IE]
Biochemisches Institut der
Universität Freiburg (FRG)

Biotransformation von Arzneimitteln. Band 4. By *S. Pfeifer.* 717 pp., bound, DM 192.00.—ISBN 3-527-25926; *Band 5.* By *S. Pfeifer* and *H.-H. Borchert.* 468 pp., bound, DM 168.00.—ISBN 3-527-26075-7, Verlag Chemie, Weinheim 1981 and 1984.

This series concerning the biotransformation of drugs has been provisionally completed since 1984. Monographs are now available concerning approximately 1000 compounds representing all significant types of active agents.

The telegraphic style and the use of many abbreviations and symbols results in compressed and not always easily readable presentations. Each monograph is set up in the same manner. A formula scheme is presented and partial structures are given for most of the metabolites—whereby no differentiation is made between the major and minor pathways of biotransformation. Details of the excretion form in animals and in man and of analysis follow. Additional information is then provided concerning pharmacokinetics and metabolic data under key headings in the section labeled "Bemerkungen"; no claims are made here to comprehensiveness. From Volume 4 the "Remarks" section has been enlarged and divided into topics. At the end, the literature surveyed is listed alphabetically according to the authors' names.

The literature to 1981 is covered in Volume 5—Volume 1 covers the literature to 1972/1973—more recent literature was included in later volumes. Furthermore, a total of over 200 monographs was compiled in supplements. With this, the total series includes the literature to at least the beginning of 1978 for important compounds.

The author has performed a remarkable feat with this series of monographs, considering the amount of information and the number of publications, which have grown considerably in recent years because of increasing requirements and technical progress. This made selection and limitation necessary and reports are included on "only" 1063 substances. It is, however, not possible to discern the criteria for selection. On the one hand, substances are described which are not yet or no longer used as drugs, and on the other, many very common pharmaceuticals are absent (e.g. reserpine, allopurinol, erythromycin, vincristine, ajmaline, norfenefrine).

The use of the monographs is made more difficult by the widespread use of Latin names (e.g. Calcii benzamidosalicylas). These terms are familiar to the phamacist and are used, among others, in the German and European pharmacopoeias; however, the majority of the users of this work

are chemists, biologists or physicians. Reference is necessary to other works for unambiguous identification. The problem could have been avoided by enlarging the index and cross referencing. Once the reader has taken this hurdle successfully, he then has to deal with a large number of abbreviations that could cause difficulties to the occasional user. However, these allow a very compressed presentation in a small space.

The monographs should not be regarded as critical evaluations suitable as primary information for the non-specialist in presenting the metabolic fates of individual pharmaceuticals, because significant data are accompanied to some extent by non-confirmed data without differentiation. This work is, however, a very comprehensive collection from the literature concerning the chosen substances and provides easy access to the primary literature necessary for intensive study.

The collection of monographs is very useful as a reference work and is likely to be welcomed by all who are concerned with the biotransformation of pharmaceuticals, because even today a comprehensive literature search is often time-consuming, at least as far as the older literature is concerned.

The constantly increasing number of publications dealing with biotransformations and pharmacokinetics makes a new form of documentation necessary in order to guarantee greater topicality; the authors are now making efforts in this direction. These volumes retain their importance as basic information concerning the substances covered.

K.-O. Vollmer [NB 678 IE]
Gödecke AG, Abt. Biochemie,
Freiburg (FRG)

Cytochrome P-450. By *K. Ruckpaul* and *H. Rein*. Akademie Verlag, Berlin 1984. 405 pp., hardback, ca. DM 80.00.—Order No. 763-110-9 (6703)

"At last", you may wish to say, along with the many biochemists, pharmacologists, microbiologists or chemists who hope to find under a title like this everything they always wanted to know about cytochrome P450. There is, without doubt, a gap in the market, which no-one has been brave enough to fill yet, for a comprehensive and, above all, systematizing monograph on cytochrome P450. This may well be because of the constant development of ideas about this cytochrome which does not exist as "the" cytochrome P450, whose description as "P450" follows no rational nomenclature, and which, strictly speaking, is not even a cytochrome.

Admittedly, it is difficult to bring order into the mass of results that have been published about cytochrome P450. It is difficult to separate the wheat from the chaff so that the important findings will open the way, for specialist and interested layman alike, to the unusual enzymology, the mechanistic features—of significance to chemists also—and the physiological, pharmacological, and toxological aspects of this enzyme. This task is not made any easier when it is entrusted to 25 authors, who deal with the significant aspects in eight chapters. The first six chapters are almost exclusively concerned with the unspecific microsomal monooxygenase system of the liver. To this extent the title of the book is undeserved in that some introduction to common structural features and to mitochondrial, bacterial, and microsomal monooxygenases might have been expected, as well as a survey of the individual enzymes.

The camphor hydroxylating system, which is dealt with in only six pages in chapter 7, is surely under-represented and it would probably have been more easily understandable to the reader than the very complex drug monooxygenating system. The phenomenon of induction, which is so important for this P450 system, appears in chapter 6 but is already presupposed in chapter 2. Also, differing designations for "monooxygenases", such as MFO (mixed function oxidases) or "monooxygenatic systems" do not promote the comprehension of the student or non-specialist.

However, for the specialist the book contains a wealth of details with an almost complete literature compilation on the mechanistic aspects. Each chapter is competently written in itself, since the authors, nearly all from the central Institute for Molecular Biology at Buch in (Berlin-East), have all made appreciable contributions in their own fields. Thus, *K. Ruckpaul* and *R. Bernhardt* present a good survey of the endoplasmic reticulum, *G. R. Jänig* and *D. Pfeil* contribute an extensive treatment of the enzymology of the liver system, and *H. Rein, C. Jung, O. Ristau* and *J. Friedrich* collate all the structural data on P450.

The chapter on cytochrome P450 in microorganisms is very lucid but not comprehensive enough in its theoretical and practical significance. A contribution on steroid hydroxylases would also have been desirable. In this case it would not have been necessary to devote a special chapter to the not very meaningful NMR data and to the still less promising biotechnological aspects.

Regardless of these well meant criticisms, this book remains the first comprehensive monograph on cytochrome P450, if the 1978 publication of the same title by *Sato* and *Omura*, which is around half the length, is overlooked. The decision to buy the book is facilitated by the reasonable price. Since the paper quality is not of the best and the index still needs supplementing, it is to be hoped that a second, improved edition is planned soon.

Volker Ulrich [NB 698 IE]
Fakultät für Biologie
der Universität Konstanz (FRG)

Methoden der Analytischen Chemie. Eine Einführung. Band 2: Nachweis- und Bestimmungsmethoden, Teil 2. By *R. Bock*. Verlag Chemie, Weinheim 1984. xi, 379 pp., bound, DM 188.00.—ISBN 3-527-25865-5

The book in question is the fourth and penultimate volume of a comprehensive and systematic account of the methods and instrumentation of analytical chemistry. After "Decomposition Methods in Inorganic and Organic Chemistry" (1972), this general review of analytical methods, originally planned as a single volume by the author, turned out to be like the mythical hydra. Volume 1 was fully taken up with an account of "Separation Methods" (1975). "Methods of Detection and Determination" (Vol. 2) proved to be so comprehensive that it is now being published in three parts. The first part (1980) dealt with procedures that are based on a measurement of electromagnetic radiation. The second part, considered here, describes analytical methods involving the measurement of electrical values as well as those based on thermal effects and phase changes. The subjects of the third part, now in preparation, will include, inter alia, gravimetric, volumetric, and barometric analysis as well as analysis employing chemical reactions.

The arrangement of the work as a whole shows that the author has introduced order into the manifold results of

analytical inventiveness; he reduces methods, instruments, and variations with impressive names and confusing abbreviations to the fundamental physical phenomena on which they are based.

Basically, an electrical measurement is the common characteristic of potentiometry, coulometry, voltammetry, chronopotentiometry, and amperometric and galvanic analysis. Gas chromatographic detection that depends on electrical conductivity (flame ionization detector, thermionic detector, photoionization detector) and β absorption (electron capture detector and helium detector) are also mentioned in this context. Scintillation measurements are dealt with under this heading as are β-backscattering methods, electron diffraction, electron spectroscopy (electron spectroscopy for chemical analysis, ultraviolet photoelectron spectroscopy, Auger electron spectroscopy, electron impact spectroscopy), and the variants of mass spectrometry.

These methods are described in varying depth according to their significance. Under thermochemical methods, besides differential thermal analysis (DTA) and differential scanning calorimetry (DSC), calorimetry/enthalpimetry and the measurement of heats of adsorption and thermal conductivity are dealt with in adequate detail. The final chapter is devoted to methods involving phase changes: turbidity, micellar and solution titrations, the determination of salting-out curves and the precipitation curves of polymers as well as phase solubility analysis.

The reader repetitively experiences the feeling that "the penny has dropped" when he realizes that very different procedures are based on similar physical principles—and this is quite a desirable effect from the educational point of view. The arrangement of the book facilitates understanding and learning. The section on "electrical" methods is preceded by a chapter dealing with the fundamentals of electronics (from *a*mpère to *o*perational amplifier). The descriptions of methods are arranged clearly; a historical summary is often appended. Areas of application and the possibilities of error are critically indicated. Without losing sight of the significant, an abundance of information is introduced in tables, sketches and diagrams. The text remains readable thanks to the consciously frugal use of abbreviations. Numerous clear examples make plain the practical applications of analytical work. Each chapter is accompanied by a carefully selected and organized literature section, which enables quick access to original literature.

"Methods of Analytical Chemistry" will be much appreciated as a German language textbook by advanced students of analytical chemistry. For those working in the field, it may serve as a reference work designed to deepen their knowledge, and will be of particular use when a general index will be available with the final volume.

Jürgen Auffarth [NB 693 IE]
Bundesanstalt für Arbeitsschutz,
Dortmund (FRG)

Reactive Molecules. The Neutral Reactive Intermediates in Organic Chemistry. By *C. Wentrup*. Wiley, Chichester 1984. xi, 333 pp., bound, £ 33.20.—ISBN 0-471-87639-9

Professor *Wentrup*'s book provides a delightful and authoritative survey of the chemistry of neutral organic reaction intermediates. After a lucid presentation of basic notions concerning reaction kinetics, thermochemistry, and frontier MO theory in Chapter 1, the author discusses the various classes of highly reactive molecules in a very readable fashion: radicals in Chapter 2, biradicals in Chapter 3, carbenes and nitrenes in Chapter 4, strained ring compounds in Chapter 5, and cyclobutadienes in Chapter 6. The section on radicals, which includes an introduction to the use of ESR and CIDNP, and the section on the chemistry of carbenes and nitrenes, which is especially well done, are about three times the length of the others. Throughout, the emphasis is on chemical reactivity rather than the details of matrix-isolation or transient spectroscopy. Indeed, some of the reactive intermediates have only been characterized by trapping reactions so far. Each chapter concludes with a useful set of problems, including information permitting the reader to consult the original literature to check the answers.

The text contains a number of useful tables and up-to-date references. Those given in Chapter 1 are primarily to monographs and reviews, those given in Chapters 2–6 are mostly to original literature. They number from about fifty to well over two hundred per chapter. References to specialized monographs, at least one of which exists for every chapter, are also provided and will be useful to readers seeking in-depth information.

In spite of its general excellence, the book does contain a few errors. Some are trivial and barely worth mentioning, such as "ΔH^0(subl) for styrene" on p. 5, which should read "for stilbene", or the presence of charge on formula **161** on p. 113, which is not compatible with the rest of the equation, as well as the overabundance of hyphens, the only clue which gives away the author's continental background (as in "in the gas-phase").

A few other errors are more likely to mislead a novice. The equation for a_{N_i} on p. 38 does not make it clear that spin densities on the neighboring atoms as well as that on the atom i need to be considered; on p. 88 one might get the impression that a more exothermic reaction is always faster; on p. 110 the relation of LUMO energies to electron affinities as determined from electron transmission spectroscopy and electron photodetachment spectroscopy could have been included in addition to the mention of UV spectroscopy (whose use for the determination of LUMO energies is not straightforward); on p. 128 and 129 transition states are referred to as maxima rather than saddle points on surfaces; on p. 163 S_1 is a singly excited and S_2 a doubly excited configuration; the arguments offered to account for the inaccessibility of the cyclobutadiene dianion on p. 312 could be applied equally well to the easily accessible cyclooctatetratene dianion.

It should also be noted that the correlation energy of two electrons is not the energy required to bring them into the same orbital (p. 163, 176), that the "heavy atom effect" normally does not refer to the mass of the collision partner in collision-induced intersystem crossing (p. 183), that the internal bond of a propellane does not tend to have a zero electron density (p. 299), and that a triplet ground state is not expected for square cyclobutadiene (p. 310, 316; cf. dynamic spin polarization). Finally, although the occurrence of rapid tunneling between the two rectangular forms of cyclobutadiene may eventually indeed be excluded by photoorientation results as claimed on p. 319, our experiments are still underway and until the final verdict is in, a conclusion is premature (Ref. 34c does not exist).

All of the shortcomings I noted above are of a theoretical or physicochemical nature and somewhat peripheral to the main subject of the book, which is treated in a very nice manner. For those interested in the preparation and chemical properties of the uncharged reactive interme-

diates of organic chemistry, the book is to be recommended very highly indeed. I plan to use it in advanced undergraduate and graduate teaching of organic chemistry.

Josef Michl [NB 697 IE]
Department of Chemistry
University of Utah
Salt Lake City, Utah 84112 (USA)

Mammalian Semiochemistry. The Investigation of Chemical Signals Between Mammals. By *E. S. Albone*. Wiley, Chichester 1984. xii, 360 pp., hardback, £ 29.50.—ISBN 0-471-10253-9

It has really been known for a very long time that there are signal agents (semiomones) that affect the behavior of mammals. Yet natural product chemists and biochemists were initially more interested in insect pheromones, which are perhaps of greater economic significance. *Albone*'s excellent study shows how the unknown and often still mysterious world of signal agents has only recently begun to be investigated with the modern instrumental analytical techniques of natural product chemistry. A distinction is made between substances used for communication by mammals with one another and those used by mammals to communicate with other species in their environment (allelochemicals).

The second chapter of the book shows comprehensively, e.g. in the description of vapor analysis, the advances that have been made and the progress that new techniques will enable in the scientific investigation of the chemical ecology of mammals. It quickly becomes clear how complex is the chemistry of an emotionally charged remark like "he's in bad odor with me" when a list of 135 substances in human perspiration is presented. Not only hydrocarbons—unsaturated and branched—alcohols, ketones, acids, esters, aromatics and heterocycles were identified, but also compounds containing sulfur and even chlorine, such as dichlorobutane. When *Albone* discusses the semiomones of apes, elephants and predators, we can see that man is "only" a mammal, since we find more or less the same chemistry every time. The organs for producing and storing allomones give the author the opportunity to extend the treatment to cover allelochemicals. The significance of the skin as a particularly environmentally sensitive organ is indicated and reference is made to all glands that produce odors and, above all, to the urine. It's "imprinting power", even that of the less volatile components, is admirably discussed.

In the final chapter *G. Shirley* deals, briefly but very informatively, with the mammalian olfactory system, so restricted compared with that of insects. The author includes a discussion of the manner of information transfer in the olfactory nerves.

In every regard, *Albone*'s book is a successful presentation of an area of natural product chemistry whose significance is steadily increasing. It is to be hoped that the book will find a wide readership amongst students, teachers, and those engaged in research.

Hermann Schildknecht [NB 708 IE]
Organisch-Chemisches Institut
der Universität Heidelberg (FRG)

Oligonucleotide Synthesis. A Practical Approach. Edited by *M. J. Gait*. IRL Press, Oxford 1984. 232 pp., stitched, £ 11.00.—ISBN 0-904147-74-6

This book provides a concentrated introduction to oligonucleotide synthesis. Modern methods of DNA synthesis and analysis are introduced by competent authors in individual chapters. The following topics are comprehensively described: the preparation of protected synthetic units, solid phase synthesis by the phosphate triester and the phosphite triester methods, the purification of synthetic oligonucleotides by HPLC and polyacrylamide gel electrophoresis and sequencing by the mobility shift and *Maxam-Gilbert* methods. These are supplemented by chapters on newer methods for the synthesis of shorter oligoribonucleotide sequences and the interesting enzymatic synthesis of oligoribonucleotides. Each chapter contains a comprehensive introduction followed by a detailed experimental section which also supplies suggestions on obtaining reagents and equipment. The book scarcely offers anything new to the experienced nucleotide chemist but is an excellent introduction for those who are looking for the quickest possible experimental access to this class of natural products. An appendix provides such practical directions as are necessary for oligonucleotide synthesis by those with little chemical experience, e.g. the packing of silica gel columns, TLC on silica gel, distillation at atmospheric pressure and in vacuo and the packing of HPLC columns. Here the book is clearly intended for those who have only studied chemistry as an ancillary subject. However, it is questionable whether the "fundamental chemical techniques" presented in this book would equip, say, a biochemist or a physician sufficiently to carry out manual oligonucleotide synthesis. For those using a DNA synthesizer, however, it could supply the necessary chemical background information. The book can be recommended to all those who need a modern, straightforward introduction to oligonucleotide synthesis.

Hubert Köster [NB 707 IE]
Institut für Organische Chemie und
Biochemie der Universität Hamburg (FRG)

Registered names, trademarks, etc. used in this journal, even without specific indication thereof, are not to be considered unprotected by law.

© VCH Verlagsgesellschaft mbH, D-6940 Weinheim, 1986. - Printed in the Federal Republic of Germany by Zechnersche Buchdruckerei, Speyer/Rhein.

All rights reserved (including those of translation into foreign languages). No part of this issue may be be reproduced in any form - by photoprint, microfilm, or any other means - nor transmitted or translated into a machine language without written permission from the publishers. Only single copies of contributions, or parts thereof, may be reproduced for personal use.

Valid for users in the USA: The appearance of the code at the bottom of the first page of an article in this journal (serial) indicates the copyright owner's consent that copies of the article may be made for personal or internal use, or for the personal or internal use of specific clients. This consent is given on the condition, however, that the copier pay the stated per-copy fee through the Copyright Clearance Center, Inc., for copying beyond that permitted by Sections 107 or 108 of the U.S. Copyright Law. This consent does not extend to other kinds of copying, such as copying for general distribution, for advertising or promotional purposes, for creating new collective works, or for resale. For copying from back volumes of this journal see 'Permissions to Photo-Copy: Publisher's Fee List' of the CCC.

Editorial office: Pappelallee 3, D-6940 Weinheim, Federal Republic of Germany, Telephone (06201) 602315, Telex 465516 vchwh d, Telefax (06201) 602328.

Editor: *P. Gölitz.*

Associate editors: *D. I. Loewus, A. Stimson.* **Editorial assistant:** *E. Schweikart*

Publishers: VCH Verlagsgesellschaft mbH. (Managing Directors: *Prof. Dr. Helmut Grünewald* and *Hans Dirk Köhler*), Pappelallee 3, D-6940 Weinheim, Federal Republic of Germany. Correspondence concerning advertisements should be addressed to VCH Verlagsgesellschaft mbH. (Advertising Manager *R. J. Roth*), Boschstr. 12, P.O. Box 1260/1280, D-6940 Weinheim, Federal Republic of Germany, Telephone Weinheim (06201) 602-0, Telex 465516 vchwh d, Telefax (06201) 602328.

ANGEWANDTE CHEMIE
International Edition in English
Volume 25 · Number 4
April 1986
Pages 297–382

Adolf von Baeyer's Scientific Achievements — a Legacy**

By Rolf Huisgen*

> „Ich halte Lehre und Studium der historischen Entwicklung der Wissenschaft für unentbehrlich ... Unsere Lehrbücher versagen darin."
>
> *Richard Willstätter*

The history of chemistry has not gained any additional prominence in our curriculum since the time *Richard Willstätter* made this statement in his memoirs some 45 years ago. Whether this is due to an inadequacy of presentation or to a lack of interest on the side of the students is a question unlikely to lead to a fruitful discussion. Textbooks tend to convey a false impression of chemistry to the student: namely that of a completed edifice, where sober facts are governed and ordered by fundamental principles. Only insiders are aware of the forging force personalities had on this well-established order. *Emil Fischer* commented as follows along this line:

> "The sciences are not abstract constructions, but rather the results of human endeavor; they are closely connected with the personalities and the fates of the dedicated researchers who developed them."



Fig. 1. *Adolf von Baeyer* monument in Munich (*H. Hahn*, 1915).

1. The Setting

The conceptual evolution of chemistry during the first half of the last century could be termed "genesis of land and sea from chaos." Most historians commit a serious error in singling out only a few eminent personalities as participants in this intellectual struggle. "Time blots out small merit while fattening big glory", as the French writer *Henri de Montherlant* phrased the injustice.

In 1873, *Hermann Kopp*, a student of *Liebig*, retraced "The Development of Chemistry in the Recent Past",[2]

[*] Prof. R. Huisgen
Institut für Organische Chemie der Universität
Karlstr. 23, D-8000 München 2 (FRG)

[**] Based on a Memorial Lecture presented at the 20th Hauptversammlung der Gesellschaft Deutscher Chemiker in Heidelberg on September 16, 1985.

 © VCH Verlagsgesellschaft mbH, D-6940 Weinheim, 1986 0570-0833/86/0404-0297 $ 02.50/0

i.e., from 1780–1860, in an 850-page book. I quote from his epilog:

> "What comes as completely natural to the young generation, acquired almost playfully, was assembled through most painstaking efforts of preceding generations to form a set of lasting truths. On the other hand, what was welcomed as an important and seemingly unshakable revelation in one epoch, was often discarded as fallacy by the next."

The development was complicated by the fact that chemists did not focus on simple compounds first and leave the more complex substances to be tackled later. Toxins, medicines, and dyes aroused human curiosity quite early. In 1805 *Friedrich Sertürner* isolated morphine from opium and described it as "one of the strangest substances, bearing some resemblance with ammonia."[3] Several decades were to pass before the simple alkylamines were discovered. Illustrating the road from the complicated to the simple once again, quinoline was first obtained by treating quinine or strychnine with molten alkali; later quinoline was found in coal tar by the ton.

Moreover, the reliability of experimental observation had to reach a higher level. For example, "ethyl hydrogen" and "dimethyl" were supposed to be different compounds until *Carl Schorlemmer*[4] proved them to be identical in 1864.

These were the scientific grounds on which one of the most successful architects of organic chemistry made his appearance, namely *Adolf von Baeyer*. His monument (Fig. 1), created by *Hermann Hahn*, will continue to remind oncoming generations of his achievements.

2. A Scientist's Life

One hundred and fifty years ago, in 1835, *Adolf Baeyer* was born in Berlin (Fig. 2), the son of a Prussian general staff officer and geodesist *Johann Jakob Baeyer*. His mother was a descendant of the respected Jewish family *Hitzig*. Among the frequent visitors to the *Hitzig* household were *E. T. A. Hoffmann*, *Emanuel Geibel* and *Theodor Fontane*. The poet *Adalbert von Chamisso* was *Adolf Baeyer*'s godfather.[5] However, at the age of 70, *Baeyer* confessed in his memoirs:[6]

> "I rejected all these literary influences completely, and, even as a small boy, was only interested in the phenomena of nature."

Adolf Baeyer was precocious. As a nine-year-old he began to experiment using *Stöckhardt*'s "Schule der Chemie." In a speech on the history of the indigo synthesis,[7] presented during a ceremony in 1900, he commented on this period as follows:

> "I shall never forget the feeling of delight when I held in my hands a chunk of indigo which I had purchased in the pharmacy for a 'Two-Thaler' on my 13th birthday. With awe I sniffed the perfume of the *o*-nitrophenol while following the instructions of *Wöhler's* 'Grundriss der organischen Chemie' to convert the dye into isatin."

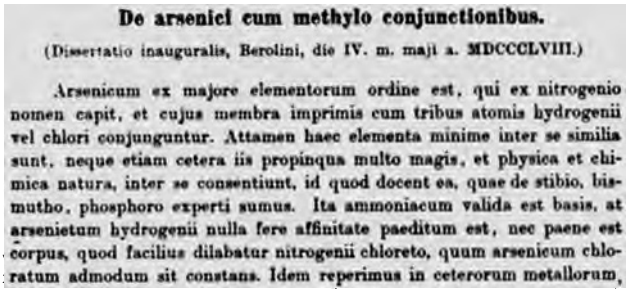
For three semesters *Baeyer* took courses in mathematics and physics at Berlin. After his obligatory military service, he switched to chemistry, and moved to Heidelberg. Even as early as his second semester, he undertook a small kinetic investigation assigned to him by *Robert Bunsen*.

Baeyer's work on his Ph. D. Thesis was carried out in the laboratory of *August Kekulé* who was a lecturer at the University of Heidelberg. *Baeyer*'s research topic, concerning organic arsenicals, originated from *Bunsen*'s field of interest. In 1858, at the age of 22, *Baeyer* submitted his thesis in Latin (Fig. 3) and obtained his degree from the University of Berlin.

Much later, in 1897, *Baeyer* participated in establishing the "Chemische Verbandsexamen". According to this new set of rules, the votaries of chemistry were no longer al-

	1835	Born October 31
		First chemical experiments at the age of 9
BERLIN		Abitur *1853* (final high school examination)
		Courses in mathematics and physics for 3 semesters
	1856	Courses in chemistry
HEIDELBERG		Ph. D. at the University of Berlin, *1858*
	1858	Assistant professorship under Kekulé, University of Gent
GENT		
	1860	Habilitation at Berlin, *1860*
		Professor at the Technical College, *1860–1872*
BERLIN		Foundation of the Deutsche Chemische Gesellschaft, *1867*
		Marriage with Lida Bendemann, *1868*
	1872	Full professorship at the University of Strassburg
STRASSBURG		
	1875	Professor at the University of Munich as successor of Liebig, *1877*
		New laboratory for the Royal Bavarian Academy of Science
MUNICH		Honors: Knighthood *1885*, Order of Maximilian *1891*,
		Order pour le mérite *1894*, Nobel Prize for Chemistry, *1905*
	1915	Retirement (successor: R. Willstätter)
STARNBERG		
	1917	Deceased on August 20

Fig. 2. A glance at *A. von Baeyer*'s curriculum vitae.



De arsenici cum methylo conjunctionibus.

(Dissertatio inauguralis, Berolini, die IV. m. maji a. MDCCCLVIII.)

Arsenicum ex majore elementorum ordine est, qui ex nitrogenio nomen capit, et cujus membra imprimis cum tribus atomis hydrogenii vel chlori conjunguntur. Attamen haec elementa minime inter se similia sunt, neque etiam cetera iis propinqua multo magis, et physica et chimica natura, inter se consentiunt, id quod docent ea, quae de stibio, bismutho, phosphoro experti sumus. Ita ammoniacum valida est basis, at arsenietum hydrogenii nulla fere affinitate paeditum est, nec paene est corpus, quod facilius dilabatur nitrogenii chloreto, quum arsenicum chloratum admodum sit constans. Idem reperimus in ceterorum metallorum,

Fig. 3. Excerpt from *A. Baeyer*'s dissertation, University of Berlin, 1858.

lowed to set their sails for research after only one semester of formal training.

When *Kekulé* received a professorship at Gent (Belgium), *Baeyer* followed him to explore the chemistry of uric acid. From there he returned to his hometown in 1860. In July he sent the following message to *Kekulé*:

> "On July 4 I presented a lecture in Latin for my 'habilitation', and since then I am a Privatdozent in full splendor."[*]

Since at that time the University of Berlin did not even have a chemical laboratory, *Baeyer* considered himself fortunate to be entrusted with a brand-new lecturer's post at the Gewerbeinstitut, i.e., an institute for vocational training which later evolved into the Technische Hochschule Charlottenburg.

The majority of research projects which we associate with *Baeyer* were launched during the twelve prolific years in Berlin. The first collaborators joined *Baeyer: Carl Graebe* and *Carl Liebermann* elucidated the structure of alizarin, the dye prepared from the madder root; its synthesis was of eminent importance for the young dye-producing industry. *Baeyer*'s contact with *Heinrich Caro*, who

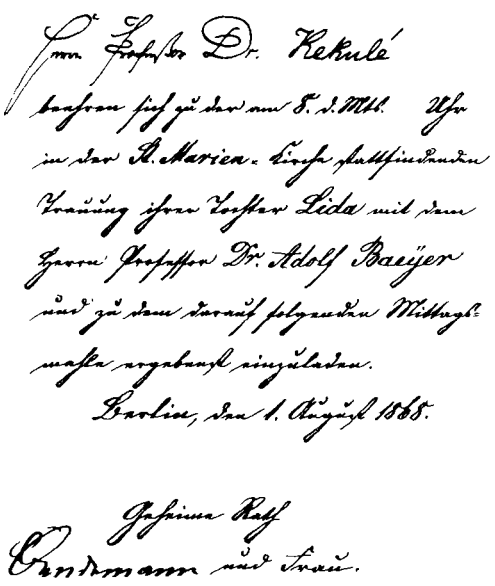


Fig. 4. Invitation received by *A. Kekulé* to attend *Baeyer*'s wedding in 1868.

[*] Part of the correspondence between *A. von Baeyer* and *A. Kekulé* can be found in the bequest of *A. Kekulé* at the Institute of Organic Chemistry, TH Darmstadt (FRG).

headed the research on dyes at the Badische Anilin- und Sodafabrik, developed into a friendship that lasted for decades.

In Berlin, *Adolf Baeyer* married *Lida Bendemann* (Fig. 4), and fathered a daughter and three sons.

August Wilhelm Hofmann and *Adolf Baeyer* played a prominent role in founding the Deutsche Chemische Gesellschaft.[8] *Baeyer* inaugurated the constituent assembly in 1867 and *Hofmann* was elected its first president. In 1868 the journal "Berichte" was established; an article by *Baeyer* on the reduction of indigo blue[9] was the first paper to be published in this journal.

Baeyer's appointment as professor at Strassburg in 1872 reflects political events: the victory of 1870/71 (Franco-German war) and the foundation of the Deutsche Reich.



Fig. 5. *A. Baeyer* in 1872.

Emil Fischer and his cousin *Otto Fischer* joined *Baeyer* as his students. In Strassburg, just as in Berlin, *Baeyer* was immediately confronted with the necessity of building a laboratory. But as soon as it was completed, *Baeyer* was asked to succeed *Justus von Liebig*, who had died in 1873, at the University of Munich.



Fig. 6. *Liebig's* auditorium and official residence in Munich around 1860 [10].

Setting up new buildings became a routine for *Baeyer*. During *Liebig*'s era, chemistry in Munich was endowed with an auditorium (Fig. 6) and research facilities, but lacked laboratories for the training of students. *Liebig*, during his years in Munich, had given priority to promot-



Fig. 7. *Baeyer's* laboratory in Munich, 1877–1906 [10].

ing chemistry and its applications to medicine and agriculture in word and print.

The only old part which was integrated into the large new building (Fig. 7) designed by *Baeyer* was *Liebig's* auditorium. Moreover, the professor's official residence was replaced by a new, almost palatial structure. When the house was taken over in 1915 by *Willstätter,* who had each of the three floors equipped with a bathroom, *Baeyer* commented with indignation:

> "Sir, you are converting my house into a public bath."

Baeyer was active in Munich from his 40th to his 80th year, finishing old projects and tackling new problems. Young chemists from all over the world crowded into *Baeyer*'s laboratory, which was one of the important centers of chemistry, then a still juvenile science. The master's scientific achievements were acknowledged with prestigious awards, some of which are recorded in Figure 2.

It appears that the art of photography in its early years singled out group-portraits as a favorite theme. From Figure 8, looking at the caps, we might deduce that heating was deficient in the winter of 1877/78. To the left of *Baeyer* we see *Jacob Volhard* who taught analytical chemistry; to the right the 25-year-old *Emil Fischer*, equipped with a prominent chapeau and striking self-confidence, having obtained his Ph.D. in Strassburg three years earlier.

3. A Brief Survey of Baeyer's Achievements

Baeyer's scientific opus covers an unprecedented range (Fig. 9). His contributions may be viewed as weighty blocks which later served as a foundation for the systematic development of numerous classes of compounds. The first two areas listed were early fields of activity to which *Baeyer* was drawn by chance. In terms of popularity and industrial importance, the leading position among his scientific ventures is clearly held by indigo, the king of the natural dyes.

Baeyer succeeded in synthesizing indigo in 1883, even before he was completely certain about its structure. A letter, dated May 1878, informs *H. Caro* that the synthesis of isatin had been accomplished (Fig. 10).

Distillation over zinc dust, a procedure introduced by *Baeyer* in 1866, was used for the conversion of oxindole, a degradation product of indigo, into its parent compound, indole;[11] the nature of this aromatic heterocycle was established in 1870.[12] Studies on related heteroaromatic compounds served as supplements. Take any of the familiar formulae of pyrrole, furan, furfural, quinoline, and cinnoline—they all originated from *Baeyer*.[12–15]



Fig. 8. Photograph of the group in the chemical laboratory of the Bavarian Academy of Sciences in the winter of 1877/78; laboratory of combustion analysis.

		Publications	
		number	pages
Organic arsenicals	1857 – 1858	4	51
Uric acid group	1860 – 1866	13	120
Indigo	1866 – 1900	36	181
N-Heteroaromatic compounds	1868 – 1883	21	105
Condensation of aldehydes and ketones with aromatic compounds	1863 – 1883	25	116
Phthaleins	1869 – 1889	24	217
Hydroaromatic compounds and the structure of benzene	1866 – 1894	40	482
Oligoacetylenes and strain theory	1865, 1885	5	45
Nitroso compounds	1869 – 1902	14	57
Dibenzalacetone and triphenylmethane	1874 – 1905	14	165
Furfural	1877 – 1879	6	18
Terpenes	1893 – 1901	27	266
Peroxides	1899 – 1902	14	97
Oxonium salts	1901 – 1915	7	60
Miscellaneous	1857 – 1905	18	138
Nomenclature	1884 – 1900	2	7

Fig. 9. *Baeyer*'s areas of research and publications.

On the occasion of *Baeyer*'s 70th birthday in 1905, his former co-workers arranged for a reprinting of all his publications; the master grouped them as indicated in Figure 9 and added "Erinnerungen aus meinem Leben".[6]

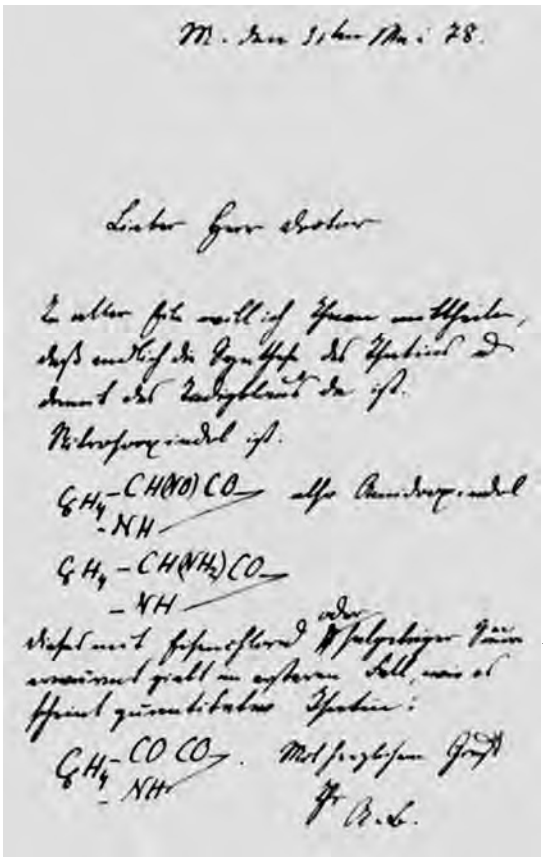


Fig. 10. *Baeyer*'s letter to *H. Caro*, 1878. [*]

The condensation of aldehydes and ketones with aromatic compounds—*Baeyer*'s serial title was "Über Wasserentziehung und Kondensation"—dealt with the linkage of two aromatic nuclei by a methylene function and was studied extensively. On allowing phenol to react with formaldehyde in 1872, *Baeyer* obtained a colorless resin[16] which he promptly discarded. This was the era of crystallizable and distillable substances; the epoch of macromolecular compounds was still to come. In 1909, the first patents on phenol-formaldehyde resins were issued to *L. H. Baekeland*. The reaction of chloral with chlorobenzene—one of a plethora of condensations—was explored by *Baeyer*'s student *O. Zeidler* in 1874.[17] The product with the acronym DDT was to trigger the development of highly active contact insecticides 70 years later.

That phthalic anhydride, like a ketone, was capable of condensing with aromatic compounds, led *Baeyer* to the discovery of the phthaleins, a prominent class of synthetic dyes.[18] Since all of *Baeyer*'s publications present information in a highly condensed form, the number of pages indicates the intensity of labor involved. From that point of view, indigo is surpassed by the phthaleins. Following this line, *Emil Fischer* centered his Ph.D. Thesis[19] on the chemistry of fluorescein.

If we measure intensity of research by the scale just mentioned, the "Chemie hydroaromatischer Verbindungen, Abbau der Mellithsäure und Konstitution des Benzols" would head the list. The field of aromatic nitroso compounds was developed by *Baeyer* from scratch, initially together with *H. Caro*.[20]

Under the heading of "Dibenzalaceton und Triphenylmethan" one finds a cache of fundamental insights into the basicity of carbon and the properties of 'carbonium salts'. *Baeyer* and *Villiger*[21] compared triphenylmethyl with the metal aluminum:

[*] *Baeyer*'s correspondence with *H. Caro* is kept in a collection at the Deutsches Museum, Munich. The author is indebted to Dr. *Otto Krätz* for his kind cooperation.

"Aluminum hydroxide does not show alkaline reaction, but yields an authentic salt when combined with sulfuric acid. Triphenylcarbinol is not a base; nevertheless it is converted to a salt by sulfuric acid."

At an age of well over 60, *Baeyer* embarked upon the investigation of terpenes, peroxides, and oxonium salts; the latter were described as derivatives of quadrivalent oxygen.

Two papers on nomenclature conclude the list of Figure 9. Who of us nowadays is aware that terms such as "carboxyl" or "carbonium salt" as well as the familiar bicyclo nomenclature originated from *Baeyer*?[22]

Let us focus on three of *Baeyer*'s sixteen fields of interest (Fig. 9), in order to illustrate a few sections of the conceptual background of our science. We will start with his contributions to the chemistry of uric acid. *Baeyer* himself regarded this work as the last phase of his apprenticeship.

4. On the Uric Acid Group

In 1838 *Friedrich Wöhler* und *Justus Liebig* published a paper entitled "Untersuchungen über die Harnsäure".[23]

"No other substance in organic chemistry attracts the attention of the physiologist and chemist to a higher degree than uric acid."

Uric acid was subjected to transformations and degradations. The resulting network of relationships between the products involved mere unknowns, until finally mesoxalic acid, oxalic acid, and urea established a bridge to simple compounds. The acids were mostly formulated as anhydrides (Fig. 11). The terms "equivalent", "atom", and "molecule" were not consistently differentiated. Moreover, all molecular formulae appeared in doubled proportions to those which later turned out to be correct. How did this come about? *Jöns Jacob Berzelius* believed that the biatomic nature of the molecules of oxygen, hydrogen, and nitrogen was preserved in their compounds; he postulated that carbon atoms occurred in pairs as well. For *Berzelius*, carbonic acid was C_2O_4.

Charles Gerhardt recognized this error in 1843, but nobody believed him. It was only at the legendary Congress

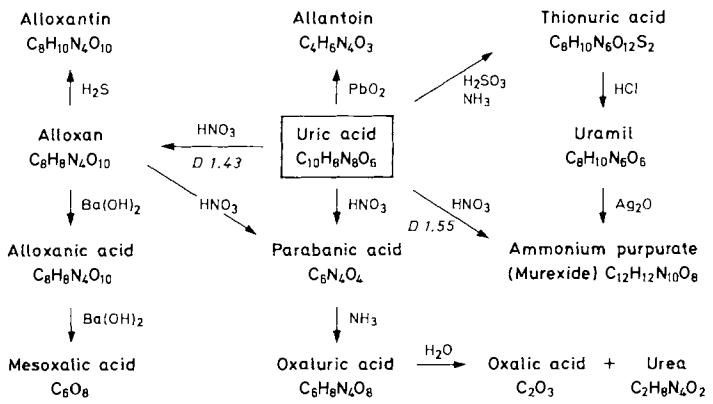


Fig. 11. Degradation scheme of uric acid according to *Wöhler* and *Liebig* [23].

of 1860 in Karlsruhe that *Stanislao Cannizzaro* persuaded his contemporaries to cut the molecular formulae in half and to double the atomic weights.

In 1861, a short paper by *Adolf Baeyer* dealt with the conversion of allantoin and alloxanic acid to hydantoin by hydrogen iodide.[24] The endearing description of hydantoin (Fig. 12) indicates that fear of chemicals had not yet surged to the mass hysteria of today.

Das Hydantoïn scheint das Glied einer Reihe von Reductionsproducten der Parabansäure zu sein :

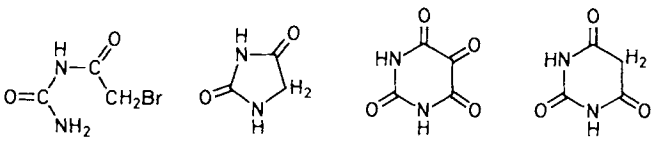
Parabansäure	$C_3H_2O_3N_2$
Leucotursäure	$C_3H_4O_3N_2 + C_3H_2O_3N_2$
Allanturs̈äure	$C_3H_4O_3N_2$
Hydantoïn	$C_3H_4O_2N_2$.

Diese Substanz krystallisirt in farblosen Krystallen, die leicht in Wasser löslich sind. Sie schmeckt schwach süfs und kracht etwas zwischen den Zähnen.

Fig. 12. From a publication by *Baeyer* on hydantoin [24].

What is the meaning of the "barred" symbols of elements in Figure 12? It is *Berzelius*' representation for double atoms, but only C and O are so designated, no longer H and N. In *Baeyer*'s next paper—one year later—the double atom spook had finally disappeared and a simple footnote declared: H=1, O=16, C=12.[25]

In 1864, *Baeyer* converted *N*-bromoacetylurea (**1**) by reaction with ammonia into hydantoin (**2**), which was regarded as glycolic acid ureide.[26] Does this mean that an underlying ring structure had been recognized? No, the idea of a cyclic arrangement of atoms in a molecule had not yet been conceived.



The first full paper on uric acid was published in the "Annalen der Chemie und Pharmazie" in 1863.[27] Its introduction disclosed an imaginative thought:

"It will become obvious that the material can be related in a simple way to the substance $N_2C_4O_3H_4$, which I will name barbituric acid, and that the problem of the constitution of uric acid can be reduced to an investigation of this substance."

Barbituric acid was still a phantom—but a phantom with a name. As in this case, *Baeyer* usually did not explain the motives for his nomenclature. Is there a "Barbara" involved somewhere along the line?

The preparation of barbituric acid from alloxan required the reduction of a carbonyl to a methylene group. Lacking a direct method, *Baeyer* elaborated a multi-step sequence with violuric acid as an intermediate;[26,27] this name was derived from the blue-violet alkali salt. In 1864, barbituric

Hiernach unterliegt es keinem Zweifel, dafs die Barbitursäure ein Amid der Kohlensäure und der Malonsäure, d. h. Malonylharnstoff ist, und es wird ihre Zersetzung durch folgende Gleichung erklärt:

$$N_2C_2H_4O_3 + 3H_2O = C_3H_4O_4 + CO_2 + 2NH_3$$

Barbitursäure — Malonsäure.

Dieses Resultat ist besonders deswegen von Interesse, weil, wie wir gesehen haben, die Barbitursäure den directen Ausgangspunkt für die Darstellung aller zur Alloxangruppe gehörigen Derivate bildet und die Constitution der letzteren somit auch nachgewiesen ist.

Fig. 13. An excerpt from *Baeyer*'s publication on the chemistry of barbituric acid [26].

acid (**4**) was born. *Baeyer* observed its alkaline hydrolysis to malonic acid, carbon dioxide, and ammonia.[26] Figure 13 shows his conclusion.

The formulae of barbituric acid and malonic acid differ from today's versions. *Baeyer* used the notation based on the "theory of types" which assembles a molecule from groups of atoms which remain unchanged or are replaced en bloc during chemical reactions.

In our time, chemical structures are first encountered in school; communicating by means of these formulae becomes as easy as using one's mother tongue. We find it hard to imagine how scientists of the past were able to exchange their insights by means of "type formulae".



Fig. 14. *August Kekulé* in 1857.

In 1864—when *Baeyer* published an article on barbituric acid—*Kekulé*'s structure theory[28] was six years old. *Kekulé* (Fig. 14) recognized that carbon is "four-atomic" and

> "that carbon atoms bind each other whereby part of the affinity of one is compensated by the same part of affinity of the other."

Why did *Baeyer* not write structural formulae? *Kekulé* himself avoided them, applying the notation of the "theory of types" instead; he justified this choice in his textbook:[29]

> "because the complete disintegration of radicals furnishes formulae of such a complexity that a clear overview is lost."

A thorny path led to current chemical notation (Fig. 15). *Kekulé* expressed the four valences of the carbon atom by a sequence of four spheres;[30] contemporaries disrespectfully termed these "sausage formulae". *Archibald Scott Couper* is usually regarded as being the father of the "valence line";[31] his fuzzy notation, however, makes me hesitate to accept this attribution. The much clearer formulae of the physicist *Josef Loschmidt* did not find the recognition they deserved, since they were not published officially. Notations similar to modern ones were adopted no earlier than the late 1860s.

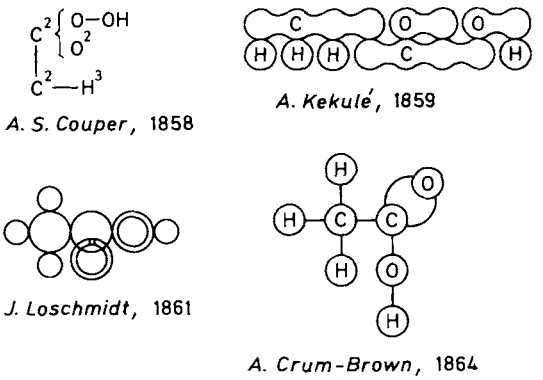


Fig. 15. Evolution of the structural formula of acetic acid.

At the age of 29, *Baeyer* turned to new hunting-grounds without having clarified the structure of uric acid. He considered the formula to be that of a cyanamido-barbituric acid;[27] *Baeyer*'s type-theoretical notation is translated into a structural formula in Figure 16. In 1868, i.e., three years after *Kekulé*'s benzene formula, *Adolf Strecker*[32] proposed a cyclic structure which borrowed the cyanamido group from *Baeyer*'s formula. By contrast, *Hermann Kolbe*'s proposal of a tartronic acid bis-cyanamide[33] was a step backward. Even in 1878, *Kolbe* dismissed the structure theory; instead, he complained about "the fantasy of the so-called chain theory and the heresy of the benzene ring".[34]

In 1875, *L. Medicus* brilliantly deduced the correct formula of uric acid[35] (Fig. 16) which was confirmed in an elegant synthesis by *Behrend* and *Roosen*[36] in 1889.

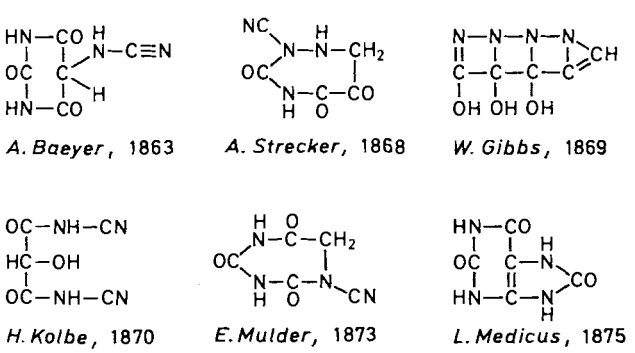


Fig. 16. Development of the formula of uric acid.

Let us branch off for a short interlude to discuss *Baeyer*'s experimental methods. Anecdotes reveal the simplicity of his lab equipment. Thus, *Baeyer* proudly told the visiting *Emil Fischer* of a marvelous new apparatus; it turned out to be a test-tube fixed on a support over a Bunsen burner.



Fig. 17. *A. Baeyer*, 1907 [10].

A photograph of the 72-year-old (Fig. 17), as well as reports of his associates in this later period of his career contributed to *Baeyer*'s reputation as a master of the test-tube experiment. While the test-tube may have dominated his late years in Munich, it does not pertain to his early activity in Berlin. Thus, the 27-year-old *Baeyer* informed *Kekulé* of the progress of his uric acid studies (Fig. 18):

> "The most painstaking part of the work was devising the preparative methods; however, I can now manufacture all these substances in large quantities, and I am all the more pleased to set to work on the second hundredweight of uric acid, since the first has passed to the fathers (guano ducks probably)."

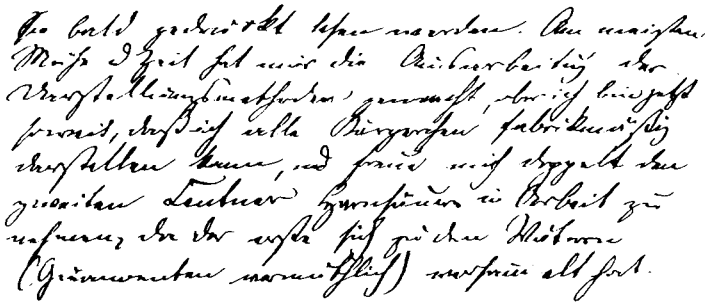


Fig. 18. From *Baeyer*'s letter to *Kekulé*, March 22, 1863.

In another letter to *Kekulé, Baeyer* discussed the constitution of the "pee compounds", as he facetiously labeled them; he then described an efficient method for converting dialuric acid to alloxantin by using sodium amalgam.[37]

> "For that purpose I need large amounts of sodium; I won't buy it here, however, because it is so expensive."

He wanted ten pounds of sodium and asked *Kekulé* to help him get it at a low price. The scale of such experiments clearly surpasses the limitations of the test-tube.

When a *Baeyer* procedure stated "was stirred for 3 hours," it really meant what it said: boring activity for the experimentalist. One morning, during his late years in Munich, the squeaking noise of two stirring devices, driven by a primitive water turbine, was heard in *Baeyer*'s laboratory. The master's anger was assuaged by his collaborator's assurance that regular stirring improves the yield. The next day, *Lida Baeyer* admired the technical progress and mused on how well this gimmick would serve in making mayonnaise.[5]

5. The Chemistry of Hydroaromatic Compounds and the Structure of Benzene

The "Benzolfest", celebrated in 1890 in honor of *August Kekulé* (Fig. 19), was one of the highlights in the history of the German Chemical Society.

> "It is imperative to express thanks and homage to the man who, 25 years ago, enriched the world of chemistry with his theory on the constitution of benzene and the aromatic compounds which proved to be so prolific. The stimulation and success which chemistry and technology owe to this single new concept remain unparalleled. As a consequence, the celebration was not limited to experts, but roused the interest of a far wider public."[38]



Fig. 19. Left: *Adolf von Baeyer*, 1890; right: *August Kekulé*, 1890.

The cyclic formula of benzene was a prerequisite to the systematic development of aromatic chemistry; the consequences for aliphatic chemistry were just as important. *Adolf von Baeyer*, the official speaker, addressed *Kekulé* emphatically:[39]

> "With your theory of benzene, you were the first to conceive the idea that carbon atoms not only can form chains, straight and branched, but also rings."

In 1865 *Kekulé* proposed "sausage formulae" for benzene and toluene (Fig. 20) which, however, only allowed

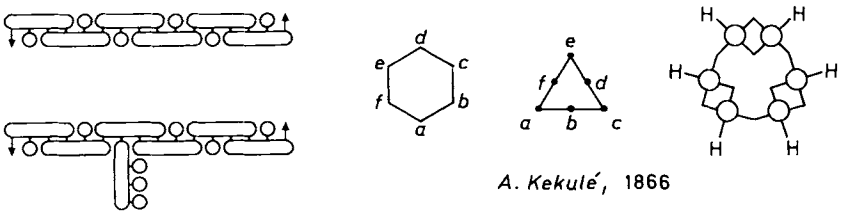


Fig. 20. Development of the formula of benzene.

the expert to decipher the alternating sequence of single and double bonds as well as the cyclic structure signaled by the terminal arrows.[40] In the next year, hexagonal and triangular representations—differing in symmetry—were recommended by *Kekulé*.[41] Late in 1866, the symbol depicted on the upper right of Figure 20 appeared in *Kekulé*'s textbook.

This did not completely solve the benzene problem, however; according to *Baeyer*,[39]

> "benzene behaves in a basically different manner than unsaturated compounds of the fatty acid series."

This difficulty was met by *Claus* with a "diagonal formula", and later by *Ladenburg* with an especially elegant prismatic image. Both notations eliminated a weak point: *Kekulé*'s benzene was expected to give isomeric *o*-disubstitution products. His own remedy was the somewhat adventurous oscillation hypothesis of 1872; the double bonds were not considered to be fixed, but rather to migrate rapidly[42] (Fig. 20).

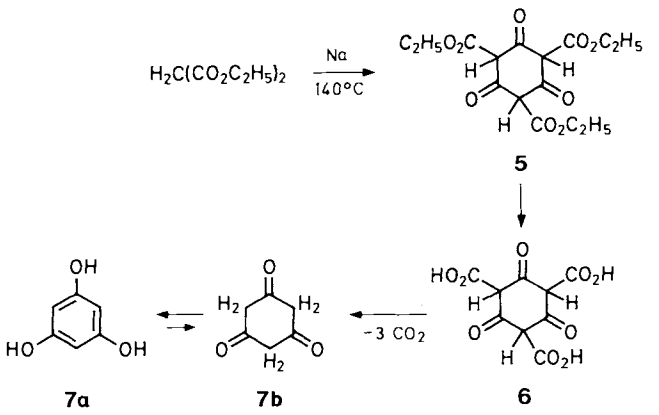
The products of the second and third substitution corresponded to those expected for a regular hexagonal structure of benzene. Many of *Kekulé*'s contemporaries indulged in the fascinating play on the "substitution piano" and in devising methods for locating the positions of the substituents.

Baeyer's concern was the bonding of benzene. He opened his *Kekulé* lecture[39] with the question:

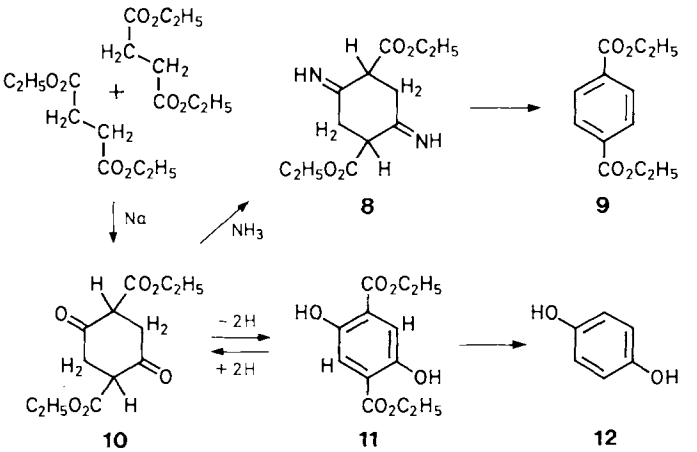
> "... was this theory correct in the first place?"

In 1866 *Baeyer* saw an endorsement of *Kekulé*'s formula in the acid condensation of three molecules of acetone yielding mesitylene; as expected, the elimination of three molecules of water resulted in an alternating sequence of double and single bonds.[43]

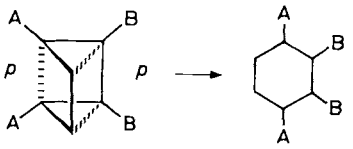
Phloroglucinol (**7a**), being a triphenol, can be alkylated three times on the oxygens. On the other hand, *Baeyer* supposed the triketo tautomer **7b** to be responsible for trioxime formation. Ester condensation was reckoned to furnish the triketo form via the tricarboxylic ester **5**. If the triketone **7b** contains a six-membered ring, the same must be true for the aromatic phloroglucinol.[44,45]



The condensation of two moles of diethyl succinate afforded the structurally secured "succinylosuccinic ester" **10**.[46] Removing two H atoms by bromine yielded the dihydroxyterephthalic ester (**11**) which was reconverted to the aliphatic dihydro form **10** by means of zinc and hydrochloric acid.[47] In short, the benzene and the cyclohexane derivatives must share the same carbon skeleton.



Baeyer demonstrated the inconsistency of *Ladenburg*'s prism formula of benzene in an ingenious way.[48] The transformation of prismane **13** to the cyclohexane ring requires the rupture of the three bonds indicated by broken lines. The substituents A define the *p*-relation in prismane;



13 14

the same is true of the two substituents B. Only *one* *p*-relation of prismane can be converted into a 1,4-disubstituted cyclohexane **14**, whereas the other *p*- give rise to 1,2-relations in **14**.

The succinylosuccinic ester **10** contains 1,4-situated ester groups; the same is true for the two keto groups. *Baeyer* proved these relative locations to be retained, since dehydrogenation furnished the diethyl dihydroxyterephthalate (**11**);[47] **10** was converted into **9** in several steps via the bis-imine **8**. The *p*-positions of the substituents in hydroquinone (**12**) and terephthalic ester (**9**) had been secured previously.

Let us go back two decades to *Baeyer*'s first encounter with aromatic compounds. Occasionally, an odd mineral, honeystone, is found in coal deposits; it is the aluminum salt of mellitic acid. *Baeyer* recognized the latter to be benzenehexacarboxylic acid[49] and wrote to his friend *Kekulé* (Fig. 21):

> "Mellitic acid is: $C_6(CO.HO)_6$, a six-basic acid. I am sending you the academy reprint of November. With sodium amalgam it yields $C_6H_6(COHO)_6$; 6-fold carboxylated benzene and 6-fold carboxylated C_6H_{12}, isn't that nice? You might use it for your textbook, the series of aromatic acids is now complete ..."

Nearly 20 years later, *Baeyer* systematically studied the reduction of benzenecarboxylic acids by sodium amalgam in aqueous medium; he expected insight into the bonding. Aromatic hydrocarbons are not reduced by sodium amalgam. Catalytic hydrogenation had not yet been discovered; it was not until 1900 that *Paul Sabatier* converted benzene into cyclohexane by hydrogen on a nickel catalyst.

On reducing terephthalic acid under mild conditions, the $\Delta^{2,5}$-dihydro acid was isolated; hence, hydrogen added to the carboxyl-bearing carbon atoms[50] (Fig. 22). Isomerization to the $\Delta^{1,5}$ acid took place in boiling water, whereas base catalysis afforded the $\Delta^{1,4}$ acid. Only the latter two acids can be reduced further by sodium amalgam. Bromine, hydrogen bromide, potassium hydroxide, and potassium permanganate: this was the entire arsenal of reagents which were applied as probes. What an amazing achievement to firmly establish the structures of the four dihydro- and the two tetrahydroterephthalic acids with so limited a set of reagents! This was the supreme art of logical deduction from a network of experimental results.

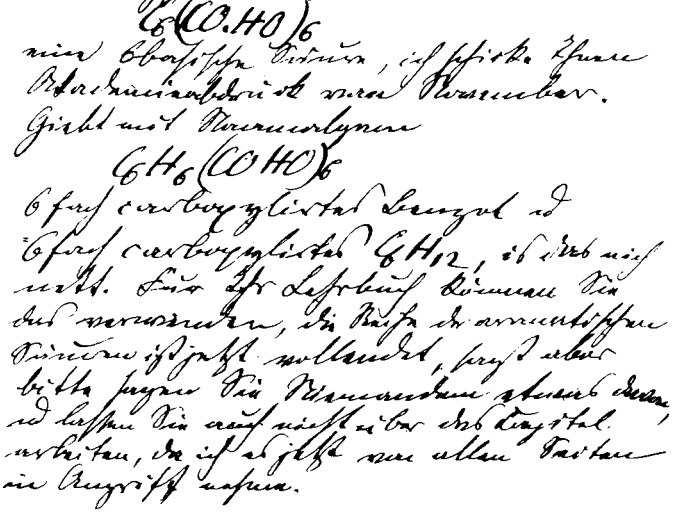


Fig. 21. From *Baeyer*'s letter to *Kekulé*, December 17, 1866.

What are the conclusions with respect to the benzene problem? The initial 1,4-addition of hydrogen corresponds to the annihilation of one *p*-bond in the *Claus* formula **15** of terephthalic acid. However, the product, the $\Delta^{2,5}$-dihydro acid **16**, does not contain the two residual *p*-bonds, but rather possesses normal olefinic double bonds instead.[50]

A key observation: The olefinic $\Delta^{1,3}$-dihydro acid **17** added hydrogen at the termini of the conjugated system.[50] Muconic acid, i.e., the *open-chain* butadiene-1,4-dicarboxylic acid, also underwent 1,4-reduction by sodium amalgam in water.[51] Here *Baeyer* prepared the ground for the studies of *Johannes Thiele* who first correctly viewed conjugated double bonds as reactive units.[52] Since *Kekulé*'s

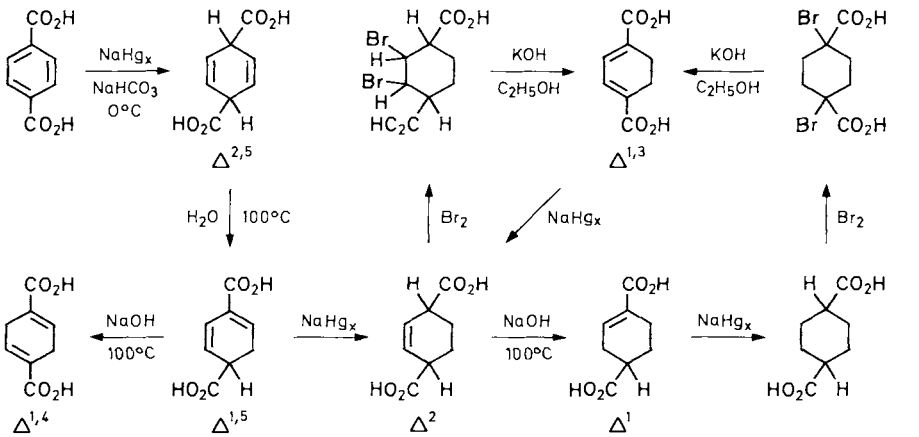
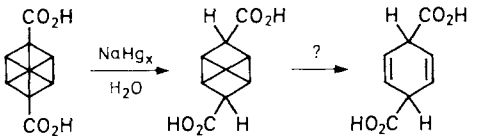
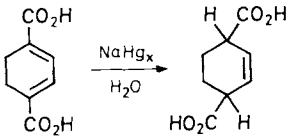


Fig. 22. Stepwise hydrogenation of terephthalic acid by sodium amalgam in water.



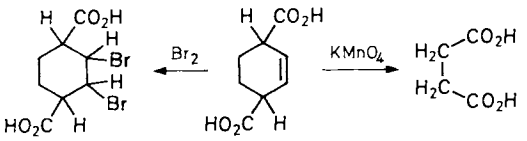
15 16

benzene contains conjugated double bonds as well, *Claus'* assumption of *p*-bonds in benzene was shown to be superfluous.

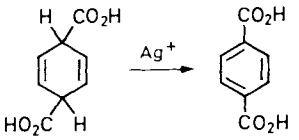


17

The olefinic reactivity of the partially hydrogenated acids towards bromine and permanganate is illustrated by the behavior of **18**. On the other hand, permanganate—



18



19

and even silver ion—converted the $\Delta^{2,5}$-dihydro acid **19** to terephthalic acid.[50] The aromatic system is energetically favored and tends to be formed easily. *Baeyer*'s comment:[39]

> "To provide an explanation for this discontinuity in the chemical properties upon introduction of the third double bond, is the task set for the theory of benzene."

The benzene anniversary of 1890 offered the opportunity for a resumé:[39]

> "The benzene ring approaches a limiting state which I propose to call the 'ideal benzene': the six CH groups are tied to each other with such extraordinary strength that the ring appears to be completely symmetric and the fourth valence of carbon vanishes from our perception."

Which of the formulae should we favor?



20 21

> "... I propose to describe the ideal benzene by the formula which I have dubbed centric; the arrows indicate the strong pressure directed inwards."

The arrows—*Henry Armstrong* and *Lothar Meyer* proposed the same symbol **20**—suggest the mutual equalization of the six residual valences, whereas the *Kekulé* formula implies a compensation in pairs.

Benzene derivatives are capable of certain addition reactions, e.g., the hydrogenation of benzenecarboxylic acids by sodium amalgam and water as discussed above. The chemistry of naphthalene, anthracene, and phenanthrene presents transitions from aromatic to olefinic reactivity. *Baeyer's* explanation strikes a downright modern note:[39]

> "The limiting states of benzene are represented by the *Kekulé* structure and the centric formula ... The nature of the benzene ring in any derivative may be intermediate between the extremes."

Even today an empirical description of aromatic bonding could hardly be more to the point.

The central valences served *Baeyer* to emphasize the special character of benzene, although their nature remained vague:[53]

> "The present state of knowledge gives us no clue to the passivity of the central valences. Whether this phenomenon ... is caused by an especially high density of the ether in the center of the ring, remains to be seen."

We are amused by the appeal to a vague, but fashionable rationalization, "ether", to account for the benzene mystery. But we need to adjust our view to the times. It was not until 1896 that *Henri Becquerel* discovered natural radioactivity. In 1890 the atom was still regarded as ἄτομος, as indivisible. Nuclei and electron clouds were unheard of. In particular, the nature of chemical bonding forces was still completely obscure. As late as 1900, *Ernst Mach* and *Wilhelm Ostwald*[54] regarded the atomic hypothesis as "univerified", and *Ostwald*'s book "Prinzipien der Chemie"[55] of 1907 got by without mention of atoms.

Adolf Baeyer, who employed molecular models of the ball and stick type, had adopted *van't Hoff*'s concepts of stereochemistry. He isolated the hydrogenated terephthalic acids in "malenoid" and "fumaroid" forms (Fig. 23); the

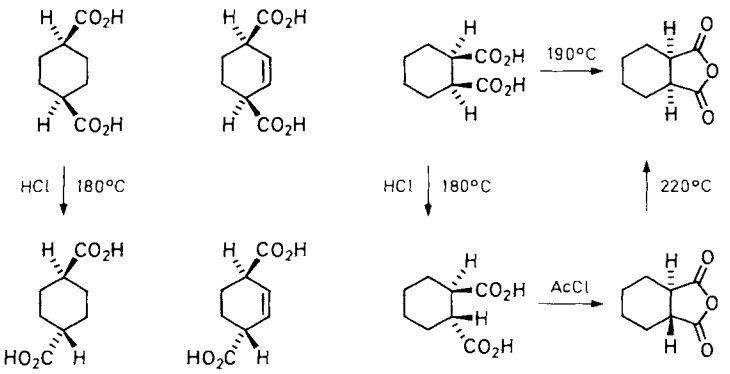


Fig. 23. Geometrical isomerism of hydrogenated benzenedicarboxylic acids; above malenoid forms, below fumaroid forms.

former were more soluble than the latter. Thus, the discovery of *cis,trans* isomerism in ring compounds was *Baeyer*'s accomplishment.[50,53,56-58]

The formation of hexahydrophthalic acid anhydrides turned out to be a valuable criterion.[58] Whereas the *cis* acid afforded the anhydride thermally, the *trans* acid required treatment with acetyl chloride[57] (Fig. 23). In contrast to fumaric acid, *trans*-hexahydrophthalic acid can form an anhydride. With unerring instinct, *Baeyer* attributed this to bond angle variations: 180° for fumaric acid, but less for hexahydrophthalic acid. The greater stability of the *cis* anhydride in comparison to that of the *trans* isomer was accounted for exactly as it is today. The concept of ring strain is *Baeyer*'s achievement.

According to *Baeyer*'s evidence, hydrogenation of phthalic acid likewise occurs at the carboxyl-bearing C-atoms[58] (Fig. 24). Let us focus on a detail. The $\Delta^{3,4}$-dihydrophthalic acid, on oxidation with copper(II) ions or

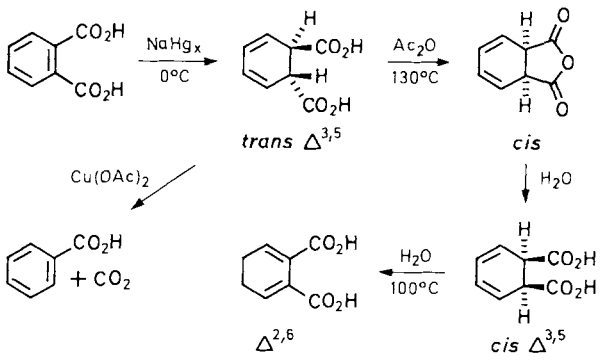


Fig. 24. The chemistry of dihydrophthalic acids.

silver ions, fragmented into benzoic acid and carbon dioxide.[58] *Baeyer*'s propensity to describe chemical behavior in terms of mechanical models turned a somersault here:

> "The elimination of carbon dioxide obviously arises from the jolt imparted to the α-carbon atom—the carrier of the carboxyl—through the abstraction of hydrogen."

The popularity of the mechanical model is easily understood. The mechanical theory of heat, associated with the names of *Clausius, Maxwell,* and *Boltzmann,* celebrated its greatest triumph in the period from 1860 to 1880. *Boltzmann* put the new trend into a nutshell:

> "Today everything is placed on the physico-mechanical loom."

That isophthalic acid does not form an anhydride, was taken by *Baeyer* to be evidence for the rigidity of the benzene nucleus (Fig. 25). In contrast, anhydride formation from *cis*-hexahydroisophthalic acid turned out to be feasible. *Baeyer* and *Villiger* concluded that a ring made up of saturated carbon atoms can be deformed as easily as an open chain.[59]

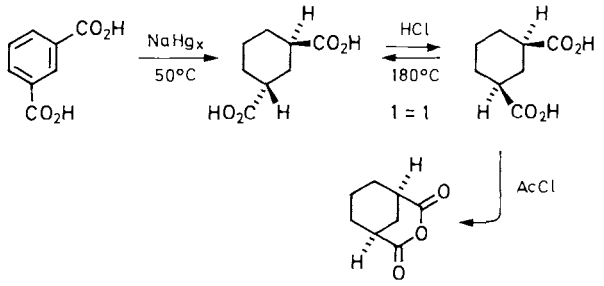
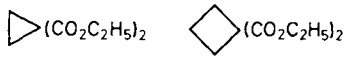


Fig. 25. Stereoisomeric hexahydroisophthalic acids.

6. The Strain Theory of Carbon Ring Compounds

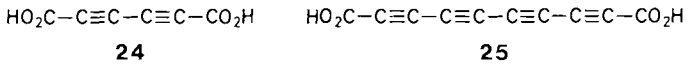
How did the strain theory of carbon rings evolve? From which sources did *Baeyer* draw his inspiration?

In 1876 *Victor Meyer* pointed out that certain reactions, expected to render 3- or 4-membered rings, took a different course. This "makes the non-existence of such rings at least highly probable."[60]



22 **23**

In 1882 *William Henry Perkin Jr.* came to Munich at the age of 22 in order to work on his thesis under *Baeyer*'s direction. *Perkin* was familiar with *Victor Meyer*'s paper, and personal debates with *V. Meyer, A. Baeyer,* and *E. Fischer* did not dissuade him from his intention to synthesize small carbon rings.[61] Applying the malonic ester synthesis, he actually succeeded in preparing diethyl tetramethylene-1,1-dicarboxylate (**23**) in 1883 and the trimethylene derivative **22** in 1884.[62] However, he observed the striking tendency of the cyclopropane rings to reopen.



24 **25**



26 **27**

Personal experience always tips the balance. *Baeyer* had prepared polyacetylenes, e.g., **24-27**, and complained about their explosive character:[63]

> "Diacetylene silver ... explodes when rubbed between the fingers —even in moist condition."

The decomposition of polyacetylenes produces "common coal". The concurrent evolution of heat indicates the unfavorable valence state of the carbon-carbon triple bond.

Baeyer's now famous "theory of ring closure" was an addendum to the polyacetylene publication.[63] Much later, in 1929, *Perkin* commented on *Baeyer*'s strain theory:[61]

> "This remarkable theory, published in August 1885, occupies only two pages of print and its description always seems to me to be a striking ex-

ample of how much can be said in a very small place."

This strain theory, now a hundred years old, was introduced by *Baeyer* as follows:

> "Whereas chains of 5 or 6 members can be closed easily, considerable difficulties are encountered in trying to do the same with shorter or longer chains. There must be steric reasons for this behavior."

Based on the tetrahedral angle of 109°28′ in methane, the inference was:

> "The direction of the attractive power can be deflected; the result is a strain that increases with growing deflection."

The planar five-membered ring involves hardly any bending at all; on the other hand, the deflection of the bond angles in smaller and larger rings—assumed to be planar as well—generates strain (Fig. 26). *Baeyer* courageously postulated that ethylene is a two-membered ring, the first member of the homologous series of cycloalkanes.

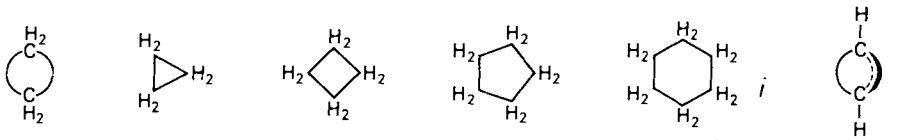


Fig. 26. Bending of the tetrahedral angle, 0.5 (109°28′−α), in carbon rings [63].

> "Dimethylene is indeed the weakest ring, opened by reactions with bromine, hydrogen bromide, or even iodine; trimethylene is forced open by hydrogen bromide, but not by bromine, whereas tetra- and hexamethylene can only be cleaved with difficulty or not at all."

The contributions of *Niels Bohr, G. N. Lewis, W. Heitler,* and *F. London* trace the development which was to lead to the quantum mechanical theory of covalence. In 1930 *Erich Hückel* viewed the CC double bond as a combination of two bonds which differ in the symmetry of their electron distributions and are denoted σ and π.[64] This interpretation proved fruitful. Is it correct? That is an all-too-simplistic question. There are various models allowing a consistent mathematical description. In 1931 *Linus Pauling*[65] declared his preference for the *Baeyer* model of ethylene with its two identical bent bonds, even though the MO treatment affords the same quantum mechanical expression for the two models. In 1958, he listed arguments in favor of the bent-bond concept, concluding:[66]

> "I contend that the σ,π description is less satisfactory than the bent-bond description, that this innovation is only ephemeral, and that the use of the σ,π description will die out before long."

In view of *Baeyer*'s passion for playing with molecular models, it is surprising that he assumed six-membered rings to be planar. In 1890 *H. Sachse* reported that two nonplanar models of cyclohexane—conformations as they were called later—do not require bending of the tetrahedral angle,[67] a discovery which was exploited and extended to larger rings by *E. Mohr*.[68] In 1905 *Baeyer* ruminated on this topic in his "Erinnerungen"[6] as follows:

> "Sachse disagreed ... with my opinion that larger rings are planar. He is certainly right from a mathematical point of view; yet in reality, strangely enough, my theory appears to be correct. The reason is not clear ..."

Let us follow *Baeyer*'s line of thought. If rings with more than six members were free of strain, why should their formation tendency be so low? Only decades later did chemists realize that more variables are involved. Not only angle bending (*Baeyer* strain), but also conformational strain and *van der Waals* repulsion contribute to the energy content of a ring.

According to *Baeyer*'s theory, the cage-like bond system of acetylene (Fig. 26) consists of three bonds, each of which deviates by 70° from the tetrahedral angle. The strain energy is set free in the explosive conversion of polyacetylenes into elementary carbon. *Baeyer* dubbed the latter "black coal" and believed it to be a stable molecular arrangement with numerous single bonds. Neither the graphitic nature of this "black coal" nor even the structure of graphite were known at that time.

7. Epilog

If we are willing to accept the number of *Baeyer*'s publications (Fig. 27) as a measure of his personal energy and productivity, we find a broad maximum from his 30th to his 50th year and a remarkably high level up to his 70th year.

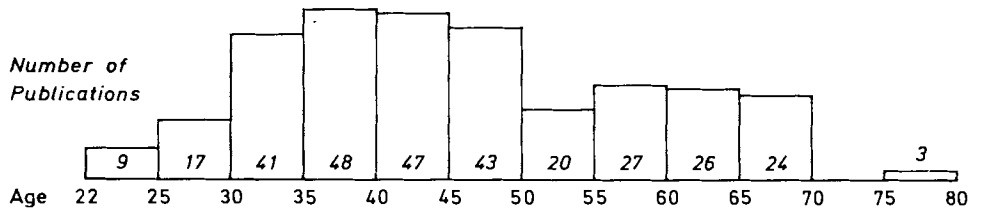


Fig. 27. Number of *Baeyer*'s papers for five-year periods plotted versus age.

Among the chemists to whom *Baeyer* introduced scientific thinking and the art of experimentation were: *G. von Brüning, W. Dieckmann, C. Duisberg, E. Fischer, O. Fischer, P. Friedländer, C. Graebe, E. Hepp, B. Homolka, W. Ipatieff, C. Liebermann, E. ter Meer, V. Meyer, W. A. Noyes, W. H. Perkin jr., H. Rupe, C. Schraube,* and *V. Villiger. Baeyer* supervised only a small group of co-workers; he carried out most of his experimental studies with his own hands.

Much larger is the illustrious group which *Willstätter* referred to as "associates in a wider sense";[69] the selection includes: *E. Bamberger, Th. Curtius, L. Claisen, O. Dimroth, A. Einhorn, M. Gomberg, K. A. Hofmann, A. F. Holleman, W. Koenigs, H. von Pechmann, W. Schlenk, J. Thiele, H. Wieland,* and *R. Willstätter.* These scientists worked in *Baeyer*'s environment, were influenced and inspired by him, and regarded themselves as members of the *Baeyer* School. Thus, *Heinrich Wieland* obtained his Ph.D. with *Johannes Thiele,* and *Alfred Einhorn* guided *Richard Willstätter*'s thesis work. Who can draw the borders of such a scientific school? Beyond doubt, the influence of *Baeyer*'s personality was amazing.



Fig. 28. Bronze bust of *A. von Baeyer* (by *A. von Hildebrand,* 1905).

Some light was shed on the secret of *Baeyer*'s success during the celebration of his 70th birthday. His students and friends presented him with a bronze bust, sculpted by *Adolf von Hildebrand,* who created, inter alia, the Wittelsbach Fountain in Munich. In his subsequent address *Baeyer* mused:[70]

> "The fact that I had such a sizable number of students and received recognition during my professional career is—so I believe—mainly due to my very timely appearance on the scientific stage."

Baeyer carried out the work for his thesis in *Kekulé*'s laboratory. Since it concerned a self-chosen topic, he sometimes claimed to be self-trained. This was not the case. In fact, *Baeyer* was *Kekulé*'s student in the most fundamental sense.

August Kekulé conceived his structural theory in Heidelberg and published it in 1858. It sparked an ignition comparable to that of *Kekulé*'s benzene theory of 1865.

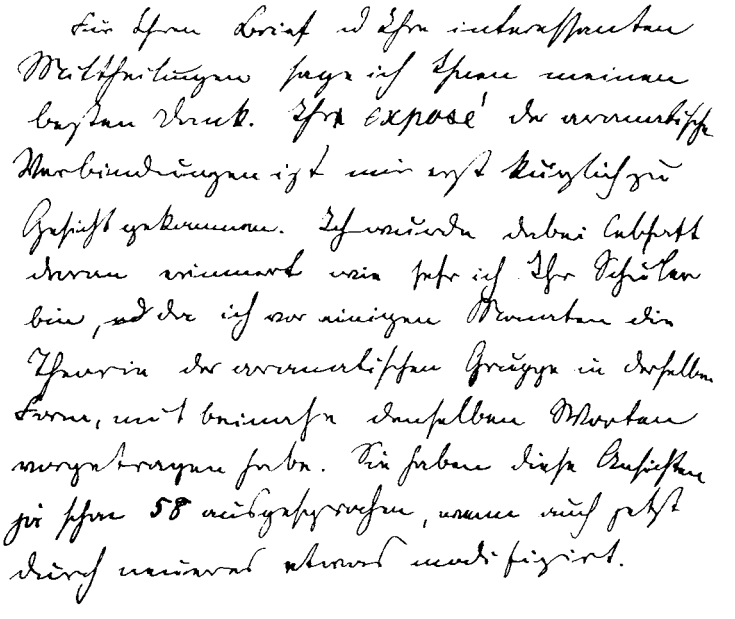


Fig. 29. From *Baeyer*'s letter to *Kekulé*, April 26, 1865.

The intellectual bond between the two scientists was unequivocally expressed in a letter dated April 26, 1865 from *Baeyer* to *Kekulé* (Fig. 29):

> "Your exposé on aromatic compounds has only recently come to my attention. It was a vivid reminder of the extent to which I am your student; my own lecture on the theory of the aromatic group a few months ago followed the same form with almost the same words."

Two more quotations from *Baeyer*'s address[70] characterize *Kekulé* in contrast to his own position.

> "*Kekulé* was not interested in the compounds themselves; his only concern was whether their behavior coincided with his concepts, and this was what he tested."
> "My own role, on the other hand, was that of a miner. I considered it my mission to reapproach nature and to look at the substances themselves, quite the way they are."

The passage of time corrects many a distortion of perspective. In my view the similarities between these two eminent personalities were more pronounced than their differences, and I hope that this opinion has been documented in my account.

Having had the first word, *Richard Willstätter* (Fig. 30) shall also have the last. A grateful student of *Baeyer*'s, he stated:[69]

> "By maintaining a close and personal interchange over many years, and by communicating his beliefs at their earliest stages of budding and maturing, *Kekulé* led his friend and junior of six years to a high level ... So provided with a new type of compass, *Baeyer* was able throughout his career to

orientate himself in the old and new domains of carbon compounds, to master the major roads, and to gain access to many a side trail as well."



Fig. 30. *R. Willstätter*, etching by *Peter Halm*.

The author wishes to express his gratitude to Professor Klaus Hafner, Darmstadt, for the kind permission to quote from the unpublished correspondence of Baeyer and Kekulé. Furthermore, the author thanks his daughters, Helga Huisgen and Professor Birge Zimmermann-Huisgen, for the preparation of the English version. Finally, he is highly indebted to Professor Paul v. R. Schleyer, Erlangen, for a careful revision.

Received: October 29, 1985 [A 572 IE]
German version: *Angew. Chem. 98* (1986) 297

[1] R. Willstätter: *Aus meinem Leben*, Verlag Chemie, Weinheim 1949.
[2] Verlag R. Oldenburg, München 1873.
[3] F. Sertürner, *Gilberts Ann. Phys. 55* (1817) 56.
[4] C. Schorlemmer, *Ann. Chem. Pharm. 131* (1864) 76.
[5] Quoted from the excellent biography by K. Schmorl: *Adolf von Baeyer*, Wissenschaftliche Verlagsgesellschaft, Stuttgart 1952.
[6] A. von Baeyer, "Erinnerungen aus meinem Leben", in: *Gesammelte Werke*, F. Vieweg, Braunschweig 1905.
[7] A. von Baeyer, *Ber. Dtsch. Chem. Ges. 33* (1900) LI.
[8] W. Ruske: *100 Jahre Deutsche Chemische Gesellschaft*, Verlag Chemie, Weinheim 1967.
[9] A. Baeyer, *Ber. Dtsch. Chem. Ges. 1* (1868) 17.
[10] Photographs from W. Prandtl: *Die Geschichte des Chemischen Laboratoriums der Bayerischen Akademie der Wissenschaften in München*, Verlag Chemie, Weinheim 1952.
[11] A. Baeyer, *Ann. Chem. Pharm. 140* (1866) 295; *ibid. Suppl. 7* (1870) 56.
[12] A. Baeyer, A. Emmerling, *Ber. Dtsch. Chem. Ges. 3* (1870) 514.
[13] A. Baeyer, *Ber. Dtsch. Chem. Ges. 10* (1877) 1358.
[14] A. Baeyer, *Ber. Dtsch. Chem. Ges. 12* (1879) 1320.
[15] V. von Richter, *Ber. Dtsch. Chem. Ges. 16* (1883) 677.
[16] A. Baeyer, *Ber. Dtsch. Chem. Ges. 5* (1872) 1094.
[17] A. Baeyer, O. Zeidler, *Ber. Dtsch. Chem. Ges. 7* (1874) 1180.
[18] A. Baeyer, *Ber. Dtsch. Chem. Ges. 4* (1871) 658.
[19] E. Fischer, *Ber. Dtsch. Chem. Ges. 7* (1874) 1211; A. Baeyer, *Justus Liebigs Ann. Chem. 183* (1876) 1.
[20] A. Baeyer, H. Caro, *Ber. Dtsch. Chem. Ges. 7* (1874) 809.
[21] A. Baeyer, V. Villiger, *Ber. Dtsch. Chem. Ges. 35* (1902) 1189.
[22] A. von Baeyer, *Ber. Dtsch. Chem. Ges. 33* (1900) 3771.
[23] F. Wöhler, J. Liebig, *Ann. Chem. Pharm. 26* (1838) 241.
[24] A. Baeyer, *Ann. Chem. Pharm. 117* (1861) 178; *119* (1861) 126.
[25] A. Baeyer, *Z. Chem. Pharm. 1862*, 289.
[26] A. Baeyer, *Ann. Chem. Pharm. 130* (1864) 129.
[27] A. Baeyer, *Ann. Chem. Pharm. 127* (1863) 1, 199.
[28] A. Kekulé, *Ann. Chem. Pharm. 106* (1858) 129.
[29] A. Kekulé: *Lehrbuch, Bd. II*, pp. 249–250 (1864); quoted from C. Graebe: *Geschichte der Organischen Chemie, Bd. I*, J. Springer, Berlin 1920, p. 234.
[30] A. Kekulé, as [29], *Bd. I*, pp. 150–165.
[31] A. S. Couper, *Ann. Chim. (Paris) [3] 53* (1858) 469.
[32] A. Strecker: *Lehrbuch der organischen Chemie*, 1868, p. 800, quoted by L. Medicus [35].
[33] H. Kolbe, *J. Prakt. Chem. [2] 1* (1870) 134.
[34] H. Kolbe, *J. Prakt. Chem. [2] 17* (1878) 139.
[35] L. Medicus, *Justus Liebigs Ann. Chem. 175* (1875) 230.
[36] R. Behrend, O. Roosen, *Justus Liebigs Ann. Chem. 251* (1889) 235.
[37] Letter of November 2, 1861.
[38] Report by G. Schultz, *Ber. Dtsch. Chem. Ges. 23* (1890) 1265.
[39] A. von Baeyer, *Ber. Dtsch. Chem. Ges. 23* (1890) 1272.
[40] A. Kekulé, *Bull. Soc. Chim. Fr. [2] 3* (1865) 98.
[41] A. Kekulé, *Ann. Chem. Pharm. 137* (1866) 129.
[42] A. Kekulé, *Ann. Chem. Pharm. 162* (1872) 77.
[43] A. Baeyer, *Ann. Chem. Pharm. 140* (1866) 306.
[44] A. Baeyer, *Ber. Dtsch. Chem. Ges. 18* (1885) 3454; *19* (1886) 159.
[45] A. Baeyer, *Ber. Dtsch. Chem. Ges. 19* (1886) 1797.
[46] F. Herrmann, *Justus Liebigs Ann. Chem. 211* (1882) 306; W. Wedel, *ibid. 219* (1883) 71; C. Duisberg, *Ber. Dtsch. Chem. Ges. 16* (1883) 133.
[47] A. Baeyer, *Ber. Dtsch. Chem. Ges. 19* (1886) 428.
[48] A. Ladenburg, *Ber. Dtsch. Chem. Ges. 2* (1869) 140, 272; *Justus Liebigs Ann. Chem. 172* (1874) 331; *179* (1875) 163.
[49] A. Baeyer, *Ann. Chem. Pharm. 141* (1867) 271; *ibid. Suppl. 7* (1870) 1.
[50] A. Baeyer, *Justus Liebigs Ann. Chem. 251* (1889) 257.
[51] A. Baeyer, H. Rupe, *Justus Liebigs Ann. Chem. 256* (1890) 1.
[52] J. Thiele, *Justus Liebigs Ann. Chem. 306* (1899) 87.
[53] A. Baeyer, *Justus Liebigs Ann. Chem. 245* (1888) 103.
[54] W. Ostwald, Die Überwindung des wissenschaftlichen Materialismus (Lecture), *Z. Phys. Chem. 18* (1895) 305.
[55] W. Ostwald: *Prinzipien der Chemie*, Akademische Verlagsgesellschaft, Leipzig 1907.
[56] A. Baeyer, J. Herb, *Justus Liebigs Ann. Chem. 258* (1890) 1.
[57] A. Baeyer, *Justus Liebigs Ann. Chem. 258* (1890) 145.
[58] A. Baeyer, *Justus Liebigs Ann. Chem. 269* (1892) 145.
[59] A. Baeyer, V. Villiger, *Justus Liebigs Ann. Chem. 276* (1893) 255; see also W. H. Perkin Jr., *J. Chem. Soc. 59* (1891) 798.
[60] V. Meyer, *Justus Liebigs Ann. Chem. 180* (1876) 192.
[61] W. H. Perkin Jr., *J. Chem. Soc. 1929*, 1347.
[62] W. H. Perkin Jr., *Ber. Dtsch. Chem. Ges. 16* (1883) 1787; *17* (1884) 54.
[63] A. Baeyer, *Ber. Dtsch. Chem. Ges. 18* (1885) 2269.
[64] E. Hückel, *Z. Phys. 60* (1930) 423; *Z. Elektrochem. 43* (1937) 752.
[65] L. Pauling, *J. Am. Chem. Soc. 53* (1931) 1367.
[66] L. Pauling: *Theoretical Organic Chemistry (Kekulé Symposium, London)*, Butterworths, London 1959, p. 1; see also L. Pauling: *The Nature of the Chemical Bond*, 3rd Ed., Cornell University Press, 1960.
[67] H. Sachse, *Ber. Dtsch. Chem. Ges. 23* (1890) 1363; *Z. Phys. Chem. 10* (1892) 203.
[68] E. Mohr, *J. Prakt. Chem. [2] 98* (1918) 315.
[69] R. Willstätter, "Adolf von Baeyer" in G. Bugge (Ed.): *Das Buch der grossen Chemiker, Vol. 2*, 6th reprint of the 1st edition of 1929, Verlag Chemie, Weinheim 1984, p. 329.
[70] *A. von Baeyer, Vorfeier des 70. Geburtstages am Oktober 2, 1905*, Dr. Wildsche Buchdruckerei, München 1905.

The Concept of Strain in Organic Chemistry

By Kenneth B. Wiberg*

"Die Ringschließung ist offenbar diejenige Erscheinung, welche am meisten über die räumliche Anordnung der Atome Auskunft geben kann. Wenn eine Kette von 5 und 6 Gliedern sich leicht, eine von weniger oder mehr Gliedern sich schwierig oder auch gar nicht schließen läßt, so müssen dafür offenbar räumliche Gründe vorhanden sein. ... Die vier Valenzen des Kohlenstoffatoms wirken in den Richtungen, welche den Mittelpunkt der Kugel mit den Tetraederecken verbinden, und welche miteinander einen Winkel von 109°28′ machen. Die Richtung der Anziehung kann eine Ablenkung erfahren, die jedoch eine mit der Größe der Letzteren wachsende Spannung zur Folge hat." [**] This is the quintessence of the "ring-strain theory" formulated by *Adolf von Baeyer* over one hundred years ago. Although it is today only one facet of the many aspects of strain theory, it has repeatedly stimulated experimental and theoretical chemists. Among the most spectacular of the recent successes in synthetic chemistry are the syntheses of tetra-*tert*-butyltetrahedrane and [1.1.1]propellane. The reasons for the great stability of these two highly strained compounds are completely different. The experimental findings as well as the results of theoretical analysis by means of molecular mechanics and ab initio calculations have contributed decisively to our present state of knowledge of the structure, energy, and reactivity of organic compounds.

1. Introduction

The second half of the nineteenth century was a period of rapid development for the structural theory of organic chemistry. The Karlsruhe conference of 1860 finally established the atomic weights of hydrogen, oxygen, and nitrogen, and led to the general acceptance of the molecular formula of water as H_2O and not HO or H_2O_2. In 1858, *Kekulé* and *Couper* independently proposed that carbon is tetravalent, and shortly thereafter *Crum Brown* proposed a carbon–carbon double bond for ethylene and *Erlenmeyer* proposed a carbon–carbon triple bond for acetylene. In 1865 *Kekulé* suggested that carbon chains could form rings and in 1874 *van't Hoff* and *LeBel* independently proposed that a four-coordinate carbon has a tetrahedral geometry.

As a result of these developments, the structures of a large number of organic compounds were correctly determined, and it was observed that whereas many compounds had five-or six-membered rings, other ring sizes were rarely found. This led *Adolf von Baeyer* in 1885 to propose his strain theory.[1] He correctly deduced that compounds with three- and four-membered rings would be less stable because of the deviation in bond angles from the normal tetrahedral values. His application of this concept to larger rings proved to be incorrect because it was not recognized at that time that these rings would be nonplanar. Nevertheless, strain is present in the medium rings (C_7–C_{12}), although for a reason different from that originally proposed.

Perkin worked in *von Baeyer*'s laboratory at the time the strain theory was being developed, and in 1884 he reported the first directed syntheses of cyclopropane and cyclobutane derivatives.[2] Many years passed before the strain in these compounds could be experimentally determined, but in 1949 and 1950 the heats of combustion of cyclopropane and cyclobutane, respectively, were determined[3] and allowed the calculation of their heats of formation and strain energies. The strain energy is the difference between the observed heat of formation and that expected for a strain-free molecule with the same number of atoms.

The concept of strain has been expanded from *von Baeyer*'s original idea[4] and is now discussed in terms of bond length and bond angle distortions as well as torsional terms and nonbonded interactions. Strain energies have proven to be very valuable quantities with which to examine organic compounds having unusual geometries or intramolecular interactions. They also provide a convenient way in which to examine a major component of the driving force for some reactions. The heats of formation of compounds with different numbers of atoms are difficult to compare directly, but the strain energy factors out the contribution to the energy derived from the number of bonds and atoms present and gives a value which is more easily compared among compounds.

2. Origin of Strain

Steric strain, which results from nonbonded interactions, is present in most compounds. In methane, as with all

[*] Prof. K. B. Wiberg
Department of Chemistry, Yale University
New Haven, CT 06511 (USA)

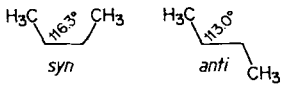
[**] Ring formation is evidently the reaction that can provide the most important information on the spatial arrangement of atoms. Steric reasons should explain the observation that a 5- or 6-membered chain undergoes ready closure, whereas a shorter or longer chain undergoes difficult or no closure.... The four valences of the carbon atom act in the directions that connect the center of a sphere with the corners of a tetrahedron and form angles of 109°28′ with one another. The direction of the attraction can deviate, but this results in increasing strain as the sizes of the latter increase.

compounds, the total energy is made up of contributions from the kinetic (T) and potential (V_1) energies of the electrons, the electron repulsion (V_{12}), and the nuclear repulsion (V_N) [Eq. (a)].

$$V_T = T + V_1 + V_{12} + V_N \qquad (a)$$

The first three of these terms may be considered to be electronic terms, and the equilibrium structure (i.e., that with the lowest value of V_T) will result from a balance between the electronic terms and nuclear repulsion term. For example, a distortion from tetrahedral geometry that maintains one of the C_3 axes leads to a decrease in the electronic energy. This is opposed, however, by a larger increase in V_N.[5] Thus, the tetrahedral geometry of methane results largely from the repulsive interaction between the hydrogen nuclei and is the one that maximizes the distance between hydrogens for a given C–H bond length.

When two of the hydrogens of methane are replaced by methyl groups, forming propane, the C–C–C bond angle is found to be larger than tetrahedral (112°).[6] Clearly, the repulsive interaction between the methyl groups is greater than that between the methylene hydrogens, leading to an increased angle. The repulsion between methyl groups also may be seen in the *syn* and *anti* conformations of *n*-butane:[7] the C–C–C bond angle in the *syn* conformer is considerably larger than that in the more stable *anti* conformer.

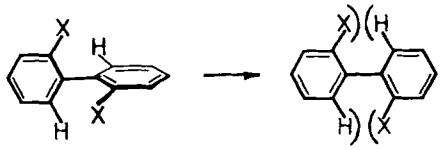


In one of the first quantitative studies of nonbonded interactions, *Brown* et al. examined the equilibrium constants for the reaction of tertiary amines with trimethylboron [Eq. (b)].[8]

$$R_3N: + B(CH_3)_3 \rightleftharpoons R_3\overset{\oplus}{N}-\overset{\ominus}{B}(CH_3)_3 \qquad (b)$$

As the size of the alkyl groups attached to nitrogen increased, the equilibrium constant decreased. This was attributed in part to the repulsive interaction between the alkyl groups, which increased as the pyramidal amine was converted into the ammonium salt with smaller C–N–C bond angles, and was termed B (back) strain. The same effect is seen in the increased rate of solvolysis of tertiary alkyl halides having bulky alkyl substituents[9] and in addition to carbonyl groups.[10] The latter reaction is probably the most widely studied example of this general effect, in which the conversion of a trigonal into a tetrahedral center is retarded (or the reverse reaction accelerated) by the increased repulsion of alkyl groups in the sterically more crowded tetrahedral species. The free energy changes for such processes are frequently well correlated by *Taft*'s E_s values, which were derived from the rates of acid-catalyzed hydrolysis of esters, a reaction that exhibits little sensitivity to polar effects.[11]

The problem of quantitatively accounting for steric strain led *Westheimer* and *Mayer*[12] to perform the first calculation of the type that is now referred to as molecular mechanics. They calculated the activation energies for the racemization of *ortho*-substituted, optically active biphenyls. The racemization requires that the molecules pass through a planar activated complex in which the *ortho*-substituents must come close to the *ortho*-hydrogen (or other substituents) on the other ring. By using reasonable



values for the nonbonded interactions, along with force constants derived from IR spectroscopy, they were able to reproduce the observed activation energy. Molecular mechanics has been developed considerably since that time, particularly as a result of the availability of fast computers, and has been applied to a variety of conformational problems and to the dynamics of conformational change.[13] The intramolecular potential functions used in this procedure will be discussed in Section 4.

If we return to propane and consider the hypothetical reaction in which the two methyl groups are brought together with the elimination of hydrogen to form cyclopropane, it can be seen that considerable energy must be expended in the constriction of the C–C–C bond angle, leading to angle strain. Although the cyclopropane bond angle is conventionally given as 60°, this is misleading. It is known that the bending of bond angles results in limited orbital following.[14] Thus, the nuclei move ahead of the overlap or bonding electron density in the bond. As a result, bent bonds are formed. This is easily seen in an electron density diagram for cyclopropane. The total electron densities (Fig. 1a) are not very revealing because they are

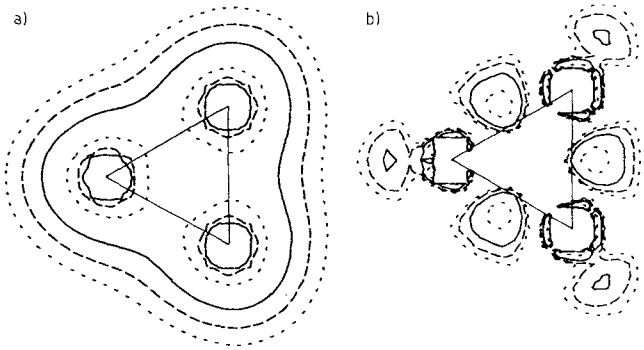


Fig. 1a) Total electron density in the three-carbon plane of cyclopropane. b) Regions of positive deformation density for cyclopropane (i.e., regions of greater electron density than would be expected for three carbon atoms in the same positions).

dominated by the density near the nuclei. However, if we subtract the electron density that would be expected for three carbon atoms at the same locations, we obtain the more interesting difference density map shown in Figure

1b. Here, it can be seen that the extra electron density in the bonding regions (deformation density) lies outside of lines drawn between the carbon nuclei. The bonds are indeed bent! It is possible to define a bond path between two carbon atoms that is the path of maximum electron density between the nuclei.[15] It is colinear with the nominal C-C bond for acyclic or unstrained compounds, but is markedly curved in the case of cyclopropane or cyclobutane. The angle between the C-C bond paths is 78° compared to the conventional 60° bond angle. Bonds of this type are weaker than normal C-C bonds; whereas the bond dissociation energy for ordinary C-C bonds is on the order of 84 kcal/mol,[16] the bond dissociation energy in cyclopropane appears to be 65 kcal/mol.[17]

As noted above, bond angle deformation is not the only source of strain. Torsional interactions also are of importance. In planar cyclobutane, the methylene groups would be eclipsed, which is a relatively high energy arrangement. Puckering will improve the torsional angles and lead to a decrease in torsional strain, but at the same time, the C-C-C bond angles are reduced leading to an increase in angle strain.[18] The two effects find a balance when the ring is puckered about 35° out of planarity, leading to torsional angles of 24° and bond angles of 88°.[19]

The two most important components of the total strain energy are usually bond angle distortion and nonbonded repulsion. The latter is commonly referred to as a steric effect. An examination of these components of the strain energy will be presented in Section 4.

3. Strain Energies

The strain energy of a molecule is derived from its heat of formation from the elements (ΔH_f) by comparison with a hypothetical "strainless" model. Any model of this type will have some arbitrary features. For example, we might take cyclohexane to be a strain-free model. Its heat of formation is −29.5 kcal/mol,[3] which is equivalent to −4.92 kcal/mol per methylene group. Cyclopropane, with three methylene groups, would then be expected to have $\Delta H_f = -14.75$ kcal/mol. The observed ΔH_f is +12.73 kcal/mol.[3] The difference between these values, 27.5 kcal/mol, is the strain energy. Similarly, cyclobutane would be expected to have $\Delta H_f = 4 \times -4.92 = -19.7$ kcal/mol, which when compared with the observed value, +6.8 kcal/mol, gives a strain energy of 26.5 kcal/mol.

If one wished to be precise, one would recognize that cyclohexane is not entirely strain free. The C-C-C-C torsional angles are 59°, corresponding to the *gauche* conformation of *n*-butane, which is less stable than the *anti* conformer by about 0.9 kcal/mol.[10] The observation that the normal methylene increment for a straight-chain hydrocarbon, −4.926 kcal/mol,[21] is very close to the methylene value for cyclohexane simply reflects the fact that relatively few molecules of a linear hydrocarbon are in the *anti* conformation. The *gauche* conformations, although energetically disfavored, predominate because, whereas there is only one *anti* conformer, there are many possible *gauche* conformers. It can be seen that the methylene increment for an alkane which is completely in the *anti* conformation will be somewhat more negative than −4.926 kcal/mol.

This is, however, of little consequence. Strain energies are used in a comparative fashion, and thus any reasonable and consistent definition will be satisfactory. The simplest approach is to use *Franklin*'s group equivalents[21] (Table 1) in determining the energy of the strain-free model.

Table 1. *Franklin*'s group equivalents for the calculation of the energies of model compounds.

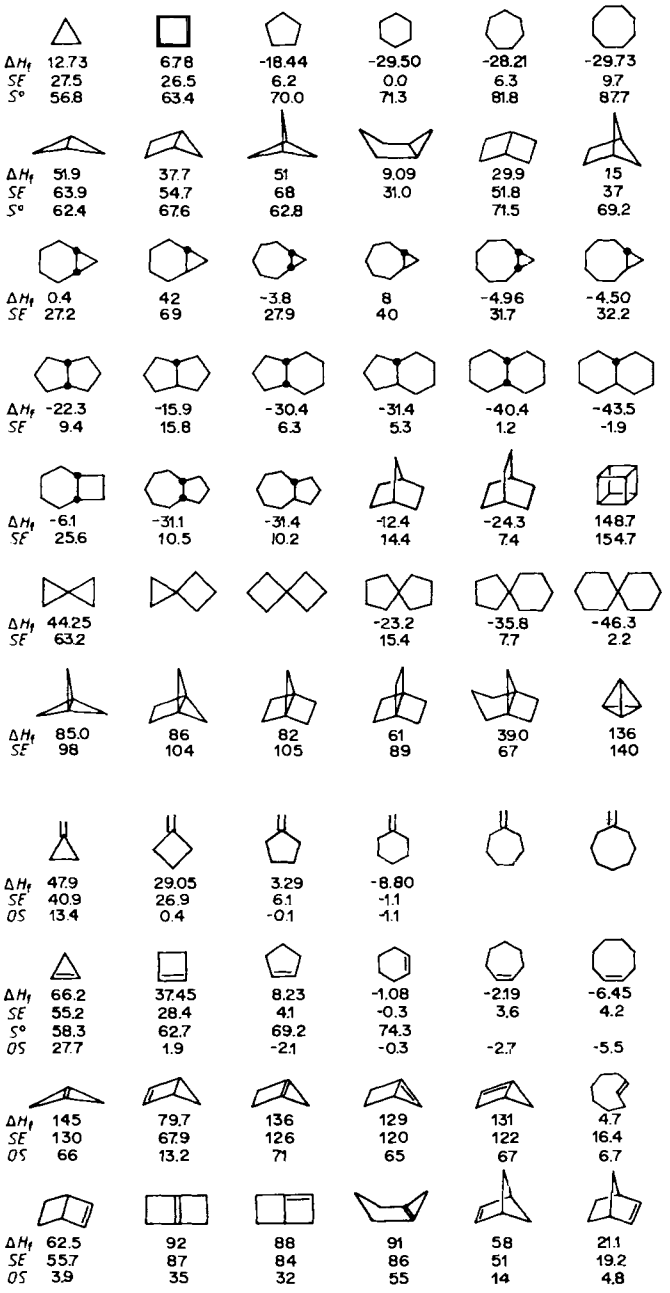
Group	Equivalent [kcal/mol]	Group	Equivalent [kcal/mol]
CH_3	−10.12	$\diagdown CH{=}CH_2$	+15.00
CH_2	− 4.926	$\diagdown CH{=}CH\diagup$	+18.88
CH	− 1.09	$\diagup CH{=}CH\diagup$	+20.19
C	+ 0.80	$\gtrdot C{=}CH\diagup$	+20.19
		$\gtrdot C{=}C\lessdot$	+24.57

Table 2 gives the heats of formation[3] and strain energies for a variety of cyclic hydrocarbons. In the cases in which the experimental error was ≤0.3 kcal/mol, ΔH_f is given to the nearest 0.01 kcal/mol, and where it was >0.3 kcal/mol it is given to the nearest 0.1 kcal/mol. The values are not available for many interesting cyclic hydrocarbons. It is unfortunate that only a few laboratories are presently determining the heats of combustion from which the heats of formation are derived. Moreover, even if such measurements were more frequently carried out, it would be of little use for compounds that can only be obtained in small amount or can only be observed under unusual conditions such as matrix isolation. In these cases, theoretical calculations frequently provide very useful information. It has been shown that the total energies obtained by ab initio molecular orbital calculations with the 6-31G* basis set may be converted into ΔH_f values with an average error of only ±1 kcal/mol using a set of group equivalents.[22] When these values are included in the table, they are given to the nearest 1 kcal/mol.

The interplay of the various components of the strain energy is nicely illustrated by the homologous series of cycloalkanes. Cyclohexane is generally taken as "strain free" (although it does have six *gauche* C-C-C-C torsional angles). In the case of cyclopentane, the planar conformation would have a low strain energy if angle strain were the only important component. However, the planar conformer has five eclipsed methylene groups. If each contributed a torsional strain of 3 kcal/mol (as in ethane), cyclopentane would have an additional 15 kcal/mol of strain. In order to minimize the torsional strain, cyclopentane assumes puckered conformations (C_s and C_2), which are rapidly interconverted by pseudorotation.[23]

Cyclobutane cannot avoid considerable angle strain since even the planar conformer has formal bond angles of 90°. Besides the angle strain, there is also the torsional strain arising from four eclipsed methylene groups. In order to minimize the total strain, cyclobutane adopts a puckered conformation. This results in a small increase in angle strain (88°), but a considerable reduction in torsional

Table 2. Experimentally determined heats of formation (ΔH_f), calculated strain energies (SE), and entropies ($S°$) of cycloalkanes, methylenecycloalkanes, and cycloalkenes [a]. For methylenecycloalkanes and cycloalkenes, an olefinic strain (OS) is also given.



[a] The data were taken from [3], [22], [55], and W. R. Roth, F.-G. Klärner, H.-W. Lennartz, *Chem. Ber. 113* (1980) 1818.

strain (C-C-C-C=24°). The puckered conformer is 1.5 kcal/mol lower in energy than the planar conformer.[19]

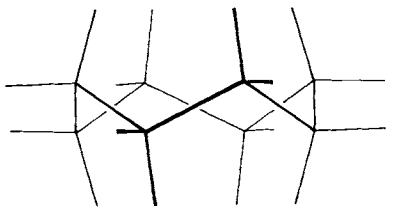
The angle strain in cyclopropane is considerably larger than that in cyclobutane. It may therefore appear strange that cyclopropane has essentially the same strain energy as cyclobutane, especially since the torsional strain cannot be relieved in any way. However, cyclopropane has two sources of stabilization. In all cycloalkanes larger then cyclobutane there are as many 1,3-repulsive interactions as there are bond angles; both terms are lumped together in the bond angle distortion energy. In cyclobutane, the number of 1,3-interactions is reduced to one-half the number of angles, and in cyclopropane, there are no 1,3-nonbonded interactions (Scheme 1). Thus, one source of destabilization is not present in cyclopropane.

Scheme 1.



Furthermore C-H bonds in cyclopropane have larger bond dissociation energies than those of other cycloalkanes.[24] The experimental value for cyclopropane is 106 kcal/mol. The normal value for a methylene C-H bond is 98 kcal/mol,[25] and it is unlikely that the value for cyclobutane is greater than 100 kcal/mol.The bond dissociation energy for a cyclopropane C-H bond is therefore 8 kcal/mol greater than that for open-chain methylene groups. A part of this difference is probably due to the difficulty of introducing a trigonal center into a three-membered ring,[36] but some is almost surely due to a stronger and shorter bond.[27] If the latter contribution were only 2 kcal/mol, it would lead to a total stabilization of 12 kcal/mol for the six bonds! The corrected strain would then be about 40 kcal/mol. This estimate should not be taken too seriously, especially since bond energies and bond dissociation energies are not directly related. However, it is clear that cyclopropane compensates for its weaker C-C bonds by increasing the strength of its C-H bonds, leading to a smaller strain energy than might otherwise be expected.

A contrary situation is found with the larger rings. With cyclooctane, for example, one can readily find a conformation that has good C-C-C bond angles and torsional angles, namely, the crown conformation. However, another problem arises—some hydrogens point in toward the center of the ring, resulting in very short nonbonded distances and a larger nonbonded strain term. Cyclooctane is thus forced to adopt a conformation (Scheme 2) that is a compromise between the angle, torsional, and nonbonded terms.[23]



Scheme 2.

Many of the larger cycloalkanes could adopt an ideal diamond-lattice arrangement for the carbons, but again, such conformations would have strong H-H nonbonded interactions.[29]

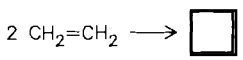
The strain energy of many bicyclic compounds is close to the sum of the strain of the monocyclic components. Thus, bicyclo[2.1.0]pentane and bicyclo[2.2.0]hexane have essentially the same strain energy, which is twice the strain in cyclopropane or cyclobutane. This is presumably the re-

sult of compensating increases in angle strain and a decrease in torsional strain since one bond is common to both rings. The interesting cases are those in which the strain energy is greater than this estimate. For example, the strain energy of bicyclobutane is 9 kcal/mol greater than expected. A similar and generally larger strain increase is found with the small-ring propellanes. These are cases in which there is an unusual degree of angular deformation at the bridgehead positions. The [1.1.1]- through [2.2.1]propellanes are forced to have "inverted" tetrahedral geometries at the bridgehead positions.[30] It is interesting to note that bicyclobutane also assumes this geometry although it is not required by structural constraint,[31] and that the strain energy of bicyclobutane is the average of those of cyclopropane and [1.1.1]propellane.

The spiro compounds also have increased strain energies. Spiropentane has 8 kcal/mol of extra strain. The central carbon, having four identical C-C bonds, is required to be sp^3 hybridized and therefore introduces considerable extra destabilization. The other cases with considerable extra strain are those having relatively small *trans*-fused rings. *trans*-Bicyclo[4.1.0]heptane is calculated to have 41 kcal/mol of extra strain[32] and readily undergoes *trans-cis* isomerization.[33] The extra strain decreases to 6 kcal/mol with *trans*-bicyclo[5.1.0]octane, and with bicyclo[6.1.0]nonane, the strain energies of the *cis* and *trans* isomers are smaller and essentially the same.[32]

It is interesting that the strain energy of cubane is just 6 times that of cyclobutane. However, the strain energy of tetrahedrane is 30 kcal/mol greater than 4 times the strain of cyclopropane. This would be expected since the strain in bicyclobutane is more than 2 times the strain in cyclopropane. The heat of dissociation of tetrahedrane to two acetylenes is calculated to be −40 kcal/mol, which is in good accord with the experimental studies.[34]

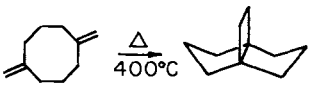
The carbon-carbon double bond is one of the more important of the functional groups in chemistry. The double bond in ethylene is commonly taken as strain free. Here, an examination of the thermochemistry of the dimerization of ethylene to cyclobutane is instructive.



$\Delta H_r = -18.2$ kcal/mol (25 °C)
$\Delta S_r = -41.5$ cal · K^{-1} · mol^{-1}
$\Delta G_r = -5.8$ kcal/mol
$K = 1.8 \times 10^4$

The reaction is quite exothermic at room temperature, despite the strain energy of cyclobutane; the results would require that ethylene be destabilized by about 22 kcal/mol. This is in good accord with the observation that whereas the dissociation energy of a carbon-carbon single bond is about 84 kcal/mol,[16] the energy of its π-bond (as determined from the barrier to rotation in *cis*-dideuterioethylene) is only 64 kcal/mol.[35]

Why isn't the dimerization of ethylene a practical synthesis for cyclobutane? The thermal interconversion requires a relatively high temperature, and the strongly negative entropy change leads, therefore, to a positive ΔG_r and an unfavorable equilibrium constant. If the entropy factor can be minimized, as when the two double bonds are in the same molecule, the thermal dimerization is successful; an example is the synthesis of [3.3.2]propellane from 1,5-dimethylenecyclooctane.[36]

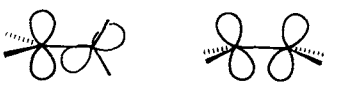


In the case of ethylene, a catalyst that would allow the equilibrium to be set up at a lower temperature is required. If it could be found, cyclobutane would become one of the most common organic compounds. Despite these considerations, for convenience in the following discussion we will adopt the conventional view that ethylene is strain free.

The introduction of a trigonal center may lead to either an increase or a decrease in strain. Here, it is useful to define the *olefinic strain* (*OS*) as the difference in strain energy between the alkene and its corresponding alkane (cf. Table 1).[37] In the case of cyclopropane, one trigonal center leads to a 13 kcal/mol increase in strain, and two trigonal centers increase the strain by 28 kcal/mol.[26] The normal bond angle at a trigonal center is ca. 120°, and a decrease to 60° would lead to a much larger increase in strain than found with cyclopropane. The larger C-C-C angle in cyclobutane should lead to a smaller increase in strain energy; indeed, it is 1 and 3 kcal/mol for one and two trigonal centers, respectively.

Cyclopentane provides a much different case. Here, the main problem is the torsional interaction. Removal of two hydrogens to form a double bond relieves part of the torsional interaction and results in a decrease in strain. Thus, whereas cyclopentane has a strain energy of 6.2 kcal/mol, in cyclopentene it is decreased to 4.1 kcal/mol.

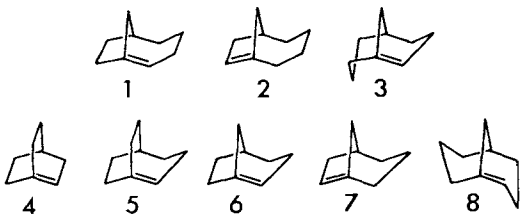
In the above examples, there is no important deformation of the π-electron system, and the strain is largely associated with the σ-bonds. There is, however, another large group of alkenes in which distortion of the π-system is responsible for much of the strain. The π-system may be deformed in two quite different fashions—twisting and bending (or pyramidalization) (Scheme 3).[38] The twisting distortion is found in small *trans*-fused alkenes such as *trans*-cyclooctene,[39] in the bridgehead alkenes that violate Bredt's rule,[40] and in alkenes with bulky substituents.



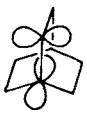
Scheme 3.

The *trans*-cycloalkenes have received considerable study.[41] For cyclopentene, cyclohexene, and cycloheptene, the *trans* isomers are too reactive to be isolated, but may be obtained and used as reactive intermediates.[42] The difference in energy between *cis*- and *trans*-cyclooctene has been determined from their heats of hydrogenation;[43] the *trans* compound is 11 kcal/mol less stable than the *cis*. With larger rings, the difference in energy decreases, and for cycloundecene, the *trans* isomer is more stable.[44] The twisting distortion is well seen in the structure of *trans*-cyclooctene as determined by electron diffraction.[39] The π-system is twisted out of planarity by 44°.

The bicyclic alkenes with bridgehead double bonds are a very interesting group, and many of these compounds have been prepared.[45] Examples include compounds **1**–**8**.

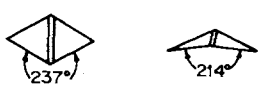


Compounds **1**–**3**, which have the *trans* double bond in an eight-membered ring, can be isolated,[46] but compounds **4**–**8**, with the *trans* double bond in a smaller ring, can only be utilized as reactive intermediates.[45,47] The problem with these compounds is easily seen by examining bicyclo[2.2.2]oct-1-ene **4**. The p-orbital at C-2 should be approximately orthogonal to the p-orbital at the bridgehead. In order to achieve any degree of π-bonding, the σ-system must be strongly twisted, and even then, the π-bond will be weak. It has been estimated that bridgehead alkenes with olefinic strain greater than about 21 kcal/mol will not be observable at room temperature.[37]



Steric interactions also may lead to twisted double bonds. Even in *cis*-2-butene, the repulsion between the alkyl groups can be seen in the C-C-C angle of 127°.[48] With *cis*-1,2-di-*tert*-butylethylene, the angle is increased to about 135° leading to a strain energy of 11 kcal/mol.[49] The introduction of a third *tert*-butyl group will oppose the increase in bond angle and would lead to greatly increased strain for a planar conformation. The strain could be partially relieved by twisting the double bond; the calculated torsional angle is 16°.[50] The synthesis of tetra-*tert*-butylethylene has not as yet been accomplished.[51]

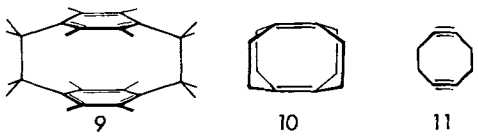
There also are many examples of bent (pyramidalized) alkenes. One of the more remarkable cases is bicyclo[1.1.0]but-1(3)-ene.[52] Theoretical calculations led to the prediction that it should be bent. An orbital analysis has been presented to explain this result, but the bent structure also may be viewed as an attempt to minimize σ-strain. In the planar form, one of the C-C-C bond angles at the bridgehead would be 237°; this can be reduced to a more reasonable 214° by bending.

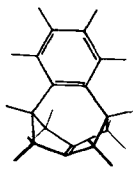


Bicyclo[2.1.0]pent-1(4)ene also is calculated to be nonplanar with a large barrier to inversion. Despite their high strain energies and unusual structures, derivatives of both of these alkenes have been formed as reaction intermediates.[53] It has not as yet proven possible to examine them via matrix isolation.

Bending of double bonds is found in less extreme cases. Norbornene is calculated to be bent out of plane by 5°,[54] and this has been explained as resulting from torsional interactions with the bridgehead position.[55] The bending distortion has been suggested as an explanation for the unusually high reactivity of norbornene in cycloaddition reactions.[56]

There are a number of compounds in which bending is forced by structural constraints. Some of the best known examples are found with the cyclophanes.[57] [2.2]Paracyclophane **9** would have an impossibly small distance between the benzene rings if they were planar. A bending distortion relieves part of the strain. Similar examples are tricyclo[4.2.2.2^{2,5}]dodeca-1,5-diene **10**[58,59] and 1,5-cyclooctadiyne **11**.[60] The distance between the double bonds in **10** could be increased to 2.4 Å by bending, and even this distance is a full 1 Å smaller than the normal shortest contact between π-systems. Another type of bending at a double bond is found with the bridged alkene **12**.[61] Unfortunately, relatively little is known about the energies of these bent alkenes.





The above examples represent only a small selection of the large number of compounds that show the effect of strain. Carbocyclic compounds have been selected because almost no information is presently available concerning the strain energies of heteroatom-containing systems.[62]

4. Quantitative Analysis of Strain

The contributions to the total strain in a molecule are summarized below:

(1) Bond length distortion
(2) Bond angle distortion
(3) Torsional strain
(4) Nonbonded interactions
(5) Energy changes due to rehybridization

The bond length distortions are usually relatively unimportant. The energy change for stretching or compressing a bond is given by Equation (c).

$$V = k_r(\Delta r)^2 \qquad \text{(c)}$$

k_r is the stretching force constant and Δr is the change in length from a "normal" value. The constant k_r for C–H and C–C bonds, as determined by IR spectroscopy, is on the order of 5 mdyn/Å or 360 kcal · mol^{-1} · Å^{-2}. Thus, a change in bond length causes a large change in energy, and changes in other geometrical parameters are generally to be preferred to bond stretching. There are, however, some notable exceptions.[63]

The distortion of bond angles leads to much smaller increases in energy. In this case, the energy change is given by Equation (d).

$$V = k_\theta(\Delta\theta)^2 \qquad \text{(d)}$$

k_θ is the force constant and $\Delta\theta$ the change from the "normal" bond angle. Analysis of IR data shows that the C–C–C force constant for cyclohexane and similar compounds is 0.8 mdyn/Å or 0.0175 kcal · mol^{-1} · degree^{-2}. Thus, an angle can be distorted by a few degrees without much increase in energy. The force constants are appropriate for small changes in angle and might reasonably be used for angles between 105 and 115° (i.e, tetrahedral ±5°). A change to 90° as in cyclobutane or 60° as in cyclopropane will result in a change in hybridization and a change in force constant. These compounds must be treated as special cases.[64]

The torsional strain for C–C–C–C angles is reasonably well understood. The potential function may be written as a sum of onefold, twofold, and threefold terms [Eq. (3)].

$$V = \frac{V_1^\circ}{2}(1+\cos\tau) + \frac{V_2^\circ}{2}(1+\cos 2\tau) + \frac{V_3^\circ}{2}(1+\cos 3\tau) \qquad \text{(e)}$$

τ is the torsional angle, and V_1°, V_2°, and V_3° are the potential terms for the onefold, twofold, and threefold barriers, respectively. The experimental data for *n*-butane may be used to obtain these terms for alkanes.[65]

Barriers to rotation for single bonds adjacent to double bonds are somewhat different. Here, alkyl groups are known to prefer to eclipse C=O groups.[66] A similar tendency is found for bonds adjacent to carbon–carbon double bonds,[67] but it is not as pronounced. Again, the total energy may be represented by one-, two-, and threefold terms.[68]

It is possible to obtain direct experimental data for each of the above intramolecular potentials, and they are therefore reasonably well understood. The other main term that dictates energies and conformations is the nonbonded interaction. However, it is much more difficult to establish the magnitude of this interaction. It is generally believed that the nonbonded interaction is well approximated by the Buckingham potential [Eq. (f)], which is shown in Figure 2.[69]

$$V = Ae^{-Br} - C/r^6 \qquad \text{(f)}$$

r is the distance between the nonbonded atoms, and A, B and C are constants that depend on the atoms involved in the interaction. In terms of the minimum in the energy curve (r_0) and the depth of the well (ε_0) and assuming a twelfth power repulsion curve, the constants may be written as follows:

$A = \varepsilon_0 e^{12}$
$B = 12/r_0$
$C = 2\varepsilon_0 r_0^6$

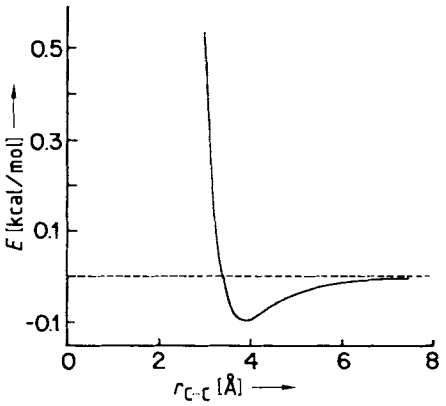


Fig. 2. Interaction energy as a function of distance for two nonbonded carbon atoms.

One way in which to obtain these constants is via an analysis of the intermolecular interactions in crystals, along with the heats of sublimation.[70] In the case of hydrocarbons, the nonbonded interactions are the only important terms. The sum of all the interactions between one molecule and all of its neighbors will be twice the heat of sublimation, and if the terms are chosen correctly, the observed intramolecular spacing between molecules will correspond to the calculated minimum energy arrangement. Constants that give good fits to the experimental data have been obtained.[70]

It is more difficult to obtain parameters for other atoms because here another term becomes significant. When an atom other than hydrogen is bonded to carbon, a bond dipole is created. These bond dipoles interact via a coulombic term, and must also be included in calculating the intermolecular interaction energy. In some cases, the bond dipoles may be estimated from the total dipole moment, and in other cases they may be estimated using the results of theoretical calculations.[71]

Once one has the necessary values for the potential functions, one may start with a guess as to the structure, and calculate the bond lengths, bond angles, torsional angles, and nonbonded distances. The application of the above functions will yield a total steric energy. The structure may then be adjusted in a systematic fashion until a minimum, corresponding to the most stable conformation, is reached. This procedure is commonly known as *molecular mechanics* and generally gives quite good results for compounds that are similar to those used in determining the parameters.[13]

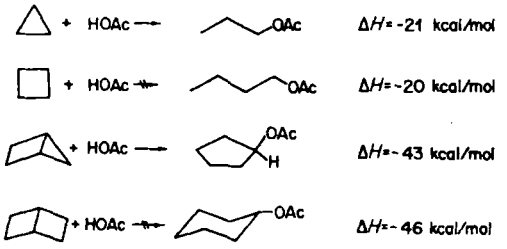
As a semi-empirical method, molecular mechanics is limited in the types of compounds for which it is applicable. Adequate experimental data are required in order to fix the parameters used, and such data are largely limited to hydrocarbons and their simple derivatives. Ab initio molecular orbital theory is much more general in its applicability and does not depend on any experimental data.[72]

Geometry optimization is now routinely carried out for many types of compounds, making use of the analytical procedure for calculating the rate of change in the energy with changes in coordinates.[73] The total energies that are calculated may be converted into heats of formation with reasonable accuracy,[22] and the structures that are calculated are, with few exceptions, in very good agreement with the experimental structures.[72] These calculations require large amounts of computer time and become impractical for molecules with more than about 10–12 atoms other than hydrogens. It seems likely that the results of ab initio calculations will prove useful in improving the parameters for molecular mechanics calculations, and a synergetic relationship will allow the study of a wider range of compounds with useful accuracy (±1 kcal/mol, ±0.01 Å, and ±1°).[74]

5. Chemical Consequences of Strain

One might reasonably expect that increased strain would lead to increased reactivity. This is, however, not always the case. Factors that must be considered include the location of the activated complex along the reaction coordinate and the strain energies of the compounds that are formed as products or reaction intermediates. If the activated complex resembles the reactants, little of the strain energy would be released in the rate-determining step, and there would be little rate acceleration. Similarly, if the products or intermediates have large strain energies, there would be little driving force to help accelerate the reaction.

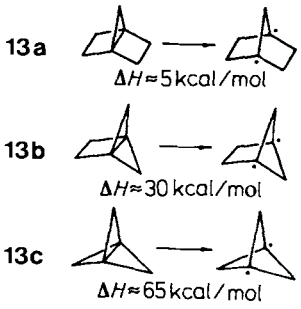
The first case is illustrated by the electrophilic reactions of cyclopropanes and cyclobutanes. Here, the strain energy relief is essentially the same, but whereas the cyclopropanes are quite reactive, the cyclobutanes are essentially inert (Scheme 4).[75]



Scheme 4.

A study of the kinetics of the acetolysis of cyclopropanes found a kinetic solvent hydrogen isotope effect wherein the reaction with CH_3COOH was significantly faster than that with CH_3COOD. This shows that proton transfer is the rate-determining step, leading to the formation of a protonated cyclopropane. Since there is little change in geometry in the rate-determining step, there is essentially no driving force from strain relief. The difference in reactivity between cyclopropanes and cyclobutanes results from the difference in their basicities, which, in turn, is related to the different bonding in these two hydrocarbons.

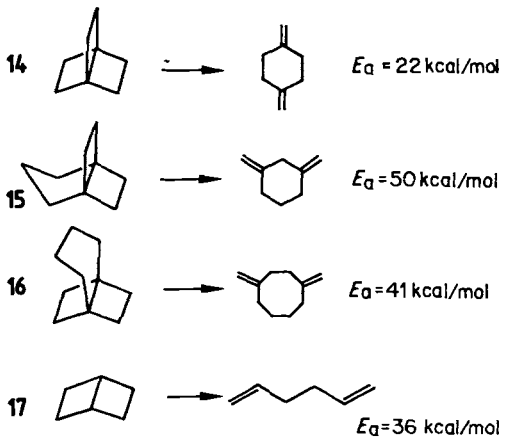
The second case is well illustrated by [1.1.1]propellane.[76] The strain energies of [1.1.1]-, [2.1.1]-, and [2.2.1]propellane are essentially the same and, therefore, these compounds might be expected to have similar reactivities. However, whereas [1.1.1]propellane is thermally stable to ca. 100 °C, the other propellanes polymerize at 50 °K![30] The reason for the difference in reactivity is easily seen by considering the energy required to "dissociate" the central bonds (Scheme 5).



Scheme 5.

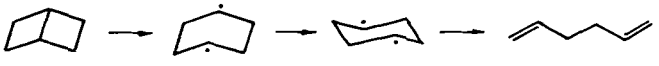
The differences in energy are mainly a result of the differences in strain between the bicycloalkanes from which the diradicals are derived. Bicyclo[1.1.1]pentane has two small rings, which, along with extra distortion, lead to a large strain energy, whereas norbornane with no small rings has a relatively low strain energy.

There are, of course, many reactions in which the strain energy of the reactant is important. One particularly interesting example is the thermolysis of [2.2.2]propellane **14**.[77] Here, a formally orbital-symmetry-forbidden reaction occurs at room temperature and may be contrasted with related compounds (Scheme 6).[73] Starting with bicyclo[2.2.0]hexane **17**, 1,4-bridging first increases the activation energy for ring opening (**15**, **16**), and then, with [2.2.2]propellane **14**, decreases it markedly.



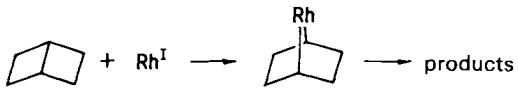
Scheme 6.

The increase in activation energy on going from **17** to **15** or **16** is easily understood. The cleavage of **17** involves the following series of steps:[79]



The final cleavage of the chair diyl is orbital symmetry allowed and occurs with the predicted stereochemistry.[80] When a 1,4-bridge is introduced, the conversion of the boat diyl to the chair form is no longer possible, and cleavage must occur via a symmetry-forbidden process which has a larger activation energy. There is no reason to think that **14** should react via a mechanism different from that for **16**. The decrease in activation energy may be accounted for by the difference in strain energy between **14** and **16** (estimated to be 34 kcal/mol). This large increase in strain in the reactant leads to a marked decrease in activation energy since there is little strain in either diyl.

Another case in which strain relief is important is in the transition-metal-induced cleavage of cyclopropanes and cyclobutanes. In contrast to the reaction with electrophiles, in which the former are reactive and the latter are almost inert, both types of compounds will react with reagents such as $[\{Rh(CO)_2Cl\}_2]$.[81] This shows that whereas the activated complex is found early along the reaction coordinate in electrophilic cleavage, it is found well along toward products in the reaction with the rhodium reagent. In the latter case, oxidative insertion occurs, leading to considerable relief of strain.

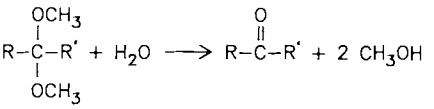


Substituents that cause steric strain may also cause low reactivity by hindering the attack by an external reagent. Thus, tri-*tert*-butylethylene reacts with bromine only slowly,[82] and tetraneopentylethylene is inert to bromine.[83] The most spectacular examples of stabilization of a compound by large alkyl groups are found with tetra-*tert*-butylcyclobutadiene[84] and tetra-*tert*-butyltetrahedrane.[84] Cyclobutadiene itself dimerizes quickly even at low temperatures,[85] and tetrahedrane, which has not been prepared, appears to cleave easily to acetylene.[34] Both of the tetra-*tert*-butyl compounds are quite stable. The large groups prevent bimolecular reactions and hinder the motions required to convert the tetrahedrane derivative into other more stable compounds.

The above examples are mainly concerned with small-ring compounds in which angle strain—the type first considered by *von Baeyer*—is of particular importance. It must, however, be recognized that strain is a controlling factor in many reactions involving quite ordinary compounds. Probably, the most common reaction of this type is addition to a carbonyl group. If bulky substituents are attached, an addition that converts the trigonal carbonyl carbon into a tetrahedral carbon will decrease the bond angle and bring the groups closer together. The effects on rates of reaction have received much attention and generally are well correlated by *Taft*'s E_s parameters.[11]

Relatively little quantitative information on energy changes has been available. One example is the hydrolysis of acetals, ketals, and ortho esters (Scheme 7).

The heats of these reactions may be measured calorimetrically,[86] and the changes in heats of hydrolysis give direct measures of the changes in steric interactions on going



Scheme 7. R' = H, CH_3, OCH_3

from the tetrahedral reactant to the trigonal product. Whereas rates of reaction (related to free energies of activation) or equilibrium constants (related to free energies of reaction) correlate well with the E_s parameters, the heats of reaction do not. This is specially noticeable in the series methyl, ethyl, *n*-propyl, where changes in rates or equilibrium constants are found, but there is essentially no change in heat of reaction. This indicates that the entropy is the major component of the steric effect for these small groups and may possibly be associated with steric inhibition of solvation.

These open-chain systems are difficult to analyze in detail because of the number of conformations with similar energies. The methyl-substituted norbornyl ketals provide a case in which the hydrocarbon residue is rigid, and the attached methyl groups should cause no conformational problems. An examination of a variety of these ketals showed large changes in heats of reaction, with the hydrolysis of the ketal of camphor being 4 kcal/mol more exothermic than that of norcamphor.[87] Examination of systems of this type should provide much of the information which is needed to gain a quantitative understanding of nonbonded interactions.

6. Conclusion

In the hundred years that have passed since the publication of *von Baeyer*'s theory, strain has been found to be a major factor in determining the structures, energies, and reactivities of organic compounds. A remarkable variety of compounds have been prepared which are significantly destabilized by one or more of the four types of strain. Studies of these compounds have led to improved understanding of chemical bonding, intramolecular interactions, and reaction mechanisms. Quantitative information is still lacking for many of these compounds, but as the capability of theoretical methods continues to improve, such information will become available via computation. The smaller compounds with large degrees of angle strain have proven to be specially useful targets for a synergistic interaction between experiment and theory. The next decade should see a marked improvement in our understanding of the role of strain in organic chemistry.

Received: July 8, 1985 [A 571 IE]
German version: *Angew. Chem. 98* (1986) 312

[1] A. von Baeyer, *Ber. Dtsch. Chem. Ges. 18* (1885) 2278.
[2] W. Perkin, Jr., *Ber. Dtsch. Chem. Ges. 17* (1884) 323.
[3] J. D. Cox, G. Pilcher: *Thermochemistry of Organic and Organometallic Compounds*, Academic Press, London 1970; J. B. Pedley, J. Rylance: *Sussex-N.P.L. Computer Analyzed Thermochemical Data; Organic and Organometallic Compounds*, University of Sussex 1977; D. R. Stull, E. F.

Westrum, Jr., C. G. Sinke: *The Chemical Thermodynamics of Organic Compounds*, Wiley, New York 1969.
[4] For reviews dealing with strain, see: A. Greenberg, J. L. Liebman: *Strained Organic Compounds*, Academic Press, New York 1978; M. D. Newton, *Mod. Theor. Chem. 4* (1977) 223; A. de Meijere, *Angew. Chem. 91* (1979) 867; *Angew. Chem. Int. Ed. Engl. 18* (1979) 809.
[5] K. B. Wiberg, G. B. Ellison, J. J. Wendoloski, *J. Am. Chem. Soc. 98* (1976) 1212.
[6] D. R. Lide, Jr., *J. Chem. Phys. 33* (1960) 4363.
[7] K. B. Wiberg, *J. Am. Chem. Soc.*, in press.
[8] H. C. Brown, R. B. Johannesen, *J. Am. Chem. Soc. 75* (1953) 16.
[9] H. C. Brown, R. S. Fletcher, *J. Am. Chem. Soc. 72* (1950) 1223.
[10] T. H. Lowry, K. S. Richardson: *Mechanism and Theory in Organic Chemistry*, 2nd ed., Harper and Row, New York 1981, chap. 8.
[11] R. W. Taft, Jr. in M. Newman (Ed.): *Steric Effects in Organic Chemistry*, Wiley, New York 1956.
[12] F. H. Westheimer, J. E. Mayer, *J. Chem. Phys. 14* (1946) 733; F. H. Westheimer in M. Newman (Ed.): *Steric Effects in Organic Chemistry*, Wiley, New York 1956.
[13] U. Burkert, N. L. Allinger: *Molecular Mechanics* (*ACS Monograph. 177*) Washington, D.C. 1980.
[14] H. Nakatsaji, *J. Am. Chem. Soc. 96* (1974) 24; H. P. Figeys, D. Berckmans, P. Geerlings, *J. Mol. Struct. 57* (1979) 271; D. M. Chipman, W. E. Palke, B. J. Kirtman, *J. Am. Chem. Soc. 102* (1980) 3377; K. B. Wiberg, J. J. Wendoloski, *J. Comput. Chem. 2* (1981) 53.
[15] R. F. W. Bader, Y. Tal, S. G. Anderson, T. T. Nguyen-Dang, *Isr. J. Chem. 19* (1980) 8.
[16] T. L. Cottrell: *The Strengths of Chemical Bonds*, 2nd ed., Butterworths, London 1958.
[17] B. S. Rabinovitch, E. W. Schlag, K. B. Wiberg, *J. Chem. Phys. 28* (1958) 504; E. W. Schlag, B. S. Rabinovitch, *ibid. 32* (1960) 5996.
[18] K. B. Wiberg, G. M. Lampman, *J. Am. Chem. Soc. 88* (1966) 4429.
[19] A. Almennigen, O. Bastiansen, P. N. Skancke, *Acta Chem. Scand. 15* (1961) 711. For a review of cyclobutane structures, see: F. A. Cotton, B. A. Frenz, *Tetrahedron 30* (1974) 1587; T. B. Malloy, Jr., W. J. Lafferty, *J. Mol. Spectrosc. 54* (1975) 20; R. M. Moriarty, *Top. Stereochem. 8* (1974) 271.
[20] A. L. Verma, U. F. Murphy, H. J. Bernstein, *J. Chem. Phys. 60* (1974) 1540.
[21] J. L. Franklin, *Ind. Eng. Chem. 41* (1949) 1070. Another set of group equivalents for use in calculating strain energies has been proposed by E. M. Engler, J. D. Andose, P. von R. Schleyer, *J. Am. Chem. Soc. 95* (1973) 8005.
[22] K. B. Wiberg, *J. Comput. Chem. 5* (1984) 197.
[23] W. J. Adams, J. J. Geise, L. S. Bartell, *J. Am. Chem. Soc. 92* (1970) 5013.
[24] M. H. Baghal-Vayjouee, S. W. Benson, *J. Am. Chem. Soc. 101* (1979) 2838.
[25] W. Tsang, *J. Am. Chem. Soc. 107* (1985) 2872.
[26] K. B. Wiberg, R. A. Fenoglio, *J. Am. Chem. Soc. 90* (1968) 3395.
[27] The C-H bond in cyclopropane is 0.01 Å shorter than that in propane, and its vibrational frequency is larger than that of the CH_2 group of propane: L. N. Ferguson: *Highlights of Alicyclic Chemistry, Part I*, Franklin Publ. Co., Palisades, NJ, USA 1973, p. 211.
[28] F. A. L. Anet, *Fortschr. Chem. Forsch. 45* (1974) 169.
[29] M. Saunders, *Tetrahedron 23* (1967) 2105.
[30] K. B. Wiberg, *Acc. Chem. Res. 17* (1985) 379.
[31] P. G. Gassman, M. L. Greenlee, D. A. Dixon, S. Richtsmeier, J. Z. Gougoutas, *J. Am. Chem. Soc. 105* (1983) 5865; K. W. Cox, M. D. Harmony, G. Nelson, K. B. Wiberg, *J. Chem. Phys. 50* (1969) 1976. (bridgehead C-H bond 11.5° below the plane formed by C-1, C-2, C-4).
[32] K. B. Wiberg, E. C. Lupton, Jr., D. J. Wasserman, A. de Meijere, S. R. Kass, *J. Am. Chem. Soc. 106* (1984) 1740.
[33] J. V. Paukstelis, J.-L. Kao, *J. Am. Chem. Soc. 94* (1972) 4783; P. Gassman, S. M. Bonser, *ibid. 105* (1983) 667.
[34] P. B. Shevlin, A. P. Wolf, *J. Am. Chem. Soc. 92* (1970) 406, 5291; H. Ona, H. Yamaguchi, S. Masamune, *ibid. 92* (1970) 7495; L. B. Rodewald, H.-K. Lee, *ibid. 95* (1973) 623, 3084.
[35] J. E. Douglas, B. S. Rabinovitch, F. S. Looney, *J. Chem. Phys. 23* (1955) 315.
[36] K. B. Wiberg, J. Caringi, unpublished results.
[37] W. F. Maier, P. von R. Schleyer, *J. Am. Chem. Soc. 103* (1981) 1891. This paper gives the strain energies of many alkenes as calculated via molecular mechanics.
[38] For a review of molecular mechanics as applied to strained alkenes, see O. Ermer: *Aspekte von Kraftfeldrechnungen*, Wolfgang Baur Verlag, Munich 1981.
[39] M. Traetteberg, *Acta Chem. Scand. B29* (1975) 29.
[40] J. Bredt, *Justus Liebigs Ann. Chem. 437* (1924) 1.
[41] J. A. Marshall, *Acc. Chem. Res. 13* (1980) 213.
[42] E. J. Corey, F. A. Carey, R. A. E. Winter, *J. Am. Chem. Soc. 87* (1965) 934; R. Bonneau, J. Joussot-Dubien, L. Salem, A. J. Yarwood, *ibid. 98* (1976) 4329.
[43] D. W. Rogers, H. von Voithenberg, N. L. Allinger, *J. Org. Chem. 43* (1978) 360.
[44] A. C. Cope, P. T. Moore, W. R. Moore, *J. Am. Chem. Soc. 82* (1960) 1744.
[45] For reviews an bridgehead double bonds, see: G. Köbrich, *Angew. Chem. 85* (1973) 494; *Angew. Chem. Int. Ed. Engl. 12* (1973) 464; R. Keese, *ibid. 87* (1975) 568 and *14* (1975) 528; G. L. Buchanan, *Chem. Soc. Rev. 3* (1974) 41; see also [37].
[46] J. R. Wiseman, *J. Am. Chem. Soc. 89* (1967) 5966.
[47] J. A. Marshall, H. Faubl, *J. Am. Chem. Soc. 89* (1967) 5965; J. R. Wiseman, H.-F. Chan, C. J. Ahola, *ibid. 91* (1969) 2812; J. R. Wiseman, J. A. Chong, *ibid. 91* (1969) 7775; *94* (1972) 8627; H. H. Grootveld, C. Blomberg, F. Bickelhaupt, *J. Chem. Soc. Chem. Commun. 1973*, 542.
[48] A. Almenningen, I. M. Anfisen, A. Haaland, *Acta Chem. Scand. 24* (1970) 43.
[49] N. L. Allinger, J. T. Sprague, *J. Am. Chem. Soc. 94* (1972) 5734.
[50] O. Ermer, S. Lifson, *Tetrahedron 30* (1974) 2425.
[51] For recent attempts at preparing tetra-*tert*-butylethylene, see: A. Krebs, W. Born, B. Kaletta, W. U. Nickel, R. Wolfgang, *Tetrahedron Lett. 24* (1983) 4821.
[52] H.-U. Wagner, G. Szeimies, J. Chandrasekhar, P. von R. Schleyer, J. A. Pople, J. S. Binkley, *J. Am. Chem. Soc. 100* (1978) 1210; K. B. Wiberg, G. Bonneville, R. Dempsey, *Isr. J. Chem. 23* (1983) 85.
[53] H.-G. Zoch, G. Szeimies, R. Römer, G. Germain, J.-P. Declercq, *Chem. Ber. 116* (1983) 2285; O. Baumgärtel, J. Harnisch, G. Szeimies, M. Van Meerssche, G. Germain, J.-P. Declercq, *ibid. 116* (1983) 2205.
[54] G. Wipff, K. Morokuma, *Tetrahedron Lett. 21* (1980) 4445; K. B. Wiberg, G. Bonneville, R. Dempsey, *Isr. J. Chem. 23* (1983) 85.
[55] N. G. Rondan, M. N. Paddon-Row, P. Caramella, J. Mareda, P. H. Mueller, K. N. Houk, *J. Am. Chem. Soc. 104* (1982) 4974.
[56] R. Huisgen, P. H. J. Ooms, M. Mingen, N. L. Allinger, *J. Am. Chem. Soc. 102* (1980) 3951.
[57] V. Boekelheide, *Acc. Chem. Res. 13* (1980) 65.
[58] K. B. Wiberg, M. G. Matturro, P. J. Okarma, M. E. Jason, *J. Am. Chem. Soc. 106* (1984) 2194.
[59] For related compounds see: N. M. Weinsheker, F. D. Greene, *J. Am. Chem. Soc. 90* (1968) 506; R. L. Viavattene, F. D. Greene, L. D. Cheung, R. Majeste, L. M. Trefonas, *ibid. 96* (1974) 4342.
[60] E. Kloster-Jensen, J. Wirtz, *Helv. Chim. Acta 58* (1975) 162.
[61] R. Greenhouse, W. T. Borden, K. Hirotsu, J. Clardy, *J. Am. Chem. Soc. 99* (1977) 1664.
[62] See ref. [4] for many examples of strained compounds containing heteroatoms. For a recent example, see J. G. Radziszewski, J. W. Downing, C. Wentrup, P. Kaszynski, M. Jawdosiuk, P. Kovacic, J. Michl, *J. Am. Chem. Soc. 106* (1984) 7996.
[63] D. A. Dougherty, H. B. Schlegel, K. Mislow, *Tetrahedron 34* (1978) 1441; K. B. Wiberg, R. D. Adams, P. J. Okarma, M. G. Matturro, B. Segmuller, *J. Am. Chem. Soc. 106* (1984) 2200; see also [37].
[64] Cyclopropane is commonly taken as having a normal bond angle of 60° and the strain of the ring is added to the final steric energy. Similarly, cyclobutane may be taken as having a normal bond angle of 90°, and the spectroscopically determined C-C-C bending force constant is used. Again, the strain in the ring is added to the final strain energy. Cf. ref. [13] and S. Chang, D. McNally, S. Dhary-Tehrany, M. J. Hickey, R. Boyd, *J. Am. Chem. Soc. 92* (1970) 3109.
[65] L. S. Bartell, *J. Am. Chem. Soc. 99* (1977) 3279; N. L. Allinger, D. Hindman, H. Hönig, *ibid. 99* (1977) 3282.
[66] For a review of conformations of carbonyl compounds, see V. Suter, *J. Am. Chem. Soc. 101* (1979) 6481.
[67] S. Kondo, E. Hirota, Y. Morino, *J. Mol. Spectrosc. 28* (1968) 471; J. R. Durig, D. A. C. Compton, *J. Phys. Chem. 84* (1980) 773.
[68] K. B. Wiberg, E. Martin, *J. Am. Chem. Soc. 107* (1985) 5035.
[69] A. D. Buckingham, B. D. Utting, *Annu. Rev. Phys. Chem. 21* (1970) 287.
[70] D. E. Williams, *J. Chem. Phys. 43* (1965) 4424; D. E. Williams, T. L. Starr, *J. Comput. Chem. 1* (1977) 173.
[71] Electron populations may be calculated by integrating the charge density over regions of space corresponding to the atoms: R. F. W. Bader, S. G. Anderson, A. J. Duke, *J. Am. Chem. Soc. 101* (1979) 1389; K. B. Wiberg, J. J. Wendoloski, *Proc. Natl. Acad. Sci. USA 78* (1981) 6561. Although these populations should not be considered point charges, they give the sense and magnitude of the bond dipole. It may be noted that the C-H bond dipole for most hydrocarbons has the direction $\overset{\delta}{C}\text{-}\overset{\delta}{H}$, which is opposite to that which has commonly been assumed.
[72] J. A. Pople, *Mod. Theor. Chem. 4* (1977) 1.
[73] P. Pulay in B. Deb (Ed.): *The Force Concept in Chemistry*. Van Nostrand, New York 1981.
[74] T. Hirano, E. Osawa, *Croat. Chem. Acta 57* (1984) 1633.
[75] K. B. Wiberg, S. R. Kass, *J. Am. Chem. Soc. 107* (1985) 988.
[76] K. B. Wiberg, F. H. Walker, *J. Am. Chem. Soc. 104* (1982) 5239; K. B. Wiberg, *ibid. 105* (1983) 1227; E. Honegger, H. Huber, E. Heilbronner, W. P. Dailey, K. B. Wiberg, *ibid. 107* (1985) 7172; K. B. Wiberg, W. P.

Dailey, F. H. Walker, S. T. Waddell, L. S. Crocker, M. Newton, *ibid. 107* (1985) 7247.
[77] P. E. Eaton, G. E. Temme III, *J. Am. Chem. Soc. 95* (1973) 7508.
[78] K. B. Wiberg, M. Matturro, *Tetrahedron Lett. 22* (1981) 3481.
[79] M. J. Goldstein, M. S. Benzon, *J. Am. Chem. Soc. 94* (1972) 5119.
[80] L. A. Paquette, J. A. Schwartz, *J. Am. Chem. Soc. 92* (1970) 3215; A. Sinnema, F. van Rantwijk, A. J. De Konig, A. M. van Wijk, H. van Bekkem, *Tetrahedron 32* (1973) 364; R. Wehrli, D. Bellus, H.-J. Hansen, H. Schmid, *Chimia 30* (1979) 416.
[81] M. Sohn, J. Blum, J. Halpern, *J. Am. Chem. Soc. 101* (1979) 2694.
[82] G. J. Abruscato, T. T. Tidwell, *J. Am. Chem. Soc. 92* (1970) 4125; *J. Org. Chem. 37* (1972) 4151.
[83] G. A. Olah, G. K. S. Prakash, *J. Org. Chem. 42* (1977) 580.
[84] G. Maier, S. Pfriem, U. Schäfer, R. Matusch, *Angew. Chem. 90* (1978) 552; *Angew. Chem. Int. Ed. Engl. 17* (1978) 520.
[85] C. Y. Lin, A. Krantz, *J. Chem. Soc. Chem. Commun. 1972,* 111; O. L. Chapman, C. L. McIntosh, J. Pacansky, *J. Am. Chem. Soc. 95* (1973) 614.
[86] K. B. Wiberg, R. R. Squires, *J. Am. Chem. Soc. 101* (1979) 5512; *ibid. 103* (1981) 4473; K. B. Wiberg, E. J. Martin, R. R. Squires, *J. Org. Chem.* 50 (1985) 4717.
[87] K. B. Wiberg, W. Cunningham, unpublished results.

Ordering of Ionic Solutes in Dilute Solutions through Attraction of Similarly Charged Solutes— A Change of Paradigm in Colloid and Polymer Chemistry**

By Norio Ise*

Dedicated to Professor Georg Manecke on the occasion of his 70th birthday

EXAFS measurements indicate the presence of a quasi lattice-like ordering of simple ions in dilute solutions. Small-angle X-ray scattering (SAXS) measurements on dilute aqueous solutions of synthetic macroions, polynucleotides, and proteins show a single broad peak; a binary mixture of synthetic macroions of different molecular weight gives a new scattering curve that is entirely different from the composite curve of the constituents before mixing. This would indicate that the macroions are distributed in a fairly regular way in the solution. The intermacroion spacing ($2D_{exp}$) obtained by the Bragg equation is found to be smaller than the average spacing ($2D_0$) calculated from the polymer concentration. Furthermore, the $2D_{exp}$ value decreases with increasing number of charges per macroion. This finding is confirmed by studies on model systems, e.g. on monodisperse ionic latex particles, which are large enough (diameter: about 3000 Å) to be seen under the ultramicroscope. It follows, from the inequality relation $2D_{exp} < 2D_0$, that there is an attraction between ionic species of like-charge. This conclusion contradicts prevailing views in colloid chemistry; it has been pointed out that such a behavior can be explained in terms of a new theory, in which counterions between the macroions or ionic latex particles play a decisive role.



This picture, painted by *Mitsuyoshi Tosa* (1539–1613), illustrates a story in the Genji monogatari (Tale of Genji),*** written by the Japanese authoress *Murasaki Shikibu*, in the early eleventh century. The two gentlemen are simultaneously attracted by the lady playing a Koto, a Japanese board zither with 13 strings. The lady is so attractive that the two gentlemen, despite their mutual repulsion, are drawn into close proximity. A similar situation seems to exist for charged solutes in dilute solutions. (Reproduced by courtesy of the Kyoto National Museum and Gakushu kenkyusha.)

1. Introduction

Elements and chemical compounds can exist in three physical states, namely solid, liquid, and gaseous states. In solids, the molecules are highly ordered, whereas in the gaseous state they are completely disordered. The distribution in the liquid state may lie between these two extremes; but our knowledge thereof is still scanty. This is also the case with solutions. When the solute concentration is high, it might not at all be surprising that the solute particles are "packed" in a more or less regular manner in the solution, provided that they have the same size and geometry. On the other hand, at low concentrations, one might expect that the solute particles behave in an irregular manner like "gas molecules". If "solid-like" ordered arrangements of the solute particles are to be found under such conditions, then we have an unexpected and interesting phenomenon which warrants careful investigation. In order to facilitate

[*] Prof. Dr. N. Ise
Department of Polymer Chemistry, Kyoto University
Kyoto 606 (Japan)

[**] Based on a plenary lecture at the Colloid and Surface Science Symposium, American Chemical Society, Toronto, Canada, June 1983.

[***] The world's first novel, according to E. O. Reischauer: *The Japanese*, Harvard University Press, Cambridge, MA, USA 1977, Chapter 4.

an understanding of this situation, let us consider balls of the same radius contained in a vessel of definite volume. When the number of balls (and hence the concentration) is sufficiently high, the space requirement forces the balls to be close-packed. In this case the distance between the centers of two balls ($2D_{exp}$) must be roughly the same as the average distance ($2D_0$) calculated from the number of the balls and the volume of the vessel. If the number of balls is relatively small, however, the average value of $2D_{exp}$, if it can be measured, is expected to be equal to $2D_0$, provided that the balls are distributed completely irregularly throughout the vessel. If a localized "solid-like" arrangement were to occur, the $2D_{exp}$ value in the ordered region would be smaller than $2D_0$. Over the past few years, it has emerged that ionic solutes (such as simple ions, synthetic macroions, proteins, polynucleotides, ionic detergent micelles, and polymer latex particles) form unexpectedly "ordered" arrays in relatively dilute solutions, irrespective of the molecular geometry and mass, and, under some conditions, $2D_{exp}$ is found to be smaller than $2D_0$. Although many related problems still remain unsolved, recent studies on dilute ionic solutions have revealed essential aspects of interionic interaction in solutions. The experimental data now available and the theoretical predictions deriving therefrom are so unexpected and contradictory to prevailing views in colloid and macromolecular science that a review of the present state-of-the-art in this sector was deemed necessary, irrespective of whether many controversies have not yet been settled.—For earlier work in this area, the reader is referred to a previous review.[1]

2. EXAFS Studies on Simple Ions

The dependence of the activity coefficient, the heat of dilution, and the viscosity on concentration suggests, though not conclusively, that simple ions form ordered structures in dilute regions.[1] A more direct argument in support of this hypothesis can now be presented on the basis of recent EXAFS (Extended X-ray Absorption Fine Structure) experiments. A French group[2,3] reported for solutions of $ZnBr_2$ that the interionic distance between Zn^{2+} and Br^- is 2.37 Å in 0.089 M aqueous solution and 2.30 Å in 0.05 M ethyl acetate. Both values are very close to that observed in the crystalline state (2.40 Å). This observation indicates that local ordering similar to that in the solid crystal persists even at these low concentrations, although the lifetime of the ordered structure would be quite short.

3. X-ray Scattering on Macroions, Proteins, and Polynucleotides in Solution

Under suitable conditions, aqueous solutions of synthetic macroions continue to show a single, broad peak in the small-angle X-ray scattering (SAXS) curves. The experimental data recently obtained for poly-L-lysine · HBr[4] and sodium polystyrenesulfonate[5] are completely consistent with those reported earlier for sodium polyacrylate:[6] When the polymer concentration and molecular weight are reasonably high and the concentration of coexisting salt is low, a scattering peak is observed which, with increasing polymer concentration and decreasing salt concentration, shifts towards larger scattering angles. This tendency is also observed with t-RNA.[7]

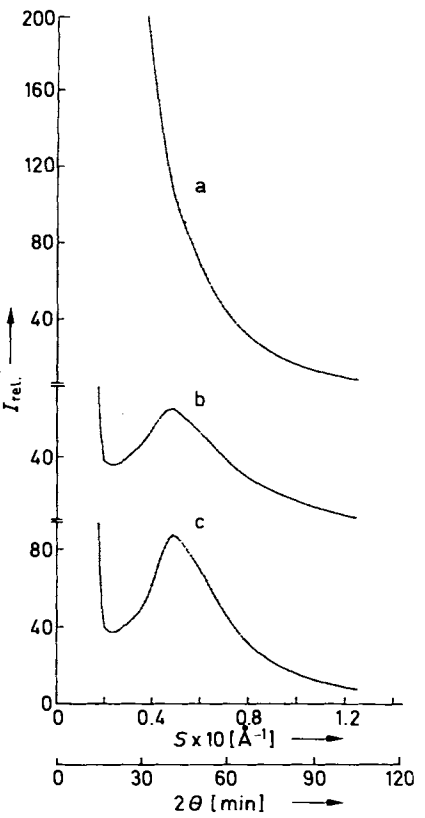


Fig. 1. Small-angle X-ray scattering of an aqueous solution of bovine serum albumin (0.075 g/mL) at 25 °C and (a) pH=5.06, (b) pH=3.44, and (c) pH=10.94. S is the scattering vector ($4\pi\sin\theta/\lambda$, where 2θ is the scattering angle and λ the wavelength of the X-rays). (Taken from Ref. [8] by courtesy of the American Institute of Physics.)

Figure 1 shows the SAXS curves for bovine serum albumin (BSA), an amphoteric polyelectrolyte.[8] A SAXS peak is observed at alkaline and at acidic pH, whereas it disappears at a pH near the isoelectric point. Unneutralized polyacrylic acid[6] and polyvinylpyrrolidone, a neutral polymer, show no scattering peak.[5,9] These findings imply that the appearance of the peak is due to electric charges on the solutes.

We shall now turn to synthetic macroions and homologues with various degrees of polymerization. The scattering vectors of the peak position of polystyrenesulfonate samples with narrow molecular weight distributions were 0.091 and 0.073 for M_W=4600 and 74000, respectively ($M_W/M_N = 1.07 - 1.17$) at the same concentration (0.04 g/ml).[5] Obviously the peak position shifts to smaller scattering vectors when the molecular weight increases, as was previously observed for sodium polyacrylate[6] and poly-L-lysine.[4] Interestingly, the scattering curves of binary mixtures of two samples of different molecular weight cannot be reproduced by a composite one drawn by the summation of two original curves.[5] This indicates that the observed peak is due to an intermolecular and not to an intramolecular ordering, otherwise the peak position would not change by mixing. In other words, the SAXS data indi-

cate the presence of an ordered array of the macroions in solution.[10]

It is now possible to estimate the approximate interparticle distance ($2D_{exp}$) with the help of the Bragg equation. Some data obtained for sodium polystyrenesulfonate are listed in Table 1.[5] The behavior of $2D_{exp}$ (e.g., dependence on polymer and salt concentrations) is essentially in agreement with previous findings.[4,6] A comparison of the results of experiments 9 and 10, or 11 and 12 (Table 1) reveals that $2D_{exp}$ decreases with increasing molecular weight when the number of macroions per unit volume remains constant. For such macroions, the ionic charge increases with increasing molecular weight. According to the usually accepted interpretation, $2D_{exp}$ might be expected to become larger with increasing charge on the macroion because of enhanced mutual repulsion of the particles. The observed tendency, however, is completely the opposite.

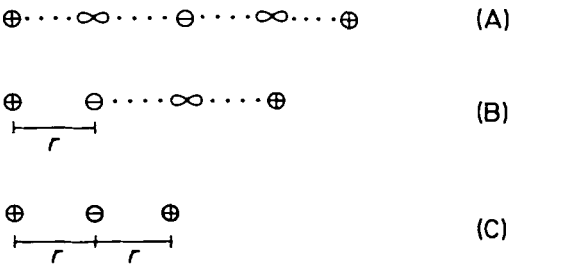
Table 1. Small-angle X-ray scattering data for aqueous solutions of sodium polystyrenesulfonate at 25°C [a]. S_m: scattering vector at the peak ($S=4\pi\sin\theta/\lambda$, 2θ: scattering angle, λ: wavelength). $2D_{exp}$: observed interparticle distance. The $2D_{exp}$ value for macroions is obtained by the Bragg equation. The uncertainty was estimated to be within ±5% from repeated runs. $2D_0$: theoretical interparticle distance calculated from the concentration by assuming uniform distribution.

No.	Polymer concn. [g/mL]	M_W	NaCl concn. [g/mL]	S_m [Å^{-1}]	$2D_{exp}$ [Å]	$2D_0$ [Å]
1	0.01	7.4×10^4	0	0.040	157	231
2	0.02	7.4×10^4	0	0.052	122	183
3	0.04	7.4×10^4	0	0.073	87	145
4	0.16	7.4×10^4	0	0.134	47	92
5	0.04	4.6×10^3	0	0.091	69	58
6	0.04	7.8×10^5	0	0.073	87	319
7	0.04	1.8×10^4	0.1	0.067	(94) [d]	91
8	0.04	1.8×10^4	0.5	0.051	(123) [d]	91
9 [b]	0.02	4.6×10^3	0	0.074	85	73
10 [b]	0.078	1.8×10^4	0	0.102	62	73
11 [c]	0.02	1.8×10^4	0	0.053	119	115
12 [c]	0.08	7.4×10^4	0	0.096	65	115

[a] M_W/M_N is 1.07, 1.14, and 1.17 for the samples with $M_W=4.6\times10^3$, 1.8×10^4, and 7.4×10^4, respectively. [b] Number of macroions per unit volume 2.6×10^{18} mL^{-1}. [c] Number of macroions per unit volume 6.6×10^{17} mL^{-1}. [d] These values are believed to be overestimated because the intramacroion scattering must have affected the S_m value at small angles.

This implies that either the scattering measurements and the data analysis have not been carried out correctly, or that the widely accepted interpretation is incorrect. The first possibility has been considered very carefully and could be ruled out. Our positive assessment of the experimental data relies on our more direct experiments (see Section 4) on solutions of ionized latex particles, which are so large that their distribution in the solution can be observed directly with the ultramicroscope. (The resolution of a simple microscope is as large as the wavelength of the light used, whereas that of an ultramicroscope is 40 – 100 Å, depending on the refractive index of the particle.) It should be noted that macroions (studied by X-ray scattering) and polymer latices give consistent results.

The second possibility invites detailed consideration. Naturally, like charges repel each other and unlike charges attract each other. We are not, of course, questioning this axiom. If only macroions or colloidal particles of the same charge were to exist in solution, they would repel each other. However, this is not physically possible. In ionic solutions, there must exist macroions of the same charge and, *in addition*, equivalent amounts of oppositely charged counterions (such as H^+ or Na^+). The presence of the counterions between two macroions generates a Coulombic attraction between the macroions, which overwhelms the Coulombic repulsion between them. This can be illustrated quite easily in the following way: Suppose two cations and one anion each bear a charge (e) of the same magnitude. We now compare the potential energy of three systems (A, B, and C), namely free ions (A), an ion pair and a free ion (B), and a triple ion (C). The potential energy of case A is, of course, zero; that of case B is given by $-e^2/r$, where r is the distance between the cation and anion in the ion pair. The potential energy of the triple ion is $-1.5e^2/r$, since we have attraction ($-2e^2/r$) between the cation and anion (at a distance r) and naturally repulsion ($+e^2/2r$) between the two cations (at a distance $2r$). It is



immediately clear that, as far as the potential energy is concerned, the triple ion is the most stable of the three possibilities and is more stable than the ion pair plus a free ion, in spite of the repulsion between the cations. This argument can be extended to much higher ionic aggregate systems. In real solutions we cannot ignore the contribution of kinetic energy of the various particles, and we must also take into account the asymmetric nature of the ionic species, particularly in the case of highly charged macroions with monovalent counterions. Essentially, however, the stabilization can be caused by the very presence of oppositely charged species between similarly charged species: In other words, similarly charged species attract each other through the intermediary of oppositely charged species. (For readers who might be interested in an analogy taken from human behavior, we suggest the illustration of the Tale of Genji as being instructive.) This situation is lucidly described by *Feynman*, et al. who state that attraction arises "because the repulsion of likes and attraction of unlikes will tend to bring unlikes closer together and push likes farther apart".[14] For the same reason, ionic crystals such as sodium chloride are essentially stable. Ionic solutions are stabilized in the same way, that is they can exist as condensed systems. As a matter of fact, the free energy of interaction for simple ionic solutions is always negative according to the Debye-Hückel theory, despite repulsion between ions of the same sign;[15] this demonstrates that the *net* interaction is attraction. This important aspect has been almost completely ignored in some widely accepted treatises. It will be discussed in the following.

Table 2. Shortening of the intermacroion spacing in various polyelectrolyte solutions with increasing number of charges at 25 °C.

Polyelectrolyte	Degree of neutralization or pH	Concn. [g/mL]	$2D_{exp}$ [Å]	Ref.
Sodium polyacrylate	0.1	0.02	(129) [c]	[6]
	0.2	0.02	111	
	0.3	0.02	98	
	0.4	0.02	93	
	0.5	0.0221	88	
	0.65	0.02	92	
Sodium polymethacrylate [a]	0.2	0.0331	106	[16]
	0.4	0.0331	73	
	0.8	0.0331	72	
Poly-L-lysine·HBr [b]	pH = 9.8	0.04	114	[4]
	pH = 8.2	0.04	74	
Bovine serum albumin	pH = 8.08	0.073	133	[8]
	pH = 10.9	0.072	127	
	pH = 12.2	0.069	105	
	pH = 4.07	0.073	157	
	pH = 3.44	0.072	129	
	pH = 2.65	0.069	128	

[a] P_w (weight average degree of polymerization) = 590. [b] P_w = 406. [c] This value was obtained from a vague scattering peak, so that the experimental error would largely exceed the value (±5%), which is expected for other data.

Not only the data on sodium polystyrenesulfonate, but also existing data for weak macroions indicate that the $2D_{exp}$ value *decreases* with increasing charge. The $2D_{exp}$ values measured by *Dušek* et al. for sodium polymethacrylate,[16] and those found for sodium polyacrylate,[6] poly-L-lysine · HBr,[4] and bovine serum albumin[8] are listed in Table 2.

4. Microscopic Studies on Model Systems (Latex Solutions)

Although X-ray scattering experiments provide comparatively direct information about ordering phenomena, and although we believe that the conclusions drawn therefrom are basically correct, we cannot be absolutely sure about such information. One could carry out theoretical calculations of the scattering intensity using various geometrical models and then compare the results with experimental findings. In the case of ordered structures *in liquids*, however, such a strategy would be uninformative. What we are doing instead is to accumulate experimental data for dilute solutions of ionized latex particles. With these data we hope to gain insights into the behavior of macroions in solution.[17] Monodisperse polymer latex particles are not difficult to synthesize, and methods for their purification and characterization are well-established.[18] Owing to the difference in the refractive indices of the solvent and particle, aqueous polystyrene latex solutions are milky. When ionic impurities are removed, the solution becomes iridescent for latices of relatively small diameters.[19] It has been demonstrated that the iridescence is due to Bragg diffraction of visible light by an ordered array of the latex particles in soluion.[20] The most direct evidence for the ordering was obtained by *Hachisu* et al. by using a metallurgical microsope as ultramicroscope.[21]

Figure 2a shows such an ordering of latex particles. From this picture, the interparticle distance ($2D_{exp}$) can be estimated directly.

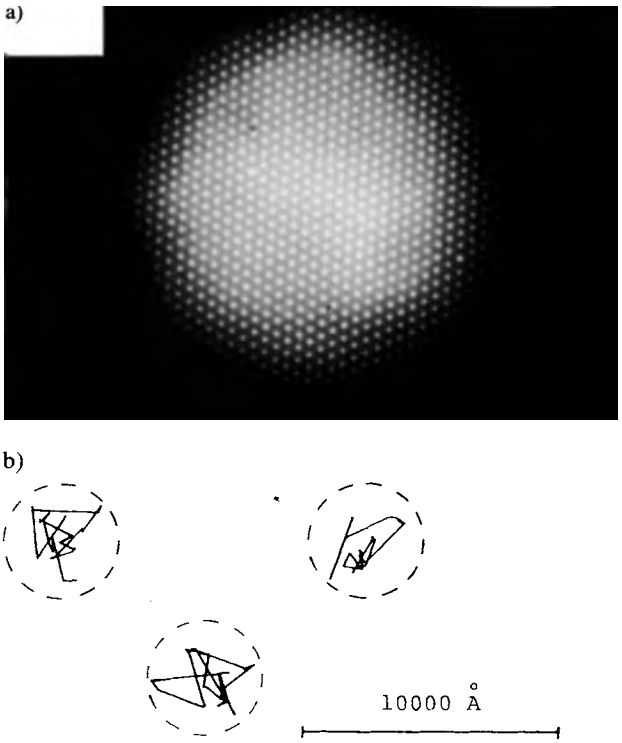


Fig. 2. Microscopic investigation of the ordering of polymer latex particles in dilute solutions. a) Static aspect of the ordering. The latex was prepared by emulsifier-free emulsion copolymerization of styrene and styrene sulfonate. Diameter: 3690 ± 100 Å, charges (SO_3H): 2.7×10^5 per particle. Latex concentration: 0.0066 g/ml. The figure, taken with a Carl-Zeiss Axiomat IAC at 25 °C, is *not* an electron micrograph. The interparticle distance ($2D_{exp}$) directly estimated from this picture is about 9000 Å, whereas that calculated from the concentration ($2D_0$) is 15000 Å. From this difference, it can be concluded that ordered regions and less dense disordered regions must coexist (cf. Fig. 3). The ordering of the latex particles in a horizontal plane is shown. b) Trajectory of the centers of the latex particles in the ordered structure [22]. Latex: SS-37, a styrene-styrenesulfonate copolymer, diameter: 4500 Å, latex concentration: 4%, charges: 1.76×10^5 per particle; film speed: 24 fps (frames per sec), exposure: 1/6s, *T*: 25 °C. The particle motion was followed using twelve consecutive film frames, i.e., for 0.5 s.

Figure 2a is indeed quite impressive, but it can lead to false conclusions. Under the microscope, the particles are not stationary but oscillate quite "rapidly" around their equilibrium positions. It is a grave mistake to presuppose something like a rigid lattice-like structure as found in solid crystals. In order to show how dynamic the ordered structure of the latex is, the particle motion was photographed with a movie camera and the trajectory of the particle center was recorded and reproduced as shown in Figure 2b.[22] By using such a technique, it is possible to estimate the *two-dimensional* standard deviation ($\Delta 2D_{exp}$) of the interparticle distance. Under the experimental conditions of Figure 2b, $\Delta 2D_{exp}$ was found to be 900–1000 Å, i.e. for an interparticle distance ($2D_{exp}$) of 10000–12000 Å. The ratio $\Delta 2D_{exp}/2D_{exp}$ amounts to about 0.1 at concentrations of 0.039 g/mL. Needless to say, these values vary with the experimental conditions. At lower latex concentrations, and naturally also for smaller particles, the ratio must be larger.

This information is of considerable significance in the case of macroion systems. As already mentioned, small-angle X-ray (and also neutron) scattering gives a single, broad peak for macroions. It is often insisted that the ob-

served scattering peak does not correspond to a Bragg diffraction, because higher peaks are lacking. In this respect, it should be remembered that the scattering intensity is strongly influenced by the size and number of the ordered structures, thermal motion, and paracrystalline disorder of the diffracting components. Thus, the observed single broad peak implies either (i) the absence of an ordered structure or (ii) substantial distortion of an ordered structure. According to a theory proposed by *Hosemann* and *Wilke*[23] for paracrystals, when the distortion factor multiplied by the order of the diffraction peak n is larger than 0.35, the n-th peak is not distinguishable. If $\Delta 2D_{exp}/2D_{exp}$ is equated to the distortion factor, though not rigorously correct, the number of observable peaks should be three for the 0.039 g/mL solution. At lower latex concentrations or for macroions, which are much lighter and smaller than latex particles, it is reasonable to anticipate much more pronounced disorder and hence one or two scattering peaks. This is a very rough estimate but might not be very far from the truth, judging from the recent work of *Kato* et al. on laser light scattering,[24] which shows only a single broad peak at a concentration of 0.00018 g/mL (much lower than that in Fig. 2b, 0.039 g/mL) for smaller latex particles (diameter: 1540 Å). A similar situation was reported for a latex solution by *Versmold* et al.[25] Although a more rigorous calculation is in progress,[8,26] it might be claimed that the lack of higher diffraction peaks does not necessarily imply the absence of an ordered structure. Due attention must be paid to paracrystalline distortion of the ordered structures.

5. Comparison of $2D_{exp}$ with $2D_0$ — Two-State Structure and Interparticle Attraction

In addition to the Bragg spacing ($2D_{exp}$), a theoretical interparticle distance ($2D_0$) calculated from the solute concentration by assuming a uniform simple cubic distribution is given in Table 1.[27] It is immediately clear that $2D_{exp}$ is smaller than $2D_0$, except for the samples with low molecular weight ($M_W = 4.6 \times 10^3$ and 1.8×10^4), if a $\pm 5\%$ error in $2D_{exp}$ is assumed. The relation $2D_{exp} < 2D_0$ was also confirmed for sodium polyacrylate[6] and poly-L-lysine · HBr.[4] In this respect, it is interesting to inquire into the case of polymer latex particles. The interparticle distance observed ($2D_{exp}$) for latex samples is compared with the theoretical values ($2D_0$) in Table 3.[28] For the sample of *Hachisu* et al.[21], which has a relatively small number of charges, the relation $2D_{exp} \approx 2D_0$ is seen to hold. On the other hand, for highly charged particles $2D_{exp} < 2D_0$ applies at low concentrations, and $2D_{exp} \approx 2D_0$ when the concentration is high. These facts, and the relation $2D_{exp} < 2D_0$ observed for the macroions, suggest that there must be an attraction between the solute particles and, furthermore, that the attraction is more intense for particles having a larger number of charges. The second aspect is consistent with the tendency for $2D_{exp}$ to become smaller with increasing molecular weight of the synthetic macroions, and hence number of charges (cf. Table 1, entries 9 and 10 or entries 11 and 12, and Table 2).

These results are unexpected, but can be rationalized if the concentration effect of charged particles and the action of counterions are properly considered. The inequality of $2D_{exp}$ and $2D_0$ suggests the coexistence of ordered and disordered regions of solute particles (namely a two-state structure) in dilute solutions. The existence of a two-state structure can be confirmed by the naked eye for latex solutions at relatively low concentrations.[17] Figure 3[30] shows the two-state structure. The difference between the coexisting ordered and disordered regions is more than obvious by comparing the trajectories of the particles in the two regions. Figure 3 provides visible evidence for the interparticle attraction, since the localized ordering seen on the left-hand side of the figure has a free boundary, and such a "condensed" or "non-space-filling" ordered structure is inconceivable unless an interparticle attraction really does exist.

Table 3. Comparison of the observed interparticle distance ($2D_{exp}$) and the theoretical average distance ($2D_0$) for charged polymer latex solutions [a]. A: *Hachisu*'s sample [21] (diameter 3410 Å, < 1000 charges per particle [b]. B: *Ise*'s sample [17] (diameter 4190 Å, 2×10^5 charges per particle) [b].

Sample	Concn. [Vol-%]	$2D_{exp} \times 10^{-3}$ [Å]	$2D_0 \times 10^{-3}$ [Å]
A	0.4	18	19.4
	0.55	15	17.5
	1.5	10	12.5
	4	8	9
B	0.75	12.6 ± 0.7	19.4
	1.40	10.7 ± 0.7	15.7
	3.72	8.9 ± 0.7	11.4
	5.59	8.2 ± 0.6	9.9
	11.2	7.1 ± 0.6	7.9

[a] The error in our measurements was estimated to be 15% at worst. The data for *Hachisu*'s sample were evaluated from a published micrograph. An error of 15% is also reasonable. [b] The diameter was determined by electron micrography and the number of charges per particle was estimated by conductometric titration. The number of charges in *Hachisu*'s sample could not be measured because of the small number. Thus, 1000 is the largest possible value estimated on the basis of the experimental precision of the conductometric measurements.

Kato et al.[24] also calculated $2D_{exp}$ for the above-mentioned small latex particles. For a 93%-sulfonated (i.e., highly charged) polystyrene latex of 1540 Å diameter, the $2D_{exp}$ values were found to be 8×10^3, 3.8×10^3, 2.9×10^3, and 2.8×10^3 Å at concentrations of 1.81×10^{-4}, 5.45×10^{-4}, 1.09×10^{-3} and 2.18×10^{-3} g/mL, respectively, while the $2D_0$ values were 1.5×10^4, 5.2×10^3, 4.1×10^3 and 3.3×10^3 Å. The relation $2D_{exp} < 2D_0$ is obviously fulfilled. This experiment is important in that it shows that the inequality holds also in the inner part of the solution, where the laser light was diffracted. When we claim the inequality relation purely on the basis of microscopic observation, it may be criticized that the relation is an artifact whose origin lies in the sedimentation of latex particles to the bottom of the solution cell. (With the microscopic method, we are forced to observe particles in the region not much further than 10^5 Å from the bottom of the cell, since an inverted microscope is used, and the solution is usually turbid (cf. Ref. 21). It must be remembered that the specific weight of our latex sphere (copolymer of styrene and styrenesulfonate) is 1.03 g/cm^3). The local concentration near the bottom can be higher than that in the upper part of the solution. If the concentration difference is very high, it may happen that $2D_{exp}$ is smaller than $2D_0$. However, the fact that $2D_{exp} < 2D_0$ was also observed by the

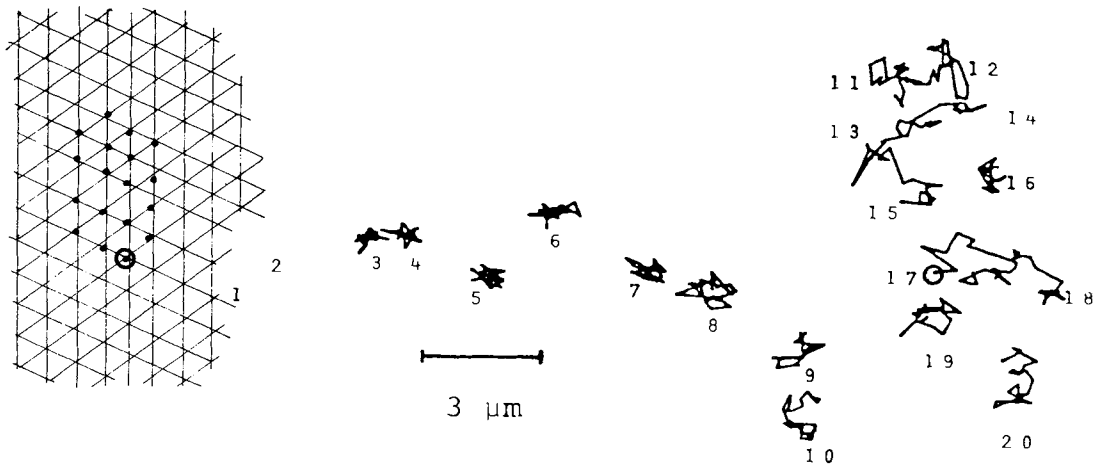


Fig. 3. Coexistence of ordered (left) and disordered regions (right) in a latex solution and trajectory of the particles in 1 s. Latex: SS-37 (the same as in Fig. 2b), concentration: 2%. On the left-hand side, a "solid"-like hexagonal array with a high density is seen, which coexists with a much less dense "gas"-like disordered region (right-hand side). $2D_{exp}$ in the ordered region is about 10^4 Å, whereas $2D_0$ is about 1.5×10^4 Å. Thus the total volume of the ordered regions in the solution amounts to $1/3.4=[(10^4/1.5 \times 10^4)^3]$ of the total solution volume, although the volume of a single ordered region has not yet been determined. The particles in the ordered region show oscillatory motion (as in Fig. 2b), but the amplitude is too small to see on the scale chosen here. The random motion of the particles in the disordered region is close to that predicted according to the Einstein theory for Brownian motion, though we would like to postpone drawing a definite conclusion until a much larger number of particles have been treated. (Taken from Ref. [30] by courtesy of the American Chemical Society.)

laser light diffraction clearly indicates that the sedimentation effect, if any, was not of considerable importance. The relatively minor role of this effect is also demonstrated in Figure 3, which shows the particle distribution in a horizontal, (not vertical) plane: if this effect were to be substantial in producing local ordered regions of latex particles (and hence in leading to $2D_{exp} < 2D_0$), we would have to admit larger acceleration of gravity on the left-hand side of Figure 3 than on the right-hand side. This is inconceivable.

A most convincing result substantiating the inequality $2D_{exp} < 2D_0$ for polymer latex solutions was recently reported by *Yoshiyama* et al.,[31] who obtained very clear Kossel images. At low latex concentrations below 2 vol-% a body-centered-cubic structure was found, whereas above 3% a face-centered-cubic lattice was identified. In both cases, lattice constants were found that were typically smaller than would be expected for a uniform particle distribution.

6. Activity of Ionic Solutes

The activity a is a measure of the non-ideality of the solution. In spite of the basic nature of this quantity, not much attention has been paid to it as far as ionic polymers and polymer latex particles are concerned. Needless to say, all concepts or conclusions drawn from experimental data must be consistent with the activity data. Thus, it would be of interest to analyze the concept of intermacroion interaction discussed in Sections 3–5 in terms of the activity. Figure 4 gives experimental data of the activities of polymer latex particles (a_{2p}) and of their counterions (protons) (a_{2g}) and the mean activity (a_z). These quantities were obtained from vapor pressure measurements, using the Gibbs-Duhem relation. Most noteworthy is the dramatically steep decrease of a_{2p} with increasing solute concentration.[33] In contrast, the counterion activity (a_{2g}) increases steadily with concentration, as is usually the case

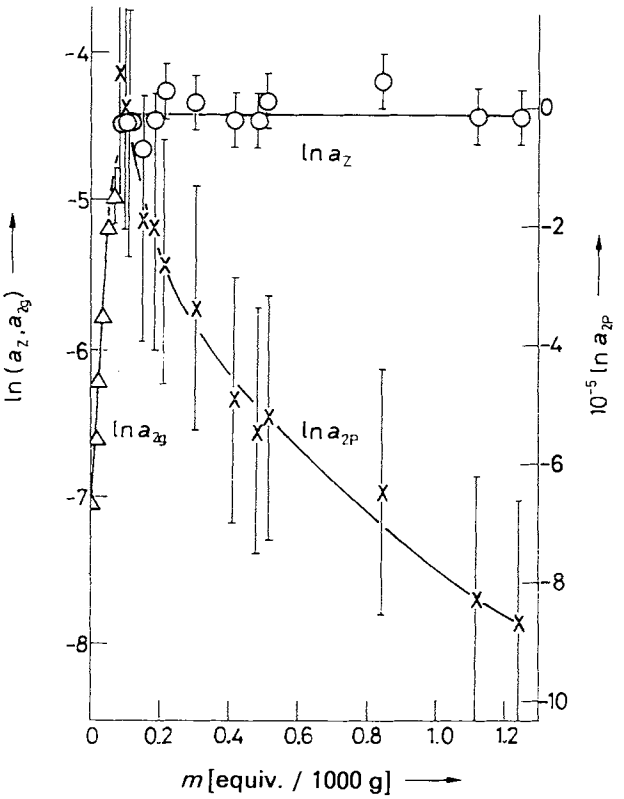


Fig. 4. Mean activity of latex particles (a_z) and ionic activities of the latex ions (a_{2p}) and of the counterions (protons) (a_{2g}) in water at 25 °C. Latex: polystyrene latex sulfonated with sulfur trioxide ("Latex No. 3"), diameter: 620 Å, charges (Z): 3.5×10^5 per particle (charge density=4.5×10^8 µC/cm^3). a_z was evaluated by the Gibbs-Duhem equation from the solvent (water) activity determined by vapor pressure measurements. a_{2g} was determined by conventional potentiometry. The a_z value at 0.1 equiv/1000 g water was set equal to the a_{2g} value so that a_{2p} was unity at this reference concentration. The vertical bar denotes the estimated error limit. (Taken from Ref. [32] by courtesy of the American Chemical Society).

with simple ions. The activity a is defined as the quotient of the vapor pressure (or more exactly fugacity) of the solute and that of a reference state. According to Roult's law, in an ideal solution, in other words in the complete absence of interaction, $a=N$, where N is the concentration. That is, in the ideal case a must increase with increasing concentration. This is readily accepted, because a signifies the volatility of a component, and the vapor pressure (and hence the number of component molecules or ions in the gas phase) may be expected to increase when the number (and hence concentration) of components in the solution increases. When taking this into consideration, the tendency of a_{2p} to decrease is at first sight perplexing. Nevertheless, it is understandable if we accept the existence of an intermacroion attraction, which prevents macroions from transferring from the solution phase to the gas phase. A similar trend is also found in the case of linear macroions.[34] The activity of the macroions decreases steeply with increasing concentration, and the rate of this decrease increases when the charge density of the macroion increases. The latter feature suggests that the attraction under discussion becomes stronger with increasing charge density. This is indeed consistent with the previous finding that $2D_{exp}$ (estimated by X-ray scattering or by microscopy) becomes smaller with increasing number of charges on the macroion (see Sections 3 and 5).[35]

7. Recent Theoretical Approach—Verification of Electrostatic Attraction between Similarly Charged Particles—Limit of the DLVO Theory of Colloidal Stability

As discussed in the preceding sections, there is indeed an attraction between macroions or ionic latex particles in solution in spite of charges of the same sign. As shown by the dependence of $2D_{exp}$ on the salt concentration,[5-7] the attraction is of an electrostatic nature. Furthermore, the attraction increases (or $2D_{exp}$ becomes smaller) with increasing charge. About 20 years ago, we realized the existence of such an intermacroion attractive interaction on the basis of the dependence of the mean activity coefficients of polyelectrolytes on concentration.[38] For colloidal systems, *Langmuir*[39] had already emphasized the importance of attraction between charged micelles and a surrounding atmosphere of ions of opposite charge; this attraction exceeds the repulsive force between the micelles. According to him, it is one of the three fallacies in the theories of colloidal systems to ignore or neglect this interaction.

Langmuir's claim was criticized by colloid scientists.[40] Similary, the electrostatic interparticle attraction, which we discuss on the basis of X-ray and microscopic studies on macroions and latex particles, appears to be judged as "unacceptable" in the light of the Derjaguin-Landau-Verwey-Overbeek (DLVO) theory of colloidal stability. According to this theory, two colloidal spherical particles immersed in a continuous medium (dielectric constant ε) should simply repel each other. The repulsive potential (V_R) is given by

$$V_R = \frac{\varepsilon x \psi_0^2}{2} \ln\left[1+\exp\left(-\kappa x\left(\frac{R}{x}-2\right)\right)\right]$$

where x is the radius of the sperical particle, R the center-to-center interparticle distance, ψ_0 the surface potential, and $1/\kappa$ the Debye radius. However, since condensed systems such as colloidal solutions or solutions of macroions can exist only by virtue of some kind of attractive interaction, V_R does not represent the total potential. As a matter of fact, a van der Waals type attraction (V_A) is assumed in the DLVO theory, which is written

$$V_A = -\frac{A}{6}\left[\frac{2x^2}{R^2-4x^2} + \frac{2x^2}{R^2} + \ln\frac{R^2-4x^2}{R^2}\right]$$

where A is the Hamaker constant. This constant is said to lie between 0 and 6×10^{-12} erg.[40] Thus, the DLVO theory indicates that the electrostatic interaction between colloidal particles must be repulsive, and that the interparticle attraction must be non-electrostatic. This contradicts our observations.

Recently, *Sogami*, a theoretical elementary particle physicist, became interested in latex solutions as classical models for atomic and molecular assemblies and has formulated a new theory.[41,42] He successfully proved the presence of an electrostatic attraction between similarly charged particles and has clarified the origin of such an attraction. The reader is referred to the original articles[41,42] for detailed calculations; here, we shall comment only briefly on the essential aspects of the theory. In Figure 5, three negatively charged colloidal particles and their counterions are illustrated. When the particles are not highly charged (Fig. 5a), the interaction between the particles and the counterions is relatively weak, so that the solution volume (V) represents the space in which the counterions can move. In the case of highly charged particles (Fig. 5b), however, the particle-counterion interactions are so intense that the counterions are forced to reside in a small space (v'). Under such conditions, there arise two basic problems. First, an interaction is generated between the particles, e.g. P-1 and P-2, because the counterions such as A, which reside in the space in between the two particles, are attracted by the two particles at the same time. Here, the readers are reminded of the analogy with the triple ion formation or with the one lady-two gentlemen relationship depicted in the Tale of Genji. It would be no wonder if attraction were to be created with other neighboring particles in succession and in a three-dimensional way. Under suitable conditions, the attraction would lead to the formation of intermacroion "linkage" according to our earlier terminology[38] and eventually to some kind of clusters of particles.

There are several factors favoring or disfavoring the intermacroion attraction: (1) Obviously, the kinetic energy disfavors it. Elevation of the solution temperature would help the counterions to escape from the sphere of influence of the particles. In other words, the volume v' increases with increasing temperature. Under such conditions, the attraction would be weakened. (2) Similarly, a lowering of the concentration of the particles (and hence of the counterions) diminishes the chances for the counterions to stay in the region near the particles. (3) In contrast, the use of multivalent counterions (as opposed to monovalent ones such as H^+ or Na^+) would intensify the inter-

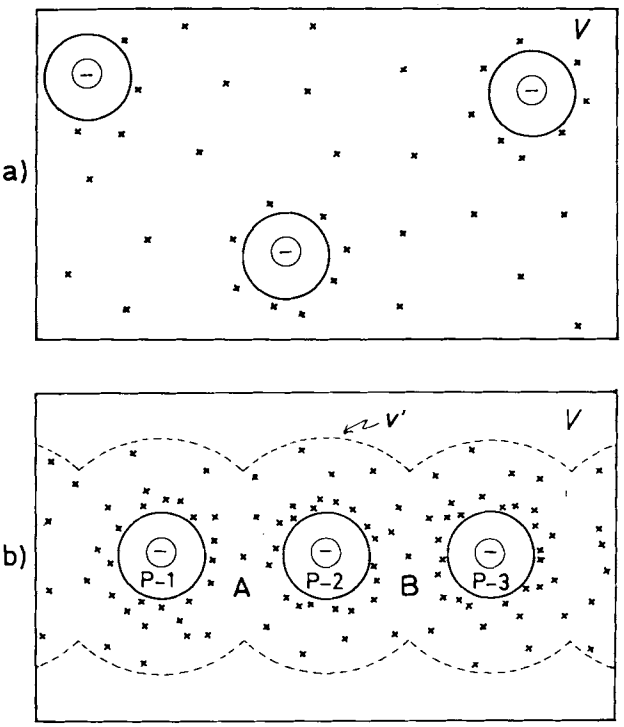


Fig. 5. Schematic representation of the distribution of counterions around charged particles. a) Distribution around low charge particles. The counterions can reside in the entire volume (V) of the solution, because the particle-counterion interaction is not strong; the number of the counterions per unit volume, however, decreases with increasing distance from the particles. b) Distribution around highly charged particles. The strong interaction between the particles and counterions restricts the freedom of motion of the latter: the counterions are confined to a small space v'. The difference $V-v'$ is expected to become larger with increasing charge of the particle. Thus, the solution volume loses its significance as the thermodynamic parameter for highly charged particles. Because of the weak particle-counterion interactions, no ordering of the particles is expected in the case (a), whereas we have ordering of the particles in the case (b).

macroion attraction, because the attraction between the particles and the counterions increases with increasing valency of the counterions. (4) Similarly, the intermacroion attraction would become stronger if the particle valency is raised, because the counterion-particle interaction would be enhanced. Although the particle-particle repulsive interaction is intensified at the same time, this interaction is operating at much larger distances than the counterion-particle interaction, so that the overall result is the intensification of the attraction. In this respect, the aforementioned statement by *Feyman*[14] is informative (cf. Section 3).

It should be pointed out that all these four changes in the attraction between macroions are predicted in *Sogami*'s theory. Also noteworthy is that these changes have, at least qualitatively, been demonstrated experimentally. For example, the ordering of polymer latex particles in solution can be destroyed by increasing the temperature.[43] Our own experiments on a soluble polyelectrolyte[5] showed that the intensity of the diffracted X-ray diminished with increasing temperature, indicating deterioration of ordering of the macroions (and hence weakening of the intermacroion attraction). It is widely recognized that the ordering of latex particles can be observed at relatively high latex concentrations. This seems to be the case with other charged species. Regarding the third factor mentioned above, namely the counterion valency, the intensified intermacroion attraction explains the autocomplex-coacervation reported by a Dutch group,[44] which was observed when the counterions of valency two or higher were involved. And with respect to the fourth factor, it was mentioned earlier (Section 5) that $2D_{exp} \approx 2D_0$ applies for low charge density latices, whereas $2D_{exp} < 2D_0$ holds for highly charged latices (Table 3). The intensification of the intermacroion attraction with increasing charge number of the macroion follows quite clearly from Table 2.

The second important feature associated with the confinement of the counterions within the small space v' is the inequality of the Gibbs and Helmholtz free energies of interaction. When ionic species have low charge numbers, as is the case for simple salts, this problem is not serious. At sufficiently low concentrations, interionic interaction is relatively weak so that the ions have the freedom to move around in the entire volume of the solution. Thus, the solution volume V has a definite thermodynamic significance. For such solutions, the free energy of interaction can be calculated with the assumption of a constant solution volume, if the compressibility of the solvent is negligibly small. Then, as *Debye* and *Hückel* carefully discussed in their original paper,[15] this is a permissible assumption as far as simple salt solutions are concerned. The Helmholtz free energy change (dF) is then equal to the Gibbs free energy change (dG). In other words, in the basic thermodynamic relation $dF = dG - p\,dV$, the second term on the right-hand side is neglected. It seems to us that the basic nature of this assumption is not given sufficient attention: a careful discussion of this problem is only to be found in a textbook by *Fowler* and *Guggenheim*.[45] The problem is not mentioned at all in most of the text-books on colloid chemistry and statistical thermodynamics. This is also true in the case of the DLVO theory on colloidal stability: dF is assumed to be equal to dG. But, in our opinion this assumption is invalid for colloidal particles, and even more so when such particles are highly charged. This is almost self-evident from Figure 5. As has already been pointed out, the solution volume V has no thermodynamic significance for highly charged particle systems, because the counterions have only volume v' at their disposal. In other words, the systems are "compressed" from V to v' by charging-up of the particles and counterions. This compression makes the term $p\,dV$ negative and sizeable, and even more so for highly charged particles[46] In other words, dF is larger than dG. It should be remembered that the difference between dF and dG has nothing to do with the compressibility of the solution, but has its origin in the high valency of the particles and hence in the intense interaction between the particles and the counterions.

Since the free energy of interaction is given as the product of the potential and the quantity of charge, the above mentioned difference in dF and dG may lead to different potential values (cf. Ref. [45] for problems relevant to the determination of the free energy of interaction in ionic solutions). Figure 6 shows a graphical representation of *Sogami*'s potentials. The potential curve derived from the Helmholtz energy (U^F) shows a monotonous decrease with increasing particle-particle distance R. This implies that

only electrostatic repulsion exists between the two particles. However, the potential from the Gibbs free energy (U^G) has a minimum point at a relatively large R value. This means that there is strong repulsion at small distances and weak attraction at large ones.

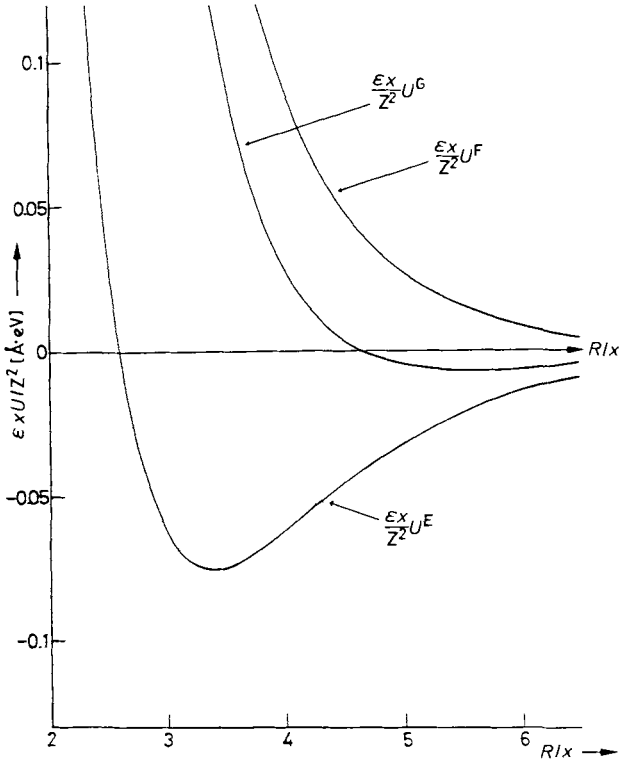


Fig. 6. Pair potential curves derived by the Sogami theory as a function of interparticle distance R. The numerical calculation was carried out for $\kappa x=1$, where κ is the screening parameter and x is the radius of the particle. ε is the dielectric constant of the solvent and Z is the number of charges the particle carries. U^E is the potential referred to the electrostatic energy; the curve shows a very strong attractive component. U^F is the potential corresponding to the Helmholtz free energy of interaction and indicates that there is only repulsive interaction between two similarly charged particles. The difference between U^E and U^F is due to entropic contributions of the counterions as discussed by *Verwey* and *Overbeek* [40]. U^G was calculated taken into account the volume contraction from V to v', which is not negligible for highly charged particles, and indicates the existence of a weak but definite attractive contribution, namely a secondary minimum. It should be remembered that this minimum is created by the equilibrium between electrostatic repulsion and electrostatic attraction; it is not due to the presence of a van der Waals type attraction. (Taken from Ref. [42] by courtesy of the American Institute of Physics.)

It is self-evident then that the experimental data obtained under isobaric conditions should be referred to dG, and not to dF. Hence, the presence of an electrostatic attraction between similarly charged ionic species can be claimed as having been proven by *Sogami*'s theory. Once again, it should be emphasized that attraction is possible through the intermediary of counterions; as expected, the attraction is particularly large when the particles are highly charged.

Therefore, the widely accepted view that colloidal particles or macroions in solution should repel each other as a result of having the same charge cannot be totally correct. It may be correct for particles of low charge density, because the "compression" is then negligible. In other words, the DLVO theory holds for the limiting case of colloids with low charge density.

The following example will serve to illustrate the results of the Sogami theory: For particles with a charge of 4×10^3 and a diameter of 1700 Å, the U^G minima lie at 1.8×10^4 and 7.2×10^3 Å at concentrations of 0.004 and 0.04 g/mL, respectively. The $2D_{exp}$ values for latex particles having similar properties[22] are 1.8×10^4 and 8.0×10^3 Å, respectively (for detailed quantitative tests see[41,42]).

One question remains to be answered: Why has the DLVO theory been regarded as satisfactory in interpreting various colloidal phenomena? One of the reasons could be that, in most cases, low charge density particles have been studied. With such particles, the attraction is usually weak, so that the particles are situated at close to the largest possible separation, namely at $2D_0$. Indeed, the value $2D_{exp}$ for *Hachisu*'s sample agrees with $2D_0$ (Table 3). A neutron-scattering study of lithium dodecyl sulfate (LDS)[48] gave 62 Å and 52 Å for the intermicellar spacing at LDS concentrations of 0.598 and 1.107 M, respectively, while $2D_0$ was found to be 66 Å and 54 Å, respectively. The agreement appears to be in favor of an interpretation of the results in terms of Coulombic repulsion. This conclusion, however, is erroneous. Particles carrying a small number of charges (such as ionic micelles) are not suitable for exploring the true nature of interactions between colloidal particles.

8. General Discussion

8.1. Conformation of Linear Synthetic Macroions

The $2D_{exp}$ and $2D_0$ values (Table 1) were calculated without any assumptions concerning the geometry of the macroions. For this reason, we find it necessary to make a brief comment on the conformation of linear synthetic macroions. It is generally believed and often claimed that linear macroions are stretched like a rod. We also have been able to demonstrate good agreement of various experimental data on soluble polyelectrolyte solutions with the Manning theory,[49] which assumed rod-like models for macroions.[50] The justification for this assumption is that α has a value close to 2 for salt-free polyelectrolyte solutions. α is the exponent in the relation $[\eta]=KM^{\alpha}$, where $[\eta]$ is the intrinsic viscosity and K a constant.[51] It should be remembered that $[\eta]$ refers to infinite dilution. *Fuoss* clearly stated that "the configuration of a polyelectrolyte at infinite dilution is an extended rod",[51] but it seems that this boundary condition is completely ignored or neglected in recent work on polyelectrolytes. The fully stretched model is justified only at infinite dilution. It may be correct, because the degree of dissociation may be large at infinite dilution. In other words, the counterions might diffuse away from the macroion domain at such a dilution, so that the ionized groups of the macroion repel each other. However, there remain two problems: The first is a technical one related to the determination of $[\eta]$ in *salt-free* polyelectrolyte solutions, which is a formidable task. As clearly demonstrated by *Conway* et al.,[52] *Fujita* and *Homma*,[53] *Eisenberg*,[54] and *Butler* et al.,[55] the η_{sp}/C–C curve (C=polymer concentration) has a maximum at a very low concentration (C_1) and a minimum at a much higher concentration (C_2).

The minimum is widely recognized, whereas the maximum has been completely ignored in recent papers on polyelectrolyte solutions. This appears to be unavoidable, since the experimental determination of the maximum is difficult, except when the highly-developed techniques of the experts such as mentioned above are available. As a matter of fact, C_1 lies at $2\text{-}3 \times 10^{-4}$ g/L, for example, for polystyrenesulfonate samples having a molecular weight of about 10^6.[55] This range is not easily accesible. Hence, the "experimental" value of $[\eta]$ that was obtained by ignoring the maximum point at C_1 must be carefully reevaluated, and the conclusion that α assumes a value close to 2 and that the macroions are consequently stretched out like rods, must be reconsidered. We believe that the linear macroions are *probably* stretched below C_1; but this is not the case above C_1. The well-known sharp drop in the η_{sp}/C value with increasing concentration in the concentration range between C_1 and C_2 might be caused by a rapid shrinking of the macroions. This in turn could be caused by an interaction between ionized groups in the same macroion, as occurs in higher ionic aggregates.

The second problem concerns the fact that the macroion domain corresponds to a very highly concentrated solution of a simple electrolyte. This point is likewise very often ignored or neglected. For example, the distance between two ionized groups of vinyl-type polyelectrolytes such as, e.g., polyacrylates or polystyrenesulfonate is ca. 3 Å, even if one supposes that the molecules are stretched. This is surprisingly small, if one recalls that the interionic distance for 1-1 type electrolytes at a concentration of 10 M is about 4 Å. Since 75% of the counterions are bound to macroions,[56] the macroion domain corresponds very roughly to a 10 M or more concentrated soution of a simple electrolyte. How can we expect, under such conditions, that the ionizable groups of a macroion are dissociated in such a way that the ionized groups repel each other to cause the stretching? It would be reasonable and meaningful to accept that the dissociation does not take place to such an extent. On the other hand, ionic association phenomena, which are known to occur in concentrated simple electrolyte solutions, may be expected in the macroion domain. For example, triple ions may be formed under such conditions. If this were to happen between two ionized groups of the same molecule and a counterion, or if one triple ion were to be formed intramolecularly, the polymer chain would not be stretched out but form a loop. For loop formation it suffices if only *0.2%* of the total ionizable groups inside a molecule of 1000 repeating units participate in the triple ion formation.

Once again, it should be emphasized that macroions are plausibly almost completely dissociated at very low concentrations (below C_1), whereby the macroions assume a rod-like structure. Probably the steep, positive slope of the η_{sp}/C-C curve observed by the above-mentioned authors[52-55] reflects this situation; above C_1, however, this is not at all certain. Such an argument of ours may be criticized as being too speculative. If this criticism were justified, however, then the reverse view, namely that such an ionic association does not take place and that the macroions are stretched out at relatively high concentrations accessible to X-ray or neutron scattering experiments, is no less speculative than ours. Under such circumstances, it is first necessary to carry out further detailed studies on the geometry and conformation of the linear macroions at the concentrations usually employed in X-ray or neutron scattering (much higher than C_1 and C_2). Secondly, we hesitate using the so-called C^* concept,[13] which is defined by the maximum length of the stretched chain, and we also hesitate adopting the rather artificial division of the concentration range into "semidilute" and "dilute" regions on the basis of C^*, since the C^* concept is in no way certain.

In this context, a recent study by *Yanagida* et al.[57] on DNA using fluorescence microscopy is quite informative. These authors successfully and directly photographed the dynamic movement of the helical strand in solution with the aid of a video system. The helix structure was clearly seen to fluctuate in shape, between that of a flexible rod, compact sphere, and prolate ellipsoid, within a short period of about 6 s. Such a dynamic situation is surprising, since we have been led to believe in the stiffness of the helical structure. The fluorescence microscopy was mainly carried out in a buffer solution, which contained a relatively high concentration of salt. Similar dynamic behavior was also observed at much lower salt concentrations.[58] It would now be less plausible to assume a highly stretched conformation for the much more flexible vinylic macroions at such concentrations as employed in X-ray and neutron scattering experiments.

8.2. The Correlation Hole Concept

There is a counterinterpretation[59] for the occurrence of a single broad peak of scattered X-rays from solutions of macroions, namely the correlation hole concept. *Weil* et al. have criticized the interpretation advanced by *Chu* et al.[7] and by us[6] (see Section 3). They stated that, "The maxima are not reminiscent of an order in the particle distribution. They are simply due to the correlation hole produced by the strong repulsive interaction both from hard sphere and electrostatic potentials." This criticism can however be refuted as follows: First, if the maximum originates from the hole by the (repulsive) interaction, it must be shifted toward smaller angles, in other words the spacing must become larger with increasing valency. This, however contradicts the experimental facts (see Tables 1 and 2). The contradiction is very definite in the case of bovine serum albumin, whose molecular conformation is more well-defined than that of the linear macroions. Specifically, for bovine serum albumin, $2D_{exp}$ decreases from 133 Å to 105 Å when the pH is raised from 8.08 to 12.2 (in other words when the (negative) charge number is increased from 20 to 80). Secondly, the correlation hole theory gives a negative scattering intensity in the small angle regions at the high BSA concentrations employed in the X-ray scattering experiments. This is particularly true when their charge number parameter is small.[60] Experimentally, positive scattering intensity was observed. Furthermore, when the charge number parameter (or the charge number) is assumed to be as high as those of typical polyelectrolytes such as sodium polystyrenesulfonate with a molecular weight of 74000, the theory shows no scattering peak for physically reasonable values of macroion radius, which is again in contradiction

to that observed in practice. Thirdly, *Weil* et al. assumed only repulsive interaction between macroions, which was claimed to produce the correlation hole. This seems to be a fundamental error, since condensed systems with free boundaries cannot physically exist without net attractive interaction. Such an assumption could be correct—if at all—only at extremely low concentrations, when counterions may diffuse away from the macroions. This basic error is probably responsible for the above mentioned discrepancy between theory and experiment. For these reasons, and also in light of the observed dependence of the scattering behavior on molecular weight, the correlation hole theory should be viewed with extreme caution, at least for ionic macromolecules.

9. Summary and Outlook

Ever since *Bernal* and *Fankuchen* postulated an equidistant distribution of rod-like tobacco mosaic virus particles in very concentrated solutions,[61] several authors such as *Oster* et al.[62] have proposed a similar ordering of other biological and synthetic macromolecules. At that time, the apparatus available for X-ray scattering experiments were not sensitive enough for the study of dilute solutions. Recent technical developments now enable us to investigate relatively low concentrations. The development of new techniques such as neutron scattering and dynamic light scattering and the refinement of well-established techniques have now provided more powerful methods for the analysis of the distribution of particles in dilute solutions. For example, *Schmitz* et al.[63] have carried out dynamic light scattering measurements on poly-L-lysine at very low polymer and salt concentrations and have concluded that there exist "regions of correlated polymer motions for sufficiently high "local" concentrations and regions of "isolated" particles for sufficiently sparse local concentrations". It is difficult to find the essential difference between this statement and terminology such as the two-state structure proposed by us some time ago.[1,6] They further describe the role of counterions as screening of the direct repulsive interaction between the polyions and providing a "fluctuating dipole" interaction. In our opinion this interaction and the intermacroion attraction through the intermediary of counterions describe one and the same situation, except of course that the former emphasizes the dynamic character of the counterions. Recent studies by *Nemoto, Kurata* et al. also appears to provide positive support for the two-state structure.[64] Classical light scattering experiments on salt-free polyelectrolyte solutions at very low concentrations showed that the scattered intensity was characterized by a single broad peak, which is quite similar to the maxima obtained by X-ray and neutron scattering at much higher concentrations.[65] *Drifford* and *Dalbiez* concluded therefrom that their result was consistent with a short and local ordering. We are of the opinion that, if paracrystalline distortion is taken into consideration, this light scattering data is also consistent with the concept of a relatively long-range ordering of macroions, which would be stretched out fairly strongly at the concentrations employed.

It becomes increasingly clear that ionic solutes are structurally organized in dilute solutions under suitable conditions. Depending on the size, shape, and weight of the solutes, the experimental techniques to be used vary from solute to solute. The mode of ordering, the lifetime, and the size of the ordered structure also varies. When the fact that an ordered structure can exist in liquid states is fully comprehended, both the static and dynamic aspects of the ordering phenomena become equally important. Ignoring either of them would lead us to completely erroneous conclusions. The study of the trajectory of latex particles in ordered structures is an important advance, though much detailed study remains to be done in the future. The polymer latex has provided much valuable information, not directly accessible from X-ray or neutron scattering.

The ordering phenomena is obviously of great significance in the physical chemistry of ionic solutions; adequate knowledge about the nature of ordering is indispensable for a complete understanding of dilute ionic solutions. Furthermore, we believe that such a phenomenon might also be relevant to some of the activities of biological macromolecules. In this connection, for example, *Srere* has pointed out that the activity of Krebs cycle enzymes might be affected by their spatial relationships in the mitochondrial matrix.[66] From kinetic data, it has been concluded that ordered enzyme arrays are able to achieve higher throughputs than random arrays of enzymes at the same substrate concentration. To date, enzymologists have mostly analyzed the behavior of individual enzyme molecules in the test tube. The kinetics of enzymes in organized states may turn out to be an interesting subject in the future.[67]

The author expresses his gratitude to his co-workers, whose names are referred to in the references. He also expresses his thanks to Professor Ikuo Sogami for helpful discussions, Dr. von Korff, Michigan Molecular Institute, for having drawn attention to Ref. [66], and Professors J. Th. G. Overbeek and Shiro Akabori for valuable comments and for calling the author's attention to the relationship between "Intermacroionic" attraction and the coacervation phenomena. This work was generously supported by the Ministry of Education, Science and Culture (Grant-in-Aid for Specially Promoted Research), the Toray Science Foundation, the Mistubishi Foundation, and the Nissan Science Foundation, to whom sincere thanks are due.

Received: November 9, 1984;
revised: February 15, 1985 [A 570 IE]
German version: *Angew. Chem. 98* (1986) 323

[1] N. Ise, T. Okubo, *Acc. Chem. Res. 13* (1980) 303.
[2] P. Lagarde, A. Fontaine, D. Raoux, A. Sadoc, P. Migliardo, *J. Chem. Phys. 72* (1980) 3061.
[3] A. Sadoc, A. Fontaine, P. Lagardo, D. Raoux, *J. Am. Chem. Soc. 103* (1981) 6287.
[4] N. Ise, T. Okubo, K. Yamamoto, H. Matsuoka, H. Kawai, T. Hashimoto, M. Fujimura, *J. Chem. Phys. 78* (1983) 541.
[5] N. Ise, T. Okubo, S. Kunugi, H. Matsuoka, K. Yamamoto, Y. Ishii, *J. Chem. Phys. 81* (1984) 3294.
[6] N. Ise, T. Okubo, K. Yamamoto, H. Kawai, T. Hashimoto, M. Fujimura, Y. Hiragi, *J. Am. Chem. Soc. 102* (1980) 7901.
[7] A. Patrowski, E. Gulari, B. Chu, *J. Chem. Phys. 73* (1980) 4178.
[8] H. Matsuoka, N. Ise, T. Okubo, S. Kunugi, H. Tomiyama, Y. Yoshikawa, *J. Chem. Phys. 83* (1985) 378.
[9] N. Ise, T. Okubo, unpublished results.

[10] Neutron scattering on macroion solutions also shows a single broad peak [11, 12], which was interpreted by an isotropic model proposed by *de Gennes* et al. [13]. The observed molecular weight dependence mentioned in the text indicates that the isotropic model is not generally valid. It should be mentioned that *Gennes* et al. did not carry out experiments on the molecular weight dependence. The statement that the scattering behavior is molecular weight independent is therefore unfounded.
[11] M. Moan, *J. Appl. Crystallogr. 11* (1978) 519.
[12] M. Nierlich, C. E. Williams, F. Boue, J. P. Cotton, M. Daoud, B. Farnoux, G. Jannink, C. Picot, M. Moan, C. Wolff, M. Rinaudo, P. G. de Gennes, *J. Phys. (Paris) 40* (1979) 701.
[13] P. G. de Gennes, P. Pincus, R. M. Velasco, *J. Phys. (Paris) 37* (1976) 1461.
[14] R. P. Feynman, R. B. Leighton, M. Sands: *The Feynman Lecture on Physics, Vol. 1*, Addison-Wesley, Reading, MA 1963, Chapt. 2, p. 2-3.
[15] P. J. W. Debye, E. Hückel, *Phys. Z. 24* (1923) 85.
[16] J. Plestil, J. Mikes, K. Dušek, *Acta Polym. 30* (1979) 29.
[17] N. Ise, T. Okubo, M. Sugimura, K. Ito, H. Nolte, *J. Chem. Phys. 78* (1983) 536.
[18] J. W. Vanderhoff, H. J. van den Hul, R. J. M. Tausk, J. T. G. Overbeek in G. Goldfinger (Ed.): *Clean Surface*, Marcel Dekker, New York 1970.
[19] T. Alfrey, Jr., E. B. Bradford, J. W. Vanderhoff, G. Oster, *J. Opt. Soc. Am. 44* (1954) 603.
[20] W. Luck, M. Klier, H. Wesslau, *Ber. Bunsenges. Phys. Chem. 67* (1963) 75.
[21] A. Kose, M. Ozaki, K. Takano, Y. Kobayashi, S. Hachisu, *J. Colloid Interface Sci. 44* (1973) 330.
[22] N. Ise, T. Okubo, K. Ito, S. Dosho, I. Sogami, *J. Colloid. Interface Sci. 103* (1985) 292.
[23] R. Hosemann, R. Wilke, *Makromol. Chem. 118* (1968) 230.
[24] T. Kato, H. Masuda, A. Takahashi, *Polym. Prepr. Jpn. 31* (1982) 2249.
[25] W. Härtl, H. Versmold, U. Wittig, *Mol. Phys. 50* (1983) 815.
[26] Y. Ishii, H. Matsuoka, N. Ise, *Ber. Bunsenges. Phys. Chem. 90* (1986) 50.
[27] By assuming an hexagonal or face-centered cubic distribution we obtained slightly larger $2D_0$ values. However, the difference in the distribution modes is small in comparison with the values of $2D_{exp}$, so it does not affect our arguments [17].
[28] The $2D_{exp}$ value for latex solutions is affected by the column height of the solution. However, our experiments were designed to make the uncertainty in $2D_{exp}$ smaller than 10%, by taking into account previous results [29].
[29] R. S. Crandall, R. Williams, *Science 198* (1977) 293.
[30] N. Ise, T. Okubo, K. Itom, S. Dosho, I. Sogami, *Langmuir 1* (1985) 176.
[31] T. Yoshiyama, I. Sogami, N. Ise, *Phys. Rev. Lett. 53* (1984) 2153.
[32] M. Sugimura, T. Okubo, N. Ise, S. Yokoyama, *J. Am. Chem. Soc. 106* (1984) 5069.
[33] The activity coefficient of simple ionic species is assumed to be unity at infinite dilution. However, in the case of macroions, interaction still persists between the ionic groups even at infinite dilution, because the ionic groups are bound to each other by covalent bonds. In the light of this property, the activity coefficient of the macroion cannot be set equal to unity at infinite dilution. In Figure 4 the a_{2p} value was conveniently assumed to be unity at 0.1 equiv./1000 g. Since we are interested in the concentration dependence of the activity, the choice of the standard does not matter. In this reference system, $\ln a_{2p}$ at 1.2 equiv/1000 g is about -8.5×10^5, whereas at 0.1 equiv/1000 g it is 0. Such a surprisingly sharp drop in $\ln a_{2p}$ is due to the fact that the stoichiometric valency (z) of the latex particle under consideration is 3.5×10^5 and a_z is defined by the thermodynamic relation $a_z^{1+z} = a_{2g}^z \times a_{2p}$. Similar drastic decreases in $\ln a_{2p}$ were also noted earlier [34] in the case of synthetic macroions.
[34] N. Ise, T. Okubo, *J. Phys. Chem. 70* (1966) 2407.
[35] The tendency for solute activity to decrease with increasing concentration is not peculiar to macroions. As a matter of fact, the activity of a neutral polymer decreases with concentration in a limited concentration range when the so-called interaction parameter χ is large according to the Flory-Huggins theory (cf. Ref. [36] and [37]).
[36] H. Tompa: *Polymer Solutions*, Butterworth, London 1956, p. 96, 310.
[37] P. J. Flory: *Principles of Polymer Chemistry*, Cornell University Press, Ithaca, NY 1953, Chapt. 12.
[38] N. Ise, T. Okubo, *J. Phys. Chem. 70* (1966) 1930, 2400; *71* (1967) 1287, 1886, 4588; *72* (1968) 1370.
[39] I. Langmuir, *J. Chem. Phys. 6* (1938) 873.
[40] J. T. G. Overbeek in H. R. Kruyt (Ed.): *Colloid Science*, Elsevier, Amsterdam 1952, Chapt. 6.
[41] I. Sogami, *Phys. Lett. A 96* (1983) 199.
[42] I. Sogami, N. Ise, *J. Chem. Phys. 81* (1984) 6320.
[43] R. Williams, R. S. Crandall, P. J. Wojtowicz, *Phys. Rev. Lett. 37* (1976) 348.
[44] J. Th. G. Overbeek, M. J. Voorn, *J. Cell. Comp. Physiol. 49 Suppl. 1* (1957) 7, and references cited therein.
[45] R. H. Fowler, E. A. Guggenheim: *Statistical Thermodynamics*, Cambridge University Press, Cambridge 1939, Chapt. 9.
[46] The discrimination between V and v' has already been pointed out to be necessary by *Einstein* [47] in a different context.
[47] A. Einstein, *Ann. Phys. 17* (1905) 549.
[48] D. Bendedouch, S. H. Chen, *J. Phys. Chem. 87* (1983) 1653.
[49] G. S. Manning, *J. Chem. Phys. 43* (1965) 4260; *51* (1969) 924.
[50] N. Ise, T. Okubo, *Macromolecules 11* (1978) 439.
[51] a) A. Katchalsky, H. Eisenberg, *J. Polym. Sci. 6* (1951) 145; b) A. Oth, P. Doty, *J. Phys. Chem. 56* (1952) 43; c) R. M. Fuoss, *Discuss. Faraday Soc. 11* (1952) 125.
[52] B. E. Conway, J. A. V. Butler, *Nature (London) 172* (1953) 153.
[53] H. Fujita, T. Homma, *J. Colloid Sci. 9* (1954) 591.
[54] H. Eisenberg, J. Pouyet, *J. Polym. Sci. 13* (1954) 85.
[55] J. A. V. Butler, A. B. Robins, K. V. Shooter, *Proc. R. Soc. London A 241* (1957) 299.
[56] J. R. Huisenga, P. F. Grieger, F. T. Wall, *J. Am. Chem. Soc. 72* (1950) 2636.
[57] M. Yanagida, Y. Hiraoka, I. Katsura, *Cold Spring Harbor Symp. Quant. Biol. 47* (1983) 177.
[58] M. Yanagida, private communication.
[59] M. Benmouna, G. Weil, H. Benoit, Z. Akcasu, *J. Phys. (Paris) 43* (1982) 1679.
[60] In Ref. [59], the Debye screening parameter is erroneously defined. When this error is corrected, the physically meaningful charge number, which may be expected from the correlation hole theory to give a positive scattering intensity, is 32 for BSA at a charge number parameter of 10.
[61] J. D. Bernal, I. Fankuchen, *J. Gen. Physiol. 25* (1941) 111.
[62] D. P. Riley, G. Oster, *Discuss. Faraday Soc. 11* (1951) 107.
[63] K. S. Schmitz, M. Lu, J. Gauntt, *J. Chem. Phys. 78* (1983) 5059; K. S. Schmitz, M. Lu, N. Singh, D. J. Ramsay, *Biopolymers 23* (1984) 1637.
[64] N. Nemoto, H. Matsuda, Y. Tsunashima, M. Kurata, *Macromolecules 17* (1984) 1731.
[65] M. Drifford, J. P. Dalbiez, *J. Phys. Chem. 88* (1984) 5368.
[66] P. A. Srere in M. A. Mehlman, R. W. Hanson (Eds.): *Energy Metabolism and the Regulation of Metabolic Processes in Mitochondria*, Academic Press, New York 1972.
[67] *Note added in proof:* In 1984, *Schellman* discussed the forces stabilizing the DNA lattice [68] and pointed out that the electrostatic interaction is one of the major factors. He states, "The repulsion of one molecule by another has been overemphasized in discussions of condensed phases containing DNA. An analogy with ionic crystals is not unreasonable. This [repulsive energy] is more than compensated for by the attractive interactions of Cl^+ lattice with the Na^+ lattice. The key point is that ions of opposite charge are nearer to one another than ions of the same charge." The situation described in this statement is basically the same as that discussed in the text.
[68] J. A. Schellman, *J. Mol. Biol. 175* (1984) 313.

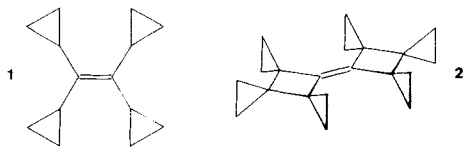
When submitting manuscripts, authors of articles intended for publication as "Communications" are requested to read the "Notice to Authors" reproduced in the January issue of the journal following the list of contents; upon request, a copy can be obtained from the editorial office.

10,10'-Bi(trispiro[2.0.2.0.2.1]decylidene): a Highly Nucleophilic Olefinic Hydrocarbon**

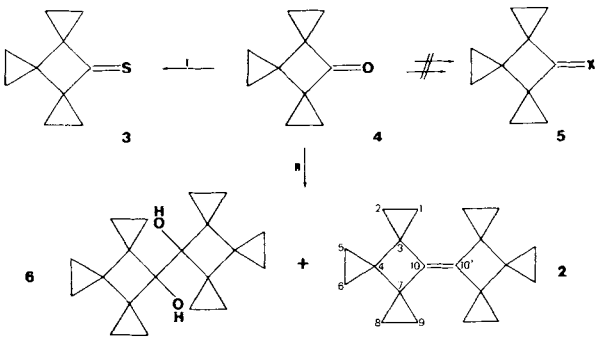
By *Horst Wenck, Armin de Meijere,* Fabian Gerson,* and *Rolf Gleiter*

Dedicated to Professor Hans Musso on the occasion of his 60th birthday

No other substituent without a heteroatom is as capable of enhancing the nucleophilicity of an olefin as the cyclopropyl group,[1] which exhibits a unique donor ability toward electron-deficient centers.[2] Tetracyclopropylethylene **1** has until now held the potential for the greatest effect of this kind, since it contains the largest number of such substituents.[3] However, because the short diagonal distance in a four-membered ring allows a 1,3-interaction,[4] both the four α- and the two β-spirocyclopropyl groups in the bi(cyclobutylidene) **2** should be able to exercise a donor effect on the double bond during electrophilic attack.



Our strategy for the synthesis of **2** started with readily available trispiro[2.0.2.0.2.1]decanone **4**.[5] Although conversion of **4** with *Lawesson*'s reagent[6] into the thioketone **3**[7] (85%) was achieved without difficulty, the preparation of the diazo compound **5a** could not be realized, despite the use of several methods. The hydrazone **5b** was very prone to azine formation, and the Bamford–Stevens reaction of the tosylhydrazone **5c** yielded only thermolysis products of the labile **5a**.[8] Thus, the "double-extrusion" route via the 2,5-dihydro-1,3,4-thiadiazole prepared from **3** and **5a**,[9] could not be employed, although this method has frequently been successful in the preparation of sterically demanding tetrasubstituted alkenes.



Scheme 1. **5a**, X=N_2; **5b**, X=NNH_2; **5c**, X=NNHTos. **I**: *Lawesson*'s reagent [6], toluene, reflux, 4 h; **II**: $TiCl_3$, $LiAlH_4$ (1:0.5), tetrahydrofuran, room temperature, 3d.

The titanium-induced reductive coupling of **4**,[10] on the other hand, was surprisingly easy, even though the yield was low. Based on a 60% conversion of **4**, the yield of **2**[7] was 8%, the major product being the pinacol **6**. The structure of **2** is unequivocally established by its spectral and physical data (see Table 1).

Table 1. Spectroscopic and physical data for **2** and **8**.

2: ^{1}H-NMR (270 MHz, $CDCl_3$): δ(TMS)=0.10 (s, 5,6,5',6'-H_2), 0.52 and 0.66 (AA'BB', 1,2,8,9,1',2',8',9'-H_2).—^{13}C-NMR (100.62 MHz, C_6D_6): δ(TMS)=5.32 (C-5,6,5',6'), 12.64 (C-1,2,8,9,1',2',8',9'), 29.77 (C-4,4'), 30.37 (C-3,7,3',7'), 136.22 (C-10,10').—IR (KBr): $\tilde{\nu}$=3160, 3010, 2870, 1460, 1425, 1010 cm^{-1}.—High-resolution MS: calcd for $C_{20}H_{24}$ 264.1878, found 264.1883 (±0.01).—M.p.=193 °C

8: ^{1}H-NMR (270 MHz, C_6D_6): δ=−0.31 (mc, 2H), −0.13 (mc, 4H), 0.02 (mc, 2H), 0.13 (mc, 4H), 0.31 (mc, 4H), 0.65 (mc, 2H), 0.77 (mc, 4H), 1.10 (mc, 2H).—IR (KBr): $\tilde{\nu}$=3060, 2980, 2920, 2850, 1760, 1660, 1460, 1370, 1280, 1255, 1100, 1010, 1000, 985, 940, 920, 870, 700, 850, 610 cm^{-1}.—High-resolution MS: calcd for $C_{20}H_{24}O$ 280.1827, found 280.1747 (±0.01)

As expected, **2** is very easily oxidized. The ESR spectrum of the radical cation $2^{\oplus\ominus}$, which was electrochemically produced at −80 °C in CH_2Cl_2 with n-Bu_4NClO_4 as the conducting salt, shows three hyperfine splittings with a_H=0.207, 0.048, and 0.014 mT, one for each set of eight equivalent protons. One of the splittings is caused by coupling with the eight protons on the β-spirocyclopropyl groups.[11]

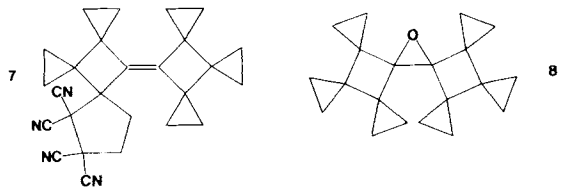
The oxidation potential of **2** ($E^{\circ\prime}$=0.74 V, determined cyclovoltammetrically vs. SCE) is far lower than that of **1** (1.13 V), let alone that of vinylcyclopropane (2.24 V).[13] This cannot be due to a twisting of the double bond in **2**, since the sterically comparable 2,2,2',2',4,4,4',4'-octamethylbi(cyclobutylidene) and the strongly twisted 2,2,2',2',5,5,5',5'-octamethylbi(cyclopentylidene) have $E^{\circ\prime}$ values of 1.81 and 1.37 V (vs. SCE), respectively.[14]

The He(I) photoelectron spectrum of **2** confirms the strong tendency to form $2^{\oplus\ominus}$. The π-ionization potential (IP(π)) of 7.3 eV for **2** is the lowest measured value for a monoolefin without heteroatom substituents;[15] the corre-

[*] Prof. Dr. A. de Meijere, Dipl.-Chem. H. Wenck
Institut für Organische Chemie der Universität
Martin-Luther-King-Platz 6, D-2000 Hamburg 13 (FRG)
Prof. Dr. F. Gerson
Institut für Physikalische Chemie der Universität
Klingelbergstrasse 80, CH-4056 Basel (Switzerland)
Prof. Dr. R. Gleiter
Institut für Organische Chemie der Universität
Im Neuenheimer Feld 270, D-6900 Heidelberg (FRG)

[**] This work was supported by the Deutsche Forschungsgemeinschaft (Project Me 405/15-1) and the Fonds der Chemischen Industrie. *H. W.* thanks the Fonds der Chemischen Industrie for a doctoral scholarship and *F. G.* thanks the Swiss National Science Foundation for support.

sponding values for tetracyclopropylethylene **1** and tricyclopropylethylene are IP(π)=7.9 and 7.48 eV, respectively.[16] Accordingly, **2** reacts smoothly with tetracyanoethylene in acetonitrile at room temperature. Presumably for steric reasons, however, attack occurs predominantly at one of the α-cyclopropyl groups to give **7** (64%), as observed for **1**.[3b] The question whether some addition also occurs at the double bond or at a β-cyclopropyl group remains open.



The oxidation of **2** with *m*-chloroperbenzoic acid (CH_2Cl_2, $NaHCO_3$) gave epoxide **8** (Table 1) without skeletal rearrangement. Compound **2** is also attacked by singlet oxygen ($^3O_2$, *hν*, tetraphenylporphin), but not by triplet oxygen, despite its low oxidation potential.

Received: October 21, 1985;
revised: Januar 9, 1986 [Z 1504 IE]
German version: *Angew. Chem. 98* (1986) 343

CAS registry numbers:
2, 101077-69-4; **2** (radical cation), 101077-71-8; **3**, 101077-64-9; **4**, 24375-15-3; **4** (azine), 101077-66-1; **5a**, 101077-68-3; **5b**, 101077-65-0; **5c**, 101077-67-2; **6**, 101077-70-7; **7**, 101144-75-6; **8**, 101077-72-9.

[1] Cf. V. J. Nowlan, T. T. Tidwell, *Acc. Chem. Res. 10* (1977) 252, and references cited therein.
[2] Review: A. de Meijere, *Angew. Chem. 91* (1979) 867; *Angew. Chem. Int. Ed. Engl. 18* (1979) 809, and references cited therein.
[3] a) This effect does not, however, result in an increase in the overall reaction rate for the addition of tetracyanoethylene; Cf. S. Nishida, *Angew. Chem. 84* (1972) 309; *Angew. Chem. Int. Ed. Engl. 11* (1972) 328. b) S. Nishida, I. Moritani, T. Teraji, *Chem. Commun. 1971*, 36.
[4] Cf. E. F. Kiefer, J. D. Roberts, *J. Am. Chem. Soc. 84* (1962) 784; M. Simonetta, S. Carrà, *Tetrahedron Lett. 1965*, 913; D. Seebach in *Houben-Weyl-Müller: Methoden der Organischen Chemie, Bd. IV/4*, p. 5, and references cited therein.
[5] L. F. Fitjer, *Chem. Ber. 115* (1982) 1047.
[6] B. S. Pederson, F. Scheibye, N. H. Nielsson, S. O. Lawesson, *Bull. Soc. Chim. Belg. 87* (1978) 223.
[7] All new compounds were fully characterized by ^{1}H-NMR, ^{13}C-NMR, and IR spectroscopy and by high-resolution mass spectrometry or satisfactory C,H elemental analysis.
[8] H. Wenck, A. de Meijere, unpublished results.
[9] D. H. R. Barton, F. S. Guziec, Jr., I. Shahak, *J. Chem. Soc., Perkin Trans. 1 1974*, 1794; T. G. Back, D. H. R. Barton, M. R. Britten-Kelly, F. S. Guziec, Jr., *ibid. 1976*, 2079. Cf. also A. Krebs, W. Rüger, B. Ziegenhagen, M. Hebold, I. Hardtke, R. Müller, M. Schütz, M. Wietzke, M. Wilke, *Chem. Ber. 117* (1984) 277.
[10] J. E. McMurry, M. P. Fleming, K. L. Kees, L. R. Krepski, *J. Org. Chem. 43* (1978) 3255; cf. also R. Dams, M. Malinowski, I. Westdorp, H. Y. Geise, *ibid. 47* (1982) 248 and references cited therein.
[11] INDO calculations [12] showed a clear trend for the hyperfine splittings, according to which the smallest corresponds to the 1(1′,2,2′,8,8′,9,9′)-H^{syn}, the largest to the 1(1′,2,2′,8,8′,9,9′)-H^{anti}, and the intermediate to the 5(5′,6,6′)-H. A definitive assignment can be made only after further experimentation. We thank Dipl.-Chem. *G. Gescheidt* for measuring the ESR spectra and Dipl.-Chem. *S. Kirchmeyer* for the INDO calculations.
[12] Cf. J. A. Pople, D. L. Beveridge, P. A. Dobosh, *J. Am. Chem. Soc. 90* (1968) 4201, and references cited therein.
[13] We thank *Dr. D. Knittel*, Institut für Physikalische Chemie, Universität Hamburg, for the cyclovoltammetric measurements.
[14] A. Krebs, W. Rüger, W.-U. Nickel, M. Wilke, U. Burkert, *Chem. Ber. 117* (1984) 310.
[15] Cf. R. Gleiter, *Top. Curr. Chem. 89* (1979) 197.
[16] S. Nishida, *J. Chem. Soc. Chem. Comnun. 1972*, 1114.

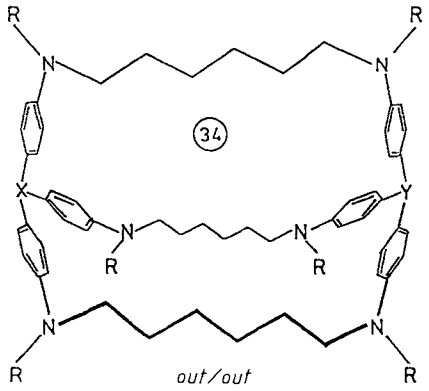
Bicyclic Host Cavities Derived from Triphenylamine—Guest Selectivity and Redox Properties**

By *Heinrich Schrage, Joachim Franke, Fritz Vögtle,** and *Eberhard Steckhan*

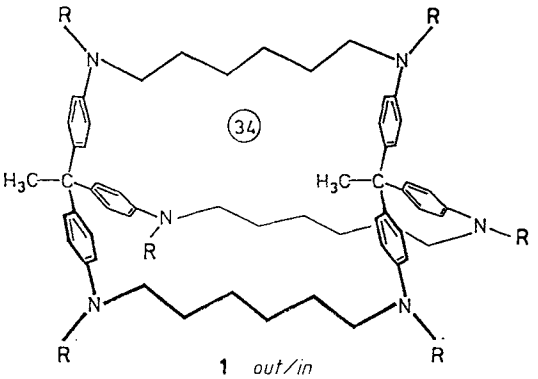
Dedicated to Professor Heinz A. Staab on the occasion of his 60th birthday

The host compounds (*out/out*)-**1** and (*out/in*)-**1**, which are derived from 1,1,1-triphenylethane are capable of forming complexes with guest molecules of varying size in aqueous acidic solution.[1] As revealed by models, the corresponding isomers of the triply bridged triphenylamine compounds **2** and **3** can undergo conformational interconversion, which obviates the necessity of separating them. Therefore, compounds **2** and **3** should be easy to synthesize and, moreover, should exhibit modified guest selectivities on account of their different bond angles. Furthermore, the triphenylamine unit is of interest because it is capable, via its radical cation, of serving as a redox catalyst that is incorporated into the ring system.

The yield obtained for the triple chain extension of **4**, Y=N, with 1,6-dibromohexane to give **5**, X=N, is slightly higher (21%) than that obtained for the synthesis of the



1: X, Y = C–CH_3; **2**: X, Y = N; **3**: X = N, Y = C–CH_3



1 *out/in*

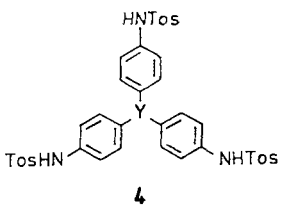
a: R = H; **b**: R = tosyl

[*] Prof. Dr. F. Vögtle, Dipl.-Chem. H. Schrage, Dr. J. Franke[+], Prof. Dr. E. Steckhan
Institut für Organische Chemie und Biochemie der Universität
Gerhard-Domagk-Strasse 1, D-5300 Bonn 1 (FRG)

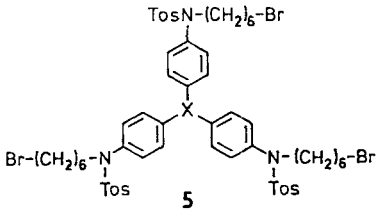
[+] Present address: Bayer AG, Wissenschaftliches Hauptlaboratorium, 5090 Leverkusen (FRG)

[**] This work was supported by the Fonds der Chemischen Industrie. We thank Mr. *T. Brettner* for his assistance.

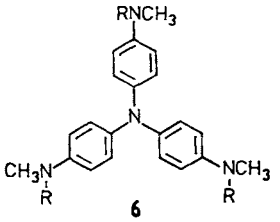
isomers **1** (17%). The crucial multiple ring closure to give the hexatosyl compound **2b** (24%) and **3b** (29%) from **4**, Y=C-CH_3, and **5**, Y=N, respectively, proceeded, however, in lower yield than that in the carbon series of equal chain length (79%). This result is presumably due to the less bent–trigonal instead of tetrahedral[2]—structure of the triphenylamine skeleton, which is less favorable for the cyclization.[3] Detosylation of **2b** and **3b** to give **2a** and **3a**, respectively, was achieved with HBr/phenol.[4]



4



5



6

Molecular models suggest that the cavities of **2** and **3** are shallower than the spherical cavity of (*out/out*)-**1** owing to the trigonal geometry of the triphenylamine nitrogen. This is confirmed by their different complexation properties. Thus, variously substituted naphthalene diols (2,7-, 2,6-, 2,3-) undergo complexation by **2a** and **3a**; however, adamantane, which undergoes complexation by (*out/out*)-**1a**, does not. The ^{1}H-NMR high-field shifts observed ($\Delta\delta$=0.25 ppm) for the host/guest complexes with **2a** are not dramatic; however, the signals of the guest undergo strong line broadening, which indicates dynamic exchange processes that are slow on the NMR time scale. With the host **3a** and 2,7-naphthalenediol as guest, on the other hand, sharp signals with marked shifts to high field are found for the guest protons ($\Delta\delta \approx 0.5$ ppm).[5]

Fluorescence spectroscopic measurements permit the study of the complexation of ANS (8-anilino-1-naphthalenesulfonate) by **2a** and **3a**:[6] the constants for complex formation so determined in each case are less than those for (*out/out*)-**1a** (lg K=4.6),[1a] and the difference between **2a** and **3a** (lg K=3.1 and 3.2, respectively) is minor within the limits of experimental error. The hydrophobicity of the cavity is supported by the observed blue shift in the wavelength maximum of emission to λ=485 nm (**2a**) and 440 nm (**3a**).[7]

The electrochemical properties of the host compounds **2** and **3** are of interest in connection with their model character for redox enzymes. Triarylamines are well known as electron-transfer reagents (mediators).[8] In these reactions, the electrochemically generated and regenerated, stable radical cations serve as the oxidizing agent. The oxidation potentials are very sensitive to the steric effects of substituents, which result in twisting and/or bending of the aryl groups.[9] Accordingly, the redox behavior of the bicyclic compounds **2** and **3**, in comparison to that of the open-chain compound **6**, may be used as a probe for steric effects.

The cyclovoltammograms of the new bicyclic compounds **2b** (Fig. 1), **3b**, and **6b** are very similar.[10, 11] They all show two redox pairs, Ox1/Red1 and Ox2/Red2, during the first potential scan; moreover, during the second potential scan, a new redox pair, Ox3/Red3, is observed at lower potentials, which, with increasing number of potential scans, increases at the expense of Ox2/Red2. The first redox step, the formation of the radical cation, exhibits electrochemical and chemical reversibility for all compounds and is diffusion controlled (Fig. 1b). The second step corresponds to the formation of a dication, which, in a chemical follow-up reaction, forms the third redox pair, Ox3/Red3, which is presumably a quinoid system. The potentials of the first oxidation steps of **2b** and **3b** are shifted by about 135 mV and 110 mV, respectively, to more positive values in comparison with the open-chain compound **6b** (see Table 1). This clearly reflects the differing steric environment, which will cause the bending or twisting of the aryl groups in the bicyclic compounds. Likewise, the slight release of strain upon replacement of a triphenylamine unit by a triphenylmethane unit is reflected in the potential. In contrast, steric factors have less effect on the potential of the second redox step.

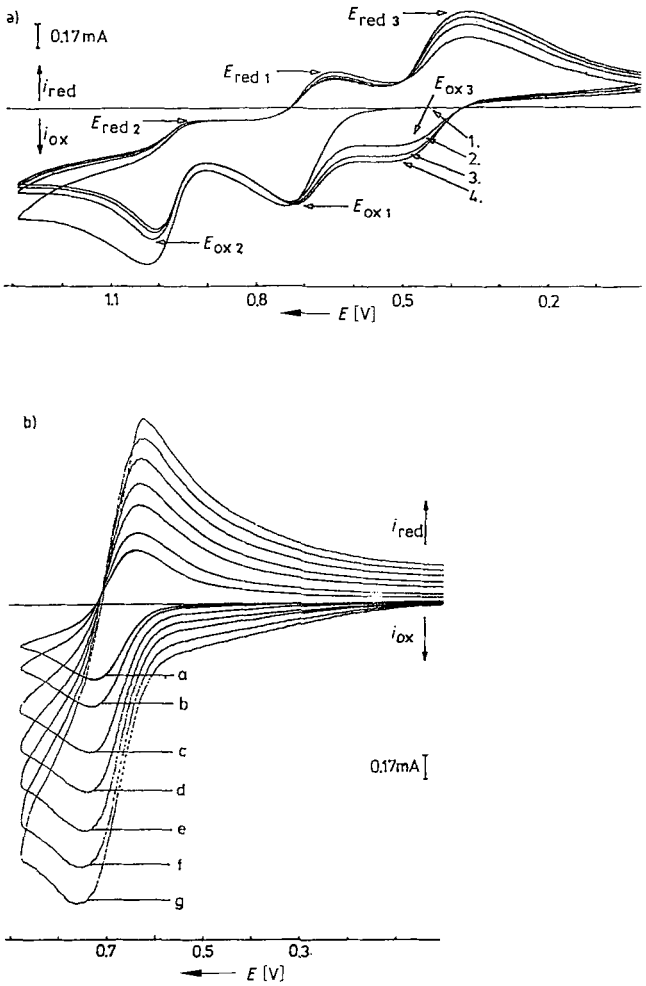


Fig. 1. Cyclovoltammogram of **2b**: a) Potential range 0–1.3 V [Ag/$AgNO_3$ (0.1 M in CH_3CN)], potential scan rate 40 mV/s, the numbering corresponds to the sequence of the scans; concentration of **2b**: 2×10^{-3} M in CH_3CN/CH_2Cl_2 (1:1) (0.1 M $LiClO_4$). b) Potential range 0–900 mV [Ag/$AgNO_3$ (0.1 M in CH_3CN)], potential scan rate (a–g): 20, 40, 90, 160, 250, 360, 490 mV/s, concentration as in a). The Ag/$AgNO_3$ reference electrode has a potential of 590 mV versus the normal hydrogen electrode (NHE).

Table 1. Potentials of compounds **2b**, **3b**, **6b** [a].

	E_{ox1}/E_{red1}	E_{ox2}/E_{red2}	E_{ox3}/E_{red3}
2b	725/660	1010/– [b]	525/370
3b	700/640	1030/– [b]	500/350
6b	590/530	965/880	445/380

[a] Potentials in mV relative to the $Ag/AgNO_3$ reference electrode. [b] Reduction signal too weak for exact determination.

Compounds **2** and **3** are, therefore, two of the most easily prepared water-soluble hosts with a high inclusion ability whose electronic state and reactivity and, possibly, cavity shape, can be influenced electrochemically. Since **2** and **3**, as well as guest compounds, are capable of undergoing redox reactions, possibilities exist for novel substrate-selective redox reactions.[12]

Received: October 31, 1985;
revised: December 12, 1985 [Z 1517 IE]
Publication delayed at authors' request
German version: *Angew. Chem. 98* (1986) 335

CAS registry numbers:
2a, 100814-17-3; **2a** · XHCl, 100814-19-5; **2b**, 100814-15-1; **3a**, 100814-18-4; **3a** · XHCl, 100814-20-8; **3b**, 100814-16-2; **4** (Y = C–CH_3), 95274-90-1; **4** (Y = N), 100814-13-9; **5** (X = N), 100814-14-0; **6b**, 100814-21-9; $Br(CH_2)_6Br$, 629-03-8; 2,3-naphthalenediol, 92-44-4; 2,6-naphthalenediol, 581-43-1; 2,7-naphthalenediol, 582-17-2; 8-anilino-1-naphthalenesulfonate, 82-76-8.

[1] a) J. Franke, F. Vögtle, *Angew. Chem. 97* (1985) 224; *Angew. Chem. Int. Ed. Engl. 24* (1985) 219; b) cf. D. O'Krongly, S. R. Denmeade, M. Y. Chiang, R. Breslow, *J. Am. Chem. Soc. 107* (1985) 5544.

[2] D. Hellwinkel, M. Melan, C. R. Degel, *Tetrahedron 29* (1973) 1895; K. S. Hayes, M. Nagumo, J. F. Blount, K. Mislow, *J. Am. Chem. Soc. 102* (1970) 2773.

[3] F. Vögtle, J. Winkel, *Tetrahedron Lett. 1979*, 161.

[4] The structures given are supported by elemental analysis and by NMR and mass spectra.—**2a** (hydrochloride): m.p. > 330 °C; ^{1}H-NMR (400 MHz, $\delta(D_2O)$=3.8): δ = 1.28–1.60 (m, 24H, CH_2), 3.38 (t, 12H, CH_2N, J=6 Hz), 7.12, 7.40 (AA'BB', 24H, aromat. H, J=9 Hz); ^{13}C-NMR (200 MHz, D_2O, trimethylsilyl propionate ext.): δ=25.57, 26.86 (CH_2), 52.75 (CH_2N), 126.89, 127.75, 131.70, 149.94 (aromat. C); MS: m/z 826 (M^+, 100%).—**2b**: m.p. > 330 °C; ^{1}H-NMR (400 MHz, CD_2Cl_2/TMS int.): δ=1.13–1.30 (m, 24H, CH_2), 2.41 (s, 18H, tosyl-CH_3), 3.40 (t, 12H, CH_2N, J=6 Hz), 6.82 (s, 24H, aromat. H), 7.24, 7.44 (AA'BB', 24H, aromat. H); ^{13}C-NMR (400 MHz, CD_2Cl_2/TMS int.): δ=21.35 (tosyl-CH_3), 26.00, 27.23 (CH_2), 50.00 (CH_2N), 124.04, 127.7, 129.49, 129.69, 133.81, 135.21, 143.73, 146.43 (aromat. C).—**3a** (hydrochloride): m.p. > 330 °C; ^{1}H-NMR (400 MHz, $\delta(D_2O)$=4.8); δ=1.16–1.58 (m, 24H; CH_2), 2.10 (s, 3H, CH_3-*out*), 3.30, 3.38 (dt, 12H, CH_2N), 7.00–7.42 (AB system, 24H, aromat. H); MS: m/z 839 (M^+, 100%).—**3b**: m.p. = 158–159 °C; ^{1}H-NMR (400 MHz, CD_2Cl_2/TMS int.): δ=1.10–1.32 (m, 24H, CH_2), 2.16 (s, 3H, CH_3-*out*), 2.41 (s, 18H, tosyl-CH_3), 3.36–3.50 (m, 12H, CH_2N), 6.80–6.86 (s, 24H, aromat. H), 7.22–7.48 (AB system, 24H, aromat. H).

[5] Exact assignment of the proton signals is difficult on account of overlapping of the host and guest signals. Measurement conditions: 400 MHz, D_2O/DCl, pD=1.2, T=20 °C; standard: HDO at δ=4.8; concentrations: host: 2.5×10^{-2} M, guest: 2.5×10^{-2} M.

[6] Hitachi 204-A fluorescence spectrometer, excitation wavelength: λ=390 nm (**2a**), 360 nm (**3a**), emission measurement at λ = 485 nm (**2a**), 440 nm (**3a**), medium 0.5 M KCl/0.015 M HCl buffer, concentration of ANS: 2×10^{-6} M; the concentrations of **2a** and **3a** were varied from 0 to 10^{-3} M.

[7] Cf. F. Diederich, K. Dick, *J. Am. Chem. Soc. 106* (1984) 8024.

[8] K. H. Grosse-Brinkhaus, E. Steckhan, W. Schmidt, *Acta Chem. Scand. B37* (1983) 499; M. Platen, E. Steckhan, *Chem. Ber. 117* (1984) 1679, and references cited therein.

[9] W. Schmidt, E. Steckhan, *Chem. Ber. 113* (1980) 577.

[10] Although the free amines **2a**, **3a**, and **6a** could be analyzed electrochemically, as we were able to show for **2a**, the tosyl derivates **2b**, **3b**, and **6b** were chosen on account of their high chemical stability. The steric effects on the potential should be similar for the two types of compound.

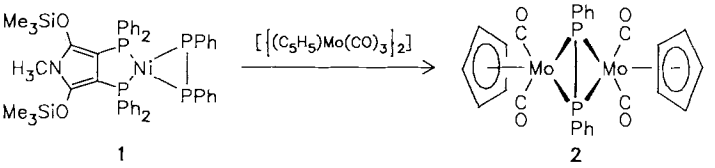
[11] Potentiostat Wenking-Potentioscan POS 73 (Bank Elektronik), combined with a Hewlett-Packard 7045A xy-printer. A Metrohm EA-876-5 cell served as the electrolysis vessel. It was equipped with a platinum working electrode (0.18 cm^2) and a platinum counter electrode as well as a $Ag/AgNO_3$ reference electrode.

[12] A step in this direction is the substitution of β-cyclodextrin in the 6-position with a catalytically active redox group: C. Z. Smith, J. H. P. Utley, *Chem. Soc. Chem. Commun. 1981*, 792. General examples of catalytically redox-active macrocycles: A. G. Talma, P. Jouin, J. G. De Vries, C. B. Troostwijk, G. H. Werumeus Buning, J. K. Waninge, J. Visscher, R. M. Kellogg, *J. Am. Chem. Soc. 107* (1985) 3981; W. Geuder, S. Hünig, A. Suchy, *Angew. Chem. 95* (1983) 501; *Angew. Chem. Int. Ed. Engl. 22* (1983) 489.

$[(\eta^5\text{-}C_5H_5)_2Mo_2(CO)_4(PPh)_2]$, a Diphosphene Complex with a Butterfly Structure**

By *Dieter Fenske** and *Kurt Merzweiler*

We recently described the reaction of $PhE(SiMe_3)_2$ (E = P, As) with [2,3-bis(diphenylphosphino)-*N*-methylmaleimide]nickel(II) chloride,[1] which results in migration of two $SiMe_3$ substituents to the CO groups of the maleimide and formation of the complex **1** as well as its analogue with $(AsPh)_2$ instead of $(PPh)_2$, the $(EPh)_2$ ligands having a *trans* configuration. In attempts to prepare heterometallic clusters, we allowed **1** to react with $[\{CpMo(CO)_3\}_2]$ in toluene. This resulted in the evolution of CO and the formation of an insoluble nickel-containing precipitate of unknown structure. When pentane was added to the filtrate, the dark brown, diamagnetic diphosphene complex **2** crystallized in a yield of 30%.[2]



1 **2**

The IR spectrum (KBr) of **2** exhibits four $\tilde{\nu}$(CO) bands (1950, 1930, 1861, and 1845 cm^{-1}). The P atoms of the $(PPh)_2$ ligands give rise to a singlet at $\delta = -94$ in the ^{31}P-NMR spectrum (tetrahydrofuran); the ^{1}H-NMR spectrum exhibits a multiplet at δ = 7.10 (Ph) and a singlet at δ = 5.50 (Cp).

According to the crystal structure analysis,[3] **2** (Fig. 1) consists of a *cis*-diphosphene unit, which bridges two Mo atoms. In addition, two terminal CO groups and an η^5-C_5H_5 ligand are bonded to each Mo atom. The Mo–P bond lengths are significantly different (Mo1–P1, Mo2–P1: 246.6, 247.0; Mo2–P2, Mo1–P2: 254.2, 254.6 pm).

Most of the $(ER)_2$ complexes known to date contain the ligands in the *trans* configuration.[4] However, compounds containing a *cis*-$(PR)_2$ group, e.g., **3**–**5**, are also known.[5]

$[Fe_2(CO)_6(PtBu)_2]$ **3**

$[Ni_5(CO)_6\{[(Me_3Si)_2CHP]_2\}_2]Cl$ **4**

$[(mesityl\text{-}P)_2\{Mo(CO)_5\}_2]$ **5**

$[Cp_2Mo_2(CO)_4P_2]$ **6**

[*] Prof. Dr. D. Fenske, Dipl.-Chem. K. Merzweiler
Institut für Anorganische Chemie der Universität
Engesserstrasse, Geb. Nr. 30.45, D-7500 Karlsruhe (FRG)

[**] This work was supported by the Deutsche Forschungsgemeinschaft and the Fonds der Chemischen Industrie. We thank the Institut für Kristallographie der Universität Karlsruhe for measurement of the crystal data.

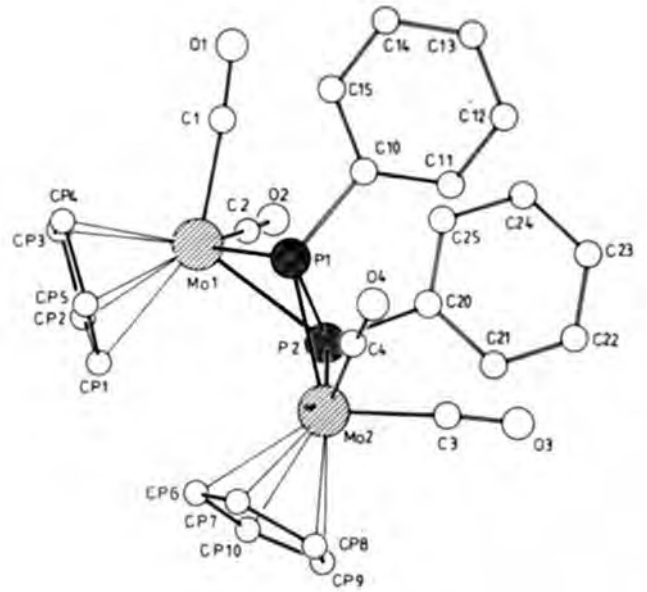


Fig. 1. Structure of **2** in the crystal. Important bond lengths (±0.2 pm) and bond angles (±0.1°): Mo1-P1 246.6, Mo1-P2 254.6, Mo1-C1 193.1, Mo1-C2 196.2, C-O 114.2-114.8, Mo-C(Cp) 229-238, C(Cp)-C(Cp) 138.5-142.2, P1-P2 213.6, Mo2-P1 247.0, Mo2-P2 254.2, Mo2-C3 193.6, Mo2-C4 195.9; P1-Mo1-P2 50.4, Mo1-P-Mo2 110.8-116.0, P-P-Mo 62.9-66.7, Mo-C-O 174.1-177.6, P1-Mo2-P2 50.4.

The P1-P2 distance (213.6 pm) is significantly shorter than a P-P bond and is similar to the values that have also been found for other "side-on"-coordinated $(PR)_2$ complexes.[4] It is noteworthy that the P-P bond in **2** is longer than that in **3** (205.9 pm), **4** (208.5, 209.8 pm), and **5** (202.6 pm). The angle between the planes Mo1, P1, P2 and Mo2, P1, P2 is 135°. The distance between the Mo atoms is 418.7 pm; i.e., they are not bonded to each other.

M_2P_2 clusters with tetrahedral structure were found, e.g., in **3** and in **6**.[6] In these cases, 14e and 15e complex fragments are bridged by a 6e donor $(PR)_2$ and a 4e donor (P_2), respectively. In order to attain a filled 18e shell at the metal center, a metal-metal bond is formed (Fe-Fe in **3**: 274.0 pm, Mo-Mo in **6**: 302.2 pm). In contrast, the 18e rule is fulfilled for **2** without the formation of a Mo-Mo bond. Comparison of **2** and **6** clearly shows that the Mo_2P_2 cluster in **2** is formed by opening of the Mo-Mo bond in **6**, resulting in a butterfly structure for the Mo_2P_2 skeleton.

According to the isolobal terminology of *Roald Hoffmann*, **3** and **6** can be regarded as derivatives of tetrahedrane.[7] **2** is then a derivative of bicyclobutane. Accordingly, a formal analogy exists between **2** and E_2 complexes (E = P, As) such as $(diphos)_2Ni_2P_2$ (diphos = bis(diphenylphosphino)ethane and $[\{(C_5Me_5)(CO)_2Mn\}_2As_2]$.[8,9] The formation of **2** is one of the first examples for the transfer of a coordinated diphosphene to another metal.

Received: November 25, 1985;
revised: January 17, 1986 [Z 1552 IE]
German version: *Angew. Chem. 98* (1986) 357

[1] D. Fenske, K. Merzweiler, *Angew. Chem. 96* (1984) 600; *Angew. Chem. Int. Ed. Engl. 23* (1984) 635.

[2] *Experimental procedure*: **1** (2.70 g, 0.030 mol) and $[\{(C_5H_5)Mo(CO)_3\}_2]$ (1.58 g, 0.032 mol) were dissolved in 100 mL of toluene and heated for 1 h at 100°C. After filtration, the solution was covered with a layer of pentane. **2** crystallizes at the phase boundary in a yield of 0.60 g (30%).

[3] Crystals of **2** from toluene/pentane. Space group $P\bar{1}$, lattice constants (180 K): $a = 1027.9(3)$, $b = 1105.2(3)$, $c = 1207.0(3)$ pm, $\alpha = 86.54(2)$, $\beta = 74.30(2)$, $\gamma = 67.23(2)°$; $Z = 2$, $\mu(Mo_{K\alpha}) = 12.2$ cm^{-1}, empirical absorption correction; Syntex R3, $2\theta = 3.5$-$56.0°$, 6484 reflections, 6100 with $I > 2\sigma(I)$; Patterson methods, Mo, P, C, O anisotropic, H isotropic, $R_1 = 0.035$, $R_2 = 0.041$. Further details of the crystal structure investigation may be obtained from the Fachinformationszentrum Energie, Physik, Mathematik GmbH, D-7514 Eggenstein-Leopoldshafen 2 (FRG), on quoting the depository number CSD-51756, the names of the authors and the journal citation.

[4] J. C. Green, M. L. H. Green, G. E. Morris, *J. Chem. Soc. Chem. Commun. 1974*, 212; E. Cannilo, A. Coda, K. Prout, J. C. Daran, *Acta Crystallogr. B33* (1977) 2608; A. H. Cowley, J. E. Kilduff, J. G. Lasch, N. C. Normann, M. Pakulski, F. Ando, T. C. Wright, *J. Am. Chem. Soc. 105* (1983) 7751; J. Borm, L. Zsolnai, G. Huttner, *Angew. Chem. 95* (1983) 1018; *Angew. Chem. Int. Ed. Engl. 22* (1983) 977; *Angew. Chem. Suppl.* 1477; H. Schäfer, *Z. Naturforsch. B34* (1979) 1358; B. Deppisch, H. Schäfer, *Z. Anorg. Allg. Chem. 490* (1982) 129; B. Deppisch, H. Schäfer, *Acta Crystallogr. B38* (1982) 748; A. H. Cowley, *Polyhedron 3* (1984) 389; O. J. Scherer, *Angew. Chem. 97* (1985) 905; *Angew. Chem. Int. Ed. Engl. 24* (1985) 924.

[5] H. Vahrenkamp, D. Wolters, *Angew. Chem. 95* (1983) 152; *Angew. Chem. Int. Ed. Engl. 22* (1983) 154; M. M. Olmstead, P. P. Power, *J. Am. Chem. Soc. 106* (1984) 1495; H. Lang, O. Orama, G. Huttner, *J. Organomet. Chem. 291* (1985) 293.

[6] O. J. Scherer, H. Sitzmann, G. Wolmershäuser, *J. Organomet. Chem. 268* (1984) C9.

[7] R. Hoffmann, *Angew. Chem. 94* (1982) 725; *Angew. Chem. Int. Ed. Engl. 21* (1982) 711.

[8] H. Schäfer, D. Binder, D. Fenske, *Angew. Chem. 97* (1985) 523; *Angew. Chem. Int. Ed. Engl. 24* (1985) 522.

[9] W. A. Herrmann, B. Koumbouris, T. Zahn, M. L. Ziegler, *Angew. Chem. 96* (1984) 802; *Angew. Chem. Int. Ed. Engl. 23* (1984) 812.

Simple Synthesis of Anthracyclinones by Cyclization of an Intermediate Hydroxynitronate**

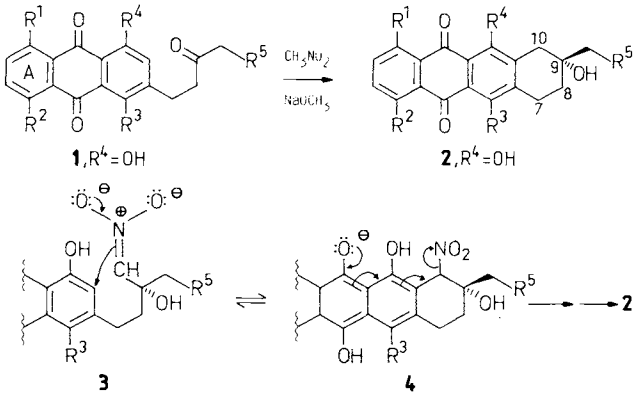
By *Karsten Krohn** and *Wahyudi Priyono*

The possibility of introducing side chains regioselectively by the Marschalk reaction or the Claisen rearrangement has made hydroxylated anthraquinones valuable starting materials in the synthesis of anthracyclinones.[2] Thus, the oxoalkyl anthraquinones **1b-f**, for example, can be prepared in over 50% yield from industrially manufactured 1,4,5-trihydroxy-9,10-anthraquinone.[3,4] The C atom required for the cyclization to anthracyclinones was introduced previously via acyl anion equivalents such as lithio-1,3-dithiane[3] or lithiodichloromethane[4] in a multistep reaction sequence. We have now found that the condensation of the ketones **1a-f** with nitromethane offers a preparatively simple, one-pot procedure for the synthesis of the anthracyclinones **2a-f**.

Sutherland et al.[5] have employed the addition of a long-chain nitroalkane building block for the synthesis of 9-deoxydaunomycinone. In our method, the incorporation of the C_1 building block into the ketone **1** and the formation of the 9-OH group of the anthracyclinone are carried out simultaneously. The procedure is generally applicable to a wide variety of substituted 1,4-dihydroxy anthraquinones, such as **1b-e**. Compounds without hydroxyl groups on C-4 cyclize equally well, as shown by the conversion of **1f** into the new anthracyclinone **2f**. However, the presence of the phenolic hydroxyl group on C-1 is necessary: compounds of type **1** ($R^1 = R^5 = H$, $R^2 = R^3 = OH$, $R^4 = H$ or OCH_3) cannot be converted into tetracycles with nitromethane. These findings reveal at the same time the mechanism of this remarkable cyclization. We propose that the ketones **1** exist in equilibrium with the nitromethane adducts **3**, which, as indicated by the arrows, undergo intramolecu-

[*] Prof. Dr. K. Krohn, Dr. W. Priyono
Institut für Organische Chemie der Technischen Universität
Hagenring 30, D-3300 Braunschweig (FRG)

[**] Synthetic Anthracyclinones, Part 30.—Part 29: [1].



	R^1	R^2	R^3	R^5	**2**, yield [%]
a	H	H	OH	CH_3	66
b	H	OH	OH	H	80
c	H	OH	OH	CH_3	92
d	H	OCH_3	OH	H	81
e	H	OCH_3	OH	CH_3	83
f	OH	H	H	H	81

lar *nucleophilic* addition resulting in cyclization to the quinones **4**. Tautomeric forms of the anthraquinones, in which the quinoid function is shifted to the outer ring A, may play a role in this reaction.[6] In the final step, the primary cyclization product **4** stabilizes itself by elimination of the nitro group and simultaneous reoxidation to the products **2**. This intramolecular redox process with elimination of leaving groups in the benzylic position is well established for the anthrahydroquinones.[2,7,8]

By hydroxylation at C-7 of **1b**,**c** and **1d**,**e**, the racemic natural products belonging to the rhodomycinones and feudomycinones, respectively, are obtained;[4b] **1c** or **1e** can be converted into β-rhodomycinones via elimination of the tertiary hydroxyl group on C-9.[9]

Experimental Procedure

2: A solution of sodium (92 mg, 4 mmol) in 100 mL of anhydrous ethanol was treated with 3 mL of nitromethane and 1 mmol of **1** [4, 10] and then refluxed under nitrogen for 24–48 h until all the starting material had reacted (as followed by tlc). After neutralization with acetic acid, the solution was concentrated, and the residue was dissolved in ca. 50 mL of dichloromethane, washed with water, and dried over sodium sulfate. The solution was then concentrated again and the product recrystallized from a small amount of dichloromethane/ether. **2f**: m.p. = 183 °C; IR: $\tilde{\nu}$ = 3400 (OH), 1675, 1662, 1621 (C=O); UV (CH_3OH): λ_{max} (lg ε) = 224 (4.20), 259 (4.11), 286 (3.85), 431 (3.66), 450 nm (3.62); ^{1}H-NMR (400 MHz): δ = 1.29 (s; 1H, 9_{ax}-OH), 1.45 (s; 3H, 9_{eq}-CH_3), 1.80 (ddd, $J(8_{ax,eq})$ = 13.4 Hz, $J(8_{ax},7_{ax})$ = 10.5 Hz, $J(8_{ax},7_{eq})$ = 6.0 Hz; 1H, 8_{ax}-H), 1.95 (dddd, $J(8_{eq,ax})$ = 13.4 Hz, $J(8_{eq},7_{ax})$ = 6.5 Hz, $J(8_{eq},7_{eq})$ = 4.5 Hz, $J(8_{eq},10_{eq})$ = 2.0 Hz; 1H, 8_{eq}-H), 2.77 (d, $J(10_{ax,eq})$ = 18.5 Hz; 1H, 10_{ax}-H), 2.90 (ddd, $J(7_{eq,ax})$ = 18.5 Hz, $J(7_{eq},8_{ax})$ = 10.5 Hz, $J(7_{eq},8_{eq})$ = 4.5 Hz; 1H, 7_{eq}-H), 2.95 (dd, $J(10_{eq,ax})$ = 18.5 Hz, $J(10_{eq},8_{eq})$ = 2.0 Hz; 1H, 10_{eq}-H), 1.16 (ddd, $J(7_{ax,eq})$ = 18.5 Hz, $J(7_{ax},8_{ax})$ = 10.5 Hz, $J(7_{ax},8_{eq})$ = 6.5 Hz; 1H, 7_{ax}-H), 7.28 (dd, $J(2,3)$ = 8.3 Hz, $J(2,4)$ = 1.0 Hz; 1H, 2-H), 7.63 (s; 1H, 6-H), 7.66 (t; 1H, 3-H), 7.28 (dd, $J(4,3)$ = 7.1 Hz, $J(4,2)$ = 1.0 Hz; 1H, 4-H), 12.15 and 12.48 (each s; each 1H, each OH); MS (180 °C): *m/z* 324 (70%, M^+), 306 (55, $M^+ - H_2O$), 296 (100, $M^+ - CO$), 291 (49, $M^+ - CH_3 - H_2O$), 281 (83), 266 (61).

Received: November 28, 1985 [Z 1558 IE]
German version: *Angew. Chem. 98* (1986) 338

CAS registry numbers:
1a, 72817-84-6; **1b**, 88100-93-0; **1c**, 75963-98-3; **1d**, 95384-68-2; **1e**, 75963-97-2; **1f**, 100929-19-9; **2a**, 75963-80-3; **2b**, 88101-19-3; **2c**, 63640-62-0; **2d**, 95384-76-2; **2e**, 63605-05-0; **2f**, 100929-20-2; $MeNO_2$, 75-52-5.

[1] K. Krohn, K. Tolkiehn, V. Lehne, H. W. Schmalle, H.-F. Grützmacher, *Liebigs Ann. Chem. 1985*, 1311.
[2] Review: K. Krohn, *Angew. Chem.*, in press.
[3] K. Krohn, B. Behnke, *Chem. Ber. 113* (1980) 2994.
[4] a) K. Krohn, B. Behnke, *Liebigs Ann. Chem. 1983*, 1818; b) K. Krohn, W. Priyono, *Tetrahedron 40* (1984) 4609.
[5] A. E. Ashcroft, D. T. Davies, J. K. Sutherland, *Tetrahedron 40* (1984) 4579.
[6] K. Krohn, W. Baltus, *Synthesis*, submitted.
[7] C. Marschalk, F. Koenig, N. Ourousoff, *Bull. Soc. Chim. Fr. 3* (1936) 1545.
[8] K. Bredereck, S. A. Metwally, *Liebigs Ann. Chem. 1974*, 1536.
[9] A. S. Kende, Y.-G. Tsay, *J. Chem. Soc. Chem. Commun. 1977*, 140.
[10] The ketone **1f** was prepared from aloe emodin in analogy to a published procedure [4]: K. Krohn, J. Köhle, unpublished results.

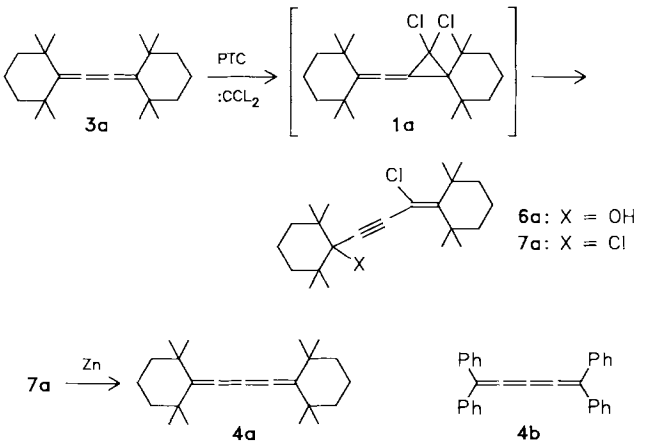
Structure Determinations of Pentatetraenes—Comparison of the Structures of Cumulenes**

By *Hermann Irngartinger** and *Wolfgang Götzmann*

Dedicated to Professor Heinz A. Staab on the occasion of his 60th birthday

For our studies on the structures of cumulenes,[1] we synthesized the pentatetraene **4a**.[2] The addition of dichlorocarbene to the butatriene **3a** (phase-transfer conditions (PTC)[3]) did not afford the expected[2b,4] adduct **1a** but rather the rearranged enynol **6a**. The X-ray structure analysis[5] revealed a lengthening of the double bond to 1.348(3) Å, which is due to strong repulsive interactions between the chlorine atom and the two neighboring methyl groups (Cl···C 3.170(3) and 3.213 (3) Å). In comparable enyne units the double bonds are 1.305–1.338 Å long.[6] Because the chlorine atom is locked in place by the two methyl groups, twisting of the double bond is not possible (torsional angle only 4.5°). The weakening of the bond is also shown by the C=C vibrational absorption, which is shifted to longer wavelengths (IR 1540, Raman 1544 cm^{-1}). The pentatetraene **4a** was ultimately obtained by exchange of the OH group of **6a** for Cl followed by cleavage of chlorine from **7a** with zinc dust.[7]

The structures of **4a**[7] and its tetraphenyl analogue **4b**[8] were determined by X-ray diffraction. Both cumulenes are



[*] Prof. Dr. H. Irngartinger, Dr. W. Götzmann
Organisch-chemisches Institut der Universität
Im Neuenheimer Feld 270, D-6900 Heidelberg 1 (FRG)

[**] This work was supported by the Deutsche Forschungsgemeinschaft and the Fonds der Chemischen Industrie.

linear (Fig. 1). In each case, the terminal substituents are oriented perpendicularly to each other (with the exception of a deviation of 10° in **4a** caused by packing effects). Owing to the differing hybridization of the C atoms, the terminal C(sp^2)=C(sp) double bonds in both molecules are longer than the central C(sp)=C(sp) bonds. The terminal double bonds of **4b** are significantly lengthened by conjugation with the phenyl rings; in contrast, the central double bonds in **4a** and **4b** have approximately the same lengths (Fig. 1). Only *one* of the phenyl groups at each end of the tetraene system **4b** adopts an orientation that is favorable for the conjugation. The twist angles of the phenyl rings with respect to the plane of the terminal double bonds are 16.4° and 28.2° for rings **A** and **C**, respectively (51.3° and 42.5° for rings **B** and **D**, respectively, Fig. 1).

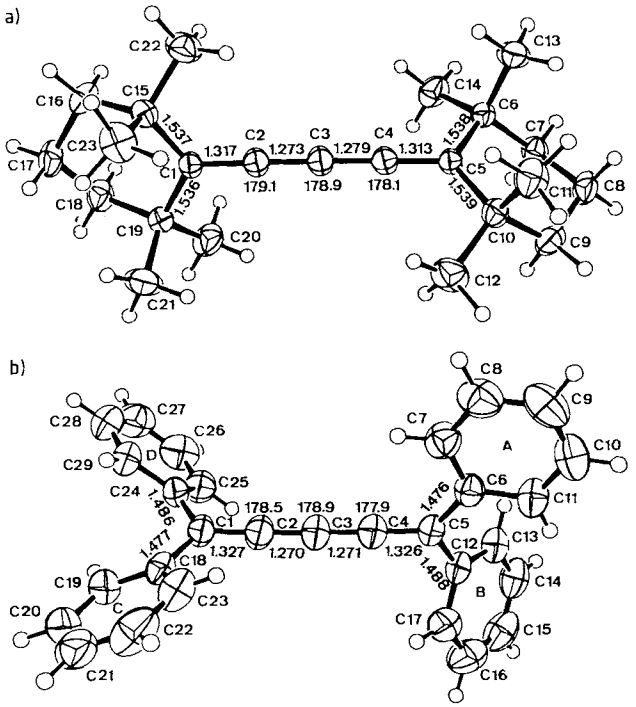
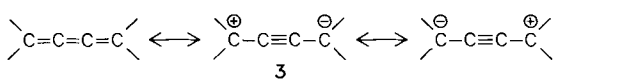
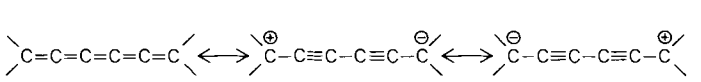


Fig. 1. Molecular structure of pentatetraenes in the crystal. Bond lengths [Å], bond angles [°]. a) **4a**: Standard deviation 0.002 Å and 0.1°; b) **4b**: standard deviation 0.002 Å and 0.1–0.2°.

Comparison of the cumulative double bonds of homologous systems reveals a clear difference between cumulenes with an even number and those with an odd number of double bonds. In the cumulenes with an odd number of double bonds (trienes **3**, pentaenes **5**; Table 1), the terminal bonds are approximately 0.02 Å longer and the neighboring bonds about 0.02 Å shorter than the corresponding bonds in cumulenes with an even number of double bonds (allenes **2**, tetraenes **4**; Table 1). Accordingly, the bonds marked x in cumulenes with an odd number of double bonds have some single-bond character and the bonds marked y have some triple-bond character.



3



5

Table 1. Bond lengths [Å] of the double bonds in **2a–5a** and **2b–4b** (averaged in the case of multiple determinations).

2a–5a, > = ⟨⟩; **2b–4b**, > = Ph/Ph

Compd.	x	y	z	Ref.
2a	1.305			[1]
3a	1.328	1.256		[1]
4a	1.315	1.276		
5a	1.329	1.259	1.299	[1]
2b	1.310			[9]
3b	1.345	1.246		[10]
4b	1.327	1.271		

These cumulenes contain a 1,3-butadiene system (trienes **3**) or 1,3,5-hexatriene system (pentaene **5a**) with resonance along the entire length of the cumulene chain, so that a phenyl ring at either end of the chain can also participate in the resonance. Therefore, the x bond in the triene **3b** is about 0.02 Å longer and the y bond 0.01 Å shorter than the corresponding bonds in the triene **3a** with aliphatic substituents.

For the cumulenes with an even number of double bonds, resonance involving triple bonds is not possible. Such systems have two perpendicular π systems, which cannot interact. The substituents of the allene **2** have no significant effect on the length of the double bonds. In the tetraene **4b**, which has two perpendicularly oriented 1,3-butadiene systems, the x bond is lengthened by a small amount (ca. 0.01 Å) compared with that in the aliphatic substituted tetraene **4a** on account of the substituent effect of the phenyl ring.

Received: December 5, 1985;
revised: January 31, 1986 [Z 1567/1568 IE]
German version: *Angew. Chem. 98* (1986) 359

CAS registry numbers:
3a, 60004-34-4; **4a**, 101165-59-7; **4b**, 1674-27-7; **6a**, 101165-60-0; **7a**, 101165-61-1; $:CCl_2$, 1605-72-7.

[1] H. Irngartinger, H.-U. Jäger, *Angew. Chem. 88* (1976) 615; *Angew. Chem. Int. Ed. Engl. 15* (1976) 562; H. Irngartinger, E. Kurda, H. Rodewald, A. Berndt, R. Bolze, K. Schlüter, *Chem. Ber.* 115 (1982) 967.
[2] Syntheses according to modified procedures: a) F. Bohlmann, K. Kieslich, *Chem. Ber. 87* (1954) 1363; b) G. Karich, J. C. Jochims, *ibid. 110* (1977) 2680.
[3] C. M. Starks, C. Liotta: *Phase Transfer Catalysis*, Academic Press, New York 1978; E. V. Dehmlow, S. S. Dehmlow: *Phase Transfer Catalysis*, Verlag Chemie, Weinheim 1980.
[4] L. Skattebøl, *Tetrahedron Lett. 1965*, 2175; E. V. Dehmlow, J. Schönfeld, *Justus Liebigs Ann. Chem. 744* (1971) 42.
[5] **6a**: M.p.=89–90 °C; colorless platelets from acetonitrile. Space group *C2/c*; $Z=8$; $a=44.507(6)$, $b=8.155(1)$, $c=11.976(2)$ Å; $\beta=99.10(1)°$; $\rho_{calcd}=1.13$ gcm $^{-3}$. $Mo_{K\alpha}$ radiation, Enraf-Nonius CAD4 diffractometer,

graphite monochromator, $\sin\theta/\lambda < 0.66$ Å^{-1}; 5162 independent reflections, 2876 of which observed ($I > 3\,\sigma(I)$); $R = 0.05$.

[6] Y. Gopichand, F. J. Schmitz, J. Shelly, A. Rahman, D. van der Helm, *J. Org. Chem. 46* (1981) 5192.

[7] **4a**: M.p. = 68–69 °C, ^{1}H-NMR (90 MHz, $CDCl_3$): $\delta = 1.13$ (s, 24H, CH_3), 1.30–1.70 (m, 12H, CH_2); IR (KBr): $\tilde{\nu} = 2060$ cm^{-1} (C=C=C); UV (cyclohexane): $\lambda_{max} = 234$, 256, 302, 342 nm ($\varepsilon = 85000$, 32300, 481, 94).—Space group $P2_1/c$; $Z = 4$; $a = 12.702(2)$, $b = 7.588(1)$, $c = 21.557(3)$ Å; $\beta = 93.06(1)°$; $\rho_{calcd} = 1.00$ gcm^{-3}. Measuring temperature: -83 ± 1 °C; $Mo_{K\alpha}$-radiation, Enraf-Nonius CAD4 diffractometer, graphite monochromator; $\sin\theta/\lambda \leqq 0.60$ Å^{-1}; 4989 independent reflections, 3321 of which observed ($I > 2.5\sigma(I)$); $R = 0.041$. Further details of the crystal structure investigation may be obtained from the Fachinformationszentrum Energie, Physik, Mathematik GmbH, D-7514 Eggenstein-Leopoldshafen 2 (FRG), on quoting the depository number CSD 51796, the names of the authors and the journal citation.

[8] Synthesis of **4b**: R. Kuhn, H. Fischer, H. Fischer, *Chem. Ber. 97* (1964) 1760.—Space group $P\bar{1}$; $Z = 2$; $a = 8.646(2)$, $b = 11.217(2)$, $c = 11.818(1)$ Å; $\alpha = 100.55(1)$, $\beta = 106.92(1)$, $\gamma = 74.96(1)°$; $\rho_{calcd} = 1.16$ gcm^{-3}. Measurement at room temperature. The usual conditions as described in [7], $\sin\theta/\lambda \leqq 0.66$ Å^{-1}; 5065 independent reflections, 2530 of which observed ($I > 2.5\sigma(I)$), $R = 0.038$.

[9] H.-U. Jäger, Dissertation, Universität Heidelberg 1967.

[10] Z. Berkovitch-Yellin, L. Leiserowitz, *Acta Crystallogr. B 33* (1977) 3657.

The Elucidation of the Constitution of Glycopeptides by the NMR Spectroscopic COLOC Technique

By *Horst Kessler,* Wolfgang Bermel, Christian Griesinger,* and *Cenek Kolar*

In the elucidation of the constitution of organic compounds by NMR spectroscopy, it is usually easy to identify the scalar-coupled proton spin systems, e.g., by means of H,H-COSY[1] or H-relayed H,H-COSY.[2] If these spin systems are separated by quaternary carbon atoms or heteroatoms that bear no protons, however, the determination of the connectivity is difficult. Frequently, interpretation of the nuclear Overhauser effects is useful (e.g., to assign the NMR signals of biopolymers such as peptides[3] and oligosaccharides[4]); however, in order to avoid circular reasoning, these should only be used to elucidate the stereochemistry (configuration and conformation).[5] As we recently found, the two-dimensional heteronuclear correlation via long-range coupling (COLOC) may be employed for the determination of the sequences of amino acids in peptides.[6] We show here the potential of this technique as applied to the disaccharide derivative **1** (see Fig. 2), for which it was possible to solve simultaneously three structural problems:

—The 3-1′ connectivity of the sugar moieties was established by means of the detection of a $^3J_{H,C}$ coupling through the oxygen atom.[7]

—The connectivity of C-1 of the sugar with the amino group of the amino acid through a urethane carbonyloxy group was confirmed.

—The positions of the acetyl and benzoyl groups were established by means of the couplings of the carbonyl C atoms of the acyl group to the protons of the sugar and acyl moieties. At the same time, it was possible to assign the ^{13}CO signals and the ^{1}H signals of the acetyl groups.

[*] Prof. Dr. H. Kessler, Dipl.-Chem. C. Griesinger
Institut für Organische Chemie der Universität
Niederurseler Hang, D-6000 Frankfurt am Main 50 (FRG)
Dr. W. Bermel
Bruker Analytische Meßtechnik GmbH
Silberstreifen, D-7512 Rheinstetten (FRG)
Dr. C. Kolar
Behring Werke
Postfach 1140, D-3550 Marburg (FRG)

Upon attempted glycosylation of Ddz-serine benzyl ester (Ddz=α,α-dimethyl-3,5-dimethoxybenzyloxycarbonyl), a surprising migration of the α,α-dimethyl-3,5-dimethoxybenzyl group to the β-hydroxyl group of the serine took place with the formation of a glycosyl urethane.[8] Although this connectivity was suggested by a signal of a urethane carbonyl C atom in the ^{13}C-NMR spectrum of the substance *after* cleavage of the putative Ddz protecting group and by the unusual low-field shift of the ^{1}H-NMR signal of H-1 as well as by mass spectroscopic analysis of the glycosyl urethane,[8] unequivocal proof of the structure of **1** was desired.

The assignment of the sugar protons and the determination of the relative configuration of both pyranose rings was achieved by analysis of the ^{1}H-NMR spectrum of **1** (Fig. 1a) and of an H,H-COSY spectrum.[11] The nonquaternary C atoms were, as usual, assigned by means of an H,C-COSY spectrum.[9] In order to establish the connectivity of the sugar moieties, a COLOC spectrum for the aliphatic C

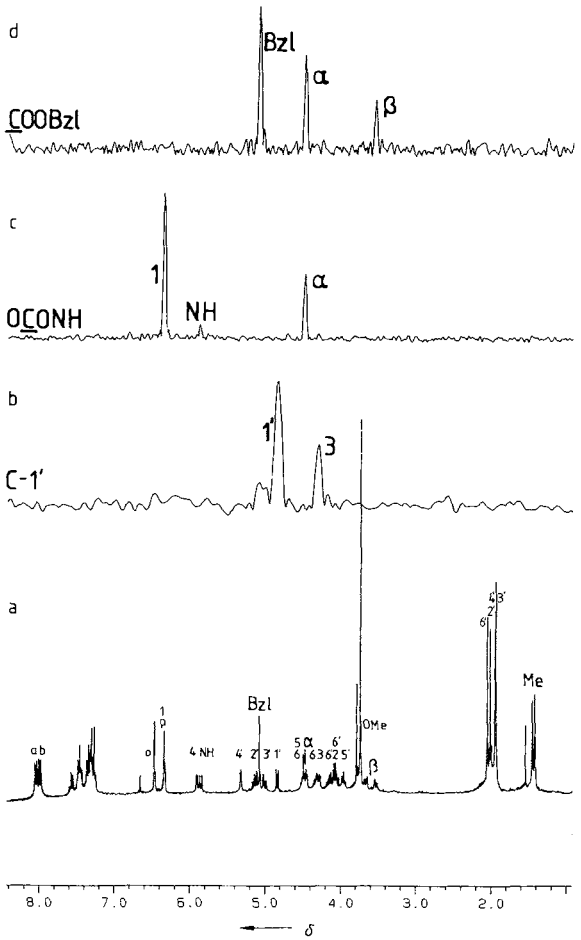


Fig. 1. 300-MHz ^{1}H-NMR spectrum of **1** (440 mg in 3 mL of $CDCl_3$) (a) and cross sections through the COLOC spectra (b–d). b: Cross section at the signal of C-1′. The signal to H-3 gives information on the connectivity of the sugar moiety. c: Cross section at the signal of the urethane C atom. In addition to a weak $^2J_{C,H}$ correlation to the NH proton, the proximity of H-1 and the α-proton of the serine in clearly observed. d) Cross section at the signal of the carbonyl C atom of the ester.—The COLOC spectrum was recorded with the following pulse sequence: $\pi/2(^1H)(t_1/2)\pi(^1H, ^{13}C)(\Delta_1 - t_1/2)\ \pi/2$ (^{1}H, ^{13}C) Δ_2 acquis. (^{13}C) ^{1}H-broadband decoupling. Measuring conditions: b: 140 experiments, 128 scans each with 8 K data points; acquisition time, 0.45 s; relaxation delay; 1.5 s; $\Delta_1 = \Delta_2 = 63$ ms; total measuring time, 13 h. Spectral width in F2, 9091 Hz; in F1, 2994 Hz; ^{1}H measuring frequency, 300 MHz.—c, d: 330 experiments, 64 scans each with 4 K data points; acquisition time, 0.5 s; relaxation delay, 1.5 s; $\Delta_1 = \Delta_2 = 90$ ms; total measuring time, 13 h. Spectral width in F2, 4032 Hz; in F1, 2439 Hz; ^{1}H measuring frequency, 270 MHz.

atoms[10] was recorded. The cross section at the chemical shift of C-1′ shows a coupling from C-1′ to H-3 ($^3J_{CH}$ coupling, Fig. 1b) in addition to a correlation between C-1′ and H-1′. For the signal of C-3, on the other hand, only $^2J_{CH}$ and $^3J_{CH}$ couplings to protons of the same sugar ring are observed. Furthermore, the COLOC spectrum exhibits a large number of cross signals to each carbon atom, thereby providing independent confirmation of the assignment of the ^{1}H-NMR and ^{13}C-NMR spectra.

The ^{13}C-NMR signal of the urethane carbonyl group at $\delta = 153.38$ was identified in a second COLOC spectrum for quaternary carbon atoms[6, 11] by means of its coupling to the NH and α-proton of the serine (Fig. 1c). The α-proton is coupled to only one additional quaternary C atom at $\delta = 169.86$, which, however, could be characterized as the signal of the ester carbonyl group by means of its coupling to a β-proton of the serine and to a methylene proton of the benzyl moiety (Fig. 1d). Of particular importance is the coupling of the urethane carbonyl C atom with H-1 of the sugar moiety (Fig. 1c).

All remaining carbon atoms can be assigned unequivocally in this spectrum (Table 1). The positions of the acetyl and benzoyl protecting groups can be determined by couplings of their carbonyl C atoms to the protons of the sugar moiety *and* the acyl groups (CH_3 and C_6H_5, respectively) (Fig. 2). Hence, the COLOC technique allows the easy determination of the positions of protecting groups, which is of use in the characterization of intermediates and in the structural elucidation of natural products.

We have thus demonstrated that the ^{13}C-NMR signals of quaternary and nonquaternary C atoms can be assigned unequivocally with the COLOC spectra. Further, the assignment of the signals in the ^{1}H-NMR spectra is considerably facilitated; even protons that show no resolved couplings to other protons or that are separated by non-proton-bearing carbon atoms or heteroatoms can be connected with one another by means of the COLOC experiment.

Table 1. Chemical shifts (δ values) in **1**.

Position	Sugar		Protecting group	
	δ(H)	δ(C)	δ(H)	δ(CO)
1	6.34	92.13		
2	4.08	59.07		
3	4.28	75.61		
4	5.91	69.87	8.04 *(ortho)*	165.26
5	4.45	69.43		
6	4.45, 4.34	62.82	8.00 *(ortho)*	165.94
1′	4.84	101.50		
2′	5.15	68.73	2.01	169.10
3′	5.01	70.76	1.94	169.93
4′	5.33	66.64	1.95	170.04
5′	3.96	70.76		
6′	4.12 [a]	61.06	2.05	170.25
Ser α	4.46	54.42		
β	3.53, 3.67	62.48		
NH	5.86			
urethane CO		153.38		
ester CO		169.86		

[a] Broad.

Received: November 4, 1985;
revised: January 8, 1986 [Z 1518 IE]
German version: *Angew. Chem.* 98 (1986) 352

CAS registry number:
1, 100842-24-8.

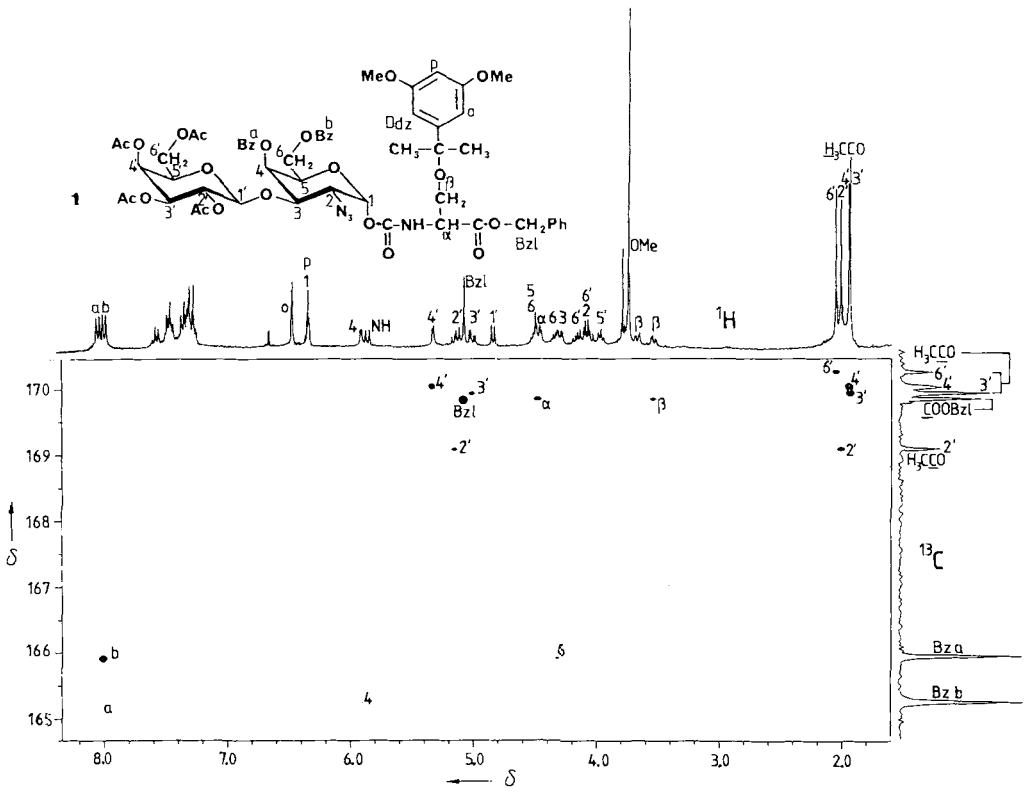


Fig. 2. Section of the 300-MHz COLOC NMR spectrum for the quaternary carbon atoms. The carbonyl groups are identified by means of cross peaks to the protons of the a and b benzoyl groups and the acetyl groups. Cross peaks to the signals of the sugar moieties give the position of the protecting groups. Measuring conditions: see Fig. 1c, d.

[1] W. P. Aue, E. Bartholdi, R. R. Ernst, *J. Chem. Phys. 64* (1976) 2229.
[2] G. Eich, G. Bodenhausen, R. R. Ernst, *J. Am. Chem. Soc. 104* (1982) 3731.
[3] W. A. Gibbons, D. Crepaux, J. Delayre, J. J. Dunand, G. Hajdukovic, H. R. Wyssbrod in R. Walter (Ed.): *Peptides*. Ann Arbor Science Publ., Ann Arbor, MI, USA, 1975, p. 127; G. Wagner, K. Wüthrich, *J. Mol. Biol. 155* (1982) 347.
[4] J. Dabrowski, P. Hanfland, H. Egge, U. Dabrowski, *Arch. Biochem. Biophys. 210* (1981) 405; H. Thøgersen, R. U. Lemieux, K. Bock, B. Meyer, *Can. J. Chem. 60* (1982) 44.
[5] H. Kessler, H. Oschkinat, H. R. Loosli in R. M. Carlson, W. R. Croasmun (Eds.): *2D NMR Spectroscopy*. VCH Publ., Deerfield Beach, FL, USA, chap. 4. in press.
[6] H. Kessler, C. Griesinger, J. Zarbock, H. R. Loosli, *J. Magn. Reson. 57* (1984) 331.
[7] A coupling between C-2 of the fructose ring and H-1 of the glucose ring was detected earlier in saccharose by means of a H,C COSY spectrum that was optimized for small couplings (the pulse sequence differs from that of the COLOC experiment): W. E. Hull (see Bruker brochure "Two-Dimensional NMR," December 1982, Fig. 18b).
[8] C. Kolar, U. Knödler, F. Seiler, H. Paulsen, V. Sinnwell, M. Schultz, W. Fehlhaber, unpublished results.
[9] G. Bodenhausen, R. Freeman, *J. Magn. Res. 28* (1977) 471.
[10] H. Kessler, W. Bermel, C. Griesinger, *J. Am. Chem. Soc. 107* (1985) 1083.
[11] H. Kessler, C. Griesinger, J. Lautz, *Angew. Chem. 96* (1984) 434. *Angew. Chem. Int. Ed. Engl. 23* (1984) 444.

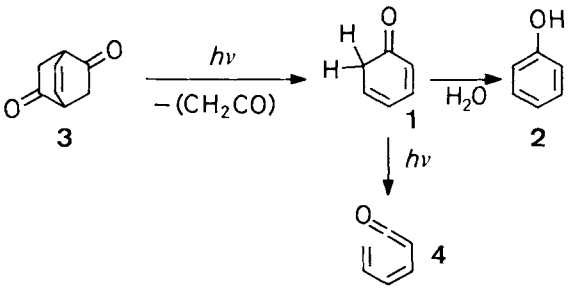
The Phenol ⇌ 2,4-Cyclohexadienone Equilibrium in Aqueous Solution**

By *Marco Capponi, Ivo Gut,* and *Jakob Wirz**

Cyclohexadienones were long ago proposed[1] and were recently detected[2,3] as transient intermediates in electrophilic substitution reactions of phenols. Keto tautomers of phenols are frequently postulated to occur as intermediates in the isomerization of arene oxides, and an important criterion to determine the routes of metabolism of aromatic compounds ("NIH shift"[4]) relies on indirectly determined kinetic isotope effects attributed to the enolization of α-H isotopomeric ketone intermediates. It is therefore surprising that the equilibria and mechanisms of phenol tautomerization have so far hardly been investigated,[5] in sharp contrast to the reverse enolization of simple ketones, which is one of the most documented reactions in organic chemistry.[6]

If a thermodynamically unstable tautomer can be generated photochemically from a suitable precursor, its rate of conversion to the stable isomer can be determined directly by the method of flash photolysis. By combining the rate constants for the forward and back reactions, we have recently obtained the first purely experimental and accurate equilibrium constants both for the enolization and for the acid dissociation (enolate formation) of simple ketones in aqueous solution.[7] We have now developed a method to monitor the tautomerization of 2,4-cyclohexadienone **1** to phenol **2** and report here the pH profile of the rate constant $k_{1\to2}$ (H_2O, 25 °C) as well as preliminary estimates for the equilibrium constant of tautomerization, K = [**1**]/[**2**], and for the acidity constant K_a of the carbon acid **1**.

The phenol tautomer **1** is formed by a retro-Diels-Alder reaction in the gas phase pyrolysis of suitable bicyclic ketones.[8] Bicyclo[2.2.2]oct-7-ene-2,5-dione **3** yields phenol upon irradiation in solution.[9] It seemed likely that this reaction also proceeds via **1**. This was confirmed by photolysis of **3** (λ = 313 nm) in a glassy solution at 77 K. In agreement with a previous observation,[10] very little **1** accumulated under these conditions because of its highly efficient conversion into the dienyl ketene **4** by secondary photolysis, a reaction with ample precedent.[11] Compound **4** was characterized by its absorption spectrum [λ_{max} (rel. int.) = 284 (1), 274 (1.2), 265 nm (1.0, sh.)] and identified by trapping with ethanol upon thawing of the rigid glass.



Flash photolysis of **3** at 25.0 ± 0.5 °C in aqueous solution, using either an excimer laser operated on XeCl (200 mJ, 25-ns pulses at 308 nm) or a conventional electric discharge flash lamp (1000 J, 20 μs), produced a weak transient absorption in the wavelength range of 280 to 330 nm, as expected for **1**.[11] The decay of the intermediate obeyed first-order kinetics. The rate constants $k_{1\to2}$ as a function of pH are shown in Figure 1. The points within the pH range of 4 to 6 were obtained with sodium acetate buffer solutions by extrapolating to zero buffer concentration; the ionic strength was kept constant at I = 0.1 M by the addition of sodium chloride. Plots of the observed decay rate constants $k_{1\to2}$ vs. the total buffer concentration at a given buffer ratio were linear and the slopes indicated general base catalysis, $k_{AcO^-} = (9.2 \pm 0.5) \times 10^3\ M^{-1}\ s^{-1}$, but no significant contribution by general acid catalysis, $k_{HOAc} < 5 \times 10^2\ M^{-1}\ s^{-1}$. Similar measurements with α-amino-α-(hydroxymethyl)-1,3-propanediol (Tris)/HCl buffers in the pH range of 7 to 9 gave $k_{Tris} = (2.0 \pm 0.1) \times 10^5\ M^{-1}\ s^{-1}$.

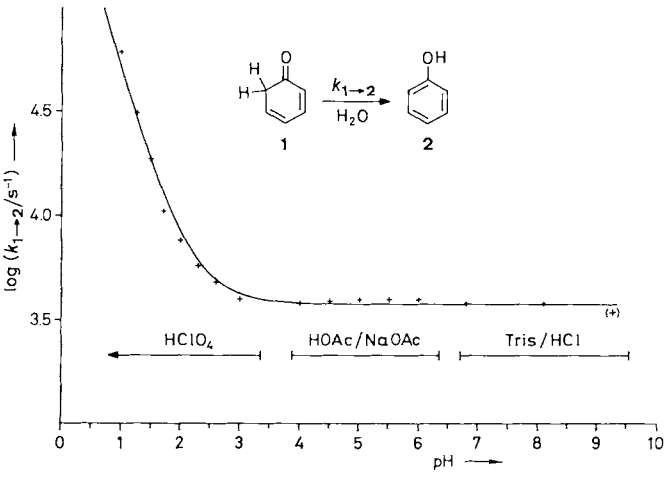


Fig. 1. Measured rate constants $k_{1\to2}$ in aqueous solution at 25 °C as a function of pH. The ionic strength was kept constant at I = 0.1 M by the addition of NaCl. The solid line was found by least-squares fitting of the function $k_{1\to2} = k_0 + k_H \cdot [H^+]$ (see text).

[*] Prof. Dr. J. Wirz, Dipl.-Chem. M. Capponi, I. Gut
Institut für Physikalische Chemie der Universität
Klingelbergstrasse 80, CH-4056 Basel (Switzerland)

[**] This work was supported by the Swiss National Science Foundation. We thank Priv.-Doz. Dr. *M. Demuth*, and Prof. Dr. *C. A. Grob* for kindly providing samples of 5,7-dioxobicyclo[2.2.2]octane-2,3-dicarboxylic acid.

As is evident from Figure 1, the tautomerization of **1** is dominated by an uncatalyzed reaction, $k_0=(3.8\pm0.2)\times10^3$ s^{-1}, in the pH range of 3 to 9. A reaction rate of this order of magnitude is expected for the *protonation of water by the strong carbon acid* **1**: inserting k_{AcO^-} and k_{Tris} into the Brønsted relation

$$\log(k_{Tris}/k_{AcO^-})=\beta[pK_a(HTris^+)-pK_a(HOAc)]$$

yields $\beta\approx0.4$ and, assuming $pK_a(H_3O^+)=-1.74$, one obtains $k_{H_2O}\approx30\ M^{-1}s^{-1}$ or $k_0\approx2\times10^3\ s^{-1}$. At pH values below 3, the reaction rate is dominated by acid catalysis, $k_{H^+}=(4.6\pm0.2)\times10^5\ M^{-1}s^{-1}$.

The rate of deuteration of phenol in 1 N D_2SO_4 at 80 ± 1 °C was measured by intermittent ^{1}H-NMR analysis at 25 °C. On a 400-MHz spectrometer the NMR signals of the *ortho* and *para* hydrogen atoms could be integrated separately yielding $k(ortho)=(1.1\pm0.1)\times10^{-5}\ s^{-1}$ and $k(para)=(2.3\pm0.2)\times10^{-5}\ s^{-1}$. In order to derive the rate constant of ketonization, $k_{2\to1}$, from the observed rate of *ortho*-deuteration, several isotope effects and statistical factors need to be accounted for. A comparison with isotope effects observed in related reactions[3, 12] yields the prediction $k_{2\to1}\approx5k(ortho)$. This estimate is likely to be correct within one order of magnitude (±0.5 log units); experimental investigations of the kinetic isotope effects of the reaction **1** $\rightleftharpoons$ **2** are in progress. The rate constant of the reverse reaction under similar conditions (1 N $HClO_4$, 80 °C) was determined by the method of flash photolysis: $k_{1\to2}=(5.6\pm0.6)\times10^6\ s^{-1}$.

The ratio of these rate constants then gives $pK\approx11.0\pm0.8$ for the equilibrium **2** $\rightleftharpoons$ **1** at 80 °C. The equilibrium constant at 25 °C may be estimated by neglecting the contribution of entropy to the highly exothermic reaction **1** → **2** (for an estimate of the error involved in this approximation we assume $|\Delta S_{1\to2}|\leq20\ J\ mol^{-1}\ K^{-1}$). Thus, $d(T\cdot pK)/dT\approx0$ and $pK(25\,°C)=13\pm1$. Finally, the acidity of **1** as a carbon acid in water (25 °C) is $pK_a(\mathbf{1})=-pK+pK_a(\mathbf{2})\approx-3\pm1$.

Received: December 5, 1985;
revised: January 13, 1986 [Z 1566]
German version: *Angew. Chem. 98* (1986) 358

CAS registry numbers:
1, 24599-57-3; **2**, 108-95-2; **3**, 17660-74-1; **4**, 101055-58-7.

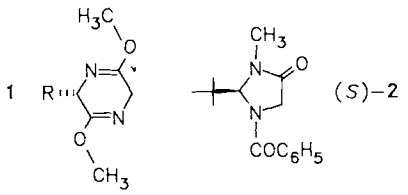
[1] A. Lapworth, *J. Chem. Soc. 79* (1901) 1265.
[2] P. B. D. de la Mare, *Acc. Chem. Res. 7* (1974) 361; J. M. Brittain, P. B. D. de la Mare in S. Patai (Ed.): *The Chemistry of Functional Groups, Suppl. D*, Wiley, New York 1983, chapter 12, p. 481.
[3] O. S. Tee, N. R. Iyengar, *J. Am. Chem. Soc. 107* (1985) 455.
[4] J. W. Daly, D. M. Jerina, B. Witkop, *Experientia 28* (1972) 1129.
[5] R. H. Thomson, *Q. Rev. Chem. Soc. 10* (1956) 27; S. Forsén, M. Nilsson in S. Patai (ed.): *The Chemistry of the Carbonyl Group*, Wiley, New York 1970, p. 168; H. Hart, *Chem. Rev. 79* (1979) 515.
[6] J. Toullec, *Adv. Phys. Org. Chem. 18* (1982) 1.
[7] P. Haspra, A. Sutter, J. Wirz, *Angew. Chem. 91* (1979) 652; *Angew. Chem. Int. Ed. Engl. 18* (1979) 617; Y. Chiang, A. J. Kresge, Y. S. Tang, J. Wirz, *J. Am. Chem. Soc. 106* (1984) 460; Y. Chiang, A. J. Kresge, J. Wirz, *ibid. 106* (1984) 6392.
[8] M.-C. Lasne, J.-L. Ripoll, J.-M. Denis, *Tetrahedron Lett. 21* (1980) 463.
[9] P. H. Schippers, H. P. J. M. Dekkers, *J. Chem. Soc. Perkin Trans. 2 1982*, 1429.
[10] D. M. Jerina, B. Witkop, C. L. McIntosh, O. L. Chapman, *J. Am. Chem. Soc. 96* (1974) 5578.
[11] G. Quinkert, *Pure Appl. Chem. 33* (1973) 285.
[12] R. P. Bell: *The Proton in Chemistry*, 2nd ed., Chapman and Hall, London 1973, chapter 12; D. J. Hupe, E. R. Pohl, *J. Am. Chem. Soc. 106* (1984) 5634; A. J. Kresge, R. A. More, O'Ferrall, M. F. Powell: *Isotopes in Organic Chemistry, Vol. 7*, Elsevier, Amsterdam 1985.

Enantiomer Separation of (*R,S*)-2-(*tert*-Butyl)-3-methyl-4-imidazolidinone, a Chiral Building Block for Amino Acid Synthesis**

By *Robert Fitzi* and *Dieter Seebach*

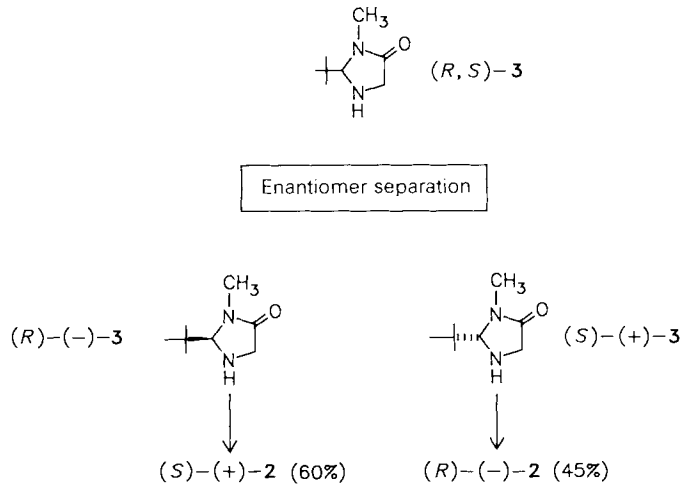
Owing to their possible biological activity, enantiomerically pure nonprotein α-amino acids have become increasingly important. For their preparation various methods have been employed.[2-4] These afford a 1:1 mixture of enantiomers or—if additional chirality centers are present—diastereomeric pairs of enantiomers, thereby necessitating enantiomer separation.[5, 6]

Among the recently developed stereoselective α-amino acid syntheses, the α-alkylation of chiral glycine derivatives is especially attractive.[7] The highest selectivities have been observed with the bislactim ethers **1**[8] and with the imidazolidinone **2**.[9]



The six-membered heterocycle **1** is obtained from glycine and another amino acid via the diketopiperazine, which is *O*-methylated by Meerwein salt. Its use requires the separation of two amino acids in the final step. When the five-membered heterocycle **2** is employed, it is only necessary to separate the desired product from benzoic acid, methylamine, and pivalaldehyde, and almost all derivatives of **2** can be conveniently purified by crystallization. So far, enantiomerically pure **2** was only available by degradation of a substituent in the 5-position.

We have now succeeded in separating the enantiomers of the nonbenzoylated glycine derivative **3** by crystallization of the mandelate salt. *Both* enantiomers of **2**, and thus the (*R*)- *or* (*S*)-amino acids, thereby become readily available on a preparative scale.



[*] Prof. Dr. D. Seebach, Dipl.-Natw. R. Fitzi
Laboratorium für Organische Chemie
der Eidgenössischen Technischen Hochschule
ETH-Zentrum, Universitätsstrasse 16, CH-8092 Zürich (Switzerland)
[**] Part of the projected dissertation of *R. F.*, ETH Zürich.

The (*R,S*)-aminal **3**, prepared from glycine methyl ester hydrochloride, methylamine, and pivalaldehyde,[10] was treated with 14 chiral carboxylic or sulfonic acids. In two cases one of the two possible diastereomeric salts crystallized selectively: the salt from (−)-2,3:4,6-di-*O*-isopropylidene-2-ketogulonic acid [(−)-diacetone-2-ketogulonic acid] and (*S*)-**3**, and that from (*S*)-(−)-mandelic acid and (*R*)-**3**. For preparative resolution a single crystallization with mandelic acid gave enough enrichment so that *N*-benzoylation and recrystallization of **2** produced the two enantiomers with greater than 98% *ee*. Mandelic acid is recovered in 95% yield without detectable racemization.

Experimental Procedure

(*R,S*)-**3**: Glycine methyl ester hydrochloride (125.6 g, 1 mol) was added to 375 mL of 8 M ethanolic methylamine (ice-cooled) with stirring. After 15 h at room temperature, the suspension was concentrated in a rotatory evaporator (water aspirator). A slurry of the resulting viscous material in 200 mL of CH_2Cl_2 was prepared and concentrated three times. A solution of the residue, pivalaldehyde (235 mL, 1.5 mol, Fluka pract.), and triethylamine (209 mL, 1.5 mol) in 1 L of CH_2Cl_2 was then heated at reflux for 10 h with separation of water. After cooling, the mixture was filtered through a sintered-glass filter and the filter cake was washed with 500 mL of ether. Concentration of the filtrate gave an oil, which was dissolved in 300 mL of CH_3OH. The resulting solution was combined (with cooling and stirring) with 600 mL of methanol that had been saturated with HCl gas at 0 °C. After 30 min of stirring at 0 °C and 2 h at room temperature, the mixture was concentrated to a syrup, dissolved in 800 mL of CH_2Cl_2, washed with 670 mL of 3 M aqueous NaOH, and then evaporated to give the crude product **3** (107.5 g, 69%; yellow oil, which crystallizes upon cooling; for characterization of (*R,S*)-**3** see [10].

Enantiomeric resolution: A mixture of (*R,S*)-**3** (70.0 g, 0.448 mol) and (*S*)-(−)-mandelic acid (70.0 g, 0.460 mol) was dissolved in boiling acetone (ca. 170 mL, saturation!). The solution was stirred in order to spread the initially formed crystals in the insulated flask, which was then allowed to cool slowly (in ca. 6 h to ambient temperature), resulting in the separation of the (*R,S*)-diastereomeric salt. After 15 h in a refrigerator (5 °C), the crystal cake was pressed and filtered. Drying in vacuo afforded 54.5 g of light yellow, fine crystals.

(*S*)-(+)-**2**: A suspension of the (*R,S*)-diastereomeric salt (54.5 g, 0.177 mol) in 200 mL of CH_2Cl_2 was shaken with 92 mL of 2 M aqueous NaOH. For recovery of mandelic acid, the aqueous layer was acidified with 50% H_2SO_4, whereupon the acid crystallized and was filtered off or extracted into ethyl acetate. The aminal **3** remaining in the CH_2Cl_2 layer was *N*-benzoylated by addition of benzoyl chloride (20.1 mL, 0.173 mol) and 195 mL of 1 M NaOH with ice cooling. This afforded 45.8 g of a yellow crystalline material with $[\alpha]_D$ +107 (c=1, CH_2Cl_2).

(*R*)-(−)-**2**: The mother liquor from the crystallization above was concentrated (syrup, ca. 0.27 mol of diastereomeric salts) and then dissolved in 300 mL of CH_2Cl_2. The resulting solution was first treated with 2 M NaOH (140 mL) and then with benzoyl chloride (30 mL, 0.26 mol)/1 M NaOH (280 mL) for removal of mandelic acid and *N*-benzoylation, respectively, as described above for the (+)-enantiomer. The lumps of brown crystals obtained upon concentration of the CH_2Cl_2 phase were recrystallized from 45 mL of ethanol to give 33.6 g of a brownish material with $[\alpha]_D$ −109 (c=1, CH_2Cl_2).

Further purification of **2**: Each enantiomer was recrystallized twice from ethanol. Although the crystals were pulverized, the material dissolved only very slowly in refluxing ethanol (ca. 1.43 mL/g). Finally, the product was precipitated from a CH_2Cl_2 solution by addition of pentane and dried for at least 12 h at 60 °C/0.1 torr. This afforded 34.7 g (0.133 mol) of (*S*)-(+)-**2** (60%) with $[\alpha]_D$ +127 (c=1, CH_2Cl_2) and 26.4 g (0.101 mol) of (*R*)-(−)-**2** (45%) with $[\alpha]_D$ −126 (c=1, CH_2Cl_2). A sample was recrystallized several more times and sublimed (135 °C/0.01 torr) to give material with $[\alpha]_D$ +127.5 and m.p. = 143–144 °C. For spectroscopic data of (*R,S*)-**2** and (*R,S*)-**3** see [9, 10]. The enantiomeric excess of the derivatives was therefore greater than 98% and 99%, respectively.

Received: December 13, 1985 [Z 1585 IE]
German version: *Angew. Chem. 98* (1986) 363

[1] G. Nass, K. Poralla, H. Zähner, *Naturwissenschaften 58* (1971) 603; I. Wagner, H. Musso, *Angew. Chem. 95* (1983) 827; *Angew. Chem. Int. Ed. Engl. 22* (1983) 816.

[2] Malonic ester synthesis: S. P. L.Sörensen, *Hoppe-Seylers Z. Physiol. Chem. 44* (1905) 448; N. F. Albertson, S. Archer, *J. Am. Chem. Soc. 67* (1945) 308; N. F. Albertson, B. F. Tullar, *ibid. 67* (1945) 502.

[3] Strecker synthesis: A Strecker, *Justus Liebigs Ann. Chem. 75* (1850) 27; Bucherer variants: H. T. Bucherer, W. Steiner, *J. Prakt. Chem. 140* (1934) 291; H. T. Bucherer, V. A. Lieb, *ibid. 141* (1934) 5.

[4] For further methods see [6], p. 697ff.

[5] J. Jacques, A. Collet, S. H. Wilen: *Enantiomers, Racemates and Resolutions*, Wiley, New York 1981.

[6] J. P. Greenstein, M. Winitz: *Chemistry of the Amino Acids*, Wiley, New York 1961, p. 737ff.

[7] See ref. [17] in [9]; also see: D. A. Evans, E. B. Sjogren, *Tetrahedron Lett. 26* (1985) 3783; Y. N. Belokon, A. G. Bulychev, S. V. Vitt, Y. T. Struchkov, A. S. Batsanov, T. V. Timofeeva, V. A. Tsyryapkin, M. G. Ryzhov, L. A. Lysova, V. I. Backhmutov, V. M. Belikov, *J. Am. Chem. Soc. 107* (1985) 4252.

[8] U. Schöllkopf, *Tetrahedron 39* (1983) 2085; U. Schöllkopf, U. Groth, M.-R. Gull, J. Nozulak, *Liebigs Ann. Chem. 1983*, 1133; U. Schöllkopf, *Pure Appl. Chem. 55* (1984) 1799; H. J. Neubauer, J. Baeza, J. Freer, U. Schöllkopf, *Liebigs Ann. Chem. 1985*, 1508; M. Grauert, U. Schöllkopf, *ibid.* 1985, 1817.

[9] D. Seebach, D. D. Miller, S. Müller, T. Weber, *Helv. Chim. Acta 68* (1985) 9.

[10] R. Naef, D. Seebach, *Helv. Chim. Acta 68* (1985) 135.

Organic Reactions at High Pressure: Cycloaddition Reactions of 11-Methylene-1,6-methano[10]annulene**

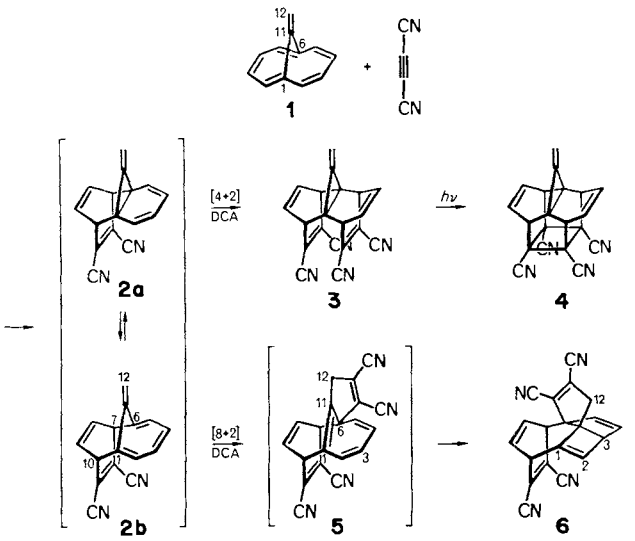
By *Frank-Gerrit Klärner,* Barbara M. J. Dogan, Richard Weider, David Ginsburg*, and *Emanuel Vogel*

The 1,6-methano[10]annulene route to cyclopropabenzenes[1] suggests 11-methylene-1,6-methano[10]annulene **1**[2] as a suitable starting material for the preparation of the still unknown methylenecyclopropabenzene[3] via cycloaddition of **1** with dicyanoacetylene (DCA) and Alder-Rickert cleavage. However, **1**, unlike the parent 1,6-methano[10]annulene, exhibits little tendency to react with DCA.[4] For this reason, we attempted to favor the cycloaddition by increasing the pressure (to 7000 bar). We report here the partly unexpected results for the reaction of **1** with DCA (Scheme 1).

At normal pressure, reaction of DCA with **1** (60 °C, pentane, 24 h in a sealed glass ampule) affords, in addition to polymers, a 3–4% yield of a crystalline 1:1 adduct (m.p. = 158 °C), which was identified as **2** by its spectral properties.[5] According to the ^{13}C-NMR spectrum (cf. Table 1), **2** exists in solution as the fluxional methylenenorcaradiene-heptafulvene system, **2a/2b**, with both components present in similar amounts. The chemical shift of C-1,6 (δ = 73.9, 32 °C) of **2** takes an intermediate position between symmetrically substituted methylenecyclopropanes (e.g., **3**: δ(C-1,6) = 39.9)[5] and heptafulvene (δ(C-1,6) = 138.3).[6] To the best of our knowledge, **2a/2b** is the first example of its kind. In contrast to **2**, the DCA adduct of 1,6-methano[10]annulene (δ(C-1,6) = 38.1) is only present as a "frozen" norcaradiene, that is, **2a** with $>CH_2$ instead of $>C=CH_2$.[1a] The similar energy content of **2a** and **2b** is presumably due to the fact that the strain energy of the methylenecyclopropane subunit,[7] which is 13.4 kcal/mol higher than that of cyclopropane, is able to compensate for the constraining effect of the 1,6-bridge. **2b** does not exhi-

[*] Prof. Dr. F.-G. Klärner, Dr. B. M. J. Dogan
Fakultät für Chemie der Universität
Postfach 102148, D-4630 Bochum 1 (FRG)
Prof. Dr. E. Vogel, R. Weider
Institut für Organische Chemie der Universität
Greinstrasse 4, D-5000 Köln 41 (FRG)
Prof. Dr. D. Ginsburg
Department of Chemistry, Israel Institute of Technology
Haifa 32000 (Israel)

[**] This work was supported by the Minister für Wissenschaft und Forschung des Landes Nordrhein-Westfalen and by the Fond der Chemischen Industrie. We thank Prof. Dr. *H. Duddeck* and Dr. *M. Kaiser*, Universität Bochum, for the recording of the high-resolution NMR spectra and the help with their interpretation.



Scheme 1. The numbering of the centers is only intended for the assignment of the spectra.

Table 1. Selected spectroscopic data for the compounds **2**, **3**, **4**, **6** [a], and dihydro-**6** [b].

2: ^{13}C-NMR (20 MHz, [D$_6$]acetone, ^{1}H broadband decoupled, 32°C): δ = 73.9 (C-1, 6); 48.2 (C-7, 10); 104.9 (C-12); 115.0 (−*C*≡N); 123.7 and 125.0 (C-2, 3, 4, 5); 134.1 (C-8, 9); 140.3 (=*C*−CN); 142.0 (C-11)

3: ^{13}C-NMR (100.6 MHz, CD_3CN): δ = 39.9 (s, C-1, 6); 45.8 (d, C-2, 5, 7, 10); 108.0 (t, C-12); 115.3 (−*C*≡N); 136.1 (s, =*C*−CN); 138.3 (d, C-3, 4, 8, 9); 144.1 (s, C-11)

4: ^{13}C-NMR (100.6 MHz, [D$_6$]acetone): δ = 39.0 (s, C-1, 6); 50.2 (d, C-2, 5, 7, 10); 59.4 (s, −*C*−CN); 125.0 (s, −*C*≡N); 128.3 (t, C-12); 129.6 (s, C-11); 139.7 (d, C-3, 4, 8, 9)

6: ^{1}H-NMR (400 MHz, [D$_6$]acetone): δ = 3.22; 3.32 (AB spectrum, 12,12′-H$_2$; J(12,12′) = 19.3 Hz); 3.59 (m, 3-H; J(3,4) = 2.2 Hz; J(3,10) = 1 Hz); 3.83 (dd, 7-H; J(7,8) = 6.1 Hz; J(7,9) = 0.9 Hz); 4.43 (d, broad; 10-H; J(9,10) = 6.2 Hz; J(8,10) = 1.2 Hz; J(2,10) = 0.8 Hz); 6.00 (d, broad; 2-H); 6.07 (d, 5-H; J(4,5) = 5.6 Hz); 6.14 (dd, 4-H); 6.62 (m, 9-H; J(8,9) = 8.5 Hz); 6.73 (m, 8-H). — ^{13}C-NMR (100.6 MHz, [D$_6$]acetone): δ = 42.6 (d, C-10; J(C−H) = 146.9 Hz); 43.1 (t, C-12; J(C−H) = 137.3 Hz); 45.8 (d, C-7; J(C−H) = 139.5 Hz); 61.2 (d, C-3; J(C−H) = 154.2 Hz); 63.9 (s, C-11); 64.4 (s, C-6); 113.1; 113.9; 115.0; 116.2 (s, −*C*≡N); 126.2; 131.8; 132.3; 135.7 (s, =*C*−CN); 129.9 (d, C-5; J(C−H) = 167.9 Hz); 131.5 (d, C-8; J(C−H) = 174.6 Hz); 132.1 (d, C-9; J(C−H) = 176.8 Hz); 135.3 (d, C-2; J(C−H) = 178.8 Hz); 135.9 (d, C-4; J(C−H) = 166.3 Hz); 140.0 (s, C-1)

Dihydro-**6**: ^{13}C-NMR (100.6 MHz, [D$_6$]acetone): δ = 27.0 (t, C-2); 36.9 (d, C-1); 43.0; 44.8 (d, C-7, 10); 51.0 (t, C-12); 51.2 (d, C-3); 55.5 (s, C-11); 66.3 (s, C-6); 112.7; 113.6; 115.8; 116.2 (s, −*C*≡N); 129.2; 131.0; 132.6; 134.7 (s, =*C*−CN); 129.0; 131.5; 133.1; 139.1 (d, C-4, 5, 8, 9)

[a] The assignment of the ^{1}H-NMR signals was made on the basis of a COSY 2D NMR spectrum. The coupling constants were determined by double resonance experiments (irradiation of the signals of H-3, H-7, and H-10 with a second RF field). A NOESY 2D NMR experiment allowed the determination of the spatial proximity of the noncoupled atom H-3 with H-2 and H-12 (*endo*) and a ^{13}C,^{1}H correlation the C,H connectivities. [b] Hydrogenated on the centers marked 1 and 2 in **6**.

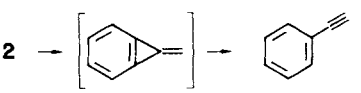
bit any significant heptafulvene character, which is understandable since the conjugation of the methylene group with the cycloheptatriene system is sterically strongly hindered.

When **1** is allowed to react with DCA at high pressure (7000 bar, 80°C, toluene, 4 h), two 2 : 1 adducts, which can be separated by fractional crystallization, are obtained in the ratio of 1 : 4 as determined by ^{1}H-NMR spectroscopy [yields of the isolated adducts: 11 and 16%, respectively; m.p. = 223°C (dec.) and 242°C, respectively].

According to its spectral and chemical properties, the high-pressure product formed in lower yield was characterized as the symmetrical 2 : 1 adduct **3**.[5] This adduct is very sensitive to light; it rearranges to the cage compound **4**, partly upon recrystallization in daylight and quantitatively upon short irradiation with a sunlamp.[5] The photochemical transformation of **3** into **4** proves that both dicyanovinylene bridges in **3** are in *anti* position with respect to the methylenecyclopropane ring.

The structural elucidation of the second 2 : 1 adduct proved to be more difficult insofar as an X-ray structure analysis led to no definitive result (presumably on account of crystallographic disorder).[8] By high-resolution ^{1}H- and ^{13}C-NMR spectroscopy along with the use of homo- and heteronuclear decoupling and 2D NMR experiments, it was possible to assign structure **6** to this adduct,[5] significant parts of which proved to be identical with those of the trapping product of 1,6-methano[10]annulene-11-ylidene with 1,3-diphenylisobenzofuran.[9] The presence of **6** is also revealed by the reduction with diimine, which gives the dihydro compound[5] (selective hydrogenation at C-1 and C-2, see Scheme 1).

The 1 : 1 adduct is formed by Diels–Alder reaction, the question remaining open whether the [10]annulene or its norcaradiene valence tautomer serves as the diene partner of DCA. The low yield of **2**, which could not be improved by high pressure, thus far has not allowed a detailed study of the thermolysis. Preliminary investigations show, however, that **2** fragments upon heating (130°C in benzene (1 h) or 400°C in a flow system), but, aside from phthalonitrile, mainly phenylacetylene is formed, which is probably a secondary product of the primarily formed methylenecyclopropabenzene.



In order to elucidate the mechanism of formation of the 2 : 1 adducts **3** and **6**, we showed by reaction of isolated **2** with DCA at 7000 bar that both adducts could arise from **2**. The course of the addition of DCA to **2** is apparently controlled by the valence tautomeric equilibrium **2a** ⇄ **2b**. As expected, **2a** reacts with DCA in a Diels–Alder type reaction, resulting in the formation of **3**. The ease with which **3** cyclizes photochemically to give **4** is a consequence of the small distance of the cyano-substituted double bonds, which, according to force-field calculations of *Ermer*[8] is only 2.98 Å. The unpredictable formation of the unsymmetrical 2 : 1 adduct **6** can only be explained by the reaction of **2b** with DCA via the intermediate **5**. The initial step **2b** → **5** may be regarded as an [8 + 2] cycloaddition, which is known to occur in the parent heptafulvene system.[10] That this cycloaddition occurs in the case of the geometrically unfavorable **2b**, however, is surprising. According to the inspection of models, the double bond between C-1 and C-11 of **5** exhibits a torsional angle of almost 90° (anti-Bredt compound). Accordingly, **5** has significant diradical character and apparently takes advantage of the sterically favorable possibility to stabilize itself by formation of **6**. Examples of such a butadiene–cyclobutene isomerization are known for *cis,cis,trans*-cycloheptatrienes[11] and related, extremely strained compounds.[12]

The preferential formation of the 2 : 1 adducts **3** and **6** upon reaction of **1** with DCA at high pressure is presumably due to the different activation volumes for the compet-

ing reactions of **2**. The bimolecular [4+2] and [8+2] cycloadditions are certain to have appreciably more negative activation volumes than the monomolecular Alder-Rickert cleavage.[13] Thus, an increase in pressure should enhance the rate of the association process strongly in comparison with the dissociation and the former process should dominate. The example described here clearly reveals the different effects of pressure and temperature on the rate of the reaction, which can result, as shown here, in the formation of unusual compounds that are not observed under normal conditions.

Received: December 16, 1985;
revised: January 28, 1986 [Z 1590 IE]
German version: *Angew. Chem. 98* (1986) 344

[1] a) E. Vogel, W. Grimme, S. Korte, *Tetrahedron Lett. 1965*, 3625; b) E. Vogel, S. Korte, W. Grimme, H. Günther, *Angew. Chem. 80* (1968) 279; *Angew. Chem. Int. Ed. Engl. 7* (1968) 289; c) B. Halton, B. R. Dent, S. Böhm, D. L. Officer, H. Schmickler, F. Schophoff, E. Vogel, *J. Am. Chem. Soc. 107* (1985) 7175; d) reviews on cyclopropabenzenes: B. Halton, *Chem. Rev. 73* (1973) 113; W. E. Billups, *Acc. Chem. Res. 11* (1978) 245; B. Halton, *Ind. Eng. Chem. Prod. Res. Dev. 1980*, 349.

[2] a) E. Vogel, F. Weyres, H. Lepper, V. Rautenstrauch, *Angew. Chem. 78* (1966) 754; *Angew. Chem. Int. Ed. Engl. 5* (1966) 732; b) R. R. Andréa, H. Cerfontain, H. J. A. Lambrechts, J. N. Louwen, A. Oskam, *J. Am. Chem. Soc. 106* (1984) 2531.

[3] Derivatives of methylenecyclopropabenzene: B. Halton, C. J. Randall, P. J. Stang, *J. Am. Chem. Soc. 106* (1984) 6108.

[4] For the cycloadditions to 1,6-methano[10]annulenes see: a) E. Vogel, *Spec. Publ. Chem. Soc. 21* (1967) 113; b) P. Ashkenazi, E. Vogel, D. Ginsburg, *Tetrahedron 33* (1977) 1169; *34* (1978) 2167; this work is regarded by *D. G.* as Part 90 of his propellane series; c) P. Ashkenazi, M. Peled, E. Vogel, D. Ginsburg, *ibid. 35* (1979) 1321; d) P. Ashkenazi, M. Kaftory, D. Ginsburg, *Helv. Chim. Acta 66* (1983) 611; e) P. Ashkenazi, E. Vogel, D. Ginsburg, *ibid. 66* (1983) 615.

[5] All new compounds were characterized by their spectra (^{1}H-NMR, ^{13}C-NMR, IR, UV, MS). Table 1 contains selected data.

[6] R. Hollenstein, A. Mooser, M. Neuenschwander, W. von Philipsborn, *Angew. Chem. 86* (1974) 595; *Angew. Chem. Int. Ed. Engl. 13* (1974) 551.

[7] S. W. Benson: *Thermochemical Kinetics*, 2nd ed., Wiley, New York 1976, p. 273, 274.

[8] We thank Prof. Dr. *O. Ermer* and Dr. *J. Lex* for the crystal structure investigations and for the force-field calculations (*O. E.*).

[9] J. Berkowitz Carlton, R. H. Levin, J. Clardy, *J. Am. Chem. Soc. 98* (1976) 6068.

[10] W. von E. Doering, D. W. Wiley, *Tetrahedron 11* (1960) 183.

[11] W. R. Roth, F.-G. Klärner, W. Grimme, H. G. Köser, R. Busch, B. Muskulus, R. Breuckmann, B. P. Scholz, H.-W. Lennartz, *Chem. Ber. 116* (1983) 2717.

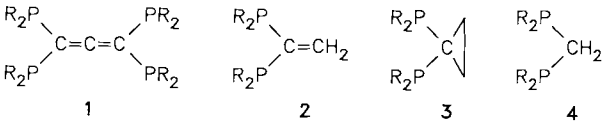
[12] M. Christl, U. Heinemann, W. Kristof, *J. Am. Chem. Soc. 97* (1975) 2299, and references cited therein.

[13] For discussions of the activation volumes of retro Diels-Alder reactions see G. Jenner, M. Papadopoulos, J. Rimmelin, *J. Org. Chem. 48* (1983) 748.

Tetrakis(diphenylphosphino)allene**

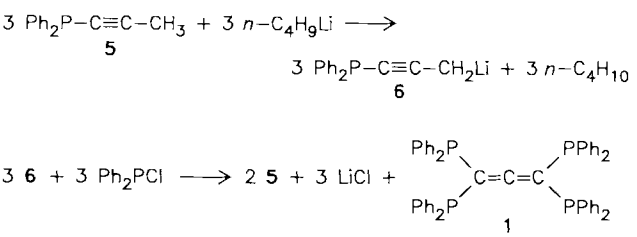
By *Hubert Schmidbaur** and *Thomas Pollok*

Little is known about phosphinoallenes at present,[11] and examples with four phosphino substituents (**1**) are totally lacking. Owing to the partly unexpected reaction behavior of 1,1-bis(diphenylphosphino)ethene **2**, R = Ph,[2] -cyclopropane **3**, R = Ph,[3] and -methane **4**, R = Ph,[4] upon quaternization,[5,6] oxidation,[7] and complex formation,[8] we have synthesized the title compound **1**, R = Ph.



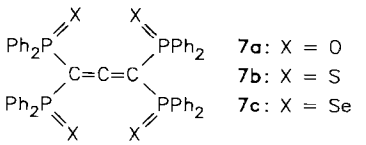
1 **2** **3** **4**

Compound **1** was prepared surprisingly easily by lithiation of 1-diphenylphosphinopropyne **5**[9] to give **6**, followed by reaction of **6** with chlorodiphenylphosphane, and isolated in highly pure form in satisfactory yield (60%).[10] The molar ratios given in the two reaction equations clearly show that several transmetalations occur. Apparently, the CH acidity of the intermediates increases with increasing number of phosphino substituents, thereby favoring the complete replacement of all propyne/allene H atoms by Ph_2P groups. In contrast, the reactions of lithium or magnesium propynide (Li_4C_3 and Mg_2C_3) with chlorodiphenylphosphane afforded only tetraphenyldiphosphane.[11]



The allene **1** forms colorless crystals with a melting point (dec.) of 224 °C, which are only sparingly soluble in halogenated hydrocarbons. The allene structural unit is revealed in the IR spectrum by an absorption at 1890 cm^{-1}. The presence of the isomeric tetrakis(diphenylphosphino)propyne is also excluded by the observation that the ^{31}P-NMR spectrum contains only one signal ($\delta = -6.9$). In the ^{13}C-NMR spectrum, the central allene C atom gives rise to a quintet ($^2J_{PC} = 9.8$ Hz) at $\delta = 209.7$; the flanking C atoms, on the other hand, give rise to a singlet at $\delta = 89.1$. In solution the Ph_2P substituents are apparently free to rotate around the P-C bonds (such as in **2**, R = Ph[2]), so that only one set of signals results from the eight phenyl groups. In the mass spectrum (electron ionization, 70 eV), the peak at *m/z* 776 is due to the molecular ion.

The allene **1** can be converted into the tetraoxide **7a** by careful oxidation with bis(trimethylsilyl)peroxide in tetrahydrofuran (THF) (87% yield, m.p. = 258–260 °C); **7a**



7a: X = O
7b: X = S
7c: X = Se

Table 1. Selected NMR and IR data for the compounds **1** and **7a–c**.

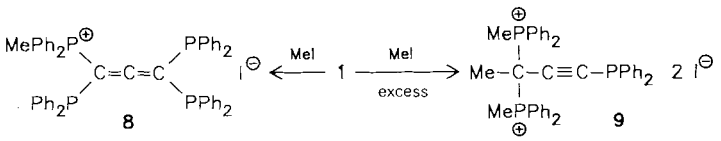
	1	**7a**	**7b**	**7c**
^{31}P-NMR ($CDCl_3$), δ values	−6.9	23.5	45.6	37.2
^{13}C-NMR ($CDCl_3$), δ values				
CP_2	89.1	96.9	102.5	99.3
CC_2	209.7	213.2	216.7	216.9
Ph-C1	135.5	130.6	138.8	covered
Ph-C2,6	134.1	132.1	133.8	134.6
Ph-C3,5	127.8	127.9	127.5	127.3
Ph-C4	128.5	131.6	131.4	131.4
IR ν(C=C=C) [cm^{-1}]	1890	1905	1880	1870

[*] Prof. Dr. H. Schmidbaur, Dipl.-Chem. T. Pollok
Anorganisch-chemisches Institut der Technischen Universität München
Lichtenbergstrasse 4, D-8046 Garching (FRG)

[**] This work was supported by the Deutsche Forschungsgemeinschaft, the Fonds der Chemischen Industrie, Hoechst AG, Knapsack and Frankfurt, and SKW Trostberg.

forms beautiful single crystals.[12] Sulfur and selenium also add to **1**, giving the chalcogenides **7b** and **7c**, respectively. Table 1 gives spectroscopic data for **1** and **7**. Moreover, an X-ray structure analysis is available for **7a**.[12]

Other reactions often proceed in a complex manner—as observed for the vinyl derivative **2**, R = Ph[5]—since the propyne/allene isomerism allows several possible sites of attack. Thus, whereas the mild quaternization with iodomethane (in benzene at 0°C) indeed gives the monophosphonium salt **8**,[13] the use of the reagent in excess leads, even at 20°C, to the totally unexpected formation of the butynylphosphonium salt **9**.[14] Presumably, ylidic intermediates play a role in the lengthening of the allene/propyne chain. The Ph_2P unit that is lost is found in the reaction mixture as $[Ph_2PMe_2]I$.



Received: January 8, 1986;
supplemented: January 24, 1986 [Z 1611 IE]
German version: *Angew. Chem. 98* (1986) 365

[1] W. Hewertson, I. C. Taylor, S. Trippett, *J. Chem. Soc. C 1970*, 1835; M.-P. Simonnin, C. Charrier, *C. R. Acad. Sci. Paris, Ser. C 267* (1968) 550. See also: P. D. Landor in S. R. Landor (Ed.): *The Chemistry of Allenes*, Academic Press, New York 1982, p. 174; H. Hopf in S. Patai (Ed.): *The Chemistry of Ketenes, Allenes and Related Compounds*, Wiley, New York 1980, p. 848.

[2] H. Schmidbaur, R. Herr, J. Riede, *Chem. Ber. 117* (1984) 2322; I. J. Colquhoun, W. McFarlane, *J. Chem. Soc. Dalton Trans. 1982*, 1915.

[3] H. Schmidbaur, T. Pollok, *Helv. Chim. Acta 67* (1984) 2175.

[4] K. Issleib, D. W. Müller, *Chem. Ber. 92* (1959) 3175; W. Hewertson, H. R. Watson, *J. Chem. Soc. 1962*, 1490.

[5] H. Schmidbaur, R. Herr, J. Riede, *Angew. Chem. 96* (1984) 237; *Angew. Chem. Int. Ed. Engl. 23* (1984) 247.

[6] H. Schmidbaur, R. Herr, T. Pollok, A. Schier, G. Müller, J. Riede, *Chem. Ber. 118* (1985) 3105.

[7] H. Schmidbaur, R. Herr, G. Müller, *Z. Chem. 24* (1984) 378.

[8] H. Schmidbaur, T. Pollok, R. Herr, F. E. Wagner, R. Bau, J. Riede, G. Müller, *Organometallics 5* (1986), in press.

[9] A. M. Aguiar, G. W. Prejean, J. R. S. Ireland, C. J. Morrow, *J. Org. Chem. 34* (1969) 4024; C. Charrier, W. Chodkiewicz, P. Cadiot, *Bull. Soc. Chim. Fr. 1966*, 1002.

[10] *Experimental Procedure*: **1**: A solution of **5** (1.99 g, 8.87 mmol) in 15 mL of THF was metalated at −70°C with the equivalent amount of *n*BuLi (in hexane). The reaction mixture was allowed to warm up to 20°C and then cooled again to 0°C after 2 h. After slow addition (1 h) of Ph_2PCl (1.96 g, 8.86 mmol) in 10 mL of THF, the mixture was stirred for ca. 15 h and the solvent was then removed; the oily residue was crystallized from ethanol and dried; yield: 1.3 g (56%). Correct elemental analyses were obtained for **1**, **7a–c**, **8**, and **9**.

[11] We thank SKW Trostberg for chemicals and advice.

[12] G. Reber, G. Müller, unpublished results.

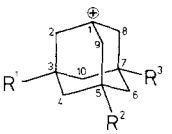
[13] The reaction of **1** (1.17 g, 1.51 mmol) with 2 mL (32.1 mmol) of iodomethane in 50 mL of benzene at 0°C affords, after 3 h, 1.20 g of **8** (87%), decomposition temperature: 203°C. IR: ν(C=C=C) = 1880 cm^{-1}. ^{1}H-NMR ($CDCl_3$): δ = 2.25 (br. d, J = 12.4 Hz, 3H, CH_3), 6.9–7.9 (m, 40H, C_6H_5). ^{13}C-NMR ($CDCl_3$): δ = 10.1 (d, J = 55.7 Hz, CH_3), 99.0 (m, CP_2), 117.9 (d, J = 86.9 Hz, C1), 207.3 (m, CC_2), signals of C2–C6 overlap.— ^{31}P-NMR ($CDCl_3$): AB_2X multiplet δ = −7 and +22. MS (FD): m/z 792 ($M^{\oplus}$).

[14] A solution of **1** (1.34 g, 1.73 mmol) and 2 mL (32.1 mmol) of iodomethane in 50 mL of THF was refluxed for 30 min. Upon cooling, **9** separates out as a yellow precipitate (yield: 1.52 g, 99%, m.p. = 225°C (dec.)). IR: ν(C≡C) = 2120 cm^{-1}. MS (FD): m/z 764 ($M^{\oplus}$ − I, 100%), 319 ($M^{\oplus}$ − 2I, 40.5). ^{1}H-NMR ($CDCl_3$): δ = 2.5–2.9 (m, 9H), 7.4–8.2 (m, 30H). ^{13}C-NMR ($CDCl_3$): δ = 13.3 (t, ^2J(PC) = 48.3 Hz, CH_3C), 18.2 (dt, ^1J(PC) = 110.3, ^3J(PC) = 4.4 Hz, CP_2), 65.4 (dt, ^1J(PC) = 191.4, ^3J(PC) = 6.3 Hz, P–C≡), 120.3 (d, ^1J(PC) = 99.6, C1 of PPh_2), 120.7 (AXX', N = 91.8 Hz, C1 of PPh_2Me), signals of C2–C6 overlap; 125.6 (dt, ^2J(PC) = 36.0, ^2J(PC) = 2.4 Hz, C–C≡). ^{31}P-NMR ($CDCl_3$): δ = 1.1 (t, ^3J(PP) = 7.3 Hz, P^{III}), 22.7 (d, P^V).

First Crystal Structure Analysis of an Aliphatic Carbocation—Stabilization of the 3,5,7-Trimethyl-1-adamantyl Cation by C–C Hyperconjugation**

By *Thomas Laube**

The 1-adamantyl cation **1a** and its derivatives **1b** and **1c**, bridgehead cations with high stability, have been the subject of numerous NMR spectroscopic,[1] theoretical,[2] and solvolytic[3] studies, because many observations can only be interpreted by assuming that the γ carbon atoms 3, 5, and 7 bear partial positive charges. Although *Olah* et al.[4] described the synthesis of solid **1a**-SbF_6 in 1973, no X-ray structure analysis of the salt of an adamantyl cation or, for that matter, of a cation that is not stabilized by a π-system or a heteroatom has been reported. By reaction of 1-fluoro-3,5,7-trimethyladamantane[5] with antimony pentafluoride (modification of the procedure in ref. [4]), it has now been possible to synthesize the salt **1c**-Sb_2F_{11}, which, after recrystallization, afforded suitable crystals[7] for the X-ray structure analysis.[6]



	R¹	R²	R³
1a	H	H	H
1b	CH_3	CH_3	H
1c	CH_3	CH_3	CH_3

No interaction between cations and anions is found in the crystal lattice, since, even though the shortest C⊕···F distance (C1···F25) is only 2.88(2) Å,[8] the Sb2–F25 bond is not lengthened[9] (Fig. 1). The bent structure of the anion does not differ from that in other Sb_2F_{11} salts.[10] The cation **1c**, however, exhibits drastic differences from the idealized structure[11] (Fig. 2).

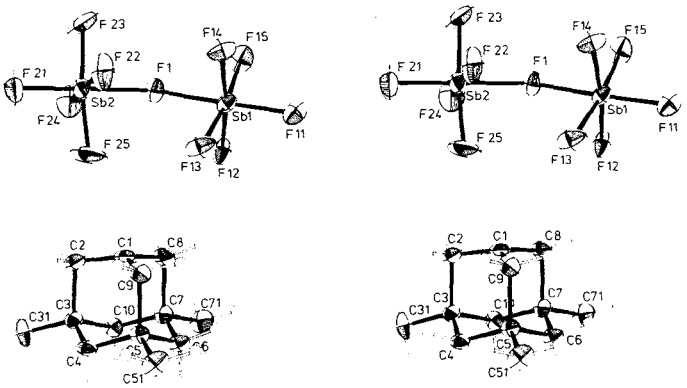


Fig. 1. ORTEP stereo plot of the crystal structure of **1c**-Sb_2F_{11}. The ellipsoids are drawn at the 50% probability level. Within the limits of error of the structure, the cation belongs to the point group C_{3v}, the anion approximately to the point group C_2. The ion pair shown forms the asymmetric unit.

The cationic center C1 is clearly flattened (the "pyramidalization"[12] is 0.21 Å); the bonds emanating from C1 are on the average 1.44(2) Å, the subsequent bonds to the qua-

[*] Dr. T. Laube
Laboratorium für Organische Chemie der Eidgenössischen Technischen Hochschule
ETH-Zentrum, Universitätstrasse 16, CH-8092 Zürich (Switzerland)

[**] I thank Prof. Dr. *D. Seebach* for his generous support and Prof. Dr. *J. D. Dunitz* for his interest and for provoding me with measuring time.

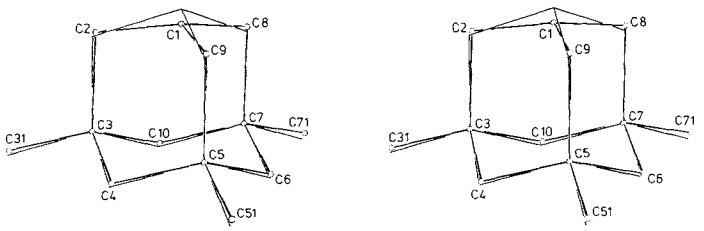


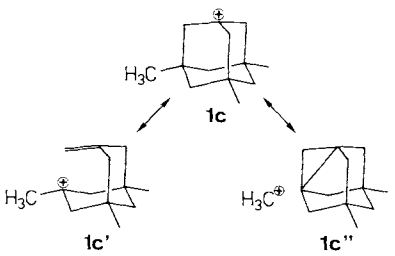
Fig. 2. Stereoprojection of the superposition of the 3,5,7-trimethyladamantyl cation **1c** (atoms drawn as circles; thick bonds) on a corresponding section of the diamond lattice (bond lengths 1.54 Å; thin bonds). Fitting to the atoms C3, C5, and C7 was carried out with 100-fold more weight compared to the other atoms.

ternary centers 1.62(2) Å long; the six-membered ring with the three methyl groups is slightly flattened (see Table 1).

Table 1. The structural data of the cation **1c** (distances in Å, angles and torsion angles in °; standard deviations of the distances 0.02 Å, of the angles and the torsion angles 1°).

C1-C2	1.43	C3-C31	1.50	C1-C2-C3	101
C1-C9	1.42	C5-C51	1.53	C1-C9-C5	99
C1-C8	1.47	C7-C71	1.54	C1-C8-C7	98
C2-C3	1.61	C1···C3	2.34	C2-C1-C9	120
C9-C5	1.62	C1···C5	2.32	C8-C1-C9	116
C8-C7	1.62	C1···C7	2.34	C2-C1-C8	118
C3-C4	1.52	C3-C4-C5	113	C3-C4-C5-C6	−56
C4-C5	1.51	C4-C5-C6	110	C4-C5-C6-C7	+55
C5-C6	1.53	C5-C6-C7	111	C5-C6-C7-C10	−55
C6-C7	1.52	C6-C7-C10	113	C6-C7-C10-C3	+54
C7-C10	1.51	C7-C10-C3	111	C7-C10-C3-C4	−53
C10-C3	1.55	C10-C3-C4	110	C10-C3-C4-C5	+55

The structure of the cation reflects the effect of hyperconjugative resonance structures of type **1c'**. Homohyperconjugation appears to play no or at most a very minor role, because resonance structures of type **1c''** are not able to explain the extreme differences in bond lengths[13] and the bonds to the methyl groups are not lengthened (Table 1). The very small C-C-C bond angles (99(1)°) around the methylene carbon atoms 2, 8, and 9 show that these atoms, like C1, are approximately sp^2 hybridized, the p-like orbital contributing in each case to the bond to the quaternary C atom.[14]



Received: February 5, 1986 [Z 1657 IE]
German version: *Angew. Chem. 98* (1986) 368

CAS registry numbers:
1c · Sb_2F_{11}, 101144-74-5.

[1] a) G. A. Olah, G. K. S. Prakash, J. G. Shih, V. V. Krishnamurthy, G. D. Mateescu, G. Liang, G. Sipos, V. Buss, T. M. Gund, P. von R. Schleyer, *J. Am. Chem. Soc. 107* (1985) 2764; b) G. A. Olah, G. K. S. Prakash, J. Sommer: *Superacids*, Wiley, New York 1985, p. 93, and references cited therein.

[2] a) D. E. Sunko, *Croat. Chem. Acta 53* (1980) 525; b) D. E. Sunko, S. Hirši-Starčević, S. K. Pollack, W. J. Hehre, *J. Am. Chem. Soc. 101* (1979) 6163.

[3] a) D. Färcaşiu, J. Jähme, C. Rüchardt, *J. Am. Chem. Soc. 107* (1985) 5717; b) C. A. Grob, B. Schaub, *Helv. Chim. Acta 65* (1982) 1720; c) W. Fischer, C. A. Grob, *ibid. 61* (1978) 1588.

[4] G. A. Olah, J. J. Svoboda, A. T. Ku, *Synthesis 1973*, 492.

[5] Synthesized from perhydrofluorene by isomerization with $AlBr_3$ (B. M. Lerman, Z. Y. Aref'eva, A. R. Kuzyev, G. A. Tolstikov, V. I. Khvostenko, A. S. Sultanov, *Izv. Akad. Nauk SSSR, Ser. Khim. 1972*, 1815), bromination (H. Stetter, M. Schwarz, A. Hirschhorn, *Chem. Ber. 92* (1959) 1629) and subsequent bromine-fluorine exchange with AgF (R. C. Fort Jr., P. von R. Schleyer, *J. Org. Chem. 30* (1965) 789).

[6] Enraf-Nonius CAD4 diffractometer, $Mo_{K\alpha}$ radiation, graphite monochromator, measurement temperature −160°C; space group *Pbca*, $a = 11.55(1)$, $b = 16.222(6)$, $c = 20.46(3)$ Å, $V = 3832.9$ Å^3, $\rho_{calcd} = 2.183$ gcm^{-3}, $\mu = 29.3$ cm^{-1} (no absorption correction), $Z = 8$, 4382 measured reflections ($\theta < 27.5°$), 3089 with $I > 3\sigma(I)$. Position of the Sb atoms determined with the Patterson option of SHELX84, all other atoms, except hydrogen atoms, by subsequent difference Fourier synthesis with SHELX76. Refinement by the least-square method (all atoms except hydrogens anisotropic, H atoms on C2 and C9 isotropic, the other H atoms were calculated and refined according to the riding model) with unit weights, finally in the XRAY system: $R = 0.070$. The tensor component U_{11} is large for F23 and F25: 0.18 and 0.28 Å^2, respectively.

[7] The X-ray structure analyses of **1a**-Sb_2F_{11} and **1b**-Sb_2F_{11} gave only poor R values on account of disorder (**1a**-Sb_2F_{11}: *C2/c*, $a = 17.072(7)$, $b = 13.263(5)$, $c = 9.017(4)$ Å, $\beta = 121.90(4)°$ at −30°C; **1b**-Sb_2F_{11}: $Pmn2_1$, $a = 14.486(8)$, $b = 7.692(4)$, $c = 8.51(1)$ Å at −40°C).

[8] Sum of the van der Waals radii of C and F: 1.70 Å + 1.47 Å = 3.17 Å; the van der Waals radius of C°, which is actually required, is unknown.

[9] W. H. Hersh, *J. Am. Chem. Soc. 107* (1985) 4599.

[10] a) A. J. Edwards, R. J. C. Sills, *J. Chem. Soc. Dalton Trans. 1974*, 1726, and references cited therein; b) R. J. Gillespie, F. G. Riddell, D. R. Slim, *J. Am. Chem. Soc. 98* (1976) 8069.

[11] The Cambridge File contains to date no structure with the 3,5,7-trimethyladamantyl fragment. X-ray structure analysis of the ordered phase of adamantane: J. Donohue, S. H. Goodman, *Acta Crystallogr. 22* (1967) 352.

[12] "Pyramidalization" means the distance of a trivalent atom from the plane formed by its three binding partners; see also K. L. Brown, L. Damm, J. D. Dunitz, A. Eschenmoser, R. Hobi, C. Kratky, *Helv. Chim. Acta 61* (1978) 3108.

[13] Structure of 1-cyano-3,5-dehydroadamantane: C. S. Gibbons, J. Trotter, *Can. J. Chem. 51* (1973) 87.

[14] Although the protons on C2 and C9 could only be determined very imprecisely, they deviated systematically in this sense from the local C_{2v} symmetry at C2 and C9 that is usually assumed. For the construction of natural hybrid orbitals from the structure of a molecule, see: M. Scholz, H.-J. Köhler: *Quantenchemie - ein Lehrgang. Bd. 3*, Hüthig-Verlag, Heidelberg 1981, p. 73.

$Ge_{4.06}I$, an Unexpected Germanium Subiodide—a Tetragermanioiodonium(III) Iodide with Clathrate Structure $[Ge_{46-x}I_x]I_8$, $x = 8/3$

By *Reinhard Nesper, Jan Curda,* and *Hans-Georg von Schnering**

The clathrate structures found for the nobel gas hydrates $Xe(H_2O)_{5.75} \triangleq Xe_8(H_2O)_{46}$[1] are characterized by a three-dimensional network of tetrahedrally bonded structural units, which enclose large and usually highly symmetric cavities. In the case of the nobel gas hydrates, the 46 H_2O molecules form a cubic E_{46} network, which is held together by hydrogen bonds and which contains (2+6) cavities of two different types, providing space for the eight Xe atoms. As was recently shown by the synthesis of the clathrasils,[2] this structural principle is also adopted by SiO_2 and may be modified in a variety of ways by the introduction of foreign substances. Further significant variants are the silicides and germanides of the alkali metals of the type K_8Si_{46}[3] and $Rb_8[In_8Ge_{38}]$,[4] respectively, and ternary halides of the type $[A_{38}B_8]X_8$ with A = Si, Ge, B = P, As, Sb, and X = Cl, Br, I;[5,6] in these cases, the E_{46} framework is

[*] Prof. Dr. H.-G. von Schnering, Dr. R. Nesper, Dipl.-Ing. J. Curda
Max-Planck-Institut für Festkörperforschung
Heisenbergstrasse 1, D-7000 Stuttgart 80 (FRG)

built up from Si and Ge/In and from $38\,A+8\,B^+$, respectively, while the alkali metal atoms and the halide ions fill the eight cavities. The formation of the nobel gas hydrates and the clathrasils, in particular, indicates that the clathrate structures, which are apparently topologically acceptable for tetrahedrally bonded units, allow the transfer of structural elements from solution to the crystalline state—even if it is metastable. For this reason, we have used high pressures of a foreign gas (Xe, CO_2; 80 atm) to influence the crystallization of Ge from the gas phase following thermal decomposition of GeI_2[7] and have indeed obtained a product with a clathrate structure. However, this product was not the desired $Ge_{46}Xe_8$ but rather the subiodide $Ge_{4.06}I$.

$Ge_{4.06}I$ is formed upon rapid thermal decomposition of GeI_2 at 660 K under extreme conditions of the chemical transport.[8] It is a black powder, which, under the electron microscope, consists of cubic crystals having edges of up to 10 μ (Fig. 1). According to inductively coupled phase (ICP) analyses, the chemical composition is $Ge_{4.1}I$, which, combined with the experimental density $\rho_{exp}=5.85$ g·cm^{-3} for the cubic unit cell ($a=10.814$ Å; $V=1264.6$ Å^3), gives the overall formula $Ge_{43.0}I_{10.5}$. Although this formula contains nearly 54 atoms, as one would expect for a clathrate structure, it includes more than eight I atoms (2+6 cages). $Ge_{4.06}I$ is a diamagnetic semiconductor ($\chi_{mol}=-114\times10^{-6}$ cm^3 per $Ge_{4.1}I$; $\Delta E\approx1$ eV). X-ray photoelectron spectroscopic (XPS) measurements reveal that two types of iodide 1s states are present in the ratio 3:1, at −619 and −623 eV, which, when compared with the known values for I^- (−619 eV) and I^{7+} in IO_3^- (−626 eV) indicate the presence of I^{1-} and I^{3+}.[9] $Ge_{4.06}I$ undergoes thermal decomposition above 780 K to give crystalline α-Ge, gaseous GeI_2, and I_2 (differential thermal analysis, thermogravimetry, mass spectra). All the findings indicate that $Ge_{4.06}I$ is thermodynamically metastable with respect to disproportionation into GeI_2 and α-Ge.

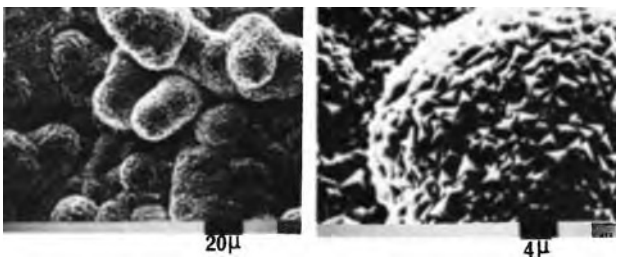


Fig. 1. Scanning electron micrographs of $Ge_{4.06}I$. The pictures show the typical dendrite-like, nodular growth of intergrown cubes around the starting compound GeI_2.

The structure elucidation was achieved by careful analysis of 80 reflections of a powder sample.[10] The surprising result is summarized in Table 1. 43.33 Ge atoms and 2.67 I atoms form the covalently bonded E_{46} framework, the cavities of which contain the remaining eight I atoms.

This distribution of the atoms was determined from the intensities of the reflections alone, independently of chemical analysis and density measurements. This is especially true for the statistical distribution of Ge1 and I3 at the position 6c (Table 1). Under the probable assumption that the I atoms in the cavities are I^- ions (cf. ref. [11]), the principle of neutrality requires that the 2.67 I atoms at 6c be I^{3+} ions, in good agreement with the results of the XPS measurements and also with the tetravalency of I^{3+}, which is necessary for a tetrahedral framework. Since each of these I atoms is coordinated by four Ge atoms, tetragermanioiodonium(III) centers are present. The overall structure may be described as a polygermanioiodonium(III) triiodide $[I(Ge_n)]I_3$ ($n=16.25$): $[I_4Ge_{65}]I_{12}$. The bond lengths (Table 1) and physical properties are in accordance with this description.

Table 1. $Ge_{43.33}I_{10.67}$; Structure parameters: space group $Pm3n$ (223); $a=10.814(3)$ Å; $Z=1$; powder sample; 80 reflections hkl; $R=0.087$. The larger U value of I1 probably results from defects (SOF = 0.85), which may also be the case for the Ge positions. On account of the method of synthesis, statistical defects in the structure are very likely. With SOF(I1) = 0.85 alone and assuming the validity of the electroneutrality rule, one obtains $Ge_{43.43}I_{10.27}\triangleq Ge_{4.23}I$, that is, only small differences from the chemical analysis. For this reason, we have preferred the composition of the fully occupied ideal structure.

Atom	Position	Parameters	U [Å^2]	Occupation	
Ge1+I3	6c	1/4 0 1/2	0.047(9)	0.55(5) Ge + 0.45(5) I	
Ge2	16i	x x x	0.024(4)	1.00 Ge	—
Ge3	24k	0 y z	0.027(7)	1.00 Ge	—
		x = 0.182(1) y = 0.311(1) z = 0.118(1)			
I1	2a	0 0 0	0.047(6)	—	1.00 I
I2	6d	1/4 1/2 0	0.015(7)	—	1.00 I

Distances [Å]

Ge1/I3-Ge3	2.50(1) 4×	Ge3-Ge1/I2	2.50(1)
Ge1/I3-I2	3.82(1) 4×	Ge3-Ge2	2.51(1) 2×
Ge2-Ge3	2.51(1) 3×	Ge3-Ge3	2.55(3)
Ge2-Ge2	2.56(1) 1×	Ge3-I1	3.60(1)
Ge2-I1	3.40(1)	Ge3-I2	3.62(1) 2×
Ge2-I2	4.40(1)	Ge3-I2	4.18(2)
I1-Ge2	3.43(1) 8×	I2-Ge3	3.62(1) 8×
I1-Ge3	3.47(2) 12×	I2-Ge1/I3	3.82(1) 4×
		I2-Ge2	4.03(1) 8×
		I2-Ge3	4.18(2) 4×

Recently, it was again confirmed that only GeI_2 and GeI_4 exist as stable phases in the Ge/I system.[12] The discovery of the subiodide $Ge_{4.06}I$ in no way changes this situation insofar as it involves thermodynamically controlled reactions. The thermal decomposition of GeI_2 was carried out under conditions, however, under which $Ge_{4.06}I$ is only observed as an intermediate. Thermodynamic data for $Ge_{4.06}I$ are still not available. The equilibrium temperature for the reaction $GeI_2(g)=0.50\ Ge(s)+0.50\ GeI_4(g)$ is 670 K.[8] The value for the decomposition $GeI_2(g)=0.13\ Ge_{4.06}I(s)+0.47\ GeI_4\ (g)$ should be similar. In fact, the mean deposition temperature of $Ge_{4.06}I$ is $T_d=645$ K. Using the entropy increments for Ge and I (47.2 and 56.4 JK^{-1} mol^{-1}[13]) and the standard values ΔH_f^{298} and ΔS_f^{298} for $GeI_2(g)$ and $GeI_4(g)$ (+53.9 and −37.6 kJ mol^{-1} and 338 and 428 JK^{-1} mol^{-1}, respectively[14, 15]), one obtains at T_d the realistic value ΔH_f^{645} ($Ge_{4.06}I$,f) = +4 kJ mol^{-1}.

Experimental Procedure

$Ge_{4.06}I$ was synthesized by thermal decomposition of GeI_2 and by chemical transport. The thermal decomposition was carried out at $T=650$ K and $p=10^{-1}$ Pa in a glass ampule opened at one end. GeI_2 (0.5 g, 1.5 mmol) was converted into $Ge_{4.06}I$ in a yield of about 50% within 5 to 10 min. $Ge_{4.06}I$ was only formed in a vacuum. Under argon atmosphere (100 Pa), mixtures of GeI_2 and α-Ge were always obtained. The chemical transport was carried out in a sealed quartz ampule (28 cm × 0.27 cm) between $T_1=1070$ K and $T_2=625$ K. α-Ge (3.0 g, 0.04 mol) was transported with I_2 (0.25 g, 0.001 mmol) to the cold side within ca. 20 h. $Ge_{4.06}I$ appears as a black powder in a zone between ca. 635 K and 685 K. Despite numerous synthetic attempts, the crystal size could not be increased to more than 10 μ.

Received: December 2, 1985;
revised: January 17, 1986 [Z 1561 IE]
German version: *Angew. Chem.* 98 (1986) 369

 © VCH Verlagsgesellschaft mbH, D-6940 Weinheim, 1986 0570-0833/86/0404-0351 $ 02.50/0

CAS registry numbers:
$Ge_{4.06}I$, 37348-82-6; GeI_2, 13573-08-5; Ge, 7440-56-4; I_2, 7553-56-2.

[1] M. von Stackelberg, H. R. Müller, *Z. Elektrochem. 58* (1954) 25.
[2] H. Gies, F. Liebau, H. Gerke, *Angew. Chem. 94* (1982) 214; *Angew. Chem. Int. Ed. Engl. 21* (1982) 206.
[3] J. Gallmeier, H. Schäfer, A. Weiss, *Z. Naturforsch. B 24* (1969) 665.
[4] H.-G. von Schnering, H. Menke, *Z. Anorg. Allg. Chem.*, in press.
[5] H. Menke, H.-G. von Schnering, *Z. Anorg. Allg. Chem. 395* (1973) 223.
[6] H.-G. von Schnering, H. Menke, *Z. Anorg. Allg. Chem. 424* (1976) 108.
[7] T. Karantossis, L. Captos, *C. R. Acad. Sci. 201* (1935) 74.
[8] H. Schäfer: *Chemische Transportreaktionen*, Verlag Chemie, Weinheim 1962; Chemical Transport Reactions, Academic Press, New York 1964.
[9] H. Geyer Lippmann, Stuttgart, private communication.
[10] Powder diffractometer STOE STADI PL2; Debye geometry with $R = 130$ mm; $Cu_{K\alpha 1}$ radiation; $10° \leq 2\theta \leq 100°$; Ge monochromator; intensities were obtained twice by means of the peak-fit procedure (PEAK program, STOE) and measurement of the powder scans and then averaged. The structure factors of overlapping reflections were approximated by iteration starting from a trial model.
[11] R. Nesper, H.-G. von Schnering, *Tschermaks Mineral. Petrogr. Mitt. 32* (1983) 195.
[12] H. Oppermann, *Z. Anorg. Allg. Chem. 504* (1983) 95.
[13] R. F. Lever, *J. Electrochem. Soc. 110* (1963) 775.
[14] O. Kubaschewski: *Thermochemical Properties of Inorganic Substances*, Springer, Berlin 1977, p. 285.
[15] A. C. Loonam, *J. Electrochem. Soc. 106* (1959) 238.

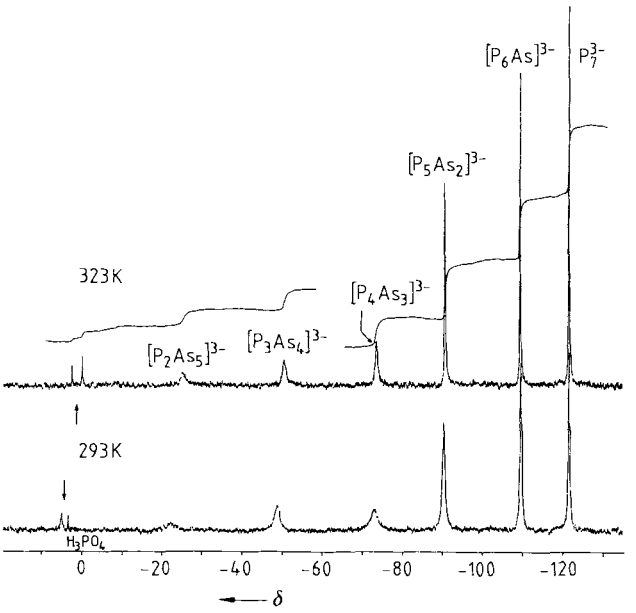
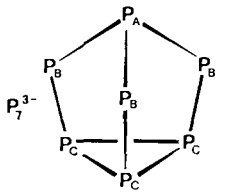


Fig. 1. $^{31}P\{^1H\}$-NMR spectrum of $Rb_3[P_{7-x}As_x]$ in en at 293 and 323 K ($x \approx 3$). The signals at $\delta \approx 5$ (arrow) are assigned to $H_2PO_4^-$ and HPO_4^{2-} [11], which are introduced inadvertently in the preparation procedure. The signal of $[PAs_6]^{3-}$ could coincide with these signals (cf. text).

Valence Tautomerism of the Heptaheteronortricycles $[P_{7-x}As_x]^{3-}$**

By *Wolfgang Hönle* and *Hans-Georg von Schnering**

Several years ago, *Baudler* et al.[1] described the valence tautomerism of the polycyclic heptaphosphane(3) anion P_7^{3-} in tetrahydrofuran solutions of solvated $Li_3P_7(solv)_3$ at 80 °C. Furthermore, we found that all solvent-free poly-



phosphides M_3P_7 (M = Li–Cs) dissolve in ethylenediamine (en) and, even at room temperature, undergo valence tautomerism.[2] The unequivocal identification of the arsenides M_3As_7 (M = Na–Cs) containing As_7^{3-} ions[3] was the motivation for undertaking an investigation of mixed crystals $M_3[P_{7-x}As_x]$, which we consider ideal for verifying the concept of topological charge stabilization.[4] According to *Gimarc* and *Joseph*, particularly stable structures are formed when the positions of highest charge density in a homoatomic isoelectronic reference system are replaced by heteroatoms with greater electronegativity.[4] In P_7^{3-}, the bridge P atoms have the greatest charge density.[5] According to *Allred* and *Rochow* as well as *Sanderson*, the electronegativity of arsenic is greater than that of phosphorus.[6] Accordingly, in mixed crystals $M_3[P_{7-x}As_x]$ the arsenic atoms should preferentially occupy the bridge positions, thereby favoring a polycycle $[P_4As_3]^{3-}$. The results of our investigations on the polymeric heptaphosphides $MP_{7-x}As_x$ (M = Li, Na)[7] fulfill these expectations, but not the results on the mixed crystals of the type $Eu[P_{3-x}As_x]$.[8]

Mixed crystals $Rb_3[P_{7-x}As_x]$ are synthesized from the elements in a stoichiometric ratio in sealed Ta ampules at 900 K. The dark red mixed crystals ($x \approx 3$) are air-sensitive and dissolve completely in en. The ^{31}P-NMR spectrum[9] of the intense red solutions exhibits six singlets at room temperature (Fig. 1), the halfwidths of which decrease with increasing temperature. The spectrum is surprisingly easy to explain if one assumes that a series of compounds are present, all of which can interconvert by valence tautomerism. The positions of the coalescence signals are derived from the weighted averages of the chemical shifts δ_i of the atoms involved in the rearrangement.

For the AB_3C_3 spin system of P_7^{3-}, the chemical shifts $\delta(P_A) = -57$, $\delta(P_B) = -103$, and $\delta(P_C) = -162$ are observed for the three structurally different P atoms P_A, P_B, and P_C, respectively.[1] Their weighted average $[\delta(P_A) + 3\delta(P_B) + 3\delta(P_C)]/7 = -121.7$ is in agreement with the signal of the highest shift at $\delta = -121.4$ (Fig. 1). The further coalescence signals are not equidistant, but their shifts in position to lower field correspond to the stepwise deshielding of the P atom by the As atom. If the signal at $\delta = 121.4$ is assigned to P_7^{3-}, in agreement with the observations of *Baudler* et al.,[1] the signals at $\delta = -109.5$, -90.2, -72.9, -48.7, and -22.4 correspond to the anions $[P_6As]^{3-}$, $[P_5As_2]^{3-}$, $[P_4As_3]^{3-}$, $[P_3As_4]^{3-}$, and $[P_2As_5]^{3-}$.

The chemical shifts are unequivocally correlated with the number of P atoms and are each separated by about 12–26 ppm with an average value of $\Delta\delta = 19.8$, which is close to the value $\delta(P_7^{3-})/7 = 17.3$. An analogous continuous series of shifts was observed by *Rudolph* et al.[10] for the heteronuclear clusters $[Sn_{9-x}Pb_x]^{4-}$; for $[Sn_{9-x}Ge_x]^{4-}$, however, a reversal in the shifts at $x = 4$ was observed. In specific cases, therefore, deviations should be expected. For this reason, it is also not possible to decide whether the anion $[PAs_6]^{3-}$ is absent or whether its chemical shift happens to coincide with the signal group at $\delta = 5$ (Fig. 1),

[*] Prof. Dr. H.-G. von Schnering, Dr. W. Hönle
Max-Planck-Institut für Festkörperforschung
Heisenbergstrasse 1, D-7000 Stuttgart 80 (FRG)

[**] The Chemistry and Structures of Phosphides and Polyphosphides, Part 40.—Part 39: H.-G. von Schnering, D. Vu, *J. Less-Common Met. 116* (1986) 257.

which would be in agreement with the (irregular) increase in the differences $\Delta\delta = |\delta(x) - \delta(x+1)|$ in the series $[P_{7-x}As_x]^{3-}$ with increasing x. It is also possible, however, that this heteroanion is unstable and decomposes into As_7^{3-} and, for example, $[P_2As_5]^{3-}$, because incorporation of the small P atom into the large As_7 cage is unfavorable. The ^{31}P-NMR spectra of solutions of mixtures of the pure compounds Rb_3P_7 and Rb_3As_7 exhibit, even after several weeks, only the signal of P_7^{3-}, so that no exchange between P_7^{3-} and As_7^{3-} occurs in solution.

The intensities of the ^{31}P-NMR signals—after correction with respect to the number of P atoms involved in the heteroanion—indicate a preference for the groups $[P_6As]^{3-}$ and $[P_5As_2]^{3-}$, but none for $[P_4As_3]^{3-}$, as would have been expected based on the concept of topological charge stabilization. With increasing content of arsenic, the valence tautomerism becomes slower, as shown by the increasing halfwidths of the signals. The question remains open, therefore, whether As_7^{3-} also has a fluxional structure in solution.

Received: December 10, 1985;
revised: January 17, 1986 [Z 1575 IE]
German version: *Angew. Chem. 98* (1986) 370

CAS registry numbers:
P, 7723-14-0; As, 7440-38-2; Rb, 7440-17-7.

[1] M. Baudler, H. Ternberger, W. Faber, J. Hahn, *Z. Naturforsch. B 34* (1979) 1690.
[2] W. Hönle, V. Manriquez, C. Mujica, D. Weber, H.-G. von Schnering, *29th IUPAC Congr., Coll. Abstr.*, Köln 1983, p. 36.
[3] W. Hönle, M. Somer, H.-G. von Schnering, unpublished results.
[4] B. M. Gimarc, P. J. Joseph, *Angew. Chem. 96* (1984) 518; *Angew. Chem. Int. Ed. Engl. 23* (1984) 506.
[5] W. Hönle, H.-G. von Schnering, *Z. Anorg. Allg. Chem. 440* (1978) 171.
[6] A. L. Allred, E. G. Rochow, *J. Inorg. Nucl. Chem. 5* (1958) 264; R. T. Sanderson: *Polar Covalence*, Academic Press, New York 1983.
[7] W. Hönle, H.-G. von Schnering, *IXth Crystallogr. Congr., Coll. Abstr.*, Oxford 1978, p. 552.
[8] B. Olés, H. J. Stolz, H.-G. von Schnering, *Phys. Status Solidi (b) 106* (1981) 157.
[9] The $^{31}P\{^1H\}$-NMR spectra were recorded with a 300-MHz instrument (121.49 MHz) in ethylenediamine with C_6D_6 and 85% H_3PO_4 as external standard. The high-field shift is indicated by −, the low-field shift by +.
[10] W. Rudolph, W. L. Wilson, R. C. Taylor, *J. Am. Chem. Soc. 103* (1981) 2480.
[11] E. Fluck: *Die kernmagnetische Resonanz und ihre Anwendung in der anorganischen Chemie*, Springer, Berlin 1963.

$[NbAs_8]^{3-}$, a Novel Type of Complex and an Unexpected One-Dimensional Chain Structure: $^1_\infty[Rb\{NbAs_8\}]^{2-}$

By *Hans-Georg von Schnering,* Juliana Wolf, Dieter Weber, Rafael Ramirez,* and *Teodoro Meyer*

In recent years, polyphosphides and polyarsenides of the alkali metals have been used, on the one hand, to synthesize a variety of polycyclic phosphanes and arsanes[1-3] and, on the other hand, to generate quasi-isolated ions such as P_7^{3-}, P_{11}^{3-}, As_7^{3-}, As_{11}^{3-}, and Sb_7^{3-}. This was achieved by complexation of the cations by large ligands (e.g., formation of cryptates) in order to prevent direct interactions between the cations and anions.[4-6] Pure metal compounds are required for both types of reaction. Alkali metal arsenides are usually synthesized from the elements in sealed quartz ampules. Recently, niobium ampules have been shown to be well suited for the suppression of reactions on the walls, in particular in the case of arsenic-rich polyarsenides.[7] However, here too, problems can arise as the amount of alkali metal is increased. Normally, such side reactions are undesired, although they often lead to especially beautiful compounds that are totally unexpected, to say nothing of being unpredicted. We report here one such case.

During the synthesis of Rb_3As_7 in a sealed niobium tube, rubidium was mistakenly added in too large an excess. The reaction product, primarily RbAs having helical $^1_\infty[As^-]$ chains,[8] was dissolved in a solution of 4,7,13,16,21,24-hexaoxa-1,10-diazatricyclo[8.8.8]hexacosane (2,2,2-crypt) in ethylenediamine (en). Red, transparent crystals separated out of the deep red solution and were identified as compound **1**:[9]

$[Rb(2,2,2\text{-crypt})]_2[Rb\{NbAs_8\}]$ **1**

In **1**, only two of the three Rb atoms are enclosed in the cryptands. The third forms a one-dimensional chain $^1_\infty[Rb\{NbAs_8\}]^{2-}$ with the complex anion $[NbAs_8]^{3-}$ (Fig. 1). The η^8-cyclooctaarsenidoniobate(v) trianion $[NbAs_8]^{3-}$ present in this chain, with the symmetry $\bar{8}2m$-D_{4d}, represents a novel type of complex, consisting of a monocyclic, crown-shaped polyanion $(As^-)_8$ with a Nb^V ion in the center. In accordance with the Zintl-Klemm rule (cf. ref. [1]), the ligand is isoelectronic and isostructural with the S_8 molecule (Nb-As 261.9, As-As 243.4 pm; bond angle at As: 93.7°; dihedral angle: 111.8°). The topology of the complex anion is unusual, because the donor functions of an $(As^-)_8$ crown should be directed outward, as has been observed up to now.[10] In this case, these donor functions bind the third Rb atom with formation of one-dimensional chains (Rb-As 392 pm). Evidently, the Rb-As interactions in these chains are able to compete with those between Rb^+ and the solvent en (ethylenediamine) as well as with those between Rb^+ and 2,2,2-crypt. This is remarkable since RbCl dissolves immediately in cryptand solutions, and sufficient 2,2,2-crypt was available in this reaction.

INDO calculations[11] afforded an insight into the electronic structure of the complex anion and the chain; for technical reasons, however, these calculations were carried out with K instead of Rb and V instead of Nb. The order of the energy levels obtained from the calculations and the distances between them should apply, in principle, to the $^1_\infty[Rb\{NbAs_8\}]^{2-}$ system. In particular, no essential differences between the isolated complex $[M^VAs_8]^{3-}$ and the one-dimensional chain $^1_\infty[M^I\{M^VAs_8\}]^{2-}$ with M^I, M^V = K, V and Rb, Nb are expected with respect to the 24 bonding energy levels. Important details are shown in Figure 1. The calculations reveal, among other things, that the compound is diamagnetic and that the band gap is 5 eV, which is in qualitative agreement with the observations.

The electronic states in the As_8 crown can be described practically exclusively in terms of pure 4s and 4p atomic orbitals, the latter of which form the σ bonds as well as the 4p π states of the electron lone pairs. The M^V-As bonds can largely be described by combinations of these 4p π states with functions of M^V having the symmetry e_2 and e_3. An important feature of the chain is the coupling of the $3a_1$ (As, 4p) state with $M^I(ns, np_z)$ functions. This results in

[*] Prof. Dr. H.-G. von Schnering, Dipl.-Chem. J. Wolf, Dr. D. Weber, Dipl.-Chem. R. Ramirez, Dr. T. Meyer
Max-Planck-Institut für Festkörperforschung
Heisenbergstrasse 1, D-7000 Stuttgart 80 (FRG)

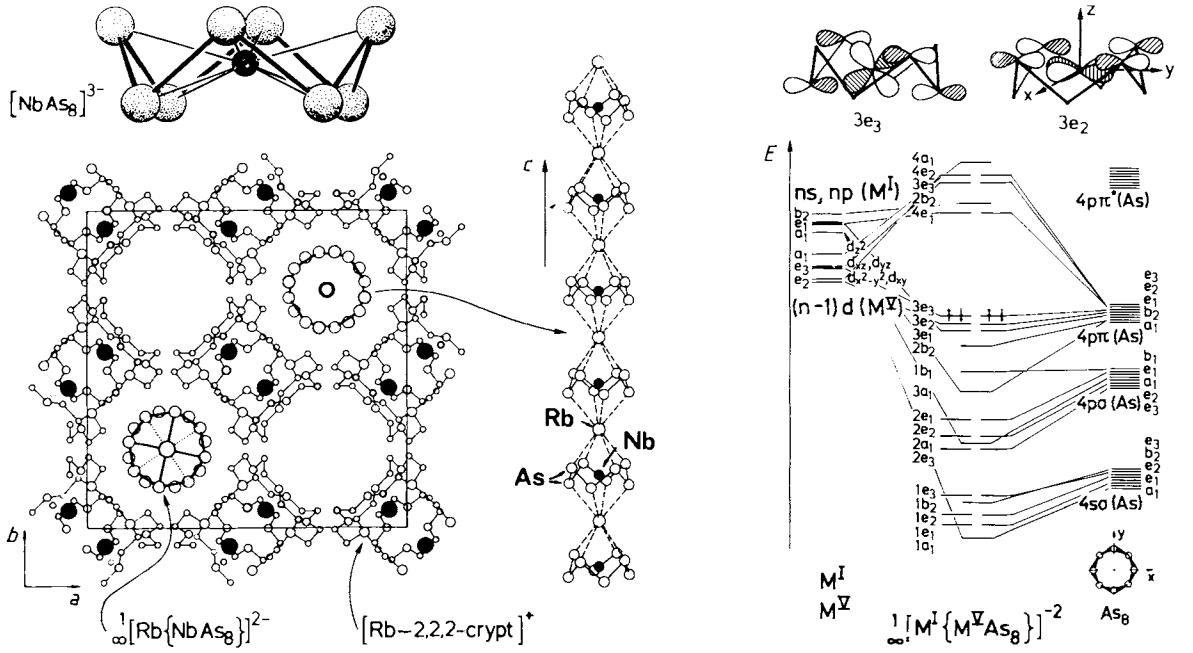


Fig. 1. Above: Structure of the complex anion $[NbAs_8]^{3-}$ in the crystal (left) and HOMOs $3e_2$ and $3e_3$ of the Nb-As bonds (one component of the e representation in each case, right). Below: Projection of the crystal structure along the chains $^1_\infty[Rb\{NbAs_8\}]^{2-}$ (left), a single chain (middle), and the electronic states of the chain $^1_\infty[M^I\{M^VAs_8\}]^{2-}$ with $M^I = K$, $M^V = V$ for the wave vector $k = 0$ (right). The irreducible representation corresponds to the point symmetry $\bar{8}2m$-D_{4d}. For technical reasons, the INDO calculations were carried out with K and V. The $3e_3$ HOMOs are indicated by arrows.

bonding M^I-As interactions along the one-dimensional chain. At the same time, the $4a_1$ orbital $(M^V, (n-1)d_{z^2})$ is destabilized and therefore direct metal-metal bonding along the chain is prevented.

With knowledge of the composition and structure of the new compound in hand, a direct synthesis was possible. To this end, Nb_2O_5 is added in the first step of the reaction.[12]

Received: December 10, 1985;
revised: January 27, 1985 [Z 1576 IE]
German version: *Angew. Chem. 98* (1986) 372

CAS registry numbers:
1, 101165-26-8; $[Rb(NbAs_8)]^{2-}$, 101165-27-9; Nb_2O_5, 1313-96-8; Rb, 7440-17-7; Nb, 7440-03-1; As, 7440-38-2.

[1] H.-G. von Schnering, *Angew. Chem. 93* (1981) 44; *Angew. Chem. Int. Ed. Engl. 20* (1981) 33; *ACS Symp. Ser. 232* ("Rings, Clusters, and Polymers of the Main Group Elements") (1983) 69.
[2] G. Fritz, K. D. Hoppe, W. Hönle, D. Weber, C. Mujica, V. Manriquez, H.-G. von Schnering, *J. Organomet. Chem. 249* (1983) 63.
[3] H.-G. von Schnering, D. Fenske, W. Hönle, M. Binnewies, K. Peters, *Angew. Chem. 91* (1979) 755; *Angew. Chem. Int. Ed. Engl. 18* (1979) 679.
[4] D. G. Adolphson, J. D. Corbett, D. J. Merryman, *J. Am. Chem. Soc. 98* (1976) 7234.
[5] C. H. E. Belin, *J. Am. Chem. Soc. 102* (1980) 6036.
[6] L. Diehl, K. Khodadadeh, D. Kummer, J. Strähle, *Z. Naturforsch. B 31* (1976) 522.
[7] W. Hönle, T. Meyer, J. Wolf, unpublished results.
[8] W. Hönle, H.-G. von Schnering, *Acta Crystallogr. A 34* (1978) S 152.
[9] Space group *P4/ncc* (No. 130); $a = 2062.1(7)$, $c = 1504.3(10)$ pm; $Z = 4$; $\rho_{calcd} = 1.768$ g·cm^{-3}; $Mo_{K\alpha}$ radiation; 2109 reflections, 1077 with $F \geq 3\sigma(F)$; $R = 0.099$. Further details of the crystal structure investigation may be obtained from the Fachinformationszentrum Energie, Physik, Mathematik GmbH, D-7514 Eggenstein-Leopoldshafen 2 (FRG), on quoting the depository number CSD-51799, the names of the authors and the journal citation.
[10] P. S. Elmes, B. M. Gatehouse, D. J. Lloyd, B. O. West, *J. Chem. Soc. Chem. Commun. 1974*, 953.
[11] M. C. Böhm, *Theor. Chim. Acta 59* (1981) 153.
[12] Experimental procedure: **1**: Freshly distilled Rb (3.08 g), vacuum-annealed As (3.33 g), and Nb_2O_5 (0.74 g) (molar ratio 16 : 16 : 1) were fused under argon in an Nb ampule (1.5 cm × 10 cm). The ampule was then heated in an evacuated quartz tube for 35 h at 925 K. After annealing for 3 d at 925 K and cooling to room temperature over 48 h, 3.8 g of the product was obtained. This was allowed to stir with 1 g of 2,2,2-crypt in 100 mL of anhydrous, oxygen-free en under argon for 3 d at room temperature (three-necked flask). After filtration and concentration of the dark red solution, fine crystals of **1** separated out. Dark red prisms formed upon counter-current diffusion with tetrahydrofuran on both sides of a G3 frit. After decantation and drying under vacuum, the yield of **1** was ca. 700 mg (15% based on 2,2,2-crypt). The product of the thermal reaction is unknown.

Intramolecular Addition of 2-(Trimethylsilyl)methyl-substituted Alkyl Cations to Double Bonds—Synthesis of Bicyclo[3.3.0]octane Derivatives**

By *Junes Ipaktschi** and *Gerald Lauterbach*

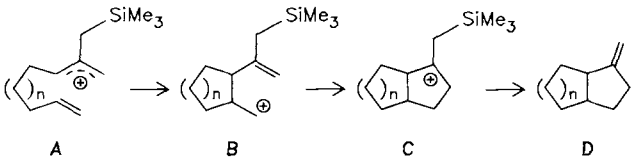
Dedicated to Professor Heinz A. Staab on the occasion of his 60th birthday

The development of methods for the synthesis of cyclopentanoid compounds continues to be a subject of intensive study.[1] An important entry to carbocyclic five-membered ring systems consists in the coupling of a C_3 unit such as, e.g., a trimethylenemethane derivative,[2] to an electron-deficient olefin. The C_3 building blocks can be prepared in a Ni^0- or Pd^0-complex-catalyzed reaction from methylenecyclopropanes[2a] or 2-[(trimethylsilyl)methyl]-allyl acetates,[2b] or by pyrolysis of pyrazoline derivatives.[2c] These reactions can also be carried out intramolecularly with formation of bicyclo[3.3.0]octane and bicy-

[*] Prof. Dr. J. Ipaktschi, Dr. G. Lauterbach
Institut für Organische Chemie der Universität
Heinrich-Buff-Ring 58, D-6300 Giessen (FRG)

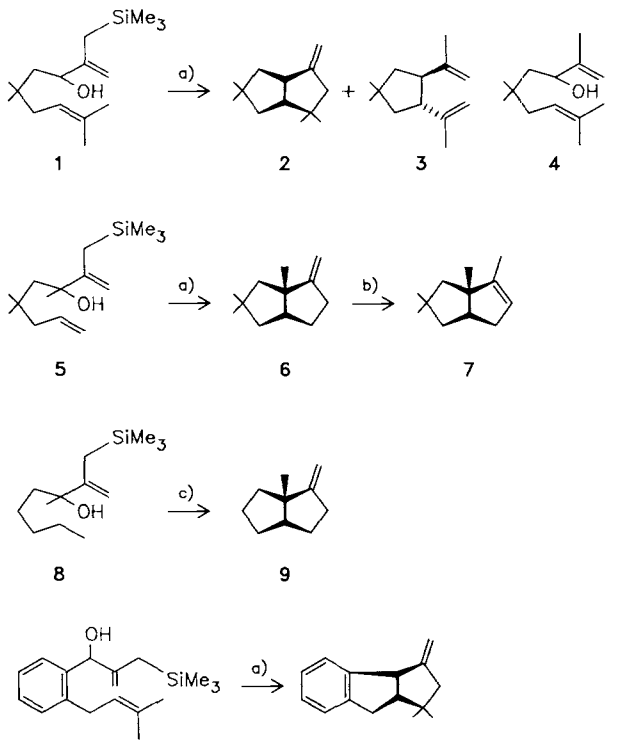
[**] This work was supported by the Fonds der Chemischen Industrie.

clo[4.3.0]nonane derivatives.[2b,c] Such systems should also be accessible if it were possible to add allyl cations intramolecularly in a [3+2]-cycloaddition to double bonds. [3+2]-Cycloadditions of allyl cations as concerted reactions are forbidden.[3] On the other hand, a multistep mechanism (Scheme 1) requires a cyclization step (**B**→**C**), which according to the Baldwin rules[4] is unfavorable. That examples of reactions of this type are rare is not surprising.[5]



Scheme 1.

We have now found that the intramolecular [3+2]-cycloaddition of 2-trimethylsilylmethyl-substituted allyl cations of type **A** to alkenes does in fact lead to bicyclo[3.3.0]octane derivatives. When $TiCl_4$/*N*-methylaniline (1:1) is allowed to react with **1** in dichloromethane at −15 °C,[6] the bicyclooctane **2** (Scheme 2, Table 1) is obtained in 55% yield. Other products include **3** (25%) and an, as yet, unidentified hydrocarbon (5%).[7]



Scheme 2. a) $TiCl_4$, *N*-methylaniline (1:1), CH_2Cl_2, −15 °C, 1 h [10]; b) TosOH (cat.), $CHCl_3$, 50 °C, 5 min; c) $TiCl_4$/*N*-methylaniline (2:1), CH_2Cl_2, −20 °C, 1 h [10].

The influence of the trimethylsilylmethyl group on the cyclization is illustrated quite well by a comparison of the reactions of **1** and **4**. When **4** is allowed to react under otherwise the same conditions with Lewis acids, the *trans*-diisopropenylcyclopentane **3** is formed as sole product in 17% yield. The cyclization of **5** proceeds astonishingly smoothly.[6] **6** was isolated as sole product in 70% yield and was converted quantitatively in a proton-catalyzed reaction into **7**. This result is remarkable inasmuch as, as in **5**—after the reaction with Lewis acid—the allyl cation initially formed is highly substituted and the alkene is only monosubstituted. As expected, reaction of **8**,[6] in which the two geminal methyl groups are missing, affords **9** (15%) in an essentially unspecific reaction. **11** could be prepared in 45% yield from **10** in the same way.[6]

These results show that the cyclization **B**→**C** (Scheme 1) is greatly facilitated by the "β-effect"[8] of the silicon and by two geminal methyl groups in the β-position. Hence, the reaction can be regarded as an extension to the Pd-assisted cycloaddition of 2-[(trimethylsilyl)methyl]allyl acetates and electron-deficient olefins, since bicyclooctanes can also be synthesized in satisfactory yields from alkyl-substituted alkenes according to Scheme 1.

Table 1. NMR data (δ values, $CDCl_3$) of the products **2**, **3**, **6**, **7**, **9**, and **11**.

	^{1}H-NMR	^{13}C-NMR
2	(500 MHz) 4.73, 4.68 (br. s, 2H), 3.02 (q, 1H), 2.33 (d, 1H), 2.20 (q, 1H), 1.78–1.86 (m, 2H), 1.12–1.22 (m, 2H), 1.03 (s, 3H), 0.92 (s, 3H), 0.87 (br. s, 6H), 0.77–0.82 (m, 1H)	156.82 (s, C-2), 105.58 (t), 54.63 (d, C-5), 47.30 (d, C-1), 45.50 (t), 43.34 (t), 40.95 (s, C-7), 38.58 (s, C-4), 29.60 (q), 29.02 (q), 26.79 (q), 24.02 (q)
3	4.66 (br. s, 4H), 2.58 (dd, 2H), 1.68 (s, 6H), 1.08 (s, 6H), 0.80–1.80 (m, 4H)	146.95 (s), 110.14 (t), 50.84 (d), 47.25 (t), 36.18 (s), 31.39 (q), 19.45 (q)
6	4.7 (m, 2H), 2.2–2.6 (m, 2H), 0.8–1.8 (m, 16H)	
7	(400 MHz) 5.01 (m, 1H, 3-H), 2.45 (m, 1H, J=16, 8.0 and 2.2 Hz, *exo*-4-H), 2.35 (ddd, 1H, J=10.0, 8.0 and 7.6 Hz, 5-H), 1.88 (d, 1H, J=16 Hz, *endo*-4-H), 1.70 (ddd, 1H, J=12.3, 7.6 and 1.7 Hz, 6-H), 1.61 (dd, 3H, J=2.2 and 1.0 Hz), 1.50 (d, 1H, J=12.9 Hz, 8-H), 1.28 (dd, 1H, J=12.9 and 1.7 Hz, 8-H), 1.16 (dd, 1H, J=12.3 and 10.0 Hz, 6-H), 1.11 (s, 3H), 1.01 (s, 3H), 0.98 (s, 3H)	146.24 (s, C-2), 120.33 (d, C-3), 58.23 (s, C-1), 51.28 (t, C-8), 50.03 (t, C-6), 49.35 (d, C-5), 39.99 (s, C-7), 36.09 (t, C-4), 29.60 (q), 28.82 (q), 26.64 (q), 12.19 (q)
9	4.7 (m, 2H), 2.3–0.8 (m, 14H)	
11	(400 MHz) 7.15, 7.29 (m, 4H, aromat.), 5.07, 4.91 (br. s, 2H, $=CH_2$), 4.07 (d, 1H, J=8.0 Hz, 1-H), 2.90 (2H, AB part of ABX with J_{AB}=16.6 Hz, J_{AX}=9.4 Hz, J_{BX}=7.5 Hz, 6-H), 2.68 (ddd, 1H, J=9.4, 8.0 and 7.5 Hz, 5-H), 2.28, 2.10 (2d, J=15.2 Hz, 2H, 3-H), 1.05 (s, 3H, 0.96 (s, 3H)	154.10 (s, C-2), 145.32 (s), 142.64 (s), 126.15 (d), 123.67 (d), 123.53 (d), 106.54 (t), 54.47 (d), 54.39 (d), 47.11 (t, C-3), 39.30 (s, C-4), 33.58 (t, C-6), 29.05 (q), 23.57 (q)

Received: October 2, 1985;
supplemented: November 5, 1985 [Z 1480 IE]
German version: *Angew. Chem. 98* (1986) 346
Publication delayed at authors' request

CAS Registry numbers:
1, 100841-62-1; (*trans*)-**2**, 100841-63-2; (*trans*)-**3**, 100841-64-3; **4**, 100841-65-4; **5**, 100841-66-5; (*trans*)-**6**, 100841-67-6; (*trans*)-**7**, 100841-68-7; **8**, 100841-69-8; (*trans*)-**9**, 100841-70-1; **10**, 100841-71-2; **11**, 100841-72-3; $TiCl_4$, 7550-45-0; PhNHMe, 100-61-8; $CH_2=CBrCH_2TMS$, 81790-10-5; $Me_2C=CHCH_2CMe_2CH_2CHO$, 13820-23-0; $CH_2=CHCH_2CMe_2CH_2Ac$, 17123-68-1; $CH_2=CH(CH_2)_3Ac$, 21889-88-3; *o*-$(Me_2C=CHCH_2)C_6H_4CHO$, 100841-73-4.

[1] Reviews: M. Vandewalle, P. De Clercq, *Tetrahedron 41* (1985) 1767; L. A. Paquette, *Top. Curr. Chem. 119* (1984) 1; cf. also *Nachr. Chem. Tech. Lab. 31* (1983) 14, 262, 360, 638, 710; *32* (1984) 429.

[2] a) P. Binger, A. Brinkmann, P. Wedemann, *Chem. Ber. 116* (1983) 2920; P. Binger, Q.-H. Lü, P. Wedemann, *Angew. Chem. 97* (1985) 333; *Angew. Chem. Int. Ed. Engl. 24* (1985) 316; b) B. M. Trost, T. N. Nanninga, *J. Am. Chem. Soc. 107* (1985) 1075; B. M. Trost, D. M. T. Chan, *ibid. 105* (1983) 2315; B. M. Trost, *Angew. Chem. 98* (1986) 1; *Angew. Chem. Int. Ed. Engl. 25* (1986) 1; c) O. Campopiano, R. D. Little, J. L. Petersen, *J. Am. Chem. Soc. 107* (1985) 3721; D. J. Stone, R. D. Little, *ibid. 107* (1985) 2495.

[3] R. B. Woodward, R. Hoffmann, *Angew. Chem. 81* (1969) 797; *Angew. Chem. Int. Ed. Engl. 8* (1969) 781.

[4] J. E. Baldwin, *J. Chem. Soc. Chem. Commun. 1976*, 734.

[5] H. Klein, H. Mayr, *Angew. Chem. 93* (1981) 1069; *Angew. Chem. Int. Ed. Engl. 20* (1981) 1027.

[6] The compounds **1**, **5**, **8**, and **10** were prepared from 1-trimethylsilylmethylvinylmagnesium bromide **9** and the corresponding carbonyl compounds. All compounds gave correct spectroscopic and analytical data.

[7] This hydrocarbon is presumably the *trans*-isomer of **2**. ^{13}C-NMR ($CDCl_3$): δ = 152.0 (s), 106.68 (t), 52.55 (d), 51.64 (t), 48.71 (d), 48.28 (t), 42.28 (t), 40.54 (s), 32.12 (s), 30.31 (q), 29.35 (q), 7.66 (q), 17.27 (q).

[8] E. Colvin: *Silicon in Organic Synthesis*, Butterworths, London 1981.

[9] N. Nishiyama, H. Yokoyama, S. Narimatsu, K. Itoh, *Tetrahedron Lett. 23* (1982) 1267; B. M. Trost, B. P. Coppola, *J. Am. Chem. Soc. 104* (1982) 6879.

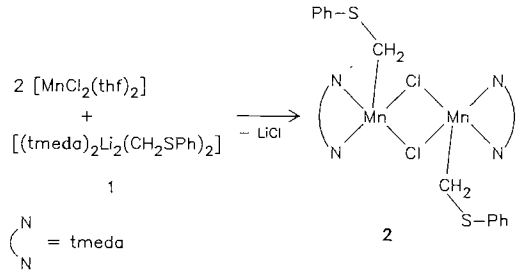
[10] T. Saito, A. Hoh, K. Oshima, H. Nozaki, *Tetrahedron Lett. 1979*, 3519.

An α-Functionalized Organomanganese(II) Derivative: a Dinuclear Manganese(II) Complex with a σ-Bonded α-Thioalkyl Ligand**

By *Edouard Marc Meyer* and *Carlo Floriani**

Alkylmetal compounds M-CH_2X containing a functional group [X = OR, NR_2, SR] in the α-position are key reagents in organic synthesis.[1] In addition, knowledge of their chemistry is essential for an understanding of several well known metal promoted catalytic processes.[2] In this context, there are two important points that must be mentioned. First, the reactivity of α-functionalized alkylmetals is different from that of non-functionalized M-CH_2-R fragments. The M-CH_2-X unit not only functions as a precursor to metal carbenes, but is also a source of free CH_2.[2,6] Secondly, M-CH_2OX compounds are formed during metal-assisted reductions of carbon monoxide and formaldehyde;[3,4] and, insertion of CO into the M-CH_2OH bond is claimed to be the main route to the catalytic syntheses of ethyleneglycol from CO/H_2.[5] α-Thio-substituted organolithium compounds, which have been the subject of a number of chemical, structural, and theoretical studies,[7] are widely used in organic synthesis. However, only a limited number of examples of organometallic compounds containing the -CH_2SR residue have been reported.[8-11] When bonded,through various bonding modes, to soft transition metal ions, this fragment is stable.[8,9,12] Except in a few cases,[7c] however, attempts to bind this unit to hard metal ions in the absence of soft ancillary ligands,[10] resulted in decomposition, with loss of the CH_2 group.[11]

Herein, we report the synthesis and structural characterization of the manganese(II) Grignard reagent [{(tmeda)(PhSCH_2)Mn(Cl)}$_2$] **2** (tmeda = *N*,*N*,*N'*,*N'*-tetramethylethylenediamine), in which a σ-bonded thioalkyl residue is the only carbon ligand bonded to manganese(II). **2** was synthesized by addition of a solution of [(tmeda)$_2$Li$_2$(CH_2SPh)$_2$] **1**[7] in tetrahydrofuran (THF) to a suspension of [$MnCl_2$(thf)$_2$] in THF at −30°C.



Solubilization of $MnCl_2$ was observed as the reaction proceeded. After evaporation to dryness, partial dissolution of the residue in toluene and addition of *n*-hexane, colorless crystals were obtained (yield ca. 65%). All operations were carried out at temperatures below 35°C. Although complex **2** can be stored for months at room temperature in the solid state, it is thermally labile in solution at temperatures above 35°C. The colorless crystals of **2** contain one molecule of toluene per dimer. The magnetic moment of 5.91 BM per Mn at 298 K is consistent with two non-interacting high-spin d^5 centers, separated by 3.806(3) Å.

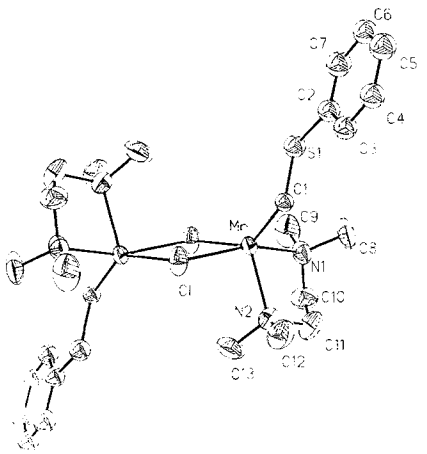


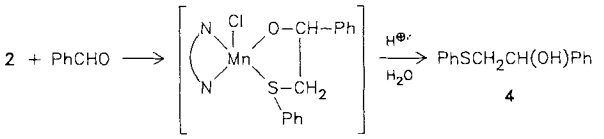
Fig. 1. ORTEP diagram of the structure of **2** in the crystal. Bond distances [Å]: Mn-N1 2.334(10), Mn-N2 2.234(9), Mn-Cl 2.701(4), Mn-Cl′ 2.411(2), Mn-C1 2.177(9), Mn···Mn′ 3.806(3), C1-S1 1.796(13), S1-C2 1.772(8); Bond angles [°]: N1-Mn-N2 79.0(3), Cl-Mn-Cl′ 83.9(1), N2-Mn-C1 110.0(4), Cl-Mn-Cl 89.6(4), Mn-C1-S1 110.5(6), C1-S1-C2 108.1(5).

The crystal structure of **2** is shown in Figure 1.[13] Mn^{II} is five coordinate with the two Mn-Cl bonds differing significantly in length (2.701(4) and 2.411(2) Å). Such an asymmetry was observed in carbon bridges in alkylmanganese(II) compounds.[14] Each Mn atom in **2** carries a σ-bonded phenylthiomethyl residue; the bond length of 2.177(9) Å, lies within the range of the few known Mn^{II}-C σ-bond distances.[14,15] Sulfur does not interact with the manganese atoms of the dimer. The structural parameters of the phenylthiomethyl ligand (C1-S1 1.796(13), S1-C2, 1.772(8) Å) compare with those found in complex **1** (1.779(2) and 1.792(2) Å)[16] and in the homoleptic derivative [{Pd(CH_2SPh)$_2$}$_4$] (1.82 and 1.80 Å),[8] in which, however, the thioalkyl ligand displays a C-S bridge-bonding mode. With regard to its coordination number of five for Mn^{II}, its single Mn-C σ-bond, and a coordination environment provided by the hard donor ligands, Cl and tmeda, complex **2** is unique in manganese(II) organometallic chemistry. Consequently, complex **2** represents an impor-

[*] Prof. Dr. C. Floriani, Dr. E. M. Meyer
Chemistry Department, Columbia University
New York, N. Y. 10027 (USA)

[**] *E. M. M.* thanks the Fonds National Suisse de la Recherche Scientifique (projet Nr. 82.099.1.83) for a fellowship.

tant addition to the chemistry, developed by *Wilkinson* et al., of alkylmanganese(II) derivatives.[14, 15]



3 4

Furthermore, complex **2** may be viewed as a manganese(II) Grignard reagent, [RMnX]. Thus, reaction of **2** with benzaldehyde in toluene furnishes the adduct **4** (77% yield).[17] The intermediate **3** was not isolated.

Received: October 15, 1985;
revised: January 31, 1986 [Z 1497 IE]
German version: *Angew. Chem. 98* (1986) 376

CAS Registry numbers:
1, 90215-81-9; **2**, 101248-13-9; **4**, 16162-51-9; $[MnCl_2(thf)_2]$, 70317-52-1; PhCHO, 100-52-7.

[1] P. von R. Schleyer, T. Clark, A. J. Kos, G. W. Spitznagel, C. Rohde, D. Arad, K. N. Houk, N. G. Rondan, *J. Am. Chem. Soc. 106* (1984) 6467, and references cited therein.

[2] W. A. Herrmann, *Angew. Chem. 94* (1982) 118; *Angew. Chem. Int. Ed. Engl. 21* (1982) 117.

[3] E. J. Crawford, C. Lambert, K. P. Menard, A. R. Cutler, *J. Am. Chem. Soc. 107* (1985) 3130; M. L. Engelhardt, E. G. Jacobsen, C. L. Raston, A. H. White, *J. Chem. Soc. Chem. Commun. 1984*, 220; S. Young, H. Hope, N. E. Shore, *Organometallics 3* (1984) 1585.

[4] P. T. Wolczanski, J. E. Bercaw, *Acc. Chem. Res. 13* (1980) 121; S. Gambarotta, C. Floriani, A. Chiesi-Villa, C. Guastini, *J. Am. Chem. Soc. 105* (1983) 1690; *104* (1982) 2019 and references cited therein.

[5] R. L. Pruett, *Science 211* (1981) 11; B. D. Dombek, *J. Am. Chem. Soc. 101* (1979) 6466; *102* (1980) 6855; *J. Organomet. Chem. 250* (1983) 467.

[6] E. J. O'Connor, P. Helquist, *J. Am. Chem. Soc. 104* (1982) 1869.

[7] a) R. Amstutz, J. D. Dunitz, D. Seebach, *Angew. Chem. 93* (1981) 487; *Angew. Chem. Int. Ed. Engl. 20* (1981) 465; b) B. T. Gröbel, D. Seebach, *Synthesis 1977*, 357; c) B. Weidmann, L. Wilder, A. G. Olivero, C. D. Maycock, D. Seebach, *Helv. Chim. Acta 64* (1981) 357.

[8] K. Miki, D. Yoshida, Y. Kai, N. Yasuoka, N. Kasei, *J. Organomet. Chem. 149* (1978) 195 and references cited therein.

[9] K. Miki, Y. Kai, N. Yasuoka, N. Kasei, *J. Organomet. Chem. 165* (1979) 79.

[10] D. Steinborn, R. Taube, *J. Organomet. Chem. 284* (1985) 395; R. Taube, D. Steinborn, W. Hobold, *ibid. 284* (1985) 385; E. A. Mintz, A. S. Ward, D. S. Tice, *Organometallics 4* (1985) 1308.

[11] D. Steinborn, R. Taube, *Z. Anorg. Allg. Chem. 521* (1985) 183.

[12] E. R. de Gil, L. F. Dahl, *J. Am. Chem. Soc. 91* (1969) 3751 and references cited therein.

[13] Space group $P\bar{1}$, $a = 8.403(2)$, $b = 11.401(4)$, $c = 11.569(4)$ Å, $\alpha = 98.19(3)$, $\beta = 110.69(2)$, $\gamma = 98.40(3)°$, $V = 1003.0(6)$ Å^3, $Z = 1$, $\rho_{calcd} = 1.24$ g cm^{-3}, $F(000) = 396$, $Cu_{K\alpha}$ radiation ($\lambda = 1.54178$ Å), $\mu = 75.09$ cm^{-1}. Intensity data were collected with an R3m Nicolet diffractometer. 4595 independent reflections ($2\theta < 110°$). Structure solved by Patterson and Fourier techniques and partly refined anisotropically. For 2507 unique observed structure amplitudes ($I > 3\sigma(I_0)$) the current R value was 0.082. H-atoms not considered. The thioalkyl residue in the centrosymmetric complex is disordered; site occupancy factor for the two configurations: 70 and 30%, respectively (in isotropic refinements). Further details of the crystal structure investigation are available on request from the Fachinformationszentrum Energie, Physik, Mathematik GmbH, D-7514 Eggenstein-Leopoldshafen 2 (FRG), on quoting the depository number CSD-51776, the names of the authors, and the full citation of the journal.

[14] C. G. Howard, G. Wilkinson, M. Thornton-Pett, M. B. Hursthouse, *J. Chem. Soc. Dalton Trans. 1983*, 2025.

[15] P. M. Treichel in G. Wilkinson, F. G. A. Stone, E. W. Abel (Eds.): *Comprehensive Organometallic Chemistry*, Vol. 4, Pergamon Press, Oxford 1982, Chap. 29, pp. 68-71; C. G. Howard, G. S. Girolami, G. Wilkinson, M. Thornton-Pett, M. B. Hursthouse, *J. Chem. Soc. Dalton Trans. 1983*, 2621; G. S. Girolami, C. G. Howard, G. Wilkinson, H. M. Dawes, M. Thornton-Pett, M. Motevalli, M. B. Hursthouse, *ibid.* (1985) 921; S. Gambarotta, C. Floriani, A. Chiesi-Villa, C. Guastini, *J. Chem. Soc. Chem. Commun. 1983*, 1128.

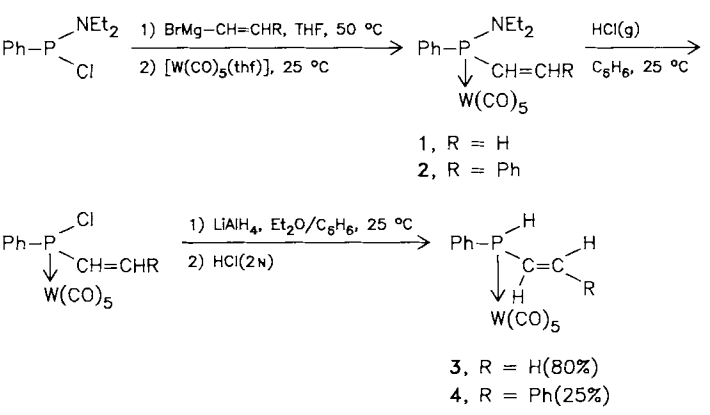
[16] R. Amstutz, T. Laube, W. B. Schweizer, D. Seebach, J. D. Dunitz, *Helv. Chim. Acta 67* (1984) 224.

[17] Benzaldehyde (0.49 g, 4.61 mmol) was added to a stirred and cooled (−78°C) solution of **2** (1.52 g, 2.31 mmol) in toluene (70 mL). After 30 min, the solution was allowed to warm up to, and to remain at room temperature for 24 hours. Hydrolysis was carried out under nitrogen at 0°C by adding 50 mL of degassed 1.4 N H_2SO_4 to the toluene solution. Separation of the two phases was followed by washing of the organic phase to neutrality, which, after drying and removal of the solvent, gave the crude product. Purification of the crude product was carried out by flash chromatography (silicagel, elution with *n*-hexane : ethylacetate 95 : 5). ^{1}H-NMR [$(CD_3)_2CO$]: $\delta = 7.10$–7.45 (m, 10H, Ph), 4.82 (t, 1H, CH), 3.26 (d, 2H, CH_2), 3.1 (bs, 1H, OH); MS: m/z 230 (M^+), 213 ($PhSC_7H_6$), 135 (C_8H_8S), 123 (C_7H_7S), 104 (C_8H_9).

η^3-1-Phosphaallyliron Complexes with Additional $W(CO)_5$-Coordination at the Phosphorus—the 1-Phosphaallyl Ligand as 5e-Donor

By *François Mercier, Jean Fischer,* and *François Mathey**

Whereas the initial claim for stable η^3-silaallyliron complexes[1] was subsequently discarded,[2] recently some genuine hetero analogues of the ubiquitous η^3-allyl(transition-metal) complexes have been reported in the literature. They include stable η^3-1-azaallylmolybdenum[3] and η^3-1,3-diphosphaallylcobalt[4] complexes, each of which were unambiguously characterized by X-ray crystal structure analysis. In the same vein, we wish to report here on the first characterization of a 1-phosphaallyl ligand acting as a bridging η^1,η^3 5e-donor. In a preceding paper,[5] we demonstrated that it was possible to prevent the self-condensation of secondary vinylphosphanes by complexation of the lone pair at phosphorus with $W(CO)_5$. Using this approach, we first prepared the two secondary vinylphosphane complexes **3** and **4** (an excess of $LiAlH_4$ must be used), which are quite stable and can be purified by chromatography on silica gel (hexane/toluene); in the case of **4** the yield is based on crude **2**.



Reaction of complex **3** with $[\{CpFe(CO)_2\}_2]$ (Cp = cyclopentadienyl) in boiling xylene then afforded the η^1,η^3-1-phosphaallyl complex **5** together with other products.

Complex **5** was completely characterized by NMR, IR, and mass spectroscopy (Table 1), but we were unable to obtain good crystals for a full X-ray crystal structure anal-

[*] Dr. F. Mathey, Dr. F. Mercier
Laboratoire CNRS-SNPE
2-8 rue Henry Dunant, F-94320 Thiais (France)
Prof. J. Fischer
Laboratoire de Cristallochimie, Institut Le Bel
Université Louis Pasteur
F-67070 Strasbourg (France)

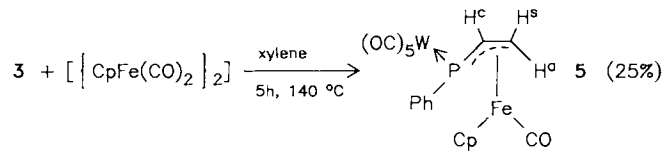


Table 1. Physical and spectroscopic data of **3**–**8**.

3: ^{1}H-NMR ($CDCl_3$): $\delta = 5.50$–6.80 (m, 3H, vinyl), 6.35 (dd, 1H, PH, $^1J(H,P) = 345$ Hz, $^3J(H,H) = 4.6$ Hz); ^{31}P-NMR ($CDCl_3$, 85% H_3PO_4, ext.): $\delta = -26.7$ ($^1J(^{31}P,^{183}W) = 229.5$ Hz); mass spectrum (EI, 70 eV, ^{184}W): *m/z* 460 (M^+, 24%), 318 (100%); IR (decalin): $\tilde{\nu}$(CO) = 2070 (w), 1945 (vs) cm^{-1}

4: ^{1}H-NMR ($CDCl_3$): $\delta = 6.47$ (dd, 1H, PH, $^1J(P,H) = 347$ Hz, $^3J(H,H) = 5.1$ Hz); 6.3–7.7 (m, 12H, Ph + vinyl); ^{31}P-NMR ($CDCl_3$): $\delta = -28.2$ ($^1J(^{31}P,^{183}W) = 229.5$ Hz); IR (decalin): $\tilde{\nu}$(CO) = 2070 (w), 1945 (vs) cm^{-1}

5: Orange solid, m.p. 124°C (dec.) (CH_2Cl_2, MeOH 10:90); ^{1}H-NMR ($CDCl_3$): $\delta = 1.72$ (m, 1H, H^a, $^3J(H,P) = 7.6$ Hz, $^2J(H,H) = 1.2$ Hz, $^3J(H,H) = 12.5$ Hz); 3.66 (m, 1H, H^s, $^3J(H,P) = 24.4$ Hz, $^3J(H,H) = 8.8$ Hz); 4.32 (m, 1H, H^c, $^2J(H,P) \approx 29.8$ Hz); 4.86 (s, 5H, C_5H_5); 7.10 (m, 5H, Ph); ^{13}C{^{1}H}-NMR (CD_2Cl_2): $\delta = 47.84$ (d, CH_2, $^2J(C,P) = 7.3$ Hz); 61.62 (d, CH, $^1J(C,P) = 3.7$ Hz); 83.22 (s, C_5H_5); 198.48 (d, W–CO *cis*, $^2J(C,P) = 8.5$ Hz); 201.24 (d, W–CO *trans*, $^2J(C,P) = 24.4$ Hz); 219.14 (d, Fe–CO, $^2J(C,P) = 13.4$ Hz); ^{31}P-NMR (C_6D_6): $\delta = -6.9$ ($^1J(^{31}P,^{183}W) = 224.6$ Hz); mass spectrum (EI): *m/z* 608 (M^+, 12%), 438 (100%); (CI, C_4H_{10}) *m/e* 609 ($M^+ + 1$, 100%); IR (decalin): $\tilde{\nu}$(CO) = 2060 (w), 2055 (w), 1980 (s), 1970 (sh), 1940 (vs), 1930 (vs) cm^{-1}

6: ^{1}H-NMR (CD_2Cl_2): $\delta = 4.77$ (d, 5H, C_5H_5, $^3J(H,P) = 1.2$ Hz); 6.91 (*ABX*, 1H, vinyl, $^3J(H,H) = 16.8$ Hz); 7.12 (*ABX*, 1H, vinyl); ^{31}P-NMR ($CDCl_3$): $\delta = -17.3$ ($^1J(^{31}P,^{183}W) = 208$ Hz); IR (decalin): $\tilde{\nu}$(CO) = 2060 (w), 2020 (m), 1985 (m), 1938 (vs), 1925 (vs) cm^{-1}

7: m.p. 148°C (dec.) (hexane, cyclohexane 90:10); ^{1}H-NMR (CD_2Cl_2): $\delta = 3.39$ (m, 1H, H^a, $^3J(H,H) = 12.2$ Hz, $^3J(H,P) = 7.6$ Hz); 4.59 (s, 5H, C_5H_5); 5.10 (m, 1H, H^c, $^2J(H,P) = 27$ Hz); ^{13}C-NMR (CD_2Cl_2): $\delta = 58.59$ (d, *C*HPh, $^2J(C,P) = 3.7$ Hz); 69.41 (d, *C*HP, $^1J(C,P) = 4.9$ Hz); 84.79 (s, C_5H_5); 198.51 (d, W–CO *cis*, $^2J(C,P) = 7.3$ Hz); 201.15 (d, W–CO *trans*, $^2J(C,P) = 25.6$ Hz); 219.75 (d, Fe–CO, $^2J(C,P) = 13.4$ Hz); ^{31}P-NMR ($CDCl_3$): $\delta = -20.5$ ($^1J(^{31}P,^{183}W) = 227$ Hz); mass spectrum (EI, 70 eV, ^{184}W) *m/z* 684 (M^+, 4.7%), 656 (M – CO, 40%), 516 (M – 6CO, 99%), 514 (100%); IR (decalin): $\tilde{\nu}$(CO) = 2063 (w), 1982 (m), 1945 (vs), 1937 (vs), 1930 (s) cm^{-1}

8: ^{1}H-NMR (CD_2Cl_2): $\delta = 3.45$ (m, 1H, H^a, $^3J(H,H) = 12.4$ Hz, $^3J(H,P) = 10.2$ Hz); 4.16 (s, 5H, C_5H_5); 5.86 (m, 1H, H^c, $^2J(H,P) \simeq 0$ Hz); ^{31}P-NMR ($CDCl_3$): $\delta = -37.38$ ($^1J(^{31}P,^{183}W) = 231.9$ Hz); IR (decalin): $\tilde{\nu}$(CO) = 2065 (w), 1985 (m), 1940 (vs), 1935 (sh) cm^{-1}

ysis.[6] Nevertheless, the collected data furnished valuable information concerning the stereochemistry of the compound (Fig. 1). The most notable features of the structure are the approximate coplanarity of the W–P–CH=CH_2 unit, the *cis* disposition of W and H^c (W–P–C–H^c dihedral angle ca. 6.6°) and the Fe–CO unit pointing in the opposite direction to C–H^c.

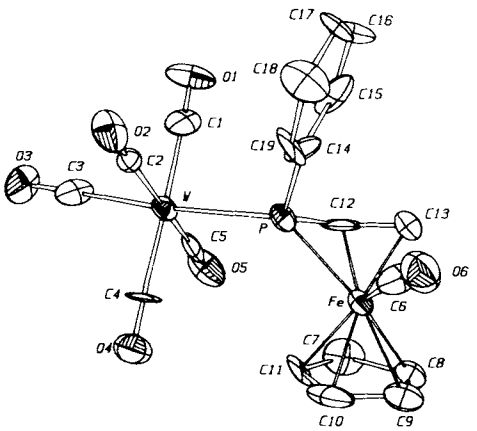
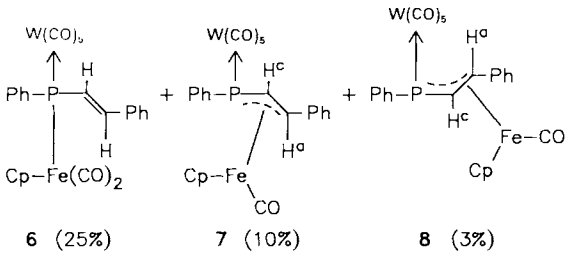


Fig. 1. Structure of **5** in the crystal [6]. Ellipsoids are scaled to enclose 50% of the electronic density. Hydrogen atoms are omitted for clarity.

When we carried out the same reaction with **4**, we obtained the complexes **6**–**8**, which could be separated by chromatography. Complex **6** is a $W(CO)_5$-complexed, ferrio-substituted vinylphosphane, whereas **7** and **8** are η^1,η^3-phosphaallyl complexes like **5** (Table 1).



Complexes **7** and **8** were also obtained in 79% overall yield (ratio **7** : **8** ≈ 1 : 3) by brief irradiation of a CH_2Cl_2 solution of **6**. At room temperature in solution, an equilibrium between **7** and **8** takes place favoring the formation of **7**. (Since the equilibration is very slow, it is possible to separate **7** and **8** by chromatography.) According to an X-ray structure analysis,[6] complex **7** has the same stereochemistry as **5** (Fig. 2) with H^c *cis* to W and pointing away from the Fe–CO unit.

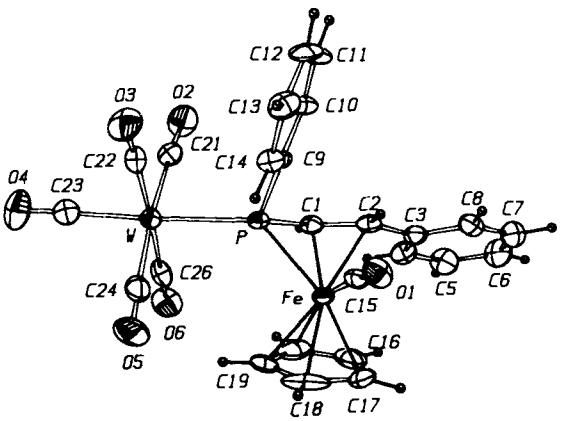


Fig. 2. Structure of **7** in the crystal [6]. Ellipsoids are scaled to enclose 50% of the electronic density. Hydrogen atoms are omitted for clarity. Important bond distances [Å] and angles [°]: W-P 2.511(1), Fe-P 2.270(1), P-C(1) 1.761(5), P-C(9) 1.819(4), C(1)-C(2) 1.380(7), C(2)-C(3) 1.489(7), $\langle$W-$C_{eq}\rangle$ 2.020(3), W-C_{ax} 1.992(6), $\langle$C-O$\rangle_W$ 1.158(3), Fe-C(15) 1.777(6), C(15)-O(1) 1.116(6), $\langle$C-C$\rangle_{Phe}$ 1.385(2), $\langle$C-C$\rangle_{Cp}$ 1.393(4), Fe-C(Cp) 2.056(6) to 2.098(6); W-P-C(1) 124.6(2), W-P-C(9) 111.7(1), W-P-Fe 130.11(6), C(1)-P-C(9) 106.5(2), C(9)-P-Fe 113.0(1), P-C(1)-C(2) 119.6(4), C(1)-C(2)-C(3) 126.4(4), $\langle$C-C-C$\rangle_{Phe}$ 120.0(1), $\langle$C-C-C$\rangle_{Cp}$ 108.0(3).

We assume that **7** and **8** equilibrate via a decoordination of the C=C double bond with subsequent 180°-rotation of the vinyl unit around the P–C(vinyl) bond. In **8**, H^c is probably *trans* to W and located close to the Fe–CO unit. This stereochemistry explains why H^c resonates at lower field than in **7**[7] and why no coupling is observed between H^c and P.[8] Finally, the short P–C(vinyl) bond of **7** [1.761(5) Å] is quite similar to those found in various η^5-phospholyl complexes[9] and in the recently described 1,3-diphosphaallyl complex.[4]

Experimental

All reactions were carried out under argon.

6–**8**: 4 (2.14 g, 4 mmol) was heated with [{CpFe(CO)$_2$}$_2$] (0.72 g, 2 mmol) in boiling xylene (25 mL) for 5 h. After filtration and evaporation, the residue

was chromatographed on a silica gel column (70–230 mesh Riedel de Haën) with a mixture of hexane and toluene (50:50). Complex **7** was eluted first ($R_f \approx 0.7$, yield 0.3 g), then complex **8** ($R_f \approx 0.5$, yield 0.1 g) and complex **6** ($R_f \approx 0.35$, yield 0.7 g).—**5** ($R_f \approx 0.6$, yield 0.75 g) was prepared from complex **3** (2.3 g, 5 mmol) by the same procedure.—**7** and **8** by irradiation of **6**: A stirred solution of complex **6** (0.7 g, 1 mmol) in 150 mL of dichloromethane was irradiated (125 W medium pressure mercury lamp) for 20 min at room temperature. After evaporation of the solvent, the residue was chromatographed. 140 mg of complex **7** and 400 mg of complex **8** were obtained.

Received: October 18, 1985;
revised: January 9, 1986 [Z 1502 IE]
German version: *Angew. Chem. 98* (1986) 347

CAS Registry numbers:
1, 101078-12-0; **2**, 101078-13-1; **3**, 101078-14-2; **4**, 101078-15-3; **5**, 101144-76-7; **6**, 101078-16-4; **7**, 101078-17-5; **8**, 101078-18-6; $[W(CO)_5P(Ph)(Cl)CH=CH_2]$, 101078-19-7; $[W(CO)_5P(Ph)(Cl)CH=CHPh]$, 101078-20-0; $PhP(Cl)NEt_2$, 4073-31-8; $[W(CO)_5(THF)]$, 36477-75-5; $[\{CpFe(CO)_2\}]$, 12154-95-9.

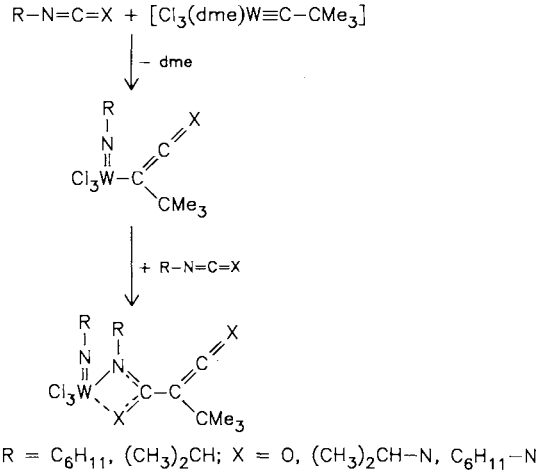
[1] H. Sakurai, Y. Kamiyama, Y. Nakadaira, *J. Am. Chem. Soc. 98* (1976) 7453.
[2] P. Radnia, J. S. McKennis, *J. Am. Chem. Soc. 102* (1980) 6349.
[3] M. Green, R. J. Mercer, C. E. Morton, A. G. Orpen, *Angew. Chem. 97* (1985) 422; *Angew. Chem. Int. Ed. Engl. 24* (1985) 422.
[4] R. Appel, W. Schuhn, F. Knoch, *Angew. Chem. 97* (1985) 421; *Angew. Chem. Int. Ed. Engl. 24* (1985) 420.
[5] F. Mercier, F. Mathey, *Tetrahedron Letters 26* (1985) 1717.
[6] Suitable single crystals of **5** and **7** were obtained by slow evaporation of CH_2Cl_2 solutions at room temperature. Data were collected at −100°C using $Mo_{K\alpha}$ radiation for **5** and $Cu_{K\alpha}$ radiation for **7** (Philips PW 1100/16 automatic diffractometer). Both crystal structures were solved by the heavy atom method using the Enraf-Nonius SDP package. Hydrogen atoms were introduced at their computed positions but not refined.—**5**: orthorhombic, space group $P2_12_12_1$, $a = 17.278(6)$, $b = 16.277(6)$, $c = 6.956(3)$ Å, $\alpha = \beta = \gamma = 90°$, $V = 1956$ Å^3, $Z = 4$, $\rho_{calc} = 2.06$ g cm^{-3}, $F(000) = 1160$, 1390 observed reflections, $R_1 = 0.048$, $R_2 = 0.078$. Unfortunately, the single crystals of **5** are highly mosaic; the quality of this data set is therefore very poor and only the overall geometry of **5** is meaningful.—**7**: triclinic, space group $P\bar{1}$, $a = 10.724(4)$, $b = 12.424(4)$, $c = 10.647(4)$ Å, $\alpha = 97.53(2)$, $\beta = 117.86(2)$, $\gamma = 72.48(2)°$, $V = 1196$ Å^3, $Z = 2$, $\rho_{calc} = 1.899$ g cm^{-3}, $F(000) = 660$, 2931 observed reflections, $R_1 = 0.027$, $R_2 = 0.047$. Further details of the crystal structure investigation are available on request from the Fachinformationszentrum Energie, Physik, Mathematik GmbH, D-7514 Eggenstein-Leopoldshafen 2 (FRG), on quoting the depository number CSD-51831, the names of the authors, and the journal citation.
[7] Strong shifts to lower fields (up to 2 ppm) due to neighboring Co–CO units have been observed with the protons of a phospholylcobalt complex, see: S. Holand, F. Mathey, J. Fischer, A. Mitschler, *Organometallics 2* (1983) 1234.
[8] A similar phenomenon has already been noted with phosphirane complexes with a $W(CO)_5$ group coordinated to the P atom. The protons located on the ring are coupled to P when they are *cis* to W and not coupled when they are *trans*, see: A. Marinetti, F. Mathey, *Organometallics 3* (1984) 456.
[9] F. Mathey, J. Fischer, J. H. Nelson, *Structure and Bonding 55* (1983) 153.

The Schrock Carbyne-Complex $[Cl_3(dme)W{\equiv}CCMe_3]$, a Highly Reactive Catalyst for the Metathesis of Alkenes**

By *Karin Weiss**

Fischer-type carbyne complexes such as *trans*-carbyne(tetracarbonyl)(halogeno)tungsten were already used by *Fischer* et al. as long ago as 1976 as catalysts for the ring-opening metathesis of cycloolefins. Metal chlorides, e.g. $TiCl_4$, WCl_6, or $SnCl_4$, were used as cocatalysts.[1] In 1984, *Katz* et al. investigated the activity of Fischer-type carbyne complexes in this reaction in the absence of metal halides. At room temperature (decomposition temperature), the carbyne complexes showed only slight activity, which, however, increased markedly in the presence of oxygen. Oxygen is also used as cocatalyst in other metatheses with transition metals.[3] That the cocatalysts have a decisive influence on the course of the reaction in the metathesis of cycloolefins follows from the stereochemistry of the polymers that are formed. For example, when using the same carbyne complex, *Fischer* et al.[1] obtained from cyclopentene a poly-1-pentenylene having predominantly *trans* double-bonds, whereas *Katz* et al.[2] obtained a poly-1-pentenylene having predominantly (70%) *cis* double bonds.

Metatheses of the W≡C triple bond of Schrock-type carbyne complexes with alkynes[4] and nitriles[5] are well known. Recently, the metathesis of the W≡C triple bond of $[Cl_3(dme(W{\equiv}CCMe_3]$ (dme = 1,2-dimethoxyethane) with the C=N double bonds of isocyanates[7] and carbodiimides[8] was also accomplished. In this metathesis, tungsten complexes with an imido ligand and a singly bonded ketenyl (X = O) or ketenimido ligand (X = NR) are formed initially. A further molecule of the heteroallene is then inserted into the W–C single bond (see Scheme 1).



Scheme 1.

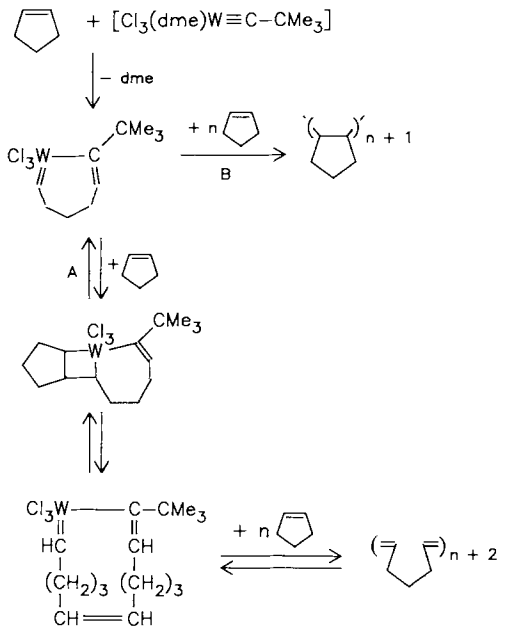
This communication is concerned with the metathetic activity of $[Cl_3(dme)W{\equiv}CCMe_3]$ towards alkenes. Reaction of cyclopentene with catalytic amounts of the carbyne complex at room temperature affords poly-1-pentenylene with predominantly (75%) *trans*-configurated double bonds as sole product and in good yields. In view of the reaction pathway of the metathesis of the heteroallenes, the most likely course for the above reaction would appear to be that depicted in Scheme 2.

Metathesis of the W≡C triple bond with the double bond of cyclopentene could initially lead to formation of a tungstacycloheptadiene containing a W=C double bond and a W–C single bond. For further reactions with cyclopentene there exist two possible routes: insertion of cyclopentene in the W–C single bond according to a Ziegler-Natta-like mechanism, leading to poly(cyclopentene) (route B); metathesis of cyclopentene with the W=C double bond, leading to poly-1-pentenylene (route A), the reaction product actually obtained.

Each additional metathetic step increases the size of the metallacycle. The original carbyne ligand ($CCMe_3$) re-

[*] Dr. K. Weiss
Laboratorium für Anorganische Chemie der Universität
Postfach 3008, D-8580 Bayreuth (FRG)

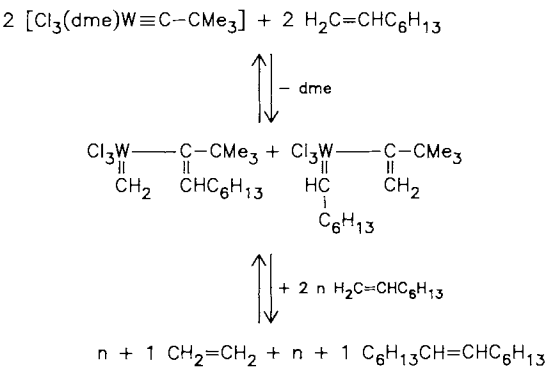
[**] *Investigations of Polymerization and Metathesis Reactions, Part 7.*—Part 6: K. Weiss, U. Schubert, R. R. Schrock, *Organometallics 5* (1986) 397.



Scheme 2.

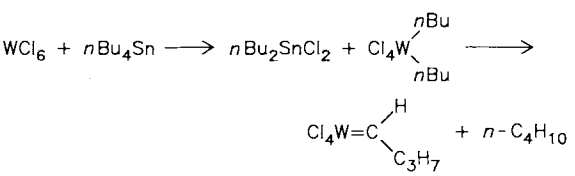
mains coordinated to the metal as an alkyl ligand in all reaction steps and can thus influence the steric course of the reaction. The metallacycle, concomitantly an alkyl- and a carbenetungsten-complex, is the active metathetic catalyst.

$[Cl_3(dme)W{\equiv}CCMe_3]$ catalyzes not only the metathesis of cycloalkenes, but also that of linear alkenes such as 1-octene (Scheme 3).[9] The products of the metathesis were found to be ethylene and 7-tetradecene (GC, GC-MS, NMR), of which the latter consisted predominantly of the *trans*-isomer.



Scheme 3.

For highly reactive metathetic catalysts, which mostly consist of WCl_6 and an alkylating agent such as nBu$_4$Sn as cocatalyst, carbene complexes, which should be formed according to the reaction formulated in Scheme 4 have been postulated as the active species.[3]



Scheme 4.

Reactions of WCl_6 with alkylating agents are often very complex.[10] However, in reactions of WCl_6 with alkyllithium or Grignard compounds no carbene complexes are formed, but only carbynetungsten complexes of the Schrock type.[6] The metathesis of alkenes with the catalyst system WCl_6/alkylating agent is therefore most likely initiated by carbyne complexes.

Since *Mayr*'s recent successful synthesis of Schrock-type carbyne complexes from Fischer-type carbyne complexes and Br_2,[11] there is now a further possibility that Schrock-type carbyne complexes are formed from Fischer-type carbyne complexes and metal chlorides (as chlorinating agent) or oxygen (as oxidizing agent), which then initiate the alkene metathesis.

Received: November 13, 1985 [Z 1536]
German version: *Angew. Chem. 98* (1986) 350

CAS Registry numbers:
$[Cl_3(dme)WCCMe_3]$, 83416-70-0; poly-1-pentenylene, 25103-85-9; 7-tetradecene, 10374-74-0; ethylene, 74-85-1; cyclopentene, 142-29-0; 1-octene, 111-66-0.

[1] E. O. Fischer, W. R. Wagner, *J. Organomet. Chem. 116* (1976) C21.
[2] T. J. Katz, T. H. Ho, N. Y. Shin, Y. Ch. Ying, I. W. Stuart, *J. Am. Chem. Soc. 106* (1984) 2659.
[3] K. J. Ivin: *Olefin Metathesis*. Academic Press, London 1983.
[4] J. Sancho, R. R. Schrock, *J. Mol. Catal. 15* (1982) 75.
[5] H. J. Freudenberger, R. R. Schrock, *Organometallics 5* (1986) 398.
[6] R. R. Schrock, D. N. Clark, J. Sancho, J. H. Wengrovius, S. M. Rocklage, S. F. Pedersen, *Organometallics 1* (1982) 1645.
[7] K. Weiss, U. Schubert, R. R. Schrock, *Organometallics 5* (1986) 397.
[8] K. Weiss, unpublished results.
[9] Procedure: Poly-1-pentenylene: A solution of $[Cl_3(dme)WCCMe_3]$ (100 mg, 0.22 mmol) in CH_2Cl_2 (5 mL) was treated at 20°C with 3 mL (32 mmol) of cyclopentene. The solution became viscous within a few minutes; after 3 h, the solution was diluted with 20 mL of CH_3OH and the poly-1-pentenylene precipitated by addition of 100 mL of CH_3OH. Yield: 1.6 g (70% referred to cyclopentene). Characterization by ^{1}H- and ^{13}C-NMR as well as IR spectroscopy. Concentration of *trans* configurated double bonds: 75% (^{13}C-NMR).—Metathesis of 1-octene: A solution of $[Cl_3(dme)WCCMe_3]$ (30 mg, 0.067 mmol) in CH_2Cl_2 (5 mL) was treated with 1 mL (6.4 mmol) of 1-octene at 20°C. The reaction was monitored by gas chromatography. After 30 min, 40% of the 1-octene was converted into 7-tetradecene (^{1}H- and ^{13}C-NMR as well as GC/MS) and ethylene (GC).
[10] R. R. Schrock, G. W. Parshall, *Chem. Rev. 76* (1976) 243.
[11] A. Mayr, G. A. McDermott, *J. Am. Chem. Soc. 108* (1986) 548.

Synthesis of *O*-Glycopeptides of the Tumor-Associated T_N- and T-Antigen Type and Their Binding to Bovine Serum Albumin**

By *Horst Kunz** and *Stefan Birnbach*

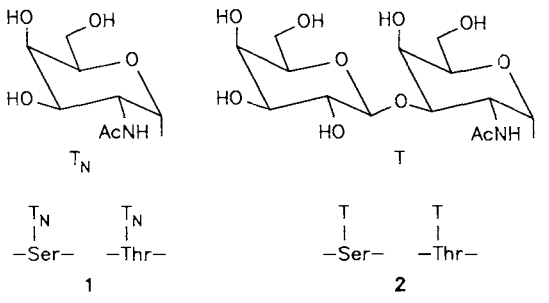
Dedicated to Professor Siegfried Hünig on the occasion of his 65th birthday

Cellular biological and biochemical investigations have shown that glycoproteins perform important functions in cell differentiation and in the regulation of cell growth.[1] Normal cells and unregulated growing tumor cells differ very much in the glycolipid and glycoprotein profiles of their cell membranes.[2] The glycoproteins of the tumor cell membranes are regarded as tumor-associated antigens.

[*] Prof. Dr. H. Kunz, Dipl.-Chem. S. Birnbach
Institut für Organische Chemie der Universität
Johann-Joachim-Becher-Weg 18-20, D-6500 Mainz (FRG)

[**] This work was supported by the Deutsche Forschungsgemeinschaft and the Fonds der Chemischen Industrie.

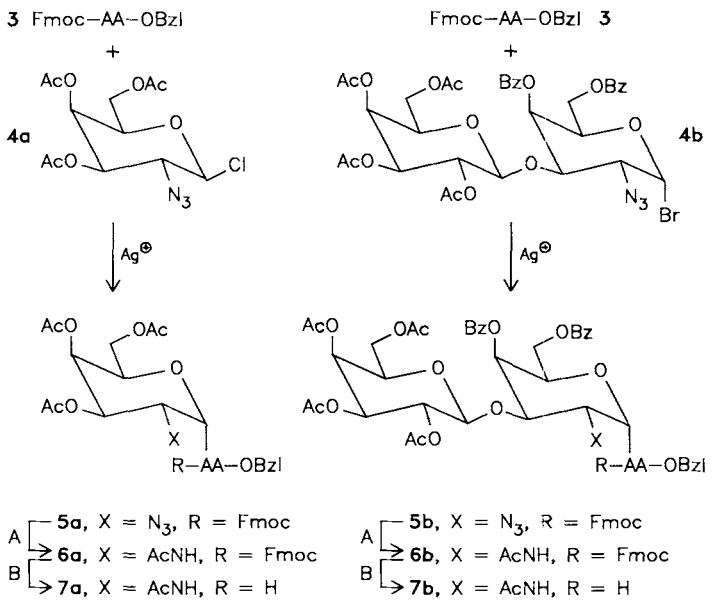
This property was demonstrated, in particular, for the T-antigen, an *O*-glycoprotein that is closely related to glycophorin A and contains the βGal(1-3)GalNAc disaccharide unit linked to serine or threonine as typical structural unit **2**.[3] Frequently, several such glycosylated amino acids are coupled together directly. The monosaccharidic structural unit **1**, the T_N-antigen, is also present in human epithelial tumor cells[3] and in the erythrocytic membranes of patients suffering from leukopenia and thrombocytopenia.[4]



Commensurate with the immunological importance of the structures **1** and **2**, glycopeptides of the T_N-[5] and T-antigen type[6,7] have already been the subjects of several studies. However, for the immunological application of synthetic antigens their conjugation with a biologically appropriate carrier is necessary.

Whereas the disaccharide β-Gal(1-3)GalNAc of the T-antigen could be bound to bovine serum albumin via artificial spacers,[8] the linking of glycopeptides of type **1** and **2** with biological carrier molecules has so far never been accomplished.

We describe here the synthesis of glycotripeptides of the tumor-associated T_N- and T-antigen type, which correspond to the *N*-terminus of glycophorin A with blood-group M activity,[9] and, for the first time, their binding to bovine serum albumin. Our synthetic strategy does not call for a spacer; that is, we can achieve a "natural" linking of the antigen structures to the biological carrier molecule.



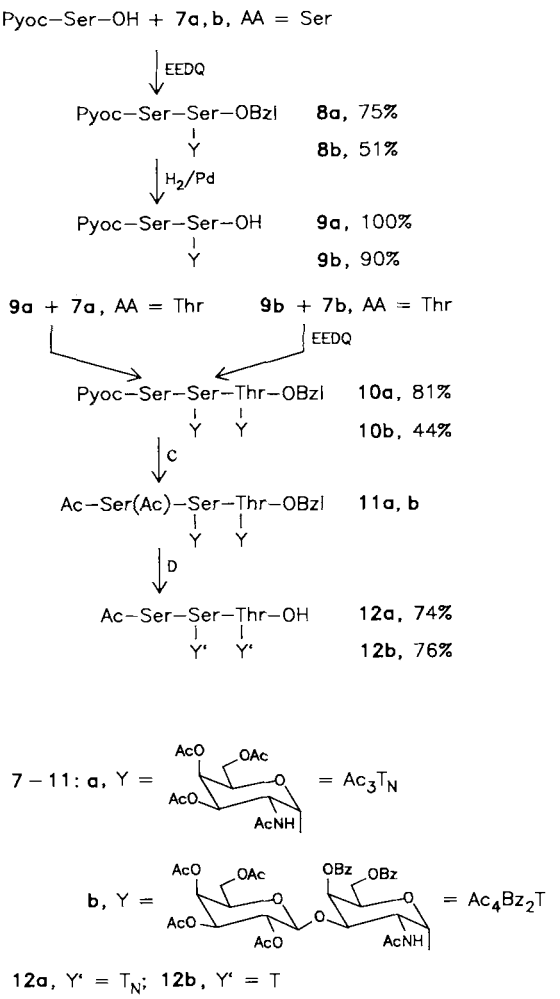
Scheme 1. AA = Ser or Thr. Bzl = benzyl, Bz = benzoyl. A: 1) $NaBH_4/NiCl_2$, 2) Ac_2O/pyridine; B: morpholine.

As protecting groups we used our tested combination[10] of *N*-terminal 9-fluorenylmethoxycarbonyl(Fmoc) group[11] and *C*-terminal benzyl ester in the glycosylation step, and in the chain-lengthening reactions the solubility-promoting 2-(4-pyridyl)ethoxycarbonyl (Pyoc) group.[12]

Table 1. Yields of compounds **5** and **6**.

Cpd.	AA	Yield [%]	Cpd.	AA	Yield [%]
5a	Ser	65 + 9% β	**6a**	Ser	86
5a	Thr	60 + 4% β	**6a**	Thr	85
5b	Ser	51 + 20% β	**6b**	Ser	70
5b	Thr	30 + 21% β	**6b**	Thr	60

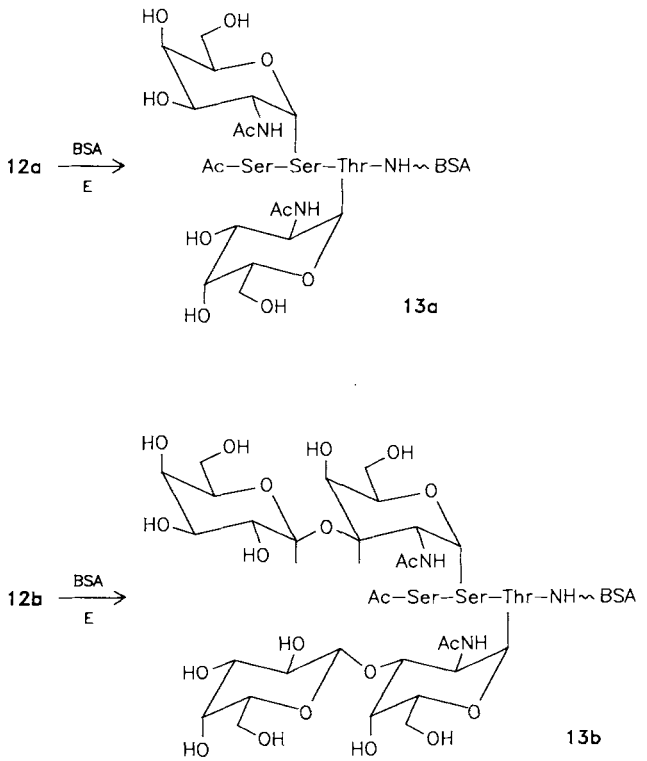
Scheme 1 outlines the synthesis of the partially protected serine and threonine derivatives having T_N- **7a** or T-antigen structure **7b** (see also Table 1). Fmoc-serine benzyl ester **3**, AA = Ser,[10] and Fmoc-threonine benzyl ester **3**, AA = Thr, react with glycosyl donors **4a**[13] and **4b**[6] to give mainly the α-glycosides **5**. The accompanying β-glycosides, particularly those in the case of the disaccharide derivatives **5b**, can be separated chromatographically.



Scheme 2. C: 1) CH_3I/CH_2Cl_2, 2) morpholine/CH_2Cl_2, 3) Ac_2O/pyridine; D: 1) H_2/Pd, 2) hydrazine hydrate/methanol. The yield of **12** is based on **10**.

After reaction of the azido function with sodium boronate/nickel chloride[13, 14] and immediate acetylation, the fully-protected *O*-glycosylamino acid derivatives **6** are obtained. The Fmoc group can be selectively removed from these sensitive compounds with morpholine.[10] It is decisive for the further steps of the synthesis that the rate of reaction of the *N*-unprotected compounds **7** thus obtained is fast enough, since they otherwise decompose by self-destructing β-elimination of the glycan moiety. Fmoc-protected carboxyl components often react too sluggishly.

The chain-lengthening steps (Scheme 2) with formation of **8** and **10**, on the other hand, can be accomplished quite effectively with Pyoc-serine[15] or with the Pyoc-protected glycopeptides **9** in the presence of ethyl 2-ethoxy-1,2-dihydroquinoline-1-carboxylate (EEDQ).[16] In the selective deblocking of the carboxyl function on the fully-protected glycodipeptides **8**, the Pyoc group shows a further advantage: In contrast to the Fmoc group[17] it is stable towards hydrogenolysis. Prior to coupling with the albumin, the Pyoc residue is selectively removed from the fully-protected glycopeptides **10** by methylation to the pyridinium form and decomposition with morpholine in dichloromethane[12] without destroying the base-sensitive *O*-glycosidic bonds of serine and threonine. The free terminal serine residue is acylated to **11**, so that the free amino functions have no effect on the base-catalyzed destruction of the *O*-glycoside bonds, and, later, also do not influence the immunological recognition of the carbohydrate-peptide linkage region.[18] After hydrogenolysis of the *C*-terminal benzyl ester and gentle cleavage of all acetates using hydrazine in methanol,[10] the glycopeptides with T_N- and T-antigen structure (**12a** and **12b**, respectively) deblocked in the carbohydrate moiety are obtained in high yields. Their structure and purity has been unequivocally confirmed by ^{13}C-NMR spectroscopy.[20]



Scheme 3. E: Bovine serum albumin (BSA), (water soluble) $EtN{=}C{=}N{-}(CH_2)_3NMe_2$, 1-hydroxybenzotriazole, 4°C [21].

The coupling of the synthetic antigen-glycopeptides **12** to bovine serum albumin (BSA)—presumably at the ε-amino functions of the lysine residues—can only be carried out in aqueous solution (Scheme 3).

The conjugates **13a** and **13b** are freed from low-molecular impurities by dialysis against water. According to a photometric carbohydrate determination[18] (*N*-acetylgalactosamine/galactose as standard) they contain ca. 130 μg of carbohydrate/1 mg conjugate (**13a**) and 280 μg of carbohydrate/1 mg conjugate (**13b**), respectively. This means that, of the ca. 60 lysine residues of BSA, 25 and 38, respectively, are conjugated with the synthetic tumor-associated T_N- and T-antigen structures. The conjugates **13** are thus the first immunologically relevant bound synthetic glycopeptides with the tumor-specific recognition structures **1** and **2**, which, moreover, are only bound via natural peptide and amide bonds to the biological carrier molecule and should be suitable for inducing formation of antibodies against the structures typical for tumor cell membranes.

Received: November 19, 1985 [Z 1541 IE]
German version: *Angew. Chem. 98* (1986) 354

CAS Registry numbers:
3 (AA = Ser), 73724-46-6; **3** (AA = Thr), 73724-48-8; **4a**, 67817-37-2; **4b**, 87376-57-6; **5a** (AA = Ser), 100929-00-8; **5a** (AA = Thr), 100938-55-4; **5b** (AA = Ser), 100929-01-9; **5b** (AA = Thr), 100929-02-0; **6a** (AA = Ser), 100929-03-1; **6a** (AA = Thr), 100938-56-5; **6b** (AA = Ser), 100929-04-2; **6b** (AA = Thr), 100929-05-3; **7a** (AA = Ser), 100929-06-4; **7a** (AA = Thr), 100938-57-6; **7b** (AA = Ser), 100929-07-5; **7b** (AA = Thr), 100929-08-6; **8a**, 100929-09-7; **8b**, 100929-10-0; **9a**, 100929-11-1; **9b**, 100929-12-2; **10a**, 100929-13-3; **10b**, 100929-14-4; **11a**, 100929-15-5; **11b**, 100929-16-6; **12a**, 100929-17-7; **12b**, 100938-78-7; Pyoc-Ser-OH, 100929-18-8.

[1] Review: R. T. Schwarz, R. Datema, *Adv. Carbohydr. Chem. Biochem. 40* (1982) 287.
[2] Cf., e.g., W. W. Young, Jr., S. Hakomori, *ACS Symp. Ser. 80* (1978) 357.
[3] G. F. Springer, P. R. Desai, M. S. Murthy, E. F. Scanlon, *ACS Symp. Ser. 80* (1978) 311.
[4] J. P. Carton, A. T. Nurdem, *Nature (London) 282* (1978) 621.
[5] B. Ferrari, A. A. Pavia, *Tetrahedron 41* (1985) 1939.
[6] H. Paulsen, M. Paal, M. Schultz, *Tetrahedron Lett. 24* (1983) 1759.
[7] V. Verez Bencomo, P. Sinay, *Glycoconjugate J. 1* (1984) 1.
[8] H. Paulsen, M. Paal, *Carbohydr. Res. 113* (1983) 203.
[9] M. Tomita, V. F. Marchesi, *Proc. Nat. Acad. Sci. USA 72* (1975) 2964.
[10] P. Schultheiss-Reimann, H. Kunz, *Angew. Chem. 95* (1983) 64; *Angew. Chem. Int. Ed. Engl. 22* (1983) 62; *Angew. Chem. Suppl. 1983*, 39.
[11] L. A. Carpino, N. Y. Han, *J. Org. Chem. 37* (1972) 3404.
[12] H. Kunz, S. Birnbach, *Tetrahedron Lett. 25* (1984) 3567.
[13] H. Paulsen, J.-P. Hölck, *Carbohydr. Res. 101* (1982) 89.
[14] K. Heyns, D. Feldmann, D. Hadamczyk, J. Schwentner, J. Thiem, *Chem. Ber. 114* (1981) 232.
[15] Prepared according to the procedure given in Ref. [12]: m.p. 145°C, $[\alpha]_D^{22} = -4.0$ ($c = 1$, DMF).
[16] G. Malek, B. Belleau, *J. Am. Chem. Soc. 90* (1968) 1651.
[17] J. Martinez, J. C. Tolle, M. Bodanszky, *J. Org. Chem. 44* (1979) 3596.
[18] We thank Herr Dr. *R. Wieser*, Institut für Toxikologie der Universität Mainz, for valuable discussions and advice regarding immunological problems, and for the carbohydrate analyses on the conjugates **13a** and **13b** according to Ref. [19].
[19] M. Dubois, K. A. Gilles, J. K. Hamilton, P. A. Rebers, F. Smith, *Anal. Chem. 28* (1956) 350.
[20] **12a**: $[\alpha]_D^{22} = +122.8$ ($c = 1.2$, H_2O): **12b**: $[\alpha]_D^{22} = +80.8$ ($c = 0.8$, H_2O). 100.6MHz-^{13}C-NMR (D_2O, CS_2 int.): **12a**: $\delta = 174.54$, 174.44, 173.72, 171.99, 171.12 (5 × C=O); 98.90 (C-1 on Thr), 97.92 (C-1, bound to Ser^2); 57.86, 55.53, 53.49 (C-α of $Ser^{1,2}$, Thr); 22.27, 22.12, 21.82 (CH_3, NAc), 17.90 (CH_3, Thr). **12b**: $\delta = 174.78$, 174.30, 174.17, 173.92, 171.60, 170.28 (6 × C=O); 104.32, 104.24 (βGal-C-1'/7, 98.58 (C-1 on Thr), 97.58 (C-1 on Ser), 58.63, 55.13, 53.21 (C-α of $Ser^{1,2}$, Thr), 22.05, 21.78, 21.44 (CH_3, NAc), 17.49 (CH_3, Thr).
[21] W. König, R. Geiger, *Chem. Ber. 103* (1970) 788.

cyclo-P_5 as Complex Ligand—the Phosphorus Analogue of the Cyclopentadienyl Ligand**

By *Otto J. Scherer,* Joachim Schwalb, Gotthelf Wolmershäuser, Wolfgang Kaim,* and *Renate Gross*

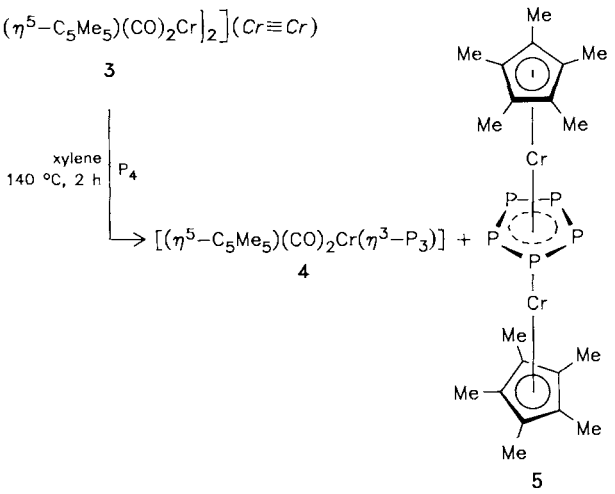
Dedicated to Professor Rolf Appel on the occasion of his 65th birthday

The recently reported successful stabilization of *cyclo*-As_5 and *cyclo*-P_6 ("hexaphosphabenzene") as bridge ligand ("middle deck") in the triple-decker complexes **1**[1] and **2**[2] respectively, signaled the possibility of also stabilizing *cyclo*-P_5 in the same way.[3]

$[\{(\eta^5\text{-}C_5H_5)Mo\}_2(\mu,\eta^4\text{-}As_5)]$ **1**

$[\{(\eta^5\text{-}C_5Me_5)Mo\}_2(\mu,\eta^6\text{-}P_6)]$ **2**

If, in analogy to the synthesis of **2**, the Cr_2-complex **3** is allowed to react with P_4, then not only traces of the yellow η^3-P_3-complex **4** are formed but also the μ,η^5-P_5 triple-decker complex **5**, which can be isolated as blackish-red, shiny-metallic crystals (dec. 250 °C).[4, 17]



5,[4] which is only sparingly soluble in pentane but moderately soluble in benzene and dichloromethane (the solutions are very air-sensitive), is a paramagnetic triple-decker complex.[5] With 27 valence electrons (3×5 and 2×6), **5** closes a gap, since up to now only examples with 26 and 28 to 34 valence electrons were known.[6, 16] In the ^{1}H-NMR spectrum (200 MHz, 293 K, $CDCl_3$, TMS int.), a broad signal (halfwidth = 30 Hz) is observed at $\delta = -7.1$ (paramagnetic shift), in the $^{31}P\{^1H\}$-NMR spectrum (80.82 MHz, [D_6]benzene, 85% H_3PO_4 ext.), a sharp singlet at $\delta = 290.5$ ($^{13}C\{^1H\}$-NMR (50.28 MHz, [D_6]benzene, TMS int.): $\delta = 80.4$ (s, C_5Me_5), -2.2 (s, CH_3)). In the mass spectrum,[7] the line for the molecular ion is the strongest-intensity line.

The paramagnetism ($S = 1/2$) of **5** can be detected ESR spectroscopically at room temperature. Under high resolution conditions, a relatively narrow, unstructured signal[7] is obtained, from which the upper limiting values $a(^1H) \le 0.15$ mT, $a(^{31}P) \le 0.5$ mT, and $a(^{53}Cr) \le 0.9$ mT can be estimated for the coupling constants. With regard to reference compounds,[8, 9] this means, on the one hand, that the P_5 ring is situated in a nodal plane of the singly occupied molecular orbital[12] (cf. the well resolved ^{31}P-NMR spectrum), and, on the other, that the splitting of ca. 1.8 mT[9] by the isotope ^{53}Cr ($I = 3/2$, 9.54% natural abundance) observed for mononuclear paramagnetic Cr^I sandwich complexes is clearly lowered, at least halved. This was to be expected in the case of equal distribution of the unpaired electron between the two chromium centers.[10] **5** can therefore be regarded as a delocalized, mixed-valence complex of class III,[11] in which two equivalent chromium centers of oxidation state +1.5 (d^4/d^5 system) are bound by a *cyclo*-$P_5^{\ominus}$ bridge ($P_5^{\ominus} \triangleq C_5H_5^{\ominus}$).

The ESR results and the ratio $g_\parallel > g_\perp \approx g_{electron}$[10] are consistent with results of MO calculations on triple-decker complexes;[12a, b] nine electrons (d^4/d^5) are located in the predominantly metal-centered bonding orbitals e_2' (δ), e_2'' (δ), a_1' (σ), and a_2'' (σ), so a non-degenerated ground state $^2A_1$ can be assumed for **5**.

Electrochemical investigations on the 27-valence-electron system **5** (cf. also [5, 16]) gave a reversible one-electron oxidation step and reduction step[7] to the 26-valence-electron cation $\mathbf{5}^{\oplus}$ and 28-valence-electron anion $\mathbf{5}^{\ominus}$, respectively; calculations using $E_{ox} = +0.07$ V and $E_{red} = -0.97$ V gives a comproportionation constant $K_c = 4\times10^{17}$.

The accuracy of the X-ray structure analysis[13] is diminished by the crystallographically conditioned disorder of one of the two independent molecules (molecule 2) and the strong anisotropy of the temperature factors of the P atoms. Furthermore, the number of the reflections categorized as observed (2126) compared to the number of parameters to be determined is low and an anisotropic refinement of the temperature factors of the C atoms is therefore not justified. A detailed discussion of the bond lengths and angles quoted in Figure 1 is therefore out of the question. A refinement of the structures in the likewise conceivable acentric space groups $P2/n$ and $P2_1$ did not lead to any significant improvement.

5, with the three planar, parallel five-membered rings (Fig. 1), has a similar conformation as the triple-decker

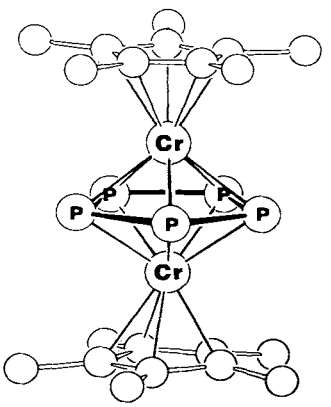


Fig. 1. Structure of **5** (molecule 1) in the crystal. Selected bond lengths [Å] and angles [°]: P-P 2.15(2)-2.21(2), P-Cr 2.29(1)-2.32(1), Cr-Cr 2.727(5); P-P-P 107.3(6)-108.9(6). Sum of angles 540, Cr-P-Cr 72.2(3)-72.7(3). The corresponding values for molecule 2 do not differ significantly.

[*] Prof. Dr. O. J. Scherer, Dipl.-Chem. J. Schwalb, Dr. G. Wolmershäuser [+]
Fachbereich Chemie der Universität
Erwin-Schrödinger-Strasse, D-6750 Kaiserslautern (FRG)
Priv.-Doz. Dr. W. Kaim, Dipl.-Chem. R. Gross
Institut für Anorganische Chemie der Universität
Niederurseler Hang, D-6000 Frankfurt am Main 50 (FRG)

[+] X-ray structure analysis.

[**] This work was supported by the Fonds der Chemischen Industrie.

complex $[\{(\eta^5\text{-}C_5H_5)Ni\}_2(\mu,\eta^5\text{-}C_5H_5)]^{\oplus}$.[14] In contrast to **1** (As_5 middle deck), in which a μ,η^4-coordination of the five-membered ring is discussed on the basis of the large differences in the As–As bond lengths (2.389(2)–2.762(3) Å),[1] in **5** the P_5 ring forms a regular pentagon (cf. the pentagonal columns of phosphorus atoms in Hittorf's phosphorus and the polyphosphides derivable therefrom[15]); the mean value of the P–P bond lengths differs very little from that in the P_6 middle deck of **2**,[2] and is of an order of magnitude which has also been found in the triple-decker complexes stabilized by triphosphorus ligands (triphos = for example 1,1,1-tris(diphenylphosphinomethyl)ethane) with μ,η^3-P_3 bridges.[16]

Received: October 31, 1985;
supplemented: December 30, 1985 [Z 1516 IE]
German version: *Angew. Chem. 98* (1986) 349
Publication delayed at authors' request

CAS Registry number:
5, 101077-62-7.

[1] A. L. Rheingold, M. J. Foley, P. J. Sullivan, *J. Am. Chem. Soc. 104* (1982) 4727.

[2] O. J. Scherer, H. Sitzmann, G. Wolmershäuser, *Angew. Chem. 97* (1985) 358; *Angew. Chem. Int. Ed. Engl. 24* (1985) 351.

[3] Cf. also the theoretical studies of $N_5^{\ominus}$, $[(N_5)Fe(CO)_3]^{\ominus}$, $[(N_5)Mn(CO)_3]$, and $[(N_5)Cr(CO)_3]^{\ominus}$ (M. T. Nguyen, M. Sana, G. Leroy, J. Elguéro, *Can. J. Chem. 61* (1983) 1435; M. T. Nguyen, M. A. McGinn, A. F. Hegarty, J. Elguéro, *Polyhedron 4* (1985) 1721) and $P_5^{\ominus}$ (N. C. Baird, *Can. J. Chem. 62* (1984) 341); mass spectrometric detection of $P_5^{\ominus}$ (from red phosphorus at ca. 325°C, negative ion mass spectrometry): T. Snodgrass, J. V. Coe, C. B. Freidhoff, K. M. McHugh, K. H. Bowen, *Chem. Phys. Lett. 122* (1985) 352.

[4] Procedure: A solution of $Cr(CO)_6$ (3.5 g, 15.9 mmol) and pentamethylcyclopentadiene (2.9 mL, 16.6 mmol) in xylene (130 mL) was stirred under reflux for 60 h. The solution was then treated at room temperature with 2.0 g (16.1 mmol) of P_4 and heated to gentle boiling for 2 h. The blackish-brown solution was decanted and the residue extracted twice with CH_2Cl_2 (2 × 10 mL). The xylene solution was evaporated to dryness in a vacuum, and, after combination with the CH_2Cl_2 extract and addition of aluminum oxide (10 g, basic, 2% H_2O), re-dried under oil-pump vacuum until just pourable. Chromatographic separation (column: 2 cm × 35 cm, alumina (basic, 2% H_2O)) with pentane as first eluent gave a weak yellow phase (which was difficult to separate from the following broad, brown phase) which contained **4** (yield 10 mg, 0.2%, referred to $Cr(CO)_6$; $^{31}P\text{-}\{^1H\}$-NMR (C_6D_6): $\delta = -269.7$ (s); IR (*n*-heptane): $\tilde{\nu}(CO) = 1975$ (vs), 1928 (vs) cm^{-1}. Elution of the brown fraction with pentane/toluene (10 : 1), followed by evaporation to dryness and recrystallization from toluene afforded blackish-red crystals of **5** (yield 350 mg, 8.3%).

[5] Cf. also: J. Edwin, M. Bochmann, M. C. Böhm, D. E. Brennan, W. E. Geiger, C. Krüger, J. Pebler, H. Pritzkow, W. Siebert, W. Swiridoff, H. Wadepohl, J. Weiss, U. Zenneck, *J. Am. Chem. Soc. 105* (1983) 2582 and [1], [12b], and [16].

[6] W. Siebert, *Angew. Chem. 97* (1985) 924; *Angew. Chem. Int. Ed. Engl. 24* (1985) 943.

[7] EI-MS (100 eV, 220°C): *m/z* 529 (M^+, $I_{rel} = 100\%$), 467 ($M^+ - 2P$, 17%) and other weak intensity lines. ESR: dilute solution in toluene (25°C), peak-to-peak distance 1.2 mT, estimation of the coupling constants by computer simulation. $g_{iso} = 2.022$; $g_{\parallel} = 2.054$, $g_{\perp} = 2.006$ (−150°C, toluene), cyclovoltammetry: CH_3CN, 0.1 M nBu_4NClO_4; glassy-carbon electrode versus saturated calomel electrode.

[8] Cf. also the dibenzophosphole dianion radical: W. Kaim, P. Hänel, H. Bock, *Z. Naturforsch. B37* (1982) 1382.

[9] C. Elschenbroich, E. Bilger, J. Koch, J. Weber, *J. Am. Chem. Soc. 106* (1984) 4297.

[10] Cf. investigations on Mn^{II}/Mn^{I} mixed-valence complexes: R. Gross, W. Kaim, *Angew. Chem. 97* (1985) 869; *Angew. Chem. Int. Ed. Engl. 24* (1985) 856; *Inorg. Chem. 25* (1986), in press.

[11] M. B. Robin, P. Day, *Adv. Inorg. Radiochem. 10* (1967) 248.

[12] a) J. W. Lauher, M. Elian, R. H. Summerville, R. Hoffmann, *J. Am. Chem. Soc. 98* (1976) 3219; b) P. T. Chesky, M. B. Hall, *ibid. 106* (1984) 5186 and [3].

[13] **5**: $P2_{1/n}$, $a = 8.347(2)$, $b = 31.600(3)$, $c = 14.203(2)$ Å, $\beta = 95.59(2)°$, $Z = 6$, $\rho_{calc} = 1.414$ g cm^{-3}. 4087 independent reflections ($Mo_{K\alpha}$, $2\theta \leq 46°$), 2126 observed with $F_0^2 \geq 3.0\sigma(F_0^2)$, 214 parameters, $R = 0.108$, $R_w = 0.123$. Further details of the crystal structure investigation are available on request from the Fachinformationszentrum Energie, Physik, Mathematik GmbH, D-7514 Eggenstein-Leopoldshafen 2, on quoting the depository number CSD-51655, the names of the authors, and the full citation of the journal.

[14] E. Dubler, M. Textor, H.-R. Oswald, A. Salzer, *Angew. Chem. 86* (1974) 125; *Angew. Chem. Int. Ed. Engl. 13* (1974) 135; H. Werner, *ibid. 89* (1977) 1, *16* (1977) 1.

[15] H. G. von Schnering in A. L. Rheingold: *Homoatomic Rings, Chains and Macromolecules of Main-Group Elements*, Elsevier, Amsterdam 1977, p. 317; *Angew. Chem. 93* (1981) 44; *Angew. Chem. Int. Ed. Engl. 20* (1981) 33.

[16] M. Di Vaira, L. Sacconi, *Angew. Chem. 94* (1982) 338; *Angew. Chem. Int. Ed. Engl. 21* (1982) 330.

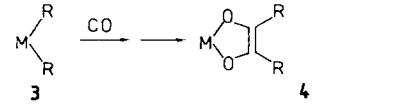
[17] Note added in proof (February 26, 1986): $[\{(\eta^5\text{-}C_5H_4R)Cr\}_2(\mu,\eta^5\text{-}P_5)]$ (R = CH_3, yield ca. 15%; $^{31}P\{^1H\}$-NMR: $\delta = -283$ (s)); R = H (eluted with CH_2Cl_2), yield ca. 20%; $\delta = -285$ (s)) has been synthesized under almost analogous experimental conditions from $[\{(\eta^5\text{-}C_5H_4R)(CO)_3Cr\}_2](Cr\text{-}Cr)$ and P_4.

Reductive Coupling of CO: Formation of a 1 : 1 Adduct of η^2-Ketone- and Enediolato-Complex upon Carbonylation of Bis(cyclopentadienyl)hafnacyclobutane**

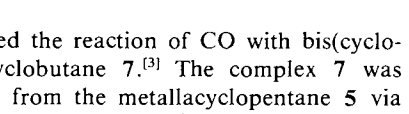
By *Gerhard Erker,* Peter Czisch, Rüger Schlund, Klaus Angermund,* and *Carl Krüger*

Dedicated to Professor Siegfried Hünig on the occasion of his 65th birthday

Alkyl and hydrido complexes of the bent metallocenes of oxygenophilic d- and f-elements can react with CO to give [(enediolato)MCp_2] compounds. Whereas the mechanism of this reductive coupling is basically understood in the case of multinuclear enediolate-bridged compounds (**1** → **2**) through the isolation of intermediates,[1] this is not so in the case of mononuclear compounds (**3** → **4**).[2]



1 **2**



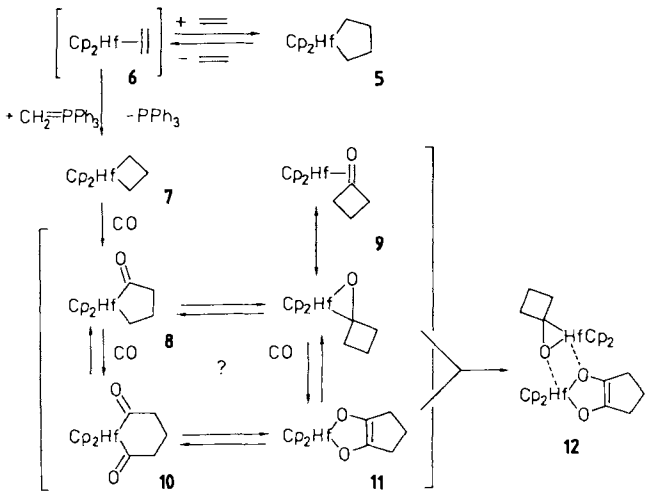
3 **4**

We have examined the reaction of CO with bis(cyclopentadienyl)hafnacyclobutane **7**.[3] The complex **7** was synthesized starting from the metallacyclopentane **5** via formation of (ethylene)hafnocene **6**[4] by extrusion of one equivalent of ethylene and reaction with methylenetriphenylphosphorane. Upon carbonylation of this very reactive alkylmetal compound we expected that the following reactions might possibly take place: Initially, CO insertion into a Hf–C σ-bond leading to formation of the metallacyclopentanone **8**,[5] followed by direct rearrangement with CC coupling to give (η^2-cyclobutanone)hafnocene **9**, or, alternatively, further uptake of a CO molecule with formation of the bis(acyl)metallocene complex **10**. **10** would be a potential intermediate for intramolecular CC coupling to yield the enediolato complex **11** (see Scheme 1).

[*] Prof. Dr. G. Erker [+], Dipl.-Chem. P. Czisch, Dipl.-Chem. R. Schlund, Dipl.-Chem. K. Angermund, Prof. Dr. C. Krüger
Max-Planck-Institut für Kohlenforschung
Kaiser-Wilhelm-Platz 1, D-4330 Mülheim a. d. Ruhr (FRG)

[+] Present address:
Institut für Organische Chemie der Universität
Am Hubland, D-8700 Würzburg (FRG)

[**] This work was supported by the Deutsche Forschungsgemeinschaft and the Fonds der Chemischen Industrie. We thank Dr. *R. Benn* and his colleagues, Max-Planck-Institut in Mülheim, for the NMR analyses.



Scheme 1.

Indeed, the hafnacyclobutane **7** rapidly takes up 1.5 equivalents of carbon monoxide under ambient conditions. The compound **12**, a 1 : 1 adduct of the two hypothetical intermediates **9** and **11**, was isolated as the sole product in good yield.[6] The NMR spectra show two Cp absorptions, the complex splitting pattern of the substituted cyclobutane moiety, and—very characteristic—the signals of the enediolato moiety (e.g. ^{13}C-NMR ([D$_6$]benzene): $\delta = 135.0$, 144.7 (s, C5, C9); the apparent C_{2v} symmetry of the building block **11** is lowered to C_s by adduct formation. In the IR spectrum, the C=C stretching vibration band of the enediolate is observed at $\tilde{\nu} = 1690\ cm^{-1}$.

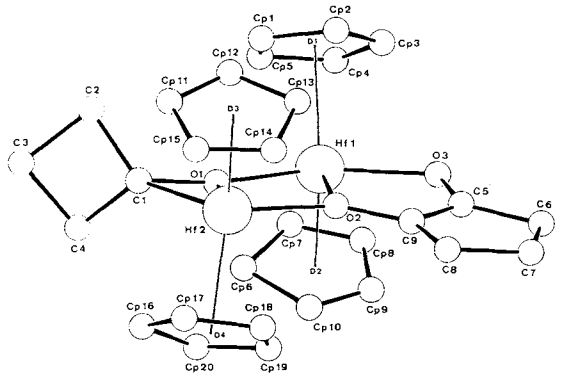


Fig. 1. Crystal structure of **12**. Selected bond lengths [Å] and angles [°]: Hf1-O1 2.138(6), Hf1-O2 2.234(5), Hf1-O3 2.097(7), Hf2-O1 2.103(6), Hf2-O2 2.163(5), Hf2-C1 2.266(8), O1-C1 1.46(1), O2-C9 1.40(1), O3-C5 1.35(1), C5-C9 1.33(1); O1-Hf1-O2 65.9(2), O2-Hf1-O3 74.2(2), O1-Hf2-O2 67.7(2), O1-Hf2-C1 38.8(3), Hf1-O1-Hf2 116.2(3), Hf1-O2-Hf2 110.0(2), Hf2-C1-O1 64.5(4).

An X-ray structure analysis of **12**[7] showed that the cyclobutane moiety is folded ($\theta = 35.8°$; C3 directed towards Hf2). As is usual for a (η^2-ketone)metallocene complex, the (η^2-cyclobutanone)hafnocene unit exhibits pronounced σ-complex character.[8] The adduct formation with the (enediolato)hafnocene substructure stabilizes in a very typical way the coordinatively unsaturated metallaoxirane moiety using both metal centers and two oxygen atoms. An almost planar Hf_2O_2 four-membered ring results, exhibiting almost equidistant Hf-O bond lengths (for further details of the structure see Fig. 1).

Adduct formation is neither unusual for the very reactive metallaoxiranes of the metallocenes of the titanium group[8] nor for metalladioxolene systems.[9] However, it is quite remarkable that we have only obtained the cross-over product **12**, and not the simple dimers of **9** and **11**. Presumably the reactive metallaoxirane traps the enediolate complex before substantial monomer concentrations of the two species are built up. As shown in Scheme 1 the monomers can, in principle, be formed via two routes. The assumption that **11** is a consecutive product of **9**, i.e., that it may be formed by a reaction path avoiding the frequently proposed bis(acyl)metallocene intermediate **10**, is an interesting mechanistic alternative.[9, 10]

Received: November 21, 1985 [Z 1545 IE]
German version: *Angew. Chem. 98* (1986) 356
Publication delayed at authors' request

CAS Registry numbers:
7, 98395-20-1; **12**, 101248-15-1; CO, 630-08-0.

[1] a) P. T. Wolczanski, J. E. Bercaw, *Acc. Chem. Res. 13* (1980) 121; P. T. Barger, B. D. Santarsiero, J. Armantrout, J. E. Bercaw, *J. Am. Chem. Soc. 106* (1984) 5178; b) G. Erker, *Acc. Chem. Res. 17* (1984) 103; c) K. G. Moloy, T. J. Marks, *J. Am. Chem. Soc. 106* (1984) 7051.

[2] J. M. Manriquez, D. R. McAlister, R. D. Sanner, J. E. Bercaw, *J. Am. Chem. Soc. 100* (1978) 2716; G. Erker, F. Rosenfeldt, unpublished; F. Rosenfeldt, *Dissertation*, Universität Bochum 1981; see also: P. Hofmann, M. Frede, P. Stauffert, W. Lasser, U. Thewalt, *Angew. Chem. 97* (1985) 693; *Angew. Chem. Int. Ed. Engl. 24* (1985) 712.

[3] G. Erker, P. Czisch, C. Krüger, J. M. Wallis, *Organometallics 4* (1985) 2059.

[4] U. Dorf, K. Engel, G. Erker, *Angew. Chem. 94* (1982) 916; *Angew. Chem. Int. Ed. Engl. 21* (1982) 913; *Angew. Chem. Suppl. 1982*, 1984.

[5] Whether the η^1- or η^2-acyl form is preferred for these compounds with enforced lateral placement of the acyl oxygen is irrelevant to this discussion; regarding this problem see: K. Tatsumi, A. Nakamura, P. Hofmann, P. Stauffert, R. Hoffmann, *J. Am. Chem. Soc. 107* (1985) 4440.

[6] Procedure. **12**: when CO (10 mL/min, 30 min) was passed through a solution of the hafnocyclobutane **7** (212 mg, 0.6 mmol) in toluene (20 mL) at room temperature, **12** was formed as a colorless precipitate; this was filtered off, washed with 2 mL of toluene and 2 × 5 mL of pentane, and dried in vacuo. Crystallization from refluxing benzene. M.p. 220°C; correct elemental analysis; MS (70 eV): $m/z = 788$ (M^+); IR (KBr): $\tilde{\nu} = 3100$, 1440, 1020, 800 (Cp), 1690 (enediolate-C=C) cm^{-1}; ^{1}H-NMR (C_6D_6, for numbering scheme see Figure 1): $\delta = 5.64$, 5.95 (s, each 10H, Cp), 2.58, 2.90 (m, each 2H, H2, H2'; $^2J_{HH} = 10.6$ Hz, $^3J(H2,H3) = 9.1$ Hz, $^3J(H2,H3') = 10.8$ Hz), 1.75, 1.50 (m, each 1H, H3, H3'; $^2J_{HH} = -9.9$ Hz, $^3J(H2',H3') = 1.4$ Hz, $^3J(H2',H3) = 7.3$ Hz), 2.38 (m, 4H, H6, H8; $^3J_{HH} = 7$ Hz), 2.06 (m, 2H, H7); ^{13}C-NMR (C_6D_6, $^1J_{CH}$ [Hz] in parenthesis): $\delta = 108.6$, 111.6 (d, 172, Cp), 40.2 (t, 127, 140, C2), 14.1 (t, 136, C3), 27.8, 27.5 (t, 131, 130, C6, C8), 21.6 (t, 128, C7), 92.7 (s, C1), 135.0, 144.7 (s, C5, C9).

[7] Cell data: $a = 9.907(1)$, $b = 15.294(1)$, $c = 16.127(4)$ Å, $\beta = 91.03(1)°$, $V = 2443.1$ Å^3, $\rho_{calc} = 2.14$ g cm^{-3}, $\mu = 84.47$ cm^{-1}, $Z = 4$, space group: $P2_1/n$. Total number of reflections: 5523; observed reflections 4425. Refined parameters: 307, $R = 0.043$, $R_w = 0.053$. Further details of the crystal structure investigation are available on request from the Fachinformationszentrum Energie, Physik, Mathematik GmbH, D-7514 Eggenstein-Leopoldshafen 2, on quoting the depository number CSD-51829, the names of the authors, and the full citation of the journal.

[8] G. Fachinetti, C. Biran, C. Floriani, A. Chiesi-Villa, C. Guastini, *Inorg. Chem. 17* (1978) 2995; D. D. Straus, R. H. Grubbs, *J. Am. Chem. Soc. 104* (1982) 5499; G. S. Bristow, P. B. Hitchcock, M. F. Lappert, *J. Chem. Soc. Chem. Commun. 1982*, 462; K. Kropp, V. Skibbe, G. Erker, C. Krüger, *J. Am. Chem. Soc. 105* (1983) 3353; G. Erker, U. Dorf, P. Czisch, J. L. Petersen, *Organometallics*, in press.

[9] S. Gambarotta, C. Floriani, A. Chiesi-Villa, C. Guastini, *J. Am. Chem. Soc. 105* (1983) 1690; see also: H. Takaya, M. Yamakawa, K. Mashima, *J. Chem. Soc. Chem. Commun. 1983*, 1283.

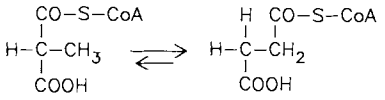
[10] C. D. Wood, R. R. Schrock, *J. Am. Chem. Soc. 101* (1979) 5422; G. Erker, K. Kropp, C. Krüger, A.-P. Chiang, *Chem. Ber. 115* (1982) 2447.

Methylmalonylcarba(dethia)-Coenzyme A as Substrate of the Coenzyme B_{12}-Dependent Methylmalonyl-CoA Mutase: Enzymatic Rearrangement of a β- to a γ-Keto Acid**

By *Martina Michenfelder* and *János Rétey**

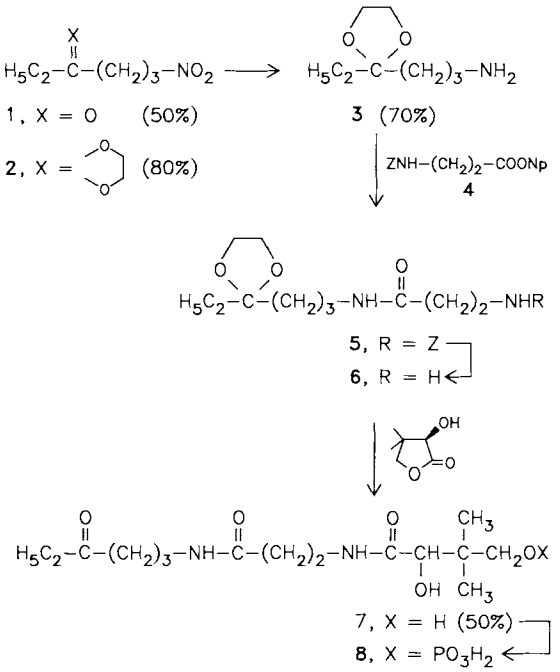
Dedicated to Professor Hans Musso on the occasion of his 60th birthday

Methylmalonyl-CoA mutase[1] is the only well-characterized coenzyme-B_{12} (AdoCbl)-dependent enzyme occurring in animal and human tissues. It catalyzes the reversible rearrangement of methylmalonyl-CoA to succinyl-CoA [Equation (a)], an important step in the metabolism of propionic acid. In spite of the revelation of interesting details,[1] the mechanism of this unusual enzyme reaction is



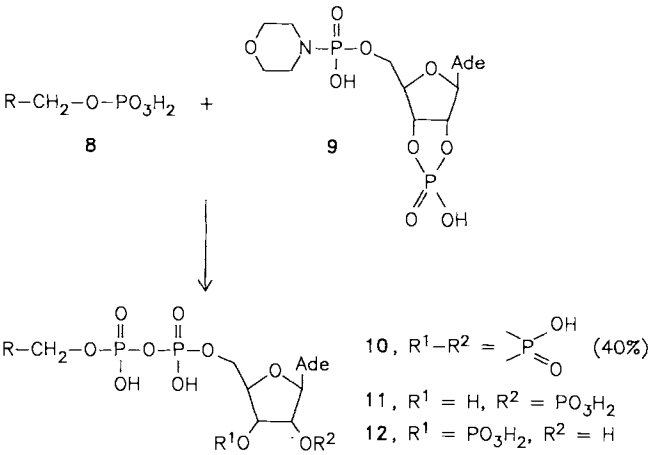
(a)

still unclear. The behavior of enzymes towards substrate analogues can often make a valuable contribution to an understanding of their mode of action. We therefore synthesized by a combination of chemical and enzymatic methods methylmalonylcarba(dethia)-CoA **13**, an analogue in which sulfur is replaced by methylene (Schemes 1 and 2).[2]



Scheme 1. Z = benzyloxycarbonyl, Np = *p*-nitrophenyl.

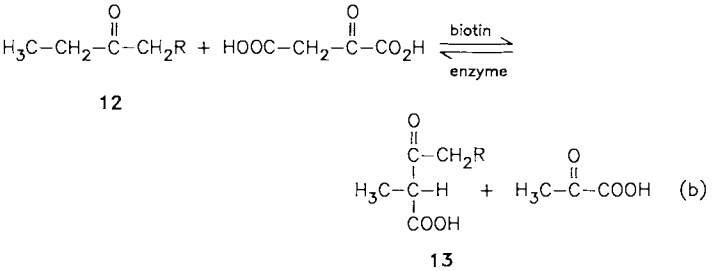
Addition of nitromethane to ethyl vinyl ketone in the presence of sodium methoxide furnished 6-nitro-3-hexanone **1**. The nitro group in the acetal **2** was reduced with Raney nickel to give **3**, which was condensed with protected β-alanine **4** according to the method described by *Stewart* and *Wieland*[2] to give the peptide **5**. The amine **6**, obtained by hydrogenolytic removal of the benzyloxycarbonyl protecting group, was condensed with (−)-(*R*)-pantolactone in the melt to give propionylcarba(dethia)pantetheine **7**.[3] The phosphorylation of **7** was accomplished with (cyanoethyl)phosphate in the presence of dicyclohexylcarbodiimide, and the cyanoethyl group was subsequently removed by alkaline hydrolysis. The barium salt of propionylcarba(dethia)phosphopantetheine **8** was characterized by ^{1}H- and ^{31}P-NMR spectra.[4]



Scheme 2. R see **8** in Scheme 1. Ade = adenine residue.

The final steps for the synthesis of the desired coenzyme A analogue **13** are outlined in Scheme 2. **8** was condensed with the known[2,5] adenosine derivative **9** to give the carba(dethia)-CoA derivative **10**, in which only the 2′,3′-phosphate ester ring had to be opened in order to obtain an almost 1:1 mixture of the 2′- and 3′-phosphates **11** and **12**. The 3′-phosphate is the target compound, namely propionylcarba(dethia)-coenzyme A **12**, while the ^{1}H-NMR spectroscopically distinguishable 2′-phosphate is the undesired propionylcarba(dethia)-isocoenzyme A **11**. The compounds **11** and **12** were almost completely separated by chromatography on DE-32 cellulose with a LiCl gradient and characterized.[6]

Whereas **11** is inert towards methylmalonyl-CoA pyruvate carboxylase (transcarboxylase), **12** reacts smoothly according to Equation (b). (The enzymatic carboxylation of **12** was not surprising since the analogous carboxylation of acetonylcarba(dethia)-CoA has already been reported.[7])



(b)

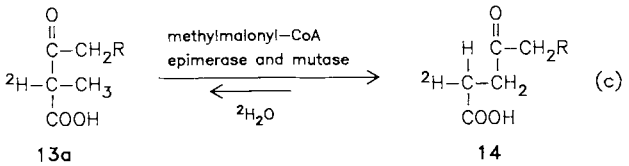
Removal of pyruvate from the equilibrium by reaction with lactate dehydrogenase led to complete conversion into (2*R*)-methylmalonylcarba(dethia)-CoA **13**, which was isolated and characterized by ^{1}H-NMR spectroscopy.[8]

[*] Prof. Dr. J. Rétey, Dipl.-Chem. M. Michenfelder
Lehrstuhl für Biochemie im Institut für Organische Chemie der Universität
Richard-Willstätter-Allee, D-7500 Karlsruhe 1 (FRG)

[**] This work was supported by the Deutsche Forschungsgemeinschaft and the Fonds der Chemischen Industrie.

The pH-dependent epimerization of **13** can be observed directly in the NMR spectrometer, since it proceeds concomitantly with the replacement of the α-H atom by deuterium. The halftime of the epimerization at p^2H 7.1 is 140 min, and is thus shorter than that for a methylmalonic acid thiolester.[9] The epimerization of **13** to **13a** is accelerated by methylmalonyl-CoA epimerase.

13a is an excellent substrate for the coenzyme B_{12}-dependent methylmalonyl-CoA mutase. The enzymatic rearrangement [Eq. (c)] could be observed directly in the NMR



13a 14

spectrometer. Most striking was the disappearance of the methyl doublet at $\delta=1.21$.[10] In a preparative experiment, the enzymatic rearrangement was carried out in unlabeled solvent and the succinylcarba(dethia)-CoA **14** was isolated. With **14** and succinyl-CoA as substrates for methylmalonyl-CoA mutase the Michaelis constants were found to be $K_M=13.6\times10^{-5}$ M and $K_M=2.5\times10^{-5}$ M, respectively. The constant for **14** is somewhat higher (i.e. the affinity for the analogue is somewhat weaker), while the maximum reaction velocity (V_{max}) is practically the same.

The enzymatic rearrangement of a β-keto acid (**13**) to a γ-keto acid (**14**) is described here for the first time: the decomposition of model cobalt complexes with migration of an acyl group has already been observed.[11]

Received: November 26, 1985;
supplemented: January 30, 1986 [Z 1553 IE]
German version: *Angew. Chem. 98* (1986) 337

CAS Registry numbers:
1, 101009-82-9; **2**, 101009-83-0; **3**, 101009-84-1; **4**, 3642-91-9; **5**, 101009-85-2; **6**, 101009-86-3; **7**, 101009-87-4; **8**, 101009-88-5; **9**, 38976-06-6; **10**, 101009-89-6; **11**, 101030-86-8; **12**, 101009-90-9; **13**, 101009-91-0; **13a**, 101141-39-3; **14**, 101009-92-1; nitromethane, 75-52-5; ethyl vinyl ketone, 1629-58-9; sodium methoxide, 124-41-4; methylmalonyl-CoA-pyruvatecarboxylase, 9029-86-1; oxalacetic acid, 328-42-7; methylmalonyl-CoA-epimerase, 9024-03-7; methylmalonyl-CoA-mutase, 9023-90-9; succinyl-CoA, 604-98-8; (R)-pantolactone, 599-04-2.

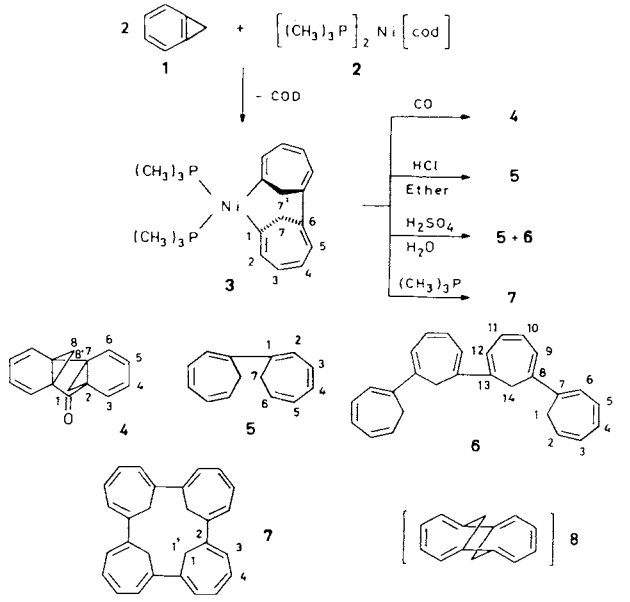
[1] Recent review: J. Rétey in D. Dolphin (ed.): *B_{12} Vol. 2*, Wiley, New York 1982, p. 357.
[2] Synthesis of acetonylcarba(dethia)-CoA: C. J. Stewart, T. Wieland, *Liebigs Ann. Chem. 1978*, 57.
[3] **7**, 250-MHz ^{1}H-NMR (^2H_2O): δ=0.78 (s, 3H), 0.81 (s, 3H), 0.90 (t, J=7.9 Hz, 3H), 1.63 (quint., J=7.7 Hz, 2H), 2.4 (m, 6H), 3.05 (t, J=7.7 Hz, 2H), AB 3.36 (J=12 Hz, 2H), 3.41 (m, 2H), 3.86 (s, 1H).
[4] **8**, 2500-MHz ^{1}H-NMR (^2H_2O): δ=0.83 (s, 3H), 0.98 (s, 3H), 1.00 (t, J=9 Hz, 3H), 1.73 (quint., J=6.5 Hz, 2H), 2.5 (m, 6H), 3.16 (t, J=6.5 Hz, 2H), 3.52 (t, J=5.5 Hz, 2H), 3.74 (m, 2H), 4.10 (s, 1H). 121.49-MHz ^{31}P-NMR (^2H_2O, H_3PO_4 ext.): δ=6.2 (s).
[5] J. G. Moffatt, H. G. Khorana, *J. Am. Chem. Soc. 83* (1961) 649, 663.
[6] **12**, 250-MHz ^{1}H-NMR (^2H_2O): δ=0.60 (s, 3H), 0.70 (s, 3H), 0.83 (t, J=6.8 Hz, 3H), 1.51 (quint., J=6.6 Hz, 2H), 2.32 (m, 6H), 2.91 (t, J=6.6 Hz, 2H), 3.30 (t, J=7.0 Hz, 2H), ABX 3.6 (J=12 Hz, J_{HP}=5 Hz, 2H), 3.9 (s, 1H), 4.1 (m, 2H), 6.09 (d, J=8.3 Hz, 1H), 8.18 (s, 1H), 8.43 (s, 1H). 121.49-MHz ^{31}P-NMR (^2H_2O, H_3PO_4 ext.): δ=−7.89 (m), 2.7 (s). — **11**, 250-MHz ^{1}H-NMR (^2H_2O): δ=6.23 (d, J=5.8 Hz, 1H), otherwise as with **12**. 121.49-MHz ^{31}P-NMR (^2H_2O): δ=−7.89 (m), +6.61 (s).
[7] J. Nikawa, S. Numa, T. Shiba, C. J. Stewart, T. Wieland, *FEBS-Lett. 91* (1978) 144.
[8] **13**, 250-MHz ^{1}H-NMR (^2H_2O): δ=0.73 (s, 3H), 0.88 (s, 3H), 1.21 (d, J=7.5 Hz, 3H), 1.71 (quint., J=6.6 Hz, 2H), 2.45 (t, J=7.4 Hz, 2H), 2.65 (m, 2H), 3.13 (t, J=6.6 Hz, 2H), 3.45 (t, J=7.4 Hz, 2H), 3.55 (m, 1H), unresolved ABX 3.66 (2H), 4.00 (s, 1H), 4.25 (m, 2H), 6.20 (d, J=6.2 Hz, 1H), 8.28 (s, 1H), 8.58 (s, 1H).
[9] P. Overath, G. M. Kellerman, F. Lynen, H. P. Fritz, H. J. Keller, *Biochem. Z. 335* (1962) 500.
[10] **14**, 250-MHz ^{1}H-NMR (^2H_2O): δ=0.55 (s, 3H), 0.72 (s, 3H), 1.50 (quint., J=5.8 Hz, 2H), 2.25 (m, 3H), 2.40 (t, J=5.8 Hz, 2H), 2.53 (d, J=6.2 Hz, 2H), 2.95 (t, J=5.8 Hz, 2H), 3.30 (t, J=6.8 Hz, 2H), ABX 3.53 (J=12 Hz, J_{HP}=6 Hz, 2H), 3.86 (s, 1H), 4.10 (m, 2H), 6.06 (d, J=7.5 Hz, 1H), 8.15 (s, 1H), 8.43 (s, 1H).
[11] M. Okabe, T. Osawa, M. Tada, *Tetrahedron. Lett. 22* (1981) 1899.

Nickel-Induced Cyclotetramerization of Cyclopropabenzene to 1,6 : 7,12 : 13,18 : 19,24-Tetrakismethano[24]annulene**

By *Richard Mynott, Richard Neidlein,* Harald Schwager,* and *Günther Wilke**

Dedicated to Professor Heinz A. Staab on the occasion of his 60th birthday

Ever since 1,6-methano[10]annulenes were first synthesized,[1] bridged annulenes have been the subject of intense theoretical and preparative interest. It seems surprising, however, that there has so far been no reported attempt at the synthesis of such compounds via organometallic intermediates. In catalytic cyclooligomerizations on "naked" nickel, numerous metallacycles—as catalytic intermediates—could be trapped and isolated.[2,3] Thus, reaction of 3,3-dimethylcyclopropene with 2,2′-bipyridyl-1,5-cyclooctadienenickel(0) affords a metallacyclopentane with two annelated three-membered rings.[4] We report here, an unusual two-step synthesis of tetrakismethano[24]annulene **7** by cyclotetramerization of cyclopropabenzene **1** via a metallacycle intermediate (Scheme 1).



Scheme 1. The (unsymmetrical) numbering merely serves for assignment of the spectra. cod = 1,5-cyclooctadiene.

[*] Prof. Dr. G. Wilke, Dipl.-Chem. H. Schwager, Dr. R. Mynott
Max-Planck-Institut für Kohlenforschung
Kaiser-Wilhelm-Platz 1, D-4330 Mülheim-Ruhr (FRG)
Prof. Dr. R. Neidlein
Pharmazeutisch-chemisches Institut der Universität
Im Neuenheimer Feld 364, D-6900 Heidelberg (FRG)

[**] This work was supported by the Deutsche Forschungsgemeinschaft and the Fonds der Chemischen Industrie.

1[5] reacts smoothly with 1,5-cyclooctadienenickel(0) **2** in pentane at $-20°C$ to give the bismethanonickelacyclotridecahexaene **3**.[6] Two cyclopropabenzene molecules are added oxidatively to **2** with displacement of the olefin ligand and C–C coupling. The liberated olefin can be removed in a high vacuum or by recrystallization. Compound **3** is stable at room temperature under argon.[7] The structure was essentially derived from a 2D-INADEQUATE ^{13}C-NMR spectrum: the chemical shift of C-7 ($\delta = 52.8$), the values of the coupling constants $^1J_{C\text{-}7,H\text{-}7} = 130$ and 140 Hz, and the geminal coupling $^2J_{H\text{-}7,H\text{-}7'} = 8.3$ Hz, indicated a bis(cycloheptatriene) system. This was confirmed by an X-ray structure analysis,[8] which, in addition, revealed a *trans* orientation of the methano bridges.

The Ni–C σ-bonds in **3** are amenable to insertion reactions with subsequent reductive elimination. Reaction of **3** with CO leads not only to formation of dicarbonylbis(trimethylphosphane)nickel(0) but also of the cyclopentanone derivative **4**,[7, 9] whose structure was determined by NMR, IR/Raman, and mass spectroscopy, and by an X-ray structure analysis.[8] The ^{13}C-NMR shift of C-8 ($\delta = 21.8$) and the values of the coupling constants $^1J_{C\text{-}8,H\text{-}8} = 168$ Hz and $^2J_{H\text{-}8,H\text{-}8'} = 3.9$ Hz, indicate that **4** is present as a norcaradiene isomer, and not—as expected—as a carbonylated bis(cycloheptatriene) derivative. The *trans* orientation of the methano bridges, which cannot be derived from the NMR spectra, was demonstrated by an X-ray structure analysis. Reaction of **3** with ethereal HCl, affords 1,1'-bi(1,3,5-cycloheptatriene) **5** in almost quantitative yield.[7, 10, 11] In contrast, when hydrolysis is carried out with H_2SO_4/H_2O, high yields of a 1:1 mixture of **5** and **6** are obtained.[7, 12] The methyl protons in **5** and **6** are, as expected, equivalent.

Upon reaction with trimethylphosphane, **3** undergoes reductive elimination to give tetrakismethano[24]annulene **7**;[13] the expected formation of 1,6:7,12-bismethano[12]annulene **8** was not observed. It follows from the NMR spectra of **7** that all four rings are in the cycloheptatriene form ($^2J_{H\text{-}1,H\text{-}1'} = 11.8$ Hz). This geminal coupling shows that, as in the case of **3** and **4**, the methano bridges do not invert. The UV spectrum of **7** points to an extended conjugated system.

With the synthesis of **7**, it has been shown for the first time that a methano-bridged annulene can be prepared by a two-step transition-metal-induced reaction. Formally, the reaction is a cyclotetramerization of cyclopropabenzene.

Received: December 9, 1985 [Z 1572 IE]
German version: *Angew. Chem. 98* (1986) 374

CAS Registry numbers:
1, 4646-69-9; **2**, 101077-61-6; **3**, 101144-73-4; **4**, 101055-11-2; **5**, 35393-05-6; **6**, 101077-59-2; **7**, 101077-60-5.

[1] E. Vogel, H. D. Roth, *Angew. Chem. 76* (1964) 145; *Angew. Chem. Int. Ed. Engl. 3* (1964) 228.
[2] G. Wilke, M. Kröner, B. Bogdanović, *Angew. Chem. 73* (1961) 755.
[3] G. Wilke, *Pure Appl. Chem. 50* (1978) 677.
[4] P. Binger, M. J. Doyle, J. McMeeking, C. Krüger, Y.-H. Tsay, *J. Organomet. Chem. 135* (1977) 405.
[5] W. E. Billups, A. J. Blakeney, W. Y. Chow, *Org. Synth. 55* (1976) 12.
[6] **3**: A solution of **2** (720 mg, 2.26 mmol) in pentane (40 mL), prepared under argon, was treated at $-20°C$ with 0.48 mL (5.52 mmol) of **1** with vigorous stirring. After 3 h at $-20°C$, the solution was cooled to $-78°C$ for 2 d to complete the crystallization and then filtered by suction through a cold frit. The crystals were dried under high vacuum, and recrystallized from Et_2O. Yield: 769 mg (1.97 mmol, 87%), orange-red crystals, m.p. 142°C (decomp.).—^1H-NMR (200 MHz, [D$_8$]tetrahydrofuran, TMS): $\delta = 6.22$ (m, H-2, $^4J(2,P) = 4.5$ Hz); 6.34 (dd, H-3); 6.13 (dd, H-4); 6.00 (d, H-5); 0.91 (dd, H-7, $^4J(7,P) = 3.6$ Hz, $^4J(7,P') = 1.0$ Hz); 2.89 (br. d, H-7', $^2J(7,7') = 8.3$ Hz); 1.37 (d, H-8, $^2J(8,P) = 7.3$ Hz).—^{13}C-NMR (75.5 MHz, [D$_8$]THF, TMS, $-30°C$): $\delta = 174.1$ (s, C-1, $^2J(P,C) + {}^2J(P,C') = 41.8$ Hz); 125.9 (d, C-2, $^3J(P,C) + {}^3J(P',C) = 13.5$ Hz); 128.4 (d, C-3); 122.3 (d, C-4); 117.1 (d, C-5); 129.6 (d, C-6); 52.8 (t, C-7); 16.4 (q, C-8, $^2J(P,C) + {}^2J(P',C) = 28.3$ Hz).—^{31}P-NMR (32 MHz, [D$_8$]THF): $\delta = -17.6$ (s).—MS: *m/z* 390 (M^+) (for ^{58}Ni).—IR (KBr): $\tilde{\nu} = 1536$, 1579, 1609 (m) (C=C) cm^{-1}.
[7] The results of an elemental analysis were in accord with the given empirical formula.
[8] C. Krüger, unpublished results.
[9] **4**: A solution of **3** (350 mg, 0.89 mmol) in THF (20 mL) was treated at $-78°C$ under argon with 59.8 mL (2.67 mmol) of CO. After several hours' stirring at RT the THF was removed and the residue taken up in pentane. After filtration through a frit, the filtrate was evaporated to dryness and the resulting residue sublimed in a high vacuum (70–90°C) and recrystallized from Et_2O. Yield: 130 mg (0.62 mmol, 70%), colorless crystals, m.p. 91°C.—^1H-NMR (200 MHz, [D$_8$]THF, TMS): $\delta = 6.48$, 6.34 (m, H-3,6, $^3J(3,4) = 9.4$ Hz, $^3J(5,6) = 9.4$ Hz, $^4J(3,5) = 0.7$ Hz, $^4J(4,6) = 0.7$ Hz); 6.00, 5.83 (m, H-4,5, $^3J(4,5) = 5.9$ Hz); 1.62 (d, H-8', $^2J(8,8') = 3.9$ Hz); 0.20 (d, H-8).—^{13}C-NMR (75.5 MHz, $CDCl_3$, TMS): $\delta = 206.5$ (s, C-1); 42.9, 40.0 (s, C-2,7); 124.4, 122.5, 122.1, 120.3 (d, C-3,5,6,4); 21.8 (t, C-8).—MS: *m/z* 208 (M^+).—IR (KBr): $\tilde{\nu} = 1719$ (s) (CO) cm^{-1}, 1545, 1627 (m) (C=C).—UV (*n*-hexane): $\lambda_{max} = 195$ nm ($\varepsilon = 13000$), 230 sh (5100), 270 (4600).
[10] **5**: A solution of **3** (660 mg, 1.68 mmol) in THF (20 mL) was treated under argon with 5 mL (1.7 M, 8.5 mmol) of etheral HCl. After 30 min, and addition of pentane (50 mL), the mixture was extracted with 30 mL of H_2O and the organic phase dried over $MgSO_4$. Subsequent filtration over silica gel and evaporation of the filtrate to dryness furnished 292 mg (1.60 mmol, 95%) of a pale-yellow oil, b.p. 30°C/10^{-3} torr.—^1H-NMR (200 MHz, $CDCl_3$, TMS): $\delta = 6.5$ (m, 3H, H-2,3,4); 6.20 (m, H-5); 5.42 (m, H-6); 2.60 (d, H-7, $^3J(6,7) = 7.2$ Hz).—^{13}C-NMR (75.5 MHz, $CDCl_3$, TMS): $\delta = 133.3$ (s, C-1); 130.7, 130.3, 127.2, 123.4, 122.5 (d, C-2,3,4,5,6); 30.8 (t, C-7).—MS: *m/z* 182 (M^+).—IR (KBr): $\tilde{\nu} = 1521$, 1581 (m) (C=C) cm^{-1}.—UV (*n*-hexane): $\lambda_{max} = 221$ nm ($\varepsilon = 18000$), 265 (3500), 340 (11000).
[11] R. S. Girens, *Tetrahedron Lett. 1969*, 663.
[12] **5** and **6**: A solution of **3** (600 mg, 1.53 mmol) in THF (20 mL) was treated under argon with 1% H_2SO_4 (10 mL) and, after 30 min, with pentane (50 mL). The organic phase was washed three times with H_2O (30 mL) and dried over $MgSO_4$. Flash chromatography on silica gel (15 cm × 3 cm Ø; eluent: pentane) yielded, besides 111 mg (0.61 mmol, 40%) of **5**, in the second fraction 153 mg (0.42 mmol, 55%) of red crystals of m.p. 114°C. **6**: ^1H-NMR (200 MHz, $CDCl_3$, TMS): $\delta = 2.51$ (d, 2H, H-1); 5.35 (br. q, 1H, H-2); 6.17 (m, 1H, H-3); 6.60 (m, 6H, H-4,5,9,10,11,12); 6.37 (br. d, 1H, H-6); 2.75 (s, 2H, H-14).—^{13}C-NMR (75.5 MHz, $CDCl_3$, TMS): $\delta = 30.6$ (t, C-1); 122.3, 123.0, 124.2, 124.5, 127.0 (d, C-2,3,6,9,12); 130.3 (d, C-4); 130.4 (2C), 130.8 (d, C-5,10,11); 132.5, 132.8, 132.9 (s, C-7,8,13); 33.2 (t, C-14).—MS: *m/z* 362 (M^+).—IR (KBr): $\tilde{\nu} = 1487$, 1518, 1577 (m) (C=C) cm^{-1}.—UV (*n*-hexane): $\lambda_{max} = 241$ nm ($\varepsilon = 37000$), 299 (20800), 340 (13500), 394 (10400).
[13] **7**: A solution of **3** (2.0 g, 5.11 mmol) in THF (300 mL) was treated at $-78°C$ under argon with 1 mL (10.22 mmol) of trimethylphosphane. The mixture was allowed to warm to RT over 4 d. After removal of the THF the residue was taken up in pentane and the resulting solution filtered through a frit; the filtrate and pentane washings were evaporated to dryness and subjected to work-up by HPLC. Crude yield: 75 mg (0.42 mmol, 8.2%). After HPLC separation: 41 mg (0.11 mmol, 4.5%) red crystals, m.p. 277°C.—^1H-NMR (400 MHz, CD_2Cl_2, TMS): $\delta = 0.65$ (d, H-1, $^2J(1,1') = 11.8$ Hz); 3.18 (d, H-1'); 6.33 (m, H-3, $^3J(3,4) = 6.8$ Hz); 6.68 (m, H-4).—^{13}C-NMR (75.5 MHz, CD_2Cl_2, TMS): $\delta = 31.0$ (t, C-1); 126.5 (s, C-2); 124.6 (d, C-3); 128.5 (d, C-4).—MS: *m/z* 360 (M^+).—IR (KBr): $\tilde{\nu} = 1570$ (m) (C=C) cm^{-1}.—UV (*n*-hexane): $\lambda_{max} = 263$ nm ($\varepsilon = 91100$), 338 (22600), 415 (3800).

Carbohydrate-Based Liquid Crystals: Mesogenic 1-*O*-Alkyl Derivatives of 2,5-Anhydrohexitols**

By *Peter Köll** and *Michael Oelting*

Although *Emil Fischer* had already reported on the perculiar melting behavior of some amphiphilic *O*-alkylglycosides at the turn of the century, and the first systematic investigations on the liquid-crystalline properties of these

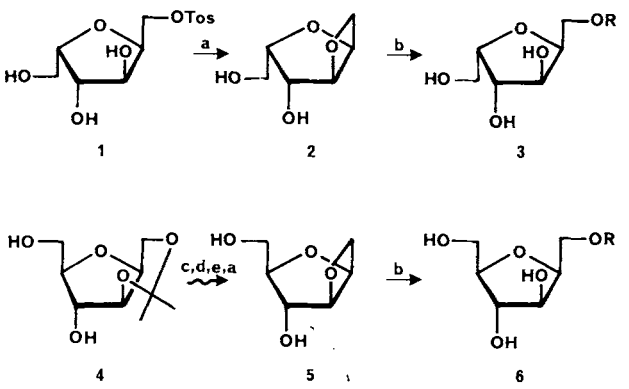
[*] Prof. Dr. P. Köll, Dipl.-Chem. M. Oelting
Fachbereich Chemie der Universität
Carl-von-Ossietzky-Str. 9–11, D-2900 Oldenburg (FRG)

[**] Carbohydrate-Based Liquid Crystals, Part 1.

compounds were carried out in the 1930s,[1] the field of thermotropic mesogenic carbohydrates can be considered as having been neglected.

Consequently, *Jeffrey*, in his recent review of the few sugar-based liquid crystals reported so far, restricted himself to *O*- and *S*-*n*-alkylglycosides.[2] There are, however, further isolated reports in the literature on mono-*O*-acyl derivatives of saccharides possibly exhibiting liquid crystalline properties.[3]

Recently, *Dahlhoff* introduced a new type of non-glycosidic stable carbohydrate mesogenes, namely 1-*O*-alkyl derivatives of sugar alcohols.[4] This prompted us to report our findings that are relevant in this connection.



Scheme 1. a) NaOMe in MeOH, 24 h, RT; b) ROH in $CHCl_3$, 48 h at 50°C in presence of trifluoromethanesulfonic acid as catalyst; c) Ac_2O in pyridine, 18 h, RT; d) 80% HOAc, 18 h, RT; e) TosCl in pyridine, 18 h, RT.

Table 1. Melting points (M.p.) and clearing points (Cl.p.) of **3** and **6**.

	R	3		6	
		M.p. [°C]	Cl.p. [°C]	M.p. [°C]	Cl.p. [°C]
a	n-C_6H_{13}	—	—	—	—
b	n-C_7H_{15}	<RT	42	<RT	32
c	n-C_8H_{17}	59	67	<RT	78
d	n-C_9H_{19}	61	82	<RT	81
e	n-$C_{10}H_{21}$	70	89	46	87
f	n-$C_{12}H_{25}$	74	115	58	102
g	n-$C_{14}H_{29}$	80	126	67	103
h	n-$C_{16}H_{33}$	87	210	74	104
i	n-$C_{18}H_{37}$	92	>210	80	101

The 1,3:2,5-dianhydrohexitols **2** and **5**, which can be synthesized from the known educts **1**[5] and **4**,[6] respectively (Scheme 1), undergo smooth reaction with alcohols to give the mono-1-*O*-alkyl ethers **3a–i** and **6a–i**, respectively.[7] Whereas the compounds of type **3** exhibit L-*ido* configuration, the derivatives **6** belong to the D-*gluco* series of the 2,5-anhydrohexitols.

When the chain length of the *n*-alkyl moiety in the 1-*O*-alkyl-2,5-anhydrohexitols **3** and **6** exceeds C_7, the latter show an anisotropic phase above the melting point that is transformed into the isotropic liquid at a distinctly higher clearing point (Table 1). The compounds **3b** and **6b–d** are already liquid-crystalline even at room temperature. We assume, on the basis of the birefringence observed under the polarizing microscope that smectic phases are formed in all cases.[8] Also in the other previously described liquid-crystalline carbohydrates, if one disregards the special case of some discotic hexa- and penta-*O*-acyl derivatives of inositols and hexoses,[9] smectic phases are presumed.[10] Aside from the phase transitions given in Table 1, further solid/solid transformations take place below the melting point in some cases.

Comparison of the two series of compounds **3** and **6**, with L-*ido* and D-*gluco* configuration, respectively, reveals in almost all cases that the *ido* derivatives **3** show higher melting and clearing points than the analogous gluco compounds **6**. This difference, which is said to be essentially due to deviating possibilities for the formation of hydrogen bridges, is already found in the parent compounds (R = H).

CC-coupled amphiphiles ("C-glycosides" of pentofuranoses) can also be synthesized from the oxetanes **2** and **5**.[11] Such compounds with alkyl chains beyond C_5 (i.e. C_6 with inclusion of the primary CH_2 group of the 2,5-anhydrohexitol) also form liquid-crystalline phases. The melting points of comparable derivatives, however, are in each case higher than in the case of the ethers **3** and **6** described here.

Received: December 10, 1985;
revised: January 30, 1986 [Z 1573 IE]
German version: *Angew. Chem. 98* (1986) 362

CAS Registry numbers:
1, 32445-71-9; **3b**, 101079-21-4; **3c**, 101079-22-5; **3d**, 101079-23-6; **3e**, 101079-24-7; **3f**, 101079-25-8; **3g**, 101223-00-1; **3h**, 101079-26-9; **3i**, 101079-27-0; **4**, 65729-81-9; **6b**, 101221-93-6; **6c**, 101221-94-7; **6d**, 101221-95-8; **6e**, 101221-96-9; **6f**, 101221-97-0; **6g**, 101079-28-1; **6h**, 101221-98-1; **6i**, 101223-01-2.

[1] E. Fischer, B. Helferich, *Justus Liebigs Ann. Chem. 383* (1911) 68; C. R. Noller, W. C. Rockwell, *J. Am. Chem. Soc. 60* (1938) 2076.
[2] G. A. Jeffrey, *Mol. Cryst. Liq. Cryst. 110* (1984) 221.
[3] K. Hess, E. Heumann, *Fette Seifen Anstrichm. 61* (1959) 928; R. Hori, T. Koizumi, *Yakugaku Zasshi 78* (1958) 1003; P. E. Pfeffer, E. S. Rothmann, G. M. Moore, *J. Org. Chem. 41* (1976) 2925.
[4] W. V. Dahlhoff, *Abstr. III. Eur. Symp. on Carbohydrates*, Grenoble, September 16–20, 1985, p. 96.
[5] L. von Vargha, T. Puskas, *Ber. Dtsch. Chem. Ges. 76* (1943) 859; J. Defaye, V. Ratovelomanana, *Carbohydr. Res. 17* (1970) 57.
[6] K. Bock, C. Pedersen, H. Thøgersen, *Acta Chem. Scand. B 35* (1981) 441; T. A. W. Koerner, Jr., R. J. Voll, E. S. Younathan, *Carbohydr. Res. 24* (1977) 403.
[7] All compounds were purified by chromatography, and, as far as possible, by subsequent crystallization. Elemental analyses and ^{1}H-NMR spectra are consistent with the proposed structures.
[8] G. W. Gray, J. W. Goodby: *Smectic Liquid Crystals*, Leonard Hill, Glasgow 1984.
[9] B. Kohne, K. Praefcke, *Angew. Chem. 96* (1984) 70; *Angew. Chem. Int. Ed. Engl. 23* (1984) 82; *Chem.-Ztg. 109* (1985) 121; R. G. Zimmermann, G. B. Jameson, R. G. Weiss, G. Demailly, *Mol. Cryst. Liq. Cryst. Lett. 1* (1985) 183.
[10] G. A. Jeffrey, S. Bhattacharjee, *Carbohydr. Res. 115* (1983) 53.
[11] P. Köll, M. Oelting, *Tetrahedron Lett.*, in press.

(*Z*)-[6]Paracycloph-3-ene**

By *Yoshito Tobe,** *Ken-ichi Ueda, Kiyomi Kakiuchi,* and *Yoshinobu Odaira*

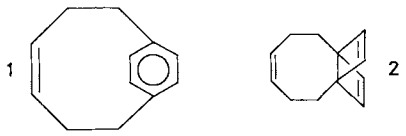
Of the [n]paracyclophanes that have been isolated, [6]Paracyclophane has the smallest-bridge; its remarkable properties are due to the severe deformation of the benzene ring.[1] Although we as well as *Bickelhaupt* et al. have recently been able to characterize the next lower homologue, [5]paracyclophane, spectroscopically as an unstable intermediate,[2] it has so far eluded isolation.

We now describe the synthesis of (*Z*)-[6]paracycloph-3-

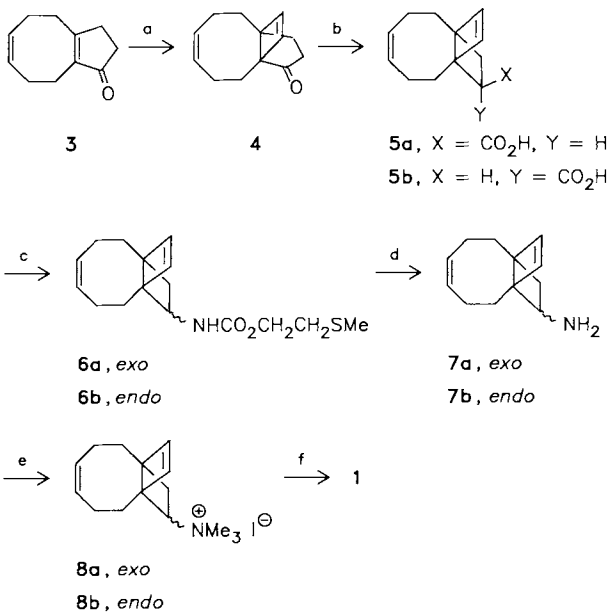
[*] Dr. Y. Tobe, K. Ueda, Dr. K. Kakiuchi, Prof. Dr. Y. Odaira
Department of Applied Fine Chemistry, Faculty of Engineering
Osaka University, Suita, Osaka 565 (Japan)

[**] We are grateful to Dr. *Y. Takai* of the Institute of Scientific and Industrial Research, Osaka University for measuring the ^{1}H-NMR spectrum and for valuable discussions.

ene **1**, which, because of the length of its bridge—the bridge consists of six carbon atoms and has one *cis* double bond at the center[3]—must be allotted a place between [6]- and [5]paracyclophane. **1** is thus the smallest isolable paracyclophane known so far.

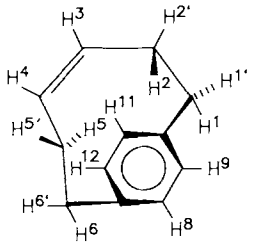


For the synthesis of **1**, we took advantage of the thermal valence isomerization of its Dewar-benzene isomer, [6.2.2]propellatriene **2**. The *exo*- and *endo*-propelladienecarboxylic acids **5a** and **5b**, respectively, were prepared from the bicyclic enone **3**[4] via the propelladienone **4** using our photocycloaddition and ring contraction strategy[1c] (yield: 26 and 17%, respectively). Reaction of **5a** with diphenylphosphoryl azide[5] and subsequent treatment with methylthioethanol afforded the methylthioethyl carbamate **6a** in 78% yield; alkaline hydrolysis[6] of the sulfonium salt of **6a** furnished the *exo*-amine **7a** (65%), which was converted into the ammonium salt **8a** (81%, m.p. 147–150°C). After conversion into the corresponding hydroxide and subsequent pyrolysis (120°C, 0.1 torr), **1** was obtained as a colorless solid (m.p. 29–33°C) in 44% yield. Although the Dewar-benzene isomer **2** was not detected at all, it is reasonable to assume that **1** was formed by thermal isomerization of **2** during pyrolysis. **5b** was transformed in an analogous way into the ammonium salt **8b** (m.p. 161–163°C), which on Hofmann degradation afforded **1** in lower yield (see Scheme 1).



Scheme 1. Synthesis of **1**: a) 1. ClHC=CHCl, *hv*; 2. $HOCH_2CH_2OH$, $H^{\oplus}$; 3. Na, NH_3; 4. $H^{\oplus}$. b) 1. HCO_2Et, EtONa; 2. $TosN_3$, Et_3N; 3. *hv*, MeOH; 4. KOH. c) $(PhO)_2PON_3$, $HOCH_2CH_2SMe$. d) 1. Me_2SO_4; 2. NaOH. e) MeI, $KHCO_3$. f) 1. Ag_2O, H_2O; 2. 120°C, 0.1 torr.

The spectroscopic properties of **1**,[7] especially its ^1H-NMR spectrum (360 MHz, $CDCl_3$, 25°C), are characteristic for the structure. The AA'XX' pattern of the signals of the aromatic protons appears at $\delta = 7.20$ and 7.07 ($^4J_{AX} = 1.0$, $^5J_{AX'} = 0.9$ Hz); decoupling and simulation experiments show that the vinyl protons exhibit an AA'BB'XX' pattern, formed by coupling to the allyl protons ($^3J_{AX} = 11.9$, $^4J_{AX'} = -0.8$, $^3J_{BX} \approx 5$, $^4J_{BX'} \approx -1$, $^3J_{XX'} = 12.2$ Hz); the signals of the two pairs of benzylic protons (H^1 and H^6, and $H^{1'}$ and $H^{6'}$) and of the two pairs of allylic protons (H^2 and H^5, and $H^{2'}$ and $H^{5'}$) appear at considerably different field strengths. Particularly noteworthy is the remarkably high-field shift (ca. 1 ppm) of the signals of the vinyl protons ($\delta = 4.68$) and one pair of the allylic protons (H^2 and H^5: $\delta = 1.01$) due to the shielding effect of the aromatic ring. Moreover, the sharp lineshapes and the temperature independence of ^1H- and ^{13}C-NMR spectra indicate conformational rigidity of the bridge in **1**.



1 exhibits a remarkable bathochromic shift in the UV spectrum (hexane, $\lambda_{max} = 310$ ($\varepsilon = 340$), 260 (3900), 227 (5400) nm) in comparison to [6]paracyclophane[8], suggesting a considerable increase in the out-of-plane deformation of the benzene ring in the former system relative to that in the latter. We are presently investigating the effect of the above strain on the reactivity of the aromatic ring and the double bond.

Received: December 17, 1985;
supplemented: January 23, 1986 [Z 1594 IE]
German version: *Angew. Chem. 98* (1986) 364

CAS Registry numbers:
1, 101055-48-5; **3**, 92007-28-8; **4**, 101055-43-0; **5a**, 101055-44-1; **5b**, 101143-53-7; **6a**, 101055-45-2; **6b**, 101221-88-9; **7a**, 101055-46-3; **7b**, 101143-54-8; **8a**, 101055-47-4; **8b**, 101143-55-9; ClCH=CHCl, 540-59-0; $MeS(CH_2)_2OH$, 5271-38-5.

[1] a) V. V. Cane, A. D. Wolf, M. Jones, Jr., *J. Am. Chem. Soc. 96* (1974) 2643; b) S. L. Kammula, L. D. Iroff, M. Jones, Jr., J. W. van Straten, W. H. de Wolf, F. Bickelhaupt, *ibid. 99* (1977) 5815; c) Y. Tobe, K. Kakiuchi, Y. Odaira, T. Hosaki, Y. Kai, N. Kasai, *ibid. 105* (1983) 1376; d) Y. Tobe, K. Ueda, K. Kakiuchi, Y. Odaira, *Chem. Lett. 1983*, 1645; e) J. Liebe, C. Wolff, W. Tochtermann, *Tetrahedron Lett. 23* (1982) 171, 2439; f) C. Krieger, J. Liebe, W. Tochtermann, *ibid. 24* (1983) 707; g) J. Liebe, W. Tochtermann, J. Weiss, *ibid. 24* (1983) 2549.

[2] L. W. Jenneskens, F. J. J. de Kanter, P. A. Kraakman, L. A. M. Turkenburg, W. E. Koolhaas, W. H. de Wolf, F. Bickelhaupt, Y. Tobe, K. Kakiuchi, Y. Odaira, *J. Am. Chem. Soc. 107* (1985) 3716; Y. Tobe, T. Kaneda, K. Kakiuchi, Y. Odaira, *Chem. Lett. 1985*, 1301.

[3] [8]Paracyclophane derivatives with a *cis* or *trans* double bond on the bridge are known: D. J. Cram, C. S. Montgomery, G. R. Knox, *J. Am. Chem. Soc. 88* (1966) 515; A. C. Cope, B. A. Pawson, *ibid. 90* (1968) 636; T. Tsuji, S. Nishida, *ibid. 95* (1973) 7519; K.-L. Noble, H. Hopf, L. Ernst, *Chem. Ber. 117* (1984) 474.

[4] G. Mehta, K. S. Rao, *Tetrahedron Lett. 25* (1984) 1839.

[5] K. Ninomiya, T. Shioiri, S. Yamada, *Chem. Pharm. Bull. 22* (1974) 1398.

[6] H. Kunz, *Chem. Ber. 109* (1976) 3639.

[7] IR: $\tilde{\nu}$ = 790, 730, 690 cm^{-1}; MS: *m/z* 158 ($M^{\oplus}$, 10%), 104 ($M^{\oplus} - C_4H_6$, 100%); ^{1}H-NMR (360 MHz, $CDCl_3$): δ = 7.20 (2H, dd, ^4J = 1.0, ^5J = 0.9 Hz, H^8, H^9), 7.07 (2H, dd, ^4J = 1.0, ^5J = 0.9 Hz, H^{11}, H^{12}), 4.68 (2H, XX' of AA'BB'XX', ^3J = 12.2, ^3J = 11.9, $^3J \approx 5$, $^4J = -0.8$, $^4J \approx -1$ Hz, H^3, H^4), 2.79 (2H, ddd, ^2J = 12.0, ^3J = 3.5, ^3J = 3.5 Hz, H^1, H^6), 2.26 (2H, ddd, ^2J = 12.0, ^3J = 12.0, ^3J = 3.0 Hz, $H^{1'}$, $H^{6'}$), 1.88 (2H, m, $H^{2'}$, $H^{5'}$), 1.01 (2H, m, H^2, H^5). Upon irradiation at δ = 4.68, the multiplets at 1.88 and 1.01 changed into ddd with ^2J = 12.0, ^3J = 3.5, ^3J = 3.0 Hz and ^2J = 12.0, ^3J = 12.0, ^3J = 3.5 Hz, respectively. ^{13}C-NMR ($CDCl_3$): δ = 142.9 (s), 136.0 (d), 132.1 (d), 132.0 (d), 35.8 (t), 34.2 (t).

[8] [6]Paracyclophane: UV (hexane): λ_{max} = 299 (ε = 460), 251 (6500), and 214 (17000) nm.

[Cp(CO)$_2$Mo{NR*[Rh(norbornadiene)]-CH(pyridyl)}], a Rhodium Complex with an Asymmetric Molybdenum Atom in the Chelate Skeleton**

By *Henri Brunner,* Joachim Wachter, Johann Schmidbauer, George M. Sheldrick,* and *Peter G. Jones*

Usually, in enantioselective catalysis, optically active chelate ligands are employed which coordinate via P or N atoms.[1] In some of these ligands the P atoms are the chirality centers; mostly, however, the inducing chirality is located in the chelate skeleton, as a rule in the form of asymmetric C atoms, but occasionally also as axial and planar chiral moieties. We now report on nitrogen chelate ligands and their rhodium complexes, which, for the first time, contain chiral transition metal atoms besides asymmetric C and N atoms in the chelate skeleton.

Reaction of the molybdenum complex **1** with sodium amalgam (20°C, 2 h, tetrahydrofuran) leads to formation of the complex **3** in 46% yield; its formation in the reaction of **1** with $LiCH_3$ has already been reported.[2,3] **3** has four chirality centers. One of them is already contained in R* [(*R*)-1-phenylethyl], the other three, at the Mo, N and C atoms of the three-membered ring, are formed during the reaction. Thus, eight stereoisomers are possible, of which only four have been detected (by ^{1}H-NMR spectroscopy) and only two isolated in pure form.

Regardless of whether one starts from the pure diastereomers **1a** and **1b** or from a **1a/1b** mixture, the reaction always leads to a 55:45 mixture of two products having different ^{1}H-NMR spectra, which can be separated chromatographically. The first red zone obtained upon chromatography on Merck-Lobar columns[4] contains the complexes **3a/3b**, while the second red zone contains the complexes **3c/3d**.

The isomers **3a** and **3b** rapidly interconvert in solution at room temperature; this manifests itself in the breadth of the ^{1}H-NMR signals. The high-temperature limiting spectrum for the **3a/3b** mixture was observed at 100°C and the low-temperature limiting spectrum with separate signals for **3a** and **3b** in the intensity ratio 96:4 at −70°C.[5] The isomeric pair **3c/3d** behaves analogously (at −70°C 90:10).[5]

At −20°C, ether/pentane solutions of **3a/3b** and **3c/3d**, afforded single crystals of **3a** and **3c**, respectively, whose absolute configurations were determined by X-ray

[*] Prof. Dr. H. Brunner, Dr. J. Wachter, Dipl.-Chem. J. Schmidbauer
Institut für Anorganische Chemie der Universität
Universitätsstr. 31, D-8400 Regensburg (FRG)
Prof. G. M. Sheldrick, Priv.-Doz. P. G. Jones
Institut für Anorganische Chemie der Universität
Tammannstr. 4, D-3400 Göttingen (FRG)

[**] Optically Active Transition Metal Complexes, Part 90. This work was supported by the Deutsche Forschungsgemeinschaft, the Fonds der Chemischen Industrie, and BASF AG. Part 89: I. Bernal, G. M. Reisner, H. Brunner, G. Riepl, *Inorg. Chim. Acta 103* (1985) 179.

crystallography[6,7] (Fig. 1 and 2). In both compounds, the substituents Cp on Mo, H on N, and pyridyl on C are located on the same side of the three-membered ring; the NH proton forms a hydrogen bridge to the pyridine N. The configurations of the chirality centers in the three-membered ring are $S_{Mo}S_NS_C$ in **3a** and $R_{Mo}R_NR_C$ in **3c**.[11]

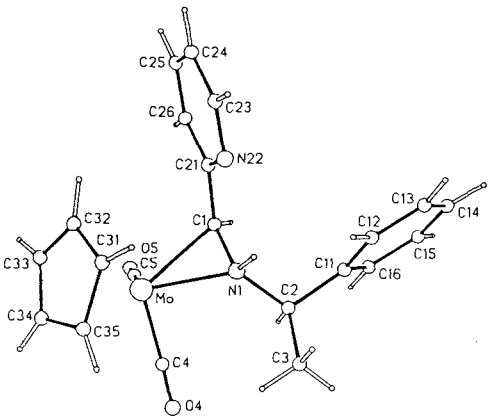


Fig. 1. Structure of **3a** in the crystal. Selected bond lengths [Å] and angles [°]: Mo-N1 2.174(4), Mo-C1 2.210(4), C1-N1 1.414(5), Mo-C4 1.921(5), Mo-C5 1.939(5), C4-O4 1.170(6), C5-O5 1.141(6), Mo-Cp 2.318–2.383, C1-C21 1.472(6), N1-C2 1.491(5), C2-C3 1.519(6), C2-C11 1.516(5), C-C(phenyl and pyridyl) 1.368–1.373, C-N22 1.339(6) and 1.340(6); N1-Mo-C1 37.6(2), Mo-N1-C1 72.6(3), Mo-C1-N1 69.8(3), N1-Mo-C5 107.4(2), N1-Mo-C4 90.7(2), C1-Mo-C4 110.9(2), C4-Mo-C5 77.3(3), C1-Mo-C5 81.1(3), Mo-N1-C2 126.2(3), Mo-C1-C21 116.3(3). Only one of two independent, very similar molecules is shown; in the second molecule the C11-C16 ring is rotated through ca. 30° compared to that in the first molecule.

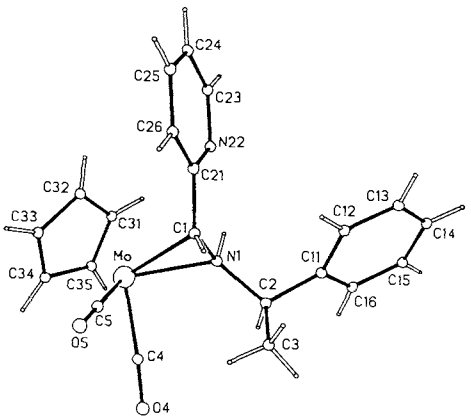


Fig. 2. Structure of **3c** in the crystal. Selected bond lengths [Å] and angles [°]: Mo-N1 2.172(3), Mo-C1 2.213(3), C1-N1 1.421(4), Mo-C4 1.938(4), Mo-C5 1.942(4), C4-O4 1.159(4), C5-O5 1.152(4), Mo-Cp 2.318–2.378, C1-C21 1.483(4), N1-C2 1.499(4), C2-C3 1.522(4), C2-C11 1.514(4), C-C (phenyl and pyridyl) 1.382–1.400, C21-N22 1.333(5), C23-N22 1.350(5); N1-Mo-C1 37.8(2), Mo-N1-C1 72.7(2), Mo-C1-N1 69.5(2), N1-Mo-C5 108.7(2), N1-Mo-C4 90.9(2), C1-Mo-C4 111.7(2), C4-Mo-C5 78.6(2), C1-Mo-C5 82.0(2), Mo-N1-C2 128.9(2), Mo-C1-C21 115.9(2).

Thus, the following picture emerges: In the reduction of **1**, the cation accepts two electrons. The anionic intermediate **2a** is formed in which the Mo–N(pyridyl) bond is broken. The chirality of the Mo atom disappears, and **1a** and **1b**, despite the contrary Mo configurations, give the same products. In the reaction **2a** → **2b** + **2c** the σ-bonded imine ligand becomes π-bonded and thereby the configuration at the C atom of the three-membered ring is established (S_C in **2b** and R_C in **2c**). The placement of the proton on **2b** and **2c** on the pyridine side via a preformed H bridge explains the *cis* orientation of the substituents H and pyridyl in **3a** and **3c**; there is no experimental evidence for a *trans* orientation. The isomer **3b**, which constitutes about 4% of the mixture with **3a** ($S_{Mo}S_NS_C$), is assigned opposite Mo configuration ($R_{Mo}S_NS_C$) whereby rapid isomerization **3a** ⇄ **3b** might arise by intramolecular rotation of the immonium ligand,[8] comparable with the rotation of an olefin in a π-complex. Correspondingly, **3c** and **3d** can be assigned the configurations $R_{Mo}R_NR_C$ and $S_{Mo}R_NR_C$, respectively. **3a** and **3c**, with *cis* oriented Cp, H, pyridyl substituents on the MoNC three-membered ring, are thermodynamically more stable than **3b** and **3d**.

Reaction of **3a/3b** with $[Rd(nbd)Cl]_2$ (nbd = norbornadiene) afforded the complex **4**, which after chromatography was isolated as a reddish-brown powder in 61% yield.[9] The same product is formed on using **3c/3d** as starting material. Crystallization from ether/pentane at −20°C furnished single crystals of **4a**, whose absolute configuration was determined by X-ray crystallography.[6,7] In **4a** the chelate ring formed via the two N atoms and the Rh atom lies on the side of the MoNC three-membered ring opposite to the cyclopentadienyl ring. This is surprising, since the substituents Cp, H and pyridyl are located on the same side of the MoNC three-membered ring in the complexes **3a** and **3c**. The reason for the chelate ring in **4a**, in contrast to the N–H–N hydrogen bridge in **3a** and **3c**, preferring that side of the three-membered ring with the CO ligands, may be sought in the formation of a bond between the Rh atom and C10 of the CO group C10-O10 (Fig. 3). This CO group (Mo-C10-O10 166.9°) deviates from linearity; the Rh-C10 distance (2.821 Å), however, points to only a weak interaction of the Rh atom with the C atom. The formation of this CO bridge is unusual, because semibridging CO groups normally only occur when metal–metal bonds are present.

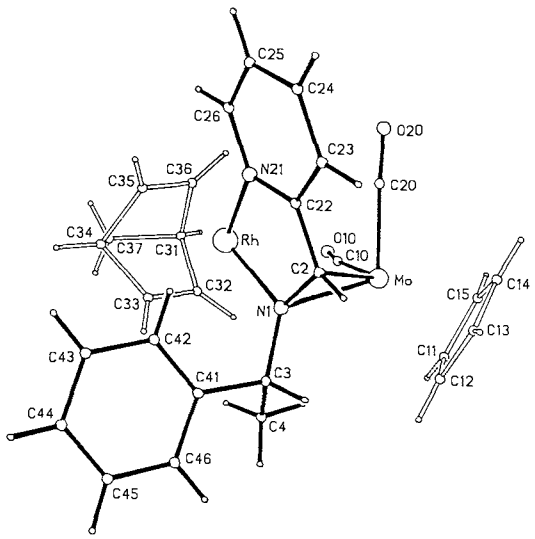


Fig. 3. Structure of **4a** in the crystal. Selected bond lengths [Å] and angles [°]: Mo-N1 2.221(5), Mo-C2 2.241(6), N1-C2 1.401(7), Mo-C10 1.966(6), Mo-C20 1.939(8), C10-O10 1.143(7), C20-O20 1.151(10), Mo-Cp 2.327–2.388, C2-C22 1.419(7), N1-C3 1.491(8), C22-N21 1.346(7), C26-N21 1.345(7), Rh-N21 2.117(5), Rh-N1 2.068(5), Rh-C32 2.122(6), Rh-C33 2.136(5), Rh-C35 2.110(6), Rh-C36 2.121(6); N1-Mo-C2 36.6(3), Mo-C2-N1 70.9(3), Mo-N1-C2 72.5(3), C10-Mo-C20 77.7(4), Mo-C10-O10 166.9(6), Mo-C20-O20 174.4(7), N1-Rh-N21 80.2(2), C22-C2-N1 118.1(5), Rh-N1-C2 109.8(4), Rh-N21-C22 112.3(4), N21-C22-C2 116.4(5).

The ^{1}H-NMR spectra show that **4** forms two diastereomers **a** and **b**, which rapidly interconvert in solution at room temperature. The high-temperature limiting spectrum for **4a/4b** is observed at 100°C, while the low-temperature limiting spectrum, with separate signals for **4a** and **4b** in the intensity ratio 98:2, is observed at −70°C.[10] It is not possible, as yet, to make any statements about the structure of **4b**.

The finding that the reactions of **3a/3b** and **3c/3d** with $[Rh(nbd)Cl]_2$ lead to the same product **4a/4b** can only be explained in terms of an intermediate **2a**. The intermediate **2a** is formed from both **3a/3b** as well as from **3c/3d**; the asymmetry of all former three-membered ring atoms is removed, leading under the strongly alkaline conditions used in the synthesis,[9] to establishment of the equilibrium **3a/3b** ⇄ **3c/3d**, even in the absence of $[Rh(nbd)Cl]_2$. It therefore follows that epimerization of the intermediates **2b** and **2c** (with π-coordinated imine ligand) via **2a** (with σ-coordinated imine ligand) is more rapid than the reaction with $[Rh(nbd)Cl]_2$: Otherwise, if the complex **4a** ($R_{Mo}R_NS_C$) is formed from **3a/3b**, then **3c/3d** would have to yield a Rh-complex **4c** with $S_{Mo}S_NR_C$ configuration, which is not observed.

Received: December 16, 1985;
revised: January 30, 1986 [Z 1586 IE]
German version: *Angew. Chem. 98* (1986) 339

[1] J. D. Morrison (Ed.): *Asymmetric Syntheses, Vol. 5*, Academic Press, London 1985.
[2] H. Brunner, H. Schwägerl, J. Wachter, G. M. Reisner, I. Bernal, *Angew. Chem. 90* (1978) 478; *Angew. Chem. Int. Ed. Engl. 17* (1978) 453.
[3] H. Brunner, H. Schwägerl, J. Wachter, *Chem. Ber. 112* (1979) 2079.
[4] Type B (310/25 mm) LiChroprep Si60 (40–63 μm), toluene/ether 50:1.
[5] **3a/3b**: IR (cyclohexane): $\tilde{\nu}$(CO) = 1940, 1850 cm^{-1}; ^{1}H-NMR (250 MHz, [D$_8$]toluene), 100°C: δ = 1.59 (d, 3H, J = 6.8 Hz, CHCH_3), 3.11 (m, 1H, CH$_3$CH), 3.72 (d, 1H, J = 6.9 Hz, MoCH), 5.29 (m, 1H, NH), 4.89 (s, 5H, Cp), 6.26–7.96 (m, 9H, phenyl and pyridyl).—**3a**, −70°C: δ = 1.51 (d, 3H), 3.04 (m, 1H), 3.67 (d, 1H), 5.38 (m, 1H), 4.70 (s, 5H), 6.18–7.86 (m, 9H).—**3b**, −70°C: δ = 4.91 (s, Cp).—**3c/3d**: IR (cyclohexane): $\tilde{\nu}$(CO) = 1940, 1850 cm^{-1}; ^{1}H-NMR (250 MHz, [D$_8$]toluene), 100°C: δ = 1.21 (d, 3H, J = 6.7 Hz, CHCH_3), 3.06 (m, 1H, CH$_3$CH), 3.76 (d, 1H, J = 7.2 Hz, MoCH), 5.37 (m, 1H, NH), 4.75 (s, 5H, Cp), 6.38–8.02 (m, 9H, phenyl and pyridyl).—**3c**, −70°C: δ = 1.05 (d, 3H), 2.51 (m, 1H), 3.61 (d, 1H), 5.30 (m, 1H), 4.59 (s, 5H), 6.27–7.93 (m, 9H).—**3d**, −70°C: δ = 4.67 (s, Cp).
[6] **3a**: Space group $P2_12_12_1$, a = 10.084(2), b = 13.516(2), c = 29.203(5) Å, Z = 8 (two independent molecules), 7237 reflections ($Mo_{K\alpha}$ radiation, $2\theta_{max}$ = 60°C), η = 1.06(7), R_w = 0.036.—**3c**: space group $P2_12_12_1$, a = 6.795(1), b = 11.744(2), c = 24.110(3) Å, Z = 4, 4422 reflections ($2\theta_{max}$ = 63°), η = −1.19(9) for the opposite configuration, R_w = 0.029.—**4a**: space group $P2_12_12_1$, a = 8.948(2), b = 14.048(3), c = 20.007(4) Å, Z = 4, 4479 reflections ($2\theta_{max}$ = 55°), η = 1.05(9), R_w = 0.034. Further details of the crystal structure investigation are available on request from the Fachinformationszentrum Energie, Physik, Mathematik GmbH, D-7514 Eggenstein-Leopoldshafen 2 (FRG) on quoting the depository number CSD-51778, the names of the authors, and the full citation of the journal.
[7] D. Rogers, *Acta Crystallogr. A 37* (1981) 734.
[8] C. W. Fong, G. Wilkinson, *J. Chem. Soc. Dalton Trans. 1975*, 1100; E. K. Barefield, D. J. Sepelak, *J. Am. Chem. Soc. 101* (1979) 6542.
[9] **4**: 0.2 mmol **3a/3b**, 0.1 mmol $[Rh(nbd)Cl]_2$, 100 mg KOH, catalytic amounts of [18]crown-6 (toluene, 2 h, 20°C). Chromatography on Al_2O_3, neutral without added water with toluene/ether 6:1.
[10] **4a/4b**: IR (cyclohexane): $\tilde{\nu}$(CO) = 1915 s, 1835 m, 1815 w sh cm^{-1}; ^{1}H-NMR (250 MHz, [D$_8$]toluene), 100°C: δ = 1.19 (s, 2H, nbd), 1.20 (d, 3H, J = 6.9 Hz, CHCH_3), 3.21 (q, 1H, CH$_3$CH), 3.48 (m, 2H, nbd), 3.57 (m, 3H, MoCH + nbd), 3.72 (m, 2H, nbd), 4.97 (s, 5H, Cp), 6.03–7.76 (m, 9H, phenyl and pyridyl).—**4a**, −70°C: δ = 0.9 (d, 3H), 1.17 (s, 2H), 2.87 (m, 1H), 3.29 (s, 1H), 3.40, 3.57, 3.83 (m, 6H), 4.82 (s, 5H), 5.83–7.94 (m, 9H).—**4b**, −70°C: δ = 5.30 (s, Cp).
[11] Priority sequence used for the specification of the Mo configuration: Cp > N(MoNC ring) > C(MoNC ring), looking at the molecule from the side opposite to the two carbonyl groups. Cf. H. Brunner, *Adv. Organomet. Chem. 18* (1980) 195.

[(α-Cyanobenzyllithium · Tetramethylethylenediamine)$_2$ · Benzene]: X-ray Structure Analysis of an α-Nitrile "Carbanion"**

By *Gernot Boche,* Michael Marsch,* and *Klaus Harms*

The synthetic importance of α-nitrile-"carbanions" extends from dinitrile cyclization[1] to the umpolung of aldehydes with trimethylsilyl cyanide.[2] However, although numerous mechanistic investigations have been carried out,[3] and both mono- as well as di-alkali-metal compounds of acetonitriles and phenylacetylnitriles have been prepared and investigated IR spectroscopically,[4, 5] an X-ray structure analysis has so far never been carried out.[6] In the following, we report on such an analysis of [(α-cyanobenzyllithium · tetramethylethylenediamine (TMEDA))$_2$ · benzene] **1** · C_6H_6[7] (Fig. 1).

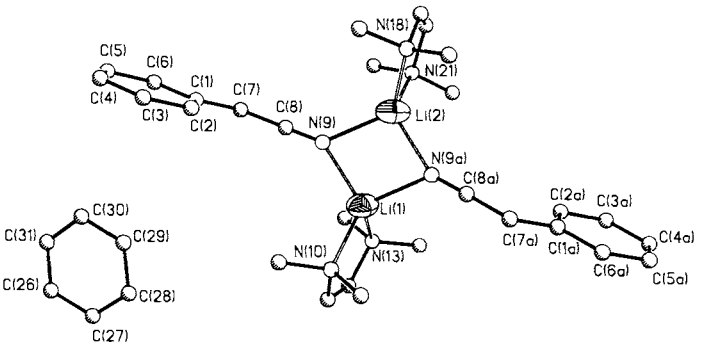
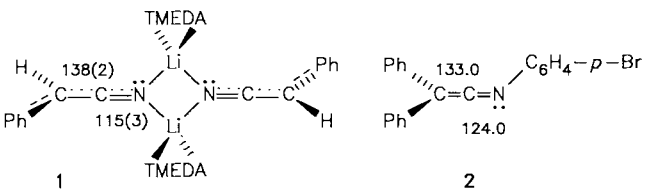


Fig. 1. Asymmetric unit of the crystal structure of **1** · C_6H_6. Space group $P2_1/n$, a = 968.0(2), b = 1583.4(4), c = 2402.9(6) pm, β = 99.46(2)°, Z = 4, R = 0.115 for 2292 reflections with $F > 3\sigma(F)$. The high R value is due to decomposition of the crystal in the X-ray beam. The H atoms on C-7 and C-7a were given a fixed C-H distance (96 pm) and a common isotropic temperature factor. All other H atoms were refined according to a riding model with C-H = 96 pm. All calculations were carried out with the SHELXTL (Rev. 5.1) program system (*G. M. Sheldrick*, Göttingen 1985). Selected bond lengths [pm] and angles [°] (mean values: Li-N(TMEDA) 205(4), Li-N(anion) 204(3), C1-C7 143(2), C7-C8 138(2), C8-N9 115(3), Li1-Li2 264(5); C1-C7-C8 124.5 (1.0), C7-C8-N9 178.4(1.0), N9-Li1-N9a 98.2(0.5), Li1-N9-Li2 80.9 (0.5), dihedral angle C6-C1-C7-C8 179.2 (0.7). Because of the small anisotropic vibration of the nitrogen atom, an analysis of the C8-C9 bond length according to a riding model [8] gave only a slight lengthening to 117(2) pm. Further details of the crystal structure investigation are available on request from the Fachinformationszentrum Energie, Physik, Mathematik GmbH, D-7514 Eggenstein-Leopoldshafen 2, on quoting the depository number CSD-51841, the names of the authors, and the full citation of the journal.

1 · C_6H_6 crystallizes as a dimer, in which Li atoms are bonded to the N atoms of the nitrile groups and the TMEDA molecules. This solid state structure may corre-



[*] Prof. Dr. G. Boche, M. Marsch
Fachbereich Chemie der Universität
Hans-Meerwein-Strasse, D-3550 Marburg (FRG)
Dr. K. Harms
Institut für Anorganische Chemie der Universität
Tammannstr. 4, D-3400 Göttingen (FRG)

[**] This work was supported by the Fonds der Chemischen Industrie, by the Deutsche Forschungsgemeinschaft, and by NATO (travel grant). We thank Prof. Dr. *K. Dehnicke*, Universität Marburg, for recording and discussing the IR spectrum of 1 · C_6H_6.

spond to the structure in solution, since $PhCH(CN)^{\ominus}Li^{\oplus}$ is likewise dimeric according to molecular weight determinations in dimethoxyethane and in dimethyl sulfoxide.[5f,9] As in the recently described [$tBu_2C{=}NLi \cdot$ hexamethylphosphoric acid triamide]$_2$,[10] μ2-N-Li bonds are present in the slightly puckered Li_2N_2 ring (torsional angle $\pm 10.2(0.5)°$). The "anions" are almost planar (greatest deviation from the least squares plane: 2 pm), so the "anionic" C atoms C-7 and C-7a should also be planar coordinated.[11] The "anion" planes are at an angle of 95.7 and 103.5°, respectively, to the least squares plane of the Li_2N_2 ring. The co-crystallized benzene molecule fills the gaps between the orthogonally oriented planes of the "anion" and the Li-TMEDA five-membered ring; the nearest intermolecular distance is 378 pm (C30-C4).

Particularly interesting is the bonding situation in the almost linear CCN unit ($\sphericalangle = 178.4\ (1.0)°$). Thus, the C7-C8 distance is 138(2) pm, whereas the C8-N9 bond length of 115(3) pm is as short as in a nitrile.[11,12]

In comparable ketenimines such as **2** one finds shorter CC distances and longer CN distances,[13] which is also consistent with the IR spectra. Thus, $\mathbf{1} \cdot C_6H_6$ (in Nujol) shows an intense band at 2065 cm^{-1} ($\tilde{\nu}_{as}(C{=}C{=}N)$),[14] whereas ketenimines absorb at $\approx$1990–2010 cm^{-1}.[13c] Hence, the structural relationship between the lithium "keteniminate" $\mathbf{1} \cdot C_6H_6$ and normal ketenimines is less than that between a lithium enolate and enol ethers: In the latter series the C=C and C-O distances are almost the same.[15] The reason for this could lie in the different stabilization of a negative charge. Whereas a carbonyl group is predominantly mesomeric, in a nitrile group the (inductive) field effect also plays an prominent role.[3,16]

Received: December 30, 1985;
supplemented: January 22, 1986 [Z 1559 IE]
German version: *Angew. Chem. 98* (1986) 373

[1] a) F. Thorpe, *J. Chem. Soc. 95* (1909) 1903; b) K. Ziegler, H. Eberle, H. Ohlinger, *Justus Liebigs Ann. Chem. 504* (1933) 94.

[2] a) U. Hertenstein, S. Hünig, H. Reichelt, R. Schaller, *Chem. Ber. 115* (1982) 261, and references cited therein; b) G. Boche, F. Bosold, M. Niessner, *Tetrahedron Lett. 23* (1982) 3255; c) see also J. C. Stowell: *Carbanions in Organic Synthesis*, Wiley, New York 1979.

[3] Review: D. J. Cram: *Fundamentals of Carbanion Chemistry*, Academic Press, New York 1965.

[4] Sodiumacetonitrile: C. Krüger, *J. Organomet. Chem. 9* (1967) 125.

[5] Mono- und dilithium(phenyl)acetonitriles: a) E. M. Kaiser, C. R. Hauser, *J. Am. Chem. Soc. 88* (1966) 2348; b) *J. Org. Chem. 33* (1968) 3402; c) D. N. Crouse, D. Seebach, *Chem. Ber. 101* (1968) 3113; d) I. Pattison, K. Wade, B. K. Wyatt, *J. Chem. Soc. 1968*, 837; e) G. Gornowicz, R. West, *J. Am. Chem. Soc. 93* (1971) 1714; f) R. Das, C. A. Wilkie, *ibid. 94* (1972) 4555.

[6] Multi-nitrile-substituted "carbanions" are known, e.g. a) $K^{\ominus}C(CN)_3^{\ominus}$: J. R. Witt, D. Britton, *Acta Cristallogr. Sect. B 27* (1971) 1835; b) $Na^{\ominus}C(CN)_3^{\ominus}$: P. Andersen, B. Keewe, E. Thom, *Acta Chem. Scand. 21* (1967) 1530, and references cited therein.

[7] $\mathbf{1} \cdot C_6H_6$: A solution of benzyl cyanide (100 mg, 0.85 mmol) in benzene (3 mL) was treated at room temperature with a solution of TMEDA (1.04 mmol) and BuLi (1.04 mmol) in hexane, and, after 1 h, with 1.2 mL of hexane. After 4 to 8 h, the whitish, needle-shaped crystals of $\mathbf{1} \cdot C_6H_6$ were freed from solvent with the aid of a drawn out pipette. They were then washed with hexane and dried at 10^{-3} torr.

[8] C. K. Johnson: *Crystallographic Computing*, Munksgaard, Kopenhagen 1970, p. 220–226.

[9] Quantum mechanical calculations gave an analogous structure; P. von R. Schleyer, private communication, April 18, 1985. Interestingly W. Bauer and D. Seebach (*Helv. Chim. Acta 67* (1984) 1972) and D. Seebach (private communication) January 6, 1986) found that $PhCH(CN)^{\ominus}Li^{\oplus}$ is present as a monomer in tetrahydrofuran at −108 °C and not, as at 18.5 °C, as a dimer [5f]. This finding is consistent with MNDO calculations by S. Schröder, Universität Marburg. Accordingly, $[PhCH(CN)^{\ominus}Li^{\oplus}(NH_3)_2]_2$ is, as model for **1**, only obout $\Delta\Delta H_f \approx 5$ kcal/mol more stable than the monomer $PhCH(CN)^{\ominus}Li^{\oplus}(NH_3)_3$; hence, entropy effects can favor the monomer at low temperatures. According to STO-3G calculations by *H.-U. Wagner*, Universität München (private communication, March 24, 1980), a bent monomer with a Li-1,3-bridge is the most stable one; see also J. B. Moffat, *J. Chem. Soc. Chem. Commun. 1980*, 1108.

[10] D. Barr, W. Clegg, R. E. Mulvey, D. Reed, R. Snaith, *Angew. Chem. 97* (1985) 322; *Angew. Chem. Int. Ed. Engl. 24* (1985) 328. Review of analogous μ_2-C-Li compounds: W. N. Setzer, P. von R. Schleyer, *Adv. Organomet. Chem. 24* (1985) 353.

[11] Since we could not localize the H atoms on C-7 and C-7a, a more suitable substitution is a prerequisite before a definite answer can be given. *Note added in proof (March 7, 1986):* A new measurement at ca. −35 °C gave the following important results: 1) The hydrogen atoms on C(7) and C(7a) could be located and refined. The sum of the bonding angles on C(7) is 359.9°, on C(7a) 359.7°. These atoms are thus planar coordinated. 2) The C(8)-N(9) was determined accurately. It is 117.4(7) pm, i.e. somewhat longer than the mean value measured at room temperature. A riding correction lengthened this bond to 119.5(10) pm. The cell constants at −35 °C are: a=968.9(2), b=1569.9(4), c=2391.4(6) pm, β=99.53(2)°. The R value is 0.094 (R_w=0.088) for 2469 reflections with $F > 3\sigma(F)$.

[12] CH_3CN: 115.7 pm; C.C. Costain, *J. Chem. Phys. 29* (1958) 864. Since the CN distance in nitrile complexes of Lewis acids is shortened to 113.5 pm, as in $CH_3CN \cdot BF_3$ (B. Swanson, D. F. Shriver, J. A. Ibers, *Inorg. Chem. 8* (1969) 2182) a similar effet caused by $Li^{\oplus}$. TMEDA could contribute to short CN-bonding in $1 \cdot C_6H_6$.

[13] a) J. J. Daly, *J. Chem. Soc. 1961*, 2801; b) R. R. Nagvi, P. J. Wheatley, *J. Chem. Soc. A 1970*, 2053; c) J. Lambrecht, B. Gambke, J. von Seyerl, G. Huttner, G. Kollmannsberger-von Nell, S. Herzberger, J. C. Jochims, *Chem. Ber. 114* (1981) 3751. d) abnormally short CN bonds ($\approx$115 pm) are found in linear(!) ketenimines such as $(CH_3SO_2)_2\overset{\ominus}{C}{-}C{\equiv}\overset{\oplus}{N}{-}CH_3$ [13a,b]; hence, their structure was compared with that of cyanamidinium salts $R^1R^2\overset{\oplus}{N}{-}C{\equiv}\overset{\oplus}{N}{-}R^3X^{\ominus}$; e) see also J. Lambrecht, L. Zsolnai, G. Huttner, J. C. Jochims, *ibid. 114* (1981) 3655.

[14] 1175 cm^{-1} ($\tilde{\nu}_s(C{=}C{=}N)$); 570 cm^{-1} ($\tilde{\nu}(Li_2N_2$-Ring)). $PhCH(CN)^{\ominus}Na^{\oplus}$ shows a similar band as $\mathbf{1} \cdot C_6H_6$ at 2080 cm^{-1} [4], whereas completely different bands have been reported for $PhCH(CN)^{\ominus}Li^{\oplus}$ in Nujol [5f].

[15] Example: $H_2C{=}C(tBu)$-OLi: C=C 134, C-O 135 pm, enol ether: C=C 132, C-O 136 pm; R. Amstutz, W. B. Schweizer, D. Seebach, J. D. Dunitz, *Helv. Chim. Acta 64* (1981) 2617.

[16] This manifests itself in the low (high) activity of cyclopropyl ketones (nitriles); J. M. Motes, H. M. Walbossky, *J. Am. Chem. Soc. 92* (1970) 3697; H.-U. Wagner, G. Boche, *Z. Naturforsch. B 37* (1982) 1339, and references cited therein.

Benzo[*c*]benzo[3,4]cinnolino[1,2-*a*]cinnoline, a Chiral Hydrazine Derivative**

By *Hans Fischer, Claus Krieger,* and *Franz A. Neugebauer**

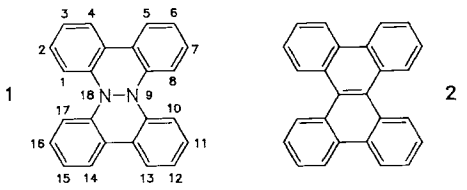
Dedicated to Professor Heinz A. Staab on the occasion of his 60th birthday

In benzo[*c*]benzo[3,4]cinnolino[1,2-*a*]cinnoline (**1**),[1] a triphenylhydrazine derivative with *ortho* linkage of the *N,N'*-phenyl substituents, the interaction of the lone-electron pairs on the nitrogen atoms with the connected π-electron system can lead to a flattening of the molecule. But even on extensive planarization the axial (*N-N*) chirality should be preserved because of the spatial requirements of the 1,17- and 8,10-hydrogen atoms; as in the case of dibenzo[*g,p*]chrysene (**2**)[2] one would expect a very low racemization barrier. Surprisingly, **1** crystallizes as separate enantiomers in the chiral space group $P2_1$. Prisms of up to a length of 4 mm (0.7 mg) were obtained on crystallization from ethyl acetate.

An X-ray structure analysis[3] of the crystals showed that the substituents on the nitrogen atoms are arranged pyram-

[*] Prof. Dr. F. A. Neugebauer, H. Fischer, C. Krieger
Abteilung Organische Chemie,
Max-Planck-Institut für medizinische Forschung
Jahnstrasse 29, D-6900 Heidelberg 1 (FRG)

[**] This work was supported by the Deutsche Forschungsgemeinschaft and the Fonds der Chemischen Industrie.



idally. As shown by the C-N-C angle (ca. 140°) of the Newman projection, the molecule as a whole is only slightly flattened. The torsional angle of the orbitals of the two lone pairs is 64°. The structure of **1** corresponds to a propellane skeleton in which a bridge is replaced by two vicinal lone pairs (Fig. 1).

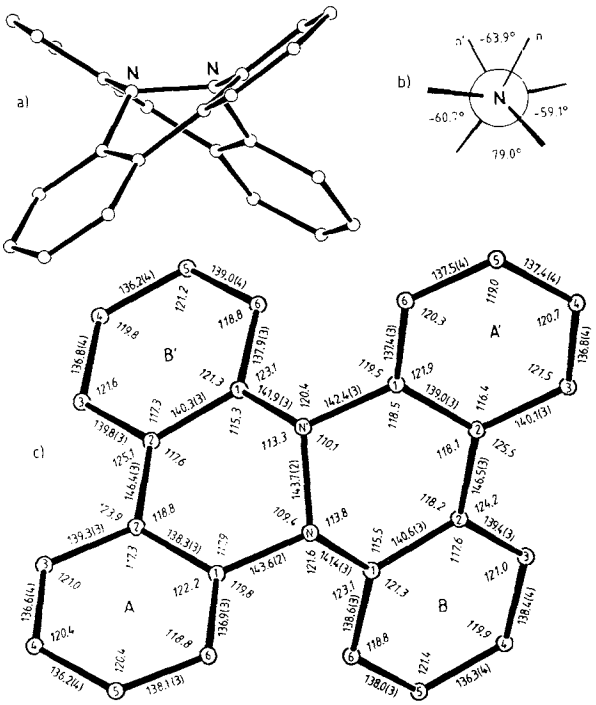


Fig. 1. a) Molecular structure of **1** in the crystal (*M* representation); b) Newman projection (*M*) with torsional angles; c) bond lengths [pm] and angles [°].

In dioxane, the enantiomers gave molar optical rotation values of $[\Phi]_D^{20}$ 2130±60 and $[\Phi]_{405}^{20}$ 24700±400 [enantiomer **A**: (+); enantiomer **B**: (−); concentrations 2×10^{-5} to 14×10^{-5} g mL^{-1}]. Figure 2 shows the respective CD spectra and the electronic spectrum. A definite assignment of the absolute configuration of the enantiomers could not be carried out, even after determination of several Cu-data sets, since the small dispersion effect of the nitrogen with $Cu_{K\alpha}$ radiation was too small compared to the error of measurement.

The rate constants for the racemization were determined by measurement of the optical rotations in decane; T [K] ($k\times10^4$ [min^{-1}]): 370 (642), 360 (233), 350 (75.6), 340 (24.7), 330 (7.34), 320 (2.01). The thermal racemization requires an activation energy of 27.1(±1) kcal mol^{-1} [113(±4) kJ mol^{-1}]; pre-exponential factor $A=6.52\times10^{14}$. Compound **1** can racemize both by rotation about the N-N axis as well as by double nitrogen-inversion. In both cases, a greater degree of planarization of the molecule is to be expected for the transition state. A comparable planarization can also be achieved by one-electron oxidation, which transforms the destabilizing interaction of the vicinal lone pairs into a bonding three-electron interaction, resulting in a planarization of the pyramidal arrangement of the substituents. $\mathbf{1}^{\odot\oplus}$ should therefore have a very low racemization barrier. This is in fact observed. Oxidation of the enantiomers affords an optically inactive radical cation.[4]

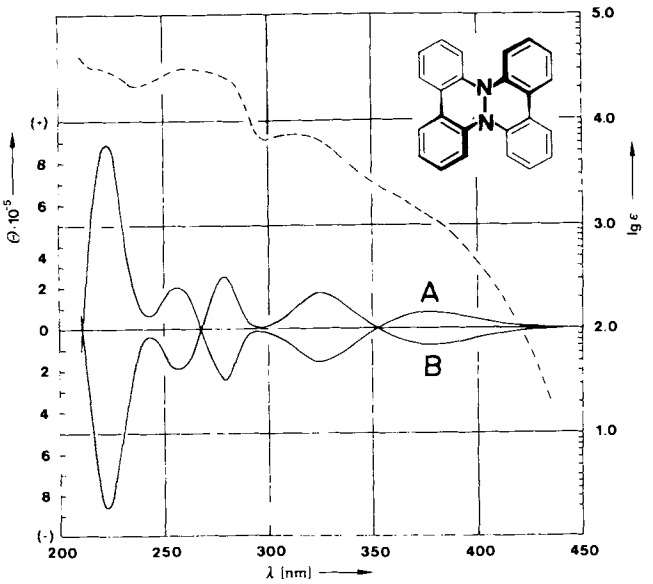


Fig. 2. Electronic spectrum (---) and CD spectra (—) (θ [grad cm^2 dmol^{-1}]) of **1** in dioxane (enantiomer **A**: $c=2\times10^{-5}$ g mL^{-1}; enantiomer **B**: $c=1.4\times10^{-4}$ g mL^{-1}; JASCO J 500).

The above findings indicate that the high racemization barrier of **1** is essentially due to the *gauche* effect[5] of the vicinal lone pairs. Their interaction with the coupled π-electron system proves to be surprisingly small.

Received: December 30, 1985 [Z 1605 IE]
German version: *Angew. Chem. 98* (1986) 341

CAS Registry numbers:
1, 100992-72-1; *ent*-**1**, 100992-73-2.

[1] F. A. Neugebauer, S. Kuhnhäuser, *Angew. Chem. 97* (1985) 589; *Angew. Chem. Int. Ed. Engl. 24* (1985) 596.
[2] F. H. Herbstein, *Acta Crystallogr. Sect. B 35* (1979) 1661.
[3] Yellow crystals (from ethyl acetate), ca. 0.2×0.2×0.4 mm, $P2_1$, $a=934.2(2)$, $b=769.2(1)$, $c=1209.2(2)$ pm, $\beta=102.37(1)°$, $\rho_{calc.}=1.301$ g cm^{-3} for $Z=2$. 2324 symmetry independent reflections measured (Nonius CAD 4 diffractometer, $Mo_{K\alpha}$ radiation). Solution of structure by direct methods. Anisotropic refinement of all non-H atoms converged at $R=0.037$ for 1514 observed reflections [$I\geq1.96\sigma(I)$]. Further details of the crystal structure investigation are available on request from the Fachinformationszentrum Energie, Physik, Mathematik GmbH, D-7514 Eggenstein-Leopoldshafen 2, on quoting the depository number CSD-51730, the names of the authors, and the full citation of the journal.
[4] F. A. Neugebauer, M. Bock, S. Kuhnhäuser, H. Kurreck, *Chem. Ber. 119* (1986) 980.
[5] S. F. Nelsen, *Acc. Chem. Res. 11* (1978) 14.

Strontium and Barium Alkoxostannates(II)—Molecules with S_6 Symmetry**

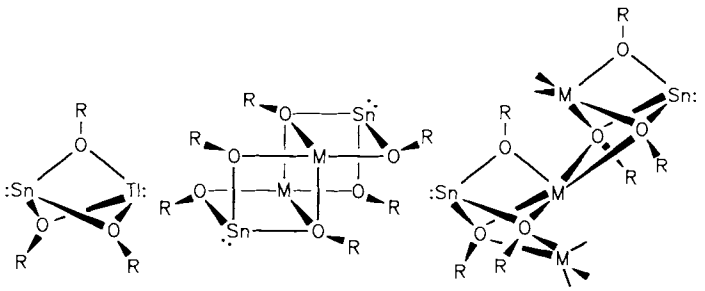
By *Michael Veith,* Dieter Käfer,* and *Volker Huch*

Tris(*tert*-butyloxo)stannates of the alkali-metals[1] and of monovalent thallium[2] exhibit a remarkable variety of structures. Whereas the stannates of thallium, **1**, as well as

[*] Prof. Dr. M. Veith, Dipl.-Chem. D. Käfer, Dr. V. Huch
Institut für Anorganische Chemie der Universität
D-6600 Saarbrücken (FRG)

[**] Alkoxostannates, Part 3. This work was supported by the Deutsche Forschungsgemeinschaft.—Part 2: [1].

those of lithium and sodium, **2**, form cage-like, molecular units, those of potassium, rubidium and cesium, **3**, form polymers. The structures are illustrated in formulas **1**–**3**, where the lines between the atoms represent, as usual, electron pairs, either in the sense of a two-center bond or a donor-acceptor bond (formal charges not shown). Our interest now turned to the question of whether these structural principles are preserved when two tris(*tert*-butyloxo)stannate ligands are available per "cation", i.e. on going to divalent metal "cations".



1 **2**, M = Li, Na **3**, M = K, Rb, Cs

R = *t*Bu

To check this we have examined the reaction of *tert*-butoxides of Mg,[3] Ca,[4] Sr,[5] and Ba,[5] which are insoluble in benzene, with a solution of tin di-*tert*-butoxide[6] [Eq. (a)]. $Mg(OtBu)_2$ and $Ca(OtBu)_2$ do not react, even in boiling benzene (^{1}H-NMR, quantitative recovery of the starting substances), whereas $Sr(OtBu)_2$ and $Ba(OtBu)_2$ undergo complete reaction in accord with Equation (a). The sharp distinction between the *tert*-butoxides of calcium and strontium is also demonstrated in the following experiment: A Ca/Sr alloy was converted into a mixture of the *tert*-butoxides, which was then treated with a benzene solution of $[Sn(OtBu)_2]_2$ (molar ratio 2:1); only the strontium salt was found to react! It dissolved completely, whereas the calcium salt remained undissolved. This procedure can be exploited without difficulty for the quantitative separation of Sr and Ca.

$$M(OtBu)_2 + [Sn(OtBu)_2]_2 \longrightarrow [Sn(OtBu)_3M(OtBu)_3Sn] \quad (a)$$

4, M = Sr; **5**, M = Ba

The compounds **4** and **5** are colorless, and crystallize isotypically (decomposition temperatures: 220 and 270°C, respectively). Both show a singlet in the ^{1}H-NMR spectrum (**4**: $\delta = 1.44$ (1.42), **5**: $\delta = 1.41$ (1.40) in benzene (toluene)), and the elemental analyses and mass spectra are consistent with the formula given in Equation (a). We have determined the structure of **4** by single-crystal X-ray structure analysis (Fig. 1).

The crystal lattice of **4** contains molecules of point symmetry $S_6(\bar{3})$, packed, internally interlocked, parallel to (001) within the layers and in the [001] direction with the layer sequence A,B,C... (the angle in the rhombohedric unit cell is 52.2°). If we consider only the skeletal atoms, then the polycycle can be built from two trigonal bipyramids connected via a common apex with retention of the threefold axis. This apical position, which at the same time is a center of inversion, is occupied by the Sr atom, which is situated in a distorted octahedral environment (O-Sr-O: 90 ± 24.4(1)°). The Sn atoms are, as in the related compounds **1**–**3**, trigonal-pyramidally coordinated (O-Sn-O: 82.3(1)°). The equatorial apices of the two bipyramids are occupied by the oxygen atoms, which, as expected, are at shorter distances from the Sn atoms than from the Sr atom (cf. Fig. 1). A striking feature is that the O atoms are not, as in **1**[2], located in a pyramidal, but in a trigonal-planar environment (sum of angles at the O atoms: 359.5°)—perhaps this arises as a result of intramolecular interactions. Actually, the *tert*-butyl groups in the molecule are in unusual close proximity (distance between the centers of the *tert*-butyl groups 511 and 550 pm); they completely shield the metal atom in the center of the molecule. If the central metal atom were to be even smaller than strontium, the *tert*-butyl groups would repel each other extremely strongly. The Ca atom is probably already too small (Ca–O in CaO: 240.5 pm[6]).

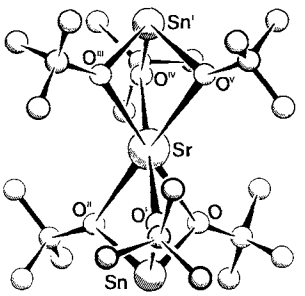
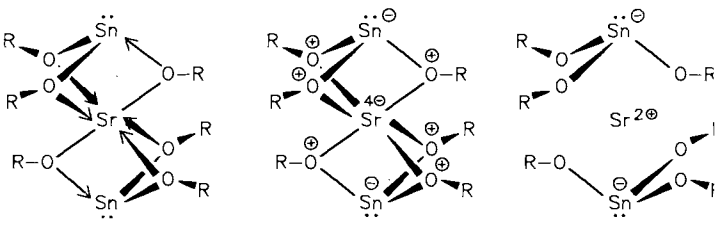


Fig. 1. Structure of **4** in the crystal. The unmarked atoms are C atoms; the H atoms are not shown. The point symmetry of **4** in the crystal is reduced from D_{3d} ($\bar{3}m$) to $S_6(\bar{3})$ by slight rotation of the *tert*-butyl groups. Cell dimensions: $a = 1017(1)$, $c = 2986(2)$ pm, space group: $R\bar{3}$; $Z = 3$. Four-circle diffractometer (Siemens) $R = 0.033$ (all atoms anisotropic) at a reflection-parameter ratio of 15.0:1. Some selected bond lengths [pm] and angles [°]: Sn-O 207.8(3), Sr-O 252.3(3), O-C 141.8(6); O-Sr-O' 65.6(1), Sn-O-C 124.9(3), Sr-O-C 142.8(3). Further details of the structure investigation are available on request from the Fachinformationszentrum Energie, Physik, Mathematik GmbH, D-7514 Eggenstein-Leopoldshafen 2, on quoting the depository number CSD-51786, the names of the authors, and the full citation of the journal.

The structure of **4**, like that of **1**–**3**, is very difficult to formulate. Besides the formulation as the donor-acceptor complex **4**, other possible formulations are those with formal charges or ionic substructures **4'** and **4''**, respectively.



4 **4'** **4''**

In **4''** the two halves of the molecule are held together by electrostatic forces, with striking similarity to strontium oxide: The SrO_6 polyhedron in **4** could be regarded as a section of the SrO structure,[6] since the Sr–O distances are also very similar (in SrO: 258.0 pm; in **4**: 252.3(3) pm). Compounds such as **4** and **5** are therefore extraordinarily remarkable in that they contain alkaline-earth metal atoms yet nevertheless are molecularly structured. **4** and **5** are soluble in non-polar solvents such as hexane, benzene, and toluene.

Procedure

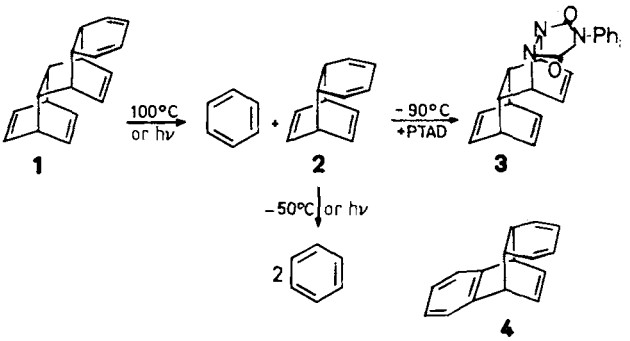
A solution of freshly sublimed $[Sn(OtBu)_2]_2$ [7] (1.2 g, 4.53 mmol) in benzene (25 mL) was added dropwise to a suspension of $M(OtBu)_2$, M = Sr, Ba (6 mmol) in benzene (10 mL). The mixture was stirred for 2 h, filtered, and the filtrate evaporated almost to dryness. The product crystallized out as colorless platelets. Yield: 1.59 g (92%) **4** or 1.71 g (93%) **5**.

Received: January 14, 1986;
revised: February 4, 1986 [Z 1622 IE]
German version: *Angew. Chem. 98* (1986) 367

CAS Registry numbers:
4, 101165-23-5; **5**, 101165-24-6.

[1] M. Veith, R. Rösler, *Z. Naturforsch. B*, in press.
[2] M. Veith, R. Rösler, *Angew. Chem. 94* (1982) 867; *Angew. Chem. Int. Ed. Engl. 21* (1982) 858.
[3] G. E. Coates, J. A. Heslop, M. E. Redwood, D. Ridley, *J. Chem. Soc. A 1968*, 1118.
[4] Synthesis in analogy to a previously described method: E. Chablay, *Ann. Chim. (Paris) 8* (1917) 415.
[5] Synthesis analogous to that of the isopropyl compounds: J. S. Smith II, R. T. Doloff, K. S. Mazdiasni, *J. Am. Ceram. Soc. 53* (1970) 91.
[6] A. R. West: *Solid State Chemistry*, Wiley, Chichester 1984, p. 235.
[7] M. Veith, F. Töllner, *J. Organomet. Chem. 246* (1983) 219.

recording the ^{1}H-NMR spectrum, signals other than that of benzene are observed, which first build up and then decrease during the course of the reaction. These signals correspond to those expected for *o,p'*-dibenzene (Fig. 1): upon heating of the sample to room temperature, they disappear in favor of the benzene signal. At −90°C, the intermediate photoproduct reacts with 4-phenyl-1,2,4-triazoledione (PTAD) to form the adduct **3**, the structure of which also confirms the presence of **2**.



Diels–Alder Adducts of Benzene with Arenes and Their [4 + 2] Cycloreversion**

By *Achim Bertsch, Wolfram Grimme,** and *Gerd Reinhardt*

A continuum of reaction pathways exists for the [4 + 2] cycloreversion, from the simultaneous breaking of two single bonds to stepwise bond cleavage. The retrocleavage of Diels–Alder adducts formed from two arenes should most closely resemble the ideal synchronous reaction. Both components lack the two singly occupied p-orbitals necessary to become aromatic, and only simultaneous formation of these two centers enables the transition state to acquire part of this stabilization. Having reported earlier the adduct **4** between benzene and naphthalene,[1] we now report the Diels–Alder adducts of benzene both with itself and with anthracene and naphthacene.

The Diels–Alder trimer **1** of benzene decomposes at 100°C to benzene without evidence for the formation of the intermediate *o,p'*-dibenzene **2**.[2,8] The retrocleavage of **1** also takes place upon irradiation with a high-pressure mercury lamp through quartz. If the reaction is carried out at −90°C in CD_2Cl_2 in an NMR tube and followed by

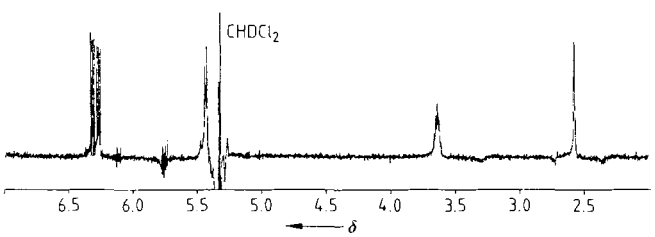


Fig. 1. 300-MHz ^{1}H-NMR spectrum of *o,p'*-dibenzene **2** in CD_2Cl_2 at −90°C. The $CHDCl_2$ signal has been truncated.

The kinetics of the [4 + 2] cycloreversion of *o,p'*-dibenzene **2** was determined by flash photolysis.[3] A solution of the tribenzene **1** in isooctane (8×10^{-5} M) was irradiated in a quartz cuvette ($l = 10$ cm) with a flash from a capacitor discharge and the transient UV absorption of the dibenzene formed, **2**, was recorded at 280 nm. The lifetime of **2** is ca. 0.5 s at room temperature; the kinetic parameters of the decomposition were derived from nine rate constants in the temperature range 20–55°C (see Table 2).

In order to synthesize the more stable adducts **5**–**7**, anthracene and naphthacene were allowed to react with *p*-benzoquinone. With anthracene, **5a** was the sole product, whereas with naphthacene a 1:1 mixture of the stereoisomers **6a** and **7a** was obtained. By hydrogenation with zinc in acetic acid, **5b** and a mixture of **6b** and **7b** were obtained; these compounds were then converted into the bistosylhydrazones **5c**–**7c**. Reaction with *n*-butyllithium in tetrahydrofuran/*n*-hexane at 0°C afforded the anthracene adduct **5**[4] and a 1:1 mixture of the isomeric naphthacene adducts **6** and **7**, respectively.

The adduct **10**, involving the outer ring of anthracene, was obtained from 4a,9,9a,10-tetrahydroanthracene **8**.[5] Cycloaddition of *p*-benzoquinone afforded the adduct **9a**, which, as described above, was converted into the hydrocarbon **9** via the intermediates **9b** and **9c**. Before dehydrogenation of the tetralin moiety in **9**, the cyclohexadiene ring must be protected by addition of 4-ethyl-1,2,4-triazoledione to give adduct **9d**. After formation of the naphthalene system in **10d** by heating with 2,3-dichloro-5,6-dicyano-*p*-benzoquinone in tetrachloroethane, the protecting group is removed by basic hydrolysis and oxidation with copper(II) chloride.

The adducts so obtained (Table 1) decompose cleanly into their aromatic components between 0 and 100°C; the nonseparated isomeric naphthacene adducts **6** and **7** have the same lifetime. In order to measure the rates of cycloreversion, a degassed solution of the compound in dodecane (10^{-5} M) was added to a thermostated polarimeter cuvette ($l = 5$ cm); the formation of naphthalene, anthracene, and naphthacene was followed by continuous re-

[*] Prof. Dr. W. Grimme, Dipl.-Chem. A. Bertsch, Dr. G. Reinhardt
Institut für Organische Chemie der Universität
Greinstrasse 4, D-5000 Köln 41 (FRG)

[**] This work was supported by the Fonds der Chemischen Industrie and BASF AG, Ludwigshafen.

cording of their long-wavelength UV absorptions. The Arrhenius parameters of the cycloreversion and the temperature range in which they were determined are given in Table 2.

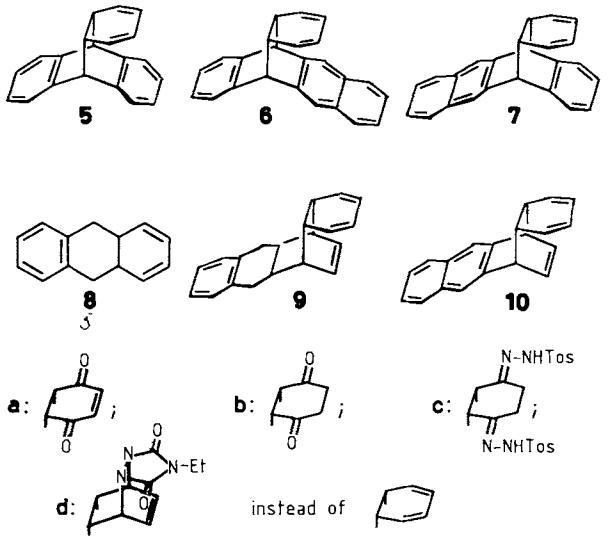


Table 1. Yields and some physical data for the compounds **2**, **3**, **5**, **6**, **7**, **9**, and **10**. The ^{1}H-NMR spectra (except for that of **2**, see Fig. 1) were recorded at 90 MHz in $CDCl_3$.

2, ^{1}H-NMR: $\delta = 6.32$ (q, 2H), 6.27 (q, 2H), 5.43 (m, 4H), 3.63 (sext, 2H), 2.58 (s, 2H)

3, M.p. = 156°C (dec.); ^{1}H-NMR: $\delta = 7.39$ (m, 5H), 6.52 (q, 2H), 6.07 (q, 2H), 5.90 (q, 2H), 4.80 (m, 2H), 3.52 (m, 2H), 2.58 (m, 2H)

5, Yield 8% from **5a**; m.p. = 150°C (dec.); ^{1}H-NMR: $\delta = 7.5$–7.0 (m, 8H), 5.38 (s, 4H), 4.21 (s, 2H), 3.06 (s, 2H)

6, **7**, Yield 4% from **6a**, **7a**; ^{1}H-NMR: $\delta = 7.8$ (m + 2s, 4H), 7.5–7.0 (m, 6H), 5.38 (m + s, 4H), 4.29 (s, 2H), 3.13 (s, 2H)

9, Yield 15% from **9a**; m.p. = 154°C; ^{1}H-NMR: $\delta = 7.1$ (m, 4H), 6.42 (q, 2H), 5.43 (AA'BB', 4H), 2.95 (s, 2H), 2.5 (m, 6H), 2.2 (m, 2H)

10, Yield 32% from **9**; m.p. = 156°C (dec.); ^{1}H-NMR: $\delta = 7.64$ (s, 2H), 7.63 (AA'BB', 4H), 6.70 (q, 2H), 5.63 (s, 4H), 4.10 (m, 2H), 2.92 (s, 2H)

The following linear relationship exists between the observed free energies of activation ΔG^+ for the cycloreversion of the adducts and the gain in resonance energy, ΔRE, calculated according to the SCF-MO method:[6]

Table 2. Activation parameters and resonance gain for the [4 + 2] cycloreversion of the adducts of benzene with arenes.

Compd	ΔT [°C]	lg$A$	E_a [kcal/mol]	ΔG^+ (77°C) [kcal/mol]	ΔRE [kcal/mol]
2	20–55	13.4 ± 0.2	16.5 ± 0.2	15.7 ± 0.1	40.0
4	0–14	12.1 ± 0.6	19.6 ± 0.8	20.8 ± 0.1	30.5
10	20–45	12.3 ± 0.2	21.8 ± 0.6	22.6 ± 0.1	26.4
5	56–80	15.5 ± 0.4	29.3 ± 0.7	25.3 ± 0.2	16.8
6, **7**	80–95	14.9 ± 0.4	30.8 ± 0.6	28.6 ± 0.2	11.5

$$\Delta G^+ = 33.3 \pm 0.9 - (0.43 \pm 0.03) \cdot \Delta RE$$

The correlation coefficient is $r = 0.995$ and the confidence level 99%. Thus, the transition state for the cycloreversion of the adducts is uniformly reduced in energy by 43% of the amount of resonance energy to be gained, ΔG^+ extending over a range of 13 kcal/mol. Structural parameters apparently have no influence on ΔG^+ in this series of closely related adducts. The linear relationship found is only in accordance with a synchronous process, since the breaking of only one bond in the rate-determining step would effect a gain of resonance energy in the intermediate diradicals over a range of only 2 kcal/mol.[7]

Received: December 5, 1985 [Z 1569 IE]
German version: *Angew. Chem. 98* (1986) 361

[1] W. Grimme, H.-G. Köser, *Angew. Chem. 92* (1980) 307; *Angew. Chem. Int. Ed. Engl. 19* (1980) 307.
[2] W. Grimme, G. Reinhardt, *Angew. Chem. 95* (1983) 636; *Angew. Chem. Int. Ed. Engl. 22* (1983) 617.
[3] We thank Prof. Dr. *J. Wirz*, Universität Basel, for the kind invitation to carry out these measurements in his laboratories.
[4] The synthesis described here: R. Waldraff, *Dissertation*, Universität Köln 1983; **5** was obtained for the first time by N. C. Yang, M. J. Chen, P. Chen, K. T. Mak, *J. Am. Chem. Soc. 104* (1982) 853; see also *ibid. 106* (1984) 7310.
[5] K. Takeda, J. Horibe, H. Minato, *J. Chem. Soc. Perkin Trans. 1 1973*, 2212.
[6] M. J. S. Dewar, C. de Llano, *J. Am. Chem. Soc. 91* (1969) 789.
[7] W. C. Herndon, *J. Org. Chem. 46* (1981) 2119.
[8] Note added in proof: *o,p'*-Dibenzene **2** has meanwhile been synthesized independently by another photochemical route and characterized by its UV spectrum (R. Braun, M. Kummer, H.-D. Martin, M. B. Rubin, *Angew. Chem. 97* (1985) 1054; *Angew. Chem. Int. Ed. Engl. 24* (1985) 1059). The half-life at 40°C reported is ca. 5 ms, which is close to that of 10.0 ms measured by us.

BOOK REVIEWS

The Chemist's English. By *Robert Schoenfeld*. VCH Verlagsgesellschaft, Weinheim 1985. xii, 173 pp., bound, DM 42.00/$ 17.95.—ISBN 3-527-26309-8 (VCH Verlagsgesellschaft), 0-89573-436-2 (VCH Publishers)

A large number of books on writing good English are available to the chemist—everything from college textbooks and usage dictionaries to handbooks and style manuals for authors of scientific papers and books. What recommends *The Chemist's English* is above all its readability. In a collection of short essays ranging from the correct use of hyphens and dashes ("Of Nuts, Muttons and Shotguns") and the choice between "that" and "which" ("On the Training of Old Dogs for Which-Hunting") to general questions of style ("Instant Stylistics," "An Investigative Examination of Driveliferous Jargonogenesis") and even "A Chemical Analysis of the English Sentence," *Robert Schoenfeld*, the former editor of the Australian Journal of Chemistry, discusses the many ingredients that go into making the chemist's English good.

Schoenfeld's avowed purpose is not to teach the skill of effective writing per se but rather to whet the appetite for good English. This modest goal he strives to achieve with a highly readable blend of fact, opinion, anecdote, and humor. What emerges from this unorthodox excursion through the English language is the amicably recounted story of one editor's experiences, filled with words of ad-

vice for the scientific author and pervaded with the message that language, like chemistry, can be fun.

The chapter on the overuse of strings of nouns ("Amazing Revelations: English Scientists Secretly Practise German Vice!") illustrates the ingenuity with which the author approaches problems of grammar. In order to explain why "ring junction carbon environment differences" is bad and "differences in the environment of the carbons at the ring junction" or "differences in the environment of the ring junction carbons" better, he introduces the "adjectival" and "genitive bonds" and proceeds to "hydrolyse" this "peptide chain of the order A_5." While perhaps a bit farfetched, the analogy is effective and certainly more entertaining than the dry discussions of most conventional books on grammar and style.

There is, unfortunately, one disturbing side to this book, namely, the inordinate number of errors (which this reviewer would like to assume are merely typographical). In the chapter "Of Nuts, Muttons and Shotguns," for example, the em dash, which may be used to set off parenthetic words or phrases, is discussed and—as in this sentence—printed correctly (i.e., it has roughly the width of a capital M and fills the space almost entirely). This is the first and only time the em dash is printed correctly in the entire book! Further examples are "undistinguishable" instead of indistinguishable (p. 50), "pronounciation" (footnote on p. 64), "commonsense" as a noun (p. 100), and "Oberhauser enhacement" (p. 127).

As the author notes in "Yes, Virginia, there *is* a Temperature," "he who writes about language skates on very thin ice indeed." *Schoenfeld,* like most editors, leaves behind a trail of opinions and pet peeves, but, fortunately, not too many cracks in the ice. Indeed, of all the books on English directed to the scientist, it is refreshing to find one that addresses the subject humorously and in terms the chemist is likely to enjoy. If *The Chemist's English* helps to elevate the chemist's appreciation of good writing, even to a small extent, it will have succeeded where many of its more pretentious relatives have often failed.

David I. Loewus [NB 731 IE]
Angewandte Chemie, Weinheim

Spectral Atlas of Polycyclic Aromatic Compounds. By *W. Karcher, R. J. Fordham, J. J. Dubois, P. G. J. M. Claude,* and *J. A. M. Lighthart.* D. Reidel Publishing Company, Dordrecht 1985. 818 pp., bound, $ 94.00.—ISBN 90-277-1652-8

Polycyclic aromatic compounds (hydrocarbons and aromatic heterocycles) arise from the pyrolysis and incomplete combustion of organic material. Since such processes occur all over the place in our environment (e.g. in motor vehicles, furnaces and in forest fires), polycyclic aromatic compounds (PACs) are ubiquitous. Some PACs have turned out to be carcinogenic in experiments on animals. These two facts explain the enormous current interest in the analysis of PACs.

The samples that the analyst has to investigate generally comprise extremely complex mixtures of PACs. Therefore, combinations of separation (chromatographic) techniques and identification (spectroscopic) methods are usually, employed. Ideally, a laboratory that carries out PAC analysis would possess highly pure reference samples, for identification and standardization purposes, of all PACs in the mixtures to be analyzed. However, the authors justly observe that "due to the enormous number of compounds which are encountered, this situation is unlikely to be attained in the foreseeable future", and they conclude that "the widespread availability of high quality molecular spectra and related data represents a more realistic and practical alternative".

This work is seen by the authors as the beginning of the realization of this alternative. The spectral atlas deals altogether with only 42 compounds (25 polycyclic aromatic hydrocarbons (PAH), eight methyl-PAHs, five thiophene benzologs, three carbazole derivatives, and 10-azabenzo[a]pyrene). The spectra were recorded by the authors on their own instruments. Many of the compounds documented, and their spectra, could be found in any laboratory that carries out PAC analysis (carbazole, anthracene, phenanthrene, fluoranthene, pyrene, benzo[a]pyrene and others). Yet the authors intend—as indicated in their preface—that further volumes should follow this book. The production of an extensive, multivolume PAC spectral atlas would indeed be a welcome and useful enterprise and would increase the significance of this volume.

The conception and realization of the spectral documentation are excellent:

- In the form of graphs and tables, the following spectra are reproduced: the UV/VIS absorption spectra, fluorescence and fluorescence-excitation spectra (room temperature, energy-corrected), Shpol'skii-fluorescence and phosphorescence spectra (15 K), mass spectra (70 eV), ^{1}H-NMR spectra (80 MHz), ^{13}C-NMR spectra, and IR spectra (KBr disk and solution).
- All spectra have been recorded under stringently standard conditions with suitably pure (>99%) samples.
- The instruments used to make the measurements and the experimental conditions are comprehensively described.
- The chemical shifts in the NMR spectra are assigned by reference to literature data and by comparison with the spectra of related compounds.
- Likewise, the IR bands are assigned to important structural characteristics of the compounds.

Only one critical observation will be made here: such an extensive collection of the spectra of PACs should not have neglected the phosphorescence spectra in solid glasses measured at 77 K; at least for quantitative analysis these are appreciably more useful than the Shpol'skii phosphorescence spectra.

In addition, the book contains the melting points of the ultra-pure compounds. In some cases, literature values for the solubility in water (25 °C) are given.

The authors see the value of their work exclusively in connection with the environmental analysis of PACs (in the reviewer's opinion this is a fully unnecessary limitation; PACs are of significance, for example, in photo- and semiconductor physics, in coal chemistry, and many other fields). Thus, it is understandable that for every compound, indications are given as to "occurrence' and "biological activity". This information is presented in tabular form, with reference to the corresponding literature. These tables should, however, only be seen as a structured literature compilation (which the authors do not make explicitly clear) and their perusal cannot replace a comparative study of the works quoted. A critical evaluation, carried out by experts, of the carcinogenic potential of most of the compounds that appear in this volume can be found in Vol. 32 of the well known IARC monographs (International Agency for Research on Cancer). It is to be wel-

comed that the "IARC classification" has been followed in the tables of this book. Yet it could have been hoped, not least in view of the high reputation of the IARC monographs and their great significance as a source of information, that the authors of the PAC spectral atlas should quote accurately. Thus, we read in Vol. 32 of the IARC monographs "The available data provide *no evidence* that *anthracene* is carcinogenic to experimental animals", while the authors of the PAC spectral atlas remark of anthracene "IARC ranking: *inadequate data*".

Summary: A good spectral atlas, whose acquisition can be recommended, and which will be of use especially to laboratories that are beginning to institute PAC analysis. As far as occurrence and biological activity of PACs are concerned, the book can facilitate literature searching, but in no way replace it.

M. Zander [NB 734 IE]
Rütgerswerke AG, Castrop-Rauxel (FRG)

Biotechnology. A Comprehensive Treatise in 8 Volumes. Series editors: *H.-J. Rehm, G. Reed.* **Vol. 6a: Biotransformations.** *K. Kieslich.* VCH Verlagsgesellschaft, Weinheim 1985. xii, 473 pp., bound, Subscription price: DM 425.00.—ISBN 3-527-25768-3

Biotransformation is the broad term for chemical reactions carried out with the help of microbes or enzymes. These reactions may utilize the microbes or enzymes in an immobilized form or otherwise. The present volume is intended for anyone who wants an overview of the variety of biotransformations of commercial or academic interest.

The volume, which is divided into eleven chapters, begins, after an introductory remark by *K. Kieslich,* with an introduction to some of the methodologies for carrying out these transformations by *H. G. W. Leuenberger.* In the second chapter, *L. L. Smith* presents an excellent summary of the reactions involving steroids. The topic is continued by *C. K. A. Martin* who discusses the selective side chain cleavage of sterols for the synthesis of C-19 or C-22 steroids and the partial degradation of the sterol ring system. As is so often the case, biotechnology here succeeds only when it can surpass the chemical methods regarding conversion efficiencies.

Terpenoid transformations, of interest to the flavor and fragrance industries, are discussed by *V. Krasnobajew.* Optimal control of the transformation processes, such that no useless compounds are formed, and economical isolation of the products are the major challenges in this area. Acyclic, monocyclic, and bicyclic monoterpenoids and ionones and related compounds are discussed. In Chapter 5, *A. Kergomard* gives a comprehensive review of the reduction, oxidation, hydrolysis, hydroxylation, degradation, and synthesis reactions which are effected by bacteria and fungi on alicyclic and heterocyclic compounds. Microbial transformations involving natural and semisynthetic alkaloids (e.g. indole, isoquinoline, quinoline, colchicine, morphine, quinolizidine, nicotine, tropane, and ephedrine alkaloids) are reviewed by *P. J. Davis.* These reactions are of interest because microbial systems offer the first level of investigation into bioactivation, bioinactivation, and detoxification in mammals.

An excellent review of reactions involved in antibiotic compounds of both academic and practical interest is provided by *O. K. Sebek.* β-Lactams, aminoglycosides and rifamycins are discussed in some detail in this chapter, which is also sprinkled with some recent references.

The degradation reactions of arenes and five- and six-membered heterocyclic structures are reviewed in an excellent chapter by *P. R. Wallnöfer* and *G. Engelhardt.* While the emphasis here is on the degradation of pesticides and other industrial pollutants, the authors also cover the possibility of using the catabolism of microbes for the production of potentially useful intermediates. *M. Bühler* and *J. Schindler* contribute a fine review on the transformation of short chain *n*-alkanes, higher aliphatic hydrocarbons, and fatty acids by microbes. The role of the monooxygenase system is discussed in detail. Also included is a survey of patents issued during 1972 to 1982 in Europe, Japan, and the United States. Finally, the investigation of recombinant DNA is also discussed briefly.

The production of amino acids and peptides with the help of microbes and enzymes is reviewed by *G. Schmidt-Kastner* and *P. Egerer.* A brief but informative section outlines the economic aspects. In the last chapter, *A. Crueger* and *W. Crueger* conclude this volume with a discussion of carbohydrates. Aldose-ketose isomerizations such as, e.g., in high fructose corn syrup production, oxidations as in ascorbic acid and gluconic acid production are briefly but accurately highlighted, as are also reductions and the hydrolysis of glycosides, above all with a view towards commercial applications.

This volume is a welcome addition to the volumes that have already appeared.[*] The overall quality of the volume is very good. However, the reader should be cautioned that most of the references cover only up to about 1982. As in the case of the volumes reviewed so far, the contents of this volume also continue to fluctuate between the objective of reviewing the research on the topic and that of providing an overview of the relevant industrial aspects. The emphasis, more often than not, is on the former.

Bhavender P. Sharma [NB 727 IE]
Genencor, South San Francisco, CA (USA)

Electroorganic Chemistry as a New Tool in Organic Synthesis. By *T. Shono.* Springer Verlag, Heidelberg 1984. xi, 171 pages, hardback, DM 128.00.—ISBN 3-540-13070-5

Electroorganic synthesis has undergone rapid and continuous redevelopment in the past two decades. It now offers versatile possibilities for the preparation of synthetically valuable intermediates; it serves as a key reaction within complex synthetic sequences and, in addition, it offers easy access to synthetic equivalents with unusual reactivity by means of redox Umpolung. Considering the relatively rare application of this method by non-electrochemists, it must be concluded that it has not been satisfactorily propagated amongst preparative organic chemists. The fear of complex apparatus and electrochemistry's very theoretical presentation to students seem to weigh heavily against it.

T. Shono, one of the most active synthetic electrochemists, tries to dispel these inhibitions in his concise monograph on electroorganic chemistry as a tool in organic synthesis. He emphasizes in his foreword that he intends to present the field exclusively from a synthetic standpoint by means of selected examples. The book does not aim at being comprehensive, nor at penetrating mechanistic analysis.

[*] Cf. *Angew. Chem. Int. Ed. Engl. 24* (1985) 436.

The book consists of three chapters: introduction, anodic oxidations and cathodic reductions. These are followed by a short appendix in which it is demonstrated that the reactions can be carried out with very moderate apparatus.

In the introduction he discusses the principle and potential of redox Umpolung, unfortunately rather scantily. This is followed by a consideration of the consequences of the heterogeneous character of the reaction upon the stereochemistry of the conversion and upon the concentration relationships of the active species that are generated. The influence of the choice of electrode material and electrolyte on product distribution are missing here. The effect of the electrochemical procedure on the stereochemical course of a reaction could easily be overestimated through the presentation of three particularly impressive examples.

Anodic oxidation, with 120 pages, occupies two thirds of the book. This chapter is organized according to the structure of the substrates. Whether this arrangement is more accomodating to a synthetic chemist than organization by reaction type is to be left undecided. Yet, having chosen this system, it would have been more sensible to use it for the reductions too. The section on amine oxidation is, in spite of its great synthetic significance, clearly over-represented with 25 pages.

The chapter on cathodic reductions seems to be rather too brief with 35 pages only. It is organized by reaction type. Even if it is admitted that at present oxidation reactions show a somewhat greater synthetic potential, this abbreviated presentation of synthetic possibilities at the cathode does not meet ones expectations. For example, there is no room for the versatile cathodic heterocycle syntheses and conversions.

It is taken for granted that the author should give preference to his own work in the choice of examples; however, there are some places where a rather more balanced presentation would have been preferred. To meet the claims of the book to present organic electrochemistry as a synthetic tool, it would have to emphasize more strongly the principal synthetic possibilities at the beginning of each section and perhaps compare these with the chemical alternatives. That would offer welcome orientation to the chemist engaged in synthesis. Unfortunately, the index cannot supply this help since it lists, essentially, only compounds, classes of compounds or technical terms and does not link compound and methods or vice-versa. Unfortunately, it is incomplete.

In spite of these reservations, the book should provide valuable and stimulating reading for all synthetically oriented chemists. This presentation of organic electrochemistry as a synthetic tool should be a suitable way to dispel inhibitions about this technique. It can only be hoped that no potential reader will be deterred by the relatively high price.

Eberhard Steckhan [NB 705 IE]
Institut für Organische Chemie und Biochemie
der Universität Bonn (FRG)

Synthetic Organic Photochemistry. Edited by *W. M. Horspool*, Plenum Press, New York 1984. xvii, 534 pp., hardback, $ 75.00.—ISBN 0-306-41449-X

The renaissance of synthesis in organic chemistry has also had a stimulating influence on photochemistry. This welcome development cannot, however, disguise the fact that photochemical reactions still play only a minor rôle in organic synthesis. One reason for this surely lies in the inadequate communication between those engaged in synthesis and those investigating mechanisms.

Up to now, only a few have mastered the interdisciplinary transfer of results from physical chemistry to modern synthesis; thus, any attempt to make the synthetic potential of photochemistry accessible to a wider circle is very much to be welcomed. However, the question ought to be raised whether the prefix "Synthetic" suffices to differentiate this book from a well known series, of which six volumes have already appeared. As the foreword trenchantly comments, the selection of material in any single volume work is bound to be incomplete. If, on this account, however, particular stress has been laid on topicality and synthetic potential, then why are such significant classes of compounds as cyclohexadienones and di-π-methane systems not covered, while topical problems like chirality transfer in cycloadditions are treated comparatively briefly and incompletely? The list of such examples could be continued.

The book does, of course, contain useful information—in some cases very much so—on the photoreactions of arenes, enones, phthalimides, azirines, benzothiophenes and furans and indoles. The same applies for the Paterno-Büchi reaction, for electron transfer reactions in particular, and for photochemical methods with protecting groups. The final chapter, on experimental techniques, does indeed offer an introduction, but this is not exhaustive. Here, every reader is strongly recommended to refer back to textbooks or to "Houben-Weyl".

Around half the topics presented here have already been extensively described elsewhere in surveys, e.g. in the series referred to above. Since most of these contributions have been written from a synthetic standpoint and thus cite similar examples and, moreover, provide more mechanistic information, the editor of this book could easily have avoided repetition and thereby made room for other items. In summary, it can be said that this book provides an introduction to the subject. The reader should, however, have prompt recourse to other books on this topic.

Jochen Mattay [NB 711 IE]
Institut für Organische Chemie der
Technischen Hochschule Aachen (FRG)

Techniques in Organic Reaction Kinetics. By *P. Zuman* and *R. C. Patel*. John Wiley, Chichester 1984. 340 pp., hardback, £ 57.25.—ISBN 0-471-103556-4

This book is based on lectures given by the authors. In four chapters it gives an easily readable insight into the kinetic methods of physical organic chemistry. The theory of chemical reaction kinetics is only brought in to the extent required for the measurement of reaction rates. After a short introduction, the physico-chemical methods of measuring the rates of slow reactions are dealt with in chapter 2 (40 pages). Chapter 3 (201 pages) is concerned with the analysis of kinetic data. It is consciously modelled on the book by *Frost* and *Pearson* (A. A. Frost, R. G. Pearson: *Kinetics and Mechanism*). It contains formal kinetics with many examples from organic chemistry; the influence of ionic strength, solvent characteristics and substituent effects are discussed in depth. Chapter 4 (82 pages) handles the study of fast reactions; it follows *E. F. Caldin*'s book

(*Fast Reactions in Solution*) and is extended by the inclusion of examples from the electrochemical kinetic work of the authors.

This book offers the reader an instructive compilation of older books on kinetics, with a slant towards organic chemistry. The inescapable disadvantage, however, is that the techniques and applications of new developments in the last ten years could not be included. The book can be recommended to students as an introduction to this subject, alongside the thematically very similar book by *K. Schwetlick* (*Kinetic Methods for the Investigation of Reaction Mechanisms*).

Hans-Heinrich Limbach [NB 718 IE]
Institut für Physikalische Chemie
der Universität Freiburg (FRG)

New Books

The following books have been received by the editor. All the publications listed are available through W & P Buchversand für Wissenschaft und Praxis, Boschstrasse 12, D-6940 Weinheim (Federal Republic of Germany). Tel. (06201) 606-0, Telex 465516 vchwh d, Telefax (06201) 602328.

Mass Spectrometry of Heterocyclic Compounds. (Series: **Wiley Series in General Heterocyclic Chemistry,** Series Editors: *E. C. Taylor* and *A. Weissberger*). 2nd Edition. By *Q. N. Porter*. A Wiley-Interscience Publication. John Wiley, Chichester 1985. xxv, 966 pp., bound, £ 289.15.—ISBN 0-471-09901-5

Einführung in die Physikalische Chemie. Teil II: Kinetik. (Series: Hochschultext). By *H. Labhart*. 2nd completely revised edition by *H. D. Breuer*. Springer-Verlag, Berlin 1985. x, 102 pp., paperback, DM 22.80.—ISBN 3-540-15257-1

ESR-Spektroskopie. Anwendungen in der Chemie (Series: Wissenschaftliche Taschenbücher). By *R. Kirmse* and *J. Stach*. Akademie-Verlag, Berlin 1985. 188 pp., paperback, ca. DM 12.50.—Order-No. 763 397 2 (7202)

Wörterbuch der Wasserchemie/Dictionary of Water Chemistry/Dictionnaire de la Chimie de l'Eau. By *F. von Ammon*. VCH Verlagsgesellschaft, Weinheim 1985. xiii, 203 pp., bound, DM 130.00.—ISBN 3-527-25956-2

Modern Practice of Gas Chromatography. 2nd Edition. Edited by *R. L. Grob*. A Wiley-Interscience Publication. John Wiley, Chichester 1985. xix, 897 pp., bound, £ 75.20.—ISBN 0-471-87157-5

A History of the Nomenclature of Organic Chemistry (Series: Chemists and Chemistry). By *P. E. Verkade*. D. Reidel Publishing Company, Dordrecht 1985. xiv, 507 pp., bound, HFl. 220.00.—ISBN 90-277-1643-9

ICSU Short Reports. Vol. 3: Third European Bioenergetics Conference. Edited by *G. Schäfer*. Cambridge University Press, Cambridge 1985. XLVII, 745 pp., bound, £ 50.00.—ISBN 0-521-30813-5

Synthetic Reagents. Vol. 6: Chloramine-T, Hydrogen Peroxide, Polyphosphoric Acid. Edited by *J. S. Pizey*. Ellis Horwood, Chichester 1985. 438 pp., bound, £ 45.00.—ISBN 0-85312-739-5

Molecular Semiconductors. Photoelectrical Properties and Solar Cells. By *J. Simon* and *J.-J. André*. Springer-Verlag, Berlin 1985. xiii, 288 pp., bound, DM 174.00.—ISBN 3-540-13754-8

Handbook of Tritium NMR Spectroscopy and Applications. By *E. A. Evans, D. C. Warrell, J. A. Elvidge,* and *J. R. Jones*. A Wiley Interscience Publication. John Wiley, Chichester 1985. xiv, 249 pp., bound, £ 25.50.—ISBN 0-471-90583-6

Structure and Spectra of Molecules. By *W. G. Richards* and *P. R. Scott*. John Wiley, Chichester 1985. ix, 172 pp., paperback, £ 6.95.—ISBN 0-471-90579-8

Symmetry and Structure. By *S. F. A. Kettle*. John Wiley, Chichester 1985. x, 330 pp., paperback, £ 8.95.—ISBN 0-471-90705-7

Specialist Periodical Reports. General and Synthetic Methods. Vol. 7. A Review of the Literature Published During 1982. Edited by *G. Pattenden*. The Royal Society of Chemistry, London 1985. xiii, 469 pp., bound, £ 88.00.—ISBN 0-85186-884-3

Corrigendum.

The title of the communication by Hans Bock and Martin Bankmann, *Angew. Chem. Int. Ed. Engl. 25* (1986) 265 should read, "$H_3C-P=CH_2$: An Ylide with Two-Coordinate Phosphorus?"

Registered names, trademarks, etc. used in this journal, even without specific indication thereof, are not to be considered unprotected by law.

© VCH Verlagsgesellschaft mbH, D-6940 Weinheim, 1986. - Printed in the Federal Republic of Germany by Zechnersche Buchdruckerei, Speyer/Rhein.

All rights reserved (including those of translation into foreign languages). No part of this issue may be be reproduced in any form - by photoprint, microfilm, or any other means - nor transmitted or translated into a machine language without written permission from the publishers. Only single copies of contributions, or parts thereof, may be reproduced for personal use.

Valid for users in the USA: The appearance of the code at the bottom of the first page of an article in this journal (serial) indicates the copyright owner's consent that copies of the article may be made for personal or internal use, or for the personal or internal use of specific clients. This consent is given on the condition, however, that the copier pay the stated per-copy fee through the Copyright Clearance Center, Inc., for copying beyond that permitted by Sections 107 or 108 of the U.S. Copyright Law. This consent does not extend to other kinds of copying, such as copying for general distribution, for advertising or promotional purposes, for creating new collective works, or for resale. For copying from back volumes of this journal see 'Permissions to Photo-Copy: Publisher's Fee List' of the CCC.

Editorial office: Pappelallee 3, D-6940 Weinheim, Federal Republic of Germany, Telephone (06201) 602315, Telex 465516 vchwh d, Telefax (06201) 602328.

Editor: *P. Gölitz.*

Associate editors: *D. I. Loewus, A. Stimson.* **Editorial assistant:** *E. Schweikart*

Publishers: VCH Verlagsgesellschaft mbH. (Managing Directors: *Prof. Dr. Helmut Grünewald* and *Hans Dirk Köhler*), Pappelallee 3, D-6940 Weinheim, Federal Republic of Germany. Correspondence concerning advertisements should be addressed to VCH Verlagsgesellschaft mbH. (Advertising Manager *R. J. Roth*), Boschstr. 12. P.O. Box 1260/1280, D-6940 Weinheim, Federal Republic of Germany, Telephone Weinheim (06201) 602-0, Telex 465516 vchwh d, Telefax (06201) 602328.

ANGEWANDTE CHEMIE
International Edition in English
Volume 25 · Number 5
May 1986
Pages 383–486

^{15}N-NMR Spectroscopy—New Methods and Applications**

New Analytical Methods (28)

By Wolfgang von Philipsborn* and Raffaello Müller

The nitrogen nucleus is the third most important probe (after ^{1}H and ^{13}C) for structural investigations of organic and bioorganic molecules by NMR spectroscopy. For a long time, however, the insufficient sensitivity and low natural abundance of the ^{15}N isotope hampered detection of the ^{15}N nucleus, and the quadrupolar ^{14}N nucleus proved unsuitable for the study of larger molecules with several nonequivalent nitrogen atoms. The advent of new techniques, such as pulse sequences and polarization transfer, in conjunction with the use of high-field magnets and large-sample probe heads largely solved the detection problem. As a result, the last few years have seen a dramatic development of ^{15}N-NMR spectroscopy as a versatile method for studying molecular structure, both in isotropic (liquid) and anisotropic (solid) phases. The scope of chemical applications extends from inorganic, organometallic, and organic chemistry to biochemistry and molecular biology, and includes the study of reactive intermediates, biopolymers, enzyme-inhibitor complexes, and nitrogen metabolism. Two-dimensional NMR techniques offer additional possibilities for detailed studies of biological systems.

1. Introduction

Nitrogen belongs to the few elements that form the skeleton of organic and bioorganic molecules, and functional groups containing nitrogen atoms are of great importance in organic and biochemical reactions. Therefore, nitrogen NMR spectroscopy provides a sensitive method for the study of chemical structure and bonding, reaction mechanisms, biosynthesis, nitrogen fixation, and metal coordination, as well as for the study of active sites in biochemical systems.

In fact, *Proctor* and *Yu*[2] carried out nitrogen NMR studies in the very early days of nuclear magnetic resonance spectroscopy and thereby discovered the chemical shift phenomenon in NH_4NO_3. For a long time, the quadrupolar ^{14}N nucleus was preferred by NMR spectroscopists because of its high natural abundance (99.63%). The introduction of FT NMR spectroscopy, however, stimulated interest in the much less abundant spin-½ ^{15}N isotope. Although the NMR receptivity of the ^{15}N nucleus (0.37% abundance) is 280 times smaller than that of ^{14}N (Table 1), there are at least two factors that compensate for this deficiency. First, the line broadening of ^{14}N signals (up to several kHz) is absent in ^{15}N resonances, and, second, the large nuclear Overhauser effect (NOE) ($\eta_0 = -4.93$) enhances the ^{15}N signal intensities of proton-bearing ^{15}N atoms when proton noise decoupling is applied. Furthermore, it is sometimes possible to shorten the

[*] Prof. Dr. W. von Philipsborn, Dipl.-Chem. R. Müller
Organisch-chemisches Institut der Universität
Winterthurerstrasse 190, CH-8057 Zürich (Switzerland)

[**] ^{15}N-NMR Spectroscopy, Part 16.—Part 15: [1].

 © VCH Verlagsgesellschaft mbH, D-6940 Weinheim, 1986 0570-0833/86/0505-0383 $ 02.50/0

Table 1. Magnetic properties of the ^{15}N, ^{14}N, ^{13}C, and ^{1}H isotopes.

Nucleus	ν/MHz [a]	Nat. abundance/%	Spin	Gyromagnetic ratio $\gamma/10^7$ rad T^{-1} s^{-1}	Relative sensitivity [b]	[c]
^{1}H	400.0	99.98	1/2	26.7510	62.91	5676
^{13}C	100.6	1.11	1/2	6.7263	1	1
^{14}N	28.9	99.63	1	1.9324	0.064	5.69
^{15}N	40.5	0.37	1/2	−2.7107	0.066	0.02

[a] At a field of 9.4 tesla. [b] For the same number of nuclei at constant field B_0. [c] For natural isotopic abundance and constant field B_0.

long spin-lattice relaxation times (T_1) of tertiary N atoms by the use of high magnetic field strengths (superconducting magnets) or, alternatively, to circumvent the problem by the use of polarization-transfer from fast-relaxing, sensitive nuclei, such as ^{1}H or ^{19}F.

^{14}N-NMR spectroscopy has been employed to study relatively small organic[3] and inorganic molecules[4,5] and to study molecular motion;[6] the quadrupole moment is an especially important nuclear property for the investigation of dynamic processes. For larger molecules with several nonequivalent N atoms, including biopolymers, only the ^{15}N isotope yields satisfactory and interpretable NMR spectra. The results obtained up to 1980 are summarized in three monographs.[7] In many cases, ^{15}N-NMR spectra can also be recorded in the proton-coupled mode, thereby yielding both chemical shift and spin-coupling information (scalar coupling in solution and dipolar coupling in the solid). Finally, the use of large sample volumes in wide-bore high-field magnets has helped considerably to overcome the hitherto bad reputation of ^{15}N-NMR spectroscopy as being insensitive, time-consuming, and unsuitable for analytical applications in structural chemistry and biochemistry. It is the purpose of this review article to discuss the experimental progress and to illustrate the broad spectrum of present and future applications of ^{15}N-NMR spectroscopy in chemistry.

2. Experimental Techniques

2.1. Standard Pulse Experiments

Conventional FT NMR experiments with a pulse-modulated high-frequency field at the ^{15}N resonance are only feasible if the spin-lattice relaxation times (T_1) are reasonably short; this is true for N atoms with directly bonded protons, e.g., in NH_2 and NH groups. In such cases (nuclear-nuclear) dipole-dipole relaxation (DD) is the dominant relaxation mechanism, and T_1 values of less than 20 s are usually observed.[7a] Figure 1 shows the spectrum of the dication **1** of 6,7-dimethyltetrahydropterin. Each N atom is bonded to at least one H atom. Moreover, the N atoms have similar relaxation times, which results in comparable signal intensities. However, even tertiary N atoms may be detected with sufficient sensitivity if measurements are conducted in strong magnetic fields (9–11 tesla) generated by superconducting magnets. In this case, a chemical shift anisotropy dependent relaxation process (CSA), which increases with the square of the field strength, may contribute significantly to the spin-lattice relaxation rate (Section 3.3). Finally, otherwise long T_1 values may be reduced by electron-nuclear dipole-dipole interaction when paramagnetic species, so-called relaxation reagents, are added. A convenient and widely used compound is chromium(III) acetylacetonate, $Cr(acac)_3$,[8] which enhances ^{15}N relaxation rates without significant line shifts (< 1 ppm).

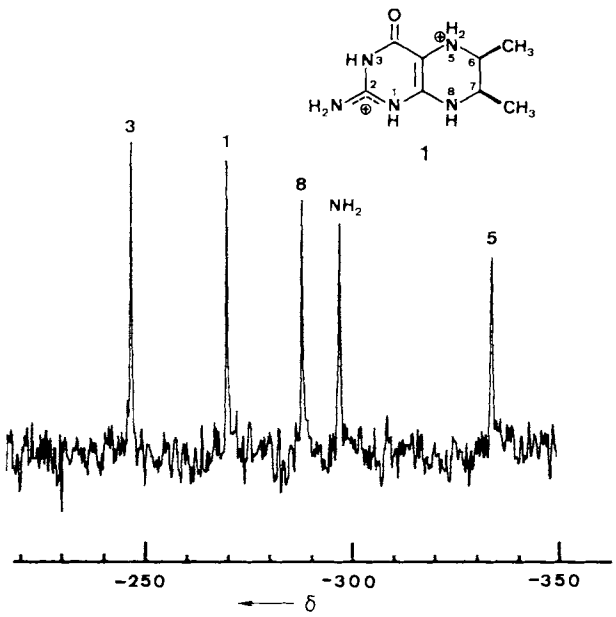


Fig. 1. Proton-noise-decoupled and phase-adjusted ^{15}N-NMR spectrum of the dication **1** of *cis*-6,7-dimethyl-5,6,7,8-tetrahydropterin (10.1 MHz; CF_3COOH, 0.7 M) [9].

^{1}H broadband-decoupling enhances the signal-to-noise ratio not only as a result of multiplet collapse but even more effectively by the large NOE factor ($\eta_0 = -4.93$) for the ^{15}N, ^{1}H system. From Equation (a) it is apparent that the full benefit of this (negative) signal enhancement is only obtained if T_1 is dominated by dipole-dipole interactions, which is the case for NH_2 and NH groups, and that it leads to signal inversion (Fig. 2) (M_z = z-magnetization; M_z^0 = z-magnetization at thermal equilibrium, T_1^{DD} = time constant of dipole-dipole relaxation).

$$\frac{M_z}{M_z^0} = 1 + 0.5\,\frac{\gamma_H}{\gamma_N}\,\frac{T_1}{T_1^{DD}} \qquad \text{(a)}$$

$$\eta_0 = 0.5 \cdot (-9.86) = -4.93$$

As shown in Figure 2a, inefficient dipolar relaxation for tertiary N atoms may result in loss of the signal. Such cases, frequently encountered in N-heterocycles, can be handled by deliberate suppression of the NOE; this is achieved by switching the decoupler power output on during acquisition and off during the pulse delay time (inverse gated decoupling). Since spin decoupling becomes effective almost instantaneously when the B_2 field is switched on whereas the NOE is built up more slowly with the time constant T_1^{DD}, ^{1}H-decoupled ^{15}N-NMR spectra may be recorded with a minimized Overhauser effect (Fig. 2b). This technique allows tertiary and proton-bearing N atoms to

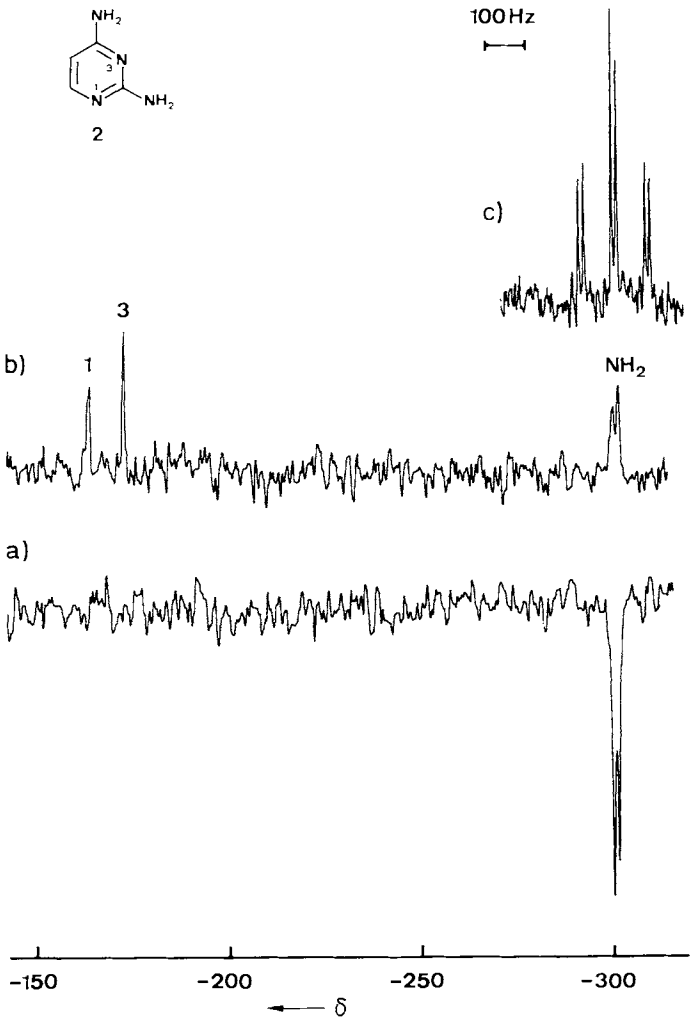


Fig. 2. ^{15}N-NMR spectra of 2,4-diaminopyrimidine **2** (10.1 MHz; $(CD_3)_2SO$): a) ^{1}H-noise-decoupled; b) "inverse-gated"-decoupled (decoupler output "on" during acquisition, "off" during acquisition delay time); c) no ^{1}H decoupling.

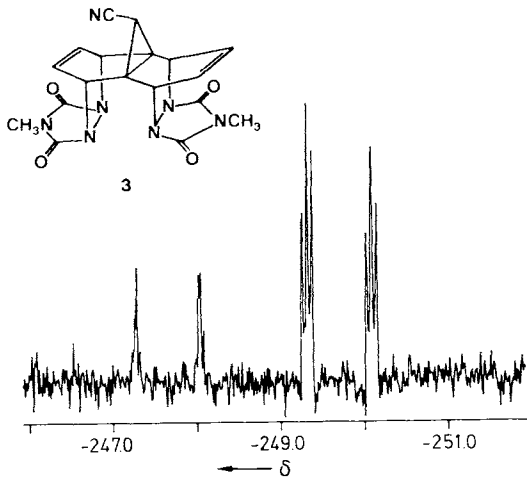


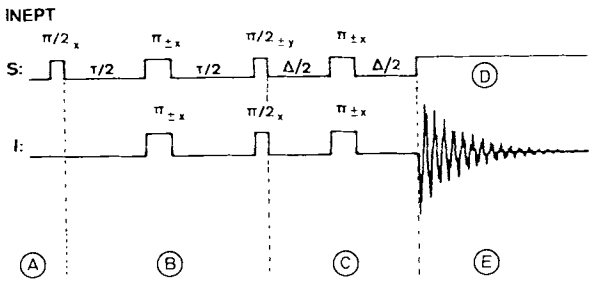
Fig. 3. Proton-coupled DEPT ^{15}N-NMR spectrum of the 1:2 adduct **3** of tricyclo[4.4.1.0^{1,6}]undeca-2,4,7,9-tetraene-11-carbonitrile with N-methyl-1,2,4-triazoledione) (40.6 MHz; $(CD_3)_2SO$). The cyano doublet ($\delta = -113.3$) is not shown. The assignment of the two weak and two strong signals to the NCH_3 and NCHCH groups, respectively, follows from the multiplicities and from the values of N,H coupling constants.

be simultaneously observed. Thus, the relative intensities of ^{1}H-decoupled ^{15}N resonances are dependent on the spin-lattice relaxation times T_1 *and* the nuclear Overhauser effects ($\eta \leq |\eta_0|$). Quenching of undesired, small Overhauser effects may also be achieved by the use of relaxation reagents.

The sensitivity of ^{15}N-NMR detection may be further enhanced by the use of large-diameter sample tubes (15–25 mm) and the application of strong magnetic fields (B_0). The excellent performance, in terms of field homogeneity and stability, of modern wide-bore superconducting magnets permits the routine measurement of ^{15}N-NMR spectra with natural isotope abundance with the techniques described above. A typical example is shown by the spectrum of the [4.4.1]propellane derivative **3** (Fig. 3).[10]

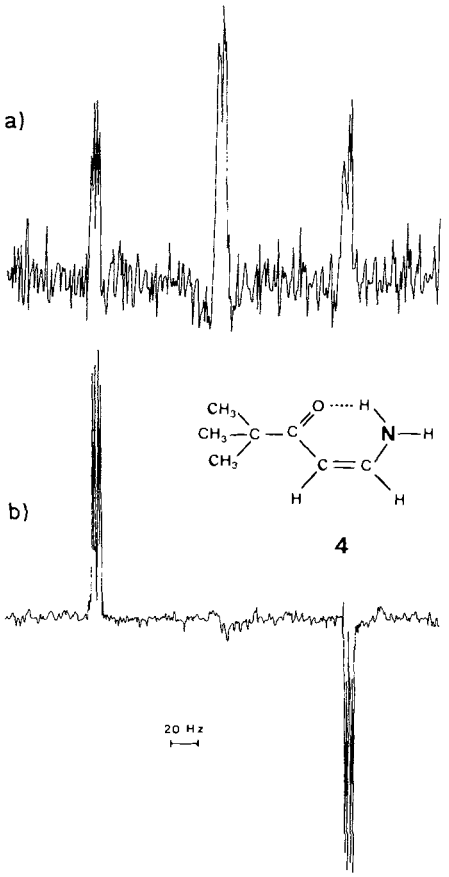
2.2. One-Dimensional Pulse Sequence Experiments (INEPT, DEPT)

The rapid development of pulse techniques and their implementation on modern spectrometers provides still more effective and versatile methods for sensitivity improvement in ^{15}N-NMR spectroscopy. In such experiments, application of a sequence of nonselective and simultaneous pulses on a scalar-coupled heteronuclear spin system leads to spin polarization transfer from the sensitive ^{1}H nuclei (large abundance, large γ) to the insensitive ^{15}N nuclei (small abundance, small γ) and a maximum enhancement factor of $|\gamma_H/\gamma_N| = 9.86$ for the intensities of the ^{15}N resonances. Furthermore, since the rate at which the entire pulse sequence can be repeated is governed by the short relaxation times of the ^{1}H nuclei, additional time is saved. A typical polarization transfer experiment, the INEPT pulse sequence (*I*nsensitive *N*uclei *E*nhanced by *P*olarization *T*ransfer) is shown in Scheme 1.[11] For a discussion of the mechanism of polarization transfer the reader is referred to the review by *Benn* and *Günther*.[12] After the polarization transfer (90° pulse) and following the ^{15}N detection pulse, antiphase signals can be detected or, by refocusing and decoupling during acquisition, the spin system can be "processed" further. Thus, proton-coupled, selectively decoupled, or fully decoupled ^{15}N-NMR spectra can be obtained, thereby increasing the information content of the spectra for structural studies.



Scheme 1. S, ^{1}H; I, ^{15}N; Ⓐ preparation, Ⓑ evolution, Ⓒ refocusing, Ⓓ ^{1}H-broadband decoupling, Ⓔ detection. See also [12].

The quality of such spectra, in terms of sensitivity and resolution, in comparison with standard pulse spectra, is exemplified in Figure 4. This example also demonstrates that the multiplicity and phases of the signals in INEPT



4

Fig. 4. ^{15}N-NMR spectra of the conformer shown of (*Z*)-1-amino-4,4-dimethyl-1-penten-3-one **4** (20.3 MHz; C_6D_6, 3.7 M): a) standard-pulse NMR spectrum (measuring time 10 h); b) INEPT ^{15}N-NMR spectrum (measuring time 1.9 h) [13]. $^1J(N,H) = 92.7$, $^2J(N,H) = 1.7$, $^3J(N,H) = 4.0$ Hz.

spectra differ from those in regular spectra. For instance, the relative intensities for NH doublets are +1 and −1, for NH_2 triplets +1, 0, and −1.[14] The phases can be adjusted by application of the above-mentioned refocusing procedure. In addition, selective ^{1}H-decoupling may lead to considerably sharper lines and, hence, to still better sensitivity. The ^{15}N-NMR spectra of 5-methylisoxazole **5** (Fig. 5) illustrate the accurate determination of $^2J(N,H)$ and $^3J(N,H)$ through selective ^{1}H-decoupling. Coupling of the ^{15}N nuclei to methyl protons often obscures the desired spin-coupling information, as shown in the case of 2-acetylpyridine **12** (Section 3.2.2), and increases the measuring time required.

Polarization transfer to an insensitive nucleus requires scalar-coupling to a sensitive nucleus. In addition to the ^{1}H nucleus, ^{19}F[17] and ^{31}P have been used; in particular, ^{31}P was used successfully to transfer spin polarization to ^{15}N,[16a] ^{57}Fe, ^{103}Rh, and ^{183}W.[16b] The substantial spin coupling between ^{19}F and ^{15}N is especially advantageous in polarization transfer experiments. Figure 6 shows the re-

5

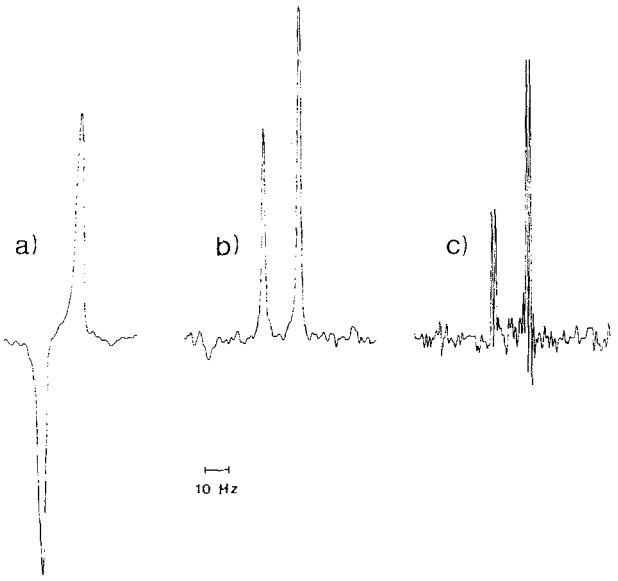


Fig. 5. INEPT ^{15}N-NMR spectra of 5-methylisoxazole **5** (20.3 MHz; $(CD_3)_2SO$): a) proton-coupled; b) refocused and selectively ^{1}H-decoupled (H-C4); c) same as b) but irradiated at the CH_3 resonance [15].

sult of such an INEPT measurement for perfluoropyridine **6**.[17] The large $^2J(N,F)$ coupling (−51.7 Hz) determines the pulse delay $\tau = 1/2J(N,F)$ in the INEPT pulse sequence (cf. Scheme 1). Here again, the central lines of the triplet are absent, so that the large splitting corresponds to $2 \times J(N,F)$.

The optimum setup of an INEPT experiment is less straightforward if there are no dominant heteronuclear

6

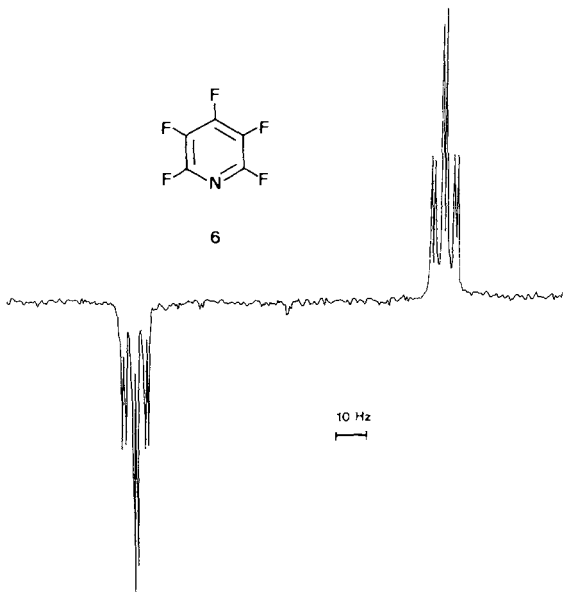


Fig. 6. INEPT ^{15}N-NMR spectrum of perfluoropyridine **6** (20.3 MHz; $(CD_3)_2CO$) with polarization transfer from the ^{19}F nuclei (188.2 MHz). The τ value for the INEPT sequence was calculated using $|^2J(N,F)| = 52$ Hz [17].

coupling constants. If the ^{15}N nucleus is coupled with several protons, which, in turn, are mutually coupled (spin systems of the type $IS^1S^2...S^n$), the optimal τ values can be determined by using analytical expressions.[18] This is shown for the nitroethene 7 in Figure 7. It should be noted

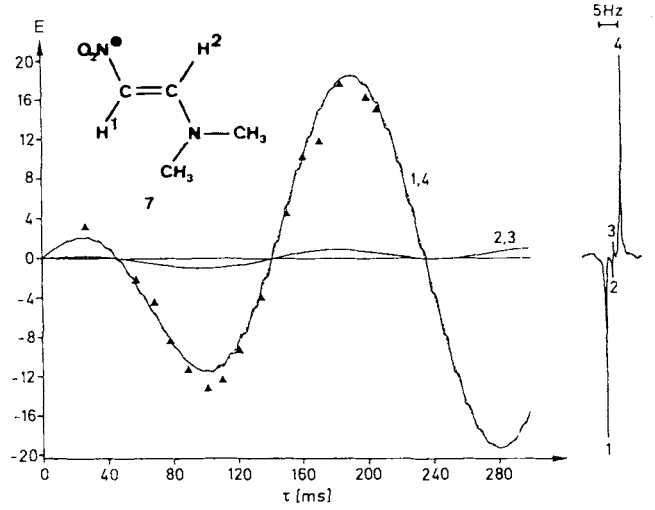
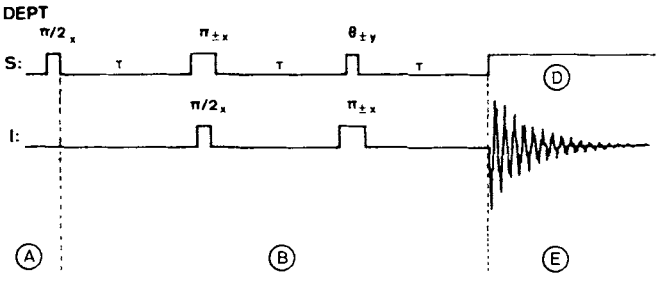


Fig. 7. Right: INEPT ^{15}N-NMR spectrum of the NO_2 group of (*E*)-*N*,*N*-dimethyl-2-nitrovinylamine 7; left: signal enhancements (E) as a function of τ. (—) calculated and (▲) experimental values [18]. $J(N,H\text{-}2)=2.2$, $J(N,H\text{-}1)=1.8$, $J(H\text{-}1,H\text{-}2)=10.6$ Hz; $\nu(H\text{-}1)-\nu(H\text{-}2)=-290$ Hz (20.3 MHz).

that τ_{opt} (190 ms) does not correspond to either $1/2J(N,H^1)$ ($\tau=278$ ms) or $1/2J(N,H^2)$ (227 ms), because the homonuclear coupling constant $^3J(H^1,H^2)$ is much larger (10.6 Hz) than the two heteronuclear values (1.8 and 2.2 Hz, respectively). Nevertheless, such spin systems are also amenable to an effective polarization transfer, which considerably extends the application of the INEPT technique beyond the detection of simple NH and NH_2 groups[14] (see also Section 4).



Scheme 2. S, I, Ⓐ, Ⓑ, Ⓒ, Ⓓ see legend to Scheme 1. See also [12].

The pulse sequence DEPT (*D*istortionless *E*nhancement by *P*olarization *T*ransfer) was developed[19] as an alternative polarization transfer technique in order to avoid the intensity and phase distortions inherent in the INEPT experiment. The DEPT sequence yields spectra (Scheme 2) with positive signals only, which thus resemble standard pulse spectra. In this technique, the sensitivity enhancement is described as a function of the delay time τ and the pulse angle θ. Only for simple spin systems of the type IS_n, however, are pure phase spectra obtained; spin systems $IS^1S^2...S^n$ with hetero- and homonuclear coupling are subject to phase distortions.[18] Further, when higher-order spin systems are involved, the intensities are also distorted. Decoupled DEPT spectra always show positive phase signals. DEPT ^{15}N-NMR spectra of thiazole **8** are shown in Figure 8. Selective decoupling allows the assignment of the small coupling constant (2.2 Hz) to the vicinal N,H interaction ($^3J(N,H)$).

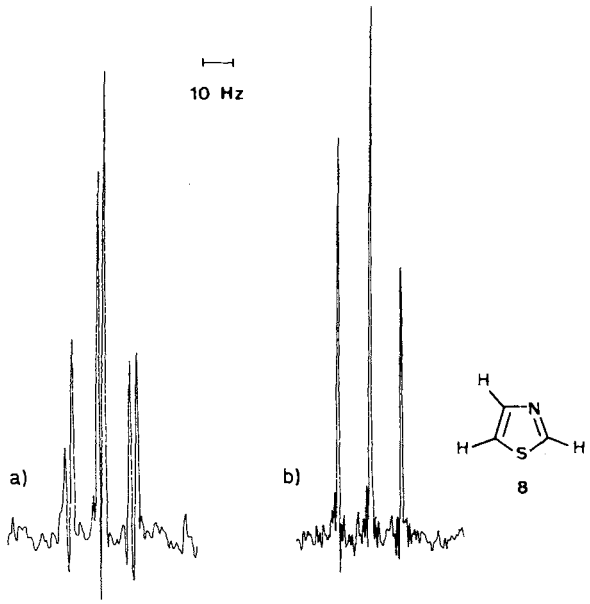


Fig. 8. DEPT ^{15}N-NMR spectra of thiazole **8** (20.3 MHz; $CDCl_3$): a) proton-coupled; b) selective irradiation of the H-5 resonance [15].

In terms of sensitivity enhancement, the INEPT pulse sequence has proven superior to the DEPT sequence;[19b] for the five-spin system of 2-methoxypyridine the enhancement is larger by a factor of 1.8.[18] The simple INEPT experiment (without refocusing) appears to be less prone to perturbation by additional homo- and heteronuclear couplings.

The advantage of the polarization transfer experiments discussed above is the nonselective nature of the ^1H-irradiation. Thus, polarization can be transferred to several nonequivalent N atoms, which allows the structural investigation of complex molecules (cf. Section 4).

An alternative way of achieving sensitivity enhancement is based on a *selective* population transfer (SPT), in which a single ^1H transition is irradiated, resulting in equalization or inversion of the populations followed by transfer to connected levels.[20] The ^{15}N sensitivity enhancement attained is the same as in the nonselective INEPT or DEPT experiments; however, the transition-selective nature of the experiment permits the determination of the relative signs of N,H coupling constants.[21] Similarly, for non-proton-bearing N atoms a modified INEPT sequence, which achieves a selective polarization transfer, was proposed. It largely suppresses homonuclear multiquantum coherence and allows neglect of N,H long-range coupling to other than the selectively irradiated proton.[22] For this purpose,

soft proton pulses (typical pulse duration 5 ms for a 90° flip angle) were used in the detection of the proline ^{15}N resonance of a hexapeptide. However, the enhancement is only large if the proton excitation is highly selective, which constitutes a serious limitation for complex molecules, even in high magnetic fields.

The largest sensitivity improvements are achieved when the ^{15}N resonance is detected indirectly via the proton resonance; theoretically, the sensitivity can be increased by a factor of $(\gamma_H/\gamma_N)^3$, i.e., by about 961. Such results have actually been obtained in multiple quantum coherence experiments on large peptides by the use of 1D and 2D data representations[23,24] (see also Section 2.3).

A critical evaluation of the advantages and disadvantages of the numerous one-dimensional pulse sequence experiments has recently been presented by *Turner*.[25]

2.3. Heteronuclear Correlated 2D NMR Spectroscopy

During the last decade, 2D NMR experiments have developed to a very high degree of versatility and sophistication and many of them can be routinely performed on commercial spectrometers. Nevertheless, the application to ^{15}N-NMR spectroscopy has been slow and, only recently, owing to improved general NMR instrumentation and the development of multiple quantum coherence experiments, has significant progress been achieved. Of the classical 2D experiments, only heteronuclear $^1H,^{15}N$ shift correlation has found application in the assignment of ^{15}N resonances via $^1J(N,H)$ and long-range $J(N,H)$. For a review of the classical 2D NMR methods the reader is again referred to the article by *Benn* and *Günther*.[12]

The correlation of ^1H and ^{15}N chemical shifts based on multiple quantum coherence has also led to a dramatic improvement in sensitivity, since determination of the ^{15}N frequencies is effected by detection of the scalar-coupled protons.[26] A third significant application of 2D NMR is found in the analysis of solid-state ^{15}N-NMR spectra with dipolar coupling.[27]

$^1H,^{15}N$ shift correlated (COSY) 2D NMR spectroscopy can be applied to oligopeptides and leads to an assignment of ^{15}N resonance lines based on known NH and $C_\alpha H$ proton frequencies.[28,29] Measurements of this kind, when carried out on nonenriched substrates, are rather time-consuming compared with $^1H,^1H$ and $^{13}C,^1H$ 2D NMR experiments. The complete assignment of all ^{15}N-NMR signals for the undecapeptide cyclosporin A has been achieved by using the COLOC pulse sequence[30] (Fig. 9). The proton shift assignments were obtained from additional COSY experiments, e.g., 2D homonuclear NH,H(α) and 2D heteronuclear C(α),H(α) correlation.

A 2D NMR experiment specifically designed for the detection of proton-coupled ^{15}N resonances utilizes the idea of a double transfer of polarization based on an INEPT pulse sequence and allows the determination of ^{15}N chemical shifts with the sensitivity of the proton resonance. The original pulse sequence used by *Bodenhausen* and *Ruben*[31] was subsequently modified and simplified by *Redfield*[32] (HAHNDOR pulse sequence) and *Bax* et al.[24] with the result that this 2D NMR multiple quantum

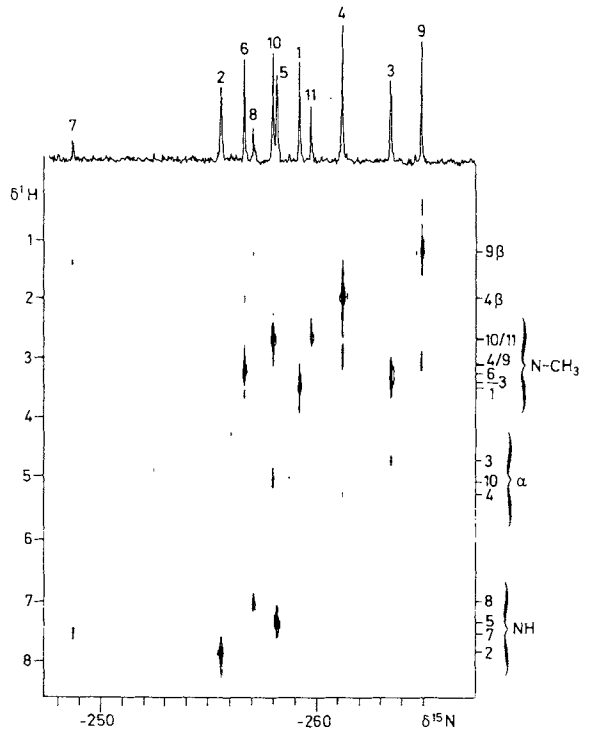


Fig. 9. COLOC $^1H,^{15}N$-heteronuclear shift correlated NMR spectrum of cyclosporin A (50.7 MHz; $CDCl_3$, measuring time 36 h). The spectrum shows correlation peaks for ^{15}N atoms with directly bonded protons (NH) and geminal protons ($N-C_\alpha-H$ and $N-CH_3$), thereby allowing a complete assignment of the eleven N atoms in one experiment [28c]. Cyclosporin A is an undecapeptide with the following amino acid sequence (MeBmt = *N*-methylbutenylmethylthreonine):

cyclo[MeBmt-Abu-Sar-MeLeu-Val-MeLeu-Ala-D-Ala-MeLeu-MeLeu-MeVal].
1 2 3 4 5 6 7 8 9 10 11

method has found wide practical use. The advantages of this experiment are a dramatic sensitivity gain by a factor of $(\gamma_H/\gamma_N)^3 = 961$ and the detection of only those ^1H resonances that are scalar-coupled to an ^{15}N nucleus. This permits detection of relevant NH groups in large biomolecules.[33a,23] The spectrum of ^{15}N-labeled *E. coli* $tRNA_f^{Met}$ (Fig. 10) demonstrates the use of this method to identify the six nucleotide units biosynthetically derived from uridine and, at the same time, the improved resolution obtainable in the 2D data representation. It was estimated that ^{15}N-NMR shifts for $^{15}N,^1H$ groups in nonenriched samples can be obtained in 2–4 h with a 100 mM sample of the biopolymer.

Recent developments in high-resolution ^{15}N-NMR spectroscopy of solids (see Section 4.6) permit the measurement of spectra of biomolecules which contain precise isotropic chemical shift and $^{15}N,^1H$ dipolar coupling information. Since such spectra may be very complex, 2D NMR spectroscopy and graphical representation of the spectra with $\delta(N)$ as the F_2 and D(N,H) as the F_1 coordinate is very useful. In one of the first applications, *DiVerdi* and *Opella*[34] reported N–H bond lengths in DNA based on the magnitude of dipolar $^{15}N,^1H$ couplings (Fig. 11). "D-resolved" $^{15}N,^1H$ spectra of oriented virus solutions, obtained by spontaneous alignment of these macromolecules in the external magnetic field B_0, have also been recorded.[35]

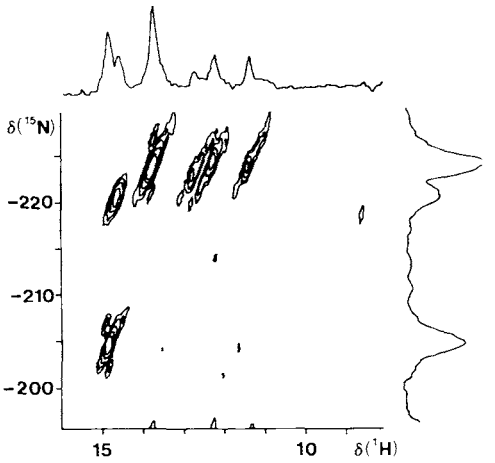


Fig. 10. Contour plot of $^{15}N,^{1}H$ heteronuclear chemical shift correlation NMR spectrum, derived from a multiple quantum coherence experiment, of ^{15}N-labeled $tRNA_f^{Met}$ from *E. coli* (36.5 MHz; $\nu(H)=360.1$ MHz; 65% enriched at N-3 of uridine and uridine-derived bases, 5 mg sample dissolved in 250 μL of aqueous buffer solution, measuring time 6 h). Projections of the ^{1}H- and ^{15}N-NMR spectra are shown opposite the respective chemical shift axes. For further experimental details and assignments of chemical shifts see [33a]. An improved method for the indirect detection of ^{15}N resonances was recently described[33b].

J-resolved 2D ^{15}N-NMR spectra are another powerful source for structure elucidation via long-range $^{15}N,^{1}H$ spin couplings. Such experiments have been performed in combination with an INEPT polarization-transfer pulse sequence applied during the preparation period of a selective 2D *J* pulse sequence.[36] In this way, long-range $^{15}N,^{1}H$ spin coupling constants have been determined, with excellent sensitivity and resolution, for aromatic and aliphatic

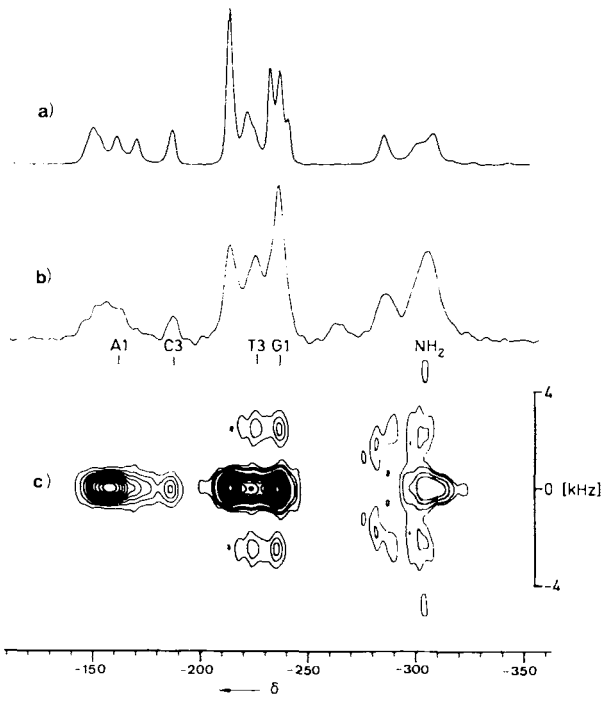


Fig. 11. CPMAS (cross polarization and magic angle spinning) ^{15}N-NMR spectra of DNA (15.24 MHz): a) isotropic chemical shifts of B-DNA; b) low-humidity DNA; c) $\delta(N)/D(N,H)$ 2D ^{15}N-NMR spectrum of low-humidity DNA. For assignments of chemical shifts see [34].

compounds, and the method has been suggested as a means to obtain precise values for $^{3}J(N,H)$ in peptides (see Section 3.2.2).

In conclusion, modern FT NMR spectroscopic techniques combined with high magnetic field strengths and large sample volumes have largely overcome the sensitivity problem and now permit the routine performance of ^{15}N-NMR experiments at natural isotope abundance. Nevertheless, depending on the type of ^{15}N resonance to be investigated, the most suitable detection technique has to be found and the experimental conditions carefully matched. This set-up procedure often requires more time than for conventional nuclei such as ^{1}H and ^{13}C. One major obstacle, the long T_1 relaxation times of tertiary N atoms and the small NOE, has been successfully removed by polarization transfer from a sensitive, fast-relaxing scalar-coupled nucleus, usually a proton. Even higher sensitivity can be achieved by indirect detection of the ^{15}N nuclei via the ^{1}H resonance, and corresponding 1D and 2D multiple quantum coherence experiments are particularly suited for large biomolecules. The ^{15}N resonance in nonlabeled low-molecular-weight compounds ($M_r<500$) can now be directly detected in a few hours with 0.1–0.2 M solutions. A variety of applications to organic and inorganic chemistry as well as to biochemistry will be discussed in Section 4.

3. Structural Dependence of Spectral Parameters

High-resolution ^{15}N-NMR spectra provide information on nuclear shielding constants (chemical shift), spin-lattice relaxation times (T_1), spin-spin relaxation times (T_2), and scalar heteronuclear spin coupling (e.g., $^{n}J(N,H)$). This constitutes a considerable improvement over ^{14}N-NMR spectroscopy, which mainly yields chemical shift information. Only in a few favorable cases can heteronuclear coupling constants be obtained and line-shape information be used to characterize exchange processes and molecular motion. In this section, the spectral parameters of ^{15}N-NMR will be discussed in terms of their structural significance and potential application in chemistry.

3.1. Chemical Shifts

The shielding range of the ^{15}N nucleus in diamagnetic molecules extends over 1000 ppm, corresponding to about 40 kHz in a field of 9.4 tesla ($\nu_0=40.5$ MHz). Taking into account a line width of 1–2 Hz and the smaller abundance of nitrogen atoms in organic and bioorganic molecules, this leads to an even better dispersion of the resonance lines than in ^{13}C-NMR spectra. This excellent dispersion is not attenuated by the fact that the resonances of the majority of N atoms in organic structures lie within a 500-ppm range. An example is provided in Figure 12 by the spectrum of a mixture of 1- and 2-methyltetrazole, **9** and **10**, respectively; well-separated lines for the eight nonequivalent N atoms are observed over a range of 170 ppm, but their assignment requires additional experiments (cf. Section 3.4).

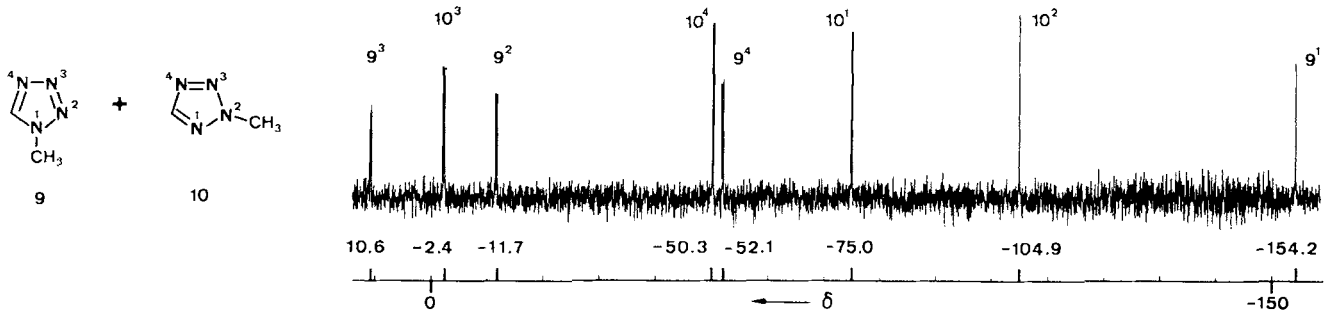


Fig. 12. ^{15}N-NMR spectrum of a mixture of 1- and 2-methyltetrazole, **9** and **10**, respectively (40.6 MHz; 200 mg in 2.5 mL of $CDCl_3$, 75 mg of $Cr(acac)_3$ added; measuring time 42 min).

3.1.1. *Standardization—Reference Compounds*

In this review, all chemical shifts (δ values) will be given relative to that of nitromethane ($CH_3{}^{15}NO_2$) as pure liquid in a capillary (external standard), without susceptibility correction and with negative signs for low-frequency and positive signs for high-frequency shifts. Literature data originally measured relative to other reference compounds, such as $NH_4{}^{15}NO_3$, $H^{15}NO_3$, or $^{15}NH_3$, are adjusted to the CH_3NO_2 scale.[7a] We have used nitromethane throughout our own work; its use allows direct comparison with the two extensive data collections compiled by *Martin* et al.[7a] and by *Witanowski* et al.[7b] The choice of CH_3NO_2 has the consequence that most δ values are negative. This fact, although quite common for other nuclei (e.g., metal nuclei), has induced some authors to adopt other references (e.g., NH_3(liq.) or $NH_4^{\oplus}$) at the low-frequency end of the nitrogen-shift scale, either as a primary reference (external standard) or as a secondary artificial reference. However, an arbitrary value for the $CH_3{}^{15}NO_2$ shift relative to NH_3 (liq.) (e.g., 380.2 ppm) should be used since the NH_3 resonance is strongly temperature dependent.[37] Moreover, as a consequence of concentration, solvent, and temperature effects, especially for different sample alignments in electromagnets and superconducting magnets, and usually neglected susceptibility corrections,[7a] the general reproducibility of ^{15}N chemical shifts is not better than ± 1 ppm. This value may be a lower limit in cases where relaxation reagents (>0.05 M) are used to measure the ^{15}N resonance.

3.1.2. *Main Trends in ^{15}N-NMR Shifts*

The ^{15}N-NMR shifts of N atoms with different oxidation states, coordination numbers, and hybridizations (sp^3, sp^2, sp) are summarized in Figure 13. As expected from the similarity of nitrogen and carbon in electronic structure and bonding, the ^{15}N-NMR shifts parallel the ^{13}C-NMR shifts in many respects. Thus, the tricoordinated N atoms (amines) appear at the low-frequency end of the scale; tetracoordinated N atoms (ammonium salts and *N*-oxides) absorb in the same range. The introduction of electronegative substituents leads to deshielding; the three principal hybridization states of nitrogen give rise to deshielding in the sequence $sp^3 < sp < sp^2$. The ranges for the resonance of carbon-substituted tricoordinated ($\delta = -400$ to -200) and dicoordinated N atoms ($\delta = -100$ to $+100$) are well separated. The carbonyl analogues $-$NO and $-NO_2$ exhibit resonance positions at the high-frequency end of the scale for organic nitrogen compounds. The characteristic position of functionalized N atoms is largely maintained when they act as ligands in metal complexes, i.e., the coordination shifts are fairly small[4] (see Section 4.4). An important feature of the N atom, the lone-pair electrons, have a pronounced influence on the shielding of ^{15}N nuclei if low-lying $n \rightarrow \pi^*$ transitions are available to affect the $(\Delta E)^{-1}$ term in the paramagnetic shielding expression. For example, protonation of the azine N atoms in pyridines and pyrimidines leads to low-frequency shifts of 100–120 ppm,[39] such effects being suitable for the study of protonation and hydrogen bonding in organic and bioorganic molecules (see Section 4.1). When the lone pair is involved in n,π-delocalization, e.g., in enamines and enamino ketones, high-frequency shifts are observed which can be correlated with the extent of conjugation in such systems.[40] Figure 14 illustrates the transition between amines, enamines, enamino ketones (vinylogous amides), and amides as reflected in the ^{15}N chemical shifts. An application of these principles to a conformational study of enamino ketones will be discussed in Section 4.3.

A less phenomenological and more detailed discussion of ^{15}N chemical shifts has to be based on the paramagnetic shielding term, σ^p, which dominates the relative line positions of the heavier nuclei. The observed ^{15}N chemical shifts have also been extensively discussed on the basis of quantum chemical calculations.[7b,41] In this context, it is important to note that the shielding values for the ^{14}N and ^{15}N isotopes may be readily compared with each other as well as with calculated data since the ratio of the resonance frequencies of a series of isotopomeric molecules was found to be constant within $\pm 8 \times 10^{-8}$.[3] All available data indicate that primary isotope effects are of the order of a few tenths of a ppm[7b] and may thus be neglected for practical purposes (see also ref. [78b]). In doing so, however, one must realize that the error limits of ^{14}N shielding data can be quite large (several ppm) depending on the line width (up to several kHz), whereas ^{15}N-NMR data are usually accurate to ± 0.5 ppm.

Both ^{15}N and ^{14}N chemical shifts are prone to medium effects, i.e., solvent, concentration, and temperature. Depending on the nature of the solvent and substrate, these effects may be as high as several tens of ppm. An example

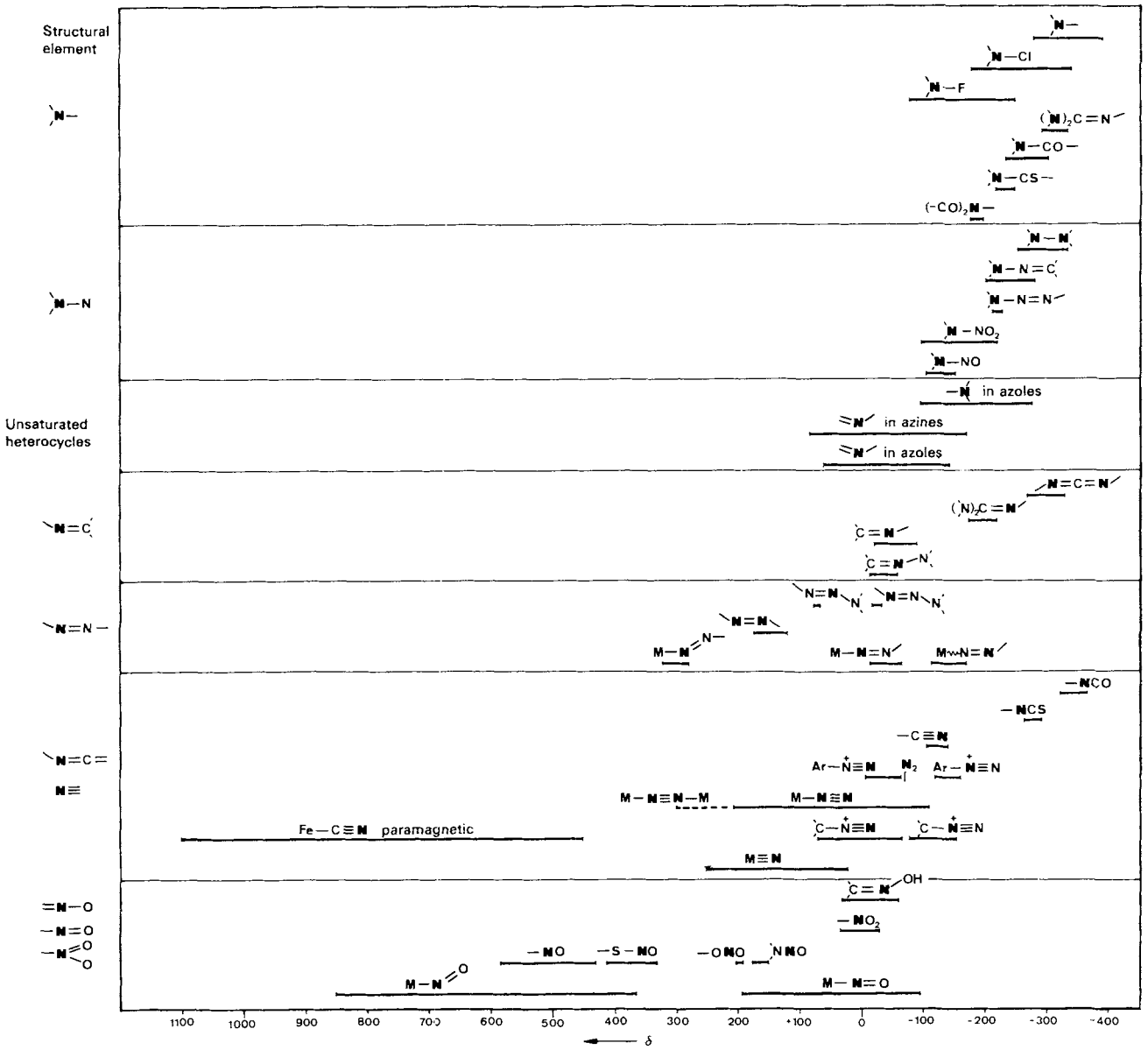


Fig. 13. ^{15}N chemical shift ranges in organic and inorganic compounds relative to CH_3NO_2; positive δ values correspond to ^{15}N resonances shifted to higher frequencies [38]. Ar = aryl.

is given in Figure 15. The substituent-induced shifts in *p*-substituted *N,N*-dimethylbenzaldehyde hydrazones **11** correlate well with Hammett substituent constants, and the slope is solvent dependent (which indicates the origin of the effects).[42] The dicoordinated N atoms of azines and azoles, frequently encountered in heterocyclic systems, are

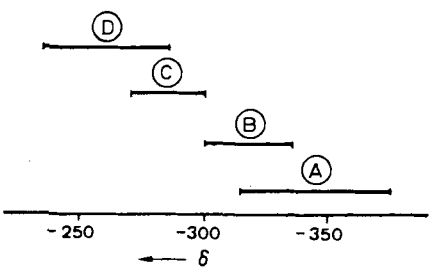


Fig. 14. ^{15}N chemical shift ranges for Ⓐ *tert.*-amines, Ⓑ enamines, Ⓒ enamino ketones, and Ⓓ amides.

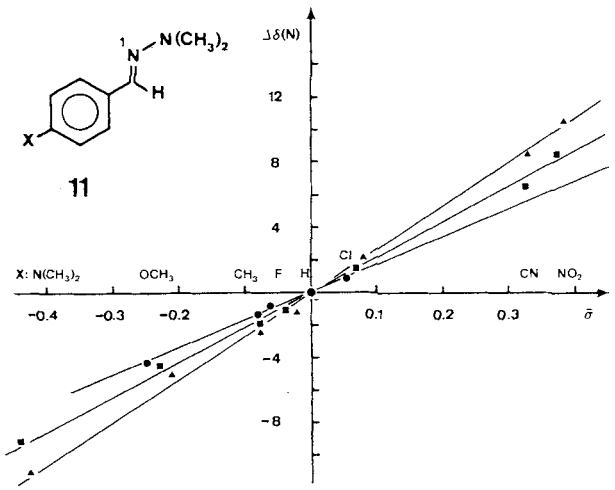


Fig. 15. Correlation between $\Delta\delta(N) = \delta_N^X - \delta_N^H$ and the substituent constants $\bar{\sigma} = (\rho_I\sigma_I + \rho_R\sigma_R)/(\rho_I + \rho_R)$ for the N-1 resonance of *p*-substituted benzaldehyde hydrazones **11**; measured in C_6H_{12} (●), $(CH_3)_2SO$ (■), and CH_3OH (▲) [42].

typical examples where the solvent-induced ^{15}N shift correlates well with the hydrogen bonding properties of the solvent[43] (Table 2). The limiting case, full protonation on the N atom, causes a low-frequency shift of approximately 120 ppm (see ref. [39] and references cited therein). An excellent overview of solvent effects on ^{15}N chemical shifts is given in ref. [7a], and some applications will be discussed in Section 4.1.

Table 2. Solvent effects $\Delta\delta$(N) for pyridine (in ppm) [93].

Gas phase	C_6H_{12}	CCl_4	C_6H_6	Neat liquid	DMSO [a]
0	−1.5	−4.3	−4.9	−6.3	−6.9
CH_2Cl_2	$CHCl_3$	CH_3OH	H_2O	TFE [b]	
−9.1	−12.5	−24.9	−28.1	−39.9	

[a] $(CH_3)_2SO$. [b] CF_3CH_2OH.

Several authors have investigated deuterium isotope effects on ^{15}N chemical shifts, although the data base is still rather small. In an early study, *Litchman* et al.[44] measured low-frequency shifts of 0.68, 1.29, and 1.96 ppm for mono-, di-, and trideuterated ammonia, respectively, and a value of −0.6 ppm per deuterium atom was observed in [^{13}C-2,3-$^{15}N_2$-guanidino]arginine.[45] Deuterium isotope effects over several bonds have been detected in enamino ketones, but they usually do not exceed 0.1 ppm.[46] If the deuteration affects a fast tautomeric equilibrium, as in 2-hydroxyazo compounds, much larger shifts (several ppm) can be observed.[47] Isotope effects may thus be useful for the detection and quantitative study of tautomeric systems.

Because of the manifold influences on ^{15}N chemical shifts, the assignment of resonance lines for structure elucidations may become a difficult problem. A variety of assignment techniques, however, are available, which will be discussed collectively in Section 3.4. The possibilities have been considerably expanded by the inclusion of N,H coupling constants, which are obtainable from INEPT, DEPT, or 2D NMR heteronuclear correlation experiments. In the course of this development our knowledge of N,H couplings over several bonds (^nJ(N,H), n = 2, 3, 4) has progressed to a point where an application to structural analysis becomes possible.

3.2. Spin-Spin Coupling Constants

Contrary to the nearly identical chemical shifts of the two nitrogen isotopes, their coupling constants to an X nucleus depend on the gyromagnetic ratios $\gamma(^{14}N) = 1.9324$ and $\gamma(^{15}N) = -2.7107$. From Equation (b), it is apparent that the ^{15}N,X coupling constants are 40% larger than the ^{14}N,X coupling constants and have an opposite sign.

$$J(^{15}N,X) = \gamma(^{15}N)/\gamma(^{14}N) \cdot J(^{14}N,X) = -1.40 \cdot J(^{14}N,X) \quad (b)$$

It may be recalled that a "reduced coupling constant" $K(X,X')$ has been defined in order to allow a comparison of coupling energies of different nuclei (isotopes or elements)[48] [Eq. (c)].

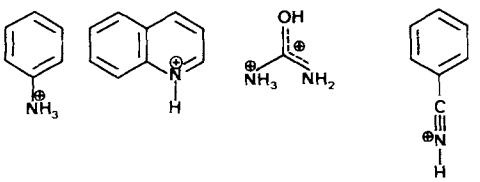
$$K(X,X') = \frac{4\pi^2}{h\gamma_X\gamma_{X'}} \cdot J(X,X') \ [N \cdot A^{-2} \cdot m^{-3}] \quad (c)$$

This definition eliminates the influence of the gyromagnetic ratio (magnitude and sign). Therefore, K reflects the coupling pathway and the mechanism of the scalar spin–spin interaction. In practice, coupling energies are always reported as J or $|J|$ values.

3.2.1. One-Bond $^{15}N,X$ Coupling (^1J(N,X))

As for C–H bonds in ^{13}C-NMR spectroscopy, the largest coupling constants in ^{15}N-NMR spectroscopy are observed for N–H bonds; moreover, they depend linearly on the s-character of the hybrid orbital involved in the N–H bond (see Scheme 3). There are several empirical equations that describe this dependence.

$$^1J(N,H) = -2.94 \cdot (\%s) \quad [Hz] \quad (d)[51]$$
$$^1J(N,H) = -2.33 \cdot (\%s) + 6 \quad [Hz] \quad (e)[52]$$
$$^1J(N,H) = -1.69 \cdot (\%s) - 17 \quad [Hz] \quad (f)[53]$$

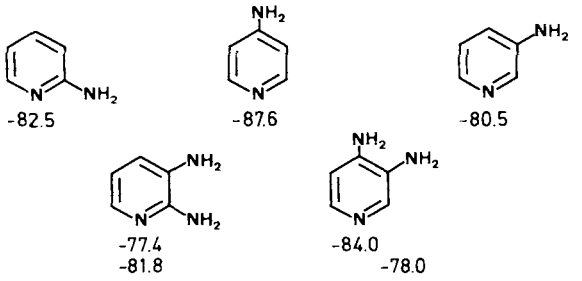


^1J(N,H) [Hz]						
	found	−76.9 [49]	−96.0 [49]	−76.5	−96.8 [50]	−136 [49]
	calcd	−73.5	−98.0	−73.5	−98.0	−147
	%s	25	33	25	33	50

Scheme 3.

Equation (d) is preferably used for charged species and reproduces the ^1J(N,H) values in Scheme 3 within ±3.5 Hz with the exception of the value for protonated benzonitrile (−11 Hz). These correlations can be used to estimate the hybridization of the N atom. For example, compared with the ^1J(N,H) value for ammonia (62 ± 2 Hz),[7a] the small values for the 1,2-disubstituted triaziridines **24** and **25** (51.7 and 58.1 Hz, respectively, see Section 4.2)[54] indicate a pyramidal geometry at N-3.

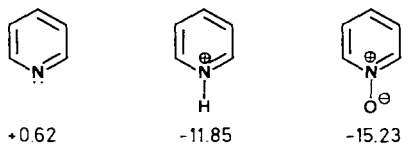
^1J(N,H) coupling constants in aminopyridines and aminopyrimidines are dependent on the position of the NH_2 group, a manifestation of the extent of conjugation and, as a consequence, loss of pyramidal geometry at the N atom (Scheme 4). This result can be used for the assignment of amino groups in azines and is consistent with the conclusions drawn from chemical shifts.[39] The barriers to internal rotation about the N–C bond[55] are 22.1 and 31.3 kJ/mol for the 3- and 4-amino groups, respectively, in 3,4-diaminopyridine, which clearly supports the weaker conjugation and more pyramidal geometry of the 3-amino group. It should be added that N,H coupling in anilines is also solvent dependent. ^1J(N,H) increases with increasing tendency of the solvent to form hydrogen bonds to the NH_2 groups; for example, $\Delta J^{DMSO}_{CDCl_3}$ is 4–5 Hz.[56]



Scheme 4. The coupling constants $^1J(N,H)$ [Hz] are given below the formulas [39].

The $^1J(N,H)$ coupling shows no significant H/D isotope effect since the same value ($^1J(N,D) = 9.45 \pm 0.2$ Hz) was measured for the three species NH_2D, NHD_2, and ND_3. This value can be used to calculate $^1J(N,H)$ in ammonia, $^1J(N,H) = \gamma_H/\gamma_D \cdot J(N,D) = 6.494 \cdot J(N,D) = 61.4$ Hz, in good agreement with direct measurements.[44]

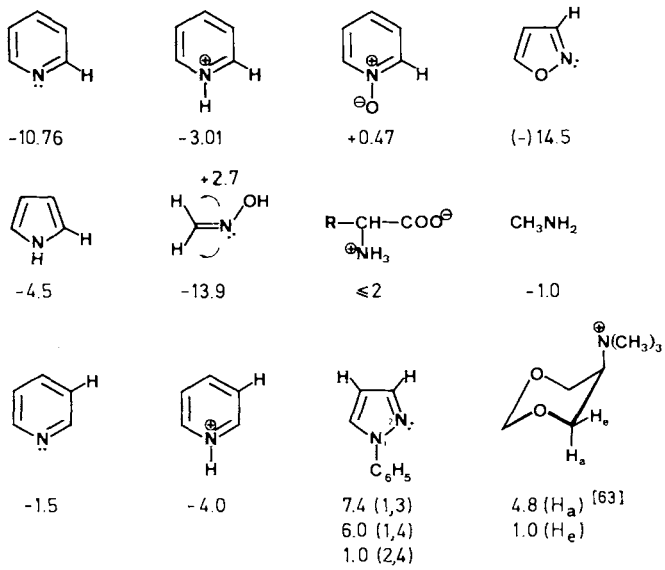
One-bond coupling of ^{15}N to other nuclei (e.g., ^{13}C, ^{15}N, ^{29}Si, ^{31}P) is expected to decrease with decreasing gyromagnetic ratio of the X nucleus since, for the lighter elements, the Fermi contact mechanism dominates this coupling.[57] In fact, $^1J(N,P)$ shows the largest values (50–95 Hz) in aminophosphanes.[58] The one-bond coupling between ^{13}C and ^{15}N nuclei is much smaller (for alkyl amines, absolute values of 2–5 Hz) but increases with increasing s-character in both the N- and C-orbitals and reaches values of -17.5 Hz in acetonitrile[59] and -20.2 Hz in diazomethane.[60] No general relationship, however, seems to hold between $^1J(N,C)$ and s-character, although the equation $^1J(N,C) = 0.0125 \cdot (\%s)_C \cdot (\%s)_N$[52] was proposed. It is evident from the extensive data collections on $^1J(N,C)$[7a,b] that factors such as the electronegativity of the substituents on nitrogen, the π-bond order, and the orientation of the lone-pair electrons contribute substantially to the coupling constant. For example, the lone-pair electrons make a positive contribution to $^1J(N,C)$ in pyridine, which results in a small coupling constant for the free base and a large, negative value for the pyridinium ion and the *N*-oxide[61] (Scheme 5). Furthermore, mechanisms other than the Fermi contact type can make considerable positive or negative contributions to coupling between ^{15}N and ^{13}C nuclei.[62]



Scheme 5. The coupling constants $^1J(N,C)$ [Hz] are given below the formulas [61].

3.2.2. Long-Range $^{15}N,X$ Coupling ($^nJ(N,X)$, $n = 2, 3$)

In this section we will restrict ourselves to the discussion of $^{15}N,^1H$ and $^{15}N,^{13}C$ coupling constants and their application in structure elucidation. Values for these interactions are usually < 20 Hz and thus in the same range as corresponding $^1H,^1H$ or $^{13}C,^1H$ coupling constants. Whereas $J(^{15}N,^1H)$ can be determined for compounds containing a natural abundance of ^{15}N, the measurement of $^{15}N,^{13}C$ coupling constants requires ^{13}C- or ^{15}N-labeled components since both nuclei have a very low natural isotope abundance (1.1% and 0.37%, respectively). $^{15}N,^1H$ coupling constants are, therefore, useful for analytical purposes (e.g., spectral assignments, configurational and conformational studies), while $^{15}N,^{13}C$ coupling constants may be expected to aid mechanistic and biosynthetic investigations. With the advent of modern pulse sequences (cf. Section 2.2), a large number of $^{15}N,X$ coupling constants have become readily available, and major trends in their structural dependence have been worked out. Scheme 6 lists some typical examples for $^2J(N,H)$ and $^3J(N,H)$ in organic structures. Geminal N,H coupling is rather large in H–C=N– systems (10–20 Hz); a significant contribution to $^2J(N,H)$ originates from nonbonding electron transfer into the antibonding σ^* orbital of the C–H bond.[64] Protonation or quaternization of the dicoordinated sp^2-hybridized N atom leads to a drastic reduction of the value of $^2J(N,H)$, as seen in pyridinium and pyrimidinium compounds (Scheme 6).[65b]



Scheme 6. The coupling constants $^nJ(N,H)$, $n = 2, 3$ [Hz], are given below and, if necessary, above the formulas [7a, b].

When the INEPT and DEPT pulse sequences were first used to measure proton-coupled ^{15}N-spectra, it was recognized that $(2 \times {}^2J(N,H))^{-1}$ is the optimal τ value for azines[65] and azoles.[15] The following example illustrates the use of $^2J(N,H\text{-}6) = 11.1$ Hz in 2-acetylpyridine **12** to obtain a fully proton-coupled refocused INEPT spectrum. The very complex spectrum (Fig. 16a) can be simplified by applying selective ^1H-decoupling during the acquisition period. These experiments (Fig. 16b) permit the determination and assignment of all long-range N,H coupling constants; corresponding studies can help to elucidate the

substitution pattern in more complex nitrogen heterocycles (see Section 4).

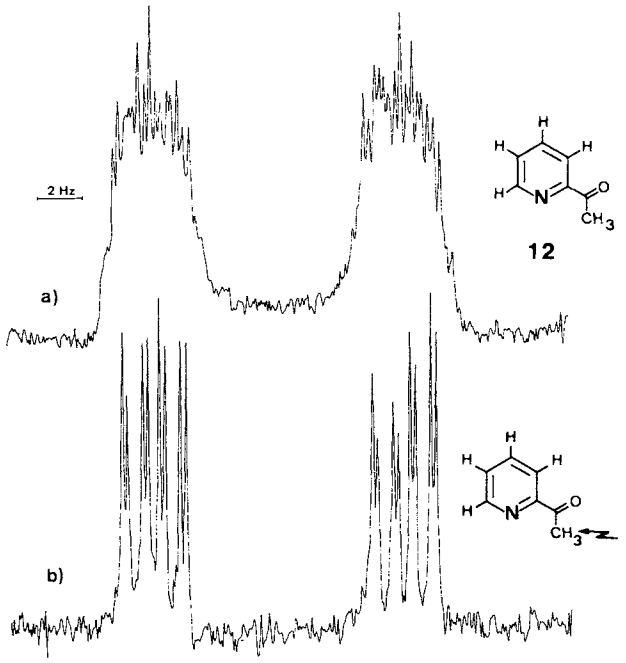
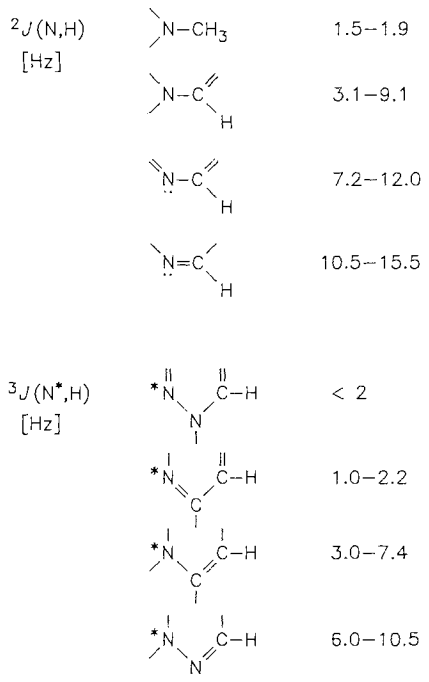


Fig. 16. INEPT ^{15}N-NMR spectra of 2-acetylpyridine **12** (20.3 MHz; 90% v/v in $(CD_3)_2CO$): a) proton-coupled, 11000 pulses; b) selective irradiation at the CH_3 resonance, 1500 pulses [65a].

A detailed investigation of N,H coupling constants in azoles[66] has revealed a subtle dependence of ^2J(N,H) and ^3J(N,H) on the coupling pathway, i.e., connectivity, geometry, and bond order (Scheme 7). Such information, even if only semiquantitative, can be useful for structural assignments and for the estimation of coupling constants in order to optimize delay times for polarization transfer experiments and for heteronuclear 2D NMR.

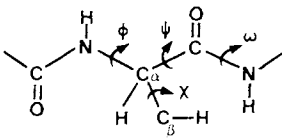


Scheme 7.

Long-range N,H coupling constants in aliphatic systems are usually small (<4 Hz) and, since the spin systems are often complex, the precise values cannot be readily determined. For example, the potential importance of ^3J(N,H) for the determination of the torsional angles ψ or χ in peptide systems has raised considerable interest (Scheme 8).[67] Although a torsional angle dependence of the type

$$^3J(N\text{–}CO\text{–}CH) = A\cos^2\psi + B\cos\psi + C$$

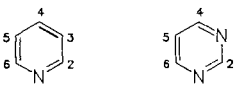
was demonstrated both theoretically[68] and experimentally,[69] the very narrow range of ^3J(N,H) is a serious limitation. The fact that small values may have either sign constitutes a further uncertainty in stereochemical applications.



Scheme 8.

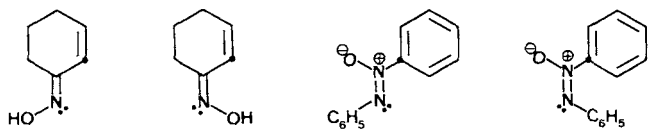
The relative signs of N,H coupling constants may be determined by standard double resonance techniques[70] or spectral analysis and simulation. As expected, the Fermi contact dominated coupling constants ^1J(N,H) are always negative, whereas ^2J(N,H) and ^3J(N,H) may show either sign; in general, N,H coupling constants > 10 Hz are negative.[71] The relative signs of all N,H coupling constants in pyridine and pyrimidine have been determined by SPT experiments[21c] and spectral simulation,[72] respectively. The consistent results are collected in Table 3.

Table 3. Magnitudes and relative signs of coupling constants ^nJ(N,H) [Hz] in pyridine [21c] and pyrimidine [72].



	H-2	H-3	H-4	H-5	H-6
Pyridine	−10.93	−1.48	+0.27	−1.48	−10.93
Pyrimidine	−14.42	—	+0.54	−1.07	−10.76

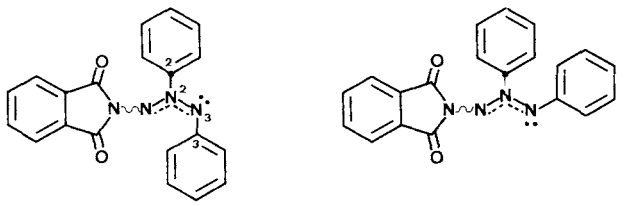
Long-range ^{15}N,^{13}C coupling constants are generally smaller than 10 Hz. The data can be best obtained from the ^{13}C-NMR spectra of ^{15}N-labeled compounds. ^2J(N,C), like ^2J(N,H), is known to depend upon the orientation of the lone-pair electrons on nitrogen relative to the geminal carbon atom, significantly larger values being observed for synperiplanar than for antiperiplanar arrangements[73] (Scheme 9). The geometrical dependence of the N-C-C coupling is not impaired by the presence of other heteroatoms, as shown by the spectra of (*E*)- and (*Z*)-azoxybenzene. This fact permitted the use of ^2J(N,C) in the structural proof of two stereoisomeric azimines, **13** and **14**, formed by addition of phthalimidonitrene to (*E*)- and (*Z*)-azobenzene, respectively (Scheme 10).[75] Since N-2 and N-3 have similar chemical shifts in **13** and **14**, their assign-



(-) 11.0 [74] (+) 1.8 [74] (-) 9.4 [75] (+) 2.5 [75]

Scheme 9. The coupling constants ^2J(N,C) [Hz] are given below the formulas.

ments are based upon the very different values of ^1J(N,C), in analogy to the azoxybenzenes and on the basis of a theoretical treatment of ^1J(N,C).[62] The (*E*)- and (*Z*)-configurations clearly follow from the ^2J(N,C) values obtained from the ^{13}C-NMR spectra of the [2,3-N_2]-labeled substrates.



13 14

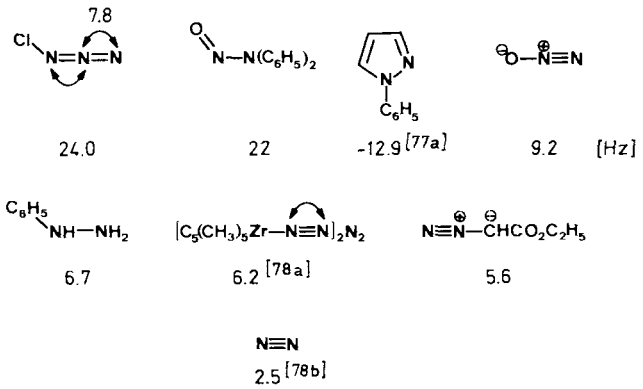
	13	14	
^1J(N-2,C-2)	13.6	12.3	[Hz]
^1J(N-3,C-3)	3.0	2.0	
^2J(N-3,C-2)	6.9	2.0	
^2J(N-2,C-3)	1.5	<0.5	

Scheme 10.

The use of N,C coupling constants in biosynthetic studies will be discussed in Sections 4.1 and 4.5.

3.2.3. $^{15}N,^{15}N$ Coupling Constants

For sensitivity reasons, ^{15}N,^{15}N coupling can only be observed in the spectra of ^{15}N-labeled compounds. Nevertheless, a considerable amount of data has accumulated and is summarized in several reviews.[76, 7a, b] The coupling constants are small (<25 Hz) since two nuclei with very small gyromagnetic ratios are involved. ^1J(N,N) does not seem to show correlations with either s-character in the bonding orbitals or N-N bond length (Scheme 11).



24.0 22 -12.9 [77a] 9.2 [Hz]

6.7 6.2 [78a] 5.6

2.5 [78b]

Scheme 11. The coupling constants ^1J(N,N) [Hz] are given below and, if necessary, above the formulas [7a, b]. The value for N_2 was calculated from the experimental value for $^{14}N^{15}N$ [78b] by means of Equation (b).

Quantum-chemical calculations have predicted that most ^1J(N,N) values should have a negative sign[79] owing to the dominant contribution of lone-pair electrons in "s-hybridized" orbitals. A pronounced dependence of the magnitude and sign of this coupling on the lone-pair dihedral angle was also predicted.[79b] A detailed interpretation of N,N coupling data should be based upon experimental determinations of the sign,[77] but such measurements are still lacking in most cases. Some structural applications of N,N coupling constants will be discussed in Section 4.

3.3. ^{15}N Relaxation Times

The two principal time constants of nuclear magnetic relaxation, T_1 and T_2, have very different significance for ^{14}N- and ^{15}N-NMR spectroscopy. For the quadrupolar nucleus ^{14}N, it is the transverse relaxation time T_2 that influences the ease of observation of the NMR signal. T_2 determines the line width $\Delta\nu_{1/2}$ of the signal, which may vary from a few Hz for a highly symmetrical electronic environment to several kHz for unsymmetrical environments and large molecules. Thus, sensitivity is lost as a result of *fast* relaxation, which results in line broadening ($T_2 = 1/\pi\Delta\nu \approx 65$ ms to 65 μs for $\Delta\nu = 5$ Hz to 5 kHz).

On the other hand, a very different situation arises for the spin-1/2 isotope ^{15}N, which lacks an effective internal relaxation mechanism. As a nucleus with a small gyromagnetic ratio, ^{15}N depends on the spatial proximity of a sensitive nucleus for fast dipolar spin-lattice relaxation rates, $(T_1^{DD})^{-1}$, or, alternatively, on high magnetic fields (B_0) to increase the contribution of the chemical shift anisotropy term to the rate of relaxation, $(T_1^{CSA})^{-1}$. The rate of spin-lattice relaxation $(T_1)^{-1}$ determines the pulse repetition rate in single-pulse experiments. Hence, it becomes evident that NH_2 and NH groups with efficient ^{1}H,^{15}N dipolar relaxation can be more readily detected than tertiary N atoms, which lack the dipolar interaction with a directly bonded proton, resulting in rather long T_1 values and the loss of a nuclear Overhauser effect (Section 2.1). With the availability of high-field magnets ($B_0 = 9.4$ or 11.7 tesla), the measurement of tertiary N atoms is less time-consuming. The CSA term, which contributes to $1/T_1$ for all larger molecules, increases proportionally to B_0^2 [Eq.(g)][80] and thus causes a significant decrease in T_1 (Table 4).

$$(T_1^{CSA})^{-1} = \tfrac{2}{15}\gamma_N^2 B_0^2(\sigma_\parallel - \sigma_\perp)^2 \cdot \bar{\tau}_c \qquad (g)$$

Table 4. Field dependence of ^{15}N spin-lattice relaxation times T_1/s.

	B_0=1.4	4.2	4.7	9.4 T
$NaNO_2$ [a]			19.0	17.5
KCN [b]	21.2	14.5		
2-chloro-pyrimidine [c]			170	114

[a] 99% ^{15}N, 1.1 M in D_2O, 25 °C [b]. 95% ^{15}N, 7.9 M in D_2O, 30 °C (from Table 2.3 in [7a]). [c] 99% $^{15}N_2$, 1.6 M in $(CD_3)_2CO$, 25 °C.

It should be mentioned that chemical shift anisotropy, $\Delta\sigma = \sigma_{\parallel} - \sigma_{\perp}$, is up to 4 times larger for ^{15}N than for ^{13}C nuclei and, consequently, the B_0^2-dependent CSA relaxation mechanism becomes more effective for ^{15}N nuclei in high-field spectrometers.

At lower field strengths very fast relaxation can be obtained by the addition of paramagnetic relaxation reagents, such as $Cr(acac)_3$, $Ni(acac)_2$, or $Gd(dpm)_3$ (dpm = dipivalomethanato)[81] or, for aqueous solutions, $[Gd(2:2:1)]^{3\oplus}$ cryptate.[82] An increase in the spin-lattice relaxation rate (T_1^{-1}) by a factor of 10-100 is frequently observed,[81] and measuring times are, therefore, dramatically reduced. The most recent and efficient technique to overcome the low sensitivity due to long T_1 relaxation times is the polarization transfer from an abundant, sensitive, fast-relaxing nucleus (e.g., ^1H, ^{19}F) to ^{15}N in the INEPT or DEPT pulse sequence experiments (Section 2.2). The repetition rate of the pulse sequence is governed by the (fast) proton relaxation and not by the (slow) ^{15}N relaxation.[11,12]

An intricate feature of spin-lattice relaxation is its dependence on molecular motion, specifically the reorientation times or correlation times τ_c. T_1 decreases linearly with increasing correlation time τ_c for small fast tumbling molecules in the so-called extreme narrowing condition ($\tau_c^2(\omega_N + \omega_H)^2 \ll 1$), approaches a minimum for $\tau_c = 10^{-9}$-10^{-8} s, and it increases again for longer correlation times (Fig. 17). This effect applies to large biomolecules, such as proteins and nucleic acids, and becomes more pronounced at high fields.

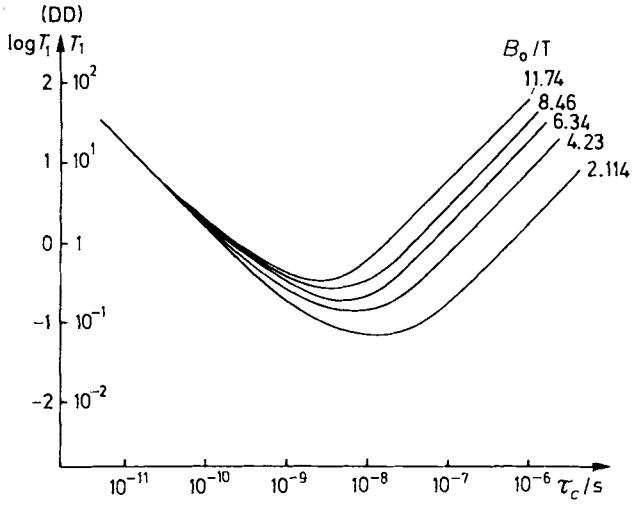


Fig. 17. Dipole-dipole relaxation (T_1^{DD}) as a function of the correlation time τ_c (for isotropic molecular reorientation) for different field strengths B_0 [7a].

In conclusion it may be emphasized that a consideration of spin-lattice relaxation is a prerequisite for the optimization of ^{15}N-NMR experiments. Since T_1 values are strongly dependent on experimental conditions (field strength, concentration, solvent, temperature) and very sensitive to the structural environment, data compilations are only of limited value. T_1 values of some typical molecules are reported in ref. [7a, c, 4].

3.4. Assignment Techniques

The assignment of ^{15}N resonances may become a considerable problem for compounds with several N atoms, in particular when repeating structural units are involved, such as in polypeptides or polynucleotides. But even in small molecules the identification of the ^{15}N-NMR signals may become a challenging task. The first difficulty arises when the true signals have to be differentiated from spurious electronic signals in spectra with low signal-to-noise ratio. As a result of variable T_1 relaxation times and (negative) nuclear Overhauser enhancements, ^{15}N-NMR intensities can be very different, and weak signals are easily lost in the noise. Application of several of the detection methods outlined in Section 2 is often necessary to ensure that all resonances are indeed detected. In particular, experiments with and without NOE should be performed and, in the case of polarization transfer experiments with pulse sequences, the delay time τ should be varied.

The second problem concerns the assignment of lines to specific N atoms. Based on the discussion of the spectral parameters in Section 3, the following criteria can be applied:

- chemical shifts, including substituent effects
- protonation effects, N-H exchange rates
- lanthanide-induced shifts (LIS)
- nuclear Overhauser effects
- N,H and N,X coupling constants
- N,H and N,X correlation experiments (1D and 2D)
- spin-lattice relaxation times
- isotopic labeling

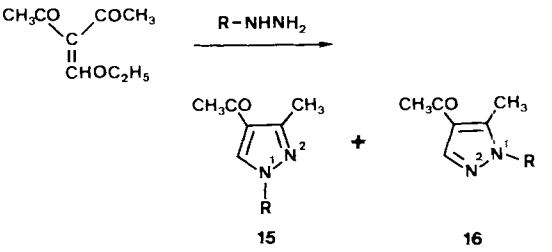
The most powerful assignment aid is the analysis of the proton-coupled ^{15}N-NMR spectra. It is this area of ^{15}N-NMR spectroscopy where rapid progress has been made in the past few years, owing to the development of modern 1D and 2D pulse sequence experiments. Paramagnetic shift reagents (lanthanide complexes) have also proven useful in several cases[83,39,84] to assign ^{15}N resonances. In oligopeptides, the different exchange rates of free and hydrogen-bonded NH groups are a useful criterion for their assignment. Moreover, additive empirical shift increments are available, e.g., for azoles[85] and azines.[86] Finally, extensive molecular orbital calculations have led to the prediction of a wide range of ^{15}N chemical shifts, which may be used for assignment purposes.[41,7b,87]

4. Chemical Applications

The increased sensitivity of ^{15}N-NMR spectroscopy together with the possibility of obtaining ^1H-coupled ^{15}N-NMR spectra has greatly enlarged the scope of applications in structural chemistry during the past few years. In this section, we will discuss selected examples from the fields of organic chemistry, biochemistry, and organometallic and coordination chemistry. They were chosen to illustrate the principles discussed in the previous Sections, the wide spectrum of applications, and the general potential of ^{15}N-NMR spectroscopy as a probe into molecular structure and reactions.

4.1. Structure and Bonding of Organic Molecules

^{15}N-NMR spectroscopy is particularly suited for studies of isomerism in nitrogen-containing heterocyclic systems. For example, isomeric acetylpyrazoles of the types **15** and **16**, which serve as precursors for biologically active substances,[88] are formed by the reaction of monosubstituted hydrazines with 3-(ethoxymethylene)-2,4-pentanedione, the product ratio depending on the nature of R (Scheme 12). Since the tricoordinated and dicoordinated nitrogen



Scheme 12.

atoms, N-1 and N-2, respectively, are readily distinguishable by their chemical shifts (Fig. 18), the geminal and vicinal N,H coupling constants obtained from an INEPT experiment allow an unambiguous assignment of the isomers.[15] As expected from the results discussed in Section 3.2.2, the pyrazoles **16** show large ^2J(N-2,H) and ^3J(N-1,H) values (e.g., **16a**, R = $CO_2C_2H_5$, 13.7 and 9.0 Hz, respectively), whereas the corresponding values for **15a** are 3.4 and 1.9 Hz, respectively. Very similar data were found for the *N*-benzyl derivatives.

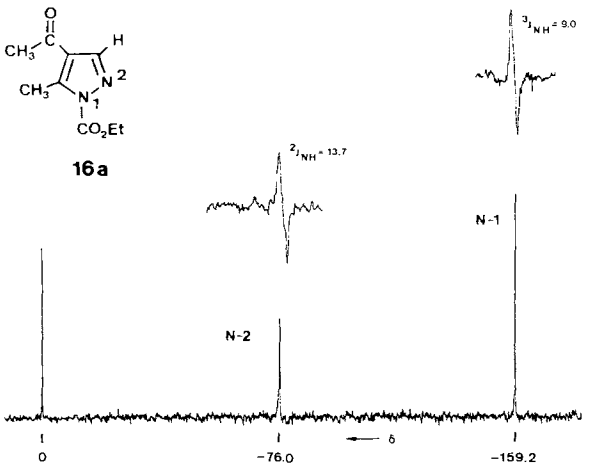
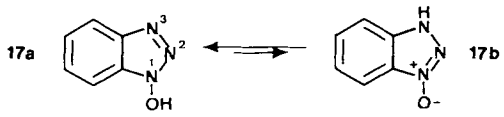


Fig. 18. Refocused and ^{1}H-decoupled INEPT ^{15}N-NMR spectrum of ethyl 4-acetyl-5-methyl-1-pyrazolecarboxylate **16a** (20.3 MHz; $(CD_3)_2SO$); without decoupling (insets) [15].

4- and 5-Nitroimidazoles present another case of regioisomerism, and their differentiation is of particular interest since *N*-substituted 5-nitro isomers are potent antiprotozoics.[88b] A reliable assignment was possible on the basis of the chemical shifts of the NO_2 group (4-NO_2, $\delta = -18 \pm 1$; 5-NO_2, $\delta = -25 \pm 1$) and ^{15}N,^{1}H coupling constants of N-1 and N-3.[15]

Intricate tautomeric equilibria are common in heterocyclic systems and their elucidation can often be achieved by ^{15}N-NMR spectroscopy. For example, the position of the fast tautomeric equilibrium of 1-hydroxybenzotriazole **17a** and its derivatives was determined as a function of solvent on the basis of the chemical shifts of N-3.[89] The range of chemical shifts for N-3 (-58 to -100 ppm) clearly shows that the *N*-hydroxy form **17a** dominates the equilibrium, the contribution of the *N*-oxide **17b** ranging from 6% (DMSO) to 26% (CH_3OH) (Scheme 13). 2-Hydroxyazines



Scheme 13.

are known to exist in the tautomeric amide form. However, an unusual iminol-amide equilibrium was recently observed for the hydroxyaza[10]annulene **18** (Scheme 14). The averaged ^{15}N chemical shift of the tautomeric system ($\delta = -204.3$, $(CD_3)_2SO$, 37 °C) was compared with data of the *N*-methyl ($\delta = -240.6$) and *O*-methyl ($\delta = -115.9$) derivatives, the results indicating an **18a/18b** ratio of about 7:3.[90] The remarkable stability of the iminol form **18b** was also evident from the ^{13}C-NMR spectrum.



Scheme 14.

Similar studies have been carried out on a series of substituted azoles[91,92,7b] with special emphasis on imidazole[93] and nucleotides, which are important for the investigation of biological systems.[94]



Scheme 15.

Hull, Künstlinger, and *Breitmaier*[95] have reported on the tetrazolo[1,5-*a*]pyrimidine **19**/2-azidopyrimidine **20** valence isomerism, which lends itself to an investigation by ^{15}N-NMR spectroscopy (Scheme 15). This exchange, studied previously by ^{1}H-NMR spectroscopy,[96] is so slow that it is possible to assign all nine signals of the nonequivalent N atoms of the *n*-butyl derivative (as a neat liquid) (Fig. 19); the equilibrium lies on the tetrazole side (85%). The ^2J(N,H) values were crucial for the correct assignment. The equilibrium was shown to be strongly solvent dependent, the tetrazolo form **19** being favored in polar solvents, while the azido form **20** predominates in chloroform.

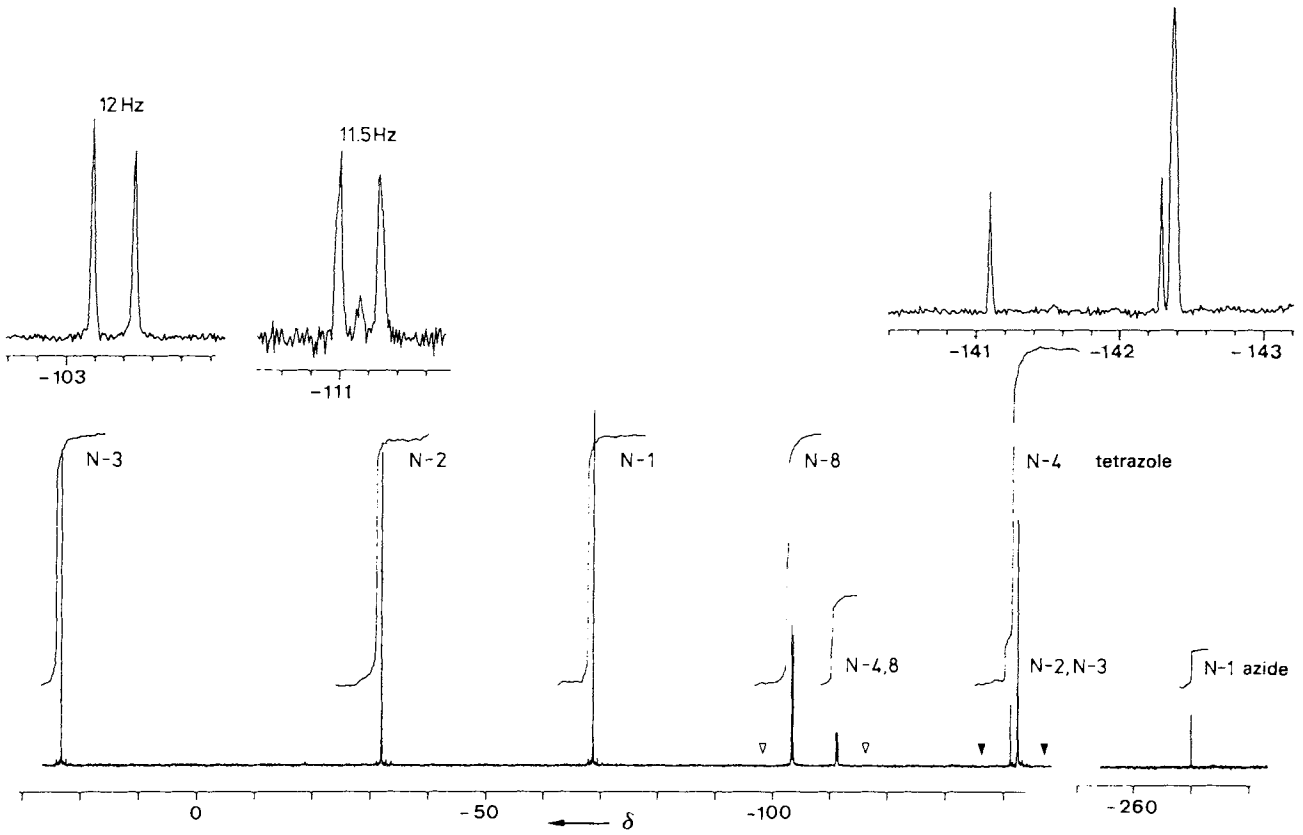
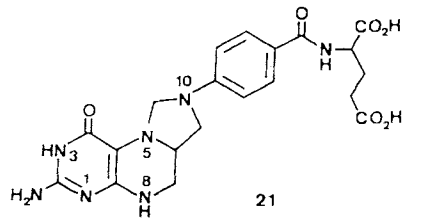


Fig. 19. ^{15}N-NMR spectrum of the equilibrium mixture of 6-butyltetrazolo[1,5-*a*]pyrimidine **19** and 2-azido-5-butylpyrimidine **20**, R = *n*-C_4H_9 (40.6 MHz; neat liquid, 15-mm sample tube). The numbering of the N atoms does not correspond to the systematic nomenclature (see Scheme 15) [95].

Substituent effects on the ^{15}N resonances were studied in pyridines,[97] pyrimidines,[97] and pyrazines,[98] and linear correlations with ^{13}C substituent effects could be established.

Extensive studies of the ^{15}N-NMR spectra of the biologically important pteridines[9] have led to a definite structure assignment of the so-called "activated formaldehyde" (Blakley cofactor), which is formed from (6*S*)-5,6,7,8-tetrahydro-L-folic acid and formaldehyde. This compound serves as a cofactor in the enzymatic conversion of glycine into serine.[99] Both the 5-hydroxymethyl- and the cyclic 5,10-methylene structure **21** have been proposed.[99, 100] The natural abundance ^{15}N-NMR spectrum of the (6*RS*) compound is shown in Figure 20. The assignments of the seven N atoms are based on the ^{15}N-NMR data of tetrahydrofolic acid derivatives,[9] but the signals of the two diastereoisomers (at 10.1 MHz) are not resolved.

The 20.3-MHz ^{15}N-NMR spectrum of the product labeled with ^{15}N in the 5- and 10-positions (Fig. 21) reveals clearly resolved doublets ($\Delta\delta = 0.24$) for the (6*R*) and (6*S*) diastereoisomers. Since the small ^{15}N-5,^{15}N-10 coupling of 2 Hz does not disprove the 5-hydroxymethyl structure, the 11-position was labeled by reaction with [^{13}C]formaldehyde. In the ^{1}H-decoupled ^{13}C-NMR spectrum the methylene carbon appears as a double doublet with $J(^{15}N,^{13}C) = 10.8$ and 4.7 Hz. Since the signal of ^{13}C-11 in the compound with natural ^{15}N isotope abundance is not split, the double doublet structure in the triply labeled product is due to ^{1}J(N,C) coupling only, thus clearly proving the *cyclic* methylene structure **21** for the activated formaldehyde[101] (cf. the other ^{13}C,^{15}N coupling constants in Scheme 16). As expected from the linear correlation between ^{1}J(N,C) and the s-character of the bonding orbitals (see Section 3.2.1), the aniline-type N-10 atom shows the largest ^{1}J(N,C) values, whereas N-5 shows smaller values, indicating a pyramidal (sp^3-type) geometry at this nitrogen



21

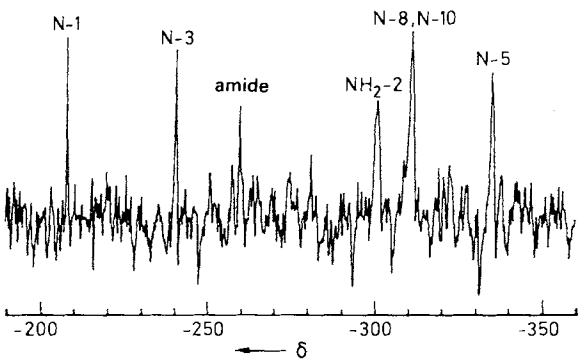


Fig. 20. ^{15}N-NMR spectrum of (6*RS*)-5,10-methylenetetrahydrofolic acid **21** (10.1 MHz; 0.8 M in H_2O/D_2O 92:8 at pH 7, 20-mm tube) [101a].

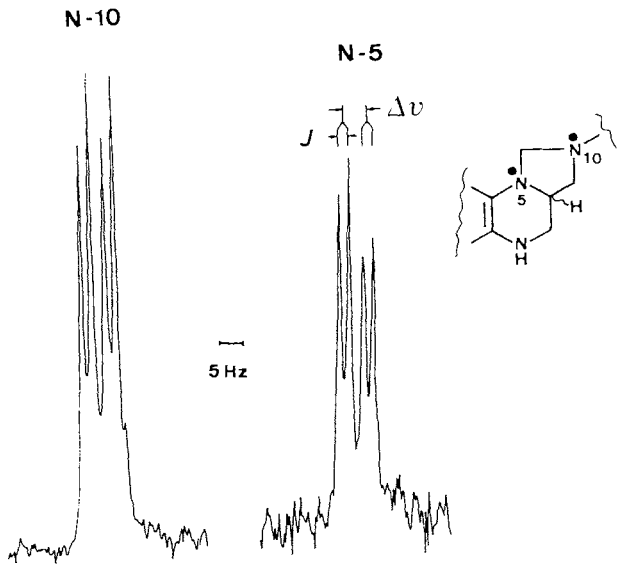
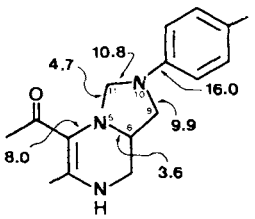
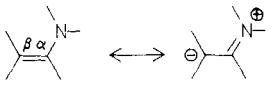


Fig. 21. ^{15}N-NMR spectrum of (5,10-$^{15}N_2$)-**21** (20.3 MHz; 0.05 M in D_2O at pD 7, 10-mm tube); for the assignments of the splittings in the resonances of N-5 and N-10 see text and [101b].

atom. For comparison, the ^1J(N,C) value for CH_3NH_2 is 4.5 Hz.[102]



Scheme 16. For numerical values see text.



Scheme 17.

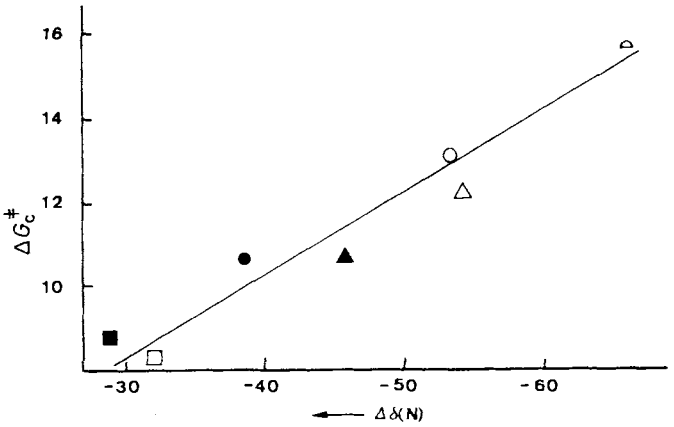
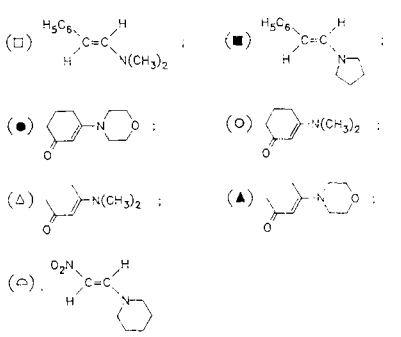


Fig. 22. Correlation of the free energy of activation $\Delta G_c^{\neq}$ for rotation about the N-C(α) bond with the differential chemical shift $\Delta\delta(^{15}N) = \delta$(amine) $-\delta$(enamine) [40].



The lone pair of electrons on the nitrogen atom is responsible for the dependence of ^{15}N chemical shifts on n,π-delocalization and hydrogen bonding. A further, directly related effect—most of the time annoying but occasionally useful—is the solvent dependence of ^{15}N shielding data (cf. Section 3.1.2). In the following discussion we will give specific examples for the successful use of ^{15}N-NMR spectroscopy in studies of electronic structure and hydrogen bonding.

The n,π-interactions in enamines and related compounds are largely responsible for the specific physical and chemical properties of enamines as synthons in organic synthesis.[103] In our laboratory, extensive studies have been carried out on ^{15}N chemical shifts in amines, enamines, enamino ketones, and other enamines with extended conjugation.[40, 46, 104, 13] The chemical shifts of ^{15}N nuclei in this class of compounds are found between those of tertiary amines (more shielded) and amides (less shielded) (Fig. 14). In order to separate the n,π-delocalization from electronic and steric substituent effects, it proved advantageous to define a differential chemical shift $\Delta\delta(^{15}N) = \delta$(amine) $-\delta$(enamine). $\Delta\delta(^{15}N)$ correlates well with the free energy of activation $\Delta G^{\neq}$ for restricted rotation about the N-C_α bond as determined from variable-temperature ^{13}C-DNMR measurements[40] (Scheme 17, Fig. 22).

Extrapolation of the data in Figure 22 gives a $\Delta G^{\neq}$ value of 15–20 kJ mol^{-1} for rotation about the N-C_α bond in a simple enamine; this is in good agreement with theoretical predictions for vinylamine (25.5 kJ mol^{-1})[105] and with experimental data on conjugative interactions in other simple enamines.[106]

In a similar study, *Martin* et al.[107] correlated activation energies E_a with ^{15}N chemical shifts in amides and thioamides and also advanced a semiempirical explanation for the validity of such correlations. Since enamino ketones may be considered as vinylogous amides, our results lend further support to this approach.

n,π-Delocalization was studied in a similar manner in substituted anilinostyrenes **22**; the $\Delta\delta$(N) values show excellent correlation with the Hammett σ constants for a series of donor and acceptor substituents (Fig. 23).[40] In this case, the ^{13}C chemical shift of C_β also exhibits a similar correlation with $\Delta\delta$(N), since this nucleus is in a similar electronic environment and no steric interactions with the substituents occur.

An excellent survey of correlations of $\delta(^{15}N)$ with E_a and $\Delta G^{\neq}$ for hindered rotation about N-X bonds and with σ values is given in ref. [7a] and covers the literature up to 1980. More recently, *Taft* et al.[108] analyzed ^{15}N-NMR shifts of amides in solution in terms of three solvent pa-

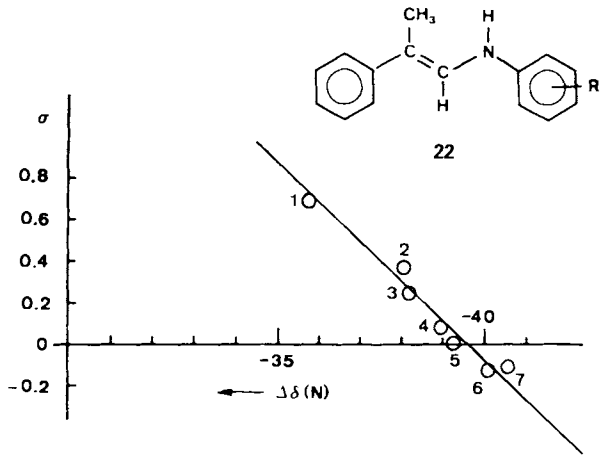


Fig. 23. Correlation of $\Delta\delta(^{15}N) = \delta_N^X - \delta_N^H$ with Hammett σ values for substituted anilinostyrenes **22**; (1) R = *m*-NO_2, (2) *m*-Cl, (3) *p*-Cl, (4) *m*-OCH_3, (5) H, (6) *p*-CH_3, and (7) *p*-OCH_3 [40].

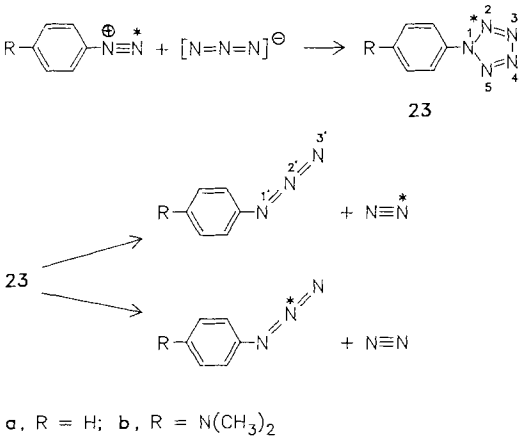
rameters, π^* (polarity/polarizability), α (hydrogen-bond donor acidity), and β (hydrogen-bond acceptor basicity) using multiparameter linear relationships with $\delta(^{15}N)$. Further linear free energy correlations involving Hammett σ constants have been reported for δ(NO) values in substituted *N*-methyl-*N*-nitrosoanilines,[109] for the three N atoms in *p*-substituted 1-phenyl-3,3-pentamethylenetriazenes,[110] and in a detailed study of ^{15}N- and ^{17}O-NMR shifts versus σ_I and σ_R constants as well as calculated electron densities in nitrobenzene derivatives.[111]

As expected from the foregoing discussion ^{15}N chemical shifts have been used successfully to monitor hydrogen-bond formation and protonation. Particularly large, low-frequency shifts are observed in systems containing the C=N group; pyridine has already been discussed in Section 3.1.2. Detailed studies on imines and oximes by *Roberts* et al.[112] showed that hydrogen-bond effects may become as large as 28 ppm (in going from $CHCl_3$ to CF_3CH_2OH as solvent), whereas full protonation (CF_3COOH) results in shifts of 110 to 150 ppm (to lower frequencies). ^{15}N chemical shifts were measured in *N*-retinylidenebutylamine and related Schiff bases as models for rhodopsin and bacteriorhodopsin in solvents of increasing hydrogen-bond donor acidity.[113] The protonation effects on the ^{15}N-NMR shifts increase with increasing length of the conjugated polyene, and it was concluded that ^{15}N-NMR spectroscopy is a most suitable method for the determination of the degree of protonation of the Schiff base linkage. In contrast, small high-frequency shifts (<25 ppm) are observed upon protonation (and hydrogen bonding) of aliphatic amines. In cases where hydrogen-bond shifts are too small to permit a reliable interpretation, ^{15}N spin-lattice relaxation times can be used to monitor restricted motion, as recently shown by *Yu* and *Levy* for 2,4-pentanediamine.[114]

The study of hydrogen bonds between NH and CO groups in peptides showed that ^{15}N chemical shifts are a sensitive indicator of *intra*molecular NH···O=C interactions and thus of the secondary structure of peptides. Gramicidin S, a cyclic decapeptide containing the sequence Phe-Leu-Orn-Val-Pro twice, is a particularly well-studied case investigated by several research groups.[115] The four hydrogen bonds between valine and leucine are indeed reflected in the ^{15}N chemical shifts of the two amino acids when the decapeptide is measured in solvents of increasing proton acidity; this is due to *inter*molecular hydrogen-bond formation between the solvent and the exposed carbonyl group of the respective peptide bond.[116] The four *intra*molecular hydrogen bonds are also demonstrated by reduced exchange rates for the protons involved, which is reflected in a distinct $^{15}N,^1H$ coupling even in basic medium. A comparison of the ^{15}N-NMR spectra of linear oligopeptides with that of gramicidin S led to the same conclusion.[117] *Inter*molecular hydrogen bonding in nucleosides, the predominant mechanism of self-association and base-pairing, is another domain in which ^{15}N-NMR spectroscopy has been successfully applied to structure elucidation.[118] An extension to the study of N-H bond lengths in DNA by solid-state ^{15}N-NMR spectroscopy has also been reported (cf. Section 4.6 and Fig. 11).

4.2. Reaction Mechanisms and Reactive Intermediates

In mechanistic studies ^{15}N-NMR spectroscopy has proven to be a powerful tool for the structure elucidation of unstable intermediates. Very recently, we reinvestigated the classic reaction of benzenediazonium chloride with lithium azide, which results in the elimination of nitrogen and the formation of phenyl azide.[1] This reaction, first described by *Hantzsch*,[119] was investigated mechanistically in 1956–1958 by *Huisgen* and *Ugi* et al.[120] They discovered that the reaction proceeds by two separate mechanisms. For one of them, it was proposed that phenylpentazole **23a** is an intermediate, since it accounts for the equal distribution of the ^{15}N-labeled, terminal N atom of the diazonium salt in the decomposition products phenyl azide and nitrogen (Scheme 18). Although a series of crystalline *p*-sub-



Scheme 18.

stituted phenylpentazoles was subsequently isolated[121] at low temperature (−30 °C) and despite the determination of the structure of *p*-dimethylaminophenylpentazole **23b** by X-ray crystallography,[122] a direct proof for the existence of the pentazole ring in solution was still lacking.

The natural abundance 40.56-MHz ^{15}N-NMR spectrum at −35 °C of **23b** is shown in Figure 24. Although even at this low temperature the pentazole had partially decomposed to the azide and N_2, its four resonance signals could be identified. The assignment was achieved by means of the ^{15}N-NMR spectrum of the [2(5)-^{15}N]pentazole **23b*** (Fig. 25a). The ^{15}N-NMR spectrum measured during decomposition of **23b*** (Fig. 25b) proves the exclusive formation of $^{15}N{\equiv}^{14}N$ and azide labeled in the N-2 position. The structural integrity and very slow decomposition of the pentazole ring at −20 °C is thus confirmed for the *p*-dimethylaminophenyl derivative **23b**.[1]

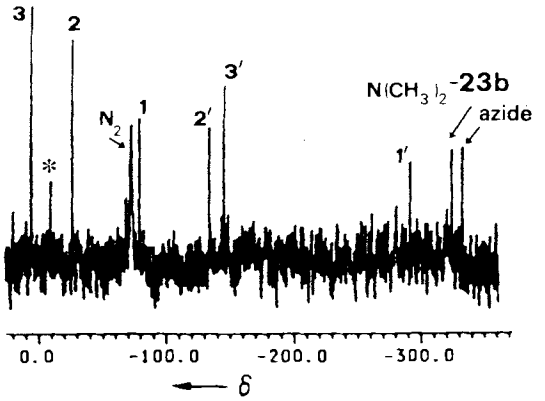


Fig. 24. ^{15}N-NMR spectrum of *p*-dimethylaminophenylpentazole **23b** (40.6 MHz; −35 °C; 0.04 M in $CDCl_3$ with 0.07 M $Cr(acac)_3$). The dashed numbers apply to the azide.

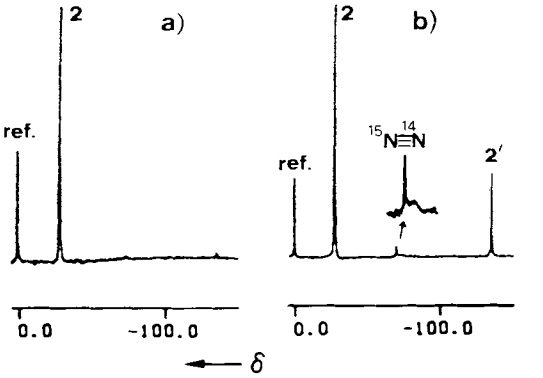
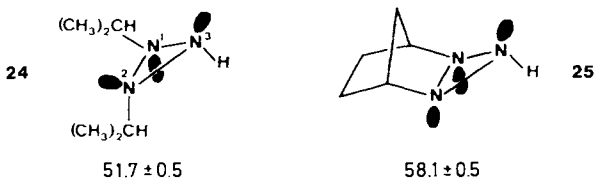


Fig. 25. ^{15}N-NMR spectra of the [2(5)-^{15}N]pentazole **23b** (40.56 MHz; −20 °C; 0.013 M in $CDCl_3$ with 0.06 M $Cr(acac)_3$); a) directly after preparation of the sample; b) during decomposition to the *N*-2-labeled azide and $^{15}N{\equiv}^{14}N$. ref = standard CH_3NO_2.

A considerably less reactive nitrogen homocycle, triaziridine, has been a target of organic synthesis for many years. *Dreiding* et al. achieved the photochemical cyclization of azimines to substituted triaziridines.[123] Subsequently, the stereochemistry of substituted triaziridines was investigated both experimentally and theoretically[124] and a series of compounds was characterized by ^{15}N-NMR spectroscopy.[54] The chemical shifts of 1,2-dialkyl-substituted triaziridines lie in the range of substituted hydrazines ($\delta = -240$ to -290) and are typical for pyramidal, tricoordinated N atoms. The N,H coupling constants, however, are unusually small (cf. Section 3.2.1 and Scheme 19). The significant increase in $|^1J(N,H)|$ in going from the 1,2-*trans*-diisopropyl derivative **24** to the *cis*-triaziridine **25** is consistent with a second hyperconjugative lone-pair effect from the inverted N-2 atom. The N,H coupling constant may thus provide a structural criterion for the still unknown all-*cis*-triaziridine, for which in the absence of any lone-pair effect a $^1J(N,H)$ value of approximately 45 Hz would be expected. These effects are in line with similar observations in N–C–H systems where a *syn*-orientation of the lone pair and the C–H bond leads to an increase of $^1J(C,H)$, e.g., in 1-methylaziridine[125a] and in peptides.[125b]



Scheme 19. The coupling constants $^1J(N,H)$ [Hz] are given below the formulas (in $CDCl_3$).

The existence of short-lived free radical intermediates in chemical reactions can be demonstrated by ^{15}N-CIDNP (*c*hemially *i*nduced *d*ynamic *n*uclear *p*olarization) effects in the stable products if radical pairs are involved.[126] This technique provided the first direct experimental proof for the formation of aromatic radical cations in the nitration of *N,N*-dimethylaniline with $H^{15}NO_3$ in 88% aqueous H_2SO_4[127] (Scheme 20). The radical cations are believed to originate in a reaction catalyzed by HNO_2.[128] As shown in Figure 26, polarization is only present in the *p*-nitro product (time-dependent negative signals), whereas the *m*-nitro product gives an absorption signal that steadily increases with time, since this product is not formed in the catalyzed reaction.

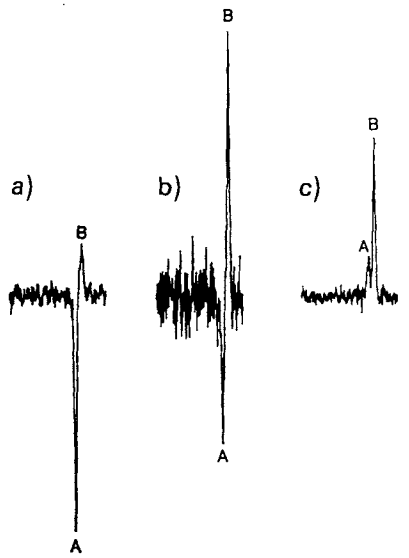
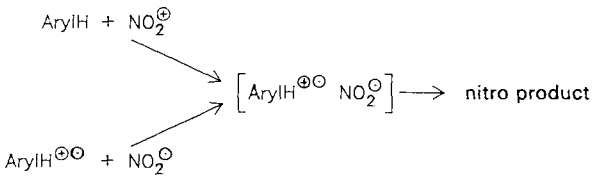


Fig. 26. ^{15}N-NMR spectra (25 °C; $H^{15}NO_3$ (0.53 M) in aqueous H_2SO_4 (88%)) as a function of time for the nitration of dimethylaniline (0.55 M): a) after 3 min; b) after 12 min; c) after 55 min; A = *p*-$O_2{}^{15}N$-C_6H_4-$N(CH_3)_2$, B = *m*-$O_2{}^{15}N$-C_6H_4-$N(CH_3)_2$ [127a].

The same authors have reported CIDNP effects in the ^{15}N-NMR spectra recorded during the acid-catalyzed rearrangement of *N*-nitroanilines to *p*-nitroanilines; their results support the intermediate formation of [ArylNH$_2^{\oplus\ominus}$NO$_2^{\ominus}$] radical pairs.[129] Because of the negative magnetic moment of the ^{15}N nucleus, a negative sign has to be inserted into Kaptein's formulas for the calculation of the sign of net polarization.[130]



Scheme 20.

^{15}N-CIDNP spectra have also been recorded during nucleophilic substitution of arenediazonium ions and indicate that the process is at least partially homolytic.[131] The ^{15}N-NMR spectrum of ^{15}N-labeled 4-chlorobenzenediazonium tetrafluoroborate subjected to decomposition in weakly alkaline aqueous solution (Fig. 27) clearly exhibits enhanced absorption and emission signals for diazonium

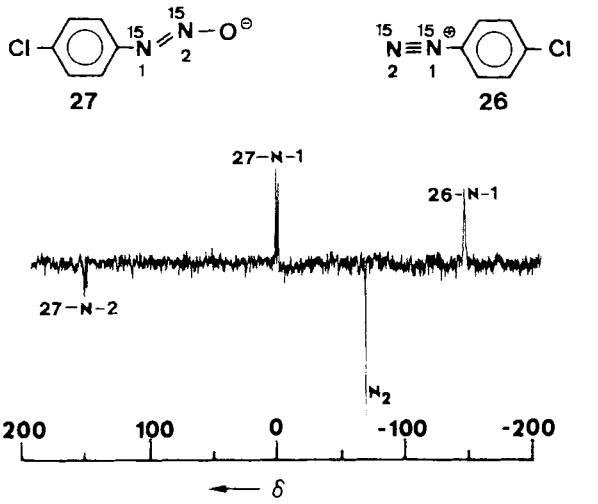


Fig. 27. ^{15}N-NMR spectrum of [1,2-^{15}N$_2$]-*p*-chlorobenzenediazonium tetrafluoroborate (9.1 MHz; 72°C, H_2O, pH 9.7) [131]. The signal for N-2 of **26** is not observed. ^1J(N,N) in **26** is <1 Hz (not resolved), whereas a value of 14.7 ± 0.5 Hz is obtained for **27**.

ion **26**, the *trans*-diazotate ion **27**, and molecular nitrogen. In a detailed interpretation, the authors conclude that the two radical pairs

[ArylN$_2^{\oplus\ominus}$ON$_2$Aryl] and [Aryl$^{\ominus\ominus}$ON$_2$Aryl]

are formed in a very complex reaction sequence. However, other radical pairs cannot be excluded and, most importantly, the experiments "do not allow determination of the extent to which the homolytic pathway contributes to the total reaction." The last statement describes one of the major limitations of the significance of CIDNP experiments for quantitative mechanistic studies.

Several other applications of ^{15}N-NMR spectroscopy to reaction mechanisms have been published, e.g., detailed investigations of the Fischer indole synthesis,[132] the rearrangement of 1,3-oxazine-2,4-diones into pyrimidines and pyrazoles,[133] and the mechanism of formation of *N*-nitrosothiourea.[134]

4.3. Stereochemistry and Dynamic Processes

Variable temperature ^{1}H- and ^{13}C-NMR studies have proven very useful in investigations of intra- and intermolecular dynamic phenomena. Measurements of ^{15}N-DNMR parameters are still hampered by the low sensitivity of the ^{15}N nucleus. However, it can be anticipated that the experimental improvements discussed in Section 2 will surmount this difficulty. Furthermore, lowering of the temperature results in a more effective spin-lattice relaxation, at least for small molecules and in magnetic fields of moderate strength.

The high sensitivity of the ^{15}N chemical shift to delocalization of the lone-pair electrons makes it a useful configurational and conformational probe for conjugated molecules. Thus, different chemical shifts were observed for the (*E*) and (*Z*) isomers of enamino ketones, esters, and amides; moreover, different conformers could be detected in the slow exchange limit.[13, 104]

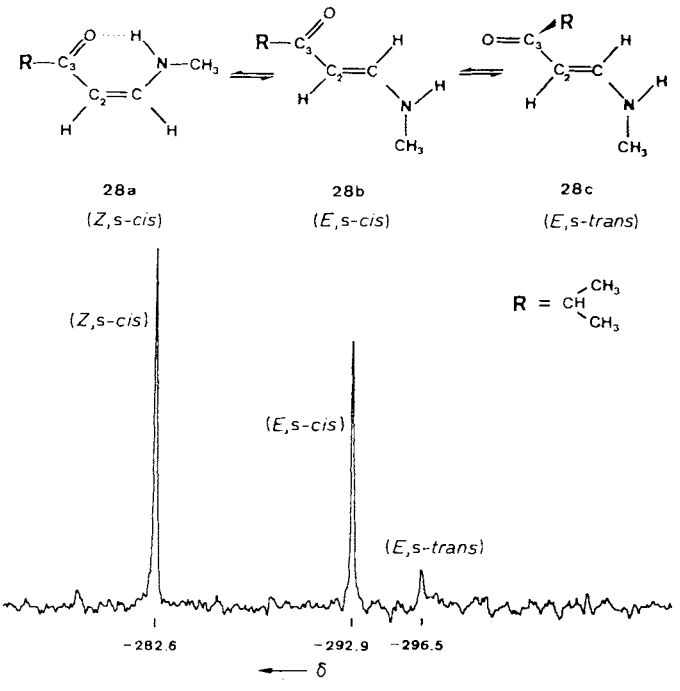


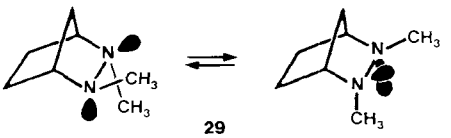
Fig. 28. INEPT ^{15}N-NMR spectrum of 4-methyl-1-(methylamino)-1-penten-3-one **28** (20.3 MHz; -65°C; [D$_8$]dioxane) [104].

For example, the low-temperature spectrum of the enamino ketone **28** (Fig. 28) exhibits signals that can be assigned to s-*cis* and s-*trans* conformers on account of restricted rotation around the C(2)–C(3) bond.[104] Whereas the high-frequency signal ($\delta = -282.6$, hydrogen bonded

(*Z*,s-*cis*) isomer **28a**) remains narrow over the entire temperature range from +24 to −60°C, the two other lines exhibit dynamic behavior and, at −60°C, show the equilibrium **28b** ⇌ **28c** in the slow-exchange limit. The weak, low-frequency signal ($\delta = -296.5$) increases in intensity with decreasing size of the *C*-alkyl group and is therefore assigned to the nonplanar (*E*,s-*trans*) conformer **28c**. The higher shielding of the N atom in **28c** (−2.6 to −4.7 ppm relative to the N atom in the (*E*,s-*cis*) conformer **28b**) is in agreement with expectations based on the paramagnetic shielding term, $\sigma^P \approx -(\Delta E)^{-1}\langle r^{-3}\rangle_{2p}\sum Q$, since inhibition of conjugation in nonplanar **28c** is expected to result in a larger ΔE value (see also Fig. 14).

It should be noted that the dependence of the chemical shift differences on solvent and temperature requires careful consideration before small chemical shift effects can be interpreted.

Nomura and *Takeuchi*[135] observed slow double inversion at two N atoms in bicyclic hydrazines by low-temperature ^{15}N-NMR spectroscopy. At −45°C, the chemical shift difference of the two diastereotopic N atoms in **29** is 1.08 ppm (10.9 Hz at 10.1 MHz) and ΔG_c^{+} ($T_c = 269 \pm 1$ K) was determined to be 58.4 kJ mol^{-1}, a value that agrees well with the data obtained from ^{1}H- and ^{13}C-NMR measurements (55.2 kJ mol^{-1}) (Scheme 21). Further conformational studies on piperidine[136] and tetraazadecalins[137] as well as on restricted C–N bond rotation in the guanidino moiety of L-arginine[138] have also been reported.



Scheme 21.

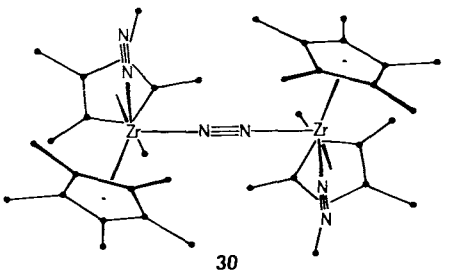
Although stereochemical applications of ^{15}N-DNMR studies are still scarce, the above-mentioned examples show that the considerable sensitivity of the ^{15}N nucleus to subtle stereochemical effects constitutes a promising basis for further investigations, particularly in biochemistry.

In this context, the ^{15}N-NMR spectroscopic investigations on chiral substances reported by *Roberts* et al.[139] are worth mentioning. The diastereotopic splittings in the ^{15}N-NMR spectrum of racemic 8-benzyl-5,6,7,8-tetrahydroquinoline in the presence of optically active carboxylic acids were found to be 3–12 Hz at 18.25 MHz and were strongly medium dependent, larger differential shifts being associated with less polar solvents and lower temperatures.

4.4. Coordination Chemistry

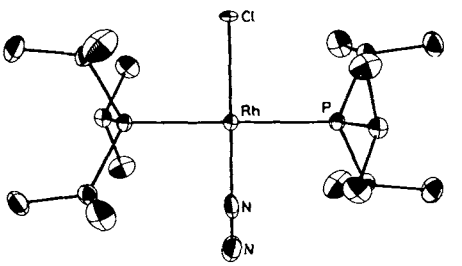
Although the number of significant structural applications of ^{15}N-NMR spectroscopy is much smaller in organometallic and inorganic chemistry then in organic chemistry, there are a few nitrogen-containing ligands that have been studied extensively with respect to metal binding, e.g., NO, CN and, most important, N_2. Whereas the differences in chemical shift due to coordination are relatively small (a few tens of ppm) for the majority of nitrogen ligands,[4] a wide range of shifts has been observed for N_2 and NO groups. In addition, the known ^{15}N chemical shifts for organic compounds are extended toward higher resonance frequencies (Fig. 13). Unsaturated ligands with direct metal–nitrogen bonds are observed between $\delta = 0$ and 900; additional deshielding effects are observed in paramagnetic molecules. Moreover, the coupling constants for ^{15}N nuclei directly bonded to metals may vary between a few and several hundred Hz. From a study of these parameters, information about the mode of coordination and the geometry of the complexed ligand can be obtained. The literature of this field up to 1980 is covered in a review by *Mason*.[4a]

The fundamental biochemical problem of nitrogen fixation and reduction has stimulated the study of dinitrogen complexes of various transition metals, and ^{15}N-NMR spectroscopy has proven a powerful tool in their structural investigation.[140] Dinitrogen was found to coordinate either in a linear *dihapto* (M–N–N–M) or in a *monohapto* (M–N–N) fashion. The structure of the first complex containing both types of dinitrogen ligands, **30**, was established by X-ray diffraction analysis[141] (Scheme 22). The



Scheme 22. [{[η^5-$C_5(CH_3)_5$]$_2$ZrN$_2$}$_2$N$_2$] **30**.

^{15}N-NMR spectrum of the fully labeled compound exhibits a singlet at $\delta = 179$ for the 1,2-η^2-bonded N_2 (μ-N_2) and doublets at $\delta = 80$ and $\delta = 11$ ($^1J(N,N) = 6.2$ Hz) for the η^1-bonded N_2. The latter signals are temperature-dependent indicating dissociative exchange between bound N_2 and free, dissolved N_2.[78] The ^{15}N chemical shifts of 1,2-η^2-N_2 complexes extend from $\delta = 300$ to 50, whereas the η^1-bound N_2 is more shielded ($\delta = 200$ to -100) with the N_α atom resonating at lower frequencies.[140a] The ^{15}N,M coupling constants provide another important criterion for the differentiation of the two binding modes of N_2, as shown in the *trans*-chloro(dinitrogen)bis(triisopropylphosphane)rhodium complex **31** ($^1J(Rh,N(1)) = 28$ Hz, $^2J(Rh,N(2)) = 4$ Hz)[142] (Scheme 23).



Scheme 23. **31**

Reduction of coordinated dinitrogen leads to the diazenido complexes M–N=N–R, which can exist in a singly bent or doubly bent configuration (Scheme 24). The transoid form is characterized by a strongly deshielded N_α nucleus ($\delta \approx 300$), which allows a differentiation from the singly bent isomer[143] (cf. Fig. 13). Further reduction products, e.g., hydrazido, nitrido, and imido complexes, have also been characterized by ^{15}N-NMR data.[140,143]

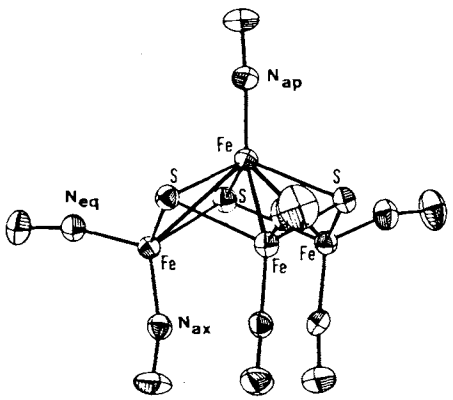


Scheme 24. Left: singly bent; right: doubly bent.

The stereochemistry of nitroso complexes was also successfully studied by means of ^{15}N chemical shifts.[144] As in the case of the M–N=N–R system, bending leads to strong deshielding effects on the ^{15}N(O) signal, and available data allow a correlation between M–N–O bond angle and ^{15}N chemical shift. Linear nitrosyl complexes exhibit shielding values of $\delta = 0 \pm 80$ and strongly bent complexes (120°) $\delta = 350$–800; intermediate cases are also known. Since the strong deshielding parallels a bathochromic shift of the UV/VIS absorption maximum, the effect can be ascribed to a lower $n \rightarrow \pi^*$ excitation energy, which results in an increase in the paramagnetic shielding term. For nitroso complexes of cobalt(III) this is also reflected in decreased shielding of the ^{59}Co nucleus.[145]

^{15}N chemical shifts of nitroso ligands were used in the structure determination of the Roussin cluster anions, **32** and **33**[146] (Scheme 25). The presence of three resonances in the spectrum of ^{15}N-enriched (99%) **32** (Fig. 29), two of which are mutually coupled, suggests a threefold symmetry axis and the presence of $Fe(NO)_2$ and Fe(NO) subunits in the cluster molecule. The ^{15}N chemical shifts of the nitroso ligands in **32** and **33** are typical for linear Fe–N=O groups ($Fe(NO)_{eq}(NO)_{ax}$: $\delta = 30$–80; $Fe(NO)_{ap}$: $\delta = 7$–20).

Spin coupling of ^{15}N nuclei to complexed metal nuclei depends on the gyromagnetic ratio of the metal and is very sensitive to the bonding orbitals involved. An interesting



32

$[Fe_4S_3(NO)_7]^{\ominus}$ **32**
$[Fe_4Se_3(NO)_7]^{\ominus}$ **33**

Scheme 25.

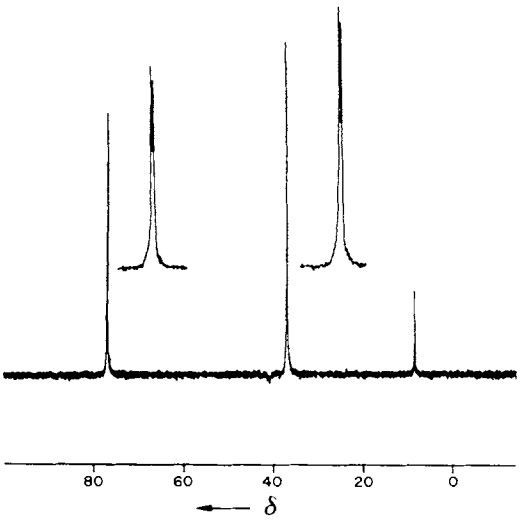
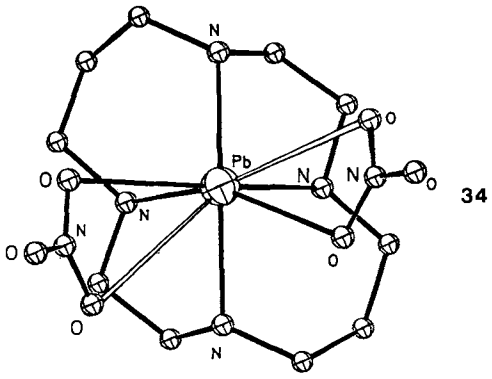


Fig. 29. ^{15}N-NMR spectrum (36.5 MHz) of the NO groups in $[(C_6H_5)_3PNP(C_6H_5)_3]^{\oplus}[Fe_4S_3(^{15}NO)_7]^{\ominus}$, a salt of the anion **32**; the equatorial and axial NO groups show a ^2J(N,N) coupling of 4.3 Hz [146].

example is provided by the lead(II) nitrate complex of 1,4,8,11-tetraazacyclotetradecane, **34**, which forms a distorted octahedral structure (Scheme 26) with strikingly different ^{207}Pb,^{15}N coupling constants (207.5 and 19.8 Hz) for the two ^{15}N resonances at $\delta = -318.8$ and $\delta = -325.5$, respectively, at the low-frequency end of the ^{15}N-NMR shift scale. Since the lengths of the equatorial and axial Pb–N bonds (2.45 ± 0.02 and 2.50 ± 0.08 Å, respectively) are not appreciably different, the large difference in ^1J(Pb,N) is ascribed to differing contributions of the Fermi contact term as a consequence of the axially distorted octahedral geometry. Hence, the assignment of 207.5 Hz to equatorial N-donor ligands (normal octahedral bonds) and 19.8 Hz to axial N-donor ligands (distorted octahedral bonds) was suggested.[147] Such differences in ^1J(M,^{15}N) values were also reported for related Cd^{II}, Hg^{II}, and Pb^{II} complexes.[148]



34

Scheme 26.

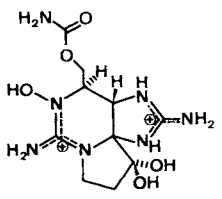
In favorable circumstances, i.e., very short electron spin relaxation times, ^{15}N resonances may even be observed in paramagnetic metal complexes, e.g., $^{15}N{\equiv}C^{\ominus}$ ligands in low-spin iron(III) cyanide complexes of porphyrin derivatives and hemoproteins. A further extension of the ^{15}N chemical shift range to higher frequencies is found for the $NC^{\ominus}$ resonance, $\delta = 450$ to 1100.[149] In low-spin iron(III)

tetraphenylporphin complexes extremely short T_1 and T_2 relaxation times (0.2–3.0 ms) were reported for the pyrrole N atoms.[150]

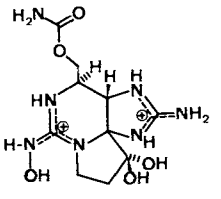
4.5. Biochemical Applications

The potential of ^{15}N-NMR spectroscopy for the study of biologically relevant molecules and molecular systems has been the major driving force for the rapid development of experimental techniques and for a steady improvement of ^{15}N-NMR sensitivity. The last few years, in particular, have seen a significant increase in biological ^{15}N-NMR studies. A recent review by *Blomberg* and *Rüterjans*[151] covers detection techniques, spectral parameters, and typical applications in the major biological fields. Further, *Kanamori* and *Roberts*[152] reported specific applications with particular emphasis on enzyme systems, nucleotides and nucleic acids, and intact cell systems. Intermolecular interactions in biomolecules were reviewed by *Kyogoku*,[153] and *Coxon* reported on ^{15}N-NMR studies of amino sugars.[154] Although not primarily biological in nature, a comprehensive account of the ^{15}N-NMR spectroscopic characterization of oligo- and polypeptides by *Krichel-dorf*[155] should be mentioned in this context. Very few studies of nonbiological polymers have so far been reported.[156]

We will focus our attention on a few examples from the recent literature in order to illustrate the possibilities and trends of ^{15}N-NMR spectroscopy in the study of biological systems. Studies of biosynthesis and metabolism are one field in which isotopic labeling combined with ^{15}N-NMR measurements allows detailed studies, which afford new insights into biochemical mechanisms. *Hori* and *Shimizu*[157] have investigated the structures of two related neurotoxins using biosynthetically enriched material. They succeeded in demonstrating that neosaxitoxin **35** is the N^1-hydroxy derivative of saxitoxin (Scheme 27). The ^{15}N-NMR spectrum (Fig. 30) of an ^{15}N-enriched (99%) toxin allows the identification and assignment of the seven N atoms, based on chemical shifts and N,H coupling constants, and the elimination of the alternative structure **36**. The correct assignment of the ^{15}N-NMR signals of complex molecules is an important prerequisite for biosynthetic studies. ^{15}N,^{13}C double labeling allows ^{15}N,^{13}C coupling constants to be measured, thus providing evidence for biosynthetic routes; for example, the biosynthetic formation of the N–C(5) bond in isopenicillin N (which is formed by cyclization of δ-(α-L-aminoadipoyl)-L-[3-^{13}C]cysteinyl-D-[^{15}N]valine) is demonstrated by the one-bond ^{15}N, ^{13}C coupling constant (4.4 Hz).[158]



35



36

Scheme 27.

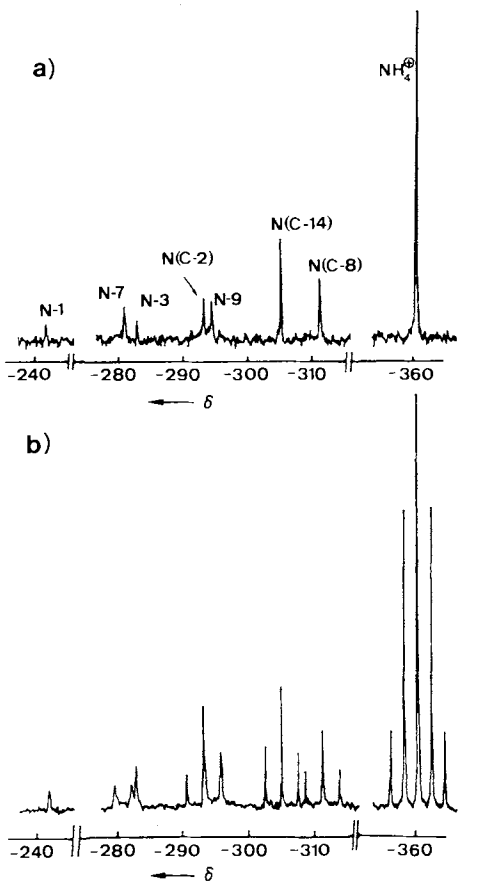


Fig. 30. ^{15}N-NMR spectra of 99% ^{15}N-enriched neosaxitoxin **35** (36.5 MHz; 1.8 mM in H_2O/D_2O 95:5): a) ^{1}H-decoupled; b) ^{1}H-coupled [157].

The in vivo study of amino acid biosynthesis in fungal and bacterial cells has proven a particularly successful domain for ^{15}N-NMR spectroscopy. In 1975 we observed that fast motion of *intra*cellular small molecules permits the measurement of narrow-line spectra in living cells of *Ustilago sphaerogena*.[159] Subsequently, the research groups of *Roberts*[160] and *Lapidot*[161] investigated the biosynthesis of amino acids in *Neurospora crassa* and *Brevibacterium lactofermentum*. The latter organism was used to monitor both nitrogen assimilation from $^{15}NH_4Cl$ and amino acid production throughout the growth cycle.[161] Under optimal growth conditions, i.e., high aeration and low biotin concentration, the glutamic-acid-producing bacteria convert about 50% of the ammonium salt into L-[^{15}N]glutamic acid. Spectra were recorded of intact cells and cell media at different stages of growth and production (Fig. 31). All ^{15}N-NMR signals can be clearly assigned to amino acids and metabolites, although a quantitative evaluation is hampered by different nuclear Overhauser effects and spin–lattice relaxation times. However, a semiquantitative comparison of the respective peaks in spectra recorded at various times in the growth cycle is possible. Two phases were distinguished during the fermentation process. At a very early stage (Fig. 31b) glutamic acid is accumulated in the cells, but practically no product is released into the growth medium. Later, the cell walls become permeable

and amino acids are excreted (Fig. 31a). The alanine/glutamic acid intracellular ratio depends on oxygen and biotin concentration; low oxygen supply leads to a release of alanine instead of glutamic acid. This sensitive and convenient ^{15}N-NMR technique has thus proven a powerful probe for monitoring both *intra-* and *inter*cellular amino acid concentrations in fermentation processes, and it may become an important analytical tool in biotechnology. Furthermore, the metabolic pathways of the intracellular amino acid pool can be followed and elucidated. A number of other studies on the metabolism of important biological precursor molecules have appeared recently.[162] The mobility and environment of intracellular glutamine, alanine, and arginine were studied using ^{15}N spin-lattice relaxation times T_1, and nuclear Overhauser effects.[163]

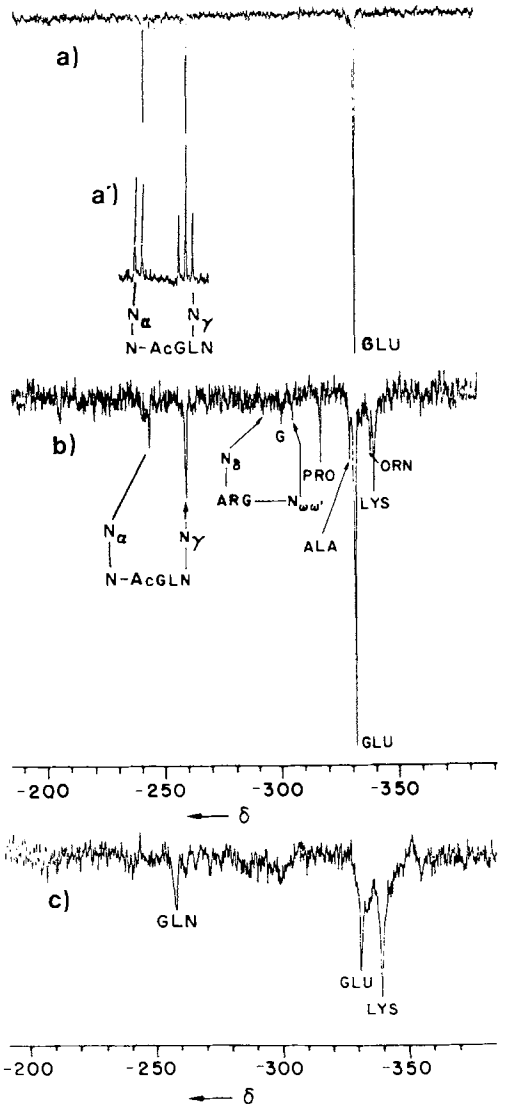


Fig. 31. Proton-decoupled ^{15}N-NMR spectra of 96.7% ^{15}N-enriched *B. lactofermentum* cells grown under conditions of high oxygen supply in normal biotin concentration (30.4 MHz). a) Spectrum of cell-free culture medium obtained after 31 h of fermentation; a') shows a spectrum from the same sample with gated ^{1}H-decoupling; b) spectrum of growth-phase cells (obtained after 10 h of fermentation); c) spectrum of early stationary phase cells (obtained after 16 h of fermentation) [161].

An important parameter characterizing the intracellular medium, the pH, can be determined from ^{15}N-NMR measurements. For example, the two ring atoms of histidine show substantial chemical shift changes between pH 4 and 8; this was used successfully to estimate the pH in the cytoplasmic and vacuolar environment of intact mycelia of *Neurospora crassa*.[164] In addition, pH-dependent line widths for the ^{15}N-NMR signals of the terminal NH_2 groups of arginine and the α-NH_2 group of alanine were used. Measurements on arginine and histidine yielded a pH value of 6.1 ± 0.4 for the vacuoles; the cytoplasmic pH determined by measurements on proline and alanine, on the other hand, was 7.2, in good agreement with other measurements.

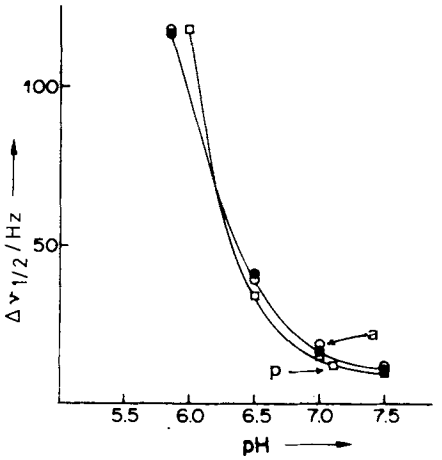


Fig. 32. Plots of the line width at half-height, $\Delta\nu_{1/2}$, of the ^{15}N-NMR signal versus pH for alanine in nitrogen-free medium: (●) 0.01 M, (○) 0.04 M, and (□) 0.005 M proline [164]. a = alanine, p = proline.

The pH dependence of the ^{15}N-NMR line widths for proline and alanine is due to base-catalyzed proton exchange between the NH_2 group and H_2O (see Fig. 32). ^{15}N-NMR experiments appear to offer definite advantages over other techniques, such as ^{31}P-NMR spectroscopy, since amino acids are regiospecifically distributed in subcellular units and their structure-dependent NMR parameters are more sensitive to pH changes in the weakly acidic region.

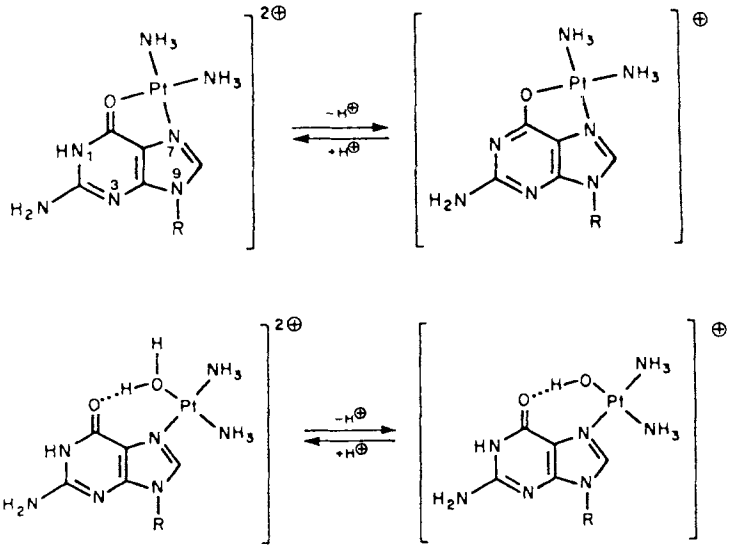
As a last example, we will discuss some ^{15}N-NMR studies on the binding of drugs to biomolecules, in particular, to proteins and nucleic acids. The antitumor activity of certain platinum(II)-amine complexes has stimulated the investigation of model systems for the presumed DNA complex.[165] Binding of ^{15}N-enriched *cis*-$[Pt(NH_3)_2Cl_2]$ to a nucleoside results in changes in the chemical shifts and (^{15}N,^{195}Pt) coupling constants in the ^{15}N-NMR spectrum. Interpretation of these spectra is facilitated by the large low-frequency shifts of the resonances for the azine nitrogen atoms (–N=, N-3) upon coordination (Table 5). Pt complexes containing one or two nucleoside ligands are formed. As expected, cytidine is complexed at N-3, whereas for guanosine, which has several possible sites of coordination, a mixture of mono-complexes is formed. Exchange of both chloride ligands affords a complex for which the structures in Scheme 28 were proposed in order

Table 5. ^{15}N chemical shifts δ of free nucleosides and of platinum-nucleoside complexes [165] [a].

	N-1	N-3	N-7	N-9	NH_2
cytidine 5'-phosphate	−227.9	−179.6			−287.6
cis-$[Pt(NH_3)_2(Cyd)_2]^{2\oplus}$	−228.0	−255.4			−276.8
guanosine 5'-phosphate	−233.5	−215.7	−145.6	−211.6	−307.9
cis-$[Pt(NH_3)_2(Guo)_2]^{2\oplus}$	−232.5	−215.8	−237.9	−207.1	−304.7

[a] Recalculated relative to CH_3NO_2.

to explain the pH dependence of the resonance of the NH_3 ligand *trans* to the oxygen ligand. The low pK_a value of 4.9 for the acidic group suggests the incorporation of a water molecule in the complex rather than deprotonation of the amide function. The most complex coordination behavior was observed for adenosine and involves all four basic N atoms (N-1, N-3, N-7, and 6'-NH_2). A few relevant studies on ^{15}N-^{195}Pt interactions have also been reported[166] (see also references cited in ref. [165]).



Scheme 28.

The binding of small molecules to large biomolecules does not necessarily lead to broad resonance lines, as might be expected from the long correlation times of these macromolecules. An example of the application of ^{15}N-NMR spectroscopy to enzyme systems was provided by *Becker* and *Roberts* in their detailed investigation of a ternary inhibitor complex, liver alcohol dehydrogenase-NAD^+-pyrazole.[167] The ^{15}N-NMR spectrum obtained at 18.25 MHz (4.2 tesla) (Fig. 33) demonstrates the nonequivalence of N-1 and N-2 in the bound [1,2-$^{15}N_2$]pyrazole. The chemical shift of N-1 ($\delta = -146.5$) is relatively close to the corresponding resonance of the adduct between pyrazole and N-benzylnicotinamide ($\delta = -140.7$), whereas that of N-2 in the enzyme complex ($\delta = -122.2$) is shifted by 41.1 ppm to lower frequencies relative to the model compound. These results were interpreted in terms of covalent bonding between N-1 of pyrazole and C-4 of the nicotinamide group and coordination of N-2 by the Zn atom at the active site of the enzyme, in agreement with a structural model proposed by *Theorell* and *Yonetani* and with X-ray crystallographic studies (see ref. [167]).

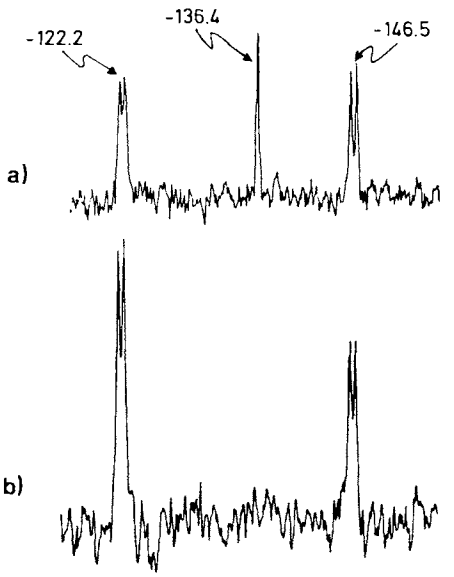


Fig. 33. ^{15}N-NMR spectra of the dehydrogenase-$NAD^{\oplus}$-pyrazole complex (18.25 MHz, prepared from 99% $^{15}N_2$-labeled pyrazole; 0.1 M sodium phosphate buffer; pH 7.0): a) before dialysis; b) after dialysis [167]. The signals at $\delta = -122.2$, -136.4, and -146.5 are assigned to N-2 of bound pyrazole, free pyrazole, and N-1 of bound pyrazole, respectively.

The formation of an enzyme-inhibitor complex is also responsible for the pharmacological activity of the dihydrofolate reductase (DHFR) inhibitors. Typical inhibitors are trimethoprim (2,4-diamino-5-(3,4,5-trimethoxybenzyl)pyrimidine, TMP) and methotrexate (MTX), the latter of which has a modified folic acid structure. The binding mode of TMP and MTX to DHFR has been the subject of extensive investigations by several interdisciplinary research groups.[168] The ternary complex between *Lactobacillus casei* DHFR, trimethoprim, and $NADP^+$ exists in solution as a mixture of approximately equal amounts of two slowly interconverting conformational states, which have been characterized by multinuclear NMR experiments. The ^{15}N-NMR spectrum[168] of a triply ^{15}N-labeled TMP in its ternary complex with DHFR and $NADP^+$ is shown in Figure 34. Comparison of this spectrum with the spectra of the binary DHFR-TMP complex and with the free protonated trimethoprim confirms the presence of two species in aqueous solution. The chemical shifts of the N-1 and 2-NH_2 ^{15}N resonances in the inhibitor complex are typical for protonated trimethoprim, which had been studied earlier by our group.[39] In another study, binding of human carbonic anhydrase B with benzenesulfonamide and cya-

nate ion, typical inhibitors, was investigated by ^{15}N-NMR spectroscopy.[169a] Recently, ^{15}N-NMR spectroscopy has also been used to study whole enzyme systems, e.g., in the study of the flavin-apoenzyme interaction.[169b]

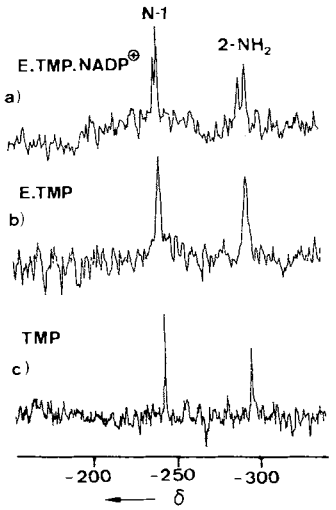


Fig. 34. ^{15}N-NMR spectra of (1,3,N^2-^{15}N$_3$)trimethoprim (TMP) (20.2 MHz): a) TMP in its ternary complex with dihydrofolate reductase (E) and NADP$^⊕$ (INEPT pulse sequence with ^{1}H-decoupling, 90% H_2O/10% D_2O); the signal of N-3 was not reported [168]. b) TMP in its binary complex with dihydrofolate reductase (conditions similar to a)). c) TMP in 0.1 M aqueous HCl.

4.6. High-Resolution ^{15}N-NMR Spectra of Solids

Whereas numerous structural studies have been concerned with ^{15}N-NMR spectroscopy of liquid samples of small, medium sized, and even large biomolecules, there are as yet only a few examples in which the ^{15}N nucleus has been used as a probe into molecular structure of the solid state, and most of these have dealt with biochemical problems. This fact is easily explained. The solid-state ^{13}C- and ^{1}H-NMR spectra of biomolecules are often difficult to interpret on account of the large number of nonequivalent ^{1}H and ^{13}C atoms. In contrast, nitrogen nuclei are favorable for solid-state NMR studies of biomolecules and biological systems since there are relatively few nonequivalent N atoms and the chemical shift differences are usually large. Thus, resolution problems are less severe. Sensitivity problems can be overcome by using selective ^{15}N isotopic enrichment and very effective cross-polarization experiments (polarization transfer from protons). The distances between N atoms in biomolecules guarantee that even with very high isotopic enrichment no problems due to homonuclear spin coupling arise. The inherent difficulties with NMR studies of solids have been successfully overcome by a combination of high-frequency magic angle spinning (MAS) to remove chemical shift anisotropy, broadband proton-decoupling to eliminate dipolar and scalar coupling, and cross polarization (CP) for sensitivity enhancement. These methods[170, 171, 27] and their chemical applications[172] have been reviewed recently. In addition, a survey of solid-state NMR as applied to biological systems has appeared.[173] Examples of CPMAS experiments on ^{15}N nuclei are given in this review.

Solid-state ^{15}N-NMR spectra have been obtained from single crystals, crystalline and amorphous powders, and whole biological systems, e.g., plant leaves. In all but the single-crystal studies, ^{15}N-enriched samples were used. The natural abundance ^{15}N-NMR single-crystal spectrum of histidine hydrochloride monohydrate is shown in Figure 35; well-resolved lines for the $NH_3^⊕$ groups and the N atoms in the ring can be recognized. Orientation-dependent NMR measurements may then be used to determine the chemical shift tensors.[174] The shift anisotropy, $\Delta\sigma$, was found to be 220 ppm for N-2 and 216 ppm for N-3, while the $NH_3^⊕$ group gave $\Delta\sigma < 12$ ppm. Since much larger $\Delta\sigma$ values were reported for unprotonated pyridine ($\approx$780 ppm),[175] such determinations of ^{15}N-NMR shift tensors can yield valuable information about the degree of protonation in solid biological systems. *Munovitz* et al.[27] have recently shown that chemical shift and dipolar tensors can be measured simultaneously with excellent resolution if the dipolar spin interaction is reintroduced and the spectra are analyzed by 2D NMR methods. The experimental techniques thus allow the study of dipolar interactions between nitrogen sites in solid biomolecules. ^{15}N and ^{13}C chemical shift tensors have been determined for the peptide bond in ^{15}N,^{13}C-labeled glycylglycine hydrochloride;[176] moreover, the authors give a discussion of $\Delta\sigma$(N) values known to date in terms of C–N π-bond order. The ^{15}N shift anisotropy for the peptide bond (155 ppm) reflects its partial double-bond character.

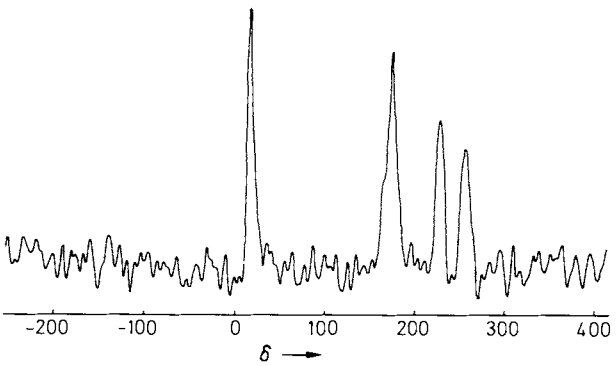


Fig. 35. ^{15}N-NMR spectrum of a single crystal obtained from L-histidine hydrochloride monohydrate. The unit cell *a* axis was approximately along the rotation axis of the NMR goniometer. Chemical shifts are relative to solid $(NH_4)_2SO_4$. The single line on the left is assigned to the $NH_3^⊕$ groups; it is indicative of very small shift tensors. The three lines on the right are due to the imidazole nitrogen atoms [174].

The protonation of and hydrogen bonding to nitrogen atoms is of central importance in many biochemical systems. A solid-state ^{15}N-NMR study of the Schiff base linkage in ε-[^{15}N]lysylbacteriorhodopsin, the only protein in purple membrane, has revealed, from the isotropic chemical shift ($\delta = -204.6$), that the imine N atom is protonated in the dark-adapted form.[177] The doublet structure of the signal (Fig. 36) suggests that the bacteriorhodopsin contains two stereoisomeric forms, which are tentatively assigned to 13-*cis*- and all-*trans*-retinal Schiff bases. The ^{15}N chemical shift of the lysylbacteriorhodopsin ($\delta = -204.6$) is similar to the values for the model all-*trans*-retinylidene-

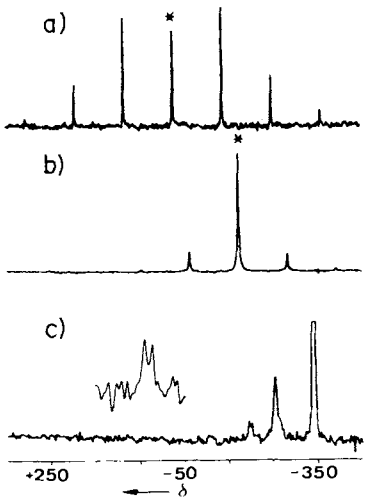


Fig. 36. Proton-decoupled MAS ^{15}N-NMR spectra of a) retinylidenebutyl[^{15}N]amine (^{15}N-RB); b) ^{15}N-RBH$^{\oplus}$Cl$^{\ominus}$; c) ε-[^{15}N]lysylbacteriorhodopsin (29.8 MHz). For clarity the center bands in a) and b) are marked with asterisks. The inset in c) is an expansion of the Schiff base signal showing the doublet structure ($\Delta\delta = 5.7$) tentatively assigned to the 13-*cis* and the all-*trans* stereoisomers. The two remaining lines in c) arise from the peptide backbone *N* atoms ($\delta = -259.3$) and the six lysine $NH_3^{\oplus}$ groups ($\delta = -344.5$). Chemical shifts originally referred to external, aqueous 5.6 M NH_4Cl [177] were recalculated relative to CH_3NO_2; conversion value −352.9 ppm [7a].

butyl[^{15}N]ammoniumchloride ($\delta = -181.2$), whereas the ^{15}N atom of the model base is strongly deshielded ($\delta = -37.6$). The chemical shift of the protonated solid is thus very similar to the one reported for the hydrochloride in solution ($\delta = -147$)[113] (see also section 4.1). Here, too, protonation of nitrogen results in a drastic narrowing of the chemical shift tensor, as shown in the ^{1}H-decoupled ^{15}N-NMR powder spectrum (Fig. 37), from $\Delta\sigma \approx 600$ ppm for the Schiff base to 270 ppm for the hydrochloride.

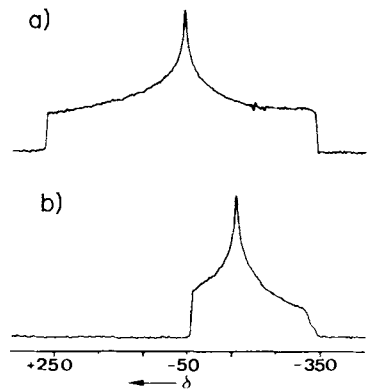


Fig. 37. Proton-decoupled ^{15}N-NMR powder spectra of all-*trans*-retinylidene butyl[^{15}N]amine; a) unprotonated; b) hydrochloride. In a) the powder pattern is ≈600 ppm (18 kHz) wide with an isotropic shift of $\delta = -38$. Protonation narrows the spectrum to a 270 ppm breadth and moves the chemical shift 142 ppm downfield. The chemical shifts were recalculated relative to CH_3NO_2 as standard (see legend to Fig. 36) [177].

Solid-state NMR studies are particularly attractive since they permit a comparison of enzyme structures in anisotropic and isotropic phase (i.e., in solid and in solution, respectively) using the same physical method, in contrast to the usual comparisons between X-ray diffraction and NMR data. For example, the structure of α-lytic protease was studied by the CPMAS technique; initially, the N^{τ} atom of His^{57} was ^{15}N-labeled, and, in a subsequent experiment, both the N^{π} and N^{τ} atoms were ^{15}N-labeled.[178] The behavior of the ^{15}N chemical shifts as a function of the pH (Fig. 38) of the solution used to prepare the lyophilized samples was found to closely parallel that observed in earlier solution studies,[179a] except for the slower proton exchange at His^{57} in the solid state. The local environment at the His^{57} close to the active site of the enzyme is shown in Scheme 29. The unusual tautomeric form of

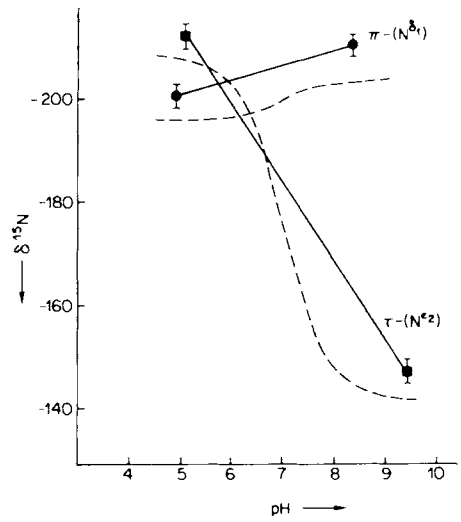
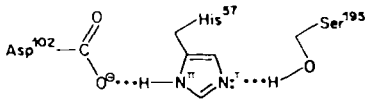


Fig. 38. The pH-dependence of the ^{15}N chemical shifts of the imidazole ring N atoms of histidine-57 in α-lytic protease in solutions (--) [179] and in lyophilized powders (—) [178].



Scheme 29.

histidine with an N^{π}–H bond was originally proposed[179a] and later confirmed[93c] on the basis of ^{15}N-NMR measurements on the enzyme in solution. The specific triad structure involving His^{57} with the closely spaced aspartate^{102} ion on the π-side and the OH group of Ser^{195} on the τ side is responsible for the stabilization of this tautomer. The good agreement between the new solid-state data and the solution results represents convincing structural evidence. A similar study employing ^{15}N-CPMAS and X-ray diffraction data was recently carried out on a carboxypeptidase A complex with glycyltyrosine.[179b]

The reduced proton exchange rates in the solid state allow the identification of protonated N atoms in biomolecules and ^{15}N-DNMR studies of proton transfer. A recent investigation by *Limbach* et al.[180a] on tautomerism in ^{15}N-enriched *meso*-tetra-*p*-tolylporphins **37** has shown that the process can be conveniently studied as a two-site exchange problem in the temperature range from 210 to 295 K. The CPMAS ^{15}N-NMR spectra are shown in Figure 39; a complete line-shape analysis gave first-order rate constants

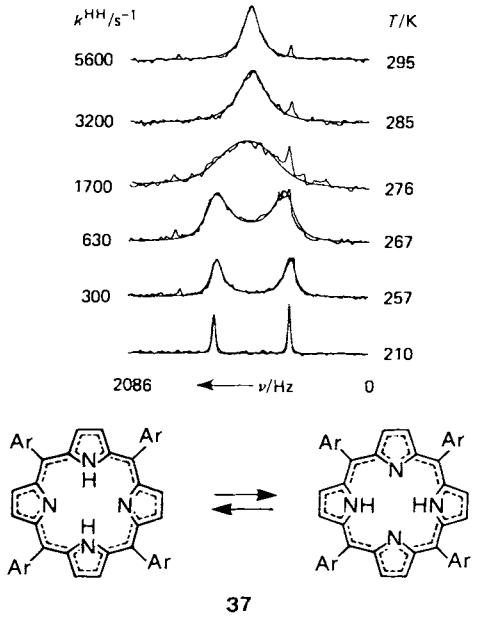


Fig. 39. CPMAS ^{15}N-DNMR spectra of *meso*-tetra-*p*-tolylporphin **37** (Ar = *p*-tolyl; 6.1 MHz; 95% ^{15}N-enriched **37**); experimental and calculated spectra are superimposed. The small sharp low-frequency line is attributed to an impurity [180].

(k^{HH}). Whereas the dynamic behavior of the *p*-tolyl- and phenylporphins was found to be the same in solution, they show very different solid-state spectra as a function of temperature. The complex cases of the arylporphins were also discussed in conjunction with the results from X-ray diffraction studies.[180b]

^{15}N-NMR spectroscopy of solids has also been applied to nucleic acids, e.g., to the study of N–H bond lengths in B-DNA[34] (see also Section 2.3, Fig. 11) and to the study of the DNA backbone structures of fd and Pfl bacteriophages.[181] The latter investigations were supported by 2D NMR analysis of the dipolar splittings in the spectra of oriented virus molecules.[35] From the same research group, several solid-state ^{15}N-NMR studies on proteins were also reported.[181, 182a]

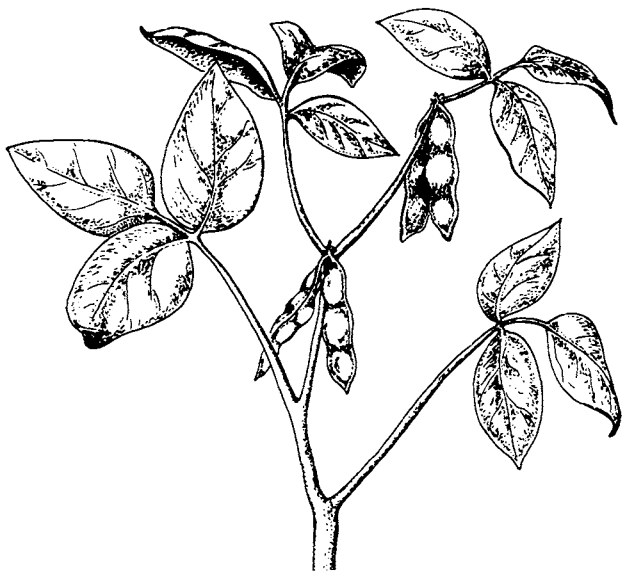


Fig. 40. Shoot of a soybean plant (Glycine soja) [184].

We will close this review by quoting a paper that demonstrates the almost unlimited potential of ^{15}N-NMR spectroscopy in biological studies.[182b] *Schaefer* et al.[183a] recorded the double cross-polarization MAS ^{15}N-NMR spectra of soybean leaves in order to determine the protein turnover number. This plant was also used to investigate the metabolism of allantoin in the early growth state.[183b] Figure 40 shows a soybean shoot as a symbol of the ever-growing applications of NMR spectroscopy to chemistry, biochemistry, and biology. New branches are expected to grow and will call for imaginative investigators.

5. Outlook

During the past few years ^{15}N-NMR spectroscopy has developed as a versatile experimental probe into the structure and reactivity of organic, bioorganic, and inorganic molecules. The majority of studies have been performed without isotopic enrichment of the substrates. Since the sensitivity of the ^{15}N-NMR technique is still improving, its application is expected to increase still further in the future. Modern 1D and 2D NMR experiments will undoubtedly make possible the structural investigations of larger molecules and more complex biomolecules in the liquid and solid states. For example, the heteronuclear "D-resolved" 2D NMR experiments recently described offer a new dimension for the quantitative study of hydrogen bonding in solids. Although many ^{15}N-NMR investigations of active sites in biological systems still require isotopic enrichment, the first successful attempts to study drug binding, i.e., the mechanism of drug action, have shown a considerable pharmacological potential. The fundamental problem of biological nitrogen fixation and metabolism may be investigated in the future by an extended use of ^{15}N-NMR techniques, and other applications may be envisaged. However, the realization of many chemical and biochemical ideas will finally depend on the availability of versatile multinuclear NMR instrumentation and flexible computing facilities. It is this area where the most significant advances can be expected for the near future.

The senior author (W. v. P.) wishes to express his gratitude and indebtedness to his co-workers who have contributed to the results from the Zürich laboratory that are described in this review: Dr. W. Schwotzer, Dr. W. Städeli, Dr. R. Hollenstein, Dr. P. Bigler, Dr. L. Kozerski, Dr. G. Cerioni, Dr. M. Tatò, B. C. Chen, C. Adams, and R. Müller. Their scientific enthusiasm, experimental skill, and endurance have had, and continue to have, a major impact on the research and spirit of our group. Generous financial support from the Government of the Kanton Zürich and the Swiss National Science Foundation is gratefully acknowledged.

Received: July 23, 1985;
supplemented: October 23, 1985 [A 576 IE]
German version: *Angew. Chem. 98* (1986) 381

[1] R. Müller, J. D. Wallis, W. von Philipsborn, *Angew. Chem. 97* (1985) 515; *Angew. Chem. Int. Ed. Engl. 24* (1985) 513.

[2] W. G. Proctor, F. C. Yu, *Phys. Rev. 77* (1950) 717; *81* (1951) 20.

[3] M. Witanowski, G. A. Webb (Eds.): *Nitrogen NMR*, Plenum Press, London 1973.

[4] a) J. Mason, *Chem. Rev. 81* (1981) 205; b) *Chem. Br. 19* (1983) 654.

[5] N. Logan in [3], chapter 6, p. 319, "Applications of ^{14}N NMR Data in the Study of Inorganic Molecules".

[6] J. M. Lehn, J. P. Kintzinger in [3], chapter. 3, p. 79, "Nitrogen-14 Nuclear Quadrupole Effects".

[7] a) G. J. Martin, M. L. Martin, J.-P. Gouesnard, "^{15}N-NMR Spectroscopy" in P. Diehl, E. Fluck, R. Kosfeld (Eds.): *NMR Basic Principles and Progress, Vol. 18*, Springer, Berlin 1981; b) M. Witanowski, L. Stefaniak, G. A. Webb, *Annu. Rep. NMR Spectrosc. 11B* (1981); c) G. C. Levy, R. L. Lichter: *Nitrogen-15 Nuclear Magnetic Resonance Spectroscopy*, Wiley, New York 1979.

[8] L. F. Farnell, E. W. Randall, A. I. White, *J. Chem. Soc. Chem. Commun. 1972*, 1159; O. A. Gansow, A. R. Burke, G. N. La Mar, *ibid. 1972*, 456; A. J. DiGioia, R. L. Lichter, *J. Magn. Reson. 27* (1977) 431.

[9] W. Schwotzer, J. H. Bieri, M. Viscontini, W. von Philipsborn, *Helv. Chim. Acta 61* (1978) 2108.

[10] P. Ashkenazi, M. Kaftory, D. Arad, Y. Apeloig, D. Ginsburg, *Helv. Chim. Acta 64* (1981) 579.

[11] G. A. Morris, R. Freeman, *J. Am. Chem. Soc. 101* (1979) 760.

[12] R. Benn, H. Günther, *Angew. Chem. 95* (1983) 381; *Angew. Chem. Int. Ed. Engl. 22* (1983) 350.

[13] L. Kozerski, K. Kamienska-Trela, L. Kania, W. von Philipsborn, *Helv. Chim. Acta 66* (1983) 2113.

[14] G. A. Morris, *J. Am. Chem. Soc. 102* (1980) 428.

[15] B. C. Chen, W. von Philipsborn, K. Nagarajan, *Helv. Chim. Acta 66* (1983) 1537.

[16] a) S. J. B. Price, M. J. DiMartino, D. T. Hill, R. Kuroda, M. A. Mazid, P. J. Sadler, *Inorg. Chem. 24* (1985) 3425; b) C. Brevard, R. Schimpf, *J. Magn. Reson. 47* (1982) 528.

[17] A. Costa, M. Tato, R. S. Matthews, *Magn. Reson. Chem.*, in press.

[18] K. V. Schenker, W. von Philipsborn, *J. Magn. Reson. 61* (1985) 294.

[19] a) D. M. Doddrell, D. T. Pegg, M. R. Bendall, *J. Magn. Reson. 48* (1982) 323; b) D. T. Pegg, D. M. Doddrell, M. R. Bendall, *J. Chem. Phys. 77* (1982) 2745; c) D. T. Pegg, M. R. Bendall, *J. Magn. Reson. 53* (1983) 229.

[20] K. G. R. Pachler, P. L. Wessels, *J. Magn. Reson. 28* (1977) 53; H. J. Jakobsen, H. Bildsøe, *ibid. 26* (1977) 183.

[21] a) H. J. Jakobsen, W. S. Brey, *J. Am. Chem. Soc. 101* (1979) 774; b) *J. Chem. Soc. Chem. Commun. 1979*, 478; c) H. J. Jakobsen, P.-I. Yang, W. S. Brey, *Org. Magn. Reson. 17* (1981) 290; d) O. W. Sørensen, S. Scheibye, S.-O. Lawesson, H. J. Jakobsen, *ibid. 16* (1981) 322.

[22] A. Bax, Ch.-H. Niu, D. Live, *J. Am. Chem. Soc. 106* (1984) 1150.

[23] D. H. Live, D. G. Davis, W. C. Agosta, D. Cowburn, *J. Am. Chem. Soc. 106* (1984) 6104.

[24] A. Bax, R. H. Griffey, B. L. Hawkins, *J. Am. Chem. Soc. 105* (1983) 7188.

[25] C. J. Turner, *Prog. Nucl. Magn. Reson. Spectrosc. 16* (1984) 311.

[26] A. Bax, R. H. Griffey, B. L. Hawkins, *J. Magn. Reson. 55* (1983) 301.

[27] M. G. Munovitz, H. H. Huang, C. M. Dobson, R. G. Griffin, *J. Magn. Reson. 57* (1984) 56.

[28] a) H. Kessler, W. Hehlein, R. Schuck, *J. Am. Chem. Soc. 104* (1982) 4534; b) H. Kessler, H. R. Loosli, H. Oschkinat, *Helv. Chim. Acta 68* (1985) 661; c) H. Kessler, H. Oschkinat, H. R. Loosli, „2D NMR Spectroscopy", in R. M. Carlson, W. R. Croasmun (Eds.): *Methods in Stereochemical Analysis*, VCH Verlagsgesellschaft, Weinheim, 1986.

[29] G. A. Gray, *Org. Magn. Reson. 21* (1983) 111.

[30] H. Kessler, C. Griesinger, J. Zarbock, H. R. Loosli, *J. Magn. Reson. 57* (1984) 331.

[31] G. Bodenhausen, D. J. Ruben, *Chem. Phys. Lett. 69* (1980) 185.

[32] A. G. Redfield, *Chem. Phys. Lett. 96* (1983) 537.

[33] a) R. H. Griffey, C. D. Poulter, A. Bax, B. L. Hawkins, Z. Yamaizumi, S. Nishimura, *Proc. Natl. Acad. Sci. USA 80* (1983) 5895; R. H. Griffey, D. Davis, Y. Yamaizumi, S. Nishimura, A. Bax, B. Hawkins, C. D. Poulter, *J. Biol. Chem. 260* (1985) 9734; b) L. Müller, R. A. Schiksnis, S. J. Opella, *J. Magn. Reson. 66* (1986) 379.

[34] J. A. DiVerdi, S. J. Opella, *J. Am. Chem. Soc. 104* (1982) 1761.

[35] T. A. Cross, P. Tsang, S. J. Opella, *Biochemistry 22* (1983) 721.

[36] D. G. Davis, W. C. Agosta, D. Cowburn, *J. Am. Chem. Soc. 105* (1983) 6189.

[37] P. R. Srinivasan, R. L. Lichter, *J. Magn. Reson. 28* (1977) 227.

[38] IUPAC Recommendations for nuclei other than ^1H, cf. *Pure Appl. Chem. 45* (1976) 219.

[39] W. Städeli, A. Wick, I. Kompiš, W. von Philipsborn, *Helv. Chim. Acta 63* (1980) 504, and references cited therein.

[40] W. Schwotzer, W. von Philipsborn, *Helv. Chim. Acta 60* (1977) 1501.

[41] K. A. K. Ebraheem, G. A. Webb, *Prog. Nucl. Magn. Reson. Spectrosc. 11* (1977) 149; M. Bremond, G. J. Martin, G. A. Webb, D. J. Reynolds, *Org. Magn. Reson. 22* (1984) 640; K. A. K. Ebraheem, G. A. Webb, M. Witanowski, *ibid. 11* (1978) 27; K. A. K. Ebraheem, G. A. Webb, *ibid. 9* (1977) 248.

[42] W. Städeli, *Dissertation*, Universität Zürich 1981.

[43] See [7a], p. 60.

[44] W. M. Litchman, M. Alei, A. E. Florin, *J. Chem. Phys. 50* (1969) 1897.

[45] R. E. London, T. E. Walker, T. W. Whaley, N. A. Matwiyoff, *Org. Magn. Reson. 9* (1977) 598.

[46] L. Kozerski, W. von Philipsborn, *Helv. Chim. Acta 65* (1982) 2077.

[47] A. Lyčka, P. E. Hansen, *Org. Magn. Reson. 22* (1984) 569.

[48] J. A. Pople, D. P. Santry, *Mol. Phys. 8* (1964) 1.

[49] See [3], p. 269.

[50] G. A. Olah, A. W. White, *J. Am. Chem. Soc. 90* (1968) 6087.

[51] A. J. R. Bourn, E. W. Randall, *Mol. Phys. 8* (1964) 567.

[52] G. Binsch, J. B. Lambert, B. W. Roberts, J. D. Roberts, *J. Am. Chem. Soc. 86* (1964) 5564.

[53] R. Wasylishen, T. Schaefer, *Can. J. Chem. 49* (1971) 3627.

[54] H. Hilpert, R. Hollenstein, *Helv. Chim. Acta. 69* (1986) 136.

[55] J. Dorie, B. Mechin, G. Martin, *Org. Magn. Reson. 12* (1979) 229.

[56] L. Paolillo, E. D. Becker, *J. Magn. Reson. 2* (1970) 168.

[57] See [7b], p. 12.

[58] See [7a], p. 310f.

[59] W. McFarlane, *Mol. Phys. 10* (1965) 603.

[60] W. Runge, J. Firl, *Z. Naturforsch. B 31* (1976) 1515.

[61] T. Bundgaard, H. J. Jakobsen, E. J. Rahkamaa, *J. Magn. Reson. 19* (1975) 345.

[62] J. M. Schulman, T. Venanzi, *J. Am. Chem. Soc. 98* (1976) 4701, 6739; T. Khin, G. A. Webb, *Org. Magn. Reson. 10* (1977) 175; J. M. Schulman, *J. Magn. Reson. 28* (1977) 137; T. Axenrod, C. M. Watnick, M. J. Wieder, S. Duangthai, G. A. Webb, H. J. C. Yeh, S. Bulusu, M. M. King, *Org. Magn. Reson. 20* (1982) 11.

[63] M. J. O. Anteunis, F. A. M. Borremans, J. Gelan, A. P. Marchand, R. W. Allen, *J. Am. Chem. Soc. 100* (1978) 4050; the $^3J(^{14}N,^1H)$ values were recalculated by use of Equation (b).

[64] R. Wasylishen in T. Axenrod, G. A. Webb (Eds.): *Nuclear Magnetic Resonance Spectroscopy of Nuclei Other Than Protons*, Wiley, New York 1974, chapter 8.

[65] a) W. Städeli, P. Bigler, W. von Philipsborn, *Org. Magn. Reson. 16* (1981) 170; b) M. Schumacher, H. Günther, *Chem. Ber. 116* (1983) 2001.

[66] R. Müller, *Diplomarbeit*, Universität Zürich 1983; R. Müller, W. von Philipsborn, unpublished.

[67] V. F. Bystrov, *Prog. Nucl. Magn. Reson. Spectrosc. 10* (1976) 41.

[68] M. Barfield, H. L. Gearhart, *Mol. Phys. 27* (1974) 899; V. N. Solkan, V. F. Bystrov, *Izv. Akad. Nauk SSSR. Ser. Khim. 1974*, 102.

[69] V. F. Bystrov, Yu. D. Gavrilov, V. N. Solkan, *J. Magn. Reson. 19* (1975) 123; J. A. Sogn, W. A. Gibbons, E. W. Randall, *Biochemistry 12* (1973) 2100; A. J. Fischman, H. R. Wyssbrod, W. C. Agosta, D. Cowburn, *J. Am. Chem. Soc. 100* (1978) 54; A. J. Fischman, D. H. Live, H. R. Wyssbrod, W. C. Agosta, D. Cowburn, *bid. 102* (1980) 2533; A. de Marco, M. Llinas, K. Wüthrich, *Biopolymers 17* (1978) 2727.

[70] W. von Philipsborn, *Angew. Chem. 83* (1971) 470; *Angew. Chem. Int. Ed. Engl. 10* (1971) 472.

[71] T. Axenrod in [3], chapter 5, p. 261.

[72] C. M. Adams, W. von Philipsborn, *Magn. Reson. Chem. 23* (1985) 130.

[73] S. Nagata, T. Yamabe, K. Hirao, K. Fukui, *J. Phys. Chem. 79* (1975) 1863.

[74] R. L. Lichter, D. E. Dorman, R. Wasylishen, *J. Am. Chem. Soc. 96* (1974) 930.

[75] W. Schwotzer, C. Leuenberger, L. Hoesch, A. S. Dreiding, W. von Philipsborn, *Org. Magn. Reson. 9* (1977) 382.

[76] H. Schultheiss, E. Fluck, *Z. Naturforsch. B 32* (1977) 257.

[77] a) T. Berkhoudt, H. J. Jakobsen, *J. Magn. Reson. 50* (1984) 323; b) Y. Kuroda, Y. Fujiwara, K. Matsushita, *ibid. 62* (1985) 218; c) M. Gruner,

D. Pfeifer, H. G. O. Becker, R. Radeglia, J. Epperlein, *J. Prakt. Chem. 327* (1985) 63.

[78] a) J. M. Manriquez, D. R. McAlister, E. Rosenberg, A. M. Shiller, K. L. Williamson, S. I. Chan, J. E. Bercaw, *J. Am. Chem. Soc. 100* (1978) 3078; b) J. O. Friedrich, R. E. Wasylishen, *J. Chem. Phys. 83* (1985) 3707.

[79] a) T. Khin, G. A. Webb, *J. Magn. Reson. 33* (1979) 159; b) J. M. Schulman, J. Ruggio, T. J. Venanzi, *J. Am. Chem. Soc. 99* (1977) 2045.

[80] J. R. Lyerla, Jr., in G. C. Levy (Ed.): *Topics in Carbon-13 NMR Spectroscopy, Vol. 1*, Wiley, New York 1974, p. 79.

[81] G. C. Levy, C. E. Holloway, R. C. Rosanske, J. M. Hewitt, C. H. Bradley, *Org. Magn. Reson. 8* (1976) 643; G. C. Levy, T. Pehk, P. R. Srinivasan, *ibid. 14* (1980) 129; see also [7a], p. 7.

[82] O. A. Gansow, K. M. Triplett, T. T. Peterson, R. E. Botto, J. D. Roberts, *Org. Magn. Reson. 13* (1980) 77.

[83] H. R. Kricheldorf, W. E. Hull, *Makromol. Chem. 181* (1980) 507.

[84] T. A. Scahill, S. L. Smith, *Org. Magn. Reson. 21* (1983) 621, 662.

[85] See [7b], p. 77.

[86] See [7b], p. 84.

[87] L. Stefaniak, J. D. Roberts, M. Witanowski, G. A. Webb, *Org. Magn. Reson. 22* (1984) 201, 215; L. Stefaniak, J. D. Roberts, M. Witanowski, B. T. Hamdi, G. A. Webb, *ibid. 22* (1984) 209.

[88] a) K. Nagarajan, V. P. Arya, *J. Sci. Ind. Res. 41* (1982) 232; b) M. D. Nair, K. Nagarajan in E. Jucker (Ed.): *Progress in Drug Research, Vol. 27*, Birkhäuser Verlag, Basel 1983, p. 163.

[89] W. Schilf, L. Stefaniak, M. Witanowski, G. A. Webb, *Magn. Reson. Chem. 23* (1985) 181.

[90] P. Schmitt, K. Finneiser, H. Günther, personal communication.

[91] E. Bojarska-Olejnik, L. Stefaniak, M. Witanowski, B. T. Hamdi, G. A. Webb, *Magn. Reson. Chem. 23* (1985) 166.

[92] D. S. Wofford, D. M. Forkey, J. G. Russell, *J. Org. Chem. 47* (1982) 5132.

[93] a) W. W. Bachovchin, J. D. Roberts, *J. Am. Chem. Soc. 100* (1978) 8041; b) I. I. Schuster, J. D. Roberts, *J. Org. Chem. 44* (1979) 3864; c) J. D. Roberts, Chun Yu, C. Flanagan, R. T. Birdseye, *J. Am. Chem. Soc. 104* (1982) 3945.

[94] N. C. Gonnella, H. Nakanishi, J. B. Holtwick, D. S. Horowitz, K. Kanamori, N. J. Leonhard, J. D. Roberts, *J. Am. Chem. Soc. 105* (1983) 2050; N. C. Gonnella, J. D. Roberts, *ibid. 104* (1982) 3162.

[95] W. E. Hull, M. Künstlinger, E. Breitmaier, *Angew. Chem. 92* (1980) 957; *Angew. Chem. Int. Ed. Engl. 19* (1980) 924.

[96] See references in [95].

[97] W. Städeli, W. von Philipsborn, *Org. Magn. Reson. 15* (1981) 106.

[98] S. Tobias, P. Schmitt, H. Günther, *Chem. Ber. 115* (1982) 2015.

[99] R. L. Blakley, *Biochem. J. 58* (1954) 448.

[100] R. L. Kisliuk, W. Sakami, *J. Am. Chem. Soc. 76* (1954) 1456; M. J. Osborn, P. T. Talbert, F. M. Huennekens, *ibid. 82* (1960) 4921; R. G. Kallen, W. P. Jencks, *J. Biol. Chem. 241* (1966) 5851.

[101] a) R. Kalbermatten, W. Städeli, J. H. Bieri, M. Viscontini, *Helv. Chim. Acta 64* (1981) 2627; b) R. Kalbermatten, *Dissertation*, Universität Zürich 1981.

[102] L. Paolillo, E. D. Becker, *J. Magn. Reson. 3* (1970) 200.

[103] S. K. Malhotra in A. G. Cook (Ed.): *Enamines*, M. Dekker, New York 1969.

[104] L. Kozerski, W. von Philipsborn, *Org. Magn. Reson. 17* (1981) 306.

[105] a) R. A. Eades, D. A. Weil, M. R. Ellenberger, W. E. Farneth, D. A. Dixon, C. H. Douglass, Jr., *J. Am. Chem. Soc. 103* (1981) 5372; b) W. von E. Doering, personal communication.

[106] J. Dorie, B. Mechin, G. Martin, *Org. Magn. Reson. 12* (1979) 229.

[107] G. J. Martin, J. P. Gouesnard, J. Dorie, C. Rabiller, M. L. Martin, *J. Am. Chem. Soc. 99* (1977) 1381.

[108] M. J. Kamlet, C. Dickinson, R. W. Taft, *J. Chem. Soc. Perkin Trans. 2 1981*, 353.

[109] R. Kupper, B. D. Hilton, M. B. Kröger-Koepke, S. R. Koepke, C. J. Michejda, *J. Org. Chem. 49* (1984) 3781.

[110] T. B. Patrick, R. P. Willaredt, *J. Org. Chem. 48* (1983) 4415.

[111] D. J. Craik, G. C. Levy, R. T. C. Brownlee, *J. Org. Chem. 48* (1983) 1601.

[112] M. Allen, J. D. Roberts, *J. Org. Chem. 45* (1980) 130, and references cited therein.

[113] D. D. Muccio, W. G. Copan, W. W. Abrahamson, G. D. Mateescu, *Org. Magn. Reson. 22* (1984) 121.

[114] C. Yu, G. C. Levy, *Org. Magn. Reson. 22* (1984) 131.

[115] For references see: D. H. Live, D. G. Davis, W. G. Agosta, D. Cowburn, *J. Am. Chem. Soc. 106* (1984) 1939.

[116] G. E. Hawkes, E. W. Randall, W. E. Hull, O. Convert, *Biopolymers 19* (1980) 1815.

[117] H. R. Kricheldorf, *Org. Magn. Reson. 15* (1981) 162.

[118] C. Dyllick-Brenzinger, G. R. Sullivan, P. P. Pang, J. D. Roberts, *Proc. Natl. Acad. Sci. USA 77* (1980) 5580.

[119] A. Hantzsch, *Chem. Ber. 36* (1903) 2056.

[120] R. Huisgen, I. Ugi, *Chem. Ber. 90* (1957) 2914; I. Ugi, R. Huisgen, *ibid. 91* (1958) 531; I. Ugi, R. Huisgen, K. Clusius, M. Vecchi, *Angew. Chem. 68* (1956) 753.

[121] I. Ugi, H. Perlinger, L. Behringer, *Chem. Ber. 91* (1958) 2324.

[122] J. D. Wallis, J. D. Dunitz, *J. Chem. Soc. Chem. Commun. 1983*, 910.

[123] L. Hoesch, C. Leuenberger, H. Hilpert, A. S. Dreiding, *Helv. Chim. Acta 65* (1982) 2682; C. Leuenberger, L. Hoesch, A. S. Dreiding, *J. Chem. Soc. Chem. Commun. 1980*, 1197.

[124] M. T. Nguyen, J. Kaneti, L. Hoesch, A. S. Dreiding, *Helv. Chim. Acta 67* (1984) 1918.

[125] a) T. Yonezawa, I. Morishima, *J. Mol. Spectrosc. 27* (1968) 210; b) H. Egli, W. von Philipsborn, *Helv. Chim. Acta 64* (1981) 976.

[126] C. Richard, P. Granger in P. Diehl, E. Fluck, R. Kosfeld (Eds.): *NMR Basic Principles and Progress, Vol. 8*, Springer, Berlin 1974.

[127] a) J. H. Ridd, J. P. B. Sandall, *J. Chem. Soc. Chem. Commun. 1981*, 402; b) A. H. Clemens, P. Helsby, J. H. Ridd, F. Al-Omran, J. P. B. Sandall, *J. Chem. Soc. Perkin Trans. 2 1985*, 1217; c) A. H. Clemens, J. H. Ridd, J. P. B. Sandall, *ibid. 2 1985*, 1227.

[128] J. C. Giffney, J. H. Ridd, *J. Chem. Soc. Perkin Trans. 2 1979*, 618.

[129] J. H. Ridd, J. P. B. Sandall, *J. Chem. Soc. Chem. Commun. 1982*, 261.

[130] N. A. Porter, G. R. Dubay, J. G. Green, *J. Am. Chem. Soc. 100* (1978) 920.

[131] E.-L. Dreher, P. Niederer, A. Rieker, W. Schwarz, H. Zollinger, *Helv. Chim. Acta 64* (1981) 488.

[132] A. W. Douglas, *J. Am. Chem. Soc. 101* (1979) 5676.

[133] M. Yogo, K. Hirota, S. Senda, *J. Chem. Soc. Perkin Trans. 1 1982*, 473.

[134] J. W. Lown, S. M. S. Chauhan, *J. Org. Chem. 48* (1983) 513.

[135] Y. Nomura, Y. Takeuchi, *J. Chem. Soc. Chem. Commun. 1979*, 295.

[136] G. T. Furst, R. L. Lichter, F. W. Vierhapper, *J. Org. Chem. 45* (1980) 1521.

[137] R. L. Willer, D. W. Moore, L. F. Johnson, *J. Am. Chem. Soc. 104* (1982) 3951.

[138] K. Kanamori, J. D. Roberts, *J. Am. Chem. Soc. 105* (1983) 4698.

[139] R. Dyllick-Brenzinger, J. D. Roberts, *J. Am. Chem. Soc. 102* (1980) 1166.

[140] a) J. R. Dilworth, S. Donovan-Mtunzi, C. T. Kan, R. L. Richards, J. Mason, *Inorg. Chim. Acta 53* (1981) L161; b) J. Chatt, M. E. Fakley, R. L. Richards, J. Mason, I. A. Stenhouse, *J. Chem. Res. (S) 1979*, 322; *J. Chem. Res. (M) 1979*, 3701.

[141] R. D. Sanner, J. M. Manriquez, R. E. Marsh, J. E. Bercaw, *J. Am. Chem. Soc. 98* (1976) 8351, 3042.

[142] D. L. Thorn, T. H. Tulip, J. A. Ibers, *J. Chem. Soc. Dalton Trans. 1979*, 2022.

[143] J. R. Dilworth, C. T. Kan, R. L. Richards, J. Mason, I. A. Stenhouse, *J. Organomet. Chem. 201* (1980) C24.

[144] a) L. K. Bell, D. M. P. Mingos, D. G. Tew, L. F. Larkworthy, B. Sandell, D. C. Povey, J. Mason, *J. Chem. Soc. Chem. Commun. 1983*, 125; D. H. Evans, D. M. P. Mingos, J. Mason, A. Richards, *J. Organomet. Chem. 249* (1983) 293; b) J. Mason, D. M. P. Mingos, J. Schäfer, D. Sherman, E. O. Stejskal, *J. Chem. Soc. Chem. Commun. 1985*, 444.

[145] J. Bultitude, L. F. Larkworthy, J. Mason, D. C. Povey, B. Sandell, *Inorg. Chem. 23* (1984) 3629.

[146] A. R. Butler, C. Glidewell, A. R. Hyde, J. McGinnis, *Polyhedron 3* (1984) 1165.

[147] N. W. Alcock, N. Herron, P. Moore, *J. Chem. Soc. Dalton Trans. 1979*, 1486.

[148] E. H. Curzon, N. Herron, P. Moore, *J. Chem. Soc. Dalton Trans. 1980*, 721.

[149] I. Morishima, T. Inubushi, *J. Am. Chem. Soc. 100* (1978) 3568; *FEBS Lett. 81* (1977) 57.

[150] E. von Goldammer, *Z. Naturforsch. C 34* (1979) 1106.

[151] F. Blomberg, H. Rüterjans in L. J. Berliner, J. Reuben (Eds.): *Biological Magnetic Resonance, Vol. 5*, Plenum Press, New York 1983, p. 21.

[152] K. Kanamori, J. D. Roberts, *Acc. Chem. Res. 16* (1983) 35.

[153] Y. Kyogoku, *Appl. Spectrosc. Rev. 17* (1981) 279.

[154] B. Coxon, *Pure Appl. Chem. 49* (1977) 1151.
[155] H. R. Kricheldorf, *Pure Appl. Chem. 54* (1982) 467.
[156] J. R. Ebdon, P. E. Heaton, T. N. Huckerby, W. T. S. O'Rourke, J. Parkin, *Polymer 25* (1984) 821; R. A. McKay, J. Schaefer, E. O. Stejskal, R. Ludicky, C. N. Matthews, *Macromolecules 17* (1984) 1124; D. E. Axelson, S. L. Blake, *J. Polym. Sci. Polym. Chem. Ed. 23* (1985) 2507; H. R. Kricheldorf, W. E. Hull, D. Müller, *Macromolecules 18* (1985) 2135.
[157] A. Hori, Y. Shimizu, *J. Chem. Soc. Chem. Commun. 1983*, 790.
[158] R. L. Baxter, C. J. McGregor, G. A. Thomson, A. I. Scott, *J. Chem. Soc. Perkin Trans. 1 1985*, 369.
[159] M. Llinas, K. Wüthrich, W. Schwotzer, W. von Philipsborn, *Nature (London) 257* (1975) 817.
[160] T. L. Legerton, K. Kanamori, R. L. Weiss, J. D. Roberts, *Proc. Natl. Acad. Sci. USA 78* (1981) 1495; K. Kanamori, T. L. Legerton, R. L. Weiss, J. D. Roberts, *J. Biol. Chem. 257* (1982) 14168.
[161] N. Haran, Z. E. Kahana, A. Lapidot, *J. Biol. Chem. 258* (1983) 12929.
[162] $NH_3/NO_2^\ominus$ (*Nitrosomonas*): K. K. Andersson, S. B. Philson, A. B. Hooper, *Proc. Natl. Acad. Sci. USA 79* (1982) 5871; D-lysine (*Neurospora crassa*): N. Fangmeier, E. Leistner, *J. Biol. Chem. 255* (1980) 10205; nitrate (*Neurospora crassa*): G. S. Jacob, J. Schaefer, E. O. Stejskal, R. A. McKay, *Biochem. Biophys. Res. Commun. 97* (1980) 1176; $NH_4^\oplus$ (*Streptomyces venezuelae*): S. Shapiro, L. C. Vining, M. Laycock, A. G. McInnes, J. A. Walter, *Can. J. Microbiol. 31* (1985) 629; Nitropropanoic acid (*Penicillium atrovenetum*): R. L. Baxter, S. L. Greenwood, *J. Chem. Soc. Chem. Commun. 1986*, 175.
[163] K. Kanamori, T. L. Legerton, R. L. Weiss, J. D. Roberts, *Biochemistry 21* (1982) 4916.
[164] T. L. Legerton, K. Kanamori, R. L. Weiss, J. D. Roberts, *Biochemistry 22* (1983) 899.
[165] M. Nee, J. D. Roberts, *Biochemistry 21* (1982) 4920.
[166] M. Alei, Jr., P. J. Vergamini, W. E. Wageman, *J. Am. Chem. Soc. 101* (1979) 5415; A. Albinati, H. Moriyama, H. Rüegger, P. S Pregosin, A. Togni, *Inorg. Chem. 24* (1985) 4430.
[167] N. N. Becker, J. D. Roberts, *Biochemistry 23* (1984) 3336.
[168] B. Birdsall, A. W. Bevan, C. Pascual, G. C. K. Roberts, J. Feeney, A. Gronenborn, G. M. Clove, *Biochemistry 23* (1983) 4733; A. W. Bevan, G. C. K. Roberts, J. Feeney, L. Kuyper, *Eur. Biophys. J. 11* (1985) 211.
[169] a) K. Kanamori, J. D. Roberts, *Biochemistry 22* (1983) 2658; b) J. Vervoort, F. Müller, J. LeGall, A. Bacher, H. Sedlmaier, *Eur. J. Biochem. 151* (1985) 49; W.-D. Beinert, H. Rüterjans, F. Müller, *ibid. 152* (1985) 573.
[170] M. Mehring: *Principles of High-Resolution NMR in Solids*, 2nd ed., Springer, Berlin 1983.
[171] C. S. Yannoni, *Acc. Chem. Res. 15* (1982) 201.
[172] J. R. Lyerla, C. S. Yannoni, C. A. Fyfe, *Acc. Chem. Res. 15* (1982) 208.
[173] S. J. Opella, *Annu. Rev. Phys. Chem. 33* (1982) 533.
[174] G. Harbison, J. Herzfeld, R. G. Griffin, *J. Am. Chem. Soc. 103* (1981) 4752.
[175] D. Schweitzer, H. W. Spiess, *J. Magn. Reson. 15* (1974) 529.
[176] G. S. Harbison, L. W. Jelinski, R. E. Stark, D. A. Torchia, J. Herzfeld, R. G. Griffin, *J. Magn. Reson. 60* (1984) 79; R. E. Stark, L. W. Jelinski, D. J. Ruben, D. A. Torchia, R. G. Griffin, *ibid. 55* (1983) 266.
[177] G. S. Harbison, J. Herzfeld, R. G. Griffin, *Biochemistry 22* (1983) 1.
[178] T.-H. Huang, W. W. Bachovchin, R. G. Griffin, Ch. M. Dobson, *Biochemistry 23* (1984) 5933.
[179] a) W. W. Bachovchin, J. D. Roberts, *J. Am. Chem. Soc. 100* (1978) 8041; b) N. E. Mackenzie, P. E. Fagerness, A. I. Scott, *J. Chem. Soc. Chem. Commun. 1985*, 635.
[180] a) H. H. Limbach, J. Hennig, R. Kendrick, C. S. Yannoni, *J. Am. Chem. Soc. 106* (1984) 4059; b) R. J. Butcher, G. B. Jameson, C. B. Storm, *ibid.* (1985) 2978; M. J. Hamor, T. A. Hamor, J. L. Hoard (1964) 1938.
[181] T. A. Cross, J. A. DiVerdi, S. J. Opella, *J. Am. Chem. Soc. 104* (1982) 1759.
[182] a) T. A. Cross, S. J. Opella, *J. Am. Chem. Soc. 105* (1983) 306; T. A. Cross, M. H. Frey, S. J. Opella, *ibid. 105* (1983) 7471; T. A. Cross, S. J. Opella, *J. Mol. Biol. 182* (1985) 367; b) F. Martin, *Physiol. Veg. 23* (1985) 463.
[183] a) J. Schaefer, T. A. Skokut, E. O. Stejskal, R. A. McKay, J. E. Varner, *J. Biol. Chem. 256* (1981) 11574; b) G. T. Coker, III, J. Schaefer, *Plant Physiol. 77* (1985) 129.
[184] H. G. Baker: *Plants and Civilization*, Macmillan, London 1970.

Organic Synthesis at High Temperatures. Gas-Phase Flow Thermolysis**

New Synthetic Methods (57)

By Martin Karpf*

The preference for carrying out synthetic organic reactions at the lowest possible temperature is due to the expectation that the selectivity often increases with decreasing temperature, as is confirmed by many examples and also theoretically justified. Selectivity, however, is not the only problem at high temperatures; further factors include the frequently limited thermal stability of the functional groups and structural elements not directly involved in the transformation. In spite of these limitations, the advantages of high temperatures and the greatly improved knowledge of the mechanisms of dynamic gas-phase processes accumulated in recent years can be exploited in directed organic synthesis. In this review the synthetic potential of gas-phase flow thermolysis will be described from the viewpoint of the synthetic chemist with the aid of typical examples of application.

1. Introduction—Pyrolysis, Thermolysis, High Temperatures

The temperature is of decisive importance for the course of a chemical reaction. The majority of organic reactions are carried out between the sublimation point of dry ice (−78.5 °C) and the boiling points of high-boiling solvents (ca. 300 °C). There are two reasons for the lower limit of this range: the solubility of the reactants decreases and the reaction time increases with decreasing temperature. The upper limit, in contrast, is determined by the usually limited thermal stability of starting materials and products. Therefore, investigations outside this range of temperatures are often treated not as an extension of existing areas but rather as independent areas of research in organic chemistry.

Whereas the preparative development of the low-temperature realm, which hitherto has been largely dominated by spectroscopic studies, has made progress only in recent times,[1] high-temperature reactions have a longer tradition, as seen in the designation of the methods and transformations used, e.g., "Brenzreaktionen" (pyrogenic reactions) or *pyrolysis*.[2]

These terms originally meant the physical and chemical separation or decomposition of materials of mostly unknown composition by means of fire and heat. Later, they were extended to include the thermal behavior of well-defined chemical compounds. Thus, in 1929, *Hurd*, in the introduction to his classic work "The Pyrolysis of Carbon Compounds,"[3] described "pyrolysis" as "the transformation of a compound into another substance, or other substances, through the agency of heat alone," specifically including both isomerizations without decomposition and synthetic thermal processes. The expansion of knowledge in the area of mechanistic organic chemistry caused *Hurd*'s definition, which was based on molecular transformations to be supplemented or even replaced by separate, more specific terms of a mechanistic origin. As a consequence of this development, the application of the term "pyrolysis" has been restricted, in particular for nondestructive processes, to the induction of chemical reactions by means of high temperatures. Thus, *Brown*'s 1980 monograph "Pyrolytic Methods in Organic Chemistry"[4] treats organic gas-phase reactions at high temperatures according to mechanistic criteria. However, *Brown* retained the term "pyrolysis" in the broader sense introduced by *Hurd*,[3] in particular as a means to distinguish these reactions from reactions and methods carried out at "normal" temperatures. Without committing himself to a too-narrow distinction between "normal" and "high" temperatures, *Brown*[4] gave the temperature region between about 350 and 900 °C as typical for organic high-temperature reactions.

The use of the term "thermolysis" for purely thermally induced reactions has become more frequent in recent times and has, for example, been proposed by *de Mayo* et al.[5] for dynamic gas-phase processes (see Section 2.2.2). However, this concept is also used, e.g., by *Kametani*,[6] for pericyclic reactions under static conditions in the temperature range of ca. 100 to 300 °C. In contrast, modern textbooks of organic chemistry[7,8] and a well-known reference work[9] use the term "pyrolysis" in its original and narrower meaning, namely, the thermal decomposition of molecules; in this context both preparative and industrially important organic high-temperature processes are treated.

2. High Temperatures in Organic Chemistry

2.1. Analytical Investigations

The characterization of organic materials through analysis of their thermal decomposition products[10] comes close to the original goal of the use of high temperatures. The combination of special pyrolysis techniques (such as Curie point, pulsed, and laser pyrolyses) with modern analytical and spectroscopic procedures (such a gas chromatography,

[*] Priv.-Doz. Dr. M. Karpf
Organisch-Chemisches Institut der Universität
Winterthurerstrasse 190, CH-8057 Zürich (Switzerland)
Present address:
Hoffmann La Roche & Co.
Zentrale Forschungseinheiten
CH-4002 Basel (Switzerland)

[**] Part of the *Habilitationsschrift*, M. Karpf, Universität Zürich 1984.

mass and infrared spectroscopy) permits the reproducible, qualitative and quantitative analysis of small amounts of a material. The efficiency of these methods is further increased by the availability of electronic data processing (spectral comparisons, statistical analysis, etc.). In particular, slightly volatile substances may often be examined—e.g., synthetic and natural polymers, geologically and biologically interesting samples, and even microorganisms (in taxonomy studies).

2.2. Preparative Reactions at High Temperatures

Preparative organic reactions at high temperatures[11] can be divided, depending on the techniques used, into static and dynamic processes.

2.2.1. Static Processes

Static processes, i.e., those in which a substrate is heated continuously in the solid phase, in solution, or in the gas phase, have long been used for a large number of classical thermal reactions. For example, eliminations, fragmentations, and rearrangements, including many pericyclic processes, have been carried out under static conditions.[12-22] The transition from normal to high temperatures is, in many cases, necessary because of the low reactivity of the substrates, which cannot always be compensated for by an increase in the reaction time. Since static conditions at not too elevated temperatures are technically easy to accomplish (sealed tubes, autoclaves) and since large quantities can be handled without difficulty, these reactions are suitable not only for mechanistic studies but also for many preparative applications.

2.2.2. Dynamic Processes

Dynamic processes, i.e., those in which a substrate is transported in its gaseous state through a heated zone, are characterized by a transient thermal excitation of the molecules in the gas phase, followed by rapid cooling of the products formed. Compared to static procedures, higher reaction temperatures are usually employed. This procedure, which was already used by *Berthelot*[23] in 1866 for the conversion of acetylene into benzene and other products, has experienced increasing popularity, especially during the past twenty years. Accordingly, a large number of variants of the method, which are united under the concept of "gas-phase flow thermolysis," are employed. These variants, which have different names, often differ only very slightly from one another.[24] Thus, in important reviews in this area the following expressions are found: "Flash Thermolysis" (*de Mayo*, 1972,[25] translated into German as "Kurzzeit-Thermolyse"); "Flash Vacuum Thermolysis" (FVT) (*Hageman* and *Wiersum*, 1973,[26] *Wiersum*, 1982[27] and 1984[28]); and "Blitzthermolyse" (*Seybold*, 1977[29]). However, in accordance with an earlier suggestion by *Hedaya*,[30] the same method is also described as "Flash Vacuum Pyrolysis" (FVP) (*Hedaya*, 1967[30] and 1963;[31] *Brown*, 1980[4]), "Flow Vacuum Pyrolysis," (*Brown*, 1980[4]), or "Flash Pyrolysis" (*Wentrup*, 1977[32]).

An important advantage of the dynamic over the static method is the possibility, through intense but transient thermal excitation of the starting materials followed by instant cooling of the products to low temperatures, of isolating and identifying by spectroscopic or chemical means even highly reactive thermal primary products. For investigations of this nature, which are usually mechanistically oriented, techniques such as matrix isolation and trapping reactions have proven to be particularly useful. The advantage of working at very low pressures using special techniques such as "Very Low Pressure Pyrolysis" (VLPP) developed by *Benson* et al.[33] is the avoidance of intermolecular secondary reactions in the hot zone. To distinguish the *flow* methods, operating at elevated, normal, or only slightly reduced pressures, from the low-pressure techniques, the latter are often called *flash* methods.

Dynamic conditions are also suitable, however, for the preparation of stable compounds. This is particularly true when product formation is hindered because of activation barriers that cannot be overcome at temperatures attainable in static systems, or when the starting materials or end products cannot withstand the thermal load. In addition, the problem of wall catalysis, which frequently arises in static systems is often less pronounced because of the short reaction times and high temperatures. For synthetic applications, gas-phase flow thermolysis methods also have the advantage that simple, often commercially available apparatus can be used,[34] which usually include an entry part for the substrate, a reactor part, and a cold trap to condense the products. In most cases the reactors consist of electrically heated, empty or packed quartz tubes.[4] Since the synthesis of stable products often permits working at normal or only slightly reduced pressure (flow conditions, see above), preparatively interesting rates of conversion can be achieved without difficulty in such apparatus. Furthermore, the method usually avoids the use of solvents and thus allows continuous operation.

2.3. Technical-Industrial Reactions at High Temperatures

The decomposition of organic compounds at high temperatures forms the basis for many technical-industrial applications.[35-38] For example, the thermal cracking of certain mineral oil fractions is at present one of the most important sources of lower olefins, which are particularly useful as starting materials in the chemical industry. Furthermore, there are also many catalytic processes of industrial significance, such as dehydration, isomerization, oxidation, and reduction. These reactions are preferentially carried out in gas-phase flow systems, which permit a continuous reaction process as well as simple reaction control.

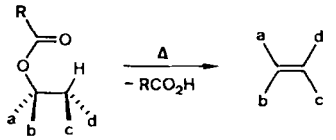
3. Gas-Phase Flow Thermolysis in Organic Synthesis

3.1. Eliminations

3.1.1. Ester Pyrolyses

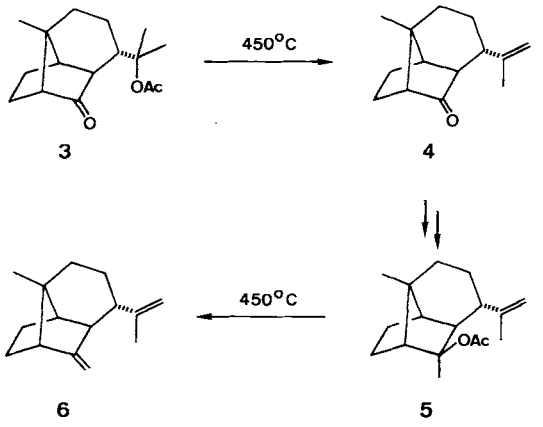
The ester pyrolysis **1** → **2** is the most common of the classical olefin-forming thermal eliminations carried out

under gas-phase flow thermolysis conditions; comparable reactions, such as the thermal decomposition of xanthate esters (Tschugaeff reaction) or amine oxides (Cope reaction), on the other hand, are usually carried out in solution at lower temperatures.[39,40] The pronounced *cis*-selectivity even at high temperatures (ca. 400–600 °C) can be explained by the intramolecular, cyclic transition state of a retro-ene type reaction (see Section 3.2.1). *Barton* et al.,[41] in the course of their classical work aimed at distinguishing between axial and equatorial substituents of cyclohexane rings, used the results of ester pyrolysis reactions as an argument for the assignment of the relative configuration of steroid hydroxyl groups.



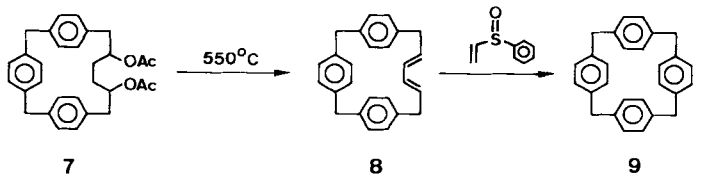
1 2

A recent example of a synthetic application of the ester pyrolysis reaction is the synthesis of the tricyclic marine natural product sinularene **6** described by *Collins* and *Wege*,[42] whereby the introduction of the two carbon–carbon double bonds was achieved through acetate pyrolysis in a stream of nitrogen. The first thermal step (**3**→**4**) led preferentially to the less substituted olefin. Only 5% of the tetrasubstituted double-bond isomer of **4** was found in the product mixture.



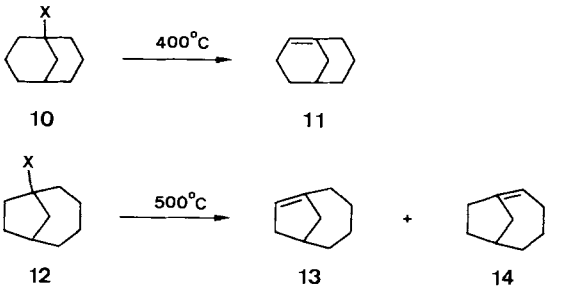
3 4 6 5

Miyahara et al.[43] succeeded in building the fourth aromatic ring in the synthesis of [1.1.1.1]paracyclophane **9** via a Diels–Alder reaction (**8**→**9**). The necessary starting diene **8** was obtained through double acetate pyrolysis of **7** at 550 °C in a yield of 38%.



7 8 9

The acetate pyrolysis of **10** or **12** (X = OAc) as described by *Becker* and *Pfluger*[44] makes possible a very simple synthesis of the strained bridgehead olefins **11**, **13**, and **14** (**13** : **14** = 8 : 1). A double-bond shift from the bridgehead position was not observed.

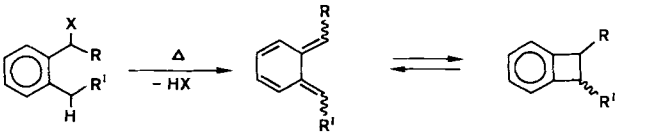


10 11 12 13 14

3.1.2. Elimination of Hydrogen Halides

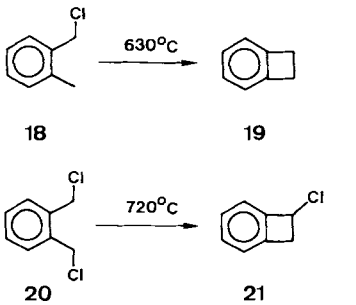
The thermal β-elimination of hydrogen halides from organohalogen compounds usually occurs with low regio- and stereoselectivity and is, therefore, of only minor synthetic use.[45] An exception is the β-elimination of hydrogen chloride from **10** and **12** (X = Cl) (see Section 3.1.1), even at lower temperatures (**10** at 250 °C and **12** at 350 °C), to give the Bredt olefins **11** and **13** or **14**, respectively, in comparable or even better yields than from the corresponding acetates. The thermolysis tube was coated with calcium carbonate to remove the liberated HCl.

The specific 1,4-elimination of hydrogen halides from *o*-alkylbenzyl halides **15** to form benzocyclobutenes **17** (1,2-dihydrocyclobutabenzene derivatives) via *o*-quinodimethanes **16** has been intensively studied. Benzocyclobutenes are synthetically interesting intermediates since, already at lower temperatures, they are in equilibrium with the *o*-quinodimethane derivatives **16**, which are particularly reactive dienes for intramolecular Diels–Alder reactions.[6,12,15,17]



15 16 17

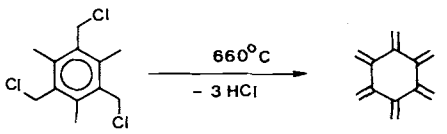
Benzocyclobutene **19** was first obtained by *Maccoll* et al.[46] from 2-methylbenzyl chloride **18** at 630 °C in 70% yield; the chloro derivative **21** was prepared by *Schiess* et al.[47] from the corresponding dichloro compound **20** in a yield of 53%. Grignard reaction allows the transformation of **21** into various benzocyclobutenes in good yields (e.g.,



18 19 20 21

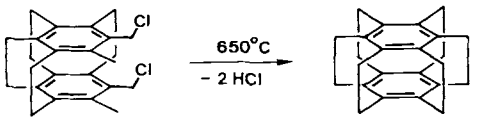
17, R=COOH, R'=H (72%) or R=CHO, R'=H (74%)),[47] which are of interest as synthetic building blocks.

A remarkable application of such 1,4-eliminations, reported by *Schiess* and *Heitzmann*[48] and by *Boekelheide* et al.,[49] is the synthesis of hexaradialene **23** from commercially available **22** by triple hydrogen chloride elimination at 660°C. Although **23** is only stable at low temperatures, the spectroscopic data and chemical behavior demonstrate that this compound exists exclusively in the tris-*o*-quinoid form and that, in spite of the presence of a cyclic 6π-electron system, no specific aromatic character is evident.



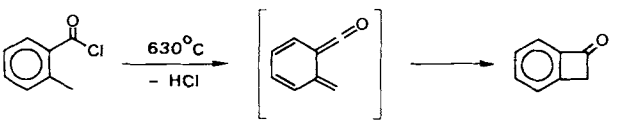
22 **23**

A further and particularly interesting example of this reaction was also reported by *Boekelheide* et al.[50] Double hydrogen chloride elimination from **24** allowed the preparation of the long-sought [2.2.2.2.2.2.](1,2,3,4,5,6)cyclophane **25** ("superphane") in a single step in a yield of 40% (see also Section 3.2.3).

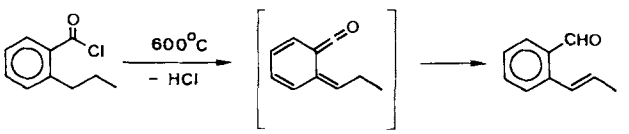


24 **25**

The synthesis of benzocyclobutenone **28** was achieved by hydrogen chloride elimination from 2-methylbenzoyl chloride **26**, whereby the *o*-quinoid ketene **27** was assumed to be the initial product.[51] Further evidence for such intermediates is provided by the thermolysis of 2-propylbenzoyl chloride **29**, which does not lead to the correspondingly substituted benzocyclobutenone. Instead, the assumed intermediate ketene **30** undergoes a [1,5]-hydrogen shift to give the aromatic aldehyde **31**.



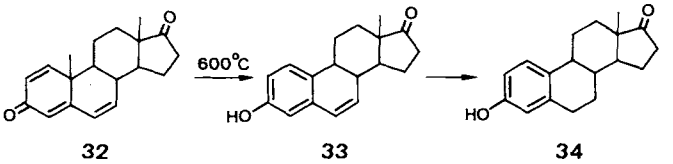
26 **27** **28**



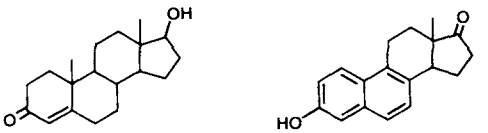
29 **30** **31**

3.1.3. Dealkylations

The aromatization of ring A is presumably the driving force for the loss of the C-19 methyl group in steroid-1,4-dien-3-ones upon gas-phase flow thermolysis. This dealkylation, discovered by *Inhoffen*[52] and mechanistically little investigated, has been used by *Djerassi* et al.[53] for the transformation of 1,4,6-androstatriene-3,7-dione **32**, obtained from the male sex hormone testosterone **35**, into 6-dehydroestrone **33**, which in turn was transformed into the female sex hormone estrone **34** by simple hydrogenation. Surprisingly, further aromatization of **33** to equilenine **36** did not take place under the conditions of flow thermolysis, although this transformation could be carried out at much lower temperatures in the condensed phase.



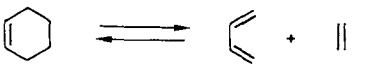
32 **33** **34**



35 **36**

3.1.4. Retro Diels–Alder Reactions

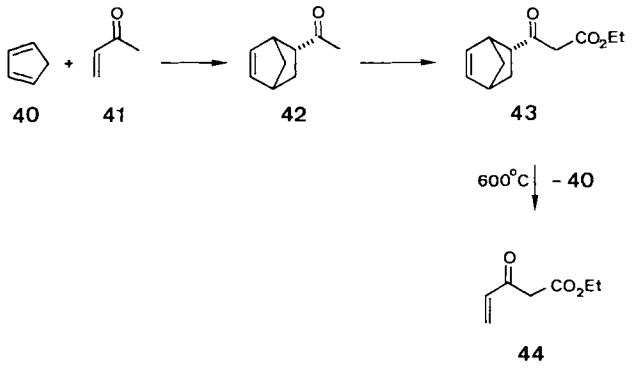
The synthetic value of the Diels–Alder reaction lies in the regio- and stereoselective addition of a diene **38** to a suitable dieneophile **39** to give a cyclohexene derivative **37**.[12-17,19] In contrast, the majority of retro Diels–Alder reactions, **37** → **38** + **39**, are used to regenerate "Diels–Alder protected" double bonds or 1,3-dienes.[54]



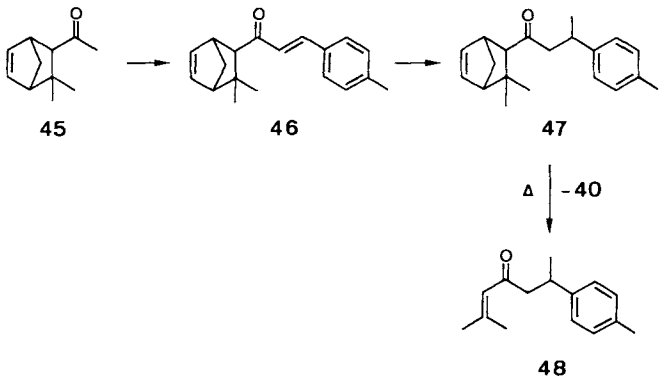
37 **38** **39**

The use of high temperatures and reduced pressure has proven valuable in achieving a high degree of retro-reaction in the gas phase. Typical examples are the syntheses of α,β-unsaturated ketones, allylic alcohols, and sensitive nonconjugated polyenes. For instance, *Stork* and *Guthikonda*[55] reported a simple route to ethyl acryloylacetate **44**, which is used as a Michael acceptor for Robinson type annelations and as a diene precursor for Diels–Alder additions. The reactivity of the α,β-unsaturated system in **41** was masked by forming the Diels–Alder adduct **42** from cyclopentadiene **40** and methyl vinyl ketone **41**. The subsequent ethoxycarbonylation to **43** proceeded under strongly basic conditions. Regeneration of the α,β-double bond to give **44** was achieved at 600°C with concomitant elimination of **40**.

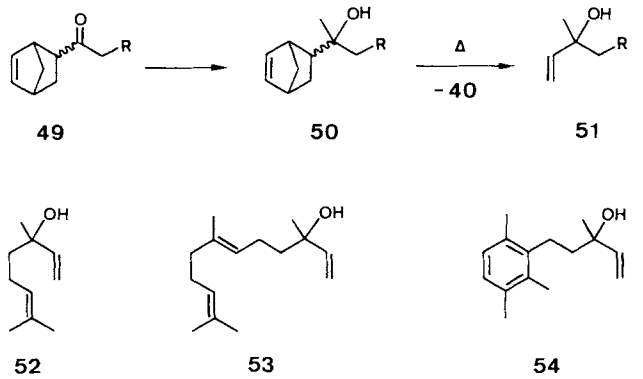
The same strategy was used by *Ho*[56] in the synthesis of turmerone **48**, in which cyclopentadiene **40** was eliminated in the last step by destructive distillation of **47** at reduced pressure. **47** itself was prepared by reaction of cyclopentadiene **40** with mesityl oxide to give the Diels–



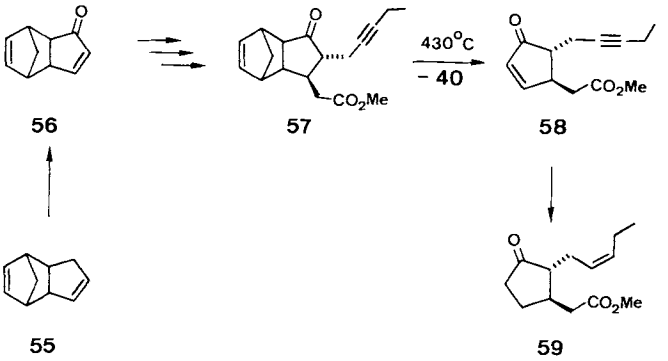
Alder adduct **45**, followed by condensation of **45** with *p*-methylbenzaldehyde to give **46** and subsequent 1,4-addition of a methyl group.



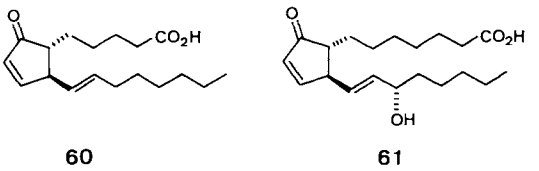
Bloch[57] used the above principle to synthesize allylic alcohols **51** starting from **49** (*endo/exo* mixtures), the alkylation products of **42**. Compounds **49** were treated with methylmagnesium iodide to give the tertiary alcohols **50** prior to thermolysis. In this way, linalool **52**, nerolidol **53**, and the sesquiterpene alcohol **54**, isolated from a Pacific algae species, were synthesized.



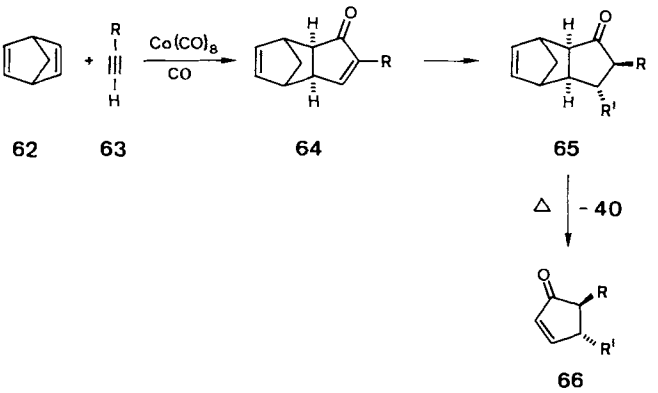
The strong tendency of cyclopentadienones to dimerize makes them less attractive for the synthesis of substituted five-membered rings.[58] An alternative to recent attempts to circumvent this problem in the condensed phase[59] is the use of **56** and its derivatives. These compounds can formally be regarded as "Diels-Alder protected" cyclopentadienones. In this manner, *Ducos* and *Rouessac*[60] succeeded in synthesizing the natural perfume component jasmone carboxylic acid methyl ester **59** starting from **56**, which is easily accessible from dicyclopentadiene **55**. After the introduction of the two side chains, which was facilitated by the 2-cyclopentenone partial structure, gas-phase flow thermolysis of **57** at 430°C led to the substituted 2-cyclopentenone **58**, which in turn was converted into the natural product **59** by selective reduction.



Wiel and *Rouessac*[61] also used **56** to synthesize other 4,5-substituted 2-cyclopentenones (e.g., **60**), which are possible intermediates for the synthesis of prostaglandins (e.g., prostaglandin A_1 **61**).

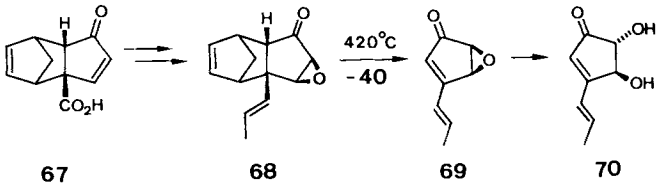


Schore,[62] with a similar goal in view, thermolyzed the compounds **65** (R = *n*Bu, R′ = H, Me, *t*Bu) to give **66**, whereby **65** was obtained by 1,4-addition of alkyl cuprates to the α,β-unsaturated system in **64**. The tricycle **64** was obtained using the Co^0-catalyzed cocyclization of acetylenes **63**, carbon monoxide, and norbornadiene **62** introduced by *Pauson* et al.[63]

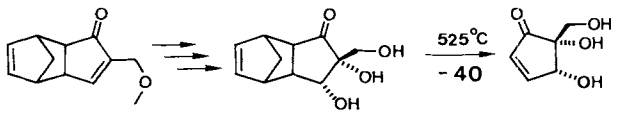


Zwanenburg et al.[66] used **67** and **71**, derivatives of **56**, for the synthesis of the cyclopentane antibiotics terrein **70** and pentenomycin **73**.[64,65] After transformation of the remaining α,β-double bonds to give **68** and **72**, respectively, the 2-cyclopentenone units of the natural products were obtained by gas-phase flow thermolysis. The fact that the free triol **72** could be directly transformed into penteno-

mycin **73** in 50% yield at 525°C demonstrates that this method can also be applied to substances with sensitive functional groups.

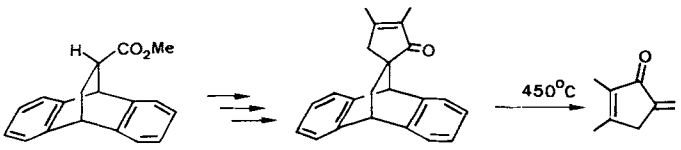


67 **68** **69** **70**

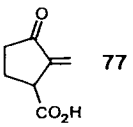


71 **72** **73**

Siwapinyoyos and *Thebtaranonth*[67] have described the synthesis of a further cyclopentane antibiotic,[64,65] methylenomycin B **76**, via the Diels–Alder/retro Diels–Alder route. After cycloaddition of anthracene with methyl acrylate to form **74** and subsequent elaboration of the dimethylcyclopentenone moiety, thermolysis of **75** furnished anthracene and the natural product **76**, which is sensitive in the condensed phase. The same principle was applied to the synthesis of sarkomycin **77**.[68]

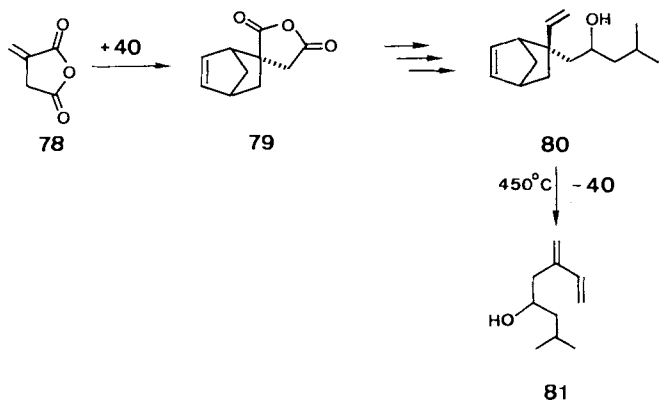


74 **75** **76**



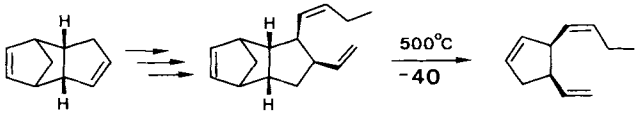
77

The cyclopentadiene adduct **79** was used by *Rouessac* and *Haslouin*[69] to protect the carbon–carbon double bond in itaconic anhydride **78** in the synthesis of the pheromone ipsenol **81**; compound **79** was converted via several steps into **80**, which underwent thermolysis at 450°C to give **81** in quantitative yield.



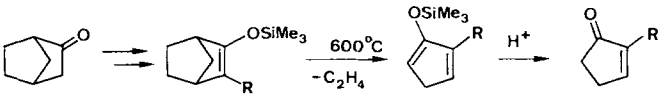
78 **79** **80** **81**

Boland and *Jaenicke*[70] synthesized the gynogamete sex attractant of a marine brown algae, multifidene **83**; dicyclopentadiene **55** was converted into the triene **82**, which underwent subsequent gas-phase flow thermolysis at 500°C to give the natural product **83** as a racemate with three nonconjugated carbon–carbon double bonds.



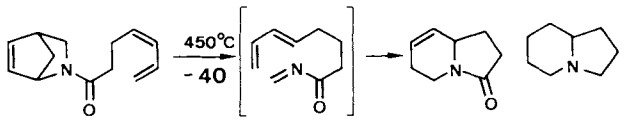
55 **82** *rac*-**83**

Bloch[71] has described an interesting variant of the application of the retro Diels–Alder reaction in which the 1,3-diene **86** formed in the thermal step is further used synthetically to give 2-substituted 2-cyclopentenones **87** (R = H, CH_3, $CH_2CH{=}CH_2$, or *n*-pentyl). Alkylation of 2-norbornanone **84** and silyl enol ether formation afforded **85**, which underwent thermolysis to furnish the cyclopentadiene derivative **86** and ethylene. The products **87** were then obtained by acid hydrolysis.



84 **85** **86** **87**

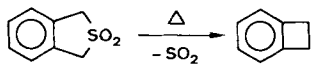
By gas-phase flow thermolysis of the azabicyclo[2.2.1]heptene **88**, *Ripoll* et al.[72] obtained the intermediate **89**, the *N*-acylimine moiety of which is extremely sensitive in the condensed phase. The formation of the lactam **90** in an intramolecular Diels–Alder addition upon warming of the thermolysate can be regarded as evidence for the intermediacy of **89**. Compound **90** in turn is a known intermediate in the synthesis of the alkaloid δ-coniceine **91**.



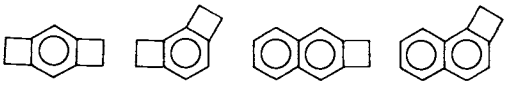
88 **89** **90** **91**

3.1.5. Elimination of Sulfur Dioxide

The thermal elimination of sulfur dioxide from cyclic sulfones under flow thermolysis conditions can be exploited synthetically in a variety of ways. Thus, in addition to the 1,4-elimination approach (see Section 3.1.2), the elimination of sulfur dioxide from dihydrobenzo[*c*]thiophene 1,1-dioxides provides a route to benzocyclobutenes. The fragmentation of the type **92** → **19** was first described by *Cava* and *Deana*[73] and was later used also in the synthesis of systems containing two four-membered-ring units such as **93**,[74] **94**,[75] and the dihydrocyclobutanaphthalenes **95** and **96**.[76] In this way *Smith* et al.[77] prepared the substituted benzocyclobutenes **17** (R = CH_3, R′ = H; R = R′ = CH_3; R = $CH_2C_6H_5$, R′ = H; R = $CH_2CH{=}CH_2$, R′ = H).

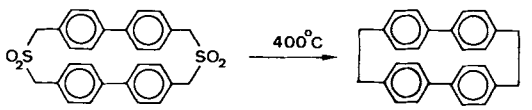


92 19



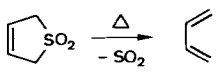
93 94 95 96

An SO_2 extrusion, possibly proceeding via benzyl radicals, was first used in the condensed phase by *Vögtle*[78] and in the gas phase by *Staab* and *Haenel*[79] for the synthesis of macrocyclic cyclophanes. Thus, the thermolysis of the disulfone **97** gave [2.2](4,4')biphenylophane **98** in 47% yield, a transformation that, in contrast to other examples,[78] was unsuccessful in both the condensed phase and in solution. Further examples of this type are found in the review by *Vögtle* and *Neumann*.[80]

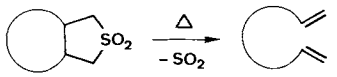


97 98

SO_2 eliminations can also be used in retro-cheletropic processes to synthesize dienes of the type **100** and **102** from di- and tetrahydrothiophene 1,1-dioxides **99** and **101**, respectively.

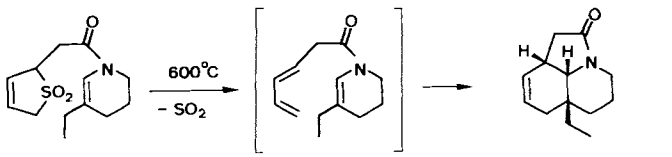


99 100

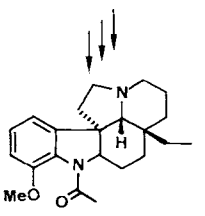


101 102

In the elegant synthesis of the indole alkaloid aspidospermine **106**, developed by *Martin* et al.,[81] the diene **104**, formed by thermal SO_2 elimination, reacts in an intramolecular Diels–Alder reaction to give the tricycle **105** selectively. In a series of steps (some already known) **105** was transformed into the natural product **106**.

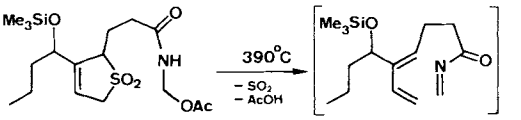


103 104 105

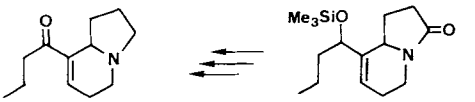


106

The same method was employed by *Weinreb* and *Schmitthenner*[82] in the synthesis of the elaeocarpus alkaloid elaeocanine A **110**, in which they succeeded in simultaneously generating the diene moiety and the acylimino moiety of **108** by SO_2 elimination and by acetate elimination, respectively.

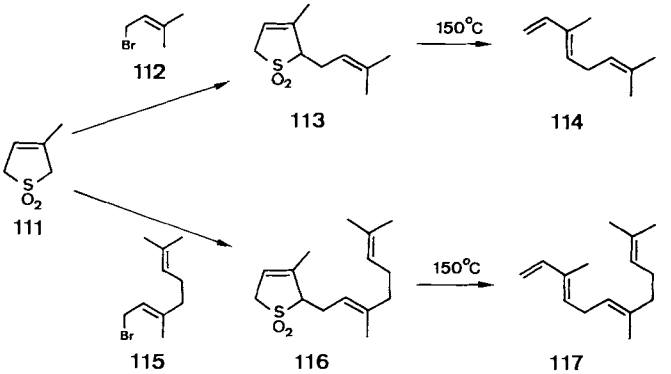


107 108



110 109

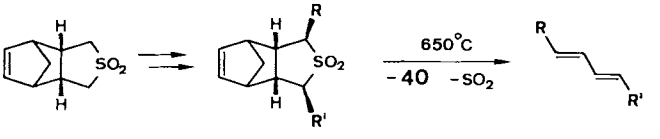
The use of 3-methyl-3-sulfolene **111** as an isoprene building block was demonstrated by *Chou* et al.[83] in the synthesis and thermolysis of the cyclic sulfones **113** and **116**, which were obtained from the anion of **111** by reaction with prenyl bromide **112** and geranyl bromide **115**, respectively. The SO_2 elimination took place already under preparative gas chromatographic conditions, leading stereoselectively to *trans*-β-ocimene **114** and α-farnesene **117**, respectively.



111 112 113 114 115 116 117

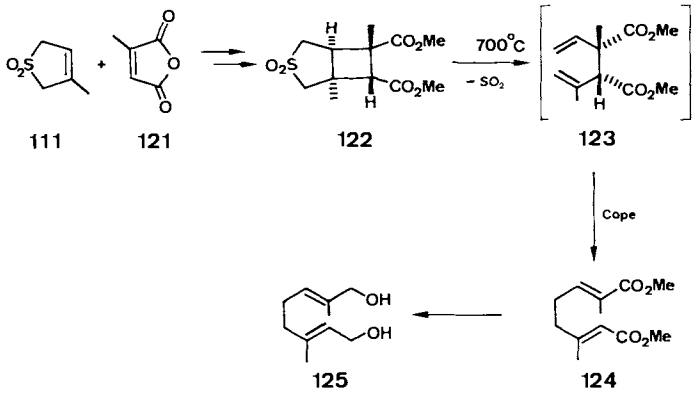
Bloch and *Abecassis*[84] effectively used a combination of retro Diels–Alder fragmentation and SO_2 extrusion to prepare the (*E,E*)-dienes **120** in a highly stereoselective manner and in good yields. Here, the exclusively *exo*-substituted tricyclic sulfone **119** was obtained by iterative alkylation of **118**. The method was applied to the synthesis of **120** (R = CH_3, R' = $(CH_2)_7OH$) and R = C_2H_5, R' = $(CH_2)_8OAc$), the sex attractants of two species of moths.

The sulfone **122**, obtained from **111** and **121** by photocycloaddition, was used by *Williams* and *Lin*[85] to prepare



118 119 120

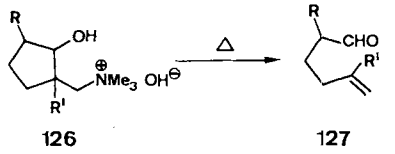
the 1,5-diene **123** by thermolytic SO_2 elimination. Under the reaction conditions, a subsequent, stereoselective Cope rearrangement to give the diester **124** took place. Lithium aluminum hydride reduction of **124** opened a simple route to 10-hydroxygeraniol **125**.



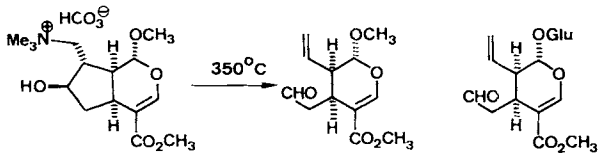
111 121 122 123 124 125

3.1.6. *Fragmentations*

Terminally unsaturated aldehydes **127**, which readily undergo condensation reactions in the solid phase or in solution, were synthesized by *Tietze* et al.[86] through gas-phase flow thermolysis of γ-hydroxyammonium hydroxides **126** (R, R′=H; R, R′=CH_3; or R=H, R′=CH_3) at 350–450°C. This method was also successfully applied to the synthesis of **129**, the aglycone *O*-methyl ether of secologanin **130**, which in turn is an important intermediate in the biogenesis of many alkaloids and monoterpenes.[87]



126 127

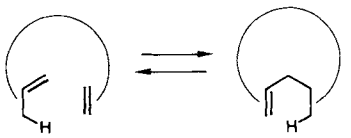


128 129 130

3.2. Rearrangements

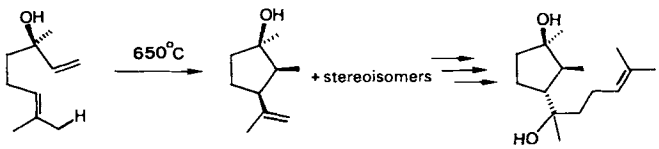
3.2.1. *Intramolecular Ene and Retro-Ene Reactions*

Cyclizations via ene reactions, i.e., involving the intramolecular addition of an olefin having an allylic hydrogen to a multiple bond (**131** → **132**), as well as the ring opening retro-ene reaction (**132** → **131**), are of particular synthetic interest and have been intensively studied in recent years by several groups.[12,13,18,22] Although the intramolecular ene addition is usually carried out under static conditions (e.g., in sealed tubes), gas-phase flow thermolysis has proven useful in some cases, particularly for retro-ene reactions.



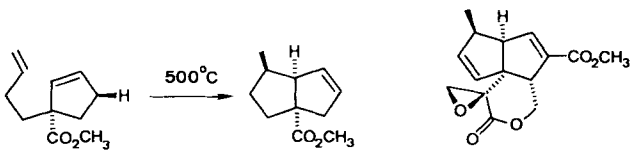
131 132

Intramolecular Ene Reactions: In experiments carried out by *Ohloff* et al.,[88] the cyclization of (−)-linalool **133** at 650°C led to a stereoisomeric mixture of plinols, the main isomer of which, (−)-plinol C **134**, was used as the starting material for enantioselective synthesis of the sesquiterpene cyclonerodiol **135**.[89]



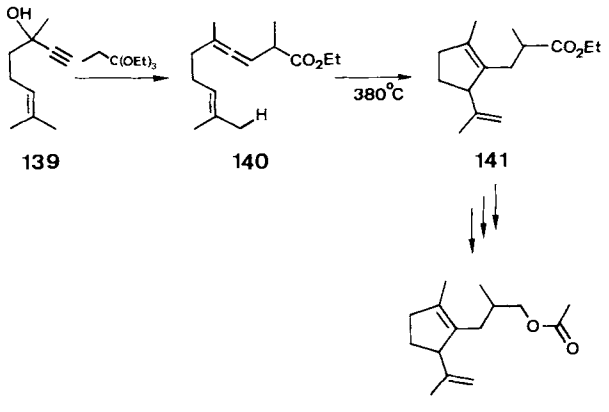
133 134 135

Searching for new ways to synthesize the ring skeleton of the antibiotic pentalenolactone **138**, *Plavac* and *Heathcock*[90] subjected the ester **136** to gas-phase flow thermolysis at 500°C and obtained an almost quantitative yield of the bicyclic product **137**. In spite of the high temperature, the ring methyl group remains in the thermodynamically unfavorable *endo* position, owing to the cyclic transition state of the ene reaction.



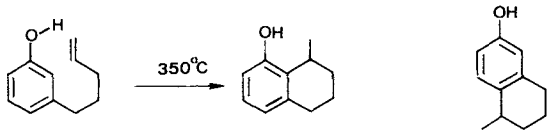
136 137 138

An industrial process consisting of a continuous gas-phase flow thermolysis at 380°C is used in the synthesis of **141**, a synthetic precursor of the cyclopentanoid perfume ingredient **142**.[18,91] The required starting material, the allene **140**, is also synthesized thermally, albeit under static conditions, from dehydrolinalool **139** and triethyl orthopropionate by Claisen ortho ester rearrangement.



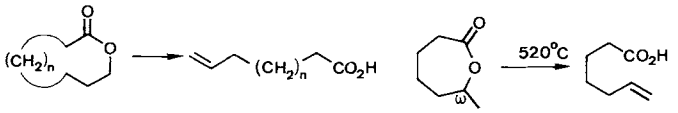
139 140 141 142

That the choice of reaction conditions used, static or dynamic, can have a considerable influence on the products of a reaction, is demonstrated by the cyclization of 3-(4-pentenyl)phenol **143**. This reaction, carried out by *Conia* et al.[91] using flow thermolysis at 350°C, led to exclusive formation of the *ortho* product **144**, whereas in the condensed phase the *para* product **145** was formed in roughly the same yield.



143 **144** **145**

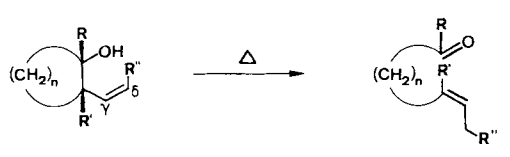
Retro-ene reactions: Apart from the eliminative retro-ene reactions such as the ester pyrolyses, which are most commonly carried out under gas-phase flow thermolysis conditions (see Section 3.1.1), there are many examples of the use of intramolecular reactions. For example, the pyrolysis of the lactones **146** has been studied by *Bailey* and *Bird*.[93] In agreement with the *syn*-specific reaction course discussed in Section 3.1.1 (**1**→**2**), the authors found that the intramolecular transformation of the lactone **146** into the terminally unsaturated acids **147** only occurred when medium-sized rings were employed (n = 4 and 6). Smaller lactones, such as **148**, reacted only when an additional methyl group was introduced into the ω-position, where it becomes available for the pericyclic process.



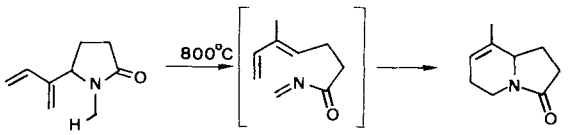
146 **147** **148** **149**

A further application of the retro-ene reaction under dynamic conditions involves the thermolysis of γ,δ-unsaturated alcohols such as **150**, which are used in the stereoselective synthesis of unsaturated aldehydes (**151**, R = H) or ketones (**151**, R = alkyl). *Arnold* and *Smolinsky*[94] found that 2-alkenylcycloalkanols (**150**, R, R′ = H, R″ = *n*-alkyl, n = 3, 4, or 5) smoothly rearrange at temperatures around 500°C to the corresponding aldehydes **151** with *E* configuration at the double bond. Later, *Marvell* and *Rusay*[95] used the same method in the thermolysis of 2-vinylcyclohexanols (**150**, R = H or CH_3, R′ = CH_3, R″ = H, n = 4) for a stereoselective synthesis of the corresponding trisubstituted unsaturated carbonyl compound **151** with E configuration.

Earl and *Vollhardt*[96] developed a process for the synthesis of bicyclic lactams (example **154**) in which the first thermal retro-ene step (**152**→**153**) gives rise simultaneously to both an acylimine and a diene partial structure, which in turn undergo an intramolecular Diels–Alder reaction to give the indolizidinone **154**. However, this reaction, in contrast to the thermolysis examples involving N-acylimines discussed in Sections 3.1.4 and 3.1.5, affords only moderate yields.

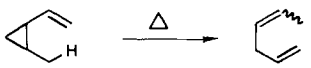


150 **151**



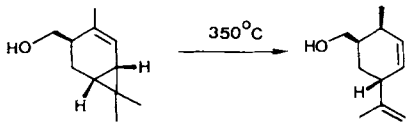
152 **153** **154**

The most common synthetic intramolecular retro-ene reaction not involving heteroatoms is the rearrangement of methylvinylcyclopropanes **155** to give 1,4-hexadienes **156**. Because of its pericyclic character, this reaction, which is favored by release of ring strain, proceeds particularly easily when the two cyclopropane substituents involved are *cis* to each other.



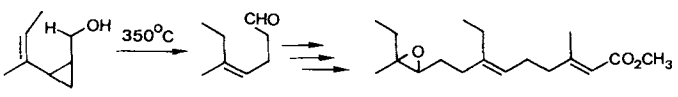
155 **156**

Already in 1960, while examining the thermal behavior of terpenes in the carane series, *Ohloff*[97] found that, upon thermolysis at 350°C, the carene derivative **157** gave the menthadiene derivative **158** stereoselectively in high yield. Later, *Gollnick* and *Schade*[98] described related examples.



157 **158**

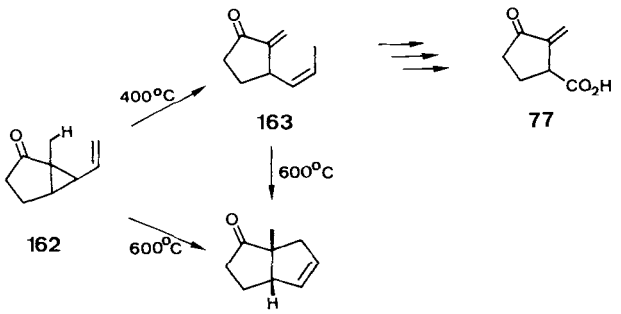
Corey et al.[99] used this transformation in the conversion of **159** into the δ-unsaturated aldehyde **160**, which is an important intermediate in the synthesis of the juvenile hormone JH-II **161**.



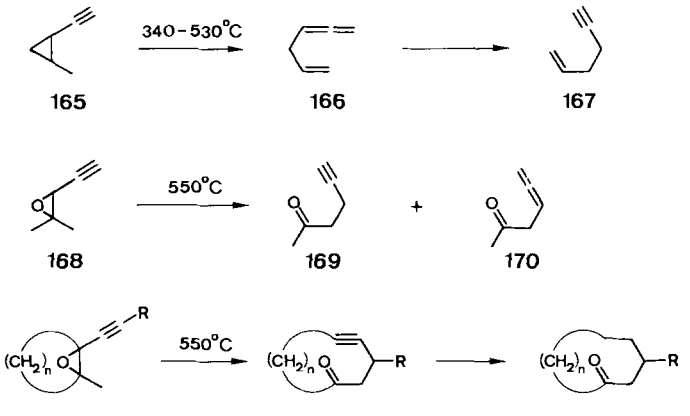
159 **160** **161**

A further example is the synthesis of the antitumor-active methylenecyclopentanone sarkomycin **77**. *Hudlicky* et al.[100] succeeded in transforming the bicyclo[3.1.0]hexanone **162** by thermolysis at 400°C into the retro-ene product **163**, which in turn was selectively oxidized to the natural product **77**.[101] At higher temperatures, **164** is formed from **162** by a vinylcyclopropane rearrangement (see Section 3.2.5); under the same conditions, **164** can also be obtained from **163**.[101] In addition to the temperature dependence of this reaction, the authors described the de-

pendence of the product ratio (**163/164**) on the surface treatment of the reactor material used.



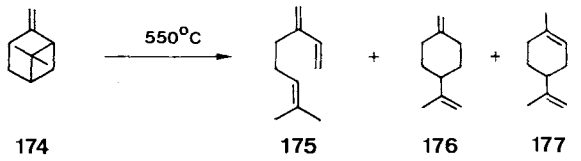
The retro-ene reaction of ethynylmethylcyclopropane **165** to give **166** followed by a Cope type rearrangement to the enyne **167**, reported by *Dalacker* and *Hopf*,[102] was applied by *Karpf* and *Dreiding*[103] to the three-atom ring expansion of acetylenic epoxides **171**. In order to demonstrate that such a transformation is possible, the reaction analogous to **165** → **167** was first carried out on **168** to give **169** and **170**. Similarly, the thermolysis of the epoxycycloalkanes **171** (R = H; n = 4, 10) gave, among other products, the corresponding ring-expanded alkynones **172**, hydrogenation of which furnished the cycloalkanones **173** (R = H; n = 4, 10). Attempted use of this reaction sequence in the synthesis of muscone **173** ($R = CH_3$, n = 10) starting from **171** ($R = CH_3$, n = 10), however, yielded only traces of the expected product.



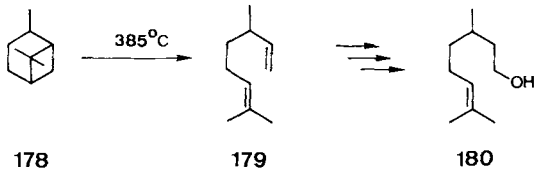
3.2.2. *Cyclobutane Ring Opening*

The use of the cyclobutane ring-opening reaction as a synthetic principle has been extensively applied to terpenes with a pinane backbone.[104] The technical process[105] for the flow thermolysis production of myrcene **175** (75–80%) from β-pinene **174** at 550°C is formally a [2+2]-cycloreversion. The pronounced regioselectivity of the cyclobutane ring opening and the simultaneous formation of the two limonenes **176** (3–4%) and **177** (10%) however, indicate a radical pathway for this transformation.

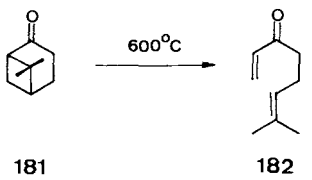
Rienäcker and *Ohloff*[106] applied this ring-opening reaction to the flow thermolysis transformation of pinane **178**



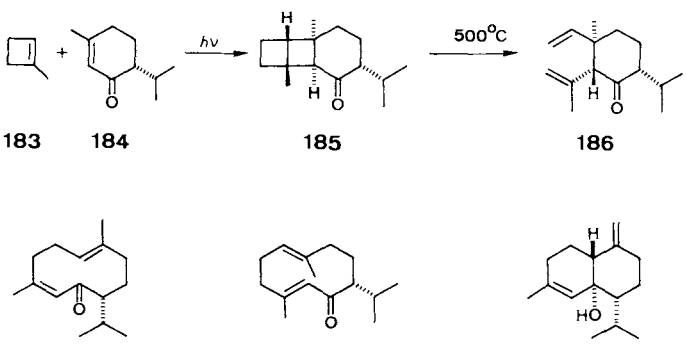
to the diene **179**. Subsequent hydroxylation of the monosubstituted double bond of **179** gave β-citronellol **180**, which is an important perfume component of ethereal oils. The use of the optically pure antipodes of pinane **178** made it possible to produce either of the known optical antipodes of the natural product **180**.



The thermal opening of nopinone **181** at 600°C was carried out in an analogous way by *Mayer* and *Crandall*[107] to yield the dienone **182**.

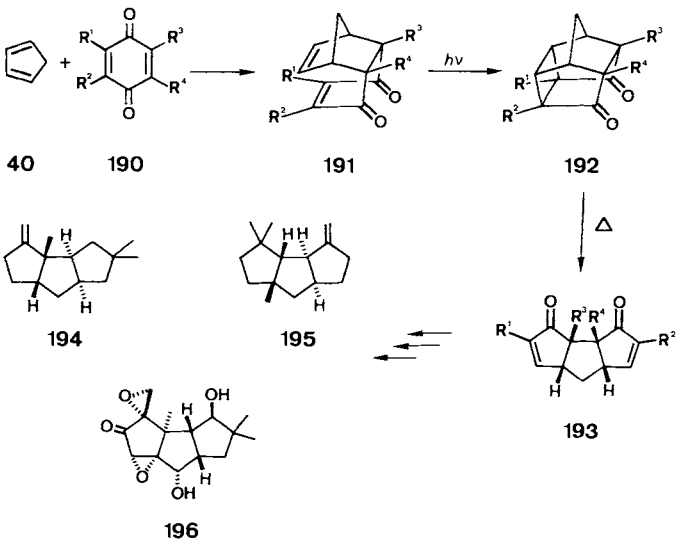


The thermal ring opening of bicyclo[2.2.0]hexanes, which in turn are formed through [2+2]-photocycloaddition reactions, can be used to advantage in synthetic sequences. *Williams* and *Callahan*[108] described the synthesis of (−)-shyobunone **186** in which the gas-phase flow thermolysis at 500°C of **185**, which itself was formed by the photochemical [2+2]-cycloaddition of methylcyclobutene **183** and (−)-piperitone **184**, led directly to products that included (−)-**186**. Three epimers of **186** were also formed as well as (+)-(*R*)-isoacoragermacrone **187**, which, according to a known reaction sequence, can be isomerized to (*R*)-acoragermacrone **188**. When **185** was heated under static conditions in the condensed phase for 30 min at 250°C, the only product isolated was the cadenane derivative **189** which is the product of an intramolecular ene reaction of **187**. This example clearly illustrates a com-



monly observed advantage of gas-phase flow thermolysis, namely, the possibility of isolating the primary thermal product.

An addition–rearrangement reaction sequence was developed by *Mehta* et al.[109] as a route to the linearly annelated triquinanes with the ring skeleton of **193**. The starting point of the sequence is the Diels–Alder addition of cyclopentadiene **40** to the substituted *p*-benzoquinones **190**. After the intramolecular photocycloaddition of **191** to give the pentacycle **192**, thermolysis, preferably under dynamic conditions, gave the *cis-syn-cis* isomer of the triquinane skeleton **193**. The two 2-cyclopentenone moieties then permitted further functionalization of the two lateral rings as well as isomerization to the known naturally occurring[110] *cis-anti-cis* configuration. So far, this strategy has led to the successful synthesis of hirsutene **194**,[111] $\Delta^{9(12)}$-capnellene **195**,[112] and the oxygenated triquinane corioline **196**.[113]



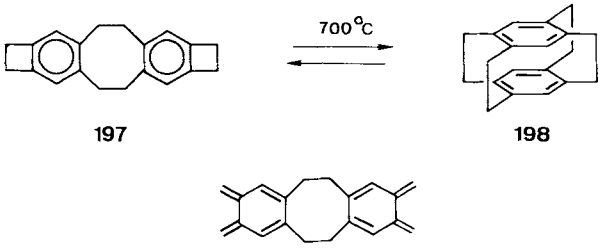
40 190 191 192

194 195 193

196

3.2.3. Benzocyclobutene Dimerizations

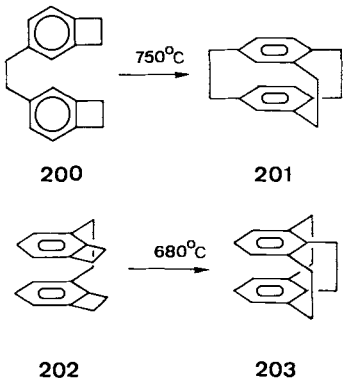
o-Quinodimethanes **16**, which are obtainable by thermolysis of benzocyclobutenes **17**, readily dimerize (see Section 3.1.2). *Boekelheide* and *Ewing*[114] were the first to recognize the importance of this property for the synthesis of cyclophanes. Thus, this group succeeded not only in synthesizing the "superphane" **25** (see Section 3.1.2) but also in transforming the benzocyclobutene derivative **197** into [2.2.2.2](1,2,4,5)cyclophane **198**. The intermediate formation of the bis-*o*-quinodimethane **199** is very probable since the retro-reaction **198** → **197** was also observed.



197 198

199

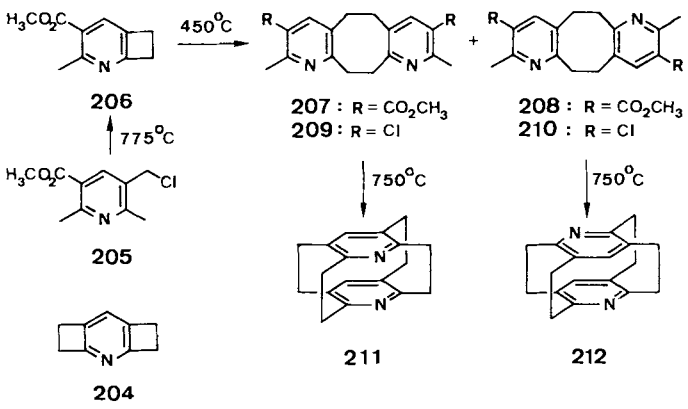
The same principle has been used by *Aalbersberg* and *Vollhardt*[115] in the flash thermolytic synthesis of the [2.2.2](1,2,4)cyclophane **201**. The bis-benzocyclobutene **200**, obtained by Co^0-catalyzed trimerization of 1,5-hexadiyne, gave **201** in 75% yield upon thermolysis at 650 °C. In benzene solution at 200 °C, on the other hand, **200** was transformed into a colorless polymer. *Neuschwander* and *Boekelheide*[116] synthesized the symmetrical [2.2.2](1,2,3)-cyclophane **203** by thermolysis of **202** at 680 °C.



200 201

202 203

The unusually strong tendency of *o*-quinodimethanes to dimerize was even applied by *Boekelheide* et al.[117] to the intermolecular synthesis of [2.2.2.2](1,2,4,5)cyclophane **198** by thermolysis of the dicyclobuta[*a*, *d*]benzene **93** (see Section 3.1.5) in a stream of nitrogen at 450 °C. The authors assume that this dimerization also proceeds via **199**. In contrast, an attempt to apply this method to the synthesis of the diaza[2.2.2.2](1,2,4,5)cyclophanes **211** and **212** by the gas-phase flow thermolysis of **204**, the aza analogue of **93**, failed.[118] The synthesis of **211** and **212** was accomplished, however, in three thermal steps. Starting from **205**, the dihydrocyclobutapyridine **206** was formed at 775 °C (10^{-2} torr) (see Section 3.1.2); **206** in turn gave the dimers **207** and **208** in a stream of nitrogen at 450 °C. After separation and transformation into **209** and **210**, respectively, thermolysis at 750 °C (10^{-3} torr) furnished the desired azacyclophanes **211** and **212**, respectively.



206

207 : R = CO_2CH_3
209 : R = Cl

208 : R = CO_2CH_3
210 : R = Cl

205

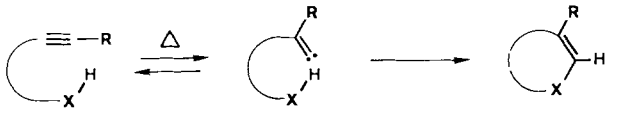
204

211 212

3.2.4. [1,2]-Rearrangements

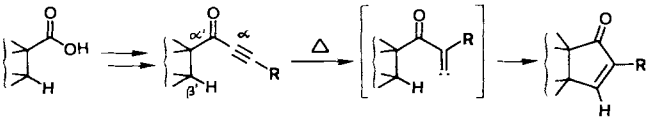
[1,2]-Rearrangements of acetylenes: The thermal [1,2]-rearrangement of acetylenes **213** to vinylidene carbenes

214, first demonstrated by *Brown* et al.[119] under gas-phase flow thermolysis conditions, can be used preparatively when the carbene **214** contains a suitable site for intramolecular insertion, e.g., an X–H bond.



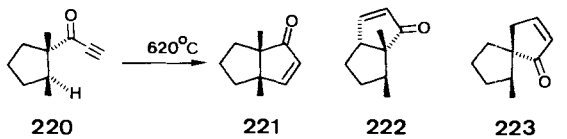
213 **214** **215**

Examples of species such as **214** are alkylidene carbenes conjugated with carbonyl groups, **218**, which are assumed to be intermediates in the flow-thermolytic isomerization of α-acetylenic ketones **217** to 2-cyclopentenones **219**. This "α-alkynone cyclization," discovered by *Karpf* and *Dreiding*,[120] is of interest as a cyclopentenone annelation sequence, because the required alkyl alkynyl ketones **217** are readily accessible from the corresponding carboxylic acids **216**; moreover, the 2-cyclopentenones **219** thus formed are synthetically useful intermediates.

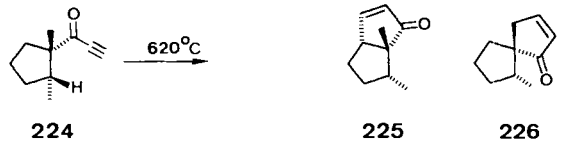


216 **217** **218** **219**

The selectivity of the cyclization step **217** → **219**, which usually takes place with good yields, in particular when R = H, allows predictions to be made about the products.[121] The cyclization takes place with exclusive five-membered-ring formation and occurs at the more highly substituted C(β′) atom, provided that the C(β′)–H bond can adopt a nearly synperiplanar relationship with the alkynone unit with respect to the C(α′)–C(β′) bond. Thus, bicyclo[3.3.0]octenone **221** was preferentially formed from the *cis*-dimethylalkynone **220** by insertion into the tertiary C(β′)–H bond, whereas in the thermolysis of the *trans*-dimethyl compound **224** a tertiary insertion product analogous to **221** was not obtained.

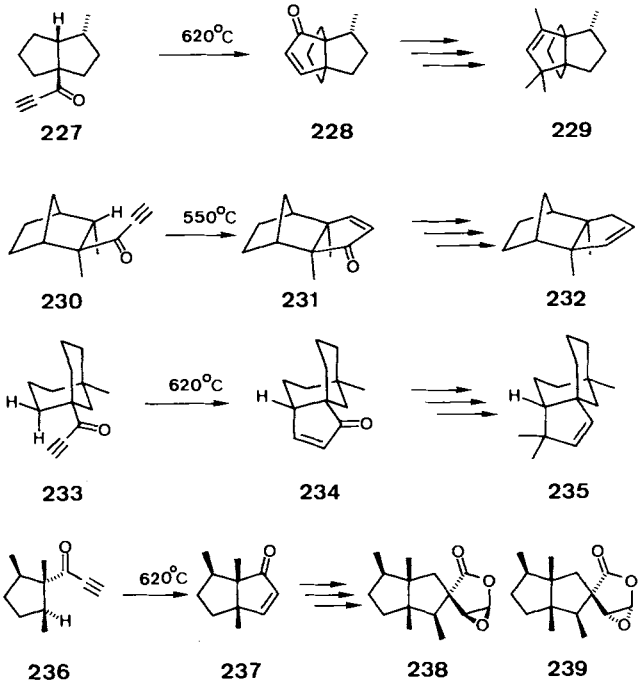


220 **221** (69 : 26) **222** **223** (5)



224 **225** (89 : 11) **226**

The "α-alkynone cyclization" permitted the construction, for example, of the carbon backbone of the cyclopentanoid natural products modhephene **229**,[122] albene **232**,[123] and clovene **235**,[124] as well as **238**,[125] a stereoisomer of ptychanolide **239**,[126] by the thermolysis of the α-alkynones **227**, **230**, **233**, and **236**, respectively.



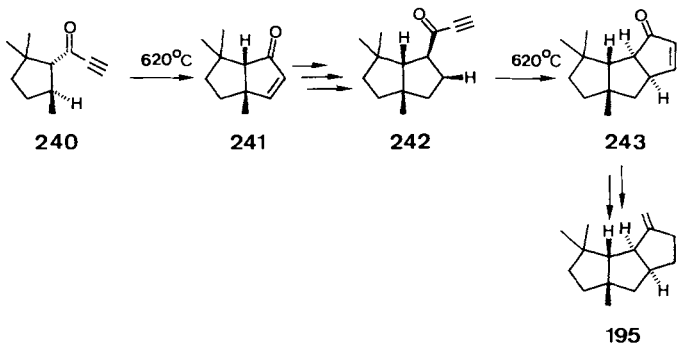
227 **228** **229**

230 **231** **232**

233 **234** **235**

236 **237** **238** **239**

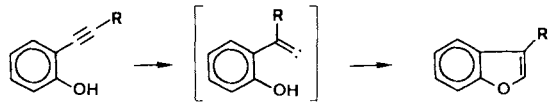
By consecutive application of this cyclopentane annelation, the synthesis of the linearly annelated marine triquinane sesquiterpene capnellene **195**[127] was achieved. In the first thermal step, the α-alkynone **240** gave exclusively the bicycle **241**. After introduction of the alkynone side chain to give **242**, a second cyclization step provided the secondary insertion product **243**, needed for the transformation to **195**, in 33% yield. **243** is the product of insertion into a secondary C–H bond.



240 **241** **242** **243**

195

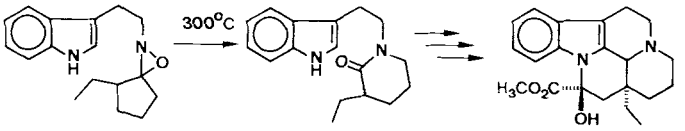
The selective rearrangement of the 2-ethynylphenol **244** (R = H) to benzofuran **246** (R = H) was explained by *Bloch* and *Orvane*[128] as the insertion of the intermediate vinylidene carbene **245** (R = H) into the O–H bond. In support of this interpretation, *Barton* and *Groh*[129] observed the formation of **246** with R = $Si(CH_3)_3$, along with other



244 **245** **246**

products, in the thermolysis of the trimethylsilyl derivative of **244** (R = $Si(CH_3)_3$).

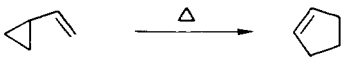
Oxazirane-lactam rearrangements: The gas-phase thermal [1,2]-rearrangement of oxaziranes (example **247**) results in ring expansion to lactams (example **248**) and, according to *Kuehne* and *Parsons*,[130] represents an alternative to the photochemical reaction. Compound **248** is a known intermediate in the synthesis of the pentacyclic indole alkaloid vincamine **249**.[131]



247 **248** **249**

3.2.5. *[1,3]-Rearrangements*

Thermal [1,3]-rearrangements usually occur only at high temperatures and are, therefore, rarely useful for synthetic purposes.[132] One exception is the thermal rearrangement of vinylcyclopropanes **250** to cyclopentenes **251**. This rearrangement was first described by *Neureiter*[133] and shortly afterwards also by *Overberger* and *Borchert*[134] and has been thoroughly investigated by several groups.[135]



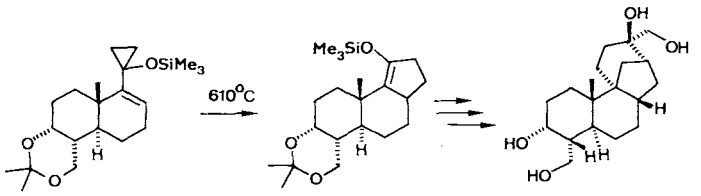
250 **251**

This reaction can be applied synthetically to the formation and annelation of five-membered rings, for example, the cyclopentane annelation sequence for cyclic ketones developed by *Trost* et al.[136] (example **252**). The reaction proceeds via addition of diphenylsulfoniocyclopropanide **253** to the ketone **252**, leading to the oxaspirononane **254**. After opening of the epoxide ring to give the trimethylsilyl ether **255**, flow thermolysis at 330 °C provided the bicyclic trimethylsilyl enol ether **256**.



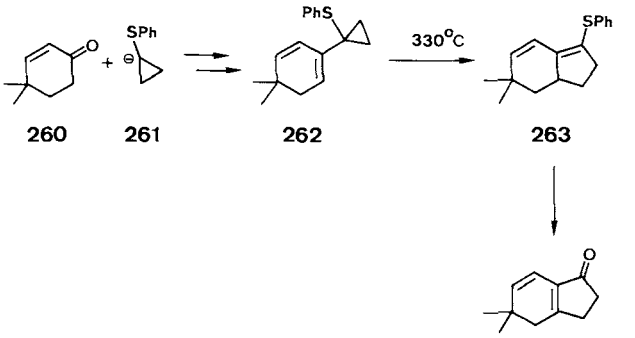
252 **253** **254** **255** **256**

The annelation of the five-membered ring of the antibiotically active compound aphidicolin **259** was achieved in this way; at 610 °C **257** was virtually quantitatively transformed into **258**.[137]



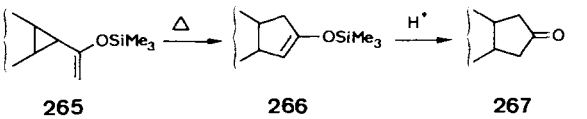
257 **258** **259**

Trost and *Keeley*[138] found an interesting variant of this oxaspiropentane route (**252** → **256**). Addition of the cyclopropyl phenyl sulfide anion **261** to **260** and subsequent dehydration yielded the vinylcyclopropane derivative **262**, which rearranged to the vinyl sulfide **263** upon gas-phase flow thermolysis. The ketone **264** was liberated in good yield by Ti^{IV}-catalyzed hydrolysis of **263**.

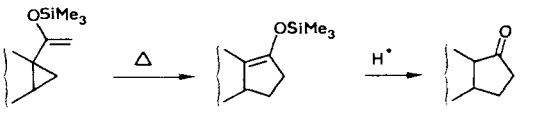


260 **261** **262** **263** **264**

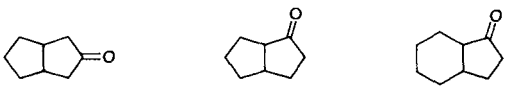
Cyclopropyl-substituted silyl enol ethers of the types **265** and **268**, respectively, have been synthesized by several pathways. Their thermolysis gives the vinylcyclopropane-rearrangement products **266** and **269**, respectively; hydrolysis furnishes the ketones **267** and **270**, respectively. The success of the thermal step developed by *Monti* et al.[139] is very strongly dependent on the particular structure of the silyl enol ethers. Thus, bicyclo[3.3.0]octanone **271** is formed by the path **265** → **267** in only 8% yield, whereas the ketones **272** and **273**, respectively, formed via **268** → **270**, are accessible in yields of 21% and 99%, respectively.



265 **266** **267**



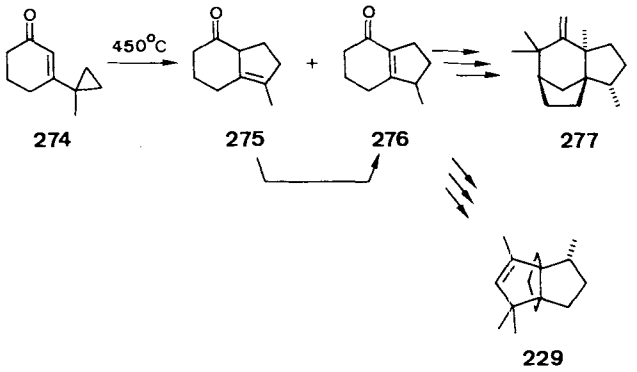
268 **269** **270**



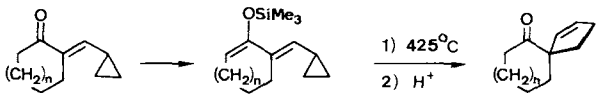
271 **272** **273**

Piers et al.[140] have developed an efficient route for the synthesis and rearrangement of β-cyclopropyl-substituted α,β-unsaturated ketones. A typical example is the synthesis of the bicyclo[4.3.0]octenone **276** by thermal vinylcyclopropane rearrangement of **274**; the simultaneously formed **275** is also converted into **276** by isomerization of the β,γ-double bond. Compound **276** was then used for the syn-

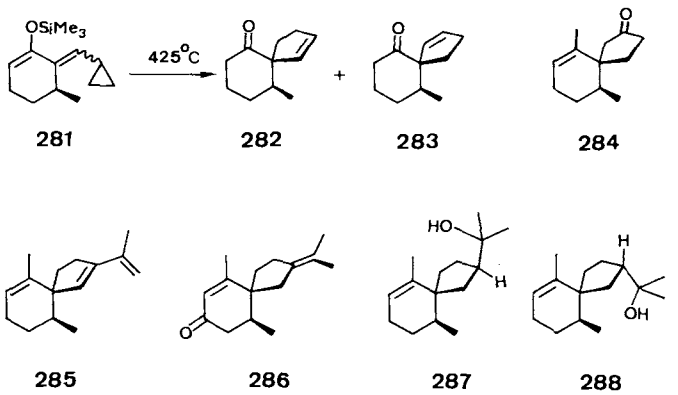
thesis of the tricyclic sesquiterpene zizaene **277**. Moreover, *Smith* and *Jerris*[141] used **276** as the starting material in their synthesis of modhephene **229**, which is the first natural product with a propellane carbon skeleton.



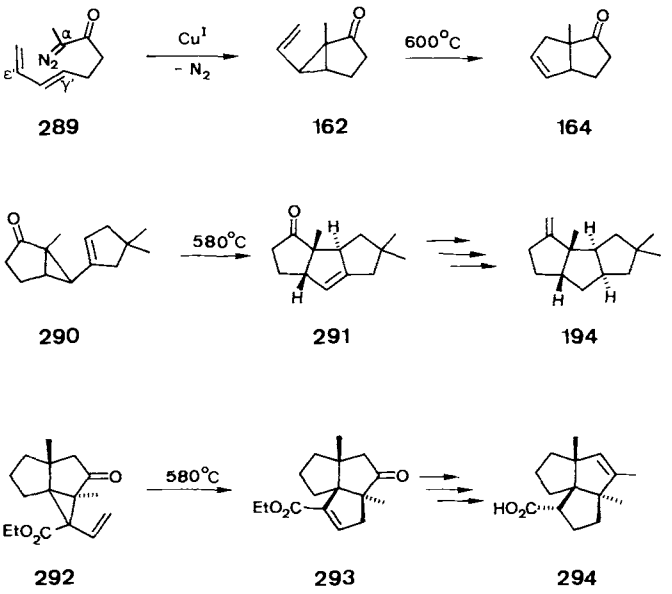
Piers et al.[142] have developed a spiroannelation of the silyl enol ether **279** (n = 1, 2) based on the vinylcyclopropane rearrangement. Acid hydrolysis of the crude thermolysate gave the spiroketones **280** in a total yield of 50–60%. Direct thermolysis of the ketones **278**, on the other hand, resulted in lower yields of the compounds **280** along with several other products.



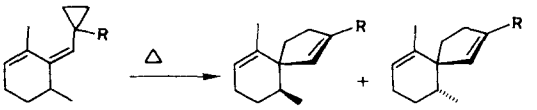
This method can be used to prepare a mixture of the diastereoisomeric spiro compounds **282** and **283** from **281**. Compound **282** is then used as starting material for **284**, thus making it possible to achieve the total synthesis of several sesquiterpenes of the spirovetivane type such as α-vetispirene **285**, β-vetivone **286**, hinesol **287**, and agarospirol **288**.[142]



The vinylcyclopropane rearrangement was used in the synthesis of polycyclopentanoid natural products by *Hudlicky* et al.[143] The required vinylcyclopropanes (example **162**) were obtained through Cu^I-catalyzed, intramolecular cyclopropanation of γ′,ε′-unsaturated α-diazoketones (example **289**). Gas-phase flow thermolysis then gave generally high yields of bicyclo[3.3.0]octenones (example **164**; cf. also Section 3.2.1). Compounds **291** and **293**, which are important as precursors in the synthesis of hirsutene **194**[144] and isocomenic acid **294**,[143] respectively, were obtained in this way.

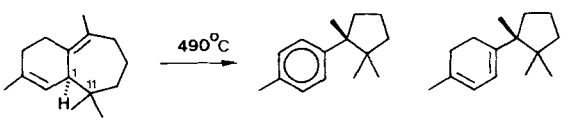


The gas-phase flow thermolysis of trimethylsilyl-substituted vinylcyclopropanes such as **295**, studied by *Paquette* et al.[145], led to synthetically interesting vinylsilanes such as **296** and **297** (6 : 1), relatively high temperatures (560 °C) being required for complete transformation. Since the vinylsilanes resisted transformation into sesquiterpenes of the spirovetivane type, **295** was transformed into the 1-methoxy-1-methylethyl derivative **298** or the cyano derivative **301**, respectively, the thermolysis of which provided the diastereoisomeric mixtures **299/300** (5 : 1) and **302/303** (4 : 1), respectively. The main components **299** and **302** opened up the way to α-vetispirene **285** and hinesol **287**, respectively, as well as β-vetivone **286**.



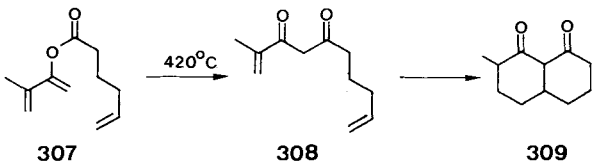
R = $SiMe_3$	: 295	560°C	296	297
R = CMe_2OMe	: 298	440°C	299	300
R = CN	: 301	470°C	302	303

A further example of the synthetic application of [1,3]-rearrangements under dynamic conditions is the thermal rearrangement described by *Sukh Dev* et al.[146] in which (+)-β-himalachene **304** yielded (+)-cuparene **305** at 490 °C, most probably via the dihydro derivative **306**. The opening of the doubly allylic 1,11-bond in **304** is particularly favored by the highly substituted intermediate radi-

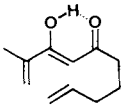


cals formed. The optical activity of the product **305** is retained to a degree of about 20%, which was interpreted with a partly concerted reaction path for the rearrangement.

Shea and *Wada*[147] observed a thermal [1,3]-acyl shift, described earlier in simpler vinyl ester systems, upon gas-phase flow thermolysis of the dienyl ester **307**. This compound is transformed at temperatures above 360 °C into the 1,3-diketone **308**, part of which reacts further to give the decalindione **309**, probably by an intramolecular Diels–Alder reaction via the enol **310**. Attempts at carrying out this transformation under static conditions failed.



307 308 309



310

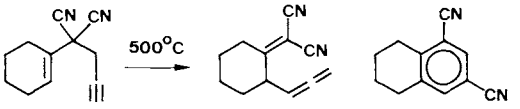
3.2.6. *[3,3]-Sigmatropic Rearrangements*

Among the preparatively most valuable pericyclic reactions, apart from Diels–Alder reactions,[12-17,19] are the [3,3]-sigmatropic rearrangements, namely, the Cope rearrangement (**311** ⇄ **312** with X = CR_2) and the Claisen rearrangement (**311** ⇄ **312** with X = O).[20,21,148] Although these processes are usually carried out under static conditions in the condensed phase or in the gas phase, there are examples known where gas-phase flow thermolysis is used.[149]



311 312

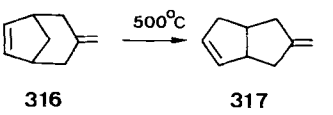
A rearrangement that gives rise to the Cope product **314** only in the gas phase, the thermolysis of the dinitrile **313**, was described by *Brown* and *McAllan*.[150] In the condensed phase **313** yielded exclusively the tetralin derivative **315**.



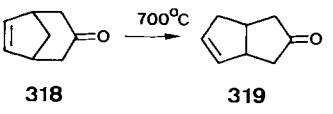
313 314 315

The bicyclo[3.2.1]octenes **316** and **318**, whose Cope systems are unfavorably arranged for a concerted rearrangement, only undergo transformation at high temperatures, according to *Klumpp* et al.,[151] to give the bicyclo[3.3.0]octenes **317** and **319**, respectively; this is indicative of a radical pathway.

An example of a synthetic application of the Claisen rearrangement under flow thermolysis conditions has been described by *Büchi* and *White*[152] in connection with the

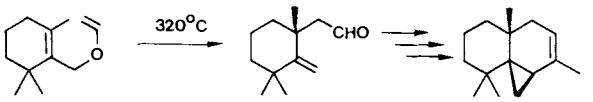


316 317



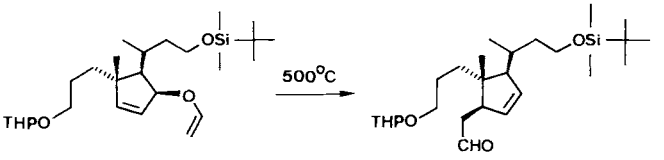
318 319

total synthesis of thujopsene **322**. The allyl vinyl ether **320** rearranged to the γ,δ-unsaturated aldehyde **321**. The vinyl ether **320**, which is readily accessible from β-cyclogeraniol, was subjected to continuous gas-phase flow thermolysis in quantities of over 100 g to give **321**.

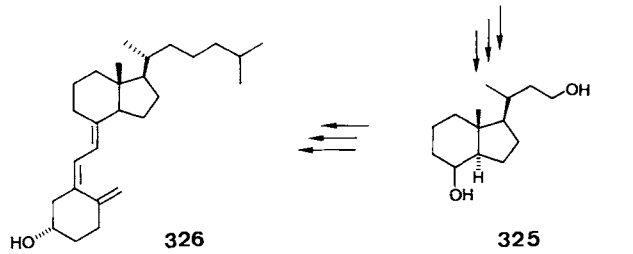


320 321 322

Flow thermolysis of the allyl vinyl ether **323** at 500 °C led stereoselectively to the aldehyde **324** in a yield of 60%.[153] Compound **324** is a precursor for the Inhoffen-Lythgoe diol **325**, which in turn is a crucial reaction intermediate in the total synthesis of vitamin D_3 **326**. It should be noted that in spite of the high temperature used in this reaction both protecting groups remained unaffected.



323 324



326 325

3.3. Conclusion

The examples presented in this article show that organic reactions at high temperatures under gas-phase flow thermolysis conditions are synthetically useful. Several of the cases discussed emphasize the fact that, depending on the reaction conditions used, whether static or dynamic, different outcomes of the reaction can be expected. The choice of special conditions is, therefore, not only dependent on the intended thermal rearrangement, but also on the functional groups and structural elements of the starting material. Furthermore, it is important to study the compatibility of the reacting substructure with the functional groups that are not directly involved in the thermal step. The knowl-

edge so obtained will greatly expand the use of flow thermolysis methods in organic synthesis.

Received: March 15, 1985 [A 573 IE]
German version: *Angew. Chem. 98* (1986) 413
Translated by Dr. *Edeline Wentrup-Byrne*, Brisbane, Australia

[1] D. Seebach, A. Hidber, *Chimia 37* (1983) 449.
[2] Derived from the Greek: pyros = fire; lysis = dissolution, separation.
[3] C. D. Hurd: *The Pyrolysis of Carbon Compounds*, Chem. Catalog Co., New York 1929.
[4] R. F. C. Brown: *Pyrolytic Methods in Organic Chemistry*, Academic Press, New York 1980.
[5] J. F. King, P. de Mayo, C. L. McIntosh, K. Piers, D. J. H. Smith, *Can. J. Chem. 48* (1970) 3704.
[6] T. Kametani, *Pure Appl. Chem. 51* (1979) 747.
[7] A. Streitwieser, C. H. Heathcock: *Organische Chemie*, Verlag Chemie, Weinheim 1980, p. 93; *Introduction to Organic Chemistry*, 2nd ed., Macmillan, New York 1980, p. 103.
[8] S. H. Pine, J. B. Hendrickson, D. J. Cram, G. S. Hammond: *Organic Chemistry*, 4th ed., McGraw-Hill, Tokyo 1980, p. 475.
[9] O.-A. Neumüller: *Römpps Chemie-Lexikon*. 2nd, ed., Franckh'sche Verlagshandlung, Stuttgart 1975, p. 2850.
[10] W. J. Irwin, *J. Anal. Appl. Pyrolysis 1* (1979) 3, 89.
[11] G. Schaden, *J. Anal. Appl. Pyrolysis 4* (1982) 83.
[12] G. Desimoni, G. Tacconi, A. Barco, G. P. Pollini: *Natural Products Synthesis Through Pericyclic Reactions (ACS Monogr. 180)* Am. Chem. Soc., Washington, D. C., USA 1983.
[13] D. F. Taber: *Intramolecular Diels-Alder and Alder Ene Reactions*, Springer, Berlin 1984.
[14] W. Oppolzer, *Pure Appl. Chem. 53* (1981) 1181.
[15] R. L. Funk, K. P. C. Vollhardt, *Chem. Soc. Rev. 9* (1980) 41.
[16] C. Brieger, J. N. Bennett, *Chem. Rev. 80* (1980) 63.
[17] W. Oppolzer, *Synthesis 1978*, 793.
[18] W. Oppolzer, V. Snieckus, *Angew. Chem. 90* (1978) 506; *Angew. Chem. Int. Ed. Engl. 17* (1978) 476.
[19] W. Oppolzer, *Angew. Chem. 89* (1977) 10; *Angew. Chem. Int. Ed. Engl. 16* (1977) 10.
[20] G. B. Benett, *Synthesis 1977*, 589.
[21] F. E. Ziegler, *Acc. Chem. Res. 10* (1977) 227.
[22] J. M. Conia, P. Le Perchec, *Synthesis 1975*, 1.
[23] M. Berthelot, *Ann. Chim. Phys. Ser. 4, 9* (1866) 445; *C. R. Hebd. Seances Acad. Sci. 62* (1866) 905.
[24] This ill-founded multitude of concepts together with the often rudimentary description of apparatus and experimental conditions used are justifiably important reasons for the skepticism of many organic chemists toward the use of these methods.
[25] P. de Mayo, *Endeavour 31* (1972) 135.
[26] H. J. Hageman, U. E. Wiersum, *Chem. Br. 9* (1973) 206.
[27] U. E. Wiersum, *Recl.: J. R. Neth. Chem. Soc. 101* (1982) 317, 365.
[28] U. E. Wiersum, *Aldrichimica Acta 17* (1984) 31.
[29] G. Seybold, *Angew. Chem. 89* (1977) 377; *Angew. Chem. Int. Ed. Engl. 16* (1977) 365.
[30] E. Hedaya, D. McNeil, *J. Am. Chem. Soc. 89* (1967) 4213.
[31] E. Hedaya, *Acc. Chem. Res. 2* (1969) 367.
[32] C. Wentrup, *Chimia 31* (1977) 258.
[33] D. M. Golden, G. N. Spokes, S. W. Benson, *Angew. Chem. 85* (1973) 602; *Angew. Chem. Int. Ed. Engl. 12* (1973) 534.
[34] *Aldrichimica Acta 16* (1983) 11.
[35] L. F. Albright, B. L. Crynes, W. H. Corcoran (Eds.): *Pyrolysis: Theory and Industrial Practice*, Academic Press, New York 1983.
[36] L. F. Albright, B. L. Crynes (Eds.): *Industrial and Laboratory Pyrolyses (ACS Symp. Ser. 32)* Am. Chem. Soc., Washington, D. C., USA 1976.
[37] K. Weissermel, H.-J. Arpe: *Industrielle Organische Chemie*, Verlag Chemie, Weinheim 1976.
[38] J. M. Tedder, A. Nechvatal, A. H. Jubb: *Basic Organic Chemistry, Part 5: Industrial Products*, Wiley, New York 1975.
[39] C. H. DePuy, R. W. King, *Chem. Rev. 60* (1960) 431.
[40] W. H. Saunders, A. F. Cockerill: *Mechanisms of Eliminiation Reactions*, Wiley, New York 1973.
[41] D. H. R. Barton, W. J. Rosenfelder, *J. Chem. Soc. 1951*, 1048; D. H. R. Barton, *ibid. 1949*, 2174.
[42] P. A. Collins, D. Wege, *Aust. J. Chem. 32* (1979) 1819.
[43] Y. Miyahara, T. Inazu, T. Yoshino, *Tetrahedron Lett. 24* (1983) 5277.
[44] K. B. Becker, R. W. Pfluger, *Tetrahedron Lett. 1979*, 3713.
[45] See [4], p. 94ff.
[46] A. G. Loudon, A. Maccoll, S. K. Wong, *J. Am. Chem. Soc. 91* (1969) 7577.
[47] P. Schiess, S. Rutschmann, V. W. Toan, *Tetrahedron Lett. 1978*, 3669.
[48] P. Schiess, M. Heitzmann, *Helv. Chim. Acta 61* (1978) 844.
[49] L. G. Haruff, M. Brown, V. Boekelheide, *J. Am. Chem. Soc. 100* (1978) 2893.
[50] Y. Sekine, M. Brown, V. Boekelheide, *J. Am. Chem. Soc. 101* (1979) 3126.
[51] P. Schiess, M. Heitzmann, *Angew. Chem. 89* (1977) 485; *Angew. Chem. Int. Ed. Engl. 16* (1977) 469; P. Schiess, P. Radimerski, *Helv. Chim. Acta 57* (1974) 2583.
[52] H. H. Inhoffen, *Naturwissenschaften 25* (1937) 125.
[53] S. Kaufmann, J. Pataki, G. Rosenkranz, J. Romo, C. Djerassi, *J. Am. Chem. Soc. 72* (1950) 4531, 4534; US-Pat. 3020294 (1961) see also: *Chem. Abstr. 57* (1962) 916.
[54] J. L. Ripoll, A. Rouessac, F. Rouessac, *Tetrahedron 34* (1978) 19.
[55] G. Stork, R. N. Guthikonda, *Tetrahedron Lett. 1972*, 2755.
[56] T. L. Ho, *Synth. Commun. 4* (1974) 189.
[57] R. Bloch, *Tetrahedron 39* (1983) 639.
[58] M. Harre, P. Raddatz, R. Walenta, E. Winterfeldt, *Angew. Chem. 94* (1982) 496; *Angew. Chem. Int. Ed. Engl. 21* (1982) 480.
[59] P. G. Baraldi, A. Barco, S. Benetti, G. P. Pollini, E. Polo, D. Simoni, *J. Chem. Soc. Chem. Commun. 1984*, 1049; F. Gavina, A. M. Costero, P. Gil, S. V. Luis, *J. Am. Chem. Soc. 106* (1984) 2077.
[60] P. Ducos, F. Rouessac, *Tetrahedron 29* (1973) 3233.
[61] J.-B. Wiel, F. Rouessac, *Bull. Soc. Chim. Fr. 1979*, 273.
[62] N. E. Schore, *Synth. Commun. 9* (1979) 41.
[63] I. U. Khand, G. R. Knox, P. L. Pauson, W. E. Watts, M. I. Foreman, *J. Chem. Soc. Perkin Trans. 1, 1973*, 977.
[64] A. B. Smith III, D. Boschelli, *J. Org. Chem. 48* (1983) 1217.
[65] R. M. Scarborough, B. H. Toder, A. B. Smith III, *J. Am. Chem. Soc. 102* (1980) 3904.
[66] A. J. H. Klunder, W. Bos, B. Zwanenburg, *Tetrahedron Lett. 22* (1981) 4557; J. M. J. Verlaak, A. J. H. Klunder, B. Zwanenburg, *ibid. 23* (1982) 5463.
[67] T. Siwapinyoyos, Y. Thebtaranonth, *J. Org. Chem. 47* (1982) 599.
[68] M. Kodpinid, T. Siwapinyoyos, Y. Thebtaranonth, *J. Am. Chem. Soc. 106* (1984) 4862.
[69] J. Haslouin, F. Rouessac, *Bull. Soc. Chim. Fr. 1977*, 1242.
[70] W. Boland, L. Jaenicke, *Chem. Ber. 111* (1978) 3262.
[71] R. Bloch, *Tetrahedron Lett. 1979*, 3945.
[72] M.-C. Lasne, J. L. Ripoll, A. Thuillier, *J. Chem. Res. Synop. 1982*, 214.
[73] M. P. Cava, A. A. Deana, *J. Am. Chem. Soc. 81* (1959) 4266.
[74] M. P. Cava, A. A. Deana, K. Muth, *J. Am. Chem. Soc. 82* (1960) 2524.
[75] E. Giovannini, H. Vuilleumier, *Helv. Chim. Acta 60* (1977) 1452.
[76] M. P. Cava, R. L. Shirley, B. W. Erickson, *J. Org. Chem. 27* (1962) 755.
[77] T. Durst, M. Lancaster, D. J. H. Smith, *J. Chem. Soc. Perkin Trans 1, 1981*, 1846.
[78] F. Vögtle, *Angew. Chem. 81* (1969) 258; *Angew. Chem. Int. Ed. Engl. 8* (1969) 274.
[79] H. A. Staab, M. Haenel, *Chem. Ber. 106* (1973) 2190.
[80] F. Vögtle, P. Neumann, *Synthesis 1973*, 85.
[81] S. F. Martin, S. R. Desai, G. W. Phillips, A. C. Miller, *J. Am. Chem. Soc. 102* (1980) 3294.
[82] H. F. Schmitthenner, S. M. Weinreb, *J. Org. Chem. 45* (1980) 3372.
[83] T.-S. Chou, H.-H. Tso, L.-J. Chang, *J. Chem. Soc. Chem. Commun. 1984*, 1323.
[84] R. Bloch, J. Abecassis, *Tetrahedron Lett. 24* (1983) 1247.
[85] J. R. Williams, C. Lin, *J. Chem. Soc. Chem. Commun. 1981*, 752.
[86] L.-F. Tietze, G. Kienast, H. C. Uzar, *Angew. Chem. 91* (1979) 576; *Angew. Chem. Int. Ed. Engl. 18* (1979) 541.
[87] A. R. Battersby, A. R. Burnett, P. G. Pearson, *J. Chem. Soc. C 1969*, 1187.
[88] H. Strickler, G. Ohloff, E. sz. Kováts, *Helv. Chim. Acta 50* (1967) 759.
[89] S. Nozoe, M. Goi, N. Morisaki, *Tetrahedron Lett. 1971*, 3701.
[90] F. Plavac, C. H. Heathcock, *Tetrahedron Lett. 1979*, 2115.
[91] V. Rautenstrauch, DOS 2657903 (1977) see also: *Chem. Abstr. 87* (1977) 167605j, *90* (1979) 186472s.
[92] C. Moreau, F. Rouessac, J. M. Conia, *Tetrahedron Lett. 1970*, 3527; C. Moreau, F. Rouessac, P. Beslin, J. M. Conia, *Chem. Lett. 1974*, 59; C. Moreau, F. Rouessac, *Bull. Soc. Chim. Fr. 1973*, 3425.
[93] W. J. Bailey, C. N. Bird, *J. Org. Chem. 42* (1977) 3895.
[94] R. T. Arnold, G. Smolinsky, *J. Am. Chem. Soc. 82* (1960) 4918.
[95] E. N. Marvell, R. Rusay, *J. Org. Chem. 42* (1977) 3336.
[96] R. A. Earl, K. P. C. Vollhardt, *Heterocycles 19* (1982) 265.
[97] G. Ohloff, *Chem. Ber. 93* (1960) 2673.
[98] K. Gollnick, G. Schade, *Tetrahedron 22* (1966) 123.
[99] E. J. Corey, H. Yamamoto, D. K. Herron, K. Achiwa, *J. Am. Chem. Soc. 92* (1970) 6635.
[100] S. V. Govindan, T. Hudlicky, F. J. Koszyk, *J. Org. Chem. 48* (1983) 3581.
[101] T. Hudlicky, F. J. Koszyk, *Tetrahedron Lett. 21* (1980) 2487.
[102] V. Dalacker, H. Hopf, *Tetrahedron Lett. 1974*, 15.
[103] M. Karpf, A. S. Dreiding, *Helv. Chim. Acta 60* (1977) 3045.
[104] B. D. Sully, *Chem. Ind. London 1964*, 263; D. V. Banthorpe, D. Whitacker, *Q. Rev. Chem. Soc. 20* (1966) 373.

[105] R. E. Kirk, D. F. Othmer (Eds.): *Encyclopedia of Chemical Technology, Vol. 19*, 2nd. ed., Interscience, New York 1969, p. 817ff.
[106] R. Rienäcker, G. Ohloff, *Angew. Chem. 73* (1961) 240.
[107] C. F. Mayer, J. K. Crandall, *J. Org. Chem. 35* (1970) 2688.
[108] J. R. Williams, J. F. Callahan, *J. Org. Chem. 45* (1980) 4475.
[109] G. Mehta, A. Srikrishna, A. V. Reddy, M. S. Nair, *Tetrahedron 37* (1981) 4543.
[110] L. A. Paquette, *Top. Curr. Chem. 119* (1984) 1.
[111] G. Mehta, A. V. Reddy, *J. Chem. Soc. Chem. Commun. 1981*, 756.
[112] G. Mehta, A. V. Reddy, A. N. Murty, *J. Chem. Soc. Chem. Commun. 1983*, 824.
[113] G. Mehta, A. V. Reddy, A. N. Murty, D. S. Reddy, *J. Chem. Soc. Chem. Commun. 1982*, 540.
[114] V. Boekelheide, G. Ewing, *Tetrahedron Lett. 1978*, 4245.
[115] W. G. L. Aalbersberg, K. P. C. Vollhardt, *Tetrahedron Lett. 1979*, 1939.
[116] B. N. Neuschwander, V. Boekelheide, *Isr. J. Chem. 20* (1980) 288.
[117] B. E. Eaton, E. D. Laganis, V. Boekelheide, *Proc. Natl. Acad. Sci. USA 78* (1981) 6564.
[118] H. C. Kang, V. Boekelheide, *J. Am. Chem. Soc. 106* (1984) 2672.
[119] R. F. C. Brown, K. J. Harrington, G. L. McMullen, *J. Chem. Soc. Chem. Commun. 1974*, 123.
[120] M. Karpf, A. S. Dreiding, *Helv. Chim. Acta 62* (1979) 852.
[121] M. Karpf, J. Huguet, A. S. Dreiding, *Helv. Chim. Acta 65* (1982) 13.
[122] M. Karpf, A. S. Dreiding, *Tetrahedron Lett. 21* (1980) 4569; *Helv. Chim. Acta 64* (1981) 1123.
[123] G. G. G. Manzardo, M. Karpf, A. S. Dreiding, *Helv. Chim. Acta 66* (1983) 627.
[124] J. Ackroyd, M. Karpf, A. S. Dreiding, *Helv. Chim. Acta 67* (1984) 1963.
[125] J. Huguet, M. Karpf, A. S. Dreiding, *Tetrahedron Lett. 24* (1983) 4177.
[126] R. Takeda, H. Naoki, T. Iwashita, K. Mizukawa, Y. Hirose, T. Isida, *Bull. Chem. Soc. Jpn. 56* (1983) 1125; R. Takeda, H. Naoki, T. Iwashita, Y. Hirose, *Tetrahedron Lett. 22* (1981) 5307.
[127] J. Huguet, M. Karpf, A. S. Dreiding, *Helv. Chim. Acta 65* (1982) 2413.
[128] R. Bloch, P. Orvane, *Tetrahedron Lett. 22* (1981) 3597.
[129] T. J. Barton, B. L. Groh, *J. Org. Chem. 50* (1985) 158.
[130] M. E. Kuehne, W. H. Parsons, *Tetrahedron 39* (1983) 3763.
[131] J. L. Herman, R. J. Cregge, J. E. Richman, C. L. Semmelhack, R. H. Schlessinger, *J. Am. Chem. Soc. 96* (1974) 3701.
[132] See [4], p. 307-310.
[133] N. P. Neureiter, *J. Org. Chem. 24* (1959) 2044.
[134] G. G. Overberger, A. E. Borchert, *J. Am. Chem. Soc. 82* (1960) 1007.
[135] J. J. Gajewski: *Hydrocarbon Thermal Isomerizations*, Academic Press, New York 1981, p. 81-87.
[136] B. M. Trost, M. J. Bogdanowicz, *J. Am. Chem. Soc. 95* (1973) 5311.
[137] B. M. Trost, Y. Nishimura, K. Yamamoto, S. S. McElvain, *J. Am. Chem. Soc. 101* (1979) 1328.
[138] B. M. Trost, D. E. Keeley, *J. Am. Chem. Soc. 98* (1976) 248.
[139] S. A. Monti, F. W. Cowherd, T. W. McAninch, *J. Org. Chem. 40* (1975) 858.
[140] E. Piers, J. Banville, C. K. Lau, I. Nagakura, *Can. J. Chem. 60* (1982) 2965.
[141] A. B. Smith III, P. J. Jerris, *J. Org. Chem. 47* (1982) 1845; *J. Am. Chem. Soc. 103* (1981) 194.
[142] E. Piers, C. K. Lau, I. Nagakura, *Can. J. Chem. 61* (1983) 288.
[143] R. P. Short, J. M. Revol, B. C. Ranu, T. Hudlicky, *J. Org. Chem. 48* (1983) 4453, and references cited therein.
[144] T. Hudlicky, T. H. Kutchen, S. R. Wilson, D. T. Mao, *J. Am. Chem. Soc. 102* (1980) 6351.
[145] L. A. Paquette, T.-H. Yan, G. J. Wells, *J. Org. Chem. 49* (1984) 3610; L. A. Paquette, G. J. Wells, K. A. Horn, T.-H. Yan, *Tetrahedron 39* (1983) 913; T.-H. Yan, L. A. Paquette, *Tetrahedron Lett. 23* (1982) 3227.
[146] H. N. Subba Rao, N. P. Damodaran, Sukh Dev, *Tetrahedron Lett. 1968*, 2213.
[147] K. J. Shea, E. Wada, *Tetrahedron Lett. 23* (1982) 1523.
[148] See [12], p. 268-338.
[149] See [4], p. 317-320.
[150] R. F. C. Brown, C. G. McAllan, *Aust. J. Chem. 30* (1977) 1747.
[151] J. Japenga, K. Kool, G. W. Klumpp, *Tetrahedron Lett. 1975*, 1029.
[152] G. Büchi, J. D. White, *J. Am. Chem. Soc. 86* (1964) 2884.
[153] B. M. Trost, P. R. Bernstein, P. C. Funfschilling, *J. Am. Chem. Soc. 101* (1979) 4378.

The Pentagonal Column and the ReO_3-Type Structure

By Bengt-Olov Marinder*

The pentagonal column (PC), consisting of MX_7 bipyramids sharing their equatorial edges with five MX_6 octahedra, is a structural feature frequently occurring in association with frameworks of the ReO_3-type, where it enables accomodation of an anion deficiency. The present article discusses the geometry of the PC and its compatibility with the ReO_3-type structure, which naturally emerges from the finding that a PC may result from twinning of an ReO_3-type structure on the unit cell level. A new symbolism is presented which facilitates visualization of a large variety of crystal and defect structures of MX_{3-x} stoichiometry. This symbolism may also serve as a convenient aid in deriving models of possible new structures that may be of value in the interpretation of HREM images.

1. Introduction

In his paper[1] that deals with the crystal structure of $W_{18}O_{49}$, *Magnéli* states that the arrangement of five W atoms close to the corners of a regular pentagon with a W atom situated in the center "is a very peculiar one". This structure is very likely the first known example of a transition metal oxide in which, according to present-day concepts of atomic arrangement, a central metal atom M is coordinated by seven oxygen atoms to form a pentagonal bipyramid [MO_7]. In turn, this bipyramid shares its equatorial edges with five [MO_6] octahedra (Fig. 1a). Further structural studies by means of X-ray diffraction techniques and High Resolution Electron Microscopy (HREM) on oxides, hydroxides and oxide fluorides of transition metals have revealed that this entity is quite common in several compounds with MX_{3-x} stoichiometry, $0.069 \leqslant x \leqslant 0.333$ (see Table 1). It has also been observed as a structural defect in a matrix of ReO_3-type structure. In all these structures such entities are linked to each other by their X vertices along a normal to the equatorial plane, and they thus form what has been called a pentagonal column or PC.[2] In the following we will also use the term PC to mean the repetitive unit of such a column.

The PC as a structure element in transition metal oxides and related compounds has been discussed by *Lundberg* et al.[2,3] *Hyde* and *O'Keeffe*[4] relate the PC to the ReO_3-type structure using the concept of cylindrical antiphase boundaries and concomitant interpolation of ...MXMX... rows in the resulting pentagonal tunnels. The ensuing structures are regarded as crystallographic shear (CS) structures with cylindrical rather than planar CS surfaces. The PC concept has been developed further by *Ekström*[5] and by *Ekström* and *Tilley*.[6]

The introduction of a PC into a matrix of the ReO_3 type always creates new types of tunnels running parallel with the PCs. Quite frequently three- or three- and five-sided tunnels are formed. If cations, appropriate in size and concentration, are inserted in the larger tunnels, these might serve as avenues for the transport of ions under the influence of an electric potential gradient, the substance thus acting as a solid electrolyte. In recent years we have been actively involved in the search for new substances of this kind;[7] those of current interest are listed in Table 1, with emphasis on substances of MX_{3-x} stoichiometry containing PCs and tunnels of various size and cross-section.

In what follows we will try to picture a PC in a convenient way, using a simple model of a PC as a building unit either alone, thereby following in the footsteps of *Lundberg*, or coupled with units of an ReO_3-type structure, i.e. with MX_6 octahedra. We shall also see how structural defects in transition metal oxides can be illustrated by the same model. First of all, however, we must discuss the geometry of a PC, and study in what way it is related to the ReO_3-type structure.

2. Some Geometric Properties of the Pentagonal Column

Figure 1a shows the idealized PC with five symmetry planes projected along a normal to the equatorial plane (which is also a symmetry plane) of the pentagonal bipyramid. In a real structure, such as that of $LiNb_6O_{15}F$[8] (see Fig. 1b) or Nb_2WO_8,[9] the five symmetry planes have been reduced to one. Figure 1c shows a slightly readjusted PC with one mirror plane perpendicular to the equatorial plane. The PC may be described in terms of a square having an edge equal to $d\sqrt{5}$, where d is the length of the diagonal of a regular MX_6 octahedron. Figure 1c also pictures the PC in an abbreviated way as a square with an inserted arrow. The same size of square will accommodate five ReO_3-type octahedra as shown in Figure 1d, which also depicts two mirror-related orientations of this grouping. The two sets are oriented at an angle of $2\,\mathrm{arctg}\,1/2$ ($=53.13°$) to each other.

Figure 2a shows squares with PCs and MO_6 octahedra joined together to form the characteristic part of a model of $4\,Nb_2O_5 \cdot 50\,WO_3$, $4\,Nb_2O_5 \cdot 22\,WO_3$,[10] and $W_{12}O_{34}$[3,11] structures. The model, in this particular case shows an intergrowth of $LiNb_6O_{15}F$- and ReO_3-type structures; the

[*] Dr. B.-O. Marinder
Department of Inorganic Chemistry
Arrhenius Laboratory, University of Stockholm
S-10691 Stockholm (Sweden)

 © VCH Verlagsgesellschaft mbH, D-6940 Weinheim, 1986 0570-0833/86/0505-0431 $ 02.50/0

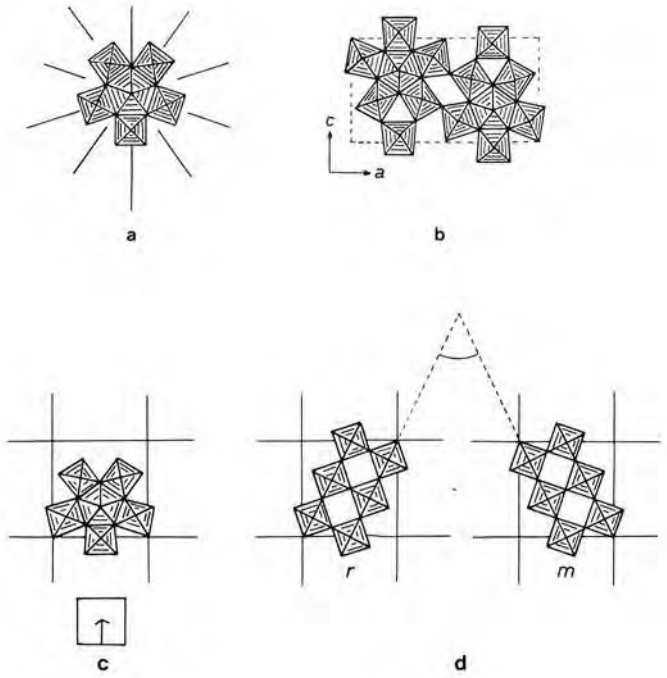


Fig. 1. a) A regular pentagonal column (PC) projected perpendicularly to its equatorial plane. Five symmetry planes are indicated. b) A structure model of $LiNb_6O_{15}F$. The unit cell contains two PCs. c) The slightly readjusted PC associated with a square, the length of whose edge is $d\sqrt{5}$; d is the diagonal of the MX_6 octahedron. A short-hand symbol of a PC is shown below: the arrow is pointing to the "top" of the PC. d) Two ReO_3 type structures, related by reflection and denoted r and m. Each of them has been assigned a square with an edge $= d\sqrt{5}$. The angle of 2 arctg 1/2 between them is shown.

two ReO_3 nets have the same orientation. As a consequence of the intergrowth, empty pentagonal tunnels (PTs)[3] are created, which render the structure a formal similarity to the tetragonal tungsten bronze (TTB) structure[12] (Fig. 2b). Figure 2c shows a model of an intergrowth between a $LiNb_6O_{15}F$-type structure and ReO_3 nets in two orientations indicated by r and m. It is a model of another kind of boundary sometimes observed as a defect in the Nb_2O_5/WO_3 system.[13] In the two models shown, both the top and bottom parts of a PC are involved in the intergrowth. Figure 2d shows two PCs joined by an isolated octahedron whose orientation, indicated by b, is halfway between m and r (see Section 3).

Figure 3 shows two PCs completely embedded in an ReO_3-type matrix. The occurrence of an $LiNb_6O_{15}F$-type structure in an ReO_3-type matrix has been observed in the system Nb_2O_5/WO_3 by *Iijima* and *Allpress*,[13] who regard it as a TTB element.

Further models of boundaries with yet other PCs participating in addition to those demonstrated in Figures 2a and 2c are shown in Figure 4. The ReO_3 structures to the left and to the right of a PC are twin related by reflection or glide. Whereas the boundaries in Figures 4a–c are made up of triangle linked PCs (for nomenclature see [3]), those in Figures 4d and 4e contain isolated PCs. PTs are formed at all boundaries except the one in Figure 4a. So far none of the structures shown in Figures 4a–d has been reported, while the one shown in Figure 4e has been found as a defect in the Nb_2O_5/WO_3 system.[10]

Before concluding this section some remarks should be

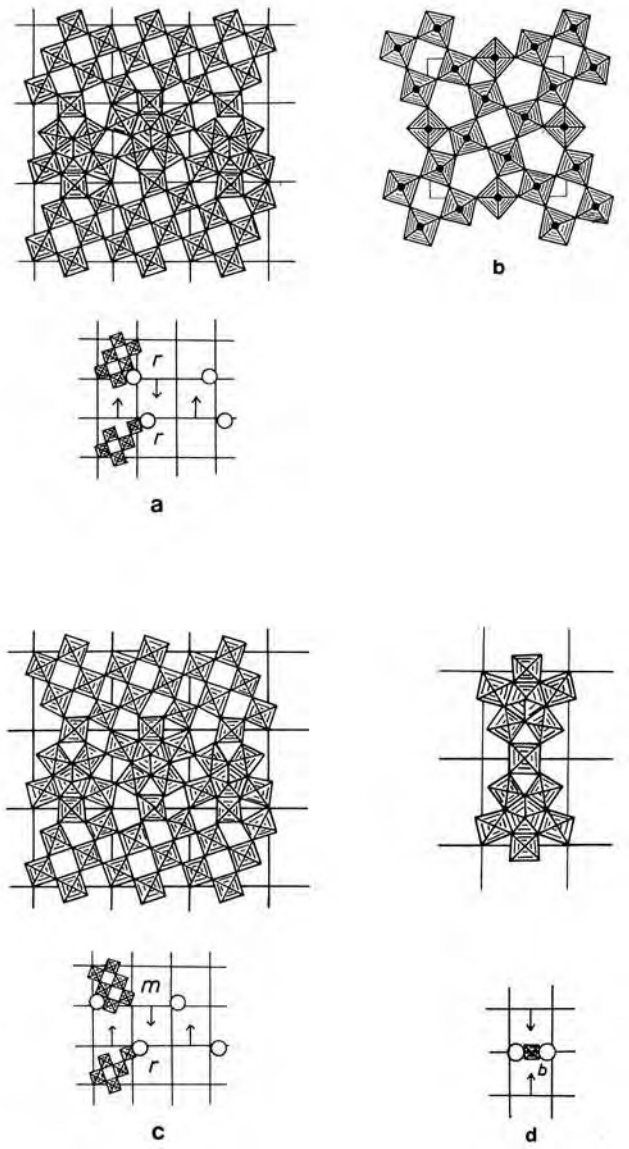


Fig. 2. a) Intergrown structures of the $LiNb_6O_{15}F$- and ReO_3-type. Below a schematic representation is given, where the rings denote pentagonal tunnels. The orientation of the ReO_3 net is the same throughout (r or m). b) A structure model of an empty, tetragonal tungsten bronze projected along the c-axis. c) As a), but with twin-related ReO_3 nets indicated by r and m; d) two PCs joined through triangle links to one octahedron whose orientation is b.

made about the structures of $LiNb_6O_{15}F$[8] (Fig. 5a) and $NaNb_6O_{15}F$[14] (Fig. 5b). In both types of structure the top of one PC is linked to the bottom of another, resulting in

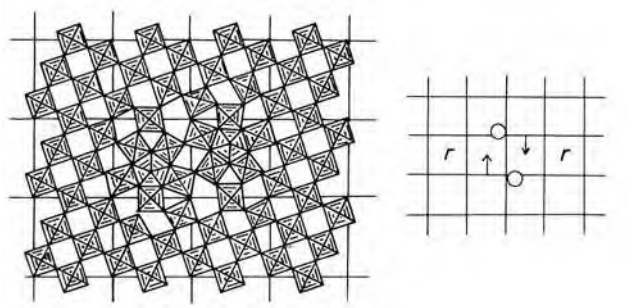


Fig. 3. A unit cell of $LiNb_6O_{15}F$ in a matrix of ReO_3 type in r orientation.

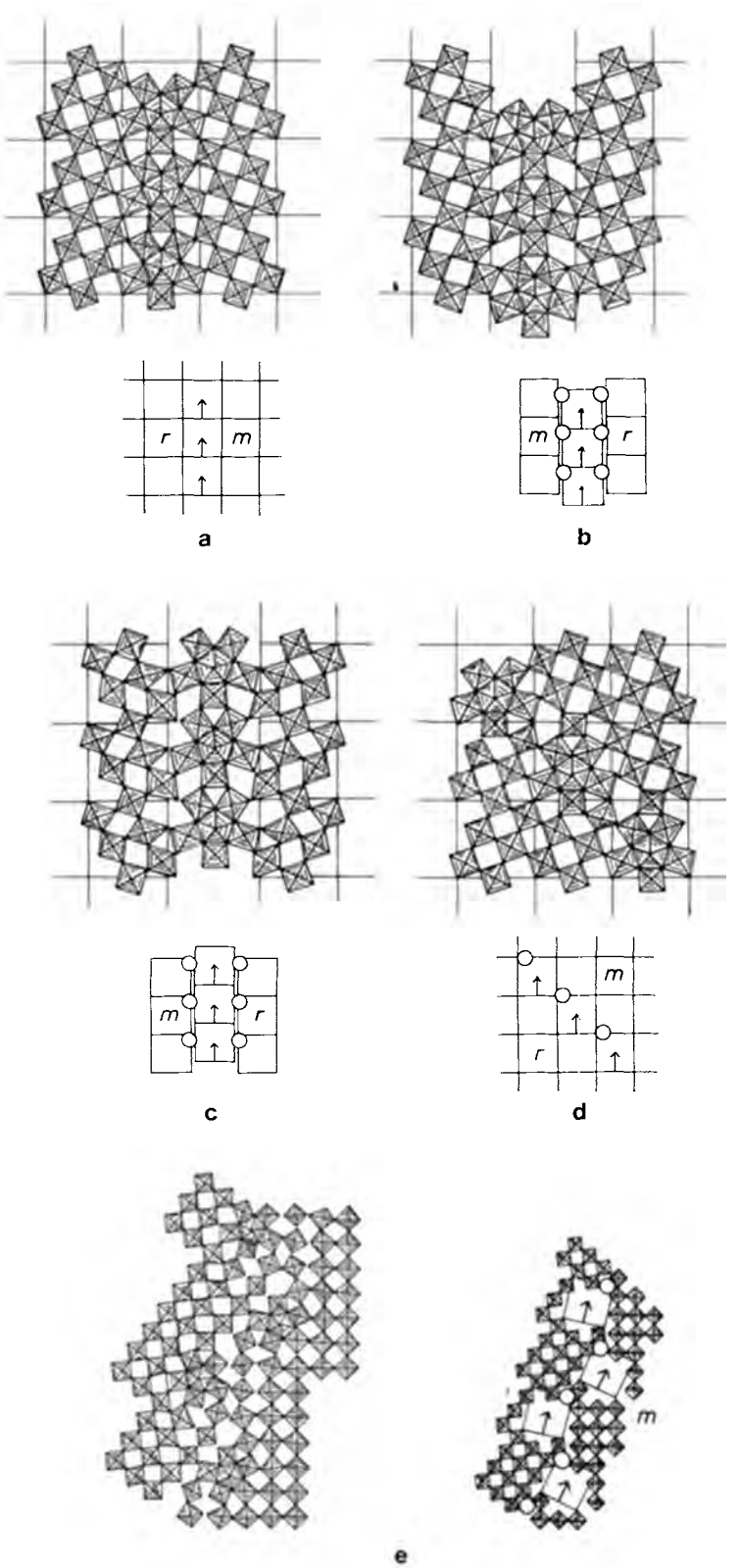


Fig. 4. Models of twin-related ReO_3-type structures with PCs. a)-c) PCs joined by triangle links; d) and e) show discrete PCs. A defect observed in $4\,Nb_2O_5 \cdot 22\,WO_3$ is shown in e).

straight slabs of triangle-linked PCs. In $LiNb_6O_{15}F$ the right edge of a square in such a slab is linked to the right edge of a square in another slab, the two slabs being antiparallel. The latter are linked among themselves in a diamond-like fashion. The idealized orthorhombic unit cell has the cell parameters[4]

$$a = 4a_R - 2c_R, \quad b = b_R \quad \text{and} \quad c = a_R + 2c_R$$

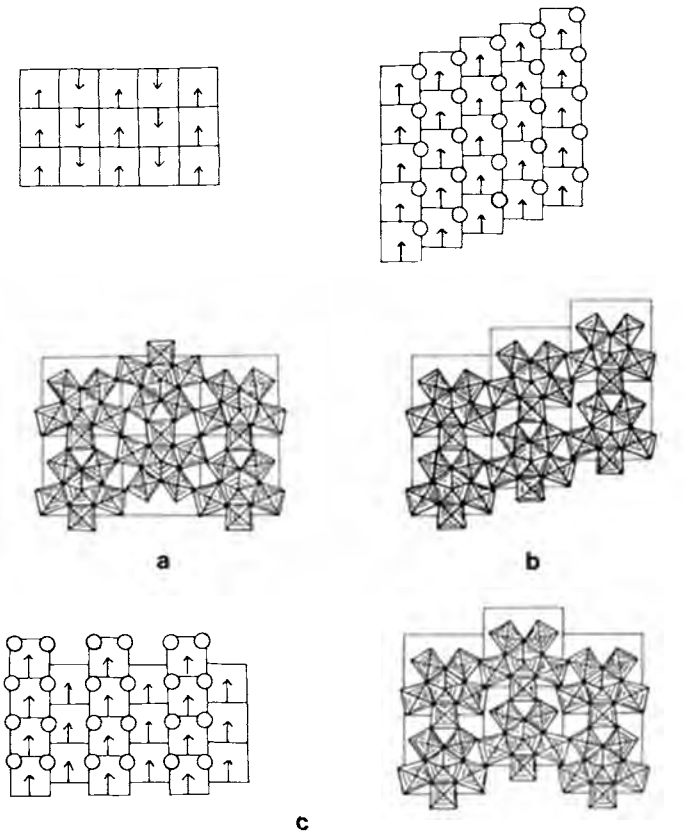


Fig. 5. Models of framework structures of a) $LiNb_6O_{15}F$, b) $NaNb_6O_{15}F$, and c) hypothetical AM_6X_{16}. Rings denote pentagonal tunnels.

(The subscript R denotes vectors of the ReO_3 subcell.) In $NaNb_6O_{15}F$ the slabs are parallel but displaced by a third of a square edge and the PCs thereby joined via a triangle link. The slabs are arranged in an abcabc... sequence. The cell parameters of the idealized monoclinic unit cell are

$$a = a_R, \quad b = 2(2/3)b_R + 1/3\,c_R \quad \text{and} \quad c = 2/3\,b_R - 3(2/3)c_R$$

In the real structure, however, the PCs are so assembled that orthorhombic symmetry is observed. It is obvious that an abab... arrangement should be possible (Fig. 5c); however, an example of such a structure has not yet been reported. The actual axial ratios are given in Table 1 and are commented on in Section 3.

3. Illustrating Structures with Pentagonal Columns

The present state of our knowledge of PCs and the ReO_3-type structure allows us to model PC-containing structures by means of the symbolism described above. We simply put together the symbols for PCs and octahedra in *m*-, *r*- or *b*-orientation. No attempt will be made to adjust the structures so as to make the polyhedra fit together properly. In most cases the adjustment needed would be

small. (When preparing the figures in this paper a template of a PC was often used. The fit between PCs or between a PC and an octahedron may therefore not always be perfect. In Figures 4e, 5b and 5c, for instance, the tunnels with a pentagonal cross-section are made up of octahedra with common corners. The actual, small misfit is in a way a measure of the adaptability of the PC to various surroundings.)

Let us now survey the structures according to the number N of octahedra per unit cell that are not part of a PC, and relate this to the number of PCs present. Let M be the number of metal atoms and P the number of PCs per unit cell. With six metal atoms in an ordinary PC, there are then $M-6P$ non-PC octahedra and $N=(M-6P)/P$ non-PC octahedra per unit cell. $M-P$ is the total number of octahedra per unit cell.

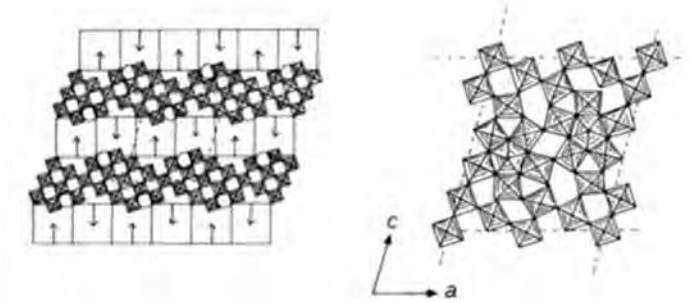


Fig. 6. Structure models of $W_{12}O_{34}$.

Figure 6 shows a model of the structure of $W_{12}O_{34}$.[11] With $M=24$ and $P=2$, N equals 6. The ideal structure has the cell parameters

$$a=4a_R+2c_R,\quad b=b_R\quad\text{and}\quad c=-a_R+5c_R$$

It can be regarded as an ordered intergrowth of structures of the $LiNb_6O_{15}F$- and ReO_3-type.[3] The structures of $4\,Nb_2O_5\cdot 50\,WO_3$, $N=23$, and $4\,Nb_2O_5\cdot 22\,WO_3$, $N=9$, are built analogously, as is immediately obvious from similarities in the unit cell parameters (see Table 1). All non-PC octahedra have the same orientation. The idealized unit cell parameters are[10]

$$a=12a_R-4c_R\quad\text{or}\quad 6a_R-2c_R,\quad b=b_R\quad\text{and}\quad c=2a_R+4c_R$$

Figures 7 and 8 show models of the structures of $2\,Nb_2O_5\cdot 7\,WO_3$, $N=5$,[15,16] and Mo_5O_{14}, $N=4$,[17] respectively. In both models non-PC octahedra are present in roughly two distinct orientations (r and m). Both structures have tetragonal symmetry and contain areas of TTB type, i.e. regions of a TTB unit cell with empty square and pentagonal tunnels. The structure of $2\,Nb_2O_5\cdot 7\,WO_3$ is an ordered intergrowth of structures of $LiNb_6O_{15}F$, ReO_3, and (empty) TTB. Its idealized unit cell parameters are[15]

$$a=6a_R+2b_R,\quad b=-2a_R+6b_R\quad\text{and}\quad c=c_R$$

The structure of Mo_5O_{14} also contains empty units of TTB, related to each other through a mirror plane. In the

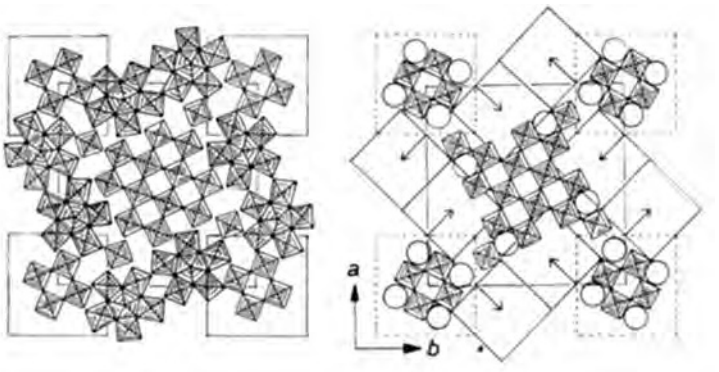


Fig. 7. Structure models of $2\,Nb_2O_5\cdot 7\,WO_3$. Note the areas of TTB structure type at the corners of the projected tetragonal unit cell.

idealized structure, the angle between the units is 2 arctg 1/2. The idealized unit cell has the lattice constants (cf. [4])

$a=6a_p$, $b=6b_p$ and $c=c_p$

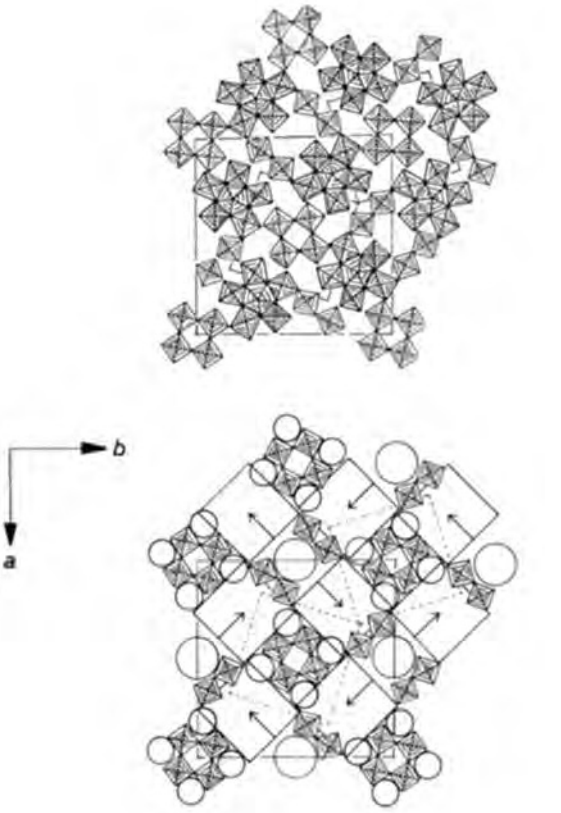


Fig. 8. Structure models of Mo_5O_{14}. Note the areas of TTB structure type at the corners and center of the projected tetragonal unit cell, and the diamond-like linked octahedra at the top of the PCs.

Note the large six-sided tunnels in Mo_5O_{14}.

In $W_{18}O_{49}$, $N=3$[1] (Fig. 9) all non-PC octahedra have the same orientation. According to the model, the structure can be described as built of slices; that is, of ordered intergrowths of the $LiNb_6O_{15}F$- and ReO_3-type structures. The slices are parallel to (100) of $W_{18}O_{49}$; the width of one slice is two squares or PCs. Between the slices, which are held together by edge-linked PCs, there are large, six-sided

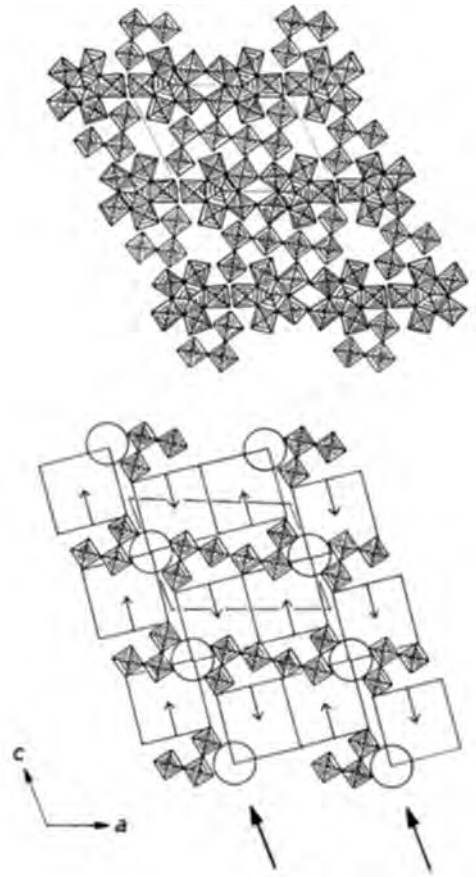


Fig. 9. Structure models of $W_{18}O_{49}$. The arrows (at the bottom) mark the width of a slice, which is made up of an $LiNb_6O_{15}F$-type structure intergrown with WO_3. The slices are parallel to (100). There are large, empty, six-sided tunnels running in the [010]-direction. The slices are held together by PCs united through edge links at the corners of the projected unit cell.

holes. The idealized monoclinic unit cell has the parameters

$$a = 5a_R + c_R, \quad b = b_R \quad \text{and} \quad c = -2a_R + 3c_R$$

In $Mo_{17}O_{47}$, $N = 2.5$[18,19] (Fig. 10), the non-PC octahedra are present in three orientations *m*, *b* and *r*. As in $W_{18}O_{49}$ the structure is built of slices parallel to (010) of $Mo_{17}O_{47}$, the slices being an ordered arrangement of PCs and MoO_6 octahedra. The width of a slice is one PC. Between the slices there are seven-sided holes; the slices are held together by edge-linked PCs. The idealized orthorhombic unit cell has the parameters

$$a = 4a_R + 4b_R, \quad b = -4a_R + 4b_R \quad \text{and} \quad c = c_R$$

Figure 11 shows a model of $Nb_8W_9O_{47}$, $N = 2.5$.[20] It is built of units of the type already discussed in Section 2 (Fig. 2d): two PCs are linked by a common MO_6 octahedron. These double PCs are then joined to each other in a diamond-like fashion. The result is a zig-zag arrangement of PCs forming slices which run parallel to (010). Between the slices there are further pentagonal holes and non-PC octahedra in *r*- and *m*-orientations. The idealized orthorhombic unit cell has[4]

$$a = 3a_R - b_R, \quad b = 3(a_R + 3b_R), \quad \text{and} \quad c = c_R$$

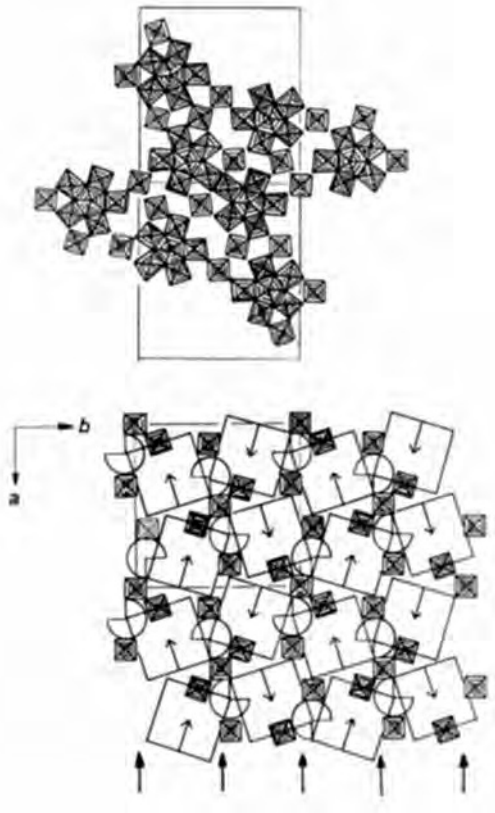


Fig. 10. Structure models of $Mo_{17}O_{47}$. The arrows (at the bottom) mark the width of a slice made up of PCs and MoO_6 octahedra. The slices are parallel to (010). Between them are seven-sided tunnels running in the [001]-direction. The slices are held together by PCs united through edge links at the midpoints of the *a* and *b* axes of the projected unit cell.

$Na_7Nb_{15}W_{13}O_{80}$, $N = 1$,[21] (Fig. 12a) is built of straight slabs consisting of PCs joined by a triangle link, just the same as in $LiNb_6O_{15}F$ and $NaNb_6O_{15}F$. The structure is

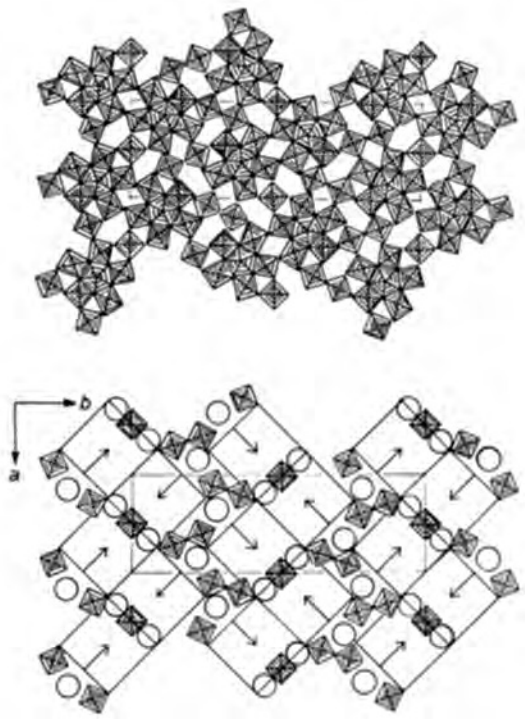


Fig. 11. Structure models of $4\,Nb_2O_5 \cdot 9\,WO_3$. Note the occurrence of two PCs united by triangle links to the same octahedron (cf. Fig. 2d).

analogous to that of lithium niobate; adjacent slabs are antiparallel. Non-PC octahedra in *r*- and *m*-orientation link the slices to each other. Between the slices tunnels with S-shaped cross-section are created, in which the sodium atoms are accomodated. A model commensurate with the ReO_3-type structure can be shown to have orthorhombic symmetry with

$$a = 6(4/5\,a_R + 2/5\,c_R), \quad b = 2(a_R + 2\,b_R), \quad \text{and} \quad c = c_R$$

Figure 12b shows a HREM image of the crystal structure of the isotypic potassium compound. The PCs are clearly recognizable, whereas the potassium atoms in the tunnels are hardly discernible.

Figure 13 surveys the various arrangements of PCs and MX_6 octahedra in the structures discussed in this section. Note that each PC is associated with N non-PC octahedra whose orientation may be *r*, *m* or *b*. In our description of the structures we find with one exception that the top part of a PC is triangle-linked either to an octahedron of another PC, as in Figures 5a and 12a, or to a non-PC octahedron. The exceptional case is the Mo_5O_{14} structure, where the top of a PC forms a diamond-like link with two non-PC octahedra (Fig. 8). The rest of the PC is bonded to four other non-PC octahedra by triangle links (Fig. 13e). This results in a structure with PCs completely separated from each other—a unique feature of the Mo_5O_{14} crystal structure. Similarly isolated PCs have been observed as defects (see Fig. 4e).

Table 1 lists some calculated cell parameters as a function of d together with the respective values observed in real structures. In order to compare these values the calculated and observed ratios of the parameters are also given. Note that in the structures discussed here there is always an observed short axis (3.8 to 3.9 Å) which corresponds to a diagonal in an MX_6 octahedron. The observed ratios are in most cases lower than the calculated ones. In general, however, the agreement seems fairly good; the largest deviations are found for $Mo_{17}O_{47}$ (*b* axis), $W_{18}O_{49}$ (*a* axis), $LiNb_6O_{15}F$ (*a* axis), and Nb_2WO_8 (*c* axis). The first and second structures are special cases in the sense that they contain edge-linked PCs with a short M–M bond across the common octahedron edge. This is likely to shorten the *a* axis of $W_{18}O_{49}$, in which the W–W bonds are parallel to this axis. The same is true in the case of $Mo_{17}O_{47}$, although the Mo–Mo bond is not quite parallel to the *b* axis. (Note also that the calculated unit cell volume (Table 1) is greater than $(M-P)d^3$ for these two compounds (see below).) As regards $LiNb_6O_{15}F$, the *a* axis is shorter than the corresponding distance in an ReO_3 structure, implying a more dense atomic arrangement and an ensuing stable configuration of the PC.

In our discussion of the geometric properties of a PC we have assumed that the volume of five octahedra and a pentagonal bipyramid equals that of five octahedra of an ReO_3-type structure (cf. Figs. 1c,d). We may now test the validity of this assumption in the following way: Given a real structure composed of PCs only or PCs and ReO_3-type units, we want to consider an average MX_3 unit cell of ReO_3 type whose volume is V_{av}. This is accomplished by dividing the unit cell volume (V) of the real structure by

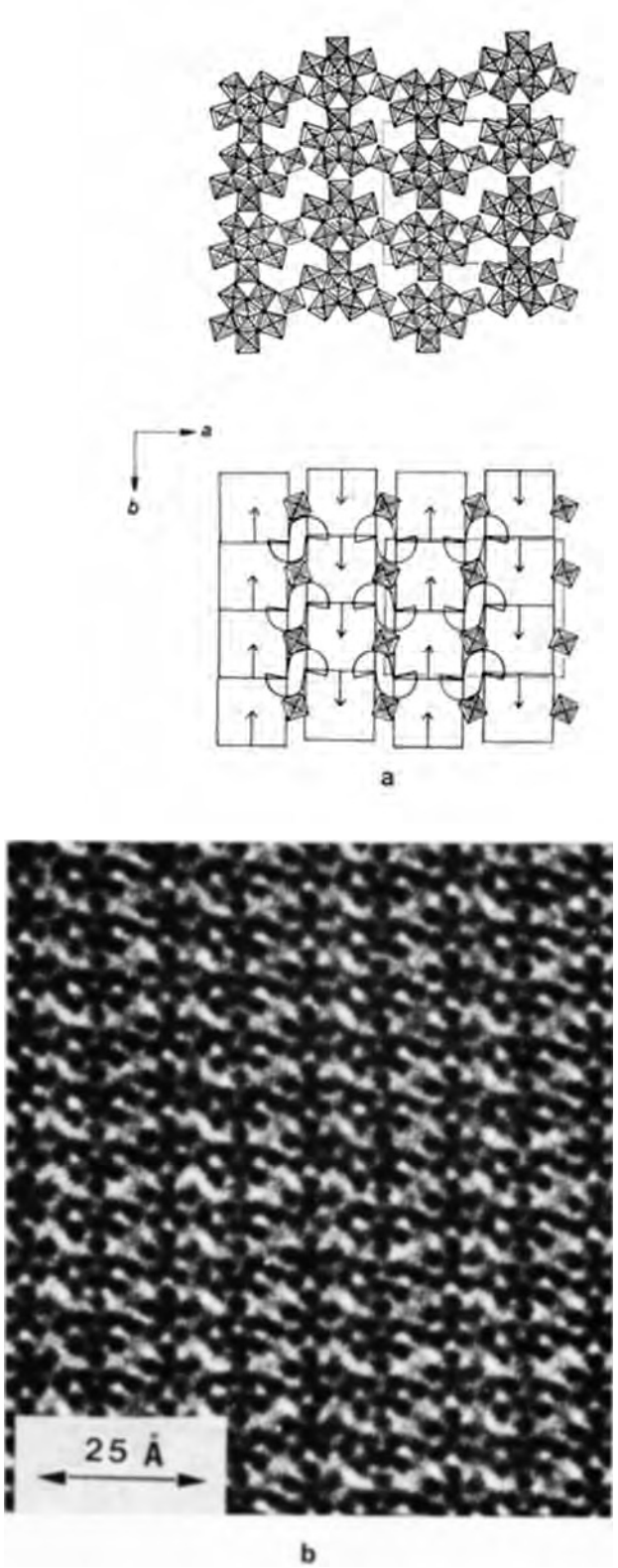


Fig. 12. a) Structure models of $Na_7Nb_{15}W_{13}O_{80}$ (sodium atoms not shown). b) HREM image of a thin crystallite of a potassium compound, isotypic with $Na_7Nb_{15}W_{13}O_{80}$. JEOL JEM 200CX microscope, accelerating voltage 200 kV, defocus ≈ -500 Å, objective-aperture 0.42 Å^{-1}. The electron beam is parallel to the (short) *c* axis.

the number M of M atoms in the unit cell, excluding those in the center of the pentagonal bipyramids. With the symbols used above this gives $V_{av} = V/(M-P)$ which has been listed in Table 1. The V_{av} values range from 54.6 Å^3 ($W_{18}O_{49}$) to 63.7 Å^3 ($Na_7Nb_{15}W_{13}O_{80}$). The values should

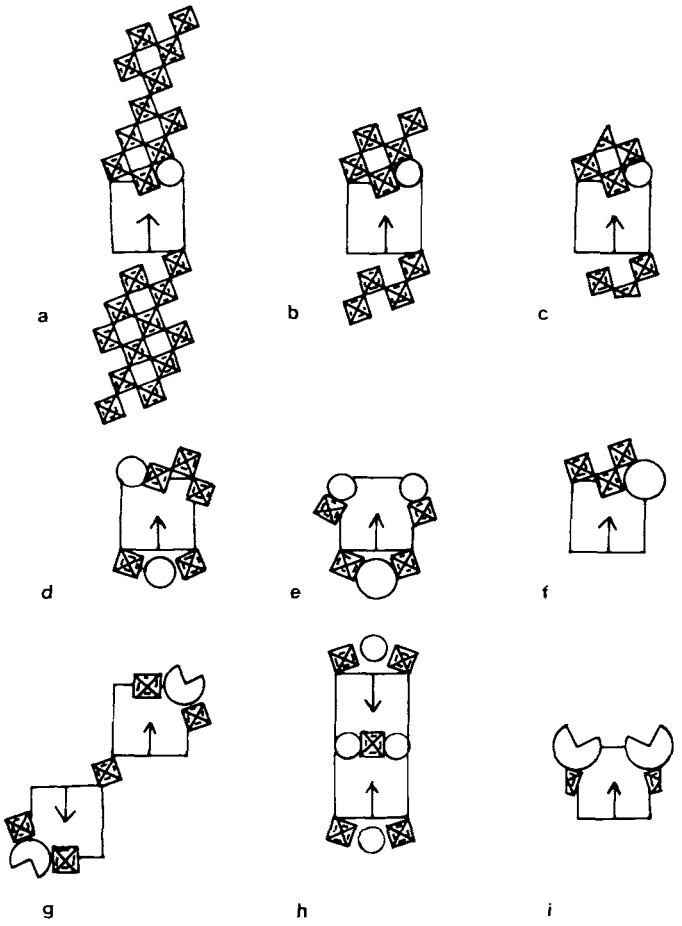


Fig. 13. Survey of structure units involved in some PC-containing compounds: a) $4Nb_2O_5 \cdot 50WO_3$; b) $4Nb_2O_5 \cdot 22WO_3$; c) $W_{12}O_{34}$; d) $2Nb_2O_5 \cdot 7WO_3$; e) Mo_5O_{14}; f) $W_{18}O_{49}$; g) $Mo_{17}O_{47}$; h) $4Nb_2O_5 \cdot 9WO_3$; i) $Na_7Nb_{15}W_{13}O_{80}$. Small rings denote pentagonal tunnels and large rings six-sided tunnels. A three-quarter ring denotes a seven-sided tunnel in g) and part of an S-shaped tunnel in i).

be compared with the corresponding unit cell volumes of ReO_3 type, or related structures. Thus, the larger niobium atom in NbO_2F and $NaNbO_3$ leads to volumes of 59.4 Å^3 and 59.5 Å^3 ($V/8$), respectively, while the smaller tungsten atom in WO_3 results in $V/4 = 52.8$ Å^3.[22, 23, 16] The deviating structure is $Na_7Nb_{15}W_{13}O_{80}$. It contains tunnels with S-shaped cross-section, which apparently make the structure quite spacious.

4. Some Defects in Structures with Pentagonal Columns

This section deals with some structural defects reported to exist in some of the compounds discussed above. Thus, Figure 14 shows domains of $2Nb_2O_5 \cdot 7WO_3$ separated by a domain containing unit cells of $4Nb_2O_5 \cdot 9WO_3$.[15] Note the six PCs arranged as in the $LiNb_6O_{15}F$ structure that traverse the domain in between, starting and ending in the domains of $2Nb_2O_5 \cdot 7WO_3$, virtually keeping them together.

Some interesting defects have been observed in $W_{18}O_{49}$.[24, 25] Figure 15a shows a model of a defect parallel to (100) in $W_{18}O_{49}$. The ordinary diamond-like link between two PCs has been replaced by a corner link at the same time as two further octahedra have been introduced into the structure. Figure 15b shows a model of an expanded defect of the same type. The latter is from a slightly oxidized sample of $W_{18}O_{49}$, as is also the defect illustrated in Figure 16. Its stoichiometry is W_9O_{25}, with Z (the number of formula units) = 2 and N (defined above) = 3, intergrown with $W_{18}O_{49}$. The W_9O_{25} structure can be regarded as an ordered intergrowth of the $LiNb_6O_{15}F$- and the ReO_3-type structures (similarly to the structure of $W_{12}O_{34}$). Figure 16 clearly demonstrates that there exists a CS relationship between W_9O_{25} and $W_{18}O_{49}$, the CS proc-

Table 1. Calculated and observed unit cell parameters in some copounds M_mX_n containing pentagonal columns (PCs).

Z = Number of formula units per unit cell
M = Number of metal atoms per unit cell
P = Number of PCs per unit cell
$M-P$ = Number of octahedra per unit cell
N = Number of non-PC octahedra per unit cell
V = Volume of a unit cell
d = Length of an octahedron diagonal
V_{av} = Average volume of a unit cell of ReO_3 type
N = $(M-6P)/P$; $V_{av} = V/(M-P)$

X/M	Compound Z $M-P$	N	Lattice constants calcd	found	Axial ratios calcd	found	V_{av} [Å^3]	Fig.	Ref.
2.931	$4Nb_2O_5 \cdot 5WO_3$	23	$a = 4\sqrt{10}\,d$	48.02 Å	12.65	12.6	55	2a, 13a	[10]
	1		$b = d$	3.8 Å	1	1			
	56		$c = 2\sqrt{5}\,d$	16.99 Å	4.47	4.5			
			$\beta = 98.13°$	98.13°					
			$V = 56d^3$	$3.07 \cdot 10^3$ Å^3					
2.867	$4Nb_2O_5 \cdot 22WO_3$	9	$a = 2\sqrt{10}\,d$	24.01 Å	6.32	6.3	55	2a, 13b	[10]
	1		$b = d$	3.8 Å	1	1			
	28		$c = 2\sqrt{5}\,d$	16.99 Å	4.47	4.5			
			$\beta = 98.13°$	98.13°					
			$V = 28d^3$	$1.53 \cdot 10^3$ Å^3					
2.833	$W_{12}O_{34}$	6	$a = 2\sqrt{5}\,d$	17.1 Å,	4.47	4.5	55	6, 13c,	[11]
	2		$b = d$	3.8 Å	1	1		18a	
	22		$c = \sqrt{26}\,d$	19.2 Å	5.10	5.0			
			$\beta = 105.25°$	105.5°					
			$V = 22d^3$	$1.20 \cdot 10^3$ Å^3					

Table 1 (continued).

X/M	Compound Z M−P	N	Lattice constants calcd	found	Axial ratios calcd	found	V_{at} [Å^3]	Fig.	Ref.
2.818	$2Nb_2O_5 \cdot 7WO_3$ 4 40	5	$a = 2\sqrt{10}\,d$ $b = 2\sqrt{10}\,d$ $c = d$ $V = 40d^3$	24.264 Å 24.264 Å 3.924 Å $2.310 \cdot 10^3$ Å^3	6.32 6.32 1	6.18 6.18 1	57.76	7, 13d, 14	[15, 16]
2.800	Mo_5O_{14} 8 (subcell) 36	5	$a = 6d$ $b = 6d$ $c = d$ $V = 36d^3$	23.00 Å 23.00 Å 3.937 Å $2.082 \cdot 10^3$ Å^3	6.00 6.00 1	5.84 5.84 1	57.85	8, 13e	[17]
2.778	W_9O_{25} 2 16	3	$a = 2\sqrt{5}\,d$ $b = d$ $c = \sqrt{13}\,d$ $\beta = 97.12°$ $V = 16d^3$	[a]	4.47 1 3.61			16, 18b	[25]
2.722	$W_{18}O_{49}$ 1 16	3	$a = \sqrt{26}\,d$ $b = d$ $c = \sqrt{13}\,d$ $\beta = 112.38°$ $V = 17d^3$	18.28 Å 3.775 Å 13.98 Å 115.14° $8.733 \cdot 10^2$ Å^3	5.10 1 3.61	4.82 1 3.70	54.58	9, 13f, 15, 16	[1]
2.778	Mo_9O_{25} 4 32	3	$a = 4\sqrt{2}\,d$ $b = 4\sqrt{2}\,d$ $c = d$ $V = 32d^3$	[b]	5.66 5.66 1			17	
2.765	$Mo_{17}O_{47}$ 2 30	2.5	$a = 4\sqrt{2}\,d$ $b = 4\sqrt{2}\,d$ $c = d$ $V = 32d^3$	21.61 Å 19.63 Å 3.951 Å $1.676 \cdot 10^3$ Å^3	5.66 5.66 1	5.47 4.97 1	55.87	10, 13g, 17	[18, 19]
2.765	$4Nb_2O_5 \cdot 9WO_3$ 2 30	2.5	$a = \sqrt{10}\,d$ $b = 3\sqrt{10}\,d$ $c = d$ $V = 30d^3$	12.251 Å 36.621 Å 3.94 Å $1.768 \cdot 10^3$ Å^3	3.16 9.49 1	3.11 9.29 1	58.9	11, 13h, 14	[20]
2.857	$Na_7Nb_{15}W_{13}O_{80}$ 1 24	1	$a = (12/\sqrt{5})d$ $b = 2\sqrt{5}\,d$ $c = d$ $V = 24d^3$	21.962 Å 17.763 Å 3.9165 Å $1.528 \cdot 10^3$ Å^3	5.37 4.47 1	5.61 4.53 1	63.66	12, 13i	[21, 33]
2.667	Nb_2WO_8 8 20	0	$a = d$ $b = 2\sqrt{5}\,d$ $c = 2\sqrt{5}\,d$ $V = 20d^3$	3.946 Å 17.616 Å 16.617 Å $1.155 \cdot 10^3$ Å^3	1 4.47 4.47	1 4.46 4.21	57.75		[9]
2.667	$LiNb_6O_{15}F$ 2 10	0	$a = 2\sqrt{5}\,d$ $b = d$ $c = \sqrt{5}\,d$ $V = 10d^3$	16.635 Å 3.964 Å 8.888 Å $5.861 \cdot 10^2$ Å^3	4.47 1 2.24	4.20 1 2.24	58.61	1b, 2a, 3, 5a, 21a	[8]
2.667	$NaNb_6O_{15}F$ 2 10	0	$a = d$ $b = (1/3)\sqrt{65}\,d$ $c = (5/3)\sqrt{5}\,d$ $\alpha = 93.18°$ $V = 10d^3$	3.949 Å 10.192 Å 14.721 Å $\pi/2$ $5.925 \cdot 10^2$ Å^3	1 2.69 3.73	1 2.58 3.73	59.25	5b, 21b	[14]
2.667	AM_6X_{16} 2 10	0	$a = d$ $b = 2\sqrt{5}\,d$ $c = \sqrt{5}\,d$ $V = 10d^3$	[c]	1 4.47 2.24			5c	

[a] Observed as a structure defect in slightly oxidized $W_{18}O_{49}$. [b] Hypothetical structure related to $Mo_{17}O_{47}$. [c] Hypothetical structure, cf. $LiNb_6O_{15}F$.

ess taking place parallel to the (100) plane of $W_{18}O_{49}$. The W_9O_{25} structure contains two pentagonal tunnels. They are formed by octahedra, two of which are shared between the two tunnels.

The $Mo_{17}O_{47}$ structure might be discussed from a similar point of view. We must then assume a hypothetical structure of the kind shown in Figure 17a. Its stoichiometry is Mo_9O_{25}, $Z=4$ and $N=3$; the unit cell is indicated (broken lines). Due to a CS process the following "reaction" takes place:

$$Mo_{36}O_{100} = Mo_{34}O_{94} + 2\,MoO_3$$

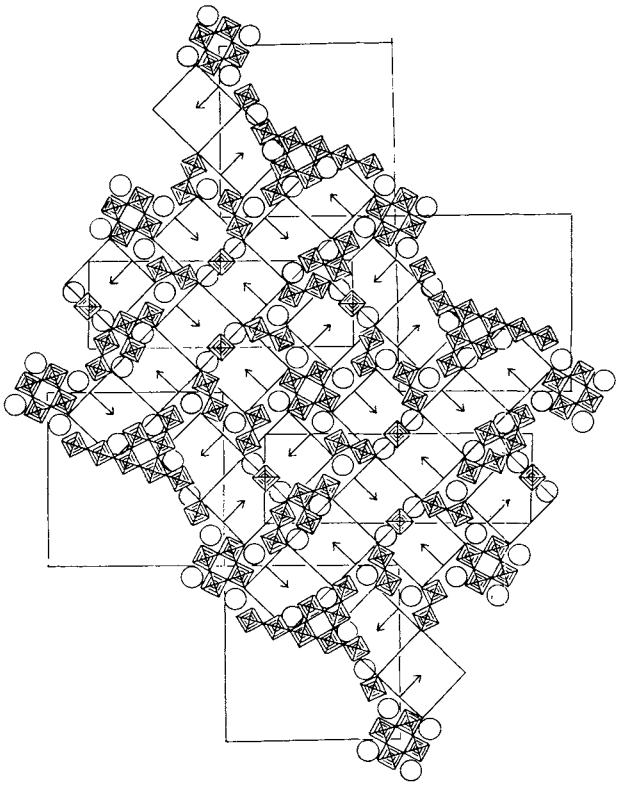


Fig. 14. Model of two domains (upper right and lower left) of $2\,Nb_2O_5 \cdot 7\,WO_3$ (see Fig. 7), in phase with each other but separated by a boundary of $4\,Nb_2O_5 \cdot 9\,WO_3$ unit cells (see Fig. 11). After the interpretation given in [15].

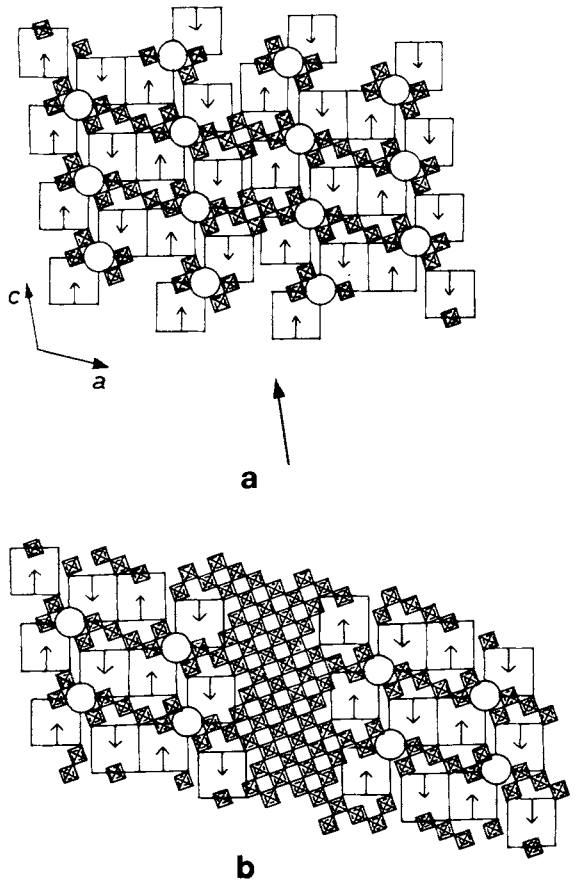


Fig. 15. a) Model of a defect (indicated by an arrow below the figure) parallel with (100) in $W_{18}O_{49}$ (cf. Fig. 9); b) Model of a wider defect of WO_3 type in $W_{18}O_{49}$. The defect is of the same kind as that shown in Fig. 15a.

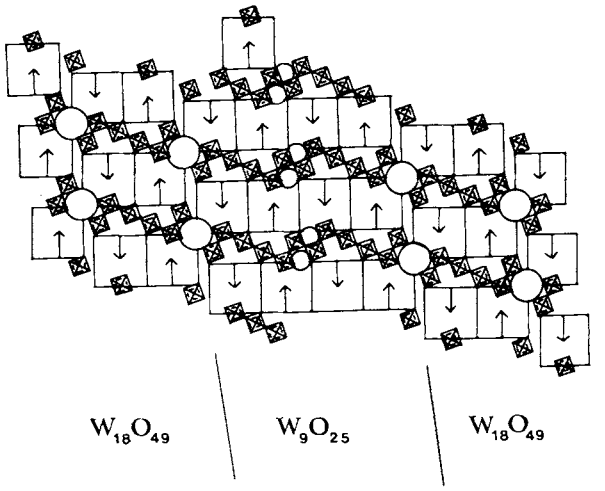


Fig. 16. Model of a structural defect in slightly oxidized $W_{18}O_{49}$. It shows an intergrowth of W_9O_{25} (in the center of the model) and $W_{18}O_{49}$. Note the pentagonal tunnels with two common octahedra in the W_9O_{25} structure.

The structural changes are modeled in Figure 17b. *Hyde* et al.[26] discuss a similar process when relating Mo_5O_{14} to $Mo_{17}O_{47}$.

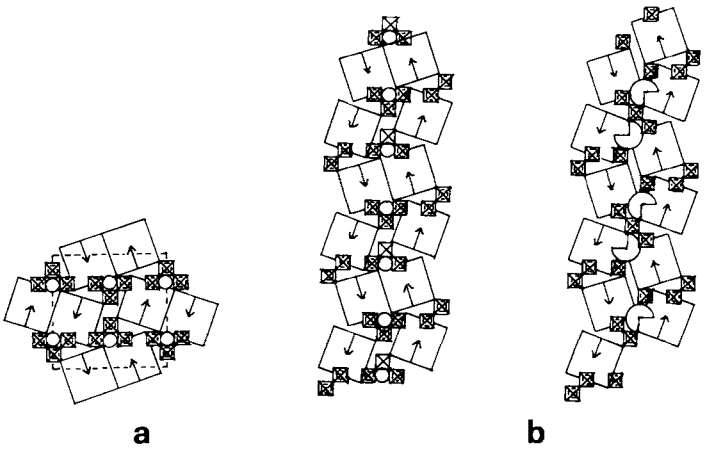


Fig. 17. a) Model of the hypothetical structure Mo_9O_{25}; b) a CS process converts the hypothetical Mo_9O_{25} (left) into $Mo_{17}O_{47}$ (right). The non-striated octahedra (left) are eliminated in the process.

5. Intergrowth of Pentagonal Columns with the ReO_3-Type Structure

It is apparent that two main structure types can be conceived when we consider the possibilities of intergrowths between PCs and the ReO_3-type structure. The first one has PCs joined by a triangle link in the direction of the arrow used in our symbolism. These slabs of PCs are straight and may be regularly interspersed with octahedra. We may interpret the structure of $Na_7Nb_{15}W_{13}O_{80}$[21] with $N=1$ in this way. Similar structures with $N>1$ can easily be imagined.

The second type of structure can be formed by joining slabs of PCs joined through a diamond-like link perpendicular to the direction of the arrow. MO_6 octahedra forming an ReO_3-type net may be regularly interspersed be-

tween these corrugated slabs.[3] This arrangement is found, e.g., in the structures of $W_{12}O_{34}$ and W_9O_{25}.

It is interesting to note that again two types of structures are possible, depending on the mutual arrangement of the slabs. When we project one slab onto a neighboring one in a direction parallel to an arrow we find that there is a more or less exact overlap of PCs (Figs. 18a, b). The emerging structure type depends on whether parallel or antiparallel PCs show the best overlap. Thus, in $4\,Nb_2O_5 \cdot 22\,WO_3$ and in the W_9O_{25} defects found in $W_{18}O_{49}$ parallel PCs overlap best, while in $4\,Nb_2O_5 \cdot 50\,WO_3$ and $W_{12}O_{34}$ the antiparallel PCs exhibit this feature. A special case is found in structures with $N=5$. Here the overlap is complete (see Figs. 18c, d). Further structural possibilities arise if *r*, *m* and *b* octahedra are included between the slabs (Fig. 19). Note the topological relationship with the TTB structure (Fig. 19b, bottom).

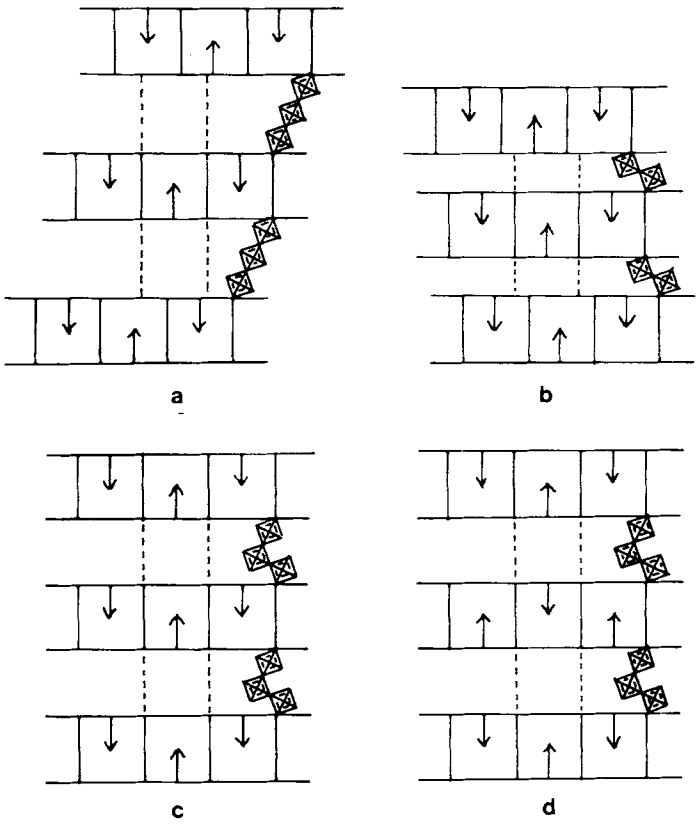


Fig. 18. Models of structures of a) $W_{12}O_{34}$ and b) W_9O_{25}. Indicated projections show best overlap of antiparallel PCs in a), while best overlap of parallel PCs is the case in b). Models of structures with $N=5$ with complete overlap of parallel PCs in c) and of antiparallel PCs in d).

The following observations are noteworthy: Given an intergrowth structure with parallel PCs overlapping, we may gradually decrease the value of N until we get the limiting structure which is that of the $LiNb_6O_{15}F$-type with $N=0$ (cf. Fig. 5a). An intergrowth with antiparallel PCs will give a limiting structure characterized by two PCs having one octahedron in common. So far, such an arrangement has not been reported, but PCs with two octahedra common with two other PCs have been found in $TlNb_7O_{18}$[27] and the isotypic rubidium compound.[28] Structure models are shown in Figure 20.

In concluding this section on intergrowth structures mention should be made of the possibilities of obtaining structures from the hypothetical Mo_9O_{25} structure discussed above (Fig. 17a). Further MoO_6 octahedra may be inserted into the structure, thereby increasing the value of N. No such structures seem to have been reported, however.

6. Some Remarks on the Formation of Pentagonal Columns

In this survey of models of ordered structures and defect structures we note that PCs may exist as isolated entities (Fig. 4e) or, as in Mo_5O_{14} (Fig. 8), surrounded by ReO_3-type elements. More common is the case, however, where PCs are coupled to each other by diamond-like, triangle or

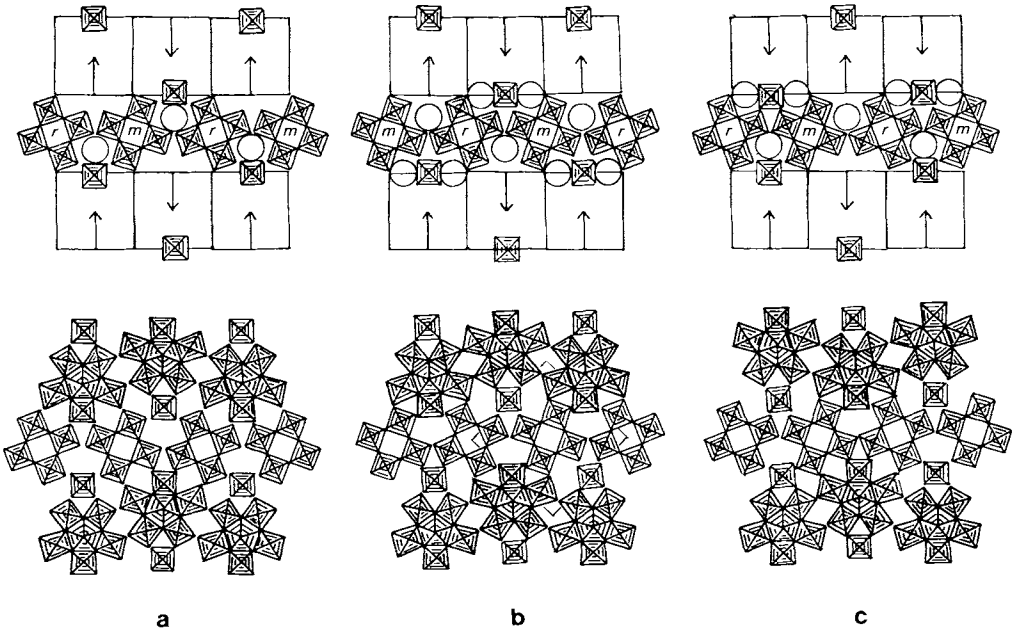


Fig. 19. a)-c), top: Models of structures with symbolic PCs; $N=5$. Note the twin planes running parallel to the arrows and perpendicular to the plane of the paper. The rings denote pentagonal tunnels. a)-c), bottom: Detailed structural models of the three structures shown at the top. Note the TTB type structure in b) (indicated by a unit cell).

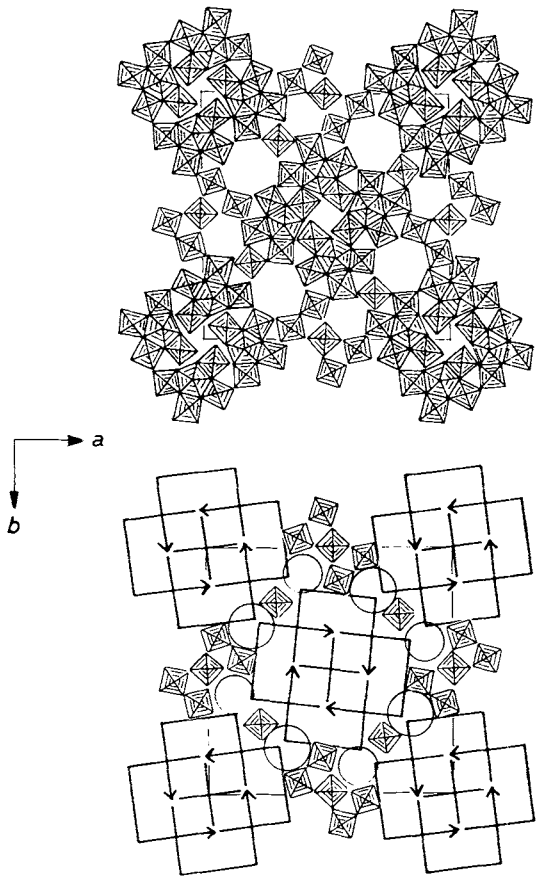


Fig. 20. Structure models of $TlNb_7O_{18}$. Note the ensembles of four PCs with common octahedra and the occurrence of six- and seven-sided tunnels in the structure.

edge links. As regards the formation of structures of this kind, it seems likely that a crystal grows in a matrix of composition MX_{3-x} to form an ReO_3-type structure with occasional dislocations in the form of PCs (and/or CS structures).[6, 29] Actually, a PC seems to be a very stable configuration of metal atoms and anions X. Due to its geometry, it is capable of attaching to itself other PCs or smaller or larger parts of an ReO_3-type structure, depending on the overall stoichiometry of the reactants. In the process, defects or ordered structures are created. In this connection it should be pointed out that the structures of $LiNb_6O_{15}F$ and $NaNb_6O_{15}F$ are examples of twinning on the unit cell level.[30] In Figure 21a a ReO_3-type structure is regularly repeated on $(2\bar{1}0)_R$. The twin blocks are $2.5d$ wide, measured along $[100]_R$. The resulting $LiNb_6O_{15}F$-type framework structure can then be symbolically written as

2.5, 2.5, 2.5, 2.5, ...

with a repeat distance of $5d$.

The structure of $NaNb_6O_{15}F$ can be derived analogously (Fig. 21b). Here the twin blocks are different, and the structure can be written as

1, 1.5, 1, 1.5, 1, 1.5, ...

The repeat distance is again $5d$. Note the angle of 2 arctg 1/2 between diagonals of octahedra in the twin sets of ReO_3 type. The hypothetical structure shown in Figure 5c can be written as

1, 1.5, 1.5, 1, 1, ...

also with a repeat distance of $5d$.

It has been emphasized that twin planes contain coordination polyhedra which are not found in the parent structure.[30] In fact, it can be stated that the PC is formed through a chemical twinning operation on the ReO_3 structure. Thus, we find the PCs centered on twin planes in $LiNb_6O_{15}F$ and $NaNb_6O_{15}F$. The coordination polyhedra

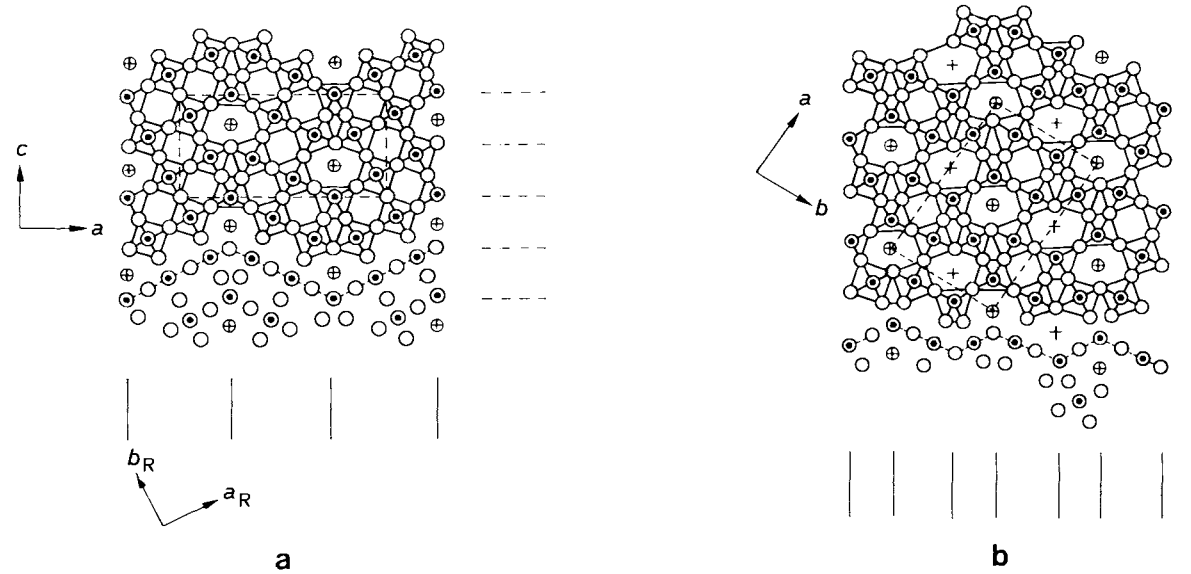


Fig. 21. The framework structures of octahedra of a) $LiNb_6O_{15}F$ and b) $NaNb_6O_{15}F$ as obtained from twinning of a parent structure of ReO_3 type. Small rings denote oxygen/fluorine, circled dots denote niobium atoms. A set of twin planes perpendicular to the plane of projection is indicated beneath the figures. The unit cells are shown. Note the glide planes indicated at the right in a). The orientation of an ReO_3 type subcell is also given in a). The center of a PC is marked with a crossed ring. The sodium positions in $NaNb_6O_{15}F$ are shown by crosses.

of the sodium atoms in the latter are also situated on these planes. The atomic arrangements shown in Figure 4 can also be easily derived through a chemical twinning operation on the ReO_3 structure.

As shown in Figure 21a, the MX_6 framework structure of $LiNb_6O_{15}F$ exhibits a set of *a*-glides perpendicular to the plane of projection. If every other glide plane is replaced by a reflection plane, the $LiNb_6O_{15}F$ structure converts into that of a TTB structure (Fig. 2b). It has been shown that the latter structure can be derived from the ReO_3-type structure through a chemical fourling operation, which is characterized by two sets of twin planes perpendicular to each other and circumscribing the fourling unit.[31] The idealized TTB unit cell dimensions have been derived from those of ReO_3.[4,32] The geometrical relation between the TTB and the $LiNb_6O_{15}F$ structures has been noted by *Lundberg* et al.[3] The intergrown structures illustrated in Figures 2a, 2c, and 3 may also be treated as chemical twinning.[33]

7. Conclusions

This paper describes a simple and general method for illustrating the structural relationships between the pentagonal column and the ReO_3-type structure. To the best of our knowledge all hitherto known compounds containing PCs and units of the ReO_3 type can be described in this way. The method enables us to discuss, in some detail, the similarities between PC-containing structures. It aids in their classification and in the search for new compounds with interesting structural features. It may also be very useful in the interpretation of lattice images of defects in such compounds.

The author wishes to thank Professors A. Magnéli and L. Kihlborg and Drs. M. Lundberg, M. Nygren and M. Sundberg for valuable discussions.—This study was supported by the Swedish Natural Science Research Council.

Received: May 20, 1985 [A 575 IE]
German version: *Angew. Chem. 98* (1986) 430

[1] A. Magnéli, *Ark. Kemi 1* (1949-50) 223.
[2] M. Lundberg, *Chem. Commun. Univ. Stockholm* (1971) No. XII.
[3] M. Lundberg, M. Sundberg, A. Magnéli, *J. Solid State Chem. 44* (1982) 32.
[4] B. G. Hyde, M. O'Keeffe, *Acta Crystallogr. A 29* (1973) 243.
[5] T. Ekström, *Chem. Commun. Univ. Stockholm* (1975) No. 7.
[6] T. Ekström, R. J. D. Tilley, *Chem. Scr. 16* (1980) 1.
[7] T. Hörlin, B.-O. Marinder, M. Nygren, *Rev. Chim. Minér. 19* (1982) 231.
[8] M. Lundberg, *Acta Chem. Scand. 19* (1965) 2274.
[9] M. Lundberg, *Acta Chem. Scand. 26* (1972) 2932.
[10] S. Iijima, *Acta Crystallogr. A 34* (1978) 922.
[11] M. Sundberg, *Chem. Scr. 14* (1978-79) 161.
[12] A. Magnéli, *Ark. Kemi 24* (1949) 213.
[13] S. Iijima, J. G. Allpress, *Acta Crystallogr. A 30* (1974) 29.
[14] S. Andersson, *Acta Chem. Scand. 19* (1965) 2285.
[15] S. Iijima, J. G. Allpress, *Acta Crystallogr. A 30* (1974) 22.
[16] R. S. Roth, J. L. Waring, *J. Res. Natl. Bur. Stand. 70A* (1966) 281.
[17] L. Kihlborg, *Ark. Kemi 21* (1963) 427.
[18] L. Kihlborg, *Acta Chem. Scand. 13* (1959) 954.
[19] L. Kihlborg, *Acta Chem. Scand. 14* (1960) 1612.
[20] A. Sleight, *Acta Chem. Scand. 20* (1966) 1102.
[21] B. O. Marinder, M. Sundberg, *Acta Crystallogr. C 40* (1984) 1303.
[22] L. K. Frevel, H. W. Rinn, *Acta Crystallogr. 9* (1956) 626.
[23] P. Vousden, *Acta Crystallogr. 4* (1951) 545.
[24] W. Sahle, *J. Solid State Chem. 45* (1982) 324.
[25] W. Sahle, *J. Solid State Chem. 45* (1982) 334.
[26] B. G. Hyde, A. N. Bagshaw, S. Andersson, M. O'Keeffe, *Annu. Rev. Mater. Sci. 4* (1974) 43.
[27] V. Bhide, M. Gasperin, *Acta Crystallogr. B 35* (1979) 1318.
[28] B. M. Gatehouse, D. J. Lloyd, B. K. Miskin, *Natl. Bur. Stand. (US) Spec. Publ. 364*, p. 15.
[29] M. Sundberg, *Chem. Commun. Univ. Stockholm* (1981) No. 5.
[30] S. Andersson, B. G. Hyde, *J. Solid State Chem. 9* (1974) 92.
[31] J.-O. Bovin, S. Andersson, *J. Solid State Chem. 18* (1976) 347.
[32] M. H. Francombe, *Acta Crystallogr. 13* (1960) 131.
[33] For a detailed account of this and related topics, see: B.-O. Marinder, to be published.

When submitting manuscripts, authors of articles intended for publication as "Communications" are requested to read the "Notice to Authors" reproduced in the January issue of the journal following the list of contents; upon request, a copy can be obtained from the editorial office.

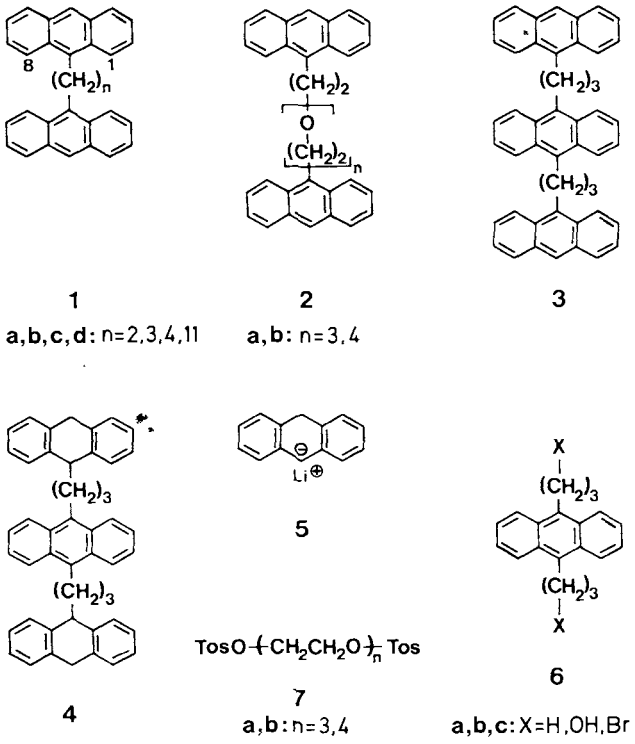
Synthesis and Redox Properties of Compounds with Several Separated Anthracene Electrophores**

By *Jürgen Fiedler, Walter Huber,* and *Klaus Müllen**

The through-space interaction of separated π-systems that are partly doped with electrons is of interest for theories of bonding[1] and for the material sciences.[2] The model dianthryl compounds **1a–c** can serve as efficient electron storage devices;[3] their ions exhibit π-system interactions[4] that are similar to those in the multilayered phanes.[5] As part of our studies directed toward the preparation of "polyelectrophoric" hydrocarbons,[6] we describe here the synthesis and reduction of the new compounds **1d**, **2a**,**b**, and **3**. Two questions arise: Is the electronic interaction between the anthracene moieties in **1** also possible for longer bridges (n = 11)? Are the electron-transfer properties of **1a–c** also evident in the higher homologues, e.g., **3**, with more than two redox groups?

1,11-Di(9-anthryl)-3,6,9-trioxaundecane **2a**[7] was prepared by reaction of the trioxaundecyleneditoluenesulfonate **7b** with the species **5** (2 equiv.) (obtained from 9,10-dihydroanthracene and *n*BuLi), followed by dehydrogenation of the tetrahydrodianthryl system.[8] The X-ray structure analysis of **2a** reveals a close approach of the anthracene moieties (preference of the *gauche* over the *anti* conformations of the CC bonds in the chain[9, 10]).[11] The C-9/C-9′ separation (ca. 10 Å) is significantly smaller than that expected for polymethylene chains with the CC *anti* conformation.

The synthesis of the hydrocarbon **1d**, which corresponds to the polyether **2a**, was achieved in an analogous manner. On account of the poor accessibility of **7**, n = 5, **2b** was prepared from **7a** and 2-(9-anthryl)ethoxide. In analogy to the synthesis of **1d** and **2a**, 9,10-bis[3-(9,10-dihydro-9-anthryl)propyl]anthracene **4** was prepared from **5** and 9,10-bis(3-bromopropyl)anthracene **6c**[12] (tetrahydrofuran, −80 °C) in 83% yield. Deprotonation of **4** (*n*BuLi/tetramethylethylenediamine, cyclohexane, 80 °C) followed by oxidation with cadmium chloride afforded the product **3**, which contains three separated anthracene moieties.[13]



1 a,b,c,d: n = 2,3,4,11 — **2** a,b: n = 3,4 — **3**

4 — **5** — **7** a,b: n = 3,4 — **6** a,b,c: X = H, OH, Br

The new compounds **1d**, **2a**,**b**, and **3** were reduced with alkali metals to the paramagnetic radical anions as well as to the polyanions. The distribution of spin density among the anthracene moieties in the radical anions (localization in one fragment or delocalization over all fragments) serves as an indication of the extent of through-space interaction. The most important experimental criteria are the size and multiplicity of the hyperfine coupling constants determined by ESR or ENDOR spectroscopy.

The coupling constants of the radical anion **1d**$^{\odot\ominus}$/$K^{\oplus}$ [a_H [mT] = 0.261 (H-1,8), 0.136 (H-2,7), 0.168 (H-3,6), 0.282 (H-4,5), 0.510 (H-10), 0.250 (α-CH_2), 0.029 (β-CH_2)] are the same as those in the 9-ethylanthracene radical anion. The spin density remains localized in one of the π-systems, as expected from the separation of the anthracene moieties. This result is independent of temperature and is valid for the solvent system dimethoxyethane (DME)/hexamethylphosphoric triamide (HMPT) as well as for 2-methyltetrahydrofuran (MTHF). As expected, solvent-separated ion pairs are present in DME/HMPT; MTHF, on the other hand, favors the formation of contact ion pairs.[3] In contrast, the hyperfine structure of the ESR spectrum of **2a**$^{\odot\ominus}$ depends markedly on the solvent, counterion, and temperature. The potassium salt proved to be "spin-localized" in MTHF. With lithium in MTHF or potassium in DME, however, the ESR line shapes were found to be reversibly dependent on temperature. At 20 °C, only a broad, S-shaped signal was observed. This exchange broadening is due to an intramolecular electron transfer between the anthracene moieties (K, DME, 60 °C: $k = 0.54 \times 10^6$ s^{-1}, $E_a = 15 \pm 2$ kJ/mol). The decrease in the electron-transfer barrier in **2a**$^{\odot\ominus}$ in comparison with that for the radical anion of the analogous hydrocarbon **1d** may be due to the helix-like chain conformation and, possibly, to the cation-coordination ability of the oxygen atoms; these factors fa-

[*] Prof. Dr. K. Müllen, Dipl.-Chem. J. Fiedler
Institut für Organische Chemie der Universität
Johann-Joachim-Becher-Weg 18–20, D-6500 Mainz 1 (FRG)
Dr. W. Huber
Institut für Physikalische Chemie der Universität
Klingelbergstrasse 80, CH-4056 Basel (Switzerland)

[**] This work was supported by the Deutsche Forschungsgemeinschaft, the Schweizerische Nationalfonds zur Förderung der wissenschaftlichen Forschung, and the Fonds der Chemischen Industrie.

vor a position of the counterion between the redox-active groups.[14, 15]

Reduction of **3** in MTHF leads to a radical anion [$K^{\oplus}$, 20°C; a_H [mT] = 0.262 (H-1,4,5,8), 0.155 (H-2,3,6,7), 0.117 (α-CH_2)], the coupling constants of which can be assigned to the protons of the inner anthracene fragment and to the protons of the two neighboring methylene groups. The coupling constants correspond to those in the radical anions of 9,10-dialkylanthracenes.[3] Under conditions that favor a strong interaction within the ion pair, the spin density of $\mathbf{3}^{\odot\ominus}$ remains localized in the central anthracene π-system.

In DME/HMPT (−85°C), $\mathbf{3}^{\odot\ominus}/K^{\oplus}$ exhibits only very small coupling constants (a_H [mT] = 0.02, 0.04, 0.06, 0.09, 0.11, 0.16). The largest of these hyperfine constants is less than one-third of the coupling constants of H-10 in $\mathbf{1d}^{\odot\ominus}$. On the time-scale of measurement, the spin density is delocalized over all the anthracene fragments of $\mathbf{3}^{\odot\ominus}$—a situation that, under the conditions of solvent-separated ion pairs, was also found for the dianthryl systems $\mathbf{1a}$–$\mathbf{1c}^{\odot\ominus}$.

Whereas in solution the primary ESR spectra of $\mathbf{3}^{\odot\ominus}$ are observed, the ESR spectra of triplet diradicals are observed in glassy rigid solutions; the latter can be assigned to the dianion $\mathbf{3}^{2\ominus}$. The zero-field splitting D measured in MTHF glass is 6.5 mT and agrees with that of the triplet dianion $\mathbf{1b}^{2\ominus}$.[3] This finding supports a structure with one electron in a terminal and one in the central anthracene moiety. In DME/HMPT glass two overlapping triplet-radical spectra are found (D = 6.5 and 9.2 mT); two structures are formed,[16] one of which agrees with the dianion structure also present in MTHF.

Upon further reduction, **1d** is converted into a stable tetraanion, the identity of which is established by NMR spectroscopy [$\mathbf{1d}^{4\ominus}/4\,Li^{\oplus}$, [$D_8$]tetrahydrofuran (THF), −50°C; δ_H = 3.58 (H-1,8), 4.38 (H-2,7), 4.18 (H-3,6), 3.36 (H-4,5), 1.90 (H-10), 0.60 (α-CH_2), 0.89 (β-CH_2), 1.00 (γ-CH_2), 1.20 ($\delta,\varepsilon,\varphi$-$CH_2$)]. Upon longer contact with the metal, the polyether **2a** undergoes reductive cleavage, as shown by the identification of ethylanthracene and anthrylethoxide fragments. In the case of **3**, the formation of a hexaanion can be shown by cyclovoltammetry (THF, sodium tetraphenylborate), i.e., each of the anthracene moieties can be charged with two electrons.[17]

This study shows that the rate of the intramolecular electron-transfer processes of compounds of type **1–3** can be specifically modified by the bridge and by the ion-pair structure and that the model system **3**, which contains three electroactive groups, behaves similarly to the "bis-electrophore" **1b**.

Received: November 21, 1985;
revised: February 24, 1986 [Z 1547 IE]
German version: *Angew. Chem. 88* (1986) 444

CAS Registry numbers:
1d, 101542-97-6; $\mathbf{1d}^{\odot\ominus}\cdot K^{\oplus}$, 101543-05-9; $\mathbf{1d}^{4\ominus}\cdot 4\,Li^{\oplus}$, 101519-19-1; **2a**, 101542-98-7; $\mathbf{2a}^{\odot\ominus}$, 101543-06-0; **2b**, 101542-99-8; **3**, 101543-00-4; $\mathbf{3}^{\odot\ominus}\cdot K^{\oplus}$, 101543-07-1; $\mathbf{3}^{2\ominus}\cdot 2K^{\oplus}$, 101628-80-2; $\mathbf{3}^{6\ominus}\cdot 6\,Na^{\oplus}$; 101519-21-5; **4**, 101543-03-7; **6c**, 101543-04-8; **7a**, 19249-03-7; **7b**, 37860-51-8; $TsO(CH_2)_{11}OTs$, 101543-01-5; 9,10-dihydroanthracene, 613-31-0; 2-(9-anthryl)ethoxide, 101543-02-6.

[1] A. J. Fry, T. A. Powers, K. Müllen, W. Irmen, *Tetrahedron Lett. 26* (1985) 4879.
[2] G. Wegner, M. Monkenbusch, G. Wieners, R. Weizenhöfer, G. Lieser, W. Werner, *Mol. Cryst. Liq. Cryst. 118* (1985) 85, and references cited therein.
[3] W. Huber, H. Unterberg, K. Müllen, *Angew. Chem. 95* (1983) 239; *Angew. Chem. Int. Ed. Engl. 22* (1983) 242; *Angew. Chem. Suppl. 1983*, 288.
[4] a) K. Itaya, A. J. Bard, M. Szwarc, *Z. Phys. Chem. NF 112* (1978) 1; b) K. Shimada, M. Szwarc, *J. Am. Chem. Soc. 97* (1975) 3313; *97* (1975) 3321.
[5] Review: F. Vögtle (Ed.): *Top. Curr. Chem. 113* (1983) 115; P. M. Keehn, S. M. Rosenfeld (Eds.): *Cyclophanes*, Academic Press, New York 1983.
[6] D. Bender, H. Unterberg, K. Müllen, *Angew. Chem. 98* (1986) 446; *Angew. Chem. Int. Ed. Engl. 25* (1986) 444.
[7] In view of the easy reductive cleavage of benzyl ethers, the planned reductions of **2a,b** required that the anthracene moieties be separated from the ether oxygen by (at least) one 1,2-ethanediyl group.
[8] M. Daney, G. F. R. Lapouyade, H. Bouas-Laurent, Fr. Pat. Appl. 2314165 (1977); L. M. Jackman, *Adv. Org. Chem. 2* (1960) 329.
[9] J. Dale, *Tetrahedron 30* (1974) 1683.
[10] I. Yamashita, M. Fujii, T. Kaneda, S. Misumi, T. Osubo, *Tetrahedron Lett. 21* (1980) 541.
[11] J. Fiedler, J. Lex, K. Müllen, unpublished results.
[12] Compound **6c** was conveniently prepared by reaction of 9,10-dilithioanthracene with oxetane (40%, based on 9,10-dibromoanthracene) followed by bromination of the diol **6b**.
[13] R. G. Harvey, L. Nazareno, H. Cho, *J. Am. Chem. Soc. 95* (1973) 2376.
[14] S. Mazur, V. M. Dixit, F. Gerson, *J. Am. Chem. Soc. 102* (1980) 5343.
[15] The intramolecular electron transfer does not require a close approach of the π-systems, which would be disfavored by repulsive forces, such as would be necessary for the formation of charge-transfer complexes or excimers; see [5b].
[16] The measured zero-field splitting depends not only on the separation of the π-systems but also on the ion-pair structure; see H. van Willigen, S. I. Weissman, *Mol. Phys. 11* (1966) 175.
[17] J. Mortensen, J. Heinze, D. Bender, J. Fiedler, K. Müllen, unpublished.

Poly(anthrylenetrimethylene) and 9,10-Bridged Anthracenes by Reductive Alkylation**

By *Dietmar Bender, Heinz Unterberg,* and *Klaus Müllen**

The synthesis of compounds consisting of several separated anthracene moieties and the study of their electron-transfer processes has directed attention to the polymer **7**.[1–3] The procedure for the synthesis of **7** and its precursor **6** consists in the alkylation of carbanions that are derived from anthracene **1** with 1,n-dibromoalkanes. Depending on the reaction conditions, this reaction can lead to the polymers **6** or to the monomers **8** (as well as their dehydrogenation products).

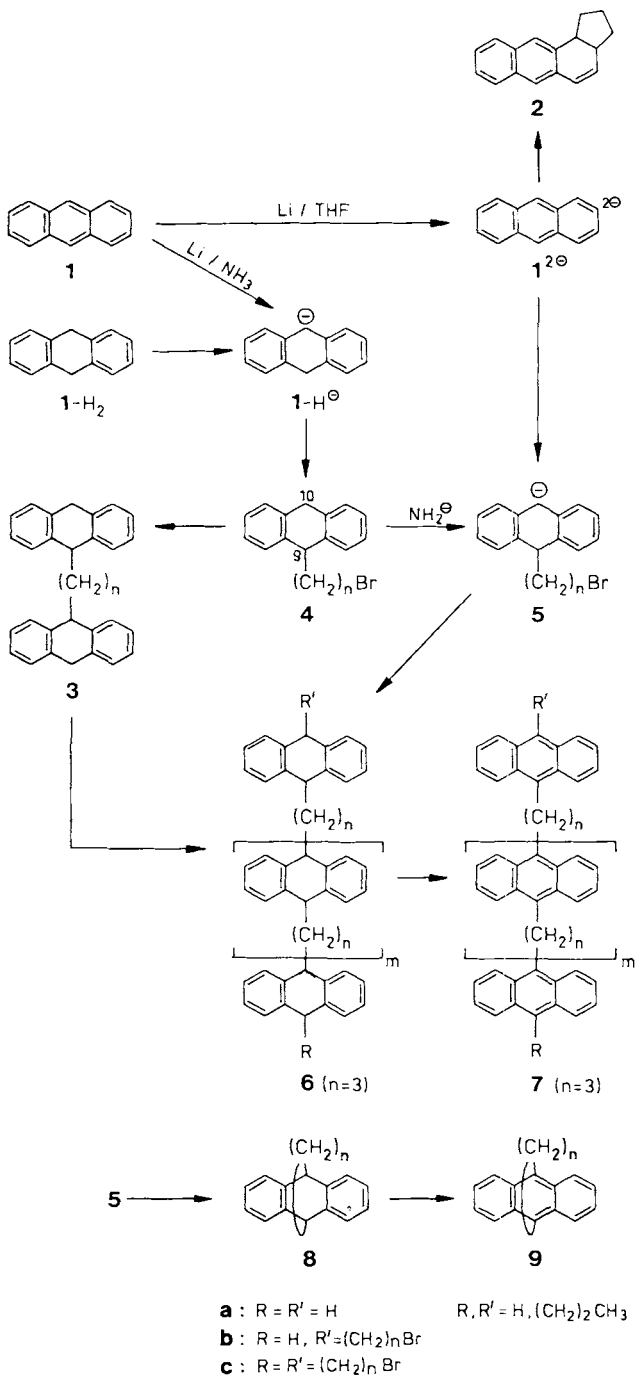
Key intermediates are 9-(n-bromoalkyl)-9,10-dihydroanthracenes **4** and the monoanions **5**. Their preparation from **1** or $\mathbf{1}\text{-}H_2$ and their reaction possibilities are summarized in Scheme 1.

When $\mathbf{1}\text{-}H^{\ominus}$[4] was generated by deprotonation of $\mathbf{1}\text{-}H_2$ and the 1,n-dibromoalkane was then added, the tetrahydrodianthrylalkane[5] **3** was formed (yield for n = 3: 80%). When the order of addition was reversed, i.e., addition of $\mathbf{1}\text{-}H^{\ominus}$ to a large excess of the alkylating agent, the substituted dihydroanthracene **4** (n = 3,[6] 60%; n = 6, 40%; n = 8, 38%; n = 10, 35%) was formed.

The isolated product **4** was then converted into the monoanion **5** by deprotonation [$LiNH_2$ or KNH_2 in NH_3/tetrahydrofuran (THF)]. The reactions of this species, which has both nucleophilic and electrophilic properties, is very much dependent on the chain length n and the concentration. If a solution of $LiNH_2$ (3 equiv.) in NH_3/THF (2:1, −33°C) was prepared and a 10^{-1} M solution of **4** (1

[*] Prof. Dr. K. Müllen, Dipl.-Chem. D. Bender, Dr. H. Unterberg
Institut für Organische Chemie der Universität
Johann-Joachim-Becher-Weg 18–20, D-6500 Mainz 1 (FRG)

[**] Reductive Transformations, Part 7. This work was supported by the Stiftung Volkswagenwerk.—Part 6: G. Neumann, K. Müllen, *Chimia 39* (1985) 275.



Scheme 1.

equiv.) in THF was added over 10 min, then the yields of cyclization product **8** were small for longer chain lengths (n = 3[7,8], 62%; n = 6, 8%; n = 8, 0%; n = 10, 8%). Reaction under dilution conditions proved more favorable. Separate solutions of **4** (THF, 2.5×10^{-2} M) and KNH_2 (NH_3, 3×10^{-2} M) were added synchronously over several hours to a NH_3/THF mixture (2:1, −33 °C). In this case, too, the smallest yield of the cyclization was obtained for n = 8 (n = 6, 34%; n = 8, 10%; n = 10, 38%). The higher homologues of **8** (n > 4) were previously unknown. **8** (n = 10) undergoes ready dehydrogenation to the known[9] anthracene derivative **9** (n = 10). The controlled conversion of **8** into **9** (n = 10) was achieved by oxidation ($CdCl_2$)[10] of the dianion obtained by deprotonation of **8**. On the basis of the ^{1}H-NMR chemical shifts of the methylene protons of **9** (n = 10) and $\mathbf{9}^{2\ominus}/2Li^{\oplus}$ (n = 10) it was possible to visually follow the anisotropy of the diamagnetic and paramagnetic ring-current effects, respectively [**9** (n = 10): $\delta_H = 3.8$ (α-CH_2), 1.8 (β-CH_2), 0.85 (γ-CH_2), 0.0 (δ,ε-CH_2); $\mathbf{9}^{2\ominus}/2Li^{\oplus}$ (n = 10), −50 °C: $\delta_H = 0.70$ (α-CH_2), 1.15 (β-CH_2), 1.70 (γ-CH_2), 2.35 (δ-CH_2), 2.70 (ε-CH_2); between −100 °C and −30 °C temperature-dependent line-shape changes are observed as a consequence of conformational transformations].

The third possible transformation of **4** and **5** consists in the polymerization to form **6**. This process can begin by bond formation between two monoanions **5** or by nucleophilic attack of the anions $\mathbf{1}\text{-}H^{\ominus}$ (in NH_3/THF) and $\mathbf{1}^{2\ominus}$ (in THF) on the bromoalkyl moiety of **4** and **5**, respectively. A high concentration of the nucleophile $\mathbf{1}\text{-}H^{\ominus}$ and $\mathbf{1}^{2\ominus}$ is guaranteed if **4** and **5**, respectively, are generated reductively from anthracene. Trapping of the dianion $\mathbf{1}^{2\ominus}$ (dilithium salt, 0.01 M in THF, −20 °C) with 1,3-dibromopropane affords the products **1**, **2**, and **8** and polymeric material (each n = 3) in 33, 20, 42, and ≤ 5% yield, respectively. The amount of polymer is small but can be increased by increasing the temperature and concentration; the reductive alkylation of anthracene is not regioselective under the conditions described above.[7,8] The relative yields of the monomeric cyclization products **2** and **8** could not be affected by varying the experimental conditions. In contrast, the reduction of **1** in NH_3 and alkylation with 1,3-dibromopropane gave up to 90% of poly(9,10-dihydroanthrylene-trimethylene) of type **6**. With 1,2-dibromoethane, instead of alkylation, oxidative coupling of $\mathbf{1}\text{-}H^{\ominus}$ occurred to give 9,9′,10,10′-tetrahydro-9,9′-bianthryl (46%).

For the fraction of the samples of **6** (n = 3) soluble in chloroform, molecular weight measurement by vapor pressure osmometry gave values between 1200 and 3500 depending on the synthesis conditions. These values are confirmed by gel-permeation chromatography[11] and FD mass spectroscopy.[12] According to the FD mass spectra, **6** (n = 3) consists of **6a**, **6b**, and **6c**. The structural proof of **6**[13,14] was accomplished by using ^{13}C-NMR spectroscopy; 9,10-dipropyl-9,10-dihydroanthracene, the tetrahydrodianthrylpropane **3**, its 10,10′-dipropyl derivative, and the model compound **6a** (m = 2, n = 3) containing four dihydroanthracene moieties (which was synthesized by us via an independent route[12]) were used as model compounds. The signals of these reference compounds agree with those of the corresponding polymers[13] within ±0.3 ppm. The NMR spectra do not provide evidence of interchain linkage by double alkylation at C-9 or C-10: the anthracene moieties are only linked through the positions 9 and 10. This is due to the high selectivity of the reductive alkylation in NH_3 (alkylation of $\mathbf{1}\text{-}H^{\ominus}$), which is not guaranteed in THF (alkylation of $\mathbf{1}^{2\ominus}$).[8,15]

The formation of **6** (n = 3) is a side reaction in the base-induced cyclization of **4** to **8**. The considerably better yields of polymer in the reductive alkylation of **1** in NH_3 confirm that the polymerization begins mainly by nucleophilic attack of $\mathbf{1}\text{-}H^{\ominus}$ on **4** or **5** and with less likelihood by reaction of two molecules of **5**. In agreement with this course of reaction is the finding that the polymer **6** (n = 3) can also be obtained from **3**, lithium amide, and dibromopropane.

The dehydrogenation of **6** to **7** (n = 3) was achieved (after removal of the bromine with $LiAlH_4$) with sulfur at 200 °C. The solubility of the brown material formed depends markedly on the molecular weight of the educt **6** and on the degree of dehydrogenation. Complete dehydro-

 © VCH Verlagsgesellschaft mbH, D-6940 Weinheim, 1986 0570-0833/86/0505-0445 $ 02.50/0

genation of higher-molecular-weight samples in organic solvents afforded insoluble products.[16]

This polymer synthesis can be considerably varied by the choice of the bridges and the reducible π-system.[12]

Received: November 21, 1985;
revised: February 24, 1986 [Z 1548 IE]
German version: *Angew. Chem. 98* (1986) 446

[1] J. Fiedler, W. Huber, K. Müllen, *Angew. Chem. 98* (1986) 444; *Angew. Chem. Int. Ed. Engl. 25* (1986) 443.
[2] W. Huber, H. Unterberg, K. Müllen, *Angew. Chem. 95* (1983) 239; *Angew. Chem. Int. Ed. Engl. 22* (1983) 242; *Angew. Chem. Suppl. 1983*, 288.
[3] J. H. Golden, *J. Chem. Soc. 1961*, 3741.
[4] K. Müllen, W. Huber, G. Neumann, C. Schnieders, H. Unterberg, *J. Am. Chem. Soc. 107* (1985) 801.
[5] M. Daney, G. F. R. Lapouyade, H. Bouas-Laurent, Fr. Pat. Appl. 2314165 (1977).
[6] E. Hobolth, H. Lund, *Acta Chem. Scand. B31* (1977) 395.
[7] D. Lipkin, G. J. Divis, R. W. Jordan, *Am. Chem. Soc. Div. Pet. Chem. Prepr. 13* (1968) D60.
[8] F. J. Burgess, A. V. Cunliffe, D. H. Richards, *Eur. Polym. J. 10* (1974) 665.
[9] F. Vögtle, P. K. T. Mew, *Angew. Chem. 90* (1978) 58; *Angew. Chem. Int. Ed. Engl. 17* (1978) 60.
[10] R. G. Harvey, L. Nazareno, H. Cho, *J. Am. Chem. Soc. 95* (1973) 2376.
[11] Column combination: μ-ultrastyragel 10^3 Å, μ-styragel 500 Å and 100 Å; mobile phase: chloroform. We thank Prof. Dr. *R. C. Schulz* and Dipl.-Chem. *K. Mühlbach* for experimental assistance.
[12] Chemical and physical properties of **6** and **7**: D. Bender, K. Müllen, M. Przybylski, unpublished results.
[13] Typical ^{13}C-NMR chemical shifts of **6** (n = 3) ($CDCl_3$, 100 MHz): δ_C for nonterminal fragments: 46.2 (–CH), 42.2 (α-CH_2), 27.0 (β-CH_2).
[14] The elemental analyses gave correct values and showed at the same time that type **6a** (with two dihydroanthracene moieties) predominates.
[15] F. J. Burgess, A. V. Cunliffe, D. H. Richards, *Eur. Polym. J. 10* (1974) 657.
[16] The dehydrogenation was also achieved with chloranil as well as with *n*BuLi/tetramethylethylenediamine and iodine; however, the reaction mixtures were difficult to purify. The structural assignment of the insoluble samples of **7** was achieved by comparison of the IR spectra with those of model compounds (see **1–3** in [1]). For the partially dehydrogenated samples, the formation of anthracene π-systems could be followed by ^{1}H- and ^{13}C-NMR spectroscopy.

Evidence for Equilibria between μ-Alkyne and Alkylidyne Complexes of Tungsten Alkoxides: $[W_2(OR)_6(\mu\text{-}C_2R'_2)] \rightleftharpoons 2[(RO)_3W{\equiv}CR']$**

By *Malcolm H. Chisholm,* Brian K. Conroy, John C. Huffman, and Nancy S. Marchant*

The cleavage of alkynes to form two alkylidyne moieties has been observed at dinuclear,[1,2] trinuclear,[3–7] and tetranuclear[8] metal centers. The reverse reaction, the coupling of two alkylidyne ligands, is also known.[6,7] In certain instances a reversible process can be induced by CO elimination or uptake.[3,4] Recently, we suggested that a dynamic equilibrium between the μ-alkyne ditungsten complex **1a** and the alkylidynetungsten complex **2a**, involving the elimination or uptake of pyridine, exists in solution at room temperature [Eq. (a)].[2] Here, we present evidence for a general equilibrium of this type for which the equilibrium constant K is dependent upon the nature of R and R′, bulky combinations favoring the alkylidyne species.

$$[W_2(OR)_6(py)_n(\mu\text{-}C_2R'_2)] \overset{K}{\rightleftharpoons} 2[(RO)_3W{\equiv}CR'] + n\ py \qquad (a)$$

1 **2**

1, 2	a	b	c	d	e
R	*t*Bu	*t*BuCH$_2$	*t*BuCH$_2$	*t*BuCH$_2$	*t*BuCH$_2$
R′	H	H	Me	Et	Ph
n	1	2	2	1	1

The addition of sterically bulky alkynes to $[W_2(O\mathit{t}Bu)_6]$ results in the formation of alkylidyne species in high yields (i.e., alkyne cleavage).[11] By reducing the steric demands of the alkoxide ligands, we were able to prepare the stable μ-alkyne complexes **1b–e** [Eq.(a)].[2]

In principal the equilibrium (a) should be observable by UV/VIS spectroscopy since the alkyne adducts are blue or green whereas the alkylidyne species are yellow and do not show an absorption maximum in the visible region of the spectrum. The alkyne adducts **1c–e** do not obey the Beer–Lambert Law for their absorptions in the visible region. Hydrolysis by traces of water or oxidation by adventitious O_2 under the high-dilution conditions employed, which are necessary to drive the equilibrium to the right, may be responsible for such behavior. This precludes determination of the equilibrium constant K. Consequently, we have used trapping reagents to obtain chemical evidence for the existence of the equilibrium (a).

The alkyne adducts **1c–e** can be used as alkylidyne sources for the preparation of alkylidyne clusters **3** according to Equation (b).

$$2[W_2(OCH_2\mathit{t}Bu)_6(py)_2] + [W_2(OCH_2\mathit{t}Bu)_6(py)_n(\mu\text{-}C_2R'_2] \xrightarrow{25\,^\circ C,\ hexane} 2[W_3(\mu_3{-}CR')(OCH_2\mathit{t}Bu)_9] + (n+4)py \qquad (b)$$

1c–e **3**

R′ = Me, Et, Ph

Addition of the alkyne to $[W_2(OCH_2\mathit{t}Bu)_6(py)_2]$ (molar ratio 1:3) results in the direct formation of the alkylidyne-capped tritungsten compounds **3**. ^{1}H-NMR studies showed that the complexes **1** were formed initially [Eq. (b)]. The rate of formation of **3** follows the order Et ≈ Ph > Me, which probably reflects the magnitude of K in Equation (a). Interestingly, no μ_3-CH cluster could be prepared by this route. Furthermore, in a double labeling experiment involving $[W_2(OCH_2\mathit{t}Bu)_6(py)_2(\mu\text{-}{}^*C_2H_2)]$ and $[W_2(OCH_2\mathit{t}Bu)_6(py)_2(\mu\text{-}C_2D_2)]$, we found no evidence for formation of $[W_2(OCH\mathit{t}Bu)_6(py)_2(\mu\text{-}H{}^*CCD)]$ (*C represents 92.5 mol-% ^{13}C).

The new compounds **3** are analogous (^{1}H-, ^{13}C-NMR) to $[W_3(\mu_3\text{-}CMe)(O\mathit{i}Pr)_9]$, which was previously prepared by the comproportionation of $[(\mathit{t}BuO)_3W{\equiv}CMe]$ **4**[9] and $[W_2(O\mathit{i}Pr)_6]$ in the presence of *i*PrOH.[10]

Further evidence for equilibrium (a) is provided by the reaction of **4** with CO. Addition of CO (1 atm) to a hexane solution of **4** results in a color change (pale yellow to blue) and the quantitative formation of complex **5** (Eq. (c)].[11]

$$2[(\mathit{t}BuO)_3W{\equiv}CMe] + CO \xrightarrow{25\,^\circ C,\ hexane} [W_2(O\mathit{t}Bu)_6(CO)(\mu\text{-}C_2Me_2)] \qquad (c)$$

4 **5**

[*] Prof. M. H. Chisholm, B. K. Conroy, Dr. J. C. Huffman, N. S. Marchant
Department of Chemistry and Molecular Structure Center, Indiana University
Bloomington IN 47405 (USA)

[**] This work was supported by the Department of Energy, Office of Basic Sciences, Chemical Division, and by the Wrubel Computing Center.

Reaction (c) is complete after 24 h (^{1}H-NMR). Under analogous conditions, the complexes [(tBuO)$_3$W≡CR′], R=Et, Ph, do not react, suggesting that, for these complexes, the equilibrium (a) lies far to the right.

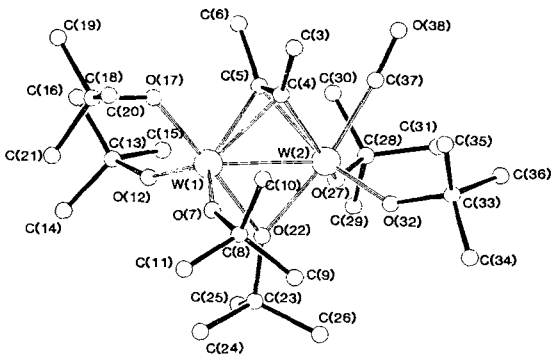


Fig. 1. Crystal structure of **5**. Selected bond distances [Å] and angles [°]: W-W 2.633(1), W(1)-C(4) 2.124(15), W(1)-C(5) 2.169(16), W(2)-C(4) 2.173(14), W(2)-C(5) 2.098(15), C(4)-C(5) 1.36(2), W-O(terminal) 1.90(2) (averaged), W-O(bridging) 2.065(10), W(2)-C(37) 1.988(15), C(4)-C(5)-C(6) 126(1), C(5)-C(4)-C(3) 130(1), W(2)-C(37)-O(38) 173(1). Further details of the crystal structure investigation are available on request from the Fachinformationszentrum Energie, Physik, Mathematik GmbH, D-7514 Eggenstein-Leopoldshafen 2 (FRG), on quoting the depository number CSD 51748, the names of the authors, and the full journal citation.

Complex **5** can be isolated as dark blue crystals from hexane. ^{1}H- and ^{13}C-NMR spectroscopic studies support the existence of a static structure, having a mirror plane of symmetry, on the NMR time scale. The molecular structure deduced from a single-crystal X-ray study is shown in Figure 1. In the IR spectrum ν(CO) occurs at 1917 cm^{-1}, which is indicative of extensive W-to-CO back-bonding. It is this π-acceptor property of CO that stabilizes the μ-C_2Me_2 adduct relative to the alkylidyne species **4**.

Theoretical studies predicted[12] that there would be virtually no energy barrier for the interconversion of $L_3M(\mu\text{-}L)(\mu\text{-}CR)_2ML_3$ and $L_6M_2(\mu\text{-}L)(\mu\text{-}C_2R_2)$ complexes where the electron count on each metal was between d^4 and d^8 (the ligands L being counted as neutral rather than charged).

Received: December 11, 1985;
revised: January 27, 1986 [Z 1581 IE]
German version: *Angew. Chem. 98* (1986) 448

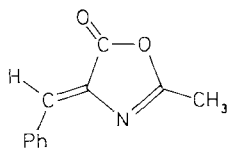
CAS Registry numbers:
1a, 87667-98-9; **1b**, 101518-65-4; **1c**, 88608-51-9; **1d**, 101077-89-8; **1e**, 101164-93-6; **2a**, 91389-20-7; **2b**, 101518-69-8; **2c**, 101077-93-4; **2d**, 101077-92-3; **2e**, 101077-91-2; **3** (R′=Me), 101518-66-5; **3** (R′=Et), 101518-67-6; **3** (R′=Ph), 101518-68-7; **4**, 82209-23-2; **5**, 101077-90-1; [W_2(OCH$_2$tBu)$_6$(py)$_2$], 88608-50-8.

[1] a) R. R. Schrock, M. L. Listemann, L. G. Sturgeoff, *J. Am. Chem. Soc. 104* (1982) 4291; b) M. L. Listemann, R. R. Schrock, *Organometallics 4* (1985) 74; c) J. H. Freudenberger, S. F. Pedersen, R. R. Schrock, *Bull Soc. Chim. Fr. 1985*, 349; d) F. A. Cotton, W. Schwotzer, E. S. Shamshoum, *Organometallics 3* (1984) 1770.
[2] a) M. H. Chisholm, K. Folting, D. M. Hoffman, J. C. Huffman, *J. Am. Chem. Soc. 106* (1984) 6794; b) M. H. Chisholm, D. M. Hoffman, J. C. Huffman, *Chem. Soc. Rev. 14* (1985) 69.
[3] a) A. D. Clauss, J. R. Shapley, C. N. Wilker, R. Hoffmann, *Organometallics 3* (1984) 619; b) Y. Chi, J. R. Shapley, *ibid. 4* (1985) 1900.
[4] D. Nuel, F. Daham, R. Mathieu, *Organometallics 4* (1985) 1436.
[5] N. T. Allison, J. R. Fritch, K. P. C. Vollhardt, E. C. Walborsky, *J. Am. Chem. Soc. 105* (1983) 1384.
[6] a) J. R. Shapley, J. T. Park, M. R. Churchill, C. Bueno, H. J. Wasserman, *J. Am. Chem. Soc. 103* (1981) 7385; b) M. R. Churchill, C. Bueno, H. J. Wackerman, *Inorg. Chem. 21* (1982) 640.
[7] a) L. Busetto, M. Green, J. A. K. Howard, B. Hessner, J. C. Jeffrey, R. M. Mills, F. G. A. Stone, P. Woodward, *J. Chem. Soc. Chem. Commun. 1981*, 1101; b) L. Buestto, J. C. Jeffery, R. M. Mills, F. G. A. Stone, M. J. Went, P. Woodward, *J. Chem. Soc. Dalton Trans. 1983*, 101; c) J. C. Jeffery, J. C. V. Laurie, F. G. A. Stone, *Polyhedron 4* (1985) 1135; d) M. Green, S. J. Porter, F. G. A. Stone, *J. Chem. Soc. Dalton Trans 1983*, 513; e) M. Green, J. C. Jeffery, S. J. Porter, H. Razay, F. G. A. Stone, *J. Chem. Soc. Dalton Trans. 1982*, 2475.
[8] J. T. Park, J. R. Shapley, M. R. Churchill, C. Bueno, *J. Am. Chem. Soc. 105* (1983) 6182.
[9] M. H. Chisholm, D. M. Hoffman, J. C. Huffman, *Inorg. Chem. 22* (1983) 2903.
[10] M. H. Chisholm, K. Folting, J. A. Heppert, D. M. Hoffman, J. C. Huffman, *J. Am. Chem. Soc. 107* (1985) 1234.
[11] *Schrock* and co-workers have studied reactions of other alkylidynes with CO: a) M. R. Churchill, H. J. Wasserman, S. J. Holmes, R. R. Schrock, *Organometallics 1* (1982) 766; b) J. H. Wengrovius, R. R. Schrock, M. R. Churchill, H. J. Wasserman, *J. Am. Chem. Soc. 104* (1982) 1739.
[12] C. N. Wilker, R. Hoffmann, O. Eisenstein, *Nouv. J. Chim. 7* (1983) 535.

C_{phenyl}–H···O and C_{phenyl}–H···N Interactions: Crystal Structure of (*Z*)-4-Benzylidene-2-methyl-5(4*H*)-oxazolone, an Intermediate for Dehydropeptide Synthesis

By *Mohamed Souhassou, André Aubry, Guy Boussard,* and *Michel Marraud**

The spatial distribution of atoms in the environment of the phenylalanine aromatic rings in protein[1] and peptide[2] crystal structures has revealed that the carbonyl oxygen atoms are preferentially situated in the plane of these aromatic rings; ab initio calculations on benzene and formamide have suggested the existence of a favorable enthalpic interaction.[1] Moreover, *Taylor* and *Kennard* have presented crystallographic evidence, obtained by neutron diffraction experiments, for hydrogen bonds involving C–H bonds and O or N atoms.[3] A C–H···O contact can be described as a hydrogen bond when the H···O distance is shorter than 2.4 Å (i.e., C···O<3.5 Å for a linear arrangement of the three atoms) and the C–H···O angle is greater than 90°.



1

We report here on the crystal structure of **1**, which contains two short C–H···O and C–H···N contacts involving aromatic H atoms.

The existence of α,β-dehydro amino acid residues in naturally occurring microbial peptides exhibiting antibiotic activity has incited chemists to introduce these modified

[*] Dr. M. Marraud, Dr. G. Boussard
Laboratoire de Chimie Physique Macromoléculaire
C.N.R.S.-UA-494, ENSIC-INPL
1 rue Grandville, F-54042 Nancy (France)
Dr. A. Aubry, M. Souhassou
Laboratoire de Minéralogie et Cristallographie
C.N.R.S.-UA-809
Université de Nancy I, BP 239, F-54506 Vandœuvre (France)

residues into a number of analogues.[4] The expected advantages are a defined orientation of the unsaturated side chain due to the rigidity of the $C^{\alpha}C^{\beta}$ double bond and increased resistance to enzymatic degradation.[5] However, both (*Z*) and (*E*) configurations of the double bond are a priori possible and their characterization is not yet straightforward.[6, 7] According to *Kono* and *Stammer*,[8] one of the most promising procedures for the introduction of an α,β-dehydro amino acid into a growing peptide chain is to prepare an intermediate containing a *C*-terminal 5(4*H*)-oxazolone ring.

The crystal structure of the title compound **1**, obtained from α,β-dehydrophenylalanine,[9] is shown in Figure 1.[10] All the atoms were located, and the hydrogen atoms were moved along the observed C–H bonds until the C–H bond lengths were equal to the usual values found in neutron diffraction experiments.

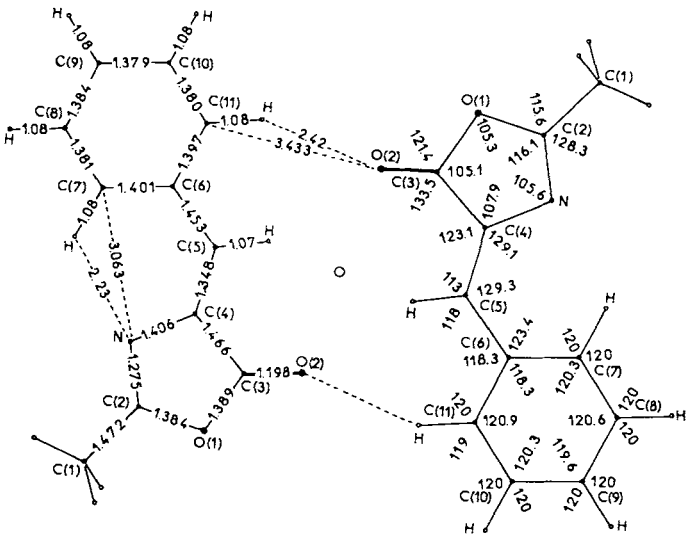


Fig. 1. Crystal structure of a "dimer" of **1** projected on the mean plane. Bond lengths (Å, left) and bond angles (°, right) are indicated, together with the C11–H···O2 and C7–H···N contacts.

The small thermal factors of the non-hydrogen atoms (B_{eq} = 3.0–4.8 Å^2) result in accurate bond lengths (σ = 0.002 Å) and bond angles (σ = 0.1°). The perfectly planar (*Z*) configuration of the molecules (maximum deviation from the mean plane: 0.027 Å) allows strong electronic conjugation, resulting in a rather short C5–C6 bond and a rather long C4–C5 bond compared to those of similar species with a twisted C5–C6 bond.[11]

In the unit cell (Fig. 2), the molecules are stacked two by two in an antiparallel disposition with the neighboring phenyl rings nearly orthogonal to each other. One intramolecular C7–H···N contact and one intermolecular C11–H···O contact are shorter than the van der Waals distances (Fig. 1). The former is probably responsible for the coplanar disposition of the oxazole and phenyl rings. In dehydropeptides, the accepting nitrogen atom of **1** is replaced by a proton-donating NH group and the C5–C6 bond is effectively rotated by an angle of up to 37°.[11] The C11–H···O interaction results in centrosymmetric "cyclic dimers" of two nearly coplanar molecules with a distance of 0.046 Å between the average planes.

We believe that these C–H···O and C–H···N interactions are not simply a consequence of the crystal packing forces; the low solubility of this molecule in an inert solvent such as CCl_4, however, prevents an NMR study of aggregation in solution. However, the low-field shift of the *o*-H signal (δ = 8.05) compared to that of the *m*- and *p*-H signals (δ = 7.40) suggests that the intramolecular C–H···N interaction is also present in solution.

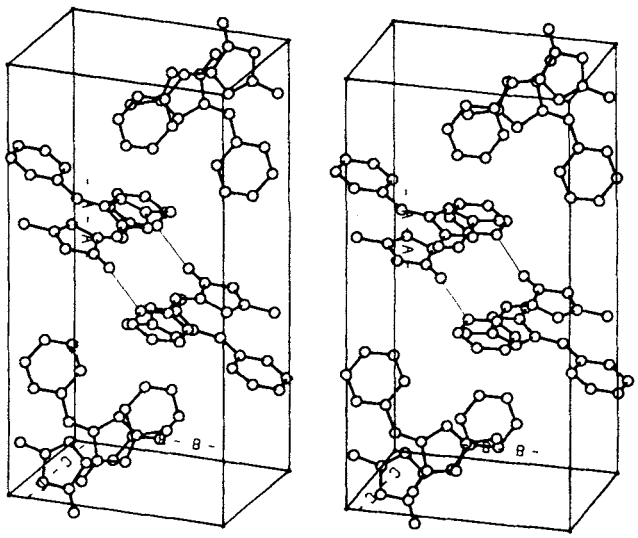


Fig. 2. Packing of the "dimers" of **1** (stereoview).

The crystal structure of **1** indicates that the phenyl ring not only experiences hydrophobic interactions and stacking forces, but is also capable of acting as a proton donor to atoms bearing a partial negative charge such as the oxygen of carbonyl groups. This type of interaction deserves to be taken into consideration in the analysis of aromatic side-chain folding in peptides and of molecular recognition in biological processes.

Received: December 16, 1985;
revised: February 7, 1986 [Z 1593 IE]
German version: *Angew. Chem. 98* (1986) 449

CAS Registry number:
1, 38879-46-8.

[1] R. O. Gould, A. M. Gray, P. Taylor, M. D. Walkinshaw, *J. Am. Chem. Soc. 107* (1985) 5921.
[2] K. A. Thomas, G. M. Smith, T. B. Thomas, R. J. Feldman, *Proc. Natl. Acad. Sci. USA 79* (1982) 4843.
[3] R. Taylor, O. Kennard, *J. Am. Chem. Soc. 104* (1982) 5063.
[4] K. Noda, Y. Shimohigashi, N. Izumiya in E. Gross, J. Meienhofer (Eds.): *The Peptides, Analysis, Synthesis, Biology, Vol. 5*, Academic Press, New York 1983, p. 285.
[5] M. L. English, C. H. Stammer, *Biochem. Biophys. Res. Commun. 83* (1978) 1464.
[6] C. G. Shin, Y. Yonezawa, T. Yamada, J. Yoshimura, *Bull. Chem. Soc. Jpn. 55* (1982) 2147.
[7] Y. Shimohigashi, T. J. Nitz, C. H. Stammer, T. Inobushi, *Tetrahedron Lett. 23* (1982) 3235.
[8] S. Kono, C. H. Stammer, *Int. J. Peptide Protein Res. 12* (1978) 222.
[9] R. M. Herbst, D. Shemin in A. H. Blatt (Ed.): *Organic Synthesis, Vol. II*, Wiley, New York 1943, p. 1.
[10] **1**: *Pbca*, a = 21.318(2), b = 10.890(1), c = 7.981(1) Å, Z = 8; ρ_{calcd} = 1.34 g cm^{-3}, 1797 unique reflections, 1448 with $I > 1.5\sigma(I)$, structure solution and refinement with the program MULTAN 80 and SHELX to R = 0.035; R_w = 0.041 ($w = 2.25/(\sigma^2(F) + 0.00026F^2)$). Further details of the crystal structure investigation can be obtained from the Fachinformationszentrum Energy, Physik, Mathematik GmbH, D-7514 Eggenstein-Leopoldshafen 2 (FRG), on quoting the depository number CSD-51767, the names of the authors, and the journal citation.
[11] A. Aubry, F. Allier, G. Boussard, M. Marraud, *Biopolymers 24* (1985) 639.

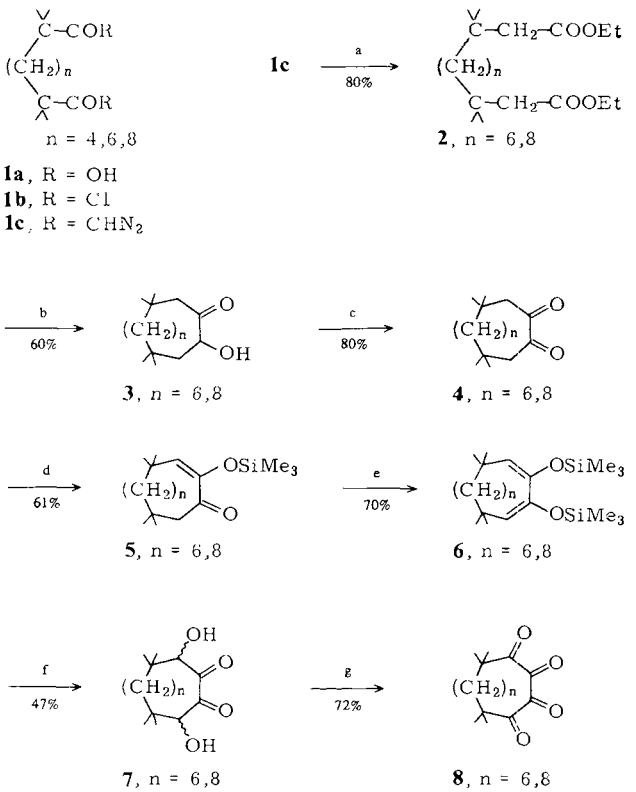
Synthesis of Cyclic, Vicinal Tetraketones**

By *Rolf Gleiter** and *Gerhard Krennrich*

Dedicated to Professor Edgar Heilbronner on the occasion of his 65th birthday

Whereas open-chain, vicinal tetraketones have long been known[1] and are well investigated,[2,3] only cyclic, vicinal tetraketones that bear strongly electron-donating substituents have been prepared to date (e.g., rhodizonic acid[4]). They are of interest because of their expected photochemistry[5] and on account of their physical-chemical properties (acceptor behavior, color).[2,3] Our initial goal was to synthesize cyclic compounds with 12 and 14 C atoms, since the syn-coplanar arrangement of the four CO groups in smaller rings results in the appreciable instability of such tetraketones. We report here the synthesis of simple, cyclic, vicinal tetraketones and bistetraketones.

The β,β′-tetramethyl diesters **2**[6] are obtained by conversion of the aliphatic α,α′-tetramethyl dicarboxylic acids **1a**[7] to the acid chlorides **1b**, followed by reaction of **1b** with diazomethane and irradiation of the products formed, the bis(diazo)ketones **1c** (Scheme 1). Subsequent acyloin condensation leads to the acyloins **3**,[6] which are oxidized with Cu^{II} to the yellow diketones **4**.[6] Reaction of **4** with sodium bistrimethylsilylamide followed by chlorotrimethylsilane[8] gives the monosilyl enol ethers **5**,[6] which smoothly react with lithium diisopropylamide (LDA) and



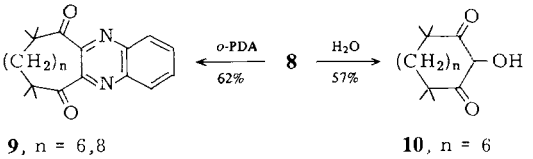
Scheme 1. a) EtOH, *hν*, 1 h; b) Na, xylene; c) $Cu(OAc)_2$, HOAc/H_2O (1:1), 100°C; d) $NaN(SiMe_3)_2$, tetrahydrofuran (THF), −70°C, Me_3SiCl; e) LDA, Me_3SiCl, THF, −78°C; f) *m*-CPBA, CH_2Cl_2; g) NBS, 2 h, 77°C.

[*] Prof. Dr. R. Gleiter, Dipl.-Chem. G. Krennrich
Institut für Organische Chemie der Universität
Im Neuenheimer Feld 270, D-6900 Heidelberg (FRG)

[**] This work was supported by the Deutsche Forschungsgemeinschaft, the Fonds der Chemischen Industrie, and BASF. We thank Priv.-Doz. Dr. *D. Spitzner* for recording the field desorption mass spectra and Mrs. *G. Rissmann* for recording the NMR spectra.

chlorotrimethylsilane to give the 2,3-bis(trimethylsiloxy)-1,3-dienes **6**.[6] Oxidation of **6** with *m*-chloroperbenzoic acid (*m*-CPBA) leads to the diols **7**[6] (*cis* and *trans* isomers), which are oxidized with *N*-bromosuccinimide (NBS) in CCl_4 in the presence of pyridine at 77°C to give **8** (violet-red oil).

The tetraketones **8** react with *o*-phenylenediamine (*o*-PDA) to give the quinoxaline derivatives **9** (Scheme 2). Traces of water result in the ring contraction of **8** (n = 6) to **10**.[3,4,6] In contrast, **8** (n = 8) reacts with water at room temperature to give only the hydrate. The most important spectroscopic data for **8** and **9** are summarized in Table 1.



Scheme 2.

Table 1. Spectroscopic data for the compounds **8** (n = 6, 8), **9** (n = 6, 8), and **15** (n = 4, 6). ^{1}H-NMR: 300 MHz, $CDCl_3$; ^{13}C-NMR: 75.46 MHz, $CDCl_3$; UV: CH_2Cl_2. Correct elemental analyses were obtained for **9** (n = 6, 8) and for the hydrates of **15** (n = 4, 6).

8 (n = 6): IR (film): $\tilde{\nu}$ = 1710 cm^{-1}; ^{1}H-NMR: δ = 1.65–1.59 (m; 4H), 1.52–1.07 (m) 1.28 (s) (20H); ^{13}C-NMR: δ = 206.5 (s), 188.1 (s),47.2 (s), 35.9 (t), 25.1 (t), 24.4 (q), 21.6 (t); UV: $\lambda_{max}(\varepsilon)$ = 507 (43), 368 nm (97)

8 (n = 8): IR (film): $\tilde{\nu}$ = 1735, 1685 cm^{-1}; ^{1}H-NMR: δ = 1.60–1.55 (m; 4H), 1.41–1.06 (m) 1.28 (s) (24H); ^{13}C-NMR: δ = 207.3 (s), 185.2 (s), 46.1 (s), 37.8 (t), 27.3 (t), 26.0 (t), 24.4 (q), 23.7 (t); UV: $\lambda_{max}(\varepsilon)$ = 533 (87), 385 nm (94)

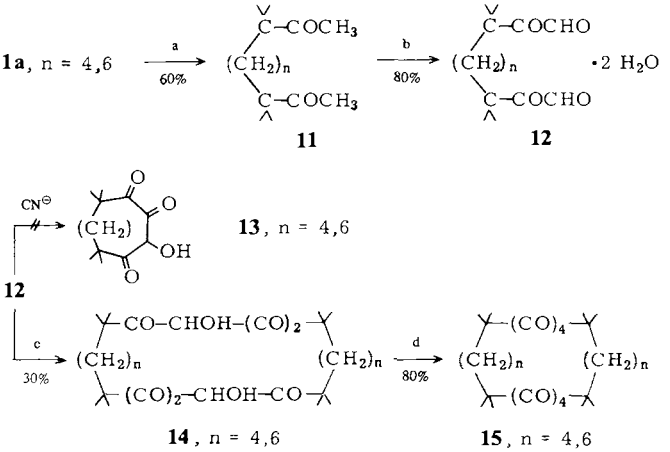
9 (n = 6): IR (KBr): $\tilde{\nu}$ = 1700, 1680 cm^{-1}; ^{1}H-NMR: δ = 8.14 (q, J = 6 Hz, 3 Hz; 2H), 7.88 (q, J = 6 Hz, 3 Hz; 2H), 1.64–1.58 (m; 4H), 1.53 (s; 12H), 1.26–1.22 (m; 4H), 0.9 (m; 4H); MS: *m/z* 352 ($M^{\oplus}$, 100%), 307, 227

9 (n = 8): IR (KBr): $\tilde{\nu}$ = 1680 cm^{-1}; ^{1}H-NMR: δ = 8.07 (q, J = 6 Hz, 3 Hz; 2H), 7.84 (q, J = 6 Hz, 3 Hz; 2H), 1.77–1.72 (m; 4H), 1.56 (s; 12H), 1.42–1.26 (m; 12H); MS: *m/z* 380 ($M^{\oplus}$), 335 (100%), 227

15 (n = 4): IR (KBr): $\tilde{\nu}$ = 1730, 1685 cm^{-1}; ^{1}H-NMR: δ = 1.69–1.64 (m; 4H), 1.30 (s) 1.39–1.16 (m) (16H); ^{13}C-NMR: δ = 204.9 (s), 187.8 (s), 46.1 (s), 38.4 (t), 29.0 (t), 23.6 (q); MS (FD): *m/z* 506, 505 ($M^{\oplus}$), 504; UV: $\lambda_{max}(\varepsilon)$ = 525 (165), 385 nm (149)

15 (n = 6): IR (KBr): $\tilde{\nu}$ = 1725, 1685 cm^{-1}; ^{1}H-NMR: δ = 1.73–1.68 (m; 4H), 1.28 (s) 1.38–1.19 (m) (20H); ^{13}C-NMR: δ = 204.4 (s), 188.1 (s), 46.1 (s), 39.1 (t), 29.6 (t), 24.1 (t), 23.8 (q); MS (FD): *m/z* 562, 561 ($M^{\oplus}$); UV: $\lambda_{max}(\varepsilon)$ = 522 (100), 380 nm (96)

A second reaction sequence, however, leads not to **8** but to the vicinal bistetraketones. Compounds **1a** (n = 4, 6)



Scheme 3. a) MeLi in THF, 0°C; b) 1. SeO_2, dioxane, 2. H_2O; c) KCN, EtOH/H_2O (1:1); d) CH_2Cl_2, HNO_3.

react with MeLi to give the ketones **11** (Scheme 3),[6] which are converted smoothly into the glyoxal derivatives **12**[6] with SeO_2. The benzoin condensation does not result in the expected 2-hydroxy-1,3,4-triketones (formoins) **13**, but rather in the dimers **14**.[6,9] Compounds **14** are oxidized with HNO_3 to the yellow dihydrates of **15**,[6] which, upon heating, afford the anhydrous, red bistetraketones **15** (data for **15**: see Table 1). The molecular weight determined by field desorption (FD) mass spectrometry supports the structure of **15**.

Received: December 30, 1985;
revised: January 22, 1986 [Z 1601 IE]
Publication delayed at authors' request
German version: *Angew. Chem. 98* (1986) 452

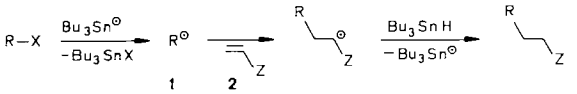
CAS Registry numbers:
1a (n=4), 16386-99-5; **1a** (n=6), 22092-62-2; **1a** (n=8), 22092-64-4; **1b** (n=6), 101671-41-4; **1b** (n=8), 101671-42-5; **1c** (n=6), 101671-43-6; **1c** (n=8), 101671-44-7; **2** (n=6), 101671-45-8; **2** (n=8), 101671-46-9; **3** (n=6), 101671-47-0; **3** (n=8), 101671-48-1; **4** (n=6), 101671-49-2; **4** (n=8), 101671-50-5; **5** (n=6), 101671-51-6; **5** (n=8), 101671-52-7; **6** (n=6), 101671-53-8; **6** (n=8), 101671-54-9; **7** (n=6, isomer 1), 101671-55-0; **7** (n=6, isomer 2), 101757-88-4; **7** (n=8, isomer 1), 101671-56-1; **7** (n=8, isomer 2), 101757-89-5; **8** (n=6), 101671-57-2; **8** (n=8), 101671-58-3; **9** (n=6), 101695-31-2; **9** (n=8), 101695-32-3; **10** (n=6), 101671-59-4; **11** (n=4), 101671-60-7; **11** (n=6), 54857-29-3; **12** (n=4), 101671-61-8; **12** (n=6), 101671-62-9; **14** (n=4), 101671-63-0; **14** (n=6), 101695-33-4; **15** (n=4), 101671-64-1; **15** (n=6), 101695-34-5; *o*-PDA, 95-54-5.

[1] P. W. Abenius, H. G. Soderbaum, *Ber. Dtsch. Chem. Ges. 24* (1891) 3033.
[2] a) L. Horner, F. Maurer, *Chem. Ber. 101* (1968) 1783; b) R. Gleiter, W. Dobler, *Chem. Ber. 118* (1985) 1917, and references cited therein.
[3] M. B. Rubin, *Chem. Rev. 75* (1975) 177.
[4] R. West (Ed.): *Oxocarbons*, Academic Press, New York 1980.
[5] M. B. Rubin, E. C. Krochmal, Jr., M. Kaftory, *Recl. Trav. Chim. Pays-Bas 98* (1979) 85.
[6] All new products gave correct elemental analyses.
[7] G. R. Newkome, *Synthesis 1975*, 517.
[8] M. T. Reetz, G. Neumeier, *Chem. Ber. 112* (1979) 2209.
[9] The spectroscopic data for the formoins **14** support a cyclic structure for the formoin fragments [2a].

Synthesis of "*C*-Disaccharides" by Radical C–C Bond Formation**

By *Bernd Giese** and *Tom Witzel*

Disaccharides linked through a carbon atom ("*C*-disaccharides")[1] are of interest on account of their possible activity as enzyme inhibitors and for the investigation of carbohydrate metabolism. It has only been possible so far, however, to link pyranosyl building blocks directly[2] either through a hydroxymethylene[3] or a CH_2–CH_2 group.[1] We have now achieved the synthesis of a "*C*-disaccharide" in which the pyranosyl rings are linked to each other through a methylene group, employing a method developed by us earlier for the formation of C–C bonds, namely, the addition of radicals **1** to alkenes **2**.[4]

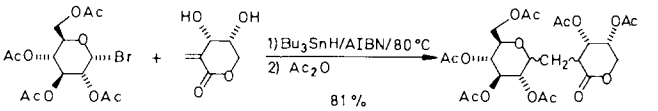


1 2

[*] Prof. Dr. B. Giese, Dipl.-Ing. T. Witzel
Institut für Organische Chemie und Biochemie
der Technischen Hochschule
Petersenstrasse 22, D-6100 Darmstadt (FRG)

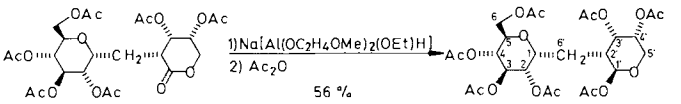
[**] This work was supported by the Deutsche Forschungsgemeinschaft and the Fonds der Chemischen Industrie.

The glycosyl radicals required as reactants can be selectively generated from glycosyl halides such as **3**.[4] The second reactant is a "carbohydrate alkene" containing an exocyclic double bond, e.g., the methylene lactone **4**, which can be synthesized diastereoselectively starting from D-glyceraldehyde.[5]



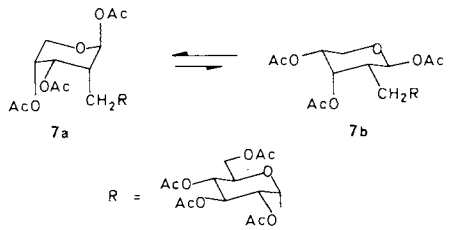
3 4 5

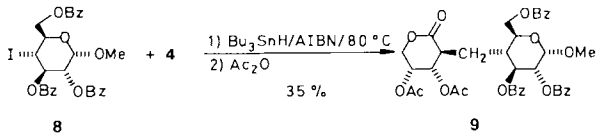
The "*C*-glycosides" **5** were obtained in an α:β ratio of 10:1 from **3** in the presence of a catalytic amount of azoisobutyronitrile (AIBN). In contrast to the high stereoselectivity observed for the reaction of alkenes and glycosyl radicals,[4] the hydrogen transfer from tri-*n*-butyltin hydride to the adduct radical exhibits only low selectivity (60:40). Upon stirring the concentrated reaction mixture with ether, the isomer **6** precipitated out in analytically pure form in 22% yield.[6] Reduction of **6** with sodium ethoxybis(2-methoxyethoxy)hydridoaluminate[7] followed by acetylation afforded the "*C*-disaccharide" **7** in 56% yield.[8]



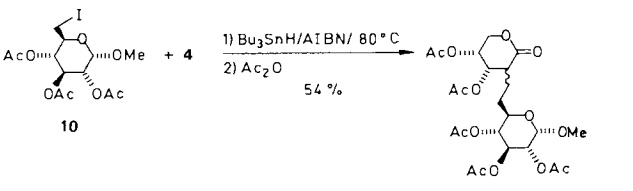
6 7

In order to determine the stereochemistry at C-1′, ^{1}H-NMR spectra were recorded at several temperatures. A doublet for H-1′ ($J(1',2')=5.1$ Hz) is observed at 20 °C, but is split up at −80 °C to give a doublet with a coupling constant of 8.5 Hz and a broad singlet. Such splitting is known for tetra-*O*-acetylribopyranoses[9] and indicates the *trans* geometry of the substituents at C-1′ and C-2′. At −80 °C, the ratio **7a** : **7b** is 70:30, i.e., the energy gain on account of the anomeric effect in **7a** is largely compensated by the energy loss on account of the axial arrangement of the CH_2R group on C-2′.





8 9



10 11

The advantage of this radical C-C bond formation is the variability of the radical building block, because it is possible to generate selectively carbohydrate radicals, with the radical center at any C atom, from xanthogenates, halides, selenides, and nitro compounds with the NO_2 group on a tertiary carbon atom.[4] Thus, the iodides **8** and **10** react with the alkene **4**, under conditions similar to those used for **3**, to give the C-C linked products **9** and **11**, respectively.

Experimental Procedure:

5: **3** (8.63 g, 21.0 mmol) and **4** (2.02 g, 14.0 mmol) were allowed to react in refluxing 1,2-dimethoxyethane with tri-*n*-butyltin hydride (6.11 g, 21.0 mmol) in the presence of a catalytic amount of AIBN. After acetylation, 6.30 g (81%) of **5** was isolated.

Received: January 15, 1986 [Z 1624 IE]
German version: *Angew. Chem. 98* (1986) 459

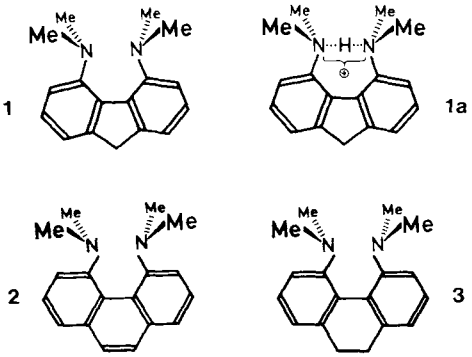
CAS Registry numbers:
3, 572-09-8; **4**, 101757-90-8; **5** (1'α,2β-isomer), 101671-65-2; **5** (1'β,2α-isomer), 101757-91-9; **5** (1'β,2β-isomer), 101757-92-0; **6**, 101757-93-1; **7**, 101671-66-3; **8**, 23487-07-2; **9**, 101671-67-4; **10**, 6304-96-7; **11** (2'α-isomer), 101671-68-5; **11** (2'β-isomer), 101757-94-2.

[1] D. Rouzaud, P. Sinaÿ, *J. Chem. Soc. Chem. Commun. 1983*, 1353.
[2] S. J. Danishefsky, C. J. Maring, M. R. Barbachyn, B. E. Segmuller, *J. Org. Chem. 49* (1984) 4564; S. J. Danishefsky, W. H. Pearson, D. F. Harvey, C. J. Maring, J. P. Springer, *J. Am. Chem. Soc. 107* (1985) 1256; B. Aebischer, R. Meuwly, A. Vasella, *Helv. Chim. Acta 67* (1984) 2236; J. Jurczak, T. Bauer, S. Jarosz, *Tetrahedron Lett. 25* (1984) 4809.
[3] B. Aebischer, J. H. Bieri, R. Prewo, A. Vasella, *Helv. Chim. Acta 65* (1982) 2251; J. M. Beau, P. Sinaÿ, *Tetrahedron Lett. 26* (1985) 6189.
[4] B. Giese, *Angew. Chem. 97* (1985) 555; *Angew. Chem. Int. Ed. Engl. 24* (1985) 553, and references cited therein.
[5] C. Papageorgiou, C. Benezra, *J. Org. Chem. 50* (1985) 157; A. Bernardi, M. G. Beretta, L. Colombo, C. Gennari, G. Poli, C. Scolastico, *ibid. 50* (1985) 4442; the δ-lactone **4** crystallizes from ethyl acetate as a single isomer, m.p. = 117-119°C.
[6] Compound **6** is the isomer of the two α-*C*-glycosides formed in smaller amount. The stereochemistry at C-1 and C-2' is derived from the axial-equatorial coupling constants $J(1,2) = 4.9$ and $J(2',3') = 3.1$ Hz. Comparison with the NMR data of the product that was obtained by C-C bond formation between *tert*-butyl iodide and the alkene **4** and for which an X-ray structure analysis is available supports the structure of **6**.
[7] R. Kanazawa, T. Tokoroyama, *Synthesis 1976*, 526.
[8] The "*C*-disaccharide" **7** is a colorless crystalline substance; m.p. = 68-70°C, $[\alpha]_D^{20}$ 29.2 ($c = 0.95$ in $CHCl_3$); ^{1}H-NMR (300 MHz, $CDCl_3$): $\delta = 2.04$, 2.05, 2.06, 2.08, 2.09, 2.12, 2.15 (each s, OAc), 1.64-1.74 (m, 1H; H-6'b), 1.86-1.96 (m, 1H; H-6'a), 2.20-2.28 (m, 1H; H-2'), 3.80 (ddd, 1H, $J(5,6a) = 5.8$, $J(5,6b) = 2.6$ Hz; H-5), 3.84 (dd, 1H, $J(4',5'b) = 6.0$, $J(5'a,5'b) = 12.2$ Hz; H-5'b), 3.95 (dd, 1H, $J(4',5'a) = 3.6$ Hz; H-5'a), 4.08 (dd, 1H, $J(6a,6b) = 12.2$ Hz; H-6b), 4.21 (dd, 1H; H-6a), 4.28 (ddd, 1H, $J(1,2) = 5.7$, $J(1,6'a) = 2.8$, $J(1,6'b) = 12.3$ Hz; H-1), 4.94 (t, 1H, $J(3,4) = J(4,5) = 9.1$ Hz; H-4), 5.04-5.12 (m, 2H; H-2, H-4'), 5.29 (t, 1H, $J(2,3) = 9.1$ Hz; H-3), 5.45 (t, 1H, $J(2',3') = J(3',4') = 3.6$ Hz; H-3'), 5.90 (d, 1H, $J(1',2') = 5.1$ Hz; H-1').
[9] N. S. Bhacca, D. Horton, *J. Am. Chem. Soc. 89* (1967) 5993.

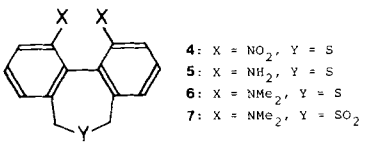
4,5-Bis(dimethylamino)phenanthrene and 4,5-Bis(dimethylamino)-9,10-dihydrophenanthrene: Syntheses and "Proton Sponge" Properties

By *Thomas Saupe, Claus Krieger,* and *Heinz A. Staab**

We have ascribed the fact that the basicity of 4,5-bis(dimethylamino)fluorene **1** is even higher than that of 1,8-bis(dimethylamino)naphthalene ("Proton Sponge")[2] to the stronger steric interaction of the two dimethylamino groups and to the formation of an especially strong, nearly linear N···H···N hydrogen bond in the monoprotonated **1a**.[3] Simple examinations of models (cf. ref. [3]) indicated that 4,5-bis(dimethylamino)phenanthrene **2** and 4,5-bis-(dimethylamino)-9,10-dihydrophenanthrene **3** might also be interesting as potential "proton sponges." In particular, a strong steric hindrance of the dimethylamino groups with unfavorable overlapping of the nitrogen lone-pairs was expected for **2**, and a nearly linear N···H···N hydrogen bond with an even shorter N···N distance than in **1a** was expected for the monocation **2a**.



In order to synthesize **2** and **3**, 2,2'-bis(bromomethyl)-6,6'-dinitrobiphenyl[4] was allowed to react with sodium sulfide (methanol/water, reflux, 5 h) to give the cyclic sulfide **4**[5] (m.p. = 173-174°C; 84% yield). Reduction of **4** with zinc dust in acetic acid (reflux, 140 min) gave the diamino compound **5**[5] (m.p. = 190-191°C; 80%), which was methylated with dimethyl sulfate in the presence of sodium hydride (tetrahydrofuran (THF), reflux, 1 h) to give **6** [5] (m.p. = 128-129°C; 36%). Oxidation of **6** with peroxytrifluoroacetic acid (trifluoroacetic acid, 0-25°C, 100 min) led selectively to the sulfone **7**[5] (m.p. = 265-266°C; 81%).

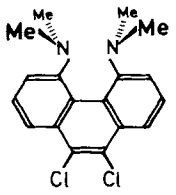


Vacuum gas-phase pyrolysis of **7** (625°C, 0.1-0.3 Pa) afforded (along with 20% of unreacted **7**) the product **3**[5] in 58% yield (m.p. = 82-84°C); ^{1}H-NMR (360 MHz, $CDCl_3$, 303 K): $\delta = 2.51$ (s, 12H), 2.57-2.74 (AA'BB', 4H), 6.75 ('d', $J \approx 7.3$ Hz, 2H), 6.85 ('d', $J \approx 8.1$ Hz, 2H), 7.08 ('dd', $J \approx 7.3$ and 8.1 Hz, 2H). The observation of an AA'BB' system for the protons in the 9- and 10-positions of **3** shows that the flipping-over of the "biphenyl moiety" in **3** is strongly hindered sterically. All attempts to dehydrogenate **3** did not lead—apparently owing to the required formation of significantly higher strain—to 4,5-bis(dimethylamino)phenanthrene **2** but rather to more or less complete decomposition of the starting material.

Although the synthesis of **2** by Ramberg-Bäcklund rearrangement of the α-chlorosulfone of **7** appeared futile in view of *Paquette*'s investigations,[6] the variant of the Ramberg-Bäcklund rearrangement described by *Meyers* et al.[7] was carried out on **7** [tetrachloromethane/*tert*-butyl alcohol (1 : 1), potassium hydroxide, 0-20°C, 1 h). Surprisingly, this reaction led indeed to the phenanthrene system of **2**;

[*] Prof. Dr. H. A. Staab, Dr. T. Saupe, C. Krieger
Abteilung Organische Chemie
Max-Planck-Institut für medizinische Forschung
Jahnstrasse 29, D-6900 Heidelberg (FRG)
[**] New "Proton Sponges," Part 3.—Part 2: [1].

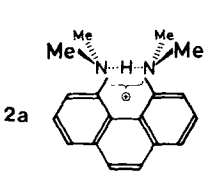
its 9,10-dichloro substitution product **8**[5] was obtained in 53% yield (m.p. = 160–161.5 °C). Halogen–metal exchange (excess lithium, THF, −55 to −35 °C, 1–1.5 h) and subsequent reaction with methanol gave **2**[5] (m.p. = 148 °C) in 27% yield (along with 10% of **3** and 46% of reisolated **8**).[8]



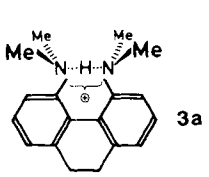
8

In the ^{1}H-NMR spectrum of **2** [(360 MHz, $CDCl_3$, 303 K): $\delta = 2.06$ (br. s, 6H), 3.13 (br. s, 6H), 7.08 ('d', $J \approx 7.8$ Hz, 2H), 7.24 ('d', $J \approx 7.5$ Hz, 2H), 7.39 ('dd', $J \approx 7.8$ and 7.5 Hz, 2H), 7.50 (s, 2H)] the pairwise nonequivalence of the methyl protons indicates a strong helical deformation of the phenanthrene system of **2**. From the coalescence of these signals ($T_c = 337$ K, $\Delta\nu_s = 370$ Hz), the enantiomerization barrier for **2** was determined to be $\Delta G^{\neq} = 64.0 \pm 0.4$ kJ/mol (in [D_5]pyridine). Similarly, for **8**, $\Delta G^{\neq} = 66.8 \pm 0.4$ kJ/mol at $T_c = 352$ K was found. These values are of the same order of magnitude as those determined for the enantiomerization of similar 4,5-disubstituted phenanthrenes.[9]

Both **2** and **3** react with perchloric acid—although used in excess—to form well-defined monoperchlorates, which contain the cations **2a** and **3a**. In the ^{1}H-NMR spectra[10] of **2a**-perchlorate[5] (m.p. = 190–191 °C) and **3a**-perchlorate[5] (m.p. = 221 °C), the strongly downfield shifted absorptions of the protons of the N···H···N hydrogen bond at $\delta = 18.37$ (**2a**) and 16.50 (**3a**) are particularly noticeable. The large positive isotope effect $\Delta\delta(^1H,^2H) = \delta(^1H) - \delta(^2H)$ that was observed for these protons supports, according to *Forsén* et al.,[11] the presence of strong but still unsymmetrical hydrogen bonds in **2a** and **3a**, as in **1a**-perchlorate. The coupling constants between the bridge proton and the methyl groups [monocation of 1,8-bis(dimethylamino)naphthalene, $J = 192$ Hz;[3] **1a**, $J = 2.03$ Hz;[3] **2a**, $J = 2.17$ Hz] also support the presence of an especially strong hydrogen bond in **2a**.



2a



3a

We obtained crystals of **2a**-perchlorate that were suitable for an X-ray structure analysis from acetone by addition of a layer of diethyl ether and subsequent slow crystal growth at the layer boundary. The structure of the **2a** part is characterized, above all, by the strong helical twisting of the phenanthrene system by 23° along the C12–C13 axis (Fig. 1B). The bond angles (Fig. 1A) at C12 and C13 reflect the considerable steric repulsion between the dimethylamino groups at C4 and C5. The bond lengths are similar to those of other phenanthrenes (with the exception of the especially short C1–C2, C7–C8, and C9–C10 bonds).[12] The hydrogen atom in the hydrogen bond is in a nearly linear arrangement (angle 168°) and unsymmetrically located between N4 and N5, which is connected with the only approximate C_2 symmetry of **2a**. The direct N···N distance in **2a** (254.4 pm) is significantly shorter than the corresponding N···N distance in **1a** (262.6 pm);[3] it is one of the shortest distances found so far for N···H···N hydrogen bonds.

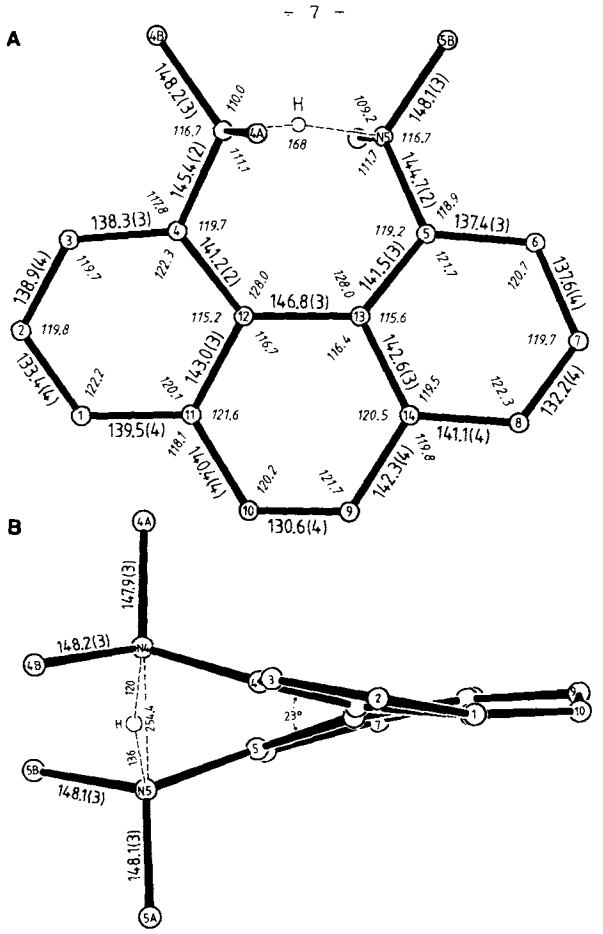


Fig. 1. Structure of the **2a** portion of **2a**-perchlorate as viewed looking down on the plane of the phenanthrene ring (A) and from the side (along the C2···C7 axis) (B). Crystal and measurement data: $a = 1293.4(3)$, $b = 1235.4(3)$, $c = 1218.4(3)$ pm, $\beta = 111.67(4)°$; space group $P2_1/c$, $Z = 4$; 4715 measured, 2402 observed reflections with $I \geq 1.96\sigma(I)$; $R = 0.058$. Further details of the crystal structure investigation may be obtained from the Fachinformationszentrum Energie, Physik, Mathematik GmbH, D-7514 Eggenstein-Leopoldshafen 2 (FRG), on quoting the depository number CSD-51758, the names of the authors and the journal citation.

The data given indicate that the N···H···N hydrogen bond in **2a** is stronger than in **1a**. Furthermore, the free base **2** should also have a shorter N···N distance than **1** and therefore a stronger destabilizing interaction between the nitrogen lone-pair electrons,[13] which is removed upon protonation. For both reasons, we expected **2** to exhibit a higher basicity than **1**. Surprisingly, however, the determination of the pK_a values in 35% (v/v) dimethylsulfoxide/water ($I = 0.1$ mol/L, 25 °C)[14] gave a significantly lower pK_a value for **2** (11.5 ± 0.1) than for **1** (12.8 ± 0.1). We ascribe this result to the fact that the hydrogen bond in **2a** is less shielded on all sides by the flanking *N*-methyl groups than that in **1a**, as shown by comparison of the X-ray structure analyses of **1a**[3] and **2a** (Fig. 1). According to examination of models, this effect should be even more pronounced for **3a** than for **2a**; this is in accord with the estimated pK_a value of 10.9 for **3a** based on proton transfer experiments.

Received: January 17, 1986 [Z 1629 IE]
German version: *Angew. Chem.* 98 (1986) 460

CAS Registry numbers:
2, 101543-79-7; **2** · $HClO_4$, 101543-86-6; **3**, 101543-80-0; **3a** · $HClO_4$, 101543-87-7; **4**, 101543-81-1; **5**, 101543-82-2; **6**, 101543-83-3; 7, 101543-84-4; **8**, 101543-85-5; 2,2'-bis(bromomethyl)-6,6'-dinitrobiphenyl, 56798-69-7.

[1] R. Gleiter, W. Schäfer, H. A. Staab, T. Saupe, *J. Org. Chem. 49* (1984) 4463.

[2] R. W. Alder, P. S. Bowman, W. R. S. Steele, D. R. Winterman, *Chem. Commun. 1968*, 723; F. Hibbert, *J. Chem. Soc. Perkin Trans. 2 1974*, 1862.

[3] H. A. Staab, T. Saupe, C. Krieger, *Angew. Chem. 95* (1983) 748; *Angew. Chem. Int. Ed. Engl. 22* (1983) 731.

[4] P. Newman, P. Rutkin, K. Mislow, *J. Am. Chem. Soc. 80* (1958) 465; D. C. Iffland, H. Siegel, *ibid. 80* (1958) 1947.

[5] Elemental analyses and spectroscopic data are in accord with the structures given.

[6] L. A. Paquette, *J. Am. Chem. Soc. 86* (1964) 4085; *Acc. Chem. Res. 1* (1968) 209.

[7] C. Y. Meyers, A. M. Malte, W. S. Matthews, *J. Am. Chem. Soc. 91* (1969) 7510; C. Y. Meyers, W. S. Matthews, G. J. McCollum, J. C. Branca, *Tetrahedron Lett. 1974*, 1105.

[8] By using a smaller excess of lithium, it was also possible to obtain the derivative of **2** monochlorinated in the 9-position [5] (m.p. ≈ 183–184°C).

[9] Cf. H. Scherübl, U. Fritzsche, A. Mannschreck, *Chem. Ber. 117* (1984) 336; and references cited therein.

[10] ^{1}H-NMR (360 MHz, [D_6]dimethylsulfoxide): **2a**-perchlorate: $\delta = 3.00$ ('d', $J = 2.17$ Hz, 12H), 7.93 ('dd', $J \approx 8.0$ and 6.5 Hz, 2H), 8.02 ('dd', $J \approx 6.5$ and 1.3 Hz, 2H), 8.03 (s, 2H), 8.18 ('dd', $J \approx 8.0$ and 1.3 Hz, 2H), 18.37 (br. s, 1H); **3a**-perchlorate $\delta = 2.5$–3.2 (m, 16H), 7.49 ('d', $J \approx 7.1$ Hz, 2H), 7.56 ('dd', $J \approx 7.1$ and 8.0 Hz, 2H), 7.62 ('dd', $J \approx 8.0$ Hz and 1.1 Hz, 2H), 16.50 (br. s, 1H).

[11] L. J. Altman, D. Laungani, G. Gunnarsson, H. Wennerström, S. Forsén, *J. Am. Chem. Soc. 100* (1978) 8264.

[12] The atoms involved in these bonds exhibit especially large anisotropic vibration parameters, which are due to a considerable vibration of the phenanthrene skeleton around an axis perpendicular to the plane of the molecule.

[13] This is supported by preliminary results of PE investigations on **2**: R. Gleiter, personal communication.

[14] Cf. also F. Hibbert, K. P. P. Hunte, *J. Chem. Soc. Perkin Trans. 2 1983*, 1895.

$[Pd_2S_{28}]^{4\ominus}$: A 30-Membered Cage Containing an Entrapped Cation**

By *Achim Müller,* Klaus Schmitz, Erich Krickemeyer, Michael Penk,* and *Hartmut Bögge*

Dedicated to Professor Marianne Baudler on the occasion of her 65th birthday

Novel, exciting metal–sulfur heterocycles and clusters can be formed from polysulfide ions and metal ions,[1] since, on the one hand, polysulfide ligands exhibit a wide range of coordination possibilities and, in addition, a large variety of combinations of rings is possible depending on the type of metal center.

We have now succeeded in obtaining orange-red crystals of **1** by reaction of palladium acetylacetonate in acetonitrile/dimethylformamide with an ethanolic solution of polysulfide in the presence of the cations $PPh_4^{\oplus}$ and $NH_2Me_2^{\oplus}$. **1** was characterized spectroscopically[2] and magnetochemically[2] as well as by elemental analysis and a complete X-ray crystal structure analysis.[3,4]

$(PPh_4)_2(NH_2Me_2)(NH_4)[Pd_2(S_7)_4]$ **1**

The anion of **1**, which exhibits approximate D_4 symmetry, has an unusual cage structure (Fig. 1). The cage is formed by linking two Pd atoms (or two PdS_4 planes, which form an approximate square antiprism) with four polysulfide chains. Alternatively, it can be described as being built up from two almost perpendicular tetradecathia-8,16-dipalladacyclohexadecanes having the Pd atoms in common. The coordination of the Pd atom corresponds to that expected for Pd^{II}-d^8.

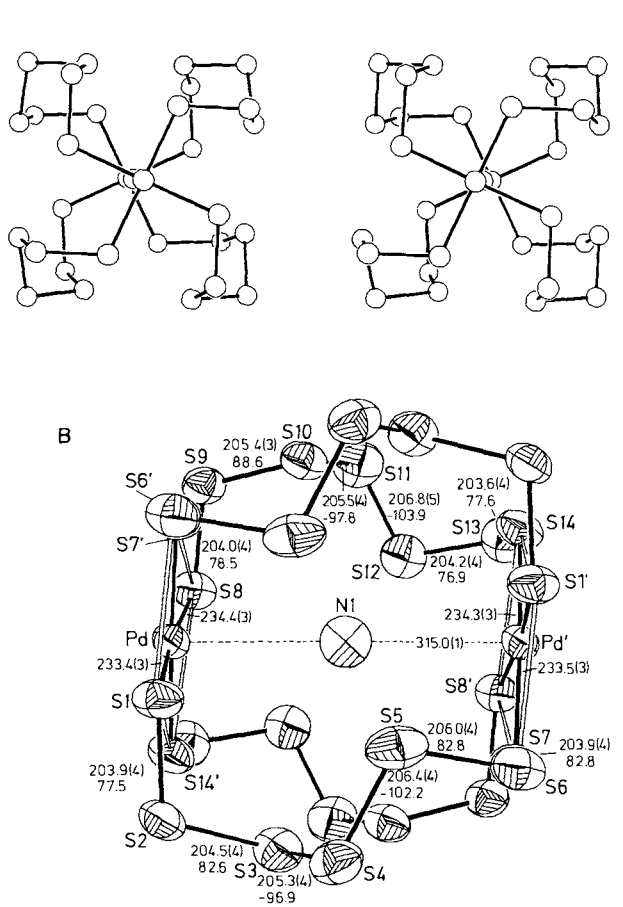


Fig. 1. Structure of the anion in crystals of **1**: A) stereoview along the Pd–Pd axis; B) viewed along the crystallographic C_2 axis with bond lengths [pm] and selected torsional angles [°]: S1-Pd-S(other ring) and S8-Pd-S(other ring) 89.5(1)–90.4(1), S1-Pd-S8 174.4(1), S7'-Pd-S14' 177.9(1), all Pd-S-S 112.5(1)–113.3(2), all S-S-S 105.6(2)–108.2(2); PdS_4 planes (S1-S14'-S8-S7' and S1'-S7-S8'-S14) in B specially marked. Definition of the rings: PdPd'S1···S14, "other" PdPd'S1'···S14'.

Since the Pd–Pd distance is 630.0(1) pm and the second coordination shell sulfur atoms lie roughly in the PdS_4 planes, the cage has a (relatively) large cavity. In its center is an $NH_4^{\oplus}$ ion, which most likely contributes to the stabilization of the cage system. The anion of **1** can, therefore, also be regarded as the "cation–anion complex" $[Pd_2\{NH_4\}(S_7)_4]^{3\ominus}$. The four equivalent $S_7^{2\ominus}$ ligands are so arranged that the sulfur atoms have alternatingly small (373.3–408.0 pm) and large (453.3–492.1 pm) distances from the center of the cage. The Pd–N distance is 315.0(1) pm. Remarkably, the cages are stacked parallel to the plane diagonals $\vec{a}+\vec{c}$ with a Pd–Pd distance of (only) 741.8 pm and the $NH_2Me_2^{\oplus}$ ions in between them.

[*] Prof. Dr. A. Müller, K. Schmitz, E. Krickemeyer, M. Penk, Dr. H. Bögge
Fakultät für Chemie der Universität
Postfach 8640, D-4800 Bielefeld 1 (FRG)

[**] We thank Degussa for the donation of platinum metal compounds.

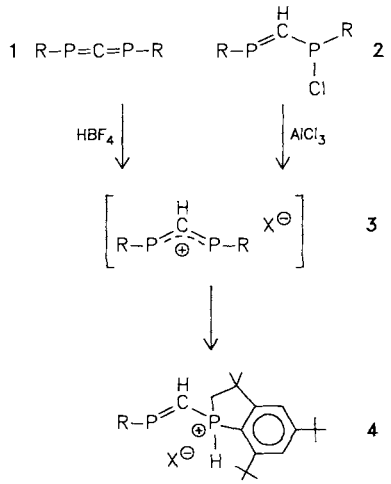
Received: February 10, 1986 [Z 1664 IE]
German version: *Angew. Chem. 98* (1986) 470

[1] A. Müller, E. Diemann, *Adv. Inorg. Chem. Radiochem. 31*, in press; M. Draganjac, T. B. Rauchfuss, *Angew. Chem. 97* (1985) 745; *Angew. Chem. Int. Ed. Engl. 24* (1985) 743.

[2] IR (solid/CsI pellet): 482 (w), 453 (w) (ν(SS)), 315 (w) cm^{-1} (ν_{as}(PdS)); Raman (solid/λ_e = 647.1 nm): 488 (s), 462 (m), 435 (w), 419 (m) (ν(SS)), 292 (s) cm^{-1} (ν_s(PdS)); (only characteristic bands below 500 cm^{-1} are listed); UV/VIS (solid/reflectance/cellulose): 475 (sh), 375 nm; **1** is diamagnetic (without correction).

[3] *C2/c*, a = 2094.9(10), b = 1469.6(6), c = 2586.9(12) pm, β = 109.89(3)°; V = 7489.1 × 10^6 pm^3; Z = 4; R = 0.075 for 5775 independent reflections ($F_o > 3.92\sigma(F_o)$); Syntex P2$_1$ diffractometer, Mo$_{K\alpha}$-radiation, graphite monochromator. The powder diffractogram calculated from single-crystal data is in agreement with the measured one. Further details of the crystal structure investigation may be obtained from the Fachinformationszentrum Energie, Physik, Mathematik GmbH, D-7514 Eggenstein-Leopoldshafen 2 (FRG), on quoting the depository number CSD-51798, the names of the authors, and the journal citation.

[4] Black [NEt$_4$]$_2$[Pd(S$_4$)$_2$] could also be obtained and characterized by crystal structure analysis.



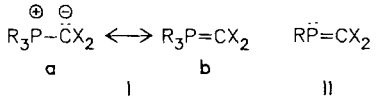
R = 2,4,6-tBu$_3$C$_6$H$_2$

a, X = AlCl$_4$; b, X = BF$_4$

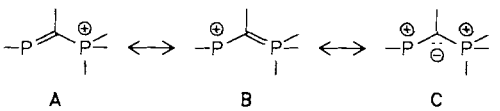
A 2-Phosphonio-Substituted 1-Phospha-1-alkene: Resonance between P^{III} Alkene and P^{V} Ylide**

By *Hans H. Karsch,* Hans-Ulrich Reisacher,* and *Gerhard Müller*

Compounds with a P^{V}C "double bond" **I** have long been known, although they are best described by the ylide form **Ia**.[1] Compounds **II** with a P^{III}C double bond, on the other hand, have only become available in recent years and their PC double bonds are substantially less polarized.[2]



We have now studied whether the introduction of 2-phosphonio substituents on a 1-phospha-1-alkene leads to a resonance relationship as described by Equation (1). Such a bonding situation would have crucial consequences for the character and reactivity of the P^{III}C double bond. We have prepared the 2-phosphonio-substituted 1-phospha-1-alkene **4** both from the diphosphaallene **1**[3] and from the phosphino-substituted phosphaalkene **2**.[3b]



(1)

Compound **4** is formed via the presumed intermediate 1,3-diphosphaallyl cation **3** by the known C,H addition of a *tert*-butyl group to a proximal electropositive center, resulting in ring formation.[4] The yellow, crystalline compounds **4a**[5] and **4b**[6] dissolve surprisingly well in toluene.

The resonance relationship shown in Equation (1) follows from the NMR data: in the ^{31}P-NMR spectrum of **4**, the resonance signal of the P^{III} atom is found at unusually low field (cf. ref. [3b]) in the range observed for phosphenium ions.[7] On the other hand, the ^{13}C-NMR signal of the bridging sp^2 C atom has the lowest chemical shift found so far for phosphaalkenes:[8] δ = + 109.94 (**4a**) and + 116.25 (**4b**).[9] The alkene hydrogen atom is also correspondingly shielded ($\delta(^1H)$ = 6.84 for **4a** in comparison with 8.56 for **2**). The magnitudes of the ^1J(PC) coupling constants also agree with expectations. These results indicate that resonance structures B and C [Eq. (1)] are of considerable importance in describing the actual structure of **4**. Structure C is a resonance-stabilized bis(σ-organo)phosphenium ion.[11] The cation/anion interaction apparently has only a minor effect. Prototropism, i.e., the existence of tautomeric forms, was not observed (ylides with hydrogen on the phosphorus atom are rare).

Compounds **4a**, **b** are thus examples of compounds having a strongly polarized P^{III}C double bond, which may be described by P^{III}=C(sp^2)/P^V=C(sp^2) resonance structures. To the best of our knowledge, such a resonance relationship was unknown until now.[12] Polarization of the double bond is also observed for vinylphosphonium salts, resulting in a deshielded β-C atom that is highly electrophilic.[13] These observations further support the analogy between carbon and phosphorus expected on the basis of the diagonal relationship.

Received: December 19, 1985;
supplemented: February 10, 1986 [Z 1596 IE]
German version: *Angew. Chem. 98* (1986) 467

CAS Registry numbers:
4a, 101519-15-7; **4b**, 101519-16-8.

[*] Priv.-Doz. Dr. H. H. Karsch, Dipl.-Chem. H.-U. Reisacher, Dr. G. Müller
Anorganisch-chemisches Institut der Technischen Universität München
Lichtenbergstrasse 4, D-8046 Garching (FRG)

[**] Compounds of Main-Group Elements with Phosphinidene Substituents, Part 3. This work was supported by the Deutsche Forschungsgemeinschaft and the Fonds der Chemischen Industrie.—Part 2: [3a].

[1] H. Schmidbaur, *Adv. Organomet. Chem. 14* (1976) 205, and references cited therein.

[2] R. Appel, F. Knoll, I. Ruppert, *Angew. Chem. 93* (1981) 771; *Angew. Chem. Int. Ed. Engl. 20* (1981) 731, and references cited therein.

[3] a) H. H. Karsch, H.-U. Reisacher, G. Müller, *Angew. Chem. 96* (1984) 619; *Angew. Chem. Int. Ed. Engl. 23* (1984) 618; b) H. H. Karsch, F. H. Köhler, H.-U. Reisacher, *Tetrahedron Lett. 25* (1984) 3687; c) R. Appel, P. Fölling, B. Josten, M. Siray, V. Winkhaus, F. Knoch, *Angew. Chem. 96* (1984) 620; *Angew. Chem. Int. Ed. Engl. 23* (1984) 619; d) M. Yoshifuji, K. Toyota, N. Inamoto, *J. Chem. Soc. Chem. Commun. 1984*, 689.

[4] a) A. H. Cowley, J. E. Kidluff, N. C. Norman, M. Pakulski, *J. Am. Chem. Soc. 105* (1983) 4845; M. Yoshifuji, I. Shiria, K. Ando, N. Inamoto, *Tetrahedron Lett. 24* (1983) 933; D. H. Champion, A. H. Cowley, *Polyhedron 4* (1983) 1791; b) H. H. Karsch, H.-U. Reisacher, unpublished, see also [3b].

[5] **4a**, m.p. = 153–155 °C; NMR ([D$_8$]toluene, 25 °C): ^{31}P: $\delta(P^{III}) = 383.3$, $\delta(P^{V}) = 11.0$ ($^2J(PP) = 111.5$ Hz; $^1J(P^{V}H) = 525$ Hz); ^{13}C: $\delta(PCHP) = 109.94$ (dd, $^1J(P^{III}C) = 7.8$ Hz, $^1J(P^{V}C) = 82.0$ Hz); ^{1}H: $\delta(PC\mathit{H}P) = 6.84$ (ddd, $^2J(P^{III}H) = 17.8$ Hz, $^2J(P^{V}H) = 9.0$ Hz, $^2J(HH) = 10.5$ Hz), $\delta(P^{V}H) = 7.76$ (d, $^1J(P^{V}H) = 525$ Hz). The constitution was confirmed by X-ray structure analysis; satisfactory refinement of the structure was not possible owing to the poor quality of the crystals. Crystal data (**4a**·2toluene): orthorhombic, $P2_12_12_1$; $a = 13.567(4)$, $b = 15.212(3)$, $c = 26.106(8)$ Å; $V = 5387.79$ Å^3, $\rho_{calcd} = 1.133$ g cm^{-3} for $Z = 4$, $\mu(Mo_{K\alpha}) = 3.24$ cm^{-1}, $F(000) = 1968$, $T = -35$ °C.

[6] **4b**, m.p. = 181–184 °C; NMR ([D$_8$]toluene, 25 °C): ^{31}P: $\delta(P^{III}) = 365.8$, $\delta(P^{V}) = 23.5$ ($^2J(PP) = 172.0$ Hz, $^1J(P^{V}H) = 535$ Hz); ^{13}C: $\delta(PCHP) = 116.25$ ($^1J(P^{III}C) = 11.0$ Hz; $^1J(P^{V}C) = 116.3$ Hz); ^{1}H: $\delta(PC\mathit{H}P)$ not determined (overlapping with aromatic region); $\delta(P^{V}H) = 8.94$ (ddd, $^1J(P^{V}H) = 535.0$ Hz, $^3J(P^{III}H) = 6.0$ Hz, $^3J(HH) = 12.0$ Hz).

[7] A. H. Cowley, *Chem. Rev. 85* (1985) 367, and references cited therein.

[8] ^{13}C-NMR data for phosphaalkenes reported up to now gave δ values of +137.1 (H(*s*Bu)NN(*s*Bu)P=C(Ph)SiMe$_3$ [10a]) to +252.5 (Me$_3$SiP=C(OSiMe$_3$)Re(NO)(CO)C$_5$Me$_5$ [10b]).

[9] For phosphaalkenes such as **2**, this value is $\delta \approx +170$ [3b]. The proximity of a phosphonium center, however, should result in deshielding of the sp^2 C atom.

[10] a) R. Appel, S. Korte, M. Halstenberg, F. Knoch, *Chem. Ber. 115* (1982) 3610; b) L. Weber, K. Reizig, *Angew. Chem. 97* (1985) 53; *Angew. Chem. Int. Ed. Engl. 24* (1985) 53.

[11] The bis(ferrocenyl)phosphenium tetrachloroaluminate ion may be considered as the only example so far for a bis(σ-organo)phosphenium ion.

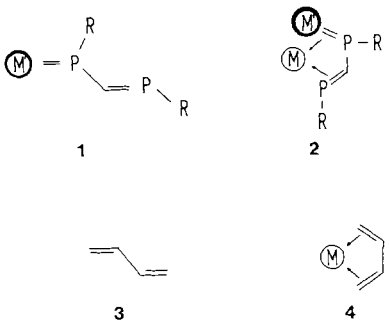
[12] Parallels may be drawn, however, with 2-phospha- and 2-phosphonioallyl cations: R. O. Day, A. Willhalm, J. M. Holmes, R. R. Holmes, A. Schmidpeter, *Angew. Chem. 97* (1985) 775; *Angew. Chem. Int. Ed. Engl. 24* (1985) 764.

[13] a) For reaction of vinylphosphonium salts with nucleophiles, see P. Keough, M. Grayson, *J. Org. Chem. 29* (1964) 631; b) for deshielding of the β-C atom in vinylphosphonium salts see T. A. Albright, S. V. De Voe, W. J. Freeman, E. E. Schweizer, *ibid. 40* (1975) 1651.

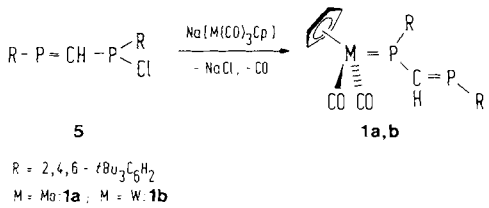
Phosphorus Analogues of Unsaturated Carbon Compounds: an (*s-trans*)-1,3-Diphospha-4-metallabutadiene and Its (*s-cis*)-Fe(CO)$_3$ Complex**

By *Hans H. Karsch,* Hans-Ulrich Reisacher, Brigitte Huber, Gerhard Müller, Wolfgang Malisch,* and *Klaus Jörg*

Analogies between phosphorus and carbon chemistry are well documented for saturated systems[1] and have been extended in recent years to the unsaturated systems.[2, 3] Until now, however, it has not been possible to isolate acyclic, conjugated 1,3-diphosphabutadienes.[3a] They are also unknown as complex ligands, even though a large number of complexes are known that contain an isolated PX multiple bond.[4] The incorporation of a metal into the heterobutadiene unit has only been achieved so far for cyclic compounds that are stabilized by complex formation.[5] Free 1,3-diphospha-4-metallabutadienes **1** and their metal complexes **2**, which contain **1** as an acyclic π-ligand, have not been described so far. They would be true analogues of butadiene **3** (which has the *s-trans* conformation in the ground state) and its *s-cis* metal complexes **4**, respectively.



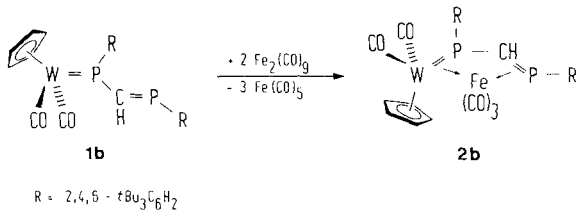
We have now succeeded in obtaining compounds of the type **1** from the recently described 2-chlorophosphino-substituted 1-phospha-1-alkene **5**.[6a] **1a**, **b**[7, 8] can be isolated as green, air-stable crystals. According to an X-ray structure analysis of **1a** (M = Mo),[7] they can be described as *s-trans* heterobutadienes (Fig. 1). In **1a**, a 1,3-diphosphaallyl fragment[6b] (which is not obtainable in its uncomplexed



form) is bonded to the metal "end-on" through the planar-coordinated P1.[9] A (noncrystallographic) mirror plane passes through Mo, P1, C1, and P2. The MoP1 bond (2.268(2) Å) is only slightly longer than other MoP double bonds and significantly shorter than MoP single bonds.[10] The P–C bond lengths differ significantly. P1–C1 corresponds to a (slightly shortened) single bond and P2–C1 to a double bond.[2] The NMR data, especially the low-field shift of the signals of the phosphorus nuclei and the large $^1J(WP)$ coupling constant, are in good agreement with reference values.[2, 6, 10]

The tricarbonyliron complex (butadiene)Fe(CO)$_3$ may be considered as a "classical" butadiene complex of the type **4**. In order to test the butadiene analogy of **1**, we allowed **1b** to react with Fe$_2$(CO)$_9$[11] and thereby obtained reddish brown crystals of **2b**.[12] According to the ^{31}P-NMR spectrum, no intermediate is formed.

The butadiene-like coordination of **1b** to the Fe(CO)$_3$ fragment requires a rotation around the PC single bond. The NMR data are in accord with a π-coordination of the ligand **1b**; in particular, the high-field shifts of the ^{31}P- and ^{13}C-NMR resonances are typical for such a coordination.[4, 5, 11]



The X-ray structure analysis[12] confirms that **2b** is a heterobutadiene complex (Fig. 1). Characteristic are the nearly planar arrangement of the ligand framework

[*] Priv.-Doz. Dr. H. H. Karsch, Dipl.-Chem. H.-U. Reisacher, cand. Chem. B. Huber, Dr. G. Müller
Anorganisch-chemisches Institut der Technischen Universität München
Lichtenbergstrasse 4, D-8046 Garching (FRG)
Prof. Dr. W. Malisch, Dipl.-Chem. K. Jörg
Institut für Anorganische Chemie der Universität
Am Hubland, D-8700 Würzburg (FRG)

[**] Compounds of Main-Group Elements with Phosphinidene Substituents, Part 4. This work was supported by the Deutsche Forschungsgemeinschaft and the Fonds der Chemischen Industrie.—Part 3: [6b].

WP1C1P2 and the partial structure WP1C1C2, the distances of the iron atom from the donor atoms W, P1, C1, and P2,[5, 11] and the near equivalence of the two P-C1 bond lengths. The $Cp(CO)_2W$ fragment is only slightly changed in comparison with the $Cp(CO)_2Mo$ fragment in **1a**. The conformation found in the solid state requires a rotation around the WP double bond during the complexation with the $Fe(CO)_3$ fragment. This finding also supports the view that **2b** is a heterobutadiene complex. These results allow, for the first time, the direct use of an uncomplexed diphosphametallaheterobutadiene as a ligand in synthesis.[13]

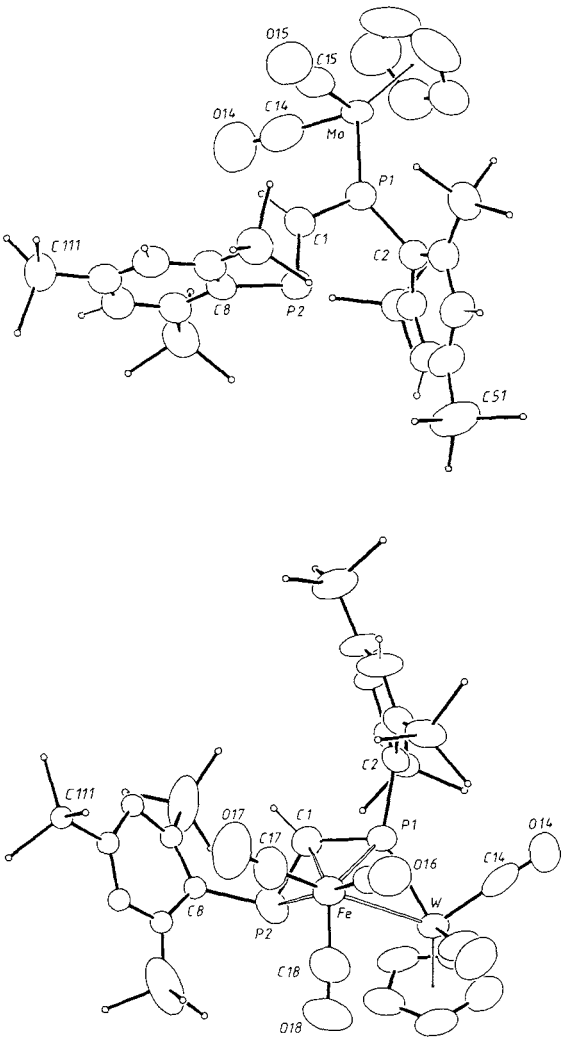


Fig. 1. Structures of **1a** (above) and **2b** (below) in the crystal; ORTEP thermal ellipsoids at the 50% probability level, methyl groups (and isotropic atoms for **2b**) drawn with arbitrary radii without H atoms. Important bond lengths [Å] and bond angles [°]: **1a**: Mo-P1 2.268(2), P1-C1 1.799(6), P2-C1 1.685(6), P1-C2 1.867(6), P2-C8 1.867(6); Mo-P1-C1 120.8(2), Mo-P1-C2 138.9(2), C2-P1-C1 100.3(3), P1-C1-P2 125.1(3), C1-P2-C8 103.4(3).—**2b**: W-P1 2.365(3), P1-C1 1.74(1), P2-C1 1.76(1), P1-C2 1.88(1), P2-C8 1.86(2), Fe-W 2.980(2), Fe-P1 2.295(3), Fe-C1 2.11(1), Fe-P2 2.441(4); W-P1-C1 117.8(4), W-P1-C2 140.4(4), C2-P1-C1 100.5(5), P1-C1-P2 120.3(6), C1-P2-C8 101.3(6).

Received: December 19, 1985;
supplemented: February 10, 1986 [Z 1597 IE]
German version: *Angew. Chem. 98* (1986) 468

CAS Registry numbers:
1a, 101518-74-5; **1b**, 101518-76-7; **2b**, 101518-75-6; $Cp(CO)_3W$-PR-CH=PR(R = $tBu_3C_6H_2$), 101711-25-5; R-P=CH-P(Cl)R(R = $tBu_3C_6H_2$), 93554-05-3; Na[Mo(Co)$_3$Cp], 12107-35-6; Na[W(CO)$_3$Cp], 12107-36-7; $Fe_2(CO)_9$, 15321.51.4.

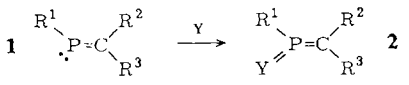
[1] M. Baudler, *Angew. Chem. 94* (1982) 520; *Angew. Chem. Int. Ed. Engl. 21* (1982) 492.
[2] R. Appel, F. Knoll, I. Ruppert, *Angew. Chem. 93* (1981) 771; *Angew. Chem. Int. Ed. Engl. 20* (1981) 731, and references cited therein.
[3] a) R. Appel, V. Barth, F. Knoch, *Chem. Ber. 116* (1983) 938; b) A. Schmidpeter, C. Leyh, K. Karaghiosoff, *Angew. Chem. 97* (1985) 127; *Angew. Chem. Int. Ed. Engl. 24* (1985) 124.
[4] O. J. Scherer, *Angew. Chem. 97* (1985) 905; *Angew. Chem. Int. Ed. Engl. 24* (1985) 924, and references cited therein.
[5] a) K. Knoll, O. Orama, G. Huttner, *Angew. Chem. 96* (1984) 989; *Angew. Chem. Int. Ed. Engl. 23* (1984) 976; b) H. Lang, L. Zsolnai, G. Huttner, *Chem. Ber. 118* (1985) 4426.
[6] a) H. H. Karsch, F. H. Köhler, H.-U. Reisacher, *Tetrahedron Lett. 25* (1984) 3687; b) H. H. Karsch, H.-U. Reisacher, G. Müller, *Angew. Chem. 98* (1986) 467; *Angew. Chem. Int. Ed. Engl. 25* (1986) 454.
[7] **1a**, m.p. = 223–225 °C; ^{31}P-NMR (C_6D_6, 25 °C): δ(P1) = 303.4, δ(P2) = 324.3 (^2J(PP) = 55 Hz); ^{13}C-NMR (C_6D_6, 25 °C): δ(C1) = 185.74 (d, ^1J(P2-C) = 65.9 Hz); IR (C_6H_6, ν(CO), cm^{-1}): 1932, 1850; Crystal structure data: triclinic, $P\bar{1}$, a = 10.078(2), b = 15.178(3), c = 15.685(1) Å; α = 95.24(1), β = 102.22(1), γ = 104.94(1)°; V = 2238.4 Å^3, ρ_{calcd} = 1.161 g cm^{-3} for Z = 2, F(000) = 832, T = 21 °C. 9919 unique reflections, of which 5996 observed with $I \geq 2.0\sigma(I)$ [(θ-2θ) scan, $\Delta\omega = 0.7 + 0.35\tan\theta$, $(\sin\theta/\lambda)_{max} = 0.646$, ±h, ±k, +l, Mo$_{K\alpha}$, λ = 0.71069 Å, graphite monochromator, CAD4]; solution by Patterson methods, R = 0.056, R_w = 0.070, $w = 1/\sigma^2(F_0)$ (anisotropic, H constant, tBu groups C51/C111 in two alternatives, 496 parameters in two blocks, GFMLS); $\Delta\rho_{max}$(final) = +1.17/−0.54 e/Å^3.—**1b**, m.p. = 200 °C (dec.); ^{31}P-NMR (C_6D_6, 25 °C): δ(P1) = 246.7, δ(P2) = 332.5 (^2J(PP) = 64 Hz, ^1J(WP) = 638 Hz); ^{13}C-NMR (C_6D_6, 25 °C): δ(C1) = 188.14 (dd, ^1J(P2-C) = 65.3, ^1J(P1-C) = 8.6 Hz); IR (C_6H_6, ν(CO), cm^{-1}): 1928, 1842.
[8] The metalated phosphane $Cp(CO)_3W$–PR–CH=PR (IR (C_6H_6, ν(CO), cm^{-1}): 2004, 1920, 1901) is the primary product formed from **1b** in benzene at 5 °C; decarbonylation occurs at room temperature.
[9] Symmetrically coordinated 1,3-diphosphaallyl fragments: R. Appel, W. Schuhn, F. Knoch, *Angew. Chem. 97* (1985) 421; *Angew. Chem. Int. Ed. Engl. 24* (1985) 420.
[10] a) E. Gross, K. Jörg, K. Fiederling, H. Göttlein, W. Malisch, R. Boese, *Angew. Chem. 96* (1984) 705; *Angew. Chem. Int. Ed. Engl. 23* (1984) 738; b) K. Jörg, W. Malisch, W. Reich, A. Meyer, U. Schubert, *ibid. 98* (1986) 103; bzw. *25* (1986) 92; c) W. Maisch, M. Schmeusser, W. Malisch, C. Alt, W. S. Sheldrick, unpublished; d) L. D. Hutchins, E. N. Duesler, R. Paine, *Organometallics 3* (1984) 399; e) D. Gudat, E. Niecke, W. Malisch, H. Hofmockel, A. H. Cowley, A. M. Arif, B. Krebs, M. Dartmann, *J. Chem. Soc. Chem. Commun. 1985*, 1687.
[11] a) The reaction of $Fe_2(CO)_9$ with metal-phosphorus double-bond systems $Cp(CO)_2M{=}PR_2$ (M = Mo, W) leads to cyclic compounds of the type $Cp(CO)_2\overline{W{-}PR_2{-}Fe(CO)_4}$, cf. [10a]; K. Jörg, E. Gross, W. Malisch, unpublished; b) for the reaction of $Fe_2(CO)_9$ with phosphorus(III)–carbon double-bond systems, see R. Appel, C. Casser, M. Immenkeppel, F. Knoch, *Angew. Chem. 96* (1984) 905; *Angew. Chem. Int. Ed. Engl. 23* (1984) 895; R. H. Neilson, R. J. Thoma, I. Vickovic, W. H. Watson, *Organometallics 3* (1984) 1132; R. R. Ford, B.-L. Li, R. H. Neilson, R. J. Thoma, *Inorg. Chem. 24* (1985) 1993.
[12] **2b**, m.p. = 120 °C (dec.); ^{31}P-NMR (C_6D_6, 25 °C): δ(P1) = 154.6 (^1J(WP) = 369.3 Hz), δ(P2) = −8.8 (^2J(PP) = 106.8 Hz); ^{13}C-NMR (C_6D_6, 25 °C): δ(C1) = 105.02 (dd, ^1J(P2-C) = 89.3, ^1J(P1-C) = 5.6 Hz); IR (C_6H_6, ν(CO), cm^{-1}): 2002, 1972, 1945, 1927, 1854; crystal structure data: monoclinic, $C2/c$; a = 47.950(14), b = 14.246(6), c = 16.508(6) Å; β = 104.99(3)°; V = 10892.8 Å^3, ρ_{calcd} = 1.232 g cm^{-3} for Z = 8, F(000) = 4128, T = 22 °C. 11583 unique reflections, empirical absorption correction, 5726 observed reflections with $I \geq 2.0\sigma(I)$ [(θ-2θ) scan, $\Delta\omega = 1.0 + 0.35\tan\theta$, $(\sin\theta/\lambda)_{max} = 0.648$, +h, +k, ±l]; solution by Patterson methods, R = 0.057, R_w = 0.050, $w = 1/\sigma^2(F_0)$ (anisotropic, phenyl ring C8–C13 and tBu group C111 isotropic, H constant, 449 parameters in two blocks, SHELX 76); $\Delta\rho_{max}$(final) = +1.79/−1.63 e/Å^3. Further details of the crystal structure investigations may be obtained from the Fachinformationszentrum Energie, Physik, Mathematik GmbH, D-7514 Eggenstein-Leopoldshafen 2 (FRG), on quoting the depository number CSD-51740, the names of the authors, and the journal citation.
[13] Formation of a cyclic 1-phospha-4-metallabutadiene ligand on the tricarbonyliron fragment by metal-centered bond formation between alkynes and phosphanediyl ligands: see ref. [5].

Dioxides of *C*-Amino-Substituted Phosphaalkenes and Phosphaallyl Cations**

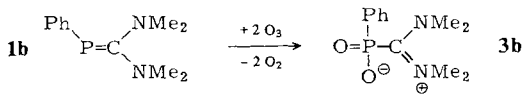
By *Alfred Schmidpeter,* Karl-Heinz Zirzow, Angela Willhalm, Joan M. Holmes, Roberta O. Day,* and *Robert R. Holmes*

Dedicated to Professor Marianne Baudler on the occasion of her 65th birthday

Phosphaalkenes **1** react as nucleophiles and are converted by chalcogens into the P^V compounds **2** (Y = O, S, Se).[1] Thus, reaction of **1a** ($R^1 = C_6H_2tBu_3$, $R^2 = Ph$, $R^3 = SiMe_3$) with ozone at −78 °C affords a stable methyleneoxophosphorane **2a** (Y = O);[2] with an excess of ozone, secondary reactions take place,[2] most likely with cleavage of the P–C bond.[3]



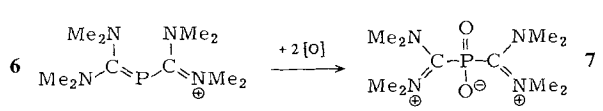
We have now found that the electron-rich phosphaalkene **1b**[4] takes up two equivalents of oxygen smoothly and selectively upon reaction with ozone at room temperature, leading directly to formation of **3b**. **2b** (Y = O) is not observed as an intermediate, since a part of **1b** remains unchanged upon reaction with less ozone, and more ozone does not lead to secondary reactions.





In the ^{13}C-NMR spectrum (CD_3CN) of **3b**[5] the downfield shift of the sp^2 C-atom observed for **1b** ($\delta = 200$, $J_{PC} = 67$ Hz[4]) is essentially retained ($\delta = 180$, $J_{PC} = 91$ Hz). This is not consistent with the epoxide **4b** (oxaphosphirane oxide), and rather suggests formation of the zwitterionic amidiniophosphinate **3b**.[6] The thiaphosphirane sulfides **5** corresponding to **4b** can be synthesized from methylenethioxophosphoranes **2** (Y = S) by (reversible) uptake of sulfur.[1] **3b** is also accessible from dimethyl phenylphosphonite and tetramethylurea dichloride.[7]

The tetrakis(dimethylamino)-2-phosphaallyl cation **6**[8] is smoothly converted into the colorless dioxide **7**, not only by ozone, but also by hydrogen peroxide or dimethyl sulfoxide (DMSO).[9] Even the perchlorate counterion effects this oxidation already under mild conditions: colorless **7**·ClO_4 crystallizes from a solution of yellow **6**·ClO_4 in acetone or acetonitrile after heating to 60 °C.



The X-ray structure analysis of the perchlorate of **7** (Fig. 1)[10] confirms the bis(amidinio)phosphinate structure of the cation (C_2 symmetry). Compared to the phosphaallyl

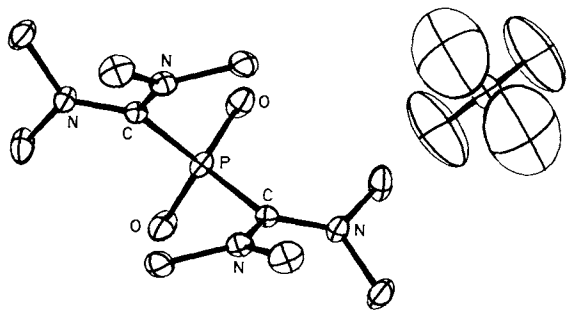


Fig. 1. ORTEP diagram of the structure of 7·ClO_4 in the crystal. The vibration ellipsoids are drawn at the 30% probability level. The hydrogen atoms have been omitted for clarity. Bond lengths [pm] and angles [°] (where necessary mean values): PO 147.8(3), PC 188.7(4), CN 133.5(5); OPO 122.5(3), OPC 102.5(3), CPC 103.8(3), PCN 119.6(3), NCN 120.6(4) [11].

cation **6**[8] the CPC angle is unchanged, while the PC bonds are lengthened from 179.6(4) to 188.7(4) pm and thus lie at the upper limit of known PC single-bond lengths. There is no contact between the $PO_2^{\ominus}$ and the $CN_2^{\oplus}$ groups; the amidinio C-atom is planar coordinated. In **6**, which has a conjugated allyl system, the spatial crowding of the two Me_2N groups turned towards each other results in the "internal" PCN angle being considerably greater than the "external" one.[8] In **7** the conjugation is no longer present, so the two amidinio groups are not kept coplanar; accordingly the two PCN angles of a group do not differ in **7**.

Received: December 6, 1985;
revised: January 24, 1986 [Z 1571 IE]
German version: *Angew. Chem. 98* (1986) 471

CAS Registry numbers:
1b, 80592-10-5; **3b**, 34959-67-6; **6**·$Cl^{\ominus}$, 86196-96-5; **6**·$ClO_4^{\ominus}$, 86196-98-7; **7**·$Cl^{\ominus}$, 101542-94-3; **7**·$ClO_4^{\ominus}$, 101542-96-5.

[*] Prof. Dr. A. Schmidpeter, Dipl.-Chem. K.-H. Zirzow, Dipl.-Chem. A. Willhalm
Institut für Anorganische Chemie der Universität
Meiserstrasse 1, D-8000 München 2 (FRG)
Prof. Dr. R. R. Holmes, Prof. Dr. R. O. Day, J. M. Holmes
Department of Chemistry
University of Massachusetts
Amherst, MA 01003 (USA)

[**] This work was supported by the Deutsche Forschungsgemeinschaft and the Fonds der Chemischen Industrie (*A. S.*), as well as by the National Science Foundation and the National Institutes of Health (*R. R. H.*).

[1] T. A. van der Knaap, F. Bickelhaupt, *J. Organomet. Chem. 277* (1984) 351, and references cited therein; M. Caira, R. H. Neilson, W. H. Watson, P. Wisian-Neilson, Z.-M. Xie, *J. Chem. Soc. Chem. Commun. 1984*, 698.

[2] R. Appel, F. Knoch, H. Kunze, *Angew. Chem. 96* (1984) 159; *Angew. Chem. Int. Ed. Engl. 23* (1984) 157.

[3] T. A. van der Knaap, T. C. Klebach, R. Lourens, M. Vos, F. Bickelhaupt, *J. Am. Chem. Soc. 105* (1983) 4026.

[4] L. N. Markovskii, V. D. Romanenko, T. I. Pidvarko, *Zh. Obshch. Khim. 52* (1982) 1925; *J. Gen. Chem. USSR 52* (1982) 1707. For the ^{13}C-NMR signal (C_6H_6) of the amidinio C-atoms, these authors give $\delta = 203.4$, $J_{PC} = 44.4$ Hz. The phosphaalkene **1b** was prepared by us via another route from $LiPhPSnPh_3$ and $(Me_2N)_2CCl_2$: A. Schmidpeter, K.-H. Zirzow, unpublished.

[5] *Procedure:* **3b**: A stream of O_3/O_2 was passed through a solution of **1a** (1 mmol) in acetonitrile (2 mL) for 5 to 60 s at room temperature and the progress of the reaction was monitored by ^{31}P-NMR spectroscopy. After evaporation to dryness and extraction with ether, **3b** was obtained from the ethereal solution as colorless highly deliquescent platelets. $^{31}P\{^1H\}$-NMR (CD_3CN): $\delta = 8$; $^{13}C\{^1H\}$-NMR (CD_3CN): $\delta = 180$ (d, $^1J_{PC} = 91$ Hz, amidinio-C), 141 (d, $^1J_{PC} = 140$ Hz, phenyl-*ipso*-C), 45 (d, $^3J_{PC} = 1.5$ Hz, CH_3).

[6] This finding is to be compared with the ease of ring-opening of (assumed) amino epoxides; see, for example, V. Nuti, M. F. Saettone, *Tetrahedron 26* (1970) 3875.

[7] G. H. Birum, J. D. Wilson, *J. Org. Chem. 37* (1972) 2730.

[8] A. Schmidpeter, A. Willhalm, *Angew. Chem. 96* (1984) 901; *Angew. Chem. Int. Ed. Engl. 23* (1984) 903; R. O. Day, A. Willhalm, J. M. Holmes, R. R. Holmes, A. Schmidpeter, *ibid. 97* (1985) 775 and *24* (1985) 764.

[9] *Procedure:* 7·Cl: A yellow solution of **6**·Cl (0.80 g, 3 mmol) in ethanol becomes hot and decolorizes within 10 min after addition of 0.60 mL of 30% hydrogen peroxide; at the same time, colorless crystalline 7·Cl precipitates. Yield: 0.83 g (93%), m.p. 194–196°C (dec.). $^{31}P\{^1H\}$-NMR (D_2O): $\delta = -3$; $^{13}C\{^1H\}$-NMR (D_2O, CD_3CN): $\delta = 170$ (d, $^1J_{PC} = 139$ Hz, amidinio-C), 45 (d, $^3J_{PC} = 2.8$ Hz, CH_3); ^1H-NMR (D_2O): $\delta = 3.30$ (CH_3).

[10] Colorless crystals from acetone, m.p. 224–226°C (dec.). Monoclinic, *P2/c*, $a = 10.419(2)$, $b = 6.958(2)$, $c = 11.959(2)$ Å, $\beta = 105.24(2)°$, $Z = 2$, Enraf-Nonius CAD4 diffractometer, $Mo_{K\alpha}$ (graphite monochromator) for $2° \leq 2\theta \leq 50°$; 1179 independent reflections with $I > 2\sigma(I)$; $R = 0.064$, $R_w = 0.094$. Further details of the crystal structure investigation are available on request from the Fachinformationszentrum Energie, Physik, Mathematik GmbH, D-7514 Eggenstein-Leopoldshafen 2, on quoting the depository number CSD-51800, the names of the authors, and the full citation of the journal.

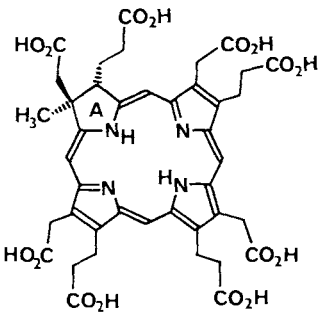
[11] The structure of the PO_2 group compares with that in the bis(tetramethylamidinio)diphosphonate: F. Sanz, J. J. Daly, *J. Chem. Soc. Dalton Trans. 1972*, 2267.

Facile Entry to Geminally Dialkylated Chlorins**

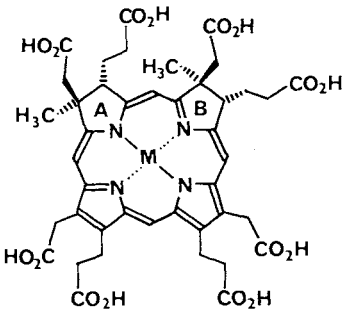
By *Franz-Peter Montforts** and *Gottfried Zimmermann*

Dedicated to Professor Burchard Franck on the occasion of his 60th birthday

Factor I **1** and sirohydrochlorin **2a** are novel porphinoid pigments with a chlorin and isobacteriochlorin structure, respectively. Their reduced derivatives occur as intermediates in the biosynthesis of vitamin B_{12} via uroporphyrinogen III.[1] Iron-containing sirohydrochlorin **2b**, moreover, functions as prosthetic group in sulfite- and nitrite-reductases of bacteria and plants.[2]



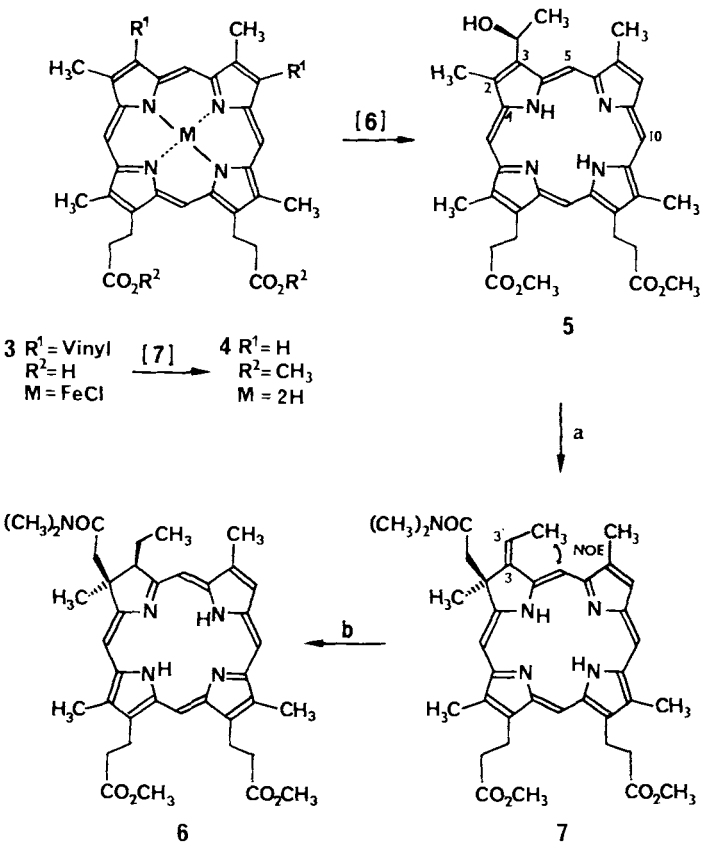
1



2a M = 2H
2b M = Fe

One of the main difficulties in model[3] and total syntheses[4] of these structure types is the construction of the geminally dialkylated moiety in the pyrrole rings A or A and B. We have now found that this moiety can be conveniently constructed starting from the readily accessible hydroxyalkylporphyrins by Claisen rearrangement with *N,N*-dimethylacetamide dimethyl acetal.[5]

A 3-hydroxyethylporphyrin **5**[6] suitable as starting compound can be obtained via deuteroporphyrin dimethyl ester **4**[7] from hemin hydrochloride **3** by a known pathway. Upon reaction with *N,N*-dimethylacetamide dimethyl acetal, **5** is converted into **7**. The *Z*-configuration of the exocyclic double bond in the product **7**, which is readily detectable by intramolecular ^1H-nuclear Overhauser effect (NOE), evidences the expected stereoselective course[8] of the rearrangement. Catalytic hydrogenation of **7** affords the chlorin **6**, whose *cis*-configuration likewise follows from a NOE experiment (Scheme 1).



Scheme 1. Reaction conditions: a) $CH_3C(OCH_3)_2N(CH_3)_2$, *o*-xylene, molecular sieve 3 Å, argon, 160°C, 1 h; flash chromatography; crystallization 76%. – b) H_2, Pd/C, CH_3OH, room temperature, 2 h; flash chromatography; crystallization 70%. – All the new compounds have been characterized by elemental analyses and UV/VIS, ^1H-NMR and mass spectroscopy. Selected spectroscopic data: **7**, UV/VIS ($CHCl_3$): $\lambda_{max} = 399$ nm ($\lg\varepsilon = 5.176$), 496 (3.99), 503 (3.95), 532 (4.03), 602 (3.56), 629 (3.48), 659 (4.61); ^1H-NMR ($CDCl_3$, 270 MHz): $\delta = -2.68$, -2.52 (2m, 2NH), 2.19 (s, 2-CH_3), 2.82 (d, $J = 7.5$ Hz, 3'-CH_3), 3.25 (AB system, 2-CH_2), 6.44 (q, $J = 7.5$ Hz, 3'-H), 8.86 (s, 20-H), 9.52 (s, 5-H); MS (200°C): *m/z* 651 (26%, M^+), 565 (100%, $M^{\oplus} - CH_2CON(CH_3)_2$). **6**, UV/VIS ($CHCl_3$): $\lambda_{max} = 392$ ($\lg\varepsilon = 5.195$), 489 (4.025), 496 (4.041), 522 (3.185), 532 (3.047), 592 (3.505), 616 (3.466), 645 (4.583); ^1H-NMR ($CDCl_3$, 270 MHz): $\delta = 1.18$ (t, $J = 7.4$ Hz, CH_3, 3-ethyl), 2.20 (s, 2-CH_3), 2.42 (m, $J = 7.4$ Hz, CH_2, 3-ethyl), 3.25 (AB system, 2-CH_2), 4.66 (t, 3-H), 8.79 (s, 20-H), 9.01 (s, 5H).

Since there are methods available for the efficient synthesis of porphyrins, and since hydroxyalkyl substituents can be readily introduced by acylation with subsequent reduction, the concept presented here should open up a route to the natural products **1** and **2**. Preliminary experiments show that hematoporphyrin dimethyl ester is converted by double Claisen rearrangement into the isobacteriochlorin structure type, but the stereochemistry involved thereby is complex and still requires clarification.

[*] Prof. Dr. F.-P. Montforts, [+] Dr. G. Zimmermann
Institut für Organische Chemie der Universität
Niederurseler Hang, D-6000 Frankfurt am Main 50 (FRG)

[+] Present address: FB-2-Chemie, Universität Bremen, Loebenstr. NW2, 2800 Bremen 33 (FRG)

[**] This work was supported by the Deutsche Forschungsgemeinschaft and the Fonds der Chemischen Industrie. We thank Prof. Dr. *D. Leibfritz* (Universität Bremen) for recording the mass spectra.

Received: December 20, 1985;
revised: February 6, 1986 [Z 1598 IE]
German version: *Angew. Chem. 98* (1986) 451

CAS Registry numbers:
1, 73528-45-7; **2a**, 65207-12-7; **5**, 63148-21-0; **6**, 101544-05-2; **7**, 101544-04-1; $Me_2NC(OMe)_2Me$, 18871-66-4.

[1] A. R. Battersby, E. McDonald in D. Dolphin (Ed.): *Vitamin B_{12}. Vol. 1*, Wiley, New York 1982, p. 107.

[2] a) L. M. Siegel, M. J. Murphy, H. Kamin, *J. Biol. Chem. 248* (1973) 251; b) M. J. Murphy, L. M. Siegel, *ibid. 248* (1973) 6911; c) M. J. Murphy, L. M. Siegel, H. Kamin, D. Rosenthal, *ibid. 248* (1973) 2801; d) M. J. Murphy, L. M. Siegel, S. R. Tove, H. Kamin, *Proc. Natl. Acad. Sci. USA 71* (1974) 612.

[3] a) A. R. Battersby, L. A. Reiter, *J. Chem. Soc. Perkin Trans. 1 1984*, 2743; b) A. R. Battersby, C. J. R. Fookes, R. J. Snow, *ibid. 1984*, 2725, 2733; c) C. K. Chang, C. Sotiriou, *J. Org. Chem. 50* (1985) 4889; d) F.-P. Montforts, U. M. Schwartz, *Liebigs Ann. Chem. 1985*, 1228. This work contains a complete list of references to corresponding model syntheses from the laboratories of *Eschenmoser* and *Battersby*.

[4] a) C. J. Dutton, C. J. R. Fookes, A. R. Battersby, *J. Chem. Soc. Chem. Commun. 1983*, 1237; b) F.-P. Montforts, U. M. Schwartz, *Angew. Chem. 97* (1985) 767; *Angew. Chem. Int. Ed. Engl. 24* (1985) 775; c) S. P. D. Turner, M. H. Block, Z. C. Sheng, S. C. Zimmermann, A. R. Battersby, *J. Chem. Soc. Chem. Commun. 1985*, 583; d) M. H. Block, S. C. Zimmermann, G. B. Henderson, S. P. D. Turner, S. W. Westwood, F. J. Leeper, A. R. Battersby, *ibid. 1985*, 1061.

[5] a) H. Meerwein, W. Florian, N. Schön, G. Stopp, *Justus Liebigs Ann. Chem. 641* (1961) 1; b) D. Felix, K. Gschwend-Steen, A. E. Wick, A. Eschenmoser, *Helv. Chim. Acta 52* (1969) 1030; c) A. E. Wick, D. Felix, K. Steen, A. Eschenmoser, *ibid. 47* (1964) 2425.

[6] a) H. Brockmann jr., K. M. Bliesner, H. H. Inhoffen, *Justus Liebigs Ann. Chem. 718* (1968) 148; b) K. M. Smith, E. M. Fujinari, K. C. Langry, D. W. Parish, H. D. Tabba, *J. Am. Chem. Soc. 105* (1983) 6638; c) P. S. Clezy, V. Diakiw, N. W. Webb, *J. Chem. Soc. Chem. Commun. 1972*, 413.

[7] R. K. DiNello, C. K. Chang in D. Dolphin (Ed.): *The Porphyrins, Vol. 1*, Academic Press, New York 1978, p. 294.

[8] R. K. Hill in J. D. Morrison (Ed.): *Asymmetric Synthesis, Vol. 3, Part B*, Academic Press, New York 1984, p. 503. On using enantiomerically pure **5** its chirality should be transferred to the geminally dialkylated center in **7**.

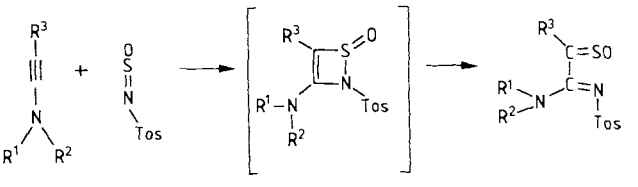
Thioketone *S*-Oxides by [2+2]-Cycloaddition of Ynamines to *N*-Sulfinyltosylamide

By *Steffen Kosack, Gerhard Himbert,** and *Gerhard Maas*

Ynamines undergo [2+2]-cycloaddition reactions with compounds that contain electrophilic C=C double bonds or carbonyl-, thiocarbonyl- or imino groups.[1] The resulting cyclobutenes are, as a rule, stable[1,2] (exceptions[3]), whereas the 1,2-dihydro-oxete, -thiete, and -azete derivatives that are formed initially isomerize by electrocyclic ring-opening to give α,β-unsaturated amides, thioamides, and amidines, respectively.[1,4]

In continuation of our studies on cycloadditions we have examined the reaction of ynamines **1a–f** with *N*-sulfinyltosylamide **2**.[5] We were able to isolate, in good yields (66–90%), the α-amidinothioketone oxides **4** (Table 1),[6] whose formation can be explained in terms of a spontaneous ring opening of the 1,2-dihydro-1,2-thiazete derivatives **3** (Scheme 1).

The constitution of the open-chain products **4** is substantiated, in particular, by their IR spectra; the *N*-sulfonylamide moiety is revealed by intense bands in the regions 1510–1560 cm^{-1} (C=N) as well as 1270–1305 and 1139–1152 cm^{-1} (SO_2), whereby the region of the asymmetric SO_2 valence vibration ($\tilde{\nu} \approx 1300\ cm^{-1}$) is especially characteristic.[7] We assign one of the intense absorptions between 1075 and 1139 cm^{-1} to the sulfinyl group.[8] Confirmation of the structure is provided by the chemical shift of the



1 **2** **3** **4**

1,3,4	a	b	c	d	e	f
R^1	Et	Et	Me	Me	Me	Ph
R^2	Et	Et	Ph	Ph	Ph	Ph
R^3	Me	Ph	H	Me	Ph	H

Scheme 1.

thioaldehyde H-atom in the ^{1}H-NMR spectra of **4c** and **4f** ($\delta > 9$; see Table 1). The position of the signal and the magnitude of the coupling constants for the thiocarbonyl C-atom in the ^{13}C-NMR spectra of **4a** ($\delta = 183.77$; q, $^2J = 8.2$ Hz), **4b** (175.28, s), and **4f** (163.86; d, $^1J = 179$ Hz)

Table 1. Melting points, assignment of configuration, and selected ^{1}H-NMR data of **4**.

4	M.p. [°C]	Configuration	^{1}H-NMR ($CDCl_3$, δ values) NR^1R^2(alkyl)	R^3
a	110–111	*E*	1.19 (t; 6H) 3.43 (4H) [a]	2.54 (s; 3H)
b	127–128	*E*	1.13 (t; 3H) 1.26 (t; 3H) 3.20–3.90 (m; 4H)	7.40 (m; 3H) 7.95 (m; 2H)
c [b]	91–92	*E*	3.40 (s; 3H)	9.39 (s; 1H)
	155–156	*Z*	3.40 (s; 3H)	9.09 (s; 1H)
d [c]	133–134	*Z*	3.39 (s; 3H)	2.21 (s; 3H)
e	140–141	*Z* [d]	3.51 (s; 3H)	[d]
f [e]	160–161	*Z*	—	9.34 (s; 1H)

[a] Unstructured broad signal. [b] The *E* isomer is obtained upon addition of **1c** to **2** followed by rapid isolation; in solution, it transforms into the *Z* isomer (e.g. in $CDCl_3$ at room temperature in ca. 1 h). [c] New signals ($\delta = 2.27$ and 3.43 < 40%) appear in the ^{1}H-NMR spectrum within 5 h; these we assign to the *E* form. [d] Unequivocal assignment of configuration impossible owing to overlapping of the aryl-proton signals. [e] The ^{1}H-NMR spectra of some crystal fractions show a second, less intense singlet at $\delta = 9.50$, which we assign to the *E*-form.

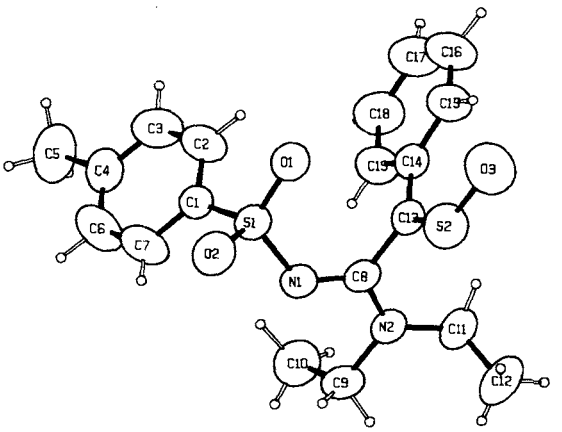


Fig. 1. ORTEP diagram of the crystal structure of **4b**. The vibration ellipsoids are drawn at the 50% probability level. Important bond lengths [Å] and angle [°]: S2-C13 1.629(3), S2-O3 1.470(4); C13-S2-O3 115.7(2) [9].

[*] Prof. Dr. G. Himbert, Dipl.-Chem. S. Kosack, Prof. Dr. G. Maas
Fachbereich Chemie der Universität
Postfach 3049, D-6750 Kaiserslautern (FRG)

are also consistent with the structure **4**. The adducts **4** exhibit the activity expected of a compound containing a sulfinyl group:[8] desulfurization on photolysis of **4a** and **4b**, Diels-Alder reactivity of the C=S double bond of **4c** and **4f** towards 2,3-dimethyl-1,3-butadiene, and hydrolysis of **4f** to the acetamidine derivative.

Assignment of configuration is based on the anisotropic effect of the sulfinyl group:[8] that the methyl protons of **4a** ($\delta = 2.51$, s) and the *ortho*-aryl protons of **4b** ($\delta = 7.93$ m) absorb at relatively low field shows that the oxygen of the SO group is near to these substituents, i.e. the C=S bond is *E*-configurated. In contrast, the *Z*-form seems to predominate in the aniline derivatives **4c-f** (see Table 1).

An X-ray structure analysis was carried out on **4b**. There is no conjugation between the π-systems of the amidine moiety and the C=S(O) bond, since the N1-C8-N2 and C14-C13-S2 planes are almost perpendicular (92.8°) to each other.

Received: December 30, 1985;
supplemented: February 4, 1985 [Z 1602 IE]
German version: *Angew. Chem. 98* (1986) 443

CAS Registry numbers:
1a, 4231-35-0; **1b**, 4231-26-9; **1c**, 4231-31-6; **1d**, 4231-29-2; **1e**, 32907-84-9; **1f**, 4231-39-4; **2**, 4104-47-6; **4a**, 101543-88-8; **4b**, 101543-89-9; (*E*)-**4c**, 101543-94-6; (*Z*)-**4c**, 101543-90-2; (*E*)-**4d**, 101543-95-7; (*Z*)-**4d**, 101543-91-3; **4e**, 101543-92-4; (*E*)-**4f**, 101543-96-8; (*Z*)-**4f**, 101543-93-5.

[1] Review: J. Ficini, *Tetrahedron 32* (1976) 1448.
[2] See also: a) M. L. M. Pennings, D. N. Reinhoudt, *J. Org. Chem. 47* (1982) 1816, and references cited therein; b) J. J. Eisch, J. E. Galle, L. E. Hallenbeck, *ibid. 47* (1982) 1608; J. Ficini, A. Guingant, J. d'Angelo, G. Stork, *Tetrahedron Lett. 24* (1983) 907, and references cited therein.
[3] a) J. Ficini, A. Duréault, G. Revial, A. M. Touzin, *Tetrahedron Lett. 1974*, 1025; b) G. Desimoni, P. Righetti, G. Tacconi, *J. Chem. Soc. Perkin Trans. 1 1979*, 856; c) G. Himbert, W. Brunn, *Chem. Ber. 117* (1984) 642.
[4] See also: a) S. I. Pennanen, *Synth. Commun. 10* (1980) 373; b) V. H. M. Elferink, H. J. T. Bos, *J. Chem. Soc. Chem. Commun. 1985*, 882; c) V. H. M. Elferink, R. G. Visser, H. J. T. Bos, *Recl.: J. R. Neth. Chem. Soc. 100* (1981) 414; d) R. Abramovitch, B. Mavunkel, J. R. Stowers, M. Wegrzyn, C. Riche, *J. Chem. Soc. Chem. Commun. 1985*, 845.
[5] Reactions of sulfinylamides with numerous compounds containing "hetero-double bonds", with enol ethers, and with a few acetylenes have already been described, but so far no reactions with ynamines; see review by R. Bussas, G. Kresze, H. Münsterer, A. Schwöbel, *Sulfur Rep. 2* (1983) 215.
[6] *Procedure:* A solution of **2** (1.09 g, 5 mmol) in ether (10 mL) was added dropwise to an ice-cooled solution of **1** (5 mmol) in ether (10 mL) and the mixture stirred for 30–50 min at 0°C. The thioketone oxides **4** that precipitated were filtered off and, with exception of (*E*)-**4c**, recrystallized from $CHCl_3$/ether.
[7] The shift of the absorption of the asymmetric SO_2 vibration to smaller wave numbers ($\Delta\tilde{\nu} = 50\ cm^{-1}$) is caused by the conjugation of the SO_2 group with the amidine system; see also: W. Logemann, P. Artini, G. Tosolini, *Chem. Ber. 91* (1958) 2566.
[8] Reviews: a) B. Zwanenburg, J. Strating, *Q. Rep. Sulfur Chem. 5* (1970) 79; b) E. Block in R. K. Freidlina, A. E. Shorova (Eds.): *Organic Sulfur Chemistry (IUPAC)*, Pergamon Press, Oxford 1981, p. 15ff; c) B. Zwanenburg, *Recl.: J. R. Neth. Chem. Soc. 101* (1982) 1; d) B. Zwanenburg, B. G. Lenz in *Houben-Weyl-Müller: Methoden der Organischen Chemie, Band E11*, Thieme, Stuttgart 1985, p. 911.
[9] **4b**: triclinic, $P\bar{1}$; $a = 9.859(2)$, $b = 13.031(2)$, $c = 8.178(3)$ Å; $\alpha = 100.16(3)$, $\beta = 95.32(3)$, $\gamma = 73.66(2)°$; $Z = 2$, $\rho_{calc} = 1.308\ g\ cm^{-3}$, Enraf-Nonius CAD4 diffractometer, $Mo_{K\alpha}$ radiation; 3098 independent reflections with $2.0 < \theta < 24.0°$. Refinement: $R = 0.0481$, $R_w = (\Sigma\Delta^2 F/\Sigma \cdot F_0^2)^{1/2} = 0.0446$ (2588 reflections with $I > 2\sigma(I)$, unit weight, full matrix refinement, heavy atoms anisotropic, H-atoms refined isotropically, 323 variables, maximum shift-error ratio finally 0.77). Further details of the crystal structure investigation are available on request from the Fachinformationszentrum Energie, Physik, Mathematik GmbH, D-7514 Eggenstein-Leopoldshafen 2, on quoting the depository number CSD-51785, the names of the authors, and the full citation of the journal.

Unusual Behavior of the Stable Paramagnetic Dihydridoiridium(IV) Complex $[Ir(H)_2(Cl)_2(iPr_3P)_2]$ in Solution**

By *Pasquale Mura** and *Annalaura Segre*

The title compound, *trans* $[Ir(H)_2(Cl)_2(iPr_3P)_2]$ **1**, whose preparation and X-ray crystal structure was reported recently,[1] failed to show any EPR signals both in the solid state and in solution, even when cooled to 110 and 193 K, respectively.

Consideration of electron spin relaxation times for systems with $T_{1e} \approx T_{2e} \lesssim 10^{-10}$ s led to the expectation that EPR lines would be so broad that they could not be readily detected, whereas the corresponding NMR line-widths should be only slightly affected by the unpaired electron.[2] Since we were unable to observe any EPR resonances for **1**, we undertook a study of its ^1H- and ^{31}P-NMR spectra.

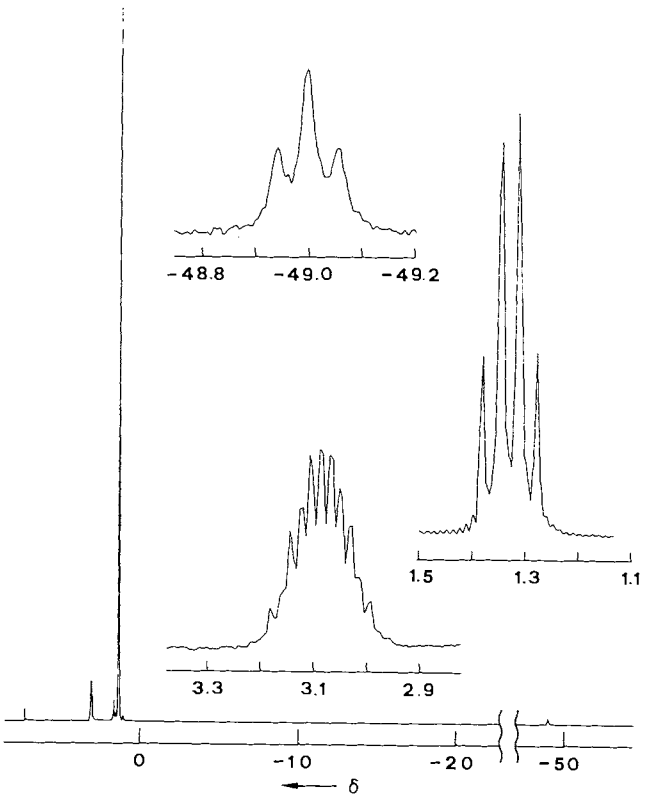
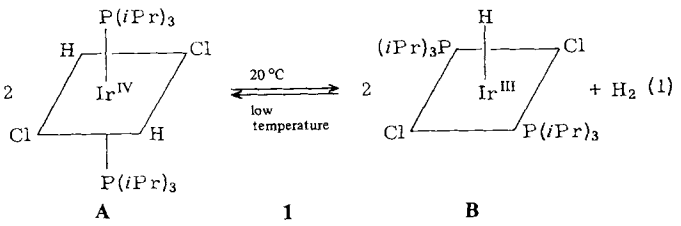


Fig. 1. ^1H-NMR spectrum of **1** at room temperature in $CDCl_3$; some sections have been enlarged.

The ^1H-NMR spectrum ($CDCl_3$, room temperature, TMS) of **1** (Fig. 1) contains three sharp, well-resolved multiplets (relative intensities 6:36:1); $\delta(PCH) = 3.11$ (m), $\delta(PCHCH_3) = 1.33$ (d, vt), and $\delta(IrH) = -49.0$ (t); $J(HH) = 7.3$ and $J(PH_{hydride}) = 11.1$ Hz. The broad-band decoupled $^{31}P\{^1H\}$-spectrum shows a sharp singlet at $\delta = 33.3$. Selective irradiation of the signals due to the CH and CH_3 protons in the region $\delta = 1$–3 converted this singlet into a doublet. Thus, it follows from the observed spectrum that a monohydride with a stereochemistry such as that of compound **B** is present in solution [reaction (1)].

[*] Dr. P. Mura, Dr. A. Segre
Istituto di Strutturistica Chimica "G. Giacomello",
Area della Ricerca di Roma
C.P. 10, I-00016 Monterotondo Stazione (RM) (Italy)

[**] We are indebted to Prof. *L. M. Venanzi* for valuable suggestions and discussions, and to the NMR service of the Research Area of Rome.



A 1 B

Another broad peak, centered at $\delta \approx 2$ ppm and of very low intensity is also always present and will be discussed below.

It must be noted that the coupling constants, chemical shifts and relative intensities of the signals are reconcilable only with the presence of a *diamagnetic* monohydrido complex such as **B**—which is in complete contrast with the X-ray structure data and magnetic susceptibility measurements performed on solid **1**.[1]

However, on lowering the temperature all peaks of the ^{1}H- and ^{31}P-NMR spectra noticeably broaden and, at 223 K, the hydrido peak disappears.

In order to clarify this behavior, a study of the ^{1}H-NMR spectrum of **1** as a function of the temperature was undertaken. On lowering the temperature to 183 K the spectrum progressively broadens; in the meantime, also the solvent peak slightly broadens. This process is reversible. At the same time, on cooling, the signal of the hydrido hydrogen, as well as that of the methyne hydrogen, undergo a paramagnetic shift (Fig. 2a, b).[3] Thus, it is reasonable to postulate that an equilibrium between a paramagnetic and a diamagnetic species exists in solution,[4] in which the paramagnetic dihydrido species **A** is evident only at low temperature; i.e., NMR data obtained as a function of the temperature point to an equilibrium of type (1) in solution.

In order to verify this hypothesis a small quantity of H_2 gas was bubbled into the NMR tube. The intensity of the broad signal at $\delta \approx 2$ strongly increased, while the hydride signals underwent a strong paramagnetic shift (≈ 5 ppm) and broadened from ≈ 4 Hz to ≈ 50 Hz, indicating that equilibrium (1) moves in favor of species **A**.[5] When D_2 gas was bubbled into the NMR tube the broad peak at $\delta \approx 2$ disappeared. Thus, the proposed equilibrium (1) would appear to be consistent with and rationalize all solution and solid state data.[1]

One explanation why the molecular H_2 formed in (1) does not leave the solution could be that H_2 is in some way linked to the monohydrido species **B**, as has recently been reported for other complexes.[6] From this point of view the equilibrium (1) could be seen as an example of a temperature-dependent reversible ligand-to-metal charge transfer (LMCT)[7] $\rightleftarrows$ metal-to-ligand charge transfer (MLCT) [Reaction (2)].

$$2\,Ir^{IV}(H)_2 \underset{MLCT}{\overset{LMCT}{\rightleftharpoons}} 2\,Ir^{III}H\cdot(H_2) \qquad (2)$$

Extremely large chemical shifts ($\delta \cong -50$) have been reported by *Shaw* et al.[8] as well as by *H. Werner* et al.[9] for several monohydrido-Ir^{III} complexes. Given the similarity of the chemical shifts between **1** (δ(IrH) $= -49.0$) and the above compounds it is possible that their behavior is analogous to that what we observe for **1**, and that paramagnetic hydrido complexes may be present in solution at low temperature.

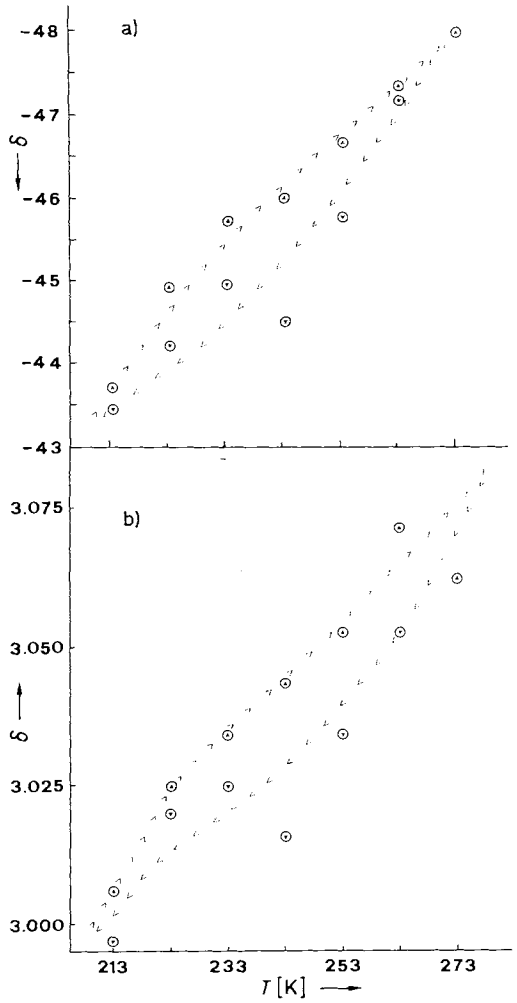


Fig. 2. Chemical shift behavior as a function of the temperature for the hydrido peak (a) and for the methyne peak (b) in the 200-MHz ^{1}H-NMR spectrum of **1**. In each case the measurements were made, starting from the lowest temperature. (The peak due to the methyl groups does not shift enough.)

The IR spectrum of **1** (in benzene at room temperature) shows one strong band at 2256 cm^{-1}, which is assigned to $\tilde{\nu}$(IrH). This value is very different from that observed for the solid compound,[1] $\tilde{\nu}$(IrH) $= 2003$ cm^{-1} (mw) (KBr pellets). Comparison of these two values strongly confirms the substantial difference between solid state and solution at room temperature.

Received: December 30, 1985;
revised: January 27, 1986 [Z 1604 IE]
German version: *Angew. Chem. 98* (1986) 453

[1] a) P. Mura, *J. Am. Chem. Soc. 108* (1986) 351; b) paper presented, in part, at the XIIth International Conference on Organometallic Chemistry, Vienna, September 8, 1985.

[2] G. N. La Mar, W. D. Horrocks, R. H. Holm (Eds.): *NMR of Paramagnetic Molecules*. Academic Press, New York 1973.

[3] The hysteresis pattern apparent in Fig. 2a, b is most probably due to the fact that only 15 minutes dead-time were given between one NMR run and the other. In fact, solutions of **1** are not stable indefinitely; thus, as soon as the temperature was stabilized a new spectrum was run. Consequently, kinetic reasons can explain the apparent hysteresis cycle, which is observable only for signals due to **1** and not, for instance, for the H_2O signal; water was present as an impurity in solution. In the case of the analogue of **1** with cyclohexyl groups instead of isopropyl groups, the same experiment does not show any evidence of the hysteresis pattern, thus confirming that kinetic reasons can explain the behavior for **1**.

 © VCH Verlagsgesellschaft mbH, D-6940 Weinheim, 1986 0570-0833/86/0505-0461 $ 02.50/0

[4] Since we could observe a ^{31}P-NMR spectrum at -90 °C, even if rather broad, the equilibrium in solution must in any case be shifted towards the diamagnetic species; thus, the rate of the paramagnetic/dimagnetic equilibrium cannot be measured.
[5] Upon bubbling H_2 into an NMR tube containing $CDCl_3$ only, a sharp peak appeared at 4.61 ppm which disappeared in 60 s.
[6] a) G. J. Kubas, R. R. Ryan, B. I. Swanson, P. J. Vergamini, H. J. Wasserman, *J. Am. Chem. Soc. 106* (1984) 451; b) R. K. Upmacis, G. E. Gadd, M. Poliakoff, M. B. Simpson, J. J. Turner, R. Whyman, A. F. Simpson, *J. Chem. Soc. Chem. Commun. 1985*, 27, and references cited therein.
[7] Y. S. Sohn, D. N. Hendrickson, H. B. Gray, *J. Am. Chem. Soc. 93* (1971) 3603.
[8] a) C. Masters, B. L. Shaw, R. E. Stainbank, *Chem. Commun. 1971*, 209; b) *J. Chem. Soc. A 1971*, 664; c) B. L. Shaw, R. E. Stainbank, *J. Chem. Soc. Dalton Trans. 1972*, 2108.
[9] H. Werner, J. Wolf, A. Hohn, *J. Organomet. Chem. 287* (1985) 395.

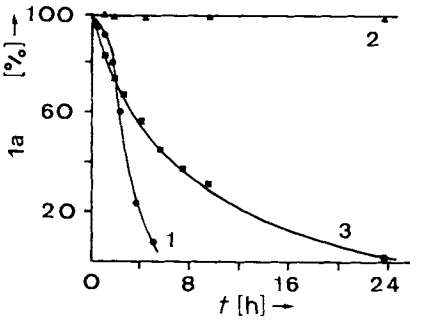
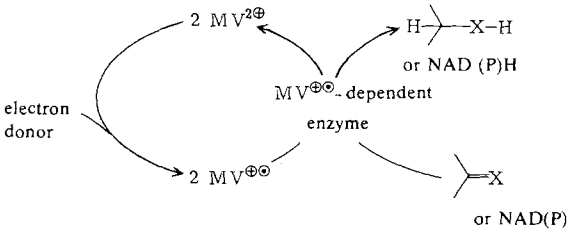


Fig. 1. Rate of hydrogenation of tiglate **1a** under the same conditions (80 mM of **1a** in 10 mL of 0.1 M potassium phosphate buffer (pH 6.5) and 4 mM methyl viologen shaken under H_2 at room temperature) but in the presence of various catalysts. Curve 1: 12 mg of Pd/C. Curve 2: 12 mg of modified Pd/C and 12 µL of Zonyl®-FSC. Curve 3: As for curve 2, but with 0.4 mg (≈6 units) enoate reductase. The reactions were monitored gas chromatographically.

Stereospecific Reductions with Hydrogen Gas, Modified Metal Catalysts, Methyl Viologen and Enzymes or Microorganisms**

By *Iordanes Thanos* and *Helmut Simon**

Reductases which can take up electrons from reduced viologens such as methyl viologen ($MV^{\oplus\odot}$) can stereospecifically reduce numerous 2-enoates and 2-oxocarboxylates.[1-3] The methyl viologen, which is present in catalytic amounts, is recycled according to Scheme 1 between the oxidized and reduced state.



Scheme 1. Methyl viologen ($MV^{2\oplus}$) is the *N,N'*-dimethyl-4,4'-bipyridine dication.

We have hitherto reduced $MV^{2\oplus}$ in three ways:[1] 1) with hydrogen in combination with a hydrogenase, 2) with formate in combination with a formate dehydrogenase, and 3) electrochemically.

We have now found that methyl viologen and other viologens can also be reduced with palladium, platinum or Raney nickel and hydrogen gas when these catalysts are

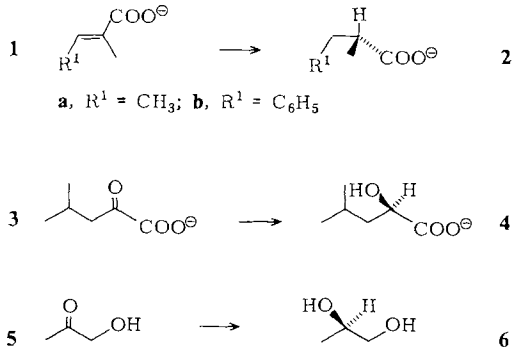


Table 1. Reduction of the substrates **1a**, **1b**, **3** and **5** with H_2, modified metal catalysts, methyl viologen, and biocatalysts (for further experimental conditions see caption to Fig. 1; enzymes, see [1]).

Experiment No.	Reaction volume [mL]	Substrate [mM]	Product [% *ee*]	MV [mM]	Catalyst [mg]	Biocatalyst	Remarks
1	10	**1a** (80)	**2a** (>97)	4	Pd [a] (12.2)	enoate reductase	≥98% product after 15 h
2	3	**1b** (80)	**2b** (>97)	4	Pd [a] (27)	1.5 units enoate reductase	
3	3.2	**1b** (70)	**2b** (>97)	3	Pt [b] (10)	1.5 units enoate reductase	
4	3.2	**1b** (70)	**2b** (>97)	3	Ni [c] (10)	2 × 1.5 units enoate reductase	
5	50	**3** (100)	**4** (>95)	4	Pd [a] (30)	2-oxocarboxylate reductase	>98% product after 50 h
6	10	**5** (100)	**6** [d]	3	Pd [a] (7)	140 mg *Candida utilis*	after 9 h at 25 °C 90% 1,2-propanediol

[a] Palladium on carbon, weight ratio 1:10 modified with Zonyl®-FSC. Weights inclusive of carrier. [b] Modified with Zonyl®-FSC after reduction of PtO_2 by H_2. [c] Raney-nickel was modified with Zonyl®-FSC and used after 3 weeks. [d] *ee* value of this material not determined. The yeast strain, however, forms (2*R*)-1,2-propanediol **6** with *ee* > 95% [1].

[*] Prof. Dr. H. Simon, Dr. I. Thanos
Organisch-chemisches Institut der Technischen Universität München
Lichtenbergstrasse 4, D-8046 Garching (FRG)

[**] This work was supported by the Deutsche Forschungsgemeinschaft (Sonderforschungsbereich 145), BASF, and the Fonds der Chemischen Industrie. We thank H. Costenoble GmbH & Co. KG, Eschborn/Ts. (FRG), for kindly supplying samples of Zonyl®. We also thank Mrs. *Christine Filser* for technical assistance and Mr. *A. S. Paxinos* for valuable discussions.

modified with fluorine-containing surfactants such as Zonyl®-FSC.[4,5] In the presence of such pretreated catalysts, 2-enoates or 2-oxocarboxylates are not reduced by hydrogen gas. When catalytic amounts of $MV^{2\oplus}$ and appropriate enzymes are added, however, the reduction proceeds exclusively enzymatically. Figure 1 shows a typical result. Tiglate **1a** is rapidly reduced by palladium and hydrogen. Palladium pretreated with surfactant was unable

to effect any hydrogen uptake from **1a**. On addition of the aforementioned $MV^{2\oplus}$ and enoate reductase, however, enantiomerically pure (*R*)-2-methyl butyrate **2a** was formed. Thus, we have here particularly simple systems containing only one enzyme, and resort to the relatively expensive electrochemical cell is circumvented. The results are listed in Table 1. For determination of the enantiomeric excess, the products **2a** and **2b** transferred to the organic phase were allowed to react with (*R*)-2-amino-2-phenylethanol according to the method described by *Helmchen*;[6] the unpurified reaction mixture was investigated by reversed phase HPLC or the optical rotation of the isolated products was measured. In each case base line separation could be achieved upon chromatography of the diastereomeric mixtures that were obtained in control experiments by reaction of *rac*-**2a** and *rac*-**2b** with (*R*)-2-amino-2-phenylethanol.

In the method previously used by us,[1,3] enoate reductase leads to products of the type **2a** and **2b** with an enantiomeric excess (*ee*) of >96–98%. (*ee* >96% means that *ee* can be practically 100%.) The experiments 1–5 show that the enantiomeric excess of the chiral acids is very high. It is irrelevant whether modified Pd, Pt or Raney nickel is used.

The catalyst pretreated with Zonyl®-FSC reduces methyl viologen at about the same rate as untreated catalyst. However, methyl viologen is more than 500 times more stable in the presence of pretreated palladium than in the presence of unmodified palladium. The modified palladium also attacks the pyridine nucleotide system. Unmodified catalysts destroy NAD(P) in ca. 1 h in a hydrogen atmosphere. This is very important if enzymatic NAD(P)H is formed with methyl viologen and is then consumed by a corresponding reductase. Experiment 6 shows that it is possible to couple yeast to hydrogen gas for bioreductions via modified catalysts and methyl viologen.

In some of the experiments listed in Table 1, relatively little biocatalyst was intentionally used in order to show that the systems have satisfactory long-term stability and that the chiral products do not racemize.

We envisage the following possible applications for the modified metal catalysts: 1) One-enzyme systems with simple regeneration of cheap mediators. 2) Coupling of many microorganisms not having any hydrogenase to hydrogen gas. This is possible, since many organisms can enzymatically reduce NAD and/or NADP with $MV^{\oplus\odot}$.[1,7] 3) Accelerating hydrogen uptake in the hydrogenation of substrates with hydrogenase-containing organisms, if the hydrogenase activity is limiting. It is, moreover, advantageous if the course of the reaction can be followed by the readily observable consumption of hydrogen.

Finally, the preparation of reduced methyl viologen with hydrogen and modified palladium or platinum in preparative enzymatic work is far superior to the methods with dithionite,[8] zinc,[9] or unmodified platinum with hydrogen as reducing agents. In the preparative application of these methods, high concentrations of sulfite or zinc ions, respectively, were introduced into the systems; both the viologen as well as the pyridine nucleotide are stable for only a short time in the presence of unmodified metal.

Received: December 30, 1985 [Z 1607 IE]
German version: *Angew. Chem.* *98* (1986) 455

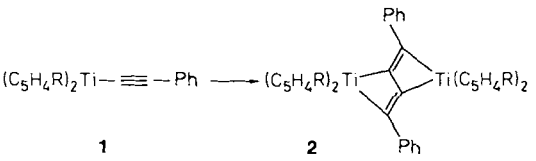
CAS Registry numbers:
1a, 80-59-1; **1b**, 140-10-3; **2a**, 107-92-6; **2b**, 501-52-0; **3**, 816-66-0; (*R*)-**4**, 20312-37-2; **5**, 116-09-6; (*R*)-**6**, 4254-14-2.

[1] H. Simon, J. Bader, H. Günther, S. Neumann, I. Thanos, *Angew. Chem.* *97* (1985) 541; *Angew. Chem. Int. Ed. Engl.* *24* (1985) 539.
[2] H. Simon, H. Günther, J. Bader, S. Neumann, *Ciba Found. Symp.* *111* (1985) 97.
[3] H. Simon, J. Bader, H. Günther, S. Neumann, I. Thanos in A. I. Laskin et al. (Eds.): "*Enzyme Engineering 7*", *Ann. N. Y. Acad. Sci.* *434* (1984) 171.
[4] Procedure: A mixture of 0.1 M phosphate buffer solution (20 mL, pH 7) and 60 mg of Pd/C (10% palladium) or 100 mg of Pt or 100 mg of Raney-Ni was first gassed with hydrogen to remove dissolved oxygen and then treated with 120 mL of Zonyl®-FSC [5]. The mixture was then shaken for 15 h at 35°C under hydrogen and treated with 2 mL of 1 M *N*-tris(hydroxymethyl)aminomethane/HCl solution (pH 7).—Before use, the catalyst can be centrifuged off and taken up in the moist state in the working buffer, containing ca. 30 ppm of Zonyl®-FSC.
[5] Zonyl®-FSC is a fluorine-containing surfactant of the composition $R_f(CH_2)_2S(CH_2)_2N^{\oplus}(CH_3)_3CH_3SO_4^{\ominus}$, where $R_f = F(CF_2)_{6-16}$.
[6] G. Helmchen, G. Nill, D. Flockerzi, W. Schühle, M. S. K. Youssef, *Angew. Chem.* *91* (1979) 64; *Angew. Chem. Int. Ed. Engl.* *18* (1979) 63.
[7] J. Bader, H. Günther, S. Nagata, H. J. Schuetz, M. L. Link, H. Simon, *J. Biotechnol.* *1* (1984) 95.
[8] K. Tsukahara, R. G. Wilkins, *J. Am. Chem. Soc.* *107* (1986) 2632. (In this work no enzymes are used, but the kinetics of the reduction of viologen by dithionite is dealt with in detail and accompanied by an up-to-date list of references.)
[9] P. A. Trudinger, *Anal. Biochem.* *36* (1970) 222.

Unusual Bridging of the Metal Centers in Dimeric Bis(η-methylcyclopentadienyl)-phenylethynylzirconium**

By *Gerhard Erker,** *Wolfgang Frömberg, Richard Mynott, Barbara Gabor,* and *Carl Krüger*

The special bonding situation in bent metallocenes $[Cp_2M]$ often leads to rather unusual complex geometries upon interaction with organic π-systems.[1] *Teuben* and *de Liefde Meijer* observed that (phenylethynyl)titanocene **1a** spontaneously dimerized under the conditions used for its preparation.[2] *Stucky* et al. elucidated the unusual CC-coupled structure of the stable dinuclear reaction product **2b**



1 **2**

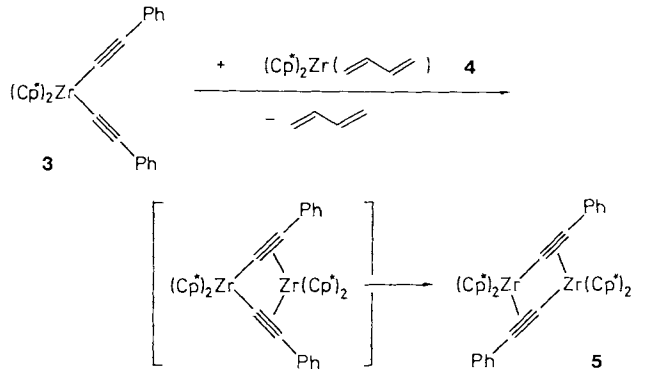
a, R=H; **b**, R=CH$_3$

by an X-ray structure analysis of the methylcyclopentadienyl analogue **1b**.[3] We have now tried to prepare the corresponding zirconium complex via a similar route. Surprisingly, we have observed that in this system the formation of the novel structure type **5** (Cp* = η-$C_5H_4CH_3$) is favored upon replacement of the 3d element titanium by the 4d element zirconium.

Reaction of the zirconocene derivative **3**[4] with **4**[5] at room temperature proceeds slowly, with liberation of butadiene, to give the sparingly soluble compound **5**. The IR spectrum immediately shows that **5** and **2** belong to different types of complexes. Whereas the titanium compound **2**

[*] Prof. Dr. G. Erker [+], Dipl.-Chem. W. Frömberg, Dr. R. Mynott, Ing. Grad. B. Gabor, Prof. Dr. C. Krüger
Max-Planck-Institut für Kohlenforschung
Kaiser-Wilhelm-Platz 1, D-4330 Mülheim a. d. Ruhr (FRG)
[+] Present address: Institut für Organische Chemie der Universität, Am Hubland, D-8700 Würzburg (FRG)

[**] This work was supported by the Fonds der Chemischen Industrie.



shows no IR absorption in the C≡C stretching vibration region,[2,3] in the case of **5** a strong band at 1780 cm^{-1} indicates the presence of a π-complexed alkynyl ligand.[6] In the ^{13}C-NMR spectrum the signal of one of the alkynyl C-atoms appears at unusually low field ($\delta = 228.9$, C2; 154.7, C1).

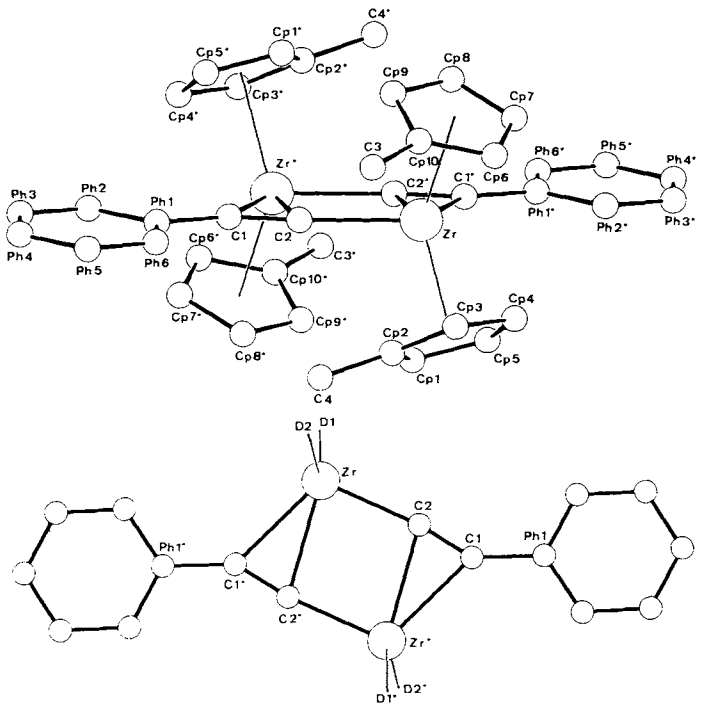
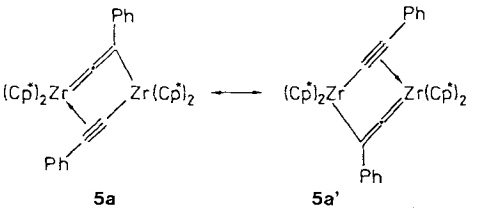


Fig. 1. Two views of the structure of **5** in the crystal. (D1 and D2 denote centroids of the cyclopentadienyl ligands.—Selected bond lengths [Å] and angles [°] C1-C2 1.261(2), C1-Ph1 1.467(2), Zr-C2 2.188(2), Zr-C2* 2.431(2), Zr-C(1*) 2.407(2); D1-Zr-C2 128.0, Zr-C2-Zr* 98.6(1), C2-Zr-C2* 81.4(1).

The X-ray structure analysis (Fig. 1)[7] shows that in the course of reaction one of the two σ-alkynyl ligands of **3** has been transferred to the $(\eta\text{-}C_5H_4CH_3)_2Zr$ fragment of **4**. Compound **5** may be regarded as a centrosymmetric dimer of formally d^1-configurated mono(alkynyl)zirconocene fragments. However, in contrast to the titanium system **2** no CC coupling of the alkynyl groups has occurred here. The two Zr centers in the diamagnetic complex **5** are neither coupled directly to each other nor by forming a CC bond but solely via the completely planar alkynyl ligand system. This can be regarded to a first approximation as a pair of bridging σ,π-alkynyl units. It should be noted, however, that the Zr-C2 bond is rather short.[8] Moreover, the Zr-C2* and Zr-C1* distances indicate that side-on coordination of the alkynyl ligands has led to metal-to-carbon bonds exhibiting a considerable σ-character.[1,8]



These findings indicate that a new type of bridging of two metal centers by alkynyl ligands is present in **5**.[9] **5** is a delocalized metallacyclic system. The bonding can be described in terms of an equivalent participation of the resonance structures **5a** and **5a'**.[10]

Received: January 8, 1985;
revised: February 20, 1985 [Z 1612 IE]
German version: *Angew. Chem. 98* (1986) 456

CAS Registry numbers:
3, 72951-38-3; **4**, 101518-70-1; **5**, 101518-71-2.

[1] G. Erker, C. Krüger, G. Müller, *Adv. Organomet. Chem. 24* (1985) 1; see, e.g.: G. Erker, W. Frömberg, J. L. Atwood, W. E. Hunter, *Angew. Chem. 96* (1984) 72; *Angew. Chem. Int. Ed. Engl. 23* (1984) 68; W. Frömberg, G. Erker, *J. Organomet. Chem. 280* (1985) 343.

[2] J. H. Teuben, H. J. de Liefde Meijer, *J. Organomet. Chem. 17* (1969) 87.

[3] D. G. Sekutowski, G. D. Stucky, *J. Am. Chem. Soc. 98* (1976) 1376.

[4] A. D. Jenkins, M. F. Lappert, R. C. Srivastava, *J. Organomet. Chem. 23* (1970) 165; R. Jimenez, M. C. Barral, V. Moreno, A. Santos, *ibid. 182* (1979) 353.

[5] 60/40 mixture of (*s-cis*- and *s-trans*-butadiene)zirconocene isomers prepared by reaction of $(\eta\text{-}C_5H_4Me)_2ZrCl_2$ with butadiene-magnesium; G. Erker, W. Frömberg, unpublished.

[6] Reaction of **3** (1.5 g, 3.3 mmol) [4] with **4** (1.0 g, 3.3 mmol) [5] in benzene at room temperature (20 h) afforded **5** in 60% yield; crystalline, from CH_2Cl_2 at 5°C. M.p. 257°C; correct elemental analysis; ^1H-NMR (C_6D_6): $\delta = 2.09$ (s, $C_5H_4\text{-}CH_3$), 4.98 (m, $C_5H_4\text{-}CH_3$), 5.34 (m, $C_5H_4\text{-}CH_3$), 7.3 (m, Ph), 7.8 (m, Ph); ^{13}C-NMR (CD_2Cl_2, 223 K, $^1J(CH)$ [Hz] in parenthesis): $\delta = 15.5$ (q, 127, $C_5H_4\text{-}CH_3$), 97.6 (d, C_5H_4-Me), 103.9 (d, C_5H_4-Me), 104.3 (d, C_5H_4-Me), 105.8 (d, C_5H_4-Me), 116.6 (s, C_5H_4-Me), 126.5 (d, Ph), 128.4 (d, Ph), 131.9 (d, Ph), 133.8 (s, Ph), 154.7 (s, C-1), 228.9 (s, C-2); IR (KBr): $\tilde{\nu}(C\equiv C) = 1780\ cm^{-1}$; MS (70 eV): *m/z* 698 (M^+), 349.

[7] **5**: $a = 10.696(1)$, $b = 8.224(1)$, $c = 17.909(1)$ Å, $\beta = 99.08(1)°$, $V = 1555.6$ Å^3, $\rho_{calc} = 1.50\ g\ cm^{-3}$, $\mu = 6.85\ cm^{-1}$, $Z = 2$, space group $P2_1/n$. 4502 independent reflections, 3514 observed, 266 refined parameters, $R = 0.021$, $R_w = 0.027$. Further details of the crystal structure investigation are available on request from the Fachinformationszentrum Energie, Physik, Mathematik GmbH, D-7514 Eggenstein-Leopoldshafen 2, on quoting the depository number CSD-51745, the names of the authors, and the full citation of the journal.

[8] Cf. a) $Cp_2ZrCl(-CH{=}CHPh)ZrCp_2$: 2.196(7) Å; G. Erker, K. Kropp, J. L. Atwood, W. E. Hunter, *Organometallics 2* (1983) 1555; b) $Cp_2Zr(-C{\equiv}C-CH_3)_2$: 2.249(3) Å; G. Erker, W. Frömberg, C. Krüger, unpublished; c) $(C_5H_4Me)_2Zr(CO)_2$: 2.145(9) Å; D. J. Sikora, M. D. Rausch, R. D. Rogers, J. L. Atwood, *J. Am. Chem. Soc. 103* (1981) 1265; d) $Cp_2Zr(CO)_2$: 2.187(4) Å; J. L. Atwood, R. D. Rogers, W. E. Hunter, C. Floriani, G. Fachinetti, A. Chiesi-Villa, *Inorg. Chem. 19* (1980) 3812.

[9] The alkynyl bridging in **5** is structurally different, not only from that observed in the dimeric alkynyl compounds of Al, In or Be, but also in the dimeric alkynyl compounds of Cp_2Er and Cp_2Sm with d^0 configuration. G. D. Stucky, A. Mootz McPherson, W. E. Rhine, J. J. Eisch, J. L. Considine, *J. Am. Chem. Soc. 96* (1974) 1941; W. Fries, W. Schwarz, H.-D. Hausen, J. Weidlein, *J. Organomet. Chem. 159* (1978) 373; N. A. Bell, I. W. Nowell, G. E. Coates, H. M. M. Shearer, *ibid. 273* (1984) 179; B. Morosin, J. Howatson, *ibid. 29* (1971) 7; J. L. Atwood, W. E. Hunter, A. L. Wayda, W. J. Evans, *Inorg. Chem. 20* (1981) 4115; W. J. Evans, I. Bloom, W. E. Hunter, J. L. Atwood, *Organometallics 2* (1983) 709.

[10] The d^1 configurated $Cp_2Zr{-}C{\equiv}C{-}R$ subunit in the bonding situation found here is isolobal to an allyl radical. Therefore, there is a formal analogy between **5** and delocalized (single minimum) Cope systems; a) W. von E. Doering, C. A. Troise, *J. Am. Chem. Soc. 107* (1985) 5739, and

references cited therein; b) R. Hoffmann, W.-D. Stohrer, *ibid. 93* (1971) 6941; M. J. S. Dewar, Z. Nàhlovska, B. D. Nàhlovský, *Chem. Commun. 1971*, 1377; M. J. S. Dewar, D. H. Lo, *J. Am. Chem. Soc. 93* (1971) 7201; c) for attempts at experimental realization with purely organic systems, see, e.g., C. Schnieders, H.-J. Altenbach, K. Müllen, *Angew. Chem. 94* (1982) 638; *Angew. Chem. Int. Ed. Engl. 21* (1982) 637; *Angew. Chem. Suppl. 1982*, 1353; Y. Kobayashi, A. Ando, K. Kawada, I. Kumadaki, *J. Am. Chem. Soc. 103* (1981) 3958; H. Quast, Y. Görlach, J. Stawitz, *Angew. Chem. 93* (1981) 96; *Angew. Chem. Int. Ed. Engl. 20* (1981) 93; d) see also: D. Cremer, E. Kraka, *J. Am. Chem. Soc. 107* (1985) 3800; D. B. Brown: *Mixed-Valence Compounds*, D. Reidel, Dordrecht 1980.

Superactive Alkali Metal Hydride Metalation Reagents: LiH, NaH, and KH**

By *Peter A. A. Klusener, Lambert Brandsma,* Hermann D. Verkruijsse, Paul von Ragué Schleyer,* Thomas Friedl,* and *Rafael Pi*

In principle, the hydrides of alkali metals should be ideal synthetic reagents for the metalation of active hydrogen compounds.[1-10] Hydrogen is the only by-product, and the course of the reaction can be conveniently followed by gas evolution. Addition reactions (e.g. of *n*-butyllithium (BuLi) to carbonyl groups) and electron transfer processes (e.g. by alkali metals) are largely (but not completely) avoided. The high lattice energies of the metal hydrides, particularly of LiH,[1] reduce their reactivity. Commercially available KH and NaH have both been used to some extent as bases,[1-6] whereas LiH has hardly been used at all.[7] Activated by tetramethylethylenediamine (TMEDA), commercial lithium hydride does metalate dibenzyl ketone, but the reaction takes four days.[8] *C. A. Brown* showed that commercial potassium hydride is more reactive than sodium hydride, but described LiH as "essentially inert".[1] We now report the preparation of extremely active NaH, KH and even LiH "superbase" reagents under mild conditions using simple procedures.

Gilman et al. found that a number of organolithium compounds as well as other organometallics could be reduced by hydrogen to give the corresponding metal hydrides.[11] Although these slow reactions can be accelerated by ethers or tertiary amines,[12] they remain "of no practical value".[9] *Bank* and others have prepared "exceedingly active" sodium hydride by hydrogen reduction of sodium naphthalene, but few reactions of this promising reagent have been reported.[13] Attempts by *Brown* to prepare KH in a similar way met without success.[1]

Enormous improvement in these procedures is achieved by hydrogenating BuLi in hexane in the presence of TMEDA. The finely suspended LiH which is produced metalates dibenzyl ketone and 1,1,2,2-tetraphenylacetone exothermically and almost instantly at room temperature; high yields (ca. 80%) of quench products (e.g. silylated enol ethers with $(CH_3)_3SiCl$) were obtained.

BuNa and BuK were prepared first by the reaction of NaO*t*Bu or KO*t*Bu with BuLi in hexane/TMEDA.[14, 15] Hydrogenation at $-25°C$ to $-10°C$ gave the highly reactive NaH and KH in suspension.[16] tBuCOCH$_3$ was metalated almost instantaneously by this KH reagent at $-20°C$; NaH reacts less vigorously, but at 0–20°C enolate formation was complete in 20 minutes. High (ca. 90%) yields of tBuC(OSiMe$_3$)=CH$_2$ were obtained in both cases with Me$_3$SiCl; only a slight amount (ca. 5%) of the addition product, tBuCH(CH$_3$)OSiMe$_3$, was formed. LiH with the same ketone gave comparable amounts of reduction and deprotonation products (after quenching with Me$_3$SiCl).

In contrast to these results, the reported yields with commercially available NaH and LiH are 20% and 2%, respectively.[1] With the difficultly enolizable dicyclopropyl ketone, reduction to the alcohol (95%) was achieved with both KH and LiH, but the rates of reduction were both much faster than those reported in the literature for commercial NaH.[7] Commercial LiH does not react at all. Our KH also metalated dibenzyl ketone instantly at $-20°C$ (80% yield of Me$_3$SiCl quench product), but refluxing for one day did not effect conversion into the known[10] dimetalated species.

Brown compared the reactivities of the alkali hydrides by measuring the rate of hydrogen evolution with, e.g., an excess of dimethyl sulfoxide.[1] At 25°C, KH reacted completely in 8 min; even at 50°C, NaH effected only partial conversion, while LiH was inert. Our reagents are indeed "superactive". Under the same conditions, but at 0°C, KH, NaH, and LiH all react within 1–5 minutes. With excess pyrrolidine at 20°C, our KH gave essentially complete metalation in one minute; LiH reacts somewhat slower and incompletely (70%). NaH leads to only 40% H_2 evolution; but this is essentially achieved in one minute. Incomplete reactions are due to solubility problems, especially with NaH. The metalated products appear to cover the metal hydride surface and prevent further reaction. Hence, use of excess hydride reagent may be needed.

Experimental

Preparation of NaH and KH Reagents. A mixture of 0.10 mol of NaO*t*Bu or KO*t*Bu and 50 mL of hexane (dried by distillation from LiAlH$_4$) was cooled to below $-20°C$. Dry TMEDA (0.10 mol) was added, and then a solution of 0.10 mol of BuLi in about 70 mL of hexane at $-30°C$ [14, 15]. After 15 min, hydrogen was introduced with vigorous stirring at such a rate that practically all gas was absorbed. Fine suspensions of KH and NaH were formed. The reactions were markedly exothermic; cooling was needed to keep the temperature between -20 and $-25°C$ (KH), and -10 to $-15°C$ (NaH). When the rate of absorption decreased, the flow of H_2 was increased to about 0.5 L/min, and the temperature allowed to rise gradually to $+10°C$ or somewhat higher. When no more hydrogen was absorbed, the reaction was stopped. ***Warning:** These active alkali hydrides are pyrophoric in air!*

Preparation of the LiH Reagent. An equimolar or small (1.2 times) excess of TMEDA was added to a solution of *n*-butyllithium in hexane at room temperature. Hydrogen was then introduced with vigorous agitation while keeping the resulting suspension between 30 and 35°C (30–60 min) until no more hydrogen was absorbed. The substrate to be metalated could then be added; the reaction could be followed by the rate and the amount of the H_2 evolved. Under the same conditions, H_2 does not react with BuLi in the absence of TMEDA.

Received: January 16, 1986;
supplemented: February 14, 1986 [Z 1626 IE]
German version: *Angew. Chem. 98* (1986) 458

CAS Registry numbers:
NaH, 7646-69-7; KH, 7693-26-7; LiH, 7580-67-8; BuLi, 109-72-8; NaO*t*-Bu, 865-48-5; KO*t*-Bu, 865-47-4; t-BuCOCH$_3$, 75-97-8; PhCH$_2$COCH$_2$Ph, 102-04-5; Ph$_2$CHCOCHPh$_2$, 7476-11-1; t-BuC(OSiMe$_3$)=CH$_2$, 17510-46-2.

[*] Prof. Dr. L. Brandsma, P. A. A. Klusener, H. D. Verkruijsse
Department of Organic Chemistry of the University of Utrecht
Padualaan 8, NL-3584 CH-Utrecht (The Netherlands)
Prof. Dr. P. von R. Schleyer, T. Friedl, Dr. R. Pi
Institut für Organische Chemie der Universität Erlangen-Nürnberg
Henkestrasse 42, D-8520 Erlangen (FRG)

[**] This work was supported at Utrecht by the Netherlands Science Foundation (S.O.N.) and at Erlangen by the Deutsche Forschungsgemeinschaft, the Fonds der Chemischen Industrie, and by an Alexander von Humboldt Fellowship (to *R. P.*). We thank *C. Schade* for his contribution in developing the BuNa and BuK reagents.

[1] C. A. Brown, *J. Am. Chem. Soc. 95* (1973) 982, 4100; *J. Org. Chem. 39* (1974) 1324, 3913, and references cited therein.

[2] J. P. Bays, *J. Org. Chem. 43* (1978) 38.
[3] A. A. Millard, M. W. Rathke, *J. Org. Chem. 43* (1978) 1834.
[4] P. Groenewegen, H. Kallenberg, A. van der Gen, *Tetrahedron Lett. 1978*, 491, 2817.
[5] D. Ladjama, J. J. Riehl, *Synthesis 1979*, 504; F. Jung, D. Ladjama, J. J. Riehl, *ibid. 1979*, 507.
[6] E. Buncel, B. Menon in E. Buncel, T. Durst (Eds.): *Comprehensive Carbanion Chemistry, Part A*, Elsevier, Amsterdam 1980, p. 112–113, 120.
[7] J.-L. Pierre, P. Arnoud, *Bull. Soc. Chim. Fr. 1967*, 2107; P. Caubère, J. Moreau, *ibid. 1971*, 3276; review, P. Caubère, *Angew. Chem. 95* (1983) 597; *Angew. Chem. Int. Ed. Engl. 22* (1983) 599.
[8] K. M. Pietrusiewicz, J. Monkiewicz, R. Bodalski, *J. Org. Chem. 48* (1983) 788; K. M. Pietrusiewicz, J. Monkiewicz, *Tetrahedron Lett. 27* (1986) 739.
[9] B. J. Wakefield: *The Chemistry of Organolithium Compounds*, Pergamon, New York 1974.
[10] D. W. Wilhelm, T. Clark, P. von R. Schleyer, *J. Chem. Soc. Perkin Trans. 2 1984*, 915; H. Dietrich, W. Mahdi, D. Wilhelm, T. Clark, P. von R. Schleyer, *Angew. Chem. 96* (1984) 623; *Angew. Chem. Int. Ed. Engl. 23* (1984) 621.
[11] H. Gilman, A. L. Jacoby, H. Ludeman, *J. Am. Chem. Soc. 60* (1938) 2336.
[12] C. G. Screttas, J. F. Eastham, *J. Am. Chem. Soc. 88* (1966) 5668; C. G. Screttas, J. F. Eastham, C. W. Kamienski, *Chimia 24* (1970) 109.
[13] S. Bank, T. A. Lois, *J. Am. Chem. Soc. 90* (1968) 4505; S. Bank, M. C. Prislopski, *Chem. Commun. 1970*, 1624, and references cited therein; active MgH_2 can also be obtained by hydrogenation. B. Bogdanović, *Angew. Chem. 97* (1985) 253; *Angew. Chem. Int. Ed. Engl. 24* (1985) 262. Active LiH can be prepared from *t*-butyllithium and hydrogen under pressure. E. C. Ashby, S. A. Noding, *J. Org. Chem. 45* (1980) 1041.
[14] C. Schade, W. Bauer, P. von R. Schleyer, *J. Organomet. Chem. 295* (1985) C25; R. Pi, W. Bauer, B. Brix, C. Schade, P. von R. Schleyer, *ibid.*, in press.
[15] L. Brandsma, H. D. Verkruijsse: *Preparative Polar Organometallic Chemistry, Vol. 1*, Springer, Berlin 1986.
[16] In this procedure, LiO*t*Bu also is present. However, BuNa and BuK can be obtained pure by filtration and washing [14]; suspension in hexane/TMEDA and hydrogenation gives LiO*t*Bu-free NaH and KH. However, these reagents are less reactive and offer no preparative advantages.

Synthesis of a Dicyclopenta[*a,e*]pentalene by [6 + 2]-Cycloaddition of 1,3-Di-*tert*-butyl-5-vinylidenecyclopentadiene and Consecutive 8π-Electrocyclic Reaction**

By *Bernd Stowasser* and *Klaus Hafner**

Dedicated to Professor Heinz A. Staab on the occasion of his 60th birthday

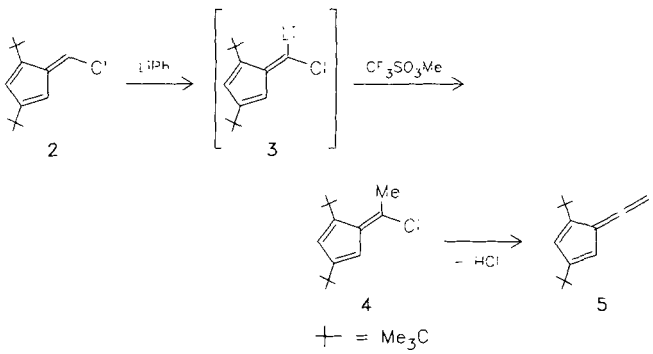
Nonbenzenoid linear annelated [4n + 2]- and [4n]-π-electron systems can be formally regarded as annulenes perturbed by central σ-bonds. According to quantum chemical investigations the bonding behavior of these polycycles should be determined by the π-perimeter as well as by its partial structures.[1] Only three examples of linear annelated hydrocarbons containing more than two exclusively nonbenzenoid rings have so far been reported, namely cyclohepta[*a*]cyclopenta[*e*]- and cyclohepta[*a*]cyclopenta[*g*]azulene as well as azuleno[2,1-*a*]azulene.[2] The partial structures of these aromatic 18π-electron systems also contain [4n + 2]-π-electrons.[3] Consequently, the bonding situation in a representative of the hitherto unknown systems with [4n + 2]-perimeter having [4n]-π-partial structures is of special interest. These prerequisites are fulfilled by dicyclopenta[*a,e*]pentalene **1**. We report here on the synthesis of its tetra-*tert*-butyl derivative **11** by a surprising, novel dimerization of the "pentafulveneallene" **5**.[4] The synthesis concomitantly opens up an entry to the hitherto largely unexplored linear annelated tetraquinanes. The 14π-electron system of **1** formally consists of a pentalene and a



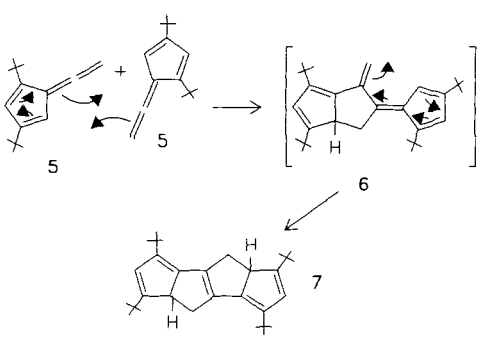
1A 1B

pentafulvene partial structure (**1A**) or two pentalene units (**1B**). According to π-SCF-MO calculations the perimeter of **1** should exhibit a pronounced double-bond fixation determined by a pseudo-Jahn-Teller effect and the π-bonding isomer **1A** (C_s symmetry) should be ca. 4 kcal·mol^{-1} lower in energy than **1B** (C_{2h} symmetry) with two overlapping pentalenoid partial structures. The delocalized 14π-electron system should have an enthalpy of formation ca. 14 kcal mol^{-1} higher than that of **1A**.[1a]

For the synthesis of the tetra-*tert*-butyl derivative **11** of the tetracycle **1** we used 1,3-di-*tert*-butyl-5-vinylidenecyclopentadiene **5** as educt. While "pentafulveneallenes" were hitherto only accessible from diradical generators by pyrolysis or photolysis,[4] we prepared **5** in 88% yield as pale yellow crystals of m.p. 43–44°C (after sublimation) by



metalation of the 6-chloropentafulvene **2**[5] with phenyllithium (tetrahydrofuran (THF), −78°C) to the carbenoid **3**, followed by methylation with methyl trifluoromethanesulfonate (−78°C) to give **4** (yellow leaflets, m.p. 71°C, yield 33%) and subsequent HCl elimination with lithium 2,2,6,6-tetramethylpiperidide (LiTMP) (−78 to 25°C).[6] **5** dimerizes in a solid-state reaction at ca. 10°C within approx. 14 days to give 1,3,5,7-tetra-*tert*-butyl-4,4a,8,8a-tetrahydrodicyclopenta[*a,e*]pentalene **7** (from *n*-hexane, pale-



[*] Prof. Dr. K. Hafner, Dipl.-Ing. B. Stowasser
Institut für Organische Chemie der Technischen Hochschule
Petersenstrasse 22, D-6100 Darmstadt (FRG)

[**] This work was supported by the Deutsche Forschungsgemeinschaft, the Fonds der Chemischen Industrie, and the Dr.-Otto-Röhm-Gedächtnisstiftung.

yellow crystals, decomp. above 114°C; yield 35%). The formation of **7** could involve a [6+2]-cycloaddition of the terminal bond of **5** to the pentafulvene moiety of a second molecule of **5** to give the tetrahydropentalene derivative **6**, which subsequently undergoes an 8π-electrocyclization to **7**.

Whereas the direct dehydrogenation of **7** with 2,3-dichloro-5,6-dicyano-*p*-benzoquinone (DDQ) in ether at 25°C affords only **8** (from *n*-hexane, brown crystals, sublimation >250°C; yield 63%),[7] the proton-catalyzed tautomerization ($CHCl_3$/HCl, 25°C) of **7** leads to the hydrocarbon **9** (from *n*-hexane, reddish-brown fine crystals, m.p. 182°C; yield 75%). Dehydrogenation with DDQ in the molar ratio 1:1 affords the dihydro compound **10** (greenish-brown powder, m.p. 131°C; yield 72%). Upon further dehydrogenation of **10** or reaction of **9** with DDQ in the molar ratio 1:2, the desired 1,3,5,7-tetra-*tert*-butyldicyclopenta[*a*,*e*]pentalene **11** is obtained as thermally stable brownish-violet crystals (chromatography on Al_2O_3 BII–III with pentane) of m.p. 136°C (decomp.) in 70% yield.

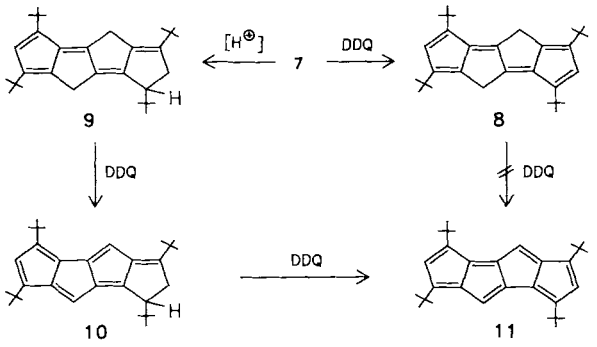


Table 1. Spectral data of **4**, **5**, **7**–**14**. ^{1}H-NMR at 300 MHz, *J* in Hz.

4: ^{1}H-NMR ($CDCl_3$): δ = 1.15 (s; 9H, *t*Bu), 1.31 (s; 9H, *t*Bu), 2.71 (s; CH_3), 6.26 (d, *J* = 2.4; 1H, 2-H or 4-H), 6.28 (d, *J* = 2.4; 1H, 2-H or 4-H); UV (*n*-hexane): λ_{max} (lgε) = 260 (4.19) sh, 266 (4.27), 272 (4.27), 281 (4.06) sh, 376 nm (2.66)

5: ^{1}H-NMR (C_6D_6): δ = 1.16 (s; 9H, *t*Bu), 1.36 (s; 9H, *t*Bu), 4.81 (d, *J* = 1.2; 2H, CH_2), 6.04 (d, *J* = 2.0; 1H, 2-H), 6.24 (dt, J_1 = 2.0, J_2 = 1.2; 1H, 4-H); ^{13}C-NMR (C_6D_6, 75.47 MHz): δ = 29.6, 31.4 ($C(CH_3)_3$), 32.3, 34.0 ($C(CH_3)_3$), 76.3 (CH_2), 110.2 ($C_{quart.}$), 116.2 ($C_{tert.}$), 124.1 ($C_{tert.}$), 149.8 ($C_{quart.}$), 153.0 ($C_{quart.}$), 211.1 ($C_{quart.}$); UV (*n*-hexane): λ_{max} (lgε) = 250 (4.13), 354 nm (2.80)

7: ^{1}H-NMR (C_6D_6): δ = 1.16 (s; 18H, *t*Bu), 1.33 (s; 18H, *t*Bu), 2.65 (m, J_1 = 12.5, J_2 = 5.8; 2H, 4/8-H), 3.25 (m, J_1 = 12.5, J_2 = 7.5; 2H, 4/8-H), 4.35 (ddd, J_1 = 7.5, J_2 = 5.8, J_3 = 1.8; 2H, 4a/8a-H), 6.38 (d, *J* = 1.8; 2H, 2/6-H); UV (*n*-hexane): λ_{max} (lgε) = 227 (4.09), 276 (3.44), 392 nm (4.19)

8: ^{1}H-NMR ($CDCl_3$): δ = 1.24 (s; 18H, *t*Bu), 1.26 (s; 18H, *t*Bu), 3.56 (s; 4H, 4/8-H), 6.36 (s; 2H, 2/6-H); UV (*n*-hexane): λ_{max} (lgε) = 255 (3.36), 264 (3.37), 305 (3.79) sh, 320 (4.14) sh, 333 (4.46), 350 (4.68), 368 (4.64), 474 nm (3.24)

9: ^{1}H-NMR ($CDCl_3$): δ = 0.96 (s; 9H, *t*Bu), 1.22 (s; 9H, *t*Bu), 1.26 (s; 9H, *t*Bu), 1.29 (s; 9H, *t*Bu), 2.68 (m; 2H, 2/3-H), 2.87 (dd, J_1 = 18.0, J_2 = 7.5; 1H, 2-H), 3.25 (d, *J* = 21.0; 1H, 4-H), 3.39 (d, *J* = 21.0; 1H, 4-H), 3.42 (s; 2H, 8-H), 6.34 (s; 1H, 6-H); UV (*n*-hexane): λ_{max} (lgε) = 244 (3.63) sh, 252 (3.70), 260 (3.69), 288 (3.62) sh, 302 (3.71) sh, 358 (4.46) sh, 369 (4.53), 382 (4.46) sh, 425 nm (3.28) sh

10: ^{1}H-NMR ($CDCl_3$): δ = 0.88 (s; 9H, *t*Bu), 1.18 (s; 9H, *t*Bu), 1.20 (s; 9H, *t*Bu), 1.22 (s; 9H, *t*Bu), 2.66 (dd, J_1 = 6.5, J_2 = 1.8; 1H, 3-H), 2.72 (dd, J_1 = 19.0, J_2 = 1.8; 1H, 2-H), 2.95 (dd, J_1 = 19.0, J_2 = 6.5; 1H, 2-H), 5.96 (br. s; 1H, 6-H or 8-H), 6.16 (s; 1H, 6-H or 8-H), 6.60 (d, *J* = 0.6; 1H, 4-H); UV (*n*-hexane): λ_{max} (lgε) = 275 (3.97) sh, 327 (4.68), 337 (4.63) sh, 435 (3.33), 497 nm (3.04) sh

11: ^{1}H-NMR ($CDCl_3$): δ = 1.31 (s; 18H, *t*Bu), 1.33 (s; 18H, *t*Bu), 6.58 (s; 2H, 2/6-H or 4/8-H), 6.72 (s; 2H, 2/6-H or 4/8-H); ^{13}C-NMR ($CDCl_3$, 75.47 MHz): δ = 29.8, 30.8 ($C(CH_3)_3$), 32.7, 33.5 ($C(CH_3)_3$), 118.3 ($C_{tert.}$), 134.3 ($C_{quart.}$), 137.3 ($C_{tert.}$), 142.7, 142.9, 145.8, 155.5 ($C_{quart.}$); UV (*n*-hexane): λ_{max} (lgε) = 226 (4.10), 249 (3.92) sh, 349 (4.58), 399 (3.68) sh, 518 (3.25), 808 nm (1.57) sh

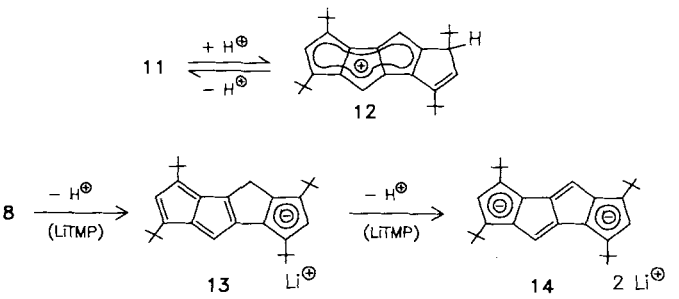
12: ^{1}H-NMR ($CDCl_3$): δ = 1.13 (s; 9H, *t*Bu), 1.44 (s; 9H, *t*Bu), 1.58 (s; 18H, *t*Bu), 3.70 (d, *J* = 1.9; 1H, 1-H), 7.42 (d, *J* = 1.9; 1H, 2-H), 7.70 (br. s; 1H, 6-H), 8.09 (s; 1H, 8-H), 8.46 (d, *J* = 0.8; 1H, 4-H); UV (CH_2Cl_2): λ_{max} (lgε) = 265 (3.83) sh, 308 (4.06), 369 (4.26), 435 (3.84) sh, 470 (3.50) sh, 547 (2.97) sh, 572 (3.06) sh, 622 (3.33) sh, 663 (3.43), 722 (3.24) sh, 862 (2.54), 974 nm (2.23)

13: ^{1}H-NMR ([D$_8$]THF): δ = 1.01 (s; 9H, *t*Bu), 1.03 (s; 9H, *t*Bu), 1.20 (s; 9H, *t*Bu), 1.22 (s; 9H, *t*Bu), 3.51 (s; 2H, 4-H), 4.42 (s; 1H, 8-H), 5.06 (s; 1H, 2-H), 5.65 (s; 1H, 6-H)

14: ^{1}H-NMR ([D$_8$]THF): δ = 1.00–1.33 (*t*Bu signals masked by LiTMP/TMP signals), 4.64 (s; 2H, 4/8-H or 2/6-H), 5.13 (s; 2H, 2/6-H or 4/8-H)

Consistent with what was to be expected on the basis of quantum mechanical calculations, the ring-proton signals at δ = 6.58 and 6.72 (in $CDCl_3$) in the ^{1}H-NMR spectrum of **11** are shifted markedly upfield compared to those of bridged [14]annulenes such as *trans*-10b,10c-dihydropyrene[8] (δ = 7.98–8.67) or *syn*-1,6:8,13-bismethano[14]annulene[9] (δ = 7.1–7.9). In comparison to the ring-proton signals of 1,3,5-tri-*tert*-butylpentalene[10] (δ = 4.72–5.07) the ^{1}H-signals of **11** are shifted to lower field. The similarity of the ring-proton signals of **10** and **11** (Table 1) reflects the cyclopolyolefin character (extensive double-bond fixation) of the new hydrocarbon **11**. The absorptions in the electronic spectrum of **11** (Table 1) correspond favorably to the singlet electron transfers calculated by *Lindner*[1a,11] and by *Toyota* and *Nakajima*[1b] for **1A** with localized double bonds.

11 can be reversibly converted by protonation with trifluoroacetic acid in $CHCl_3$ at 25°C into the stable green cation **12**,[12] whose ^{1}H-NMR data are consistent with a delocalized 10π-electron system. Deprotonation of **8** with equimolar amounts of LiTMP in THF at 25°C affords the lithium salt of the deep-green anion **13**, which can be further deprotonated with LiTMP to give the brownish-yellow dilithium salt of the 1,3,5,7-tetra-*tert*-butyldicyclopenta[*a*,*e*]pentalene dianion **14**. A comparison of the ^{1}H-NMR signals of the ring protons of **11** and **14** shows that the conversion of the 14π-perimeter into the 16π-electron system—taking into account the negative charges in **14**—does not lead to the formation of a clearly paratropic system (upfield shift: Δδ = 1.5–2).[13]



Received: January 20, 1986 [Z 1630 IE]
German version: *Angew. Chem. 98* (1986) 477

CAS Registry numbers:
2, 85655-87-4; **3**, 101671-69-6; **4**, 101671-70-9; **5**, 101671-71-0; **7**, 101671-72-1; **8**, 101671-73-2; **9**, 101671-74-3; **10**, 101671-75-4; **11**, 101671-76-5; **12**, 101654-05-1; **13**, 101671-77-6; **14**, 101671-79-8.

[1] a) H. J. Lindner, unpublished results; b) A. Toyota, T. Nakajima, *Tetrahedron 37* (1981) 2575; c) B. A. Hess, Jr., L. J. Schaad, *J. Org. Chem. 36* (1971) 3418; d) M. Randic, *J. Am. Chem. Soc. 99* (1977) 444; e) R. Zahradnik, *Angew. Chem. 77* (1965) 1097; *Angew. Chem. Int. Ed. Engl. 4* (1965) 1039.

[2] C. Jutz, H. G. Peuker, W. Kosbahn, *Synthesis 1976*, 673; Z. Yoshida, M. Shibata, E. Ogino, T. Sugimoto, *Tetrahedron Lett. 25* (1984) 3343; T. Toda, N. Shimazaki, T. Mukai, C. Kabuto, *ibid. 21* (1980) 4001.

[3] For non-benzenoid linear annelated tricyclic ions see: a) cyclopenta[*a*]azulenide: R. Fleischer, K. Hafner, J. Wildgruber, P. Hochmann, R. Zahradnik, *Tetrahedron 24* (1968) 5943; b) 1,6- and 2,6-di-*tert*-butylcyclopenta[*f*]azulenide: K. Hafner, G. F. Thiele, *Tetrahedron Lett. 26* (1985) 2567; c) cyclopenta[*e*]azulenide: Z. Yoshida, M. Shibata, A. Sakai, T. Sugimoto, *J. Am. Chem. Soc. 106* (1984) 6383; d) 2,5-di-*tert*-butylcyclopenta[*a*]pentalenide: K. Hafner, G. F. Thiele, *Tetrahedron Lett. 25* (1984) 1445.

[4] P. Schissel, M. E. Kent, D. J. McAdoo, E. Hedaya, *J. Am. Chem. Soc. 92* (1970) 2147; E. Hedaya, M. E. Kent, *ibid. 92* (1970) 2149; C. Wentrup, *Top. Curr. Chem. 62* (1976) 173; *Chimia 31* (1977) 258.

[5] H.-P. Krimmer, B. Stowasser, K. Hafner, *Tetrahedron Lett. 23* (1982) 5135; K. Hafner, H.-P. Krimmer, B. Stowasser, *Angew. Chem. 95* (1983) 496; *Angew. Chem. Int. Ed. Engl. 22* (1983) 490.

[6] All the compounds isolated gave correct elemental analyses.

[7] The electronic spectrum and ^{1}H-NMR spectra of **8** are in accordance with those of bis(2,4-di-*tert*-butylcyclopentadienylidene)ethane; R. Brand, H.-P. Krimmer, H. J. Lindner, V. Sturm, K. Hafner, *Tetrahedron Lett. 23* (1982) 5131.

[8] V. Boekelheide, *Pure Appl. Chem. 44* (1975) 807.

[9] E. Vogel, *Pure Appl. Chem. 54* (1982) 1015.

[10] K. Hafner, H. U. Süss, *Angew. Chem. 85* (1973) 626; *Angew. Chem. Int. Ed. Engl. 12* (1973) 575.

[11] H. J. Lindner: Singlet electron transitions of **1A** calculated according to the π-SCF-CI method: λ_{max} (*F*): 224 (0.210), 226 (0.151), 251 (0.031), 289 (0.040), 313 (0.009), 331 (1.045), 334 (0.479), 409 (0.199), 518 (0.003), 888 nm (0.003) (*F* = oscillator strength).

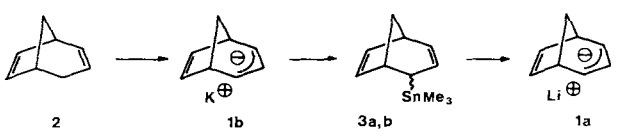
[12] In addition to **12**, small amounts of the 3*H* tautomer are also formed.

[13] In contrast to **14**, lithium-2,5-di-*tert*-butylcyclopenta[*a*]pentalenide [3d] shows a pronounced paratropic ring current.

Bicyclo[3.2.1]octa-2,6-dienyllithium**

By *Norbert Hertkorn, Frank H. Köhler,* Gerhard Müller,* and *Gabriele Reber*

The bicyclo[3.2.1]octa-2,6-dienyl anion **1** is an illustrious example for uniting differently orientated chemists in their ambition to understand a molecule. Although the existence of **1** in solution was first demonstrated more than twenty years ago[1] a lithium derivative thereof has so far never been reported; indeed, no alkali metal derivative has ever been isolated. The central question since its discovery has been: Does **1** experience a stabilization due to bishomoaromaticity or not? Many careful and elegant experiments as well as different computational methods gave diametrically opposed answers (for reviews see Refs. [2–4]). During the last five years *Grutzner* and *Jørgensen*[2a] as well as *Mayr, Schleyer* et al.[2b] concluded from their calculations that homoaromaticity should be negligible in **1**. Modified computations by *Brown* et al.[2c] were much in favor of homoaromaticity. The same was deduced by *Washburn*[3] from the experimental acidities of bicyclo[3.2.1]octa-2,6-diene **2** and similar compounds. *Christl* et al.[4a] and our group[4b] have published ^{13}C-NMR data which are in accord with (possibly slight) homoconjugation; at least, considerable charge transfer from the allylic to the olefinic part of **1** could be demonstrated. We have now been able to isolate the lithium derivative **1a** of the anion **1** as tetramethylethylenediamine (TMEDA) complex **1c**, and to obtain ^{13}C-NMR data of **1a**.



2 1b 3a,b 1a

As described earlier,[4b] **2** was converted into the potassium derivative **1b** of the anion **1**. Reaction with Me_3SnCl furnished a mixture of *exo/endo*-4-trimethylstannylbicyclo[3.2.1]octa-2,6-dienes **3a/b**,[5] and these were transformed into **1a** by methyllithium. **1a**, which according to its ^{13}C-NMR spectrum contained only small amounts of ether, was dissolved in various solvents in order to obtain the ^{13}C-NMR data listed in Table 1; new data for **1b** are also listed. The number of signals and their shifts show that in solution the anion has the same symmetry in **1a** and **1b**. We also wanted to establish how the charge transfer from the allylic to the olefinic part of **1** changes when the equilibrium between contact ion pairs and solvent separated ion pairs[6] is influenced by different alkali ions and/or solvents. As can be seen from Table 1 the average chemical shift δ^{av} is not constant. Hence the effect of the charge delocalization in the π-system on $\delta(^{13}C)$ is obscured by other effects like aggregation, participation of the σ-framework, and geometrical changes within **1**.

Table 1. ^{13}C-NMR data [a] of **1a** and **1b** in various solvents [b].

Cpd.	Solvent	C3	C6/7	C2/4	C1/5	C8	δ^{av}
1a	TMEDA	114.4	84.2	55.6	37.2	29.9	62.3
		142	*158*	*159*	*138*	*132*	
1a	Benzene	115.3	83.8	56.3	37.3	30.0	62.5
1a	Et_2O	114.9	83.0	55.3	36.9	29.4	61.8
		142	*159*	*162*	*140*	*134*	
1a	DME	114.9	85.6	56.2	37.8	30.3	63.1
		142	*158*	*162*	*137*	*131*	
1a	THF	117.6	90.1	58.1	38.8	31.3	65.4
		141	*158*	*158*	*135*	*131*	
1a	Dioxane	118.0	90.0	57.6	38.0	30.7	65.0
1b	DME	119.8	89.8	57.9	39.8	31.3	65.8
		137	*154*	*161*	*133*	*131*	
1b [c]	THF	119.5	90.0	57.9	39.8	31.4	65.8
		138	*157*	*161*	*134*	*131*	

[a] Shifts measured at 273 K (**1a** in C_6H_6: 280 K, in dioxane: 288 K) relative to internal cyclohexane ($\delta = 27.30$) and converted to the δ-scale. $^1J(^{13}C^1H)$ in Hz is given in italics. Numbering scheme cf. Figure 1. Instrument: Bruker CXP 200. [b] TMEDA (tetramethylethylenediamine), DME (1,2-dimethoxyethane), THF (tetrahydrofuran). [c] Remeasured; the deviation from our earlier results [4b] is attributed to changes for the reference (C_6H_{12} instead of [D_8]THF), the solvent (THF instead of [D_8]THF), and different concentrations.

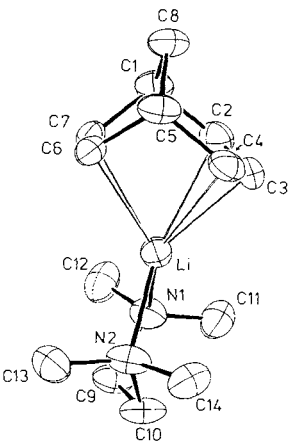


Fig. 1. Structure of bicyclo[3.2.1]octa-2,6-dienyllithium·TMEDA **1c** in the crystal (ORTEP, thermal ellipsoids 50%, hydrogens omitted). Important distances [Å] and angles [°]: C1-C2 1.520(4), C4-C5 1.517(5), C2-C3 1.394(5), C3-C4 1.384(4), C5-C6 1.508(5), C1-C7 1.512(4), C6-C7 1.354(4), C1-C8 1.542(4), C5-C8 1.538(4), Li-C2 2.515(6), Li-C4 2.440(6), Li-C3 2.194(6), Li-C6 2.399(5), Li-C7 2.429(6).

[*] Prof. Dr. F. H. Köhler, Dr. G. Müller, Dipl.-Chem. N. Hertkorn, Dipl.-Chem. G. Reber
Anorganisch-chemisches Institut der Technischen Universität München
Lichtenbergstr. 4, D-8046 Garching (FRG)

[**] This work was supported by the Fonds der Chemischen Industrie and BASF.

Upon cooling a saturated solution of **1a** in TMEDA we obtained yellow crystals that were suitable for an X-ray structure analysis.[7] Figure 1 shows that the crystals contain **1c**, bicyclo[3.2.1]octa-2,6-dienyllithium stabilized by one molecule TMEDA. **1c** is a monomer with a crystallographic symmetry (C_1) which is lower than expected for **1a** alone (C_s) because N1-N2 is not parallel to C1-C5. Lithium occupies an almost central position below the seven-membered ring, such that not only the allylic but also the olefinic part of the carbanion is engaged in metal–ligand bonding. Li-C6 and Li-C7 are even shorter than Li-C2 and Li-C4. A coordination number of seven, rarely observed for solvated lithium bound to a pure hydrocarbon,[8] is thus achieved.

According to the C_1 symmetry lithium is placed asymmetrically below the allyl part of **1**; this confirms NMR-results on allyllithium.[9] Li-C3 is the only "normal" lithium-carbon distance, the others being much longer than in most organolithium compounds.[8] In 1,3-diphenylallyllithium[10] similar Li-C distances are found for the outer allyl carbon atoms while the inner one is ca. 0.013 Å further away from lithium than in **1c**.

A still closer Li-C3 contact is to be expected in the case of an undistorted carbanion. However, the allylic plane is inclined towards C8 by 3.9° relative to the C1-C2-C4-C5 plane. This distortion is the first experimental verification that the inner substituents in an allyllithium compound are bent away from the metal, as predicted for the inner hydrogens of the parent compound C_3H_5Li.[11] There is also a similarity to the tricarbonyl(bicyclo[3.2.1]octa-2,6-dienyl)iron cation,[12] while in cyclopentadienyllithium (silylated in the five-membered ring) the π-system is planar.[13]

In view of the controversy about the homoaromaticity in **1** the results are especially enlightening. If the C1-C2-C4-C5, C1-C5-C6-C7, and C1-C5-C8 planes are termed A, B, and C then the interplanar angles A/B, A/C, and B/C are found to be 103.2°, 119.2°, and 137.6° respectively. While angles of about 120°, as for A/C, are expected,[14] it looks as if C6/7 moves towards the allyl system, thus increasing the angle for B/C and decreasing it for A/B. Correspondingly, C2 and C7 and C4 and C6 are separated by only 2.371 and 2.370 Å, respectively. The approach of the olefinic and the allylic part has been claimed to be crucial for the interaction in **1**.[2c] When the MNDO optimized geometry with C2-C7 = C4-C6 = 2.480 Å was used as a basis for ab initio calculations on **1** no homoaromatic stabilization could be found.[2a,b,15] In contrast, *Brown* et al.[2c] believe that substantial homoconjugative delocalization is responsible for the charge transfer in **1**. This follows from the orbital analysis at the equilibrium geometry of **1** with likewise 2.48 Å for C2-C7 and C4-C6. We find this distance to be even 0.11 Å shorter in **1c**. Such a shortening is expected[2b] for cyclic conjugation in **1**. On the other hand, the shortening is partly compensated by the interplanar angle A/allyl of 3.9°. As for an additional "lithium effect" on the geometry of **1**, theoretical work including the metal must be awaited.[16] Many X-ray structures[8] suggest that lithium rather accommodates itself to the constraint of ligands (cf. the long distances Li-C2/4/6/7 in **1c**) than vice versa.

Received: January 28, 1986 [Z 1644 IE]
German version: *Angew. Chem. 98* (1986) 462

CAS Registry numbers:
1a, 101671-14-1; **1b**, 87951-21-1; **1c**, 101671-15-2.

[1] a) J. M. Brown, *Chem. Commun. 1967*, 638; b) S. Winstein, M. Ogliaruso, M. Sakai, J. M. Nicholson, *J. Am. Chem. Soc. 89* (1967) 3656.
[2] a) J. B. Grutzner, W. L. Jørgensen, *J. Am. Chem. Soc. 103* (1981) 1372; b) E. Kaufmann, H. Mayr, J. Chandrasekhar, P. von R. Schleyer, *ibid. 103* (1981) 1375; c) J. M. Brown, R. J. Elliot, W. G. Richards, *J. Chem. Soc. Perkin Trans. 2 1982*, 485.
[3] W. N. Washburn, *J. Org. Chem. 48* (1983) 4287.
[4] a) M. Christl, H. Leininger, D. Brückner, *J. Am. Chem. Soc. 105* (1983) 4843; b) F. H. Köhler, N. Hertkorn, *Chem. Ber. 116* (1983) 3274.
[5] a) F. H. Köhler, N. Hertkorn, *Z. Naturforsch. B38* (1983) 407; b) F. H. Köhler, N. Hertkorn, unpublished.
[6] a) D. H. O'Brien, C. R. Russell, A. J. Hart, *J. Am. Chem. Soc. 98* (1976) 7427; b) U. Edlund, *Org. Magn. Reson. 9* (1977) 593; c) J. van der Giessen, C. Gooijer, C. Maclean, N. H. Velthorst, *Chem. Phys. Lett. 55* (1978) 33.
[7] Crystal structure data (**1c**): monoclinic, $P2_1/n$, $a = 8.437(2)$, $b = 10.006(2)$, $c = 17.648(4)$ Å, $\beta = 104.08(2)°$, $V = 1445.1$ Å^3, $\rho_{calcd} = 1.049$ g/cm^3 for $Z = 4$, $\mu(Mo_{K\alpha}) = 0.6$ cm^{-1}. 2264 independent reflections, 1858 "observed" with $F_0 \geq 4.0\,\sigma(F_0)$ (ω scans, $\Delta\omega = 0.9°$, $(\sin\vartheta/\lambda)_{max} = 0.572$, +h, +k, ±l, $Mo_{K\alpha}$, graphite monochromator, $T = -40$°C, Syntex $P2_1$). Direct methods (SHELX76), $R = 0.071$, $R_w = 0.068$, $w = 1/\sigma^2(F_0)$ for 174 refined parameters (anisotropic, H constant, CH_3 rigid groups, disordered TMEDA CH_2 groups as two alternatives 75/25, SHELX76). $\Delta\rho_{fin}(max/min) = 0.28/-0.22$ e/Å^3. Further details of the crystal structure analysis are available on request from the Fachinformationszentrum Energie, Physik, Mathematik GmbH, 7514 Eggenstein-Leopoldshafen 2, on quoting the depository number CSD-51880, the names of the authors, and the full citation of the journal.
[8] W. N. Setzer, P. von R. Schleyer, *Adv. Organomet. Chem. 24* (1985) 353.
[9] a) M. Schlosser, M. Strähle, *Angew. Chem. 92* (1980) 49; *Angew. Chem. Int. Ed. Engl. 19* (1980) 487; b) M. Strähle, M. Schlosser, *J. Organomet. Chem. 220* (1981) 277.
[10] G. Boche, H. Etzrodt, M. Marsch, W. Massa, G. Baum, H. Dietrich, W. Mahdi, *Angew. Chem. 98* (1986) 84; *Angew. Chem. Int. Ed. Engl. 25* (1986) 104.
[11] a) T. Clark, C. Rohde, P. von R. Schleyer, *Organometallics 2* (1983) 1344, and references cited therein; b) G. Decher, G. Boche, *J. Organomet. Chem. 259* (1983) 31.
[12] T. N. Margulis, L. Schiff, M. Rosenblum, *J. Am. Chem. Soc. 87* (1965) 3269.
[13] a) P. Jutzi, E. Schlüter, C. Krüger, S. Pohl, *Angew. Chem. 95* (1983) 1015; *Angew. Chem. Int. Ed. Engl. 22* (1983) 994; b) M. F. Lappert, A. Singh, L. M. Engelhardt, A. H. White, *J. Organomet. Chem. 262* (1984) 271; c) P. Jutzi, E. Schlüter, S. Pohl, W. Saak, *Chem. Ber. 118* (1985) 1959.
[14] A value of ca. 115° has been found for the corresponding angle in norbornadiene: K. Raghavachari, R. C. Haddon, H. D. Roth, *J. Am. Chem. Soc. 105* (1983) 3110, and references cited therein.
[15] The C–C distance has not been given explicitly in Ref. [2a]; it should be very similar to that in Ref. [2b].
[16] After submission of this paper Prof. *Schleyer* informed us that he has carried out MNDO calculations on **1a**.

Synthesis and Structure of the First Arsaalkenyl Complex with FeAs Single Bond**

By *Lothar Weber,* Georg Meine,* and *Roland Boese*

The chemistry of phosphaalkenes has been the subject of intensive study in the past ten years.[1] Such compounds are not only of interest from the theoretical and preparative point of view but also because they exhibit a versatile coordination chemistry.[2] In contrast, very few arsaalkenes have so far been reported. Compounds of type **1** have been prepared by *Becker* et al. from disilylarsanes and pivaloyl chloride.[3] Further, the synthesis and spectroscopic properties of the substituted α-arsastyrenes **2**,[4] **3**,[5] and **4**[6] have been described, but without quoting any X-ray structure data. Coordination compounds of arsaalkenes have, with exception of the rhodium complex **5**, so far never been reported.[7]

[*] Prof. Dr. L. Weber, G. Meine, Dr. R. Boese
Institut für Anorganische Chemie der Universität
Universitätsstr. 5–7, D-4300 Essen 1 (FRG)

[**] This work was supported by the Fonds der Chemischen Industrie.

$R-As=C(OSiMe_3)(tBu)$

1

$2,4,6\text{-}Me_3C_6H_2-As=CPh_2$ **2** $Ph-As=CH(NMe_2)$ **3**

$Ph-As=C(tBu)[(N(SiMe_3)R]$, $R=Ph, p\text{-}MeC_6H_4$

4

$[(\eta^5\text{-}C_5Me_5)(CO)Rh(\eta^2\text{-}Ph-As=CH_2)]$

5

We report here on the first arsaalkenyl complexes **9**, which can also be regarded as transition-metal substituted arsaalkenes. Complex **9a** is, moreover, the first compound to have been characterized by an X-ray structure analysis in which an As=C double bond does not belong to a conjugated system. The strategy used had previously proven successful in the synthesis of phosphaalkenyl complexes.[8,9] We obtained the title compounds **9a–c** by reaction of the disilylarsenido complex **6** with the carboxylic acid chlorides **7a–c**.

$$[(\eta^5\text{-}C_5H_5)(CO)_2Fe-As(SiMe_3)_2] \xrightarrow[-Me_3SiCl]{+RCOCl\ 7} [(\eta^5\text{-}C_5H_5)(CO)_2Fe-As(SiMe_3)(COR)] \longrightarrow [(\eta^5\text{-}C_5H_5)(CO)_2Fe-As=C(OSiMe_3)(R)]$$

6 **8** **9**

a, R = *t*Bu; **b**, R = 2,4,6-$Me_3C_6H_2$; **c**, R = 2,4,6-$tBu_3C_6H_2$

Postulated intermediates such as, e.g., **8a–c** could not be detected, either by IR or by ^{1}H-NMR spectroscopy.

The $Fe(CO)_2$ group of the complexes **9** is, in each case, recognizable by two intense bands. A medium intensity band occurs at 1180–1194 cm^{-1}; we assign this to the coupled $\tilde{\nu}$(SiOC) vibration. The characteristic downfield shift of the ^{13}C resonances of the As=C unit (δ = 216.4–232.7) is compatible with the monomeric structure of the complexes **9**. As in the case of the phosphorus analogues[8,9] of **9**, *Z*-configuration is assumed at the double bond for steric reasons.

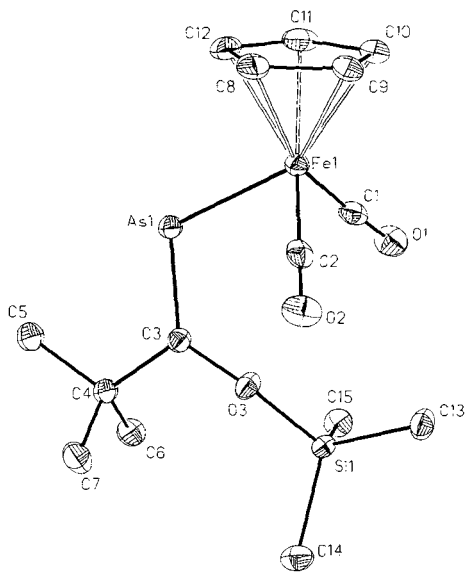


Fig. 1. Structure of **9a** in the crystal. Selected bond lengths [pm] and angles [°]: Fe-As 240.7(1), As-C3 182.1(2), C3-O3 135.6(3), C3-C4 153.3(4), Fe-C1 175.6(3), Fe-C2 176.1(3), C1-O1 114.6(4), C2-O2 114.2(3), Fe-C(Ring) 210.6(2) to 211.3(2); C1-Fe-As 88.0(1), C2-Fe-As 87.0(1), C1-Fe-C2 96.7(1), Fe-As-C3 111.4(1), As-C3-O3 124.1(2), As-C3-C4 120.6(2), C4-C3-O3 115.1(2), C3-O3-Si 144.1(2).

These assumptions were confirmed by an X-ray structure analysis of **9a** at −150°C (Fig. 1).[10] The As=C distance (182.1(2) pm) is distinctly shorter than in the arsabenzene 2,3,6-$Ph_3C_5H_2As$ (185.9, 188.4 pm)[11] and than the standard As–C single bond length (196 pm).[12] From the As=As distance in a diarsene (224.6 pm)[13] and the C=C bond length (130 pm), the length of an As=C double bond can be estimated to be 177 pm. The iron atom lies in a plane with the As, C3 and O3 atoms and is coupled to the arsenic atom by a single bond (240.7(1) pm).

The C3–O3 distance (135.6(3) pm) is significantly shorter than the calculated C(sp^2)O single bond length (141 pm).[14] We explain this in terms of delocalization of a lone electron pair of the oxygen and the electrons of the As=C double bond.

Experimental

^{1}H-NMR: In all cases 200-MHz, C_6D_6, 22°C; ^{13}C-NMR: in all cases C_6D_6, 22°C; EI-MS: in all cases 70 eV (Varian MAT 312).

6: The suspension of $[Cp(CO_3)Fe]^{\oplus}BF_4^{\ominus}$ (Cp = η^5-C_5H_5) (5.89 g, 20.2 mmol) in ether (170 mL) was treated at −55°C with 7.96 g (20.2 mmol) of solid $LiAs(SiMe_3)_2\cdot(THF)_{2.3}$ [15]; the solution immediately turned red. After 15 minutes stirring at −55°C and 30 minutes stirring at 0°C the solution was evaporated in a vacuum at 0°C. The oily dark-red residue was taken up in pentane (30 mL), filtered, and the filtrate concentrated to 10 mL and allowed to stand for 12 h at −78°C; yield 6.34 g (79%) of dark-red, crystalline **6**, m.p. 54–56°C.—^{1}H-NMR: δ = 0.48 (s, $SiMe_3$), 4.18 (s, Cp).—^{13}C{^{1}H}-NMR: δ = 4.7 (s, $SiMe_3$), 84.8 (s, Cp), 217.2 (s, Fe–C≡O).—IR (cyclopentane): 2009 s, 1956 s cm^{-1} ($\tilde{\nu}$(CO)).—EI-MS: *m/z* 399 (M^+).

9a: A solution of **7a** (0.33 g, 2.76 mmol) in THF (50 mL) was added dropwise within 1 h at 0°C to a solution of **6** (1.10 g, 2.76 mmol) in THF (100 mL). The dark-brown solution was evaporated to dryness in a vacuum. The oily, brown residue was taken up in *n*-pentane (25 mL), filtered, and the filtrate concentrated to ca. 10 mL. At −28°C, brown **9a** crystallized out; yield 0.31 g (27%), m.p. 61°C.—^{1}H-NMR: δ = 0.44 (s, $SiMe_3$), 1.42 (s, *t*Bu), 4.14 (s, Cp).—^{13}C-NMR: δ = 2.7 (s, $SiMe_3$), 30.1 (s, $C(CH_3)_3$), 48.3 (s, $C(CH_3)_3$), 85.0 (s, Cp), 215.9 (s, Fe–C≡O), 232.7 (s, As=C).—IR (cyclopentane): 2012 s, 1957 s cm^{-1} ($\tilde{\nu}$(CO)); IR (Nujol): 1194 m cm^{-1} ($\tilde{\nu}$(SiOC)).—EI-MS: *m/z* 412 (M^+ + 2H).

9b: Prepared analogously to **9a**. Brown crystals, yield 30%, m.p. 76°C.—^{1}H-NMR: δ = 0.11 (s, $SiMe_3$), 2.07 (s, *p*-Me), 2.61 (s, 6H, *o*-Me), 4.16 (s, Cp), 6.71 (s, 2H, Ph).—^{13}C-NMR: δ = 0.7 (s, $SiMe_3$), 21.2 (s, *p*-Me), 21.3 (s, *o*-Me), 84.5 (s, Cp), 128.8 (s, *m*-C–Ph), 135.3 (s, *o*-C–Ph), 137.4 (s, *p*-C–Ph), 142.0 (s, *i*-C–Ph), 215.5 (s, Fe–C≡O), 216.4 (s, As=C).—IR (cyclopentane): 2012 s, 1960 s cm^{-1} ($\tilde{\nu}$(CO)); IR (Nujol): 1180 m cm^{-1} ($\tilde{\nu}$(SiOC)).—EI-MS: *m/z* 474 (M^+ + 2H).

9c: Prepared analogously to **9a**. Dark brown crystals, yield 26%, m.p. 160–170°C.—^{1}H-NMR: δ = 0.15 (s, $SiMe_3$), 1.30 (s, *p*-*t*Bu), 1.87 (s, 18H, *o*-*t*Bu), 4.14 (s, Cp), 7.62 (s, 2H, Ph).—^{13}C-NMR: δ = 2.0 (s, $SiMe_3$), 31.5 (s, *p*-$C(CH_3)_3$), 32.6 (s, *p*-$C(CH_3)_3$), 35.0 (s, *o*-$C(CH_3)_3$), 39.0 (s, *o*-$C(CH_3)_3$), 84.9 (s, Cp), 123.7 (s, *m*-C–Ph), 139.8 (s, *p*-C–Ph), 148.2 (s, *o*-C–Ph), 149.6 (s, *i*-C–Ph), 215.2 (s, Fe–C≡O), 216.4 (s, As=C).—IR (cyclopentane): 2012 s, 1959 s cm^{-1} ($\tilde{\nu}$(CO)); IR (Nujol): 1181 m cm^{-1} ($\tilde{\nu}$(SiOC)).—EI-MS: *m/z* 600 (M^+ + 2H).

Received: January 29, 1986 [Z 1646 IE]
German version: *Angew. Chem. 98* (1986) 463

[1] Reviews: a) R. Appel, F. Knoll, I. Ruppert, *Angew. Chem. 93* (1981) 771; *Angew. Chem. Int. Ed. Engl. 20* (1981) 731; b) G. Becker, W. Becker, O. Mundt, *Phosphorus Sulfur 14* (1983) 267.

[2] O. J. Scherer, *Angew. Chem. 97* (1985) 905; *Angew. Chem. Int. Ed. Engl. 24* (1985) 924.

[3] G. Becker, G. Gutekunst, *Angew. Chem. 89* (1977) 477; *Angew. Chem. Int. Ed. Engl. 16* (1977) 463; *Z. Anorg. Allg. Chem. 470* (1980) 144.

[4] T. C. Klebach, H. van Dongen, F. Bickelhaupt, *Angew. Chem. 91* (1979) 423; *Angew. Chem. Int. Ed. Engl. 18* (1979) 395.

[5] G. Becker, A. Münch, H.-J. Wessely, *Z. Naturforsch. B36* (1981) 1080.

[6] J. Heinicke, A. Tzschach, *J. Organomet. Chem. 116* (1979) 175.

[7] H. Werner, W. Paul, R. Zolk, *Angew. Chem. 96* (1984) 617; *Angew. Chem. Int. Ed. Engl. 23* (1984) 626.

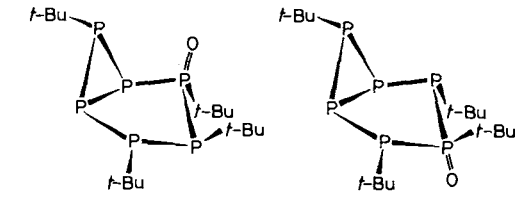
[8] L. Weber, K. Reizig, R. Boese, M. Polk, *Angew. Chem. 97* (1985) 583; *Angew. Chem. Int. Ed. Engl. 24* (1985) 604.
[9] L. Weber, K. Reizig, M. Frebel, R. Boese, M. Polk, *J. Organomet. Chem.*, in press.
[10] **9a**, $P2_1/n$, $a=675.4(2)$, $b=3175.7(8)$, $c=842.8(2)$ pm, $\beta=97.53(2)°$, $V=1792.1\times10^6$ pm^3, $Z=4$, $R=0.030$. Further details of the crystal structure investigation are available on request from the Fachinformationszentrum Energie, Physik, Mathematik GmbH, D-7514 Eggenstein-Leopoldshafen 2, on quoting the depository number CSD-51809, the names of the authors, and the full citation of the journal.
[11] F. Sanz, J. J. Daly, *Angew. Chem. 84* (1972) 679; *Angew. Chem. Int. Ed. Engl. 11* (1972) 630.
[12] Interatomic Distances Supplement Special Publ. No. 18, The Chemical Society, London 1965.
[13] A. H. Cowley, J. C. Lasch, N. C. Norman, M. Pakulski, *Angew. Chem. 95* (1983) 1019; *Angew. Chem. Int. Ed. Engl. 22* (1983) 978; *Angew. Chem. Suppl. 1983*, 1493.
[14] U. Schubert, H. Fischer, P. Hofmann, K. Weiss, K. H. Dötz, F. R. Kreissl: *Transition Metal Carbene Complexes*, Verlag Chemie, Weinheim 1983, p. 77.
[15] G. Becker, G. Gutekunst, H. J. Wessely, *Z. Anorg. Allg. Chem. 462* (1980) 113.

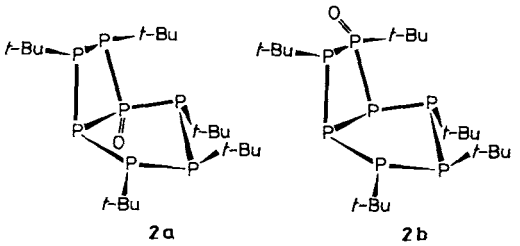
P_6tBu_4O and P_7tBu_5O— the First Polycyclophosphane Oxides**

By *Marianne Baudler,* Michael Michels, Manfred Pieroth,* and *Josef Hahn*

Dedicated to Professor Rolf Appel on the occasion of his 65th birthday

Polycyclic organophosphanes P_nR_m ($m<n$)[1] are generally susceptible to oxidative attack by atmospheric oxygen—especially in solution. But, so far, nothing has been reported about the polycyclophosphane oxides that are formed. Of particular interest is whether the oxygen reacts with insertion into the P_n-skeleton, as in the formation of P_4O_6 from P_4, or with exocyclic addition to the intact polycyclophosphane. We have now been able to isolate pure tetra-*tert*-butylbicyclohexaphosphane monoxide, **1**, and penta-*tert*-butylbicycloheptaphosphane monoxide, **2**; according to nuclear magnetic resonance investigations two constitutional isomers are formed in each case.





[*] Prof. Dr. M. Baudler, Dr. M. Michels, Dr. M. Pieroth, Dr. J. Hahn
Institut für Anorganische Chemie der Universität
Greinstrasse 6, D-5000 Köln 41 (FRG)

[**] Contributions to the Chemistry of Phosphorus, Part 165. This work was supported by the Deutsche Forschungsgemeinschaft and the Fonds der Chemischen Industrie.—Part 164: M. Baudler, L. de Riese-Meyer, *Z. Naturforsch. B*, in press.

1 and **2** were obtained by reaction of excess P_6tBu_4[2] and P_7tBu_5,[3] respectively, in solution with dry air and were separated chromatographically from unchanged polycyclophosphane.[4] When stoichiometric amounts of atmospheric oxygen were used, the corresponding dioxides and further unidentified products were also formed, thus complicating work-up of the reaction mixture. **1a** and **1b** were separately isolable (abundance ratio 4.5 : 1), whereas **2a** and **2b** (abundance ratio approx. 1 : 1) could not be separated, even by high-pressure liquid chromatography.

1a, **1b**, and the mixture **2a**,**b** are pale yellow solids (**1a**: m.p. 132 °C; **1b**: m.p. 134 °C; **2a**,**b**: softening range 122–130 °C), which are stable at room temperature in the absence of air and light. They are readily soluble in hydrocarbons, tetrahydrofuran (THF), and methanol; the solutions are more sensitive to oxidation than the solid substances. The compositions of **1a**, **1b**, and **2a**,**b** were confirmed by elemental analyses and molecular mass determinations (MS). Each show an intense band in the IR spectrum in the region of the P=O valence vibrations.

Table 1. ^{31}P-NMR parameters [a] of **1a** [b] and **1b** [c], in [D$_6$]benzene at 25 °C.



δ	J(PP)	δ	J(PP)
−103.7 (P^1)	−361.1 (P^1P^2)	−129.1 (P^1)	−363.5 (P^1P^2)
+161.9 (P^2)	−370.9 (P^2P^3)	+ 27.5 (P^2)	−385.0 (P^2P^3)
+ 25.1 (P^3)	−349.7 (P^3P^4)	+185.1 (P^3)	−385.0 (P^3P^4)
+ 68.3 (P^4)	−304.5 (P^4P^5)	+ 27.5 (P^4)	−363.5 (P^4P^5)
−167.7 (P^5)	−194.3 (P^5P^6)	−129.1 (P^5)	−168.1 (P^5P^6)
−131.5 (P^6)	−171.6 (P^1P^6)	−133.8 (P^6)	−168.1 (P^1P^6)
	−250.8 (P^1P^5)		−198.5 (P^1P^5)
	+ 48.8 (P^1P^3)		− 20.9 (P^1P^3)
	+ 24.6 (P^1P^4)		+ 23.4 (P^1P^4)
	+ 34.9 (P^2P^4)		− 57.5 (P^2P^4)
	+ 4.9 (P^2P^5)		+ 23.4 (P^2P^5)
	+ 39.3 (P^2P^6)		+123.7 (P^2P^6)
	+ 2.4 (P^3P^5)		− 20.9 (P^3P^5)
	+116.7 (P^4P^6)		+123.7 (P^4P^6)
	− 0.1 (P^3P^6)		− 2.5 (P^3P^6)

[a] J [Hz]; signs assuming negative ^1J(PP) couplings. [b] RMS value of the spectrum calculation: 1.0; all transitions assigned. [c] RMS value: 0.4; 165 of 184 transitions assigned.

Proof of the constitution of **1a**, **1b**, **2a**, and **2b** is provided by the ^{1}H-NMR data, and above all by the complete analysis of the ^{31}P{^{1}H}-NMR spectra (Tables 1 and 2). In the case of the ^{31}P{^{1}H}-NMR spectrum of the mixture **2a**,**b**, first a separation into the partial spectra of the isomers by selective population transfer experiments[6] was necessary, which also gave the signs of the coupling constants. Superposition of the calculated individual spectra very satisfactorily reproduced the experimental spectrum of the mixture **2a**,**b** (Fig. 1).

It follows from the ^{31}P-NMR parameters and especially from the ^1J(PP) coupling constants, that the oxygen in the monoxides is in each case bound exocyclically to the P_n skeleton of the parent compound. Which of the P atoms is present as λ^5-phosphorus follows from the drastic down-

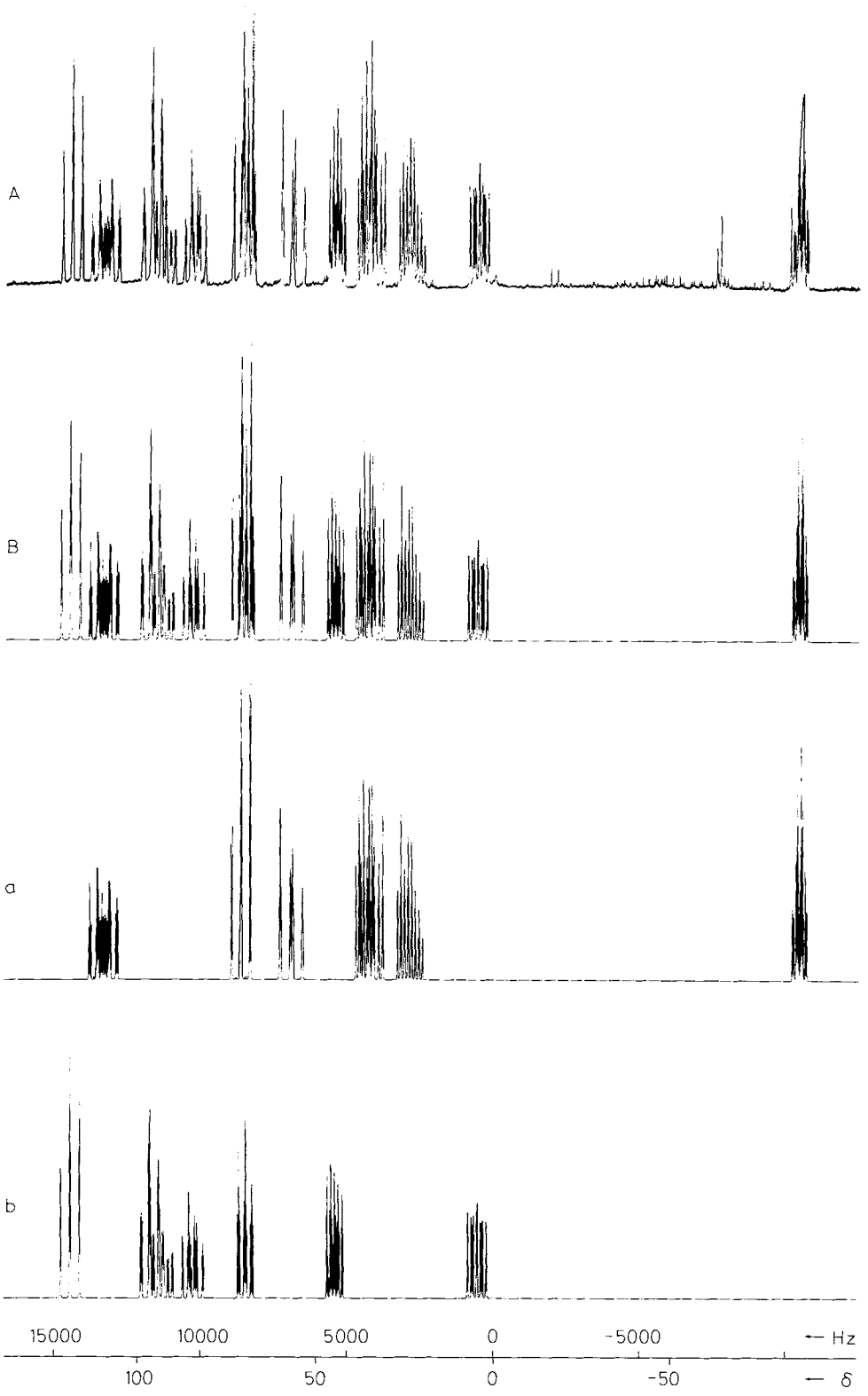
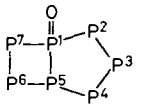


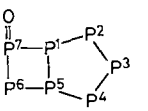
Fig. 1. Observed (A) and calculated (B) $^{31}P\{^1H\}$-NMR spectrum of **2a,b** in [D_6]benzene at 25 °C (121.497 MHz); a, b: calculated spectra of the isomers **2a** and **2b**, respectively.

Table 2. ^{31}P-NMR parameters [a] of **2a** [b] and **2b** [c] [8], isomeric mixture, in [D_6]benzene at 25 °C.



2a

δ	J(PP)
+113.5 (P^1)	−416.3 (P^1P^2)
+ 61.0 (P^2)	−334.3 (P^2P^3)
+ 74.8 (P^3)	−319.2 (P^3P^4)
+ 38.2 (P^4)	−359.2 (P^4P^5)
+ 27.6 (P^5)	−135.1 (P^5P^6)
− 82.5 (P^6)	−174.2 (P^6P^7)
+ 40.4 (P^7)	−271.9 (P^1P^7)
	−252.9 (P^1P^5)
	− 29.6 (P^1P^3)
	+ 17.6 (P^1P^4)
	+ 50.3 (P^1P^6)
	− 13.6 (P^2P^4)
	− 21.8 (P^2P^5)
	− 10.3 (P^2P^7)
	− 6.2 (P^3P^5)
	+151.1 (P^4P^6)
	+110.3 (P^5P^7)
	+ 20.9 (P^2P^6)
	− 0.9 (P^3P^6)
	+ 1.7 (P^3P^7)
	− 22.3 (P^4P^7)



2b

δ	J(PP)
+ 88.4 (P^1)	−285.3 (P^1P^2)
+100.4 (P^2)	−306.8 (P^2P^3)
+122.7 (P^3)	−325.2 (P^3P^4)
+ 97.5 (P^4)	−314.1 (P^4P^5)
+ 8.5 (P^5)	−126.2 (P^5P^6)
+ 48.5 (P^6)	−246.0 (P^6P^7)
+ 73.7 (P^7)	−223.1 (P^1P^7)
	−194.7 (P^1P^5)
	− 17.1 (P^1P^3)
	+ 5.3 (P^1P^4)
	− 25.8 (P^1P^6)
	− 16.3 (P^2P^4)
	+ 2.3 (P^2P^5)
	+ 40.4 (P^2P^7)
	− 8.2 (P^3P^5)
	+150.5 (P^4P^6)
	+ 30.0 (P^5P^7)
	+ 29.5 (P^2P^6)
	− 0.1 (P^3P^6)
	− 0.4 (P^3P^7)
	+ 37.8 (P^4P^7)

[a] See Table 1. [b] RMS value of the spectrum calculation: 0.5; 200 of 512 transitions assigned. [c] RMS value: 0.4; 122 of 484 transitions assigned.

field shift of the signal for the relevant P-nucleus compared to the starting compound (**1a**: $\Delta\delta(P^2)=46.3$; **1b**: $\Delta\delta(P^3)=41.5$; **2a**: $\Delta\delta(P^1)=62.2$; **2b**: $\Delta\delta(P^7)$[8] $=107.6$). In addition, the oxidized P atoms are recognizable by the magnitude and the sign of the $^1J(P^VP^{III})$ coupling constants.[7] Accordingly, **1a** and **1b** are 2,3,4,6-tetra-*tert*-butyl-2-oxo- and -3-oxo-bicyclo[3.1.0]hexaphosphanes, respectively, while **2a** and **2b** are 2,3,4,6,7-penta-*tert*-butyl-

1-oxo- and -6-oxo-bicyclo[3.2.0]heptaphosphanes, respectively.[8] The large positive P,P long range couplings (**1a**: $^2J(P^4P^6)$; **1b**: $^2J(P^2P^6)$, $^2J(P^4P^6)$; **2a**: $^2J(P^4P^6)$; **2b**: $^2J(P^4P^6)$) indicate that the lone electron pairs at the respective P atoms are directed towards each other;[2,3,9] i.e. the three-membered ring and four-membered ring are strongly inclined towards the five-membered ring. The organo-groups have the same spatial arrangement as in the starting compounds, as follows from the similarity of the corresponding coupling constants (e.g. **2a** (cf. [3]): $^1J(P^3P^4)$, $^2J(P^5P^7)$, $^3J(P^3P^6)$; **2b** (cf. [3]): $^1J(P^2P^3)$, $^1J(P^3P^4)$, $^3J(P^3P^6)$). As a result of the unsymmetrical substitution, the five-membered ring in **1a** is markedly distorted ($^2J(P^1P^3) \gg {}^2J(P^3P^5)$). **1a**, **2a**, and **2b** are present as enantiomeric pairs.

The findings clearly indicate that the attack of the oxygen at a polycyclic organophosphane is largely determined by steric factors. The observed isomeric abundance **1a** : **1b** = 4.5 : 1 (statistically 2 : 1) is an indication that the five-membered ring atom P^3 in P_6tBu_4 is more strongly shielded by the *tert*-butyl groups than the neighboring atoms P^2 and P^4. In P_7tBu_5 the exocyclic bonding of the oxygen at P^1 and P^7 is apparently equally favorable, but at P^2 or P^4, on the other hand, it is hindered by the *endo* position of the *t*Bu group on P^7. That no isomers with oxygen on the three-membered ring were found in the case of **1** could be due to the pronounced s-character of the lone electron pair on the respective P atoms of the parent compound.

Received: January 10, 1986 [Z 1615 IE]
German version: *Angew. Chem. 98* (1986) 465

CAS Registry numbers:
1a, 101671-16-3; **1b**, 101671-17-4; **2a**, 101671-18-5; **2b**, 101671-19-6; P_6t-Bu_4, 79593-41-2; P_7tBu_5, 96482-81-4.

[1] Reviews: a) M. Baudler, *Angew. Chem. 94* (1982) 520; *Angew. Chem. Int. Ed. Engl. 21* (1982) 492; b) M. Baudler, V. Arndt, *Z. Naturforsch. B 39* (1984) 275; c) M. Baudler, *Z. Chem. 24* (1984) 352.

[2] M. Baudler, Y. Aktalay, K.-F. Tebbe, T. Heinlein, *Angew. Chem. 93* (1981) 1020; *Angew. Chem. Int. Ed. Engl. 20* (1981) 967.

[3] M. Baudler, M. Michels, J. Hahn, M. Pieroth, *Angew. Chem. 97* (1985) 514; *Angew. Chem. Int. Ed. Engl. 24* (1985) 504.

[4] **1a**, **1b**: 6.24 L of dry air were passed into a stirred solution of P_6tBu_4 [2] (23.5 g, 56.7 mmol) in benzene (500 mL) within 2 h. The progress of the oxidation was monitored by ^{31}P-NMR spectroscopy. The solvent was removed under reduced pressure, and the residue (ca. 40% **1a**,**b**, 60% P_6tBu_4) dissolved in benzene (20 mL) and chromatographed under inert gas on Al_2O_3 (heated in vacuo). P_6tBu_4 was eluted with *n*-pentane and then **1a**,**b** with benzene/methanol (80 : 20). For separation of the isomers the solvent mixture was removed and the residue was rechromatographed with benzene on a short column (8 cm). The fractions containing the largest amounts of **1a** were combined and recrystallized from a small amount of pentane/THF (2 : 1) at −30 °C; yield 0.16 g of **1a** (0.7% referred to P_6tBu_4). A previously eluted fraction contained mainly **1b** (ca. 55%); this was isolated by preparative HPLC (Nucleosil 5-C18 column, acetonitrile, receiver −78 °C, rapid condensation of solvent at −30 °C); yield 0.11 g of **1b** (0.5%, referred to P_6tBu_4). — **2a**,**b**: The isomeric mixture was isolated as by-product (0.21 g) in the final purification of P_7tBu_5 by HPLC.[3] Separation of **2a** and **2b** was not possible because of their similar retention times.

[5] ^{1}H{^{31}P}-NMR ([D$_6$]benzene, 25 °C, 300.133 MHz): **1a**: δ = 1.44 (P^2tBu, P^4tBu), 1.21 (P^3tBu), 0.89 (P^6tBu); **1b**: δ = 1.55 (P^2tBu, P^4tBu), 1.37 (P^3tBu), 0.88 (P^6tBu); **2a**: δ = 1.62 (P^2tBu), 1.31 (P^3tBu), 1.36 (P^4tBu), 1.19 (P^6tBu), 1.40 (P^7tBu); **2b**: δ = 1.29 (P^2tBu), 1.46 (P^3tBu), 1.30 (P^4tBu), 1.36 (P^6tBu), 1.40 (P^7tBu).

[6] K. G. R. Pachler, P. L. Wessels, *J. Chem. Soc. Chem. Commun. 1974*, 1038.

[7] A marked increase in the absolute value of the negative $^1J(PP)$ coupling constants is observed for both isomers in going from H(tBu)P–P(tBu)H to H(tBu)(O)P–P(tBu)H (M. Baudler, H. Heumüller, unpublished).

[8] The designation of **2b** as a 7-oxo derivative simplifies systematic comparison with the parent compound and **2a**.

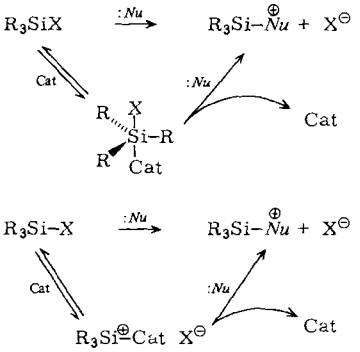
[9] a) M. Baudler, G. Reuschenbach, J. Hahn, *Chem. Ber. 116* (1983) 847; b) M. Baudler, T. Pontzen, *Z. Naturforsch. B 38* (1983) 955; c) M. Baudler, J. Hellmann, T. Schmidt, *ibid. B 38* (1983) 537.

Reactivity of Anionic Pentacoordinated Silicon Complexes towards Nucleophiles

By *Alain Boudin, Geneviève Cerveau, Claude Chuit, Robert J. P. Corriu,* and Catherine Reye*

The reactivity of pentacoordinated anionic silicon species towards nucleophiles has attracted our interest for two reasons: 1) Hypervalent anionic silicon species have been known for a long time[1] and their structures have been investigated,[2] yet reactivity studies have been carried out only in isolated cases and mainly on hexacoordinated species.[1a,3] 2) Pentacoordinated silicon complexes are of interest in connection with mechanistic studies. Nucleophilic substitution at silicon in R_3SiX compounds can be activated by nucleophiles which are good coordinating agents for Si (e.g. $F^\ominus$, HMPA, $RCO_2^\ominus$).[4] These nucleophiles catalyze the nucleophilic substitution but they do not appear in the final product. The activation of organosilicon compounds with $F^\ominus$ is very useful in organic synthesis: the $F^\ominus$-activation of Si–H,[5a] Si–O,[5a,b] Si–N,[5c] Si–C,[5d] and even P–O[6a] and P–X[6b] bonds provided some new synthetic methods.

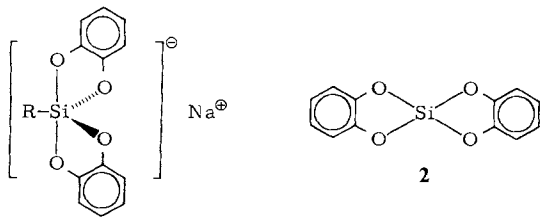
We have proposed a mechanism for the activation of Si–X bonds by nucleophiles[4a] in which the rate determining step is the attack of the nucleophile *Nu* at a pentacoordinated silicon center. This was formed in a first step by the reversible coordination of the activating nucleophile (cat) (Schema 1, top). However, at least in the case of SiCl and SiBr bonds,[7] this mechanism was considered unlikely since the silicon center of the pentacoordinated adduct should be both more sterically hindered and less electrophilic than the tetracoordinated one and consequently less susceptible to nucleophilic attack. An alternative mechanism (double displacement) was therefore proposed[8] (Scheme 1, bottom).



Scheme 1. Cat = $F^\ominus$, $RCO_2^\ominus$, HMPA, dimethyl sulfoxide (DMSO).

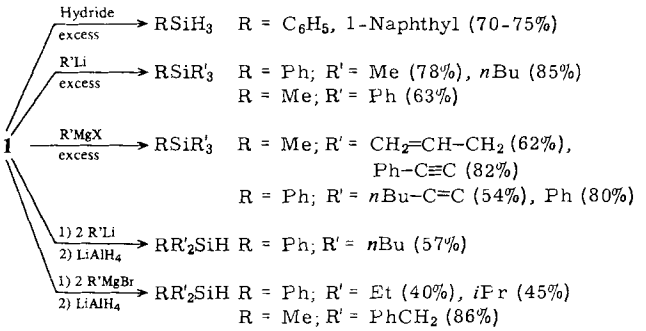
We now investigated the reaction of the complex anions **1** with nucleophiles (hydrides, R'MgX and R'Li, see Scheme 2). Stable ammonium salts and sodium salts of **1** are known.[9] Hydrides such as $LiAlH_4$, iBu_2AlH or Et_3Al/NaH react with **1** to give only trihydrogenosilanes $RSiH_3$, but Grignard reagents or organolithium derivatives are

[*] Prof. Dr. R. J. P. Corriu, A. Boudin, Dr. G. Cerveau, Dr. C. Chuit, Dr. C. Reye
Institut de Chimie Fine, Université des Sciences et Techniques du Languedoc, Unité associée C.N.R.S. U.A. 1097
Place Eugène Bataillon, F-34060 Montpellier Cédex (France)



1, R = Me, Ph, 1-Naphthyl

more selective and lead to two types of products depending on the amount of organometallic reagent: reaction of two equivalents of R'MgX or R'Li, followed by reduction with $LiAlH_4$ gives mainly silanes of type RR'_2SiH; excess of R'MgX or R'Li leads to the tetrasubstituted silanes $RSiR'_3$. Silanes of the type $RR'SiH_2$ (formation of one Si-C bond) are never obtained in yields better than 10%, whatever the experimental conditions may be. This means that the first substitution should be the rate determining step of the reaction.



Scheme 2. Hydride = $LiAlH_4$, iBu_2AlH, Et_3Al/NaH.

We have also compared the reactivity of **1** with that of the previously studied compound **2**.[10] **1** (R = Ph) reacts with 5 equivalents of PhMgBr at room temperature within 3 h to give Ph_4Si in 80% yield, whereas **2** gives only 35% of Ph_4Si after 20 hours in the presence of a large excess of Grignard reagent. Apparently the pentacoordinated anionic silicon species are more reactive than the tetracoordinated ones.

We thus have ample evidence that pentacoordinated anionic silicon species can undergo a nucleophilic attack and may be regarded as possible intermediates in nucleophilic substitutions at silicon. Hence, the mechanism proposed by us (Scheme 1, top) cannot be ruled out merely on the basis of arguments of steric hindrance or of reduced electrophilicity of silicon. These criteria do, of course, hold in the case of nucleophilic substitution at carbon, but may not be schematically extrapolated to silicon.

Experimental

RR'_2SiH: 2 equivalents of organometallic reagent were added dropwise to a suspension of 20 mmol of **1** in 100 mL of ether. The temperature of the mixture rose to 30 °C during the addition.

The mixture was refluxed for 1 h, then treated with an excess of $LiAlH_4$ and refluxed for a further hour. After hydrolysis with H_2SO_4 (25%), the silane was extracted with ether. The ethereal solution was washed with two portions each of 2 N NaOH, water, and brine, and then dried over $MgSO_4$. The ether was removed in a vacuum and the silane was purified by distillation and identified by IR, NMR, and mass spectroscopy.

$RSiR'_3$: The suspension of **1** in ether was treated with an excess (3.6 equivalents) of organometallic reagent. After the addition, the mixture was refluxed for 1 h and then hydrolyzed with H_2SO_4 (25%). The silane was then extracted as described above.

Received: December 11, 1985;
revised: February 6, 1986 [Z 1579 IE]
German version: *Angew. Chem. 98* (1986) 472

CAS Registry numbers:
$RSiH_3$ (R = C_6H_5), 694-53-1; $RSiH_3$ (R = naphthyl), 38274-75-8; $RSiR'_3$ (R = Ph, R' = Me), 768-32-1; $RSiR'_3$ (R = Ph, R' = *n*Bu), 18510-29-7; $RSiR'_3$ (R = Me, R' = Ph), 791-29-7; $RSiR'_3$ (R = Me, R' = CH_2–CH_2–CH=CH_2), 101518-72-3; $RSiR'_3$ (R = Me, R' = C≡C–Ph), 18822-97-4; $RSiR'_3$ (R = Ph, R' = C≡C–*n*Bu), 101518-73-4; $RSiR'_3$ (R = R' = Ph), 1048-08-4; RR'_2SiH (R = Ph, R' = *n*Bu), 65105-83-1; RR'_2SiH (R = Ph, R' = Et), 16545-43-0; RR'_2SiH (R = Ph, R' = *i*Pr), 18027-99-1; RR'_2SiH (R = Me, R' = CH_2Ph), 1631-71-6.

[1] a) A. Weiss, A. Herzog in G. Bendz, I. Lindqvist (Eds.): *Biochemistry of Silicon and Related Problems*, Plenum, New York 1978, p. 109; b) R. J. P. Corriu, C. Guerin, J. J. E. Moreau, *Top. Stereochem. 15* (1984) 158, and references cited therein.

[2] a) F. P. Boer, J. J. Flynn, J. W. Turley, *J. Am. Chem. Soc. 90* (1968) 6973; J. J. Flynn, F. P. Boer, *ibid. 91* (1969) 5756; b) J. J. Harland, R. O. Day, J. F. Vollano, A. C. Sau, R. R. Holmes, *ibid. 103* (1981) 5269; R. R. Holmes, R. O. Day, J. J. Harland, A. C. Sau, J. M. Holmes, *Organometallics 3* (1984) 341; R. R. Holmes, R. O. Day, V. Chandrasekhar, J. M. Holmes, *Inorg. Chem. 24* (1985) 2009.

[3] a) E. M. Soshestvenskaya, *Zh. Obshch. Khim. 22* (1952) 1122; b) M. Kumada, K. Tamao, J. I. Yoshida, *J. Organomet. Chem. 239* (1982) 115; c) R. Müller, *Z. Chem. 24* (1984) 41, and references cited therein.

[4] a) R. J. P. Corriu, G. Dabosi, M. Martineau, *J. Chem. Soc. Chem. Commun. 1977*, 649; *J. Organomet. Chem. 154* (1978) 33; *ibid. 186* (1980) 25; b) R. J. P. Corriu, C. Guerin, *Adv. Organomet. Chem. 20* (1982) 265.

[5] a) R. J. P. Corriu, R. Perz, C. Reye, *Tetrahedron 39* (1983) 999, and references cited therein; b) O. W. Welster, W. R. Hertler, D. Y. Sogah, W. B. Farnham, T. V. Rajanbabu, *J. Am. Chem. Soc. 105* (1983) 5706; J. Boyer, R. J. P. Corriu, R. Perz, C. Reye, *Tetrahedron 39* (1983) 117; R. J. P. Corriu, R. Perz, *Tetrahedron Lett. 26* (1985) 1311; I. Kuwajima, E. Nakamura, *J. Am. Chem. Soc. 97* (1975) 3257; I. Kuwajima, E. Nakamura, M. Shimizu, *ibid. 104* (1982) 1025; R. Noyori, K. Yokoyama, J. Sakata, I. Kuwajima, E. Nakamura, M. Shimizu, *ibid. 99* (1977) 1265; c) R. J. P. Corriu, V. Huynh, J. J. E. Moreau, M. Pataud-Sat, *Tetrahedron Lett. 23* (1982) 3257; d) E. Nakamura, T. Murofushi, M. Shimizu, I. Kuwajima, *J. Am. Chem. Soc. 98* (1976) 2346; A. Hosomi, A. Shirabata, H. Sakurai, *Tetrahedron Lett. 1978*, 3043; I. Kuwajima, E. Nakamura, K. Hashimoto, *Tetrahedron 39* (1983) 975.

[6] a) K. K. Ogilvie, S. L. Beaucage, N. Therault, D. W. Entwistle, *J. Am. Chem. Soc. 99* (1977) 1277; b) R. J. P. Corriu, G. F. Lanneau, J. P. Dutheil, *ibid. 106* (1984) 1060.

[7] a) J. Chojnowski, M. Cypryk, J. Michalski, *J. Organomet. Chem. 161* (1978) C31; b) A. R. Bassindale, T. Stout, *ibid. 238* (1982) C41.

[8] H. K. Chu, M. D. Johnson, C. L. Frye, *J. Organomet. Chem. 271* (1984) 327.

[9] a) C. L. Frye, *J. Am. Chem. Soc. 86* (1964) 3170; C. L. Frye, DBP 1493601 (1964); b) R. Corriu, G. Cerveau, C. Chuit, C. Reye, Fr. Pat. 5130811/*YS* (1984).

[10] S. Cabiddu, A. Maccioni, M. Secci, *Gazz. Chim. Ital. 101* (1971) 512.

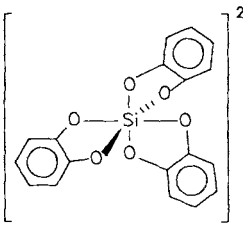
Reaction of Grignard Reagents with Dianionic Hexacoordinated Silicon Complexes: Organosilicon Compounds from Silica Gel

By *Alain Boudin, Geneviève Cerveau, Claude Chuit, Robert J. P. Corriu,** and *Catherine Reye*

Organosilicon compounds are nowadays of great importance in such diverse fields as organic synthesis[1] and ceramics.[2] Hitherto, they have been prepared from elemental silicon, either by "direct synthesis" (Rochow reaction),[3] by the organometallic route,[4] or by the hydrosilylation reaction.[5] In the search for new synthetic routes silica gel has also been used as starting material.[6] It was previously

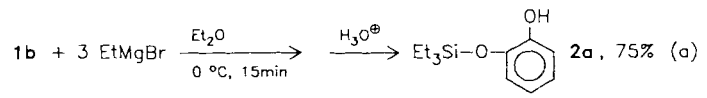
[*] Prof. Dr. R. J. P. Corriu, A. Boudin, Dr. G. Cerveau, Dr. C. Chuit, Dr. C. Reye
Institut de Chimie Fine, Université des Sciences et Techniques du Languedoc, Unité Associée C.N.R.S. U.A. 1097
Place Eugène Bataillon, F-34060 Montpellier Cédex (France)

reported that hexacoordinated silicon complexes of catechol, **1**, can be prepared directly from silica gel in water;[7] this reaction corresponds to a depolymerization of SiO_2 with formation of a monomeric silicon complex.



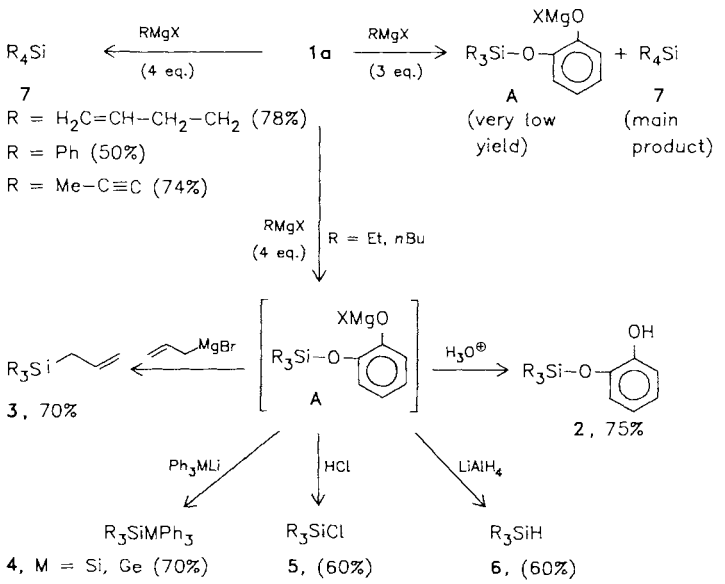
2 $M^{\oplus}$ **1a**, M = Na; **1b**, M = K

We have now investigated—as previously in the case of anionic pentacoordinated silicon complexes[8]—the reactivity of strong nucleophiles towards very stable sodium and potassium salts **1a** and **1b** prepared under anhydrous conditions.[9] We have found that these reactions lead to the formation of silicon-carbon bonds, thus providing an alternative route for the synthesis of organosilicon compounds. Compound **1b** is very reactive; for instance, it reacts with ethylmagnesium bromide to completion within 15 minutes at 0°C, giving triethylsiloxyphenol **2a** in 75% yield [Eq. (a)].



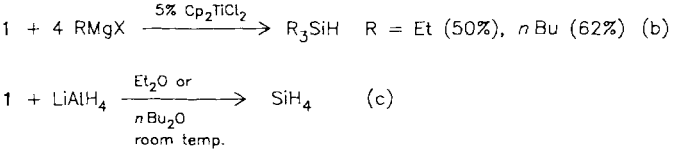
1b + 3 EtMgBr $\xrightarrow[0\,°C,\ 15min]{Et_2O}$ $\xrightarrow{H_3O^{\oplus}}$ Et_3Si-O-(OH) **2a**, 75% (a)

The reaction course depends on the nature of the Grignard reagent: When RMgX is an alkyl Grignard compound, three silicon-carbon bonds are directly formed irrespective of the ratio **1a**:Grignard compound. The siloxyphenols **2** can be isolated (Scheme 1). They react with nucleophiles to give further organosilicon compounds. Very interestingly, these products (**3**, **4**, and **6**) can also be obtained directly from the intermediate **A** (Scheme 1). In contrast, when RMgX is an allyl, phenyl, or alkyne Grignard reagent the tetraorganosilanes SiR_4 **7** are formed directly, once again independently of the ratio **1a**:Grignard compound. The intermediate **A** can also be cleaved with HCl, resulting in formation of a trialkylchlorosilane **5**.



Scheme 1.

We have reported[10] that Grignard reagents having an hydrogen atom in the β position and activated by Cp_2TiCl_2 (Cp = cyclopentadienyl) are reducing agents. Accordingly, silanes of the type R_3SiH can be prepared in one step directly from **1** and RMgX in the presence of Cp_2TiCl_2 [Eq. (b)]. Complexes **1** react with reducing agents such as $LiAlH_4$ under very mild conditions to give SiH_4 quantitatively [Eq. (c)].



1 + 4 RMgX $\xrightarrow{5\%\ Cp_2TiCl_2}$ R_3SiH R = Et (50%), *n*Bu (62%) (b)

1 + $LiAlH_4$ $\xrightarrow[n Bu_2O\ \text{room temp.}]{Et_2O\ \text{or}}$ SiH_4 (c)

The new methods enable the synthesis of organosilicon compounds directly from silica, thus circumventing the route via elemental silicon; the catechol that is employed can be quantitatively recovered and the complexes are easy to handle. Very important is the fact that the dianionic hypervalent species **1** are very reactive towards organometallic reagents. This demonstrates the synthetic potential of such hypervalent compounds, which hitherto were given very little attention.[11] Indeed, very little is known about the reactivity of hexacoordinated silicon complexes. Reports have merely been published on the basic hydrolysis of cationic species such as acetylacetone,[12] tropolone, and aminotropinimine[13] complexes. Our results and previous observations by *Kummer* et al.[14] on cationic bis-2,2′-bipyridine-, 1,10-phenanthroline- and pyridine-*N*-oxide-silicon complexes show that the reactivity of these species is unusual.

Experimental

1a: A solution of sodium methoxide (80 mmol) in methanol (40 mL) was treated with 45 mmol of silicagel (95%) and then with a solution of catechol (120 mmol) in methanol (40 mL); the resulting mixture was then heated under reflux with stirring for 18 h. After removal of methanol in a vacuum, the solid residue was washed with ether. The black solid was dissolved in 400 mL of tetrahydrofuran (THF) and the resulting solution heated for 1 h in the presence of activated charcoal. After filtration and removal of solvent **1a** was isolated as a white powder and identified by ^{13}C- and ^{29}Si-NMR spectroscopy.

2: Three equivalents of Grignard reagent were added to a suspension of 20 mmol of **1a** in 100 mL of ether at room temperature. The mixture was heated under reflux for 2 h, then hydrolyzed with H_2SO_4 (25%). After extraction with ether, the ethereal solution was washed with two portions of NaOH (2N), two portions of water, and with brine, then dried over $MgSO_4$. The ether was removed in a vacuum and the residue **2** was purified by distillation and identified by IR, NMR, and mass spectroscopy. The NaOH washings were acidified with HCl (4N), then extracted with ether. The ethereal solution was dried over $MgSO_4$ and the ether removed in a vacuum. The residue remaining was identified as crude catechol.

SiH_4: A suspension of **1a** (1 mmol) in *n*-butyl ether (10 mL) was treated with an excess of $LiAlH_4$ in *n*-butyl ether. 22.5 mL of a gas evolved, which was identified as SiH_4 by IR spectroscopy.

Received: December 11, 1985;
revised: February 6, 1986 [Z 1580 IE]
German version: *Angew. Chem. 98* (1986) 473

CAS Registry numbers:
1a, 101519-12-4; **1b**, 101519-13-5; **2a**, 101541-79-1; **2** (R=Bu), 101541-83-7; **3** (R=Et), 17898-21-4; **3** (R=Bu), 17907-83-4; **5** (R=Et), 994-30-9; **5** (R=Bu), 995-45-9; **6** (R=Et), 617-86-7; **6** (R=Bu), 998-41-4; **7** (R=CH_2–CH_2–CH=CH_2), 101541-80-4; **7** (R=Ph), 1048-08-4; **7** (R=C≡C–Me), 20143-21-9; $Et_3SiSiPh_3$, 18754-93-3; $Bu_3SiSiPh_3$, 101541-81-5; $Et_3SiGePh_3$, 18771-58-9; $Bu_3SiGePh_3$, 101541-82-6; SiH_4, 7803-62-5; pyrocatechol, 120-80-9.

[1] W. P. Weber: *Silicon Reagents for Organic Synthesis*, Springer, Berlin 1983.
[2] H. J. Sanders, *Chem. Eng. News 62* (1984) No. 28, p. 26.
[3] a) E. G. Rochow, *J. Am. Chem. Soc. 67* (1945) 963; b) *An Introduction to the Chemistry of Silicones*, Wiley, New York 1951, 2nd edit., p. 36.
[4] C. Eaborn, *Organosilicon Compounds*, Butterworths, London 1960, p. 10.
[5] a) J. L. Speier, J. A. Webster, G. H. Barnes, *J. Am. Chem. Soc. 79* (1957) 974; b) R. A. Benkeser, R. F. Cunico, S. Dunny, P. R. Jones, P. G. Nerlekar, *J. Org. Chem. 32* (1967) 2634.
[6] a) H. Kautsky, B. Bartocha, *Z. Naturforsch. B 10* (1955) 422; b) J. Wartmann, H. Deuel, *Helv. Chim. Acta 42* (1959) 1166.
[7] a) A. Rosenheim, B. Raibmann, G. Schendel, *Z. Anorg. Allg. Chem. 196* (1931) 160; b) A. Weiss, G. Reiff, A. Weiss, *ibid. 311* (1961) 151; c) D. W. Barnum, *Inorg. Chem. 9* (1970) 1942; *11* (1972) 1424.
[8] A. Boudin, G. Cerveau, C. Chuit, R. J. P. Corriu, C. Reye, *Angew. Chem. 98* (1986) 472; *Angew. Chem. Int. Ed. Engl. 25* (1986) 479.
[9] R. Corriu, G. Cerveau, C. Chuit, C. Reye, *Fr. Pat. 51308 I/YS* (1984).
[10] R. J. P. Corriu, B. Meunier, *J. Organomet. Chem. 82* (1974) 367.
[11] a) E. M. Soshestvenskaya, *Zh. Obshch. Khim. 22* (1952) 1122; b) R. Müller, *Z. Chem. 24* (1984) 41, and references cited therein.
[12] a) S. K. Dhar, V. Doron, S. Kirschner, *J. Am. Chem. Soc. 81* (1959) 6372; b) H. Kelling, H. U. Kibbel, *Z. Anorg. Allg. Chem. 386* (1971) 59.
[13] a) E. L. Muetterties, C. M. Wright, *J. Am. Chem. Soc. 86* (1964) 5132; *87* (1965) 21.
[14] a) D. Kummer, H. Köster, *Z. Anorg. Allg. Chem. 398* (1973) 279; *402* (1973) 297; D. Kummer, K. E. Gaiper, T. Seshadri, *Chem. Ber. 110* (1977) 1950; D. Kummer, T. Seshadri, *Z. Anorg. Allg. Chem. 428* (1977) 129; b) *Chem. Ber. 110* (1977) 2355; c) *Z. Anorg. Allg. Chem. 432* (1977) 147.

Enantioselective Robinson Annelations via Phase-Transfer Catalysis**

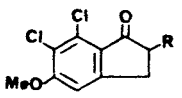
By *Apurba Bhattacharya,* Ulf-H. Dolling, Edward J. J. Grabowski, Sandor Karady, Kenneth M. Ryan,* and *Leonard M. Weinstock*

Robinson annelations have been one of the most widely used synthetic methods in organic chemistry, leading to such complex natural products as steroids, terpenes, and alkaloids.[1] However, only a few methods for accomplishing these reactions in a practical, efficient, and enantioselective manner exist to date.[2–4] Our interest in a chiral version of this reaction arose out of the need to synthesize the optically active tricyclic enone **4d**, which is currently undergoing clinical evaluation.[5]

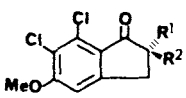
Earlier we described the first efficient, catalytic alkylation of a ketone via asymmetric phase-transfer catalysis mediated by substituted *N*-benzylcinchoninium salts.[6] 6,7-Dichloro-5-methoxy-2-phenyl-1-indanone **1a** was converted into its (*S*)-2-methyl analogue **2a** in 92% *ee* and 95% yield.[6] Herein we further demonstrate the application of this methodology to an asymmetric modification of the Robinson annelation employing 1,3-dichloro-2-butene (the Wichterle reagent[7]) as a methyl vinyl ketone surrogate.[11b]

Alkylation of **1b** with 1,3-dichloro-2-butene[8] in analogy to the procedure described earlier with *N*-(*p*-trifluoromethylbenzyl)cinchoninium bromide[9] as the chiral phase-transfer catalyst produced (*S*)-(+)-6,7-dichloro-2-(3-chloro-2-butenyl)-5-methoxy-2-propyl-1-indanone **2b** in 92% *ee*[10a] and 99% yield.[11a] On the basis of the tight ion-pair theory proposed earlier[6] we anticipated that the product resulting from the above reaction would be the (*S*)-enantiomer, which proved to be the case (see Fig. 1, **5**).[10b]

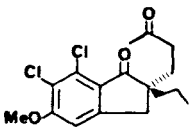
Since the enantiomorph of cinchonine is not available from natural sources, the diastereomer cinchonidine was used to synthesize the (*R*)-enantiomer **2c**. Chiral phase-transfer alkylation using *N*-(*p*-trifluoromethylbenzyl)cinchonidinium bromide[9] afforded **2c** 78% *ee* and 99% yield at 30 mol-% catalyst.[11b]



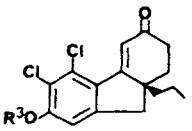
1a, R = C_6H_5
1b, R = *n*-C_3H_7



2a, $R^1 = C_6H_5$, $R^2 = CH_3$
2b, R^1 = *n*-C_3H_7, $R^2 = -CH_2CH{=}C(Cl)CH_3$
2c, $R^1 = -CH_2CH{=}C(Cl)CH_3$, R^2 = *n*-C_3H_7

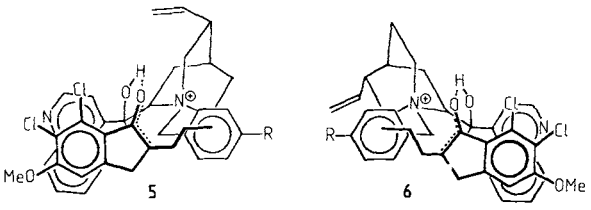


3



4a, $R^3 = CH_3$
4b, $R^3 = H$
4c, $R^3 = CH_2COOEt$
4d, $R^3 = CH_2COOH$

After the alkylation, the extremely insoluble racemate was separated from the pure enantiomer **2c** by crystallization from hexane. Compound **2c** was converted into **4d** (83% overall yield based on **2c**) without isolation of intermediates by (1) hydrolysis with concentrated sulfuric acid (0 °C, 1.5 h) to **3**, (2) cyclization with concentrated sulfuric acid (H_2O:**3** = 2:1, 70 °C, 1 h) to **4a**, (3) demethylation ($AlCl_3$, toluene, 45 °C, 2 h) to **4b**, (4) alkylation ($ClCH_2COOEt$, K_2CO_3, KI, Triton X-405, toluene, reflux) to **4c**, and (5) hydrolysis by KOH (KOH:**4c** = 2.5:1, toluene, reflux) to **4d**.[12]



5 **6**

Fig. 1. Tight ion-pairs **5** and **6** of the enolate of **1b** with *N*-(*p*-trifluoromethylbenzyl)cinchoninium and *N*-(*p*-trifluoromethylbenzyl)cinchonidinium, respectively.

As proposed for the selective formation of **2a**,[6] a tight ion-pair, **5** (Fig. 1), also accounts for the formation of **2b**. Interestingly one of the attractive π–π interactions in the ion-pair leading to **2a** is replaced by an attractive non-bonded alkyl–π interaction[13] in **5** without loss in *ee*. The remaining ionic and π–π interactions and hydrogen bond proposed for the formation of **2a** also prevail in **5**. A Hammet plot of $\lg(ee/ee_0)$ vs. σ for catalysts with a *p*-substituted phenyl ring afforded a ρ value of 0.67 as op-

[*] Dr. A. Bhattacharya, Dr. U.-H. Dolling, Dr. E. J. J. Grabowski, Dr. S. Karady, K. M. Ryan, Dr. L. M. Weinstock
Merck, Sharp & Dohme Research Laboratories, Merck & Co., Inc.
P. O. Box 2000, Rahway, NJ 07065 (USA)

[**] Efficient Catalytic Asymmetric Alkylations, Part. 2.—Part 1: [6].

posed to 0.21 obtained for **2a**. The negative charge is delocalized into the phenyl ring in the enolate anion **1a**, whereas such delocalization is absent in the 2-propyl analogue **1b**. Accordingly, the latter responds toward substituent effects in the catalyst to a greater extent.[14] A similar tight ion-pair **6** (Fig. 1) can also account for the asymmetric induction in the formation of **2c**.[15] The decrease in enantioselectivity for **2c** vs. **2b** (78% vs. 92%) must result from the relative position of the vinyl group in the two tight ion-pairs. Study of the space filling models suggests that the vinyl group in **5** buttresses the hydroxyl group of the catalyst in a position to maintain the desired hydrogen bond. The vinyl group-hydroxyl interaction is absent in **6**, which may confer greater degrees of freedom to the system and hence lower the *ee*.

This chiral Robinson annelation offers potential as a pseudo-enzymic[16] process in organic synthesis in terms of simplicity, ease of operation, and enantiospecificity.

Received: November 20, 1985;
revised: February 19, 1986 [Z 1544 IE]
German version: *Angew. Chem. 98* (1986) 442

CAS Registry numbers:
1b, 101165-82-6; **2b**, 101165-83-7; **2c**, 101165-84-8; **3**, 101165-85-9; **4a**, 101165-86-0; **4b**, 101165-87-1; **4c**, 101165-88-2; **4d**, 81997-33-3; $ClCH_2COOEt$, 105-39-5; (*E*)-$ClCH_2CH=CClCH_3$, 7415-31-8; (*Z*)-$ClCH_2CH=CClCH_3$, 10075-38-4; *N*-(*p*-trifluoromethylbenzyl)cinchoninium bromide, 95088-20-3; *N*-(*p*-trifluoromethylbenzyl)cinchonidinium bromide, 101311-12-0.

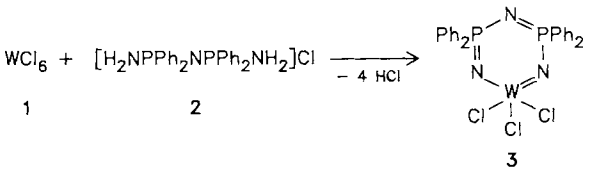
[1] a) M. E. Jung, *Tetrahedron 32* (1976) 3; b) R. E. Gawley, *Synthesis 1976*, 777.
[2] M. Pfau, G. Revial, A. Guigant, J. d'Angelo, *J. Am. Chem. Soc. 107* (1985) 273 and references therein.
[3] K. Hermann, H. Wynberg, *J. Org. Chem. 44* (1979) 2238.
[4] D. J. Cram, G. D. Y. Sogah, *J. Chem. Soc. Chem. Commun. 1981*, 625.
[5] E. J. Cragoe, Jr., G. E. Stokker, N. P. Gould, *U. S. Pat.* 4316043 (1982).
[6] U.-H. Dolling, P. Davis, E. J. J. Grabowski, *J. Am. Chem. Soc. 106* (1984) 446.
[7] P. Wichterle, J. Prochazka, J. Hofman, *Coll. Czech. Chem. Commun. 13* (1948) 300.
[8] 1,3-Dichloro-2-butene was purchased from du Pont as a mixture of isomers (*Z*: *E* 4:1).
[9] The catalysts are commercially available from Chemical Dynamics Corporation, South Plainfield, NJ, USA.
[10] a) The *ee* was determined by NMR ($CDCl_3$, tris[3-(heptafluoropropylhydroxymethylene)-*d*-camphorato]europium(III)] and/or by ketalization of the enantiomeric ketones **3** with (2*R*, 3*R*)-(−)-2,3-butanediol followed by HPLC assay of the diasteromeric ketals on a Pirkle ionic L-phenylglycine column. b) The absolute sense of asymmetric induction was determined by converting the (*R*)-(−)-indanone **2c** into the (*R*)-(+)-carboxylic acid **4d**, whose structure has been established by X-ray analysis.
[11] *Experimental procedure:* a) **2b**: **1b** (1.64 g, 6.03 mmol), 1,3-dichloro-2-butene (4.5 g, 36 mmol), and *N*-(*p*-trifluoromethylbenzyl)cinchoninium bromide (0.32 g, 0.60 mmol) in toluene (75 mL) and 50% aqueous NaOH (15 mL) were stirred at 1100 rpm under N_2 at 20 °C for 18 h in a 300-mL autoclave; b) **2c**: **1b** (9.9 g, 36.4 mmol), 1,3-dichloro-2-butene (15 g, 120 mmol), and *N*-(*p*-trifluoromethylbenzyl)cinchonidinium bromide (5.4 g, 10.1 mmol) in toluene (300 mL) and 50% aqueous NaOH (60 mL) were stirred at 1800 rpm under N_2 at 20°C for 24 h in a 500-mL autoclave.
[12] The high yield (97%) realized in the H_2SO_4-hydrolysis-cyclization sequence (**2c**→**4a**) is a key factor for the success of this synthetic sequence.
[13] For attractive nonbonded interactions see: E. R. Carter, B. Nilsson, K. Olsson, *J. Am. Chem. Soc. 97* (1975) 6155; E. R. Carter, P. Stilbs, *ibid. 98* (1976) 7515.
[14] T. H. Lowry, K. S. Richardson: *Mechanism and Theory in Organic Chemistry*. Harper and Row, New York 1976, p. 60.
[15] X-ray analysis of *N*-(*p*-trifluoromethylbenzyl)cinchonidinium bromide and *N*-benzylcinchoninium chloride clearly shows their pseudo mirror image relationship, the catalyst plane being defined by the quinoline ring, the C-O bond, and the *N*-benzyl group (private communication with Dr. *J. Springer*, Merck, Sharp & Dohme).
[16] K. B. Sharpless, S. S. Woodward, M. G. Finn in W. Bartmann, B. M. Trost (Eds.): *Selectivity—A Goal for Synthetic Efficiency*. Verlag Chemie, Weinheim 1984, p. 377.

A Transition Metal Atom as Building Block of a Cyclic Phosphazene— Synthesis and Structure of $[Cl_3WN_3(PPh_2)_2]$**

By *Herbert W. Roesky,* Kattesh V. Katti, Ulrich Seseke, Michael Witt, Ernst Egert, Regine Herbst,* and *George M. Sheldrick*

Dedicated to Professor Marianne Baudler on the occasion of her 65th birthday

In 1983 we reported the synthesis and structure of $[Cl_2VN_3S_2]$, a 1,3-dithia-2,4,6-triazine containing a metal atom as the sixth member of the ring.[1] We describe here the first cyclic phosphazene containing a metal atom in the ring. Cyclic, trimeric phosphazenes have been known since 1834 and their chemistry has been the subject of numerous investigations.[2] To date, however, only derivatives with substituents on the ring, metal complexes, or polymers have been synthesized.[3] We have now succeeded in replacing one phosphorus atom in the six-membered phosphazene ring by a transition-metal atom. Tungsten hexachloride **1** reacts with $[H_2NPPh_2NPPh_2NH_2]Cl$ **2** in chloroform with elimination of HCl to give $[Cl_3WN_3(PPh_2)_2]$ **3**.[4]



In the solid state, **3** is probably present as a chlorine-bridged polymer. Evidence for the cyclic structure of **3** was provided by both a mass spectrum and a ^{31}P-NMR spectrum. Electron impact ionization gives rise to a peak at *m/z* 668 (relative intensity 100%) corresponding to the $[M-Cl]^{\oplus}$ ion. The ^{31}P-NMR spectrum contains a signal at $\delta = 39.2$ (85% H_3PO_4) with ^{183}W satellites and a $^2J(^{31}P\text{-}^{183}W)$ coupling constant of 63 Hz.

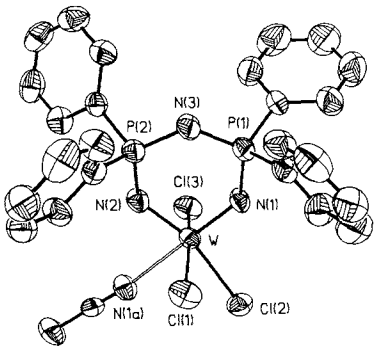


Fig. 1. Structure of **3**·$2CH_3CN$ in the crystal (without hydrogen atoms). Important bond lengths [pm]: W-N(1) 177.3(5), W-N(2) 179.8(6), W-N(1a) 236.4(6), N(1)-P(1) 166.3(7), N(2)-P(2) 164.0(7), P(1)-N(3) 158.7(7), P(2)-N(3) 159.6(6). Bond angles in central six-membered ring [°]: W 97.3(3), N(1) 134.5(4), N(2) 133.1(3), P(1) 113.4(3), P(2) 114.6(3), N(3) 126.4(5).

[*] Prof. Dr. H. W. Roesky, Dr. K. V. Katti, Dipl.-Chem. U. Seseke, Dr. M. Witt, Dr. E. Egert, R. Herbst, Prof. G. M. Sheldrick
Institut für Anorganische Chemie der Universität
Tammannstrasse 4, D-3400 Göttingen (FRG)

[**] This work was supported by the Deutsche Forschungsgemeinschaft and the Fonds der Chemischen Industrie. *K. V. K.* thanks the Alexander von Humboldt Foundation for a fellowship.

Crystals suitable for X-ray structure analysis were obtained by recrystallization from acetonitrile; two molecules of the solvent are incorporated into the crystal lattice. The single-crystal X-ray structure analysis[6] confirms the presence of a six-membered, planar ring (mean deviation of the ring atoms from the best plane: 3.4 pm) with pairwise equivalent bond lengths and angles (Fig. 1). A molecule of acetonitrile is weakly coordinated to the tungsten atom; it is surprising that the "*trans* effect" on the lengths of the W-N bonds is hardly evident. Compounds such as **3** should allow the synthesis of metal-containing polymeric phosphazenes.

Received: November 28, 1985;
revised: January 8, 1986 [Z 1554 IE]
Publication delayed at authors' request
German version: *Angew. Chem. 88* (1986) 447

CAS Registry numbers:
1, 13283-01-7; **2**, 2960-45-4; **3**, 101653-99-0; **3**·2CH_3CN, 101654-01-7.

[1] H. W. Roesky, J. Anhaus, H. G. Schmidt, G. M. Sheldrick, M. Noltemeyer, *J. Chem. Soc. Dalton Trans. 1983*, 1207; J. Hanich, M. Krestel, U. Müller, K. Dehnicke, D. Rehder, *Z. Naturforsch. B 39* (1984) 1686.

[2] J. Liebig, *Ann. Pharm. (Lemgo, Ger.) 11* (1834) 139; H. Rose, *ibid. 11* (1834) 131.

[3] H. R. Allcock: *Phosphorus Nitrogen Compounds*, Academic Press, New York 1972; H. R. Allcock in A. H. Cowley (Ed.): *Rings, Clusters, and Polymers of the Main Group Elements (ACS Symp. Ser. 232)*, Am. Chem. Soc. Washington, DC, USA 1983, p. 49; H. R. Allcock, N. M. Tollefson, R. A. Arcus, R. R. Whittle, *J. Am. Chem. Soc. 107* (1985) 5167; J. Emsley, D. Hall: *The Chemistry of Phosphorus*, Harper und Row, London 1976.

[4] *Experimental Procedure:* **3**: **2** (2.84 g, 6.3 mmol) [5] was added to a solution of **1** (2.5 g, 6.3 mmol) in 150 mL of dry $CHCl_3$ and the resulting mixture was refluxed under N_2 for 10 h. Upon cooling, a yellow powder precipitated (2.15 g), which was filtered off. The filtrate was concentrated, which resulted in the precipitation of a yellow solid (1.10 g). According to IR and ^{31}P-NMR spectra, both solids could be identified as **3**. Yield: 3.25 g (73%). **3** was recrystallized from acetonitrile to yield **3**·2CH_3CN.

[5] D. L. Herring, C. M. Douglas, *Inorg. Chem. 3* (1964) 428.

[6] Crystal structure analysis of **3**·2CH_3CN: Space group $P\bar{1}$, $a = 946.3(1)$, $b = 1151.2(1)$, $c = 1520.1(2)$ pm, $\alpha = 104.53(1)$, $\beta = 92.72(1)$, $\gamma = 98.61(1)°$, $V = 1.579$ nm^3, $Z = 2$, $\mu = 4.12$ mm^{-1} ($Mo_{K\alpha}$); 5761 measured intensities, $2\theta_{max} = 50°$, empirical absorption correction, 4578 unique reflections with $F > 4\sigma(F)$ used for the structure solution and refinement (Patterson and Fourier methods); non-hydrogen atoms anisotropic, H atoms (localized in part by difference electron density determinations) refined with a "riding" model, $R = 0.045$ ($R_w = 0.050$, $w^{-1} = \sigma_F^2 + 0.0005 \cdot F^2$). Further details of the crystal structure investigation may be obtained from the Fachinformationszentrum Energie, Physik, Mathematik GmbH, D-7514 Eggenstein-Leopoldshafen 2 (FRG), on quoting the depository number CSD-51685, the names of the authors, and the journal citation.

Synthesis of Alkyl Azides with a Polymeric Reagent**

By *Alfred Hassner** and *Meir Stern*

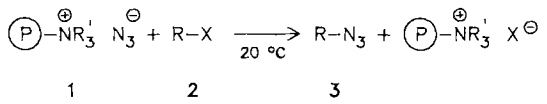
Nucleophilic substitution by azide ion is a well-established synthetic pathway to alkyl azides.[2] Some of the problems associated with this preparative method, such as the low solubility of inorganic azides in organic solvents, have been solved by the use of the more soluble tetraalkylammonium[3a] or guanidinium azides,[3] by phase-transfer conditions,[4] or by Lewis acid catalysis, the latter being mainly used with tertiary or activated alkyl halides or alcohols.[5]

[*] Prof. Dr. A. Hassner, Dr. M. Stern
Department of Chemistry, Bar-Ilan University
Ramat-Gan 52100 (Israel)

[**] Synthetic Methods, Part 22.—Part 21: [1].

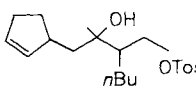
Since azides are thermally and photochemically labile and are often explosive,[6] it is preferable to avoid heating during reaction or purification. Yet this is often required for the above-mentioned methods.

We now report the use of the polymeric quaternary ammonium azide **1** as a reagent for the preparation of azides; **1** permits clean nucleophilic substitution of activated as well as nonactivated alkyl halides **2** at room temperature. Since the insoluble polymeric reagent can be used in large excess, essentially complete conversion into alkyl azide can be achieved. The progress of the reaction can be monitored by GC, TLC, etc. After filtration of the polymer, a clean solution of alkyl azide **3** in organic solvent is obtained and can be used for subsequent reactions, either directly or after removal of solvent. The polymer **1** can be regenerated easily with NaN_3 solution.



In this manner we have succeeded not only in achieving clean conversion of benzyl halides but also of hexyl bromide **2b**, cyclohexyl bromide **2c**, α-halo esters and ketones, and dihalides into their corresponding azides (Table 1).

Table 1. Synthesis of the azides **3** from the educts **2** with the polymer **1** at 20°C.

	R–X **2**	Solvent	*t* [a]	Conversion (Yield)[%][b]
a	*n*-C_4H_9–Br	CH_3CN	3 h	100
	n-C_4H_9–I	CH_3CN	1 h	100
	n-C_4H_9–OTos	CH_3CN	24 h	100
	n-C_4H_9–Cl	CH_3CN	>7 d	100
b	*n*-C_6H_{13}–Br	ether	4 d	100 (71)
c	cyclohexyl-Br	ether	11 d	94
d	$PhCH_2$–Cl	CH_2Cl_2	2 h	98 (91)
	$PhCH_2$–Br	CH_2Cl_2	1 h	100
e	*p*-Br–$C_6H_4CH_2$–Br	CH_2Cl_2	2 h	100 (93) [c]
f	Ph–CO–CH_2–Br	CH_2Cl_2	1 h	100
g	EtO–CO–CH_2–Cl	CH_3CN	2 h	100
h	$PhCH_2O$–CO–Cl	ether	24 h	95
i	$C_6H_4(CH_2–Br)_2$–(*o*)	CH_3CN	16 h	100 [d]
j	Br–$(CH_2)_4$–Br	CH_3CN	24 h	100
k	CH_2Br_2	tetrahydrofuran	16 d	60
l		CH_3CN	3 d	100

[a] Reaction time. [b] All azides were identified by IR, NMR, and, in many cases, mass spectra. 100% conversion was indicated by the absence of **2** and the presence of only **3** (GC, TLC). It is assumed that some product remains adsorbed on the polymer **1**, accounting for lower yields than conversion. [c] Yield of a dimethyl acetylenedicarboxylate adduct of **3i** was 90%.

The solvents of choice are chloroform, ether, dichloromethane (caution! see below), or acetonitrile. As expected, the reaction proceeds faster in more polar solvents such as acetonitrile and dimethylformamide (Table 2), which are especially appropriate where solvent removal is not a problem.

For comparison with other methods, butyl bromide **2a** requires heating at 100°C for 3 h in the presence of methyltrioctylammonium chloride/NaN_3 under phase-transfer conditions for its conversion into the azide (which was purified by distillation).[4] In contrast, butyl bromide **2a** or

Table 2. Relative rate of conversion of *n*-hexyl bromide **2b** into *n*-hexyl azide **3b** with the polymer **1** (after 4 h in various solvents; determined by GC).

Solvent	Conversion [%]	Solvent	Conversion [%]
toluene	23	diethyl ether	54
chloroform	26	acetone	82
methanol	32	acetonitrile	>95
tetrahydrofuran	38	dimethyl-	
pentane	52	formamide	>95

even the more sluggishly reacting hexyl bromide **2b** are converted into their azides **3a** and **3b**, respectively, by reaction with **1** at 20°C within 3 h in acetonitrile or within 24 h in dichloromethane.

Most remarkably, this method allowed us, for the first time, to convert dibromomethane **2k** or, more slowly, dichloromethane into diazidomethane **3k**, an explosive compound.[7] Although dichloromethane is a convenient, low-boiling solvent for reactions of **1** with alkyl halides (usually complete within 4–24 h), the above results indicate caution when employing this solvent (conversion into **3k** requires over two weeks). The relative rate of reactivity with the polymer **1** is R–I > R–Br > R–OTos ≫ R–Cl, which is in accord with a nucleophilic substitution process.

Experimental Procedure

Polymer **1**: Amberlite IR-400 was washed with 20% sodium azide solution, then with water, methanol, and chloroform or ether. The polymer was dried at room temperature in vacuum and found to contain 2.55 mmol of azide per gram. The friction parameter of **1** as measured on a Julius-Peter apparatus was 14.4 kg, indicative of high friction stability.

Reaction of **1** with **2e**: To 4.9 g of **1** (12.5 mmol of azide) was added 4 mL of CH_2Cl_2 and 0.265 g (1.06 mmol) of *p*-bromobenzyl bromide **2e**. After 2 h of mixing, the polymer was filtered and washed with CH_2Cl_2. Evaporation of the combined solvent mixture gave pure *p*-bromobenzyl azide **3e** as an oil in 93% yield; ^{1}H-NMR: $\delta = 7.5$ and 7.2 (AA'BB', 4H); 4.29 (s, 2H). *m/z* 212.74, 210.84.

Received: January 24, 1986 [Z 1637 IE]
German version: *Angew. Chem. 98* (1986) 479

[1] A. Hassner, J. Keogh, *J. Org. Chem. 51* (1986) in press.
[2] M. E. C. Biffin, J. Miller, D. B. Paul in S. Patai (Ed.): *The Chemistry of the Azido Group*, Interscience, London 1971, p. 57.
[3] a) A. Brandstrom, B. Lamb, I. Palmertz, *Acta Chem. Scand. B28* (1974) 699; b) A. J. Papa, *J. Org. Chem. 31* (1966) 1426; c) K. Sakai, J. P. Anselme, *ibid. 36* (1971) 2387.
[4] W. Reeves, L. Bahr, *Synthesis 1976*, 823.
[5] A. Hassner, R. Fibiger, D. Andisik, *J. Org. Chem. 49* (1984) 4237.
[6] a) *Nachr. Chem. Tech. 18* (1970) 26; b) M. J. Lelen, *Cah. Notes Doc. 91* (1978) 319.
[7] Details about this compound: A. Hassner, M. Stern, unpublished.

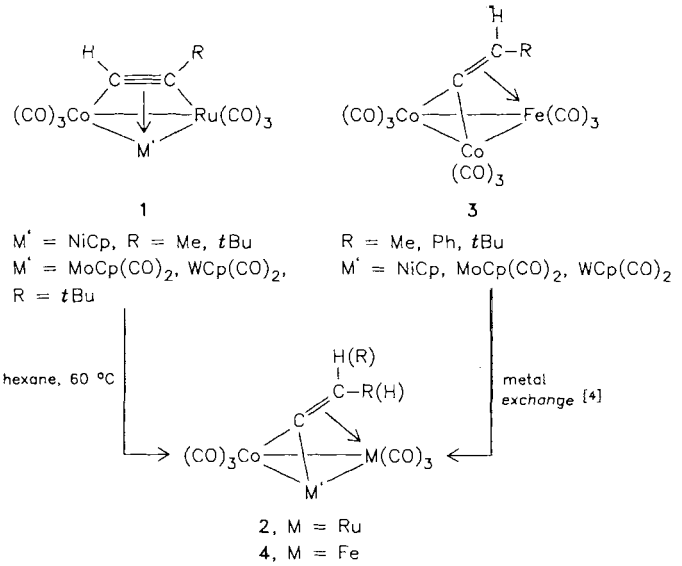
Diastereoselective Transformations on Heterometal Clusters**

By *Christine von Schnering, Thomas Albiez, Wolfgang Bernhardt,* and *Heinrich Vahrenkamp**

The phenomena of enantio- and diastereoselectivity, which are of current interest in catalysis and organic chemistry, have not yet been the objects of research in organometallic cluster chemistry; even simple isomerism has only seldom been observed for cluster frameworks.[1] Furthermore, there are only a few reported examples of isomerism in the coordination sphere of clusters,[2] and stereoselective reactions with clusters were unknown up to now. We report here reactions in which one of two possible isomers is preferentially formed.

The starting point of our studies was the acetylene–vinylidene rearrangement on trimetal clusters, which we have described for the compounds $[RuCo_2(CO)_9(\mu_3,\eta^2\text{-}L)]$, L = HC≡CR or C=CHR.[3] When the alkyne-bridged starting clusters are converted by metal exchange[4] into the chiral clusters **1**, which are then isomerized thermally to the vinylidene-bridged RuCoM′ clusters **2** (see Scheme 1), two isomers can be formed in each case, which differ in the positions of H and R. If M′ = NiCp, the isomers are formed in equal amounts regardless of the R group. If M′ = $MoCp(CO)_2$ or $WCp(CO)_2$ and R = *t*Bu, only one isomer is formed in each case.

Analogous results were obtained for FeCoM′ clusters **4**, which permit greater variation of the R groups (see Scheme 1). The alkyne-bridged binuclear complexes $[Co_2(CO)_6(HC{\equiv}CR)]$[5] react thermally with $Fe_3(CO)_{12}$, resulting in $Fe(CO)_3$ addition and H migration to give the vinylidene-bridged clusters **3**, which, in turn, can be easily converted into the corresponding clusters **4** by metal exchange.[6] In the case of the FeCoNi complexes, 1 : 1 mixtures of isomers are formed. For M′ = $MoCp(CO)_2$ and $WCp(CO)_2$, the isomers are formed in ratios of 1 : 3 to 1 : 4 when R is Me or Ph; only one isomer is formed when R is *t*Bu.



Scheme 1.

Clusters **2** and **4** each have two asymmetric centers, namely, the two vinylidene C atoms. Thus, for each of the two isomers, there exists an enantiomer, and two pairs of diastereomers are present. For R = *t*Bu, therefore, the transformations **1** → **2** and **3** → **4** are diastereospecific. However, it has not yet been possible to prepare optically active **1**.

In order to prove that the selectivity has a steric origin, an X-ray structure analysis was carried out for **2**, M′ = $WCp(CO)_2$, R = *t*Bu.[7] Surprisingly, the bulky *t*Bu group and C_5H_5 ligand were found to lie on the same side

[*] Prof. Dr. H. Vahrenkamp, Dipl.-Chem. C. von Schnering, Dipl.-Chem. T. Albiez, Dipl.-Chem. W. Bernhardt
Institut für Anorganische und Analytische Chemie der Universität Albertstrasse 21, D-7800 Freiburg (FRG)

[**] This work was supported by the Fonds der Chemischen Industrie, Heraeus, and the Rechenzentrum der Universität Freiburg.

of the molecule (Fig. 1). The shortest distance between *t*Bu and C_5H_5 (C44-C15 369 pm) indicates that practically no steric hindrance is present. This unexpected result compelled us to ascribe an electronic effect as the cause of the stereoselectivity.

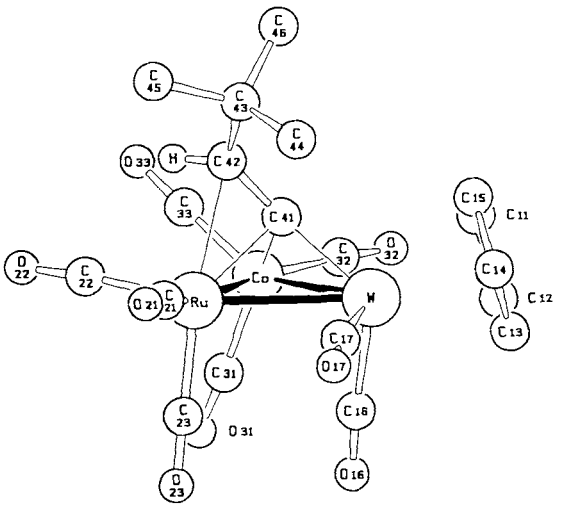


Fig. 1. Crystal structure of [RuCoWCp(CO)$_8$(μ_3,η^2-C=CH*t*Bu)] **2**. Important bond lengths [pm]: W-Ru 290.1(1), W-Co 272.3(3), Ru-Co 262.4(3), W-C41 201(1), Ru-C41 210(1), Co-C41 195(1), Ru-C42 235(2), C41-C42 129(2).

In view of the manifold possibilities for the transformation of organic multiple bond systems on clusters, for the release of transformed substrates from clusters, and for the preparation of clusters in optically active form, the results described here should point out a new way for the exploitation of variations in the inorganic part of cluster compounds, which, up to now, have been less investigated than those of the organic part.

Received: December 16, 1985 [Z 1591 IE]
German version: *Angew. Chem. 98* (1986) 474

[1] Cf. F. Richter, H. Vahrenkamp, *Chem. Ber. 115* (1982) 3224, 3243; J. R. Fox, W. L. Gladfelter, G. L. Geoffroy, I. Tavanaiepour, S. Abdel-Mequid, V. W. Day, *Inorg. Chem. 20* (1981) 3230; P. D. Williams, M. D. Curtis, D. N. Duffy, W. M. Butler, *Organometallics 2* (1983) 165; D. E. Fjare, W. L. Gladfelter, *J. Am. Chem. Soc. 106* (1984) 4799; R. Bender, P. Braunstein, A. Tiripicchio, M. Tiripicchio Camellini, *Angew. Chem. 97* (1985) 862; *Angew. Chem. Int. Ed. Engl. 24* (1985) 861.

[2] Cf. A. J. Deeming, S. Hasso, M. Underhill, *J. Chem. Soc. Dalton Trans. 1975*, 1614; R. D. Adams, *Acc. Chem. Res. 16* (1983) 67; R. J. Haines, S. Smit, personal communication (addition of C_2H_2 to [$Ru_4(CO)_{11}(PPh)_2$]); J. F. Halet, J.-Y. Saillard, R. Lissillour, M. J. McGlinchey, G. Jaouen, *Inorg. Chem. 24* (1984) 218; E. Sappa, A. Tiripicchio, P. Braunstein, *Chem. Rev.*, in press; C. Choo Yin, A. J. Deeming, *J. Organomet. Chem. 193* (1977) 123; G. Süss-Fink, L. Khan, P. Raithby, *ibid. 228* (1982) 179.

[3] E. Roland, W. Bernhardt, H. Vahrenkamp, *Chem. Ber. 118* (1985) 2858; for complexes of type **1** and **2** having the composition [RuCoMoCp(CO)$_8$(C_2H*t*Bu)] see W. Bernhardt, C. von Schnering, H. Vahrenkamp, *Angew. Chem. 98* (1986) 285; *Angew. Chem. Int. Ed. Engl. 25* (1986) 279.

[4] H. Vahrenkamp, *Comments Inorg. Chem. 4* (1985) 253.

[5] U. Krüerke, W. Hübel, *Chem. Ber. 94* (1961) 2829.

[6] All new compounds gave acceptable elemental analyses and mass spectra. Typical IR data (C_6H_{12}, $\tilde{\nu}$ [cm^{-1}]): **1** (M′ = WCp(CO)$_2$, R = *t*Bu): 2076 (s), 2054 (w), 2031 (vs), 2012 (vs), 1987 (s), 1982 (sh), 1969 (m), 1885 (w); **2** (M′ = NiCp, R = Me): 2071 (m), 2041 (vs), 2011 (vs), 1985 (sh), 1977 (m); **3** (R = Ph): 2104 (w), 2060 (vs), 2050 (vs), 2042 (sh), 2025 (w), 1982 (w), 1977 (w); **4** (M′ = MoCp(CO)$_2$, R = Me): 2074 (w), 2032 (s), 2023 (vs), 2010 (m), 1992 (s), 1985 (m), 1975 (w), 1965 (w), 1955 (sh), 1945 (m), 1885 (w). ^{1}H-NMR spectra ($CDCl_3$, TMS, δ values, J [Hz]): **1**: 9.27 (s, br., 1H), 5.43 (s, 5H), 1.18 (s, 9H); **2** (equal amounts of the two isomers, vinylidene H signals probably obscured by NiCp signals): 5.43 (s, ca. 5.5H), 5.34 (s, ca. 5.5H), 2.01 (d, 6.0, 3H), 1.86 (d, 6.0, 3H); **3**: 7.38 (m, 5H), 6.91 (s, 1H); **4** (major isomer): 5.90 (q, 6.0, 1H), 5.53 (s, 5H), 1.73 (d, 6.0, 3H); (minor isomer): 5.20 (q, 6.0, 1H), 5.27 (s, 5H), 1.95 (d, 6.0, 3H).

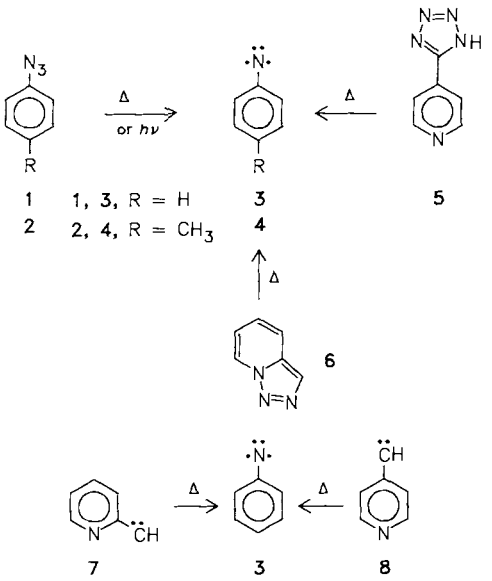
[7] Monoclinic, $P2_1/c$, $a = 1700.4(4)$, $b = 921.8(6)$, $c = 1523.7(2)$ pm, $\beta = 113.62(2)°$; $Z = 4$, 2572 reflections, $R = 0.049$. Further details of the crystal structure investigation may be obtained from the Fachinformationszentrum Energie, Physik, Mathematik GmbH, D-7514 Eggenstein-Leopoldshafen 2 (FRG), on quoting the depository number CSD-51640, the names of the authors, and the journal citation.

ESR Observation of Thermally Produced Triplet Nitrenes and Photochemically Produced Triplet Cycloheptatrienylidenes**

By *Martin Kuzaj, Holger Lüerssen*, and *Curt Wentrup**

To date all nitrenes observed by ESR[1,2] have been generated by photolysis in low-temperature glasses or matrices. We now report the thermal gas-phase production of nitrenes with subsequent matrix isolation,[3] which permits direct monitoring of thermal carbene and nitrene rearrangements that were previously only inferred from product studies.[4] Moreover, we describe the first observation of cycloheptatrienylidenes and their aza derivatives.

The pyrolysis of phenyl azide **1** at 500 °C gave a product with a strong ESR signal ($|D/hc| = 0.9896$; $|E/hc| = 0.00\ cm^{-1}$) typical of phenylnitrene **3**. The same signal was obtained on photolysis of matrix-isolated **1**. Phenylnitrene spectra were also obtained on pyrolysis of the *carbene* precursors **5** and **6**, thereby verifying the carbene-nitrene rearrangements **7** → **3** and **8** → **3**.[5,6] *p*-Tolylnitrene **4** was similarly generated from *p*-tolyl azide **2** (Table 1). The much debated thermal cycloperambulation[7] to *m*- and *o*-tolylnitrene did not take place to any measurable extent under these conditions.

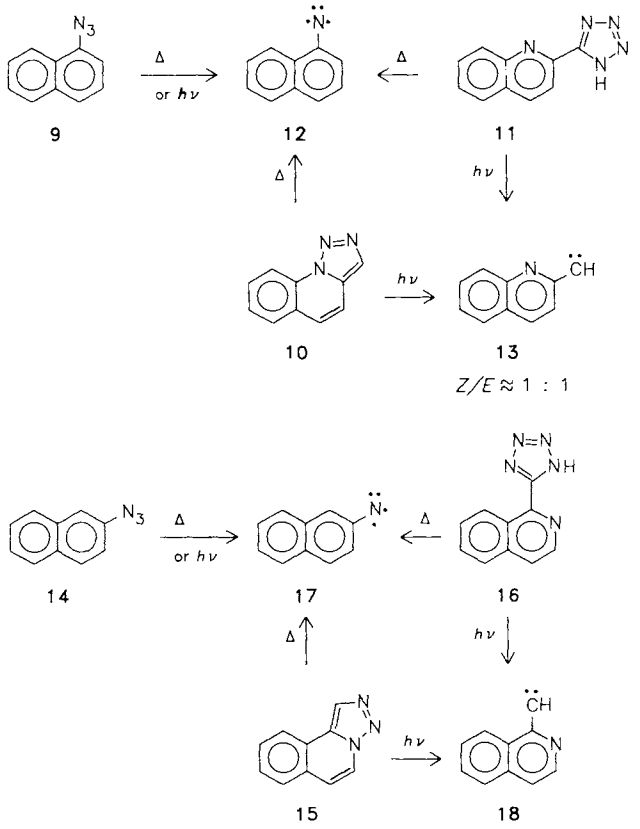


The discrete nitrenes **12** and **17** were likewise obtained from the naphthyl azides **9** and **14**, respectively, as well as

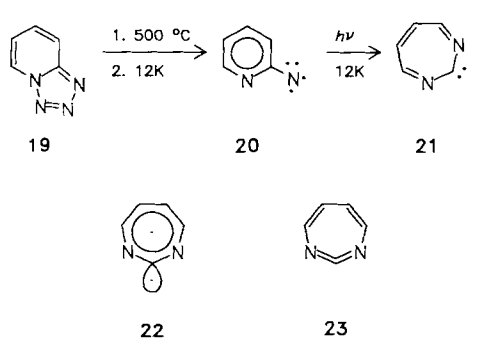
[*] Prof. Dr. C. Wentrup, Dr. M. Kuzaj, Dr. H. Lüerssen
Department of Chemistry, University of Queensland
St. Lucia, Brisbane, Queensland, Australia 4067

[**] This work was initiated at the University of Marburg (FRG) and supported by the Deutsche Forschungsgemeinschaft, the Fonds der Chemischen Industrie, and the University of Queensland, Australia.

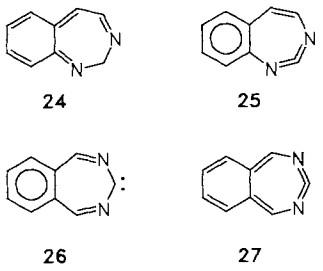
from the carbene precursors **10** and **11** or **15** and **16**. No interconversion of the 1- and 2-naphthylnitrenes **12** and **17** was observed. The *carbenes* **13**[8] and **18** were obtainable only on *photolysis* of the carbene precursors (Ar, 12 K). Both (*Z*) and (*E*) forms of **13** were observed, in a ca. 1 : 1 ratio. The fact that, in the thermal experiments, the *carbene* precursors rearrange entirely to *nitrenes* confirms our argument that nitrenes are intrinsically more stable thermodynamically than isomeric carbenes;[9] hence, the rearrangement of carbenes to nitrenes is virtually unidirectional in the gas phase.



The ring expansions interconverting carbenes and nitrenes are nowadays normally formulated in terms of cycloheptatetraenes/azacycloheptatetraenes.[2,4] The corresponding carbenes, the cycloheptatrienylidenes/azacycloheptatrienylidenes, have never been observed. If cycloheptatrienylidenes have triplet ground states,[10] it should be possible to generate such species by photolysis of triplet precursors. Indeed, this appears to have been achieved: Photolysis (200-W high-pressure Hg lamp) of thermally generated and Ar-matrix-isolated 2-pyridylnitrene **20** gave



a new triplet carbene characterized by unusually low *D* and *E* values (Table 1). These values are too low for a heteroarylcarbene, because aza substitution tends to *increase* the *D* value (Table 1); therefore, the new carbene may be 1,3-diazacycloheptatrien-2-ylidene **21**, which would be strongly delocalized, as expressed in canonical structure **22**. The *thermal* (singlet) rearrangement of **20** (as monitored by IR spectroscopy) gives only the carbodiimide **23**, which is presumably the lowest-energy form of this seven-membered ring system.[11]



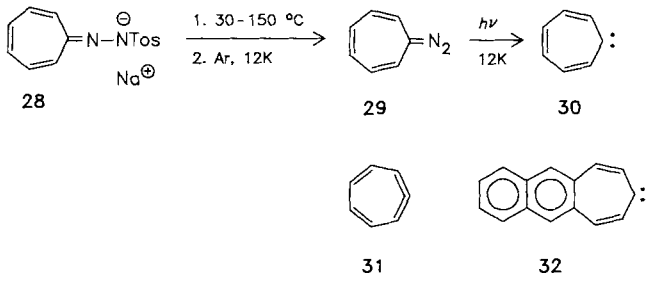
The structural assignment of **21** was tested by irradiation of 2-quinolyl- and 1-isoquinolylnitrene; both gave the *same* carbene, **24**, which is also characterized by low *D* and *E* values (Table 1). 3-Isoquinolylnitrene gave a different carbene, **26**. The corresponding carbodiimides **25** and **27** have been observed by IR spectroscopy.[4,11]

Table 1. ESR data for some nitrenes and carbenes [a].

Triplet species	$\|D/hc\|$ [cm^{-1}]	$\|E/hc\|$ [cm^{-1}]	Number of exp. [b]
3 [c, d]	0.990(5)	0.0000(0)	4
4 [d]	0.967	0.0000	1
12 [c, d]	0.793(6)	0.0025(4)	7
Z-**13** [c]	0.531(1)	0.0265(2)	7
E-**13** [c]	0.467(0)	0.0259(2)	4
17 [c, d]	0.925(2)	0.0023(3)	6
18 [c]	0.489(1)	0.0245(2)	9
20 [c, d]	1.051(8)	0.0000(0)	3
21 [c]	0.426(2)	0.0056(2)	2
2-quinolylnitrene [c-e]	1.034(2)	0.0039(1)	3
1-isoquinolylnitrene [c-e]	0.847(2)	0.0042(1)	2
24 [c]	0.386(1)	0.0150(0)	3
3-isoquinolylnitrene [c-e]	0.943(2)	0.0049(1)	4
26 [c]	0.433(0)	0.0124(0)	2
phenylcarbene [c, f]	0.517(1)	0.0245(2)	7
30 [c]	0.425(0)	0.0222(2)	2
32 [c]	0.453	0.0193	1
2-pyrazinylnitrene [c-e]	1.014(2)	0.000	3
2-pyrimidinylnitrene [c-e]	1.217(15)	0.0052(0)	4
4-quinolylnitrene [c, d, g]	0.882(3)	0.0020(2)	5
2-quinoxalylnitrene [c, e]	0.955(2)	0.0030(1)	2
2-quinoxalylcarbene [c, h]	0.474(0)	0.0261(1)	7

[a] $H_0 = h\nu/g\beta \approx 3372.0$ Gauss; the exact value of ν was measured in each experiment. Uncertainties in *D* and *E* values in units of the least significant digit. [b] Number of experiments used in averaging *D* and *E* and determining the uncertainties. [c] Photochemically produced. [d] Thermally produced. [e] From annelated tetrazoles or azides. [f] By photolysis of phenyldiazomethane or by pyrolysis of 5-phenyltetrazole followed by photolysis. [g] From 4-quinolyl azide or by thermal rearrangement of 2-quinoxalylcarbene produced by pyrolysis of either 1,2,3-triazolo[1,5-*a*]quinoxaline or 2-(5-tetrazolyl)quinoxaline. [h] Photolysis of triazoloquinoxaline or tetrazolylquinoxaline.

The above results led us to attempt the direct generation of triplet cycloheptatrienylidene **30**. Mild pyrolysis of the salt **28** gave the diazo compound **29** (IR: 2048 cm^{-1}; Ar,



12 K). Photolysis of **29** at 12 K gave a carbene, different from phenylcarbene (Table 1) and characterized by a low *D* value. The ESR signal intensity did not follow the Curie law exactly, and, when the warmed sample was cooled again, the signals failed to return to their original intensities. One intriguing possibility is that **30** has a triplet ground state and, on warming, is partly converted into the lower-energy[10] allene **31**. Repeated warming and cooling should finally remove triplet **30** from the matrix.[12] Cyclohepta[*b*]naphthalen-8-ylidene **32**, a ground-state triplet,[13] was similarly generated and gave *D* and *E* values very close to those of **30** (Table 1).

Received: December 16, 1985;
revised: February 26, 1986 [Z 1592 IE]
German version: *Angew. Chem. 98* (1986) 476

CAS Registry numbers:
1, 622-37-7; **2**, 2101-86-2; **3**, 2655-25-6; **4**, 38157-47-0; **5**, 14389-12-9; **6**, 274-59-9; **7**, 21963-51-9; **8**, 37998-87-1; **9**, 6921-40-0; **10**, 235-21-2; **11**, 101772-02-5; **12**, 3315-52-4; **13**, 78759-52-1; **14**, 20937-86-4; **15**, 34456-69-4; **16**, 59175-48-3; **17**, 3315-51-3; **18**, 101772-03-6; **19**, 274-87-3; **20**, 24843-39-8; **21**, 101772-04-7; **24**, 101772-07-0; **26**, 101772-09-2; **28**, 18870-24-1; **29**, 101418-91-1; **30**, 17476-70-9; **32**, 73794-91-9; PhCH:, 3101-08-4; PhCH = N_2, 766-91-6; 5-phenyltetrazole, 18039-42-4; 2-quinolylnitrene, 101772-05-8; 4-quinolylnitrene, 101772-12-7; 1-isoquinolylnitrene, 101772-06-9; 3-isoquinolylnitrene, 101772-08-1; 2-pyrazinylnitrene, 101772-10-5; 2-pyrimidylnitrene, 101772-11-6; 2-quinoxalylnitrene, 101772-13-8; 2-quinoxalylcarbene, 101772-14-9; 2-(5-tetrazolyl)quinoxaline, 101772-15-0; 1,2,3-triazolo[1,5-*a*]quinoxaline, 13390-30-2.

[1] E. Wasserman, *Prog. Phys. Org. Chem. 8* (1971) 319.
[2] M. S. Platz in E. F. V. Scriven (Ed.): *Azides and Nitrenes*, Academic Press, New York 1984, chapter 7, p. 359–393.
[3] Pyrolyzer housing a 10 × 0.8 cm quartz tube flanged to Air Products He cryostat CSA-202E. Product isolation in Ar matrix at 12–15 K on a copper rod. Distance between pyrolyzer exit and copper rod 2.5 cm; 10^{-4} torr); Varian E6 ESR spectrometer, AEG nuclear resonance field, and Rohde and Schwarz microwave frequency measuring units were used. *D* and *E* values calculated using iterative computer program based on *Wasserman*'s equations: E. Wasserman, L. C. Snyder, W. A. Yager, *J. Chem. Phys. 41* (1964) 1763.
[4] C. Wentrup in E. F. V. Scriven (Ed.): *Azides and Nitrenes*, Academic Press, New York 1984, chapter 8, p. 395–432.
[5] C. Wentrup, C. Mayor, R. Gleiter, *Helv. Chim. Acta 55* (1972) 2628; C. Thetaz, C. Wentrup, *J. Am. Chem. Soc. 98* (1976) 1258.
[6] For the corresponding *photochemical* interconversion of pyridylcarbenes and phenylnitrene, see O. L. Chapman, R. S. Sheridan, J.-P. LeRoux, *J. Am. Chem. Soc. 100* (1978) 6245.
[7] W. D. Crow, M. N. Paddon-Row, *Aust. J. Chem. 28* (1975) 1755.
[8] ESR of quinolylcarbenes: R. S. Hutton, H. D. Roth, M. L. M. Schilling, J. W. Suggs, *J. Am. Chem. Soc. 103* (1981) 5147. H. D. Roth, R. S. Hutton, *Tetrahedron 41* (1985) 1567.
[9] C. Wentrup, *Top. Curr. Chem. 62* (1976) 173; *Reactive Molecules*, Wiley, New York 1984, pp. 184, 230.
[10] M. Z. Kassaee, M. R. Nimlos, K. E. Downie, E. E. Waali, *Tetrahedron 41* (1985) 1579. MNDO values: **29**-S: 91.5 kcal/mol; **30**-T: 97.4 kcal/mol; **30**-S (transition state): 114.4 kcal/mol.
[11] C. Wentrup, H.-W. Winter, *J. Am. Chem. Soc. 102* (1980) 6159.
[12] The singlet **31** has been observed by IR and UV spectroscopy: P. R. West, O. L. Chapman, J.-P. LeRoux, *J. Am. Chem. Soc. 104* (1982) 1779.
[13] A. Hackenberger, H. Dürr, *Chem. Ber. 117* (1984) 2644.

BOOK REVIEWS

Analytical Solution Calorimetry. Edited by *J. K. Grime*. Wiley, Chichester 1985. xvi, 401 pp., bound, £ 69.40.—ISBN 0-471-86942-2

Calorimetry. Fundamentals and Practice. By *W. Hemminger* and *G. Höhne*. Verlag Chemie, Weinheim 1984. vi, 310 pp., bound, DM 135.00.—ISBN 3-527-25948-1

The book "Analytical Solution Calorimetry" edited by *J. K. Grime* and the English version of "Calorimetry" written by *W. Hemminger* and *G. Höhne* provide two extensive accounts of the experimental methods used in calorimetry. They describe the most important areas of calorimetric measurement techniques in accordance with the current state of development. As very few self-contained books have been published on this subject and all earlier review articles are out of date, these books make a welcome appearance. The selection and classification of their subject matter differ considerably however. The book "Analytical Solution Calorimetry" appears as volume 79 of the "Chemical Analysis" series and its concept is based on the requirements of the chemical-analytical applications of calorimetric measurement methods. The basic principles of analytical solution calorimetry, flow calorimetry and the determination of reaction enthalpies are accordingly described by competent experts and are presented in a form suitable for practical applications. This section is preceded by an introductory chapter on the thermodynamics, thermochemistry and principles of calorimetry. Further chapters provide a great deal of information on the selection of instruments and the evaluation of experimental data, as well as important examples of the applications of calorimetric methods in analysis and special studies performed in biochemical and clinical laboratories. The experimentalist will find important information for his daily work both in the text and in the large number of literature references.

"Calorimetry" is an extended English version of the book entitled "Grundlagen der Kalorimetrie" published in 1979. It summarizes the field of calorimetry including theoretical and methodological prerequisites and takes both historical development and the most recent methodological improvements into consideration. Six of the ten chapters (supplemented by an appendix) are dedicated to physical principles and evaluation procedures. Calorimeters with compensation for thermal effects are described in chapter seven and calorimetric measurements with registration of a temperature difference are treated in chapter eight. Chapter nine is especially important as regards practical applications and gives criteria for selecting suitable

calorimeters. The book is concluded by a few brief comments on possible future developments. Chapter nine has been extended in comparison with the original German edition by including sections on the influence of noise (short-term noise and long-term noise) and the functioning of the apparatus. The numbers assigned to two of the figures in section 9.2 have been corrected. This monograph written by *Hemminger* and *Höhne* is the only up-to-date book that gives a clearly presented account of methods for the determination of reaction enthalpies, procedures for measuring specific heats and applications in analytical and biophysical chemistry. Detailed examples of applications cannot, of course, be included in such a wide-ranging work but are to be found in the studies cited in the appendix. The book is a standard work which every natural science institute should have in its library, it can be recommended without any reservations to all scientists interested in thermodynamic measurements.

Theodor Ackermann [NB 750 IE]
Institut für Physikalische Chemie
der Universität Freiburg (FRG)

Methods of Enzymatic Analysis. Vol. 7. Metabolites 2: Tri- and Dicarboxylic Acids, Purines, Pyrimidines and Derivatives, Coenzymes, Inorganic Compounds. By *H. U. Bergmeyer, J. Bergmeyer,* and *M. Grassl.* 3rd Edit. VCH Verlagsgesellschaft: Weinheim 1985. xxviii, 641 pp., bound, DM 325.00.—ISBN 3-527-26047-1

The five chapters of this volume[*] describe quantitative analyses for di- and tricarboxylic acids; purines, pyrimidines and nucleosides; nucleotides, coenzymes and related materials; nucleoside diphosphate sugars; and inorganic compounds.

Much of what separates this new edition from its predecessor of 10 years ago is the wealth of information which has been added in support of the assay procedure itself. Each assay has been extensively supplemented with concise information concerning the analyte's history, physical and biological properties, biogenesis and occurrence, special properties relevant in analysis, references and standards for the analyte, and alternate methods of analysis.

Some two dozen new assay procedures have been added to this edition; a similar number from the second edition have been omitted. Although most of the deletions are alternate procedures for analytes which are still represented in this edition, some metabolites appearing in the second edition will no longer be found.

Many of the procedures in this edition are the same as those in the second edition. Some of these procedures have been altered to incorporate new information and findings but others have been incorporated unchanged as they still represent the state-of-the-art—even after more than 10 years in a rapidly advancing area of science! That the content of the second edition has required only little change in a changing field is a strong statement about the durability of this new edition.

As in the previous edition, the assay itself is detailed and covers the Method Design (the assay principle and optimum measurement conditions), Equipment, Reagents and Solutions (purity, preparation, storage and stability of reagents and solutions), Procedure (specimen collection, treatment, preparation and stability; measurement and calculations) and Validation of the Method (precision, accuracy, detection limit and sensitivity, error, specificity, and reference range).

Accompanying each assay is a thorough list of references among which many citations from 1983 and 1984 can be found, thus attesting to the text's timeliness.

The first chapter contains analytical procedures for determining di- and tricarboxylic acids. Those familiar with the second edition of "Bergmeyer" will find that assays for both D- and L-tartrate, and for D-malate have been added to the procedures for the seven acids of the citrate cycle. Delections in this chapter include several fluorimetric procedures as well as the assay for maleate.

The chapter describing analyses for purines, pyrimidines and nucleosides has been extensively changed. Among the analyses for the purine and pyrimidine bases, those for guanine/adenine and for uric acid have been improved by using superior indicator reactions, the analysis for cytosine has been omitted while the procedures for orotate, hypoxanthine, and xanthine remain the same as those in the second edition.

For nucleosides, an analysis for total nucleosides has been added to those for adenosine, guanosine and inosine. Analyses for cytidine, deoxycytidine, deoxythymidine and deoxyuridine have all been omitted.

The third chapter, containing assays for nucleotides, coenzymes and related compounds, comprises more than 50% of the book. Analyses for pantethine, coenzyme A and a variety of acyl CoA derivatives—acetyl, acetoacetyl, long chain fatty acyl, 3-hydroxy-3-methyl-glutaryl, malonyl and succinyl—are described by a mixture of new, old and modified assays. Assays for six less-common CoA derivatives which appeared in the second edition are omitted.

The coverage of NAD(P)(H) cofactors is essentially unchanged from the second edition, however a luminometric method for determining NADH/NADPH is new. The assay for flavin-adenine dinucleotide has been revised and two assays for flavin mononucleotide have been added.

Assays for diadenosine tetraphosphate, *S*-adenosylmethionine, *S*-adenosylhomocysteine and two luminometric assays for the adenosine phosphates have been added to the nucleotide section. These assays, in addition to those which have been retained from the second edition for the adenosine phosphates, bring total coverage for this important group of materials to over 70 pages. The remainder of the chapter contains assays for the guanosine-, inosine-, cytidine-, and uridine 5′-mono-, di- and triphosphates in a streamlined manner. The chapter also contains the old UV-based assays for thiamine pyrophosphate and pyridoxal phosphate and new assays for pyridoxal phosphate (radiometric method) and tetrahydrofolate.

The chapter for nucleoside diphosphate sugars has been greatly expanded and now contains assays for 5-F-UDP-glucose/5-F-UDP-galactose, UDP-glucosamine/UDP-galactosamine, UDP-2-deoxyglucose/UDP-2-deoxygalactose, and thymidine 5′-diphosphoglucose in addition to assays for adenosine-, cytidine-, and uridine-5′-diphosphoglucose, uridine 5′-diphosphogalactose and guanosine 5′-diphosphomannose.

The chapter on inorganics has been expanded to include assays for lead, arsenic, zinc, magnesium, sulfite and bicarbonate as well as those for inorganic phosphate, inorganic pyrophosphate, inorganic peroxides and nitrate, of which the latter three have been improved since appearing in the second edition.

The improvements and additions made in this edition are significant and useful. As with previous volumes, the

[*] Cf. *Angew. Chem. Int. Ed. Engl. 25* (1985) 291.

editors and publisher have put together a high-quality reference which will find almost daily use among those involved in biochemistry, biology, chemistry and related areas. This series is strongly recommended to libraries and groups where analyses are routinely done.

Philip D. Stein and *George M. Whitesides* [NB 726 IE]
Department of Chemistry, Harvard University
Cambridge, MA 02138 (USA)

Electroorganic Syntheses, Part I: Oxidations. By *S. Torii.* VCH Verlagsgesellschaft, Weinheim 1985. xi, 338 pp., bound, DM 138.00.—ISBN 3-527-26318-7

Shortly after the publication of *Shono*'s book, *S. Torii,* another important electroorganic chemist engaged in synthesis, has addressed the subject in a monograph. The first volume of this work has been published; the second part (on reductions) is planned. This volumed is based on a monograph of the author's, which appeared in 1981 in Japanese. It amounts to more than a simple translation into English, however, since it has been revised and extended. Literature references cover publications up to 1983; in a few cases there are even references from 1984. Since the author is not aiming at an exhaustive presentation of organic electrochemistry, literature from earlier than 1970 is considered only in a few cases.

This book, similarly to *Shono*'s, is directed at chemists engaged in synthesis, i.e., in the first place, at non-electrochemists. It is arranged in thirteen chapters, of which the first, "Electrooxidation and Product Selectivity", clearly gives the intention of the whole work from the outset. Chapters 2–10 and 12 deal with the electrooxidation of particular classes of compounds. Two chapters are concerned with catalytic phenomena which have achieved more and more significance lately: indirect electrooxidation and the use of electrochemically generated acids.

In these chapters, the author presents an abundance of synthetically interesting reactions, clearly arranged. Non-electrochemists are not put off by a lengthy explanation of the theoretical basis or exhaustive presentation of reaction mechanisms. Instead, the emphasis is placed on the discussion of selectivity and the steering of reactions. The author points out that high selectivity in the reactions can only be achieved through the right choice of the reaction parameters, especially of solvent, conducting salt and electrode material. Particularly in the first chapter, but also in all subsequent parts of the book, the influence of these parameters on the course of the reaction is repeatedly discussed in detail and possibilities for steering the reactions are worked out. Since this is done, to a large extent, on an empirical basis, it will appeal to synthetic chemists. It must be said, however, that this approach may perhaps distract those readers who want only to cast a quick glance at the synthetic potential of the method.

As the author points out in the foreword, he is attempting to present results in a form which makes plain the possibilities for their application in synthesis. An appendix to Chapter 1 contributes particularly to this end. Here, the possible conversions are set out schematically, arranged according to the kind of bond formation, bond splitting, rearrangement and functionalization, and linked with the appropriate reaction conditions and with references to pages and chapters of the book. Such a presentation is especially valuable, if information is required on a particular type of conversion. Synthetic chemists would surely, however, have welcomed a critical comparison of the pros and cons of electrochemical methods against current chemical alternatives. It would have been helpful for the evaluation of the potential of electroorganic synthesis by non-electrochemists had the author expounded the principle of redox-Umpolung, which underlies electrochemical reactions.

It is annoying, however, that in an otherwise very carefully edited book, the literature references in Chapter 1, contain some monographs in Japanese or translations into Japanese, while the English originals or equivalent works in English are not cited. Unfortunately, as frequently encountered, the index has not been given much attention. Not only is it incomplete, but it also suffers from the fact that the entries, mostly compounds, are not further qualified, so that their relationship to a method, type of conversion, or property is not established. This applies, for example, to the entry "anisaldehyde" in the index. If the reader were to be properly guided, the qualification "from methoxytoluene" would be necessary. As it is, the page number given refers only to the indirect electrochemical preparation, while the direct electrochemical synthesis, spanning almost two pages in Chapter 3, is not mentioned.

It is to be welcomed that, with these books by *Shono* and *Torii,* there are now two monographs available on the subject of electroorganic synthesis that are directly aimed at synthetic chemists. In both cases, it is not so much the electrochemical method itself which is given prominance to, but rather the great synthetic potential of this method, which is still underestimated. The books are written in a style which makes this fascinating area accessible to every reader. Thus, it is to be hoped that both books will achieve the largest possible circulation amongst synthetically oriented chemists. The length of the two books, in one case 171 pages and, in the other, 338 pages for volume 1 alone, shows quite clearly that the intended readership is different for each. *Shono*'s monograph is especially suitable for those who want a brief survey of the manifold possibilities of electrosynthesis, who want to kindle an interest or who are looking for new synthetic concepts. Students majoring in chemistry should belong to this group, if they are not put off by the relatively high price. On account of its strong emphasis on selectivity and the steering of electrochemical reactions, *Torii*'s book is not only suitable as a source of general information, but also offers a lot of concrete suggestions as to the most favorable procedure and the most suitable reaction conditions to those who want to incorporate electrochemical steps into their synthetic plans. It presents to the interested reader a good survey of the present state of the art and makes it clear that the high expectations on selectivity of modern synthetic operations can be fulfilled by electrosynthesis. It is, therefore, a book that can convince the synthetic chemist of the advantages of organic electrochemistry so that he will refer to it again and again.

Eberhard Steckhan [NB 705a IE]
Institut für Organische Chemie und Biochemie
der Universität Bonn (FRG)

Structure and Spectra of Molecules. By *W. G. Richards* and *P. R. Scott.* John Wiley, Chichester 1985. ix, 172 pp., paperback, £ 6.95.—ISBN 0-471-90575-0

In this brief introduction, the authors are principally concerned with illustrating the physical relationships of spectroscopic quantities with the electronic and geometric

structure of a molecule. The basic models are defined, energy values and quantum numbers are given, and eigenfunctions are qualitatively described. In contrast to some "practical" guides to instrumental analysis, this book does indeed contain many schematic, but only a few, simple, real spectra and hardly any empirical "rules".

53 pages serve for the introduction to the physical foundations of the subject. Proficiency in mathematics is not required: only the short section on symmetry and selection rules needs somewhat deeper understanding. A qualitative concept of H atom orbitals is taken for granted; antisymmetrized product eigenfunctions are illustrated. On this basis, the following topics are described: LCAO molecular orbitals and their symmetries, MO diagrams, term symbols, Walsh diagrams, the Jahn-Teller effect, hybridization, and crystal field splitting. These are followed by potential curves, then eigenvalues for the anharmonic oscillator, the non-rigid diatomic rotator and for the symmetric top.

In the spectroscopic part, the experimental methods are illustrated with block diagrams; term diagrams and spectra are mostly presented schematically. This part begins with pure rotational spectra, including the Stark effect and rotational Raman spectra. Then follow rotation-vibration spectra, Fortrat diagrams and classification aids for normal vibrations that are not, as such, more closely defined. Typical vibration-rotation structures of the electron bands of diatomic molecules are explained; predissociation, fluorescence, and Rydberg transitions are also mentioned. The following 18 pages deal with line intensities, transition probabilities, occupation numbers, Franck-Condon factors, symmetry selection rules, including hyperfine interactions, line widths and, finally, the laser principle. Alongside UV and X-ray photoelectron spectroscopy, spin-orbit coupling and the Auger effect are touched on and Koopman's theorem is critically illustrated. 12 pages are devoted to electronic spectra in the condensed phase (absorption, fluorescence, phosphorescence). Several types of chromophore are described here and a few empirical rules are stated. ^{1}H-NMR spectroscopy is more extensively handled, with references to temperature effects; solid state NMR spectra, ^{13}C-NMR spectra, Fourier techniques and double resonance methods are mentioned. The work concludes with the electron spin resonance of organic radicals.

The presentation is concise, informative and easily readable. I found no errors of fact. A few exercises are appended to each chapter. A good qualitative survey is given of the methods dealt with. Some important concepts are missing from the subject index, even though they are included in the text. The literature references at the end comprise 15 titles; apart from the three classical volumes by Herzberg, the rest are by British authors.

Friedrich Dörr [NB 728 IE]
Institut für Physikalische und Theoretische Chemie
der Technischen Universität München, Garching (FRG)

Stripping Analysis. Principles, Instrumentation, and Applications. By *J. Wang*. VCH Verlagsgesellschaft, Weinheim 1985. viii, 160 pp., bound, DM 120.00.—ISBN 3-527-26192-3

Voltammetric "Stripping Analysis" (inverse voltammetry) was introduced by *W. Kemula* in the mid 1950's. In spite of strong competition from atomic spectrometry and activation analysis methods it can no longer be dismissed from the arsenal of trace analysis. Not only does it allow, in its various forms, the determination of many elements with a very high power of detection, it also is capable of speciation. A further advantage lies in the fact that, with relatively modest instrumentation, most environmentally relevant elements (e.g. Hg, Cu, Pb, Cd, Bi, Tl, As, Se, Sb, Sn, Ni, Co) can be determined very reliably down to the pg/g region, above all in aquatic and biotic systems. If there are any reservations felt about the rôle of inverse voltammetry in analytical practice, these are certainly not objectively founded. Lacking in adequate information, many people unjustifiably regard electrochemical methods as more difficult and less reliable than, for example, oven-AAS, which is more intensively marketed by powerful manufacturers.

The author has based the book on established monographs (e.g. by *Neeb, Brainina* and *Vydra, Stulik, Julakova*). However, he discusses classical inverse voltammetric methods together with newer developments, e.g. "differential pulse stripping voltammetry", "square wave stripping voltammetry" and "potentiometric stripping analysis", which have enabled considerable improvements with regard to reproducibility and reliability.

All these established electrochemical methods of analysis, in which the actual determination step is preceded by electrolytic enrichment of the element in question, are clearly discussed. Modern types of instrumentation and their applications, above all in the fields of environmental, clinical and foodstuff analysis are included. Some 500 literature references, of which most are very recent, ensure that the work is thoroughly up to date.

Unfortunately, the author was not bold enough to highlight critically the advantages of inverse voltammetry, especially when these are obvious with respect to other possible methods. Admirably, much valuable information has been packed into 150 pages, but the high price will hamper wide circulation. This brief monograph is simply too expensive, especially for the purpose of education in analytically chemistry. Indeed, it may prove very difficult to introduce this work, whose content is very valuable, to those circles where its use would be most appropriate.

Günther Tölg [NB 729 IE]
Institut für Spektrochemie,
Dortmund (FRG)

Analytical Methods in Human Toxicology. Part 1. Edited by *A. S. Curry*. VCH Verlagsgesellschaft, Weinheim 1985. x, 319 pp., hardback, DM 148.00.—ISBN 3-527-26284-9

In the past two decades enormous progress has been made in methods of separation and detection as well as in the qualitative registration of trace substances. This has been of especial value in toxicological practice and research. The field of toxicological investigation is so wide that it can scarcely be straddled by individual toxicologists. In consequence, the current state of knowledge can only be described by a group of experts in the form of a monograph.

In this, the first volume of a two volume monograph, specialists address the following subjects: *N. Morley* describes the detection of medicaments in cell samples, primarily with fluorescence or immunofluorescence methods. The following chapter by *R. J. Flanagan* and *B. Widdop* is concerned with the topic of poisoning through medicament overdoses. *R. J. Metcalfe* deals with the search for

drug receptors with the aid of labelled ligands and discusses "radioreceptor analysis". *J. S. Oliver*'s chapter describes the detection of solvent residues in those prone to solvent abuse. This is followed by *L. V. Jones*' treatment of mass spectrometry. *R. Whelpton* describes the analysis of tricyclic antidepressants and neuroleptics while *G. T. Tucker* and *M. S. Lennard* tackle the analysis of anesthetics. *A. V. Kovatsis* outlines the quantitative recovery of toxic compounds by chelation and subsequent determination of the metals by atomic absorption. In the following chapter *B. S. Thomas* and *E. Bailey* discuss the significance of glass capillary chromatography to toxicology. The final chapter of this volume, by *D. J. Harvey*, is concerned with the investigation of the constituents of hashish.

In my opinion the editor must have made things very easy for himself in compiling this book—he obviously ordered the chapters according to their date of arrival or some equally unfathomable system. How else could chapters on methodology be interspersed with those describing the analysis of particular classes of compounds? This external impression of disorganization is reinforced by the widely differing standard of the individual contributions: while Chapter 10, on cannabinoids, is comprehensive and profound, Chapter 5, on mass spectrometry, is concerned far too much, in my opinion, with the question of construction of the apparatus, surely of secondary importance to the toxicologist, and the crucial question of how and where the technique can be applied to toxicology is only marginally handled. This deficiency is evident in the scanty literature references.

In many of the chapters the specialists concerned to not make the comparative assessment of methods and their applicability which is important for the less experienced researcher. In my view this cannot be compensated for by a list of literature references, however extensive.

A few chapters, above all those on the analysis of individual classes of compounds, fulfil all requirements and expectations. Thanks to them this book is to be regarded as an important reference work for toxicology, in spite of the reservations expressed above.

Gerhard Spiteller [NB 710 IE]
Laboratorium für Organische Chemie
der Universität Bayreuth (FRG)

Superacids. By *G. A. Olah, G. K. S. Prakash,* and *J. Sommer.* Wiley, Chichester 1985. xv, 372 pp., bound, £ 67.00.—ISBN 0-471-88469-3

This is a timely and very useful review of a fascinating and rapidly growing field of chemistry. It deals with acid systems that are stronger than 100% sulfuric acid, i.e. superacid systems, and their applications. The development since the early 1960s of $HFSO_3/SbF_5$ (Magic acid), HF/SbF_5 (fluoroantimonic acid) and related conjugate superacids which are 10^7 to 10^{19} times stronger than sulfuric acid have been truly spectacular. The discovery that stable, long-lived, electron deficient ions, such as carbocations, acidic oxonium ions, halonium ions and halogen cations can be obtained in these highly acidic systems has played an important role in this development in which *G. A. Olah* has been an outstanding leader. This work has provided a detailed insight into the structures and mechanisms of reactions of carbocations.

The superacid systems, which all contain superacid/very weak base pairs, allow the extension of acid catalyzed reactions to include substrates such as extremely weak basic substrates like hydrocarbons (including methane) in which σ-bonds are attacked. Applications of superacids are foreseen to expand in catalysis, synthetic chemistry, as well as in the preparation and study of reactive ionic intermediates.

The first two chapters (60 pages) of the book deal with general aspects including techniques for acidity measurements and the description of superacid systems, i.e. Brønsted superacids, Lewis superacids, conjugate Brønsted-Lewis superacids and solid superacids. Chapter 3 (112 pages) reviews some carbocations including tricoordinated as well as penta- and hexacoordinated and degenerate carbocations. A brief account of the methods and techniques used in the study of carbocations is also given. Heterocations are reviewed in Chapter 4 (66 pages). Ions included are onium ions, enium ions, homo- and heteropolycations and miscellaneous cations like $H_3^{\oplus}$. The last chapter (101 pages) is devoted to superacid catalyzed reactions: conversion of saturated hydrocarbons, alkylation of aromatic hydrocarbons, alkylation of aromatics, carboxylation, formylation, nitration, oxyfunctionalization, polymerization etc. Friedel-Crafts systems are not treated in the present book since they have already been reviewed.

Altogether, the chapters contain more than one thousand references to original publications. The overall impression of the authors' presentation is favorable despite some misreferencing, errors in structural formulas, misprints and that IUPAC-nomenclature is not strictly obeyed.

It is clear that the book will be most useful not only to the specialists but also to other chemists that want to enter the field or make use of superacids. Therefore, the book is strongly recommended and is expected to find a place on the book shelves of a large number of chemists as well as in the majority of the chemistry libraries.

Per Ahlberg [NB 745 IE]
Department of Organic Chemistry
University of Göteborg (Sweden)

Registered names, trademarks, etc. used in this journal, even without specific indication thereof, are not to be considered unprotected by law.

© VCH Verlagsgesellschaft mbH, D-6940 Weinheim, 1986. - Printed in the Federal Republic of Germany by Zechnersche Buchdruckerei, Speyer/Rhein.

All rights reserved (including those of translation into foreign languages). No part of this issue may be be reproduced in any form - by photoprint, microfilm, or any other means - nor transmitted or translated into a machine language without written permission from the publishers. Only single copies of contributions, or parts thereof, may be reproduced for personal use.

Valid for users in the USA: The appearance of the code at the bottom of the first page of an article in this journal (serial) indicates the copyright owner's consent that copies of the article may be made for personal or internal use, or for the personal or internal use of specific clients. This consent is given on the condition, however, that the copier pay the stated per-copy fee through the Copyright Clearance Center, Inc., for copying beyond that permitted by Sections 107 or 108 of the U.S. Copyright Law. This consent does not extend to other kinds of copying, such as copying for general distribution, for advertising or promotional purposes, for creating new collective works, or for resale. For copying from back volumes of this journal see 'Permissions to Photo-Copy: Publisher's Fee List' of the CCC.

Editorial office: Pappelallee 3, D-6940 Weinheim, Federal Republic of Germany, Telephone (06201) 602315, Telex 465516 vchwh d, Telefax (06201) 602328.

Editor: *P. Gölitz.*

Associate editors: *D. J. Loewus, A. Stimson.* **Editorial assistant:** *E. Schweikart*

Publishers: VCH Verlagsgesellschaft mbH. (Managing Directors: *Prof. Dr. Helmut Grünewald* and *Hans Dirk Köhler*), Pappelallee 3, D-6940 Weinheim, Federal Republic of Germany. Correspondence concerning advertisements should be addressed to VCH Verlagsgesellschaft mbH. (Advertising Manager *R. J. Roth*), Boschstr. 12, P.O. Box 1260/1280, D-6940 Weinheim, Federal Republic of Germany, Telephone Weinheim (06201) 602-0, Telex 465516 vchwh d, Telefax (06201) 602328.

ANGEWANDTE CHEMIE
International Edition in English
Volume 25 · Number 6
June 1983
Pages 487–582

Second-Sphere Coordination—a Novel Rôle for Molecular Receptors

By Howard M. Colquhoun, J. Fraser Stoddart,* and David J. Williams

Although it has been appreciated for most of this century that the coordinating influence of many transition metal complexes extends beyond their covalently-bonded first-sphere ligands to non-covalently bound chemical species in the so-called second-sphere, it is only recently that the fundamental importance of the phenomenon has been recognized and researched in its most general context. Rapid progress has been possible in this relatively new area of supramolecular chemistry by appealing to the symbiotic relationship that exists between X-ray crystallographic investigations and synthetic work. The gamut of non-covalent bonds, including electrostatic forces, hydrogen bonding, charge transfer, and van der Waals interactions are available for exploitation in choosing or designing suitable molecular receptors for particular transition metal complexes. Crown ethers are the synthetic macrocycles *par excellence* for forming adducts with neutral and cationic complexes carrying protic ligands (NH_3, H_2O, CH_3CN, etc.) in their first coordination spheres. Anionic complexes with electron-rich first-sphere ligands (e.g. $CN^{\ominus}$) form adducts with polyammonium macrocyclic receptors. In both situations, hydrogen bonds and electrostatic interactions provide the dominant sources of supramolecular stabilization. Spectroscopic studies (UV, IR, and NMR) reveal that the structural integrity of the adducts is usually maintained in solution. The transition metal complexes can be organometallic as well as inorganic. In complexes supporting organic ligands, such as 1,5-cyclooctadiene, norbornadiene, cyclopentadiene, 2,2′-bipyridine, and trimethylphosphane, the opportunity exists to match their steric and electronic characteristics with appropriate binding sites in the molecular receptor. With these ligands, the weaker categories of non-covalent bonding, e.g. charge transfer and van der Waals interactions, assume considerable importance. The phenomenon is also observable with naturally-occurring receptors such as the cyclodextrins and polyether antibiotics. Moreover, it extends beyond the territory of transition metal complexes to main group complexes such as ammonia-borane. As far as applications are concerned, it finds expression in areas as diverse as separation science and drug delivery systems.

[*] Dr. J. F. Stoddart
Department of Chemistry, The University
Sheffield S3 7HF (England)
Dr. H. M. Colquhoun
New Science Group, Imperial Chemical Industries PLC
The Heath, Runcorn WA7 4QE (England)
Dr. D. J. Williams
Chemical Crystallography Laboratory
Department of Chemistry, Imperial College
London SW7 2AY (England)

1. Introduction

With the greater awareness amongst contemporary chemists of the importance of the non-covalent bond in chemistry, the opportunity exists to examine old concepts in new contexts. One concept, which has been around since almost the turn of the century, relates to the ability of transition metal complexes to confer some degree of struc-

 © VCH Verlagsgesellschaft mbH, D-6940 Weinheim, 1986 0570-0833/86/0606-0487 $ 02.50/0

tural order beyond the first sphere of ligands directly coordinated to the metal. These marshalling influences, which invariably involve weak intermolecular interactions, are usually referred to under the umbrella of second-sphere coordination.[1] More recently, the rapidly expanding availability[2] of a wide range of low molecular weight molecular receptors, both natural[3] and synthetic,[4] has provided the potential for a range of interdisciplinary discoveries to be realized.[5] Although much of the story that follows has unfolded in our midst during the last five years, some advances of relevance to the theme of this tale happened in other places at different times. Presently, we reflect on our observations and experiences against the backcloth of historical and present-day activities that characterize this fascinating corner of chemical science.

The color code which has been employed in illustrating the X-ray crystal structures is as follows:

H (white)	B (green)	C	(grey)
N (blue)	O (red)	F	(green)
P (pink)	Cl (green)	All metals	(yellow)

The identity of the atoms in green is clear from their context in the structures.

2. Historical Background

The idea that ligands in the primary coordination sphere of a transition metal complex can interact in an ordered manner with neutral molecules or charged species to give a second-sphere or outer-sphere complex was first advanced by *Alfred Werner*[6] in 1912. He found the concept necessary in order to explain[7] a number of phenomena, which included (i) the formation of addition compounds between amines and coordinatively-saturated trisacetylacetonato complexes, (ii) the presence of solvents (e.g. H_2O) of so-called crystallization in complexes, such as $[Co(en)_3 \cdot 3H_2O][Cl]_3$, where $en = H_2NCH_2CH_2NH_2$, and (iii) the observation that the molar optical rotations of chiral complexes depend strongly on the nature of the solvents and the counterion, if present. Understandably, however, the nature of the forces involved in solvation were not at all well-understood at that stage.

Since *Werner*'s original proposal, however, developments in optical, spectroscopic, crystallographic, and theoretical techniques have revealed a very wide range of other phenomena which can only be accounted for on the basis of second-sphere coordination either in the solid state or in solution, or indeed, in both. The forces responsible include the whole range of non-covalent interactions, i.e. hydrogen bonding—probably the single most important stabilizing interaction in second-sphere coordination chemistry, polar and dipolar attractions, dispersion forces, and charge-transfer interactions.

An early observation (1931) in the field of transition metal chemistry, which is now attributable to second-sphere coordination, is the so-called Pfeiffer effect.[8] One manifestation[9] of this effect is the ability of an optically-inactive transition metal complex—either achiral or a racemic modification—to display circular dichroism of one or more electronic transitions ($d \rightarrow d$), when it is dissolved in a medium containing an optically-active *environment* species, capable of interacting with its first-sphere ligands. Although the effect is independent of time for achiral and optically-stable racemic transition metal complexes, it is overlaid by an additional time-dependent change when an optically-labile transition metal complex is employed. This latter phenomenon is a result of the preferential second-sphere coordination of the *environment* species to *one* of the two enantiomeric complexes. In an optically-labile system, this second-sphere perturbation can disturb the enantiomeric equilibrium, shifting it away from its original 1 : 1 position to produce a slow increase in optical activity, a phenomenon which is generally referred to[9] as *anti-racemization*.

Although chiroptical methods are extremely sensitive tools for investigating second-sphere coordination by transition metal complexes, probing the phenomenon with other techniques, such as electronic and vibrational spectroscopes, has also proved to be very informative. Electronic spectroscopy provides[10] a straightforward method of distinguishing between second-sphere coordination and ligand-exchange. Thus, whereas the positions and/or intensities of charge-transfer bands are strongly affected by changes in both the first and second coordination spheres, *d-d* absorptions are normally shifted only by addition or exchange of ligands in the primary sphere. Vibrational spectroscopy has been employed by *Chatt* et al.[11,12] to detect hydrogen bonding associated with first-sphere coordinated ligands, both directly by the effect[11] on N-H stretching and deformation modes, and indirectly, by the effect[12] on co-ligand frequencies such as $\tilde{\nu}(C{\equiv}O)$ and $\tilde{\nu}(N{\equiv}N)$.

Kinetic data often indicate[13] the occurrence of second-sphere coordination in solution. In particular, the rates of certain anation reactions are found to be independent of anion concentration over a very wide range, suggesting rapid and extensive ion-pairing to give [Equation (1)] a second-sphere complex which is presumably stabilized by hydrogen bonding. This species can then undergo [Equation (2)] slow intramolecular rearrangement with loss of an aqua ligand.

$$[Co(NH_3)_5(H_2O)]^{3\oplus} + [SO_4]^{2\ominus} \overset{\text{fast}}{\rightleftharpoons} [\{Co(NH_3)_5(H_2O)\}\{SO_4\}]^{\oplus} \quad \ldots(1)$$

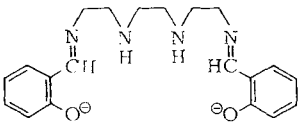
$$[\{Co(NH_3)_5(H_2O)\}\{SO_4\}]^{\oplus} \xrightarrow{\text{slow}} [Co(NH_3)_5(SO_4)]^{\oplus} + H_2O \ldots \quad (2)$$

Nuclear magnetic resonance spectroscopy has been employed extensively in the study of second-sphere coordination of transition metal complexes, particularly by *Nekipelov* et al.[14] Their investigations have depended heavily on ^{1}H-NMR spectroscopic measurements in solutions containing neutral, *paramagnetic*, transition metal complexes, since variations in chemical shifts and relaxation rates of solvent molecules in the second-sphere are then large enough to be measured reliably. Second-sphere stability constants, lifetimes, coordination numbers, and possible geometries have been estimated using this technique. However, as these results have been reviewed[14] recently in some detail, they will not be discussed further here.

An alternative ^{1}H-NMR spectroscopic technique uses the well-known aromatic-solvent-shift effect. This shift to

lower frequencies (i.e. to high field) of resonances associated with protons located within the aromatic ring-current shielding zone of solvating arene molecules has been used—to cite but one example—to study[15] the orientation of solvating benzene molecules with respect to the diamagnetic zinc complex, $[Zn(Me_2NCH_2CH_2NMe_2)Cl_2]$. It has also proved to be an extremely valuable tool in our investigations (see Sections 4 and 5) of second-sphere coordination by macrocyclic polyethers containing fused aromatic rings.

Second-sphere coordination has recently been shown[16] to have significant influence on the position of the high-spin/low-spin equilibrium for the complex, $[Fe(sal)_2(trien)]^{\oplus}$, and some related species. In the solid state, the equilibrium position is strongly dependent on the nature of the counterion and on the presence of solvents of crystallization which can hydrogen bond to the two NH groups of the hexadentate ligand, $[(sal)_2(trien)]$. In solution, the nature of the solvent influences the position of the spin-equilibrium in similar fashion. Low-spin is favored increasingly as the hydrogen bonding (electron donor) character of the solvent increases.



$(sal)_2(trien)$

In the past, second-sphere coordination has often been regarded simply as an aspect of solvation. Thus, it is relevant at this point to note that a *host*—or *receptor molecule*—has been *defined*[17] as one which provides "an assembly of solvation sites, tied together by covalent bonds". We therefore posed[5] the question: can we use molecular receptors to provide an insight into the nature of second-sphere coordination by studying their interactions with transition metal complexes, both in solution and in the solid state?

3. 3*n*C*n*-Type Crown Ethers as Receptors in the Second-Sphere

3.1. Adduct Formation involving Ammine Ligands

Macrocyclic polyethers such as [18]crown-6 (18C6) have long been known[18] to form[4,17-22] discrete hydrogen bonded complexes with primary alkylammonium ions, $[RNH_3]^{\oplus}$. It was the recognition[5] of a simple geometric and electronic analogy between an $[RNH_3]^{\oplus}$ ion and a transition metal ammine complex, $[ML_x(NH_3)]^{n\oplus}$, which led to our initial investigation of crown ether receptor molecules as second-sphere ligands. However, before discussing the interactions of $[ML_x(NH_3)]^{n\oplus}$ complexes with 18C6, we shall comment briefly on the binding of some complexes of main-group compounds by 18C6.

The borane complexes, $[BX_3NH_3]$ (X = H or halogen), are amongst the very simplest ammine complexes. In fact, $[BH_3NH_3]$ is strictly isoelectronic with the methylammonium ion, $[CH_3NH_3]^{\oplus}$. It follows that, just as $[CH_3NH_3][ClO_4]$ forms[23] a crystalline 1:1 complex with 18C6, so $[BH_3NH_3]$ affords[24] a well-defined crystalline 1:1 adduct[25] with 18C6. X-ray crystallographic studies reveal[23,24] the existence of a close structural relationship between the adduct and the complex—and, for that matter, most of the closely related $[RNH_3 \cdot 18C6][X]$ complexes.[26] In both cases, the 18C6 ring adopts an all-*gauche* conformation with pseudo D_{3d} symmetry, which is quite different from that found[27] in its free state. Figure 1 shows the X-ray structures of free 18C6,[27] of $[CH_3NH_3 \cdot 18C6]^{\oplus}$ as its $ClO_4^{\ominus}$ salt,[23] and of $[BF_3NH_3 \cdot 18C6]$ as its CH_2Cl_2 solvate.[24] In both $[CH_3NH_3 \cdot 18C6]^{\oplus}$ and $[BF_3NH_3 \cdot 18C6]$, three strong N-H···O hydrogen bonds ($[N \cdots O] \leqq 2.95$ Å) link the $NH_3^{\oplus}$ center to the alternate oxygen atoms in the 18C6 ring which are closer to the $NH_3^{\oplus}$ group. This geometry corresponds to the so-called[23] perching mode of binding.

The first adducts of transition metal complexes with 18C6 to be investigated[28,29] by X-ray crystallography involved the neutral ammine-platinum(II) complexes, [*trans*-$Pt(PR_3)Cl_2(NH_3)$] (R = Me or Et).[30] Unlike the ammineboranes, however, the platinum complexes form adducts with 18C6 in which both faces of the macrocycle are involved simultaneously in binding to the ammine ligands.

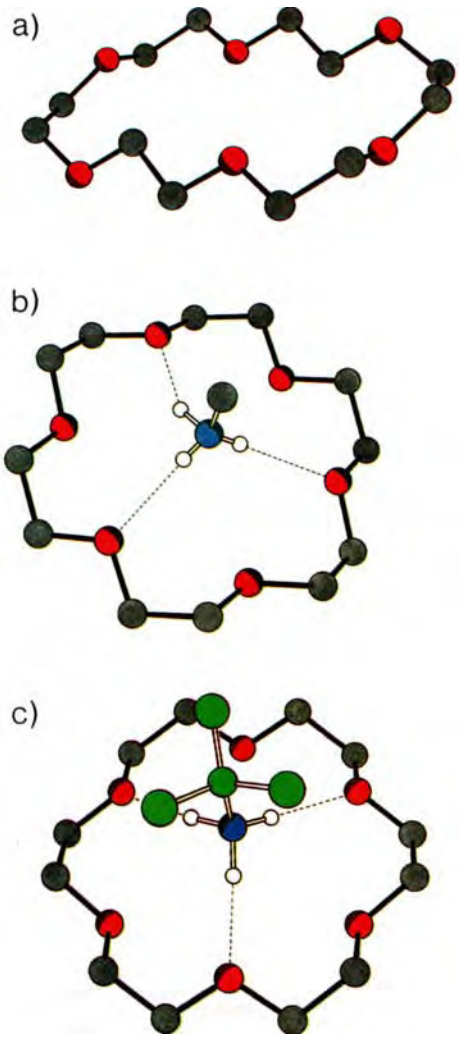


Fig. 1. Skeletal representations of the X-ray structures of (a) 18C6, (b) $[CH_3NH_3 \cdot 18C6]^{\oplus}$ ($ClO_4^{\ominus}$-salt), and (c) $[BF_3NH_3 \cdot 18C6]$ (CH_2Cl_2-solvate).

This phenomenon results in the crystallization of adducts having 2 : 1 (complex: 18C6) stoichiometry, even from solutions containing equimolar amounts of the transition metal complex and 18C6. As revealed[28,29] by the X-ray structure of [{*trans*-$Pt(PMe_3)Cl_2(NH_3)$}$_2$ · 18C6] (Fig. 2), the macrocycle still retains the familiar all-*gauche* conformation, characteristic[23,24,26] of $[RNH_3]^{\oplus}$ and $[BX_3NH_3]$ binding to 18C6. However, all six oxygen atoms in 18C6 are hydrogen bonded in approximately trigonal fashion via perching modes to the two NH_3 ligands on the neutral platinum complex. The [N···O] distances of the N-H···O hydrogen bonds (3.31, 3.21, and 3.04 Å) are significantly longer—by up to 0.4 Å—than in [BF_3NH_3 · 18C6]. Indeed, it will become increasingly apparent that long hydrogen bonds (3.0–3.4 Å) are a feature of many second-sphere complexes involving ammine-metal complexes and crown ethers.

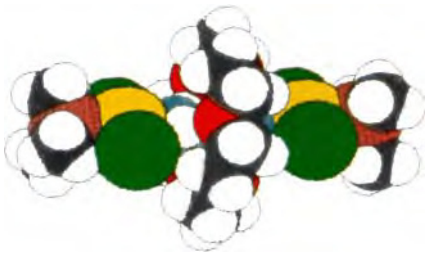


Fig. 2. Space-filling representation of the X-ray structure of [{*trans*-$Pt(PMe_3)Cl_2(NH_3)$}$_2$ · 18C6].

Although the factors favoring crystallization of either a 1 : 1 or 2 : 1 complex or adduct from a solution initially of 1 : 1 stoichiometry are not yet fully understood, it seems reasonable to expect that two $[RNH_3]^{\oplus}$ ions, in which the NH_3 groups carry essentially localized positive charges, should tend to repel one another as they approach each other from opposite faces of 18C6. This simple explanation accounts for the observed preference for discrete 1 : 1 stoichiometry. Conversely, a pair of *neutral* transition metal complexes with ligating ammonia [$M \leftarrow NH_3^{\delta\oplus}$] can obviously approach[31] within hydrogen bonding distances of each face of 18C6. Moreover, although 18C6 has an unfavorable conformation[27] for adduct formation in its free state, the unused face of a 1 : 1 adduct with its preorganized all-*gauche* conformation could provide an energetically-preferred binding site leading to adducts with the observed 2 : 1 stoichiometry. Alternatively, adduct solubilities and/or crystal packing forces may be more significant in dictating stoichiometries in the solid state.

The potential bireceptor nature of 18C6 suggested[28,29] that interaction with *trans*-diammines should generate a novel type of linear hydrogen bonded polymer. Indeed, this is so. On mixing dimethylformamide (DMF) solutions of 18C6 and [*trans*-$Pt(NH_3)_2Cl_2$], a highly insoluble 1 : 1 adduct is precipitated instantly. This material can only be dissolved in dipolar aprotic solvents (e.g. DMF) at high temperatures (e.g. 120 °C). Although crystallographic confirmation of the structure is not available because of crystal-twinning, the stoichiometry and extreme insolubility of the adduct strongly support a polymeric superstructure as indicated diagrammatically in Figure 3.

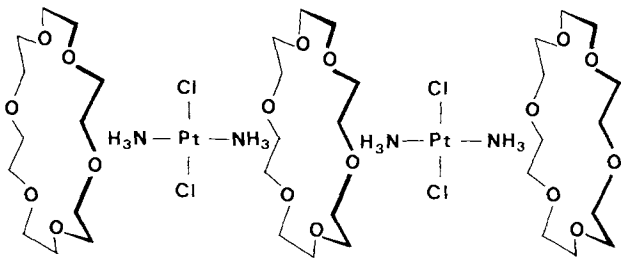


Fig. 3. Diagrammatic representation of the proposed structure of [*trans*-$Pt(NH_3)_2Cl_2$ · 18C6]$_n$.

In contrast, the isomer [*cis*-$Pt(NH_3)_2Cl_2$], the antitumor drug[32] Cisplatin, interacts with 18C6 in dimethylacetamide (DMA) to give[33] a soluble 2 : 1 adduct with a structure (Fig. 4) very similar to that described for [{*trans*-$Pt(PMe_3)Cl_2(NH_3)$}$_2$ · 18C6]. Again, both faces of 18C6 are involved in binding but, this time, the ammine ligands on platinum, which are oriented *cis* to those hydrogen-bonded in the normal trigonal manner to each face of 18C6, form additional N-H···O hydrogen bonds ([N···O] = 3.11 Å), also to each face. This additional hydrogen bonding tilts each complex with respect to the mean plane of the 18C6 macrocycle so that the Pt-N vectors of the two triply hydrogen bonded ammine ligands are no longer collinear nor, for that matter, orthogonal to the mean plane. The remaining ammine hydrogen atoms in this structure (Fig. 4) are, in fact, also involved in hydrogen bonds—one symmetry-related pair to solvating DMA molecules and the other pair to chlorine ligands in adjacent Cisplatin molecules.

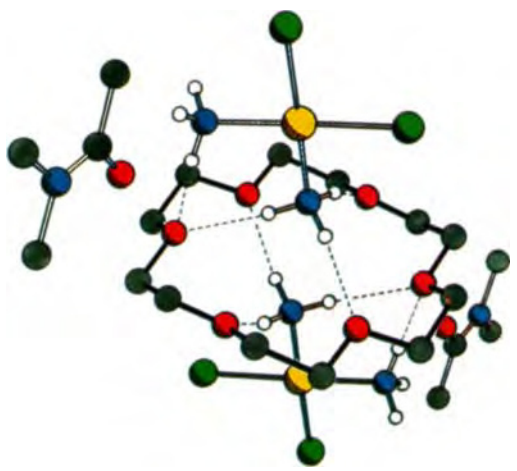


Fig. 4. Skeletal representation of the X-ray structure of [{*cis*-$Pt(NH_3)_2Cl_2$ · dma}$_2$ · 18C6].

A further increase in structural complexity is observed[29,34] when 18C6 interacts with the dicationic copper(II) complex, $[Cu(NH_3)_4(H_2O)]^{2\oplus}$ as its $PF_6^{\ominus}$-salt. The resulting polymeric 1 : 1 adduct crystallizes readily from aqueous solution, and an X-ray structural investigation (Fig. 5 and 6) has shown that the hydrogen bonding may be regarded as an extension of that already described above for [{*cis*-$Pt(NH_3)_2Cl_2$}$_2$ · 18C6]. Thus, each macrocycle not only interacts with two ammine ligands (one on each face) employing the normal three-point binding mode, but it also

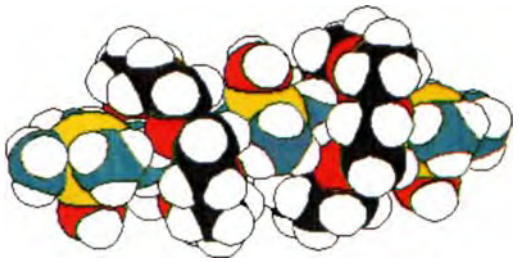


Fig. 5. Space-filling representation of the X-ray structure of $[Cu(NH_3)_4(H_2O)\cdot 18C6]_n^{2n\oplus}$.

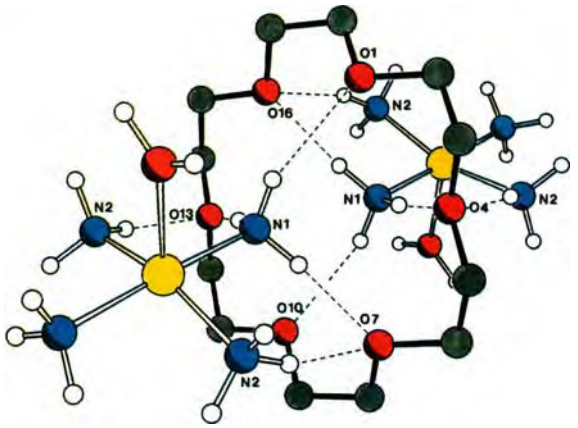


Fig. 6. Skeletal representation of the X-ray structure of $[Cu(NH_3)_4(H_2O)\cdot 18C6]_n^{2n\oplus}$ showing the hydrogen bonding pattern associated with an 18C6 ring.

forms single hydrogen bonds (two to each face) to ammine ligands which are oriented *cis* to the triply hydrogen bonded ammine ligands. The hydrogen bond distances are again relatively long (3.06–3.28 Å) and each macrocycle is involved in no fewer than ten hydrogen bonds. Oxygen atoms O1 and O10 each form one hydrogen bond with approximately trigonal approach geometry while O4, O7, O13, and O16 each accept two hydrogen bonds, one from N1 with approximately trigonal approach geometry, and the other from N2 with approximately tetrahedral approach geometry. The aqua ligand does not interact with 18C6 but it may hydrogen bond weakly to a $PF_6^{\ominus}$ counterion.

Clearly, simple metal complexes containing ammine ligands possess a strong affinity for 18C6. The examples of adduct formation quoted in this Section could probably be expanded upon almost indefinitely. However, given the limited range of hydrogen bonding patterns already established, it seems unlikely that many new binding modes will be uncovered for this particular class of adduct. For example, one might predict that the crystalline 1:1 adduct formed[35] between $[Pt(bpy)(NH_3)_2][PF_6]_2$ (bpy = 2,2′-bipyridyl) and 18C6, which has not yet been structurally characterized, will have a four-point binding pattern (Fig. 7) similar to that found in $[\{cis\text{-}Pt(NH_3)_2Cl_2\}_2\cdot 18C6]$.

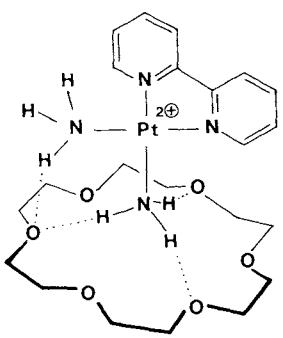


Fig. 7. Diagrammatic representation of the proposed structure of $[Pt(bpy)(NH_3)_2\cdot 18C6]^{2\oplus}$.

The opportunity remains (i) to alter the nature of the monodentate ammine ligands (e.g. to RNH_2 or R_2NH) and (ii) to examine a range (say n = 4, 5, 7, 8, etc.) of 3*n*C*n* crown ethers as potential second-sphere ligands. So far, we have not pursued these possibilities. However, we have examined[29,36] the ability of $[Pt(en)_2][PF_6]_2$, containing a bidentate diamino ligand ($en = H_2NCH_2CH_2NH_2$), to interact with 18C6 in aqueous solution. A colorless crystalline 1:1 adduct is formed and X-ray crystallography reveals (Fig. 8) a polymeric structure in which only one hydrogen atom of each NH_2 group and only four crown ether oxygen atoms are involved in hydrogen bonding. There are also weak interactions between the en ligands and $PF_6^{\ominus}$ counterions.

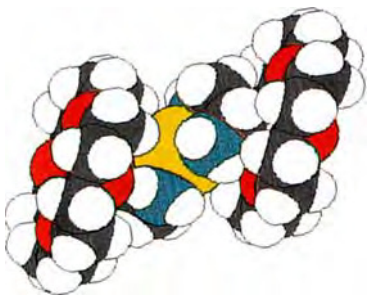


Fig. 8. Space-filling representation of the X-ray structure of $[Pt(en)_2\cdot 18C6]_n^{2n\oplus}$.

3.2. Adduct Formation involving Aqua Ligands

Just as ammine ligands on transition metals are activated towards second-sphere coordination of crown ethers, so aqua ligands coordinated to electropositive metals $[M{\leftarrow}OH_2^{\delta\oplus}]$ show an enhanced dipole and increased acidity. This phenomenon finds expression in the numerous crystalline adducts that have been isolated[37–44] between 18C6, other 3*n*C*n* crown ethers (e.g. 12C4 and 15C5)—as well as benzo[15]crown-5 and dibenzo[18]crown-6—and

Table 1. Some aqua complexes for which X-ray crystal data are available in the literature.

Structure	Repeating Polymeric Unit	Ref.
1	$[UO_2(NO_3)_2(H_2O)_2\cdot 18C6][H_2O]_2$	[37]
2	$[UO_2(NO_3)_2(H_2O)_2\cdot 18C6]$ [a]	[38]
3	$[Mn(NO_3)(H_2O)_5\cdot 18C6][NO_3][H_2O]$	[39]
4	$[Mn(H_2O)_6\cdot 18C6][ClO_4]$	[40]
5	$[Co(H_2O)_6\cdot 18C6][CoCl_4]$ [b]	[41]
6	$[U(SCN)_4(H_2O)_4\cdot(18C6)_{1.5}][H_2O]_3$ [c]	[42]
7	$[SnCl_4(H_2O)_2\cdot 18C6][H_2O]_2$ [d, e]	[43]
8	$[\{SnMe_2Cl_2(H_2O)\}_2\cdot 18C6]$	[44]

[a] Structural studies supported by infrared (IR) and ^{1}H-NMR spectroscopic data. [b] Me_2CO solvate. [c] Solvated with methyl isobutyl ketone. [d] $CHCl_3$ solvate. [e] The structure and bonding in this adduct and related adducts are discussed in terms of IR and ^{119}Sn-Mössbauer spectroscopic data.

aqua complexes of $U^{VI}O_2$, Mn^{III}, Co^{II}, Th^{IV}, U^{IV}, Sn^{IV}, etc. Although the characterization (Table 1) by X-ray crystallography of many of these polymeric adducts preceded our own investigations on transition metal ammines, there did not appear to be any widespread recognition of the generality of the phenomenon. The 18C6 rings in all the structures, except **8** listed in Table 1, adopt the normal all-*gauche* conformations with pseudo D_{3d} symmetry. With the exception of structure **7**, *trans*-aqua ligands are invariably hydrogen bonded to the macrocyclic ring faces to afford linear polymeric arrays of alternating metal complex and 18C6 macrocycle. An example (Structure **4**) is illustrated in Figure 9. Structure **7** (Fig. 10) is unique insofar as, although the H_2O molecules within the octahedral $[SnCl_4(H_2O)_2)]$ units are *cis* to each other, they still support a hydrogen bonded polymeric structure by involving non-coordinated H_2O molecules bound to each face of the 18C6 rings.



Fig. 9. Skeletal representation of the X-ray structure of $[Mn(H_2O)_6 \cdot 18C6]_n^{n\oplus}$ ($ClO_4^{\ominus}$ salt) **4**.

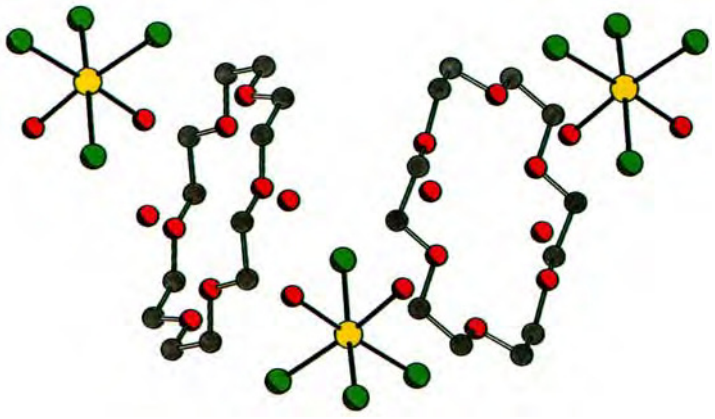


Fig. 10. Skeletal representation of the X-ray structure of $[SnCl_4(H_2O)_2 \cdot 18C6][H_2O]_2$ **7**.

3.3. Adduct Formation involving Other Ligands

In addition to NH- and OH-acidic species, CH-acidic organic compounds form[31] crystalline complexes with 18C6. Since 18C6 is readily purified[45] as such a complex with CH_3CN, we reasoned that coordination of acetonitrile $[M \leftarrow N \equiv C - CH_3]$ to a transition metal should render the CH_3 group more acidic and hence more prone to hydrogen bonding with 18C6. Indeed, in marked contrast to [*trans*-$Ir(CO)(NH_3)(PPh_3)_2][PF_6]$ where the ammine ligand is sterically quite inaccessible to 18C6, [*trans*-$Ir(CO)(CH_3CN)(PPh_3)_2][PF_6]$ forms[46] a crystalline 2:1

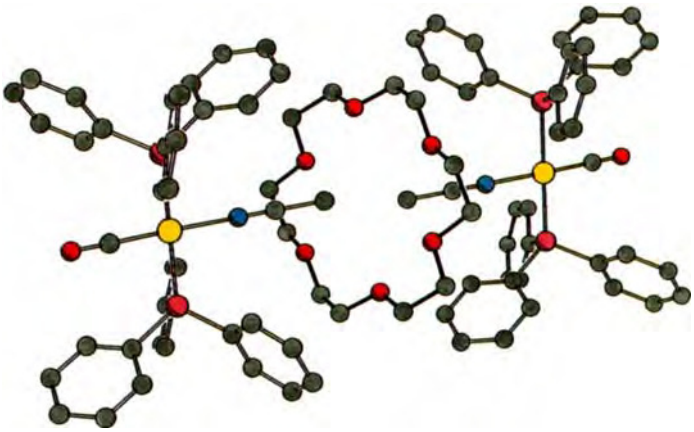


Fig. 11. Skeletal representation of the X-ray structure of $[\{trans\text{-}Ir(CO)(CH_3CN)(PPh_3)_2\}_2 \cdot 18C6]^{2\oplus}$.

complex with 18C6. X-ray crystallography has revealed (Fig. 11) the anticipated structure, with C–H···O hydrogen bonds ([C···O] = 3.24, 3.26, and 3.38 Å) between the more elongated CH_3CN ligands and the macrocycle in its ubiquitous conformation. Addition of excess of NaCl to equivalent amounts of $[Ir(CO)(CH_3CN)(PPh_3)_2][PF_6]$ and 18C6 in CH_2Cl_2 gave exclusively $[Ir(CO)(PPh_3)_2Cl]$. This promotion of the displacement of CH_3CN by $Cl^{\ominus}$ ion is reminiscent of a situation which exists in the reaction[47] of [*trans*-$Co(en)_2(CH_3CN)(NO_2)][ClO_4]_2$ with D_2O at pD 4.4 in the presence of either 18C6 or 15C5, where the small observed rate enhancements have been ascribed to adduct formation between the crown ether and the acidic CH_3 group of the CH_3CN ligand. However, it should be pointed out that the crown ethers will probably interact more strongly by N–H···O hydrogen bonding to the en ligands in this Co complex. Spectroscopic evidence also indicates interactions between CH_3CN ligands and crown ethers. Copper iodide reacts[48] in acetonitrile solution with dibenzo[18]crown-6 to form a crystalline adduct $[(CuI)_4(CH_3CN)_4 \cdot DB18C6]$: the luminescence spectrum of the adduct is red shifted, indicating some interaction between the crown ether and the acetonitrile copper iodide.

It is obvious that second-sphere coordination of transition metal complexes by 3*n*C*n* crown ethers could involve an extensive range of first-sphere ligands [e.g. PH_3, $CS(NH_2)_2$, $(H_2NCS)_2$, $H_2NCS_2^{\ominus}$, $CH_3N^{\oplus} \equiv C^{\ominus}$, CH_3, and even H] which are potentially able to enter into hydrogen bonding because of their acidic character.

4. Dibenzo Crown Ethers of Type DB3*n*C*n* as Receptors in the Second-Sphere

4.1. Adduct Formation involving Monoammine-Transition Metal Complexes

Our first evidence for interactions between crown ethers and ammine-metal complexes in solution was pro-

vided[5,29] by the shift to lower frequency of the two $\tilde{\nu}$(C≡O) bands in the IR spectrum of $[Fe(\eta^5\text{-}C_5H_5)(CO)_2(NH_3)]^{\oplus}$ when a molar equivalent of dibenzo[18]crown-6 (DB18C6) was added to a solution of the complex as its $BPh_4^{\ominus}$ salt in dichloromethane. This shift was not observed for $[Fe(\eta^5\text{-}C_5H_5)(CO)_2(C_5H_5N)][PF_6]$, thus confirming that hydrogen bonding to the ammine ligand was responsible for the carbonyl frequency shift. Since hydrogen bonding involves a net donation of charge to the metal complex, this change in frequency clearly reflects increased d→(C≡O)π* electron transfer as a result of the increased density at the metal center.

Although dynamic ^{1}H-NMR spectroscopic studies indicate an activation free energy of ca. 45 kJ mol^{-1} for dissociation of $[Fe(\eta^5\text{-}C_5H_5)(CO)_2(NH_3)\cdot DB18C6][BPh_4]$, no crystalline adduct could be isolated from solution. However, the neutral monoammines, [*trans*-$Pt(PR_3)Cl_2(NH_3)$]



Fig. 12. Space-filling representation of the X-ray structure of [*trans*-$Pt(PMe_3)Cl_2(NH_3)\cdot DB18C6$].

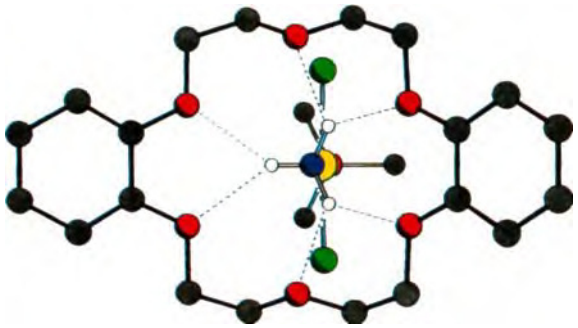
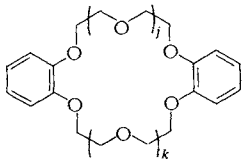


Fig. 13. Skeletal representation of the X-ray structure of [*trans*-$Pt(PMe_3)Cl_2(NH_3)\cdot DB18C6$] showing the three bifurcated hydrogen bonds.

(R = Me or Et) and $[W(CO)_5(NH_3)]$ do yield isolable 1:1 adducts with DB18C6. The tungsten derivative has been characterized spectroscopically (IR and $^{13}C\{^1H\}$-NMR) and the platinum derivative (with R = Me) crystallographically (Fig. 12 and 13). The benzene rings on the macrocycle in [*trans*-$Pt(PMe_3)Cl_2(NH_3)\cdot DB18C6$] are folded *away* from the Pt–N vector and the six oxygen atoms form three bifurcated hydrogen bonds to the ammine ligand (Fig. 13). The directions of approach of the hydrogen bonds result in approximately trigonal geometries at the aryl oxygen atoms, whereas the aliphatic oxygen atoms enter into essentially orthogonal hydrogen bonding interactions. Variable temperature ^{1}H-NMR spectroscopy in CD_2Cl_2 solution indicates a dissociation free energy of 33 kJ mol^{-1} for this neutral second-sphere adduct, i.e. it is a considerably weaker adduct than that formed in solution by the cationic iron derivative.

4.2. Adduct Formation involving Rhodium Complexes

Virtually all the results described so far in this review were obtained using commercially-available crown ethers with a ring size of 18 atoms or less. However, when a transition metal complex contains more than one protic ligand, larger macrocyclic polyethers with 21- to 36-membered rings become attractive second-sphere ligands, since one can envisage several ammine ligands, for example, being bound simultaneously within the extended cavities provided by the larger ring sizes. The dibenzo[3n]crown-n (DB3*n*C*n*) ethers (n = 6–12) are especially attractive candidates[49] for investigation as they are reasonably straightforward to synthesize and, moreover, have the potential for inducing aromatic ring-current shifts in the ^{1}H-NMR resonances of transition metal complexes containing organic ligands, thus providing a sensitive means of probing the stereochemical aspects of second-sphere coordination in solution.



DB3*n*C*n*	*n*	*j*	*k*
DB18C6	6	1	1
DB21C7	7	2	1
DB24C8	8	2	2
DB27C9	9	3	2
DB30C10	10	3	3
DB33C11	11	4	3
DB36C12	12	4	4

The cationic rhodium(I) complexes $[Rh(cod)(NH_3)_2]^{\oplus}$ (cod = 1,5-cyclooctadiene) and $[Rh(nbd)(NH_3)_2]^{\oplus}$ (nbd = norbornadiene) have been extensively studied by us[50] in this stereochemical context since they provide (i) a pair of *cis*-ammine ligands for hydrogen bond participation and (ii) an organic ligand with three sets of protons in heterotopic environments (Fig. 14). Any ring current shifts in-

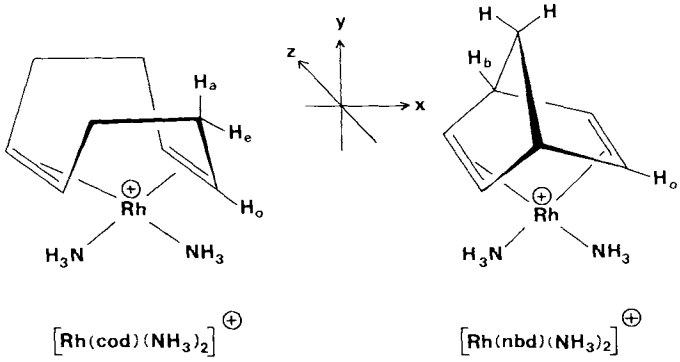


Fig. 14. Structural formulas of $[Rh(cod)(NH_3)_2]^{\oplus}$ and $[Rh(nbd)(NH_3)_2]^{\oplus}$

duced by a molecular receptor can therefore be related to the position of the shielding arene units relative to the heterotopic protons on the organic ligands.

The organometallic cations are readily isolated from aqueous solution as crystalline hexafluorophosphates. Both salts are insoluble in hydrocarbon and halocarbon solvents but dissolve freely in halocarbons on addition of crown ethers such as 18C6 or DB3*n*C*n* ($n=6$–12). The ^{1}H-NMR spectra of the complexes in CD_2Cl_2 solutions containing equimolar amounts of certain of the DB3*n*C*n* ethers—especially DB21C7 and DB24C8—show dramatic upfield shifts of the diene resonances relative to their positions when 18C6 is used as the solubilizing agent. The chemical shift data for both the cod and nbd complexes are summarized in Figure 15. It shows that the most dramatic

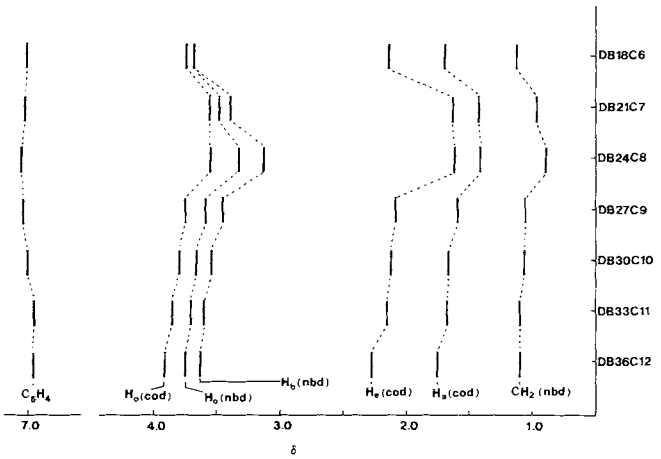


Fig. 15. The partial ^{1}H-NMR line spectra for the complexes [Rh(cod)$(NH_3)_2$·DB3*n*C*n*][PF_6] and [Rh(nbd)$(NH_3)_2$·DB3*n*C*n*][PF_6]. The signals (singlets) for the aromatic protons refer to [Rh(cod)$(NH_3)_2$·DB3*n*C*n*][PF_6] only.

shifts are experienced by the equatorial methylene protons of the cod ligand and the bridgehead methine protons of the nbd ligand. The olefinic protons are also shifted significantly upfield in both cases but the other ligand resonance in each case is influenced much less so. This difference in magnitude of the ring-current shifts of the probe protons strongly suggests an adduct geometry in which one or both aromatic ring systems of the receptor molecules approach the rhodium complexes "face on" along the sterically unhindered *z* axis (Fig. 14). In this super-structure, the olefinic, the equatorial methylene (cod), and the bridgehead-methine (nbd) protons, but not the remaining ligand protons, lie well within (Fig. 16) the aromatic ring-current shielding zones of the benzene rings in the molecular receptors.

Further evidence for a close association between the benzene rings in DB24C8 and the cod ligand in [Rh(cod)$(NH_3)_2$·DB24C8]$^{\oplus}$ was provided by the observation of intermolecular nuclear Overhauser effects (NOE's) between the aromatic protons on the receptor and the equatorial methylene and olefinic protons on the cod ligand. In accordance with the superstructure proposed (Fig. 16), intermolecular NOE's are *not* observed for the

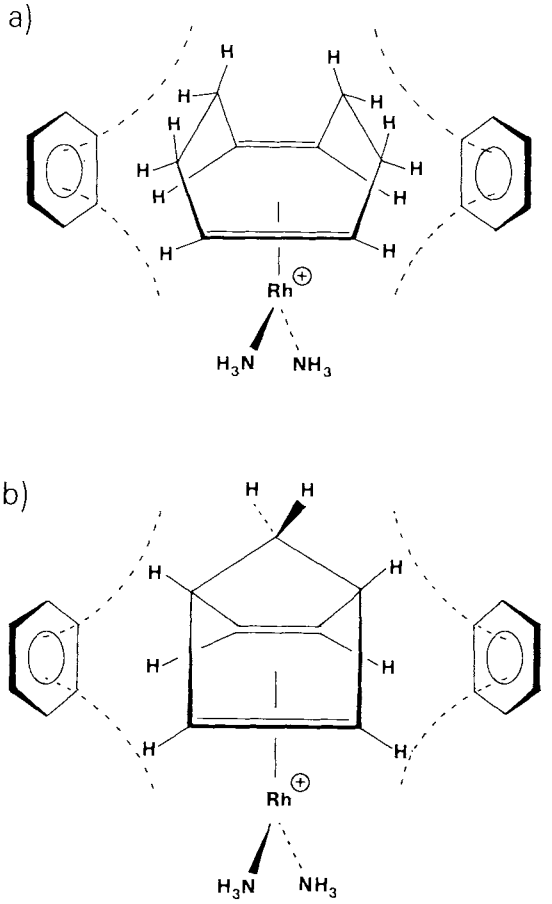


Fig. 16. A diagrammatic representation of the shielding effect of the annelated benzene rings of the dibenzo crown ethers DB3*n*C*n* ($n=7$–10) on (a) the cod ligand and (b) the nbd ligand of the Rh complexes of Figure 14.

axial-methylene protons on the cod ligand. This implies that these protons are more distant from the benzene groups of the crown ether than are the equatorial methylene and olefinic protons of the cod ligand.

The supramolecular structural features indicated by ^{1}H-NMR spectroscopic investigations have been amply confirmed by a series of X-ray structure determinations performed on adducts crystallized from halocarbon (CH_2Cl_2 or $C_2H_4Cl_2$) solutions. Four of the five adducts, which have been characterized in the solid state, are of 1 : 1 stoichiometry. They have many features in common, including a characteristic V-shaped conformation for the receptor, within which the rhodium complex is bound. Space-filling representations of the supramolecular structures of [Rh(cod)$(NH_3)_2$·DB21C7]$^{\oplus}$ and [Rh(nbd)$(NH_3)_2$·DB24C8]$^{\oplus}$ are shown in Figure 17. Figure 18 presents skeletal representations of the 1 : 1 adducts between [Rh(cod)$(NH_3)_2$]$^{\oplus}$ and the receptors, DB24C8 and DB30C10. These X-ray structural studies reveal that, without exception, the two *cis*-ammine ligands on the complexes straddle one chain of the macrocycle—the longer chain in the case of DB21C7—so that, in fact, only *one* ammine ligand is hydrogen bonded *within* the cavity while the other interacts with the oxygen atoms in the straddled chain. In both DB24C8 adducts, one of the four aryloxymethylene units is distorted from its customary coplanarity[51] with the benzene ring plane so

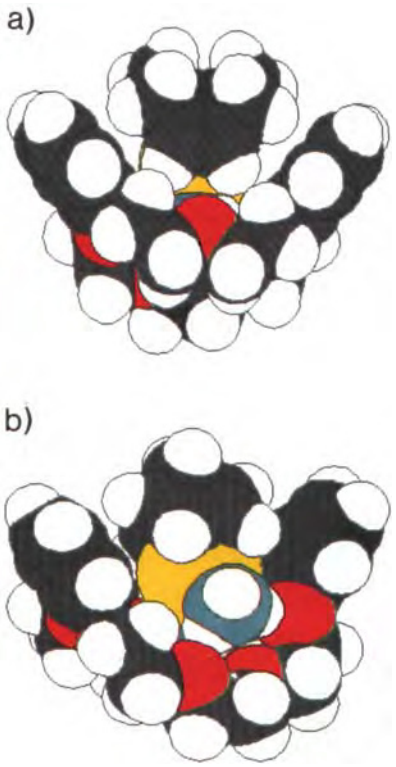


Fig. 17. Space-filling representations of the X-ray structures of (a) $[Rh(cod)(NH_3)_2 \cdot DB21C7]^{\oplus}$ and (b) $[Rh(nbd)(NH_3)_2 \cdot DB24C8]^{\oplus}$.

that the oxygen atom can form a hydrogen bond to one of the ammine ligands with an approximately trigonal approach to the oxygen. N–H···O hydrogen bond distances ([N···O]) in this collection of adducts are in the range 2.95–3.38 Å though the vast majority lie (Table 2) between 3.10 and 3.20 Å.

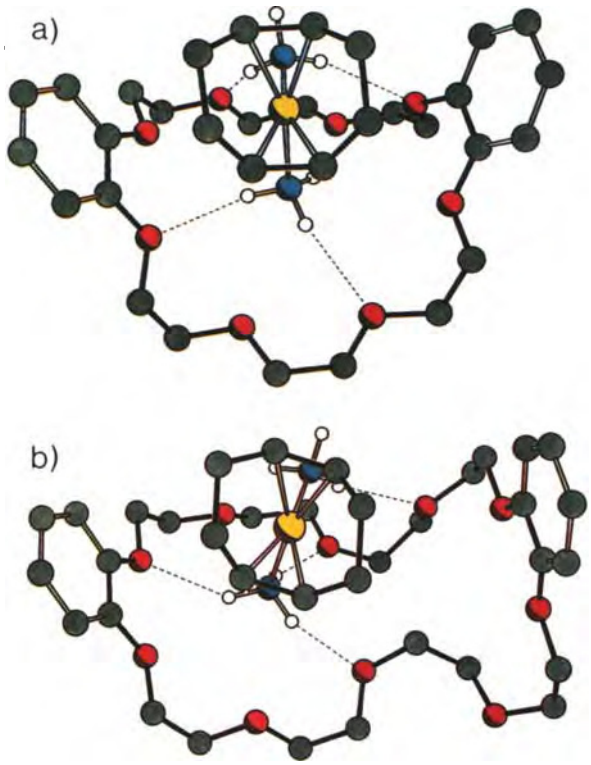


Fig. 18. Skeletal representations of the X-ray structures of (a) $[Rh(cod)(NH_3)_2 \cdot DB24C8]^{\oplus}$ and (b) $[Rh(cod)(NH_3)_2 \cdot DB30C10]^{\oplus}$.

Table 2. Selected hydrogen bond distances ([N···O]) in the 1:1 adducts of $[Rh(L)(NH_3)_2]^{\oplus}$ (L = cod or nbd) and DB3*n*C*n* (*n* = 7, 8 and 10).

$[Rh(L)(NH_3)_2 \cdot DB3nCn]^{\oplus}$ L	*n*	*R* [N···O] [Å]
cod	7	3.04, 3.12, 3.12, 3.17, 3.19, 3.19, 3.20, 3.22, 3.23, 3.31
cod	8	3.03, 3.13, 3.21, 3.34
nbd	8	2.95, 3.01, 3.27, 3.38
cod	10	2.96, 3.16, 3.18, 3.19

Although the primary binding forces between DB3*n*C*n* crown ethers (*n* = 7–10) and the rhodium complexes undoubtedly arise from hydrogen bonds, there also exist (Table 3) a large number of contacts ([Rh···O] and [Rh···C])

Table 3. Selected contact distances to rhodium ([Rh···O] and [Rh···C]) in the 1:1 adducts of $[Rh(L)(NH_3)_2]^{\oplus}$ (L = cod or nbd) and the aromatic O–C–C–O units of DB3*n*C*n* (*n* = 7 and 8) [a].

$[Rh(L)(NH_3)_2 \cdot DB3nCn]^{\oplus}$ L	*n*	*R* [Rh···O] [Å]	*R* [Rh···C] [Å]
cod	7	3.80, 3.87	4.04, 4.06
cod	8	3.59, 3.65, 4.01, 4.07	3.87, 3.87, 4.06, 4.12
nbd	8	3.50, 3.74, 3.78, 4.08	3.68, 3.86, 3.86, 4.06

[a] In $[Rh(cod)(NH_3)_2 \cdot DB30C10]^{\oplus}$, because of the larger ring size of the macrocycle, there are no contacts of less than 4 Å between the aromatic O–C–C–O units and the Rh atom.

at about van der Waals distances, which may provide weak, additional binding as a result of Coulombic and dispersion forces. Not only could these forces contribute to the overall stabilization of the adducts but they could also be largely responsible for ordering their superstructures. In particular, it is noticeable that, in all four adducts, the diene ligand is sandwiched between the two aromatic rings of the crown ether so that a number of allylic and vinylic C–H groups are brought into close contact with the π-arene systems of the receptor. As yet, there is no direct evidence that these contacts ([H···benzene ring plane] = 2.6–3.3 Å) enhance the stability of the adducts to any significant extent. However, there is considerable literature precedent for the existence of attractive [CH···arene] interactions at distances of 2.5–3.5 Å. The dimer of benzene, for example, has been shown[52] to have a T-shaped geometry in the gas phase with a binding energy of 14.7 kJ mol^{-1} derived almost entirely from dispersion forces between the C–H groups of one ring and the π-electron system of the other. An interaction of this type was, in fact, recently demonstrated crystallographically,[53] and more general evidence for attractive [CH···arene] interactions has been obtained for a wide range of different systems containing aromatic and aliphatic units from conformational studies,[54] gas-liquid chromatography,[55] molecular mechanics calculations,[56] and association constant measurements.[57] Whatever the form and relative strengths of these weak attractive interactions involving the benzene rings of the DB3*n*C*n* crown ethers and the rhodium(I) complexes, there is no doubt that both DB24C8[58] and DB30C10[59] undergo considerable conformational changes from their

rather flat extended structures (Fig. 19) in the free states[58, 59] to their V-shaped conformations in the 1 : 1 adducts.

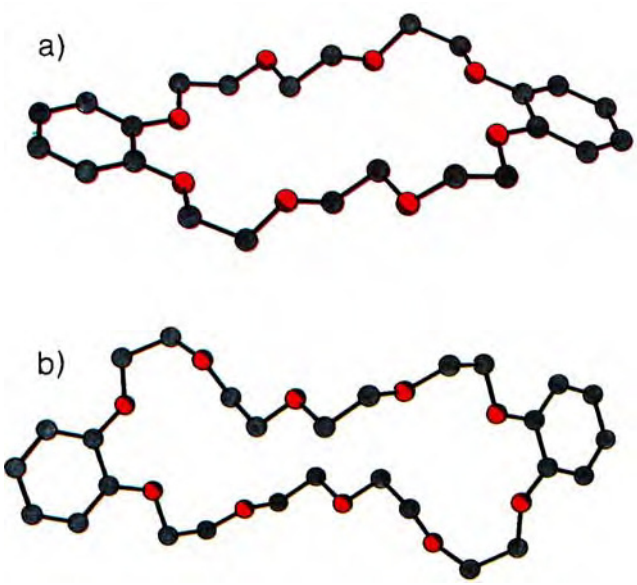


Fig. 19. Skeletal representations of the X-ray structures of (a) DB24C8 and (b) DB30C10.

In only one of the rhodium-based adducts is a significantly different solid state structure observed. DB36C12 forms a 2 : 1 (complex : receptor) adduct in which the macrocycle adopts a relatively flat, extended conformation (Fig. 20) with two $[Rh(cod)(NH_3)_2]^{\oplus}$ ions hydrogen-bonded centrosymmetrically to opposite faces of the receptor. Again, the characteristic straddling relationship of the two *cis*-ammine ligands with respect to the polyether chains is adopted. In accordance with the virtual absence (Fig. 15) of ring current shifts for the 1 : 1 adduct, the benzene rings of the receptor in the crystalline 2 : 1 adduct do not even begin to approach the diene ligand. The relatively flattened conformation adopted by the 36-membered ring in this adduct seems to be quite characteristic of DB36C12 (cf. its 2 : 1 complexes formed with sodium hexafluorophosphate[60] and lithium picrate).[61]

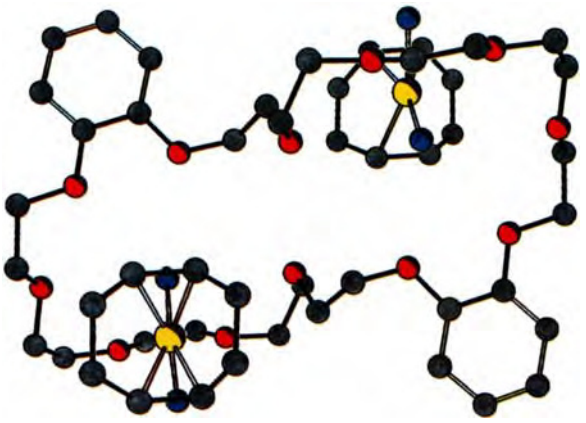


Fig. 20. Skeletal representation of the X-ray structure of $[\{Rh(cod)(NH_3)_2\}_2 \cdot DB36C12]^{2\oplus}$.

4.3. Adduct Formation involving a Platinum Complex

In view of the major rôle played by hydrogen bonding in second-sphere coordination we sought to enhance the hydrogen bonding potential of ammine ligands on transition metals by incorporation of π-acceptor co-ligands such as 2,2-bipyridyl into the primary coordination sphere of an ammine complex. It is known[62] that π-acceptor groups increase significantly the acidity of protic ligands on the same metal center by allowing partial delocalization of the increased electron density resulting from deprotonation. In this context, we may regard hydrogen bonding as a form of incipient deprotonation.

Although the square-planar platinum(II) complex, $[Pt(bpy)(NH_3)_2][PF_6]_2$ is insoluble in hydrocarbon or halocarbon solvents, it dissolves[35] in dichloromethane to give a pale yellow solution when a molar equivalent of 18C6 is added. A similar effect is produced by addition of the DB3*n*C*n* crown ethers ($n = 6$–12) to the complex. However, we noticed (eventually!) that solutions containing DB3*n*C*n* ethers (particularly $n = 7$–11) are markedly stronger in color than the solution obtained with 18C6 at the same concentration. Moreover, deep yellow, crystalline 1 : 1 adducts may be isolated from solutions containing the DB3*n*C*n* ethers when $n = 8$, 10, and 11. Single crystal X-ray diffraction studies[35] of two ($n = 8$ and 10) of these second-sphere adducts have revealed the source of this enhanced absorption in the visible region. Skeletal structures of the adducts are shown in Figure 21. A space-filling representation of $[Pt(bpy)(NH_3)_2 \cdot DB30C10]^{2\oplus}$ is given in Figure 22.

Three major features of the second-sphere coordination of the platinum complex are immediately apparent. Firstly, as anticipated, the ammine ligands lie within the cavity of the V- and U-shaped receptor and form hydrogen bonds to some of the crown ether oxygen atoms. Once again, the characteristic straddling disposition of the *cis*-ammine ligands with respect to one of the polyether chains is evident. Secondly, there is undoubtedly some stabilization provided by favorable electrostatic interactions of a charge-dipole type between the dicationic complex and the oxygen atoms of the macrocycle. Thirdly, the parallel arrangement and close contact (3.48–3.52 Å) between the relatively π-electron deficient bpy ligand and one or both of the π-electron rich catechol units of the receptor strongly suggest the existence of a $\pi \rightarrow \pi$ charge-transfer interaction. The associated electronic charge-transfer absorption, which was found to be centered at ca. 350 nm in acetonitrile solution, is clearly responsible for the enhanced depth of color of this type of adduct.

This charge-transfer absorption provides good evidence that the adduct-stereochemistry observed in the solid state is also retained in solution. Further proof of a close association of the crown ethers and the platinum complex in solution is provided by the observation (Fig. 23) of substantial upfield shifts (up to 0.7 ppm) for the ^{1}H-NMR resonances associated with the aromatic protons in both the complex and the receptor. As in the corresponding adducts involving rhodium-diene complexes, the shifts of the bpy ligand resonances can be ascribed to diamagnetic shielding by ring currents associated with the benzene rings of the macrocycle. On this occasion, however, the effect is recip-

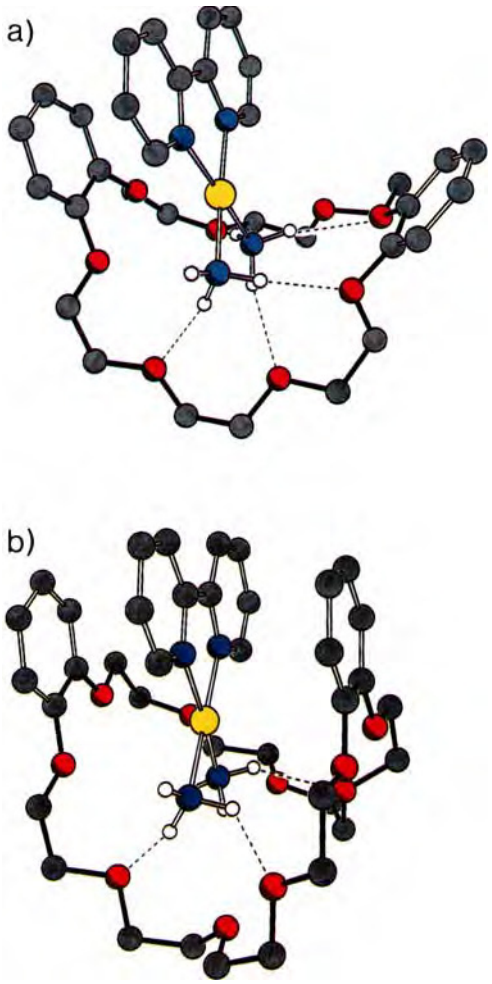


Fig. 21. Skeletal representations of the X-ray structures of (a) $[Pt(bpy)(NH_3)_2 \cdot DB24C8]^{2\oplus}$ and (b) $[Pt(bpy)(NH_3)_2 \cdot DB30C10]^{2\oplus}$.



Fig. 22. Space-filling representation of the X-ray structure of $[Pt(bpy)(NH_3)_2 \cdot DB30C10]^{2\oplus}$.

rocated and the aromatic protons of the receptor are also shielded by ring-currents associated with the bpy ligand in the complex. As shown in Figure 23, these upfield shifts increase with the ring size of the macrocycle up to a maximum for $n = 10$ or 11 and then decrease markedly for $n = 12$. The same general trend is followed by the intensity of the charge-transfer absorption band at 350 nm. This agreement is to be expected since the magnitudes of ring-current shielding and charge-transfer should both become

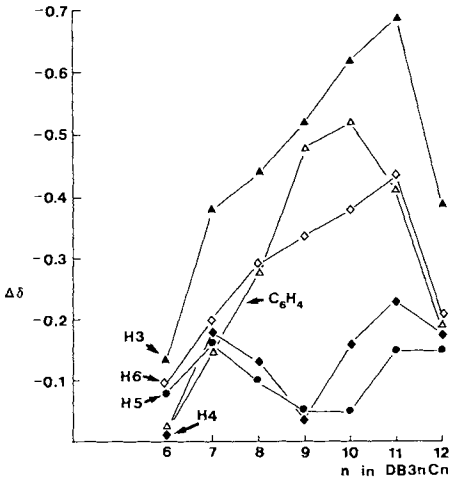


Fig. 23. A plot of ^{1}H-NMR chemical shifts ($\Delta\delta$) for crown ethers of the type DB3*n*C*n* in the formation of 1:1 adducts with $[Pt(bpy)(NH_3)_2][PF_6]_2$ in CD_2Cl_2 against the ring size ($n = 6$–12) of DB3*n*C*n*. Note that a negative $\Delta\delta$ value corresponds to an upfield shift.

optimal when the geometrical overlap of the π-systems is greatest and the inter-ring separations are least.

Analysis of the concentration dependence of the charge-transfer absorption can be used[63] to derive association constants (K_a) and free energies of binding (ΔG^0) for these adducts. The values for $n = 9$, 10, and 11 are $K_a = 66000$, 191000, and 69000 M^{-1} corresponding to $-\Delta G^0 = 27.7$, 30.2, and 27.7 kJ mol^{-1}, respectively. Thus, DB30C10 forms the most stable second-sphere adduct in solution. This particular receptor-complex match presumably reflects an optimum combination of hydrogen bonding and charge-transfer.

The relative significance of charge-transfer interactions in second-sphere coordination is probably best illustrated by examining the solid state structure of an adduct only recently obtained (Fig. 24) between $[Pt(bpy)(NH_3)_2][PF_6]_2$ and a dinaphtho[30]crown-10 (DN30C10) derivative.[64] This solid state structure reveals that the platinum complex is significantly tilted from its position in the corresponding

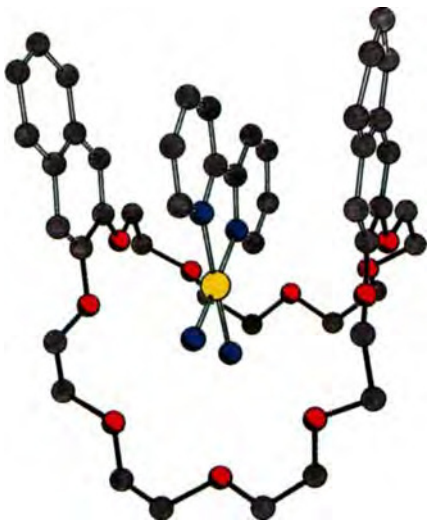


Fig. 24. Skeletal representation of the X-ray structure of $[Pt(bpy)(NH_3)_2 \cdot DN30C10]^{2\oplus}$.

DB30C10 adduct, apparently in order to maximize the overlap between the π-systems of the bpy ligand and those of the two naphthalene units. Clearly, a balance is being struck between N-H···O hydrogen bonding, pole-dipole interactions, and the dispersive forces that constitute a significant component of all charge-transfer interactions.

In conclusion, it should be mentioned that these investigations on the second-sphere coordination of $[Pt(bpy)(NH_3)_2]^{2\oplus}$ by DB3*n*C*n* crown ethers were directly responsible for initiating our research programme on the complexation of the bipyridinium herbicides, Diquat[49,65] and Paraquat[66] by the same and related molecular receptors.

5. Macrobicyclic and Macropolycyclic Polyether Receptors in the Second-Sphere

In the previous Section, we have witnessed, without exception, how the two ammine ligands in *cis*-diammine transition metal complexes straddle one of the polyether chains in the DB3*n*C*n* ether receptors. Thus, the receptor constitution is failing to make full use of the hydrogen bonding potential of these ammine ligands. For this reason, we decided to prepare macrobicyclic polyethers containing aromatic rings in which two crown ether rings are placed side-by-side such that each ring can bind one ammine ligand. The design concept and synthetic outcomes are summarized in Figure 25.

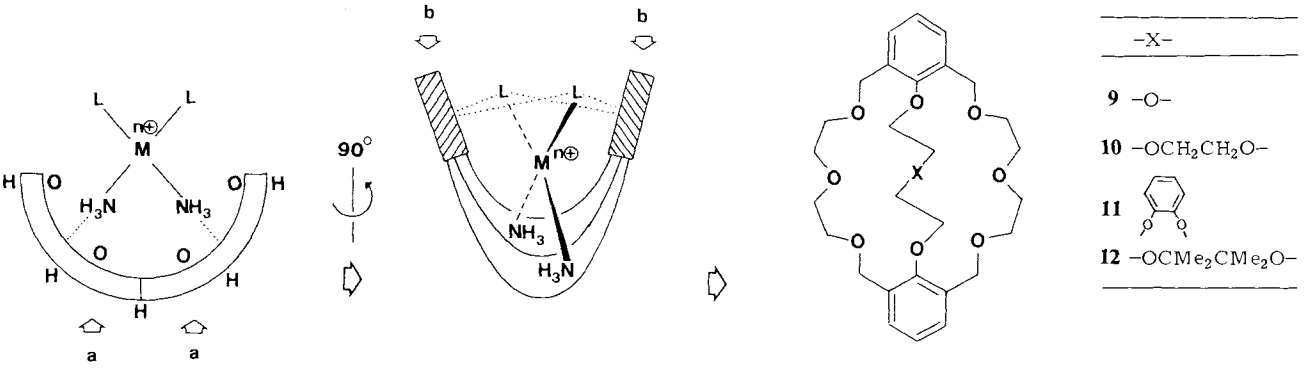


Fig. 25. The design concept behind macrobicyclic polyether receptors for *cis*-diammine transition metal complexes. a: receptor binding center; b: aromatic ring.

5.1. Adduct Formation involving a Rhodium Complex

The X-ray crystal structure analysis (Fig. 26) of the macrocycle **10** reveals[67] immediately that this receptor offers a more preorganized cavity for binding $[Rh(cod)(NH_3)_2]^{\oplus}$ than do the DB3*n*C*n* crown ethers. Although the three polyether chains have to undergo considerable conformational change prior to any adduct formation, the required V-shaped conformation of the receptor is already established. The suitability of the macrocycle **10**—and also the closely related derivative **11**—for adduct formation is confirmed by the solid state structures (Fig. 27 and 28) of their 1:1 adducts with the rhodium complex. The 24-membered macroring is clearly ideal for optimal hydrogen bonding of two *cis*-ammine ligands. The macroring encircles them by

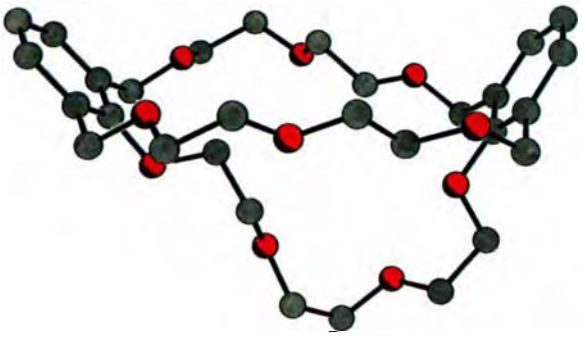


Fig. 26. Skeletal representation of the X-ray structures of the macrocycle **10**.

adopting a conformation with alternating *gauche* helicities for the C–C bonds and both structures are clearly stabilized by N-H···O hydrogen bonding: in each case, there are eight [N···O] distances lying within the range 3.00–3.26 Å and the N atoms of the ammine ligands are actually inserted below (0.53–0.63 Å) the mean planes of the six peripheral oxygen atoms. In both adducts, the middle two oxygen atoms in the central polyether chains are redundant as far as hydrogen bonding to the ammine ligands is

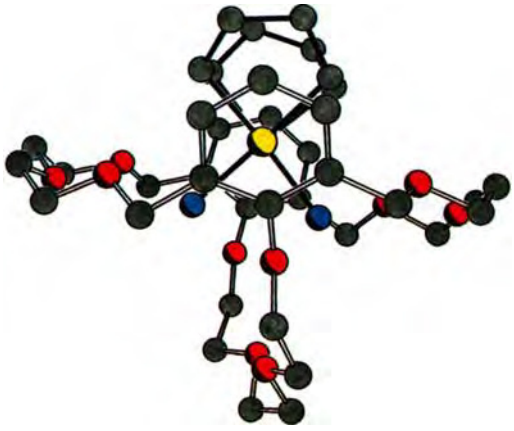


Fig. 27. Skeletal representation of the X-ray structure of $[Rh(cod)(NH_3)_2 \cdot \mathbf{10}]^{\oplus}$.

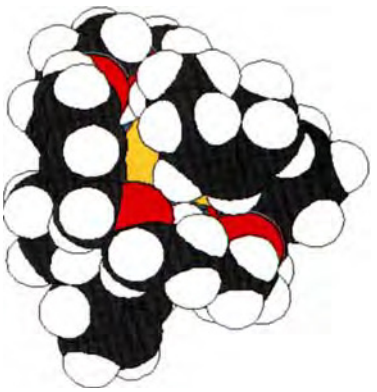


Fig. 28. Space-filling representation of the X-ray structure of $[Rh(cod)(NH_3)_2 \cdot \mathbf{11}]^{2\oplus}$.

concerned. Nonetheless, it has not been possible to obtain a crystalline 1:1 adduct of the macrocycle **9** and $[Rh(cod)(NH_3)_2]^{\oplus}$, and ^{1}H-NMR chemical shift data (Table 4) for all the 1:1 adducts in CD_2Cl_2 solutions suggest that binding is somewhat weaker in this case than it is in the $[Rh(cod)(NH_3)_2]^{\oplus}$ adducts of **10**, **11**, or **12**. As in the case of the $[Rh(cod)(NH_3)_2 \cdot DB3nCn]^{\oplus}$ adducts, upfield shifts of the signals for the cod protons were accompanied by downfield shifts in the signals for the aromatic protons in the receptors. Dynamic ^{1}H-NMR spectroscopy on the conformationally-mobile receptors **9** and **10** indicates that inversion of the receptors (i.e. passage of the central polyether chain through the middle of the 24-membered ring) is impeded on forming the 1:1 adducts with $[Rh(cod)(NH_3)_2][PF_6]$. The barriers to conformational inversion obtained from studying the temperature dependences of the signals—in each case, an AB system at low temperature coalescing to a singlet at higher temperature—for the benzylic methylene protons on the receptors are increased by 12.1 kJ mol^{-1} (from 32.6 to 44.7 kJ mol^{-1}) for **9**, and by 13.4 kJ mol^{-1} (from 43.5 to 56.9 kJ mol^{-1}) for **10**, respectively, on adduct formation. These values, which represent a minimum estimate of the binding free energies within the adducts reveal that **9** is a poorer receptor than **10** for $[Rh(cod)(NH_3)_2]^{\oplus}$.

Table 4. Selected ^{1}H-NMR data (δ- and $\Delta\delta$-values) for the 1:1 adduct of $[Rh(cod)(NH_3)_2][PF_6]$ and the macrobicyclic receptors **9**–**12** in CD_2Cl_2.

Resonance	**9**	**10**	**11**	**12**
NH_3 [a]	2.00	2.22	2.22	2.20
	(−0.39)	(−0.17)	(−0.17)	(−0.19)
(cod)-H_e [a]	2.00	1.32	1.52	1.48
	(−0.39)	(−1.07)	(−0.87)	(−0.91)
(cod)-H_a [a]	1.59	1.13	1.27	1.24
	(−0.26)	(−0.72)	(−0.58)	(−0.61)
(cod)-H_o [a]	3.54	3.60	[c]	[c]
	(−0.53)	(−0.47)	[c]	[c]
p-H [b]	7.18	7.27	7.20	7.28
	(+0.17)	(+0.27)	(+0.15)	(+0.26)
m-H [b]	7.39	7.50	7.51	7.50
	(+0.14)	(+0.25)	(+0.23)	(+0.22)

[a] The values in parantheses indicate the extent to which signals of the cod protons (H_e = equatorial methylene protons, H_a = axial methylene protons, H_o = olefinic protons) are shifted relative to the corresponding signals in $[Rh(cod)(NH_3)_2 \cdot 18C6][PF_6]$ where NH_3, (cod)-H_e, (cod)-H_a and (cod)-H_o have δ values of 2.39, 2.39, 1.85 and 4.07, respectively. [b] The values in parentheses indicate the extent to which the signals for *p*-H- and *m*-H are shifted relative to the corresponding signals in **9** (δ = 7.01 and 7.25, respectively), **10** (δ = 7.00 and 7.25, respectively), **11** (δ = 7.05 and 7.28, respectively), and **12** (δ = 7.02 and 7.28, respectively). [c] Signals obscured by signals for OCH_2 protons.

5.2. Adduct Formation involving a Platinum Complex

One of our objectives in this investigation was to encapsulate the antitumor agent, Cisplatin, in a molecular receptor. Although this goal still eludes us at the time of writing, we have discovered[68] that **10** forms a crystalline 1:1 adduct with $[Pt(NH_3)_4][PF_6]_2$. The X-ray structural analysis reveals that there are *two* independent adducts which differ subtly in the conformations adopted by the central polyether chain and in the relative orientations of the ammine ligands on platinum. One of the two independent adducts is illustrated in skeletal form in Figure 29. Compared with the monocationic $[Rh(cod)(NH_3)_2]^{\oplus}$ complex, the dicationic $[Pt(NH_3)_4]^{2\oplus}$ complex penetrates further into the receptor cavity, with all four ammine ligands involved in hydrogen bonding to the polyether chains. As a consequence, even the middle two oxygen atoms in the central polyether chain are no longer redundant as hydrogen bond acceptors.

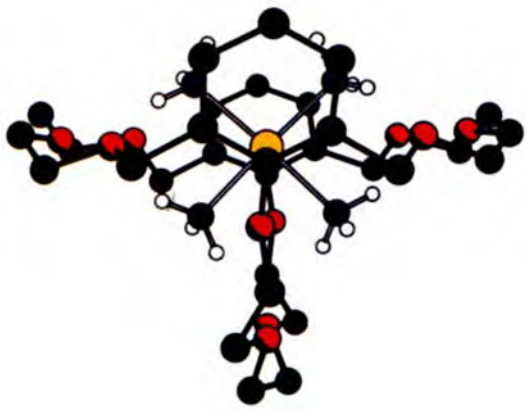
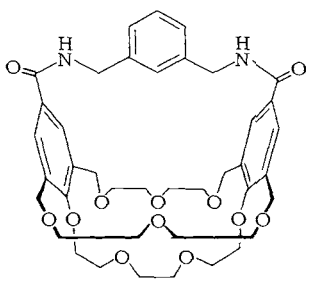


Fig. 29. Skeletal representation of the X-ray structure of $[Pt(NH_3)_4 \cdot \mathbf{10}]^{2\oplus}$.

In the knowledge that N–H···Cl hydrogen bonds exist[69] between adjacent Cisplatin molecules in the solid state, we have turned our attention to utilizing the hydrogen bonding potential of the Cl ligands in Cisplatin by synthesizing appropriately designed macropolycyclic polyether receptors. One of these is the bisamide **13**. The X-ray crystal structure (Fig. 30) of the free receptor confirmed[70] that there is indeed a cleft in the molecule into



13

which Cisplatin could fit. Alas, Cisplatin is not solubilized in halocarbon solvents containing the receptor despite the fact that $[Rh(cod)(NH_3)_2][PF_6]$ dissolves in CD_2Cl_2 in the presence of equimolar amounts of the bisamide receptor. However, the rhodium complex clearly does not enter the receptor cleft, since no significant changes in ^{1}H-NMR

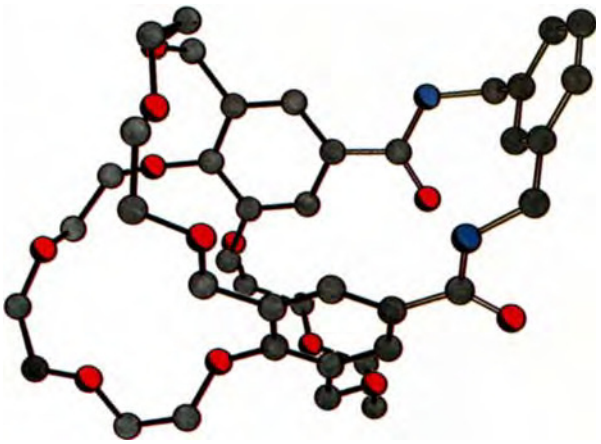


Fig. 30. Skeletal representation of the X-ray structure of the macrotricycle **13**.

chemical shifts are observed in the resonances for either the complex or receptor protons. Believing this to be for a simple steric reason, we examined the ability of $[Pt(NH_3)_4][PF_6]_2$ to form a crystalline adduct with the bisamide **13**. Crystals appeared almost immediately in methanol/acetone. However, X-ray crystallography revealed (Fig. 31) that, unexpectedly, a 2:1 (receptor:complex) adduct is formed in the solid state as an acetone solvate. Although this centrosymmetric adduct is undoubtedly stabilized by electrostatic interactions, N–H···O hydrogen bonds between *trans*-related ammine ligands and the amide oxygen atoms ([N···O]=2.90 and 3.01 Å) are obviously highly significant sources of adduct stabilization. The four ammine ligands are also involved in hydrogen bonding to oxygen atoms in one of the polyether chains of the bisamide receptor. This is the first example we have met where two receptor molecules coordinate simultaneously to the second-sphere of a transition metal complex in a discrete manner.

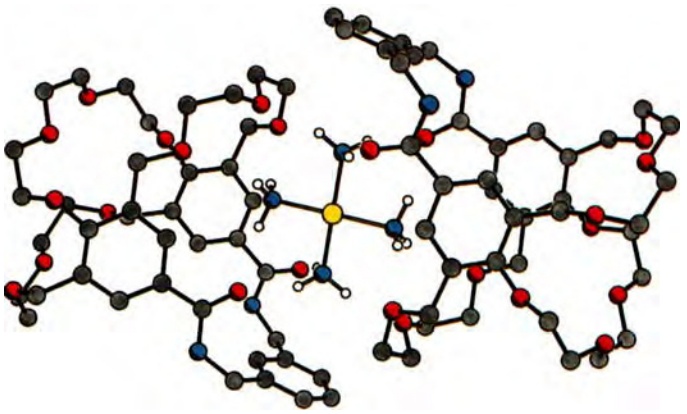


Fig. 31. Skeletal representation of the X-ray structure of $[Pt(NH_3)_4 \cdot \mathbf{13}]^{2\oplus}$.

6. Simultaneous First- and Second-Sphere Coordination

At present, there are only two well-characterized systems in which a receptor-type molecule interacts with a metal complex such that a ligand occupies sites in *both* the first *and* the second coordination spheres of the transition metal. The first such crystalline complex was reported[71] in 1974 as the product of a reaction between the phosphino-ether **14** and tetracarbonyldirhodium dichloride, followed by treatment of the neutral complex, **15**, in dichloromethane with silver tetrafluoroborate in the presence of adventitious water to give the salt **16**.

$$\underset{\mathbf{14}}{Ph_2P(CH_2CH_2O)_3CH_2CH_2PPh_2} \longrightarrow \underset{\mathbf{15}}{[Rh(CO)Cl \cdot \mathbf{14}]} \longrightarrow [Rh(CO)(H_2O) \cdot \mathbf{14}][PF_6]$$
$$\mathbf{16}$$

The X-ray crystal structure (Fig. 32) demonstrates the existence of a macrocyclic aqua-complex. The cavity formed by *trans*-coordination of the phosphino-ether is sterically and electronically perfect for binding a molecule of water, since coordination of the aqua-oxygen atom to a cationic metal center increases the polarization of the O–H bonds,

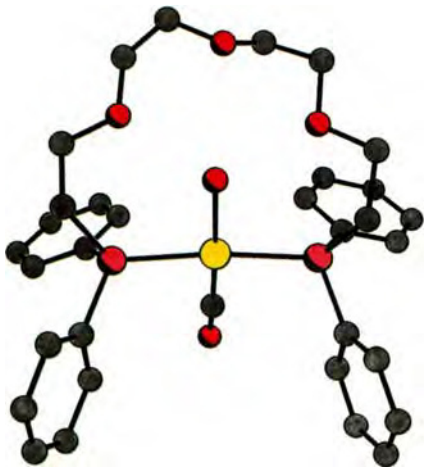


Fig. 32. Skeletal representation of the X-ray structure of $[RhCO(H_2O)\{Ph_2P(CH_2CH_2O)_3CH_2CH_2PPh_2\}]^{\oplus}$.

which are then directed to form strong linear O–H···O hydrogen bonds to two of the ether oxygen atoms ([O···O]=2.68 Å) in the chelate chain which adopts an almost ideal conformation. Although molecular modelling indicates that coordination of a polyether oxygen atom *directly* to rhodium is quite feasible, the water molecule is so strongly bound by the cooperative effects of first- and second-sphere coordination that it cannot be removed even after several cycles of dissolution in chloroform and evacuation at 10^{-3} torr. The second example[72] also emerged somewhat unexpectedly from an investigation of the second-sphere coordination 1,4,10,13-tetraoxa-7,16-diazacyclooctadecane (diaza-18C6) to $[Rh(cod)(NH_3)_2][PF_6]$. The rhodium complex is readily solubilized in halocarbons by

18C6 and we anticipated that the diaza-18C6 analogue would form an even more strongly hydrogen-bonded second-sphere adduct. Indeed, rapid solubilization of the metal complex was observed in dichloromethane on addition of an equimolar amount of diaza-18C6. Initially, ^{1}H-NMR spectroscopic data were consistent with the formation of a 1:1 adduct. However, slow crystallization over 36 hours yielded a compound which was clearly *not* the expected adduct. Single-crystal X-ray analysis revealed that the first-formed second-sphere adduct had, in fact, decomposed with loss of ammonia to give a novel complex in which the amino groups of the diaza-18C6 are directly coordinated to rhodium. The structure (Fig. 33) shows that the macrocyclic ligands not only bind to rhodium in the first coordination sphere but also coordinate in the second sphere via N-H···O hydrogen bond formation to the remaining ammine ligand on the metal. Although the [N···O] distances are relatively long (3.22, 3.45, and 3.50 Å), the orientation of the ammine ligands directly over the faces of the macrocycle and the appreciable tilting of the Rh-N bonds in the same direction (Rh-N-C angles are 116° and 117° rather than the expected tetrahedral value) are both clearly indicative of significant interactions in the second sphere.

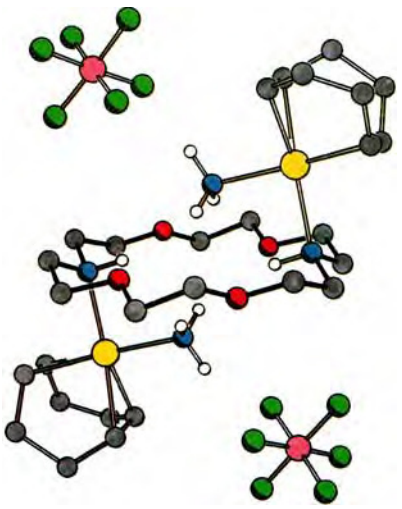
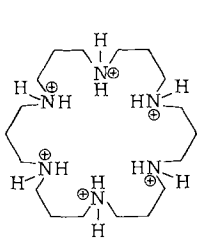


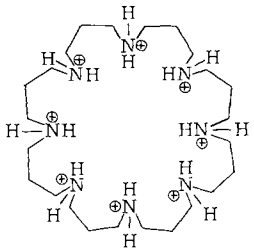
Fig. 33. Skeletal representation of the X-ray structure of diamminebis-(1,5-cyclooctadiene)(μ-1,4-10,13-tetraoxa-7,16-diazacyclooctadecane-N^7,N^{16})-dirhodium bis(hexafluorophosphate).

7. Other Synthetic Molecular Receptors as Second-Sphere Ligands

The binding of anions like $[Fe(CN)_6]^{4\ominus}$, $[Ru(CN)_6]^{4\ominus}$, $[Co(CN)_6]^{3\ominus}$, and other complex anions of transition metals by polyammonium macrocyclic receptors[73,74] such as 24-$N_6H_6^{6\oplus}$ and 32-$N_8H_8^{8\oplus}$ may be considered as yet another example of second-sphere coordination, since the central metal cation is complexed by cyanide anions, which are, in turn, bound to the receptors by multiple $N^{\oplus}$-H···NC-$M^{\ominus}$ hydrogen bonds. Although adduct formation does not influence the UV spectroscopic properties of the $[M(CN)_6]^{n\ominus}$ anions (cf. Section 2), it does affect the electrochemical properties of the anions by stabilizing the



24-$N_6H_6^{6\oplus}$



32-$N_8H_8^{8\oplus}$

more highly charged forms, i.e. the lower oxidation state of the metal. Electrochemical measurements show[75] that $[Fe(CN)_6]^{4\ominus}$ and $[Ru(CN)_6]^{4\ominus}$ both form 1:1 adducts with 24-$N_6H_6^{6\oplus}$ and 32-$N_8H_8^{8\oplus}$, and that the anions are more difficult to oxidize in the presence of the polyammonium macrocycles than in their absence. Changes observed in the redox potential of a given $[M(CN)_6]^{3\ominus}/[M(CN)_6]^{4\ominus}$ couple indicate that the resulting adduct exchanges one electron reversibly *without dissociation* of the complex. The lower stabilities (Table 5) of the adducts of the oxidized

Table 5. Stability constants, log K_a (±0.2) for binding of complex anions by the polyammonium macrocycles in aqueous solution containing 0.1 M Me_4NCl.

	24-$N_6H_6^{6\oplus}$	32-$N_8H_8^{8\oplus}$
$[Fe(CN)_6]^{4\ominus}$	6.9	8.9
$[Fe(CN)_6]^{3\ominus}$	4.2	5.0
$[Co(CN)_6]^{3\ominus}$	3.9	6.0

anions in aqueous solution are consistent with the interactions between the anion and the protonated second-sphere ligand being mainly Coulombic in nature. Although second-sphere coordination of $[M(CN)_6]^{n\ominus}$ anions does not affect their spectroscopic energy levels, it does modify their photochemical properties by inhibiting those nuclear motions (i.e. metal-ligand stretching) responsible for chemical change. Thus, irradiation of $[Co(CN)_6 \cdot 32\text{-}N_8H_8]^{5\oplus}$ in aqueous solution at 313 nm results[76-78] in the same $CN^{\ominus}/H_2O$ photoaquation as undergone by free $[Co(CN)_6]^{3\ominus}$:

$$[Co(CN)_6 \cdot 32\text{-}N_8H_8]^{5\oplus} \xrightarrow[H_2O]{h\nu} [Co(CN)_5(H_2O) \cdot 32\text{-}N_8H_8]^{6\oplus} + CN^{\ominus} \ldots \quad (3)$$

However, the quantum yield of the reaction in Equation (3) is only one-third that for the photoaquation of free $[Co(CN)_6]^{3\ominus}$. This result implies that in the adduct two-thirds (i.e. four out of six) of the cyanide groups of the first coordination sphere cannot dissociate. This suggests a structure (Fig. 34) for the adduct in which four coplanar equatorial cyanide ligands are hydrogen bonded to alternate $NH_2^{\oplus}$ centers on the macrocycle leaving two axial cyanide ligands free to react. The practical importance of this finding will be discussed briefly in Section 11. To our knowledge, although a crystalline 1:1 adduct of $[Pt(CN)_4]^{2\ominus}$ and 32-$N_8H_8^{8\oplus}$ has been isolated,[73] an X-ray analysis in support of the above structural proposal has yet to appear in the literature.

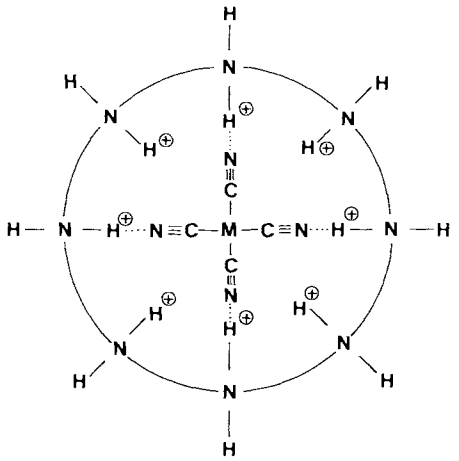
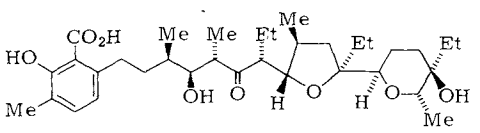


Fig. 34. A possible structure for the $[Co(CN)_6 \cdot 32\text{-}N_8H_8]^{5\oplus}$ adduct. The two $CN^{\ominus}$ ligands, which are perpendicular to the plane of the macrocycle, are not shown.

Just as anionic transition metal complexes can be coordinated by positively-charged macrocycles in aqueous solution, so it should be possible to coordinate cationic transition metal complexes with negatively-charged macrocycles in aqueous solution. Indeed, it has been claimed[79] that a macrocyclic hexacarboxylate receptor fulfils[80] this function.

8. Second-Sphere Coordination of Ammine-Transition Metal Complexes by a Natural Ionophore

The acyclic carboxylic ionophore, Lasalocid A, not only has the ability to transport mono-, di-, and trivalent metal cations across natural and artificial membranes, but also is capable of binding and transporting substituted ammonium cations.[3] An X-ray crystallographic investigation of the Lasalocid A complex of (*R*)-1-(4-bromophenyl)ethylamine reveals[81] that an $NH_3^{\oplus}$ center binds the Lasalocid A anion via three N-H···O hydrogen bonds.

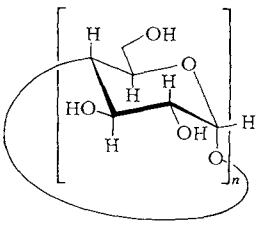


Lasalocid A

Very recently, crystalline adducts with the stoichiometry $[Cation^{n\oplus}][Lasalocid\ A^{\ominus}]_n$ have been isolated and characterized[82] for the inorganic cations, $[Co(NH_3)_6]^{3\oplus}$, $[Cr(NH_3)_6]^{3\oplus}$, $[Pt(NH_3)_6]^{4\oplus}$, $[Co(NH_3)_5Cl]^{2\oplus}$, and Δ- and Λ-$[Co(en)_3]^{3\oplus}$. The crystalline adducts are highly soluble in chloroform and dichloromethane. All the spectroscopic data (UV/visible and ^{13}C-NMR, and circular dichroism in the case of the Δ- and Λ-$[Co(en)_3]^{3\oplus}$ adducts) indicate that the structural integrity of the adducts is maintained in solution, a fact supported by vapor pressure osmometry in chloroform solutions. Adduct formation with Lasalocid A anions does not cause any rupture or rearrangement of the M-N bonds associated with the first coordination sphere of the cations, which are believed to interact with the anions through N-H···O hydrogen bonds involving one or two ammine ligands on the metal of the cation and possibly the oxygen atoms of the anion. Once again, Coulombic interactions presumably contribute substantially to adduct stabilities. No doubt, other transition metal complex adducts of natural ionophores await discovery and investigation.

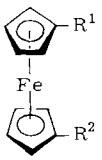
9. Cyclodextrins as Second-Sphere Receptors

Although the cyclodextrins, α-, β-, and γ-CD are promiscuous in their role as receptors towards a wide range of chemical species,[3] only relatively few examples of adduct formation with organometallic compounds have been described in the literature. Since the initial brief report[83] in 1975 that ferrocene (FcH) forms a 1:1 adduct with β-CD in both dimethylformamide (DMF) ($K_a = 67\ M^{-1}$) and dimethyl sulfoxide (DMSO) ($K_a = 50\ M^{-1}$), no further investigations appear to have been carried out until quite recently when a range of crystalline adducts were characterized[84] in which FcH, acetylferrocene (FcAc) and, 1,1'-diacetylferrocene [$Fc(Ac)_2$] are believed to be included within the cavities of the cyclodextrins. Treatment of β- and γ-CDs with FcH and its derivatives, FcAc and $Fc(Ac)_2$, yielded only 1:1 adducts whereas α-CD formed 2:1 (CD:FcR) adducts with FcH and FcAc. It is of interest that the [FcH·(α-CD)$_2$] and [FcH·β-CD] are thermally stable and do not liberate FcH on heating *in vacuo* at 100°C. In addition, [FcH·(α-CD)$_2$] and [FcH·β-CD)] can be recrystallized from water giving yellow crystals. It would appear that, although FcH and FcAc are too large to be accommodated within a single α-CD cavity, they will fit into two juxtapositioned α-CD cavities. Additionally, circular dichroism spectra indicate that the orientation of FcH in β-CD is different from that of FcH in γ-CD. All these observations taken together have led to the general structural proposals for the adducts shown in Figure 35.



α-CD: $n = 6$
β-CD: $n = 7$
γ-CD: $n = 8$

The relatively strong binding of the ferrocene nucleus by β-CD in DMSO/H_2O (3:2) has encouraged[85] the use of the *p*-nitrophenyl esters **21** and **22** of ferrocene-2-acrylic acid and ferrocenepropiolic acid as suitably optimized substrates in studying the acylation of β-CD by bound substrates. The results in terms of the rate accelerations of acylation relative to hydrolysis have been quite spectacular. Further attempts at the optimization of metallocene substrates for β-CD acylation prompted the investigation of the ruthenocene analogue of **21** only to discover that it is an inferior substrate (ruthenocene is ca. 10% thicker than ferrocene) for the reaction. The oxidation of ferrocenecar-



	FcR	R^1	R^2
17	FcH	H	H
18	FcAc	COMe	H
19	$Fc(Ac)_2$	COMe	COMe
20		CO_2H	H
21		$CH{=}CHCO_2C_6H_4{-}p{-}NO_2$	H
22		$C{\equiv}CCO_2C_6H_4{-}p{-}NO_2$	H

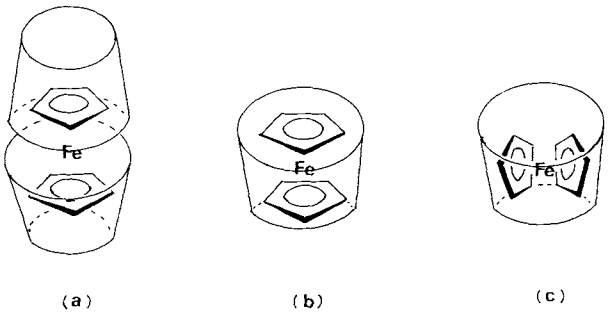


Fig. 35. The proposed structures for the adducts of (a) [FcH·(α-CD)$_2$], (b) [FcH·β-CD], and (c) [FcH·γ-CD].

boxylic acid (FcCA) in the presence of β-CD has been investigated[86] at pH 9.2 in aqueous buffer by cyclic voltammetry and the following conclusions were drawn: (i) the oxidation of the carboxyclic acid **20** proceeds by prior dissociation of the complex followed by electron transfer from free FcH, and (ii) there is no direct electron transfer from the complexed FcH within the accessible range of potentials.

The preparation and properties of several [rotaxane·CD] adducts have been described[87] in which α- or β-CD are threaded by α,ω-diaminoalkanes with a cobalt(III) complex coordinated to the terminal amino groups. The reaction yields (Scheme 1) were surprisingly high (1.9–19%) producing good evidence that the CDs are binding the α,ω-diaminoalkanes during the reactions.

It is only recently that a 1:1 crystalline adduct between a *cationic* transition metal complex and a CD has been characterized by X-ray crystallography. Despite the fact that [Rh(cod)$(NH_3)_2$][PF_6] undergoes slow hydrolysis of its ammine ligands in an aqueous solution of α-CD, it proved possible[88] to obtain good single crystals of the 1:1 adduct. A space-filling plan view of [Rh(cod)$(NH_3)_2$·α-CD]$^{\oplus}$ is shown in Figure 36. The cod ligand is inserted partly into the α-CD cavity and the complex is tilted so that the two ammine ligands can enter into N-H···O hydrogen bonding ([N···O]=3.24, 3.25, 3.31, 3.46 Å) with four of the secondary hydroxyl groups on two of the six α-D-glucopyranoside units in the receptor. ^{1}H-NMR spectroscopy indicates that the adduct exists in D_2O solution but decomposes slowly with time as ammonia is released from the first coordination sphere. Replacement of the two ammine ligands by a bidentate en ligand afforded a rhodium com-

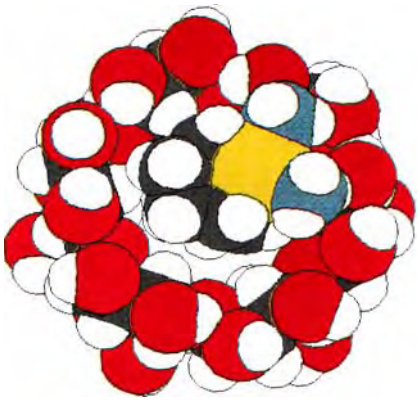


Fig. 36. Space-filling representation of the X-ray structure of [Rh(cod)$(NH_3)_2$·α-CD]$^{\oplus}$.

plex stable in aqueous solution in the presence of α-CD. A K_a value of 520±80 mol^{-1} kg was obtained from a quantitative ^{1}H-NMR spectroscopic analysis of the concentration dependence of [Rh(cod)(en)·α-CD][PF_6] in D_2O solution. Microcalorimetry and ^{1}H-NMR spectroscopy have also established[89] that the neutral antitumour drug diammine-1,1-cyclobutanedicarboxylatoplatinum(II) and α-CD form a 1:1 adduct in water with a standard free energy change ($-\Delta G^0$) in the region of 10.4–13.0 kJ mol^{-1} at 22–25°C. Slow cooling (starting from 80°C) of an aqueous solution of α-CD saturated with respect to the platinum complex afforded single crystals suitable for X-ray structural investigation.[90] A side-on view of the skeletal representation (Fig. 37) reveals that stabilization of the adduct is achieved by the cyclobutane ring of the complex penetrating into the α-CD cavity leaving the two ammine ligands to form two N-H···O hydrogen bonds ([N···O]=2.94, 3.14 Å) with secondary hydroxyl groups on neighboring α-D-glucopyranosidic units of the α-CD.

The binding of organometallic compounds to chemically-modified CDs awaits detailed investigations.[91] However, circular dichroism measurements show[92] that 6-deoxy-

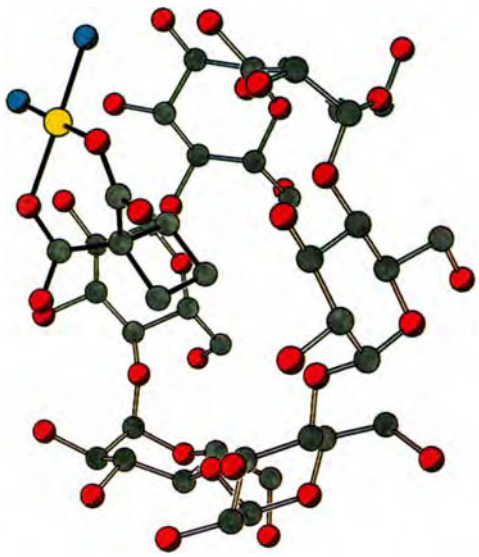


Fig. 37. Skeletal representation of the X-ray structure of [diammine-1,1-cyclobutanecarboxylatoplatinum(II)·α-CD].

6-(2-methoxyethylamino)-β-CD has a strong binding ability ($K_a = 600 \pm 44\ M^{-1}$) for ferrocenecarboxylic acid **20** in DMSO because of a Coulombic [$-CO_2^{\ominus} \cdots {}^{\oplus}H_2N<$] interaction.

10. Adduct Formation involving Ammonia-Borane

We have already noted in Section 3.1 that the borane complexes $[BX_3NH_3]$ (X = H, F) form[24] crystalline 1 : 1 adducts with 18C6. Because of the formal positive charge on the nitrogen atom, we concluded that the formation of 2 : 1 adducts with two neutral $[BX_3NH_3]$ molecules binding to opposite faces might be disfavored by Coulombic repulsion. However, it transpires that this is not necessarily the case when the 18C6 ring carries substituents. Thus, both the octamethyl[18]crown-6 derivative[93] Me_8-18C6 and the *trans-syn-trans*-tetraphenyl[18]crown-6 derivative[94] (*RRSS*)-Ph_4-18C6 form crystalline 2 : 1 adducts. Their X-ray crystal structures (Fig. 38) reveal that, in each case, the two $[BH_3NH_3]$ molecules are hydrogen bonded in a centrosymmetric manner to the opposite faces of the macrocycle which adopts a characteristic all-*gauche* conformation.

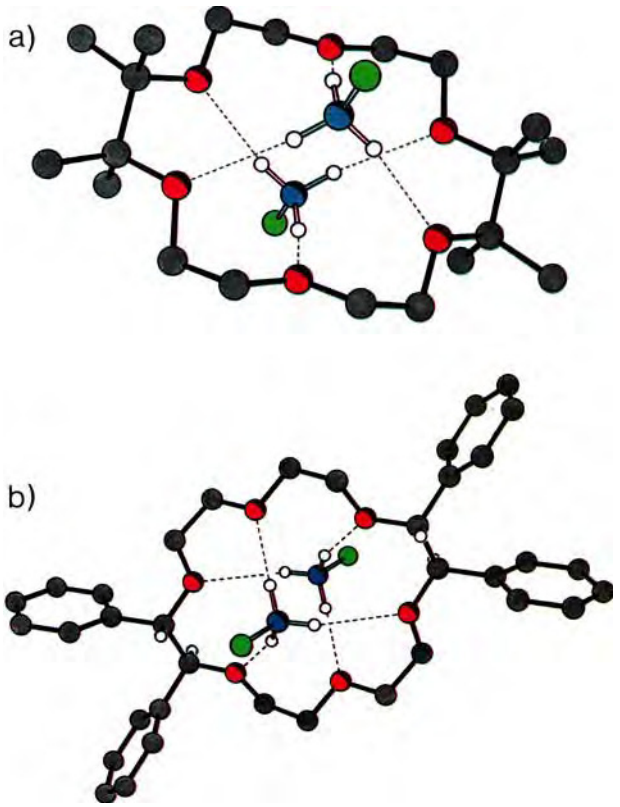
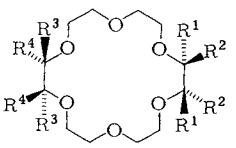


Fig. 38. Skeletal representation of the X-ray structure of (a) $[(BH_3NH_3)_2 \cdot Me_8\text{-}18C6]$ and (b) $[(BH_3NH_3)_2 \cdot (R,R,S,S)\text{-}Ph_4\text{-}18C6]$.

In $[(R,R,S,S)\text{-}Ph_4\text{-}18C6 \cdot (BH_3NH_3)_2]$, the four phenyl substituents are equatorially oriented. Interestingly, however, in the chiral *trans-anti-trans*-derivative (*R,R,R,R*)-{*p*-MeO−C_6H_4}$_4$-18C6,[95] although, once again, the characteristic all-*gauche* conformation—this time carrying two axial and two equatorial anisyl substituents—is adopted, only one $[BH_3NH_3]$ molecule is bound in the crystalline



	R¹	R²	R³	R⁴
Me_8-18C6	Me	Me	Me	Me
(*R,R,S,S*)-Ph_4-18C6	H	Ph	Ph	H
(*R,R,R,R*)-Ph_4-18C6	Ph	H	Ph	H
(*R,R,R,R*)-{*p*-MeO−C_6H_4}$_4$-18C6	*p*-MeO−C_6H_4	H	*p*-MeO−C_6H_4	H

adduct (Fig. 39). Clearly, the stoichiometry in the solid state varies, possibly reflecting the lattice requirements of the particular adduct. Nonetheless, high crystallinity is a feature of all the adducts involving $[BH_3NH_3]$ and crown ethers we have prepared and characterized in our laboratories.[95,96]

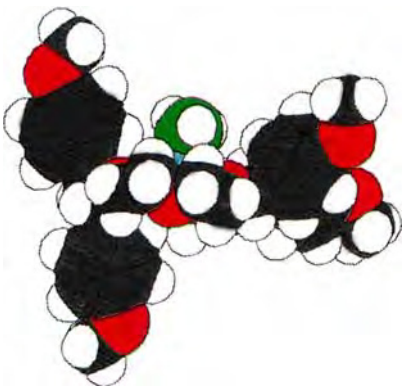


Fig. 39. Space-filling representation of the X-ray structure of $[(BH_3NH_3) \cdot (R,R,R,R)\text{-}\{p\text{-MeO}-C_6H_4\}_4\text{-}18C6]$.

11. Applications

These already exist and the potential for their growth is large and broad.

The purification of receptor molecules which are occasionally oils themselves can often be transformed from a difficult to an easy task by the formation of highly crystalline adducts. Thus, $[BH_3NH_3]$ has been used[96] successfully to purify and characterize a wide range of chiral crown ethers incorporating carbohydrate residues. Another *selective* crystallization procedure (Fig. 40) provides[29] a novel approach to the separation of *copper* from *cobalt*. The stability of the polymeric 1 : 1 adduct formed by $[Cu(NH_3)_4(H_2O)][PF_6]_2$ and 18C6 is such that it will precipitate almost quantitatively from aqueous solution, even in the presence of competing ions such as $[NH_4]^{\oplus}$ and $[Co(NH_3)_6]^{3\oplus}$.

Selectivity can also be observed in reactions of very different kinds. For example, enantioselective reductions of prochiral phenyl ketones PhCOR (R = Me, Et, *i*Pr, *t*Bu) with the chiral adduct (Fig. 40) formed between $[BH_3NH_3]$ and (*R,R,R,R*)-Ph_4-18C6 in toluene at −78 to −40 °C have afforded the corresponding secondary benzyl alcohols with 22–67% excess of the (*S*)-enantiomer. These re-

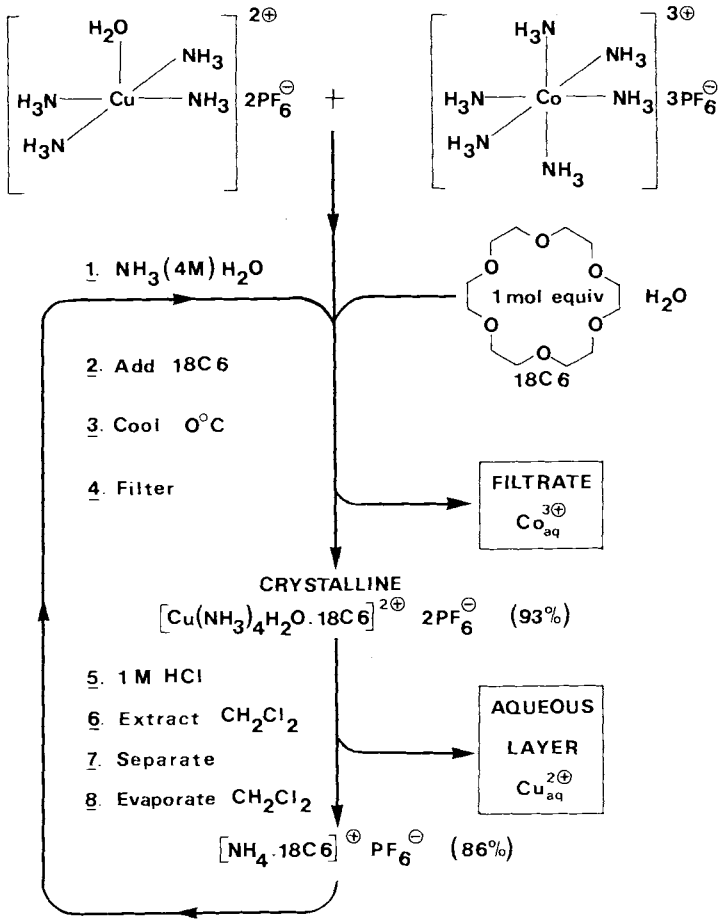


Fig. 40. A cyclic process for the separation of copper(II) from cobalt(III).

sults have been improved[97] by changing the reaction conditions. In a completely different context, the possibility exists of protecting coordinated $[M(CN)_6]^{n\ominus}$ anions against ligand photodissociation by using appropriate polyammonium macrocyclic receptors.[76–78] This combination of novel protecting group chemistry and photochemistry could be applied to the synthesis of substituted cyano complexes of transition metals.

Cyclodextrins have numerous and different applications. The interaction between β-CD and α-diimineruthenium(II) complexes containing phenanthroline ligands with phenyl substituents protects[98] the metal-to-ligand charge-transfer excited state from oxygen quenching and therefore modifies their properties as sensitizers. Perhaps most significantly of all, the formation of a 1 : 1 adduct between α-CD and Carboplatin provides an opportunity[99] for developing a drug delivery system for this promising anticancer agent.

12. Outlook

As in most interdisciplinary research areas, unexpected and exciting results are not difficult to come by, and pleasant surprises are often just waiting round the corner. Studying the second-sphere coordination of transition metal complexes by molecular receptors is proving to be a satisfying and rewarding pursuit. There is no doubt that, although the future in this field of chemistry offers many new challenges of a conceptual and practical nature, it also holds much promise of many new discoveries of technological importance. In a recent review article[100] where *Chatt* presents his reminiscences of scientific progress from academic backwater to industrial importance in the context of *A Half Century of Platinum Metal Chemistry*, he concludes:

> "Scientific discovery is not yet predictable. If you have an exciting road to follow do not be put off by those who say there is nothing at the end of it; they do not know. Persevere, and enjoy the excitement of exploring the unknown."

We draw strength and inspiration from the work of this scientist who, among his many pioneering contributions to coordination chemistry, sowed the seeds for the development of the second-sphere coordination of neutral and cationic metal complexes of the platinum group by molecular receptors.

We wish to thank our numerous students and coworkers for their contributions to the research program. Without their dedicated and enthusiastic involvement, only a very small part of the work we have reviewed here would have been accomplished. Their names are cited in many of the references. We thank ICI plc, Johnson Matthey plc, and the Agricultural and Food, and Science and Engineering Research Councils in the United Kingdom for their support. We are especially grateful to Dr. John Kendrick of the New Science Group at ICI Runcorn for his computer-assisted production of the color space-filling molecular illustrations.

Received: October 28, 1985 [A 577 IE]
German version: *Angew. Chem. 98* (1986) 483

[1] J. Bjerrum, *Adv. Chem. Ser. 62* (1967) 178.
[2] J. F. Stoddart, *Annu. Rep. Prog. Chem. B 1983* (1984) 353.
[3] M. L. Bender, M. Komiyama: *Cyclodextrin Chemistry*, Springer, Berlin 1978; W. Saenger, *Angew. Chem. 92* (1980) 343; *Angew. Chem. Int. Ed. Engl. 19* (1980) 344; J. Szejtli: *Cyclodextrins and their Inclusion Complexes*, Akademiai Kiado 1982; R. Breslow, *Chem. Br. 19* (1983) 126; J. L. Atwood, J. E. D. Davies, D. D. MacNicol (Eds.): *Inclusion Compounds, Vols. 1-3*, Academic Press, London 1984; M. Dobler: *Ionophores and Their Structures*, Wiley, New York 1981; J. W. Westley: *Polyether Antibiotics: Naturally Occurring Acid Ionophores, Vols. I and II*, Marcel Dekker, Basel 1982; D. H. Williams, *Acc. Chem. Res. 17* (1984) 364.
[4] R. M. Izatt, J. J. Christensen (Eds.): *Synthetic Multidentate Macrocyclic Compounds*, Academic Press, New York 1978; R. M. Izatt, J. J. Christensen (Eds.): *Progress in Macrocyclic Chemistry*, Wiley, New York, *Vol. 1*, 1979; *Vol. 2*, 1981; S. Patai (Ed.): *The Chemistry of the Functional Groups. Supplement E. The Chemistry of Ethers, Crown Ethers, Hydroxyl Groups, and their Sulphur Analogues, Part 1*, Wiley, Chichester 1980; M. Hiraoka: *Crown Compounds*, Elsevier, New York 1982; G. W. Gokel, S. H. Korzeiowski: *Macrocyclic Polyether Synthesis*, Springer, Berlin 1982; F. Vögtle, E. Weber (Eds.): *Host Guest Complex Chemistry. Macrocycles*, Springer, Berlin 1985; P. M. Keehn, S. M. Rosenfield (Eds.): *Cyclophanes I and II*, Academic Press, New York 1983; F. Vögtle (Ed.): *Cyclophanes I and II* (Topics in Current Chemistry 113, 115), Springer, Berlin 1983.
[5] H. M. Colquhoun, J. F. Stoddart, *J. Chem. Soc. Chem. Commun. 1981*, 612.
[6] A. Werner *Ann. Chem. 386* (1912) 1; *Neuere Anschauungen auf dem Gebiete der anorganischen Chemie*, 3rd edit., Vieweg, Braunschweig 1913.
[7] A. Werner, *Ber. Dtsch. Chem. Ges. 45* (1912) 121.
[8] P. Pfeiffer, K. Quehl, *Ber. Dtsch. Chem. Ges. 64* (1931) 2667; *65* (1932) 560.

[9] S. Kirschner, N. Ahmad, C. Munir, R. J. Pollock, *Pure Appl. Chem. 51* (1972) 913; A. F. Drake, J. R. Levey, S. F. Mason, T. Prosperi, *Inorg. Chim. Acta 57* (1982) 151.
[10] J. M. Smithson, R. J. P. Williams, *J. Chem. Soc. 1958*, 457.
[11] J. Chatt, L. A. Duncanson, L. M. Venanzi, *J. Chem. Soc. 1956*, 2712.
[12] J. Chatt, G. J. Leigh, N. Thankarajan, *J. Chem. Soc. A 1971*, 3168.
[13] H. Taube, F. A. Posey, *J. Am. Chem. Soc. 75* (1953) 1463.
[14] V. M. Nekipelov, K. I. Zamaraev, *Coord. Chem. Rev. 61* (1985) 185 and references cited therein.
[15] R. S. Armstrong, M. J. Aroney, R. K. Duffin, H. J. Stootman, R. J. W. Le Fevre, *J. Chem. Soc. Perkin Trans. 2 1973*, 1272.
[16] M. F. Tweedle, L. J. Wilson, *J. Am. Chem. Soc. 98* (1976) 4824; E. Sinn, G. Sim, E. V. Dose, M. F. Tweedle, L. J. Wilson, *ibid. 100* (1978) 3375.
[17] D. J. Cram, R. C. Helgeson, L. R. Sousa, J. M. Timko, M. Newcomb, F. de Jong, G. W. Gokel, D. H. Hoffman, L. A. Domeier, S. C. Peacock, K. Madan, L. Kaplan, *Pure Appl. Chem. 43* (1975) 327.
[18] C. J. Pedersen, *J. Am. Chem. Soc. 89* (1967) 7017.
[19] D. J. Cram, J. M. Cram, *Science 183* (1974) 803; *Acc. Chem. Res. 11* (1978) 8.
[20] J.-M. Lehn, *Acc. Chem. Res. 11* (1978) 49; *Pure Appl. Chem. 51* (1979) 979; *52* (1980) 2303, 2441; in K. J. Laidler (Ed.): *IUPAC Frontiers of Chemistry*, Pergamon Press, Oxford 1982, p. 265.
[21] J. F. Stoddart, *Chem. Soc. Rev. 8* (1979) 85; in M. I. Page (Ed.): *The Chemistry of Enzyme Action*, Elsevier, Amsterdam 1984, p. 529.
[22] F. de Jong, D. N. Reinhoudt, *Adv. Phys. Org. Chem. 17* (1980) 279.
[23] K. N. Trueblood, C. B. Knobler, D. S. Lawrence, R. V. Stevens, *J. Am. Chem. Soc. 104* (1982) 1355.
[24] H. M. Colquhoun, G. Jones, J. M. Maud, J. F. Stoddart, D. J. Williams, *J. Chem. Soc. Dalton Trans. 1984*, 63.
[25] Second-sphere coordination of transition metal complexes affords complexes of complexes. We find it convenient to refer to these complexes of complexes as *adducts*.
[26] The X-ray crystal structures of $[PhCH_2NH_3 \cdot 18C6][SCN]$ (M. J. Bovill, D. J. Chadwick, I. O. Sutherland, D. Watkin, *J. Chem. Soc. Perkin Trans. 2 1980*, 1529) and $[PhCOCH_2NH_3 \cdot 18C6][PF_6]$ (J. M. Maud, J. F. Stoddart, D. J. Williams, *Acta Crystallogr. C41* (1985) 137) indicate face-to-face complexation in the perching mode of the $[RNH_3]^{\oplus}$ ions to 18C6 in its all-*gauche* conformation with pseudo D_{3d} symmetry. For a discussion of the crystalline complex formed between $NH_4^{\oplus}$ ions and 18C6, see O. Nagano, A. Kobayashi, Y. Sasaki, *Bull. Chem. Soc. Jpn. 51* (1978) 790 and D. A. Pears, J. F. Stoddart, M. E. Fakley, B. L. Allwood, D. J. Williams, unpublished.
[27] J. D. Dunitz, P. Seiler, *Acta Crystallogr. B30* (1974) 2739.
[28] H. M. Colquhoun, J. F. Stoddart, D. J. Williams, *J. Chem. Soc. Chem. Commun. 1981*, 847.
[29] H. M. Colquhoun, D. F. Lewis, J. F. Stoddart, D. J. Williams, *J. Chem. Soc. Dalton Trans. 1983*, 607.
[30] As an aside, it is an interesting historical fact that these complexes were prepared in 1980 at the ICI Corporate Laboratory from samples of $[Pt(PR_3)_2Cl_2]$, synthesized by *Chatt*'s Research Group working at The Frythe (ICI) some 25 years earlier!
[31] Later, in Section 7, we shall see that $[BH_3NH_3]$ can form 2:1 complexes with 18C6 derivatives. There are numerous examples (e.g. $[\{CH_2(CN)_2\}_2 \cdot 18C6]$ and $[(CH_3NO_2)_2 \cdot 18C6]$) of 2:1 complexes involving *neutral* organic molecules with 18C6 in the literature (J. A. A. de Boer, D. N. Reinhoudt, S. Harkema, G. J. Hummel, F. de Jong, *J. Am. Chem. Soc. 104* (1982) 4073; A. Elbasyouny, H. J. Brügge, K. von Deuten, M. Dickel, A. Knöchel, K. U. Koch, J. Kopf, D. Melzer, G. Rudolph, *ibid. 105* (1983) 6568; W. H. Watson, J. Galloy, D. A. Grossie, F. Vögtle, W. M. Müller, *J. Org. Chem. 49* (1984) 347). More often than not, the macrocycle adopts the familiar all-*gauche* conformation with pseudo D_{3d} symmetry, but not always (e.g. $[(PhSO_2NH_2)_2 \cdot 18C6]$). Organic cations can (B. L. Allwood, H. M. Colquhoun, J. Crosby, D. A. Pears, J. F. Stoddart, D. J. Williams, *Angew. Chem. 96* (1984) 806; *Angew. Chem. Int. Ed. Engl. 23* (1984) 824; B. L. Allwood, J. Crosby, D. A. Pears, J. F. Stoddart, D. J. Williams, *ibid. 96* (1984) 987 and *23* (1984) 977; D. A. Pears, J. F. Stoddart, J. Crosby, B. L. Allwood, D. J. Williams, unpublished) also form 2:1 complexes provided the formal positive charge is not directly associated with the binding group (e.g. $[\{Ph_3PMe\}_2 \cdot 18C6][PF_6]_2$, $[\{Ph_2SMe\}_2 \cdot 18C6][Hg_2I_6]$ and $[\{PhCOCHPhSMe_2\}_2 \cdot 18C6][PF_6]_2$). The bireceptor nature of 18C6 manifests itself structurally in yet another manner. Neutral (e.g. $MeO_2CC{\equiv}CCO_2Me$) and cationic (e.g. $[PhCOCH_2SMe_2]^{\oplus}$) organic molecules containing *two binding groups* can form polymeric hydrogen bonded structures with alternating 18C6 units.
[32] A. W. Prestayko, S. T. Crooke, S. K. Carter (Eds.): *Cisplatin, Current Status and New Developments*, Academic Press, New York 1980; P. J. Sadler, *Chem. Br. 18* (1982) 182; S. J. Lippard, *Am. Chem. Soc. Symp. Ser. 209* (1983); K. R. Harrup, *Platinum Met. Rev. 28* (1984) 14.
[33] D. R. Alston, J. F. Stoddart, D. J. Williams, *J. Chem. Soc. Chem. Commun. 1985*, 532.
[34] H. M. Colquhoun, J. F. Stoddart, D. J. Williams, *J. Chem. Soc. Chem. Commun. 1981*, 849.
[35] H. M. Colquhoun, J. F. Stoddart, D. J. Williams, J. B. Wolstenholme, R. Zarzycki, *Angew. Chem. 93* (1981) 1093; *Angew. Chem. Int. Ed. Engl. 20* (1981) 1051; H. M. Colquhoun, S. M. Doughty, J. M. Maud, J. F. Stoddart, D. J. Williams, J. B. Wolstenholme, *Isr. J. Chem. 25* (1985) 15.
[36] H. M. Colquhoun, J. F. Stoddart, D. J. Williams, *J. Chem. Soc. Chem. Commun. 1981*, 851.
[37] R. M. Costes, G. Folcher, N. Keller, P. Plurien, P. Rigny, *Inorg. Nucl. Chem. Lett. 11* (1975) 469; P. G. Eller, R. A. Penneman, *Inorg. Chem. 15* (1976) 2439.
[38] B. Bombieri, G. de Paoli, A. Cassol, A. Immirzi, *Inorg. Chim. Acta 18* (1976) L23; R. M. Costes, G. Folcher, P. Plurien, P. Rigny, *Inorg. Nucl. Chem. Lett. 12* (1976) 13; J. Klimes, A. Knöchel, G. Rudolph, *ibid. 13* (1977) 45; G. Bombieri, G. de Paoli, A. Immirzi, *J. Inorg. Nucl. Chem. 40* (1978) 799.
[39] A. Knöchel, J. Klines, J. Oehler, G. Rudolph, *Inorg. Nucl. Chem. Lett. 11* (1975) 787; A. Knöchel, J. Kopf, J. Oehler, G. Rudolph, *ibid. 14* (1978) 61.
[40] T. B. Vance, Jr., E. M. Holt, D. L. Varie, S. L. Holt, *Acta Crystallogr. B36* (1980) 153.
[41] T. B. Vance, Jr., E. M. Holt, C. G. Pierpont, S. L. Holt, *Acta Crystallogr. B36* (1980) 150.
[42] P. Charpin, R. M. Costes, G. Folcher, P. Plurien, A. Navaza, C. de Rango, *Inorg. Nucl. Chem. Lett. 13* (1977) 341.
[43] U. Russo, A. Cassol, A. Silvestri, *J. Organomet. Chem. 260* (1984) 69; G. Valle, A. Cassol, U. Russo, *Inorg. Chim. Acta 82* (1984) 81; P. A. Cusack, B. N. Patel, P. J. Smith, D. W. Allen, I. W. Nowell, *J. Chem. Soc. Dalton Trans. 1984*, 1239.
[44] M. M. Amini, A. L. Rheingold, R. W. Taylor, J. J. Zuckerman, *J. Am. Chem. Soc. 106* (1984) 7289.
[45] G. W. Gokel, D. J. Cram, C. L. Liotta, H. P. Harris, F. L. Cook, *J. Org. Chem. 39* (1974) 2445.
[46] H. M. Colquhoun, J. F. Stoddart, D. J. Williams, *J. Am. Chem. Soc. 104* (1982) 1426.
[47] G. L. Blacker, M. D. Nordyke, T. M. Vickrey, R. A. Bartsch, R. A. Holwerda, *Inorg. Chem. 17* (1978) 3310.
[48] H. D. von Hardt, H.-J. Stoll, *Z. Anorg. Allg. Chem. 442* (1978) 221.
[49] H. M. Colquhoun, E. P. Goodings, J. M. Maud, J. F. Stoddart, J. B. Wolstenholme, D. J. Williams, *J. Chem. Soc. Chem. Commun. 1983*, 1140; *J. Chem. Soc. Perkin Trans. 2 1985*, 607.
[50] H. M. Colquhoun, S. M. Doughty, J. F. Stoddart, D. J. Williams, *Angew. Chem. 96* (1984) 232; *Angew. Chem. Int. Ed. Engl. 23* (1984) 235; J. F. Stoddart, S. E. Fuller, S. M. Doughty, P. C. Y. K. Ning, D. J. Williams, B. L. Allwood, A. M. Z. Slawin, H. M. Colquhoun in J. Streith, H. Prinzbach, G. Schill (Eds.): *Organic Synthesis: An Interdisciplinary Challenge*, Blackwell, Oxford 1985, p. 529; H. M. Colquhoun, S. M. Doughty, A. M. Z. Slawin, J. F. Stoddart, D. J. Williams, *J. Chem. Soc. Dalton Trans.*, in press.
[51] G. M. Anderson III, P. A. Kollman, L. N. Dommelsmith, N. K. Houk, *J. Am. Chem. Soc. 101* (1979) 2344; L. N. Dommelsmith, T. A. Eaton, N. K. Houk, G. M. Anderson III, R. A. Glennon, A. T. Shulgin, N. Castagnoli, Jr., P. A. Kollman, *J. Med. Chem. 24* (1981) 114; A. Makriyannis, S. Fesik, *J. Am. Chem. Soc. 104* (1982) 6462; L. I. Kruse, J. K. Cha, *J. Chem. Soc. Chem. Commun. 1982*, 1329; J. D. Mersh, J. K. M. Saunders, S. A. Matlin, *ibid. 1983*, 306.
[52] J. Pawliszyn, M. M. Szczesniak, S. Schreiner, *J. Phys. Chem. 88* (1984) 1726.
[53] E. Dubler, U. K. Haring, K. H. Scheller, P. Baltzer, H. Sigel, *Inorg. Chem. 23* (1984) 3785.
[54] J. Uzawa, S. Zushi, Y. Kodama, Y. Fukuda, K. Nishihata, K. Umemura, M. Nishio, M. Hirota, *Bull. Chem. Soc. Jpn. 53* (1980) 3623.
[55] T. Endo, M. M. Ito, Y. Yamada, H. Saito, K. Miyazawa, M. Nishio, *J. Chem. Soc. Chem. Commun. 1983*, 1430.
[56] Y. Kodama, K. Nishihata, M. Nishio, N. Nakagawa, *Tetrahedron Lett. 1977*, 2105.
[57] H. Sigel, B. E. Fischer, E. Farkas, *Inorg. Chem. 22* (1983) 925.
[58] I. R. Hanson, D. L. Hughes, M. R. Truter, *J. Chem. Soc. Perkin Trans. 2 1976*, 972.
[59] M. A. Bush, M. R. Truter, *J. Chem. Soc. Perkin Trans. 2 1972*, 345.
[60] J. M. Maud, J. F. Stoddart, H. M. Colquhoun, D. J. Williams, *Polyhedron 3* (1984) 675.
[61] S. M. Doughty, J. F. Stoddart, H. M. Colquhoun, D. J. Williams, *Polyhedron 4* (1985) 567.
[62] G. W. Watt, D. G. Upchurch, *J. Am. Chem. Soc. 90* (1968) 914.
[63] R. Foster: *Organic Charge-Transfer Complexes*, Academic Press, London 1969, p. 128; A. Ray, *J. Am. Chem. Soc. 93* (1971) 7146.
[64] B. L. Allwood, H. M. Colquhoun, S. M. Doughty, F. H. Kohnke, A. M. Z. Slawin, J. F. Stoddart, D. J. Williams, R. Zarzycki, unpublished.
[65] F. H. Kohnke, J. F. Stoddart, B. L. Allwood, D. J. Williams, *Tetrahedron Lett. 26* (1985) 1681; F. H. Kohnke, J. F. Stoddart, *ibid. 26* (1985)

1685; B. L. Allwood, F. H. Kohnke, A. M. Z. Slawin, J. F. Stoddart, D. J. Williams, *J. Chem. Soc. Chem. Commun. 1985*, 311; F. H. Kohnke, J. F. Stoddart, *ibid. 1985*, 314; B. L. Allwood, F. H. Kohnke, J. F. Stoddart, D. J. Williams, *Angew. Chem. 97* (1985) 584; *Angew. Chem. Int. Ed. Engl. 24* (1985) 581.

[66] B. L. Allwood, H. M. Colquhoun, H. Shahriari-Zavareh, J. F. Stoddart, D. J. Williams, unpublished.

[67] D. R. Alston, A. M. Z. Slawin, J. F. Stoddart, D. J. Williams, *Angew. Chem. 96* (1984) 804; *Angew. Chem. Int. Ed. Engl. 23* (1984) 821.

[68] D. R. Alston, J. F. Stoddart, A. M. Z. Slawin, D. J. Williams, unpublished.

[69] G. H. W. Milburn, M. R. Truter, *J. Chem. Soc. A 1966*, 1609.

[70] D. R. Alston, A. M. Z. Slawin, J. F. Stoddart, D. J. Williams, unpublished.

[71] N. W. Alcock, J. M. Brown, J. C. Jeffrey, *J. Chem. Soc. Chem. Commun. 1974*, 829; *J. Chem. Soc. Dalton Trans. 1976*, 583.

[72] H. M. Colquhoun, S. M. Doughty, A. M. Z. Slawin, J. F. Stoddart, D. J. Williams, *Angew. Chem. 97* (1985) 124; *Angew. Chem. Int. Ed. Engl. 24* (1985) 135.

[73] B. Dietrich, M. W. Hosseini, J. M. Lehn, R. B. Sessions, *J. Am. Chem. Soc. 103* (1983) 1282.

[74] B. Dietrich, M. W. Hosseini, J. M. Lehn, R. B. Sessions, *Helv. Chim. Acta 66* (1983) 1262.

[75] F. Peter, M. Gross, M. W. Hosseini, J. M. Lehn, R. B. Sessions, *J. Chem. Soc. Chem. Commun. 1981*, 1067; F. Peter, M. Gross, M. W. Hosseini, J. M. Lehn, *J. Electroanal. Chem. 144* (1983) 279.

[76] M. F. Manfrin, N. Sabbatini, L. Moggi, V. Balzani, M. W. Hosseini, J. M. Lehn, *J. Chem. Soc. Chem. Commun. 1984*, 555.

[77] M. F. Manfrin, L. Moggi, V. Caselvetro, V. Balzani, M. W. Hosseini, J. M. Lehn, *J. Am. Chem. Soc.*, in press.

[78] V. Balzani, N. Sabbatini, F. Scandola, unpublished.

[79] J. M. Lehn, P. Vierling, R. Hayward, *J. Chem. Soc. Chem. Commun. 1979*, 296.

[80] J. M. Lehn, private communication.

[81] J. W. Westley, R. H. Evans, Jr., J. F. Blount, *J. Am. Chem. Soc. 99* (1977) 6057.

[82] J. Shaw, G. W. Everett, *Inorg. Chem. 24* (1985) 1917.

[83] B. Siegel, R. Breslow, *J. Am. Chem. Soc. 97* (1975) 6869.

[84] A. Harada, S. Takahashi, *J. Chem. Soc. Chem. Commun. 1985*, 645.

[85] M. F. Czarniecki, R. Breslow, *J. Am. Chem. Soc. 100* (1978) 7771; R. Breslow, M. F. Czarniecki, J. Emert, H. Hamaguchi, *ibid. 102* (1980) 762; R. Breslow, G. Trainor, A. Ueno, *ibid. 105* (1983) 2739; W. J. le Noble, S. Srivastava, R. Breslow, G. Trainor, *ibid. 105* (1983) 2739, 2745.

[86] T. Matsue, D. H. Evans, T. Osa, N. Kobayashi, *J. Am. Chem. Soc. 107* (1985) 3411.

[87] H. Ogino, *J. Am. Chem. Soc. 103* (1981) 1303; H. Ogino, K. Ohata, *Inorg. Chem. 23* (1984) 3312.

[88] D. R. Alston, A. M. Z. Slawin, J. F. Stoddart, D. J. Williams, *Angew. Chem. 97* (1985) 771; *Angew. Chem. Int. Ed. Engl. 24* (1985) 786.

[89] D. R. Alston, T. H. Lilley, J. F. Stoddart, *J. Chem. Soc. Chem. Commun. 1985*, 1600.

[90] D. R. Alston, A. M. Z. Slawin, J. F. Stoddart, D. J. Williams, *J. Chem. Soc. Chem. Commun. 1985*, 1602.

[91] If the suggested structure of a binuclear copper(II) complex of α-CD involving cross-linking of contiguous glucose residues in the cyclodextrin by a $Cu(OH)_2Cu$ bridge (Y. Matsui, T. Kurita, Y. Date, *Bull. Chem. Soc. Jpn. 45* (1972) 3229; Y. Matsui, T. Kurita, M. Yagi, T. Okayama, K. Mochida, Y. Date, *ibid. 48* (1975) 2187; Y. Matsui, D. Suemitsu, *ibid. 58* (1985) 1658) is supported subsequently by firm structural evidence, then it could constitute an interesting example of simultaneous first- and second-sphere coordination of copper(II) by α-CD.

[92] A. Ueno, F. Moriwaki, T. Osa, F. Hamada, K. Murai, *Tetrahedron Lett. 26* (1985) 899.

[93] D. R. Alston, J. F. Stoddart, J. B. Wolstenholme, B. L. Allwood, D. J. Williams, *Tetrahedron 41* (1985) 2923.

[94] B. L. Allwood, H. Shahriari-Zavareh, J. F. Stoddart, D. J. Williams, *J. Chem. Soc. Chem. Commun. 1984*, 1461.

[95] J. Crosby, D. A. Pears, J. F. Stoddart, B. L. Allwood, D. J. Williams, unpublished.

[96] H. Shahriari-Zavareh, J. F. Stoddart, M. K. Williams, B. L. Allwood, D. J. Williams, *J. Inclusion Phenom. 3* (1985) 355.

[97] J. Crosby, D. A. Pears, H. Shahriari-Zavareh, J. F. Stoddart, B. L. Allwood, D. J. Williams, B. Koppenhöfer, unpublished results.

[98] J. I. Cline III, W. J. Dressick, J. N. Demas, B. A. DeGraff, *J. Phys. Chem. 89* (1985) 94.

[99] D. R. Alston, J. F. Stoddart, Br. Pat. Appl. 8427747 (November 2, 1984).

[100] J. Chatt, *Platinum Met. Rev. 29* (1985) 126.

The Palladium-Catalyzed Cross-Coupling Reactions of Organotin Reagents with Organic Electrophiles

New Synthetic Methods (58)

By John K. Stille*

The cross-coupling of organotin reagents with a variety of organic electrophiles, catalyzed by palladium, provides a novel method for generating a carbon-carbon bond. Because this mild, versatile reaction is tolerant of a wide variety of functional groups on either coupling partner, is stereospecific and regioselective, and gives high yields of product, it is ideal for use in the synthesis of elaborate organic molecules. When the coupling reaction is carried out in the presence of carbon monoxide, instead of a direct coupling, carbon monoxide insertion takes place, stitching the two coupling partners together and generating a ketone.

1. Introduction

There are relatively few basic reaction types that generate a new carbon-carbon bond, although this is one of the most critical operations in the synthesis of organic molecules. Group VIII transition metals, particularly nickel and palladium, are effective in catalyzing the cross-coupling of organometallic reagents with organic halides and related electrophiles [Eq. (1)].[1-10]

$$RM + R'X \xrightarrow{M'} R-R' + MX \qquad (1)$$

In order for the coupling reaction to be useful, it should be relatively straightforward and require only a small amount of catalyst. Moreover, the reaction conditions and reagents, particularly the organometallic partner, should tolerate a wide variety of functional groups so that tedious protection-deprotection reactions are not necessary. Of the organometallic reagents available, many will not tolerate sensitive functionality on the coupling partners, are difficult to prepare, or are air or moisture sensitive, and few can be purified and stored.

Various organometallic reagents, RM, have been used in coupling reactions with disparate success. High conversions often are not obtained with lithium or Grignard reagents, neither of which will tolerate a wide variety of functional groups on either coupling partner,[2,3] and often homocoupling of the organic halide is observed. The copper-promoted coupling of alkenyl or aryl compounds is more successful, but it often results in extensive homocoupling.[11] In addition, the methods of synthesis of copper reagents do not always allow the presence of the more reactive functional groups on the organocopper partner.

The use of organometallic reagents containing metals of intermediate electropositive character generally leads to higher yields of coupled product and fewer side reactions. Many of these organometallic compounds tolerate a wide range of functional groups in either or both of the coupling partners. Organozinc compounds are particularly good in this regard, although the methods of synthesis limit the variety of structures that can be incorporated into the organic portion of the organozinc reagent. Organomercurials also tolerate functionality, but the methods for their synthesis are somewhat limiting; moreover, methods for the alkylation of organomercurials are unfortunately limited to a few examples with organic halides.[12,13] Organometallic partners in which the metal is boron or aluminum often are not conveniently synthesized or the structure of the organic portion is limited by the methods of synthesis available, usually hydroboration or hydroalumination.[4-7] Organozirconium reagents have the advantage that ether or acetal groups are tolerated in the hydrozirconation reaction and carbonyl and ester groups may be present in the alkenyl halide partner.[14] In coupling reactions, low turnovers of catalyst are observed, however.

One of the most versatile organometallic reagents in palladium-catalyzed coupling reactions is the organotin reagent. Organotin compounds containing a variety of reactive functional groups can be prepared by a number of routes; moreover, these reagents are not particularly oxygen or moisture sensitive. Because of their value in coupling reactions, a brief survey of their syntheses, particularly some of the more recent ones, is presented.

In the palladium-catalyzed coupling of organic electrophiles with organotin reagents, essentially only one of the groups on tin enters into the coupling reaction [Eq. (2)].

$$RX + R'SnR''_3 \xrightarrow{[PdL_n]} R-R' + XSnR''_3 \qquad (2)$$

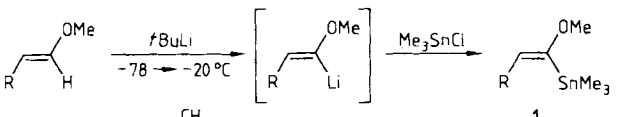
This is not a problem if a relatively simple organic group, for example, methyl, is to be transferred, since tetramethyltin can be used. If the group is more expensive or difficult to synthesize, however, then the utilization of only one of four identical groups would be a distinct disadvantage. Fortunately, different groups are transferred with different selectivities from tin, the simple alkyl group having the slowest transfer rate (see Section 3.1). Thus, an unsymmetrical organotin reagent containing three simple alkyl groups (such as methyl or butyl) is chosen; the fourth group, which undergoes transfer, is usually an alkynyl, alkenyl, aryl, benzyl, or allyl group.

[*] Prof. Dr. J. K. Stille
Department of Chemistry, Colorado State University
Fort Collins, CO 80523 (USA)

2. Synthesis of Organotin Reagents

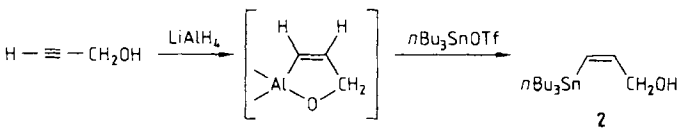
2.1. Synthesis from Electrophilic and Nucleophilic Triorganotin Compounds

A variety of methods for the synthesis of unsymmetrical organostannanes are known.[15-18] Although the reaction of a triorganotin halide with an organometallic compound is widely used, its scope of application is limited since the organometallic compound (usually M = Li, Al, Mg) does not allow a large variety of functional groups to be introduced into the organotin product. There are a number of valuable synthetic procedures involving organic anions, however. Lithiation of an enol ether followed by reaction with trimethyl- or tributyltin chloride gives a vinyltin reagent **1** that can serve as an acyl anion equivalent.[19,20]

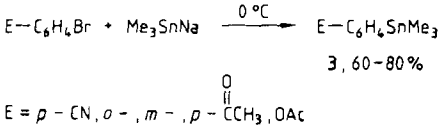


R = H, CH_2=CH, CH_2=C(CH$_3$), Ph

The reaction of propargyl alcohol with lithium aluminum hydride followed by tributyltin trifluoromethanesulfonate (triflate) yields the *Z*-vinyltin reagent **2**.[21] Cuprates also undergo *cis* addition to acetylenes, generating a vinyl metal compound, which reacts with tributyltin triflate to yield the (*Z*)-vinyltin compound.[22]

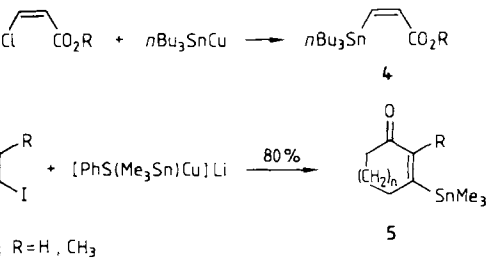


The inverse reaction of a trimethyl- or tributyltin anion with an organic electrophile is more versatile. The displacement of a halide or tosylate by a trimethyltin anion can be made to take place with inversion of configuration at an sp^3 carbon. Reaction of sodium trimethylstannate with an aryl bromide takes place under mild conditions, without reaction at other electrophilic substituents, to yield aryltin reagents **3**.[16,17]



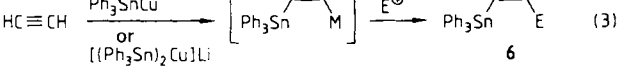
E = *p*-CN, *o*-, *m*-, *p*-C(=O)CH$_3$, OAc

The reaction of lithium tributylstannate with (*Z*)-β-chlorostyrene occurs with retention of configuration of the double bond. This reaction provides a method of synthesis of either pure (*E*)- or (*Z*)-β-tributyltin acrylates **4** from the corresponding (*E*)- and (*Z*)-β-chloroacrylates.[23] The reaction of a tin cuprate with an α,β-unsaturated β-iodo ketone gives high yields of the corresponding tin reagent **5**.[17,18]

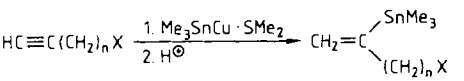


n = 2, 3; R = H, CH_3

An especially useful reaction is the stereospecific addition of a complex containing a copper–tin bond across a triple bond. The stereochemistry of addition depends on the particular copper reagent and the reaction conditions. Acetylene undergoes a *cis* addition with the copper(I) reagents Ph_3SnCu and $[(Ph_3Sn)_2Cu]Li$ [Eq. (3)].[24] The initially

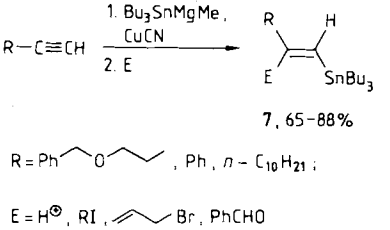


(3)



n = 1–4, 6; X = OH, OTHP, OSi*t*BuMe$_2$, Cl

formed anion can be trapped with a variety of electrophiles to yield the substituted vinyltin reagents **6**. When $Me_3SnCu \cdot SMe_2$ is used, the regiochemistry of addition to a monoalkyl-substituted acetylene is that expected for anionic addition; the alkyne can bear a variety of alkyl groups (THP = tetrahydropyranyl).[25] Methylmagnesium tributylstannate in the presence of copper(I) cyanide, however, yields product **7** of opposite regiochemistry. A variety of electrophiles may be used to trap the vinyl anion.[26]



R = Ph(THP), Ph, *n*-$C_{10}H_{21}$;

E = H$^{\oplus}$, RI, allyl bromide, PhCHO

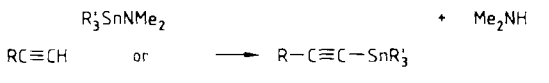
Either *cis* or *trans* addition of trimethylstannyl copper reagents to substituted and unsubstituted propiolate esters can be achieved to yield either (*E*)-**8** or (*Z*)-**9**, depending on the cuprate and the reaction conditions (THF = tetrahydrofuran).[27,28]



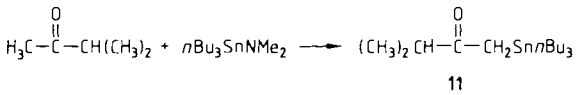
		8		**9**
R = Me	[$Me_3SnCuSPh$]Li, −78 °C, MeOH/THF	99	:	1
R = Me	[$Me_3SnCuSPh$]Li, −48 °C, THF	2	:	98
R = Me	[$Me_3SnCuC{=}CR$]Li or $Me_3SnCu \cdot LiBr \cdot Me_2S$, −48 °C, THF	99	:	1
R = H	[$Me_3SnCuSPh$]Li, −100 °C, EtOH/THF	97	:	3

2.2. Synthesis from Tin Amides and Oxides

Weakly acidic hydrogen can be replaced by tin in a reaction with tin amides or oxides.[15-17,29] This serves as a mild method for the synthesis of acetylenic tin reagents **10** and α-stannyl ketones **11**.

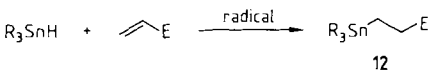


R = alkyl, aryl, CN, CH=CHOMe, OEt



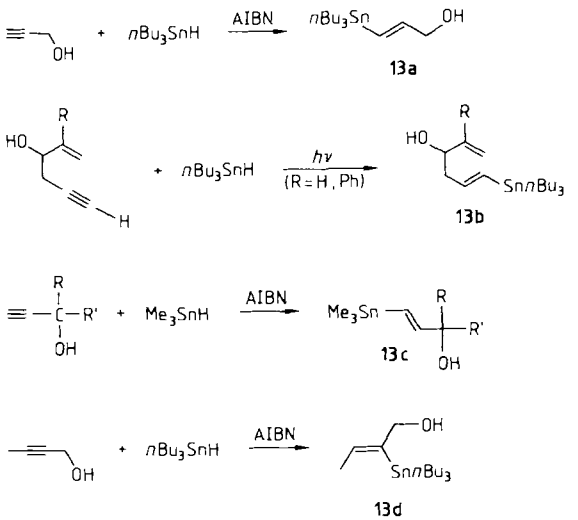
2.3. Tin Hydride Additions to Alkenes and Alkynes

The free radical addition of triorganotin hydrides to olefins takes place regiospecifically.[15] This reaction has limited use, however, since the product **12** is a mixed alkyltin reagent, which will not necessarily transfer the newly added group exclusively in a catalytic coupling reaction.

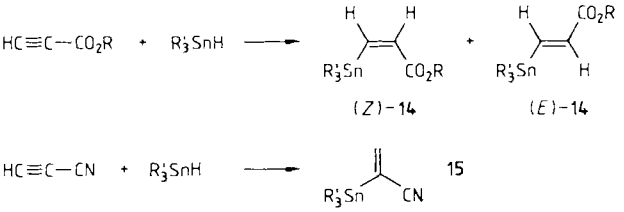


E = $CONH_2$, $CH(OEt)_2$, CH_2OH, CN

The radical addition of triorganotin hydrides to monosubstituted acetylenes to give substituted vinylstannanes **13** is mostly regiospecific, the (*E*)-isomer being favored, although an (*E*)/(*Z*) mixture is often obtained (AIBN = azobisisobutyronitrile).[30-34]



Radical addition to propiolate esters generally yields one regioisomer **14** as an (*E*)/(*Z*) mixture.[15,35] In the absence of catalyst, especially in polar solvents, cyanoacetylene yields the vinyltin reagents **15**.

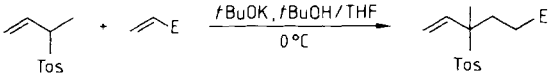


Triorganotin hydrides also react with diazoalkanes, giving the tin reagents **16** containing various functional groups.[15] However, these tin reagents will be useful in coupling reactions only if selective transfer of the added alkyl group is realized.

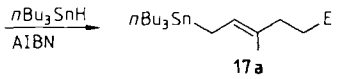


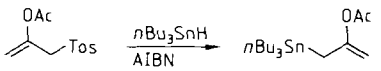
R' = CO_2Et, $COCH_3$, COC_6H_5, CN

The radical addition of tributyltin hydride to an olefin containing an allylic tosylate leaving group leads to the allyltin reagents **17a**, bearing a nitrile, ester, or tosyl group, or **17b**, bearing an enolacetate group.[36]



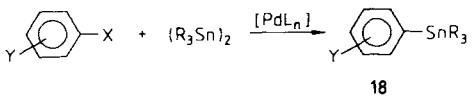
E = CN, CO_2Me, Tos





2.4. Reactions of Hexaalkyldistannanes with Organic Halides

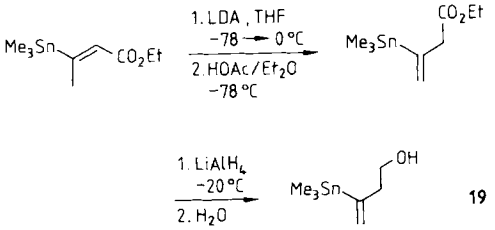
The mild, palladium-catalyzed coupling of hexaalkyldistannanes with aryl, benzyl, or allyl halides provides a unique method of synthesis of organotin reagents in which the organic group derived from the organic halide can have reactive substituents.[37-39] This synthetic procedure is especially valuable for the synthesis of trialkylaryltin reagents **18**.



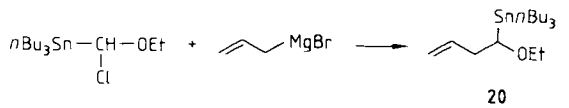
X = Br, I; Y = C(=O)-CH_3, CN, NO_2; R = Me, *n*Bu

2.5. Elaboration of Organotin Reagents

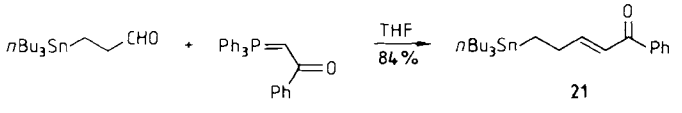
Tin–carbon bonds in organotin reagents are relatively stable, the bond energy being about 50 kcal/mol.[15] Thus, it is not surprising that a wide variety of reactions can be performed at other functional groups in the molecule without breaking the Sn–C bond. For example, the permanganate oxidation of primary alcohols to carboxylic acids[15] and the chromium trioxide oxidation of secondary alcohols to ketones,[16,17] as well as the lithium aluminum hydride reduction of esters, nitriles, and ketones to alcohols and amines,[15–17,40] can be carried out without cleavage of the carbon–tin bonds. Thus, the substituted vinyltin reagent **19**, containing a primary OH group, was obtained by an isomerization–reduction sequence (LDA = lithiumdiisopropylamide).[41]



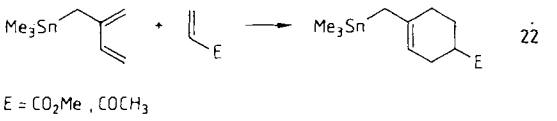
The Sn–C bond survives reactions of Grignard reagents, either when the Grignard reagent is allowed to react with an organotin compound containing an appropriate functional group or when a halogen-containing organotin compound is converted into a Grignard reagent.[15,17] Cyano and carbonyl groups on one of the organic groups of an unsymmetrical organotin reagent undergo Grignard reactions in the usual manner. An unsymmetrical organotin compound containing an α-chloroether function reacts with allylmagnesium bromide, for example, to yield the allylic tin reagent **20**.[42]



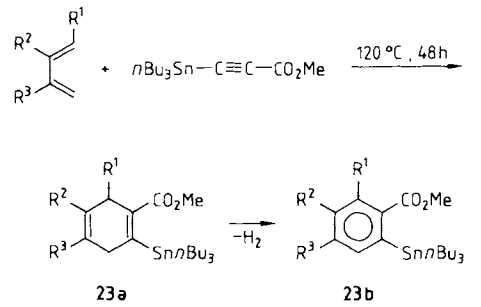
The NH_2 group undergoes typical reactions with various electrophiles;[43] for example, amines may be converted into isocyanates with phosgene.[16] Unsymmetrical organostannanes undergo the Wittig reaction, either by reaction of an aldehyde function on the organotin compound with methylenetriphenylphosphorane[15,16] or by reaction of an organotin-containing Wittig reagent with an aldehyde.[17] This reaction has been used in the synthesis of the organotin reagent **21** containing an α,β-unsaturated ketone.[44]



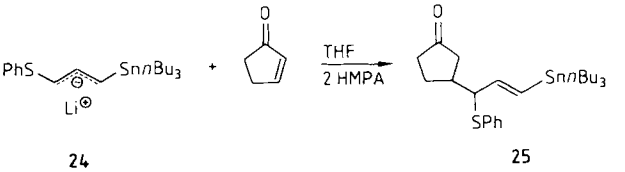
Olefinic groups on an organotin reagent can be hydroborated[17] and acetylenic groups add alkylboranes.[16] Cyclopropanation of an acetylenic group can be achieved with diazoalkanes.[16] A 1,3-diene containing a trimethylstannylmethyl group in the 2-position will undergo the Diels–Alder reaction with an electron-poor dienophile,[45] thereby providing a new allylic tin reagent **22**.



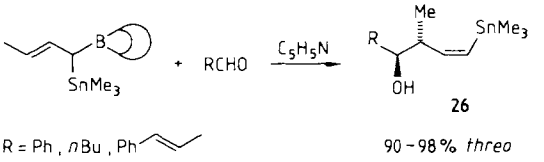
A Diels–Alder reaction between methyl tributylstannylpropiolate and substituted butadienes at 120 °C gives good yields of the 1,4-cyclohexadiene adduct **23a**, which can be dehydrogenated to the aryltin reagent **23b**.[46]



The ability to generate relatively stable anions on an organic group attached to tin, without carbon–tin bond cleavage, provides a versatile method of elaboration of organostannanes. The stabilized allyl anion **24**, for example, undergoes 1,4-addition to cyclopentenone to yield the vinyltin reagent **25** (HMPA = hexamethylphosphoramide).[47]

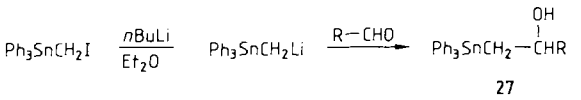


In a related reaction, aldehydes react with 9-borabicyclononane(9-BBN)-substituted organotin compounds with allylic rearrangement to yield the vinyltin reagents **26**.[48]



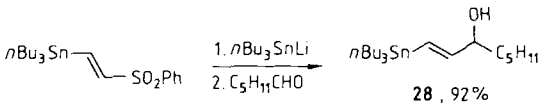
An anionic center in the α-position to tin reacts with a variety of electrophiles (such as aldehydes, ketones, and

allyl bromides) to give the organostannanes **27**.[49] In the example shown, however, the alkyl group could not necessarily be expected to undergo selective transfer in transition-metal-catalyzed coupling reactions. A tributyltin-substituted vinyl anion also adds to aldehydes to give an al-



27

lylic alcohol **28** in which the Sn-C(sp^2) bond could be expected to undergo preferential cleavage in coupling reactions.[50]



28, 92%

2.6. Separation and Purification of Organotin Compounds

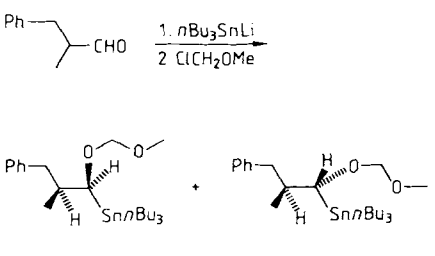
Since organotin reagents are relatively stable, it should not be surprising that some can be purified by distillation. Higher-molecular-weight compounds can sometimes be crystallized. Most importantly, many of the reagents withstand chromatography on silica gel.

The separation of an (*E*)/(*Z*) mixture of benzyl tributylstannylacrylate **29**, obtained from the addition of tributyltin hydride to benzyl propiolate, can be achieved on a preparative scale by medium pressure liquid chromatography (MPLC) on silica gel. The (*Z*)-isomer elutes first and can be reisomerized to an (*E*)/(*Z*) mixture, thereby providing a means of converting nearly all of the product into the (*E*)-isomer.



(*E*)-**29** (*Z*)-**29**

The reaction of 2-methyl-3-phenylpropanal with lithium tributylstannate followed by chloromethyl methyl ether yields two stereoisomers, **30a**, **b**, which also have been separated on an MPLC column.[51]

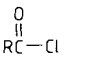
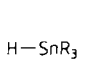
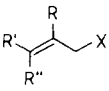
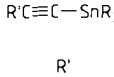
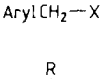
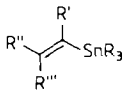
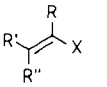
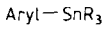
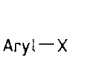
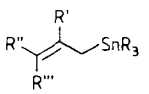
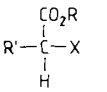
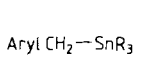
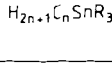


30a **30b**

3. Reactions with Organotin Compounds

The coupling reaction of organotin reagents with organic electrophiles catalyzed by palladium takes place under mild conditions in high yields. A wide variety of organic halides and organotin compounds can be coupled, either directly or in the presence of carbon monoxide (to yield a ketone, RCOR′, see Section 3.2) (Table 1). Moreover, a wide variety of functional groups (e.g., CO_2R, CN, OH, and even CHO) are tolerated on either partner. In addition, the reaction is regioselective in coupling reactions of allyl partners and occurs stereospecifically with inversion of configuration at sp^3 carbon centers bound to tin and/or halogen. Usually retention of configuration of the double bond is observed regardless of which reactant contains the double bond.

Table 1. Organotin reagents and electrophilic compounds suitable for coupling reactions.

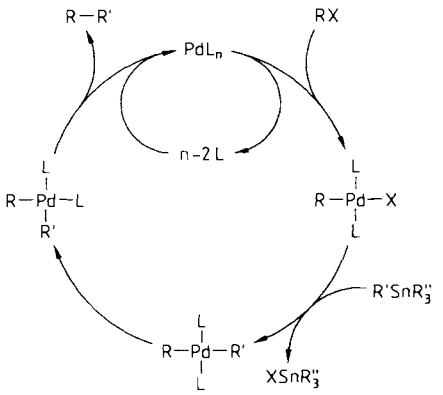
Electrophile		Organotin reagent
		
	[X = Cl, Br]	
	[X = Cl, Br]	
	[X = I, OTf]	
	[X = Br, I]	
	[X = Br, I]	
		

In the following discussion, the direct coupling reaction of organotin compounds with acid chlorides, organic halides, and vinyl triflates will be treated separately from the carbonylative coupling (Section 3.2).

3.1. Direct Coupling

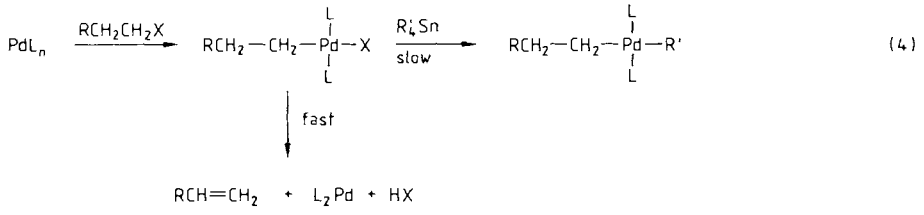
The catalytic cycle in Scheme 1 serves as a working model for the direct coupling reaction. Although this cycle has yet to be established for the coupling, many of the individual steps in the cycle have been documented;[52–57] a more detailed mechanistic discussion of certain of the coupling reactions is given in Section 4.

Notably absent from the list of electrophiles in Table 1 are those organic compounds with a hydrogen on an sp^3 carbon in the β-position to the carbon bearing the leaving group. This limitation is imposed because the slowest step

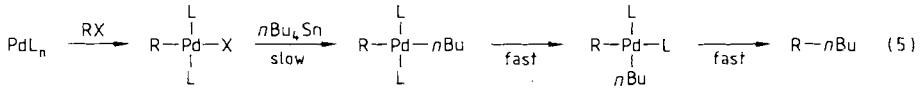


Scheme 1. Mechanism of the catalyzed, direct coupling.

in the catalytic cycle, the transmetalation step, is much slower than the β-elimination that takes place in the alkylpalladium halide complex [Eq. (4)]. This limitation is not imposed on the organotin partner, however, since the catalytic steps taking place after transmetalation—*trans/cis* isomerization and reductive elimination—are faster than β-elimination [Eq. (5)]. Nevertheless, the direct palladium-catalyzed coupling reactions of acid chlorides, benzyl halides, allyl halides, vinyl halides, vinyl triflates, and aryl halides with various organotin reagents have been reasonably well worked out.



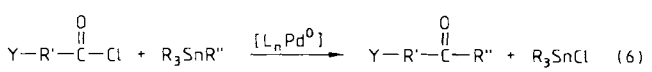
(4)



(5)

3.1.1. Acid Chlorides

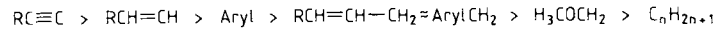
The synthesis of ketones from acid chlorides [Eq. (6)] [58–61] is quite general with respect to the organotin reagent and the acid chloride.[60,61] Aromatic, aliphatic, and heterocyclic acid chlorides give high yields of product (75–100%) in 15 min–1 h under very mild (25 °C), neutral reaction conditions, and catalytic turnovers of 1000 have been achieved. Sterically hindered acid chlorides react normally and α,β-unsaturated acid chlorides do not undergo 1,4-addition; dicarboxylic acid dichlorides can also be employed. There is no further addition to the product ketone, and a wide variety of functional groups (Y) are tolerated, including nitro, nitrile, haloaryl, methoxy, ester, and even aldehyde groups.



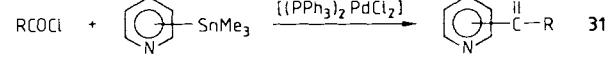
(6)

There are virtually no side reactions and the workup is simple. The end of the reaction is clearly visualized by the precipitation of palladium, and there is no need to run the reaction under an inert atmosphere.

The tetraorganostannane transfers the first group rapidly, but the second leaves about 100 times slower from R_3SnCl. Thus, with a stoichiometric amount of tetraorganostannane, only one group is transferred. This single transfer of an organic group from tin is not a problem if a relatively simple organic group, for example, methyl, is to be transferred, since tetramethyltin can be used. If the partner on tin to be transferred is more expensive or difficult to synthesize, however, then the utilization of only one of those four partners would be a distinct advantage. Fortunately, different types of groups transfer selectively from tin, the simple alkyl group having the slowest transfer rate.[62] Thus, by using a trimethyl or tributylorganotin reagent, the group other than the methyl or butyl groups transfers exclusively:



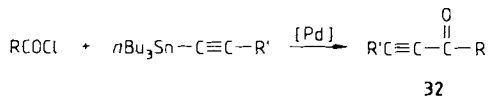
In many cases, the trimethylorganostannane is preferred, since the by-product, trimethyltin chloride, can be easily removed from the reaction mixture by a water wash. Allyl transfer takes place predominantly with allylic rearrangement, coupling at a benzylic carbon takes place with inversion,[63] and coupling of an alkenyl group takes place with retention of double-bond configuration.[26,63] A number of trimethyltin derivatives of aromatic nitrogen heterocycles (pyridine, quinoline, isoquinoline) undergo transfer, leading to high yields of aromatic heterocyclic ketones such as **31**.[64] The conversion of alkynyltin reagents into



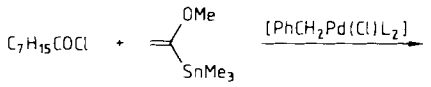
31

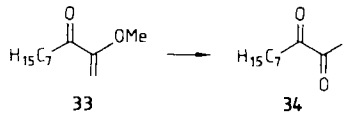
alkynyl ketones **32** is one of the best methods for the synthesis of these valuable intermediates.[65] The use of vinyltin reagents derived from enol ethers yields a vinyl ketone **33** that is easily converted into the 1,2-diketone **34**.[66] A variety of palladium catalysts have been used in these coupling reactions, including π-allylpalladium chloride dimer.

Symmetrical 1,2-diketones can be made from aroyl chlorides in a palladium-catalyzed coupling reaction that evidently involves conversion of half the acid chloride into an



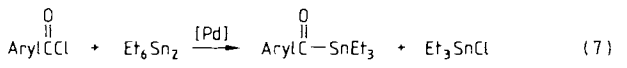
32



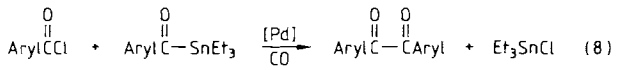


33 34

acyltin reagent [Eq. (7)], which then couples with the remaining acid chloride [Eq. (8)].[67] Decarbonylation of the intermediate aroylpalladium complexes is minimized by running the reaction under CO (8 atm).

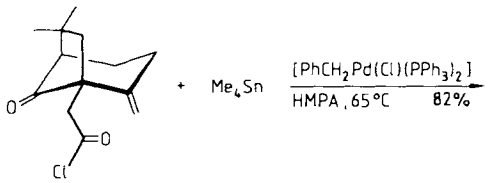


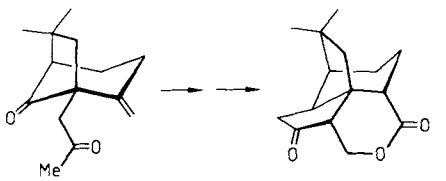
(7)



(8)

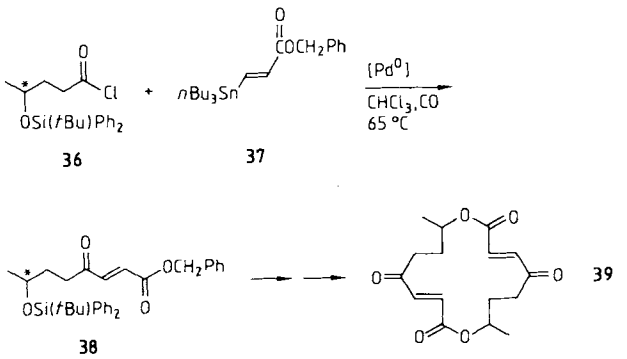
The conversion of an acid chloride into a ketone has been used in a number of syntheses of more complicated organic molecules, for example, in the synthesis of (±)-quadrone **35**.[68]





35

The coupling reaction of the acid chloride **36** with the substituted vinyltin reagent **37** gave the ketone **38**, which is a key intermediate in the synthesis of the antibiotic pyrenophorin **39** (Scheme 2).[69,70] Since the Mitsunobu coupling reaction proceeds with inversion of configuration at the chiral C atom and since the (*S*)-enantiomer of the starting lactone (precursor for **36**) is available, the synthesis of the naturally occurring (*R,R*)-pyrenophorin can be carried out. The synthesis illustrates the utility of the coupling reaction, even for the synthesis of more complicated ketones.

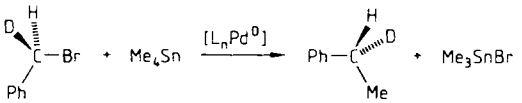


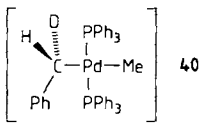
36 37 38 39

Scheme 2. Synthesis of pyrenophorin.

3.1.2. Benzyl Halides

In the direct catalytic coupling reaction between benzyl bromide and tetramethylstannane, an intermediate benzyl(methyl)palladium complex **40** is formed in the catalytic cycle.[71] The reductive-elimination reaction from this intermediate is stereospecific, proceeding with retention of configuration at the chiral center. Overall, inversion of configuration takes place as a result of inversion in the oxidative-addition step. High yields of cross-coupled products are obtained.[72]

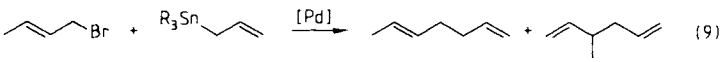




40

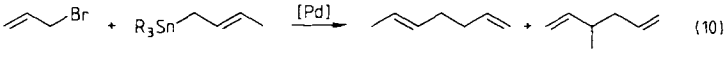
3.1.3. Allyl Halides and Acetates

The coupling of allyl bromides with allyltin reagents[73] takes place without homocoupling and allylic rearrangement takes place to a greater extent in the organotin reagent than in the allyl halide [Eq. (9) and (10)].[73,74] The ratios of coupled products are dependent on the R group of the tin reagent and on both the solvent and the catalyst. Generally, allylic acetates do not react, cinnamyl acetate[75] and allyl acetate[76,77] being exceptions.



(9)

1 : 1.8

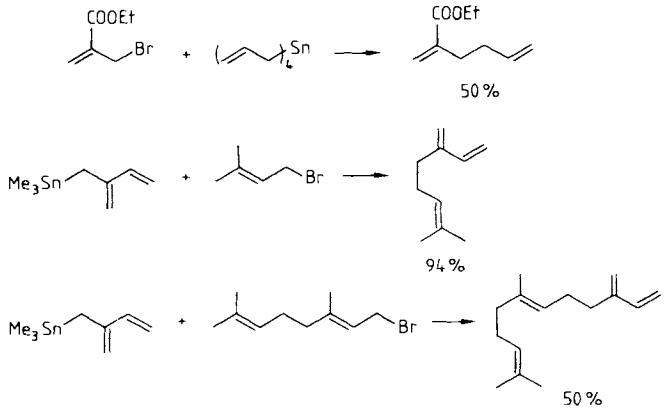


(10)

1 : 3

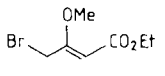
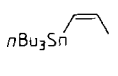
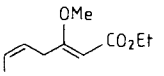
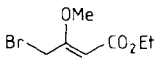
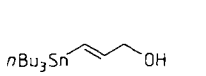
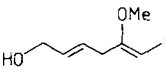
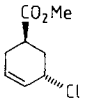
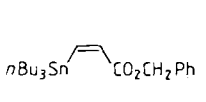
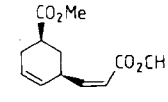
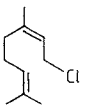
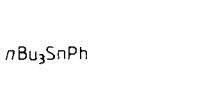
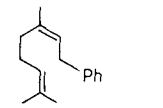
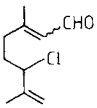
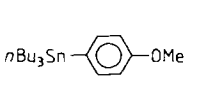
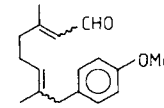
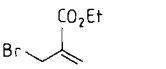
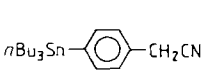
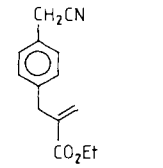
Nevertheless, with allylic bromides and particularly allylic tin reagents in which the product of allylic rearrangement is identical with the starting material, useful coupling reactions can be achieved (Scheme 3). In the latter two examples, coupling takes place more readily in the presence of zinc chloride[74] and no allylic rearrangement takes place in the allyl (prenyl-type) bromide.

The palladium-catalyzed coupling of allyl bromides or chlorides with alkenyl- or aryltin reagents leads to 1,4-dienes in high yields (Table 2).[78,79] The reaction is quite mild and is tolerant of a wide variety of functional groups,



Scheme 3. Coupling of two allyl compounds.

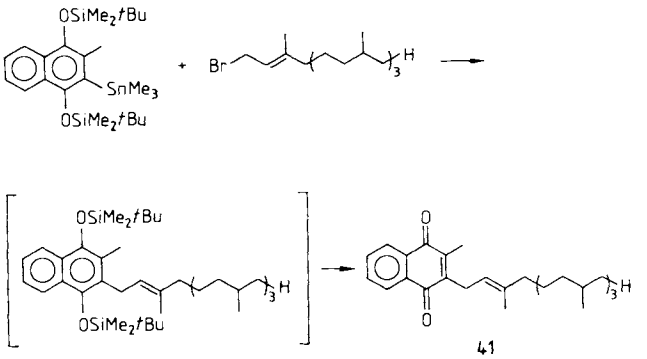
Table 2. Palladium-catalyzed coupling of allyl halides with alkenyltin compounds [a].

Reaction	Allyl halide	Organotin reagent	Product	Yield [%] [b]
1				86
2				82
3				80
4				90
5				87
6				81

[a] The reactions were carried out in dry THF at 50°C for 24–48 h, using equimolar amounts of allyl halide and alkenyltin reagent in the presence of 3 mol-% bis(dibenzylideneacetone)palladium(0) ([Pd(dba)$_2$]) and 6 mol-% PPh_3. [b] Isolated yields.

including CO_2R, CN, OH, and CHO. The reaction also proceeds with retention of double-bond configuration in the alkenyl compound (No. 1–3) as well as of the (*Z*)-configuration of neryl chloride (No. 4). The allyl halide undergoes regioselective coupling at the primary allylic carbon (No. 5; compare also No. 1, 2, and 4). Thus, this reaction exhibits stereospecific and regioselective carbon–carbon bond formation.

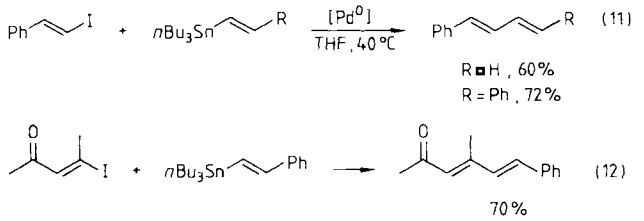
The coupling of allyl chlorides and bromides with aryltin reagents yields allyl-substituted arenes.[79,80] This reaction has been used in the synthesis of vitamin K_1 **41**; zinc chloride was again a better catalyst than palladium.[74]



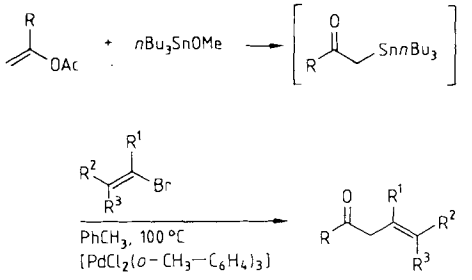
41

3.1.4. Substituted Vinyl Halides and Triflates

Substituted vinyl halides undergo direct, palladium-catalyzed cross-coupling with alkenyltin reagents to give good yields of conjugated dienes. Although the scope of this reaction has not been explored, it appears that retention of double-bond configuration in the vinyl partners occurs. Vinyl iodides [Eq. (11) and (12)] react readily at 25–40°C; vinyl bromides require higher temperatures (100°C) for the oxidative-addition step to take place readily.

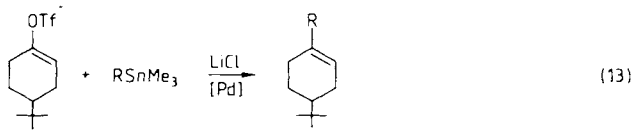


The palladium-catalyzed coupling of vinyl bromides with stannanes generated in situ from enol acetates yields allyl ketones **42**.[81]



42

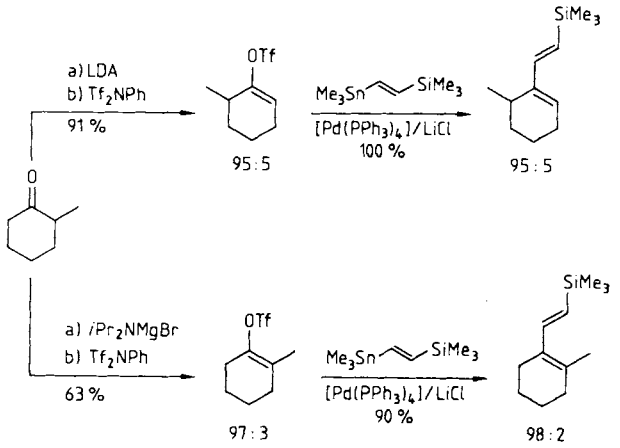
Vinyl triflates can be made to undergo palladium-catalyzed coupling reactions [Eq. (13)] provided lithium chlo-



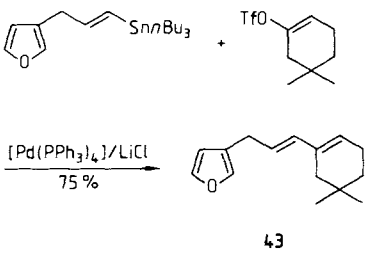
R = H, $CH{=}CH_2$, $CH{=}CHSiMe_3$, *n*Bu, Me, $CH_2CH{=}CH_2$, $C{\equiv}C{-}SiMe_3$

ride is added to the reaction.[82] Apparently the vinyl palladium chloride complex is required for the transmetalation reaction, since the palladium triflates will not undergo transmetalation with vinyltin compounds.

The discovery that vinyl triflates undergo coupling with a variety of tin reagents has proven to be very valuable. Since the triflates can be obtained from ketones, enolate chemistry is available and triflates are formed selectively from an unsymmetrical ketone by generating either the kinetic or thermodynamic enolate (Scheme 4).[82] This methodology has been used in a short synthesis of pleraplysillin-1 **43**.[82]



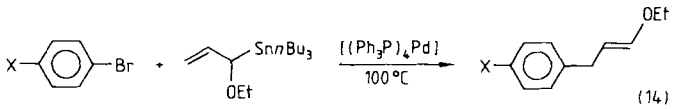
Scheme 4. Coupling of vinyl triflates.



43

3.1.5. *Aryl Halides*

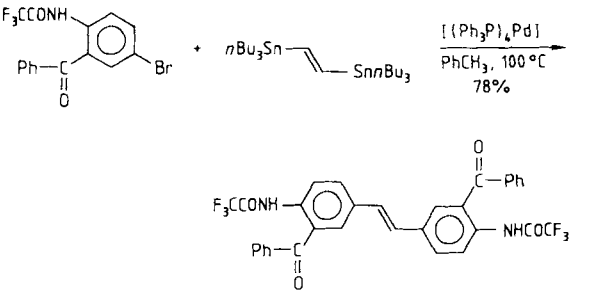
Because aryl iodides and bromides undergo oxidative addition to palladium(0) complexes at moderate temperatures, these halides are suitable for coupling with tin reagents; in contrast, aryl chlorides require activation with electron-withdrawing substituents on the ring. These coupling reactions take place with a wide variety of tin reagents.[83-89] Coupling reactions take place between aryl bromides and allyltin reagents at 100 °C with tetrakis(triphenylphosphane)palladium(0) as the catalyst [Eq. (14)].[42,83]



(14)

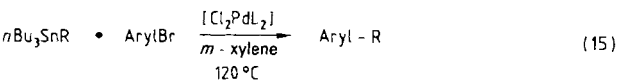
X = H, Cl, F 88–91 %

The bis-coupling of an aryl bromide with a vinylenedistannane proceeded at 100 °C to give a 78% yield of the stilbene derivative **44**.[89]



44

When ligandless catalysts generated from such palladium complexes as $LiPdCl_3$ or $[(CH_3CN)_2PdCl_2]$ in solvents that exhibit weak donor properties (such as HMPA, dimethylformamide (DMF), or acetone) are used, the coupling reactions with aryl iodides take place at ambient temperature as a result of a more facile oxidative addition with a coordinatively unsaturated d^{10} complex.[87] In addition to allyltin and vinyltin reagents, hydroxymethyl- and methoxymethyltin[90] compounds as well as α-acetonitrile-,[91] acetonyl-,[92] and cyanotin[93,94] compounds, can undergo the coupling reaction with aryl halides [Eq. (15)], although the mechanism of the reaction involving trimethyltin cyanide is evidently different from that shown in Scheme 1. Aromatic diazonium salts also undergo the palladium-catalyzed coupling with tetramethylstannane.[95]

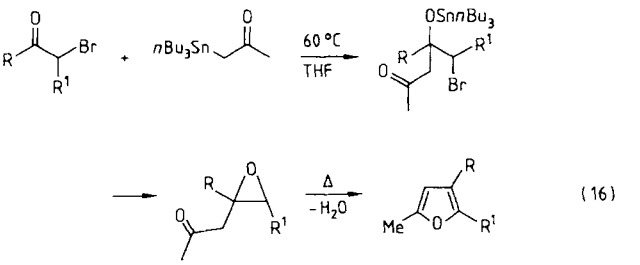


(15)

R = CH_2OH, CH_2OMe, CH_2CN, CH_2COMe, CN

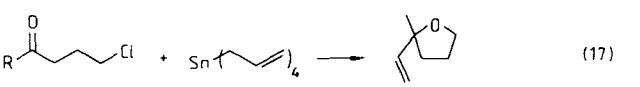
3.1.6. *α-Haloketones and α-Haloesters*

The reaction of a variety of α-haloketones with acetonyl- and allyltin reagents catalyzed by palladium gives cyclic ethers in good yield.[96] Oxiranes, oxetanes, and tetrahydrofurans can be obtained under mild conditions when the catalyst is introduced as benzyl(chloro)bis(triphenylphosphane)palladium(II) [Eq. (16) and (17)]. The catalyst is required both for the addition of the organotin reagent across the carbonyl group and for the epoxide generation. Thermal rearrangement of these initially formed acetonyl



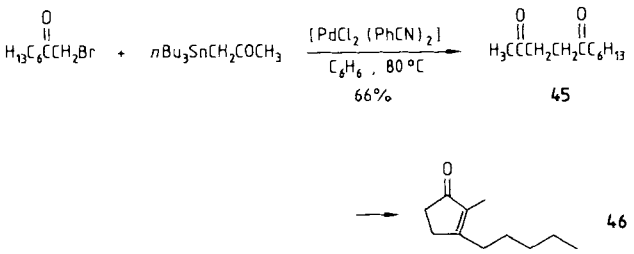
(16)

R = Me, Ph

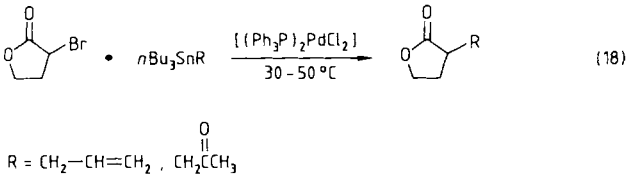


(17)

oxiranes leads to substituted furans. If a catalyst that does not contain phosphane ligands is used, a 1,4-diketone is formed, apparently through an initial oxidative addition step at the α-halo position.[97] The coupling reaction of 1-bromo-2-octanone with acetonyltributylstannane gives the 1,4-diketone **45**, a key intermediate in the synthesis of dihydrojasmone **46**.



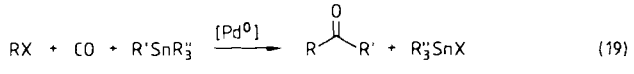
α-Bromo-γ-butyrolactones undergo palladium-catalyzed coupling with allyl- or acetonyltin reagents to give good yields of α-allyl- or α-acetonyl-γ-butyrolactones [Eq. (18)].[98] Only moderate yields of coupled product could be obtained with ethyl α-bromoacetate, however. The coupling reaction of α-iodolactone involves a radical process and does not require a palladium catalyst.



(18)

3.2. Carbonylative Coupling

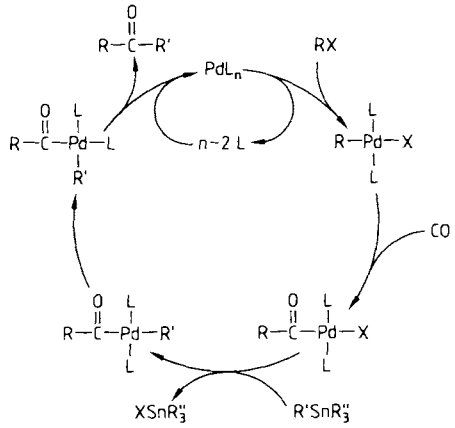
The palladium-catalyzed carbonylative coupling reaction of organic halides with organotin compounds in the presence of carbon monoxide [Eq. (19)] is an especially valuable synthetic procedure for a number of reasons.



(19)

First, if the acid chloride is not readily available for a ketone synthesis by a direct coupling, then the organic halide having one less carbon can be used, since the same acylpalladium intermediate is generated. Second, since an acid chloride is not involved in the synthesis, presumably other functional groups such as OH and NH_2, suitably placed, can be present in the organic halide. Although our original efforts to achieve this transformation were not particularly successful,[60,61] this type of reaction was reported later to proceed with symmetrical tetraalkyltin reagents under severe reaction conditions (120°C, HMPA, 30 atm CO).[99]

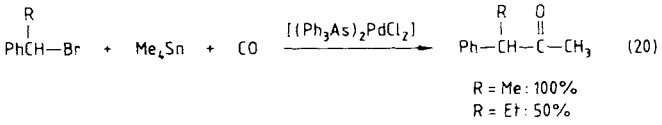
The probable catalytic cycle for this carbonylative coupling reaction (Scheme 5) is analogous to the direct coupling except that carbon monoxide insertion takes place after the oxidative addition step and prior to the transmetalation step.



Scheme 5. Mechanism of the catalyzed, carbonylative coupling.

3.2.1. *Benzyl Halides*

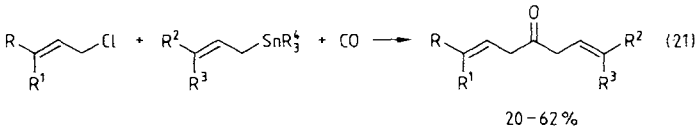
The carbonylative coupling of benzyl bromides and tetramethylstannane takes place to yield benzyl methyl ketones [Eq. (20)].[99,100] The insertion of carbon monoxide into the benzyl-palladium bond must be faster than β-elimination, at least under 20 atm of carbon monoxide.



(20)

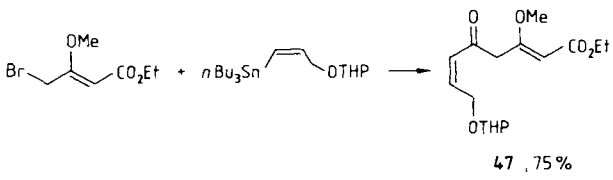
3.2.2. *Allyl Chlorides*

Bis-allylic ketones were synthesized by the reaction of allyl chlorides and allyltin reagents in the presence of CO (3 atm) at 25°C.[101] Higher temperatures resulted in the further addition of the allyltin reagent to the ketone to yield a tertiary alcohol (after hydrolysis). Rearrangement to give the α,β-unsaturated carbonyl compounds can be avoided. In contrast to direct coupling, carbonylative coupling occurs without allylic rearrangement of the organotin compound, and CO insertion takes place exclusively at the least hindered site of the allyl halide partner. This reaction [Eq. (21)] also tolerates other functional groups, including CO_2R, OH, and even CHO, at least on the allyl halide partner.



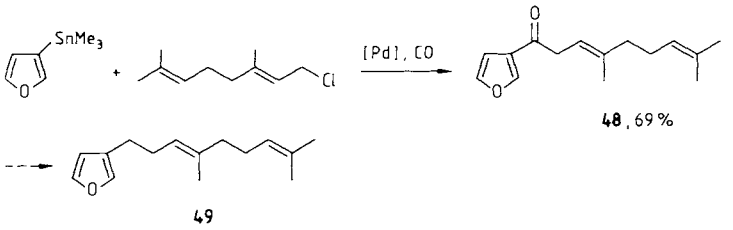
(21)

The use of alkenyltin reagents under 3 atm of carbon monoxide gives high yields of the carbonylated product **47**.[78,79]

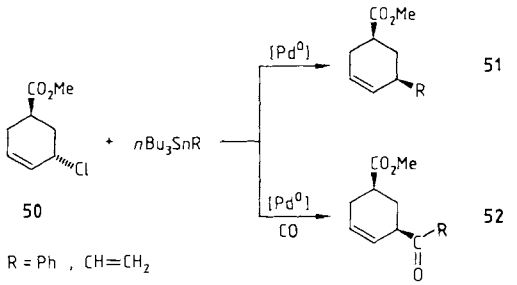


47, 75%

Aryltin compounds also yield carbonylative coupling products. This reaction type was the basis for the high-yield synthesis of egomaketone and a precursor, **48**, to dendrolasin **49** by the carbonylative coupling between 3-furanyltrimethylstannane and prenyl chloride or geranyl chloride, respectively.[79]



The cross-coupling of **50** with either tributylphenyl- or tributylvinylstannane proceeded with inversion of configuration at the allylic carbon center to yield **51** (see also Table 2, No. 3). In the presence of carbon monoxide, the carbonylated *cis* product **52** was obtained.[78,79] Thus, the coupling of this allyl halide either in the absence or presence of carbon monoxide takes place with 100% net inversion of configuration at the allylic center.



3.2.3. *Substituted Vinyl Halides and Triflates*

The palladium-catalyzed reaction of substituted vinyl iodides with vinyl-, alkenyl-, alkynyl-, and phenyltin compounds in the presence of carbon monoxide (3 atm) proceeds under mild reaction conditions to yield the corresponding ketones[102] (Table 3).

The reaction tolerates carbonyl groups in both partners as well as an acetylenic group in the tin partner. Under these mild reaction conditions, no further addition of the tin reagent to the product ketone takes place. Generally, the preparation of unsymmetrical ketones by transition-metal-catalyzed cross-coupling reaction is severely limited, since the organometallic partners often react with the product ketone.

The (*E*)-configuration of the double bond, both in the vinyl iodide and in the stannane, is retained in the product. The (*Z*)-configuration of the double bond in the stannane, however, is lost under the usual reaction conditions and the (*E*)-isomer of the product predominates. (*E*)/(*Z*)-Isomerization of vinyl ketones is very facile, however.

Vinyl triflates also will undergo the palladium-catalyzed carbonylative coupling reaction provided lithium chloride is added to the reaction mixture (Table 4).[103] As in the direct coupling of vinyl triflates with organotin compounds, the lithium chloride apparently is necessary since the palladium triflate complex will not undergo transmetalation with the tin reagent. In coupling reactions with vinyltin reagents, the configuration of the double bond is maintained. An important aspect of this work is the ability to prepare a vinyl triflate regioselectively, using well-known enolate chemistry, and to couple the triflate with an organostannane under a carbon monoxide atmosphere to give only one regioisomeric product (Scheme 6).

The carbonylative coupling reaction followed by a Nazarov cyclization was used for a sequential annulation to assemble the fused five-membered-ring structure of (±)$\Delta^{9(12)}$-capnellene **53** (Scheme 7, L-Selectride = $LiBHsBu_3$).[103]

Table 3. Carbonylative coupling of vinyl iodides with organostannanes.

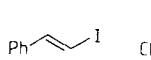
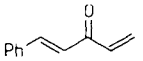
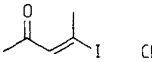
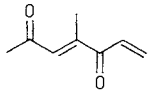
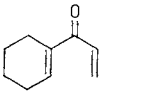
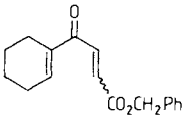
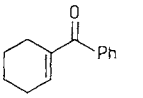
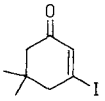
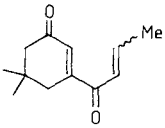
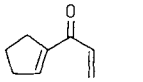
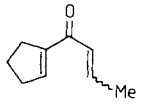
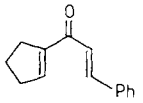
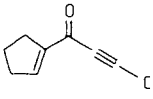
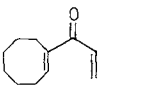
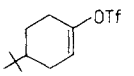
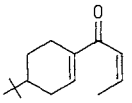
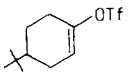
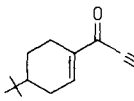
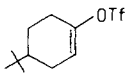
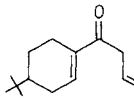
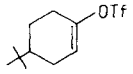
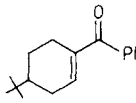
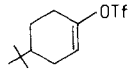
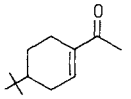
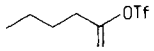
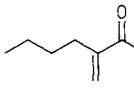
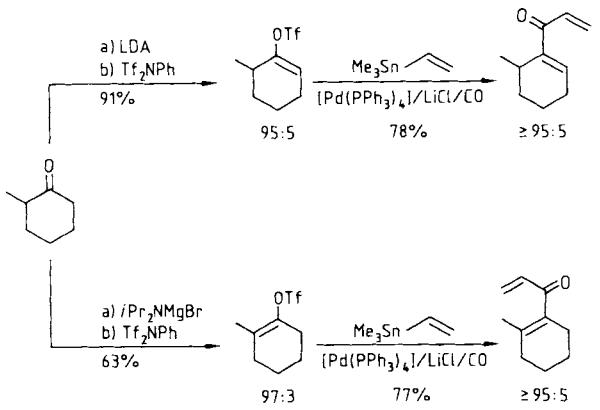
Vinyl iodide	R in nBu_3SnR	Ketone	Yield [%]
	CH=CH$_2$		65
	CH=CH$_2$		50
	CH=CH$_2$		93
	(*Z*)–CH=CHCO$_2$R		45
	Ph		40
	(*Z*)–CH=CHMe		71
	CH=CH$_2$		90
	(*Z*)–CH=CHMe		63
	(*E*)–CH=CHPh		60
	C≡C–C$_3$H$_7$		54
	CH=CH$_2$		74

Table 4. Carbonylative coupling of vinyl triflates with organostannanes.

Reaction	Vinyl triflate	R in Me_3SnR	Product	Yield [%]
1		(*Z*)—CH=CHCH$_3$		70
2		C≡C—SiMe$_3$		95
3		CH$_2$—CH=CH$_2$		95
4		Ph		93
5		Me		73
6		(*E*)—CH=CHSiMe$_3$		77



Scheme 6. Carbonylative coupling of vinyl triflates.

3.2.4. *Aryl Halides*

The carbonylative coupling reaction of aryl iodides and bromides can be carried out with a variety of palladium catalysts and tin reagents as coupling partners. The first reported aryl iodide carbonylative coupling reactions required high temperatures (120°C) and high pressures of carbon monoxide (30 atm),[99] even with nickel catalysts.[104] The reaction can be carried out under much milder reaction conditions (1 atm CO, 20°C) [Eq. (22)], particularly with ligandless catalysts.[105]

$$\text{Aryl I} + \text{RSnMe}_3 + \underset{1\,\text{bar}}{\text{CO}} \xrightarrow[72\,\text{h}]{[(C_3H_5)PdCl]_2} \text{Aryl}\overset{\overset{\text{O}}{\|}}{\text{C}}\text{—R} \qquad (22)$$

Aryl = *p*-C_6H_4X ; X = NO_2, CO_2Me, CN, Cl, I, H

R = Me, $CH{=}CH_2$,  , *p*-C_6H_4X, C_6F_5, C≡CPh,

(X = OMe, Me, H, Cl, NO_2)

3.2.5. *Aldehyde Synthesis*

Organic halides may be converted into aldehydes in the presence of a palladium catalyst, carbon monoxide, and tributyltin hydride under mild reaction conditions [Eq. (23)].[106] Aryl, benzyl, alkenyl, and allyl halides can be

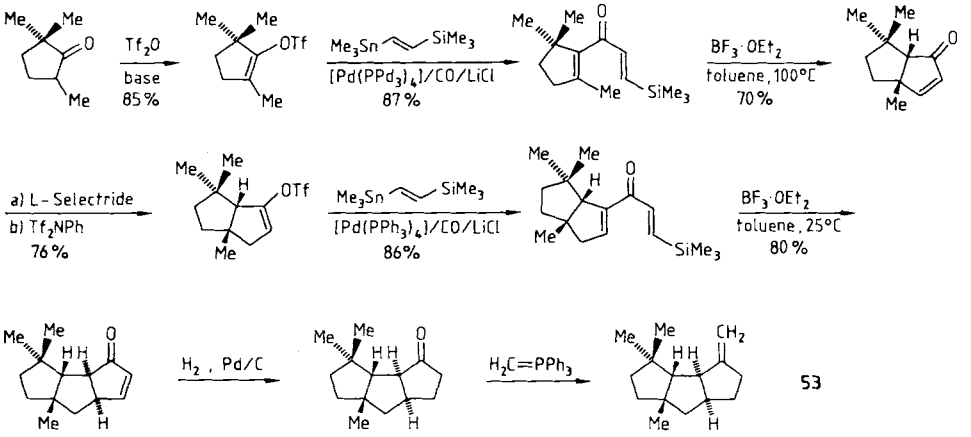
$$\text{RX} + \text{CO} + n\text{Bu}_3\text{SnH} \xrightarrow[50\,^\circ\text{C}]{[\text{Pd}^0]} \text{RCHO} + n\text{Bu}_3\text{SnX} \qquad (23)$$

converted into aldehydes; other functional groups in the molecule remain unaffected under these reaction conditions (Table 5).

4. Mechanisms

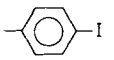
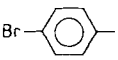
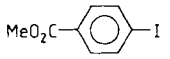
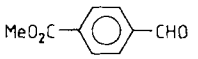
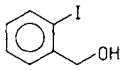
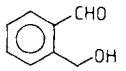
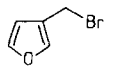
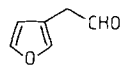
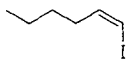
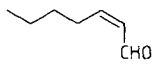
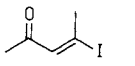
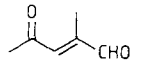
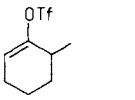
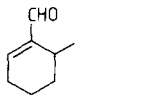
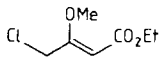
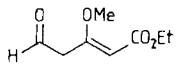
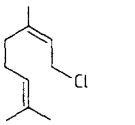
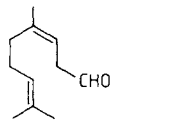
4.1. Coupling of Acid Chlorides with Organotin Compounds

The catalytic cycle for the coupling reaction of acid chlorides with organotin reagents is shown in Scheme 8.

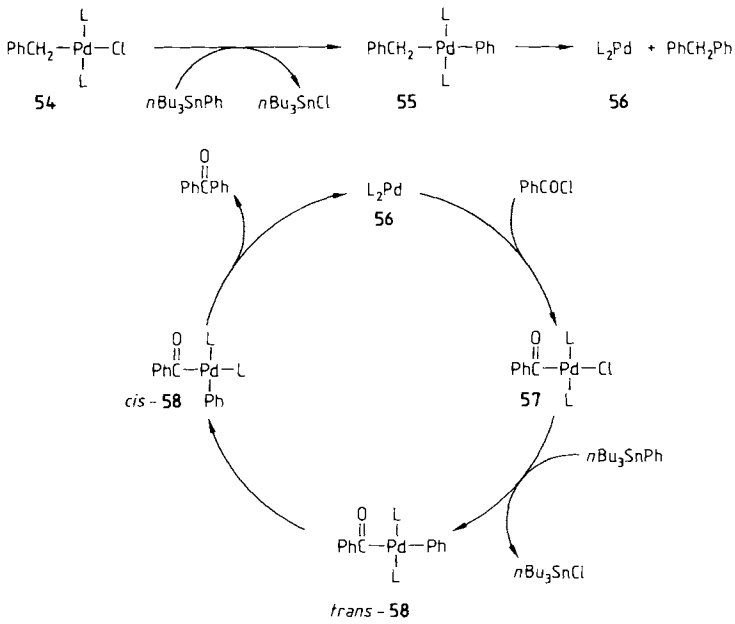


Scheme 7. Synthesis of capnellene.

Table 5. Formylation of organic halides [a].

Halide	Solvent	Aldehyde	Yield [%]
	THF		87
	THF		91
	$PhCH_3$		55
	THF		67
	THF		88
	THF		95
	THF [b]		96
	THF		86
	THF		59

[a] 50°C, $[(Ph_3P)_4Pd]$. [b] LiCl added.

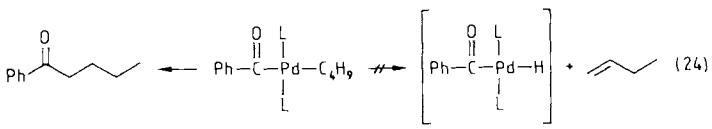


Scheme 8. Mechanism of the catalytic coupling of acid chlorides with organotin compounds. L = PPh_3.

Palladium was introduced into the reaction as benzyl(chloro)bis(triphenylphosphane)palladium(II) **54** (L = PPh_3) with the expectation that it would be reduced (via a transmetalation reaction to yield **55**, followed by a reductive elimination sequence) to reactive bis(triphenylphosphane)palladium(0) **56**.[62] The benzyl catalyst **54** was allowed to react with equimolar amounts of tributyl(phenyl)stannane and benzoyl chloride, and the reaction was followed at 65°C by ^{31}P-NMR spectroscopy. The signal for the benzyl catalyst disappeared concomitantly with the appearance of the acylpalladium species **57**.

When both benzoyl chloride and tributyl(phenyl)stannane are used in excess over the benzyl catalyst **54**, only the ^{31}P-NMR signals for **54** and **57** could be observed, those for **54** eventually disappearing. No additional signals for **56** or **58** could be detected, even though benzophenone was produced.

These results are consistent with the catalytic cycle shown in Scheme 8 if the transmetalation reaction is the slow step, with oxidative addition, isomerization, and reductive elimination occurring rapidly. The oxidative addition of benzoyl chloride to tetrakis(triphenylphosphane)palladium(0) in THF has a half-life of 10 min at 30 °C.[107] A fast reductive-elimination step is consistent with the observation that in coupling reactions with tetrabutylstannane, high yields of phenyl butyl ketone are obtained, and no butene resulting from a β-hydride elimination is observed [Eq. (24)].



Although the mechanisms of the oxidative-addition and reductive-elimination sequences have been individually studied, and are reasonably well understood,[52-57] much less is known about the transmetalation reaction. The existing data support an electrophilic cleavage of the Sn-C bond with the palladium(II) complex **57** acting as the electrophile. Several lines of evidence support this.

First, since the reductive elimination of an alkenyl group attached to tin is known[56] to take place with retention of configuration, overall retention of configuration in the coupling reactions of vinyltin compounds requires retention in the transmetalation step. Retention of configuration at the double bond is also observed in the cleavage reactions of alkenyltin compounds with electrophiles.[108]

Second, the order (relative rates) of transfer of organic groups is consistent with electrophilic cleavage. The reactions of trimethylorganotin compounds by mercury(II) chloride follow the order shown.[109] Further, the transfer order is the same as that observed for transmetalation reactions with platinum(II) complexes.[110, 111]

$PhC\equiv C$	>	$CH_2=CH$	>	Ph	>	Me
very fast		5		1		0.007

Third, the transfer of a benzyl group is accelerated by electron-withdrawing groups on the ring. A slightly positive ρ value (+1.2, Fig. 1) was obtained. These results are consistent with electrophilic attack at the benzylic carbon.

The relatively low ρ value indicates that there is little direct conjugation of the substituent group with the incipient benzyl anion and that carbon-palladium bond formation may precede carbon-tin bond breaking.

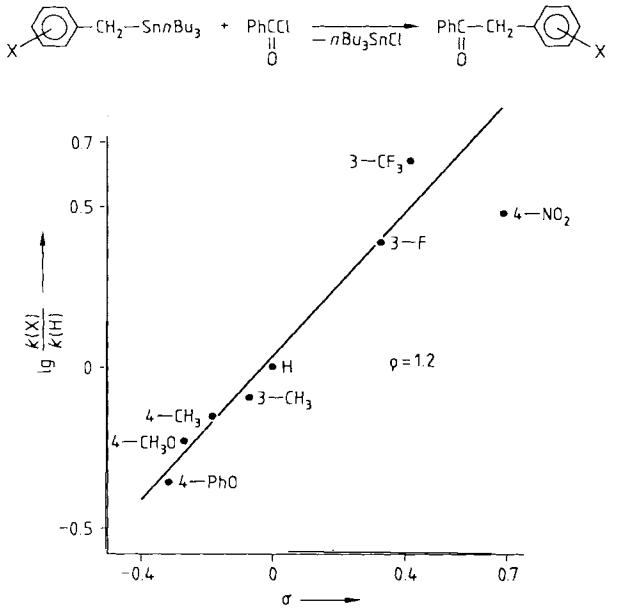
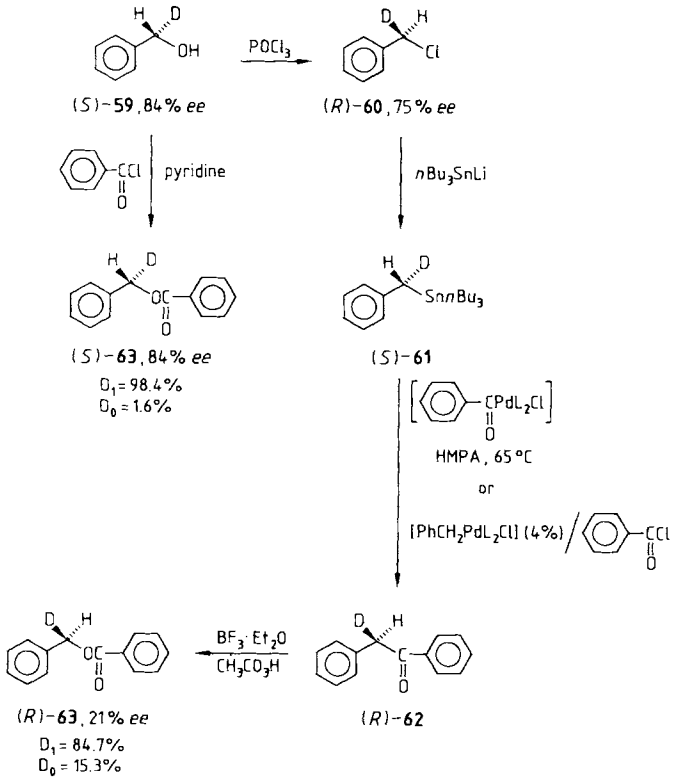


Figure 1. Linear free-energy relationship for the coupling of benzyltin compounds with benzoyl chloride.

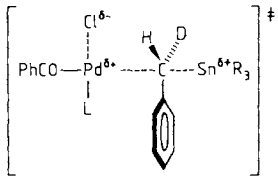
Finally, the inversion of configuration at an sp^3 carbon atom attached to tin is consistent with electrophilic cleavage and an open transition state (Scheme 9).[59-63] The reaction of (*S*)-(+)-[1-^{2}H]benzyl alcohol (*S*)-**59** (84% *ee*) with $POCl_3$ gave (*R*)-(−)-[1-^{2}H]benzyl chloride (*R*)-**60** (75% *ee*).



Scheme 9.

The addition of lithium tributylstannate to a solution of (*R*)-**60** gave (*S*)-**61** of unknown optical purity. Although there is controversy concerning the degree of nucleophilic vs. radical (electron-transfer) reaction,[112-116] the net inversion of configuration is high, often greater than 90%.[114-116]

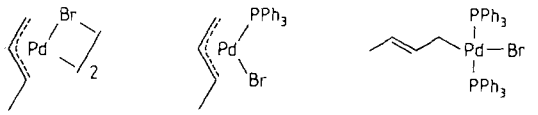
When the reaction of equimolar amounts of (*S*)-**61** with benzoyl chloride in the presence of catalytic amounts of benzyl(chloro)bis(triphenylphosphane)palladium(II) was carried out, desoxybenzoin (*R*)-**62** was obtained. The reaction of equal amounts of (*S*)-**61** and benzoyl(chloro)bis(triphenylphosphane)palladium(II) also gave **62**. The CD spectra of **62** are consistent with the (*R*)-configuration. The Baeyer-Villiger oxidation of **62** afforded the (*R*)-(−)-benzyl ester **63**; retention of configuration at the benzylic carbon atom occurs in this oxidation.[117] Conversion of (*S*)-**59** to the benzyl ester (*S*)-**63** and comparison of the optical rotation of the two esters allowed an assessment of the optical purity of (*R*)-**63**. Taking into consideration that the deuterium content in (*R*)-**63** is 85% compared to 98% in (*S*)-**63** and that any enolization would racemize **62** (independent of the deuterium content) and assuming a primary deuterium isotope effect of 2, it is possible to estimate at least 65% net inversion in the transmetalation reaction. This is based on the knowledge that reductive elimination takes place with retention of configuration at carbon[71,62] and that all steps other than the transmetalation step in proceeding from **60** to **62** take place without any racemization. This is not the case, of course, so the transmetalation reaction probably takes place highly stereospecifically, certainly with more than 65% net inversion. These results are consistent with a transmetalation reaction taking place by an S_E2 mechanism[118] and an open transition state **64** in which the electrophile is the palladium complex.



64

4.2. Allyl Coupling

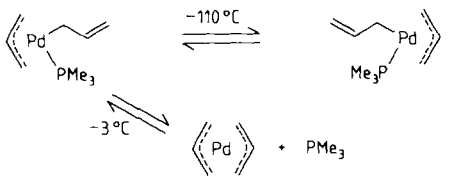
The mechanism of the coupling reaction of an allyl halide with an allyltin reagent is much more obscure, although presumably the same type of catalytic cycle as in the reaction of acid halides with organotin compounds is operative (see previous Section). In the reaction of allylpalladium complexes **65**–**67** with tetraallyltin, only **66** produced the yields observed in the catalytic coupling. The σ-complex **67** would be expected to be formed in the oxidative-addition reaction of $(CH_2{=}CH{-}CH_2)_4Sn$ with $[(Ph_3P)_2Pd]$ **56**, but excess crotyl bromide could be expected to scavenge an equivalent of phosphane to give **66** when only catalytic amounts of the palladium complex are used. Indeed, when a second molar equivalent of allyl bromide was present in the reaction with **67**, the yield of coupled products matched that of the catalytic reaction.[119]



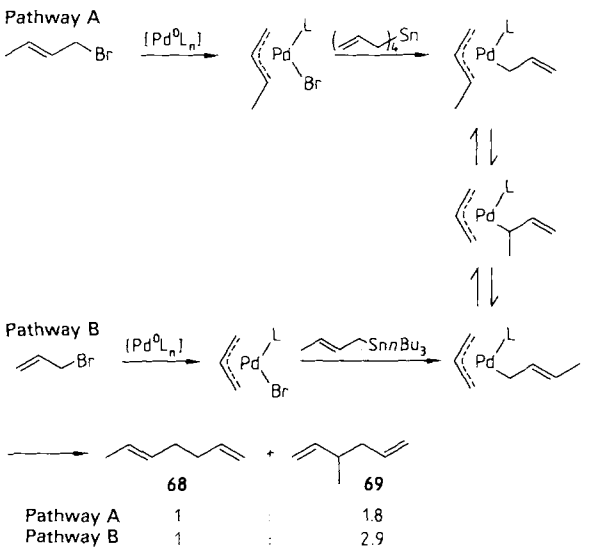
65 66 67

Unfortunately, the ratio of regioisomers **68** and **69** produced in the stoichiometric reactions of **66** with tetraallyl tin was different (5 : 4) from that obtained in the catalytic reaction (1 : 2).

Whether a bisallylpalladium species is the key intermediate leading to the coupled product also is not clear. It has been shown that a rapid equilibration takes place between η^1- and η^3-bound allyl groups in the bisallylpalladium complex (Scheme 10).[120] Thus, if bisallyl intermediates of this type are involved in the palladium-catalyzed coupling reactions, the reactions of either crotyl bromide and tetraallylstannane or of allyl bromide and tributyl(crotyl)stannane should lead to the same ratios of coupled products **68** and **69**. The ratios found, however, are different (Scheme 11).



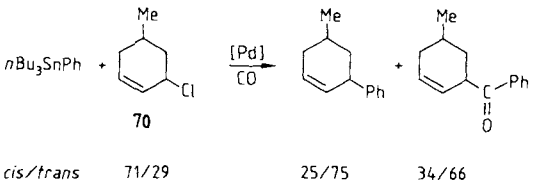
Scheme 10. Isomerization of bisallylpalladium complexes.



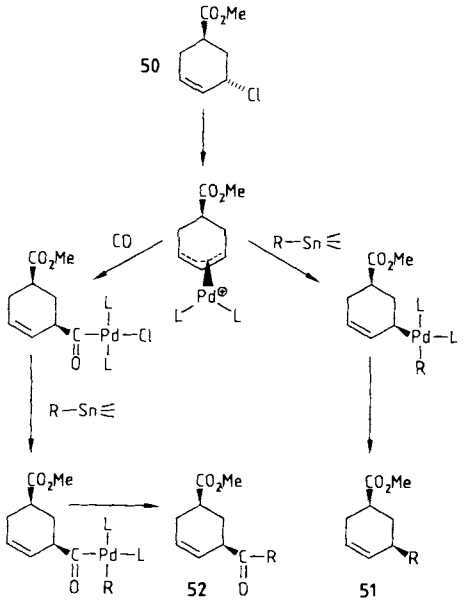
Scheme 11.

The stereochemistry of the coupling reaction of allylic chlorides with vinyl- or phenyltin reagents is unequivocal, however. The reaction of *trans*-methyl 5-chloro-3-cyclohexenecarboxylate **50** with tributyl(phenyl)- or tributylvinylstannanes catalyzed by benzyl(chloro)bis(triphenylphosphane)palladium(II) gave the cross-coupled product **51** in which complete inversion of configuration had taken place.[78,79] Similarly, reaction of a *cis-trans* mixture (42 : 58) of **50** gave *trans*-**51** and *cis*-**51** in a 41 : 59 ratio. Under carbon monoxide (3 atm), both the products of direct coupling and of carbonylative coupling were obtained. Both products, **51** and **52**, had the *cis* configuration.

In order to ensure that the stereochemical course of the reaction with the chloride **50** was not due to participation of the methoxycarbonyl substituent in directing the approach of the palladium, the analogous 3-chloro-5-methylcyclohexene **70** was allowed to react with tributyl(phenyl)stannane in the presence of carbon monoxide. Similar results were obtained.



These results suggest a sequence of events outlined in Scheme 12. Oxidative addition, which takes place with inversion of configuration for allylic esters[121] and benzyl chloride[122], also takes place with inversion in the allylic chloride system. This is confirmed by the fact that carbon monoxide, which is known to insert into the Pd–C bond with retention of configuration at carbon,[123] freezes the stereochemistry of the oxidative-addition reaction. The presence of carbon monoxide does not modify the stereochemistry since both directly coupled products **51** and ketones **52** are produced at intermediate carbon monoxide pressures, and the *cis/trans* ratio of the cross-coupled product **51** is unaffected by the presence of carbon monoxide. Carbon monoxide simply diverts the allylpalladium (II) complex toward formation of the ketone **52**. Transmetalation and reductive elimination, which proceed with retention of configuration at carbon,[71,72] complete the sequence.



Scheme 12. Coupling of an allyl chloride.

The catalytic cycles shown (Schemes 1, 2, and 8) have made use of $Pd^0 \rightleftharpoons Pd^{II}$ oxidation states, although there is some evidence that coupling reactions take place via $Pd^{II} \rightleftharpoons Pd^{IV}$ states.[52, 71, 72] The stoichiometric coupling reactions between benzyl(iodo)bis(triphenylphosphane)palladium(II) and aryltrimethylstannane give coupled product, although higher yields are obtained when an equivalent of aryl iodide is present, suggesting some involvement of a Pd^{IV} complex.[124] Alternatively, the aryl halide, particularly iodobenzenes containing electron-withdrawing substituents, may promote reductive elimination by charge transfer.[125]

Our research in this area was supported by the National Science Foundation (Grant CHE-8305468), whose assistance is greatfully acknowledged. The research was carried out by a number of able graduate students and postdoctoral research associates, whose names appear in the references.

Received: June 20, 1985 [A 574 IE]
German version: *Angew. Chem. 98* (1986) 504

[1] R. Baker, *Chem. Ind. London 1980,* 816.
[2] M. Kumada, *Pure Appl. Chem. 52* (1980) 669.
[3] T. Hayashi, M. Konishi, M. Fukushima, T. Mise, M. Kagotani, M. M. Tajika, M. Kumada, *J. Am. Chem. Soc. 104* (1982) 180, and references cited therein.
[4] E. Negishi, *Acc. Chem. Res. 15* (1982) 340.
[5] E. Negishi in H. Nozaki (Ed.): *Current Trends in Organic Synthesis,* Pergamon, New York 1983, p. 269.
[6] E. Negishi, *Pure Appl. Chem. 53* (1981) 2333.
[7] E. Negishi in T. H. Brewster (Ed.): *Aspects of Mechanisms in Organometallic Chemistry,* Plenum, New York 1978, p. 285.
[8] R. Noyori in H. Alper (Ed.): *Transition Metal Organometallics in Organic Synthesis, Vol. 1,* Academic Press, New York 1976, p. 84.
[9] A. P. Kozikowski, H. F. Wetter, *Synthesis 1976,* 561.
[10] M. Kumada in Y. Ishi, M. Tsutsui (Eds.): *Organotransition Metal Chemistry,* Plenum, New York 1975, p. 211.
[11] G. H. Posner: *An Introduction to Synthesis Using Organocopper Reagents,* Wiley-Interscience, New York 1980.
[12] R. C. Larock, *Angew. Chem. 90* (1978) 28; *Angew. Chem. Int. Ed. Engl. 17* (1978) 27.
[13] R. C. Larock, *Tetrahedron 38* (1982) 1713.
[14] J. Schwartz, *Pure Appl. Chem. 52* (1980) 733.
[15] W. P. Neumann: *The Organic Chemistry of Tin,* Wiley-Interscience, New York 1970.
[16] M. Gielen, B. de Poorter, *Rev. Silicon Germanium Tin Lead Compd. 3* (1977) 9.
[17] M. Gielen, *Rev. Silicon Germanium Tin Lead Compd. 5* (1981) 6.
[18] J.-P. Quintard, M. Pereyre, *Rev. Silicon Germanium Tin Lead Compd. 4* (1980) 151.
[19] J. A. Soderquist, A. Hassner, *J. Am. Chem. Soc. 102* (1980) 1577.
[20] J. A. Soderquist, G. J.-H. Hsu, *Organometallics 1* (1982) 830.
[21] E. J. Corey, T. M. Eckrich, *Tetrahedron Lett. 25* (1984) 2415.
[22] E. J. Corey, T. M. Eckrich, *Tetrahedron Lett. 25* (1984) 2419.
[23] D. E. Seitz, S.-H. Lee, *Tetrahedron Lett. 22* (1981) 4909.
[24] H. Westmijze, K. Ruitenberg, J. Meijer, P. Vermeer, *Tetrahedron Lett. 23* (1982) 2797.
[25] E. Piers, J. M. Chong, *J. Chem. Soc. Chem. Commun. 1983,* 934.
[26] J. Hibino, S. Matsubara, Y. Morizawa, K. Oshima, H. Nozaki, *Tetrahedron Lett. 25* (1984) 2151.
[27] E. Piers, J. M. Chong, H. E. Morton, *Tetrahedron Lett. 22* (1981) 4905.
[28] E. Piers, J. M. Chong, *J. Org. Chem. 47* (1982) 1602.
[29] B. Wrackmeyer, *Rev. Silicon Germanium Tin Lead Compd. 6* (1982) 75.
[30] M. E. Jung, L. A. Light, *Tetrahedron Lett. 23* (1982) 3851.
[31] G. H. Posner, T. P. Kogan, S. R. Haines, L. L. Frye, *Tetrahedron Lett. 25* (1984) 2627.
[32] R. H. Newman-Evans, B. K. Carpenter, *Tetrahedron Lett. 26* (1985) 1141.
[33] A. Amamria, T. N. Mitchell, *J. Organomet. Chem. 199* (1980) 49.
[34] H. E. Ensley, R. R. Buescher, K. Lee, *J. Org. Chem. 47* (1982) 404.
[35] J.-P. Quintard, M. Dequeil-Castaing, G. Dumartin, A. Rahm, M. Pereyre, *J. Chem. Soc. Chem. Commun. 1980,* 1004.
[36] Y. Ueno, M. Ohta, M. Okawara, *J. Organomet. Chem. 197* (1980) C 1.
[37] H. Azizian, C. E. Eaborn, A. Pidcock, *J. Organomet. Chem. 215* (1981) 49.
[38] A. N. Kashin, I. G. Bumagina, N. A. Bumagin, V. N. Bakunin, I. P. Beletskaya, *J. Org. Chem. USSR 17* (1981) 789.
[39] N. A. Bumagin, I. G. Bumagina, I. P. Beletskaya, *Dokl. Akad. Nauk SSSR 274* (1984) 1103.
[40] G. J. M. van der Kerk in J. J. Zuckerman (Ed.): *Organotin Compounds: New Chemistry and Applications (ACS Adv. Chem. Ser. 157,* 1, Washington, D.C., USA 1976).
[41] E. Piers, V. Karunaratne, *J. Org. Chem. 48* (1983) 1774.
[42] J.-P. Quintard, B. Elissondo, M. Pereyre, *J. Organomet. Chem. 212* (1981) C 31.
[43] H. Weichmann, A. Tzschach, *Z. Anorg. Allg. Chem. 458* (1979) 291.
[44] Y. Ueno, M. Ohta, M. Okawara, *Tetrahedron Lett. 23* (1982) 2577.
[45] A. Hosomi, M. Siato, H. Sakurai, *Tetrahedron Lett. 21* (1980) 355.
[46] B. Jousseaume, *J. Chem. Soc. Chem. Commun. 1984,* 1452.
[47] M. R. Binns, R. K. Haynes, T. L. Houston, W. R. Jackson, *Tetrahedron Lett. 21* (1980) 573.
[48] Y. Yamamoto, H. Yatagai, K. Maruyama, *J. Am. Chem. Soc. 103* (1981) 3229.
[49] T. Kauffmann, R. Kriegesmann, B. Altepeter, F. Steinseifer, *Chem. Ber. 115* (1982) 1810.
[50] M. Ochiai, T. Ukita, E. Fujita, *Tetrahedron Lett. 24* (1983) 4025.
[51] W. C. Still, C. Sreekumar, *J. Am. Chem. Soc. 102* (1980) 1201.
[52] A. Moravskiy, J. K. Stille, *J. Am. Chem. Soc. 103* (1981) 4182.
[53] J. K. Stille, K. S. Y. Lau, *Acc. Chem. Res. 10* (1977) 434.
[54] J. K. Stille in F. R. Hartley, S. Patai (Eds.): *The Chemistry of the Metal-Carbon Bond, Vol. 2,* Wiley, New York 1985, p. 625.
[55] A. Gillie, J. K. Stille, *J. Am. Chem. Soc. 102* (1980) 4933.
[56] M. K. Loar, J. K. Stille, *J. Am. Chem. Soc. 103* (1981) 4174.
[57] K. Tatsumi, R. Hoffmann, Y. Yamamoto, J. K. Stille, *Bull. Chem. Soc. Jpn. 54* (1981) 1857.
[58] M. Kosugi, Y. Shimizu, T. Migita, *Chem. Lett. 1977,* 1423.
[59] M. Kosugi, Y. Shimizu, T. Migita, *J. Organomet. Chem. 129* (1977) C 36.
[60] D. Milstein, J. K. Stille, *J. Am. Chem. Soc. 100* (1978) 3636.
[61] D. Milstein, J. K. Stille, *J. Org. Chem. 44* (1979) 1613.
[62] J. W. Labadie, J. K. Stille, *J. Am. Chem. Soc. 105* (1983) 6129.
[63] J. W. Labadie, J. K. Stille, *J. Am. Chem. Soc. 105* (1983) 669.
[64] Y. Yamamoto, A. Yanagi, *Chem. Pharm. Bull. 30* (1982) 2003.
[65] M. W. Logue, K. Teng, *J. Org. Chem. 47* (1982) 2549.
[66] J. A. Soderquist, W. W.-H. Leong, *Tetrahedron Lett. 24* (1983) 2361.
[67] N. A. Bumagin, Yu. V. Gulevich, I. P. Beletskaya, *J. Organomet. Chem. 282* (1985) 421.
[68] A. S. Kende, B. Roth, P. J. Sanfilippo, T. J. Blacklock, *J. Am. Chem. Soc. 104* (1982) 5808.
[69] J. W. Labadie, J. K. Stille, *Tetrahedron Lett. 24* (1983) 4283.
[70] J. W. Labadie, D. Tueting, J. K. Stille, *J. Org. Chem. 48* (1983) 4634.
[71] D. Milstein, J. K. Stille, *J. Am. Chem. Soc. 101* (1979) 4981.
[72] D. Milstein, J. K. Stille, *J. Am. Chem. Soc. 101* (1979) 4992.
[73] J. Godschalx, J. K. Stille, *Tetrahedron Lett. 21* (1980) 2599.
[74] J. Godschalx, J. K. Stille, *Tetrahedron Lett. 24* (1983) 1905.
[75] B. M. Trost, E. Keinan, *Tetrahedron Lett. 21* (1980) 2595.
[76] I. P. Beletskaya, A. N. Kasatkin, S. A. Lebedev, N. A. Bumagin, *Izv. Akad. Nauk SSSR Ser. Khim. 1981,* 2414.
[77] N. A. Bumagin, A. N. Kasatkin, I. P. Beletskaya, *Dokl. Akad. Nauk SSSR 266* (1982) 862.
[78] F. K. Sheffy, J. K. Stille, *J. Am. Chem. Soc. 105* (1983) 7173.
[79] F. K. Sheffy, J. Godschalx, J. K. Stille, *J. Am. Chem. Soc. 106* (1984) 4833.
[80] N. A. Bumagin, I. G. Bumagina, A. N. Kashin, I. P. Beletskaya, *Zh. Obshch. Khim. 52* (1982) 714.
[81] M. Kosugi, I. Hagiwara, T. Migita, *Chem. Lett. 1983,* 839.
[82] W. J. Scott, G. T. Crisp, J. K. Stille, *J. Am. Chem. Soc. 106* (1984) 4630.
[83] M. Kosugi, K. Sasazawa, Y. Shimizu, T. Migita, *Chem. Lett. 1977,* 301.
[84] A. N. Kashin, I. G. Bumagina, N. A. Bumagin, I. P. Beletskaya, *J. Org. Chem. USSR 47* (1981) 18.
[85] N. A. Bumagin, A. N. Kasatkin, I. P. Beletskaya, *Izv. Akad. Nauk SSSR Ser. Khim. 1984,* 636.
[86] A. N. Kashin, I. G. Bumagina, N. A. Bumagin, I. P. Beletskaya, O. A. Reutov, *Izv. Akad. Nauk SSSR Ser. Khim. 1980,* 479.
[87] I. P. Beletskaya, *J. Organomet. Chem. 250* (1983) 551.
[88] N. A. Bumagin, I. G. Bumagina, I. P. Beletskaya, *Dokl. Akad. Nauk SSSR 274* (1984) 818.

[89] E. K. Zimmermann, J. K. Stille, *Macromolecules 18* (1985) 321.
[90] M. Kosugi, T. Sumiya, T. Ogata, H. Sano, T. Migita, *Chem. Lett. 1984*, 1225.
[91] M. Kosugi, M. Ishiguro, Y. Negishi, H. Sano, T. Migita, *Chem. Lett. 1984*, 1511.
[92] M. Kosugi, M. Suzuki, I. Hagiwara, K. Goto, K. Saitoh, T. Migita, *Chem. Lett. 1982*, 939.
[93] I. P. Beletskaya, A. N. Kashin, A. Ts. Malkhasyan, A. A. Solov'yanov, E. Yu. Bekhli, O. A. Reutov, *J. Org. Chem. USSR 10* (1974) 682.
[94] M. Kosugi, Y. Kato, K. Kiuchi, T. Migita, *Chem. Lett. 1981*, 69.
[95] K. Kikukawa, K. Kono, F. Wada, T. Matsuda, *J. Org. Chem. 48* (1983) 1333.
[96] I. Pri-Bar, P. S. Pearlman, J. K. Stille, *J. Org. Chem. 48* (1983) 4629.
[97] M. Kosugi, I. Takano, M. Sakurai, H. Sano, T. Migita, *Chem. Lett. 1984*, 1221.
[98] J. H. Simpson, J. K. Stille, *J. Org. Chem. 50* (1985) 1759.
[99] M. Tanaka, *Tetrahedron Lett. 1979*, 2601.
[100] T. Kobayashi, M. Tanaka, *J. Organomet. Chem. 205* (1981) C27.
[101] J. H. Merrifield, J. Godschalx, J. K. Stille, *Organometallics 3* (1984) 1108.
[102] W. F. Goure, M. E. Wright, P. D. Davis, S. S. Labadie, J. K. Stille, *J. Am. Chem. Soc. 106* (1984) 6417.
[103] G. T. Crisp, W. J. Scott, J. K. Stille, *J. Am. Chem. Soc. 106* (1984) 7500.
[104] M. Tanaka, *Synthesis 1981*, 47.
[105] N. A. Bumagin, I. G. Bumagina, A. N. Kashin, I. P. Beletskaya, *Dokl. Akad. Nauk SSSR 261* (1981) 1141.
[106] V. P. Baillargeon, J. K. Stille, *J. Am. Chem. Soc. 105* (1983) 7175; *ibid., 108* (1986) 452.
[107] P. Four, F. Guibe, *J. Org. Chem. 46* (1981) 4439.
[108] J. C. Cochran, S. C. Bayer, J. T. Bilbo, M. S. Brown, L. B. Colen, F. J. Gaspirini, D. W. Goldsmith, M. D. Jamin, K. A. Nealy, C. T. Resnick, G. J. Schwartz, W. M. Short, K. R. Skarda, J. P. Spring, W. L. Strauss, *Organometallics 1* (1982) 586.
[109] A. N. Kashin, I. P. Beletskaya, A. T. Malkhaysan, O. A. Reutov, *J. Org. Chem. USSR 10* (1974) 677.
[110] C. J. Cardin, D. J. Cardin, M. F. Lappert, *J. Chem. Soc. Dalton Trans. 1977*, 767.
[111] C. Eaborn, K. J. Odell, A. Pidcock, *J. Chem. Soc. Dalton Trans. 1978*, 357.
[112] M. Newcomb, A. R. Courtney, *J. Org. Chem. 45* (1980) 1707.
[113] H. G. Kuivila, M. S. Alnajjar, *J. Am. Chem. Soc. 104* (1982) 6146.
[114] E. C. Ashby, R. DePriest, *J. Am. Chem. Soc. 104* (1982) 6144.
[115] J. San Filippo, Jr., J. Silbermann, *J. Am. Chem. Soc. 104* (1982) 2831.
[116] W. Kitching, H. A. Olszowy, K. Harvey, *J. Org. Chem. 47* (1982) 1893.
[117] R. Kaiser, D. Lamparsky, *Helv. Chim. Acta 61* (1978) 2671.
[118] J. M. Fukuto, F. R. Jensen, *Acc. Chem. Res. 16* (1983) 177.
[119] J. Godschalx, *Ph. D. Thesis*, Colorado State University, Fort Collins, CO, USA 1983.
[120] B. Henc, P. W. Jolly, R. Salz, S. Stobbe, G. Wilke, R. Benn, R. Mynott, K. Seevogel, R. Goddard, C. Krüger, *J. Organomet. Chem. 191* (1980) 449.
[121] B. M. Trost, L. Weber, *J. Am. Chem. Soc. 97* (1975) 1611.
[122] P. K. Wong, K. S. Y. Lau, J. K. Stille, *J. Am. Chem. Soc. 96* (1974) 5956.
[123] L. F. Hines, J. K. Stille, *J. Am. Chem. Soc. 94* (1972) 485.
[124] N. A. Bumagin, I. G. Bumagina, I. P. Beletskaya, *J. Org. Chem. USSR 20* (1984) 411.
[125] A. Goliaszewski, J. Schwartz, *Organometallics 4* (1985) 415.

Orthophosphates in the Ternary System Al_2O_3-P_2O_5-H_2O

By Rüdiger Kniep*

Orthophosphates of aluminum have been the subject of numerous studies since the middle of the nineteenth century. They have acquired importance in such diverse fields as the earth sciences, chemical engineering, and medicine. The chemical problems associated with this Al_2O_3-P_2O_5-H_2O system mainly arise from the marked tendency to form polymeric aluminum orthophosphate complexes in solution; equilibrium is reached only with difficulty, and crystallization of single phases is the exception rather than the rule. However, the crystal structures of several aluminum orthophosphates (including minerals) have been elucidated, and it is now possible to give a systematic description of this class of compounds and the conditions necessary for their formation.

1. Introduction

The three-component system Al_2O_3-P_2O_5-H_2O encompasses several intermediate orthophosphates, the variety of which stems from the many ways of combining the cationic coordination polyhedra of aluminum with anionic phosphate species ($H_2PO_4^{\ominus}$, $HPO_4^{2\ominus}$, $PO_4^{3\ominus}$). Referred to the ternary system, these compounds occur only within the shaded area in Figure 1, with boundary conditions of 1 : 3 and 3 : 1 for the Al : P ratio. The Al : P ratio also determines the general classification into acid (Al : P < 1), neutral (Al : P = 1) and basic (Al : P > 1) phases.

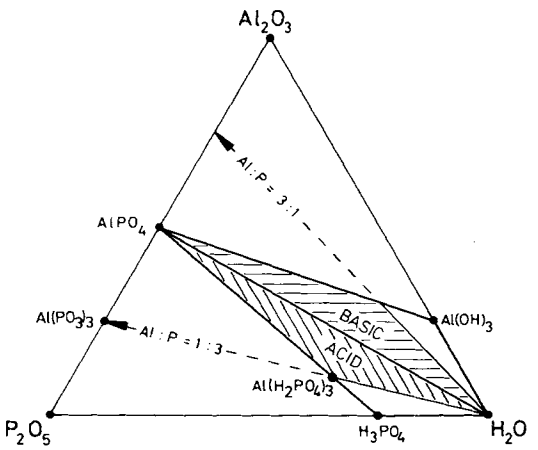


Fig. 1. The three-component system Al_2O_3-P_2O_5-H_2O; the shaded region comprises orthophosphate species.

Aluminum orthophosphates (henceforth AOPH) are of wide-ranging importance and application, and thus of interest over a wide spectrum of disciplines. Although this is a promising factor for the interdisciplinary exchange of information, such an exchange has not yet taken place to any great extent. In this article an attempt will be made to summarize current knowledge on the composition, structure and conditions of formation of AOPH.

[*] Prof. Dr. R. Kniep
Institut für Anorganische Chemie und Strukturchemie der Universität
Universitätsstrasse 1, D-4000 Düsseldorf (FRG)

Many applications of AOPH are based on their capacity to lose water on heating, being converted into compounds on the Al_2O_3-P_2O_5 edge of Figure 1. Of these, neutral, anhydrous $AlPO_4$ is of especial importance because it is closely related to silicon dioxide, both chemically and structurally: $AlPO_4$ is isoelectronic with SiO_2 (formally Si-SiO_4) and is known in all SiO_2-analogous modifications (quartz, cristobalite, tridymite) including their α- and β-forms, which are reversibly interconvertible.[1-3] The low-temperature modification α-$AlPO_4$ (berlinite) can be obtained as large single crystals by hydrothermal methods[4] and is of interest because of its dielectric and piezoelectric properties.[5] At normal pressure, $AlPO_4$ shows negligible decomposition up to 1100 °C;[6] this fact, taken together with its insolubility and chemical inertness, accounts for its application in refractories, in ceramics, and in impregnating or insulating surface coatings.

The starting material for the preparation of such *inorganic binding or coating agents* is often aluminum dihydrogenphosphate $Al(H_2PO_4)_3$,[7-9] which undergoes a setting reaction with basic oxides such as $Al(OH)_3$ [Eq. (1)] or condenses by thermal dehydration[10] to $Al(PO_3)_3$ [Eq. (2)]; the reactions (1) and (2) are simplified limiting cases and do not take into account intermediate phases.

$$Al(H_2PO_4)_3 + 2\,Al(OH)_3 \longrightarrow 3\,AlPO_4 + 6\,H_2O \quad (1)$$

$$Al(H_2PO_4)_3 \longrightarrow Al(PO_3)_3 + 3\,H_2O \quad (2)$$

As can be seen from Figure 1, the course of reaction (1) intersects the regions of acidic, neutral and basic AOPH, whereas reaction (2) proceeds through the region P_2O_5-$AlPO_4$-H_3PO_4 (the condensed aluminum phosphates[11,12]); again it is not at all clear which particular compounds of this class actually exist. $Al(PO_3)_3$ is formed from aluminum dihydrogenphosphate via at least one intermediate (probably $Al_2(H_2P_2O_7)_3$[13]) and is obtained as either a cubic crystalline tetrametaphosphate[14] or as a monoclinic polyphosphate with hexameric chains,[15] depending on the reaction temperature (500° or 800 °C, respectively). Above 1300 °C the crystalline phase is converted into a molten glass, which is used as a ceramic binding agent[7-9] and in the preparation of optical fluorophosphate glasses.[16] At still higher temperatures the melt decomposes, releasing P_2O_5 and depositing $AlPO_4$, which at

temperatures up to 1800°C is converted into α-Al_2O_3, again with release of P_2O_5.[17] These decomposition reactions are of importance in the production of *highly refractory materials*.[18]

AOPH also find applications in the field of *corrosion protection*. Amorphous AOPH coatings, in contrast to corresponding oxide coatings, can be deposited from solution at relatively low temperatures;[19] undesirable hydration (boehmite formation) of oxide layers generated by anodic oxidation at aluminum can be extensively suppressed by surface phosphatization;[20,21] porous Al_2O_3 layers, required because of their good adhesion properties with respect to subsequently applied coatings,[22] are generated by anodic oxidation in the presence of phosphoric acid.

The adsorption properties and surface-active donor-acceptor centers of aluminum phosphates, and of phases generated from AOPH by reaction with Al_2O_3 or SiO_2, make these materials suitable for *catalysis* (cracking processes, hydrogenation, oxidation).[23-26] In this context a new group of substances should be mentioned, namely those containing neutral $AlPO_4$ networks with cavities of a specific size. These phases are analogous to zeolites; they find application as molecular sieves, catalysts, or catalyst supports and can be prepared hydrothermally in the presence of organic molecules (amines or quaternary ammonium salts) that determine the cavity size.[27] A recent report describes the synthesis and characterization of corresponding mixed silicon/aluminum phosphates.[28]

In the *medical and pharmaceutical field*, aluminum phosphate has been used for a long time as a regulator of stomach acidity.[29-31] Pure $Al(OH)_3$ is certainly a better neutralizer, but phosphate ions have a pharmacologically more favorable effect on the stomach lining.[32]

Neutral and basic AOPH occur naturally as (relatively scarce) minerals.[33] The formation of such mineral phases is of importance in *soil science*, since the effectiveness of phosphate fertilizers is considerably reduced by phosphate fixation (formation of sparingly soluble AOPH) to $Al(OH)_3$-containing soil components (e.g. clay minerals).[34-38] This effect can however be turned to advantage in the *purification* of phosphate-containing *waste water*.[39-41]

2. The Variety of Compounds

The AOPH in the ternary system Al_2O_3-P_2O_5-H_2O that have so far been identified are shown in Figure 2. Table 1 gives their chemical composition, the mineral names of the basic and neutral phases, and, where applicable, information concerning polymorphism. The large number of compounds and their abundance within a small segment of the complete system serve to demonstrate that the formation of single-phase products can only be realized by a precise knowledge of, and adhesion to, exact conditions for their synthesis. A further difficulty in the case of acid AOPH is that the solutions needed for crystallization experiments are highly viscous, because of the formation of "aggregation polymers"[69] (see also Section 4). Unambiguous characterization of single phases can only be achieved by studies of single crystals; it thus follows that the existence of those AOPH listed in Figure 2 and Table 1, but not confirmed by single crystal methods, cannot be regarded as absolutely certain.

The problem of identifying AOPH phases will be illustrated by some concrete examples: Only as recently as

Table 1. Orthophosphates in the ternary system Al_2O_3-P_2O_5-H_2O; XA = X-ray structure analysis, CA = chemical analysis, XP = X-ray powder studies, W = Weissenberg studies, EM = electron microscopy, DTA = differential thermal analysis, TG = thermogravimetry.

No.	Composition	Mineral name/Polymorphism	Crystal system	Ref.	Identification
Basic (Al:P > 1)					
1	$Al_4(OH)_3(PO_4)_3$	Trolleite	Monoclinic	[42]	XA
2	$Al_2(OH)_3(PO_4)$	Augelite	Monoclinic	[43]	XA
3	$Al_2(OH)_3(PO_4)\cdot H_2O$	Senegalite	Orthorhombic	[44]	XA
4	$Al_3(OH)_3(PO_4)_2\cdot 5H_2O$	Wavellite	Orthorhombic	[45, 46]	XA
5	$Al_4(OH)_3(PO_4)_3\cdot 11H_2O$	Vashegyite	Orthorhombic	[47]	CA, XP, W
6	$Al_3(OH)_3(PO_4)_2\cdot 9H_2O$	Kingite	Triclinic	[48]	CA, EM
7	$Al_2(OH)_3(PO_4)\cdot 4.75H_2O$	Bolivarite	(amorphous to X-rays)	[49, 50]	CA, DTA, TG
8	$Al_3(OH)_6(PO_4)\cdot 6H_2O$	Evansite	(amorphous to X-rays, opalescent glass)	[51]	CA, DTA, TG
Neutral (Al:P = 1)					
9	$AlPO_4\cdot 2H_2O$	Variscite-Lucine (VL)	Orthorhombic	[52]	XA
		Variscite-Messbach (VM)	Orthorhombic	[53]	XP
		Metavariscite (MV)	Monoclinic	[54, 55]	XA
Acid (Al:P < 1)					
10	$Al(H_2PO_4)_3$	A	Trigonal	[56, 57]	XA
		B		[56]	XP
		C	Rhomboedral	[56, 58]	XA
11	$Al(H_2PO_4)(HPO_4)\cdot H_2O$		Monoclinic	[59, 60]	XA
12	$H_3O[Al_3(H_2PO_4)_6(HPO_4)_2]\cdot 4H_2O$		Monoclinic	[61]	XA
13	$Al_2(HPO_4)_3\cdot 3.5H_2O$			[10, 63]	CA
14	$Al_2(HPO_4)_3\cdot 4H_2O$			[64]	CA, DTA, TG, XP
15	$Al(H_2PO_4)(HPO_4)\cdot 2.5H_2O$			[10, 65, 66]	CA
16	$Al_2(H_{2-x}PO_4)_3(H_{3x}PO_4)\cdot 6H_2O$	$(0 \le x \le 1)$	Trigonal	[59, 67]	XA
17	$Al_2(HPO_4)_3\cdot 6.5H_2O$			[66]	CA
18	$Al_2(HPO_4)_3\cdot 8H_2O$			[10, 65, 68]	CA

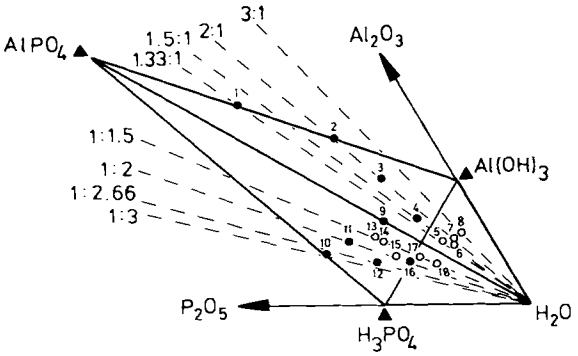


Fig. 2. Orthophosphates of the three-component system Al_2O_3-P_2O_5-H_2O. The chemical composition of the phases 1-18 is given in Table 1. Broken lines connect phases with equal Al : P ratio. Filled circles indicate phases for which crystal structure analyses have been performed.

1979 it was demonstrated[64] that the compounds $Al_2(H_2PO_4)_4(HPO_4)\cdot 2H_2O$,[70] $Al_4(H_2PO_4)_2(HPO_4)_5$,[70] $Al_2O_3\cdot 2P_2O_5\cdot 3H_2O$[71] and $Al_2(HPO_4)_3\cdot 2.5H_2O$,[72] formerly referred to in the literature as independent phases, in fact consist of mixtures of several phases. It must also be remembered that the presence of extraneous ions (such as alkali metal ions, which are added as their hydroxides to regulate the pH of the solution) can affect the preparation of AOPH by promoting the formation of quaternary compounds, of which the added ions form part. $AlH(H_2PO_4)_4\cdot 2H_2O$,[73] prepared in the presence of $Na^{\oplus}$, was later shown[64] to be a mixture of at least three phases (Na : Al : P = 1 : 1 : 4, 1 : 3 : 8 (see [59]), and 3 : 1 : 5), while $Al_3(H_2PO_4)_7(HPO_4)\cdot 6H_2O$,[73] crystallized from solutions containing $K^{\oplus}$, has been shown by X-ray powder methods[64] to be the potassium compound isotypic with phase 12 of Table 1. Non-existent compounds have also been introduced into the literature by simple transcription errors; the phases $Al(H_2PO_4)_3\cdot 1.5H_2O$ (see Addendum) and $Al_2(HPO_4)_3\cdot 3H_2O$[74] were mentioned as a result of an error in a list of AOPH.[64]

3. Crystal Structures and Their Classification

The classification of AOPH on the basis of the Al : P ratio into basic (> 1), neutral (= 1), and acid (< 1) phases finds its counterpart in structural studies.

The AOPH are not only classified according to the nature of the phosphate ions, but also according to the coordination polyhedra of aluminum (cation coordination polyhedra, CCP) and the types of linkage between them.[75-79] In all the AOPH investigated, excepting augelite and senegalite, $Al^{3\oplus}$ is octahedrally coordinated (see, however, Section 6); the oxygen donor atoms of the ligands may be defined as O_{H_2O} (from water), O_P (from phosphate anions) or O_{OH} (from hydroxyl groups). O_{OH} ligands always lead to further linkage between the CCP, whereas O_{H_2O} are always terminal. All non-protonated oxygen atoms of phosphate ions function as O_P ligands in the formation of CCP, the linkage type always being vertex-bridging. Protonated oxygens of phosphate groups are always terminal and do not contribute to further CCP-phosphate bridging (except for the formation of hydrogen bonds).

These general structural principles serve as a basis for the following summary of the fundamental differences between basic, neutral, and acid phases: basic AOPH contain condensed CCP aggregates and $PO_4^{3\ominus}$ units; neutral AOPH contain isolated CCP and $PO_4^{3\ominus}$ units; acid AOPH contain isolated CCP and protonated phosphate groups.

CCP linkages in basic AOPH are illustrated in Figure 3. Trolleite contains dimeric units $Al_2(O_{OH})_3(O_P)_6$; these face-bridged octahedra act as structure-generating CCP elements, being vertex-bridged to symmetry-equivalent dimers via O_{OH} and thus forming an infinite one-dimensional CCP double chain of composition $Al_2(O_{OH})_3(O_P)_{12}$. The CCP double chains are linked by common O_P-vertices of PO_4 tetrahedra, resulting in a dense three-dimensional network of octahedra and tetrahedra with even distribution of strong Al-O-P-O bonds. Augelite displays a less

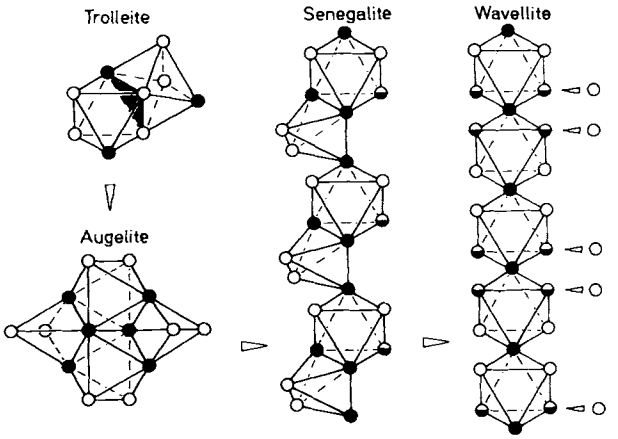


Fig. 3. Linkage of the coordination polyhedra of aluminum in basic AOPH. ●: oxygen atoms of hydroxide ions (O_{OH}); ○: oxygen atoms of phosphate ions (O_P); ◒: oxygen atoms of H_2O molecules (O_{H_2O}). The arrows to the right of the wavellite structure show the water positions which are replaced by O_P in the second chain-like structural unit. For the position of the fifth H_2O molecule, see text.

densely packed structure that contains tetrameric CCP units $Al_4(O_{OH})_6(O_P)_8$, in turn consisting of two $Al(O_{OH})_4(O_P)_2$ octahedra and two $Al(O_{OH})_3(O_P)_2$ trigonal bipyramids linked by common O_{OH}-O_{OH} edges. PO_4 tetrahedra bind the tetramers via O_P vertices to form the final three-dimensional structure. Senegalite contains coordination octahedra ($Al(O_{OH})_3(O_P)_2(O_{H_2O})$) and trigonal bipyramids ($Al(O_{OH})_3(O_P)_2$), condensed to dimeric units via common O_{OH}-O_{OH} edges; further bridging via O_{OH} vertices forms infinite chains of the dimers. Neighboring chains are united in a layer structure by vertices shared with PO_4 tetrahedra. Wavellite contains two different types of octahedra: $Al(O_{OH})_2(O_P)_3(O_{H_2O})$ and $Al(O_{OH})_2(O_P)_2(O_{H_2O})_2$, in the ratio 2 : 1; each type of CCP is incorporated into infinite one-dimensional chains via O_{OH} in *trans* positions. The chains are linked via common vertices shared with PO_4 tetrahedra, forming a three-dimensional structure with broad canals (Fig. 4) parallel to the crystallographic *a* axis. These canals contain disordered water molecules with relatively high mobility. The disorder can be reasonably described in terms of two half-occupied, mutually exclusive water sites. Between room

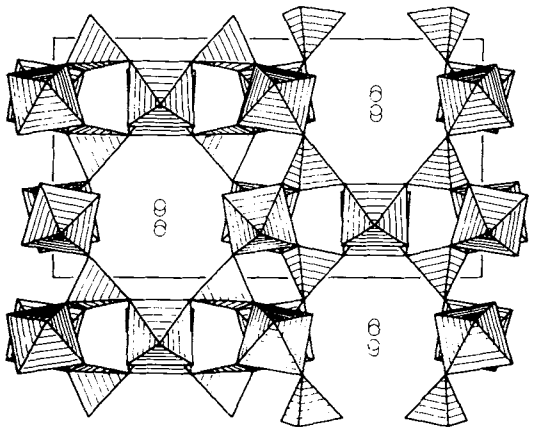


Fig. 4. Part of the crystal structure of wavellite (polyhedral representation). The double circles in the otherwise empty canals indicate disordered water molecules in mutually exclusive positions 0.88 Å apart.

temperature and 100 °C, this water can be completely removed; the process is reversible in single crystals, and wavellite thus shows a temperature-dependent phase range with respect to the water of crystallization.[79] Vashegyite and kingite have not yet been subjected to complete crystal structure analyses, because the crystals are extremely small. It is however clear that both are layer structures, and it has been suggested that they are structurally similar to kaolinite.[80] Bolivarite, whose average composition is given in Table 1, is amorphous to X-rays. Evansite is an opal-like, basic phosphate glass and displays the largest Al : P ratio yet observed (3 : 1). It may be assumed that this phase contains extensive aggregates of condensed CCP (fragments of the layer structures of gibbsite or bayerite[81]) that cannot be connected into a regular lattice structure because of the small number of phosphate tetrahedra available for bridging.

The tendency of basic AOPH to form crystalline phases decreases with increasing water content.[79,82,83] The AOPH that form well-characterized crystalline phases show a decreasing degree of CCP-condensation (Fig. 3) with increasing water content (in the order 1→4, see Fig. 2 and Table 1) and therefore also a decreasing density: trolleite (face- and vertex-bridging) 3.08 g cm^{-3}, augelite (edge-bridging) 2.70 g cm^{-3}, senegalite (edge- and vertex-bridging) 2.55 g cm^{-3}, wavellite (vertex-bridging) 2.35 g cm^{-3}.

The crystal structures of the neutral AOPH variscite-lucine (VL) and metavariscite contain $Al(O_P)_4(O_{H_2O})_2$ octahedra, connected via vertices shared with PO_4 tetrahedra to form a three-dimensional structure. The O_{H_2O} are mutually *cis* at aluminum. CCP polymerization, as is observed in the case of basic AOPH, does not occur in the neutral phases. Figure 5 shows comparable projections of the structures of VL and metavariscite; the linkage of CCP via phosphate tetrahedra is similar but not identical, as can be seen from the orientation of the shaded tetrahedron. Therefore, any interconversion of phases would, despite identical coordination polyhedra in both compounds, have to take place reconstructively.[84] No crystal structure analysis of variscite-messbach (VM) has been carried out, because this phase is only known in cryptocrystalline form. IR and X-ray powder investigations[53] suggest a close relationship to VL, with a doubled *b*-axis in VM but otherwise

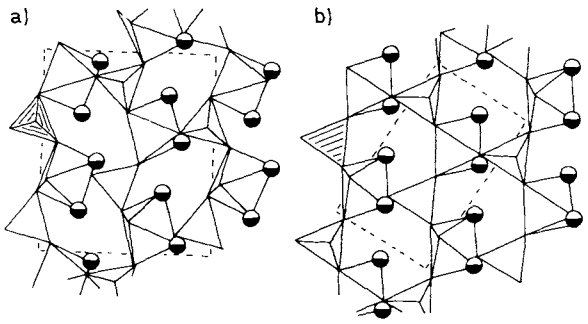


Fig. 5. Part of the crystal structures of (a) variscite-lucine (VL) and (b) metavariscite (polyhedral representation). The unit cells are indicated by broken lines. The shaded tetrahedra serve to emphasize the difference in the otherwise identical connectivities.

unchanged symmetry. VM can be regarded as a precursor in the formation of VL from amorphous neutral precipitates[53,79,85] (see also Section 4).

Thermal dehydration of the neutral AOPH variscite-lucine and metavariscite leads to tridymite-$AlPO_4$, but intermediate $AlPO_4$ phases, which correspond to none of the SiO_2-isotypic $AlPO_4$ modifications, are formed first.[79,85-88] Variscite-lucine is first converted under 600 °C to the crystalline phases $AlPO_4$-A and $AlPO_4$-B, the metric lattices of which are very similar to that of the starting hydrate. The dehydration of metavariscite leads below 450 °C to a phase $AlPO_4$-C. The fact that these primary dehydration products give sharp X-ray patterns and are capable of reversibly reabsorbing water—at least partially—suggests that the topology of the starting phases is largely unaltered by the initial dehydration; the coordination sphere of aluminum will however change from octahedral ($Al(O_P)_4(O_{H_2O})_2$) to tetrahedral ($Al(O_P)_4$). The simplification of the metavariscite crystal structure to its Al and P positions and their linear connections to each other results in the three-dimensional network shown in Figure 6,[79] which may be assumed to represent the topology of the three-dimensional structure of the phase $AlPO_4$-C. The structural model contains 4-, 6- and 8-membered rings of vertex-linked coordination tetrahedra, such as are found in the aluminosilicate framework of paracelsian;[89] the anion in paracelsian ($Al_2Si_2O_8^{2\ominus}$) is isoelectronic with the neutral aluminum phosphate

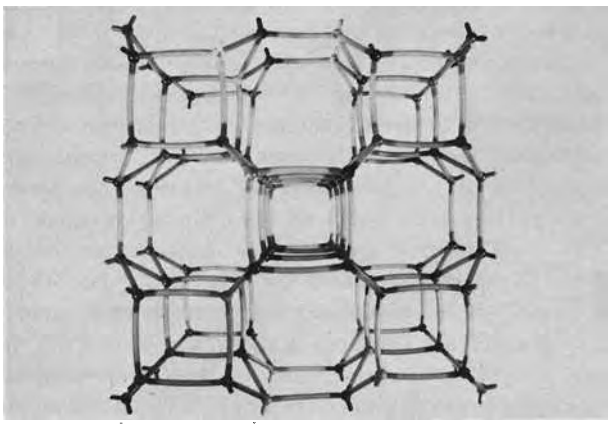


Fig. 6. Three-dimensional network structure assumed for $AlPO_4$-C; each "bond" corresponds to an ideally extended Al-O-P unit.

($Al_2P_2O_8$). The crystal structure of β-BeO[90,91] affords another topological model for comparison with that of $AlPO_4$-C; the linkage of tetrahedra as depicted in Figure 6 is precisely that of the Be-O bonding framework.[92]

Five phases of the group of acid AOPH (Nos. 10–18 in Fig. 2 and Table 1) have already been structurally analyzed. Figure 7 shows details of the crystal structures of

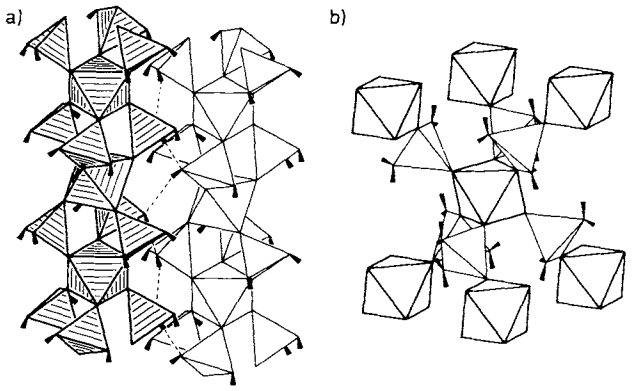


Fig. 7. Part of the crystal structures of (a) $Al(H_2PO_4)_3$-C and (b) $Al(H_2PO_4)_3$-A (polyhedral representation). One structural unit of $Al(H_2PO_4)_3$-C is indicated by shading. The hydrogen atom positions are shown by wedges; in $Al(H_2PO_4)_3$-A the hydrogen atoms are disordered, with two independent half-occupied sites at each P-OH group.

modifications A and C of $Al(H_2PO_4)_3$. Both structures contain $Al(O_P)_6$ octahedra, linked by common vertices to $O_2P(OH)_2$ tetrahedra; in $Al(H_2PO_4)_3$-C this results in an infinite one-dimensional structure, while in $Al(H_2PO_4)_3$-A a three-dimensional Al-O-P network results. With respect to their heavy atom positions alone, phases A and C are almost centrosymmetric. However, C is rendered significantly acentric (with a polar axis) by the observed directionality of the hydrogen atoms. In A, on the other hand, the hydrogen atoms are disordered at room temperature, with two half-occupied positions at each P-OH moiety, such that centrosymmetry is preserved. C is of interest because it may be ferroelectric; a phase transition observed at 60°C, associated with only minor changes in the X-ray diffraction diagram, could be considered as the transition to the paraelectric state. Whether the crystal structure of A thus represents a paraelectric state at room temperature, and A can become ferroelectric at lower temperatures, is still unclear.

Figure 8 shows details of the structures of the two-dimensional Al-O-P-linked phases $Al(H_2PO_4)(HPO_4)\cdot H_2O$ and $H_3O[Al_3(H_2PO_4)_6(HPO_4)_2]\cdot 4H_2O$. The former contains isolated $Al(O_P)_5(O_{H_2O})$ octahedra linked by common vertices to $O_2P(OH)_2$ and $O_3P(OH)$ tetrahedra, resulting in a macromolecular layer structure. Within each layer the octahedra are bridged in one dimension by both $H_2PO_4^{\ominus}$ and $HPO_4^{2\ominus}$ groups, in the other dimension only by $HPO_4^{2\ominus}$. Hydrogen bonds link the layers in the third dimension.

In $H_3O[Al_3(H_2PO_4)_6(HPO_4)_2]\cdot 4H_2O$, $Al(O_P)_6$ octahedra are linked by common vertices to $O_2P(OH)_2$ and $O_3P(OH)$ tetrahedra, forming layers with trigonal symmetry. The layers contain "holes", in the centers of which $H_3O^{\oplus}$ ions are located. Water molecules are held between the layers by hydrogen bonds. The trigonal symmetry of each individual layer is not a feature of the overall structure because of the particular displacements of the layers relative to each other. This oxonium salt could, according to the suggested transport mechanism of proton conduction in the solid state,[93] function as such a proton conductor. The particular position of the $H_3O^{\oplus}$ ions in the "holes" of the layers is a key to understanding the isotypy already suggested for compounds of the type $M^{I}M^{III}_3H_{14}(PO_4)_8\cdot 4H_2O$ ($M^{I}=H_3O^{\oplus}$, $Na^{\oplus}$, $K^{\oplus}$, $NH_4^{\oplus}$; $M^{III}=Al^{3\oplus}$, $Fe^{3\oplus}$).[94] It should be mentioned here that the compound $Al_2(H_2PO_4)(HPO_4)\cdot 2H_2O$ reported by *Erlenmeyer*[70] in 1878 is in fact none other than this oxonium salt, so that the true identity of the compound was finally determined more than a century after it was first described.

The structure of $Al_2(H_{2-x}PO_4)_3(H_{3x}PO_4)\cdot 6H_2O$ ($0\leq x\leq 1$) contains two different components stacked in the direction of the crystallographic *c* axis (Fig. 9): isolated PO_4 tetrahedra and larger groupings of two $Al(O_P)_3(O_{H_2O})_3$ octahedra linked through common vertices to three phosphate tetrahedra. The hydrogen positions could not be determined experimentally. If an ordered proton distribution is assumed, then two alternative limiting formulas are possible: $Al_2(H_2PO_4)_3(PO_4)\cdot 6H_2O$ and $Al_2(HPO_4)_3$-

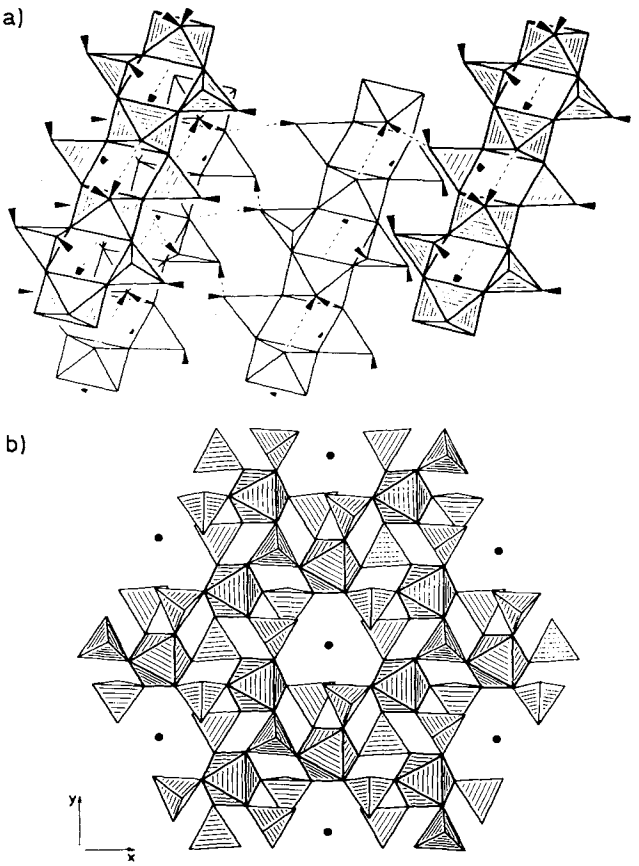


Fig. 8. Part of the crystal structures of two-dimensional Al-O-P connected acid AOPH (polyhedral representation). (a) $Al(H_2PO_4)(HPO_4)\cdot H_2O$; polyhedron linkages directed upwards in this projection are indicated by shading. The hydrogen sites are shown by wedges. Inter- and intramolecular hydrogen bonds are shown by broken lines. (b) $H_3O[Al_3(H_2PO_4)_6(HPO_4)_2]\cdot 4H_2O$; the filled circles in the middle of the "holes" represent the $H_3O^{\oplus}$ sites.

$(H_3PO_4)\cdot 6H_2O$. However, neither formulation seems very realistic, since they involve phosphate species differing by two in their degree of protonation. In addition, "free" phosphate oxygens, neither protonated nor coordinating, have never been observed, either in acid, neutral or basic AOPH. Since even a detailed analysis of the bond lengths and angles does not favor either of the limiting formulas, it is assumed that the true structure lies between both these states. Proton conduction was considered likely for this phase with its disordered protons,[67] but could not be confirmed experimentally;[95] our present understanding of the mechanism of proton conduction[93] in the solid state, however, suggests that such conduction here is not to be expected.

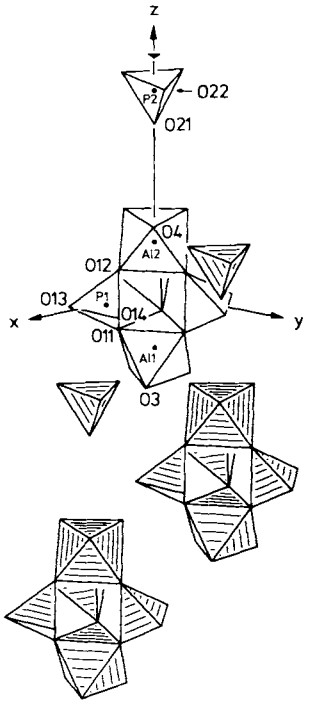


Fig. 9. Part of the crystal structure of $Al_2(H_{2-x}PO_4)_3(H_{3x}PO_4)\cdot 6H_2O$ (polyhedral representation).

Although only five crystal structures are known from the whole range of acid AOPH (see Fig. 2, Table 1), it is already clear that there is no restriction on the number of dimensions involved in the linking of the Al-O-P units: three-dimensional linking in $Al(H_2PO_4)_3$-A, two-dimensional in $Al(H_2PO_4)(HPO_4)\cdot H_2O$ and $H_3O[Al_3(H_2PO_4)_6(HPO_4)_2]\cdot 4H_2O$, one-dimensional in $Al(H_2PO_4)_3$-C, and isolated units in $Al_2(H_{2-x}PO_4)_3(H_{3x}PO_4)\cdot 6H_2O$. It remains to be seen to what extent further successful crystal structure determinations of acid AOPH are made possible by crystal-growing experiments; it has not yet proved possible to obtain suitable single crystals of acid AOPH with an Al : P ratio of 1 : 1.5 (phases 13, 14, 17, 18 in Fig. 2 and Table 1). In this connection it is interesting to note a recent high-field ^{27}Al-NMR study of solid aluminum phosphates,[96] which allowed definite conclusions concerning the coordination geometry of aluminum and also, to a certain extent, the nature of the ligands at aluminum; however, the AOPH with Al : P = 1 : 1.5 were not investigated in this study.

4. Stability Relationships and Conditions of Formation of AOPH

AOPH are obtained from aqueous solutions (pH ≤ 6). The conditions for the formation of trolleite, augelite, senegalite and wavellite correspond to hydrothermal syntheses, whereas all other AOPH can be obtained at normal pressure.

In aqueous solution, the aluminum cation exists in the form of an octahedral hexaaqua complex, which functions as a weak cation acid[97] and is subject to the dissociation equilibrium formulated in Equation (3) as a first step:

$$[Al(H_2O)_6]^{3\oplus} \rightleftharpoons [Al(OH)(H_2O)_5]^{2\oplus} + H^{\oplus} \quad (3)$$

The initially monomeric complexes condense via common OH groups (olation) to give polynuclear units; the dimeric, edge-bridged cation formed according to Equation (4) has been identified in the crystal structure of its sulfate salt.[98]

$$2[Al(OH)(H_2O)_5]^{2\oplus} \rightleftharpoons [(Al(OH)(H_2O)_4)_2]^{4\oplus} + 2H_2O \quad (4)$$

Further condensation, at pH values >4, leads mostly to ring-shaped hexanuclear cationic complexes with bridging along O_{OH}-O_{OH} edges,[99] which may be regarded as fragments of the layers of crystalline $Al(OH)_3$ phases. It may take several days to establish equilibrium, and intermediate phases, once precipitated, redissolve extremely slowly. Larger, probably metastable complexes have been isolated as their sulfate or selenate salts.[100, 101]

In phosphate-containing solutions the tendency of the aluminum octahedra to condense with each other is additionally influenced by complex formation with phosphate species. At the beginning of this century it was reported[102–104] that the mixing of $Al^{3\oplus}$- and $H_2PO_4^{\ominus}$-solutions causes a spontaneous lowering of the pH. The release of protons is consistent with the formation of stable, soluble aluminum phosphate complexes, in which (as Eq. (5) shows in schematic and simplified form) at least one ligand site of the octahedrally coordinated aluminum is occupied by the oxygen atom of a phosphate tetrahedron, forming an Al-O-P unit.

$$[Al(H_2O)_6]^{3\oplus} + H_2PO_4^{\ominus} \rightleftharpoons [Al(OPO_3H)(H_2O)_5]^{\oplus} + H_3O^{\oplus} \quad (5)$$

These complexes may be neutral, anionic or cationic depending on the nature and number of the phosphate ligands.[69, 103, 106–112] In concentrated solutions these complexes can form three-dimensional cross-linked "aggregation polymers",[69] thus leading to a highly viscous medium. Such highly viscous solutions may be obtained, for example, by dissolving aluminum in 60–85% H_3PO_4; the maximum attainable Al concentration in a still transparent solution corresponds to an Al : P ratio of ca. 1 : 2.[64]

Stock solutions with Al : P ratios $\leqq 1:2$ are used for the preparation and crystallization of acid AOPH; these solutions are themselves prepared by the reaction of $AlPO_4 \cdot 2H_2O$, $Al(OH)_3$ or aluminum with 60–85% H_3PO_4.[56, 59, 64, 113–117] Reproducible results in crystallization experiments (usually by evaporation between 25 and 100 °C) can only be obtained by the use of "matured" solutions that have been left untouched for a long time to reach equilibrium. The process by which equilibrium is reached is clearly an ordering or preliminary structure formation; the complex aggregates that are present in the crystalline materials are first formed in solution. Table 2 shows schematically which crystalline phases are preferentially

Table 2. Relationship between the Al : P ratios in concentrated solutions and those in the acid AOPH crystallizing from them. The phases are numbered as in Table 1.

	Al : P in solution							
T [°C]	1:7	1:6	1:5	1:4	1:3	1:2	Phase	Al : P
80							10-A	1:3
40–100							10-C	1:3
50–80							12	1:2.66
80–100							11	1:2
30–70							16	1:2
<65							14	1:1.5

formed for given Al : P ratios in solution; phase 10(C), $^1_\infty[Al(H_2PO_4)_3]$, can be regarded as a relatively stable, "everpresent" species, whereas the other phases crystallize only in restricted concentration ranges. Figure 10 shows the effect of temperature on the formation of crystalline phases from a stock solution with a constant Al : P ratio of 1 : 3.[116]

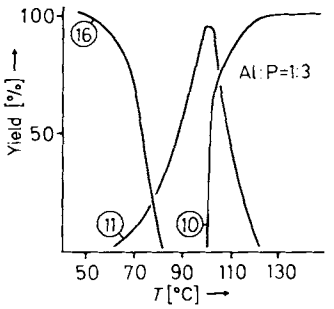


Fig. 10. Crystallization and yield of acid AOPH from solutions with an Al : P ratio of 1 : 3, as a function of temperature [116]. The phases are numbered as in Table 1.

The tendency to form products consisting of many phases (as already mentioned in the introduction) on crystallization from concentrated solutions can be observed in this system. The polymeric aggregates present in solution are responsible for this phenomenon, since they hinder the formation of crystallization centers and can cause supersaturation even to the extent of forming glasses. In addition, the high viscosity leads to marked concentration gradients in the neighborhood of growing crystals and thus to the crystallization of other phases around the crystal originally formed.

In contrast to the acid AOPH, which crystallize from highly concentrated solutions, the neutral AOPH are obtained from dilute aluminum phosphate solutions;[64, 85, 118–124] the temperatures required lie between 80 and 130 °C. When using solutions prepared from aluminum salts and phosphate salts it should be remembered that the presence of impurities (notably the cations $K^\oplus$ and $NH_4^\oplus$) can often have a serious effect on the products, sometimes leading to the precipitation of phases incorporating the impurities.[121] Metavariscite crystallizes directly from solution at $pH \approx 1$, whereas variscite-lucine is formed at pH 2-4 via an amorphous precipitate after long digestion. Many different intermediate stages with differing water content and degree of crystallinity are involved.[85] Variscite-messbach should be considered as a crystalline precursor of variscite-lucine (see Section 3).

Basic AOPH can be obtained at pH values of 4–6 and temperatures that increase with decreasing water content of the solid phases formed.[124–129] This is consistent with the expected increase of thermal stability, in the order $O_{(H_2O)} < O_{(OH)} < O_{(P)}$, of oxygen ligands coordinated to aluminum.[130, 131] In trolleite and augelite, $O_{(H_2O)}$ are not involved in the aluminum polyhedra, and these phases are thus the most thermally stable AOPH. Under hydrothermal conditions the stability ranges of trolleite and augelite are determined by various equilibrium processes[129] in which the even more stable phases berlinite ($AlPO_4$) and corundum (Al_2O_3) are involved [Eq. (6)–(9)].

$$\text{trolleite} \rightleftharpoons \text{augelite} + 2\,\text{berlinite} \quad (6)$$

$$\text{trolleite} \rightleftharpoons 3\,\text{berlinite} + 1/2\,\text{corundum} + 3/2\,H_2O \quad (7)$$

$$\text{augelite} \rightleftharpoons \text{berlinite} + 1/2\,\text{corundum} + 3/2\,H_2O \quad (8)$$

$$\text{augelite} \rightleftharpoons 1/3\,\text{trolleite} + 1/3\,\text{corundum} + H_2O \quad (9)$$

Figure 11 shows the course of the four univariant curves in the p/T diagram for reactions (6)–(9); the intersection of the equilibrium lines defines an invariant point at 4.70 kbar (p_{H_2O}) and 542 °C.[129]

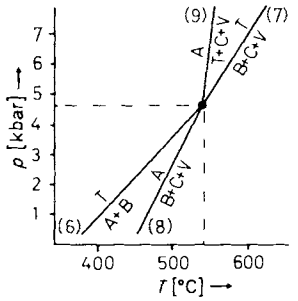


Fig. 11. p/T diagram showing the course of the equilibrium reactions (6)–(9) about their invariant point ($p_{H_2O} = 4.70$ kb; $T = 542$ °C) [129]. T = trolleite, A = augelite, B = berlinite, C = corundum, V = H_2O.

The thermal stability of the isolated "dry" AOPH (Fig. 12) varies over a wide temperature range according to the water content; the heavily hydrated phase 16 ($Al_2(H_{2-x}PO_4)_3(H_{3x}PO_4) \cdot 6H_2O$) decomposes at 70 °C, whereas the phase with the least water (trolleite,

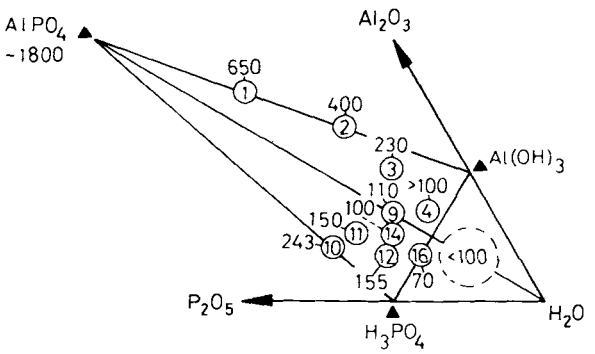


Fig. 12. The thermal stability of isolated ("dry") AOPH; temperatures in °C. The phases are numbered as in Table 1.

$Al_4(OH)_3(PO_4)_3$) is stable to 650°C. Higher hydrates can in general be converted into their corresponding less-hydrated phases by thermal dehydration. This preparative procedure is particularly suitable (given a constant Al : P ratio) when the higher hydrate decomposes below 100°C (generally by incongruent melting) and the lower hydrate decomposes at a temperature higher than the temperature of evaporation of water from the saturated solution. The principle of crystallization by evaporation finds an application here. In this way phase 16, for example, can be quantitatively converted into phase 11 [Eq. (10)].[60, 67, 113]

$$\underset{\text{Phase 16, m.p. (incong.)} = 70\,^{\circ}\text{C}}{Al_2(H_{2-x}PO_4)_3(H_{3x}PO_4)\cdot 6H_2O} \xrightarrow[-4\,H_2O]{120\,^{\circ}\text{C}} \underset{\text{Phase 11, decomp. temp.} = 150\,^{\circ}\text{C}}{2\,Al(H_2PO_4)(HPO_4)\cdot H_2O} \qquad (10)$$

Phase 15, which might occur as an intermediate (Fig. 2, Table 1), is in fact not observed in this thermal decomposition.

5. Summary and Concluding Remarks

The small segment $AlPO_4$–$Al(OH)_3$–H_2O–H_3PO_4 of the three-component system Al_2O_3–P_2O_5–H_2O encompasses several orthophosphate hydrates that can be classified as basic, neutral or acid phases according to chemical and structural principles. Their variety stems from the different condensation and linkage processes that are possible between the coordination polyhedra of aluminum and anionic phosphate species. The structural elements of the solid phases are preformed in concentrated aqueous solutions as complex "aggregation polymers"; if sufficiently extended, these may give rise to highly viscous solutions. This in turn leads to special problems in crystal growth, and single-phase products are the exception rather than the rule. Studies of single crystals are therefore of great importance for the identification of the AOPH phases.

The interest in, and applications of, AOPH extend to many regions of natural sciences, earth sciences, technology and medicine; a prominent role is played by single phases and their specific properties, such as behavior on heating, thermal stability, insolubility, chemical inertness, insulator properties, catalytic activity, acid or base capacity, ferroelectricity, and proton conduction.

On the basis of their peculiar structural characteristics and chemical composition, AOPH can be assigned to a wider group of compounds, to which iron(III) orthophosphate hydrates and also the corresponding arsenates belong; some are isotypic with AOPH. Thus variscite-lucine ($AlPO_4\cdot 2H_2O$) is isotypic with strengite ($FePO_4\cdot 2H_2O$), mansfieldite ($AlAsO_4\cdot 2H_2O$) and skorodite ($FeAsO_4\cdot 2H_2O$);[79, 132, 133] $Al(H_2PO_4)_3$-A and $Fe(H_2PO_4)_3$-A are also isotypic.[56, 57] In some cases isotypy in the strict sense is not observed, but the structural units display the same arrangement; for example, $Fe(H_2AsO_4)_3\cdot 5H_2O$[134] displays a one-dimensional structure type also seen in $Al(H_2PO_4)_3$-C, but with additional interstitial water molecules. The possible existence of an analogous pentahydrate of $Al(H_2PO_4)_3$ (possibly at low temperature) has not been investigated, and indeed the existence of further AOPH in general cannot be ruled out. It is however clear that AOPH represent the best-studied type of compound within this larger group of compounds. The main reason for this is that the arsenic compounds are too toxic, and the iron(III) compounds too susceptible to reduction, to have found wide application. An additional factor is that the hydrogen atom positions, although difficult to determine by X-ray methods, are generally more easy to determine in the absence of heavier elements.

6. Addendum

In the course of recent intensive work on $AlPO_4$-based molecular sieves[27] (see also Section 1) a neutral AOPH of composition $AlPO_4\cdot 1.5H_2O$ has been synthesized (probably under hydrothermal conditions).[62] The unusual crystal structure of this compound contains two different kinds of two-dimensional nets, which are stacked alternately and which are joined via common oxygen atoms to form a three-dimensional framework.[135] One kind of layer corresponds to an arrangement of $Al(O_P)_4(O_{H_2O})_2$-octahedra and PO_4-tetrahedra that is also present in variscite and metavariscite ($AlPO_4\cdot 2H_2O$) (see Fig. 5). The other kind of layer is built up from $Al(O_P)_4$- and PO_4-tetrahedra that are connected to four- and eight-membered rings, an arrangement proposed for the primary product ($AlPO_4$-C) of the metavariscite-dehydration (cf.[79] and Fig. 6). The resulting topology of the $AlPO_4\cdot 1.5H_2O$-framework is given schematically in Figure 13. The circles are $Al(O_P)_4(O_{H_2O})_2$-octahedra, and the composition of the four-connected net is thus $AlPO_4\cdot 1H_2O$; the remaining $0.5H_2O$ is loosely bonded within cavities of the structure and is readily released even at lower temperatures.

In an earlier work[85] on the dehydration and rehydration of neutral AOPH a low hydrate of composition $AlPO_4\cdot 1.67H_2O$ was described; this phase, however, is in fact the new 1.5-hydrate described here.[135] Generally, the reactions that take place upon dehydration and (partial) rehydration of neutral AOPH are rather complex, and involve a number of intermediate phases (see Section 3 and

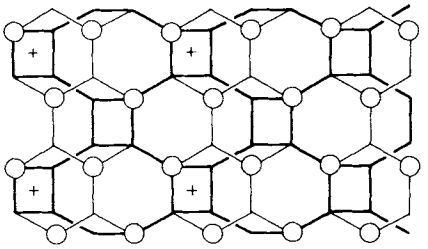


Fig. 13. Topology of the framework (linkage of the layers; projection along [100]) in $AlPO_4 \cdot 1.5\,H_2O$. Al- and P-positions (alternating) with tetrahedral coordination at the corners of the nets; open circles represent Al in octahedral coordination ($Al(O_P)_4(O_{H_2O})_2$) with terminal O_{H_2O}. Upper layer in the projection: net of condensed six-membered rings (6.6.6.-net); lower layer: net of condensed four- and eight-membered rings (4.8.8.-net). Linkage of the layers (coinciding edges of the nets) produces four-membered rings. The + sign indicates the corner point of the unit cell in this projection.

Ref. [105]), so that further investigations are necessary for definite clarification. Here again, the investigation of single crystals should be the most rewarding.

This work was supported by the Minister für Wissenschaft und Forschung des Landes Nordrhein-Westfalen and the Fonds der Chemischen Industrie. I wish to thank Prof. Dr. D. Mootz for cooperation and fruitful discussions.

Received: August 7, 1985;
supplemented: March 10, 1986 [A 578 IE]
German version: *Angew. Chem. 98* (1986) 520
Translated by Dr. *P. G. Jones*, Göttingen (FRG)

[1] O. W. Flörke, *Sci. Ceram. 3* (1965).
[2] J. H. Nicola, J. F. Scott, *Phys. Rev. B: Condens. Mater. 18* (1978) 1972.
[3] C. Ecolivet, H. Poignant, *Phys. Status Solidi A 63* (1981) K 107.
[4] L. E. Drafall, R. F. Belt, *Gov. Rep. Announce Index (U. S.) 80* (1980) 4847.
[5] E. D. Kolb, A. M. Glass, R. L. Rosenberg, J. C. Grenier, R. A. Laudise, *Ultrason. Symp. Proc. 1981*, 332.
[6] O. W. Flörke, *Z. Kristallogr. Kristallgeom. Kristallphys. Kristallchem. 125* (1967) 134.
[7] H. Bechtel, G. Ploss, *Ber. Dtsch. Keram. Ges. 40* (1963) 399.
[8] V. Köhne, W. Peek, *Sprechsaal Keram. Glas Email Silik. 100* (1967) 830; *101* (1968) 507.
[9] J. H. Morris, P. G. Perkins, A. E. A. Rose, W. E. Smith, *Chem. Soc. Rev. 6* (1971) 173.
[10] H. Guerin, R. Martin, *C. R. Hebd. Seances Acad. Sci. 234* (1952) 1777.
[11] F. d'Yvoire, *Bull. Soc. Chim. Fr. 1962*, 1224.
[12] F. d'Yvoire, *Bull. Soc. Chim. Fr. 1962*, 1237.
[13] V. F. Tikavyi, K. N. Lapko, A. N. Lobanok, A. N. Chnewkov, A. A. Sokol'chik, *Vestsi Akad. Navuk BSSR Ser. Khim. Navuk 1972*, 74.
[14] L. Pauling, J. Sherman, *Z. Kristallogr. Kristallgeom. Kristallphys. Kristallchem. 96* (1937) 481.
[15] H. van der Meer, *Acta Crystallogr. Sect. B 32* (1976) 2423.
[16] F. Gan, Y. Jiang, F. Jiang, *J. Non-Cryst. Solids 52* (1982) 263.
[17] V. M. Medvedeva, A. A. Medvedeva, I. V. Tananaev, *Izv. Akad. Nauk SSSR Neorg. Mater. 1* (1965) 211.
[18] R. N. Rickles, *J. Appl. Chem. 1965*, 74.
[19] R. N. Rothon, *Thin Solid Films 77* (1981) 149.
[20] G. D. Davis, T. S. Sun, J. S. Ahearn, J. D. Venables, *J. Mater. Sci. 17* (1982) 1807.
[21] H. Konno, S. Kobayashi, H. Takahashi, M. Nagayama, *Corros. Sci. 22* (1982) 913.
[22] J. A. Marceau, R. H. Firminhac, Y. Moji, Br. Pat. 1555940 (1979).
[23] A. Krzywicki, M. Marczewski, *React. Kinet. Catal. Lett. 13* (1980) 45.
[24] W. L. Kehl, US-Pat. 4407730 (1983).
[25] S. F. Yushchenko, Z. V. Gryaznova, A. M. Dimitriev, N. N. Greben'ko, *Vestn. Mosk. Univ. Ser. 2: Khim. 24* (1983) 490.
[26] P. M. Deya, M. Capo, A. Costa, J. V. Sinisterra, J. M. Marinas, *An. Quim. 77* (1981) 153.
[27] S. T. Wilson, B. M. Lok, C. A. Messina, T. R. Cannan, E. M. Flanigen, *J. Am. Chem. Soc. 104* (1982) 1146.
[28] B. M. Lok, C. A. Messina, R. L. Patton, T. G. Richard, T. R. Cannan, E. M. Flanigen, *J. Am. Chem. Soc. 106* (1984) 6092.
[29] K. Metza, W. Rösch, *Z. Gastroenterol. 19* (1981) 212.
[30] C. Walther, P. Herzog, K. H. Hissnauer, H.-J. Köhl, K.-H. Holtermüller, *Z. Gastroenterol. 20* (1982) 263.
[31] R. Kniep, Dtsch. Pat.-Anm. 3330944.2 (1983).
[32] R. Wegmann, Y. Bergerot-Blondel, *Ann. Histochim. 21* (1976) 1.
[33] J. O. Nriagu, P. B. Moore (Eds.): *Phosphate Minerals*, Springer, Berlin 1984.
[34] A. Shayan, B. G. Davey, *Soil Sci. Soc. Am. J. 42* (1978) 878.
[35] W. Robarge, R. B. Corey, *Soil Sci. Soc. Am. J. 43* (1979) 481.
[36] K. C. Park, K. W. Park, *Yo Op Hoe Chi 18* (1981) 192.
[37] J. T. Sims, *Dissertation*, Michigan State University 1982.
[38] J. T. Sims, B. G. Ellis, *Soil Sci. Soc. Am. J. 47* (1983) 912.
[39] L. Lijklema, *Environ. Sci. Technol. 14* (1980) 537.
[40] D. Donnert, S. H. Eberle, P. Gruber, H. Metzger, H. P. Sapandowski, *Z. Wasser Abwasser Forsch. 14* (1981) 188.
[41] N. Narkis, M. Meiri, *Environ. Pollut. Ser. B 2* (1981) 327.
[42] P. B. Moore, T. Araki, *Am. Mineral. 59* (1974) 974.
[43] T. Araki, J. J. Finney, T. Zoltai, *Am. Mineral. 53* (1968) 1069.
[44] T. D. Keegan, T. Araki, P. B. Moore, *Am. Mineral. 64* (1979) 1243.
[45] T. Araki, T. Zoltai, *Z. Kristallogr. Kristallgeom. Kristallphys. Kristallchem. 127* (1968) 21.
[46] R. Kniep, *Diplomarbeit I*, Technische Universität Braunschweig 1970.
[47] Z. Johan, E. Slanski, P. Povondra, *Can. Mineral. 21* (1983) 489.
[48] T. Kato, *Am. Mineral. 55* (1970) 515.
[49] P. van Tassel, *Mineral. Mag. J. Mineral. Soc. 32* (1960) 419.
[50] L. van Wambeke, *Mineral. Mag. 38* (1971) 418.
[51] J. Melon, J. Touissant, *Ann. Soc. Geol. Belg. Bull. 80* (1957) B 497.
[52] R. Kniep, D. Mootz, A. Vegas, *Acta Crystallogr. B 33* (1977) 263.
[53] P. S. Salvador, J. Fayos, *Am. Mineral. 57* (1972) 36.
[54] R. Kniep, D. Mootz, *Acta Crystallogr. B 29* (1973) 2292.
[55] J. Boresztajn, *Bull. Soc. Fr. Mineral. Cristallogr. 89* (1966) 428.
[56] F. d'Yvoire, *Bull. Soc. Chim. Fr. 1961*, 2277.
[57] D. Brodalla, R. Kniep, D. Mootz, *Z. Naturforsch. B 36* (1981) 907.
[58] R. Kniep, M. Steffen, *Angew. Chem. 90* (1978) 286; *Angew. Chem. Int. Ed. Engl. 17* (1978) 272.
[59] F. d'Yvoire, *Bull. Soc. Chim. Fr. 1961*, 2283.
[60] R. Kniep, D. Mootz, A. Wilms, *Z. Naturforsch. B 33* (1978) 1047.
[61] D. Brodalla, R. Kniep, *Z. Naturforsch. B 35* (1980) 403.
[62] S. T. Wilson, B. M. Lok, E. M. Flanigen, unpublished.
[63] R. F. Jameson, J. E. Salmon, *J. Chem. Soc. 1954*, 4013.
[64] D. Brodalla, *Diplomarbeit*, Universität Düsseldorf 1979.
[65] M. Millot, *Bull. Soc. Chim. Fr. 22* (1874) 242.
[66] M. Millot, *C. R. Hebd. Seances Acad. Sci. 82* (1876) 89.
[67] R. Kniep, A. Wilms, *Z. Naturforsch. B 34* (1979) 750.
[68] Travers, Perron, *Ann. Chim. Phys. 1924*, 332.
[69] C. F. Callis, J. R. van Wazer, P. G. Arvan, *Chem. Rev. 54* (1954) 777.
[70] E. Erlenmeyer, *Justus Liebigs Ann. Chem. 194* (1878) 178.
[71] F. d'Yvoire, *C. R. Hebd. Seances Acad. Sci. 247* (1958) 297.
[72] N. N. Sveshnikova, *Zh. Neorg. Khim. 5* (1960) 477.
[73] E. Zirngiebl, *Dissertation*, Universität Erlangen-Nürnberg 1957.
[74] A. D. F. Toy in J. C. Bailar, H. J. Emeléus, R. Nyholm, A. F. Trotman-Dickenson (Eds.): *Comprehensive Inorganic Chemistry, Vol. 2*, Pergamon Press, Oxford 1973.
[75] D. E. C. Corbridge: *The Structural Chemistry of Phosphorus*, Elsevier, Amsterdam 1974.
[76] F. Liebau, *Fortschr. Mineral. 42* (1966) 266.
[77] P. B. Moore, *Am. Mineral. 55* (1970) 135.
[78] P. Keller, *Neues Jahrb. Mineral. Abh. 117* (1972) 217.
[79] R. Kniep, *Habilitationsschrift*, Universität Düsseldorf 1978.
[80] D. McConnell, *Mineral. Mag. 39* (1974) 802.
[81] K. Wefers, G. M. Bell, *Tech. Pap. Alcoa Res. Lab. 19* (1972).
[82] R. Kniep, *Diplomarbeit II*, Technische Universität Braunschweig 1971.
[83] D. McConnell, *Mineral. Mag. 40* (1976) 609.
[84] F. Liebau, *Fortschr. Mineral. 61* (1983) 29.
[85] F. d'Yvoire, *Bull. Soc. Chim. Fr. 1962*, 1762.
[86] B. M. Kobtsev, A. G. Kotlova, N. I. Shchepochkina, B. V. Strizhkov, *Izv. Akad. Nauk SSSR Neorg. Mater. 8* (1972) 396.
[87] A. G. Kotlova, N. I. Shchepochkina, *Russ. J. Inorg. Chem. Engl. Transl. 1972*, 165.
[88] E. Z. Arlidge, V. C. Farmer, B. D. Mitchell, W. A. Mitchell, *J. Appl. Chem. 13* (1963) 17.

[89] J. V. Smith, *Acta Crystallogr. 6* (1953) 613.
[90] D. K. Smith, C. F. Cline, S. B. Austermann, *Acta Crystallogr. 18* (1965) 393.
[91] A. F. Wells: *Structural Inorganic Chemistry*, Clarendon Press, Oxford 1984, p. 539.
[92] D. Mootz, J. Fayos, private communication.
[93] K.-D. Kreuer, A. Rabenau, W. Weppner, *Angew. Chem. 94* (1982) 224; *Angew. Chem. Int. Ed. Engl. 21* (1982) 208.
[94] P. Remy, A. Boulle, *C. R. Hebd. Seances Acad. Sci. Ser. C271* (1971) 360.
[95] K.-D. Kreuer, unpublished.
[96] D. Müller, L. Grunze, E. Hallas, G. Ladwig, *Z. Anorg. Allg. Chem. 500* (1983) 80.
[97] C. Brosset, *Acta Chem. Scand. 6* (1952) 910.
[98] G. Johansson, *Acta Chem. Scand. 16* (1962) 403.
[99] C. Brosset, G. Biedermann, L. G. Sillen, *Acta Chem. Scand. 8* (1954) 1917.
[100] G. Johansson, G. Lundgren, L. G. Sillen, R. Söderquist, *Acta Chem. Scand. 14* (1960) 769.
[101] G. Johansson, *Acta Chem. Scand. 14* (1960) 771.
[102] L. Dede, *Z. Anorg. Allg. Chem. 125* (1922) 28.
[103] N. Bjerrum, C. R. Dahmen, *Z. Phys. Chem., Bodenstein-Festband* (1931) 627.
[104] K. A. Jensen, *Z. Anorg. Allg. Chem. 221* (1934) 1.
[105] M. Sato, E. Kobayashi, M. Matsumoto, S. Matsuda, *Rev. Chim. Miner. 22* (1985) 37.
[106] A. Holroyd, J. E. Salmon, *J. Chem. Soc. 1956*, 269.
[107] J. R. van Wazer: *Phosphorus and its Compounds, Vol. 1*, Wiley-Interscience, New York 1966.
[108] J. E. Salmon, J. G. L. Wall, *J. Chem. Soc. 1958*, 1128.
[109] G. Kuhl, *J. Inorg. Nucl. Chem. 31* (1969) 1043.
[110] J. W. Akitt, N. N. Greenwood, G. D. Lester, *J. Chem. Soc. A 1971*, 2450.
[111] V. F. Tikavyi, K. N. Lapko, I. A. Zakharov, E. P. Antonyuk, L. I. Dorozhkina, *Russ. Inorg. Mater. 7* (1971) 1446.
[112] S. J. Karlik, G. A. Elgavish, R. P. Pilai, G. L. Eichorn, *J. Magn. Reson. 49* (1982) 164.
[113] A. Wilms, *Diplomarbeit*, Universität Düsseldorf 1978.
[114] R. Martin, C. Duc-Maugé, H. Guerin, *Bull. Soc. Chim. Fr. 1966*, 851.
[115] F. d'Yvoire, *Bull. Soc. Chim. Fr. 1962*, 1243.
[116] M. Tsuhako, T. Matsuo, I. Motooka, M. Kobayashi, *Chem. Lett. 1978*, 777.
[117] M. Tsuhako, *Kagaku no Ryoiki 37* (1983) 194.
[118] C. V. Cole, M. L. Jackson, *J. Phys. Colloid Chem. 54* (1950) 128.
[119] C. V. Cole, M. L. Jackson, *Soil Sci. Soc. Am. Proc. 15* (1950) 84.
[120] J. M. Axelrod, M. K. Carron, C. Milton, T. P. Thayer, *Am. Mineral. 37* (1952) 883.
[121] J. F. Haseman, J. R. Lehr, J. P. Smith, *Soil. Sci. Soc. Am. Proc. 15* (1950) 76.
[122] A. M. Golub, I. I. Boldog, *Russ. J. Inorg. Chem. Engl. Transl. 21* (1976) 45.
[123] A. Yu. Kudeyarova, A. I. Trubin, *Pochvovedenie 1978*, 137.
[124] N. V. Greben'ko, L. S. Eshchenko, V. V. Pechkovskii, *Izv. Akad. Nauk SSSR Neorg. Mater. 14* (1978) 136.
[125] S. R. Zamyatkin, P. S. Mamykin, T. P. Knyazeva, *Zh. Prikl. Khim. (Leningrad) 45* (1972) 956.
[126] W. S. Wise, S. E. Loh, *Am. Mineral. 61* (1976) 409.
[127] T. Goldshmid in A. J. Rubin (Ed.): *Chemistry of Wastewater Technology*, Ann Arbor Science, Naples, FL (USA) 1978, p. 59.
[128] S.-S. Feng, T. J. Rockett, *J. Am. Ceram. Soc. 62* (1979) 430.
[129] J. D. Bass, C. B. Sclar, *Am. Mineral. 64* (1979) 1175.
[130] P. B. Moore, *Neues Jahrb. Mineral. Monatsh. 1970*, 39.
[131] P. B. Moore, *Mineral. Rec. 4* (1973) 103.
[132] W. Kleber, K.-L. Weiner, *Neues Jahrb. Mineral. Abh. 90* (1958) 253.
[133] K. Kitahama, R. Kiriyama, Y. Baba, *Acta Crystallogr. B31* (1975) 322.
[134] A. Boudjadea, J. C. Guitel, *Acta Crystallogr. B37* (1981) 1402.
[135] J. J. Pluth, J. V. Smith, *Nature (London) 318* (1985) 165.

High-Pressure Liquid Chromatography (HPLC) of Proteins

New Analytical Methods (29)

By Gerhard Seipke,* Hubert Müllner, and Ulrich Grau

The application of high-pressure liquid chromatography (HPLC) to proteins has undergone a dramatic development in recent years. Nowadays its many variants expand the repertoire of high-performance analysis methods available to the protein chemist, which, until now, have been dominated by electrophoretic techniques. The advent of gene technology has resulted in a renaissance of protein chemistry. The new analytical and preparative problems that have thereby emerged are often ideally solved by HPLC methods. HPLC has long since ceased to be solely a laboratory technique; HPLC systems are now being developed for the separation of proteins—particularly those of great pharmaceutical interest—on a 100-g scale. The range of applications of analytical and preparative HPLC will be illustrated by two examples of pharmaceutical importance—insulin and interleukin 2.

1. Introduction

Liquid chromatography has become one of the most important biochemical separation methods since its discovery more than eighty years ago. A differential distribution of biopolymers between a stationary and a mobile phase can be achieved by exploiting differences in molecular size, ionic properties, solubility, and polar or nonpolar character as well as specific interactions with other molecules (e.g., enzyme-inhibitor interactions). Earlier, however, the packing materials available precluded rapid high-resolution separations, so that these methods were mainly employed at low pressure for preparative purposes. The analytical sector was dominated by electrophoretic methods.

High-resolution chromatography requires microparticulate column packings with a narrow particle size distribution.[1,2] Although this concept was known very early, its realization in practice took decades since it was necessary to solve several technical problems:

- Pump systems providing constant flow rates at high pressures had to be developed.
- The "soft" gels previously used had to be replaced by pressure-stable materials.
- Columns had to be reproducibly and evenly packed with these fine particles.

Once the instrumental requirements had been fulfilled, the application of HPLC in biochemistry underwent a dramatic development. Within a few years a wide range of new analytical methods have become available to protein chemists. The applications of HPLC (Table 1) are not restricted to analysis, however. The new techniques are being increasingly employed preparatively as well—both in the laboratory and in industrial production.

2. The Construction and Operation of an HPLC Unit

HPLC is of itself not a new method, but rather a refinement of known methods combined with greater instrumental complexity and precision. The successful application of HPLC as a quantitative analytical method requires great care in the choice and purity of the solvent, a highly constant flow rate, and continual checks of column performance.

Table 1. Some applications of HPLC in the chemistry of amino acids, peptides, and proteins.

Analysis
— Amino acid analysis
— Purity control of synthetic peptides, optimization of reaction conditions
— Identification of multiple or mutant forms of proteins
— Molecular weight determination
— Analytical peptide mapping
— Sequence analysis (identification of degradation products)
— Chemical or enzymatic modification (process control and optimization, product characterization)
— Determination of enzyme specificity
— Metabolism studies, identification of prohormones
Preparative separation
— Isolation of natural products from extracts
— Purification of products obtained from chemical synthesis or gene technology
— Purification of modified peptides or proteins, for example, radioactively labeled substances
— Separation of diastereomers
— Isolation of protein fragments for sequence studies

A typical HPLC apparatus (Fig. 1) consists of a high-pressure pumping system, a sample applicator (injector and preinjector), a column, and a detector. It is also possible to include a fraction collector and/or a microcomputer for data processing. Automation is desirable if the instrument is to be employed for routine analytical or preparative purposes.

2.1. Pumps

All HPLC pumps on the market[3] are capable of delivering both organic solvents and aqueous buffer solutions with equally high precision. The pumps must provide a constant flow with little pulsation. These requirements are ideally fulfilled by a non-reciprocating pump resembling a large hypodermic syringe, whose delivery is free of pulsation and almost independent of the back pressure of the column and the viscosity of the solvent. Its use is relatively restricted, however, because of its design, which involves a fixed, relatively large internal volume.

[*] Dr. G. Seipke, Dr. H. Müllner, Dr. U. Grau
Pharma Forschung Biochemie der Hoechst AG
Postfach 800320, D-6230 Frankfurt am Main 80 (FRG)

 © VCH Verlagsgesellschaft mbH, D-6940 Weinheim, 1986 0570-0833/86/0606-0535 $ 02.50/0

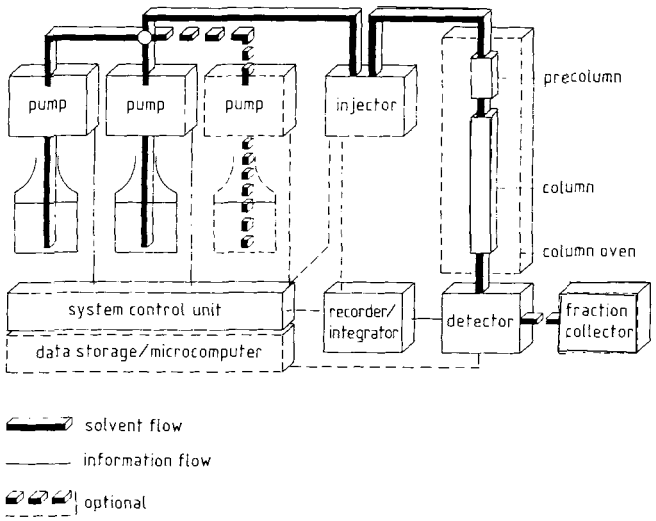


Fig. 1. Basic design of an HPLC system.

The delivery systems most frequently in use employ either short-stroke piston pumps or membrane piston pumps. Complex electronic controls are employed to ensure that the delivery volume set is maintained under changing back pressure (altered compressibility). Optimized pump design reduces the pulsation caused by the movement of the pistons. Further smoothing is usually achieved by hydraulic damping.

2.2. Gradient Formers

The composition of the mobile phase can be varied during the analysis by mixing two or more solvents continuously (gradient elution). This technique predominates in the separation of proteins by adsorption chromatography. Gradient elutions yield peaks of equal sharpness throughout the whole course of elution. In contrast to isocratic elution, in which the solvent composition remains unchanged, gradient elution results in the same detection sensitivity for strongly retarded components as well as a shorter analysis time.[47] Proteins bind cooperatively to more than one portion of the stationary phase.[5-7] Only the simultaneous effect of a corresponding number of molecules of the "displacing agent" (for example, salt in ion-exchange chromatography, organic solvent in reversed-phase chromatography) is able to displace them. From this it can be deduced that there will be an increasingly concave dependence of retention on the elution composition with increasing molecular weight.[4,8,9] In practice, if the displacer concentration is slowly increased, extremely strong adsorption (that is, minimal migration) of the proteins is initially observed. As the concentration is further increased, adsorption and thus retention strongly decreases within a range that becomes narrower with increasing molecular weight and whose position can be extremely different from protein to protein.[7-10] Gradient elution is therefore essential for the separation of complex mixtures of proteins, but its use places great demands on the precision of such delivery systems.

In the great majority of cases the solvents are mixed by employing two separate, adjustable pumps. Binary gradients are sufficient for most applications. A third solvent can be useful for the application of larger volumes of sample in preparative work or for the addition of a second, more strongly eluting solvent at the end of a gradient in reversed-phase chromatography.[11]

2.3. Eluents

The choice of eluents depends, above all, on the separation principle (see Section 3); further limitations are set by the compatibility of the eluents with the stationary phase (see Section 2.5) and with the materials from which the HPLC equipment is constructed. Warnings are often given against the use of buffer solutions containing halides. In practice, however, it is possible to avoid corrosion of the pumps and columns.[12] The choice of buffer components and organic solvents is also dictated by the method and required sensitivity of detection (see Section 2.6). The viscosity must also be taken into account since it not only contributes to the back pressure of the column, but also influences the separation efficiency of a column (measured in theoretical plates N[2,13]).

Filtration of all eluents through a 0.2- or 0.45-μm membrane filter not only protects the pumps, but also improves the long-term stability of the separation columns. Subsequent thorough degassing removes dissolved oxygen, which would make sensitive detection at low wavelengths impossible and could lead to problems when mixing gradients (formation of air bubbles). Sparging with helium is very effective and does not significantly affect the composition of the mobile phase.[14] In the case of pump designs that are sensitive to dissolved helium, degassing can be performed under vacuum or ultrasonically.

2.4. Sample application

The analysis of complex protein mixtures and the re-equilibration of the columns requires a relatively long time. Automatic injection of the samples ensures economical use of the expensive setup. As in the case of manual application, the choice is between fixed sample size (sample loop) and variable sample size (syringe).

2.5. Columns

The chromatographic column is the centerpiece of every HPLC unit. Its design and the type and quality of its packing are decisive for good separation and minimal dispersion of the sample components. In general, steel columns with minimal dead-volume, fixed end-fittings are employed. In addition, economically priced cartridge systems are available, in which ready-packed exchange cartridges are compressed in a corresponding module. Radially compressible plastic cartridges offer the additional advantages that wall effects[15] are avoided and that it is possible to repack the matrix after the formation of cracks.

Most of the commercially available analytical steel columns have a diameter of 4.0–4.6 mm and a length of 10–30 cm. Larger columns are sometimes employed for gel filtration, and, in the case of adsorptive techniques, signifi-

cantly smaller columns have been employed with success.[16-19] The resolution of a column (proportional to $N^{0.5}$[4]) is, in fact, not very greatly dependent on its length. However, from the special elution behavior of macromolecules (see Section 2.2) and simple trial separations, the conclusion should not be drawn that long columns generally fail to offer advantages for the separation of proteins using gradient elution.[20?] According to the gradient theory of *Snyder* et al.,[4] this is only true when short elution times (i.e., steep gradients) are chosen. However, when difficult separation problems require longer elution times (i.e., a shallower gradient), then there is a drastic increase in the influence of column length on the performance of the system.[2,22] If short columns can be employed, they have the advantage of less back pressure (higher long-term stability) and less dilution of the sample.

Theoretically, the column diameter has no influence on the separation performance of the column if the flow rate is suitably adjusted.[21] Because, in addition, the wall effect[15] is of less significance for larger diameters, there is a great potential for increasing the loading capacity for preparative work. Reducing the diameter leads to smaller peak volumes and, hence, to lower detection limits;[21] the "micro-bore" technique (column diameter < 1 mm) has found only occasional application in the protein field so far[23,24] and, like the use of short columns mentioned above, requires increased care with respect to possible peak broadening by the other system components. Suitable prepacked columns are only available with packing materials of low pore diameter (ca. 100 Å), which are less suitable than packing materials with larger pore-size particles (> 300 Å) for proteins with molecular weights of more than 20000.[25-27]

As far as the particle size of the packing is concerned, a compromise must be reached between the highest possible resolution, which improves as the particle size decreases, and the long-term stability of the column packing. At present, the minimum particle diameter is 5 μm for the large pore-size packings needed for the separation of high-molecular-weight biological samples.[21]

Silica gel largely fulfills the most important criteria for a packing material: very small particle size, high mechanical stability, and high porosity. However, it is only stable at pH values between 2 and 7. Organic polymers are suitable for use with basic buffers, but are not yet available with similar small particle sizes and with equivalent pressure stabilities. An easily exchangeable precolumn is highly recommended when working with complicated mixtures (such as cell homogenates). Filtrations or irreversible adsorptions take place at this stage, thus protecting the main column.

Many protein separations can be performed at ambient temperature. However, the temperature affects the resolution, retention, and recovery in all adsorptive techniques.[28-30]

Commercially available ready-packed columns, which are delivered with a test chromatogram, are employed most often. However, columns that are specially supplied for protein chromatography are seldom tested by the manufacturers with appropriate sample mixtures under relevant elution conditions. In practice each user has to test the quality of the column packing, the performance of the whole system, and, in particular, the recovery rate of the proteins. Various model mixtures have been proposed for this purpose in the literature.[31]

2.6. Detectors

UV detection is by far the most commonly applied method of detection in protein separation.[32] The peptide bond absorbs at $\lambda = 210$–230 nm, the absorbance being independent of the amino acid composition.[33] At 210 nm, moreover, the secondary structure is without influence.[34] The sensitivity is 10- to 20-fold higher than at $\lambda = 250$–280 nm, where only the aromatic amino acids absorb. However, working at lower wavelengths restricts the choice of solvent, places greater demands on its purity, and requires the effective exclusion of oxygen. It is scarcely possible to avoid a drifting baseline in gradient elution. Programmable detectors (e.g., diode arrays) can scan the whole available spectrum at various points (usually the peak maxima) in a very short time. This can be of particular value in the analysis of short peptides (e.g., from enzymatic or chemical degradations).[35-37]

In particular cases, the intrinsic fluorescence can be employed with sufficient sensitivity for the identification of peptides rich in aromatic amino acids.[38] Fluorescent detection with on-line, post-column derivatization is of more universal application.[39] With *o*-phthalaldehyde[40] or fluorescamine,[41] derivatives are formed that absorb at higher wavelengths and thus allow unhindered detection in the presence of strongly UV-absorbing buffers. For preparative work, only an aliquot is diverted for detection by means of a switching valve (splitting technique). A cysteine-specific method has also been described.[42]

3. Principles of Separation

3.1. Gel Filtration

Gel filtration occupies a special place among chromatographic separation methods. The separation does not take place on the basis of interaction between the sample, the stationary phase, and the mobile phase, but depends on "sorting" according to molecular size. In ideal gel filtration, proteins are separated on the basis of their distribution between mobile liquid phase and the liquid situated in the pores of the matrix.[43] The elution volume available for separation thus lies between two limiting volumes: the volume of liquid between the particles (V_o) and the total diffusion volume as the sum of V_o and the pore volume V_i. The peak capacity is, therefore, strictly limited. The elution volume V_e of a substance peak is given by

$$V_e = V_o + K_D \times V_i$$

The distribution coefficient K_D is virtually 0 for very large molecules. These cannot diffuse into the pores and are, therefore, eluted most rapidly. For small molecules K_D is 1; they migrate unhindered into all the available pores and are thus subjected to the greatest delay.

In general, a linear relationship between the distribution coefficient and the logarithm of the molecular weight exists in the range $K_D = 0.15$–0.80. Gel filtration can, therefore, be employed for the characterization of proteins when interactions between the protein molecules and the surfaces of the particles can be excluded and the protein is regular in form and not aggregated. Nonideal column behavior can be investigated by means of simple tests.[44]

The resolution of the column depends on its dimensions, the density of the packing, the pore volume, the pore-size distribution, and the peak width. Since the separation only takes place within a limited elution volume, efforts must be made to restrict the volumes of the individual peaks as much as possible.

The peak width is associated with the molecular transport between the phases and reaches its optimum at small particle sizes,[45] low flow rate and viscosity of the mobile phase, and high diffusion coefficient for the protein. From these relationships it can be understood that the limits for sample volume and concentration are lower (ca. 100 μg and 10 μL per mL of column volume) than is the case for adsorption methods.[46]

All the other parameters mentioned are fixed properties of the column packing. Spherical particles can be packed significantly more densely than can irregular ones, so that V_0—the column volume that is not available for separation—only makes up 37% of the total column volume.[44] The maximum volume available for separation is achieved by increasing the pore volume V_i. Here a compromise has to be reached between optimal pore volume and high mechanical stability.[44,46] A narrow pore-size distribution is advantageous for high resolution, but the packing process itself evidently also plays an important role in determining the efficiency of the column.[44]

Of the organic polymer particles developed for gel filtration, the TSK-PW series (Biorad) is finding increasing use; the hydrophobic interactions that are unavoidable in all materials of this type (see Section 3.3) are apparently minimized, thereby allowing very efficient protein separations, particularly in the high-molecular-weight range.[47]

Silica gels exhibit better separation performance in narrow molecular-weight ranges.[48,49] The surface may be treated with hydrophilic organosilanes[50,51] or organic polymers[52] to block silanol groups and prevent adsorption effects. However, the treatment is never complete for steric reasons,[53] so that these materials always exhibit residual ion-exchanger properties. This can be compensated for by the presence of salts in the eluent.[44] Too high a salt concentration should be avoided, however, since it would increase hydrophobic interactions. A new surface treatment variant that imparts greater pH stability to the support is also worthy of mention.[54]

Silica gels are also very stable in the presence of chaotropic salts and detergents. It is possible to employ guanidinium chloride, sodium dodecyl sulfate, urea, and organic solvents to denature the proteins before separation, thereby preventing self-association and increasing solubility.[55–58] However, this can greatly increase the hydrodynamic radius of the protein, which results in displacement of the fractionation range to lower molecular weight. Figure 2 shows the gel filtration chromatograms of two protein standards with two different eluents.

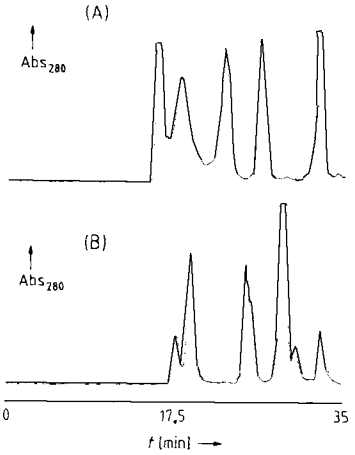


Fig. 2. Gel permeation chromatography of protein standards. HPLC system: Bio Sil TSK, 7.5 mm × 60 cm (Bio Rad), 0.7 mL/min, ambient temperature, Abs_{280} = absorption at $\lambda = 280$ nm; t = retention time. (A): 20 mM phosphate buffer, 0.1 M sodium sulfate, pH 6.8, peaks in the order of elution: thyroglobulin (MW 670000), γ-globulin (MW 158000), ovalbumin (MW 44000), myoglobin (MW 17000), vitamin B_{12} (MW 1350). MW = molecular weight. (B): 20% acetic acid/30% acetonitrile, pH 3.0, peaks in the order of elution: myoglobin (MW 17000), 17.8 min; cytochrome c (MW 12500), 19.1 min; insulin (MW 5850), 24.9 min; insulin B-chain (MW 3400), 25.5 min; phenylazo-Z-Pro-Leu-Gly-Pro-D-Arg (MW 777), 28.7 min; sodium azide (MW 65), 32.7 min). Z = benzyloxycarbonyl.

3.2. Ion-Exchange Chromatography

Because of its amphoteric character, a protein can exist in either cationic or anionic form depending on the pH. A characteristic parameter of proteins is, therefore, the isoelectric point at which the net charge of the protein is zero. The isoelectric point determines the pH of the medium and the choice of the type of ion exchanger. The strength of binding is determined by the number of cooperatively effective ionic groups on the protein, the charge density of the ion exchanger (theoretical capacity), and the ionic strength of the mobile phase. Thus, elution of the proteins can be brought about by a gradient of increasing ionic strength, a pH gradient, or a combination of both. The user has a wide range of possibilities available for influencing retention and selectivity.

Silica gel and its derivatives were the most commonly used ion-exchange supports for a long time and were used in the great majority of systematic investigations of ion-exchange HPLC of proteins.[59] Organic methacrylate-based polymers, which are only available in relatively large pore sizes and which are partially hydrophobic, did not prove to be as useful.[60] Recently, however, hydrophilic organic polymers, such as the above-mentioned TSK-PW series, have become available and provide good results in analytical and preparative separations, at a somewhat lower flow rate and pressure.[61–65] Their stability in the alkaline pH range allows a wide selection of buffer solutions and more efficient regeneration methods, thereby increasing the working lives of the columns, even when crude extracts are separated.[62]

Silica gels are available in a wide range of pore sizes and with a large variety of organic ligands. Strongly acidic and basic exchangers are usually characterized by higher resolution and detection sensitivity, because the better desorption leads to smaller peak volumes. The range of variation of the pH of the mobile phase does not affect the degree of ionization of the exchanger, so that the optimization problem is less complex.[29,66] A particularly stable and efficient masking of nonspecific binding sites on the silica gel surface and a high ion-exchange capacity is achieved when the ionic ligands are cross-linked within a thin polymer film.[67-70] The theoretical capacity in this case is proportional to the total surface area of the particles and, hence, highest for small pore-size material. However, ion-exchangers with wide pores are more accessible to high-molecular-weight proteins and, hence, exhibit a higher effective capacity. The optimization of peak sharpness also plays a crucial role, because diffusion is as unhindered as possible. The best choice for most protein separation problems is a pore size of 300 Å, whereas for molecules with a molecular weight larger than 150000 a pore size of 1000 Å or more is preferred.[16,27,66]

It is usual to elute by means of a salt gradient at a constant pH. Since the displacing power of a range of ions can be completely different for different proteins,[29] the exchange of one displacing ion for another can result in different selectivities. Thus, an astute choice of the salt type can optimize the distribution of all sample components and the resolution of early eluting components as well as improve the recovery of particularly strongly adsorbed proteins.[29]

The retention time of a protein increases as the difference between its isoelectric point and the pH of the buffer increases.[62] The selectivity can also be influenced by varying this parameter, since the shape of the titration curve is characteristic for each protein. A good starting point is often pH 7, which leads, on the average, to the best selectivity in anion- and cation-exchange chromatography.[29] A different pH can be more advantageous for the separation of a particular pair of proteins. This can often only be determined empirically and cannot necessarily be deduced from the titration curves of the proteins.[7]

Other conditions are easier to optimize than the composition of the mobile phase. The total volume of the salt gradient is generally between 5 and 15 column volumes. A reduction of the flow rate and of the steepness of the gradient improve the resolution considerably.[16,59] An increase in the temperature also has a positive effect.[16] The load that present-day columns can accept is high; 2–3 mg of protein per mL of packing volume can easily be separated without loss of resolution.[16,63] Apart from a few exceptions, the recovery rates are greater than 90%.[29,71]

3.3. Hydrophobic-Interaction Chromatography

Hydrophobic interactions play an important role in the folding of proteins and in the stabilization of their tertiary structures.[72] The nonpolar amino-acid side chains of soluble proteins are largely shielded inside the three-dimensional structure. Nonetheless, proteins possess a few hydrophobic points of contact on the surface, which lead to adsorption to a nonpolar stationary phase. This effect was at first observed as abnormal retention behavior in conventional affinity chromatography and then later deliberately exploited for the separation of proteins on alkylated agarose gels.[73-75] Hydrophobic adsorption of proteins on HPLC gel filtration columns has been observed under certain conditions.[44,76] Special phases based on silica gel[77-80] or organic polymer particles[81,82] were later developed for performing this type of separation by HPLC.

The hydrophobic interaction is strong in the presence of high concentrations of ions.[73,74] The type and concentration of the salt are decisive for the retention, which is greater for salts exerting a larger *salting-out* effect on proteins.[79,82-84] The strength of the hydrophobic interaction increases with increasing temperature;[30,79] on the other hand, the retention is reduced by the addition of small quantities of organic solvent or chaotropic reagents (urea, guanidinium chloride).[30,82] Theoretically, the bonding ought to be strongest at the isoelectric point;[85] in practice, however, the pH can affect the retention of different proteins, depending on the matrix, to differing degrees and in different ways, which is probably attributable to the effect of charges on the stationary phase.[82,83] The selectivity of the separation can also be strongly affected by changing the temperature and by addition of organic solvents to the eluent.[30,82,83]

The type of salt is also important for the resolution. Neutral salts with a high salting-out effect are preferred for hydrophilic (weakly binding) proteins, whereas those with a low salting-out effect are preferable for hydrophobic (strongly binding) proteins.[78] The resolution can also be improved by longer columns,[22,82] lower flow rates,[82] and shallower gradients (longer gradient elution time),[22,82] and by the addition of chaotropic agents or organic solvents.[30,82] Lower temperatures are also advantageous,[30,49] Denaturation caused by matrix contact is rare in this method.[22,86] The sample load that the columns can carry and the recovery rate are about the same as those in *ion-exchange chromatography*.

3.4. Reversed-Phase Chromatography

Reversed-phase (RP) chromatography was introduced as early as 1950[87] and has become the preferred method of HPLC because of its wide scope of application.[88] It is basically a variant of hydrophobic chromatography (see Section 3.3). In both cases binding takes place between a nonpolar surface of the protein and the stationary phase, thereby shielding the stationary phase from the polar (aqueous) mobile phase.[89-91] In contrast to hydrophobic chromatography, significantly more nonpolar, i.e., more heavily alkylated, stationary phases, are employed here, so that the proteins bind to the matrix even in aqueous buffers of low ionic strengths. Differential desorption is achieved by applying a gradient with an increasing concentration of organic solvent. On the one hand, this lowers the surface tension of the mobile phase and favors the formation of a solvent shell around the molecule that has been desorbed;[89-91] on the other hand, it favors desorption by means of direct competitive interaction with the protein and the matrix. Several theoretical models are un-

der discussion for the quantitative description of the complex thermodynamic and kinetic phenomena involved in the interaction between stationary phase, eluent components, and sample molecules and particularly the relationship between retention and solvent composition.[92-94]

Many binding sites can participate in the interaction of a protein with the matrix.[5,6,17,95] Hence, adsorption effects predominate rather than a distribution between stationary and mobile phases.[95,96] During gradient elution, the relatively more weakly binding solvent molecules first occupy free contact sites on the matrix and the protein surfaces not involved in binding. When a critical concentration is reached,[9,10,94,97] the protein is suddenly displaced from the matrix surface. This concept of a competitive interaction between matrix, protein, and solvent molecules is the basis of a newer stoichiometric displacement model[8] that explains very well the observed influences of molecular size and solvent composition and is in agreement with the general theory of gradient elution.[4]

The retention of a sample molecule depends on the ratio of the polar to nonpolar amino-acid side chains on the part of the surface that is involved in binding to the stationary phase. In the case of smaller polypeptides (<20 amino acids), it is possible to calculate the retention time accurately in advance from the sum of the relative hydrophobicities of the individual amino acids.[98-101] However, predictions are difficult for some proteins on account of the tertiary structure. Even in the case of B30 analogues of insulin (see Section 4.1 and Fig. 5), the incorporation of particular amino acids leads to a change in the retention time from the predicted value. In addition, under the usual elution conditions for RP-HPLC, possible conformational changes must also be taken into account,[105] which depend on the composition of the eluent and other parameters. In extreme cases they can lead to multiple peaks (native and denatured forms).[106-109]

The behavior of a silica-gel-based matrix is not just influenced by the nonpolar ligands but also, to a considerable extent, by the free silanol groups. This leads to the following phenomenon: with increasing organic solvent concentration, the retention of a given protein first decreases, as expected for nonpolar interactions, but then increases again owing to the silanophilic contribution.[97] Ionic components in the eluent suppress these interactions, leading to the formation of sharper peaks with higher resolution and, in the case of certain ion-pair reagents, allowing milder elution conditions. Only when these factors were included in the optimization of the separation conditions was it possible to overcome the initial difficulties[110] experienced in the RP-HPLC of proteins.

The HPLC user today finds himself confronted with a bewildering array of stationary phases, in which silica gel derivatives predominate. Two wide-pore materials based on organic polymers have recently appeared on the market.[112,113] Their advantage lies in the possibility of effective regeneration by washing with dilute sodium hydroxide solution. Stationary phases with a pore size of ca. 300 Å are best suited for proteins with molecular weights greater than 20000 with respect to loading capacity, resolution, and recovery.[25,26,96,104,114-116] The retention of most proteins is essentially independent of the chain length of the alkyl ligand for the same density of occupation.[115,117,118] The degree of alkylation, on the other hand, is critical for the resolving power and the gentle elution of proteins.[92,93,119-122] Wide-pore particles have the advantage that, because of the limited surface area, an optimal coating density (ca. 3–4 μmol alkyl residue/m^2) is obtained even at a low carbon content (2–4% wt-% C).[120,121] This allows the elution of proteins at low concentrations of organic solvent.[92,93,120] Octyl or octadecyl ligands lead to better masking of residual silanol groups than do ultrashort alkyl residues ($<C_4$).[120] It is recommended that silanophilic interactions be further suppressed by treating the alkylated silica gel with reactive silanes of small size ("end-capping").[93,120]

Electrostatic interactions with free silanol groups lead to very asymmetrical peaks or even to irreversible adsorption of the proteins to the RP matrix. Since the dissociation of the silanol groups is largely suppressed at low pH (<pH 4),[123] the best results are generally obtained in this region.[26,93,103,116,124] Thus, satisfactory protein separations are possible even in dilute hydrochloric acid.[12,23,104,116,117] Various buffer substances, however, are able to change the retention characteristics of proteins owing to ion-pair formation.[92,93,111,125] Examples include phosphoric acid, perchloric acid, perfluorinated carboxylic acids, and alkyl sulfonic acids and their salts. Phosphoric acid decreases[126] and perfluorinated carboxylic acids increase the retention time.[95,127] Cationic components in the eluent affect the matrix properties directly. Ammonium, alkylammonium, pyridinium, and morpholinium ions deactivate silanol groups by hydrogen bonding and electrostatic interactions.[92,128] High concentrations (>0.1 M) of chaotropic salts (e.g., $NaClO_4$, Na_2SO_4) lead to increased peak sharpness and improved elution, particularly on account of the electrostatic shielding of the silanol groups.[100,129-131]

Dilute trifluoroacetic acid has found the greatest application of all buffer systems,[17-19,83,95,96,132-137] whereas longer-chain perfluorinated carboxylic acids have been employed much more seldomly.[95,104,133,138] Trifluoroacetic acid is UV-transparent and easily evaporated and, hence, is also suitable for preparative work. It is particularly recommended, as is dilute formic acid,[139] for the separation of hydrophobic proteins or protein fragments.[95,127] On the other hand, the elution of the structural proteins of polio virus was not possible with any of these systems, but only with highly concentrated formic acid.[140] Pyridine acetate or pyridine formate are also volatile buffers, which have been employed with great success in the pH 3–5 range, that is, for work with acid-labile proteins.[141-145] A disadvantage is that their low UV-transparency necessitates detection at $\lambda = 280$ nm or post-column derivatization (see Section 2.6). Eluents with even higher pH values include ammonium hydrogen carbonate (pH 7.8)[147] and hexafluoroacetone/ammonia (pH 7.2).[148]

The most frequently reported nonvolatile buffer is phosphate,[28,98,100,103,111,149] very often in the form of the tri- or tetraalkylammonium salts[111,150-153] and with the addition of sodium perchlorate.[25,100,129-131] Usually the separations are performed below pH 4, more rarely at higher pH.[154] Separations have also been reported with Tris buffer at pH 7.5.[155]

The organic component must be sufficiently nonpolar to effect desorption of the protein from the matrix; on the other hand, it must be polar enough that the protein does not precipitate. This virtually restricts the choice to acetonitrile and alcohols. Dioxane has been used in the purification of interferon.[156] The eluting capacity increases in the order methanol, ethanol, acetonitrile, propanol, butanol.[93] Changing or combining the solvents allows different selectivities to be obtained.[98, 131, 148, 157–160] Small additions of methoxymethanol can improve the resolution.[92, 149] Propanol is recommended for larger, hydrophobic proteins. Since the concentration of the organic component in the eluate can be kept low, fewer problems are to be expected with precipitation and denaturation.[127, 141] Occasionally, however, peak broadening is observed,[100, 112, 148] which can be reduced by raising the temperature, provided that the proteins are sufficiently stable.[28] In general, both improvements[98] and deteriorations[103, 116, 128] in the resolution have been observed on raising the temperature. The resolution improves for reduced flow rates and shallower gradients.[26, 92, 119, 142]

The elution conditions of RP-HPLC not only reduce the solubility of many proteins, but also can result in conformational changes.[105] In the case of labile proteins this can lead to complete denaturation with irreversible adsorption or precipitation. This is not just a preparative problem, it can also bring into question the accuracy of a quantitative analysis. Examples are available for the successful isolation of functionally intact proteins by RP-HPLC in the presence of stabilizing cofactors or by special treatment of the fractions obtained.[136, 155, 161–163] In some cases, furthermore, certain proteins are eluted with low yield or are initially inactivated.[12] Recent investigations[86, 106, 122, 164, 165] of the mechanism of this process have revealed that, depending on the protein, denaturation processes can occur at various rates during column contact; the degree of denaturation depends on how long the protein is in contact with both the matrix and the solvent. Desorption initiates a refolding to the natural tertiary structure. The kinds of peaks obtained are determined by the relationship between the kinetics of unfolding and refolding and the separation kinetics: a) individual peaks of narrow width are observed when the protein is either especially stable (no denaturation) or the refolding is greatly inhibited (only denaturation product); b) multiple[106–109, 112, 165] or extremely asymmetrical[28, 112, 121, 122, 164, 165] peaks are observed when native and (several) denatured forms are present in equilibrium. Strongly eluotropic solvents, hydrophilic ion-pair reagents, reduced concentrations of the perfluorinated carboxylic acids, or steeper gradients inhibit the denaturation on the stationary phase.[106, 112] This leads to higher recovery rates and a high degree of retention of the native biologically active form.[28, 112, 116, 166] High salt concentrations, on the other hand, can have a negative effect[28, 116] since they intensify the interaction with the matrix. High flow rates and temperatures do not allow sufficient refolding to occur, so that, in the extreme case, only the denatured form is eluted[164, 165] or irreversible binding takes place (memory effect).[112, 165] In those cases high resolutions are obtained,[28] but the recovery is sometimes small.[116]

RP-HPLC is unquestionably one of the most efficient methods of separation. Its greatest potential lies in the separation of closely related proteins and protein derivatives, since selectivity and resolution can be manipulated in many different ways. However, the protein-chemical consequences of the elution conditions must be reevaluated in each case.

3.5. Other Techniques

Adsorption to hydroxylapatite is a central component of one system for the purification of monoclonal antibodies;[167] however, it can also be employed for other separation problems.[168] Affinity chromatography[169] involves biospecific selection from complex mixtures and, thus, places no great demands on elution techniques. The HPLC version of this method, therefore, emphasizes high speed rather than high resolution. Stationary phases are prepared by the user himself by coupling the appropriate ligand to glass,[170] silica gel,[171, 172] or organic polymers.[173] Some ligands have a variety of applications; these include adenosine monophosphate,[171] protein A,[170] lectins,[174] and the pseudo-affinity ligand Cibacron Blue.[175] Ready-to-use columns can be envisaged here. In view of the wide variety of other specific ligands, the use of self-made columns is inevitable. However, the process can be simplified by the use of a pre-packed, pre-activated column, which is then treated by allowing a solution containing the ligand to flow slowly through the column.[176] Chromatofocusing can be carried out with commercially available ion exchangers and buffer solutions.[177, 178] Like its electrophoretic counterpart, the separation depends strictly on the isoelectric point.

4. Insulin

The blood-sugar-lowering hormone insulin is a small protein. It has a molecular weight of 5800 and consists of two peptide chains: the A chain, with 21 amino acid residues, and the B chain, with 30. The two peptide chains are cross-linked by two disulfide bridges. A third disulfide bridge links the cysteine residues at positions 6 and 11 within the A chain.[179, 180]

Insulin has a relatively rigid structure[181] and therefore exhibits relatively high stability. Consequently, it poses a simple problem for HPLC analysis,[182–186] and insulins separated by HPLC generally remain biologically and immunologically active.[187–189] Moreover, insulin is of eminent importance in pharmaceutical research. For these reasons, insulin is ideal for demonstrating the scope of application of HPLC of proteins.

In this connection, it is important for preparative and analytical work that insulin is insoluble near to its isoelectric point at pH 5.4 and dissociates at acidic pH, whereas it forms dimers and hexamers at neutral pH. The hexamer is stabilized by zinc. Separations above the isoelectric point are only successful with zinc-chelating and dissociating additives such as ethylenediaminetetraacetate (EDTA) and alcohols,[190] urea,[191] or detergents.[192]

Insulin is nowadays produced by two important methods, isolation from animal pancreas[193] and genetic engi-

neering. The insulin from the pancreases of three pigs satisfies the requirements of one diabetic for about ten days. Insulin with human sequence can also be produced by semisynthesis from porcine insulin. In contrast to this, the production of human insulin by genetically altered microorganisms, whose carbon source is glycerin or simple sugars, is virtually unlimited.[194-197]

4.1. Semisynthesis of Human Insulin

Human insulin only differs from porcine insulin in the amino acid at position 30 of the B chain. Since lysine occurs at position B29, replacement of alanine (porcine insulin) by threonine (human insulin) is possible using the enzyme trypsin (Fig. 3). Although, in an aqueous medium at a neutral pH, trypsin catalyzes the cleavage of peptide bonds at basic amino acids, at a lower pH and in a suitable

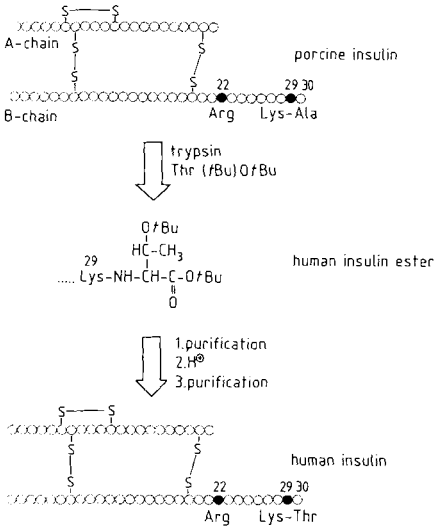


Fig. 3. Semisynthesis of human insulin from porcine insulin.

medium, it can also catalyze the formation of peptide bonds[198] or even directly catalyze the replacement of an amino acid without the formation of an intermediate hydrolysis product.[199-201] This replacement is formally equivalent to aminolysis of the acyl-enzyme intermediate. HPLC analysis of reaction mixtures suggests a direct exchange mechanism in human insulin semisynthesis (Fig. 4): After reaction with threonine *tert*-butyl ester, the OH group of which is protected by a *t*Bu group, des-(B30) insulin is not detectable; only the desired side-chain-etherified human insulin ester (III), nonconverted porcine insulin (II), and des-(B23-B30) insulin (I) are in evidence. The latter is an unwanted by-product originating from proteolysis at arginine (B22) and, for steric reasons, is apparently only formed in small amounts.[202]

A series of B30 derivatives, whose behavior in reversed-phase HPLC corresponds exactly with the change in hydrophobicity[100] of the *C*-terminal region of the B chain (Fig. 5), have been produced by semisynthesis.[201] However, two derivatives—thr(B30) insulin and tyr(B30) insulin—for which local structural changes (e.g., the presence of an additional hydrogen bond) can be postulated, do not follow the linear relationship.

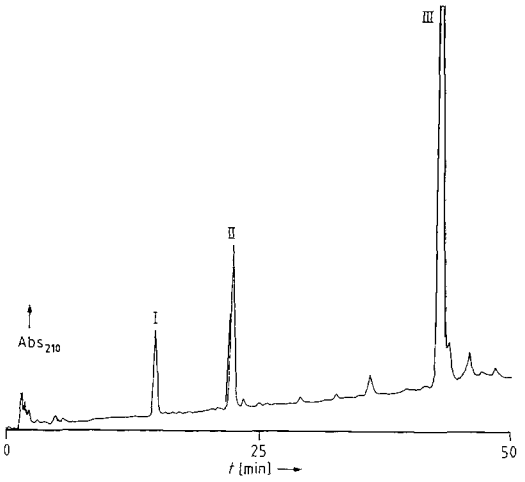


Fig. 4. HPLC chromatogram of the crude reaction mixture obtained in the semisynthesis of human insulin. HPLC system: Rad Pak C8, 10 μm, 8 × 10 mm (Waters), 50 mM tetraethylammonium phosphate, 0.25 M sodium perchlorate, 10% acetonitrile, pH = 3.0 (buffer A), and 50 mM tetraethylammonium phosphate, 90% acetonitrile, pH = 3.0 (buffer B), gradient from 28% to 40% B, 1.5 mL/min, ambient temperature, detection at $\lambda = 210$ nm; t = retention time. I-III: see text.

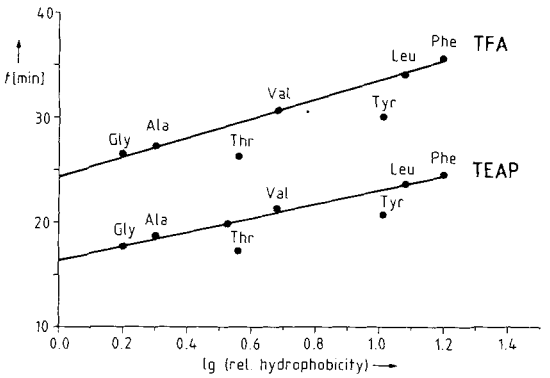


Fig. 5. Retention time of various B30 derivatives of insulin as a function of relative hydrophobicity of the amino acid at position B30 in the following RP-HPLC systems: **TFA**: Nucleosil 300-7 protein-RP, 4.6 × 125 mm (Macherey-Nagel), 0.1% trifluoroacetic acid, pH = 2.1, gradient from 30% to 40% acetonitrile, 0.8 mL/min, ambient temperature. **TEAP**: Rad Pak C18, 5 μm, 8 × 100 mm (Waters), composition of buffers and other conditions as for Figure 4.

4.2. Production of Human Insulin by Gene Technology

Except for the final purification steps, the procedure used to produce human insulin from microorganisms by gene technology differs fundamentally from that used to isolate it from pancreas. The insulin from pancreas is present in the biologically active, native spatial structure in all isolation steps. The preliminary stages in gene technology, on the other hand, involve inactive and generally poorly soluble precursors, which, for instance in the *E. coli* cell, are deposited in large quantity in the form of inclusion bodies (Fig. 6). These precursors have to be converted into the native structure by sophisticated protein chemistry—supported by appropriate chemical analysis (Fig. 6). The proinsulin concept presented here exploits the natural folding tendency of the physiological insulin precursor,[203,204] in which the A and B chain are connected by a

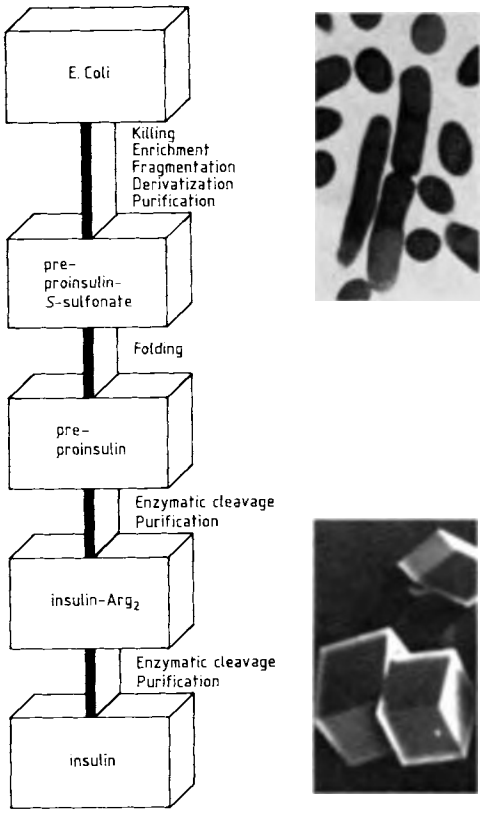


Fig. 6. Left: Principal steps in the production of human insulin from genetically engineered microorganisms. Right: Electron micrographs of *E. coli* cells (above) producing the insulin precursor and of the rhombohedral insulin crystals (zinc-stabilized hexamer) obtained by this process (below).

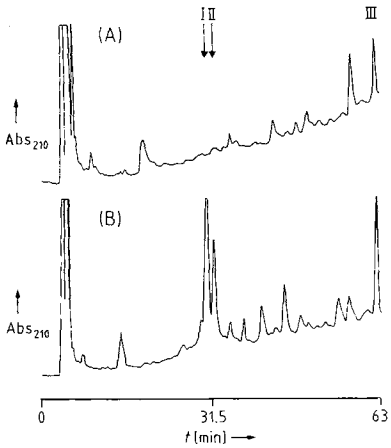


Fig. 7. HPLC chromatogram of the reaction mixtures obtained in the preparation of human insulin by gene technology: after chemical fragmentation of the insulin precursor (A) and after further modification by oxidative sulfitolysis and fractional precipitation (B). HPLC system: PLRP-S 300 A, 4.6 × 250 mm (Latek), 0.1 M hexafluoroacetone/NH_3, 2% butanol, 8% acetonitrile, pH = 7.0 (buffer A), 0.1 M hexafluoroacetone/NH_3, 9% butanol, 81% acetonitrile, pH = 7.0 (buffer B), gradient from 20% to 35% buffer B in 60 min, 0.8 mL/min, 40°C. I–III: see text.

peptide segment, the C peptide. The alternative concept, namely, separate production of the A and B chains, results, on recombination of these two chains, in a low yield and numerous by-products. Nevertheless, this was historically the first method for producing human insulin by gene technology and was also successfully used on a technical scale.[194]

For the isolation of insulin, the following procedure can be used: the microorganisms are harvested following fermentation, and the insulin precursor is enriched. The precursor is then cleaved chemically at methionine residues, thereby resulting in the formation of "preproinsulin"—a proinsulin with an *N*-terminal extension consisting of several amino acids. The six cysteine residues of preproinsulin, which are initially present in a form not precisely defined (*E. coli* lacks an enzyme system that specifically links the disulfides), are converted by sulfitolysis[205] to *S*-sulfonates. At this stage, the product is detectable by HPLC for the first time. In the reaction mixtures available prior to this, there are either too many by-products or the molecules of interest become irreversibly adsorbed on the reversed-phase support. This clearly demonstrates one of the limitations of HPLC analysis (Fig. 7A).

The preproinsulin *S*-sulfonate is a markedly acidic molecule. For reasons of solubility, the acid-mobile phases normally used in reversed-phase HPLC are therefore not feasible. A neutral hexafluoroacetone system,[148] in which the preproinsulin *S*-sulfonate (I) can be analyzed separately even from a precursor fragment (II) that is chemically very similar, is used instead (Fig. 7B). In contrast to fragments I and II, fragment III does not contain a cysteine residue and therefore elutes as a sharp peak without prior derivatization (Fig. 7A).

The preproinsulin *S*-sulfonate is not only an intermediate with a key role for purification and chemical analysis; the naturally folded preproinsulin is also available from it in high yields.[206,207] The folding and correct linking of the two interchain disulfide bridges can be examined by fingerprint analysis. The following requirements must be met:

- the formation of a limited number of fragments of interest
- a minimum of nonspecific reactions
- the identification of individual fragments
- a rapid and efficient method of separation and detection

Proteolytic fragmentation by *Staphylococcus aureus* protease V8 under special conditions in connection with HPLC analysis fulfills these requirements.[208] *S. aureus* protease V8 cleaves *C*-terminally at glutamate; the theoretical—and also experimentally verified—fragmentation pattern is shown in Figure 8. Fragments I, II, and III are of particular importance for the analysis. Fragment III contains the *C*-terminal region of the B chain and is present irrespective of whether preproinsulin *S*-sulfonate, disulfide-bridged preproinsulin or other species of the same sequence are present. It serves as internal standard for quantification purposes. In contrast, fragments I and II are only found in full amount when their disulfide bridges are present to the full extent. By-products, such as incorrectly disulfide-bridged species, would produce new peaks at the expense of peaks I and II. Fingerprint analysis of preproinsulin *S*-sulfonate does not produce either fragment I or II. Preproinsulin *S*-sulfonate, reduced with an excess of mercaptan, shows correspondingly low proportions of

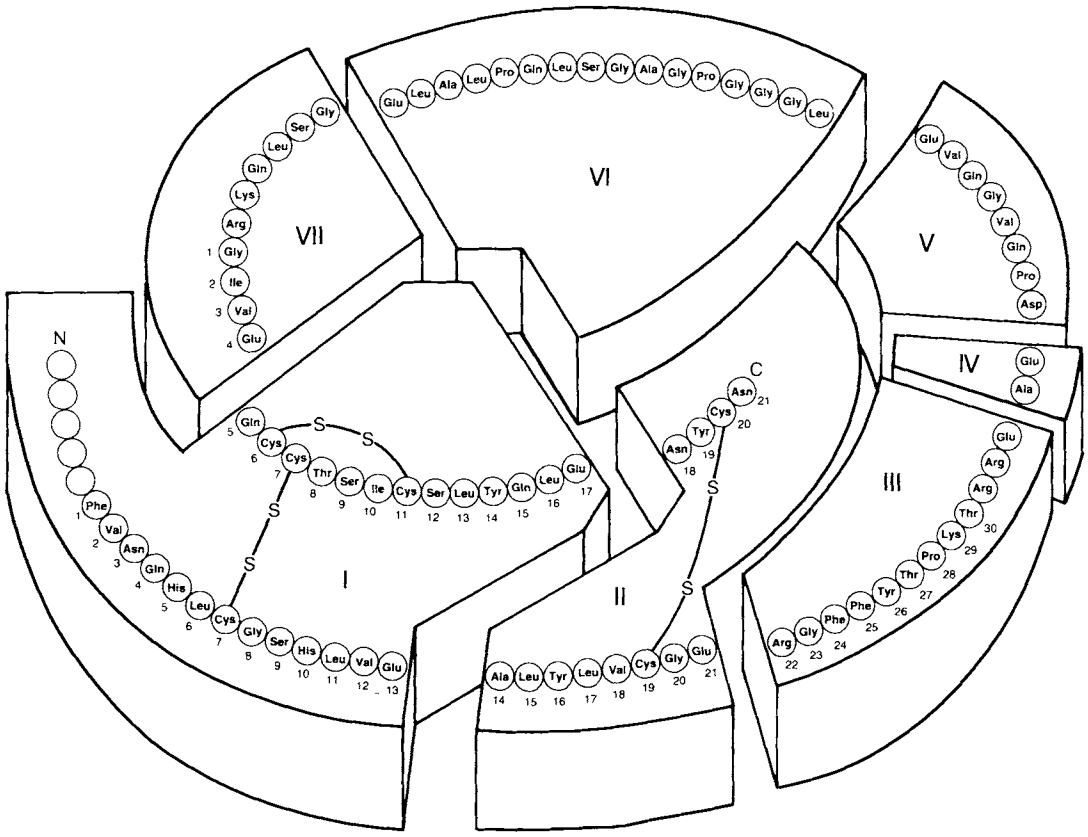


Fig. 8. Peptide fragments of preproinsulin formed by proteolysis with *S. aureus* protease V8. The prefix pre indicates that the proinsulin is lengthened at the *N*-terminal end by five amino acids (white circles).

both fragments. For comparison, an *S. aureus* protease V8 fingerprint of correctly folded preproinsulin is shown in Figure 9.

HPLC analysis is also essential in the next step, namely, in following the enzymatic processing of preproinsulin to insulin-Arg_2 and insulin-Arg (Fig. 10). Proteolysis of preproinsulin with trypsin occurs mainly at six arginine or lysine residues (see Fig. 8). However, cleavage at arginine(A0) at the *N*-terminal end of the A chain, at arginine(B0) at the *N*-terminal end of the B chain, and at arginine(B32) are preferred kinetically. Cleavage at lysine(B29) yields des-Thr(B30) insulin in small amount, while cleavage at arginine(B22) to give des-(B23-30) insulin—as found in semisynthesis—virtually does not occur, apparently for steric reasons.

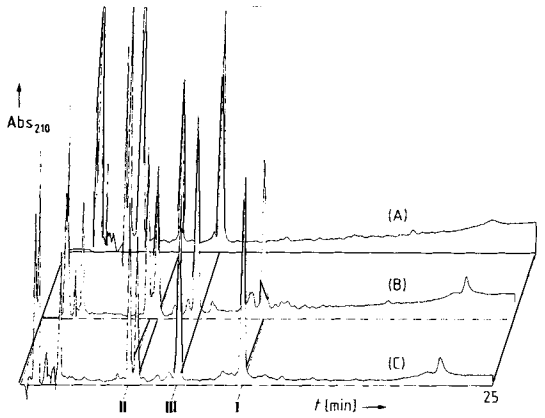


Fig. 9. HPLC analysis (fingerprints) of *S. aureus* protease V8 digests of (A) preproinsulin *S*-sulfonate, (B) preproinsulin reduced with excess thiol, and (C) correctly folded preproinsulin. HPLC system: Rad Pak C 18, 5 μm, 8 × 100 mm (Waters), buffers as in Figure 4, gradient from 20% to 45% buffer B in 25 min. I–III correspond to the fragments in Figure 8.

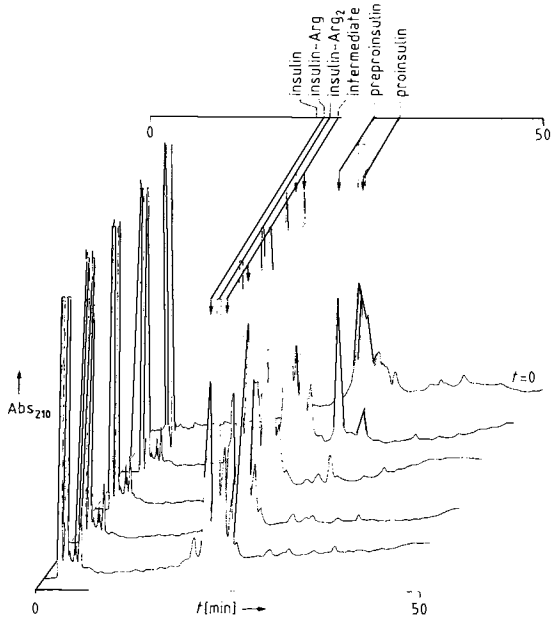


Fig. 10. HPLC chromatogram of samples taken at various times after incubation of preproinsulin with trypsin. HPLC system: Rad Pak C 18, 5 μm, 8 × 100 mm (Waters), buffers, gradients, and other conditions as in Figure 4.

Separation of des-Thr(B30) insulin, human insulin-Arg_2, and human insulin by reversed-phase HPLC is dependent to a large extent on whether perchlorate is present in the eluent. When a triethylammonium phosphate system without perchlorate is used as the mobile phase (Fig. 11), the sequence of the elution of these species is the reverse of that obtained when a tetraethylammonium phosphate system containing perchlorate is used (Fig. 10). However, HPLC analysis of the product mixture obtained by cleavage of purified human insulin-Arg_2 with carboxypeptidase B, which was performed using the perchlorate-free triethylammonium system (Fig. 11), affords distinctly less sharp peaks than analysis with the system containing perchlorate (see also Section 3.4).

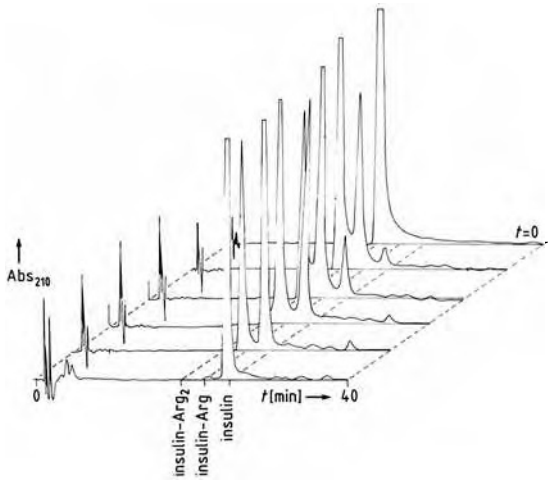


Fig. 11. HPLC chromatogram of samples taken at various times after incubation of human insulin-Arg_2 with carboxypeptidase B. HPLC system: Rad Pak C 18, 6 μm; buffer A: 0.25 M triethylammoniumphosphate, 20% acetonitrile, pH = 3.0; buffer B: 0.25 M triethylammonium phosphate, 50% acetonitrile, pH = 3.0, gradient from 19% to 32% buffer B in 40 min, 1.5 mL/min, 35 °C.

4.3. Purity Assessment and Quality Control

In order to ensure optimum tolerance and minimum immunogenicity, all insulins used in therapy nowadays are of high purity. In 1925, a few years after the discovery of insulin, a preparation containing 5 units per mg was used therapeutically; in 1935, the insulin content was about 20 units per mg. The highly purified insulin available at present has 28 units per mg. Foreign proteins in the end product are consistently in the ppm range or less and are only detectable by radioimmunoassay. The same applies to proinsulin, which is very efficiently separated by gel and ion-exchange chromatography. Ion-exchange chromatography (Fig. 12) yields a product that, moreover, is largely free of insulin derivatives formed during production and storage. For instance, under the acidic conditions of ethanol extraction, the acid amide groups of asparagines—in particular those of Asn(A21)—are hydrolyzed to aspartate, the desamido insulins[209] or their ethyl esters being formed.

HPLC permits identification of the individual products and the isolation of high-purity fractions (Fig. 12). It may likewise be used for quality control of the pure substance (e.g., with respect to species identity) or of the finished pharmaceutical as well as for checking the stability of insulins to storage at different temperatures and over several years.

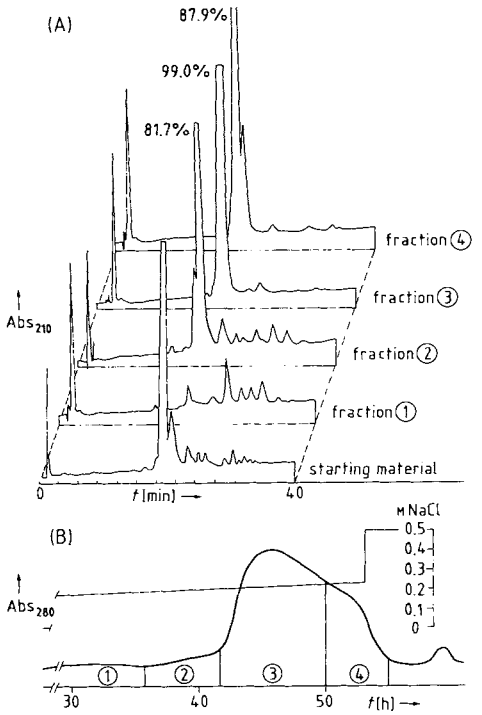


Fig. 12. Ion-exchange chromatography of crude, semisynthetic human insulin (B) and HPLC analysis of pooled fractions (A). The conditions of the ion-exchange purification on a diethylaminoethyl(DEAE)-cellulose matrix with detergent-containing eluents and a sodium chloride gradient are described elsewhere [192]. HPLC system: see Figure 4.

Gel-permeation HPLC is nowadays also used routinely for quality control and stability tests (Fig. 13); by this method, high-molecular-weight insulin derivatives, such as dimers originating as a result of transamidation, can be detected. For clinical therapy only highly purified insulins are used—for instance, they must not contain more than 10 ppm of proinsulin or more than 1% of high-molecular-weight derivatives.[210]

Detection of the absence of porcine insulin in semisynthetic human insulin poses a somewhat complicated analytical problem. Although it is possible to separate human and porcine insulin by HPLC, desamido(A21) human insulin, which can be a companion substance, coelutes with porcine insulin. Detection can be successfully carried out, however, at the preliminary stage of the human insulin es-

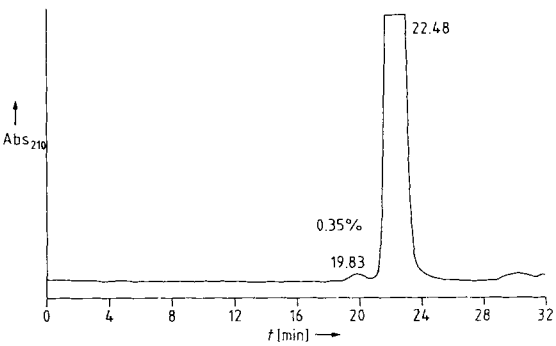


Fig. 13. Gel permeation HPLC of human insulin-Arg_2 obtained by gene technology. HPLC system: Bio Sil TSK 125, 7.5 × 600 mm (Bio Rad), 20% acetic acid, 30% acetonitrile, pH = 3.0, 0.7 mL/min, ambient temperature, detection at $\lambda = 280$ nm, sample load 200 μg.

ter,[199] or by the *S. aureus* protease V8 fingerprint method. If porcine insulin is present in the human insulin, fragment III (Fig. 8) will exhibit a small after-peak. On the other hand, if desamido(A21) human insulin is present, this after-peak will occur at fragment II (Fig. 14).

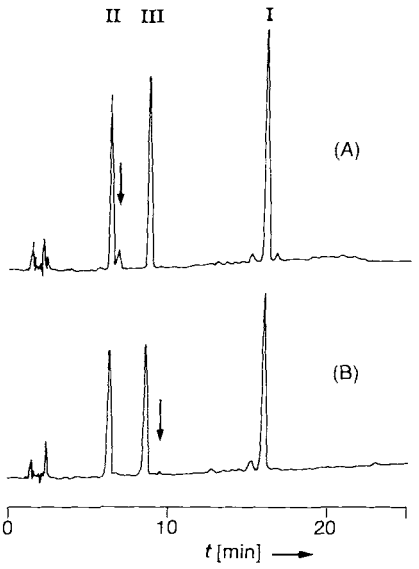


Fig. 14. HPLC chromatogram of *S. aureus* protease V8 digests of mixtures of (A) human insulin contaminated with desamido(A21) insulin and (B) human insulin contaminated with porcine insulin. HPLC system: see Figure 9.

4.4. Stability of Insulin in Dosage Devices

The pharmacokinetics of insulin in healthy individuals is extremely complex. The pancreas excretes a small amount of insulin as basal supply and larger amounts after glucose intake. Although the blood sugar then increases slightly, it settles down very rapidly at approximately 80 mg/dL. Substitution therapy with insulin administered subcutaneously can only very inadequately imitate these kinetics. Nowadays, a relatively constant blood-sugar level of 150–200 mg/dL is considered to be ideal. Such a profile (Fig. 15) is only possible when insulin preparation and food intake are well adapted to each other. Such high blood-sugar values, however, are considered at least partly responsible for various late complications of diabetes.[211–213]

The normal excretion of insulin in healthy individuals can be simulated by means of an infusion system (Fig. 15, right). Such infusion systems, in miniaturized form, are now in clinical trial. Externally worn devices, by means of which insulin is supplied subcutaneously via a catheter, are commercially available,[214] while implants are still at the development stage.[215] With implants, insulin is delivered into the abdominal cavity or vascular system, the reservoir being refilled from time to time through the skin.

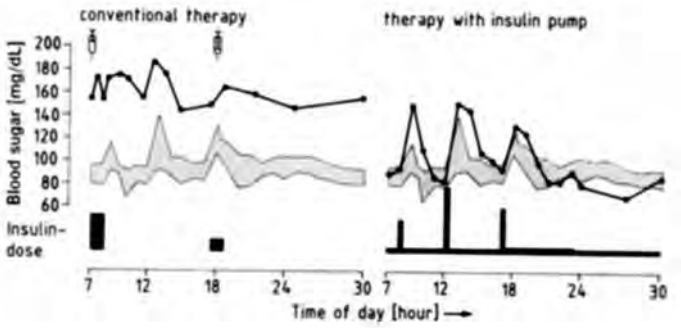


Fig. 15. Comparison of average blood-sugar levels of twelve type I diabetics under conventional therapy with Depot-H-Insulin Hoechst® (left, Prof. Skrabalo, Zagreb 1982) and of a different group of patients under therapy with external infusion devices (right, adapted from *Rizza* et al. [223]). The range of blood-sugar levels in healthy subjects is shown as shaded area.

Early in the development of these systems, however, a severe problem emerged: insulin is not stable in neutral solution under the conditions found in dosage systems. Denatured, biologically inactive insulin usually precipitates within a few days.[216,217]

Acidic insulin solutions (pH = 3) are comparatively stable physically (i.e., against denaturation). Under the conditions in implants, however, a number of modified products form within a refill cycle of four weeks; consequently, native insulin is ultimately only present in traces (Fig. 16). The stability of insulin in acidic solutions in dosage devices, as shown by HPLC analysis, is accordingly insufficient for human administration.[218]

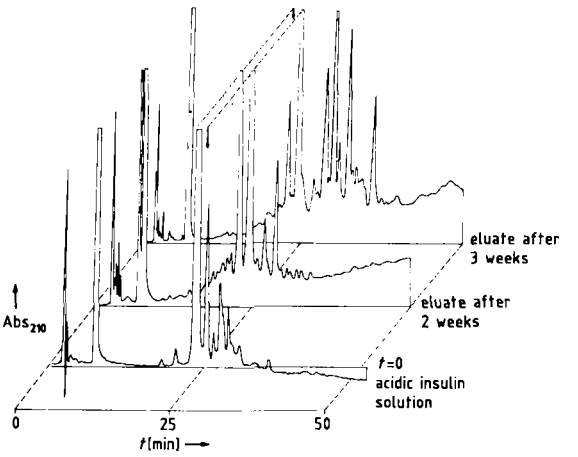


Fig. 16. HPLC chromatograms of acid porcine insulin (pH = 3.0) at refill and after passage through an implantable dosing device (240 μL/day) with 2 and 3 weeks of constant shaking at 37°C. The arrows indicate native (retention time 24 min) and desamido(A21) insulin (retention time 25 min). The latter is present in small amounts at $t = 0$ (arrow) and increases initially due to the acidic medium; native insulin decreases continuously, with the formation of several new species different from desamido(A21) insulin. HPLC system: see Figure 4.

Adsorption can be regarded as the initial step in surface denaturation of proteins.[219] Adsorption of insulin to hydrophobic interfaces can be prevented in neutral medium by the addition of a small amount of a surface-active substance.[219,220] Such an insulin solution is comparatively stable not only physically but also chemically, on account of the neutral pH. HPLC analyses have shown that insulin delivered through a pump at 37°C undergoes hardly any more changes than would be the case under conditions of elevated temperature alone (Fig. 17). A specific derivative eluting in HPLC with a retention time of 1.25 relative to insulin is thereby formed and can be isolated by preparative HPLC in a butanol/ethanol/water system.[208] It is a monomeric insulin, which is modified in the *N*-terminal region of the B chain, possibly at B3[221] and which has full biological activity and an immunogenicity as low as that of human insulin.[222]

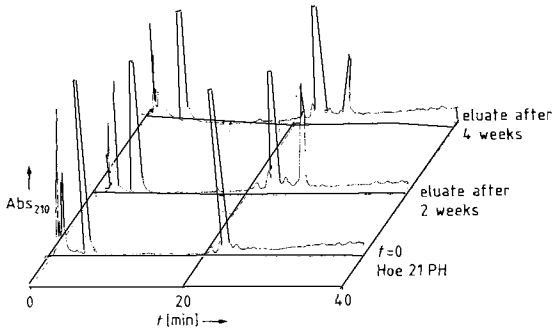


Fig. 17. HPLC chromatograms of a stabilized, neutral human insulin preparation (Hoe 21 PH) tested under identical conditions as described in Figure 16.

5. Further Applications of Analytical and Semipreparative HPLC in Protein Chemistry

At the present state of development, all conventional column-chromatographical methods are transferable to the HPLC version. Column materials and pumps also tolerate buffer systems such as those used in gel filtration, ion-exchange (Fig. 18), hydrophobic-interaction (Fig. 19), or affinity chromatography (Fig. 20). The resolution attainable is, in many cases, comparable in every way to that of the electrophoretic method. However, separation by HPLC is not restricted to size and charge differences. Furthermore, HPLC enables a smooth transition to the preparative scale with good recovery and, except in gel filtration, enrichment from very dilute solutions.

A good example is the isolation of colony stimulating factor (CSF) from human urine by hydrophobic-interaction HPLC.[224] Thymosin β4 could be detected in various cell culture extracts after rough preenrichment and subsequent RP-HPLC.[146] Several separation principles are generally combined; direct recovery of inhibin from follicular fluid was successfully carried out by gel filtration and RP-HPLC,[225] and ion-exchange and reversed-phase HPLC proved to be appropriate for isolating γ-interferon.[226] Semipreparative techniques are widely used for the characterization of proteins. The speed, reliability, and sensitivity of sequence analysis of proteins was decisively improved by HPLC methods; nowadays, the primary structure of proteins can be determined with sample sizes in the microgram range. Again, these amounts can be optimally obtained by HPLC.[18,23,227]

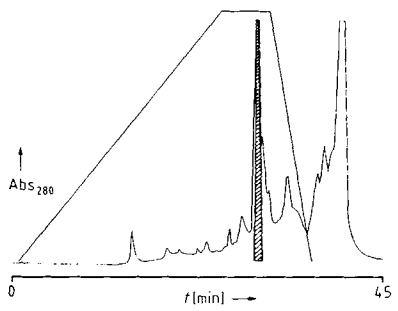


Fig. 18. Isolation of glucose-6-phosphate dehydrogenase by ion-exchange chromatography of a crude bacterial extract (300 μg). HPLC system: Protein Pak 5 PW, 7.5 mm × 7.5 cm (Waters), linear gradient from 0.02 M Tris/HCl, pH = 8.5, to 0.02 M Tris/HCl, 0.5 M NaCl, pH = 8.5, in 25 min, 5 mL/min, detection at $\lambda = 280$ nm; 0.1 absorption units full. Recovery of activity and protein was 100% and 81%, respectively (with permission of Millipore-Waters, Eschborn, FRG).

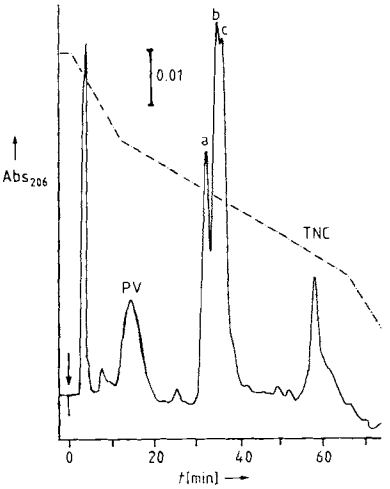


Fig. 19. Separation of various Ca^{2+}-binding proteins by hydrophobic-interaction chromatography. HPLC system: TSK-Phenyl-5PW, 7.5 mm × 7.5 cm (LKB), gradient from 1.5 M Na_2SO_4 in 0.1 M phosphate buffer, pH = 7.0, 1 mM Ca^{2+} to 0.1 M phosphate buffer, pH = 7.0, 1 mM Ca^{2+} in 74 min as indicated (---), 0.75 mL/min, detection at $\lambda = 206$ mm. Parvalbumin (PV), troponin C (TNC), and calmodulins from bovine brain (a), tetrahymena pyriformis (b), and paramecium (c) were recovered with more than 90% (from [258] with permission of Academic Press).

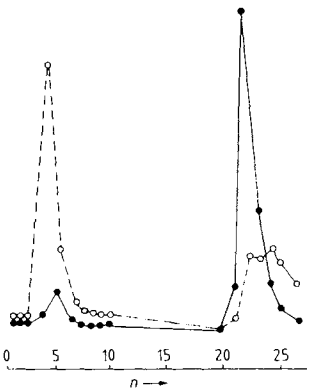


Fig. 20. Affinity chromatography of acetylcholinesterase (AChE) from a crude extract (1 mL). n = fraction number. HPLC system: Ultraaffinity-EP, 4.6 mm × 5.0 cm (Beckman), derivatized with procainamide (8 mg); sample loading (1 mL) with 0.1 M potassium phosphate, pH = 7.0; elution with 0.1 M decamethonium salt in 0.1 M potassium phosphate, pH = 7.0, 0.15 mL/min, detection at $\lambda = 280$ nm (○---○) or by measurement of AChE activity (●---●). Fivefold enrichment with 75% recovery in 2.5 h. (With permission of Beckman Instruments, Munich, FRG.)

The isolation of membrane-bound proteins is somewhat more problematic; the resolutions customarily obtained with water-soluble proteins are rarely achieved here. Successful use of ion-exchange chromatography in the presence of nonionic or zwitterionic detergents has been described.[228,229] Antigenicity is preserved by such mild separating conditions.[230] This can be of particular importance in isolating viral proteins, which are of use in obtaining antisera for diagnosing viral infections or in developing synthetic vaccines.[231,232] However, there are also reports that, under drastic RP-HPLC conditions, the isolated pro-

teins were still suitable for producing antisera to native viral proteins even though they could no longer be identified by antibodies to the native structure.[140,231,232]

HPLC is meanwhile also being widely used in the purification of radioactively labeled polypeptide hormones and antibodies for radioimmunological determinations. The high selectivity of RP-HPLC can be utilized to separate molecules labeled at different positions and, consequently, to optimize the reaction conditions, remove by-products, and isolate individual species.[233,234] A high degree of specific activity and stability is thereby obtained. The purification of antibodies can be carried out equally efficiently by hydroxylapatite[167] or hydrophobic-interaction chromatography,[49] or by ion-exchange chromatography alone[235] or in combination with gel filtration.[236]

The purely analytical application of protein HPLC is much less common. In the most recent European pharmacopeial directives, HPLC methods are included in the case of insulin only. This will definitely change, however, when, as a result of gene technology, a number of new pharmaceutically useful polypeptides and proteins become available. The insulin example shows what possibilities are offered by HPLC for process optimization and quality control, in particular for the separation of microheterogeneities caused by processing.

The wide range of applications in the diagnostic field have still not been fully explored. Interesting examples are the identification of abnormal insulins and proinsulins in hyperinsulinemic patients,[183,237] the analysis of genetically dependent hemoglobin variants,[238,239] the characterization of glycosylated hemoglobins caused by metabolic disorders,[240] the separation of receptor isoforms,[241] and the determination of immunoglobulin E in serum by affinity chromatography.[242] Certain isoforms of transferases may be connected with myocardial infarction;[243] specific growth factors were detected by HPLC in the sera of cancer patients.[244] In qualitative serum screening, electrophoresis, with its high sample throughput, is unparalleled; HPLC, however, may be employed irrespective of the sample concentration and is particularly of advantage where quantitative analyses are concerned.[239,240,242]

6. Preparative Separation of Proteins by HPLC

Large-pore silica gels with minimal carbon coating[92,93,115,116,119–222,245] are one of the basic prerequisites of preparative RP-HPLC.

The TP material from Vydac (TP = totally porous) particularly meets the requirements for the preparative separation of proteins.[17,246] Due to the minimal carbon coating and residual saturation of silanol groups by double bonding (i.e., a second derivatization with very short ligands), this material permits selective separations to be performed, and, despite low capacity, the yield obtained is good. The spherical 15–20-μm particles can be dry-packed. With radially compressible plastic cartridges, a simple but efficient separation system is obtained.

For preparative purposes, volatile buffers are most commonly used as solvent systems. The trifluoroacetic acid/acetonitrile system is most often used, with considerable success.[17,127,136] The counterion effect results in sharp peaks, and the products can be obtained salt-free after freeze drying. Relatively sensitive proteins can be separated by pyridine/acetic acid or by pyridine/formic acid[26,247] at pH 4–5. Here too, the proteins can be isolated salt-free. Although acetonitrile is one of the best eluents (sharp peaks), the less toxic propanol, which is stronger in eluotropic power, and mixtures of propanol and butanol are being used to an ever increasing extent[25,115,166] in order to keep the impact of the denaturing organic phase on the protein as low as possible.

Interleukin 2 will be used to exemplify that direct transference of an analytical separation to the preparative scale is possible.

6.1. Interleukin 2

Interleukin 2 (IL-2) is an immunologically active protein that, like γ-interferon, interleukin 1, and CSF, is now attracting great attention as a result of the progress achieved in gene technology. It plays a central role in the immune system during an immune reaction (Fig. 21). IL-2 is the proliferation factor that is necessary for the increase in activated T and B lymphocytes—the blood cells responsible for specific immune reaction. When the body comes in contact with an antigen, e.g., with a virus-transformed cell or fragments thereof, the antigen is first eliminated by the macrophages. The macrophages digest the antigen and express parts of it on their surface, together with other essential indicator proteins. At the same time, they release a signal protein, interleukin 1, which activates the lymphocytes. By means of interleukin 1 and the antigen on the macrophage surface, the T-helper lymphocytes specific to this antigen are activated; they react to this activation by production of a number of messenger substances, including interleukin 2. Interleukin 2 binds to the lymphocytes, which, subsequent to activation by the antigen and interleukin 1, express the receptor for interleukin 2. The binding of IL-2 to the receptor drives the cells to proliferation as long as IL-2 is present.

The cell division initiated by IL-2 binding leads to the specific defense reaction of the immune system. The number of reactive cells is increased by a factor of 100–1000. IL-2 is consequently an immunostimulator and is of interest for a whole series of therapeutic applications. Studies

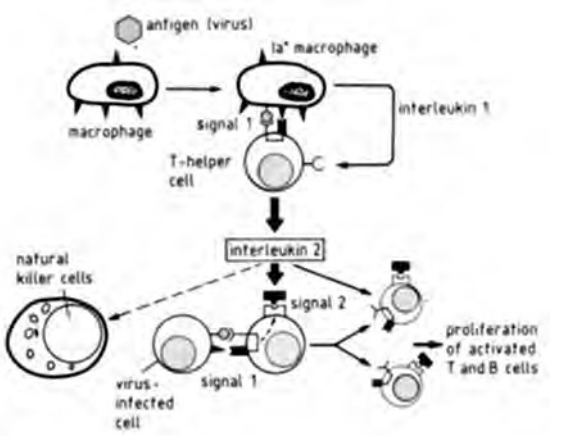


Fig. 21. Role of interleukin 2 in immune response (adapted from [259]).

performed at the National Cancer Institute of the United States of America have shown that IL-2 can also be successfully used in the treatment of tumors.

Human IL-2 was initially enriched in trace amounts from supernatants of activated lymphocytes and partially purified by RP-HPLC.[249-251] Elucidation of the nucleotide sequence by *Taniguchi* et al.[252] made possible the production of human IL-2 by gene technology. The protein consists of 133 amino acids with a molecular weight of about 15000. Two of the three cysteine residues form a disulfide bridge[253] (Fig. 22), which is essential for biological activity. After the nucleotide sequence—and hence the amino acid sequence—had been elucidated, human IL-2 was cloned and expressed[252, 254, 255] and has ever since been available in therapeutic quantities. IL-2 has also been obtained from yeast, as well as from *E. coli*. The specific activity of the natural molecule glycosylated at Thr3 (Fig. 22) is identical to that of glycosylated IL-2 from yeast and to that of nonglycosylated IL-2 from *E. coli*. It is clear from this that glycosylation is not essential to the activity.

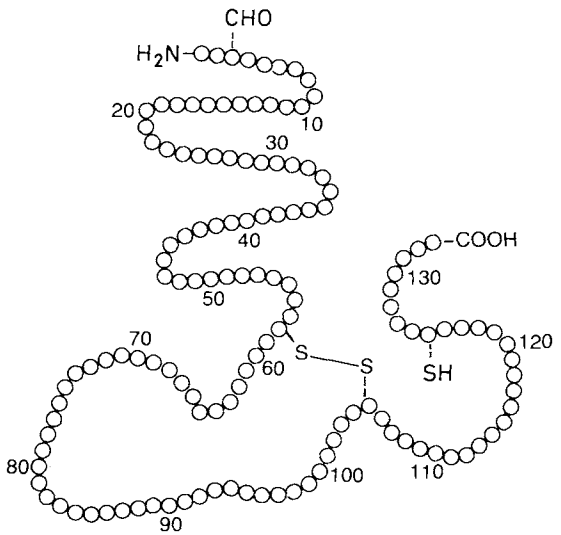


Fig. 22. Primary structure of IL-2 with the essential disulfide bond and the glycosylation site (CHO).

The physical properties of the nonglycosylated protein, however, complicate purification by traditional methods since, in *E. coli*, the protein is present as an aggregate in inclusion bodies. It is insoluble in conventional buffers and can therefore be relatively easily enriched. This is achieved by washing the material with buffers of different ionic strength, with and without detergents or organic solvents; foreign proteins and other cell constituents are thereby flushed out and IL-2 is enriched. This raw material is then extracted with a mixture of acetic acid and alcohols. Such an extract contains up to 40% IL-2, which is subsequently purified directly by RP-HPLC. Due to the considerable hydrophobicity of IL-2, the protein is only eluted after all impurities.

The initial studies using an analytical column and the trifluoroacetic acid/acetonitrile solvent system gave excellent separations and showed no memory effect (i.e., elution of protein, strongly bound in denatured form, in the subsequent runs) by precipitated IL-2, despite the large concentration of acetonitrile required for the elution. Rechromatography of 20 μg of IL-2 led to an elution of approximately 18 μg, i.e., a recovery of 90%.

The conditions of the analytical separation were first transferred to a semipreparative scale (2-cm column). After optimization of flow rate and elution gradient, we were already able to isolate IL-2 in milligram amounts. For preparative separation, we used radially compressible plastic cartridges (5.7 cm × 30.0 cm) filled with large-pore Vydac material. Despite the larger particles (15–20 μm), the quality of separation of IL-2 on such a cartridge is comparable to that on analytical columns (Fig. 23). About 60 mg of high-purity pyrogen-free interleukin 2 was obtained per run.

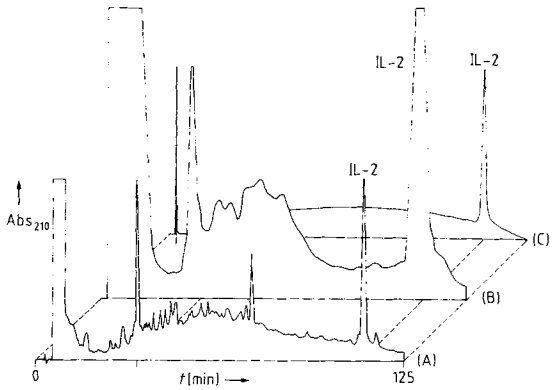


Fig. 23. Analytical and preparative HPLC separation of recombinant IL-2 from *E. coli*. (A) Analytical HPLC of an extract obtained with acetic acid/butanol. HPLC system: Hipore C18, 4.6 mm × 25.0 cm with guard column (Bio Rad); eluent A: 0.1% trifluoroacetic acid in water; eluent B: 0.1% trifluoroacetic acid/80% acetonitrile in water; gradient from 35% to 85% B in 60 min, 1.5 mL/min, detection at $\lambda = 210$ nm. (B) Preparative HPLC of 60 mg crude IL-2. HPLC system: Prep Pak radially compressed cartridge, 5.7 cm × 30.0 cm (Waters) with TP 218, 15–20 μ, 300 Å (Vydac), gradient as described for (A), 50 mL/min, detection with a 1/50 split. (C) Analytical HPLC of the material obtained in (B). HPLC system as in (A). The curved baseline results from an overlapping of the n-π* transition of the free acid with the π-π* transition of the $CF_3CO_2^{\ominus}$ anion [257].

It is well known that, in chromatography, the recovery of hydrophobic proteins can be increased when a coating of silica gel with relatively short alkyl chains, such as C_3, C_4, or C_6, is used. The proteins are less strongly bound and also often require a smaller proportion of organic phase for the elution.

The advantage of shorter alkyl chains could also be demonstrated in the case of IL-2. On C_{18} material, the yield decreased substantially after a single overload. The initial separating characteristics and initial yield could only be reestablished by regeneration with 60% acetic acid/guanidinium hydrochloride. In contrast, the C_4 material was relatively insensitive to overloading. Accordingly, for preparative, routine purification work, C_4 material should be given preference to C_{18} material.

6.2. Other Protein Purifications on a Preparative Scale

In contrast to IL-2, which can be obtained by means of preparative HPLC in pure and highly active form, many other proteins undergo partial unfolding and denaturation upon RP-HPLC owing to the pH conditions, organic eluents, and adsorption effects. By careful choice of the stationary phase and elution system and by appropriate

further treatment of the fractions, it is also possible, however, to purify enzymes such as trypsin and alkaline phosphatase without loss of activity.[135,256] For instance, a preparation of trypsin purified on RP-18 is free of other proteolytic activities to the extent that it can be used for highly selective peptide cleavages, as in sequence analysis.

Whereas the preparative separation of proteins with a molecular weight greater than 20000 is still limited to a few examples, the isolation and purification of antibodies with a molecular weight of around 180000 by high-pressure ion-exchange and hydroxylapatite chromatography has become generally accepted. A complete system for purifying monoclonal antibodies is available commercially under the name MAPS.[167]

7. Summary and Outlook

Within the last few years, HPLC versions of all conventional chromatographic techniques have been utilized in protein chemistry. Efficient separation systems have been developed and are now being used increasingly in fields that previously were a domain of electrophoretic methods. While the advantages of electrophoresis lie in the huge number of parallel analyses possible (e.g., in serum screening), HPLC impresses by the speed of the individual analyses with direct detection of the components. Newly developed supporting materials made of extremely small nonporous particles ($<2\,\mu m$) promise even further improvements. The high-resolution separations can also be extended to preparative HPLC. The development here is aimed at offering, at as reasonable a price as possible, stationary phases with relatively coarse particles, which can easily be packed into large columns by the user and can be operated with considerable long-term stability.

A crucial problem is the biocompatibility of stationary and mobile phase. Gel filtration and ion-exchange chromatography are carried out under approximately physiological conditions. Separations on reversed phase, however, still involve the risk of protein denaturation, even if considerable efforts have been made to reduce this problem, e.g., by using detergents. Solutions of this kind are often specific for a particular protein and can rarely be generalized. Hydrophobic-interaction chromatography separates according to criteria similar to those of RP-HPLC but, in principle, under milder conditions. By this means, higher recovery rates of biologically active proteins are achieved. For this reason, considerable further progress can be expected in this relatively new field.

We wish to thank Dr. H.-H. Schöne for his interest in these studies and for helpful discussions. We also wish to thank C. Müller and R. Lohfink for their help in preparing the manuscript.

Received: March 3, 1986 [A 579 IE]
German version: *Angew. Chem. 98* (1986) 530
Translated by Dr. *Frank Hampson*, Saarbrücken, and by *G. McConaghy*, Hoechst AG, Frankfurt.

[1] A. J. P. Martin, R. L. M. Synge, *Biochem. J. 35* (1941) 1358.
[2] J. C. Giddings: *Dynamics of Chromatography*, Marcel Dekker, New York 1965.
[3] H. Funke, *LaborPraxis 8* (1984) 18.
[4] L. R. Snyder, M. A. Stadalius, M. A. Quarry, *Anal. Chem. 55* (1983) 1412A.
[5] N. K. Boardman, S. M. Partridge, *Biochem. J. 59* (1955) 543.
[6] H. P. Jennissen, *J. Chromatogr. 159* (1978) 71.
[7] W. Kopaciewicz, M. A. Rounds, J. Fausnaugh, F. E. Regnier, *J. Chromatogr. 266* (1983) 3.
[8] X. Geng, F. E. Regnier, *J. Chromatogr. 296* (1984) 15.
[9] M. A. Stadalius, H. S. Gold, L. R. Snyder, *J. Chromatogr. 296* (1984) 31.
[10] J. M. Di Bussolo, J. R. Gant, *J. Chromatogr. 327* (1985) 67.
[11] M. Hermodson, W. C. Mahoney, *Methods Enzymol. 91* (1983) 352.
[12] J. Luiken, R. van der Zee, G. W. Welling, *J. Chromatogr. 284* (1984) 482.
[13] L. R. Snyder, J. J. Kirkland: *Introduction to Modern Liquid Chromatography*, Wiley-Interscience, New York 1979.
[14] L. R. Snyder, *J. Chromatogr. Sci. 21* (1983) 65.
[15] P. A. Bristow, J. H. Knox, *Chromatographia 10* (1977) 279.
[16] G. Vanecek, F. E. Regnier, *Anal. Biochem. 109* (1980) 345.
[17] J. D. Pearson, N. T. Lin, F. E. Regnier, *Anal. Biochem. 124* (1982) 217.
[18] J. W. Crabb, L. M. G. Heilmeyer, *J. Chromatogr. 296* (1984) 129.
[19] R. M. Moore, R. R. Walters, *J. Chromatogr. 317* (1984) 119.
[20] F. E. Regnier, *Science 222* (1983) 245.
[21] M. A. Stadalius, M. A. Quarry, L. R. Snyder, *J. Chromatogr. 327* (1985) 93.
[22] N. T. Miller, B. L. Karger, *J. Chromatogr. 326* (1985) 45.
[23] E. C. Nice, C. J. Lloyd, A. W. Burgess, *J. Chromatogr. 296* (1984) 153.
[24] R. van der Zee, G. W. Welling, *J. Chromatogr. 325* (1985) 187.
[25] K. J. Wilson, E. van Wieringen, S. Klauser, M. W. Berchtold, G. J. Hughes, *J. Chromatogr. 237* (1982) 407.
[26] R. V. Lewis, A. Fallon, S. Stein, K. D. Gibson, S. Udenfried, *Anal. Biochem. 104* (1980) 153.
[27] G. Vanecek, F. E. Regnier, *Anal. Biochem. 121* (1982) 156.
[28] K. A. Cohen, K. Schellenberg, K. Benedek, B. L. Karger, B. Grego, M. T. W. Hearn, *Anal. Biochem. 140* (1984) 223.
[29] W. Kopaciewicz, F. E. Regnier, *Anal. Biochem. 133* (1983) 251.
[30] S. C. Goheen, S. C. Engelhorn, *J. Chromatogr. 317* (1984) 55.
[31] F. E. Regnier, *Methods Enzymol. 91* (1983) 137.
[32] R. P. W. Scott: *Liquid Chromatography Detectors*, Elsevier, New York 1977.
[33] C. J. R. Thorne in H. L. Kornberg (Ed.): *Techniques in Life Sciences, B104*, Elsevier, Amsterdam 1978, p. 1.
[34] W. B. Gratzer in G. D. Fasman (Ed.): *Poly-α-amino acids, Biological Macromolecule Series*, Marcel Dekker, New York 1967, p. 177.
[35] J. L. Di Cesare, *Chromatogr. Newsl. 9* (1981) 16.
[36] C. Y. Yang, H. J. Pownall, A. M. Gotto, *Anal. Biochem. 145* (1985) 67.
[37] L. Servillo, G. Colonna, C. Balestieri, R. Ragone, G. Irace, *Anal. Biochem. 126* (1982) 251.
[38] T. D. Schlabach, T. C. Wehr, *Anal. Biochem. 127* (1982) 222.
[39] G. Schwedt: *Chemische Reaktionsdetektoren für die schnelle Flüssigkeitschromatographie*, Hüthig Verlag, Heidelberg 1981.
[40] J. R. Benson, *Anal. Biochem. 71* (1976) 459.
[41] P. Böhlen, S. Stein, J. Stone, S. Udenfried, *Anal. Biochem. 67* (1975) 438.
[42] H. Nika, *J. Chromatogr. 297* (1984) 261.
[43] G. K. Ackers, *Adv. Protein Chem. 24* (1970) 343.
[44] E. Pfannkoch, K. C. Lu, F. E. Regnier, H. G. Barth, *J. Chromatogr. Sci. 18* (1980) 430.
[45] G. Guiochon, M. Martin, *J. Chromatogr. 326* (1985) 3.
[46] T. V. Alfredson, C. T. Wehr, L. Tallman, F. Klink, *J. Liq. Chromatogr. 5* (1982) 489.
[47] M. Okazaki, Y. Ohno, I. Hara, *J. Chromatogr. 221* (1980) 257.
[48] Y. Kato, K. Komiya, H. Sasaki, T. Hashimoto, *J. Chromatogr. 193* (1980) 311.
[49] S. C. Goheen, R. S. Matson, *J. Chromatogr. 326* (1985) 235.
[50] F. E. Regnier, R. Noel, *J. Chromatogr. Sci. 14* (1976) 316.
[51] H. Engelhardt, D. Mathes, *J. Chromatogr. 142* (1977) 311.
[52] Y. Kato, K. Komiya, H. Sasaki, T. Hashimoto, *J. Chromatogr. 190* (1980) 297.
[53] P. Roumeliotis, K. K. Unger, *J. Chromatogr. 149* (1978) 211.
[54] R. W. Stout, J. J. De Stefano, *J. Chromatogr. 326* (1985) 63.
[55] Y. Kato, K. Komiya, H. Sasaki, T. Hashimoto, *J. Chromatogr. 193* (1980) 29.
[56] Y. Kato, K. Komiya, H. Sasaki, T. Hashimoto, *J. Chromatogr. 193* (1980) 458.
[57] J. E. Rivier, *J. Chromatogr. 202* (1980) 211.
[58] B. S. Welinder in W. S. Hancock (Ed.): *Handbook of HPLC for the Separation of Amino Acids, Peptides and Proteins, Vol. II*, CRC Press, Boca Raton, FL, USA 1984, p. 413.
[59] F. E. Regnier, *Anal. Biochem. 126* (1982) 1.
[60] O. Mikes, *Int. J. Pept. Protein Res. 14* (1979) 393.

[61] Y. Kato, K. Nakamura, T. Hashimoto, *J. Chromatogr. 294* (1984) 207.
[62] T. Kadoya, T. Isobe, Y. Amano, Y. Kato, K. Nakamura, T. Okuyama, *J. Liq. Chromatogr. 8* (1985) 635.
[63] K. Nakamura, Y. Kato, *J. Chromatogr. 333* (1985) 29.
[64] J. Richey, *Am. Lab. 14* (1982) 104.
[65] L. Fägerstam, L. Söderberg, L. Wahlström, *Protides Biol. Fluids 30* (1982) 621.
[66] K. M. Gooding, M. N. Schmuck, *J. Chromatogr. 327* (1985) 139.
[67] S. H. Chang, R. Noel, F. E. Regnier, *Anal. Chem. 48* (1976) 1839.
[68] A. J. Alpert, F. E. Regnier, *J. Chromatogr. 185* (1979) 375.
[69] S. Gupta, E. Pfannkoch, F. E. Regnier, *Anal. Biochem. 128* (1983) 196.
[70] Y. Kato, K. Komiya, T. Hashimoto, *J. Chromatogr. 246* (1982) 13.
[71] Y. Kato, K. Nakamura, T. Hashimoto, *HRC & CC, J. High Resolut. Chromatogr. Chromatogr. Commun. 8* (1985) 154.
[72] C. Tanford, *Science 200* (1978) 1012.
[73] Z. Er-el, Y. Zaidenzaig, S. Shaltiel, *Biochem. Biophys. Res. Commun. 49* (1972) 383.
[74] H. A. Arfmann, S. Shaltiel, *Eur. J. Biochem. 70* (1976) 269.
[75] S. Shaltiel, *Methods Enzymol. 104* (1984) 69.
[76] H. Engelhardt, D. Mathes, *Chromatographia 14* (1981) 325.
[77] Y. Kato, T. Kitamura, T. Hashimoto, *J. Chromatogr. 266* (1983) 49.
[78] J. L. Fausnaugh, E. Pfannkoch, S. Gupta, F. E. Regnier, *Anal. Biochem. 137* (1984) 464.
[79] N. T. Miller, B. Feibush, B. L. Karger, *J. Chromatogr. 316* (1984) 519.
[80] D. L. Gooding, M. N. Schmuck, K. M. Gooding, *J. Chromatogr. 296* (1984) 107.
[81] Y. Kato, T. Kitamura, T. Hashimoto, *J. Chromatogr. 292* (1984) 418.
[82] Y. Kato, T. Kitamura, T. Hashimoto, *J. Chromatogr. 298* (1984) 407.
[83] J. L. Fausnaugh, L. A. Kennedy, F. E. Regnier, *J. Chromatogr. 317* (1984) 141.
[84] W. R. Melander, D. Corradini, C. Horvath, *J. Chromatogr. 317* (1984) 67.
[85] W. R. Melander, C. Horvath, *Arch. Biochem. Biophys. 183* (1977) 393.
[86] R. H. Ingraham, S. Y. M. Lau, A. K. Taneja, R. S. Hodges, *J. Chromatogr. 327* (1985) 77.
[87] G. A. Howard, A. J. P. Martin, *Biochem. J. 46* (1950) 532.
[88] R. E. Majors, *J. Chromatogr. Sci. 18* (1980) 488.
[89] C. Horvath, W. Melander, I. Molnar, *J. Chromatogr. 125* (1976) 129.
[90] C. Horvath, W. Melander, I. Molnar, *Anal. Chem. 49* (1977) 142.
[91] C. Horvath, W. Melander, *J. Chromatogr. Sci. 15* (1977) 393.
[92] W. S. Hancock, J. T. Sparrow in C. Horvath (Ed.): *High-Performance Liquid Chromatography: Advances and Perspectives, Vol. 3*, Academic Press, New York 1983, p. 49.
[93] M. T. W. Hearn, *Methods Enzymol. 104* (1984) 190.
[94] R. A. Barford, B. J. Sliwinski, A. C. Breyer, H. L. Rothbart, *J. Chromatogr. 235* (1982) 281.
[95] W. C. Mahoney, *Biochim. Biophys. Acta 704* (1982) 284.
[96] J. D. Pearson, W. C. Mahoney, M. A. Hermodson, F. E. Regnier, *J. Chromatogr. 207* (1981) 325.
[97] M. T. W. Hearn, B. Grego, *J. Chromatogr. 255* (1983) 125.
[98] M. J. O'Hare, E. C. Nice, *J. Chromatogr. 171* (1979) 209.
[99] S.-J. Su, B. Grego, B. Niven, M. T. W. Hearn, *J. Liq. Chromatogr. 4* (1981) 1745.
[100] J. L. Meek, Z. L. Rossetti, *J. Chromatogr. 211* (1981) 15.
[101] T. Sasagawa, T. Okuyama, D. C. Teller, *J. Chromatogr. 240* (1982) 329.
[102] E. Keshavarz, S. Nakai, *Biochim. Biophys. Acta 576* (1979) 269.
[103] S. Terabe, H. Nishi, T. Ando, *J. Chromatogr. 212* (1981) 295.
[104] E. C. Nice, M. W. Capp, N. Cooke, M. J. O'Hare, *J. Chromatogr. 218* (1981) 569.
[105] A. J. Sadler, R. Micanovic, G. E. Katzenstein, R. V. Lewis, C. R. Middaugh, *J. Chromatogr. 317* (1984) 93.
[106] K. Benedek, S. Dong, B. L. Karger, *J. Chromatogr. 317* (1984) 227.
[107] A. R. Kerlavage, C. J. Weitzmann, T. Hasan, B. S. Cooperman, *J. Chromatogr. 266* (1983) 225.
[108] S. A. Cohen, K. Benedek, S. Dong, Y. Tapuhi, B. L. Karger, *Anal. Chem. 56* (1984) 217.
[109] P. G. Stanton, B. Grego, M. T. W. Hearn, *J. Chromatogr. 296* (1984) 189.
[110] W. S. Hancock, C. A. Bishop, M. T. W. Hearn, *FEBS Lett. 72* (1976) 139.
[111] W. S. Hancock, C. A. Bishop, R. L. Prestidge, D. R. K. Harding, M. T. W. Hearn, *Science 200* (1978) 1168.
[112] Y. Kato, T. Kitamura, T. Hashimoto, *J. Chromatogr. 333* (1985) 93.
[113] Technical bulletin: *Polymeric HPLC-columns for proteins and peptides*, Polymer Laboratories, 1985 (Latek GmbH).
[114] F. V. Warren, B. A. Bidlingmeyer, *J. Liq. Chromatogr. 8* (1985) 619.
[115] R. V. Lewis, D. De Wald, *J. Liq. Chromatogr. 5* (1982) 1367.
[116] M. J. O'Hare, M. W. Capp, E. C. Nice, N. H. C. Cooke, B. G. Archer, *Anal. Biochem. 126* (1982) 17.
[117] E. C. Nice, M. W. Capp, M. J. O'Hare, *J. Chromatogr. 185* (1979) 413.
[118] J. D. Pearson, F. E. Regnier, *J. Liq. Chromatogr. 6* (1983) 497.
[119] N. H. C. Cooke, B. G. Archer, M. J. O'Hare, E. C. Nice, M. W. Capp, *J. Chromatogr. 255* (1983) 115.
[120] H. Engelhardt, H. Müller, *Chromatographia 19* (1984) 77.
[121] M. T. W. Hearn, B. Grego, *J. Chromatogr. 282* (1983) 541.
[122] M. T. W. Hearn, B. Grego, *J. Chromatogr. 296* (1984) 61.
[123] I. Molnar, C. Horvath, *J. Chromatogr. 142* (1977) 263.
[124] M. T. W. Hearn, B. Grego, W. S. Hancock, *J. Chromatogr. 185* (1979) 429.
[125] M. T. W. Hearn, *Adv. Chromatogr. 18* (1980) 59.
[126] W. S. Hancock, C. A. Bishop, L. J. Meyer, D. R. K. Harding, M. T. W. Hearn, *J. Chromatogr. 161* (1978) 291.
[127] W. C. Mahoney, M. A. Hermodson, *J. Biol. Chem. 255* (1980) 11199.
[128] J. E. Rivier, *J. Liq. Chromatogr. 1* (1978) 343.
[129] J. B. Shelton, J. R. Shelton, W. A. Schröder, *J. Liq. Chromatogr. 4* (1981) 1381.
[130] U. Certa, G. von Ehrenstein, *Anal. Biochem. 118* (1981) 147.
[131] G. Szepesi, M. Gazdag, *J. Chromatogr. 218* (1981) 597.
[132] M. Kehl, F. Lottspeich, A. Henschen, *Hoppe-Seyler's Z. Physiol. Chem. 363* (1982) 1501.
[133] H. P. J. Bennett, C. A. Browne, S. Solomon, *J. Liq. Chromatogr. 3* (1980) 1353.
[134] C. A. Browne, H. P. J. Bennett, S. Solomon, *Anal. Biochem. 124* (1982) 201.
[135] J. J. L'Italien, J. E. Strickler, *Anal. Biochem. 127* (1982) 198.
[136] K. Titani, T. Sasagawa, K. Resing, K. A. Walsh, *Anal. Biochem. 123* (1982) 408.
[137] H. P. Nick, R. E. H. Wettenhall, M. T. W. Hearn, F. J. Morgan, *Anal. Biochem. 148* (1985) 93.
[138] M. van der Rest, P. Fietzek, *Eur. J. Biochem. 125* (1982) 491.
[139] G. E. Gerber, H. G. Khorana, *Methods Enzymol. 88* (1982) 56.
[140] J. Heukeshoven, R. Dernick, *J. Chromatogr. 326* (1985) 91.
[141] M. Rubinstein, *Anal. Biochem. 98* (1979) 1.
[142] B. N. Jones, R. V. Lewis, S. Pääbo, K. Kojima, S. Kimuro, S. Stein, *J. Liq. Chromatogr. 3* (1980) 1373.
[143] M. Green, K. H. Brackmann, *Anal. Biochem. 124* (1982) 209.
[144] A. Fallon, R. V. Lewis, K. D. Gibson, *Anal. Biochem. 110* (1981) 318.
[145] K. J. Wilson, A. Honegger, R. P. Stölzel, G. J. Hughes, *Biochem. J. 199* (1981) 31.
[146] E. Hannappel, W. Leibold, *Protides Biol. Fluids 32* (1984) 1093.
[147] B. Grego, G. S. Baldwin, J. A. Knessel, R. J. Simpson, F. J. Morgan, M. T. W. Hearn, *J. Chromatogr. 297* (1984) 21.
[148] G. E. Tarr, J. W. Crabb, *Anal. Biochem. 131* (1983) 99.
[149] S. W. Herring, R. K. Enns, *J. Chromatogr. 266* (1983) 249.
[150] W. S. Hancock, J. D. Capra, W. A. Bradley, J. T. Sparrow, *J. Chromatogr. 206* (1981) 59.
[151] W. S. Hancock, J. T. Sparrow, *J. Chromatogr. 206* (1981) 71.
[152] R. J. Ferris, C. A. Cowgill, R. R. Traut, *Biochemistry 23* (1984) 3434.
[153] J. Spiess, J. E. Rivier, C. Rivier, M. Vale, *Proc. Natl. Acad. Sci. USA 78* (1981) 6517.
[154] W. Richter, P. Schwandt, *J. Neurochem. 36* (1981) 1279.
[155] M. W. Berchthold, K. J. Wilson, C. W. Heizmann, *Biochemistry 21* (1982) 6552.
[156] E. Rinderknecht, B. H. O'Connor, H. Rodriguez, *J. Biol. Chem. 259* (1984) 6790.
[157] B. Larsen, B. L. Fox, M. F. Burke, V. J. Hruby, *Int. J. Pept. Protein Res. 13* (1979) 12.
[158] J. A. Smith, M. J. O'Hare, *J. Chromatogr. 299* (1984) 13.
[159] H. Gazdag, G. Szepesi, *J. Chromatogr. 218* (1981) 603.
[160] R. van der Zee, S. Welling-Wester, G. W. Welling, *J. Chromatogr. 266* (1983) 577.
[161] A. R. Kerlavage, T. Hasan, B. S. Cooperman, *J. Biol. Chem. 258* (1983) 6313.
[162] G. S. Baldwin, B. Grego, M. T. W. Hearn, J. A. Knessel, F. J. Morgan, R. J. Simpson, *Proc. Natl. Acad. Sci. USA 80* (1983) 5276.
[163] M. P. Strickler, J. Kintzios, M. J. Gemski, *J. Liq. Chromatogr. 5* (1982) 1921.
[164] S. A. Cohen, K. Benedek, Y. Tapuhi, J. C. Ford, B. L. Karger, *Anal. Biochem. 144* (1985) 275.
[165] M. T. W. Hearn, A. N. Hodder, M. I. Aguilar, *J. Chromatogr. 327* (1985) 47.
[166] J. P. Chang, W. R. Melander, C. Horvath, *J. Chromatogr. 318* (1985) 11.
[167] T. L. Brooks, A. Stevens, *Int. Lab. 15* (1985) No. 9, p. 72.
[168] S. van der Wal, J. F. K. Huber, *Anal. Biochem. 105* (1980) 219.
[169] R. R. Walters, *Anal. Chem. 57* (1985) 1099A.
[170] T. M. Phillips, W. D. Queen, N. S. Moore, A. M. Thompson, *J. Chromatogr. 327* (1985) 213.
[171] S. Ohlson, L. Hansson, P. O. Larsson, K. Mosbach, *FEBS Lett. 93* (1978) 5.
[172] J. R. Sportsman, G. S. Wilson, *Anal. Chem. 52* (1980) 2013.
[173] M. E. Robers, M. W. Adlard, G. Saunders, G. Holt, *J. Chromatogr. 326* (1985) 163.

[174] A. Borchert, P. O. Larsson, K. Mosbach, *J. Chromatogr. 244* (1982) 49.
[175] C. R. Lowe, M. Glad, P. O. Larsson, S. Ohlson, D. A. P. Small, T. Atkinson, K. Mosbach, *J. Chromatogr. 215* (1981) 303.
[176] *Fast Affinity Chromatography* (Bulletin 5933) Beckman Instruments, San Ramon, CA, USA, 1985.
[177] G. Wagner, F. E. Regnier, *Anal. Biochem. 126* (1982) 37.
[178] T. W. Hutchens, H. E. Dunaway, P. K. Besch, *J. Chromatogr. 327* (1985) 247.
[179] F. Sanger, H. Tuppy, *Biochem. J. 49* (1951) 481.
[180] F. Sanger, E. O. P. Thompson, *Biochem. J. 53* (1953) 366.
[181] G. Bentley, E. Dodson, G. Dodson, D. Hodgkin, D. Mercola, *Nature London 261* (1976) 166.
[182] A. McLeod, S. P. Wood, *J. Chromatogr. 285* (1984) 319.
[183] H. S. Tager, *Diabetes 33* (1984) 693.
[184] B. S. Welinder, S. Linde in W. S. Hancock (Ed.): *Handbook of HPLC for the Separation of Amino Acids, Peptides and Proteins, Vol. II*, CRC Press, Boca Raton, FL, USA 1984, p. 357.
[185] E. P. Kroeff, R. E. Chance in J. L. Guerigian (Ed.): *Proc. of the FDA Workshop on Insulins, Growth Hormone and Recombinant DNA Technology*, The U. S. Pharmacopeial Convention Inc., Rockville, MD, USA 1982, p. 148.
[186] B. S. Welinder, F. H. Andresen, *ibid.*, p. 163.
[187] S. Linde, B. Hansen, O. Sonne, J. J. Holat, J. Gliemann, *Diabetes 30* (1981) 1.
[188] B. H. Frank, D. E. Peavy, C. S. Hooker, W. C. Duckworth, *Diabetes 32* (1983) 705.
[189] B. S. Welinder, S. Linde, B. Hansen, *J. Chromatogr. 265* (1983) 301.
[190] K. H. Joergensen, DBP 1940130 C2, Novo Terapeutisk Laboratorium 1983.
[191] R. D. Cole, *Fed. Proc. Fed. Am. Soc. Exp. Biol. 18* (1959) 206.
[192] M. Zoltobrocki, DOS 2659568 C3, Hoechst AG 1981.
[193] W. Burgermeister, F. Enzmann, H. H. Schöne in A. Hasselblatt, F. von Bruchhausen (Eds.): *Handbuch der experimentellen Pharmakologie*, Springer, Berlin 1975, p. 715.
[194] D. V. Goeddel, D. G. Kleid, F. Bolivar, H. C. Heyneken, D. G. Yansura, R. Crea, T. Hirose, A. Kraszewski, K. Itakura, A. D. Riggs, *Proc. Natl. Acad. Sci. USA 76* (1979) 106.
[195] R. E. Chance, E. P. Kroeff, J. A. Hoffmann in J. L. Guerigian (Ed.): *Insulins, Growth Hormone and Recombinant DNA Technology*, Raven Press, New York 1981, p. 71.
[196] I. S. Johnson, *Science 219* (1983) 632.
[197] F. Wengenmeyer, *Angew. Chem. 95* (1983) 874; *Angew. Chem. Int. Ed. Engl. 22* (1983) 842.
[198] J. Fruton, *Adv. Enzymol. Relat. Areas Mol. Biol. 53* (1982) 239.
[199] H.-D. Jakubke, P. Kuhl, A. Könnecke, *Angew. Chem. 97* (1985) 79; *Angew. Chem. Int. Ed. Engl. 24* (1985) 85.
[200] a) R. Obermeier, G. Seipke, U. Grau in K. G. Petersen, K. J. Schlüter, L. Kerp (Eds.): *Neue Insuline*, Freiburger Graphische Betriebe, Freiburg 1982, p. 32; b) J. Markussen, *ibid.*, p. 38.
[201] R. Obermeier, G. Seipke, *Process Biochem. 19* (1984) 29.
[202] J. D. Young, F. H. Carpenter, *J. Biol. Chem. 236* (1961) 743.
[203] D. F. Steiner, *Trans. N. Y. Acad. Sci. 30* (1967) 60.
[204] D. F. Steiner, J. L. Clark, C. Nolan, A. H. Rubenstein, E. Margoliash, B. Aten, P. E. Oyer in S. Baba, T. Kaneko, N. Yanaihara (Eds.): *Proinsulin, Insulin, C-Peptide*, Excerpta Medica, Amsterdam 1979, p. 267.
[205] J. M. Swan, *Nature London 180* (1957) 643.
[206] G. H. Dixon, A. C. Wardlaw, *Nature London 188* (1960) 721.
[207] B. H. Frank, Eur. Pat. Appl. 0037255, Eli Lilly and Company 1981.
[208] U. Grau, *Diabetes 34* (1985) 1174.
[209] F. H. Carpenter, A. Crambach, *J. Biol. Chem. 237* (1962) 404.
[210] *United States Pharmacopeia*, 21st Revision, U. S. Pharmacopeial Convention Inc., Rockville, MD, USA 1985, p. 536.
[211] H. Ross, G. Bernstein, H. Rifkin in M. Ellenberg, H. Rifkin (Eds.): *Diabetes Mellitus, Theory and Practice*, Medical Examination Publishing Corp., New York 1983, p. 907.
[212] M. Brownlee, H. Vlassara, A. Cerami, *Ann. Intern. Med. 101* (1984) 527.
[213] P. Rastein in M. Ellenberg, H. Rifkin (Eds.): *Diabetes Mellitus, Theory and Practice*, Medical Examination Publishing Corp., New York 1983, p. 941.
[214] J. C. Pickup, D. Rothwell, *Med. Biol. Eng. Comput. 22* (1984) 385.
[215] K. Irsigler, H. Kritz, R. Lovett (Eds.): *Diabetes Treatment with Implantable Insulin Infusion Systems*, Urban und Schwarzenberg, Munich 1983.
[216] K. Irsigler, H. Kritz, *Diabetes 28* (1979) 196.
[217] W. D. Lougheed, H. Woulfe Flanagan, J. R. Clement, A. M. Albisser, *Diabetologia 19* (1980) 1.
[218] U. Grau, *Diabetologia 28* (1985) 458.
[219] U. Grau in K. D. Hepp, R. Renner (Eds.): *Continuous Insulin Infusion Therapy. Experience from One Decade*, Schattauer, Stuttgart 1985, p. 33.
[220] U. Grau, G. Seipke, R. Obermeier, H. Thurow in K. G. Petersen, K. J. Schlüter, L. Kerp (Eds.): *Neue Insuline*, Freiburger Graphische Betriebe, Freiburg 1982, p. 441.
[221] J. Brange, L. Langkjaer, S. Havelund, E. Sørensen, *Diabetologia 25* (1983) 143.
[222] U. Grau, P. Jährling, *Diabetologia*, submitted for publication; H. P. Neubauer, Hoechst AG, unpublished results.
[223] R. A. Rizza, J. E. Gerich, M. W. Haymond, R. E. Westland, L. D. Hall, A. H. Clemens, I. J. Service, *N. Engl. J. Med. 303* (1980) 1313.
[224] P. V. Byrne, *J. Chromatogr. 283* (1984) 459.
[225] M. Dobos, H. G. Burger, M. T. W. Hearn, F. J. Morgan, *Mol. Cell. Endocrinol. 31* (1983) 187.
[226] D. Novick, D. G. Fischer, Y. Mory, M. Revel, M. Rubinstein, *Protides Biol. Fluids 32* (1984) 1049.
[227] M. W. Hunkapiller, J. E. Strickler, K. J. Wilson, *Science 226* (1984) 304.
[228] P. Lundahl, E. Greijer, H. Lindblom, L. G. Fägerstam, *J. Chromatogr. 297* (1984) 129.
[229] H. Ikigai, T. Nakae, Y. Kato, *J. Chromatogr. 322* (1985) 212.
[230] P. Lambotte, J. van Snick, T. Boon, *J. Chromatogr. 297* (1984) 139.
[231] G. W. Welling, G. Kroen, K. Slopsema, S. Welling-Wester, *J. Chromatogr. 326* (1985) 173.
[232] R. van der Zee, G. W. Welling, *J. Chromatogr. 327* (1985) 377.
[233] B. H. Frank, M. J. Beckage, K. A. Willey, *J. Chromatogr. 266* (1983) 239.
[234] B. S. Welinder, S. Linde, B. Hansen, O. Sonne, *J. Chromatogr. 298* (1984) 41.
[235] J. R. Deschamps, J. E. K. Hildreth, D. Deer, J. T. August, *Anal. Biochem. 147* (1985) 451.
[236] M. J. F. Schmerr, K. R. Goodwin, H. D. Lehmkuhl, R. C. Cutlip, *J. Chromatogr. 326* (1985) 225.
[237] S. Seino, A. Funakoshi, Z. Z. Fu, A. Vinik, *Diabetes 34* (1985) 1.
[238] T. H. J. Huismans, J. B. Wilson, *Protides Biol. Fluids 32* (1984) 1029.
[239] A. Kutlar, F. Kutlar, J. B. Wilson, M. G. Headlee, T. H. J. Huismans, *Am. J. Hematol. 17* (1984) 39.
[240] E. C. Toren, D. N. Vacik, P. B. Mockridge, *J. Chromatogr. 266* (1983) 207.
[241] D. M. Boyle, R. D. Wiehle, N. A. Shahabi, J. L. Wittcliff, *J. Chromatogr. 327* (1985) 369.
[242] T. M. Phillips, N. S. Moore, W. D. Queen, A. M. Thompson, *J. Chromatogr. 327* (1985) 205.
[243] S. W. Rabkin, P. Desjarduis, *Clin. Chim. Acta 138* (1984) 245.
[244] E. S. Kimball, W. H. Bohn, K. D. Cockley, T. C. Warren, S. A. Sherwin, *Cancer Res. 44* (1984) 3613.
[245] L. E. Henderson, R. Sowder, S. Oroszlan in T. Liu, A. Schechter, R. Heinrikson, P. Condliffe (Eds.): *Chemical Synthesis and Sequenzing of Peptides and Proteins*, Elsevier/North-Holland, Amsterdam 1981, p. 251.
[246] J. E. Rivier, R. McClintock, R. Galyean, H. Anderson, *J. Chromatogr. 288* (1984) 303.
[247] H. J. Friesen, S. Stein, M. Evinger, P. C. Familletti, J. Moschera, J. Meienhofer, J. Shively, S. Pestka, *Arch. Biochem. Biophys. 206* (1981) 432.
[248] S. A. Rosenberg, M. T. Lotze, L. M. Muul, S. Leitman, A. E. Chang, S. E. Ettingshausen, Y. L. Matory, J. M. Skibber, E. Shiloni, J. T. Vetto, C. A. Seipp, C. Simpson, C. M. Reichert, *N. Engl. J. Med. 313* (1985) 1485.
[249] K. Welte, C. Y. Wang, R. Mertelmann, V. Salvatore, S. P. Feldman, M. A. S. Moore, *J. Exp. Med. 156* (1982) 454.
[250] E. M. Kniep, B. Kniep, W. Grote, H. S. Conradt, D. A. Monner, P. F. Mühlradt, *Eur. J. Biochem. 143* (1984) 199.
[251] A. Godard, J. Naulet, M. A. Peyrat, H. Vie, J. F. Moreau, J. D. Bignon, J. P. Soullilou, *J. Immunol. Methods 70* (1984) 233.
[252] T. Taniguchi, M. Matsui, T. Fujita, C. Takaoka, N. Kashima, R. Yoshimoto, J. Hamuro, *Nature London 302* (1983) 305.
[253] R. J. Robb, R. M. Kutny, M. Panico, H. R. Morris, V. Chowdry, *Proc. Nat. Acad. Sci. USA 81* (1984) 6486.
[254] R. Devos, G. Plaetinck, M. Cheroute, G. Simons, W. Degrave, J. Tavernier, E. Remaut, W. Fiers, *Nucleic Acids Res. 11* (1983) 4307.
[255] K. Kato, T. Yamada, K. Kawahara, H. Onda, T. Asano, H. Sugino, A. Kakinuma, *Biochem. Biophys. Res. Commun. 130* (1985) 692.
[256] M. P. Strickler, M. J. Gemski, B. P. Doctor, *J. Liq. Chromatogr. 4* (1981) 1765.
[257] G. Winkler, P. Wolschan, P. Briza, F. X. Heinz, C. Kunz, *J. Chromatogr. 347* (1985) 83.
[258] D. Guerini, J. Krebs, *Anal. Biochem. 150* (1985) 178.
[259] H. Wagner, M. Röllinghoff, *Behring Inst. Mitt. 67* (1980) 2.

When submitting manuscripts, authors of articles intended for publication as "Communications" are requested to read the "Notice to Authors" reproduced in the January issue of the journal following the list of contents; upon request, a copy can be obtained from the editorial office.

Reduced Cobalt-*meso*-Tetraphenylporphyrin Complexes: Synthesis and Structure of $[Na(thf)_3]_2[Co(TPP)]$

By *Stefano Ciurli, Sandro Gambarotta, Carlo Floriani,* Angiola Chiesi-Villa,* and *Carlo Guastini*

In cobalt-porphyrin chemistry it is generally assumed that the diamagnetic anion $[Co(TPP)]^{\ominus}$ with d^8-Co^I is formed as sole reduction product of cobalt(II)-*meso*-tetraphenylporphyrin [Co(TPP)] **1**—independent of the amount and nature of the reducing agent and the reaction conditions.[1] This anion is one of the most popular metallic nucleophiles used in inorganic chemistry, and the experimental conditions under which it can be generated without forming other reduced species requires definition.[2] Only very recently an X-ray structure analysis of $[Co(TPP)]^{\ominus}$ in the salt $[(2,2,2\text{-crypt})K]_4[Co(TPP)]Cl_3 \cdot H_2O$ was reported.[3] We now report on the product that is formed upon reduction of [Co(TPP)] with two equivalents of sodium sand.

When a solution of **1** in tetrahydrofuran (THF) was stirred with two equivalents of sodium sand until all sodium disappeared, a brown solution formed; upon subsequent addition of Et_2O, $[Na(thf)_3]_2[Co(TPP)]$ **2** crystallized as a brown solid[4] (yield ca. 52%).

$$\underset{\mathbf{1}}{[Co(TPP)]} + 2\,Na \xrightarrow{THF} \underset{\mathbf{2}}{[Na(thf)_3]_2[Co(TPP)]}$$

At 298.0 K, complex **2** has a magnetic moment μ_{eff} of 2.22 BM, thus indicating one unpaired electron. Reaction of **2** in THF with an equimolar amount of **1** led to formation of a red-brown solution; upon addition of Et_2O and cooling at −8 °C, $[Na(thf)_3][Co(TPP)]$ **3** was obtained as a violet diamagnetic crystalline solid (yield ca. 83%).[5]

$$\underset{\mathbf{2}}{[Na(thf)_3]_2[Co(TPP)]} + \underset{\mathbf{1}}{[Co(TPP)]} \longrightarrow 2\underset{\mathbf{3}}{[Na(thf)_3][Co(TPP)]}$$

Complex **2** poses two fundamental questions: 1. Is the formulation of the Co^0 complex correct? 2. Which d-configuration describes the ground state? An analysis of the structural parameters can help in answering these questions.[6]

Figure 1 shows an ORTEP plot of complex **2**, which is isomorphous with the recently reported iron(0) complex $[Na(thf)_3]_2[Fe(TPP)]$.[7] The cobalt atom is a crystallographic center of symmetry; the two $[Na(thf)_3]^{\oplus}$ ions are located at equal distances above and below the plane of the porphinato ligand. Some bond lengths of the anion are given in Table 1.

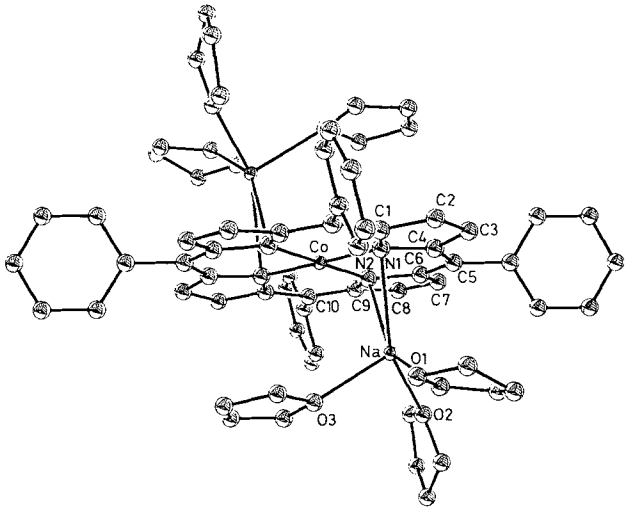


Fig. 1. Perspective ORTEP diagram of the structure of $[Na(thf)_3]_2[Co(TPP)]$ **2** in the crystal.

Table 1. Comparison of the bond lengths (average) [Å] of [M(TPP)] complexes (M = Co, Cu) [a].

Bond	$[Co(TPP)(Pip)_2]$ [10] [b]	$[Co(TPP)]^{\ominus}$ [3]	$[Co(TPP)]^{2\ominus}$	[Cu(TPP)] [11]
$M-N_p$	1.987(2)	1.942(3)	1.971(3)	1.981(7)
$N-C_\alpha$	1.380(2)	1.397(3)	1.400(5)	1.383(12)
$C_\alpha-C_\beta$	1.444(3)	1.434(3)	1.422(6)	1.427(16)
$C_\beta-C_\beta$	1.344(3)	1.337(7)	1.356(6)	1.335(23)
$C_\alpha-C_m$	1.393(2)	1.380(3)	1.390(6)	1.398(13)

[a] C_α and C_β are the α- and β-C atoms of a pyrrole ring; C_m is a methine C atom. [b] Pip = piperidine.

The conformation of the porphinato core in $[Co(TPP)]^{2\ominus}$, whose maximum deviation from planarity is −0.0105(6) Å for C2, is not unusual. The dihedral angles between the peripheral phenyl rings and the core are 75.7 and 76.1°. The interaction between the two $[Na(thf)_3]^{\oplus}$ ions and the $[Co(TPP)]^{2\ominus}$ ion is that of a contact ion-pair. The rather long Na-N distances (Na-N1, 2.766(5); Na-N2, 2.757(5) Å) are comparable with those in the iron(0) complex[7] and with those in a cryptate complex.[8] We can assume here also that they correspond to a bonding interaction.[7] The plane through Na-N1-N2 forms a dihedral angle of 83.4(1)° with that of the anion. The Na-O distances are unusual, ranging from 2.312(5) to 2.341(4) Å.[9]

In Table 1 averaged bond distances are compared for $[Co(TPP)(Pip)_2]$,[10] $[Co(TPP)]^{\ominus}$,[3] $[Co(TPP)]^{2\ominus}$, and [Cu(TPP)].[11] Following the arguments used by *Reed* et al.[7] for the reduced forms of [Fe(TPP)], complex **2** can be viewed as a resonance hybrid of a porphinate with d^9-co-

[*] Prof. Dr. C. Floriani, Dr. S. Gambarotta, S. Ciurli
Chemistry Department, Columbia University,
Havemeyer Hall, Box 307, New York, NY 10027 (USA)
Dr. A. Chiesi-Villa, Dr. C. Guastini
Istituto di Strutturistica Chimica, Centro di Studio
per la Strutturistica Diffrattometrica del CNR
Università di Parma, I-43100 Parma (Italy)

balt(0) at the center and a porphinate radical anion with d^8-cobalt(I) as central atom:

$$[Co^{0}(TPP)]^{2\ominus} \longleftrightarrow [Co^{I}(TPP^{\odot})]^{2\ominus}$$

For final confirmation of the radical anion character of complex **2**, further studies are necessary. Present considerations, however, suggest that the cobalt(0) designation should be used as a label of convenience only. The above findings closely parallel those in iron chemistry concerning the two reduced forms $[Fe(TPP)]^{\ominus}$ and $[Fe(TPP)]^{2\ominus}$,[7] though a significant difference exists between the stability of the reduced form as a function of the metal.[1,3,7] A significant aspect of these structures which can be deduced from the structural determinations of the doubly reduced species $[M(TPP)]^{2\ominus}$ [M = Fe, Co], is that the reduction products occur in tightly ion-paired forms in the solid state. Current efforts are aimed at finding a relationship between the structure in the solid state and in solution. Such ion-pairs have already been found to exist in salen-type compounds (salen = *N,N'*-ethylenebis(salicylideneaminato)) both in solution[12,13] and in the solid state.[7,9,13,14] In these complexes, the simultaneous presence of acidic (alkali cation) and basic (cobalt) sites close together in the same molecular structure is responsible for the so-called 'bifunctional' fixation of CO_2 and other reactions,[13,15] which are not observed in the case of such complexes with only a single reactive site.

Received: December 10, 1985;
revised: March 14, 1985 [Z 1577 IE]
German version: *Angew. Chem. 98* (1986) 553

[1] H. W. Whitlock, B. K. Bower, *Tetrahedron Lett. 1965*, 4827; H. Kobayashi, T. Hara, Y. Kaizu, *Bull. Chem. Soc. Jpn. 45* (1972) 2148; D. A. Clarke, D. Dolphin, R. Grigg, A. W. Johnson, H. A. Pinnock, *J. Chem. Soc. C 1968*, 881; M. Momenteau, M. Fournier, M. Rougée, *J. Chim. Phys. Phys.-Chim. Biol. 67* (1970) 926.

[2] For related supernucleophilic systems see: U. Eckert, I. Ugi, *Angew. Chem. 88* (1976) 717; *Angew. Chem. Int. Ed. Engl. 15* (1976) 681; *ibid. 87* (1975) 847 and *14* (1975) 825.

[3] P. Doppelt, J. Fischer, R. Weiss, *Inorg. Chem. 23* (1984) 2958 and references therein. The 2,2,2-crypt ligand is 4,7,13,16,21,24-hexaoxa-1,10-diazabicyclo[8.8.8]hexacosane.

[4] The solid is highly crystalline and homogeneous. The quoted yield can be improved if a less crystalline material is desired. The IR spectrum is significantly different from those of the three complexes **1**, **2**, **3** and can be used for identification. Since **2** is extremely air-sensitive, particularly in dilute solutions, an electronic spectrum of **2** in which oxidized products are not present could not be recorded.

[5] The number of thf molecules in **3** was deduced from the ^{1}H-NMR spectrum.

[6] Space group $P\bar{1}$, $a = 13.172(3)$, $b = 11.905(2)$, $c = 11.293(2)$ Å, $\alpha = 110.29(2)$, $\beta = 113.74(2)$, $\gamma = 77.49(1)°$; $V = 1514.3(6)$ Å^3; $Z = 1$; $\mu(Mo_{K\alpha}) = 3.48$ cm^{-1}. 5314 unique reflections [$I > 3\sigma(I)$, $6 < 2\theta < 50°$, $\lambda(Mo_{K\alpha}) = 0.71069$ Å] were measured on a Philips PW 1100 diffractometer. The structure was solved by Patterson and Fourier syntheses and refined anisotropically by full-matrix least-squares to $R = 0.055$. Further details of the crystal structure investigation are available on request from the Fachinformationszentrum Energie, Physik, Mathematik GmbH, D-7514 Eggenstein-Leopoldshafen 2, on quoting the depository number CSD-51788, the names of the authors, and the full citation of the journal.

[7] T. Mashiko, C. A. Reed, K. J. Haller, W. R. Scheidt, *Inorg. Chem. 23* (1984) 3192; C. A. Reed, *Adv. Chem. Ser. 201* (1984) 333.

[8] D. Moras, R. Weiss, *Acta Crystallogr. Sect. B 29* (1973) 396; R. G. Teller, R. G. Finke, J. P. Collman, H. B. Chin, R. Bau, *J. Am. Chem. Soc. 99* (1977) 1104.

[9] J. H. Noordik, H. M. Doesburg, P. A. Prick, *Acta Crystallogr. Sect. B 37* (1981) 1659; N. Bresciani-Pahor, M. Calligaris, P. Delise, G. Nardin, L. Randaccio, E. Zotti, G. Fachinetti, C. Floriani, *J. Chem. Soc. Dalton Trans. 1976*, 2310.

[10] W. R. Scheidt, *J. Am. Chem. Soc. 96* (1974) 84.

[11] E. B. Fleischer, C. K. Miller, L. E. Webb, *J. Am. Chem. Soc. 86* (1964) 2342.

[12] A. Giacomelli, T. Rotunno, L. Senatore, *Inorg. Chem. 24* (1985) 1303.

[13] S. Gambarotta, F. Arena, C. Floriani, P. F. Zanazzi, *J. Am. Chem. Soc. 104* (1982) 5082.

[14] G. Fachinetti, C. Floriani, P. F. Zanazzi, A. R. Zanzari, *Inorg. Chem. 18* (1979) 3469.

[15] S. Gambarotta, F. Arena, C. Floriani, A. Gaetani-Manfredotti, *J. Chem. Soc. Chem. Commun. 1982*, 835.

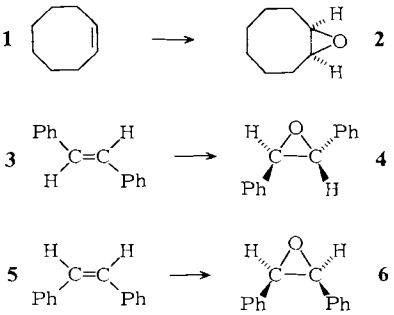
Epoxidation of Olefins with Elemental Fluorine in Water/Acetonitrile Mixtures

By *Shlomo Rozen** and *Michael Brand*

In the last few years we have shown that elemental fluorine, which, since its discovery one-hundred years ago, had been in a state of hibernation as far as organic chemistry was concerned, can in fact be a versatile fluorinating reagent.[1-7] We report here a general reaction of F_2 that leads, in contrast, to fluorine-free derivatives, namely, the facile synthesis of epoxides from olefins using fluorine in water/acetonitrile mixtures.

There are several methods for the synthesis of epoxides, including the reaction of olefins with peracids, H_2O_2, or XOH (X = Cl, Br; subsequent elimination of HX).[8] Most of these reactions, however, proceed slowly, need strongly basic or acidic medium, and often afford unsatisfactory yields.

When dilute fluorine (10% in N_2) is passed through dry acetonitrile or distilled water at 0°C, only a small amount of oxidizing agent is produced, which is inactive toward olefins. When a similar N_2/F_2 mixture is passed through a well-agitated solution containing 400 mL of acetonitrile and 20 mL of distilled water, however, an oxidizing solution is obtained. When it was added to *cis*-cyclooctene **1** in $CHCl_3$ at −15°C, reaction was complete within 1 min. After neutralizing the reaction mixture with $NaHCO_3$, we were able to isolate *cis*-epoxycyclooctane **2** in 85% yield. The epoxidation is stereospecific, as is evident from the conversion of *trans*- and *cis*-stilbene, **3** and **5**, respectively, into *trans*- and *cis*-2,3-diphenyloxirane, **4** and **6**, respectively.[9] Both reactions were complete within one minute in a yield of over 80%.



7 $CH_3(CH_2)_9CH{=}CH_2 \longrightarrow CH_3(CH_2)_9{-}CH{-}CH_2$ **8**

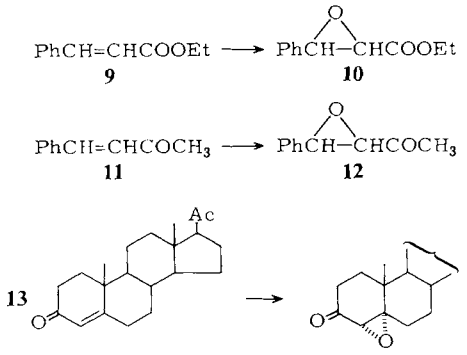
Terminal olefins are usually more sensitive toward strong oxidizing agents. However, even such olefins react

[*] Prof. Dr. S. Rozen, M. Brand
School of Chemistry, Raymond and Beverly Sackler Faculty
of Exact Sciences, Tel-Aviv University
Tel-Aviv 69978 (Israel)

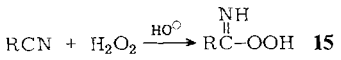
[**] This work was supported by the Fund for Basic Research of the Israel Academy of Science and Humanities.

practically instantaneously to give the corresponding oxiranes in high yields: for example, 1-dodecene **7** was converted into **8** in a yield of over 90%.

Conjugated enones, which are much more resistant to epoxidation, undergo oxidation if the ratio of oxidizing agent to alkene is increased from 1.2:1 to 2.5:1. Thus, ethyl cinnamate **9** was converted into the corresponding epoxide **10**[10] within one minute in 80% yield. Benzylideneacetone **11** and progesterone **13** underwent rapid epoxidation to give **12** (m.p. = 45 °C[11]) and **14** (m.p. = 177 °C[12]), respectively, in yields of 85% and 80%.



Acetonitrile is known to act as a carrier for an oxidizing agent. It reacts with H_2O_2 to form peroxyimidic acid **15**, an intermediate that has not been isolated, but which reacts with some olefins to form epoxides.[13] This epoxidation reaction, however, usually requires several hours at elevated temperatures, and electron-poor olefins such as enones do not react.



Since no oxidizing solutions are formed with fluorine unless both CH_3CN and H_2O are present, CH_3CN must be essential for the formation of the oxidizing agent. A crucial step is presumably the formation of hypofluorous acid, HOF,[14] which then reacts with CH_3CN. The $F_2/CH_3CN/H_2O$ system offers promise as a useful method for fast, low-temperature, high-yield epoxidations.

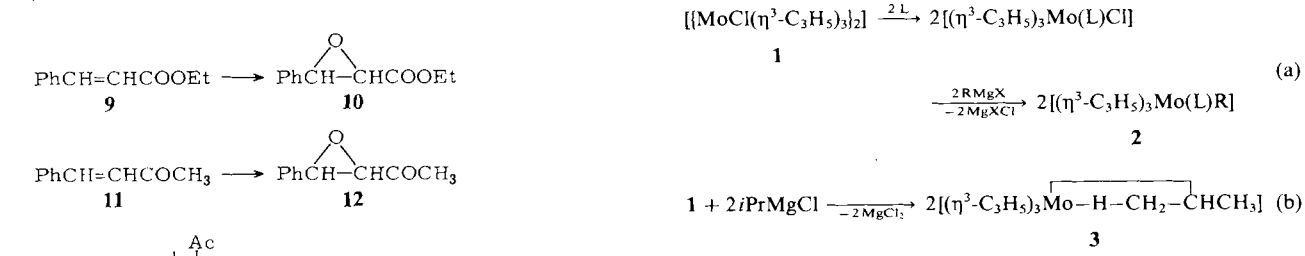
Received: January 21, 1986;
revised: March 13, 1986 [Z 1631 IE]
German version: *Angew. Chem. 98* (1986) 565

[1] C. Gal, S. Rozen, *Tetrahedron Lett. 26* (1985) 2793.
[2] S. Rozen, O. Lerman, *J. Org. Chem. 45* (1980) 672.
[3] O. Lerman, S. Rozen, *J. Org. Chem. 45* (1980) 4122; D. F. Persico, G. E. Gerhardt, R. J. Lagow, *J. Am. Chem. Soc. 107* (1985) 1197.
[4] J. L. Adcock, M. L. Robin, *J. Org. Chem. 49* (1984) 1442.
[5] O. Lerman, Y. Tor, D. Hebel, S. Rozen, *J. Org. Chem. 49* (1984) 806.
[6] S. Rozen, M. Brand, *Synthesis 1985*, 665.
[7] S. Rozen, M. Brand, *J. Org. Chem. 50* (1985) 3342.
[8] A. Y. Zapevalov, T. I. Filyakova, I. P. Kolenko, N. V. Peschanskii, M. I. Kodess, *Zh. Org. Khim. 20* (1984) 2267.
[9] G. Ceccarelly, G. Berti, G. Lippi, B. Macchia, *Org. Magn. Reson. 2* (1970) 379.
[10] J. Baldas, Q. N. Parter, *Aust. J. Chem. 20* (1967) 2655.
[11] R. D. Temple, *J. Org. Chem. 35* (1970) 1275.
[12] H. B. Henbest, W. R. Jackson, *J. Chem. Soc. C 1967*, 2459.
[13] R. D. Bach, J. W. Knight, *Org. Synth. 60* (1981) 63, and references cited therein.
[14] E. H. Appelman, R. C. Thompson, *J. Am. Chem. Soc. 106* (1984) 4167.

$[MoR(\eta^3\text{-}C_3H_5)_3]$, R = Alkyl: Alkylmolybdenum Complexes with Agostic C–H→Mo Bond**

By *Reinhard Benn, Sigrid Holle, Peter W. Jolly,* Richard Mynott,* and *Carlos C. Romão*

Earlier we reported the conversion of the binuclear molybdenum complex **1** into the ligand-stabilized alkylmolybdenum complexes **2** [Eq. (a)].[1,2] We discuss here the reactions of **1** with Grignard reagents in the absence of stabilizing ligands [Eq. (b)].



Treatment of **1** with isopropylmagnesium chloride in ether at −78 °C results in the formation of a yellow compound $[MoiPr(\eta^3\text{-}C_3H_5)_3]$ **3**, which decomposes in solution above ca. −10 °C. The ^{1}H-NMR spectra at various temperatures indicate that **3** contains an alkyl group having an agostic hydrogen atom (Fig. 1):[3] at −120 °C the three H atoms of one of the methyl groups are magnetically inequivalent with the agostic H atom absorbing at $\delta = -8.43$. At higher temperatures exchange of these protons occurs and at −50 °C only one signal is observed ($\delta = -2.90$). The second methyl group is not involved in this process (the associated doublet is sharp at all temperatures). Furthermore, there is no evidence for transfer of the agostic H atom to the metal—at least within the temperature range studied (−30 °C to −120 °C).

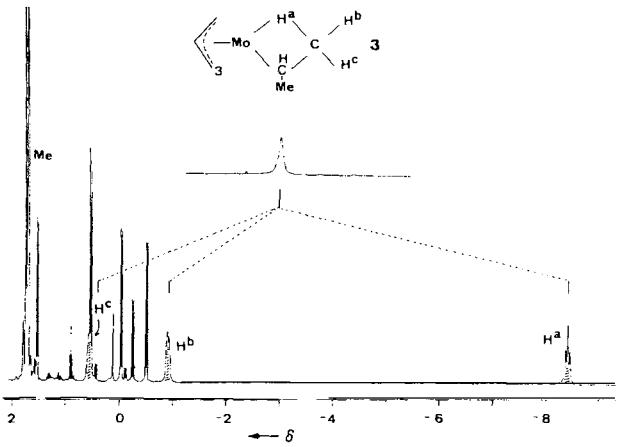


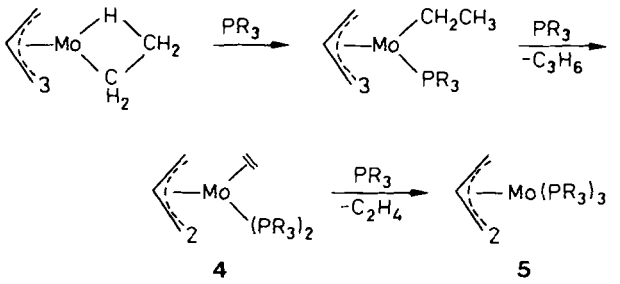
Fig. 1. Part of the ^{1}H-NMR spectrum of **3** (400 MHz, [D$_8$]toluene) at −120 °C (below) and −50 °C (above).

[*] Dr. P. W. Jolly, Priv.-Doz. Dr. R. Benn, S. Holle, Dr. R. Mynott, Prof. Dr. C. C. Romão [+]
Max-Planck-Institut für Kohlenforschung
Postfach 10 13 53, D-4330 Mülheim a. d. Ruhr (FRG)
[+] Present address: Instituto Superior Técnico
Lissabon (Portugal)

[**] *C. C. R.* thanks the Alexander von Humboldt Stiftung for a stipendium.

The effect of the agostic interaction is also observed in the ^{13}C-NMR spectrum of **3**: as expected, two signals are observed for the diastereotopic isopropyl methyl groups, but one of them experiences an unusually large upfield shift relative to the other ($\delta = 7.3$ and 27.5). The ^{13}C chemical shifts are not temperature dependent (down to $-115\,^{\circ}C$), but, whereas at $-60\,^{\circ}C$ in the proton-coupled spectrum a quartet is observed for the high-field group, ($^1J_{C,H} = 122$ Hz), at $-115\,^{\circ}C$ this becomes a triplet of doublets ($^1J_{C,H} = 138$ Hz (t), $^1J_{C,H} = 88$ Hz (d)).

We have prepared a series of related [MoR(η^3-C_3H_5)$_3$] complexes where R = Et, *n*Pr, *i*Pr, *n*Bu, *t*Bu, *cyclo*-C_6H_{11}, $(CH_2)_2CH{=}CH_2$, and $(CH_2)_3CH{=}CH_2$. In all cases the agostic interaction β-C-H → Mo is observed. In the absence of β-H atoms, either no reaction is observed (e.g., **1**/Me_3CCH_2MgCl) or a binuclear complex is formed (e.g., **1**/MeMgI or **1**/MeLi), while the reaction of **1** with 2-methylallylmagnesium chloride leads to the formation of [Mo(η^3-2-MeC_3H_4)(η^3-C_3H_5)$_3$].



R = CH_3, OCH_3

Scheme 1.

Treatment of the ethylmolybdenum complex with trimethylphosphane or trimethylphosphite leads to the cleavage of the agostic bond to give [(η^3-C_3H_5)$_3$Mo(L)Et], which reacts with a second ligand molecule to give the η^2-ethylenemolybdenum complex **4**,[5] as the result of what is presumably an intramolecular transfer of a β-H atom to an η^3-allyl group. The ethylene molecule can be displaced by a third ligand molecule to give **5**, which we previously prepared by reacting **1** with lithium in the presence of excess ligand.[2]

Experimental Procedure

3: **1** (3.2 g, 12.58 mmol) was dissolved in ether (50 mL) and *i*PrMgCl (12.58 mmol in ether) was added slowly at $-78\,^{\circ}C$. After the initially pink suspension had turned yellow, it was filtered to give a bright yellow solution, which was evaporated to dryness at $-78\,^{\circ}C$. Yield: 2.1 g (65%); correct elemental analysis. ^1H-NMR ([D$_8$]tetrahydrofuran (THF), $-60\,^{\circ}C$): allyl group 1: $\delta = 3.91$ (*meso*), 3.38 (*syn*, $^3J = 7.7$ Hz), 1.75 (*syn*, $^3J = 7.7$), 2.36 (*anti*, $^3J = 12.6$), -0.49 (*anti*, $^3J = 11.0$); allyl group 2: $\delta = 3.82$ (*meso*), 2.43 (*syn*, $^3J = 8.2$), 1.53 (*syn*, $^3J = 8.4$), 3.42 (*anti*, $^3J = 12.9$), -0.02 (*anti*, $^3J = 10.5$); allyl group 3: $\delta = 3.34$ (*meso*), 2.84 (*syn*, $^3J = 8.2$), 3.28 (*syn*, $^3J = 7.5$), 0.57 (*anti*, $^3J = 11.4$), 2.68 (*anti*, $^3J = 10.7$); isopropyl group $-120\,^{\circ}C$; $\delta = 2.49$ (C_α-H, ^3J(H,Me) = 6.6), 1.72 (Me), 0.54 (C_β-H^b), -0.93 (C_β-H^c), -8.43 (Mo-H^a); $^2J(H^a,H^b) = 8.0$, $^2J(H^a,H^c) = 8.4$.

Received: January 22, 1986;
supplemented: March 6, 1986 [Z 1632 IE]
German version: *Angew. Chem. 98* (1986) 555

CAS Registry numbers:
1, 89922-74-7; **2**, 101981-43-5; **4**, 101981-44-6; *i*PrMgCl, 1068-55-9; [MoEt(η^3-C_3H_5)$_3$].

[1] P. W. Jolly, C. Krüger, C. C. Romão, M. J. Romão, *Organometallics 3* (1984) 939.

[2] R. Benn, S. Holle, P. W. Jolly, C. Krüger, C. C. Romão, M. J. Romão, A. Rufińska, G. Schroth, *Polyhedron 5* (1986) 461.

[3] The term *agostic* has been introduced [4] to describe the various degrees of interaction between a carbon-bonded H atom and a transition-metal atom (C-H → M).

[4] M. Brookhart, M. L. H. Green, *J. Organometal. Chem. 250* (1983) 395; for further examples see G. F. Schmidt, M. Brookhart, *J. Am. Chem. Soc. 107* (1985) 1443 and references cited therein.

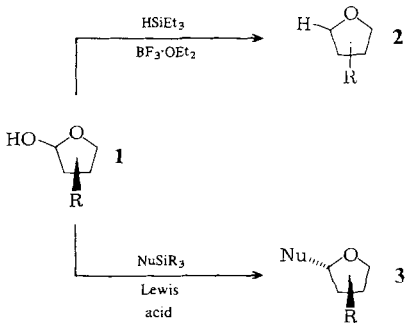
[5] **4**, R = Me: ^1H-NMR (400 MHz, [D$_8$]THF, $-80\,^{\circ}C$): $\delta = 4.37$ (m, *meso*-H), 1.89 (br. s, *syn*-H), 1.23 (m, $=CH_2$), 1.10 (t, Me), 0.94 (m, *anti*-H), 0.76 (m, *anti*-H), 0.54 (d, $=CH_2$), 0.38 (m, *syn*-H). ^{31}P-NMR (32.4 MHz, [D$_6$]acetone, $-30\,^{\circ}C$): $\delta = 12.1$.

Diastereoselective Synthesis of Functionalized Tetrahydrofuran Derivatives from γ-Lactols**

By *Christiane Brückner, Hiltrud Lorey,* and *Hans-Ulrich Reissig**

Dedicated to Professor Siegfried Hünig on the occasion of his 65th birthday

Cyclic hemiacetals of type **1** (γ-lactols) can be smoothly reduced to the cyclic ethers **2** with triethylsilane/$BF_3 \cdot OEt_2$,[1] a method that we employed in the synthesis of methyl 3-tetrahydrofurancarboxylates.[2] Other silylated nucleophiles, such as allyltrimethylsilane **4**, cyanotrimethylsilane **5**, or silyl enol ethers, were only used in special cases for the direct reaction of hemiacetals according to **1** → **3**.[3]

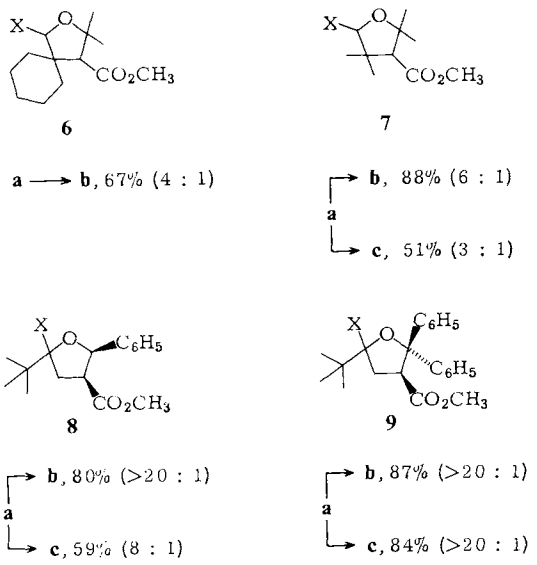


The large number of recent reports in which the substitution of RO and RS groups as well as halogens on anomeric C atoms—especially of sugar derivatives—was described is evidence of the large interest in this type of reaction.[4] We show now that the free OH group can also be substituted effectively and sometimes with high diastereoselectivity.

When the readily available γ-lactols **6a**–**9a**[2,5] are allowed to react with allyltrimethylsilane **4** or cyanotrimethylsilane **5** in the presence of $BF_3 \cdot OEt_2$ (dichloromethane, $-78 \rightarrow 20\,^{\circ}C$), the 5-allyl- or 5-cyano-substituted meth-

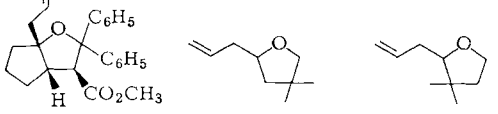
[*] Priv.-Doz. Dr. H.-U. Reissig, Dipl.-Chem. C. Brückner, H. Lorey
Institut für Organische Chemie der Universität
Am Hubland, D-8700 Würzburg (FRG)

[**] This work was supported by the Deutsche Forschungsgemeinschaft, the Fonds der Chemischen Industrie, and the Universitätsbund Würzburg. *H.-U. R.* thanks the Karl-Winnacker Stiftung (Hoechst AG) for a fellowship.



Scheme 1. Synthesis of methyl 5-allyl-3-tetrahydrofurancarboxylates **6b–9b** ($X=CH_2-CH=CH_2$) and methyl 5-cyano-3-tetrahydrofurancarboxylates **7c–9c** ($X=C\equiv N$) from the γ-lactols **6a–9a** (X = OH) and allyltrimethylsilane **4** or cyanotrimethylsilane **5**, respectively, in the presence of $BF_3\cdot OEt_2$ as promoter. The *trans* : *cis* ratios of the products are given after the yields in parentheses.

yl 3-tetrahydrofurancarboxylates **6b–9b** and **7c–9c**, respectively, are isolated in good yields (Scheme 1).[6] Because boron trifluoride etherate has been successfully used until now, the effect of other Lewis acids on yields and on the stereochemical course of the substitution has not yet been investigated. The reaction of **7a** and **9a** with silyl enol ethers or with trimethylvinylsilane was unsuccessful even in the presence of $TiCl_4$. That both bicyclic compounds and simple tetrahydrofuran derivatives can be synthesized is demonstrated by the preparation of the allylated products **10–12**[6] (yields in parentheses), which were obtained analogously from the corresponding γ-lactols with allyltrimethylsilane **4**/$BF_3\cdot OEt_2$.



10 (85%) **11** (57%) **12** (40%)

The substitution might take place via oxonium ions, which are formed upon treatment of the γ-lactols with Lewis acids. Preferential attack of the nucleophile from the more accessible side would then lead to the observed products. Because the structural assignments of **6b**, **7b**, **7c**, and **8c** appear to be well established on the basis of the spectroscopic data,[7] we assume that the other main products in Scheme 1 also have the *trans* configuration. In the case of **7** and **8**, cyanotrimethylsilane **5** is less selective than allyltrimethylsilane **4** (even switching from **5** to *tert*-butyl(cyano)dimethylsilane does not change the *trans* : *cis* ratio in the case of **7c**).

Because γ-lactols are readily accessible[8] and allyl or cyano groups are easy to modify, the synthetic method described here should allow access to a variety of tetrahydrofuran derivatives.[9]

General Experimental Procedure

The γ-lactol was dissolved in dry dichloromethane (5 mL per mmol of γ-lactol) and treated first with 2 equivalents of **4** or **5** (1.1 equivalents are sufficient for **6** and **7**) under N_2 at −78 °C and then with 2 equivalents of $BF_3\cdot OEt_2$. The stirred reaction mixture was allowed to warm over ca. 16 h to room temperature. After aqueous workup, drying ($MgSO_4$), concentration, and distillation or chromatography, the substitution products shown in Scheme 1 as well as **10–12** were obtained.

Received: January 23, 1986;
revised: March 3, 1986 [Z 1635 IE]
German version: *Angew. Chem. 98* (1986) 559

[1] a) G. A. Kraus, K. A. Frazier, B. D. Roth, M. J. Taschner, K. Neuenschwander, *J. Org. Chem. 46* (1981) 2417; b) review: D. N. Kursanov, Z. N. Parnes, M. M. Loim, *Synthesis 1974*, 633.
[2] C. Brückner, H.-U. Reissig, *J. Chem. Soc. Chem. Commun. 1985*, 1512.
[3] To the best of our knowledge, only a few sugar derivatives have been tested: a) M. D. Lewis, J. K. Cha, Y. Kishi, *J. Am. Chem. Soc. 104* (1982) 4976; b) F. D. DeLasHeras, A. SanFelix, P. Fernàndez-Resa, *Tetrahedron 39* (1983) 1620; c) J. Farkas, I. Fric, *Collect. Czech. Chem. Commun. 50* (1985) 1291.
[4] a) Allylsilane: A. Giannis, K. Sandhoff, *Tetrahedron Lett. 26* (1985) 1479; A. P. Kozikowski, A. K. Ghosh, *J. Org. Chem. 50* (1985) 3217, and references cited therein; b) silyl enol ethers: A. Hosomi, Y. Sakata, H. Sakurai, *Chem. Lett. 1983*, 405; M. T. Reetz, H. Müller-Starke, *Liebigs Ann. Chem. 1983*, 1726, and references cited therein; c) various silylated nucleophiles: M. G. Hoffmann, R. R. Schmidt, *Liebigs Ann. Chem. 1985*, 2403, and references cited therein; d) new developments in the nucleophilic addition to acetals: R. Imwinkelried, D. Seebach, *Angew. Chem. 97* (1985) 781; *Angew. Chem. Int. Ed. Engl. 24* (1985) 765, and references cited therein.
[5] H.-U. Reissig, *Tetrahedron Lett. 22* (1981) 2981, and unpublished results.
[6] All new compounds isolated gave satisfactory elemental analyses and appropriate spectra.
[7] Characteristic is, for example, the low-field shift of the ^{1}H-NMR signals of 3-H and 5-H by 0.11 and 0.73, respectively, on going from *cis*- to *trans*-**7c**. This assignment is supported by the ^{13}C-NMR spectrum ($CDCl_3$, 22.6 MHz): *trans*-**7c**: δ = 169.7 (s, C=O), 117.4 (s, C≡N), 84.6 (s, C-2), 75.9 (d, C-5), 60.8 (d, C-3), 51.5 (q, OCH_3), 46.4 (s, C-4), 30.8, 25.7, 24.7, 21.7 (4q, $4CH_3$); *cis*-**7c**: δ = 169.3 (s, C=O), 117.4 (s, C≡N), 83.5 (s, C-2), 75.1 (d, C-5), 61.9 (d, C-3), 51.5 (q, OCH_3), 46.3 (s, C-4), 29.5, 25.5, 25.3, 19.3 (4q, $4CH_3$). Similar arguments hold also for **6b**, **7b**, and **8c**.
[8] γ-Lactols are most easily prepared by addition of nucleophiles (e.g., hydride from diisobutylaluminum hydride) to γ-lactones.
[9] Tetrahydrofuran substructures are found in many antibiotic natural products of the polyether type: R. E. Ireland, D. Häbich, *Chem. Ber. 114* (1981) 1418, and references cited therein.

Complex-Induced Fragmentation of As_4S_4: Stabilization of an As_2S_3 Ligand

By *Henri Brunner, Heike Kauermann, Bernd Nuber, Joachim Wachter,** and *Manfred L. Ziegler*

The system arsenic/sulfur provides a treasure chest of new ligands for transition-metal complexes. As_2S_3 and As_4S_4 have been employed to obtain compounds with AsS_3,[1] AsS,[2] and As_2S[3] ligands. However, cage molecules as ligands were lacking, even though they are known in the phosphorus/sulfur system (P_4S_3[4]). During a search for complexes with AsS cage molecules as ligands, we allowed **1**, **4**, and **7** to react with As_4S_4. Of the products **2**, **3**, **5**, **6**, and **8**, complex **8** contains an As_2S_3 ligand, the largest fragment of the As_4S_4 cage reported so far.

The complexes **2** (green) and **3** (red-violet) can be prepared by reaction of As_4S_4 with $[(C_5Me_5)_2Fe_2(CO)_4]$ **1** in

[*] Dr. J. Wachter, Prof. Dr. H. Brunner, Dr. H. Kauermann
Institut für Anorganische Chemie der Universität
Universitätsstrasse 31, D-8400 Regensburg (FRG)
Prof. Dr. M. L. Ziegler, Dr. B. Nuber
Institut für Anorganische Chemie der Universität
Im Neuenheimer Feld 270, D-6900 Heidelberg (FRG)

boiling toluene. On the other hand, $[(C_5Me_5)_2Co_2(CO)_2]$ (*Co=Co*) **4** reacts with As_4S_4 in toluene (80 °C) to form the carbonyl-containing complex **5** and the black-brown cluster **6**.

$$[(C_5Me_5)_2Fe_2(CO)_4] + As_4S_4 \xrightarrow[115\,°C]{\text{toluene}} [(C_5Me_5)_2Fe_2As_2S_2] + [(C_5Me_5)_2Fe_2As_2S_3]$$

1 → **2** + **3**

$$[(C_5Me_5)_2Co_2(CO)_2] + As_4S_4 \xrightarrow[80\,°C]{\text{toluene}} [(C_5Me_5)_2(CO)Co_2As_2S_2] + [(C_5Me_5)_3Co_3As_2S_4]$$

4 → **5** + **6**

$$[C_5Me_5Co(CO)_2] + As_4S_4 \xrightarrow[h\nu]{\text{THF}} [(C_5Me_5)_2Co_2As_2S_3]$$

7 → **8**

The photochemical reaction of **1** and **7** with As_4S_4 in tetrahydrofuran (THF) gives **3** and the violet-brown complex **8**, respectively.[5] The compositions of the diamagnetic complexes **2**, **3**, **5**, **6**, and **8** were established by field-desorption mass spectroscopy and, for **2**, **6**, and **8**, by complete elemental analysis. The reaction of $[(C_5Me_5)_2W_2(CO)_4]$ (*W≡W*) with As_4S_4, on the other hand, affords solely the already known, exclusively sulfur-containing complexes $[(C_5Me_5)_2W_2(\mu\text{-}S_2)S_2]$ and $[(C_5Me_5)_2W_2(\mu\text{-}S)_2S_2]$.[6] Common to **2**, **3**, and **5** is a side-on bonded As_2 ligand as four-electron donor,[7] which, along with the sulfur ligands required for electron balance, appears to be better suited than mixed AsS ligands for the stabilization of lower metal oxidation states.

An X-ray structure analysis of **8**[8] revealed that in this complex a novel As_2S_3 ligand is present as a 4e donor with two *cis*-arranged η^2-bonded AsS units that are bridged by an S atom. This results in a "basket" with a C_2 axis through S(2) and the midpoint of the Co_2S_2 square. The structure differs from the sulfur-arsenic chains of the As_2S_3 layer lattice primarily in the all-*cis* geometry that is forced upon the molecule by the two C_5Me_5Co units. Comparison of the bond lengths for both kinds of As–S bonds reveals a surprisingly narrow range of variation of As–S distances. The mean value (2.231 Å) corresponds to that (2.237 Å) of the μ_2,η^2-AsS ligand in $[(C_5Me_5)_2Mo_2AsS_3Co(CO)_2]$[2] and is comparable to those in realgar (As_4S_4) and orpiment (As_2S_3).[9] The bond angles at S and As, although slightly expanded, more resemble those in As_2S_3 than in As_4S_4.

The results presented here underline the importance of As_4S_4 as a starting material for new As–S ligands, but also show the difficulties in controlling the complex-induced cage fragmentation, which appears to depend crucially on the transition-type complex used.

Received: January 24, 1986 [Z 1636 IE]
German version: *Angew. Chem. 98* (1986) 551

CAS Registry numbers:
1, 35344-11-7; **3**, 102284-25-3; **4**, 6965752-9; **7**, 12129-77-0; **8**, 102284-26-4; As_4S_4, 12279-90-2.

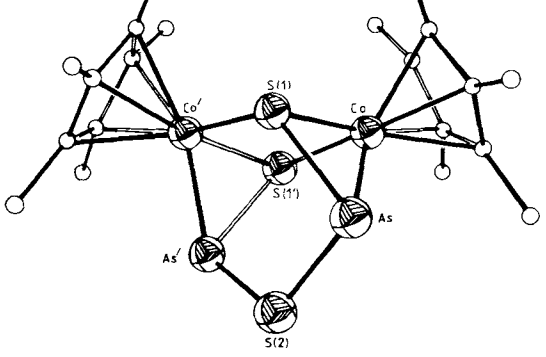


Fig. 1. ORTEP plot of the crystal structure of **8**. Selected bond lengths [Å] and bond angles [°]: Co-S1 2.224(4), Co-As 2.324(3), Co'-S1 2.267(4), As-S1 2.237(4), As-S2 2.226(2); As-Co-S1 58.3(1), S1-Co-S1' 86.3(2), Co-S1'-As' 112.4(1), As-S2-As' 104.8(1), S1-As-S2 103.3(2).

[1] G. A. Zank, T. B. Rauchfuss, S. R. Wilson, A. L. Rheingold, *J. Am. Chem. Soc. 106* (1984) 7621.
[2] H. Brunner, H. Kauermann, U. Klement, J. Wachter, T. Zahn, M. L. Ziegler, *Angew. Chem. 97* (1985) 122; *Angew. Chem. Int. Ed. Engl. 24* (1985) 132.
[3] I. Bernal, H. Brunner, W. Meier, H. Pfisterer, J. Wachter, M. L. Ziegler, *Angew. Chem. 96* (1984) 428; *Angew. Chem. Int. Ed. Engl. 23* (1984) 438; M. di Vaira, F. Mani, S. Moneti, M. Perruzini, L. Sacconi, P. Stoppioni, *Inorg. Chem. 24* (1985) 2230.
[4] R. Jefferson, H. F. Klein, J. F. Nixon, *Chem. Commun. 1969*, 536; A. W. Cordes, R. D. Joyner, R. D. Shores, E. D. Dill, *Inorg. Chem. 13* (1974) 132; M. di Vaira, M. Perruzini, P. Stoppioni, *ibid. 22* (1983) 2196.
[5] **8**: $[C_5Me_5Co(CO)_2]$ 7 (530 mg, 2.12 mmol) and As_4S_4 (907 mg, 2.12 mmol) in 230 mL of THF were irradiated for 19 h in an immersion lamp apparatus (125-W Hg lamp). The solvent was removed and the dark brown crude product was dissolved in 15 mL of CH_2Cl_2 and chromatographed on SiO_2 (column: 40 cm × 3 cm). **8** was eluted with toluene as a dark brown band. Re-purification on SiO_2 (column: 10 cm × 1.5 cm; eluent: toluene/petroleum ether 1:1) afforded 16% of **8**, which was recrystallized from toluene/pentane (5:1).—^{1}H-NMR ($CDCl_3$): $\delta(CH_3) = 1.70$. MS (70 eV): $M^{\oplus}$ (42%), $[M-AsS]^{\oplus}$ (100).—Complexes **2**, **3**, **5**, 6 were prepared analogously [10].
[6] H. Brunner, W. Meier, J. Wachter, E. Guggolz, T. Zahn, M. L. Ziegler, *Organometallics 1* (1982) 1107.
[7] G. Huttner, B. Sigwarth, O. Scheidsteger, L. Zsolnai, O. Orama, *Organometallics 3* (1985) 326.
[8] The structure was determined with a SIEMENS-STOE AED2 diffractometer ($Mo_{K\alpha}$), $2.5 \leq 2\theta \leq 60°$, MULTAN (As, Co) and Fourier methods. $P4_12_12$ (D_4^4), $a = 8.996(5)$, $c = 29.92(1)$ Å, $V = 2421.4$ Å^3, $Z = 4$ (dimer); 1072 reflections, 1055 reflections with $I > 3.0\sigma(I)$; anisotropic refinement, $R_w = 0.05$. Further details of the crystal structure investigation may be obtained from the Fachinformationszentrum Energie, Physik, Mathematik GmbH, D-7514 Eggenstein-Leopoldshafen 2 (FRG), on quoting the depository number CSD 51759, the names of the authors, and the journal citation.
[9] D. J. E. Mullen, W. Nowacki, *Z. Kristallogr. Kristallgeom. Kristallphys. Kristallchem. 136* (1972) 48, and references cited therein.
[10] H. Kauermann, *Dissertation*, Universität Regensburg 1985.

Heterogeneous Catalysis of Ammonia Synthesis at Room Temperature and Atmospheric Pressure

By *Ken-ichi Aika**

The artificial fixation of nitrogen at ambient temperature and under atmospheric pressure is one of the most important goals of chemical technology. The first step toward this goal has been achieved: for example, a large number of organometallic dinitrogen complexes have been prepared,[1] and the dissociative adsorption of N_2 occurs easily on a clean single-crystal surface of Mo[2] or Fe[3] at about room temperature. However, the catalytic synthesis of ammonia from N_2 and H_2 has not been achieved at am-

[*] Prof. Dr. K. Aika
Research Laboratory of Resources Utilization
Tokyo Institute of Technology
4259 Nagatsuta, Midori-ku, Yokohama 227 (Japan)

bient temperature and under atmospheric pressure. The solid catalyst described herein—potassium-containing ruthenium on active carbon—produces ammonia from N_2 and H_2 at room temperature under atmospheric pressure; however, its activity is much lower than that of nitrogenases.

Recently, several heterogeneous solids[4,5] and clean metal surfaces[6,7] have been reported to be efficient catalysts for the synthesis of ammonia. One of the most active catalysts,[4,5] ruthenium (4.5 wt-%) on active carbon with 32 wt-% metallic potassium (Ru-K/C), contains Ru particles with diameters of ca. 10 nm. In order to check the reproducibility of the catalytic activity, the ammonia synthesis was carried out with 1 g of Ru-K/C (2.5 cm^3) in a conventional glass circulation reactor for one week at 190 to 233 °C under a pressure of 600 torr (molar ratio $N_2:H_2=1:3$). The products were collected in a liquid nitrogen trap. For an estimated flow rate of 5.3 $dm^3\ h^{-1}$, the rate of NH_3 production at 190 °C was 3.4 $cm^3\ h^{-1}$ (g-catalyst)$^{-1}$ (gas analysis under standard conditions). The apparent activation energy was 22 to 23 kcal mol^{-1}, which agrees with the value reported earlier above 200 °C.[4,5] The reaction also occurs at 31 °C under atmospheric pressure (760 torr). The time course of the decrease in gas volume (measured with a gas burette) is shown in Figure 1. A constant rate of decrease was observed, although there was some fluctuation

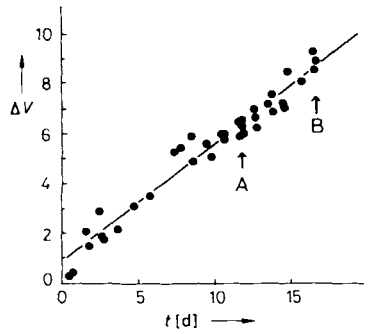


Fig. 1. Time course of the decrease of the volume ΔV [cm^3(g-catalyst)$^{-1}$] of the N_2/H_2 mixture (molar ratio 1:3) during reaction over the Ru-K/C catalyst at 31 °C under atmospheric pressure. The trapped product was identified to be ammonia.

owing to variations in the room temperature. At times A and B, the trapped gas was released and identified to be ammonia by mass spectrometry. The amount of ammonia produced between A and B (116 h) was 0.92 cm^3, which roughly corresponds to consumption of half of the N_2/H_2 mixture initially present (2.3 cm^3). The observed reaction rate, 0.23 $cm^3\ NH_3\ d^{-1}$ (g-catalyst)$^{-1}$, corresponds to 0.011 mmol $NH_3\ d^{-1}$ (g-catalyst)$^{-1}$ or 0.010 $cm^3\ NH_3\ h^{-1}$ (g-catalyst)$^{-1}$. The rate at 31 °C, calculated from the kinetic data above 190 °C, is approximately 1×10^{-5} $cm^3\ NH_3\ h^{-1}$ (g-catalyst)$^{-1}$, which was 10^3 times less than the observed result. Thus the reaction mechanism at ambient temperature might be different from that at higher temperatures, where the cleavage of the N–N bond is the rate-determining step. Nitrogenases have much higher activities: for example, the nitrogenase from *Klebsiella pneumoniae* has an activity of 0.25 mmol min^{-1} (g-protein)$^{-1}$,[8] which is 10^5 times higher than that of Ru-K/C. However, the results presented here demonstrate that a solid heterogeneous catalyst can also produce ammonia from H_2 and N_2 at room temperature under atmospheric pressure.

Received: January 31, 1986 [Z 1648 IE]
German version: *Angew. Chem. 98* (1986) 556

CAS Registry numbers:
K, 7440-09-7; Ru, 7440-18-8; C, 7440-44-0; N_2, 7727-37-9; H_2, 1333-74-0; NH_3, 7664-41-7.

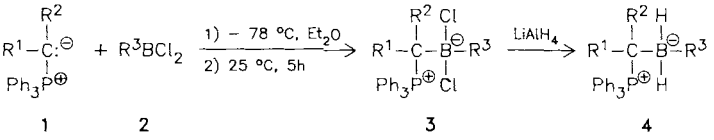
[1] M. M. Taqui Khan, A. E. Martell: *Homogeneous Catalysis by Metal Complexes*, Academic Press, New York 1974.
[2] F. C. Tompkins: *Chemisorption of Gases on Metals*, Academic Press, New York 1978.
[3] G. Ertl, S. B. Lee, M. Weiss, *Surf. Sci. 114* (1982) 515, 527.
[4] K. Aika, H. Hori, A. Ozaki, *J. Catal. 27* (1972) 424.
[5] K. Aika, A. Ohya, A. Ozaki, Y. Inoue, I. Yasumori, *J. Catal. 92* (1985) 305; A. Ohya, K. Aika, A. Ozaki, *J. Chem. Soc. Chem. Commun. 1984*, 321.
[6] N. D. Spencer, R. C. Schoonmaker, G. A. Somorjai, *J. Catal. 74* (1982) 129.
[7] N. D. Spencer, G. A. Somorjai, *J. Catal. 78* (1982) 142.
[8] R. R. Eady, B. E. Smith in R. W. F. Hardy, F. Bottomley, R. C. Burns (Eds.): *A Treatise on Dinitrogen Fixation, Sections 1 and 2*, Wiley, New York 1979, p. 466.

Reaction of Phosphonium Ylides with Alkyldichloroboranes**

By *Hans-Jürgen Bestmann** and *Thomas Arenz*

We recently reported on the reaction between phosphonium ylides **1**, $R^2=H$, and dialkylchloroboranes, which leads via transylidation to boron-substituted ylides and phosphonium salts such as **6**.[1] ^{31}P-NMR studies show that **3**, $R^2=H$, $^{\ominus}BClR^3_2$ instead of $^{\ominus}BCl_2R^3$, probably occurs as intermediate. It decomposes above 0 °C into the starting compounds and is not isolable.[2]

We have now examined the reaction of phosphonium ylides **1** with alkyldichloroboranes **2**. Compounds **1** and **2** react in the molar ratio 1:1 at −78 °C in ether to give the alkyltriphenylphosphonio-alkyldichloroborates **3** (for examples cf. Table 1). Unlike the chlorine-deficient analogues, these are stable at room temperature and are isolable under protective gas.



1 2 3 4

Table 1. Examples of alkyltriphenylphosphonioalkyldichloroborates **3** and -alkylborates **4**.

	R^1	R^2	R^3 [a]	Yield [%]	NMR (δ) ^{31}P [b]	^{11}B [c]	IR [cm^{-1}]	M.p. [°C] [d]
3a	H	H	*c*-C_6H_{11}	78	+26.5	+ 5.7		144–146
3b	CH_3	H	*c*-C_6H_{11}	86	+33.6	+10.1		170 (decomp.)
3c	CH_3	H	thexyl	71	+35.7	+10.1		75 (decomp.)
3d	CH_3	CH_3	*c*-C_6H_{11}	77	+40.8	+ 1.4		130
3e	H	H	thexyl	76	+27.9	− 8.4		[e]
4a	H	H	*c*-C_6H_{11}	73	+31.5	−19.8	2230	120
4b	CH_3	H	*c*-C_6H_{11}	75	+43.1	−15.0	2220	105–110

[a] *c*-C_6H_{11} = cyclohexyl, thexyl = $-(CH_3)_2C-C(CH_3)_2H$. [b] In $CDCl_3$, H_3PO_4 as external standard. [c] In $CDCl_3$, $BF_3\cdot OEt_2$ as external standard. [d] Under N_2 in sealed tube. [e] Still contains impurities.

The ate-onium complexes[3] **3** are crystalline compounds, some of which melt sharply, while others melt with decomposition. The ^{1}H-, ^{11}B-, ^{13}C-, and ^{31}P-NMR

[*] Prof. Dr. H. J. Bestmann, Dr. T. Arenz
Institut für Organische Chemie der Universität Erlangen-Nürnberg
Henkestrasse 42, D-8520 Erlangen (FRG)

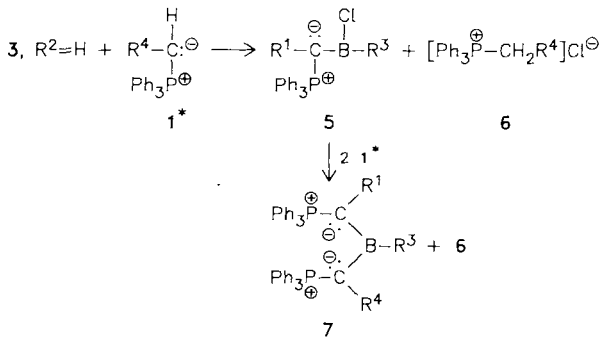
[**] This work was supported by the Deutsche Forschungsgemeinschaft.

 © VCH Verlagsgesellschaft mbH, D-6940 Weinheim, 1986 0570-0833/86/0606-0559 $ 02.50/0

spectra as well as the mass spectra of complexes **3** were consistent with what was expected for such compounds. With $LiAlH_4$ in slight excess,[4] the compounds **3** are reduced to the monoalkylborane-alkylidenetriphenylphosphorane adducts **4**[5] (for examples cf. Table 1).

We now allowed the adducts **3**, $R^2=H$, which were formed from **1**, $R^2=H$, and **2**, to react with one equivalent of **1***, $R^2=H$ (**1** and **1*** contain the substituents R^1 and R^4, respectively; $R^1 \neq R^4$). Transylidation to **5** and **6** occurred. Attempts to remove HCl from **5**, $R^1=H$, with bases, in order to obtain ylides with P=C=B-partial structure (cf. [6]), met without success. **5** is again transylidated with **1*** as base (molar ratio 1:2), and affords **7** and **6**. The boron-containing bisylides **7**, $R^1 \neq R^4$, obtained in this way (A) could be interesting complex ligands. Reaction of **1**, $R^2=H$, with **2** (molar ratio 4:1), leads via route (B) directly to **7**, $R^1=R^4$, and **6** (for examples cf. Table 2). The compounds **7** are sensitive toward atmospheric oxygen and moisture.

(A) 1, R^2=H + 2 ⟶ 3, R^2=H



(B) 4x1, R^2=H + 2 ⟶ 7, $R^1=R^4$ + 2x6

Table 2. Borandiylbis(triphenylphosphonioalkanides) **7** and triphenylphosphonio-1-[chloro(2,2,6,6-tetramethylpiperidineboryl]alkanides **5**.

	R^1	R^3 [a]	R^4	Yield [%]	NMR (δ) ^{31}P [b]	^{11}B [c]	Route
7a	H	*c*-C_6H_{11}	H	94.4	+17.37	+52.25	A, B
7b	H	*c*-C_6H_{11}	CH_3	82.8			A
					+21.07, +15.62	+49.2	
7b	CH_3	*c*-C_6H_{11}	H	76.7			A
7c	H	thexyl	H	89.8	+15.92	+44.13	A, B
7d	H	TMP	H	79.8	+11.64, +16.0	+45.57	A
5e	CH_3	TMP	—	90	+28.6	+40.9	
5f	C_2H_5	TMP	—	85	+27.6	+40.9	

[a] TMP=2,2,6,6-tetramethylpiperidino. [b] In C_6D_6, H_3PO_4 as external standard. [c] In C_6D_6, $BF_3 \cdot EtO_2$ as external standard.

The ^{1}H-, ^{11}B-, ^{13}C-, and ^{31}P-NMR and mass spectra as well as the elemental analyses were once again consistent with our expectations.[1] The intermediate **5**, which is sensitive to atmospheric oxygen and moisture, is isolable by reaction of **1**, $R^1 \neq H$, $R^2=H$, with dichloro (2,2,6,6-tetramethylpiperidino)borane **2**, R^3=TMP, in the molar ratio 2:1 (cf. Table 2). A transylidation with further **1** to give **7** is not observed in this case.

Experimental

7, $R^1=R^4$, route (B): A solution of **1**, $R^2=H$, (4 mmol) in ca. 100 mL of benzene was treated with 1 mmol of **2** and the resulting mixture stirred for 12 h at room temperature. After removal of the phosphonium salt **6** by vacuum filtration, the red filtrate was evaporated down to ca. one quarter of its original volume and then slowly covered with hexane (ca. 50 mL) and allowed to stand for about 12 h. The crystals of the bisylide **7** were filtered off and dried by suction (oil-pump vacuum) for 10 h at room temperature.

Received: February 3, 1986 [Z 1650 IE]
German version: *Angew. Chem. 98* (1986) 571

CAS Registry numbers:
1 ($R^1=R^2=H$), 3487-44-3; **1** ($R^1=CH_3$, $R^2=H$), 1754-88-7; **1** ($R^1=R^2=CH_3$), 16666-80-1; **2** (R=*c*-$C6H_{11}$), 39105-81-2; **2** (R=thexyl), 79200-82-1; **3a**, 102150-45-8; **3b**, 102150-46-9; **3c**, 102150-47-0; **3d**, 102150-48-1; **3e**, 102150-49-2; **3** ($R^1=R^2=H$, R^3=TMP), 102150-52-7; **4a**, 102150-50-5; **4b**, 102150-51-6; **5e** (phosphorane), 102150-33-4; **5e** (ylide), 102150-39-0; **5f** (phosphorane), 102-150-34-5; **5f** (ylide), 102150-40-3; **6** ($R^4=H$), 1031-15-8; **6** ($R^4=CH_3$), 896-33-3; **7a** (phosphorane), 102150-35-6; **7a** (ylide), 102150-41-4; **7b** (phosphorane), 102150-36-7; **7b** (ylide), 102150-42-5; **7c** (phosphorane), 102150-37-8; **7c** (ylide), 102150-43-6; **7d** (phosphorane), 102150-38-9; **7d** (ylide), 102150-44-7.

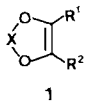
[1] H. J. Bestmann, T. Arenz, *Angew. Chem. 96* (1984) 363; *Angew. Chem. Int. Ed. Engl. 23* (1984) 381.
[2] H. J. Bestmann, T. Arenz, unpublished; T. Arenz, *Dissertation*, Universität Erlangen-Nürnberg 1985.
[3] Cf. also: R. Köster in *Houben-Weyl-Müller: Methoden der Organischen Chemie, 4. Aufl., Bd. XIII/3b*, Thieme, Stuttgart 1982, p. 702ff.
[4] For the reduction cf.: D. Seyferth, S. O. Grim, *J. Am. Chem. Soc. 83* (1961) 1613.
[5] a) M. F. Hawthorne, *J. Am. Chem. Soc. 83* (1961) 367; b) H. J. Bestmann, G. Günther, unpublished; G. Günther, *Dissertation*, Universität Erlangen-Nürnberg 1985.
[6] H. J. Bestmann, *Angew. Chem. 89* (1977) 361; *Angew. Chem. Int. Ed. Engl. 16* (1977) 349.

2-Substituted 1,3,2-Dioxaboroles as Synthetic Equivalents for the Glycolaldehyde Anion**

By *Günter Wulff** and *Achim Hansen*

Dedicated to Professor Leonhard Birkofer on the occasion of his 75th birthday

The glycolaldehyde anion $^{\ominus}$:CHOH-CHO plays an important role as a synthon since it can be exploited strategically through an Aldol reaction for the synthesis of α,β-dihydroxyaldehydes, in particular for carbohydrates.



1

1a, X=P(OMe)$_3$; **1b**, X=B–Ph; **1c**, X=Sn
R^1=alkyl, aryl
R^2=H, alkyl, aryl

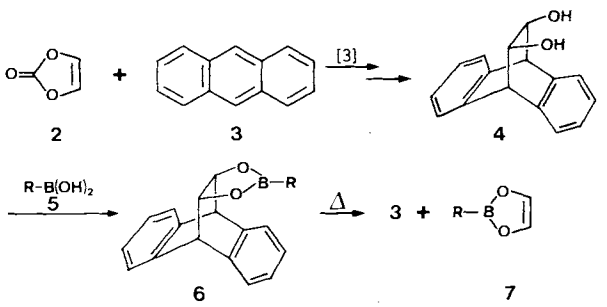
Cyclic enediolates **1**, $R^1=R^2=H$, should be suitable as synthetic equivalents. So far, only their 4- and 4,5-substituted derivatives have proven to be useful from a preparative point of view. *Ramirez*[1] was able to prepare α,β-dihydroxyketones by the reaction of 1,3,2-dioxaphospholes **1a** with aldehydes and ketones. *Mukaiyama* et al.[2] have similarly prepared α,β-dihydroxyketones by Aldol reactions of the boron- and tin-enediolates **1b** and **1c**.

We have been interested in the application of the previously unknown 1,3,2-dioxaboroles **7a–e**, having substi-

[*] Prof. Dr. G. Wulff, Dipl.-Chem. A. Hansen
Institut für Organische Chemie II der Universität
Universitätsstrasse 1, D-4000 Düsseldorf (FRG)

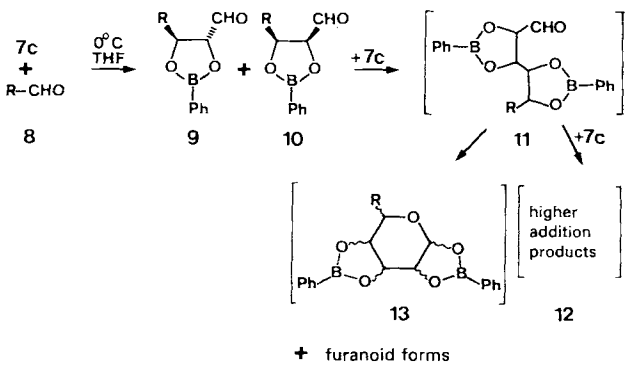
[**] This work was supported by the Deutsche Forschungsgemeinschaft and the Fonds der Chemischen Industrie.

tuents only in the 2-position, as building blocks for the synthesis of carbohydrates. We have now been able for the first time to synthesize these interesting compounds in excellent yields in the following manner: esters **6a–e** were synthesized by reaction of the boronic acids **5a–e** with the diol **4**, which was obtained from vinylene carbonate **2** and anthracene **3** by Diels-Alder reaction and subsequent hydrolysis.[3] These were sublimable at 160–220°C/10^{-2} mbar and could be converted almost quantitatively by thermolysis in the gas phase at 550°C/10^{-2} mbar into the analytically pure 1,3,2-dioxaboroles **7a–e**.[4] The total yields with respect to **2** were over 80%.



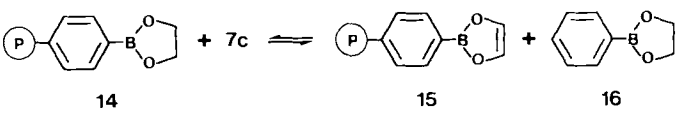
a, R = cyclohexyl; **b**, R = methoxy; **c**, R = phenyl; **d**, R = 2-methylphenyl; **e**, R = 2,6-dimethylphenyl

The addition of 2-phenyl-1,3,2-dioxaborole **7c** to the aldehydes **8f–k** proceeds in a manner similar to the addition of the 4- and 4,5-substituted dioxaboroles **1b**, as described by *Mukaiyama* et al.[2a] We obtained a diastereomeric mixture of **9f–k** and **10f–k** in the ratio 1:2 to 1:3.[5] Unlike the products obtained from **1b** and aldehydes, these products contain a keto group instead of an aldehyde group and therefore could undergo further reaction with **7c**. Thus, in reactions with **8f–k**, mixtures of pyranoid (and furanoid) isomers **13**, which were formed from **11** by ring closure, were isolable in yields of 8–40%, in addition to larger amounts of not yet fully characterized, high molecular weight addition products **12**.

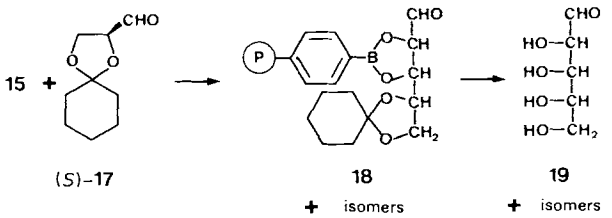


f, R = methyl; **g**, R = ethyl; **h**, R = isopropyl; **i**, R = *tert*-butyl; **j**, R = (*R*)-2,2-dimethyl-1,3-dioxolan-4-yl; **k**, R = phenyl. THF = tetrahydrofuran.

In order to restrict the reaction at a single addition to aldehydes, **7c** was immobilized on a cross-linked polymer; this strategy for site separation inhibits any further reaction of the primary addition products. Polymer bound **7c** (≡ **15**) could be obtained quite easily by triethylamine-catalyzed, rapid transesterification.



As a first example of the applications of **15** we describe here the synthesis of L- and D-ribose. 2,3-*O*-cyclohexylidene-L-glyceraldehyde (*S*)-**17** or the D-form (as 2,3-*O*-isopropylidene derivative (*R*)-**20**) was allowed to react with **15**[6] (CH_2Cl_2, room temperature, 12–36 h). The addition products could be isolated from the polymer using methanol/water. Removal of the protecting group (by ion exchanger) furnished the aldopentoses of the L- or the D-series in 70–95% yield with respect to the 1,3,2-dioxaborole units, or 75% with respect to (*S*)-**17** and (*R*)-**20**.



Product ratios:
L-Ribose : L-Lyxose : L-Arabinose : L-Xylose = 53.8 : 10.5 : 32.5 : 3.2
D-Ribose : D-Lyxose : D-Arabinose : D-Xylose = 56.0 : 6.6 : 35.2 : 2.2

Enantiomerically pure L-ribose was obtained by liquid chromatographic separation (LiChrosorb-NH_2, acetonitrile/water 85 : 15; $[\alpha]_D^{20} = +19.7$ ($c = 0.22$, H_2O)).[7] The nucleophilic attack of the enediolate **15** at the aldehyde group of **17** is controlled *ul*-selectively (1,2-induction ca. 9 : 1) by the diastereofacial influence of the isopropylidenedioxy- or the cyclohexylidenedioxy residue according to the Felkin-Anh model.[8] An enantiofacial control (1,3-induction) was seldom observed. The *threo-erythro* ratio at C-2 and C-3 was 1 : 2, similar to that found with achiral aldehydes.

The synthetic procedure described here enables the lengthening of sugar chains by two C atoms and thus offers a novel possibility for the synthesis of rare sugars.[9]

Received: February 3, 1986;
revised: March 19, 1986 [Z 1653 IE]
German version: *Angew. Chem. 98* (1986) 552

CAS Registry numbers:
4, 2732-95-8; **5a**, 4441-56-9; **5b**, 68498-84-0; **5c**, 98-80-6; **5d**, 16419-60-6; **5e**, 100379-00-8; **6a**, 102150-53-8; **6b**, 102150-54-9; **6c**, 102150-55-0; **6d**, 102150-56-1; **6e**, 102150-57-2; **7a**, 102150-58-3; **7b**, 102150-59-4; **7c**, 4406-78-4; **7d**, 102150-60-7; **7e**, 102-150-61-8; **8f**, 75-07-0; **8g**, 123-38-6; **8h**, 78-84-2; **8i**, 630-19-3; **8j**, 15186-48-8; **8k**, 100-52-7; **9f**, 102150-62-9; **9g**, 102150-63-0; **9h**, 102210-60-6; **9i**, 102210-61-7; **9j**, 102150-64-1; **9k**, 102150-65-2; **10f**, 102150-66-3; **10g**, 102150-67-4; **10h**, 102210-62-8; **10i**, 102210-63-9; **10j**, 102281-25-4; **10k**, 102150-68-5; **13f**, 102281-26-5; **13g**, 102150-71-0; **13h**, 102150-72-1; **13i**, 102150-73-2; **13j**, 102150-74-3; **13k**, 102150-75-4; **14**, 4406-72-8; *(S)-17*; 99744-77-1; *(R)-17*; 78008-36-3; **18**, 102150-69-6; **18** *isomer* 102150-70-9; **19**, 24259-59-4; **19** *isomer* 50-69-1.

[1] F. Ramirez, *Synthesis 1974*, 90.
[2] a) T. Mukaiyama, M. Yamaguchi, *Chem. Lett. 1982*, 509; b) J. Ichikawa, T. Mukaiyama, *ibid. 1985*, 1009, and references cited therein.
[3] Synthesis of **4**: T. L. Patton, US-Pat. 2857434 (1958); *Chem. Abstr. 53* (1959) 7127h; retro-Diels-Alder reaction of **4**-derivatives: N. D. Field, *J. Am. Chem. Soc. 83* (1961) 3504.
[4] **7a–e**: **6a–e** (2–20 g) were converted by sublimation (160–220°C/10^{-2} mbar) in a quartz thermolysis apparatus (U. L. Wiersum, *Recl. Trav.*

Chim. Pays Bas. 101 (1982) 317, S. 323, Fig. 1) into the vapor phase and thermolyzed at 550°C/10^{-2} mbar in a quartz tube. The anthracene **3** formed during thermolysis separated out in the cooler portion of the tube, while the 1,3,2-dioxaboroles **7a–e** were collected in a cold-trap. Yield 95%; consistent ^{1}H-NMR, ^{13}C-NMR, MS, and elemental analysis data. Representative ^{1}H-NMR and ^{13}C-NMR data of the vinylic protons and C atoms ($CDCl_3$/TMS): $\delta(^1H)/\delta(^{13}C)$: **7a**: 6.93/132.75; **7b**: 6.76/132.57; **7c**: 6.99/133.33; **7d**: 7.08/133.14; **7e**: 7.06/132.57.

[5] Ratio of amounts determined by ^{13}C-NMR spectroscopy. The yields obtained upon reaction of **7c** with acetaldehyde (**8f**) (molar ratio 1:2) are: 10% of **9f** + **10f**, 40% of **13**, 20% of the products by triple addition of **7c**, 30% of unidentified high molecular addition products. By using a large excess of **8f**, yields of up to 30% of **9f** + **10f** could be obtained.

[6] Copolymer **14**: Preparation by radical polymerization from styrene, 12% *m*-diisopropenylbenzene, 2.5% 2-(4-vinylphenyl)-1,3,2-dioxaborolane.

[7] L-Ribose: $[\alpha]_D$ + 18.8 (c = 1.5, H_2O); W. A. Van Ekenstein, J. J. Banksma, *Chem. Weekbl. 6* (1909) 373.

[8] a) M. Cherest, H. Felkin, N. Prudent, *Tetrahedron Lett. 1968*, 2199; b) N. T. Anh, *Top. Curr. Chem. 88* (1980) 145.

[9] When carried out in the D-series, the very elegant synthesis described by *Sharpless* and *Masamune* et al. (A. W. M. Leej, V. S. Martin, S. Masamune, K. B. Sharpless, F. J. Walker, *J. Am. Chem. Soc. 104* (1982) 3515), using 2,3-*O*-isopropylidene-(*R*)-glyceraldehyde as starting material gave the protected D-ribose derivative in a five-step reaction (42% yield).

N-Aryl-*O*-(diphenylphosphinoyl)hydroxylamines: Electrophilic Amination of Amines to Hydrazines; a Model Reaction for the Carcinogenicity of Aromatic Amines**

By *Gernot Boche,* Reinhard H. Sommerlade,* and *Ferdinand Bosold*

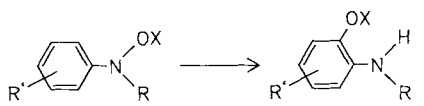
The carcinogenicity of aromatic amines Aryl-NH_2 is due to their reactive metabolites, the *N*-arylhydroxamate esters **1** and the *N*-arylhydroxylamine esters **2**, which react with nucleophilic centers in nucleic acids and peptides.[1,2]

Aryl–N($COCH_3$)–OX Aryl–NH–OX

1 **2**

X = $SO_3^{\ominus}$, $COCH_3$, $PO_3^{2\ominus}$

The rearrangement of the species **3a–d** to the *o*-aminophenol derivatives **4a–d**[3a,4,5,6a–c] is regarded as confirmation[3a] that the nitrenium (aminylium) ion Aryl–$\overset{\oplus}{N}$–R is the ultimate carcinogen.[1] Furthermore, it is known that, upon solvolysis of **3a**, R′ = *p*-CH_3, in methanol[3b] and of **3e**, R′ = *p*-CH_3 or *p*-OCH_3, in water,[6d,e] the nucleophiles attack the phenyl ring of **3**.[8]



3 **4**

3, 4	R	X	Ref.
a	$COCH_3$	SO_2CH_3	[3a]
b	H	SO_2R''	[4]
c	COC_6H_5	SO_2R''	[5]
d	$COCH_3$	$SO_3^{\ominus}$	[6a–c]
e	$COCH_3$	$COC(CH_3)_3$	[6d, e]

R′ = H, CH_3, CO_2CH_3, CF_3, CN, Cl, Br, OCH_3, NO_2

[*] Prof. Dr. G. Boche, Dipl.-Chem. R. H. Sommerlade, F. Bosold
Fachbereich Chemie der Universität
Hans-Meerwein-Strasse, D-3550 Marburg (FRG)

[**] This work was supported by the Fonds der Chemischen Industrie and the Deutsche Forschungsgemeinschaft.

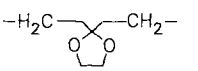
We report here on the reaction of the *N*-aryl-*O*-(diphenylphosphinoyl)hydroxylamines **5**[9] with the amines **6**. In contrast to **3a–e**, neither a rearrangement to the *o*-aminophenol derivatives nor a reaction of the nucleophile with the phenyl ring of **5** was observed. Instead, exclusive electrophilic amination to give the hydrazines **7** took place (Table 1).[10]



5 **7**

5a, R^1 = H; **5b**, R^1 = *p*–Cl; **5c**, R^1 = *m*–CN; **5d**, R^1 = *p*–CH_3

Table 1. Reaction of the *N*-aryl-*O*-(diphenylphosphinoyl)hydroxylamines **5a–d** with the amines **6** to give the hydrazines **7** [a].

No.	R^1	R^2	R^3	Yield [%]
1	H	*n*-C_4H_9	H	45 [b]
2	H	$CH_2C_6H_5$	H	46 [c]
3	H	$CH_2CO_2C_2H_5$	H	38
4	H	*c*-C_6H_{11}	H	25
5	H	$CH(CH_3)_2$	H	0
6	H	C_6H_4–$CO_2C_2H_5$-(*m*)	H	94
7	H	C_6H_4–$CO_2C_2H_5$-(*p*)	H	32
8	H	C_6H_4–CH_3-(*o*)	H	83
9	H	$C_5H_4FeC_5H_5$	H	54
10	*p*-Cl	C_6H_4–$CO_2C_2H_5$-(*m*)	H	97
11	*p*-Cl	C_6H_4–CH_3-(*o*)	H	93
12	*m*-CN	C_6H_5	H	94
13	*p*-CH_3	C_6H_5	H	40
14	H	CH_3	CH_3	80
15	H	C_6H_5	CH_3	56
16	H	*n*-C_4H_9	C_2H_5	85
17	H	H_2C–CH=CH_2	H_2C–CH=CH_2	69
18	H	H_2C–C≡CH	CH_3	80
19	H	–$CH_2CH_2OCH_2CH_2$–		48
20	H			85
21	H	$CH_2C_6H_5$	CH_3	58
22	H	–*rac*-$CH_2CH_2CH_2CH_2CH(CH_3)$–		60
23	H	–(*R*)-$CH_2CH_2CH_2CH(CH_3)$–		34
24	H	C_2H_5	C_2H_5	60
25	*p*-Cl	C_2H_5	C_2H_5	87
26	*m*-CN	C_2H_5	C_2H_5	62

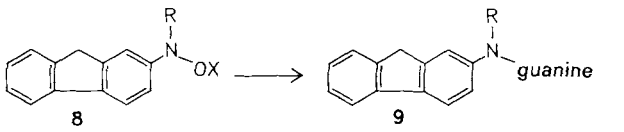
[a] The hydrazines **7** were characterized by ^{1}H-NMR spectroscopy—and, if they were new compounds—by elemental analysis and mass spectroscopy. [b] Isolated as the azo compound. [c] Isolated as *N*-benzylidene-*N*′-phenylhydrazine.

Notes to Table 1:

Reactions 1–5: Primary aliphatic amines **6** afford the hydrazines **7** in only moderate yields; branching at the α-C atom of **6** lowers the yields still further.

Reactions 6–13: Primary aromatic amines **6** give the hydrazines **7** (also called hydrazo compounds) usually in good yields. Since hydrazo compounds can be easily oxidized to azo compounds,[11] this provides a new route to symmetric and unsymmetric azo compounds.

Reactions 14–26: With secondary amines **6**, trisubstituted hydrazines **7** bearing virtually any substituents R^2 and R^3 are formed. In addition, deprotonation and subsequent alkylation can be used to introduce a fourth substituent R^4.[12] In this way, R^2, R^3, and R^4 can be introduced regioselectively without the use of protecting groups and *N*-nitroso compounds and without the formation of hydrazinium salts.



8 9

	R	X		R
8a	$COCH_3$	H	**9**	$COCH_3$, H
8b	$COCH_3$	$PO_3^{\ominus}$		
8c	$COCH_3$	$SO_3^{\ominus}$, $COCH_3$		
8d	H	H		
8e	H	$COCH_3$		

For the investigation of the carcinogenicity of aromatic amines, the *N*-aryl-*O*-(diphenylphosphinoyl)hydroxylamines **5** and the reaction of their electrophilic N atom with amines **6** are important for the following reasons:

1. The compounds **5** are the first models for the product **8b**, which is formed when the extremely carcinogenic *N*-(2-fluorenyl)acetohydroxamic acid **8a** (and related compounds) undergo in vivo activation with phosphate.[13]

2. *N*-arylhydroxamate esters such as **3a**, **c–e** and **8b**, **c** are in general considerably more stable that the corresponding hydroxylamine compounds; **3b** is not isolable. With the synthesis of **5a–d**, *O*-substituted *N*-arylhydroxylamines without second substituents on the N atoms are now easily accessible.[14] They are of interest, because, for example, **8a** can be enzymatically activated not only by transformation to **8b**, **c**, etc., but also by deacylation to **8d** or transacylation to **8e**.[1, 13]

3. The carcinogenic **8a** reacts with guanine-containing substances such as guanosine or DNA in vivo and in vitro under a variety of conditions, giving predominantly the fluorenylamino (or amido) guanine derivatives **9**, i.e., the products of an electrophilic amination. Precisely this reaction, which is apparently crucial for the carcinogenicity of **8a**,[1, 13] can be simulated by the reactions of **5a–d** described here.

Received: February 10, 1986;
revised: February 28, 1986 [Z 1661 IE]
German version: *Angew. Chem. 98* (1986) 563

[1] a) J. A. Miller, *Cancer Res. 30* (1970) 559; b) E. Kriek, *Biochim. Biophys. Acta 335* (1974) 177; c) E. Miller, *Cancer Res. 38* (1978) 1479; d) E. C. Miller, J. A. Miller, *Cancer (Amsterdam) 47* (1981) 2327.

[2] Reactions of *N*-(acyloxy)purines with nucleophiles: a) U. Wolcke, W. Pfleiderer, T. J. Delia, G. B. Brown, *J. Org. Chem. 34* (1969) 981; b) J. C. Parham, M. A. Templeton, *ibid. 47* (1982) 652, and references cited therein.

[3] a) P. G. Gassman, J. E. Granrud, *J. Am. Chem. Soc. 106* (1984) 1498; b) *ibid. 106* (1984) 2448.

[4] G. T. Tisue, M. Grassmann, W. Lwowski, *Tetrahedron 24* (1968) 999.

[5] U. Gessner, A. Heesing, L. Keller, W. Kleine Homann, *Chem. Ber. 115* (1982) 2865, and references cited therein.

[6] a) M. Novak, M. Pelecanou, A. K. Roy, A. F. Andronico, F. M. Ploude, T. M. Olefirowicz, T. J. Curtin, *J. Am. Chem. Soc. 106* (1984) 5623; b) M. Novak, A. K. Roy, *J. Org. Chem. 50* (1985) 571; c) M. Pelecanou, M. Novak, *J. Am. Chem. Soc. 107* (1985) 4499; d) M. Novak, A. K. Roy, *J. Org. Chem. 50* (1985) 4884; e) M. Novak, M. Pelecanou, L. Pollack, *J. Am. Chem. Soc. 108* (1986) 112; see also [7].

[7] *N,O*-Diacyl-*N*-arylhydroxylamines undergo radical rearrangement to *N,O*-diacylated *o*-aminophenols: L. Horner, H. Steppan, *Justus Liebigs Ann. Chem. 606* (1957) 24, and references cited therein.

[8] See also J. D. Scribner, *J. Am. Chem. Soc. 99* (1977) 7383.

[9] The compounds **5a–d** were prepared analogously to other *O*-(diphenylphosphinoyl)hydroxylamines: M. Bernheim, G. Boche, *Angew. Chem. 92* (1980) 1043; *Angew. Chem. Int. Ed. Engl. 19* (1980) 1010.

[10] Until now only the electrophilic amination of amines with H_2N reagents was known: a) F. Raschig, *Chem. Ber. 40* (1907) 4580; b) Y. Tamura, J. Minamikawa, M. Ikeda, *Synthesis 1977*, 1; c) R. G. Wallace, *Aldrichimica Acta 13* (1980) 3; d) W. Klötzer, H. Baldinger, E. M. Karpitschka, J. Knoflach, *Synthesis 1982*, 592.

[11] K. H. Schündehütte in *Houben-Weyl-Müller: Methoden der Organischen Chemie, Band X/3*, Thieme, Stuttgart 1965, p. 377.

[12] U. Lerch, J. König, *Synthesis 1983*, 157.

[13] P. D. Lotlikar, M. B. Wasserman, *Biochem. J. 120* (1970) 661, and references cited therein.

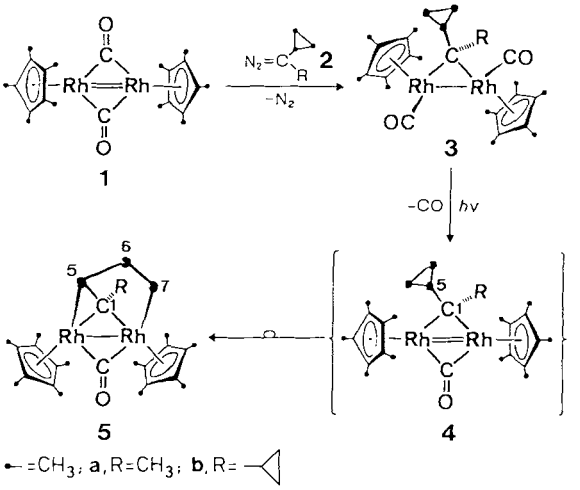
[14] *O*-Arenecarbonyl-*N*-arylhydroxylamines: S. Prabhakar, A. M. Lobo, M. M. Marques, *Tetrahedron Lett. 23* (1982) 1391; see also W. P. Jencks, *J. Am. Chem. Soc. 80* (1958) 4581.

Spontaneous Intramolecular Ring Opening of the Cyclopropyl Group at a Metal-Metal Double Bond**

By *Wolfgang A. Herrmann,* Eberhardt Herdtweck,* and *Cornelia Weber*

Cyclopropane occupies a special position among the alkanes even in organometallic reactions. Although systematic investigations of its behavior toward metal-complex fragments are lacking, it may be assumed as a working hypothesis that electron-rich metal centers cleave CH bonds by nucleophilic attack, whereas electron-deficient metal centers cleave CC bonds by electrophilic attack.[1–3] However, the latter reactions are only commonly observed for the C_3 structural unit as a building block of strained, polycyclic hydrocarbons; e.g., quadricyclane undergoes isomerization to norbornadiene at Rh^I and Pt^{II} centers.[3] We have now observed, for the first time, a spontaneous carbon–carbon bond breaking process at an (electrophilic) metal–metal double bond, namely, in a cyclopropyl group anchored to a binuclear μ-alkylidene complex.

Treatment of the binuclear rhodium complex **1** with the diazo compounds **2a** and **2b**, generated in situ from their hydrazone precursor compounds, results in the formation of the new dimetallacyclopropanes **3**,[4] once again confirming the generality of our well-documented synthetic strategy for the preparation of μ-alkylidene complexes.[5]



[*] Prof. Dr. W. A. Herrmann, Dr. E. Herdtweck, Dr. C. Weber
Anorganisch-chemisches Institut der Technischen Universität München
Lichtenbergstrasse 4, D-8046 Garching (FRG)

[**] Transition Metal Methylene Complexes, Part 62. This work was supported by the Deutsche Forschungsgemeinschaft, the Fonds der Chemischen Industrie, BASF AG, Hüls AG, DEGUSSA AG, and the Bundesministerium für Forschung und Technologie. Part 61: W. A. Herrmann, C. Weber, M. L. Ziegler, O. Serhadli, *J. Organomet. Chem. 297* (1985) 245.

According to the IR and NMR data, the complexes **3a**, **b** have the same constitution as the many other derivatives of this class whose structures have been established by X-ray diffraction analyses: characteristic are the two terminally bonded carbonyl groups and the two π-bonded pentamethylcyclopentadienyl ligands in *trans* positions with respect to the three-membered Rh_2C core structure.[5] In general, such compounds are thermally stable, but lose one of the two CO ligands rapidly upon irradiation. This results in the formation once again of a (highly reactive) double bond between the metal atoms (complexes of type **4**), to which small, reactive species may add (e.g., CO, CH_2, C_2H_2, Se, AgCl).[5,6]

The behavior of complexes **3a** and **3b** deviates fundamentally from this well-established reaction scheme. Although carbon monoxide is, in fact, cleaved off, the resulting species **4a** and **4b**, respectively, cannot be isolated. Even under mild reaction conditions (−50°C), a novel, spontaneous rearrangement takes place. The products **5a** and **5b**, respectively, having the same net composition as **4a** and **4b**, are isolated as deep red, lustrous crystals, which are stable to at least 250°C and are only soluble in very polar solvents such as acetone.[4] In contrast to its precursors **3b** (C_2 symmetry) and **4b** (mirror-plane symmetry), the stable end product **5b** is asymmetric. The absence of molecular symmetry is reflected in the ^{1}H-NMR spectra (300 MHz, $CDCl_3$, +28°C), not only in two different C_5Me_5 signals ($\delta = 1.68, 1.77, 2 \times d$; $^3J(Rh,H) = 0.6$ Hz) but also in numerous sets of signals for the CH and CH_2 protons. Of particular value in assignment of the structure is the group of signals centered at $\delta = 0.19$, which, on the basis of the chemical shift and the coupling ($^2J(Rh,H) = 0.8$ Hz) is assigned to the C5 protons. Without attempting a detailed interpretation of the spectra,[4] it is possible to locate an intact cyclopropyl group (C2, C3, C4) by spectral comparisons ($\delta = 0.46, 0.53, 0.90, 1.05, 1.30$; $5 \times m$).[6a] The molecule does not contain metal-bonded hydride ligands.

A single-crystal X-ray structure analysis of **5b** also revealed that the rearrangement involves cleavage of an α carbon-carbon bond of the cyclopropyl group, which was still intact in the precursor species **3a** and **3b**. As shown in Figure 1, a tricyclic Rh_2C_4 skeleton is formed in which C1 is the original μ-methylene carbon atom. Whereas the dimetallacyclopropane structure of the precursor species **3** is retained (Rh-C1 = 205.0(5) and 203.6(5) pm), the atoms involved in the CC bond cleavage form single bonds to the metal atoms (209(1) and 216(1) pm) in order to satisfy their valence requirements. This results in the formation of a dimetalladihydrobenzvalene structure. Since two possibilities exist for the α-cleavage of the cyclopropyl group, a disorder is observed for the tricyclic Rh_2C_4 skeleton, with C5 bonded to either Rh1 or Rh2; furthermore, the C_5Me_5 ligand of Rh1 is also disordered.[7] On account of the disorders, the structure alternatives that are in principle possible do not agree with the NMR data and are not reasonable in terms of bonding theory.

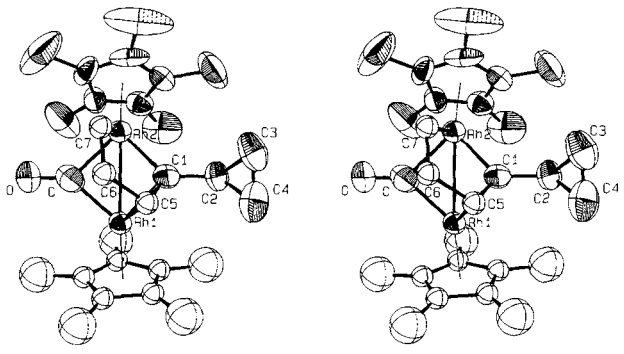
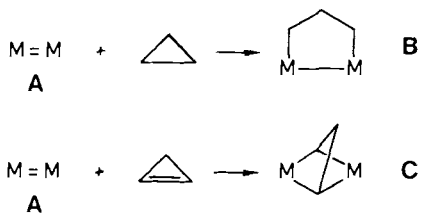


Fig. 1. ORTEP plot (stereoview) of the crystal structure of **5b** (50% probability; without hydrogen atoms; disordered atoms represented as balls). The compound was crystallized at −25°C from acetone; monoclinic, space group $P2_1/c$ ($Z = 4$), $a = 817.2(1)$, $b = 1766.8(3)$, $c = 1847.1(6)$ pm, $\beta = 98.14(2)°$, $V = 2640 \times 10^6$ pm^3.—Selected bond lengths [pm] and bond angles [°]: C1-C5 145(1), C1-Rh1 205.0(5), C5-C6 162(2), C6-C7 144(1), Rh2-C7 216.5(9), C1-C2 150.5(8), Rh1-C 195.4(7), Rh2-C 199.1(7); Rh-C-Rh2 85.0(3), Rh1-C1-Rh2 81.5(2); C5 lies 105 pm below the best plane of the atoms Rh1, C6, C7, and Rh2. Further details of the crystal structure investigation may be obtained from the Fachinformationszentrum Energie, Physik, Mathematik GmbH, D-7514 Eggenstein-Leopoldshafen 2 (FRG), on quoting the depository number CSD 51873, the names of the authors, and the journal citation.

Particularly noteworthy is the simple formation of the dimetallapentane system **B**. It was achieved here, for the first time, by the ring-opening addition of a cyclopropane to a metal-metal double bond **A**, which in turn is transformed into a single bond (266.7(1) pm). Whereas dimetallacyclopentanes are usually thermally labile, either eliminating ethylene and undergoing ring contraction to form dimetallacyclopropane derivatives or undergoing β-hydrogen migration to form α-olefins (propene in the case of **B**),[8] complexes **5** probably owe their stability to the incorporation of the C_3 bridge into a polycyclic framework. Ring-opening of cyclopropene at the metal-to-metal double bond of **1** (type **A**) leads primarily to dicarbenoid species **C**, which, however, undergo rapid subsequent reaction (e.g., with CO insertion).[9] The ring opening of methylenecyclopropanes, which has been observed repeatedly, begins with π-complexation of the intact molecule;[10] in other cases, cyclopropyl groups remain intact, even at coupling-active compounds (e.g., allylidenecyclopropanes).[11]



Received: February 10, 1986;
revised: March 24, 1986 [Z 1662 IE]
German version: *Angew. Chem. 88* (1986) 557

[1] R. G. Bergman, P. F. Seidler, T. T. Wenzel, *J. Am. Chem. Soc. 107* (1985) 4358, and references cited therein.
[2] C. F. H. Tipper, *J. Chem. Soc. 1955*, 2043.
[3] Review: R. H. Crabtree, *Chem. Rev. 85* (1985) 245, and references cited therein.
[4] *Experimental procedure:* The complexes **3a** and **3b** were synthesized according to known procedures by reaction of **1** with cyclopropylmethyl ketone hydrazone and dicyclopropyl ketone hydrazone, respectively, in the presence of activated MnO_2 in >80% yield and were recrystallized from *n*-hexane after chromatographic workup on Florisil (−35°C). Ruby-red crystals (**3a**, m.p. = 140°C; **3b**, m.p. = 122-125°C).—Spectroscopic data for **3b**: IR ($\tilde{\nu}$(CO) [cm^{-1}]): 1927 (THF); 1945 m, 1921 s (KBr); ^{1}H-NMR (270 MHz, $CDCl_3$, +28°C: $\delta = 1.87$ (s, CH_3, 30 H), 1.34 (m, CH, 2 H), 0.60, 0.45 (2 m, CH_2, 2×4 H).—In order to synthesize the metallacycles **5a** and **5b**, THF solutions of **3a** and **3b** were irradiated at 0°C in an immersion-well apparatus constructed of DURAN glass with a high-pressure mercury lamp (125 W) (3 mmol of complex in 150 mL of THF), CO evolution terminating after ca. 30 min. The initially bright red solution turned dark red. The solvent was removed under vacuum and the solid residue was recrystallized from a small amount of acetone (−30°C); yield 85%.—Spectroscopic data for **5b**: IR ($\tilde{\nu}$(CO)

[5] R. H. Crabtree, *Acc. Chem. Res. 12* (1979) 331.
[6] R. H. Crabtree, *J. Organomet. Chem. 234* (1982) 331.
[7] R. H. Crabtree, *Angew. Chem. 93* (1981) 307; *Angew. Chem. Int. Ed. Engl. 20* (1981) 296.
[8] R. H. Crabtree, *J. Organomet. Chem. 135* (1977) 395.
[9] R. H. Crabtree, *J. Organomet. Chem. 141* (1977) 205.
[10] R. H. Crabtree, *J. Organomet. Chem. 135* (1977) 329.
[11] R. H. Crabtree, *J. Organomet. Chem. 135* (1977) 319.

[cm^{-1}]): 1785 (THF); 1780 vs, 1742 vw (sh) (KBr); ^{1}H-NMR (300 MHz, $CDCl_3$, +28°C): δ = 1.68, 1.77 (2d, CH_3, 2 × 15 H; ^3J(Rh,H) = 0.5–0.6 Hz), 0.46, 0.53, 0.90, 1.05, 1.30 (5m, cyclopropyl-H, 5 × 1 H), 0.19 (m, ^2J(Rh,H) = 0.8 Hz, 1 H), 1.52 (m, 2 H), 2.58 (m, 1 H), 2.73 (m, 1 H) (together $Rh_2C_3H_5$). A correct elemental analysis (C, H, O, Rh) was obtained. MS: m/z 598 (molecular ion for $C_{28}H_{40}ORh_2$; EI and FD spectra).

[5] Review: a) W. A. Herrmann, *Pure Appl. Chem. 54* (1982) 65; *J. Organomet. Chem. 250* (1983) 319; *Adv. Organomet. Chem. 20* (1982) 159.

[6] More recent examples: a) W. A. Herrmann, C. Weber, M. L. Ziegler, C. Pahl, *Chem. Ber. 117* (1984) 875, and references cited therein; b) W. A. Herrmann, C. Bauer, J. Weichmann, *J. Organomet. Chem. 243* (1983) C21; c) W. Kalcher, W. A. Herrmann, *Chem. Ber. 118* (1985) 3861, and references cited therein.

[7] CAD-4 (Enraf-Nonius), $Mo_{K\alpha}$, graphite monochromator, ω-scan ($\Delta\omega = 1.0° + 0.35 \tan\theta$, $2° \leq \theta \leq 20°$), $t_{max} = 60$ s, $h(-7/7)$, $k(0/17)$, $l(-17/17)$, 5096 measured reflections, 4069 of which with $I > 1\sigma(I)$; after averaging, 2146 reflections remained.—Structure solution: Patterson and difference Fourier methods; all atoms with the exception of hydrogen and all nondisordered carbon atoms were anisotropically refined; ideal positions were assumed for the hydrogen atoms and used in calculating the structure factors; however, they were not refined. $R = 0.040$, $R_w = 0.041$.

[8] Example: K. M. Motyl, J. R. Norton, C. K. Schauer, O. P. Anderson, *J. Am. Chem. Soc. 104* (1982) 7325.

[9] C. J. Schaverien, M. Green, A. G. Orpen, I. D. Williams, *J. Chem. Soc. Chem. Commun. 1982*, 912.

[10] a) P. Binger, M. J. Doyle, R. Benn, *Chem. Ber. 116* (1983) 1; b) P. Binger, A. Brinkmann, P. Wedemann, *ibid. 116* (1983) 2920.

[11] Example: H. M. Büch, P. Binger, R. Benn, C. Krüger, A. Rufinska, *Angew. Chem. 95* (1983) 814; *Angew. Chem. Int. Ed. Engl. 22* (1983) 774.

Direct Aminolysis of Unactivated Esters at High-Pressure**

By *Kiyoshi Matsumoto,* Shiro Hashimoto,* and *Shinichi Otani*

In memoriam Ryozo Goto

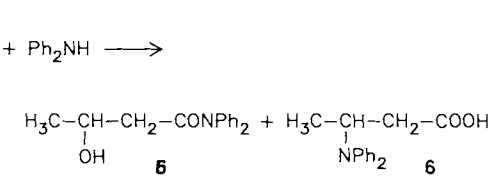
The direct conversion of esters into acid amides is known to be a difficult reaction,[1] though it potentially constitutes a useful synthetic strategy and several methods designed to facilitate it have been reported.[2–5] Uncatalyzed aminolysis with primary amines requires temperatures in excess of 200°C,[6] while the corresponding reaction with secondary amines has never been reported.

We have now found that even secondary amines **2** react in high yield at room temperature or 35–45°C with a wide variety of unactivated esters **1** to give acid amides **3** if the reactions are carried out under a few kbar (Table 1).[7] Neither an inert atmosphere nor dry solvents are required. The reaction is extremely clean and therefore the work-up procedure is straightforward; even the hydrolysis procedure used in the excellent method with alkylaluminum amide reagents is unnecessary. Usually, the solution of the products **3** contains only the esters **1**, if the yield is not quantitative, and excess amine **2**. Naturally, this method is also applicable to primary amines (see Table 1).

The reaction of β-butyrolactone **4** at 45°C with an extremely unreactive amine such as diphenylamine[8] further illustrates the utility and mildness of the method. The desired amide **5** is obtained in 28% yield, along with 35% 3-(*N,N*-diphenylamino)butyric acid **6**. Under conventional conditions at 180–190°C—without use of pressure—only 0.8% of the acid is formed.

[*] Prof. Dr. K. Matsumoto, S. Hashimoto, Prof. Dr. S. Otani
College of Liberal Arts and Sciences, Kyoto University
Kyoto 606 (Japan)

[**] This work was supported by the Japanese Ministry of Education (No. 61840017).



Because of its broad applicability and the low temperatures, the method presented here appears to be superior to reactions with alkylaluminum amides.[9] Whereas these reagents often react with such a valuable functional group as a cyano group,[10] this is not the case in our method. The high acceleration of the aminolysis of esters by application of pressure would suggest that the formation of a tetrahedral zwitterion is rate-determining.[11]

Received: February 11, 1986 [Z 1666 IE]
German version: *Angew. Chem. 98* (1986) 569

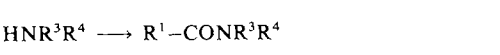


Table 1. Aminolysis of unactivated esters **1** to acid amides **3** at 8 kbar with primary and secondary amines **2** [7] [a].

R^1	R^2	R^3	R^4	T [b] [°C]	Yield [%][c]	M.p. [°C]
$H(CH_2)_8CH{=}CH(CH_2)_7$	Me [d]	$-(CH_2)_4-$		35	100	oil
		$-(CH_2)_5-$		35	100	oil
$PhCH_2$	Me	$-(CH_2)_4-$		35	100	oil
		$-(CH_2)_5-$		35	100	oil
		Et	Et	45	67	oil
		$PhCH_2$	H	35	100	118–119
Ph	Et [e]	$-(CH_2)_4-$		RT	100	oil
		$-(CH_2)_5-$		35	81	oil
PhCH(OH)	Me	$-(CH_2)_4-$		35	96	94–95
		$-(CH_2)_5-$		35	100	77
		$PhCH_2$	H	35	90	99–100
c-C_6H_{11}	Me [e]	$-(CH_2)_4-$		45	89	67–68
		$-(CH_2)_5-$		45	98	oil
$NCCH_2CH_2$	Me	$-(CH_2)_4-$		35	100	oil
		$-(CH_2)_5-$		35	100	oil

[a] Reaction conditions not optimized. [b] Temperatures: 35 ± 2°C, 45 ± 2°C, room temperature. [c] Yields of pure isolated amides **3**; all amides gave correct CHN analyses and IR, ^{1}H-NMR, and ^{13}C-NMR spectra. [d] When octylamine is used instead of pyrrolidine at normal pressure, then heating to 230°C is necessary [6]. [e] Does not react under vapor-phase chromatography conditions at 190°C [5].

[1] Review: A. L. J. Beckwith in J. Zabicky (Ed.): *The Chemistry of Amides*, Interscience, New York 1970, p. 96.

[2] Strong alkali metal catalysts: a) $NaOCH_3$: R. J. De Feo, P. D. Strickler, *J. Org. Chem. 28* (1963) 2915; E. L. Allred, M. D. Hurwitz, *ibid. 30* (1965) 2376; b) $NaNH_2$ or KNH_2: E. S. Stern, *Chem. Ind. (London) 1956*, 277; C. F. Huebner, R. Lucas, H. B. MacPhillamy, H. A. Troxell, *J. Am. Chem. Soc. 77* (1955) 469; c) *n*BuLi: K. W. Young, J. G. Cannon, J. G. Rose, *Tetrahedron Lett. 1970*, 1791; d) NaH: B. Singh, *Tetrahedron Lett. 1971*, 321; d) $LiAlH_4$: J. Petit, R. Poisson, *C. R. Hebd. Séances Acad. Sci. 247* (1958) 1628; D. A. Evans, *Tetrahedron Lett. 1969*, 1573; e) RMgX: H. L. Bassett, C. R. Thomas, *J. Chem. Soc. (London) 1954*, 1188.

[3] Milder catalysts: a) 2-Pyridone: T. Openshaw, N. Whittaker, *J. Chem. Soc. (London) C 1969*, 89; b) BBr_3: H. Yazawa, K. Tanaka, K. Kariyone, *Tetrahedron Lett. 1974*, 3995.

[4] Metal amide reagents: a) R_3SnNMe_2: T. A. George, M. F. Lappert, *J. Chem. Soc. (London) A 1969*, 992; G. Chandra, T. A. George, M. F. Lappert, *ibid. 1969*, 2565; b) $Me_2AlNR^1R^2$: A. Basha, M. Lipton, S. M. Weinreb, *Tetrahedron Lett. 1977*, 4171.

[5] Unusually facile aminolysis of β-ketoesters: M. Labelle, D. Gravel, *J. Chem. Soc. Chem. Commun. 1985*, 105.

[6] E. T. Roe, J. T. Scanlan, D. Swern, *J. Am. Chem. Soc. 71* (1949) 2215; R. Crossley, A. C. W. Curran, D. G. Hill, *J. Chem. Soc. Perkin Trans. 1 1976*, 977.

[7] Procedure: A mixture of the ester **1** (5 mmol) and the amine **2** (10 mmol) was diluted with acetonitrile in an 8-mL Teflon capsule, which was then stored for 3 d at 8 kbar. After evaporation of the solvent and amine, the residue was dissolved in dichloromethane and extracted with dilute HCl (saturated with ammonium sulfate in the case of water-soluble amides **3**). In the case of incomplete reaction, the amide was readily separated by flash chromatography.—For reviews on organic syntheses under high-pressure, including a description of the high-pressure equipment used in this study, see: K. Matsumoto, A. Sera, T. Uchida, *Synthesis 1985*, 1; K. Matsumoto, A. Sera, *ibid. 1985*, 999.

[8] Y. Iwakura, K. Nagakubo, J. Aoki, A. Yamada, *Nippon Kagaku Zasshi 75* (1954) 315; *Chem. Abstr. 51* (1957) 11246b.

[9] M. F. Lipton, A. Basha, S. M. Weinreb, *Org. Synth. 59* (1980) 49.

[10] H. Hoberg, J. B. Mur, *J. Organomet. Chem. 17* (1969) P30; T. Hirabayashi, K. Itoh, S. Sakai, Y. Ishii, *ibid. 21* (1970) 273.

[11] For a recent mechanistic study on the aminolysis of esters: I. M. Kovach, M. Belz, M. Larson, S. Rousy, R. L. Schowen, *J. Am. Chem. Soc. 107* (1985) 7360.

Red, Transparent Alkali Metal Silicides with Si_4 Tetrahedrons

By *Hans Georg von Schnering,* Martin Schwarz,* and *Reinhard Nesper*

In memoriam Herbert Schäfer

The theoretically predicted structure of the fourfold μ_3-coordinated tetralithiotetrahedrane Li_4C_4[1] has not yet been experimentally confirmed. The homologous silicide is unknown,[2] and the germanide LiGe does not have Ge_4 tetrahedrons as anions.[3] The tetrahedral arrangement, however, has been long established for all higher homologues of the first and fourth main groups.[4–6] We have therefore attempted to determine, by the synthesis of ternary and quaternary silicides M*Si (M* = mixed alkali metal), whether lithium can at least be partially present as a μ_3-bonded metal atom on Si_4 tetrahedra. These experiments were successful and led, surprisingly, to the first red, transparent metal silicides.

Reaction of an alkali metal mixture, Li + M (M = Na–Cs) with silicon results in the formation of both red, transparent and metallic grey, opaque silicides. It is still unclear which conditions with respect to M* : Si and Li : M and which structures are characteristic for either of the two types. We have established, however, that the light absorption of the red silicides K_3LiSi_4 and $K_7Li(S_4)_2$ is an intrinsic property of these compounds. (*Preparation:* stoichiometric mixture of the elements; sealed Nb ampoule in a quartz ampoule; 4 h heating at 800 °C; 4 h annealing at 800 °C; slow cooling over 12 h.) These red silicides are also flammable in air and form flammable silanes with protic solvents.

The structures of the new silicides (Fig. 1) belong to the types already known or are variants of these. Thus, $K_7Li(Si_4)_2$ belongs to the $Rb_7Na(Ge_4)_2$ type,[7] and K_3LiSi_4 exhibits the polymeric chain $^1_\infty[M'(Y_4)]$ known for the $Cs_2Na_2Ge_4$ type.[8] In K_3LiSi_4, the Si_4^{4-} tetrahedra are linked by the Li atoms to form infinite one-dimensional chains $^1_\infty[Li(Si_4)]^{3-}$, thereby functioning twice as μ_3-ligands. Li is thus bonded to six Si atoms with d(Li–Si) = 258.8–294.7 pm ($\bar{d}$ = 272.9 pm), and, at the same time, two triangular faces of the Si_4^{4-} tetrahedron are capped by Li. In contrast to $Cs_2Na_2Ge_4$,[8] however, only one other face is capped by a K atom as μ_3-ligand; the other K atoms bridge only edges or coordinate only corners of the Si_4 tetrahedron (coordination number 6 and 7, respectively, with K–Si = 339.4–356.9 pm and 354.6–380.7 pm, respectively). The bond lengths in the anion are on the average $\bar{d}$(Si–Si) = 242.4 pm (236.3–244.9 pm) and are thus larger than in NaSi (240.9 pm[9]). The Si_4 tetrahedra in $K_7Li(Si_4)_2$, with the dumb-bell-shaped unit $[Li(Si_4)_2]^{7-}$, are also larger than in NaSi: $\bar{d}$(Si–Si) = 241.8 pm; $\bar{d}$(Li–Si) = 271.4 pm. In this structure, six of the K atoms serve as further μ_3-ligands (K–Si = 338.5–351.2 pm with $\bar{d}$ = 343.9 pm), whereas one of the K atoms exhibits no K–Si contacts.

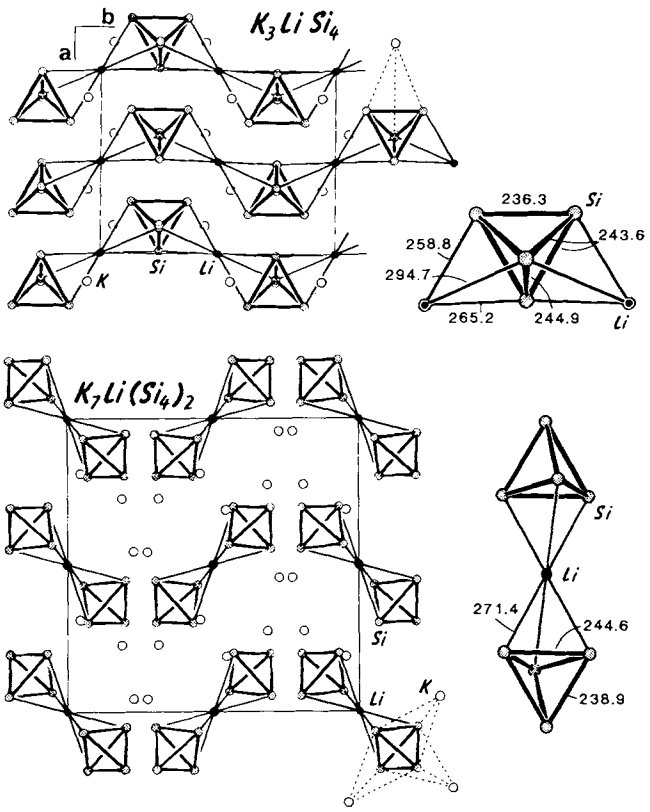


Fig. 1. Crystal structures of K_3LiSi_4 and $K_7Li(Si_4)_2$ with the bond lengths in the polymeric chain $^1_\infty[Li(Si_4)]^{3-}$ and in the dumb-bell-shaped structural group $[(Si_4)Li(Si_4)]^{7-}$. In both structures, the additional μ_3-coordinations by the K atoms are given on the right margin (hatched lines).—Crystallographic data: K_3LiSi_4: *Pnma* (No. 62); a = 765.1(4), b = 980.5(4), c = 1222.1(9) pm; Z = 4; 1253 reflections; R(aniso) = 0.033.—$K_7Li(Si_4)_2$: *Pa3* (No. 205); a = 1249.5(3) pm; Z = 4; 495 reflections, R(aniso) = 0.026. Further details of the crystal structure investigation may be obtained from the Fachinformationszentrum Energie, Physik, Mathematik GmbH, D-7514 Eggenstein-Leopoldshafen 2 (FRG), on quoting the depository number CSD 51899, the names of the authors, and the journal citation.

Some of the structural details could be of importance for theoretical understanding. Thus, in $K_7Li(Si_4)_2$, the Si–Si distances in the tetrahedral faces bonded to μ_3(Li) are large (244.6 pm) and those in the faces bonded to μ_3(K) small (238.9 pm). In K_3LiSi_4, the Si_4^{4-} tetrahedra are also distorted. The one edge of the tetrahedron not involved in a μ_3(Li) cap structure has the smallest Si–Si distance (236.3 pm) and the edge involved in two μ_3(Li) cap structures the largest Si–Si distance (244.9 pm). Apparently, the strongly covalent Li–Si interaction of the μ_3-bonded Li atom weakens the Si–Si bonds of the Si_4^{4-} tetrahedron. Even the noted deformations due do incomplete μ_3-coordination can no longer permit a doubt as to the favoring of the T_d form for Li_4Si_4 as well.[10] Although *Ritchie* et al. predict a higher stability for the D_{2d} form,[11] more detailed

[*] Prof. Dr. H. G. von Schnering, Dipl.-Chem. M. Schwarz, Dr. R. Nesper
Max-Planck-Institut für Festkörperforschung
Heisenbergstrasse 1, D-7000 Stuttgart 80 (FRG)

calculations with inclusion of electron correlations confirm the T_d symmetry for Li_4C_4.[12]

Received: February 11, 1986;
supplemented: March 19, 1986 [Z 1667 IE]
German version: *Angew. Chem. 98* (1986) 558

CAS Registry numbers:
K_3LiSi_4, 102210-64-0; $K_7Li(Si_4)_2$, 102210-65-1; Si, 7440-21-3; Li, 7439-93-2; K, 7440-09-7.

[1] P. von R. Schleyer, *Pure Appl. Chem. 50* (1984) 151; G. Rauscher, T. Clark, D. Poppinger, P. von R. Schleyer, *Angew. Chem. 90* (1978) 306; *Angew. Chem. Int. Ed. Engl. 17* (1978) 276.
[2] H. G. von Schnering, R. Nesper, K.-F. Tebbe, J. Curda, *Z. Metallkd. 71* (1980) 357.
[3] E. Menges, V. Hopf, H. Schäfer, A. Weiss, *Naturforsch. B 24* (1969) 1351; A. Grüttner, *Dissertation*, Universität Stuttgart 1982.
[4] E. Busmann, *Naturwissenschaften 47* (1960) 82.
[5] J. Witte, H. G. von Schnering, *Z. Anorg. Allg. Chem. 327* (1964) 260.
[6] R. E. Marsh, D. P. Shoemaker, *Acta Crystallogr. 6* (1953) 197.
[7] J. Llanos, R. Nesper, H. G. von Schnering, *Angew. Chem. 95* (1983) 1026; *Angew. Chem. Int. Ed. Engl. 22* (1983) 998.
[8] J. Llanos, R. Nesper, H. G. von Schnering, *Acta Crystallogr. A 40* (1984) Suppl. C-228, Abstr. 08.2-40.
[9] H. G. von Schnering, R. Nesper, T. Chattopadhyay, D. Stoilova, unpublished refinement of the NaSi structure (cf. [5]).
[10] A. Savin, K. Vogel, H. Preuss, H. Stoll, R. Nesper, H. G. von Schnering, unpublished.
[11] J. P. Ritchie, *J. Am. Chem. Soc. 105* (1983) 2083; R. L. Disch, J. Schulman, J. P. Ritchie, *ibid. 106* (1984) 6246.
[12] K. Raghavachari, P. von R. Schleyer, private communication (1986).

A Stable 1,2,4-Thiadiphosphole ("2,4-Diphosphathiophene")**

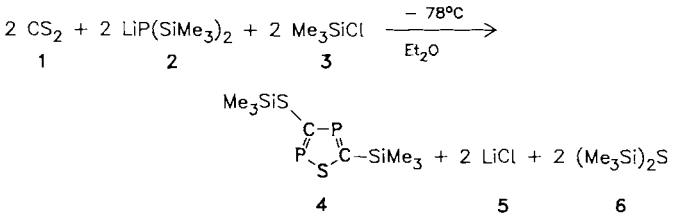
By *Rolf Appel** and *Rainer Moors*

Dedicated to Professor Marianne Baudler on the occasion of her 65th birthday

Investigations carried out in the past few years have revealed that there is a definite and, in some cases, amazing relationship between the P=C and C=C double bond.[1] This relationship manifests itself in the reaction behavior of the phosphaalkenes and alkenes as well as in the synthesis of phosphabenzene,[2] phosphaazulenes,[3] and various phospholes containing heteroatoms. Among these, only one incompletely characterized thiadiphosphole has been described as reactive intermediate[5] aside from aza-, oxaza-, and thiazaphospholes.[4]

We have now been able to synthesize the stable thiadiphosphole derivative **4** containing a conjugated P=C–P=C sequence by reaction of carbon disulfide **1** with lithium bis(trimethylsilyl)phosphide **2** and chlorotrimethylsilane **3**.

5-Trimethylsilyl-3-trimethylsilylthio-1,2,4-thiadiphosphole **4** is a yellow liquid that can be distilled under high vacuum (b.p. 75–78 °C/10^{-3} torr). Its composition has been confirmed by an elemental analysis and a molar mass determination; its constitution by an analysis of the spectroscopic data.



The ^{31}P-NMR spectrum shows an AB system at $\delta = 309.8$ and 304.3 in the characteristic PC double bond region with a PP coupling constant of 59.1 Hz. In the ^{13}C-NMR spectrum, the ring C-atoms appear as a doublet of doublets at $\delta = 194.84$ ($^1J_{CP} = 82.4$ Hz, $^2J_{CP} = 1.0$ Hz) and 189.96 ($^1J_{CP} = 88.5$ Hz, $^1J_{CP} = 87.5$ Hz) in the region for sp^2-hybridized carbon atoms. The signal at $\delta = 1.54$ (d, $^3J_{CP} = 5.3$ Hz) is assigned to the trimethylsilyl carbon atoms. Due to very similar coupling constants, the carbon atoms of the trimethylsilylthio group appear with the chemically different phosphorus atoms as a pseudo-triplet at $\delta = 0.66$ with a coupling constant $^4J_{CP} = 1.4$ Hz.

A double-doublet with two small Si–P coupling constants of 5.8 and 3.0 Hz is observed at $\delta = 18.32$ in the ^{29}Si-NMR spectrum. On the basis of the characteristic value of the shift, this signal can be assigned to the trimethylsilylthio-silicon atom. The silicon atom of the trimethylsilyl group bound to the carbon appears as a double doublet at $\delta = -2.03$ ($^2J_{SiP} = 25.8$ Hz, $^3J_{SiP} = 3.2$ Hz).

Experimental

All operations were carried out under inert gas using anhydrous solvents.

A solution of **2**·2THF (12 g, 37 mmol) in diethyl ether (80 mL) was slowly added dropwise to a solution of CS_2 (2.5 mL, 41 mmol) in 80 mL diethyl ether cooled with methanol/dry ice. After 15 minutes' stirring the dark-red mixture was treated with **3** (5.2 mL, 41 mmol) and allowed to warm to room temperature. The solvent was then removed and the residue was taken up in 50 mL of pentane, filtered, and the LiCl washed several times with pentane. After removal of the pentane under vacuum, the crude product **4** was distilled under vacuum (mercury diffusion pump); yield 2.5 g (45% referred to **2**); MS (70 eV 90 °C (selection)): *m/z* 296 ($M^{\oplus}$, 47.7%), 281 ($M^{\oplus} - CH_3$, 15.2%), 233 ($M^{\oplus} - PS$, 6.0%), 73 $(CH_3)_3Si$, 100%).

The thioether **6** was collected in a cold trap, distilled (b.p. 65 °C/15 torr), and identified ^{1}H-NMR spectroscopically by comparison with authentic samples.

Received: February 13, 1986 [Z 1668 IE]
German version: *Angew. Chem. 98* (1986) 570

[1] R. Appel, F. Knoll, I. Ruppert, *Angew. Chem. 93* (1981) 771; *Angew. Chem. Int. Ed. Engl. 20* (1981) 731.
[2] A. J. Ashe, *J. Am. Chem. Soc. 93* (1971) 3293.
[3] G. Märkl, E. Seidl, *Angew. Chem. 95* (1983) 58; *Angew. Chem. Int. Ed. Engl. 22* (1983) 57; *Angew. Chem. Suppl. 1983*, 75; G. Märkl, E. Seidl, I. Trötsch, *Angew. Chem. 95* (1983) 891; *Angew. Chem. Int. Ed. Engl. 22* (1983) 879.
[4] A. Schmidpeter, K. Karaghiosoff, *Nachr. Chem. Tech. Lab. 33* (1985) 793 (review of azaphospholes), and references cited therein.
[5] Y. Kobayashi, S. Fujino, I. Kumadaki, *J. Am. Chem. Soc. 103* (1981) 2465.

Anionic Host Molecules with Bicyclic Carbon Skeletons— Synthesis and Guest Inclusion in Aqueous Solution**

By *Thomas Merz, Herbert Wirtz,* and *Fritz Vögtle**

Macro*bi*cyclic molecules with *carbon* skeletons that can act as water-soluble host molecules, such as **1**, were unknown up to now.[1] The corresponding monocyclic carbon

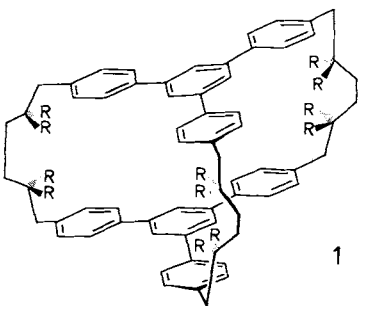
[*] Prof. Dr. R. Appel, R. Moors
Anorganisch-chemisches Institut der Universität
Gerhard-Domagk-Str. 1, D-5300 Bonn 1 (FRG)

[**] Lower Coordinated Phosphorus Compounds, Part 50.—Part 49: R. Appel, F. Knoch, C. Porz, *Chem. Ber.*, in press.

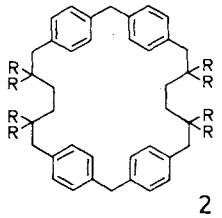
[*] Prof. Dr. F. Vögtle, Dipl.-Chem. T. Merz, Dr. H. Wirtz
Institut für Organische Chemie und Biochemie der Universität
Gerhard-Domagk-Strasse 1, D-5300 Bonn 1 (FRG)

[**] We thank Prof. *F. W. Röllgen* and Dipl.-Chem. *S. S. Wong* (Bonn), Prof. *H. Egge* (Bonn), and Dr. *G. Eckhardt* (Bonn) for the mass spectra, and Dr. *B. Steffan* and Mr. *C. Schmidt* (Bonn) for the 400-MHz ^{1}H-NMR spectra.

compounds, such as **2**, have become known only recently.[2] The investigation of guest inclusion in molecules such as **1**, which has a disk-shaped cavity (Fig. 1), offers promise of progress in the preparation of artificial receptors and membrane channels and—by selection of appropriate functional groups—in the development of synthetic catalysts.[1]



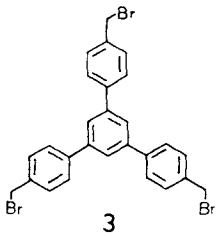
1



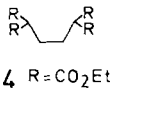
2

a R=CO_2Et
b R=CO_2H
c R=$CO_2^{\ominus}Na^{\oplus}$

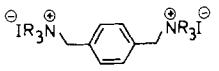
We have now prepared the first example of this type of molecule, the dodecaester **1a** (m.p. = 285 °C),[3] from simple starting materials—the trifunctional bromo compound **3** and the tetraethyl carboxylate **4**[2]—in a single synthetic step under dilution conditions (sixfold bond formation; 0.6% yield). The dodecacarboxylic acid **1b**[4] (m.p. > 320 °C), obtained from **1a** by hydrolysis with KOH in ethanol, is particularly soluble in water at pH > 7. In aqueous NaOH, **1c** is formed.



3



4 R=CO_2Et

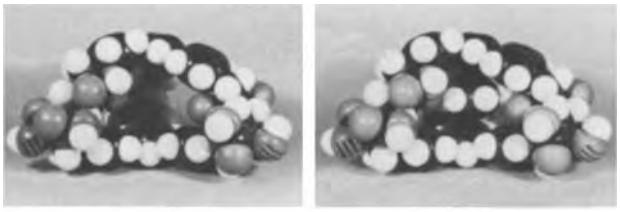


5 R=CH_3

On account of the macrobicyclic effect,[5] it was of interest to compare the strength and selectivity of the binding of guest substances by the new bicyclic host **1b** (as the sodium salt **1c**) with those of the monocyclic host **2b** (as the sodium salt **2c**).[2] In contrast to the findings for **2c**,[2] the doubly charged guest compound **5**, which, according to examination of molecular models, should fit into the cavity of **1b**, does not exhibit ^{1}H-NMR high-field shifts in aqueous solution. This points to an unexpected and significant difference in the recognition of guests by the macrobicyclic host **1c** compared with the macromonocycle **2c**. We propose that the guest dication is already "trapped" at the anionic periphery[6] of the sodium salt **1c** (cf. Fig. 1) and, owing to the formation of strong ion pairs as well as the relatively rigid skeleton, does not enter the cavity. In contrast, the conformationally more flexible host **2c** offers the same guest **5** both the possibility of analogous ion-pair formation and access to a directly neighboring cavity, which results in high-field shifts for the enclosed guest compound on account of anisotropy effects.

In view of these findings, it was at first surprising that an association constant of $\lg K_{ass} = 2.1$ (pH 11) was found by fluorescence spectroscopy for the reaction of **1c** (concentration between 0 and 10^{-3} mol/L) with 1,8-ANS (1,8-anilinonaphthalenesulfonate) in aqueous solution, since **1c** therefore binds this guest with an association constant ($\lg K_{ass} = 2.0$ at pH 7) similar to that of **2c** ($\lg K_{ass} = 2.3$ at pH 7). Examination of models provides an explanation for this finding; namely, neither cavity offers sufficient space for the entire ANS molecule. Only the anilino moiety of ANS fits into the cavity of **1c**. Presumably, the charges of the peripheral carboxylate groups have less effect on the guest ANS than on positively charged guest molecules.

Taking into consideration these results, we expanded the search for guests that fit into the cavity of **1c** to electrically uncharged guest molecules that, moreover, do not exhibit high-field shifts on association with the monocyclic host **2c**.[3] In fact, after addition of benzene to an aqueous solution of **1c** (and ultrasonication over several hours), we observed in the ^{1}H-NMR spectrum, in addition to the usual benzene absorption at $\delta = 7.34$, a strongly high-field shifted signal ($\Delta\delta = 0.65$ ppm!), which we assign to benzene enclosed in the cavity of **1c**. Evaporation to dryness and pumping at 50 °C removes all traces of benzene; subsequent addition of toluene and ultrasonication leads to inclusion of this guest, the aromatic and aliphatic protons of which appear at very high field besides in the usual region ($\Delta\delta(H_{aromat.}) = 0.5$, $\Delta\delta(CH_3) = 0.6$ ppm). Mesitylene also undergoes inclusion in **1c** in aqueous solution upon ultrasonication, as was demonstrated analogously ($\delta = 6.2$ and 1.8; $\Delta\delta(H_{aromat.}) = 0.6$ ppm, $\Delta\delta(CH_3) = 0.5$ ppm).



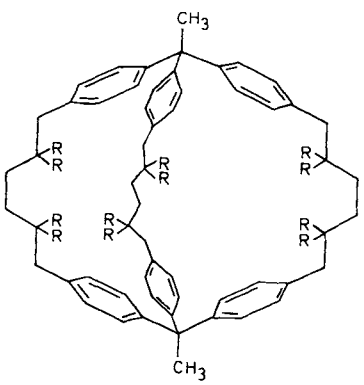
a) b)

Fig. 1. Space-filling model of the host **1b**: a) empty; b) with enclosed benzene.

Thus, whereas the monocycle **2c** does not bind uncharged guest molecules to a significant extent, **1c** does, owing to its ability to enclose the guest on all sides in a preformed cavity.

As demonstrated by the preparation of the analogous host compound **6a** (0.8% yield),[7] which contains a modified cavity, the one-step synthesis strategy chosen for **1a** is also applicable to other building blocks.

The differences observed in the binding of cationic, anionic, and uncharged guests by the bicyclic guest **1c** opens up possibilities for influencing the complexation in cavi-



6a R=CO_2Et
6b R=CO_2H
6c R=$CO_2^{\ominus}Na^{\oplus}$

ties by the use of pH-dependent charged groups on the periphery. Moreover, on account of their relevance for the control of the passage of molecules through membrane openings,[8] the host compounds described here appear to us to be of great interest with respect to guest selection.[9]

Received: February 18, 1986;
revised: March 14, 1986 [Z 1672 IE]
German version: *Angew. Chem. 98* (1986) 549

[1] F. Vögtle, W. M. Müller, *J. Inclusion Phenom. 2* (1984) 369; D. O'Krongly, S. R. Denmeade, M. Y. Chiang, R. Breslow, *J. Am. Chem. Soc. 107* (1985) 5544; F. Diederich, K. Dick, *ibid. 106* (1984) 8024; J. R. Moran, S. Karbach, D. J. Cram, *ibid. 104* (1982) 5826; M. Dhaenens, L. Lacombe, J. M. Lehn, J.-P. Vigneron, *J. Chem. Soc. Chem. Commun. 1984*, 1098; J. Rebek, Jr., B. Askew, N. Islam, M. Killoran, D. Nemeth, R. Wolak, *J. Am. Chem. Soc. 107* (1985) 6736; H. Schrage, J. Franke, F. Vögtle, E. Steckhan, *Angew. Chem. 98* (1986) 335; *Angew. Chem. Int. Ed. Engl. 25* (1986) 336, and references cited therein.

[2] F. Vögtle, T. Merz, H. Wirtz, *Angew. Chem. 97* (1985) 226; *Angew. Chem. Int. Ed. Engl. 24* (1985) 221. In the meantime, an X-ray structure analysis of **2a** has been carried out. The dimensions of the cavity plausibly account for the inclusion of a benzene ring.

[3] **1a**: ^{1}H-NMR ($CDCl_3$/TMS int.): $\delta = 1.29$ (t, 36H, CH_3), 1.80 (s, 12 aliphat. H), 3.24 (s, 12 benzyl. H), 4.25 (m, ABX, 24 OCH_2), 6.78, 6.82, 7.08, 7.12 (AA'BB', 24 aromat. H), 7.26 (s, 6 aromat. H).—^{13}C-NMR (CD_2Cl_2): $\delta = 171.4$, 141.9, 139.7, 131.6, 129.3, 127.3, 124.8, 61.6, 58.1, 36.5, 25.2, 14.1.—FAB-MS: *m/z* 1723 $[M+H]^{\oplus}$.

[4] **1b**: ^{1}H-NMR (D_2O standard): $\delta = 1.65$ (s, 12 aliphat. H), 3.15 (s, 12 benzyl. H), 6.9, 7.05 (AA'BB', 24 aromat. H), 7.3 (s, 6 aromat. H).

[5] A. Caron, J. Guilhelm, C. Riche, C. Pascarol, B. Alpha, J. M. Lehn, J. C. Rodriguez-Ubis, *Helv. Chim. Acta 68* (1985) 1577.

[6] Compare the open-chain hexanoic acids: a) F. M. Menger, M. Takeshita, J. F. Chow, *J. Am. Chem. Soc. 103* (1981) 5939; b) S. Shinkai, S. Mori, T. Tsubaki, T. Sone, O. Manabe, *Tetrahedron Lett. 25* (1984) 5315; high-field shifts were not reported in this case.

[7] **6a**: ^{1}H-NMR ($CDCl_3$/TMS int.): $\delta = 1.25$ (t, 36H, CH_3), 1.89 (s, 12 aliphat. H), 2.05 (s, 6H, bridgehead CH_3), 3.33 (s, 12 benzyl. H), 4.22 (q, 24 OCH_2), 7.24, 7.64 (24 aromat. H).—EI-MS: *m/z* 1622.

[8] Review: D. W. Urry, *Top. Curr. Chem. 128* (1985) 175.

[9] For transport of molecules with or against a pH gradient, see [8].

$[Cu_{36}I_{56}]^{20\ominus}$—a Novel Polyanion in the Compound $(pyH)_2[Cu_3I_5]$**

By *Hans Hartl** and *Joachim Fuchs*

Dedicated to Professor Georg Manecke on the occasion of his 70th birthday

In iodocuprates(I) $[Cu_mI_n]^{(n-m)\ominus}$, trigonal-planar and tetrahedrally coordinated Cu atoms are present; the CuI_3 units may be joined by common edges and the CuI_4 tetrahedrons by common corners, edges, and faces (!) to form higher condensed iodocuprate(I) ions. This results in a surprisingly wide range of possibilities in the structural chemistry of iodocuprates(I), from low-molecular-weight units such as $[CuI_3]^{2\ominus}$[1] or the binuclear ions $[Cu_2I_4]^{2\ominus}$, $[Cu_2I_5]^{3\ominus}$, and $[Cu_2I_6]^{4\ominus}$ and higher condensed units such as $[Cu_4I_6]^{2\ominus}$, $[Cu_4I_8]^{4\ominus}$, $[Cu_5I_7]^{2\ominus}$, $[Cu_6I_{11}]^{5\ominus}$, or $[Cu_8I_{13}]^{5\ominus}$ to polymeric anions such as $^1_\infty[CuI_2^{\ominus}]$, $^1_\infty[Cu_2I_3^{\ominus}]$, $^1_\infty[Cu_3I_4^{\ominus}]$, or $^2_\infty[Cu_2I_3^{\ominus}]$.[2] Such a variety of structures is not encountered for other iodometalates. The structure and degree of condensation of the iodocuprates(I) is determined by the size, form, and charge distribution of the cations involved.

[*] Prof. Dr. H. Hartl, Prof. Dr. J. Fuchs
Institut für Anorganische und Analytische Chemie
der Freien Universität
Fabeckstrasse 34/36, D-1000 Berlin 33 (FRG)

[**] Synthesis and Structural Investigation of Iodocuprates(I), Part 7. This work was supported by the Fonds der Chemischen Industrie.—Part 6: [2].

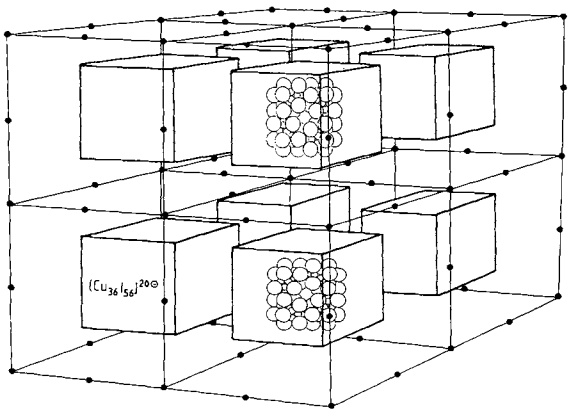


Fig. 1. Structure and arrangement of the anion $[Cu_{36}I_{56}]^{20\ominus}$ in the crystal.

In the system pyridinium iodide/CuI, it has now been possible to isolate the largest discrete iodocuprate(I) ion to date. The structural determination of a compound having the composition $(pyH)_2[Cu_3I_5]$ revealed that the correct formulation was $(pyH)_{24}([Cu_{36}I_{56}]I_4)$.[3] In addition to isolated $I^{\ominus}$ ions at the positions 8b and 24d of the cubic space group *Fm3c*, eight iodocuprate(I) ions $[Cu_{36}I_{56}]^{20\ominus}$ are present in the unit cell (Fig. 1). 36 CuI_4 tetrahedrons joined by two or three common edges form a structure having the extremely rare molecule symmetry 432 (=O). The 56 I atoms of the anion can be regarded ideally as a section of a cubic close-packing of spheres (Fig. 2a); eight cubes, face-centered on all sides, combine to form a larger cube, which lacks the I atoms in the middle of the faces and in the center. The Cu atoms occupy 36 tetrahedral gaps of the iodine partial lattice in such a way that 24 Cu atoms occupy the corners of a cube with octahedral habit, i.e., the positions formed by cutting off the corners of a cube. The 12 remaining Cu atoms lie at the middle of the edges of this cube; the centers of the faces and of the cube itself are unoccupied (Fig. 2b). If a van der Waals radius of 2.2 Å is assumed for $I^{\ominus}$, a diameter of approximately 7 Å is obtained for the cavity in the center of the anion. The holes in the centers of the faces have a diameter of about 1.5 Å and are therefore too small to allow guest molecules or cations to enter the cavity of the cube; the compound crystallizes without molecules of solvent.

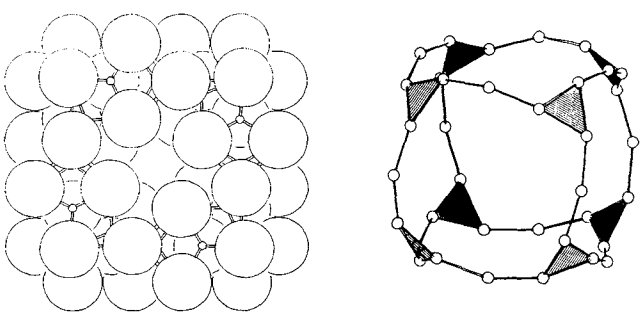


Fig. 2. a) View along an axis perpendicular to a face of the cube, showing the anion $[Cu_{36}I_{56}]^{20\ominus}$; large circles, I; small circles, Cu; distances [pm]: Cu-I 264.9(5)-270.8(5), Cu···Cu 278.9(5)-285.4(7); angle [°]: I-Cu-I 103.6(2)-113.7(1). b) Cu partial structure of the anion $[Cu_{36}I_{56}]^{20\ominus}$ (cube with octahedral habit). Hatched triangles: front side; black triangles: rear side.

The pyridinium ion $C_5H_6N^{\oplus}$, which is isosteric with benzene, often appears to have the high molecule symmetry of benzene on account of the disorder of the NH positions, which results in unusual crystal structures likewise exhibiting high symmetry.[4] In the present case, the 192 pyridinium rings of the unit cell are situated around their center of gravity in 0 0.19 0.11 and 0 0.22 0.23 and form, together with the 32 $I^{\ominus}$ ions, a suitable matrix for the eight $[Cu_{36}I_{56}]^{20\ominus}$ ions.

Experimental Procedure

Pyridinium iodide (1.38 g, 6.7 mmol) was allowed to react with CuI (1.9 g, 10 mmol) in 150 mL of acetone for 2–3 h at reflux and the reaction mixture was then filtered while still hot. Yellow-brown cube-shaped crystals precipitated upon slow cooling and addition of anhydrous ether or chloroform (1–2 drops/min).

Received: February 18, 1986;
revised: March 14, 1986 [Z 1673 IE]
German version: *Angew. Chem. 98* (1986) 550

[1] G. A. Bowmaker, G. R. Clark, D. A. Rogers, *J. Chem. Soc. Dalton Trans. 1984*, 37.

[2] H. Hartl, I. Brüdgam, F. Mahdjour-Hassan-Abadi, *Z. Naturforsch. B 40* (1985) 1032, and references cited therein; G. A. Bowmaker, G. R. Clark, D. K. P. Yuen, *J. Chem. Soc. Dalton Trans. 1976*, 2329; N. P. Rath, E. M. Holt, *J. Chem. Soc. Chem. Commun. 1985*, 665; S. Andersson, S. Jagner, *Acta Chem. Scand. A 39* (1985) 181.

[3] *Fm3c*, $a = 3825.2(8)$ pm, $\varrho_{calcd} = 2.69$ g·cm^{-3}, $Z = 96 \times [(pyH)_2(Cu_3I_5)]$, $\mu = 94.9$ cm^{-1} ($Mo_{K\alpha}$). 1197 unique reflections, 651 with $I > 2\sigma(I)$, were used for the structure determination by means of Patterson and Fourier methods [5]. $R = 0.058$. Further details of the crystal structure investigation may be obtained from the Fachinformationszentrum Energie, Physik, Mathematik GmbH, D-7514 Eggenstein-Leopoldshafen 2 (FRG), on quoting the depository number CSD 51893, the names of the authors, and the journal citation.

[4] Examples: S. Geller, *Science 176* (1972) 1016; S. Geller, P. M. Skarstad, S. A. Wilber, *J. Electrochem. Soc. 122* (1975) 332; L. Y. Y. Chan, S. Geller, P. C. Skarstad, *J. Solid State Chem. 25* (1978) 85.

[5] P. Luger, J. Fuchs, *Acta Crystallogr. Sect. A*, in press.

Transition-Metal Clusters as Catalysts of Unconventional Reactions: Reductive C–N Coupling of Alkyl Isocyanates**

By *Georg Süss-Fink** and *Gerhard Herrmann*

Despite the great expectations that are placed in the catalytic potential of transition-metal clusters,[1] the use of such compounds has been limited up to now almost exclusively to conventional catalytic reactions.[2] An unconventional application, which we had found for the first time, was the spirocyclization of alkyl isocyanates to spiroheterocycles catalyzed by the cluster anion $[HRu_3(CO)_{10}(SiEt_3)_2]^{\ominus}$.[3]

Herein we report a novel reductive C–N coupling of alkyl isocyanates **1** to give *N*-formylureas **2**. The reaction takes place in the presence of the tetranuclear cluster anion $[H_3Ru_4(CO)_{12}]^{\ominus}$[4] as catalyst (precursor) (Table 1). The products **2a–c** can be isolated by preparative thin layer chromatography (silica gel, diethyl ether). When D_2 is used in place of H_2, the primary product formed from methyl isocyanate **1a** is presumably the expected product **2d**; chromatographic workup, however, affords the species **2e**, deuterated specifically in the formyl position. In every case, the reaction mixture contains the intact cluster anion, the catalytic activity of which remains unchanged.

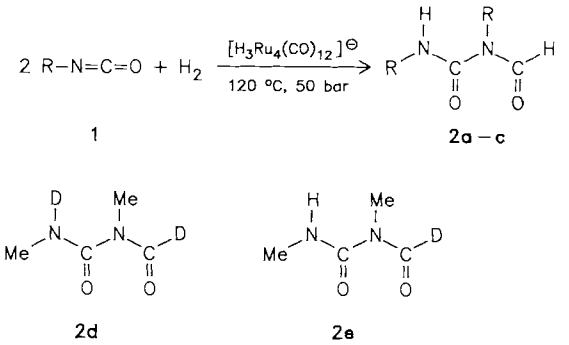


Table 1. Preparation of **2a–c**: **1a–c** (50 mmol) and $[N(PPh_3)_2][H_3Ru_4(CO)_{12}]$ (0.05 mmol) were allowed to react under 50 bar of H_2 in 25 mL of tetrahydrofuran at 120°C in a 100-mL autoclave.

	R	Reaction time [h]	Yield [%]	Turnover number [5]
2a	Me	20	46	230
2b	Et	40	41	205
2c	*n*Pr	40	56	280

The diphenyl derivative **2**, R = Ph, was assumed to be an intermediate in the protonolysis of the tetramethylethylenediamine adduct of 1,4-diphenyl-1,4-diaza-2-nickela-3,5-cyclopentanedione: instead of **2**, R = Ph, however, the decarbonylation product *N,N'*-diphenylurea was isolated.[6] In agreement with these results, exclusively *N,N'*-diphenylurea is found in the reductive C–N coupling of phenyl isocyanate in the presence of $[H_3Ru_4(CO)_{12}]^{\ominus}$; also isocyanates with branched alkyl groups, such as *i*PrNCO, give only the symmetrical urea. Whereas the corresponding ureas are always present as side products for EtNCO **1b** and *n*PrNCO **1c**, *N,N'*-dimethylurea is not observed in the reaction of MeNCO **1a**.

The composition of the new *N*-formylureas (*N*-carbamoylformamides) **2** was established by elemental analysis and (high-resolution) mass spectrometry. The IR and nuclear magnetic resonance data are in agreement with the given structures (Table 2).

Table 2. Characteristic IR and NMR data for the *N*-formylureas **2a–c** and **2e**.

		2a	**2b**	**2c**	**2e**
IR [a]	$\tilde{\nu}$(CO)	1707, 1673	1708, 1670	1707, 1672	1684, 1658
	$\tilde{\nu}$(NH)	3376	3316	3314	3376
^{1}H-NMR [b]	δ(CH$_3$)	2.84 (d, 3)	1.18 (t, 3)	0.90 (t, 3)	2.85 (d, 3)
		3.13 (s, 3)	1.24 (t, 3)	0.94 (t, 3)	3.18 (s, 3)
	δ(CH$_2$)		3.33 (dq, 2)	1.60 (m, 4)	
			3.68 (q, 2)	3.27 (dt, 2)	
				3.57 (t, 2)	
	δ(CHO)	8.40 (br, 2)	8.45 (s, 1)	8.44 (s, 1)	
	δ(NH)		8.51 (br, 1)	8.60 (br, 1)	8.40 (br, 1)
^{13}C-NMR [c]	δ(CH$_3$)	26.4	14.7	10.8	26.2
		32.1	16.0	11.2	31.9
	δ(CH$_2$)		34.9	22.5, 23.3	
			40.4	41.5, 46.8	
	δ(CO)	154.0	152.7	152.8	153.9
		164.5	164.7	164.9	164.2 (t)

[a] KBr disk (**2a**, **2e**); film (**2b**, **2c**); [cm^{-1}]. [b] $CDCl_3$, 25°C, 250 MHz. [c] $CDCl_3$, 30°C, 22.5 MHz.

[*] Priv.-Doz. Dr. G. Süss-Fink [+], Dipl.-Chem. G. Herrmann
Laboratorium für Anorganische Chemie der Universität
Universitätsstrasse 30, D-8580 Bayreuth (FRG)

[+] New address:
Institut für Anorganische Chemie der Technischen Hochschule
Templergraben 55, D-5100 Aachen (FRG)

[**] This work was supported by the Deutsche Forschungsgemeinschaft, the Fonds der Chemischen Industrie, and Johnson Matthey Chemicals Limited.

Since, in all cases, the corresponding formamides can be detected in the reaction solution by gas chromatography, the role of the catalyst is possibly to hydrogenate the isocyanate.[7]

Received: February 10, 1986;
revised: March 19, 1986 [Z 1665 IE]
German version: *Angew. Chem. 98* (1986) 568

CAS Registry numbers:
1a, 624-83-9; **1b**, 109-90-0; **1c**, 110-78-1; **2a**, 101981-14-0; **2b**, 101981-15-1; **2c**, 101981-16-2; **2e**, 101981-17-3; PhNCO, 103-71-9; $(PhNH)_2CO$, 102-07-8; *i*-PrNCO, 1795-48-8; $(i\text{-PrNH})_2CO$, 4128-37-4; $(EtNH)_2CO$, 623-76-7; $(i\text{-PrNH})_2CO$, 623-95-0; $[N(PPh_3)_2][H_3Ru_4(CO)_{12}]$, 70073-17-5.

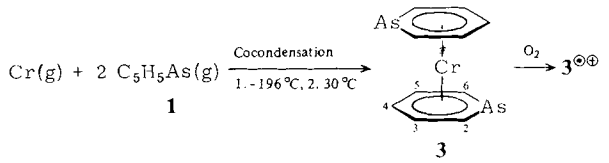
[1] E. L. Muetterties, *Science 196* (1977) 839; *Bull. Soc. Chim. Belg. 84* (1975) 959; B. F. G. Johnson, J. Lewis, *Pure Appl. Chem. 44* (1975) 229; R. Whyman in B. F. G. Johnson (Ed.): *Transition Metal Clusters*, Wiley, Chichester 1980.
[2] E. L. Muetterties, M. J. Krause, *Angew. Chem. 95* (1983) 135; *Angew. Chem. Int. Ed. Engl. 22* (1983) 135.
[3] G. Süss-Fink, G. Herrmann, U. Thewalt, *Angew. Chem. 95* (1983) 899; *Angew. Chem. Int. Ed. Engl. 22* (1983) 880; *Angew. Chem. Suppl. 1982*, 71.
[4] J. W. Koepke, J. R. Johnson, S. A. R. Knox, H. D. Kaesz, *J. Am. Chem. Soc. 97* (1975) 3947.
[5] Turnover number (catalytic turnover): mole product/mole catalyst.
[6] H. Hoberg, B. W. Oster, C. Krüger, Y. H. Tsay, *J. Organomet. Chem. 252* (1983) 365.
[7] G. Süss-Fink, G. Herrmann, unpublished results; cf. G. Herrmann, *Dissertation*, Universität Bayreuth 1986.

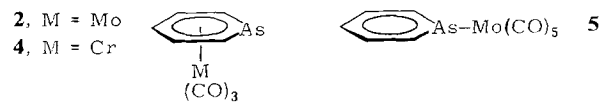
Bis(η^6-arsabenzene)chromium(0)**

By *Christoph Elschenbroich,* Jörg Kroker, Werner Massa, Martin Wünsch,* and *Arthur J. Ashe III*

Compared to the extensively documented organic chemistry of six-membered ring heterocycles only very few studies on the synthesis and properties of bis(η^6-heteroarene)metal complexes have so far been reported in the literature.[2] The reasons for this are the limited number of synthetic routes to such complexes as well as the ambident nature of many heteroarenes. The latter aspect requires for the synthesis of an η^6-complex the donor ability of lone pairs, which favors classical η^1-coordination, to be suppressed.[3] In the case of pyridine the lone pair on the nitrogen atom could be sterically blocked by 2,6-dialkyl substitution, thus enabling the synthesis of bis(2,6-dimethyl-η^6-pyridine)chromium as the first binary sandwich complex of a neutral heteroarene.[2e, f] In our attempts to prepare the unsubstituted parent compounds $(\eta^6\text{-}C_5H_5E)_2Cr$ (E = Group 5B element) we first selected arsabenzene **1** as ligand, since the σ-basicity of **1** is much lower than that of pyridine,[4] and, furthermore, the ability of **1** to undergo η^6-coordination has already been demonstrated in the formation of the complex $[(\eta^6\text{-}C_5H_5As)Mo(CO)_3]$ **2**.[5]

We have now synthesized bis(η^6-arsabenzene)chromium(0) **3** in 15% yield by metal atom-ligand cocondensation. The reddish-black, air-sensitive crystals of **3** are sublimable under high vacuum without decomposition.[6]





The cyclovoltammetrically determined redox potential $E_{1/2}(\mathbf{3}/\mathbf{3}^{\odot\oplus}) = -0.51$ V (reversible, at 25°C in 1,2-dimethoxyethane (DME)/tetra-*n*-butylammonium perchlorate (TBAP) versus saturated calomel electrode) displays an anodic shift of 0.17 V compared to that of bis(η^6-benzene)chromium. **3** can also be reduced, albeit not completely reversibly ($E_{1/2}(\mathbf{3}/\mathbf{3}^{\odot\ominus}) = -1.36$ V, 25°C, 100 mV s^{-1}, $\Delta E_p = 94$ mV, $I_{pa}/I_{pc} = 0.6$). Comparison with the electrochemical data for free arsabenzene **1** ($E_{1/2}(\mathbf{1}/\mathbf{1}^{\odot\ominus}) = -1.10$ V, irrev., $E_{1/2}(\mathbf{1}/\mathbf{1}^{\odot\ominus}) = -2.08$ V[8]) shows that the shifts of the redox potentials due to complexation are similar in magnitude for the transitions from the neutral molecule to the radical cation and to the radical anion (+0.59 V and +0.72 V, respectively).

An η^6-coordination of the two heteroarenes in **3** can already be inferred from the NMR spectra (Table 1): As has already been observed in the case of **2**, the unusually large difference in the shielding of the protons H-2,6 and H-3,4,5 in the free ligand **1** is reduced in the sandwich complex **3**. According to the ^{1}H-NMR data of $[(C_6H_5As)Mo(CO)_5]$ **5** this does not occur upon η^1-coordination.[9] The NMR spectra of **3** show no signs of freezing-in of ring rotation down to $T = -70$°C. Such a freezing-in could not be ruled out a priori, since a rotational barrier had been found for open metallocenes.[10]

To answer the related question as to whether a certain conformation is preferred, a single crystal of **3**, twinned along (001), was subjected to an X-ray crystallographic analysis (space group $P2_1/n$; $a = 658.8(5)$, $b = 783.1(5)$, $c = 963.8(4)$ pm; $\beta = 94.78(5)°$; $Z = 2$; $T = -90$°C). The analysis revealed a high degree of disorder of the whole complex. In this context, note that no refined crystal structure investigations of sandwich complexes with unsubstituted heterocycles have thus far been reported in the liter-

Table 1. ^{1}H- and ^{13}C-NMR parameters of the ligand **1** and the complexes **3** and **4** [a].

	1	**3**	**4** [d]
^{1}H-NMR			
δ(H-2,6); ($\Delta\delta$) [b]	9.79	4.22 (−5.57) [c]	5.99 (−3.80)
^3J(H-2,H-3)	11.1	7.0	9.5
δ(H-3,5); ($\Delta\delta$)	7.90	5.10 (−2.80)	5.55 (−2.35)
^3J(H-3,H-4)	8.4	6.2	7.0
δ(H-4); ($\Delta\delta$)	7.60	4.86 (−2.74)	5.98 (−1.62)
^{13}C-NMR			
δ(C-2,6); ($\Delta\delta$)	168.4	86.8 (−81.6)	114.9 (−53.5)
^1J(C-2,H-2)	158.7	164.8	167.9
δ(C-3,5); ($\Delta\delta$)	133.8	84.8 (−49.0)	95.6 (−38.2)
^1J(C-3,H-3)	156.8	163.2	170.3
δ(C-4); ($\Delta\delta$)	129.0	75.7 (−53.3)	91.1 (−37.9)
^1J(C-4,H-4)	159.4	164.4	171.6

[a] In [D$_8$]THF at 30°C, 400 and 100 MHz, resp., δ values relative to TMS, coupling constants in Hz. [b] $\Delta\delta$ = coordination shift. [c] δ(H-2,6) is temperature dependent: 4.25 (+30°C), 4.16 (−10°C), 4.06 (−40°C). [d] **4** was synthesized analogously to **2** [5].

[*] Prof. Dr. C. Elschenbroich, Dipl.-Chem. J. Kroker, Priv.-Doz. Dr. W. Massa, Dipl.-Chem. M. Wünsch
Fachbereich Chemie der Universität
Hans-Meerwein-Strasse, D-3550 Marburg 1 (FRG)
Prof. Dr. A. J. Ashe III
Department of Chemistry, University of Michigan
Ann Arbor, MI 48109 (USA)

[**] Metal π-Complexes of Benzene Derivatives, Part 27. This work was supported by the Deutsche Forschungsgemeinschaft and the Fonds der Chemischen Industrie.—Part 26: [1].

ature. In the case of **3**, the disorder can be described to a good approximation in terms of a model in which half of the As atoms occupy position 1 of the ring and the other half position 4 of the ring ($R_g = 0.086$ for 424 reflections). The chromium atom is located 25 pm from a crystallographic center of symmetry, so that the two alternative orientations of the complex are slightly displaced from each other. It is therefore impossible to infer structural details of the coordinated arsabenzene rings. However, from the positions of the As atoms it can be concluded that either the *cis*- or the *trans*-eclipsed form is present, and, from the maximum Cr–As distance of 252 pm that genuine η^6-coordination prevails.[11]

A first indication of the electronic structure of **3** is provided by the ESR spectra of the radical cation $\mathbf{3}^{\odot\oplus}$: Whereas the data obtained for $\mathbf{3}^{\odot\oplus}$ in fluid solution (dimethylformamide (DMF)/$CHCl_3$ = 1:1, 30°C, $\langle g \rangle = 1.9892$, $a(^{53}Cr) = 19.3$ G, ligand hyperfine structure only partially resolved) are consistent with the parameters of bis(η^6-arene)chromium(d^5) cations,[12] the spectrum of $\mathbf{3}^{\odot\oplus}$ recorded in rigid solution (DMF/$CHCl_3$ = 1:1, −135°C, $g_\parallel = 1.9730$, $g_\perp = 1.9980$, $A_\perp(^{53}Cr) \approx 20$ G) shows a g-anisotropy, typical for bis(η^6-arene)chromium anions.[13] In the latter, an MO with dominant π-ligand character is singly occupied. The similar g-anisotropy thus suggests that—in contrast to cations of the corresponding carbocyclic arene complex—the singly occupied HOMO in $\mathbf{3}^{\odot\oplus}$ has considerable ligand character.

Received: December 30, 1985;
revised: March 17, 1986 [Z 1600 IE]
German version: *Angew. Chem. 98* (1986) 562

CAS Registry numbers:
1, 289-31-6; **3**, 101934-66-1; $\mathbf{3}^{\odot\oplus}$, 101934-67-2; Cr, 7440-47-3.

[1] C. Elschenbroich, J. Schneider, H. Prinzbach, W.-O. Fessner, *Organometallics*, in press.

[2] a) G. E. Herberich, G. Greiss, H. F. Heil, J. Müller, *J. Chem. Soc. Chem. Commun. 1971*, 1328; b) G. E. Herberich, G. Greiss, *Chem. Ber. 105* (1972) 3413; c) G. E. Herberich, M. J. Becker, G. Greiss, *ibid. 107* (1974) 3780; d) A. J. Ashe III, E. Myers, P. Shu, T. V. Lehmann, *J. Am. Chem. Soc. 97* (1975) 6865; e) L. M. Simmons, P. E. Riley, R. E. Davies, J. J. Lagowski, *ibid. 98* (1976) 1044; f) P. E. Riley, R. E. Davies, *Inorg. Chem. 15* (1976) 2735; g) A. J. Ashe III, W. Butler, H. F. Sandford, *J. Am. Chem. Soc. 101* (1979) 7066; h) binary transition metal complexes of the λ^4-phosphorin anions 1-R-2,4,6-R'$_3$-$C_5H_2P^{\ominus}$ undergo η^5-coordination and are to be regarded as 2,6-bridged open metallocenes: T. Dave, S. Berger, E. Bilger, H. Kaletsch, J. Pebler, J. Knecht, K. Dimroth, *Organometallics 4* (1985) 1565; G. Baum, W. Massa, *ibid. 4* (1985) 1572; i) an η^6-bonded phosphabenzene derivative is present in the mixed sandwich complex [(1,3,5-Ph_3-η^6-C_5H_2P)(η^5-C_5H_5)Mn]: F. Nief, C. Charrier, F. Mathey, M. Simalty, *J. Organomet. Chem. 187* (1980) 277; J. Fischer, A. De Cian, F. Nief, *Acta Crystallogr. Sect. B 37* (1981) 1067.

[3] a) J. Deberitz, H. Nöth, *Chem. Ber. 103* (1970) 2542; *106* (1973) 2222; *J. Organomet. Chem. 49* (1973) 453; b) H. Vahrenkamp, H. Nöth, *Chem. Ber. 105* (1972) 1148; *106* (1973) 2227; H.-G. Biedermann, K. Öfele, J. Tajtelbaum, *Z. Naturforsch. B: Anorg. Chem. Org. Chem. 31* (1976) 321.

[4] a) A. J. Ashe III, *Top. Curr. Chem. 105* (1982) 125; b) R. V. Hodges, J. L. Beauchamp, A. J. Ashe III, W.-T. Chan, *Organometallics 4* (1985) 457.

[5] A. J. Ashe III, J. C. Colburn, *J. Am. Chem. Soc. 99* (1977) 8099.

[6] Procedure: The vapors of arsabenzene **1** (3 g, 36 mmol) [7] and chromium (0.3 g, 5.8 mmol) were cocondensed over a period of 1.5 h onto the walls of an evacuated, cooled (−196°C) reaction vessel. After warming to room temperature under N_2, the dark red co-condensate was taken up in tetrahydrofuran and the solution filtered over silanated silica gel. The solvent and unchanged **1**, which can be recovered in this way, were removed in a high vacuum. Recrystallization of the residue from toluene afforded **3** in the form of reddish-black, analytically pure crystals (yield: 290 mg (0.87 mmol), 15% referred to vaporized Cr). M.p. 253°C (dec.); MS (EI, 70 eV): m/z 332 (26%, $M^{\oplus}$), 192 (39%, $M^{\oplus} - L$), 140 (58%, $L^{\oplus}$), 52 (100% $^{52}Cr^{\oplus}$).

[7] A. J. Ashe III, W.-T. Chan, *J. Org. Chem. 44* (1979) 1409.

[8] M. Wünsch, C. Elschenbroich, unpublished.

[9] ^{1}H-NMR data of **5**: $\delta = 9.6$ (H-2,6), 7.8 (H-3,5), 7.5 (H-4) [5]; cf. also A. J. Ashe III, R. R. Sharp, J. W. Tolan, *J. Am. Chem. Soc. 98* (1976) 5451.

[10] D. R. Wilson, R. D. Ernst, T. H. Cymbaluk, *Organometallics 2* (1983) 1220.

[11] Other Cr–As distances: 252 pm in [$(CO)_5CrAs(Me)_2Mn(CO)_5$] (H. Vahrenkamp, *Chem. Ber. 105* (1972) 1486), 238 pm in [$C_6H_5As\{Cr(CO)_5\}_2$] (G. Huttner, J. von Seyerl, M. Marsili, H.-G. Schmid, *Angew. Chem. 87* (1975) 455; *Angew. Chem. Int. Ed. Engl. 14* (1975) 434).

[12] C. Elschenbroich, R. Möckel, U. Zenneck, D. Clack, *Ber. Bunsenges. Phys. Chem. 83* (1979) 1008.

[13] C. Elschenbroich, E. Bilger, J. Koch, J. Weber, *J. Am. Chem. Soc. 106* (1984) 4297, and references cited therein.

Dihydropyrazolopyridine and Bis(dihydroindolizine)—Novel Mono- and Bifunctional Photochromic Systems**

By *Heinz Dürr,* Charles Schommer,* and *Thomas Münzmay*

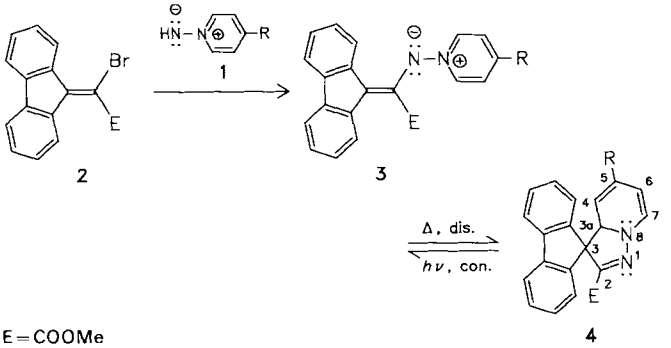
Dedicated to Professor Heinz A. Staab on the occasion of his 60th birthday

Photochromic systems have long claimed worldwide interest.[1] They are not only of great importance in fundamental research but also in practice, where they find application as light-filters, chemical actinometers, silver-free materials for display devices in reprotechnology and more recently in computer chips.[1] We recently reported on a photochromic system based on a 1,5-electrocyclization of spirodihydroindolizine.[2] The aim of our present work is to prepare new systems that can undergo 1,5-electrocyclizations as well as molecules containing two chromophores.

We now report on the extraordinary reactivity of 1-pyridinioamides ("pyridin-*N*-imines") **1** towards pentafulvenes such as **2**. The deep-colored betaines initially formed are converted in a 1,5-electrocyclic reaction into the novel dihydropyrazolo[1,5-*a*]pyridines **4**; these are the first dihydropyrazole-based photochromic systems (Type 2,3-systems[3]).

For the synthesis of **4**, the *N*-imines **1** were generated from the corresponding *N*-aminopyridinium salts[4] with potassium carbonate in anhydrous dimethylformamide and allowed to react directly with **2** without prior isolation.[4d]

The deep-red to violet products transform within a few hours into the yellow title compounds **4**, whose structure



[*] Prof. Dr. H. Dürr, Dipl.-Chem. C. Schommer, Dipl.-Chem. T. Münzmay
Fachrichtung 14.1 Organische Chemie der Universität
D-6600 Saarbrücken 11 (FRG)

[**] Photochromic Systems, Part 11. This work was supported by the Deutsche Forschungsgemeinschaft and the Fonds der Chemischen Industrie.—Part 10: H. Dürr, V. Bach, *Tetrahedron Lett.*, in press.

Table 1. Some data of the dihydropyrazolo[1,5-*a*]pyridines **4** (UV/VIS data: see Table 2; for ^{1}H-NMR of **4a** see [5]).

	R	Yield [%]	M.p. [°C]	IR (KBr) [cm^{-1}] $\tilde{\nu}$(C=O)	$\tilde{\nu}$(C=N)
4a	H	67	154	1710	1505
4b	CH_3	30	150	1700	1505
4c	Ph	94	155	1715	1518
4d	CN	35	162	1702	1505
4e	COPh	15	176	1705 1650	1510

was derived from the spectroscopic data (Table 1). The assignment of the ^{1}H-NMR signals of the dihydropyridine protons (H-3a to H-7)[5] was accomplished by double resonance experiments, by a (^{1}H,^{1}H)-COSY experiment, and by comparison with the spectra of dihydroindolizines. The structure of **4** could be further verified by ^{13}C-DEPT spectroscopy and by a ^{13}C,^{1}H-correlated 2D-NMR experiment.—The structure of the intermediates **3** was elucidated by ^{1}H-NMR of the long-lived betaine **3g**. The conversion of **3** into **4** is a thermal disrotatory 1,5-electrocyclic ring-closure.

Table 2. Some UV/VIS data of **3** and **4**, as well as kinetic data [a] for the cyclization **3**→**4**.

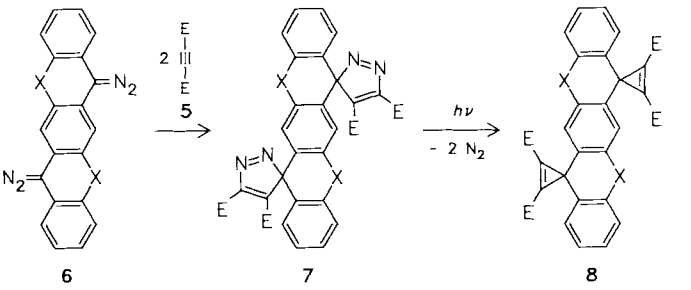
	λ_{max} [nm] (lgε) **3**	**4**	10^3 k [s^{-1}]	$\tau_{1/2}$ [s]
a	511	401 (3.95)	2.17	320
b	511	399 (3.96)	1.89	367
c	547	406 (3.96)	2.46	282
d	527	406 (3.96)	5.14	135
e	556	414 (3.81) 365 (3.80)	4.21	165

[a] At 25°C in CH_2Cl_2.

Table 2 shows the absorption maxima in the electronic spectrum of the betaines **3** and the dihydropyrazolopyridines **4**. The compounds **4** are converted in a photochemical controtatory 1,5-electrocyclic ring-opening reaction into **3**. The half-lives $\tau_{1/2} = \ln 2/k$ are also listed in Table 2. The compounds **3** and **4**, which can undergo reversible interconversion, thus form a novel photochromic system whose central reaction is 1,5-electrocyclic ring-opening.

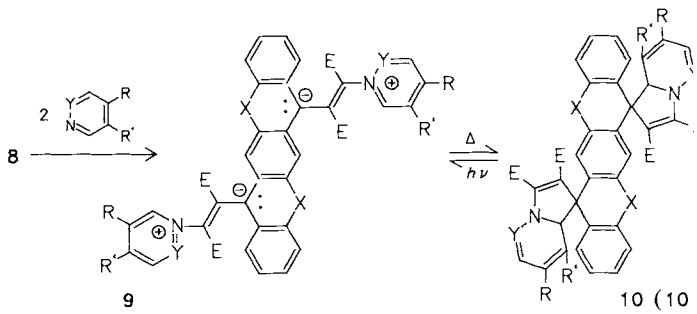
We also report on the novel dichromophoric bis(dihydroindolizines) **10**. Based on the synthesis for monofunctional dihydroindolizines, the bifunctional 3*H*-pyrazoles **7** were generated first by 1,3-dipolar cycloaddition of the bis(diazo) compounds **6** to acetylenedicarboxylates **5**.[6a,b] The structure of **7** could be verified by ^{1}H-NMR, IR, and mass spectroscopy and by elemental analysis.

The bis(pyrazoles) **7** are cyclic *cis*-azo compounds, which can be converted photochemically with loss of nitrogen into cyclopropenes[6c] (in ether, pyrex filter, Hg high-pressure lamp HPK 125W; yield: **8a** 10%, **8c** 50%). Recrystallization of the solvent-free residue (ether) afforded the bis(cyclopropenes) **8**, which showed the strong IR bands characteristic for the cyclopropenes at 1850 cm^{-1}. For the synthesis of the photochromic bis(dihydroindolizines) **10**, the electrophilic bis(cyclopropenes) **8** were allowed to react with six-membered N-heterocycles in the molar ratio 1:2 (room temperature, ether). In all cases the deep-colored betaines **9** (or **9'**) occurred as intermediates which thermally cyclized to the yellow bis(dihy-

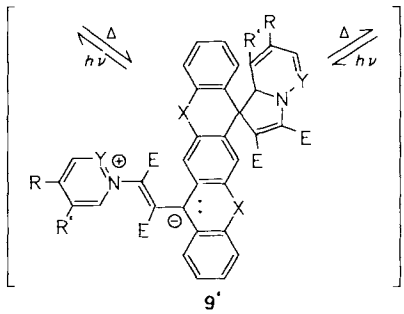


6 **7** **8**

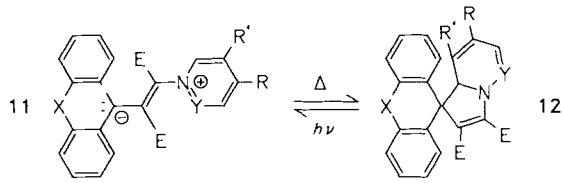
a, X = H, H; b ≡ a; c, X = —



9 **10** (10



9'



11 **12**

Table 3. Some data of the products **9** and **10** (**10'**), as well as some data for comparison of **11** and **12**.

9, **10**	R, R'	X	Y	Yield [%]	M.p. [°C]	λ_{max} [nm] ($\varepsilon \cdot 10^{-3}$) [a] **9**	**10**	10^4 k [s^{-1}]
a	Benzo	H, H	CH	13	210	577 (13) [b]	396 (14)	2.0
b	Benzo	H, H	N	4	180	481 —	378 (16)	1.8
c [c]	H, H	—	N	56	240	526 —	387 (15)	103.0
11, **12**	R, R'	X	Y	Yield [%]		λ_{max} [nm] ($\varepsilon \cdot 10^{-3}$) [a] **11**	**12**	10^4 k [s^{-1}]
a	Benzo	H, H	CH	52		574 (9) [b]	383 (9.0)	1.3
b	Benzo	H, H	N	39		478 —	378 (9.4)	2.8
c	H, H	—	N	74		525 —	388 (9.0)	86.0

[a] At 25°C in CH_2Cl_2. [b] Determined by the Fischer method [7]. [c] Only **10c** and **10c'** could be separately isolated.

droindolizines) **10**. The adducts **10** were purified by column chromatography and recrystallized from ether. The assignment of the structures of **10** was possible on the basis of the ^{1}H-NMR, IR, and UV data.

The ^{1}H-NMR spectra of **10a, b** showed a sixfold splitting of the characteristic methyl ester signals and a complex splitting of the dihydropyridine and dihydropyridazine protons, respectively, thus indicating that both substances consist of inseparable diastereomers. **10c** and **10c'** (dihydropyridazine rings either *syn* or *anti* to the planar *trans*-fluoreneacene skeleton) could be isolated from the reaction mixture formed upon reaction of **8c** with pyridazine. According to the ^{1}H-NMR spectrum the isomers **10c** and **10c'** can interconvert by photochemical 1,5-electrocyclic ring opening and subsequent thermal cyclization.

The maxima in the UV/VIS region of **10a–c** lie between 378 and 396 nm (Table 3) and do not differ very greatly from those of the analogous monofunctional systems **12**[2a,b] (Table 3). The extinction coefficients of the bisadducts **10a–c** are about a factor of 1.5 to 1.7 greater than those of the monomers **12**. In solution, the compounds **10a, c** could be converted into the colored forms **9a–c** by irradiation with polychromatic light. A comparison of the bis(betaines) **9** with the analogous monobetaines **11** likewise shows good agreement of the maxima. The ε-values of **9a** and **11a** were determined from the degree of conversion using the Fischer method[7] (Table 3). Since the bisadduct **9a** has an ε-value 1.4 times higher for the longest-wavelength absorption than the monomer **11a**, it is very likely that both rings of the bisadduct can be opened. This photochemical ring opening **10** → **9'** → **9** should proceed in two one-photon steps (cf. also [8]). The rate constants of the cyclization of the betaines **9** → **10** points in all cases to a 1st order reaction; actually more complicated kinetics had been expected. The rate constants of the reaction **9** → **10** were increased in comparison to those of the monofunctional systems. The spiro bridge in **9c** causes a drastic increase in the rate constant compared to that of the mobile unbridged species **9a** and **9b**. The ΔH^+ values for the cyclization of **9** lie between 14 and 19 kcal/mol, the ΔS^+ values between -25 and -6 cal mol^{-1} K^{-1}. Hence, the ΔG^+_{298} values for all the compounds **9** are ca. 20 kcal/mol. That is, the novel bis(dihydroindolizines) **10** exhibit photochromic properties that are due to a 1,5-electrocyclic reversion to the betaines **9**.

Received: January 10, 1986;
revised: March 14, 1986 [Z 1617/1618 IE]
German version: *Angew. Chem. 98* (1986) 565

CAS Registry numbers:
1a, 25275-41-6; **1b**, 57156-85-1; **1c**, 102149-96-2; **1d**, 102149-97-3; **1e**, 102149-98-4; **2**, 18083-75-5; **3a**, 102149-99-5; **3b**, 102150-00-5; **3c**, 102150-01-6; **3d**, 102150-02-7; **3e**, 102150-03-8; **4a**, 102210-48-0; **4b**, 102210-49-1; **4c**, 102210-50-4; **4d**, 102210-51-5; **4e**, 102210-52-6; **6a**, 102150-04-9; **6b**, 102150-05-0; **7a**, 102210-53-7; **7b**, 102150-06-1; **8a**, 102150-07-2; **8b**, 102210-54-8; **9a**, 102210-55-9; **9b**, 102150-08-3; **9c**, 102150-09-4; **10a**, 102210-56-0; **10b**, 102210-57-1; **10c**, 102233-40-9; **11a**, 102150-10-7; **11b**, 102150-1-8; **11c**, 72206-53-2; **12a**, 102210-58-2; **12b**, 102210-59-3; **12c**, 72206-64-5; EC≡CE, 762-42-5; Isoquinoline, 119-65-3; Phthalazine, 253-52-1; Pyridazine, 289-80-5.

[1] a) N. Y. C. Chu, *Proc. X-th Symp. Photochem.*, Interlaken 1984; b) R. C. Bertelson in H. G. Brown (Ed.): *Photochromism*, Wiley-Interscience, New York 1971; c) R. Dessauer, J. P. Paris, *Adv. Photochem. 1* (1963) 275; d) H. Sixl, *Umschau 83* (1983) 474.

[2] a) G. Hauck, H. Dürr, *Angew. Chem. 91* (1979) 1010; *Angew. Chem. Int. Ed. Engl. 18* (1979) 945; b) H. Gross, H. Dürr, *Angew. Chem. 94* (1982) 204; *Angew. Chem. Int. Ed. Engl. 21* (1982) 216; *Angew. Chem. Suppl. 1982*, 559.

[3] a) C. R. Hardy, *Adv. Heterocycl. Chem. 36* (1984) 343; b) R. Huisgen, *Angew. Chem. 92* (1980) 979; *Angew. Chem. Int. Ed. Engl. 19* (1980) 947. Heteroatoms in 2,3-position of the hetero-pentadienyl anion.

[4] a) A. Meuwsen, R. Gösl, *Chem. Ber. 92* (1959) 2521; b) Y. Tamura, J. Minamikawa, M. Ikeda, *Synthesis 1977*, 1; c) Y. Tamura, J. Minamikawa, Y. Miki, S. Matsugashita, M. Ikeda, *Tetrahedron Lett. 1972*, 4133; d) T. L. Gilchrist, C. W. Rees, *J. Chem. Soc. C 1968*, 779.

[5] **4a**: ^{1}H-NMR ($CDCl_3$): $\delta = 3.51$ (s, 3H, CH_3), 4.62 (m, 1H, H-4), 5.21 (m, 1H, H-6), 5.56 (m, 1H, H-3a), 5.79 (m, 1H, H-5), 7.03 (m, 1H, H-7), 7.22 (m, 1H, arom.), 7.3–7.45 (m, 4H, arom.), 7.50 (m, 1H, arom.), 7.76 (m, 2H, arom.).

[6] a) R. W. Murray, A. M. Trozzolo, *J. Org. Chem. 26* (1961) 3109; b) J. van Alphen, *Recl. Trav. Chim. Pays-Bas 62* (1943) 483; c) L. Schrader, *Chem. Ber. 104* (1971) 941.

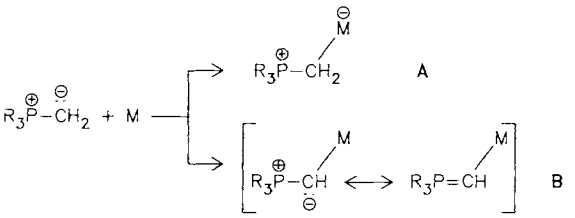
[7] E. Fischer, *J. Phys. Chem. 71* (1967) 3704.

[8] P. Spang, H. Dürr, *Angew. Chem. 96* (1984) 227; *Angew. Chem. Int. Ed. Engl. 23* (1984) 241.

A Polyfunctional Dititanacyclobutane

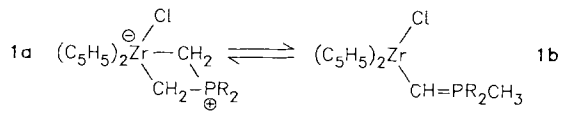
By *Hubert Schmidbaur,* Reinhard Pichl,* and *Gerhard Müller*

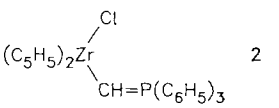
Whereas the chemistry of the metal complexes of phosphorus ylides (type **A**) has developed into a rapidly growing field of research[1] with important applications,[2] the chemistry of metal-substituted ylides (type **B**) has been relatively little investigated. All the examples that have been studied in detail are derived from the electron-deficient p- and d-block elements.[3]



Apparently, absolutely no compounds of type **B** containing electron-rich metal centers (such as the late transition-metal elements in low oxidation states) have been accessible. All attempts led only to isomeric products.[1] Moreover, even for the early transition metals, prototropism accompanied by the formation of a second metal–carbon bond between an R group of R_3P and the metal center is possible.

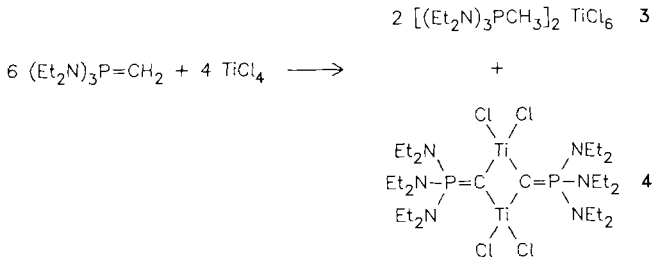
Thus, for example, an equilibrium mixture **1a/b** is found for the zirconium complex **1** ($R = N(C_2H_5)_2$) in solution. Only when no acidic H atom is present in the α-position to the P atom (e.g., in **2**) does the complex exist exclusively as an ylide.[4]





By the introduction of bulky diethylamino groups on the P atom, it has now been possible to replace both H atoms

[*] Prof. Dr. H. Schmidbaur, Dipl.-Chem. R. Pichl, Dr. G. Müller
Anorganisch-chemisches Institut der Technischen Universität München
Lichtenbergstrasse 4, D-8046 Garching (FRG)



on the ylidic C atom by Ti atoms. Reaction of $(Et_2N)_3P{=}CH_2$ with $TiCl_4$ in diethyl ether results in immediate formation of a violet solution, from which the bis(phosphoranylidene)dititanacyclobutane **4** can be isolated in over 70% yield. The formation of the by-product tris(diethylamino)methylphosphonium hexachlorotitanate **3** (yield 80%) proves the stoichiometry of the transylidation. The structure of the analogous hexachlorozirconate was recently established by X-ray diffraction analysis.[5] The cyclic double ylide **4** is even soluble in solvents of low polarity. The $^{31}P\{^1H\}$-NMR spectrum of **4** in benzene exhibits a singlet at $\delta = 26.22$. The ^1H- and ^{13}C-NMR spectra establish the equivalence of all 12 ethyl groups.[6] The signal of the ylidic C atom could not be located with certainty. Black-violet crystals form from toluene at $-78\,^\circ C$; the X-ray structure analysis gave the centrosymmetric molecular structure shown in Figure 1.[7]

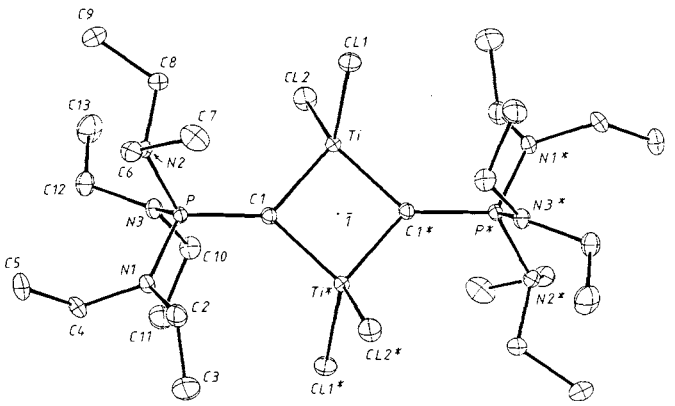


Fig. 1. Crystal structure of **4** (ORTEP, thermal ellipsoids 50%, without H atoms). Selected bond lengths [Å] and angles [°]: Ti-Cl1 2.278(1), Ti-Cl2 2.280(1), Ti-C1 1.957(2), Ti-C1* 1.957(2), P-C1 1.729(2), P-N1 1.656(2), P-N2 1.665(2), P-N3 1.644(2); Cl1-Ti-Cl2 110.69(3), Cl1-Ti-C1 116.32(7), Cl1-Ti-C1* 113.12(7), Cl2-Ti-C1 110.76(7), Cl2-Ti-C1* 117.04(7), C1-Ti-C1* 87.27(9), Ti-C1-Ti* 92.73(9), Ti-C1-P 128.0(1), Ti*-C1-P 136.9(1).

The most important detail of this structure, which has a nearly planar $PCTi_2CP$ framework, is the existence of four equal, remarkably short Ti–C distances (1.957(2) Å). This finding can be explained by the delocalization of the negative charge of the ylidic carbon atom into the Ti_2C_2 four-membered ring. The four Cl atoms are not completely symmetrically arranged with respect to the four-membered ring; this is revealed in part by the significantly different Cl-Ti-Cl1(2) angles.

The easily accessible complex **4** should prove to be an important starting material for numerous reactions.

Received: January 24, 1986 [Z 1638 IE]
German version: *Angew. Chem. 98* (1986) 572

CAS Registry numbers:
3, 101981-46-8; **4**, 101998-21-4; $(Et_2N)_3P{=}CH_2$, 98297-72-4; $TiCl_4$, 7550-45-0.

[1] H. Schmidbaur, *Angew. Chem. 95* (1983) 980; *Angew. Chem. Int. Ed. Engl. 22* (1983) 907; W. C. Kaska, *Coord. Chem. Rev. 48* (1983) 1; L. Weber in F. R. Hartley, S. Patai (Eds.): *The Chemistry of the Metal-Carbon Bond*, Wiley, Chichester 1982, p. 91.

[2] W. Keim, F. H. Kowaldt, R. Goddard, C. Krüger, *Angew. Chem. 90* (1978) 493; *Angew. Chem. Int. Ed. Engl. 17* (1978) 466; W. Keim, A. Behr, B. Limääcker, C. Krüger, *ibid. 95* (1983) 505 and *22* (1983) 503; *Angew. Chem. Suppl. 1983*, 655; K. A. Ostoja Starzewski, J. Witte, *Angew. Chem. 97* (1985) 610; *Angew. Chem. Int. Ed. Engl. 24* (1985) 599.

[3] Ylides with substituents from the main groups of the periodic table: H. Schmidbaur, *Acc. Chem. Res. 8* (1975) 62; *Adv. Organomet. Chem. 14* (1976) 205; derivatives of early-transition-metal elements: a) H. Schmidbaur, W. Scharf, H.-J. Füller, *Z. Naturforsch. B32* (1977) 858; b) H. Schmidbaur, R. Pichl, *ibid. 40* (1985) 352; c) J. C. Baldwin, N. L. Keder, C. E. Strouse, W. C. Kaska, *ibid. 35* (1980) 1289; d) K. I. Gell, J. Schwartz, *Inorg. Chem. 19* (1981) 3207; e) G. W. Rice, G. B. Ansell, M. A. Modrick, S. Zentz, *Organometallics 2* (1983) 154; f) G. Erker, P. Czisch, C. Krüger, J. M. Wallis, *ibid. 4* (1985) 2059; g) R. E. Cramer, R. B. Maynard, J. W. Gilje, *J. Am. Chem. Soc. 103* (1981) 3589; *100* (1978) 5562; *Inorg. Chem. 20* (1981) 2466; *19* (1980) 2564.

[4] See also [3a–f]; this is also in agreement with unpublished results (R. Pichl, Munich 1985).

[5] H. Schmidbaur, R. Pichl, G. Müller, *Z. Naturforsch. B41* (1986) 395.

[6] *Experimental procedure:* $TiCl_4$ (1.33 mL, 2.30 g, 12.1 mmol), dissolved in 20 mL of toluene, was added slowly to a solution of $(Et_2N)_3P{=}CH_2$ (5 mL, 4.76 g, 18.2 mmol) in 30 mL of diethyl ether at room temperature. The reaction mixture immediately turned violet. Upon cooling the reaction mixture to $-78\,^\circ C$, **3** precipitated out (yield 3.8 g, 79%) and was filtered off and then washed with toluene. The solvent was removed from the filtrate and the residue was recrystallized from toluene (1.6 g, 69%). The product **4** gave a correct elemental analysis, dec. temp. = 180 °C.—^1H-NMR (C_6D_6): $\delta = 1.07$ (t, $^3J(HCCH) = 7.2$ Hz; CH_3), 3.04 (dq, $^3J(PNCH) = 10.4$ Hz; CH_2). ^{13}C-NMR (C_6D_6): $\delta = 36.22$ (d, $^3J(PC) = 3.7$ Hz; CH_3), 62.18 (d, $^2J(PC) = 2.4$ Hz; CH_2). $^{31}P\{^1H\}$-NMR (C_6D_6): $\delta = 26.22$ (s).—**3**: ^1H-NMR ($CDCl_3$): $\delta = 1.12$ (t, $^3J(HCCH) = 7.4$ Hz; CH_3), 2.45 (d, $^2J(PCH) = 12.2$ Hz; CH_3P), 3.01 (dq, $^3J(PNCH) = 10.8$ Hz; CH_2). $^{31}P\{^1H\}$-NMR ($CDCl_3$): $\delta = 58.89$ (s).

[7] Crystal structure data: orthorhombic, space group *Pbca* (No. 61), $a = 14.827(1)$, $b = 16.399(1)$, $c = 16.223(1)$ Å, $V = 3944.6$ Å^3, $Z = 4$, $\rho_{calcd} = 1.273$ g cm^{-3}, $\mu = 7.8$ cm^{-1}, $F(000) = 1600$. 5723 unique reflections, of which 3388 observed with $I \geq 2.0\sigma(I)$. ($(\theta - 2\theta)$ scans, $\Delta\omega = 1.0 + 0.35\tan\theta$, $(\sin\theta/\lambda)_{max} = 0.703$, *hkl*: +20, +23, +22, $Mo_{K\alpha}$, $\lambda = 0.71069$ Å, $T = 22\,^\circ C$, CAD4). Direct methods (MULTAN 82), $R = 0.041$, $R_w = 0.052$, GOF: 1.32 for 181 refined parameters (anisotropic, H constant, SDP-PLUS), $\Delta\rho_{fin}(max) = 0.35$ eÅ^{-3}. Further details of the crystal structure investigation may be obtained from the Fachinformationszentrum Energie, Physik, Mathematik GmbH, D-7514 Eggenstein-Leopoldshafen 2 (FRG), on quoting the depository number CSD 51739, the names of the authors, and the journal citation.

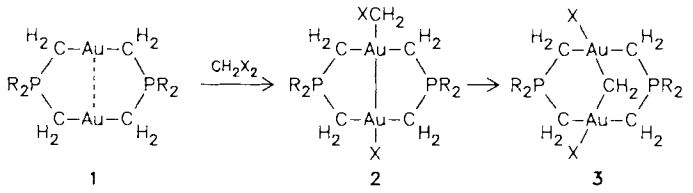
Methylene-Bridged Dinuclear Gold(III) Complexes with Terminal and Bridging Ylide Ligands**

By *Hubert Schmidbaur** and *Christoph Hartmann*

Cyclic Au^I-ylide complexes **1**[1–3] are important model compounds for the oxidative addition of alkyl halides to multinuclear metal complexes.[4,5] Spectroscopic findings and structural data indicate the occurrence of an Au···Au interaction in **1**, which facilitates both metal atoms assuming the unusual oxidation state +II. Both monohaloalkanes as well as geminal di- and trihaloalkanes and even tetrahalomethanes add to the ring system in such a way that a genuine transannular metal–metal bond is first formed (**2**), which, in the case of polyfunctionalized halo-

[*] Prof. Dr. H. Schmidbaur, Dipl.-Chem. C. Hartmann
Anorganisch-chemisches Institut der Technischen Universität München
Lichtenbergstrasse 4, D-8046 Garching (FRG)

[**] This work was supported by the Deutsche Forschungsgemeinschaft, the Fonds der Chemischen Industrie, and by Hoechst AG and Degussa AG.



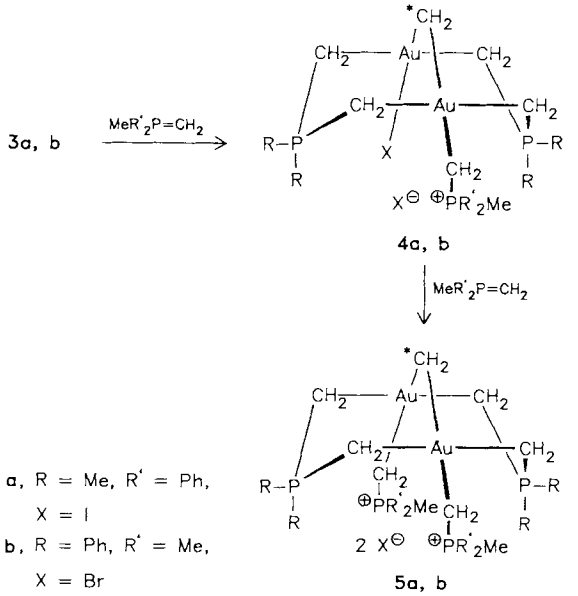
1 2 3

alkanes is readily transformed in a subsequent step into a methylene bridge (**3**).[5] With suitable substrates these processes are at least partly reversible: thus, after methylation of the gold atoms in **3**, propane can be eliminated during the thermolysis.[6]

We have now tried to replace the substituents X in **3** by phosphorus ylides in order to obtain cationic complexes, which, with the exception of the CH_2-bridges, contain only onium-stabilized Au–C bonds. In the thermolysis of mononuclear cationic Au^{III} complexes the non-ylidic Au–C bonds proved to be the more labile centers [Eq. (a)].[7]

$$[R_2Au(CH_2PR_3)_2]^{\oplus} \xrightarrow{\Delta} [Au(CH_2PR_3)_2]^{\oplus} + R_2 \qquad (a)$$

The reactions of **3a** (R = Me, X = I) and **3b** (R = Ph, X = Br) with $MePh_2P{=}CH_2$[8] and $Me_3P{=}CH_2$[9] smoothly afforded the products of double substitution **5a** and **5b**, respectively, in good yields. With reaction partners in the stoichiometric ratio 1 : 1, formation of the intermediates **4a** and **4b**, respectively, is also observed.[10]



3a, b 4a, b 5a, b

a, R = Me, R' = Ph, X = I

b, R = Ph, R' = Me, X = Br

5a, **b** are colorless, air stable salts which are soluble in chloroform and methanol, but insoluble in diethyl ether, toluene, and pentane. Since the structures of **1–3** were already known,[4,5] the constitution of **5a**, **b** could easily be deduced from the analytical and spectroscopic data: The signals of the high resolution ^1H-, ^{13}C-, and ^{31}P-NMR spectra can be unequivocally assigned to the individual structural units[11] and are consistent with a C_{2v} symmetry for the cations in solution (mirror planes through P*CH_2P and Au*CAu). An essentially rigid boat conformation can be assumed for the eight-membered ring.[4,5] This and the location of the *CH_2 bridge on one side of the eight-membered ring give rise to a non-equivalence of the H-atoms ($A_2A_2'B_2B_2'XX'$ system) and substituents R on the eight-membered ring (A_3B_3X system when R = CH_3). In contrast the H-atoms of the *CH_2 bridge and of the exocyclic CH_2 groups are in each case equivalent. Accordingly, the ^{197}Au-Mossbauer spectra of **5a**, **b** show in each case a doublet with almost equal values for the isomeric shift IS and the quadrupole coupling constants QS (Fig. 1), thus also providing proof of the equivalence of the metal atoms and their oxidation state (+III).[12]

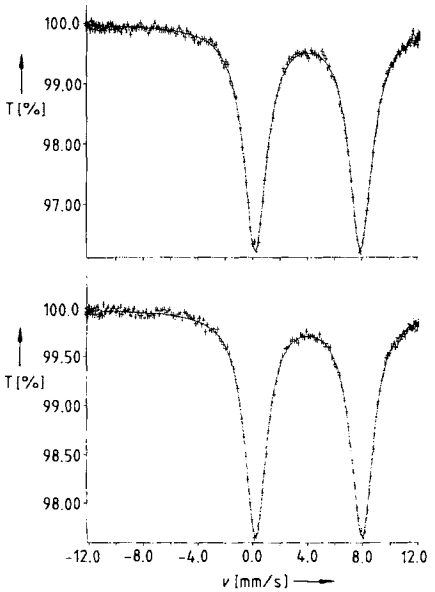
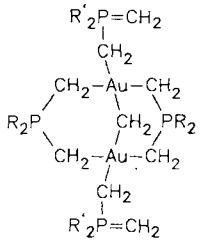


Fig. 1. ^{197}Au-Mössbauer spectra of **5a** (top) and **5b** (bottom) at 4 K (I = relative transmission, v = relative rate). **5a**: IS = 4.04 mm/s, QS = 7.72 mm/s. **5b**: IS = 4.10 mm/s, QS = 7.73 mm/s.

The constitutional isomerism of the complex cations of **5a**, **b** is recognizable in the field desorption mass spectra. In the case of **5a**, not only the dication (*m/z* 508) is observable, but also the monocation (*m/z* 1141) associated with an iodide ion. Observation of the unexpected cation $[Me_3PCH_2AuCH_2PMe_3]^{\oplus}$ demonstrates the ready formation and stability of these cations, which are also formed according to equation (a). The mass spectra of **5a**, **b** also contain the signals of the cations of the heterocycles **1** (R = Me and Ph, respectively). The IR spectra of **5a**, **b** do not show any typical bands for Au–X vibrations.



6a, R = Me, R' = Ph

6b, R = Ph, R' = Me

The corresponding ylides **6a**, **b** can be generated from the salts **5a**, **b** by reaction with strong bases under mild conditions. In solution the ylides are yellow, have different ^{31}P-NMR spectra, and can be reconverted into the salts by treatment with hydrogen haloacids. A rearrangement of the cation of **5a** into that of **5b** via an ylidic intermediate, with the terminal ylide taking up the bridge position and vice versa, could not be detected.

Received: January 24, 1986;
supplemented: March 14, 1986 [Z 1639 IE]
German version: *Angew. Chem.* 98 (1986) 573

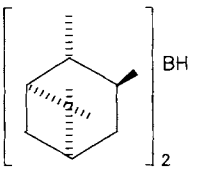
CAS Registry numbers:
3a, 80387-83-3; **3b**, 90742-64-6; **4a**, 102234-12-8; **4b**, 102234-13-9; **5a**, 102260-73-1; **5b**, 102260-74-2; $MePh_2P{=}CH_2$, 4554-22-7; $Me_3P{=}CH_2$, 14580-91-7.

[1] H. Schmidbaur, *Angew. Chem. 95* (1983) 980; *Angew. Chem. Int. Ed. Engl. 22* (1983) 907.
[2] H. Schmidbaur in *Gmelin Handbuch der Anorganischen Chemie, Organogold Compounds*, Springer, Berlin 1980, p. 263.
[3] H. Schmidbaur, *Inorg. Synth. 18* (1980) 136.
[4] a) H. Schmidbaur, R. Franke, *Inorg. Chim. Acta 13* (1975) 84; b) P. Jandik, U. Schubert, H. Schmidbaur, *Angew. Chem. 94* (1982) 74; *Angew. Chem. Int. Ed. Engl. 21* (1982) 73; *Angew. Chem. Suppl. 1982*, 1; c) H. Schmidbaur, P. Jandik, *Inorg. Chim. Acta 74* (1983) 97.
[5] H. H. Murray III, J. P. Fackler, Jr., D. A. Tocher, *J. Chem. Soc. Chem. Commun. 1985*, 1278; H. H. Murray III, J. P. Fackler, Jr., A. M. Mazany, *Organometallics 3* (1984) 1310.
[6] H. Schmidbaur, C. Hartmann, J. Riede, B. Huber, G. Müller, *Organometallics*, in press.
[7] H. Schmidbaur, R. Franke, *Inorg. Chim. Acta 13* (1975) 79.
[8] H. Schmidbaur, M. Heimann, *Z. Naturforsch. B 29* (1974) 485.
[9] H. Schmidbaur, W. Tronich, *Chem. Ber. 101* (1968) 595.
[10] Procedure: When the reaction is carried out in tetrahydrofuran with the reactants in the molar ratio 1:2, the salts **5a**, **b** separate out as colorless precipitates, which after washing with benzene and drying in vacuo are analytically pure. The yields are almost quantitative. **5a**: m.p. 158–162°C (decomp.); **5b**: m.p. 187–192°C (decomp.). The intermediates **4** can be characterized ^{31}P-NMR spectroscopically ($CDCl_3/CD_3OD$). **4a**: $\delta = 38.7$, 30.5 (2:1); **4a**: $\delta = 38.6$, 27.9 (2:1).
[11] **5a** ($CDCl_3/CD_3OD$): ^{31}P-NMR: $\delta = 37.1$, 27.0 (each s; 1:1). ^{1}H-NMR: $\delta = 0.66$ ($N = 13.0$ Hz; $AuCH_2P$(ring)), 1.07 (s; $*CH_2$), 1.42 (d, $^2J(PH) = 16$ Hz; $AuCH_2PPh_2Me$), 1.25, 1.45 (each d, $^2J(PH) = 12.1$ and 12.8 Hz; $P(CH_3)_2$), 2.00 (d, $^2J(PH) = 13$ Hz; PPh_2CH_3), 7.15–7.50 (m; C_6H_5). ^{13}C-NMR: $\delta = 9.8$ (d, $^1J(PC) = 33$ Hz; CH_2PPh_2Me), 10.6 (d, $^1J(PC) = 62.3$ Hz; $AuCH_2P$(ring)), 12.9, 18.9 ($N = 50.4$ and 46.7 Hz; $P(CH_3)_2$), 13.6 (d, $^1J(PC) = 64.2$ Hz; PPh_2CH_3), 38.2 (br. s; $*CH_2$), 126.1, 128.7, 131.5 and 132.6 ($J = 81.6$, 11.9, 10.1 and 2.8 Hz; C_6H_5).—**5b** ($CDCl_3/CD_3OD$): ^{31}P-NMR: $\delta = 41.1$, 27.0 (each s; 1:1). ^{1}H-NMR: $\delta = 0.66$ (d, $^2J(PH) = 15.4$ Hz; CH_2PMe_3), 1.42 (s; $*CH_2$), 1.57 (d, $^2J(PH) = 13.2$ Hz; $P(CH_3)_3$), 1.78 ($N = 13$ Hz; $AuCH_2P$(ring)), 7.0–7.5 (m; C_6H_5). ^{13}C-NMR: $\delta = 10.5$ ($N = 48.2$ Hz; $AuCH_2P$(ring)), 13.6 (d, $^1J(PC) = 55.5$ Hz; $P(CH_3)_3$), 14.3 (d, $^1J(PC) = 36.0$ Hz; CH_2PMe_3), 38.9 (br. s; $*CH_2$), 134.9–123.7 (C_6H_5) (N = average coupling constant).
[12] H. Schmidbaur, J. R. Mandl, F. E. Wagner, D. F. van de Vondel, G. P. van der Kelen, *J. Chem. Soc. Chem. Commun. 1976*, 170; see also [6].

Secondary Deuterium Kinetic Isotope Effects in Enantioselective Hydroborations with (+)-Diisopinocampheylborane**

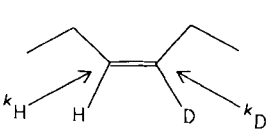
By *Brian E. Mann, Peter W. Cutts, James McKenna,* Jean M. McKenna,* and *Catriona M. Spencer*

High degrees of regio- and/or stereo-selectivity in organic reactions are often achieved through the effect of differential strong non-bonded interactions in competitive transition states, where the geometrical arrangements of reacting bonds are controlled by stereoelectronic factors. The non-bonded interactions typically involve hydrogen atoms in alkyl or other groups. In such cases highly selective reactions would be expected to exhibit large inverse secondary hydrogen kinetic isotope effects associated with isotopic replacement at the compressed hydrogen atoms. A method for precisely locating the positions of important compressive interactions is therefore available, and we have successfully applied this method to investigate the relevant transition-state characteristics for enantioselective hydroborations of alkenes using (+)-diisopinocampheylborane, **1**, prepared from (−)-α-pinene.

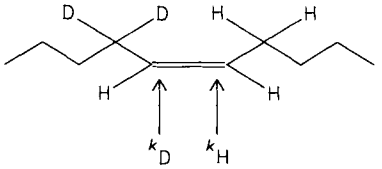


1

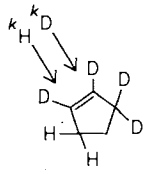
Various detailed models, qualitative and (more recently) quantitative have been suggested[1] for this interesting reaction, which gives high enantioselectivity notably with simple acyclic non-terminal (*Z*)-alkenes, and which may be regarded as perhaps the most important early example[2] of the range of highly enantioselective reactions of great current interest in preparative organic chemistry. In every model, strong steric interactions between alkyl or other groups in the alkene and in the hydroborating reagent are envisaged, which serve to differentiate the free energies of competitive diastereoisomeric transition states. We now wish to report new and significant experimental evidence with which any satisfactory detailed model must accord.



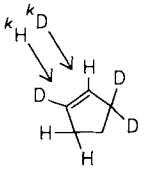
2



3



4



5

The deuteriated (*Z*)-alkenes **2** through **5** were synthesized, hydroborated at −10°C in diglyme with **1**, and subsequently oxidized with aqueous Na_2O_2 at 25–40°C. The resultant reaction mixtures were analyzed by ^{1}H-NMR spectroscopy in presence of the lanthanoid shift reagent[3] $Eu(fod)_3$ to estimate in each case the relative proportions of structurally isomeric secondary alcohols. (Example: **6a** and **6b** were formed from **2**.) The enantiomeric purity of the isomers was not measured. The product ratios are equated to the competitive rate constant ratios, k_D/k_H, where k_D and k_H are defined as the overall rate constants for the attachment of the B-atom of **1** to the particular alkene C-atoms indicated by the arrows in the structural formulas. For substrates **2** through **5** we evaluate the kinetic isotope effects k_D/k_H as follows: **2**, 1.00 ± 0.17; **3**, 2.86 ± 0.24; **4**, 1.45 ± 0.16; and **5**, 1.41 ± 0.35. Precision limits quoted are standard deviations.

$$\mathbf{2} \longrightarrow \underset{\mathbf{6a}}{H_5C_2{-}CHOH{-}CDH{-}C_2H_5} + \underset{\mathbf{6b}}{H_5C_2{-}CH_2{-}CDOH{-}C_2H_5}$$

Hydroborations of simple acyclic non-terminal (*Z*)-alkenes with **1** are independently known[1,2] to be highly (up to 98%) enantioselective, so our results for **2** and **3**, and, by extrapolation for **4** and **5**, may be interpreted in terms of the characteristics of transition states leading to the expected[4] preferred enantiomers. Two important conclu-

[*] Dr. J. McKenna, Dr. B. E. Mann, Dr. P. W. Cutts, Dr. J. M. McKenna, Dr. C. M. Spencer
Chemistry Department, The University
Sheffield S3 7HF (England)

[**] This work was supported by the Science and Engineering Research Council.

sions regarding the preferred transition states for hydroboration of such (*Z*)-alkenes emerge. Firstly, during the reactions there is no appreciable steric compression at the vinylic hydrogens; this conclusion follows from the absence of a secondary kinetic isotope effect for substrate **2** and from the similar values for this effect for **4** and **5**. Secondly, there is very strong steric compression at the allylic hydrogens during the reaction; this follows from the *exceptionally large* inverse kinetic isotope effect for **3**. The values for **4** and **5** are smaller (but still substantial), presumably because the allylic CH_2 (or CD_2) groups are partly bent back away from the reaction area by incorporation into the cyclopentene ring.

In an investigation of the enantioselective hydroboration of some deuteriated terminal alkenes, reaction of **1** with (*E*)- and (*Z*)-1-deuterio-1-hexene followed by oxidation had previously been reported[5] to yield active 1-deuterio-1-hexanols with 86% and 42% enantiomeric purity respectively, the enantiomeric ratios being assessed both biochemically and by asymmetric synthesis with ethylphenylacetic anhydride. We have repeated this work, but determined the enantiomeric purities by the more convenient modern procedure using NMR spectroscopy in presence of the chiral shift reagent[3] $Eu(hfbc)_3$. We found enantiomeric purities of 65% and 46%, respectively. This substantial difference is clearly due to a combination of several kinetic isotope effects, but it is not in this case algebraically possible to calculate absolute values of isotope effects, analogous to those given above, for enantioselective hydroboration in one or other chiral sense.

Received: February 5, 1986;
revised: March 24, 1986 [Z 1659 IE]
German version: *Angew. Chem. 98* (1986) 567

[1] Reviews: H. C. Brown, P. K. Jadhav, A. K. Mandal, *Tetrahedron 37* (1981) 3547; K. N. Houk, N. G. Rondau, Yun-Dong Wu, J. T. Metz, M. N. Paddon-Row, *ibid. 40* (1984) 2257.

[2] H. C. Brown, N. R. Ayyangar, G. Zweifel, *J. Am. Chem. Soc. 86* (1964) 397.

[3] $Eu(fod)_3$: tris(6,6,7,7,8,8,8-heptafluoro-2,2-dimethyl-3,5-octanedionato)europium(III). $Eu(hfbc)_3$: tris[(3-heptafluorobutyryl)-(+)-camphorato]europium(III). For a review on the use of chiral lanthanoid shift reagents such as $Eu(hfbc)_3$ see G. R. Sullivan, *Top. Stereochem. 10* (1978) 287.

[4] The enantioselective addition of the chiral borane **1** to each of the alkenes is taken to be stereochemically analogous to known additions [1, 2] of **1** to simple acyclic alkenes, which yield after oxidation (*S*)-alcohols of very high optical purity.

[5] H. Weber, P. Loew, D. Arigoni, *Chimia 19* (1965) 595; D. Arigoni, private communication.

A Novel Entry to Dendralene Systems

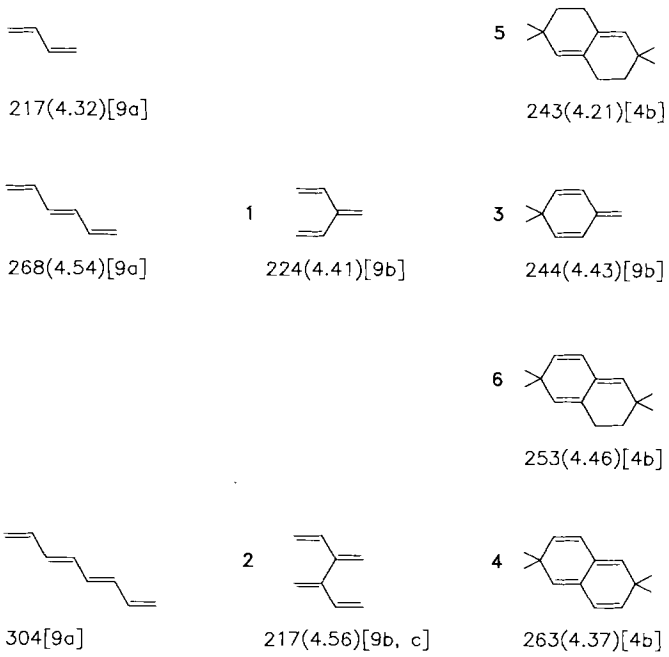
By *Thomas Loerzer, Ralf Gerke,* and *Wolfgang Lüttke**

Dedicated to Professor Edgar Heilbronner on the occasion of his 65th birthday

Of the four groups of polyenes—linear polyenes, annulenes, radialenes, dendralenes[1]—the parent compounds of the dendralenes have been the subject of very few studies, even though the clarification of their conjugative behavior and the properties determined by their topology[2] deserve interest. The first two known members **1** and **2** exhibit the light absorption of the butadiene chromophore (cf. Table 1); that is, they must be twisted, for steric reasons.

[*] Prof. Dr. W. Lüttke, Dr. T. Loerzer, R. Gerke
Institut für Organische Chemie der Universität
Tammannstrasse 2, D-3400 Göttingen (FRG)

Table 1. UV absorption data (λ_{max} (lg ε); cyclohexane) of linear polyenes and dendralenes.

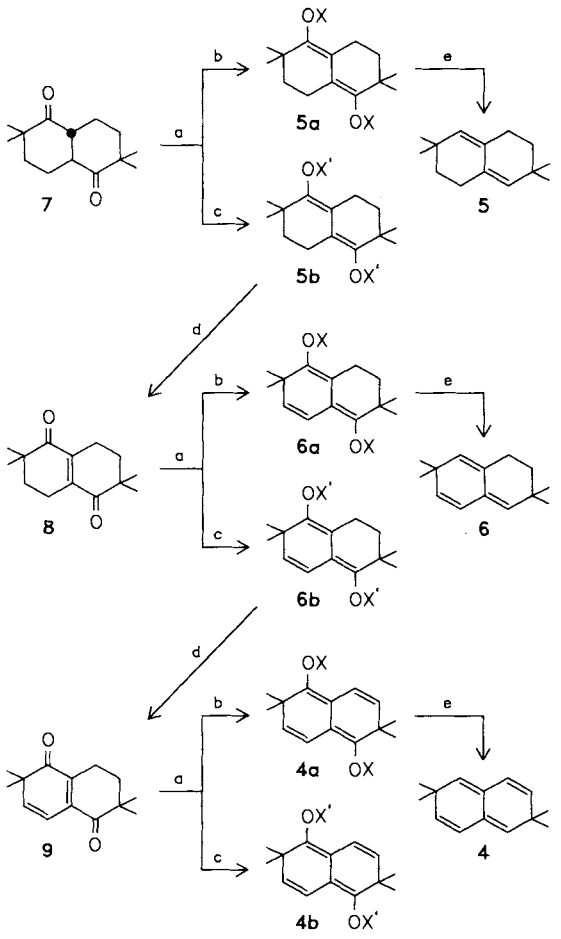


In order to determine the "true" structural properties of the dendralenes we therefore had to prepare fixed planar compounds of this type. In the case of the triene **1** a corresponding substance **3** is already known.[3] We report here on the synthesis of the fixed tetraene **2**, the dendralene **4**, and its partially hydrogenated analogues **5** and **6**, each of which carry two pairs of geminal dimethyl groups for protection against hydrogen shifts.

The synthetic strategy chosen by us, which involves the use of tetramethyldiketone **7** as starting material, enabled successive incorporation of the double bonds, exploiting the trick of completely enolizing a carbonyl compound (step a). The resulting enediolate ions were either converted into the reducible enol phosphates **5a**, **6a**, **4a** (step b) or oxidized via the trimethylsilyl enol ethers **5b**, **6b** (steps c and d) (Scheme 1).

The starting compound **7** (m.p. 163 °C; overall yield 34%)[4] can be readily obtained by a previously described three-step synthesis[5] from 1,5-decalindione. For the complete enolization of **7** and its dehydro compounds **8** and **9** the base system potassium hydride/[18]crown-6[6] is, to our knowledge, the most suitable. The enolates are subsequently trapped in situ with chlorodiethyl phosphate and chlorotrimethylsilane, respectively; the enol ether derivatives **5a**, **6a**, **4a** and **5b**, **6b**, **4b** are obtained in yields of more than 60%. These compounds are stabilized by the geminal dimethyl groups to such an extent that they can be purified even by column chromatography (basic alumina; pentane).

The bistrimethylsilyl enol ethers **5b** and **6b** can—formally—be oxidatively desilylated at room temperature with *N*-bromosuccinimide.[7] We assume that this proceeds in each case via the 1-oxa-8a-bromotrimethylsilyl enol ether, which spontaneously loses bromotrimethylsilane. It is thus possible to dehydrogenate the dicarbonyl compounds



Scheme 1. a) KH/[18]crown-6, THF, RT, 15 h; molar ratio **7**, **8** or **9**: KH = 1:4. b) Reaction in situ with $(EtO)_2POCl/Et_3N$, RT, 3 h; 80–95%. c) Reaction in situ with Me_3SiCl/Et_3N, RT, 30 min; 60–85%. d) *N*-bromosuccinimide, THF, RT, 15 min; 95%. e) Ti^0, THF, reflux, 2 h; 5–20%. – X = $P(O)(OC_2H_5)_2$, X' = $Si(CH_3)_3$.

7 and **8** extraordinarily smoothly via the intermediates **5b** and **6b**, respectively.

Reduction of the enol phosphates **5a**, **6a**, **4a** with zerovalent titanium (prepared from titanium trichloride and potassium) afforded the diene **5** and the dendralenes **4** and **6**.[8] The yields decreased sharply with increasing number of double bonds. This is, in part, due to overreduction. **4**, **5**, and **6** could be isolated in pure form by gas-chromatographic separation (15% FFAP on Chromosorb W/AW-DMCS; 180°C) (**4**: m.p. 68°C, 5%; **5**: m.p. 44°C, 20%; **6**: m.p. 43°C, 15%).

For characterization of the bonding properties we consider here only the UV absorption data (Table 1). Other than in the case of the open-chain dendralenes **1** and **2**, in the fixed cyclic species **3**, **6** and **4** a bathochromic shift of the absorption maximum of ca. 10 nm per double bond is observed with increasing number of double bonds. The shift is—regardless of the alkyl substitution—essentially smaller than in the analogous linear polyenes. Consistent with PPP calculations[4b] and with the molecular topology[2] the π-delocalization in the dendralenes is obviously much more weaker than in the linear polyenes.

Received: February 21, 1986 [Z 1678 IE]
German version: *Angew. Chem. 98* (1986) 560

[1] Review: H. Hopf, *Angew. Chem. 96* (1984) 947; *Angew. Chem. Int. Ed. Engl. 23* (1984) 948.
[2] I. Gutman, B. Ruščić, N. Trinajstić, C. F. Wilcox, *J. Chem. Phys. 62* (1975) 3399.
[3] K. Auwers, K. Müller, *Ber. Dtsch. Chem. Ges. 44* (1911) 1595; H. E. Zimmerman, P. Hackett, D. F. Juers, J. M. McCall, B. Schröder, *J. Am. Chem. Soc. 93* (1971) 3653.
[4] a) All the new compounds were unequivocally characterized by ^1H-NMR, ^{13}C-NMR, IR and mass spectra as well as by elemental analyses; b) T. Loerzer, *Dissertation*, Universität Göttingen 1983.
[5] Regiospecific geminal dimethylation of ketones: R. M. Coates, S. K. Chung, *J. Org. Chem. 38* (1973) 3677; R. M. Coates, R. L. Sowerby, *J. Am. Chem. Soc. 93* (1971) 1027.
[6] Cf. C. A. Brown, *J. Org. Chem. 39* (1974) 3913; A. A. Millard, M. W. Rathke, *ibid. 43* (1978) 1834; C. A. Brown, *ibid. 39* (1974) 1324.
[7] Cf. Preparation of α-bromoketones from trimethylsilyl enol ethers: R. H. Reuss, A. Hassner, *J. Org. Chem. 39* (1974) 1785; L. Blanco, P. Amice, J. M. Conia, *Synthesis 1976*, 194.
[8] Reduction of simple enol phosphates with Ti^0: S. C. Welch, M. E. Walters, *J. Org. Chem. 43* (1978) 2715.
[9] a) E. S. Stern, C. J. Timmons: *Gillam and Stern's Introduction to Electronic Absorption Spectroscopy in Organic Chemistry*, 3rd. edit. Edward Arnold, London 1970, p. 31; b) W. J. Bailey, N. A. Nielsen, *J. Org. Chem. 27* (1962) 3088; c) A. Cassens, *Dissertation*, Universität Göttingen 1979.

BOOK REVIEWS

Reductions in Organic Chemistry. By *M. Hudlicky*. Ellis Horwood Ltd., Chichester 1984. xvi, 309 pp., hardback, £ 35.00.—ISBN 0-85312-345-4

This book claims to present a comprehensive coverage of all types of reduction reactions. The author attempts to link the numerous classes of compounds and the various different methods of reduction in a sort of matrix in order to reach his difficult goal. With the choice of predominantly very simple model compounds, the neglect of stereochemical problems and the uncritical juxtaposition of important and unimportant methods, the author pays a high price to achieve his aim.

The introductory chapter covers catalytic hydrogenations, reductions with hydrides and hydrido-complexes, electroreductions, and reductions with metals and non-metallic reagents.

For the sake of clarity, it would have been better to dispense with experimental details and large-scale diagrams of apparatus at this point, especially since these are presented again, at some length, in an experimental appendix. The reductions of nearly all classes of compounds are listed in the main part of the book, accompanied by an abundance of examples. In this way completeness is achieved, but a discussion of problems of regio- and stereoselectivity and their basis in reaction mechanisms, which would have been appropriate, is lost. The field of reductions with chiral reagents, which has been the focus of much recent attention, is indeed broached here and

there in the book but surely deserves a more detailed treatment.

Preparative chemists will find useful the tables that follow the main chapter, in which are grouped important types of educt, reduction reagents and products. These tables refer back into the main body of the text and thence to an extensive literature index.

The last part of the book consists of fifty experimental procedures for the preparation of special reduction reagents and for the reduction of representative compounds. Since the compounds chosen have got quite simple structures, these procedures can serve only as a guide; for more complicated molecules it would certainly be advisable to consult the original literature.

This book does not, then, offer a critical view, but simply a superficial description of the extensive arsenal of reduction methods. For the practical chemist there is useful guidance, especially in the numerous tables and experimental procedures. The very high price is bound to stand in the way of purchase for everyday use.

Franz-Peter Montforts [NB 712 IE]
Institut für Organische Chemie
der Universität Frankfurt (FRG)

Handbuch der Gaschromatographie. Edited by *E. Leibnitz* and *G. Struppe*. Akademische Verlagsgesellschaft Geest & Portig, Leipzig 1984. 828 pages, hardback, DM 198.00. Order No. 669-628-5 (Sole distributors for the FRG: W & P Buchversand für Wissenschaft und Praxis, Weinheim, ISBN 3-89141-001-8)

This handbook, compiled by an authors' collective, amounts to a comprehensive treatment of all aspects of gas chromatography, which is certainly not lacking in detailed information. This is an area of chemistry which is rapidly developing and even a freshly published work is bound to be partly out of date at the time of publication; however, the new edition of this handbook does cover in supplements more recent techniques for sample introduction (e.g. "on column injection"), modern methods of coupling, column connections, flexible quartz capillaries, chemically immobilized stationary phases etc., even if not in close detail.

There are successful chapters on the principles and development of gas chromatography, capillary columns, detectors, quantitative analysis (albeit almost exclusively on "packed" columns) and the coupling of gas chromatography with spectroscopic methods. Packed columns, whose significance is diminishing these days, are rather overemphasized in two extensive chapters. It may be a drawback of this new edition that the increasing trend towards use of capillary gas chromatography is not sufficiently recognized. The admittedly difficult problems encountered in quantitative analysis with capillary columns are only briefly discussed.

The treatment of stationary phases is very comprehensive but a supplement covering newer literature on the use of chiral stationary phases would not have come amiss. Likewise, there is no reference to complexation gas chromatography and the work of *V. Schurig*. The chapter on derivatization reactions is also in need of supplementation: much of the newer literature is not included here. However, the handbook does contain chapters on such industrial aspects as process control, process regulation and automation. The physico-chemical basis of the different methods, the theory of temperature programming and many fundamental concepts are given detailed and comprehensible treatment.

This handbook not only offers the user, whether involved in industrial or academic research, many hints for the optimization and the solution of separation problems, it also provides fundamental knowledge in this area of physical chemistry.

Wilfried A. König [NB 716 IE]
Institut für Organische Chemie
der Universität Hamburg (FRG)

Macrolide Antibiotics. Chemistry, Biology and Practice. Edited by *S. Ōmura*. Academic Press, Orlando 1984, 635 pages, hardback, $ 89.50.—ISBN 0-12-526450-X

Professor *Satoshi Ōmura* (Kitasato University Tokyo) is surely currently by far the best authority on the chemistry and biochemistry of macrolides. His book on the chemistry, biology and applications of macrolide antibiotics is correspondingly comprehensive. He has succeeded in gathering a group of renowned authors about him so that the content of this book goes far beyond his own field of interest, and even includes the application of macrolides in human and veterinary medicine.

A good half of the book is devoted to classical macrolides of the erythromycin and carbomycin type, the subgroup of macrolides which has found the broadest medical application. The chapters on the determination of constitution and configuration, on chemical modifications and structure/activity relationships, and on regulation of biosynthesis and the genetics of macrolide production are sound and contain extensive literature references. Especially penetrating is the description by *S. Masamune* of the total synthesis of macrolides. An easily grasped model of the structure and mode of function of ribosomes serves as the basis for *J. W. Corcoran*'s chapter on the mode of action and resistance mechanisms. This section gives some idea how much fundamental research in biochemistry and molecular biology owes to the use of antibiotics. The sections on macrolides in clinical *(I. Nakayama)* and veterinary *(R. C. Wilson)* use may be too brief for medical practitioners. However, they provide a valuable survey of the application of macrolide antibiotics for the chemist or biochemist.

The quite appreciable second part of the book is devoted to fungicidal polyene macrolides, of which some (e.g. amphotericin B, nystatin) have found medical application, albeit limited. This part is arranged similarly to the first and owes its completeness to the contributions of *H. Tanaka* (structure and fungicidal activity), *J. F. Martin* (biosynthesis, regulation and genetics), *E. F. Gale* (mode of action and resistance mechanisms) and *C. P. Schaffner* (clinical practice).

To keep the size of the book under control, the "macrolide-like" antibiotics from actinomycetes have been handled in a much more condensed way, even though a series of biogenetically and structurally most interesting compounds have recently been discovered here. To these belong, e.g., chlorothricin and nargenicin, as well as metabolites with high fungicidal and cytotoxic activity, like oligomycins, venturicidins and concanamycins. However, a good literature register enables access to these compounds as well. This applies too for the numerous fungal macrolides with quite diverse biological effects, for macrodiolides

(e.g. the boron containing boromycin), and for the macrotetrolides, which complex alkali metal ions specifically. In contrast, avermectins and milbemycins are dealt with in a chapter of their own (by *M. H. Fisher* and *H. Mrozik*), no doubt on account of their promising antiparasitic properties.

This book will be a useful aid, above all to natural products chemists, biochemists and microbiologists. It may also have much to offer medical personnel with an interest in chemistry.

Walter Keller-Schierlein [NB 713 IE]
Laboratorium für Organische Chemie
der ETH Zürich (Switzerland)

Vom Würfelspiel zum Naturgesetz. Simulation und Modelldenken in der Physikalischen Chemie. By *G. Marsch*. VCH Verlagsgesellschaft, Weinheim 1985. x, 269 pp., bound, DM 58.00.—ISBN 3-527-26226-1

There has been no lack of attempts to present the difficult material of physical chemistry in a simple and didactically skillful manner in the past. The author has nevertheless been successful in finding a new approach which is particularly addressed to the mathematically less experienced reader. He presents a selection of dice and board games in order to illustrate some of the fundamental concepts of statistical thermodynamics and reaction kinetics.

Individual chapters deal with game models for the Maxwell distribution of velocities, the Boltzmann distribution, the concept of entropy, and various aspects of chemical reactions. The final chapter includes games for the illustration of several problems from different fields including the theory of chromatography, light absorption, crystallization, and phase separation of liquids.

The compilation under consideration is a success, reflecting the author's long experience in university instruction. Little more than a knowledge of the most elementary mathematical concepts and operations is assumed. The reader learns more difficult concepts, such as that of entropy, "as a player." Historical details of the development of statistical thermodynamics enrich the book decidedly. In the chapter on chemical reaction kinetics, the author also includes quite recent examples taken from oscillating reactions and processes of molecular selection. In this chapter, the algorism developed by *Gillespie* of the simulation of chemical processes would have fit in well, above all since it is well suited to illustrate the extrapolation from the extremely small numbers of statistical events in the games to the laws of kinetics in real systems. The section covering games played on a pocket calculator will surely be very useful to the reader. It is unfortunate that the author has not included microcomputers too, which are accessible almost everywhere nowadays, and on which many aspects of university instruction can be quickly demonstrated in a didactically effective manner.

On the whole, this excellent monograph is an enrichment of the literature used in physical-chemistry instruction. It can be warmly recommended to students and university teachers alike. Senior physicists and chemists will also discover much of interest in this work: old, familiar material appears in a new light when looked at through "game-glasses."

Peter Schuster [NB 736 IE]
Institut für Theoretische Chemie und Strahlenchemie
der Universität, Vienna (Austria)

Orbital Interactions in Chemistry. By *T. A. Albright, J. K. Burdett,* and *M. H. Whangbo*. Wiley, Chichester 1985. xv, 447 pp., bound, £ 63.25.—ISBN 0-471-87393-4

As preface, let me say that in spite of the large number of books on the market dealing with the principles, methods, and applications of MO models in various fields of chemistry, the book under consideration could fill a gap that has been recognized not only by those who are engaged in teaching this area of theoretical chemistry, but also and especially by all those—whether advanced students or research colleagues—who want to learn MO theory as a "tool".

The content and presentation of this book are obviously strongly influenced by the theoretical approach and by the didactic example of the scientific mentor of the three authors, *Roald Hoffmann*, whose Preface to the book is well worth reading. Within the realm of the possible, this work comes very close to satisfying its very high aim: the transmission of a qualitative, sound understanding of the electronic structure, geometry, and reactivity of compounds, ranging from simple molecules to solids. This understanding is based on a model that is as universally useful as possible, the model of interacting orbitals. The consequent utilization of the fragment-orbital formalism runs like a red thread through the entire book. According to this formalism, the orbitals of complex molecules are built up from simple orbital building blocks, or fragments, using a few, straightforward interaction rules from perturbation theory.

In the beginning chapters, the theoretical foundations and formalisms are discussed in the necessary depth. Only little mathematical knowledge is required, a consideration that is not totally unimportant for a book's wide acceptance by chemists. The treatment is neither tiring nor unnecessarily extensive, considering the aims of the book. Here, chapters are found covering AO's and MO's, as well as the qualitative rules for orbital interactions and for the construction of correlation diagrams based on perturbation theory; group theory, orbital symmetry, and an introduction to the fragment-orbital approach are also included. In this section, hybridization, perturbations based on electronegativity and geometry, Walsh diagrams, and Jahn-Teller distortions are treated. In an extraordinarily thorough and detailed manner, and by means of many examples, the qualitative derivation of the "appearance" of molecular orbitals and of their relative energies is presented and made clear to the reader using qualitative, pictorial representations. Thus, he learns to "think in orbitals", progressing from simple, two-atom systems to complex molecules and finally to solids. The chapter on the electronic structure of solids is especially attractive: the correspondence between the MO picture of molecular entities, on the one hand, and the band structures of crystalline solids, on the other, as well as quasi analogous concepts and phenomena, are elaborated very well didactically. A bridge between molecular chemistry and solid-state physics can thus be recognized. A clearly written chapter, immediately accessible even to non-theorists, dealing with the limitations of the one-electron model in molecules, with electron-electron interactions, state energies, etc., including CI-wave functions, has not been overlooked. This is important, since most of the book is deliberately kept at the simple one-electron valence-MO level.

Whereas the basic theory and applications presented in the first half of the book are illustrated using organic molecules and light atoms as examples, it is predominantly the series of chapters on the application of MO theory to

inorganic and organometallic transition-metal compounds, following a chapter on so-called hypervalent species and their MO theory, that make the book worth reading. A survey like the one that the three authors give here has until now been lacking in the textbook field. A very thorough treatment, not only of the basic types of organometallic fragments, ML_n, and their bonding capability, but also of questions concerning the electronic structure, molecular geometry, structural dynamics, and reactivity of metal complexes, is provided using numerous qualitative MO and interaction diagrams. *Hoffmann's* Isolobal Analogy, treated at the end of this part of the book, serves to overlap and link inorganic with organic chemistry. This concept has recently received wide application as a structural and even as a synthetic guideline, especially in the organometallic field. It would have perhaps been useful if the authors had pointed out a little more clearly that transition-metal fragments and complexes with the same orbital characteristics may nevertheless differ in their chemistry, depending on the position of the respective metal atom within its group, on the actual charge, and on the appearance of special problems (relativistic effects, spin-orbit coupling, etc.) with the heavier transition metals. A chapter on cluster compounds closes the book.

The authors have chosen the subject matter and examples, especially in the section on transition metals, in such a way that the book can be considered a review at the textbook level of the research performed in this field by *Hoffmann* and his co-workers over the past ten years. Didactically, the book is a masterful achievement, and in this respect, the graphic work (formulas, MO diagrams, etc.) is in no way inferior to the text. Misprints, inevitable in a first edition, are not worth going into here. The references are sufficiently numerous and suitably chosen considering the aim of the book.

This book could be of great benefit to teachers and students alike. It could contribute to the understanding of modern chemistry as an integrated whole, rather than as a rigidly compartmentalized system. Much would be gained if university teachers gave this book the same attention as has been given to the original publications on which it is based. It is unfortunate that the book's price can only be regarded as an unreasonable demand and that students as a rule will be prevented from purchasing it. As is so often the case, a moderately priced, paperback edition would have been more appropriate and more conducive to the wider circulation and use of the book.

Peter Hofmann [NB 720 IE]
Anorganisch-chemisches Institut
der Technischen Universität München (FRG)

Common Fragrance and Flavor Materials. By *K. Bauer* and *D. Garbe*. VCH Verlagsgesellschaft, Weinheim 1985, 213 pages, hardback, DM 112.00.—ISBN 3-257-26038-2

In seven chapters of a monograph of 213 pages, the two authors try to give an overview of the chemistry of flavors and fragrances. The authors are predestined to do so by their profession, but succeed only partly. The classification of odorous compounds according to their structure is of course a possibility, but certainly not the clearest. This leads to curious situations. Macrocyclic odorants can thus be found in three different places, e.g. civetone on p. 56, 15-pentadecanolide on p. 104, and ambrettolide on p. 137. A classification by odors would have shown the reader the molecular similarities and structural variety that can cause a typical type of odor. Also elsewhere such present knowledge of the relationship between structure and odor is not covered. The relevant remarks in chapter 1 "Introduction" are totally insufficient. The information about the sources and the detailed descriptions of the odors of compounds that are listed in the voluminous chapter 2 "Single Fragrance and Flavor Compounds" are an agreeable surprise, but to give the boiling points, refractive indexes, and densities would have been justified 30 years ago, not today. This is aggravated by the fact that modern analytical data such as IR, NMR and MS are not given. As an extreme, chapter 3 "Essential Oils", lists the above "classical" physical constants of oils of different provenience in tabular form. Pages 152 and 171 could have been omitted together with another ten pages. Instead one would have wished modern analytical data and also information about important oils not treated at all. If physical data are to be compared, why not GC-fingerprints?

Specialists will miss the trade names for quite a number of odorants. 1,1,2,3,3,8-hexamethyl-6-oxa-2,3,5,6,7,8-hexahydro-1*H*-benzo[f] (p. 102) will be meaningless whereas the name Galaxolide® will recall the odorous power of an extraordinary musk substance. Lyral® (p. 58), Hedione® (p. 62) and Lilial® (p. 71) are some further examples. Even names that can be found in most textbooks like Exaltolide® are not given. Exaltone® and a number of other modern odorants are not treated at all. Flavor compounds have been specially neglected. The extraordinary richness of flavor compounds found, for example in the area of *N*- and *S*-heterocycles has been compressed into two pages. Literature references are cited in a very liberal manner. Half of them come from works called ISO and EOA, which will mean nothing to chemists, who, according to the introduction, are included in the potential readership. The layout and legibility are excellent, as is also the translation into English.

Günther Ohloff [NB 715 IE]
Firmenich AG, Geneva (Switzerland)

Registered names, trademarks, etc. used in this journal, even without specific indication thereof, are not to be considered unprotected by law.

© VCH Verlagsgesellschaft mbH, D-6940 Weinheim, 1986. - Printed in the Federal Republic of Germany by Zechnersche Buchdruckerei, Speyer/Rhein.

All rights reserved (including those of translation into foreign languages). No part of this issue may be be reproduced in any form – by photoprint, microfilm, or any other means – nor transmitted or translated into a machine language without written permission from the publishers. Only single copies of contributions, or parts thereof, may be reproduced for personal use.

Valid for users in the USA: The appearance of the code at the bottom of the first page of an article in this journal (serial) indicates the copyright owner's consent that copies of the article may be made for personal or internal use, or for the personal or internal use of specific clients. This consent is given on the condition, however, that the copier pay the stated per-copy fee through the Copyright Clearance Center, Inc., for copying beyond that permitted by Sections 107 or 108 of the U.S. Copyright Law. This consent does not extend to other kinds of copying, such as copying for general distribution, for advertising or promotional purposes, for creating new collective works, or for resale. For copying from back volumes of this journal see 'Permissions to Photo-Copy: Publisher's Fee List' of the CCC.

Editorial office: Pappelallee 3, D-6940 Weinheim, Federal Republic of Germany, Telephone (06201) 60 23 15, Telex 465 516 vchwh d, Telefax (06201) 602 328.

Editor: *P. Gölitz.*

Associate editors: *D. I. Loewus, A. Stimson.* **Editorial assistant:** *E. Schweikart*

Publishers: VCH Verlagsgesellschaft mbH. (Managing Directors: *Prof. Dr. Helmut Grünewald* and *Hans Dirk Köhler*), Pappelallee 3, D-6940 Weinheim, Federal Republic of Germany. Correspondence concerning advertisements should be addressed to VCH Verlagsgesellschaft mbH. (Advertising Manager *R. J. Roth*), Boschstr. 12, P.O. Box 1260/1280, D-6940 Weinheim, Federal Republic of Germany, Telephone Weinheim (06201) 602-0, Telex 465 516 vchwh d, Telefax (06201) 602 328.

ANGEWANDTE CHEMIE
International Edition in English
Volume 25 · Number 7
July 1986
Pages 583–660

A Receptor-Mediated Pathway for Cholesterol Homeostasis (Nobel Lecture)**

By Michael S. Brown* and Joseph L. Goldstein*

In 1901 a physician, *Archibald Garrod*, observed a patient with black urine. He used this simple observation to demonstrate that a single mutant gene can produce a discrete block in a biochemical pathway, which he called an "inborn error of metabolism." *Garrod*'s brilliant insight anticipated by 40 years the one gene–one enzyme concept of *Beadle* and *Tatum*. In similar fashion the chemist *Linus Pauling* and the physician *Vernon Ingram*, through study of patients with sickle cell anemia, showed that mutant genes alter the amino acid sequences of proteins. Clearly, many fundamental advances in biology were spawned by perceptive studies of human genetic diseases.[1]

We began our work in 1972 in an attempt to understand a human genetic disease, familial hypercholesterolemia or FH. In these patients the concentration of cholesterol in blood is elevated many fold above normal and heart attacks occur early in life. We postulated that this dominantly inherited disease results from a failure of end-product repression of cholesterol synthesis. The possibility fascinated us because genetic defects in feedback regulation had not been observed previously in humans or animals, and we hoped that study of this disease might throw light on fundamental regulatory mechanisms.

Our approach was to apply the techniques of cell culture to unravel the postulated regulatory defect in FH. These studies led to the discovery of a cell surface receptor for a plasma cholesterol transport protein called low density lipoprotein (LDL) and to the elucidation of the mechanism by which this receptor mediates feedback control of cholesterol synthesis.[2,3] FH was shown to be caused by inherited defects in the gene encoding the LDL receptor, which disrupt the normal control of cholesterol metabolism. Study of the LDL receptor in turn led to the understanding of receptor-mediated endocytosis, a general process by which cells communicate with each other through internalization of regulatory and nutritional molecules.[4] Receptor-mediated endocytosis differs from previously described biochemical pathways because it depends upon the continuous and highly controlled movement of membrane-embedded proteins from one cell organelle to another in a process termed receptor recycling.[4]

Many of the mutations in the LDL receptor that occur in FH patients disrupt the movement of the receptor between organelles. These mutations define a new type of cellular defect that has broad implications for normal and deranged human physiology.

In this lecture we first discuss the peculiar problem of plasma cholesterol transport. We then present some historical aspects of FH and the origin of the LDL receptor concept. Next, we summarize current knowledge of this receptor and the mechanism by which it functions in cells. Finally, we relate these findings to the pathogenesis of FH and to the common clinical problem of high blood cholesterol levels and atherosclerosis in human subjects.

The Problem of Cholesterol Transport

Cholesterol is the most highly decorated small molecule in biology. Thirteen Nobel Prizes have been awarded to

[*] Prof. M. S. Brown, Prof. J. L. Goldstein
Department of Molecular Genetics
University of Texas Health Science Center
Southwestern Medical School
5323 Harry Hines Boulevard, Dallas, TX 75235 (USA)

[**] Copyright © The Nobel Foundation 1986.—We thank the Nobel Foundation, Stockholm, for permission to print this article.

scientists who devoted major parts of their careers to cholesterol.[5] Ever since it was first isolated from gallstones in 1784, almost exactly 200 years ago, cholesterol has exerted a hypnotic fascination for scientists from the most diverse domains of science and medicine. Organic chemists have been fascinated with cholesterol because of its complex four-ring structure. Biochemists have been fascinated because cholesterol is synthesized from a simple two-carbon substrate, acetate, through the action of at least 30 enzymes, many of which are coordinately regulated. Physiologists and cell biologists have been fascinated with cholesterol because of its essential function in membranes of animal cells, where it modulates fluidity and maintains the barrier between cell and environment, and because cholesterol is the raw material for the manufacture of steroid hormones and bile acids. And finally, physicians have been fascinated because elevated levels of blood cholesterol accelerate the formation of atherosclerotic plaques, leading to heart attacks and strokes. The studies of cholesterol therefore embrace almost all disciplines of modern biology. If the role of cholesterol in biomedicine is to be elucidated, all of these disciplines must be employed.

Cholesterol is a Janus-faced molecule. The very property that makes it useful in cell membranes, namely its absolute insolubility in water, also makes it lethal. For when cholesterol accumulates in the wrong place, for example within the wall of an artery, it cannot be readily mobilized, and its presence eventually leads to the development of an atherosclerotic plaque. The potential for errant cholesterol deposition is aggravated by its dangerous tendency to exchange passively between blood lipoproteins and cell membranes. If cholesterol is to be transported safely in blood, its concentration must be kept low, and its tendency to escape from the bloodstream must be controlled.

Multicellular organisms solve the problem of cholesterol transport by esterifying the sterol with long-chain fatty acids and packaging these esters within the hydrophobic cores of plasma lipoproteins (Fig. 1). With its polar hydroxyl group esterified, cholesterol remains sequestered within this core, which is essentially an oil droplet composed of cholesteryl esters and triglycerides, solubilized by a surface monolayer of phospholipid and unesterified cholesterol and stabilized by protein. The small amounts of unesterified cholesterol on the surface of the particle are maintained in equilibrium exchange with the cholesterol of cell membranes, but the larger amounts of cholesteryl esters remain firmly trapped in the core of the particle and leave the particle only as the result of highly controlled processes.

The major classes of plasma lipoproteins were delineated in the 1950s and 1960s through work in many laboratories, most notably those of *Oncley*,[6] *Gofman*,[7] and *Fredrickson*.[8] The four major classes are very low density lipoprotein (VLDL), intermediate density lipoprotein (IDL), low density lipoprotein (LDL), and high density lipoprotein (HDL). A schematic representation of LDL, the most abundant cholesterol-carrying lipoprotein in human plasma, is shown in Figure 1.

Packaging of cholesteryl esters in lipoproteins solves the problem of nonspecific partitioning of cholesterol into cell membranes, but it creates another problem, namely one of

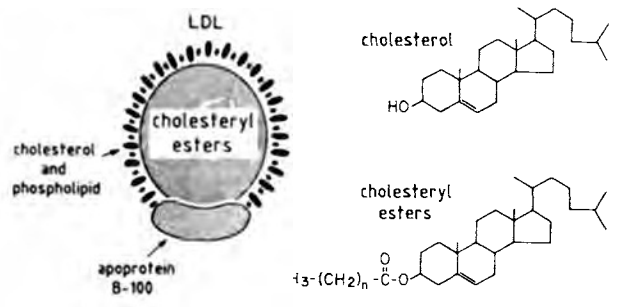


Fig. 1. Structure of plasma LDL (left) and its cholesterol and cholesteryl ester components (right). LDL is a spherical particle with a mass of 3×10^6 daltons and a diameter of 22 nanometers. Each LDL particle contains about 1500 molecules of cholesteryl ester in an oily core that is shielded from the aqueous plasma by a hydrophilic coat composed of 800 molecules of phospholipid, 500 molecules of unesterified cholesterol, and 1 molecule of a 387000-dalton protein called apoprotein B-100 [129]. Elevations in blood cholesterol are usually attributable to an increase in the number of LDL particles.

delivery. Cholesteryl esters are too hydrophobic to pass through membranes. How then can esterified cholesterol be delivered to cells? The delivery problem is solved by lipoprotein receptors, of which the prototype is the LDL receptor.[9] Strategically located on the surfaces of cells, these receptors bind LDL and carry it into the cell by receptor-mediated endocytosis. The internalized lipoprotein is delivered to lysosomes where its cholesteryl esters are hydrolyzed. The liberated cholesterol is used by the cell for the synthesis of plasma membranes, bile acids, and steroid hormones, or stored in the form of cytoplasmic cholesteryl ester droplets. Two properties of the receptor—its high affinity for LDL and its ability to cycle multiple times in and out of the cell—allow large amounts of cholesterol to be delivered to body tissues, while at the same time keeping the concentration of LDL in blood low enough to avoid the buildup of atherosclerotic plaques. When LDL receptor function is inappropriately diminished as a result of genetic defects or in response to regulatory signals, the protective mechanism is lost, cholesterol builds up in plasma, and atherosclerosis ensues.[10]

Familial Hypercholesterolemia: Origin of the LDL Receptor Concept

As a disease, FH has a rich clinical history. It was first described in 1938 by *Carl Müller*, a clinician at the Oslo Community Hospital in Norway, as an "inborn error of metabolism" that produced high blood-cholesterol levels and myocardial infarctions in young people.[11] *Müller* astutely concluded that FH is transmitted as a single gene-determined autosomal dominant trait. In the mid-1960s and early 1970s, *Khachadurian*[12] at the American University in Beirut, Lebanon, and *Fredrickson* and *Levy*[13] at the National Institutes of Health showed that FH exists clinically in two forms: the less severe heterozygous form and the more severe homozygous form.

FH heterozygotes, who carry a single copy of a mutant LDL receptor gene, are quite common, accounting for one out of every 500 persons among most ethnic groups throughout the world.[14] These individuals have a twofold

increase in the number of LDL particles in plasma from the time of birth. They begin to have heart attacks at 30 to 40 years of age. Among people under age 60 who suffer myocardial infarctions, about 5% have the heterozygous form of FH, a 25-fold enrichment over the incidence in the general population.[15-17]

The attractiveness of FH as an experimental model stems from the existence of homozygotes. These rare individuals, who number about one in one million persons, inherit two mutant genes at the LDL receptor locus, one from each parent. Their disease is much more severe than that of heterozygotes. They have six- to tenfold elevations in plasma LDL levels from the time of birth, and they often have heart attacks in childhood.[12-14] The severe atherosclerosis that develops in these patients without any other risk factors is formal proof that high levels of plasma cholesterol can produce atherosclerosis in humans. Experimentally, the availability of FH homozygotes permits study of the manifestations of the mutant gene without any confounding effects from the normal gene.

At the time that our studies began in 1972, it was generally felt that all important events in cholesterol metabolism take place in the liver or intestine.[18] It was obviously impossible to perform meaningful studies in livers of humans with FH. Our only chance to explain its mysteries depended on the mutant phenotype being faithfully manifest in long-term cultured cells such as skin fibroblasts. Techniques for growing such cells had been established over the preceeding two decades. Moreover, inherited enzyme defects were known to be expressed in cultured fibroblasts from patients with rare recessive diseases such as galactosemia, the Lesch Nyhan syndrome, and Refsum's syndrome. By 1970, *Neufeld*'s classic studies of the mucopolysaccharidoses, a form of lysosomal storage disease, were beginning to establish the value of cultured skin fibroblasts in elucidating complex cellular pathways.[19]

There was some reason to believe that the FH derangement might be manifest in cultured skin fibroblasts. Studies in the 1960s by *Bailey*[20] and *Rothblat*[21] had demonstrated that several types of cultured animal cells synthesize cholesterol and that this synthesis is subject to negative feedback regulation. When serum was present in the medium, cultured cells produced little cholesterol from radioactive acetate. When serum lipoproteins were removed from the culture medium, cholesterol synthesis increased.

Regulation of HMG CoA Reductase by LDL in Fibroblasts

We began our work by setting up a microassay for 3-hydroxy-3-methylglutaryl coenzyme A reductase (HMG CoA reductase), the rate-determining enzyme of cholesterol biosynthesis. This assay was used to measure HMG CoA reductase activity in extracts of cultured fibroblasts.[2,22] Earlier studies in rat livers by *Bucher* and *Lynen*[23] and by *Siperstein*[24] had shown that the activity of this enzyme was reduced when rats ingested cholesterol and that this reduction limited the rate of cholesterol synthesis. We soon found that the activity of HMG CoA reductase was subject to negative regulation in fibroblasts.[2,22] As shown in Figure 2A, when normal human fibroblasts were grown in the presence of serum, HMG CoA reductase activity was low. When the lipoproteins were removed from the culture medium, the activity of HMG CoA reductase rose by at least 50-fold over a 24-hour period. The induced enzyme was rapidly suppressed when lipoproteins were added back to the medium (Fig. 2B).

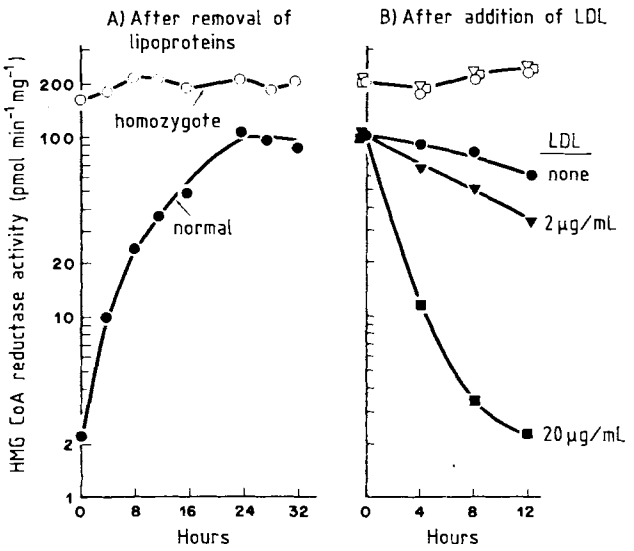


Fig. 2. Regulation of HMG CoA reductase activity in fibroblasts from a normal subject (●) and from an FH homozygote (○). A) Monolayers of cells were grown in dishes containing 10% fetal calf serum. On day 6 of cell growth (zero time), the medium was replaced with fresh medium containing 5% human serum from which the lipoproteins had been removed. At the indicated time, extracts were prepared and HMG CoA reductase activity was measured. B) At 24 hours after addition of 5% human lipoprotein-deficient serum, human LDL was added to give the indicated cholesterol concentration. HMG CoA reductase activity was measured in cell-free extracts at the indicated time. (Reprinted from ref. [2].)

Not all lipoproteins could suppress HMG CoA reductase activity. Of the two major cholesterol-carrying lipoproteins in human plasma, LDL and HDL, only LDL was effective.[22,25] This specificity was the first clue that a receptor might be involved. The second clue was the concentration of LDL that was required. The lipoprotein was active at concentrations as low as 5 µg of protein per milliliter, which is less than 10^{-8} M.[22,25] A high-affinity receptor mechanism must be responsible for enzyme suppression.

The key to this mechanism emerged from studies of cells from patients with homozygous FH.[2,25] When grown in serum containing lipoproteins, the homozygous FH cells had HMG CoA reductase activities that were 50- to 100-fold above normal (Fig. 2A). This activity did not increase significantly when the lipoproteins were removed from the serum, and there was no suppression when LDL was added back. Clearly, the genetic defect was expressed in cell culture (Figs. 2A and 2B).

The simplest interpretation of these results was that FH homozygotes had a defect in the gene encoding HMG CoA reductase that rendered the enzyme resistant to feedback regulation by LDL-derived cholesterol. This working hypothesis was immediately disproved by the next experi-

ment. Cholesterol, dissolved in ethanol, was added to normal and FH homozygote cells. When mixed with albumin-containing solutions, cholesterol forms a quasi-soluble emulsion that enters cells passively, apparently by diffusion through the plasma membrane. When cholesterol was added in this form, the HMG CoA reductase activities of normal and FH homozygote fibroblasts were suppressed at the same rate and to the same extent.[25]

Clearly, the defect in the FH homozygote cells must reside in their ability to extract cholesterol from the lipoprotein, and not in the ability of the cholesterol, once extracted by the cells, to act. But how do normal cells extract the cholesterol of LDL? The high affinity of the process suggested that a cell surface receptor was involved. The existence of cell surface receptors for protein hormones and other chemical messengers had been known for many years. It was generally thought that these receptors acted by binding the ligand at the surface and then generating a "second messenger" on the intracellular side of the plasma membrane. The classic second messenger was cyclic adenosine monophosphate (cyclic AMP).[26] Perhaps LDL was binding to a receptor and generating some second messenger that suppressed HMG CoA reductase.

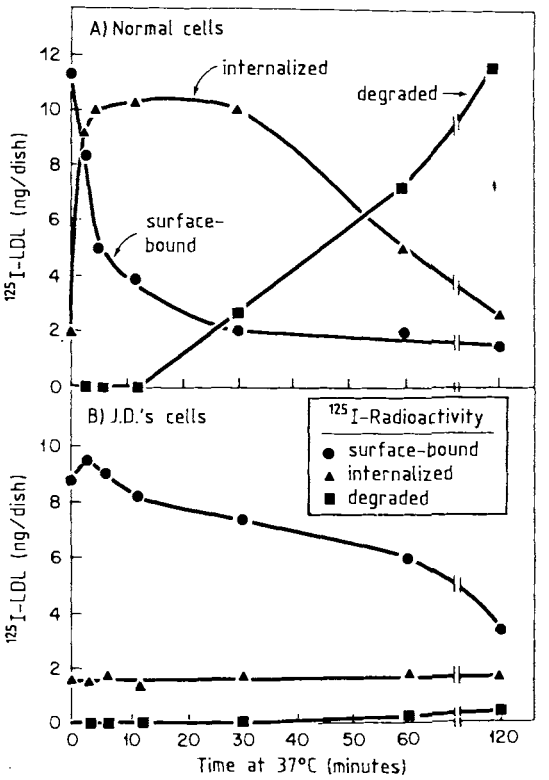


Fig. 3. Internalization and degradation at 37°C of ^{125}I-LDL previously bound to the LDL receptor at 4°C in fibroblasts from a normal subject (A) and from J. D., a patient with the internalization-defective form of FH (B). Each cell monolayer was allowed to bind ^{125}I-LDL (10 μg protein/mL) at 4°C for 2 hours, after which the cells were washed extensively. In one set of dishes, the amount of ^{125}I-LDL was determined by measuring the amount of ^{125}I-LDL that could be released from the surface by treatment with heparin. Each of the other dishes then received warm medium, after which they were incubated at 37°C. After the indicated interval, the dishes were rapidly chilled to 4°C, and the amounts of surface-bound (heparin-releasable) ^{125}I-LDL (●), internalized (heparin-resistant) ^{125}I-LDL (▲), and degraded (trichloroacetic acid-soluble) ^{125}I-LDL (■) were measured. (Reprinted with permission from ref. [41].)

Delineation of the LDL Receptor Pathway

The existence of an LDL receptor was confirmed when LDL was radiolabeled with ^{125}I and incubated with normal and FH homozygote fibroblasts. These studies showed that normal cells had high-affinity binding sites for ^{125}I-LDL, whereas FH homozygote cells lacked high-affinity receptors.[3,27] This seemed to explain the genetic defect in FH, but it did not reveal how LDL generated the signal that suppressed HMG CoA reductase. The answer came from studies of the fate of the surface-bound ^{125}I-LDL. Techniques were developed to distinguish surface-bound from intracellular ^{125}I-LDL,[28] and these revealed that the receptor-bound LDL remained on the surface for less than 10 minutes on average (Fig. 3A). Within this time most of the surface-bound LDL particles entered the cell; within another 60 minutes the protein component of ^{125}I-LDL was digested completely to amino acids and the ^{125}I, which had been attached to tyrosine residues on LDL, was released into the culture medium as ^{125}I-monoiodotyrosine.[27,28] Meanwhile, the cholesteryl esters of LDL were hydrolyzed, generating unesterified cholesterol which remained within the cell.[29]

The only cellular organelle in which LDL could have been degraded so completely and rapidly was the lysosome. Originally described by *de Duve*,[30] lysosomes were known to contain a large number of acid hydrolases that could easily digest all of the components of LDL. The hypothesis of lysosomal digestion of LDL was confirmed through the use of inhibitors such as chloroquine,[31] which raises the pH of lysosomes and inhibits lysosomal enzymes,[32] and through studies of cultured fibroblasts from patients with a genetic deficiency of lysosomal acid lipase.[29] Cells from the latter patients bound and internalized LDL but failed to hydrolyze its cholesteryl esters, even though they were able to degrade its protein component.

The cholesterol that was generated from LDL within the lysosome proved to be the second messenger responsible for suppressing HMG CoA reductase activity. We now know that cholesterol (or an oxygenated derivative that is formed within the cell) acts at several levels, including suppression of transcription of the HMG CoA reductase gene[33] and acceleration of the degradation of the enzyme protein.[34] The LDL-derived cholesterol also regulates two other cellular processes in a coordinated action that stabilizes the cell's cholesterol content. It activates a cholesterol-esterifying enzyme, acyl CoA: cholesterol acyltransferase (ACAT), so that excess cholesterol can be stored in the cytoplasm as cholesteryl ester droplets.[35] It also suppresses synthesis of LDL receptors by lowering the concentration of receptor mRNA.[36,37] The latter action allows cells to adjust the number of LDL receptors to provide sufficient cholesterol for metabolic needs without causing cholesterol overaccumulation.[9] Through these regulatory mechanisms, cells keep their level of unesterified cholesterol remarkably constant despite wide fluctuations in cholesterol requirements and exogenous supply.

Receptor-Mediated Endocytosis of LDL: Binding Coupled to Internalization in Coated Pits

The rapidity of internalization of receptor-bound LDL and the completeness with which the protein of LDL was hydrolyzed implied that fibroblasts have a special mechanism for transport of the lipoprotein from the cell surface to the lysosome. The likely mechanism was endocytosis, the process by which surface membranes pouch inward and pinch off to form vesicles that eventually fuse with lysosomes. Endocytosis was first demonstrated by cinematography of phagocytic cells in the 1930s, and its universal occurrence in all cells was established in the 1950s by the electron microscopic studies of *Palade*.[38] Endocytosis was felt to be a nonspecific process that transported bulk fluid and its contents into cells. There was no precedent for entry of specific receptors into cells by this route.

To determine whether endocytosis was involved in LDL uptake, we began in 1975 a collaboration with *Richard G. W. Anderson*, a cell biologist at our medical school in Dallas. Through the use of LDL coupled to electron-dense ferritin, we found that receptor-bound LDL was internalized by endocytosis. More important, however, these morphological studies explained the efficiency of internalization: efficiency was contingent upon the clustering of the LDL receptors in small pockets on the surface called coated pits.[39] Coated pits had been described in detail by *Roth* and *Porter*[40] in 1964 during electron microscopic studies of the uptake of yolk proteins by mosquito oocytes. These investigators showed that coated pits pinch off from the surface to form coated endocytic vesicles that carry extracellular fluid and its contents into the cell.

The finding that LDL receptors were clustered in coated pits raised the general possibility that these structures serve as gathering-places for cell surface receptors that are destined for endocytosis.[4] Other cell surface proteins, being excluded from coated pits, could not rapidly enter the cell.

This interpretation of coated-pit function was strengthened by study of fibroblasts from a unique FH homozygote. Cells from most of these subjects simply failed to bind LDL, but cells from one FH patient, whose initials are J. D., bound LDL, but failed to internalize it (Fig. 3B).[41,42] In collaboration with *Anderson*, we showed that the receptors in these mutant cells were excluded from coated pits.[43] This was an important finding, for it established the essential role of coated pits in the high-efficiency uptake of receptor-bound molecules.[4]

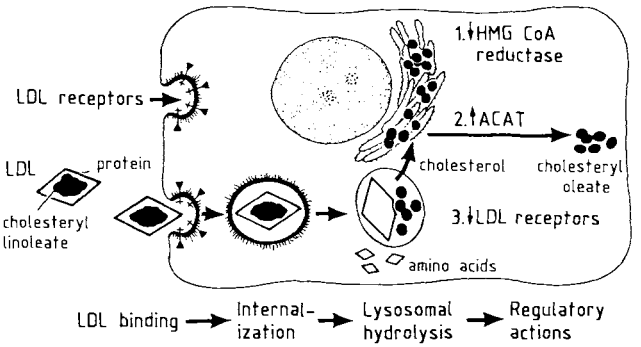


Fig. 4. Sequential steps in the LDL receptor pathway of mammalian cells. HMG CoA reductase denotes 3-hydroxy-3-methylglutaryl CoA reductase; ACAT denotes acyl-CoA: cholesterol acyltransferase. Vertical arrows indicate the directions of regulatory effects. (Reprinted from ref. [130].)

Figure 4 summarizes the sequential steps in the LDL receptor pathway as deduced from the biochemical, genetic, and ultrastructural studies performed between 1972 and 1976. Figure 5 shows the striking "all-or-none" biochemi-

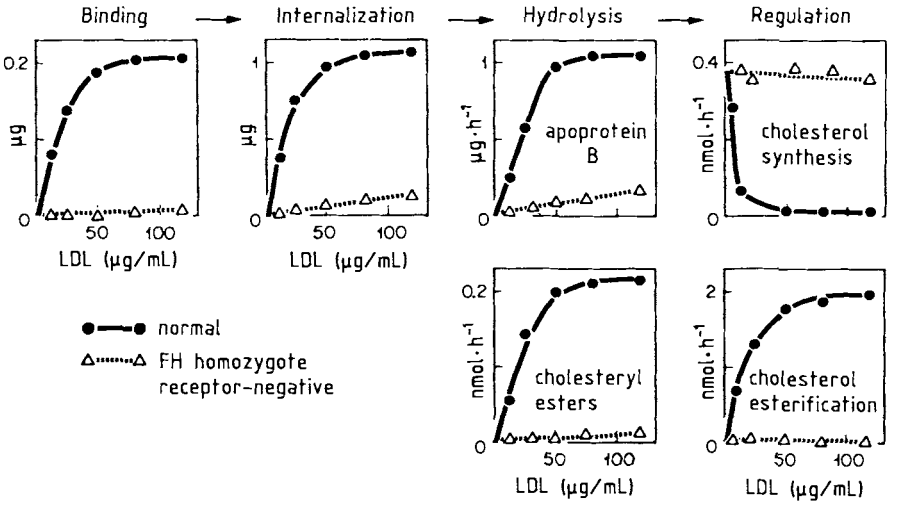


Fig. 5. Actions attributable to the LDL receptor in fibroblasts from a normal subject (●) and from a homozygote with the receptor-negative form of FH (△). The cells were incubated with varying concentrations of ^{125}I-LDL or unlabeled LDL at 37 °C for 5 hours. Assays were performed in growing cells in monolayers as previously described [128]. All data are normalized to 1 mg of total cell protein. The units for each assay are as follows: *binding*, μg of ^{125}I-LDL bound to cell surface; *internalization*, μg of ^{125}I-LDL contained within the cell; *hydrolysis of apoprotein B-100*, μg of ^{125}I-LDL degraded to ^{125}I-monoiodotyrosine per hour; *hydrolysis of cholesteryl esters*, nmol of [^{3}H]cholesterol formed per hour from the hydrolysis of LDL labeled with [^{3}H]cholesteryl linoleate; *cholesterol synthesis*, nmol of [^{14}C]acetate incorporated into [^{14}C]cholesterol per hour by intact cells; *cholesterol esterification*, nmol of [^{14}C]oleate incorporated into cholesteryl [^{14}C]oleate per hour by intact cells. (Reprinted from ref. [130].)

cal differences in the metabolism of LDL and its regulatory actions in fibroblasts derived from a normal subject and from an FH homozygote with a complete deficiency of LDL receptors.

Soon after the initial studies of the LDL receptor pathway, *Pearse*[44] purified coated vesicles and found that the cytoplasmic coat was composed predominantly of a single protein that she named clathrin. At the same time, *Cohen* and his collaborators performed their elegant studies of the action of epidermal growth factor (EGF) on cultured fibroblasts.[45] They found that this peptide hormone was internalized by cells in a manner that was indistinguishable from that of LDL. Similar observations were made by *Terris* and *Steiner*[46] with insulin in hepatocytes, by *Neufeld* and co-workers[47] and by *Sly* and co-workers[48] with lysosomal enzymes in fibroblasts, and by *Ashwell, Morell,* and co-workers[49] with asialoglycoproteins in hepatocytes. Moreover, *Helenius, Simons,* and their co-workers[50] showed that several lipid-enveloped viruses enter cells by this route. Clearly, receptor-mediated endocytosis did not exist solely for cholesterol delivery: it was a general process by which cells internalized and degraded many extracellular molecules.[4,51] In all instances in which adequate morphologic studies were performed, this internalization was attributable to clustering of receptors in coated pits. Indeed, *Pastan* and *Willingham*[51] and *Carpentier* et al.[52] showed that receptors for several different ligands colocalize in the same coated pit.

The early LDL receptor studies also exposed another feature of receptor-mediated endocytosis—namely, that receptors can be recycled.[4,28] After internalization the receptors dissociate from their ligands. From the work of *Maxfield*[53] and of *Helenius* and co-workers,[54] we now know that such dissociation is triggered by a drop in pH within a special class of endocytic vesicles called endosomes (discussed below). After dissociation, the receptors find their way back to the cell surface. The LDL receptor makes one round-trip into and out of the cell every 10 minutes for a total of several hundred trips in its 20-hour life span.[4,28]

The LDL Receptor: Structure Adapted to Function

The LDL receptor is a cell surface glycoprotein that contains approximately two asparagine-linked (*N*-linked) oligosaccharide chains of the complex type and approximately 18 serine/threonine-linked (*O*-linked) oligosaccharide chains.[55,56] About two-thirds of the *O*-linked sugars are clustered in one region of the molecule.[57] The LDL receptor binds two proteins: (1) apo B-100, the 387000-dalton glycoprotein that is the sole protein of LDL;[27] and (2) apo E, a 34000-dalton protein that is found in multiple copies in intermediate density lipoprotein (IDL) and a subclass of HDL.[58,59] *Innerarity* and *Mahley*[59] demonstrated that lipoproteins that contain multiple copies of apo E bind to LDL receptors with up to 20-fold higher affinity than LDL, which contains only one copy of apo B.

Figure 6 illustrates the circuitous itinerary followed by the LDL receptor from its site of synthesis to its site of internalization in coated pits and its site of recycling in endosomes. The receptor is synthesized in the rough endoplasmic reticulum (ER) as a precursor[60] that contains high-mannose *N*-linked carbohydrate chains and the core sugar (*N*-acetylgalactosamine) of the *O*-linked chains.[56] The *O*-linked core sugars are added before the mannose residues of the *N*-linked chains are trimmed, i.e., while the receptor is still in the endoglycosidase H-sensitive stage. Thus, the *O*-linked sugars must be added either in the ER or in a transitional zone between the ER and the Golgi apparatus. The receptor precursor migrates on sodium dodecyl sulfate (SDS) polyacrylamide gel electrophoresis as a

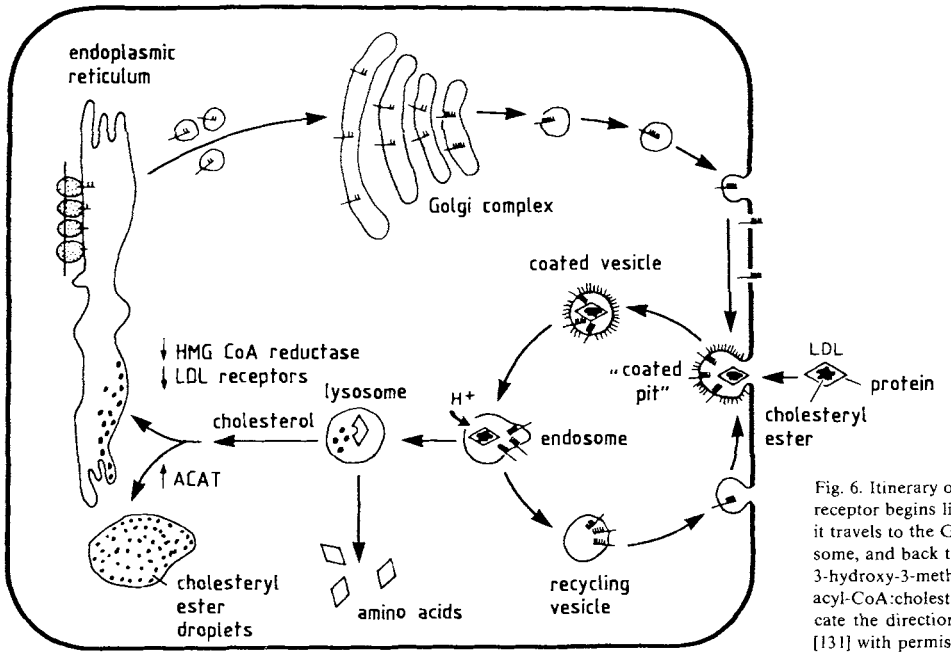


Fig. 6. Itinerary of the LDL receptor in mammalian cells. The receptor begins life in the endoplasmic reticulum from which it travels to the Golgi complex, cell surface, coated pit, endosome, and back to the surface. HMG CoA reductase denotes 3-hydroxy-3-methylglutaryl CoA reductase; ACAT denotes acyl-CoA:cholesterol acyltransferase. Vertical arrows indicate the direction of regulatory effects. (Reprinted from ref. [131] with permission.)

single band corresponding to an apparent molecular weight of 120000.[60]

Within 30 minutes after its synthesis, the LDL receptor decreases in mobility on SDS gels. The apparent molecular weight increases from 120000 to 160000.[60] This change is coincident with the conversion of the high-mannose *N*-linked oligosaccharide chains to the complex endoglycosidase H-resistant form.[56] At the same time, each *O*-linked chain is elongated by the addition of one galactose and one or two sialic acid residues.[56] The amount of carbohydrate is not sufficient to account for an increase in molecular mass of 40000 daltons. Rather, the decrease in electrophoretic mobility is primarily caused by a change in conformation of the protein that results from the elongation of the clustered *O*-linked sugars.[56,57]

About 45 minutes after synthesis, LDL receptors appear on the cell surface, where they gather in coated pits. Within 3 to 5 minutes of their formation, the coated pits invaginate to form coated endocytic vesicles. Very quickly, the clathrin coat dissociates. Multiple endocytic vesicles then fuse to create larger sacs of irregular contour called endosomes or receptosomes.[4,61] The pH of the endosomes falls below 6.5, owing to the operation of ATP-driven proton pumps in the membrane.[53,54,61] At this acid pH, the LDL dissociates from the receptor. The latter returns to the surface, apparently by clustering with other receptors in a segment of the endosomal membrane that pinches off to form a recycling vesicle. Once it reaches the surface, the receptor binds another lipoprotein particle and initiates another cycle of endocytosis.[4] Each LDL receptor makes one round-trip every 10 minutes in continuous fashion whether or not it is occupied with LDL.[4,62] The LDL that dissociates from the receptor is delivered to a lysosome when the membranes of the endosome and lysosome fuse. There the protein component of LDL is hydrolyzed to amino acids and the cholesteryl esters are hydrolyzed by an acid lipase, liberating cholesterol (discussed above).

The striking feature of this pathway is that it requires the continuous movement of a membrane-embedded protein from one organelle to another in a highly ordered fashion. Each time it moves, the receptor must be segregated from neighboring membrane proteins that do not follow the same route. This raises a crucial question: What are the signals that direct the highly selective movement of receptors from one membrane organelle to another? Clearly, the signals must lie in the structures of the receptors. What do we know about the structure of the LDL receptor?

The LDL Receptor: A Multi-Domain Protein

The LDL receptor was purified from bovine adrenal cortex by *Wolfgang Schneider* in our laboratory.[55] A partial amino acid sequence was obtained, and this sequence was used by *David Russell* and *Tokuo Yamamoto* to isolate a full-length cDNA for the human LDL receptor.[37,63] Biochemical studies of the receptor protein, coupled with the amino acid sequence that was deduced from the nucleotide sequence of the cDNA, have provided insight into the structural domains of the LDL receptor (Fig. 7).[63–65]

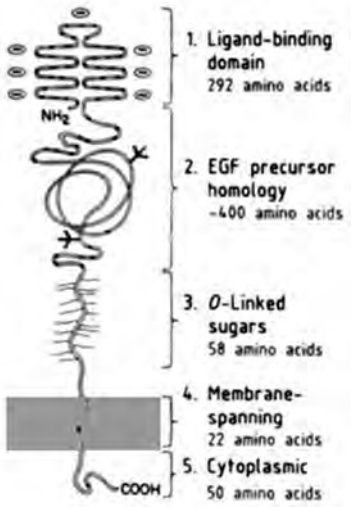


Fig. 7. The LDL receptor: a single protein with five domains. The significance of each domain is discussed in the text.

At the extreme NH_2-terminus of the LDL receptor, there is a hydrophobic sequence of 21 amino acids that is cleaved from the receptor immediately after it is translated. This segment functions as a classic signal sequence to direct the receptor-synthesizing ribosomes to the ER membrane. Because it does not appear in the mature receptor, the signal sequence is omitted from the structural domain that is described below. The mature receptor (without the signal sequence) consists of 839 amino acids.[63]

The *first domain* of the LDL receptor consists of the NH_2-terminal 292 amino acids, which is composed of a sequence of 40 amino acids that is repeated with some variation seven times.[65,66] Studies of anti-peptide antibody binding to intact cells revealed that this domain is located on the external surface of the plasma membrane.[67] Each of the seven 40-amino-acid repeats contains six cysteine residues, which are in register for all of the repeats. The receptor cannot be labeled with [^{3}H]iodoacetamide without prior reduction, suggesting that all of these cysteines are disulfide-bonded.[65] This region of the receptor must therefore exist in a tightly cross-linked, convoluted state. This explains the extreme stability of the binding domain of the receptor; the receptor can be boiled in strong denaturants and still retain its binding activity as long as the disulfide bonds are intact.[65]

A striking feature of each cysteine-rich repeat sequence is a cluster of negatively charged amino acids near the COOH-terminus of each repeat.[65,66] The charges on these sequences are complementary to a cluster of positively charged residues that are believed to occupy one face of a single α-helix in apo E, the best studied ligand for the LDL receptor.[68] Elegant studies by *Mahley* and *Innerarity*[68] with mutant and proteolyzed forms of apo E and with monoclonal antibodies against different regions of apo E showed that the positively charged region contains the site whereby this protein binds to the LDL receptor. It is therefore tempting to speculate that the negatively charged clusters of amino acids within the cysteine-rich repeat se-

quence of the LDL receptor constitute multiple binding sites, each of which binds a single apo E molecule by attaching to its positively charged α-helix.[65]

The *second domain* of the LDL receptor, consisting of approximately 400 amino acids, is 35% homologous to a portion of the extracellular domain of the precursor for epidermal growth factor (EGF).[63,64,69] The EGF precursor is a molecule of 1217 amino acids that appears to span the plasma membrane once, like the LDL receptor.[69-72] Analysis of the amino acid sequence of the EGF precursor, as revealed from the sequence of the cloned cDNA,[70,71] suggests that EGF, a peptide of 53 amino acids, is liberated from the EGF precursor by proteolysis. The sequence of EGF is not homologous to the LDL receptor. Rather, the homology involves a part of the EGF precursor that is on the NH_2-terminal side of EGF itself. The function of this region in either the LDL receptor or the EGF precursor is unknown.

The *third domain* of the LDL receptor lies immediately external to the membrane-spanning domain and consists of a stretch of 58 amino acids that contains 18 serine or threonine residues.[63,66] This domain is encoded within a single exon. Proteolysis studies reveal that this region contains the clustered *O*-linked sugar chains.[64]

The *fourth domain* consists of a stretch of 22 hydrophobic amino acids that span the plasma membrane, as demonstrated by proteolysis experiments.[63,64] Comparison of the amino acid sequences of the human and bovine LDL receptors reveals that the membrane-spanning region is relatively poorly conserved.[65] Of the 22 amino acids in this region, seven differ between human and cow, but all of the substitutions retain a hydrophobic character.

The *fifth domain* is the cytoplasmic tail. The human and bovine LDL receptors each contain a COOH-terminal segment of 50 amino acids that projects into the cytoplasm.[63,64] Localization of this domain to the cytoplasmic side of the membrane was determined through the use of an anti-peptide antibody directed against the COOH-terminal sequence.[64] When inside-out membrane vesicles containing receptor were digested with pronase, the antibody-reactive material was removed, and the molecular weight of the receptor was reduced by approximately 5000. The cytoplasmic sequence is strongly conserved among species. Of the 50 amino acids in this region, only four differ between human and cow, and each of these substitutions is conservative with respect to charge.[65]

The cytoplasmic domain of the LDL receptor plays an important role in clustering in coated pits, either through interaction with clathrin itself or with some protein that is associated with clathrin on the cytoplasmic side of the membrane.[4] This conclusion is based on a molecular analysis of three naturally occurring mutations at the LDL receptor locus that produce receptors that bind LDL normally but fail to cluster in clathrin-coated pits. All three of these mutations produce defects in the cytoplasmic tail (discussed below).[65,73]

The LDL Receptor: A Mosaic Gene

The haploid human genome contains a single copy of the LDL receptor gene[66] on chromosome 19.[74] Sequences representing almost the entire gene were isolated from bacteriophage lambda and cosmid libraries by *Thomas Südhof* and *David Russell*.[66] The position of each intron within the gene was mapped, and the sequence of each exon-intron junction was determined.

The LDL receptor gene spans approximately 45000 bases and is made up of 18 exons separated by 17 introns.[66] There is a striking correlation between the exons in the gene and the functional domains of the protein (Fig. 8). The first intron is located just at the end of the DNA encoding the cleaved signal sequence. The binding domain is encoded by exons 2 to 6. Within this domain (which contains the seven cysteine-rich repeats), introns occur precisely at the ends of repeats I, II, V, VI, and VII (Fig. 8). Repeats III, IV, and V are included in one exon. The binding domain is terminated by an intron at amino acid 292, the last residue in the seventh repeat. Thus, the binding domain is composed of a single exon that has been duplicated multiple times to produce seven repeats of a single 40-amino-acid sequence. Each of these seven repeats in the LDL receptor is strongly homologous with a stretch of 40 amino acids that occurs in the middle of the C9 component of complement, a plasma protein of 537 amino acids that participates in the complement cascade.[66,75]

The next eight exons in the LDL receptor gene (exons 7 to 14) encode the region that is homologous with the EGF precursor (Fig. 8). The gene for the EGF precursor con-

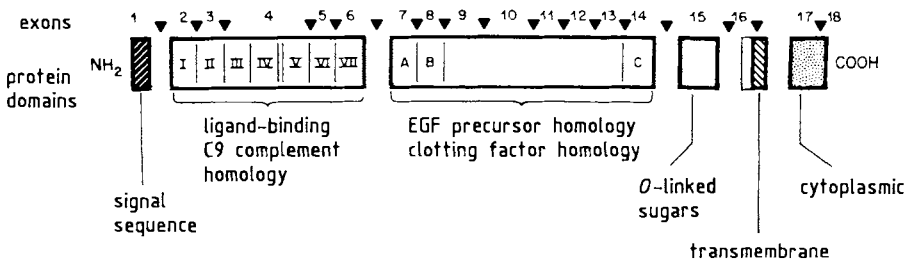


Fig. 8. Correlation of exon organization with protein domains in the human LDL receptor. The domains of the protein are delimited by thick black lines and are labeled in the lower portion. The seven cysteine-rich, 40-amino-acid repeats in the LDL binding domain (Fig. 7) are assigned roman numerals I to VII. Repeats IV and V are separated by eight amino acids. The three cysteine-rich repeats in the domain that is homologous with the EGF precursor are lettered A to C. The positions at which introns interrupt the coding region are indicated by arrowheads. Exon numbers are shown between the arrowheads. (Reprinted with permission from ref. [66].)

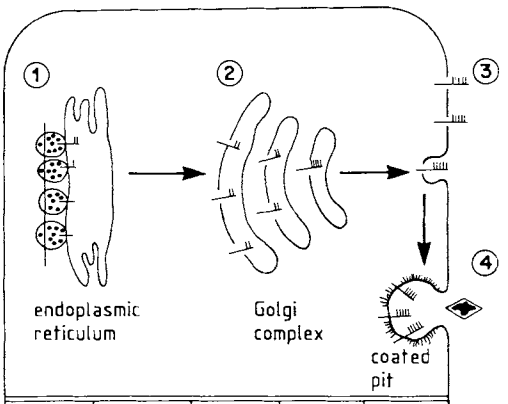
tains the same eight exons.[69] These exons form a cassette that has been lifted out of some ancestral gene during evolution and placed in the middle of the EGF precursor gene and the LDL receptor gene. Three of these exons have also been used by another class of genes. These exons encode a cysteine-rich sequence of 40 amino acids (labeled A, B, and C in Fig. 8) that is repeated three times in the LDL receptor and occurs once in several proteins of the blood clotting system, including factor IX, factor X, and protein C.[69,76] Thus, these exons have been used by members of at least three different gene families.

The *O*-linked sugar domain is also encoded by a single exon (exon 15). However, not all domains of the protein are encoded by single exons. Thus, the membrane-spanning region is encoded by parts of two exons (exons 16 and 17). The cytoplasmic tail is also encoded by two exons (exons 17 and 18) (Fig. 8).

The sharing of exons between the LDL receptor gene and other genes provides strong evidence to support *Gilbert*'s hypothesis concerning the nature and function of introns.[77] As originally proposed by *Gilbert*, introns permit functional domains encoded by discrete exons to shuffle between different proteins, thus allowing proteins to evolve as mosaic combinations of preexisting functional units. The LDL receptor is a vivid example of such a mosaic protein.[66,78] It seems likely that other cell surface receptors will also be found to be mosaic structures assembled from exons shared with other genes.

Genetic Defects in the LDL Receptor

The mutations in the LDL receptor gene in FH patients have helped to delineate the crucial steps of receptor-mediated endocytosis. So far, we have studied fibroblasts from 110 patients with the clinical phenotype of homozygous FH. All of them show evidence of defects in the LDL receptor, but not all defects are the same. At least ten different mutations can be distinguished by structural criteria.[65] These fall into four classes as shown in Figure 9. Many of the apparent FH homozygotes are actually compound heterozygotes who inherit different mutant alleles from each parent.



Class of mutation	Synthesis	Transport from ER to Golgi	Binding of LDL	Clustering in coated pits
1	X			
2	→	X		
3	→	→	X	
4	→	→	→	X

Fig. 9. Four classes of mutations that disrupt the structure and function of the LDL receptor and cause FH. Each class of mutation affects a different region in the gene and thus interferes with a different step in the process by which the receptor is synthesized, processed in the Golgi complex, and transported to coated pits. Each class of mutation can be further subdivided into different mutant alleles that are described in detail in ref. [65]. (Reprinted with permission from ref. [132].)

Class 1 Mutations: No Receptors Synthesized

This is the most common class of mutant alleles, accounting for approximately half of the mutations so far analyzed. These genes produce either no LDL receptor protein or only trace amounts as determined by reaction with polyclonal or monoclonal antibodies. One of these alleles has been analyzed by molecular cloning; the gene bears a large deletion that extends from exon 13 to an *Alu* repetitive element in intron 15.[79] This deletion is easily recognized on Southern blots of genomic DNA. We have not found evidence of a similar deletion in any other individual with the receptor-negative phenotype, so this particular deletion must be rare.

Class 2 Mutations: Receptor Synthesized, but Transported Slowly from ER to Golgi Complex

This is the second most common class of mutations. These alleles produce receptors that are synthesized as precursors whose apparent molecular weights vary from 100000 to 135000. Most have an apparent molecular weight similar to that of the normal precursor (120000). These receptors contain high-mannose *N*-linked sugars and the core *N*-acetylgalactosamine of the *O*-linked sugars.[56,80] However, the *N*-linked sugars are not converted to the complex endoglycosidase H-resistant form nor are the *O*-linked sugar chains elongated. These mutant receptors do not appear on the surface of the cell; rather, they seem to remain in the ER until they are eventually degraded. Some mutations in this class are complete, i.e., there is no detectable processing of carbohydrate. Others are partial, i.e., some of the receptors are processed and move to the surface at a rate that is one-tenth of normal.[80,81] The molecular defect in this class of mutations has not been determined.

Class 3 Mutations: Receptors are Processed and Reach Cell Surface, but Fail to Bind LDL Normally

In the mature form, these mutant receptors can have a normal apparent molecular weight of 160000 or aberrant apparent molecular weights of 140000 or 210000.[65] They are all synthesized as precursors that appear to be 40000 daltons smaller than the mature form. They all undergo normal carbohydrate processing and reach the cell surface, and they bind a variety of antibodies directed against the LDL receptor. However, they have a markedly reduced ability to bind LDL. We suspect that these mutations may involve amino acid substitutions, deletions, or duplications

in the cysteine-rich LDL binding domain or the EGF precursor region, but none has yet been fully elucidated at the molecular level.

Class 4 Mutations: Receptors Reach Cell Surface and Bind LDL, but Fail to Cluster in Coated Pits

Study of these internalization-defective mutations at the cellular level originally revealed the importance of coated pits in receptor-mediated endocytosis.[42,43] Three of the mutations have now been elucidated in molecular detail. All involve alterations in the cytoplasmic tail of the receptor, i.e., the 50 amino acids at the COOH-terminus that project into the cytoplasm (Fig. 10). The mutations have been unraveled through the preparation of genomic DNA libraries and the subsequent isolation and sequencing of exons 17 and 18, which encode the cytoplasmic domain. In the most drastic case, a tryptophan codon has been converted to a nonsense (stop) codon at a position that is two residues distal to the membrane-spanning region.[73] This produces a receptor with only two amino acids in the cytoplasmic tail. Another mutation involves a duplication of four nucleotides following the codon for the sixth amino acid of the cytoplasmic tail.[73] This duplication alters the reading frame and leads to a sequence of eight random amino acids followed by a stop codon. This receptor has only six of the normal amino acids in the cytoplasmic domain. Protein-chemistry studies have confirmed that these two proteins lack the normal COOH-terminus.[73]

The third mutation is the most informative. In this patient, who was the original internalization-defective subject to be described (J. D., see Fig. 3), a single base change leads to the substitution of a cysteine for a tyrosine residue at position 807, which is in the middle of the cytoplasmic tail domain (Fig. 10). We have recently reproduced this amino acid substitution in the normal LDL receptor cDNA by oligonucleotide-directed mutagenesis. When the altered cDNA was introduced into Chinese hamster ovary cells by gene transfer techniques, it produced a receptor that bound LDL but did not cluster in coated pits, confirming that the single base change is responsible for the internalization defect in J. D.'s cells.[82]

Inasmuch as all three internalization-defective mutations involve the cytoplasmic tail, this region must normally play a crucial role in the clustering of LDL receptors in coated pits. It is likely that the cytoplasmic tail binds to clathrin or some other protein that is itself linked to clathrin. The puzzling feature at the moment is that other cell surface receptors that cluster in coated pits do not show obvious homology with the LDL receptor in the amino acid sequences of their cytoplasmic tails.[65] Thus, the precise structure that links receptors to coated pits remains a mystery.

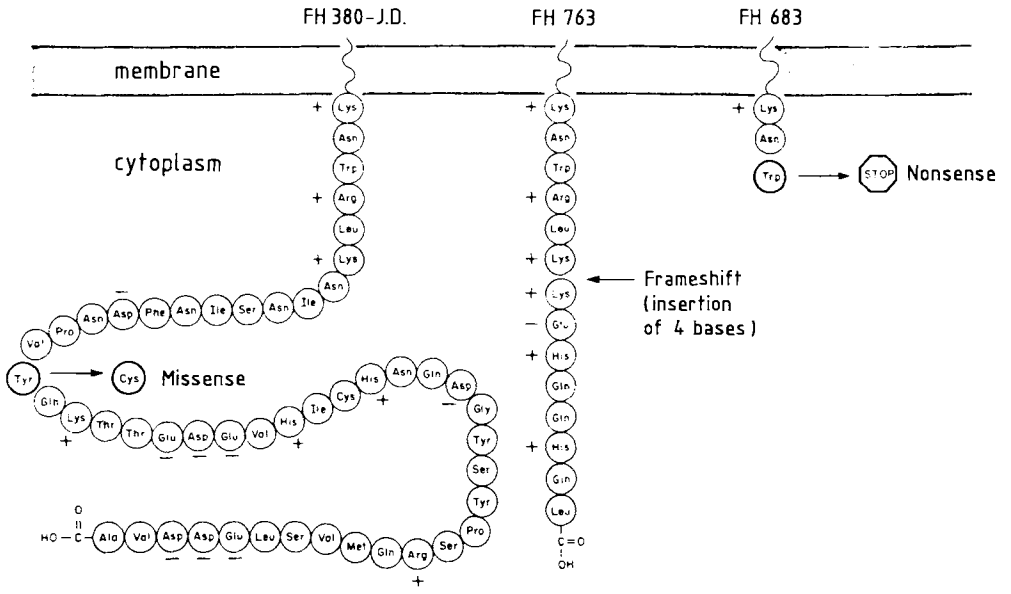


Fig. 10. Mutations affecting the cytoplasmic domain of the LDL receptor in three FH homozygotes with the internalization-defective form of FH.

We have identified several interesting variants of the class 4 mutations in which the mutant genes produce LDL receptors that are secreted into the culture medium. In two mutants of this class (each from an unrelated family), the responsible mutation is a large deletion that results from a recombination between two repetitive *Alu* sequences, one in intron 15 and the other in the 3′ untranslated region of exon 18. The deletion joints in the two mutants are similar but not identical, indicating that the two mutations arose by independent events (ref. [83] and unpublished observations). In each mutant, the deletion removes the exons encoding the membrane-spanning region as well as the cytoplasmic tail. Presumably these prematurely terminated proteins have a short random sequence of amino acids at the COOH-terminus, owing to read-through of an unspliced mRNA. The receptors are transported to the surface, where some of them remain bound to the membrane. The vast majority, however, are released into the culture medium (ref. [83] and unpublished observations). The few receptors that remain on the surface bind LDL, but do not

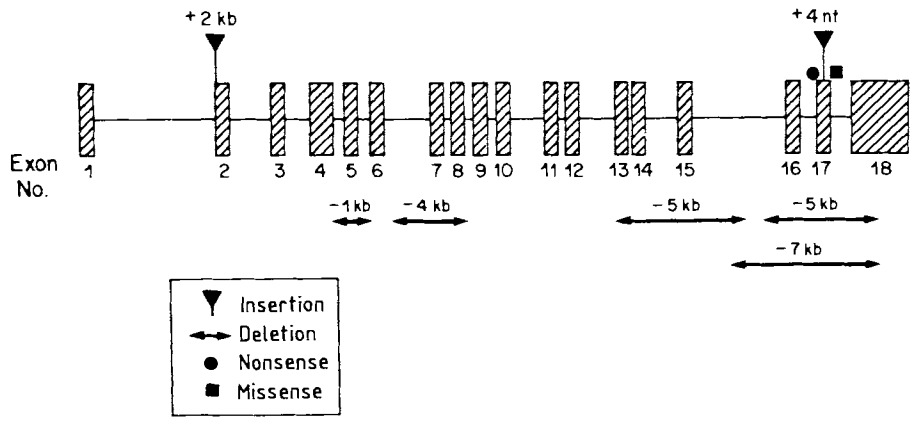


Fig. 11. Location of mutations in the LDL receptor gene. To date, nine mutations have been identified by molecular cloning and DNA sequence analysis or by restriction endonuclease analysis of genomic DNA. Five of the nine mutations are described in detail in refs. [73, 79, 82, 83]. kb denotes kilobases; nt denotes nucleotides.

migrate to coated pits, thus giving rise to an internalization-defective phenotype. These findings emphasize the importance of the membrane-spanning region in anchoring the LDL receptor to the plasma membrane.

Figure 11 shows the location of nine mutations in the LDL receptor gene that have been analyzed at the molecular level. Each FH family examined to date has had a different mutation, and multiple types of mutational events have occurred. Of the nine mutations, two involve single base substitutions, two involve insertions (one small and one large), and five involve large deletions. Many of the deletion joints occur in *Alu* repetitive elements.

Functions of the LDL Receptor in the Body

The LDL receptor was elucidated by an investigative route that is opposite to the one usually employed to uncover metabolic pathways in animals. These pathways are usually observed first in intact animals or tissues and then they are studied in isolated cells. The LDL receptor was first observed in a totally artificial environment—namely, tissue culture. The question immediately arose: What tissues express LDL receptors in the body, and how do they work? We knew at the outset that the receptor must play some role in the body as evidenced by the devastating consequences of LDL receptor deficiency in FH homozygotes and the proportionately less severe abnormalities in FH heterozygotes. Clearly, the receptor must be functioning somewhere. But where?

Detection of LDL Receptor Expression In Vivo

The first cells that were demonstrated to have LDL receptor activity in vivo were circulating blood lymphocytes. In the initial studies carried out with *Y. K. Ho* in 1975, we isolated lymphocytes from the bloodstream and incubated them for 67 hours in vitro in the absence of exogenous cholesterol so as to "derepress" receptor synthesis.[84] Under these conditions the lymphocytes expressed abundant LDL receptors as determined by measurements of the high-affinity uptake and degradation of ^{125}I-LDL (Fig. 12A). Lymphocytes from FH homozygotes did not express

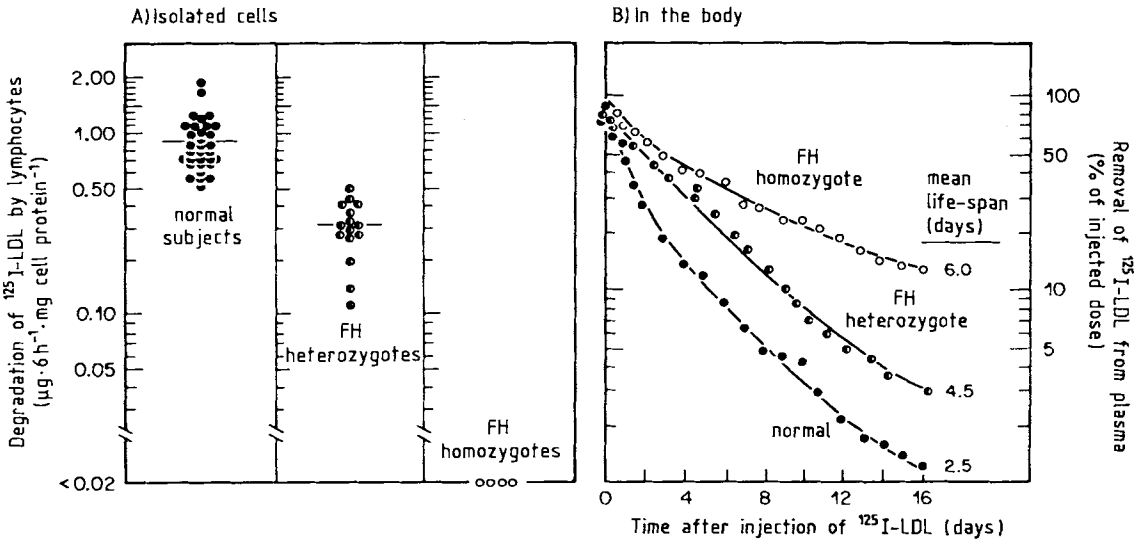


Fig. 12. Measurement of the number of LDL receptors in blood lymphocytes (A) and in living subjects (B). A) Lymphocytes were isolated from venous blood of 32 normal subjects (●), 15 FH heterozygotes (◐), and 4 FH homozygotes (○). After incubation for 67 hours at 37°C in medium containing 10% lipoprotein-deficient serum, LDL receptor activity was assessed by measurement of the high-affinity degradation of ^{125}I-LDL at 37°C. (Data replotted from ref. [85].) B) In the whole-body assay, a tracer amount of ^{125}I-LDL was injected intravenously, and the radioactivity remaining in the circulation over the next 16 days was measured in samples of venous blood [87, 89]. The higher the number of LDL receptors on body cells (A), the faster the removal of ^{125}I-LDL from the blood (B).

detectable LDL receptor activity, and lymphocytes from FH heterozygotes had an intermediate level consistent with the presence of only a single functional gene.[85] LDL receptors were also detectable on lymphocytes immediately after their isolation from the bloodstream, although the level of activity was lower than it was after derepression for 67 hours. Thus, LDL receptors were expressed in at least one cell type in vivo.

Another early clue to the function of LDL receptors in vivo came from studies of the rate of disappearance of intravenously injected ^{125}I-LDL from plasma (Fig. 12B). Such LDL is removed from the circulation more slowly in FH heterozygotes than it is in normal individuals.[86,87] In FH homozygotes the removal defect is even more profound.[87-89] The sluggishness of LDL catabolism in vivo correlates with the relative deficiency of LDL receptors as determined in isolated lymphocytes.

More detailed demonstrations of LDL receptor function in vivo have been obtained in experimental animals. Together with *Sandip K. Basu*, we established an assay for the binding of ^{125}I-LDL to membranes from homogenates of cultured cells and various tissues of the cow and other animals.[90] Using this assay, *Petri Kovanen* found that most tissues of the cow had detectable high-affinity ^{125}I-LDL binding; the adrenal gland and ovarian corpus luteum had the highest activity on a per gram basis.[91] When the weight of the organ was taken into consideration, the liver was found to produce by far the largest number of LDL receptors. Similar results were obtained in studies of human fetal tissues.[91] In collaboration with *Havel*'s laboratory, we showed that ^{125}I-LDL was taken up by perfused rat livers by a high-affinity receptor-mediated process that could be markedly accelerated by administration of the estrogenic hormone 17α-ethinyl estradiol.[92]

High levels of hepatic LDL receptors were also observed when radiolabeled LDL was injected into the circulation of experimental animals and its uptake into various tissues was compared. *Steinberg* and co-workers[93] and *Dietschy* and co-workers[94] showed that approximately 70% of the total-body uptake of radiolabeled LDL took place in the liver by LDL receptor-dependent pathways, but that the highest rates of uptake on a weight basis were seen in the adrenal gland. Various other tissues also showed receptor-mediated uptake of LDL in excess of that seen with nonspecific bulk-phase markers such as radiolabeled albumin.

Measurements of receptor-mediated LDL uptake by tissues of animals were made more practical as a result of two developments: (1) *Steinberg* and co-workers developed a method to label LDL with radioactive sucrose and later with tyramine-cellobiose.[95] In contrast to ^{125}I-labeling of tyrosines, the latter methods produced a radioactive marker that remained trapped in lysosomes after uptake and degradation, thus allowing slow rates of uptake to be quantified cumulatively over long periods. (2) *Shepherd* and *Packard*[96] showed that LDL whose arginine residues were modified by reaction with cyclohexanedione was cleared from the human circulation much more slowly than was native LDL. The rationale for these latter studies lay in previous work from our laboratory[97] and from *Mahley*'s laboratory,[98] which showed that modification of arginine or lysine residues on LDL abolished its ability to bind to the LDL receptor. These observations provided a crude estimate of the fraction of LDL clearance that was attributable to LDL receptors.

We had earlier estimated the fraction of total LDL clearance that was receptor-dependent by comparing the rate of catabolism of intravenously injected ^{125}I-LDL in normal individuals and in FH homozygotes.[99] The fractional catabolic rate for LDL, i.e., the fraction of the total plasma pool of LDL removed per unit time, was threefold higher in normal subjects than in FH homozygotes.[87] From this observation we reasoned that approximately two-thirds of LDL clearance is normally mediated through the LDL receptor.[99] This conclusion has generally been borne out by a number of studies comparing the degradation rates for native versus lysine-modified or arginine-modified LDL both in normal human subjects and in a wide variety of experimental animals.[100]

The WHHL Rabbit and the Role of the LDL Receptor in Clearance of IDL

One of the most important functions of LDL receptors in vivo was appreciated only in the past few years as a result of studies performed in Watanabe Heritable-Hyperlipidemic (WHHL) rabbits. This strain of mutant rabbits was discovered in the late 1970s by *Yosio Watanabe*, a veterinarian in Kobe, Japan.[101] These rabbits have a mutation in the LDL receptor gene that is similar to the class 2 mutations in human FH.[81,102] When present in the homozygous form, this mutation gives rise to extremely high LDL-cholesterol levels; the rabbits develop atherosclerosis early in life.[101,102]

The WHHL rabbits proved invaluable in explaining a previously puzzling feature of homozygous FH. Kinetic studies of ^{125}I-LDL metabolism by *Myant* and co-workers[88] and by *Bilheimer* and *Grundy*[87,89] indicated that FH subjects have a dual defect. In addition to degrading LDL more slowly, FH homozygotes and heterozygotes also appeared to overproduce LDL. How does a genetic defect in the LDL receptor lead simultaneously to overproduction and reduced degradation of LDL? The answer lies in the complex biosynthetic pathway for LDL.

Early studies by *Gitlin*[103] and later those of *Bilheimer, Levy*, and *Eisenberg*[104] suggested that LDL is not secreted directly from the liver, but rather produced in the circulation from a blood-borne precursor, very low density lipoprotein (VLDL) (Fig. 13A). VLDL is a large, triglyceride-rich lipoprotein that is secreted by the liver; it transports triglyceride to adipose tissue and muscle. The triglycerides in VLDL are removed in capillaries by the enzyme lipoprotein lipase, and the VLDL returns to the circulation as a smaller particle with a new name, intermediate density lipoprotein (IDL). The IDL particles have lost most of their triglyceride, but they retain cholesteryl esters. Some of the IDL particles are rapidly taken up by the liver; others remain in the circulation where they undergo further triglyceride hydrolysis and are converted to LDL. A distinguishing feature of the IDL particles is their content of multiple copies of apo E in addition to a single copy of apo B-100.

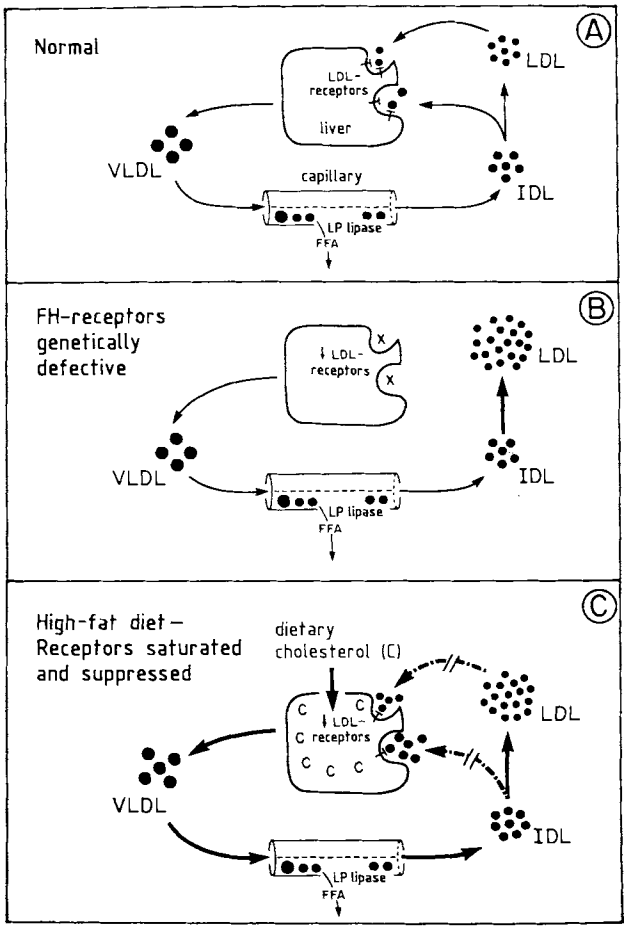


Fig. 13. Schematic model of the mechanism by which LDL receptors in the liver control both the production and catabolism of plasma LDL in normal human subjects (A), in individuals with FH (B), and in individuals consuming a diet rich in saturated fats and cholesterol (C). VLDL denotes very low density lipoprotein; IDL denotes intermediate density lipoprotein; FFA denotes free fatty acid. (Modified from ref. [132] with permission.)

The multiple copies of apo E allow IDL to bind to the LDL receptor with very high affinity. When IDL is converted to LDL, the apo E leaves the particle and only apo B-100 remains. Thereafter, the affinity for the LDL receptor is much reduced.[102]

With *Toru Kita*, we showed that the apparent overproduction of LDL in WHHL rabbits is due to the failure of IDL to be removed from the plasma[102, 105] (Fig. 13B). Thus, when ^{125}I-VLDL was administered to WHHL rabbits, the resultant IDL was not taken up by the liver, as it was in normal rabbits.[105] Rather it remained in the circulation and was converted in increased amounts to LDL. These findings strongly suggest that IDL is normally cleared from plasma by binding to LDL receptors in the liver. Although experiments of similar detail cannot be carried out in humans, the observations of *Soutar*, *Myant*, and *Thompson*[106] are consistent with the notion that enhanced conversion of IDL to LDL also occurs in FH homozygotes, thus accounting for much of the apparent overproduction of LDL.

Figure 13A illustrates the dual role of the LDL receptor in LDL metabolism as determined from the studies of WHHL rabbits. First, the receptor limits LDL production by enhancing the removal of the precursor, IDL, from the circulation. Second, it enhances LDL degradation by mediating cellular uptake of LDL. A deficiency of LDL receptors causes LDL to accumulate as a result both of overproduction and of delayed removal (Fig. 13B). By this quirk of dual functionality, LDL receptors become crucially important modulators of plasma LDL levels in humans and animals.

Perspectives

Receptor Regulation: Therapeutic Implications

Knowledge of the fundamental properties of the LDL receptor has important implications for the therapy of FH and other hypercholesterolemic states. This knowledge also provides fuel for certain speculations about the role of the LDL receptor as a protective factor against atherosclerosis in human beings.

The therapeutic implications of the LDL receptor studies center on strategies for increasing the production of LDL receptors in the liver, thereby lowering plasma LDL-cholesterol levels. In FH heterozygotes this goal can be attained by stimulating the normal gene to produce more than its usual number of LDL receptors, thus compensating for the defective allele.[107] The rationale for such therapy emerged from studies of cultured fibroblasts, which showed that the production of LDL receptors is driven by the cell's demand for cholesterol.[9, 36] When demands for cholesterol are high, the cells have high levels of mRNA for the LDL receptor. Conversely, when demands for cholesterol are reduced, excess cholesterol accumulates in cells, and the amount of receptor mRNA falls.[36, 37]

Inasmuch as the liver is the major site of expression of LDL receptors, the therapeutic problem is reduced to the development of methods to increase hepatic demands for cholesterol. This can be achieved by two techniques: (1) inhibition of the intestinal reabsorption of bile acids; and (2) inhibition of cholesterol synthesis. These techniques can be used alone or in combination, as illustrated in Figure 14.

The liver requires cholesterol for conversion into bile acids, which constitute the major route by which cholesterol is excreted from the body.[18] However, only a fraction

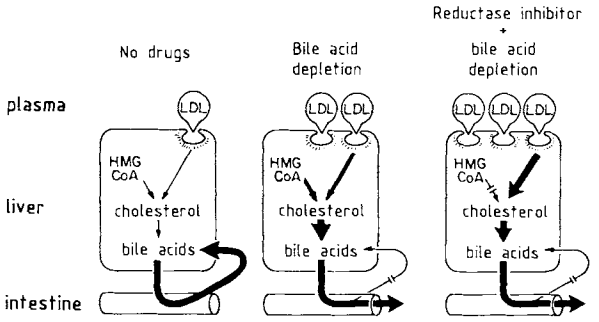


Fig. 14. Rationale for the use of a bile acid-binding resin and an inhibitor of 3-hydroxy-3-methylglutaryl coenzyme A reductase in the treatment of FH heterozygotes. A detailed discussion of this figure is presented in the text.

of the bile acids secreted by the liver actually leaves the body. The vast bulk of bile acids are reabsorbed in the terminal ileum and returned to the liver for reutilization. As a result, the liver converts only a minimal amount of cholesterol into bile acids (Fig. 14, left). The liver's demand for cholesterol can be enhanced by the ingestion of resins that bind bile acids in the intestine and prevent their reabsorption. Since the liver can no longer reuse old bile acids, it must continually make new bile acids and the liver's demand for cholesterol increases. In order to obtain this cholesterol, the liver makes a dual response: (1) it synthesizes increased amounts of cholesterol through an increase in the activity of HMG CoA reductase; and (2) it attempts to take up additional plasma cholesterol by increasing the production of LDL receptors. The increased LDL receptor activity causes plasma LDL levels to fall (Fig. 14, center). The problem with bile acid resin therapy (and the physiologically equivalent procedure of ileal bypass surgery) is that the effects are not profound. The increase in cholesterol production partially offsets the hepatic demand for cholesterol and so there is only a 15 to 20% increase in the synthesis of LDL receptors and only a 15 to 20% drop in plasma LDL-cholesterol levels.

The second method for increasing LDL receptor production, namely, inhibition of hepatic cholesterol synthesis, is much more powerful than bile acid depletion. The technique emerged from the discovery in 1976 of a class of fungal metabolites that inhibit HMG CoA reductase. The original compound, discovered by *Akira Endo* at the Sankyo Drug Company in Japan, is called compactin.[108] A more recent version, developed by the Merck, Sharp and Dohme Research Laboratories in the United States, is called mevinolin.[109] These two agents are potent competitive inhibitors of HMG CoA reductase; the inhibitory constant is approximately 10^{-9} M.[108]

When given to experimental animals, compactin or mevinolin initially inhibit cholesterol synthesis in the liver, and this triggers a complex regulatory mechanism that lowers the plasma LDL-cholesterol level. With *Kovanen* and *Kita*, we showed that the inhibition of cholesterol synthesis elicits a dual compensatory response: (1) hepatocytes synthesize increased amounts of HMG CoA reductase; and (2) they synthesize increased numbers of LDL receptors.[110] When a new steady state is attained, the increase in HMG CoA reductase is almost sufficient to overcome the inhibitory effects of compactin. Total body cholesterol synthesis is only slightly reduced.[111] Meanwhile, the plasma LDL level has fallen as a result of the increase in LDL receptors. The fall in plasma LDL levels is balanced by the increase in LDL receptors, and so the absolute amount of cholesterol entering the liver through the receptor pathway is the same as it was earlier. The difference, however, is that this delivery is now occurring at a lower plasma LDL level.[107]

When given as a single agent to FH heterozygotes, mevinolin routinely produces a 30% fall in plasma LDL-cholesterol levels. When given together with cholestyramine, mevinolin blocks the compensatory increase in cholesterol synthesis, and the increase in LDL receptors is even more profound (Fig. 14, right). Plasma LDL cholesterol levels fall by 50 to 60%.[112]

The important principle to emerge from these studies is that stimulation of LDL receptor activity lowers the plasma LDL-cholesterol level without grossly distorting cholesterol delivery.[107, 111] At present mevinolin and related compounds are in the early stages of clinical testing. Their efficacy in lowering plasma LDL-cholesterol levels has been well established, but there is no information regarding long-term toxicity in man. If these drugs turn out to be nontoxic, they will have an important role in the therapy of FH heterozygotes and probably of other hypercholesterolemic individuals as well.

The principles applied to treatment of FH heterozygotes cannot, unfortunately, be applied to homozygotes, especially those who have totally defective LDL receptor genes. These individuals do not respond to the abovementioned drugs because they cannot synthesize LDL receptors.[113] Current therapy for these individuals involves removal of LDL from plasma extracorporeally through repeated plasmapheresis.[114] Such procedures, which must be repeated every two to three weeks, are technically difficult and are very demanding of patient and physician.

Recently, a more direct therapeutic approach was taken in an FH homozygote, whose initials are S. J. and who has two mutant genes at the LDL receptor locus. This six-year-old girl, who is a patient of our colleague *David Bilheimer* in Dallas, had a total plasma cholesterol level over 1,000 mg/dL (greater than six times above normal limits), and she sustained repeated episodes of myocardial infarction. After she failed to respond to two coronary bypass procedures plus a mitral valve replacement, she was subjected to combined heart-liver transplantation by a team of surgeons led by *Thomas E. Starzl* at the University of Pittsburgh.[115] The liver transplant was designed to provide a source of LDL receptors. The heart transplantation was necessitated because of the poor condition of her own heart as a result of the atherosclerotic process.

Immediately after the operation, S. J.'s total plasma cholesterol level fell from 1100 mg/dL to the range of 200 to 300 mg/dL, and it remained in that range for the succeeding 13 months (Fig. 15A). Thereafter she was started on the HMG CoA reductase inhibitor mevinolin, and her cholesterol fell further to the range of 150 to 200 mg/dL (Fig. 15A). Liver transplantation not only lowered the plasma cholesterol level but it also restored responsiveness to mevinolin, which requires a normal LDL receptor gene in order to act. Lipoprotein turnover studies performed six months after surgery confirmed that the new LDL receptors furnished by the transplanted liver were responsible for the dramatic drop in plasma cholesterol level (Fig. 15B). S. J. remains asymptomatic at the time of this writing, and her cutaneous xanthomas have resolved. However, she requires continuous therapy with cyclosporin to prevent rejection of the transplanted organs, and her long-term prognosis is uncertain.

The response to liver transplantation in S. J. underscores the importance of hepatic LDL receptors in vivo and raises the possibility that other FH homozygotes may respond to similar transplantation procedures. Hopefully, in appropriate cases liver transplantation can be performed before heart transplantation becomes necessary.

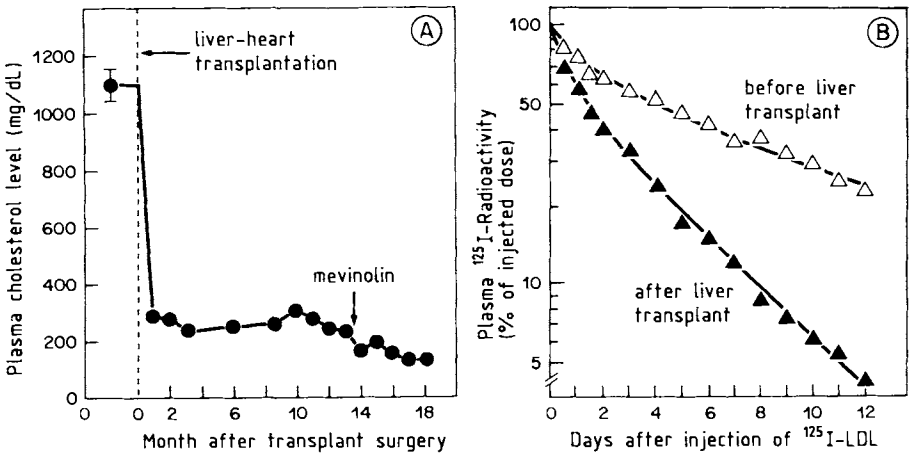


Fig. 15. LDL metabolism in S. J., a patient with homozygous FH, before and after liver-heart transplantation. A) Total cholesterol levels in plasma. B) Plasma decay curves of ^{125}I-LDL after intravenous injection of tracer amounts of ^{125}I-LDL before (△) and after (▲) liver-heart transplantation. (Data in B reprinted with permission from ref. [115].)

Speculations: LDL Receptors and the General Problem of Atherosclerosis

We now leave the realm of solidly established scientific fact and enter the much more controversial realm of speculation about the relation between cholesterol levels, LDL receptors, and atherosclerosis in the general population. After all, FH heterozygotes account for only 5% of myocardial infarctions in patients under the age of 60. What causes the other 95% of heart attacks?

Extensive epidemiologic studies performed in many populations in many countries over the past three decades have pointed strongly to a general association of high blood cholesterol levels with heart attacks. Among the most striking examples is the seven-country study of coronary artery disease directed by *Ansel Keys*.[116] A similar correlation has been observed within a single population in the extensive studies in Framingham, Massachusetts.[117]

These studies have all shown that the incidence of myocardial infarction rises in proportion to the plasma cholesterol level, more specifically the plasma level of LDL-cholesterol. When LDL-cholesterol levels are below 100 mg/dL (equivalent to a total plasma cholesterol level of approximately 170 mg/dL), heart attacks are rare. When LDL-cholesterol levels are above 200 mg/dL (equivalent to a total plasma cholesterol level of approximately 280 mg/dL), heart attacks are frequent. Controversy arises over the middle ground, i.e., individuals with plasma LDL-cholesterol levels between 100 and 200 mg/dL (total plasma cholesterol of 170 to 280 mg/dL). This is the range in which most heart attacks occur. Somewhere within this range there is a threshold value of cholesterol at which heart attacks begin to become more frequent. In this middle ground, how much of the heart attack burden is attributable to plasma cholesterol? There is no definitive answer. In addition to cholesterol, heart attacks in this group are aggravated by smoking, hypertension, stress, diabetes mellitus, and poorly understood genetic factors. However, it seems reasonable to propose that plasma cholesterol does have something to do with heart attacks in these subjects and that the incidence of heart attacks would be reduced if plasma cholesterol could be lowered.[10]

The LDL receptor studies lend experimental support to the epidemiologists' suggestion that the levels of plasma cholesterol usually seen in Western industrialized societies are inappropriately high.[9] This support derives from knowledge of the affinity of the LDL receptor for LDL. The receptor binds LDL optimally when the lipoprotein is present at a cholesterol concentration of 2.5 mg/dL.[28] In view of the 10-to-1 gradient between concentrations of LDL in plasma and interstitial fluid, a level of LDL-cholesterol in plasma of 25 mg/dL would be sufficient to nourish body cells with cholesterol.[118] This is roughly one-fifth of the level usually seen in Western societies (Fig. 16).[119] Several lines of evidence suggest that plasma levels of LDL-cholesterol in the range of 25 to 60 mg/dL (total plasma cholesterol of 110 to 150 mg/dL) might indeed be physiologic for human beings. First, in other mammalian species that do not develop atherosclerosis, the plasma LDL-cholesterol level is generally less than 80 mg/dL (Fig. 16).[120] In these animals the affinity of the LDL receptor for their own LDL is roughly the same as the affinity of the

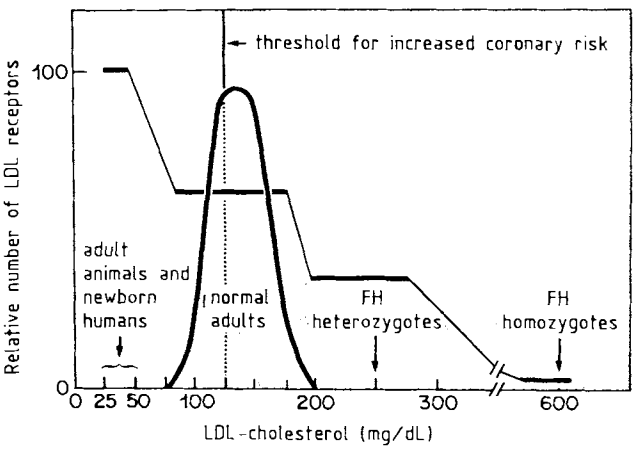


Fig. 16. Range of LDL levels in "normal" adults in Western industrial societies, indicated by the bell-shaped curve [127], is compared with the range in adult animals [120] and human infants [121] and with the levels seen in FH patients [14]. Levels in the shaded region of the chart are above the threshold associated with accelerated atherosclerosis; more than half of the adults have LDL levels above this threshold. The LDL level is inversely associated with the number of LDL receptors. (Modified from ref. [10] with permission.)

human LDL receptor for human LDL, implying that these species are designed by evolution to have similar plasma LDL levels.[9, 119] Second, the LDL level in newborn humans is approximately 30 mg/dL,[121] well within the range that seems to be appropriate for receptor binding (Fig. 16). Third, when humans are raised on a low-fat diet, the plasma LDL-cholesterol tends to stay in the range of 50 to 80 mg/dL. It only reaches levels above 100 mg/dL in individuals who consume a diet rich in saturated animal fats and cholesterol that is customarily ingested in Western societies.[116, 122]

What is the mechanism for the high levels of plasma LDL that are so frequent in Western industrialized societies? Extensive evidence implicates two major factors: diet and heredity. When people habitually consume diets low in animal fats, their plasma LDL-cholesterol levels generally tend to remain low. When even moderate amounts of animal fat are introduced into the diet, the plasma cholesterol level rises.[116, 122] However, the level does not rise equally in every person. Clearly, genetic as well as dietary factors play a role.

How might a diet rich in animal fats and cholesterol elevate the plasma LDL-cholesterol level? Here we believe that two properties of the LDL receptor play a role—saturation and suppression. As the plasma LDL level rises, the receptors become saturated. This saturation of receptors sets an upper limit on the rate at which LDL can be removed efficiently from plasma.[123] Each receptor can handle only one particle of LDL at a time. Once the receptors become saturated, the rate of removal of LDL can be accelerated only by an increase in clearance by non-receptor pathways that operate at low efficiency. In order to drive these alternate pathways, the LDL level must be quite high.[99] At ordinary levels of LDL, the major factor that limits the removal of LDL from plasma is saturation of the LDL receptor.[123]

Once LDL receptors become saturated, the removal rate of LDL is proportional to the number of receptors. Whenever the number of receptors is reduced, plasma LDL levels must rise. Experiments in animals indicate that the consumption of a high-fat diet decreases the number of LDL receptors in the liver.[123, 124] We believe that this mechanism operates through feedback suppression as described above. That is, when excess dietary cholesterol accumulates in the liver, the liver responds by decreasing the production of LDL receptors (Fig. 13C). The entry of dietary cholesterol into the liver is mediated by a receptor, termed the chylomicron remnant receptor, whose activity is genetically distinct from the LDL receptor.[125] The chylomicron remnant receptor is unaffected by cholesterol accumulation,[126] and it causes cholesterol to accumulate to high levels in liver when the diet contains excess fat.

The combination of saturation and suppression of hepatic LDL receptors contributes in a major way to the buildup of LDL in plasma when a diet rich in saturated fats and cholesterol is ingested. Insofar as such a diet also may increase production of LDL in the face of a fixed or declining removal capacity, the LDL level would rise even higher.

If the LDL receptor does limit the removal of LDL from plasma, then maneuvers that increase LDL receptor activity might be effective in individuals who have high plasma LDL-cholesterol levels, but who do not have defective LDL receptor genes. Such therapy seems feasible with the development of HMG CoA reductase inhibitors. However, it is still too early to tell whether such therapy would decrease the incidence of myocardial infarctions in individuals with moderately elevated plasma LDL-cholesterol levels in the range of 100 to 200 mg/dL. There is much circumstantial evidence to expect such improvement,[127] but unequivocal data are simply not there. Hopefully, with the availability of powerful receptor-stimulating drugs, the hypothesis should be susceptible to testing in the near future.

In considering the role of diet and drugs in treatment of high cholesterol levels, physicians and public health authorities must bear in mind the genetic variability between individuals. This variability exists at three levels: (1) The degree of increase in plasma cholesterol upon ingestion of a high cholesterol diet is variable. Not all people develop hypercholesterolemia. Some people, such as the Pima Indians, maintain low plasma cholesterol levels despite ingestion of a high-fat diet.[10] (2) Even when the plasma cholesterol level becomes elevated, the propensity for atherosclerosis varies. For example, a substantial proportion of FH heterozygotes (10 to 20%) escape myocardial infarction until the eight or ninth decade despite pronounced hypercholesterolemia from birth.[14] (3) Genetic susceptibility to contributory risk factors is variable. Some people can withstand hypertension and cigarette smoking for decades without developing atherosclerotic complications; others are highly sensitive.

In view of this genetic variability in susceptibility, dietary and drug recommendations must be individualized. The family history of the individual must be constantly borne in mind, particularly the familial incidence of premature heart attacks or strokes. An important goal of future research will be to dissect this genetic variability. Hopefully, it will become possible to identify the genes that determine such predispositions and to analyze them in each individual. For example, are there alleles that produce subtle defects in the LDL receptor that predispose to "garden-variety," diet-responsive hypercholesterolemia? Are there subtle abnormal alleles at other loci such as those governing cholesterol absorption, cholesterol synthesis, or bile acid synthesis? It seems likely that variability at such loci exists; the scientific challenge is to expose it.

Receptor Recycling: A Novel Cellular Pathway

The studies of the LDL receptor have revealed a new process by which membrane-embedded receptors cycle continuously into and out of cells. The receptors move from one organelle to another as a result of two sequential events: (1) segregation from other proteins by lateral movement in the plane of the membrane, and (2) pinching off of receptor-enriched membranes to form vesicles that eventually fuse with a different organelle. These receptors have been designated as "migrant" membrane proteins to distinguish them from "resident" membrane proteins that do not move in this fashion.[4] The purpose of such intracellular traffic is to integrate the behavior of multiple orga-

nelles to form coherent biochemical pathways. Thus, the movement of the LDL receptor links the cell surface to the endosome and to the lysosome. The cholesterol liberated from LDL in lysosomes exerts regulatory effects in two other organelles, the endoplasmic reticulum and the nucleus. Selective movement of membrane proteins from one organelle to another allows such multi-organelle regulation to occur.

What are the signals that dictate the path that each migrant membrane protein must follow? We are beginning to obtain some insight into the signals necessary for LDL receptors to be incorporated into one sorting structure, the coated pit. However, there is still no information with regard to signals that cause proteins to leave other organelles such as the endoplasmic reticulum and move to different organelles such as the Golgi complex. Delineation of these sorting signals is a major challenge facing the field of cell biology.

Concluding Remarks

In his Nobel Lecture of 1964, *Konrad Bloch* summarized his brilliant studies on the biological synthesis of cholesterol. At the end of his talk, Bloch predicted that the next era in cholesterol research would involve the elucidation of homeostatic control mechanisms.[128] A decade later, in 1973, the LDL receptor concept was advanced to explain the homeostasis of plasma cholesterol and to account for regulatory abnormalities in cholesterol metabolism that were observed in patients with familial hypercholesterolemia. During the next 12 years, the LDL receptor was transformed from a genetic abstraction to a well-characterized protein whose structural domains have been defined. Studies of this receptor taught us about receptor-mediated endocytosis and the novel route by which receptors cycle into and out of cells. We have learned that receptors contain multiple functional domains that direct each step in this movement and that these domains are encoded on exons that can be shared among many proteins. We have learned that genetic defects in the receptor can cause cholesterol to accumulate in plasma, producing premature atherosclerosis. Together with others, we have also learned that the liver is the most important site of action of LDL receptors and that liver replacement can offer a successful form of therapy for children with homozygous FH. Finally, we have learned that regulation of this receptor through drugs and diet can profoundly change the LDL-cholesterol level and that saturation and suppression of receptors may contribute to the high incidence of hypercholesterolemia in industrialized society. It is hoped that these insights will lead to a deeper understanding of the biology of cells and thereby to more effective forms of treatment for diseases such as familial hypercholesterolemia.

We wish to express our deepest appreciation to Dr. Donald W. Seldin, chairman of the Department of Internal Medicine at the University of Texas Southwestern Medical School for more than 30 years and creator of the intellectual environment that made our work possible. We are grateful for the contributions of many students, postdoctoral fellows, and faculty members who have advanced this effort over the past 12 years. Finally, we acknowledge the National Heart, Lung, and Blood Institute of the National Institutes of Health, the Moss Heart Foundation, and the Leland Fikes Foundation for their long-term financial support.

Received: January 30, 1986 [A 581 IE]
German version: *Angew. Chem. 98* (1986) 579

[1] A. E. Garrod: *Inborn Errors of Metabolism*, Oxford University Press, London 1923, 2nd ed., p. 1-216; G. W. Beadle, Genes and chemical reactions in neurospora, *Science 129* (1959) 1715-1719; E. L. Tatum, A case history in biological research, *ibid. 129* (1959) 1711-1714; L. Pauling, H. A. Itano, S. J. Singer, I. C. Wells, Sickle cell anemia: A molecular disease, *ibid. 110* (1949) 543-548; V. M. Ingram, Gene mutations in human haemoglobin: The chemical difference between normal and sickle cell haemoglobin, *Nature (London) 180* (1957) 326-328.

[2] J. L. Goldstein, M. S. Brown, Familial hypercholesterolemia: Identification of a defect in the regulation of 3-hydroxy-3-methylglutaryl coenzyme A reductase activity associated with overproduction of cholesterol, *Proc. Natl. Acad. Sci. USA 70* (1973) 2804-2808.

[3] M. S. Brown, J. L. Goldstein, Familial hypercholesterolemia: Defective binding of lipoproteins to cultured fibroblasts associated with impaired regulation of 3-hydroxy-3-methylglutaryl coenzyme A reductase activity, *Proc. Natl. Acad. Sci. USA 71* (1974) 788-792.

[4] J. L. Goldstein, R. G. W. Anderson, M. S. Brown, Coated pits, coated vesicles, and receptor-mediated endocytosis, *Nature (London) 279* (1979) 679-685; M. S. Brown, R. G. W. Anderson, J. L. Goldstein, Recycling receptors: The round-trip itinerary of migrant membrane proteins, *Cell 32* (1983) 663-667.

[5] *Heinrich O. Wieland* (1928), *Adolf O. R. Windaus* (1928), *Leopold Ruzicka* (1939), *Robert Robinson* (1947) and *Otto P. H. Diels* (1950) were awarded the Nobel Prize in Chemistry in part for work that led to the elucidation of the structure of cholesterol, a brilliant chapter in the history of organic chemistry. *Konrad Bloch* and *Feodor Lynen* were awarded the Nobel Prize in Medicine or Physiology in 1964 for their landmark studies of the cholesterol biosynthetic pathway, a complex sequence involving at least 30 steps. *Robert B. Woodward*, who pioneered the stereochemical synthesis of cholesterol, received the Nobel Prize in Chemistry in 1965 "for his outstanding achievement in the art of organic synthesis." *Derek H. R. Barton* and *Odd Hassel*, were awarded the Nobel Prize in Chemistry in 1969 "for developing and applying the principles of conformation in chemistry," which included establishing the *all chair* conformation of cholesterol. *John W. Cornforth*, who collaborated with *George Popjak* to establish the orientation of all of the hydrogen atoms in the cholesterol molecule, received the Nobel Prize in Chemistry in 1975 "for his work on the stereochemistry of enzyme-catalyzed reactions."

[6] J. L. Oncley, Lipoproteins of human plasma, *Harvey Lect. 50* (1956) 71-91.

[7] J. W. Gofman, O. Delalla, F. Glazier, N. K. Freeman, F. T. Lindgren, A. V. Nichols, B. Strisower, A. R. Tamplin, The serum lipoprotein transport system in health, metabolic disorders, atherosclerosis and coronary heart disease, *Plasma 2* (1954) 413-484.

[8] D. S. Fredrickson, Plasma lipoproteins and apolipoproteins, *Harvey Lect. 68* (1974) 185-237.

[9] J. L. Goldstein, M. S. Brown, The low-density lipoprotein pathway and its relation to atherosclerosis, *Annu. Rev. Biochem. 46* (1977) 897-930.

[10] M. S. Brown, J. L. Goldstein, How LDL receptors influence cholesterol and atherosclerosis, *Sci. Am. 251* (1984) No. 5, 58-66; *Spektrum Wiss. 1985*, No. 1, 96-109.

[11] C. Müller, Xanthomata, hypercholesterolemia, angina pectoris, *Acta Med. Scand. 89* (1938) (Suppl.) 75-84.

[12] A. K. Khachadurian, The inheritance of essential familial hypercholesterolemia, *Am. J. Med. 37* (1964) 402-407.

[13] D. S. Fredrickson, R. I. Levy, Familial hyperlipoproteinemia, chapter 28 in J. B. Stanbury, J. B. Wyngaarden, D. S. Fredrickson (Eds.): *The Metabolic Basis of Inherited Disease*. 3rd ed., McGraw-Hill, New York 1972, p. 545-614.

[14] J. L. Goldstein, M. S. Brown, Familial hypercholesterolemia, chapter 33 in J. B. Stanbury, J. B. Wyngaarden, D. S. Fredrickson, J. L. Goldstein, M. S. Brown (Eds.): *The Metabolic Basis of Inherited Disease*, 5th ed., McGraw-Hill, New York 1983, p. 672-712.

[15] J. L. Goldstein, H. G. Schrott, W. R. Hazzard, E. L. Bierman, A. G. Motulsky, Hyperlipidemia in coronary heart disease. II. Genetic analysis of lipid levels in 176 families and delineation of a new inherited disorder, combined hyperlipidemia, *J. Clin. Invest. 52* (1973) 1544-1568.

[16] D. Patterson, J. Slack, Lipid abnormalities in male and female survivors of myocardial infarction and their first-degree relatives, *Lancet i 1972*, 393-399.

[17] E. A. Nikkila, A. Aro, Family study of serum lipids and lipoproteins in coronary heart-disease, *Lancet i 1973*, 954-958.

[18] J. M. Dietschy, J. D. Wilson, Regulation of cholesterol metabolism, *N. Engl. J. Med. 282* (1970) 1128–1138, 1179–1183, 1241–1249.
[19] E. F. Neufeld, J. C. Fratantoni, Inborn errors of mucopolysaccharide metabolism, *Science 169* (1970) 141–146.
[20] J. M. Bailey, Regulation of cell cholesterol content, in R. Porter, J. Knight (Eds.): *Atherogenesis: Initiating Factors*, Ciba Found. Symp., Vol. 12, Elsevier, Amsterdam 1973, p. 63–92.
[21] G. H. Rothblat, Lipid metabolism in tissue culture cells, *Adv. Lipid Res. 7* (1969) 135–162.
[22] M. S. Brown, S. E. Dana, J. L. Goldstein, Regulation of 3-hydroxy-3-methylglutaryl coenzyme A reductase activity in human fibroblasts by lipoproteins, *Proc. Natl. Acad. Sci. USA 70* (1973) 2162–2166.
[23] N. L. R. Bucher, K. McGarrahan, E. Gould, A. V. Loud, Cholesterol biosynthesis in preparations of liver from normal, fasting, x-irradiated, cholesterol-fed, triton, or Δ^4-cholesten-3-one-treated rats, *J. Biol. Chem. 234* (1959) 262–267; N. L. R. Bucher, P. Overath, F. Lynen, β-Hydroxy-β-methylglutaryl coenzyme A reductase, cleavage and condensing enzymes in relation to cholesterol formation in rat liver, *Biochim. Biophys. Acta 40* (1960) 491–501.
[24] M. D. Siperstein, Regulation of cholesterol biosynthesis in normal and malignant tissues, *Curr. Top. Cell. Regul. 2* (1970) 65–100.
[25] M. S. Brown, S. E. Dana, J. L. Goldstein, Regulation of 3-hydroxy-3-methylglutaryl coenzyme A reductase activity in cultured human fibroblasts: Comparison of cells from a normal subject and from a patient with homozygous familial hypercholesterolemia, *J. Biol. Chem. 249* (1974) 789–796.
[26] E. W. Sutherland, Studies on the mechanism of hormone action, *Science 177* (1972) 401–408.
[27] J. L. Goldstein, M. S. Brown, Binding and degradation of low density lipoproteins by cultured human fibroblasts: Comparison of cells from a normal subject and from a patient with homozygous familial hypercholesterolemia, *J. Biol. Chem. 249* (1974) 5153–5162.
[28] J. L. Goldstein, S. K. Basu, G. Y. Brunschede, M. S. Brown, Release of low density lipoprotein from its cell surface receptor by sulfated glycosaminoglycans, *Cell 7* (1976) 85–95.
[29] J. L. Goldstein, S. E. Dana, J. R. Faust, A. L. Beaudet, M. S. Brown, Role of lysosomal acid lipase in the metabolism of plasma low density lipoprotein: Observations in cultured fibroblasts from a patient with cholesteryl ester storage disease, *J. Biol. Chem. 250* (1975) 8487–8495.
[30] C. de Duve, Lysosomes revisited, *Eur. J. Biochem. 137* (1983) 391–397.
[31] J. L. Goldstein, G. Y. Brunschede, M. S. Brown, Inhibition of the proteolytic degradation of low density lipoprotein in human fibroblasts by chloroquine, concanavalin A, and Triton WR 1339, *J. Biol. Chem. 250* (1975) 7854–7862.
[32] C. de Duve, T. DeBarsy, B. Poole, A. Trouet, P. Tulkens, F. Van Hoof, Lysosomotropic agents, *Biochem. Pharmacol. 23* (1974) 2495–2534.
[33] K. L. Luskey, J. R. Faust, D. J. Chin, M. S. Brown, J. L. Goldstein, Amplification of the gene for 3-hydroxy-3-methylglutaryl coenzyme A reductase, but not for the 53-kDa protein, in UT-1 cells, *J. Biol. Chem. 258* (1983) 8462–8469.
[34] G. Gil, J. R. Faust, D. J. Chin, J. L. Goldstein, M. S. Brown, Membrane-bound domain of HMG CoA reductase is required for sterol-enhanced degradation of the enzyme, *Cell 41* (1985) 249–258.
[35] J. L. Goldstein, S. E. Dana, M. S. Brown, Esterification of low density lipoprotein cholesterol in human fibroblasts and its absence in homozygous familial hypercholesterolemia, *Proc. Natl. Acad. Sci. USA 71* (1974) 4288–4292.
[36] M. S. Brown, J. L. Goldstein, Regulation of the activity of the low density lipoprotein receptor in human fibroblasts, *Cell 6* (1975) 307–316.
[37] D. W. Russell, T. Yamamoto, W. J. Schneider, C. J. Slaughter, M. S. Brown, J. L. Goldstein, cDNA cloning of the bovine low density lipoprotein receptor: Feedback regulation of a receptor mRNA, *Proc. Natl. Acad. Sci. USA 80* (1983) 7501–7505.
[38] G. E. Palade, Fine structure of blood capillaries, *J. Appl. Phys. 24* (1953) 1424.
[39] R. G. W. Anderson, J. L. Goldstein, M. S. Brown, Localization of low density lipoprotein receptors on plasma membrane of normal human fibroblasts and their absence in cells from a familial hypercholesterolemia homozygote, *Proc. Natl. Acad. Sci. USA 73* (1976) 2434–2438; R. G. W. Anderson, M. S. Brown, J. L. Goldstein, Role of the coated endocytic vesicle in the uptake of receptor-bound low density lipoprotein in human fibroblasts, *Cell 10* (1977) 351–364.
[40] T. F. Roth, K. R. Porter, Yolk protein uptake in the oocyte of the mosquito *Aedes aegypti. L, J. Cell Biol. 20* (1964) 313–332.
[41] M. S. Brown, J. L. Goldstein, Analysis of a mutant strain of human fibroblasts with a defect in the internalization of receptor-bound low density lipoprotein, *Cell 9* (1976) 663–674.
[42] J. L. Goldstein, M. S. Brown, N. J. Stone, Genetics of the LDL receptor: Evidence that the mutations affecting binding and internalization are allelic, *Cell 12* (1977) 629–641.
[43] R. G. W. Anderson, J. L. Goldstein, M. S. Brown, A mutation that impairs the ability of lipoprotein receptors to localise in coated pits on the cell surface of human fibroblasts, *Nature (London) 270* (1977) 695–699.
[44] B. M. F. Pearse, Clathrin: A unique protein associated with intracellular transfer of membrane by coated vesicles, *Proc. Natl. Acad. Sci. USA 73* (1976) 1255–1259.
[45] G. Carpenter, S. Cohen, ^{125}I-labeled human epidermal growth factor: Binding, internalization, and degradation in human fibroblasts, *J. Cell Biol. 71* (1976) 159–171.
[46] S. Terris, D. F. Steiner, Binding and degradation of ^{125}I-insulin by rat hepatocytes, *J. Biol. Chem. 250* (1975) 8389–8398.
[47] E. F. Neufeld, G. N. Sando, A. J. Garvin, L. H. Rome, The transport of lysosomal enzymes, *J. Supramol. Struct. 6* (1977) 95–101.
[48] A. Gonzalez-Noriega, J. H. Grubb, V. Talkad, W. S. Sly, Chloroquine inhibits lysosomal enzyme pinocytosis and enhances lysosomal enzyme secretion by impairing receptor recycling, *J. Cell Biol. 85* (1980) 839–852.
[49] G. Ashwell, J. Harford, Carbohydrate-specific receptors of the liver, *Annu. Rev. Biochem. 51* (1982) 531–554; R. J. Stockert, D. J. Howard, A. G. Morell, I. H. Scheinberg, Functional segretation of hepatic receptors for asialoglycoproteins during endocytosis, *J. Biol. Chem. 255* (1980) 9028–9029.
[50] A. Helenius, J. Kartenbeck, K. Simons, E. Fries, On the entry of Semliki Forest virus into BHK-21 cells, *J. Cell Biol. 84* (1980) 404–420.
[51] I. H. Pastan, M. C. Willingham, Journey to the center of the cell: Role of the receptosome, *Science 214* (1981) 504–509.
[52] J. L. Carpentier, P. Gorden, R. G. W. Anderson, J. L. Goldstein, M. S. Brown, S. Cohen, L. Orci, Co-localization of ^{125}I-epidermal growth factor and ferritin-low density lipoprotein in coated pits: A quantitative electron microscopic study in normal and mutant fibroblasts, *J. Cell Biol. 95* (1982) 73–77.
[53] F. R. Maxfield, Weak bases and ionophores rapidly and reversibly raise the pH of endocytic vesicles in cultured mouse fibroblasts, *J. Cell. Biol. 95* (1982) 676–681.
[54] M. Marsh, E. Bolzau, A. Helenius, Penetration of Semliki forest virus from acidic prelysosomal vacuoles, *Cell 32* (1983) 931–940.
[55] W. J. Schneider, U. Beisiegel, J. L. Goldstein, M. S. Brown, Purification of the low density lipoprotein receptor, an acidic glycoprotein of 164,000 molecular weight, *J. Biol. Chem. 257* (1982) 2664–2673.
[56] R. D. Cummings, S. Kornfeld, W. J. Schneider, K. K. Hobgood, H. Tolleshaug, M. S. Brown, J. L. Goldstein, Biosynthesis of the N- and O-linked oligosaccharides of the low density lipoprotein receptor, *J. Biol. Chem. 258* (1983) 15261–15273.
[57] C. G. Davis, A. Elhammer, D. W. Russell, W. J. Schneider, S. Kornfeld, M. S. Brown, J. L. Goldstein, Deletion of clustered O-linked carbohydrates does not impair function of low density lipoprotein receptor in transfected fibroblasts, *J. Biol. Chem. 261*(1986) 2828–2838.
[58] T. P. Bersot, R. W. Mahley, M. S. Brown, J. L. Goldstein, Interaction of swine lipoproteins with the low density lipoprotein receptor in human fibroblasts, *J. Biol. Chem. 251* (1976) 2395–2398.
[59] T. L. Innerarity, R. W. Mahley, Enhanced binding by cultured human fibroblasts of apo-E-containing lipoproteins as compared with low density lipoproteins, *Biochemistry 17* (1978) 1440–1447.
[60] H. Tolleshaug, J. L. Goldstein, W. J. Schneider, M. S. Brown, Post-translational processing of the LDL receptor and its genetic disruption in familial hypercholesterolemia, *Cell 30* (1982) 715–724.
[61] A. Helenius, I. Mellman, D. Wall, A. Hubbard, Endosomes, *Trends Biochem. Sci. 8* (1983) 245–250; I. Pastan, M. C. Willingham, Receptor-mediated endocytosis: Coated pits, receptosomes and the Golgi, *ibid. 8* (1983) 250–254.
[62] M. S. Brown, R. G. W. Anderson, S. K. Basu, J. L. Goldstein, Recycling of cell surface receptors: Observations from the LDL receptor system, *Cold Spring Harbor Symp. Quant. Biol. 46* (1981) 713–721; S. K. Basu, J. L. Goldstein, R. G. W. Anderson, M. S. Brown, Monensin interrupts the recycling of low density lipoprotein receptors in human fibroblasts, *Cell 24* (1981) 493–502.
[63] T. Yamamoto, C. G. Davis, M. S. Brown, W. J. Schneider, M. L. Casey, J. L. Goldstein, D. W. Russell, The human LDL receptor: A cysteine-rich protein with multiple Alu sequences in its mRNA, *Cell 39* (1984) 27–38.
[64] D. W. Russell, W. J. Schneider, T. Yamamoto, K. L. Luskey, M. S. Brown, J. L. Goldstein, Domain map of the LDL receptor: Sequence homology with the epidermal growth factor precursor, *Cell 37* (1984) 577–585.
[65] J. L. Goldstein, M. S. Brown, R. G. W. Anderson, D. W. Russell, W. J. Schneider, Receptor-mediated endocytosis: Concepts emerging from the LDL receptor system, *Annu. Rev. Cell Biol. 1* (1985) 1–39.
[66] T. C. Südhof, J. L. Goldstein, M. S. Brown, D. W. Russell, The LDL receptor Gene: A mosaic of exons shared with different proteins, *Science 228* (1985) 815–822.
[67] W. J. Schneider, C. J. Slaughter, J. L. Goldstein, R. G. W. Anderson, D. J. Capra, M. S. Brown, Use of anti-peptide antibodies to demonstrate external orientation of NH_2-terminus of the LDL receptor in the plasma membrane of fibroblasts, *J. Cell Biol. 97* (1983) 1635–1640.

[68] R. W. Mahley, T. L. Innerarity, Lipoprotein receptors and cholesterol homeostasis, *Biochim. Biophys. Acta 737* (1983) 197-222; T. L. Innerarity, K. H. Weisgraber, K. S. Arnold, S. C. Rall, Jr., R. W. Mahley, Normalization of receptor binding of apolipoprotein E2: Evidence for modulation of the binding site conformation, *J. Biol. Chem. 259* (1984) 7261-7267.

[69] T. C. Südhof, D. W. Russell, J. L. Goldstein, M. S. Brown, R. Sanchez-Pescador, G. I. Bell, Cassette of eight exons shared by genes for LDL receptor and EGF precursor, *Science 228* (1985) 893-895.

[70] J. Scott, M. Urdea, M. Quiroga, R. Sanchez-Pescador, N. Fong, M. Selby, W. J. Rutter, G. I. Bell, Structure of a mouse submaxillary messenger RNA encoding epidermal growth factor and seven related proteins, *Science 221* (1983) 236-240.

[71] A. Gray, T. J. Dull, A. Ullrich, Nucleotide sequence of epidermal growth factor cDNA predicts a 128,000-molecular weight protein precursor, *Nature (London) 303* (1983) 722-725.

[72] R. F. Doolittle, D.-F. Feng, M. S. Johnson, Computer-based characterization of epidermal growth factor precursor, *Nature (London) 307* (1984) 558-566.

[73] M. A. Lehrman, J. L. Goldstein, M. S. Brown, D. W. Russell, W. J. Schneider, Internalization-defective LDL receptors produced by genes with nonsense and frameshift mutations that truncate the cytoplasmic domain, *Cell 41* (1985) 735-753.

[74] U. Francke, M. S. Brown, J. L. Goldstein, Assignment of the human gene for the low density lipoprotein receptor to chromosome 19: Synteny of a receptor, a ligand, and a genetic disease, *Proc. Natl. Acad. Sci. USA 81* (1984) 2826-2830.

[75] K. K. Stanley, H.-P. Kocher, J. P. Luzio, P. Jackson, J. Tschopp, The sequence and topology of human complement component C9, *EMBO J. 4* (1985) 375-382.

[76] R. F. Doolittle, The genealogy of some recently evolved vertebrate proteins, *Trends Biochem. Sci. 10* (1985) 233-237.

[77] W. Gilbert, Why genes in pieces? *Nature (London) 271* (1978) 501.

[78] W. Gilbert, Genes-in-pieces revisited, *Science 228* (1985) 823-824.

[79] M. A. Lehrman, D. W. Russell, C. G. Davis, J. L. Goldstein, M. S. Brown, *Proc. Natl. Acad. Sci. USA 83* (1986) 3679-3683.

[80] H. Tolleshaug, K. K. Hobgood, M. S. Brown, J. L. Goldstein, The LDL receptor locus in familial hypercholesterolemia: Multiple mutations disrupting the transport and processing of a membrane receptor, *Cell 32* (1983) 941-951.

[81] W. J. Schneider, M. S. Brown, J. L. Goldstein, Kinetic defects in the processing of the LDL receptor in fibroblasts from WHHL rabbits and a family with familial hypercholesterolemia, *Mol. Biol. Med. 1* (1983) 353-367.

[82] C. G. Davis, M. A. Lehrman, D. W. Russell, R. G. W. Anderson, M. S. Brown, J. L. Goldstein, The J. D. mutation in familial hypercholesterolemia: Substitution of cysteine for tyrosine in cytoplasmic domain impedes internalization of LDL receptors, *Cell 45* (1986) 15-24.

[83] M. A. Lehrman, W. J. Schneider, T. C. Südhof, M. S. Brown, J. L. Goldstein, D. W. Russell, Mutation in LDL receptor: Alu-Alu recombination deletes exons encoding transmembrane and cytoplasmic domains, *Science 227* (1985) 140-146.

[84] Y. K. Ho, M. S. Brown, D. W. Bilheimer, J. L. Goldstein, Regulation of low density lipoprotein receptor activity in freshly isolated human lymphocytes, *J. Clin. Invest. 58* (1976) 1465-1474.

[85] D. W. Bilheimer, Y. K. Ho, M. S. Brown, R. G. W. Anderson, J. L. Goldstein, Genetics of the low density lipoprotein receptor: Diminished receptor activity in lymphocytes from heterozygotes with familial hypercholesterolemia, *J. Clin. Invest. 61* (1978) 678-696.

[86] T. Langer, W. Strober, R. I. Levy, The metabolism of low density lipoprotein in familial type II hyperlipoproteinemia, *J. Clin. Invest. 51* (1972) 1528-1536.

[87] D. W. Bilheimer, N. J. Stone, S. M. Grundy, Metabolic studies in familial hypercholesterolemia: Evidence for a gene-dosage effect *in vivo*, *J. Clin. Invest. 64* (1979) 524-533.

[88] L. A. Simons, D. Reichl, N. B. Myant, M. Mancini, The metabolism of the apoprotein of plasma low density lipoprotein in familial hyperbetalipoproteinaemia in the homozygous form, *Atherosclerosis 21* (1975) 283-298.

[89] D. W. Bilheimer, J. L. Goldstein, S. M. Grundy, M. S. Brown, Reduction in cholesterol and low density lipoprotein synthesis after portacaval shunt surgery in a patient with homozygous familial hypercholesterolemia, *J. Clin. Invest. 56* (1975) 1420-1430.

[90] S. K. Basu, J. L. Goldstein, M. S. Brown, Characterization of the low density lipoprotein receptor in membranes prepared from human fibroblasts, *J. Biol. Chem. 253* (1978) 3852-3856.

[91] P. T. Kovanen, S. K. Basu, J. L. Goldstein, M. S. Brown, Low density lipoprotein receptors in bovine adrenal cortex. II. Low density lipoprotein binding to membranes prepared from fresh tissue, *Endocrinology 104* (1979) 610-616; M. S. Brown, P. T. Kovanen, J. L. Goldstein, Receptor-mediated uptake of lipoprotein-cholesterol and its utilization for steroid synthesis in the adrenal cortex, *Recent Prog. Horm. Res. 35* (1979) 215-257.

[92] Y. S. Chao, E. E. Windler, G. C. Chen, R. J. Havel, Hepatic catabolism of rat and human lipoproteins in rats treated with 17α-ethinyl estradiol, *J. Biol. Chem. 254* (1979) 11360-11366; P. T. Kovanen, M. S. Brown, J. L. Goldstein, Increased binding of low density lipoprotein to liver membranes from rats treated with 17α-ethinyl estradiol, *ibid. 254* (1979) 11367-11373.

[93] R. C. Pittman, T. E. Carew, A. D. Attie, J. L. Witztum, Y. Watanabe, D. Steinberg, Receptor-dependent and receptor-independent degradation of low density lipoprotein in normal rabbits and in receptor-deficient mutant rabbits, *J. Biol. Chem. 257* (1982) 7994-8000.

[94] D. K. Spady, D. W. Bilheimer, J. M. Dietschy, Rates of receptor dependent and independent low density lipoprotein uptake in the hamster, *Proc. Natl. Acad. Sci. USA 80* (1983) 3499-3503.

[95] D. Steinberg, Lipoproteins and atherosclerosis: A look back and a look ahead, *Arteriosclerosis 3* (1983) 283-301.

[96] J. Shepherd, S. Bicker, A. R. Lorimer, C. J. Packard, Receptor mediated low density lipoprotein catabolism in man, *J. Lipid Res. 20* (1979) 999-1006.

[97] S. K. Basu, J. L. Goldstein, R. G. W. Anderson, M. S. Brown, Degradation of cationized low density lipoprotein and regulation of cholesterol metabolism in homozygous familial hypercholesterolemia fibroblasts, *Proc. Natl. Acad. Sci. USA 73* (1976) 3178-3182.

[98] R. W. Mahley, T. L. Innerarity, R. E. Pitas, K. H. Weisgraber, J. H. Brown, E. Gross, Inhibition of lipoprotein binding to cell surface receptors of fibroblasts following selective modification of arginyl residues in arginine-rich and B apoproteins, *J. Biol. Chem. 252* (1977) 7279-7287; K. H. Weisgraber, T. L. Innerarity, R. W. Mahley, Role of the lysine residues of plasma lipoproteins in high affinity binding to cell surface receptors on human fibroblasts, *ibid. 253* (1978) 9053-9062.

[99] J. L. Goldstein, M. S. Brown, Atherosclerosis: The low-density lipoprotein receptor hypothesis, *Metabolism 26* (1977) 1257-1275.

[100] M. S. Brown, J. L. Goldstein, Lipoprotein receptors in the liver: Control signals for plasma cholesterol traffic, *J. Clin. Invest. 72* (1983) 743-747.

[101] Y. Watanabe, Serial inbreeding of rabbits with hereditary hyperlipidemia (WHHL-rabbit). Incidence and development of atherosclerosis and xanthoma, *Atherosclerosis 36* (1980) 261-268.

[102] J. L. Goldstein, T. Kita, M. S. Brown, Defective lipoprotein receptors and atherosclerosis: Lessons from an animal counterpart of familial hypercholesterolemia, *N. Engl. J. Med. 309* (1983) 288-295.

[103] D. Gitlin, D. G. Cornwell, D. Nakasato, J. L. Oncley, W. L. Hughes, Jr., C. A. Janeway, Studies on the metabolism of plasma proteins in the nephrotic syndrome. II. The lipoproteins, *J. Clin. Invest. 37* (1958) 172-184.

[104] D. W. Bilheimer, S. Eisenberg, R. I. Levy, The metabolism of very low density lipoprotein proteins. I. Preliminary *in vitro* and *in vivo* observations, *Biochim. Biophys. Acta 260* (1972) 212-221.

[105] T. Kita, M. S. Brown, D. W. Bilheimer, J. L. Goldstein, Delayed clearance of very low density and intermediate density lipoproteins with enhanced conversion to low density lipoprotein in WHHL rabbits, *Proc. Natl. Acad. Sci. USA 79* (1982) 5693-5697.

[106] A. K. Soutar, N. B. Myant, G. R. Thompson, The metabolism of very low density and intermediate density lipoproteins in patients with familial hypercholesterolaemia, *Atherosclerosis 43* (1982) 217-231.

[107] M. S. Brown, J. L. Goldstein, Lowering plasma cholesterol by raising LDL receptors (editorial), *N. Engl. J. Med. 305* (1981) 515-517.

[108] A. Endo, M. Kuroda, K. Tanzawa, Competitive inhibition of 3-hydroxy-3-methylglutaryl coenzyme A reductase by ML-236A and ML-236B fungal metabolites, having hypocholesterolemic activity, *FEBS Lett. 72* (1976) 323-326; A. Endo, Compactin (ML-236B) and related compounds as potential cholesterol-lowering agents that inhibit HMG-CoA reductase, *J. Med. Chem. 28* (1985) 401-405.

[109] A. W. Alberts, J. Chen, G. Kuron, V. Hunt, J. Huff, C. Hoffman, J. Rothrock, M. Lopez, H. Joshua, E. Harris, A. Patchett, R. Monaghan, S. Currie, E. Stapley, G. Albers-Schonberg, O. Hensens, J. Hirshfield, K. Hoogsteen, J. Liesch, J. Springer, Mevinolin, a highly potent competitive inhibitor of HMG-CoA reductase and cholesterol lowering agent, *Proc. Natl. Acad. Sci. USA 77* (1980) 3957-3961.

[110] T. Kita, M. S. Brown, J. L. Goldstein, Feedback regulation of 3-hydroxy-3-methylglutaryl coenzyme A reductase in livers of mice treated with mevinolin, a competitive inhibitor of the reductase, *J. Clin. Invest. 66* (1980) 1094-1100; P. T. Kovanen, D. W. Bilheimer, J. L. Goldstein, J. J. Jaramillo, M. S. Brown, Regulatory role for hepatic low density lipoprotein receptors *in vivo* in the dog, *Proc. Natl. Acad. Sci. USA 78* (1981) 1194-1198.

[111] S. M. Grundy, D. W. Bilheimer, Inhibition of 3-hydroxy-3-methylglutaryl-CoA reductase by mevinolin in familial hypercholesterolemia heterozygotes: Effects on cholesterol balance, *Proc. Natl. Acad. Sci. USA 81* (1984) 2538-2542.

[112] H. Mabuchi, T. Sakai, Y. Sakai, A. Yoshimura, A. Watanabe, T. Wakasugi, J. Koizumi, R. Takeda, Reduction of serum cholesterol in heterozygous patients with familial hypercholesterolemia: Additive effects of compactin and cholestyramine, *N. Engl. J. Med. 308* (1983) 609-613; D. W. Bilheimer, S. M. Grundy, M. S. Brown, J. L. Goldstein, Mevinolin stimulates receptor-mediated clearance of low density lipoprotein from plasma in familial hypercholesterolemia heterozygotes, *Proc. Natl. Acad. Sci. USA 80* (1983) 4124-4128; D. R. Illingworth, Mevinolin plus colestipol in therapy for severe heterozygous familial hypercholesterolemia, *Ann. Intern. Med. 101* (1984) 598-604.

[113] A. Yamamoto, H. Sudo, A. Endo, Therapeutic effects of ML-236B in primary hypercholesterolemia, *Atherosclerosis 35* (1980) 259-266.

[114] G. R. Thompson, N. B. Myant, D. Kilpatrick, C. M. Oakley, M. J. Raphael, R. E. Steiner, Assessment of long-term plasma exchange for familial hypercholesterolaemia, *Br. Heart J. 43* (1980) 680-688.

[115] D. W. Bilheimer, J. L. Goldstein, S. C. Grundy, T. E. Starzl, M. S. Brown, Liver transplantation provides low density lipoprotein receptors and lowers plasma cholesterol in a child with homozygous familial hypercholesterolemia, *N. Engl. J. Med. 311* (1984) 1658-1664.

[116] A. Keys: *Seven countries: A multivariate analysis of death and coronary heart disease,* Harvard University Press, Cambridge, MA 1980, p. 1-381.

[117] W. B. Kannel, W. P. Castelli, T. Gordon, P. M. McNamara, Serum cholesterol, lipoproteins, and the risk of coronary heart disease: The Framingham Study, *Ann. Intern. Med. 74* (1971) 1-12.

[118] D. Reichl, N. B. Myant, M. S. Brown, J. L. Goldstein, Biologically active low density lipoprotein in human peripheral lymph, *J. Clin. Invest. 61* (1978) 64-71.

[119] J. L. Goldstein, M. S. Brown, Lipoprotein receptors: Genetic defense against atherosclerosis, *Clin. Res. 30* (1982) 417-426.

[120] G. L. Mills, C. E. Taylaur, The distribution and composition of serum lipoproteins in eighteen animals, *Comp. Biochem. Phys. 40B* (1971) 489-501; G. D. Calvert, Mammalian low density lipoproteins, in C. E. Day, R. S. Levy (Eds.): *Low Density Lipoproteins,* Plenum Press, New York 1976, p. 281-319.

[121] P. O. Kwiterovich, Jr., R. I. Levy, D. S. Fredrickson, Neonatal diagnosis of familial type-II hyperlipoproteinaemia, *Lancet i* (1973) 118-122.

[122] S. J. Connor, W. E. Connor, The interactions of genetic and nutritional factors in hyperlipidemia, in A. Velazquez, H. Bourges: *Genetic Factors in Nutrition,* Academic Press, Orlando, FL 1984, p. 137-155; D. Applebaum-Bowden, S. M. Haffner, E. Hartsook, K. H. Luk, J. J. Albers, W. R. Hazzard, Down-regulation of the low-density lipoprotein receptor by dietary cholesterol, *Am. J. Clin. Nutr. 39* (1984) 360-367.

[123] P. T. Kovanen, M. S. Brown, S. K. Basu, D. W. Bilheimer, J. L. Goldstein, Saturation and suppression of hepatic lipoprotein receptors: A mechanism for the hypercholesterolemia of cholesterol-fed rabbits, *Proc. Natl. Acad. Sci. USA 78* (1981) 1396-1400.

[124] D. Y. Hui, T. L. Innerarity, R. W. Mahley, Lipoprotein binding to canine hepatic membranes: Metabolically distinct apo-E and apo B,E receptors, *J. Biol. Chem. 256* (1981) 5646-5655; D. K. Spady, S. D. Turley, J. M. Dietschy, Rates of low density lipoprotein uptake and cholesterol synthesis are regulated independently in the liver, *J. Lipid Res. 26* (1985) 465-472.

[125] T. Kita, J. L. Goldstein, M. S. Brown, Y. Watanabe, C. A. Hornick, R. J. Havel, Hepatic uptake of chylomicron remnants in WHHL rabbits: A mechanism genetically distinct from the low density lipoprotein receptor, *Proc. Natl. Acad. Sci. USA 79* (1982) 3623-3627.

[126] B. C. Sherrill, J. M. Dietschy, Characterization of the sinusoidal transport process responsible for uptake of chylomicrons by the liver, *J. Biol. Chem. 253* (1978) 1859-1867.

[127] Lipid Research Clinics Program. The lipid research clinics coronary primary prevention trial results: I. Reduction in incidence of coronary heart disease, *J. Am. Med. Assoc. 251* (1984) 351-364; Lipid Research Clinics Program. The lipid research clinics coronary primary prevention trial results: II. The relationship of reduction in incidence of coronary heart disease to cholesterol lowering, *ibid. 251* (1984) 365-374.

[128] K. Bloch, The biological synthesis of cholesterol, *Science 150* (1965) 19-28; German version: Die Biosynthese des Cholesterins, *Angew. Chem. 77* (1965) 944-954.

[129] R. J. Deckelbaum, G. G. Shipley, D. M. Small, Structure and interactions of lipids in human plasma low density lipoproteins, *J. Biol. Chem. 252* (1977) 744-754; J. Elovson, J. C. Jacobs, V. N. Schumaker, D. L. Puppione, Molecular weights of apoprotein B obtained from human low-density lipoprotein (apoprotein B-PI) and from rat very low density lipoprotein (apoprotein B-PIII), *Biochemistry 24* (1985) 1569-1578.

[130] M. S. Brown, J. L. Goldstein, Receptor-mediated endocytosis: Insights from the lipoprotein receptor system, *Proc. Natl. Acad. Sci. USA 76* (1979) 3330-3337.

[131] M. S. Brown, J. L. Goldstein, The LDL receptor and HMG-CoA reductase - Two membrane molecules that regulate cholesterol homeostasis, *Curr. Top. Cell. Regul. 26* (1985) 3-15.

[132] J. L. Goldstein, M. S. Brown, Progress in understanding the LDL receptor and HMG CoA reductase, two membrane proteins that regulate the plasma cholesterol, *J. Lipid Res. 25* (1984) 1450-1461.

Direct Methods and Anomalous Dispersion (Nobel Lecture)**

By Herbert Hauptman*

1. Introduction

The electron density function, $\rho(\mathbf{r})$, in a crystal determines its diffraction pattern, i.e. both the magnitudes and phases of its X-ray diffraction maxima, and conversely. Since, however, only magnitudes are available from the diffraction experiment, then the density function $\rho(\mathbf{r})$ cannot be recovered. If one invokes prior structural knowledge, usually that the crystal is composed of discrete atoms of known atomic numbers, then the observed magnitudes are, in general, sufficient to determine the positions of the atoms, i.e. the crystal structure.

It should be noted here that the recognition that observed diffraction data are in general sufficient to determine crystal structures uniquely was an important milestone in the development of the direct methods of crystal structure determination. The erroneous contrary view, that crystal structures could not, even in principle, be deduced from diffraction intensities, had long been held by the crystallographic community prior to ca. 1950 and constituted a psychological barrier which first had to be removed before real progress could be made.

2. The Traditional Direct Methods

2.1. The Phase Problem

Denote by $\phi_{\mathbf{H}}$ the phase of the structure factor $F_{\mathbf{H}}$:

$$F_{\mathbf{H}} = |F_{\mathbf{H}}| \exp(i\phi_{\mathbf{H}}) \tag{1}$$

where $\mathbf{H}$ is a reciprocal lattice vector (having three integer components) which labels the corresponding diffraction maximum. The relationship between the structure factors $F_{\mathbf{H}}$ and the electron density function $\rho(\mathbf{r})$ is then given by

$$F_{\mathbf{H}} = \int_V \rho(\mathbf{r}) \exp(2\pi i\, \mathbf{H}\cdot\mathbf{r})\, dV \tag{2}$$

and

$$\rho(\mathbf{r}) = \frac{1}{V}\sum_{\mathbf{H}} F_{\mathbf{H}} \exp(-2\pi i\, \mathbf{H}\cdot\mathbf{r}) = \frac{1}{V}\sum_{\mathbf{H}} |F_{\mathbf{H}}| \exp i(\phi_{\mathbf{H}} - 2\pi\, \mathbf{H}\cdot\mathbf{r}) \tag{3}$$

in which V represents the unit cell or its volume. Thus the structure factors $F_{\mathbf{H}}$ determine $\rho(\mathbf{r})$. The X-ray diffraction experiment yields only the magnitudes $|F_{\mathbf{H}}|$ of a finite number of structure factors, but the values of the phases $\phi_{\mathbf{H}}$, which are also needed if one is to determine $\rho(\mathbf{r})$ from Eq. (3), cannot be determined experimentally. If arbitrary values for the phases $\phi_{\mathbf{H}}$ are specified in Eq. (3), then density functions $\rho(\mathbf{r})$ are defined, which, when substituted into Eq. (2) yield structure factors $F_{\mathbf{H}}$, the magnitudes of which agree with the observed magnitudes $|F_{\mathbf{H}}|$. It follows that the diffraction experiment does not determine $\rho(\mathbf{r})$. It was this argument which led crystallographers, prior to 1950, to the erroneous conclusion that diffraction intensities could not, even in principle, determine crystal structures uniquely. What had been overlooked was the fact that the phases $\phi_{\mathbf{H}}$ could not be arbitrarily specified if Eq. (3) is to yield density functions characteristic of real crystals.

Crystals are composed of discrete atoms. One exploits this prior structural knowledge by replacing the real crystal, with continuous electron density $\rho(\mathbf{r})$, by an ideal one, the unit cell of which consists of N discrete, non-vibrating, point atoms located at the maxima of $\rho(\mathbf{r})$. Then the structure factor $F_{\mathbf{H}}$ is replaced by the normalized structure factor $E_{\mathbf{H}}$ and Eq. (1) to (3) are replaced by

$$E_{\mathbf{H}} = |E_{\mathbf{H}}| \exp(i\phi_{\mathbf{H}}) \tag{4}$$

$$E_{\mathbf{H}} = \frac{1}{\sigma_2^{1/2}} \sum_{j=1}^{N} f_j \exp(2\pi i\, \mathbf{H}\cdot\mathbf{r}_j) \tag{5}$$

$$\langle E_{\mathbf{H}} \exp(-2\pi i\, \mathbf{H}\cdot\mathbf{r})\rangle_{\mathbf{H}} = \frac{1}{\sigma_2^{1/2}} \left\langle \sum_{j=1}^{N} f_j \exp[2\pi i\, \mathbf{H}\cdot(\mathbf{r}_j - \mathbf{r})] \right\rangle_{\mathbf{H}}$$
$$= \frac{f_j}{\sigma_2^{1/2}} \quad \text{if} \quad \mathbf{r} = \mathbf{r}_j$$
$$= 0 \quad \text{if} \quad \mathbf{r} \neq \mathbf{r}_j \tag{6}$$

where f_j is the zero-angle atomic scattering factor, $\mathbf{r}_j$ is the position vector of the atom labelled j, and

$$\sigma_n = \sum_{j=1}^{N} f_j^n \quad (n = 1, 2, 3, \ldots) \tag{7}$$

In the case of X-ray diffraction the f_j are equal to the atomic numbers Z_j and are thus presumed to be known. From Eq. (6) it follows that the normalized structure factors $E_{\mathbf{H}}$ determine the atomic position vectors $\mathbf{r}_j$ ($j = 1, 2, \ldots, N$), i.e. the crystal structure.

In practice a finite number of magnitudes $|E_{\mathbf{H}}|$ of normalized structure factors $E_{\mathbf{H}}$ are obtainable (at least approximately) from the observed magnitudes $|F_{\mathbf{H}}|$, while the phases $\phi_{\mathbf{H}}$, as defined by Eq. (4) and (5), cannot be determined experimentally. Since one now requires only the 3N components of the N position vectors $\mathbf{r}_j$, rather than the much more complicated electron density function $\rho(\mathbf{r})$, it turns out that, in general, the known magnitudes are more than sufficient. This is most readily seen by equating the magnitudes of both sides of Eq. (5) in order to

[*] Prof. Dr. H. Hauptman
Medical Foundation of Buffalo, Inc.
73 High Street, Buffalo, NY 14203 (USA)

[**] Copyright © The Nobel Foundation 1986.—We thank the Nobel Foundation, Stockholm, for permission to print this article.

obtain a system of equations in which the only unknowns are the 3N components of the position vectors $\mathbf{r}_j$. Since the number of such equations, equal to the number of reciprocal lattice vectors $\mathbf{H}$ for which magnitudes $|E_{\mathbf{H}}|$ are available, usually greatly exceeds the number, 3N, of unknowns, this system is redundant. Thus, observed diffraction intensities usually over-determine the crystal structure, i.e. the positions of the atoms in the unit cell. In short, by merely replacing the integral of Eq. (2) by the summation of Eq. (5), i.e. taking Eq. (5) as the starting point of our investigation rather than Eq. (2), one has transformed the problem from an unsolvable one into one which is solvable, at least in principle.

In summary then, the intensities (or magnitudes $|E_{\mathbf{H}}|$) of a sufficient number of X-ray diffraction maxima determine a crystal structure. The available intensities usually exceed the number of parameters needed to describe the structure. From these intensities a set of numbers $|E_{\mathbf{H}}|$ can be derived, one corresponding to each intensity. However, the elucidation of the crystal structure requires also a knowledge of the complex numbers $E_{\mathbf{H}} = |E_{\mathbf{H}}| \exp(i\phi_{\mathbf{H}})$, the normalized structure factors, of which only the magnitudes $|E_{\mathbf{H}}|$ can be determined from experiment. Thus, a "phase" $\phi_{\mathbf{H}}$, unobtainable from the diffraction experiment, must be assigned to each $|E_{\mathbf{H}}|$, and the problem of determining the phases when only the magnitudes $|E_{\mathbf{H}}|$ are known is called the "phase problem". Owing to the known atomicity of crystal structures and the redundancy of observed magnitudes $|E_{\mathbf{H}}|$, the phase problem is, in principle, solvable.

2.2. The Structure Invariants

Equation (6) implies that the normalized structure factors $E_{\mathbf{H}}$ determine the crystal structure. However, Eq. (5) does not imply that, conversely, the crystal structure determines the values of the normalized structure factors $E_{\mathbf{H}}$ since the position vectors $\mathbf{r}_j$ depend not only on the structure but on the choice of origin as well. It turns out nevertheless that the magnitudes $|E_{\mathbf{H}}|$ of the normalized structure factors are in fact uniquely determined by the crystal structure and are independent of the choice of origin but that the values of the phases $\phi_{\mathbf{H}}$ depend also on the choice of origin. Although the values of the individual phases depend on the structure and the choice of origin, there exist certain linear combinations of the phases, the so-called structure invariants, whose values are determined by the structure alone and are independent of the choice of origin.

It follows readily from Eq. (5) that the linear combination of three phases

$$\psi_3 = \phi_{\mathbf{H}} + \phi_{\mathbf{K}} + \phi_{\mathbf{L}} \tag{8}$$

and that the linear combination of four phases

$$\mathbf{H} + \mathbf{K} + \mathbf{L} = 0 \tag{9}$$

the linear combination of four phases

$$\psi_4 = \phi_{\mathbf{H}} + \phi_{\mathbf{K}} + \phi_{\mathbf{L}} + \phi_{\mathbf{M}} \tag{10}$$

is a structure invariant (quartet) provided that

$$\mathbf{H} + \mathbf{K} + \mathbf{L} + \mathbf{M} = 0 \tag{11}$$

etc.

2.3. The Structure Seminvariants

If a crystal possesses elements of symmetry then the origin may not be chosen arbitrarily if the simplifications permitted by the space group symmetries are to be realized. For example, if a crystal has a center of symmetry it is natural to place the origin at such a center, whereas if a two-fold screw axis, but no other symmetry element is present, the origin would normally be situated on this symmetry axis. In such cases the permissible origins are greatly restricted and it is therefore plausible to assume that many linear combinations of the phases will remain unchanged in value when the origin is shifted only in the restricted ways allowed by the space group symmetries. One is thus led to the notion of the structure seminvariant, those linear combinations of the phases whose values are independent of the choice of permissible origin.

If the only symmetry element is a center of symmetry, for example (space group $P\bar{1}$), then it turns out (again from Eq. (5)) that a single phase $\phi_{\mathbf{H}}$ is a structure seminvariant provided that the three components of the reciprocal lattice vector $\mathbf{H}$ are even integers; the linear combination of two phases $\phi_{\mathbf{H}} + \phi_{\mathbf{K}}$ is a structure seminvariant provided that the three components of $\mathbf{H} + \mathbf{K}$ are even integers; etc.

If the only symmetry element is a two-fold rotation axis (or twofold screw axis) then one finds from Eq. (5) that the single phase ϕ_{hkl} is a structure seminvariant provided that h and l are even integers and $k = 0$; the linear combination of two phases

$$\phi_{h_1 k_1 l_1} + \phi_{h_2 k_2 l_2}$$

is a structure seminvariant provided that $h_1 + h_2$ and $l_1 + l_2$ are even and $k_1 + k_2 = 0$; etc.

The structure invariants and seminvariants have been tabulated for all the space groups.[13-15, 19, 21] In general the collection of structure invariants is a subset of the collection of structure seminvariants. If no element of symmetry is present, that is the space group is $P1$, then the two classes coincide.

2.3.1. Origin and Enantiomorph Specification

The theory of the structure seminvariants leads in a natural way to space group dependent recipes for origin and enantiomorph (i.e. the handedness, right or left) specification.

In general the theory identifies an appropriate set of phases whose values are to be specified in order to fix the origin uniquely. For example, in space group $P1$ (no elements of symmetry) the values of any three phases

$$\phi_{h_1 k_1 l_1},\ \phi_{h_2 k_2 l_2},\ \phi_{h_3 k_3 l_3} \tag{12}$$

for which the determinant Δ satisfies

$$\Delta = \begin{vmatrix} h_1 & k_1 & l_1 \\ h_2 & k_2 & l_2 \\ h_3 & k_3 & l_3 \end{vmatrix} = \pm 1 \qquad (13)$$

may be specified arbitrarily, thus fixing the origin uniquely. Once this is done then the value of any other phase is uniquely determined by the structure alone. For enantiomorph specification it is sufficient to specify arbitrarily the sign of any enantiomorph sensitive structure invariant, i.e. one whose value is different from 0° or 180° (for further details see ref. [6], pages 28–52).

In the space group $P\bar{1}$ one again specifies arbitrarily the value (0° or 180°) of three phases (see (12)), but now the condition is that the determinant Δ [defined by Eq. (13)] be odd. Similar recipes for all the space groups are now known and are to be found in the literature cited.

2.4. The Fundamental Principle of Direct Methods

It is known that the values of a sufficiently extensive set of cosine seminvariants (the cosines of the structure seminvariants) lead unambiguously to the values of the individual phases.[6] Magnitudes |E| are capable of yielding estimates of the cosine seminvariants only or, equivalently, the magnitudes of the structure seminvariants; the signs of the structure seminvariants are ambiguous because the two enantiomorphous structures permitted by the observed magnitudes |E| correspond to two values of each structure seminvariant differing only in sign. However, once the enantiomorph has been selected by specifying arbitrarily the sign of a particular enantiomorph sensitive structure seminvariant (i.e. one different from 0 or π), then the magnitudes |E| determine both signs and magnitudes of the structure seminvariants consistent with the chosen enantiomorph. Thus, for a fixed enantiomorph, the observed magnitudes |E| determine unique values for the structure seminvariants; the latter, in turn, lead to unique values of the individual phases. In short, the structure seminvariants serve to link the observed magnitudes |E| with the desired phases ϕ (the fundamental principle of direct methods). It is this property of the structure seminvariants which accounts for their importance and which justifies the stress placed on them here.

By the term "direct methods" is meant that class of methods which exploits relationships among the structure factors in order to go directly from the observed magnitudes |E| to the needed phases ϕ.

2.5. The Neighborhood Principle

It has long been known that, for a fixed enantiomorph, the value of any structure seminvariant ψ is, in general, uniquely determined by the magnitudes |E| of the normalized structure factors. In recent years it has become clear that, for a fixed enantiomorph, there corresponds to ψ one or more small sets of magnitudes |E|, the neighborhoods of ψ, on which, in favorable cases, the value of ψ most sensitively depends; that is to say that, in favorable cases, ψ is primarily determined by the values of |E| in any of its neighborhoods and is relatively insensitive to the values of the great bulk of remaining magnitudes. The conditional probability distribution of ψ, assuming as known the magnitudes |E| in any of its neighborhoods, yields an estimate for ψ which is particularly good in the favorable case that the variance of the distribution happens to be small.[7,8]

The study of appropriate probability distributions (compare Section 2.7) leads directly to the definition of the neighborhoods of the structure invariants. Definitions are given here only for the triplet ψ_3 and the quartet ψ_4, but recipes for defining the neighborhoods of all the structure invariants are now known.[3,10,11]

2.5.1. *The First Neighborhood of the Triplet ψ_3*

Let **H**, **K**, **L** be three reciprocal lattice vectors which satisfy Eq. (9). Then ψ_3 [Eq. (8)] is a structure invariant and its first neighborhood is defined to consist of the three magnitudes:

$$|E_{\mathbf{H}}|, |E_{\mathbf{K}}|, |E_{\mathbf{L}}|. \qquad (14)$$

2.5.2. *Neighborhoods of the Quartet ψ_4*

The First Neighborhood

Let **H**, **K**, **L**, **M** be four reciprocal lattice vectors which satisfy Eq. (11). Then ψ_4 [Eq. (10)] is a structure invariant and its first neighborhood is defined to consist of the four magnitudes:

$$|E_{\mathbf{H}}|, |E_{\mathbf{K}}|, |E_{\mathbf{L}}|, |E_{\mathbf{M}}| \qquad (15)$$

The four magnitudes in (15) are said to be the main terms of the quartet ψ_4.

The second Neighborhood

The second neighborhood of the quartet ψ_4 is defined to consist of the four magnitudes in (15) plus the three additional magnitudes:

$$|E_{\mathbf{h}+\mathbf{K}}|, |E_{\mathbf{K}+\mathbf{L}}|, |E_{\mathbf{L}+\mathbf{H}}| \qquad (16)$$

i.e. seven magnitudes |E| in all. The three magnitudes in (16) are said to be the cross-terms of the quartet ψ_4.

2.6. The Extension Concept

By embedding the structure seminvariant T and its symmetry related variants in suitable structure invariants Q one obtains the extensions Q of the seminvariant T. Owing to the space group dependent relations among the phases, T is related in a known way to its extensions. In this way the theory of the structure seminvariants is reduced to that of the structure invariants. In particular, the neighborhoods of T are defined in terms of the neighborhoods of its extensions. The procedure will be illustrated in some detail only for the two-phase structure seminvariant in the space group $P\bar{1}$ which serves as the prototype for the structure

seminvariants in general, in all space groups, noncentrosymmetric as well as centrosymmetric.

2.6.1. The Two-Phase Structure Seminvariant in $P\bar{1}$

It has already been seen (Section 2.3) that the linear combination of two phases

$$T=\phi_{\mathbf{H}}+\phi_{\mathbf{K}} \tag{17}$$

is a structure seminvariant in $P\bar{1}$ if and only if the three components of the reciprocal lattice vector $\mathbf{H}+\mathbf{K}$ are all even. Then the components of each of the four reciprocal lattice vectors $\frac{1}{2}(\pm\mathbf{H}\pm\mathbf{K})$ are all integers. Note also that in this space group the structure factors are real and all phases are 0° or 180°.

2.6.2. The Extensions of T

One embeds the two-phase structure seminvariant T [Eq. (17)] and its symmetry related variant

$$T_1=\phi_{-\mathbf{H}}+\phi_{\mathbf{K}} \tag{18}$$

in the respective quartets

$$Q=T+\phi_{-\frac{1}{2}(\mathbf{H}+\mathbf{K})}+\phi_{-\frac{1}{2}(\mathbf{H}+\mathbf{K})} \tag{19}$$

$$Q_1=T_1+\phi_{-\frac{1}{2}(-\mathbf{H}+\mathbf{K})}+\phi_{-\frac{1}{2}(-\mathbf{H}+\mathbf{K})} \tag{20}$$

From Eq. (17) and (18) and the space group-dependent relationships among the phases, it is readily verified that Q and Q_1 are in fact (special) four-phase structure invariants (quartets) and

$$T=T_1=Q=Q_1 \tag{21}$$

The quartets Q and Q_1 are said to be the extensions of the seminvariant T. In this way the theory of the two-phase structure seminvariant T is reduced to that of the quartets. In particular, the neighborhoods of T are defined in terms of the neighborhoods of the quartet.

2.6.3. The First Neighborhoods of the Extensions

Since two of the phases of the quartet Q [Eq. (19)] are identical, only three of the four main terms are distinct. The first neighborhood of Q is accordingly defined to consist of the three magnitudes

$$|E_{\mathbf{H}}|, |E_{\mathbf{K}}|, |E_{\frac{1}{2}(\mathbf{H}+\mathbf{K})}| \tag{22}$$

(since $|E_{-\frac{1}{2}(\mathbf{H}+\mathbf{K})}|=|E_{\frac{1}{2}(\mathbf{H}+\mathbf{K})}|$)

In a similar way the first neighborhood of the extension Q_1 [Eq. (20)] is defined to consist of the three magnitudes

$$|E_{\mathbf{H}}|, |E_{\mathbf{K}}|, |E_{\frac{1}{2}(\mathbf{H}-\mathbf{K})}| \tag{23}$$

2.6.4. The First Neighborhood of T

The first neighborhood of the two-phase structure seminvariant T is defined to consist of the set-theoretic union of the first neighborhoods of its extensions, i.e., in view of (22) and (23), of the four magnitudes

$$|E_{\mathbf{H}}|, |E_{\mathbf{K}}|, |E_{\frac{1}{2}(\mathbf{H}+\mathbf{K})}|, |E_{\frac{1}{2}(\mathbf{H}-\mathbf{K})}| \tag{24}$$

2.7. The Solution Strategy

One starts with the system of equations (5). By equating real and imaginary parts of (5) one obtains two equations for each reciprocal lattice vector $\mathbf{H}$. The magnitudes $|E_{\mathbf{H}}|$ and the atomic scattering factors f_j are presumed to be known. The unknowns are the atomic position vectors $\mathbf{r}_j$ and the phases $\phi_{\mathbf{H}}$. Owing to the redundancy of the system (5), one naturally invokes probabilistic techniques in order to eliminate the unknown position vectors $\mathbf{r}_j$, and in this way to obtain relationships among the unknown phases $\phi_{\mathbf{H}}$ having probabilistic validity.

Choose a finite number of reciprocal lattice vectors $\mathbf{H}$, $\mathbf{K}$, ... in such a way that the linear combination of phases

$$\psi=\phi_{\mathbf{H}}+\phi_{\mathbf{K}}+\cdots \tag{25}$$

is a structure invariant or seminvariant whose value we wish to estimate. Choose satellite reciprocal lattice vectors $\mathbf{H}'$, $\mathbf{K}'$, ... in such a way that the collection of magnitudes

$$|E_{\mathbf{H}}|, |E_{\mathbf{K}}|, \ldots; \quad |E_{\mathbf{H}'}|, |E_{\mathbf{K}'}|, \ldots \tag{26}$$

constitutes a neighborhood of ψ. The atomic position vectors $\mathbf{r}_j$ are assumed to be the primitive random variables which are uniformly and independently distributed. Then the magnitudes $|E_{\mathbf{H}}|, |E_{\mathbf{K}}|, \ldots; |E_{\mathbf{H}'}|, |E_{\mathbf{K}'}|, \ldots$; and phases $\phi_{\mathbf{H}}, \phi_{\mathbf{K}}, \ldots; \phi_{\mathbf{H}'}, \phi_{\mathbf{K}'}, \ldots$ of the complex, normalized structure factors $E_{\mathbf{H}}, E_{\mathbf{K}}, \ldots; E_{\mathbf{H}'}, E_{\mathbf{K}'}, \ldots$, as functions [Eq. (5)] of the position vectors $\mathbf{r}_j$, are themselves random variables, and their joint probability distribution P may be obtained. From the distribution P one derives the conditional joint probability distribution

$$P(\Phi_{\mathbf{H}}, \Phi_{\mathbf{K}}, \ldots | |E_{\mathbf{H}}|, |E_{\mathbf{K}}|, \ldots; |E_{\mathbf{H}'}|, |E_{\mathbf{K}'}|, \ldots), \tag{27}$$

of the phases $\phi_{\mathbf{H}}, \phi_{\mathbf{K}}, \ldots$, given the magnitudes $|E_{\mathbf{H}}|, |E_{\mathbf{K}}|, \ldots; |E_{\mathbf{H}'}|, |E_{\mathbf{K}'}|, \ldots$, by fixing the known magnitudes, integrating with respect to the unknown phases $\Phi_{\mathbf{H}'}, \Phi_{\mathbf{K}'}, \ldots$ from 0 to 2π, and multiplying by a suitable normalizing parameter. The distribution (27) in turn leads directly to the conditional probability distribution

$$P(\Psi | |E_{\mathbf{H}}|, |E_{\mathbf{K}}|, \ldots; |E_{\mathbf{H}'}|, |E_{\mathbf{K}'}|, \ldots) \tag{28}$$

of the structure invariant or seminvariant ψ, assuming as known the magnitudes of (26) constituting a neighborhood of ψ. Finally, the distribution (28) yields an estimate for ψ which is particularly good in the favorable case that the variance of (28) happens to be small.

2.8. Estimating the Triplet in $P1$

Let the three reciprocal lattice vectors **H**, **K**, and **L** satisfy Eq. (9). Refer to Section 2.5.1 for the first neighborhood of the triplet ψ_3 [Eq. (8)] and to Section 2.7 for the probabilistic background.

Suppose that R_1, R_2, and R_3 are three specified non-negative numbers. Denote by

$$P_{1/3} = P(\psi | R_1, R_2, R_3)$$

the conditional probability distribution of the triplet ψ_3, given the three magnitudes in its first neighborhood:

$$|E_{\mathbf{H}}| = R_1, |E_{\mathbf{K}}| = R_2, |E_{\mathbf{L}}| = R_3 \tag{29}$$

Then, carrying out the program described in Section 2.7, one finds[11]

$$P_{1/3} = P(\Psi | R_1, R_2, R_3) \approx \frac{1}{2\pi I_0(A)} \exp(A \cos \Psi) \tag{30}$$

where

$$A = \frac{2\sigma_3}{\sigma_2^{3/2}} R_1 R_2 R_3 \tag{31}$$

I_0 is the modified Bessel function, and σ_n is defined by Eq. (7). Since $A > 0$, $P_{1/3}$ has a unique maximum at $\Psi = 0°$, and it is clear that the larger the value of A the smaller is the variance of the distribution (see Fig. 1, where $A = 2.316$; Fig. 2, where $A = 0.731$). Hence, in the favorable case that A is large, say, for example, $A > 3$, the distribution leads to a reliable estimate of the structure invariant ψ_3, zero in this case:

$$\psi_3 \approx 0 \text{ if A is large} \tag{32}$$

Furthermore, the larger the value of A, the more likely is the probabilistic statement (32). It is remarkable how useful this relationship has proven to be in the applications; and yet (32) is severely limited because it is capable of yielding only the zero estimate for ψ_3, and only those estimates are reliable for which A is large, the favorable cases.

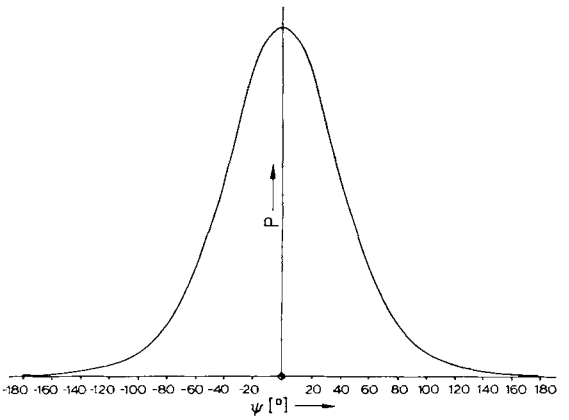


Fig. 1. The distribution $P_{1/3}$ [Eq. (30)] for $A = 2.316$.

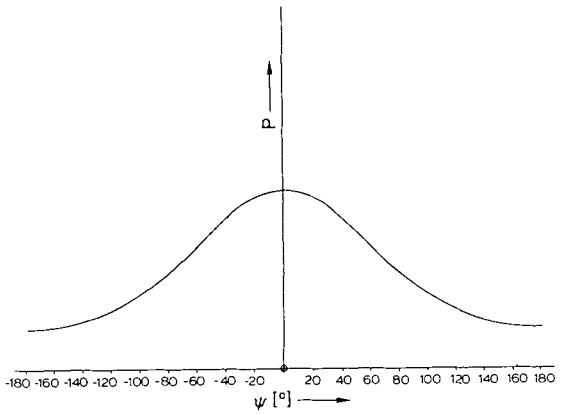


Fig. 2. The distribution $P_{1/3}$ [Eq. (30)] for $A = 0.731$.

It should be mentioned in passing that a distribution closely related to (30) leads directly to the so-called tangent formula[18] which is universally used by direct methods practitioners:

$$\frac{\sin\phi_{\mathbf{h}}}{\cos\phi_{\mathbf{h}}} = \tan\phi_{\mathbf{h}} = \frac{\langle |E_{\mathbf{K}} E_{\mathbf{h}-\mathbf{K}}| \sin(\phi_{\mathbf{K}} + \phi_{\mathbf{h}-\mathbf{K}}) \rangle_{\mathbf{K}}}{\langle |E_{\mathbf{K}} E_{\mathbf{h}-\mathbf{K}}| \cos(\phi_{\mathbf{K}} + \phi_{\mathbf{h}-\mathbf{K}}) \rangle_{\mathbf{K}}} \tag{33}$$

in which **h** is a fixed reciprocal lattice vector, the averages are taken over the same set of vectors **K** in reciprocal space, usually restricted to those vectors **K** for which $|E_{\mathbf{K}}|$ and $|E_{\mathbf{h}-\mathbf{K}}|$ are both large, and the sign of $\sin\phi_{\mathbf{h}}$ ($\cos\phi_{\mathbf{h}}$) is the same as the sign of the numerator (denominator) on the right hand side. The tangent formula is usually used to refine and extend a basis set of phases, presumed to be known.

2.9. Estimating the Quartet in $P1$

Two conditional probability distributions are described, one assuming as known the four magnitudes |E| in the first neighborhood of the quartet, the second assuming as known the seven magnitudes |E| in its second neighborhood.

2.9.1. The First Neighborhood

Suppose that **H**, **K**, **L**, and **M** are four reciprocal lattice vectors which satisfy Eq. (11). Refer to Section 2.5.2 for the first neighborhood of the quartet ψ_4 [Eq. (10)] and to Section 2.7 for the probabilistic background. Suppose that R_1, R_2, R_3, and R_4 are four specified non-negative numbers. Denote by

$$P_{1/4} = P(\Psi | R_1, R_2, R_3, R_4)$$

the conditional probability distribution of the quartet ψ_4, given the four magnitudes in its first neighborhood:

$$|E_{\mathbf{H}}| = R_1, |E_{\mathbf{K}}| = R_2, |E_{\mathbf{L}}| = R_3, |E_{\mathbf{M}}| = R_4 \tag{34}$$

Then

$$P_{1/4} = P(\Psi | R_1, R_2, R_3, R_4) \approx \frac{1}{2\pi I_0(B)} \exp(B \cos \Psi) \tag{35}$$

where

$$B = \frac{2\sigma_4}{\sigma_2^2} R_1 R_2 R_3 R_4$$

and σ_n is defined by Eq. (7). Thus $P_{1/4}$ is identical with $P_{1/3}$, but B replaces A. Hence similar remarks apply to $P_{1/4}$. In particular, (35) always has a unique maximum at $\Psi = 0°$ so that the most probable value of ψ_4, given the four magnitudes (34) in its first neighborhood, is zero, and the larger the value of B the more likely it is that $\psi_4 = 0°$. Since B values, of order $1/N$, tend to be less than A values, of order $1/\sqrt{N}$, at least for large values of N, the estimate (zero) of ψ_4 is in general less reliable than the estimate (zero) of ψ_3. Hence the goal of obtaining a reliable non-zero estimate for a structure invariant is not realized by Eq. (35). The decisive step in this direction is made next.

2.9.2. *The Second Neighborhood*

Employ the same notation as in Section 2.9.1 and refer again to Section 2.5.2 for the second neighborhood of the quartet ψ_4. Suppose that R_1, R_2, R_3, R_4, R_{12}, R_{23}, and R_{31}, are seven non-negative numbers. Denote by

$$P_{1/7} = P(\Psi | R_1, R_2, R_3, R_4;\ R_{12}, R_{23}, R_{31})$$

the conditional probability distribution of the quartet ψ_4, given the seven magnitudes in its second neighborhood:

$$|E_H| = R_1,\ |E_K| = R_2,\ |E_L| = R_3,\ |E_M| = R_4 \tag{36}$$

$$|E_{H+K}| = R_{12},\ |E_{K+L}| = R_{23},\ |E_{L+H}| = R_{31} \tag{37}$$

Then[7,9]

$$P_{1/7} \approx \frac{1}{L} \exp(-2B' \cos \Psi) \times I_0\left[\frac{2\sigma_3}{\sigma_2^{3/2}} R_{12} X_{12}\right] I_0\left[\frac{2\sigma_3}{\sigma_2^{3/2}} R_{23} X_{23}\right] I_0\left[\frac{2\sigma_3}{\sigma_2^{3/2}} R_{31} X_{31}\right] \tag{38}$$

where

$$B' = \frac{1}{\sigma_2^3}(3\sigma_2^3 - \sigma_2\sigma_4) R_1 R_2 R_3 R_4 \tag{39}$$

$$X_{12} = [R_1^2 R_2^2 + R_3^2 R_4^2 + 2 R_1 R_2 R_3 R_4 \cos \Psi]^{1/2} \tag{40}$$

$$X_{23} = [R_2^2 R_3^2 + R_1^2 R_4^2 + 2 R_1 R_2 R_3 R_4 \cos \Psi]^{1/2} \tag{41}$$

$$X_{31} = [R_3^2 R_1^2 + R_2^2 R_4^2 + 2 R_1 R_2 R_3 R_4 \cos \Psi]^{1/2} \tag{42}$$

σ_n is defined by Eq. (7), and L is a normalizing parameter, independent of Ψ, which is not needed for the present purpose.

Figures 3–5 show the distribution (38) (solid line —) for typical values of the seven parameters (36) and (37). For comparison the distribution (35) (broken line ---) is also shown. Since the magnitudes |E| have been obtained from a real structure with N = 29, comparison with the true value of the quartet is also possible. As already emphasized, the distribution (35) always has a unique maximum at $\Psi = 0°$. The distribution (38), on the other hand, may have a maximum at $\Psi = 0°$ or 180°, or any value between these extremes, as shown by Figures 3–5. Roughly speak-

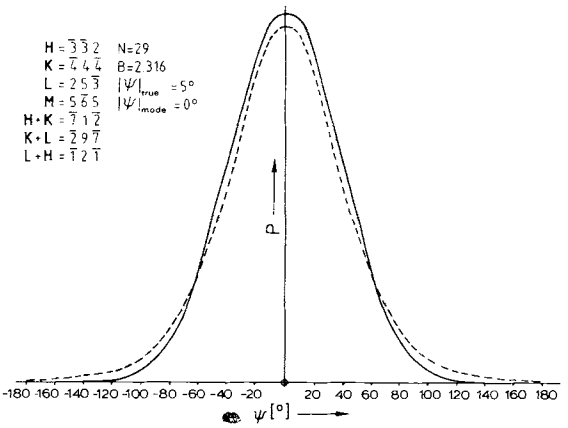


Fig. 3. The distributions (38) (—) and (35) (---) for the values of the seven parameters (36) and (37): $R_1 = 3.034$, $R_2 = 2.766$, $R_3 = 2.217$, $R_4 = 1.805$, $R_{12} = 2.918$, $R_{23} = 0.933$, $R_{31} = 2.863$. The mode of (38) is here $\Psi = 0°$, of (35) always $\Psi = 0°$.

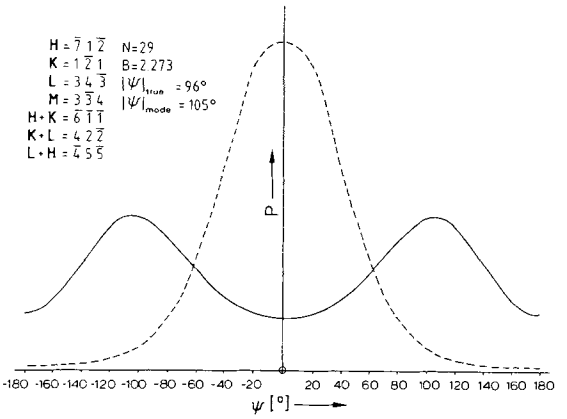


Fig. 4. The distributions (38) (—) and (35) (---) for the values of the seven parameters (36) and (37): $R_1 = 2.918$, $R_2 = 2.863$, $R_3 = 2.276$, $R_4 = 1.733$, $R_{12} = 1.631$, $R_{23} = 0.223$, $R_{31} = 1.540$. The mode of (38) is here $\Psi = \pm 105°$, of (35) always $\Psi = 0°$.

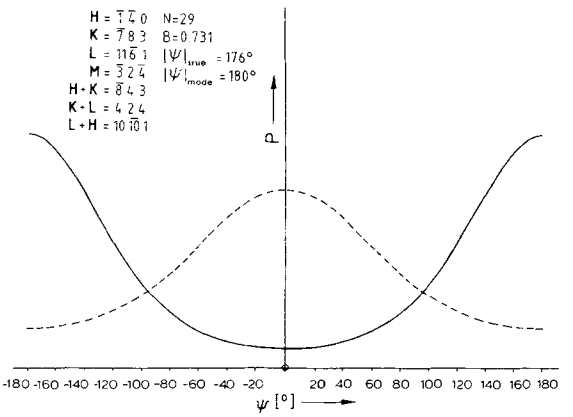


Fig. 5. The distributions (38) (---) and (35) (- ·) for the values of the seven parameters (36) and (37): $R_1 = 1.408$, $R_2 = 1.592$, $R_3 = 2.672$, $R_4 = 1.770$, $R_{12} = 0.157$, $R_{23} = 0.425$, $R_{31} = 0.385$. The mode of (38) is here $\Psi = 180°$, of (35) always $\Psi = 0°$.

ing, the maximum of (38) occurs at 0° or 180° according as the three parameters R_{12}, R_{23}, R_{31} are all large or all small, respectively. These figures also clearly show the improvement which may result when, in addition to the four magnitudes (36), the three magnitudes (37) are also assumed to be known. Finally, in the special case that

$$R_{12} \approx R_{23} \approx R_{31} \approx 0 \tag{43}$$

the distribution (38) reduces to

$$P_{1/2} \approx \frac{1}{L} \exp(-2B' \cos \Psi) \tag{44}$$

which has a unique maximum at $\Psi = \pi$ (Fig. 5).

2.10. Estimating the Two-Phase Structure Seminvariant in $P\bar{1}$

Suppose that **H** and **K** are two reciprocal lattice vectors such that the three components of $\mathbf{H} + \mathbf{K}$ are even integers. Then the linear combination T of two phases [Eq. (17)] is a structure seminvariant. Refer to Section 2.6.4 for the four magnitudes (24) in the first neighborhood of T and to Section 2.7 for the probabilistic background. Suppose that R_1, R_2, r_{12}, and $r_{1\bar{2}}$ are four non-negative numbers. In this space group every phase is 0° or 180° so that $T = 0°$ or 180° and the conditional probability distribution of T, assuming as known the four magnitudes in its first neighborhood, is discrete. Denote by $P_+(P_-)$ the conditional probability that $T = 0°$ (180°), given the four magnitudes in its first neighborhood:

$$|E_{\mathbf{H}}| = R_1,\ |E_{\mathbf{K}}| = R_2,\ |E_{\frac{1}{2}(\mathbf{H}+\mathbf{K})}| = r_{12},\ |E_{\frac{1}{2}(\mathbf{H}-\mathbf{K})}| = r_{1\bar{2}} \tag{45}$$

In the special case that all N atoms in the unit cell are identical, the solution strategy described in Section 2.7 leads to[2]

$$P_\pm \approx \frac{1}{M} \exp\left\{\mp \frac{R_1 R_2 (r_{12}^2 + r_{1\bar{2}}^2)}{2N}\right\} \cosh\left\{\frac{r_{12} r_{1\bar{2}} (R_1 \pm R_2)}{\sqrt{N}}\right\} \tag{46}$$

where upper (lower) signs go together and

$$M = \exp\left\{-\frac{R_1 R_2 (r_{12}^2 + r_{1\bar{2}}^2)}{2N}\right\} \cosh\left\{\frac{r_{12} r_{1\bar{2}} (R_1 + R_2)}{\sqrt{N}}\right\} + \exp\left\{+\frac{R_1 R_2 (r_{12}^2 + r_{1\bar{2}}^2)}{2N}\right\} \cosh\left\{\frac{r_{12} r_{1\bar{2}} (R_1 - R_2)}{\sqrt{N}}\right\} \tag{47}$$

It is easily verified that, under the assumption that R_1 and R_2 are both large, $P_+ \gg 1/2$ if r_{12} and $r_{1\bar{2}}$ are both large, but $P_+ \ll 1/2$ if one of r_{12}, $r_{1\bar{2}}$ is large and the other is small. Hence $T \approx 0°$ or 180° respectively (the favorable cases of the neighborhood principle for T).

3. Combining Direct Methods with Anomalous Dispersion

3.1. Introduction

The overview of the traditional direct methods described in Sections 1 and 2 is readily generalized to the case that the atomic scattering factors are arbitrary complex-valued functions of $(\sin\theta)/\lambda$, thus including the special case that one or more anomalous scatterers are present. Once again the neighborhood concept plays an essential role. Final results from the probabilistic theory of the two- and three-phase structure invariants are briefly summarized. In particular, the conditional probability distributions of the two- and three-phase structure invariants, given the magnitudes |E| in their first neighborhoods, are described. The distributions yield estimates for these invariants which are particularly good in those cases where the variances of the distributions happen to be small (the neighborhood principle). It is particularly noteworthy that these estimates are unique in the whole range from −180° to +180°. An example shows that the method is capable of yielding unique estimates for tens of thousands of structure invariants with unprecedented accuracy, even in the macromolecular case. It thus appears that this fusion of the traditional techniques of direct methods with anomalous dispersion will facilitate the solution of those crystal structures which contain one or more anomalous scatterers.

Most crystal structures containing as many as 80–100 independent nonhydrogen atoms are more or less routinely solvable nowadays by direct methods. On the other hand, it has been known for a long time[22–24] that the presence of one or more anomalous scatterers facilitates the solution of the phase problem; and some recent work[16,20] employing Bijvoet inequalities and the double Patterson function, leads in a similar way to estimates of the sines of the three-phase structure invariants. Again, some early work of *Rossmann*[25], employing the difference synthesis $(|F_{\mathbf{H}}| - |F_{\bar{\mathbf{H}}}|)^2$ in order to locate the anomalous scatterers and recently used[17] for the solution of the crambin structure, shows that the presence of anomalous scatterers facilitates the determination of crystal structures. This work strongly suggests that the ability to integrate the techniques of direct methods with anomalous dispersion would lead to improved methods for phase determination. The fusion of these techniques is described here. That the anticipated improvement is in fact realized is shown in Tables 1 and 2 and Figure 6. Not only do the new formulas lead to improved estimates of the structure invariants but, more important still, because the distributions derived here are unimodal in the whole interval from −180° to +180°, the twofold ambiguity inherent in all the earlier work is removed. It is believed that this resolution of the twofold ambiguity results from the ability now to make use of the individual magnitudes in the first neighborhood of the structure invariant and the avoidance of explicit dependence on the Bijvoet differences; the explicit use of the Bijvoet differences, as had been done in all previous work, leads apparently to a loss of information resulting in a twofold ambiguity in estimates of the structure invariants. It may be of some interest to observe that in the earlier work with anomalous dispersion only the sine of the invariant may be estimated; in the absence of anomalous scatterers only the cosine of the invariant may be estimated; as a result of the work described here both the sine and the cosine, that is to say the invariant itself, may be estimated. Since, in the presence of anomalous scatterers, the observed intensities are known to determine a unique enan-

tiomorph, and therefore unique values for all the structure seminvariants, formulas of the kind described here should not be unexpected; nevertheless not even their existence appears to have been anticipated.

3.2. The Normalized Structure Factors

In the presence of anomalous scatters the normalized structure factor

$$E_{\mathbf{H}} = |E_{\mathbf{H}}| \exp(i\phi_{\mathbf{H}}) \tag{48}$$

is defined by

$$E_{\mathbf{H}} = \frac{1}{\alpha_{\mathbf{H}}^{1/2}} \sum_{j=1}^{N} f_{j\mathbf{H}} \exp(2\pi i\, \mathbf{H}\cdot\mathbf{r}_j) \tag{49}$$

$$= \frac{1}{\alpha_{\mathbf{H}}^{1/2}} \sum_{j=1}^{N} |f_{j\mathbf{H}}| \exp|i(\delta_{j\mathbf{H}} + 2\pi\, \mathbf{H}\cdot\mathbf{r}_j| \tag{50}$$

where

$$f_{j\mathbf{H}} = |f_{j\mathbf{H}}| \exp(i\delta_{j\mathbf{H}}) \tag{51}$$

is the (in general complex) atomic scattering factor (a function of $|\mathbf{H}|$ as well as of j) of the atom labeled j, $\mathbf{r}_j$ is its position vector, N is the number of atoms in the unit cell, and

$$\alpha_{\mathbf{H}} = \sum_{j=1}^{N} |f_{j\mathbf{H}}|^2 \tag{52}$$

For a normal scatter, $\delta_{j\mathbf{H}} = 0$; for an atom which scatters anomalously, $\delta_{j\mathbf{H}} \neq 0$. Owing to the presence of the anomalous scatterers, the atomic scattering factors $f_{j\mathbf{H}}$, as functions of $(\sin\theta)/\lambda$, do not have the same shape for different atoms, even approximately. Hence the dependence of the $f_{j\mathbf{H}}$ on $|\mathbf{H}|$ cannot be ignored, in contrast to the usual practice when anomalous scatterers are not present. For this reason the subscript $\mathbf{H}$ is not suppressed in the symbols $f_{j\mathbf{H}}$ and $\alpha_{\mathbf{H}}$ [Eq. (52)].

The reciprocal-lattice vector $\mathbf{H}$ is assumed to be fixed, and the primitive random variables are taken to be the atomic position vectors $\mathbf{r}_j$ which are assumed to be uniformly and independently distributed. Then $E_{\mathbf{H}}$, as a function [Eq. (50)], of the primitive random variables $\mathbf{r}_j$, is itself a random variable and, as it turns out,

$$\langle |E_{\mathbf{H}}|^2 \rangle_{\mathbf{r}_j} = 1 \tag{53}$$

3.3. The Two-Phase Structure Invariant

The two-phase structure invariant, which has no analogue when no anomalous scatterers are present, is defined by

$$\psi = \phi_{\mathbf{H}} + \phi_{\overline{\mathbf{H}}} \tag{54}$$

3.3.1. The First Neighborhood

The first neighborhood of the two-phase structure invariant ψ [Eq. (54)] is defined to consist of the two magnitudes

$$|E_{\mathbf{H}}|,\ |E_{\overline{\mathbf{H}}}| \tag{55}$$

which, because of the breakdown of Friedel's law, are in general distinct.

3.3.2. Estimating the Two-Phase Structure Invariant

Define $C_{\mathbf{H}}$ and $S_{\mathbf{H}}$ by means of

$$C_{\mathbf{H}} = \frac{1}{\alpha_{\mathbf{H}}} \sum_{j=1}^{N} |f_{j\mathbf{H}}|^2 \cos(2\delta_{j\mathbf{H}}) \tag{56}$$

$$S_{\mathbf{H}} = \frac{1}{\alpha_{\mathbf{H}}} \sum_{j=1}^{N} |f_{j\mathbf{H}}|^2 \sin(2\delta_{j\mathbf{H}}) \tag{57}$$

where $f_{j\mathbf{H}}$, $\delta_{j\mathbf{H}}$, and $\alpha_{\mathbf{H}}$ are defined in (51) and (52). Define X and ξ by means of

$$X\cos\xi = C_{\mathbf{H}}, \qquad X\sin\xi = -S_{\mathbf{H}} \tag{58}$$

$$X = (C_{\mathbf{H}}^2 + S_{\mathbf{H}}^2)^{\frac{1}{2}} \qquad \tan\xi = -S_{\mathbf{H}}/C_{\mathbf{H}} \tag{59}$$

Suppose that R and $\overline{R}$ are fixed non-negative numbers. In view of (48) to (50) the two-phase structure invariant $(\phi_{\mathbf{H}} + \phi_{\overline{\mathbf{H}}})$, as a function of the primitive random variables $\mathbf{r}_j$, is itself a random variable. Denote by $P(\Psi|R,\overline{R})$ the conditional probability distribution of the two-phase structure invariant $(\phi_{\mathbf{H}} + \phi_{\overline{\mathbf{H}}})$, given the two magnitudes in its first neighborhood:

$$|E_{\mathbf{H}}| = R,\ |E_{\overline{\mathbf{H}}}| = \overline{R} \tag{60}$$

Then[5, 12]

$$P(\Psi|R,\overline{R}) \approx \left[2\pi I_0\left(\frac{2R\overline{R}X}{1-X^2}\right)\right]^{-1} \exp\left[\frac{2R\overline{R}X}{1-X^2}\cos(\Psi+\xi)\right] \tag{61}$$

where X and ξ, defined by (56)–(59), are seen to be functions of the (complex) atomic scattering factors $f_{j\mathbf{H}}$, which are presumed to be known. It should be noted that the distribution (61) has the same form as (30) but is centered at $-\xi$ instead of 0. Since (61) has a unique maximum at $\Psi = -\xi$, it follows that

$$\phi_{\mathbf{H}} + \phi_{\overline{\mathbf{H}}} \approx -\xi \tag{62}$$

provided that the variance of the distribution is small, i.e. provided that

$$A = \frac{2R\overline{R}X}{1-X^2} \tag{63}$$

is large. It should be noted that, while A depends on R, $\overline{R}$, and $|\mathbf{H}|$, for a fixed chemical composition ξ depends only on $|\mathbf{H}|$ (or $(\sin\theta)/\lambda$) and is independent of R and $\overline{R}$.

3.4. The Three-Phase Structure Invariant

It will be assumed throughout that $\mathbf{H}$, $\mathbf{K}$, and $\mathbf{L}$ are fixed reciprocal-lattice vectors satisfying

$$\mathbf{H} + \mathbf{K} + \mathbf{L} = 0 \tag{64}$$

Owing to the breakdown of Friedel's law there are, in sharp contrast to the case that no anomalous scatterers are present, eight distinct three-phase structure invariants:

$$\psi_0 = \phi_{\mathbf{H}} + \phi_{\mathbf{K}} + \phi_{\mathbf{L}} \quad (65)$$

$$\psi_1 = -\phi_{\overline{\mathbf{H}}} + \phi_{\mathbf{K}} + \phi_{\mathbf{L}} \quad (66)$$

$$\psi_2 = \phi_{\mathbf{H}} - \phi_{\overline{\mathbf{K}}} + \phi_{\mathbf{L}} \quad (67)$$

$$\psi_3 = \phi_{\mathbf{H}} + \phi_{\mathbf{K}} - \phi_{\overline{\mathbf{L}}} \quad (68)$$

$$\psi_{\bar{0}} = \phi_{\overline{\mathbf{H}}} + \phi_{\overline{\mathbf{K}}} + \phi_{\overline{\mathbf{L}}} \quad (69)$$

$$\psi_{\bar{1}} = -\phi_{\mathbf{H}} + \phi_{\overline{\mathbf{K}}} + \phi_{\overline{\mathbf{L}}} \quad (70)$$

$$\psi_{\bar{2}} = \phi_{\overline{\mathbf{H}}} - \phi_{\mathbf{K}} + \phi_{\overline{\mathbf{L}}} \quad (71)$$

$$\psi_{\bar{3}} = \phi_{\overline{\mathbf{H}}} + \phi_{\overline{\mathbf{K}}} - \phi_{\mathbf{L}} \quad (72)$$

3.4.1. The First Neighborhood

The first neighborhood of each of the three-phase structure invariants [Eq. (65)–(72)] is defined to consist of the six magnitudes:

$$|E_{\mathbf{H}}|, |E_{\mathbf{K}}|, |E_{\mathbf{L}}|, |E_{\overline{\mathbf{H}}}|, |E_{\overline{\mathbf{K}}}|, |E_{\overline{\mathbf{L}}}| \quad (73)$$

which, again owing to the breakdown of Friedel's law, are not in general equal in pairs.

3.4.2. The Probabilistic Background

Fix the reciprocal-lattice vectors **H**, **K**, and **L**, subject to Eq. (64). Suppose that the six non-negative numbers R_1, R_2, R_3, $R_{\bar{1}}$, $R_{\bar{2}}$, and $R_{\bar{3}}$ are also specified. Define the N-fold Cartesian product W to consist of all ordered N-tuples $(\mathbf{r}_1, \mathbf{r}_2, \ldots, \mathbf{r}_N)$, where $\mathbf{r}_1, \mathbf{r}_2, \ldots, \mathbf{r}_N$ are atomic position vectors. Suppose that the primitive random variable is the N-tuple $(\mathbf{r}_1, \mathbf{r}_2, \ldots, \mathbf{r}_N)$ which is assumed to be uniformly distributed over the subset of W defined by

$$|E_{\mathbf{H}}| = R_1, |E_{\mathbf{K}}| = R_2, |E_{\mathbf{L}}| = R_3 \quad (74)$$

$$|E_{\overline{\mathbf{H}}}| = R_{\bar{1}}, |E_{\overline{\mathbf{K}}}| = R_{\bar{2}}, |E_{\overline{\mathbf{L}}}| = R_{\bar{3}} \quad (75)$$

where the normalized structure factors E are defined by Equation (49). Then the eight structure invariants [Eq. (65)–(72)]

$$\psi_j, \psi_{\bar{j}} \quad (j = 0, 1, 2, 3) \quad (76)$$

as functions of the primitive random variables $(\mathbf{r}_1, \mathbf{r}_2, \ldots, \mathbf{r}_N)$ are themselves random variables.

Our major goal is to determine the conditional probability distribution of each of the three-phase structure invariants [Eq. (65)–(72)], given the six magnitudes (74) and (75) in its first neighborhood, which, in the favorable case that the variance of the distribution happens to be small, yields a reliable estimate of the invariant (the neighborhood principle).

3.4.3. Estimating the Three-Phase Structure Invariant

Denote by

$$P_j(\Psi | R_1, R_2, R_3, R_{\bar{1}}, R_{\bar{2}}, R_{\bar{3}}) = P_j(\Psi) \quad (j = 0, 1, 2, 3, \bar{0}, \bar{1}, \bar{2}, \bar{3}) \quad (77)$$

the conditional probability distribution of each ψ_j, assuming as known the six magnitudes (73) in its first neighborhood. Then the final formula, the major result of this article, is simply[5, 12]

$$P_j(\Psi) \approx \frac{1}{K_j} \exp[A_j \cos(\Psi - \omega_j)], \quad (j = 0, 1, 2, 3, \bar{0}, \bar{1}, \bar{2}, \bar{3}) \quad (78)$$

where the parameters K_j, A_j, and ω_j are expressible in terms of the complex scattering factors $f_{j\mathbf{H}}$, $f_{j\mathbf{K}}$, $f_{j\mathbf{L}}$, presumed to be known, and the observed magnitudes $|E_{\mathbf{H}}|$, $|E_{\mathbf{K}}|$, $|E_{\mathbf{L}}|$, $|E_{\overline{\mathbf{H}}}|$, $|E_{\overline{\mathbf{K}}}|$, $|E_{\overline{\mathbf{L}}}|$ in the first neighborhood of the invariant. Since the K_j and A_j values are positive, the maximum of distribution (78) occurs at $\Psi = \omega_j$. Hence when the variance of the distribution (78) is small, i.e. when A_j is large, one obtains the reliable estimate

$$\psi_j = \omega_j \quad (j = 0, 1, 2, 3, \bar{0}, \bar{1}, \bar{2}, \bar{3}) \quad (79)$$

for the structure invariant ψ_j. It should be emphasized that the estimate (79) is unique in the whole range from $-180°$ to $+180°$. No prior knowledge of the positions of the anomalous scatterers is needed, nor is it required that the anomalous scatterers be identical.

3.4.4. The Applications

Using the presumed known coordinates of the $PtCl_4^{2\ominus}$ derivative of the protein Cytochrome c_{550} from *Paracoccus denitrificans*[26] (molecular weight $M_r \approx 14\,500$, space group $P2_12_12_1$) some 8300 normalized structure factors E were calculated (to a resolution of 2.5 Å). In addition to the anomalous scatterers Pt and Cl, this structure contains one Fe and six S atoms which also scatter anomalously at the wavelength used ($Cu_{K\alpha}$). Using the 4000 phases ϕ_{hkl} corresponding to the 4000 largest $|E_{hkl}|$ values with $hkl \neq 0$, the three-phase structure invariants ψ_j [Eq. (65)–(72)] were generated and the parameters ω_j and A_j, needed to define the distributions (78), were calculated. All calculations were done on the VAX 11/780 computer; double precision (approximately 15 significant digits) was used in order to eliminate round-off errors. The A_j values were arranged in descending order and the first 2000, sampled at intervals of 100, were used in the construction of Table 1; the top 60000 were used for Table 2.

Table 1 lists 21 values of A_j, sampled as shown from the top 2000, the corresponding estimates ω_j of the invariants ψ_j, the true values of the ψ_j, and the magnitude of the error, $|\omega_j - \psi_j|$. Also listed are the six magnitudes |E| in the first neighborhood of the corresponding invariant.

Table 2 gives the average magnitude of the error,

$$\langle |\omega_j - \psi_j| \rangle \quad (80)$$

in the nine cumulative groups shown, for the 60000 most reliable estimates ω_j of the invariants ψ_j.

Tables 1 and 2 show firstly that, owing to the unexpectedly large number of large values of A_j, our formulas yield reliable (and unique) estimates of tens of thousands of the three-phase structure invariants. Secondly, the invariants which are most reliably estimated lie anywhere in

Table 1. Twenty-one estimates ω_j of the structure invariants ψ_j sampled from the top 2000 for the $PtCl_4^{2\ominus}$ derivative of Cytochrome c_{550}.

j	$\lvert E_H \rvert$	$\lvert E_H \rvert$	$\lvert E_K \rvert$	$\lvert E_K \rvert$	$\lvert E_L \rvert$	$\lvert E_L \rvert$	A_j	Estimated value ω_j of ψ_j [°]	True value of ψ_j [°]	Mag. of the Error $\lvert\omega_j - \psi_j\rvert$ [°]
1	2.17	2.04	0.89	1.03	0.85	0.67	6.92	− 58	− 88	30
100	1.91	2.06	1.61	1.49	0.85	0.67	5.62	148	130	18
200	1.91	2.06	1.96	2.06	1.41	1.57	4.83	− 79	−121	42
300	2.36	2.48	1.56	1.69	0.82	0.68	4.52	52	2	50
400	2.17	2.04	1.34	1.48	1.28	1.15	4.31	79	96	17
500	1.85	1.94	0.85	0.67	0.78	0.92	4.21	56	42	14
600	2.17	2.04	0.92	1.04	0.86	0.70	4.10	146	148	2
700	1.39	1.28	0.85	0.67	0.87	0.75	4.02	− 72	− 68	4
800	1.41	1.57	1.61	1.49	0.71	0.85	3.93	70	50	20
900	1.88	1.98	1.28	1.15	0.85	0.67	3.87	104	96	8
1000	1.29	1.43	0.79	0.71	0.85	0.67	3.80	− 88	−138	50
1100	1.34	1.48	1.34	1.22	1.25	1.16	3.76	− 72	−126	54
1200	1.56	1.69	1.41	1.57	0.98	0.90	3.72	73	78	5
1300	1.98	2.07	2.08	1.94	1.08	1.21	3.68	−161	−124	37
1400	1.56	1.67	1.41	1.57	1.24	1.33	3.63	− 72	− 3	69
1500	2.38	2.50	1.91	2.06	0.74	0.64	3.59	84	77	7
1600	1.91	2.06	1.34	1.22	0.72	0.83	3.55	− 64	− 94	30
1700	1.91	2.06	2.02	2.12	2.15	2.24	3.51	− 64	− 72	8
1800	2.38	2.50	1.61	1.49	0.78	0.90	3.46	78	82	4
1900	2.38	2.50	1.63	1.70	1.81	1.93	3.43	63	123	60
2000	0.85	0.67	0.97	0.83	1.02	1.09	3.42	− 96	−126	30

Table 2. Average magnitude of the error in the top 60000 estimated values of the three-phase structure invariants, cumulated in nine groups, for the $PtCl_4^{2\ominus}$ derivative of Cytochrome c_{550}.

Group No.	Number of A values in Group	Average Value of A	Average Mag. of Error [°]
1	100	6.01	27.9
2	500	4.90	29.3
3	1000	4.44	28.8
4	2000	4.02	28.0
5	5000	3.49	31.4
6	10000	3.09	33.8
7	20000	2.71	36.1
8	40000	2.35	38.6
9	60000	2.15	39.8

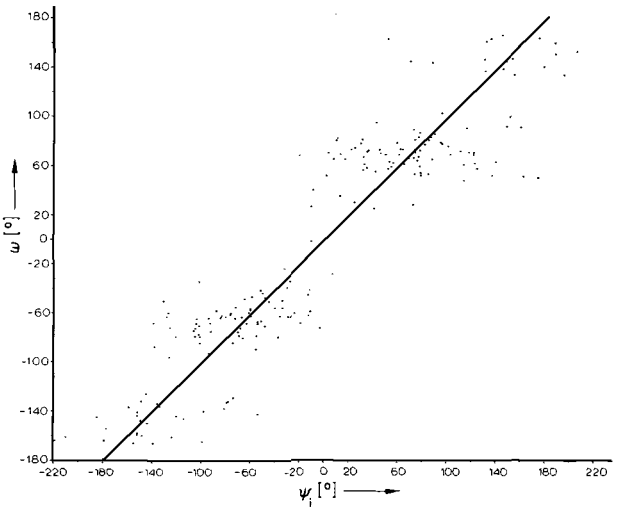


Fig. 6. A scatter diagram of ω_j versus ψ_j, using 201 invariants sampled at intervals of ten from the top 2000, for the $PtCl_4^{2\ominus}$ derivative of Cytochrome c_{550}, as well as the line $\omega_j = \psi_j$.

the range from -180 to $+180°$, and appear to be uniformly distributed in this range (Columns 9 and 10 of Table 1). Finally, in sharp contrast to the case that no anomalous scatterers are present, the most reliable estimates are not necessarily of invariants corresponding to the most intense reflections but of those corresponding instead to reflections of only moderate intensity (Columns 2–7 of Table 1).

Figure 6 shows a scatter diagram of ω_j versus ψ_j for the $PtCl_4^{2\ominus}$ derivative of Cytochrome c_{550}, using 201 invariants sampled at intervals of length ten from the top 2000, as well as the line $\omega_j = \psi_j$. Since the line falls evenly among the points, it appears that the ω_j are unbiased estimates of the invariants ψ_j.

3.4.5. Concluding Remarks

In this article the goal of integrating the techniques of direct methods with anomalous dispersion is realized. Specifically, the conditional probability distribution of the three-phase structure invariant, assuming as known the six magnitudes in its first neighborhood, is obtained. In the favorable case that the variance of the distribution happens to be small, the distribution yields a reliable estimate of the invariant (the neighborhood principle). It is particularly noteworthy that, in strong contrast to all previous work, the estimate is unique in the whole interval $(-180°, +180°)$ and that any estimate in this range is possible (even, for example, in the vicinity of $\pm 90°$ or $180°$). The first applications of this work using error-free diffraction data have been made, and these show that in a typical case some tens of thousands of three-phase structure invariants may be estimated with unprecedented accuracy, even for a macromolecular crystal structure. Some preliminary calculations on a number of structures, not detailed here, show that the accuracy of the estimates depends in some complicated way on the complexity of the crystal structure, the number of anomalous scatterers, the strength of the anomalous signal, and the range of $(\sin\theta)/\lambda$. With smaller

structures the accuracy may be greatly increased, average errors of only three or four degrees for thousands of invariants being not uncommon.

It should be stated in conclusion that the availability of reliable estimates for large numbers of the three-phase structure invariants implies that the traditional machinery of direct methods, in particular the tangent formula [Eq. (33)], suitably modified to accommodate the non-zero estimates of the invariants, may be carried over without essential change to estimate the values of the individual phases and thus to facilitate structure determination via anomalous dispersion. In view of the calculations summarized in Tables 1 and 2 and Figure 6, it seems likely that, in time, even macromolecules will prove to be solvable in this way. It is clear too, that, owing to the ability to estimate both the sine and cosine invariants, that is to say both the signs and magnitudes of the invariants, the unique enantiomorph determined by the observed intensities is automatically obtained. In fact the first application of these techniques using experimental diffraction data has already facilitated the solution of an unknown macromolecular structure.[4]

Received: January 30, 1986 [A 580 IE]
German version: *Angew. Chem. 98* (1986) 600

[1] W. Cochran, *Acta Crystallogr. 8* (1955) 473.
[2] E. Green, H. Hauptman, *Acta Crystallogr. A 32* (1976) 940.
[3] S. Fortier, H. Hauptman, *Acta Crystallogr. A 33* (1977) 694.
[4] W. Furey, A. H. Robbins, L. L. Clancy, D. R. Winge, B. C. Wang, C. D. Stout, *Science 231* (1986) 704.
[5] C. Giacovazzo, *Acta Crystallogr. A 39* (1983) 585.
[6] H. Hauptman: *Crystal Structure Determination: The Role of the Cosine Seminvariants*, Plenum, New York 1972.
[7] H. Hauptman, *Acta Crystallogr. A 31* (1975) 671.
[8] H. Hauptman, *Acta Crystallogr. A 31* (1975) 680.
[9] H. Hauptman, *Acta Crystallogr. A 32* (1976) 877.
[10] H. Hauptman, *Acta Crystallogr. A 33* (1977) 553.
[11] H. Hauptman, *Acta Crystallogr. A 33* (1977) 568.
[12] H. Hauptman, *Acta Crystallogr. A 38* (1982) 632.
[13] H. Hauptman, J. Karle, *Solution of the Phase Problem I. The Centrosymmetric Crystal (Am. Crystallogr. Assoc. Monogr. 3)* (1953).
[14] H. Hauptman, J. Karle, *Acta Crystallogr. 9* (1956) 45.
[15] H. Hauptman, J. Karle, *Acta Crystallogr. 12* (1959) 93.
[16] J. J. L. Heinerman, H. Krabbendam, J. Kroon, A. L. Spek, *Acta Crystallogr. A 34* (1978) 447.
[17] W. A. Hendrickson, M. M. Teeter, *Nature (London) 290* (1981) 107.
[18] J. Karle, H. Hauptman, *Acta Crystallogr. 9* (1956) 635.
[19] J. Karle, H. Hauptman, *Acta Crystallogr. 14* (1961) 217.
[20] J. Kroon, A. L. Spek, H. Krabbendam, *Acta Crystallogr. A 33* (1977) 382.
[21] L. Lessinger, H. Wondratschek, *Acta Crystallogr. A 31* (1975) 521.
[22] Y. Okaya, R. Pepinsky, *Phys. Rev. 103* (1956) 1645.
[23] A. F. Peerdeman, J. M. Bijvoet, *Proc. K. Ned. Akad. Wet. Ser. B: Phys. Sci. 59* (1956) 312.
[24] G. N. Ramachandran, S. Raman, *Curr. Sci. 25* (1956) 348.
[25] M. G. Rossmann, *Acta Crystallogr. 14* (1961) 383.
[26] R. Timkovich, R. E. Dickerson, *J. Biol. Chem. 251* (1976) 4033.

Recovering Phase Information from Intensity Data (Nobel Lecture)**

By Jerome Karle*

The concept of a crystal is that of a solid body in which the atomic or molecular units are so arranged as to form an array having three dimensional periodicity. Because of the periodicity, it is possible to describe the arrangements of the atomic composition by means of Fourier series. The type of Fourier series that is used in crystal structure analysis represents the electron density distribution in a crystal. This is indeed equivalent to representing the structure of a crystal since the atomic locations are represented by the regions of highest electron density in the electron distributions.

The experimental technique used for examining the structure of crystals is called diffraction. In a diffraction experiment, rays are made to impinge on a crystalline substance of interest and, given the proper geometric conditions, the rays are scattered as if they were bouncing off large numbers of different planes imagined to be cutting through the crystal. The collected intensities of scattering (often 5000–10000 in number) are called a scattering pattern or diffraction pattern and comprise the experimental data from which the structure of the crystal of interest is to be elucidated. The most commonly used rays are Roentgen rays or X-rays, as they are usually called. Other rays, composed of neutrons or electrons, also have their purposes.

It is possible to obtain an insight into the character and sense of a diffraction experiment by imagining some experimental circumstances on the macroscopic scale. Let us suppose that we would like to probe the shape of some large object, hidden from view, by using balls that are hurled in a precise way at the object of interest and interact with the surface with essentially perfect restitution. Let us also suppose that it is possible to minimize and correct for the gravitational effects on the impinging balls. We assume that we can observe the results of the bouncing of the balls from the surface of the object. If a large area were scanned perpendicular to the direction in which the balls were hurled and each time the bouncing pattern were essentially parallel but in the opposite direction to that of the impinging balls, we would conclude that the object had a face with a high degree of flatness that was perpendicular to the direction of the impinging balls. Evidently, by varying the orientation of an arbitrarily shaped object and observing the patterns of the bouncing balls or, equivalently, the scattering pattern, knowledge of the shape of the object could be developed in quite some detail. On the submicroscopic scale, the situation is somewhat different. Crystals are quite porous to X-rays and the interactions between the rays and the atomic composition of the crystal are different than that of a ball bouncing off a surface such that, as noted, certain geometric conditions need to be fulfilled before it appears that reflection of the rays has taken place. The nature of the interactions is understood, however, and the relevance of the comparison with the macroscopic thought experiment involving bouncing balls maintains. In the case of X-rays and a crystal, the X-rays replace the bouncing balls and the way the X-rays interact with electron density distributions within the crystal gives rise to a scattering pattern unique to each crystalline substance. The problem that the analyst faces is to be able to take the diffraction pattern and from it determine the atomic architecture of the crystal which cannot be observed directly.

There is a special problem in taking the intensity information from a diffraction pattern and calculating from it the electron density distribution of a crystal by use of the Fourier series. The coefficients in the Fourier series are, in general, complex numbers. Only the magnitudes of the complex numbers appear to be available from the measured intensities of scattering. The required phases of the complex numbers seem to be lost in an ordinary X-ray diffraction experiment. It was therefore generally thought that it was not possible to go directly from a diffraction pattern to a determination of a crystal structure. The impasse was overcome in a series of steps that involved recognition that the required phase information was contained in the experimental intensity information, the derivation of a foundation mathematics that displayed relationships between phases and magnitudes and even among phases alone and, finally, the development of practical procedures for structure determination, strategies that brought together in a more or less optimal fashion the mathematical relationships with suitably adjusted and refined experimental data.

The results of structure determinations have been playing a valuable role in a number of areas of scientific endeavor. Crystallization, for example, is a very common phenomenon and many types of substances form crystals ranging from metals and minerals to huge macromolecules such as viruses. Knowledge of structure allows one to relate structure to function, i.e., understand physical, chemical or biological properties and activities, provides the chemist with useful information for syntheses, modifications and reaction mechanisms and can also be used to identify very small quantities of scarce material. It often provides the theoretical chemist with a starting point for his calculations. Structural research provides a conceptual basis for many associated scientific disciplines and it is the opportunity to interact with a variety of such disciplines that has made structural research particularly appealing to me.

[*] Prof. Dr. J. Karle
Laboratory for the Structure of Matter, Naval Research Laboratory
Washington, DC 20375-5000 (USA)

[**] Copyright © The Nobel Foundation 1986.—We thank the Nobel Foundation, Stockholm, for permission to print this article.

As this article proceeds, it will elaborate on a number of the items discussed in this introductory part, describe some interesting applications, and discuss briefly some research paths and opportunities for the future.

Electron Density Distribution

The electron density distribution, $\rho(\mathbf{r})$, is expressed in terms of the three-dimensional Fourier series

$$\rho(\mathbf{r}) = V^{-1} \sum_{-\infty \mathbf{h}}^{\infty} F_{\mathbf{h}} \exp(-2\pi \mathbf{h} \cdot \mathbf{r}) \tag{1}$$

where V is the volume of the unit cell of the crystal, the basic structural unit from which, through three-dimensional periodicity, the crystal is formed. The coefficients

$$F_{\mathbf{h}} = |F_{\mathbf{h}}| \exp(i\phi_{\mathbf{h}}) \tag{2}$$

are the crystal structure factors associated with the planes labeled with the vectors $\mathbf{h}$. The $\mathbf{h}$ have integer components, h, k and l, the Miller indices, whose values are inversely proportional to the intercepts on the x, y and z axes, respectively, of planes cutting through the crystal. The angle $\phi_{\mathbf{h}}$ is the phase associated with $F_{\mathbf{h}}$ and $\mathbf{r}$ labels the position of any point in the unit cell. $F_{\mathbf{h}}\mathbf{E}$ is the amplitude of the scattered wave associated with the plane labeled by $\mathbf{h}$, where $\mathbf{E}$ is the electric field vector of the incident beam. The measured intensities of X-ray scattering are proportional to $|F_{\mathbf{h}}|^2$. If the values of the $\phi_{\mathbf{h}}$ were also obtained directly from experiment, structures could be immediately calculated from equation (1). The seeming absence of this information gave rise to the so-called "phase problem".

The Fourier inversion of equation (1) followed by the replacement of the integral by the sum of contributions from the N discrete atoms in the unit cell gives, for the Fourier coefficient,

$$|F_{\mathbf{h}}| \exp(i\phi_{\mathbf{h}}) = \sum_{j=1}^{N} f_{j\mathbf{h}} \exp(2\pi i \mathbf{h} \cdot \mathbf{r}_j) \tag{3}$$

where $f_{j\mathbf{h}}$ represents the amplitude of scattering of the jth atom in the unit cell and $\mathbf{r}_j$ is its position vector.

Overdeterminacy

A system of simultaneous equations is formed by the definition of the crystal structure factors given by equation (3) since the values of the scattered intensities are measured for a large number of $\mathbf{h}$. The unknown quantities in equation (3) are the phases $\phi_{\mathbf{h}}$ and the atomic positions $\mathbf{r}_j$. The known quantities are the $|F_{\mathbf{h}}|$ obtained from the measured intensities and the $f_{j\mathbf{h}}$ which differ little from the theoretically calculated atomic scattering factors for free atoms. Since each equation (3) involves complex quantities, there are really two equations, one for the real and one for the imaginary part. In order to determine the overdeterminacy, a comparison is made of the number of unknown quantities with the number of independent data available. With the use of $Cu_{K\alpha}$ radiation, the overdeterminacy can be as great as a factor of about 50 for crystals that have a center of symmetry and about 25 for those that do not. In practice, somewhat fewer than the maximum available data are measured, but the overdeterminacy is still quite high.

Some Attempts, Some Successes

There were some early attempts to obtain structural information or phase information from the structure factor equations. *Ott*[1] made use of the structure factor equation (3) to derive relationships among the structure factors and atomic positions and he showed that in some simple cases atomic coordinates could be obtained directly from the relationships. *Banerjee*[2] devised a trial and error self-consistency routine based on *Ott*'s results for finding the phases of structure factors that are centric and therefore the phases have values that are limited to zero or π. The number of trials increased rapidly with complexity, limiting applications to rather simple structures. *Avrami*[3] worked with equations that relate intensities to interatomic vectors [eq. (4)]. Solutions to these equations were given in terms of the roots of a polynomial equation whose degree increases rapidly as the complexity of the crystal increases. In all these approaches, the increase in computational demands with complexity, sensitivity to experimental errors and inherent ambiguities in the results prevented their application to any but the simplest structures. Even though present day computational facility is enormously greater than when this work was done originally, the limitations cannot be suitably overcome even now.

A significant advance in the attempt to obtain structural information from the measured intensities was made in 1934 by *A. L. Patterson*. He developed a Fourier series which has as its coefficients the magnitude of the square of the structure factors rather than the structure factors themselves. The phases may be eliminated from equation (3) by multiplying by the corresponding complex conjugates to obtain

$$|F_{\mathbf{h}}|^2 = \sum_{j=1}^{N} \sum_{k=1}^{N} f_{j\mathbf{h}} f_{k\mathbf{h}} \exp[2\pi i \mathbf{h} \cdot (\mathbf{r}_j - \mathbf{r}_k)] \tag{4}$$

The Fourier transform of (4) is known as the Patterson function,[4,5]

$$P(\mathbf{r}) = \sum_{-\infty \mathbf{h}}^{\infty} |F_{\mathbf{h}}|^2 \exp(-2\pi i \mathbf{h} \cdot \mathbf{r}) \tag{5}$$

The maxima of a Patterson function represent the interatomic vectors in a structure. Evidently the values of the coefficients are directly obtainable from the measured intensities of scattering. This function has been very useful in locating the heavier atoms in a structure, if they are not too numerous, since the interatomic vectors associated with them would predominate in a map computed from equa-

tion (5) and the atomic positions for them could then be readily deduced. The coordinates for the heavy atoms may be used with equation (3) to compute an initial set of approximate phases. Depending upon the scattering power of the heavy atoms, such a computation may be suitable for structures containing up to a few hundred atoms. There are numerous procedures for developing a complete structure from the initial phase information obtained from the heavy atoms. The use of the Patterson function with structures containing heavy atoms has found widespread application and remains one of the major methods of crystal structure determination.

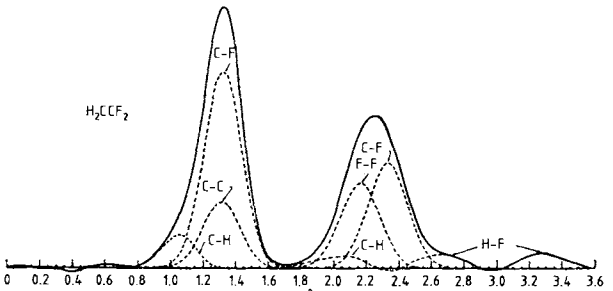
The difficulty with using the Patterson function with experimental data in a general way in the absence of heavy atoms arises from the lack of resolution that occurs for the $N(N-1)$ interatomic vectors as well as inaccuracies. The Patterson function becomes somewhat accessible when it is used in combination with known atomic groupings.[6-8]

The fact that the Patterson function could be used to solve simple structures made a positive contribution to the background atmosphere in which progress in phase determination was made. Once a structure was solved, it was possible to use equation (3) to calculate values for the phases. In effect then, phase values were determined from the measured intensities. In the case of the Patterson function, this happened through the intermediary step of first determining the structure. It was however conceivable that the process could be reversed, namely, to obtain phase information directly from the intensities and then to compute the structure by use of equation (1). This is indeed what happened. So far, except for special cases involving heavy atoms, it has turned out to be easier to obtain phase values directly from the measured intensities and then compute the structure than to obtain the structure directly from the intensities without the use of phases.

Relationships between phases and magnitudes that anticipated the later developments were the inequalities of *Harker* and *Kasper*.[9] They derived a number of inequalities by application of the Schwarz and Cauchy inequalities to the structure factor equations (3) in the presence of crystallographic symmetry. The Harker-Kasper inequalities have provided valuable insights. For example, the simple inequality expressions can provide useful phase information, as shown by *Kasper, Lucht* and *Harker*[10] in their solution of the structure of decaborane. In addition, work with the inequalities indicated that they may have probabilistic characteristics. *Gillis*,[11] for example, noted that the implication of an inequality was probably correct even when the magnitudes of the structure factors were too small to permit a definitive conclusion to be drawn. *Gillis* speculated that the smallness of the structure factor magnitudes may have been due to thermal effects and employed an appropriate function to increase the values of the structure factor magnitudes so that the inequalities could be applied. The probabilistic interpretation, however, remained a possible alternative, namely, that although an inequality does not quite determine the value of a phase definitively, it still does so with a high probability that the value is correct. This could be important because it would imply that the inequalities have probabilistic implications that could extend their range of usefulness.

Non-Negativity and General Inequalities

The initial motivation to investigate the mathematics of crystal structure determination arose from experiences in the development of an analytical procedure for obtaining accurate radial distribution functions for determining the structures of gaseous molecules by electron diffraction. A problem arose; namely, to find an accurate background intensity so that the molecular interference intensity could be accurately extracted from the total intensity of scattering. The Fourier transform of the molecular intensity can be interpreted as representing the probability of finding interatomic distances in a molecule. Therefore, this transform must be non-negative and the non-negativity imposed a very useful constraint on the shape of the background intensity.[12, 13] Figure 1 shows a radial distribution function for H_2CCF_2[14] derived from application of the non-negativity constraint and the component distances in the molecule. The attendant accuracy of the result permitted not only equilibrium interatomic distances to be determined but also estimates of the root-mean-square amplitudes of vibration associated with the interatomic distances.



Distance	C-H	C-C	C-F	C-H	F-F	C-F	H-F	H-F
nZ_iZ_j	4	12	36	4	27	36	6	6
Actual area	4.2	12.1	36.0	4.1	27.2	36.0	5.4	7

Fig. 1. The essentially non-negative radial distribution function (solid curve) for H_2CCF_2, computed from the experimental molecular intensity data extracted by use of a properly formed background intensity curve. The solid curve is a probability density that gives the probability of finding interatomic distances in some distance interval along the horizontal axis. The dashed lines represent the decomposition of the main peaks into their component individual interactomic distances. The individual peaks have a definite width related to the internal vibrations in the molecule. nZ_iZ_j are the theoretical values for the areas under the curves representing the various interatomic distances. Z_i is the atomic number of atom i and n denotes the number of times a particular distance occurs in the molecule.

At about the time this work in gas electron diffraction was proceeding, *Herbert Hauptman* joined our group at the Naval Research Laboratory and, in view of the success of the non-negativity criterion, we decided to explore the possibility that this criterion might be useful in other areas of structural research. This led us to investigate the determination of electron density distributions around free atoms,[15] which found a very fine application in the determination of the electron distribution about argon by *Bartell* and *Brockway*.[16]

We were also quite interested in seeing what the consequences of the application of non-negativity would be for crystal structure analysis, since the electron density distri-

bution defined in equation (1) is constrained not to be negative. This brought in the work of *Toeplitz*[17] early in this century on non-negative Fourier series and subsequent developments by others. We discussed the theory in three-dimensions and wrote it in a form that would have particular relevance to crystallographic data.

The fundamental result was that the necessary and sufficient condition for the electron density distribution in a crystal to be non-negative is that an infinite system of determinants involving the crystal structure factors be non-negative. A typical determinant is[18]

$$\begin{vmatrix} F_{000} & F_{-\mathbf{k}_1} & F_{-\mathbf{k}_2} & \dots F_{-\mathbf{h}} \\ F_{\mathbf{k}_1} & F_{000} & F_{\mathbf{k}_1-\mathbf{k}_2} & \dots F_{\mathbf{k}_1-\mathbf{h}} \\ F_{\mathbf{k}_2} & F_{\mathbf{k}_2-\mathbf{k}_1} & F_{000} & \dots F_{\mathbf{k}_2-\mathbf{h}} \\ \vdots & \vdots & \vdots & \vdots \\ F_{\mathbf{h}} & F_{\mathbf{h}-\mathbf{k}_1} & F_{\mathbf{h}-\mathbf{k}_2} & \dots F_{000} \end{vmatrix} \geq 0 \qquad (6)$$

The subscripts in the first column start with 0,0,0 but are otherwise arbitrary. The subscripts in the first row are the same but of opposite sign. The subscript of the element in the ith row and jth column is the sum of the subscripts of the elements of the ith row and first column and the first row and jth column. The third order inequality

$$\begin{vmatrix} F_{000} & F_{-\mathbf{k}} & F_{-\mathbf{h}} \\ F_{\mathbf{k}} & F_{000} & F_{\mathbf{k}-\mathbf{h}} \\ F_{\mathbf{h}} & F_{\mathbf{h}-\mathbf{k}} & F_{000} \end{vmatrix} \geq 0 \qquad (7)$$

contains a relationship among the structure factors that has played a most important role in direct crystal structure analysis. This may be seen by rewriting (7) in the form,[18]

$$\left| F_{\mathbf{h}} - \frac{F_{\mathbf{k}} F_{\mathbf{h}-\mathbf{k}}}{F_{000}} \right| \leq \frac{\left| \begin{matrix} F_{000} & F_{-\mathbf{k}} \\ F_{\mathbf{k}} & F_{000} \end{matrix} \right|^{\frac{1}{2}} \left| \begin{matrix} F_{000} & F_{-\mathbf{h}+\mathbf{k}} \\ F_{\mathbf{h}-\mathbf{k}} & F_{000} \end{matrix} \right|^{\frac{1}{2}}}{F_{000}} \qquad (8)$$

For structure factors of unusually large magnitude, the right side of (8) becomes quite small, and then

$$F_{\mathbf{h}} \approx F_{\mathbf{k}} F_{\mathbf{h}-\mathbf{k}} / F_{000} \qquad (9)$$

One evident conclusion from (9) is

$$\phi_{\mathbf{h}} \approx \phi_{\mathbf{k}} + \phi_{\mathbf{h}-\mathbf{k}} \qquad (10)$$

This states that for large structure factor magnitudes, the value of $\phi_{\mathbf{h}}$ may be defined in terms of the values of two other phases. This may also be seen from a construction based on (8), Figure 2, in which $\delta = F_{\mathbf{k}} F_{\mathbf{h}-\mathbf{k}} / F_{000}$ and r is equal to the right side of (8). The form for (8) is then

$$|F_{\mathbf{h}} - \delta| \leq r \qquad (11)$$

It can be readily shown[18] that all determinants (6) can be written in the form of inequality (11). As the order of the determinants increases, there is a tendency for r to decrease in size, making the determination of $\phi_{\mathbf{h}}$ rather definitive.

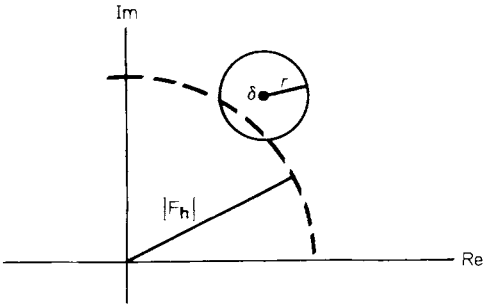


Fig. 2. The determinantal inequalities can be written in the general form $|F_{\mathbf{h}} - \delta| \leq r$. This means that $F_{\mathbf{h}}$ is bounded by a circle of radius r in the complex plane centered at δ. If $|F_{\mathbf{h}}|$ is known, then $F_{\mathbf{h}}$ is confined to a line within the circle.

Formula (10) has found wide application beyond the range of usefulness of inequality (8). This is because of the probabilistic characteristics of the inequalities[19] which imply that the most likely value of $\phi_{\mathbf{h}}$ is that of $\phi_{\mathbf{k}} + \phi_{\mathbf{h}-\mathbf{k}}$ and the probability decreases the farther the value of $\phi_{\mathbf{h}}$ deviates from that of $\phi_{\mathbf{k}} + \phi_{\mathbf{h}-\mathbf{k}}$. Therefore, even when the radius, r, of the bounding circle is large, the most likely value of $\phi_{\mathbf{h}}$ is $\phi_{\mathbf{k}} + \phi_{\mathbf{h}-\mathbf{k}}$.

The structure factors in inequalities (6) can be replaced by quasi-normalized structure factors, $\mathscr{E}$, that represent point atoms (to an approximation when atoms of unequal atomic number are present) rather than atoms with electron distributions,

$$\mathscr{E}_{\mathbf{h}} = F_{\mathbf{h}} \Big/ \left(\sum_{j=1}^{N} f_{j\mathbf{h}}^2 \right)^{\frac{1}{2}} \qquad (12)$$

Structure factors representing point atoms are the type of quantity normally used in phase-determining procedures. Instead of formula (9), we have

$$\mathscr{E}_{\mathbf{h}} \approx \mathscr{E}_{\mathbf{k}} \mathscr{E}_{\mathbf{h}-\mathbf{k}} / \mathscr{E}_{000} \qquad (13)$$

For centrosymmetric crystals, we have

$$s\mathscr{E}_{\mathbf{h}} \approx s\mathscr{E}_{\mathbf{k}} \mathscr{E}_{\mathbf{h}-\mathbf{k}} \qquad (14)$$

where s means "sign of", a plus sign implying that the phase is equal to zero and a minus sign that it is equal to π. A one-term tangent formula also follows from (13),

$$\tan\phi_{\mathbf{h}} \simeq \frac{|\mathscr{E}_{\mathbf{k}} \mathscr{E}_{\mathbf{h}-\mathbf{k}}| \sin(\phi_{\mathbf{k}} + \phi_{\mathbf{h}-\mathbf{k}})}{|\mathscr{E}_{\mathbf{k}} \mathscr{E}_{\mathbf{h}-\mathbf{k}}| \cos(\phi_{\mathbf{k}} + \phi_{\mathbf{h}-\mathbf{k}})} \qquad (15)$$

The tangent formula composed of the sum of terms over **k** both in the numerator and the denominator is another formula that has played a major role in the practical applications of the theory for structure determination.

After the set of determinantal inequalities (6) were obtained on the basis of the non-negativity of the electron density distribution in a crystal, it was of interest to investigate their relationship to the inequalities derived by *Harker* and *Kasper*[9] from use of the Schwarz-Cauchy in-

equalities. It was shown that,[18] when the appropriate symmetry was introduced into the third order determinantal inequality by means of certain relationships among the structure factors, the Harker-Kasper inequalities could be derived. Examination of the derivation of the Harper-Kasper inequalities shows, as would be expected, that the nonnegativity of the electron density distribution is a requirement for their validity.

The variety of phase determining formulas contained within the determinantal inequalities (6) have their counterpart in probability theory, i.e., similar formulas can be derived with the use of probability theory. Their virtue is that measures of reliability can be attached to them and the judicious use of such measures was an important feature in bridging the gap between mathematical theory and practical application.

It had been pointed out that the determinants have inherent probabilistic characteristics[19] that can, in fact, be directly read out from inequality (11). This was not, however, how the first probability formulas were derived. The pursuit of such formulas was motivated by the expectation that the usefulness of the formulas from the inequalities could be extended because of the great overdeterminacy of the structure problem, the expectation that the points within the bounding circle of radius r and center δ (Fig. 2) would not be uniformly probable and the experience of *Gillis*[11] with structure factor magnitudes that were too small to elicit definitive conclusions from the inequalities but which, when made larger artifically, led to correct conclusions.

In order to characterize the probabilistic aspects of this subject, we initially decided to develop a facility in the use of the random walk,[20] but subsequently changed to the joint probability distribution,[21,22] which culminated in a monograph[23] that contained for the first time, a set of probabilistic formulas and measures for attacking the phase problem, in this case limited to crystals that have a center of symmetry. It was in this monograph[23] also that the theory of invariants and semi-invariants was introduced for the purpose of solving the problem concerning how many and what types of phases to specify to fix the origin in a crystal and what values are permitted. The practical aspects of solving crystals that lack a center of symmetry were developed later on and it was not until 1964 that the structure of the first crystal lacking a center of symmetry was solved[24] by the "direct method" for obtaining phase information by direct use of the measured intensities of scattering. It is interesting that fairly recent developments in the mathematics of the random walk have made this technique quite accurate, stimulating revived interest in its application to the probabilistic aspects of phase determining formulas.[25]

Formulas for Phase Determination

The main formulas for phase determination are now listed. They will suffice to characterize the nature of the phase determining procedures. There are additional formulas that play a variety of helpful roles and may be found in the referenced literature of this article.

Centrosymmetric Crystals

The Σ_2 formula is,[23]

$$s E_{\mathbf{h}} \approx s \sum_{\mathbf{k}_r} E_{\mathbf{k}} E_{\mathbf{h}-\mathbf{k}} \tag{16}$$

where s means the "sign of" and $\mathbf{k}_r$ represents restricted values of $\mathbf{k}$ for which the corresponding $|E_{\mathbf{k}}|$ and $|E_{\mathbf{h}-\mathbf{k}}|$ values are large. A plus sign refers to a phase of zero and a minus sign to a phase of π, the only two values possible for a centrosymmetric crystal when an origin in the crystal is properly chosen. The quantities, E, are normalized structure factors which arise as appropriate quantities to use with probability theory and are the same as the quasi-normalized structure factors, $\mathscr{E}$, except for a reweighting[26] of certain subsets of the E. The treatment of the intensity data to obtain normalized structure factors[27] arises from the work of *Wilson*,[28,29] the earliest application of probability methods to crystal structure analysis. Equation (16) is the probability equivalent of the set of inequalities (8) as $\mathbf{k}$ varies over the set $\mathbf{k}_r$. The appropriate probability function, $P_+(\mathbf{h})$, which represents the probability that the sign of $E_{\mathbf{h}}$ be positive was given in the above mentioned monograph.[23] It is conveniently applied in the form derived by use of the central limit theorem by *Woolfson*[30] and *Cochran* and *Woolfson*,[31]

$$P_+(\mathbf{h}) \approx \frac{1}{2} + \frac{1}{2} \tanh \sigma_3 \sigma_2^{-\frac{3}{2}} |E_{\mathbf{h}}| \sum_{\mathbf{k}} E_{\mathbf{k}} E_{\mathbf{h}-\mathbf{k}} \tag{17}$$

where

$$\sigma_n = \sum_{j=1}^{N} Z_j^n \tag{18}$$

and Z_j is the atomic number of the jth atom in the unit cell containing N atoms.

Noncentrosymmetric Crystals

The sum of angles and tangent formulas are, respectively,

$$\phi_{\mathbf{h}} \approx \langle \phi_{\mathbf{k}} + \phi_{\mathbf{h}-\mathbf{k}} \rangle_{\mathbf{k}_r} \tag{19}$$

$$\tan \phi_{\mathbf{h}} \approx \frac{\sum_{\mathbf{k}} |E_{\mathbf{k}} E_{\mathbf{h}-\mathbf{k}}| \sin(\phi_{\mathbf{k}} + \phi_{\mathbf{h}-\mathbf{k}})}{\sum_{\mathbf{k}} |E_{\mathbf{k}} E_{\mathbf{h}-\mathbf{k}}| \cos(\phi_{\mathbf{k}} + \phi_{\mathbf{h}-\mathbf{k}})} \tag{20}$$

The expressions (19) and (20) are comparable to (10) and (15), respectively, and result from combining a number of individual terms as $\mathbf{k}$ varies over some chosen set. An appropriate measure of the reliability of (19) and (20) is a variance, V,[32] given by,

$$V = \frac{\pi^2}{3} + [I_0(\alpha)]^{-1} \sum_{n=1}^{\infty} (I_{2n}(\alpha)/n^2) - 4[I_0(\alpha)]^{-1} \sum_{n=0}^{\infty} [I_{2n+1}(\alpha)/(2n+1)^2] \tag{21}$$

where I_n is a Bessel function of imaginary argument,[33]

$$\alpha = \left\{ \left[\sum_{\mathbf{k}_r} \kappa(\mathbf{h},\mathbf{k}) \cos(\phi_{\mathbf{k}} + \phi_{\mathbf{h}-\mathbf{k}}) \right]^2 + \left[\sum_{\mathbf{k}_r} \kappa(\mathbf{h},\mathbf{k}) \sin(\phi_{\mathbf{k}} + \phi_{\mathbf{h}-\mathbf{k}}) \right]^2 \right\}^{\frac{1}{2}} \quad (22)$$

and

$$\kappa(\mathbf{h},\mathbf{k}) = 2\sigma_3\sigma_2^{-\frac{3}{2}} |E_{\mathbf{h}} E_{\mathbf{k}} E_{\mathbf{h}-\mathbf{k}}| \quad (23)$$

Expression (21) gives the variance of $\phi_{\mathbf{h}}$ as determined from a given set of $\phi_{\mathbf{k}} + \phi_{\mathbf{h}-\mathbf{k}}$. This variance formula has its origin in a probability distribution (in somewhat different notation) of *Cochran*[34] for $\phi_{\mathbf{h}}$, given a particular $\phi_{\mathbf{k}} + \phi_{\mathbf{h}-\mathbf{k}}$ and the accompanying |E| values. The tangent formula (20) can be derived in many ways. It has arisen, for example, in theoretical investigations of noncentrosymmetric space groups by use of the joint probability distribution[35] and can be shown to occur[32] in a generalization of the Cochran formula[34] for a particular $\phi_{\mathbf{h}}$ to take into consideration a set consisting of several or more $(\phi_{\mathbf{k}} + \phi_{\mathbf{h}-\mathbf{k}})$ rather than just one.[32,34] The average in (19) is to be taken in the context of maximum clustering i.e. a minimum deviation of the contributions of individual addition pairs, $\phi_{\mathbf{k}} + \phi_{\mathbf{h}-\mathbf{k}}$ from the average value. All ϕ are kept in a range $-\pi < \phi \leq \pi$ and maximum clustering requires the addition of 0, 2π or -2π to each addition pair. A practical method for effecting appropriate clustering has been described.[32]

Practical Phase Determination

In this part, the various aspects of practical phase determination will be outlined in terms of the first procedure that had broad practical applications to both centrosymmetric and noncentrosymmetric crystals, the symbolic addition procedure.[24,32,36,37] It arose mainly from the efforts of my wife, *Isabella Karle,* to bridge the gap between the mathematics of phase determination and the world of experimental data and practical application. By about 1956, we had acquired apparatus for carrying out X-ray diffraction experiments with crystals and *Isabella Karle* taught herself with the aid of a book written by *Martin Buerger* how to collect and interpret diffraction photographs. Working with crystal diffraction data was quite different then than now; computer-aided collection of diffraction data was essentially nonexistent and, by present standards, computers were very primitive. The thousands of diffraction data collected in the experiments were measured by eye with the use of a calibrated comparison strip. At the present time, data are collected by automatic diffractometers that measure and record the data after some modest, preliminary human intervention and the largest computers are many orders of magnitude superior in speed and capacity than thirty years ago. Technical advances in the recent past, as exemplified by synchrotron sources of X-radiation and area detectors, promise even greater advances in the near future in terms of the speed and facility with which data can be collected. They provide experimental opportunities that otherwise could not be contemplated.

Once the intensity data are collected, they are transformed into normalized structure factor magnitudes defined by,

$$|E_{\mathbf{h}}| = |F_{\mathbf{h}}| \Big/ \left(\varepsilon \sum_{j=1}^{N} f_{j\mathbf{h}}^2 \right)^{\frac{1}{2}} \quad (24)$$

where ε reweights certain subsets of the data.[26] A procedure for doing this is described in the International Tables for X-ray Crystallography.[38]

It is apparent on examining (16), (19) and (20) that it is necessary to know the values of some phases before additional ones can be evaluated. There are several sources of such information, from certain phase specifications associated with establishing an origin in the crystal,[38] the assignment of symbols to some phases for later evaluation and the use on occasion of auxiliary formulas, such as Σ_1 and Σ_3, that define individual phases in terms of structure factor magnitudes alone.[38] The number and types of phases to be used for specifying the origin in a crystal has been determined by use of the theory of invariants and semi-invariants that was developed for this purpose. Depending upon the type of space group involved, the number can vary from none at all to as many as three. Suitable tables[38] are available for carrying out this task.

The phase determining procedure is a stepwise one with few contributors to (16) or (19) at the start. Use at the start of phases associated with the largest possible values of the normalized structure factor magnitudes, |E|, will assure that the probability measures (17) and (21) will be as optimal as possible. The large overdeterminacy of the problem helps to ensure that initial probabilities will be large enough to proceed in a stepwise fashion to build up a sufficiently reliable set of phase values to effect a solution to the structure problem. Because the nature of phase determination is inherently probabilistic and contingent in a stepwise and interdependent fashion, the problem of establishing optimal procedures based on experimental data was not at all straightforward. There are a very large number of paths through a phase determination. Among many of them are pitfalls in which there arise, for example, temptations to take paths in which the interconnections between phase evaluations flow easily at the expense somewhat of the probability measures. Such paths are more likely to lead to missteps and cumulative errors that could damage or defeat a phase determination than ones that are based only on the highest values of the probability measures.

There is also an ambiguousness inherent in procedures for phase determination which is controlled by the use of symbols. The symbols can assume more than one value. For centrosymmetric crystals, they can have only two phase values, zero or π. For noncentrosymmetric crystals, experience has shown that whereas phase values for the general reflections can have any value in the range from $-\pi$ to π, it is usually sufficient to use only four possible values for the symbols spaced $\pi/2$ apart. One of the virtues

of using symbols is that, as the phase determination develops, relationships develop among the symbols reducing the number to be assigned values. Here again, one must proceed with caution so that reliable relationships are distinguished from those that are not. With centrosymmetric crystals, the entire phase determination is carried through before the remaining symbols are given alternative numerical values and tested to see which set yields a Fourier series that makes good chemical sense and reproduces the measured intensities well. For noncentrosymmetric crystals the symbolic addition procedure initially makes use only of equation (19). After about 100 phases have been evaluated, the remaining symbols are given alternative numerical values after which equation (20) is applied to further extend the phase set. Again, the correct phase set is the one whose Fourier series makes good chemical sense and yields a structure that is in fine agreement with the measured intensities. When a satisfactory result is not obtained, it is appropriate to try an alternative path through the phase determination.

An additional specification, whose character also derives from the theory of invariants and semi-invariants, is required for most noncentrosymmetric space groups. In making the specification, a choice is made of enantiomorph or axis direction or both. A good way in which this specification is achieved in the symbolic addition procedure is to find that a symbolic representation of a phase value most likely has a magnitude that differs significantly from 0 and π. The specification is accomplished by assigning a plus or minus sign arbitrarily to the magnitude of the phase. The enantiomorph ambiguity for noncentrosymmetric crystals arises from the fact that such a crystal gives the same diffraction pattern as its mirror image in the absence of detectable anomalous dispersion effects.

In the course of phase determinations, particularly in the case of noncentrosymmetric crystals, it may turn out that only a partial structure will appear in a Fourier map based on the determined phase values. This occurs because the phase determination went somewhat awry but not altogether so. The partial structure would be recognized as possibly being a correct fragment because it would make chemical sense, i.e., the fragment would have connectedness and acceptable interatomic distances and angles. A method has been developed for deriving a complete structure from a partial structure[39] that is based on the use of the tangent formula (20) and has been used in many applications. It may happen that a partial structure is not placed correctly with respect to a proper origin in the unit cell of a crystal. Under such circumstances, the use of a translation function[40–43] to place the fragment properly may be helpful.

The symbolic addition procedure[24, 32, 36, 37] was developed as an outgrowth of the experiences in applying the procedure for phase determination for centrosymmetric crystals described in the 1953 monograph.[23] In the monograph, the procedures proposed for sign determination involved the initial use of auxiliary phase formulas such as Σ_1 and Σ_3.[23] The application of preliminary phase information obtained from these formulas along with probability measures associated with individual indications from the phase-determining formulas facilitated the use of the Σ_2 relation (16). The combination of auxiliary formulas and probability theory greatly reduced to a practicable level the ambiguousness that would be obtained in the employment of the Σ_2 relation by itself along with some rather insensitive and often misleading criterion such as internal consistency.

In the course of applying the procedures of the monograph,[23] two important features were found that ultimately played an important role in the symbolic addition procedure. The first feature was that if probability measures were carefully employed at each step of a phase determination, it was possible to carry out the procedure with a small set of starting phases. It was also apparent that the use of symbols could greatly increase the efficiency of the procedure by carrying along in their alternative values a residual ambiguity that could not be easily overcome. A sufficient number of reliable relationships among the symbols usually developed in the course of a phase determination to reduce the alternative possible sets of phases to consider to just a few. A further reduction could be obtained, if desired, by applying auxiliary phase determining formulas at the end of a phase determination to help evaluate the remaining symbols. If an evaluation were incorrect, as occasionally happened with the auxiliary formulas, no great harm would be done. The alternative value could be tried without the necessity of repeating the phase determination. The symbolic addition procedure for centrosymmetric crystals is thus the procedure of the monograph[23] facilitated by the use of symbols and the application of auxiliary formulas at the end, if needed, instead of at the beginning of a phase determination.

The symbolic addition procedure for centrosymmetric crystals has several features in common with the procedure of *Zachariasen*.[44] The main distinction from the latter procedure was the application of probability measures to guide each step of the phase determination, especially in the beginning, the consequent use of a minimal number of symbols, and the resulting minimization of the ambiguousness of the determination and the optimization of the reliability of the result. There were efforts by others in the 1950's, e.g. *Rumanova*[45] and *Cochran* and *Douglas*[46] that met with some success. *Rumanova* developed a systematic method for using symmetry relations in the centrosymmetric space groups with equation (16). She used it in connection with *Zachariasen*'s procedure.[44] *Cochran* and *Douglas* used a variant of (16) based on a formula derived by *Sayre*[47] in a procedure that generated a very large number of sets of signs from which the correct one had to be selected under highly ambiguous circumstances.

The procedural features of the symbolic addition procedure for centrosymmetric crystals were extended, in the main by the efforts of *Isabella Karle*, to noncentrosymmetric crystals[24] with the use of equations (19), (20) and (21). Several problems arose in developing the technique for phase determination for noncentrosymmetric crystals concerning, for example, the assignment and handling of symbols, the use of the probability measure (21), the number of possible values to assign to the symbols that represent phase values that range continuously from $-\pi$ to π, the combined use of (19) and (20) for phase determination, the proper use of the tangent formula for the processes of

phase refinement and phase extension, the development of techniques for specifying an enantiomorph or axis directions or both, and special considerations such as the avoidance of certain troublesome triplet phase invariants involving one and two-dimensional centric reflections. These various aspects of the symbolic addition procedure are to be found in references [32] and [38] and in the papers concerning the applications described further on.

A considerable virtue of the symbolic addition procedure is that, because of its efficiency, a main part of the procedure for phase determination can be carried through by hand. For many years, the procedure for centrosymmetric crystals was carried out in our laboratory completely by hand. In the case of noncentrosymmetric crystals, the first stage, which involved the use of equation (19), was performed by hand until about 100 phases were evaluated and useful relationships developed among the symbols. Only after selected numerical values were assigned to the few remaining symbols was the tangent formula (20) applied with the aid of a computer. The benefits of this aspect of the efficiency of symbolic addition have been the opportunity for those with modest computing facilities to carry out structure determinations, the possibility of close interaction with the phase determination as it progresses, and the educational value for those newly learning about phase determination to be able to witness and carry through the procedure by hand.

As the application of direct phase determination began to increase during the 1960's and structure determination became more and more a part of research programs, there began to be developed at the end of the 1960's "program packages", software for determining structures from X-ray diffraction data. Among the ones that are widely used, alternative numerical values have been used instead of symbolic phases in the case of noncentrosymmetric crystals, although there are some programs that retain the use of symbols for such types of crystals. For those programs that use alternative numerical values for phases, large numbers of alternative phase sets are generated by use of the tangent formula (20) and the selection of the most likely solutions is dependent upon the use of an elaborate set of probability formulas, auxiliary formulas and acceptance criteria. Other computational techniques have also evolved. For example, random sets of phases have been used as starting sets to be refined by application of the tangent formula (20). By considering large numbers of alternative starting sets it is often practicable to obtain a correct answer, although a large amount of computing is involved. There are also special programs for specific purposes such as the development of a structural fragment into a complete structure.

The computer programs are quite successful with centrosymmetric crystals and also do fairly well with noncentrosymmetric crystals having up to 100 independent (nonhydrogen) atoms to be placed in the unit cell. On occasion an answer will not be forthcoming from the use of a program package. In that case, crystallographers may pursue the problem with special techniques and the application of insights and acumen that have been too special to be found in current programs.

Some names that have been associated with the preparation and dissemination of computer programs for various aspects of automated, direct structure determination are *Ahmed, Andrianov, Beurskens, Germain, Gilmore, Hall, Main, Schenk, Sheldrick, Stewart, Viterbo,* and *Woolfson.* Among them, some of their programs have enjoyed a broader range of popularity than others. Insight into the contents and philosophy of the programs can be obtained from several publications of the Commission on Crystallographic Computing of the International Union of Crystallography.[48, 49, 50, 51, 52]

Applications

This section will be devoted to illustrating the broad range of applications that have been made accessible by the development of direct structure determination. The examples will be mainly taken from my laboratory but will be seen to be representative of activities that now produce thousands of structural investigations each year.

The earliest applications after the publication of the monograph[23] were collaborations with colleagues at the U.S. Geological Survey on colemanite[53] and meyerhofferite.[54] This was followed by the initial investigations based on the experimental work of *Isabella Karle,* for example, on *p,p'*-dimethoxybenzophenone[55] and *N*-benzyl-1,4-dihydronicotinamide[56] that, in time, led to the symbolic addition procedure.

Early Applications of the Symbolic Addition Procedure

The first application of the symbolic addition procedure concerned cyclohexaglycyl, a synthetic polypeptide in which six glycine residues form an eighteen-membered ring. The polypeptide crystallizes as a hemihydrate in the triclinic space group $P\bar{1}$ with eight molecules in the unit cell[36] (Fig. 3). An interesting characteristic of this structure is that the eighteen-membered ring occurs in the unit cell in four different conformations. Another feature is that all hydrogen atoms capable of forming hydrogen bonds are so involved.

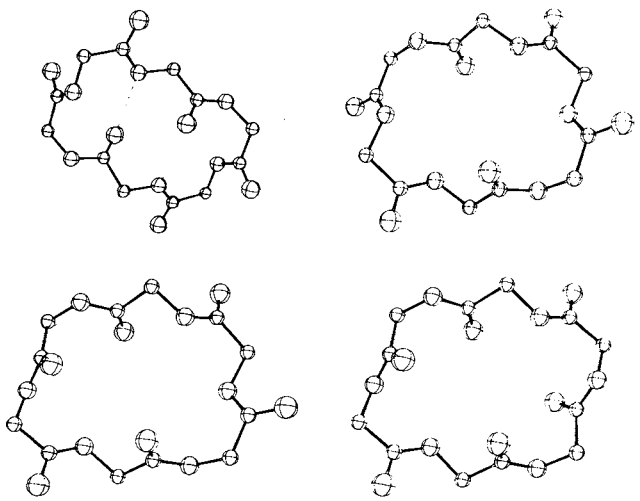


Fig. 3. The four co-crystallizing conformers of cyclohexaglycyl. The conformer at the upper left occurs four times in the unit cell, the one at the lower left occurs twice and the other two occur once.

Noncentrosymmetric crystals are quite common among substances of biochemical interest. The determination of the structure of the dihydrate of the amino acid L-arginine,[24] which crystallizes in space group $P2_12_12_1$, is the first noncentrosymmetric structure determined by the direct method. As seen in the diagram of the contents of the unit cell (Fig. 4), the hydrogen-bonding indicated by the dashed lines is extensive. As a consequence of this hydrogen-bonding the molecules of arginine form an infinite chain. In addition, water molecules also form hydrogen bonded infinite chains which are perpendicular to the plane of the figure.

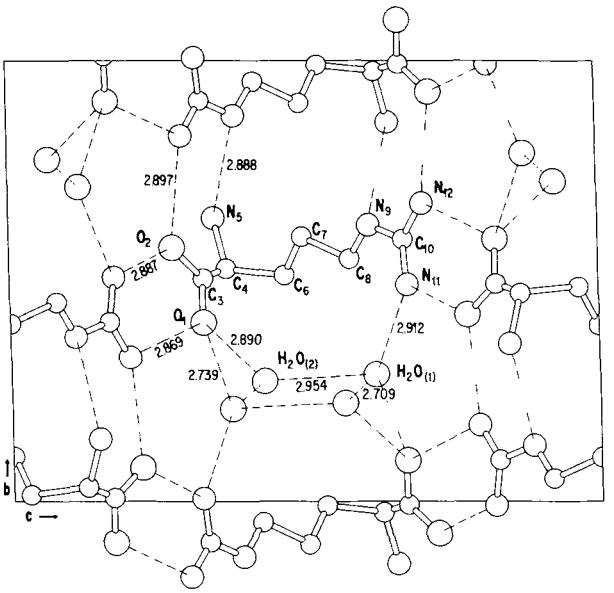


Fig. 4. The structure of L-arginine dihydrate viewed along the *a* axis. Hydrogen bonding is shown by the dashed lines.

The stereochemistry of reserpine, a drug that has been used to control hypertension and nervous disorders, had been determined by chemical means. It was of interest, however, to establish the spatial arrangement of the atoms in the molecule. Reserpine was found to crystallize in the noncentrosymmetric space group, $P2_1$.[57] In this investigation, the symbolic addition procedure yielded a partial structure which was developed into a complete structure (Fig. 5) by use of the recycling procedure[39] involving the tangent formula. Figure 5 shows sections from an electron density map projected down the *b*-axis. The trimethoxybenzoate group at the bottom is nearly perpendicular to the rest of the molecule. The indole group at the top of the diagram is planar and the dihedral angle between least-squares planes for the indole group and the benzoate group is 82°.

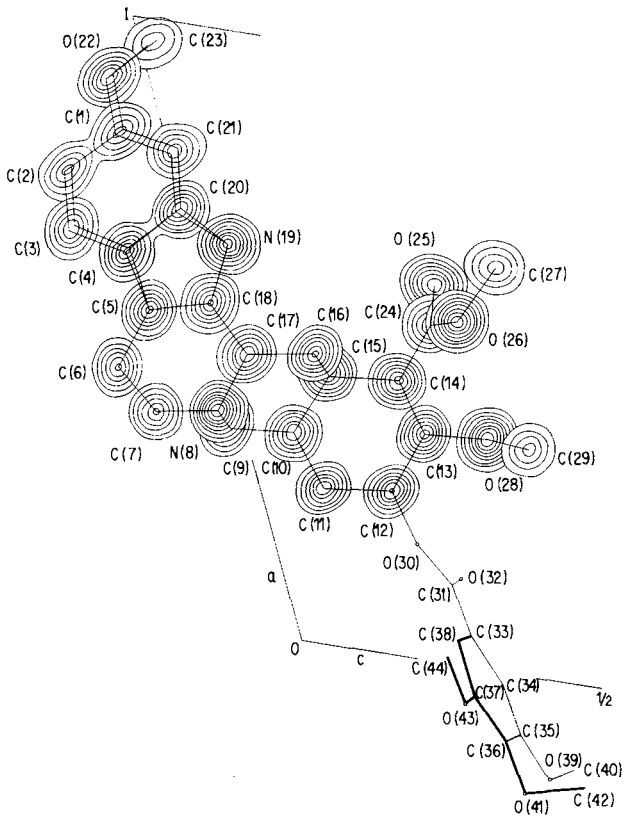


Fig. 5. Sections from a three-dimensional electron density map for the alkaloid reserpine projected down the *b* axis. The electron density contours are equally spaced at $1\,e\,Å^{-3}$ starting with the $1\,e\,Å^{-3}$ contour.

Identification and Stereoconfiguration

The problems concerning the determination of molecular formula and stereoconfiguration can become especially acute when the amount of sample available is very small, when the chemical linkages are new and unusual, or when the number of asymmetric centers is large. Under such circumstances, the use of crystal structure analysis can be not only quite helpful but also essential. An example of this is provided by batrachotoxin, a powerful neurotoxin that can be extracted from the skin of the frog, *Phyllobates aurotaenia*, from tropical America. It is used by native Indians to tip blow darts for hunting. Purified congeners were obtained from ethanol extracts of the skins of about 8000 frogs. The amounts were insufficient to permit the determination of the structural formulae by standard methods. A few, very small crystals of the *O-p*-bromobenzoate derivative of batrachotoxinin A, one of the congeners, were grown and one crystal was selected for structure analysis. It was found to crystallize in space group $P2_12_12_1$. The specialized position of the Br atom (at 1/5, 0, 0) and the restricted amount of data available limited the amount of information derivable from knowledge of the location of the Br atom. The structure was determined by use of the tangent formula to develop partial structural information into a complete structure. It showed that batrachotoxinin A was a steroidal alkaloid with several novel features[58] (Fig. 6). Other information obtained was the stereoconfiguration at the nine asymmetric centers, the conformations of the six rings, including the seven-membered ring containing the alkaloid function, values of bond lengths, bond angles and torsional angles, the location of intermolecular hydrogen bonds, and the packing of the models in the unit cell. The absolute configuration was established by mea-

urement of the anomalous scattering of the Br atom.[59] From the information obtained from the structural analysis, the structure and absolute configuration of batrachotoxin and many other congeners were readily deduced.[60]

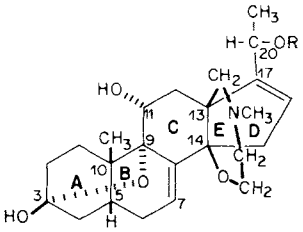


Fig. 6. The molecular formula and absolute stereoconfiguration for batrachotoxinin A (R = H) (heavy solid lines are above plane of paper and dashed ones behind).

Another small frog, *Dendrobates aurotaenia*, occurring in Columbia and Ecuador, secretes from its skin defensive substances among which are two major toxic alkaloids, histrionicotoxin and dihydroisohistrionicotoxin. These alkaloids are quite unique, having a spiropiperidine system with acetylenic and allenic moieties (Fig. 7). The molecular structures, stereoconfigurations and absolute configurations were established by crystal structure analyses of a hydrochloride and hydrobromide of the histrionicotoxin and a hydrochloride of the dihydroiso compound.[61,62] Space groups $C2$ and $P2_12_12_1$ were involved in the analyses. The histrionicotoxins appear to offer the first examples of the occurrence of acetylene and allene moieties in the animal kingdom. Other congeners that occur in smaller quantities were shown, subsequently, by means of mass and NMR spectra to differ only in the saturation of the two side chains.[63] The spiro ring system, with the intramolecular NH···O hydrogen bond, remained unchanged.

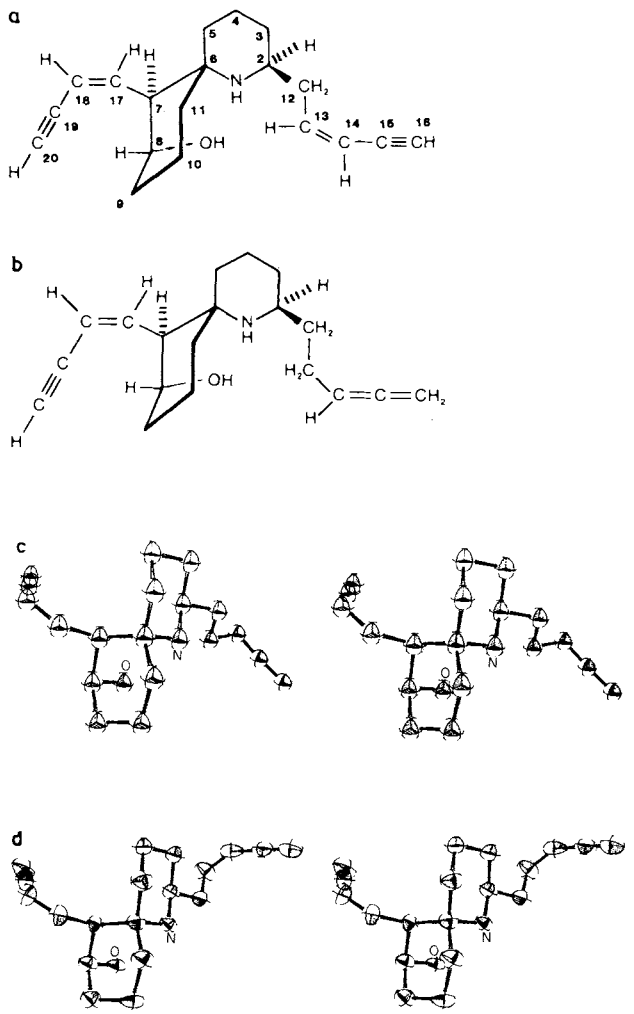


Fig. 7. Histrionicotoxin: a) structural formula; d) stereodiagram. Dihydroisohistrionicotoxin: b) structural formula; c) stereodiagram.

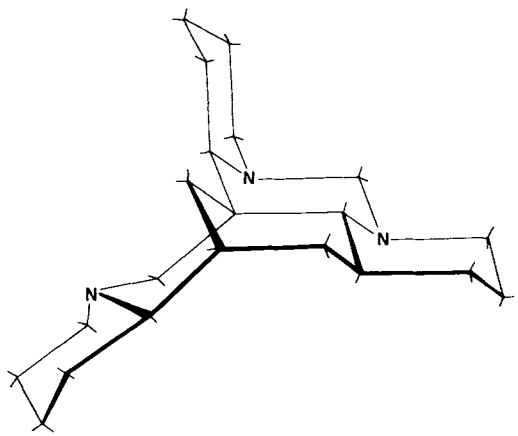


Fig. 8. The stereoconfiguration of jamine.

Another example of the application of X-ray crystal structure analysis to the determination of structural formula and stereoconfiguration of an unknown substance is illustrated by the investigation of an alkaloid derived from an *Ormosia* plant, namely the alkaloid jamine, which crystallizes in the triclinic space group $P\bar{1}$.[64] The configuration determined for the molecule is shown in Figure 8. The connectivity was found to comprise six six-membered rings, five of which were in the chair configuration and one in the boat configuration. There were six asymmetric carbon atoms and the stereoconfiguration about each was, evidently, readily apparent. The identification of the nitrogen atoms was also readily made in the course of the structure determination.

Brassinolide[65-67] is a very potent plant growth promoter. It is active in very small amounts, 1–10 ng/plant. Brassinolide generates cell enlargement and stimulates cell division in many food plants and plants grown in arid regions that yield oil and other energy related materials. The yield from extraction from plant pollen is very low and therefore large-scale testing awaited chemical synthesis. Evidently, chemical synthesis would be facilitated by structural information. A few crystals of brassinolide became available for crystal structure determination. The crystallization took place in space group $P2_1$ and the analysis[66] established that the steroid nucleus of the molecule had a seven atom B-ring lactone, an unprecedented feature for a natural ste-

roid (Fig. 9). The presence of the lactone appears to be responsible for promoting the plant growth. Subsequent synthesis has shown that compounds analogous to brassinolide are easier to prepare in large quantities and have adequate plant-growth regulating properties. Field evaluation of these regulators are currently under way.

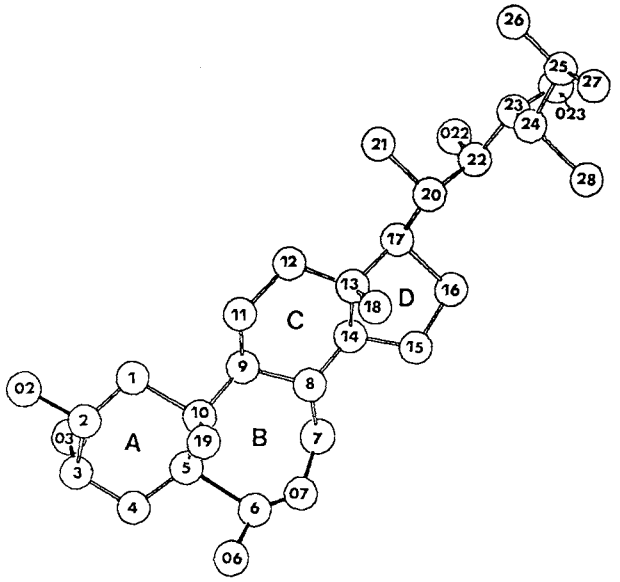


Fig. 9. The molecular formula (only C and O atoms) and stereoconfiguration of brassinolide. Note that the B ring is a seven-membered lactone ring.

There are very large numbers of examples that could be discussed under the heading of this section. It is noteworthy, however, that the implications of only a small number of definitive structure determinations can be extended far beyond the immediate results of the particular determinations. An outstanding example is given by some fundamental structural investigations on frog toxins which have provided the information on which was based the subsequent establishment of molecular formulas and stereoconfigurations of over 200 related frog toxins.[68,69]

Rearrangements

In the case of rearrangement reactions, crystal structure determination can again play a particularly useful role because many rearrangement reactions give products that are the result of vast and unanticipated changes in the starting materials. The following examples provide illustrations of such changes.

A photorearrangement reaction in which a major rearrangement takes place is illustrated by the reaction shown in Figure 10. A crystal structure investigation of a single optically active crystal, selected from a racemic conglomerate established the structural formula and configuration of the photoproduct.[70,71] The substance crystallized in space group $P2_12_12_1$. The structure analysis showed that the photoproduct consisted of four ring systems, namely two five-membered and two four-membered rings.

Ultraviolet irradiation of *N*-chloracetyltyramine, where there is a hydroxyl group on the phenyl ring in contrast to the two methoxy groups in the previous example, yields entirely different photorearrangement products. HCl was eliminated and two unusual photodimers, shown in Figure 11, were produced. Their molecular formulas and stereoconfigurations have been identified by use of crystal structure analysis.[72] It is interesting to note that dimer **II** is the more stable since it is produced from dimer **I** by use of additional ultraviolet radiation. Dimer **I** crystallizes in space group $P2_1/c$ and dimer **II** crystallizes in space group *Pbca*. Dimer **I** is seen to have a central cage bounded by four six-membered rings and two four-membered rings. Each four-membered ring is puckered, with the torsion angles around the ring bonds having values of about 20°. The six-membered rings assume distorted boat conformations. Dimer **II** is seen to have a more complex, partially open, cage bounded by one three-, two five-, two six-, and one seven-membered ring. The six-membered rings are again in a distorted boat conformation. Once the structural characteristics of the photoproducts are known, it is possible to

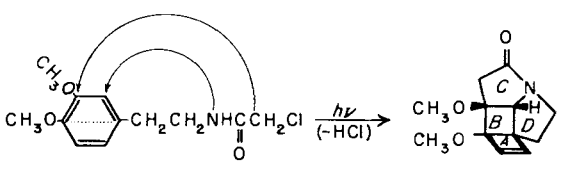


Fig. 10. The photorearrangement of *N*-(3,4-dimethoxyphenethyl)chloracetamide to a fused ring system consisting of two four- and two five-membered rings.

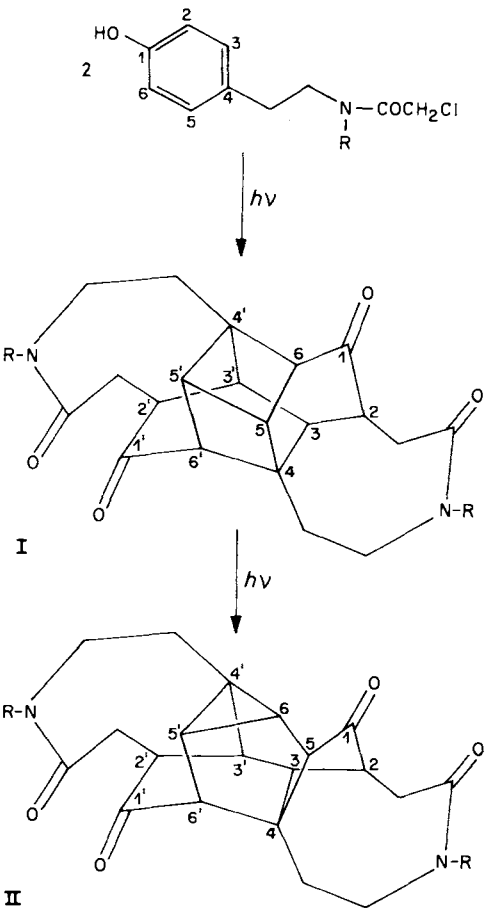


Fig. 11. The configurations of two dimers formed by photorearrangement from *N*-chloroacetyltyramine. Dimer **II** is seen to be formed from dimer **I** by continued irradiation with ultraviolet light (R = H or CH_3).

consider possible reaction mechanisms that describe the intermediate changes that occur in the rearrangements of the initial materials resulting in the final products. Postulated mechanisms for the formation of dimers **I** and **II** have been presented.[73]

Irradiation of a solution containing 5-methyl-1,2-diaza-4,6-cyclohexadien-3-one **III** and 2-propen-1-ol with ultraviolet light produces a cyclobutane addition compound **IV**, which, upon further irradiation, opens and switches bonds to form a tricyclic molecule **V** (Fig. 12). The crystal structure analysis[74] of **V**, which crystallizes in space group $P\bar{1}$, established that the final photoproduct was composed of a fused ring system, one three-membered ring, and two five-membered rings.

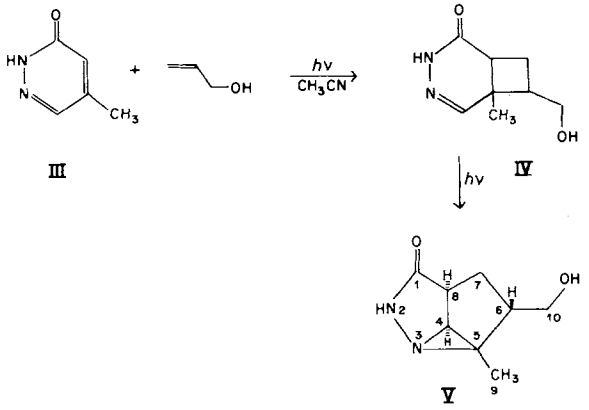


Fig. 12. Irradiation with ultraviolet light of a solution of 5-methyl-1,2-diaza-4,6-cyclohexadien-3-one **III** and 2-propenol leads to a cyclobutane addition product **IV**. On further irradiation, **IV** rearranges to a tricyclic product **V**.

Conformation

The conformations of molecules can be importantly related to their chemical and physiological behavior. Crystal structure investigations can be helpful in providing conformational information. It may be argued, and rightly so, that biologically active materials may assume conformations in the crystalline state that they would not assume in solution. There are, however, numerous instances of conformational studies in which the results of crystal structure analyses are either highly suggestive or rather definitive. The following examples are such instances.

One way in which the crystalline state can imitate the circumstances found in solution is to include in the crystallization relatively large amounts of solvent. Such a crystal is formed by [Leu^5]enkephalin (Tyr-Gly-Gly-Phe-Leu) grown from *N,N*-dimethylformamide (DMFA)/water. Endogenous enkephalin is a linear pentapeptide that occurs in the brain as [Leu^5]enkephalin and [Met^5]enkephalin in varying proportions depending upon the species.[75] Both are quite flexible and the structural study of [Leu^5]enkephalin was undertaken in the hope that insight into probable conformations would be so derived. The crystallization took place in space group $P2_1$ and it turned out that there were four molecules of the peptide in the asymmetric unit of the unit cell, each having a different conformation[76] (Fig. 13). The large amount of solvent surrounding the molecules suggests that the conformations may be relevant to the circumstances in solution. The four conformers with

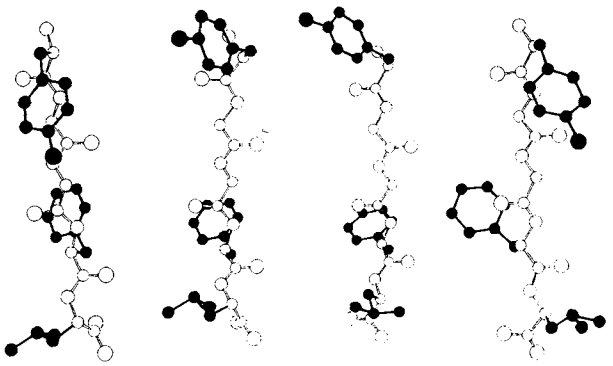


Fig. 13. Four conformations of [Leu^5]enkephalin that occur in *N,N*-dimethylformamide/water. Note the similarities in the backbone conformations and the differences in the (black) side chains.

extended backbones form an infinite antiparallel β-sheet. β-sheets related by the twofold screw axis are separated by a 12 Å spacing. Side groups protrude above and below the β-sheets and are entirely immersed in a thick layer of solvent that fills the volume between the β-sheets. The crystal was stable only in contact with the mother liquor. Structurally, it consisted of rather rigid sheets of peptide molecules separated by spaces filled with mobile solvent. Many of the solvent molecules appeared from the X-ray analysis to be completely disordered. An asymmetric unit of the unit cell contained four enkephalin molecules, eight water molecules, eight DMFA molecules, and an unknown number of disordered solvent molecules.

The crystal of enkephalin contains more than 210 independent C, N and O atoms and is of a size that lies between what is normally considered small-structure crystallography (up to 100 nonhydrogen atoms or so) and protein crystallography (about 500 nonhydrogen atoms or more).

The visual chromophores, 11-*cis*- and all-*trans*-retinal are present in both rod and cone cells of vertebrate retinas and in the corresponding organs of insects and crustacea.[77] The photochemical isomerization of the 11-*cis* isomer to the *trans* form is an important step in the visual process with the 11-*cis* isomer acting as a photochemical sensor. In the dark, 11-*cis*-retinal is covalently linked to proteins in the retina known as opsins. They differ in different species and may differ in different cells of the retina. The details of the geometry of the retinals had not been determined and, in view of their importance to biological function, a crystal structure investigation was undertaken on the 11-*cis* and all-*trans* forms. Special precautions had to be observed with the 11-*cis*-retinal. It is unstable towards light and oxygen and its stability is favored by lower temperatures. In solution, the *cis* isomer isomerizes to the *trans* form very readily at 20°C. Fortunately, crystals of the *cis* isomer are more stable than its solution. The diffraction data for the *cis* form were collected in a light-tight container that was continuously purged with dry nitrogen and maintained at 16–17°C. Crystal structure analyses[78,79] of

the 11-*cis* and all-*trans* forms revealed the detailed geometry of both (Fig. 14). An additional, independent structure

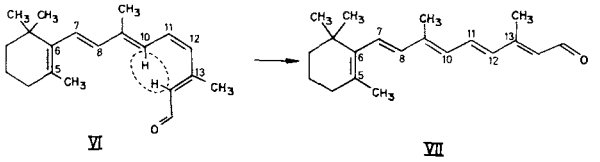


Fig. 14. Two isomers of retinal, the 11-*cis* (**VI**) and all-*trans* (**VII**) forms.

analysis of all-*trans*-retinal was also reported.[80] Of particular interest was the conformation of the *cis* form as there had been much speculation and theoretical work concerning its conformation. The 11-*cis*-retinal crystallized in space group $P2_1/c$ and the *trans* isomer in space group $P2_1/n$. The all-*trans*-retinal chain is planar with the six-membered ring inclined to the plane of the chain. The inclination is given by the torsional angle of the 5-6-7-8 segment, which is found to be 59°. The torsion angle of a planar *trans* conformation is 180° and that of a planar *cis* conformation is 0°. The conformation for the all-*trans* isomer is typical of carotenoids. In forming the 11-*cis*-retinal from the all-*trans* form, there is not only a rotation of 180° about the C11=C12 double bond, but also a rather unexpected rotation of 141° about the C12–C13 single bond. This additional rotation relieves the difficulty of too close a contact in the absence of the additional rotation between the hydrogen atom on C10 and the hydrogen atoms of the methyl group attached to C13 (see the diagram in Fig. 15). At the time that the manuscript concerning the crystal structure determination of 11-*cis*-retinal was being prepared, a theoretical calculation was published by *Honig* and *Karplus*[81] in which a ground-state configuration for 11-*cis*-retinal was proposed that closely resembled the result of the crystal structure determination.

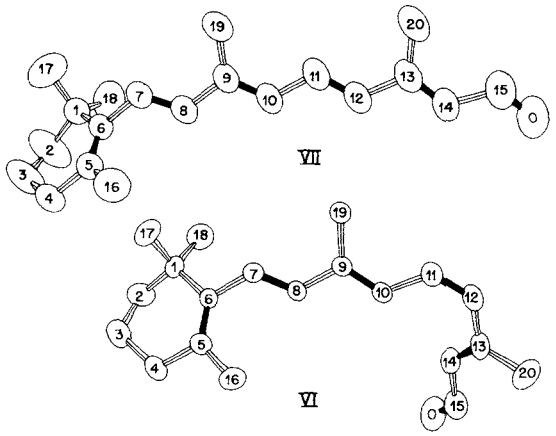


Fig. 15. Conformations of 11-*cis*-retinal **VI** and all-*trans* retinal **VII**.

The cyclic decapeptide antamanide acts as an antidote to the toxin phalloidin found in the deadly poisonous mushroom *Amanita phalloides*. Antamanide can also be isolated from the same mushroom but occurs in much smaller quantities. The synthetic analog of antamanide in which all four phenylalanyl residues are hydrogenated to cyclohexylalanyl residues (Cha), cyclic (ValProProAlaCha-ChaProProChaCha), has no antitoxic potency despite its ability to form ion complexes in the same manner as antamanide. A conformational analysis of the hydrogenated antamanide was carried out by means of a crystal structure analysis of Li-perhydroantamanide, which crystallizes in space group $P2_12_12_1$[82] (Fig. 16). The backbone encapsulates a Li ion in quite the same fashion as in Li-antamanide. In the Li-antamanide, however, the four phenyl groups are folded against the backbone, thus providing a hydrophobic surface for the complex, whereas in Li-perhydroantamanide the four cyclohexyl moieties are extended away from the folded backbone, with the consequent exposure of large portions of the polar backbone to the sur-

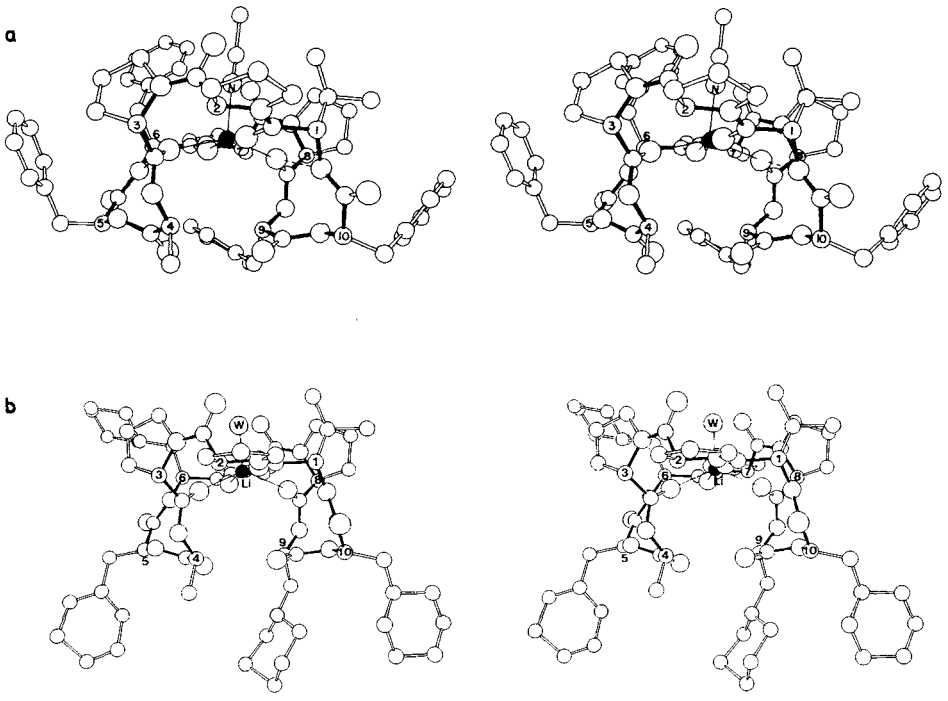


Fig. 16. a) Phenyl rings folded up around the backbone of a biologically active antamanide complex with Li^+ or Na^+ providing a lipophilic surface. b) In the inactive analogue, Li-perhydroantamanide, the cyclohexyl groups are folded down, thus exposing the peptide backbone to the environment.

rounding environment. As a result, elements of the backbone that would be otherwise shielded from the environment were found to make hydrogen bonds and ligands that would not occur in the Li-antamanide complex. It would appear that the large change of hydrophobicity around the backbone in the perhydroantamanide complex is related to the loss of biological activity.

These few applications represent only a minuscule portion of the broad range of topics and individual studies represented by the thousands of structural investigations performed each year. They do illustrate, however, how structure determination can play a useful and often indispensable role in the progress of many research disciplines.

Analysis of a Macromolecular Structure: Recent Interests

The analysis of structures of macromolecules, molecules that consist of at least about 500 nonhydrogen atoms and more, is facilitated by use of specialized heavy-atom techniques that have the titles anomalous dispersion and isomorphous replacement. Heavy atoms can often be soaked into a macromolecular crystal without seriously disturbing the structure. As a consequence, the technique of anomalous dispersion and isomorphous replacement have enjoyed considerable success in the determination of the structure of native (unsubstituted) macromolecules.

Anomalous dispersion effects arise from the fact that the atomic scattering factors, f, as would be used in equation (3), are in general complex numbers defined by

$$f = f^n + f' + if'' \tag{25}$$

where f′ and f″ are the real and imaginary parts, respectively, of the correction to f^n and are considered the contributions of anomalous dispersion. The scattering factor f^n is obtained from computations in which it is assumed that the frequency of the radiation is much larger than the absorption frequencies for the constituent atoms. The consequence of having atomic scattering factors with a significant imaginary part, as occurs with the heavier atoms at commonly used wavelengths, is that the intensity measured for an acentric reflection $\mathbf{h}$ is, in general, different than that for $-\mathbf{h}$. The fact that $I_{\mathbf{h}} \neq I_{\bar{\mathbf{h}}}$ has been the basis of a technique that has broad applications[83] in the field of structure research.

Crystals that have the same unit cell geometry but differ in chemical composition are called isomorphous. Since it is often possible to substitute heavy atoms into macromolecules with relatively minor perturbations on the structure, the criterion for isomorphicity can be fairly readily achieved to good approximation for such molecules. The method of phase determination based on one substituted isomorphous structure is called the single isomorphous replacement method (SIR) and if several isomorphous structure are available it is called the multiple isomorphous replacement method (MIR). If two isomorphous structures are centrosymmetric, the signs of the structure factors for both crystals can be determined. In practice, some signs would remain indeterminate because of experimental errors and the presence of structure factors of small magnitude. When two noncentrosymmetric crystals form an isomorphous pair, analysis shows that a twofold ambiguity occurs in the evaluation of the phases. It can be readily shown, however, that in the case of noncentrosymmetric crystals many individual phases can be unambiguously evaluated when the structure of the substituted atoms is known.[84] Such phases are either close to the value of the corresponding phases for the substituted atoms or are shifted by π from those values. There are a number of ways to resolve the ambiguity from isomorphous replacement. They involve, for example, the use of a second isomorphous substitution or, instead, the additional use of anomalous dispersion data.

Multiple isomorphous substitution with the occasional additional use of anomalous dispersion data has been the technique that has led to the enormous progress in macromolecular structure research of biological importance for the past 25 years. The early theoretical work that supported the advances in this field was that of *Patterson*[4, 5] and *Bijvoet*.[85] With the types of heavy atoms that are usually substituted into macromolecular structures, there can be significant effects from anomalous dispersion, so that data collection for both anomalous dispersion and isomorphous replacement can be, in effect, combined.

My interest in the techniques of anomalous dispersion and isomorphous replacement was rekindled by a development in my laboratory that demonstrated the considerable potential of the anomalous dispersion technique in structure determination. In an application of the anomalous dispersion technique to the structure determination of the protein, crambin, *Hendrickson* and *Teeter*[86] solved the structure by use of the anomalous scattering from six sulfur atoms occurring in three disulfide bridges. The experiment was performed as a single-wavelength experiment with $Cu_{K\alpha}$ radiation, which is far from the absorption edge for S at 5.02 Å. The success with the use of the relatively weak anomalous scattering from the S atoms coupled with the great span in wavelength between that of the absorption edge and the wavelength of $Cu_{K\alpha}$ radiation stimulated me to initiate a program to investigate various theoretical aspects of the single- and multiple-wavelength anomalous dispersion techniques and also, in time, isomorphous replacement.

One investigation concerned an exact algebraic analysis of single- and multiple-wavelength anomalous dispersion[87] by use of the structure factor equations (3) in which the atomic scattering factors are complex according to equation (25). The appropriate structure factor equations are treated as simultaneous equations and the key to obtaining the final form in which the equations were expressed was the separation of the contributions from the normal atomic scattering factors f^n from those of the real and imaginary corrections to f^n, f′ and f″, respectively.

A simple result of the algebraic analysis that concerns the case when a structure is composed of atoms that scatter normally and one type of atom that scatters anomalously is as follows,

$$\begin{aligned}|F_{\lambda\mathbf{h}}|^2 = {} & |F^n_{1,\mathbf{h}}|^2 + \{1 + (f^a_{\lambda 2,\mathbf{h}}/f^n_{2,\mathbf{h}})[(f^a_{\lambda 2,\mathbf{h}}/f^n_{2,\mathbf{h}}) + 2\cos\delta_{\lambda 2,\mathbf{h}}]\}|F^n_{2,\mathbf{h}}|^2 \\ & + 2[1 + (f^a_{\lambda 2,\mathbf{h}}/f^n_{2,\mathbf{h}})\cos\delta_{\lambda 2,\mathbf{h}}]|F^n_{1,\mathbf{h}}||F^n_{2,\mathbf{h}}|\cos(\phi^n_{1,\mathbf{h}} - \phi^n_{2,\mathbf{h}}) \\ & + 2(f^a_{\lambda 2,\mathbf{h}}/f^n_{2,\mathbf{h}})\sin\delta_{\lambda 2,\mathbf{h}}|F^n_{1,\mathbf{h}}||F^n_{2,\mathbf{h}}|\sin(\phi^n_{1,\mathbf{h}} - \phi^n_{2,\mathbf{h}})\end{aligned} \tag{26}$$

where $|F_{\lambda \mathbf{h}}|^2$ is the square of the measured magnitude of the structure factor at the wavelength λ, $|F^n_{1,\mathbf{h}}|^2$ is the square of the magnitude of the structure factor for the non-anomalously scattering atoms and $|F^n_{2,\mathbf{h}}|^2$ is the square of the magnitude of the structure factor for the anomalously scattering atoms, but scattering as if they were doing so normally. The measured $|F_{\lambda \mathbf{h}}|^2$ are corrected for vibrational effects and the latter are also absent from $|F^n_{1,\mathbf{h}}|^2$ and $|F^n_{2,\mathbf{h}}|^2$. The quantities $f^a_{\lambda j,\mathbf{h}}$ and $\delta_{\lambda j,\mathbf{h}}$ are defined for a particular λ,

$$f^a_{\lambda j,\mathbf{h}} = [(f'_{\lambda j,\mathbf{h}})^2 + (f''_{\lambda j,\mathbf{h}})^2]^{\frac{1}{2}} \tag{27}$$

and

$$\delta_{\lambda j,\mathbf{h}} = \tan^{-1}(f''_{\lambda j,\mathbf{h}}/f'_{\lambda j,\mathbf{h}}) \tag{28}$$

The f′ and f″ are tabulated in International Tables.[88] The phase angles $\phi^n_{1,\mathbf{h}}$ and $\phi^n_{2,\mathbf{h}}$ are the angles associated with $|F^n_{1,\mathbf{h}}|$ and $|F^n_{2,\mathbf{h}}|$, respectively.

Four equations can be formed from (26) by performing anomalous dispersion experiments at two different wavelengths and making measurements of the intensities of reflections associated with $\mathbf{h}$ and $-\mathbf{h}$. The equations are linear if the four quantities, $|F^n_{1,\mathbf{h}}|^2$, $|F^n_{2,\mathbf{h}}|^2$, $|F^n_{1,\mathbf{h}}||F^n_{2,\mathbf{h}}|\cos(\phi^n_{1,\mathbf{h}} - \phi^n_{2,\mathbf{h}})$ and $|F^n_{1,\mathbf{h}}||F^n_{2,\mathbf{h}}|\sin(\phi^n_{1,\mathbf{h}} - \phi^n_{2,\mathbf{h}})$ are chosen as the unknowns. It is worthwhile to add the quadratic relationship, $\sin^2\phi + \cos^2\phi = 1$, and treat the defining equations in a least-squares fashion.

A general analysis[87] has also been carried out which is appropriate for any number and type of anomalous scatterers. This general formulation has a number of favorable characteristics that are illustrated by the simple set of simultaneous equations formed from (26) by using multiple wavelengths and measuring the intensities at $\mathbf{h}$ and $-\mathbf{h}$. The unknown quantities are intensities of scattering and phase differences, all associated with the non-anomalous scattering. The intensities are those that would be obtained from individual types of atoms as if each type were present in isolation from all the rest. Knowledge of the intensities for the structure of an individual type of atom can facilitate the determination of the structure associated with this type of atom. Once this is known, the entire structure can be readily determined. The anomalous scattering enters the simultaneous equations as separate factors in terms of known, tabulated quantities. With appropriate definitions of unknown quantities, the simultaneous equations are linear. It is useful to introduce also quadratic relationships that exist among the unknown phase differences. The systems of simultaneous equations involve no approximations and remain exact for any number or type of anomalous scatterers.

There are some additional features of the equations (26). One concerns the fact that the usual analysis of single-wavelength anomalous scattering leads to the conclusion that there would be a twofold ambiguity in the evaluation of certain phase differences. It has recently been shown[89] that information that is inherent in the measured intensities $|F_{\lambda \mathbf{h}}|^2$ and $|F_{\lambda \bar{\mathbf{h}}}|^2$ that gives approximate information concerning $|F^n_{1,\mathbf{h}}|^2$ and $|F^n_{2,\mathbf{h}}|^2$ can be used with equation (26) for $\mathbf{h}$ and $-\mathbf{h}$ to obtain unique or essentially unique values for the phase differences that occur in (26) with potentially useful accuracy. This was specifically shown for a one-wavelength experiment for the case of one type or one predominant type of anomalously scattering atoms in the presence of essentially non-anomalously scattering atoms. It should be more generally true. *Hauptman*[90] showed earlier the uniqueness of a one-wavelength anomalous dispersion experiment in terms of unique values for triplet phase invariants.

A second feature of equations (26) and their generalization to many kinds of anomalous scatterers concerns the fact that anomalous scatterers in the form of heavy atoms are often substituted into a native substance that scatters essentially non-anomalously. In that case, intensity data for the native material corresponds to $|F^n_{1,\mathbf{h}}|^2$ in (26), thus reducing the number of unknown quantities.

Another type of theoretical study designed to elicit phase information from anomalous dispersion and isomorphous replacement concerns the development of formulas for evaluating the so-called triplet phase invariants. Triplet phase invariants are sums of three phases whose subscripts add to zero, e.g., $\phi_{\mathbf{h}} + \phi_{\mathbf{k}} + \phi_{\bar{\mathbf{h}}+\bar{\mathbf{k}}}$. In general, the sum of subscripts is carried out by attaching the sign associated with the corresponding phase to each subscript, e.g., $\phi_{\mathbf{h}} + \phi_{\mathbf{k}} - \phi_{\mathbf{h}+\mathbf{k}}$ is also an invariant. Note that there are triplet phase invariants in equations (10) and (19) forming the "sum of angles" formula.

Recently, there have been two main approaches to the evaluation of triplet phase invariants from isomorphous replacement and anomalous dispersion data. One involves the use of the mathematics of the joint probability distribution by *Hauptman* for isomorphous replacement[91] and for anomalous dispersion,[90] a similar theory for anomalous dispersion by *Giacovazzo*[92] and a theory for both techniques by *Pontenagel, Krabbendam, Peerdeman* and *Kroon*.[93] A recent investigation by *Fortier, Moore* and *Fraser*[94] of the evaluation of triplet phase invariants for isomorphous replacement when the heavy-atom structure is known indicates the potential of this approach for good accuracy.

A second approach to the evaluation of triplet phase invariants from isomorphous replacement and anomalous dispersion data has interested me for the past few years. It involved initially the development of formulas by use of approximate but simple algebraic manipulations that were based on certain mathematical and physical characteristics of the two techniques.[95,96] This was followed by algebraic analyses[84,97,98] that indicated a potential for good accuracy for many of a large number of formulas proposed.

The development of optimal strategies for the use of triplet phase invariants awaits practical experience. If the heavy-atom (anomalously scattering) substructure is known, there are a number of techniques for obtaining values for individual phases.[84,87,89] In that case, it is quite possible that the triplet phase invariants would be used mainly for phase extension and refinement. In those circumstances when the heavy-atom (anomalously scattering) substructure is not known and resists analysis, the triplet phase invariants may be able to play a primary role in reaching a solution to the structure, since the triplet phase invariants

can be evaluated without knowledge of the substructure.

The enhanced opportunities to carry out multiple-wavelength anomalous dispersion experiments with high intensity and tunable synchrotron X-ray sources should facilitate the development of applications of the new theoretical formulations. Coupled with the major advances in computing, the new theories have the potential to improve the facility with which macromolecular structure research is performed.

Received: January 30, 1986 [A 582 IE]
German version: *Angew. Chem. 98* (1986) 611

[1] H. Ott, *Z. Kristallogr. Kristallgeom. Kristallphys. Kristallchem. 66* (1928) 136.
[2] K. Banerjee, *Proc. R. Soc. London Ser. A 141* (1933) 188.
[3] M. Avrami, *Phys. Rev. 54* (1938) 300.
[4] A. L. Patterson, *Phys. Rev. 46* (1934) 372.
[5] A. L. Patterson, *Z. Kristallogr. Kristallgeom. Kristallphys. Kristallchem. 90* (1935) 517.
[6] W. Hoppe, *Z. Elektrochem. 61* (1957) 1076.
[7] C. E. Nordman, K. Nakatsu, *J. Am. Chem. Soc. 85* (1963) 353.
[8] R. Huber, W. Hoppe, *Chem. Ber. 98* (1965) 2403.
[9] D. Harker, J. S. Kasper, *Acta Crystallogr. 1* (1948) 70.
[10] J. S. Kasper, C. M. Lucht, D. Harker, *Acta Crystallogr. 3* (1950) 436.
[11] J. Gillis, *Acta Crystallogr. 1* (1948) 174.
[12] I. L. Karle, J. Karle, *J. Chem. Phys. 17* (1949) 1052.
[13] J. Karle, I. L. Karle, *J. Chem. Phys. 18* (1950) 957.
[14] I. L. Karle, J. Karle, *J. Chem. Phys. 18* (1950) 963.
[15] H. Hauptman, J. Karle, *Phys. Rev. 77* (1950) 491.
[16] L. S. Bartell, L. O. Brockway, *Phys. Rev. 90* (1953) 833.
[17] O. Toeplitz, *Rend. Circ. Mat. Palermo* (1911) 191.
[18] J. Karle, H. Hauptman, *Acta Crystallogr. 3* (1950) 181.
[19] J. Karle, *Acta Crystallogr. Sect. B 27* (1971) 2063.
[20] H. Hauptman, J. Karle, *Acta Crystallogr. 5* (1952) 48.
[21] J. Karle, H. Hauptman, *Acta Crystallogr. 6* (1953) 131.
[22] H. Hauptman, J. Karle, *Acta Crystallogr. 6* (1953) 136.
[23] H. Hauptman, J. Karle, *Solution of the Phase Problem I. The Centrosymmetric Crystal (Am. Crystallogr. Assoc. Monogr. 3)* (1953).
[24] I. L. Karle, J. Karle, *Acta Crystallogr. 17* (1964) 835.
[25] U. Shmueli, G. H. Weiss, J. E. Kiefer, A. J. C. Wilson, *Acta Crystallogr. Sect. A 40* (1984) 651.
[26] J. M. Stewart, J. Karle, *Acta Crystallogr. Sect. A 32* (1976) 1005.
[27] J. Karle, H. Hauptman, C. L. Christ, *Acta Cystallogr. 11* (1958) 757.
[28] A. J. C. Wilson, *Nature (London) 150* (1942) 151.
[29] A. J. C. Wilson, *Acta Crystallogr. 2* (1949) 318.
[30] M. M. Woolfson, *Acta Crystallogr. 7* (1954) 61.
[31] W. Cochran, M. M. Woolfson, *Acta Crystallogr. 8* (1955) 1.
[32] J. Karle, I. L. Karle, *Acta Crystallogr. 21* (1966) 849.
[33] G. N. Watson: *Theory of Bessel Functions*, Cambridge University Press, Cambridge 1945.
[34] W. Cochran, *Acta Crystallogr. 8* (1955) 473.
[35] J. Karle, H. Hauptman, *Acta Crystallogr. 9* (1956) 635.
[36] I. L. Karle, J. Karle, *Acta Crystallogr. 16* (1963) 969.
[37] I. L. Karle, K. S. Dragonette, S. A. Brenner, *Acta Crystallogr. 19* (1965) 713.
[38] J. Karle in J. A. Ibers, W. Hamilton (Eds.): *International Tables for X-ray Crystallography, Vol. IV*, The Kynoch Press, Birmingham 1974, pp. 337–358.
[39] J. Karle, *Acta Crystallogr. Sect. B 24* (1968) 182.
[40] P. Tollin, *Acta Crystallogr. 21* (1966) 613.
[41] R. A. Crowther, D. M. Blow, *Acta Crystallogr. 23* (1967) 544.
[42] J. Karle, *Acta Crystallogr. Sect. B 28* (1972) 820.
[43] D. A. Langs, *Acta Crystallogr. Sect. A 41* (1985) 578.
[44] W. H. Zachariasen, *Acta Crystallogr. 5* (1952) 68.
[45] I. M. Rumanova, *Dokl. Akad. Nauk SSSR 98* (1954) 399.
[46] W. Cochran, A. S. Douglas, *Proc. R. Soc. London Ser. A 227* (1955) 486.
[47] D. Sayre, *Acta Crystallogr. 5* (1952) 60.
[48] F. R. Ahmed, S. R. Hall, C. P. Huber (Eds.): *Crystallographic Computing*, Munksgaard, Copenhagen 1970.
[49] F. R. Ahmed, K. Huml, B. Sedlacek (Eds.): *Crystallographic Computing Techniques*, Munksgaard, Copenhagen 1976.
[50] R. Diamond, S. Ramaseshan, K. Venkatesan (Eds.): *Computing in Crystallography*, Indian Academy of Sciences, Bangalore 1980.
[51] D. Sayre (Ed.): *Computational Crystallography*, Clarendon Press, Oxford 1982.
[52] S. R. Hall, T. Ashida (Eds.): *Methods and Applications in Crystallographic Computing*, Clarendon Press, Oxford 1984.
[53] C. L. Christ, J. R. Clark, H. T. Evans Jr., *Acta Crystallogr. 7* (1954) 453.
[54] C. L. Christ, J. R. Clark, *Acta Crystallogr. 9* (1956) 830.
[55] I. L. Karle, H. Hauptman, J. Karle, A. B. Wing, *Acta Crystallogr. 11* (1958) 257.
[56] I. L. Karle, *Acta Crystallogr. 14* (1961) 497.
[57] I. L. Karle, J. Karle, *Acta Crystallogr. Sect. B 24* (1968) 81.
[58] I. L. Karle, J. Karle, *Acta Crystallogr. Sect. B 25* (1969) 428.
[59] R. D. Gilardi, *Acta Crystallogr. Sect. B 26* (1970) 440.
[60] T. Tokuyama, J. Daly, B. Witkop, *J. Am. Chem. Soc. 91* (1969) 3931.
[61] J. W. Daly, I. Karle, C. W. Myers, T. Tokuyama, J. A. Waters, B. Witkop, *Proc. Natl. Acad. Sci. USA 68* (1971) 1870.
[62] I. L. Karle, *J. Am. Chem. Soc. 95* (1973) 4036.
[63] T. Tokuyama, K. Uenoyama, G. Brown, J. W. Daly, B. Witkop, *Helv. Chim. Acta 57* (1974) 2597, and references cited therein.
[64] I. L. Karle, J. Karle, *Acta Crystallogr. 17* (1964) 1356.
[65] J. W. Mitchell, N. Mandava, J. F. Worley, J. R. Plimmer, N. V. Smith, *Nature (London) 225* (1970) 1065.
[66] N. Mandava, M. Kozempel, J. F. Worley, D. Matthews, J. D. Warthen, Jr., N. Jacobson, G. L. Steffens, H. Kenny, M. D. Grove, *Ind. Eng. Chem. Prod. Res. Dev. 17* (1978) 351.
[67] M. D. Grove, G. F. Spencer, W. K. Rohwedder, N. Mandava, J. F. Worley, J. D. Warthen, Jr., G. L. Steffens, J. L. Flippen-Anderson, J. C. Cook, Jr., *Nature (London) 281* (1979) 216.
[68] B. Witkop, E. Gössinger in A. Brossi (Ed.): *The Alkaloids, Vol. XXI*, Academic Press, New York 1983, pp. 139–254.
[69] J. W. Daly in W. Herz, H. Grisebach, G. W. Kirby: *Progress in the Chemistry of Organic Natural Products, Vol. 41*, Springer, New York 1982, pp. 206–340.
[70] O. Yonemitsu, Y. Okuno, Y. Kanaoka, I. L. Karle, B. Witkop, *J. Am. Chem. Soc. 90* (1968) 6522.
[71] I. L. Karle, J. W. Gibson, J. Karle, *Acta Crystallogr. Sect. B 25* (1969) 2034.
[72] D. S. Jones, I. L. Karle, *Acta Crystallogr. Sect. B 30* (1974) 617.
[73] T. Iwakuma, H. Nakai, O. Yonemitsu, D. S. Jones, I. L. Karle, B. Witkop, *J. Am. Chem. Soc. 94* (1972) 5136.
[74] I. L. Karle, *Acta Crystallogr. Sect. B 38* (1982) 1022.
[75] J. Hughes, T. W. Smith, H. W. Kosterlitz, L. A. Fothergill, B. A. Morgan, H. R. Morris, *Nature (London) 258* (1975) 577.
[76] I. L. Karle, J. Karle, D. Mastropaolo, A. Camerman, N. Camerman, *Acta Crystallogr. Sect. B 39* (1983) 625.
[77] G. Wald, *Nature (London) 219* (1968) 800.
[78] R. Gilardi, W. Sperling, I. L. Karle, J. Karle, *Nature (London) 232* (1971) 187.
[79] R. D. Gilardi, I. L. Karle, J. Karle, *Acta Crystallogr. Sect. B 28* (1972) 2605.
[80] T. Hamanaka, T. Mitsui, T. Ashida, M. Kakudo, *Acta Crystallogr. Sect. B 28* (1972) 214.
[81] B. Honig, M. Karplus, *Nature (London) 229* (1971) 558.
[82] I. L. Karle, *Proc. Natl. Acad. Sci. USA 82* (1985) 7155.
[83] S. Ramaseshan, S. C. Abrahams (Eds.): *Anomalous Scattering*, Munksgaard, Copenhagen 1975.
[84] J. Karle, *Acta Crystallogr. Sect. A 42* (1986) 246.
[85] J. M. Bijvoet, *Nature (London) 173* (1954) 888.
[86] W. A. Hendrickson, M. Teeter, *Nature (London) 290* (1981) 107.
[87] J. Karle, *Int. J. Quantum Chem. Quantum Biol. Symp. 7* (1980) 357.
[88] D. T. Cromer in J. A. Ibers, W. Hamilton (Eds.): *International Tables for X-ray Crystallography, Vol. IV*, The Kynoch Press, Birmingham 1974, pp. 148–151.
[89] J. Karle, *Acta Crystallogr. Sect. A 41* (1985) 387.
[90] H. Hauptman, *Acta Crystallogr. Sect. A 38* (1982) 632.
[91] H. Hauptman, *Acta Crystallogr. Sect. A 38* (1982) 289.
[92] C. Giacovazzo, *Acta Crystallogr. Sect. A 39* (1983) 585.
[93] W. M. G. F. Pontenagel, H. Krabbendam, A. F. Peerdeman, J. Kroon, *Eighth Eur. Crystallogr. Meet. August 8–12, 1983 Abstract 4.01P*, p. 257.
[94] S. Fortier, N. J. Moore, M. E. Fraser, *Acta Crystallogr. Sect. A 41* (1985) 571.
[95] J. Karle, *Acta Crystallogr. Sect. A 39* (1983) 800.
[96] J. Karle, *Acta Crystallogr. Sect. A 40* (1984) 374.
[97] J. Karle, *Acta Crystallogr. Sect. A 40* (1984) 526.
[98] J. Karle, *Acta Crystallogr. Sect. A 41* (1985) 182.

When submitting manuscripts, authors of articles intended for publication as "Communications" are requested to read the "Notice to Authors" reproduced in the January issue of the journal following the list of contents; upon request, a copy can be obtained from the editorial office.

Synthesis and Properties of 1,3,5,7-Tetra-*tert*-butyl-*s*-indacene**

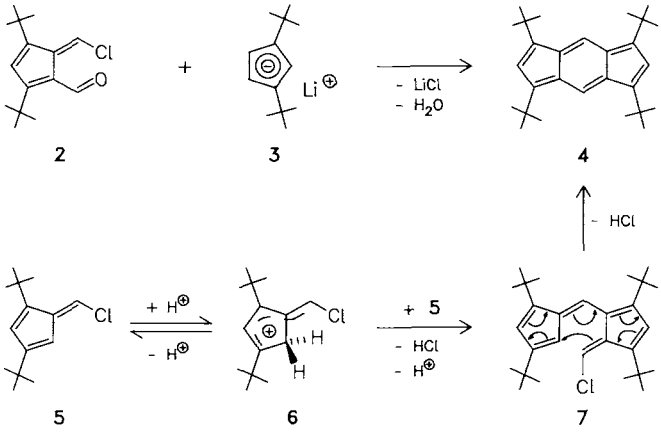
By *Klaus Hafner,* Bernd Stowasser, Hans-Peter Krimmer, Stefanie Fischer, Michael C. Böhm,* and *Hans Jörg Lindner*

According to quantum chemical calculations (MINDO/3 method) on *s*-indacene **1**[1]—a [12]annulene perturbed by two σ-bonds—substituents can be expected to have a strong influence on the bonding situation of the 12π perimeter. The enthalpy of formation for the localized structure **1A** with C_{2h}-symmetry and the corresponding structure of the 2,4,6,8-tetraalkyl derivatives is calculated ca. 10 kcal·mol^{-1} less than that for the delocalized structure **1B**



with D_{2h}-symmetry. For the 1,3,5,7-tetraalkyl-*s*-indacenes this energy gap should only be 2 kcal·mol^{-1}, whereas in the case of 4,8-diamino-*s*-indacenes a completely delocalized π-electron system should be preferred. Even nitrile groups in the 2- and 6-position can be expected to lower the energy difference between **1A** and **1B** to ca. 6 kcal·mol^{-1}. A similarly significant alkyl group effect, changing the bonding situation of the 12π perimeter of **1**, has so far never been reported in the case of other [4n]-π-electron systems. This effect is due to enhanced coupling between the π-electron system and the substituents in the case of the delocalized structure **1B**. The quantum chemical predictions could be experimentally established in the case of the stable 4,8-bis(dimethylamino)-*s*-indacene and the 4-dimethylamino-2,6,8-tri-*tert*-butyl derivative.[2,3] These results encouraged us to check the calculations also for pure alkyl derivatives of **1**, to gain more detailed information about the 12π-electron system. 1,3,5,7-Tetra-*tert*-butyl-*s*-indacene **4** seemed to be especially suitable for this purpose since it should be additionally stabilized kinetically by the bulky alkyl groups compared to the thermally extremely unstable **1**.[1]

In analogy to the synthesis of 4,8-bis(dimethylamino)-*s*-indacene, **4** can be obtained as red needles (decomp. 190°C; yield 30%)[3] by reaction of 2,4-di-*tert*-butyl-6-chloro-1-formylpentafulvene **2**[4] with lithium 1,3-di-*tert*-butylcyclopentadienide **3**[5] (CH_2Cl_2, 0°C). Recently we found an even more simple and rational entry to **4**, namely the protic acid-catalyzed condensation of 1,3-di-*tert*-butyl-6-chloropentafulvene **5**[6] in boiling methanol. The cation **6** formed on reversible protonation could be combined with **5** to give the 6-chloro-1-(6-pentafulvenyl)pentafulvene derivative **7**, whose 12π-electrocyclization with subsequent elimination of HCl led to **4** in 90% yield. Solid **4** is thermally stable as well as air-stable, but in solution it is extremely sensitive towards oxygen and traces of acid.[7]



The signals of the ring protons in the simple ^{1}H-NMR spectrum of **4** (see Table 1) are shifted to higher field in comparison to those of the dihydro derivative **9** ($\Delta\delta = 0.66$–0.81). This indicates a weak antiaromatic character of the *s*-indacene system. The ^{13}C-NMR spectrum, with four signals for the twelve perimeter C-atoms shows no temperature-dependence of the line shapes down to −130°C (in CS_2/COS (1 : 1)).[8] This suggests that either—in agreement with quantum chemical calculations—there is a low energy barrier between the two π-bond isomers, or the π-electron system is delocalized.

The crystal structure analysis of **4** at room temperature (see Fig. 1) gives CC-bond lengths for the perimeter that

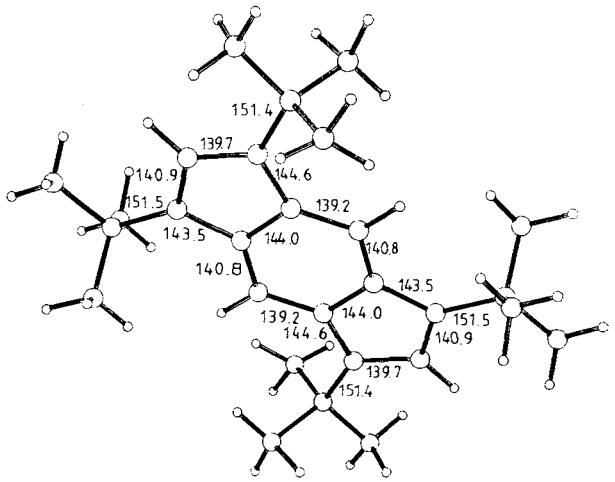


Fig. 1. Structure of **4** in the crystal at room temperature; bond lengths in pm (standard deviations $\sigma_r = 0.5$ pm). [10]

[*] Prof. Dr. K. Hafner, Dipl.-Ing. B. Stowasser, Dr. H.-P. Krimmer, S. Fischer, Dr. M. C. Böhm, Prof. Dr. H. J. Lindner
Institut für Organische Chemie der Technischen Hochschule
Petersenstrasse 22, D-6100 Darmstadt (FRG)

[**] This work was supported by the Deutsche Forschungsgemeinschaft, the Fonds der Chemischen Industrie, and the Dr.-Otto-Röhm-Gedächtnisstiftung.

are consistent with a delocalized state. However, as in the case of tetra-*tert*-butylcyclobutadiene,[9] an unequivocal proof of the structure can only be expected from a diffraction experiment at low temperatures.

An electronic spectrum calculated for the localized structure of **4** according to a modified INDO variant[11] (CI method) is in good agreement with the measured data (see Table 1).[12]

Table 1. Spectral data of the compounds **4**, **8**–**10**, and **13**–**15**. ^{1}H-NMR ($CDCl_3$, 300 MHz), ^{13}C-NMR ($CDCl_3$, 75.47 MHz), UV (*n*-hexane).

4: ^{1}H-NMR: $\delta = 1.18$ (s; 36 H, 4 *t*Bu), 5.29 (s; 2 H, 2,6-H), 6.90 (s; 2 H, 4,8-H); ^{13}C-NMR: $\delta = 31.2$ (q; *t*Bu), 34.0 (s; *t*Bu), 124.9 (d; C-2,6 or C-4,8), 129.1 (d; C-2,6 or C-4,8), 132.0 (s; C-3a,4a,7a,8a), 164.3 (s; C-1,3,5,7); UV: λ_{max} (lg ε) = 224 (4.10), 234 (4.03) sh, 278 (4.23) sh, 284 (4.37) sh, 289 (4.48) sh, 294 (4.61), 301 (4.66), 307 (4.77), 330 (3.45) sh, 340 (3.48), 451 (3.41) sh, 486 (3.83) sh, 500 (3.96) sh, 505 (4.01), 519 (4.11) sh, 527 (4.26) sh, 539 (4.51) sh, 545 nm (4.64)

8: ^{1}H-NMR: $\delta = 0.94$ (s; 9 H, *t*Bu), 1.00 (s; 9 H, *t*Bu), 1.26 (s; 3 H, Me), 1.36 (s; 9 H, *t*Bu), 1.38 (s; 9 H, *t*Bu), 3.09 (d, $J = 2.0$ Hz; 1 H, 7-H), 6.04 (s; 1 H, 2-H), 6.11 (d, $J = 2.0$ Hz; 1 H, 6-H), 7.53 (s; 1 H, 8-H), 7.66 (s; 1 H, 4-H); UV: λ_{max} (lg ε) = 230 (4.17) sh, 237 (4.43), 245 (4.65), 254 (4.64), 274 (3.64), 284 (3.63), 296 (3.60), 302 (3.53) sh, 308 (3.56), 313 (3.38) sh, 322 nm (3.27)

9: ^{1}H-NMR: $\delta = 0.67$ (d, $J = 6.7$ Hz; 3 H, Me), 1.22 (s; 9 H, *t*Bu), 1.29 (s; 9 H, *t*Bu), 1.30 (s; 9 H, *t*Bu), 1.32 (s; 9 H, *t*Bu), 3.40 (br. d, $J = 4.5$ Hz; 1 H, 3a-H), 3.89 (qd, $J_1 = 6.7$ Hz; $J_2 = 4.5$ Hz; 1 H, 4-H), 6.10 (s; 1 H, 6-H), 6.36 (d, $J = 1.2$ Hz; 1 H, 2-H), 7.56 (s; 1 H, 8-H); UV: λ_{max} (lg ε) = 235 (3.95), 241 (3.95), 286 (3.20) sh, 386 (4.30), 471 nm (2.76) sh

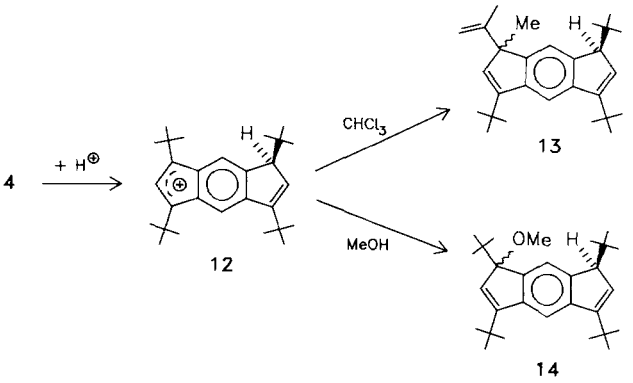
10: ^{1}H-NMR: $\delta = 1.01$ (s; 18 H, 2 *t*Bu), 1.40 (s; 18 H, 2 *t*Bu), 3.09 (d, $J = 1.9$ Hz; 2 H, 1,7-H), 6.13 (d, $J = 1.9$ Hz; 2 H, 2,6-H), 7.67 (s; 1 H, 4-H or 8-H), 7.73 (s; 1 H, 4-H or 8-H); UV: λ_{max} (lg ε) = 223 (4.06) sh, 230 (4.19) sh, 236 (4.43) 245 (4.61), 253 (4.55), 286 (3.82), 290 (3.82), 296 (3.84), 301 (3.78) sh, 307 (3.68) sh, 312 (3.53) sh, 321 nm (3.17)

13: ^{1}H-NMR: $\delta = 0.97$ (s; 9 H, *t*Bu), 1.38–1.40 (24 H, 2 *t*Bu, 2 Me), 3.10 (d, $J = 2.0$ Hz; 1 H, 7-H), 4.90 (m; 1 H, $=CH_2$), 5.10 (m; 1 H, $=CH_2$), 5.86 (s; 1 H, 2-H), 6.13 (d, $J = 2.0$ Hz; 1 H, 6-H), 7.32 (s; 1 H, 8-H), 7.70 (s; 1 H, 4-H); UV: λ_{max} (lg ε) = 229 (4.02) sh, 237 (4.26), 244 (4.49), 253 (4.50), 268 (3.50) sh, 278 (3.46) sh, 283 (3.43) sh, 296 (3.38), 301 (3.29) sh, 308 (3.40), 313 (3.14) sh, 321 nm (320)

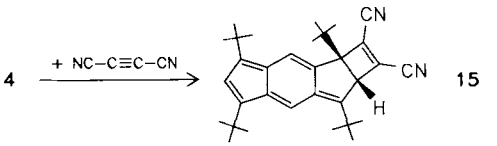
14: ^{1}H-NMR: $\delta = 0.99$ (s; 9 H, *t*Bu), 1.00 (s; 9 H, *t*Bu), 1.37 (s; 9 H, *t*Bu), 1.39 (s; 9 H, *t*Bu), 2.92 (s; 3 H, OMe), 3.09 (d, $J = 2.0$ Hz; 1 H, 7-H), 5.84 (s; 1 H, 2-H), 6.15 (d, $J = 2.0$ Hz; 1 H, 6-H), 7.48 (s; 1 H, 8-H), 7.60 (s; 1 H, 4-H); UV: λ_{max} (lg ε) = 227 (4.07) sh, 233 (4.23) sh, 240 (4.44), 248 (4.67), 257 (4.68), 281 (3.38), 288 (3.37) sh, 300 (3.27), 312 (3.20), 326 nm (3.03)

15: ^{1}H-NMR: $\delta = 1.12$ (s; 9 H, *t*Bu), 1.33 (s; 18 H, *t*Bu), 1.49 (s; 9 H, *t*Bu), 4.64 (s; 1 H, 2a-H), 6.41 (s; 1 H, 6-H), 7.31 (s; 1 H, 8-H), 7.74 (s; 1 H, 4-H); ^{13}C-NMR: $\delta = 26.0$–35.5 (*t*Bu), 60.5 ($C_{tert.}$), 67.4 ($C_{quart.}$), 111.2, 111.6 (C≡N), 121.4, 123.2 ($C_{tert.}$), 124.1, 129.5, 130.4 ($C_{quart.}$), 130.7 ($C_{tert.}$), 134.0, 137.8, 145.0, 145.4, 148.4, 155.3 ($C_{quart.}$); UV: $\lambda_{max} = 227$, 234 sh, 258 sh, 289, 308 sh, 358 sh, 369, 564, 582 sh, 650 nm sh

In its reaction with nucleophilic partners, **4** behaves—with exception of the formation of **9**—similarly to the 4,8-bis(dimethylamino)-*s*-indacene derivatives,[3] but contrary to these it is incapable of reversible protonation or Michael addition to electron-deficient alkynes. Whereas the addition of methyllithium (ether, 25 °C) leads to formation of 1,3,5,7-tetra-*tert*-butyl-1-methyl-1,7-dihydro-*s*-indacene **8** (colorless crystals, m.p. 200 °C; yield 46%) and its isomer **9** (brown crystals, m.p. 125 °C; yield 20%), the reduction with $LiAlH_4$ (tetrahydrofuran, 25 °C) gives 1,3,5,7-tetra-*tert*-butyl-1,7-dihydro-*s*-indacene **10** as major product along with 15% of the isomer **11** (both colorless crystals, subl. 218 °C). Protonation of **4** with methanesulfonic acid at room temperature affords the indenyl cation **12**,[13]



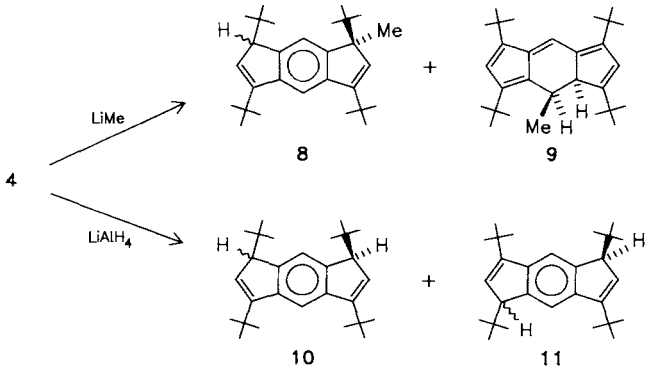
which rapidly undergoes a Wagner-Meerwein rearrangement in $CHCl_3$ to **13** (colorless crystals, m.p. 152 °C; yield 43%). In methanolic solution **12** can be trapped as the methyl ether **14** (colorless crystals, m.p. 195 °C; yield 62%). In boiling benzene, **4** combines with dicyanoacetylene to give



the [12+2]-cycloadduct **15** (blue powder, decomp. 40 °C; yield 9%), whose ring opening to the corresponding cyclohepta[*f*]indene has so far not been accomplished.

Received: February 20, 1986 [Z 1675 IE]
German version: *Angew. Chem. 98* (1986) 646

CAS Registry numbers:
2, 101998-69-0; **3**, 101998-78-1; **4**, 101998-70-3; **5**, 85655-87-4; **8**, 101998-71-4; **9**, 101998-72-5; **10**, 101998-73-6; **11**, 101998-74-7; **13**, 101998-75-8; **14**, 101998-76-9; **15**, 101998-77-0; NCC≡CCN, 1071-98-3.



[1] K. Hafner, *Angew. Chem. 75* (1963) 1041; *Angew. Chem. Int. Ed. Engl. 3* (1964) 165; *Pure Appl. Chem. Suppl. 2* (1971) 1.
[2] K. Hafner, H.-P. Krimmer, *Angew. Chem. 92* (1980) 202; *Angew. Chem. Int. Ed. Engl. 19* (1980) 199.
[3] K. Hafner, *Pure Appl. Chem. 54* (1982) 939.
[4] H.-P. Krimmer, *Dissertation*, Technische Hochschule Darmstadt 1983.
[5] L. Knothe, H. Prinzbach, E. Hädicke, *Chem. Ber. 114* (1981) 1656.
[6] H.-P. Krimmer, B. Stowasser, K. Hafner, *Tetrahedron Lett. 23* (1982) 5135; K. Hafner, H.-P. Krimmer, B. Stowasser, *Angew. Chem. 95* (1983) 496; *Angew. Chem. Int. Ed. Engl. 22* (1983) 490.
[7] The data on the stability of **4** in [3] refer to solutions in organic solvents.
[8] We thank Prof. *K. Müllen*, Mainz, for recording the low-temperature ^{13}C-NMR spectra of **4**.
[9] H. Irngartinger, M. Nixdorf, *Angew. Chem. 95* (1983) 415; *Angew. Chem. Int. Ed. Engl. 22* (1983) 403.

[10] 4: Monoclinic, space group $P2_1/c$, $Z=2$, $a=982.8(1)$, $b=1186.6(1)$, $c=1222.0(1)$ pm, $\beta=121.92(1)°$, $V=1.209\times10^9$ pm^3, $\rho_{calc}=1.142$ g/cm^3; $3°<2\theta<40°$ ($Mo_{K\alpha}$, $\lambda=71.07$ pm), 1052 independent reflections, Lorentz and polarization corrections, molecule at crystallographic inversion center, position of the hydrogen atoms calculated according to ideal geometry and optimized, anisotropic refinement of the carbon atoms, $R=0.070$, $R_w=0.048$ for 1048 structure factors ($|F|_0>0$). Further details of the crystal structure investigation are available on request from the Fachinformationszentrum Energie, Physik, Mathematik GmbH, D-7514 Eggenstein-Leopoldshafen 2 (FRG) on quoting the depository number CSD-51911, the names of the authors, and the full citation of the journal.

[11] M. C. Böhm, R. Gleiter, *Theor. Chim. Acta 59* (1981) 127; calculated singlet-electron transitions of **4**: λ_{max}(oscillator strength) = 525 (0.15), 380 (0.02), 320 (0.36), 299 (0.75), 273 (0.07), 269 (0.27), 264 nm (0.30).

[12] T. Nakajima, T. Saijo, H. Yamaguchi, *Tetrahedron 20* (1964) 2119.

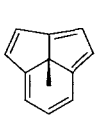
[13] Deuteration experiments show that **4** is protonated in the 2-position and the resulting cation then rapidly rearranges to **12**.

9b-Methyl-9b*H*-benzo[*cd*]azulene—A Novel Antiaromatic 12π-Electron System**

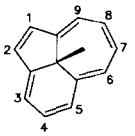
By *Klaus Hafner** and *Volker Kühn*

Dedicated to Professor Edgar Heilbronner on the occasion of his 65th birthday

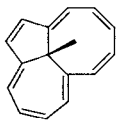
Of the hitherto reported cyclic conjugated 12π-electron systems, only 1,7-methano-[12]annulene[1] allows conclusions to be drawn about the expected antiaromaticity of the planar 12π perimeter, since [12]annulene[2] and 1,6-methano-[12]annulene[3] are conformationally mobile and the π-perimeters deviate considerably from the planar geometry. In cycl[3.3.3]azine (9b-azaphenalene) and cycl[4.3.2]-azine[4] the properties of the perimeters are influenced by electronic interactions with the central nitrogen atom. Contrary to singly bridged annulenes multiple bridging of the perimeter should result in an increased planarity due to less transannular interactions and therefore allow a substantial delocalization of the peripheral π-electron system. In the case of the 10π-perimeter this expectation was confirmed by *Rees* et al.[5] with the synthesis of 7b-methyl-



1



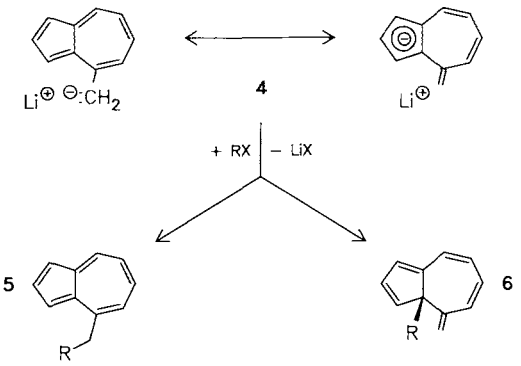
2



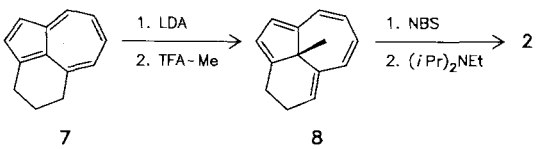
3

7b*H*-cyclopenta[*cd*]indene **1**. An unexpected reaction of 4-alkylideneazulenide salts **4** with electrophiles recently opened up a simple access to 9b-methyl-9b*H*-benzo[*cd*]-azulene **2**, the first tricyclic [12]annulene,[6] which proves to be an antiaromatic [12]annulene *par excellence* among the 12π-electron systems. At the same time, **2** fills the gap between the tricyclic annulenes **1** and **3**.[7]

Whereas reaction of the resonance-stabilized lithium 4-methyleneazulenide **4**[8] with primary alkyl halides in diethyl ether affords exclusively the 4-alkylazulenes **5**, reactions with *sec*- and *tert*-alkyl halides as well as with dimethyl sulfate or methyl trifluoromethanesulfonate (TFA-Me) lead chiefly to 3a-alkyl-3a,4-dihydro-4-methyleneazulenes **6** and small amounts of **5**, with removal of the azulenoid 10π-electron system.[9] The different regiochemical course of these reactions could be due to competing substitution mechanisms (S_N, SET).[10]



Also 4,5-dihydro-3*H*-benz[*cd*]azulene **7**,[11] after deprotonation with lithium diisopropylamide (LDA), reacts, like **4**, with dimethyl sulfate or TFA-Me to give the tricyclic pentaene **8** (yellow oil, yield 52%).[12] Bromination of **8**



with *N*-bromosuccinimide (NBS) in CCl_4 at 0°C yields an unstable bromo-derivative (yellow, oil), which is dehydrobrominated to **2** with diisopropylethylamine in tetrahydrofuran at room temperature without further purification. Thereby, the blue hydrocarbon **2** is obtained in ca. 30% yield; **2** is stable in solution up to 80°C. Solid **2** rapidly transforms into yellow high molecular products, even at −30°C.

Table 1. Spectral data of **2**, **8**, and **9**.

2A: 300-MHz ^{1}H-NMR ([D$_6$]DMSO): $\delta=3.88$ (d, $J=7.1$ Hz; 1H, 6-H), 3.98 (d, $J=5.8$ Hz; 1H, 3-H), 4.01 (d, $J=9.5$ Hz; 1H, 5-H), 4.18 (d, $J=6.7$ Hz; 1H, 9-H), 4.27–4.41 (m: $\delta=4.30$ (7-H), 4.37 (8-H), 4.39 (4-H)), 4.67, 4.69 (AB system, $J=5.8$ Hz; 2H, 1,2-H), 4.75 (s; 3H, Me); UV (*n*-hexane) (qualitative): $\lambda_{max}=262$, 286, 351, 368, 387 sh, 491 sh, 559 sh, 567 nm

8: 300-MHz ^{1}H-NMR ($CDCl_3$): $\delta=0.76$ (s; 3H, Me), 2.42–2.56 (m; 2H, 3-H), 2.81–2.93 (m; 2H, 4-H), 5.86–6.05 (m; 4H, 6-H or 9-H and 5,7,8-H), 6.18 (dd, $J=1.7$ Hz, $J=2.0$ Hz; 1H, 2-H), 6.43 (d, $J=1.7$ Hz; 1H, 1-H), 6.66 (d, $J=10.7$ Hz; 1H, 6-H or 9-H); UV (*n*-hexane): λ_{max}(lgε) = 262 (4.25), 266 (4.25), 289 sh (3.23), 304 sh (3.04), 350 sh (3.39), 370 sh (3.53), 384 (3.59), 402 sh (3.45) nm

9: 300-MHz ^{1}H-NMR ([D$_6$]DMSO): $\delta=1.07$ (s; 3H, Me), 5.87 (d, $J=10.4$ Hz; 1H, 9-H), 6.15 (dd, $J=6.5$ Hz, $J=10.4$ Hz; 1H, 8-H), 6.44 (dd, $J=6.5$ Hz, $J=11.5$ Hz; 1H, 7-H), 6.71 (d, $J=5.5$ Hz; 1H, 1-H), 6.79 (d, $J=5.5$ Hz; 1H, 2-H), 7.03 (d, $J=11.5$ Hz; 1H, 6-H), 7.20 (dd, $J=1.1$ Hz, $J=7.7$ Hz; 1H, 3-H or 5-H), 7.28 (dd, $J=7.1$ Hz, $J=7.7$ Hz; 1H, 4-H), 7.44 (dd, $J=1.1$ Hz, $J=7.1$ Hz; 1H, 3-H or 5-H); UV (*n*-hexane): λ_{max}(lgε) = 211 (4.12), 257 (4.34), 265 (4.38), 375 (3.61) nm

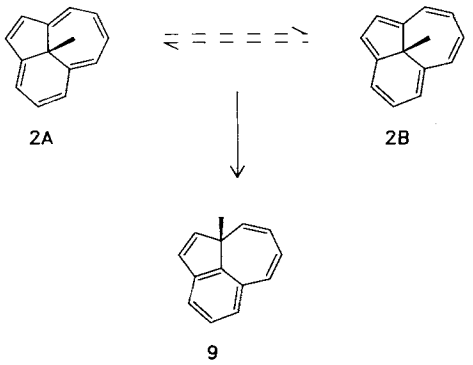
Proof of the structure of **2** is provided, in particular, by its ^{1}H-NMR spectrum[13] (see Table 1), which, at the same time, provides interesting insights into the bonding structure of this [12]annulene, which according to model considerations has a rigid planar structure. From the spec-

[*] Prof. Dr. K. Hafner, Dipl.-Ing. V. Kühn
Institut für Organische Chemie der Technischen Hochschule
Petersenstrasse 22, D-6100 Darmstadt (FRG)

[**] This work was supported by the Deutsche Forschungsgemeinschaft, the Fonds der Chemischen Industrie, and the Dr.-Otto-Röhm-Gedächtnisstiftung, Darmstadt.

trum, which is temperature-independent up to 80°C, the structure of the π-bond isomer **2A** could be deduced on the basis of the coupling constant $J = 5.8$ Hz for the AB system of 1 H and 2 H and the vicinal coupling constants of 3-H, 5-H, 6-H, and 9-H. In comparison to the spectrum of the dihydro derivative **8**, in the spectrum of **2** the signals of the central methyl group and of the peripheral ring protons appear in the opposite sequence. The signals of the perimeter protons exhibit a strong upfield shift of about 2 ppm in the range $\delta = 3.88$–4.69, whereas the methyl group singlet experiences a substantial downfield shift of about 4 ppm to $\delta = 4.75$. The extremely high-field resonances of the ring protons of **2** compared to the ^{1}H-NMR shifts of the perimeter protons of [12]annulene ($\delta = 5.91$), 1,7-methano[12]annulene ($\delta = 5.1$–5.8) and 1,6-methano[12]annulene ($\delta = 5.50$–6.17) are consistent with a pronounced paramagnetic ring current in the 12π-perimeter of **2**.

The electronic spectrum of **2** (see Table 1), like those of the mono- and bicyclic [12]annulenes and the dehydro[12]annulenes,[14] shows a strong absorption in the region of 260 nm and, in contrast to these, an additional long-wave absorption at 567 nm. The absorption corresponds to the singlet-electron transitions calculated by *Lindner*[15a] for the localized 12π-electron system **2A**.



According to π-SCF force field calculations,[15b] the standard enthalpies of formation of **2A** and **2B** should be about the same, and the activation enthalpies for the π-bond shift should be more than 25 kcal·mol^{-1}. However, contrary to expectations based on these calculations, isomer **2B** was not detected. Hence, the equilibrium may lie further to the side of **2A** than predicted by the calculations, or a higher barrier between **2A** and **2B** is involved. At elevated temperatures a, presumably sigmatropic, methyl-group shift takes place in **2** — as is found in the case of **1**;[5] the 9a-methyl-9a*H*-benz[*cd*]azulene **9** (yellow oil) having a benzenoid partial structure is formed. In contrast to **1**, this isomerization already occurs at 80°C (in dimethyl sulfoxide) in case of **2**, and proceeds quantitatively within 15 min in boiling xylene.

Received: February 20, 1986 [Z 1676 IE]
German version: *Angew. Chem. 98* (1986) 648

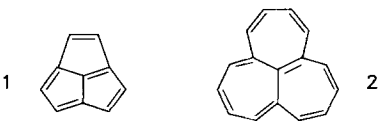
CAS Registry numbers:
7, 101998-44-1; **8**, 101998-45-2; **2**, 101998-46-3; **9**, 101998-47-4.

[1] E. Vogel, H. Königshofen, K. Müllen, J. F. M. Oth, *Angew. Chem. 86* (1974) 229; *Angew. Chem. Int. Ed. Engl. 13* (1974) 281.
[2] J. F. M. Oth, H. Röttele, G. Schröder, *Tetrahedron Lett. 1970*, 61; J. F. M. Oth, J.-M. Gilles, G. Schröder, *ibid. 1970*, 67.
[3] E. Vogel, M. Mann, Y. Sakata, K. Müllen, J. F. M. Oth, *Angew. Chem. 86* (1974) 231; *Angew. Chem. Int. Ed. Engl. 13* (1974) 283.
[4] D. Farquhar, T. T. Gough, D. Leaver, *J. Chem. Soc. Perkin Trans. 1 1976*, 341, and references cited therein; W. Flitsch, A. Gurke, B. Müter, *Chem. Ber. 108* (1975) 2969.
[5] R. McCague, C. J. Moody, C. W. Rees, *J. Chem. Soc. Perkin Trans. 1 1984*, 165 and following publications.
[6] Attempts to synthesize 9b-Methyl-9b*H*-phenalene have been reported by M. Moore, A. Amaro, P. D. Noire, K. G. Grohmann, *Abstr. 4. Int. Symp. Chem. Novel Aromatic Compounds*, Jerusalem 1981.
[7] K. Müllen, *Pure Appl. Chem. 58* (1986) 177.
[8] K. Hafner, H. Pelster, H. Patzelt, *Justus Liebigs Ann. Chem. 650* (1961) 80; K. Hafner, *Pure Appl. Chem. 28* (1971) 153; K. Hafner, K.-P. Meinhardt, W. Richarz, *Angew. Chem. 86* (1974) 235; *Angew. Chem. Int. Ed. Engl. 13* (1974) 204.
[9] V. Kühn, K. Hafner, unpublished.
[10] N. Kornblum, *Angew. Chem. 87* (1975) 797; *Angew. Chem. Int. Ed. Engl. 14* (1975) 734.
[11] W. Treibs, H. Froitzheim, *Justus Liebigs Ann. Chem. 564* (1949) 43; R. N. McDonald, N. L. Wolfe, H. E. Petty, *J. Org. Chem. 38* (1973) 1106; M. Müller, *Dissertation*, Technische Hochschule Darmstadt 1982.
[12] Correct elemental analyses or mass spectra were obtained for all the compounds described.
[13] We thank Dr. *S. Braun* for recording and discussing a 2D-^{1}H-NMR spectrum (COSY) of **2**.
[14] K. G. Untch, D. C. Wysocki, *J. Am. Chem. Soc. 88* (1966) 2608; F. Sondheimer, R. Wolovsky, P. J. Garratt, I. C. Calder, *ibid. 88* (1966) 2610.
[15] a) H. J. Lindner: Singlet transitions of **2A** calculated according to the π-SCF-CI method: λ_{max}(oscillator strength) = 244 (1.873), 255 (0.941), 297 (0.003), 580 nm (0.005); b) H. J. Lindner, *Tetrahedron 30* (1974) 1127; Program PIMM 82, unpublished, Technische Hochschule Darmstadt 1982.

Synthesis and Dynamic Properties of Substituted Cyclohepta[*ef*]heptalene**

By *Klaus Hafner,* Günter L. Knaup,* and *Hans Jörg Lindner*

As in the case of the mono- and bicyclic [4n]-π-electron systems cyclobutadiene,[1a] cyclooctatetraene,[1b] pentalene[1c] and heptalene,[1d] which contain localized double bonds in the ground state, a π-bond shift should also be observed in polycyclic non-alternating [4n]-π-electron systems. However, all previously reported *peri*-annelated tri- and tetracyclic compounds[2] with [4n]-π-electrons contain either benzenoid or azulenoid partial structures, which impede this dynamic process. The still unknown tricycles cy-



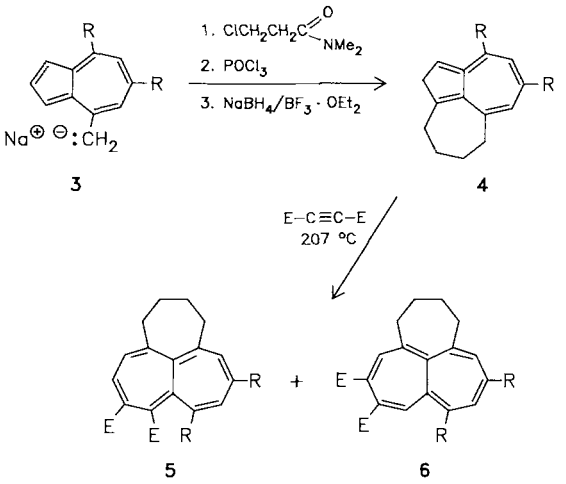
clopenta[*cd*]pentalene **1** and cyclohepta[*ef*]heptalene **2**,[3,4] on the other hand, do not have any aromatic structural elements. In contrast to the mono- and bicyclic [4n]-π-systems, in the case of **1** and **2** three isodynamic structures with localized double bonds should be in equilibrium with each other. Furthermore, the seven-membered rings of cyclohepta[*ef*]heptalene (pleiaheptalene) **2** should prefer a boat conformation, so that a ring inversion also could occur as a further dynamic process in this tricycle, as in the case of cyclooctatetraene[1b] and heptalene.[5] With the synthesis of substituted cyclohepta[*ef*]heptalenes we have now

[*] Prof. Dr. K. Hafner, Dr. G. L. Knaup, Prof. Dr. H. J. Lindner
Institut für Organische Chemie der Technischen Hochschule
Petersenstrasse 22, D-6100 Darmstadt (FRG)

[**] This work was supported by the Deutsche Forschungsgemeinschaft, the Fonds der Chemischen Industrie, and Degussa AG, Frankfurt am Main (FRG).

succeeded for the first time in investigating the dynamic processes of a tricyclic 16π-electron system.

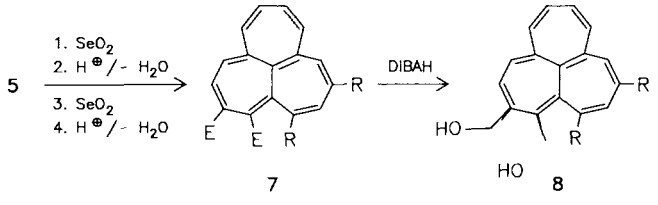
Alkylation of the sodium 4-methyleneazulenides **3a** and **3b**[6] with 3-chloropropionic acid *N,N*-dimethylamide (tetrahydrofuran (THF), −70°C), subsequent intramolecular Vilsmeier reaction with phosphoryl chloride (THF, 67°C) and reduction of the keto group with $NaBH_4/BF_3 \cdot OEt_2$ (1,2-dimethoxyethane, 0°C) afforded the tetrahydroace-



3 4 5 6

a: R = H; b: R = Me; E = CO_2Me

heptylenes **4a**[7] (blue platelets, m.p. 66°C; yield 39%) and **4b** (blue crystals, m.p. 52°C; yield 40%), respectively, whose reactions with dimethyl acetylenedicarboxylate (tetralin, 207°C) lead to the heptalene derivatives **5a** (yellow platelets; m.p. 128–129°C; yield 35%) and **6a** (yellow crystals, m.p. 133°C; yield 53%) as well as **5b** (yellow rhombs, m.p. 158°C; yield 23%) and **6b** (yellow crystals, m.p. 135°C; yield 1%), respectively. Since dehydrogenation of **5a** and **5b** with chloroanil or 2,3-dicyano-5,6-dichloro-*p*-benzoquinone proved unsuccessful, the missing double bonds were successively introduced by oxidation with selenium dioxide (dioxane, 90°C) to give the hydroxy compounds and subsequent elimination of water (TosOH/C_6H_6/80°C).[8] The completely unsaturated tricycles **7a** (orange-red platelets, m.p. 173–175°C; yield 18%) and **7b** (red crystals, m.p. 147–148°C; yield 7%) are stable towards heat and atmospheric oxygen.



7 8

a: R = H; b: R = Me; E = CO_2Me

As shown by the result of the X-ray structure analysis[9] of **7a** (Fig. 1), the achiral tricycle **2** has C_s symmetry and alternating bond lengths. Due to the puckering of the seven-membered rings, the molecule adopts a saddle shaped conformation.

Table 1. Spectral data of compounds **4–8**. ^{1}H-NMR (300 MHz): **4a**, **4b**, **5a**, **5b**, **6a**, **6b** in $CDCl_3$, **7aA**, **7bA**, **8bA**, **8bB** in [D_6]DMSO; UV: **4a**, **4b**, **5a**, **6a** in *n*-hexane, **5b**, **6b**, **7aA**, **7bA**, **8bA** in dioxane.

4a: ^{1}H-NMR: δ = 1.98–2.20 (m; 4H, 4,4′,5,5′-H), 3.26 (m; 4H, 3,3′,6,6′-H), 6.81 (dd, J = 10.2, 9.5 Hz; 1H, 9-H), 6.82 (d, J = 10.1 Hz; 1H, 7-H), 7.16–7.22 (br. s; 1H, 1-H), 7.26 (td, J = 10.1, 1.0 Hz; 1H, 8-H), 7.56 (br. s; 1H, 2-H), 8.09 (dd, J = 9.5, 1.3 Hz; 1H, 10-H); UV: λ_{max} (lgε) = 245 (4.30), 269 sh (4.27), 274 sh (4.47), 279 sh (4.58), 283 (4.66), 288 sh (4.64), 293 sh (4.45), 302 (4.02), 322 sh (3.25), 327 sh (3.36), 335 (3.53), 347 sh (3.64), 350 (3.70), 363 (3.22), 393 sh (1.18), 502 sh (1.94), 520 sh (2.14), 540 sh (2.30), 563 sh (2.44), 582 (2.52), 604 (2.60), 631 (2.54), 660 (2.56), 693 (2.22), 732 (2.19) nm

4b: ^{1}H-NMR: δ = 1.94–2.14 (m; 4H, 4,4′,5,5′-H), 2.51 (s; 3H, 10-Me), 2.76 (s; 3H, 8-Me), 3.21 (m; 4H, 3,3′,6,6′-H), 6.77, 6.80 (2s; each 1H, 7,9-H), 7.18 (d, J = 3.8 Hz; 1H, 1-H), 7.38 (d, J = 3.8 Hz; 1H, 2-H); UV: λ_{max} (lgε) = 216 (4.09), 247 (4.40), 290 (4.69), 295 (4.67), 307 sh (4.08), 327 sh (3.33), 341 (3.57), 351 sh (3.62), 357 (3.71), 368 sh (3.00), 522 sh (2.37), 545 sh (2.52), 567 sh (2.61), 582 (2.65), 603 (2.61), 631 (2.58), 663 sh (2.30), 695 (2.14) nm

5a: ^{1}H-NMR: δ = 1.10–2.78 (m; 8H, $-(CH_2)_4-$), 3.66, 3.70 (2s; each 3H, $2CO_2Me$), 6.07 (dm, J = 10.6 Hz; 1H, 12-H), 6.29 (d, J = 5.8 Hz; 1H, 4-H), 6.30 (ddd, J = 10.6, 5.6, 1.5 Hz; 1H, 11-H), 6.47 (ddd, J = 11.3, 5.6, 0.8 Hz; 1H, 10-H), 6.54 (dm, J = 11.3 Hz; 1H, 9-H), 7.48 (d, J = 5.8 Hz; 1H, 3-H); UV: λ_{max} (lgε) = 214 (4.35), 272 (4.32), 329 (3.56) nm

5b: ^{1}H-NMR: δ = 1.11–2.70 (m; 8H, $-(CH_2)_4-$), 1.95 (d, J = 1.2 Hz; 3H, 12-Me), 2.04 (d, J = 1.2 Hz; 3H, 10-Me), 3.69, 3.70 (2s; each 3H, $2CO_2Me$), 5.99 (quint, J = 0.9 Hz; 1H, 11-H), 6.13 (br. s; 1H, 9-H), 6.30 (d, J = 6.1 Hz; 1H, 4-H), 7.52 (d, J = 6.1 Hz; 1H, 3-H); UV: λ_{max} (lgε) = 274 (4.24), 324 sh (3.56), 386 sh (2.91) nm

6a: ^{1}H-NMR: δ = 1.18–2.80 (m; 8H, $-(CH_2)_4-$), 3.76, 3.78 (2s; each 3H, $2CO_2Me$), 5.76 (dm, J = 6.5 Hz; 1H, 12-H), 6.27 (d, J = 6.2 Hz; 1H, 9-H), 6.34 (dd, J = 11.2, 6.2 Hz; 1H, 10-H), 6.45 (dd, J = 11.2, 6.5 Hz; 1H, 11-H), 6.66 (br. s; 1H, 1-H), 7.45 (br. s; 1H, 4-H); UV: λ_{max} (lgε) = 253 sh (4.23), 266 (4.29), 341 (3.79) nm

6b: ^{1}H-NMR: δ = 1.18–2.70 (m; 8H, $-(CH_2)_4-$), 1.80 (d, J = 1.0 Hz; 3H, 10-Me), 1.98 (s; 3H, 12-Me), 3.75, 3.77 (2s; each 3H, $2CO_2Me$), 6.03 (s; 1H, 11-H), 6.12 (s; 1H, 9-H), 6.68 (s; 1H, 1-H), 7.41 (s; 1H, 4-H); UV: λ_{max} (lgε) = 225 sh (4.27), 239 sh (4.42), 275 (4.30), 340 (3.80), 404 sh (3.01) nm

7aA: ^{1}H-NMR: δ = 3.57, 3.64 (2s; each 3H, $2CO_2Me$), 5.73 (dd, J = 6.3, 1.1 Hz; 1H, 4-H), 6.10–6.35 (m; 5H, 5,6,7,9,10-H), 6.42 (ddd, J = 11.5, 5.5, 1.0 Hz; 1H, 11-H), 6.56 (d, J = 10.5 Hz; 1H, 8-H), 6.59 (d, J = 11.5 Hz; 1H, 12-H), 7.49 (d, J = 6.3 Hz; 1H, 3-H); UV: λ_{max} (lgε) = 233 (4.44), 257 sh (4.25), 308 (4.09), 372 sh (3.35) nm

7bA: ^{1}H-NMR: δ = 1.91 (d, J = 1.1 Hz; 3H, Me), 1.93 (d, J = 0.9 Hz; 3H, Me), 3.59, 3.64 (2s; each 3H, $2CO_2Me$), 5.73 (dd, J = 6.6, 1.1 Hz; 1H, 4-H), 5.95 (br. s; 1H, 11-H), 6.10–6.20 (m; 2H, 6,7-H), 6.21 (br. s; 1H, 9-H), 6.31 (dm, J = 10.7 Hz; 1H, 8-H), 6.55 (dd, J = 10.6, 1.2 Hz; 1H, 5-H), 7.51 (d, J = 6.6 Hz; 1H, 3-H); UV: λ_{max} (lgε) = 222 (4.43), 233 (4.44), 260 sh (4.26), 318 (3.94) nm

8bA: ^{1}H-NMR: δ = 1.85 (d, J = 0.9 Hz; 3H, 12-Me), 2.09 (d, J = 1.1 Hz; 3H, 10-Me), 3.98–4.01 (m; 2H, 1-CH_2O), 4.10 (dd, J = 13.3, 2.4 Hz; 1H, 2-CH_2O), 4.33 (ddd, J = 13.3, 5.2, 0.7 Hz; 1H, 2-CH_2O), 4.65 (t, J = 4.5 Hz; 1H, 1-OH), 4.93 (dd, J = 6.2, 5.2 Hz; 1H, 2-OH), 5.46 (d, J = 6.6 Hz; 1H, 4-H), 5.89, 5.99 (2br. s; each 1H, 9,11-H), 5.94–6.07 (m; 3H, 6,7,8-H), 6.35 (d, J = 11.4 Hz, 1H, 5-H), 6.46 (d, J = 6.6 Hz, 1H, 3-H); UV: λ_{max} (lgε) = 240 (4.48), 258 sh (4.29), 287 sh (3.94), 318 sh (3.67), 363 sh (3.34) nm

8bB: ^{1}H-NMR: δ = 1.57 (s; 3H, 12-Me), 1.90 (d, J = 1.1 Hz; 3H, 10-Me), 3.92 (dd, J = 12.9, 6.0 Hz; 1H, CH_2O), 3.98–4.19 (m; 2H, CH_2O), 4.30–4.38 (m; 1H, CH_2O), 4.71 (dd, J = 5.9, 5.0 Hz; 1H, OH), 4.81 (t, J = 5.6 Hz; 1H, OH), 5.30 (br. s; 1H, 9-H), 5.87 (d, J = 11.1 Hz; 1H, 8-H), 5.94–6.07 (m; 3H, 6,7,11-H), 6.23 (d, J = 11.8 Hz; 1H, 3-H), 6.35 (dd, J = 8.4, 3.0 Hz; 1H, 5-H), 6.36 (d, J = 11.8 Hz, 1H, 4-H)

X-ray analysis of **7a** and low temperature ^{1}H-NMR spectra of solutions of **7a** and **7b**, prepared at low temperatures, indicate that, as in **5** and **6**, only the π-bond-shift isomers with a single bond between the ester-substituted positions exist in solution and in the crystalline state. On the other hand, at room temperature there are signals of other isomers in the ^{1}H-NMR spectra with ratios of 9 : 2 : 1 in **7a** and 12 : 1 in **7b**. The complexity of the spectra as well as the unfavorable isomer distribution have so far thwarted any unequivocal structural assignments of the additional isomers formed at room temperature.

Reduction of the diester **7b** with diisobutylaluminum hydride (DIBAH) (THF, 0°C) affords the pure π-bond-

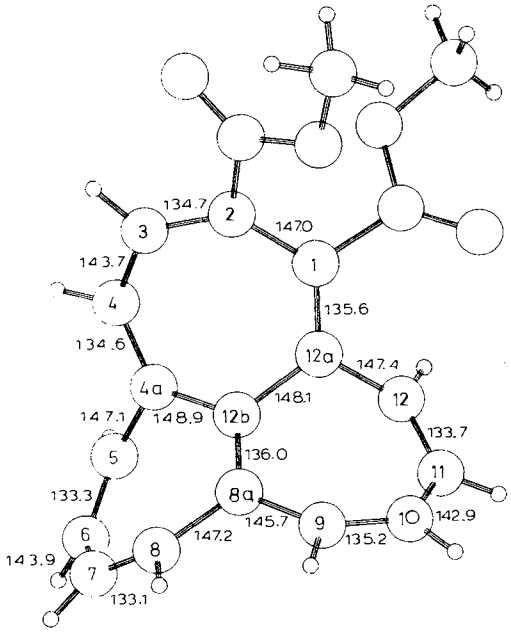
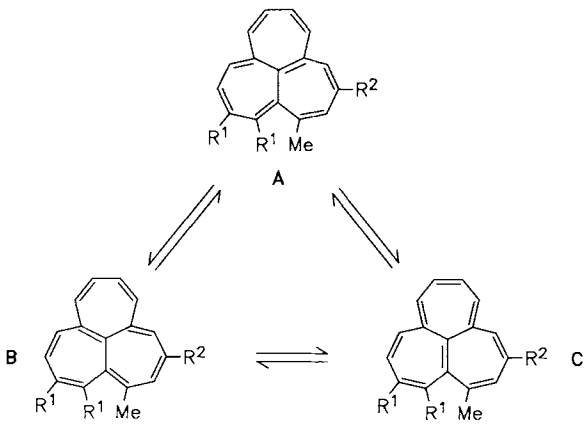


Fig. 1. Structure of **7a** in the crystal; bond lengths in pm (standard deviations: $\sigma_l = 0.4$ pm) [8].

shift isomer **A** of the diol **8b** (orange crystals, m.p. 178–179°C); in solution at room temperature an equilibrium is slowly established with the π-bond-shift isomer **B** (Table 1). Even at 150°C only the valence isomers **8bA** and **8bB** (1:1) are detectable in the ^{1}H-NMR spectrum. The free activation enthalpy for the isomerization **8bA** → **8bB** was found to be 24.1 kcal·mol^{-1} in [D$_6$]DMSO at 33°C.



8b: R^1 = CH_2OH, R^2 = Me; **9**: R^1 = Me, R^2 = H

These experimental results are consistent with π-SCF force field calculations[10] for the dynamics of the 1,2,12-trimethylcyclohepta[*ef*]heptalene **9**. Accordingly, the π-bond-shift isomer **9C**, in which the central double bond causes a partial planarization of the substituent-bearing carbon atoms, has an enthalpy of formation ca. 5 kcal·mol^{-1} higher than the other two isomers. Whereas the direct conversion of **9A** into **9B** should require an activation enthalpy of 38 kcal·mol^{-1}, the value for the isomerization of **9A** to **9C** is only 28 kcal·mol^{-1} and for the isomerization of **9C** to **9B** only 18 kcal·mol^{-1}. Hence, the observed conversion of **8bA** into **8bB** seems to proceed via the thermodynamically unstable isomer **8bC**. On the other hand, for a planarization of the tricycle **9**, i.e. for the transition state of the ring inversion, activation energies of ca. 70 kcal·mol^{-1} have been calculated. Consequently, a ring inversion in case of **7b** and **8b** may require temperatures at which these compounds are presumably no longer stable.

Received: February 20, 1986 [Z 1677 IE]
German version: *Angew. Chem. 98* (1986) 650

CAS-Registry numbers:
3a, 51381-34-1; **3b**, 51381-54-5; **4a**, 7140-38-7; **4b**, 101998-79-2; **5a**, 101998-80-5; **5b**, 101998-81-6; **6a**, 101998-82-7; **6b**, 101998-83-8; **7a**, 101998-84-9; **7b**, 101998-85-0; **8b**, 102046-58-2; $Cl(CH_2)_2CONMe_2$, 17268-49-4; $MeO_2CC{\equiv}CCO_2Me$, 762-42-5.

[1] a) H. Irngartinger, M. Nixdorf, *Angew. Chem. 95* (1983) 415; *Angew. Chem. Int. Ed. Engl. 22* (1983) 403; G. Maier, H.-O. Kalinowski, K. Euler, *ibid. 94* (1982) 706 and *21* (1982) 693; b) J. F. M. Oth, *Pure Appl. Chem. 25* (1971) 573, and references cited therein; L. A. Paquette, *ibid. 54* (1982) 982, and references cited therein; c) K. Hafner, H. U. Süss, *Angew. Chem. 85* (1973) 626; *Angew. Chem. Int. Ed. Engl. 12* (1973) 575; B. Kitschke, H. J. Lindner, *Tetrahedron Lett. 1977*, 2511; P. Bischof, R. Gleiter, K. Hafner, K. H. Knauer, J. Spanget-Larsen, H. U. Süss, *Chem. Ber. 111* (1978) 932; d) E. Vogel, J. Wassen, H. Königshofen, K. Müllen, J. F. M. Oth, *Angew. Chem. 86* (1974) 777; *Angew. Chem. Int. Ed. Engl. 13* (1974) 732; L. A. Paquette, *Isr. J. Chem. 20* (1980) 233; K. Hafner, H. Diehl, H. U. Süss, *Angew. Chem. 88* (1976) 121; *Angew. Chem. Int. Ed. Engl. 15* (1976) 104.

[2] D. Lloyd: *Nonbenzenoid Conjugated Carbocyclic Compounds*, Elsevier, Amsterdam 1984, and references cited therein.

[3] Theoretical studies: A. Streitwieser, Jr.: *Molecular Orbital Theory for Organic Chemists*, Wiley, New York 1961, p. 290f; T. Nakajima: *Molecular Orbitals in Chemistry, Physics, and Biology*, Academic Press, New York 1964, p. 451; R. Zahradník in J. P. Snyder (Ed.): *Nonbenzenoid Aromatics, Vol. 2*, Academic Press, New York 1971, p. 1; B. A. Hess, Jr., L. J. Schaad, *J. Org. Chem. 36* (1971) 3418; F. Tomas, J. I. Fernandez-Alonso, *An. Quim. 72* (1976) 122; I. Gutman, M. Milun, N. Trinajstić, *J. Am. Chem. Soc. 99* (1977) 1692; J. P. Gastmans, D. F. Gastmans, M. H. Mendes Ferraz, *Tetrahedron 33* (1977) 2205.

[4] Unsuccessful attempted syntheses: R. B. Woodward, T. Fukunaga, R. C. Kelly, *J. Am. Chem. Soc. 86* (1964) 3162; H. Butenschön, A. de Meijere, *Tetrahedron Lett. 25* (1984) 1693.

[5] K. Hafner, G. L. Knaup, H. J. Lindner, H.-C. Flöter, *Angew. Chem. 97* (1985) 209; *Angew. Chem. Int. Ed. Engl. 24* (1985) 212; W. Bernhard, P. Brügger, J. F. Daly, P. Schönholzer, R. H. Weber, H.-J. Hansen, *Helv. Chim. Acta 68* (1985) 415; W. Bernhard, P. Brügger, P. Schönholzer, R. H. Weber, H.-J. Hansen, *ibid. 68* (1985) 429.

[6] K. Hafner, H. Pelster, H. Patzelt, *Justus Liebigs Ann. Chem. 650* (1961) 80; K. Hafner, *Pure Appl. Chem. 28* (1971) 153; K. Hafner, K.-P. Meinhardt, W. Richarz, *Angew. Chem. 86* (1974) 235; *Angew. Chem. Int. Ed. Engl. 13* (1974) 204.

[7] All the compounds gave correct elemental analyses.

[8] G. L. Knaup, *Dissertation*, Technische Hochschule Darmstadt 1985.

[9] **7a**: Monoclinic, space group $P2_1/n$, $Z = 4$, $a = 1442.4(4)$, $b = 785.6(2)$, $c = 1462.4(4)$ pm, $\beta = 95.56(1)°$, $V = 1.649 \times 10^9$ pm^3, $\rho_{calc} = 1.290$ g/cm^3; $3° \le 2\theta \le 45°$; ($Mo_{K\alpha}$; $\lambda = 71.07$ pm); 2009 independent reflections, Lorentz and polarization corrections, position of the hydrogen atoms refined; disorder in the region of ester group at C1 (two positions for one oxygen with occupation numbers 0.9 and 0.1), $R_1 = 0.045$, $R_2 = 0.042$ for 1862 structure factors ($|F_o| \ge 2\sigma_F$). Further details of the crystal structure investigation are available on request from the Fachinformationszentrum Energie, Physik, Mathematik GmbH, D-7514 Eggenstein-Leopoldshafen 2 on quoting the depository number CSD-51912, the names of the authors, and the full citation of the journal.

[10] H. J. Lindner, *Tetrahedron 30* (1974) 1127; Program PIMM 82, unpublished, Technische Hochschule Darmstadt 1982.

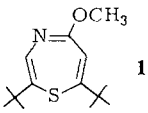
A Stable Monocyclic 1,4-Thiazepine: Synthesis and Characterization of 2,7-Di-*tert*-butyl-5-methoxy-1,4-thiazepine

By *Kagetoshi Yamamoto, Shoko Yamazaki, Hiroki Osedo,* and *Ichiro Murata**

Currently, there is a great deal of interest in seven-membered heterocycles such as oxepins, azepines, and thie-

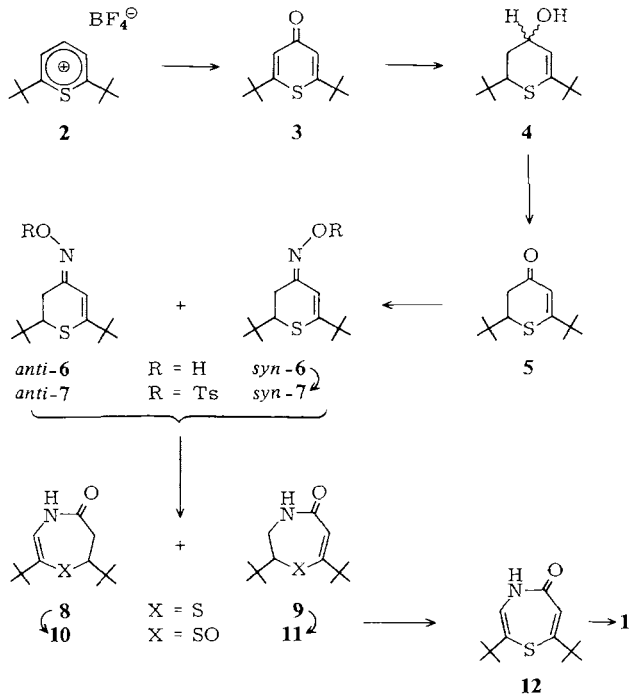
[*] Prof. Dr. I. Murata, Prof. Dr. K. Yamamoto, Dipl.-Chem. S. Yamazaki, H. Osedo
Department of Chemistry, Faculty of Science, Osaka University
Toyonaka, Osaka 560 (Japan)

pins.[1] Of these molecules, the parent thiepin still remains unknown owing to its thermal instability, although the parent oxepin[2] and azepine[3] have already been synthesized. We have recently demonstrated that monocyclic thiepins having two bulky groups at the 2- and 7-positions are surprisingly stable.[4,5] By comparison, 2,7-diisopropyl-5-ethoxycarbonyl-4-methylthiepin[6] extrudes sulfur even at −78 °C, whereas its 2,7-di-*tert*-butyl counterpart is stable up to 130 °C.[4,5] This increase in stability most likely rests on the severe nonbonding steric repulsion between the two *tert*-butyl groups in the corresponding thianorcaradiene proposed as an intermediate in the sulfur extrusion reaction.[7] Bulky groups may also stabilize the thiazepine ring system, the known examples of which have been confined to the annelated derivatives.[8,9] We report here the first synthesis of a stable monocyclic 1,4-thiazepine, 2,7-di-*tert*-butyl-5-methoxy-1,4-thiazepine **1**.



1

2,6-Di-*tert*-butylthiopyrylium tetrafluoroborate **2**, prepared from 2-*tert*-butyl-5-pivaloylthiophene in four steps by our previously reported procedure,[4] was oxidized by Sarett reagent to 2,6-di-*tert*-butylthiopyran-4-one **3**[10] in 56% yield. Formation of the seven-membered thiazepine ring by Beckmann rearrangement of the oxime of **3** (or its tosylate) failed.[11] It was necessary to reduce one double bond in **3** for the subsequent Beckmann rearrangement.



Reduction of **3** in tetrahydrofuran (THF) with a large excess of sodium borohydride gave a mixture of the dihydro alcohols **4**, which, without separation, were oxidized with Sarett reagent to dihydrothiopyranone **5** in 43% yield (based on **3**). Reaction of **5** with hydroxylamine gave a mixture of the oximes *syn*-**6** and *anti*-**6** in 92% yield in a ratio of 1:2 (comparison of the relative areas of the ^{1}H-NMR signals of the olefinic protons; see Table 1). The mixture was converted into the tosylates *syn*-**7** and *anti*-**7**, which underwent Beckmann rearrangement in 70% aqueous dioxane with Et_3N at 80 °C within 5 h to give a mixture of lactams, which could easily be separated into **8** (48%) and **9** (25%) by column chromatography on silica gel (deactivated with 5% H_2O) with benzene/ether.

Table 1. Some physical data of the compounds **1**, **3**, **5**, *syn*-**6**, *anti*-**6**, *syn*-**7**, *anti*-**7**, **8**, **9**, **12**, and **13**.

1: Pale yellow oil; ^{1}H-NMR (100 MHz, $CDCl_3$): $\delta = 1.20$ (s, 9H; $C(CH_3)_3$), 1.21 (s, 9H; $C(CH_3)_3$), 3.73 (s, 3H; OCH_3), 6.02 (d, $^5J(6,3) = 1.0$ Hz, 1H; *H*-6), 6.78 (d, 1H; *H*-3); ^{13}C-NMR (22.5 MHz, $CDCl_3$): $\delta = 29.59$, 30.21, 37.99, 40.15, 52.91, 120.7 (*C*-6), 133.4 (*C*-3), 134.7 (*C*-5), 163.3 (*C*-7), 167.1 (*C*-2); IR (film): $\tilde{\nu} = 1640$ cm^{-1} (C=N); MS (70 eV): *m/z* 253 ($M^{\oplus}$, 28%), 238 ($M^{\oplus} - CH_3$, 24%), 211 (54%), 181 (100%); high-resolution MS: $M^{\oplus} = 253.1493$ (calcd. 253.1499). UV (cyclohexane): $\lambda_{max}(\log\varepsilon) = 244$ (3.77), 340 (2.36) nm

3: Colorless needles, m.p. = 97–99 °C (from hexane); ^{1}H-NMR (60 MHz, $CDCl_3$): $\delta = 1.37$ (s, 18H; $C(CH_3)_3$), 6.87 (s, 2H); IR (KBr): $\tilde{\nu} = 1610$ cm^{-1} (C=O)

5: Colorless crystals, m.p. = 52.5–53.5 °C (from hexane); ^{1}H-NMR (100 MHz, $CDCl_3$): $\delta = 1.04$ (s, 9H; 2-$C(CH_3)_3$), 1.24 (s, 9H, 6-$C(CH_3)_3$), 3.21 (dd, $^3J(2,3a) = 3.4$, $^3J(2,3b) = 13.5$ Hz; *H*-2), 2.71 (dd, $^2J(3a,3b) = 16.1$ Hz; *H*-3a), 2.42 (dd; *H*-3b), 6.20 (s, *H*-5); IR (KBr): $\tilde{\nu} = 1640$ cm^{-1} (C=O); MS (70 eV): *m/z* 226 ($M^{\oplus}$, 5%)

syn-**6** + *anti*-**6**: ^{1}H-NMR (100 MHz, $CDCl_3$): $\delta = 6.84$ (s; *H*-5 of *syn*-**6**, relative intensity = 1), 6.22 (s, *H*-5 of *anti*-**6**, relative intensity = 2), the remaining signals are overlapped; MS (70 eV): *m/z* 241 ($M^{\oplus}$, 81%)

syn-**7** + *anti*-**7**: ^{1}H-NMR (60 MHz, $CDCl_3$): $\delta = 0.97$ (s, 9H), 1.11 (s, 9H), 2.00–3.50 (m, 3H), 7.13–7.38 (m, 2H), 7.72–7.88 (m, 2H), 2.38 (s, aryl-CH_3 of *anti*-**7**, relative intensity = 2), 2.43 (s, aryl-CH_3 of *syn*-**7**, relative intensity = 1), 6.07 (s, *H*-5 of *anti*-**7**, relative intensity = 2), 6.55 (s, *H*-5 of *syn*-**7**, relative intensity = 1)

8: Colorless crystals, m.p. = 147–147.5 °C (from methanol); ^{1}H-NMR (100 MHz, $CDCl_3$): $\delta = 1.04$ (s, 9H, 7-$C(CH_3)_3$), 1.22 (s, 9H, 2-$C(CH_3)_3$), 2.69 (d, $^3J(6,7) = 7.3$ Hz, 2H; *H*-6), 3.60 (t; *H*-7), 6.32 (d, $^3J(3,NH) = 3.6$ Hz; H-3), 7.15 (br. s, NH); IR (KBr): $\tilde{\nu} = 1665$ cm^{-1} (C=O); MS (70 eV): *m/z* 241 ($M^{\oplus}$, 100%)

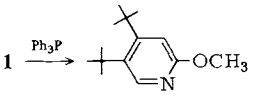
9: Colorless crystals, m.p. = 141–142 °C (from hexane); ^{1}H-NMR (100 MHz, $CDCl_3$): $\delta = 1.04$ (s, 9H; 2-$C(CH_3)_3$), 1.26 (s, 9H; 7-$C(CH_3)_3$), 3.32–3.64 (m, 3H; H-2,3a,3b), 6.15 (d, $^4J(6,NH) = 1.4$ Hz; *H*-6), 6.82 (br. s, NH); IR (KBr): $\tilde{\nu} = 1650$ cm^{-1} (C=O); MS (70 eV): *m/z* 241 ($M^{\oplus}$, 82%)

12: Colorless crystals, m.p. = 125–126 °C (from hexane); ^{1}H-NMR (100 MHz, $CDCl_3$): $\delta = 1.18$ (s, 9H, $C(CH_3)_3$), 1.22 (s, 9H, $C(CH_3)_3$), 6.17 (d, $^4J(6,NH) = 1.8$ Hz; *H*-6), 6.27 (d, $^3J(3,NH) = 4.6$ Hz; *H*-3), 7.12 (br. s, NH); IR (KBr): $\tilde{\nu} = 1662$, 1640 cm^{-1} (−NH−CO−); MS (70 eV): *m/z* 239 ($M^{\oplus}$, 33%), 182 ($M^{\oplus} - 57$, 100%)

13: Colorless oil; ^{1}H-NMR (100 MHz, $CDCl_3$): $\delta = 1.49$ (s, 9H; $C(CH_3)_3$), 1.52 (s, 9H; $C(CH_3)_3$), 3.92 (s, 3H; OCH_3), 6.91 (s, 1H; *H*-3), 8.35 (s, 1H; *H*-6); MS (70 eV): *m/z* 221 ($M^{\oplus}$, 16%), 206 ($M^{\oplus} - CH_3$, 68%); high-resolution MS: $M^{\oplus} = 221.1755$ (calcd. 221.1778)

In order to introduce the additional double bond, Pummerer reaction[12] of the sulfoxide **10**, derived from the major isomer **8** in 91% yield by oxidation with *m*-chloroperbenzoic acid, was examined. This reaction, however, resulted in the formation of a complex mixture of unidentified products. Unlike **10**, the sulfoxide **11**, obtained quantitatively from the lactam **9**, reacted smoothly under the same reaction conditions (F_3CCO_2H in H_2CCl_2, RT, 3 h) to give the desired diene **12** in 79% yield.[13] **12** was converted into the lactim **1**, a pale yellow oil, in 65% yield by treatment with $Me_3O^{\oplus}BF_4^{\ominus}$ in CH_2Cl_2. The elemental analysis and spectral data are in full accord with the thiazepine structure **1**. The thiazepine **1** is stable up to 130 °C; no detectable sulfur extrusion could be observed within 20 h (^{1}H-NMR monitoring in [D_8]toluene). However, thermolysis of **1** in benzene (110 °C, 7 h, sealed tube) in the presence of an equimolar amount of triphenylphosphane gave

4,5-di-*tert*-butyl-2-methoxypyridine **13** as a colorless oil in 77% yield.



13

The thermal stability of **1** is presumably due to the steric effect of two *tert*-butyl groups; however, the effect of the methoxy group on the thermal stability of **1** is still unclear.

Received: March 3, 1986 [Z 1688 IE]
German version: *Angew. Chem. 98* (1986) 639

[1] Reviews: a) E. Vogel, H. Günther, *Angew. Chem. 79* (1967) 429; *Angew. Chem. Int. Ed. Engl. 6* (1967) 385; b) L. A. Paquette in J. P. Snyder (Ed.): *Nonbenzenoid Aromatics, Vol. 1*, Academic Press, New York 1969, p. 249; c) L. Field, D. L. Tuleen, V. J. Traynelis in A. Rosowsky (Ed.): *Heterocyclic Compounds, Vol. 26*, Wiley, New York 1972, chapters X and XI; d) T. Mukai, T. Kumagai, Y. Yamashita, *Heterocycles 15* (1981) 1569; e) D. M. Jerina, H. Yagi, J. W. Daly, *ibid. 1* (1973) 267; f) U. Eisner, Krishnamurthy, *Int. J. Sulfur Chem. 6* (1971) 267; g) I. Murata, K. Nakasuji, *Top. Curr. Chem. 97* (1981) 33.

[2] E. Vogel, R. Schubart, W. A. Böll, *Angew. Chem. 76* (1964) 535; *Angew. Chem. Int. Ed. Engl. 3* (1964) 510; H. Prinzbach, M. Arguelles, E. Druckrey, *ibid. 78* (1966) 1057 and *5* (1966) 1039.

[3] E. Vogel, J.-J. Altenbach, J.-M. Drossard, H. Schmickler, H. Stegelmeier, *Angew. Chem. 92* (1980) 1053; *Angew. Chem. Int. Ed. Engl. 19* (1980) 1016.

[4] K. Nishino, S. Yano, Y. Kohashi, K. Yamamoto, I. Murata, *J. Am. Chem. Soc. 101* (1979) 5059; I. Murata, K. Nishino, S. Yano, Y. Kohashi, K. Yamamoto, *Croatica Chem. Acta 53* (1980) 615.

[5] K. Yamamoto, S. Yamazaki, Y. Kohashi, I. Murata, Y. Kai, N. Kanehisa, K. Miki, N. Kasai, *Tetrahedron Lett. 23* (1982) 3195.

[6] S. Yano, K. Nishino, K. Nakasuji, I. Murata, *Chem. Lett. 1978*, 723.

[7] R. Gleiter, G. Krennrich, D. Cremer, K. Yamamoto, I. Murata, *J. Am. Chem. Soc. 107* (1985) 6874.

[8] K.-H. Wünsch, A. Ehlers, *Z. Chem. 10* (1970) 361.

[9] Highly substituted monocyclic 1,3-thiazepines: R. R. Schmidt, G. Berger, *Synthesis 1974*, 187.

[10] Alternative synthesis of **3**: K. Kawamura, H. Katsuyama, H. Sato, DOS 3011279; *Chem. Abstr. 94* (1981) 141207a; M. R. Detty, J. W. Hassett, B. J. Murray, G. A. Reynolds, *Tetrahedron 41* (1985) 4853.

[11] We examined, without success, the Beckmann rearrangement of 2,6-di-*tert*-butylthiopyranone oxime (pale yellow crystals, m.p. = 138–140°C; ^{1}H-NMR ($CDCl_3$): $\delta = 1.28$ (s, 9H), 1.33 (s, 9H), 6.41 (s, 1H), 7.67 (s, 1H); MS: *m/z* 239 ($M^{\oplus}$)) and its tosylate (colorless prisms, m.p. = 151–152°C (benzene), ^{1}H-NMR ($CDCl_3$): $\delta = 1.26$ (s, 9H), 1.32 (s, 9H), 2.43 (s, 3H), 6.49 (d, $J = 1.3$ Hz, 1H), 7.07 (d, $J = 1.3$ Hz, 1H), 7.31 (d, $J = 8.2$ Hz, 2H), 7.91 (d, $J = 8.2$ Hz, 2H) obtained from **3** via the corresponding thioketone (red prisms, m.p. = 138–139°C (hexane); ^{1}H-NMR ($CDCl_3$): $\delta = 1.40$ (s, 18H), 6.80 (s, 2H).

[12] Successful Pummerer reaction in a seven-membered-ring compound: K. Yamamoto, S. Yamazaki, I. Murata, *Angew. Chem. 97* (1985) 206; *Angew. Chem. Int. Ed. Engl. 24* (1985) 214.

[13] The diphenyl derivative corresponding to **11** gave a pyridine and a 1,2-thiazolidone derivative under the Pummerer reaction conditions.

$[U_3(\mu^3\text{-}Cl)_2(\mu^2\text{-}Cl)_3(\mu^1,\eta^2\text{-}AlCl_4)_3(\eta^6\text{-}C_6Me_6)_3][AlCl_4]$— A Trinuclear Arene Complex of U^{III}**

By *F. Albert Cotton,* Willi Schwotzer,* and *Charles Q. Simpson II*

The reaction of halides of early transition metals under reducing Friedel-Crafts conditions was successfully employed by *E. O. Fischer* et al. for the synthesis of trinuclear cluster compounds of the general type $[M_3(\eta^6\text{-}C_6Me_6)_3(\mu^2\text{-}Cl)_6]^{n+}$.[1] X-ray crystallographic and physicochemical studies have shown[2] that there is metal-metal bonding in these clusters. We have tried to emulate this seemingly generic reaction type in the chemistry of uranium and worked out reaction conditions for the synthesis of the first dinuclear and trinuclear arene complexes of U^{IV}, **1** and **2**, respectively.[3] **1** and **2** resemble the arene complexes of low-valent elements of the third and fourth main groups.[4]

$[U(C_6Me_6)Cl_2(\mu\text{-}Cl)_3UCl_2(C_6Me_6)][AlCl_4]$ **1**[3a]
$[U(C_6Me_6)Cl_2(\mu\text{-}Cl)_3UCl_2(\mu\text{-}Cl)_3UCl_2(C_6Me_6)]$ **2**[3b]

We now have found that a trinuclear cluster compound of U^{III}, **3**, can also be prepared under reducing Friedel-Crafts conditions [Eq. (a)].

$$3\,UCl_4 + 3\,AlCl_3 + 3\,C_6Me_6 + Al \longrightarrow [U_3(\mu^3\text{-}Cl)_2(\mu^2\text{-}Cl)_3(\eta^2\text{-}AlCl_4)_3(\eta^6\text{-}C_6Me_6)_3][AlCl_4] \quad (a)$$

3

The structure of the complex cation of **3** is depicted in Figure 1.[5] The three uranium atoms define approximately

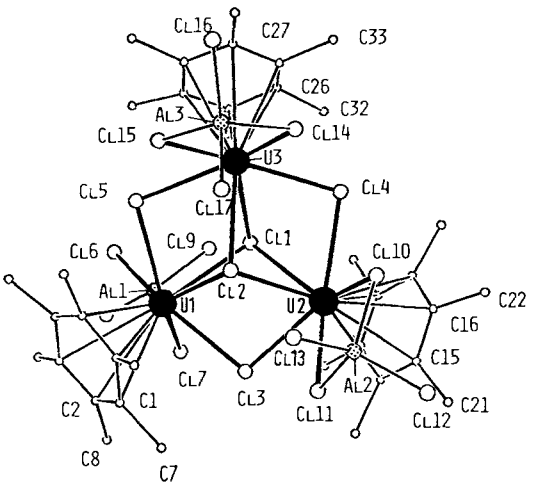


Fig. 1. Perspective drawing of the structure of the cation of **3** in the crystal.

an equilateral triangle. Three chlorine atoms bridge the edges of the triangle, while two additional chlorine atoms cap the triuranium fragment on each side in μ^3-fashion. The coordination polyhedron of each U atom is best described as a distorted pentagonal bipyramid. The equatorial plane is defined by two Cl atoms of the bridges, two Cl atoms of $AlCl_4$, and one μ^3-Cl atom of the caps. The apical positions are occupied by the other capping μ^3-Cl atom and the C_6Me_6 moiety. Important distances and angles of the structure of **3** are given in Table 1. For comparison, some selected structure data for the other known uranium arene complexes and for some uranium compounds with anionic π-ligands are summarized in Table 2. The U–C distances involving neutral π-ligands are systematically longer than those involving anionic ligands. This supports the view that the ionic contribution to the bonding of cyclopentadienyl, allyl, or cyclooctatetraenyl ligands is an im-

[*] Prof. F. A. Cotton, Dr. W. Schwotzer, C. Q. Simpson II
Department of Chemistry and Laboratory for Molecular Structure and Bonding, Texas A & M University
College Station, TX 77843 (USA)

[**] We are grateful to the Robert A. Welch Foundation (Grant No. A-494) for financial support.

Table 1. Important distances and angles for **3** in the crystal.

Distances [Å]					
U1-U2	4.216(3)	U2-U3	4.199(3)	U3-Cl1	3.054(14)
U1-U3	4.270(3)	U2-Cl1	2.99(2)	U3-Cl2	2.89(2)
U1-Cl1	2.850(15)	U2-Cl2	2.854(15)	U3-Cl4	2.792(14)
U1-Cl2	3.05(2)	U2-Cl3	2.782(15)	U3-Cl5	2.801(15)
U1-Cl3	2.76(2)	U2-Cl4	2.76(2)	U3-Cl14	2.95(2)
U1-Cl5	2.758(14)	U2-Cl10	2.92(2)	U3-Cl15	2.95(2)
U1-Cl6	2.93(2)	U2-Cl11	2.90(2)	U3-C(hmb)[a]	2.90[6]
U1-Cl7	3.01(2)	U2-C(hmb)[a]	2.93[5]		
U1-C(hmb)[a]	2.94[9]				

Angles [°]	
U-U-U	59.3-61
Cl1-U1-hmb(1)-center	171.6
Cl1-U1-Cl2	68.1
Cl1-U1-Cl-3(5,6,7)	75.4-84.3
hmb(1)-center-U1-Cl-2(3,5,6,7)	101.8-103.5
Cl2-U2-hmb(2)-center	172.7
Cl2-U2-Cl1	68.9
Cl2-U2-Cl-3(4,10,11)	74.9-80.7
hmb(2)-center-U2-Cl-1(3,4,10,11)	100.1-106.5
Cl2-U3-hmb(3)-center	171.4
Cl2-U3-Cl1	67.6
Cl2-U3-Cl-4(5,14,15)	72.6-81.0
hmb(3)-center-U3-Cl-4(5,14,15)	101.5-105.0

[a] hmb = hexamethylbenzene; mean value.

Table 2. Structure data for uranium π-complexes.

Compound	U-Cl [Å]	U-C [Å]	Ref.
$[U(\eta^6\text{-}C_6H_6)(\eta^2\text{-}AlCl_4)_3]$	2.88 [a]	2.91	[7]
1	2.75 [b] 2.58 [c]	2.92	[3a]
2	2.78 [b] 2.53 [c]	2.94	[3b]
3	2.78 [b] 2.99 [d] 2.94 [a]	2.92	
$[U(\eta^8\text{-}C_8H_8)_2]$(uranocene)		2.56	[8]
$[U(C_5H_5)_4]$		2.81	[9]
$[\{U(\eta^3\text{-}C_3H_5)_2(O\text{i}Pr)_2\}_2]$		2.68	[10]

[a] η^2-$AlCl_4$. [b] Bridging. [c] Terminal. [d] Capping.

portant one, although our compounds with neutral π-ligands clearly indicate that covalent bonding is not to be neglected.[11] Moreover, while there is no simple correlation between bond length and bond strength, the large U–C separation is in agreement with our experience that the arene ligands are easily displaced by σ-donor molecules even though the arene complexes are fairly stable in a thermodynamic sense. The U–Cl distances vary according to the bonding situation (terminal, bridging, or capping) but fall into the expected ranges observed in many other uranium chlorides.

The relative orientation of the hexamethylbenzene ligands with respect to the triangular plane is *anti* for the ligands on U1 and U2 as well as for U1 and U3 but *syn* for the pair U2/U3. This could be explained by steric arguments assuming facile site interchange between hexamethylbenzene and $AlCl_4$ in solution and selective crystallization of the diastereomer with the most favorable steric interaction, including crystal packing. There is, however, an alternative explanation. The substructures containing the *anti* arrangement, for example, the fragment $[(C_6Me_6)(AlCl_4)U1(\mu^2\text{-}Cl)_3U2(C_6Me_6)(AlCl_4)]$, bear a very close structural resemblance to the dinuclear precursor **1**. All it takes to complete the trinuclear unit of **3** with correct stereochemistry is to attach, in our example, the fragment $[(C_6Me_6)(AlCl_4)U3(Cl)_2]$ via two of the bridging chlorine atoms, which consequently become caps. Unfortunately, NMR experiments to probe possible isomerization processes at the metal centers are not feasible because of paramagnetic line broadening.

The observed U–U distance (> 4.2 Å, Table 1) probably rules out a direct M–M interaction.[12] Therefore, the electron configurations of the U atoms are expected to be f^3, leading to a paramagnetic complex. This is in agreement with our observation that in the solid-state ^{13}C-NMR spectrum of **3** only very broad lines are observed, as opposed to the also paramagnetic (f^2-configuration) compound **2**.[3b]

Well-defined complexes of U^{III} and U^{IV} are thus accessible by a modified Friedel-Crafts procedure.[1,3,7] They represent the first examples of complexes of an actinide metal with neutral π-ligands. Meanwhile we have succeeded in extending our work to a lanthanide element and have isolated a hexamethylbenzene complex of samarium.[13] Such donor-acceptor complexes of f-block elements are gaining increasing attention. There are recent reports on compounds with other π-ligands, most notably CO[14] and olefins,[15] as well as with electron-rich transition metals.[16]

Experimental Procedure

All reactions were carried out under scrupulous exclusion of air and moisture in Schlenk-type glassware. Solvents were distilled under N_2 from appropriate drying agents. UCl_4 was prepared by published procedures [6].—**3**: Reaction of a mixture of UCl_4 (380 mg, 1 mmol), $AlCl_3$ (150 mg), and C_6Me_6 (200 mg) in refluxing toluene yielded a green solution with very little precipitate within 30 min. The green product, **1**, was isolated by slow cooling of the filtered solution. An excess (ca. 100 mg) of aluminum powder was then added from a dump tube without prior isolation of **1**. The solution gradually turned red-brown. It was then heated under reflux for 4 h and filtered hot; the residue was extracted twice with hot toluene. *Very slow* cooling of the combined extracts afforded the trinuclear compound **3**; yield: 410 mg (55%). On several occasions oily precipitates, which were converted into brown powders by washing with hexane, were formed. The precipitate, once formed, was no longer soluble in hot toluene or halocarbon solvents. It was soluble in polar donor solvents where it appeared to undergo chemical transformation. Crystalline products have been obtained from acetonitrile and are presently under investigation. **3** is exceedingly sensitive to air and moisture. Heating in vacuum (10^{-4} torr) leads to decomposition at ca. 160°C with concomitant sublimation of C_6Me_6.

Received: February 24, 1986;
supplemented: April 15, 1986 [Z 1679 IE]
German version: *Angew. Chem. 98* (1986) 652

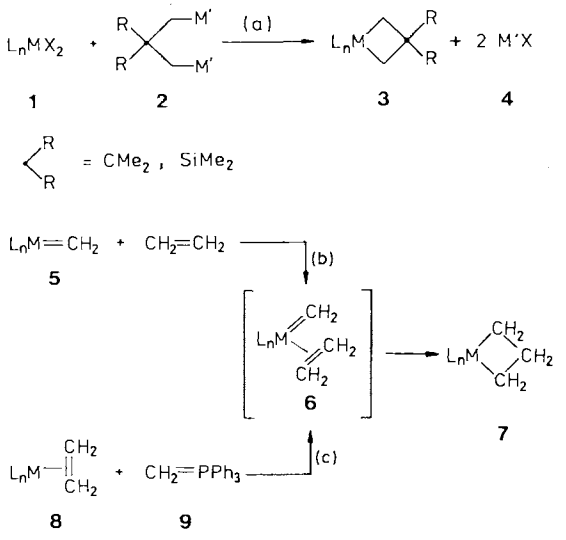
[1] a) E. O. Fischer, F. Röhrschied, *J. Organomet. Chem. 6* (1966) 53; b) F. Stollmaier, U. Thewalt, *ibid. 208* (1981) 327; c) S. Z. Goldberg, B. Spivack, G. Stanley, R. Eisenberg, D. M. Braitsch, J. S. Miller, M. Abkowitz, *J. Am. Chem. Soc. 99* (1977) 110.
[2] F. A. Cotton, R. Jostes, A. Müller, *Angew. Chem. 92* (1980) 921; *Angew. Chem. Int. Ed. Engl. 19* (1980) 875.
[3] a) F. A. Cotton, W. Schwotzer, *Organometallics 4* (1985) 942; b) G. C. Campbell, J. F. Haw, F. A. Cotton, W. Schwotzer, *ibid. 5* (1986) 274.
[4] H. Schmidbaur, *Angew. Chem. 97* (1985) 893; *Angew. Chem. Int. Ed. Engl. 24* (1985) 893.
[5] Crystal data: dark red-brown crystals; monoclinic $P2_1/n$; $a = 12.566(3)$, $b = 23.224(7)$, $c = 27.141(7)$ Å, $\beta = 102.47(3)°$, $R = 0.072$ ($R_w = 0.065$); 331 parameters from 2107 data. The hexamethylbenzene molecules were treated as rigid groups during the final cycles of refinement. Further details of the crystal structure investigation may be obtained from the Fachinformationszentrum Energie, Physik, Mathematik GmbH, D-7514 Eggenstein-Leopoldshafen 2 (FRG), on quoting the depository number CSD 51874, the names of the authors, and the journal citation.
[6] T. A. Herman, J. F. Suttle, *Inorg. Synth. 5* (1957) 143.
[7] M. Cesari, U. Pedretti, A. Zazetta, G. Lugli, W. Marconi, *Inorg. Chim. Acta 5* (1971) 439.
[8] A. Zalkin, K. N. Raymond, *J. Am. Chem. Soc. 91* (1969) 5667.
[9] H. J. Burns, *J. Organomet. Chem. 69* (1974) 225.
[10] M. Brunelli, G. Perego, G. Lugli, A. Mazzei, *J. Chem. Soc. Dalton Trans. 1979*, 861.
[11] K. Tatsumi, R. Hoffmann, *Inorg. Chem. 23* (1984) 1633.

[12] We estimate, based on M-M distances in similar clusters of d-transition elements [1b, 2], a U-U distance of 3.5 Å to be an upper limit for a bonding interaction. In a dinuclear uranium alkoxide with a U-U separation of 3.63 Å, the interaction is clearly repulsive (F. A. Cotton, D. O. Marler, W. Schwotzer, *Inorg. Chem. 23* (1984) 4211).
[13] F. A. Cotton, W. Schwotzer, *J. Am. Chem. Soc.*, in press.
[14] J. G. Brennan, R. A. Andersen, J. L. Robbins, *J. Am. Chem. Soc. 108* (1986) 335.
[15] G. M. Smith, H. Suzuki, D. C. Sonnenberger, V. W. Day, T. J. Marks, *Organometallics 5* (1986) 549.
[16] a) J. M. Ritchey, A. J. Zozulin, D. A. Wrobleski, R. R. Ryan, H. J. Wasserman, D. C. Moody, R. T. Paine, *J. Am. Chem. Soc. 107* (1985) 501; b) P. J. Hay, R. R. Ryan, K. V. Salazar, D. A. Wrobleski, A. L. Sattelberger, *ibid. 108* (1986) 313; c) R. S. Sternal, C. P. Brock, T. J. Marks, *ibid. 107* (1985) 8270.

Metallacyclic Four-Membered Ring Systems: Two Independent Routes to Bis(cyclopentadienyl)titanacyclobutabenzene**

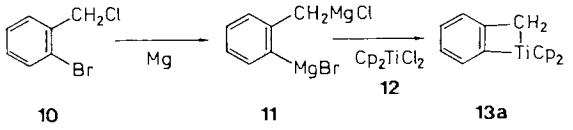
By *Henricus J. R. de Boer, Otto S. Akkermann, Friedrich Bickelhaupt,* Gerhard Erker,* Peter Czisch, Richard Mynott, Julian M. Wallis,* and *Carl Krüger*

Metallacyclobutanes of the early transition metals[1] are accessible via two routes (Scheme 1): by reaction of metal halides with suitably substituted 1,3-propanediyl dianion-equivalents [route (a)][2] or by the electrocyclic ring closure of carbene(olefin)metal complexes. The latter are usually obtained by reaction of carbene-metal complexes with olefins [route (b)],[1c] but more recently they have been prepared from organic alkylidene donors and reactive olefin-metal complexes [route (c)].[3] We have now found that

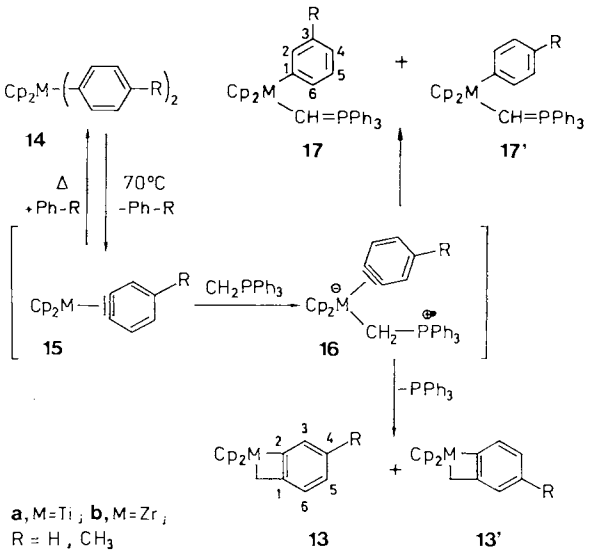


Scheme 1.

otherwise difficultly and rarely accessible metallacyclobutabenzene compounds[4] can be prepared by variants of routes (a) and (c). We have been able to demonstrate this, for example, in the case of bis(cyclopentadienyl)titanacyclobutabenzene **13a**.



The novel, double Grignard reagent **11** was obtained by reaction of *o*-bromobenzyl chloride with magnesium in tetrahydrofuran (THF). Reaction of a THF suspension of **11** with Cp_2TiCl_2 (**12**, equimolar amount) at -20 °C afforded the titanacyclobutabenzene **13a**.[5] **13a** can, however, also be prepared via the cycloaddition route (c) (Scheme 1). (Aryne)$ZrCp_2$ **15b**, generated thermally from diphenylzirconocene, reacts with $CH_2{=}PPh_3$ to give the metallocene-substituted ylide **17b**.[6] In the analogous titanocene system, transfer of the entire methylene group of the reagent with formation of **13a** and PPh_3 competes with H-transfer (**17a** : **13a** = 2 : 1).[7] A labeling experiment showed that both of the products are formed by an aryne mechanism[8] (Scheme 2).



Scheme 2. The (non-systematical) numbering merely serves for assignment of the NMR signals.

17a was characterized by an X-ray structure analysis (Fig. 1).[9] Like **17b**, in the crystal it exhibits a preferred conformation that allows for maximal π-interaction of the formally coordinatively unsaturated metal center[10] with the trigonal-planar ylide carbon atom. The Ti-C7 bond length (2.033(6) Å) is remarkably short.[11] The metal-C(ylide) π-interaction in the titanium compound **17a** ($\Delta d(M) = d[M\text{-}C1] - d[M\text{-}C7]$; $\Delta d(Ti) = 0.22$ Å) is stronger than in the zirconium compound **17b** ($\Delta d(Zr) = 0.18$ Å). **17a** and **17b** show dynamic NMR spectra in solution: In **17a** the activation barrier for rotation about the M-C7 bond ($\Delta G^{\ddagger}_{34\,°C} = 12.0 \pm 0.2$ kcal/mol) is considerably higher than in the case of **17b** ($\Delta G^{\ddagger}_{102\,°C} = 8.6 \pm 0.3$ kcal/mol),[6] suggesting a stronger π-interaction in **17a**. The methylene transfer to give **13** would be favored by a similarly enhanced M-C π-interaction in the intermediate **16**.

[*] Prof. Dr. F. Bickelhaupt, Dr. H. J. R. de Boer, Dr. O. S. Akkerman
Scheikundig Laboratorium, Vrije Universiteit Amsterdam
De Boelelaan 1083, NL-1081 HV Amsterdam (The Netherlands)
Prof. Dr. G. Erker [+], Dipl.-Chem. P. Czisch, Dr. R. Mynott, Dr. J. M. Wallis, Prof. Dr. C. Krüger
Max-Planck-Institut für Kohlenforschung
Kaiser-Wilhelm-Platz 1, D-4330 Mülheim a. d. Ruhr (FRG)
[+] Present address:
Institut für Organische Chemie der Universität
Am Hubland, D-8700 Würzburg (FRG)

[**] This work was supported by the Deutsche Forschungsgemeinschaft and the Fonds der Chemischen Industrie (*G. E.*), and by the Netherlands Foundation for Research (SON) and the Netherlands Organization for the Advancement of Pure Research (ZWO) (*H. J. R. de B.*).

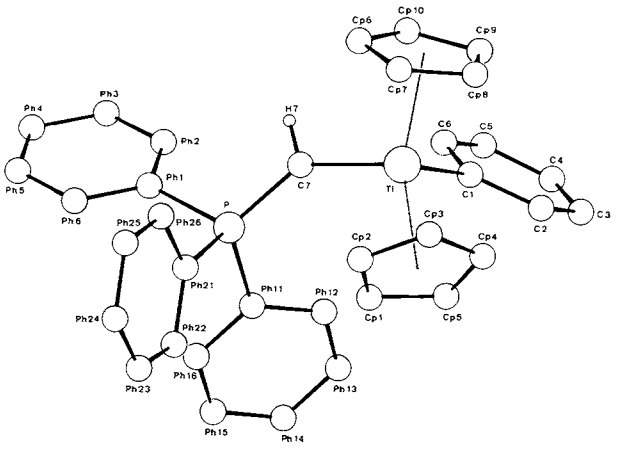


Fig. 1. Crystal structure of **17a**, R = H.

Experimental

A suspension of doubly sublimed magnesium (576 mg, 24 mmol, particle size 1–2 mm) in THF (4 mL) was treated with dibromoethane (21 mg, 0.1 mmol), and the mixture stirred for 15 min. A solution of **10** (492 mg, 2.4 mmol)[12] in THF (30 mL) was then added dropwise to the mixture within 2 h, and stirring continued for a further 1 h. To remove excess magnesium, the mixture was filtered through glass wool. This furnished a suspension of a green precipitate in a greenish-yellow solution, with the precipitate containing the greater part of the organomagnesium compound. The yield of **11** was almost quantitative. This was ascertained by hydrolysis and titration of the base and the magnesium ions with HCl and ethylenediamine tetraacetate (EDTA), respectively, and by determination of the α,*o*-dideuteriotoluene (99%) after deuteriolysis (GC/MS). Derivatization with CO_2, Me_3GeCl, and Me_3SnCl also afforded the expected disubstitution products in 92–94% yield.

For the synthesis of **13a**, **12** (198 mg, 0.795 mmol) was added to a THF-suspension of a molar equivalent of **11** (0.0199 M) at −20°C in a sealed glass system and stirred for 2 h. The grey precipitate dissolved and a deep red solution resulted. After removal of the THF by distillation at 4°C the solution was treated with dioxane (10 mL); after 15 minutes' stirring and removal of a white precipitate (magnesium salts), the filtrate was evaporated to dryness. The residue was virtually pure **13a** (red powder; 93% yield, determined by ^{1}H-NMR spectroscopy with cyclopentane as standard).

Received: March 4, 1986;
revised: May 15, 1986 [Z 1690 IE]
German version: *Angew. Chem. 98* (1986) 641

[1] a) J. B. Lee, G. L. Gajda, W. P. Schaefer, T. R. Howard, T. Ikariya, D. A. Straus, R. H. Grubbs, *J. Am. Chem. Soc. 103* (1981) 7358; A. K. Rappe, W. A. Goddard III, *ibid. 104* (1982) 297; W. R. Tikkanen, J. W. Egan, Jr., J. L. Petersen, *Organometallics 3* (1984) 1646; b) F. N. Tebbe, G. W. Parshall, D. W. Ovenall, *J. Am. Chem. Soc. 101* (1979) 5074; T. R. Howard, J. B. Lee, R. H. Grubbs, *ibid. 102* (1980) 6876; D. A. Straus, R. H. Grubbs, *J. Mol. Catal. 28* (1985) 9; c) K. A. Brown-Wensley, S. L. Buchwald, L. Cannizzo, L. Clawson, S. Ho, D. Meinhardt, J. R. Stille, D. Straus, R. H. Grubbs, *Pure Appl. Chem. 55* (1983) 1733, and references cited therein.

[2] a) J. W. F. L. Seetz, B. J. J. van de Heisteeg, G. Schat, O. S. Akkerman, F. Bickelhaupt, *J. Mol. Catal. 28* (1985) 71, and references cited therein; B. J. J. van de Heisteeg, G. Schat, O. S. Akkerman, F. Bickelhaupt, *Tetrahedron Lett. 25* (1984) 5191; *Organometallics 4* (1985) 1141; b) W. R. Tikkanen, J. Z. Liu, J. W. Egan, Jr., J. L. Petersen, *ibid. 3* (1984) 825; c) for other modes of formation of metallacyclobutanes see, e.g., P. Foley, G. M. Whitesides, *J. Am. Chem. Soc. 101* (1979) 2732; M. Ephritikhine, M. L. H. Green, R. E. MacKenzie, *J. Chem. Soc. Chem. Commun. 1976*, 619.

[3] G. Erker, P. Czisch, C. Krüger, J. M. Wallis, *Organometallics 4* (1985) 2059.

[4] T. H. Tulip, D. L. Thorn, *J. Am. Chem. Soc. 103* (1981) 2448; L. Dahlenburg, V. Sinnwell, D. Thoennes, *Chem. Ber. 111* (1978) 3367; V. F. Traven, M. Yu. Eismont, V. V. Redchenko, B. I. Stepanov, *Zh. Obshch. Khim. 50* (1980) 2007; *Chem. Abstr. 94* (1981) 29681z; T. Behling, G. S. Girolami, G. Wilkinson, R. G. Somerville, M. B. Hursthouse, *J. Chem. Soc. Dalton Trans. 1984*, 877; J. A. Stotler, G. Wilkinson, M. Thornton-Pett, M. B. Hursthouse, *ibid.* 1731; R. Neidlein, A. Rufińska, H. Schwager, G. Wilke, *Angew. Chem. 98* (1986) 643; *Angew. Chem. Int. Ed. Engl. 25* (1986) 640.

[5] **13a**: MS (70 eV): *m/z* 268 ($M^{\oplus}$), 178 (Cp_2Ti); ^{1}H-NMR (for numbering see Scheme 1): δ (CD_2Cl_2) = 5.85 (s, 10H; C_5H_5), 3.17 (s, 2H; CH_2), 7.06, 7.28 (d, in each case $^3J_{HH}$ = 7 Hz, each 1H; *H3*, *H6*), 6.90 (m, 2H; *H4*, *H5*); δ (C_6D_6) = 5.50 (C_5H_5), 3.30 (CH_2); ^{13}C-NMR (CD_2Cl_2): δ = 111.8 (d, $^1J_{CH}$ = 174 Hz; C_5H_5), 63.4 (t, $^1J_{CH}$ = 140 Hz; CH_2), 105.1 (s; *C1*), 208.9 (s; *C2*), 128.9 (d; *C6*), 132.6 (d, $^1J_{CH}$ = 157 Hz; *C3*), 125.5, 125.2 (d, $^1J_{CH}$ = 158 Hz; *C4*, *C5*).

[6] a) G. Erker, P. Czisch, R. Mynott, Y.-H. Tsay, C. Krüger, *Organometallics 4* (1985) 1310; b) for further examples of this type of compound see: G. Erker, P. Czisch, R. Mynott, *Z. Naturforsch. B40* (1985) 1177; H. Schmidbaur, R. Pichl, *ibid.* 352; R. E. Cramer, R. B. Maynard, J. W. Gilje, *Inorg. Chem. 20* (1981) 2466; K. I. Gell, J. Schwartz, *ibid. 19* (1980) 3207; c) J. C. Baldwin, N. L. Keder, C. F. Strouse, W. C. Kaska, *Z. Naturforsch. B35* (1980) 1289.

[7] A mixture of 3.6 g (10.9 mmol) of Cp_2TiPh_2 and 3.3 g (12 mmol) of $H_2C{=}PPh_3$ in 250 mL of heptane after heating at 70°C for 7 h and subsequent crystallization afforded 3.6 g (95%) of pure **17a**. The solution contained up to 80–90% of pure **13a** together with PPh_3 (1:1). **17a**: M.p. 163°C; correct elemental analysis; MS (70 eV): *m/z* 530 ($M^{\oplus}$), 453 ($M^{\oplus}$ − Ph), 275 ($CHPPh_3^{\oplus}$); IR (KBr): $\tilde{\nu}$ = 3040, 1430, 1100, 800 (C_5H_5), 920 (C-P) cm^{-1}; ^{1}H-NMR (C_6D_6, for numbering see Scheme 1): δ = 5.71 (s, 10H; C_5H_5), 8.78 (d, $^2J_{HP}$ = 5 Hz, 1H; *CH*=P), 6.85–7.20 and 7.40–7.85 (m, 20H; $4C_6H_5$); ^{13}C-NMR (CD_2Cl_2): δ = 108.8 (d, $^1J_{CH}$ = 173 Hz; C_5H_5), 165.2 (dd, $^1J_{CH}$ = 122 Hz, $^1J_{CP}$ = 20 Hz; *CH*=P), 187.7 (s; *C1*), 144.0 (d, $^1J_{CH}$ = 156 Hz; *C2*), 125.5 (d, $^1J_{CH}$ = 153 Hz; *C3*), 121.5 (d, $^1J_{CH}$ = 157 Hz; *C4*), signals of the PPh_3 group: δ = 133.7 (d, $^1J_{CP}$ = 80.5 Hz; *i-C*), 133.7 (dd, $^1J_{CH}$ = 163 Hz, $^2J_{CP}$ = 9.2 Hz; *o-C*), 128.8 (dd, $^1J_{CH}$ = 163 Hz, $^3J_{CP}$ = 11.1 Hz; *m-C*), 131.4 (dd, $^1J_{CH}$ = 160 Hz, $^4J_{CP}$ = 2.6 Hz; *p-C*).

[8] Starting from bis(*p*-tolyl)titanocene, the aryltitanocene ylides **17a** (methyl at C3) and **17a'** (methyl at C4) were obtained in a 60:40 ratio together with a mixture of the substituted titanacyclobutabenzenes **13a** (methyl at C5) and **13a'** (methyl at C4). In this particular case, H-transfer is favored over CH_3-transfer to the extent of 3:1.

[9] Crystal structure analysis of **17a**: *a* = 10.872(1), *b* = 17.928(3), *c* = 28.643(4) Å; *V* = 5583.1 Å^3; ρ_{calc} = 1.26 g cm^{-3}, μ = 3.79 cm^{-1}, *Z* = 8; space group *Pbca*, 2151 of 6290 independent reflections observed, 458 parameters refined, *R* = 0.049, R_w = 0.042. Selected bond lengths [Å] and angles [°]: Ti-C1 2.254(5), Ti-C7 2.033(6), P-C7 1.709(6); C1-Ti-C7 95.5(2), Ti-C7-P 138.5(3); C6-C1-Ti-C7 31.5, C1-Ti-C7-P 99.5. Further details of the crystal structure investigation are available on request from the Fachinformationszentrum Energie, Physik, Mathematik GmbH, D-7514 Eggenstein-Leopoldshafen 2, on quoting the depository number CSD-51937, the names of the authors, and the full citation of the journal.

[10] For the special stereoelectronic properties of the bent metallocene moiety see J. W. Lauher, R. Hoffmann, *J. Am. Chem. Soc. 98* (1976) 1729; G. Erker, F. Rosenfeldt, *Angew. Chem. 90* (1978) 640; *Angew. Chem. Int. Ed. Engl. 17* (1978) 605.

[11] Almost identical with *d*(Ti-C) in dicarbonyltitanocene (2.030(11) Å): J. L. Atwood, K. E. Stone, H. G. Alt, D. C. Hrncir, M. D. Rausch, *J. Organomet. Chem. 132* (1977) 367; Ti-C bond lengths: W. E. Hunter, J. L. Atwood, G. Fachinetti, C. Floriani, *ibid. 204* (1981) 67; I. W. Bassi, G. Allegra, R. Scordamaglia, G. Chiccola, *J. Am. Chem. Soc. 93* (1971) 3787; J. L. Calderon, F. A. Cotton, B. G. De Boer, J. Takats, *ibid.* 3592; G. P. Pez, *ibid. 98* (1976) 8072.

[12] Prepared from *o*-bromobenzyl alcohol according to the method described by D. Landin, F. Monetari, F. Rolla, *Synthesis 1974*, 37.

Nickelacyclobutabenzene Compounds by Oxidative Addition of Cyclopropabenzene to Nickel(0) Compounds**

By *Richard Neidlein,* Anna Rufińska, Harald Schwager,* and *Günther Wilke**

Dedicated to Professor Hans-Herloff Inhoffen on the occasion of his 80th birthday

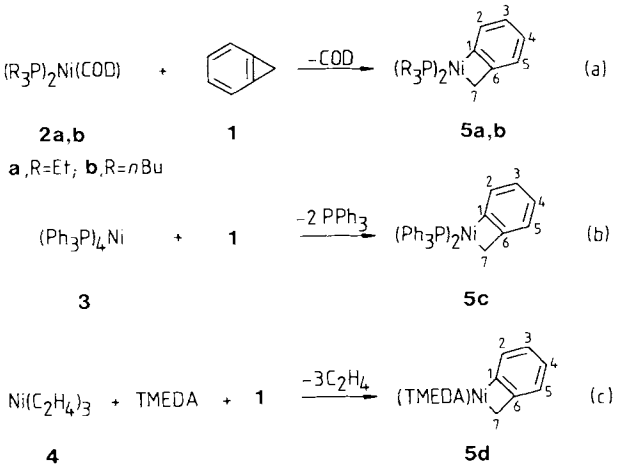
Metallacyclobutanes, which are so far known for only a few transition metals,[1] have developed into an important

[*] Prof. Dr. G. Wilke, Dr. A. Rufińska, Dipl.-Chem. H. Schwager
Max-Planck-Institut für Kohlenforschung
Kaiser-Wilhelm-Platz 1, D-4330 Mülheim a.d. Ruhr (FRG)
Prof. Dr. R. Neidlein
Pharmazeutisch-chemisches Institut der Universität
Im Neuenheimer Feld 364, D-6900 Heidelberg (FRG)

[**] This work was supported by the Deutsche Forschungsgemeinschaft and the Fonds der Chemischen Industrie.

class of organometallic compounds on account of their importance as intermediates in olefin metathesis reactions.[2] Metallacyclobutenes, on the other hand, have not yet been isolated, although metallacyclobutabenzene compounds of some transition metals (but not of nickel) are known.[3] Higher-membered, multiply unsaturated metallacycles may be prepared, for example, by oxidative addition of biphenyls to nickel(0) compounds, whereby a CC σ-bond that is activated by ring strain undergoes cleavage.[4] As we recently showed, oxidative addition of cyclopropabenzene **1** to $[(Me_3P)_2Ni(cod)]$ (COD = *cis,cis*-1,5-cyclooctadiene) results in the formation of a bis-methano-bridged nickela[12]annulene.[5] Here we report a novel and flexible approach to metallacyclobutabenzenes, which was discovered in the course of those investigations.

When **1**[6] is allowed to react with the nickel(0) complexes **2**[7,8] and **3**[9] [Eq. (a) and (b), respectively] or with a 1:1 mixture of trisethenenickel(0) **4**[10] and tetramethylethylenediamine (TMEDA)[11] [Eq. (c)], the corresponding nickelaannulenes are not formed.[5] Instead, the crystalline nickel(II) compounds **5**, i.e., nickelacyclobutabenzene derivatives, are produced in high yields as the result of insertion of a Ni atom into one of the CC σ-bonds of the three-membered ring of **1**. The ligands thereby released can be removed by recrystallization or under high vacuum. The complexes with $(n\text{Bu})_3P$ and Ph_3P ligands (**5b** and **5c**, respectively) are stable at room temperature, whereas those with the ligands Et_3P and TMEDA (**5a** and **5d**, respectively) decompose slowly, turning black.[12]



The nuclear magnetic resonance spectra are in agreement with the structures given[13] (Tables 1 and 2). The following features were observed for each of the compounds **5a–c**. In the ^{31}P-NMR spectrum, the splitting pattern of an AX spin system is observed. In the $^{13}C\{^1H\}$-NMR spectrum, the signal of the Ni-bonded C atom of the methylene group (C-7) is a doublet of doublets at high field; the differing magnitudes of the coupling constants $^2J(P,C\text{-}1)$ and $^2J(P',C\text{-}1)$ (as well as $^2J(P,C\text{-}7)$ and $^2J(P',C\text{-}7)$) (see Table 2) indicate a square-planar geometry at the Ni atom. The C-6 atom of the aromatic ring gives rise to a signal at markedly low field ($\delta = 158\text{–}160$). In the ^1H-NMR spectrum, the nonequivalent, aromatic protons (H-2 to H-5) appear as an ABCD spin system, and the protons of the CH_2 group appear as a broad signal at $\delta = 0$. For **5d**, the chelating ligand assumes a preferred conformation at $T = -120\,^\circ C$. This causes the Ni atom to become a center of chirality, and the protons on C-7 are thus diastereotopic ($\delta = -0.24$ and -0.34, $^2J = 9$ Hz). The NMR spectra of **5d** differ clearly from those of **5a–c** in the high-field shifts of the atoms C-1 and C-7, which are directly bonded to the Ni atom, as well as of the proton H-7. We ascribe this to the stronger shielding of these nuclei on account of the large electron density at the Ni atom; the ligand TMEDA acts only as an electron donor without taking part in back bonding.

Table 1. ^1H-NMR data for the nickelacyclobutabenzene fragment of the compounds **5** (400 MHz [a], $[D_8]THF$, $-80\,^\circ C$ [b], δ values with respect to TMS).

	H-2 1H	H-3 1H	H-4 1H	H-5 1H	H-7 2H
5a	7.17(m)	6.58(m)	6.70(m)	6.24(m)	0.41(d)
5b	7.18(m)	6.59(m)	6.70(m)	6.23(m)	0.38(br. d)
5c	6.17(m)	6.57(m)	6.16(m)	5.99(m)	0.55(dd)
5d	7.03(dd)	6.34(dt)	6.53(dt)	6.00(dd)	−0.26(br. s)

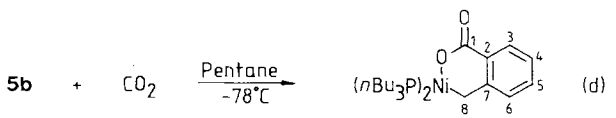
[a] **5a** at 200 MHz. [b] **5c** at $-10\,^\circ C$.

Table 2. ^{13}C-NMR data for the nickelacyclobutabenzene fragment of the compounds **5** (75.5 MHz, $[D_8]THF$, $-80\,^\circ C$ [a]).

	5a	**5b**	**5c**	**5d**
δ values relative to TMS, $J(C,H)$ multiplicities in parentheses				
C-1	134.7 (s)	134.2 (s)	134.5 (s) [b]	128.6 (s)
C-2	122.4 (d)	122.5 (d)	122.8 (d)	121.7 (d)
C-3	124.3 (d)	124.2 (d)	124.3 (d)	122.3 (d)
C-4	125.4 (d)	125.6 (d)	123.8 (d)	123.4 (d)
C-5	129.4 (d)	129.5 (d)	— [c]	128.1 (d)
C-6	160.5 (s)	160.7 (s)	158.0 (s)	159.1 (s)
C-7	−6.3 (t)	−7.1 (t)	0.5 (t)	−17.8 (t)
$\lvert J(P,C)\rvert$ in Hz				
$^2J(P,C\text{-}1)$	25.0	24.9	−[b]	
$^2J(P',C\text{-}1)$	78.2	78.8	−[b]	
$^2J(P,C\text{-}7)$	23.0	23.4	18.3	
$^2J(P',C\text{-}7)$	55.4	56.0	50.9	

[a] **5c** at $-40\,^\circ C$, **5d** at $-60\,^\circ C$. [b] Signal not identified unequivocally. [c] Signal overlapped.

Evidence for the structures of **5a–d** is also provided by chemical reactions. Protolysis of **5b** with HCl in ether results in the nearly quantitative formation of toluene. As expected on account of the ring strain, **5a–d** readily undergo ring expansion: **5b** already undergoes reaction at $-78\,^\circ C$



with carbon dioxide to form the six-membered cyclic carboxylate **6** in high yield [Eq. (d)], which could be characterized unequivocally.[14] Protolysis of **6** with HCl in ether affords *o*-methylbenzoic acid in nearly quantitative yield.

Received: March 6, 1986 [Z 1694 IE]
German version: *Angew. Chem. 98* (1986) 643

[1] a) P. W. Hall, R. J. Puddephatt, C. F. H. Tipper, *J. Organomet. Chem. 84* (1975) 407, and references cited therein; b) M. Ephrithikine, M. L. H. Green, *J. Chem. Soc. Chem. Commun. 1976*, 926, and references cited therein; c) G. Erker, P. Czisch, C. Krüger, J. M. Wallis, *Organometallics 4* (1985) 2059, and references cited therein.
[2] R. H. Grubbs, *Prog. Inorg. Chem. 24* (1978) 1.

[3] T. H. Tulip, D. L. Thorn, *J. Am. Chem. Soc. 103* (1981) 2448; L. Dahlenburg, V. Sinnwell, D. Thoennes, *Chem. Ber. 111* (1978) 3367; V. F. Traven, M. Yu. Eismont, V. V. Redchenko, B. I. Stepanov, *Zh. Obshch. Khim. 50* (1980) 2007; *Chem. Abstr. 94* (1981) 29681z; T. Behling, G. S. Girolami, G. Wilkinson, R. G. Somerville, M. B. Hursthouse, *J. Chem. Soc. Dalton Trans. 1984*, 877; J. A. Statler, G. Wilkinson, M. Thornton-Pett, M. B. Hursthouse, *J. Chem. Soc. Dalton Trans. 1984*, 1731; H. J. R. de Boer, O. S. Akkerman, F. Bickelhaupt, G. Erker, P. Czisch, R. Mynott, J. M. Wallis, C. Krüger, *Angew. Chem. 98* (1986) 641; *Angew. Chem. Int. Ed. Engl. 25* (1986) 639.

[4] J. J. Eisch, A. M. Piotrowski, K. I. Han, C. Krüger, Y.-H. Tsay, *Organometallics 4* (1985) 224.

[5] R. Mynott, R. Neidlein, H. Schwager, G. Wilke, *Angew. Chem. 98* (1986) 374; *Angew. Chem. Int. Ed. Engl. 25* (1986) 367.

[6] W. E. Billups, A. J. Blakeney, W. Y. Chow, *Org. Synth. 55* (1976) 12.

[7] **5a**: **1** (0.5 mL, 4.85 mmol) was added to a vigorously stirred solution of **2a** (1.67 g, 4.14 mmol) in 60 mL of pentane under argon at −20°C. The reaction mixture was then allowed to warm to room temperature and stirred for 30 min. After the reaction mixture had been concentrated to 20 mL and a slightly amorphous precipitate removed, the filtrate was cooled slowly to −78°C and allowed to stand for 1 week at this temperature. The crystals that separated out were filtered off, washed once with cold pentane, and dried at a maximum temperature of −20°C under high vacuum. Yield: 1.21 g (3.14 mmol, 76%) greenish brown crystals.

[8] **5b**: Synthesized analogously to **5a**. Green crystals, yield 68%.

[9] **5c**: **1** (0.5 mL, 4.85 mmol) was added to a solution of **3** (1.92 g, 1.74 mmol) in 50 mL of toluene at −20°C under argon. The reaction mixture was then stirred over night at room temperature, during which time a finely crystalline, yellow precipitate separated out. After 1 d at −20°C, the yellow crystals were collected on a D_4 frit, washed with ether, and then dried at room temperature under high vacuum. Yield: 936 g (1.39 mmol, 80%) of yellow microcrystals.

[10] K. Fischer, K. Jonas, G. Wilke, *Angew. Chem. 85* (1973) 620; *Angew. Chem. Int. Ed. Engl. 12* (1973) 525.

[11] TMEDA (0.62 mL, 4.15 mmol) was added to a freshly prepared solution of CDT-Ni (CDT = all-*trans*-1,5,9-cyclododecatriene) [15] **4** in 20 mL of Et_2O at −78°C. **1** (0.75 mL, 5.03 mmol) was then added to the clear solution at −78°C and the reaction mixture was allowed to warm over 3 h to −20°C. The reaction mixture turned cloudy and ethylene evolved. In order to achieve complete crystallization, the mixture was cooled for 1 d at −78°C. The precipitate was filtered under suction while still cold, washed twice with cold Et_2O, and dried at −20°C under high vacuum. Yield: 770 mg (2.91 mmol, 70%) of greenish brown microcrystals.

[12] The elemental analyses are in agreement with the empirical formulas.

[13] NMR data collection, NMR-Labor, Max-Planck-Institut für Kohlenforschung, Kaiser-Wilhelm-Platz 1, D-4330 Mülheim a. d. Ruhr (FRG).

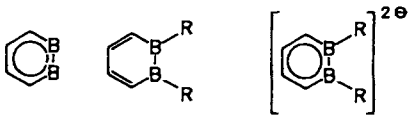
[14] **6**: **5b** (770 mg, 1.39 mmol) was dissolved in 50 mL of pentane under argon and allowed to react at −78°C with 200 mL (8.9 mmol) of CO_2. During the course of CO_2 addition, a yellow, crystalline material separated out. In order to achieve complete crystallization, the reaction mixture was allowed to stand for 1 d at −78°C. The crystals were then collected on a cooled frit by suction filtration, washed twice with cold pentane, and dried under high vacuum. Yield: 670 mg (1.12 mmol, 81%) of yellow crystals; correct elemental analysis. ^{1}H-NMR (400 MHz, [D$_8$]THF, −80°C, selected): δ = 7.49 (d, 1H; H-3), 7.0 (m, 3H; H-4, H-5, H-6), 2.29 (br, 2H; H-8); ^{13}C-NMR (75.5 MHz, [D$_8$]THF, −50°C, selected): δ = 169.8 (s, C-1), 138.2 (s, C-2), 129.4 (d, C-3), 123.1 (d, C-4), 129.9 (d, C-5), 125.9 (d, C-6), 145.0 (s, C-7), 27.4 (t, C-8, ^2J(P,C) = 28.0 Hz, ^2J(P′,C) = 53.9 Hz); ^{31}P-NMR (32 MHz, [D$_8$]THF, −80°C): δ = 9.3, 18.4 (^2J(P′,P) = 13.4 Hz); IR (KBr): $\tilde{\nu}$ = 1631 (s, C=O) cm^{-1}.

[15] B. Bogdanovic, M. Kröner, G. Wilke, *Justus Liebigs Ann. Chem. 699* (1966) 1.

A 1,2-Diboratabenzene: Lithium Salt and Transition Metal Complexes**

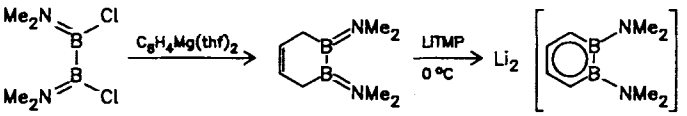
By *Gerhard E. Herberich,* Bernd Hessner,* and *Martin Hostalek*

1,2-Diborabenzene **1** and its derivatives have so far never been reported in the literature. Possibly the most important representatives of **1** are the 1,2-dibora-3,5-cyclohexadienes **2**, the 1,2-diboratabenzene ions **3**, and transition-metal complexes in which **2** and **3** are stabilized as ligands. We report here on the first entry to 1,2-diboratabenzene derivatives.



1 **2** **3**

The diborane(4) $Cl(Me_2N)BB(NMe_2)Cl$[1] smoothly reacts with $C_4H_6Mg(THF)_2$[2] (THF = tetrahydrofuran) to give the liquid 1,2-dibora-4-cyclohexene derivative **4**.[3,4] Metalation of **4** with lithium 2,2,6,6-tetramethylpiperidide (LiTMP) affords the sparingly soluble lithium 1,2-diboratabenzene derivative **5**;[4,5] this can be converted by reaction with *N,N,N′,N′*-tetramethylethylenediamine (TMEDA) into the readily crystallizable salt $[Li(TMEDA)]_2[1,2\text{-}C_4H_4(BNMe_2)_2]$ **6**, which is soluble in THF.



4 **5**

The salt **6** has a triple-decker structure with crystallographic C_2 symmetry (Fig. 1).[6] The structure can be interpreted as a contact ion triple. The 1,2-diboratabenzene ring is virtually planar (twist conformation; maximum vertical deviation 4.2 pm). The bonding pattern in the C_4B_2 ring is that of a delocalized 6π-electron system. As can be expected, the Li(TMEDA) groups are shifted from the B atoms in the direction of the atoms C2 and C2′; the acentricity of the bonding (slip distortion) is 14.9 pm.[7]

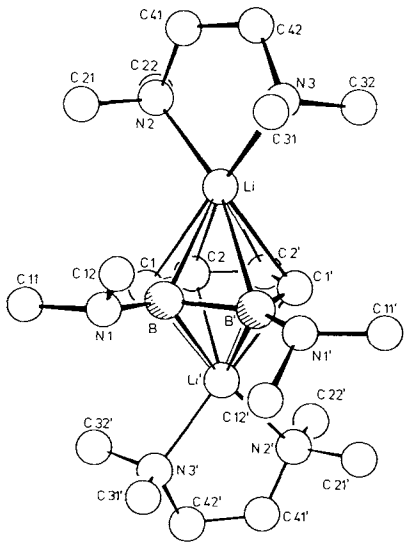
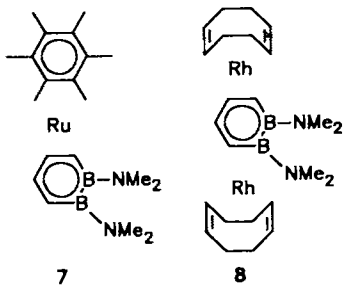


Fig. 1. Structure of **6**. Selected bond lengths [pm]: Li-C2 228.8(9), Li-C2′ 226.3(8), Li-C1 235.1(8), Li-C1′ 236.8(7), Li-B 247.1(8), Li-B′ 255.3(8), Li-N2 216.4(7), Li-N3 216.2(8); in the anion: B-B′ 170.6(8), B-C1 150.5(6), C1-C2 141.3(6), C2-C2′ 141.7(8), B-N1 149.5(5).

[*] Prof. Dr. G. E. Herberich, Dr. B. Hessner, Dipl.-Chem. M. Hostalek
Institut für Anorganische Chemie der Technischen Hochschule
Professor-Pirlet-Strasse 1, D-5100 Aachen (FRG)

[**] Derivatives of 1,2-Diborabenzene, Part 1. This work was supported by the Fonds der Chemischen Industrie.

Reaction of **5** with transition-metal halides affords sandwich and triple-decker complexes. For example, reaction with $[\{(C_6Me_6)RuCl_2\}_2]$ furnishes the yellow 18e complex **7**,[4,8] while reaction with $[\{(1,5\text{-cod})RhCl\}_2]$ leads to formation of the dark-red, 30e triple-decker complex **8**.[4,9]



7 **8**

The constitution of the new compounds **4–8** follows from their NMR data. In **4**, the rotation of the Me_2N groups about the B–N bond is, as expected, slow, while in **6–8** it is rapid. The π-interaction between the lone pair on the nitrogen atom and the p_z orbital of the boron atom is thus reduced in **6–8**. The same interaction also weakens the boron–metal interaction in **7** and **8**. The ^{11}B-NMR resonances of **7** and **8** therefore lie on the low-field limit of the range expected for facially bonded boron heterocycles.[10]

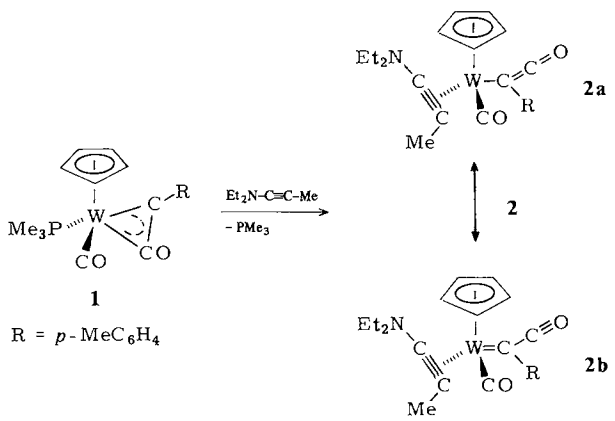
Received: February 27, 1986;
supplemented: April 25, 1986 [Z 1684 IE]
German version: *Angew. Chem. 98* (1986) 637

[1] H. Nöth, H. Schick, W. Meister, *J. Organomet. Chem. 1* (1964) 401.
[2] K. Fujita, Y. Ohnuma, H. Yasuda, H. Tani, *J. Organomet. Chem. 113* (1976) 201.
[3] Procedure: $Cl(Me_2N)BB(NMe_2)Cl$ **1** (21.1 g, 117 mmol) was added dropwise at −80°C to a stirred solution of $C_4H_6Mg(THF)_2$ [2] (38.7 g, 174 mmol) in Et_2O (300 mL). The mixture was slowly warmed to room temperature and stirred for a further 2 h. Filtration, washing of the residue with 3 × 80 mL of Et_2O, and subsequent distillation of the filtrate and washings under vacuum (finally at 10^{-6} bar) afforded 13.2 g (81 mmol, 69%) of **4**; colorless, air- and moisture-sensitive liquid, b.p. 27°C/10^{-6} bar.—^{1}H-NMR (80 MHz, $CDCl_3$, 30°C): $\delta = 5.63$ (t, $J = 2$ Hz; 4-H/5-H), 2.88 (s, 2Me), 2.76 (s, 2Me), 1.61 (d, $J = 2$ Hz; $2CH_2$). ^{11}B-NMR ($CDCl_3$): $\delta = 51$. ^{13}C-NMR ($CDCl_3$, −70°C): $\delta = 129.8$ (dm, $^1J = 153.2$ Hz; C-4/C-5), 45.4 (qq, $^1J = 133.7$, $^3J = 4.5$ Hz; $2CH_3$), 38.5 (qq, $^1J = 134.2$, $^3J = 4.5$ Hz; $2CH_3$), 23.9 (t, br, $^1J = 114$ Hz; $2CH_2$). MS (70 eV): *m/z* 164 ($M^{\oplus}$, 100%).
[4] Correct C,H analysis.
[5] Procedure: **5**: Mixing of the reactants in THF at 0°C, 3 h stirring at 20°C, filtration, washing with pentane, and drying in a high vacuum afforded **5** as a white, pyrophoric, extremely moisture-sensitive powder; yield 92%.—**6**: To a solution of 1.35 g (9.2 mmol) of LiTMP in THF (15 mL) at −80°C were added 1.07 g (9.2 mmol) of TMEDA and 0.75 g (4.6 mmol) of **4**. The mixture was slowly warmed and kept at room temperature for 3 h and then treated with 25 mL of pentane. Cooling to −70°C afforded 0.95 g (2.33 mmol; 51%) of **6** as large, yellowish-white crystals; dec. 96°C; air- and moisture-sensitive, readily soluble in THF.—^{1}H-NMR (80 MHz, [D$_8$]THF, 30°C): $\delta = 6.05$ (m, 4-H/5-H), 5.34 (m, 3-H/6-H), 2.69 (s, 4Me), 2.18 (s, $4CH_2$), 2.09 (s, 8Me). ^{11}B-NMR ([D$_8$]THF): $\delta = 37$ (br.). ^{13}C-NMR ([D$_8$]THF, −70°C): $\delta = 108.5$ (dd, $^1J = 146.5$, $^3J = 8.3$ Hz; C-4/C-5), 104.6 (d, $^1J = 127.5$ Hz; C-3/C-6), 56.5 (t, $^1J = 132.2$ Hz; $4CH_2$), 46.1 (q, $^1J = 131.3$ Hz; $4CH_3$), 43.5 (q, $^1J = 129.8$ Hz; $8CH_3$).
[6] CAD4, $Cu_{K\alpha}$ radiation, temperature of measurement: −65°C. **6**: $P4_32_12$ (No. 96), $a = 954.3(4)$, $c = 3016.5(8)$ pm; $V = 2.747(3)$ nm^3; $Z = 4$; $\rho_{calc} = 0.987$ g cm^{-3}; 1657 independent reflections with $I > 3\sigma(I)$; non-hydrogen atoms refined anisotropically, H-atoms placed at calculated positions; 136 parameters, $R = 0.087$, $R_w = 0.085$ with $w = 1$; the C-atoms of the TMEDA ligands show increased temperature factors. Further details of the crystal structure investigation are available on request from the Fachinformationszentrum Energie, Physik, Mathematik GmbH, D-7514 Eggenstein-Leopoldshafen 2, on quoting the depository number CSD-51866, the names of the authors, and the full citation of the journal.
[7] The acentricity is the distance of the projection of the lithium atom onto the ring plane from the geometric centroid of the C_4B_2 ring.
[8] Procedure: **7**: Reaction in THF, crystallization from hexane at −30°C, yield 20%; yellow needles, m.p. 162–164°C, air- and moisture-sensitive, readily soluble in all common organic solvents.—^{1}H-NMR (80 MHz, CD_2Cl_2, 30°C): $\delta = 4.56$ (m, 4-H/5-H), 2.95 (m, 3-H/6-H), 2.78 (s, 4Me), 2.12 (s, C_6Me_6). ^{11}B-NMR (CD_2Cl_2): $\delta = 30.4$. ^{13}C-NMR (CD_2Cl_2, 30°C): $\delta = 92.8$ (s, C_6Me_6), 88.0 (d, $^1J = 159.2$ Hz; C-4/C-5), 73.4 (d, Br, $^1J \approx 125$ Hz; C-3/C-6), 42.6 (q, $^1J = 130.0$ Hz; $4CH_3$), 17.4 (q, $^1J = 127.4$ Hz; $C_6(CH_3)_6$). MS (70 eV): *m/z* 426 ($M^{\oplus}$, 41%), 371 ($M^{\oplus} - BNMe_2$, 100%).
[9] Procedure: **8**: Reaction in THF, crystallization from hexane at −80°C (twice), yield 58%; dark-red crystals, m.p. 104–106°C, air- and moisture-sensitive, readily soluble in all common organic solvents.—^{1}H-NMR (80 MHz, CD_2Cl_2, 30°C): $\delta = 4.99$ (m, 4-H/5-H), 4.16 (m, 8CH), 3.70 (m, 3-H/6-H), 2.88 (s, 4Me), 2.33–1.60 (m, $8CH_2$). ^{11}B-NMR (CD_2Cl_2): $\delta = 19$. ^{13}C-NMR (CD_2Cl_2, 30°C): $\delta = 78.6$ (d, br, $^1J = 144$ Hz; C-3/C-6), 74.9 (d, $^1J = 170.6$ Hz; C-4/C-5), 71.7 (dd, $^1J = 158.2$, $^3J = 6.9$ Hz; 8CH), 42.6 (q, $^1J = 135.9$ Hz; $4CH_3$), 32.0 (t, $^1J = 126.9$ Hz; $8CH_2$). MS (70 eV): *m/z* 584 ($M^{\oplus}$, 100%).
[10] H. Nöth, B. Wrackmeyer in P. Diehl, E. Fluck, R. Kosfeld (Eds.): *NMR Basic Principles and Progress, Vol. 14*, Springer, Berlin 1978.

Variable Electron-Donor Ability of Alkyne Ligands—Synthesis and Structure of Carbonyl(η^5-cyclopentadienyl)(η^2-1-diethylamino-1-propyne)(η^1-*p*-methylphenylketenyl)tungsten**

By *Fritz R. Kreissl,* Gabriele Reber,* and *Gerhard Müller*

Depending on the electronic requirements of the metal atom, the ketenyl ligand −C(R)=C=O in transition metal complexes is η^1-[1,2] or η^2-coordinated.[3] In both cases it characteristically exhibits pronounced electrophilicity. Consequently, electron-rich ynamines such as 1-diethylamino-1-propyne should undergo a cycloaddition reaction with the C=C or C=O double bond of the ketenyl ligand.[4] Surprisingly, however, the reaction of carbonyl(η^5-cyclopentadienyl)(*p*-methylphenylketenyl)(trimethylphosphane)tungsten **1** with the aforementioned ynamine leads via replacement of trimethylphosphane and concomitant opening of the WC_2 three-membered ring in **1** to the alky-



[*] Priv.-Doz. Dr. F. R. Kreissl, Dipl.-Chem. G. Reber, Dr. G. Müller
Anorganisch-chemisches Institut der Technischen Universität München
Lichtenbergstr. 4, D-8046 Garching (FRG)

[**] Transition Metal-Ketene Compounds, Part 27. This work was supported by the Deutsche Forschungsgemeinschaft and the Fonds der Chemischen Industrie. We thank Mr. *J. Riede* for assistance with the X-ray structure investigation.—Part 26: W. J. Sieber, D. Neugebauer, F. R. Kreissl, *Z. Naturforsch. B40* (1985) 1500.

neketenyl complex **2**, which, according to spectroscopic findings (IR, NMR), contains an η^1-bonded *p*-methylphenylketenyl ligand.

The ketenyl ligand in **2** ought to function as a 1e-donor, whereas the ynamine ligand should act as a 4π-electron donor, if one assumes an 18e-configuration at the tungsten atom. However, the X-ray structure analysis[5] surprisingly indicates a weaker donor action of the ynamine ligand and a stronger donor action of the ketenyl ligand. The pseudotetrahedral structure of **2** (Fig. 1) is characterized by a

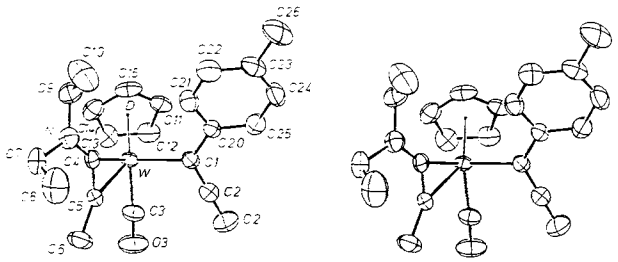


Fig. 1. Stereoplot of the molecular structure of **2** (ORTEP, thermal ellipsoids 50%, without H atoms). Important bond lengths [Å] and angles [°]: W-C1 2.171(6), W-C3 1.963(6), W-C4 2.032(6), W-C5 2.038(6), C1-C2 1.301(8), C2-O2 1.173(7), C1-C20 1.467(8), C4-C5 1.339(8), C4-N 1.354(7), N-C7 1.462(9), N-C9 1.459(8), C3-O3 1.158(7); W-C1-C2 107.3(5), W-C1-C20 129.7(4), C1-C2-O2 179.5(7), W-C3-O3 175.9(7), C20-C1-C2 122.9(6), C4-C5-C6 140.7(6), N-C4-C5 136.7(6).

short W-$C1_{ketene}$ bond (2.171(6) Å), whose length lies in the range found for W=$C_{carbene}$ bonds.[6,7] It is distinctly shorter than the W-C_{ketene} bond in the related *p*-methylphenylketenyl complex **3** (2.27(2) Å).[1]



3, R = *p*-MeC_6H_4

That the structure of **2** should be described in terms of the resonance structures **2a** and **2b** is underscored by the bond lengths C1-C2 (1.301(8) Å) and C2-O2 (1.173(7) Å), which are markedly longer and shorter, respectively, than the corresponding bonds in **3** (1.24(3) and 1.21(3) Å).[1] Moreover, the C1-C20 bond is also relatively short, and the aromatic ring is tilted by only 24.2° with respect to the W,C1,C2,C20 plane, so that an effective π-electron delocalization should be possible. The fact that the ketenyl ligand in **2** can donate more than one electron to the metal center is all the more surprising, since the planar geometry at the nitrogen atom and the interplanar angle C4,N,C7,C9/W,C4,C5 of only 7.3° in the ynamine ligand allow for optimal *p*-orbital overlap.[8]

It was hitherto usual, on the basis of an 18e-configuration for the central metal atom, to classify acetylene ligands as 2e- or 4e-donors.[9-11] It seems to us, however, that these are merely limiting cases, where the 4e-donor extreme could hardly ever be completely realized!

Experimental

A solution of **1** (0.48 g, 1 mmol) in toluene (30 mL) was treated under inert gas (argon) with 0.17 g (1.5 mmol) of 1-diethylamino-1-propyne and stirred for ca. 2 h at 25 °C. The solution slowly changed color from violet to reddish-orange. After removal of solvent, the residue was taken up in dichloromethane (10 mL); subsequent addition of pentane led to precipitation of the complex **2**. Repeated recrystallization from dichloromethane/pentane gave 0.42 g (81% yield) of the red crystals.

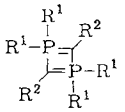
Received: March 4, 1986 [Z 1689 IE]
German version: *Angew. Chem. 98* (1986) 640

[1] F. R. Kreissl, A. Frank, U. Schubert, T. L. Lindner, G. Huttner, *Angew. Chem. 88* (1976) 649; *Angew. Chem. Int. Ed. Engl. 15* (1976) 632.
[2] F. R. Kreissl, K. Eberl, W. Uedelhoven, *Chem. Ber. 110* (1977) 3782.
[3] F. R. Kreissl, P. Friedrich, G. Huttner, *Angew. Chem. 89* (1977) 110; *Angew. Chem. Int. Ed. Engl. 16* (1977) 102.
[4] H. G. Viehe: *The Chemistry of Acetylenes*, Marcel Decker, New York 1969.
[5] Crystal structure data: $C_{22}H_{25}NO_2W$, $M_r = 519.3$, monoclinic, $P2_1/n$, $a = 8.138(1)$, $b = 13.895(5)$, $c = 18.104(3)$ Å, $\beta = 98.23(1)°$, $V = 2026.1$ Å^3, $\rho_{calc} = 1.702$ g/cm^3 for $Z = 4$. 22°C. 4720 measured reflections, of which 4384 independent ($R_{int} = 0.01$) and 3404 observed with $I \geq 2\sigma(I)$ ($\theta - 2\theta$ scan, $\Delta\omega = 1.0 + 0.35 \tan\theta$, $1 \leq \theta \leq 27.4°$, $\pm h$, $+k$, $+l$, $Mo_{K\alpha}$, $\lambda =$ 0.71069 Å, Enraf-Nonius CAD4). Lp and empirical absorption correction (rel. transmission = 50.7-99.8%). Solution by Patterson methods, $R = 0.027$, $R_w = 0.029$, $w = 1/\sigma^2(F_0)$ (anisotropic, H constant, 235 parameters, SHELX 76). $\Delta\rho_{fin}$(max/min) = +0.64/−1.06 e/Å^3. Further details of the crystal structure investigation are available on request from the Fachinformationszentrum Energie, Physik, Mathematik GmbH, D-7514 Eggenstein-Leopoldshafen 2, on quoting the depository number CSD-51869, the names of the authors, and the full citation of the journal.
[6] W=C = 2.15(1) Å in $[(CO)_5W{=}C(C_6H_5)_2]$: C. P. Casey, T. J. Burkhardt, C. A. Bunnell, J. C. Calabrese, *J. Am. Chem. Soc. 99* (1977) 2127.
[7] The length of the W-CH_3 bond in $[(C_5H_5)_2W(CH_3)C_2H_4P(CH_3)_2C_6H_5][PF_6]$ is 2.25 Å: R. A. Forder, G. D. Gale, K. Prout, *Acta Crystallogr. B31* (1975) 307.
[8] The approximate colinearity and coplanarity of the C≡C axis with the CO ligand (the deviation of the atoms W, C3, O3, C4, C5 from the best plane through them is maximally 0.04 Å) is a common feature of CO-containing alkyne complexes and maximizes the back-bonding to these ligands: B. E. R. Schilling, R. Hoffmann, J. W. Faller, *J. Am. Chem. Soc. 101* (1979) 592. Cf. [9].
[9] L. Ricard, R. Weiss, W. E. Newton, G. J.-J. Chen, J. W. McDonald, *J. Am. Chem. Soc. 100* (1978) 1318.
[10] B. Capelle, A. L. Beauchamp, M. Dartiguenave, Y. Dartiguenave, *J. Chem. Soc. Chem. Commun. 566* (1982).
[11] H. G. Alt, H. I. Hayen, *Angew. Chem. 95* (1983) 1030; *Angew. Chem. Int. Ed. Engl. 22* (1983) 1008; *Angew. Chem. Suppl. 1983*, 1364.

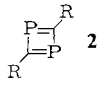
1,3-Diphosphacyclobutadienecobalt(I) Complexes from Phosphaalkynes**

By *Paul Binger,* Roman Milczarek, Richard Mynott, Manfred Regitz,* and *Wolfgang Rösch*

In the past few years the synthesis of a number of λ^5-1,3-diphosphetes **1** has been accomplished by dimerization steps which presumably involve participation of λ^5-phosphaalkynes.[1] In contrast, λ^3-1,3-diphosphetes ("1,3-diphosphacyclobutadienes"), which should be antiaromat-



1



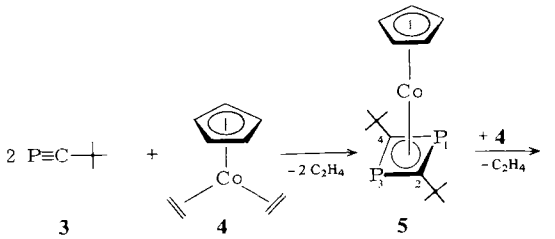
2

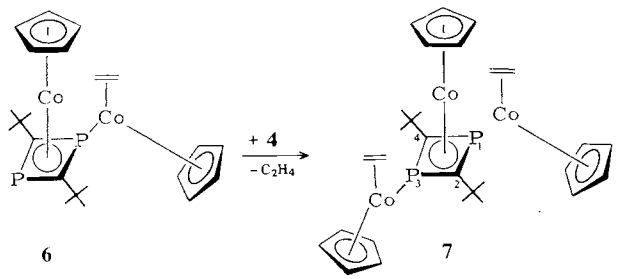
[*] Priv.-Doz. Dr. P. Binger, Dipl.-Chem. R. Milczarek, Dr. R. Mynott
Max-Planck-Institut für Kohlenforschung
Kaiser-Wilhelm-Platz 1, D-4330 Mülheim a. d. Ruhr (FRG)
Prof. Dr. M. Regitz, Dipl.-Chem. W. Rösch
Fachbereich Chemie der Universität
Erwin-Schrödinger-Strasse, D-6750 Kaiserslautern (FRG)

[**] Phosphorus Compounds of Unusual Coordination, Part 11. This work was supported by the Fonds der Chemischen Industrie and the Landesregierung von Rheinland-Pfalz.—Part 10: H. Keller, G. Maas, M. Regitz, *Tetrahedron Lett. 27* (1986) 1903.

ic, have so far never been reported. They could possibly be prepared and stabilized by cyclodimerization of λ^3-phosphaalkynes such as **3** on suitable transition metal complexes. It is known, e.g., that **3**[2] forms side-on complexes with platinum[3] and can function as a bridging ligand in metal clusters.[4] We chose the cobalt complex **4**,[5] since its ethylene ligands can be replaced by alkynes and it is capable of undergoing alkyne-cyclooligomerization.[6]

When **4** is allowed to react with **3** in ether/pentane at -30°C, the monocobalt complex **5**, the dicobalt complex **6**, or the tricobalt complex **7** is obtained, depending upon the molar ratio of the reactants; **5**, **6**, and **7** are red to reddish-brown, crystalline compounds, a common feature of which is the novel λ^3-1,3-diphosphete structural unit. The complexes **6** and **7** can also be prepared by reaction of **5** and of **5** or **6**, respectively, with **4**.





The compounds **5**, **6**, and **7** gave correct elemental analyses. The molar mass of **5** was determined mass spectrometrically (*m/z* 324, 96% relative intensity). **6** and **7** are less stable: the first fragment in the case of **7** has *m/z* 572 (7%) and is formed by loss of two ethylene units.

Consistent with the structures of **5**[10] and **7**, the atoms of the four-membered ring each give rise to only one signal in the ^{31}P-NMR (**5**: $\delta = 38.1$; **7**: $\delta = 85.9$) and ^{13}C-NMR spectra (**5**: $\delta = 107.55$, t, $J(P,C) = 54.4$ Hz; **7**: $\delta = 99.38$, t, $J(P,C) = 22.1$ Hz). In contrast, the ^{31}P-NMR spectrum of **6** shows two resonance signals ($\delta = 134.9$, -32.0), the downfield signal being somewhat broadened (halfwidth 35 Hz, σ-bonded to Co). However, in the ^{13}C-NMR spectrum C-2/C-4 give rise to only one signal, a doublet of doublets [$\delta = 102.8$, $J(P,C) = 58.7$, 19.6 Hz].[7] Thus, it follows that for each phosphorus atom the bond to both former phosphaalkyne-carbon atoms in the dicobalt complex **6** must be the same. Alternative structures such as diphosphacobaltacyclopentadienes or complexes with σ- and π-bonded phosphaalkynes can therefore be ruled out. The signal multiplicities for C-2/C-4 in the ^{13}C-NMR spectra of **5** and **7** are also consistent with a diphosphete structure, but do not conclusively prove the chemical and magnetic equivalence of the two phosphorus atoms, since an ABX spin system (A, B = ^{31}P, X = ^{13}C) with a large coupling constant J_{AB} could also explain the splitting pattern.[8] (Since both phosphorus atoms would then not be directly bonded to the ^{13}C-atom, they would form an AB spin system with a very small chemical shift difference due to the isotope effect.)

Monocobalt complexes of the type **5** were also obtained from bisethylene(indenyl)cobalt and **3** or 2-methylpropylidinephosphane (**3**, $CH(CH_3)_2$ instead of $C(CH_3)_3$).[12]

Experimental

5: A solution of **3** [2] (2.0 g, 20.0 mmol) in ether/pentane (10 mL, anhydrous) was added dropwise with stirring (under argon) at -30°C to a solution of **4**[5] (1.4 g, 7.8 mmol) in ether/pentane (1:1; 20 mL, anhydrous). After stirring for one hour at -5°C, the mixture was evaporated to dryness, the crystalline residue dissolved in 10 mL of pentane (anhydrous), filtered over Florisil, and cooled to -78°C for 12 h, whereupon **5** crystallized out. The solvent was removed with a glass siphon and the crystals of **5** dried at 10^{-3} torr. Yield 1.70 g (67%) of reddish-brown crystals, m.p. 54°C.

6: As described for **5**; 0.7 g (3.7 mmol) of **4** [5] and 0.4 g (4.0 mmol) of **3** [2] furnish 0.4 g (50%) of **6** as reddish-brown crystals, m.p. 125°C (decomp.).

7: As described for **5**; 1.6 g (8.9 mmol) of **4** [5] and 0.6 g (6.0 mmol) of **3** [2] afford 0.8 g (43%) of **7** as red needles, m.p. 135°C (decomp.).

Received: March 10, 1986;
Supplemented: April 18, 1986 [Z 1697 IE]
German version: *Angew. Chem. 98* (1986) 645

[1] **1**, $R^1 = Ph$, $R^2 = PPh_3^{\oplus}Cl^{\ominus}$: R. Appel, F. Knoll, H. D. Wihler, *Angew. Chem. 89* (1977) 415; *Angew. Chem. Int. Ed. Engl. 16* (1977) 402; **1**, $R^1 = NMe_2$, $R^2 = H$: J. Svava, E. Fluck, H. Riffel, *Z. Naturforsch. B40* (1985) 1258; **1**, $R^1 = Ph$, $R^2 = PO(NiPr_2)_2$ etc.: H. Keller, G. Maas, M. Regitz, *Tetrahedron Lett. 27* (1986) 1903.

[2] G. Becker, G. Gresser, W. Uhl, *Z. Naturforsch. B36* (1981) 16.

[3] J. C. T. R. Burckett-St. Laurent, P. B. Hitchcock, H. W. Kroto, J. F. Nixon, *J. Chem. Soc. Chem. Commun. 1981*, 1141; S. J. Al-Resayes, P. B. Hitchcock, M. F. Meidine, J. F. Nixon, *J. Chem. Soc. Chem. Commun. 1984*, 1080.

[4] Review: O. J. Scherer, *Angew. Chem. 97* (1985) 905; *Angew. Chem. Int. Ed. Engl. 24* (1985) 924.

[5] K. Jonas, E. Defense, D. Habermann, *Angew. Chem. 95* (1983) 729; *Angew. Chem. Int. Ed. Engl. 22* (1983) 716.

[6] K. Jonas, *Angew. Chem. 97* (1985) 292; *Angew. Chem. Int. Ed. Engl. 24* (1985) 295.

[7] **5**: ^{1}H-NMR (400 MHz, [D$_8$]toluene): $\delta = 0.91$ (s, 18H; $C(CH_3)_3$), 4.92 (s, 5H; C_5H_5); ^{13}C-NMR (75.5 MHz, [D$_8$]toluene, -50°C): $\delta = 31.21$ ($J(H,C) = 125$ Hz, $J(P,C) = 4.1$ Hz; $C(CH_3)_3$), 34.33 ($J(P,C) = 7.1$ Hz; $C(CH_3)_3$), 81.53 ($J(H,C) = 177$ Hz; C_5H_5), 107.55 ($J(P,C) = 54.4$ Hz, C-2,4). —**6**: ^{1}H-NMR (400 MHz, [D$_8$]toluene): $\delta = 1.01$ (s, 18H; $C(CH_3)_3$), 2.06, 2.67 (each m, each 2H; C_2H_4), 4.62, 4.84 (each s, each 5H; C_5H_5); ^{13}C-NMR (75.5 MHz, [D$_8$]toluene, -50°C): $\delta = 26.81$ ($J(H,C) = 154$ Hz; C_2H_4), 30.81 ($J(H,C) = 126$ Hz; $C(CH_3)_3$), 32.75 ($J(P,C) = 3.7$ and 7.1 Hz; $C(CH_3)_3$), 80.31 ($J(H,C) = 177$ Hz; η-C_5H_5-Co(η)), 82.35 ($J(H,C) = 177$ Hz, $J(P,C) = 2.4$ Hz; η-C_5H_5-Co(σ)), 102.82 ($J(P,C) = 58.7$ and 19.6 Hz; C-2,4).—**7**: ^{1}H-NMR (200 MHz, [D$_8$]toluene): $\delta = 1.15$ (s, 18H; $C(CH_3)_3$), 2.04, 2.81 (each m, each 4H; C_2H_4), 4.48 (s, 5H; C_5H_5), 4.57 (s, 10H; C_5H_5); ^{13}C-NMR (75.5 MHz, [D$_8$]toluene, -30°C): $\delta = 27.08$ ($J(H,C) = 154$ Hz; C_2H_4), 30.65 ($J(H,C) = 126$ Hz, $J(P,C) = 5.0$ Hz; $C(CH_3)_3$), 33.02 ($J(P,C) = 4.2$ Hz; $C(CH_3)_3$), 80.26 ($J(H,C) = 176$ Hz; η-C_5H_5-Co(η)), 82.67 ($J(H,C) = 174$ Hz; η-C_5H_5-Co(σ)), 99.38 ($J(P,C) = 22.1$ Hz; C-2,4).

[8] D. A. Redfield, V. H. Nelson, L. W. Cary, *Inorg. Nucl. Chem. Lett. 10* (1974) 727; P. W. Jolly, R. Mynott, *Adv. Organomet. Chem. 19* (1981) 257.

[9] W. Rösch, U.-J. Vogelbacher, T. Allspach, M. Regitz, *J. Organomet. Chem. 306* (1986) 39.

[10] *Note added in proof* (April 16, 1986): In the meantime the structure of **5** has also been confirmed by a crystal structure analysis, according to which the 1,3-diphosphacyclobutadiene is almost planar and the PC distances are all equal [11].

[11] C. Krüger, Y.-H. Tsay (Mülheim a. d. Ruhr), private communication.

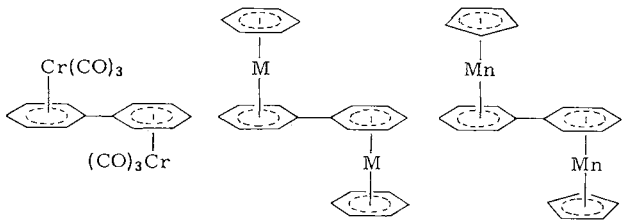
[12] Editorial note: The synthesis and characterization of **5** has also been reported elsewhere very recently: M. J. Maah, J. F. Nixon, *J. Chem. Soc. Chem. Commun. 1986*, 737.

$[\{(\eta^5\text{-}C_5Me_5)Co\}_3C_{12}H_{10}]$—A Complex of Biphenyl with Kekulé Structure

By *Herbert Lehmkuhl,* Hans Nehl, Reinhard Benn,* and *Richard Mynott*

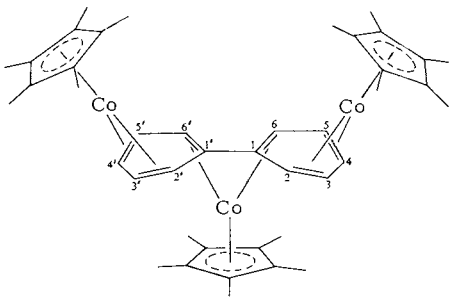
Only a few examples of transition-metal complexes with π-bonded biphenyl are known; in these compounds the biphenyl can function as a singly or, as in **1**-**3**,[1-4] as a doubly η^6-bonded ligand.

Complex **1** is obtained along with (η^6-biphenyl)tricarbonylchromium directly by heating $[Cr(CO)_6]$ with biphenyl,[1] but in the preparation of complexes **2** and **3**, the biphenyl is formed only in the course of the reaction. Compounds **2** are prepared starting from $[(\eta^6\text{-}C_6H_6)(\eta^6\text{-}C_6H_5Li)M]$ and $[(\eta^6\text{-}C_6H_6)(\eta^6\text{-}C_6H_5Br)M]$,[2,3] and compounds **3** are formed via the intermediacy of $[CpMn(C_6H_5)]$ (Cp = cyclopentadienyl).[4]



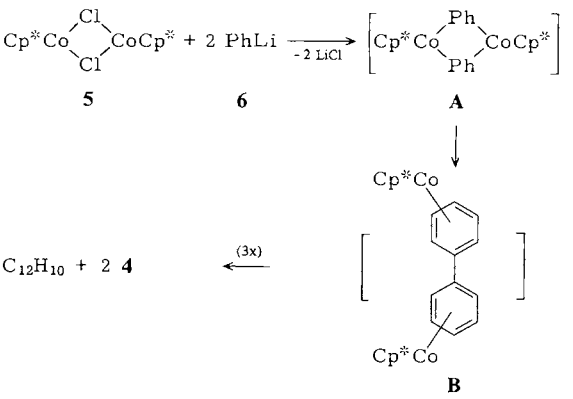
1 **2**, M = Cr, V **3**

We have now prepared a novel trinuclear metal complex, $[(Cp^*Co)_3C_{12}H_{10}]$ **4**, in which the 12-electron biphenyl ligand functions as three η^4-coordinated diene units ($Cp^* = \eta^5$-pentamethylcyclopentadienyl).



4

Complex **4** was obtained as black crystals in 69% yield along with free biphenyl upon reaction of dimeric (η^5-pentamethylcyclopentadienyl)cobalt chloride **5**[5] with phenyllithium **6**. In analogy to the formation of **3** from [CpMnPh], prepared in situ,[4] compound **5** probably reacts with PhLi in the first step to give **A** followed by reductive coupling of the two phenyl moieties to form **B**. However, in contrast to the stable complex **3**, containing the ligand η^6-coordinated to manganese, the cobalt in **B** has two additional electrons and will strive to achieve an η^4-coordination. Thus, **B** retains a free conjugated diene system, to which a third Cp*Co fragment is complexed when **B** disproportionates to form biphenyl and complex **4**.



Although it has not yet been possible to obtain suitable single crystals of **4** for an X-ray structure analysis, NMR investigations provide unequivocal confirmation of the structure shown. The ^{1}H-NMR spectrum (Table 1) exhibits five signals for the ten pairwise equivalent ligand protons (H2,2′ to H6,6′), which is in accord with a biphenyl ligand consisting of two identical phenyl moieties. In addition, two resonance signals with the intensity ratio 2:1 are observed for the methyl protons of the three Cp* groups, as expected for the suggested structure with three η^4-coordinated Cp*Co fragments, two of which are identical.

The assignment of the proton signals obtained from analysis of the chemical shifts and the H,H couplings was confirmed by observation of nuclear Overhauser effects (NOE) between the corresponding vicinal protons. On the other hand, no NOE signal enhancement was observed between the nonequivalent Cp* moieties, nor between H2 and H6′, as would have been expected if the inner diene moiety were s-*trans* (i.e., if the molecule had C_2 symmetry).[6]

The twelve pairwise equivalent C atoms of the ligand (C1,1′ to C6,6′) give rise to six ^{13}C-NMR signals (Table 1). All the C atoms are involved in the complexation. As is typical for (η^4-diene)metal systems, the terminal atoms (C2, C5, and C6) of the diene units are more strongly shielded, relative to those of noncoordinated ligands, than the inner atoms (C1, C3, and C4). Also consistent with the known properties of (η^4-diene)metal complexes is the find-

Table 1. NMR data of **4**.

Proton	^{1}H-NMR [a] δ	Intensity	$J_{H,H}$ [Hz]	^{13}C-NMR [c] C Atom [d]	δ	$^1J_{C,H}$ [Hz]
H2,2′	1.89 (d)	2	$^3J_{2,3}=6.2$	C1,1′	93.9 (s)	
H3,3′	5.92 (m)	2	$^3J_{3,4}=4.0$	C2,2′	52.4 (d)	157
H4,4′	5.51 (m)	2	$^3J_{4,5}=6.0$	C3,3′	81.9 (d)	168
H5,5′	1.7 [b]		$^3J_{5,6}=5.7$	C4,4′	80.1 (d)	167
			$^4J_{3,5}=1.4$	C5,5′	63.4 (d)	156
H6,6′	0.17 (d)	2		C6,6′	51.8 (d)	160
CH_3(Cp*)	1.76 (s)	10		Cp*	88.9 (s)	
CH_3(Cp*′) [e]	1.47 (s)	5		Cp*′ [e]	87.9 (s)	
				CH_3(Cp*)	10.5 (q)	126
				CH_3(Cp*′) [e]	10.7 (q)	126

[a] 400 MHz; [D$_8$]THF ($\delta \equiv 3.58$; α-H); 300 K. [b] Obscured by signals of residual [D$_8$]THF protons (β-H). [c] 75.4 MHz; [D$_8$]THF ($\delta \equiv 25.3$; β-C); 313 K. [d] The resonances C2 to C6 were assigned by transferring the ^{1}H-NMR assignment to the ^{13}C-NMR spectrum by means of a 2D ^{13}C,^{1}H-correlated spectrum. [e] Cp*′ is coordinated to the Co atom that is located above the center of the biphenyl fragment.

[*] Prof. Dr. H. Lehmkuhl, Dr. H. Nehl, Priv.-Doz. Dr. R. Benn, Dr. R. Mynott
Max-Planck-Instutut für Kohlenforschung
Kaiser-Wilhelm-Platz 1, D-4330 Mülheim a. d. Ruhr (FRG)

ing that the $^1J_{C,H}$ coupling constants for the inner atoms (C3, C4) are larger than those for the terminal atoms (C2, C5, and C6).[7] In analogy to the known CpCo(η^4-1,3-diene) compounds, we assume that each diene unit is planar[8] but that the two outer diene units are slightly bent with respect to the inner diene.[8]

The electron delocalization in **4** is essentially suppressed, which means that biphenyl in **4** is best described by a Kekulé structure. Although there are numerous examples of the reduction or suppression of the aromaticity of benzene, naphthalene, or anthracene by η^2-, η^3-, or η^4-complexation to a suitable metal complex fragment,[8-22] compound **4** is, to the best of our knowledge, the first example for the transformation of an aromatic system with 12 π-electrons into a system of three η^4-bonded dienes.

Experimental Procedure

A solution of **5** (4.9 g, 10.7 mmol) and **6** (1.8 g, 21.4 mmol) in 80 mL of ether was prepared at −80°C and then allowed to warm over several hours to 20°C. After 24 h, the ether was removed under vacuum and the residue was extracted with pentane. After filtration to remove the LiCl, the solvent was removed from the filtrate under vacuum. The remaining LiCl was removed by extraction with pentane, filtration, and removal of the pentane from the filtrate. This procedure was carried out three times. Finally, the residue was dried at 20°C/10^{-4} torr to remove the biphenyl. The residue was dissolved in 200 mL of pentane and filtered, and the filtrate was concentrated to 40 mL. Upon standing at −80°C, the concentrated solution slowly afforded **4** (3.6 g, 4.9 mmol, 69%) as black crystals. Correct elemental analysis and mass spectrum.

Received: January 13, 1986;
revised: March 27, 1986 [Z 1619 IE]
German version: *Angew. Chem. 98* (1986) 628

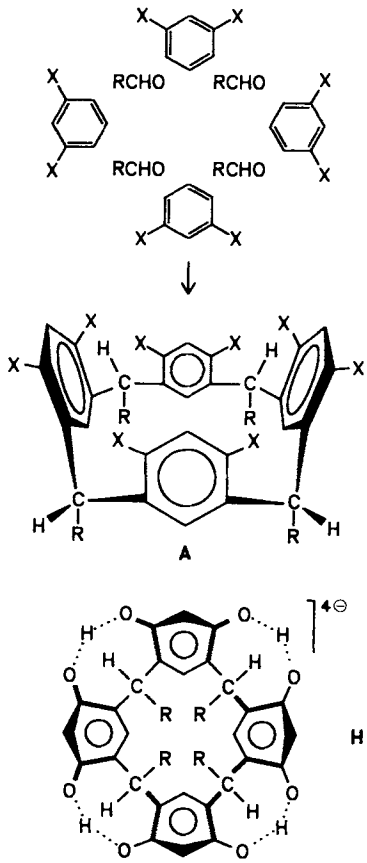
[1] S. Top, G. Jaouen, *J. Organomet. Chem. 182* (1979) 381.
[2] C. Elschenbroich, J. Heck, *Angew. Chem. 89* (1977) 497; *Angew. Chem. Int. Ed. Engl. 16* (1977) 479.
[3] C. Elschenbroich, J. Heck, *Angew. Chem. 93* (1981) 278; *Angew. Chem. Int. Ed. Engl. 20* (1981) 267.
[4] E. O. Fischer, S. Breitschaft, *Chem. Ber. 99* (1966) 2213.
[5] U. Kölle, F. Khouzami, B. Fuss, *Angew. Chem. 94* (1982) 132; *Angew. Chem. Int. Ed. Engl. 21* (1982) 131; *Angew. Chem. Suppl. 1982*, 230.
[6] Comparison of the ^{13}C-NMR data of **4** with those of the s-*cis*/*trans* isomers of [$Cp_2Zr(\eta^4$-butadiene)] also indicates that the inner diene unit has the s-*cis* configuration; see also G. Erker, J. Wicher, K. Engel, F. Rosenfeldt, W. Dietrich, C. Krüger, *J. Am. Chem. Soc. 102* (1980) 6344.
[7] P. W. Jolly, R. Mynott, *Adv. Organomet. Chem. 19* (1981) 257, 278, and references cited therein.
[8] M. R. Churchill, R. Mason, *Proc. R. Soc. London Ser. A 279* (1964) 191. For [CpCo(1–4-η)-5-phenyl-1,3-cyclopentadiene], the angle between the plane of the diene unit and C5 is 36.5°.
[9] K. Jonas, *Angew. Chem. 97* (1985) 292; *Angew. Chem. Int. Ed. Engl. 24* (1985) 295, and references cited therein.
[10] K. Jonas, *Pure Appl. Chem. 56* (1984) 63.
[11] D. J. Brauer, C. Krüger, *Inorg. Chem. 16* (1977) 884.
[12] W. E. Silverthorn, *Adv. Organomet. Chem. 13* (1975) 47, and references cited therein.
[13] G. Huttner, S. Lange, E. O. Fischer, *Angew. Chem. 83* (1971) 579; *Angew. Chem. Int. Ed. Engl. 10* (1971) 556.
[14] K. Jonas, G. Koepe, L. Schieferstein, R. Mynott, C. Krüger, Y.-H. Tsay, *Angew. Chem. 95* (1983) 637; *Angew. Chem. Int. Ed. Engl. 22* (1983) 620; *Angew. Chem. Suppl. 1983*, 920.
[15] M. R. Churchill, R. Mason, *Proc. Chem. Soc. London 1963*, 365.
[16] H.-F. Klein, K. Ellrich, S. Lamac, G. Lull, L. Zsolnai, G. Huttner, *Z. Naturforsch. B 40* (1985) 1377.
[17] G. Allegra, G. Tettamanti Casagrande, A. Immirzi, L. Porri, G. Vitulli, *J. Am. Chem. Soc. 92* (1970) 289.
[18] W. D. Jones, F. J. Feher, *J. Am. Chem. Soc. 106* (1984) 1650.
[19] J. R. Sweet, W. A. G. Graham, *Organometallics 2* (1983) 135.
[20] H. van der Hejden, A. G. Orpen, P. Pasman, *J. Chem. Soc. Chem. Commun. 1985*, 1576.
[21] J. Browning, M. Green, B. R. Penfold, J. L. Spencer, F. G. A. Stone, *J. Chem. Soc. Chem. Commun. 1973*, 31.
[22] P. Mues, R. Benn, C. Krüger, Y.-H. Tsay, E. Vogel, G. Wilke, *Angew. Chem. 94* (1982) 879; *Angew. Chem. Int. Ed. Engl. 21* (1982) 868; *Angew. Chem. Suppl. 1982*, 1891.

A Macrobicyclic Polyphenoxide as Receptor Analogue for Choline and Related Ammonium Compounds**

By *Hans-Jörg Schneider,* Detlev Güttes,* and *Ulrich Schneider*

The use of water-soluble, synthetic macrocycles as simple models for enzymes and receptors has been the focus of interest of many chemists in recent years.[1] We have now found that anions of the condensation products of resorcinol with aldehydes,[2] which have long been known and are preparable in large quantities, are by far the strongest complexing agents for methylammonium derivatives[3] discovered up to now. Interesting structural and salt effects influence the electrostatic interactions that are responsible for this behavior.

The reactions of resorcinol with aldehydes, which were already investigated by *Adolf von Baeyer*,[2a] lead, under certain conditions (for example, with acetaldehyde), to macrocyclic products such as **A**[2b-d] (Scheme 1). Their configuration and conformation has largely been elucidated for the esters (**A**, X = OOCR′ instead of OH) by means of NMR spectroscopy[2e,f] and X-ray crystallography.[2g,h] The system **A**, which was most recently studied by *Högberg*[2e] in the form of the octaacetate and octapropionate, exhibits



Scheme 1. R = CH_3, X = OH.

[*] Prof. Dr. H.-J. Schneider, Dipl.-Chem. D. Güttes, cand. chem. U. Schneider
Fachrichtung 14.1—Organische Chemie der Universität
D-6600 Saarbrücken (FRG)

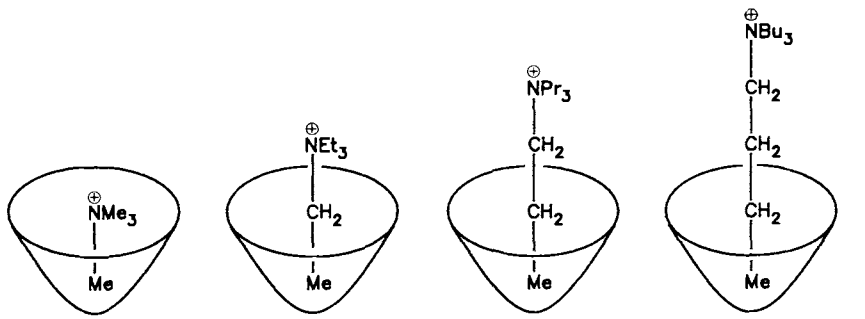
[**] Host-Guest Chemistry, Part 6. This work was supported by the Deutsche Forschungsgemeinschaft and the Fonds der Chemischen Industrie. Part 5: H.-J. Schneider, R. Busch, *Chem. Ber. 119* (1986) 747.

six ^{13}C-NMR and four ^{1}H-NMR signals in alkaline solution (e.g., 0.01 M **A**, 0.05 M NaOD in D_2O), besides signals for rapidly exchanging OH protons; the number and intensities of the signals are those expected for the highly symmetric host structure **H**.[4] That each of the four resorcinol units is only singly deprotonated, even with a large excess of NaOD, is confirmed by the deprotonation effect on the ^{13}C-NMR and ^{1}H-NMR chemical shifts, which are nearly the same for **A**/**H** and resorcinol. The high stability of the tetraphenoxide **H** is also reflected in the pK_a value, which is 11.4 in dimethylformamide (DMF)/H_2O (4:1) as opposed to 13.5 for resorcinol. The formation of four hydrogen bonds and the delocalization of the negative charge are responsible for the fact that even sodium methoxide is unable to deprotonate the tetraanion **H**.

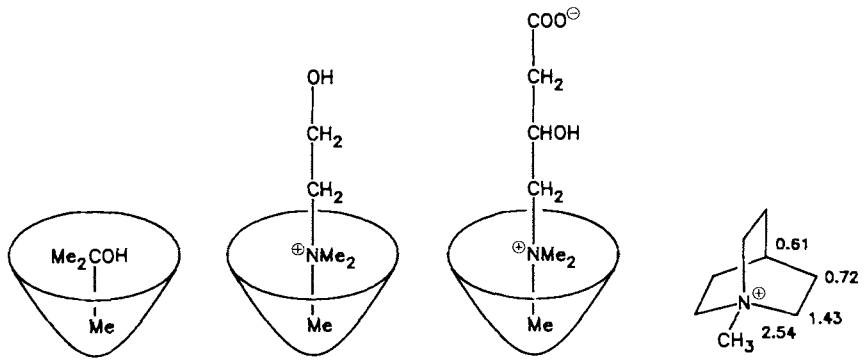
By measuring the ^{1}H-NMR chemical shifts as a function of the ratio of **H** to substrate and by numerical simulation,[5] we obtained the chemical shifts of the completely complexed substrate **S** as well as the equilibrium constants K, which were converted to the corresponding $\Delta G°$ values (Scheme 2). The predominating electrostatic interactions are characterized by the marked decrease of $\Delta G°$ with increasing separation of the positive center in the substrate from the negatively charged macrocycle as well as by the small binding constants of electroneutral substances (cf. *tert*-butyl alcohol **5**).

As in the case of the electrostatically complementary complexes between cationic host and anionic guest molecules,[5] electrolytes such as NaOH (NaOD) (Scheme 2) or NaCl weaken the interactions considerably. The strong complexation of methylammonium ions such as **1** or **6** results, even at room temperature, in considerable line broadening, which, on the one hand, makes precise determinations of K difficult, but, on the other hand, allows the determination of the rate constants of dissociation, k_d, by means of line-shape analysis. The k_d value so obtained for **1**, $2000 \pm 200\ s^{-1}$, along with $K = 3 \times 10^4$ L/mol (in 0.5 N NaOD solution; in 0.01 N NaOD, $K \cong 3 \times 10^5$ L/mol), gives a rate constant of association for complex formation of $k_a \cong 10^8\ s^{-1}$, which indicates a diffusion-controlled reaction. The changes in ^{1}H-NMR shifts upon complexation, Δ (Scheme 2), are the result of ring current anisotropy and electrical field effects and support the geometry of the complexes shown in Scheme 2.

As shown by space-filling models, **H** has a relatively open, bowl-shaped structure; this explains the strong binding of **8** and the absence of strong hydrophobic or lipophilic interactions with electroneutral guest molecules such as **5**. These findings show that, *without* extensive enclosure, the electrostatic attraction between an anionic host molecule and a singly positively charged organic cation can lead to almost micromolar binding constants, even in water, taking into consideration the strong dependence of complexation on the concentration of electrolyte. The tetraphenoxide **H** is a highly effective complexing agent not only for choline derivatives such as **6** but also



	1	2	3	4
$\Delta G°$(0.5 N)	6.1	4.8	2.0	1.3
$\Delta G°$(0.01 N)	(7.5)	6.1	3.1	–
Δ(CH_3)	1.83	1.19	0.43	–



	5	6	7	8
$\Delta G°$(0.5 N)	1.1	6.4	5.2	5.3
$\Delta G°$(0.01 N)	–	(7.7)	–	–
Δ(CH_3)	0.36	2.02	2.07	2.54

Scheme 2. Complexation free energies $\Delta G°$ and selected ^{1}H-NMR chemical shift changes upon complexation Δ (ppm). From measurements in D_2O at 25 (± 1)°C in the presence of 0.5 N or 0.01 N NaOH; counterions to ammonium: $Cl^{\ominus}$, $Br^{\ominus}$, or $I^{\ominus}$ (give the same values for $\Delta G°$ and Δ). $\Delta G°$ in kcal/mol, ±0.1 (for **1** and **6**: ±0.15); $\Delta G°$ values in parentheses by comparison with measurements on **2** and **3**.—The cyclic structures indicate inner surfaces and positions of the anionic macrocycle **H** relative to the substrates. **6** is choline, **7** carnitine. For **8**, the extrapolated Δ values are given.

for numerous related agonists and other biologically active organic ammonium compounds such as carnitine **7**.

Received: February 24, 1986;
supplemented: March 17, 1986 [Z 1680 IE]
German version: *Angew. Chem. 98* (1986) 635

CAS Registry numbers:
1, 102682-61-1; **2**, 102682-62-2; **3**, 102682-63-3; **4**, 102682-64-4; **5**, 102682-65-5; **6**, 102682-66-6; **7**, 102682-67-7; **8**, 102682-68-8.

[1] Recent reviews: a) F. Vögtle, H.-G. Löhr, J. Franke, D. Worsch, *Angew. Chem. 97* (1985) 721; *Angew. Chem. Int. Ed. Engl. 24* (1985) 727; b) J.-M. Lehn, *Science 227* (1985) 849.

[2] a) A. von Baeyer, *Ber. Dtsch. Chem. Ges. 5* (1872) 25; b) J. B. Niederl, H. J. Vogel, *J. Am. Chem. Soc. 62* (1940) 2512; c) A. Zinke, E. Ziegler, *Ber. Dtsch. Chem. Ges. 77* (1944) 264; A. Zinke, R. Ott, F. H. Garanna, *Monatsh. Chem. 89* (1958) 135; d) H. Erdtman, F. Haglid, R. Ryhage, *Acta Chem. Scand. 18* (1964) 1249; e) A. G. S. Högberg, *J. Org. Chem. 45* (1980) 4498; f) *J. Am. Chem. Soc. 102* (1980) 6046; g) B. Nilsson, *Acta Chem. Scand. 22* (1968) 732; h) K. J. Palmer, R. Y. Wong, L. Jurd, K. Stevens, *Acta Crystallogr. 32 B* (1976) 847.

[3] The most strongly binding water-soluble anionic receptors so far reported bind choline with $K \cong 500$: z. B. M. Dhaenens, L. Lacombe, J.-M. Lehn, J.-P. Vigneron, *J. Chem. Soc. Chem. Commun. 1984*, 1097.

[4] The conformation **H** is similar to those of certain condensation products of *para*-substituted phenols and formaldehyde (J. W. Cornforth, P. D'Arcy Hart, G. A. Nicholls, R. J. W. Rees, J. A. Stock, *Br. J. Pharmacol. 10* (1955) 73; G. Happel, B. Mathiasch, H. Kämmerer, *Makromol. Chem. 176* (1975) 3317; C. D. Gutsche, *Acc. Chem. Res. 16* (1983) 161, and references cited therein). Constants of complexation for these cyclophanes, called calixarenes by *Gutsche*, have been determined for only one case and are relatively small (for toluene in chloroform, $K = 1.1$ (L. J. Bauer, C. D. Gutsche, *J. Am. Chem. Soc. 107* (1985) 6063); the compounds are only sparingly water soluble compared to the products derived from resorcinol.

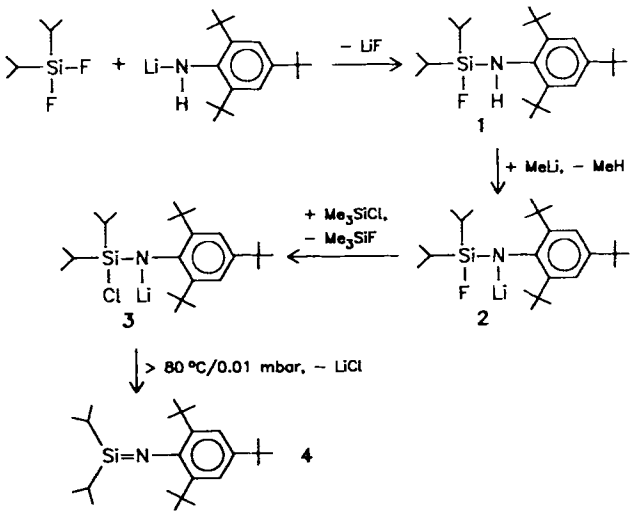
[5] Cf. H.-J. Schneider, K. Philippi, J. Pöhlmann, *Angew. Chem. 96* (1984) 907; *Angew. Chem. Int. Ed. Engl. 23* (1984) 908.

Diisopropyl(2,4,6-tri-*tert*-butylphenylimino)silane—a very Stable, Free Silaimine**

By *Michael Hesse* und *Uwe Klingebiel**

It has been known for several years that lithium salts of the aminofluorosilanes that are sufficiently sterically shielded are stable compounds, exhibiting no tendency to undergo cleavage of LiF.[1] The synthesis of a silaimine, therefore, requires a suitable salt with, for example, LiCl as leaving group. Such a LiCl elimination was recently used successfully for the preparation of a tetrahydrofuran (THF)-containing silaketimine.[2] Silaimines, moreover, have already been identified in solution at low temperature.[3]

We present here a four-step procedure for the synthesis of a stable, free silaimine. The lithium salt **2**[4] is formed in nearly quantitative yield by treatment of the aminofluorosilane **1**[5] with methyllithium; **2** is then converted into the lithiated aminochlorosilane **3**[6] by treatment with Me_3SiCl. Owing to the synthetic procedure used, **3** crystallizes as the THF adduct;[7] its ^{29}Si-NMR signal is shifted to high field with respect to $(CH_3)_4Si$ as expected for such lithium salts. These lithium salts react with carbonyl compounds and dienes as well as with unsaturated compounds.[8] In the field desorption mass spectrum of **3**, the molecular peak of the silaimine **4** is observed.



When **3** is heated in a vacuum at 0.01 mbar, it loses THF, and the silaimine **4**[9] sublimes at a bath temperature of approximately 80 °C. **4** is an orange, crystalline solid, which melts without decomposition to give a deep red liquid. This stability is due to the good steric shielding of the Si=N bond. Neither in solution nor as a solid does **4** exhibit the often common tendency to undergo dimerization.[10] However, **4** is very sensitive to water and air. The strongly low-field-shifted ^{29}Si-NMR resonance of **4** at $\delta = 60.3$ is significant for unsaturated silicon compounds. Thus, in contrast to the recently described THF-containing silaketimine,[2] **4** fits easily into the series of known silaethenes[11] and disilenes.[12] **4** is analytically pure and its structure is in agreement with the mass of $M^{\oplus}$ in the high-resolution mass spectrum. The large coupling constant, $^1J_{CC} = 58$ Hz, of the isopropyl substituents on silicon is further evidence of bonding to an sp^2-hybridized atom.

Experimental Procedure

$LiNHC_6H_2(CMe_3)_3$ (5.35 g, 0.02 mol) in 50 mL of THF/*n*-hexane was added quickly to 3.05 g (0.02 mol) of $(Me_2CH)_2SiF_2$. The reaction was followed by ^{19}F-NMR spectroscopy and was complete after 2 h. After purification by distillation, **1** (3.95 g, 0.01 mol) was lithiated with MeLi in diethyl ether. **2** was characterized by NMR spectroscopy and then treated with 50 mL of THF. The isolation of **2** was thereby circumvented. Immediately after addition of 1.09 g (0.01 mol) of Me_3SiCl, the signal of Me_3SiF ($\delta = 4.7$) was observed in the ^{19}F-NMR spectrum. The reaction was complete after 1 h. **3** was isolated and characterized as a crystalline THF adduct. Heating **3** at 0.01 mbar to approximately 80 °C results in loss of THF and LiCl and the sublimation of **4**. Compound **4** was purified by crystallization from *n*-hexane. The NMR spectra of **1**–**4** were recorded on a 250-MHz instrument.

Received: March 3, 1986;
revised: April 8, 1986 [Z 1687 IE]
German version: *Angew. Chem. 98* (1986) 638

CAS Registry numbers:
1, 102745-20-0; **2**, 102745-21-1; **3**, 102745-22-2; **4**, 102745-23-3; $(Me_2CH)_2SiF_2$, 426-05-1; $LiNHC_6H_2(CMe_3)_3$, 102745-24-4.

[*] Prof. Dr. U. Klingebiel, Dr. M. Hesse
Institut für Anorganische Chemie der Universität
Tammannstrasse 4, D-3400 Göttingen (FRG)

[**] Silaimines, Part 1. This work was supported by the Deutsche Forschungsgemeinschaft and the Fonds der Chemischen Industrie. Note added in proof: Recently, another free silaimine ($tBu_2Si=N-SitBu_3$) was reported: N. Wiberg, K. Schurz, G. Reber, G. Müller, *J. Chem. Soc. Chem. Commun. 1986*, 591.

[1] U. Klingebiel, A. Meller, *Angew. Chem. 88* (1976) 304; *Angew. Chem. Int. Ed. Engl. 15* (1976) 313.

[2] N. Wiberg, K. Schurz, G. Fischer, *Angew. Chem. 97* (1985) 1058; *Angew. Chem. Int. Ed. Engl. 24* (1985) 1053.

[3] G. Raabe, J. Michl, *Chem. Rev. 85* (1985) 419.

[4] **2**: ^{19}F-NMR (C_6D_6, Et_2O, int. C_6F_6): $\delta = 31.2$; ^{29}Si-NMR (C_6D_6, Et_2O, int. TMS): $\delta = -26.9$ ($^1J_{SiF} = 296.5$ Hz); MS (FD measurement): $m/z = 409$ $[M - Li + H]^{\oplus}$, 373 ($M^{\oplus}$ of **4**).

[5] **1**: Yield 7.1 g (90%); b.p. = 106 °C/0.01 mbar; MS (70 eV): m/z 393 ($M^{\oplus}$); IR (film): $\tilde{\nu} = 3410$ cm^{-1} (NH); ^{13}C-NMR (C_6D_6, int. TMS): $\delta = 12.76$ (SiCH, $^2J_{CF} = 20.13$ Hz), 17.63 ($CH(CH_3)_2$, $^3J_{CF} = 35.85$ Hz), 31.71 (*p*-$C(CH_3)_3$), 32.94 (*o*-$C(CH_3)_3$, $^6J_{CF} = 1.26$ Hz), 34.64 (*p*-$C(CH_3)_3$),

37.08 (*o*-*C*(CH_3)$_3$), 123.00 (*m*-*C*), 137.78 (N*C*, $^3J_{CF}$ = 1.9 Hz), 145.49, 147.3 (*o*-/*p*-*C*); ^{19}F-NMR (C_6D_6, int. C_6F_6): δ = 17.1; ^{29}Si-NMR (C_6D_6, int. TMS): δ = −4.7 ($^1J_{SiF}$ = 307.3 Hz).

[6] **3**·THF: Yield from **1** >90%; ^{13}C-NMR (C_6D_6, int. TMS): δ = 19.55, 20.14 (CH(*C*H_3)$_2$), 25.60, 68.02 (THF), 32.18 (C(*C*H_3)$_3$), 34.42 (*p*-*C*(CH_3)$_3$), 37.11 (*o*-*C*(CH_3)$_3$), 122.5 (*m*-*C*), 136.6, 142.3, 154.0 (*i*-/*o*-/*p*-C); ^{7}Li-NMR (C_6D_6, ext. 1M LiCl): δ = −0.5, ^{29}Si-NMR (C_6D_6, int. TMS): δ = −12.25.

[7] According to a preliminary X-ray diffraction analysis carried out by *R. Böse* and *D. Bläser*, Essen, **3** is a monomer and has the smallest SiN distance (164.9 pm) observed thus far.

[8] U. Klingebiel, *Chem. Ber. 111* (1978) 2735; *Z. Naturforsch. B33* (1978) 950; J. Neemann, U. Klingebiel, *Liebigs Ann. Chem. 1980*, 1978.

[9] **4**: Yield (based on 0.01 mol of **3**) 3.6 g (98%); m.p. = 97°–99°C; sublimation: >80°C/0.01 mbar; MS (70 eV): *m/z* 373 (90%, $M^{\oplus}$), 358 (100, $[M-CH_3]^{\oplus}$), 330 (92, $[M-CH(CH_3)_2]^{\oplus}$), molecular weight for $M^{\oplus}$ calcd 373.31648, found 373.31648; ^{1}H-NMR (C_6D_6): δ = 1.01 (CH(CH_3)$_2$, d), 1.2 (C*H*(CH_3)$_2$, m), 1.42 (*p*-C(CH_3)$_3$), 1.64 (*o*-C(CH_3)$_3$), 7.44 (*m*-*H*); ^{13}C-NMR (C_6D_6): δ = 17.78 (CH(CH_3)$_2$), 18.67 (Si*C*H, $^1J_{SiC}$ 55 Hz, $^1J_{CC}$ = 58 Hz), 31.66 (*o*-C(CH_3)$_3$), 32.29 (*p*-C(CH_3)$_3$), 34.60 (*p*-*C*(CH_3)$_3$), 36.46 (*o*-*C*(CH_3)$_3$), 121.22, 134.21, 137.31, 147.65 (benzene *C*); ^{29}Si-NMR (C_6D_6): δ = 60.33.

[10] U. Klingebiel, A. Meller, *Angew. Chem. 88* (1976) 307; *Angew. Chem. Int. Ed. Engl. 15* (1976) 312; W. Clegg, U. Klingebiel, C. Krampe, G. M. Sheldrick, *Z. Naturforsch. B35* (1980) 275.

[11] A. G. Brook, K. D. Safa, P. D. Lickiss, K. M. Baines, *J. Am. Chem. Soc. 107* (1985) 4335; N. Wiberg, G. Wagner, G. Müller, *Angew. Chem. 97* (1985) 220; *Angew. Chem. Int. Ed. Engl. 24* (1985) 229.

[12] M. J. Michalczyk, R. West, J. Michl, *J. Am. Chem. Soc. 106* (1984) 821.

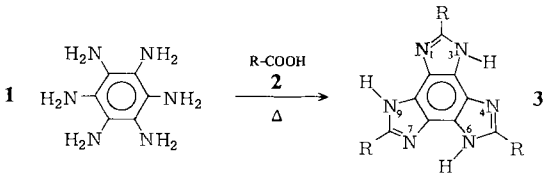
Benzotri(imidazole)—a New Ring System Derived from Benzenehexamine**

By *Bernd Kohne, Klaus Praefcke,* Thomas Derz, Thomas Gondro,* and *Felix Frolow*

Recently, two research groups[1,2] reported the "rediscovery" of benzenehexamine **1**, a polyfunctional building block that was first reported over 50 years ago.[3] **1** has in the meantime become readily available[4] and has been used for the syntheses of new heteropolycycles (derivatives of a hexaazacoronene[1,5] and a hexaazatriphenylene[2]). We have now found that the ring-closure reaction for the synthesis of benzimidazole derivatives—condensation of, for example, carboxylic acids with 1,2-benzenediamine[6]—can be carried out three times with **1**. Condensation with, for example, hexanoic acid **2c** results in formation of the tripentyl derivative **3c** of the benzotri(imidazole) ring system, which has not been described previously.

The condensation steps leading to the formation of the symmetric, trigonal compounds **3** can take place either simultaneously or in an alternating fashion; in the latter case, the intermediate, unsymmetric analogue of **3** must undergo tautomerism in one imidazole segment.[7]

According to the elemental analysis, **3c** crystallizes with water in a molar ratio of 1 : 2. The crystals melt over a wide temperature range (138–154°C). According to the thermoanalysis,[4] **3c** has two sharp transition points (endothermic); the light yellow, highly viscous, glasslike melt does not undergo crystallization after cooling to room temperature, even after standing for several weeks.



a, R = CH_3; **b**, R = C_2H_5; **c**, R = C_5H_{11}

The mass spectrum of **3c**[4] exhibits, among other peaks, a very intense molecular ion peak ($C_{24}H_{36}N_6$, *m/z* 408) and a base peak at *m/z* 352 (β-cleavage of one side chain). A characteristic feature of the ^{1}H-NMR spectrum[4] is a very broad signal at δ = 12.64 (imino protons,[8] which are apparently strongly deshielded by the formation of hydrogen bonds). The ^{13}C-NMR spectrum[4] exhibits one singlet for the six central carbon atoms (δ = 123.20) and one for the three peripheral ring carbon atoms (δ = 150.44). The analytical and spectroscopic data are in accord with the results of an X-ray structure analysis[9] (Fig. 1).

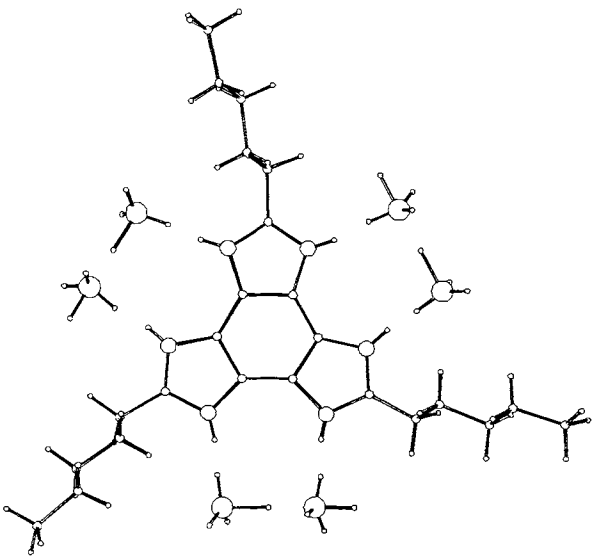


Fig. 1. Crystal structure of **3c**·2 H_2O [9]. The structure shows the disorder in the imidazole rings, resulting from tautomerism, and the statistical disorder of the hydrogen atoms of water.

The molecule has crystallographic C_3 symmetry. The thermal motions of the aliphatic side chains are large and increase toward the end of the chains. The N1–C2 and N3–C2 distances (1.33 and 1.34 Å, respectively) show that two tautomers are present in the crystal; this is supported by the presence of two hydrogen atoms with population parameters of 0.5 bonded to the nitrogen atoms (difference Fourier analysis). The central six-membered ring and the imidazole rings are nearly planar, with a deviation of 0.01 Å. The angles between the six-membered ring and the imidazole rings and between the imidazole rings themselves are 2 and 4°, respectively. The line joining the first

[*] Prof. Dr. K. Praefcke, Dr. B. Kohne, T. Derz, T. Gondro
Institut für Organische Chemie der Technischen Universität
Strasse des 17. Juni 135, D-1000 Berlin 12
Dr. F. Frolow
Chemical Services, The Weizmann Institute of Science
Rehovot 76100 (Israel)

[**] This work was supported by the Fonds der Chemischen Industrie and by the Technische Universität Berlin (FIP 5/11 and PA 1). We thank Mrs. *S. Völzke* for analytical-chemical assistance and Dr. *G. Pötzscher* for an ONLINE literature search of the ring system of the title compound. *K. P.* thanks the Minerva Komitee, Heidelberg, for a stipendium to study at the Weizmann Institute of Science.

and the last carbon atom of the alkyl chains is at an angle of 118° to the plane of an imidazole ring. The molecule thus has a bowl or crown shape in the crystal. Each molecule of **3c** is surrounded in the crystal by six molecules of H_2O (water clathrate), which in turn each lie on a threefold symmetry axis and thus form hydrogen bonds both among themselves and with the nitrogen atoms of three molecules of **3c**.

Received: January 9, 1986;
revised: April 11, 1986 [Z 1614 IE]
German version: *Angew. Chem. 98* (1986) 627

CAS Registry numbers:
1, 4444-26-2; **2a**, 142-62-1; **3c**, 102780-30-3; **3c**·2 H_2O, 102780-29-0; 2,4,6-trinitro-1,3,5-benzenetriamine, 3058-38-6.

[1] R. Breslow, P. Maslak, J. S. Thomaides, *J. Am. Chem. Soc. 106* (1984) 6453.

[2] B. Kohne, K. Praefcke, *Liebigs Ann. Chem. 1985*, 522.

[3] The only earlier reports on the synthesis, structure elucidation, and some alkylation and acylation reactions of **1**: a) B. Flürscheim, E. L. Holmes, *J. Chem. Soc. 1929*, 330; b) I. E. Knaggs, *Proc. R. Soc. London, Ser. A 131* (1931) 612; c) H. J. Backer, S. van der Baan, *Recl. Trav. Chim. Pays-Bas 56* (1937) 1175.

[4] *Experimental procedure:* **3c**: Bright yellow 2,4,6-trinitro-1,3,5-benzenetriamine [2] (3.1 g, 12 mmol) in 150 mL of freshly distilled ethyl acetate was hydrogenated in a shaking flask for approximately 80 h at room temperature (approximately 4–5 bar H_2—cf. [1]—catalyst: 450 mg of 10% Pd/active carbon). The suspension, which contains **1**,—upon complete hydrogenation, the solvent is colorless—was evaporated first under water-aspirator vacuum and then under oil-pump vacuum to remove the ethyl acetate and the water of reaction. The Pd/active carbon-containing residue reacted with 11.6 g (0.1 mol) of hexanoic acid **2c** in 1 h at 160°C under pure nitrogen to give, after workup (dissolving in ether, neutralization with aqueous potassium hydroxide solution, washing with water, etc.), approximately 3.0 g of a reddish brown crude product. Column chromatography on silica gel with chloroform/methanol (50 + 1) afforded 45 mg (8.4%) of a yellow solid; purification by HPLC (Knauer HPLC pump 64 equipped with variable wavelength detector, $\lambda = 254$ nm; reversed phase column; $l = 250$ mm, $d = 16$ mm, Polygosil 10 μm; methanol: 40 mL/min) and recrystallization from ethyl acetate afforded 327 mg (6.1%, both yields are based on the trinitrobenzenetriamine) of pure **3c**·2 H_2O as yellowish needles [7]. Melting range 138–154°C (Leitz Laborlux 12 Pol polarization microscope with a Mettler hot stage FP 2); thermoanalysis (Mettler system TA 3000): two sharp phase transitions: 1) 144.9°C ($\Delta H = 42.7$ kJ/mol) and 2) 162.4°C ($\Delta H = 30.6$ kJ/mol).—^{1}H-NMR ($(CD_3)_2SO$, 270 MHz): $\delta = 0.85$ (t, CH_3), 1.2–1.45 (m, γ- and δ-CH_2), 1.8 (quin., β-CH_2), 2.83 (t, α-CH_2), 12.64 (s, very broad, N-H).—$^{13}C\{^1H\}$-NMR ($(CD_3)_2SO$, 20 MHz): $\delta = 13.85$, 21.88, 27.78, 28.46, and 30.86 (aliph.), 123.20 (s, central aromat.), 150.44 (s, peripheral aromat.). MS: *m/z* 408 ($M^{\oplus}$, 82%), 379 ($M^{\oplus} - C_2H_5$, 14), 365 ($M^{\oplus} - C_3H_7$, 36), 352 ($M^{\oplus} - C_4H_8$, 100), ≤350 no further peaks >10%.—A correct elemental analysis was obtained for $C_{24}H_{36}N_6 \cdot 2H_2O$.

[5] B. Kohne, K. Praefcke, A. Reichmann, *Chem.-Ztg. 109* (1985) 17.

[6] Cf. E. C. Wagner, W. H. Millett, *Org. Synth. Coll. Vol. II* (1943) 65, and references cited therein, as well as numerous examples in *Beilsteins Handbuch der Organischen Chemie 23 E III* and *IV* (1980) 1070 and 1112.

[7] Acetic acid **2a** and propionic acid **2b** also react with **1** to give analogous products as yellowish crystals: **3a** ($C_{12}H_{12}N_6$): yield 36%; m.p. >350°C; MS: *m/z* 240 ($M^{\oplus}$, 100%), 239 ($M^{\oplus} - H$, 48).—**3b** ($C_{15}H_{18}N_6$): yield 2.6%; m.p. 191.3°C; MS: *m/z* 282 ($M^{\oplus}$, 40%), 281 ($M^{\oplus} - H$, 14), 267 ($M^{\oplus} - CH_3$, 40).—**3a** and **3b** gave appropriate ^{1}H- and ^{13}C-NMR spectra.

[8] Cf. $\delta_{NH} = 10.1$ in benzimidazole (solvent: $CHCl_3$ or CCl_4): E. Pretsch, T. Clerc, J. Seibl, W. Simon: *Tabellen zur Strukturaufklärung organischer Verbindungen mit spektroskopischen Methoden*, Springer, Berlin 1976, H 325.

[9] Cubic, space group $P2_13$, $a = 13.956(1)$ Å, $V = 2718.2(3)$ Å^3, $\rho_{calcd} = 1.067$ g·cm^{-3}, 3176 measured, 1062 independent and 1047 observed reflections, $R = 0.029$, $R_w = 0.031$. The measurement was carried out at 85°K with an Enraf-Nonius CAD-4 diffractometer ($Cu_{K\alpha}$ radiation, $\lambda = 1.5418$ Å). The structure solution was achieved by direct determination of the phases. All atoms except hydrogen were refined anisotropically. The hydrogen atoms were placed at newly calculated ideal positions after each refinement. All calculations were carried out with the SHELX program (G. M. Sheldrick: *SHELX 76 A Program for Crystal Structure Determination*, University Cambridge, England 1976). Further details of the crystal structure investigation may be obtained from the Fachinformationszentrum Energie, Physik, Mathematik GmbH, D-7514 Eggenstein-Leopoldshafen 2 (FRG), on quoting the depository number CSD 51927, the names of the authors, and the journal citation.

Si_6H_6: Is the Aromatic Structure the Most Stable One?

By *Alexander Sax* and *Rudolf Janoschek**

The theoretical predictions prior to the first synthesis of a compound containing a Si=Si bond[1] encouraged theoretical chemists to study other, still unknown silicon compounds, especially those whose carbon analogues are known. Studies of silaaromaticity, which has long been a subject of theoretical speculation,[2] have regained importance since the discovery of the Si=Si bond.[3] Prior to 1981, a series of theoretical studies predicted the existence of a stable Si=Si bond:[4] the disilene molecule, H_2SiSiH_2, should be effectively planar, with a SiSi bond length of 215 pm and a π-bond energy of approximately 125 kJ mol^{-1}. The first synthesis of a compound containing this new double bond was then achieved[1]—despite the double-bond rule—and X-ray diffraction experiments confirmed the calculated structure.[5] Further calculations on Si_2H_4 also confirmed the known properties of the Si=Si bond and showed, in addition, that the silanediyl(silylene) structure, $HSiSiH_3$, is nearly isoenergetic with the ethylene-like structure.[6]

Theoretical studies of silaaromatic structures were restricted until now to silabenzene C_5SiH_6 and 1,4-disilabenzene $C_4Si_2H_6$; reliable theoretical predictions[7] and experimental confirmation[8] occurred more or less simultaneously. Only recently was a silaaromatic structure in pure form investigated for the first time:[9] for the system with the overall formula Si_6H_6, detailed quantum chemical calculations have given three stable isomers so far (Fig. 1), taking only the valence electrons into consideration. A set of three s- and three p-functions was employed for the val-

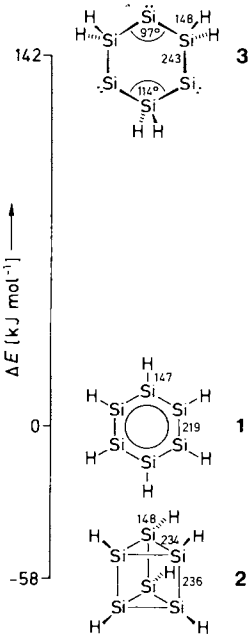


Fig. 1. Relative stabilities of three Si_6H_6 isomers; bond lengths in pm. For comparison with C_6H_6: prismane lies 543 kJ mol^{-1} higher in energy than benzene.

[*] Prof. Dr. R. Janoschek, Dr. A. Sax
Institut für Theoretische Chemie der Universität
Mozartgasse 14, A-8010 Graz (Austria)

ence shell of the Si atom (3s/3p); for those of the H atoms, a set of three s-functions was used. This basis set was extended with d-functions for the Si atoms and p-functions for the H atoms. The two lowest energy isomers were identified by calculation of the corresponding complete sets of vibrational frequencies as minima on the Si_6H_6 energy hypersurface.

Hexasilabenzene **1** should be planar (D_{6h} symmetry) with a SiSi bond length of 219 pm, which lies between those of disilane (236 pm) and disilene (215 pm) (analogous to C_2H_6, C_6H_6, C_2H_4). The extremely low wave number of 60 cm^{-1} was obtained for the ring-puckering vibration, so that a nonplanar molecule would almost be energetically equivalent. The stability of **1** with respect to alternation of the SiSi bonds (D_{3h} symmetry) is revealed in the relatively high harmonic vibrational frequency of 580 cm^{-1}.[*] In hexasilaprismane **2** (D_{3h} symmetry), the SiSi bond lengths in the three-membered rings (234 pm) are only marginally smaller than the SiSi bond lengths between the two three-membered rings (236 pm). In view of the isoenergetic structures H_2SiSiH_2 and $HSiSiH_3$, **3** would be an interesting candidate for an isomer that might be energetically comparable to **1**. For **3**, a relatively long SiSi bond length was found (243 pm), similar to that in $HSiSiH_3$. Other isomers, such as hexasila Dewar benzene, hexasilabenzvalene, and hexasilaoctahedrane are higher in energy according to preliminary calculations.

The pronounced difference between the structures of Si_6H_6 and C_6H_6 is revealed in the relative stabilities of the isomers **1** and **2**. Whereas benzene is by far the most stable form for C_6H_6, hexasilaprismane is the most stable isomer for Si_6H_6. Taking into consideration electron correlation does not change the energetic ordering of the isomers **1** and **2**. A qualitatively similar result was obtained by means of a theoretically less rigorous procedure.[11] Not the differences in ring strain energies of prismane and hexasilaprismane (606[12] and 418 kJ mol^{-1}, respectively) but rather the energy differences between sp^2- and sp^3-hybridized C and Si atoms are the essential causes of the differences in stability. The "resonance stabilization" of the π-electrons is only 30% smaller for hexasilabenzene (84 kJ mol^{-1}) than for benzene, the estimate being based on the following homodesmotic reaction:

$$Si_6H_6 + 3\,H_2Si{=}SiH_2 \longrightarrow 3\,H_2Si{=}SiH{-}SiH{=}SiH_2$$

This fact, together with the greater stability of hexasilaprismane, demonstrates once again how little aromaticity has to do with the resonance stabilization of a magic π-electron sextet. Crucial for the marked stability of the planar six-membered carbon ring is instead the energetic preference for sp^2-hybridized compared with sp^3-hybridized C atoms, both in bonding of the C atoms among themselves and in bonding to the H atoms. In the case of silicon, such a preference is absent.[13]

Received: February 19, 1986;
revised: April 1, 1986 [Z 1674 IE]
German version: *Angew. Chem. 98* (1986) 634

CAS Registry number:
1, 99759-72-5.

[*] After submission of this communication, a theoretical study on hexasilabenzene appeared in which nearly identical structural data and vibrational frequencies were reported, but the problems of aromaticity and isomers were not discussed [10].

[1] R. West, M. J. Fink, J. Michl, *Science (Washington DC) 214* (1981) 1343.
[2] H. Schmidbaur, *Chem. Unserer Zeit 1* (1967) 184.
[3] G. Raabe, J. Michl, *Chem. Rev. 85* (1985) 419.
[4] R. Daudel, R. E. Kari, R. A. Poirier, J. D. Goddard, I. G. Csizmadia, *J. Mol. Struct. 50* (1978) 115; F. F. Roelandt, D. F. van de Vondel, G. P. van der Kelen, *J. Organomet. Chem. 165* (1979) 151; L. C. Snyder, Z. R. Wasserman, *J. Am. Chem. Soc. 101* (1979) 5222; R. A. Poirier, J. D. Goddard, *Chem. Phys. Lett. 80* (1981) 37.
[5] M. J. Fink, M. J. Michalczyk, K. J. Haller, R. West, J. Michl, *J. Chem. Soc. Chem. Commun. 1983*, 1010; K. W. Zilm, D. M. Grant, J. Michl, M. J. Fink, R. West, *Organometallics 2* (1983) 193.
[6] H. J. Köhler, H. Lischka, *J. Am. Chem. Soc. 104* (1982) 5884; *Chem. Phys. Lett. 112* (1984) 33; H. Lischka, H. J. Köhler, *ibid. 85* (1982) 467; K. Krogh-Jespersen, *J. Phys. Chem. 86* (1982) 1492; *J. Am. Chem. Soc. 107* (1985) 537; K. Ohta, E. R. Davidson, K. Morokuma, *ibid. 107* (1985) 3466; A. Sax, *J. Comput. Chem. 6* (1985) 469.
[7] H. B. Schlegel, B. Coleman, M. Jones, *J. Am. Chem. Soc. 100* (1978) 6499; M. S. Gordon, P. Boudjouk, F. Anwari, *ibid. 105* (1983) 4972; P. H. Blustin, *J. Organomet. Chem. 166* (1979) 21; H. Bock, P. Rosmus, B. Solouki, G. Maier, *ibid. 271* (1984) 145; K. K. Baldridge, M. S. Gordon, *ibid. 271* (1984) 369; J. Chandrasekhar, P. von R. Schleyer, *ibid. 289* (1985) 51; B. Solouki, P. Rosmus, H. Bock, G. Maier, *Angew. Chem. 92* (1980) 56; *Angew. Chem. Int. Ed. Engl. 19* (1980) 51; J. Chandrasekhar, P. von R. Schleyer, R. O. W. Baumgärtner, M. T. Reetz, *J. Org. Chem. 48* (1983) 3453.
[8] G. Maier, G. Mihm, H. P. Reisenauer, *Angew. Chem. 92* (1980) 58; *Angew. Chem. Int. Ed. Engl. 19* (1980) 52; A. Sekiguchi, A. Tanikawa, W. Ando, *Organometallics 4* (1985) 584; T. J. Barton, G. T. Burns, *J. Am. Chem. Soc. 100* (1978) 5246; H. Bock, R. A. Bowling, B. Solouki, T. J. Barton, G. T. Burns, *ibid. 102* (1980) 429; J. D. Rich, R. West, *ibid. 104* (1982) 6884.
[9] A. Sax, R. Janoschek, *Proc. Fourth Int. Symp. Inorg. Ring Syst. Paris-Sud 1985* (*Phosphorus Sulfur*, in press).
[10] D. A. Clabo, H. F. Schaefer, *J. Chem. Phys. 84* (1986) 1664.
[11] S. Nagase, T. Kudo, M. Aoki, *J. Chem. Soc. Chem. Commun. 1985*, 1121.
[12] J. M. Schulman, R. L. Disch, *J. Am. Chem. Soc. 107* (1985) 5059.
[13] R. Janoschek, *Naturwiss. Rundsch. 37* (1984) 486.

Rearrangement of 4*H*-1,2,4-Triazolium Salts to 4-Acyl-5-aminoimidazoles

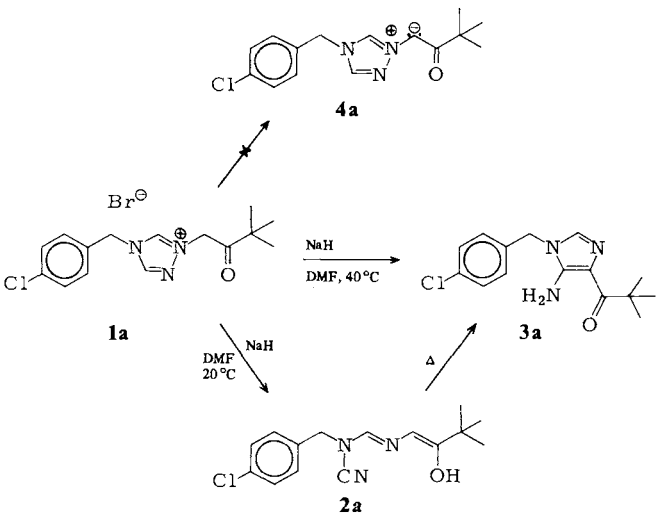
By *Costin N. Rentzea**

Dedicated to Professor Heinz A. Staab on the occasion of his 60th birthday

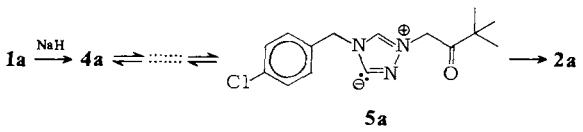
The stable *N*-ylides[1] of *as*-triazoles[1,2] or *s*-triazoles[3] that are required for 1,3-dipolar cycloadditions are usually prepared from phenacyltriazolium salts with ammonia or amines in water, C_6H_6, CH_2Cl_2, or $CHCl_3$ at room temperature.[1-3] The attempt to generate the triazolium ylide **4a** from the *as*-triazolium salt **1a**[4] with NaH in dimethylformamide (DMF), however, led to a surprising result: instead of the expected reaction, the rearrangement of **1a** to 5-amino-1-*p*-chlorobenzyl-4-pivaloylimidazole **3a** was observed to take place at 40 °C in 25% yield.

At 20 °C, the *N*-cyanoformamidine **2a** (m.p. = 120 °C) could be isolated in 35% yield; it is present mainly in the enol form. After short heating to 120 °C, **2a** affords a quantitative yield of the Thorpe product[5] **3a** (*5-exo-dig*-cyclization[6]). Under the reaction conditions for **1a** → **3a**, it is possible that an equilibrium exists between the ylide **4a** and the dipole **5a**, which is formed by deprotonation of **1a** on C-3 of the triazole ring; on account of the facile ring opening[7] of **5a** to give the cyanoformamidine **2a**, the

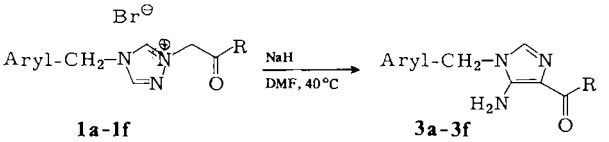
[*] Dr. C. N. Rentzea
BASF Aktiengesellschaft, Hauptlaboratorium
D-6700 Ludwigshafen (FRG)



equilibrium would be continuously driven to the right. However, the direct deprotonation of **1a** to **5a**, followed by the ring-opening to **2a** is more plausible, since analogous deprotonations of cyclic =N–CH=N–N= systems with cleavage to a >N–CN derivative are known.[7]



The reaction **1a** → **3a** can be generalized: At 40°C, the triazolium salts **1a–1f** undergo direct rearrangement to the new aminoimidazoles **3a–3f** in yields of 20–60% (not optimized) (see Table 1).[8]



The novel rearrangement of 4*H*-1,2,4-triazolium salts reported herein makes possible a simple synthesis of 4-acyl-5-aminoimidazoles from readily accessible starting materials. 4-Acetyl-5-amino-1-methylimidazole[10] was previously synthesized, for example, by saponification of 6,9-dimethylpurine 1-oxide.

Received: March 10, 1986;
revised: April 10, 1986 [Z 1698 IE]
German version: *Angew. Chem. 98* (1986) 644

Table 1. Physical data for the 4-acyl-5-amino-1-arylmethylimidazoles **3a–3f**.

3a: M.p. = 158°C (from AcOEt); IR (KBr): $\tilde{\nu}$ = 3438, 3320, 1624, 1614, 1459, 918 cm^{-1}; ^{1}H-NMR ($CDCl_3$, TMS): δ = 1.36 (s, 9H), 4.84 (s, 2H), 5.47 (s, 2H), 6.88 (s, 1H), 6.9–7.1 (d, 2H), 7.15–7.4 (d, 2H); ^{13}C-NMR ($CDCl_3$): δ = 201.99, 146.33, 134.58, 132.69, 129.52 (×2), 128.25 (×2), 120.57, 46.48, 43.09, 27.24 (×3)

3b, Aryl = *p*-FC_6H_4, R = *t*Bu: M.p. = 107°C (AcOEt); yield 21%; ^{1}H-NMR ($CDCl_3$, TMS): δ = 1.38 (s, 9H), 4.9 (s, 2H), 5.5 (br. s, 2H), 6.92 (s, 1H), 7.0–7.35 (m, 4H)

3c, Aryl = *p*-BrC_6H_4, R = *t*Bu: M.p. = 130°C (AcOEt); yield 35%; ^{1}H-NMR ($CDCl_3$:$(CD_3)_2SO$ 1:1, TMS): δ = 1.28 (s, 9H), 4.42 (s, 2H), 6.2–6.8 (br. s, 2H), 7.1–7.3 (d, 2H), 7.4–7.6 (d, 2H), 7.82 (s, 1H)

3d: Aryl = *p*-$F_3CC_6H_4$, R = *t*Bu: M.p. = 163°C (AcOEt); yield 25%; ^{1}H-NMR ($CDCl_3$, TMS): δ = 1.37 (s, 9H), 4.92 (s, 2H); 5.38 (s, 2H), 6.91 (s, 1H), 7.05–7.25 (d, 2H), 7.4–7.6 (d, 2H).

3e, Aryl = 3,4-$Cl_2C_6H_3$, R = *t*Bu: M.p. = 112°C (AcOEt); yield 32%; ^{1}H-NMR ($CDCl_3$, TMS): δ = 1.42 (s, 9H), 5.03 (s, 2H), 6.37 (s, 2H); 7.0–7.4 (m, 4H)

3f, Aryl = *p*-ClC_6H_4, R = 2,4-$Cl_2C_6H_3$: M.p. = 220°C (AcOEt); yield 60%; ^{1}H-NMR ($CDCl_3$:$(CD_3)_2SO$ 1:1, TMS): δ = 5.1 (s, 2H), 6.6–6.95 (br. s, 2H), 7.0–7.55 (m, 8H)

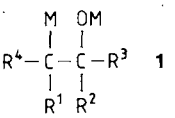
[1] M. Petrovanu, C. Luchian, C. Surpateanu, V. Barboiu, M. Constantinescu, *Tetrahedron 39* (1983) 2417, and references cited therein.
[2] C. Surpateanu, A. Lablache-Combier, M. Constantinescu, J. Marko, *Tetrahedron Lett. 25* (1984) 5751.
[3] H. J. Timpe, V. Schröder, R. Worschech, *Rev. Roum. Chim. 25* (1980) 407.
[4] **1a**: M.p. = 197°C (acetonitrile); quantitatively prepared from 3,3-dimethyl-1-(1,2,4-triazol-1-yl)-2-butanone [9] and *p*-chlorobenzyl bromide (6 h, 70°C, acetonitrile).
[5] K. Gewald, C. Heinhold, *Monatsh. Chem. 107* (1976) 1413.
[6] J. E. Baldwin, *J. Chem. Soc. Chem. Commun. 1976*, 734.
[7] R. Fusco, P. Dalla Croce, A. Salvi, *Gazz. Chim. Ital. 98* (1968) 511.
[8] Elemental analyses and molecular weights are in agreement with the formulas given.
[9] M.p. = 69°C (diethyl ether); 0.1 mol 1-bromo-3,3-dimethyl-2-butanone and 0.15 mol sodium triazolide in 150 mL of THF, 12 h stirring at 60°C, 65% yield.
[10] F. L. Lam, J. C. Parham, *J. Am. Chem. Soc. 97* (1975) 2839.

Organometallic Derivatives of Epoxides**

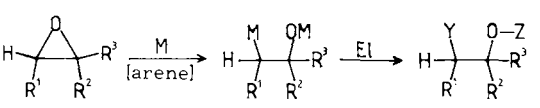
By *Ekkehard Bartmann**

Dedicated to Professor Rudolf Gompper on the occasion of his 60th birthday

Organometallic compounds RM, e.g. with M = Li, Mg, can be formed not only by the usual insertion of a metal atom into a carbon–halogen bond, but also by the cleavage of bonds between carbon and other leaving groups (even of less reactive bonds like those of ethers and amines).[1] It is especially remarkable, however, that in the case of such a reactive and frequently applied class of compounds as the epoxides no analogous reaction—with formation of β-metalated alkoxides **1**—has so far been reported in the literature,[2] except for a few specific systems with stabilizing substituents.[3]



The majority of these synthetically interesting organometallic compounds are stable only at low temperature and could be obtained by *Barluenga* et al. only via organomercury compounds or via β-chlorohydrins.[4]



[*] Dr. E. Bartmann
Fachbereich Chemie der Universität
Hans-Meerwein-Strasse, D-3550 Marburg (FRG)
Present address: E. Merck, Abt. FO IC OC
Frankfurter Strasse 250, D-6100 Darmstadt 1 (FRG)

[**] Experimental assistance: *Angelika Bartmann, Frauke Ettl,* and *Jutta Rausch.*

Although we have so far been unable to accomplish the direct conversion of epoxides into **1** at low temperatures with the metals themselves (even with highly activated forms[5]), we have had success on using the radical anion salts of aromatic hydrocarbons.[6] Table 1 contains the results of some of our experiments.

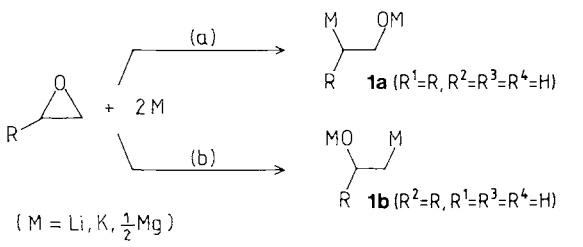
Table 1. Overview of the β-metallo-alkoxides **1** that have been prepared, and their reactions with electrophiles [d].

No.	R^1	R^2	R^3	M	Arene	El	Y	Z	Yield [%]
1	H	H	Me	Li	bi	H_2O	H	H	39 [a, b]
2	H	H	Me	Li	bi	H_2O	H	H	61 [a, b, c]
3	H	H	Me	Li	bi	$(MeS)_2$	SMe	H	57 [c]
4	H	H	Me	Mg	na	CO_2	CO_2H	H	53 [a]
5	H	H	Et	Li	bi	H_2O	H	H	45 [a, b]
6	H	H	Et	Mg	na	H_2O	H	H	72 [a, b]
7	H	Me	Me	Li	bi	H_2O	H	H	31 [a, b]
8	$(CH_2)_4$		H	Li	na	D_2O	D	H	72 (82 [a])
9	$(CH_2)_4$		H	Li	bi	$(PhS)_2$	SPh	H	70
10	Et	Et	H	Li	na	H_2O	H	H	68 [a, b]
11	Ph	H	H	Li	na	D_2O	D	H	59 (87 [a])
12	Ph	H	H	K	bi	MeI	Me	Me	74
13	Ph	H	H	K	bi	$Br(CH_2)_3Br$	$(CH_2)_3$		22
14	CO_2Et	H	H	K	bi	H_2O	H	H	69 [a]
15	CO_2Et	Me	H	Li	na	MeI	Me	Me	56

[a] Yield determined gas-chromatographically; [b] see 16; [c] metalation with addition of LiBr (equimolar amounts); [d] bi = biphenyl, na = naphthalene.

Thus, cyclohexene oxide (No. 8 and 9) is smoothly converted at −80 to −90°C by biphenyl- or naphthalene-lithium in tetrahydrofuran (THF) into the β-lithiated cyclohexanolate. Formally, two asymmetric centers are formed. The subsequent deuteration, however, is not stereoselective: according to the ^{13}C-NMR spectrum, *cis*- and *trans*-[2-D]cyclohexanol are obtained in the ratio of about 1 : 1.[7] On the other hand, with a more bulky electrophile such as diphenyl sulfide, apparently only the *trans* compound[8] is formed.

The regioselectivity of the ring opening can be investigated with the monosubstituted epoxides, since the two C–O bonds are now different (see Scheme 1). In all the experiments carried out so far, only one product could be detected: if the substituent is a phenyl or ester group, then only the neighboring C–O bond is cleaved (route (a));[9] this indicates a stabilizing effect of the substituents already during the formation of the carbanion.[10] Not only the lithium compounds but also the corresponding potassium compounds are accessible from these epoxides.



Scheme 1.

If, on the other hand, the substituent is an alkyl group, then exclusively the more distant C–O bond will be cleaved (route (b)): the formal primary alkyl anion thus formed is more stable than a secondary "alkyl anion" expected to be formed via route (a).[10] These epoxides readily undergo side reactions, which greatly reduces the yields of **1**.[11] A better yield is obtained by addition of lithium bromide (No. 1 and 2) or if naphthalenemagnesium[12] is used as metalating agent (No. 5 and 6).

Preparatively useful secondary reactions of **1** are naturally not limited to the derivatizations listed in Table 1:[13] In the reactions of these bifunctional anionic compounds with bifunctional electrophiles there emerges a novel ring expansion reaction of epoxides (see No. 13 as preliminary example).

Received: January 30, 1986;
revised: March 25, 1986 [Z 1647 IE]
German version: *Angew. Chem. 98* (1986) 629

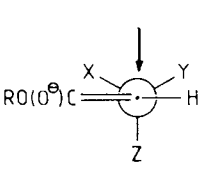
CAS Registry numbers:
K bi, 29385-16-8; Li bi, 26263-91-2; Li na, 27939-69-1; Mg na, 102745-25-5; OCH_2CHMe, 75-56-9; OCH_2CHEt, 106-88-7; OCH_2CMe_2, 558-30-5; $OCHEtCHEt$, 4468-66-0; OCH_2CHPh, 96-09-3; OCH_2CHCO_2Et, 4660-80-4; $OCHMeCHCO_2Et$, 19780-35-9; D_2O, 7789-20-0; *i*-PrOH, 67-63-0; $MeSCH_2CHMeOH$, 6943-87-9; $HO_2CCH_2CHMeOH$, 300-85-6; *s*-BuOH, 78-92-2; *t*-BuOH, 75-65-0; EtPrCHOH, 623-37-0; $PhCHDCH_2OH$, 92400-88-9; $PhCHMeCH_2OMe$, 65738-46-7; $EtO_2C(CH_2)_2OH$, 623-72-3; $MeOCHMeCHMeCO_2Et$, 6411-20-7; *(cis)*-hexanol-2-bi, 931-14-6; *(trans)*-hexanol-2-bi, 49676-90-6; *(trans)*-2-phenylthiohexanol, 35550-80-2; 3-phenylperhydropyran, 16765-32-5; 7-oxabicyclo[4.1.0]heptane, 286-20-4.

[1] *Houben-Weyl-Müller: Methoden der Organischen Chemie, Band XIII/1, XIII/2a*, Thieme-Verlag, Stuttgart 1970 and 1973.
[2] The reductions of epoxides by metals (in protic solvents) described in the literature are used for the preparation of simple alkoxides: J. G. Smith, *Synthesis 1984*, 629, and references cited therein; possibly dianions of the type **1** are formed as intermediates.
[3] a) Epoxyketones: J. D. McChesney, T. N. Thompson, *J. Org. Chem. 50* (1985) 3473; b) phenyl-substituted epoxides: E. M. Kaiser, C. G. Edmonds, S. D. Grubb, J. W. Smith, D. Tramp, *J. Org. Chem. 36* (1971) 330.
[4] a) J. Barluenga, F. J. Fañanás, M. Yus, *J. Org. Chem. 46* (1981) 1281; b) J. Barluenga, J. Flórez, M. Yus, *J. Chem. Soc. Perkin Trans. 1 1983*, 3019; c) C. Nájera, M. Yus, D. Seebach, *Helv. Chim. Acta 67* (1984) 289.
[5] For the cleavage of ethers with activated metals see: E. Bartmann, *J. Organomet. Chem. 284* (1985) 149.
[6] In the meantime this reaction has also been detected by *T. Cohen* et al.: T. Cohen, private communication, Pittsburgh.
[7] Two triplets of equal intensity appear at $\delta = 35.01$, 35.06 (rel. to TMS) for the deuterated C-atoms in the $^{13}C\{^1H\}$-NMR spectrum (in $CDCl_3$).
[8] ^1H-NMR (400 MHz, $CDCl_3$): $\delta = 1.15$–1.50 (m, 4H), 1.55–1.9 (m, 2H), 2.11 (mc, 2H), 2.78 (td, 1H), 3.33 (td, 1H), 7.2–7.4 (m, 3H), 7.4–7.6 (m, 2H).
[9] This regioselectivity was also observed (with other metalating reagents) in the cases described in the literature [3].
[10] Here, as in the cleavage of other carbon-heteroatom bonds,
$R{-}X \xrightarrow{+e^\ominus} R^\ominus + X^\ominus \xrightarrow{+e^\ominus} R^\ominus + X^\ominus$
the product might be formed in the second, non-rate-determining step. Important for the regioselectivity is that C–X bonds in general are more easily cleaved the more the C-atom is substituted. This, of course, is related to the stability of the radicals formed as intermediates[14]. The opposite regioselectivity in the case of alkyl epoxides, on the other hand, correlates with the ability of the respective C–O bond (i.e. its σ* orbital) to accept electrons, or in other words with the tendency of formation of the respective radical anion, which should be similarly influenced by substituents as the stability of the final product. In the case of acceptor- or phenyl-substituted systems a transfer of electrons into π*-orbitals of these substituents must also be taken into consideration.
[11] **1**: A solution of the epoxide (50 mmol) in THF (20 mL) is introduced within ca. 30 min by means of a syringe into the immediate neighborhood of the stirring bar in a vigorously stirred (magnetic stirrer) solution of biphenyllithium (prepared from 0.75 g (108 mmol) of lithium and 15.4 g (100 mmol) of biphenyl in 200 mL of THF [15]) at ca. −90°C. After stirring at −80°C for one hour a solution of the electrophile (quantity as calculated for reaction with **1**; in the case of H_2O and D_2O in large excess) in 20 mL THF was added dropwise to the solution, which was then warmed to RT and worked-up in the usual way by distillation or chromatography.
[12] Prepared by reaction of naphthalenepotassium [15] with magnesium bromide in THF at −70°C.
[13] For reactions of **1** with other electrophiles, especially carbonyl compounds, see [4].
[14] C. P. Andrieux, I. Gallardo, J.-M. Savéant, K.-B. Su, *J. Am. Chem. Soc. 108* (1986) 638.
[15] H. F. Ebel in *Houben-Weyl-Müller: Methoden der Organischen Chemie, Band XIII/1*, Thieme-Verlag, Stuttgart 1970, p. 377, 438, 706.
[16] The formation of the alcohol by side reactions prior to the protonation of **1** with H_2O can be ruled out. If addition of water takes place after warming to RT, the alcohol is detectable only in traces; in its place, olefin (elimination of metal oxide from **1** at temperatures above −70°C [4]) is formed.

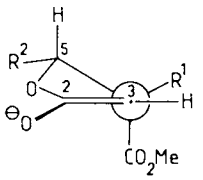
Stereocontrolled Synthesis of Paraconates from β-Lactones; Stereochemistry of Electrophilic Additions to Endocyclic Paraconate-Enolates**

By *Johann Mulzer** and *Alexander Chucholowski*

The diastereoselectivity of electrophilic additions to ester-enolates of type **1** was recently a subject of intensive study; from the results it was concluded that a perpendicularly oriented *electron-donating* substituent Z directs the attack of an electrophile to the opposite face of the double bond.[1] The informational value of the experiments described in the literature, however, was considerably impaired by the conformational mobility of the systems and the undefined (*E*)/(*Z*) geometry of the enolates. In addition, the *syn*-directing influence of a perpendicularly oriented electron-withdrawing substituent Z also had to be demonstrated in order to support the postulated stereoelectronic effect. It occurred to us that the paraconate-enolates **2** would be suitable model systems for this purpose. Here, *Z* is the inductive electron-withdrawing CO_2CH_3 group; it is fixed perpendicularly to the rest of the molecule, such that the molecule as a whole assumes an envelope conformation with equatorial R^2.[2] The residue R^1 provides for unambiguous formation of the endocyclic (*Z*)-configurated enolate.



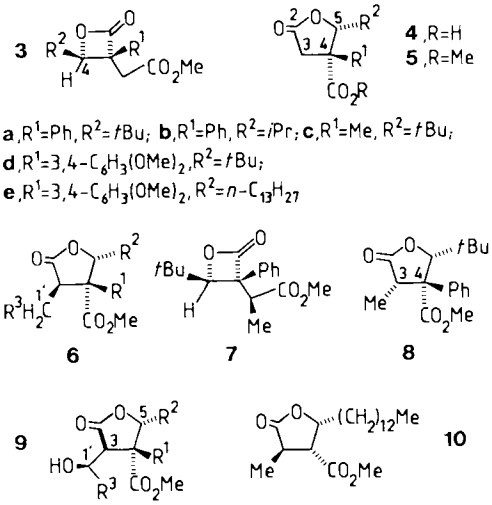
1



2

The paraconic acids **4** required for the generation of **2** were obtained diastereomerically pure by acid-catalyzed (conc. hydrochloric acid, dioxane, 120°C, 4 h) isomerization of the β-lactones **3**.[3] The driving force behind the isomerization, which proceeds with retention of configuration at C-4, is the release of strain in the four-membered ring. During the rearrangement, the orientation of the R^1/R^2 pair changes from the *cis*-vicinal to *trans*-vicinal, which in the case of R^1 = aryl is indicated by a downfield shift of the ^{1}H-NMR signals of protons in R^2 by ca. 0.3 ppm.[4] The esters **5**, obtained from **4** by reaction with diazomethane (Et_2O, 25°C), were converted with S_N2-active alkyl halides R^3CH_2X in the presence of hexamethylphosphoric triamide (HMPT) into the ^{1}H-NMR pure (>95%) products **6** (Table 1), via the enolates **2** (lithium diisopropylamide) (LDA), tetrahydrofuran (THF), −78°C).

We clarified the steric course of the methylation by unambiguous synthesis of the derivative **8**, which is 3-epimeric with **6a**. The enolate generated from **3a** (LDA, THF, −78°C) adds methyl iodide diastereoselectively to give **7**,[5] which can be isomerized to **8** in an analogous way to **3a–3f**. The ^{1}H-NMR signal of the methyl group in position 3 is characteristically different in the case of **6a** ($\delta = 0.73$) and **8** ($\delta = 1.13$); the values suggest *cis*- and *trans*-arrangements of 3-Me and 4-Ph, respectively. In a similar way, the 1′-CH_2 signals in **6b–6h** are clearly shifted upfield compared to their "normal position"[6] (Table 1).



3, **4**, R=H, **5**, R=Me

a, R^1=Ph, R^2=*t*Bu; **b**, R^1=Ph, R^2=*i*Pr; **c**, R^1=Me, R^2=*t*Bu;
d, R^1=3,4-$C_6H_3(OMe)_2$, R^2=*t*Bu;
e, R^1=3,4-$C_6H_3(OMe)_2$, R^2=*n*-$C_{13}H_{27}$

6 **7** **8**

9 **10**

Table 1. Melting points, yields (**5**→**6**), and characteristic ^{1}H-NMR shifts of some derivatives **6** [a].

6	R^1	R^2	R^3CH_2X	M.p. [°C]	Yield [%]	^{1}H-NMR δ(1′-CH_2)
a	Ph	*t*Bu	CH_3I	111–112	87	0.73
b	Ph	*t*Bu	CH_2=$CHCH_2Br$	120–121	91	1.74
c	Ph	*t*Bu	$PhCH_2Br$	oil	87	2.25
d	Ph	*t*Bu	MeO_2CCH_2Br	142–143	87	1.98
e	Ph	*i*Pr	CH_3I	76–77	76	0.73
f	Ph	*i*Pr	CH_2=$CHCH_2Br$	oil	75	1.80
g	3,4-$C_6H_3(OMe)_2$	*t*Bu	CH_3I	136–137	92	0.74
h	3,4-$C_6H_3(OMe)_2$	*n*-$C_{13}H_{27}$	CH_3I	oil	72	0.77

[a] Correct elemental analyses were obtained for **6a–6h**.

In the reaction of **2** with aldehydes (R^3CHO) (Table 2), it is also clear that the 4-CO_2CH_3 group promotes a *trans* attack of the electrophile. That is, the adducts **9** do not close the second lactone ring, as is inevitable in the case of a *cis* arrangement;[5,7] this follows from the elemental analysis and the position of the ^{1}H-NMR signals of 1′-H, which are shifted ca. 1.7 ppm upfield compared to those of 5-H. The exocyclic chirality center is also configurationally uniform when R^3 = *i*Pr and Ph; on the basis of the small ^{1}H-NMR coupling constants $J_{3,1'} = 1.9$–4.3 Hz, a "*syn*" conformation can be assumed.[8] When R^3 = Me, both "*syn*" and "*anti*"-**9** are formed (**9c**: *syn*/*anti* = 77/23; **9g**: 69/31).

The diastereoselective formation of **6** and **9** from **2** can be explained in terms of the sum of the steric effects of the

Table 2. Melting points (**5**→**9**) and characteristic ^{1}H-NMR data (80 MHz, $CDCl_3$, TMS) of some aldol adducts **9** [a].

9	R^1	R^2	R^3	M.p. [°C]	Yield [%]	^{1}H-NMR δ(1′-H)	δ(5-H)	$J_{3,1'}$ [Hz]
a	Ph	*t*Bu	Ph	198–199	86	4.02	5.70	2.5
b	Ph	*t*Bu	*i*Pr	168–169	82	3.89	5.57	1.9
c [b]	Ph	*t*Bu	Me	142–146	79	3.0–3.6	4.89/5.55	—
d	Ph	*i*Pr	Ph	127–128	78	4.70	5.02	4.3
e	Ph	*i*Pr	*i*Pr	145–146	74	3.80	5.34	2.5
f	3,4-$C_6H_3(OMe)_2$	*t*Bu	*i*Pr	188–189	82	3.77	5.49	2.0
g [b]	3,4-$C_6H_3(OMe)_2$	*t*Bu	Me	134–137	87	2.8–3.6	4.78/5.45	—

[a] Correct elemental analyses were obtained for **9a–9g**. [b] *syn*-*anti* mixture.

[*] Prof. Dr. J. Mulzer, Dr. A. Chucholowski
Institut für Organische Chemie der Freien Universität
Takustrasse 3, D-1000 Berlin 33

[**] This work was supported by the Deutsche Forschungsgemeinschaft and the Fonds der Chemischen Industrie.

substituents R^1, R^2 and CO_2CH_3; the attack is directed to the overall less-shielded ring plane. R^1 and R^2 are equatorial, and thus will contribute only slightly and almost compensatingly to the stereodifferentiation.[9] This is due, in the first place, to the influence of the 4-CO_2CH_3 group, which is clearly *anti*-directing. To postulate a *syn*-control on the basis of a stereoelectronic effect, as a logical consequence of what has been quoted in the literature,[1] is not defensible. The experiments described here, apart from being mechanistically informative, are also of preparative interest and open up a short, three-stereocenter-controlling entry to paraconic acids.[10] **6h** has been prepared as a 4-aryl derivative of the nephromopsinic acid methyl ester **10**.[11]

Received: February 5, 1986;
revised: March 27, 1986 [Z 1658 IE]
German version: *Angew. Chem. 98* (1986) 632

[1] G. J. McGarvey, J. M. Williams, *J. Am. Chem. Soc. 107* (1985) 1435; cf. also the somewhat deviating interpretation by W. Bernhard, I. Fleming, D. Waterson, *J. Chem. Soc. Chem. Commun. 1984*, 28.
[2] Crystal structure investigations on paraconic esters of type **5** show that the 4-CO_2CH_3 group is oriented almost perpendicular to the C2-C3-C4 plane (G. Huttner, I. Jibril, J. Mulzer, A. Chucholowski, unpublished).
[3] J. Mulzer, T. Kerkmann, *J. Am. Chem. Soc. 102* (1980) 3620.
[4] Thus, $\delta(C(CH_3)_3)$ in **3a** is 0.75, in **4** 1.05, in **3d** 0.81, and in **4d** 1.10. Because of the *cis*-vicinal Ph group, the $CH(CH_3)_2$ group in **3** gives two doublets ($J=6$ Hz) at $\delta=0.67$ and 0.84, whereas in **4b** it gives only one doublet at $\delta=1.02$.
[5] J. Mulzer, P. de Lasalle, A. Chucholowski, U. Blaschek, G. Brüntrup, I. Jibril, G. Huttner, *Tetrahedron 40* (1984) 2211.
[6] See, for example, T. Clerk, E. Pretsch: *Kernresonanz-Spektroskopie*, Part I, 2nd Edit., Akademische Verlagsgesellschaft, Frankfurt am Main 1973, p. 51.
[7] M. Kato, M. Kageyama, R. Tanaka, K. Kuwahara, A. Yoshikoshi, *J. Org. Chem. 40* (1975) 1932; Y. Tamaru, H. Higashimura, K. Naka, M. Hojo, Z. Yoshida, *Angew. Chem. 97* (1985) 1070; *Angew. Chem. Int. Ed. Engl. 24* (1985) 1045.
[8] *D. A. Widdowson, G. H. Wiebecke,* and *D. J. Williams* (*Tetrahedron Lett. 23* (1982) 4245) found $J=3$ Hz for the *syn*- and $J=8$ Hz for the *anti*-adduct of benzaldehyde and 2-oxolanone. The addition in this case is not stereocontrolled.
[9] According to [2] the C3-C4-C5-R^2 torsional angle in **5** is ca. 167°. Some examples of stereocontrolled additions to γ-butyrolactone-enolates have been described. See D. A. Evans in J. D. Morrison (Ed.): *Synthesis, Vol. 3B*, Academic Press, New York 1984, p. 40f. see also D. Seebach, R. Naef, G. Calderari, *Tetrahedron 40* (1984) 1313.
[10] E. E. van Tamelen, S. Rosenberg-Bach, *J. Am. Chem. Soc. 80* (1958) 3079; S. Hunek, G. Follmann, *Z. Naturforsch. B 22* (1967) 666; R. M. Carlson, A. R. Oyler, *J. Org. Chem. 41* (1976) 4065.
[11] M. Asano, T. Azumi, *Ber. Dtsch. Chem. Ges. 72* (1939) 35.

Isomorphism of Tris(cyclopentadienyl)lutetium(III) and Tris(cyclopentadienyl)scandium(III): An Unexpected Consequence of the Lanthanoid Contraction**

By *Stefan H. Eggers, Holger Schultze, Jürgen Kopf,* and *R. Dieter Fischer**

Dedicated to Professor Erwin Weiss on the occasion of his 60th birthday

It is known[1] that the "total hapticity" $\sum_i \eta_i^n$ of all four Cp ligands in the series of complexes Cp_4M **1** ($Cp=C_5H_5$) first passes through a maximum[2] in the case of **1b**, viz: **1a** 12, **1b** 16, **1c** 12. The drastic drop in the "total hapticity" in going from **1b** to **1c** is likely to result in part from the lanthanoid contraction, and in part from a theoretically well understood[6a] preference of the frequently formed[6b] complex type $[(\eta^5\text{-Cp})_2M(\eta^1\text{-X})_2]$ (M = transition metal, X = e.g. halide, pseudohalide, alkyl etc.). The occurrence of analogous changes in structure and hapticity is to be expected in related series of complexes.

Cp_4M **1**
a, M = Ti[3], **b**, M = Zr[4], **c**, M = Hf[5]

Indeed, within the series Cp_3M **2** (M = Sc, Ti, Y, La–Lu) where the "total hapticity" reaches a maximum of 17 for the structure type A ($[(\eta^5\text{-Cp})_2M(\mu\text{-}\eta^5:\eta^2\text{-Cp})]_\infty$) with M = La[7] and Pr,[8] this quantity decreases again, as we have now found for M = Lu (**2a**), to the minimum value of 12 as already observed for **2b** and **2c**.[12]

Cp_3M **2**
a, M = Lu[9], **b**, M = Sc[10], **c**, M = Ti[11], **d**, M = Tm, **e**, M = Yb

A single-crystal X-ray structure analysis of **2a**[13] confirms that here, as in the crystal of **2b**,[10] polymeric zig-zag chains of type B $[(\eta^5\text{-Cp})_2M(\mu\text{-}\eta^1:\eta^1\text{-Cp})]_\infty$ are present (Fig. 1).

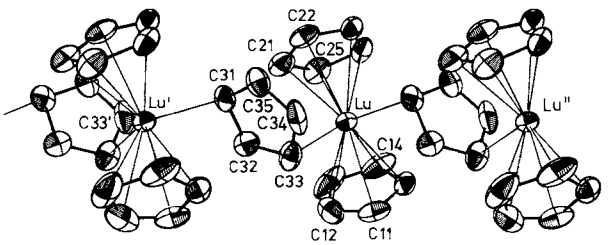


Fig. 1. ORTEP diagram of the structure of **2a** in the crystal. Selected bond lengths [Å] and angles [°]: Lu-Cent1 2.285, Lu-Cent2 2.321, Lu-Cent3 3.116, C31-C32 1.447(16), C32-C33 1.405(20), C33-C34 1.443(21), C34-C35 1.379(20), C31-C35 1.448(20), Lu-Lu' 6.163; C31-Lu'-C33' 89.0(8), Lu'-Lu-Lu'' 107.7 [25].

The structure of **2a** differs, on the other hand, from those of **2d** and Cp_3Er, whose crystals contain practically non-associated $(\eta^5\text{-Cp})_3M$ molecules ("total hapticity" 15, type C).[14]

The LuC distances found for the η^5-coordinated Cp rings (mean value 2.602 Å) and the cent1-Lu-cent2 angle (126.9(8)°) (cent = centroid of an η^5-coordinated Cp ring) resemble the corresponding data for the complex systems $[(\eta^5\text{-Cp})_2LuR(thf)]$ ($R=C(CH_3)_3$, $CH_2Si(CH_3)_3$, C_6H_4-4-CH_3, (thf) = tetrahydrofuran). Unlike in the polymers of type A[7,8] and in **2b**, the two shortest[16] LuC distances for the bridging Cp ring (Lu'-C31 2.519, Lu-C33 2.654 Å) are only slightly shorter and longer, respectively, than the two extreme $LuC(\eta^5\text{-Cp})$ contacts (Lu-C14 2.542 and Lu-C25 2.648 Å). The Lu'-C31 contact exceeds the longest hitherto known length of a LuC σ-bond (2.47 Å[15a]). The Lu'-C31 and Lu-C33 vectors form angles of 66.5 and 79.9° (**2b**: 61 and 73°,[10] respectively; **1b**: 49°[4b]) with the μ-Cp plane,

[*] Prof. Dr. R. D. Fischer, Dipl.-Chem. S. H. Eggers, Dipl.-Chem. H. Schultze, Dr. J. Kopf
Institut für Anorganische und Angewandte Chemie der Universität Martin-Luther-King-Platz 6, D-2000 Hamburg 13 (FRG)

[**] Coordination Behavior in Base-Free Tris(cyclopentadienyl)lanthanoid(III) Compounds, Part 3. We thank Prof. *H.-D. Amberger* for supplying us with a sample of **4**. – Part 2: [7].

and the spatial arrangement of the μ-Cp ligands in **2a** and **2b** resembles that in the main group metal complex $[(\eta^1\text{-Cp})_2\text{In}(\mu\text{-}\eta^1\text{:}\eta^1\text{-Cp})]_\infty$.[17] The practically non-alternating C-C distances in the μ-Cp ligand (cf. Fig. 1) essentially rule out a diene character of this ligand.

Interestingly, the enthalpy of sublimation ΔH_{subl} of **2a** markedly exceeds the ΔH_{subl} values of the Cp_3M compounds with M = Y and Tb–Yb.[18] A further consequence of the comparatively strong self-association of **2a** is its noticeably sparing solubility in toluene, CH_2Cl_2 and THF, compared to that of **2e**,[19] which even facilitates the separation of Yb and Lu via their base-free triscyclopentadienyl complexes.—The temperature-dependent ^{1}H-NMR spectra of **2a** in CD_2Cl_2 and [D$_8$]toluene in the resonance range $\delta = 5.5$–6.5 (cf. Fig. 2) indicate the presence of at least one dissolved species with non-equivalent Cp ligands.[20]

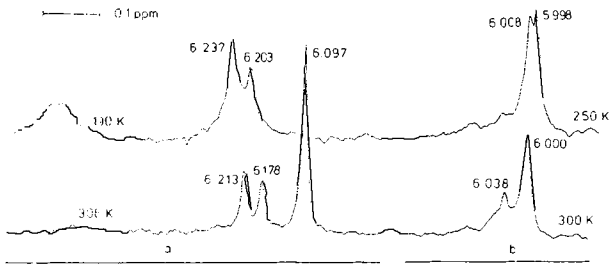


Fig. 2. ^{1}H-NMR spectra of **2a** in CD_2Cl_2 (a) and [D$_8$]toluene (b) at two temperatures (Bruker WP-80).

The difference $\Delta\{M\text{–}C(\eta^5\text{-Cp})\}$ in the MC distances (for the η^5-coordinated Cp rings in the case of **2a** and **2b**, mean value: 0.112 Å) correlates well with the difference in the metal-ion radii ($\Delta r(M^{3\oplus}) = 0.107$ Å[21]), while the corresponding MC distances for the μ-coordinated Cp ring (of **2a** and **2b**) are practically the same ($\Delta\{M'\text{-C31}\}$: 0.00 Å; $\Delta\{M\text{-C33}\}$: 0.025 Å). Hence, the MC(μ-Cp) distances in **2b** turn out to be relatively long, which feature might, in the first instance, be due to stronger interligand interactions in the coordination sphere of the smaller Sc^{III} ion.[22] Nevertheless, in view of the X-ray crystallographically confirmed existence of complexes of the type $[(\eta^5\text{-Cp})_3\text{Lu}\cdot\text{L}]$ with a "total hapticity" of 16, the observed isomorphism of **2a** and **2b** is completely unexpected.[23] The comparatively close relationship of Lu (instead of La) with Sc and Y, and the consequently more meaningful location of Lu in Group 3A of the Periodic System has, however, been hinted at on a number of earlier occasions.[24]

Received: January 27, 1986;
supplemented: February 21, 1986 [Z 1640 IE]
German version: *Angew. Chem. 98* (1986) 631

CAS Registry numbers:
2a, 102724-39-0; **2b**, 39384-99-1.

[1] Cf., e.g., F. A. Cotton, G. Wilkinson: *Advanced Inorganic Chemistry*, Wiley, New York 1980, pp. 705, 831, 1167.

[2] A second maximum with $\sum_i \eta_i^5 = 20$ is reached when M = U: J. H. Burns, *J. Organomet. Chem. 69* (1974) 225.

[3] J. L. Calderon, F. A. Cotton, B. G. DeBoer, J. Takats, *J. Am. Chem. Soc. 93* (1971) 3592.

[4] a) V. I. Kulishov, E. M. Brainina, N. G. Bokly, Yu. T. Struchkov, *Chem. Commun. 1970*, 475; b) R. D. Rogers, R. Vann Bynum, J. L. Atwood, *J. Am. Chem. Soc. 100* (1978) 5238; c) a second $[(\eta^5\text{-Cp})_3\text{Zr}(\eta^1\text{-X})$ system that has been confirmed X-ray crystallographically is $(C_5H_5)_3\text{Zr}(\mu\text{-H})\text{Al}(C_2H_5)_3]$: J. Kopf, H.-J. Vollmer, W. Kaminsky, *Cryst. Struct. Commun. 9* (1980) 985.

[5] V. I. Kulishov, N. G. Bokly, Yu. T. Struchkov, *J. Struct. Chem. (Engl. Transl.) 13* (1972) 1029; V. I. Kulishov, E. M. Brainina, N. G. Bokly, Yu. T. Struchkov, *J. Organomet. Chem. 36* (1972) 333.

[6] a) J. W. Lauher, R. Hoffmann, *J. Am. Chem. Soc. 98* (1976) 1729; b) as demonstrated, e.g., by the unusually broad span of the $M^{n\oplus}$ ionic radii (n = 3 and 4): from 0.74 (**1a** [1]) up to ca. 1.08 Å ($[Cp_2Sm^{III}(SiMe_3)_2]^\ominus$ ion, cf. H. Schumann, S. Nickel, E. Hahn, M. Heeg, *Organometallics 4* (1985) 800).

[7] S. H. Eggers, J. Kopf, R. D. Fischer, *Organometallics 5* (1986) 383.

[8] W. Hinrichs, D. Melzer, M. Rehwoldt, W. Jahn, R. D. Fischer, *J. Organomet. Chem. 251* (1983) 299.

[9] E. O. Fischer, H. Fischer, *J. Organomet. Chem. 3* (1965) 181.

[10] J. L. Atwood, K. D. Smith, *J. Am. Chem. Soc. 95* (1973) 1488.

[11] C. R. Lucas, M. Green, R. A. Forder, K. Prout, *J. Chem. Soc. Chem. Commun. 1973*, 97.

[12] In contrast, the two complexes $[Cp_3ZrH]$ and $[Cp_3HfH]$ appear to be isomorphous: B. V. Lokshin, Z. S. Klemenkova, M. G. Ezernitskaya, L. I. Strunkina, E. M. Brainina, *J. Organomet. Chem. 235* (1982) 69.

[13] a) Structure of **2a** (after [9]); for a check on the m.p. and the mass and IR spectra, see [14b].—Suitable single crystals (ca. 0.4 × 0.5 × 1.8 mm) were obtained by high-vacuum sublimation of **2a** (180–210 °C); b) structural data (25 °C): orthorhombic, $Pbc2_1$ (non-standard setting of $Pca2_1$ (No. 29, Int. Tab.); $a = 13.178(4)$, $b = 8.930(1)$, $c = 9.953(2)$ Å; $Z = 4$; $\rho_c = 2.10$ g cm^{-3}; SYNTEX P2$_1$ four-circle diffractometer ($Mo_{K\alpha}$, graphite monochromator, $\lambda = 0.709261$ Å), measuring range: $4.5 \le 2\theta \le 60.0°$; 1550 observed reflections with $|F| > 3\sigma(F)$, numerical absorption correction (SHELX, $\mu = 80.28$ cm^{-1}); use of the atomic coordinates of **2b** [10] as starting parameters for the least squares refinement (unit weights), refinement to $R = 0.033$ (unweighted), anisotropic temperature factors; H positions not determined.—Further details of the crystal structure investigation are available on request from the Fachinformationszentrum Energie, Physik, Mathematik GmbH, D-7514 Eggenstein-Leopoldshafen 2, on quoting the depository number CSD-51744, the names of the authors, and the full citation of the journal.

[14] a) S. H. Eggers, W. Hinrichs, J. Kopf, W. Jahn, R. D. Fischer, *J. Organomet. Chem.*, in press; b) in contrast to what has been stated earlier [9], the IR spectra of **2a** and **2d** differ slightly.

[15] a) $R = C(CH_3)_3$: W. J. Evans, A. L. Wayda, W. E. Hunter, J. L. Atwood, *J. Chem. Soc. Chem. Commun. 1981*, 292; b) $R = CH_2Si(CH_3)_3$ and $C_6H_4\text{-}4\text{-}CH_3$: H. Schumann, W. Genthe, N. Bruncks, J. Pickardt, *Organometallics 1* (1982) 1194.

[16] Other LuC(μ-Cp) distances < 3.5 Å: Lu-C32 3.043; Lu'-C35 3.133; Lu-C34 3.245; Lu'-C32 3.263 Å.

[17] F. W. B. Einstein, M. M. Gilbert, D. G. Tuck, *Inorg. Chem. 11* (1972) 2832.

[18] G. G. Devyatykh, G. K. Borisov, L. F. Zyuzina, S. G. Krasnova, *Dokl. Akad. Nauk SSSR 212* (1973) 127. Surprisingly, however, it was found that $\Delta H_{subl}(\mathbf{2b}) < \Delta H_{subl}(\mathbf{2a})$: G. G. Devyatykh, I. B. Rabinovich, V. I. Tel'noi, G. K. Borisov, L. F. Zyuzina, *ibid. 217* (1974) 609.

[19] Solubility in mg·mL^{-1}: **2a** in $C_6H_5CH_3$ 4.2, CH_2Cl_2 11.5; **2d** in $C_6H_5CH_3$ 14.2, CH_2Cl_2 29.8; for THF as solvent, see G. K. Borisov, S. G. Chugunova, G. G. Devyatykh, *Russ. J. Inorg. Chem. (Engl. Transl.) 20* (1975) 1579.

[20] Cf. the likewise temperature-dependent NMR behavior of **2b**: P. Bougeard, M. Nancini, B. G. Sayer, M. J. McGlinchey, *Inorg. Chem. 24* (1985) 93, and the ^{1}H- and ^{13}C-NMR spectra of **2a**·THF [15b].

[21] Cf. R. D. Shannon, *Acta Crystallogr. Sect. A 32* (1976) 751; in each case values for the coordination number 8 were considered.

[22] a) Cf. also the difference in structure of **2b** and **2c**, which appears to be based on the different ionic radii ($\Delta r(M^{3\oplus}) = 0.075$ [21]) [10, 11]; b) some pronounced covalency as already assumed in the case of **2b** [10] can not be ruled out in the case of **2a**, either.

[23] a) $[Cp_3Lu(thf)]$: Ch.-Z. Ni, D.-L. Deng, Ch.-T. Qian, *Inorg. Chim. Acta 110* (1985) L7; b) $[(Cp_3Lu)_2H]^\ominus$-Ion: H. Schumann, W. Genthe, E. Hahn, M. B. Hossain, D. van der Helm, *J. Organomet. Chem. 299* (1986) 67; c) $\Delta r(M^{3\oplus})$ of Tm^{III} and Lu^{III}: 0.017 Å [21].

[24] a) F. Seel, *Bild Wiss. 6* (1969) 45; b) W. B. Jensen, *J. Chem. Educ. 59* (1982) 634, and literature cited therein.

[25] **2a** and the complex $[(Cp^*Lu)_2(\mu\text{-}\eta^2\text{:}\eta^2\text{-}C_6H_4)]$ ($Cp^* = C_5Me_5$) with two pairs of Lu-C(C_6H_4) contacts of different lengths (2.364 and 2.690 Å) and Lu atoms lying outside the C_6 ring plane, also appear, in our opinion, to be distantly related: cf. T. J. Marks, plenary lecture, NATO Advanced Study Institute on Fundamental and Technological Aspects of Organo-f-Element Chemistry, Acquafredda di Maratea (Italy), September 10–21, 1984; P. L. Watson, G. W. Parshall, *Acc. Chem. Res. 18* (1985) 51.

Remarks on the Review Article "Replication and Evolution in Inorganic Systems" by *Armin Weiss*[1]

By *Gustaf Arrhenius*,* *Alexander G. Cairns-Smith*,* *Hyman Hartman*,* *Stanley L. Miller*,* and *Leslie E. Orgel**

Professor *Armin Weiss* in a paper published in 1981 in *Angewandte Chemie* has claimed observations with potential importance for the origin and early evolution of life.[1] This paper has been widely cited since it claimed experimental proof of clay mineral replication, mutational variability in replicating clay crystals, and specific catalytic effects. The results have been invoked in support of the idea that an inorganic evolution through natural selection preceded the evolution of organic life.

The information given in the Weiss 1981 paper is altogether inadequate for others to repeat the key experiments that are said to be "proof of replication". A single reference in this section reads: "Unpublished results: published in part in *G. Mai*, Dissertation, Universität München 1969; *P. Brunner*, ibid. 1978; *S. Fritz*, ibid. 1978".

We have been unable to trace the first and third of these theses, while the second contains nothing which we consider of special relevance to clay replication. Nor have repeated attempts to obtain experimental protocol from Professor *Armin Weiss* been successful.

We now ask Professor *Armin Weiss* to provide us a published account of the procedures used to obtain the important results reported in his 1981 paper so that they can be confirmed or disproved. In the meantime, his conclusions should be accepted with caution.

Received: March 14, 1986 [Z 1721 IE]
German version: *Angew. Chem. 98* (1986) 654

[*] Prof. Dr. G. Arrhenius
A-020 Scripps Institution of Oceanography
University of California, San Diego
La Jolla, CA 92093 (USA)
Dr. A. G. Cairns-Smith
Chemistry Department
The University
Glasgow G12 8QQ (UK)
Prof. Dr. H. Hartman
Department of Earth Sciences, 54-1820
Massachusetts Institute of Technology
Cambridge, MA 02139 (USA)
Prof. Dr. S. L. Miller
B-017 Department of Chemistry
University of California, San Diego
La Jolla, CA 92093 (USA)
Prof. Dr. L. E. Orgel
Salk Institute for Biological Studies
P.O. Box 85800, San Diego, CA 92138 (USA)

[1] Armin Weiss, *Angew. Chem. 93* (1981) 843; *Angew. Chem. Int. Ed. Engl. 20* (1981) 850.

BOOK REVIEWS

Applications of Dynamic NMR Spectroscopy to Organic Chemistry. By *M. Oki*. VCH Verlagsgesellschaft, Weinheim 1985. xii, 423 pp., bound, DM 208.00.—ISBN 3-527-26166-4

Why has a new book on dynamic NMR spectroscopy been published when, in addition to a number of review articles, three books are already available—the standard work by *Jackman* and *Cotton* (1975), *Kaplan* and *Fraenkel*'s more theoretically orientated book (1980) and *Sandström*'s recent introduction (1983) to DNMR analysis? The title of the present book indicates that it is concerned with applications in organic chemistry. Do the contents justify the need for a new publication?

The introductory section describes the exchange broadening phenomenon of NMR signals, gives methods (especially approximations) which can be used to determine rate constants, and provides typical examples of mechanisms that can result in spin exchange. Rotations around bonds (from sp^2-sp^2 to sp^3-sp^3) are then dealt with in detail (five chapters). The following sections concern flexible conformations in rings, the inversion and rotation of amines and imines, and applications for studying chemical reactions.

No such survey can hope to be complete, but the author has nevertheless managed to compile a surprising variety of examples from extremely different areas of organic chemistry. They reflect the current state of DNMR spectroscopy; only a few fundamental innovations have been introduced in the last decade, but the technique has become an important tool for the chemist. The book serves its purpose because it draws the reader's attention to possible applications in his own research work and can also be used as a reference work for literature published up to 1983.

Several topics are, however, missing. For example, ligand permutations at central atoms, DNMR phenomena in solids, comments on the mechanistic information obtained in multi-site exchange systems and 2D-DNMR techniques. The computer simulation of spectra is also dealt with very briefly, although six pages of the introductory chapter are dedicated to approximation solutions. This somewhat underestimates the flexibility of organic chemists as regards using new techniques.

A number of inaccurate formulations become evident on going through the book. In the first chapter, for example, "..., the lifetime of a nucleus in one site, ..., is a function of the external magnetic field.". This is impossible—what is meant is that the lower limit of the half-life times at which exchanging nuclei can still be separately observed is a function of the magnetic field. Later, the diastereotopic CH_2 protons in a molecule $XYZC\text{-}CH_AH_BW$ are considered and the three possible staggered conformations are illustrated. This is followed by the statement: "If the free energies of the three conformations are equal, it will be seen readily that the magnetic environments of H_A and H_B are completely equivalent on the average because ...". This

is incorrect; diastereotopic protons remain diastereotopic, the shift difference between H_A and H_B may be very small or almost zero depending on the population of conformers present, but equal energies of the conformers are neither necessary nor sufficient for this.

These criticisms should not, however, destroy the positive overall impression made by the book. The reader's first impression is of a useful compendium of literature. He may then be fascinated by a single topic and finally he is successfully made aware of the possibilities offered by DNMR spectroscopy for his own research.

Martin Feigel [NB 748 IE]
Institut für Organische Chemie
der Universität Erlangen-Nürnberg (FRG)

Vibronic Coupling. By *G. Fischer*. Academic Press, London 1984. viii, 222 pp., bound, $ 42.00. - ISBN 0-12-257240-8

In recent years, the significance of vibronic coupling (i.e., the interaction between electronic and nuclear motion in molecules) for spectroscopy and for many dynamic processes has become increasingly evident, as reflected in the growing number of publications on this subject. Accordingly, there is keen interest in a book that documents the current status of research in this field and also gives the nonspecialist guidance.

The monograph under consideration is primarily intended for the nonspecialist. It therefore begins in Chapter 1 with an elementary demonstration of the separation of variables in several systems, which should facilitate an understanding of the adiabatic approximation. In the following two chapters, this approximation is discussed for di- and polyatomic molecules. In order to extend the treatment and be able to describe "intensity borrowing" and nonadiabatic effects, variants of the adiabatic approximation and other methods, mainly from perturbation theory, come up for discussion. Two approaches to the calculation of transition intensities in electronic spectra (that of dipole length and that of dipole velocity) are compared in Chapter 4. Chapter 5 concludes the general part of the book with a presentation of two symmetry-dependent degeneracies, the Jahn-Teller and the Renner-Teller effects, which are classical examples of vibronic coupling. In Chapters 6-8, the most important applications come up for discussion: the calculation of vibronic-coupling effects using semiempirical (CNDO) methods as well as the manifestation and detection of these effects in electronic spectra and in multiphoton processes. Important dynamic processes in which vibronic coupling plays a role—in particular, radiationless decay—are discussed in Chapter 9. The book closes with a survey of analogous effects in molecular crystals.

On the whole, one can recognize the effort that the author has made to present the manifold applications of vibronic coupling in a way that is also understandable to the nonspecialist. Nevertheless, this effort cannot be considered successful for several reasons.

First and foremost, attention must be called to the selection and organization of the material. Questions that are only very loosely related to the subject of the book, such as local modes, energy transfer, and unimolecular reactions, are discussed. On the other hand, important newer developments, such as the concept of the so-called diabatic electronic wave functions, the appearance of strong nonadiabatic effects when potential surfaces intersect conically, and the calculation of vibronic-coupling effects using truly ab-initio methods, are not even referred to. Furthermore, many standard references are missing, and only little experimental material is presented to illustrate the meaning of the effects discussed.

The material is not very clearly organized. Thus, the basic coupled equations of electronic and nuclear motion are newly derived in each of the Chapters 2, 3, and 5; the so-called Herzberg-Teller expansion for the transition moment in each of the Chapters 3, 4, and 6. Without cross-references, such repetitions are not only superfluous, but also, at least for the beginner, even disorienting. The assignment of the material to the individual chapters is in part illogical; Chapter 7, for example, seems out of place—thematically, it belongs to either Chapter 6 or 8. The unsystematic arrangement of the material makes it extraordinarily difficult to obtain a general view of the effects of vibronic coupling and of their connection. Why, for example, in Chapter 5, which is on the Jahn-Teller effect, is the opportunity not taken to make its relation to adiabatic potential surfaces clear by discussing calculated model spectra? On the whole, the book gives the impression (though unfounded) that one can almost always describe nonadiabatic effects using perturbation theory, and it is incomprehensible, for example, why an example is cited in Section 6.5 of the "Breakdown of the Born-Oppenheimer approximation," precisely where this approximation does *not* break down.

The list of shortcomings is rounded out by the numerous minor oversights and mistakes, which have crept into the text. One example is the false definition of the term "electrical anharmonicity" on p. 106; a more serious example is the discussion of the potential surfaces of a vibronic system with several nuclear vibrations, where the multimode effect is simply overlooked (p. 84). In summary, a book that is only marginally suited for the introduction of the beginner to the field in question.

Horst Köppel [NB 721 IE]
Physikalisch-Chemisches Institut
der Universität Heidelberg (FRG)

Thermodynamik irreversibler Prozesse. Eine Einführung. By *H.-W. Kammer* and *K. Schwabe*. VCH Verlagsgesellschaft, Weinheim 1985. 114 pp., Brochure, DM 28.00.— ISBN 3-527-21104-7

This thin volume addresses physicists and chemists who wish to acquire first knowledge about thermodynamically irreversible processes. After the Introduction, which outlines the contents of the book very briefly, a short summary of equilibrium thermodynamics is given. Next, the fundamental concept of entropy production is introduced by means of two examples (solidification of supercooled water and thermal conductivity) and then generalized to processes with a single order parameter as well as to chemical reactions. In the short, fourth chapter, the dynamics of irreversible processes are discussed using the example of glass transitions in polymers. This chapter seems to me to be too complicated for an introductory text; furthermore, the mathematical treatment does not impart any knowledge that could not be equally well obtained in a simple qualitative manner. The next chapter deals with Onsager's reciprocal relationships. Thermoelectrical effects and thermodiffusion are thoroughly discussed; on the other hand,

the most important other interference effects are only briefly presented. Here, a more thorough treatment would have perhaps been appropriate. In the sixth chapter, stationary states are discussed. The theorem of minimal entropy production is derived, whereby the stability of the stationary state in the linear region is demonstrated. The last chapter is devoted to irreversible processes in the nonlinear region. Following a discussion of the general criteria for stability according to *Prigogine* and *Glansdorff*, the stability of simple, far-from-equilibrium, chemical reactions is dealt with in terms of the kinetic potential. Next, the Lotka model is presented as an example of an oscillating reaction. A qualitative discussion of several hydrodynamic instabilities closes this chapter. On the whole, this book is didactically successful and it can be recommended to every beginner.

Max Teubner [NB 740 IE]
Max-Planck-Institut für Biophysikalische Chemie,
Göttingen (FRG)

Gruppentheorie für Chemiker. By *D. Wald*. VCH Verlagsgesellschaft, Weinheim 1985. ix, 234 pp., brochure, DM 48.00.—ISBN 3-527-26300-4

Group theory is an abstract branch of mathematics that is far from easy to understand. The chemist normally encounters it in vibrational and electron spectroscopy, quantum chemistry and crystallography. This book is intended "above all for chemistry students who have taken their Bachelor's degree" and, according to the advertising literature of the publishing company, "explains the group theory to the chemist in an understandable way".

The book is a direct copy of the original typewritten manuscript and contains rather simply presented figures. It is divided into six sections, the short introduction being counted as a separate chapter. Chapter 2 introduces basic group theoretical terms and deals with symmetry operations and point groups. Chapter 3 presents basic principles of the representation theory. Chapter 4 gives some applications of the material discussed in the previous chapters, the most important being the construction of character tables, the derivation of irreducible representations for various point groups, the selection rules used in vibrational spectroscopy of molecules and solids, the determination of the 230 space groups, the formulation of group-subgroup relationships in solid state chemistry and the Woodward-Hoffmann rules. Chapter 5 contains the solutions to the problems presented at the end of Chapters 2–4. Chapter 6 is a 13-part appendix.

I read the book with the intention of refreshing my memory and furthering my limited knowledge of group theory and its applications. It soon became apparent, however, that the book was not very well suited to my taste. It can be described as a collection of group theoretical definitions, rules and calculations supplemented by practice problems and (this is undoubtedly a positive feature) a large number of precalculated examples from the field of point and space groups, some of these having been performed in great detail. Proofs and explanations of mathematical (or physical) relationships have seldom been included with the comment that they can be looked up in a mathematics text book. I feel, however, that one of the purposes of a book of this type should be to explain these relationships to the non-mathematician, but this is certainly a matter of opinion.

More serious is the fact that sometimes important information is presented in such a way that it is almost unintelligible. The text is often simply too short, i.e. explanations are inadequate (e.g. p. 25, 73, 86, 120). The book also contains grammatical errors as well as a number of unclear formulations which miss the point in question (e.g. p. 32, 34, 115, 148). Furthermore the reader is unnecessarily harrassed by the appearance of symbols and terms in the text and tables which are then first explained pages or chapters later, if at all (e.g. p. 26, 29, 75, 116). A subjective "experimental" finding: I was only able to understand some of the topics dealt with in the book (e.g. cycles or a subject as important as irreducible representations) after I had consulted another text book (also intended for the chemist).

A few final remarks on individual points: a "slanted mirror plane" appears in a stereographic projection as a circle and not as an ellipse (p. 34); a factor of 1/2 is apparently missing on the left-hand side of some of the equations given on p. 110/111; Figure 2-21 (p. 37) is geometrically incorrect; whether the so-called "unit cell group" satisfies the group axioms or not surely depends on the formulation of the combination rules for the elements (p. 208); the statement that a group is isomorphic with the group of its inner automorphisms (p. 55) contradicts the statements presented on p. 60.

Enough fault-finding! It is also certainly true that the book contains a wealth of relevant material. In my opinion the book will be of value to the practicing chemist, especially the vibrational spectroscopist, in providing a compact summary of group theoretical facts, many detailed calculated examples, and a comprehensive list of references. I feel, however, that the book is less suitable as an introductory text on group theory and its chemical applications.

Egbert Keller [NB 746 IE]
Kristallographisches Institut
der Universität Freiburg (FRG)

Registered names, trademarks, etc. used in this journal, even without specific indication thereof, are not to be considered unprotected by law.

© VCH Verlagsgesellschaft mbH, D-6940 Weinheim, 1986. – Printed in the Federal Republic of Germany by Zechnersche Buchdruckerei, Speyer/Rhein.

All rights reserved (including those of translation into foreign languages). No part of this issue may be be reproduced in any form – by photoprint, microfilm, or any other means – nor transmitted or translated into a machine language without written permission from the publishers. Only single copies of contributions, or parts thereof, may be reproduced for personal use.

Valid for users in the USA: The appearance of the code at the bottom of the first page of an article in this journal (serial) indicates the copyright owner's consent that copies of the article may be made for personal or internal use, or for the personal or internal use of specific clients. This consent is given on the condition, however, that the copier pay the stated per-copy fee through the Copyright Clearance Center, Inc., for copying beyond that permitted by Sections 107 or 108 of the U.S. Copyright Law. This consent does not extend to other kinds of copying, such as copying for general distribution, for advertising or promotional purposes, for creating new collective works, or for resale. For copying from back volumes of this journal see 'Permissions to Photo-Copy: Publisher's Fee List' of the CCC.

Editorial office: Pappelallee 3, D-6940 Weinheim, Federal Republic of Germany. Telephone (06201) 602315, Telex 465516 vchwh d, Telefax (06201) 602328.

Editor: *P. Gölitz.*

Associate editors: *D. I. Loewus, A. Stimson.* **Editorial assistant:** *E. Schweikart*

Publishers: VCH Verlagsgesellschaft mbH. (Managing Directors: *Prof. Dr. Helmut Grünewald* and *Hans Dirk Köhler*), Pappelallee 3, D-6940 Weinheim, Federal Republic of Germany. Correspondence concerning advertisements should be addressed to VCH Verlagsgesellschaft mbH. (Advertising Manager *R. J. Roth*), Boschstr. 12, P.O. Box 1260/1280, D-6940 Weinheim, Federal Republic of Germany. Telephone Weinheim (06201) 602-0, Telex 465516 vchwh d, Telefax (06201) 602328.

ANGEWANDTE CHEMIE
International Edition in English
Volume 25 · Number 8
August 1986
Pages 661–766

185-nm Photochemistry of Olefins, Strained Hydrocarbons, and Azoalkanes in Solution

By Waldemar Adam* and Thomas Oppenländer

Dedicated to Professor Dietrich Schulte-Frohlinde on the occasion of his 60th birthday

The possibility to excite *directly* at 185 nm chromophores that absorb in the vacuum-UV has stimulated increased activity during the last decade in this field of photochemistry. Whereas photochemical reactions at $\lambda < 200$ nm have been thoroughly investigated in the gas phase, only recently have intensive studies on the 185-nm photochemistry of organic compounds in *solution* provided new insights. Despite the high excitation energies, *selective* photoreactions are promoted in the short-lived singlet excited states (Rydberg photochemistry). In contrast to conventional photochemistry ($\lambda > 220$ nm), 185-nm irradiation preferentially results in *intramolecular* rearrangement, fragmentation, and isomerization reactions. Intermolecular radical couplings and abstractions as well as dimerizations (π,π^*-excitation) compete minimally. Besides the straightforward denitrogenation of photoresistant ("reluctant") azoalkanes, important applications of the short-wavelength photolysis are also found in technology (photolithography) and medicine (193-nm laser). Broadening the scope of the synthetic potential of the 185-nm photochemistry, which so far has been limited to direct *cis/trans* isomerizations, presents a challenge for the chemist.

1. Why 185-nm Photochemistry?

The photon as a "reagent" plays an important role in synthetic organic chemistry. During the last 15 years this has been particularly exemplified in the elegant syntheses of ring systems, especially four-membered rings and natural products.[1] The development of new photochemical equipment makes it possible to perform photoreactions over a wide range of wavelengths. For example, the continuous output of a synchrotron extends from the near infrared to X-ray radiation.[2]

For the organic chemist, however, it is essential to perform photochemistry as economically as possible. In 185-nm photochemistry this is accomplished by using Suprasil equipment and low-pressure mercury lamps. Such apparatus is comparably cheap and allows vacuum-UV photochemistry to be performed in solution[3] with *n*-pentane or other UV-transparent hydrocarbons as solvents. Despite the high excitation energy of 6.7 eV (647.8 kJ/mol), 185-nm photolysis of suitable substrates leads to defined products. Their formation can be rationalized according to defined mechanistic concepts. Besides the few preparative applications using 185-nm radiation, e.g., the syntheses of (*E*)-cyclooctene[4] and (*Z*)-2,2,5,5-tetramethyl-3-hexene ("di-*tert*-butylethylene"),[5] the main focus of research in

[*] Prof. Dr. W. Adam, Dr. T. Oppenländer
Institut für Organische Chemie der Universität
Am Hubland, D-8700 Würzburg (FRG)

 © VCH Verlagsgesellschaft mbH, D-6940 Weinheim, 1986 0570-0833/86/0808-0661 $ 02.50/0

this stimulating field of organic photochemistry is on mechanistic studies. One of the principle goals of these studies is to describe the nature of the electronic states that are reached by high-energy excitation with 185-nm photons.

Recently, *Srinivasan* et al.[6] investigated whether UV radiation ($\lambda < 200$ nm) could be used for practical purposes. For example, laser photolysis (193 nm) might prove useful for photolithographic processes or in medicine. Since the excess energy can be converted into the translational energy of small molecular fragments, a process called ablation, the surrounding material is not burned. In medical applications, this should be of considerable advantage over the usual laser techniques.

2. Mechanistic Concepts in 185-nm Photochemistry

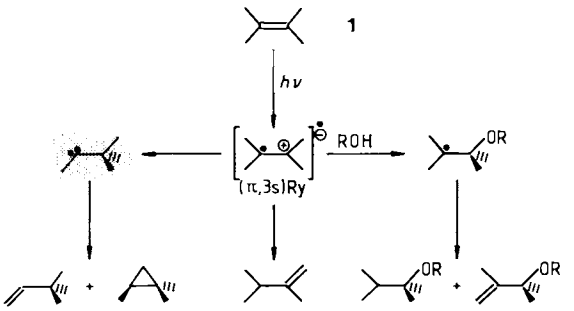
Organic photochemistry with vacuum-UV radiation is not limited to the well-examined alkenes[3a,7] and cyclopropanes.[8] Endoperoxides,[9] azoalkanes,[10] unsaturated ketones,[11] acetylenes,[12] alcohols, amines, ethers,[13] and trihalomethanes,[13f] and other bichromophoric systems such as oxacycloalkenes[14] and tetrahydropyridines[15] have been investigated in detail. Especially the degradation of halocarbons on 185-nm irradiation of aqueous solutions[13f] should acquire substantial significance in the treatment of waste water. The 185-nm photolysis of hexamethyldisiloxane[16] yields a multitude of photoproducts, the formation of which can be explained by means of radical intermediates. The gas-phase photolysis ($\lambda < 200$ nm) of olefins is described elsewhere.[17] However, there are significant differences[3c] between 185-nm photolyses in the gas phase and in solution.

The photoreversible $(Z)/(E)$ isomerization of cyclooctene,[18] which can be monitored by quantitative capillary gas chromatography, is the most commonly used chemical actinometer for the calibration of low-pressure mercury lamps. It is thereby possible to determine the absolute light output (I_0^{185}) of the UV lamp employed.[19] This method enables reproducible quantum yields Φ to be obtained for the diverse compounds employed in 185-nm photolyses.

In this article we present the mechanistic knowledge acquired during the last decade on 185-nm photochemistry in liquid media. Because mainly photoinduced isomerizations, rearrangements, and fragmentations have been investigated, we will limit the discussion to the intensively investigated olefins, cyclopropanes, and azoalkanes.

2.1. Olefins

Since the early studies by *Kropp* et al.[3d,20] the formation of rearrangement products on 185-nm photolysis of olefins has been interpreted in terms of carbene intermediates. These are formed via a 1,2-carbon shift from the excited (π,3s) Rydberg state of the olefin (Scheme 1). Experimental evidence for the involvement of Rydberg states in vacuum-UV excitation of olefins is provided by nucleophilic trapping reactions[20,21] with alcohols, leading to ethers (Scheme 1), and by the remarkable pressure dependence of the vacuum-UV spectra of alkenes.[22] Furthermore, on excitation with 185-nm photons, olefins exhibit a weak, but measurable fluorescence[23] with quantum yields of about 10^{-4} to 10^{-6}. This fluorescence results presumably from the (π,3s) Rydberg state.



Scheme 1. Rearrangements and subsequent reactions of olefins such as 2,3-dimethyl-2-butene **1** on irradiation. Ry = Rydberg.

In contrast to the simple triplet-state photochemistry of olefins,[21] their photoreactivity on direct 185-nm excitation is often more complex. This is due to strong coupling of different excited states (Fig. 1). In spite of the similar energies of the π,π^*, (π,3s) Rydberg, and π,σ^*_{CH} singlet states of olefins (Fig. 1), distinct photoreactivity of each excited

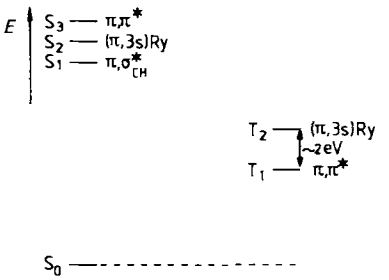
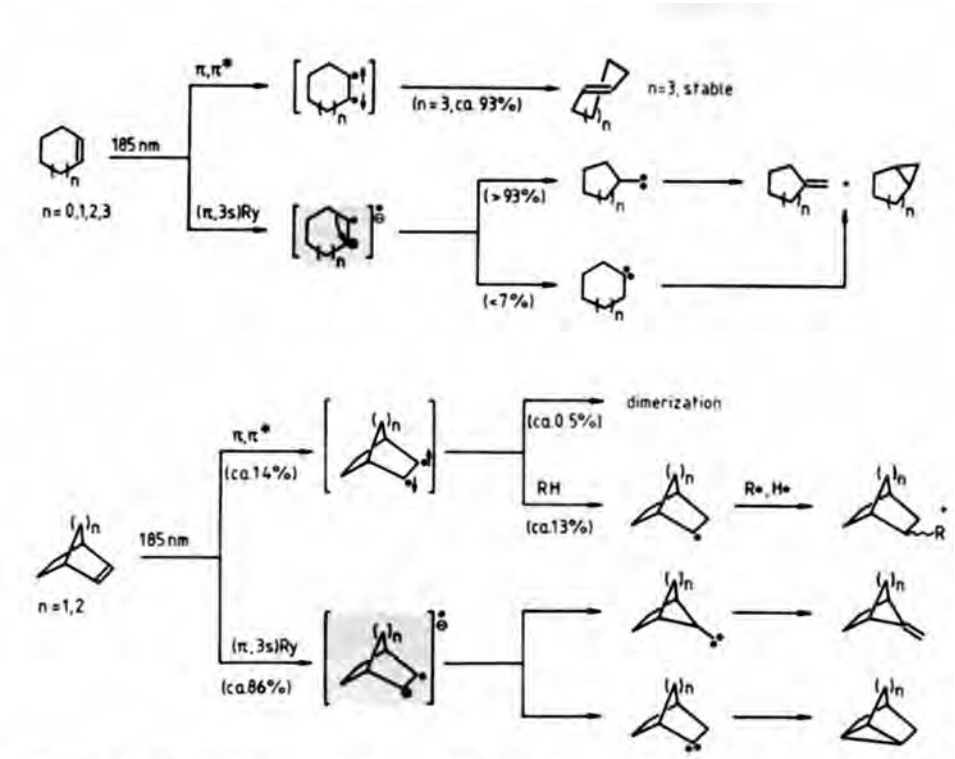


Fig. 1. Electronic states of olefins [21].

state can be observed. For example, the product distribution in the UV photolysis of 2,3-dimethyl-2-butene **1** is strongly dependent on the excitation wavelength.[24] Furthermore, there exists a direct connection between the wavelength dependence and the quantum yield of fluorescence[23] of the alkene. With increasing wavelength of excitation the chemical yield of the carbene products (Scheme 1) and the fluorescence quantum yield increase. This is a direct indication for the involvement of a Rydberg state as precursor to the intermediary carbene. The π,π^* excited state leads to $(Z)/(E)$ isomerizations and hydrogen abstractions.[24]

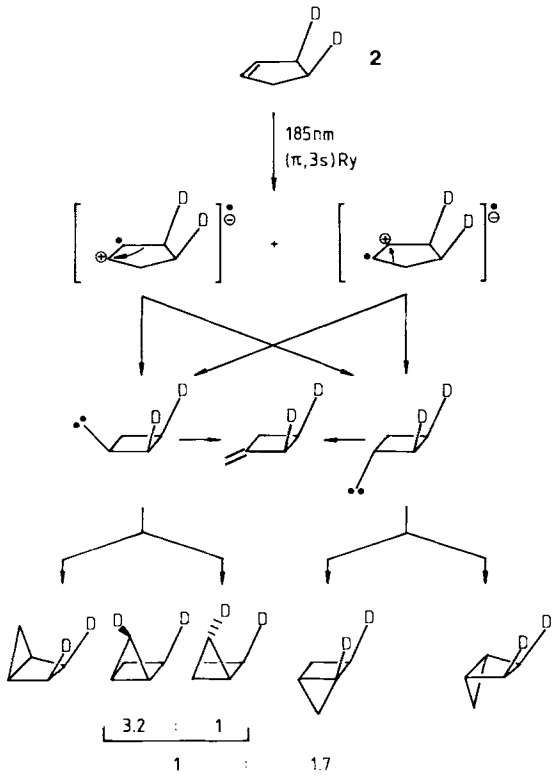
In general, the 185-nm photoreactivity of cyclic and bicyclic olefins can be summarized according to Scheme 2. Many examples that fit this scheme have been extensively investigated by *Inoue* et al.[3c,25] and by *Srinivasan* et al.[3a] In monocyclic olefins a 1,2-alkyl versus a 1,2-hydrogen shift is clearly favored (93%).[3a] A typical, recently studied[26] example is cyclopentene, which reacts with the formation of bicyclo[2.1.0]pentane and methylenecyclobutane.

A carbene intermediate is in accord with the recent results of the 185-nm photolysis of *cis*-3,4-dideuteriocyclo-

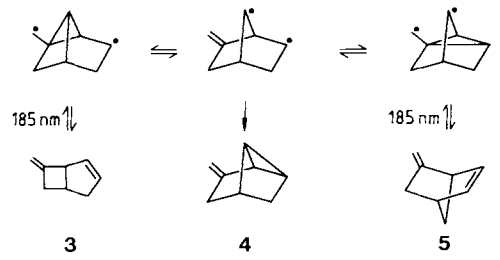


Scheme 2. 185-nm Photochemistry of mono- and bicyclic olefins [3a, 25].

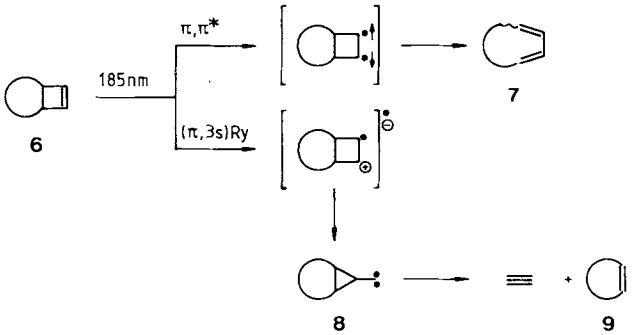
pentene **2** (Scheme 3).[26e] In bridged bicyclic olefins (Scheme 2), however, both processes compete.[7,25] The bichromophoric diolefins **3** and **5** represent exceptions, because they rearrange efficiently into one another on 185-nm irradiation and transform irreversibly to the tricyclic compound **4**.[27] This photoreactivity does not correspond to that of Scheme 2, but rather involves di-π-methane rearrangements.[28] Carbene reactivity seems to be of no importance for such dienes.



Scheme 3. 185-nm Photochemistry of *cis*-3,4-dideuteriocyclopentene **2**.



The 185-nm photochemistry of annelated cyclobutenes **6**[29] can again be described according to the general mechanism of Scheme 2. The π,π* excited state of cyclobutene **6** undergoes Woodward-Hoffmann allowed electrocyclic ring opening[30] to give the 1,3-diene **7**. On the other hand, the (π,3s) Rydberg state rearranges to the carbene **8**, which subsequently fragments into acetylene and the cycloalkene **9**.[31]



The 185-nm photolysis of cyclobutene[26a,d] provides important mechanistic insights into this process. The corresponding photoproducts can be rationalized in terms of the intermediacy of cyclopropylmethylene **10** and cyclobutylidene **11**.[31] Additional evidence for these carbenes comes from comparison of the behavior of the thermally generated carbenes with those resulting from the 185-nm irradiation of olefins (Table 1). The similar product ratios of methylenecycloalkane to bicycloalkane in the 185-nm photolysis of the homologous alkenes and the thermolysis of the corresponding tosylhydrazones proves convincingly this conjecture.

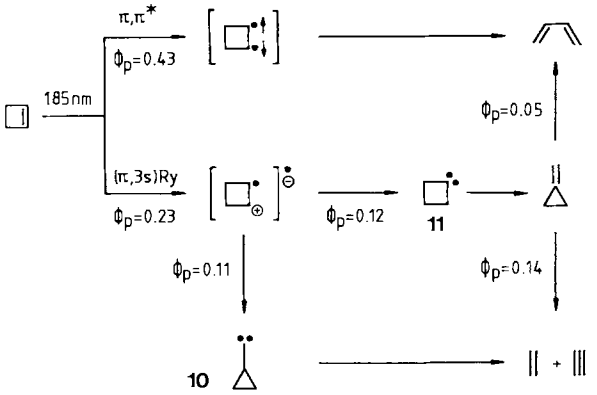
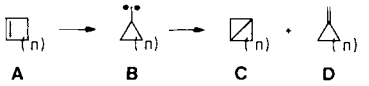


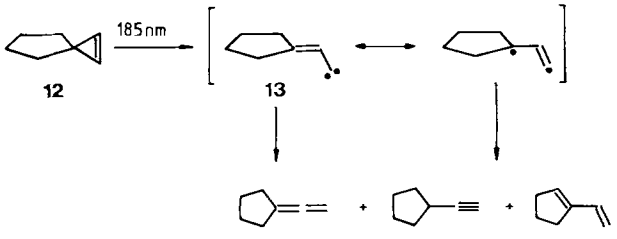
Table 1. 185-nm-Photochemistry of the homologous cycloalkenes **A**; formation of the bicyclic compounds **C** and the methylenecycloalkanes **D** from the cycloalkylmethylenes **B**.

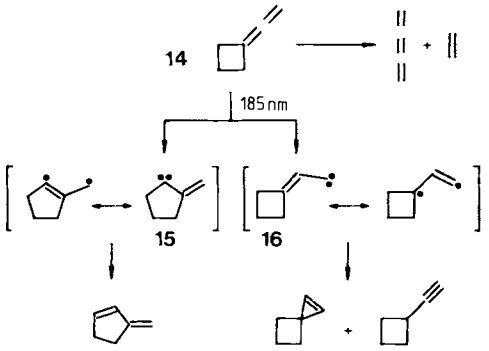


n	Quantum yields				Product ratios	
	Φ_S [a]	Φ_P [b] C	Φ_P [b] D	$\Sigma\Phi_P$	D/C 185 nm	D/C therm. [c]
5	—	0.008	0.007	0.015	0.9	—
4	—	0.02	0.10	0.12	5.0	11.5
3	—	0.07	0.05	0.12	0.7	0.4
2	0.15	0.03	0.04	0.07	1.3	1.4
1	0.71	[d]	0.12	0.12	—	—

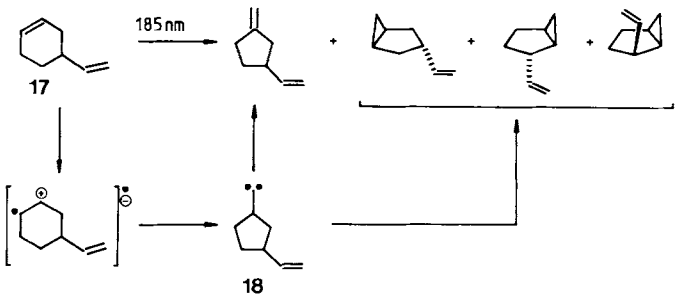
[a] Φ_S = quantum yield of substrate consumption. [b] Φ_P = quantum yield of product formation. [c] The cycloalkylmethylenes (carbenes) **B** were generated via basic decomposition of the corresponding tosylhydrazones [31]. The basic decomposition of cyclopropylcarbaldehyde tosylhydrazone did not lead to bicyclo[1.1.0]butane **C**, n = 1 [31]. [d] Not formed.

The essential step in the transformation of cyclopropenes such as **12**[32] and allenes such as **14**[33] on 185-nm irradiation corresponds to a cyclopropene–vinylcarbene rearrangement.[34] The UV photolysis of spiro[2.4]hept-1-ene **12**[32] yields as primary product the vinylcarbene **13**, which rearranges to the observed photoproducts. Similar intermediates have been proposed in the 185-nm photolysis of vinylidenecyclobutane **14**.[33] Besides the rearranged products that are formed from the two possible vinylcarbenes **15** and **16**, butatriene and ethene are produced via a [2+2] cycloreversion.



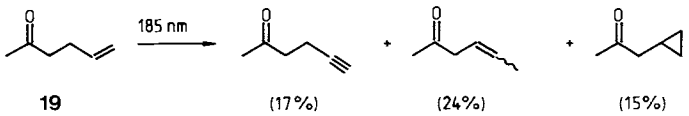


Intramolecular interactions between nonconjugated chromophores seem not to exist on 185-nm activation, but selective reactivity of the isolated chromophores can be observed. The 185-nm photolysis of 4-vinylcyclohexene **17**[35] leads to products that are formed by selective excitation of the endocyclic double bond. The photoproducts



can be explained in terms of carbene **18**. This carbene is formed from the (π,3s) Rydberg state of the cyclohexene double bond[35] since the photoproducts still contain the vinyl group intact. One would have expected a more complex product mixture had interaction between the chromophores in the excited vinylcyclohexene taken place.

Analogous selectivity can be observed in the 185-nm photolysis of γ,δ-unsaturated enones such as **19**.[11] Instead

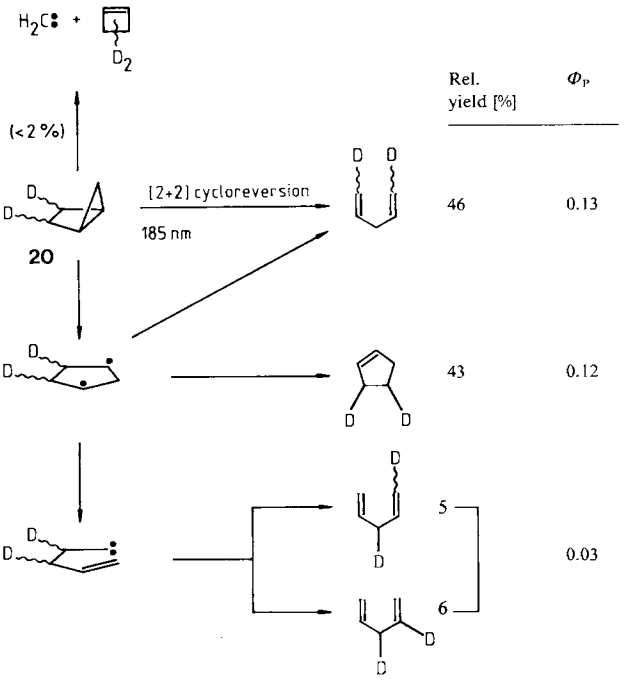


of the usual carbonyl photochemistry, such as intermolecular formation of oxetanes, the products are mainly derived from excitation of the C=C bond with preservation of the carbonyl functionality. Therefore, intramolecular energy transfer from the C=C bond to the carbonyl group is unlikely.[11]

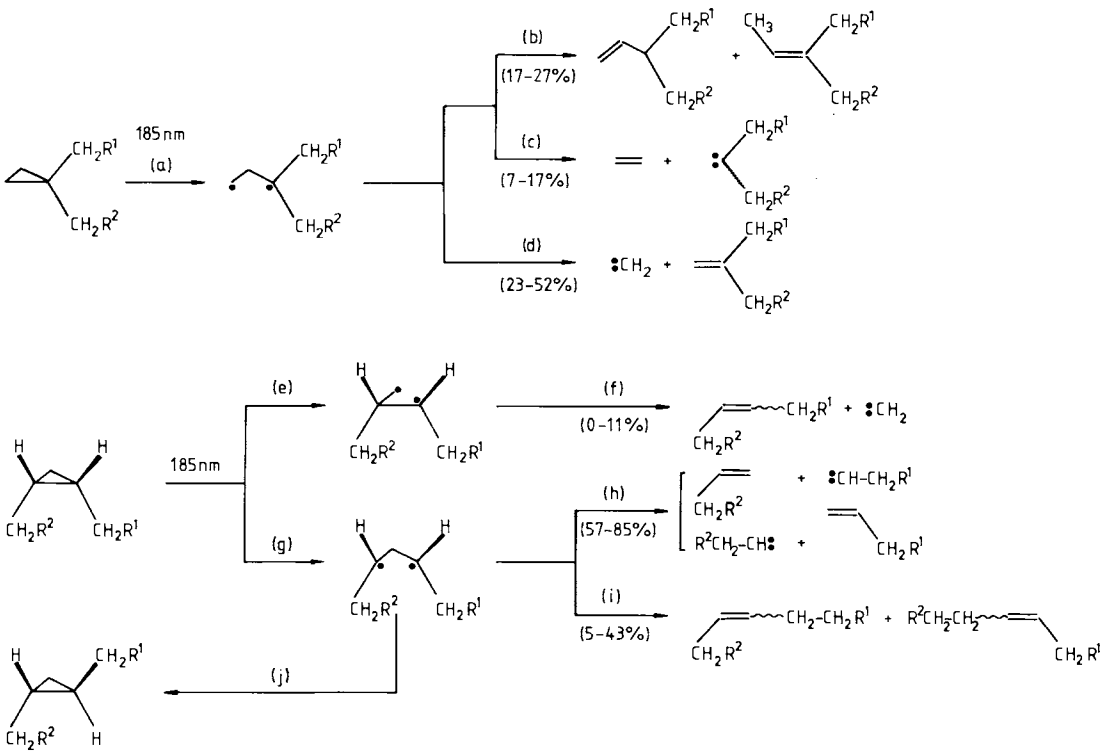
2.2. Cyclopropanes

Identification of the electronic state that is formed on 185-nm excitation of cyclopropanes is not easy. Besides very weak Rydberg transitions, cyclopropanes exhibit measurable σ,σ* transitions in the vacuum-UV region.[36] The gas-phase photolysis (147 nm and 163 nm) of cyclopropane[37] itself yields ethene and methylene (69%) via cleavage of two C–C bonds. This type of fragmentation is favored as the main reaction path in the direct 185-nm photolysis of substituted cyclopropanes in solution[8] (Scheme 4).

The photoreactivity of alkylcyclopropanes is a function of the substitution pattern. 1,1-Disubstituted[8] as well as 1,2-disubstituted[38] mono- or bicyclic alkylcyclopropanes react mainly via breakage of two bonds of the cyclopropane chromophore. Spirocyclopropanes[8] and 1,1-disubstituted cyclopropane derivatives cleave principally to form methylene (path a, d; 23–52%), whereas the related process in 1,2-disubstituted cyclopropanes[38] (path e, f; ≦11%) competes very little with fragmentation into the corresponding substituted carbenes (path g, h; 57–85%). The theoretical calculations of *Rossi*[39] show that the cleavage of two C–C bonds is not concerted, but follows a stepwise



Scheme 5. 185-nm Photochemistry of 2,3-dideuteriobicyclo[2.1.0]pentane **20**.



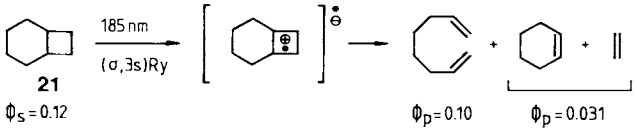
Scheme 4. 185-nm Photochemistry of 1,1- and 1,2-disubstituted alkylcyclopropanes [8, 38]. For (a)–(j) see text.

mechanism (paths a, c and a, d or paths e, f and g, h). Normally, the most substituted cyclopropane ring bond cleaves first. The stereoisomerization of *cis*-1,2-diethylcyclopropane[40] (path g, j; $R^1 = R^2 = Me$) takes place to about 10%, but it is of subordinate importance compared with the fragmentation process. Generally, the isomerization products, which are formed via cleavage of one C–C bond of the cyclopropane chromophore (paths a, b and g, i), are clearly disfavored compared with the corresponding fragmentation products.

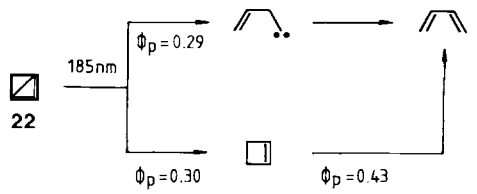
Bicyclo[2.1.0]pentane (cf. **20**) behaves differently, because mostly (about 89%) homolysis of the bridge bond of the cyclopropane chromophore takes place (Scheme 5).[126a] This behavior was attributed to a Woodward-Hoffmann

allowed [2+2] cycloreversion. Such a process is not possible in the higher homologous bicyclo[n.1.0]alkanes.

The efficient fragmentation of cyclobutanes on 185-nm excitation could be demonstrated for bicyclo[4.2.0]octane **21**.[26a,h] Possibly a radical cation mechanism can account for these fragmentations, because on 185-nm irradiation Rydberg transitions are possible. In contrast to bicyclo[2.1.0]pentane (cf. **20**), the homologous bicyclo[1.1.0]butane **22**[26a] fragments via one-bond and two-bond cleavages to the same extent.



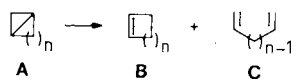
Srinivasan et al.,[26c] on the other hand, found by means of deuterium-labeling experiments a 10:1 ratio of butadiene and cyclobutene. Possibly, no corrections were made for the appreciable photolability of cyclobutene. However, the observed deuterium distribution in the photoproducts is in agreement with the results of *Adam* et al.[26d] and supports the mechanism shown in Scheme 6.



Scheme 6. 185-nm Photochemistry of bicyclo[1.1.0]butane **22**.

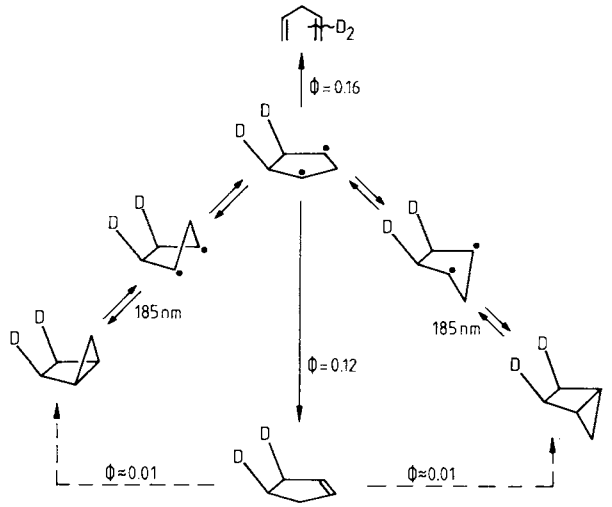
Comparison of the 185-nm photoreactivity of the homologous bicyclo[n.1.0]alkanes (Table 2) convincingly shows that bicyclo[2.1.0]pentane (n=2) is a special case. The *exo/endo* isomerization (Scheme 7)[26a] supports this fact. The isomerization is, however, quite inefficient ($\Phi_{iso}=0.03$) compared with the fragmentation into 1,4-pentadiene ($\Phi_p=0.16$) and with the formation of cyclopentene ($\Phi_p=0.12$). Already these few examples show that the conversion of bicyclo[n.1.0]alkanes into the corresponding cycloalkenes on 185-nm irradiation seems to be a general reaction.

Table 2. 185-nm Photochemistry of the homologous bicyclo[n.1.0]alkanes **A** to the cycloalkenes **B** and the 1,n+2-alkadienes **C**.

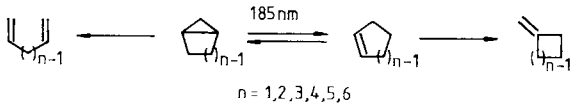


n	Quantum yields			Product ratio	Homolysis [a] [%]	
	Φ_S	Φ_P B	Φ_P C	C/B	one-bond	two-bond
6	—	—	—	—	≈17	≈83
5	0.54	0.06	0.48	8.0	12	88
4	0.21	[b]	0.14	—	—	[c]
3	0.51	0.22	0.29	1.3	43	57
2	0.25	0.12	0.16	1.3	89	11
1	0.65	0.30	0.29	1.0	51	49

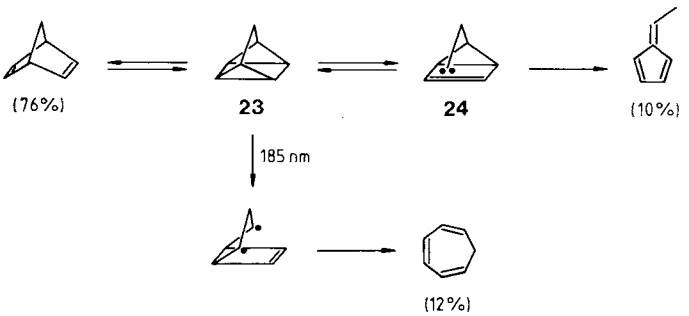
[a] One-bond and two-bond cleavages of the C–C bonds of the cyclopropane chromophore. [b] Not formed. [c] The fragmentation of two bonds of the cyclopropane chromophore seems to be the main reaction path [38].



Scheme 7. Photochemical isomerization of *cis*-2,3-dideuteriobicyclo[2.1.0]pentane (cf. Scheme 3 and Scheme 5).

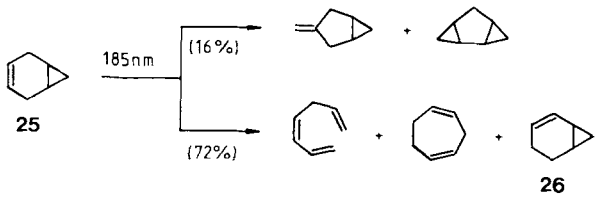


Surprisingly, the carbene elimination in quadricyclane **23**[41] plays an insignificant role, although **23** contains two cyclopropane chromophores. The formation of carbene **24** on 185-nm irradiation of quadricyclane could be reversible, so that re-addition to the double bond could regenerate the starting material and thereby account for the inefficiency ($\Phi=0.02$) of this process.[41] The side products, 6-methylfulvene and 1,3,5-cycloheptatriene, are also formed in traces in the direct 254-nm (<5%) and triplet-sensitized (<0.5%) photolyses of quadricyclane. Therefore, the use of the quadricyclane–norbornadiene system as an efficient solar energy storage system[42] has been questioned.[41]

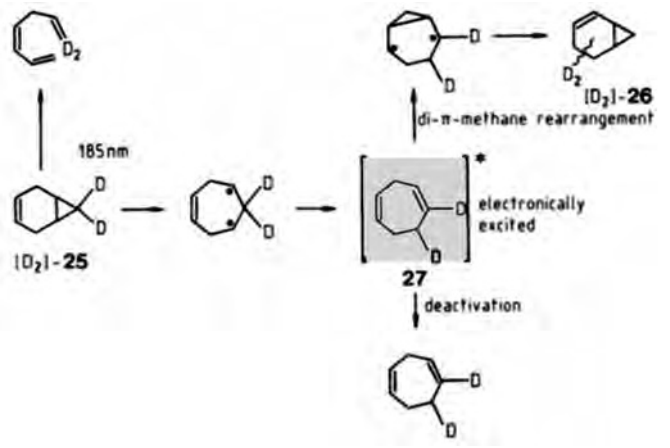


The 185-nm photolysis of compounds containing two different chromophores, e.g., cyclopropanes and olefins, provides evidence for intramolecular interactions between the excited chromophores and thus distinctive photochemical behavior of the excited states. The wavelength dependence of the UV photolysis of bicyclo[4.1.0]hept-3-ene **25**[43]

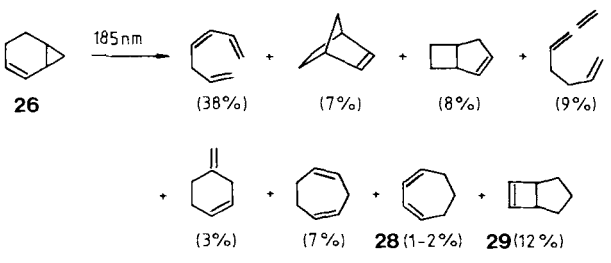
once again indicates that two or more different excited singlet states participate in one and the same molecule. Decreasing the photon energy ($\lambda = 185$, 193, and 214 nm) results in an increase of those products that are formed by selective excitation of the C=C bond of **25** and a corresponding decrease in the photoproducts derived from excitation of the cyclopropane chromophore. This observation becomes understandable when it is recognized that the first excited singlet state (S_1) of cyclopropanes lies higher in energy than the first singlet (π,3s) Rydberg state of olefins.[36]



The formation of product **26** during photolysis of the bichromophoric compound **25** can possibly be rationalized in terms of an intermediary electronically excited 1,4-diene (cf. **27**).[44] The excited intermediate **27** undergoes subsequent di-π-methane rearrangement to the isomer [D_2]-**26**. Indeed, these interesting speculations about the reaction mechanism of the 185-nm photolysis of **25** were verified through deuterium-labeling experiments.[44] Besides the formation of vibrationally excited or "hot" photoproducts,[40,45] an adiabatic reaction path is also possible.[46]



In contrast to these results, the product distribution in the 185-nm photolysis of bicyclo[4.1.0]hept-2-ene **26**[47] is independent of the excitation wavelength. In compound **26** the double bond is in conjugation with the cyclopropane ring. Therefore, no differentiation between the olefin and cyclopropane reactivity should be expected. Consequently, the 185-nm photochemistry of **26** is more complex than that of its isomer **25**.

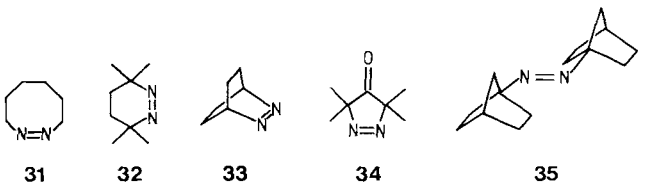


Analogous behavior is observed for 1,3-cycloheptadiene **28**,[47b] which, independent of the excitation wavelength ($\lambda = 185$, 229, or 254 nm), reacts mainly (88–99%) to give bicyclo[3.2.0]hept-6-ene **29**. However, substitution at C-7 in **26** with a methyl group (**30**) leads to *exo/endo* isomerization[48] as a side reaction.



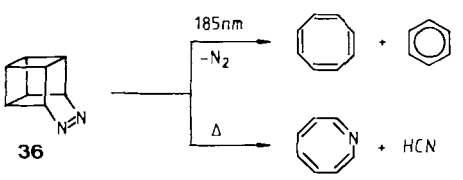
2.3. Azoalkanes

The thermal and photochemical reactivity of azoalkanes strongly depends on their structure.[49] Thus, to the group of photoresistant azoalkanes belong the structures **31** to **35**.[10,50] Their quantum yields of denitrogenation at the usual wavelengths ($\lambda > 300$ nm) are generally lower than

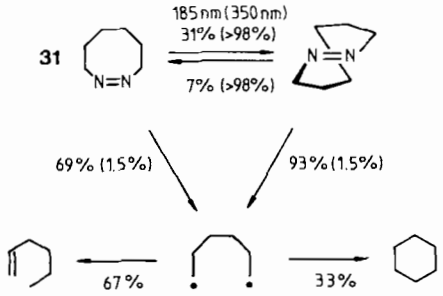


0.05.[51] In the case of six-membered azoalkanes, the quantum yield appears to be independent of whether the azo chromophore is part of a mono-, bi-, or polycyclic structure. The most important deactivation processes responsible for the photostability of these azoalkanes are fluorescence, radiationless deactivation, (*Z*)/(*E*) isomerization, intramolecular cyclizations, and phototautomerism.[52]

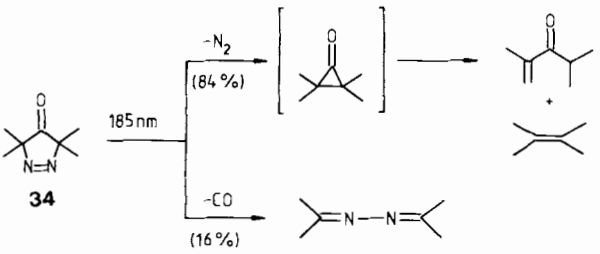
Photostable azoalkanes are of no synthetic value, because the crucial nitrogen elimination step cannot be realized to form the desired new C–C bond. A classical example for this is the attempt to synthesize cubane[53] by photolysis of diazabasketene **36**, which failed to undergo nitrogen elimination. As was shown in 1980,[51] the 185-nm photolysis of diazabasketene leads to efficient denitrogenation. However, instead of cubane,[54] cyclooctatetraene and benzene were formed. Moreover, the quantum yield of nitrogen elimination was about 1000 times higher at $\lambda = 185$ nm than at $\lambda > 300$ nm. 1,2-Diaza-1-cyclooctene **31**[26a,g] was recently shown to be effectively denitrogen-



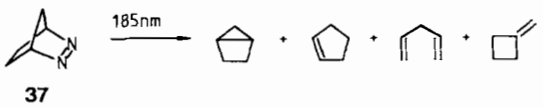
ated on 185-nm excitation. Again, the efficiency of the denitrogenation was increased by about 26- to 42-fold, depending on the configuration about the N=N bond.



An interesting bichromophoric substrate is 3,3,5,5-tetramethyl-3,5-dihydropyrazol-4-one **34**.[55] The 185-nm irradiation of **34** leads to denitrogenation and decarbonylation.[55] In this case the nitrogen elimination is six times more efficient than the CO elimination. The intermediary tetramethylcyclopropanone rearranges via ring opening to the enone or eliminates carbon monoxide to form dimethyl-2-butene.



A definitive assignment of the excited states that are involved in 185-nm excitation of azoalkanes is difficult.[36,51] These may be π,π^*, n_+,π^*, n_+,σ^*, or diverse Rydberg transitions[56] (Fig. 2). Nevertheless, 185-nm photolysis of simple azoalkanes might enable predictions to be made about the excited states that are involved in such photochemistry. In this connection it is of interest that the 185-nm excitation of 2,3-diazabicyclo[2.2.1]hept-2-ene **37**[19a,26b] is quite



different from the 350-nm photolysis. In the latter case only traces (<1%) of cyclopentene could be identified, whereas bicyclo[2.1.0]pentane was formed in >99% yield. As shown in Figure 3, on 185-nm photolysis, denitrogenation affords considerable quantities of cyclopentene, presumably via zwitterionic species. Such intermediates should have a considerable influence on the product distribution.

From this perspective, the photochemistry of the bicyclic azoalkanes 2,3-diazabicyclo[2.2.1]hept-2-ene **38a**[57] and spiro[cyclopropane-1',7-2,3-diazabicyclo[2.2.1]hept-2-ene] **38b**[58] and of their *exo*-dideutero derivatives was examined in detail. Depending on the reaction conditions of the denitrogenation, the azoalkanes **38** preferred to undergo double inversion to give the bicyclo[2.1.0]pentanes **39**.[57]

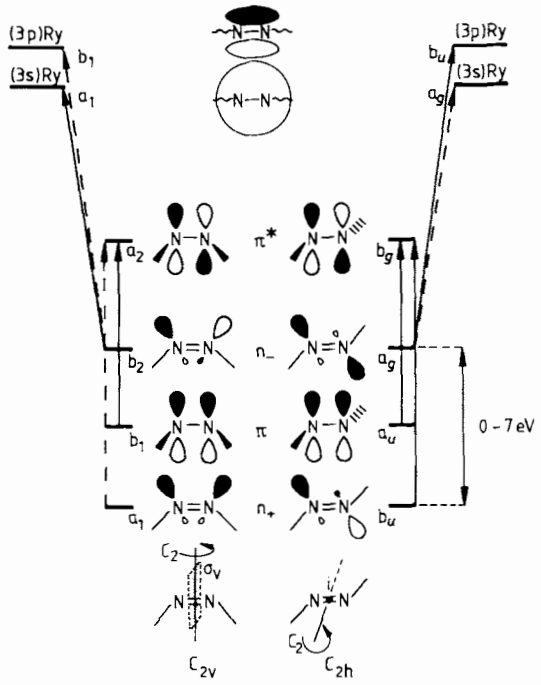


Fig. 2. High-energy electron transitions in (*Z*)- and (*E*)-azoalkanes. ——→, symmetry-allowed transition; – – →, symmetry-forbidden transition.

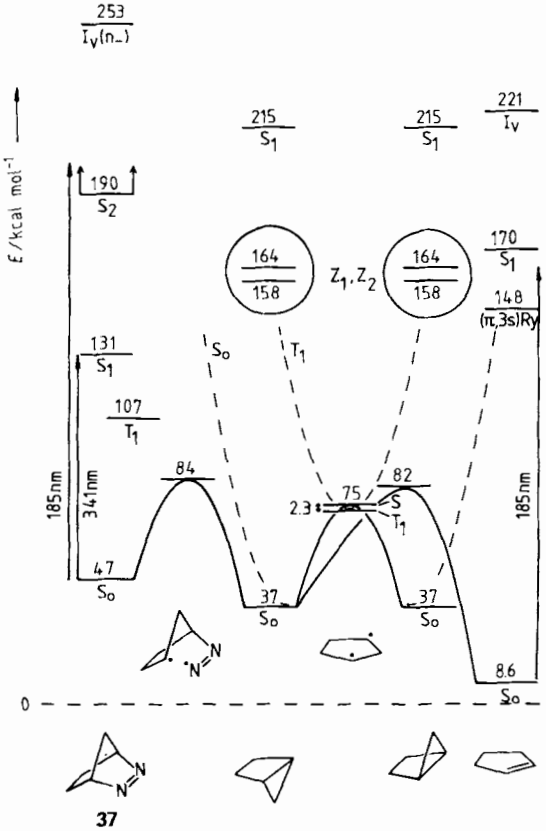
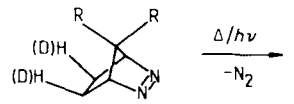
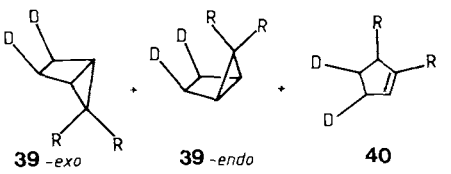


Fig. 3. Relative energies of 2,3-diazabicyclo[2.2.1]hept-2-ene, **37**, bicyclo[2.1.0]pentane, and cyclopentene.



37, R=H
38, R+R=-CH_2-CH_2-



39-*exo* **39**-*endo* **40**
a, R=H; **b**, R+R=-CH_2-CH_2-

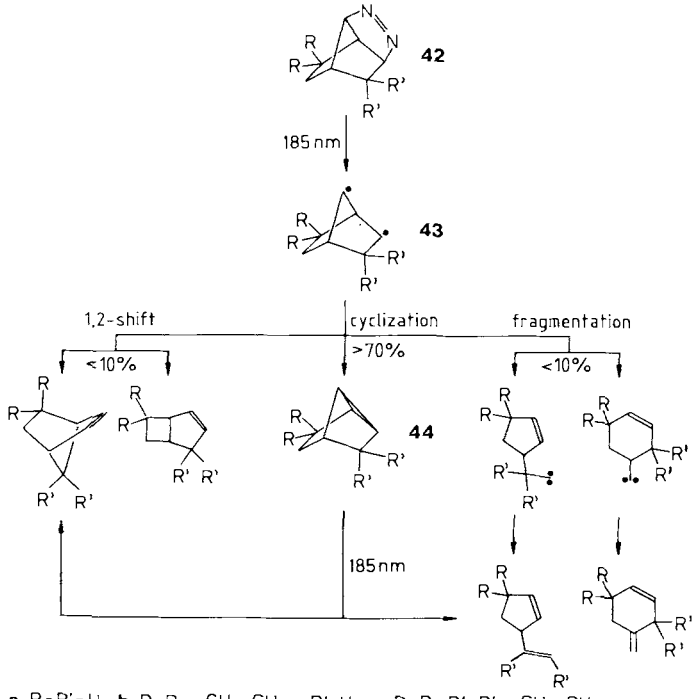
The rearrangement to the olefins **40** depends on the spin state and energy of the intermediary 1,3-cyclopentadiyl. In addition, the reaction path involving the zwitterionic species **41**, formed on 185-nm irradiation via concerted nitrogen elimination, might be possible.[26a]



41

In the long-wavelength ($\lambda > 300$ nm) photolysis of **38**, one-bond cleavage was postulated,[26f] the initially formed diazenyl diradical subsequently loses nitrogen, giving 1,3-cyclopentanediyl. Presumably, in the long-wavelength ($\lambda > 300$ nm) photolysis of azomethane,[26j] the primary step also involves one-bond cleavage to the corresponding diazenyl radical. Thus, the 185-nm photochemistry allows valuable mechanistic insights to be obtained into the denitrogenation of azoalkanes.

Attractive substrates for the examination of intramolecular interactions of distinct chromophores are the tricyclic azoalkanes **42**.[59] Their 185-nm photolysis results in denitrogenation and mainly formation of the tricyclic product **44**. In addition, the 1,3-diradical **43** undergoes a 1,2-carbon shift (<10%) and fragmentation (<10%), so that numerous photoproducts are formed.[59]



42 **43** **44**
a, R=R'=H; **b**, R+R=-CH_2-CH_2-, R'=H; **c**, R+R=R'+R'=-CH_2-CH_2-

3. Prospects

On the basis of this brief review it is apparent that 185-nm photolysis *in solution*, still a rather young branch of organic photochemistry, offers a broad spectrum of challenging mechanistic problems. At first sight one gathers the impression that the complex product mixtures reflect a multitude of mechanistic processes. This is surely the case when hydrogen abstraction occurs and entry into the usual chemistry of free radicals ensues. However, the thorough mechanistic investigations of the last decade have shown that a definite regularity obtains in the behavior of the higher excited states that are reached on irradiation with 185-nm photons. The photochemistry of alkenes (Scheme 2), cyclopropanes (Scheme 4), and azoalkanes clearly supports this observation. However, when one considers what is still unknown about such complex photochemical processes, the gratifying progress appears quite modest. In order to motivate the interest of the novice as well as the expert, Table 3 summarizes those substances that have been investigated so far. Only a few purely radical processes have been included, because the main emphasis of this review concerns unimolecular transformations, such as isomerizations, rearrangements, and fragmentations, induced by means of 185-nm excitation.

Intensive efforts are required on all fronts before short-wavelength ($\lambda < 250$ nm) photochemistry achieves the status presently enjoyed by long-wavelength photochemistry ($\lambda > 250$ nm). Innovation is highly desirable, especially from the point of view of apparatus design. The present light sources (low-pressure mercury lamps) radiate mainly 254-nm light, so that many interesting problems, e.g., the behavior of substrates with coupled chromophores, can hardly be investigated. It is essential that convenient and efficient filters or monochromatic light sources with *sufficient* intensity be developed for such studies. Laser technology should provide important contributions. An ideal situation would obtain if a broad range of intense laser lines at regular intervals would become available in the 180- to 250-nm region, so that the wavelength dependence of the product formation could be assessed. Studies of this type are essential for recognizing the nature of the higher excited states, such as Rydberg, π-π^*, and σ-σ^* transitions.

This brings us to another problem, namely, the spectroscopy of the higher excited states. Despite some efforts,[36] our knowledge and understanding is rather modest in this area. Coupled with theoretical calculations, spectroscopic investigations (such as absorption, fluorescence, and photoelectron spectroscopy) on model substrates should be helpful.

Whether the 185-nm photochemistry will prove itself in preparative work is undoubtedly of interest to the organic chemist. Until now the utility has been modest, but 185-nm photochemistry represents presently the most direct and convenient entry into strained *trans*-cycloalkenes, e.g.,

Table 3. 185-nm Photoreactions in *n*-pentane as solvent. The quantum yield Φ_P or the product yield is given for each product.

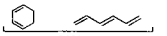
Substrate	Empirical formula	Photoproducts	Ref.
CH_3OD	CDH_3O	CH_4 0.05; CH_3CH_3 0.007; CH_2O 0.31; CH_3CH_2OH 0.025	[13d]
$CHCl_3/H_2O/O_2$	CCl_3H	CO_2 [a]; HCl [a]	[13f]
$CHBr_nCl_{3-n}/H_2O$ n=1,2,3		CO [a]; HBr [a]; HCl [a]	[13f]
	C_4H_6	 0.43;  0.12; $H_2C{=}CH_2$ 0.07; HC≡CH 0.04	[26a]
	C_4H_6	 0.05;  <0.01; $H_2C{=}CH_2$ 0.08; HC≡CH 0.06	[26a]
	C_4H_6	 0.29;  0.02; $H_2C{=}CH_2$ 0.03; HC≡CH 0.02;  0.30	[26a]
	C_5H_8	 0.04;  0.03;  0.01;  0.001;  0.006; $C_{10}H_{22}$ 0.005	[7,19a]
	C_5H_8	 32%;  7.5%; 2%	[26b]
	C_5H_8	 0.12;  0.16; 0.01	[19a,26]
	C_6H_8	 30.2%;  39.6%;  30%	[45b]
	C_6H_8	 0.054;  0.044;  0.078; = = = $H_2C{=}CH_2$ 0.12; 0.14;  6%	[33]
	C_6H_{10}	 0.05;  0.07	[3a,c]
	C_6H_{10}	 0.22;  0.29	[8,26a]
	C_6H_{12}	OOH 70%; OH 18.3%; O 11.7%	[60]
	C_6H_{12}	2.6%; 3.9%; 38%; [a]	[24]
	C_6H_{12}	19%; 4%; $C_{10}H_{22}$ 8%; Me-≡-C_3H_7 5%	[3e]
	C_6H_{12}	$H_2C{=}CH_2$ 29%; 29%; 32%	[40]
	C_7H_8	76%; 12%; 10%	[41]
	C_7H_{10}	0.07; 0.07; 0.005; 0.24%; 0.06%; <<0.01%; 0.01%; $C_{10}H_{22}$ 0.003	[7]
	C_7H_{10}	HC≡CH 0.054; 0.16	[29]
	C_7H_{10}	38%; 7%; 8%; 9%; 3%; 7%; 1-2%; 12%	[47]
	C_7H_{10}	11.6%; 3.9%; 16.7%; 37.5%; 17.4%	[43,44]
	C_7H_{10}	0.11; 0.093; 0.029	[32]
	C_7H_{10}	8.4%; 42%	[59]
	C_7H_{10}	0.18; 0.05; 0.01	[26a]
	C_7H_{10}	88-99%	[47b]
	C_7H_{12}	0.10; 0.02	[3a,c,25]
	C_7H_{12}	0.13	[8,38a]

Table 3. (Continued)

Substrate	Empirical formula	Photoproducts	Ref.
	C_7H_{14}	26%; 24%; 23%; 27%	[40]
	C_7H_{14}	44%; 44%; 1%; 2%; 4%; 6%	[40]
	C_7H_{14}	42%; 46%; 2%; [b]; 10%; ?	[40]
	C_8H_{10}	[a]; [a]	[46]
	C_8H_{10}	[a]; [a]; [a]	[46]
	C_8H_{10}	87%; 13%	[27]
	C_8H_{10}	50%; 50%	[27]
	C_8H_{12}	HC≡CH [a]; 0.15; 0.053; 0.018	[29]
	C_8H_{12}	27.6%; 11.6%; 37.8%; 23%	[35]
	C_8H_{12}	12%; 5%; 18%; 5%; 3%; 9%; 33%	[48]
	C_8H_{12}	27%; 16%; 6%; 6%; 6%; 14%; 16%	[48]
	C_8H_{12}	0.20; 0.01	[3a]
	C_8H_{12}	0.09; 0.02	[3a]
	C_8H_{12}	0.74; 0.35	[38a]
	C_8H_{12}	64-99%; 3-10%; 2-4%; 0.5-1%	[47b]
	C_8H_{14}	0.03; $H_2C{=}CH_2$ [c]; 0.10	[26a]
	C_8H_{14}	0.03; 0.008; 0.007; 0.004; 0.003; 0.001; 0.0001	[3c,4, 18,19b]
	C_8H_{14}	84%; 2.1%; 3.6%	[3c]
	C_8H_{14}	52%; 7%; 14%; 13%	[8]
	C_8H_{14}	0.06; 0.48	[8,38a]
	C_8H_{16}	C_8H_{16} isomers 54%; 18%	[11]
	C_8H_{16}	15%; 18%; 27%; $C_{10}H_{22}$ [a]	[3e]
	C_9H_{12}	[a]; [a]	[46]
	C_9H_{12}	[a]	[46]

Table 3. (Continued)

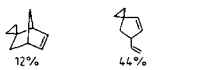
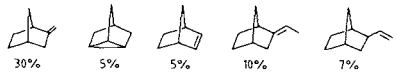
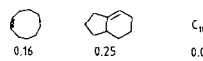
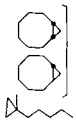
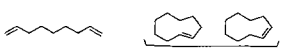
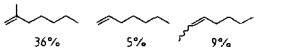
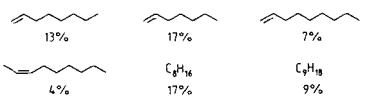
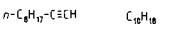
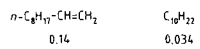
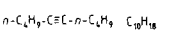
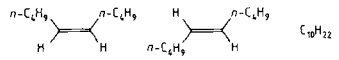
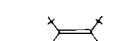
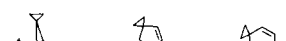
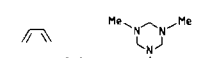
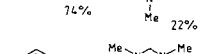
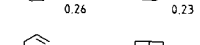
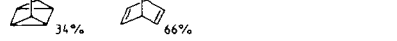
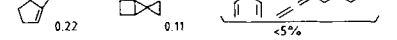
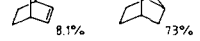
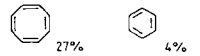
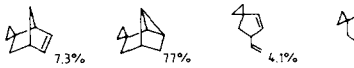
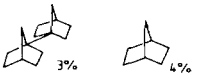
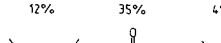
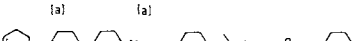
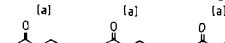
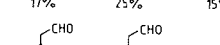
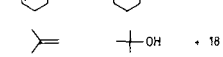
Substrate	Empirical formula	Photoproducts	Ref.
	C_9H_{12}	 12% 44% 12%	[59]
	C_9H_{12}	 30% 5% 5% 10% 7%	[8]
	C_9H_{14}	 0.16 0.25 $C_{18}H_{22}$ 0.034	[12]
	C_9H_{16}	 ≈ 83% ≈ 17%	[38b]
	C_9H_{18}	 36% 5% 9% C_9H_{18} 22%	[8]
	C_9H_{18}	 13% 17% 7% 4% C_8H_{16} 17% C_9H_{18} 9%	[8]
	$C_{10}H_{18}$	 0.14 $C_{10}H_{22}$ 0.034	[12]
	$C_{10}H_{18}$	 0.10 0.16 $C_{10}H_{22}$ 0.068	[12]
	$C_{10}H_{20}$	 40% (isolated)	[5]
	$C_{11}H_{14}$	 21% 40% 1%	[59]
	$C_8H_{13}N$	 74% 22%	[15]
	$C_8H_{13}N$	 [a] [a]	[15]
	$C_8H_{13}N$	 >90%	[15]
	$C_5H_6N_2$	 0.26 0.23 0.03 <0.01	[19a,26]
	$C_6H_{10}N_2$	 18% 9%	[51]
	$C_6H_{12}N_2$	 0.14 0.20 0.11	[26a]
	$C_6H_{12}N_2$	0.03 0.25 0.13	[26a]
	$C_7H_8N_2$	 44% 56%	[26a]
	$C_7H_8N_2$	 34% 66%	[26a]
	$C_7H_{10}N_2$	 0.22 0.11 <5%	[26a]
	$C_7H_{10}N_2$	 8.1% 73% 4.9% 4.4%	[59]
	$C_8H_8N_2$	 27% 4%	[51]
	$C_8H_{10}N_2$	 22% 12%	[51]

Table 3. (Continued)

Substrate	Empirical formula	Photoproducts	Ref.
	$C_9H_{12}N_2$	 7.3% 77% 4.1% 3.9%	[59]
	$C_{17}H_{14}N_2$	 5.4% 88% 2.5% 1.7%	[59]
	$C_{14}H_{22}N_2$	 3% 4% [c]	[10]
	$C_{16}H_{24}N_2$	 5% 37% 0.3%	[10]
	$C_{18}H_{30}N_2$	 3% 44% 0.2%	[10]
[d]	$C_{20}H_{18}N_2$	Ad-Ad 12% Ad-H 35% Ad-C_5H_{11} 4%	[10]
	$C_7H_{12}N_2O$	 15% 48% 29%	[55]
CH_3CH_2OH [e]	C_2H_6O	H_2 [a] CH_3CHO [a] CH_3-CH(OH)-CH_3 [a]	[13a]
	C_4H_6O	[a] $CH_3CH=CHCHO$ [a]	[14]
Me_3C-OH [e]	$C_4H_{10}O$	 0.306 0.256 Me_3C-O- 0.059 =O 0.031 O 0.026 OH 0.0044 Me 0.001	[13a]
	C_5H_6O	 [a] [a]	[14]
	$C_6H_{10}O$	 17% 25% 15%	[11]
	$C_7H_{10}O$	 [a] [a]	[13b]
	$C_7H_{12}O$	 62% 4% 6% 2% 2%	[11]
	$C_8H_{12}O$		[13b]
Me_3C-O-CMe_3	$C_8H_{18}O$	 0.87 OH 0.84 + 18 products	[13c]
	$C_{10}H_{16}O_2$	 [a] [a] [a] [a]	[9]

[a] Quantum yield or product yield unknown. [b] Traces detectable. [c] The product was not determined quantitatively. [d] Ad=1-Adamantyl. [e] In cyclohexane as solvent.

trans-cyclooctene, or sterically congested *cis*-alkenes, e.g., *cis*-2,2,5,5-tetramethyl-3-hexene ("*cis*-di-*tert*-butylethene").

For such synthetic problems, which until now could only be realized by means of long-wavelength photochemistry in an indirect manner, short-wavelength photochemistry offers attractive possibilities. We regard the future of 185-nm photochemistry optimistically. Undoubtedly, the main sphere of action will lie in mechanistic studies.

We thank the Deutsche Forschungsgemeinschaft for generous financial support of our work and the Fonds der Chemischen Industrie for a fellowship (T. O.).

Received: January 4, 1985;
revised: January 21, 1986 [A 583 IE]
German version: *Angew. Chem. 98* (1986) 659

[1] a) G. Pattenden, *Chem. Ind. (London) 1980,* 812; b) H. Parlar, *Chem.-Ztg. 107* (1983) 357.
[2] Y. I. Dorofeev, V. E. Skurat, *Russ. Chem. Rev. 51* (1982) 527.
[3] a) R. Srinivasan, K. H. Brown, *J. Am. Chem. Soc. 100* (1978) 4602; b) D. Sänger, C. von Sonntag, *Tetrahedron 26* (1970) 5489; c) Y. Inoue, S. Takamuku, H. Sakurai, *J. Chem. Soc. Perkin Trans. 2, 40* (1977) 1635; d) P. J. Kropp, E. J. Reardon, Jr., Z. L. F. Gaibel, K. F. Williard, J. H. Hattaway, Jr., *J. Am. Chem. Soc. 95* (1973) 7058; e) Y. Inoue, T. Mukai, T. Hakushi, *Chem. Lett. 1984,* 1725.
[4] Y. Inoue, S. Takamuku, H. Sakurai, *Synthesis 1977,* 111.
[5] W. Adam, F. Yany, *Z. Naturforsch. B 36* (1981) 658.
[6] a) R. Srinivasan, *Chem. Eng. Sci. 1983,* 4; b) R. Srinivasan, W. J. Leigh, *J. Am. Chem. Soc. 104* (1982) 6784; c) S. Lazare, P. D. Hoh, J. M. Baker, R. Srinivasan, *ibid. 106* (1984) 4288.
[7] Y. Inoue, T. Mukai, T. Hakushi, *Chem. Lett. 1982,* 1045.
[8] R. Srinivasan, T. Baum, J. A. Ors, *Tetrahedron Lett. 22* (1981) 4795.
[9] R. Srinivasan, K. H. Brown, J. A. Ors, L. S. White, W. Adam, *J. Am. Chem. Soc. 101* (1979) 7424.
[10] W. Adam, F. Mazenod, Y. Nishizawa, P. S. Engel, S. A. Baughman, W.-K. Chae, D. W. Horsey, H. Quast, B. Seiferling, *J. Am. Chem. Soc. 105* (1983) 6141.
[11] W. J. Leigh, R. Srinivasan, *J. Am. Chem. Soc. 104* (1982) 4424.
[12] Y. Inoue, Y. Ueda, T. Hakushi, *J. Am. Chem. Soc. 103* (1981) 1806.
[13] a) C. von Sonntag, H.-P. Schuchmann, *Adv. Photochem. 10* (1977) 59; b) J. Studebaker, R. Srinivasan, J. A. Ors, T. Baum, *J. Am. Chem. Soc. 102* (1980) 6872; c) H.-P. Schuchmann, C. von Sonntag, *Tetrahedron 29* (1973) 3351; d) R. J. Buenker, G. Olbrich, H.-P. Schuchmann, B. L. Schürmann, C. von Sonntag, *J. Am. Chem. Soc. 106* (1984) 4362; e) Y. Inoue, K. Goan, T. Hakushi, *Bull. Chem. Soc. Jpn. 58* (1985) 2217; f) T. Ogita, H. Hatta, I. Kagiya, *Nippon Kagaku Kaishi 1983,* 1664.
[14] a) Y. Inoue, N. Matsumoto, T. Hakushi, R. Srinivasan, *J. Org. Chem. 46* (1981) 2267; b) H. Frauenrath, T. Philipps, *Liebigs Ann. Chem. 1985,* 1303.
[15] R. Srinivasan, J. Studebaker, K. H. Brown, *Tetrahedron Lett. 1979,* 1955.
[16] H.-P. Schuchmann, A. Ritter, C. von Sonntag, *J. Organomet. Chem. 148* (1978) 213.
[17] a) G. J. Collin, H. Deslauriers, *Can. J. Chem. 61* (1983) 1970; b) G. J. Collin, *Rev. Chem. Intermed. 2* (1979) 377; c) G. J. Collin, H. Deslauriers, A. Wieckowski, *J. Phys. Chem. 85* (1981) 944.
[18] R. Srinivasan, K. H. Brown, *J. Am. Chem. Soc. 100* (1978) 2589.
[19] a) W. Adam, T. Oppenländer, *Photochem. Photobiol. 39* (1981) 719; b) H.-P. Schuchmann, C. von Sonntag, R. Srinivasan, *J. Photochem. 15* (1981) 159.
[20] T. R. Fields, P. J. Kropp, *J. Am. Chem. Soc. 96* (1974) 7559.
[21] P. J. Kropp in A. Padwa (Ed.): *Organic Photochemistry, Vol. 4.* Marcel Dekker, New York 1979, chapter 1.
[22] a) M. B. Robin, N. A. Kuebler, *J. Mol. Spectrosc. 33* (1970) 274; b) C. Sandorfy, P. J. Ausloos, M. B. Robin: *Chemical Spectroscopy and Photochemistry in the Vacuum-Ultraviolet,* D. Reidel, Dordrecht 1974.
[23] F. Hirayama, S. Lipsky, *J. Chem. Phys. 62* (1975) 576.
[24] Y. Inoue, T. Mukai, T. Hakushi, *Chem. Lett. 1983,* 1665.
[25] Y. Inoue, S. Takamuku, H. Sakurai, *J. Chem. Soc. Chem. Commun. 1975,* 577.
[26] a) T. Oppenländer, *Dissertation,* Universität Würzburg 1984; b) W. Adam, T. Oppenländer, *Tetrahedron Lett. 23* (1982) 5391; c) A. F. Becknell, J. Berson, R. Srinivasan, *J. Am. Chem. Soc. 107* (1985) 1076; d) W. Adam, T. Oppenländer, G. Zang, *ibid. 107* (1985) 3921; e) W. Adam, T. Oppenländer, *ibid. 107* (1985) 3924; f) W. Adam, T. Oppenländer, G. Zang, *J. Org. Chem. 50* (1985) 3303; g) W. Adam, T. Oppenländer, *Can. J. Chem. 63* (1985) 1829; h) *Angew. Chem. 96* (1984) 599; *Angew. Chem. Int. Ed. Engl. 23* (1984) 641; i) T. Baum, A. Rossi, R. Srinivasan, *J. Am. Chem. Soc. 107* (1985) 4411; j) P. L. Holt, K. E. McCurdy, J. S. Adams, K. A. Burton, R. B. Weisman, P. S. Engel, *ibid. 107* (1985) 2880.
[27] K. Hill, *Dissertation,* Universität Würzburg 1984.
[28] H. E. Zimmermann, R. J. Boettcher, N. E. Buehler, G. E. Keck, M. G. Steinmetz, *J. Am. Chem. Soc. 98* (1976) 7680.
[29] Y. Inoue, M. Sakae, T. Hakushi, *Chem. Lett. 1983,* 1495.
[30] a) N. J. Turro: *Modern Molecular Photochemistry.* Benjamin/Cummings, Menlo Park 1978, p. 209; b) J. Saltiel, L.-S. Ng Lim, *J. Am. Chem. Soc. 91* (1969) 5404.
[31] J. A. Smith, H. Shechter, J. Bayless, L. Friedmann, *J. Am. Chem. Soc. 87* (1965) 659.
[32] M. G. Steinmetz, Y.-P. Yen, G. K. Poch, *J. Chem. Soc. Chem. Commun. 1983,* 1504.
[33] M. G. Steinmetz, E. J. Stark, Y.-P. Yen, R. T. Mayes, R. Srinivasan, *J. Am. Chem. Soc. 105* (1983) 7209.
[34] A. Padwa, *Acc. Chem. Res. 12* (1979) 310.
[35] R. Srinivasan, K. H. Brown, *Tetrahedron Lett. 1978,* 3645.
[36] M. B. Robin: *Higher Excited States of Polyatomic Molecules, Vol. 1 and 2.* Academic Press, New York 1975.
[37] K. Shibuya, K. Obi, J. Tanaka, *Bull. Chem. Soc. Jpn. 48* (1975) 1974.
[38] a) R. Srinivasan, J. A. Ors, *J. Am. Chem. Soc. 100* (1978) 7089; b) R. Srinivasan, J. A. Ors, T. Baum, *J. Org. Chem. 46* (1981) 1950.
[39] A. R. Rossi, *J. Phys. Chem. 83* (1979) 2554.
[40] R. Srinivasan, J. A. Ors, *J. Org. Chem. 44* (1979) 3426.
[41] R. Srinivasan, T. Baum, G. Epling, *J. Chem. Soc. Chem. Commun. 1982,* 437.
[42] M. J. Mirbach, M. F. Mirbach, R. Vartan-Boghossian, A. Saus, *Nouv. J. Chim. 5* (1981) 113.
[43] R. Srinivasan, T. Baum, K. Brown, J. Ors, L. S. White, A. R. Rossi, G. A. Epling, *J. Chem. Soc. Chem. Commun. 1981,* 973.
[44] R. Srinivasan, J. A. Ors, *J. Am. Chem. Soc. 101* (1979) 3411.
[45] a) H.-P. Schuchmann, C. von Sonntag, D. Schulte-Frohlinde, *J. Photochem. 3* (1974/75) 267; b) R. Srinivasan, L. S. White, A. R. Rossi, G. A. Epling, *J. Am. Chem. Soc. 103* (1981) 7299.
[46] R. Srinivasan, J. A. Ors, K. H. Brown, T. Baum, L. S. White, A. R. Rossi, *J. Am. Chem. Soc. 102* (1980) 5297.
[47] a) W. J. Leigh, R. Srinivasan, *J. Am. Chem. Soc. 105* (1983) 514; b) Y. Inoue, Y. Daino, S. N. Hagiwara, H. Akamura, T. Hakushi, *J. Chem. Soc. Chem. Commun. 1985,* 804.
[48] W. J. Leigh, R. Srinivasan, *J. Org. Chem. 48* (1983) 3970.
[49] a) W. Adam, O. De Lucchi, *Angew. Chem. 92* (1980) 815; *Angew. Chem. Int. Ed. Engl. 19* (1980) 762; b) P. S. Engel, *Chem. Rev. 80* (1980) 99.
[50] C. G. Overberger, M.-S. Chi, *J. Org. Chem. 46* (1981) 303.
[51] W. Adam, F. Mazenod, *J. Am. Chem. Soc. 102* (1980) 7131.
[52] P. S. Engel, C. Steel, *Acc. Chem. Res. 6* (1973) 275.
[53] D. W. McNeil, M. E. Kent, E. Hedaya, P. F. D'Angelo, P. O. Schissel, *J. Am. Chem. Soc. 93* (1971) 3817.
[54] We thank Prof. *P. Eaton* for a sample of cubane.
[55] W. Adam, A. Fuss, F. P. Mazenod, H. Quast, *J. Am. Chem. Soc. 103* (1981) 998.
[56] a) M. B. Robin in S. Patai (Ed.): *The Chemistry of the Hydrazo, Azo and Azoxy Groups, Vol. 1,* Wiley, New York 1975, p. 1; b) H. Meier, K.-P. Zeller, *Angew. Chem. 89* (1977) 876; *Angew. Chem. Int. Ed. Engl. 16* (1977) 835.
[57] W. R. Roth, M. Martin, *Justus Liebigs Ann. Chem. 702* (1967) 1.
[58] W. R. Roth, E. Enderer, *Justus Liebigs Ann. Chem. 733* (1970) 44.
[59] G. Zang, *Diplomarbeit,* Universität Würzburg 1984.
[60] R. Srinivasan, L. S. White, *J. Am. Chem. Soc. 101* (1979) 6389.

Understanding Reaction Dynamics in Coordination Chemistry—Application of High Pressure Techniques

By Rudi van Eldik*

In order to understand the dynamics of chemical reactions in general, detailed information on electronic, structural and kinetic properties is required. The key questions on how chemical reactions actually occur can in many cases only be answered in terms of information obtained from kinetic studies. In conventional kinetic studies of chemical reactions in solution, the variables usually selected include concentration, acidity, solvent, and temperature. In recent years, pressure has become an additional selected variable in such studies. It enables the measurement of the volume of activation and the construction of reaction volume profiles and thus assists in the elucidation of the underlying mechanism; it also completes the comprehension of reaction kinetics by adding another kinetic parameter that the suggested reaction mechanism must account for. Furthermore, the volume of activation is the only transition state property that can be correlated with the corresponding ground state property in an experimentally simple manner. In this paper, the insights so gained in our understanding of the dynamics of reactions involving coordination complexes will be presented. Such reactions are of fundamental interest to chemists since they often form the basis of catalytic, biological, environmental and energy related processes. Any additional information that will add to the understanding of the reaction dynamics is therefore of exceptional importance.

1. Introduction

1.1. Fundamental Principles

High pressure kineticists measure not only the usual kinetic parameters but also the pressure dependence of the rate constants. From this data and the partial molar volumes of reactant and product species, obtainable from density measurements, it is possible to construct a volume profile for the reaction investigated. For a reaction of the type

$$A + B \xrightarrow{k} AB$$

the simplest conceivable mechanism that can be formulated according to the transition state theory is

$$A + B \rightleftharpoons (A\text{---}B)^{\ddagger} \longrightarrow AB \qquad (1)$$

for which a possible volume profile is given in Figure 1. The magnitude and sign of the reaction volume, $\Delta\bar{V} = \bar{V}_{AB} - \bar{V}_A - \bar{V}_B$, and of the activation volume, $\Delta V^{\ddagger} = \bar{V}_{\ddagger} - \bar{V}_A - \bar{V}_B$, depend on the nature of the chemical species involved and their environment. The transition state volume (Fig. 1) does not necessarily have to be between that of the reactant and product states; it can be a minimum during a bond formation process (see, e.g., Fig. 5). Whereas $\bar{V}$ and $\Delta\bar{V}$ data are obtainable from partial molar volumes (density measurements) and dilatometric results, $\Delta V^{\ddagger}$ can only be determined from the pressure dependence of the rate constant k of the reaction under investigation, viz.

$$\Delta V^{\ddagger} = -RT(\partial \ln k/\partial p)_T$$

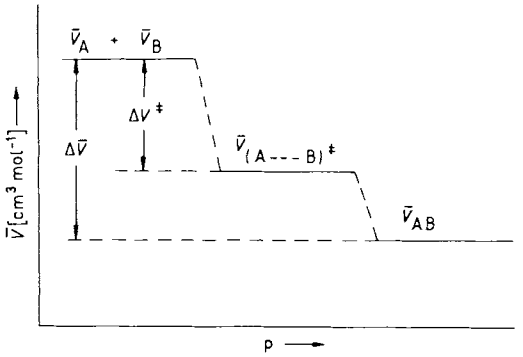


Fig. 1. Volume profile for reaction (1). $\bar{V}$ = partial molar volume, p = reaction coordinate.

In principle $\Delta V^{\ddagger}$ is not independent of pressure, i.e. the slope of $\ln k$ versus p plots depends on pressure, and the compressibility coefficient of activation, $\Delta\beta^{\ddagger}$, has been defined as

$$\Delta\beta^{\ddagger} = -(\partial \Delta V^{\ddagger}/\partial p)_T$$

Various mathematical descriptions to account for the pressure dependence of $\Delta V^{\ddagger}$ have been proposed.[1-3] However, for mechanistic purposes, the value of $\Delta V^{\ddagger}$ at ambient pressure alone is required for the above-mentioned correlation with partial molar volume data measured under such conditions. In most cases, $\Delta V^{\ddagger}$ is almost pressure independent up to 100 MPa (= 1 kbar).

[*] Priv. Doz. Dr. R. van Eldik
Institut für physikalische und theoretische Chemie der Universität
Niederurseler Hang, D-6000 Frankfurt (FRG)

 © VCH Verlagsgesellschaft mbH, D-6940 Weinheim, 1986 0570-0833/86/0808-0673 $ 02.50/0

In general, $\Delta V^{\neq}$ may be thought of as the sum of two components: an intrinsic part ($\Delta V^{\neq}_{intr}$), which represents the change in volume due to changes in bond lengths and angles, and a solvational part ($\Delta V^{\neq}_{solv}$), which represents the change in volume due to changes in the surrounding medium. An important part of this volume change is often due to changes in electrostriction, i.e. the interaction that occurs when an ion is submerged in a dielectric. It is of course principally the $\Delta V^{\neq}_{intr}$ part that is the mechanistic indicator in terms of changes in bond lengths and angles. Schematic representations of these components for typical bond formation and cleavage processes, are given in Figure 2. It follows that mechanistic assignments for processes in which no major solvational changes occur are very straightforward. In reactions with large polarity changes, $\Delta V^{\neq}_{solv}$ may be much larger than $\Delta V^{\neq}_{intr}$, and it can in fact counteract and swamp the $\Delta V^{\neq}_{intr}$ term; examples will be discussed. Nevertheless, a consistent picture arises from such studies, demonstrating the suitability of $\Delta V^{\neq}$ for mechanistic discrimination, even in extreme cases.

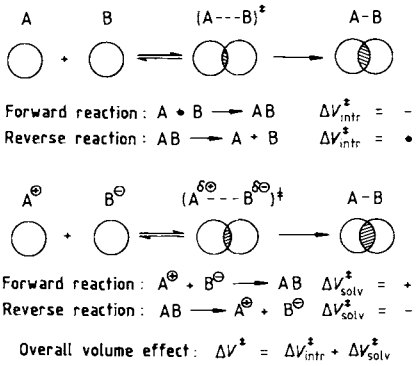


Fig. 2. Schematic presentation to illustrate the sign and components of $\Delta V^{\neq}$.

1.2. Instrumentation

Initial high pressure kinetic studies of coordination complexes in solution were conducted in a batch reactor (autoclave) either in situ, for instance by monitoring the reaction through optical windows and employing UV-VIS detection,[4] or by the use of a sampling technique. Advances in understanding the reaction dynamics of the coordination compounds described in this paper have resulted from developments in recent years which enable the pressure dependence of reactions to be studied on the milli-, micro- and nanonsecond time scales: stopped-flow[5–9] and T-jump methods[10–12], NMR spectroscopy,[13,14] and pulsed lasers.[15,16] With the increasing availability of such instrumental techniques, the output of high pressure kinetic information has increased significantly, as can be seen from a recent compilation of volume of activation data for reactions of coordination compounds.[17]

2. Reaction Dynamics in Coordination Chemistry

The effect of pressure on the reaction rates of coordination complexes has been studied for a variety of species and types of chemical reactions.[1,17] In general, such studies have been justified on the grounds that they can elucidate reaction mechanisms and resolve mechanistic discrepancies. In addition, however, pressure effects constitute important phenomena and complete our comprehension of chemical kinetics in that the suggested reaction mechanism must also account for these effects.[18] The examples selected in the following sections will clearly demonstrate both viewpoints. These include substitution, electron-transfer, and a series of miscellaneous reactions of coordination compounds. They are presented in this sequence, since substitution reactions form the basis for many of the other reaction types.

2.1. Substitution Reactions

Consider a substitution reaction of the type

$$[ML_nX] + Y \longrightarrow [ML_nY] + X \qquad (2)$$

in which M is the metal center, L the non-participating ligand, and X and Y the leaving and entering groups, respectively. Such reactions are generally discussed in terms of a dissociative (D), interchange (I) or associative (A) mechanism, depending on the degree of bonding of X and Y in the transition state of the process. The schematic presentation in Figure 3 is a useful aid to visualizing the nature of these mechanisms. If bond making is predominant, a significant decrease in molar volume of the reactants is expected (negative $\Delta V^{\neq}$); in contrast, a significant increase in volume will occur in a dissociatively activated process (positive $\Delta V^{\neq}$). In the case of an interchange process, bond breakage and bond formation occur simultaneously in varying degrees and small effects are expected, viz. a slightly negative $\Delta V^{\neq}$ for I_a and a slightly positive $\Delta V^{\neq}$ for I_d. These trends are predicted to show up in systems where no major solvational changes accompany the ligand substitution process, viz., in solvent exchange reactions; however, when charged ligands are substituted, major solvational changes are expected to influence the value of $\Delta V^{\neq}$.

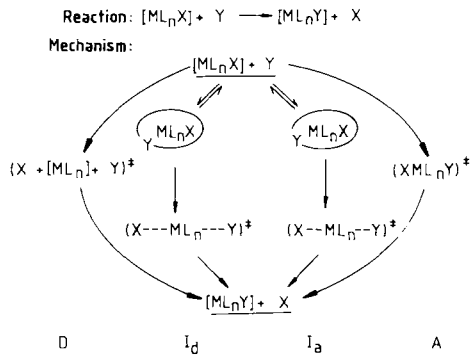


Fig. 3. Schematic presentation of the possible mechanisms of reaction (2).

2.1.1. Solvent Exchange Reactions

In a series of papers, *Merbach* and co-workers[19] reported $\Delta V^{\neq}$ data for solvent exchange reactions of diva-

Table 1. $\Delta V^{\ddagger}$ [cm^3 mol^{-1}] for solvent exchange on $[ML_6]^{2\oplus}$ ions [19]. DMF = dimethylformamide.

L \ M	$V^{2\oplus}$	$Mn^{2\oplus}$	$Fe^{2\oplus}$	$Co^{2\oplus}$	$Ni^{2\oplus}$
H_2O	−4.1	−5.4	+3.8	+6.1	+ 7.2
H_3COH		−5.0	+0.4	+8.9	+11.4
H_3CCN		−7.0	+3.0	+7.7	+ 9.6
DMF				+6.7	+ 9.1
Mechanism:	I_a	I_a	I	I_d	I_d

lent octahedral first-row transition-metal ions. This information is of fundamental importance in understanding the general substitution behavior of such metal centers. The trend in the $\Delta V^{\ddagger}$ data (Table 1) was interpreted in terms of a gradual mechanistic changeover from I_a to I_d in this series.

A similar trend was observed for solvent exchange on high spin $[ML_6]^{3\oplus}$ ions by the use of NMR techniques.[19] The results are summarized in Figure 4. The trends can be rationalized according to the following complementary ideas:[19] A decrease in ionic radius (Fig. 4) will increase the dissociative character, due to steric crowding in the transition state. For an octahedral complex, the t_{2g} orbitals are nonbonding and the e_g orbitals σ^* antibonding. From $Mn^{2\oplus}$ to $Ni^{2\oplus}$ the t_{2g} orbitals are gradually filled, which makes the approach of a seventh ligand towards the face of the octahedron less favorable electrostatically, and could explain the tendency towards less associative behavior.

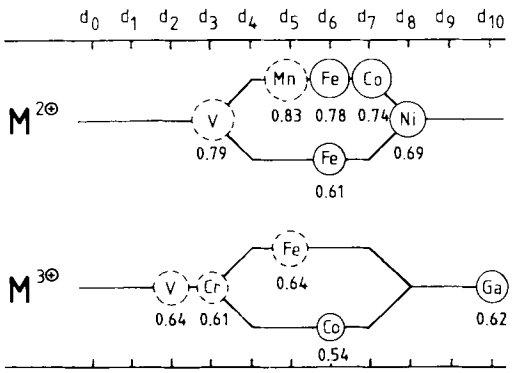


Fig. 4. First row octahedral transition metal ions (high and low spin) solvent exchange mechanisms (radii quoted in Å; Ⓜ = mechanisms A, I_a; Ⓜ = mechanisms D, I_d) taken from ref. [19].

2.1.2. Complex Formation Reactions

A logical question is whether complex formation reactions exhibit the same trend as discussed above for solvent exchange reactions. If this is indeed the case it will be of direct importance to all reactions involving such substitution processes at these metal centers. At the time the above mentioned solvent exchange work was reported,[19] only a few pressure dependence studies of fast complex formation reactions of these metal ions had been described, and the available data for complex formation with Ni^{II} and Co^{II}[20] seemed to be in good agreement with the solvent exchange data (Table 1). It was crucial to measure $\Delta V^{\ddagger}$ for complex formation of Mn^{II} or V^{II}, in order to determine whether a changeover in mechanism could be observed similar to that for the solvent exchange reactions. The first data came from a high-pressure temperature-jump study of the complexation of Mn^{II} with 2,2′-bipyridine (bpy) and 2,2′:6′,2″-terpyridine (terpy).[21,22] The presently available results (Table 2) clearly demonstrate that the activation volumes for complex formation reactions parallel those for solvent exchange, and underline the suggested changeover in mechanism along the first-row transition-metal ions.

Table 2. $\Delta V^{\ddagger}$ [cm^3 mol^{-1}] for complexation of first-row transition-metal elements in aqueous solution.

L \ M	$V^{2\oplus}$	$Mn^{2\oplus}$	$Fe^{2\oplus}$	$Co^{2\oplus}$	$Ni^{2\oplus}$	Ref.
NH_3				+4.8±0.7	+6.0±0.3	[10]
pada [a]				+7.2±0.2	+7.7±0.3	[10]
bpy		−1.2±0.2 [21]		+4.3±1.0	+5.5±0.3	[23] [b]
				+7.5±1.4	+5.1±0.4	[23] [c]
terpy		−3.4±0.7 [22]	+3.4±0.6	+4.5±0.8	+6.7±0.2	[23] [b]
			+3.7±0.8	+3.7±1.3	+4.5±0.4	[23] [c]
$SCN^{\ominus}$	−2.1±0.8					[24]

[a] pada = 4-*N*,*N*-Dimethylaminobenzene-1-azo-2′-pyridine. [b] Experimental conditions such that $[L] \gg [M^{2\oplus}]$. [c] Experimental conditions such that $[M^{2\oplus}] \gg [L]$.

In one case, it was possible to measure $\Delta V^{\ddagger}$ for the reverse aquation process; this allowed the construction of a volume profile (Fig. 5). The reaction volume estimated from the activation volumes of the forward and reverse reactions is in close agreement with that determined directly from the pressure dependence of the equilibrium constant. The transition state is significantly denser than both the reactant and product states, emphasizing the associative nature of the process. Prior to this work the dissociative nature of such reactions, i.e., the traditional "Eigen-Wilkins" (or I_d) mechanism, had never been seriously questioned. The $\Delta V^{\ddagger}$ data, however, strongly support an I_a substitution mechanism for the earlier members of the first-row transition-metal elements.

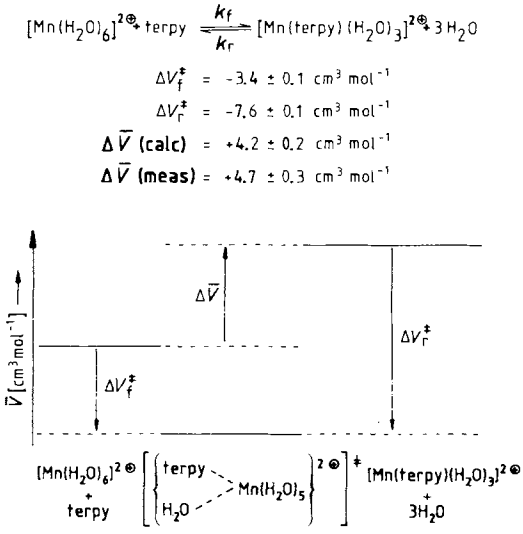


Fig. 5. Typical example of a volume profile for a complex formation reaction of Mn^{II}.

2.1.3. *Ligand Substitution Reactions of Square-Planar Complexes*

Such reactions are of general importance in the catalytic and cytostatic behavior of square-planar complexes. In general, substitution reactions of complexes of Pd^{II} and Pt^{II} follow an associative mechanism via a five-coordinate transition state. This is true for the solvolysis reaction (k_1), the subsequent rapid anation reaction (replacement of a H_2O ligand by another ligand), and the direct substitution (k_2) (see Fig. 6). The general question has been raised by

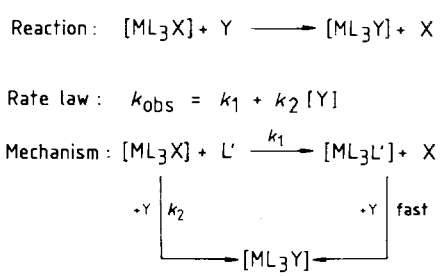


Fig. 6. A typical square planar substitution reaction; these reactions are usually associative (L' = solvent).

many investigators whether sterically hindered square-planar complexes could undergo substitution via a dissociative reaction mode. By increasing steric hindrance around the metal center, it may be possible to hinder the direct attack of the entering ligand or solvent molecule. Such a changeover in mechanism should clearly be seen in $\Delta V^{\neq}$ data. We have gradually increased the steric hindrance on a series of Pd^{II} complexes by introducing methyl and ethyl groups on the diethylenetriamine(dien) ligand. The data in Table 3 for the solvolysis/anation reaction of these complexes at 25 °C [Reaction (3)] nicely demonstrate that steric hindrance alone cannot induce a changeover in mechanism[25] even though the solvolysis rate constant decreases by up to five orders of magnitude. This reflects a gradual increase in $\Delta H^{\neq}$, but no trend is visible in $\Delta S^{\neq}$ and $\Delta V^{\neq}$.

$$[Pd(L)Cl]^{\oplus} + H_2O \xrightarrow[\text{slow}]{k_1} [Pd(L)H_2O]^{2\oplus} + Cl^{\ominus} \xrightarrow[\text{fast}]{+1^{\ominus}} [Pd(L)I]^{\oplus} + H_2O \quad (3)$$

$L = R^1R^2N-CH_2-CH_2-N(R^3)-CH_2-CH_2-NR^4R^5$

The average volume of activation (-12 ± 2 cm^3 mol^{-1}) is close to the maximum value expected for the associative entrance of a water molecule. This value, which is expected mainly to represent the intrinsic component, is significantly more negative than those (between -3 and -4 cm^3 mol^{-1}) reported[26] recently for similar solvolysis reactions involving NH_3 and pyridine as leaving ligands, and than those reported[27,28] for the solvent exchange on $[Pd(H_2O)_4]^{2\oplus}$ and $[Pt(H_2O)_4]^{2\oplus}$ (-2.2 and -4.6 cm^3 mol^{-1}, respectively). These tendencies in fact indicate that the values in Table 3 must arise partly from solvational changes probably involving dipole interactions with the charged leaving group. Such solvational contributions also show up in the data reported in Table 4 for the anation reaction (4), where partial charge neutralization during the associative reaction will result in a more positive $\Delta V^{\neq}$ value.[6,29,30] Furthermore, the volumes of activation become more negative with increasing size of the entering ligand, demonstrating the effect of the overlap of the van der Waals radii during the bond formation process.

$$[Pd(L)H_2O]^{2\oplus} + X^{\ominus} \xrightarrow{k_{anation}} [Pd(L)X]^{\oplus} + H_2O \quad (4)$$

$L = R^1R^2N-CH_2-CH_2-N(R^3)-CH_2-CH_2-NR^4R^5$

Table 3. Kinetic parameters for the reaction (3) at 25 °C [25].

R^1	R^2	R^3	R^4	R^5	k_1 [s^{-1}]	$\Delta H^{\neq}$ [kJ mol^{-1}]	$\Delta S^{\neq}$ [J K^{-1} mol^{-1}]	$\Delta V^{\neq}$ [cm^3 mol^{-1}]
H	H	H	H	H	43.8 ±0.5	43±3	− 69±12	−10.0±0.6
Me	H	Me	Me	H	25.0 ±4.2	38±4	− 87±15	− 9.2±0.6
Et	H	Et	Et	H	10.0 ±0.1	41±5	− 86±18	−10.8±1.0
Me	Me	H	Me	Me	0.99±0.02	49±1	− 79± 3	−13.4±1.9
Et	Et	Et	H	H	0.77±0.01	51±1	− 76± 3	−14.5±1.2
Me	Me	Me	Me	Me	(2.76±0.04)·10^{-1}	50±1	− 88± 3	−10.9±0.3
Et	Et	H	Et	Et	(2.1 ±0.4)·10^{-3}	69±2	− 67± 8	−14.9±0.2
Et	Et	Me	Et	Et	(6.8 ±0.1)·10^{-4}	66±7	− 84±25	−14.3±0.6
Et	Et	Et	Et	Et	(6.7 ±0.1)·10^{-4}	59±3	−106± 9	−12.8±0.8

Table 4. Kinetic parameters for the reaction (4) at 25 °C [6, 29, 30].

R^1	R^2	R^3	R^4	R^5	X	$k_{anation}$ [M^{-1} s^{-1}]	$\Delta H^{\neq}$ [kJ mol^{-1}]	$\Delta S^{\neq}$ [J K^{-1} mol^{-1}]	$\Delta V^{\neq}$ [cm^3 mol^{-1}]
Me	Me	H	Me	Me	Cl	1908±50	40±2	−49±6	− 7.2±0.2
					Br	3126±120	39±1	−47±5	− 7.6±0.3
					I	8081±890	34±2	−55±6	− 9.3±0.8
Et	Et	Et	H	H	Cl	1558± 7	44±3	−36±10	− 2.7±0.2
Me	Me	Me	Me	Me	Cl	629± 19	44±2	−42±8	− 4.9±0.4
					Br	1087± 20	40±2	−54±7	− 7.3±0.4
					I	4162±140	33±5	−63±17	− 9.9±1.2
					N_3	6678±440	31±2	−66±9	−11.7±1.2
Et	Et	H	Et	Et	Cl	4.19±0.06	56±2	−45±5	− 3.0±0.02
Et	Et	Et	Et	Et	Cl	2.27±0.01	70±2	− 1±5	− 7.7±0.5

2.1.4. Ligand Substitution Reactions of Octahedral Complexes

A number of reactions involving the substitution of ligands other than solvent molecules will be presented in this section. Such reactions occur mainly in non-coordinating solvents. For instance, the exchange of phosphane in the four-coordinated species $[Co(PPh_3)_2Br_2]$ in $CDCl_3$ exhibits a $\Delta V^{\neq}$ value of -12.1 ± 0.3 cm^3 mol^{-1}, which clearly underlines the associative nature of the substitution process.[31] Conversely, $\Delta V^{\neq}$ for the substitution of acetate in $Ni(OAc)_2$ by 2-hydroxynaphthalene-1-azo-2'-pyridine in acetic acid as solvent is $+15.5 \pm 2.6$ cm^3 mol^{-1}, demonstrating the dissociative nature of that process.[32] In the latter case, charge formation is involved so that $\Delta V^{\neq}_{intr}$ must be even more positive than the reported number. A recent study[33] of substitution reactions of the type

$$[cis\text{-}Mo(CO)_4(py)_2] + N\frown N \longrightarrow [Mo(CO)_4(N\frown N)] + 2\,py$$

where $N\frown N$ is bpy, 1,10-phenanthroline (phen) or *N,N'*-diphenyl-2,3-butanediimine (dab), resulted in $\Delta V^{\neq}$ values of $+3.6$ to $+4.5$ cm^3 mol^{-1}. These results are consistent with the rate-limiting step being the dissociation of pyridine:

$$[cis\text{-}Mo(CO)_4(py)_2] \rightleftharpoons [Mo(CO)_4py] + py$$

$$[Mo(CO)_4py] + N\frown N \longrightarrow [Mo(CO)_4(py)N\frown N] \longrightarrow [Mo(CO)_4(N\frown N)] + py$$

Many organometallic kineticists have run into problems with the interpretation of $\Delta S^{\neq}$ data in terms of the suggested reaction mechanisms. (The general fact that $\Delta S^{\neq}$ data are not very reliable for mechanistic assignments will be treated in the final section of this paper.) Positive volumes of activation have been found for systems in which other kinetic evidence, such as a negative $\Delta S^{\neq}$, points to an associative mechanism. Substitution of $[Cr(CO)_4(bte)]$ by $P(OEt)_3$ in 1,2-dichloroethane (bte = bis(*tert*-butylthio)-ethylene (2,2,7,7-tetramethyl-3,6-dithiaoctane)) is a typical example of such a case. The volume of activation of $+14.0 \pm 0.6$ cm^3 mol^{-1} clearly supports the dissociative nature of the process and emphasizes the value of this kinetic parameter. A similar value of $+14.7 \pm 0.7$ cm^3 mol^{-1} was found for the corresponding 3,6-dithiooctane complex.[34] In a recent study[35] a $\Delta V^{\neq}$ value of $+20.6 \pm 0.4$ cm^3 mol^{-1} was found for the rate-determining loss of CO in the reaction

$$[Mn(CO)_5Cl] + dab \longrightarrow [Mn(CO)_3(Cl)(dab)] + 2\,CO$$

This is indeed a very exciting result and motivates further study.

2.1.5. Base-Catalyzed Hydrolysis Reactions

Volumes of activation and volume profiles reveal significant mechanistic detail not only in the case of relatively simple chemical systems such as those discussed in the previous sections, but also for significantly more complicated processes. One of these concerns base-catalyzed hydrolysis reactions in which various complex species participate. In the case of Co^{III}-ammine complexes, base catalysis increases the rate of aquation from the hour to the millisecond time scale. Such reactions are generally accepted to proceed according to a S_N1CB mechanism which can be summarized as follows:

$$[Co(NH_3)_5X]^{(3-n)\oplus} + OH^{\ominus} \overset{K}{\rightleftharpoons} [Co(NH_3)_4(NH_2)X]^{(2-n)\oplus} + H_2O$$

$$[Co(NH_3)_4(NH_2)X]^{(2-n)\oplus} \xrightarrow{k} [Co(NH_3)_4NH_2]^{2\oplus} + X^{n\ominus}$$

$$[Co(NH_3)_4NH_2]^{2\oplus} + H_2O \xrightarrow{fast} [Co(NH_3)_5OH]^{2\oplus}$$

Net reaction:

$$[Co(NH_3)_5X]^{(3-n)\oplus} + OH^{\ominus} \longrightarrow [Co(NH_3)_5OH]^{2\oplus} + X^{n\ominus}$$

In this mechanism, formation of the conjugate base species is followed by rate-determining dissociation of $X^{n\ominus}$ to produce the five-coordinate $[Co(NH_3)_4NH_2]^{2\oplus}$ species, which rapidly reacts with the solvent to produce the hydrolysis product. The volume profile expected for this reaction scheme is given in Figure 7.

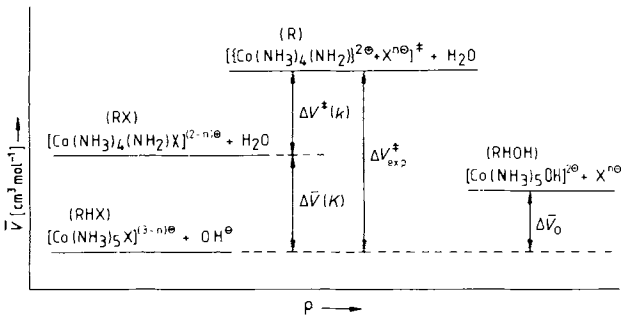


Fig. 7. Volume profile for the base hydrolysis of $[Co(NH_3)_5X]^{(3-n)\oplus}$ according to a S_N1CB mechanism.

Solvational effects are expected to significantly influence the values of $\Delta V^{\neq}_{exp}$ (consisting of $\Delta \bar{V}(K)$ and $\Delta V^{\neq}(k)$, since $k_{obs} = kK[OH^{\ominus}]$ for these reactions) and $\Delta \bar{V}_0$ (the overall volume change), since significant charge formation will be present when $X^{n\ominus}$ is a charged leaving group. This was indeed found to be the case,[36] and typical $\Delta V^{\neq}_{exp}$ values are ($X^{n\ominus}$): 40.2 ± 0.5 (Me_2SO); 31.0 ± 0.8 ($NO_3^{\ominus}$); 33.6 ± 1.0 ($I^{\ominus}$); 32.5 ± 1.4 ($Br^{\ominus}$); 33.0 ± 1.4 ($Cl^{\ominus}$); 26.4 ± 1.0 ($F^{\ominus}$); and 22.2 ± 0.7 ($SO_4^{2\ominus}$) cm^3 mol^{-1} at 25 °C. The decrease in $\Delta V^{\neq}_{exp}$ in this series is ascribed to the change in charge formation. A similar trend is seen in $\Delta \bar{V}_0$.[36] These data not only underline the validity of the suggested reaction mechanism, but reveal other interesting information. For instance, it is now possible for the first time to estimate the partial molar volume of the five-coordinate intermediate, on the assumption that the rate-determining step has a late (product-like) transition state in the case of a limiting dissociative mechanism. This volume should be independent of the nature of $X^{n\ominus}$. It turns out that the volume of the five-coordinate intermediate has an average value of 71 ± 4 cm^3 mol^{-1}, which is remarkably

close to the value of 68 $cm^3\ mol^{-1}$ for the six-coordinate $[Co(NH_3)_5OH]^{2\oplus}$ species. Furthermore, the quantity $\Delta V^{+}_{exp} - \Delta \bar{V}_0$ should also be independent of the nature of $X^{n\ominus}$ since it only involves the reaction of water with $[Co(NH_3)_4NH_2]^{2\oplus}$ to produce $[Co(NH_3)_5OH]^{2\oplus}$. It was found[36] that this volume difference is indeed constant and has an average value of 20 ± 2 $cm^3\ mol^{-1}$. This essentially equals the molar volume of water (viz. 18 $cm^3\ mol^{-1}$), which demonstrates that the water molecule is completely "absorbed" by the five-coordinate species during the final step of the reaction. In addition, this is also in line with the similarity found between the partial molar volumes of $[Co(NH_3)_4NH_2]^{2\oplus}$ and $[Co(NH_3)_5OH]^{2\oplus}$. Recent work[37] has demonstrated that similar trends exist for larger five-coordinate species, in which substituents were introduced on the ammine ligands.

2.2. Electron-Transfer Reactions

Mechanistic studies on electron transfer reactions of coordination complexes have been a popular research area for kineticists over the past decade, and the progress made and general importance of this work were recently emphasized by the award of a Nobel prize to *Henry Taube*. And yet, the mechanistic assignment in terms of inner- and outer-sphere mechanisms [Eq. (a)] has not been unambiguous. These mechanisms only differ with respect to the nature of the precursor intermediate species, Ox//Red, in the overall reaction scheme; it can be either an ion-pair or an encounter species in the case of the outer-sphere process, or a bridge intermediate in the case of an inner-sphere process. The electron-transfer [Eq. (b)] is then followed by dissociation of the successor complex [Eq. (c)]. In many systems, reaction (b) is rate-determining and in the presence of excess reducing agent, $k_{obs} = k_{ET} K[Red]/(1 + K[Red])$.

$$Ox + Red \overset{K}{\rightleftharpoons} Ox//Red \qquad (a)$$

$$Ox//Red \xrightarrow{k_{ET}} Ox^{\ominus}//Red^{\oplus} \qquad (b)$$

$$Ox^{\ominus}//Red^{\oplus} \rightleftharpoons Ox^{\ominus} + Red^{\oplus} \qquad (c)$$

The interpretation of the kinetic parameters is usually complicated by the fact that K is rather small, such that $k_{obs} = k_{ET} K[Red]$ and the observed second-order rate constant ($k_{ET} K$) is a composite quantity. However, the occurrence of bond formation and/or bond breakage in the inner-sphere mechanism should be clearly reflected in the volume of activation of the process as compared to that for outer-sphere reactions.

Halpern et al.[38] studied the pressure dependence of some typical inner-sphere electron-transfer reactions of the type

$$[Co(NH_3)_5X]^{2\oplus} + [Fe(H_2O)_6]^{2\oplus} \longrightarrow Co^{2\oplus} + 5\,NH_3 + [Fe(H_2O)_5X]^{2\oplus} + H_2O$$

They reported ΔV^{+} values of $+11$ (X = F), $+8$ (X = Cl, Br) and $+14$ $cm^3\ mol^{-1}$ (X = N_3). These values are expected to involve significant contributions from ΔV^{+}_{solv} and indeed, the data in Me_2SO as solvent were found to be $+10.3 \pm 0.4$ (X = F), $+3.8 \pm 0.7$ (X = Cl), 0.0 ± 0.4 (X = Br) and $+6.5 \pm 0.2$ $cm^3\ mol^{-1}$ (X = N_3).[39,40] In later work, *Stranks*[41] studied the effect of pressure on some typical outer-sphere electron-transfer reactions, and indeed found quite large negative values for ΔV^{+}. He developed a theoretical treatment based on the theories of *Marcus* and *Hush* and demonstrated that ΔV^{+} can be calculated by considering contributions from coulombic interaction, solvent rearrangement, internal metal-ligand rearrangement, and a Debye-Hückel component. His success is seen in the examples $[Co(en)_3]^{2\oplus}/[Co(en)_3]^{3\oplus}$ (en = ethylenediamine), for which ΔV^{+} is -19.8 ± 1.5 (exp.), and -18.4 (theor.) $cm^3\ mol^{-1}$, and $Fe(H_2O)_6^{2\oplus}/Fe(H_2O)_6^{3\oplus}$, for which ΔV^{+} is -12.2 ± 1.5 (exp.) and -14.4 (theor.) $cm^3\ mol^{-1}$. In contrast, the observed[41] ΔV^{+} values for inner-sphere electron transfer between $[Fe(H_2O)_5OH]^{2\oplus}$ and $[Fe(H_2O)_6]^{2\oplus}$ (-0.4 ± 0.4 $cm^3\ mol^{-1}$), and between $[Cr(H_2O)_5OH]^{2\oplus}$ and $[Cr(H_2O)_6]^{2\oplus}$ ($+4.2 \pm 1.1$ $cm^3\ mol^{-1}$) are significantly more positive than the values predicted for an outer-sphere electron-transfer process, viz. -11.4 and -11.6 $cm^3\ mol^{-1}$, respectively. This difference was ascribed to the dissociative release of a solvent molecule during the formation of the hydroxy-bridged inner-sphere intermediate. This trend is also in line with the data quoted above for the reduction of $[Co(NH_3)_5X]^{2\oplus}$ with $[Fe(H_2O)_6]^{2\oplus}$ and $[Fe(Me_2SO)_6]^{2\oplus}$.[38-40]

However, *Wherland*[42] recently pointed out that *Stranks*' theoretical treatment contained an error in the sign of the Debye-Hückel component, and that the close correlation between predicted and experimentally observed volumes of activation is only apparent. We[43] recently studied the outer-sphere electron-transfer reaction between $[Co(terpy)_2]^{2\oplus}$ and $[Co(bpy)_3]^{3\oplus}$ (terpy = 2,2′:6′,2″-terpyridine; bpy = 2,2′-bipyridine) in various solvents and found a ΔV^{+} value of -9.4 ± 0.9 $cm^3\ mol^{-1}$ for the reaction in water. This is in good agreement with the value of -7.3 $cm^3\ mol^{-1}$ theoretically predicted on the basis of *Wherland*'s treatment.[42]

The pressure dependence of a series of outer-sphere electron-transfer reactions in which significant ion-pair formation occurs, was also investigated.[44,45] In this case, K and k_{ET} can be determined separately.

$$[Co(NH_3)_5X]^{3\oplus} + [Fe(CN)_6]^{4\ominus} \overset{K}{\rightleftharpoons} ([Co(NH_3)_5X]^{3\oplus} \cdot [Fe(CN)_6]^{4\ominus}) \downarrow k_{ET} \quad Co^{2\oplus} + 5\,NH_3 + X + [Fe(CN)_6]^{3\ominus}$$

X = H_2O, Me_2SO, pyridine

The pressure dependence of k_{ET} results in large positive volumes of activation, viz., $+26.5 \pm 2.4$ (X = H_2O), $+29.8 \pm 1.4$ (X = py), and $+34.4 \pm 1.1$ $cm^3\ mol^{-1}$ (X = Me_2SO). Partial molar volume considerations showed[45] that these volume increases are due to the large volume increase in going from the precursor to the successor ion-pairs, e.g. 65 $cm^3\ mol^{-1}$ when $[Fe(CN)_6]^{4\ominus}$ is oxidized to $[Fe(CN)_6]^{3\ominus}$, and $[Co(NH_3)_5X]^{3\oplus}$ is reduced to

$[Co(NH_3)_5X]^{2\oplus}$. This means that on a volume basis the transition state for the electron-transfer step is approximately halfway between the two ion-pairs, and that the metal centers have a geometry halfway between the oxidation states involved. This simplified picture indicates how the molecular dimensions adjust prior to the actual electron-transfer step, which must obey the Franck-Condon restriction.

2.3. Miscellaneous Thermal Reactions

High pressure kinetic measurements have also assisted in the understanding of racemization and geometrical and linkage isomerization reactions of coordination compounds. Various mechanisms have been proposed for the racemization of octahedral complexes, and these are presented schematically in Figure 8. Although it is in many cases not possible to distinguish between all of these mechanisms, some racemization reactions exhibit very distinct pressure effects. For instance, $\Delta V^{\neq}$ for the racemization of $[Fe(phen)_3]^{2\oplus}$ (phen = 1,10-phenanthroline) is $+15.6 \pm 0.3$ $cm^3\ mol^{-1}$ compared to a value of -12.3 ± 0.3 $cm^3\ mol^{-1}$ reported for the racemization of $[Cr(C_2O_4)_2(phen)]^{\ominus}$.[46] The former result indicates a dissociative mechanism, and the latter an intramolecular one-ended ring-opening of the oxalate ligand. The large negative $\Delta V^{\neq}$ originates mainly from the increase in electrostriction during ring-opening of the oxalate chelate. A similar conclusion was drawn from the $\Delta V^{\neq}$ value of -16.6 ± 0.5 $cm^3\ mol^{-1}$ reported[47] for the geometrical isomerization of *trans*-$[Cr(C_2O_4)_2(H_2O)_2]^{\ominus}$. On the other hand, a $\Delta V^{\neq}$ value of $+14.3 \pm 0.2$ $cm^3\ mol^{-1}$ for the *trans* to *cis* isomerization of $[Co(en)_2(H_2O)_2]^{3\oplus}$ clearly supports the dissociative release of a water molecule to produce a five-coordinate intermediate.[48] A similar result was recently reported[49] for the *trans* to *cis* isomerization of $[Co(en)_2(CH_3COO)(H_2O)]^{2\oplus}$, in which the dissociation of the aqua ligand is believed to proceed according to an I_d mechanism since $\Delta V^{\neq}$ is between $+5.6$ and $+7.9$ $cm^3\ mol^{-1}$.

Linkage isomerization reactions are usually concerted intramolecular processes, and in general exhibit small pressure effects and volumes of activation.[1,17] This is understandable since such reactions, viz. M–ONO→M–NO_2, M–OSO_2→M–SO_3, and M–SCN→M–NCS, are expected to proceed via a transition state in which both coordination sites of the ligand are weakly bonded to the metal center. However, base-catalyzed isomerization reactions of $[Co(NH_3)_5ONO]^{2\oplus}$ and *cis*- and *trans*-$[Co(en)_2(ONO)_2]^{\oplus}$ exhibit large positive volumes of activation,[50,51] indicating that a S_N1CB mechanism is operative in these cases (see Section 2.1.5).

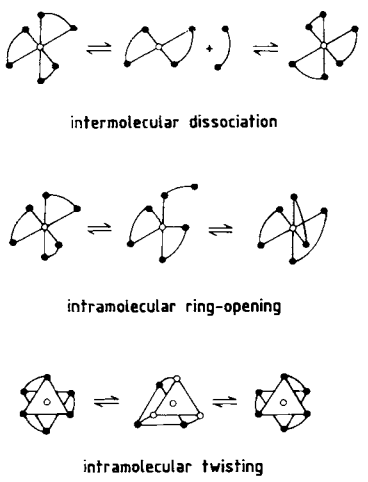


Fig. 8. Schematic representation of different racemization mechanisms of octahedral species.

Processes that involve addition or elimination reactions are expected mainly to exhibit intrinsic volumes of activation. For instance, CO_2 uptake by complexes of the type $[M(NH_3)_5OH]^{2\oplus}$ ($M = Co^{III}$, Rh^{III}, Ir^{III}) to produce the corresponding carbonato complexes, is characterized by negative volumes of activation.[52] Similarly, the reactions of [Ir(cod)(phen)]$^{\oplus}$ and [Ir(cod)(phen)I] (cod = cycloocta-1,5-diene, phen = 1,10-phenanthroline) with oxygen to produce $[Ir(cod)(phen)O_2]^{\oplus}$ exhibit volumes of activation of -31.1 ± 1.7 and -44.4 ± 1.6 $cm^3\ mol^{-1}$, respectively.[53] The more negative value for the reaction of the [Ir(cod)(phen)I] species is due to charge formation with the release of iodide. Large negative volumes of activation of this sort demonstrate the significance of bond formation in such addition reactions, and also demonstrate the significant catalytic effect pressure would have in such processes. On the other hand, decarboxylation reactions of complexes of the type $[M(NH_3)_5OCO_2H]^{2\oplus}$ all exhibit positive volumes of activation, in agreement with the release and elimination of CO_2.[52] A typical volume profile for such CO_2 uptake and elimination [Reaction (5)] is given in Figure 9, and the corresponding transition state for CO_2 uptake is illustrated schematically in Figure 10. These results are in good agreement with the volume profile reported[54] for the hydrolysis of CO_2 and the dehydration of carbonic acid.

$$[Co(NH_3)_5OH]^{2\oplus} + CO_2 \rightleftharpoons [Co(NH_3)_5OCO_2H]^{2\oplus} \quad (5)$$

Based on the results reported for organic systems,[55–57] homolytic and heterolytic decomposition reactions of coordination complexes are expected to exhibit character-

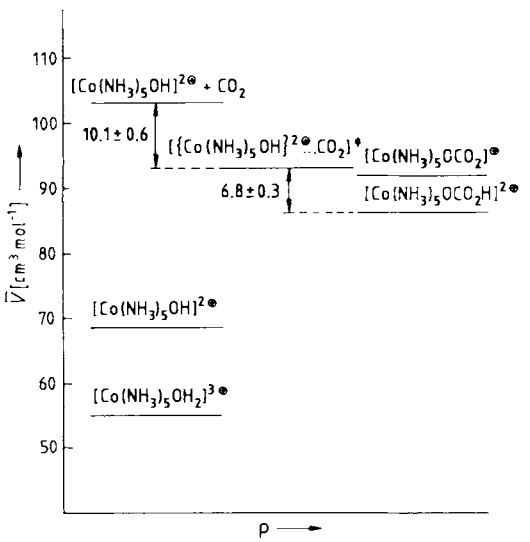


Fig. 9. Volume profile for the reaction (5).

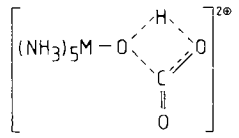


Fig. 10. Suggested transition state during CO_2 uptake and decarboxylation [Reaction (5)].

istic pressure dependencies. Such reactions were investigated for two organochromium(III) complexes of the type $[Cr(H_2O)_5R]^{2\oplus}$, where $R = C(CH_3)_2OH$ and $CH(CH_3)_2$.[58] The heterolytic decomposition path exhibited volumes of activation of $+0.3 \pm 0.2$ and -0.2 ± 0.2 cm^3 mol^{-1}, respectively. These small effects point to a transition state (I in Figure 11) which involves no net development of charge or major net changes in bond lengths. On the contrary, the volumes of activation for the homolysis reaction to produce $[Cr(H_2O)_6]^{2\oplus}$ and $R^{\odot}$ are $+15.1 \pm 1.6$ and $+26 \pm 2$ cm^3 mol^{-1} for the 2-hydroxyprop-2-yl and 2-propyl complexes, respectively. These large positive effects are ascribed to massive desolvation, i.e. breakup of the solvent cage, as the organic radicals separate from $Cr^{2\oplus}$ in the transition state (II in Figure 11).[55] Such mechanistic detail could not be obtained with conventional kinetic techniques.

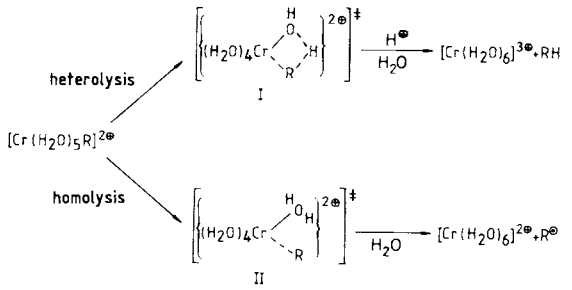


Fig. 11. Heterolytic and homolytic reactions of organochromium(III) complexes.

2.4. Photochemical reactions

The examples discussed in the preceeding sections have demonstrated how insight into reaction dynamics can be obtained from the pressure dependence of a rate constant. In photochemical reactions of coordination compounds we are dealing with the chemistry of excited state species. Since so little is known about the molecular dynamics of such reactions, the pressure dependence of the photochemical reaction step may help reveal the intimate nature of this process. The interpretation of such data can be expected to be more difficult than for ground state thermal processes.[56] Nevertheless, the results obtained so far for the photosolvolysis reactions of a series of rhodium(III)-ammine complexes are very reasonable and deserve to be mentioned in this paper.

The photosolvolysis reactions investigated all proceed according to the overall scheme:[16,60-62]

$$\begin{array}{l} [Rh(NH_3)_5X]^{(3-n)\oplus} \\ \quad + \\ \quad L \end{array} \xrightarrow[LF]{h\nu} \begin{cases} \longrightarrow [Rh(NH_3)_5L]^{3\oplus} + X^{n\ominus} \\ \longrightarrow \textit{trans}\text{-}[Rh(NH_3)_4(L)X]^{(3-n)\oplus} + NH_3 \end{cases} \quad (d)$$

LF = ligand field excitation

Earlier studies by *Ford* et al. (see literature cited in ref. [16]) indicate that the lowest energy excited state is a ligand field triplet state from which the primary photoreaction (k_p), nonradiative (k_n) and radiative deactivation (k_r) occur. Since $k_r \ll (k_p + k_n)$ it can be shown that $\Phi = k_p/(k_p + k_n) = k_p \tau$, from which it follows that the quantum yield Φ and the lifetime of the lowest excited state τ must both be measured to yield k_p at any pressure. A typical example of the pressure dependence of Φ is given in Figure 12, which clearly shows different dependencies for the two photosolvolysis reactions.

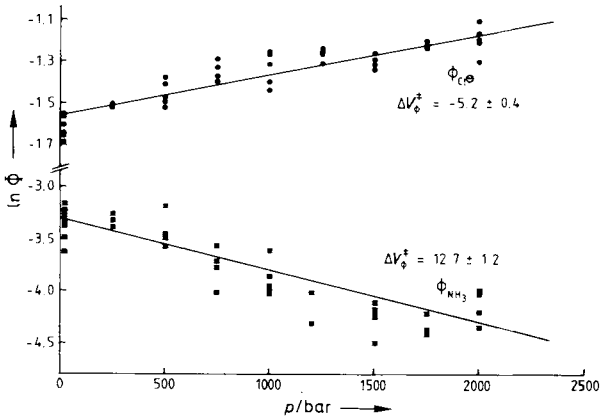


Fig. 12. Pressure dependence of the reaction (d). X = Cl, L = H_2O.

Pulsed laser techniques were employed to measure the pressure dependence of τ^{-1},[16,62] and the corresponding volumes of activation are summarized in Table 5. Throughout the series of complexes the solvolysis of NH_3 is accompanied by a positive $\Delta V_p^{\neq}$ value, which underlines the dissociative nature of the ligand substitution process. The negative $\Delta V_p^{\neq}$ values reported for the solvolysis of $X^{n\ominus}$ are attributed to electrostriction due to charge formation during the dissociative release of $X^{n\ominus}$. This is also in line with the more positive values found for the solvolysis of chloride in *trans*-$[Rh(NH_3)_4Cl_2]^{\oplus}$, for which significantly less electrostriction is expected to occur. These data also enable the calculation of $\Delta V_n^{\neq}$, the volume of activation for the non-radiative deactivation process, and throw more light on the nature of this step.[16,62] It follows that such studies can provide insight into the dynamics of the excited state processes.[59] The method can equally well be applied to study charge transfer photochemical processes, as illustrated by a series of studies[63-65] recently performed in our laboratories. The construction of volume profiles, however, is complicated by the lack of data on the partial molar volume of ligand field and charge transfer excited species.[59]

3. Concluding Remarks

We have described in the preceeding sections how the application of high pressure techniques can contribute to the understanding of thermal and photochemical reaction dynamics in coordination chemistry.[66] Such data can help

Table 5. Volumes of activation from photochemical and photophysical measurements on the photosolvolysis reactions of rhodium(III)ammine complexes at 25°C, FMA = formamide.

Solvent	Complex	Photosolvolysis product	$\Delta V^{\neq}$	$\Delta V_{r}^{\neq}$	$\Delta V_{\Phi}^{\neq}$ [a]	$\Delta V_{\Phi}^{\neq}$ [b]	Ref.
H_2O	$[Rh(NH_3)_5Cl]^{2\oplus}$	$[Rh(NH_3)_5H_2O]^{3\oplus}$	-5.2 ± 0.4	(-3.4) [c]	-8.6 ± 1.6	(-2.6) [c]	[16]
		trans-$[Rh(NH_3)_4(H_2O)Cl]^{2\oplus}$	$+12.7\pm1.2$		$+9.3\pm1.9$		
D_2O	$[Rh(ND_3)_5Cl]^{2\oplus}$	$[Rh(ND_3)_5D_2O]^{3\oplus}$	-4.2 ± 0.5	-3.5 ± 1.1	-7.7 ± 1.6	-2.6 ± 1.0	[16]
		trans-$[Rh(ND_3)_4(D_2O)Cl]^{2\oplus}$	$+9.5\pm1.6$		$+6.0\pm2.2$		
H_2O	$[Rh(NH_3)_5Br]^{2\oplus}$	$[Rh(NH_3)_5H_2O]^{3\oplus}$	-10.3 ± 1.2	$(+3.5)$ [c]	-6.8 ± 1.6	$(+2.5)$ [c]	[16]
		trans-$[Rh(NH_3)_4(H_2O)Br]^{2\oplus}$	$+4.6\pm0.6$		$+8.1\pm1.2$		
D_2O	$[Rh(ND_3)_5Br]^{2\oplus}$	$[Rh(ND_3)_5D_2O]^{3\oplus}$	-9.4 ± 1.5	$+4.1\pm0.6$	-5.3 ± 1.8	$+2.5\pm1.2$	[16]
		trans-$[Rh(ND_3)_4(D_2O)Br]^{2\oplus}$	$+3.4\pm0.5$		$+7.5\pm1.1$		
H_2O	*trans*-$[Rh(NH_3)_4Cl_2]^{\oplus}$	*trans*-$[Rh(NH_3)_4(H_2O)Cl]^{2\oplus}$	$+2.5\pm0.5$	[d]	$+2.8\pm0.6$	≈0 [c]	[60]
H_2O	*trans*-$[Rh(NH_3)_4Br_2]^{\oplus}$	*trans*-$[Rh(NH_3)_4(H_2O)Br]^{2\oplus}$	$+3.4\pm0.7$	[d]	$+2.9\pm0.7$	≈0 [c]	[60]
H_2O	$[Rh(NH_3)_6]^{3\oplus}$	$[Rh(NH_3)_5H_2O]^{3\oplus}$	$+3.7\pm0.5$	[d]	$+3.9\pm0.5$	≈0 [c]	[61]
H_2O	$[Rh(NH_3)_5I]^{2\oplus}$	*trans*-$[Rh(NH_3)_4(H_2O)I]^{2\oplus}$	$+0.3\pm0.1$	[d]	$+1.4\pm0.9$	≈0 [c]	[61]
H_2O	$[Rh(NH_3)_5SO_4]^{\oplus}$	$[Rh(NH_3)_5H_2O]^{3\oplus}$	-2.7 ± 0.4	[d]	-3.9 ± 0.6	≈0 [c]	[61]
FMA	$[Rh(NH_3)_5Cl]^{2\oplus}$	$[Rh(NH_3)_5FMA]^{3\oplus}$	-4.6 ± 0.7	-0.3 ± 0.4	-4.9 ± 1.1	$+0.2\pm0.5$	[62]
		trans-$[Rh(NH_3)_4(FMA)Cl]^{2\oplus}$	$+4.2\pm0.9$		$+3.9\pm1.3$		
DMF	$[Rh(NH_3)_5Cl]^{2\oplus}$	*trans*-$[Rh(NH_3)_4(DMF)Cl]^{2\oplus}$	$+6.3\pm0.9$	$+1.3\pm0.2$	$+7.6\pm1.1$	$+0.7\pm0.3$	[62]
Me_2SO	$[Rh(NH_3)_5Cl]^{2\oplus}$	$[Rh(NH_3)_5Me_2SO]^{3\oplus}$	-7.8 ± 1.8	-1 ± 1	-8.9 ± 2.7	-1 ± 1	[62]
		trans-$[Rh(NH_3)_4(Me_2SO)Cl]^{2\oplus}$	$+4.4\pm0.9$		$+3.3\pm1.8$		

[a] $\Delta V_{\Phi}^{\neq} = \Delta V_{\Phi}^{\neq} + \Delta V_{r}^{\neq}$. [b] $\Delta V_{\Phi}^{\neq} = \Delta V_{r}^{\neq} - \frac{\Phi_1 \Delta V_{\Phi_1}^{\neq} + \Phi_2 \Delta V_{\Phi_2}^{\neq}}{1-\Phi_1-\Phi_2}$. [c] Estimated value. [d] Not measured.

solve mechanistic questions by providing direct information on the size (volume) of transition state species. The interpretation of $\Delta V^{\neq}$ data offers a pictorial presentation of the chemical process on a volume basis that usually supports the mechanistic interpretation in an intuitive way. The occurrence of large solvational contributions may complicate the interpretation of $\Delta V^{\neq}$, and additional measurements in other solvents or for differently charged species are then helpful.

Some investigators have called attention to the apparent correlation between $\Delta V^{\neq}$ and $\Delta S^{\neq}$ data,[1,67-69] although there is no thermodynamic function that links these parameters directly. It would be misleading to use such a generalized correlation since there are numerous exceptions. In many of these $\Delta V^{\neq}$ and $\Delta S^{\neq}$ have opposite signs and it is therefore wrong to generalize this "correlation". It is important to note that $\Delta S^{\neq}$ is usually subject to large error limits since it is determined by extrapolating the experimental data to $1/T \rightarrow 0$. In contrast, $\Delta V^{\neq}$ can usually be determined with good accuracy since it results from the slope of the $\ln k$ versus p plot, similar to $\Delta H^{\neq}$.

Our present activities in this area are focussed on the thermal and photochemical dynamics of organometallic species, a research area in which many mechanistic uncertainties still persist. The advantage of such systems is the low oxidation states of the metal centers such that minor solvational contributions are expected to influence $\Delta V^{\neq}$ in most cases. The method described in this paper should also enable one to distinguish between the various reaction modes of metal clusters in solution.

Finally, these results find practical application in various areas. A better understanding of the intimate mechanism of a chemical reaction assists the design of modified systems with special behavior, for instance for use in catalytic cycles. Such information can also be applied directly in synthetic work where the application of pressure may favor a particular reaction product (see for instance Figure 12) or reduce the reaction time required; especially in organic chemistry there are numerous examples of the application of high pressure to assist the synthesis of particular species or isomers. In addition, such techniques are being applied to biochemical and environmental processes, in order to contribute to the understanding of the underlying mechanisms.

The author gratefully acknowledges financial support from the Deutsche Forschungsgemeinschaft, the Fonds der Chemischen Industrie and the Scientific Affairs Division of NATO. He sincerely appreciates the very fine collaboration with graduate students, post-doctoral fellows and visiting scientists during recent years; their names appear on the papers cited from this laboratory. This paper is dedicated to Prof. Dr. Hartwig Kelm in recognition of his pioneering work in this area, and for his continued interest and support over the last six years during which he served as President of the University.

Received: November 18, 1985;
revised: January 27, 1986 [A 585 IE]
German version: *Angew. Chem. 98* (1986) 671

[1] D. A. Palmer, H. Kelm, *Coord. Chem. Rev. 36* (1981) 89.
[2] S. Balt, W. E. Renkema, H. Ronde, *Inorg. Chim. Acta 86* (1984) 87.
[3] T. Asano, T. Okada, *J. Phys. Chem. 88* (1984) 238.
[4] W. J. le Noble, H. Kelm, *Angew. Chem. 92* (1980) 887; *Angew. Chem. Int. Ed. Engl. 19* (1980) 841.
[5] K. Heremans, *Rev. Sci. Instrum. 51* (1980) 806.
[6] R. van Eldik, D. A. Palmer, R. Schmidt, H. Kelm, *Inorg. Chim. Acta 50* (1981) 131.
[7] S. Funahashi, K. Ishihara, M. Tanaka, *Inorg. Chem. 20* (1981) 51.
[8] K. Ishihara, S. Funahashi, M. Tanaka, *Rev. Sci. Instrum. 53* (1982) 1231.
[9] Y. Ducommun, P. J. Nichols, L. Helm, L. I. Elding, A. E. Merbach, *J. Phys. (Orsay Fr.) 45 C8* (1984) 221.
[10] E. F. Caldin, M. W. Grant, B. B. Hasinoff, P. A. Tregloan, *J. Phys. E6* (1973) 349.
[11] A. Jost, *Ber. Bunsenges. Phys. Chem. 78* (1974) 300.
[12] R. Doss, R. van Eldik, H. Kelm, *Rev. Sci. Instrum. 53* (1982) 1592.
[13] H. Vanni, W. L. Earl, A. E. Merbach, *J. Magn. Reson. 29* (1978) 11.
[14] J. Jonas, D. L. Hasha, W. J. Lamb, G. A. Hoffman, T. Eguchi, *J. Magn. Reson. 42* (1981) 169.

[15] A. D. Kirk, G. B. Porter, *J. Phys. Chem. 84* (1980) 2998.
[16] W. Weber, R. van Eldik, H. Kelm, J. DiBenedetto, Y. Ducommun, H. Offen, P. C. Ford, *Inorg. Chem. 22* (1983) 623, and references cited therein.
[17] R. van Eldik in M. Twigg (Ed.): *Mechanisms of Inorganic and Organometallic Reactions, Vol. 3,* Plenum, New York 1985, p. 399.
[18] T. W. Swaddle in D. B. Rorabacher, J. F. Endicott (Eds.): *Mechanistic Aspects of Inorganic Reactions (ACS Symp. Ser. 198)* 1982, p. 39.
[19] A. E. Merbach, *Pure Appl. Chem. 54* (1982) 1479.
[20] E. F. Caldin, M. W. Grant, B. B. Hasinoff, *J. Chem. Soc. Faraday Trans. 1 68* (1972) 2247.
[21] R. Doss, R. van Eldik, *Inorg. Chem. 21* (1982) 4108.
[22] R. Mohr, L. A. Mietta, Y. Ducommun, R. van Eldik, *Inorg. Chem. 24* (1985) 757.
[23] R. Mohr, R. van Eldik, *Inorg. Chem. 24* (1985) 3396.
[24] P. J. Nichols, Y. Ducommun, A. E. Merbach, *Inorg. Chem. 22* (1983) 3993.
[25] E. L. J. Breet, R. van Eldik, *Inorg. Chem. 23* (1984) 1865.
[26] M. Kotowski, R. van Eldik, Inorg. Chem., in press.
[27] L. Helm, L. I. Elding, A. E. Merbach, *Helv. Chim. Acta 67* (1984) 1453.
[28] L. Helm, L. I. Elding, A. E. Merbach, *Inorg. Chem. 24* (1985) 1719.
[29] D. A. Palmer, R. Schmidt, R. van Eldik, H. Kelm, *Inorg. Chim. Acta 29* (1978) 261.
[30] E. L. J. Breet, R. van Eldik, H. Kelm, *Polyhedron 2* (1983) 1181.
[31] F. K. Meyer, W. L. Earl, A. E. Merbach, *Inorg. Chem. 18* (1979) 888.
[32] A. Hoiki, S. Funahashi, M. Tanaka, *Inorg. Chim. Acta 76* (1983) L151.
[33] H.-T. Macholdt, R. van Eldik, *Transition Met. Chem. (Weinheim, FRG.) 10* (1985) 323.
[34] H.-T. Macholdt, R. van Eldik, G. R. Dobson, *Inorg. Chem. 25* (1986) 1914.
[35] G. Schmidt, H. Elias, R. van Eldik, unpublished results.
[36] Y. Kitamura, R. van Eldik, H. Kelm, *Inorg. Chem. 23* (1984) 2038.
[37] Y. Kitamura, R. van Eldik, C. R. Piriz Mac-Coll, Inorg. Chem., in press.
[38] J. P. Candlin, J. Halpern, *Inorg. Chem. 4* (1965) 1086.
[39] R. van Eldik, D. A. Palmer, H. Kelm, *Inorg. Chim. Acta 29* (1978) 253.
[40] R. van Eldik, *Inorg. Chem. 21* (1982) 2501.
[41] D. R. Stranks, *Pure Appl. Chem. 38* (1974) 303.
[42] S. Wherland, *Inorg. Chem. 22* (1983) 2349.
[43] P. Braun, R. van Eldik, *J. Chem. Soc. Chem. Commun. 1985,* 1349.
[44] R. van Eldik, H. Kelm, *Inorg. Chim. Acta 73* (1983) 91.
[45] I. Krack, R. van Eldik, *Inorg. Chem., 25* (1986) 1743.
[46] G. A. Lawrance, D. R. Stranks, *Acc. Chem. Res. 12* (1979) 403.
[47] P. L. Kendall, G. A. Lawrance, D. R. Stranks, *Inorg. Chem. 17* (1978) 1166.
[48] D. R. Stranks, N. Vanderhoek, *Inorg. Chem. 15* (1976) 2639.
[49] G. A. Lawrance, S. Suvachittanont, *Aust. J. Chem. 33* (1980) 1649.
[50] W. G. Jackson, G. A. Lawrance, P. A. Lay, A. M. Sargeson, *Inorg. Chem. 19* (1980) 904.
[51] W. Rindermann, R. van Eldik, *Inorg. Chim. Acta 68* (1983) 35.
[52] U. Spitzer, R. van Eldik, H. Kelm, *Inorg. Chem. 21* (1982) 2821.
[53] D. J. A. de Waal, T. I. A. Gerber, W. J. Louw, R. van Eldik, *Inorg. Chem. 21* (1982) 2002.
[54] R. van Eldik, D. A. Palmer, *J. Solution Chem. 11* (1982) 339.
[55] R. C. Neuman, G. A. Binegar, *J. Am. Chem. Soc. 105* (1983) 134.
[56] R. C. Neuman, G. D. Lockyer, *J. Am. Chem. Soc. 105* (1983) 3982.
[57] R. van Eldik, H. Kelm, M. Schmittel, C. Rüchardt, *J. Org. Chem. 50* (1985) 2998.
[58] M. J. Sisley, W. Rindermann, R. van Eldik, T. W. Swaddle, *J. Am. Chem. Soc. 106* (1984) 7432.
[59] J. DiBenedetto, P. C. Ford, *Coord. Chem. Rev. 64* (1985) 361.
[60] L. H. Skibsted, W. Weber, R. van Eldik, H. Kelm, P. C. Ford, *Inorg. Chem. 22* (1983) 541.
[61] W. Weber, R. van Eldik, *Inorg. Chim. Acta 85* (1984) 147.
[62] W. Weber, J. DiBenedetto, H. Offen, R. van Eldik, P. C. Ford, *Inorg. Chem. 23* (1984) 2033.
[63] W. Weber, R. van Eldik, *Inorg. Chim. Acta, 111* (1986) 129.
[64] W. Weber, H. Maecke, R. van Eldik, Inorg. Chem., in press.
[65] G. Stochel, R. van Eldik, Z. Stasicka, Inorg. Chem., in press.
[66] R. van Eldik (Ed.): *Inorganic High Pressure Chemistry: Kinetics and Mechanisms,* Elsevier, Amsterdam 1986, 448 pp.
[67] M. V. Twigg, *Inorg. Chim. Acta 24* (1977) L84.
[68] J. C. Phillips, *J. Chem. Phys. 81* (1984) 478.
[69] J. C. Phillips, *J. Phys. Chem. 89* (1985) 3060.

Indirect Electroorganic Syntheses— A Modern Chapter of Organic Electrochemistry

New Synthetic Methods (59)

By Eberhard Steckhan*

The electrochemical formation and regeneration of redox agents for organic syntheses (*indirect electrolysis*) widens the potential of electrochemistry, as higher or totally different selectivities can often be obtained while at the same time the energy input can be lowered significantly. Higher current densities can also be obtained by preventing otherwise often encountered electrode inhibition. New types of redox catalysts can be formed in-situ and can be regenerated after reaction with the substrates. This principle is of increasing importance also for the application of already known redox agents with regard to environmental protection, since large amounts of a product can be generated in a closed circuit using only relatively small amounts of the redox reagent. Consequently the operation of such a process can be greatly simplified, and the release of ecologically objectionable spent reagents into the environment can be prevented. The broad spectrum of redox catalysts currently in use includes, inter alia, metal salts in very low or high oxidation states, halogens in various oxidation states, and, in particular, a wide variety of transition-metal complexes. A great deal of progress has recently been made in the application of organic electron transfer agents, since compounds have been found that are sufficiently stable in both the reduced as well as the oxidized state.

1. Introduction

In organic syntheses electrochemical reductions and oxidations offer numerous advantages over conventional methods: mild reaction conditions, which often guarantee a high selectivity; independence of a chemical redox reagent, which leads to a drastic reduction of environmental problems; better use of raw materials; easier isolation of products; simplification of continuous processing. One method that occupies a position between direct electrochemical and homogeneous-chemical redox processes and which under ideal conditions combines the advantages of both procedures is indirect electrolysis. Although at one stage almost forgotten this method has a long tradition,[1] and in some cases has found industrial application.[2,3] For example, one of the earliest electroorganic syntheses to be employed on an industrial scale was the oxidation of glucose to gluconic acid with bromide as redox catalyst [Eq. (1)]. In this process the bromine that is released at the anode is the oxidizing agent.[2]

$$2C_6H_{12}O_6 + CaCO_3 + H_2O \xrightarrow[\text{anode}]{Br^{\ominus}} Ca(C_6H_{11}O_7)_2 + CO_2 + 2H_2 \quad (1)$$

As shown in Figure 1, the indirect electrolysis combines a heterogeneous step (the production and regeneration of the redox catalyst (Med = mediator) in its active form) with the homogeneous redox reaction of Med and the substrate RH.

This electrochemical method has recently experienced a sudden revived interest,[4-10] stimulated in particular by its advantages in diminishing environmental hazards, lowering energy consumption, and, last but not least, by its ability to make extremely high selectivities possible. Moreover, the inhibition of the heterogeneous electron transfer that is often encountered in direct electrochemical processes can also be prevented by mediator-catalyzed electrochemical reactions, thus making useful current densities possible. The purpose of this article is not to summarize the scope and limitations of an already exhausted reaction principle, but rather to outline the changes and prospects of a field that is still developing and to encourage participation in its evolution and in the exploitation of its potential.

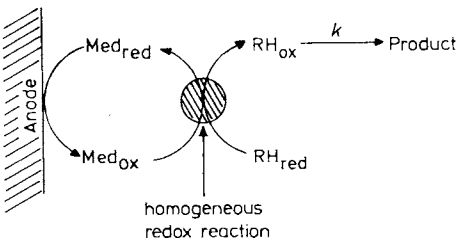


Fig. 1. The principle of indirect electrolysis exemplified by an oxidation.

2. Basic Principles

2.1. The Principle of Indirect Electrolysis

Indirect electrochemical processes are, in a certain sense, hybrids: They combine an electrochemical and therefore heterogeneous electron transfer reaction with a homogeneous redox process. The redox agent reacts with the substrate in a homogeneous reaction and is subsequently regenerated in its active form at the electrode (see Fig. 1).

The electrochemical regeneration can be performed in three different ways:[3,6,11] The most well known[12] consists

[*] Prof. Dr. E. Steckhan
Institut für Organische Chemie und Biochemie der Universität
Gerhard-Domagk-Str. 1, D-5300 Bonn 1 (FRG)

in separating and isolating the redox agent, which has been converted in the chemical reactor, and in regenerating it *externally* in an electrolysis cell. This so called "ex-cell" method[3,6] (see Fig. 2) possesses the following advantages:[7,13] chemical and electrochemical steps can be optimized independently of each other and neither substrates nor products can adversely affect the electrode reaction, nor can the electrode interfere with the homogeneous reaction. Despite this method being technically complicated most of the processes used on an industrial scale are two-stage processes of this kind, like, e.g. the external regeneration of chromic acid.

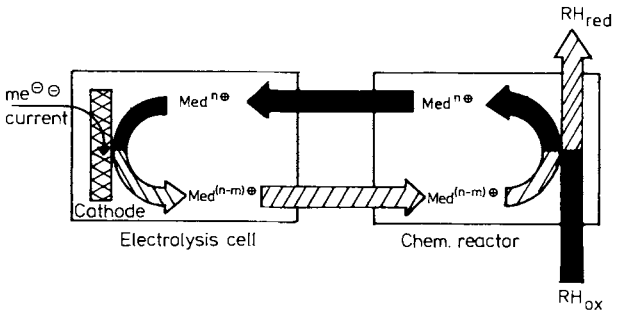


Fig. 2. Principle of indirect electrochemical synthesis with external regeneration of the redox catalyst ($Med^{(n-m)\oplus}$) exemplified by a reduction.

A second way of electrochemical regeneration consists in the continuous *internal* electrochemical retransformation of the electron transfer agent into its active form without isolating it, i.e. within the reaction vessel ("in-cell" process, Fig. 3).[3,6] The electron transfer agent, often also called mediator, that is inserted between electrode and substrate undergoes a homogeneous chemical reaction with the substrate and is subsequently regenerated at the electrode. Thus, it serves as a catalyst for the electron transfer between electrode and substrate.

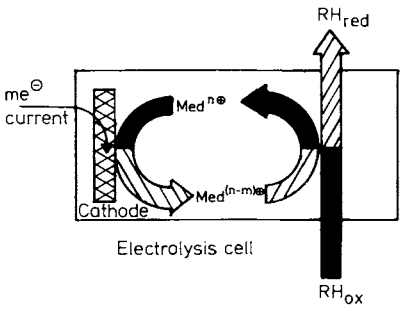


Fig. 3. Principle of indirect electrochemical synthesis with internal regeneration of the redox catalyst ($Med^{(n-m)\oplus}$) exemplified by a reduction.

Because of the coupling of two very different reactions in one reactor, however, the one-step process is much more difficult to realize than the two-step process, since conditions have to be found under which the organic substrates, reactive intermediates, and products do not hinder the electrochemical regeneration of the reagent or they themselves are not attacked electrochemically. That is why this method has only recently found more successful application. Aside from the advantage of lower investment costs, it is of great importance for the industrial application of this method that a continuous reaction processing is facilitated, since the products can be separated from catalytic amounts of the redox reagent far more easily than from an excess of reagent. It is, however, more advantageous if the process can be carried out in a two-phase system in which the product concentrates in the substrate phase.[14-16]

In the third type of indirect electrolysis the redox agent that is formed at the electrode does not react homogeneously in the solution, but remains fixed at the electrode surface, where it is continuously regenerated. Such an activation of the electrode surface can, on the one hand, take place "in-situ" by the continuous regeneration of the redox agent in its active form on the electrode surface during the electrolysis. This is the situation, e.g., both in the case of the nickel(III) oxide-hydroxide electrode, which is formed in alkaline medium during anodic polarization of a nickel electrode, and which is especially suited for the oxidation of primary alcohols to carboxylic acids and of primary amines to nitriles,[17] and in the case of the amalgam electrode, which is formed in the reduction of sodium or tetraalkylammonium salts at mercury cathodes and can, for example, be employed for the hydrodimerization of activated olefins.[5,18] On the other hand, the electrode can be chemically modified first by fixation of the redox catalyst to the electrode surface by adsorption, polymeric coating, or covalent binding. As the stability of such electrodes is not yet satisfactory enough for preparative purposes, and as this aspect of indirect electrochemical processes has already been extensively reviewed elsewhere,[19-23] it will not be discussed any further here.

2.2. The Redox Catalyst

The redox catalyst holds a key position in indirect electrolysis since it is involved in both the heterogeneous as well as the homogeneous redox reaction. To be suitable for both types of reactions the mediators must fulfill the following conditions:

1. Both reduced and oxidized forms must be chemically stable. Even a slight side-reaction to give compounds no longer convertible into the active form leads to a rapid loss of catalytic activity.
2. Electron exchange with the electrode and reaction with the substrate must be fast and as reversible as possible, otherwise larger and therefore more expensive electrode surfaces are necessary. In addition, side reactions are often favored.
3. Redox reactions with other than the desired compounds, for instance with the solvent, must not take place or must be suppressed.
4. Both redox states must be sufficiently soluble in the chosen supporting electrolyte (exception: two-phase systems).

Inorganic ions, metal salts and some metal complexes usually fulfill the condition of chemical stability more easily than organic mediators, however the electron transfer is often too slow, as it is in many cases connected with a change in the complex structure. On the other hand, metal

ions often have the advantage of moderating the reactivity of intermediates that are formed during the electron transfer by coordination or complexation and thereby enable specific and selective reactions. Moreover, in the case of transition metal complexes, the redox potential can easily be influenced by choice of the central atom or the ligands.

Organic mediators in their active form, e.g. as radical ions, are sometimes not sufficiently stable in many media. They often react irreversibly with the solvent, with the electrolyte, or with the intermediates that are formed during the redox reaction. The number of stable organic electron transfer agents is therefore limited and their availability is often restricted to certain electrolytes. Nevertheless, great progress has been made in this field recently.

In principle the redox catalysts can be classified into two groups according to the reaction mechanisms they undergo in the homogeneous redox step.

Mechanism A: The homogeneous redox reaction consists of a pure electron transfer. Such a process is called "redox catalysis" in its more stricter sense by *Savéant* et al.,[28] while *Shono*[8] has coined the expression "homomediatory system". This mechanism is represented schematically in equations (2) to (4). The radical anions and cations of aromatics, heteroaromatics and triaryl amines, for example, fall into this category of redox catalysts.

$$\text{Med} \xrightarrow[-e]{\text{anode}} \text{Med}^{\odot\oplus} \tag{2}$$

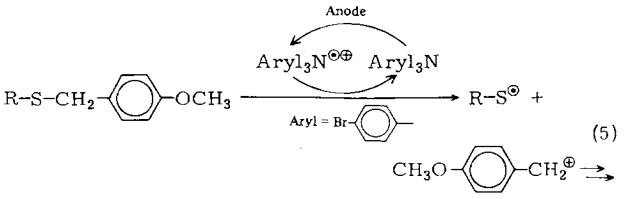
$$\text{Med}^{\odot\oplus} + \text{RH} \underset{\text{ET}}{\overset{K}{\rightleftharpoons}} \text{Med} + \text{RH}^{\odot\oplus} \tag{3}$$

$$\text{RH}^{\odot\oplus} \xrightarrow[\text{e.g. } -\text{H}^{\oplus}]{k} \text{R}^{\odot} \longrightarrow \longrightarrow \text{products} \tag{4}$$

ET = electron transfer

Electrode reactions that are often characterized by irreversible, i.e. slow electron transfer, can in this way be accelerated, and the more or less large overvoltages, that occur especially in conversions on a preparative scale, can be removed.[25] Hence, not only is the energy consumption thereby reduced but also the selectivity increased. With this type of reaction, electron transfer reactions in solution can often be carried out even with redox reagents whose potentials are up to 600 mV lower than the electrode potentials of the substrates. These redox reactions "opposite to the standard potential gradient"[25-27] can take place if a thermodynamically unfavorable electron transfer equilibrium [Eq. (3)] is followed by a fast and irreversible reaction step [Eq. (4)] that removes the product of the electron transfer from the equilibrium. In this case the overall reaction rate is determined by the equilibrium constant K, i.e. by the difference between the standard potentials of the partners of the redox step, and by the rate constant k of the follow-up reaction. In addition to the advantage of lowering the potential, which is accompanied by a gain in energy and selectivity, the number of the transferred electrons can be controlled by choice of the redox catalyst.

Decisive for the selectivity of the reaction are the potential differences between the various functional groups of the substrate and the mediator, as are also the rates of the respective chemical follow-up reactions. A typical example of such a reaction is the oxidative cleavage of a carbon-sulfur bond in *p*-methoxybenzyl sulfides with tris(*p*-bromophenyl)amine as mediator [Eq. (5)].[189]



(5)

The reductive and oxidative power, respectively, of the mediators and acceptors generated at low potentials can be enhanced by photochemical excitation during the electrochemical generation,[29,30] since a higher molecular orbital is occupied thereby, and an electron gap is generated in a lower orbital. The principle of this type of reaction is outlined in the following equations for an oxidation.

$$\text{Med} \xrightarrow[-e^{\ominus}]{\text{anode}} \text{Med}^{\odot\oplus} \tag{2}$$

$$\text{Med}^{\odot\oplus} \xrightarrow{h\nu} [\text{Med}^{\odot\oplus}]^{*} \tag{6}$$

$$[\text{Med}^{\odot\oplus}]^{*} + \text{RH} \underset{}{\overset{\text{ET}}{\rightleftharpoons}} \text{Med} + \text{RH}^{\odot\oplus} \tag{7}$$

$$\text{RH}^{\odot\oplus} \xrightarrow[\text{e.g. } -\text{H}^{\oplus}]{} \text{R}^{\odot} \longrightarrow \longrightarrow \text{products} \tag{4}$$

Mechanism B: The homogeneous redox reaction is combined with a chemical reaction, for instance a hydrogen or hydride atom abstraction. In the terminology of *Savéant* et al.[28] this process is referred to as "chemical catalysis", while *Shono*[8] speaks of a "heteromediatory system." The following equations illustrate the principle of this type of reaction for a hydrogen abstraction (oxidation).

$$\text{Med} \xrightarrow[-e^{\ominus}]{\text{anode}} \text{Med}^{\odot\oplus} \tag{2}$$

$$\text{Med}^{\odot\oplus} + \text{RH} \longrightarrow \text{MedH}^{\oplus} + \text{R}^{\odot} \tag{8}$$

$$\text{MedH}^{\oplus} + \text{B} \longrightarrow \text{Med} + \text{HB}^{\oplus} \tag{9}$$

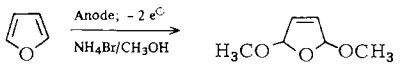
$$\text{R}^{\odot} \longrightarrow \longrightarrow \text{products} \tag{10}$$

B = base

If transition metal compounds are employed as redox catalysts, mechanism A can be regarded as outer-sphere and mechanism B as inner-sphere electron transfer. Here, the chemical step [Eq. (8)] determines the selectivity of the reaction. In addition, substantially higher potential differences can be overcome, as the chemical step [Eq. (8)] is not directly dependent upon the potential of the mediator.

The problem is, however, to find a chemical follow-up reaction in accord with equation (9) that can make the reagent electrochemically regenerable. In the case of organometallic reagents this is usually not easy to achieve, as mostly a ligand exchange has to occur first.[31,32] Some of the most frequently used redox catalysts in this category besides transition metal ions are halogen cations, hypohal-

ite ions, and molecular halogen, which are electrochemically generated from halide ions.[8] One of the oldest reactions, which is also used on an industrial scale, is the anodic methoxylation of furan in the presence of bromide ions [Eq. (11)].[33]



(11)

3. Indirect Electrochemical Syntheses with Inorganic and Organometallic Redox Catalysts

The largest group of inorganic redox catalysts comprises metal ions, especially transition metal ions, and their complexes. These reagents are often capable of undergoing selective redox reactions with a large number of organic substrates. By simply varying the reaction conditions a large variety of products can be obtained, since such redox processes are usually not simple electron transfer reactions. Rather, the substrates, reactive intermediates, or intermediate products are generally linked to the metal atom by complexation, coordination, or even by bond formation, so that their reactivity is reduced, and the selectivity thereby enhanced (mechanism B, Section 2.2).

In most cases the use of these reagents is reasonable from an economic and ecological point of view only if the redox catalysts can be regenerated. Regeneration by means of chemical reducing or oxidizing agents such as $LiAlH_4$ or $[Fe(CN)_6]^{3\ominus}$ is no solution, since it merely shifts the problem to another stage. Consequently, attempts were already made at a relatively early date to find ways of electrochemically regenerating the redox agents. In principle, it should be possible in all cases to use indirect electrolysis instead of stoichiometric amounts of inorganic redox agents. Prerequisite, however, is that the number of regenerative cycles is large and the current yield for the generation of the reagent remains constant at an acceptable order of magnitude over a long period of time.[13,24] Otherwise, the energy consumption is too high. But even in those cases where indirect electrolysis is more expensive than the comparable non-electrochemical process, the electrochemical regeneration can still be economically attractive, that is when a recycling of the reagent solution is necessary for ecological reasons, e.g. in the electrochemical recovery of chromic acid.[35]

In the meantime, results of electrochemical regeneration have been documented for the following inorganic oxidizing agents: Cr^{VI}-, Ce^{IV}-, Mn^{III}-, V^{V}-, Fe^{III}-, Hg^{II}-, Pd^{II}-, Tl^{III}-, Ag^{II}-, Os^{VIII}-compounds, $[Fe(CN)_6]^{3\ominus}$, Ru^{IV}-complexes, RuO_4, as well as the nonmetallic ions $BrO^{\ominus}$, $ClO^{\ominus}$, $IO_4^{\ominus}$, $I^{\oplus}$, $Br^{\oplus}$, $Cl^{\oplus}$, and the halogens I_2, Br_2 and Cl_2. The following electrochemically regenerated reducing agents have also been studied: Fe^{II}-, Ti^{II}-, Sn^{II}-, Sn^{II}-, V^{III}-, Cr^{II}-compounds, Pd^{0}-, Ni^{0}-, Ni^{I}-, Co^{I}-, Rh^{I}- and Fe^{0}-complexes, and the nonmetallic reagent $O_2^{\ominus\ominus}$. In addition, the alkali metal and alkaline earth metal amalgams[5,18] and solvated electrons fall into this category. An idea of the oxidative and reductive power of some of the redox agents can be gleaned from their standard potentials listed in Table 1.

Table 1. Standard redox potentials of some inorganic redox agents vs. the normal hydrogen electrode (NHE) [34].

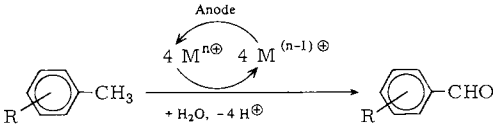
Reduction			E° [V]
$Co^{3\oplus} + e^{\ominus}$	⟶	$Co^{2\oplus}$	1.83
$Ce^{4\oplus} + e^{\ominus}$	⟶	$Ce^{3\oplus}$	1.61
$Mn^{3\oplus} + e^{\ominus}$	⟶	$Mn^{2\oplus}$	1.54
$MnO_4^{\ominus} + 8H^{\oplus} + 5e^{\ominus}$	⟶	$Mn^{2\oplus} + 4H_2O$	1.51
$RuO_4 + 4H^{\oplus} + 4e^{\ominus}$	⟶	$RuO_2 + 2H_2O$	1.39
$Cr_2O_7^{2\ominus} + 12H^{\oplus} + 6e^{\ominus}$	⟶	$2Cr(OH)^{2\oplus} + 5H_2O$	1.26
$MnO_2 + 4H^{\oplus} + 2e^{\ominus}$	⟶	$Mn^{2\oplus} + 2H_2O$	1.22
$Tl(OH)_3 + 3H^{\oplus} + 2e^{\ominus}$	⟶	$Tl^{\oplus} + 3H_2O$	1.19
$Fe^{3\oplus} + e^{\ominus}$	⟶	$Fe^{2\oplus}$	0.77
$OsO_4 + 2e^{\ominus}$	⟶	$OsO_4^{2\ominus}$	0.43
$Fe(CN)_6^{3\ominus} + e^{\ominus}$	⟶	$Fe(CN)_6^{4\ominus}$	0.36
$Sn^{4\oplus} + e^{\ominus}$	⟶	$Sn^{2\oplus}$	0.15
$Ti^{3\oplus} + e^{\ominus}$	⟶	$Ti^{2\oplus}$	−0.37
$V^{3\oplus} + e^{\ominus}$	⟶	$V^{2\oplus}$	−0.26
$Cr^{3\oplus} + e^{\ominus}$	⟶	$Cr^{2\oplus}$	−0.41
Cl_2 (sol.) $+ 2e^{\ominus}$	⟶	$2Cl^{\ominus}$	1.40
$ClO^{\ominus} + 2H^{\oplus} + 2e^{\ominus}$	⟶	$Cl^{\ominus} + H_2O$	1.70
$ClO_2 + 4H^{\oplus} + 5e^{\ominus}$	⟶	$Cl^{\ominus} + 2H_2O$	1.51
$HClO + H^{\oplus} + 2e^{\ominus}$	⟶	$Cl^{\ominus} + H_2O$	1.48
$ClO^{\ominus} + H_2O + 2e^{\ominus}$	⟶	$Cl^{\ominus} + 2OH^{\ominus}$	0.84
Br_2 (sol.) $+ 2e^{\ominus}$	⟶	$2Br^{\ominus}$	1.09
$BrO^{\ominus} + 2H^{\oplus} + 2e^{\ominus}$	⟶	$Br^{\ominus} + H_2O$	1.59
$HBrO + H^{\oplus} + 2e^{\ominus}$	⟶	$Br^{\ominus} + H_2O$	1.33
$BrO^{\ominus} + H_2O + 2e^{\ominus}$	⟶	$Br^{\ominus} + 2OH^{\ominus}$	0.76
$I_2 + 2e^{\ominus}$	⟶	$2I^{\ominus}$	0.62
$I^{\oplus} + 2e^{\ominus}$	⟶	$I^{\ominus}$	0.95
$IO^{\ominus} + 2H^{\oplus} + 2e^{\ominus}$	⟶	$I^{\ominus} + H_2O$	1.31
$3HIO + 3H^{\oplus} + 4e^{\ominus}$	⟶	$I_3^{\ominus} + 3H_2O$	1.21
$IO^{\ominus} + H_2O + 2e^{\ominus}$	⟶	$I^{\ominus} + 2OH^{\ominus}$	0.49

3.1. Oxidations with Metal Salts as Redox Catalysts

3.1.1. *Oxidation of Aromatics in the Side-Chain*

The electrochemical recovery of inorganic oxidizing agents such as Cr^{VI}-, V^{V}-, Ce^{IV}- and Co^{III}-, and, to a smaller extent, Ag^{II}-compounds for the side-chain oxidation of aromatics has been the subject of very intensive studies.

Synthesis of benzaldehydes and substituted benzaldehydes: The use of electrochemically regenerated Mn^{III}- and Ce^{IV}-compounds as "oxygen transfer agents" for the formation of benzaldehydes from the corresponding methyl substituted aromatics was proposed at a very early date and later reviewed by *Fichter*[1] [Eq. (12)]. With the ions $Mn^{3\oplus}$,[36,39,44,46] $Ce^{4\oplus}$,[7,37,38,41-43] or $Co^{3\oplus}$ as redox



(12)

catalysts for the oxidation of alkyl aromatics, only the two-step process with recycling of the electrolyte has so far led to acceptable results, whereas in the catalysis by $Ag^{2\oplus}$ ions internal regeneration is especially favored, since the cur-

rent yield is reduced drastically when higher concentrations of $Ag^{2\oplus}$ ions are produced.[40] In a fundamentally different way alkyl-substituted aromatics can also be oxidized in the benzylic position with Fenton's reagent that is formed in situ [Eq. (13)–(19)].[45]

$$\text{Cathode: } Fe^{3\ominus} + e^{\ominus} \longrightarrow Fe^{2\oplus} \quad (13)$$

$$\text{Cathode: } O_2 + 2e^{\ominus} + 2H^{\oplus} \longrightarrow H_2O_2 \quad (14)$$

$$Fe^{2\oplus} + H_2O_2 \longrightarrow Fe^{3\oplus} + {}^{\ominus}OH + {}^{\ominus}OH \quad (15)$$

$$Ph{-}CH_3 + {}^{\ominus}OH \longrightarrow Ph{-}\overset{\ominus}{C}H_2 + H_2O \quad (16)$$

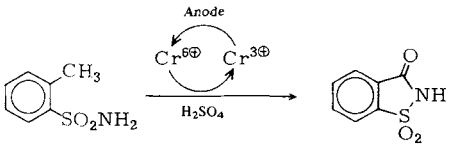
$$Ph{-}\overset{\ominus}{C}H_2 + O_2 \longrightarrow Ph{-}CH_2OO^{\ominus} \quad (17)$$

$$Ph{-}CH_2OO^{\ominus} \longrightarrow Ph{-}\overset{\oplus}{C}H{-}OOH \quad (18)$$

$$Ph{-}\overset{\oplus}{C}H{-}OOH + Fe^{2\oplus} \longrightarrow Ph{-}CHO + Fe^{3\oplus} + {}^{\ominus}OH \quad (19)$$

The redox pair $Fe^{2\oplus}/Fe^{3\oplus}$ can also be replaced by $V^{4\oplus}/V^{3\oplus}$ or $Cu^{2\oplus}/Cu^{\oplus}$.

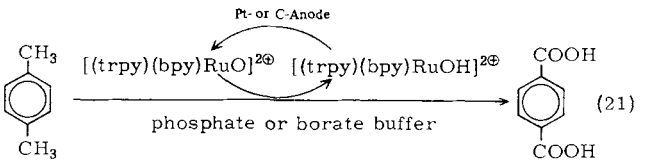
Synthesis of aromatic carboxylic acids: The oxidation of arylalkanes to arylcarboxylic acids with electrochemically regenerated chromic acid[47] has been studied intensively by *Kuhn* et al. in the case of the transformation of *o*-toluenesulfonamide to saccharin [Eq. (20)].[24,28] The yields are about 80%. The main problems encountered are the incomplete separation of the organic material and the poisoning of the lead dioxide electrode, which leads to a decrease in the current yields. These problems are not only met with in this particular case but are characteristic for all processes in which an external electrochemical regeneration of chromic acid takes part.



(20)

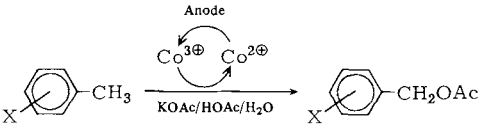
The indirect electrochemical oxidation of *p*-nitrotoluene[49,50] and 2,4-dinitrotoluene[51] to the corresponding nitrobenzoic acids and the transformations of toluene as well as *p*-xylene, *p*-toluic acid and *p*-tolualdehyde into benzoic acid and terephthalic acid[11,52–54], respectively, by electrochemically generated chromic acid have also been studied.

Recently, great hopes have been put on the use of Ru^{IV}-complexes as mediators for the oxidation of arylalkanes to carboxylic acids with internal electrochemical regeneration. Thus, with the electrochemically produced complex $[(trpy)(bpy)RuO]^{2\oplus}$ (trpy = terpyridine, bpy = bipyridine) it is possible to convert *p*-toluic acid and *p*-xylene into terephthalic acid [Eq. (21)] and toluene into benzoic acid.[75] The current yield is almost quantitative. After 100 cycles, 75% of the redox catalyst can still be recovered, which corresponds to an estimated number of 400 possible cycles.



(21)

Side-chain acetoxylations: The selective side-chain acetoxylation of arylalkanes with internal electrochemically generated cobalt^{III} acetate to give monoacetoxylated products was already patented in 1969[55] [Eq. (22)]. Further patents have recently been granted for procedures using Cu-, Fe-, Co-, Mn- and Pb-acetates as catalysts.[56,57]



(22)

3.1.2. Oxidations at the Aromatic Nucleus

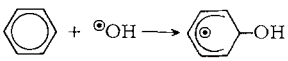
The oxidation of arenes to quinones, especially the oxidation of anthracene to anthraquinone, is usually performed with electrochemically regenerated Ce^{IV} or Cr^{VI}, even on an industrial scale,[2,3,58–60] but this method has lost importance since the development of catalytic processes. With regard to a hydroquinone synthesis, the oxidation of benzene to benzoquinone could be of industrial importance but the methods developed so far[40,61] are not yet competitive enough. Aside from the above-mentioned redox systems, Mn^{II} and Ag^{II} salts are also being investigated as catalysts.[62]

Another interesting application is the selective oxidation of benzene to phenol in the presence of iron salts, whereby the "in-situ" formation of Fenton's reagent is presumed to take place. Not only have reactions been studied in which hydrogen peroxide is added and the concentration of $Fe^{2\oplus}$ ions kept constant electrochemically[15] but also systems in which H_2O_2 is produced simultaneously at the cathode.[63–65] The addition of Cu^{II} salts is favorable, as $Cu^{2\oplus}$ ions are especially effective for the oxidation of carbon radicals [Eq. (23)–(29)]. A similar reaction sequence can also be achieved with the $Cu^{\oplus}/Cu^{2\oplus}$ redox pair alone.[66,67]

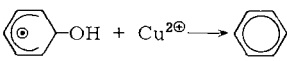
$$\text{Cathode: } Fe^{3\oplus} + e^{\ominus} \longrightarrow Fe^{2\oplus} \quad (23)$$

$$\text{Cathode: } O_2 + 2e^{\ominus} + 2H^{\oplus} \longrightarrow H_2O_2 \quad (24)$$

$$Fe^{2\oplus} + H_2O_2 \longrightarrow Fe^{3\oplus} + {}^{\ominus}OH + {}^{\ominus}OH \quad (25)$$

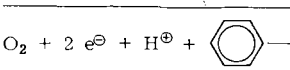


(26)



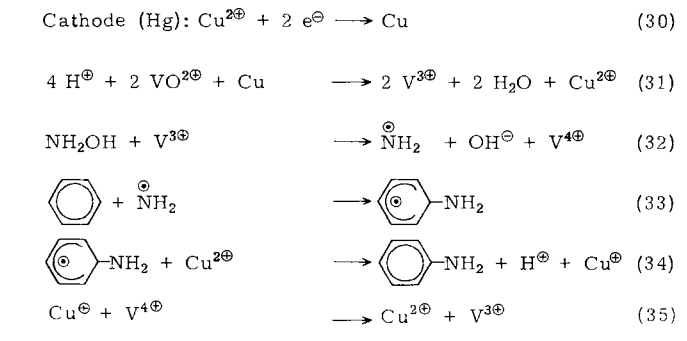
(27)

$$Cu^{\oplus} + Fe^{3\oplus} \longrightarrow Cu^{2\oplus} + Fe^{2\oplus} \quad (28)$$



(29)

Phenol is obtained with a current yield of 60%,[63] and a material yield of 64% with respect to hydrogen peroxide,[15] whereby it is especially favorable to perform the oxidation in a two-phase benzene/water system.[15] Chlorobenzene, fluorobenzene and benzonitrile have been hydroxylated in this way as well.[15] Fluorophenol is formed in particularly high yields (80% material yield; *o*/*p* = 85 : 15).

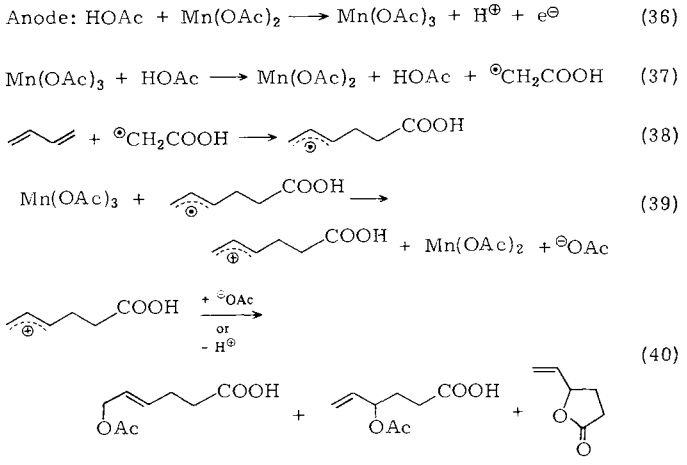


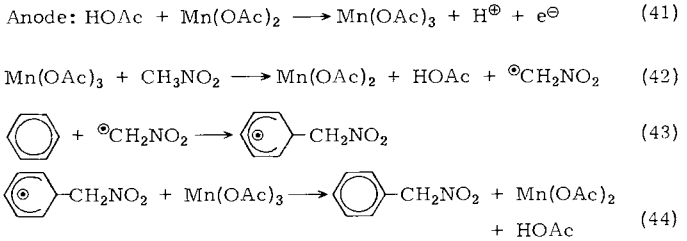
Aminations of aromatic compounds are possible in an analogous way by indirect electrochemical reduction of hydroxylamine [Eq. (30)–(35)].[68]

In a sulfuric acid/water/dioxane system, aniline is obtained from benzene with a 70% current yield and toluidines from toluene with a 50% current yield.

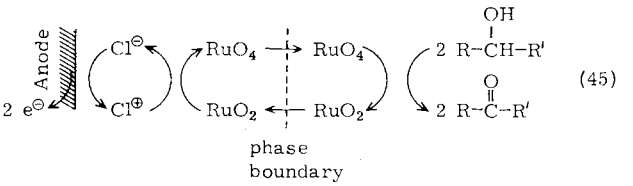
3.1.3. Oxidations with Electrochemically Generated Mn^{III}-, Ce^{IV}- or Ru^{VIII}-Compounds

The conversion of carbonyl compounds[69] and nitroalkanes[70] into carboxymethyl- [Eq. (37)] and nitromethyl-radicals [Eq. (42)], respectively, with Mn^{III}-salts is a preparatively very valuable method. These radicals are trapped by olefins such as 1,3-butadiene or by aromatics to give synthetically interesting products, whereby the in-situ regeneration of the $Mn^{3\oplus}$ ions is especially favorable. On the basis of this procedure a method was developed by Monsanto Co. for the synthesis of sorbic acid via γ-vinyl-γ-butyrolactone.[71,72] The decisive steps are summarized in equations (36)–(40). The nitromethylation of benzene can be carried out similarly [Eq. (41)–(44)][73] (current yield 78%).





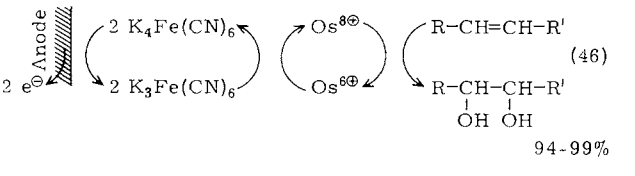
Electrochemically produced and regenerated Ce^{IV}-sulfate is employed for the cleavage of D-gluconic acid to D-arabinose.[74] The electrochemically generated complex $[(trpy)(bpy)RuO]^{2\oplus}$ already mentioned in Section 3.1.1 is capable of converting 2-propanol into acetone (current yield 100%) as well as of oxidizing ethanol to acetaldehyde or acetic acid.[75] *Torii* et al. recently reported on the internal electrochemical production and regeneration of RuO_4.[76] A double mediator system is used in this case. RuO_4 is not formed at the anode directly, but via reaction with "$Cl^{\oplus}$" ions derived electrochemically from $Cl^{\ominus}$ ions [Eq. (45)]. The reaction takes place in neutral medium in a two-phase system. Secondary alcohols furnish ketones (90%), 1,2-diols are cleaved to carboxylic acids (75%), 1,4- and 1,5-diols afford lactones (75%), and amines are oxidized to amides.



3.1.4. Olefin Oxidations with Electrochemically Generated Metal Salts as Redox Catalysts

Electrochemically produced Tl^{III}-, Pd^{II}-, Hg^{II}- and Os^{VIII}-compounds are especially suitable for indirect electrochemical olefin oxidations; these preferentially lead to formation of carbonyl compounds ($Tl^{3\oplus}$-,[77–80] $Pd^{2\oplus}$-,[81–83] $Hg^{2\oplus}$-ions[84,85]), diols ($Tl^{3\oplus}$-, $Os^{8\oplus}$-ions[86]), or carboxylic acids ($Hg^{2\oplus}$-,[84,85] $Ru^{4\oplus}$-ions[75]).

OsO_4 can be generated internally at the anode most favorably by a double mediator system [Eq. (46)].[86] With the redox catalyst $[(trpy)(bpy)RuO]^{2\oplus}$, allylic methylene groups are oxidized to keto-groups while allylic methyl groups are converted into carboxylic groups.[75]



3.2. Oxidations with Inorganic Anions as Redox Catalysts

Of the various mediator systems the halide ions are of special importance, for they have a broad spectrum of applicability. The molecular halogens, hypohalite ions, and halide cations formulated as oxidizing agents can be generated without problem by the "in-cell" method. As the redox reaction with these mediator systems is generally coupled with a chemical reaction (mechanism B, Section 2.2), very high potential differences between mediator- and substrate-redox systems can be overcome. Thus, secondary alcohols with oxidation potentials of about +2.8 V (vs. SCE) can be oxidized to ketones at +0.6 to +0.8 (vs. SCE) via

anodically generated $I^{\oplus}$-ions, which corresponds to a potential gain of about 2.0 V.[108]

The dimethoxylation of furan and its derivatives to 2,5-dimethoxy-2,5-dihydrofuran [see Eq. (11)][33,87,88] and the oxidation of aldoses to saccharic acids [see Eq. (1)][2,90,91] have achieved industrial importance. The anodic coupling of activated methylene components like malonic esters and β-keto esters in the presence of 0.01 mol-% potassium iodide,[89] in which the cathodic generation of metallic potassium can be used for the anionization of the methylene component, has also proven very successful [Eq. (47)–(51)].

Cathode: $2K^{\oplus} + 2e^{\ominus} \longrightarrow 2K$ (47)

Anode: $2I^{\ominus} \longrightarrow I_2 + 2e^{\ominus}$ (48)

Solution: $2K + 2CH_2X_2 \longrightarrow 2K^{\oplus} + 2\,^{\ominus}CHX_2 + H_2$ (49)

$2\,^{\ominus}CHX_2 + I_2 \longrightarrow X_2CH{-}CHX_2 + 2I^{\ominus}$ (50)

$2CH_2X_2 \longrightarrow X_2CH{-}CHX_2 + H_2$ (51)

The combination of this anode reaction with the cathodic hydrodimerization of acrylic acid esters[89] has also been the subject of numerous studies.

The synthesis of propylene oxide by way of heterogeneous catalysis has so far never been realized in satisfactory yield. Therefore the indirect electrochemical synthesis via intermediate formation of propylene chloro- or bromohydrin by anodically produced hypochlorite or hypobromite, respectively, was studied in great detail. The propylene halohydrins are saponified either externally or internally to propylene oxide by the sodium hydroxide formed at the cathode[92–94] [Eq. (52)–(57)]. This procedure, however, has not as yet been used on an industrial scale.

Anode: $2\,Br^{\ominus} \longrightarrow Br_2 + 2\,e^{\ominus}$ (52)

Cathode: $2\,H_2O + 2\,e^{\ominus} \longrightarrow H_2 + 2\,OH^{\ominus}$ (53)

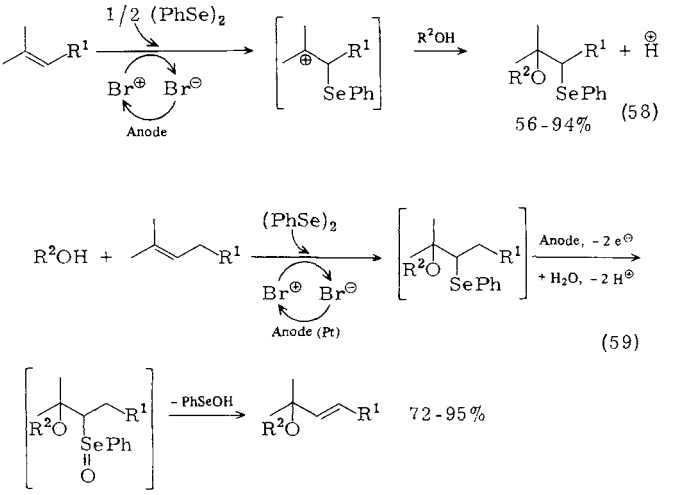
Solution: $Br_2 + H_2O \longrightarrow HOBr + HBr$ (54)

$H_3C{-}CH{=}CH_2 + HOBr \longrightarrow H_3C{-}\underset{OH}{CH}{-}CH_2{-}Br$ (55)

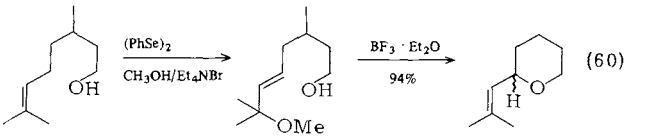
$H_3C{-}\underset{OH}{CH}{-}CH_2{-}Br + OH^{\ominus} \longrightarrow H_3C{-}\underset{O}{CH}{-}CH_2 + Br^{\ominus} + H_2O$ (56)

$H_3C{-}CH{=}CH_2 + H_2O \longrightarrow H_3C{-}\underset{O}{CH}{-}CH_2 + H_2$ (57)

Polyisoprenoids can be epoxidized regioselectively in the ω-position to functional groups in a similar way; in this case "$Br^{\oplus}$" ions are formulated as the oxidizing species.[95] Polymer bound mediators such as anion exchange resins in their bromide form can also be employed for the synthesis of epoxides.[96] The bromide ion-catalyzed anodic oxyselenation of olefins with diphenyl diselenide [Eq. (58)] made it possible to dispense with the use of positively charged selenating reagents like PhSeBr.[97] Under certain conditions even the oxyselenation-deselenation sequence can be carried out in one step [Eq. (59)].[98,99]

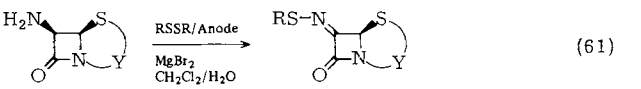


For example, an effective synthesis of D,L-rose oxide is based on this method [Eq. (60)].[98]

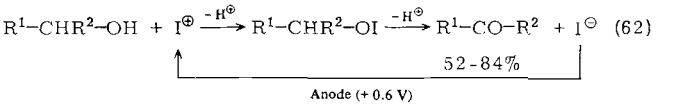


In a similar way carbonyl compounds can also be selenized in the α-position.[100]

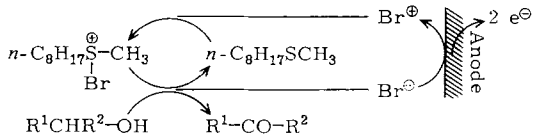
Indirect electrochemical oxidation with sodium bromide or iodide not only enables the formation of carbon-hetero atom bonds, but also of hetero-hetero atom bonds, e.g. the nitrogen-sulfur bond in sulfenimides,[101] the phosphorus-sulfur bond in phosphoric acid monothiol esters,[103] and the phosphorus-nitrogen bond in N-substituted phosphoramidates,[104] as well as the sulfur-nitrogen bond in sulfenimines. The latter bond formation is of special importance for the sulfenylation of penicillin and cephalosporin [Eq. (61)].[102]



Since the direct electrochemical conversion of simple aliphatic alcohols occurs only at potentials of far more than +2.0 V (vs. SCE), indirect electrolysis is of great importance here. With sodium bromide or potassium iodide as mediator, oxidations can already be performed at +0.6 V (vs. SCE). Thereby, secondary alcohols produce ketones, while primary alcohols mainly furnish esters [Eq. (62)].[16,105–109]



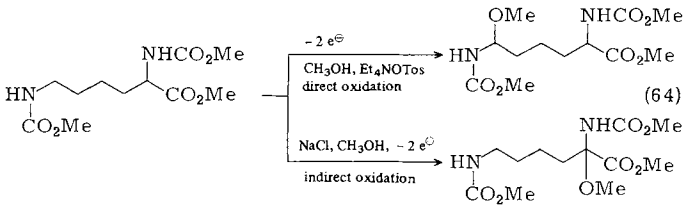
With the polymeric mediator poly-4-vinylpyridine hydrobromide it is possible to oxidize secondary hydroxyl groups selectively in the presence of primary ones.[107] The previously mentioned oxidation of alcohols with



(63)

$RuO_4/Cl^{\ominus}$[Section 3.1.3, Eq. (45)][76] is also possible with the double mediator system tetraethylammonium bromide and *n*-octylmethyl sulfide [Eq. (63)].[109] Primary amines can be converted into nitriles in an undivided cell with the system $NaBr/CH_3OH$.[110]

Methoxylation at the α-position to the nitrogen of an amide function can only be performed electrochemically in good yields, and affords valuable synthetic building blocks. This type of reaction is also possible by indirect electrolysis via catalysis by NaCl, but a decisively different regioselectivity is observed. This can be demonstrated quite neatly with a derivative of lysine methyl ester as example [Eq. (64)].[111]



(64)

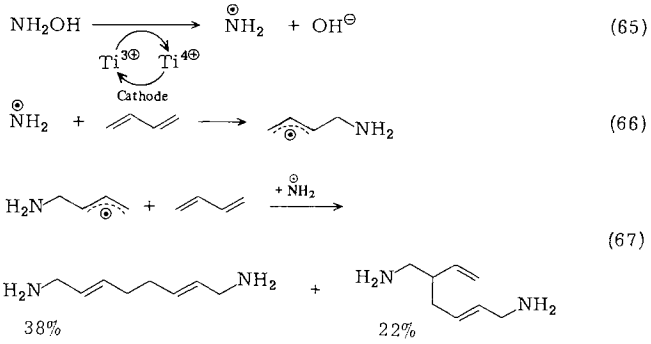
Indirect electrochemical oxidations with the nitrate ion proceed via the NO_3-radical and are suitable for the oxidation of secondary OH-groups[112] and of alkyl aromatic compounds in the side-chain.[113] The periodate regeneration has also been used on an industrial scale for the production of dialdehyde starch from starch[114] and has recently been employed for the generation of acetaldehyde from 2,3-butanediol.[115]

3.3. Reductions with Metal Salts and Metal Complexes as Redox Catalysts

3.3.1. Reductions by Electrochemically Produced Low-Valent Metal Ions and Base Metals

Low-valent metal ions such as $Ti^{3\oplus}$, $V^{3\oplus}$, $Sn^{2\oplus}$ and $Cr^{2\oplus}$ are common reducing agents for many organic compounds.[122,123] Their use in stoichiometric amounts, however, gives rise to problems, especially if they are to be used on an industrial scale. The most important problem is the removal of spent metal salts in such a way that the environment is not endangered. But also the chemical formation of the low-valent ions gives rise to problems, since the reducing agents have to be separated after conversion, thus making a continuous reaction impossible. One way of circumventing these problems is resort to the indirect electrochemical reaction, and the ever increasing number of publications relating to this approach bear witness of the great interest now being shown in this method.

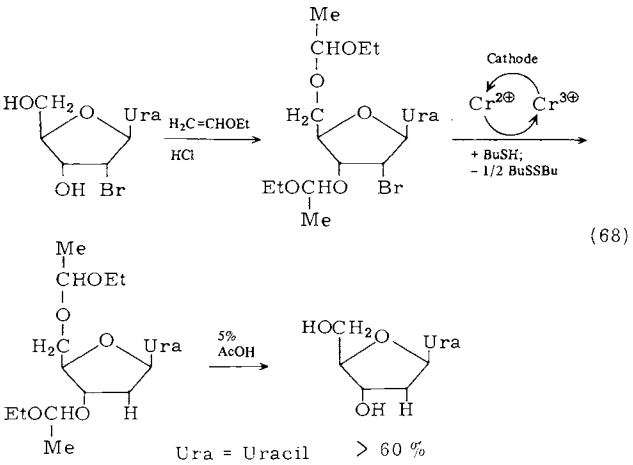
Thus, the reductive cleavage of hydroxylamine and its derivatives by electrochemically generated $Ti^{3\oplus}$- or $V^{3\oplus}$-ions with formation of aminyl radicals and hydroxide ions has been the subject of detailed investigations. The aminyl radical is preferably trapped with alkenes and aromatic compounds. Examples are the synthesis of aspartic acid from maleic acid[117] and of diamines with elongated chains from 1,3-butadiene [Eq. (65)–(67)].[116]



(65)
(66)
(67)

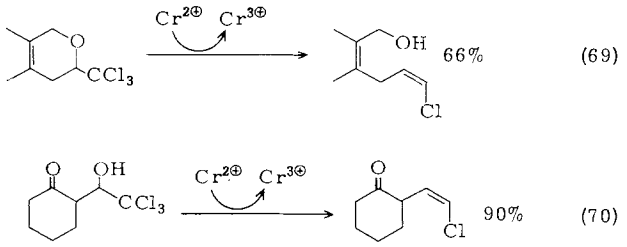
The reduction of aromatic nitro groups with electrochemically generated $Ti^{3\oplus}$ ions has also been investigated intensively, especially in India. Aniline derivatives can be generated in this way in high yields.[118–120] Because of the structure of the chemical industry in India this method evidently has some advantages compared with the otherwise conventional catalytic hydrogenation. Electrochemically produced $Sn^{2\oplus}$ ions are also used for the reduction of nitro groups. In the case of nitrobenzene the reduction can be stopped at the stage of phenylhydroxylamine,[121] which rearranges to *p*-aminophenol.

Cr^{II} reagents are known for their selectivity in organic reductions. With the in-situ formation and regeneration of Cr^{II}-chloride, allylic and benzylic halides could be coupled in anhydrous dimethylformamide (DMF) in yields comparable with those obtained by other coupling methods.[124] The dehalogenation of α-hydroxyhalides and their ethers can be realized in a similar way. The reagent, the ethylenediamine complex of $Cr(ClO_4)_2$, is electrochemically generated in moist dimethylformamide. Butanethiol acts as hydrogen donor for the trapping of the intermediate radicals.[125] To avoid elimination reactions, the α-hydroxyl group has to be protected. This method has proved to be a good alternative to the tributyltin hydride method for the synthesis of deoxynucleotides [Eq. (68)].

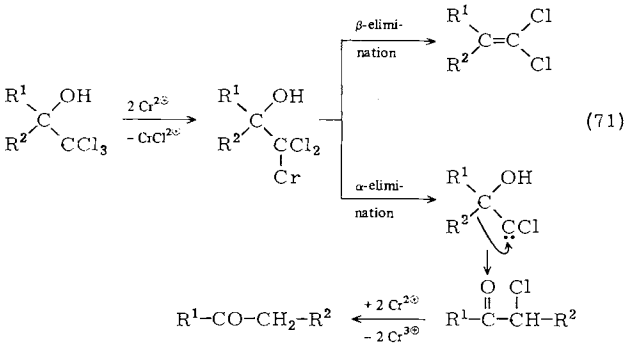


(68)

The α-trichloromethyl-substituted alcohols or ethers, which are readily accessible in a great structural variety, can be reduced to preparatively interesting products by $CrCl_2$ in water or water/DMF as electrolyte. In the case of secondary hydroxyl groups, the reaction leads to formation of (*Z*)-configurated alkenyl chlorides in one step [Eq. (69), (70)].[126] Should the alcohols have a hydroxyl group

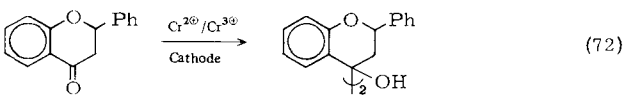


attached to a tertiary C-atom, then, depending on the reaction conditions, either formation of alkylidene dichlorides or rearrangement with formation of carbonyl compounds is preferred.[126]

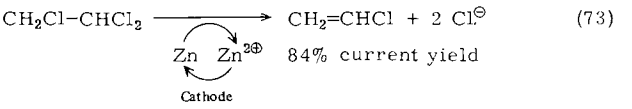


Geminal dibromocyclopropanes can be reduced to allenes in anhydrous DMF with externally generated and regenerated $Cr^{2\oplus}$ ions by an inner-sphere electron transfer mechanism.[127] If the reaction is carried out with internal regeneration, only monobromocyclopropanes are obtained via an outer-sphere electron transfer mechanism after the first regenerative cycle. This means that the Cr^{III} complex that is formed after the first conversion must contain different ligands than the originally employed chromium(III)-halogen dimethylformamide complex. Such problems also arise with other metal complexes as redox catalysts if the redox reaction proceeds via an inner-sphere electron transfer (mechanism B, Section 2.2).[31,32,128]

Electrochemically generated $Cr^{2\oplus}$ ions can even effect the pinacolization of otherwise unsatisfactorily dimerizing carbonyl compounds.[129,130] Here, the $Cr^{2\oplus}$ ions do not act as redox agent but catalyze the formation of a Cr^{III}-complex of the carbonyl compound, which is directly hydrodimerized at the cathode with formation of the pinacol. Thus, for instance, β-jonylideneacetaldehyde[129] and flavanone [Eq. (72)][130] can be pinacolized in 60% and 78% yield, respectively.

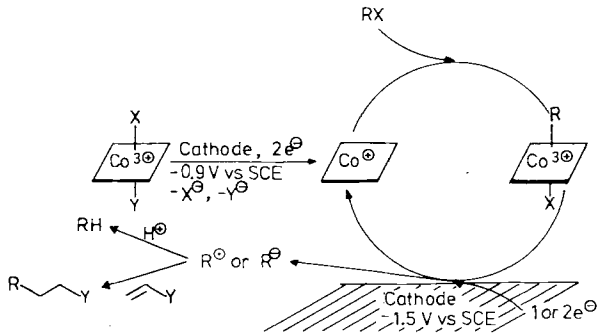


Suspensions of base metals can be generated at the cathode at high current densities (>0.5 A cm^{-2}) in two-phase systems. Since very small particles with oxygen-free surfaces are generated, the reactivity of these metal suspensions clearly surpasses that of the metals that are usually employed.[131,132] Thus, zinc, copper, iron, and tin powders have been generated in high current yields and have been used for the reduction of nitro compounds and halogenated hydrocarbons [Eq. (73)].



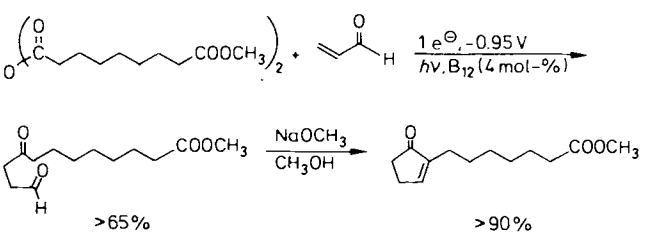
3.3.2. *Indirect Electrochemical Reductions with Transition Metal Complexes*

Transition metal complexes are finding increasing application as redox catalysts, especially for reductions. The cathodically generated active forms such as Ni^0-, Ni^I-, Co^I-, Sn^0-, Pd^0-, or Rh^I-complexes react with alkylating agents such as halides via oxidative addition. By electrochemical reduction of the alkyl complex the metal-carbon bond can be cleaved with regeneration of the active form of the complex. Such a catalytic cycle is presented in Scheme 1 for



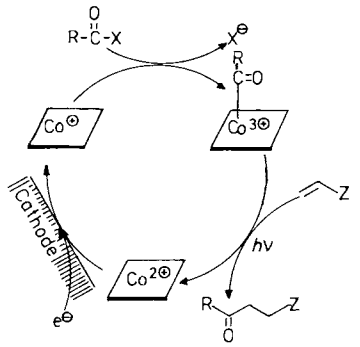
Scheme 1. Principle of the indirect electrochemical reduction of alkyl halides by a Co^I/Co^{III}-complex system.

cobalt complexes, such as vitamin B_{12}.[133] In the case of the alkylcobalt(III) complexes the reduction potential can be lowered to a value of -0.9 V (vs. SCE) by irridiation with visible light, so that the generally highly selective and specific reaction can proceed under very mild conditions.[133–136,139]



A particularly suitable catalyst is vitamin B_{12}, which not only catalyzes allyl halide coupling[141] and the dehalogenation of alkyl halides,[133,138,142] but is also excellently

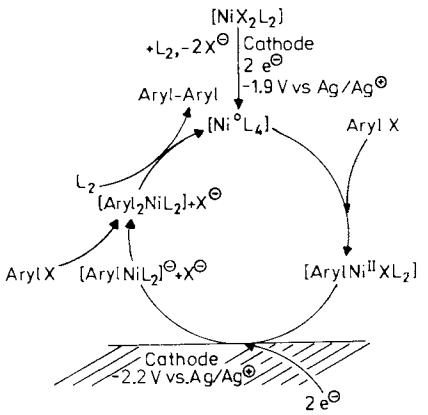
suited for the alkylation and acylation of Michael systems [Eq. (74)].[133, 134, 137] The latter proceeds via photochemically supported electrochemical cleavage of the intermediate acylcobalt(III) complex (Scheme 2).[135, 139]



Scheme 2. Nucleophilic acylation by photochemically supported electrochemical cleavage of acylcobalt(III) complexes (indirect electrochemical acylation).

This technique can be used for the synthesis of natural products such as optically active pheromones, 3-substituted steroids, cyclopentanoids, sugars, etc.[139, 140]

Ni^0-complexes can be used in a similar way as the Co^I-complexes. Thus, e.g., the formation of bisaryl by reduction of aryl halides with electrochemically generated Ni^0-complexes has been reported on in detail. The reaction mechanism, which closely resembles that presented for the cobalt system (Scheme 1), is reproduced in Scheme 3. The reaction involves the intermediates $[ArylNiXL_2]$, which react at the electrodes. Phosphanes have proved to be useful ligands.[31, 143, 144]

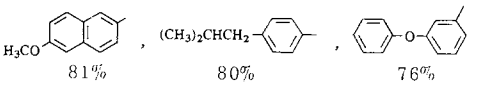


Scheme 3. Bisaryl formation via electrochemically generated and regenerated Ni^0-complexes ($L = PR_3$).

Poly-*para*-phenylenes are obtained on a preparative scale when aromatic dihalides are used as starting compounds.[148] The electrochemical generation and reduction of $[ArylNiXL_2]$ in the presence of CO_2 or $H_2C{=}CH_2$ leads to the formation of benzoic acids,[145] or 1,1-diarylethanes[147] and styrene derivatives.[146] Ni^0-complexes also catalyze the reductive carboxylation of 1-arylethyl halides to 2-arylpropionic acids.[145] In this way, the pharmaceutically effective 2-arylpropionic acids are accessible in high yields with cycle numbers of 20 to 40 for the catalyst [Eq. (75)].[145]

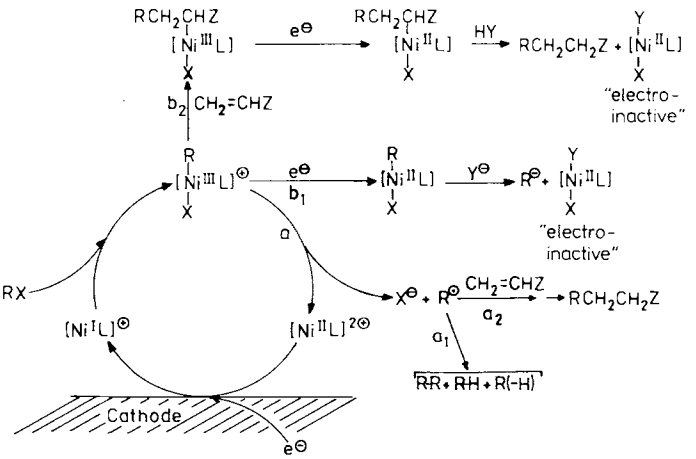
$$Aryl{-}CH(CH_3){-}Cl + CO_2 \xrightarrow[THF/HMPT/Bu_4NBF_4,\ +2\,e^{\ominus}]{NiCl_2/Ph_2P(CH_2)_3PPh_2/COD} Aryl{-}CH(CH_3){-}COOH \qquad (75)$$

COD = 1,5-cyclooctadiene, THF = tetrahydrofuran, HMPT = hexamethylphosphoric acid triamide



Aryl iodides and bromides can not only be reductively cleaved under catalysis by Ni^0-complexes but also by electrochemically generated and regenerated triphenylphosphanepalladium(0) complexes. Thus, bisaryls are obtained in material yields of 50–99%,[149] or, in presence of unsaturated compounds (styrene, 1,3-butadiene derivatives, phenyl acetylene), the products of ArH addition are obtained in yields of 20–78%.[150] The mechanism is in accordance with the one presented in Scheme 3, with palladium being substituted for nickel. Cycle numbers of 15 have been reported.

Besides phosphanenickel(0) complexes,[144] Ni^I-complexes are also suitable for the indirect electrochemical reduction of alkyl halides. They react via an organonickel(III) intermediate. The Ni^I-complexes are electrogenerated from the square planar Ni^{II}-complexes of macrocyclic quadridentate ligands[32, 151] (see Scheme 4).



Scheme 4. Reduction of alkyl halides in presence (a_2, b_2) and absence (a_1, b_1) of activated olefins by electrochemically produced and regenerated Ni^I-complexes of macrocyclic quadridentate ligands.

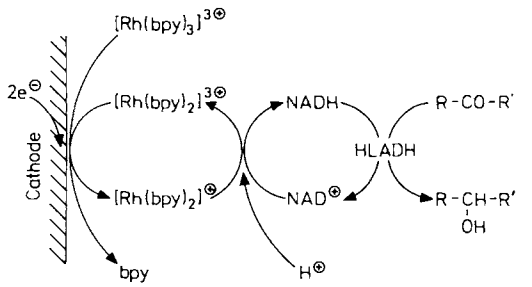
The stability of the newly formed nickel–carbon bond is decisive for the subsequent course of the reaction: If it is not very stable, the complex decomposes into an alkyl radical and the original Ni^{II}-complex (path a); the result is a large number of cycles. This is the case, e.g., with secondary and tertiary alkyl bromides. If the bond is relatively stable, however, as for instance in the case of primary alkyl bromides, the alkylnickel(III) complex is reduced to an alkylnickel(II) complex, which loses an alkyl anion and is

converted into an *electroinactive* Ni^{II}-complex (path b); the cycle number is accordingly low. The structure of the ligand also influences the lifetime of the organonickel(III) complex. Thus, a less stable complex is formed with [*N,N'*-ethylenebis(salicylideneiminato)]nickel(II) ([Ni(salen)]) than with (5,5,7,12,12,14-hexamethyl-1,4,8,11-tetraazacyclotetradecane)nickel(II) ($[Ni(teta)]^{2\oplus}$); hence, [Ni(salen)] favors the reaction via the radical path with high cycle numbers, even with primary alkyl bromides (path a). Primary halides essentially afford dimers (R–R), whereas disproportionation (R–H + R(–H)) predominates in the case of tertiary halides.

The organonickel(III) complex that is formed from alkyl bromides and the electrochemically generated $[Ni(teta)]^{\oplus}$ complex can undergo insertion reactions with added activated olefins via path b_2 (Scheme 4) thereby forming a new nickel-carbon bond. Further reduction leads to cleavage of the complex with release of the Michael adduct and a Ni^{II}-complex that is no longer "electroactive". The more labile Ni(salen) complex, on the other hand, yields the Michael adducts via the radical path a_2 with regeneration of the original Ni^{II}-complex. In this case the reaction is catalytic.[39, 152]

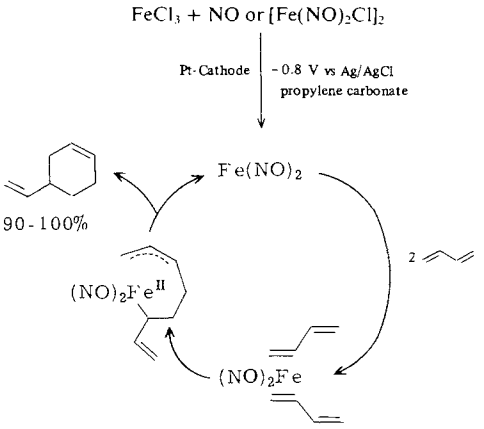
The electrochemical allylation of carbonyl compounds by electroreductive regeneration of a diallyltin reagent from allyl bromide and an Sn^0 compound leads in methanol or methanol/water to formation of homoallylic alcohols in yields of 70–90%.[153]

Using a cathodically generated and regenerated bis(bipyridine)rhodium(I) complex as two-electron transfer agent it was possible for the first time to achieve the nonenzymatically coupled selective regeneration of NADH from $NAD^{\oplus}$. The direct cathodic reduction leads mainly to NAD dimers while the indirect electrochemical reduction by the rhodium complex as two-electron transfer agent provides almost exclusively enzymatically active NADH, and only traces of dimers. If the reaction is carried out in presence of alcohol dehydrogenase, carbonyl compounds can be transformed into the respective alcohols in-situ (Scheme 5).[154] With 2,2'-bipyridine-5-sulfonic acid as ligand, the electrode covering that would be otherwise observed can be avoided and the reduction potential can be shifted in an positive direction by 200 mV to a value of −720 mV vs. Ag/AgCl. The result is complete prevention of NAD-dimer formation.[155]



Scheme 5. Regeneration of NADH from $NAD^{\oplus}$ by electrochemically generated $[Rh(bpy)_2]^{\oplus}$ as electron transfer agent.

Indirect electrolysis is very useful for the in-situ generation of transition metal catalysts. Following the basic studies carried out by ***Lehmkuhl*** et al.,[156] some very interesting results have emerged recently. Thus, dinitrosyliron(0) complexes can be generated electrochemically and used for the cyclodimerization of conjugated dienes (Scheme 6).[157, 158]



Scheme 6. Electrochemical generation and application of the dinitrosyliron(0) complex as catalyst for the cyclodimerization of conjugated dienes.

The C_4-fraction obtained in petroleum cracking can thus be used directly as substrate. In the case of butadiene, turnover rates of 20000 per hour can be achieved with complete selectivity regarding the formation of 4-vinylcyclohexene.

Highly active catalysts for olefin metathesis can be obtained in a similar way by electrochemical reduction of WCl_6 or $MoCl_5$ [Eq. (76)].[159] Since the oxidation state of the catalyst generated in this way can be stabilized by potential control, these reactions are very highly selective. Aluminum is used as anode material because it furnishes the required Lewis acid with formation of aluminum trichloride. Hydroformylation reagents can also be generated electrochemically.[160]

$$n\,e^{\ominus} + WCl_6 \xrightarrow[\text{Al-anode, } CH_2Cl_2]{\text{Pt-Cathode, } -0.9\text{ V vs SCE}} n\,Cl^{\ominus} + WCl_{(6-n)} \quad (76)$$

$WCl_{(6-n)}$ —(2-pentene)→ 2-butene + 3-hexene, 2160 cycles/h

4. Indirect Electrochemical Syntheses with Organic Redox Catalysts

The most important prerequisite for the suitability of a compound as mediator is its stability in all the oxidation states being passed through, otherwise a rapid loss in catalytic activity will take place. This condition is rarily fulfilled by organic molecules, as their active forms, mostly radical cations or anions, react irreversibly in many media. Only in recent years has there been a distinct increase in the number of known stable organic mediators. Thus, radical anions and dianions of mostly aromatic compounds have been used for reductions in aprotic solvents, whereas

viologens and violens are suitable as electron transfer agents for reductions in protic solvents; however, they can only be used at potentials of up to about -1.0 V.

For oxidations, the radical cations of compounds like 9,10-diphenylanthracene, thianthrene, phenoxathiine or dibenzodioxine are likely candidates as one-electron acceptors; however, because of their reactivity they can only be used in media of low nucleophilicity. Triarylamines behave differently, if their reactive *para*-positions are blocked by substituents from attack by nucleophiles. Thus, many of these triarylamine radical cations show an excellent stability even in solvents like methanol. Aside from pure electron transfer agents, other mediators are being employed that react by way of a hydrogen or hydride abstraction (mechanism B, Section 2.2). Methods for the theoretical treatment of the homogeneous redox catalysis of electrochemical reactions were mainly developed by *Savéant* et al.[165]

4.1. Reductions with Radical Anions and Dianions of Organic Compounds

Radical anions and dianions of a great number of organic compounds, mostly aromatics, have been tested as mediators for reductions. Table 2 gives an overview of the potentials of some organic mediators frequently used for reductions.

Table 2. Reduction potentials of common mediator systems.

Compound	$-E_{1/2}$[V] (vs. SCE)	Ref.	Compound	$-E_{1/2}$[V] (vs. SCE)	Ref.
Perylene	1.67	[a]	Methylbenzoate	2.17	[165]
Phthalonitrile	1.69	[165]	2,2'-Binaphthyl	2.21	[a]
4-Methoxybenzophenone	1.75	[165]	Benzonitrile	2.24	[165]
			Chrysene	2.25	[a]
9,10-Diphenylanthracene	1.85	[a]	*m*-Toluonitrile	2.27	[165]
			p-Toluonitrile	2.34	[165]
Anthracene	1.96	[a]	2-Methylnaphthalene	2.46	[a]
Phenanthridine	2.00	[165]	Phenanthrene	2.45	[a]
Benzo[*f*]quinoline	2.08	[165]	1,1'-Binaphthyl	2.45	[a]
Pyrene	2.09	[a]	Naphthalene	2.50	[a]
Benzo[*h*]quinoline	2.12	[165]	Biphenyl	2.70	[a]

[a] C. K. Mann, K. K. Barnes: *Electrochemical Reactions in Nonaqueous Systems*, Marcel Dekker, New York 1970.

Alkyl and aryl halides, sulfonates, sulfonamides, sulfones, sulfides, onium compounds and epoxides can be cleaved by electrochemical reduction with organic mediators at potentials that can be much more positive than those of the substrates. The driving force of this reaction opposite to the standard potential gradient[26] is generally the fast and irreversible cleavage of the carbon-hetero atom bond. The essential reaction steps (77)–(87) correspond to those that are also observed with sodium naphthalenide.

As products, either the hydrocarbons RH or the coupling products RR are obtained via the carbanions $R^{\ominus}$ or via the radicals $R^{\odot}$. Second order reactions of the radicals such as dimerizations or disproportionations [Eq. (81)] are, however, unlikely under the conditions of indirect electrolysis, since the radicals are formed in homogeneous solution and therefore occur only in low stationary concentrations. The coupling of the radicals $R^{\odot}$ with the radical anions of the mediators [Eq. (84)] results in the alkylation products $MR^{\ominus}$, which are either protonated (HMedR) or form the bisalkylation product RMedR. With naphthalene as mediator the following alkylation products could be identified:[161]

$$\text{Cathode Med} \overset{+e^{\ominus}}{\rightleftharpoons} \text{Med}^{\odot\ominus} \quad (77)$$

$$\text{Med}^{\odot\ominus} + \text{RX} \overset{\text{ET}}{\rightleftharpoons} \text{Med} + \text{RX}^{\odot\ominus} \quad (78)$$

$$\text{RX}^{\odot\ominus} \longrightarrow \text{R}^{\odot} + \text{X}^{\ominus} \quad (79)$$

$$\text{Med}^{\odot\ominus} + \text{R}^{\odot} \longrightarrow \text{R}^{\ominus} + \text{Med} \quad (80)$$

$$2\,\text{R}^{\odot} \longrightarrow \text{R}-\text{R or RH} + \text{R}(-\text{H}) \quad (81)$$

$$\text{R}^{\odot} + \text{SolvH} \longrightarrow \text{RH} + \text{Solv}^{\odot} \quad (82)$$

$$\text{R}^{\ominus} + \text{SolvH} \longrightarrow \text{RH} + \text{Solv}^{\ominus} \quad (83)$$

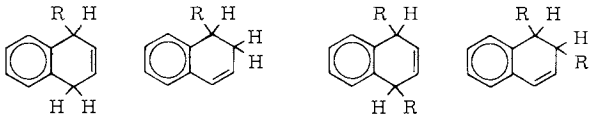
$$\text{Med}^{\odot\ominus} + \text{R}^{\odot} \longrightarrow \text{MedR}^{\ominus} \quad (84)$$

$$\text{MedR}^{\ominus} + \text{SolvH} \longrightarrow \text{HMedR} + \text{Solv}^{\ominus} \quad (85)$$

$$\text{MedR}^{\ominus} + \text{RX} \longrightarrow \text{RMedR} + \text{X}^{\ominus} \quad (86)$$

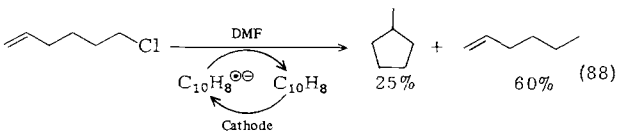
$$\text{R}^{\ominus} + \text{RX} \longrightarrow \text{RR} + \text{X}^{\ominus} \quad (87)$$

HMedR = monoalkylation product,
RMedR = dialkylation product of the mediator



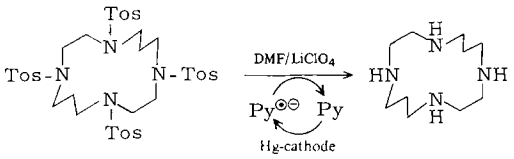
The indirect electrochemical cleavage of halides has been studied analytically in detail, especially by *Lund* and *Simonet* et al.[161–169] The course of the reaction strongly depends on the structure of the substrates. Thus, aryl and benzyl halides do not form alkylation products of the mediators, whereas these products dominate with aliphatic halides. In the latter case primary halides favor the formation of monoalkylation products, while tertiary halides favor the formation of dialkylation products. As a result of its alkylation, the mediator is naturally withdrawn from further reaction, so that stoichiometric amounts are required and the reaction sequence cannot be referred to as an "indirect electrolysis" in the fullest sense of the word. *Simonet* et al.[164] therefore coined the term "perturbed redox-catalysis".

In a number of cases the reductive halogen-hydrogen exchange has been studied on a preparative scale: If, for example, 6-chloro-1-hexene is reduced in the presence of naphthalene as redox catalyst, besides 1-hexene also methylcyclopentane is obtained as product of the radical cyclization [Eq. (88)].



(88)

Also the indirect reductive deblocking of tosylamide, tosyl ester, benzyloxycarbonyl, *o*-nitrobenzyloxycarbonyl, benzyl ester, and benzyl ether groups have been studied in

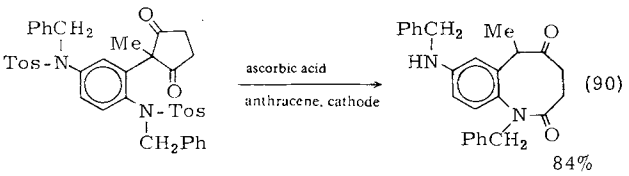


(89)

Py = Pyrene
Tos = *p*-toluene-sulfonyl

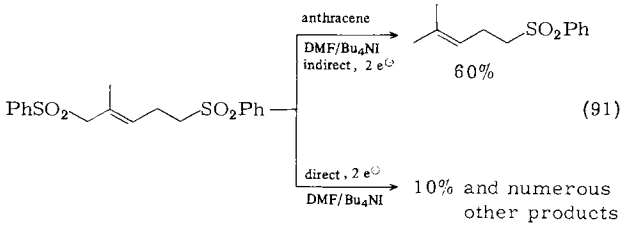
great detail.[26, 166-168] Thus, *Simonet* et al.[167] used pyrene as mediator for the release of polyaza-macrocycles from poly-*p*-toluenesulfonamides [Eq. (89)].

A very effective cleavage of a tosyl-nitrogen bond is apparently facilitated by the combined effect of the electrochemically generated anthracene radical anion as electron transfer agent with ascorbic acid as proton donor and additional reducing agent [Eq. (90)].[168]



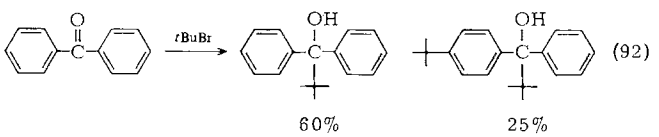
(90)

The indirect electrochemical cleavage of sulfones convincingly demonstrates that the selectivity of this method is superior to that of the direct electrolysis [Eq. (91)].[169]

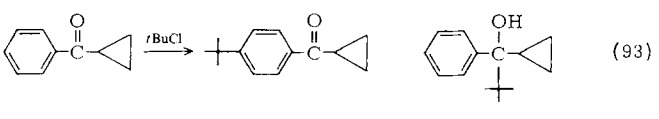


(91)

The perturbed redox catalysis, i.e. the mono- or bisalkylation of the electron transfer agent by the intermediary alkyl radicals [Eq. (77)-(79) and (84)-(86)], has been exploited for the production of arylalkanes that are difficult to obtain by Friedel-Crafts alkylation. The most suitable alkylating agent is *tert*-butyl chloride (or bromide),[161, 170-173] which can also be used for the alkylation of ketones. Tertiary alcohols and the compounds that are alkylated exclusively or additionally in the aryl moiety are formed [Eq. (92), (93)].[174]



(92)

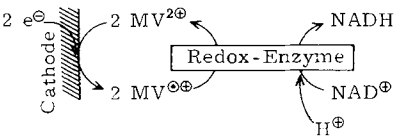


(93)

Radicals which lead to the alkylation of the mediator can also be released by electron transfer from the mediator radical anion to sulfonium or ammonium ions.[175]

4.2. Reductions by Viologen Radical Cations

Viologens, i.e. *N,N*-dialkyl-2,2'- or -4,4'-bipyridinium salts, were already used some time ago as electron transfer agents in the coulometric titration of redox-enzymes.[176] Hence, it was a logical step to apply the same principle to reductions on a preparative scale. The electrochemical reduction of $NAD^{\oplus}$ to NADH presented itself as an especially interesting problem (see also Section 3.3.2). Since the direct electrochemical reduction of $NAD^{\oplus}$ never affords NADH exclusively, a number of authors chose the detour via an enzyme-coupled indirect electrolysis with methyl viologen ($MV = N,N'$-dimethyl-4,4'-bipyridinium dichloride) as mediator (see Scheme 7). The intercalated redox enzyme must be able to take up two electrons successively from the electrochemically generated $MV^{\odot\oplus}$ and then to transfer them at one and the same time to $NAD^{\oplus}$. It was possible to carry out the NADH and NADPH regeneration with the enzyme systems ferredoxin reductase,[177] lipoamide dehydrogenase,[178] as well as 2-oxocarboxylate reductase and enoate reductase.[179]



Scheme 7. Indirect electrochemical reduction of $NAD^{\oplus}$ assisted by a redox enzyme.

With enoate reductase, enoates can also be hydrogenated stereospecifically without intermediate NADH formation. This reaction also succeeds without isolation of the enzyme, by use of intact clostridium cells. *Simon* et al. were even able to generate (*R*)-1,2-propanediol "electromicrobially" from hydroxyacetone via indirect electrochemical formation of NADH using whole yeast cells [Eq. (94)-(97)].[179]

$$2\,MV^{2\oplus} \xrightarrow[+2e^{\ominus}]{\text{cathode}} 2\,MV^{\odot\oplus} \quad (94)$$

$$2\,MV^{\odot\oplus} + H^{\oplus} + NAD^{\oplus} \xrightarrow{\text{yeast}} NADH + 2\,MV^{2\oplus} \quad (95)$$

$$H^{\oplus} + NADH + CH_3COCH_2OH \xrightarrow{\text{yeast}} NAD^{\oplus} + CH_3CH(OH)CH_2OH \quad (96)$$

sum:

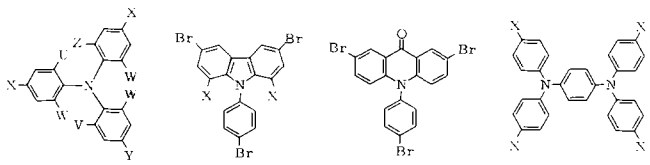
$$CH_3COCH_2OH + 2\,H^{\oplus} + 2\,e^{\ominus} \longrightarrow CH_3CH(OH)CH_2OH \quad (97)$$

4.3. Oxidations with Triarylamine Radical Cations

Oxidation reactions catalyzed by organic mediators attracted very little attention from chemists for some time, for it was a foregone conclusion that organic molecules would not be stable enough to reach an acceptable number of cycles. *Nelson* et al., however, were able to prove that the radical cations of triarylamines[180] and the related *N*-phenylcarbazoles[181] are very stable, if the *para* positions of the phenyl rings are blocked by substituents from attack

by nucleophiles. The suitability of triarylamines as mediators has for instance been demonstrated in the oxidation of cyanide ions with electrochemically generated trianisylamine radical cations as electron transfer agents.[182] We[183] and others[180, 184, 185] have in the meantime synthesized a large variety of substituted triarylamines and have tested their suitability as redox catalysts.[183] The compounds cover a potential range from +0.76 V to 1.96 V (vs. NHE), so that one should be able to find a suitable mediator for every reaction (see Table 3). It should be pointed out, however, that the stability of the triarylamine radical cations strongly depends on the reaction medium. Bromine- and chlorine-substituted compounds have proven to be especially reliable. Tris(2,4-dibromophenyl)amine, for example, is extremely stable. In methanolic solution 2500 cycles could be performed without any appreciable consumption of the mediator.[186]

Table 3. Standard potentials for the oxidation of triarylamines and related compounds to the radical cations.

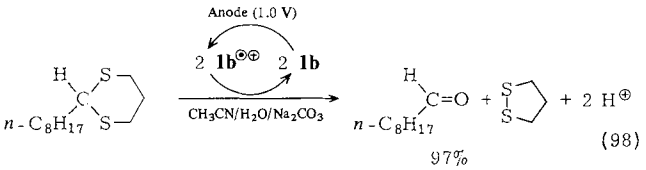


1 2 3 4

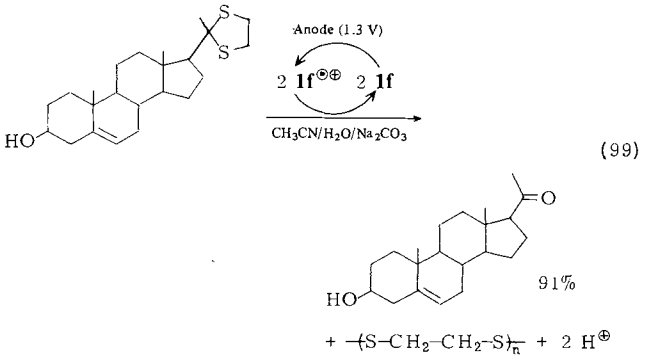
Compound number	Substituents U	V	W	X	Y	Z	E^0 [V] vs. NHE
4a	—	—	—	H	—	—	0.75
1a	H	H	H	OCH_3	OCH_3	H	0.76
4b	—	—	—	Br	—	—	0.91
1b	H	H	H	CH_3	CH_3	H	1.00
1c	H	H	H	$SiMe_3$	$SiMe_3$	H	1.08
1d	H	H	H	I	I	H	1.27
1e	H	H	H	Br	$H_2C=C(CF_3)$	H	1.28
1f	H	H	H	Br	Br	H	1.30
1g	CO_2H	H	H	Br	Br	H	1.41
1h	CO_2CH_3	H	H	Br	Br	H	1.42
1i	Br	H	H	Br	Br	H	1.42
1k	H	H	H	Br	$COCF_3$	H	1.45
1l	H	H	H	$COCH_3$	$COCH_3$	H	1.50
1m	Br	Br	H	Br	Br	H	1.56
1n	H	H	H	CF_3	CF_3	H	1.60
1o	H	H	H	NO_2	Br	H	1.64
1p	H	H	H	C_2F_5	C_2F_5	H	1.64
1q	H	H	H	CN	CN	H	1.68
1r	H	H	H	$COCF_3$	$COCF_3$	H	1.68
1s	Br	Br	H	Br	$H_2C=C(CF_3)$	Br	1.72
2a	—	—	—	H	—	—	1.72
1t	Br	Br	H	Br	Br	Br	1.74
1u	H	H	H	NO_2	NO_2	H	1.80
2b	—	—	—	Br	—	—	1.83
3	—	—	—	—	—	—	1.85
1v	Br	Br	H	Br	$COCF_3$	Br	1.86
1w	Br	Br	Br	Br	Br	Br	1.96

Compounds with potentials that are several hundered millivolts more positive than those of the mediators (electrochemical oxidation opposite to the standard potential gradient; see Section 2.2) can be oxidized with electrochemically generated triarylamine radical cations, since a fast and irreversible bond cleavage usually follows the primary electron transfer. Especially favorable follow-up reactions are deprotonations in the benzyl- or allyl-position or in the α-position to hetero atoms. The irreversible cleavage of carbon-sulfur bonds in sulfides also shifts the electron transfer equilibrium in favor of the products. In addition, in many cases the reaction between substrate and triarylamine radical cation does not proceed as a simple homogeneous electron transfer (mechanism A, Section 2.2), but presumably an interaction (complex formation or even bond formation) between mediator and substrate facilitates the electron transfer, so that potential differences higher than 600 mV can be overcome. *Eberson* came to the same conclusion in an analysis on the basis of the Marcus theory.[187]

In this way oxidation reactions are possible under very mild conditions and with high selectivity, which makes the method especially useful for the oxidative cleavage of protective groups. Thus, carbonyl compounds could be deprotected in high yields from 1,3-dithianes and 1,3-dithiolanes with **1b** or **1f** in moist acetonitrile in the presence of sodium carbonate [Eq. (98), (99)].[188] The cleavage conditions are so mild that hydroxy groups and double bonds can be tolerated without any problems.



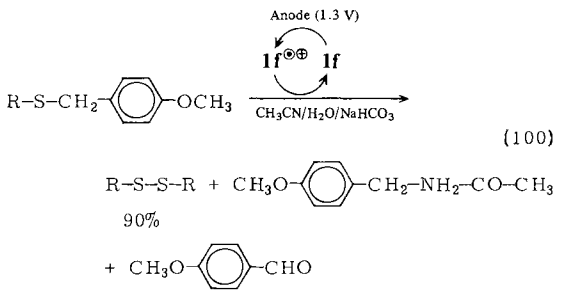
(98)



(99)

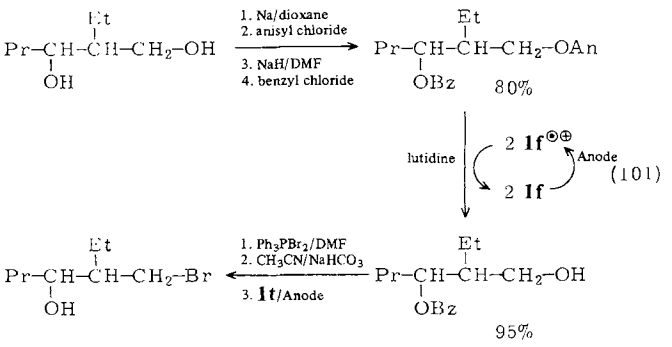
The cleavage of the carbon-sulfur bond in *p*-methoxybenzyl thioethers with formation of disulfides and secondary products of the *p*-methoxybenzyl cations [Eq. (100)] has been exploited for the directed incorporation of disulfide bridges in poly-cystinyl peptides via *S*-(4-methoxybenzyl)cysteine units in combination with *S*-tritylcysteine groups.[189]

Substituted benzyl ethers[190] and benzyl esters[191] can also be deblocked with formation of alcohols and carbox-



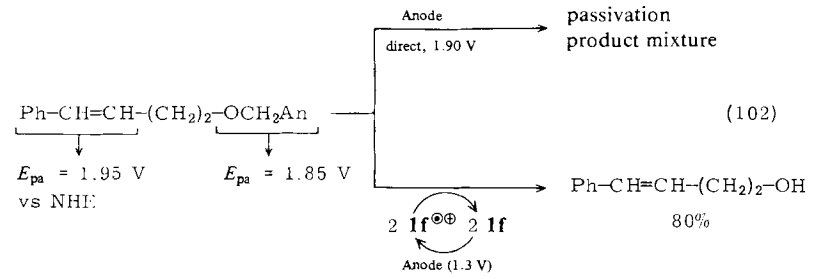
(100)

ylic acids, respectively. If a suitable mediator is selected these cleavages can be performed in a multifunctional molecule selectively and in a directed manner depending on the substitution pattern of the protective groups. Thus, the directed protection and selective deblocking of hydroxy groups attached to primary and secondary C-atoms in polyhydroxy compounds can be realized without any problem [Eq. (101)].[190b]

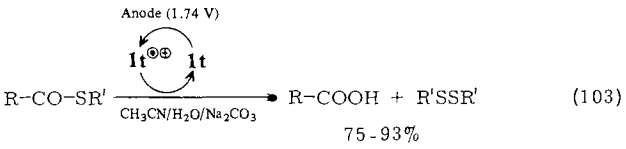


An = 4-methoxybenzyl, Bz = benzyl

Even substantially milder reaction conditions are possible, if the anisyl ether function as permanent protective group is combined with the 3,4-dimethoxybenzyl ether function as intermediate protective group.[190d] The selectivity of the reaction can be demonstrated with the anisyl ether of 4-phenyl-3-buten-1-ol [Eq. (102)].[190c] The educt contains two electrophores, whose potentials differ only by 100 mV. The direct electrolysis therefore proceeds unselectively, while the indirect electrolysis leads only to attack at the easier oxidizable function. Non-activated OH-groups are stable towards triarylamine radical cations with potentials up to 1.6 V (vs. NHE).



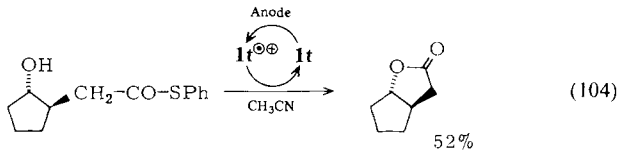
The indirect electrochemical deblocking of benzyl esters by triarylamine radical cations not only differentiates highly selectively between unsubstituted benzyl esters and 4-methoxybenzyl, 2,4-dimethoxybenzyl or benzhydryl esters, but, other than in previous methods, also between the acid labile 2,4-dimethoxybenzyl esters and the likewise acid labile 4-methoxybenzyl and benzhydryl esters.[191] The *N*-*t*-butoxycarbonyl(Boc)- and *N*-benzyloxycarbonyl(*Z*)-protective groups are stable under these conditions. In contrast, the *N*-*p*-methoxybenzyloxycarbonyl(MOZ)-protecting group can be cleaved smoothly by $\mathbf{1t}^{\odot\oplus}$. Thiol esters can also be cleaved by indirect electrolysis in good yield with **1t** as a mediator [Eq. (103)].[191b]



(103)

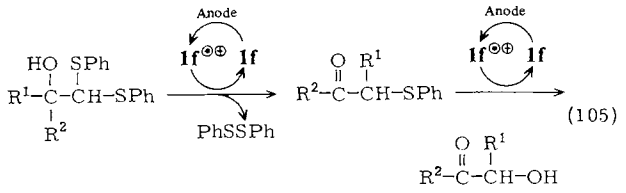
R' = Ph, $H_3CO-C_6H_4$, Ph–CH_2, n-C_8H_{17}

Starting from *S*-phenyl *trans*-2-hydroxycyclopentylthioacetate, this reaction can be used for the synthesis of an otherwise difficultly accessible cyclopentano-γ-lactone with the *trans*-configuration [Eq. (104)].[192] Rearrange-

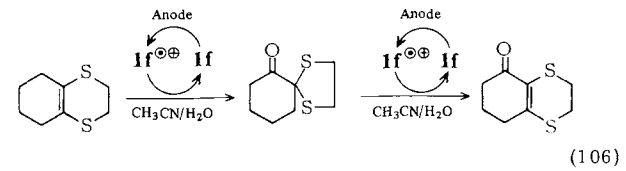


(104)

ments can be initiated by the indirect anodic cleavage of carbon-sulfur bonds [Eq. (105) and (106)].[193]



(105)

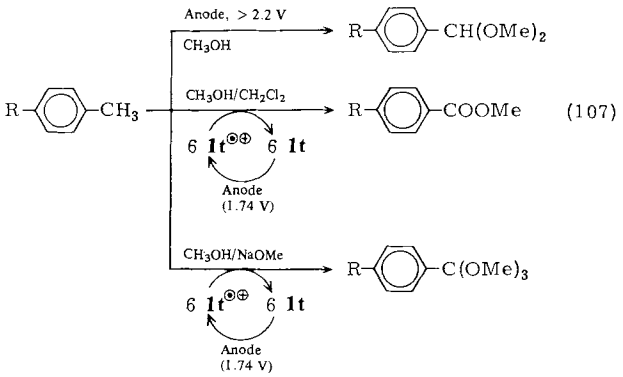


(106)

Interesting from the industrial point of view are the indirect electrochemical oxidations of benzylic alcohols, benzaldehyde dimethyl acetals and arylalkanes with **1t** as mediator. We were able to show that benzylic alcohols can be oxidized with high selectivity to benzaldehydes or their dimethyl acetals not only in acetonitrile in a divided cell but also in methanol in an undivided cell.[194a]

Arylalkanes that are oxidizable only to the stage of the benzaldehyde dimethyl acetals by direct anodic electrolysis in methanol are oxidized to methyl benzoates under mildly acidic conditions and at very low potentials with **1t** as mediator [eq. (107)].[186, 194b] Even toluene with a standard potential of 2.64 V (vs. NHE) can be transformed into

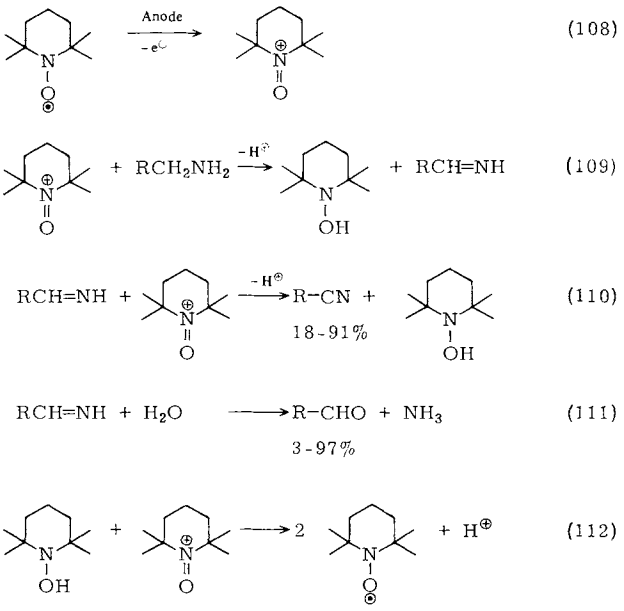
methyl benzoate in 95% material yield. If the reaction is carried out in presence of Na_2CO_3 or small amounts of NaOMe as base, trimethylorthobenzoates are obtained in good selectivity [Eq. (107)].[186, 194b] When benzaldehyde dimethyl acetals are used as starting compounds in a $CH_3OH/LiClO_4$ electrolyte in presence of low concentrations of NaOMe, orthoesters are obtained almost exclusively (selectivity > 90%). The current yields are especially good in all cases, if the substrate is used as a co-solvent.[186, 194b]



(107)

4.4. Oxidations with Electrochemically Regenerable Hydride or Hydrogen Atom Abstracting Reagents

As already demonstrated in Section 2.2, even those oxidation reagents that effect a hydrogen or hydride abstraction can be regenerated electrochemically. Hydrogen, for example, can be abstracted by in-situ electrochemically oxidized *N*-hydroxyphthalimide.[195] The presence of a base like pyridine is necessary. In this way alcohols, arylalkanes, benzyl ethers and olefins can be oxidized. The cycle numbers, however, are still very low. Electrochemically regenerable hydride abstracting agents are 2,3-dichloro-5,6-dicyano-*p*-benzoquinone (DDQ), as well as the oxoammonium ion accessible from 2,2,6,6-tetramethylpiperidyl oxide (TEMPO). DDQ has been regenerated both externally,[196] that is after the isolation of the hydroquinone, and internally.[197] TEMPO is oxidized in-situ in acetonitrile containing lutidine. Thus, primary alcohols can be converted into aldehydes, while secondary alcohols are scarcely attacked.[198] Under these conditions, primary amines preferably form nitriles; in the presence of water, hydrolysis of the intermediate azomethines with generation of carbonyl compounds is favored [Eq. (108)-(112)].[199]



5. Outlook

The optimism sparked off by euphoric predictions on the future development of electroorganic syntheses in the early sixties was suddenly displaced by a certain disillusionment during the seventies. In the meantime, however, there has been a gradual but distinct revival of interest in electrosynthesis, both in the laboratory and in industry. Responsible for this fresh impetus are new insights into chemical mechanisms and the development of new materials and new techniques.[201] One of these techniques, namely indirect electrochemical synthesis, has become a subject of intensive study and it is expected that a host of new possibilities for its application will emerge in the future. The particular advantages of this technique are its low burden on the environment, the favorable exploitation of energy because of the acceleration of electrode reactions, and the high selectivity of many of the syntheses. Special chances of development are foreseen for indirect electrolysis with transition metal complexes as redox catalysts, since these mediators are accessible in large variety, can easily be modified, and mostly undergo specific reactions. The in-situ regeneration of metal ions in low oxidation states opens up new possibilities for the use of reactive and highly sensitive reagents. Some organic mediators, in particular triarylamines, have proved to be surprisingly stable and even fulfill the prerequisites for use on an industrial scale, with cycle numbers of several thousands, Even some present day environmental problems can be reduced by resort to indirect electrochemical processes. Thus, the dehalogenation of polychlorinated biphenyls (PCB's) could be carried out with 9,10-diphenylanthracene as redox catalyst.[200] Entirely new reactions can be expected to emerge from the photochemical excitation of electrochemically generated and regenerated mediators. New insights into this field are also of great importance for the photoelectrochemical conversion of light into electrical or chemical energy.

My own results quoted in this article were only possible through the great efforts of motivated co-workers, which are mentioned in the references, and by generous support of the Deutsche Forschungsgemeinschaft, the Fonds der Chemischen Industrie, the Arbeitsgemeinschaft industrieller Forschungsvereinigungen, and the BASF Aktiengesellschaft. My sincere thanks to all of them!

Received: January 2, 1985;
revised: October 2, 1985 [A 586 IE]
German version: *Angew. Chem. 98* (1986) 681

[1] F. Fichter: *Organische Elektrochemie*, Steinkopf, Dresden 1942, p. 13ff and 75ff (in the earlier literature one speaks of "oxygen" and "hydrogen" carriers instead of redox-catalysts).

[2] C. Jackson, A. T. Kuhn in A. T. Kuhn (Ed.): *Industrial Electrochemical Processes*, Elsevier, Amsterdam 1971, p. 513–519, and references cited therein.

[3] R. Clarke, A. T. Kuhn, E. Okoh, *Chem. Br. 11* (1975) 59.

[4] J. Simonet in M. M. Baizer, H. Lund (Eds.): *Organic Electrochemistry*, 2nd edition, Marcel Dekker, New York 1983, p. 843.

[5] H. Lund in Ref. [4], p. 829.

[6] M. D. Birkett, R. L. Clarke, A. T. Kuhn, *Chem. Weekbl. Mag. 1977*, 533.

[7] N. Ibl, K. Kramer, L. Ponto, P. Robertson, *AIChE Symp. Ser. 75* (185) (1979) 45.

[8] T. Shono, *Tetrahedron 40* (1984) 841.

[9] K. Yoshida: *Electrooxidation in Organic Chemistry*, Wiley, New York 1984, p. 269.

[10] S. Torii: *Yuki Denkai Gosei (Electroorganic Synthesis)*, Kodansha Scientific, Tokyo 1981; *Electroorganic Syntheses. Methods and Applications. Part 1: Oxidations*, VCH Verlagsgesellschaft, Weinheim 1985.

[11] I. M. Dalrymple, A. R. Jones, J. P. Millington, *149th Meet. Electrochem. Soc.* (Washington 1976) Abstr.-No. 275.

[12] Ref. [1], p. 14, 15.

[13] J. P. Millington, *Chem. Ind. (London) 1975*, 780.

[14] R. A. C. Rennie (ICI), DBP 1804726 (1969); *Chem. Abstr. 71* (1969) 35535.

[15] E. Steckhan, J. Wellmann, *Angew. Chem. 88* (1976) 306; *Angew. Chem. Int. Ed. Engl. 15* (1976) 294; J. Wellmann, E. Steckhan, *Chem. Ber. 110* (1977) 3561.

[16] D. Pletcher, N. Tomov, *J. Appl. Electrochem. 7* (1977) 501.

[17] P. Seiler, P. M. Robertson, *Chimia 36* (1982) 305; J. Kaulen, H. J. Schäfer, *Tetrahedron 38* (1982) 3299; *Synthesis 1979*, 513; U. Feldhues, H. J. Schäfer, *ibid. 1982*, 145; P. M. Robertson, P. Berg, H. Reimann, K. Schleich, P. Seiler, *J. Electrochem. Soc. 130* (1983) 591, and references cited therein.

[18] L. Horner, R. E. Schmidt, *Z. Naturforsch. B37* (1982) 1163; K. E. Swenson, D. Zemach, C. Nanjundiah, E. Kariv-Miller, *J. Org. Chem. 48* (1983) 1777; E. Kariv-Miller, C. Nanjundiah, J. Eaton, K. E. Swenson, *J. Electroanal. Chem. Interfacial Electrochem. 167* (1984) 141.

[19] R. W. Murray, *Acc. Chem. Res. 13* (1980) 135.

[20] M. S. Wrighton, *Acc. Chem. Res. 12* (1979) 303.

[21] A. Merz, *Nachr. Chem. Techn. Lab. 30* (1982) 16.

[22] K. D. Snell, A. G. Keenan, *Chem. Soc. Rev. 8* (1979) 259.

[23] J. S. Miller (Ed.): *Chemically Modified Surfaces in Catalysis and Electrocatalysis (ACS Symp. Ser. 192)*, ACS, Washington, DC 1982.

[24] A. T. Kuhn, M. Birkett, *J. Appl. Electrochem. 9* (1979) 777.

[25] E. Steckhan, *Habilitationsschrift*, Münster 1978.

[26] V. G. Mairanovsky, *Angew. Chem. 88* (1976) 283; *Angew. Chem. Int. Ed. Engl. 15* (1976) 281.

[27] E. Steckhan, W. Schmidt, *J. Electroanal. Chem. Interfacial Electrochem. 89* (1978) 215.

[28] C. P. Andrieux, J.-M. Dumas-Bouchiat, J.-M. Savéant, *J. Electroanal. Chem. Interfacial Electrochem. 87* (1978) 39.

[29] H. Lund, H. S. Carlsson, *Acta Chem. Scand. Ser. B32* (1978) 505; H. S. Carlsson, H. Lund, *ibid. 34* (1980) 409; J. Eriksen, H. Lund, A. N. Nyvad, *ibid. 37* (1983) 459; P. Nelleborg, J. Eriksen, H. Lund, *XI. Sandbjerg Meet. Org. Electrochem.* (Sandbjerg 1984), Abstr. p. 76.

[30] J. C. Moutet, G. Reverdy, *Tetrahedron Lett. 1979*, 2389; *J. Chem. Soc. Chem. Commun. 1982*, 654; *Nouv. J. Chim. 7* (1983) 105; P. Labbé, J. C. Moutet, M. Paltrier, G. Reverdy, *ibid. 8* (1984) 627; M. Genies, J. C. Moutet, G. Reverdy, *Electrochim. Acta 26* (1981) 931.

[31] J. Perichon, J. F. Fauvarque et al., *J. Chem. Res. Synop. 1979*, 50; *ibid. 1980*, 24, 26, 147, 268; *J. Organomet. Chem. 202* (1980) 435.

[32] D. Pletcher et al., *J. Chem. Soc. Dalton Trans. 1978*, 972; *J. Organomet. Chem. 161* (1978) 109; *ibid. 186* (1980) 401; *J. Electroanal. Chem. Interfacial Electrochem. 117* (1981) 87, 101.

[33] D. Degner in N. L. Weinberger, B. V. Tilak (Eds.): *Techniques of Chemistry, Vol. 5, Part 3*, Wiley, New York 1982, Chap. V, p. 273, and references cited therein.

[34] G. Milazzo, S. Caroli: *Tables of Standard Electrode Potentials*, Wiley, Chichester 1978.

[35] M. Käppel, *Chem. Ing. Tech. 35* (1963) 386.

[36] Electrochemical regeneration of Mn^{III}: A. T. Kuhn, T. H. Randle, *J. Chem. Soc. Faraday Trans. 1, 79* (1983) 417.

[37] Electrochemical regeneration of Ce^{IV} with $Ag^{\oplus}$ or $Co^{2\oplus}$ ions as catalysts, see: K. H. Oehr (British Columbia Research Council, US-Pat. 4313804; *Chem. Abstr. 96* (1982) 94013p; US-Pat. 4312721; *Chem. Abstr. 96* (1982) 94014q; Can. CA 1166600; *Chem. Abstr. 101* (1984) 179923g.

[38] K. Kramer, P. M. Robertson, N. Ibl, *J. Appl. Electrochem. 10* (1980) 29.

[39] S. Chidambaram, M. S. V. Pathy, H. V. K. Udupa, *J. Electrochem. Soc. India 17* (1968) 95; *Chem. Abstr. 70* (1969) 25168u.

[40] M. Fleischmann, D. Pletcher, A. Rafinski, *J. Appl. Electrochem. 1* (1971) 1.

[41] S. Torri, H. Tanaka, T. Inokuchi, S. Nakane, M. Akada, N. Saito, T. Sirakawa, *J. Org. Chem. 47* (1982) 1647.

[42] S. Torii, S. Nakane, T. Shirakawa, M. Adada (Otsuku Chem. Co.), DOS 3028758 (1980); *Chem. Abstr. 95* (1981) 24553v; Jpn. Kokai Tokkyo Koho 80 85 682 (1980); *Chem. Abstr. 93* (1980) 194462r.

[43] S. Torii, S. Nakane, T. Shirakawa, M. Akada (Otsuka Chem. Co.), DOS 3028757 (1980); *Chem. Abstr. 95* (1981) 24552u.

[44] H. A. Halter, T. P. Malloy (U.O.P. Inc.), US-Pat. 4212711 (1979); *Chem. Abstr. 93* (1980) 140062s.

[45] R. Tomat, A. Rigo, *J. Appl. Electrochem. 6* (1976) 257; *ibid. 9* (1979) 301; *ibid. 14* (1984) 1.

[46] J. P. Millington, I. M. Dalrymple, Br. Pat. Appl. GB2140034 (1984); *Chem. Abstr. 102* (1985) 122088e.

[47] Electrochemical regeneration of chromic acid: Ref. [35], and references cited therein; S. Chidambaram, M. S. V. Pathy, H. V. K. Udupa, *Indian J. Technol. 6* (1968) 12; *Chem. Abstr. 68* (1968) 118799z; L.-C. Jiang, D. Pletcher, *J. Electroanal. Chem. Interfacial Electrochem. 152* (1983) 157 (Use of Ag ions as co-catalyst); N. Shuster, A. D. Babinsky, W. E. Kidon (Diamond Shamrock Co.), US-Pat. 4290864 (1981); *Chem. Abstr. 95* (1981) 194488v; J. P. Millington, I. M. Dalrymple (Electricity Co., London), Eur. Pat. Appl. 64417 (1982); *Chem. Abstr. 98* (1983) 62164p.

[48] A. T. Kuhn, R. Clarke, *J. Appl. Chem. Biotechnol. 26* (1976) 407, and references cited therein.

[49] S. Chidambaram, S. Balagopalan, R. Kanakam, A. P. Shakunthara, M. S. V. Pathy, H. V. K. Udupa, *Res. Ind. 15* (1970) 215; *Chem. Abstr. 75* (1971) 93944x.

[50] M. S. V. Pathy, H. V. K. Udupa, *Indian Chem. J. Annu. 1972*, 67; *Chem. Abstr. 80* (1974) 120461z.

[51] O. W. Brown, A. E. Brown, *Trans. Electrochem. Soc. 75* (1939) 393; *Chem. Abstr. 33* (1939) 28161.

[52] R. K. Srinivasan, M. S. V. Pathy, *J. Electrochem. Soc. India 30* (1981) 94; *Chem. Abstr. 95* (1981) 186792z.

[53] R. M. Engelbrecht, J. C. Hill, R. N. Moore (Monsanto Co.), US-Pat. 3714003 (1973); *Chem. Abstr. 78* (1973) 118570z.

[54] R. M. Engelbrecht, J. C. Hill, R. N. Moore (Monsanto Co.), US-Pat. 3726914 (1973); *Chem. Abstr. 79* (1973) 18399c.

[55] W. J. Koehl, Jr. (Mobil Oil Co.), US-Pat. 3448021 (1969); *Chem. Abstr. 71* (1969) 49605f.

[56] S. Torii, H. Tanaka, M. Akada (Otsuka Pharm. Co.), Jpn. Kokai Tokkyo Koho 80 50 472 (1980); *Chem. Abstr. 93* (1980) 176066k; S. Torii, H. Tanaka, T. Sroi, M. Akada, *J. Org. Chem. 44* (1979) 3305.

[57] Soda Aromatic Co., Jpn. Kokai Tokkyo Koho 80 148 781 (1980); *Chem. Abstr. 94* (1981) 129502k.

[58] R. A. C. Rennie (ICI), DOS 1804727 (1969); *Chem. Abstr. 71* (1969) 81034e.

[59] R. A. C. Rennie (ICI), Br. Pat. 1203434 (1970); *Chem. Abstr. 73* (1970) 109496z.

[60] R. A. C. Rennie (ICI), DOS. 2301803 (1973); *Chem. Abstr. 79* (1973) 115357o.

[61] F. Goodridge, E. O. Umeh, *Electrochim. Acta 20* (1975) 991.

[62] G. A. Kokarev, M. Ya. Fioshin, E. V. Gromova, *Elektrokhimiya 17* (1981) 1380; *Chem. Abstr. 95* (1981) 194363a.

[63] R. Tomat, E. Vecchi, *J. Appl. Electrochem. 1* (1971) 185.

[64] J. M. Maissant, C. Bouchoule, P. Canesson, M. Blanchard, *J. Mol. Catal. 18* (1983) 189.

[65] Y. Matsuda, K. Nishi, T. Azuma, *Denki Kagaku oyobi Kogyo Butsuri Kagaku 52* (1984) 635; *Chem. Abstr. 102* (1985) 24212w.

[66] B. Fleszar, A. Sobkowiak, *Electrochim. Acta 26* (1981) 1699; *ibid. 28* (1983) 1315.

[67] K. Sasaki, S. Ito, Y. Saheki, T. Kinoshita, T. Yamasaki, J. Harada, *Chem. Lett. 1983*, 37, 445; T. Kinoshita, J. Harada, S. Ito, K. Sasaki, *Angew. Chem. 95* (1983) 504; *Angew. Chem. Int. Ed. Engl. 22* (1983) 502; *Angew. Chem. Suppl. 1983*, 599.

[68] R. Tomat, A. Rigo, *J. Electroanal. Chem. Interfacial Electrochem. 63* (1975) 329; *ibid. 75* (1975) 629.

[69] E. I. Heiba, R. M. Dessau, P. G. Rodewald, *J. Am. Chem. Soc. 96* (1974) 7977.

[70] M. E. Kurz, T. Y. R. Chen, *J. Org. Chem. 43* (1978) 239.

[71] R. M. Dessau, E. I. Heiba, US-Pat. 3992417; *Chem. Abstr. 86* (1977) 54999.

[72] J. P. Coleman, R. C. Hallcher, D. E. McMackins (Monsanto Co.), Eur. Pat. Appl. 55934 (1982); *Chem. Abstr. 97* (1982) 146549k; Eur. Pat. Appl. 55936 (1982); *Chem. Abstr. 97* (1982) 135550d; *165 Meet. Electrochem. Soc.* (Cincinnati, OH 1984), Abstr.-No. 328.

[73] A. J. Bellamy, *Acta Chem. Scand. Ser. B33* (1979) 208.

[74] Noguchi Institute, Jpn. Kokai Tokkyo Koho 82128767 (1982); *Chem. Abstr. 97* (1982) 216620c; Y. Nakamura, *Nippon Kagaku Kaishi 1982*, 1727; Y. Nakamura, *Noguchi Kenkyusho Jiho 25* (1982) 26; *Chem. Abstr. 98* (1983) 126495g; Noguchi Institute, Jpn. Kokai Tokkyo Koho 58 39 695 (1983); *Chem. Abstr. 99* (1983) 5966y.

[75] B. A. Moyer, M. S. Thompson, T. J. Meyer, *J. Am. Chem. Soc. 102* (1980) 2310; M. S. Thompson, W. F. De Giovani, B. A. Moyer, T. J. Meyer, *J. Org. Chem. 49* (1984) 4972.

[76] S. Torii, T. Inokuchi, T. Sugiura, *J. Org. Chem. 51* (1986) 155; Jpn. Kokai Tokkyo Koho JP 59129790 (1984); *Chem. Abstr. 102* (1985) 35365z; Jpn. Kokai Tokkyo Koho JP 59166687 [84166687] (1984); *Chem. Abstr. 103* (1985) 29218h.

[77] A. F. McLean, A. L. Stautzenberger (Celanese Co.), US-Pat. 3479262 (1969); *Chem. Abstr. 72* (1970) 21323j.

[78] V. A. Shepelin, *Elektrokhimiya 11* (1975) 1767; *Chem. Abstr. 84* (1976) 43189v.

[79] F. Goodridge, C. J. H. King, *J. Appl. Chem. Biotechnol. 21* (1971) 208.

[80] R. Favier, C. Freppel, J.-C. Richer, M. Zador, *Can. J. Chem. 49* (1971) 2590.

[81] D. L. Klass (Pure Oil Co.), US-Pat. 3147203 (1964); *Chem. Abstr. 61* (1964) 13195h; (Union Oil Co.), US-Pat. 3245890 (1966); *Chem. Abstr. 64* (1966) 17427e.

[82] A. R. Blake, J. G. Sunderland, A. T. Kuhn, *J. Chem. Soc. A 1969*, 3015.

[83] F. Goodridge, C. J. H. King, *Trans. Faraday Soc. 66* (1970) 2889; *Chem. Abstr. 73* (1970) 136739n.

[84] M. Fleischmann, D. Pletcher, G. M. Race, *J. Electroanal. Chem. Interfacial Electrochem. 23* (1969) 369.

[85] M. Fleischmann, D. Pletcher, G. M. Race, *J. Chem. Soc. B 1970*, 1746.

[86] J. S. Mayell, *Ind. Eng. Chem. Prod. Res. Dev. 7* (1968) 129.

[87] T. Atsuno, Jpn. Kokai Tokkyo Koho 5803988 (1983); *Chem. Abstr. 98* (1983) 224280c.

[88] T. Iwasaki, T. Nishitani, H. Horikawa, I. Inoue, *J. Org. Chem. 47* (1982) 3799.

[89] D. A. White, *Org. Synth. 60* (1981) 78; D. K. Johnson, R. E. W. Jansson, *J. Chem. Technol. Biotechnol. 30* (1980) 200, and references cited therein.

[90] P. N. Pintauro, D. K. Johnson, K. Park, M. M. Baizer, K. Nobe, *J. Appl. Electrochem. 14* (1984) 209; *165th Meet. Electrochem. Soc.* (Cincinnati, OH 1984) Abstr.-No. 322.

[91] F. Barba, P. A. Garcia, A. Guirado, A. Zapata, *Carbohydr. Res. 105* (1982) 158.

[92] N. Ibl, A. Selvig, *Chem. Ing. Tech. 42* (1970) 180, and references cited therein.

[93] K. H. Simmrock, *Chem. Ing. Tech. 48* (1976) 1085; *Hydrocarbon Process. 57* (1978) 105; *Chem. Abstr. 90* (1979) 63490p.

[94] K. G. Ellis, R. E. W. Jansson, *Chem. Ind. (London) 1980*, 864; *J. Appl. Electrochem. 11* (1981) 531; *ibid. 13* (1983) 651.

[95] S. Torii, K. Uneyama, H. Tanaka, T. Yamanaka, T. Yasuda, M. Ono, Y. Kohmoto, *J. Org. Chem. 46* (1981) 3312, and references cited therein.

[96] J. Yoshida, J. Hashimoto, N. Kawabata, *J. Org. Chem. 47* (1982) 3575.

[97] S. Torii, K. Uneyama, M. Ono, *Tetrahedron Lett. 21* (1980) 2741.

[98] S. Torii, K. Uneyama, M. Ono, *Tetrahedron Lett. 21* (1980) 2653.

[99] S. Torii, K. Uneyama, M. Ono, T. Bannou, *J. Am. Chem. Soc. 103* (1981) 4606.

[100] S. Torii, K. Uneyama, K. Handa, *Tetrahedron Lett. 21* (1980) 1863.

[101] S. Torii, H. Tanaka, M. Ukida, *J. Org. Chem. 44* (1979) 1554.

[102] S. Torii, H. Tanaka, S. Hamano, N. Tada, J. Nokami, M. Sasaoka, *Chem. Lett. 1984*, 1823.

[103] S. Torii, H. Tanaka, N. Sayo, *J. Org. Chem. 44* (1979) 2938.

[104] S. Torii, N. Sayo, H. Tanaka, *Tetrahedron Lett. 1979*, 4471.

[105] R. E. W. Jansson, N. R. Tomov, *J. Appl. Electrochem. 10* (1980) 583.

[106] G. Dixit, R. Rastogi, K. Zutshi, *Electrochim. Acta 27* (1982) 561; M. Thomas, G. Dixit, R. Rastogi, K. Zutshi, *J. Electrochem. Soc. India 33* (1984) 213; *Chem. Abstr. 102* (1985)•131640f.

[107] J. Yoshida, R. Nakai, N. Kawabata, *J. Org. Chem. 45* (1980) 5269.

[108] T. Shono, Y. Matsumura, J. Hayashi, M. Mizoguchi, *Tetrahedron Lett. 1979*, 165; T. Shono, Jpn. Kokai Tokkyo Koho 8050473 und 8054583 (1980); *Chem. Abstr. 93* (1980) 157867f und 103843b.

[109] T. Shono, Y. Matsumura, J. Hayashi, M. Mizoguchi, *Tetrahedron Lett. 21* (1980) 1867.

[110] T. Shono, Y. Matsumura, K. Inoue, *J. Am. Chem. Soc. 106* (1984) 6075.

[111] T. Shono, Y. Matsumura, K. Inoue, *J. Org. Chem. 48* (1983) 1388.

[112] J. E. Leonard, P. C. Scholl, T. P. Steckel, *Tetrahedron Lett. 21* (1980) 4695.

[113] Y. Matsuda, T. Nishiki, K. Nakagawa, M. Dehara, *Nippon Kagaku Kaishi 1984*, 1832; (Sugai Chemical Ind. Co.), Jpn. Kokai Tokkyo Koho JP 59211585 (1984); *Chem. Abstr. 102* (1985) 122074x.

[114] H. F. Conway, E. B. Lancaster, V. E. Sohns, *Electrochem. Technol. 2* (1964) 43; C. L. Mehltretter, C. S. Wise, *Ind. Eng. Chem. 51* (1959) 511; H. F. Conway, V. E. Sohns, *ibid.* 637; V. F. Pfeifer, V. E. Sohns, H. F. Conway, E. B. Lancaster, S. Dabic, E. L. Griffin, *ibid. 52* (1960) 201; R. Ramaswamy, M. S. Venkatachalapathy, H. V. Udupa, *Indian J. Technol. 1* (1963) 115.

[115] A. Yoshiyama, T. Nonaka, M. Baizer, T. C. Chou, *Bull. Chem. Soc. Jpn. 58* (1985) 201.

[116] T. Chiba, Y. Takata, *Bull. Chem. Soc. Jpn. 51* (1978) 1418.

[117] G. Farnia, G. Sandona, E. Vianello, *J. Electroanal. Chem. Interfacial Electrochem. 88* (1978) 147.

[118] P. N. Anantharaman, H. V. K. Udupa, *Trans. SAEST 15* (1980) 41.

[119] M. Noel, P. N. Anantharaman, H. V. K. Udupa, *Electrochim. Acta 25* (1980) 1083.

[120] M. Noel, P. N. Anantharaman, H. V. K. Udupa, *J. Appl. Electrochem. 12* (1982) 291.

[121] H. C. Rance, J. M. Coulson, *Electrochim. Acta 14* (1969) 283.

[122] J. P. Hanson, *Synthesis 1974*, 1.

[123] T. L. Ho, *Synthesis 1979*, 1.

[124] J. Wellmann, E. Steckhan, *Synthesis 1978*, 901.

[125] J. Wellmann, E. Steckhan, *Angew. Chem. 92* (1980) 47; *Angew. Chem. Int. Ed. Engl. 19* (1980) 46.

[126] R. Wolf, E. Steckhan, *J. Chem. Soc. Perkin Trans. 1, 1986*, 733.

[127] R. Wolf, E. Steckhan, *J. Electroanal. Chem. Interfacial Electrochem. 130* (1981) 367.

[128] R. Wolf, E. Steckhan, unpublished.

[129] D. W. Sopher, J. H. P. Utley, *J. Chem. Soc. Chem. Commun. 1979*, 1087; *J. Chem. Soc. Perkin Trans. 2 1984*, 1361, and references cited therein.

[130] F. Fournier, J. Berthelot, Y. L. Pascal, *Tetrahedron 40* (1984) 339; *Can. J. Chem. 61* (1983) 2121; *C. R. Hebd. Scéances Acad. Sci. Ser. B 294* (1982) 849.

[131] D. Pletcher, M. Razaq, G. D. Smilgin, *J. Appl. Electrochem. 11* (1981) 601.

[132] N. E. Gunawardena, D. Pletcher, *Acta Chem. Scand. Ser. B 37* (1983) 549.

[133] Review: R. Scheffold, G. Rytz, L. Walder, *Mod. Synth. Methods 3* (1983) 355.

[134] R. Scheffold, G. Rytz, L. Walder, R. Orlinski, Z. Chilmanczyk, *Pure Appl. Chem. 55* (1983) 1791.

[135] R. Scheffold, R. Orlinski, *J. Am. Chem. Soc. 105* (1983) 7200.

[136] R. Scheffold, E. Amble, *Angew. Chem. 92* (1980) 643; *Angew. Chem. Int. Ed. Engl. 19* (1980) 629.

[137] R. Scheffold, M. Dike, S. Dike, T. Herold, L. Walder, *J. Am. Chem. Soc. 102* (1980) 3642.

[138] L. Walder, G. Rytz, K. Meier, R. Scheffold, *Helv. Chim. Acta 61* (1978) 3013.

[139] R. Scheffold, *Chimia 39* (1985) 203.

[140] S. Torii, T. Inokuchi, T. Yukawa, *J. Org. Chem. 50* (1985) 5875.

[141] S. Margel, F. C. Anson, *J. Electrochem. Soc. 125* (1978) 1232.

[142] D. Lexa, J.-M. Savéant, J. P. Soufflet, *J. Electroanal. Chem. Interfacial Electrochem. 100* (1979) 159.

[143] M. Mori, Y. Hashimoto, Y. Ban, *Tetrahedron Lett. 21* (1980) 631.

[144] G. Schiavon, G. Bontempelli, M. de Nobili, B. Corain, *Inorg. Chim. Acta 42* (1980) 211; G. Schiavon, G. Bontempelli, B. Corain, *J. Chem. Soc. Dalton Trans. 1981*, 1074; G. Bontempelli, F. Magno, B. Corain, G. Schiavon, *J. Electroanal. Chem. Interfacial Electrochem. 103* (1979) 243.

[145] M. Troupel, Y. Rollin, J. Perichon, J. F. Fauvarque, *Nouv. J. Chim. 5* (1981) 621; J. F. Fauvarque, C. Chevrot, A. Jutand, M. Francois, J. Perichon, *J. Organomet. Chem. 264* (1984) 273; J. F. Fauvarque, A. Jutand, C. Chevrot, F. Pfluger, M. Troupel (Compagnie Générale d'Électricité S.A.), Fr. Demande 2530266 (1984); *Chem. Abstr. 101* (1984) 14051h; J. F. Fauvarque, A. Jutand, M. Francois, *XI. Sandbjerg Meet. Org. Electrochem.* (Sandbjerg 1984) Abstr. p. 21.

[146] Y. Rollin, G. Meyer, M. Troupel, J. F. Fauvarque, J. Perichon, *J. Chem. Soc. Chem. Commun. 1983*, 793.

[147] Y. Rollin, G. Meyer, M. Troupel, J. F. Fauvarque, *Tetrahedron Lett. 23* (1982) 3573.

[148] J. F. Fauvarque, M. A. Petit, F. Pfluger, A. Jutand, C. Chevrot, M. Troupel, *Makromol. Chem. Rapid Commun. 4* (1983) 455.

[149] S. Torii, H. Tanaka, K. Morisaki, *Tetrahedron Lett. 26* (1985) 1655.

[150] S. Torii, H. Tanaka, K. Morisaki, *Chem. Lett. 1985*, 1353.

[151] D. Pletcher, *Rev. Port. Quim. 23* (1981) 59.

[152] K. P. Healy, D. Pletcher, *J. Organomet. Chem. 161* (1978) 109.

[153] K. Uneyama, H. Matsuda, S. Torii, *Tetrahedron Lett. 25* (1984) 6017.

[154] R. Wienkamp, E. Steckhan, *Angew. Chem. 94* (1982) 786; *Angew. Chem. Int. Ed. Engl. 21* (1982) 782; *Angew. Chem. Suppl. 1982*, 1739.

[155] M. Franke, E. Steckhan, unpublished.

[156] H. Lehmkuhl in M. M. Baizer (Ed.): *Organic Electrochemistry*, Marcel Dekker, New York 1973, p. 621; *Synthesis 1973*, 377; H. Lehmkuhl, W. Leuchte, W. Eisenbach, *Justus Liebigs Ann. Chem. 1973*, 692; D. De-Montauzon, R. Poilblanc, P. Lemoine, M. Gross, *Electrochim. Acta 23* (1978) 1247.

[157] E. Le Roy, F. Petit, J. Hennion, J. Nicole, *Tetrahedron Lett. 1978*, 2403; D. Huchette, J. Nicole, F. Petit, *ibid. 1979*, 1035; D. Huchette, B. Thery, F. Petit, *J. Mol. Catal. 4* (1978) 433; E. Le Roy, D. Huchette, A. Mortreux, F. Petit, *Nouv. J. Chim. 4* (1980) 173; A. Mortreux, J. C. Bavay, F. Petit, *ibid. 4* (1980) 671.

[158] D. Ballivet-Tkatchenko, M. Rivecchio, N. El Murr, *J. Am. Chem. Soc. 101* (1979) 2763; *Inorg. Chim. Acta 30* (1978) L289.

[159] M. Gilet, A. Mortreux, J. Nicole, F. Petit, *J. Chem. Soc. Chem. Commun. 1979*, 521; M. Gilet, A. Mortreux, J.-C. Folest, F. Petit, *J. Am. Chem. Soc. 105* (1983) 3876.
[160] J. Grobe, H. Zimmermann, *Z. Naturforsch. B 39* (1984) 962.
[161] J. Simonet, M.-A. Michel, H. Lund, *Acta Chem. Scand. Ser. B 29* (1975) 489, and references cited therein.
[162] H. Lund, J. Simonet, *J. Electroanal. Chem. Interfacial Electrochem. 65* (1975) 205, and references cited therein.
[163] Yu. Bendersky, V. G. Mairanaovsky, *J. Electroanal. Chem. Interfacial Electrochem. 79* (1977) 401; *ibid. 97* (1979) 1.
[164] J. Simonet, A. Orliac, J. Delaunay, *XI. Sandbjerg Meet. Org. Electrochem.* (Sandbjerg 1984), Abstr. p. 23; J. Simonet, G. le Guillanton, *Bull. Soc. Chim. Fr. 1985*, 190.
[165] C. P. Andrieux, C. Blocman, J.-M. Dumas-Bouchiat, J.-M. Savéant, *J. Am. Chem. Soc. 101* (1979) 3431; *J. Electroanal. Chem. Interfacial Electrochem. 87* (1978) 39; 55; *ibid. 113* (1980) 1, 19; C. P. Andrieux, C. Blocman, J.-M. Dumas-Bouchiat, F. M'Halla, J.-M. Savéant, *J. Am. Chem. Soc. 102* (1980) 3806.
[166] H. L. S. Maia, M. J. Medeiros, M. I. Montenegro, D. Court, D. Pletcher, *J. Electroanal. Chem. Interfacial Electrochem. 164* (1984) 347.
[167] R. Kossai, J. Simonet, G. Jiminet, *Tetrahedron Lett. 1979*, 1059.
[168] K. Oda, T. Ohnuma, Y. Ban, *J. Org. Chem. 49* (1984) 953.
[169] J. Simonet, H. Lund, *Acta. Chem. Scand. Ser. B 31* (1977) 909.
[170] H. Lund, L. Kristensen, *Acta Chem. Scand. Ser. B 33* (1979) 495.
[171] C. Degrand, H. Lund, *Acta Chem. Scand. Ser. B 31* (1977) 593.
[172] C. Degrand, D. Jacquin, P.-L. Compagnon, *J. Chem. Res. Synop. 1978*, 246; *J. Chem. Res. Miniprint 1978*, 3272.
[173] P. E. Hansen, A. Berg, H. Lund, *Acta Chem. Scand. Ser. B 30* (1976) 267.
[174] L. H. Kristensen, H. Lund, *Acta Chem. Scand. Ser. B 33* (1979) 735.
[175] P. Martigny, J. Simonet, *J. Electroanal. Chem. Interfacial. Chem. 101* (1979) 275.
[176] E. Steckhan, T. Kuwana, *Ber. Bunsenges. Phys. Chem. 78* (1974) 253.
[177] R. J. Day, S. J. Kinsey, E. T. Seo, N. Weliky, H. P. Siverman, *Trans. NY Acad. Sci. 34* (1972) 588, 647; M. Ito, T. Kuwana, *J. Electroanal. Chem. Interfacial Electrochem. 32* (1971) 415.
[178] R. DiCosimo, C.-H. Wong, L. Daniels, G. M. Whitesides, *J. Org. Chem. 46* (1981) 4622.
[179] H. Simon, J. Bader, H. Günther, S. Neumann, J. Thanos, *Angew. Chem. 97* (1985) 541; *Angew. Chem. Int. Ed. Engl. 24* (1985) 539.
[180] E. T. Seo, R. F. Nelson, J. M. Fritsch, L. S. Marcoux, D. W. Leedy, R. N. Adams, *J. Am. Chem. Soc. 88* (1966) 3498.
[181] J. F. Ambrose, L. L. Carpenter, R. F. Nelson, *J. Electrochem. Soc. 122* (1975) 876.
[182] L. Papouchado, R. N. Adams, S. W. Feldberg, *J. Electroanal. Chem. Interfacial Electrochem. 21* (1969) 408.
[183] W. Schmidt, E. Steckhan, *Chem. Ber. 113* (1980) 577; K. H. Grosse-Brinkhaus, S. Dapperheld, E. Steckhan, unpublished.
[184] T. N. Baker III, W. P. Doherty, Jr., W. S. Kelley, W. Newmeyer, J. E. Rogers, Jr., R. E. Spalding, R. I. Walter, *J. Org. Chem. 30* (1965) 3714; R. I. Walter, *J. Am. Chem. Soc. 77* (1955) 5999; *ibid. 88* (1966) 1923.
[185] H. Wieland, E. Wecker, *Ber. Dtsch. Chem. Ges. 43* (1910) 699; D. H. R. Barton, R. K. Haynes, G. Leclerc, P. D. Magnus, I. D. Menzies, *J. Chem. Soc. Perkin Trans. 1 1975*, 2055.
[186] K. H. Grosse-Brinkhaus, E. Steckhan, *Tetrahedron 42* (1986) 553.
[187] L. Eberson, *Adv. Phys. Org. Chem. 18* (1982) 79.
[188] M. Platen, E. Steckhan, *Tetrahedron Lett. 21* (1980) 511; *Chem. Ber. 117* (1984) 1679.
[189] M. Platen, E. Steckhan, *Liebigs Ann. Chem. 1984*, 1563.
[190] a) W. Schmidt, E. Steckhan, *Angew. Chem. 90* (1978) 717; *Angew. Chem. Int. Ed. Engl. 17* (1978) 673; *ibid. 91* (1979) 850 and *18* (1979) 801; b) *ibid. 91* (1979) 851 and *18* (1979) 802; c) W. Schmidt, E. Steckhan, unpublished; d) T. Esch, E. Steckhan, unpublished.
[191] a) S. Dapperheld, E. Steckhan, *Angew. Chem. 94* (1982) 785; *Angew. Chem. Int. Ed. Engl. 21* (1982) 780; *Angew. Chem. Suppl. 1982*, 1730; b) S. Dapperheld, *Dissertation*, Bonn 1984.
[192] S. Töteberg-Kaulen, E. Steckhan, unpublished.
[193] K. Schumacher, M. Platen, E. Steckhan, unpublished.
[194] a) K. H. Grosse-Brinkhaus, E. Steckhan, W. Schmidt, *Acta Chem. Scand. Ser. B 37* (1983) 499; b) H. Grosse-Brinkhaus, *Dissertation*, Bonn 1984.
[195] M. Masui, T. Ueshima, S. Ozaki, *J. Chem. Soc. Chem. Commun. 1983*, 479; M. Masui, S. Hara, T. Ueshima, T. Kawaguchi, S. Ozaki, *Chem. Pharm. Bull. 31* (1983) 4209; M. Masui (Yoshitomi Pharmaceutical Ind. Ltd.), Jpn. Kokai Tokkyo Koho JP 59 185 787 (1984); *Chem. Abstr. 107* (1985) 139 817q.
[196] U. H. Brinker, M. Tyner III, W. M. Jones, *Synthesis 1975*, 671.
[197] J. R. Behling, *4th Eur. Conf. Org. Organomet. Electrochem.* (Lioujas (Rodez), France 1980); internal electrochemical regeneration of 2,3,5,6-tetrafluoro-*p*-benzoquinone: F. Bedioui, P. L. Fabre, J. Devynck, *J. Chem. Soc. Chem. Commun. 1982*, 290.
[198] M. F. Semmelhack, C. S. Chou, D. A. Cortes, *J. Am. Chem. Soc. 105* (1983) 4492.
[199] M. F. Semmelhack, C. R. Schmidt, *J. Am. Chem. Soc. 105* (1983) 6732.
[200] *Chem. Eng. News 62* (1984) No. 37, p. 39.
[201] R. Jansson, *Chem. Eng. News 62* (1984) No. 47, p. 43.

[m.m]Metallocenophanes: Synthesis, Structure, and Properties

By Ulrich T. Mueller-Westerhoff*

Metallocenophanes are metallocenes in which the cyclopentadienyl ligands are linked intramolecularly through C_mH_n or C_mH_nX (X = heteroatom) chains. Two main classes of metallocenophanes are known: in [m]metallocenophanes the ligands of *one* metallocene are connected by a bridge (or by several bridges); in [m.n]metallocenophanes *two* (or more) metallocenes are brought together into one molecule by bridging groups. This article briefly describes the first class (mononuclear complexes) and then concentrates on the second (binuclear complexes). The [1.1]metallocenophanes, which are produced by linking two metallocene moieties through two C_1 bridges, are of particular interest and are characterized by a variety of unusual and useful properties: they are very flexible conformationally; hydride abstraction from the CH_2 bridges produces carbenium ions that are greatly stabilized by the adjacent metallocene moieties; deprotonation of one of the CH_2 bridges is surprisingly easy and leads to the unusual situation that an intramolecular C–H···C hydrogen bond stabilizes a carbanion; protonation of both metallocene moieties causes the liberation of one mole of hydrogen per mole of [1.1]metallocenophane, thereby allowing the use of these compounds as catalysts for the formation of hydrogen in acidic aqueous solutions.

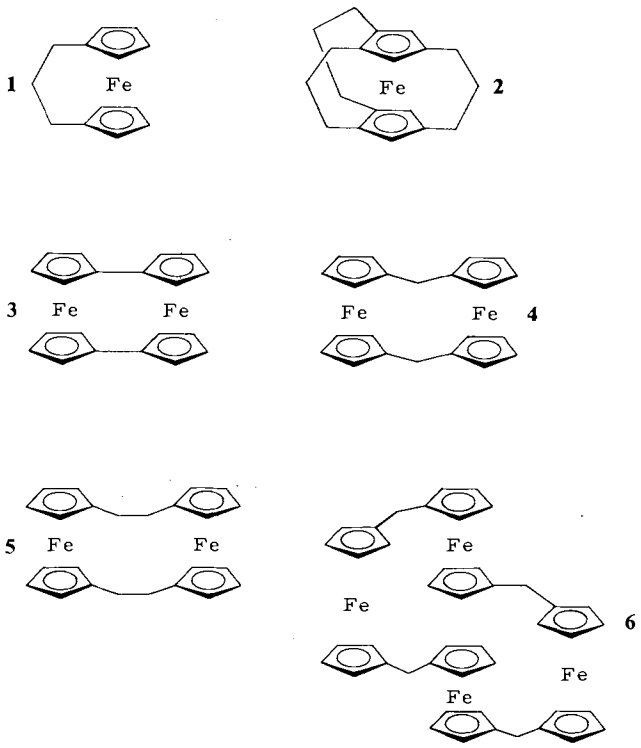
1. Introduction

1.1. General

Although some metallocenophanes have been known for close to twenty years, this class of compounds has been the subject of intensive studies only in the last few years. The development of specific syntheses and the associated study of the physical properties of the new compounds were the initial focus of investigations, which rapidly expanded to include such phenomena as metal basicity, the effects of structural deformation on the properties of metallocenes, intervalence transfer of electrons in binuclear species, electrical conductivity, and even the occurrence of intramolecular C–H···C hydrogen bonds.

There exist two main classes of metallocenophanes, exemplified here by derivatives of the classical metallocene ferrocene: the mononuclear complexes with one (**1**) or several (**2**) bridging groups and the multinuclear systems **3**–**6**, of which bis(fulvalene)diiron **3** is a special (and interesting) case because it contains no bridging groups. There also exist a large number of metallocenophanes with heteroatomic bridges, but they have been omitted from this discussion.

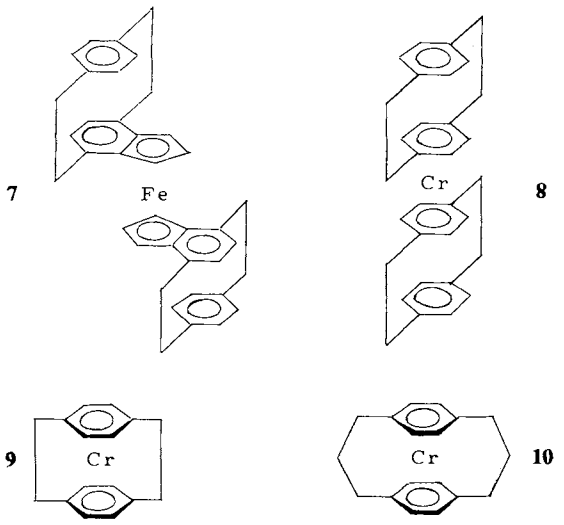
Loosely related to metallocenophanes in the sense of this definition are systems containing cyclic structures of a different type. For example, compounds **7** and **8** have been prepared[1,2] in which two cyclophane moieties coordinate a metal atom, resulting in the formation of a substituted ferrocene or bis(arene)chromium complex. Such compounds do not contain bridged metallocenes. Much more directly related are systems such as **9** and **10** in which paracyclophanes coordinate metal atoms in their cavities.[2,3] These systems are isoelectronic with similarly bridged ferrocenophanes, but they will only be mentioned here in passing.



The focus of this article is on binuclear metallocenophanes and their unusual properties; the most typical characteristics of related systems will only be discussed in connection with those of binuclear metallocenophanes. The fascination of organometallic compounds containing more than one transition-metal atom stems from the promise that these materials may show cooperative effects in which the metal centers may assist each other in redox processes and other reactions, with or without the existence of direct metal–metal interactions, and that this may

[*] Professor Dr. U. T. Mueller-Westerhoff
Department of Chemistry, University of Connecticut
Storrs, CT 06268 (USA)

 © VCH Verlagsgesellschaft mbH, D-6940 Weinheim, 1986 0570-0833/86/0808-0702 $ 02.50/0

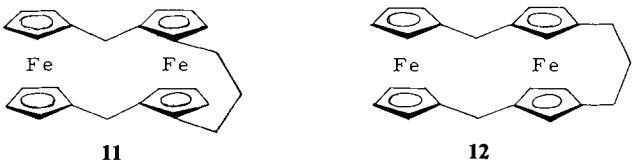


help our understanding of, for example, a variety of catalytic processes.

After several remarks concerning the nomenclature of these systems, we will discuss some of the important properties of metallocenes and of the mononuclear metallocenophanes and then focus on the chemistry and uses of the binuclear and multinuclear systems. The reader is referred to a review published nearly twenty years ago by *Watts*[4] on metallocenophanes, which emphasizes the mononuclear systems.

1.2. Nomenclature

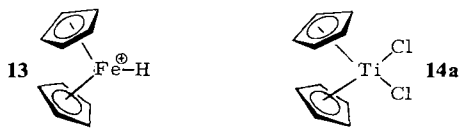
The few examples in the previous section already indicate that there does not exist a uniform nomenclature for the metallocenophanes. A widely accepted nomenclature[5] for purely organic cyclophanes[6] was used[4,7-9] rather early for bi- and multinuclear ferrocenophanes.[10] This notation appears to be the choice of the majority of researchers in this area. The ferrocenophanes (FCPs) are designated [m][n][o][p]FCP and [m.n.o.p]FCP, where the numbers in square brackets denote the length of the bridges: **1**, [3]FCP; **2**, [3][3][3]FCP;[*] **3**, [0.0]FCP; **4**, [1.1]FCP; **5**, [2.2]FCP; **6**, [1.1.1.1]FCP. This system is not sufficient, however, to indicate the exact location of the bridges, a deficiency that causes problems only in the case of multibridged FCPs or of compounds with other ring substituents. Such cases require a slightly more complex system of nomenclature, which is exemplified for **2**, a triply bridged ferrocene: although **2** can be unambiguously named, according to the IUPAC rules, as 1,1′;2,2′;4,4′-tris(trimethylene)ferrocene, its name according to metallocenophane nomenclature is [3](1,1′)[3](2,2′)[3](4,4′)ferrocenophane. In the name for **4**, [1.1]ferrocenophane, the nature of the linkages is only specified by the number of carbon atoms in the bridges. Where needed, the more complete nomenclature can be used, namely, [1.1](1,1″;1′,1‴)ferrocenophane. Interesting examples where both types of metallocenophanes have been combined into one structure were recently described by *Hillman* et al.:[11] in **11** and **12** both the [3]FCP and the [1.1]FCP structures are found. The complete name of compound **11** is [3](2,2′)[1.1](1,1″;1′,1‴)FCP and of **12** [3](3,3′)[1.1](1,1″;1′,1‴)FCP, but here it seems indeed simpler to refer to these compounds as 2,2′-trimethylene[1.1]FCP and 3,3′-trimethylene[1.1]FCP, respectively.



1.3. Important Properties of Metallocenes

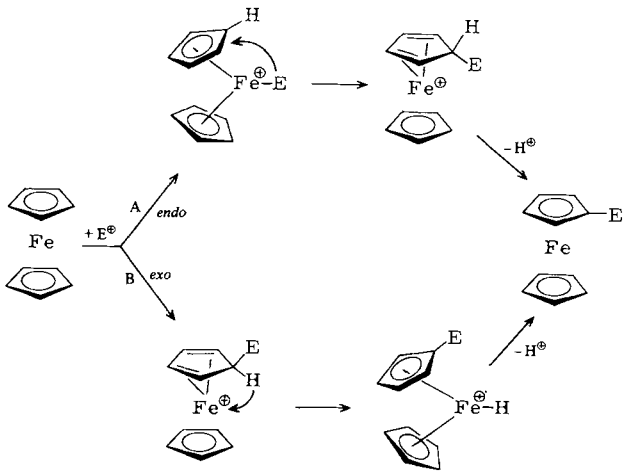
Ferrocene, known since 1952,[12] is the parent of all "sandwich" complexes. There exist many thousands today, predominantly with cyclopentadienyl ligands, although very interesting sandwich complexes are known with ligands ranging in size from C_3 (cyclopropenyl) to C_9 (cyclononatetraenyl) and with almost all of the main-group and transition metals, as well as lanthanides and actinides. The ligands in ferrocene are planar and lie in parallel planes with a separation of 330 pm;[13] this distance is comparable to the van der Waals thickness of an aromatic ring, e.g., the interplanar distance of approximately 340 pm found in crystalline arenes, so that ferrocene can roughly be thought of as a dimer of two aromatic systems within which an iron atom is "hidden," but still reveals its presence through the variety of properties of ferrocene. The C_5H_5 ligands are almost free to rotate with respect to each other: according to experimental and theoretical data,[14-17] the activation barrier to this rotation is of the order of 4-8 kJ/mol, the eclipsed conformation being slightly preferred over a staggered arrangement of the rings. Ferrocene is diamagnetic and has fully covalent bonds; it is stable toward air and nonoxidizing acids, sublimable, and soluble in most organic solvents. It can be reversibly oxidized to the deep green ferrocenium radical cation, which is more labile toward dissociation or exchange reactions than neutral ferrocene. Ferrocene acts as a very weak base: it undergoes protonation in extremely strong nonoxidizing acids to form a cation, which is slowly oxidized in air to the ferrocenium ion. In analogy to the known structures of other protonated metallocenes, the protonated ferrocene is assumed to have the bent structure **13**. Such bent structures are found frequently in compounds such as titanocene dichloride **14a**.

Related to the mechanism of protonation at the metal atom of metallocenes is the ease with which they—par-



[*] An alternative is to give the number of identical bridges in mononuclear complexes as subscripts, e.g., **2**, [3_2]FCP.

ticularly ferrocene—can undergo electrophilic substitution: compared with benzene, ferrocene is substituted several orders of magnitude faster. One of the most often (albeit incorrectly) cited reasons for this is that ferrocene coordinates the electrophile at the metal, thereby facilitating the ring substitution (path A in Scheme 1, *endo* attack). Alternatively, however, *exo* attack by the electrophile (path B) could explain the ease of substitution, because transfer of a proton of the ligand to the iron atom (the intermediate would be analogous to protonated ferrocene **13**) and its subsequent elimination are plausible; such a mechanism is not available to benzene.



Scheme 1. Alternative mechanisms for the electrophilic substitution of ferrocene (see text). Both pathways make use of the ability of the iron atom to coordinate an additional ligand.

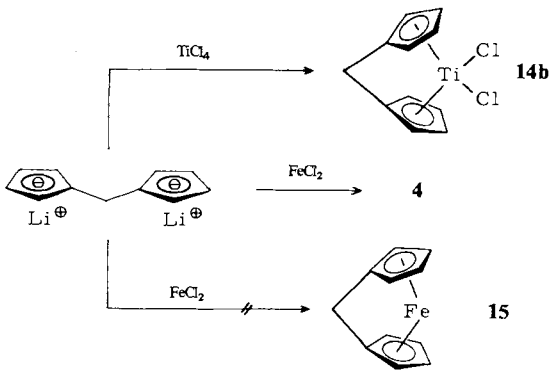
Ferrocene analogues of other transition metals show a wide range of properties. A few key properties of relevance to the discussion of metallocenophanes are related to the 18-electron rule: metallocenes with a total of 18 valence electrons (metal valence electrons plus ligand valence electrons minus total charge of the compound) are stable and have ferrocene-like sandwich structure: ruthenocene, osmocene, and the cobaltocenium ion are typical examples. The distance between the rings in ruthenocene (370 pm) is larger than in ferrocene; ruthenocene cannot be oxidized to a monocation, but a dication is known. The cobaltocenium ion is formed rapidly from its 19-electron precursor cobaltocene in aqueous acidic media upon exposure to oxygen (air). It is stable toward the strongest acids and does not undergo any of the typical electrophilic substitution reactions known for ferrocene.

2. [m]Metallocenophanes

When metallocenes and some of their simple derivatives were discovered, one of the more astonishing findings was that the cyclopentadienyl ligands lie in strictly parallel planes and can rotate easily about the symmetry axis. This is of course no longer true when the two ligands are joined by a bridge: the dihedral angle between the planes of the rings will depend to a large degree on the length of the bridge(s), and, instead of an almost free rotation, only vibration is possible. The ease of electrophilic substitution reactions should also be greatly influenced in going from ferrocenes to [m]ferrocenophanes: the tilt of the rings facilitates coordination to the metal, which in turn influences the reaction mechanism (path A or path B, see Scheme 1). Such considerations have prompted the study of [m]FCP systems having different bridge sizes and of ferrocenes with more than one bridge. Most of the present literature is still concerned with the synthesis and structural characterization of these compounds, only a few mechanistic studies having been reported. By far, most of the publications on [m]metallocenophanes concern ferrocene derivatives, although a comparison between systems involving different metals and thus varying distances between the rings is of great interest.

2.1. [1]Metallocenophanes

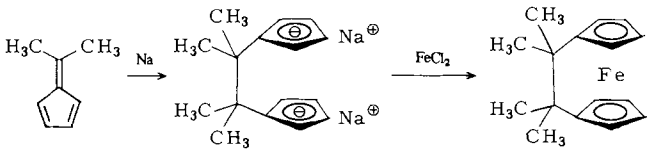
No examples exist of [1]ferrocenophanes such as **15**, because a C_1 bridge would presumably force the rings to tilt so much that the ferrocene system would no longer be stable. Precisely this tilt, however, is the preferred arrangement for the titanocene dichloride system **14a**. It is thus not surprising that the reaction of the dilithium salt of dicyclopentadienyl methane with iron(II) chloride does not lead to **15**, but instead produces **4** together with its oligomers;[9] its reaction with $TiCl_4$, on the other hand, cleanly produces **14b** (Scheme 2).[18]



Scheme 2. Reactions of dicyclopentadienylmethane dianion with $FeCl_2$ and $TiCl_4$.

2.2. [2]Metallocenophanes

The first [2]metallocenophane, 6,6,7,7-tetramethyl[2]ferrocenophane **18**, was prepared in low yield by reacting 6,6-dimethylfulvene **16** with sodium to give the disodium salt **17**, followed by addition of $FeCl_2$. This reaction (Scheme 3), first reported by *Rinehart* et al.,[19] is typical of the approach by which many [m]metallocenophanes have been prepared. The rings in **18** are tilted with respect to each other, a structure that corresponds to the one assumed for protonated ferrocene **13**. It is not surprising, therefore, that [2]ferrocenophane is easier to protonate than ferrocene.[20]

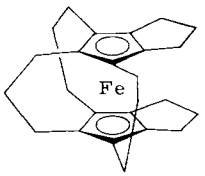


16 17 18

Scheme 3. Synthesis of 6,6,7,7-tetramethyl[2]ferrocenophane **18** from 6,6-dimethylfulvene **16**.

2.3. [3]Metallocenophanes

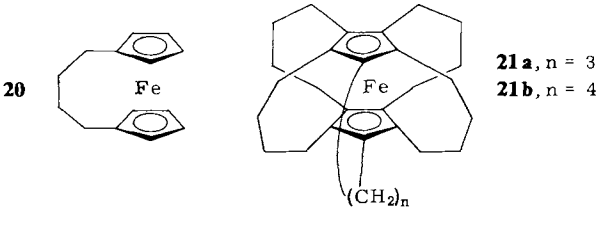
[3]Metallocenophanes are by far the best represented of the [m]metallocenophanes, both because these compounds are accessible by several routes (including some of the typical condensation reactions well-known in organic chemistry) and because the C_3 bridge causes relatively little distortion in the system. Although the C_3 bridge is too short to span the distance between the cyclopentadienyl ligands in ferrocene without any strain, the construction of multibridged systems is still possible. [3]Ferrocenophanes with one, two, three, or four bridges are known;[21,22] only the fully bridged [3][3][3][3][3]FCP ([3_5]FCP) has so far eluded all synthetic efforts. In several attempts to synthesize such a system, cyclization involving only one cyclopentadienyl ligand occurred instead of the desired bridge formation between the two sandwich moieties. Compound **19** is an example of such a product.[23]



19

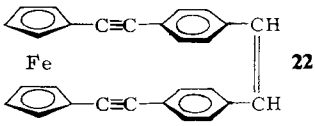
2.4. [4]Metallocenophanes and Larger Systems

The [4]ferrocenophane **20**, prepared by *Lüttringhaus* et al. in 1958,[24] was the first example of a bridged ferrocene. The synthesis, starting from a dicyclopentadienide reagent, produced a variety of oligomers. In the meantime, a large number of FCPs with C_n bridges ($n \geq 4$) have been prepared. Noteworthy are the homologues of **20**, such as the [4][4][4]- and [5][5][5]ferrocenophanes with bridges in the 1-, 2-, and 4-positions.[25] In 1982, *Hisatome* et al.[26a] reported the first example of a fully enclosed ferrocene system, [3][4][4][4][4]ferrocenophane, which contains one C_3 and four C_4 bridges. Its structure, despite disorder in the crystal, has been characterized. Recently, the same group reported the synthesis of the symmetrical [4][4][4][4][4]ferrocenophane ([4_5]FCP), which, in analogy to superphane, was named "superferrocenophane."[26b]



20 **21a**, n = 3 **21b**, n = 4

[m]Ferrocenophanes with extremely long bridges have also been prepared by *Hisatome* et al., but the current record, held by a Swedish group,[27] appears to be the synthesis of a partially conjugated [24]ferrocenophane. One further example from another Japanese group combines the [m]metallocenophane structure with that of a typical paracyclophane: compound **22** was reported by *Kasahara* et al.[28]

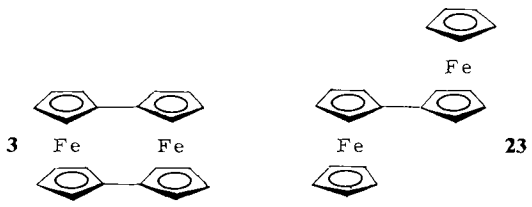


22

3. [m.m]Metallocenophanes

The concept of linking two or more metallocenes by simple hydrocarbon bridges offers a number of interesting possibilities, including various interactions between the two metallocenes, the nature and extent of which will clearly depend on the size and nature of the bridges. Such interactions may be transmitted either through the ligands (through-bond) or directly (through-space) or by combinations of the two possibilities. This concept thus allows, in principle, the construction of compounds with novel redox properties. Owing to the availability of two or more coordination sites and the existence of controllable cooperative effects in their redox chemistry, [m.m]metallocenophanes may find applications in catalytic processes where their mononuclear counterparts are of little or no use.

In any compound containing more than one metal center, the possibility exists that, through oxidation or reduction, different oxidation states of the metal may be present in the same molecule. Such "mixed valence" compounds are found in many areas of organometallic and coordination chemistry. However, the metallocenophanes have played an especially important role in contributing to our understanding of this class of substances. The presence of a mixed valence compound is revealed by usually broad but relatively intense near-IR (NIR) absorptions, often called intervalence transfer bands. These are exemplified in Figure 1 by the NIR spectra of the monocations of bis(fulvalene)diiron **3** and its singly bridged analogue biferrocene **23**.[41]



3 **23**

The electronic process giving rise to these absorptions is the transfer of an electron from the metal atom with the lower oxidation state to that with the higher oxidation state, thus reversing the order of oxidation states: in iron-containing species, for example, such an excitation corre-

sponds to the process $Fe^{II}/Fe^{III} \rightarrow Fe^{III}/Fe^{II}$. Because the local environment in different oxidation states is usually not the same, this electron-transfer process leaves both metals in a vibrationally excited state. In symmetric molecules, relaxation from this state leads to a ground state that is identical to the initial one. Metallocenophanes are excellent models for the investigation of such phenomena, because their structural parameters can be selectively varied.

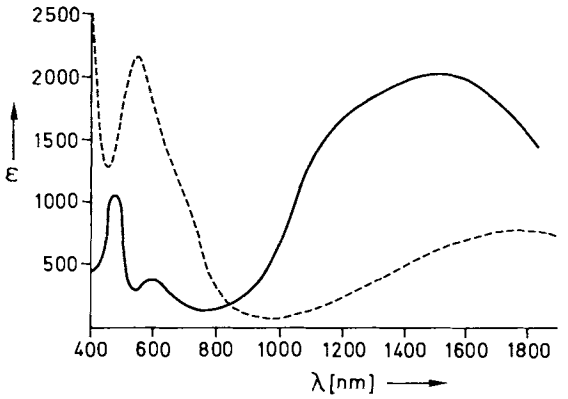


Fig. 1. The NIR spectra of the mixed valence monocations of **3** (solid line) and **23** (dashed line). Intervalence transfer bands are the broad, long-wavelength bands. For **3**, two absorptions with maxima at 1140 and 1550 nm overlap [41].

A classification of mixed valence systems based on the extent of intramolecular interaction was proposed very early by *Robin* and *Day*[29] and served as a guide to understand some of the phenomena. In compounds of class I, no interaction between the two metals exists, and such compounds show properties typical of the independent molecules. Compounds of class II show a moderate degree of interaction so that these compounds possess new properties in addition to those of their components. Class III refers to those compounds in which strong interactions between the two metals exist, so that none of the properties of the components remain and a new, delocalized species exists. This is reminiscent of the familiar picture of resonance in organic chemistry.

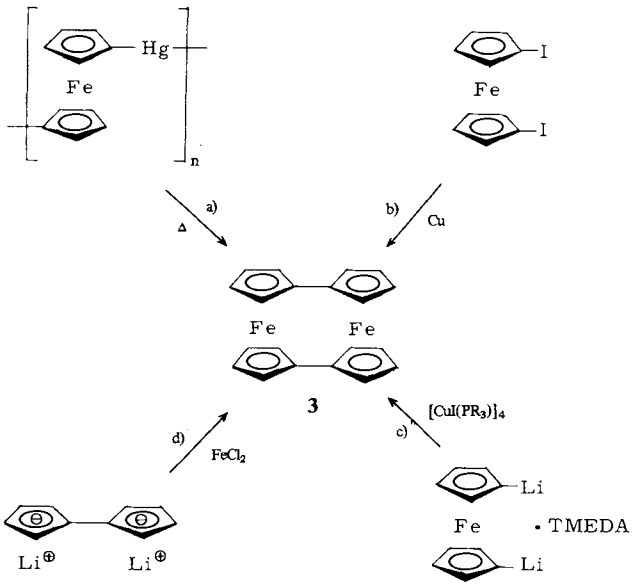
A theoretical model developed by *Hush*[30] provides a more quantitative parametrization of these systems. More recently, another model, based on the vibrational coupling of the two metals, was developed.[31] It is in good agreement with the experimental data for many systems. No clear borders exist between these classes; instead, many gradations of intramolecular exchange interactions can exist.

Most of the work on [m.m]metallocenophanes has focused on dimeric ferrocenes, but compounds containing other metals have begun to receive attention as the unique properties of these systems have been recognized. The focus on iron-containing species in this article is not an arbitrary limitation but reflects the current state of development. The [0.0]metallocenophanes are a major exception in this regard, because they are known for almost all first-row transition metals.

3.1. [0.0]Metallocenophanes

The first example of this type of binuclear metallocene was [0.0]ferrocenophane **3**, which has been named biferrocenylene, 1,1′-biferrocenylene, and, most frequently, bis(fulvalene)diiron. Many comparisons have been made between **3** and its singly bridged analogue biferrocene **23**.

There now exist four methods for the preparation of **3** (Scheme 4): pyrolysis of polymercury ferrocenes (path a),[32] Ullmann coupling of 1,1′-diiiodoferrocene (path b),[33] coupling of 1,1′-dilithioferrocene via organocuprates (path c),[34] and direct synthesis by reaction of the fulvalene dianion with $FeCl_2$ (path d).[35]



Scheme 4. Four synthetic routes to [0.0]ferrocenophane **3** (see text). TMEDA = *N,N,N′,N′*-tetramethylethylenediamine.

The yields obtained by paths a–c are low (11% for path c). The direct synthesis (path d) now affords a maximum yield of 40%.[41] This is surprisingly high in view of the potential of this reaction to produce oligomeric and polymeric material. Since polymeric materials are formed to a greater or lesser extent in all of these methods, separation of the only moderately soluble **3** was initially a problem. Indeed, the first syntheses were deemed to be failures, because such poor solubility was unexpected and the product **3** was assumed to be polymeric. Considering that biferrocene **23** can be recrystallized from hexane, it is indeed surprising that the solubility of **3** in benzene[32] is only 200 mg/L. The reason for this must be sought in the rigidity of **3**, which leaves little opportunity for adequate solvation.

The structure of **3** (Fig. 2) was expected to exhibit a larger Fe-Fe distance than a fully symmetric structure with two ferrocenes would dictate.[36] This expectation was based on the unusually large (1.5 ppm) chemical shift difference between the two kinds of protons.[32] Surprisingly, however, two completely "normal" ferrocenes were found in **3**: the two atoms lie at the center of the two ferrocene

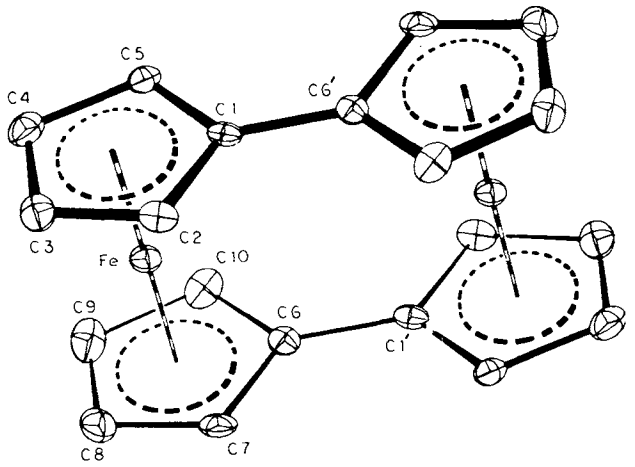


Fig. 2. The crystal structure of [0.0]ferrocenophane **3**. The ligands are coplanar and consist of regular, undistorted ferrocene moieties with a Fe-Fe distance of 398 pm. (Reprinted from ref. [36] with permission of the American Chemical Society.)

units and are 398 pm apart, the distance dictated by the C–C single bonds (148 pm) connecting the two units.

The difference between the singly connected biferrocene **23** and the doubly connected [0.0]ferrocenophane **3**, which already manifests itself in their differing solubilities, becomes very apparent when these two compounds are oxidized to their radical cations and dications. From electrochemical data[37,38] (with a saturated calomel electrode, SCE, as reference electrode, **23** is oxidized at 0.31 and 0.64 V, **3** at 0.13 and 0.72 V), it is apparent that **3** is much more easily oxidized to the monocation than **23**, but that the oxidation to the dications requires a similar, more positive potential. Why is $\mathbf{3}^{\odot\oplus}$ much more stable that $\mathbf{23}^{\odot\oplus}$? Mössbauer and X-ray photoelectron spectroscopy (XPS)[39,40] provide a first answer: whereas the iron atoms in $\mathbf{3}^{\odot\oplus}$ are identical, they are different in $\mathbf{23}^{\odot\oplus}$. The biferrocene monocation $\mathbf{23}^{\odot\oplus}$ is a typical example of a mixed valence compound of class II, according to the system of *Robin* and *Day*.[29] One iron atom has the environment of a neutral ferrocene, whereas the other is part of a ferrocenium cation; a limited degree of interaction between the two iron atoms occurs, giving rise to an intervalence transfer absorption (see Fig. 1). On the other hand, the cation $\mathbf{3}^{\odot\oplus}$ is a fully delocalized compound of class III with either a symmetric ground state or with such an extremely rapidly occurring intervalence transfer—faster than 10^{18} s^{-1} according to the XPS data—that this differentiation becomes meaningless. Of relevance, however, is the question whether the apparently very strong coupling of the iron atoms in $\mathbf{3}^{\odot\oplus}$ occurs by direct metal–metal interactions or occurs through the ligands.[41] A large number of studies and discussions suggest that both types of interactions are important.

That the ligands do play an important role is revealed by the finding that the two dications $\mathbf{3}^{2\oplus}$ and $\mathbf{23}^{2\oplus}$ are also very different: the biferrocene dication $\mathbf{23}^{2\oplus}$ is a diradical containing two noninteracting ferrocenium units,[42] whereas the [0.0]ferrocenophane dication $\mathbf{3}^{2\oplus}$ is diamagnetic (its NMR spectrum[43] is very similar to that of the neutral compound **3**). The initial explanation given for this diamagnetism was a strong intramolecular interaction through the ligands.[43] Direct metal–metal bonding was held to be unlikely on account of the accumulation of positive charge in this system, which would not be expected to allow a significantly close approach of the two iron atoms to facilitate such interaction.

That direct metal–metal interactions are also important is shown by the crystal and molecular structure of a complex salt of the [0.0]ferrocenophane radical cation $\mathbf{3}^{\odot\oplus}$ (Fig. 3).[44] The distance between the iron atoms is 364 pm (compared with 398 pm in neutral **3**); the ligands accommodate this shortening of the Fe–Fe distance by a tilting of 10°. However, the direct metal–metal interactions alone cannot account for the presence of two identical iron atoms. Arguments to the contrary have been given, but they were either shown later to be in error or repudiated by other evidence. For example, the delocalization found in the cation of [2.2]ferrocenophanediyne (see Section 3.3), in which the iron atoms are separated by more than 600 pm, can only be caused by interactions through the ligands. Molecular orbital calculations have indicated the importance of direct metal–metal interactions, but have not excluded interactions through the ligands.[45] Both interactions appear to be of varying significance in different cases, with the balance between them being dominated by structural factors which otherwise are not too obvious. This is also supported by the high degree of delocalization that some derivatives of biferrocene **23** exhibit.[46] The detailed reasons are not understood, but an analysis based on the vibronic coupling model[31] of *Piepho, Krausz,* and *Schatz* (PKS model) has once more emphasized that the differences are quantitative but not qualitative in nature.[47]

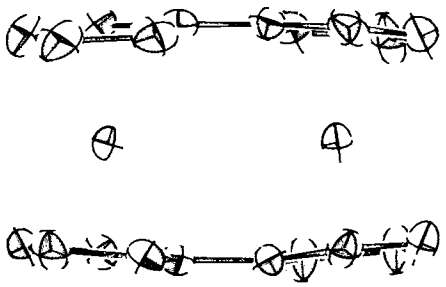


Fig. 3. Structure of the [0.0]ferrocenophane radical cation $\mathbf{3}^{\odot\oplus}$ in crystals of [0.0]ferrocenophanium picrate hemihydrate. The ligand rings tilt up toward the center, allowing the iron–iron distance to shrink by 34 pm compared with the distance in the neutral compound. (Reprinted from ref. [44] with permission of the American Chemical Society.)

Through the work of *Smart* et al.[48] and others, [0.0]metallocenophanes are now known for almost all first-row transition metals. An X-ray structure of the nickel compound has been reported (Fig. 4).[49] The compound exemplifies well the 18-electron rule: in contrast to the [0.0]ferrocenophane with its two fully symmetric ferrocene ligands, the nickel atoms are coordinated predominantly to the butadiene units of the fulvalene ligands and are consequently further apart than the combination of two nickelocenes would predict; the central C–C bond takes on considerable double-bond character and the bond lengths in the cyclopentadienyl ligands alternate significantly.

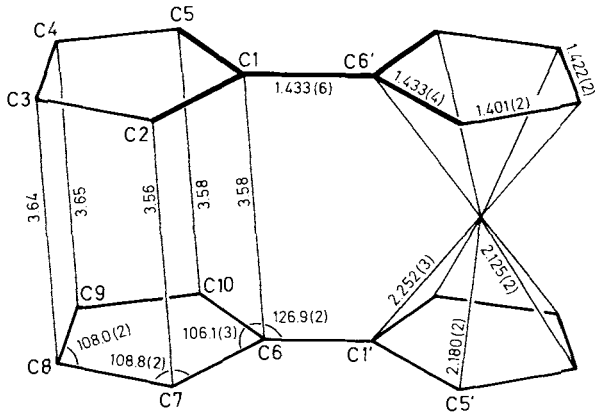
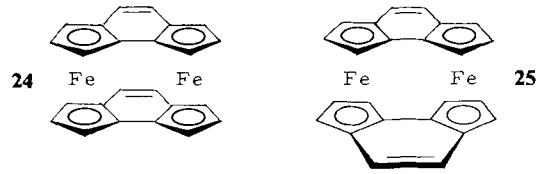


Fig. 4. Schematic drawing of the crystal structure of the ligand framework of [0.0]nickelocenophane [49] with distances [Å] and angles [°].

So far, no [0.0]metallocenophanes with two different metal atoms are known. Their preparation would require novel synthetic strategies.

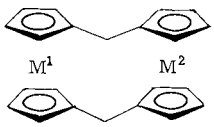
A special case in the group of [0.0]metallocenophanes is the doubly bridged system with *as*-indacenyl dianions as ligands. Bis(*as*-indacenyl)diiron is a [0.0]ferrocenophane containing ethylene groups as bridges; it exists as a mixture of the *syn* and *anti* configurations **24** and **25**, respectively.[50]



The ease with which [0.0]metallocenophanes can be oxidized to stable radical cations allows such systems to react with electron acceptors such as tetracyanobenzoquinodimethane (TCNQ) to form ionic charge-transfer complexes. The TCNQ complexes of a large number of donors have been investigated, and many of them exhibit high and strongly anisotropic electrical conductivity.[51] The one-dimensionality of the electrical conductivity is related to the tendency of TCNQ to form segregated radical anion stacks, along which electrons can move throughout the entire length of the crystal, and to its tendency to impose such one-dimensional order onto the donors as well. The first such complex was that of TCNQ with tetrathiafulvalene (TTF). [0.0]Ferrocenophane reacts with TCNQ to form a salt of the composition [0.0]FCP$(TCNQ)_2$, in which [0.0]FCP exists as the radical cation. Two TCNQ molecules share one negative charge. Compressed pellets of this complex show the same electrical conductivity as that of pellets of TTF-TCNQ. This stimulated many attempts to grow large single crystals of [0.0]FCP$(TCNQ)_2$. However, a slight mismatch between the thickness of the donor molecule and the periodicity of the TCNQ stack results in felt-like, massively interwoven crystals. Although, for this reason, the exact magnitude of the electrical conductivity in this complex could never be established, the initial findings prompted the investigation of several related materials, such as the TCNQ complex of [0.0]FCP-containing polymers.[52] The work of *Katz* et al.[53] on helical metallocenophanes was also motivated in part by the search for electronically conducting complexes. It is surprising that many different salts of the organic donor TTF are known, but that only a few salts of [0.0]FCP have been investigated for their conductive properties in spite of the fact that a large spectrum of charge-transfer salts of ferrocene and other metallocenes are known, some of which show considerable electrical conductivity.

3.2. [1.1]Metallocenophanes

In addition to the system **4**, derived from ferrocene, the [1.1]metallocenophanes also include systems containing ruthenium and cobalt (**26**–**29**).



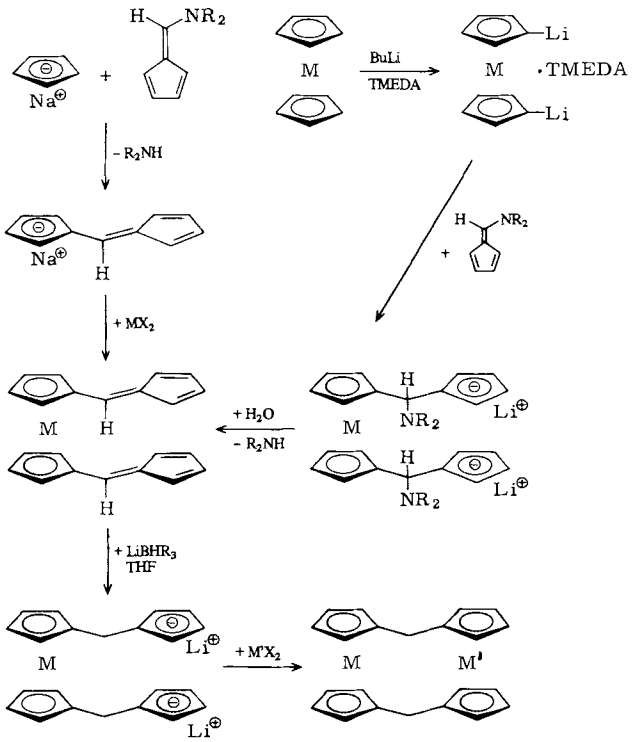
4, $M^1 = M^2 = Fe$
26, $M^1 = Fe$, $M^2 = Ru$
27, $M^1 = Fe$, $M^2 = Co$
28, $M^1 = M^2 = Ru$
29, $M^1 = M^2 = Co$

3.2.1. Syntheses

Two different and independent synthetic routes to [1.1]ferrocenophane **4** were reported in the late 1960s: *Watts*[8] prepared **4** via the corresponding diketone and *Katz* et al.[9] obtained it from the ligand dianion and iron(II) chloride; the latter route also leads to [1.1]FCP oligomers containing three, four, or five ferrocene units, including [1.1.1.1]FCP **6** cited in the introduction. Both of these routes afforded only very low yields, so that [1.1]FCP remained scarce in spite of some indications that it exhibited unusual properties. A derivative that was methylated once in each of the bridges was obtained by yet another route, but, unfortunately, also in only very modest yield.[8]

Because we required larger amounts of [1.1]FCP **4**, we developed a variant of the synthesis used by *Watts*[8] via the then unknown 1,1'-difulvenyl ferrocenes[54,55] (maximum yield 60%) (Scheme 5).[56] It's advantage is that one ferrocene unit and the entire carbon skeleton of the final product already exist in the precursor. In contrast to the original synthesis from dicyclopentadienyl methane, this route only allows the formation of oligomers with an even number of ferrocene units. Conversion of the difulvenyl ferrocene into the dicyclopentadienide was best achieved by using lithium triisobutyl borohydride. The relatively unreactive trialkyl borohydride is formed as by-product, but does not interfere with the subsequent addition of a transition-metal salt.

Since the reduction step may be followed by the addition of transition-metal salts other than iron(II) chloride, this route also offers the first useful entry to the class of metallocenophanes with different metals. In this way, the Fe/Ru and Fe/Co complexes **26** and **27**, respectively, were prepared. Bridge-substituted [1.1]FCP derivatives are also accessible. For example, reaction of the difulvenyl ferrocene with methyllithium, and $FeCl_2$ leads to a mixture of *endo,exo*- and *exo,exo*-dimethyl[1.1]ferrocenophanes (see



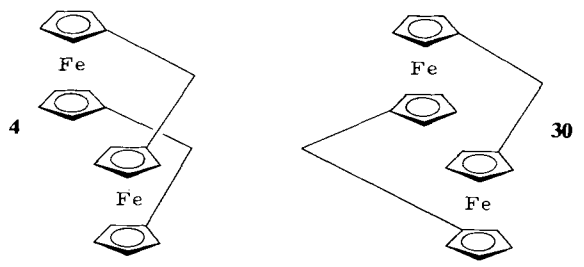
Scheme 5. The synthesis of [1.1]metallocenophanes via difulvenyl metallocenes, which are available by two different routes, both of them efficient. Their conversion to metallocenophanes involves reduction to the ligand dianion and reaction with metal(II) chlorides. Yields are surprisingly high. THF = tetrahydrofuran, R = *i*Bu.

Section 3.2.2). This route was also used for the synthesis of the [1.1]metallocenophanes **26** and **28** containing ruthenium.[57]

For [1.1]cobaltocenophane **29**, however, this route is not suited, because the lithiation of cobaltocene is not possible. Here, the original synthesis via the dianion of dicyclopentadienyl methane has to be used. The blue-green initial product **29** can be oxidized to a mixture of the more stable cobaltocenium salts, from which a salt of the dication $\mathbf{29}^{2\oplus}$ can be obtained by fractional crystallization. As expected, the yields are very low (maximum yield 2%).[58]

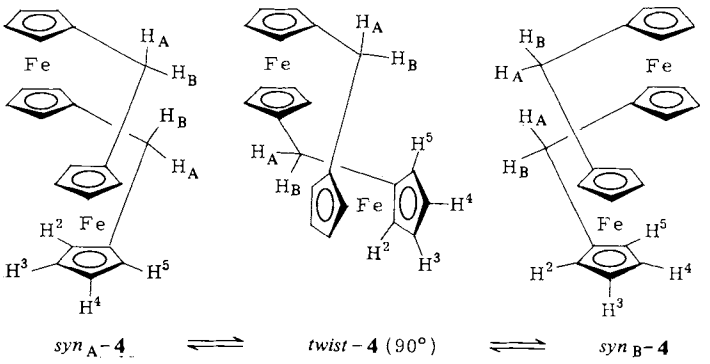
3.2.2. *Structure and Properties*

Dreiding models of [1.1]ferrocenophane **4** are helpful in understanding the structure of this compound. Intuitively, one would be tempted to assume that this compound should exist as two isomers: like bis(*as*-indacenyl)diiron, which exists in *syn* and *anti* forms, **24** and **25**, respectively, [1.1]FCP should also exhibit two configurations. In both



forms, **4** and **30**, the inner protons in the 2-position severely crowd each other (a problem that does not exist in the *as*-indacene complexes).

The models demonstrate that the *anti* isomer **30** is rigid and is not able to relieve the overcrowding, but that the *syn* isomer **4** is amazingly flexible and can easily twist to relieve all steric problems. This flexibility is directly linked to the low activation barrier for the rotation of the two ligands in the two ferrocene units. These rotations are coupled owing to the methylene links between the ferrocene units. This allows the molecule to undergo synchronized motion from one *syn* conformation to its mirror image. Although it is nearly impossible to give an adequate two-dimensional description of this motion, an attempt is made in Scheme 6.



Scheme 6. Degenerate isomerization of [1.1]ferrocenophane **4**, which results in "exchange" of the *exo*- and *endo*-protons as well as the protons in the 2- and 5-positions as well as those in the 3- and 4-positions. This exchange is very rapid and has a low activation barrier.

The unprecedented conformational flexibility of [1.1]FCP **4** is also revealed in its ^{1}H-NMR spectrum,[7,8] which exhibits peaks for only three types of protons: the bridge protons appear as one sharp singlet; the eight protons in the 2- and 5-positions and the eight protons in the 3- and 4-positions each give rise to only one multiplet. Investigations in our laboratory have shown that this motion still occurs rapidly even below $-80°$ (Fig. 5), establishing an upper limit of 10 kJ/mol for the barrier to this *syn*–*syn* exchange.[56] The name "molecular acrobats" ascribed[59] to the [1.1]ferrocenophanes is thus not too much of an exaggeration.

The isomerization can be inhibited or even suppressed by substituents either on the rings or on the bridges. Whereas an ethyl group in the 3-position does not affect the isomerization, one in the 2-position completely suppresses it.[60] The conformational flexibility has also been studied in the hybrid metallocenophanes **11** and **12**.[11] Whereas in 2,2′-trimethylene[1.1]FCP **11** the *syn*–*syn* exchange is suppressed, it occurs in the 3,3′-isomer, although not as rapidly as in **4**.

Substitution at the bridges also affects the *syn*–*syn* exchange because the two *syn* conformations, syn_A-**4** and syn_B-**4**, are no longer equivalent. The *exo,endo*- and *exo,exo*-dimethyl compounds **31** and **32**, respectively, are good examples.[56] In **31**, the two conformations are identical; the methyl groups offer little steric hindrance to the

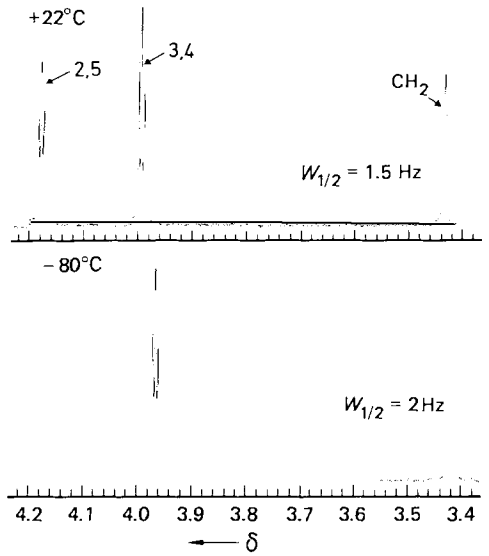
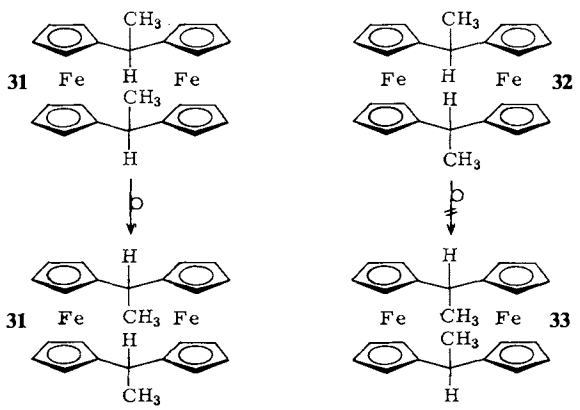
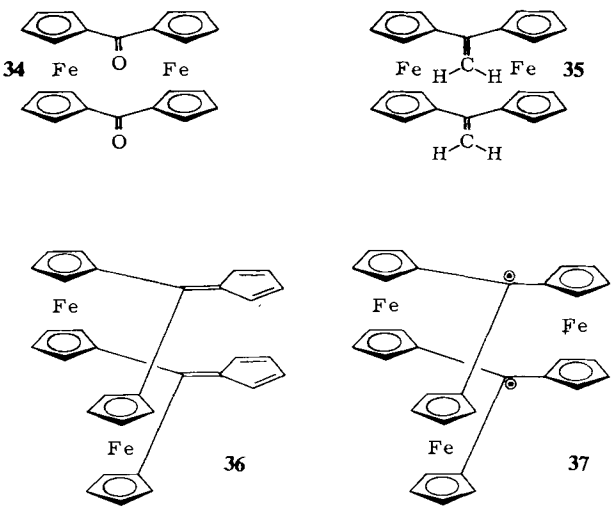


Fig. 5. 360-MHz ^{1}H-NMR spectrum of [1.1]ferrocenophane **4** in CS_2 at +22°C (above) and −80°C (below).

isomerization. For the *exo,exo* isomer **32**, on the other hand, the isomerization would give the sterically impossible *endo,endo* isomer **33**. Although the ^{1}H-NMR spectra reveal some motion in this system as well, it is limited to an opening of the *exo,exo* form to the transition state and a return to the starting conformation. As a consequence of rapid *syn,syn* exchange, there exist no isomers of the [1.1]FCP with a methyl group on only one of the bridges.



Electronic factors such as conjugation between the ferrocene units and unsaturated bridge substituents appear to be less important than steric factors in influencing this exchange. This becomes apparent from the ^{1}H-NMR spectra of the diketone **34** and the bis(methylene) compound **35**,[61] which both show the very simple two-multiplet structure for the ring protons. Even in the bis(fulvene) derivative **36**, which we recently prepared as a precursor to several trinuclear metallocenophanes, including the target "ferrous wheel" **37**, we see the same equivalence of these protons. The rapid motion of the fulvene substituents, reminiscent of the opening and closing of a crocodile's mouth, makes **36** useful for the synthesis of multinuclear metallocenes (**35** is also a potentially useful precursor).



The fact that [1.1]FCP **4** exists only in the *syn* conformation has been confirmed by X-ray crystallography. Since **4** tends to crystallize as very thin leaflets that are unsuitable for crystallography, the first structural characterization was carried out on the *exo,exo*-dimethyl derivative **32** and confirmed the expected arrangement, including a significant twist to eliminate the repulsion between the inner protons in the 2-positions.[62] We recently succeeded in obtaining suitable single crystals of the parent compound **4** and in carrying out its structure determination (Fig. 6). The ferrocene units are twisted to alleviate the steric repulsion, and the bridges are slightly opened from a fully parallel arrangement. Single crystals of the Fe/Ru system **26** were also investigated: a very similar structure was found, but with the expected dissymmetry imposed by the different ring–ring distances of the ferrocene and ruthenocene moieties.[63]

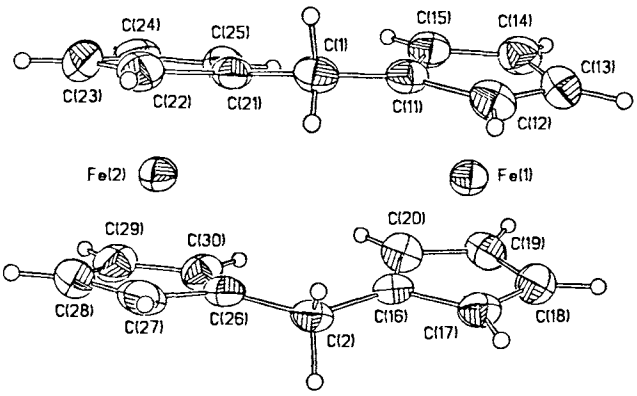


Fig. 6. Crystal structure of [1.1]ferrocenophane **4**. The molecule is twisted; this lengthens the distance between the bridge atoms and thereby avoids repulsion between the *endo*-protons of the bridge and between the ring-protons pointing toward the center of the molecule [63].

Although this article is not concerned with metallocenophanes whose bridges contain non-carbon atoms, one such compound must be mentioned here because of its direct relevance to the structure of the [1.1]metallocenophanes. In *Sn,Sn,Sn',Sn'*-tetrabutyldistanna[1.1]ferrocenophane[64] (Fig. 7), the steric bulk of the *n*-butyl groups prevents the normal *syn*-orientation; owing to the greater length of the

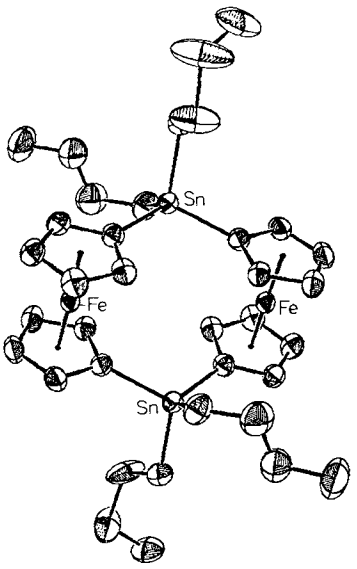


Fig. 7. Crystal structure of *Sn,Sn,Sn',Sn'*-tetra-*n*-butyldistanna[1.1]ferrocenophane (see text) [64]. The figure was taken from [64] with the permission of the authors and Elsevier Sequoia S.A., Lausanne.

C–Sn bonds (215 pm vs. 148 pm for a C–C bond), the inner protons experience less repulsion than in the *syn*-[1.1]metallocenophanes. As a consequence, the tin analogue adopts the *anti*-configuration and a nearly coplanar structure of the ferrocene units. From the structural data,[64] the distance between the inner protons can be calculated to be approximately 185 pm. The ^{1}H-NMR spectrum, which was reported without further comment, shows only two triplets with $J = 1.8$ Hz at $\delta = 4.15$ and 4.37. This pairwise equivalence of the protons in the 2- and 5- as well as 3- and 4-positions is an enigma and contradicts the behavior of typical ferrocenophanes.

Rapid *syn-syn* exchange also occurs in the other unsubstituted [1.1]metallocenophanes **26**, **27**$^{\oplus}$, **28**, and **29**$^{2\oplus}$.[65] The NMR spectra of these compounds are very simple and show the typical sharp singlet of the methylene bridges.

The yellow-orange color of ferrocene is responsible for the color of the Fe/Fe and Fe/Ru [1.1]metallocenophanes **4** and **26**, respectively. Both ruthenocene and ruthenocenophane **28** are colorless. The [1.1]cobaltocenophane dication **29**$^{2\oplus}$ is isoelectronic with [1.1]ferrocenophane **4**, a fact reflected by its yellow color. While these metallocenophanes are stable under the usual conditions, they are easily oxidized, particularly in solution, to the mono- and diketones. The ketones can be sulfurized with P_4S_{10} to produce the synthetically useful thiones.[61]

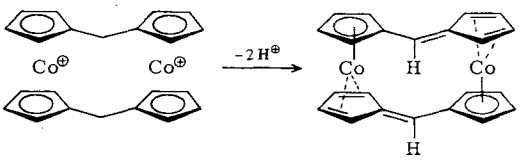
Electrochemical oxidation follows, with one remarkable exception, the normal trends found in metallocenes (Table 1).[66] Ferrocene shows a reversible one-electron oxidation at relatively low potential; ruthenocene undergoes an irreversible two-electron oxidation at a much more positive potential. In [1.1]FCP **4** the oxidation waves of the two ferrocene moieties are separated by 200 mV; the first occurs at slightly lower potential than that for ferrocene, whereas the second is at a slightly higher potential on account of Coulomb repulsion. In the Fe/Ru system **26**, the ferrocene-based one-electron oxidation is observed first; the ruthenocene-based two-electron oxidation occurs at higher potential. Astonishing is the behavior of [1.1]ruthenocenophane **28**: instead of showing an irreversible oxidation at high potential, it exhibits a reversible two-electron oxidation at the surprisingly low potential of 380 mV. The reasons for this stabilization of the resulting dication are not fully understood. However, chemical oxidation of **28** leads to a diamagnetic cation, whose ^{1}H-NMR spectrum shows four multiplets ($\delta = 5.50$, 5.66, 5.93, and 6.14) for the ring protons and a sharp singlet ($\delta = 3.55$) for the four bridge protons. Since the latter signal indicates rapid isomerization between two *syn* conformations, the nonequivalence of the ring protons (one set of which is shifted downfield by 1.0 ppm and the other by 1.5 ppm from the values for ruthenocenophane **28**: $\delta = 4.41$ and 4.60) must stem from a dissymmetry in the dication.

Table 1. Cyclovoltammetric redox potentials of metallocenes and [1.1]metallocenophanes (C_6H_5CN solution with tetrabutylammonium fluoroborate as electrolyte; SCE reference).

	E_0 [mV]	$E_c - E_a$ [mV]	e
ferrocene	500	60	1
ruthenocene	920	[a]	2
4	410	80	1
	610	80	1
26	400	80	1
	920	[a]	2
28	380	80	2

[a] Irreversible oxidation.

The dications of [1.1]metallocenophanes are strong CH acids, losing one or two protons from the bridge CH_2 groups.[58] The cobaltocenophane dication **29**$^{2\oplus}$, when treated with a weak base, loses two protons to form a diamagnetic, blue-green compound (λ_{max} 670 ($\varepsilon = 11300$), 450 (2800), and 260 (42300)), the ^{1}H-NMR data of which (two-proton singlet at $\delta = 4.22$ and four four-proton multiplets at $\delta = 4.90$, 4.99, 5.09, and 5.46) support the presence of **38** (^{1}H-NMR data of **29**$^{2\oplus}$: $\delta = 3.74$ (4H), 5.69, 5.75 (each 8H)). **38** is an 18-electron cobalt(I) species with one cyclopentadienide- and one butadiene-type ligand.



29$^{2\oplus}$ **38**

Deprotonation of the dication derived from [1.1]ferrocenophane **4** leads to a diamagnetic monocation **39**, identical to the one obtained from **4** by hydride abstraction using Ph_3CBF_4. This stabilized carbocation is described in the following Section.

3.2.3. Carbenium Ions

The bridge carbenium ion **39** is totally rigid, as shown by its room temperature ^{1}H-NMR spectrum (Fig. 8). The top and bottom halves of the cation are nonequivalent and there are now four types of protons in the rings; the proton of the carbenium ion center appears as a singlet, and the two protons on the now rigidly fixed second bridge are no longer equivalent and appear as doublets ($J = 22$ Hz).[67]

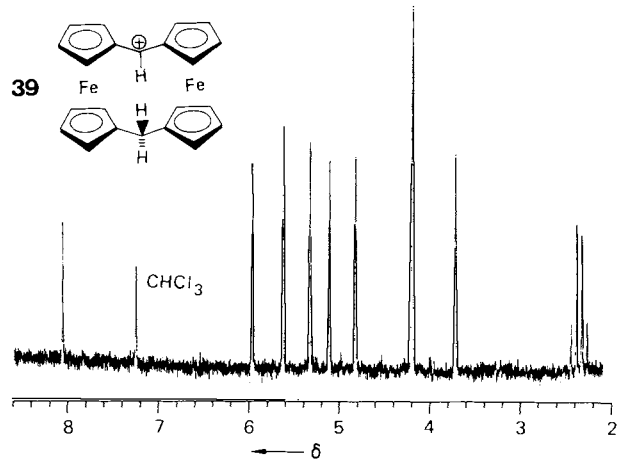


Fig. 8. 360-MHz ^{1}H-NMR spectrum of the [1.1]ferrocenophanylium ion **39** [67].

The X-ray structure analysis of **39** (Fig. 9) also revealed that direct interactions between the carbenium ion center and the two iron atoms are an important factor in the stabilization of this and, by extension, other α-ferrocenyl carbenium ions. These interactions contribute to the conformational rigidity of the carbocation. As shown by Mössbauer spectroscopy, each iron atom takes up one-third of the positive charge. This charge delocalization leads to a significant increase in the double-bond character of the bonds between the carbenium ion center and the neighboring ring carbons, resulting in a stiffening of the molecule and a dramatic reduction in the rate of isomerization. Although the spatial arrangement should favor hydride transfer between the bridges, the ^{1}H-NMR spectrum clearly shows that such a transfer does not occur. This is another consequence of charge delocalization.[67]

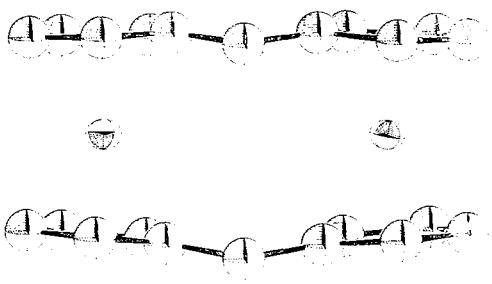
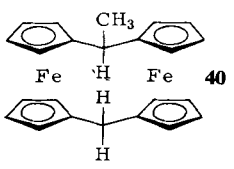


Fig. 9. Structure of the [1.1]ferrocenophanylium ion **39** in the crystal of the $BF_4^\ominus$ salt [67]. The positively charged bridge carbon is pulled toward the center of the molecule to allow direct Fe-C interactions. As in the bis(fulvalene)diiron radical cation $3^{\odot\oplus}$, the ligand rings tilt to allow a closer approach of the iron atoms. As a consequence of this, the CH_2 bridge is pushed away from the center.

Since tertiary carbenium ions are more stable than secondary ones, it is not surprising that hydride abstraction from the [1.1]FCP **40**, having a methyl substituent in one



40

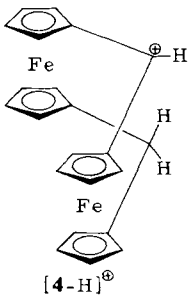
bridge, occurs from the substituted bridge. The dimethyl derivatives (both **31** and **32**) also undergo hydride abstraction to produce the same carbenium ion, which is particularly stable.[68]

Hydride abstraction from the Fe/Ru and Ru/Ru systems **26** and **28**, respectively, also leads to stable carbenium ions,[65] both of them rigid. Owing to the rigid, unsymmetrical molecular structure, the ^{1}H-NMR spectrum of $[\mathbf{26} - H]^\oplus$ exhibits a total of 16 different signals for the ring protons, the typical low-field signal for a proton at a carbenium ion center, and two doublets for the two nonequivalent protons of the methylene bridge. The carbenium ion derived from [1.1]ruthenocenophane **28** is very similar to the [1.1]FCP carbenium ion, but is clearly different from the dication $\mathbf{28}^{2\oplus}$ formed by oxidation of **28** (see preceding Section).

The carbocations discussed in this section have played an important role in understanding the structure of the mono- and dications derived from [1.1]ferrocenophane **4**. Early Mössbauer data[46] indicated the existence of diamagnetic *and* paramagnetic [1.1]FCP dications. This was taken as evidence for direct metal-metal interactions in the dications. However, it is now clear that the metallocenes in the mono- and dications are noninteracting: the monocations are trapped valence species, and the dications are paramagnetic with two unpaired electrons. The initial confusion[39,46] was a result of the very high CH acidity of the CH_2 bridges in the dications: as described in the preceding Section, diamagnetic monocations are formed by proton abstraction. The Mössbauer spectroscopic data for the carbenium ion formed from **31** or **32** agree closely with those of the diamagnetic species found to be present in the corresponding dication. The monocation of this system has recently been reinvestigated.[69] The X-ray structure shows the coexistence of one ferrocene and one ferrocenium ion unit, and there exists no intervalence transfer band in the NIR spectrum; thus, this compound should be placed into class I of the *Robin* and *Day* classification.[29] These results give a final answer to the question whether the interactions occur through the saturated ligands or through space in these compounds.[69]

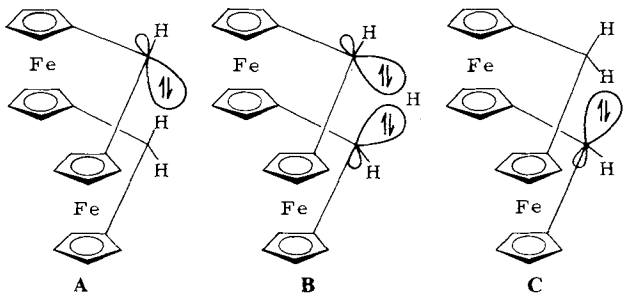
3.2.4. Carbanions

When *n*-butyllithium is added to [1.1]ferrocenophane **4** in THF, the color of the solution turns from yellow (ferrocene) to intense red. Subsequent addition of methyl iodide gives the derivative **40**, which is methylated on the bridge. Under similar conditions, diferrocenyl methane does not react with *n*-butyllithium. Since the reactivity toward alkyllithium compounds should be comparable in these two systems, the apparent difference must be due to the stability of the products: the formation of the diferrocenyl methane carbanion is an uphill reaction, whereas the reaction of **4** leads to a stabilized species. This surprising finding has found an even more surprising explanation: the carbanion of **4** is stabilized by an intramolecular hydrogen bond between the carbon atoms of the methylene bridges (Scheme 7). Because such C–H···C/C···H–C bonds had not been documented before, we undertook a closer study of this situation.[70]



[4-H]$^{\oplus}$

[1.1]FCP carbenium ion



[4-H]$^{\ominus}$

[1.1]FCP carbanion

Scheme 7. Carbenium ion and carbanion of [1.1]ferrocenophane **4**. The charge in the carbenium ion is delocalized, only one-third of the charge remaining at the carbenium center; the cation is thereby rigidly fixed in the *syn* conformation and no intramolecular hydride transfer occurs. The carbanion contains a hydrogen bond between the two bridge carbon atoms, which gives this anion a rigid structure as well. The symmetric structure **B** may be the transition state between the extremes **A** and **C** or it may be the ground state of this system.

The essential bonding situation in these carbanions is best described by contrasting them with the previously discussed carbocations. We have seen that the carbocation is rigid both in solution and in the solid; this rigidity is attributed to delocalization of the positive charge into the ferrocene moieties and to direct Fe-C bonding. Like the structure of the carbenium ion, that of the carbanion is totally rigid, owing to the C···H···C bond and possibly also to delocalization. A detailed examination, based in part on ^{1}H- and ^{13}C-NMR coupling constants (Table 2), shows that the carbenium carbon atom is sp^2 hybridized and that the rigid CH_2 bridge gives rise to a doublet of doublets in the ^{1}H-NMR spectrum with a geminal coupling constant of 22 Hz. In contrast, the carbanion has two sp^3-hybridized bridge carbon atoms; the C,H_{exo} coupling constant corresponds to the normal sp^3 value, whereas the

Table 2. Chemical shifts and coupling constants in the ^{1}H- and ^{13}C-NMR spectra of [1.1]ferrocenophane carbenium ion and carbanion (CO_2Cl_2 and [D$_8$]THF, respectively).

	δ Values		J [Hz]	
	C	H	C, H	H, H
carbenium ion				
$C^{\oplus}$–H	163.3 (d)	7.71 (s)	162.3	–
CH_2	20.4 (t)	2.05 (d)	127.0	22.0
		2.49 (d)		22.0
carbanion				
CH_{exo}	29.5 (dd)	3.09 (d)	130.4	9.0
CH_{endo}		4.51 (t)	63.9	9.0

endo-hydrogen atom, which is involved in the bridge, exhibits a C,H_{endo} coupling constant of only 63.9 Hz, about half the normal $J(C_{sp^3},H)$ value. The C···H···C bridge therefore appears to be symmetrical on the NMR time scale, but this does not allow any conclusion whether the symmetric form **B** is the ground state or the transition state for a rapid exchange between forms **A** and **C** (Scheme 7). Between +30 to −70°C, no change in the ^{1}H-NMR spectrum was observed. In the solid state, an unsymmetrical location of the THF-solvated lithium ion could induce a dissymmetry in the bridge; magic-angle-spinning ^{13}C-NMR spectroscopy has indeed shown an unsymmetrical structure, but conclusions about the structure of the carbanion in solution cannot be drawn from this result.

The carbanion formed by deprotonation of **40** shows an ^{1}H-NMR spectrum that is typical for proton exchange between two species (strongly asymmetric double-well potential). Since a negative charge is more stable on a secondary than on a tertiary carbon atom, most of the charge indeed resides on the secondary carbon atom. Proton decoupling experiments clearly show that a C···H···C bond exists in this case as well. Although this interaction does not lead to population of the higher-energy minimum (on the NMR time scale), this C···H···C bond is strong enough to introduce total rigidity into the anion. Reaction of this unsymmetric carbanion with methyl iodide leads to the exclusive formation of the *exo,exo*-dimethyl derivative **32**.

The same carbanion is formed from the *exo,endo*- and *exo,exo* dimethyl compounds **31** and **32**, respectively. Its bridging proton interacts equally with both methyl groups, which thereby give rise to one doublet in the ^{1}H-NMR spectrum. The bridging proton appears as a symmetric septet.

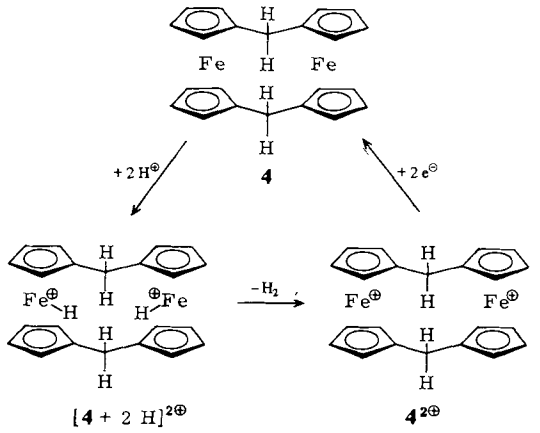
Since the ring–ring distance in [1.1]ferrocenophane **4** is 330 pm, this value is presumably also a favorable distance for the separation between the C atoms in a C···H···C bond. Extrapolation from the known distances of O···H···O, O···H···N, and N···H···N bonds further supports a value of about 330 to 350 pm. This finding explains the fact that the Fe/Ru analogue **26**, in which the bridge carbon atoms are separated by a distance of approximately 350 pm, reacts readily with *n*-butyllithium to form a bridge carbanion,[65] whereas [1.1]ruthenocenophane **28**, in which the ring–ring distance is 370 pm, does not. This result supports the suggestion that C···H···C bonds of this type are much stronger than expected. Previous estimates, derived from intermolecular hydrogen bonds between strong CH acids such as acetylenes and strong proton acceptors such as isocyanides, suggested a C···H···C bond strength of ≤8–10 kJ/mol. Although our results cannot provide an estimate of the upper or lower limits to the C···H···C bond strength, more than just a few kJ/mol are certainly involved.

3.2.5. Protonation

Ferrocene reacts with oxidizing acids to give the ferrocenium ion, a paramagnetic, green species; very strong non-oxidizing acids, on the other hand, lead to protonation without (subsequent) oxidation. In the protonated ferro-

cene **13**, the additional proton resides on the metal.[71] In the ^{1}H-NMR spectrum of ferrocene in, for example, boron trifluoride hydrate (HBF_3OH), the ten ring protons appear as a doublet ($J < 1$ Hz) at $\delta = 5.2$ (compared with $\delta = 4.1$ in ferrocene), and the proton on the iron atom appears near $\delta = -2$ as a broad signal. Although this signal should have eleven peaks resulting from the coupling to the ten ring protons, it is broadened by exchange with the solvent and shows only barely discernible structure. In the ^{1}H-NMR spectrum of ruthenocene in HBF_3OH, no coupling between ring protons and the hydridic H atom is observed; sharp singlets are observed for both types of protons. In contrast to earlier studies,[71] we found the integral ratio of the two types of signals to be exactly 10 : 1.

When [1.1]ferrocenophane **4** is added to HBF_3OH, double protonation is the main reaction, followed by immediate H_2 elimination to give $\mathbf{4}^{2\oplus}$ (Scheme 8).[72] While this reaction may not appear to be particularly unusual—Zn reacts with acids to produce H_2 and the $Zn^{2\oplus}$ ion—it is of considerable importance, because the dication $\mathbf{4}^{2\oplus}$ is easily reduced to neutral **4** and the system thus promises to be useful as a catalyst in processes where H_2 evolution is involved.[75]



Scheme 8. Catalysis of H_2 evolution in the system $\mathbf{4}/H^{\oplus}$. Double protonation of **4** leads to a dication with two almost neutral hydrogen atoms held close together. Elimination of H_2 results in the formation of $\mathbf{4}^{2\oplus}$, which can be easily reduced to neutral FCP.

A study of this reaction[73] has established the following facts: many protonation-deprotonation steps occur before a diprotonated species is formed; subsequent H_2 elimination is rapid; the resulting dication $\mathbf{4}^{2\oplus}$ can react with neutral **4**, undergoing synproportionation to form a monocation, which no longer participates in the hydrogen-producing steps; protonation of **4** does not occur directly, but rather proceeds through *exo*-attack on the ligands and subsequent proton transfer to the iron atom. These conclusions are supported by the following results. When **4** is dissolved in DBF_3OD (D_2O saturated with BF_3), the reaction product (after elimination of a mixture of H_2, HD, and D_2) contains, on the average, eight deuterium atoms in all possible ring positions, whereas the CH_2 bridges remain untouched.[73] If only direct deuteration of the iron atoms occurred, the gas evolved would be pure D_2 and no ring deuteration should occur. *Exo*-attack by deuterium on one of the rings leads to a transition state from which a proton can easily be transferred to the metal atom and ring deuteration can occur. This simple mechanism (see also Scheme 1) is complicated, however, by the low basicity of the ferrocene units. Only when the two metal atoms each bear a proton at the same time, which has a low probability, can H_2 evolution occur; many single protonations may occur in the meantime (deuteration). Addition of a small amount of a reductant such as tin leads to complete deuteration of all ring positions, because the dication is reduced to both the monocation and neutral **4**. The monocation can undergo many deuteration-dedeuteration steps without ever producing a diprotonated species that can eliminate H_2, HD, or D_2. Both pathways can lead to complete deuteration of **4**. Path B is thus the preferred one for the protonation of **4**. It is reasonable to assume that this path is not only limited to the case of the proton as electrophile, and that the generally accepted path A may not be as clearly established as some textbooks indicate. This reaction has been investigated by means of semiempirical quantum chemical methods.[74]

The reduction of the dication $\mathbf{4}^{2\oplus}$ by tin indicates that **4** can be of use as a catalyst in H_2-generating processes. Many metals such as tin and lead are more electropositive than hydrogen and should therefore react with acids, but, in fact, they are fully inert (lead acid battery!). This is a consequence of their overpotentials: the reaction is thermodynamically allowed, but one or several steps (for example, desolvation, adsorption and desorption, or the formation of an adsorbed H_2 molecule from two adsorbed H atoms) in the rather complicated reaction

$$2\,H^{\oplus}_{(solv)} + M_{(s)} \longrightarrow H_{2(g)} + M^{2\oplus}_{(solv)}$$

are inhibited. An additional potential is therefore required for the reaction to occur. Lead is a sufficiently strong reducing agent to effect the reduction of $\mathbf{4}^{2\oplus}$ to neutral **4**, which can reenter the cycle in Scheme 8. This process continues until all of the lead has dissolved. In several experiments we were able to dissolve 5 g of lead in HBF_3OH using as little as 10 mg of **4**. Compound **4** is therefore a catalyst for H_2-generating reactions where overpotentials would otherwise prevent the reaction from occurring.

For mercury, another metal with a significant overpotential to H_2 evolution, hydrogen can also be evolved from acidic media at much less negative potential in the presence of $\mathbf{4}^{2\oplus}$ (dropping mercury electrode).

Some results on the catalytic properties of **4** in H_2-generating processes are shown in Figure 10. Current flows in an electrolysis cell when the potential V (vs. SCE) is sufficiently negative to liberate hydrogen at the cathode. The amount of current at a given voltage is directly proportional to the amount of hydrogen generated. Cathodes made of polished platinum, having only a very small overpotential, will produce H_2 at potentials below -200 mV, but even this small overpotential can be eliminated by the addition of **4** to the solution. Of greater significance is the catalysis of H_2 evolution by **4** in systems involving silicon photocathodes (the use of solar energy).

The p-type silicon electrode is a poor conductor in the dark and cannot be used for the electrochemical formation of H_2. The irradiated photocathode is also unable to do so,

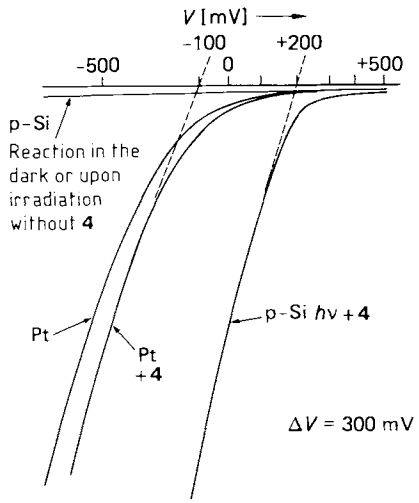


Fig. 10. Electrochemical data for HBF_3OH solutions with or without **4**. On a platinum cathode, hydrogen is evolved below -200 mV. The slight overpotential for hydrogen evolution on Pt is eliminated by the addition of **4** to the solution, which leads to current flow below -150 mV. A p-Si cathode in the dark does not evolve hydrogen and no current flows, whether or not **4** has been added. Hydrogen cannot be generated on an irradiated p-Si cathode unless **4** is added to the electrolyte solution.

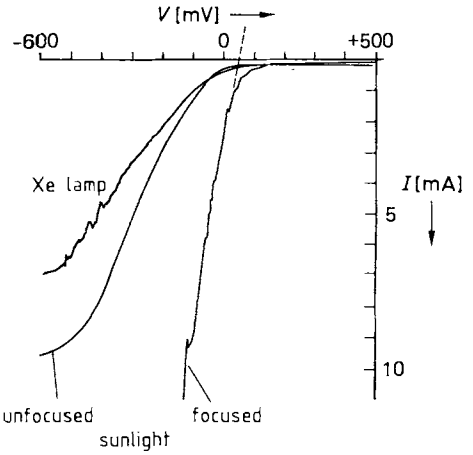


Fig. 11. H_2 evolution from a 1 M $HClO_4$ solution on p-type silicon photocathodes modified by polymer-bound **4** (see text). Noteworthy is the steep increase in current when the light is focused on the electrode. In the experiment with unfocused light, the current levels off because the number of light-generated charge carriers is small. Increasing the level of illumination increases the limiting current.

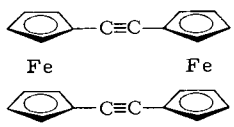
because silicon has a high overpotential. Irradiation of a p-type silicon cathode in a cell containing a Pt anode and a SCE reference electrode does not result in evolution of H_2 from HBF_3OH even at -1.0 V. If, however, **4** is added to the acid, hydrogen generation can be observed at potentials below $+200$ mV. The evolution of hydrogen at potentials more positive than those for reductions at platinum electrodes means that, through irradiation of the semiconductor electrode, light has been converted into an additional potential, which lowers the energy required for H_2 generation.

Using the [1.1]FCP carbanion (Scheme 7), we have been able to prepare a polymer-bound [1.1]FCP derivative: reaction of the carbanion with chloromethyl polystyrene produces a polymer containing enough [1.1]FCP structural units to make it catalytically active. Coating of silicon photocathodes with this polymer has led to active and stable, modified electrodes, which, in an electrochemical cell containing HBF_3OH as electrolyte, evolve hydrogen already at very positive potentials (400–450 mV) upon irradiation. Although the protonation of ferrocenes requires very strong acids, the polymer-modified silicon photocathodes, when irradiated either by a Xenon arc lamp or by sunlight, generate hydrogen efficiently even from 1 M acids (Fig. 11), although the potentials are more negative. The magnitude of the underpotentials (i.e., the difference between the potential required for H_2 generation at a Pt electrode and that required at other electrodes) is related to the efficiency of this conversion of solar energy into chemical energy in the form of hydrogen.

The reaction of [1.1]ferrocenophane **4** with acids to produce hydrogen is possible only because the dication $\mathbf{4}^{2\oplus}$ is energetically accessible. If in related systems a dication does not exist, hydrogen elimination from the diprotonated species should not be possible. This speculation has found experimental support in the case of the Fe/Ru system, for which a ferrocene-based one-electron oxidation to the monocation is followed by a ruthenocene-based two-electron oxidation to the trication. The reaction of the Fe/Ru system with HBF_3OH leads to a cationic species that can be observed by NMR spectroscopy and that indeed does not appear to lose hydrogen.[73] Protonation of [1.1]ruthenocenophane, which forms an unusually stable dication, has so far not been successfully achieved. New investigations of this compound are still needed.

3.3. [2.2]Metallocenophanes

To date, only [2.2]ferrocenophanes are known, although compounds containing other metals should be accessible. In **41**, the most interesting [2.2]ferrocenophane, the ferrocene units are connected through two acetylene bridges.[76] The diyne **41** was oxidized to a monocation and a dication. Of significance to the question of how electrons can



41

delocalize in mixed valence systems is the observation that the unpaired electron in the monocation is fully delocalized, even though the iron atoms are more than 600 pm apart.[77,78] This underlines the importance of interactions through conjugated ligands.

3.4. Larger [m.m]Ferrocenophanes

As the first [m.m]ferrocenophane to be prepared, [4.4]ferrocenophane has mainly historical significance. It was obtained in very small yield along with a variety of other products in the reaction of the ligand dianion with iron(II) chloride carried out by *Lüttringhaus* et al. in 1958.[24] Meanwhile, a number of [m.m]ferrocenophanes with long hydrocarbon bridges as well as with bridges containing heteroatoms have been prepared. No particularly

unusual properties appear to have been found in these systems.

3.5. [m^n]Metallocenophanes

The [m^n]metallocenophanes comprise the oligomeric systems in which more than two metallocene units are connected by hydrocarbon bridges (n is the number of bridges, m the number of CH_2 groups in the bridges). All synthetic routes to [1.1]metallocenophanes also produce these oligomers, but, except for the ferrocene-based systems, little effort has been made in characterizing these species. The [1^n]ferrocenophanes with n = 1 to 4 (for example, compound **6**) were described relatively early by *Katz* et al.,[9] but until recently not much new information was presented. In our work on heteronuclear metallocenophanes, we have obtained several Fe/Ru oligomers, of which the [1.1.1.1]metallocenophane containing two irons and two ruthenium atoms (analogue of **6**) is noteworthy: the two ferrocene units are on opposite sides of the ring and may approach closely. This is reflected in the ability of this system to generate H_2 upon protonation in strong acids. The reaction is slower than that of **4**. Similar studies of [1.1.1.1]FCP **6** have apparently not been carried out. The PF_6 salt of the analogous Fe_2Co_2 dication has been isolated as single crystals and its structure (Fig. 12) determined.[79] This salt was first thought to be the [1.1]metallocenophane because of its good solubility. It is formed by reduction of bis(fulvenyl) ferrocene and reaction of the dianion with hexamminecobalt(III) chloride. Undistorted ferrocene and cobaltocenium ions are arranged in such a way that Fe–Fe and Co–Co distances are minimized.

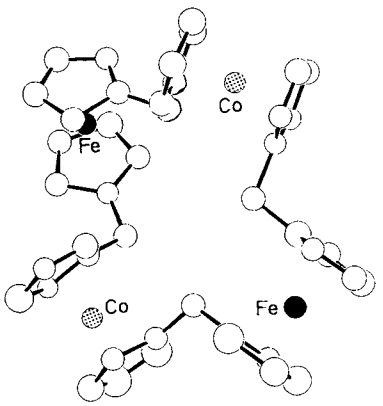


Fig. 12. Structure of the Fe_2Co_2 [1.1.1.1]metallocenophane dication in crystals of the PF_6 salt [79].

4. Summary

The chemistry of [m.m]metallocenophanes has proven to be interesting, instructive, and useful: not only have new synthetic approaches allowed the preparation of specifically tailored molecules, they have also produced materials with many unexpected properties. The structural features determined by the distance between the ligands of metallocenes, the ease with which the ligands can rotate, the availability of both flexible and rigid systems, and the presence of two or more metal atoms in an environment where interactions between them can be tuned make [m.m]metallocenophanes a fascinating class of potentially very useful materials. The first uses, for example, as catalysts for H_2 generation from acidic aqueous solution, have already been found, but many more applications of these materials can be expected, for instance in the area of conducting molecular solids and in the catalysis of C–C bond forming reactions. Only the first steps have been taken in this direction and many opportunities await to be explored.

In the work of our research group, we have benefited from very good and open communication with other groups. I would like to emphasize the importance of many discussions with Professors Cowan, Hendrickson, Watts, and Bitterwolf on many different aspects of this work. A large portion of our work was carried out at the IBM Research Laboratory in San Jose, California, where I have enjoyed the able cooperation of Adel Nazzal and of many postdoctoral fellows, whose work is acknowledged in the references. At the University of Connecticut, I enjoy the interaction with graduate students and postdoctoral fellows. Their so far unpublished contributions are noted with gratitude. I would also like to thank Professor Rheingold, University of Delaware, for his consent to include the structure of [1.1]ferrocenophane in this article before its publication.

Received: November 12, 1985 [A 584 IE]
German version: *Angew. Chem. 98* (1986) 700

[1] S. El-Tamany, F. W. Raulfs, H. Hopf, *Angew. Chem. 95* (1983) 631; *Angew. Chem. Int. Ed. Engl. 22* (1983) 633.
[2] C. Elschenbroich, R. Möckel, U. Zenneck, *Angew. Chem. 90* (1978) 560; *Angew. Chem. Int. Ed. Engl. 17* (1978) 531.
[3] A. R. Koray, M. L. Ziegler, N. E. Blank, M. W. Haenel, *Tetrahedron Lett. 1979*, 2465; R. Benn, N. E. Blank, M. W. Haenel, J. Klein, A. R. Koray, K. Weidenhammer, M. L. Ziegler, *Angew. Chem. 92* (1980) 45; *Angew. Chem. Int. Ed. Engl. 19* (1980) 44.
[4] W. E. Watts, *Organomet. Chem. Rev. 2* (1967) 231.
[5] F. Vögtle, P. Neumann, *Tetrahedron 26* (1970) 5847.
[6] B. H. Smith: *Bridged Aromatic Compounds*, Academic Press, New York 1964.
[7] W. E. Watts, *J. Am. Chem. Soc. 88* (1966) 855.
[8] W. E. Watts, *J. Organomet. Chem. 10* (1967) 191.
[9] T. J. Katz, N. Acton, G. Martin, *J. Am. Chem. Soc. 91* (1969) 2804.
[10] The name "metallocenophane" is somewhat misleading, because the suffix "phane" and its relative "phen" mean "like," "appearing," or "resembling" (as in Cellophane or epiphanie and in phenomenon and phantasy), so that "metallocenophane" has the unfortunate connotation of metallocene-like. The word cyclophane (*cyclo-phenyl-alkane*) was coined to describe cyclic structures consisting of arenes and aliphatic bridges, but its creators apparently were unaware of the coincidence that it also means "resembling a ring." Since "phane" is now the generic term for cyclic structures, the name metallocenophanes should be used.
[11] N. J. Singletary, M. Hillman, H. Dauplaise, A. Kvick, R. C. Kerber, *Organometallics 3* (1984) 1427.
[12] T. J. Kealey, P. L. Pauson, *Nature (London) 168* (1951) 1039; S. A. Miller, J. A. Tebboth, J. F. Tremaine, *J. Chem. Soc. 1952*, 632.
[13] P. Seiler, J. D. Dunitz, *Acta Crystallogr. B 35* (1979) 1068, 2020.
[14] A. Haaland, *Acc. Chem. Res. 12* (1979) 415.
[15] A. J. Campbell, C. A. Fyfe, D. Harold-Smith, K. R. Jeffrey, *Mol. Cryst. Liq. Cryst. 36* (1976) 1.
[16] S. Carter, J. N. Murrell, *J. Organomet. Chem. 192* (1980) 399.
[17] M. C. Zerner, G. H. Loew, R. F. Kirchner, U. T. Mueller-Westerhoff, *J. Am. Chem. Soc. 102* (1980) 589.
[18] T. J. Katz, N. Acton, *Tetrahedron Lett. 1970*, 2497.
[19] K. L. Rinehart, Jr., A. K. Frerichs, P. A. Kittle, L. F. Westman, D. H. Gustafson, R. L. Pruett, J. E. McMahon, *J. Am. Chem. Soc. 82* (1960) 4111.
[20] H. L. Lentzner, W. E. Watts, *Chem. Commun. 1970*, 26.
[21] M. Hisatome, N. Watanabe, T. Sakamoto, K. Yamakawa, *J. Organomet. Chem. 125* (1977) 79.
[22] M. Hillman, E. Fujita, H. Dauplaise, A. Kvick, R. C. Kerber, *Organometallics 3* (1984) 1170, and references cited therein.

[23] L. D. Spaulding, M. Hillman, G. J. B. William, *J. Organomet. Chem. 155* (1978) 109, and references cited therein.
[24] A. Lüttringhaus, W. Kullick, *Angew. Chem. 70* (1958) 438.
[25] M. Hisatome, Y. Kawajiri, J. Watanabe, M. Yoshioka, K. Yamakawa, *J. Organomet. Chem. 266* (1984) 147, and references cited therein.
[26] a) M. Hisatome, Y. Kawajiri, K. Yamakawa, Y. Harada, Y. Iitaka, *Tetrahedron Lett. 23* (1982) 1713; b) M. Hisatome, J. Watanabe, K. Yamakawa, Y. Iitaka, *J. Am. Chem. Soc. 108* (1986) 1333.
[27] D. Tanner, O. Wennerstroem, *Acta Chem. Scand. 4* (1980) 529.
[28] A. Kasahara, T. Izumi, I. Shimizu, *Chem. Lett. 1979*, 1119; I. Shimizu, Y. Kamei, T. Tezuka, T. Izumi, A. Kasahara, *Bull. Chem. Soc. Jpn. 56* (1983) 192; A. Kasahara, T. Izumi, I. Shimizu, T. Oikawa, H. Umezawa, I. Hishino, *ibid. 56* (1983) 1143.
[29] M. B. Robin, P. Day, *Adv. Inorg. Chem. Radiochem. 10* (1967) 247.
[30] N. S. Hush, *Prog. Inorg. Chem. 8* (1967) 391.
[31] S. B. Piepho, E. R. Krausz, P. N. Schatz, *J. Am. Chem. Soc. 100* (1978) 2996.
[32] F. I. Hedberg, H. Rosenberg, *J. Am. Chem. Soc. 91* (1969) 1258.
[33] M. D. Rausch, R. F. Kovar, C. S. Kraihanzel, *J. Am. Chem. Soc. 91* (1969) 1261.
[34] A. Davison, A. W. Rudie, *Synth. React. Inorg. Met.-Org. Chem. 10* (1980) 391.
[35] U. T. Mueller-Westerhoff, P. Eilbracht, *J. Am. Chem. Soc. 94* (1972) 9272.
[36] M. R. Churchill, J. Wormwald, *Inorg. Chem. 8* (1969) 1970.
[37] W. H. Morrison, S. Krogsrud, D. N. Hendrickson, *Inorg. Chem. 12* (1973) 1998.
[38] T. Matsomoto, M. Sato, A. Ichimura, *Bull. Chem. Soc. Jpn. 44* (1971) 1720.
[39] W. H. Morrison, D. N. Hendrickson, *J. Chem. Phys. 59* (1973) 380.
[40] D. O. Cowan, C. LeVanda, R. L. Collins, G. A. Candela, U. T. Mueller-Westerhoff, P. Eilbracht, *J. Chem. Soc. Chem. Commun. 1973*, 329.
[41] C. LeVanda, K. Bechgaard, D. O. Cowan, U. T. Mueller-Westerhoff, P. Eilbracht, G. A. Candela, R. L. Collins, *J. Am. Chem. Soc. 98* (1976) 3181.
[42] D. O. Cowan, R. L. Collins, F. Kaufman, *J. Phys. Chem. 75* (1971) 2025.
[43] U. T. Mueller-Westerhoff, P. Eilbracht, *Tetrahedron Lett. 1973*, 1855.
[44] M. Hillman, A. Kvick, *Organometallics 2* (1983) 1780.
[45] R. F. Kirchner, G. H. Loew, U. T. Mueller-Westerhoff, *Theor. Chim. Acta 41* (1976) 1; *Inorg. Chem. 15* (1976) 2665.
[46] W. H. Morrison, D. N. Hendrickson, *Inorg. Chem. 14* (1975) 2331.
[47] D. R. Talham, D. O. Cowan, *Organometallics 3* (1984) 1712, and references cited therein.
[48] J. C. Smart, B. Pinsky, *J. Am. Chem. Soc. 99* (1977) 956; see also G. J. Olthoff, *J. Organomet. Chem. 128* (1977) 367.
[49] P. R. Sharp, K. N. Raymond, J. C. Smart, R. J. McKinney, *J. Am. Chem. Soc. 103* (1981) 753.
[50] T. J. Katz, V. Balogh, J. Schulman, *J. Am. Chem. Soc. 90* (1968) 734; R. Gitany, I. C. Paul, N. Acton, T. J. Katz, *Tetrahedron Lett. 1970*, 2723.
[51] Review: J.-J. Andre, A. Bieber, F. Gauthier, *Ann. Phys. (Paris) 1976*, 145.
[52] C. U. Pittman, B. Surynarayanan, Y. Sasaki, *Adv. Chem. Ser. 150* (1976) 46 ("Inorganic Compounds with Unusual Properties").
[53] T. J. Katz, J. Pesti, *J. Am. Chem. Soc. 104* (1982) 346.
[54] A. Cassens, P. Eilbracht, U. T. Mueller-Westerhoff, A. Nazzal, M. Neuenschwander, W. Prössdorf, *J. Organomet. Chem. 205* (1981) C 17.
[55] U. T. Mueller-Westerhoff, A. Nazzal, W. Prössdorf, *J. Organomet. Chem. 205* (1981) C 21.
[56] A. Cassens, P. Eilbracht, A. Nazzal, W. Prössdorf, U. T. Mueller-Westerhoff, *J. Am. Chem. Soc. 103* (1981) 6367.
[57] U. T. Mueller-Westerhoff, A. Nazzal, M. Tanner, *J. Organomet. Chem. 236* (1982) C 41.
[58] U. T. Mueller-Westerhoff, A. Cassens, unpublished results.
[59] R. Dagani, *Chem. Eng. News 60* (1982) No. 9, p. 23–27.
[60] V. K. Kansal, W. E. Watts, U. T. Mueller-Westerhoff, A. Nazzal, *J. Organomet. Chem. 243* (1983) 443.
[61] W. Prössdorf, A. Nazzal, U. T. Mueller-Westerhoff, unpublished results.
[62] J. S. McKechnie, C. A. Maier, N. Bersted, I. C. Paul, *J. Chem. Soc. Perkin Trans. 2 1973*, 138.
[63] Work in progress in cooperation with Professor *A. Rheingold*, University of Delaware.
[64] A. Clearfield, C. J. Simmons, H. P. Withers, Jr., D. Seyferth, *Inorg. Chim. Acta 75* (1983) 139.
[65] M. Tanner, U. T. Mueller-Westerhoff, unpublished results.
[66] A. Diaz, U. T. Mueller-Westerhoff, A. Nazzal, M. Tanner, *J. Organomet. Chem. 236* (1982) C 45.
[67] U. T. Mueller-Westerhoff, A. Nazzal, W. Prössdorf, J. J. Mayerle, R. L. Collins, *Angew. Chem. 94* (1982) 313; *Angew. Chem. Int. Ed. Engl. 21* (1982) 293; *Angew. Chem. Suppl. 1982*, 686–695.
[68] A. Nazzal, U. T. Mueller-Westerhoff, unpublished results.
[69] M. F. Moore, S. R. Wilson, D. N. Hendrickson, U. T. Mueller-Westerhoff, *Inorg. Chem. 23* (1984) 2918.
[70] U. T. Mueller-Westerhoff, A. Nazzal, W. Prössdorf, *J. Am. Chem. Soc. 103* (1981) 7678; A. Waleh, M. L. Cher, G. H. Loew, U. T. Mueller-Westerhoff, *Theor. Chim. Acta 65* (1984) 167.
[71] G. Cerichelli, G. Illuminati, G. Ortaggi, A. M. Guiliani, *J. Organomet. Chem. 127* (1977) 357, and references cited therein.
[72] T. E. Bitterwolf, A. C. Ling, *J. Organomet. Chem. 57* (1973) C 15.
[73] K. C. Coleson, T. Haas, U. T. Mueller-Westerhoff, unpublished results.
[74] A. Waleh, G. H. Loew, U. T. Mueller-Westerhoff, *Inorg. Chem. 23* (1984) 2859.
[75] U. T. Mueller-Westerhoff, A. Nazzal, *J. Am. Chem. Soc. 106* (1984) 5381.
[76] M. Rosenblum, N. Brown, J. Papenmeier, M. Applebaum, *J. Organomet. Chem. 24* (1970) 469.
[77] C. LeVanda, K. Bechgaard, D. O. Cowan, *J. Org. Chem. 41* (1976) 2700.
[78] J. A. Kramer, D. N. Hendrickson, *Inorg. Chem. 19* (1980) 3330.
[79] U. T. Mueller-Westerhoff, J. J. Mayerle, A. Nazzal, unpublished. The unit cell of the crystal contains three cations and six disordered anions. Refinement to a satisfactory R_F value was not possible and exact bond lengths and bond angles were not determined.

When submitting manuscripts, authors of articles intended for publication as "Communications" are requested to read the "Notice to Authors" reproduced in the January issue of the journal following the list of contents; upon request, a copy can be obtained from the editorial office.

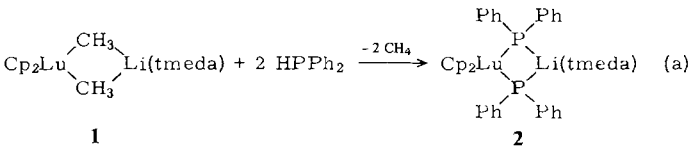
$[(Cp_2Lu\{\mu\text{-}PPh_2\}_2Li(tmeda)] \cdot 1/2\,C_6H_5CH_3$, the First Organolanthanoid-Phosphane Compound to be Characterized by X-Ray Structure Analysis**

By *Herbert Schumann*,* *Eftimios Palamidis*, *Günther Schmid*, and *Roland Boese*

Dedicated to Professor Georg Manecke on the occasion of his 70th birthday

The organolanthanoid-phosphane compounds $[Cp_2LnPtBu_2]$,[1,2] $[Cp_2LnP(C_6H_{11})_2]$,[3] $[Cp_2LnP(Ph)tBu]$,[2] and $[(H_3CC_5H_4)_2SmPPh_2]$[4] (Cp = cyclopentadienyl) are among the first compounds in which dicyclopentadienyllanthanoid fragments are bound to elements other than carbon or halogen. The structure of these compounds was hitherto derived from analytical and spectroscopic data alone, since all attempts to carry out X-ray structure analyses failed: either the compounds were too sensitive, or only disordered crystals could be obtained. Hence, the proposed structures have always been suspect, and an unequivocal elucidation of the bonding was therefore not only of theoretical interest, but also necessary in view of the potential use of such organolanthanoid-phosphane compounds in organic syntheses as mild and specific R_2P-transfer agents.

Excellently crystalline organolanthanoid-phosphane compounds are very conveniently accessible from the dicyclopentadienyllutetium-lithium complex **1**[5] and diorganophosphanes. The complex **1** reacts with $HPPh_2$ in toluene at room temperature with elimination of methane to give the dicyclopentadienyllutetium-phosphane compound **2** · $1/2\,C_6H_5CH_3$ [Eq. (a)].[6]



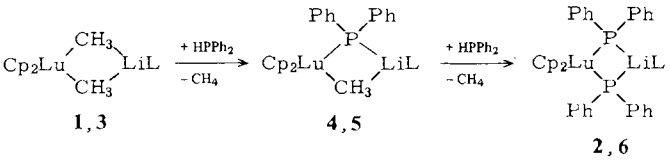
1 **2**

tmeda = *N*, *N*, *N'*, *N'*-tetramethylethylendiamine

In an analogous way, reaction of the tetrahydrofuran (THF) complex **3**[7] with $HPPh_2$ in ether at room temperature affords the complex **6**.[6]

$HPtBu_2$ does not react with **1** or **3**, even in boiling benzene, whereas reaction of $HPMe_2$ with **1** or **3** not only leads to liberation of methane but also to cleavage of the cyclopentadienyl ligand.

When this reaction [Eq. (a)] was monitored by NMR spectroscopy, it was observed that only one CH_3-bridge is initially replaced by a Ph_2P group; the singlet for the ten cyclopentadienyl H atoms ($\delta = 6.26$ for **1**, 6.31 for **3**) is replaced by a doublet ($\delta = 6.22$, $J(HP) = 0.45$ Hz for **4**, $\delta = 6.24$, $J(HP) = 0.45$ Hz for **5**), which upon further addition of $HPPh_2$, is finally converted into a triplet, indicating the substitution of both CH_3 bridges [Eq. (b)].[6]



1, **3** **4**, **5** **2**, **6**

1, **2**, **4**: L = (tmeda); **3**, **5**, **6**: L = $(thf)_2$

According to the X-ray structure analysis, **2** is a bis(diphenylphosphino)-bridged, dinuclear lutetium-lithium complex (Fig. 1).[8] The lutetium atom is surrounded by a

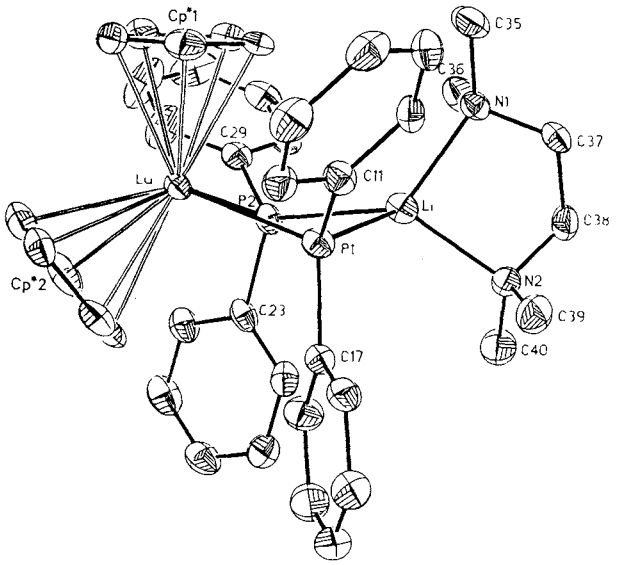
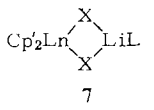


Fig. 1. Crystal structure of **2** (H atoms and solvent molecules omitted for clarity; vibration ellipsoids at the 50% probability level). Selected bond lengths [Å] and angles [°] (Cp* signifies the centroid of the cyclopentadienyl ligand): Lu···Li 3.771(1), P1···P2 3.845(2), Lu-P1 2.782(1), Lu-P2 2.813(2), Lu-Cp*1 2.311, Lu-Cp*2 2.299, mean value Lu-C(η^5) 2.602, P1-C11 1.844(3), P1-C17 1.851(4), P1-Li 2.692(14), P2-C23 1.857(3), P2-C29 1.859(4), P2-Li 2.691(8), Li-N1 2.098(12), Li-N2 2.124(12); Cp*1-Lu-Cp*2 131.2, P1-Lu-P2 86.8, Lu-P1-Li 87.1(2), Lu-P2-Li 86.5(3), P1-Li-P2 91.2(4), N1-Li-N2 87.8(5), dihedral angle between the P1-Lu-P2 and P1-Li-P2 planes 148.7.

[*] Prof. Dr. H. Schumann, Dipl.-Chem. E. Palamidis
Institut für Anorganische und Analytische Chemie
der Technischen Universität
Strasse des 17. Juni 135, D-1000 Berlin 12
Prof. Dr. G. Schmid, Dr. R. Boese
Institut für Anorganische Chemie der Universität
Universitätsstrasse 5-7, D-4300 Essen 1

[**] Organometallic Compounds of the Lanthanoids, Part 37. This work was supported by the Fonds der Chemischen Industrie, the Deutsche Forschungsgemeinschaft, and by special funds from the TU Berlin. – Part 36: H. Schumann, I. Albrecht, J. Loebel, E. Hahn, M. B. Hossain, D. van der Helm, *Organometallics*, in press.

distorted tetrahedral array of the centroids of the two cyclopentadienyl rings and the two bridging phosphorus atoms. At the same time, these two phosphorus atoms together with the two nitrogen atoms of the tmeda ligand coordinate the lithium atom tetrahedrally. In addition, the crystal contains one molecule of toluene (disordered) per two molecules of **2**. The P1-Lu-P2 and P1-Li-P2 planes form an angle of 148.7°, i.e., a bent four-membered ring is formed, as observed in compounds with sulfur[9] or selenium ($[Cp_2Lu(\mu\text{-}SePh)_2Li(thf)]$[10]) in place of phosphorus, By contrast, in the already well-known complexes **7**, the



7

Ln	Cp'	X	L	Ref.
Yb	C_5Me_5	Cl	$(Et_2O)_2$	[11]
Yb	C_5Me_5	I	$(Et_2O)_2$	[11]
Er	C_5H_5	CH_3	tmeda	[7]
Lu	C_5H_5	CH_3	tmeda	[5]

$Ln(\mu\text{-}X)_2Li$ moieties are planar. The Cp*1-Lu-Cp*2 angle and the mean value of the ten Lu-C(η^5) distances in **2** lie in the expected range; the cyclopentadienyl rings are planar. The lengths of the organolutetium-phosphorus bonds (measured for the first time) are 2.782 and 2.813 Å.

Received: March 13, 1986 [Z 1700 IE]
German version: *Angew. Chem. 98* (1986) 726

CAS Registry numbers:
1, 93895-53-5; **2**, 103349-56-0; **2** · $\frac{1}{2}C_6H_5CH_3$, 103349-57-1; **3**, 93895-55-7; **4**, 103349-58-2; $HPPh_2$, 829-85-6.

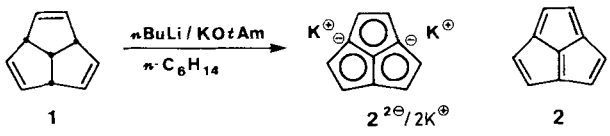
[1] H. Schumann, H. Jarosch, *Z. Anorg. Allgem. Chem. 426* (1976) 127.
[2] H. Schumann, G. M. Frisch, *Z. Naturforsch. B36* (1981) 1294.
[3] G. Bielang, R. D. Fischer, *J. Organomet. Chem. 161* (1978) 335.
[4] W. J. Evans, I. Bloom, W. E. Hunter, J. L. Atwood, *Organometallics 2* (1983) 709
[5] H. Schumann, F. W. Reier, E. Hahn, *Z. Naturforsch. B40* (1985) 1289.
[6] **2** and **6** gave correct elemental analysis. The NMR spectra were measured at 25°C in C_6D_6 with a 80-MHz instrument ($\delta(^1H, ^{13}C)$ relative to TMS, $\delta(^{31}P)$ relative to 85% H_3PO_4). **2**: decomposition point = 13°C; ^{1}H-NMR: $\delta = 1.67$ (s; NCH_2), 1.86 (s; NCH_3), 6.12 (t, $J(HP) = 0.8$ Hz; C_5H_5), 7.0-7.9 (m; C_6H_5); ^{13}C-NMR: $\delta = 46.28$ (s; NCH_3), 56.96 (s; NCH_2), 109.25 (s; C_5H_5), 130 (m; C_6H_5); ^{31}P-NMR: $\delta = 9.46$. **6**: decomposition point = 122°C; ^{1}H-NMR: $\delta = 1.31$ and 3.52 (m; THF), 6.14 (t, $J(HP) = 0.8$ Hz; C_5H_5), 7.0-7.9 (m; C_6H_5); ^{13}C-NMR: $\delta = 25.33$ and 68.65 (THF), 109.54 (s; C_5H_5), 130 (m; C_6H_5); ^{31}P-NMR: $\delta = 5.68$.
[7] H. Schumann, H. Lauke, E. Hahn, M. J. Heeg, D. van der Helm, *Organometallics 4* (1985) 321.
[8] **2** ($[(\mu^5\text{-}C_5H_5)_2Lu\{P(C_6H_5)_2\}_2Li\{(CH_3)_2NCH_2CH_2N(CH_3)_2\} \cdot \frac{1}{2}C_6H_5CH_3]$): $C2/c$, $a = 36.211(13)$, $b = 11.843(3)$, $c = 24.008(8)$ Å, $\alpha = \gamma = 90$, $\beta = 128.92(2)°$, $V = 8011(4)$ Å^3, $Z = 8$, $\rho_{calc} = 1.40$ g cm^{-3}; $Mo_{K\alpha}$ radiation, graphite monochromator, 0.8° ω-scans in the 2θ range up to 50° at −150°C, 7003 independent reflections, 5744 observed ($F_0 \geq 3.5\sigma(F)$), empirical absorption correction (min/max-transmission = 0.48/0.94). Solution by direct methods and subsequent difference-Fourier techniques, structure refinement by block-cascade methods with idealized geometry for C_5H_5- and C_6H_5-rings and CH_3- and CH_2-groups with 1.2-fold isotropic temperature factors for the H-atoms corresponding to the V_{ij} tensor of the respective C-atoms (391 parameters). All calculations with the SHELXTL program system; $R = 0.0382$, $R_w = 0.0378$ ($w^{-1} = \sigma^2(F) + 0.00037F^2$). Further details of the crystal structure investigation are available on request from the Fachinformationszentrum Energie, Physik, Mathematik GmbH, D-7514 Eggenstein-Leopoldshafen 2, on quoting the depository number CSD-51847, the names of the authors, and the full citation of the journal.
[9] H. Schumann, I. Albrecht, E. Hahn, *Angew. Chem. 97* (1985) 991; *Angew. Chem. Int. Ed. Engl. 24* (1985) 985.
[10] H. Schumann, M. Gallagher, C. Kolax, unpublished.
[11] P. L. Watson, J. F. Whitney, R. L. Harlow, *Inorg. Chem. 20* (1981) 3271.

Dihydroacepentalenediide, the Dianion of Acepentalene**

By *Thomas Lendvai, Thomas Friedl, Holger Butenschön, Timothy Clark,** and *Armin de Meijere**

Dedicated to Professor Edgar Heilbronner on the occasion of his 65th birthday

Dihydroacepentalenediide ($\mathbf{2}^{2\ominus}$), formally an ethenobridged dihydropentalenediide,[1,2] should, according to semiempirical calculations, in analogy to the latter be a closed-shell system.[3] However, the high strain energy in the cyclic and cross-conjugated skeleton with three angularly annelated five-membered rings could preclude its formation.[4] Apparently all attempts to generate $\mathbf{2}^{2\ominus}$ have thus far failed, despite the keen interest long shown by theoretical chemists in acepentalene (cyclopenta[*cd*]pentalene) **2**.[5] The most recent attempts to reductively eliminate the two dialkylamino groups from the potentially suitable precursor 4,7-bis(dialkylamino)tricyclo[5.2.1.0^{4,10}]deca-1(10),2,5,8-tetraenes[3] merely led to 1,4,7-tris(dialkylamino)-substituted monoanions.[3,6] It is therefore all the more surprising that $\mathbf{2}^{2\ominus}$ can be prepared quite simply and directly from triquinacene **1**.



1 $\mathbf{2}^{2\ominus}/2K^{\oplus}$ **2**

When **1** is added to a suspension of *n*-butyllithium and potassium *tert*-amyl alkoxide[7] in *n*-hexane,[8] the mixture turns deep red within 24 h at room temperature. To complete the reaction, the mixture is boiled under reflux for 24 h. The solvent is then removed from the mixture by suction through a fritted glass under nitrogen, and the excess base is then removed by washing five times with hexane.

The reddish-brown powder that is recovered along with potassium hydride on the filter (corresponding to 130–135% yield) can be dissolved in tetrahydrofuran (THF). Its ^{1}H-NMR spectrum shows only one singlet (Table 1), and,

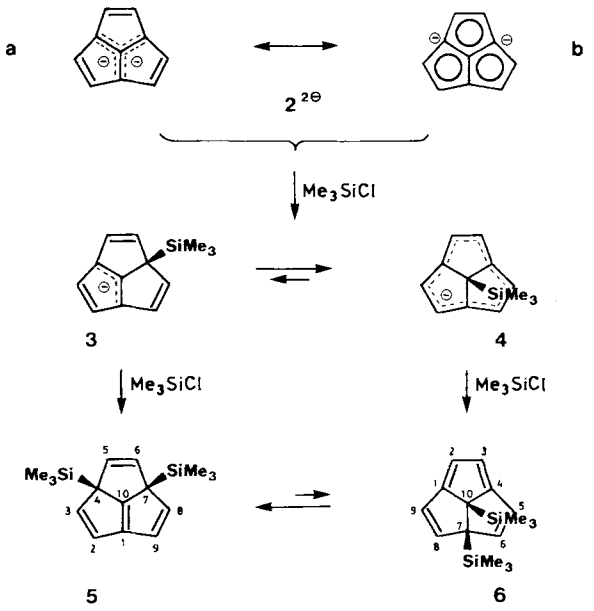
Table 1. Some characteristic data of the dipotassium acepentalenediide $\mathbf{2}^{2\ominus}/2K^{\oplus}$ and its trapping products **5** and **6**.

$\mathbf{2}^{2\ominus}$: ^{1}H-NMR (400 MHz, [D$_8$]THF): $\delta = 6.16$ (s, 6H).—^{13}C-NMR (100.63 MHz, [D$_8$]THF): $\delta = 109.87$ (d, $^1J_{C,H} = 148.8$ Hz, C-2,3,5,6,8,9), 121.79 (s, C-1,4,7), 140.64 or 159.89 (s, C-10) (see text)
5: ^{1}H-NMR (270 MHz, C_6D_6): $\delta = 0.07$ (s, 18H), 5.26 (s, 5,6-H), 5.44 (d, $^3J_{3(8),2(9)} = 5.4$ Hz, 3,8-H), 5.65 (d, 2,9-H).—MS: $M^{\oplus}$ calc. 272.14166, obs. 272.13976
6: ^{1}H-NMR (270 MHz, C_6D_6): $\delta = 0.08$ (s, 9H), 0.20 (s, 9H), 5.37 (s, 2,3-H), 5.56 (d, $^3J_{6(8),5(9)} = 5.4$ Hz, 6,8-H), 5.65 (d, 5,9-H).—MS (NH_3—Cl): m/z 273 (100%, $M^{\oplus} + H$)

[*] Prof. Dr. A. de Meijere, Dr. H. Butenschön, Dipl.-Chem. T. Lendvai
Institut für Organische Chemie der Universität
Martin-Luther-King-Platz 6, D-2000 Hamburg 13 (FRG)
Dr. T. Clark, Dipl.-Chem. T. Friedl
Institut für Organische Chemie der Universität Erlangen-Nürnberg
Henkestrasse 42, D-8520 Erlangen (FRG)

[**] This work was supported by the Stiftung Volkswagenwerk and the Fonds der Chemischen Industrie.

according to the ^{13}C-NMR spectrum, the constitution of the product recovered is indeed that of the dipotassium dihydroacepentalenediide $2^{2\ominus}/2K^{\oplus}$ (Table 1).[9] But the assignment of the very weak signal of C-10 is not absolutely certain because $2^{2\ominus}/2K^{\oplus}$ slowly decomposes in THF, even at $-40\,^{\circ}C$, and hence signals of other products appear in the spectrum. An unequivocal proof of the constitution was, however, provided by the trapping reaction with chlorotrimethylsilane. When a suspension of $2^{2\ominus}/2K^{\oplus}$ in *n*-hexane is stirred at room temperature for 48 h with an approximately equimolar amount of Me_3SiCl, decolorization of the mixture occurs, and, after the usual work-up, a product can be isolated (60–70% yield based on **1**) in which two components with $M_r = 272$ can be detected by combined GC-MS. According to the ^{1}H-NMR spectrum (Table 1) the components are the isomeric bis(trimethylsilyl)tricyclo[5.2.1.$0^{4,10}$]decatetraenes **5** and **6** (ratio 61:39).



It is especially remarkable that **6** is formed along with **5**, since the tricyclo[5.2.1.$0^{4,10}$]deca-1,3,5,8-tetraene skeleton of **6**, according to force field calculations, is about 18.2 kcal/mol more strained[4] than the skeleton of **5**, which is easily accessible in the form of 4,7-bis(dialkylamino)-derivatives.[3] According to MNDO calculations the charge distribution in dihydroacepentalenediide $2^{2\ominus}$ is best explained in terms of the structure **a**, a trisetheno-bridged trimethylenemethane dianion; structure **b** plays only a subordinate role.[3] Hence, the 4-trimethylsilyl anion **3** should be formed first in a kinetically controlled reaction of $2^{2\ominus}$ with Me_3SiCl; this could partially rearrange into the thermodynamically more stable 10-trimethylsilyl anion **4** with a 10π-perimeter by 1,2- or 1,5-silatropic shift,[10] before it reacts further to give the bis(trimethylsilyl) derivative. As expected, **5** is thermodynamically more stable than **6**; under modified conditions **5** and **6** are formed in the ratio 83:17 or 100:0. The isomer **6** rearranges into **5**, rapidly upon MeSiCl-catalysis at room temperature, but at best only slowly upon heating above 90 °C.[11]

Received: March 24, 1986 [Z 1708 IE]
German version: *Angew. Chem. 98* (1986) 734

CAS Registry numbers:
1, 6053-74-3; **2**, 103148-72-7; **5**, 103148-69-2; **6**, 103148-70-5.

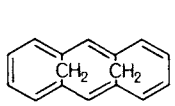
[1] Contrary to the IUPAC rules for nomenclature the dihydropentalenediide has often been called pentalenediide in the literature, cf. T. G. Katz, M. Rosenberger, *J. Am. Chem. Soc. 84* (1962) 865.
[2] J. J. Stezowski, H. Hoier, D. Wilhelm, T. Clark, P. von R. Schleyer, *J. Chem. Soc. Chem. Commun. 1985*, 1263.
[3] H. Butenschön, A. de Meijere, *Helv. Chim. Acta 68* (1985) 1658.
[4] Cf. H. Butenschön, A. de Meijere, *Chem. Ber. 118* (1985) 2557.
[5] a) A. Streitwieser, Jr.: *Molecular Orbital Theory for Organic Chemists*, Wiley, New York 1961, p. 290f.; b) R. Zahradník, J. Michl, J. Koutecký, *Coll. Czech. Chem. Commun. 29* (1964) 1932; c) R. Zahradník, J. Michl, *ibid. 30* (1965) 3529; d) B. A. Hess, Jr., L. J. Schaad, *J. Org. Chem. 36* (1971) 3418; e) F. Tomas, J. I. Fernandez-Alonso, *An. Quim. 72* (1976) 122; f) I. Gutman, N. Trinajstić, *Croat. Chem. Acta 47* (1975) 35; g) I. Gutman, M. Milun, N. Trinajstić, *J. Am. Chem. Soc. 99* (1977) 1692.
[6] K. Müllen, H. Butenschön, A. de Meijere, unpublished, results.
[7] Cf. L. Lochmann, J. Pospisil, D. Lim, *Tetrahedron Lett. 1966*, 257; cf. M. Schlosser, S. Strunk, *ibid. 25* (1984) 741.
[8] Analogous to the synthesis of numerous polyanions by metalation-elimination: D. Wilhelm, T. Clark, T. Friedl, P. von R. Schleyer, *Chem. Ber. 116* (1983) 751; D. Wilhelm, T. Clark, P. von R. Schleyer, *Tetrahedron Lett. 23* (1982) 4077.
[9] All experimental findings with other systems are consistent with the presence of a dipotassium salt. Cf. D. Wilhelm, T. Clark, P. von R. Schleyer, J. L. Courtneidge, A. G. Davies, *J. Organomet. Chem. 273* (1984) C1.
[10] According to MNDO calculations the 10-Me_3Si anion **4** is about 2.9 kcal/mol more stable than the 4-Me_3Si anion **3**. Accordingly, **4** shows hardly any bonding alternance in the 10π-perimeter. T. Clark, unpublished results.
[11] This is surprising in view of the reports that the silatropic 1,5-shift of cyclopentadienes is 10^6 times more rapid than the prototropic shift. C. A. J. Asche III, *J. Am. Chem. Soc. 92* (1970) 1233; S. McLean, G. W. B. Reed, *Can. J. Chem. 48* (1970) 3110; C. W. Spangler, *Chem. Rev. 76* (1976) 187.

Bridged [14]Annulenes with a Phenanthrene-Perimeter: *syn*-1,6:7,12-Bismethano[14]annulene**

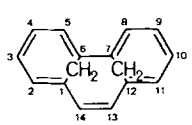
By *Emanuel Vogel,* Wilhelm Püttmann, Walter Duchatsch, Thomas Schieb, Hans Schmickler,* and *Johann Lex*

Dedicated to Professor Heinz A. Staab on the occasion of his 60th birthday

The *syn/anti*-isomeric 1,6:8,13-bismethano[14]annulenes **1**[1] and **2**[2] with an anthracene-perimeter are exemplary models for correlating aromaticity and molecular geometry.[3] On the basis of spectral[4] and structural chemical criteria, the *syn*-isomer **1** clearly qualifies as an aromatic compound, even though the annulene ring is noticeably bent—mainly as a result of steric repulsion of the internal bridge hydrogen atoms. In the *anti*-isomer **2**, on the other hand, the annulene ring is strongly puckered, so that the cyclic π-electron delocalization can no longer be sustained, and consequently **2** constitutes a highly reactive olefinic molecule.



1, *syn*
2, *anti*



3, *syn*
4, *anti*

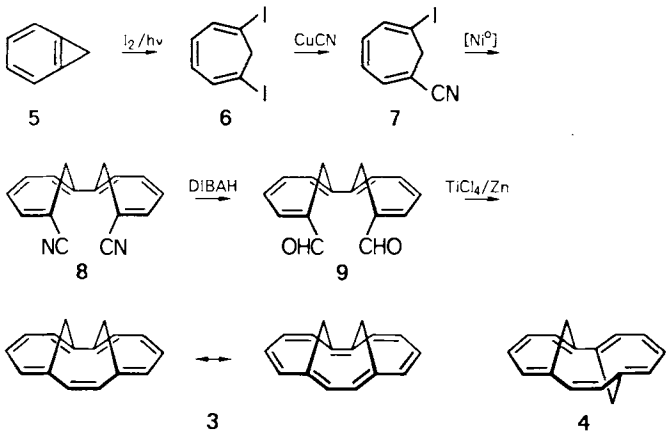
[*] Prof. Dr. E. Vogel, Dr. W. Püttmann, Dr. W. Duchatsch, Dr. T. Schieb, Dr. H. Schmickler, Dr. J. Lex
Institut für Organische Chemie der Universität
Greinstrasse 4, D-5000 Köln 41 (FRG)

[**] This work was supported by the Deutsche Forschungsgemeinschaft.

A similar geometrically induced loss of aromaticity as observed with **1**/**2** should, according to model considerations, occur in the case of the *syn/anti*-isomeric 1,6:7,12-bismethano[14]annulenes **3** and **4** derived from phenanthrene. The annulene ring of **3** appears to be more deformed than that of its counterpart **1**, yet aromatic character should still be associated with **3**, since the torsional angles of the CC bonds do not exceed values of 40–50°.[5] In the case of **4** the annulene ring is puckered to about the same extent as that in **2**, so one can safely assume that **4** is also olefinic.[6] The experimental verification of this concept is the subject of this and the following communication.[7]

The stepwise coupling of terminally suitably substituted cycloheptatrienes, preferentially of—hitherto unknown—6-halogeno-1,3,5-cycloheptatriene-1-carboxylic acid derivatives (cf. **7**), promised a relatively simple entry to **3** and/or **4**. Using this strategy we succeeded, first of all, in synthesizing the *syn*-1,6:7,12-bismethano[14]annulene **3**, which, because of non-bonding interactions between the internal bridge hydrogen atoms, is a sterically very demanding species.

As cycloheptatriene synthetic building block we chose 6-iodocycloheptatriene-1-carbonitrile **7**. The preparation of **7** was based on our previous observation that cyclopropabenzene **5**[8] upon reaction with iodine affords 1,6-diiodocycloheptatriene **6**.[8a] As the yield of **6** reached in the original procedure is maximally 5%, advantage had to be taken of the efficient synthesis of **5** by *Billups*[8b] and of the finding that the iodination of **5** is a radical process optimizable by UV irradiation.[9] **6** is thus accessible on a preparative scale.



Upon heating the diiodide **6** together with copper(I) cyanide (molar ratio 1:1) in dimethylformamide (DMF) at 120 °C (6 h) a mixture of **7** and 1,6-cycloheptatrienedicarbonitrile[9] was obtained, from which **7** could be readily separated by chromatography on silica gel (pentane/ether 3:1) [colorless rhombs (from pentane/ether 1:1); m.p. 73 °C; yield 28%]. When **7** is slowly added to the Ni^0-reagent prepared from bis(triphenylphosphane)nickel(II) chloride, triphenylphosphane and activated zinc in DMF,[10] reductive CC coupling with formation of the dinitrile **8** is achieved [m.p. 188–189 °C; yellow needles (from methanol); yield 69%]. Reduction of **8** with diisobutylaluminum hydride (DIBAH) in toluene smoothly affords the dialdehyde **9** [m.p. 132 °C; orange-colored needles (from ether); yield 82%]. Upon reaction with titanium tetrachloride/zinc/pyridine[11] in tetrahydrofuran (THF) under high dilution conditions (the more advantageous method) or with tungsten hexachloride/butyllithium,[12] **9** undergoes annulene ring closure to give, surprisingly, the *syn*-isomer **3** stereoselectively in both cases (yield 35–40% and 10%, respectively). After work-up by chromatography on alumina (Brockmann act. IV; pentane) the annulene **3**, which is air-stable, is recrystallized from pentane thus furnishing orange-colored rhombs of m.p. 93–94 °C.

The ^{1}H-NMR spectrum of **3** (see Fig. 1 and Table 1) indicates—as would be expected for an aromatic compound—the presence of a diamagnetic ring current (signals for the annulene and bridge protons at relatively low and high field, respectively), which, however, is weaker than that in **1**, and even more so than that in bridged [14]annulenes with essentially planar annulene rings. Comparison of the mean positions of the signals of the annulene protons of **3** ($\delta = 7.19$), **1** (7.59) and **4**[7] (6.45) places **3** intermediate between **1** and **4**, which according to all its

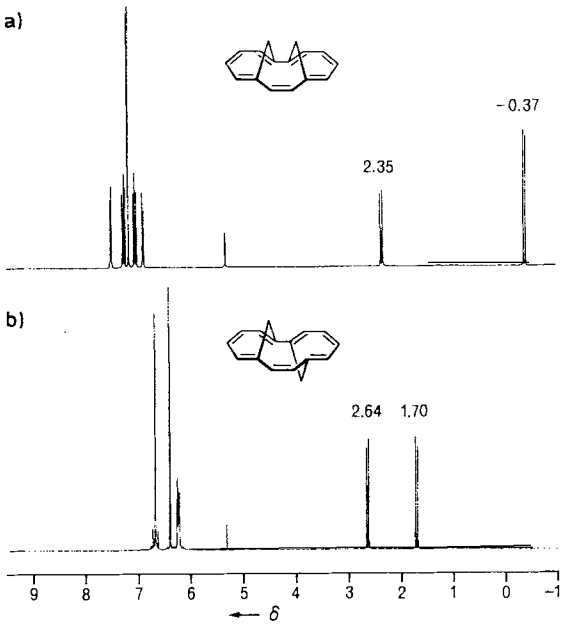


Fig. 1. ^{1}H-NMR spectra of a) *syn*-1,6:7,12-bismethano[14]annulene **3** and b) *anti*-1,6:7,12-bismethano[14]annulene **4** (300 MHz, CD_2Cl_2).

Table 1. ^{1}H-NMR data (δ values and vicinal coupling constants [Hz]) of the bridged [14]annulenes **3** and **4** and of phenanthrene [a] at 300 MHz in CD_2Cl_2.

	H-2	H-3	H-4	H-5	H-13	H-15a	H-15i
3	6.91	7.06	7.27	7.52	7.18	−0.37	2.35
4	6.23	6.67	6.69	6.26	6.40	1.70	2.64
Phenanthrene	7.99	7.71	7.75	8.76	7.84	—	—

	J(2,3)	J(3,4)	J(4,5)	J(13,14) [b]
3	6.96	10.26	7.11	11.8
4	5.94	11.03	5.27	11.2
Phenanthrene	8.00	7.04	8.44	8.8

[a] For comparison, the annulene nomenclature has been used for phenanthrene. The NMR analysis was carried out in connection with this work; for data published earlier, see R. C. Fahey, G. C. Graham, *J. Phys. Chem.* **69** (1965) 4417. [b] The J(13,14) coupling could be determined from the ^{13}C-satellites of the ^{1}H-resonance.

properties is to be regarded as a purely olefinic compound. **3** also takes a position between **1** and **4** with respect to the ratio of the vicinal coupling constants $^3J_{H,H}$, that is a measure of the degree of bond alternation.[13] From the $^3J_{H,H}$ values it can be concluded that of the two nonequivalent resonance structures of the annulene **3** that with cycloheptatriene units has special weight. This finding conforms with the observation that the π-bonds in the olefinic species **4** are localized as shown in the structural formula.[7] The downfield position of the signals of the internal bridge protons (H-15i, H-16i) of **3** must largely be due to a proximity effect, which, as inferred from the analogous case of **1**, should cause a deshielding of the order of 1–2 ppm.[1]

The electronic spectrum of **3** (in cyclohexane, see Table 2) is of the same type as that of benzene and as the spectra of other delocalized [4n+2]annulenes.[14] Apart from the extinction of the most intense band being reduced and the longest wavelength band being relatively weak, it closely agrees with the spectrum of **1**, whereas it is markedly different[15] from the spectrum of its *anti*-isomer **4**.[7]

The X-ray structure analysis[16] of **3** (Fig. 2) not only provides unequivocal proof of the *syn* arrangement of the bridges, but also confirms the conclusion drawn from models that π-orbital overlap in the annulene ring is less favorable in **3** than in **1**. Torsional angles of up to 45° are observed for the CC bonds of the ring, as compared to 34° for those in **1** and 84° for those in **4**.[7] The bond alternation ensuing from the coupling constants $^3J_{H,H}$ locally varies in its degree quite noticeably. In the cycloheptatriene units the alternation lies within the range of lengths for aromatic CC bonds, whereas in the ring segment C12-C13-C14-C1 it approximates to those in polyenes, such as the *anti*-isomer **4**. This dichotomy apparently has its origin in the steric forces which the repulsion of the internal bridge hydrogen atoms (H,H distance ca. 1.87 Å) imposes on the annulene ring.

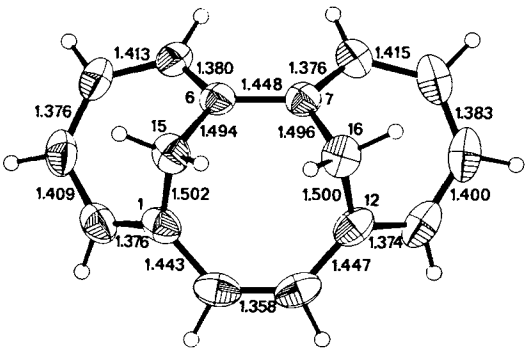
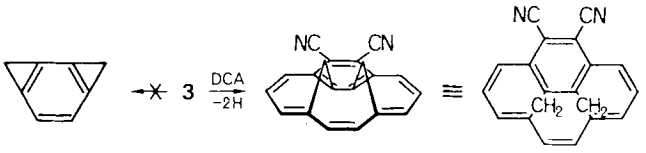


Fig. 2. Molecular structure of **3** in the crystal; selected bond lengths [Å]. Transannular CC distances: C1 ··· C6 ≙ C7 ··· C12 2.336 Å; bridge bond angles: C1-C15-C6 ≙ C7-C16-C12 102.6° (mean values for the four independent molecules in the unit cell).

From the investigations on the π-electron structure of **3** one arrives at the conclusion that the physical methods employed—especially ^{1}H-NMR spectroscopy, electron spectroscopy and X-ray structure analysis—respond with different sensitivity to the steric hindrance of resonance in **3** and other nonplanar (4n+2)π-electron systems.

The availability of **3** stimulated attempts to use this hydrocarbon, in analogy to the conversion of 1,6-methano[10]annulene to cyclopropabenzene,[8a] for a synthesis of the extremely strained di(cyclopropa)benzene **10**. The target molecule, however, did not materialize since **3** reacts



10 **11**

with acetylenedicarbonitrile (DCA) (in boiling acetone) with formation of **11** [decomp. above 235 °C; yellow rhombs (from chloroform); yield 85%].

Table 2. Some spectral data of the new compounds. ^{1}H-NMR: 300 MHz, ^{13}C-NMR: 75.5 MHz, both in $CDCl_3$ (exception: **3** in CD_2Cl_2); MS: 70 eV; UV/VIS in dioxane (exception: **3** in cyclohexane).

3: ^{1}H-NMR see Table 1; ^{13}C-NMR: δ = 33.51, 113.97, 115.98, 127.78, 128.27, 129.04, 130.53, 131.53; MS: *m/z* 206 ($M^{\oplus}$, 72%), 191 (100); IR (CsI): 3030, 1573, 1488 cm^{-1}; UV/VIS: λ_{max} = 245 nm (ε = 8300), 300 (47100), 367 (7400), 450 (340) sh

7: ^{1}H-NMR: δ = 3.14 (s, 2H), 6.49 (dd, 1H), 6.57 (dd, 1H), 6.82 (d, 1H), 6.90 (d, 1H); ^{13}C-NMR: δ = 44.33, 83.89, 100.56, 118.80, 128.53, 136.07, 137.59, 138.59; MS: *m/z* 243 ($M^{\oplus}$, 7%), 116 (100); IR (KBr): 2198 (C≡N) cm^{-1}; UV/VIS: λ_{max} = 320 nm (ε = 4500)

8: ^{1}H-NMR: δ = 2.82 (s, 4H), 6.62 (dd, 2H), 6.71 (d, 2H), 6.87 (d, 2H), 6.95 (dd, 2H); ^{13}C-NMR: δ = 31.97, 102.20, 119.08, 125.14, 128.98, 132.87, 136.07, 138.53; MS: *m/z* 232 ($M^{\oplus}$, 100%), IR (KBr): 2204 (C≡N) cm^{-1}; UV/VIS: λ_{max} = 237 nm (ε = 54400), 294 (3600), 377 (11400)

9: ^{1}H-NMR: δ = 2.79 (s, 4H), 6.74 (dd, 2H), 6.95 (d, 2H), 7.01 (dd, 2H), 7.10 (d, 2H), 9.42 (s, 2H); ^{13}C-NMR: δ = 25.70, 124.43, 128.86, 132.58, 135.23, 137.14, 142.02, 191.19; MS: *m/z* 238 ($M^{\oplus}$, 97%), 165 (100); IR (CsI): 1662 (C=O) cm^{-1}; UV/VIS: λ_{max} = 245 nm (ε = 49500), 305 (3400), 410 (9300)

11: ^{1}H-NMR: δ = 1.33 and 3.54 (AX, 4H, ^2J = −11.71 Hz), 6.06 (d, 2H), 6.72 (s, 2H), 7.07 (dd, 2H), 7.88 (d, 2H); ^{13}C-NMR: δ = 34.52, 110.09, 115.05, 124.20, 126.59, 128.53, 130.44, 132.29, 134.23, 138.15; MS: *m/z* 280 ($M^{\oplus}$, 88%), 265 (100); IR (KBr): 2220 (C≡N) cm^{-1}; UV/VIS: λ_{max} = 223 nm (ε = 41100), 280 (29600), 325 (10300) sh

Received: March 17, 1986 [Z 1703 IE]
German version: *Angew. Chem. 98* (1986) 727

CAS Registry numbers:
3, 85385-68-8; **5**, 4646-69-9; **6**, 4642-24-4; **7**, 103148-65-8; **8**, 103148-66-9; **9**, 103148-67-0; **11**, 103148-68-1; 1,6-cycloheptatrienedicarbonitrile 73172-88-0; acetylenedicarbonitrile (DCA) 1071-98-3.

[1] a) E. Vogel, J. Sombroek, W. Wagemann, *Angew. Chem. 87* (1975) 591; *Angew. Chem. Int. Ed. Engl. 14* (1975) 564; b) for the X-ray structure analysis, see: R. Destro, T. Pilati, M. Simonetta, *Acta Crystallogr. B33* (1977) 940; c) the transition from **1** to *syn*-1,6-ethano-8,13-methano[14]annulene is—analogously to that from **1** to **2**—associated with a loss of aromaticity: E. Vogel, H. M. Deger, P. Hebel, J. Lex, *Angew. Chem. 92* (1980) 943; *Angew. Chem. Int. Ed. Engl. 19* (1980) 913; H. Günther, H. von Puttkamer, H. M. Deger, P. Hebel, E. Vogel, *ibid. 92* (1980) 944 and 19 (1980) 921; d) the question as to how the π-orbital conjugation in a bridged annulene is influenced by rehybridization has recently been investigated by R. C. Haddon, L. T. Scott, *Pure Appl. Chem. 58* (1986) 137.

[2] a) E. Vogel, U. Haberland, H. Günther, *Angew. Chem. 82* (1970) 510; *Angew. Chem. Int. Ed. Engl. 9* (1970) 513; b) X-ray structure analysis of the 7-carboxylic acid methyl ester of **2**: C. M. Gramaccioli, A. S. Mimun, A. Mugnoli, M. Simonetta, *J. Am. Chem. Soc. 95* (1973) 3149; M. Simonetta, *Pure Appl. Chem. 52* (1980) 1597.

[3] **1** and **2** are conformationally stable even at 400 °C in the gas phase (flow apparatus).

[4] J. Dewey, H. M. Deger, W. Frölich, B. Dick, K. A. Klingensmith, G. Hohlneicher, E. Vogel, J. Michl, *J. Am. Chem. Soc. 102* (1980) 6412.

[5] 1,5-Methano[10]annulene may be regarded as an extreme case of a deformed [4n+2]annulene still qualifying as aromatic according to spectroscopic criteria: a) S. Masamune, D. W. Brooks, *Tetrahedron Lett. 1977*, 3239; b) L. T. Scott, W. R. Brunsvoid, *J. Am. Chem. Soc. 100* (1978) 4320; c) for the resonance energy of bridged [10]annulenes, see: W. R. Roth, M. Böhm, H.-W. Lennartz, E. Vogel, *Angew. Chem. 95* (1983) 1011; *Angew. Chem. Int. Ed. Engl. 22* (1983) 1007; *Angew. Chem. Suppl. 1983*, 1379.

[6] a) Irrespective of their configuration (*cis* or *trans*), the bridged [14]annulenes with "pyrene perimeter" are aromatic: V. Boekelheide, J. B. Phillips, *J. Am. Chem. Soc. 85* (1963) 1545; *89* (1967) 1695; R. H. Mitchell, V. Boekelheide, *ibid. 96* (1974) 1547; R. H. Mitchell, T. K. Vinod, G. J.

Bodwell, K. S. Weerawarna, W. Anker, R. V. Williams, G. W. Bushnell, *Pure Appl. Chem. 58* (1986) 15; b) the same holds for the bridged [14]annulenes with "azupyrene perimeter" (annelated systems of two azulene units): W. Huber, J. Lex, T. Meul, K. Müllen, *Angew. Chem. 93* (1981) 401; *Angew. Chem. Int. Ed. Engl. 20* (1981) 391; W. Huber, W. Irmen, J. Lex, K. Müllen, *Tetrahedron Lett. 23* (1982) 3889.

[7] E. Vogel, T. Schieb, W. H. Schulz, K. Schmidt, H. Schmickler, J. Lex, *Angew. Chem. 98* (1986) 729; *Angew. Chem. Int. Ed. Engl. 25* (1986) 723.

[8] Cyclopropabenzene syntheses: a) E. Vogel, W. Grimme, S. Korte, *Tetrahedron Lett. 1965*, 3625; b) W. E. Billups, A. J. Blakeney, W. Y. Chow, *Chem. Commun. 1971*, 1461; *Org. Synth. 55* (1976) 12.

[9] R. Okazaki, M. O-oka, N. Tokitoh, Y. Shishido, N. Inamoto, *Angew. Chem. 93* (1981) 833; *Angew. Chem. Int. Ed. Engl. 20* (1981) 799.

[10] a) A. S. Kende, L. S. Liebeskind, D. M. Braitsch, *Tetrahedron Lett. 1975*, 3375; b) M. Zembayashi, K. Tamao, J. Yoshida, M. Kumada, *ibid. 1977*, 4089; c) R. H. Mitchell, M. Chaudhary, T. W. Dingle, R. V. Williams, *J. Am. Chem. Soc. 106* (1984) 7776, and references cited therein.

[11] a) T. Mukaiyama, T. Sato, J. Hanna, *Chem. Lett. 1973*, 1041; b) J. E. McMurry, M. P. Fleming, *J. Am. Chem. Soc. 96* (1974) 4708; J. E. McMurry, *Acc. Chem. Res. 16* (1983) 405; c) D. Lenoir, *Synthesis 1977*, 553. We thank *W. H. Schulz* for the optimization of the reductive coupling of **9** with titanium tetrachloride/zinc/pyridine.

[12] a) K. B. Sharpless, M. A. Umbreit, M. T. Nieh, T. C. Flood, *J. Am. Chem. Soc. 94* (1972) 6538; b) E. Vogel in H. Nozaki (Ed.): *Current Trends in Organic Synthesis*. Pergamon Press, Oxford 1983, p. 379.

[13] H. Günther, *Tetrahedron Lett. 1967*, 2967. The statements about the bond alternation in **3** still hold when taking into account the dependence of the coupling constants $^3J_{H,H}$ on the dihedral angle; see hereto: M. Karplus, *J. Am. Chem. Soc. 84* (1962) 2458.

[14] H.-R. Blattmann, W. A. Böll, E. Heilbronner, G. Hohlneicher, E. Vogel, J.-P. Weber, *Helv. Chim. Acta 49* (1966) 2017.

[15] Electronic spectra of **3** and **4**: B. Boersch-Pulm, M. Demmer, P. S. Murthy, J. Lex, T. Schieb, G. Hohlneicher, J. Michl, E. Vogel, *J. Am. Chem. Soc.*, submitted for publication.

[16] **3** crystallizes in the triclinic system; space group $P\bar{1}$, $a=9.503(1)$, $b=11.210(1)$, $c=21.919(1)$ Å, $\alpha=84.31(1)$, $\beta=83.27(1)$, $\gamma=76.53(1)°$, $Z=8$; 6716 reflections, $R=0.052$. Further details of the crystal structure investigation are available on request from the Fachinformationszentrum Energie, Physik, Mathematik GmbH, D-7514 Eggenstein-Leopoldshafen 2, on quoting the depository number CSD-51939, the names of the authors, and the full citation of the journal.

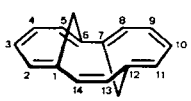
Bridged [14]Annulenes with a Phenanthrene-Perimeter: *anti*-1,6:7,12-Bismethano[14]annulene**

By *Emanuel Vogel,* Thomas Schieb, Wolfgang H. Schulz, Klaus Schmidt, Hans Schmickler,* and *Johann Lex*

The *syn*-1,6:7,12-bismethano[14]annulene **1** derived from phenanthrene, a bridged [14]annulene with a markedly bent annulene ring, is kind of a borderline case of an aromatic molecule regarding its π-electron structure.[1] In the case of the still unknown *anti*-1,6:7,12-bismethano[14]annulene **2** the predictions are that one is dealing with an olefinic molecule since, according to models, **2** possesses a puckered annulene ring in which the CC bonds are, in part, strongly twisted (maximum torsional angle 80–85 °). Following the successful synthesis of **1**[1b] we are now also able to report the synthesis of **2**.



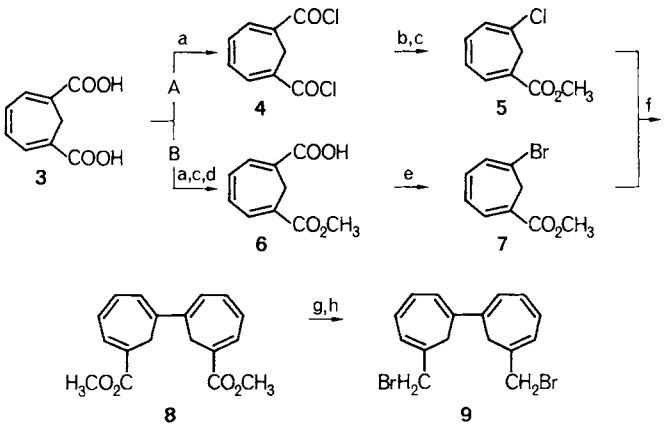
1



2

The surprising observation that reductive coupling of 1,1′-bis(cycloheptatrienyl)-6,6′-dicarbaldehyde exclusively affords the *syn*-isomer **1** suggested the idea of approaching **2** by way of its dihydro derivative **11**. Compound **11** should be formed, albeit not necessarily stereoselectively, by reductive cyclization of 6,6′-bis(bromomethyl)-1,1′-bis(cycloheptatrienyl) **9**.

The diester **8** could be obtained—more advantageously than via the cyclopropabenzene route[1]—from the readily accessible cycloheptatriene-1,6-dicarboxylic acid **3**,[2] either A) via the dicarboxylic acid dichloride **4**, or B) via the methyl half ester **6**[2b] (Scheme 1).[3] Route A): The compound **4** (m.p. 63 °C; yield 80%), prepared by reaction of **3** with sulfinyl chloride, undergoes selective monodecarbonylation on heating with tris(triphenylphosphane)rhodium(I) chloride[4] as catalyst to give 6-chlorocycloheptatriene-1-carboxylic acid chloride, which after distillation from the reaction mixture is allowed to react with methanol yielding **5**. Upon chromatographic isolation (silica gel, ether/pentane 1:9), **5** is obtained as an NMR-spectroscopically pure oil, so that for practical purposes a distillation (yellowish liquid of b.p. 62–63 °C/0.2 torr; m.p. 26 °C; yield 65%) is not required. Treatment of **5** with bis(triphenylphosphane)nickel(II) chloride (catalytic amounts) and zinc in tetrahydrofuran (THF) in the presence of tetraethylammonium iodide,[5] brings about reductive CC coupling to give **8**, which after purification by chromatography (silica gel, ether) and recrystallization (from methanol) is obtained in the form of yellow rhombs (m.p. 126–127 °C; yield 70%). Route B): The half ester **6**, best prepared by hydrolysis of the dimethyl ester[2b] with aqueous methanolic sodium hydroxide (yield 45%), can be decarboxylatively brominated to **7** according to the method of *Barton*[6] (an alternative to the Hunsdiecker degradation) in that it is converted by reaction with *N*-hydroxypyridine-2(1*H*)-thione and dicyclohexylcarbodiimide into the thiohydroxamic ester and the latter then heated in bromotrichloromethane. After isolation by chromatography (silica gel, ether/pentane 1:9) and subsequent distillation, **7** is collected as a yellowish liquid (b.p. 75–76 °C/0.1 torr; m.p. ≈ 22 °C; yield 48%). Reductive coupling of **7**, carried out as in the case of **5**, affords **8** in 70% yield (no increase in yield on going from the chloro to the bromo



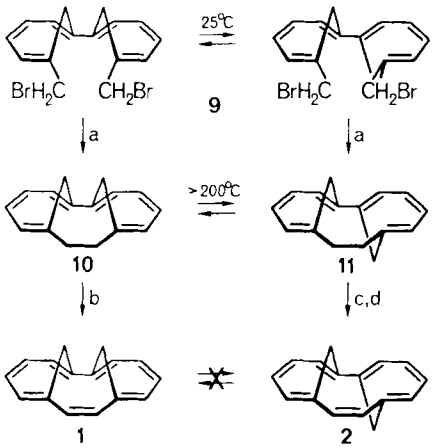
Scheme 1. A, B see text. **a**: $SOCl_2$, CH_2Cl_2, reflux, 8 h; **b**: tris(triphenylphosphane)rhodium(I) chloride (Wilkinson catalyst), 165 °C, 3 h; **c**: methanol, CH_2Cl_2, RT, 1 h; **d**: NaOH, methanol/water, RT, 24 h; **e**: *N*-hydroxypyridine-2(1*H*)-thione, dicyclohexylcarbodiimide, $CBrCl_3$, 120 °C, 4 h; **f**: bis(triphenylphosphane)nickel(II) chloride, tetraethylammonium iodide, Zn, THF, RT, 18 h; **g**: DIBAH, ether, RT, 1 h; **h**: PBr_3, pyridine, benzene, 70 °C, 5 h.

[*] Prof. Dr. E. Vogel, Dr. T. Schieb, W. H. Schulz, K. Schmidt, Dr. H. Schmickler, Dr. J. Lex
Institut für Organische Chemie der Universität
Greinstrasse 4, D-5000 Köln 41 (FRG)

[**] This work was supported by the Deutsche Forschungsgemeinschaft.

compound). The diester **8** can be readily converted into the dibromide **9** [light-sensitive, yellow cubes (from hexane); decomp. above 115 °C; yield 85%] by reduction with diisobutylaluminum hydride (DIBAH) in ether [diol isolated: m.p. 132–133 °C; yellow platelets (from ether); yield 95%] followed by bromination with phosphorus tribromide in benzene.

For the intramolecular CC coupling in **9** (Scheme 2), we resorted to the use of new reductive methods based on low-valent derivatives of sub-group metals.[7] The most convenient method proved to be the reaction of **9** with titanium tetrachloride/zinc/pyridine in THF, since a hydrocarbon mixture consisting mainly of *syn*- and *anti*-13,14-dihydro-1,6:7,12-bismethano[14]annulene (**10** and **11**, respectively) is formed,[8] in which **11** predominates. The separation of the two isomers was accomplished by chromatography on alumina (pentane), whereby **11** was collected as first fraction and **10** as second fraction [**11**: m.p. 68–69 °C; colorless rhombs (from pentane); yield 52%; **10**: m.p. 75–76 °C; yellow needles (from pentane); yield 6%]. The assignment of conformation was confirmed by X-ray structure analyses of **10** and **11**.[9]



Scheme 2. **a**: $TiCl_4$, Zn, pyridine, THF, reflux, 15 h; **b**: DDQ, anisole, 120 °C, 15 h; **c**: *N*-bromosuccinimide, CCl_4, reflux, 25 h; **d**: NaI, acetone, 60 °C, 2 h.

The *anti*-isomer **11** is dehydrogenated (with considerable losses) to **2** by reaction with 2,3-dichloro-5,6-dicyano-*p*-benzoquinone (DDQ) at 250 °C in anisole; surprisingly, **1** is also found to be a product (yields: in each case ca. 5%). In contrast, the *syn*-isomer **10** experiences DDQ-dehydrogenation already at 120 °C, the product being sterically uniform **1** (yield 75%) (likewise in anisole). These findings stimulated a study of the thermolysis of **10**/**11** and **1**/**2**. As it turned out, **10** and **11** interconvert with bridge inversion at 400 °C in the gas phase (flow apparatus) until an equilibrium (approximate composition: 25% **10** and 75% **11**) is established, whereas **1** and **2** are conformationally stable[10] under these conditions (above 400 °C irreversible rearrangements take place). In order to improve the introduction of the 13,14-double bond, **11** was allowed to react with *N*-bromosuccinimide (molar ratio 1:2.5) in carbon tetrachloride, and the resulting bromide mixture then heated with sodium iodide in acetone. Chromatography on silica gel (pentane), followed by short-path distillation (0.3 torr; bath temperature 80 °C) yielded **2** as a pale yellow liquid (yield 20%).

As expected, *anti*-1,6:7,12-bismethano[14]annulene **2** is borne out as an olefinic compound by spectral data and structural chemical findings. In the ^{1}H-NMR spectrum of **2** the signals of the annulene protons appear further upfield and those of the bridge protons further downfield than in the spectrum of **1** [$\Delta\delta$ (mean position of the signals) = 0.74 and 1.18 ppm, respectively] (Table 1). The relatively small shift of the signals of the internal bridge protons is understandable, since the signals of the corresponding protons in **1** appear at unusually low field as a result of the proximity effect.[11] In parallel with the changes in the chemical shifts one finds that the alternation of the vicinal H,H-coupling constants has increased markedly. In fact, the NMR parameters of **2** relevant to the π-electron structure of the molecule closely agree with those of its dihydro derivative **11**.

Table 1. ^{1}H-NMR data (δ-values and vicinal H,H-coupling constants [Hz]) of the [14]annulene derivatives **1**, **2**, **10**, and **11** at 300 MHz in CD_2Cl_2.

	H-2	H-3	H-4	H-5	H-13 [a]	H-15a	H-15i
1	6.91	7.06	7.27	7.52	7.18	−0.37	2.35
2	6.23	6.67	6.69	6.26	6.40	1.70	2.64
10	6.00	6.65	6.66	6.51	2.70	1.00	3.77
11	6.13	6.66	6.81	6.28	2.41	1.44	2.47

	J(2,3)	J(3,4)	J(4,5)
1	6.96	10.26	7.11
2	5.94	11.03	5.27
10	5.75	10.74	6.00
11	5.72	10.77	5.17

[a] The protons H-13/H-14 of **10** and **11** appear as an AA'BB' system (data refer to the mean position of the signals).

Especially informative is the electronic spectrum of **2**, for this, in contrast to that of **1**, no longer exhibits the three bands[12] typical for aromatic [4n + 2]annulenes, but shows only two pronounced bands (Table 2). On the other hand, the spectra of **2** and *anti*-1,6:8,13-bismethano[14]annulene[13] (polyene with fluctuating π-bonds) are strikingly similar.

For the X-ray structure analysis we used the oxime derivative of *anti*-1,6:7,12-bismethano[14]annulene-2-carbaldehyde.[14] The outcome of the structure determination[15] conforms with the image of the molecule that derives from an inspection of models (Fig. 1). The CC bonds of the annulene ring are, with few exceptions, twisted; the torsional angles of most of the bonds lie in the range of 22–35 °, but

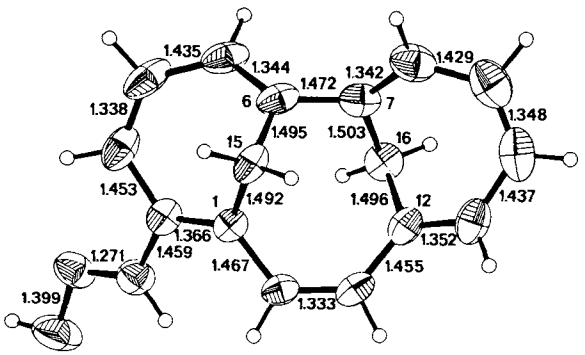


Fig. 1. Molecular structure of *anti*-1,6:7,12-bismethano[14]annulene-2-carbaldehyde oxime in the crystal; selected bond lengths [Å]. Transannular CC distances: C1 · · · C6 2.420 Å, C7 · · · C12 2.407 Å; bridge angles: C1-C15-C6 108.2°, C7-C16-C12 106.8°.

Table 2. Some spectral data of the new compounds. ^{1}H-NMR: 300 MHz, ^{13}C-NMR: 75.5 MHz, both in $CDCl_3$ (exceptions: **2**, **10**, **11** in CD_2Cl_2); MS: 70 eV (exceptions: **5**, **7**, 75 eV).

2: ^{1}H-NMR see Table 1; ^{13}C-NMR: $\delta = 43.32$, 117.71, 122.93, 129.40, 129.98, 131.82, 132.15, 135.06; MS: *m/z* 206 ($M^{\oplus}$, 38%), 89 (100); IR (film): 3010, 2976, 2906, 1637, 1601 cm^{-1}; UV/VIS (cyclohexane): $\lambda_{max} = 243$ nm ($\varepsilon = 27200$), 275 (11900) sh, 345 (5400)

5: ^{1}H-NMR: $\delta = 3.04$ (s, 2H), 3.76 (s, 3H), 6.34 (m, 1H), 6.56 (m, 1H), 6.58 (m, 1H), 7.21 (m, 1H); ^{13}C-NMR: $\delta = 35.40$, 52.16, 121.06, 124.23, 125.26, 128.34, 132.90, 133.45, 165.80; MS: *m/z* 186/184 ($M^{\oplus}$, 15/44%), 169 (100); IR (film): 2948, 1707 (C=O) cm^{-1}; UV/VIS (CH_3CN): $\lambda_{max} = 220$ nm ($\varepsilon = 7900$), 275 (3350) sh, 302 (3850)

7: ^{1}H-NMR: $\delta = 3.17$ (s, 2H), 3.78 (s, 3H), 6.51 (dd, 1H), 6.56 (d, 1H), 6.62 (dd, 1H), 7.21 (d, 1H); ^{13}C-NMR: $\delta = 37.60$, 52.25, 113.91, 121.32, 128.56, 128.63, 133.45, 133.67, 165.79; MS: *m/z* 230/228 ($M^{\oplus}$, 43/46%), 215 (100); IR (film): 3005, 2955, 1717 (C=O) cm^{-1}; UV/VIS (CH_3CN): $\lambda_{max} = 215$ nm ($\varepsilon = 13100$), 278 (3550) sh, 305 (4200)

8: ^{1}H-NMR: $\delta = 2.87$ (s, 4H), 3.71 (s, 6H), 6.61 (dd, 2H), 6.93 (dd, 2H), 7.09 (d, 2H), 7.24 (d, 2H); ^{13}C-NMR: $\delta = 28.86$, 51.83, 122.46, 124.87, 128.98, 133.53, 134.50, 135.81, 166.05; MS: *m/z* 298 ($M^{\oplus}$, 1%), 179 (100); IR (KBr): 3025, 3000, 2948, 1694 (C=O) cm^{-1}; UV/VIS (dioxane): $\lambda_{max} = 240$ nm ($\varepsilon = 51800$), 295 (4100), 385 (10900)

9: ^{1}H-NMR: $\delta = 2.67$ (s, 4H), 3.98 (s, 4H), 6.30 (d, 2H), 6.53 (dd, 2H), 6.62 (d, 2H), 6.76 (dd, 2H); ^{13}C-NMR: $\delta = 31.78$, 38.54, 123.84, 125.39, 129.40, 129.93, 131.69, 132.61; MS: *m/z* 370/368/366 ($M^{\oplus}$, 5/11/6%), 178 (100); IR (KBr): 3014, 2986, 2861 cm^{-1}; UV/VIS (dioxane): $\lambda_{max} = 238$ nm ($\varepsilon = 38600$), 282 (5600), 360 (12000)

10: ^{1}H-NMR see Table 1; ^{13}C-NMR: $\delta = 35.75$, 121.13, 122.55, 123.33, 128.34, 129.61, 130.50; MS: *m/z* 208 ($M^{\oplus}$, 40%), 178 (100); IR (KBr): 3010, 2976, 2906, 1637, 1601 cm^{-1}; UV/VIS (cyclohexane): $\lambda_{max} = 258$ nm ($\varepsilon = 14700$), 352 (8100)

11: ^{1}H-NMR see Table 1; ^{13}C-NMR: $\delta = 43.16$, 48.40, 120.47, 121.05, 129.56, 130.37, 132.28, 133.51; MS: *m/z* 208 ($M^{\oplus}$, 50%), 178 (100); IR (KBr): 3030, 3002, 2905, 1607, 1587 cm^{-1}; UV/VIS (cyclohexane): $\lambda_{max} = 243$ nm ($\varepsilon = 10100$), 285 (7100)

in the case of the C6-C7 bond the torsional angle reaches the extreme value of 84°. As a consequence, the 2p π-orbital overlap at the C6-C7 bond is only barely minimal, and this obviously accounts for the loss of aromaticity, which manifests itself in the pronounced alternation of single and double bonds. The existence of *anti*-1,6:7,12-bismethano[14]annulene as the double-bond isomer **2** with cycloheptatriene partial structures[16] follows equally so from model considerations and force field calculations.[17]

Received: March 17, 1986 [Z 1704 IE]
German version: *Angew. Chem. 98* (1986) 729

CAS Registry numbers:
1, 85385-68-8; **2**, 85440-62-6; **3**, 73875-01-1; **4**, 73875-02-2; **5**, 103149-59-3; **6**, 75538-94-2; 7, 103149-60-6; **8**, 103149-61-7; **8** reduction product (diol), 103149-62-8; **9**, 103149-63-9; **10**, 103149-64-0; **11**, 103238-76-2; *anti*-1,6:7,12-bismethano[14]annulene-2-carbaldehyde 1031-49-65-1; *anti*-1,6:7,12-bismethano[14]annulene-2-carbaldehyde oxime 103149-66-2.

[1] a) E. Vogel in H. Nozaki (Ed.): *Current Trends in Organic Synthesis*, Pergamon Press, Oxford 1983, p. 379; b) E. Vogel, W. Püttmann, W. Duchatsch, T. Schieb, H. Schmickler, J. Lex, *Angew. Chem. 98* (1986) 727; *Angew. Chem. Int. Ed. Engl. 25* (1986) 720.

[2] a) E. Vogel, H. M. Deger, J. Sombroek, J. Palm, A. Wagner, J. Lex, *Angew. Chem. 92* (1980) 43; *Angew. Chem. Int. Ed. Engl. 19* (1980) 41; b) the acid **3**, its methyl half ester **6** and its dimethyl ester were first described by R. Darms. T. Threlfall, M. Pesaro, A. Eschenmoser, *Helv. Chim. Acta 46* (1963) 2893.

[3] A new route from cyclopropabenzene to bridged annulenes with cycloheptatriene partial structures [including potential precursors of **2**] mediated by transition-metal complexes was recently described by R. Mynott, R. Neidlein, H. Schwager, G. Wilke, *Angew. Chem. 98* (1986) 374; *Angew. Chem. Int. Ed. Engl. 25* (1986) 367; b) for the conversion of cyclopropabenzene into 1,6-methano[10]annulenes via cycloaddition, see: E. Vogel, J. Ippen, V. Buch, *Angew. Chem. 87* (1975) 592; *Angew. Chem. Int. Ed. Engl. 14* (1975) 566; E. Vogel, *Proc. Robert A. Welch Found. Conf. Chem. Res. 12* (1968) 215.

[4] J. Blum, *Tetrahedron Lett. 1966*, 1605; J. Blum, E. Oppenheimer, E. D. Bergmann, *J. Am. Chem. Soc. 89* (1967) 2338; J. Tsuji, K. Ohno, *Tetrahedron Lett. 1966*, 4713; *Synthesis 1969*, 157.

[5] M. Iyoda, K. Sato, M. Oda, *J. Chem. Soc. Chem. Commun. 1985*, 1547.

[6] D. H. R. Barton, D. Crich, W. B. Motherwell, *Tetrahedron Lett. 24* (1983) 4979; for examples of the decarboxylative bromination of aromatic and α,β-unsaturated carboxylic acids, see: D. H. R. Barton, B. Lacher, S. Z. Zard, *ibid. 26* (1985) 5939; in the meantime, *Barton*'s method has also proven useful in the field of bridged annulenes; for example, the conversion of 2,7-methanoaza[10]annulene-9-carboxylic acid into 9-bromo-2,7-methanoaza[10]annulene; yield 40% (according to experiments carried out in collaboration with *W. Haas*).

[7] CuCl/dimethyl sulfoxide: H. Nozaki, T. Shirafuji, Y. Yamamoto, *Tetrahedron 25* (1969) 3461; $TiCl_4/LiAlH_4$: G. A. Olah, G. K. S. Prakash, *Synthesis 1976*, 607; $VCl_3/LiAlH_4$: T.-L. Ho, G. A. Olah, *ibid. 1977*, 170; $WCl_6/LiAlH_4$: Y. Fujiwara, R. Ishikawa, S. Teranishi, *Bull. Chem. Soc. Jpn. 51* (1978) 589. Reductive coupling with formation of **10** and **11** was observed only with the first two methods. The reaction of **9** with sodium iodide/acetone leads primarily to heptaenes, which on heating undergo electrocyclization to **10** and **11**.

[8] Reaction conditions of the Mukaiyama variant of the McMurry reaction: T. Mukaiyama, T. Sato, J. Hanna, *Chem. Lett. 1973*, 1041; D. Lenoir, *Synthesis 1977*, 553.

[9] B. Boersch-Pulm, M. Demmer, P. S. Murthy, J. Lex, T. Schieb, G. Hohlneicher, J. Michl, E. Vogel, *J. Am. Chem. Soc.*, submitted for publication.

[10] For the conformational stability of *syn*- and *anti*-1,6:8,13-bismethano[14]annulenes and their 7,14-dihydro derivatives, see E. Vogel, W. Tückmantel, K. Schlögl, M. Widhalm, E. Kraka, D. Cremer, *Tetrahedron Lett. 25* (1984) 4925.

[11] H. Günther: *NMR-Spektroskopie*, Thieme, Stuttgart 1983, p. 90.

[12] a) H.-R. Blattmann, W. A. Böll, E. Heilbronner, G. Hohlneicher, E. Vogel, J.-P. Weber, *Helv. Chim. Acta 49* (1966) 2017; b) H. J. Dewey, H. Deger, W. Frölich, B. Dick, K. A. Klingensmith, G. Hohlneicher, E. Vogel, J. Michl, *J. Am. Chem. Soc. 102* (1980) 6412.

[13] E. Vogel, U. Haberland, H. Günther, *Angew. Chem. 82* (1970) 510; *Angew. Chem. Int. Ed. Engl. 9* (1970) 513.

[14] Reaction of **2** with dichloromethyl *n*-butyl ether in the presence of tin tetrachloride [A. Rieche, H. Gross, E. Höft, *Chem. Ber. 93* (1960) 88] afforded mainly *anti*-1,6:7,12-bismethano[14]annulene-2-carbaldehyde, which was isolated by thin-layer chromatography (silica gel, pentane/ether 20:1) as an orange-colored oil (yield 13%). Reaction of the aldehyde with hydroxylamine hydrochloride/pyridine furnished the oxime; bright yellow rhombs (from dichloromethane) of m.p. 172–173 °C.

[15] *anti*-1,6:7,12-Bismethano[14]annulene-2-carbaldehyde oxime crystallizes monoclinically, space group $P2_1/c$, $a = 16.768(4)$, $b = 6.039(1)$, $c = 13.270(2)$ Å, $\beta = 99.99(1)°$, $Z = 4$; 1290 reflections, $R = 0.036$. Further details of the crystal structure investigation are available on request from the Fachinformationszentrum Energie, Physik, Mathematik GmbH, D-7514 Eggenstein-Leopoldshafen 2, on quoting the depository number CSD-51940, the names of the authors, and the full citation of the journal.

[16] See, however, the double-bond configuration of 1,6:9,14-bismethano[16]annulene: D. Tanner, O. Wennerström, E. Vogel, *Tetrahedron Lett. 23* (1982) 1221; E. Vogel, U. Kürschner, H. Schmickler, J. Lex, O. Wennerström, D. Tanner, U. Norinder, C. Krüger, *ibid. 26* (1985) 3087.

[17] According to calculations with a modified MM2 force field (W. R. Roth, F.-G. Klärner, G. Siepert, H.-W. Lennartz, unpublished) **2** is favored over its double-bond isomer by no less than 41.2 kcal/mol. In the case of **1**, this value drops to 3.6 kcal/mol (W. R. Roth, private communication).

Synthesis of Glycosphingolipids and Psychosines**

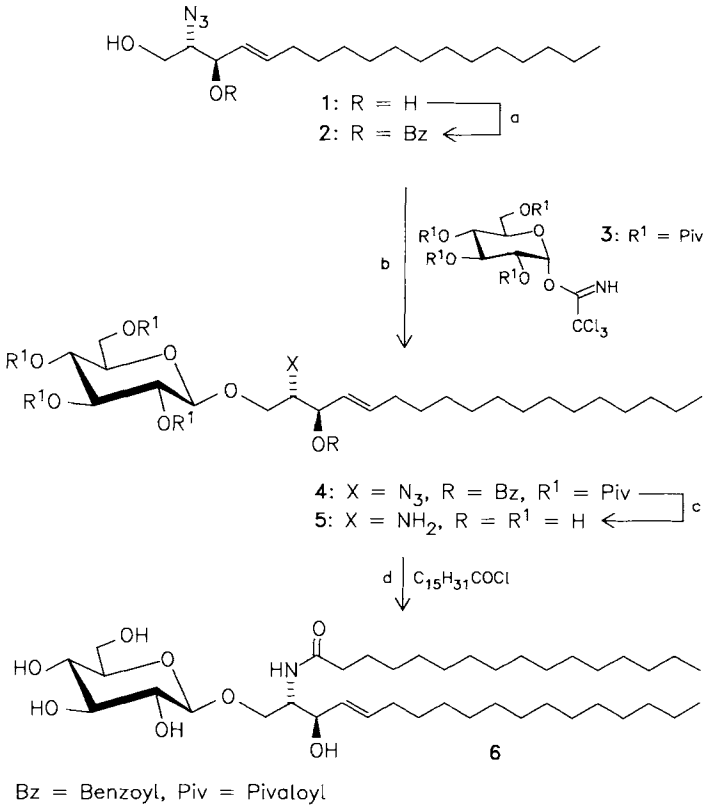
By *Richard R. Schmidt** and *Peter Zimmermann*

Glycosphingolipids have acquired great importance as components of biological membranes.[1] In order to explore their role and function in membranes, the synthesis of isomerically pure compounds that are otherwise only

[*] Prof. Dr. R. R. Schmidt, Dipl.-Chem. P. Zimmermann
Fakultät für Chemie der Universität
Postfach 5560, D-7750 Konstanz (FRG)

[**] Glycosylimidates, Part 23. This work was supported by the Deutsche Forschungsgemeinschaft and the Fonds der Chemischen Industrie.—Part 22: R. R. Schmitt, G. Effenberger, *Carbohydr. Res.*, in press.

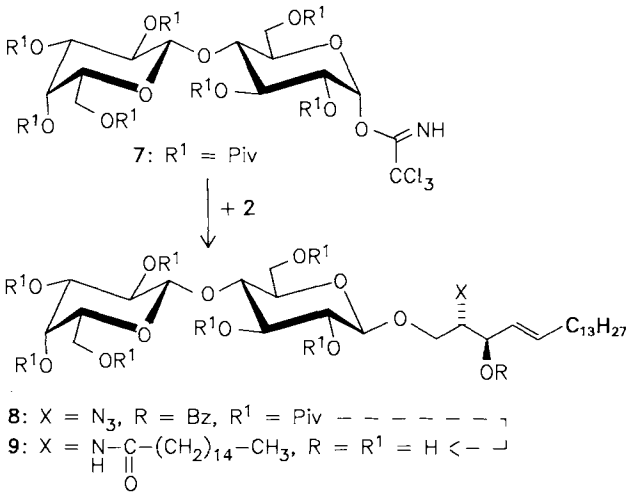
difficultly obtainable from biological materials is necessary.[1] For their synthesis, the reaction of *O*-glycosyltrichloroacetimidates (see **3** and **7**) as glycosyl donors with 3-*O*-protected or 3-*O*-unprotected ceramides as acceptors has proven to be the best approach,[2-4] but even then the yields are far from satisfactory.[2,3] We have therefore developed a new and productive entry to this class of compounds, based on our sphingosine synthesis,[5] in which the glycosylation takes place at the sphingosine stage and not, as previously, at the ceramide stage[6] (see Scheme 1).



Scheme 1. Synthesis of *O*-D-glucopsychosine **5** and D-glucocerebroside **6**. a) TrtCl (1.5 eq.), pyridine/$CHCl_3$/tetrahydrofuran (THF) (1:1:1), RT, 48 h (90%); BzCl (2 eq.), pyridine/toluene (1:4), RT, 12 h (91%); $BF_3 \cdot OEt_2$ (1.3 eq.), MeOH/toluene (1:3), RT, 5 h (90%). b) $BF_3 \cdot OEt_2$ (0.1 eq.), CH_2Cl_2, RT (94%). c) NaOMe (0.1 eq.), MeOH/CH_2Cl_2 (2:1), RT, 72 h (78%); H_2S, pyridine/H_2O (1:1), RT, 24 h (94%). d) 8 M NaOAc, THF/H_2O (1:1), RT, 1 h (81%).

The azido derivative **1** of the D-*erythro*-C_{18} sphingosine,[6] which is conveniently obtainable from D-galactose, was converted via 1-*O*-tritylation, 3-*O*-benzoylation and detritylation into the 3-*O*-benzoyl derivative **2** in high yields.[7] *O*-Pivaloylated *O*-α-D-glucosyl trichloroacetimidate **3**, which upon reaction with $BF_3 \cdot OEt_2$ as catalyst in dichloromethane affords the glucoside **4**[7] in 94% yield, proved to be most suitable for the β-specific 1-*O*-glycosylation. Removal of the *O*-acyl protecting groups with sodium methoxide/methanol and reduction of the azido group with hydrogen sulfide in pyridine/water gave as intermediate the glucopsychosine **5**, which plays an important role as metabolic product in Gauchers disease.[8]

The glucopsychosine **5** is a convenient starting compound for the synthesis of D-glucocerebrosides with different fatty acid residues on the amino group, as occur in nature.[1] For example, the D-glucocerebroside **6** previously prepared by us[2] was synthesized by reaction of **5** with palmitic acid chloride/sodium acetate. The lactosyl ceramide **9** could be prepared as the glycosphingolipid in a similar way and in comparable yields from per-*O*-pivaloylated



O-lactosyl trichloroacetimidate **7** and azidosphingosine **2** via the glycoside **8**[7] and the corresponding "lactopsychosine"; this compound, which had likewise been synthesized on a previous occasion by the "ceramide method" was characterized structurally by comparison with the authentic compound.[9]

Received: March 23, 1986;
revised: May 15, 1986 [Z 1717 IE]
German version: *Angew. Chem. 98* (1986) 722

[1] N. Sharon, H. Lis, *Chem. Eng. News 58*, No. 13 (1981) 21; S. Hakamori, *Annu. Rev. Biochem. 50* (1981) 733; Y.-T. Li, S.-C. Li, *Adv. Carbohydr. Chem. Biochem. 40* (1982) 235; H. Paulsen, *Angew. Chem. 94* (1982) 184; *Angew. Chem. Int. Ed. Engl. 21* (1982) 155; S. Hakamori in J. N. Kaufer, S. Hakamori (Ed.): *Handbook of Lipid Research, Vol. 3*, Plenum Press, New York 1983, p. 1-150; F. Sarmientos, G. Schwarzmann, K. Sandhoff, *Eur. J. Biochem. 146* (1985) 59; R. R. Schmidt, *Angew. Chem. 98* (1986) 213; *Angew. Chem. Int. Ed. Engl. 25* (1986) 212.

[2] R. R. Schmidt, R. Kläger, *Angew. Chem. 97* (1985) 60; *Angew. Chem. Int. Ed. Engl. 24* (1985) 65.

[3] M. Sugimoto, T. Ogawa, *Glycoconjugate J. 2* (1985) 5; K. Koike, M. Sugimoto, Y. Nakahara, T. Ogawa; *ibid. 2* (1985) 105; M. Sugimoto, T. Horisaki, T. Ogawa, *ibid. 2* (1985) 11.

[4] The trichloroacetimidate method affords better yields than the Koenigs-Knorr or Helferich-Weiss methods; see also Ref. [2, 3].

[5] R. R. Schmidt, P. Zimmermann, *Tetrahedron Lett. 27* (1986) 481.

[6] R. R. Schmidt, unpublished results.

[7] ^{1}H-NMR data (250 MHz, $CDCl_3$, TMS int.): **2**: 8.14 (m, 2H, Bz), 7.58 (m, 1H, Bz), 7.47 (m, 2H, Bz), 5.87-6.05 (m, 1H, CH_2-CH=), 5.53-5.69 (m, 2H, =CH-CH-OBz), 3.57-3.86 (m, 3H, CH_2-O, CH-N_3), 1.95-2.15 (m, 3H, OH, =CH-CH_2), 1.13-1.47 (m, 22H, aliphat), 0.86 (t, 3H, CH_3).—**4**: 8.05 (m, 2H, Bz), 7.58 (m, 1H, Bz), 7.45 (m, 2H, Bz), 5.83-5.99 (m, 1H, CH_2-CH=), 5.45-5.65 (m, 2H, =CH-CH-OBz), 5.02-5.37 (m, 3H, H-2, H-3, H-4), 4.58 (d, 1H, H-1, J=7.9 Hz), 3.58-4.25 (m, 6H, H-6, H-6', H-5, CH-N_3, CH_2-O), 2.06 (m, 2H, =CH-CH_2), 1.04-1.45 (m, 58H, Piv, aliphat.), 0.89 (t, 3H, CH_3).—**8**: 8.05 (m, 2H, Bz), 7.58 (m, 1H, Bz), 7.47 (m, 2H, Bz), 5.82-5.98 (m, 1H, CH_2-CH=), 5.43-5.59 (m, 2H, =CH-CH-OBz), 5.40 (d, 1H, H-4, or H-4', J=7.6 Hz), 5.08-5.27 (m, 2H), 4.82-5.03 (m, 2H), 4.50-4.63 (m, 3H, H-1, H-1', H-4 or H-4'), 3.71-4.26 (m, 7H), 3.50-3.63 (m, 2H), 2.06 (m, 2H, =CH-CH_2), 1.03-1.45 (m, 85H, Piv., aliphat), 0.89 (t, 3H, CH_3).

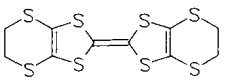
[8] O. Nilsson, J.-E. Månnson, G. Håkansson, L. Svennerholm, *Biochim. Biophys. Acta 712* (1982) 453; O. Nilson, L. Svennerholm, *J. Neurochem. 39* (1982) 709; H. Igisu, K. Suzuki, *J. Lipid Res. 25* (1984) 1000; M. Vaccaro, M. Muscillo, K. Suzuki, *Eur. J. Biochem. 146* (1985) 315.

[9] R. Kläger, *Dissertation*, Universität Konstanz 1985.

ζ-$(ET)_2AuBr_2$, a New Type of Structure for the Organic Radical Cation Salts $(ET)_2AuX_2$**

By *Eberhard Amberger*,* *Kurt Polborn*, and *Helmut Fuchs*

In 1980 the first organic superconductor, the hexafluorophosphate of the radical cation of tetramethyltetraselenafulvalene $(TMTSF)_2PF_6$[1] was synthesized. The salts $(TMTSF)_2X$ ($X = PF_6^{\ominus}$, $AsF_6^{\ominus}$, $TaF_6^{\ominus}$, $ReO_4^{\ominus}$,[2] and $FSO_3^{\ominus}$[3]) become superconducting at approximately 10 kbar; only $(TMTSF)_2ClO_4$[4] is a superconductor at ambient pressure. Five normal-pressure superconductors of bis(ethylenedithio)tetrathiafulvalene 1 ("BEDT-TTF" or "ET") have been reported to date: β-$(ET)_2X$ ($X = I_3^{\ominus}$,[5] $IBr_2^{\ominus}$,[6] $AuI_2^{\ominus}$[6a,7]), γ-$(ET)_3(I_3)_{2.5}$,[5a,b] and ε-$(ET)_2I_3(I_8)_{0.5}$.[5a,b] The transition temperature T_c (transition from metallic to superconducting behavior) extends from 0.9 to 2.0 K in the $(TMTSF)_2X$ system and from 1.2 to 4 K in the β-$(ET)_2X$ systems at ambient pressure.[10] By subsequent treatment of $(ET)_2I_3$ crystals, it has even been possible to attain $T_c = 8$ K.[5a,b,8,9]



1

In contrast to the $(TMTSF)_2X$ compounds, the $(ET)_2X$ compounds display a wide variety of structures, owing to the following two factors: (1) On account of the ethylene groups, which do not lie in the plane of the molecule, ET does not form "face-to-face stacks," as is found for the one-dimensional organic conductors with planar donors and/or acceptors. The most noteworthy feature of the ET structure is the two-dimensional "side-to-side arrangement" of the ET molecules to form layers: weak S···S interactions are observed within the stacks and strong ones between the stacks. (2) The complex anions are located between the ET layers along with molecules of solvent in some cases. By variation of the anions (size), it is possible to study their effect on the electrical properties, on T_c, and on the structure of the salts.

ET is at present the most promising donor in the search for new metallic or superconducting radical cation salts. We report here the synthesis of ζ-$(ET)_2AuBr_2$ and *t*-$(ET)_2AuBr_2$ (*t* = *twist*) as well as the structure of the ζ-phase. The rods of ζ-$(ET)_2AuBr_2$, obtained by electrocrystallization from tetrahydrofuran, are formed under certain conditions instead of the preferentially formed *t*-$(ET)_2AuBr_2$ crystals with twistlike overlapping of the ET molecules.

The structure of ζ-$(ET)_2AuBr_2$ can be best described by referring to that of β-$(ET)_2IBr_2$. Both are triclinic: in ζ-$(ET)_2AuBr_2$, the *a* axis is ca. 0.7 Å shorter and thus the shortest of all triclinic ET radical-cation salts. The *c* axis is 1.2 Å longer, not shorter, as might have been expected for a smaller anion (Table 1). Replacement of the linear anions $AuI_2^{\ominus}$ (9.4 Å) and $IBr_2^{\ominus}$ (9.3 Å) by the $AuBr_2^{\ominus}$ anion (8.7 Å), which is ca. 7% shorter, therefore leads to two ET salts having the same stoichiometry but fundamentally different structures: a ζ-phase that is remotely related to the superconducting β-phase, and a t-phase with opposed twisting of the ET molecules.[19] This twist arrangement has only been observed to date in one $(ET)_2X$ salt with linearly symmetric interhalide or halometalate ions, namely, δ-$(ET)_2I_3$.[5b] Otherwise, it has only been found for $(ET)_2ClO_4(C_4H_8O_2)$[12] and $(ET)PF_6$[13] salts with tetrahedral or octahedral anions. All of these salts are semiconductors.

Table 1. Crystal data and T_c of superconducting and nonsuperconducting ET compounds with the anions $IBr_2^{\ominus}$, $AuI_2^{\ominus}$, and $AuBr_2^{\ominus}$.

	β-$(ET)_2AuI_2$ [6a, 7a]	β-$(ET)_2IBr_2$ [6a]	ζ-$(ET)_2AuBr_2$ [18]	t-$(ET)_2AuBr_2$ [19]
a [Å]	6.600(3)	6.5907(9)	5.706(2)	6.708(2)
b [Å]	8.986(3)	8.977(2)	9.014(2)	7.816(3)
c [Å]	15.364(3)	15.093(2)	16.349(2)	31.708(5)
α [°]	95.07(2)	93.84(1)	92.05(1)	93.48(2)
β [°]	96.18(3)	94.96(1)	97.65(1)	90.01(2)
γ [°]	110.66(3)	110.44(2)	102.95(2)	90.00(3)
V [Å^3]	839.79	829.09	810.30	1659.4
space group	$P\bar{1}$	$P\bar{1}$	$P\bar{1}$	$P2/n$
Z	1	1	1	2
ρ_{calcd} [gcm^{-3}]	2.41	-	2.32	2.25
T_c [K]	3.2-4	1.9-2.8	<0.5	semiconductor

In the crystal, the ET cations of ζ-$(ET)_2AuBr_2$ form stacks along the *b* axis (weak pair formation) (Fig. 1). The smallest S···S contact in the stack (<3.8 Å, average 3.797 Å and 3.777 Å) are larger than the S···S van der Waals distance (3.7 Å), as is the case for β-$(ET)_2IBr_2$. Still more important are the short S···S contacts between the stacks, which result in the formation of ET layers and give the compound a two-dimensionality (Fig. 2). Planes of $AuBr_2^{\ominus}$ ions join the ET layers. A view along the *c* axis into the two-dimensional network with S···S contacts smaller than 3.7 Å is shown in Figure 3. Between the side-to-side arranged ET molecules of a layer (Fig. 2: black ETs from the projection on the *a*,*c* plane), there are only two short

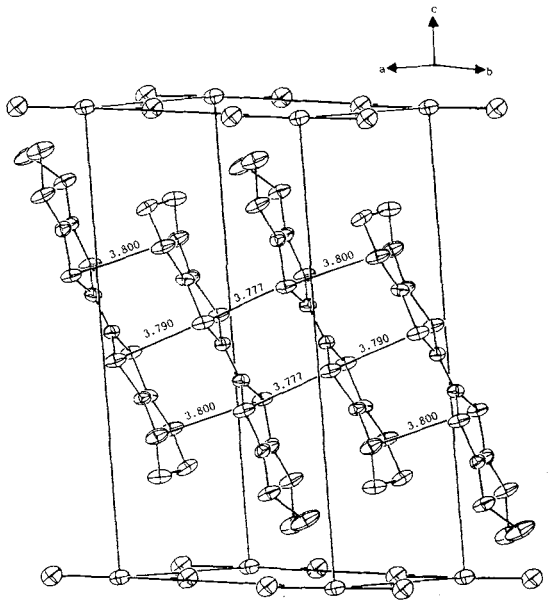


Fig. 1. Structure of ζ-$(ET)_2AuBr_2$ in the crystal; S···S contacts in the stack ≤3.8 Å.

[*] Prof. Dr. E. Amberger, Dr. K. Polborn, Dipl.-Chem. H. Fuchs
Institut für Anorganische Chemie der Universität
Meiserstrasse 1, D-8000 München 2 (FRG)

[**] We thank Dipl.-Phys. *C. P. Heidmann*, *H. Veith*, and Prof. Dr. *K. Andres*, Walther-Meissner-Institut für Tieftemperaturforschung, D-8046 Garching, for the measurement of the electrical conductivity and the T_c investigations.

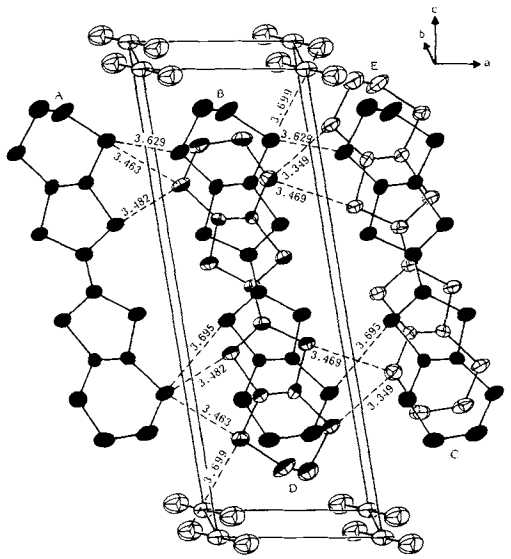


Fig. 2. "Side-to-side" layer arrangement of the ET molecules in ζ-$(ET)_2AuBr_2$ (50% ellipsoids) with unit cell. The molecules A, B, and C (black) form the upper layer of ET and the molecules, A, D (black-white), and E (white) the diagonal layer.

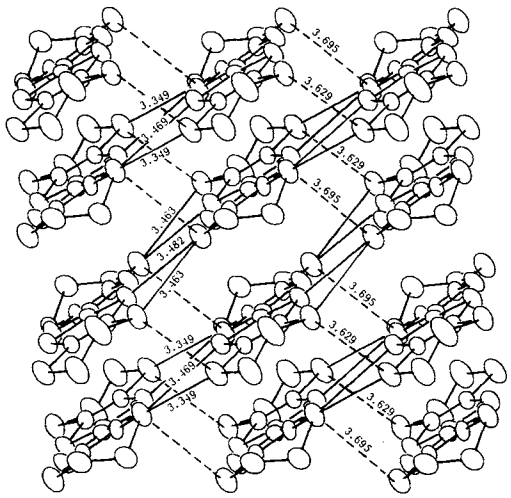


Fig. 3. Two-dimensional S···S network (distances <3.7 Å) in ζ-$(ET)_2AuBr_2$ (along the c axis).

S···S contacts (3.629 and 3.695 Å); in β-structures such as β-$(ET)_2IBr_2$, on the other hand, there are four (average value 3.587 Å).[14]

The crucial difference from the β-structure are the four very short S···S contacts between the stacks (3.349–3.482 Å, shown in Fig. 2 by the diagonal ET sequence black, black-white, and white). In β-$(ET)_2I_3$ and β-$(ET)_2IBr_2$, the short distances between the ET stacks are always larger than 3.56 Å, although the differences between the distances are less. That ζ-$(ET)_2AuBr_2$ is not superconducting could be due to the marked shortening of the S···S contacts. This results in weakening of the other S···S contacts in the plane of the layer of the ETs, which lie directly "side-to-side" (Fig. 2: linking of the black molecules), and reduces the two-dimensionality of the S···S network, which is important for electrical conductivity. In the side-to-side arrangement of the ET molecules, the sulfur atoms of the six-membered ring play an important role. All interstack distances between the S atoms of the five-membered ring are larger than 3.8 Å.

In examining the cation–anion interaction, so far only the $CH_2\cdots X$ contact (X = anion) has been considered.[15] One S···Br contact (3.699 Å) occurs per ET molecule in ζ-$(ET)_2AuBr_2$: this distance is shorter than the van der Waals distance of 3.8 Å. The twist stacks of t-$(ET)_2AuBr_2$[19] exhibit two short S···Br contacts (3.541 and 3.793 Å) per ET; however, the two-dimensional arrangement of the ET molecules, which is apparently necessary (but not sufficient) for superconductivity, is absent. These sulfur–halogen interactions could, along with the size, form, and symmetry of the anion, determine the type of structure and therefore the electrical properties.

As already observed in the case of α- and β-$(ET)_2I_3$, small changes in the experimental conditions for the synthesis of t- and ζ-$(ET)_2AuBr_2$ result in the growth of a non-superconducting and/or a superconducting phase. With the linear anions $I_3^\ominus$ (10.2 Å),[5d] $AuI_2^\ominus$ (9.4 Å), and $IBr_2^\ominus$ (9.3 Å), normal conditions of electrocrystallization (current density 1–5 μA/cm²) result in the growth of only α- and β-structures of $(ET)_2X$; with anions smaller than 9.3 Å ($Au(CN)_2^\ominus$: 9.2 Å,[19] $ICl_2^\ominus$: 8.7 Å,[11,15] $AuBr_2^\ominus$: 8.7 Å), only the β′-, ζ-, and t-structures are formed.

Experimental Procedure

ET [16] and n-Bu_4NAuBr_2 [17] were synthesized according to established procedures. Electrocrystallization: neutral ET (2×10^{-3} mol/L) in 25 mL of tetrahydrofuran (THF) or 1,1,2-trichloroethane (TCE) was galvanostatically oxidized in the presence of n-Bu_4NAuBr_2 (9×10^{-3} mol/L) with a current density of 0.5 μA/cm². After one week, thin black platelets (maximum $6\times0.5\times0.1$ mm³) were obtained at platinum electrodes from the TCE solution. These were identified by X-ray crystallography [19] as the twist phase. When THF solutions and gold or platinum electrodes were used, both the rodlike ζ-phase ($1\times0.5\times0.5$ mm³) and (usually) the twist phase (coffinlike or platelets, $1.3\times1.08\times0.18$ mm³) were obtained. Crystals obtained by a variety of procedures exhibited no volume superconductivity up to 0.5 K in a superconducting quantum magnetometer (SQUID).

Received: April 1, 1986 [Z 1718 IE]
German version: *Angew. Chem. 98* (1986) 749

CAS Restistry numbers:
ET, 66946-48-3; $(ET)_2AuBr_2$, 101897-60-3; n-Bu_4NAuBr_2, 50481-01-1.

[1] D. Jerome, A. Mazaud, M. Ribault, K. Bechgaard, *J. Phys. Lett. (Paris) 41* (1980) L95.
[2] K. Bechgaard, *Mol. Cryst. Liq. Cryst. 79* (1982) 1.
[3] a) R. C. Lacoe, S. A. Wolf, P. M. Chaikin, F. Wudl, E. Aharon-Shalom, *Phys. Rev. B27* (1983) 1947; b) F. Gross, H. Schwenk, K. Andres, F. Wudl, S. D. Cox, J. Brennan *ibid. B30* (1984) 1282.
[4] K. Bechgaard, F. B. Rasmussen, M. Olsen, G. Rindorf, C. S. Jacobsen, H. J. Pedersen, J. C. Scott, *J. Am. Chem. Soc. 103* (1981) 2440.
[5] a) E. B. Yagubskii, J. F. Shchegolev, V. N. Laukhin, L. J. Buravov, *Pis'ma Zh. Eksp. Teor. Fiz. 39* (1984) 12; b) R. P. Shibaeva, V. F. Kaminskii, E. B. Yagubskii, *Mol. Cryst. Liq. Cryst. 119* (1985) 361; c) H. Schwenk, C. P. Heidmann, F. Gross, E. Hess, K. Andres, D. Schweitzer, H. J. Keller, *Phys. Rev. 31* (1985) 3138; d) J. M. Williams, T. J. Emge, H. H. Wang, M. A. Beno, P. T. Copps, L. N. Hall, K. D. Carlson, G. W. Crabtree, *Inorg. Chem. 23* (1984) 2558.
[6] a) C. P. Heidemann, H. Veith, K. Andres, H. Fuchs, K. Polborn, E. Amberger, *Solid State Commun. 57* (1986) 161; b) J. M. Williams, H. H. Wang, M. A. Beno, T. J. Emge, L. M. Sowa, P. T. Copps, F. Behroozi, L. N. Hall, K. D. Carlson, G. W. Crabtree, *Inorg. Chem. 23* (1984) 3839; c) E. B. Yagubskii, J. F. Shchegolev, R. P. Shibaeva, D. N. Fedutin, L. P. Rosenberg, E. M. Sogomonyan, R. M. Lobkovskaya, V. N. Laukhin, A. A. Ignatiev, A. V. Zvarykina, L. J. Buravov, *Pis'ma Zh. Eksp. Teor. Fiz. 42* (1985) 167.
[7] a) E. Amberger, H. Fuchs, K. Polborn, *Angew. Chem. 97* (1985) 968; *Angew. Chem. Int. Ed. Engl. 24* (1985) 968; b) H. H. Wang, M. A. Beno, U. Geiser, M. A. Firestone, K. S. Webb, L. Nuñez, G. W. Crabtree, K. D. Carlson, J. M. Williams, L. J. Azevedo, J. F. Kwak, J. E. Shirber, *Inorg. Chem. 24* (1985) 2465.
[8] a) E. B. Yagubskii, J. F. Shchegolev, V. N. Laukhin, R. P. Shibaeva, E. E. Kostyuchenko, A. G. Khomenko, Yu. V. Sushko, A. V. Zvarykina, *Pis'ma Th. Eksp. Teor. Fiz. 40* (1984) 387; b) H. Veith, C. P. Heidmann,

F. Gross, A. Lerf, K. Andres, D. Schweitzer, *Solid State Commun. 56* (1985) 1015; c) V. N. Laukhin, E. E. Kostyuchenko, Yu. V. Sishko, J. F. Shchegolev, E. B. Yagubskii, *Pis'ma Zh. Eksp. Teor. Fiz. 41* (1985) 68; d) M. Tokumoto, K. Murata, H. Bando, H. Anzai, G. Saito, K. Kajimura, T. Ishiguro, *Solid State Commun. 54* (1985) 1031.

[9] V. A. Merzhanov, E. E. Kostyuchenko, V. N. Laukhin, R. M. Lobkovskaya, M. M. Makova, R. P. Shibaeva, J. F. Shchegolev, E. B. Yagubskii, *Pis'ms Th. Eksp. Teor. Fiz. 41* (1985) 146.

[10] Reviews on organic conductors and superconductors: a) D. Jérome, H. Schulz, *Adv. Phys. 31* (1982) 299; b) J. S. Miller: *Extended Linear Chain Compounds*, Plenum Press, New York 1982; c) K. Bechgaard, D. Jérome, Sci. Am. (1982) No 7, p. 50; *Spektrum Wiss. 1982*, No. 9, p. 38; d) F. Wudl, *Acc. Chem. Res. 17* (1984) 227; e) J. M. Williams, *Prog. Inorg. Chem. 33* (1985) 183.

[11] H. Kobayashi, R. Kato, A. Kobayashi, G. Saito, M. Tokumoto, H. Anzai, T. Ishiguro, *Chem. Lett. 1986*, 89.

[12] H. Kobayashi, R. Kato, T. Mori, A. Kobayashi, Y. Sasaki, G. Saito, T. Enoki, H. Inokuchi, *Mol. Cryst. Liq. Cryst. 107* (1984) 33.

[13] S. S. P. Parkin, *Mol. Cryst. Liq. Cryst. 119* (1985) 357.

[14] H. Endres, M. Miller, H. J. Keller, K. Bender, E. Gogu, I. Heinen, D. Schweitzer, *Z. Naturforsch. B40* (1985) 1664.

[15] P. C. W. Leung, T. J. Emge, A. J. Schultz, M. A. Beno, K. D. Carlson, H. H. Wang, M. A. Firestone, J. M. Williams, *Solid State Commun. 57* (1986) 93.

[16] M. Mizuno, A. F. Garito, M. P. Cava, *J. Chem. Soc., Chem. Commun. 1978*, 18.

[17] P. Braunstein, R. J. H. Clark, *J. Chem. Soc. Dalton Trans. 1973*, 1845.

[18] Four-circle diffractometer CAD4, Enraf-Nonius, 28°C, $Mo_{K\alpha}$ radiation, graphite monochromator, $\omega-2\theta$ scans in the range $1.0° \leq \theta \leq 30°$, 4842 independent intensities. Data reduction with Lorentz and polarization correction, empirical absorption correction ($\mu = 80.2\ cm^{-1}$), 7 ψ-scans in the range $7.51 \leq \theta \leq 14.79°$ (Enraf-Nonius Structure Determination Package). Solution with Patterson and Fourier techniques (SHELX-76), $R = 0.057$, $R_w = 0.046$ defined by $R_w = [\Sigma w(|F_o| - |F_c|)^2 / \Sigma w |F_o|^2]^{0.5}$, $w = 1.73/\sigma^2|F_o|$ for 3299 observed reflections $I \geq 3\sigma(I)$ and 178 refined parameters. Further details of the crystal structure investigation may be obtained from the Fachinformationszentrum Energie, Physik, Mathematik GmbH, D-7514 Eggenstein-Leopoldshafen 2 (FRG), on quoting the depository number CSD 51896, the names of the authors, and the journal citation.

[19] E. Amberger, H. Fuchs, K. Polborn, *Angew. Chem. 98* (1986) 751; *Angew. Chem. Int. Ed. Engl. 25* (1986) 729.

t-$(ET)_2Au(CN)_2$ and t-$(ET)_2AuBr_2$, Organic Radical Cation Salts with Twist Stucture**

By *Eberhard Amberger,* Helmut Fuchs,* and *Kurt Polborn*

Bis(ethylenedithio)tetrathiafulvalene (ET) (see **1** in ref. [3]) is currently the most promising organic donor for radical cation salts $(ET)_2X$ having metallic or superconducting properties.[1,2,11] Characteristic of the structures of all $(ET)_2X$ salts is the formation of layered structures of the ETs, whereby the π-systems overlap. The ethylene groups, which project from the planes, prevent close "face-to-face stacking," which would lead to undesired one-dimensionality. The size and shape of the anion X, as well as the "Pearson softness" of its periphery determine the kind of two-dimensional ET stack arrangement and thus the conductivity properties.

We report here the synthesis of t-$(ET)_2Au(CN)_2$ and η-$(ET)_2Au(CN)_2$[7] and the structures of the isotypic twist phases t-$(ET)_2Au(CN)_2$ and t-$(ET)_2AuBr_2$. The lengths of the anions of these t- and η-phases and of ζ-$(ET)_2AuBr_2$[3] are related to those of the anions of the known β-$(ET^{0.5\oplus})_2X^{\ominus}$ normal-pressure superconductors (T_c)[1,2,4-6] as follows: $X = I_3^{\ominus}$: 10.2 Å (1.2-1.6 K); $AuI_2^{\ominus}$: 9.4 Å (3.2-4 K); $IBr_2^{\ominus}$: 9.3 Å (1.9-2.8 K); $Au(CN)_2^{\ominus}$: 9.2 Å; $AuBr_2^{\ominus}$: 8.7 Å.

Upon anodic oxidation of ET in the presence of $nBu_4NAu(CN)_2$ or nBu_4NAuBr_2 in tetrahydrofuran (THF) or 1,1,2-trichloroethane, the following new phases crystallize out (often together): monoclinic η-$(ET)_2Au(CN)_2$[7] and monoclinic t-$(ET)_2Au(CN)_2$;[8a] monoclinic t-$(ET)_2AuBr_2$[8b] and triclinic ζ-$(ET)_2AuBr_2$.[3] Triclinic β-phases are not formed with $Au(CN)_2^{\ominus}$ and $AuBr_2^{\ominus}$.

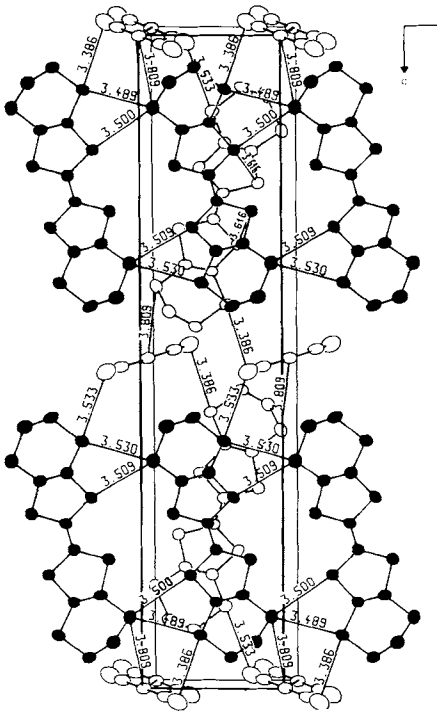


Fig. 1. Structure of t-$(ET)_2Au(CN)_2$; perpendicular to the plane of the ET molecules. "Side-to-side band arrangement" of the ET molecules along the *b* axis (S···S distances ≤3.7 Å and Au/N···S distances ≤4.0 Å). The black molecules form the upper band; only the ETs (white) in the unit cell are shown for the lower band.

In the β- and ζ-structures, the ETs are always parallel and arranged "side-to-side" (stacks and layers); they are characterized by short S···S distances between the stacks (i.e., within the layers) (≤3.7 Å; van der Waals distance 3.7 Å) and longer S···S distances within the stacks (>3.7 Å). In the new twist phases, on the other hand, the ETs are pairwise twisted in opposite directions with respect to the normals to the ET surfaces Fig. 1). These dimeric ET cations (S···S distances in the pair ca. 3.6 Å, Fig. 2, upper) are stacked parallel along the *a* axis (S···S distances between the pairs ca. 3.7 Å). Short S···S distances between the stacks (ca. 3.5 Å) of the ET molecules lying "side-to-side" parallel to the *b* axis result in an ET double band structure (Fig. 2, upper) in the twist phases. In the few known twist structures, δ-$(ET)_2I_3$,[4] $(ET)_2ClO_4(C_4H_8O_2)$,[9] and $(ET)PF_6$,[10] the twisting of the ET molecules only occurs in the direction of the stack. In t-$(ET)_2Au(CN)_2$ and t-$(ET)_2AuBr_2$, the ETs are also oppositely displaced with respect to the long ET axis (Fig. 1, black and white ETs). Planes of $Au(CN)_2^{\ominus}$ and $AuBr_2^{\ominus}$ ions join these ET bands.

For comparison, Figure 2 shows the differing S···S distances of the semiconducting t-$(ET)_2AuBr_2$ (above) and the superconducting β-$(ET)_2AuI_2$ (below) as viewed approxi-

[*] Prof. Dr. E. Amberger, Dipl.-Chem. H. Fuchs, Dr. K. Polborn
Institut für Anorganische Chemie der Universität
Meiserstrasse 1, D-8000 München 2 (FRG)

[**] We thank Dipl.-Phys. *C. P. Heidmann* and Prof. Dr. *K. Andres*, Walther-Meissner-Institut für Tieftemperaturforschung, D-8046 Garching, for the measurement of the electrical conductivity.

mately along the c axis. The two-dimensional structure that is necessary (but not sufficient) for superconductivity is not present in t-$(ET)_2Au(CN)_2$ and t-$(ET)_2AuBr_2$.

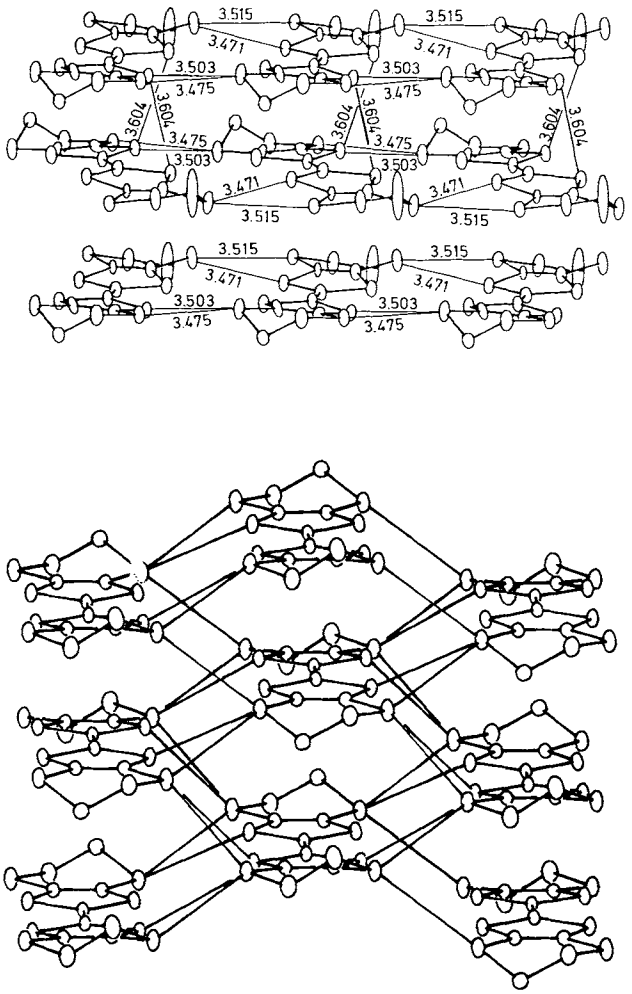


Fig. 2. Comparison of the quasi one-dimensional double band arrangement in t-$(ET)_2AuBr_2$ (above) with the steplike two-dimensional ET layers (two-dimensional network of S atoms) in β-$(ET)_2AuI_2$ (below). The view is along the c axis in each case (the S···S distances ≤ 3.7 Å are indicated).

In the highest occupied molecular orbital, the p_z orbital of sulfur predominates.[9, 10] The overlap integral of the wave functions of ET molecules having their S atoms in close proximity is therefore much larger when the S atoms of the "side-to-side" oriented ETs are arranged in a σ instead of a π configuration. The overlap in the direction of the stack (σ configuration) should be largest were it not hindered by the ethylene groups projecting from the molecular planes of the ETs. The smallest overlap occurs for the "side-to-side arrangement" (π configuration) of the ET molecules, as found for t-$(ET)_2Au(CN)_2$ and t-$(ET)_2AuBr_2$ (Fig. 2, above). The "dimerization" in the direction of the stack, the twist stacking, and the weak overlap of the S orbitals (despite the short S···S distances) of the ET bands arranged in the π configuration are thus responsible for the nonmetallic character[11,12] of the twist structures. In β-$(ET)_2AuI_2$, the steplike (diagonal) arrangement of the ET molecules (Fig. 2, below) leads to a two-dimensional S···S network and superconductivity.

In the β-phases, the transition temperature T_c (transition from metallic to the superconducting state) increases in going from β-$(ET)_2IBr_2$ to β-$(ET)_2AuI_2$,[1,11] the anion of which is 0.1 Å longer. Replacement of $IBr_2^{\ominus}$ in β-$(ET)_2IBr_2$ by $Au(CN)_2^{\ominus}$, which is 0.1 Å shorter, does not lead to "β-$(ET)_2Au(CN)_2$" with a smaller T_c. In addition to the length of the anions, therefore, the lesser "Pearson softness" in the case of $Au(CN)_2^{\ominus}$ and $AuBr_2^{\ominus}$ could also be important for the formation of the new type of structure. No t-, η-, or ζ-structures are formed with the interhalide ions $IBrCl^{\ominus}$ (9.0 Å) and $ICl_2^{\ominus}$ (8.7 Å, same length as $AuBr_2^{\ominus}$); instead, α- and β'-phases are obtained.[5] The smallest Au···S distance in t-$(ET)_2Au(CN)_2$ (3.809 Å) is significantly shorter than in β-$(ET)_2AuI_2$ (>4.1 Å; van der Waals distance 4.0 Å). In t-$(ET)_2AuBr_2$, the smallest S···Br distance (3.541 Å) is significantly shorter than the van der Waals distance (3.8 Å). The cell volumes of the twist phases, unlike those of the β-phases, are not functions of the length of the anions. t-$(ET)_2AuBr_2$ has a cell volume that is 17 Å^3 larger than that of t-$(ET)_2Au(CN)_2$, even though the $AuBr_2^{\ominus}$ anion is ca. 5% shorter than $Au(CN)_2^{\ominus}$. The η-phase with four ET molecules in the unit cell and a similar steplike arrangement of the ET molecules along the b axis, which grows only seldomly, is not superconducting.[7]

Experimental Procedure

$Et_4NAu(CN)_2$ was synthesized from AuCN and Et_4NCN (molar ratio 1:1) in THF and was precipitated with Et_2O as colorless crystals (m.p. = 89 °C; yield 92%). Electrocrystallization: Galvanostatic oxidation was carried out on neutral ET (2×10^{-3} mol/L) and $Et_4NAu(CN)_2$ (13×10^{-3} mol/L) in 30 mL of THF with 0.5 μA/cm^2 current density (electrode voltage 0.5 V) at platinum electrodes (current yield 90%). After 5 d, distorted six-sided platelets of the η-phase along with coffinlike rods (maximum size $2.45\times0.43\times0.25$ mm^3) of the t-phase were obtained.

Received: April 30, 1986;
supplemented: May 27, 1986 [Z 1753 IE]
German version: *Angew. Chem. 98 (1986)* 751

CAS Registry numbers:
ET, 66946-48-3; t-$(ET)_2Au(CN)_2$, 101897-58-9; t-$(ET)_2AuBr_2$, 101897-60-3; *n*-$Bu_4NAu(CN)_2$, 42523-89-7; *n*-Bu_4NAuBr_2, 50481-01-1.

[1] E. Amberger, H. Fuchs, K. Polborn, *Angew. Chem. 97* (1985) 968; *Angew. Chem. Int. Ed. Engl. 24* (1985) 968.
[2] C. P. Heidmann, H. Veith, K. Andres, H. Fuchs, K. Polborn, E. Amberger, *Solid State Commun. 57* (1986) 161.
[3] E. Amberger, K. Polborn, H. Fuchs, *Angew. Chem. 98* (1986) 749; *Angew. Chem. Int. Ed. Engl. 25* (1986) 727.
[4] R. P. Shibaeva, V. F. Kaminskii, E. B. Yagubskii, *Mol. Cryst. Liq. Cryst. 119* (1985) 361.
[5] P. C. W. Leung, T. J. Emge, A. J. Schulz, M. A. Beno, K. D. Carlson, H. H. Wang, M. A. Firestone, J. M. Willams, *Solid State Commun. 57* (1986) 93.
[6] H. Kobayashi, R. Kato, A. Kobayashi, G. Saito, M. Tokumoto, H. Anzai, T. Ishiguro, *Chem. Lett. 1986*, 89.
[7] Crystal data (27 °C) of η-$(ET)_2Au(CN)_2$: space group $C2/c$ $Z=4$, $a=36.517(7)$, $b=4.254(1)$, $c=22.117(4)$ Å, $\alpha=90.00(2)$, $\beta=111.38(2)$, $\gamma=90.00(2)°$, $V=3199.3$ Å^3. E. Amberger, H. Fuchs, K. Polborn, unpublished results.
[8] Four-circle diffractometer CAD4, Enraf-Nonius, 27 °C, $Mo_{K\alpha}$ radiation, graphite monochromator. a) Crystal data of t-$(ET)_2Au(CN)_2$: space group $P2/n$, $Z=2$, $a=7.912(3)$, $b=6.714(1)$, $c=30.919(4)$ Å, $\alpha=90.00(1)$, $\beta=91.20(3)$, $\gamma=90.00(3)°$, $V=1642.1$ Å$_3$, $\rho_{calcd}=2.060$ gcm^{-3}, ω-2θ scans in the range $1.0°\leq\theta\leq30°$ 2955 independent intensities. Data reduction with Lorentz and polarization correction, empirical absorption correction ($\mu=54.72$ cm^{-1}), $R=0.038$, $R_w=0.047$ defined by $R_w=\{\sum w(|F_o|-|F_c|)^2/\sum w|F_o|^2\}^{0.5}$, $w=1$, for 2094 observed reflections $I\geq3\sigma(I)$ and 190 refined parameters.—b) Crystal data of t-$(ET)_2AuBr_2$: space group $P2/n$, nonstandard setting of $P2/c$, $Z=2$, $a=7.816(3)$, $b=6.708(2)$, $c=31.708(5)$ Å, $\alpha=90.01(2)$, $\beta=93.48(2)$, $\gamma=90.00(3)°$,

$V = 1659.4$ Å^3, $\rho_{calcd} = 2.254$ gcm^{-3}. ω-2θ scans in the range $1 \leq \theta \leq 25°$, 2496 independent intensities, empirical absorption correction ($\mu = 77.97$ cm^{-1}), 8ψ scans in the θ range with $5.23 \leq \theta \leq 13.2°$. $R = 0.050$ and $R_w = 0.067$ ($R_w = \{\sum w(|F_o| - |F_c|)^2 / \sum w|F_o|^2\}^{0.5}$, $w = 1$ for $F <$ threshold, $w = (\text{threshold}/F)^2$ for $F \geq$ threshold; threshold = 479.9) for 1903 observed reflections $I \geq 3\sigma(I)$ and 181 refined parameters. Further details of the crystal structure investigation may be obtained from the Fachinformationszentrum Energie, Physik, Mathematik GmbH, D-7514 Eggenstein-Leopoldshafen 2 (FRG), on quoting the depository number CSD 51944, the names of the authors, and the journal citation.

[9] H. Kobayashi, R. Kato, T. Mori, A. Kobayashi, Y. Sasaki, G. Saito, T. Enoki, H. Inokuchi, *Mol. Cryst. Liq. Cryst. 107* (1984) 33.

[10] S. S. P. Parkin, *Mol. Cryst. Liq. Cryst. 119* (1985) 357.

[11] H. H. Wang, M. A. Beno, U. Geiser, M. A. Firestone, K. S. Webb, L. Nuñez, G. W. Crabtree, K. D. Carlson, J. M. Williams, L. J. Azevedo, J.. F. Kwak, J. E. Schirber, *Inorg. Chem. 24* (1985) 2465.

[12] Electrical conductivity of t-$(ET)_2Au(CN)_2$ at room temperature: $\sigma = 0.005$–0.006 $(\Omega cm)^{-1}$, energy gap $\Delta = 1825$ K $= 0.16$ eV.

Syntheses and Spectroscopic Properties of Triafulvalene Derivatives**

By *Richard Neidlein,* Volker Poignée, Walter Kramer,* and *Christian Glück*

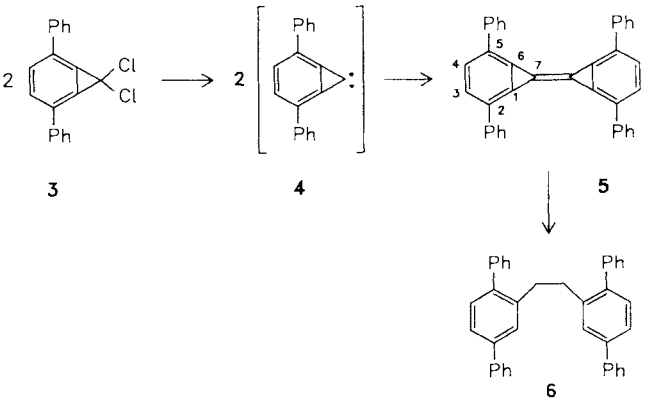
Dedicated to Professor Siegfried Hünig on the occasion of his 65th birthday

Although triafulvene **1**, the simplest cyclic cross-conjugated molecule, was recently synthesized,[1,2] triafulvalene **2** is still unknown.[3] Of its derivatives, only the benzophenanthrotriafulvalene radical cation has been postulated on the basis of mass spectrometric investigations.[4] In the course of our studies on new reactions of cyclopropabenzene and its derivatives, we have succeeded in synthesizing substituted dibenzotriafulvalenes.

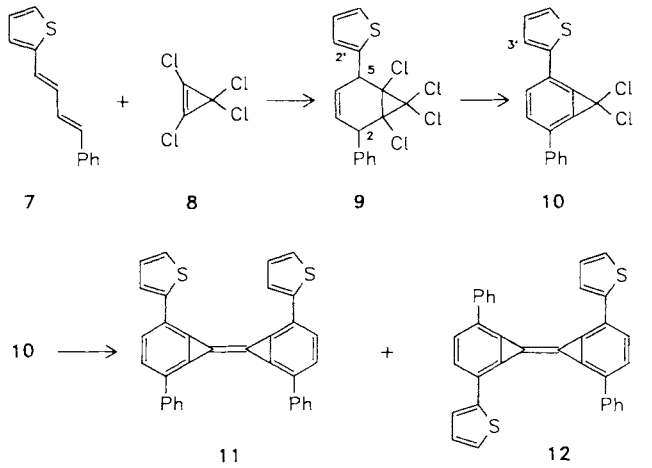


We used 7,7-dichloro-2,5-diphenylbicyclo[4.1.0]hepta-1,3,5-triene **3**[5] as the starting material for the first synthesis. Treatment of **3** with a suitable base resulted in the formation of the carbene **4**, which undergoes dimerization to give 7,7′-bis(2,5-diphenylbicyclo[4.1.0]hepta-1,3,5-trienylidene) **5**. This reaction depends strongly on the base selected. With methyllithium, **3** reacts to give products that do not include the desired ones;[6] with *n*-butyllithium, on the other hand, the triafulvalene derivative **5** is obtained. Compound **5** is characterized by poor solubility. CS_2, in which the compound exhibits a strong yellow fluorescence, was used to record the ^{1}H-NMR spectrum, which is in agreement with the structure given. The aromatic protons are similar to those of **3**, H_2 instead of Cl_2, with respect to chemical shift and splitting pattern.[7] ^{13}C-NMR investigations of **5** failed on account of the low solubility.

Hydrogenation of **5** with Pd/C and hydrogen at room temperature gave a good yield of the expected 1,2-bis(1,1′:4′,1″-terphenyl-2′-yl)ethane **6**.



Two isomeric triafulvalene derivatives can be synthesized via 7,7-dichloro-2-phenyl-5-(2-thienyl)bicyclo[4.1.0]hepta-1,3,5-triene **10**. Compound **10** is obtained by allowing 2-(4-phenyl-1,3-butadienyl)thiophene **7** to react with tetrachlorocyclopropene **8**.



The Diels–Alder product **9** thereby formed is converted into **10** by treatment with potassium *tert*-butoxide at −78 °C. In analogy to **3**, treatment of **10** with *n*-butyllithium at −78 °C affords a 1:1 mixture of **11** and **12**. On account of their likewise low solubility, it was not possible to isolate the pure isomers **11** and **12**. The isomeric ratio was determined on the basis of ^{1}H-NMR spectroscopy.

Experimental Procedure

5: **3** (625 mg, 2 mmol) was dissolved in 50 mL of dry tetrahydrofuran (THF) under argon. *n*BuLi in hexane (0.65 mL, 1.6 M) was then added to the solution at −78 °C. After 15 min, the solution was allowed to thaw; the intense red precipitate was filtered under suction through a porcelain frit and washed with diethyl ether. After drying in air, **5** (110 mg, 23%) was obtained as a microcrystalline powder, m.p. = 240–242 °C (dec.); recrystallization from 1-bromonaphthalene gave fine deep-red needles, m.p. = 245 °C (dec.). ^{1}H-NMR (250 MHz, CS_2/CD_2Cl_2 4:1): δ(relative to $CDHCl_2$) = 7.34 (m, 4H, *p*-H), 7.45 (m, 8H, *m*-H, *m*′-H), 7.67 (s, 4H, H-3,4), 7.95 (m, 8H, *o*-H, *o*′-H). MS (100 eV, 280 °C): *m/z* 481 (32%), 480 (100, $M^{\oplus}$), 479 (24), 403 (22), 241 (26), 240 (7), 78 (25); M_r calcd 480.18780, found 480.18791.

6: A suspension of **5** (48 mg, 0.1 mmol) and Pd/C (10 mg) in THF was allowed to stir under H_2 at room temperature for 48 h, until the fluorescence had vanished. The reaction mixture was then filtered and the solvent was removed under vacuum. Recrystallization of the residue from $CHCl_3$/hexane (1:1 v:v) afforded **6** (46 mg, 95%) as colorless crystals, m.p. = 242 °C. ^{1}H-NMR (250 MHz, CD_2Cl_2): $\delta = 7.55$–7.09 (m, 26H, arom. H), 2.84 (s, 4H, CH_2). MS (100 eV, 180 °C): *m/z* 487 (3%), 486 (5, $M^{\oplus}$), 244 (23), 243 (100), 166 (9), 165 (25), 115 (12), 91 (23), 77 (2).

[*] Prof. Dr. R. Neidlein, Dipl.-Chem. V. Poignée, Dr. W. Kramer, C. Glück
Pharmazeutisch-Chemisches Institut der Universität
Im Neuenheimer Feld 364, D-6900 Heidelberg (FRG)

[**] This work was supported by the Deutsche Forschungsgemeinschaft and the Fonds der Chemischen Industrie.

9: 7 (9 g, 42 mmol), **8** (5.2 mL, 42 mmol), and hydroquinone (100 mg) were dissolved in 60 mL of toluene. The reaction mixture was heated at 110 °C for 12 h. The solvent was then removed, the residue dissolved in methanol, and the insoluble matter separated off. The brown solid that crystallized was washed carefully with a small amount of acetone, dried, and recrystallized from 1-propanol. **9** (5.5 g, 33%) was obtained as almost colorless crystals, m.p. = 167 °C. ^{1}H-NMR (250 MHz, $CDCl_3$): δ = 4.1 (m, 1H, H-2), 4.5 (m, 1H, H-5), 5.77 (m, 2H, H-3,4), 7.2–7.43 (m, 8H, arom. H). ^{13}C-NMR (62.89 MHz, $CDCl_3$): δ = 41.67 (d, C-4 or C-3), 46.92 (d, C-3 or C-4), 56.40 (s, C-6 or C-1), 56.46 (s, C-1 or C-6), 70.11 (s, C-7), 125.73 (CH), 125.83 (CH), 126.58 (CH), 127.43 (CH), 127.57 (CH), 128.43 (CH), 128.50 (CH), 129.78 (CH), 140.28 (s, C-1′ or C-2′), 143.34 (s, C-2′ or C-1′).

10: KO*t*Bu (2.25 g, 20 mmol) was dissolved under argon in 100 mL of dry THF. The solution was cooled to −78 °C and a solution of **9** (3.9 g, 10 mmol) in 50 mL of dry THF was added over 15 min. After 1 h at −30 °C, the reaction mixture was allowed to thaw. The solvent was removed in vacuum and the residue was dissolved in 50 mL of $CHCl_3$. After filtration, the solution was concentrated to a third of its initial volume, treated with the same amount of *n*-hexane, and cooled to induce crystallization. **10** (890 mg, 28%) was obtained as colorless prisms, m.p. = 105–107 °C (dec.). ^{1}H-NMR (250 MHz, $CDCl_3$): δ = 7.19 (dd, 1H, H-4′), 7.45 (m, 2H, *p*-H, H-3′ or H-5′), 7.55 (m, 2H, *m*-H, *m*′-H), 7.65 (dd, 1H, H-5′ or H-3′), 7.71 (d, 1H, H-3 or H-4), 7.86 (d, 1H, H-4 or H-3), 7.91 (m, 2H, *o*-H, *o*′-H).

11, **12**: **10** (635 mg, 2 mmol) was dissolved in 50 mL of dry THF under argon. *n*BuLi in hexane (0.65 mL, 1.6 M) was then added to the solution at −78 °C. The reaction mixture was allowed to thaw and the violet microcrystals were collected under suction on a porcelain frit. After washing with diethyl ether and drying in the air, 95 mg (19%) of a 1:1 mixture of **11** and **12** was obtained, m.p. = 210 °C (dec.). ^{1}H-NMR (250 MHz, CS_2/CD_2Cl_2 4:1): δ (relative to $CDHCl_2$) = 7.17–7.78 (m, 32H), 7.98 (m, 4H, *o*-H (**11**), *o*′-H (**11**) or *o*′-H (**12**)), 8.07 (m, 4H, *o*-H (**12**), *o*′-H (**12**) or *o*′-H (**11**)). MS (100 eV, 240 °C): *m/z* 492 (2%, $M^{\oplus}$), 414 (1), 247 (2), 91 (2), 84 (6), 78 (4), 77 (4), 44 (100). M_r calcd 492.100646, found 492.1007767.

Received: March 24, 1986;
supplemented: May 2, 1986 [Z 1709 IE]
German version: *Angew. Chem. 98* (1986) 735

CAS Registry numbers:
3, 33253-76-8; **5**, 103348-54-5; **6**, 103348-55-6; 7, 52380-84-4; **8**, 6262-42-6; 9, 103348-56-7; **10**, 103348-57-8; **11**, 103348-58-9; **12**, 103437-34-9.

[1] W. E. Billups, L.-J. Lin, E. W. Casserly, *J. Am. Chem. Soc. 106* (1984) 3698.
[2] S. W. Staley, T. D. Norden, *J. Am. Chem. Soc. 106* (1984) 3699.
[3] J. Aihara, *Bull. Chem. Soc. Jpn. 56* (1983) 1935.
[4] J. Agranat, *Org. Mass Spectrom. 7* (1973) 907.
[5] B. Halton, P. J. Milsom, *Chem. Commun. 1971*, 814.
[6] B. Halton, A. D. Woolhouse, P. J. Milsom, *J. Chem. Soc. Perkin Trans. 1 1977*, 735.
[7] P. Müller, *Helv. Chim. Acta 57* (1974) 704.

(*R*)-2-Isopropenylcyclopropane-1,1-dicarboxylic Acid: Absolute Configuration and Stereospecific Ring Expansion of Its Dimethyl Ester**

By *Gerhard Quinkert*,* *Hans-Günther Schmalz*, *Egon Walzer*, *Stefan Gross*, *Gerd Dürner*, and *Jan W. Bats*

Dedicated to Edgar Heilbronner on the occasion of his 65th birthday

Recently, we reported the preparation of enantiomerically pure (*R*)-2-vinylcyclopropane-1,1-dicarboxylic acid **6a** by chirality-inducing cyclopropanation.[1] The predicted but not yet proven (*R*)-sense of chirality of **6a** is based on an analysis of the stereoelectronic factors[2] for the formation of the three-membered ring (see Scheme 1) and for the ring expansion of the diester **8a**[1,2] leading to the enantiomerically pure five-membered ring ketones **13a** + **14a** (see Scheme 2) with known absolute configuration.

We now report the analogous preparation of enantiomerically pure (*R*)-2-isopropenylcyclopropane-1,1-dicarboxylic acid **6b** by chirality-inducing cyclopropanation (see Scheme 1) and the ring expansion of its dimethyl ester **8b** to give the enantiomerically pure five-membered ring ketones **13b** + **14b** (see Scheme 2) and provide proof of the absolute configuration of both **6b** and **13b**. What **13a** + **14a**[3] already are for the total synthesis of enantiomerically pure steroids without a methyl group at C(10),[1,2] **13b** + **14b**[3] could become for the total synthesis of enantiomerically pure pseudoguaianolides.[4]

The absolute configuration of *ent*-**6b**,[5] and thus also of **6b**, was determined by an X-ray structure analysis (see Fig. 1)[6,7] of the salt obtained from one equivalent each of *ent*-**6b** and (*S*)-(−)-1-phenylethylamine.

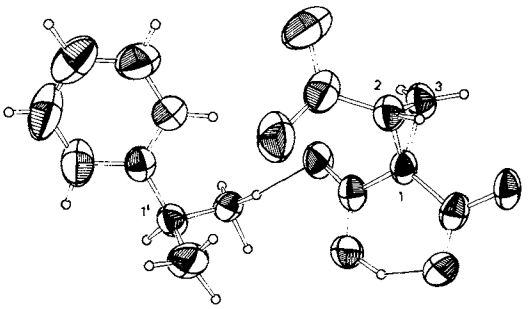


Fig. 1. Structure of the complex obtained from 1 equivalent each of *ent*-**6b** and (*S*)-(−)-1-phenylethylamine.

The absolute configuration of **13b** (obtained from **6b** according to Scheme 2) or of *ent*-**13b** (obtained from *ent*-**6b** according to Scheme 2) follows from a comparison of their CD spectra (see Fig. 2) with those of the configurationally

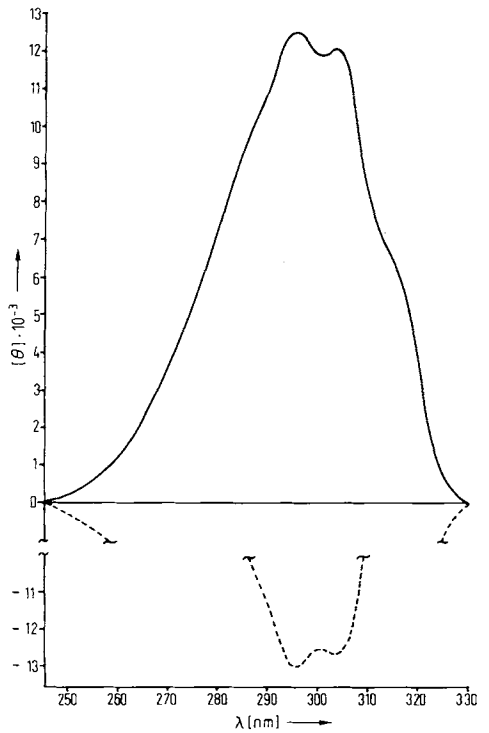
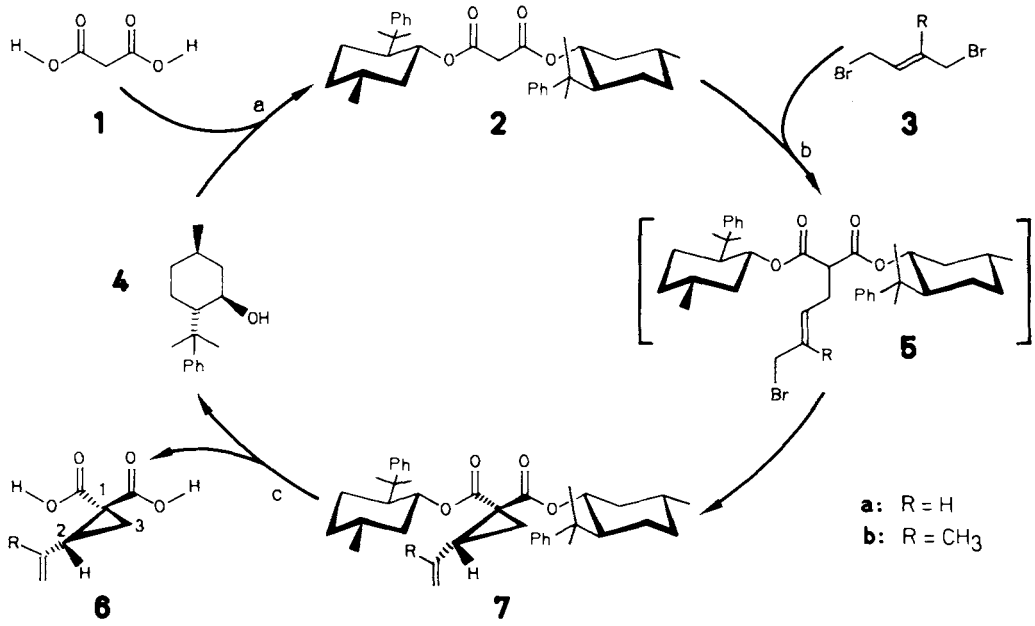


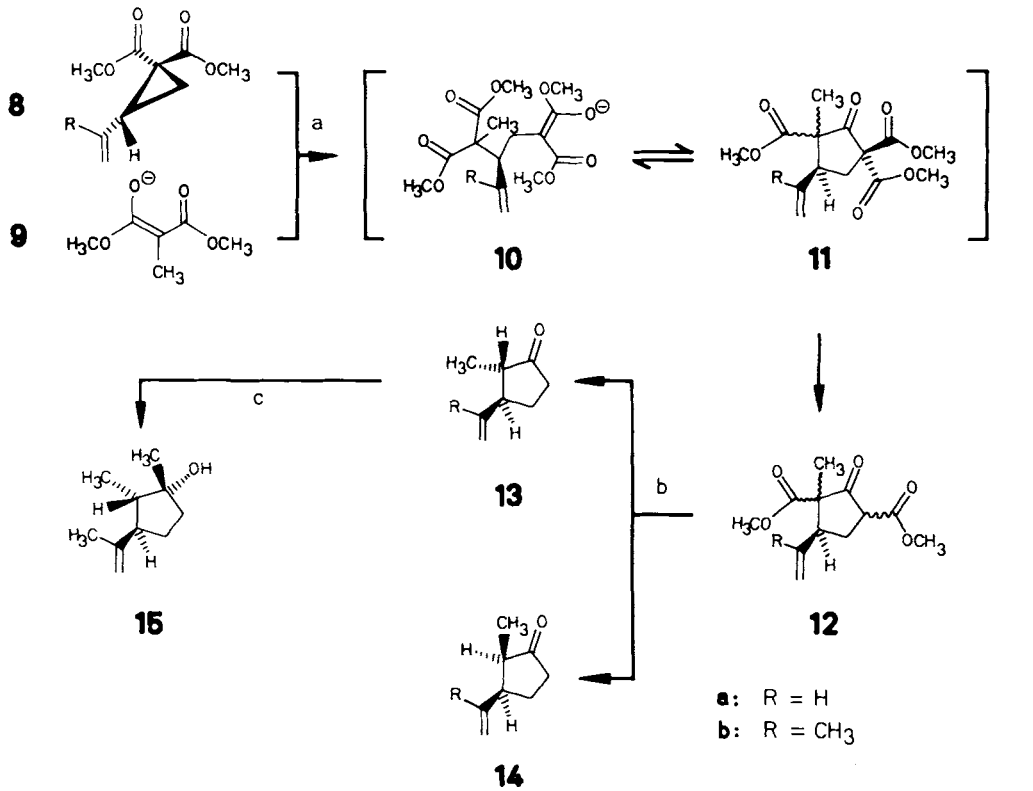
Fig. 2. CD spectra of **13b** (——) and *ent*-**13b** (----) in dioxane.

[*] Prof. Dr. G. Quinkert, Dr. H.-G. Schmalz, Dipl.-Chem. E. Walzer, Dr. S. Gross, Dr. G. Dürner, Dr. J. W. Bats
Institut für Organische Chemie der Universität
Niederurseler Hang, D-6000 Frankfurt am Main 50 (FRG)

[**] This work was supported by the Deutsche Forschungsgemeinschaft (Project 15/21-1 and 2), the Fonds der chemischen Industrie, and Hoechst AG.



Scheme 1. Simple preparation of the enantiomerically pure three-membered ring building blocks **6a** and **6b** from **1**. Synthesis of **6a**: a) see [1]; b) 1 equiv. of **3a**, Aliquat 336, Fluka AG (catalytic), hexane/50% aqueous NaOH, 14h stirring at RT; **7a**:2-*epi*-**7a** = 98:2; preparative HPLC, **7a** (67%); c) KOH; hydroquinone (catalytic), EtOH/H_2O (4:1), 16h reflux, **6a** (65%) and **4** (72%).—Synthesis of **6b**: a) see [1]; b) 1.1 equiv **3b** (mixed with (*Z*)-isomer, 78:22), Aliquat 336, Fluka AG (catalytic), hexane/50% aqueous NaOH, 65 h stirring at RT; **7b**:2-*epi*-**7b** = 84:16; preparative HPLC, **7b** (63%); c) KOH, hydroquinone (catalytic), EtOH/H_2O (4:1), 100 h reflux, **6b** (71%) and **4** (70%).



Scheme 2. Simple preparation of the enantiomerically pure five-membered ring building blocks **13a** + **14a**, **13b** + **14b** and **15** from **8**. Synthesis of **13a** + **14a**: see [1].—Synthesis of **13b** + **14b**: a) 1 equiv. of **9**, MeOH; 1.5 h at 130°C; **12b** (78%); b) 10 equiv of LiCl, dimethyl sulfoxide, 4 equiv. of H_2O, 4h at 140°C; **13b**:**14b** = 92:8 (65%).—Synthesis of **15**: c) 2 equiv. of MeLi, ether, −10°C, 45 min; **15** (38%).

known[1] compounds **13a** and *ent*-**13a**, respectively. This assignment is supported by a comparison of the optical rotation of *ent*-**15** (obtained from *ent*-**13** according to Scheme 2; $[\alpha] = +44.6$ in CCl_4) with that of plinol A (**15**; $[\alpha] = -39.5$ without solvent[8]).

At the same time as having proven the absolute configuration of **6b** we have also established that the conversion of the chiral three-membered building block of type **8** into the chiral five-membered building block of type **13** + **14** takes place with complete inversion. Still more important, however, is the fact that the (*R*)-sense of chiralty predicted for the enantiomerically pure three-membered ring compounds of type **6** on the basis of stereoelectronic considerations[1] actually is correct.

Received: March 14, 1986 [Z 1702 IE]
German version: *Angew. Chem. 98* (1986) 732

[1] G. Quinkert, U. Schwartz, H. Stark, W.-D. Weber, F. Adam, H. Baier, G. Frank, G. Dürner, *Liebigs Ann. Chem. 1982*, 1999.

[2] a) G. Quinkert, H. Stark, *Angew. Chem. 95* (1983) 651; *Angew. Chem. Int. Ed. Engl. 22* (1983) 637; b) G. Quinkert in W. Bartmann, B. M. Trost (Ed.), *Selectivity—a Goal for Synthetic Efficiency*, Verlag Chemie, Weinheim 1984; c) H. Baier, G. Dürner, G. Quinkert, *Helv. Chim. Acta 68* (1985) 1954.

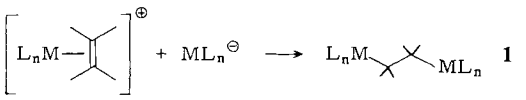
[3] The same enolate anion is obtained from both diastereomers.
[4] For the total synthesis of pseudo guaianolides, cf. C. H. Heathcock, S. L. Graham, M. C. Pirrung, F. Plavac, C. T. White in J. ApSimon (Ed): *The Total Synthesis of Natural Products, Vol. 5*, Wiley, New York 1983; M. Vandewalle, P. De Clercq, *Tetrahedron 41* (1985) 1767.
[5] Compound *ent*-**6b** is readily accessible by separation of *rac*-**6b** with (−)-brucine.
[6] Salt obtained from one equivalent each of *ent*-**6b** and (*S*)-(−)-1-phenylethylamine: monoclinic, space group $P2_1$; $a=9.2714(9)$, $b=6.178(2)$, $c=14.1140(8)$ Å, $\beta=93.902(8)°$; $V=806.5(5)$ Å^3; $Z=2$, $\rho_{calc}=1.200$ g/cm^3; Enraf-Nonius CAD4 diffractometer; $Cu_{K\alpha}$ radiation; quadrant up to $2\theta=120°$, 1311 independent reflections with $I>\sigma(I)$; structure determination by direct methods; hydrogen atom positions on the disordered isopropenyl group not localizable, all other H atoms incorporated in the refinement; $R(f)=0.043$, $\omega R(F)=0.042$; SDP program system.
[7] Further details of the crystal structure investigation are available on request from the Fachinformationszentrum Energie, Physik, Mathematik GmbH, D-7514 Eggenstein-Leopoldshafen 2, on quoting the depository number CSD-51814, the names of the authors, and the full citation of the journal.
[8] H. Strickler, G. Ohloff, E. Sz. Kovats, *Helv. Chim. Acta 78* (1967) 759.

Directed Synthesis of Rhenamolybdatetrahedranes: Nucleophilic Addition of Pentacarbonylrhenate(1-) to Alkyne Ligands in Cationic Molybdenum Complexes**

By *Wolfgang Beck,* Hans-Joachim Müller,* and *Ulrich Nagel*

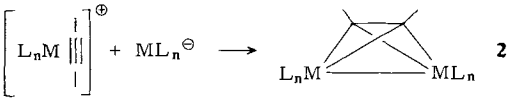
Dedicated to Professor Marianne Baudler on the occasion of her 65th birthday

The nucleophilic addition of carbonyl metalates to coordinated olefins (e.g., ethylene, butadiene) results in the formation of binuclear hydrocarbon-bridged complexes,[1] for example, of type **1**.



1

We have found, furthermore, that organometallic nucleophiles such as $Re(CO)_5^{\ominus}$ add to the coordinated alkyne of cationic molybdenum complexes with formation of dimetallatetrahedranes of type **2**.

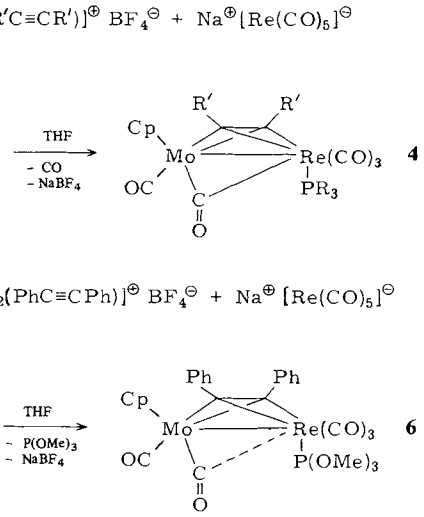


2

The addition of organic nucleophiles to cationic alkyne complexes was reported earlier.[2]

The dimetallatetrahedranes **4** and **6** are obtained by reaction of **3**[3] and **5**,[3] respectively, according to Scheme 1.

The alkyne functions as a 4-electron donor in the educts **3** and **5**;[4] this explains the formation of the μ-η^2,η^2-alkyne-bridged complexes **4** and **6**, respectively, in which each of the metal centers has a nobel-gas configuration.



Scheme 1. Cp = η^5-C_5H_5; THF = tetrahydrofuran.

	PR_3	R'CCR'		PR_3	R'CCR'
4a	PPh_3	MeCCMe	**4d**	PEt_3	PhCCPh
4b	PPh_3	MeCCPh	**4e**	PMe_2Ph	PhCCPh
4c	PPh_3	PhCCPh	**4f**	PPh_3	MeCC*n*Pr

The migration of the PR_3 ligand from the Mo to the Re atom occurs for steric reasons. The structures of the compounds **4a** and **6** are shown in Figures 1 and 2.

The known dimetallatetrahedranes with two different metals, $NiCoC_2$,[5] $NiCrC_2$, $NiMoC_2$, $NiWC_2$,[6] and $NiFeC_2$[7], have been obtained from neutral carbonyl complexes and alkynes, along with other products, or, surprisingly, from alkylidyne complexes.[8] The type of reaction presented here, on the other hand, is, to the best of our knowledge, the first *directed* synthesis of dimetallatetrahe-

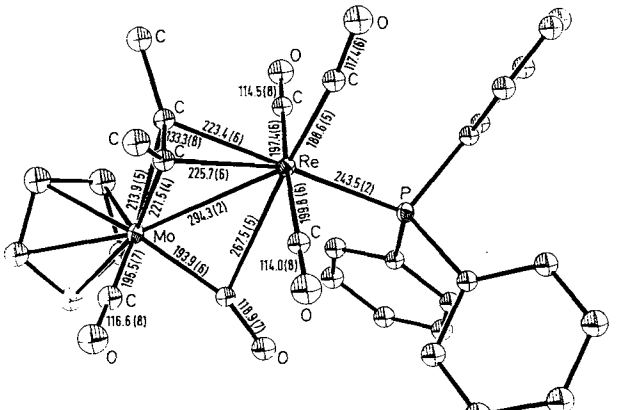


Fig. 1. Molecular structure of **4a** at −50 °C in the crystal, 20% probability level (H atoms omitted), interatomic distances [pm]. $P\bar{1}$, $a=852.4(2)$, $b=1160.2(3)$, $c=1605.0(4)$ pm, $\alpha=100.02(2)$, $\beta=104.76(2)$, $\gamma=100.88(2)°$, $V=1.4655(6)$ nm^3, $Z=2$. $\lambda(Mo_{K\alpha})=71.069$ pm; ω scan, $\Delta\omega=1.6°$, $4\leq\dot{\omega}\leq29.3°$ min^{-1}; $4°\leq2\theta\leq50°$; 10013 measured, 5120 unique reflections, of which 4904 were observed ($I\geq2\sigma(I)$), 131 parameters. The absorption ($\mu=46.9$ cm^{-1}) was corrected (crystal size $0.2\times0.1\times0.35$ mm^3, elipsoid, 250 measured values); $R=0.031$, $R_w=0.033$, $w=(\sigma^2(F_0)+0.0001\,F_0^2)^{-1}$. The hydrogen atoms are placed at calculated positons; the C_5H_5 and C_6H_5 rings were treated as regular rigid groups. Mo, Re, and P were anisotropically refined [13].

[*] Prof. Dr. W. Beck, Dipl.-Chem. H. J. Müller
Dr. U. Nagel (X-ray structure analysis)
Institut für Anorganische Chemie der Universität
Meiserstrasse 1, D-8000 München 2 (FRG)

[**] Organometallic Lewis Acids, Part 24. This work was supported by the Deutsche Forschungsgemeinschaft and the Fonds der Chemischen Industrie.—Part 23: H. Bauer, W. Beck, *J. Organomet. Chem. 308* (1986) 73.

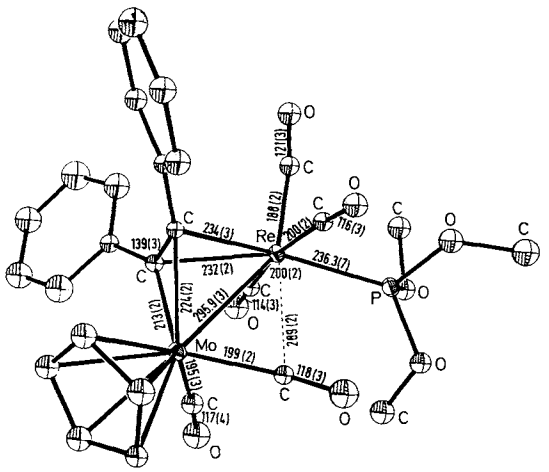


Fig. 2. Molecular structure of **6** at −50 °C in the crystal, 20% probability level (H atoms omitted), interatomic distances [pm]. $P\bar{1}$, $a=915.1(3)$, $b=1069.0(4)$, $c=3063(1)$ pm, $\alpha=85.90(3)$, $\beta=86.32(3)$, $\gamma=70.15(3)°$, $V=2.808(2)$ nm^3, $Z=4$. $\lambda(Mo_{K\alpha})=71.069$ pm; ω scan, $\Delta\omega=1.2°$, $4\leq\dot{\omega}\leq29.3°$ min^{-1}; $4°\leq2\theta\leq50°$; 10447 measured, 8947 unique reflections, of which 8237 were observed ($I\geq2\sigma(I)$), 269 parameters. The absorption ($\mu=49.0$ cm^{-1}) was corrected (crystal size $0.45\times0.4\times0.3$ mm^3); $R=0.112$, $R_w=0.131$, $w=(\sigma^2(F_o)+0.001\,F_o^2)^{-1}$. One of two crystallographically independent molecules is shown; in the other molecule, the two methoxy groups are disordered. For further details, see the caption to Figure 1 [13].

dranes of this kind.[9] The use of unsymmetrical alkynes affords intrinsically chiral tetrahedranes such as **4b** and **4f**. Numerous chiral dimetalla-[5,6,10] and trimetallatetrahedranes[11] are known; in some cases, it has been possible to separate the enantiomers.[10,11]

As revealed by the ^{1}H-NMR (Table 1) and ^{31}P-NMR data, **4a**, **b**, **c** are formed as mixtures of configurationally stable diastereomers; the Mo and Re atoms are asymmetric.

Table 1. ^{1}H-NMR data for **4** and **6** in CD_2Cl_2 (int. TMS) and IR data [$\tilde{\nu}$ (CO) bands] for **4** and **6** in CH_2Cl_2 (in cm^{-1}).

4a: $\delta=7.23$–7.46 (m, 15H, 3Ph), α isomer: $\delta=5.24$ (s, 5H, Cp), 2.82 (s, 6H, Me), β isomer: $\delta=5.20$ (s, 5H, Cp), 2.73 (s, 6H, Me); α: β ≈ 10.—**4b**: $\delta=7.23$–7.38 (m, 20H, 4Ph), α isomer: $\delta=5.36$ (s, 5H, Cp), 3.07 (s, 3H, Me), β isomer: $\delta=5.27$ (s, 5H, Cp), 2.91 (s, 3H, Me) α:β ≈ 10.—**4c**: $\delta=7.28$–7.57 (m, 25H, 5Ph), α isomer: $\delta=5.47$ (s, 5H, Cp), β isomer: $\delta=5.34$ (s, 5H, Cp); α:β ≈ 10.—**4d**: $\delta=7.21$–7.29 (m, 10H, 2Ph), 5.25 (s, 5H, Cp), 2.03 (q, 6H, $3CH_2CH_3$), 1.01 (9H, $3CH_2CH_3$).—**4e**: $\delta=7.21$–7.36 (m, 15H, 3Ph), 5.26 (s, 5H, Cp), 2.02 (d, 6H, $2CH_3$, $^2J_{H,P}=9$ Hz).—**4f**: $\delta=7.27$–7.55 (m, 15H, 3Ph), 5.33 (s, 5H, Cp), 3.04 (s, br, 3H, Me), 2.84–3.17 (m, 2H, CH_2–C_2H_5), 1.43–1.79 (m, 2H, CH_2–CH_3), 0.96–1.16 (m, 3H, $(CH_2)_2$–CH_3).—**6**: $\delta=7.2$–7.32 (m, 10H, 2Ph), 5.26 (s, 5H, Cp), 3.61 (d, 9H, 3Me).
4a: $\tilde{\nu}=2060$ w, 2037 m, 2020 vw, sh, 1992 m, 1960 vs, 1898 s, br, 1756 m, br.—**4b**: $\tilde{\nu}=2084$ w, 2044 m, 2027 w, 2003 m, 1970 vs, 1928 s, 1902 s, 1770 m, br.—**4c**: $\tilde{\nu}=2083$ w, 2043 m, sh, 2025 m, 2003 m, 1973 vs, 1934 m, 1900 m, 1770 m.—**4d**: $\tilde{\nu}=2104$ vw, 2039 m, 2000 w, 1968 vs, 1925 m, 1893 s, 1747 m.—**4e**: $\tilde{\nu}=2083$ vw, 2041 m, 2029 w, sh, 1967 vs, 1905 s, br, 1738 m.—**4f**: $\tilde{\nu}=2079$ w, 2037 m, 2025 w, sh, 1989 m, 1958 vs, 1900 s, br, 1755 m.—**6**: $\tilde{\nu}=2114$ w, 2026 s, sh, 2012 s, 1976 vs, 1935 m, 1900 s, 1848 m, sh

The Mo–Re distance in **4a** and **6** is comparable to that in $[MoRe(CO)_3Cp_3]$[12] (296 pm). As expected,[9] the CC bond of the μ,η^2,η^2-alkyne in **4a** and **6** is lengthened to 136 pm, compared with the CC bond of an alkyne that is only coordinated to *one* metal center (ca. 130 pm), and lies orthogonally above the Mo–Re bond. Like $[Cp_2NiMo(CO)_2(\mu\text{-}\eta^2,\eta^2\text{-RCCR}]$,[5b,6] **4a** and **6** contain a semibridging carbonyl group [∢Mo-C-O: **4a** 160.6(4), **6** 166(2)°], which absorbs in the IR spectrum at 1756 and 1848 cm^{-1}, respectively (Table 1).

Experimental Procedure

All reactions were carried out under argon with carefully dried solvents.

4a: The orange solution (4 mL THF, −30 °C) of $NaRe(CO)_5$, obtained by reaction of 230 mg (0.35 mmol) of $Re_2(CO)_{10}$ with sodium amalgam, was added to a violet suspension of **3a** [3] (250 mg, 0.42 mmol) in 3 mL of THF (−30 °C). After 15 min, the solvent was removed from the brownish yellow suspension and the residue ($NaBF_4$) was digested with 5 mL of CH_2Cl_2. After centrifugation, the mother liquor was decanted and the residue was washed three times with 5 mL of CH_2Cl_2. The combined CH_2Cl_2 solutions were concentrated to 3 mL (vacuum) and a layer of Et_2O (10 mL) was added. The yellow precipitate of **4a** was centrifuged off, washed three times with 5 mL of cold Et_2O, and dried under high vacuum for several hours; yield 230 mg (68%), decomposition above 163 °C.—The yellow complexes **4b**–**4f** and **6** were obtained analogously in yields of 60 to 85%.

Received: April 1, 1986;
revised: May 9, 1986 [Z 1719 IE]
German version: *Angew. Chem. 98* (1986) 739

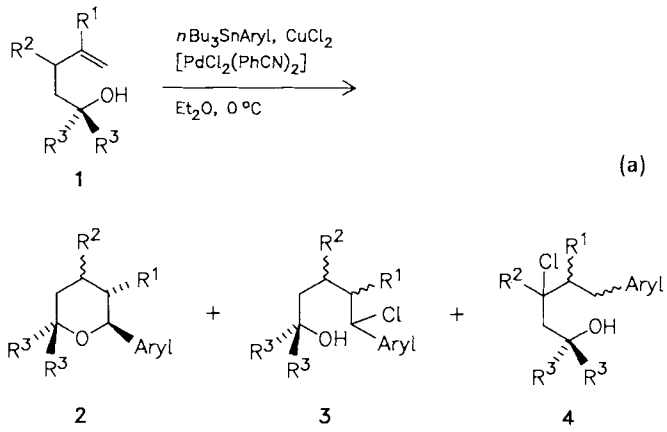
[1] W. Beck, B. Olgemöller, *J. Organomet. Chem. 127* (1977) C 45; K. Raab, U. Nagel, W. Beck, *Z. Naturforsch. B 38* (1983) 1466; W. Beck, K. Raab, U. Nagel, W. Sacher, *Angew. Chem. 97* (1985) 498; *Angew. Chem. Int. Ed. Engl. 24* (1985) 505.
[2] a) M. H. Chisholm, H. C. Clark, *Inorg. Chem. 10* (1971) 1711; D. L. Reger, K. A. Belmore, E. Mintz, P. J. McElligott, *Organometallics 3* (1984) 134; S. R. Allen, P. K. Baker, S. G. Barnes, M. Bottrill, M. Green, A. G. Orpen, I. D. Williams, A. J. Welch, *J. Chem. Soc. Dalton Trans. 1983*, 927; b) $[Mo(CO)Cp(MeCCMe)_2]^{\oplus}$ reacts with the nucleophile $[Fe(CO)_2Cp]^{\ominus}$ in a redox reaction to give $[Fe_2(CO)_4Cp_2]$ and $[Mo_2(MeCCMe)_4Cp_2]$ (M. Green, N. C. Normann, A. G. Orpen, *J. Am. Chem. Soc. 103* (1981) 1269).
[3] M. Bottrill, M. Green, *J. Chem. Soc. Dalton Trans. 1977*, 2365; S. R. Allen, P. K. Baker, S. G. Barnes, M. Green, L. Trollope, L. Manojlovic-Muir, K. W. Muir, *ibid. 1981*, 873; K. Sünkel, U. Nagel, W. Beck, *J. Organomet. Chem. 222* (1981) 251.
[4] P. S. Braterman, J. L. Davidson, D. W. A. Sharp, *J. Chem. Soc. Dalton Trans. 1976*, 241; J. L. Templeton, B. C. Ward, *J. Am. Chem. Soc. 102* (1980) 3288.
[5] a) B. H. Freeland, J. E. Hux, N. C. Payne, K. G. Tyers, *Inorg. Chem. 19* (1980) 693; b) G. Jaouen, A. Marinetti, J. Y. Saillard, B. G. Sayer, M. J. McGlinchey, *Organometallics 1* (1982) 225.
[6] M. C. Azar, M. J. Chetcuti, C. Eigenbrot, K. A. Green, *J. Am. Chem. Soc. 107* (1985) 7209.
[7] K. Yasufuku, H. Yamazaki, *Bull. Chem. Soc. Jpn. 45* (1972) 2664; K. Yasufuku, K. Aoki, H. Yamazaki, *J. Organomet. Chem. 84* (1975) C 28.
[8] J. C. Jeffery, J. C. V. Laurie, F. G. A. Stone, *Polyhedron 4* (1985) 1135.
[9] D. M. Hoffman, R. Hoffmann, C. R. Fisel, *J. Am. Chem. Soc. 104* (1982) 3858.
[10] H. Brunner, M. Muschiol, *J. Organomet. Chem. 248* (1983) 233.
[11] F. Richter, H. Vahrenkamp, *Angew. Chem. 90* (1978) 916; *Angew. Chem. Int. Ed. Engl. 17* (1978) 864; R. Blumhofer, H. Vahrenkamp, *Chem. Ber. 119* (1986) 683, and references cited therein.
[12] R. I. Mink, J. J. Welter, P. R. Young, G. D. Stucky, *J. Am. Chem. Soc. 101* (1979) 6928.
[13] Further details of the crystal structure investigations may be obtained from the Fachinformationszentrum Energie, Physik, Mathematik GmbH, D-7514 Eggenstein-Leopoldshafen 2 (FRG), on quoting the depository number CSD 51941, the names of the authors, and the journal citation.

Pd^{II}-Catalyzed Regioselective Arylchlorination and Oxyarylation of Unsaturated Alcohols

By *Yoshinao Tamaru, Makoto Hojo, Hideyuki Higashimura,* and *Zen-ichi Yoshida**

Palladium-catalyzed arylation of olefins (Heck reaction)[1] is of great value, provided that the elimination and addition reactions of the hydridopalladium species HPdX can be regioselectively terminated. Arylation of norbornene[2] (no elimination of HPdX, since a strained olefin

[*] Prof. Dr. Z. Yoshida, Dr. Y. Tamaru, M. Hojo, H. Higashimura
Department of Synthetic Chemistry, Kyoto University
Yoshida, Kyoto 606 (Japan)



endo methylene carbon atom does not bear the hydrogen atom *syn* to the Pd–C bond.[8] The tetrahydropyrans are presumably derived from **8** directly since **3** undergoes intramolecular ether formation very sluggishly under rather drastic conditions (e.g., **2f** was isolated in only 25% yield by treatment of **3f** with NaH, nBu$_4$N$^{\oplus}$I$^{\ominus}$ in refluxing THF for 10 h). This suggestion is further supported by the observation that the *trans*-2-(*p*-methoxyphenyl)-3-methyltetrahydropyrans **2g** and **2h** (reactions 8 and 9, respectively) are formed stereospecifically, whereas 6-chloro-2,5-dimethyl-6-phenyl-2-hexanol **3i** (reaction 10) is obtained as a 1:1 diastereomeric mixture. The stereospecific formation of **2g** and **2h** can be explained in one of two ways: either one of the two diastereomers **8** ($R^1 = CH_3$) which equilibrate via **7**, cyclizes to form the *trans* isomer **2g** or **2h** or

Table 1. Palladium-catalyzed, regioselective 1,1- and 1,3-difunctionalization of 4-penten-1-ols.

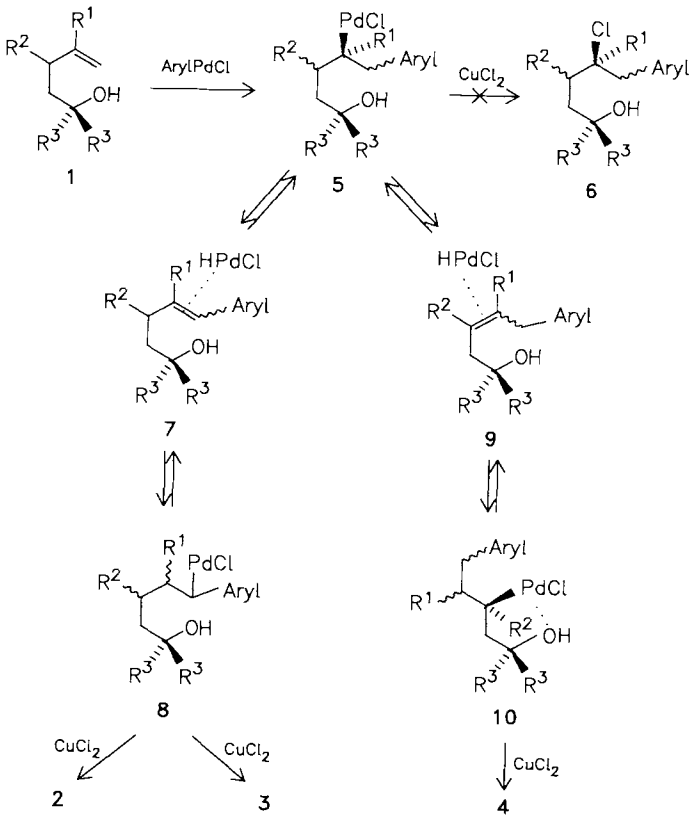
Reaction	1 R^1	1 R^2	1 R^3	Aryl in nBu$_3$SnAryl	Reaction conditions [a]	2	Yield [%] [b] 3	4
1	H	H	H	*p*-methoxyphenyl	0 °C, 7 h	**a** 86	—	—
2	H	H	H	phenyl	0 °C, 9 h	**b** 33	38	29
3	H	Me	H	*p*-methoxyphenyl	0 °C, 5 h	**c** 90 [c]	—	—
4	H	Ph	H	*p*-methoxyphenyl	0 °C, 5 h	**d** 74	—	—
5	H	H	Me	*p*-methoxyphenyl	0 °C, 6 h	**e** 82	—	—
6	H	H	Me	phenyl	0 °C, 6 h	**f** 14	37	31
7	H	H	Me	phenyl [d]	0 °C, 6 h 25 °C, 3 h	**f** 9	34	35
8	Me	H	H	*p*-methoxyphenyl	0 °C, 4 h 25 °C, 20 h	**g** 55 [e]	—	—
9	Me	H	Me	*p*-methoxyphenyl	0 °C, 4 h 25 °C, 20 h	**h** 59 [e]	—	—
10	Me	H	Me	phenyl	0 °C, 6 h 25 °C, 20 h	**i** —	59	7

[a] Reaction temperature and reaction time. [b] After column chromatography. [c] *cis/trans* 82:18. [d] PhHgCl instead of nBu$_3$SnPh. [e] *trans* Isomer.

would thereby be formed) and of allylic alcohols[3] (formation of geminal hydroxypalladium complexes[4] or enols and thus carbonyl compounds) are typical examples. Here we describe a new type of regioselective termination of such reactions.

4-Penten-1-ols **1** [Eq. (a)] react, irrespective of their pattern of substitution (Table 1), with tri-*n*-butyl(*p*-methoxyphenyl)stannane (1.3–1.5 equivalents) and $CuCl_2$ (3 equivalents) in the presence of a catalytic amount of bis(benzonitrile)palladium(II) chloride (0.05 equivalents) to give 2-(*p*-methoxyphenyl)tetrahydropyrans **2** as the sole products (reactions 1, 3–5, 8, 9). The reaction of **1** with tri-*n*-butyl(phenyl)stannane, on the other hand, generally gives rise to two types of products (reactions 2, 6, 10): 1,1-difunctionalized products (**2** and **3**) and 1,3-difunctionalized products (**4**).[5,6] Phenylmercuric chloride (reaction 7) reacts analogously. The complete absence of 1,2-arylchlorination products contrasts sharply with the results of the Heck reaction (PhHgCl, Li_2PdCl_4, $CuCl_2$, 90% AcOH).[7] Indeed, under our reaction conditions ([$PdCl_2(PhCN)_2$], $CuCl_2$, ether), 1-aryl-1-chlorooctane was obtained from 1-octene almost exclusively, irrespective of the arylation agent (n-Bu$_3$SnPh, n-Bu$_3$Sn (*p*-MeOC$_6$H$_4$), PhHgCl).

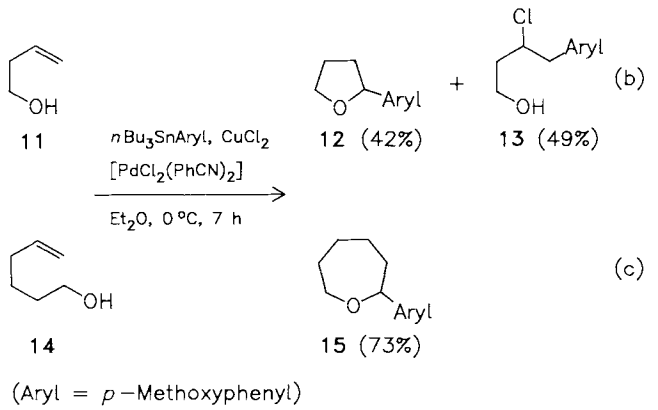
The above regioselectivity may be rationalized according to Scheme 1. The primary adduct **5** equilibrates with intermediates **8** and **10** via a series of eliminations (to give **7** and **9**, respectively) and additions of HPdX. Further equilibration to form eventually an intermediate with the Pd atom in the α position to the hydroxyl group is presumably suppressed, because in the cyclic intermediate **10** the



Scheme 1. Postulated mechanism of the selective 1,1- and 1,3-difunctionalization of 4-penten-1-ols **1**.

both diastereomers react selectively, one with inversion and the other with retention of configuration.[9]

The difference in regioselectivity (1,1- and 1,3-arylchlorination in our system vs. 1,2-arylchlorination in the Heck reaction) may stem from the different polarities of the reaction media. In ether, the intermediate **5** is too stable to undergo a heterolytic cleavage of the Pd–C bond to form **6**.[10] In view of the similarity of the Pd–C bonds of **5** and **10**, the transformation of **10** to **4** might also be slow; therefore, a high concentration of **10** is presumably responsible for the formation of **4**. Other unsaturated alcohols with chain lengths of one less or one more C atom react in a similar fashion [Eq. (b) and (c)].[11, 12]



(Aryl = *p*-Methoxyphenyl)

The detailed mechanism responsible for the regioselectivity, stereoselectivity, and partition among **2**, **3**, and **4** and the application of this reaction to systems involving other nucleophilic heteroatoms or C atoms in the molecule remain to be investigated.

Received: April 7, 1986;
revised: May 12, 1986 [Z 1722 IE]
German version: *Angew. Chem. 98* (1986) 740

CAS Registry numbers:
1 (R^1, R^2, R^3 = H), 821-09-0; **1** (R^1 = R^3 = H, R^2 = Me), 51174-44-8; **1** (R^1 = R^3 = H, R^2 = Ph), 80816-30-4; **1** (R^1 = R^2 = H, R^3 = Me, 16744-89-1; **1**(R^1 = Me, R^2 = R^3 = H), 22508-64-1; **1** (R^1 = R^3 = Me, R^2 = H), 75066-99-8; **2a**, 31526-39-3; **2b**, 4203-44-5; **2c** (*cis* isomer), 103348-68-1; **2c** (*trans* isomer), 103348-79-4; **2d**, 103348-69-2; **2e**, 103348-70-5; **2f**, 4535-54-0; **2g**, (*trans* isomer), 103348-73-8; **2h** (*trans* isomer), 103348-74-9; **3b**, 85696-67-9; **3f**, 103348-71-6; **3i**, 103348-75-0; **4b**, 103348-67-0; **4f**, 103348-72-7; **4i**, 103348-76-1; **11**, 627-27-0; **12**, 79623-15-7; **13**, 103348-77-2; **14**, 821441-0; **15**, 103348-78-3; tri-*n*-butyl-(*p*-methoxyphenyl)stannane, 70744-47-7; tri-*n*-butyl(phenyl)stannane, 960-16-7.

[1] a) R. F. Heck: *Palladium Reagents in Organic Syntheses*, Academic Press, New York 1985; b) P. Maitlis: *The Organic Chemistry of Palladium, Vol. 2*, Academic Press, New York 1971.

[2] R. C. Larock, S. Babu, *Tetrahedron Lett. 26* (1985) 2763.

[3] a) J. B. Melpolder, R. F. Heck, *J. Org. Chem. 41* (1976) 265; b) A. J. Chalk, S. A. Magennis, *ibid. 41* (1976) 273; c) Y. Tamaru, Y. Yamada, Z. Yoshida, *Tetrahedron 35* (1979) 329.

[4] a) J. Hillis, J. Francis, M. Ori, M. Tsutsumi, *J. Am. Chem. Soc. 96* (1974) 4800; b) M. Kosaki, M. Isemura, Y. Kitaura, S. Shinoda, Y. Saito, *J. Mol. Catal. 2* (1977) 351.

[5] For Pd^{II}-catalyzed 1,2-oxyarylation of a C=C bond, see H. Horino, N. Inoue, *J. Chem. Soc. Chem. Commun. 1976*, 500.

[6] All products were purified by means of column chromatography and characterized spectroscopically (IR, ^{1}H-NMR, ^{13}C-NMR) and by high-resolution mass spectrometry. Moreover, **2b** was prepared by an independent route (R. Paul, *Bull. Soc. Chim. Fr. Mem. 2* (1935) 311) and **4f** was converted into 6,6-dimethyl-4-phenethyl-2-phenylimino-1-oxa-3-thiacyclohexane by reaction with NaH and PhNCS in dry tetrahydrofuran (THF) at room temperature; compounds **3** were converted into the cyclic compounds **2** (see text).

[7] R. F. Heck, *J. Am. Chem. Soc. 90* (1968) 5538. Under similar conditions to those of *Heck*, a mixture of 1,1-acetoxyarylated and 1,2-arylchlorinated product is obtained: J.-E. Bäckvall, R. E. Nordberg, *J. Am. Chem. Soc. 102* (1980) 393; see also R. C. Larock, C.-L. Liu, H. H. Lau, S. Varaprath, *Tetrahedron Lett. 25* (1984) 4459.

[8] For the related arguments, see B. M. Trost, J. Y. L. Chung, *J. Am. Chem. Soc. 107* (1985) 4586.

[9] Several precedents indicate that O and N atoms react *intermolecularly* with inversion of configuration. To the best of our knowledge, the stereochemical outcome of the *intra*molecular substitution reactions is not yet known: J.-E. Bäckvall, *Acc. Chem. Res. 16* (1983) 335.

[10] A. Heumann, J.-E. Bäckvall, *Angew. Chem. 97* (1985) 228; *Angew. Chem. Int. Ed. Engl. 24* (1985) 207, and references cited therein.

[11] Formation of the 1,2-addition product **13** from **11** [Eq. (b)] appears to be an exception. These results, however, might be uniformly explained by selective chlorination of the C atom in the γ position to the hydroxyl group to form five-membered-ring intermediates analogous to **10**. Furthermore, it should be noted that the products shown in Equation (b), which are general for other homoallylic alcohols (unpublished), contrast with those obtained by the Heck arylation of homoallylic alcohols, namely, arylated ketones or aldehydes [3a].

[12] The 1,1-oxyarylation reported here, coupled with the Sharpless RuO_4-catalyzed oxidation of a phenyl to a carboxyl group, might be regarded as an equivalent to 1,1-oxycarbonylation of olefins: R. H. J. Carlsen, T. Katsuki, V. S. Martin, K. B. Sharpless, *J. Org. Chem. 46* (1981) 3936.

Carbyne-Iridium Complexes: Evidence for an Equilibrium between Alkenylidene(hydrido) and Carbyne Isomers

By *Arthur Höhn* and *Helmut Werner**

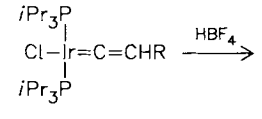
A number of mononuclear carbyne-metal complexes have been reported, particularly for the elements of the vanadium, chromium, and manganese subgroups.[1] A relatively new method of synthesis—as yet limited to octahedral complexes—has been reported which involves the conversion of an alkenylidene ligand into a carbyne ligand by addition of an electrophile.[2] MO calculations predict that the regioselectivity of the reaction, generally described by Equation (a) (where M is, e.g., $[(C_5H_5)Mo(P(OMe)_3)_2]^{\oplus}$ or $[W(CO)_{5-n}L_n]$), is governed by a significant charge localization on the β-C atom of the M=C=CHR unit, which should therefore undergo electrophilic attack.[3] We have now found that this pattern of reactivity does not hold true for square-planar alkenylidene-iridium complexes; instead, these complexes—at least for $E^{\oplus}=H^{\oplus}$—behave similarly to their carbonyl analogues and undergo electrophilic addition at the metal.

$$M{=}C{=}CHR \xrightarrow{E^{\oplus}} [M{\equiv}C{-}CH(E)R]^{\oplus} \qquad (a)$$

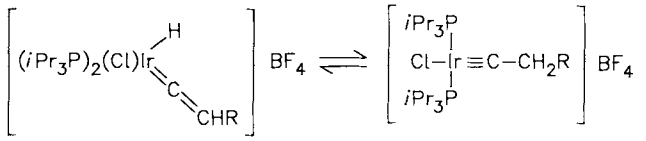
Treatment of a solution of **1a–c**[4] with HBF_4 in ether results in spontaneous formation of an orange-yellow precipitate.[5a] The ^{1}H-NMR spectrum, recorded immediately after dissolving the product obtained from **1c** in CD_3NO_2, shows a triplet at $\delta = -23.48$ ($J_{PH} = 13.2$ Hz), which is typical of a hydrido–metal bond. After 30 seconds (at room temperature), this signal, which we assign to compound **2c** has disappeared. The spectrum now corresponds to that expected for the carbyne complex **3c**.[5b] In the case of the corresponding compounds obtained from **1a** and **1b**,[5a] the ^{1}H-NMR spectra in either CD_3NO_2 or CH_3NO_2 showed no signal at high field. Nevertheless, we assume that an alkenylidene(hydrido) complex (**2a**, **b**) is also initially formed, because a characteristic band for an Ir–H stretching frequency (at ca. 2250 cm^{-1}) and a band for a C=C stretching frequency (at ca. 1640 cm^{-1}) are observed

[*] Prof. Dr. H. Werner, Dipl.-Chem. A. Höhn
Institut für Anorganische Chemie der Universität
Am Hubland, D-8700 Würzburg (FRG)

in the IR spectra of the initially obtained products for both R=Ph and R=H, Me.[6] **2a, b** appear to be very labile in solution and smoothly rearrange by a 1,3-hydride shift to form the isomers **3a** and **3b**, respectively.



1a–c

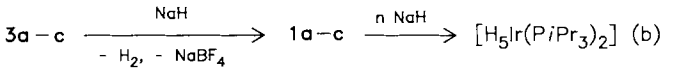


2a–c **3a–c**

a, R = H; b, R = Me; c, R = Ph

The IR spectra of the solid products obtained from nitromethane solutions of **3** after removal of the solvent surprisingly also show the characteristic bands of **2**. This indicates that an *equilibrium* exists between the cationic alkenylidene(hydrido) complexes and the carbyne complexes, which in solution (CH_3NO_2) almost completely lies on the side of the carbyne complex. By removing the solvent, the equilibrium is shifted toward the alkenylidene(hydrido) isomers **2**, which precipitate together with **3**.

The transformation of **1** to **3** is *reversible*. Upon addition of NaH to a suspension of **3a**, **3b**, or **3c** in benzene, smooth evolution of H_2 begins and is complete after ca. 10 min [Eq. (b)]. From the intensely colored (red for **1a, b** and violet for **1c**) solutions, the alkenylidene complexes **1**[4] can be isolated in nearly quantitative yield. If an excess of NaH is used and the reaction mixture stirred for a longer period of time, compounds **1a–c** further react to give the pentahydrido complex $[H_5Ir(PiPr_3)_2]$ [Eq. (b)],[7] which is also obtained from **1a–c** and other hydride sources.[8] Deprotonation of **3** to form **1** also occurs with NaOMe in methanol or with MeLi in ether but these reactions are accompanied by decomposition.



Two important conclusions emerge from these studies: (1) It has been shown for the first time that alkenylidene metal complexes do not always react with electrophiles by attack at the β-C atom of the alkenylidene ligand. In contrast to octahedral complexes $[L_nM{=}C{=}CHR]$,[2] the corresponding square-planar iridium complexes behave—at least toward Brønsted acids—as Vaska-type complexes; the metal basicity dominates.[9] (2) The reactivity of the square-planar carbyne complexes **3** differs considerably from that of comparable Fischer-type carbyne complexes. Complexes **3** do not react with nucleophiles such as $MeO^{\ominus}$ by nucleophilic addition at the carbyne C atom (with formation of a carbene ligand);[1] instead, they undergo deprotonation and regeneration of the alkenylidene complexes **1** used as starting materials for the preparation of **3**. Whether soft Lewis bases behave in a similar way remains to be investigated.

Received: April 10, 1986;
revised: May 2, 1986 [Z 1726 IE]
German version: *Angew. Chem. 98* (1986) 745

CAS Registry numbers:
1a, 95935-86-7; **1b**, 95935-85-6; **1c**, 95935-84-5; **2a**, 103349-13-9; **2b**, 103349-15-1; **2c**, 103349-17-3; **3a**, 103349-09-3; **3b**, 103366-78-5; **3c**, 103349-11-7.

[1] U. Schubert, H. Fischer, P. Hofmann, K. Weiss, K. H. Dötz, F. R. Kreissl: *Transition Metal Carbene Complexes*, Verlag Chemie, Weinheim 1983, p. 151.

[2] a) R. G. Beevor, M. Green, A. G. Orpen, I. D. Williams, *J. Chem. Soc. Chem. Commun. 1983*, 673; b) K. R. Birdwhistell, S. J. Nieter-Burgmayer, J. L. Templeton, *J. Am. Chem. Soc. 105* (1983) 7789; c) A Mayr, K. C. Schaefer, E. Y. Huang, *ibid. 106* (1984) 1517; d) K. R. Birdwhistell, T. L. Tonker, J. L. Templeton, *ibid. 107* (1985) 4474.

[3] N. M. Kostić, R. F. Fenske, *Organometallics 1* (1982) 974.

[4] F. J. Garcia Alonso, A. Höhn, J. Wolf, H. Otto, H. Werner, *Angew. Chem. 97* (1985) 401; *Angew. Chem. Int. Ed. Engl. 24* (1985) 406.

[5] *Experimental procedure:* A 54% ether solution of HBF_4 was added dropwise to a rapidly stirred solution of **1** (0.2 mmol) in 10 mL of ether. The orange-yellow precipitate that formed after a few seconds was filtered off, washed with ether, and dried in vacuo; quantitative yield; correct elemental analyses; equivalent conductivity (in CH_3NO_2): 101.7 (**3a**), 92.8 (**3b**), 95.7 (**3c**) $cm^2\Omega^{-1}mol^{-1}$. b) NMR spectra (^1H, ^{13}C: 400 MHz; ^{31}P: 90 MHz) in CD_3NO_2: **3a**: ^1H-NMR: $\delta=2.96$ (m; PCH), 1.46 (dvt, $J_{HH}=7.2$, $N=15.3$ Hz; $PCHCH_3$), −0.60 (s; $\equiv CCH_3$); ^{13}C-NMR: $\delta=261.47$ (t, $J_{PC}=8.2$ Hz; Ir≡C), 37.87 (s, q in off-resonance; CCH_3), 27.43 (vt, dvt in off-resonance, $N=29.7$ Hz; PCH), 20.50 (s, q in off-resonance; $PCHCH_3$); ^{31}P-NMR: $\delta=53.51$ (s). **3b**: ^1H-NMR: $\delta=3.00$ (m; PCH), 1.54 (dvt, $J_{HH}=7.2$, $N=15.3$ Hz; $PCHCH_3$), 1.50 (t, $J_{HH}=7.3$ Hz; CH_2CH_3), 0.39 (q, $J_{HH}=7.3$ Hz; CH_2CH_3); ^{13}C-NMR: $\delta=265.67$ (t, $J_{PC}=8.3$ Hz; Ir≡C), 44.34 (s, t in off-resonance; CCH_2), 27.84 (vt, dvt in off-resonance, $N=28.5$ Hz; PCH), 20.68 (s, q in off-resonance; $PCHCH_3$), 0.28 (s, q in off-resonance; CH_2CH_3); ^{31}P-NMR: $\delta=54.21$ (s). **3c**: ^1H-NMR: $\delta=7.30$ (m; C_6H_5), 3.01 (m; PCH), 1.54 (dvt, $J_{HH}=7.2$, $N=15.3$ Hz; $PCHCH_3$), 1.25 (s; CH_2); ^{13}C-NMR: $\delta=131.2$, 129.8, 122.0 (each s; C_6H_5), 66.84 (s; CCH_2), 28.14 (vt, $N=27.5$ Hz; PCH), 20.53 (s; $PCHCH_3$), signal of Ir≡C not observed; ^{31}P-NMR: $\delta=54.86$ (s) (N = virtual coupling constant).

[6] IR(KBr): $\tilde{\nu}=2248$, 1640 (**2a**); 2272, 1653 (**2b**); 2236, 1632 cm^{-1} (**2c**).

[7] a) M. G. Clerici, S. Di Gioacchino, F. Maspero, E. Perrotti, A. Zanobi, *J. Organomet. Chem. 84* (1975) 379; b) L. Garlaschelli, S. I. Khan, R. Bau, G. Longoni, T. F. Koetzle, *J. Am. Chem. Soc. 107* (1985) 7212.

[8] A. Höhn, H. Werner, unpublished results; see A. Höhn, H. Werner, *XIIth Int. Conf. Organomet. Chem.* (Vienna 1985) Abstr. p. 411.

[9] a) D. F. Shriver, *Acc. Chem. Res. 3* (1970) 231; b) H. Werner, *Angew. Chem. 95* (1983) 932; *Angew. Chem. Int. Ed. Engl. 22* (1983) 927.

Dimeric Chloro[dicyclopentadienyl(dimethyl)silyl]-ytterbium(III), a Rare Example of a Complex Involving Metal-Bridging instead of Chelating $[Me_2Si(\eta^5\text{-}C_5H_4)_2]$ Ligands**

By *Nils Höck, Wolfgang Oroschin, Gino Paolucci,** and *R. Dieter Fischer**

The ligands $[Me_2Si(\eta^5\text{-}C_5R_4)_2]^{2\ominus}$ (R = H, Me) are known to bond to early d-transition,[1] lanthanoid,[2] and actinoid[3] metals exclusively in a metal-chelating fashion. They are, however, metal-bridging in, e.g., the dimeric iron complexes **1**[4] and **2**.[5] We report here on the synthesis and the structure of the first correspondingly metal-bridged lanthanoid(III) complex **3**.

$[Fe_2L_2(\mu\text{-}CO)_2\{\mu\text{-}Me_2Si(\eta^5\text{-}C_5H_4)_2\}]$

1, L = CO; **2**, $L_2=(Ph_2P)_2(CH_2)_n$, n = 1–3

$[\{Yb(\mu\text{-}Cl)[\mu\text{-}Me_2Si(\eta^5\text{-}C_5H_4)_2]\}_2]$ **3**

[*] Prof. Dr. R. D. Fischer, Dipl.-Chem. N. Höck, Dr. W. Oroschin, Institut für Anorganische und Angewandte Chemie der Universität Martin-Luther-King-Platz 6, D-2000 Hamburg 13 (FRG)

Prof. G. Paolucci
Dipartimento de Chimica, Università di Venezia
Calla Large S. Marta 2137, I-30123 Venice (Italy)

[**] We thank the C.N.R. Institute (Padova, Italy) for allowing us to carry out the mass spectrometric measurements and Prof. *P. Traldi* for helpful discussions.

Reaction of $YbCl_3$ with $Na_2[Me_2Si(C_5H_4)_2]$ (1:1) in tetrahydrofuran (THF) affords primarily a THF-containing mixture of products. From its burgundy-red, saturated solution in toluene/cyclohexane, uniformly needle-shaped red crystals precipitate slowly at $-30°C$. [6] The single-crystal X-ray structure analysis[7] proves selective crystallization of the THF-free dimer, **3** (cf. Fig. 1); its isomer with chelating dicyclopentadienylsilyl ligands was not observed.

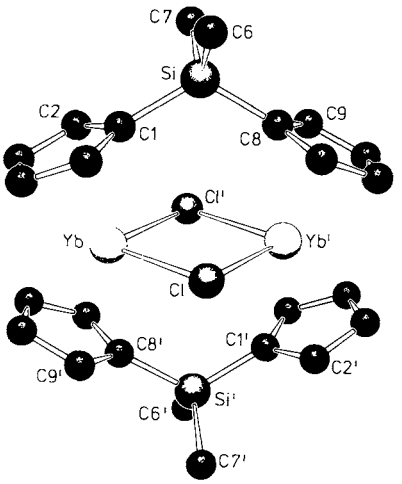


Fig. 1. SCHAKAL plot of the crystal structure of **3**. Selected angles: C(Me)-Si-C(Me) 106.6°; C(ring)-Si-C(Me) 111.4°; Cent-Yb-Cent' 135.3° (Cent and Cent': midpoints of unlinked C_5H_4Si rings); see also [10], [11], and text.

The Yb_2Cl_2 skeleton of **3** is practically a square (angles Cl-Yb-Cl' 89.3°, Yb-Cl-Yb' 90.8°), the Yb-Yb' distance (3.750 Å) being significantly shorter than in two $[\{Yb(\mu\text{-}Cl)Cp'_2\}_2]$ systems[8] with a rhombic Yb_2Cl_2 arrangement. Other remarkable features are the unusually widened C(ring)-Si-C(ring') angles of 118.7° (**1**: 105.7°[4b]), the Si-C(ring)-Cent angles (Cent: midpoint of Cp ring) of $174\pm0.5°$ which make the Si atoms point away from their Yb atoms, and a location of the C(ring)-Si-C(ring') linkages somewhat outside the $Yb_2(Cent)_4$ plane[10], so that this plane cannot function as a second mirror[9] plane of **3**. The Yb-C, Yb-Cl, and C-C distances in **3** correspond to those found in related complexes.[8]

Although the yield of pure **3** from the initially formed mixture of products[6] was rather poor, mass spectrometric findings[12, 13] indicate that **3** is preferentially formed in the reaction of $YbCl_3$ and $Na_2[Me_2Si(C_5H_4)_2]$ in toluene.[14] In contrast to the mass spectra of some exclusively Cl-bridged dimers, $[\{Yb(\mu\text{-}Cl)Cp'_2\}_2]$,[15] where the signals of mononuclear fragments ($m/z<450$) predominate,[16] the mass spectrum of **3**, prepared in toluene, exhibits numerous signals with $m/z>600$, but practically no signal in the region of mononuclear fragments. The B/E scan[17] of the ion with $m/z=790$ confirms its assignment to the most intense $M^{\oplus}$ signal ($M^{\oplus}$ with two ^{35}Cl atoms).[18] From this $M^{\oplus}$, the two binuclear primary fragments $M^{\oplus}-CH_3$ (m/z 775) and $M^{\oplus}-{}^{35}Cl_2$ (m/z 720) originate,[19] but none of the likewise conceivable fragments, $M^{\oplus}-{}^{35}Cl$, $M^{\oplus}/2$, $M^{\oplus}/2-CH_3$, and $M^{\oplus}/2-{}^{35}Cl$, could be observed.

Despite its apparently weak tendency to undergo thermal gas-phase isomerization, **3** readily adds $[D_8]THF$ in toluene (IR detection) — presumably accompanied by skeletal rearrangements.

Received: April 14, 1986;
revised: May 30, 1986 [Z 1732 IE]
German version: *Angew. Chem. 98* (1986) 748

CAS Registry numbers:
3, 103439-81-2; $Na_2[MeSi(C_5H_4)_2]$, 103457-56-3; $YbCl_3$, 10361-91-8.

[1] C. S. Bajgur, W. R. Tikkanen, J. L. Petersen, *Inorg. Chem. 24* (1985) 2539; Note added in proof (July 7, 1986): Recently, the complex $[W_2\{\mu\text{-}Me_2Si(\eta^5\text{-}C_5H_4)_2\}(CO)_6]$, in which two W atoms are bridged by the dicyclopentadienyl(dimethyl)silyl ligand, was reported: W. Abriel, J. Heck, *J. Organomet. Chem. 302* (1986) 363.

[2] G. Jeske, L. E. Schock, P. N. Swepston, H. Schumann, T. J. Marks, *J. Am. Chem. Soc. 107* (1985) 8103.

[3] C. M. Fendrick, E. A. Mintz, L. D. Schertz, T. J. Marks, V. W. Day, *Organometallics 3* (1984) 819.

[4] a) J. Weaver, P. Woodward, *J. Chem. Soc. Dalton Trans. 1973*, 1439; b) P. A. Wegner, V. A. Uski, R. P. Kiester, S. Dabestani, V. W. Day, *J. Am. Chem. Soc. 99* (1977) 4846.

[5] M. E. Wright, T. M. Mezza, G. O. Nelson, N. R. Armstrong, *Organometallics 2* (1983) 1711.

[6] *Experimental procedure:* **3**: $YbCl_3$ (1.0 g, 3.57 mmol) and $Na_2[Me_2Si(C_5H_4)_2]$ (0.83 g, 3.57 mmol) were stirred in 45 mL of THF for ca. 3 h at −50°C. After removal of the solvent at room temperature, the residue was dissolved in toluene (60 mL). After filtration and removal of the solvent from the filtrate, an oily, red residue was obtained, which, after repeated "conditioning" with small amounts of *n*-hexane and drying under oil-pump vacuum, afforded a burgundy-red powder. Crude yield: ca. 50%. Recrystallization from toluene/cyclohexane (5:1) gave **3** in the form of red crystalline needles (dec. in high vacuum above 150°C).

[7] SYNTEX $P2_1$ four-circle diffractometer ($Mo_{K\alpha}$, graphite monochromator, $\lambda=0.71969$), crystal data for **3** (25°C, $0.1\times0.1\times0.1$ mm^3): monoclinic, space group $C2/c$, $a=20.15(1)$, $b=8.29(1)$, $c=15.96(3)$ Å, $\beta=108.0(1)°$, $Z=4$, $\rho_{calcd}=2.07$ g·cm^{-3}, range of measurement: $5.0\leq2\theta\leq50°$; 1667 reflections with $|F|>4\,\sigma(F_0)$, no absorption correction ($\mu=76.24$ cm^{-1}), SHELX 76, anisotropic temperature factors (H positions not determined); $R=0.047$, $R_w=0.039$. Further details of the crystal structure investigation may be obtained from the Fachinformationszentrum Energie, Physik, Mathematik GmbH, D-7514 Eggenstein-Leopoldshafen 2 (FRG), on quoting the depository number CSD-51886, the names of the authors, and the journal citation.

[8] a) $Cp'=C_5H_4Me$: $Yb\cdots Yb'=3.979$ Å (E. C. Baker, L. D. Brown, K. N. Raymond, *Inorg. Chem. 14* (1975) 1376); b) $Cp'=C_5H_3(SiMe_3)_2$: $Yb\cdots Yb'=4.06$ Å (M. F. Lappert, A. Singh, J. L. Atwood, W. E. Hunter, *J. Chem. Soc. Chem. Commun. 1981*, 1191).

[9] The only mirror plane of **3** coincides with the Yb_2Si_2 plane (point group C_{2h}).

[10] For example, Si-Cl ≠ Si-Cl' (4.169(7) and 3.890(9) Å, respectively, and Cl-Cl ≠ Cl-Cl' (3.65(1) and 3.55(1) Å, respectively); however, Si-Yb ≈ Si-Yb' (4.052(6) and 4.035(6) Å, respectively).—For the same reason, the $Fe_2(Cent)_2$ plane in **1** cannot be a mirror plane of this molecule [4a].

[11] $\overline{Yb\text{-}C}=2.617$, $(Yb\text{-}C)_{min}=2.572$, $(Yb\text{-}C)_{max}=2.647$ Å; $Yb\text{-}Cl=2.636$ Å; $(C\text{-}C)_{min}=1.411$, $(C\text{-}C)_{max}=1.452$ Å; C(ring)-Si = 1.892, C(Me)-Si = 1.905 Å.

[12] Electron impact ionization, 70 eV, source: 200°C, sample: 100°C, direct inlet technique, resolution (based on the "10% minimum") 20000.

[13] X-ray powder diffraction patterns of **3**, prepared in toluene, could not be used for identification because of the poor scattering ability of **3**.

[14] *Experimental procedure:* $YbCl_3$ (1.0 g, 3.57 mmol) and $Na_2[Me_2Si(C_5H_4)_2]$ (0.83 g, 3.57 mmol) were allowed to react in 20 mL of toluene at room temperature. After the reaction mixture had been stirred for 24 h, it was filtered and the solvent was removed under vacuum; the remaining wine-red solid (crude yield: 60%) was dried for 3 h under high vacuum. Elemental analysis: ($C_{12}H_{14}ClSiYb$): calcd: C 36.50, H 3.57%; found: C 36.3, H 3.6%.

[15] a) $Cp'=C_5H_5$: J. Müller, *Chem. Ber. 102* (1969) 152; b) $Cp'=C_5H_3(SiMe_3)_2$, cf. [8b]; c) $Cp'=C_5H_4SiMe_3$: M. F. Lappert, P. I. W. Yarrow, J. L. Atwood, R. Shakir, J. Holton, *J. Chem. Soc. Chem. Commun. 1980*, 987; prepared from $YbCl_3$ and $K[C_5H_4SiMe_3]$ in toluene for the mass spectrometric investigations. We thank *M. Adam* for a sample of the substance.

[16] Intense signals of $[\{Yb(C_5H_4SiMe_3)_2(\mu\text{-}Cl)\}_2]$: $(M^{\oplus}/2-CH_4)$, $(M^{\oplus}/2)$, $(M^{\oplus}/2-Cl)$.

[17] A. P. Pruins, K. R. Jennings, S. Evans, *Int. J. Mass Spectrom. Ion Phys. 26* (1978) 395.

[18] The complete isotope pattern of $M^{\oplus}$ consists of 22 signals, 18 of which were actually observed.

[19] a) $I_{rel}(M^{\oplus}-{}^{35}Cl_2)\approx2/3\,I_{rel}(M^{\oplus})$; base peak: $(M^{\oplus}-Me-Me_3SiCl)$; b) The apparently selectively formed fragment $M^{\oplus}-Cl_2$ corresponds formally to the cation $[\{[\mu\text{-}Me_2Si(\eta^5\text{-}C_5H_4)_2]Yb\}_2]^{\oplus}$ with a $Yb\cdots Yb$ one-electron bond. This cation should be largely free of strain in the C(ring)-Si-C(ring') linkage.

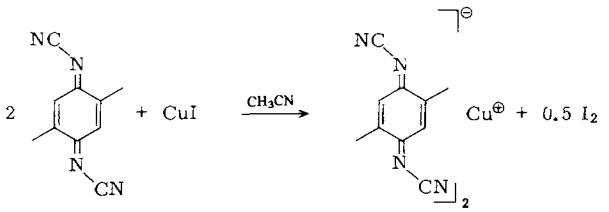
 © VCH Verlagsgesellschaft mbH, D-6940 Weinheim, 1986 0570-0833/86/0808-0739 $ 02.50/0

A Radical Anion Salt of 2,5-Dimethyl-*N,N'*-dicyanoquinonediimine with Extremely High Electrical Conductivity**

By *Alexander Aumüller, Peter Erk, Gerhard Klebe, Siegfried Hünig,* Jost Ulrich von Schütz,* and *Hans-Peter Werner*

Tetracyanoquinonedimethane (TCNQ) and its 2,5-dimethyl derivative (2,5-DM-TCNQ) have hitherto played the most important role as electron acceptors for "organic metals".[1] In 2,6- or higher substituted TCNQs and naphthalene derivatives the rigid Y-shaped $=C(CN)_2$ group is tilted from the plane of the molecule to such an extent that the requisite stacking arrangement of the acceptor in the crystal is forestalled.[2] Furthermore, TCNQs are only obtainable via tedious multistep syntheses.[3] In contrast, a new class of acceptors, the *N,N'*-dicyanoquinonediimines (DCNQIs) with various substituents, are accessible in one step from the corresponding quinones.[4] Owing to the small angle formed by the =N—CN group in this class of compounds the planarity of the molecule remains virtually unaltered, even upon tetrasubstitution.[5] This is the reason, e.g., why *syn-N,N'*-dicyano-1,4-naphthoquinonediimine reacts with tetrathiafulvalene to give a charge-transfer (CT) complex that exhibits high electrical conductivity.[6] Herein we describe a radical anion salt with metallic character derived from DCNQI.

When acetonitrile solutions of 2,5-dimethyl-*N,N'*-dicyanoquinonediimine (2,5-DM-DCNQI) and copper(I) iodide are combined, a black crystalline powder of the composition $(2,5\text{-DM-DCNQI})_2Cu$[7] precipitates, which has a powder conductivity of 0.4 Scm^{-1}. Presumably the contact resistances between the crystallite surfaces limits the conductivity.



Single crystals of this composition are obtainable by electrolysis of 2,5-DM-DCNQI and copper(II) bromide in acetonitrile.[8] They already show a conductivity of 800 S cm^{-1} at 295 K, which *continually increases* as the temperature is lowered to 1.3 K (Fig. 1).[9] This behavior clearly demonstrates the metallic character of the salt, which is not interrupted by a phase transition (Peierls distortion) at any temperature.[10] Very pure crystals show a conductivity of 500000 S cm^{-1} at 3.5 K. Radical anions with such extremely high conductivities were hitherto unknown. The analogous $(TCNQ)_2Cu$ salt is only a semiconductor, whose conductivity drops from 1.5×10^{-5} S cm^{-1} at 530 K to 2×10^{-6} S cm^{-1} at 290 K.[11]

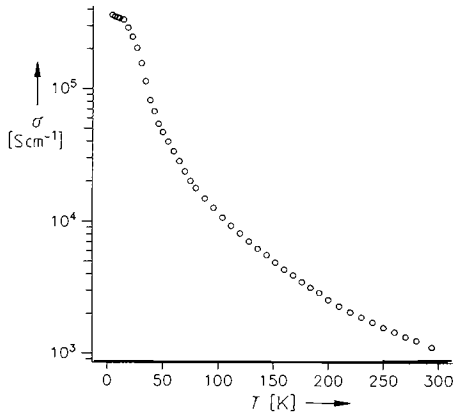


Fig. 1. Temperature dependence of the electrical conductivity σ of $(2,5\text{-DM-DCNQI})_2Cu$ single crystals [9].

As shown by a projection of the crystal structure onto the *a, b* plane, the copper atoms are coordinated in a slightly distorted tetrahedral fashion to the N-atoms of four *N*-cyano groups, with the Cu-N distances being almost equal (Fig. 2). A comparison with the stable tetrahedral complex $[(CH_3CN)_4Cu]ClO_4$[12] reveals that the bonding forces between the partners are almost the same in both cases (Table 1).

Table 1. Space groups, N-Cu distances, and N-Cu-N angles in the complexes $[(CH_3CN)_4Cu]ClO_4$ and $(2,5\text{-DM-DCNQI})_2Cu$.

Compound	Space group	Bond length N-Cu [pm]	Bond angle N-Cu-N [°]
$(2,5\text{-DM-DCNQI})_2Cu$	$I4_1$	198—199	101—126
$[(CH_3CN)_4Cu)ClO_4$ [12]	$Pn2_1a$	195—202	106—113

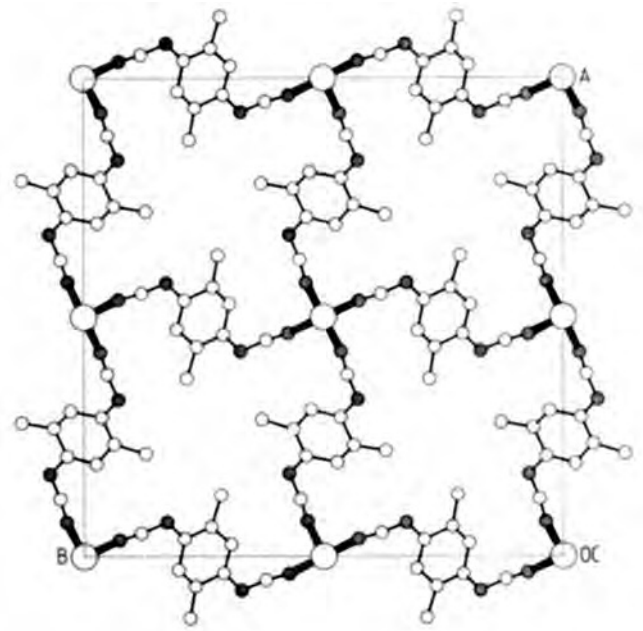


Fig. 2. *a, b*-Projection of the crystal structure of $(2,5\text{-DM-DCNQI})_2Cu$ (H atoms omitted for clarity). ○ = Cu, ○ = C, ○ = N.

[*] Prof. Dr. S. Hünig, Dr. A. Aumüller, Dipl.-Chem. P. Erk
Institut für Organische Chemie der Universität
Am Hubland, D-8700 Würzburg (FRG)
Dr. J. U. von Schütz, Dipl.-Phys. H.-P. Werner
(physical measurements)
Physikalisches Institut der Universität (Teil 3)
Pfaffenwaldring 57, D-7000 Stuttgart 80 (FRG)
Dr. G. Klebe (crystal structure analysis)
BASF AG, ZHV/D, D-6700 Ludwigshafen (FRG)

[**] This work was supported by the Stiftung Volkswagenwerk, the Fonds der Chemischen Industrie, and BASF AG, Ludwigshafen.

In the crystals of $(2,5\text{-DM-DCNQI})_2Cu$ the copper ions are arranged in chains, each surrounded by four stacks of the dicyanoquinonediimine (Fig. 3).[13] An electronic con-

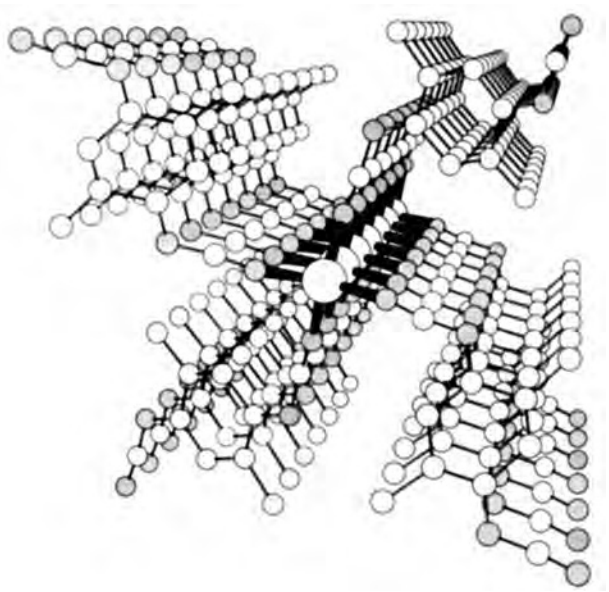


Fig. 3. Perspective view of the crystal structure along the c axis; the chain of copper atoms is surrounded by four stacks of 2,5-DM-DCNQI molecules (H atoms not shown). ○ = Cu, ○ = C, ○ = N.

ductivity along the chain of copper ions is most unlikely because of the large Cu-Cu distance (Cu-Cu 388 pm, Cu(metal) 256 pm). This could more likely take place along the stacks of the π-electron systems. The copper ions apparently take on the function of a conductivity bridge between the individual stacks. The fact that no ESR signal can be recorded (very large broadening) and the high conductivity with no phase transition both point to a multidimensional conductor.[14]

Received: May 5, 1986;
supplemented: June 6, 1986 [Z 1757 IE]
German version: *Angew. Chem. 98* (1986) 759

CAS Registry numbers:
2,5-DM-DCNQI, 98507-06-3; $[2,5\text{-DM-DCNQI}]_2Cu$, 103420-86-6.

[1] Single-crystal conductivities: tetrathiafulvalene (TTF)/TCNQ: $\sigma(66\ K) = 14700\ S\ cm^{-1}$. J. Ferraris, D. O. Cowan, V. Walatka, J. H. Perlstein, *J. Am. Chem. Soc. 95* (1973) 948; Tetramethyltetraselenafulvalene (TMTSF)/2,5-DM-TCNQ: σ (10 K; 13 kbar) = $10^3\ S\ cm^{-1}$ (A. Andrieux, P. M. Chaikin, C. Duroure, D. Jerome, C. Weyl, K. Bechgaard, J. R. Andersen, *J. Phys. (Les Ulis, Fr.) 40* (1979) 1199.

[2] F. Iwasaki, *Acta Crystallogr. B27* (1971) 1360; *I. Silverman, N.* F. Yannoni, *J. Chem. Soc. B 1967*, 1941; B. Rosenau, C. Krieger, H. A. Staab, *Tetrahedron Lett. 26* (1985) 2081.

[3] Best Synthesis of TCNQ: R. J. Crawford, *J. Org. Chem. 48* (1983) 1366. Substituted TCNQ's: R. C. Wheland, E. L. Martin, *ibid. 40* (1975) 3101.

[4] A. Aumüller, S. Hünig, *Angew. Chem. 96* (1984) 437; *Angew. Chem. Int. Ed. Engl. 23* (1984) 447; *Liebigs Ann. Chem. 1986*, 142, 165.

[5] S. Hünig, A. Aumüller, U. Schubert, *Liebigs Ann. Chem. 1985*, 1216.

[6] A. Aumüller, E. Hädicke, S. Hünig, A. Schätzle, J. U. von Schütz, *Angew. Chem. 96* (1984) 439; *Angew. Chem. Int. Ed. Engl. 23* (1984) 449.

[7] Procedure: Boiling solutions of 2,5-DM-DCNQI (184 mg, 1.00 mmol) in CH_3CN (20 mL) and CuI (128 mg, 672 mmol) in CH_3CN (10 mL) were combined, allowed to cool, and the black precipitate filtered off under suction. Yield: 188 mg (87%) $(2,5\text{-DM-DCNQI})_2Cu$; m.p. 229 °C (decomp.); correct C, H, N analyses.

[8] Procedure: A solution of 2,5-DM-DCNQI (46 mg, 250 mmol) and $CuBr_2$ (223 mg, 1.00 mmol) in CH_3CN (60 mL) was electrolyzed with a current density of 53 μA cm^{-1} for 72 h in a cell furnished with diaphragms and Pt electrodes. 17 mg (30%) of up to 6-cm long black needles of $[2,5\text{-DM-DCNQI}]_2Cu$ separated at the cathode. M.p. 229 °C (decomp.); correct C, H, N analysis.

[9] Four-point conductivity measurements with vaporized gold strips perpendicular to the crystal axis. Measurements of the anisotropy of the conductivity with reduced contact dimensions are presently under way.

[10] R. E. Peierls: *Quantum Theory of Solids*, Oxford University Press, London 1955, p. 108.

[11] H. H. Afifiy, F. M. Abdel-Kerim, H. F. Aly, A. A. Shabaka, *Z. Naturforsch. A 33* (1978) 344.

[12] F. Csöregh, P. Kierkegaard, R. Norrestan, *Acta Crystallogr. 31* (1975) 314.

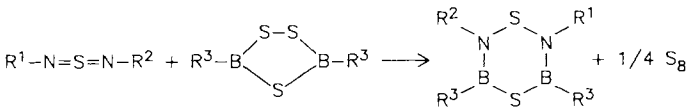
[13] Further details of the crystal structure investigation are available on request from the Fachinformationszentrum Energie, Physik, Mathematik GmbH, D-7514 Eggenstein-Leopoldshafen 2, on quoting the depository number CSD-51963, the names of the authors, and the full citation of the journal.

[14] J. U. von Schütz, H. P. Werner, H. C. Wolf, A. Aumüller, P. Erk, S. Hünig, *Proc. Colloq. AMPERE 23* (1986), in press.

Synthesis and Molecular and Crystal Structure of a New Tricyclic $B_3N_4S_2Si_2$ System**

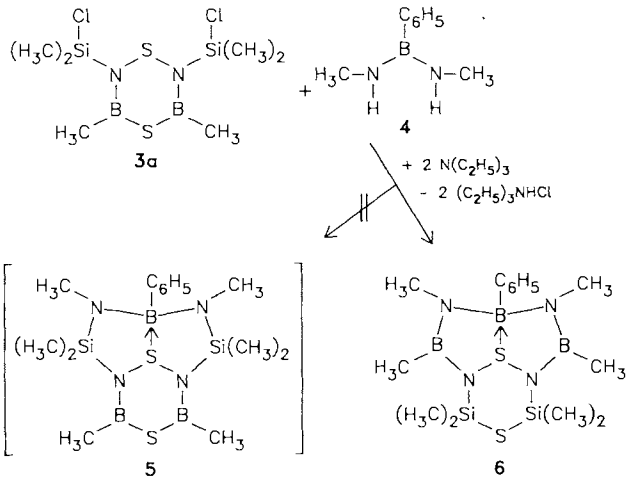
By *Carl Habben, Anton Meller, Mathias Noltemeyer*, and *George M. Sheldrick**

Acyclic sulfur diimides **1** undergo reaction with 1,2,4,3,5-trithiadiborolanes **2** to give the cyclic 1,4,2,6,3,5-dithiadiazadiborinane system **3**.[1,2]



1 2 3

The difunctional 2,6-bis(chlorodimethylsilyl)-3,5-dimethyl derivative **3a** reacts with bis(methylamino)phenylborane **4** to give not the product **5**, as might have been expected, but rather the tricyclic system **6**,[3] the structure of which was established by X-ray crystallography. The structure **6** (and **5**) is favored by the coordination of sulfur to boron; it is unclear whether **6** is a rearrangement product of **5**.



3a **4** **5** **6**

[*] Prof. G. M. Sheldrick, Dr. C. Habben, Prof. Dr. A. Meller, Dr. M. Noltemeyer
Institut für Anorganische Chemie der Universität
Tammannstrasse 4, D-3400 Göttingen (FRG)

[**] This work was supported by the Deutsche Forschungsgemeinschaft and the Fonds der Chemischen Industrie.

The molecule **6** contains two nearly planar systems (the two five-membered rings with $Si(CH_3)_2$ and methyl groups), which form an angle of 111.4° to each other. If the phenyl groups are excluded, the molecule has a mirror plane through C11, B1, S11, and S6 (see Fig. 1).

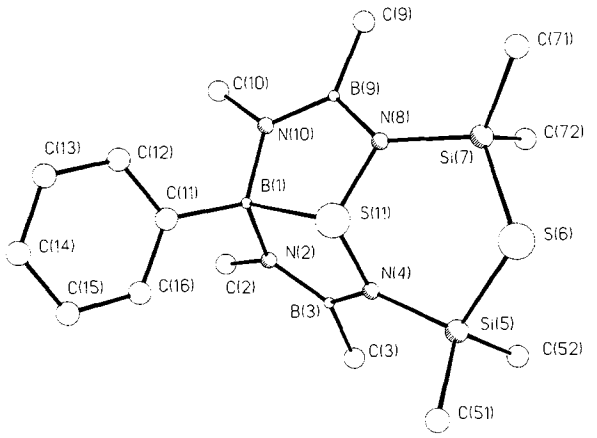


Fig. 1. Crystal structure of **6** (unsymmetrically numbered). Space group $P2_12_12_1$, $a = 715.4(1)$, $b = 1573.3(4)$, $c = 2017.0(5)$ pm, $V = 2.2702$ nm^3, $Z = 4$, $\mu(Mo_{K\alpha}) = 0.33$ mm^{-1}; $R_w = 0.046$, $R = 0.051$ for 1490 unique reflections with $F > 3\,\sigma(F)$; $Mo_{K\alpha}$ radiation, $2\theta_{max} = 45°$. Important bond lengths [pm]: B1-S11 204.4(8). S11-N4 168.1(5), S11-N8 167.8(5), B3-N4 147.6(9), B9-N8 148.1(9), N2-B3 140.0(9), N10-B9 139.2(9), B1-N2 152.4(9), B1-N10 152.4(9), N4-Si5 174.6(5), N8-Si7 176.3(5), Si5-S6 215.1(3), Si7-S6 214.6(3). — Further details of the crystal structure investigation may be obtained from the Fachinformationszentrum Energie, Physik, Mathematik GmbH, D-7514 Eggenstein-Leopoldshafen 2 (FRG), on quoting the depository number CSD 51938, the names of the authors, and the journal citation.

The B1–S11 distance (204.4 pm) is almost the longest so far found for tetracoordinated boron (186–207 pm[4]). Although the NS distances (167.8 and 168.1 pm) are shorter than those found in monocyclic compounds of type **3** (ca. 172 pm[1]), they are in good agreement with those in the bicyclic tetrasulfur hexanitrogen hexafluoroarsenates (168–169 pm[5]), which also contain three-coordinate sulfur. The BN bonds can be divided into three groups: single bonds between both N2 and N10 and the tetracoordinated B1 (152.4 pm); bonds having considerable double bond character when both atoms bear methyl substituents (139.2, 140.0 pm, compare 139–144 pm in borazines[6,7]); and the B3–N4 and B9–N8 bonds (147.6, 148.1 pm), which have intermediate lengths.

In the ^{1}H-NMR spectrum,[8] the methyl groups on the Si atoms give rise to two singlets; two types of $Si-CH_3$ groups are also apparent in the ^{13}C-NMR spectrum.[8] ^{11}B-NMR signals appear for three-coordinate boron[9] at $\delta = 35.7$ and for four-coordinate boron at $\delta = 13.7$ ($CDCl_3$/$BF_3 \cdot O(C_2H_5)_2$ ext., intensity ratio ca. 2:1; no changes in the chemical shifts or in the intensity ratios were observed at +60°C). The ^{14}N-NMR and ^{29}Si-NMR spectra show a broad singlet (^{14}N: $CDCl_3/H_3CNO_2$ ext., $\delta = -285.7$) and a sharp singlet (^{29}Si: $CDCl_3$/TMS int., $\delta = 19.39$), respectively. Compound **6** sublimes at 100°C and 2×10^{-3} mbar. Heating of **6** over several hours under argon in a sealed tube at 150°C results in partial decomposition. Protic solvents result in decomposition of **6** with the formation of H_2S.

Experimental Procedure

A mixture of **4** (1.90 g, 12.8 mmol) and triethylamine (5.18 g, 51 mmol), dissolved in 50 mL of CCl_4, was added to a solution of **3a** [2] (4.24 g, 12.8 mmol) in 150 mL of CCl_4. After 12 h of heating at reflux, the reaction mixture was filtered to separate the solvent, and **6** was sublimed at 100°C/2×10^{-3} mbar; colorless crystals, m.p. = 102°C, yield 33%.

Received: February 4, 1986;
revised: May 27, 1986 [Z 1655 IE]
German version: *Angew. Chem. 98* (1986) 717

CAS Registry numbers:
3a, 94411-17-3; **4**, 19125-66-7; **6**, 103348-98-7; **6** B(III), 103348-97-6.

[1] C. Habben, A. Meller, M. Noltemeyer, G. M. Sheldrick, *J. Organomet. Chem. 288* (1985) 1.
[2] C. Habben, A. Meller, *Z. Naturforsch. B39* (1984) 1022.
[3] Systematic name of **6**: 2,3,5,6,8,8,10,10-octamethyl-4-phenyl-9,11-dithia-1,3,5,7-tetraaza-8,10-disila-2,4,6-triboratricyclo[5.3.1.$0^{4,11}$]undecane.
[4] H. Nöth, R. Staudigl, *Chem. Ber. 115* (1982) 813.
[5] W. Isenberg, R. Mews, *Z. Naturforsch. B37* (1982) 1388.
[6] *Gmelins Handbuch der Anorganischen Chemie, Bd. 51, Borverbindungen Teil 17*, Springer, Berlin 1978.
[7] H. Nöth, *Z. Naturforsch. B38* (1983) 692.
[8] NMR, Bruker AM 250, ^{1}H ($CDCl_3$/TMS int.): $\delta = 0.38$ (s, B–CH_3, 6H), 0.53 (s, Si–CH_3, 6H), 0.61 (s, Si–CH_3, 6H), 2.76 (s, N–CH_3, 6H), 7.25-7.42 (br., C_6H_5, 5H). — ^{13}C ($CDCl_3$/TMS int.): $\delta = -1.21$ (B–CH_3), 5.30 (Si–CH_3), 6.83 (Si–CH_3), 31.81 (N–CH_3), 127.21-127.85, 133.86-142.81 (B–C/C_6H_5).
[9] H. Nöth, B. Wrackmeyer: *Nuclear Magnetic Resonance Spectroscopy of Boron Compounds*, Springer, Berlin 1978.

Cyclo[*d.e.d.e.e.d.e.d.e.e.*]decakisbenzene, a New Cycloarene**

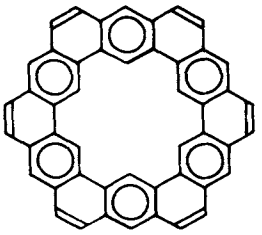
By *Dirk J. H. Funhoff* and *Heinz A. Staab**

The only example known so far for the class of cycloarenes has been kekulene,[1] for which spectroscopic investigations and X-ray diffraction studies revealed a remarkably limited π-electron delocalization in the planar macrocyclic system (formula **1**).[2] Other cycloarenes, which are of interest with regard to their electronic structure, have not yet been prepared.[3,4] For instance, the attempt to synthesize cyclo[*d.e.d.e.e.d.e.d.e.e*]decakisbenzene **2**[5] by photocyclization of [2.2](3,10)benzo[*c*]phenanthrenophane-1,15-diene resulted only in ring closure on one side to give a helical system, the rigid structure of which presumably hinders the second ring closure to give **2**.[3] A modified synthetic strategy based on this assumption has now allowed us to prepare **2**, which contains the [14]annulene skeleton as the inner ring system and, as in the case of **1**, can be formulated with an outer and an inner [4n+2] π perimeter (**2a**).

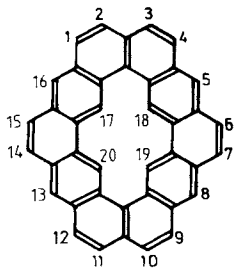
The key reaction for the synthesis of **2** should be the double photocyclization of the partially hydrogenated [2.2](3,10)benzo[*c*]phenanthrenophanediene **3**, which would result in formation of the carbon skeleton of **2**; subsequent dehydrogenation should then give **2**. Compound **3** was obtained, starting from bis(4-chlorophenyl)chloromethane via the following 18-step route. The product (m.p. = 99–100°C; 70%)[6] obtained by reaction of the starting material with diethyl malonate (sodium hydride, dimethylformamide (DMF), 3 h, 100°C) was reduced with

[*] Prof. Dr. H. A. Staab, Dipl.-Chem. D. J. H. Funhoff
Abteilung Organische Chemie,
Max-Planck-Institut für medizinische Forschung
Jahnstrasse 29, D-6900 Heidelberg

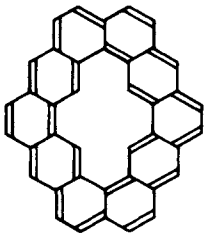
[**] Cycloarenes, a New Class of Aromatic Compounds, Part 5.—Part 4: [4].



1

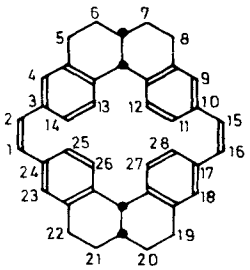


2

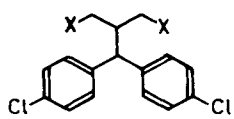


2a

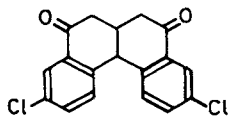
$LiAlH_4$ in tetrahydrofuran (THF) to give the diol **4** (m.p. = 118 °C)[6] in 78% yield; **4** was then converted, by reaction of the corresponding bis(methanesulfonate) **5**[6] (methanesulfonyl chloride, pyridine, −5 °C; m.p. = 143–144 °C; 89%) with potassium cyanide (DMF/water; 66%), into the dinitrile **6** (m.p. = 107–108 °C).[6] Hydrolysis (sodium hydroxide, ethanediol, 6 h, 160 °C; 90%) afforded the dicarboxylic acid **7** (m.p. = 118 °C),[6] which was cyclized with polyphosphoric acid to give 3,10-dichloro-5,8-dioxo-5,6,6a,7,8,12b-hexahydrobenzo[*c*]phenanthrene **8** (m.p. = 227–231 °C, dec.; *cis-trans* mixture 6a,12b-H)[6] in 90% yield.



3

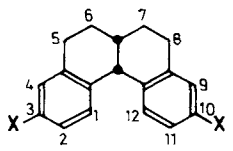


4: X = OH
5: X = OSO_2Me
6: X = CN
7: X = COOH

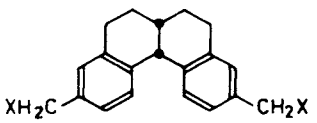


8

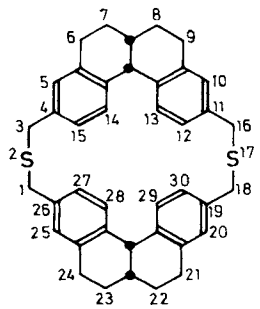
Reduction of **8** (red phosphorus, hydrogen iodide, glacial acetic acid, 5 d, reflux) gave a mixture of the *cis* compound **9** and its *trans* isomer (1:2, total yield 88%), which could be separated by crystallization (*cis*: m.p. = 138–139 °C; *trans*: m.p. = 151 °C).[6] When **8** was reduced and then heated with potassium hydroxide in ethanediol for 1 h at 160 °C, only the *cis* compound **9** was formed—as is the case for the Wolff-Kishner reduction of **8**. Compound **9** was converted into the dicyano compound **10** (m.p. = 181–183 °C)[6] by reaction with copper(I) cyanide in *N*-methyl-2-pyrrolidone (24 h, reflux; 78%); **10** reacted with hydrogen chloride in methanol/chloroform to give the dimethyl ester **11** (m.p. = 136–137 °C; 95%).[6] Reduction of **11** ($LiAlH_4$, THF; 93%) led to **13** (m.p. = 108–111 °C),[6] which was converted into the bis(bromomethyl) compound **14** (m.p. = 114–115 °C; 69%)[6] by treatment with hydrogen bromide/glacial acetic acid. Compound **14** is the first cyclization component required for the synthesis of the dithiaphane **17**. The double isothiuronium salt **15** (m.p. = 144 °C, dec.)[6], the second cyclization component, was obtained by treatment of **14** with thiourea (ethanol, 30 min, reflux; 84%).



9: X = Cl
10: X = CN
11: X = COOMe
12: X = CHO



13: X = OH
14: X = Br
15: X = $[SC(NH_2)_2]Br$
16: X = $[P(C_6H_5)_3]Br$



17

The cyclization was carried out by simultaneous addition of solutions of **14** in toluene and **15** in methanol to boiling methanol containing potassium hydroxide; a 30% yield of 6,7,7a,8,9,13b,21,22,22a,23,24,28b-dodecahydro-2,17-dithia[3.3](3,10)benzo[*c*]phenanthrenophane (m.p. = 267–269 °C, dec.)[6] was obtained. Only one of the two possible isomers was isolated, the assignment of which was not possible on the basis of the NMR spectra;[7] the X-ray structure analysis of the phanediene **3** obtained from this dithiaphane, however, showed that **17** must be present.

In order to synthesize **3**, compound **17** was converted into the 2,17-dimethyl-2,17-dithioniabis(fluorosulfonate) (m.p. = 189 °C, dec.) by reaction with methyl fluorosulfonate. The product then underwent rearrangement to give the carbocyclic 1,15- and 1,16-bis(methylthio)-substituted [2.2]phanes (m.p. = 161–175 °C, dec.; 96%)[6] upon treatment with potassium *tert*-butoxide in THF. Subsequent treatment with *m*-chloroperbenzoic acid in dichloromethane at −25 °C gave the double sulfoxide, which was pyrolyzed (sealed tube, 6 h, 170 °C, under argon atmosphere). [2.2](3,10)-5,6,6a,7,8,12b,19,20,20a,21,22,26b-dodecahydrobenzo[*c*]phenanthrenophane-1,15-diene **3** (m.p. = 226–230 °C)[6] was thereby obtained in 17% yield.

The synthesis of **3** was also attempted by double Wittig reaction (lithium hydroxide, dichloromethane/water[8]) of **12** (obtained from **13** with pyridinium chlorochromate, 55%)[9] with **16** (obtained from **14** with triphenylphos-

phane in DMF; 98%).[6] However, **3** was obtained in only 5% yield; in addition, the second possible isomer (m.p. = 295–302 °C, dec.)[6] was isolated in 2% yield.

The structure of **3** cannot be unequivocally established from the ^{1}H-NMR spectrum;[10] X-ray structure analysis, on the other hand, proved successful.[11] As revealed in Figure 1, the molecule is not strained; this was predicted from examination of models and force field calculations. In the crystal, the distance between the atom pairs C11/C28 and C14/C25 in the two *cis*-stilbene units is relatively short (342 pm); it is between these two pairs of atoms where bond formation is expected to occur photochemically.

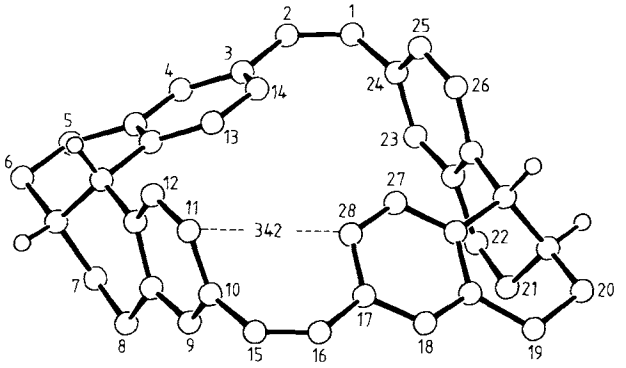


Fig. 1. Molecular model of **3** based on the X-ray structure analysis [11].

In order to carry out the photocyclization, **3** was irradiated in *n*-propylamine under argon for 6.5 h at −32 °C with a low-pressure mercury lamp; a mixture of various hydrogenated derivatives of **2** was obtained in 35% yield (after chromatography). Dehydrogenation with 2,3-dichloro-5,6-dicyano-*p*-benzoquinone (DDQ) in *m*-xylene (54 h, 90 °C) afforded a 13% overall yield of **2** in the form of yellow crystals (m.p. > 330 °C, dec.). The mass spectrum exhibits the molecular ion peak *m/z* 500 as the base peak in addition to the peak of the multiply charged molecular ions [*m/z* 250 (M^{2+}, 15.5%), 166.7 (M^{3+}, 1.9) and 125 (M^{4+}, 7.0)]. The high-resolution mass spectrum confirms the composition (calcd 500.1565; found 500.1575). Of interest, moreover, is the $(M-4)^+$ peak (*m/z* 496, 13.6%; high-resolution spectrum: calcd 496.1252, found 496.1250); it apparently arises by cleavage of the four inner hydrogen atoms with transannular C–C bond formation.

The ^{1}H-NMR spectrum of **2** (360 MHz) was recorded at 150 °C in [D_2]1,2,4,5-tetrachlorobenzene. In accordance with the symmetry of **2**, only five signals of equal intensity are observed: $\delta = 8.11$ (s; 6,7,14,15-H), 8.11 (d, $J = 8.3$ Hz; 2,3,10,11-H), 8.29 (d, $J = 8.3$ Hz; 1,4,9,12-H), 8.65 (s; 5,8,13,16-H), and 9.56 (s; 17,18,19,20-H); the signals were assigned on the basis of NOE experiments. The low-field shift of the inner protons shows that, as in the case of kekulene, no significant diatropism of the macrocyclic system exists.

The UV spectrum is similar to the UV spectra of benzo[*c*]phenanthrene and pentaphene and is therefore in accord with the benzenoid character of **2**. The zero-field splitting parameter, $|D|$, determined from the phosphorescence emission by the ODMR method, is significantly smaller for **2** (0.0881 cm^{-1} in [D_2]1,2,4,5-tetrachlorobenzene, 1.3 K)[12] than for kekulene (0.10622 cm^{-1}). This indicates a less pronounced localization of sextets and double bonds than in kekulene. Indeed, it is possible to write more than one formula for **2** with the maximum number of possible sextets, whereas this is not so for kekulene in formula **1**. We hope to further clarify the electronic structure of **2** by X-ray structure analysis and by additional spectroscopic investigations.

Received: May 28, 1986 [Z 1793 IE]
German version: *Angew. Chem. 98* (1986) 757

CAS Registry numbers:
1, 15123-47-4; **2**, 15123-45-2.

[1] a) H. A. Staab, F. Diederich, *Chem. Ber. 116* (1983) 3487; b) see also F. Diederich, H. A. Staab, *Angew. Chem. 90* (1978) 383; *Angew. Chem. Int. Ed. Engl. 17* (1978) 372.
[2] H. A. Staab, F. Diederich, C. Krieger, D. Schweitzer, *Chem. Ber. 116* (1983) 3504; see also C. Krieger, F. Diederich, D. Schweitzer, H. A. Staab, *Angew. Chem. 91* (1979) 733; *Angew. Chem. Int. Ed. Engl. 18* (1979) 699; D. Schweitzer, K. H. Hausser, H. Vogler, F. Diederich, H. A. Staab, *Mol. Phys. 46* (1982) 1141.
[3] H. A. Staab, F. Diederich, V. Čaplar, *Liebigs Ann. Chem. 1983*, 2262.
[4] H. A. Staab, M. Sauer, *Liebigs Ann. Chem. 1984*, 742.
[5] For the nomenclature of cycloarenes, see ref. [1a]. According to Chemical Abstracts rules, **2** is named 13,19:14,18-dimethenoanthra[1,2-*a*]benzo[*o*]pentaphene, which, however, reveals only poorly the structure and geometry of **2**. There are no IUPAC rules that apply to this class of compounds.
[6] Elemental analyses and spectroscopic data are in accord with the structure given.
[7] **17**: ^{1}H-NMR (360 MHz, $CDCl_3$): $\delta = 1.36$–1.46 (m, 4H; 7,8,22,23-H_{ax}), 1.84–1.92 (m, 4H; 7,8,22,23-H_{eq}), 2.29–2.35 (m, 2H; 7a,22a-H), 2.61–2.77 (m, 8H; 6,9,21,24-H), 3.51 and 3.76 (AB, $J_{AB} = 13.5$ Hz, 8H; 1,3,16,18-H), 3.86 (d, $J = 5.0$ Hz, 2H; 13b,28b-H), 6.67 (dd, $J = 7.9$ Hz and 2.0 Hz, 4H; 12,15,27,30-H), 6.89 (d, $J = 2$ Hz, 4H; 5,10,20,25-H), 6.97 (d, $J = 7.9$ Hz, 4H; 13,14,28,29-H). — ^{13}C-NMR (90.6 MHz, $CDCl_3$): $\delta = 27.1$, 27.9, 32.4, 36.0, 42.3, 126.4, 129.1, 130.4, 136.8, 137.2, 137.5. — MS (selected): *m/z* 584 (50%, M^+), 292 (12), 291 (17), 261 (17), 259 (100).
[8] A. Minsky, M. Rabinovitz, *Synthesis 1983*, 497.
[9] G. Rohlfs, *Diplomarbeit*, Universität Heidelberg 1985.
[10] **3**: ^{1}H-NMR (360 MHz, C_6D_6): $\delta = 1.08$–1.18 (m, 4H; 6,7,20,21-H_{ax}), 1.52–1.56 (m, 4H; 6,7,20,21-H_{eq}), 2.08–2.14 (m, 2H; 6a,20a-H), 2.21–2.28 (m, 4H; 5,8,19,22-H_{ax}), 2.39–2.48 (m, 4H; 5,8,19,22-H_{eq}), 3.65 (d, $J = 5.0$ Hz, 2H; 12b,26b-H), 6.74 (d, $J = 7.8$ Hz, 4H; 12,13,26,27-H), 6.77 (s, 4H; 1,2,15,16-H), 6.87 (d, $J = 1.9$ Hz, 4H; 4,9,18,23-H), 6.99 (dd, $J = 7.8$ and 1.9 Hz, 4H; 11,14,25,28-H).
[11] C. Krieger, D. J. H. Funhoff, H. A. Staab, unpublished results.
[12] D. Schweitzer, unpublished results.

An Isocyanide Radical as Complex Ligand**

By *Friedrich Seitz, Helmut Fischer,* Jürgen Riede, Thomas Schöttle,* and *Wolfgang Kaim*

Structurally, the $CNCR_2$ ligand in complexes of the type $[L_nM(CNCR_2)]^{\oplus}$ is unusually flexible. In the pentacarbonyl cations

$[(CO)_5M(CNCR_2)]^{\oplus}$ (M = W, Cr; compare **1** and **5**, respectively)

the M–C–N–C fragment is nearly linear;[1] these cations are best described as resonance hybrids of the structures **A** and **B**.

$$(CO)_5M{=}C{=}\overset{\oplus}{N}{=}CR_2 \quad \longleftrightarrow \quad (CO)_5M^{\ominus}{-}C{\equiv}\overset{\oplus}{N}{-}\overset{\oplus}{C}R_2$$
A **B**

[*] Priv.-Doz. Dr. H. Fischer, Dr. F. Seitz, J. Riede, Dr. T. Schöttle
Anorganisch-chemisches Institut der Technischen Universität München
Lichtenbergstrasse 4, D-8046 Garching (FRG)
Priv.-Doz. Dr. W. Kaim
Institut für Anorganische Chemie der Universität
Niederurseler Hang, D-6000 Frankfurt am Main 50 (FRG)

[**] Metallaheterocumulenes, Part 6. This work was supported by the Deutsche Forschungsgemeinschaft and the Fonds der Chemischen Industrie. — Part 5: [9].

$$[(CO)_5W{=}C{=}N{=}CR_2]^{\oplus}\,AlBr_4^{\ominus} \xrightarrow[-\ \text{"}AlBr_3\cdot THF\text{"}]{+\ THF} \begin{cases} \underset{\mathbf{2}}{trans\text{-}Br(CO)_4W{=}C{-}N{=}CR_2} + CO \\ + \\ \underset{\mathbf{3}}{(CO)_5W{-}C{\equiv}N{-}CR_2{-}CR_2{-}N{\equiv}C{-}W(CO)_5} + \ldots \end{cases}$$

1-$AlBr_4$

Increasing the back-bonding ability of the metal carbonyl fragment with M = W by exchange of the *trans* CO group for the weak π-donor $Br^{\ominus}$ results in a dramatic change in the bonding relationships. The $CNCR_2$ ligand of **2** is much more bent (C-N-C angle: 135.4° for CR_2 = 9-xanthenylidene = $C(C_6H_4)_2O$), and the W-C distance is typical for that of complexes with a formal W-C triple bond.[2]

The synthesis of **2** is accompanied by the formation of the binuclear diisocyanide complexes **3**, which are the products of a reductive dimerization of **1**. The product ratio **2**/**3** is strongly dependent on the reaction conditions—a preliminary indication for the involvement of paramagnetic intermediates. For R = mesityl, we have now been able to isolate and characterize such a radical intermediate.

$$[(CO)_5Cr\{C(OEt)N{=}CR_2\}] + 2\ AlBr_3 \longrightarrow$$

4

$$[(CO)_5Cr{=}C{=}N{=}CR_2]^{\oplus}\,AlBr_4^{\ominus} \xrightarrow[-\ \text{"}AlBr_3\cdot THF\text{"}]{+\ THF}$$

5-$AlBr_4$

$$[(CO)_5Cr{-}C{\equiv}N{-}\overset{\odot}{C}R_2] + \{Br^{\odot}\} + \ldots$$

6

$$[(CO)_5W{=}C{=}N{=}CR_2]^{\oplus}\,BF_4^{\ominus} \xrightarrow[CH_2Cl_2]{Br^{\ominus}}$$

1-BF_4

$$[(CO)_5W{-}C{\equiv}N{-}\overset{\odot}{C}R_2] + \{Br^{\odot}\} + \ldots$$

7

R = 2,6-dimethylphenyl (mesityl)

The complex **5**-$AlBr_4$, which can be prepared from **4** and $AlBr_3$ in CH_2Cl_2,[3] reacts at room temperature in CH_2Cl_2 with tetrahydrofuran (THF) in 30 min to give the neutral, paramagnetic isocyanide complex **6**.[4]

The reduction of **5**-$AlBr_4$ is reversible, as shown by cyclovoltammetric measurements ($E_p = +0.58$ V versus sat. $Ag^{\oplus}/AgCl$, −30 °C, 0.3 M NBu_4BF_4 in CH_2Cl_2).

The violet compound **6** is surprisingly stable: the crystals are stable for days under nitrogen at room temperature. Analysis of the ESR spectrum (Fig. 1) and comparison of the results with published data[5] indicates that the unpaired electron is largely delocalized in the CNC(mesityl)$_2$ ligand. The X-ray structure analysis (Fig. 2) confirms that **6** is an isocyanide complex with the Cr-C, C-N, and N-C bond lengths characteristic of this class of compounds.[6] The C-N-C angle of 171.2° is similar to the values found for $(CO)_5Cr{-}C{\equiv}N{-}C{\equiv}N$ (168.5°)[7] and $(CO)_5Cr{-}C{\equiv}N{-}C{\equiv}NCo_3(CO)_9$ (176.0°).[8] The C7 atom is nearly planar coordinated, the sum of the angles being 348.3°. The planes of the two mesityl groups form angles of 31.9° and 64.4° with the C81-C7-C91 plane. The stability of this diarylmethyl(isocyano) radical complex is therefore presumably due to the effective steric shielding of C7 by the *o*-methyl substituents.

The reaction of the tungsten analogue of **5**-$AlBr_4$ (= **1**-$AlBr_4$, R = mesityl) with THF does not afford the radical

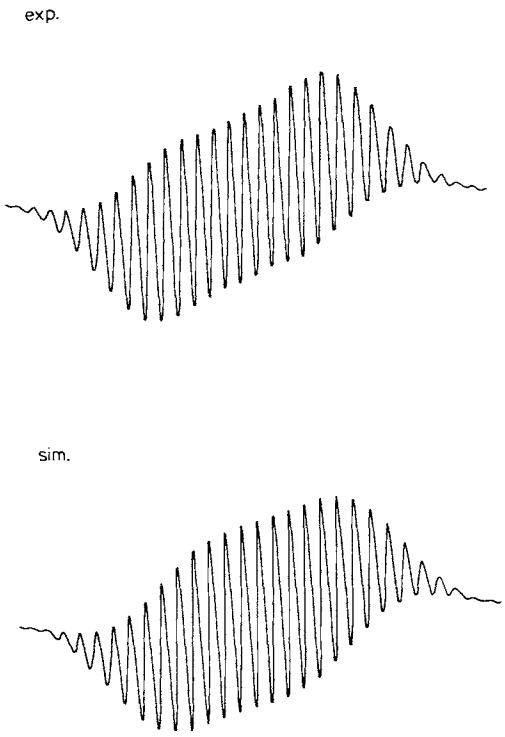


Fig. 1. ESR spectrum of **6** at room temperature in hexane (above) and simulated spectrum (below; $a(^{14}N) = 5.60$ G, $a(H)^{Me\text{-}p} = 2.30$ G, $a(H)^{Me\text{-}o} = a(H)^{H\text{-}m} = 1.15$ G; 0.77 G line width).

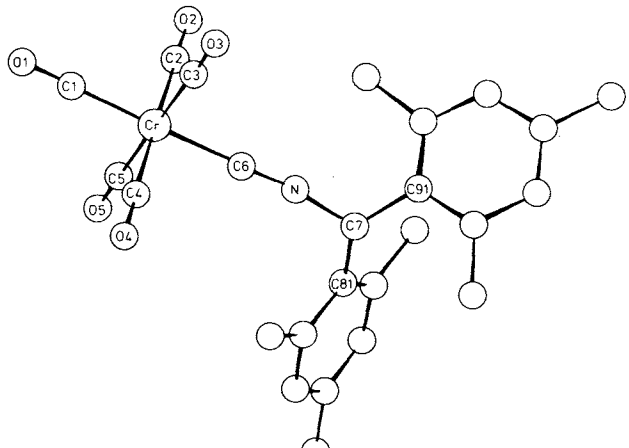
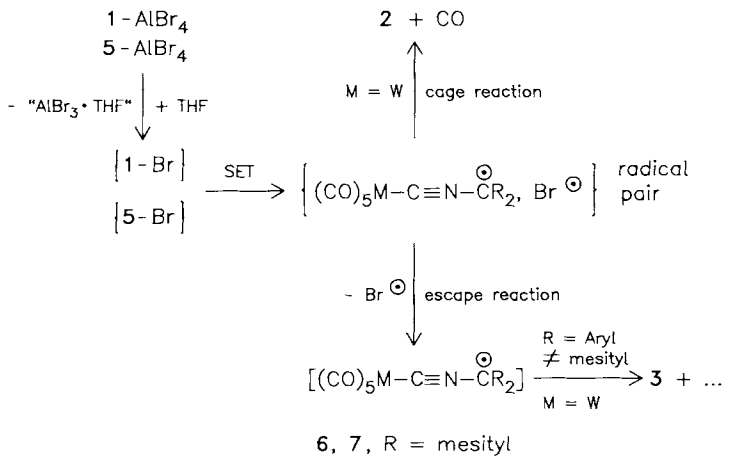


Fig. 2. Crystal structure of **6**. Selected bond lengths [pm] and angles [°]: Cr-C6 198.2(4), C6-N 115.7(5), N-C7 142.9(6), C7-C81 151.9(7), C7-C91 149.1(6); Cr-C6-N 179.0(4), C6-N-C7 171.2(4), N-C7-C81 110.5(4), N-C7-C91 116.4(4).

complex 7, which is analogous to **6**, but rather **2**, R = mesityl.[9] Compound 7, however, is formed as a by-product in the reaction of **1**-BF_4, R = mesityl, with diethyl ether and $Br^{\ominus}/CH_2Cl_2$.[10] Compound 7 can be generated cyclovoltammetrically by reversible reduction of the cation **1**, R = mesityl ($E_p = +0.66$ V versus sat. $Ag^{\oplus}/AgCl$, $-30\,^{\circ}C$, 0.3 M NBu_4BF_4 in CH_2Cl_2). At room temperature, 7 reacts rapidly (in less than one minute) with Br_2 to give **2**, R = mesityl; yield ca. 40% for $7:Br_2 = 1:1$. In contrast, 7 reacts with $Br^{\ominus}$ only very slowly upon prolonged standing of the solution at room temperature.



Scheme 1.

The reaction sequence summarized in Scheme 1 is thus an impressive example for SET (single-electron-transfer) reactivity:[11] the species **1**-Br and **5**-Br, formed by removal of $AlBr_3$ undergo an intramolecular SET reaction to form a radical pair, presumably on account of the very positive redox potentials of the cations and the easy oxidation of bromide in CH_2Cl_2; both cage products[11] (**2** in the case of the tungsten complex) and primary (**6, 7**) and secondary (**3**) escape products are detectable. We are currently investigating the fate of the $Br^{\ominus}$ species. To the best of our knowledge, **6** and **7** are the first complexes in which an isocyanide radical functions as complex ligand.[12]

Received: March 14, 1986 [Z 1701 IE]
German version: *Angew. Chem. 98* (1986) 753

[1] H. Fischer, F. Seitz, J. Riede, J. Vogel, *Angew. Chem. 97* (1985) 131; *Angew. Chem. Int. Ed. Engl. 24* (1985) 121.
[2] H. Fischer, F. Seitz, J. Riede, *J. Chem. Soc. Chem. Commun. 1985*, 537.
[3] F. Seitz, H. Fischer, J. Riede, J Vogel, *Organometallics*, in press.
[4] *Experimental procedure:* **6**: **4** (750 mg, 1.5 mmol) was added to a solution of $AlBr_3$ (1.0 g, 3.7 mmol) in CH_2Cl_2 at $-30\,^{\circ}C$ and the reaction mixture was then stirred for 45 min at room temperature. The reaction mixture was subsequently cooled to $-30\,^{\circ}C$, 2 mL of THF was added, and stirring was continued for 30 min at 20 °C. The solvent was removed and the residue chromatographed at $-20\,^{\circ}C$ on SiO_2. The complex **6** was eluted with pentane/CH_2Cl_2 (10:1) and recrystallized from pentane; violet crystals, yield 46%. IR (hexane): $\tilde{\nu}$(CO) = 2084 (m), 1962 (vs), 1964 (m, sh) cm^{-1}; $\tilde{\nu}$(CN): 2148 cm^{-1}. UV/VIS (hexane): $\lambda_{max} = 568$ ($\lg\varepsilon = 3.77$), 358 nm (4.17). MS: *m/z* 468 ($M^{\oplus}$) and peaks for $[M - n(CO)]^{\oplus}$ (n = 1, 2, 4, and 5).
[5] Cf. A. Berndt in: *Landolt-Börnstein, Neue Serie, II/9b 4*, p. 342.
[6] **6**: $P\bar{1}$, $a = 1181.7(3)$, $b = 1134.8(3)$, $c = 1198.7(3)$ pm, $\alpha = 71.23(2)°$, $\beta = 114.78(2)°$, $\gamma = 109.51(2)°$, $V = 1344 \times 10^6$ pm^3, $\rho_{calcd} = 1.26$ g · cm^{-3}, $Z = 2$, 3035 reflections ($I > 1.96\,\sigma(I)$), $R_1 = 0.056$ (Syntex $P2_1$, $Mo_{K\alpha}$). The crystals contain strongly disordered CH_2Cl_2 (occupation factor ≤ 0.5). Further details of the crystal structure investigation may be obtained from the Fachinformationszentrum Energie, Physik, Mathematik GmbH, D-7514 Eggenstein-Leopoldshafen 2 (FRG), on quoting the depository number CSD-51868, the names of the authors, and the journal citation.
[7] G. Christian, H. Stolzenberg, W. P. Fehlhammer, *J. Chem. Soc. Chem. Commun. 1982*, 184.
[8] W. P. Fehlhammer, F. Degel, H. Stolzenberg, *Angew. Chem. 93* (1981) 184; *Angew. Chem. Int. Ed. Engl. 20* (1981) 214.
[9] H. Fischer, F. Seitz, J. Riede, *Chem. Ber.*, in press.
[10] 7: $\tilde{\nu}$(CO) = 2088 (w), 1960 (sh), 1957 (vs) cm^{-1}; $\tilde{\nu}$(CN) = 2153 (vw) cm^{-1} (hexane).
[11] W. Kaim, *Nachr. Chem. Tech. Lab. 32* (1984) 436; *Acc. Chem. Res. 18* (1985) 160.
[12] W. Kaim, *Coord. Chem. Rev.*, in press.

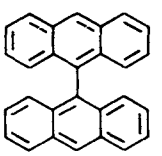
Selective Inclusion and Separation of Isomeric and Homologous Hydrocarbons by Hydrocarbon Host Lattices**

By *Edwin Weber,* Jochen Ahrendt, Mátyás Czugler,* and *Ingeborg Csöregh*

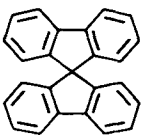
Dedicated to Professor Heinz A. Staab on the occasion of his 60th birthday

Crystalline inclusion compounds that only consist of hydrocarbons are rare.[1] We have now found new types of host compounds that make possible such "crystal inclusions" in many cases and with high selectivities.

Characteristic of compounds such as **1** and **2** is the scissor-like molecular shape and the absence of functional groups;[2] in the coordinatoclathrate-forming molecules described earlier by us, on the other hand, the presence of functional groups is essential.[3] The enclosure of guest molecules in the crystal lattices of **1** and **2** can therefore only occur by "lattice imprisonment" (clathrate formation in its original meaning).[1] The inclusion selectivity presumably depends to a significant extent on the spatial accommodation between the guest and the host molecule.



1



2

Apparently, 9,9′-bianthryl **1** and 9,9′-spirobifluorene **2** have a favorable molecular structure for the inclusion, in the crystal lattice, of isomeric and homologous hydrocarbons, as well as other uncharged organic molecules, with high selectivity. The inclusion compounds listed in Table 1 can be obtained selectively by simple crystallization of **1** or **2** from the guest compounds. As expected on the basis of the polarity of the host compounds **1** and **2**, the inclusion of aprotic and relatively nonpolar guest molecules, including alicyclic hydrocarbons as well as simple arenes and heterocycles, occurs as a rule.

[*] Prof. Dr. E. Weber, Dr. J. Ahrendt
Institut für Organische Chemie und Biochemie der Universität
Gerhard-Domagk-Strasse 1, D-5300 Bonn 1 (FRG)
Dr. M. Czugler
Central Research Institute for Chemistry, Hungarian Academy of Sciences
P. O. Box 17, H-1525 Budapest 114 (Hungary)
Dr. I. Csöregh
Arrhenius Laboratory, Department of Structural Chemistry
University of Stockholm
S-10691 Stockholm (Sweden)

[**] This work was supported by the Deutsche Forschungsgemeinschaft and the Fonds der Chemischen Industrie.

Table 1. Formation of crystalline inclusion compounds of the host substances **1** and **2** with guest molecules (which also serve as solvent).

Guest (= solvent)	Largest extension [Å] [a]	Inclusion compound [b] 1: guest	2: guest
n-pentane to *n*-octane	8.7–11.2	—	—
2,3-dimethylbutane	7.6	—	—
2,3-dimethyl-2-butene	7.3	1:1	—
cyclopentane	6.0	2:1	1:1
cyclohexane	7.0	2:1	1:1
cycloheptane	7.2	[c]	[d]
cyclooctane	7.8	[d]	—
cyclopentene	6.0	[d]	1:1
cyclohexene	6.9	2:1	1:1
cycloheptene	7.2	[c]	2:1
cyclooctene	7.7	[c]	—
1,3-cyclohexadiene	6.9	1:1	1:1
1,4-cyclohexadiene	6.9	1:1	1:1
benzene	6.9	1:1	1:1
cycloheptatriene	7.2	1:1	1:1
methylcyclopentane	7.3	—	—
methylcyclohexane	7.9	—	—
1-methylcyclohexene	7.9	—	—
3-methylcyclohexene	8.1	—	—
toluene	7.8	1:1	—
o-xylene	8.2	1:1	—
m-xylene	8.7	[c]	—
p-xylene	8.8	1:1	2:1
mesitylene	8.7	—	—
bromobenzene	8.7	—	—
cyclopentanone	6.6	[c]	1:1
cyclohexanone	7.8	1:1	1:1
2-methylcyclohexanone	7.9	—	—
cyclohexene oxide	7.1 [e]	1:1	1:1
tetrahydrofuran (THF)	6.0	1:1	1:1
1,3-dioxolane	5.9	—	—
dioxane	6.8	1:1	1:1
morpholine	6.8	1:1	1:1
piperidine	6.9	1:1	1:1
pyridine	6.9	1:1	1:1

[a] Guest molecules; van der Waals radii from space-filling models, taking into consideration the most probable conformations [4]. [b] Stoichiometry by ^{1}H-NMR integration; the substances were uniformly dried (12 h, room temperature, 15 torr). [c] Nonstoichiometric; inclusion compound decomposes under normal conditions. [d] Traces of solvent. [e] Estimated value.

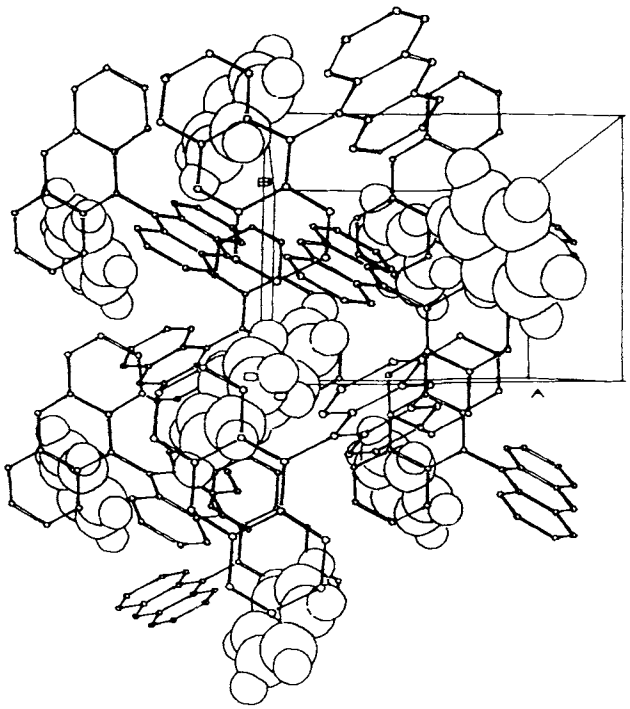


Fig. 1. Crystal packing of **1** · C_6H_6. Projection along the *c* axis. Host compound **1** represented as ball-and-stick model, guest compound benzene as space-filling model. For clarity, the H atoms of the host molecule are omitted. Important bond lengths [Å] in **1**: anthryl C-C 1.340–1.434, average 1.395(32); bianthryl C-C 1.480. Angles between the best planes [°] in **1** · C_6H_6: anthracene-A/-B 85.5, anthracene-A/benzene 48.2, anthracene-B/benzene 49.2.

The unexpected thermal stability of some of the inclusion compounds formed from hydrocarbons as both guest and host components[1] (e.g., **1** · C_6H_6, dec. > 85 °C at 760 torr) and the pronounced selectivity of the host compounds (see below) prompted us to carry out a structure investigation. The X-ray structure analysis[5] of **1** · C_6H_6 (Fig. 1) shows that the benzene molecules are enclosed pairwise with nearly perfect fit in almost completely closed cages (edge length $\approx 6.5 \times 7 \times 12$ Å), which are formed by the flat fragments of a total of eight host molecules. Consequently, no disorder is found for the benzene molecules, as might have been expected.[6] The general structure of the heteromolecular lattice is similar to that found for aromatic hydrocarbons.[7]

The cage geometry appears to be typical for the host lattice of **1** and to exhibit only minor deviations, an observation supported by the inclusion selectivity and the van der Waals dimensions of the guest molecules (Table 1). Inclusion compounds with **2** presumably exhibit similar cavity dimensions (compare Table 1). Thus, with the exception of 2,3-dimethyl-2-butene (in the case of **1**), only cyclic guest molecules having a specific ring size (five- to eight-membered) and extension in the lattice of the host compounds **1** and **2** are enclosed. In the case of cycloheptane, the maximum allowable size of a guest molecule appears to have been just achieved or just exceeded, depending on the host. By the introduction of double bonds and the resulting flattening of the ring (compare cycloheptene, cycloheptatriene), the steric relations (molecular thicknesses) are gradually improved and inclusions (2:1 and 1:1 stoichiometries) are again possible. Thus, in the case of cyclic guest compounds, it is possible to distinguish between saturated and unsaturated (or aromatic) compounds (compare methylcyclohexane/toluene).

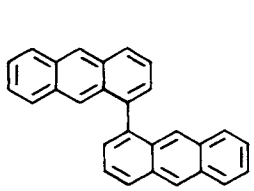
Differentiation is also achieved between substituted and unsubstituted alicyclic compounds (compare cyclohexane/methylcyclohexane and cyclopentane/methylcyclopentane), only the unsubstituted hydrocarbons being incorporated into the crystal lattices of **1** and **2**. This also holds true for cycloalkenes (compare cyclohexene/methylcyclohexene), but not for benzene. However, even in the latter case, only a limited number and arrangement of methyl groups are tolerated (Table 1). These findings open up interesting possibilities for separations, for example, of benzene from toluene or of isomeric xylenes.

A further important finding is that, for suitable van der Waals dimensions, cyclic ketones and cyclohexene oxide, but not the corresponding alcohols or amines, also form inclusion compounds with **1** and **2**. Also for the heterocyclic guest compounds, the exact fitting into the cage is presumably the crucial factor.

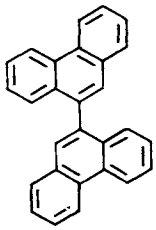
With respect to their host behavior, **1** and **2** are similar but not identical. For example, **2** is apparently capable of better spatial discrimination (compare benzene derivatives) and usually forms inclusion compounds that are more thermally stable (some of the inclusion compounds with **1** are already thermally labile under normal conditions, compare Table 1). We ascribe this observation to the rigid molecular geometry of **2**; compound **1**, on the other

hand, is capable, to a certain extent, of adjusting itself sterically on account of the flexible scissor-like hinge.[8]

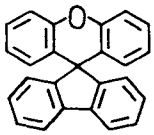
The inclusion ability of the new host compounds opens up several practical uses, e.g., comparable to the crystal inclusions of urea.[9] Whereas urea is employed for the separation of unbranched from branched and cyclic hydrocarbons,[10] the advantage of the new inclusion-forming compounds **1** and **2** lies in the separation of cyclic hydrocarbons from mixtures containing chain-like hydrocarbons or of unsubstituted cyclic hydrocarbons from mixtures containing substituted cyclic hydrocarbons (e.g., cyclohexane from *n*-hexane or *n*-hexenes or from methylcyclopentane or methylcyclohexane; compare also Table 1).[11] They could thus provide a welcome addition to existing procedures. For future applications (e.g., encapsulation of labile substances, topochemistry), it is also of importance that the ready accessibility of the new host compounds opens up the possibility of synthesizing a wide variety of structures (compare **3**–**6**).[12]



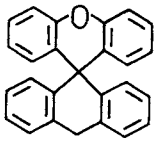
3



4



5



6

Received: February 26, 1986;
revised: May 9, 1986 [Z 1682 IE]
German version: *Angew. Chem. 98* (1986) 719

CAS Registry numbers:
1 · ½ cyclopentane, 103149-12-8; **1** · ½ cyclohexane, 103149-14-0; **1** · x cycloheptane, 103149-16-2; **1** · ½ cyclohexene, 103149-18-4; **1** · x cycloheptene, 103149-49-1; **1** · x cyclooctene, 103149-50-4; **1** · benzene, 103149-25-3; **1** · cycloheptatriene, 103149-27-5; **1** · toluene, 103149-29-7; **1** · *O*-xylene, 103149-30-0; **1** · x *m*-xylene, 103149-48-0; **1** · *p*-xylene, 103149-31-1; **1** · x cyclopentanone, 103149-33-3; **1** · cyclohexanone, 103149-35-5; **1** · cyclohexene oxide, 103149-37-7; **1** · tetrahydrofuran, 103191-45-3; **1** · dioxane, 103149-40-2; **1** · morpholine, 103149-42-4; **1** · piperidine, 103149-44-6; **1** · pyridine, 103149-46-8; **1** · 1,3-cyclohexadiene, 103149-21-9; **1** · 1,4-cyclohexadiene, 103149-23-1; **1** · 2,3-dimethyl-2-butene, 103149-11-7; **2** · cyclopentane, 103149-13-9; **2** · cyclohexane, 103149-15-1; **2** · cyclopentene, 103149-17-3; **2** · cyclohexene, 103149-19-5; **2** · ½ cycloheptene, 103149-20-8; **2** · benzene, 103149-26-4; **2** · cycloheptatriene, 103149-28-6; **2** · ½ *p*-xylene, 103149-32-2; **2** · cyclopentanone, 103149-34-4; **2** · cyclohexanone, 103149-36-6; **2** · cyclohexene oxide, 103149-38-8; **2** · tetrahydrofuran, 103149-39-9; **2** · dioxane, 103149-41-3; **2** · morpholine, 103149-43-5; **2** · piperidine, 103149-45-7; **2** · pyridine, 103149-47-9; **2** · 1,4-cyclohexadiene, 103149-24-2; **2** · 1,3 cyclohexadiene, 103149-22-0.

[1] J. L. Atwood, J. E. D. Davies, D. D. MacNicol (Eds.): *Inclusion Compounds, Vol. I–III*, Academic Press, London 1984; H. Hart, L. T. W. Lin, D. L. Ward, *J. Am. Chem. Soc. 106* (1984) 4043.

[2] Synthesis of **1**: F. Bell, D. H. Waring, *J. Chem. Soc. 1949*, 267, 1579; synthesis of **2**: R. G. Clarkson, M. Gomberg, *ibid 52* (1930) 2881; G. Haas, V. Prelog, *Helv. Chim. Acta 52* (1969) 1202.

[3] E. Weber, I. Csöregh, B. Stensland, M. Czugler, *J. Am. Chem. Soc. 106* (1984) 3297; M. Czugler, E. Weber, J. Ahrendt, *J. Chem. Soc. Chem. Commun. 1984*, 1632.

[4] J. Dale (Ed.): *Stereochemie und Konformationsanalyse*, Verlag Chemie, Weinheim 1978.

[5] **1** · C_6H_6: monoclinic, $P2_1/n$, $a=11.704(3)$, $b=8.790(5)$, $c=22.658$ Å, $\beta=95.80°$, $Z=4$, $\rho_{calcd}=1.239$ g cm^{-3}. Enraf-Nonius CAD4 diffractometer, $Mo_{K\alpha}$ (graphite monochromator) for $\lambda=0.71069$ Å; 1179 unique reflections with $I>2\sigma(I)$. Direct methods; $R=0.045$.—Further details: M. Czugler, I. Csöregh, E. Weber, unpublished results.

[6] I. Csöregh, A. Sjögren, M. Czugler, M. Cserzö, E. Weber, *J. Chem. Soc. Perkin Trans. 2 1986*, 507.

[7] S. Oikawa, M. Tsuda, H. Kato, T. Urabe, *Acta Crystallogr. B41* (1985) 437.

[8] Formation of crown ethers with 1,1′-binaphthyl: D. J. Cram, K. N. Trueblood, *Top. Curr. Chem. 98* (1981) 43; with 9,9′-spirobifluorene: M. Dobler, M. Dumić, M. Egli, V. Prelog, *Angew. Chem. 97* (1985) 793; *Angew. Chem. Int. Ed. Engl. 24* (1985) 792.

[9] W. Schlenk, Jr., *Chem. Unserer Zeit 3* (1969) 120.

[10] L. C. Fetterly in L. Mandelcorn (Ed.): *Non-Stoichiometric Compounds*, Academic Press, New York 1964, p. 491.

[11] Further important separation results (two-component solvent mixtures, enclosed compound in italics) with **1**: *cyclohexane*/toluene, *cyclohexane*/xylene, *cyclohexane*/pyridine, *pyridine*/toluene, *pyridine*/THF, *dioxane*/toluene; with **2**: *cyclohexane*/*p*-xylene, *p-xylene*/benzene. **1** and **2** only differentiate partially between cyclohexane and cyclohexene and between cyclohexane and benzene.

[12] Examples: **4**: selective inclusion of benzene, THF; **5**: of cyclohexane, benzene, pyridine, THF, dioxane, morpholine, piperidine (no inclusion of toluene or methylcyclohexane).

Synthesis and Structure of $[(Ph_3P)_3Ir(\mu_3\text{-}H)(\mu\text{-}H)_2Ag_2(OSO_2CF_3)(H_2O)](CF_3SO_3)$, a Complex with a Bent Ag–Ir–Ag Chain**

By *Pierre Braunstein,* Tania Mara Gomes Carneiro, Dominique Matt, Antonio Tiripicchio,* and *Marisa Tiripicchio Camellini*

The $Ag^{\oplus}$ ion is often used for one-electron oxidations of transition-metal complexes, but it is also able to form stable adducts in which it is bonded to fragments of other transition-metal complexes.[1] Until now, such adducts have only been reported with Ag:M ≤ 1. This ratio was believed to be limited by the oxidative stability of the transition-metal fragment, which functions in these complexes as a Lewis base. We report here a unique reaction in which an Ir complex binds *two* $Ag^{\oplus}$ ions with metal–metal bond formation.

When *mer*-$[IrH_3(PPh_3)_3]$ **1** was allowed to react with two equivalents of CF_3SO_3Ag in acetone, a new complex was formed in quantitative yield.[2] Recrystallization from dichloromethane afforded the aqua complex $[(Ph_3P)_3IrH_3Ag_2(OH_2)](CF_3SO_3)_2$ **2**. Attempts to grow crystals from completely anhydrous media were unsuccessful.

The structure of **2** (Fig. 1)[3] shows a bent Ag1-Ir-Ag2 chain with the Ir atom coordinated by three PPh_3 ligands and with the Ag1–Ir–Ag2 plane almost orthogonal to the mean plane passing through Ir,P1,P2, and P3. From the structural and NMR results (see below), it appears that the Ir atom is octacoordinated, with the two Ag atoms inserted between the hydrido ligands in the H_3IrP2 plane. This results in longer Ir–P distances in **2** than in **1**.[4] Striking features of **2** include the presence of a monodentate $CF_3SO_3^{\ominus}$

[*] Dr. P. Braunstein, T. M. Gomes Carneiro, Dr. D. Matt
Laboratoire de Chimie de Coordination, UA 416 CNRS,
Université Louis Pasteur
4 rue Blaise Pascal, F-67070 Strasbourg Cédex (France)
Prof. A. Tiripicchio, Prof. M. Tiripicchio Camellini,
Istituto di Chimica Generale ed Inorganica, Università di Parma,
Centro di Studio per la Strutturistica Diffrattometrica del CNR
Via M. D'Azeglio 85, I-43100 Parma (Italy)

[**] Financial support from CNRS (Paris), CNR (Rome) and from NATO (under Grant 257/83 to *P. B.* and *A. T.*) is gratefully acknowledged. We thank the CNPq (Brazil) for a grant to *T. M. G. C.*

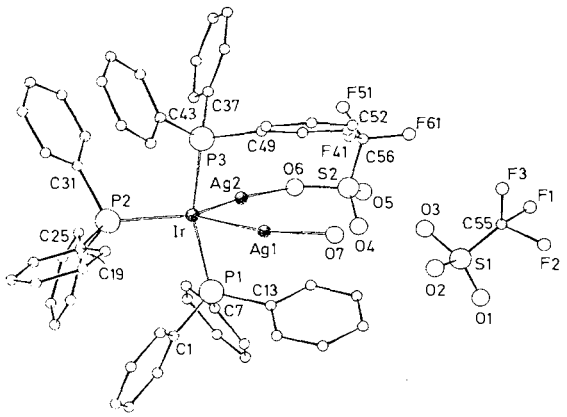


Fig. 1. Crystal structure of **2** (hydrido ligands omitted). Selected distances [Å] and angles [°]: Ir-Ag1 2.808(4), Ir-Ag2 2.764(4), Ag1 ··· Ag2 4.424(4), Ir-P1 2.357(10), Ir-P2 2.387(10), Ir-P3 2.329(9), Ag1-O7 2.23(3), Ag2-O6 2.14(4); Ag1-Ir-Ag2 105.1(1), P1-Ir-P2 99.2(3), P1-Ir-P3 161.0(4), P2-Ir-P3 99.0(3), P1-Ir-Ag1 80.8(3), P1-Ir-Ag2 82.6(3), P2-Ir-Ag1 130.9(2), P2-Ir-Ag2 123.7(3), P3-Ir-Ag1 83.3(2), P3-Ir-Ag2 91.7(3), Ir-Ag1-O7 162.6(9), Ir-Ag2-O6 164.7(9).

ion coordinated to Ag2 and of an H_2O molecule (probably hydrogen bonded with O3 and O6 according to ^{1}H-NMR and X-ray crystallographic results[5]) coordinated to Ag1.[6]

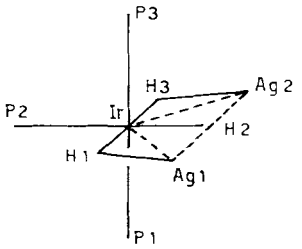


Fig. 2. Idealized positions of the hydrido ligands in **2**. Two of them bridge two different metal atoms, the third one bridges the Ir atom and the two Ag atoms (in an approximately T-shaped fashion).

The idealized positions of the hydrido ligands in Figure 2 were inferred from the ^{1}H- and ^{31}P-NMR results. At 25 °C, the ^{1}H-NMR spectrum of **2** in CD_2Cl_2 shows two resonances typical for hydrido ligands at $\delta = -9.11$ (br. s, H1 and H3) and -10.28 (br. d, $^2J_{P2H} = 88$ Hz, H2). The ^{31}P-{^{1}H}-NMR spectrum of **2** in CH_2Cl_2/CD_2Cl_2 consists of two broad signals at $\delta = 4.6$ (complex m, $\Delta\nu_{1/2} = 60$ Hz, P2) and 2.6 (s, $\Delta\nu_{1/2} = 45$ Hz, P1 and P3).[2] These data are consistent with the presence of a *mer*-[$IrH_3(PPh_3)_3$] moiety in **2**, reminiscent of **1**.[4] Upon decreasing the temperature, the ^{1}H- and ^{31}P{^{1}H}-NMR signals become more complex and at -50 °C a splitting of the H1,3 and P1,3 signals, respectively, is observed. Therefore, the equivalence of H1 and H3 and of P1 and P3 at 25 °C results from a dynamic behavior in solution during which H2 remains *trans* bonded to P2. This could occur, for instance, by an exchange of the *O*-bonded ligands at Ag1 and Ag2.

It is noteworthy that the reaction reported here does not involve $H^{\oplus}$ elimination from the hydrido complex, in contrast to other reactions between hydrido transition-metal complexes and cations of Cu, Ag, and Au.[7] This reaction also represents the first example of a double $Ag^{\oplus}$ addition to a *single* metal center. Although bimetallic Ag–Ir complexes have recently been reported,[8] we have been able to determine, for the first time, the precise Ag–Ir bond lengths.

Received: March 6, 1986;
revised: May 23, 1986 [Z 1693 IE]
German version: *Angew. Chem. 98* (1986) 721

CAS Registry numbers:
1, 18660-47-4; **2**, 103346-69-6; Ir, 7439-88-5; Ag, 7440-22-4.

[1] See, for example, B. T. Heaton, L. Strona, S. Martinengo, D. Strumolo, V. G. Albano, D. Braga, *J. Chem. Soc. Dalton Trans. 1983*, 2175; b) N. G. Connelly, J. A. K. Howard, J. L. Spencer, P. K. Woodley, *ibid. 1984*, 2003; c) R. Uson, A. Laguna, M. Laguna, B. R. Manzano, P. G. Jones, G. M. Sheldrick, *ibid. 1984*, 285; d) J. A. Ladd, H. Hope, A. L. Balch, *Organometallics 3* (1984) 1838; e) G. Bruno, S. Lo Schiavo, P. Piraino, F. Faraone, *ibid. 4* (1985) 1098; f) F. Bachechi, J. Ott, L. M. Venanzi, *J. Am. Chem. Soc. 107* (1985) 1760, and references cited therein.

[2] *Experimental procedure:* All reactions and operations, including the distillation of the solvents, were carried out under N_2. A solution of CF_3SO_3Ag (0.110 g, 0.43 mmol) in 3 mL of acetone was added to a suspension of **1** (0.210 g, 0.21 mmol) in 5 mL of acetone. After stirring for 20 min at room temperature, the solution was filtered and the solvent removed in vacuo. The solid was recrystallized from 5 mL of CH_2Cl_2 at -20 °C, affording **2** as colorless single crystals. Yield 0.261 g (83%); m. p. 145 °C (dec.) Correct elemental analysis. Since the integration of the observed ^{1}H-NMR H_2O resonance ($\delta = 1.63$, assigned by addition of D_2O) was always higher than predicted, traces of free water (which has a similar chemical shift) are presumably present. The occurrence of unresolved $^{107/109}$Ag coupling causes broadening of the hydride and phosphorus NMR resonances. ^{19}F-NMR (CD_2Cl_2, 84.67 MHz, 25 °C, external $CFCl_3$): $\delta = -76.2$ ppm.

[3] Siemens AED diffractometer, $Mo_{K\alpha}$: monoclinic space group $P2_1/n$, $Z = 4$, $a = 14.073(7)$, $b = 32.510(15)$, $c = 13.391(7)$ Å, $\beta = 93.32(3)°$, $V = 6116(5)$ Å^3, $3 \le \theta \le 23°$, 8549 unique reflections, 3461 observed reflections with $I \ge 2\sigma(I)$, $R = 0.083$, $R_w = 0.113$. Further details of the crystal structure investigation can be obtained from the Fachinformationszentrum Energie Physik Mathematik GmbH, D-7514 Eggenstein-Leopoldshafen 2 (FRG), by quoting the depository number CSD 51929, the names of the authors, and the journal citation.

[4] G. R. Clark, B. W. Skelton, T. N. Waters, *Inorg. Chim. Acta 12* (1975) 235.

[5] The O7 atom is involved in two short contacts with oxygen atoms of both anions (O7-O3 2.56(5), O7-O6 ($\frac{1}{2}+x$, $\frac{1}{2}-y$, $\frac{1}{2}+z$) 2.80(5) Å); these contacts resemble hydrogen bonds.

[6] Very few structures with Ag···OH_2 bonds have been reported; this is probably the first one in which an H_2O molecule is bonded to a Ag atom in an approximately linear fashion.

[7] P. Braunstein, H. Lehner, D. Matt, A. Tiripicchio, M. Tiripicchio Camellini, *Angew. Chem. 96* (1984) 307; *Angew. Chem. Int. Ed. Engl. 23* (1984) 304.

[8] a) A. T. Hutton, P. G. Pringle, B. L. Shaw, *Organometallics 2* (1983) 1889; b) L. F. Rhodes, J. C. Huffman, K. G. Caulton, *J. Am. Chem. Soc. 106* (1984) 6874; c) H. Lehner, D. Matt, L. Venanzi, Congrès National de la Société Française de Chimie (Nancy 1984) Abstract 5A29.

Synthesis and Crystal Structure of μ-Thiobis[tris(diethyldithiocarbamato)molybdenum(IV)]-Toluene 1:1, a Compound Containing a Rare Mo-S-Mo Core

By *Khalid S. Jasim, Chung Chieh,** and *Thomas C. W. Mak*

Interest in molybdenum-containing enzymes has prompted intensive investigation of sulfur-containing molybdenum compounds, and recent studies have revealed

[*] Prof. Dr. C. Chieh, Dr. K. S. Jasim,
Guelph-Waterloo Centre for Graduate Work in Chemistry
University of Waterloo
Waterloo, Ontario, Canada N2L 3G1
Prof. Dr. T. C. W. Mak
Department of Chemistry
The Chinese University of Hong Kong
Shatin, New Territories (Hong Kong)

 © VCH Verlagsgesellschaft mbH, D-6940 Weinheim, 1986 0570-0833/86/0808-0749 $ 02.50/0

the existence of common cores such as $Mo_2(\mu_2\text{-}S)_2$, $Mo_3(\mu_3\text{-}S)(\mu_2\text{-}S)_3$, and $Mo_4(\mu_3\text{-}S)_4$ in complexes of halides, cyanides, dithiocarbamates (dtc), and dithiophosphates.[1-2] Although there are abundant complexes with a Mo-O-Mo linkage, e.g., **1**,[4] we are aware of only one known species that contains a sulfido ligand bridging two Mo^{IV} atoms, namely, **2**.[5]

$[Mo_2(\mu\text{-}O)(dtc)_6]BF_4$ **1** $\quad$ $K_6[Mo_2(\mu\text{-}S)(CN)_{12}]$ **2**

Previously, we reported that the cubane-like complex **3**[2] was formed when a toluene solution containing $[Mo(CO)_6]$ and tetraethylthiuram disulfide was refluxed for an extended period in an inert atmosphere, whereas $[Mo_2(dtc)_6]$ was isolated if the reflux was carried out for only 3 h.[6] When the latter air-sensitive complex was dissolved in toluene and the stirred solution was aerated at 295 K, the title compound **4** was obtained.

$[Mo_4(\mu_3\text{-}S)_4(dtc)_6]\cdot$ **3** $\quad$ $[Mo_2(\mu\text{-}S)(dtc)_6]\cdot C_7H_8$ **4**

The IR, NMR, and UV/VIS spectra of **4** differ from those of the starting material. In particular, the sharp IR peak at 603 cm^{-1} beside a strong ν(CS) band at 581 cm^{-1} may be assigned to ν_{as}(Mo-S-Mo) by analogy to the corresponding band (620 cm^{-1}) in **2**[5] and the μ-oxo band (665 cm^{-1}) in **1**.[4] The ^{1}H-NMR spectrum of **4** (C_6D_6) showed that all dtc groups are equivalent: $\delta = 0.90$ ($J = 8$ Hz, CH_3), 3.35 (CH_2). Five bands were observed in the UV/VIS region: $\lambda = 526$ w, 461 ($\varepsilon = 13840$), 405 (14026), 375 (240), 280 nm (39710). The two weak bands may be due to d-d transitions, the others to charge transfer.

$[Mo(CO)_6]$ did not react with tetraethylthiuram disulfide in toluene at 295 K. When the mixture was refluxed in the atmosphere, $[Mo(dtc)_4]$ was always formed. The intermediate compound $[Mo_2(dtc)_6]$ seemed essential for the formation of the title compound **4** (major product, 60% yield). Aerating a chloroform solution of $[Mo_2(dtc)_6]$ yielded, instead of **4**, compounds **5** and **6**,[7] which were completely characterized. Redox reactions therefore occur between the solvent chloroform and the molybdenum dithiocarbamates; the use of inert toluene as a solvent seems critical for the formation of the compound containing the Mo-S-Mo core.

$[Mo(dtc)_4][Mo_6O_{19}]$ **5** $\quad$ $[Mo(dtc)_4](Cl\cdot H_2O)\cdot 0.88\ CHCl_3$ **6**

Complex **4** is insoluble in aliphatic hydrocarbons, sparingly soluble in benzene and toluene, but very soluble in chlorinated solvents such as chloroform. Black crystals of **4** grown by slow evaporation of a toluene solution quickly lost their crystallinity and solvent of crystallization upon exposure to air, yet the spectra of all samples exhibited IR bands due to the solvated toluene (700, 739, 1003 cm^{-1}). However, a freshly prepared crystal enclosed inside a 0.5-mm Lindemann glass capillary under a toluene atmosphere remained stable throughout the duration of the X-ray study.[8]

The partial crystal structure of **4** is shown in Figure 1. The preferred pentagonal bipyramidal geometry is retained by both seven-coordinated Mo^{IV} centers. The Mo-S(dtc) bond lengths range from 2.496(2) to 2.570(2) Å, the axial ones being the longest. The two Mo-S(bridging)

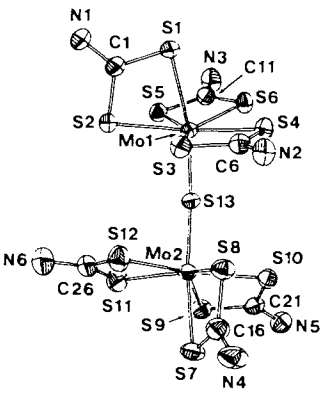


Fig. 1. ORTEP plot (35% probability thermal ellipsoids) of the crystal structure of $[Mo_2(\mu\text{-}S)(S_2CNEt_2)_6]\cdot C_7H_8$ **4**; ethyl groups and toluene are omitted. The crystals are monoclinic, space group $P2_1/c$, $a = 12.360(4)$, $b = 26.000(7)$, $c = 17.122(5)$ Å, $\beta = 92.42°$, $Z = 4$. The structure was refined to $R = 0.063$ using 8851 observed $Mo_{K\alpha}$ data [8].

bonds are 2.187(1) and 2.194(1) Å, and the Mo-S-Mo angle is 157.2°; the corresponding values for **2** are 2.173(1) Å (symmetric) and 169.5°.[5] The short Mo-S distances in the Mo-S-Mo system of **4** have been attributed to multiple bonding:

$$\sigma[Mo(d_{z^2}) + S(p_z)] + \pi[Mo(d_{xz}, d_{yz}) + S(p_x, p_y)]$$

The difference in Mo-S bond lengths in **4** and **2** is probably due to the degree of deviation of their Mo-S-Mo linkages from linearity, since the Mo atoms have the same oxidation state (+4) in both structures.

Although the symmetry of the molecule is not dictated by that of the space group, it approximates that of the point group C_2, with a twofold axis passing through S(13) and the midpoint of the line joining S(3) and S(12) (Fig. 1). The overall geometry is the same as that of the cation of **1**, which, however, has mixed Mo oxidation states and a nearly linear bridge (Mo-O-Mo = 175.7°).[4]

Received: February 4, 1986;
revised: May 5, 1986 [Z 1654 IE]
German version: *Angew. Chem. 98* (1986) 718

CAS Registry numbers:
4, 103004-17-7; $[Mo_2(dtc)_6]$, 103004-18-8.

[1] A. Müller, R. Jostes, W. Eltzner, C.-S. Nie, E. Diemann, H. Bögge, M. Zimmermann, M. Dartmann, U. Reinsch-Vogell, S. Che, S. J. Cyvin, B. N. Cyvin, *Inorg. Chem. 24* (1985) 2872; F. A. Cotton, M. P. Diebold, Z. Dori, R. Llusar, W. Schwotzer, *J. Am. Chem. Soc. 107* (1985) 6735.

[2] T. C. W. Mak, K. S. Jasim, C. Chieh, *Angew. Chem. 96* (1984) 352; *Angew. Chem. Int. Ed. Engl. 23* (1984) 391; *Inorg. Chem. 24* (1985) 1587.

[3] Y. Jian, A. Tang, R. Hoffmann, J. Huang, J. Lu, *Organometallics 4* (1985) 27.

[4] J. A. Broomhead, M. Sterns, C. G. Young, *J. Chem. Soc. Chem. Commun. 1981*, 1262; C. D. Garner, N. C. Howlander, F. E. Mabbs, A. T. McPhail, K. D. Onan, *J. Chem. Soc. Dalton Trans. 1979*, 962; D. Coucouvanis, *Prog. Inorg. Chem. 26* (1979) 301.

[5] A. Müller, P. Christophliemk, *Angew. Chem. 81* (1969) 752; *Angew. Chem. Int. Ed. Engl. 8* (1969) 753; M. G. B. Drew, P. C. H. Mitchell, C. F. Pygall, *J. Chem. Soc. Dalton Trans. 1979*, 1213.

[6] D. A. Brown, W. K. Glass, K. S. Jasim, *Inorg. Chim. Acta 45* (1980) L97.

[7] K. S. Jasmin, C. Chieh, T. C. W. Mark, *J. Crystallogr. Spectrosc. Res. 15* (1985) 403; *Inorg. Chim. Acta 116* (1986) 37; T. C. W. Mak, S. P. So, C. Chieh, K. S. Jasmin, *J. Mol. Struct. 127* (1985) 375.

[8] Two methyl C atoms belonging to different ligands exhibit twofold positional disorder. The toluene molecule is also disordered, and most of its scattering was accounted for by two half-weighted benzene rings. Further details of the crystal structure investigation may be obtained from the Fachinformationszentrum Energie, Physik, Mathematik GmbH, D-7514 Eggenstein-Leopoldshafen 2 (FRG), on quoting the depository number CSD-51900, the names of the authors, and the journal citation.

Bilayer-Immobilized Films Containing Mesogenic Azobenzene Amphiphiles—Electrically Controllable Permeability**

By *Yoshio Okahata,* Shinsuke Fujita, and Noami Iizuka*

Immobilization of synthetic or natural lipid bilayers facilitates their use as novel functional materials, such as permeability-controllable membranes.[1] Previously, we prepared a bilayer-corked capsule membrane[2] and a bilayer-immobilized film from dialkylammonium amphiphiles and polyanions,[3] and were able to control their permeability by application of an electric field across the membrane (Fig. 1, method B). The electrical field generates transient pores in the bilayer of the capsule membrane or film, resulting in a large increase in the permeability of the membrane. We report here the preparation of bilayer-immobilized films from the liquid-crystalline-type amphiphiles **1a–c** containing an azobenzene chromophore. The permeability of the film can be controlled by application of an electric field *parallel to the membrane* (Fig. 1, method A), which causes the orientation of the chromophores in the bilayer film to change.

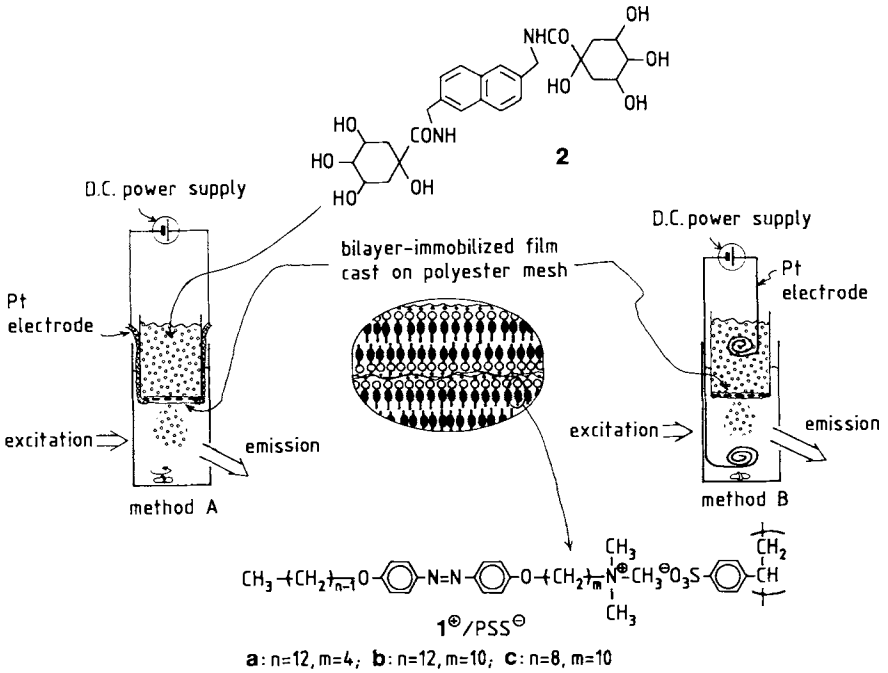


Fig. 1. Schematic drawing of the experimental setup (see text).

The preparation of the azobenzene-containing amphiphiles **1a–c** has been described elsewhere,[4] and the films were prepared according to the previously reported method.[3] An aqueous dispersion (2 mL) of azobenzene amphiphiles **1a–c** (3×10^{-5} mol) and an aqueous solution (2 mL) of sodium polystyrenesulfonate (NaPSS) ($M_r=2\times10^6$, 3×10^{-5} mol) were mixed at 70 °C. The precipitate was washed, dissolved in chloroform, and reprecipitated with ethanol. The dried, yellow powder (recovery: 80%) was dissolved in chloroform and cast on a polyester minigrid (270 mesh, 38 mm^2). The thickness of the cast film was estimated to be 100 μm from scanning electron microscopic observations. The polyionic film was transparent, mechanically stable, and water-insoluble.

The bilayer characteristics of the polyionic film were confirmed by X-ray diffraction analysis of **1a**: a strong diffraction pattern with 3.5-nm spacing was observed, which is consistent with the bimolecular length of tilted **1a**. The structural data are similar to those obtained for aqueous dispersions and cast films prepared from **1**.[5] These results clearly indicate that the films formed from azobenzene amphiphiles have extended lamellar structure like that observed for dialkylamphiphile-immobilized film.[3] The films obtained from the azobenzene amphiphiles were shown by DSC (differential scanning calorimetry) measurements to have the following phase-transition temperatures for transformation from the solid to the liquid-crystalline state: **1a**, 25 °C; **1b**, 56 °C; **1c**, 64 °C.

The permeation of the water-soluble, nonionic fluorescent probe **2**[6] (10^{-3} M) through the $1^{\oplus}/PSS^{\ominus}$ film cast on a polyester mesh was followed fluorophotometrically at $\lambda=340$ nm (excitation at $\lambda=280$ nm) (Fig. 1). Permeation rates were obtained both in the absence and presence of an electric field, which was applied either parallel (method A) or perpendicular (method B) to the film plane. The results are summarized in Table 1. The nonionic compound **2** was chosen to avoid the effect of electrostatic interaction with the electrodes and the polyionic, bilayer films.

The permeation of **2** through the $1^{\oplus}/PSS^{\ominus}$ film was very slow in the absence of an electric field, irrespective of both the chain length of the spacer and the alkyl end group of $1^{\oplus}$. When a potential of 4 V (250 μA) was applied between two electrodes with the field gradient parallel to the membrane (method A), however, the permeability was immediately increased by a factor of 5.0–10; it reverted to the original low value ($P=(1.8\text{–}2.2)\times10^{-9}$ cm^2 s^{-1}) when the potential was turned off, even after 5–10 min, irrespective

[*] Dr. Y. Okahata, S. Fujita, N. Iizuka
Department of Polymer Chemistry, Tokyo Institute of Technology, Ookayama, Meguro-ku, Tokyo 152 (Japan)

[**] Permeability-Controllable Membranes, Part 6. We thank Prof. *M. Shimomura*, Tokyo University of Agriculture and Technology, for helpful discussions.—Part 5: Y. Okahata, K. Ariga, O. Shimizu, *Langmuir*, in press.

Table 1. Permeation rates (P) of the water-soluble dye **2** across bilayer-immobilized films upon application of an electric field (4 V between two Pt electrodes) at 50 °C.

Film	P [10^{-9} cm^2 s^{-1}]					
	Method A			Method B		
	P_0 [a]	P	$\frac{P}{P_0}$	P_0 [a]	P	$\frac{P}{P_0}$
1a$^{\oplus}$/PSS$^{\ominus}$	2.0	10	5.0	2.0	3.5	1.8
1b$^{\oplus}$/PSS$^{\ominus}$	1.8	11	6.1	1.8	2.2	1.4
1c$^{\oplus}$/PSS$^{\ominus}$	1.6	16	10	1.6	2.1	1.3
$2C_{18}\overset{\oplus}{N}2C_1$/PSS$^{\ominus}$	12	12	1.0	12	120	10

[a] P_0 = permeation rate in the absence of an electric field.

of the chain length of the spacer and the alkyl end groups. The permeability change occurred within 30 s after application of the electric field, and there was no induction period due to swelling of the membrane. This permeability change could be observed at various temperatures (between 10 and 60 °C), irrespective of the phase-transition temperature of the bilayers, and could be reproduced repeatedly without damaging the films. The increase in permeability was observed only above 1.5 V (50 μA) and increased linearly with increasing potential in the range 1.5–8.0 V (50–500 μA).

When a potential of 4 V was applied across the membrane (method B), the permeability of the **1**$^{\oplus}$/PSS$^{\ominus}$ films was only slightly increased by a factor of 1.3–1.8. For films prepared from dimethyldioctadecylammonium ($2C_{18}N^{\oplus}2C_1$) amphiphile and PSS$^{\ominus}$, the permeability is largely enhanced (10 times) when the electric field is applied across the membrane (method B).[3a] In the latter case, the film acts as a capacitor because of its poor conductivity; the electric transmembrane potential can produce transient pores in the fluid bilayers by electrically induced "breakdown," which results in permeability enhancement. In contrast, the **1**$^{\oplus}$/PSS$^{\ominus}$ films contain highly conductive chromophores in the bilayers, so that a high transmembrane potential cannot form and no "breakdown" occurs.

When a potential is applied parallel to the **1**$^{\oplus}$/PSS$^{\ominus}$ films, the orientation of the azobenzene chromophore in the bilayers presumably changes, and the permeability of the resulting disordered bilayers increases. The orientation of mesogenic azobenzene chromophores in bilayers of **1**$^{\oplus}$ is well known to be sensitive to temperature changes; moreover, the UV/VIS spectra of the chromophores change upon phase transition of the bilayers.[5] The absorption spectra of the **1**$^{\oplus}$/PSS$^{\ominus}$ films, however, do not change, irrespective of whether the electric field is parallel or perpendicular to the film plane. The permeability of $2C_{18}N^{\oplus}2C_1$/PSS$^{\ominus}$ films does not change when the electric field is applied parallel to the membrane because the poorly conductive, "dialkyl" bilayers are not oriented by the electric field. Thus, the permeability of the bilayer-immobilized film containing the conductive, liquid-crystalline chromophores changes when the electric field is applied parallel to the membrane; on the contrary, the permeability of the film from the poorly conductive, dialkyl bilayers changes when the electric field is applied perpendicular to the membrane.

The fluid bilayer structure is very important for the electrically controlled change in permeability, because the change is not observed when rigid, polymeric liquid crystals such as poly(benzyl glutamate) are employed. The bilayers of **1**$^{\oplus}$ are immobilized at the hydrophilic head groups by contact with the polyanions, but still have the fluid bilayer properties. These artificial membranes, whose permeability is controllable by application of an electric field, may provide a new tool to study transport mechanisms in biological membranes.

Received: February 17, 1986;
revised: Apirl 15, 1986 [Z 1671 IE]
German version: *Angew. Chem. 98* (1986) 723

CAS Registry numbers:
1a$^{\oplus}$/PSS$^{\ominus}$, 103368-69-0; **1b**$^{\oplus}$/PSS$^{\ominus}$, 103368-71-4; **1c**/PSS$^{\ominus}$, 103368-73-6; **2**, 103368-74-7; $2C_{18}N2C_1^{\oplus}$/PSS$^{\ominus}$, 99742-69-5.

[1] Y. Okahata, *Acc. Chem. Res. 19* (1986) 57; T. Kunitake, A. Tsuge, N. Nakashima, *Chem. Lett. 1984*, 1783; T. Kajiyama, A. Kumano, M. Takayanagi, T. Kunitake, Y. Okahata, *Ber. Bunsenges. Phys. Chem. 88* (1984) 1216.

[2] Y. Okahata, S. Hachiya, T. Seki, *J. Chem. Soc. Chem. Commun. 1985*, 1377; Y. Okahata, S. Hachiya, K. Ariga, T. Seki, *J. Am. Chem. Soc. 108* (1986) 2863.

[3] a) Y. Okahata, K. Taguchi, T. Seki, *J. Chem. Soc. Chem. Commun. 1985*, 1122; b) Y. Okahata, G. En-na, K. Taguchi, T. Seki, *J. Am. Chem. Soc. 107* (1985) 5300.

[4] T. Kunitake, Y. Okahata, M. Shimomura, S. Yasunami, K. Takarabe, *J. Am. Chem. Soc. 103* (1981) 5401; M. Shimomura, R. Ando, T. Kunitake, *Ber. Bunsenges. Phys. Chem. 87* (1983) 1134.

[5] T. Kunitake, S. Shimomura, T. Kajiyama, A. Harada, K. Okuyama, M. Takayanagi, *Thin Solid Films 121* (1984) 89.

[6] Y. Okahata, N. Iizuka, G. Nakamura, T. Seki, *J. Chem. Soc. Perkin Trans. 2 1985*, 1591.

E_3Te_3Hal, Mixed Valency Tellurohalides of Gallium and Indium with One-Dimensional Structural Units**

By *Sabine Paashaus* and *Rüdiger Kniep**

The ternary systems E-Te-Hal (E = Ga, In; Hal = Cl, Br, I) contain the phases ETeHal, having incongruent melting behavior, on the E_2Te_3–$EHal_3$ sections.[1] Along the sections from these ternary phases to the binary chalcogenides ETe[2] we have been able to identify thermodynamically stable, mixed valency compounds of the formula E_3Te_3Hal. The following compounds have so far been obtained in pure form: Ga_3Te_3Cl (m.p. = 718 °C, congruent), Ga_3Te_3Br (m.p. = 733 °C, congruent), and Ga_3Te_3I (m.p. = 692 °C, congruent) by crystallization from the melt according to the Bridgman method and In_3Te_3Br (m.p. = 381 °C, incongruent) and In_3Te_3I (m.p. = 394 °C, incongruent) by annealing of stoichiometric mixtures at 240 °C. The intense red crystals have high reflecting power and an acicular habit and are very easily cleaved along the fibers.

The first crystal structure analysis was carried out on $GaTe_3I$.[3] Figure 1 shows the macromolecular elements of the structure, in which $GaTe_{3/3}I$ tetrahedra and $Ga_2Te_{6/3}$ structural units (staggered conformation) are linked. The shortest Ga–Ga distances in the central six-membered rings (2.454(2) Å) are comparable to the corresponding bond lengths in Ga_2I_3 ($Ga^{I}_2Ga^{II}_2I_6$; 2.388(5) Å[4]) and GaTe (2.434 Å[2]), so that the oxidation state +2 has to be assumed for these Ga atoms; on the other hand, for the iodine-bonded Ga atoms (Ga-I: 2.536(1) Å) the oxidation

[*] Prof. Dr. R. Kniep, Dipl.-Chem. S. Paashaus
Institut für Anorganische Chemie und Strukturchemie der Universität
Universitätsstrasse 1, D-4000 Düsseldorf (FRG)

[**] This work was supported by the Deutsche Forschungsgemeinschaft and the Fonds der Chemischen Industrie.

state is +3. Thus, Ga_3Te_3I is the first mixed valency compound that contains an element of the third main group with the oxidation states +2 *and* +3. The macromolecular connection corresponds to the following structural formula:

$$^{1}_{\infty}\{(Te_{3/3}(Ga^{II})_2Te_{3/3})(Te_{3/3}Ga^{III}I)\}_2$$

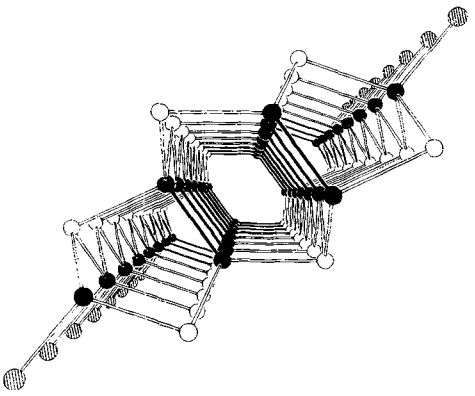


Fig. 1. View along [001] in the one-dimensional structural element of Ga_3Te_3I: Ga = ●, I = ⊘, Te = ○; each tellurium atom forms a trigonal pyramid with three gallium atoms (bond lengths Ga-Te: 2.633(1) to 2.693(5) Å).

In the structural arrangement, the strands that are extended parallel in the [001] direction are approximately hexagonally close-packed with respect to their central axes. The successive macromolecules are each translationally equivalent in the [100] direction. The shortest intermolecular distances (3.863(5) Å) are found between the terminal iodine atoms and between those tellurium atoms that are involved in the tetrahedral coordination of the Ga^{III} centers.

Received: March 10, 1986;
revised: May 6, 1986 [Z 1696 IE]
German version: *Angew. Chem. 98* (1986) 725

[1] InTeHal: R. Kniep, A. Wilms, H.-J. Beister, K. Syassen, *Z. Naturforsch. B36* (1981) 1520; GaTeHal: R. Kniep, A. Wilms, H.-J. Beister, *Mater. Res. Bull. 18* (1983) 615.

[2] InTe: J. H. C. Hogg, H. H. Sutherland, *Acta Crystallogr. Sect. B32* (1976) 2689; GaTe: M. Julien-Pouzol, S. Jaulmes, M. Guittard, F. Alpini, *ibid. B35* (1979) 2848.

[3] Crystallographic data of Ga_3Te_3I: 1408 (1462) reflections; $R = 4.8\%$; $Pna2_1$; $a = 11.168(4)$, $b = 19.529(10)$, $c = 4.102(2)$ Å; $Z = 3$; $\rho_{calcd} = 4.00$ g/cm³. Further details of the crystal structure investigation may be obtained from the Fachinformationszentrum Energie, Physik, Mathematik GmbH, D-7514 Eggenstein-Leopoldshafen 2 (FRG), on quoting the depository number CSD-52010, the names of the authors, and the journal citation.

[4] G. Gerlach, W. Hönle, A. Simon, *Z. Anorg. Allg. Chem. 486* (1982) 7.

Nature of Ni and Cu Species in Reduced Bimetallic Ni–Cu/Al_2O_3 Catalysts

By *Gopinathan Sankar* and *C. N. Ramachandra Rao**

It is well known that $Ni^{2\oplus}$ ions in calcined Ni/γ-Al_2O_3 catalysts are in a spinel-like phase, occupying both tetrahedral and octahedral sites,[1-3] and are not reduced on treatment with H_2 even at high temperatures (770 K). In calcined Cu/γ-Al_2O_3 catalysts, copper is similarly present in a spinel-like phase,[1,2,4] CuO segregating out at high copper loadings;[5] in this catalyst, however, the $Cu^{2\oplus}$ ions are reducible on treatment with H_2. We considered it worthwhile investigating the nature of species in reduced samples of bimetallic Ni–Cu/γ-Al_2O_3, which are used as catalysts for hydrogenation and other reactions. It has been reported that the presence of copper favors the formation of Ni^0 in reduced samples.[6] Presence of nickel similarly seems to promote the reduction of supported copper. The actual nature of the nickel and copper species in reduced bimetallic catalysts has not been described hitherto except for the identification of the Ni^0 species in Ni23–Cu77/γ-Al_2O_3 samples by *Ertl* et al.[1]

We have investigated Ni–Cu/γ-Al_2O_3 catalysts over the entire composition range by means of X-ray photoelectron spectroscopy (XPS) and Auger electron spectroscopy (AES).[7] The total metal loading in the catalysts studied was 5 wt-%; samples with Cu to Ni ratios 75:25, 50:50, 25:75, were studied along with the catalysts containing only Cu and Ni. The catalyst samples were first calcined at 870 K for 8 h in air. The spectra of the catalysts were recorded after reducing them in situ in the sample preparation chamber of the spectrometer (720 K, 6 h, 300-torr hydrogen pressure). The 2p level of Al_2O_3 (74.0 eV) and the $4f_{7/2}$ level of Au (83.6 eV) were used as references for the XPS binding energies.

Calcined Ni–Cu/γ-Al_2O_3 catalysts show the presence of $Ni^{2\oplus}$ in the form of $NiAl_2O_4$ with a Ni($2p_{3/2}$) binding energy of ~856.6 eV. The Cu($2p_{3/2}$) binding energy in the calcined samples was close to that of $CuAl_2O_4$. On reduction, XPS in the core level region clearly reveals the nature of the nickel species. The Ni($2p_{3/2}$) spectra show the presence of both Ni^0 and $Ni^{2\oplus}$ with binding energies of 853.2 eV and 856.3 eV respectively, in samples with high copper content (Fig. 1). The relative concentration of Ni^0 increases with increasing copper content, the Ni^0 being totally absent in reduced Ni/γ-Al_2O_3. Variation of the rela-

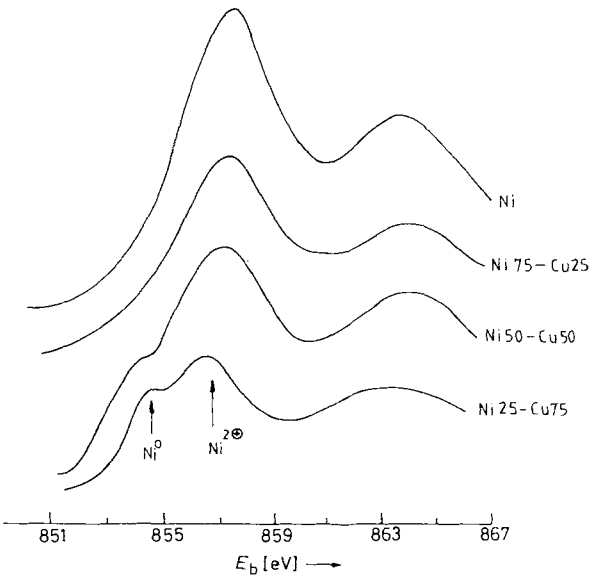


Fig. 1. Ni($2p_{3/2}$) spectra (ESCA) of reduced Ni–Cu/γ-Al_2O_3 catalysts; E_b = binding energy.

[*] Prof. Dr. C. N. R. Rao, G. Sankar
Solid State and Structural Chemistry Unit
Indian Institute of Science
Bangalore 560 012 (India)

 © VCH Verlagsgesellschaft mbH, D-6940 Weinheim, 1986 0570-0833/86/0808-0753 $ 02.50/0

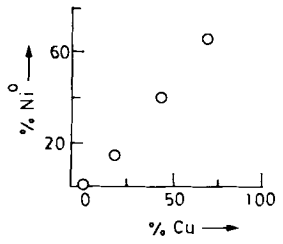


Fig. 2. Variation of the relative concentration of Ni^0 with copper content.

tive concentration of Ni^0 with copper content is shown in Figure 2. In contrast, the $Cu(2p_{3/2})$ spectra of the reduced $Cu-Ni/\gamma-Al_2O_3$ catalysts show little change with composition. From the XPS data it cannot be decided whether $Cu^{\oplus}$ is formed in addition to Cu^0, as noted earlier by *Ertl* et al.[1] Formation of $Cu^{\oplus}$ has been suggested in the literature[8] in the case of reduced $Cu/\gamma-Al_2O_3$ catalysts. We have employed Auger electron spectroscopy to examine the presence of $Cu^{\oplus}$ and Cu^0 in reduced $Ni-Cu/\gamma-Al_2O_3$ catalysts. The spectra do indeed show the presence of both species (Fig. 3). The relative proportion of $Cu^{\oplus}$ increases with the increasing copper content; accordingly, the AES spectrum of $Cu25-Ni75/\gamma-Al_2O_3$ does not show the presence of $Cu^{\oplus}$.

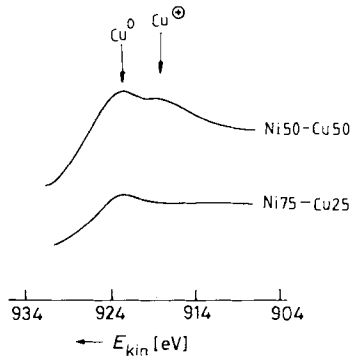


Fig. 3. $Cu(L_3M_{4,5}M_{4,5})$ Auger electron spectra of reduced $Ni-Cu/\gamma-Al_2O_3$ catalysts; E_{kin} = kinetic energy of the electrons.

The present study not only establishes the presence of Ni^0, $Ni^{2\oplus}$, Cu^0 and $Cu^{\oplus}$ in the reduced bimetallic $Ni-Cu/\gamma-Al_2O_3$ catalysts, but also shows how the relative proportion of Ni^0 increases with increasing copper content just as that of Cu^0 increases with increasing nickel content. We are presently carrying out EXAFS (*E*xtended *X*-ray *A*bsorption *F*ine *S*tructure) studies on these bimetallic catalysts.

Received: March 24, 1986;
supplemented: June 3, 1986 [Z 1710 IE]
German version: *Angew. Chem. 98* (1986) 736

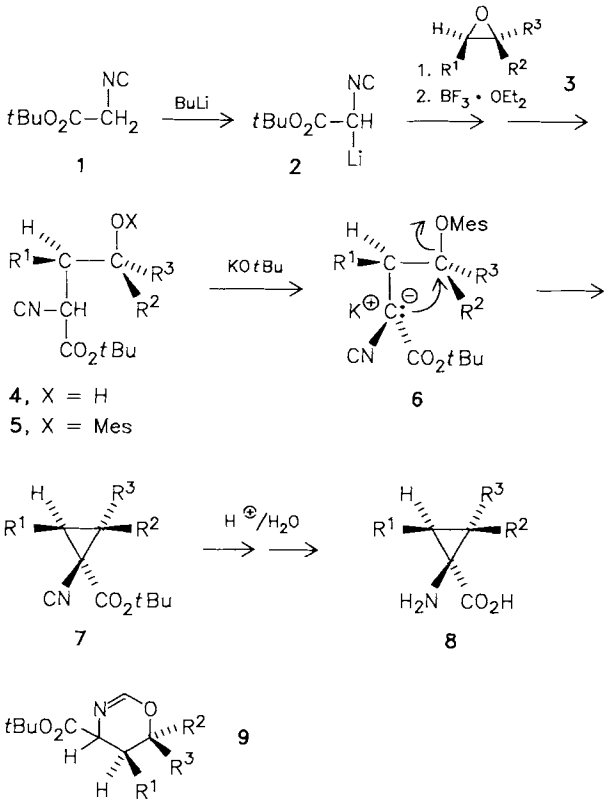
CAS Registry numbers:
Ni, 7440-02-0; Cu, 7440-50-8.

[1] G. Ertl, R. Hierl, H. Knözinger, N. Thiele, H. P. Urbach, *Appl. Surf. Sci. 5* (1980) 49.
[2] R. Hierl, H. Knözinger, H. P. Urbach, *J. Catal. 69* (1981) 475.
[3] M. Lo Jacono, M. Schiavello, A. Cimino, *J. Phys. Chem. 75* (1971) 1044.
[4] R. M. Friedman, J. J. Freeman, F. W. Lytle, *J. Catal. 55* (1978) 10.
[5] M. Lo Jacono, M. Schiavello in B. Delmon, P. A. Jacobs, G. Ponchelet (Eds.): *Preparation of Catalysts*, Elsevier, Amsterdam 1976, p. 473.
[6] A. Roman, B. Delmon, *J. Catal. 30* (1973) 333.
[7] ESCA-3 Mark II Spectrometer, VG Scientific.
[8] M. Lo Jacono, A. Cimino, M. Inversi, J. Catal. 76 (1982) 320.

Simple Synthesis of 1-Amino-1-cyclopropanecarboxylic Acids from *tert*-Butyl Isocyanoacetate and Epoxides; Synthesis of Alkyl 5,6-Dihydro-4*H*-1,3-oxazine-4-carboxylates

By *Ulrich Schöllkopf*,* *Bernd Hupfeld* and *Reinhold Gull*

1-Amino-1-cyclopropanecarboxylic acids **8** are currently attracting attention, mainly because of their proven or potential biological activity.[1] Although methods for the synthesis of this class of compounds have already been described in the literature,[1,2] a relatively simple, inexpensive and productive synthetic method is still lacking. We describe here a synthesis starting from *tert*-butyl isocyanoacetate **1** and from (inexpensive) epoxides **3**.[3] The lithiated ester **2** reacts with the epoxides **3** in the presence of boron trifluoride ether[4] to give the *tert*-butyl 4-hydroxy-2-isocyanoalkanoates **4**. The substitution takes place with inversion of configuration at the less hindered carbon atom of the epoxide. The compounds **4** are then mesylated to compounds **5**. The mesylates readily undergo base-induced cyclization to the *tert*-butyl 1-isocyano-1-cyclopropanecarboxylates **7**. Owing to the considerably large difference in size between the isocyano group and the *tert*-



3–9	R^1	R^2	R^3	7, 8 *trans*:*cis* [a,b]	Yields [%] [c] 4	5	7	8	9
a	H	H	H	-	54	80	63	60	93
b	H	CH_3	H	6.5:1	66	77	66	62	89
c	H	C_2H_5	H	6.5:1	76	85	33	62	89
d	CH_3	H	CH_3	-	72	84	66	69	91
e	$-(CH_2)_4-$		H	>95:5	80	90	67	68	89

[a] Referred to CO_2tBu and R^1, R^2. [b] Racemates; one enantiomer shown. [c] Yields referred to **1**, **4**, **5**, **7** and **4**.

[*] Prof. Dr. U. Schöllkopf, Dipl.-Chem. B. Hupfeld, Dr. R. Gull
Institut für Organische Chemie der Universität
Tammannstrasse 2, D-3400 Göttingen (FRG)

butoxycarbonyl group, this cyclization via the anion **6** proceeds highly diastereoselectively. Thus, e.g., with cyclohexene oxide **3e** as starting compound, the ester **7e** with *endo* isocyano groups is formed almost exclusively. The conversion of the isocyano-*tert*-butyl esters **7** into the amino acids **8** was accomplished in good yields by heating **7** with concentrated hydrochloric acid. Herein lies one advantage of this method, for the hydrolysis of 1-amino-1-cyclopropanecarboxylates, usually the last step of most known methods for the synthesis of **8**,[1,2] is often problematic because of the ease with which the cyclopropane ring can be opened.

The *tert*-butyl 5,6-dihydro-4*H*-1,3-oxazine-4-carboxylates **9**, which are of interest as starting materials for the total synthesis of structural variants of the cephalosporins, are obtainable from **4** by heating with copper(I) oxide in toluene. This variant of the synthesis can be accomplished equally as well with methyl isocyanoacetate instead of **1**, whereas for the synthesis of **7**, the *tert*-butyl ester **1** is more advantageous.—As example we describe here the synthesis of *endo*-7-aminobicyclo[4.1.0]heptane-7-carboxylic acid **8e**.

Experimental

4e: *n*-Butyllithium (10.5 mmol; 6.6 mL of a 1.6 N solution in hexane) was added dropwise at −78 °C to a solution of **1**[5] (1.41 g, 10.0 mmol) in tetrahydrofuran (THF) (20 mL). The mixture was stirred for 10 min at this temperature then treated, first with 1.03 g (10.5 mmol) of **3e** and secondly dropwise with 1.3 mL (10.5 mmol) of boron trifluoride-ether. After a further 10 minutes' stirring, phosphate buffer solution (20 mL, pH 7) was added and the mixture was allowed to warm to room temperature. The solvent was removed in vacuo, and the residue shaken with water (20 mL) and ether (40 mL). The layers were separated and the water layer extracted with ether (2 × 40 mL). The combined extracts were dried over $MgSO_4$. After removal of the solvent in a vacuum the resulting **4e** was purified by Kugelrohr distillation. B.p. 90–95 °C/0.01 torr, yield 1.91 g (80%). IR (film): $\tilde{\nu}$ = 1740 (CO), 2130 (NC), 3200–3600 (OH) cm^{-1}. ^1H-NMR ($CDCl_3$): δ = 1.20–2.20 (m, cyclohexyl-H), 1.51 (s, C_4H_9), 2.40 (OH), 3.40–3.70 (m, CH and CHOH), 2.40 (d, CH−NC).

5e: Mesyl chloride (0.63 g, 5.5 mmol) was added dropwise at −10 °C to a solution of **4e** (1.25 g, 5.0 mmol) and triethylamine (7.5 mL) in anhydrous dichloromethane (20 mL). This mixture was stirred for 30 min at −5 °C, poured onto 30 mL of water/ice, and the phases separated. The organic phase was washed with 10% hydrochloric acid, then with saturated $NaHCO_3$ solution and saturated NaCl solution, and finally dried over Na_2SO_4. The solvent was removed in a vacuum and the resulting **5e** (1.47 g, 90%) used directly without purification.

7e: A solution of **5e** (0.98 g, 3.0 mmol) in THF (10 mL) was added dropwise at −78 °C to a suspension of KO*t*Bu (0.37 g, 3.3 mmol) in THF (20 mL). The mixture was stirred at this temperature for 2 h and then allowed to warm to −20 °C and treated with 20 mL of phosphate buffer (pH 7). After further warming of the mixture to room temperature, the solvent was removed in a vacuum. The residue was shaken with water (20 mL) and ether (40 mL), the phases separated, and the aqueous phase extracted twice with ether (2 × 40 mL). The ether solution was dried over $MgSO_4$, the solvent removed in a vacuum and the crude **7e** purified by Kugelrohr distillation. B.p. 75–80 °C/0.01 torr, yield 0.44 g (67%). **7e** solidifies on standing; m.p. 62–63 °C. IR (KBr): $\tilde{\nu}$ = 1730 (CO), 2120 cm^{-1} (NC). ^1H-NMR ($CDCl_3$): δ = 1.20–2.10 (m, cyclohexyl-H), 1.49 (s, C_4H_9).

8e: **7e** (0.44 g, 2.0 mmol) was added to conc. hydrochloric acid (20 mL) at 5 °C. The mixture was then stirred and heated under reflux for 2 h. The temperature was allowed to reach 50 °C and the hydrochloric acid was removed in a vaccum. The **8e**-hydrochloride remaining behind was dried at 60 °C/10 torr, dissolved in 10 mL of anhydrous ethanol, and heated under reflux with 2 mL of epoxypropane for 3h. Analytically pure **8e** precipitated, and was recovered by suction filtration. M.p. 185 °C (decomp.), yield 0.21 g (68%). IR (KBr): $\tilde{\nu}$ = 1580, 1690 (C=O), 2800–3200 cm^{-1} (NH_3). ^1H-NMR (D_2O): δ = 0.90–1.51 and 1.50–1.70 (m, cyclohexyl-H), 1.72–2.10 (m, H-1 and H-6).

Received: March 25, 1986 [Z 1715 IE]
German version: *Angew. Chem. 98* (1986) 755

CAS Registry numbers:
1, 2769-72-4; **3a**, 75-21-8; **3b**, 75-56-9; **3c**, 106-88-7; **3d**, 6189-41-9; **3e**, 286-20-4; **4a**, 103348-80-7; **4b**, 103348-81-8; **4c**, 103366-75-2; **4d**, 103348-82-9; **4e**, 103366-60-5; **5a**, 103348-83-0; **5b**, 103348-84-1; **5c**, 103366-61-6; **5d**, 103348-85-2; **5e**, 103366-62-7; **7a**, 103348-86-3; **7b**, 103348-87-4; **7c**, 103366-63-8; **7d**, 103348-88-5; **7e**, 103348-89-6; **8a**, 22059-21-8; **8b**, 93621-77-3; **8c**, 65878-54-8; **8d**, 103348-90-9; **8e**, 103348-91-0; **9a**, 103348-92-1; **9b**, 103348-93-2; **9c**, 103348-94-3; **9d**, 103348-95-4; **9e**, 103348-96-5.

[1] a) K. Shiraishi, K. Konoma, H. Sato, A. Ichihara, K. Sakamura, N. Nishiyama, R. Sakai, *Agric. Biol. Chem. 43* (1979) 1753; D. H. Rich, J. P. Tam, *Synthesis 1978*, 46; I. Arenal, M. Bernabé, E. F. Alvarez, A. M. Gibello, *An. Quim. C79* (1983) 65; C. Walsh, R. A. Pascal, M. Johnston, R. Raines, D. Dikskit, A. Krantz, M. Homma, *Biochemistry 20* (1981) 7509; M. C. Pirrung, *J. Am. Chem. Soc. 105* (1983) 7207; b) M. C. Pirrung, G. M. McGeehan, *Angew. Chem. 97* (1985) 1074; *Angew. Chem. Int. Ed. Engl. 24* (1985) 1044.

[2] U. Schöllkopf, R. Harms, D. Hoppe, *Justus Liebigs Ann. Chem. 1973*, 611; I. Arenal, M. Bernabé, E. Fernandez-Alvarez, M. L. Izquierdo, S. Penades, *J. Heterocycl. Chem. 20* (1983) 607; S. W. King, J. M. Riordan, E. M. Holt, C. H. Stammer, *J. Org. Chem. 47* (1982) 3270; H. Kimura, C. H. Stammer, *ibid 48* (1983) 2440; B. Gallenkamp, R. Schröder, K. Luerssen, Eur. Pat.-Anm. 30287 (1979); *Chem. Abstr. 95* (1981) 150043s; J. E. Baldwin, R. M. Adlington, B. J. Rawlings, *Tetrahedron Lett. 26* (1985) 481; M. L. Izquierdo, I. Arenal, M. Bernabé, *Tetrahedron 40* (1985) 215; U. Schöllkopf, M. Hauptreif, J. Dippel, M. Niger, E. Egert, *Angew. Chem. 98* (1986) 187; *Angew. Chem. Int. Ed. Engl. 25* (1986) 192.

[3] After completion of our studies, *M. C. Pirrung* and *G. M. McGeehan* reported in [1b] in a footnote (*J. Org. Chem.*, in press) on an analogous synthesis of 1-amino-2-alkylcyclopropanecarboxylic acids from 1,2-dibromoalkanes and methyl isocyanoacetate. However, our method has the advantage that epoxides (e.g. cycloalkene oxides) are usually more readily available than vicinal dibromides. Moreover, secondary vicinal dibromoalkanes or -cycloalkanes could react predominantly by E_2 with deprotonated isocyanoacetates.

[4] In the absence of BF_3-ether, **2** does not react with **3** (cf. U. Schöllkopf, R. Jentsch, K. Madawinata, *Justus Liebigs Ann. Chem. 1976*, 2105).

[5] Prepared from *tert*-butyl *N*-formylglycinate (I. Ugi, W. Betz, U. Fetzer, K. Offermann, *Chem. Ber. 94* (1961) 2814) by elimination of water according to the method of R. Obrecht, R. Hermann, I. Ugi, *Synthesis 1985*, 400.

Transition Metal-Induced CO-Insertion in the P=P Bond of Diphosphenes with Formation of Diphosphinomethanone Derivatives**

By *Lothar Weber,* Klaus Reizig,* and *Roland Boese*

SbSb multiple bonds in distibene transition metal complexes are cleaved by Lewis bases such as PPh_3 with formation of stibanediyl complexes.[2] A comparable reaction has so far not been observed in the case of the homologous diarsene and diphosphene complexes.[3] In contrast, the reverse process—the formation of a diphosphene complex in the thermolysis of a phosphanediyl complex—has already been described.[4]

We describe here the first transition metal-induced carbonylation of a stable diphosphene **1** with cleavage of the P=P bond. *P*-metalated diphosphinomethanones ("diphospho-ureas") **3** are obtained.

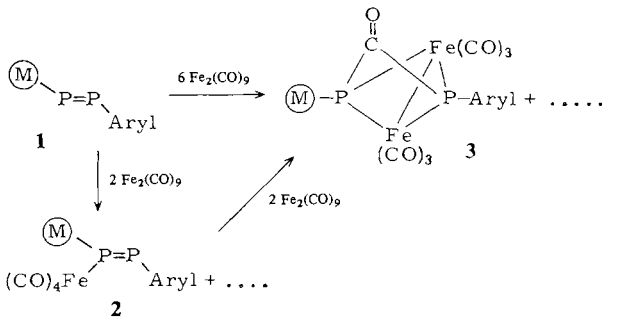
The iron-substituted diphosphene **1a**[1] reacts with $Fe_2(CO)_9$ in the molar ratio 1:6 in toluene at 20 °C to give the yellow complex **3a** in 45% yield together with small amounts of a brown byproduct identified as **2a**.

2a is formed as main product in the reaction of **1a** with $Fe_2(CO)_9$ in the molar ratio 1:2, and is to be regarded as the first intermediate in the conversion of **1a** → **3a**.[6] Logically, **2a** is converted by excess $Fe_2(CO)_9$ into **3a**. The ru-

[*] Prof. Dr. L. Weber, Dipl.-Chem. K. Rezig, Dr. R. Boese
Institut für Anorganische Chemie der Universität
Universitätsstr. 5-7, D-4300 Essen 1 (FRG)

[**] Transition Metal-Substituted Diphosphenes. Part 2. This work was supported by the Fonds der Chemischen Industrie, the Deutsche Forschungsgemeinschaft, and Degussa AG, Hanau.—Part 1: [1].

thenium derivatives **2b** and **3b** can be prepared analogously.



Aryl = 2,4,6-tBu$_3$C$_6$H$_2$; **a**, Ⓜ = C$_5$Me$_5$(CO)$_2$Fe; **b**, Ⓜ = C$_5$Me$_5$(CO)$_2$Ru

The P–CO–P functions of **3a** and **3b** each give rise to a medium strength band at 1692 cm^{-1} in the IR spectrum cyclopentane); in the ^{13}C-NMR spectrum they give rise to double doublets at $\delta = 209.82$ and $\delta = 208.60$, respectively. The two nonequivalent phosphorus atoms are recorded in the ^{31}P-NMR spectrum as doublets at $\delta_{P_1} = 234.3$, $\delta_{P_2} = 155.1$ and $\delta_{P_1} = 202.7$, $\delta_{P_2} = 157.5$, respectively (see experimental).

The X-ray structure analysis underscores the diphosphinomethanone character of **3a** (Fig. 1).[5] The two phosphorus atoms no longer coupled directly to each other (d P(1)...P(2) 2.605 Å) are bridged by a carbonyl group with P–C single bonds. The C=O bond length in the bridge is 1.187(7) Å; the P1-C7-P2 angle at the sp^2-hybridized carbon atom with a value of 88.3(2)° is strongly compressed. The Fe–P bonds, as also the Fe1–Fe2 bond, may be interpreted as single bonds.[6]

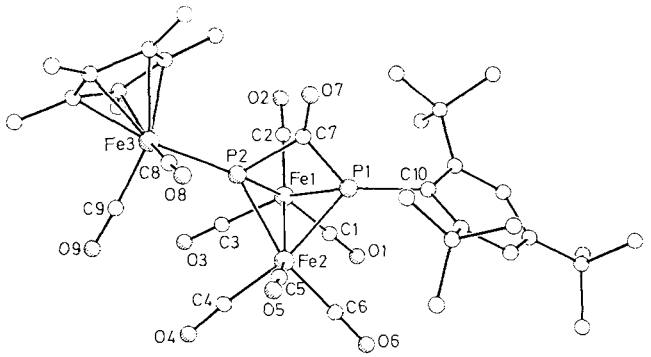


Fig. 1. Molecular structure of **3a**. Selected bond lengths [Å] and angles [°]: Fe1-Fe2 2.568(1), Fe1-P1 2.272(2), Fe1-P2 2.278(2), Fe2-P1 2.272(1), Fe2-P2 2.288(1), Fe3-P2 2.249(2), P1-C7 1.855(5), P2-C7 1.884(5), C7-O7 1.187(7); P1-C7-P2 88.3(2), P1-C7-O7 137.7(4), P2-C7-O7 133.9(4), Fe1-P1-Fe2 68.8(1), Fe1-P2-Fe2 68.4(1), P1-Fe1-P2 69.9(1), P1-Fe2-P2 69.7(1).

The complexes **2** are of interest as primary products in the formation of **3** from **1** and $Fe_2(CO)_9$. Their IR spectra show only the CO stretching vibrations of terminal ligands. The downfield shift of the ^{31}P-NMR signals ($\delta = 495.9$–546.3) and the coupling constants J of the AB spin systems (**2a**: 581.9 Hz; **2b**: 571.6 Hz) are typical for unsymmetrically substituted diphosphenes with free P=P bonding, thus suggesting coordination of the Fe(CO)$_4$ moiety to the lone pair of P1 in both compounds. This is confirmed by the X-ray structure analysis of **2a** (Fig. 2).[7] The P1-P2 distance of 2.032 Å is practically the same as that in **1a** and reflects the double bond character. The angle Fe1-P1-P2 is compressed to 106.0(2)° (in **1a**: 109.9(4)°) by the coordination of the Fe(CO)$_4$ group to P1 (P1 forms almost the apex of a trigonal bipyramid). The P1-P2-C7 angle (112.2(4)°) in **2a**, however, is considerably wider than that in **1a** (103.5(8)°).

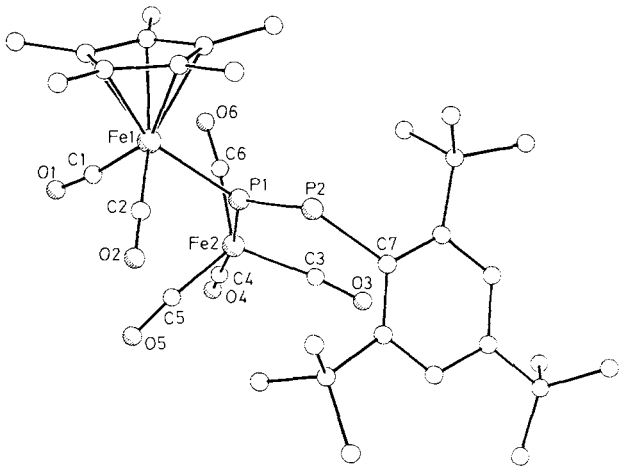
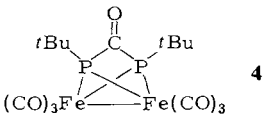


Fig. 2. Molecular structure of **2a**. Selected bond lengths [Å] and angles [°]: Fe1-P1 2.302(4), Fe2-P1 2.268(4), P1-P2 2.032(5), P2-C7 1.862(3); Fe1-P1-Fe2 122.8(2), Fe1-P1-P2 106.0(2), Fe2-P1-P2 130.3(2), P1-P2-C7 112.2(4).

The disphosphinomethanones have hitherto been the subject of very few studies. Recently, aside from the unstable $(Ph_2P)_2CO$,[8] the stable cyclic $(t\text{BuP})_4C{=}O$ was described.[9] Also only recently, complexes with diphosphinomethanone ligands analogous to **3** were surprisingly obtained upon reaction of Cl_2PNR_2 with $Na_2Fe(CO)_4$ ($NR_2 = N(i\text{Pr})_2$, $N(c\text{-}C_6H_{11})_2$, 2,2,6,6-tetramethylpiperidino).[10] Usually, reactions of Cl_2PR with carbonylmetalates lead to diphosphene- and/or phosphanediyl-complexes.[11] *Vahrenkamp* et al. synthesized the complex **4** some time ago from the corresponding diphosphene complex by carbonylation at 80 °C.[12]



4

Experimental

NMR spectra in C_6D_6 at 22 °C; ^{1}H-NMR: 200 MHz; IR: in cyclopentane.

2a: A mixture of **1a** (0.86 g, 1.56 mmol) and $Fe_2(CO)_9$ (1.01 g, 3.12 mmol) in toluene (80 mL) was stirred for 1 h at 45 °C. All volatile components were removed in a vacuum and the dark-brown residue was taken up in 80 mL of cyclopentane and filtered. The filtrate was evaporated down to 20 mL and stored for ca. 12 h at −28 °C. Dark-brown **2a** precipitated; this was isolated, and recrystallized twice from cyclopentane at −28 °C. Yield 0.62 g (55%), m.p. 150 °C (decomp.).—^{1}H-NMR: $\delta = 1.40$ (s, 9H, p-tBu), 1.45 (s, 15H, $C_5(CH_3)_5$), 1.73 (s, 18H, o-tBu), 7.65 (s, 2H, aryl).—^{31}P{^{1}H}-NMR: AB signal: $\delta_B = 546.26$ (P1); $\delta_A = 514.56$ (P2), $J_{AB} = 581.9$ Hz.—IR (cm^{-1}): $\tilde{\nu} = 2048$ s, 2025 s, 2018 s, 1980 s, 1973 m, 1961 m, 1948 m, 1942 m, 1927 m [$\tilde{\nu}$(CO)].—CI-MS (Varian MAT 312): m/z 723 ($M^+ + H$).

2b: 0.46 g (24%) of red, microcrystalline **2b**, m.p. 155 °C (decomp.) was obtained analogously from 1.52 g (2.53 mmol) of **1b** and 1.64 g (5.06 mmol) of $Fe_2(CO)_9$.—^{1}H-NMR: $\delta = 1.39$ (s, 9H, p-tBu), 1.58 (s, 15H, $C_5(CH_3)_5$), 1.76

(s, 18H, *o*-*t*Bu), 7.65 (s, 2H, aryl).—^{31}P-{^{1}H}-NMR: AB signal: $\delta_B = 503.86$ (P1), $\delta_A = 495.93$ (P2), $J_{AB} = 571.6$ Hz.—IR (cm^{-1}): $\tilde{\nu} = 2052$ vs, 2036 s, 1990 s, 1973 m, 1950 m, 1928 m, [$\tilde{\nu}$(CO)].—CI-MS: *m/z* 768 ($M^+ + H$).

3a: A mixture of **2a** (1.54 g, 2.13 mmol) and $Fe_2(CO)_9$ (1.50 g, 4.09 mmol) in toluene (50 mL) was stirred for 96 h at 22 °C and then filtered. The filtrate was evaporated to dryness and the residue chromatographed (alumina Woelm TSC). After elution of an orange-red front with petroleum ether/toluene (95:5), yellow **3a** was eluted with toluene (yield 1.13 g, 59%), m.p. decomp. above 215 °C.—^{1}H-NMR: $\delta = 1.18$ (s, 9H, *p*-*t*Bu), 1.44 (s, 15H, $C_5(CH_3)_5$), 1.72 (s, 18H, *o*-*t*Bu), 7.35 (d, 2H, $^4J_{PH} = 2.5$ Hz, aryl).—^{13}C{^{1}H}-NMR: 209.82 (dd, $^1J_{(PC)} = 81.5$ and 60.2 Hz, P_2CO), 211.99 (d, $^2J_{(PC)} = 13.8$ Hz, $C_5Me_5Fe(CO)$), 214.36 (m, br, $Fe_2(CO)_6$).—^{31}P{^{1}H}-NMR: $\delta = 234.3$ (d, $^2J_{(PP)} = 66.0$ Hz, P1), 155.1 (d, $^2J_{(PP)} = 66.0$ Hz, P2).—IR (cm^{-1}): 2060 vs, 2031 vs, 2013 vs, 1995 vs, 1977 s, 1957 m, 1943 s [$\tilde{\nu}$(CO)$_{term}$], 1692 m [$\tilde{\nu}$(CO)$_{acyl}$].—CI-MS: *m/z* 863 ($M^+ + 2H$).

3b: In the same way, reaction of 1.10 g (1.25 mmol) of **2b** with 0.81 g (2.50 mmol) of $Fe_2(CO)_9$ furnished 0.36 g (32%) of yellow, finely crystalline **3b**, m.p. 220 °C (decomp.).—^{1}H-NMR: $\delta = 1.18$ (s, 9H, *p*-*t*Bu), 1.58 (d, $^4J_{(PH)} = 1.6$ Hz, 15H, $C_5(CH_3)_5$), 1.71 (s, 18H, *o*-*t*Bu), 7.35 (d, 2H, $^4J_{(PH)} = 2.5$ Hz, aryl).—^{13}C{^{1}H}-NMR: 197.97 (d, $J_{(PC)} = 11.0$ Hz, Ru(*C*O)), 208.60 (dd, $J_{(PC)} = 79.5$, 57.5 Hz, P_2CO), 214.56 (m, Fe(*C*O)).—^{31}P{^{1}H}-NMR: $\delta = 202.7$ (d, $^2J_{(PP)} = 69.6$ Hz, P1, 157.5 (d, $^2J_{(PP)} = 69.6$ Hz, P2).—IR (cm^{-1}): $\tilde{\nu} = 2063$ vs, 2040 s, 2014 vs, 1979 s, 1957 m, 1942 m [$\tilde{\nu}$(CO)$_{term}$], 1692 m, [$\tilde{\nu}$(CO)$_{acyl}$].

Received: April 3, 1986;
revised: May 9, 1986 [Z 1720 IE]
German version: *Angew. Chem. 98* (1986) 737

CAS Registry numbers:
1a, 98088-31-4; **1b**, 98088-32-5; **2a**, 103671-25-6; **2b**, 103671-27-8; **3a**, 103693-29-4; **3b**, 103671-26-7; $Fe_2(CO)_9$, 15321-51-4; Fe, 7439-89-6.

[1] L. Weber, K. Reizig, *Angew. Chem. 97* (1985) 868; *Angew. Chem. Int. Ed. Engl. 24* (1985) 865.

[2] U. Weber, G. Huttner, O. Scheidsteger, L. Zsolnai, *J. Organomet. Chem. 289* (1985) 357.

[3] H. Lang, G. Huttner, B. Sigwarth, L. Zsolnai, I. Jibril, O. Orama, *Z. Naturforsch. B41* (1986) 191.

[4] J. Borm, G. Huttner, L. Zsolnai, *Angew. Chem. 97* (1985) 1069; *Angew. Chem. Int. Ed. Engl. 24* (1985) 1069; *ibid. 95* (1983) 1083 and *22* (1983) 977.

[5] **3a**: Crystal dimensions: $0.34 \times 0.28 \times 0.16$ mm^3; space group $P2_1/c$; $a = 1255.1(4)$, $b = 1440.8(5)$, $c = 2272.3(6)$ pm, $\beta = 98.75(2)°$, $V = 4.0613(21) \times 10^9$ pm^3, $Z = 4$, $\rho_{calc} = 1.41$ $g\,cm^{-3}$; $2\theta_{max} = 50°$; $\mu(Mo_{K\alpha}$, graphite monochromator$) = 11.8$ cm^{-1}; no absorption correction, ω-scan data collection at room temperature, 7167 independent intensities, 5179 ($F_0 \geq 3.5\sigma(F)$) observed, solution of structure by direct methods (SHELXTL), structure refinement of 362 parameters with hydrogen atoms as rigid groups ($U_{iso} = 1.2$ times the respective C atom); $R = 0.061$, $R_w = 0.062$, $w^{-1} = \sigma(F_0)^2 + 0.00064\,F_0^2$; maximum residual electron density 0.67e/Å^3. Further details of the crystal structure investigation are available on request from the Fachinformationszentrum Energie, Physik, Mathematik GmbH, D-7514 Eggenstein-Leopoldshafen 2, on quoting the depository number CSD-51916, the names of the authors, and the full citation of the journal.

[6] G. Huttner, G. Mohr, B. Pritzlaff, J. von Seyerl, L. Zsolnai, *Chem. Ber. 115* (1982) 2044.

[7] **2a**: Crystal dimensions $0.32 \times 0.25 \times 0.13$ mm^3; space group $P\bar{1}$; $a = 1032.5(5)$, $b = 1268.8(9)$, $c = 1457.3(8)$, pm, $\alpha = 98.87(5)$, $\beta = 100.77(4)$, $\gamma = 98.66(5)°$, $V = 1.8212(18) \times 10^9$ pm^3, $Z = 2$, $\rho_{calc} = 1.31$ $g\,cm^{-3}$; $2\theta_{max} = 50°$; $\mu(Mo_{K\alpha}$, graphite monochromator$) = 9.2$ cm^{-1}; no absorption correction, ω-scan data collection at room temperature, 5415 independent intensities, 3492 ($F_0 \geq 7.50\sigma(F)$) observed, solution of structure by direct methods (SHEXTL), structure refinement of 424 parameters with H atoms as rigid groups ($U_{iso} = 1.2$ times the respective C atom); C18 to C20 (atoms in the *p*-*t*Bu group) disordered and isotropically refined with half the occupation factor, but disorder resolved; $R = 0.095$, $R_w = 0.100$, $w^{-1} = \sigma(F_0)^2 + 0.0004\,F_0^2$; maximum residual electron density 1.42 e/Å^3.

[8] H. J. Becher, E. Langer, *Angew. Chem. 85* (1973) 910; *Angew. Chem. Int. Ed. Engl. 12* (1973) 842.

[9] R. Appel, W. Paulen, *Chem. Ber. 116* (1983) 109.

[10] R. B. King, F.-J. Wu, N. D. Sadanani, E. M. Holt, *Inorg. Chem. 24* (1985) 4449.

[11] a) K. M. Flynn, M. M. Olmstead, P. P. Power, *J. Am. Chem. Soc. 105* (1983) 2085; b) K. M. Flynn, B. D. Murray, M. M. Olmstead, P. P. Power, *ibid. 105* (1983) 7460; c) K. M. Flynn, H. Hope, B. D. Murray, M. M. Olmstead, P. P. Power, *ibid. 105* (1983) 7750; d) M. M. Olmstead, P. P. Power, *ibid. 106* (1984) 1495; e) A. H. Cowley, J. E. Kilduff, J. G. Lasch, N. C. Norman, M. Pakulski, F. Ando, T. C. Wright, *ibid. 105* (1983) 7751; f) H. Lang, O. Orama, G. Huttner, *J. Organomet. Chem. 291* (1985) 293.

[12] R. Lal De, D. Wolters, H. Vahrenkamp, *Z. Naturforsch. B 41* (1986) 283.

$[C_6H_3(CH_3)_3][BiCl_3]$ and $[C_6(CH_3)_6][BiCl_3]_2$, Arene Complexes of Bismuth with Half-Sandwich and "Inverted" Sandwich Structures**

By *Annette Schier, Julian M. Wallis, Gerhard Müller,* and *Hubert Schmidbaur**

For a long time the coordination of neutral arenes to metal atoms appeared to be a domain of the d-block elements, where even simple valence theory models can give a plausible explanation of the nature of the interactions present[1]. For the p- and f-block elements, the few arene adducts of Sn^{II},[2] Pb^{II},[3] Sb^{III},[4], U^{III},[5a] and U^{IV}[5b] have remained rather as exceptions.

Meanwhile, with the systematic investigation of novel arene complexes of the earlier main group elements gallium, indium and thallium, it has been recognized that a large area of organometallic chemistry has lain neglected in the post-d-block elements. Even with the simplest of experimental methods, further rapid developments are possible.[6–9]

In the case of the heavier elements, theoretical considerations indicated, inter alia, that a relativistic effect probably also plays a role in the bonding.[10] A natural extension to the investigations already carried out on thallium[9] and lead[3] was to examine the ability of the element bismuth to form arene complexes. Not only the "Menshutkin complexes" of the antimony halides,[4, 11] known for more than a century, but also the results of experiments performed in the sixties would indicate such an ability; it was shown, for example, that BiX_3 compounds form arene adducts, the structures of which, however, were never elucidated.[12, 13] Indeed, simple dissolution of anhydrous $BiCl_3$ in mesitylene or in a solution of hexamethylbenzene in toluene produces homogeneous phases, from which the crystalline arene complexes **1** and **2**, respectively, can be obtained on cooling.[14]

$$BiCl_3 + 1,3,5\text{-}(CH_3)_3C_6H_3 \longrightarrow [1,3,5\text{-}(CH_3)_3C_6H_3][BiCl_3]$$

1

$$2\,BiCl_3 + (CH_3)_6C_6 \xrightarrow{\text{toluene}} [(CH_3)_6C_6][BiCl_3]_2$$

2

The crystals of **1**[15] consist of alternating, crystallographically independent sheets of $BiCl_3$ networks, which, in turn, each contain two non-equivalent bismuth atoms (Bi1, Bi3 and Bi2, Bi4). A section from one of the sheets is reproduced in Figure 1. Six $BiCl_3$ units are seen to form a ring structure. The coordination sphere of each Bi atom can be described as pseudo-octahedral, (Fig. 2): three strongly bound chlorine atoms (Cl11–Cl13), and two more loosely bound, bridging chlorine atoms (Cl13* and Cl32) occupy five of the coordination sites, while the sixth coordination site is screened by an η^6-bound mesitylene molecule. The angles between the ring normals and the metal-to-ring center vectors lie between 2.1 and 7.3°, thus confirming the

[*] Prof. Dr. H. Schmidbaur, Dr. A. Schier, Dr. J. M. Wallis, Dr. G. Müller,
Anorganisch-chemisches Institut der Technischen Universität München
Lichtenbergstrasse 4, D-8046 Garching (FRG)

[**] This work was supported by the Fonds der Chemischen Industrie and the Deutsche Forschungsgemeinschaft (DFG). We thank Ms. *B. Huber* and Mr. *J. Riede* for the X-ray crystallographic measurements. *J. M. W.* thanks the Royal Society (Great Britain) and the DFG for a post-doctoral fellowship.

hexahapto nature of the bonding. Figure 1 also shows that the mesitylene rings are bound alternately above and below the $BiCl_3$ sheets.

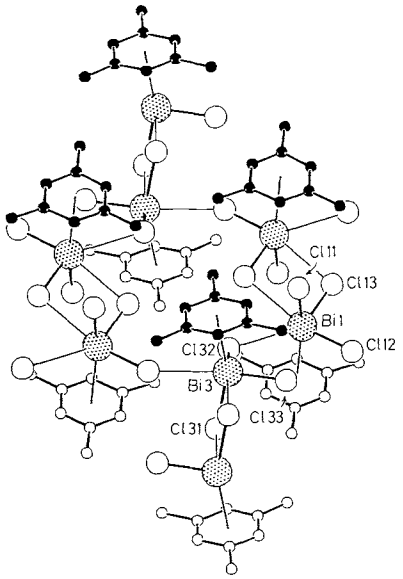


Fig. 1. Section from one of the two crystallographically independent $[(arene)BiCl_3]_n$ sheets in the crystal of **1**. In each sheet two non-equivalent centrosymmetric $[(arene)_2Bi_2Cl_6]$-units (Bi1, Bi3) are coupled via chloro bridges to each other to give strands, whereby the Bi3-dimers additionally cross-link the strands to give a sheet. Of the three Cl ligands of each Bi atom one (Cl13, Cl31) serves for the centrosymmetric coupling with an equivalent Bi atom, a second (Cl12, Cl32) forms the bridge to the nearest $[(arene)_2Bi_2Cl_6]$-dimer, while the third (Cl11, Cl33) is a terminal ligand. The mesitylene ligands are alternately bound above (black) and below (white) the sheet.

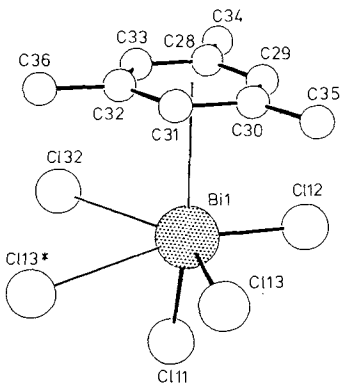


Fig. 2. Coordination sphere of one of the four crystallographically non-equivalent Bi atoms in **1** (Bi1). Bond lengths [Å]: Bi1-Cl11 2.465(5), Bi1-Cl12 2.489(4), Bi1-Cl13 2.483(5); Bi1-Cl13* 3.302(5), Bi1-Cl32 3.368(5); Bi-D4 (center of the arene) 3.11(2) Å. There is also a loose Bi1···Cl33 contact (4.050(7) Å, cf. Fig. 1).

1 is the first structurally characterized arene complex of bismuth. It differs fundamentally from the Menshutkin complexes of antimony, whose metal atoms are invariably acentrically η^2- or η^3-bound.[4]

In the crystals of **2**,[16] the centric η^6-coordination is further extended in a spectacular way. The structure consists of tetrameric $(BiCl_3)_4$ units of $\bar{4}2m$ (D_{2d}) symmetry, where each of the four crystallographically equivalent Bi atoms coordinate a hexamethylbenzene ligand (Fig. 3). Each metal atom is also bound to two nearest neighbor chlorine atoms (Cl1 and Cl2, Bi-Cl1 2.404(8), Bi-Cl2 2.438(8) Å), and to two symmetry-equivalent bridging chlorine atoms at greater distance (Cl3 and Cl3*, Bi-Cl3 2.887(6) Å). Two chlorine atoms from neighboring units also make loose contact (Cl2* and Cl2**, Bi-Cl2* 3.716(8) Å) (Fig. 4). The centers of the arene molecules form crystallographic inversion centers, so that the same bismuth halide unit is found on the other side of the ring (total symmetry $2/m$ (C_{2h}), Fig. 4; in Fig. 3 only the respective metal atoms Bi*, and not their halogen environments, are shown). Hence **2** can be regarded as an arene complex with an "inverted" sandwich structure, a structure which is extremely rare in the complex chemistry of neutral aromatic hydrocarbon compounds.[17] The tetramers in Figure 3 are coupled through the Bi(arene)Bi coordination, so that a three-dimensional framework results. Thus, the bonding between individual Bi_4Cl_{12} units is only maintained through the arene bridges.

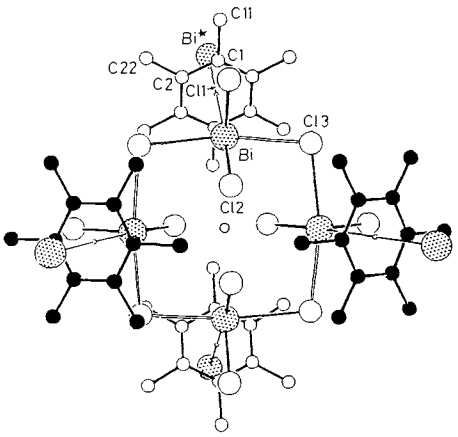


Fig. 3. Tetrameric units with $\bar{4}2m$ (D_{2d}) symmetry in the structure of **2**, as seen along the $\bar{4}$ (S4) axis, which generates the symmetry-equivalent $[(arene)Bi_2Cl_6]$ structural groups. The midpoints of the hexamethylbenzene rings are crystallographic inversion centers. The four symmetry-equivalent Bi-atoms are each components of four further tetrameric units which run screw-shaped with 4_2 symmetry through the crystal. The linkage is exclusively via mutual η^6-coordination to the arene ligand.

In this respect **2** is surprisingly similar to the complexes of the gallium subhalides with cyclophanes, where two metal atoms are not bound to one and the same arene (**A**), but

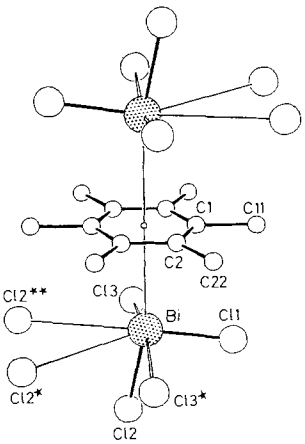
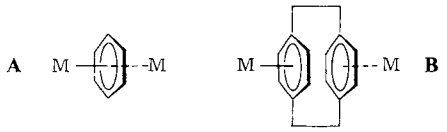


Fig. 4. The $[(arene)Bi_2Cl_6]$ unit of **2** with crystallographic $2/m$ (C_{2h}) symmetry. The Bi-Cl1/Cl2 (2.404(8)/2.438(3) Å) and Bi-Cl3 (2.887(6) Å) distances are strikingly different. In addition there are two further loose Bi-Cl2*/Cl2** contacts (3.716(8) Å). Bi-D (center of the arene) 3.07(2) Å.

to the parallel arene rings (which are inaccessible from the rear side) of the cyclophane (**B**).[6, 18]



By virtue of the η^6-bonding, **2** differs markedly from the analogous Menshutkin complexes, in which there is no central coordination.[4] The bonding in **2** can be explained quite well, however, in terms of the MO models already used in the case of the corresponding Tl^{I} and Pb^{II} complexes—dominance of the interaction between the HOMOs of the arenes and the p-orbitals of the metal atoms, which have the same symmetry.[6] It is significant that no stereochemical activity of the lone pair in the sense of ligand-free polyhedral corners is recognizable, either in **1** or in **2**. Here—and in the η^6-bonding—the stabilization of the $6s^2$ level, known as the inert pair effect, manifests itself. Due to the excessively long Bi—C bond lengths the new complexes must be classed among compounds with "weak interactions". The influence of the arene ligand is so great, however, that a relationship with the structure of $BiCl_3$ no longer exists in **1** and **2**.

Received: April 8, 1986;
revised: May 22, 1986 [Z 1723 IE]
German version: *Angew. Chem. 98* (1986) 742

CAS Registry numbers:
1, 18796-88-8; **2**, 103349-18-4; $BiCl_3$, 7787-60-2; mesitylene, 108-67-8; hexamethylbenzene, 87-85-4.

[1] E. O. Fischer, H. P. Fritz, *Angew. Chem. 73* (1961) 353.
[2] P. F. Rodesiler, T. Auel, E. L. Amma, *J. Am. Chem. Soc. 97* (1975) 7405; P. F. Rodesiler, E. L. Amma, *Inorg. Chem. 18* (1979) 751.
[3] A. G. Gash, P. F. Rodesiler, E. L. Amma, *Inorg. Chem. 13* (1974) 2429.
[4] a) H. H. Perkampus: *Wechselwirkungen von π-Elektronensystemen mit Metallhalogeniden*, Springer, Berlin 1973, and references cited therein; b) D. Mootz, V. Händler, *Z. Anorg. Allg. Chem. 533* (1986) 23, and references cited therein.
[5] a) F. A. Cotton, W. Schwotzer, C. Q. Simpson II, *Angew. Chem. 98* (1986) 652; *Angew. Chem. Int. Ed. Engl. 25* (1986) 637; b) M. Cesari, U. Pedretti, A. Zazzetta, G. Lugli, W. Marconi, *Inorg. Chim. Acta 5* (1971) 439; F. A. Cotton, W. Schwotzer, *Organometallics 4* (1985) 942.
[6] Review: H. Schmidbaur, *Angew. Chem. 97* (1985) 893; *Angew. Chem. Int. Ed. Engl. 24* (1985) 893.
[7] Gallium: H. Schmidbaur, U. Thewalt, T. Zafiropoulos, *Organometallics 2* (1983) 1550.
[8] Indium: J. Ebenhöch, G. Müller, J. Riede, H. Schmidbaur, *Angew. Chem. 96* (1984) 367; *Angew. Chem. Int. Ed. Engl. 23* (1984) 386.
[9] Thallium: H. Schmidbaur, W. Bublak, J. Riede, G. Müller, *Angew. Chem. 97* (1985) 402; *Angew. Chem. Int. Ed. Engl. 24* (1985) 414.
[10] H. Schmidbaur, Centenary Lecture, London 1984; Dwyer Memorial Lecture, Sydney 1986.
[11] W. Smith, G. W. Davis, *J. Chem. Soc. 41* (1882) 411; B. N. Menshutkin, *Zh. Russ. Fiz. Khim. Ova. 43* (1911) 1298, 1786.
[12] G. Peyronel, S. Buffagni, I. M. Vezzosi, *Gazz. Chim. Ital. 98* (1968) 147.
[13] T. Auel, E. L. Amma, *J. Am. Chem. Soc. 90* (1968) 5941.
[14] *Procedure.* **1**: A suspension of $BiCl_3$ (0.25 g, 0.79 mmol) in mesitylene (25 mL) was heated to 60°C and then filtered. A colorless filtrate was obtained, from which **1** (0.3 g; 87%) crystallized in the form of colorless platelets; m.p. 157°C (decomp.). **1** can be briefly dried in vacuo at 25°C without decomposition—**2**: Addition of the same amount of $BiCl_3$ to a solution of hexamethylbenzene (3 g) in toluene (50 mL) led under the same conditions to formation of bright yellow crystals of **2** [(0.29 g, 92%; m.p. 212—215°C (decomp.)]. **2** is stable in a vacuum at 25°C.—Both complexes gave correct elemental analyses. Their IR and NMR data differ very little from those of the components.
[15] $C_9H_{12}BiCl_3$ (435.54), triclinic, space group $P\bar{1}$, $a = 8.716(2)$, $b = 14.150(3)$, $c = 21.740(5)$ Å, $\alpha = 108.64(2)$, $\beta = 101.24(2)$, $\gamma = 88.88(1)°$; $V = 2489.2$ Å^3, $Z = 8$, $\rho_{calc} = 2.324$ g cm^{-3}; $F(000) = 1600$, $\mu(Mo_{K\alpha}) = 147.3$ cm^{-1}, $T = -5$°C. 6479 measured reflections, of which 6441 independent and 5042 "observed" with $I \geq 2.0\sigma(I)$, (ω scan, $\Delta\omega = 0.8°$, $(\sin\theta/\lambda)_{max} = 0.538$, $+h$, $\pm k$, $\pm l$, $Mo_{K\alpha}$, $\lambda = 0.71069$ Å, graphite monochromator, Syntex $P2_1$): Lp and empirical absorption correction, solution by direct methods (SHELX 76), $R = 0.051$, $R_w = 0.042$, $w = 1/\sigma^2(F_0)$ (Bi and Cl anisotropic, C isotropic, 289 parameters, $\Delta\rho_{max}$(fin) = +0.67/−0.66 e/Å^3, SHELX 76).
[16] $C_{12}H_{18}Bi_2Cl_6$ (792.96), tetragonal, space group, $P4_2/nnm$, $a = b = 12.599(3)$, $c = 12.315(3)$ Å; $V = 1954.8$ Å^3, $Z = 4$, $\rho_{calc} = 2.694$ g cm^{-3}, $F(000) = 1432$; $\mu(Mo_{K\alpha}) = 187.5$ cm^{-1}, $T = 22$°C. 2530 measured reflections, of which 1185 independent and 552 observed ($I \geq 2.0\sigma(I)$) ($\theta - 2\theta$ scan, $\Delta\omega = 0.85 + 0.35 \tan\theta$, $(\sin\theta/\lambda)_{max} = 0.648$, $+h$, $+k$, $+l$, Enraf-Nonius CAD4). Solution by Patterson methods, $R = 0.070$, $R_w = 0.048$, $w = 1/\sigma^2(F_0)$ (Bi and Cl anisotropic, C isotropic, 38 parameters, $\Delta\rho_{max}$(fin) = +3.48/−2.60 e/Å^3 at Bi, SHELX 76).—Further details of the crystal structure investigations are available on request from the Fachinformationszentrum Energie, Physik, Mathematik GmbH, D-7514 Eggenstein-Leopoldshafen 2, on quoting the depository number CSD 51870, the names of the authors, and the full citation of the journal.
[17] K. Jonas, *Angew. Chem. 97* (1985) 292; *Angew. Chem. Int. Ed. Engl. 24* (1985) 295.
[18] H. Schmidbaur, W. Bublak, B. Huber, G. Müller, *Organometallics 5* (1986) in press.
[19] C. Nyburg, G. A. Ozin, J. T. Szymanski, *Acta Crystallogr. B27* (1971) 2298.

Early Members of a Homologous Series Based on Linked GeM_2 Triangles, (M = Co, Fe): Structures of $[Ge_2Co_4Fe_2(CO)_{21}]$ and $[Ge_3Co_8(CO)_{26}]$

By *Skelte G. Anema, Kenneth M. Mackay,* Laurie C. McLeod, Brian K. Nicholson,** and *Jan M. Whittaker*

A spiro-linking of two GeM_2 triangles (M = transition metal) has been reported recently in the isoelectronic molecules $Ge[Co_2(CO)_7]_2$[1] and $Ge[Fe_2(CO)_8]_2$.[2, 3] Also known are a number of species containing two GeM_2 triangles sharing the M—M edge.[4]

Thus, it is possible to envisage a homologous series formed by extended chains of triangles linked alternately through Ge and M—M. There is good spectroscopic evidence[5] for such a structure in $Ge_2Co_6(CO)_{20}$, but so far we have been unable to grow any single crystals. In the iron series, linked-ring structures have been established[4] but these involve four-membered rings.

We report here on the structures of the title compounds **2**—isoelectronic with $Ge_2Co_6(CO)_{20}$— and **3**, which contain four and six GeM_2 triangles, respectively, and may therefore be regarded as the second and third members of the series headed by $Ge[Co_2(CO)_7]_2$.

Reaction[6] of $Co_2(CO)_8$ with the four-membered ring compound **1**[7] leads to the usual[1, 4] replacement of GeH_2 by the $GeCo_2$ triangle. The formation of the Fe—Fe bond, bridged by CO, across the Fe_2Ge_2 ring apparently occurs as a slower step since a second product was isolated which slowly lost CO to form **2**.

$$[Fe(CO)_4GeH_2]_2 + 2\,Co_2(CO)_8 \longrightarrow 2\,H_2 + 2\,CO + \text{intermediate}$$
1

$$\text{intermediate} \longrightarrow CO + Ge_2Co_4Fe_2(CO)_{21}$$
2

2 consists of the central $Fe_2(CO)_7$ unit with two links through Ge to $Co_2(CO)_7$ groups (Fig. 1a).[8]

[*] Prof. K. M. Mackay, Dr. B. K. Nicholson, S. G. Anema, L. C. McLeod, J. M. Whittaker
Department of Chemistry, University of Waikato
Hamilton (New Zealand)

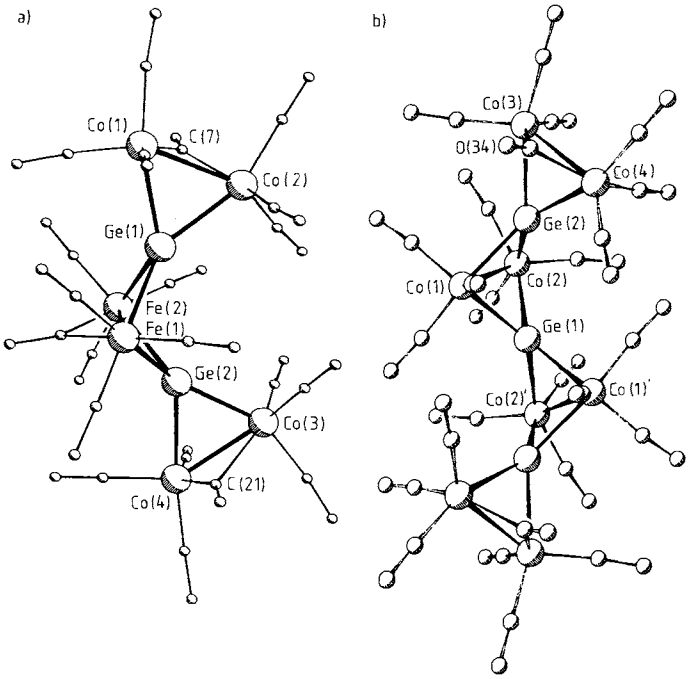


Fig. 1. a) Crystral structure of **2**. Bond lengths [pm]: Ge1-Fe1 236.5(1), Ge1-Fe2 243.7(1), Ge1-Co1 238.3(1), Ge1-Co2 235.1(1), Ge2-Fe1 242.1(1), Ge2-Co3 230.9(1), Ge2-Co4 240.0(1), Fe1-Fe2 267.8(1), Co1-Co2 252.8(1), Co3-Co4 249.1(1), Ge1···Ge2 330, Ge1···C7 260, Ge2···C21 271; Dihedral angles [°]: Ge1-Co1-Co2/Ge1-Fe1-Fe2 84, Ge2-Co3-Co4/Ge2-Fe1-Fe2 88, Ge1-Fe1-Fe2/Ge2-Fe1-Fe2 111.— b) Crystal structure of **3**, viewed down the crystallographic diad. Bond lengths [pm]: Ge1-Co1 236.1(1), Ge1-Co2 239.3(2), Ge2-Co1 238.8(2), Ge2-Co2 233.8(2), Ge2-Co3 240.7(2), Ge2-Co4 235.7(2), Co1-Co2 266.4(2), Co3-Co4 251.9(2), Ge1···Ge2 322, Ge2···C34 275. Dihedral angles [°]: Ge1-Co1-Co2/Ge1-Co1'-Co2' 70.7, Ge2-Co1-Co2/Ge2-Co3-Co4 85.3, Ge1-Co1-Co2/Ge2-Co1-Co2 110.4.

Reaction of any of the accessible germanes with $Co_2(CO)_8$[9] yields mixtures of the homologues **3**, **4** and **5**, with the yield of **3** optimized at a Ge:Co ratio of ca. 1:2.5. The reaction is cleanest with trigermane:

$$Ge_3H_8 + 4\,Co_2(CO)_8 \longrightarrow$$

$$4\,H_2 + 6\,CO + \underset{\mathbf{3}}{Ge_3Co_8(CO)_{26}} + \{\underset{\mathbf{4}}{Ge[Co_2(CO)_7]_2} + \underset{\mathbf{5}}{Ge_2Co_6(CO)_{20}}\}$$

The yields of recrystallized **3** were 30–60% based on Ge_3H_8. **3** consists of two central $Co_2(CO)_6$ and two terminal $Co_2(CO)_7$ units linked through three Ge atoms (Fig. 1b).[8]

The compounds **2** and **3** are sterically crowded with Ge···Ge and Ge···μ-C non-bonded distances less than the Van der Waals distances, and with a number of O···O interactions between adjacent $M_2(CO)_6$ moieties at distances of less than 3.0 Å. As a result of attempts to minimize these nonbonded interactions, the structures show (i) unsymmetric GeM_2 and $M_2(\mu\text{-C})$ triangles, (ii) dihedral angles between adjacent triangles linked at Ge of less than 90°, and (iii) dihedral angles between triangles with a common Co–Co edge which maintain Ge···Ge distances of 3.2–3.3 Å.

The simpler chain clusters readily lose CO and form closed clusters. Thus, $Ge[Co_2(CO)_7]_2$ loses CO at ca. 50°C to give quantitatively $(CO)_4CoGeCo_3(CO)_9$,[1,10] while $Ge_2Co_6(CO)_{20}$ similarly gives $[(CO)_4CoGe]_2Co_4(CO)_{11}$[5] with a pseudo-octahedral core. Similar rearrangements may be expected for **2** and **3**.

Finally, we note that these Ge species should have analogues with other elements of the carbon group; the first member of the Si series, $Si[Co_2(CO)_7]_2$ has been prepared,[11] and the related $Sn[Fe_2(CO)_8]_2$ has been known for years.[12] Wider correlations of this group of compounds have been explored in a recent view.[13]

Received: April 9, 1986 [Z 1724 IE]
German version: *Angew. Chem. 98* (1986) 744

[1] R. F. Gerlach, K. M. Mackay, B. K. Nicholson, W. T. Robinson, *J. Chem. Soc. Dalton Trans. 1981*, 80.
[2] A. S. Bastonov, L. V. Rybin, M. I. Rybinskaya, Yu. T. Struchkov, I. M. Salimganeeva, N. G. Bogatova, *J. Organomet. Chem. 249* (1983) 319.
[3] D. Melzer, E. Weiss, *J. Organomet. Chem. 255* (1983) 335; cf. also: W. A. Herrmann, *Angew. Chem. 98* (1986); *Angew. Chem. Int. Ed. Engl. 25* (1986) 56.
[4] K. M. Mackay, B. K. Nicholson in G. Wilkinson, F. G. A. Stone, E. W. Abel (Eds.): *Comprehensive Organometallic Chemistry, Vol. 6*, Pergamon Press, London 1982.
[5] S. P. Foster, K. M. Mackay, B. K. Nicholson, *Inorg. Chem. 24* (1985) 909.
[6] **2**: In hexane under vacuum at room temperature, $[Fe(CO)_4GeH_2]_2$ **1** (240 mg, 0.49 mmol) and $Co_2(CO)_8$ (330 mg, 0.96 mmol) formed CO and H_2 steadily for 30 h and then evolution slowed down. Work-up yielded total gases (2.20 mmol, $CO:H_2 = 1.4:1$, $H_2 = 92.6\%$ yield), hexane-extractable $HCo(CO)_4$ (0.02 mmol), $Co_2(CO)_8$ (0.03 mmol), $Co_4(CO)_{12}$ (0.06 mmol), and a dark brown solid. Extraction with CH_2Cl_2 gave dark orange $Ge_2Co_4Fe_2(CO)_{21}$, **2**, (213 mg, 0.19 mmol, 39%: $\tilde{\nu}_{CO}$ [cm^{-1}] = 2086 s, 2064 vs, 2050 vs, 2020 m, br, 2008 m, br, 1844-26 w, br (hexane/CH_2Cl_2). The light-brown, insoluble residue was provisionally identified as $Ge_2Co_4Fe_2(CO)_{22}$ (213 mg, 0.19 mmol, 39%; the compound forms CO and **2** in 1.07:1 ratio in a few hours at 20–30°C; $\tilde{\nu}_{CO}$ [cm^{-1}] = 2084 s, 2070 s, 2059 s, 2049 s, 2029 sh, 2021 vs, 2006 s, 2001 sh, 1992 s, 1984 sh, 1828 s (KBr disk).
[7] J. Christie, *D. Phil. Thesis*, University of Waikato 1981.
[8] **2**: *C2/c*, $a = 3859.7(7)$, $b = 925.7(3)$, $c = 1912.1(2)$ pm, $\beta = 107.41(1)°$, $Z = 8$, Enraf-Nonius CAD4, 3985 reflections, $1° < \theta < 25°$, 1371 with $I > 2\sigma(I)$ after absorption correction, metal atoms anisotropic, $R = 0.0524$, $R_w = 0.0498$.— **3**: *C2/c*, $a = 2605.9(2)$, $b = 1403.4(2)$, $c = 1173.9(2)$ pm, $\beta = 100.696(9)°$, $Z = 4$, Enraf-Nonius CAD4, 2900 reflections, $1° < \theta < 25°$, 1692 with $I > 2\sigma(I)$ after absorption correction, all atoms anisotropic, $R = 0.0369$, $R_w = 0.0350$. Further details of the crystal structures can be obtained from the Fachinformationszentrum Energie, Physik, Mathematik GmbH, D-7514 Eggenstein-Leopoldshafen 2, by quoting the depository number CSD-51936, the names of the authors, and the journal citation. We thank Dr. *C. Rickard*, University of Auckland, for the collection of X-ray data.
[9] **3**: Ge_3H_8 (144 mg, 0.635 mmol) and $Co_2(CO)_8$ (813 mg, 2.38 mmol) were sealed, together with hexane (10 ml), in a 40 ml ampoule and kept in subdued light for 12 weeks. Uncondensable gas (5.70 mmol, $H_2:CO = 2:3$) was removed and the hexane fraction contained $HCo(CO)_4$ (trace) and a little Ge_3H_8. The solid contained **3**, **4** and **5** in the approximate ratio 80:15:5 (IR analysis). Repeated washing with hexane, followed by recrystallization from CH_2Cl_2, gave pure **3** (437 mg, 0.309 mmol, 52%); $\tilde{\nu}_{CO}$ [cm^{-1}] = 2094 vs, 2073 vs, 2063 sh, 2059 vs, 2050 vvs, 2036 vs, 2023 vs, 2014 vs, 2005 vs, 1992 s, 1985 sh, 1837 m, 1831 m (nujol mull).
[10] G. Schmid, G. Etzrodt, *J. Organomet. Chem. 137* (1977) 367; R. Boese, G. Schmid, *J. Chem. Soc. Chem. Commun. 1979*, 349.
[11] K. M. Mackay, B. K. Nicholson, A. W. Sims, C. C. Tan, *Acta Crystallogr.*, in press.
[12] P. F. Lindley, P. Woodward, *J. Chem. Soc. A, 1967* 382.
[13] W. A. Herrmann, *Angew. Chem. 98* (1986) 57; *Angew. Chem. Int. Ed. Engl. 25* (1986) 56.

The Alkylation of Epoxides with New Organoyttrium and Organolanthanoid Reagents

By *Ishita Mukerji, Andrea Wayda,* Gary Dabbagh*, and *Steven H. Bertz**

We wish to report that a new class of organoyttrium and organolanthanoid reagents, prepared from organolithium

[*] Dr. S. H. Bertz, Dr. A. L. Wayda, I. Mukerji, G. Dabbagh
AT&T Bell Laboratories
Murray Hill, NJ 07974 (USA)

[**] We thank *S. M. Vincent* for X-ray fluorescence analyses.

or Grignard reagents and yttrium or lanthanoid tris(isopropoxides) or tris[bis(trimethylsilyl)amides], alkylate epoxides with synthetically useful yields and regiochemistries. These reagents are especially interesting due to the observation that styrene oxide and butadiene monoxide are alkylated with regioselectivities complementary to those obtained with organocuprates, currently the standard reagents for epoxide alkylation. Previous work on C-C bond formation with organolanthanoids has involved principally the alkylation of carbonyl compounds with RYbI,[1a] RX/SmI_2,[1b] and RX/Ce(Hg) or $RLi/CeCl_3$.[1c]

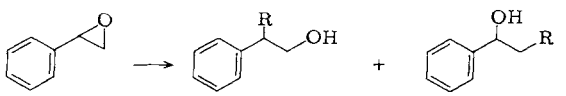
The tris(isopropoxides), $M(OiPr)_3$,[2] and tris[bis(trimethylsilyl)amides], $M[N(SiMe_3)_2]_3$,[3] are easily prepared and handled by standard dry-box techniques. Addition of 1 equivalent of RLi or RMgBr at $-78°C$ gives the active reagent, to which is added 1 equivalent of epoxide. Reaction occurs upon warming to 25°C. Initial experiments with cyclohexene oxide (**1**) demonstrated that ether was much superior to pentane or tetrahydrofuran as a reaction solvent, and it was therefore used for all the experiments reported.



1 **2**

The yields of *trans*-2-methylcyclohexanol (**2**) obtained upon adding **1** to the reagent prepared[4] from MeLi and $Sm[N(SiMe_3)_2]_3$ or $Y[N(SiMe_3)_2]_3$ were 100% and 97%, respectively, after 2 h at room temperature. Under the same conditions, the corresponding isopropoxides gave 52% and 80% yields of **2**, respectively, after 23 h at room temperature. No significant amounts of **2** resulted when **1** was treated with MeLi or $CH_3Li/Al(OiPr)_3$, and no *cis*-2-methylcyclohexanol was detected by capillary GLC in any of the reaction mixtures.

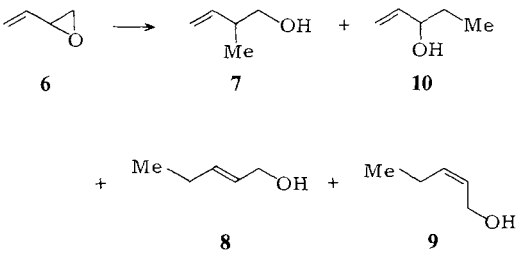
In the case of an unsymmetrical epoxide such as styrene oxide (**3**), two products are possible: a methylating reagent can give either 2-phenyl-1-propanol (**4a**) or 1-phenyl-1-propanol (**5a**) and a butylating reagent can afford either 2-phenyl-1-hexanol (**4b**) or 1-phenyl-1-hexanol (**5b**). As far as the ratio of **4a/5a** is concerned, the best methylating conditions involved $MeLi/Sm[N(SiMe_3)_2]_3$ or $MeLi/Y[N(SiMe_3)_2]_3$. The yields of **4a** obtained after 2 h at ~25°C with these reagents were 71% and 73%, respectively, while the corresponding yields of **5a** were only 0.7% and <0.1%. The best butylating reagent was prepared from two equivalents of BuMgBr and one equivalent of $Y[N(SiMe_3)_2]_3$ and yielded 80% of **4b** and <0.1% of **5b** after 2 h at ~25°C.



3 **4a**, R = Me; **4b**, R = Bu **5a**, R = Me; **5b**, R = Bu

In contrast, organocopper reagents preferentially attack **3** at the least-hindered C of the epoxide, although the ratio of products is not nearly as high as we observe. For example, we have found that **3** is opened by $Me_2CuLi \cdot LiI$ to give 19% of **4a** and 44% of **5a**. Similarly, *Lipshutz* et al.[5] found that **3** is opened by $Bu_2CuLi \cdot LiCN$ to yield 8% of **4b** and 85% of **5b**. Further, *Ganem* et al.[6] recently reported that **3** is opened by $BuLi/BF_3$ to yield 36% of **4b** and 64% of **5b**. The more substituted product (benzylic attack) is observed upon treating **3** with two equivalents of trialkylaluminum reagent.[7] The utility of this chemistry is limited, however, by the availability of the Al reagent and the fact that five potentially valuable organic groups must be wasted in order to incorporate one into the product.

Butadiene monoxide (**6**) presents an especially challenging problem, as there are three potenital sites of alkylation. A priori, methylation could occur at the allylic carbon to give 2-methyl-3-buten-1-ol (**7**), at the terminus of the double bond (S_N2' displacement) to give *trans*-2-penten-1-ol (**8**) or *cis*-2-penten-1-ol (**9**), or at the least hindered epoxide carbon to give 1-penten-3-ol (**10**). Treatment of **6** with $MeLi/Sm[N(SiMe_3)_2]_3$ yielded 81% of **7** and 2% of **10**, in analogy with the styrene oxide result. No **8** or **9** were detected by capillary GLC. Essentially the same yield of **7** was obtained with $MeLi/Er[N(SiMe_3)_2]_3$ or $MeLi/Y[N(SiMe_3)_2]_3$, and with these reagents none of **8**-**10** was detected. The Sm- and Y-alkoxides produced mixtures of **7** and **8** also containing small amounts of **9** and **10** (see Table 1).



6 **7** **10**

8 **9**

Table 1. Methylation of butadiene monoxide **6** [a].

Reagent	Yield [%]			
	7	**8**	**9**	**10**
$MeLi/Sm[N(SiMe_3)_2]_3$	81	<1	<1	2
$MeLi/Er[N(SiMe_3)_2]_3$	78	<1	<1	<1
$MeLi/Y[N(SiMe_3)_2]_3$	77	<1	<1	<1
$MeLi/Sm(OiPr)_3$	31	19	2	3
$MeLi/Y(OiPr)_3$	23	31	3	<1
$MeLi/SmCl_3$	16	10	1	1
$MeLi/CeCl_3$	10	1	5	1
MeYbI	1	1	1	1
$2\,Me_3Al$	46	6	<1	<1
$Me_2CuLi \cdot LiI$	1	67	5	<1

[a] 23 h, room temperature.

For comparison: Treatment of **6** with $Me_2CuLi \cdot LiI$ yielded 67% of **8**,[8] along with 5% of **9** and 1% of **7**. Treatment of **6** with two equivalents of $AlMe_3$ in hexane[7] gave 46% of **7** and 6% of **8**. Other, previously known organolanthanoid reagents[1] proved unsatisfactory (see Table 1).

Several other substrates and reagents have also been investigated. For example reaction of 1,2-epoxybutane with $MeLi/Sm[N(SiMe_3)_2]_3$ furnished 3-pentanol in 74% yield. *Johnson* et al.[9] obtained an 84% yield when they used two equivalents of $Me_2CuLi \cdot LiI$ to effect this transformation. Finally, reaction of $PhLi/Y(OiPr)_3$ and cyclopentene oxide afforded *trans*-2-phenylcyclopentanol in 42% yield.

Received: April 21, 1986;
revised: June 9, 1986 [Z 1738 IE]
German version: *Angew. Chem.* 98 (1986) 756

 © VCH Verlagsgesellschaft mbH, D-6940 Weinheim, 1986 0570-0833/86/0808-0761 $ 02.50/0

CAS Registry numbers:
1, 286-20-4; **2**, 7443-52-9; **3**, 96-09-3; **4a**, 1123-85-9; **4b**, 25755-73-1; **5a**, 93-54-9; **5b**, 4471-05-0; **6**, 930-22-3; **7**, 4516-90-9; **8**, 764-37-4; **9**, 764-38-5; **10**, 616-25-1; MeLi, 917-54-4; $Sm(OiPr)_3$, 3504-40-3; $Y(OiPr)_3$, 2172-12-5; $SmCl_3$, 10361-82-7; $CeCl_3$, 7790-86-5; MeYbI, 88068-44-4; Me_3Al, 75-24-1; BuMgBr, 693-038; PhLi, 591-51-5; $Sm[N(SiMe_3)_2]_3$, 35789-01-6; $Er[N(SiMe_3)_2]_3$, 103457-72-3; $Y[N(SiMe_3)_2]_3$, 41836-28-6; Me_2CuLi, 15681-48-8; *trans*-2-phenylcyclopentanol, 42086-64-6; 1,2-epoxybutane, 106-88-7; 3-pentanol, 584-02-1; cyclopentene oxide, 285-67-6.

[1] a) D. F. Evans, G. V. Fazakerley, R. F. Phillips, *J. Chem. Soc. A 1971*, 1931; T. Fukagawa, Y. Fujiwara, K. Yokoo, H. Taniguchi, *Chem. Lett. 1981*, 1771; *ibid. 1982*, 601; b) P. Girard, J. L. Namy, H. B. Kagan, *J. Am. Chem. Soc. 102* (1980) 2693; c) T. Imamoto, T. Kusumoto, Y. Tawarayama, Y. Sugiura, T. Mita, Y. Hatanaka, M. Yokoyama, *J. Org. Chem. 49* (1984) 3904.

[2] All isopropoxides were synthesized as described in S. N. Misra, T. N. Misra, R. N. Kapoor, R. C. Mehrotra, *Chem. Ind. (London) 1963*, 120, and were purified by repeated pentane extraction. The resulting products were free of Cl (X-ray fluorescence), gave satisfactory metal analyses and exhibited infrared and NMR spectra identical to those given in the literature (see K. S. Mazdiyasni, C. T. Lynch, J. S. Smith, *Inorg. Chem. 5* (1966) 342).

[3] All amides were prepared by minor modification of the original procedure: D. C. Bradley, J. S. Ghortra, F. A. Hart, *J. Chem. Soc. Dalton Trans. 1973*, 1021. Use of the lithium reagent, $LiN(SiMe_3)_2$ in the metatheses resulted in products which contained residual chloride. However, $NaN(SiMe_3)_2$ yielded chloride-free, pure amides which gave satisfactory analyses (see ref. [2]).

[4] *Procedure:* The reagents were prepared under Ar by adding the organolithium or Grignard reagent to 1 mmol of the lanthanoid amide or alkoxide suspended in 5 mL of ether at −78°C. After 15 min, the epoxide and internal standard (decane) dissolved in 5 mL of ether at −78°C was added. The reaction mixtures were sampled after stirring for 1 h at −78°C, 2 h at room temperature, and 23 h at room temperature. Quenching with 3 M aqueous ammonium chloride removed the inorganics and left a virtually colorless organic layer. Analysis by GLC calibrated with authentic materials gave the yields quoted.

[5] B. H. Lipshutz, J. Kozlowski, R. S. Wilhelm, *J. Am. Chem. Soc. 104* (1982) 2305.

[6] M. J. Eis, J. E. Wrobel, B. Ganem, *J. Am. Chem. Soc. 106* (1984) 3693.

[7] J. L. Namy, E. Henry-Basch, P. Freon, *Bull. Soc. Chim. Fr. 6* (1970) 2249; J. L. Namy, D. Abenhaim, G. Boireau, *ibid. 8* (1971) 2943.

[8] See also R. J. Anderson, *J. Am. Chem. Soc. 92* (1970) 4978.

[9] R. W. Herr, D. M. Wieland, C. R. Johnson, *J. Am. Chem. Soc. 92* (1970) 3813.

Thermally Induced Redox Reaction of Carbonyl Compounds and Alcohols in a Radical Chain Reaction: Comproportionation to Two Hydroxyalkyl Radicals

By *Dietmar Malwitz* and *Jürgen O. Metzger**

The reduction of carbonyl compounds to alcohols is a very important reaction in organic chemistry.[1] But reductions with alcohols also play an important role and, commencing with the Meerwein-Ponndorf-Verley reduction, numerous variants have been described in the literature.[2] *Ponndorf*[3] pointed out in his classical work more than half a century ago the possibility of a thermally-induced redox reaction, but so far no mechanism has been described for this reaction. Two routes are conceivable: a) a comproportionation of carbonyl compound and alcohol to two hydroxyalkyl radicals and their further reaction to give the products, or b) a pericyclic reaction in which two hydrogen atoms are transferred from the alcohol to the carbonyl group in one step.

We have found that aldehydes **1** are reduced by 2-propanol **2** in a thermal reaction to the alcohols **3**, whereby **2** is oxidized to acetone **4**.[4] Instead of **2**, methanol, primary alkyl alcohols and benzyl alcohols can also be used, whereas tertiary alcohols are not reducing.

$$\underset{\mathbf{1}}{RCH{=}O} + \underset{\mathbf{2}}{(H_3C)_2HCOH} \rightleftharpoons \underset{\mathbf{3}}{RCH_2OH} + \underset{\mathbf{4}}{(H_3C)_2C{=}O}$$

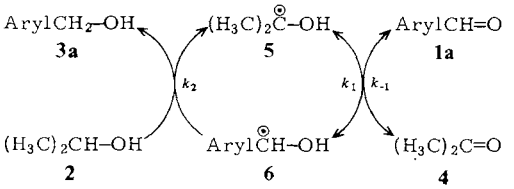
a, R = 4-*i*Pr-C_6H_4; **b**, R = C_6H_5

To elucidate the reaction mechanism we investigated the kinetics of the reaction of **2** and 4-isopropylbenzaldehyde **1a**. Preliminary experiments showed that the reaction proceeds as a radical chain reaction: active carbon as radical trapping agent completely inhibits it; radical formers such as di-*tert*-butyl peroxide[5] or atmospheric oxygen accelerate it; as soon as the radical formers are consumed, the rate is the same as for the reaction without radical former. Under the conditions used for the kinetic measurements,[6] no secondary reactions were observed. The rate law for the reaction is described by equation (1), and the Arrhenius equation is fulfilled quite well in the temperature range investigated (Eq. (2), $\Theta = 2.303\ [RT\ \mathrm{kJmol^{-1}}]$).

$$-\frac{d[\mathbf{1a}]}{dt} = \frac{d[\mathbf{3a}]}{dt} = k_{exp}[\mathbf{1a}][\mathbf{2}] \qquad (1)$$

$$\log k_{exp} = 7.56 \pm 0.05 - (125 \pm 1)/\Theta \qquad (2)$$

With deuteriated **2**, an almost temperature-independent kinetic isotope effect is obtained, both when **2** is *O*-deuteriated ($k_H/k_D = 2.06$), as well as *C*-deuteriated ($k_H/k_D = 2.61$). For perdeuteriated **2** one obtains $k_H/k_D = 5.34$.[7] A Hammet correlation gave a reaction constant $\beta = -0.62$.[8]



Start: **1a** + **2** $\xrightarrow{k_i}$ **5** + **6**

1a + **3a** $\xrightarrow{k_i'}$ 2 **6**

5 + **6** $\xrightarrow{k_t}$ chain termination

Aryl = 4-*i*Pr–C_6H_4

Scheme 1.

$$-\frac{d[\mathbf{1a}]}{dt} = \frac{d[\mathbf{3a}]}{dt} = (k_i'/k_t)^{1/2} \cdot (k_1/k_{-1})^{1/2} \cdot k_2[\mathbf{1a}][\mathbf{2}] \qquad (3)$$

All results are consistent with a radical chain reaction as shown in Scheme 1: Chain initiation starts with the formation of the hydroxyalkyl radicals **5** and **6** from **1a** and **2**. The radical **5** is converted by H-transfer to **1a** into the oxidation product **4**, a reaction which is already known from the analogous photochemical[10] and radical-induced[5] reactions, and which here is thermodynamically controlled; further reaction of the radical **6** to give the prod-

[*] Priv.-Doz. Dr. J. O. Metzger
Fachbereich Chemie der Universität
Carl-von-Ossietzky-Str. 9-11, D-2900 Oldenburg (FRG)
Dr. D. Malwitz
Meistermarken-Werke GmbH
Rembertiring 39, D-2800 Bremen 1 (FRG)

uct **3a** by H-abstraction from **2** is the rate-determining step in the radical chain reaction. Reaction of the two chain-carrying radicals **5** and **6** with each other leads to chain termination. After a relatively small conversion of ca. 5%, the comproportonation of **3a** and **1a** dominates as initiation reaction, since this reaction requires an activation energy about 45 kJ mol^{-1} less than the original initiation reaction because of the formation of two hydroxybenzyl radicals **6**.[11]

With this mechanism the experimental rate law is easy to simulate [Eq. (3)], both regarding the reaction order [Eq. (1)] as well as the Arrhenius parameter [Eq. (2)].[13] The isotope effect[14] and the reaction constant[15] are also consistent with this mechanism, a mechanism which is remarkable in two ways: 1) It describes a radical chain reaction with a "kinetic chain length" of ca. 10^7 at 200 °C.[16] In contrast, the analogous photochemical[10] and the radical-induced[5] reduction are not chain reactions. 2) The initiation reaction is the back reaction of the known disproportionation of hydroxyalkyl radicals and thus is analogous to the comproportionation of alkanes and alkenes to alkyl radicals.[17] Decisive is the "molecule-induced" homolysis[18] of a C-H bond [Eq. (4)] with a markedly reduced activation energy in comparison to the monomolecular bond cleavage.

$$RCH{=}O + HCR'_2OH \rightleftharpoons RCH{=}O\cdots H\cdots CR'_2OH \rightleftharpoons \overset{\oplus}{R}\overset{\ominus}{C}H{-}OH + \overset{\oplus}{C}R'_2{-}\overset{\ominus}{O}H \qquad (4)$$

In comparison, a pericyclic transfer of two H-atoms would be considerably slower[19] and, in view of the observed kinetics, highly unlikely, since according to equation (4) a radical chain reaction can be initiated. Our results are consistent with equation (4) most likely being the initiation reaction of the radical chain reaction.

Received: April 11, 1986
revised: May 10, 1986 [Z 1730 IE]
German version: *Angew. Chem. 98* (1986) 747

CAS Registry numbers:
1a, 122-03-2; **1b**, 100-52-7; **2**, 67-63-0; D_2, 7782-39-0.

[1] Houben-Weyl-Müller: *Methoden der organischen Chemie, Vol. VI, 1b*. Thieme, Stuttgart 1984.

[2] a) K. Krohn in [1], p. 289; b) P. Margaretha, *ibid.* p. 432.

[3] W. Ponndorf, *Angew. Chem. 39* (1926) 138.

[4] Typical reaction conditions: **2**:**1** = 100:1; 200 °C; 24-72 h; yields of **3** ca. 90%; increasing the temperature accelerated the reactions. Practically no secondary reactions occur up to 350 °C.

[5] E. S. Huyser, D. C. Neckers, *J. Am. Chem. Soc. 85* (1963) 3641.

[6] Duran glass ampules; exclusion of atmospheric oxygen; analysis: GC with on-column injection, mass balance referred to **1a** > 98%. a) Determination of reaction order at 200 °C; in the case of **1a**: 0.02–0.24 mol/L **1a** with 8.74 mol/L **2**; in the case of **2**: 8.74–1.7 mol/L **2** (variation by addition of *t*BuOH) with 0.02–0.05 mol/L **1a**. Evaluation according to pseudo 1st-order gave $k_{exp}/[\mathbf{2}] = k_{exp}$; b) temperature dependence: **2**/**1a** = 250:1; 175–230 °C (5 °C steps).

[7] The kinetics of the reactions of **1a** with $(H_3C)_2HCOD$, $(D_3C)_2DCOH$, and $(D_3C)_2DCOD$ were investigated in the temperature range 175–225 °C as described in [6].

[8] The following substituted benzaldehydes X-C_6H_4-CHO (X-**1b**) were measured for the Hammett correlation [9] in a competition reaction with **1b** at 160 °C: X = *p*-CN, *p*-Cl, *p*-Ph, *p*-*i*Pr, *p*-CH_3O. Conversions < 5 mol %; $\log([X\text{-}\mathbf{3b}]/[\mathbf{3b}]) = -0.62\sigma$ ($r = 0.999$).

[9] L. P. Hammett: *Physikalische Organische Chemie*, Verlag Chemie, Weinheim 1973, p. 352.

[10] D. I. Schuster, P. B. Karp, *J. Photochem. 12* (1980) 333.

[11] $\log(k_i/k_t) = \pm 0\text{-}217/\Theta$; $\log(k'_i/k_t) = -0.7\text{-}172/\Theta$; $\log(k_1/k_{-1}) = -1.4 + 52/\Theta$. Calculated for **1b** from thermochemical data according to *Benson* [12]. Substitution in equation (3) gives $\log k_2 \approx 8.6\text{-}65/\Theta$. The values of the A factor and of the activation energy are of the expected order of magnitude.

[12] S. W. Benson: *Thermochemical Kinetics*, Wiley, New York 1976.

[13] Other conceivable reaction sequences are not concomitantly consistent with both the observed rate law [Eq. (1)] and the experimental Arrhenius paramerers [Eq. (2)].

[14] The results evidence two different H-transfers: a) the cleavage of the O-H bond affects only k_1/k_{-1}; b) the cleavage of the C-H bond affects only k_2.

[15] In the competition reaction, the competition constant

$$k = \frac{k_1^X}{k_{-1}^X} \cdot k_2^X \Big/ \left(\frac{k_1}{k_{-1}} \cdot k_2\right)$$

is measured. A value of $\rho_1 > 0$ is to be expected for k_1/k_{-1} and $\rho_2 < 0$ for k_2, since electron-withdrawing substituents X in the aryl moiety stabilize the radical **6**. Since $\rho_{exp} < 0$ it follows that $|\rho_1| < |\rho_2|$.

[16] Kinetic chain lengths $= v_{exp}/v_i = k_{exp}[\mathbf{2}]/k'_i[\mathbf{3a}]$; $\log k'_i \approx 8.3\text{-}172/\Theta$; estimated from data in [11] with $\log k_t \approx 9.0 \pm 0/\Theta$ [12].

[17] a) J. O. Metzger, *Angew. Chem. 95* (1983) 914; *Angew. Chem. Int. Ed. Engl. 22* (1983) 889; *Angew. Chem. Suppl. 1983*, 1256; b) J. Hartmanns, K. Klenke, J. O. Metzger, *Chem. Ber. 119* (1986) 488.

[18] J. A. K. Harmony, *Methods Free-Radical Chem. 5* (1974) 101.

[19] D. F. Feller, M. W. Schmidt, K. Ruedenberg, *J. Am. Chem. Soc. 104* (1982) 960.

BOOK REVIEWS

Is Industrial Chemistry Still Presentable in Encyclopedic Form?

Ullmann's Encyclopedia of Industrial Chemistry has had a long and distinguished history beginning with the first edition which appeared in 1914. Since then, it has continued to be revised, updated and expanded at regular intervals leading to the fourth edition (1972–1984).[*] As is fitting, given the tremendous expansion in Chemistry and its impact on current technology, the time interval between successive editions has been decreasing and the number of volumes/edition has been increasing steadily. Now, less than two years after the publication of the last volume of the 4th edition, the first volumes of a new and updated 5th edition have appeared. This is a remarkable feat given the magnitude of the task.

[*] *Angew. Chem. Int. Ed. Engl. 23* (1984) 536.

Ullmann's Encyclopedia of Industrial Chemistry. 5th completely revised edition. Edited by *W. Gerhartz, Y. S. Yamamoto, F. T. Campbell, R. Pfefferkorn*, and *J. F. Rounsaville*. VCH Verlagsgesellschaft, Weinheim 1985. **Vol. A1: Abrasives to Aluminum Oxide:** xiv, 594 pp., bound, DM 430.00.—ISBN 3-527-20101-7

The 5th edition will ultimately include thirty six volumes and is divided into an A (Vol. A1–A28) and B (Vol. B1–B8) series. The latter series deals with a variety of basic knowledge topics, which by virtue of their general applicability

are not restricted to any single class of materials but are relevant to many different topics. An advantage of this "dual" volume approach is that it reduces the topical redundancy and permits more space to be devoted to the detailed description of specific products and processes.

One major difference in the 5th edition is that it is in English rather than German. This should greatly expand the audience and enhance its utility to scientists and engineers outside of the European technological community. This decision by the editorial board recognizes the truly international nature of industrial chemistry and technology. This trend is reflected not only by the composition of the editorial board, but also in the selection of contributing authors. For each topic discussed a specific location of previous and continuing expertise was selected and specific authors were chosen from that site. Where no single firm could be identified as dominant, authors have been selected from a number of competitive firms. This policy assures high quality, topical coverage and correctly recognizes the multinational contributions to Science and Technology.

I have personally reviewed the first volume of the 5th edition and was favorably impressed. The text is remarkably error free and maintains the high quality and standards of the previous editions. The subject matter selected for discussion is well organized and is treated in considerable detail. For highly specialized topics enough background data is provided to satisfy even the casual reader. Volume 1A provides a reasonably detailed and consistent treatment of twenty six separate topics ranging from Abrasives to Aluminum Oxide. All major compounds and most important derivatives are accompanied by the appropriate chemical abstract registry number to facilitate subsequent in-depth literature searches. Industrially important chemicals such as acetic acid, acetic anhydride, acetone, acetaldehyde, acetylene, etc. all receive a thorough treatment covering physical and chemical properties, manufacture and production engineering, major derivatives, reactivity, toxicology and industrial safety, transportation restrictions, economics, etc. The section on acetylene is particularly rich in details as befits a material with such a long chemical history and industrial importance. I was pleased to find a brief discussion of the formation of linear polymers by Ziegler Natta techniques, since these materials and their derivatives are of current scientific and industrial interest. Due to the industrial importance and diverse physical and chemical properties of aluminum compounds, this section is divided into a series of separate discussions of aluminum metal, aluminum alloys, inorganic aluminum compounds, organoaluminum derivatives and aluminum oxide. The last contribution describes the commercial uses of aluminum oxide except for its abrasive applications which are treated extensively in a separate section. In recognition of their considerable pharmacological importance there is a section on alkaloid derivatives. The major alkaloid groups are reviewed and many specific examples within each group are described. This section, which is quite long, is adequately indexed both by class and by compound. The organization of the sections dealing with acrylic materials (i.e. acrylic acid, acrylates, acrylonitrile) is unusual in that the respective polymers, which comprise the major industrial products, are not included in the same volume. While this makes the reading a little discontinuous, the location of the respective polymers and copolymers is adequately cross-referenced at the end of each subject article. One possible advantage of grouping the individual polymers under a broader more general polymer heading (e.g. fibers-synthetic organic, rubber-synthetic etc.) is that one can more easily see how each individual polymer product fits into the overall picture of a particular commercial polymer field.

Although I am admittedly not an expert in all of the twenty-six fields covered in volume 1A, I found all of the contributions to be quite readable and complete. Consistent with stated editorial board policy, the authorship of the first volume is internationally distributed to locations of demonstrated expertise. Although this often results in somewhat varying emphasis, the authors have all conformed to the basic editorial format which gives the volume consistency in spite of the great diversity of topics.

Regarding the format, I found the topical outline which precedes each contribution to be particularly valuable. If so desired, allows the casual reader to go easily and directly to sections of interest without wading through the entire article. This is particularly useful for someone who is interested in surveying related properties of a diverse group of materials. The text of each article is compiled in an appealing manner which seems to provide "something for everyone" whether they are interested in physical and/or chemical properties, chemical reactivity, production engineering, industrial safety or economics. I was particularly impressed with the extensive reference list provided for each topical discussion. In general these lists are composed of a mixture of accessible books, journals, patents, trade publications, etc. many of which are surprisingly current. In this regard, it was not unusual to find references as recent as 1982–83, which is somewhat unusual for a volume of this size. This currency will become increasingly important in future volumes dealing with emerging technologies in rapidly evolving fields such as genetic engineering, biotechnology, photoresists and microlithography, electronic materials etc., where reviews are often outdated by the time they appear.

In summary, I find that volume 1A of the 5th edition of Ullmann's Encyclopedia of Chemical Technology upholds in every fashion the high standards and traditions previously established. The concept is such that the articles provide something for both the casual reader as well as the skilled practitioner. The international authorship is a welcome innovation which is consistent with the multinational contributions to science and technology. The overall quality of this series is such that no Science and Engineering library should be without it.

Robert D. Miller [NB 756 IE]
IBM Almaden Research Center
San Jose, CA (USA)

Biotechnology. A Comprehensive Treatise in 8 Volumes. Edited by *H.-J. Rehm* and *G. Reed*. **Vol. 2. Fundamentals of Biochemical Engineering.** Volume Editor: *H. Brauer*. VCH Verlagsgesellschaft, Weinheim 1985. xvi, 819 pp., bound, subscription price: DM 425.00.—ISBN 3-527-25764-0

Biotechnology is an interdisciplinary field, the progress of which relies on close cooperation among professionals from various sub-disciplines within the areas of biology, chemistry, and engineering. The aim of this volume of the series[*] is to outline the fundamentals of biochemical engineering. It deals with the planning, design, and develop-

[*] Cf. *Angew. Chem. Int. Ed. Engl. 24* (1985) 436.

ment, as well as the optimization and operation of biochemical processes.

The volume contains 30 chapters in all, grouped in 5 sections. A relatively difficult philosophical question is, "what constitutes fundamentals for a diverse field like biochemical engineering". The editors seem to have decided to place a very strong emphasis on the fundamental concepts and the mathematics of transport phenomena, reaction kinetics, and reactors. About two-thirds of the book is devoted to these topics. The remaining one-third addresses the field from the practical point of view. Some very useful concepts are covered in stoichiometry, mechanical stress, measurement and control, and some selected unit operations. The quality of all the contributions is excellent; but at the risk of sounding parochial, I should share some additional observations. This volume is authored almost exclusively by experts from West Germany (19 of the 22 authors). In addition, most of the authors come from an academic environment (17 out of 22).

The first nine chapters give a review of momentum, mass, and heat transport phenomena, similarly as is to be found in *Transport Phenomena* by *R. B. Bird, W. E. Stewart,* and *E. N. Lightfoot* (Wiley 1960). The treatment is concise, but without omission of essential details. The philosophy and theory of reaction engineering form the subject of the following eight chapters. Concepts such as enzyme kinetics, batch and continuous fermentation kinetics, and reaction and mass transfer interactions are treated. Admittedly a difficult task to accomplish, yet it is a pity that practical examples of where and how these concepts are used are not presented to the reader in this volume.

Bioreactors are discussed in seven chapters. The present volume provides an extensive coverage of the "loop reactor"; interestingly, the type of reactor shown on the jacket of the volume. Loop reactors are typically fluidized reactors with at least one definitely directed circulation flow or "loop". The reader will note that there are some overlaps in what are considered "bubble" reactors, "tower" reactors, and "loop" reactors. Three chapters deal with the fundamental mathematics of stirred vessel reactors, bubble column reactors, and biochemical loop reactors. Fluid flow behavior, heat and mass transfer aspects, and gas dispersion are analyzed from a sound conceptual viewpoint. Several other chapters build on these fundamentals and provide a (somewhat redundant) comprehensive review of about 18 impressive installations, many in the Federal Republic of Germany. Examples are, the Imperial Chemical Industry's 2000–3000 m^3 (500000 to 800000 US gal) volume reactors for Single Cell Protein production; and smaller units of 20–40 m^3 at Mitsubishi and Hoechst-Uhde. Very large systems (several are 18–30 m high and 20–30 m diam) for wastewater treatment are the Hoechst BIOHOCH reactors and the Bayer "Tower Biology". Another concept presented is the "reciprocating jet" reactor which has shown promise in pilot-scale tests.

There are places in this volume where a fine attempt is made to link theory and practice. An example is a chapter on modeling and scale-up. Some important concepts are presented which are useful in determining whether kinetics or mass transfer is decisive in scale-up or other experiments. Such aspects deserve even more coverage.

Several chapters in this volume are of great practical value, and the editors are to be commended for the topics they have selected. There is an excellent chapter on the effect of mechanical stress on microbial cultures which also includes some micrographs. Gas solubility and stoichiometry are presented in two useful chapters for the reader interested in the practice of biochemical engineering. One should not, however, expect an in-depth treatment of these areas in this "Fundamentals" volume.

It must be mentioned that a chapter is included on "how to" run comparative tests for fermenters based on the recommendations of the DECHEMA working committee for biochemical engineering. Preparation of fermentation media is reviewed in another chapter that includes some 43 tables of information. The literature is a good blend of that from the US, Europe, and the USSR; and the chapter in itself constitutes a good practical starting point for the reader. In a chapter on "recovery operations," an account is given of those operations which are required in order to transform the (generally dilute) whole cell broth from the fermenter into the final product. Centrifugation and liquid-liquid extraction are dealt with very satisfactorily; however, the treatment of the other "downstream" operations is only cursory.

Finally, the editors are also to be commended for having included chapters on sterilization, measurement and control, as well as on process control and optimization. Here, the reader should expect an overview of the concepts involved and not a "how to" or "how it is done" discussion.

In summary, this volume provides a very good perspective on the kinds of activities in which the academicians and practitioners of biochemical engineering are engaged. The publication of this volume also takes us past the halfway point in this ambitious series. I wish those involved in its compilation continued success in this arduous task.

Bhavender P. Sharma [NB 757 IE]
Genencor, South San Francisco, CA (USA)

Dictionary of Organometallic Compounds. Edited by *J. Buckingham.* Chapman and Hall, London 1984. 3 Volumes, 2576 pp., £ 575.00.—ISBN 0-412-24710-0

Organometallic chemistry has increasingly developed into a discipline that, rather than being of interest only to the specialist, now attracts general attention. Therefore the appearance of an extensive compilation of the most important organometallic compounds, the brief description of their synthesis, characteristics, and physical properties, as well as (exemplary) applications, is of great interest. Entries on approximately 15000 compounds of the main-group and transition metals, including f-block elements, are presented in the *Dictionary of Organometallic Compounds* in a well organized and graphically clear manner. The editor showed his skill in not giving the authors of individual chapters any fixed rules for the selection of the compounds included. Thus, a balanced and useful presentation of the (sometimes very) different compound classes of the various metals was attained.

In general, the molecular formula, the name (often supplemented with common synonyms), the Chemical Abstracts Service Registry Number, and a very clearly drawn structural formula are given for every compound. These are followed by an enumeration of the more important physical and chemical properties. References to possible stereoisomers as well as derivatives (for which important data are in turn given) are well chosen. An important feature is that information concerning the toxicity and possible dangers of working with the given substance is provided. Finally, reference is made to important original papers and

to further literature; short statements of their contents reinforce the impression that the material presented has been carefully worked on.

The first two volumes of the "Dictionary" contain the entries on the individual compounds. These reports are organized into chapters according to the respective metal atom involved. As a result, the size of the chapters vary considerably (e.g., Fe, Ru, Os: ca. 3000; Si: ca. 2000; Cu, Ag, Au: ca. 200 entries). An index is provided at the beginning of each chapter, which in a compact form presents excellently drawn structural formulas of the compounds to be described. The corresponding entry is easily found on the basis of the simple code number that accompanies the formula. The third volume, which was prepared with great care, consists of separate name, formula, and CAS Registry Number indexes and contributes substantially to the good overall impression that the "Dictionary" makes.

The literature is covered until 1983. Yearly supplemental volumes are planned, which are to appear every eighteen months after the "copy dead-line." Unfortunately, it is to be feared that the imposing price will preclude the purchase of this useful reference work except by libraries. The announced publication of separate sections for the reader who is interested only in the compounds of a given metal is therefore very welcomed.

Gerhard Erker [NB 737 IE]
Institut für Organische Chemie
der Universität Würzburg (FRG)

Polymer Colloids. By *R. Buscall, T. Corner,* and *J. F. Stageman.* Elsevier Applied Science Publishers, London 1985. xii, 324 pp., bound, £ 38.00.—ISBN 0-85334-312-8

This book—which could equally as well have been entitled "Polymer Dispersions" or "Polymer Latexes"—discusses the synthesis, properties, and some of the methods of characterization of these materials.

In Chapter 1, methods of polymerization are briefly summarized, where the patent literature is also taken into account. In Chapter 2, using emulsion polymerization as an example, kinetic and mechanistic aspects of polymerization are considered in greater detail. The next two chapters, which are devoted to adsorption and adsorptive phenomena in polymer colloids, together with the discussion of the stability of polymer latexes (Chapter 5), constitute the most informative part of the book, at least from a scientific point of view. Rheological investigations (Chapter 6), designed to characterize flow behavior, are treated very briefly. After an explanation of the underlying principles, reference is made to equations, now considered almost classical, that take into account, inter alia, particle form. The discussion of the dependence of viscosity on concentration is followed by an account of non-Newtonian flow behavior. The introduction of dimensionless groups in order to reduce the number of variables necessary is very helpful; here electronically and sterically stabilized dispersions are handled separately. The last two chapters bring plastic materials into focus. Their great significance in technical applications is given detailed consideration using the examples of rubber and polyvinyl chloride.

To be sure, this book is not without weaknesses: this refers not only to the comprehensiveness of the literature references, but more importantly, to the scope of the individual topics, which has evidently been consciously restricted. The strength of the book lies in the broad treatment of polymer dispersions, especially with regard to the special features of their synthesis, characterization, and properties. The reader is thus given the possibility of rapidly becoming familiar with this interesting field. The reading and consultation of this book can be recommended for beginning and advanced students; for the specialist, however, only with reservation.

Werner-Michael Kulicke [NB 719 IE]
Institut für Technische und Makromolekulare Chemie
der Universität Hamburg (FRG)

Corrigendum

The following corrections should be made to the communication entitled: "Enantiomer Separation of (*R*,*S*)-2-(*tert*-Butyl)-3-methyl-4-imidazolidinone, a Chiral Building Block for Amino Acid Synthesis" by R. Fitzi and D. Seebach (*Angew. Chem. Int. Ed. Engl. 25* (1986) 345): On page 346, left-hand column, in lines 7 and 32 "(*S*)-(−)-mandelic acid" should read "(*R*)-(−)-mandelic acid," and in lines 36 and 39 "(*R*,*S*)-diastereomeric salt" should read "(*R*,*R*)-diastereomeric salt."

Registered names, trademarks, etc. used in this journal, even without specific indication thereof, are not to be considered unprotected by law.

© VCH Verlagsgesellschaft mbH, D-6940 Weinheim, 1986. – Printed in the Federal Republic of Germany by Zechnersche Buchdruckerei, Speyer/Rhein.

All rights reserved (including those of translation into foreign languages). No part of this issue may be reproduced in any form – by photoprint, microfilm, or any other means – nor transmitted or translated into a machine language without written permission from the publishers. Only single copies of contributions, or parts thereof, may be reproduced for personal use.

Valid for users in the USA: The appearance of the code at the bottom of the first page of an article in this journal (serial) indicates the copyright owner's consent that copies of the article may be made for personal or internal use, or for the personal or internal use of specific clients. This consent is given on the condition, however, that the copier pay the stated per-copy fee through the Copyright Clearance Center, Inc., for copying beyond that permitted by Sections 107 or 108 of the U.S. Copyright Law. This consent does not extend to other kinds of copying, such as copying for general distribution, for advertising or promotional purposes, for creating new collective works, or for resale. For copying from back volumes of this journal see 'Permissions to Photo-Copy: Publisher's Fee List' of the CCC.

Editorial office: Pappelallee 3, D-6940 Weinheim, Federal Republic of Germany, Telephone (06201) 602315, Telex 465516 vchwh d, Telefax (06201) 602328.

Editor: *P. Gölitz.*

Associate editors: *D. J. Loewus, A. Stimson.* **Editorial assistant:** *E. Schweikart*

Publishers: VCH Verlagsgesellschaft mbH. (Managing Directors: *Prof. Dr. Helmut Grünewald* and *Hans Dirk Köhler*), Pappelallee 3, D-6940 Weinheim, Federal Republic of Germany. Correspondence concerning advertisements should be addressed to VCH Verlagsgesellschaft mbH. (Advertising Manager *R. J. Roth*), Boschstr. 12, P.O. Box 1260/1280, D-6940 Weinheim, Federal Republic of Germany, Telephone Weinheim (06201) 602-0, Telex 465516 vchwh d, Telefax (06201) 602328.

ANGEWANDTE CHEMIE
International Edition in English
Volume 25 · Number 9
September 1986
Pages 767–852

Protein Crystallography and Computer Graphics—toward Rational Drug Design

By Wim G. J. Hol*

"The coincidence of the ideal of progress with the advance of science is not a mere coincidence. Before this advance men placed the golden age in remote antiquity. Now they face the future with a firm belief that intelligence properly used can do away with evils once thought inevitable. To subjugate devasting disease is no longer a dream; the hope of abolishing poverty is not utopian."

John Dewey in
"Democracy and Education" (1916)

1. Introduction

Diseases have diverse origins. They may come from outside, for example, by infection with viruses, bacteria, protozoa, helminths, or other parasites. They may come from inside, for example, through hereditary diseases such as juvenile diabetes, sickle cell anemia, and Down's syndrome. Or they may arise from damage incurred during the course of life, as in the case of cancer.

For millennia people have depended on chance discoveries in their fight against disease. Keen observation led to the remarkable variety of useful herbs known to ancient man. In the last three or four centuries such observation has been supported by scientific reasoning. Nevertheless, the number of new drugs brought on the world market each year is perhaps not even half a dozen, even though such debilitating diseases as leprosy, leishmaniasis, and arthritis are still widespread. Moreover, malaria is making an incredible upsurge and cancer still slowly destroys the lives of many humans, both old and young.

Despite the many possibilities now available for abolishing disease, this goal remains elusive. One of the reasons is the intrinsic difficulty in developing safe and reliable drugs. However, the current explosion of knowledge in understanding the biochemical machineries of both man and pathogens, down to the atomic level, provides grounds for optimism that new drugs will indeed be discovered. This optimism is based on the tremendous progress being made in a number of disciplines: protein purification methods, gene and protein sequencing procedures, recombinant DNA techniques, oligonucleotide synthesis, protein crystallography, computer graphics, and theoretical biochemistry.

We will show in this overview that close and mutually stimulating collaborations between laboratories engaged in medicinal chemistry and those making advances in biochemical techniques open up fascinating possibilities for developing new drugs. Let us see how this may happen and, in fact, is already happening (see also ref. [1]), albeit on a limited scale.

[*] Prof. Dr. W. G. J. Hol
Laboratory of Chemical Physics
University of Groningen
Nijenborgh 16, NL-9747 AG Groningen (The Netherlands)

 © VCH Verlagsgesellschaft mbH, D-6940 Weinheim, 1986 0570-0833/86/0909-0767 $ 02.50/0

2. A New Strategy for the Design of Drugs

Until recently the design or discovery of new drugs has largely been based on the following strategies:

1. in-depth investigations of active substances in herbs and plants traditionally considered to be of medical importance;
2. follow-up of the unexpected results of modern physiological and biochemical investigations;
3. massive screening programs;
4. exploitation of known key metabolic pathways, or other biochemical activities, in man and pathogens.

Penicillin is a prime example of the second category. The treatment of malaria provides examples of the other three categories. *Quinine* and *qinghaosu* (artemisin), from the Chinese herb *Artemisia annua*, are the active substances in plants traditionally used for medical purposes.[2,3] *Mefloquine*, commercial production of which may be too expensive, is the result of a major screening effort at the Walter Reed Army Hospital.[3] *Pyrimethamine* is a selective inhibitor of the dihydrofolate reductase of the malaria parasite. Its discovery resulted from biochemical investigations of a key step in parasite metabolism.[4]

Despite the ingenuity and sophistication often employed in these four approaches, they all suffer from the fact that their target is invisible. It is somewhat like boxing blindfolded—only by trial-and-error does one discover where the opponent is and how he can be knocked out. Being able to see one's opponent would be a big help (although one may still face a formidable problem!). This is precisely what the new strategy initiated in several laboratories aims to achieve.

The cornerstone of this new approach is the accurate knowledge of the three-dimensional structure of potential target proteins and other biomacromolecules, for example, DNA. This requires *X-ray crystallography*, which is the only method available so far to obtain accurate information regarding the three-dimensional structure of biomacromolecules ranging in molecular weight from a few thousand to more than a million. *Computer graphics* is also required, because it is the only way to visualize the complex structures so elucidated. This technique also provides a convenient interface with data bases of known structures and with hypothetical structures generated by *molecular mechanics* and *molecular dynamics* calculations.

If the potential of these recently developed techniques is to be fully exploited, there must be an ample supply of the proteins being studied. Until a few years ago this was a major bottleneck of the whole strategy because often only minute amounts of material were available. However, *recombinant DNA* and *gene cloning* techniques came to the rescue, assisted by powerful *protein microsequencing* procedures and a continual increase in the sophistication of *protein purification* methods. Although the details of each investigation differ, the overall process is illustrated by the following example. Biochemists succeed in isolating small amounts of a medically important protein. A gas-phase sequence analysis establishes the amino-acid sequence of the first 20 to 80 residues. This is followed by *oligonucleotide synthesis* of a series of DNA fragments that can hybridize with the gene encoding this particular protein. Once the gene has been identified, it is transferred into another organism where it is expressed, that is, this organism produces large quantities of the desired protein. Purification, which can sometimes be astonishingly simple if suitable *monoclonal antibodies* are available, affords gram amounts of the protein. This is the starting point for a full biochemical and kinetic characterization as well as for the growth of suitable crystals for X-ray crystallography.

This process, which is here grossly over-simplified, is the prelude to the application of X-ray crystallography, computer graphics, quantum mechanics, molecular mechanics, and molecular dynamics. These latter techniques result in numerous suggestions as to which kinds of molecules might be useful drugs. These molecules must then be synthesized and tested for their effectiveness. Although this route is little different from ongoing approaches to drug design, knowledge of the three-dimensional structure of target proteins allows an important feedback procedure. Because protein crystals contain roughly 50% solvent, small molecules can often diffuse through channels in the protein crystals and reach their binding sites. In such cases, the difference Fourier technique allows rapid determination of the structure of the complex formed between the protein and the small molecule. Even if complexes are not formed in the crystal, cocrystallization experiments may lead to formation of the complex in solution prior to crystallization. The structure determination of the complex is usually greatly speeded up by knowing the three-dimensional structure of the uncomplexed protein, since the so-called "molecular replacement method"[5] can then be used.

Accurate three-dimensional structures of a protein complexed with various small molecules provide a powerful starting point for the design of new molecules that will bind to this protein. This is especially true if the small molecules bind differently from predictions based on imperfect theories. Moreover, such structures may reveal major or minor conformational changes of the protein, which might be exploited in the design of new compounds. In this "rational drug design cycle" (Fig. 1), the structure of each new complex between the protein and a new compound expands the data base, resulting in the generation of ever better ideas for pharmaceutically active compounds. The ultimate goal is, of course, to leave the cycle as soon as possible by obtaining an effective new drug.

3. Three Cases

Three cases for the development of a new drug on the basis of potential target protein structures are possible.

1. A human protein is not functioning properly or its activity has to be modified for other reasons. In this case, only the three-dimensional structure of this particular protein is required. No proteins from infectious organisms need to be considered.

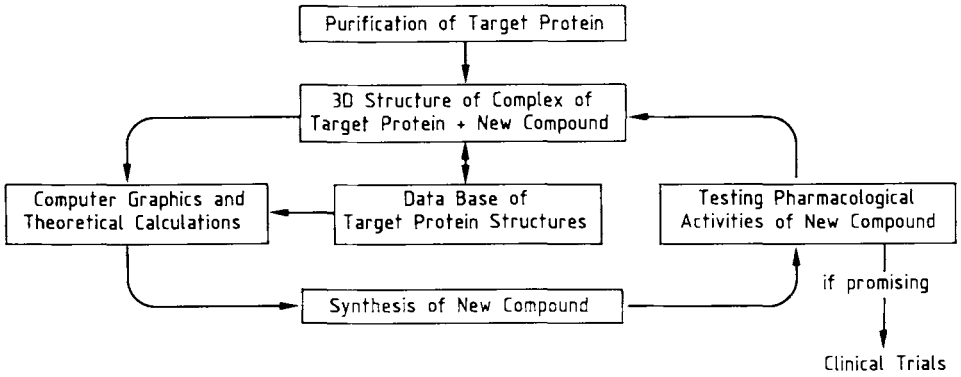


Fig. 1. A "rational drug design cycle" employing three-dimensional structures of complexes formed between target proteins and a range of small molecules (ligaands).

2. The potential target is a key protein from an infectious organism and has no counterpart in humans. In this case, the three-dimensional structure of the selected protein in the pathogen is the starting point and no human protein structures have to be taken into account.
3. The target is a protein from a harmful organism and a homologous human protein exists. In this case, the target protein must be inhibited selectively so that the human counterpart is not impaired. The three-dimensional structures of both proteins are required in order to design the desired selective inhibitors (Fig. 2).

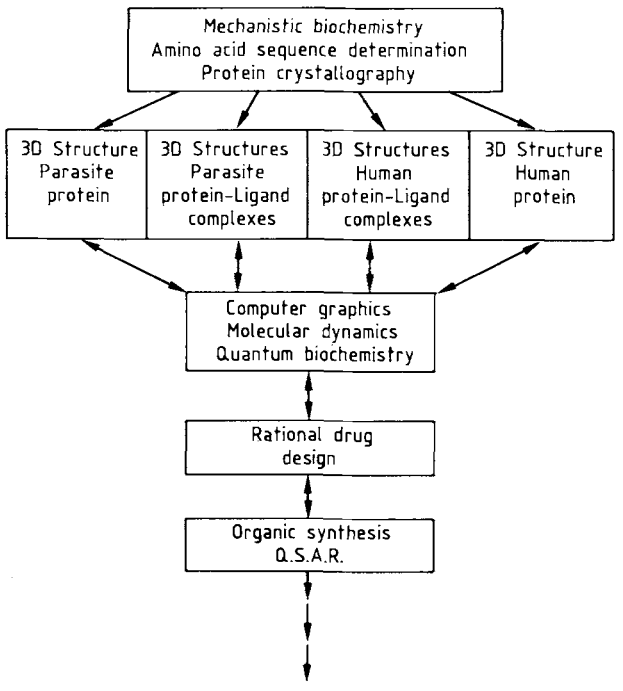


Fig. 2. Flow diagram of successive steps in a drug design strategy where detailed knowledge of the structure of key proteins plays a central role. Q.S.A.R.: quantitative structure-activity relationship.

The boundaries between these cases are by no means strict. Two of these cases are often considered simultaneously. Nevertheless, the distinction is quite useful, as shown in the following three sections.

4. Drugs that Affect Human Proteins

4.1. Sickle Cell Anemia

Hemoglobin was one of the first proteins to be structurally elucidated. Moreover, its structure was one of the first to be employed for designing new compounds that produce predicted physiological effects. The binding site for the natural effector substance, 2,3-diphosphoglycerate, in the deoxy conformation of human hemoglobin[6] was chosen as a model receptor site by *Beddell* et al.[7] They designed and synthesized a series of bibenzyl dialdehyde derivatives that produced the desired effect, namely, the stabilization of the deoxy conformation and the resulting right-shift of the oxygen saturation curve of hemoglobin.

These initial experiments were followed by an attempt to design compounds that alleviate the clinical symptoms caused by sickle hemoglobin, HbS.[8]. Substituted benzaldehydes were designed to bind preferentially to the oxy conformation of human hemoglobin at a site between the amino terminal residues of the α subunits. The compounds indeed produced the desired effect: left-shifting of the oxygen saturation curve of dilute hemoglobin solutions and of whole blood. Most interestingly, one of the predicted compounds is also a potent inhibitor of the sickling of erythrocytes of patients suffering from sickle cell disease. It may prove to be a clinically useful anti-sickling agent.[8]

Designing anti-sickling agents is difficult because a balance has to be struck between two somewhat conflicting requirements: (1) deoxy HbS fibers must not form, since they would thereby prevent the passage of erythrocytes through blood capillaries; (2) the oxygen transport capacity of the blood must not be diminished too severely.

Several groups, e.g., *Walder* et al.[9] and *Abraham* et al.[10], are using the three-dimensional structure of the hemoglobin molecule for designing anti-sickling agents. The work of *Abraham* et al. has already revealed the structures of a series of compounds complexed with hemoglobin, several of which appear to be bound in a rather unexpected manner.[11]

Future efforts to design anti-sickling compounds will be further assisted by the high-resolution structures of human oxy- and deoxy hemoglobin which are now available.[12] Also, the accuracy of the deoxy HbS structure has recently been considerably improved.[13,14] This is especially impor-

tant since the structure of the HbS aggregate in these crystals is believed to be closely similar to that of the polymer in the erythrocyte.[13, 14]

Hemoglobin is one of the very few human proteins of great interest for drug design for which an accurate three-dimensional structure is now known. However, even knowledge of the three-dimensional structure of a homologous protein from another organism may provide a starting point for obtaining the structure of a human protein—although one always has to bear in mind that more or less subtle changes in conformation may arise from amino-acid substitutions. Several such potentially useful structures are included in Table 1, a few of which are discussed further below.

Table 1. Proteins with known three-dimensional structures, which may be useful for the rational design of drugs that interact with human proteins only.

Protein	Source	Disease	Potential human target protein	Refs.
hemoglobin	human	sickle cell anemia	hemoglobin S	[8-14]
phospholipase A_2	pancreatic, snake venom	inflammation	intracellular phospholipase A_2	[55-59]
dihydrofolate reductase	bacterial	cancer	dihydrofolate reductase	[33]
carboxypeptidase A	bovine	hypertension	angiotensin-converting enzyme (ACE)	[15, 18-20]
thermolysin	bacterial			[16, 21-24]
aspartyl proteases	bacterial	hypertension	renin	[25-27, 30, 121, 122]
elastase	porcine	emphysema	leucocyte elastase	[123]
subtilisin: eglin	bacterial			
α_1-proteinase inhibitor	human	emphysema thrombosis	α_1-proteinase inhibitor anti-thrombin	[124]
calmodulin	rat	psychosis	calmodulin	[125, 126]
troponin C	chicken, turkey		troponin C	[127-129]

4.2. Hypertension

Hypertension is a major health problem in industrial societies, contributing to cardiovascular disease, stroke, and renal failure. Although its mode of action is not fully understood, the hormone angiotensin II is an important factor in regulating blood pressure, with higher concentrations of the hormone leading to higher blood pressures. The hormone is produced in the body via two steps (Fig. 3). First, the enzyme *renin* catalyzes the cleavage of angiotensin I from the inactive prohormone angiotensinogen. Second, the *angiotensin-converting enzyme* (ACE) catalyzes the removal of the carboxyl-terminal dipeptide from angiotensin I, releasing angiotensin II. Inhibition of either renin or ACE, or both, would lead to a smaller concentration of angiotensin II and contribute to lowering the blood pressure. No three-dimensional structure of ACE has been reported as yet, but the enzyme is known to be a zinc-peptidase and the structures of two such proteases have been determined with great accuracy: carboxypeptidase A and thermolysin.[15, 16]

The analogy between the active sites of ACE and carboxypeptidase A has been used by *Cushman* et al.[17] to guide the design of specific ACE inhibitors. The first carboxyalkanoyl amino acid synthesized, succinyl-L-proline, had an I_{50} value of 330 μM for inhibition of rabbit lung ACE. In the meantime, many modified compounds have been synthesized, the general architecture of the carboxypeptidase A active site having been kept constantly in mind. Replacement of the carboxyl group yielded 1-(3-mercaptopropanoyl)-L-proline with an I_{50} value of 0.2 μM. Further modifications gave the most potent inhibitor found, 1-(D-3-mercapto-2-methylpropanoyl)-L-proline, with an I_{50} of 0.023 μM.[17] This inhibitor is now on the market under the name Captopril and may be considered as the first generally available drug designed, albeit partly, on the basis of the known crystal structure of a protein molecule. This success has been one of the reasons for further investigations into the mode of binding of inhibitors to both carboxypeptidase A[18-20] and thermolysin.[21-24]

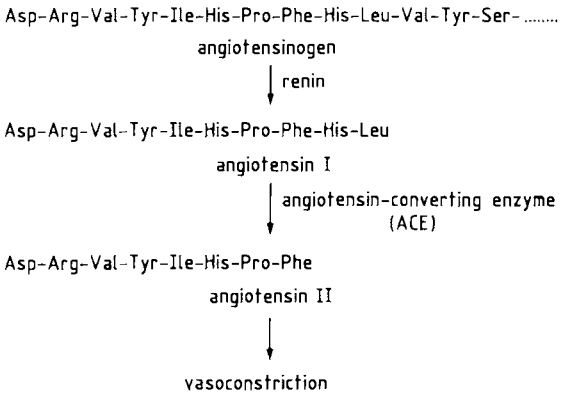


Fig. 3. Release of the oligopeptide angiotensin II catalyzed by the proteolytic enzymes renin and angiotensin-converting enzyme. Angiotensin II is involved in the regulation of blood pressure.

The aspartyl protease renin is considered a promising alternative target for inhibition of the conversion of angiotensinogen to angiotensin II, because the enzyme exhibits great specificity. Owing to the availability of high-resolution X-ray structures of several bacterial aspartyl proteases[25-27] and to the knowledge of the amino-acid sequence of human renin,[28, 29] it has been possible to use computer graphics methods to derive models of the human

enzyme. These models have formed the basis for making predictions of substrate binding.[30] Detailed crystallographic data on the structure of an aspartyl protease complexed with an inhibitor showed that the predictions made were essentially correct.[31]. The considerable activity going on in this area is further illustrated by the reported crystallization of mouse renin and renin-inhibitor complexes by a drug company in the United States.[32]

4.3. Cancer

Cancer falls squarely into the category of diseases for which successful drugs have to interact specifically with human proteins only. Although the detailed structure of a complex formed between the widely used anticancer drug methotrexate and bacterial dehydrofolate reductase is known,[33] it is hard to see how such knowledge can aid the design of better anticancer drugs: dihydrofolate reductase is too essential for *all* dividing cells. This key role of the target protein in nontransformed cells explains the serious side effects of methotrexate. For similar reasons, enormous problems exist with other anticancer drugs.

The "ideal" cancer drug should interact with a *specific* feature of the cancer cell crucial for its uncontrolled proliferation. Such a specific difference between normal and cancer cells may be provided by the point mutations observed in the *ras* "oncogene," which give rise to the transforming properties of its product, the p21 protein.[34-36] *Wierenga* and *Hol* observed an analogy between the amino-acid sequence of the first 30 residues of p21 and the sequences of a family of dinucleotide binding proteins and were able to construct a hypothetical model for this fragment of p21 (Fig. 4).[37] These residues might fold into a compact βαβ unit with the glycine at position 12 close to the phosphate group of a bound nucleotide. In several kinds of cancer cells, this glycine happens to have undergone mutation to form another residue.[34-36,38-41] In the hypothetical βαβ model[37] this would result in steric hindrance between the side chain of the non-glycine residue and the nucleotide phosphate and, therefore, in an altered mode of binding, improper functioning of p21, and loss of control of cell proliferation. If this model is correct then it might be possible to design compounds that bind to the mutated p21 of transformed cells in such a manner that their disastrous properties are suppressed. The mechanism of action of such compounds would depend on a crucial difference between cancer cells and normal cells and hence should not cause the side effects commonly associated with current anticancer drugs.

It is only fair to say that the prediction of *Wierenga* and *Hol* for the structure of p21 is by no means the only one.[42-46] Moreover, elegant site-directed mutagenesis experiments have shown that all non-glycine residues introduced at position 12, with the exception of proline, impart carcinogenic properties to p21.[47] This is difficult to reconcile with the predicted mode of binding of the dinucleotide to a βαβ unit. However, even if p21 has a structure different from all predictions made so far, the ideas discussed in the previous paragraph remain correct: a unique feature of a protein crucial for the rapid proliferation of a transformed cell provides, in principle, the basis for designing new and perhaps "ideal" drugs for certain kinds of cancer.

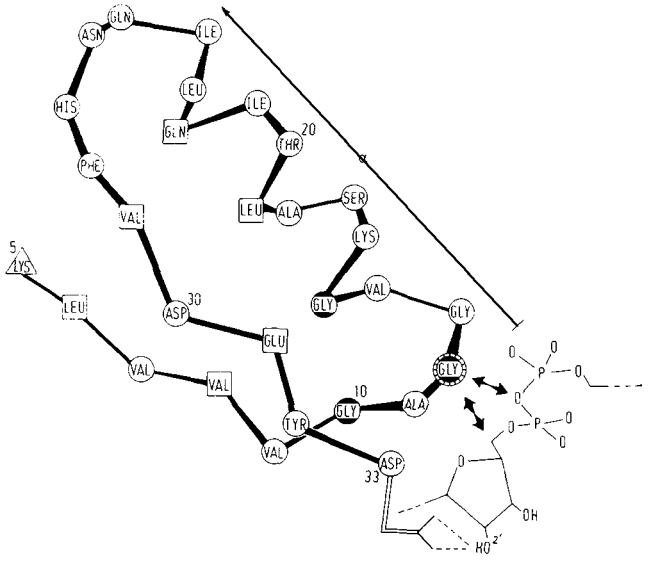


Fig. 4. Hypothetical model for the residues 5 to 33 of the p21 protein, encoded by the *ras* oncogene. Also indicated is the predicted ribose diphosphate moiety of a bound nucleotide. Mutations of glycine 12 would necessarily introduce a side chain at this position which would affect the postulated mode of binding of the nucleotide [37].

4.4. Inflammation and Asthma

Prostaglandins, thromboxanes, and leukotrienes are mediators of hypersensitivity reactions and inflammation.[48-52] They are formed via complex metabolic pathways in response to various stimuli; the formation of arachidonic acid is a central step (Fig. 5), which is catalyzed by the enzyme phospholipase A_2, or, more precisely, the intracellular $Ca^{2\oplus}$-dependent phospholipase A_2. In spite of its great importance, relatively little is known about this enzyme. However, *Okamoto* et al.[53] showed recently that the intracellular phospholipase A_2 is immunologically related to the secretory phospholipase A_2, several examples of which have been characterized in great detail (see, e.g., ref.

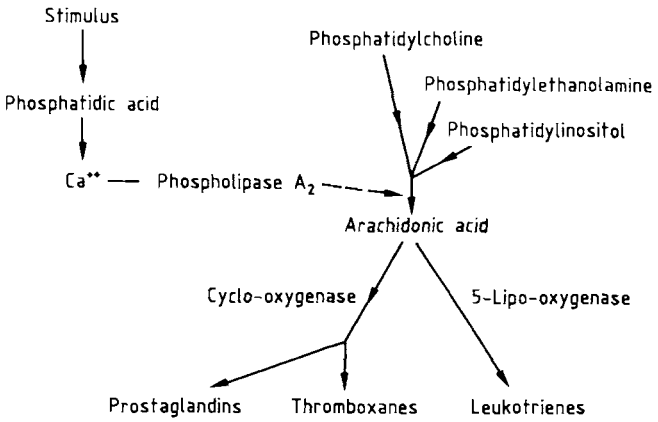


Fig. 5. Schematic drawing of the key step, catalyzed by cellular phospholipase A_2, in the biosynthesis of prostaglandins, thromboxanes, and leukotrienes.

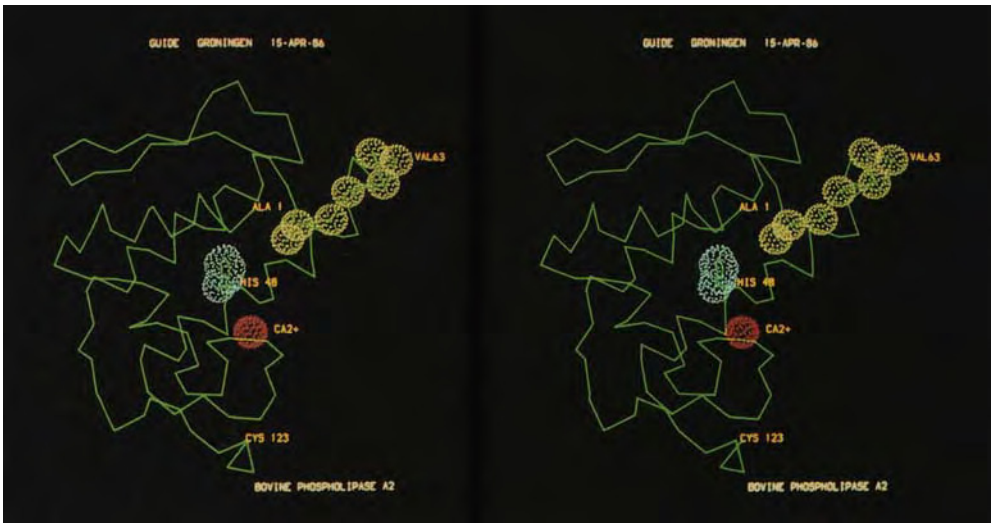


Fig. 6. Stereopicture of the structure of bovine pancreatic phospholipase A_2, which may resemble the cellular phospholipase A_2 to a considerable degree. The essential His-48 (blue) and the calcium ion (red), which is necessary for activity, are indicated. The "sixties-loop" is highlighted by yellow dot surfaces at the C_α positions. This loop has special properties: depending on the phospholipase, it is either disordered or adopts a conformation quite different from the one shown for the bovine enzyme [55–59].

[54]). The three-dimensional structures of pancreatic phospholipase A_2 from several sources are known (Fig. 6);[55–58] the structures of the snake venom and pancreatic enzymes are extremely similar.[59] Clearly, this structural information can be a starting point for designing inhibitors of intracellular phospholipase A_2, because the immunological relationship[53] almost certainly implies a considerable similarity in the active-site regions. It would be of great help if the structure of a phospholipase A_2 complexed with a phospholipid analogue were known, but this has not yet been achieved. A possible explanation is the surprising conformational sensitivity of the pancreatic enzyme to even minute alterations.[58] Nevertheless, the structure of the covalent inhibitor *p*-bromophenacyl bromide bound to the active-site histidine is currently known at 3.0 Å resolution—despite the fact that only a single suitable crystal was available.[60] This example of an inhibitor binding mode may provide an experimental starting point for designing specific inhibitors.

Even more recently, the amino-acid sequence of the protein macrocortin, or lipocortin,[61] an inhibitor of phospholipase A_2 induced by glucocorticoids,[48] was elucidated. The structure of a lipocortin:phospholipase A_2 complex would obviously be a marvelous source of inspiration for designing new compounds that interfere with arachidonic acid synthesis. A large number of laboratories are already engaged in attempts to design inhibitors using the information currently available for the structure of phospholipase A_2.

5. Inhibition of Proteins that are Unique to Infectious Organisms

5.1. Inhibition of Bacterial Cell Wall Synthesis

Penicillin is undoubtedly the best known example of a compound that inhibits, in an infectious agent, a vital metabolic step that has no counterpart in humans. The penicillin family has been enlarged by cephalosporins and other chemically related compounds (see, e.g., ref. [62]), so that a wide range of antibacterial compounds that interfere with cell wall synthesis is now available. This has caused a revolution in the treatment of bacterial infections in the twentieth century.[62] Nevertheless, drug resistance remains a severe problem. In several cases, this resistance is caused by enzymes such as β-lactamases that are able to degrade members of the penicillin family, rendering them harmless to the pathogen.

Penicillin interferes with the final steps of the synthesis of peptidoglycan, an important component of the cell wall:

$$\text{enzyme} + \text{R-D-Ala-D-Ala-COOH} \longrightarrow \text{enzyme—CO-Ala-R} + \text{D-Ala-COOH} \quad (1)$$

$$\text{enzyme—CO-Ala-R} + \text{R'NH}_2 \longrightarrow \text{R'NHCO-Ala-R} + \text{enzyme} \quad (2)$$

where R and R′ are the two polysaccharides to be cross-linked. Some of the enzymes involved are bifunctional. They can carry out both steps, acting as carboxypeptidase-transpeptidases, or they can accept water as the acceptor in step (2) and function as carboxypeptidases. Other enzymes are monofunctional and act solely as D-alanyl carboxypeptidases.[63]

The structure of a $Zn^{2\oplus}$-containing D-alanyl-D-alanyl carboxypeptidase from *Streptomyces albus* has been solved at 2.5 Å resolution by *Dideberg* et al.[64] This enzyme is penicillin-insensitive; only the β-iodopenicillinate binds irreversibly to its active site.[64] Once the structures of this enzyme and of complexes with its inhibitor are known in greater detail, they may suggest further possible modifications of the penicillin molecule, particularly those that would enable it to block a wide range of carboxypeptidases responsible for resistance.

The structure of a penicillin-sensitive D-alanyl carboxypeptidase-transpeptidase, solved by *Kelly* et al.,[65] is also of great interest. Moreover, these investigators reported the

first crystallographic binding studies of four species derived from penicillin: three β-lactams and a cyclobutanone.[66]

While this review article was being completed the first details of β-lactamase I from *Bacillus cereus* became available. Extensive regions of the tertiary structure of this enzyme are similar to those of the penicillin-sensitive D-Ala-D-Ala carboxypeptidase-transpeptidase.[67] Although details of the β-lactamase structure require further model building and refinement, it is evident that important structural information on penicillin-sensitive and penicillin-degrading enzymes is just becoming available. In due course it may become possible to design compounds that fit tightly into the active site of carboxypeptidases catalyzing the synthesis of cell walls and which, at the same time, have precisely tailored substituents that prevent inactivation by lactamases. Alternatively, efficient inhibitors of the β-lactamases may be designed. However, despite the detailed knowledge of the three-dimensional structures of proteins provided by X-ray crystallography, converting this knowledge into useful drugs, or combinations of drugs, remains a formidable challenge.

5.2. Virus Coats

High-resolution structures of viruses and of viral coat proteins are of tremendous importance for the development of new vaccines against several widespread human diseases. But also from the point of view of rational drug design, the crystallographic studies on rhino- and poliovirus,[68,69] as well as on the influenza virus coat proteins hemagglutinin[70] and neuraminidase,[71] are of potential practical use. For instance, inspection of the intricate subunit–subunit interactions of the viral coat proteins may reveal binding sites for small molecules that might interfere with the assembly of the viral particles. Alternatively, such knowledge may direct the design of precisely tailored cross-linking reagents—in analogy to the development of bivalent anti-sickling compounds.[8] Extensive cross-linking could render viruses into harmless entities. A third possibility is the design of compounds that fit tightly into the receptor binding sites of the rhino- and poliovirus and thereby prevent their entrance into the cell. The impressive results obtained by protein crystallography are therefore rich sources of inspiration for medicinal chemists designing new antiviral agents.

5.3. Bacterial Toxins

Some bacteria affect their hosts by the excretion of one or more toxins. The best characterized toxins include diphtheria toxin (DT), excreted by *Corynebacterium diphtheriae*, choleratoxin (CT), excreted by *Vibrio cholerae*, and the closely related, heat-labile enterotoxin (LT), excreted by enterotoxic *Escherichia coli* strains.[72–75]

Diphtheria toxin is synthesized as a single polypeptide chain of $M_r = 62000$, which is then split into an A chain of $M_r = 21000$ and a B chain of $M_r = 40000$. The A chain is an enzyme catalyzing the ADP-ribosylation of elongation factor 2, while the B chain is essential for entrance of the A chain into the cell. A similar mode of action has been observed for CT and LT, although their architecture and the precise point of cell deregulation differ from those of DT. CT and LT, like DT, consist of an A chain ($M_r \approx 27000$) and a B chain ($M_r = 13000$), but they form an AB_5 complex. The B chains are responsible for binding to the cell surface, where they interact with GM_1 gangliosides (Fig. 7). The A chain catalyzes an ADP-ribosylation, but the target is this time the regulatory G_s component of the adenylate cyclase system. This ribosylation sets the G_s protein in a permanent "on" state, which, in turn, stimulates adenylate cyclase to produce cAMP, resulting in a massive outflow of water and nutrients through the intestinal cell wall. This sequence of events has severe consequences, ranging from inconvenience in the northern hemisphere to child death in many less developed areas.

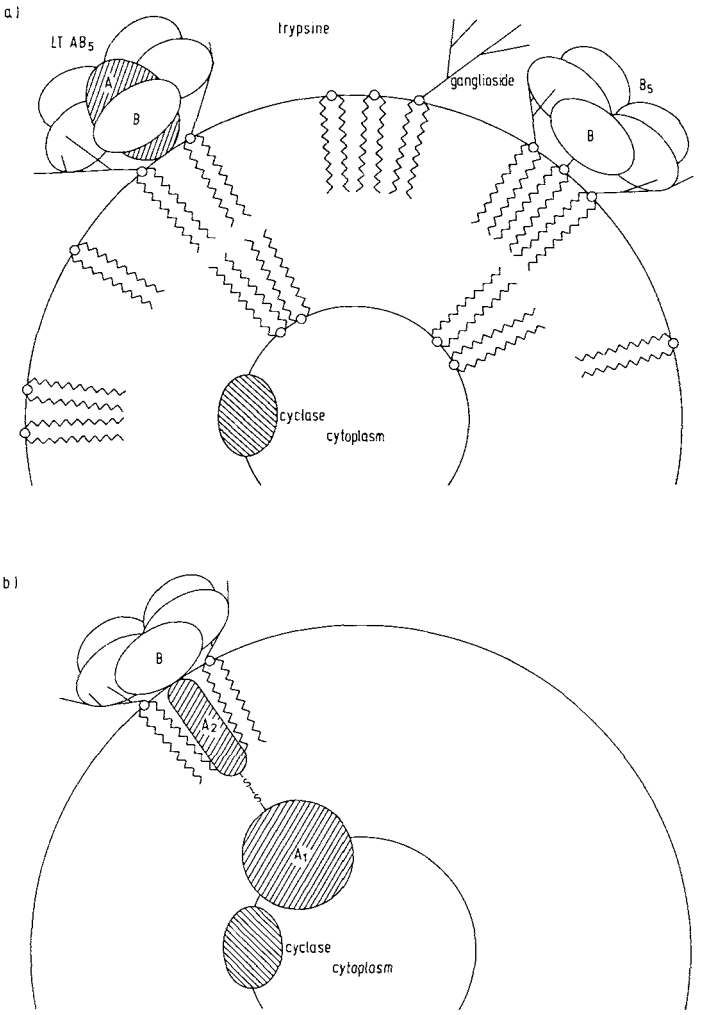


Fig. 7. The mode of action of the heat-labile enterotoxin from *E. coli*, which is virtually identical to that of choleratoxin. a) Attachment of AB_5 and B_5 complexes to gangliosides (GM_1) in the membrane of epithelial cells of the gut; b) translocation of the A1 fragment ($M_r = 22000$) across the membrane, followed by an ADP-ribosylation of the G_s component of the adenylate cyclase system (Drawing kindly provided by *Sylvia Pronk*). LT means heat-labile enterotoxin.

The amino-acid sequences of these toxins have recently become available,[76–80] and X-ray investigations are under way for DT, CT, and LT.[81–84] Once these investigations

have yielded high-resolution structures, compounds can be designed to interfere selectively with the key steps in the mode of action of these toxins; for example,

1. assembly of the AB_5 complex of CT and LT and the AB complex of DT;
2. binding to the cell surface receptors;
3. entry of the A chain into the cell;
4. ADP-ribosylation catalyzed by the A chain once it is inside the cell.

The rational design of drugs will have to compete, of course, with the development of vaccines, based either on recombinant DNA technologies or on fragment peptide synthesis, which is being carried out presently in a number of laboratories. Moreover, oral rehydration therapy appears to provide a cheap and effective method to combat child death due to enterotoxic *E. coli* and *V. cholerae* infections in developing countries. Nevertheless, accurate three-dimensional structures of the "moonlander-like" bacterial toxins, in particular the structures of their complexes with GM_1 and NAD analogues, may prove to be a starting point for the development of a variety of new pharmaceuticals.

6. Selective Inhibition of Proteins from Infectious Organisms

There are only a few examples in the literature of crystallographic projects involving the inhibition of an enzyme from a pathogen in cases where an analogous enzyme in the human host must be protected from inhibition. One well-known example is provided by the bacterial dihydrofolate reductases. Another example is that of the glycolytic enzymes from *Trypanosoma brucei*, the causative agent of sleeping sickness.

6.1. Dihydrofolate Reductase

Dihydrofolate reductase (DHFR) is a key enzyme in the metabolism of numerous organisms and the target protein of several widely employed drugs. The enzyme is vital for proliferating cells because it is required for maintaining adequate levels of fully reduced folate, which, in turn, is necessary for the synthesis of thymidylate (Fig. 8).

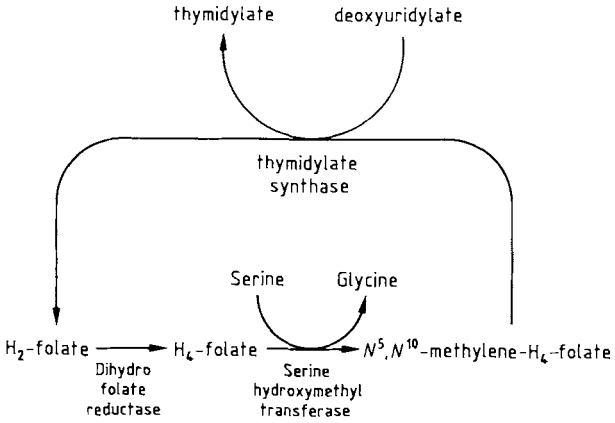


Fig. 8. Pathway involving three enzymes that are crucial for the synthesis of thymidylate and thus nucleic acids. The differences in the properties of dihydrofolate reductase from different organisms form the basis for several important antibacterial and antimalarial drugs currently in use. Human dihydrofolate reductase is, in addition, the target of the cancer drug methotrexate.

Three classes of dihydrofolate reductases have been described so far (see, e.g., refs. [85, 86] and references cited therein):

1. Chromosomal DHFRs have a molecular weight of about 15000 and, despite amino acid homologies of less than 30%, appear to share a common architecture (Fig. 9). Three-dimensional structures are known for the *E. coli*, *Lactobacillus casei*, and chicken enzymes.[33, 87, 88] A preliminary report on the structure of a second vertebrate DHFR, the enzyme from the L1210 mouse lymphoma, has appeared from the Wellcome Laboratories in the United Kingdom.[89]
2. Plasmid-encoded DHFRs occur in certain bacterial strains resistant to the antibacterial drug trimethoprim. Three types of resistant DHFRs can be distinguished:[85]
   - type I: dimeric molecules with subunits having molecular weights of about 17500; their resistance to trimethoprim is due mainly to a lowered affinity for the drug;
   - type II: a tetrameric molecule with a reported subunit molecular weight of about 8500;
   - type III: monomeric proteins with molecular weights of about 18000; their resistance to trimethoprim is due to a combination of weaker binding of the drug and enhanced affinity for the substrate.

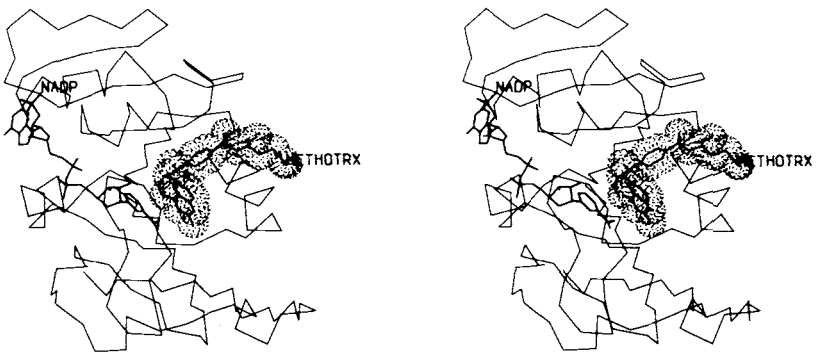


Fig. 9. Stereopicture of the structure of the complex of dihydrofolate reductase from *Lactobacillus casei* with the coenzyme NADP and the drug methotrexate (labeled METHOTRX) (coordinates kindly provided by *D. A. Matthews* and *J. Kraut*).

Amino acids crucial for the functioning of chromosomal DHFRs are conserved in type I and type III plasmid-encoded DHFRs, which suggests a common ancestry and similar overall architecture. The type II DHFRs have an entirely different folding pattern as shown by the crystal structure of apo R67 DHFR: each 78-residue subunit is folded into a six-stranded antiparallel β-barrel.[85]

3. Protozoal DHFRs have molecular weights of about 110000. These large enzymes have been found in the rodent malaria parasite *Plasmodium berghei*, in *Leishmania tropica*, and in *Trypanosoma cruzi*.[90-92] Most intriguingly, this protozoan enzyme is bifunctional, exhibiting both DHFR and thymidilate synthetase activities.[91-92] No structural information about this class of DHFRs is available yet, despite the great importance of such information for the treatment of several major tropical diseases. The need for new drugs is dramatically shown by the rapid increase of resistance against one of the most important antimalarial drugs, pyrimethamine.[2] This drug is a DHFR inhibitor, binding 1400 times more tightly to the *Plasmodium* enzyme than to the human enzyme;[93] however, the resistant malaria strains are somehow able to avoid the drug's action.

In a most interesting article, the group of *Matthews* and *Kraut* in San Diego recently described X-ray structures of complexes formed between dihydrofolate reductase and not less than ten compounds.[94] The structures of these complexes, together with the structures of the antibacterial drug trimethoprim bound to chicken and *E. coli* DHFR,[95] provided an explanation for the different binding of the drug to bacterial and mammalian DHFRs at the atomic level: amino acid residues on opposite sites of the active site cleft in the *E. coli* enzyme are approximately 1.5–2.0 Å closer to each other than the corresponding residues in the chicken enzyme.

Space does not permit further details to be presented regarding this series of DHFR structures; these studies have afforded marvelously detailed insight into the mode of action of drugs and their derivatives. They will almost certainly lead, via the rational drug design cycle (Fig. 1), to new antibacterial compounds in the near future. Reports on several investigations along these lines have already appeared (e.g., refs. [96–98]).

6.2. Glycolytic Enzymes and Sleeping Sickness

Sleeping sickness, or human trypanosomiasis, in sub-Saharan Africa is considered by the World Health Organization as one of the six most important current tropical diseases.[2] The disease is caused by the protozoal parasite *Trypanosoma brucei*. Only three drugs, each of which causes serious side effects, are presently available for treatment of the disease.[99] New and better drugs are therefore urgently needed.

Trypanosomes have several characteristic features, one of which is the variable surface glycoprotein (VSG), which enables the parasite to outwit the human immunological defense system.[100] The three-dimensional structure of a VSG has been reported at low resolution;[101] work at high resolution is in progress. The VSG structure shares a basic feature with that of influenza virus hemagglutinin, namely, long coiled α helices perpendicular to the membrane surface. Once detailed knowledge, in particular about subunit interactions, becomes available for the VSG protein, it may become possible to pursue strategies similar to those discussed above (Section 5.2) for the viral coat proteins. Compounds may be designed that either interfere with the assembly of the VSGs or bind to specific sites formed by two neighboring VSGs, thereby cross-linking them. The latter approach is not without problems, since damage to human macromolecules must be avoided.

In another project, three groups—in Amsterdam, Brussels, and Groningen—are collaborating in an attempt to design new drugs against sleeping sickness. These groups are focusing on another unique feature of *Trypanosomatidae*, namely, the presence of glycosomes. These peroxisome-like organelles are vital for the energy supply of the bloodstream form of the trypanosome.[102-104] The major glycosomal proteins are nine enzymes involved in glucose and glycerol metabolism. All nine enzymes are now available in pure form.[105, 106] Moreover, the amino acid sequences of five glycolytic trypanosomal enzymes have been determined by sequencing the corresponding genes.[107-110] Crystallization of trypanosomal enzymes is unusually difficult owing to the small amounts of material available. Nevertheless, high-quality crystals of the enzyme triose phosphate isomerase (TIM) were obtained from approximately 1 mg of protein,[110] and have allowed the solution of its three-dimensional structure.[111] Fortunately, TIM is also one of the enzymes for which the *T. brucei* sequence is available.[107] Moreover, the three-dimensional structure of the chicken enzyme[112] gives a good idea of the structure of the human enzyme owing to the high sequence homology. The *T. brucei* TIM structure still needs considerable refinement before it provides a solid basis for rational drug design. However, it is already obvious that the design of compounds that inhibit catalysis of the trypanosomal enzyme while leaving the human TIM undisturbed will not be trivial. The reason is the great similarity of the active site regions of the human and parasite proteins (Fig. 10). One of the differences closest to the active site resides in residues 101–103, which are Ala-Tyr-Tyr in *T. brucei* and His-Val-Phe in man.[107] To exploit this difference for the design of selective inhibitors, a distance of approximately 20 Å must be bridged between the substrate binding site and residue 102. This can certainly not be achieved in a single shot. However, via the rational drug design cycle, it might be possible to increase gradually the size of the compounds synthesized, see how they bind, and deduce new modifications which eventually may provide the necessary selectivity.

For another glycosomal enzyme, phosphoglycerate kinase (PGK), the amino-acid sequence is available;[108] moreover, three-dimensional structures of the horse and yeast enzymes are known.[113, 114a,b] Unfortunately, PGK from *T. brucei* does not show the slightest tendency to crystallize. However, model building on a computer graphics system coupled with energy minimization has given approximate models of the *T. brucei* and human en-

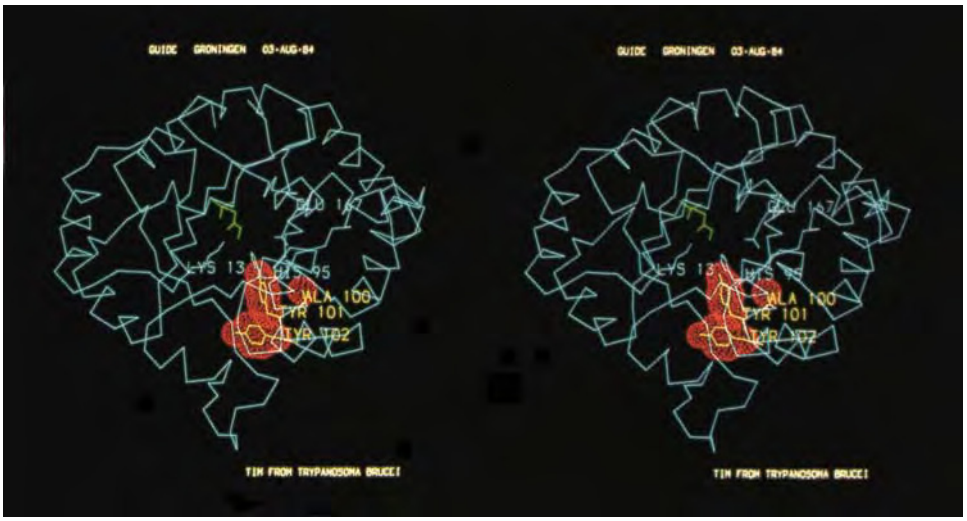


Fig. 10. Stereopicture of the structure of triose phosphate isomerase (TIM) from *Trypanosoma brucei* (coordinates kindly provided by *R. K. Wierenga*). Superpositions of TIM from *T. brucei* and yeast complexed with the substrate dihydroxyacetone phosphate (DHAP) (coordinates generously made available by *G. Petsko*) yielded an approximate position of DHAP bound to *T. brucei* TIM (center of the picture, green). For clarity, only C_α coordinates are shown except for six residues of which the side chains are outlined: the three catalytic residues Lys-13, His-95, and Glu-167, and the three residues near the active site that differ from those in the human enzyme, namely, Ala-100, Tyr-101, and Tyr-102 (yellow surrounded by a van der Waals surface in red). In the human enzyme, the latter three are His-100, Val-101, and Phe-102.

zymes.[114c] The active site regions appear to differ more from each other than in the case of triose phosphate isomerase and, hence, the design of selective inhibitors might be easier to achieve.

Selective enzyme inhibition is not the only way, however, by which the presence of glycosomes can be exploited for the rational design of drugs against sleeping sickness. Unlike their human counterparts, glycosomal enzymes have to enter the glycosome, thereby providing opportunities to interfere with the mechanism of import. Analysis of the sequences of glycosomal enzymes, together with the known three-dimensional structures of triose phosphate isomerase, phosphoglycerate kinase, and glyceraldehydephosphate dehydrogenase has led to a proposal for the mechanism of glycosome import:[115] two areas of high positive charge, approximately 40 Å apart, are considered to be essential elements of the import signal. Interestingly, this suggests a possible mode of action of suramin, one of the few drugs effective against sleeping sickness.[99] Suramin is a very complex molecule that has two trisulfonated naphthalene ring systems, which are approximately 40 Å apart in the extended conformation. The drug, which is known to interfere with glycolysis, might exert its therapeutic effect by preventing import of enzymes into glycosomes. Further investigations, currently in progress, are required, to prove these hypotheses. Whether or not these speculations are correct, the glycosomal import mechanism is an interesting target for rational drug design because there may be no closely analogous system in human beings.

7. Protein Crystallography

The methodology of X-ray crystallography of proteins is not given much attention in this article for two reasons. First, it would take up too much space. Second, several extensive accounts of the procedures required have been published (e.g., refs. [116, 117]). These monographs also give due attention to the major hurdle that has to be surmounted before a structure can be elucidated, namely, the growth of high quality crystals. This step is sometimes solved in a month, sometimes in one or two years, and sometimes not at all. Thus, it is hard to predict if and when a structure will be solved. However, with the gradual increase in the number of crystallization procedures and with the large amounts, up to grams, of very pure protein that are often made available by gene-cloning techniques, the prospects of obtaining crystals are becoming better all the time. The future may see the use of "protein-engineering-for-crystal-growth," that is, generating mutant enzymes that remain active but crystallize more readily. This will, obviously, have to be a trial-and-error process but it may be the only solution in cases where one absolutely needs to know a crystal structure. In difficult cases, it might be possible to crystallize proteins complexed with monoclonal antibodies. Once crystals are obtained, sophisticated software and hardware for data collection and phase determination allows structure determinations with increasing speed and accuracy.

8. Concluding Remarks

The drug design approach outlined here can be expanded in two ways. First, other biomacromolecules can be used as drug targets, which has already been alluded to in the introduction. In particular, X-ray crystallography of *oligonucleotides* has afforded detailed insight into the structure of DNA. For instance, the recent structure of a DNA:netropsin (congocidin) complex[118] may prove to be the starting point for the rational design of pharmaceuticals active against specific DNA sequences. It is also conceivable that differences in the tRNA, the ribosomal RNA, or the nuclear RNA structures of pathogen and host might be used for designing pharmaceutically useful compounds.

Second, the rational drug design strategy discussed here may be applied equally well to the design of new herbicides and pesticides. Indeed, the fantastic structure determination of the photosynthetic reaction center has already allowed the location of the herbicide terbutryn at its site of action.[119]

Amidst all this optimism it is good to remember the long list of obstacles to be overcome before a compound showing a desired activity in a test tube can be sold on the market as a useful drug. Drug delivery and safety, the possibility of metabolic alterations, and the economics of production all need to be given great attention and are, moreover, time-consuming. In this respect the approach outlined in the work described here and elsewhere (e.g., ref. [1]) differs little from existing procedures. However, in the initial stages of drug design, the approach discussed here is vastly different—not only because it allows one to "see" which compounds might be effective but also because three-dimensional structures of target proteins often immediately show which modifications of a compound *cannot* lead to a more active molecule, because the modified compound would simply not fit into the active site. *Freudenreich* et al.[120] give a beautiful example of these points in their rational design of alcohol dehydrogenase inhibitors on the basis of the three-dimensional structure of the enzyme.

In summary, a new drug design strategy has emerged during the last decade based upon accurate three-dimensional structures of biomacromolecules that have to be specifically affected by pharmaceutically active compounds. In view of the great advantage of this strategy over existing ones, it is not hard to predict that a considerable percentage of new drugs coming on the market by the turn of the century will be based on approaches outlined in this article.

It is a pleasure to acknowledge stimulating discussions with Rik Wierenga, Bauke Dijkstra, Jan Drenth, and Sylvia Pronk from the Groningen protein crystallography group, and Klaus Müller from Hoffmann-La Roche in Basel. I also would like to thank Randy Read for numerous suggestions for improving the text, and Dave Matthews for sending a preprint of the dihydrofolate reductase review. Roeline Hogenkamp has given excellent assistance in the preparation of the manuscript.

Received: May 30, 1986 [A 590 IE]
German version: *Angew. Chem. 98* (1986) 765

[1] P. J. Goodford, *J. Med. Chem. 27* (1984) 557.
[2] World Health Organization: *Tropical Disease Research - Seventh Programme Report*, Geneva 1985.
[3] T. H. Maugh, *Science 196* (1977) 413; D. L. Klayman, *ibid. 228* (1985) 1049.
[4] E. A. Falco, L. G. Goodwin, G. H. Hitchings, I. M. Rollo, P. B. Russell, *Br. J. Pharmacol. 6* (1951) 185.
[5] M. G. Rossmann: *The Molecular Replacement Method*, Gordon and Breach, New York 1972.
[6] A. Arnone, *Nature (London) 237* (1972) 146.
[7] C. R. Beddell, P. J. Goodford, F. E. Norrington, S. Wilkinson, R. Wootton, *Br. J. Pharmacol. 57* (1976) 201.
[8] C. R. Beddell, P. J. Goodford, G. Kneen, R. D. White, S. Wilkinson, R. Wootton, *Br. J. Pharmacol. 82* (1984) 397.
[9] J. A. Walder, R. Y. Walder, A. Arnone, *J. Mol. Biol. 141* (1980) 195.
[10] D. J. Abraham, M. F. Perutz, S. E. V. Phillips, *Proc. Natl. Acad. Sci. USA 80* (1983) 324.
[11] M. F. Perutz, personal communication.
[12] B. Shaanan, *J. Mol. Biol. 171* (1983) 31; G. Fermi, M. F. Perutz, B. Shaanan, R. Fourme, *ibid. 175* (1984) 159.
[13] E. A. Padlan, W. E. Love, *J. Biol. Chem. 260* (1985) 8272.
[14] E. A. Padlan, W. E. Love, *J. Biol. Chem. 260* (1985) 8280.
[15] D. C. Rees, M. Lewis, W. N. Lipscomb, *J. Mol. Biol. 168* (1983) 367.
[16] M. A. Holmes, B. W. Matthews, *J. Mol. Biol. 160* (1982) 623.
[17] D. W. Cushman, H. S. Cheung, E. F. Sabo, M. A. Ondetti, *Biochemistry 16* (1977) 5484.
[18] D. C. Rees, W. N. Lipscomb, *J. Mol. Biol. 160* (1982) 475.
[19] L. C. Kuo, J. M. Fukuyama, M. W. Makinen, *J. Mol. Biol. 163* (1983) 63.
[20] D. C. Rees, W. N. Lipscomb, *Proc. Natl. Acad. Sci. USA 80* (1983) 7151.
[21] W. R. Kester, B. W. Matthews, *Biochemistry 16* (1977) 2506.
[22] A. F. Monzingo, B. W. Matthews, *Biochemistry 21* (1982) 3390.
[23] A. F. Monzingo, B. W. Matthews, *Biochemistry 23* (1984) 5724.
[24] D. G. Hangauer, A. F. Monzingo, B. W. Matthews, *Biochemistry 23* (1984) 5730.
[25] M. N. G. James, A. R. Sielecki, *J. Mol. Biol. 163* (1983) 299.
[26] E. Subramanian, I. D. A. Swan, M. Liu, D. R. Davies, J. A. Jenkins, I. J. Tickle, T. L. Blundell, *Proc. Natl. Acad. Sci. USA 74* (1977) 556.
[27] R. Bott, E. Subramanian, D. R. Davies, *Biochemistry 21* (1982) 6956.
[28] F. Soubrier, J.-J. Panthier, P. Corvol, F. Rougeon, *Nucleic Acids Res. 11* (1983) 7181.
[29] T. Imai, H. Miyazaki, S. Hirose, H. Hori, T. Hayashi, R. Kageyama, H. Ohkubo, S. Nakanishi, K. Murakami, *Proc. Natl. Acad. Sci. USA 80* (1983) 7405.
[30] a) T. Blundell, B. L. Sibanda, L. Pearl, *Nature (London) 304* (1983) 273; b) B. L. Sibanda, T. Blundell, P. M. Hobart, M. Fogliano, J. S. Bindra, B. W. Dominy, J. M. Chirgwin, *FEBS Lett. 174* (1984) 102.
[31] T. L. Blundell, personal communication.
[32] M. A. Navia, J. P. Springer, M. Poe, J. Boger, K. Hoogsteen, *J. Biol. Chem. 259* (1984) 12714.
[33] J. T. Bolin, D. J. Filman, D. A. Matthews, R. C. Hamlin, J. Kraut, *J. Biol. Chem. 257* (1982) 13650.
[34] C. J. Tabin, S. M. Bradley, C. I. Bargmann, R. A. Weinberg, *Nature (London) 300* (1982) 143.
[35] E. P. Reddy, R. K. Reynolds, E. Santos, M. Barbacid, *Nature (London) 300* (1982) 149.
[36] E. Taparowsky, Y. Suard, O. Fasano, K. Shimizu, M. Goldfarb, M. Wigler, *Nature (London) 300* (1982) 762.
[37] R. K. Wierenga, W. G. J. Hol, *Nature (London) 302* (1983) 842.
[38] E. Santos, D. Martin-Zanca, E. P. Reddy, M. A. Pierotti, G. Della Porta, M. Barbacid, *Science 223* (1984) 661.
[39] D. J. Capon, P. H. Seeburg, J. P. McGrath, J. S. Hayflick, U. Edman, A. D. Levinson, D. V. Goeddel, *Nature (London) 304* (1983) 507.
[40] I. Guerrero, A. Villasante, V. Corces, A. Pellicer, *Science 225* (1984) 1159.
[41] H. Zarbl, S. Sukumar, A. V. Arthur, D. Martin-Zanca, M. Barbacid, *Nature (London) 315* (1985) 382.
[42] N. J. Gay, J. E. Walker, *Nature (London) 301* (1983) 262.
[43] M. R. Pincus, J. Van Renswoude, J. B. Harford, E. H. Chang, R. P. Carty, R. D. Klausner, *Proc. Natl. Acad. Sci. USA 80* (1983) 5253.
[44] E. Santos, E. P. Reddy, S. Pulciani, R. J. Feldmann, M. Barbacid, *Proc. Natl. Acad. Sci. USA 80* (1983) 4679.
[45] F. Jurnak, *Science 230* (1985) 32.
[46] F. McCormick, B. F. C. Clark, T. F. M. La Cour, M. Kjeldgaard, L. Norskov-Lauritsen, J. Nyborg, *Science 230* (1985) 78.
[47] P. H. Seeburg, W. W. Colby, D. J. Capon, D. V. Goeddel, A. D. Levinson, *Nature (London) 312* (1984) 71.
[48] R. Flower, *Trends Pharmacol. Sci. 2* (1981) 186.
[49] E. G. Lapetina, *Trends Pharmacol. Sci. 3* (1982) 115.
[50] J. L. Marx, *Science 215* (1982) 1380.
[51] J. W. Weiss, J. M. Drazen, N. Coles, E. R. McFadden, P. F. Weller, E. J. Corey, R. A. Lewis, K. F. Austen, *Science 216* (1982) 196.
[52] B. Samuelsson, *Science 220* (1983) 568.
[53] M. Okamoto, T. Ono, H. Tojo, T. Yamano, *Biochem. Biophys. Res. Commun. 128* (1985) 788.
[54] H. M. Verhey, A. J. Slotboom, G. H. De Haas, *Rev. Physiol. Biochem. Pharmacol. 91* (1981) 91.
[55] B. W. Dijkstra, K. H. Kalk, W. G. J. Hol, J. Drenth, *J. Mol. Biol. 147* (1981) 97.
[56] B. W. Dijkstra, G. J. H. Van Nes, K. H. Kalk, N. P. Brandenburg, W. G. J. Hol, J. Drenth, *Acta Crystallogr. Sect. B38* (1982) 793.
[57] B. W. Dijkstra, R. Renetseder, K. H. Kalk, W. G. J. Hol, J. Drenth, *J. Mol. Biol. 168* (1983) 163.
[58] B. W. Dijkstra, K. H. Kalk, J. Drenth, G. H. De Haas, M. R. Egmond, A. J. Slotboom, *Biochemistry 23* (1984) 2759.
[59] S. Brunie, J. Bolin, D. Gewirth, P. B. Sigler, *J. Biol. Chem. 260* (1985) 9742; R. Renetseder, S. Brunie, B. W. Dijkstra, J. Drenth, P. B. Sigler, *ibid. 260* (1985) 11627.
[60] R. Renetseder, B. W. Dijkstra, J. Drenth, personal communication.
[61] B. P. Wallner, R. J. Mattaliano, C. Hession, R. L. Cate, R. Tizard, L. K. Sinclair, C. Foeller, E. Pingchang Chow, J. L. Browning, K. L. Ramachandran, R. B. Pepinsky, *Nature (London) 320* (1986) 77.
[62] E. P. Abraham, *Sci. Am. 244* (6) (1981) 64; *Spektrum Wiss. 1981* (8) 46.
[63] J.-M. Frère, B. Joris, *CRC Crit. Rev. Microbiol. 11* (1985) 299.
[64] O. Dideberg, P. Charlier, G. Dive, B. Joris, J.-M. Frère, J.-M. Ghuysen, *Nature (London) 299* (1982) 469.

[65] J. A. Kelly, P. C. Moews, J. R. Knox, J.-M. Frère, J.-M. Ghuysen, *Science 218* (1982) 479.
[66] J. A. Kelly, J. R. Knox, P. C. Moews, G. J. Hite, J. B. Bartolone, H. Zhao, B. Joris, J.-M. Frère, J.-M. Ghuysen, *J. Biol. Chem. 260* (1985) 6449.
[67] B. Samraoui, B. J. Sutton, R. J. Todd, P. J. Artymiuk, S. G. Waley, D. C. Phillips, *Nature (London) 320* (1986) 378.
[68] M. G. Rossmann, E. Arnold, J. W. Erickson, E. A. Frankenberger, J. P. Griffith, H.-J. Hecht, J. E. Johnson, G. Kamer, M. Luo, A. G. Mosser, R. R. Rueckert, B. Sherry, G. Vriend, *Nature (London) 317* (1985) 145.
[69] J. M. Hogle, M. Chow, D. J. Filman, *Science 229* (1985) 1358.
[70] I. A. Wilson, J. J. Skehel, D. C. Wiley, *Nature (London) 289* (1981) 366.
[71] J. N. Varghese, W. G. Laver, P. M. Colman, *Nature (London) 303* (1983) 35.
[72] J. L. Middlebrook, R. B. Dorland, *Microbiol. Rev. 48* (1984) 199.
[73] J. Holmgren, *Nature (London) 292* (1981) 413.
[74] A. M. Pappenheimer, *Annu. Rev. Biochem. 46* (1977) 69.
[75] S. Van Heyningen, *Biosci. Rep. 2* (1982) 135.
[76] R. J. Collier, D. A. Kaplan, *Sci. Am. 250* (7) (1983) 44.
[77] A. Kurosky, D. E. Markel, J. W. Peterson, W. M. Fitch, *Science 195* (1977) 299; C.-Y. Lai, *J. Biol. Chem. 252* (1977) 7249.
[78] E. K. Spicer, J. A. Noble, *J. Biol. Chem. 257* (1982) 5716.
[79] W. S. Dallas, S. Falkow, *Nature (London) 288* (1980) 499.
[80] T. Yamamoto, T. Tamura, T. Yokota, *J. Biol. Chem. 259* (1984) 5037.
[81] R. J. Collier, E. M. Westbrook, D. B. McKay, D. Eisenberg, *J. Biol. Chem. 257* (1982) 5283.
[82] P. B. Sigler, M. E. Druyan, H. C. Kiefer, R. A. Finkelstein, *Science 197* (1977) 1277.
[83] J. A. Zelano, E. Westbrook, A. Yonath, M. E. Druyan, P. B. Sigler in M. Balaban (Ed.): *Molecular Mechanism of Biological Recognition*, Elsevier, Amsterdam 1979, p. 157–163.
[84] S. E. Pronk, H. Hofstra, H. Groendijk, J. Kingman, M. B. A. Swarte, F. Dorner, J. Drenth, W. G. J. Hol, B. Witholt, *J. Biol. Chem. 260* (1985) 13580.
[85] J. Kraut, D. A. Matthews in F. Jurnak, A. McPherson (Eds): *Biological Macromolecules and Assemblies, Vol. 3*, Wiley, New York 1986, in press.
[86] R. L. Blakley in R. L. Blakley, S. J. Benkovic (Eds.): *Chemistry and Biochemistry of Folates, Vol. 1*, Wiley, New York 1984, p. 191–253.
[87] D. J. Filman, J. T. Bolin, D. A. Matthews, J. Kraut, *J. Biol. Chem. 257* (1982) 13663.
[88] K. W. Volz, D. A. Matthews, R. A. Alden, S. T. Freer, C. Hansch, B. T. Kaufman, J. Kraut, *J. Biol. Chem. 257* (1982) 2528.
[89] D. K. Stammers, J. N. Champness, J. G. Dann, C. R. Beddell in J. A. Blair (Ed.): *Chemistry and Biology of Pteridines*, de Gruyter, Berlin/New York 1983, p. 567–571.
[90] R. Ferone, J. J. Burchall, G. H. Hitchings, *Mol. Pharmacol. 5* (1969) 49.
[91] C. E. Garett, J. A. Coderre, T. D. Meek, E. P. Carvey, D. M. Claman, S. M. Beverley, D. V. Santi, *Mol. Biochem. Parasitol. 11* (1984) 257.
[92] R. Ferone, S. Roland, *Proc. Natl. Acad. Sci. USA 77* (1980) 5802.
[93] J. J. Jaffe, J. J. McCormack, W. E. Gutteridge, *Exp. Parasitol. 25* (1969) 311.
[94] D. A. Matthews, J. T. Bolin, J. M. Burridge, D. J. Filman, K. W. Volz, J. Kraut, *J. Biol. Chem. 260* (1985) 392.
[95] D. A. Matthews, J. T. Bolin, J. M. Burridge, D. J. Filman, K. W. Volz, B. T. Kaufman, C. R. Beddell, J. N. Champness, D. K. Stammers, J. Kraut, *J. Biol. Chem. 260* (1985) 381.
[96] L. F. Kuyper, B. Roth, D. P. Baccanari, R. Ferone, C. R. Beddell, J. N. Champness, D. K. Stammers, J. G. Dann, F. E. A. Norrington, D. J. Baker, P. J. Goodford, *J. Med. Chem. 25* (1982) 1120.
[97] B. Birdsall, J. Feeney, C. Fascual, G. C. K. Roberts, I. Kompis, R. L. Then, K. Müller, A. Kroehn, *J. Med. Chem. 27* (1984) 1672.
[98] R. L. Tansik, D. R. Averett, B. Roth, S. J. Paterson, D. Stone, D. P. Baccanari, *J. Biol. Chem. 19* (1984) 12299.
[99] W. W. Gutteridge, *Br. Med. Bull. 41* (1985) 162.
[100] M. J. Turner, *Adv. Parasitol. 21* (1982) 69.
[101] D. M. Freymann, P. Metcalf, M. Turner, D. C. Wiley, *Nature (London) 311* (1984) 167.
[102] F. R. Opperdoes, P. Borst, *FEBS Lett. 80* (1977) 360.
[103] A. H. Fairlamb, F. R. Opperdoes, P. Borst, *Nature (London) 256* (1977) 270.
[104] F. R. Opperdoes, *Br. Med. Bull. 41* (1985) 130.
[105] O. Misset, F. R. Opperdoes, *Eur. J. Biochem. 144* (1984) 475.
[106] O. Misset, O. J. M. Bos, F. R. Opperdoes, *Eur. J. Biochem.*, in press.
[107] B. W. Swinkels, W. C. Gibson, K. A. Osinga, A. Kramer, P. Borst, G. H. Veeneman, J. H. Van Boom, *EMBO J.*, in press.
[108] K. A. Osinga, B. W. Swinkels, W. C. Gibson, P. Borst, G. H. Veeneman, J. H. Van Boom, P. A. M. Michels, F. R. Opperdoes, *EMBO J. 4* (1985) 3811.
[109] P. A. M. Michels, A. Poliszczak, K. A. Osinga, O. Misset, J. Van Beeumen, R. K. Wierenga, P. Borst, F. R. Opperdoes, *EMBO J.*, in press; C. E. Clayton, *ibid. 4* (1985) 2997.
[110] R. K. Wierenga, W. G. J. Hol, O. Misset, F. R. Opperdoes, *J. Mol. Biol. 178* (1984) 487.
[111] R. K. Wierenga, personal communication.
[112] T. Alber, D. W. Banner, A. C. Bloomer, G. A. Petsko, D. Phillips, P. S. Rivers, I. A. Wilson, *Philos. Trans. R. Soc. London B 293* (1981) 159.
[113] D. W. Rice, *Acta Crystallogr. Sect. A 37* (1981) 491.
[114] a) H. C. Watson, N. P. C. Walker, P. J. Shaw, T. N. Bryant, P. L. Wendell, L. A. Fothergill, R. E. Perkins, S. C. Conroy, M. J. Dobson, M. F. Tuite, A. J. Kingsman, S. M. Kingsman, *EMBO J. 1* (1982) 1635; b) C. C. F. Blake, D. W. Rice, *Philos. Trans. R. Soc. London B. 293* (1981) 93; c) T. Sixma, R. K. Wierenga, unpublished results.
[115] R. K. Wierenga, B. Swinkels, P. A. M. Michels, K. Osinga, O. Misset, W. Gibson, J. P. M. Postma, P. Borst, F. R. Opperdoes, W. G. J. Hol, submitted for publication.
[116] T. L. Blundell, L. N. Johnson: *Protein Crystallography*, Academic Press, London 1976.
[117] A. McPherson: *Preparation and Analysis of Protein Crystals*, Wiley, New York 1982.
[118] M. L. Kopka, C. Yoon, D. Goodsell, P. Pjura, R. E. Dickerson, *J. Mol. Biol. 183* (1985) 553; *Proc. Natl. Acad. Sci. USA 82* (1985) 1376.
[119] J. Deisenhofer, O. Epp, K. Miki, R. Huber, H. Michel, *Nature (London) 318* (1985) 618.
[120] C. Freudenreich, J.-P. Samama, J.-F. Biellmann, *J. Am. Chem. Soc. 106* (1984) 3344.
[121] L. Sawyer, D. M. Shotton, J. W. Campbell, P. L. Wendell, H. Muirhead, H. C. Watson, R. Diamond, R. C. Ladner, *J. Mol. Biol. 118* (1978) 137.
[122] D. L. Hughes, L. C. Sieker, J. Bieth, J.-L. Dimicoli, *J. Mol. Biol. 162* (1982) 645.
[123] C. A. McPhalen, H. P. Schnebli, M. N. G. James, *FEBS Lett. 188* (1985) 55; W. Bode, E. Papamokos, D. Musil, U. Seemueller, H. Fritz, *EMBO J. 5* (1986) 813.
[124] H. Loebermann, R. Takuoka, J. Deisenhofer, R. Huber, *J. Mol. Biol. 177* (1984) 531.
[125] Y. S. Babu, J. S. Sack, T. J. Greenhough, C. E. Bugg, A. R. Means, W. J. Cook, *Nature (London) 315* (1985) 37.
[126] D. L. Newton, M. D. Oldewurtel, M. H. Krinks, J. Shiloach, C. B. Klee, *J. Biol. Chem. 259* (1984) 4419.
[127] O. Herzberg, M. N. G. James, *Nature (London) 313* (1985) 653.
[128] M. Sundaralingam, R. Bergstrom, G. Strasburg, S. T. Rao, P. Roychowdhury, M. Greaser, B. C. Wang, *Science 227* (1985) 945.
[129] J. Gariépy, R. S. Hodges, *Biochemistry 22* (1983) 1586.

Microbial Degradation of Halogenated Hydrocarbons: A Biological Solution to Pollution Problems?

By Rudolf Müller and Franz Lingens*

In memoriam Konrad Bernhauer

Chlorinated hydrocarbons are widely used because of their chemical and thermal stability as well as their fungicidal, herbicidal, and insecticidal properties. Unfortunately, it is just this stability that makes the compounds persistent in nature; half-lives of more than 15 years are not uncommon. In many countries the use of some chlorinated compounds has been prohibited, even though many such compounds (e.g., DDT) exhibit exactly the desired spectrum of effects. Surprisingly, microbial systems that can degrade most chlorinated hydrocarbons have been found in nature. Indeed, it is possible, in many cases, to isolate pure cultures of bacteria that can utilize these compounds as the sole source of carbon and energy. Even polychlorinated compounds, such as the wood preservative and herbicide pentachlorophenol, can be utilized as a source of carbon by some bacteria. The study of the biodegradation of halogenated hydrocarbons has led to the discovery of novel catabolic pathways in which unusual and previously undescribed enzymatic activities have been detected. Bacterial enzymes have even been isolated that can replace halogen substituents in aliphatic and aromatic compounds with hydroxyl groups or hydrogen atoms. Improved understanding of the biodegradation of halogenated hydrocarbons, as described in this article, will almost certainly result in new biotechnological applications, especially in the area of waste-water treatment.

1. Introduction

Halogenated hydrocarbons are used in many aspects of our daily life. They have applications as solvents (e.g., chloroform, trichloroethylene, and chlorobenzene), as insulating liquids (polychlorinated biphenyls), as wood preservatives (pentachlorophenol), and as herbicides and fungicides. As a result, vast quantities of these compounds enter our environment both accidentally and intentionally. The sensitive methods for chemical analysis now available have revealed that few areas on earth remain uncontaminated.[1,2] Newspaper reports of the existence and associated dangers of chlorinated hydrocarbon pollutants are commonplace; consequently, the general public is aware and concerned about this issue. In contrast to most man-made compounds, which are rapidly degraded upon introduction into the environment, chlorinated hydrocarbons are often highly persistent.[3] This lack of degradation is thought by some biologists to reflect the inability of nature to adapt, through the evolution of appropriate biodegradative microorganisms, to the dramatic increase in the number of new compounds resulting from man's industrial activities in this century. However, since nature itself produces a variety of chlorinated compounds in large amounts, it would be surprising if mechanisms for their biodegradation did not exist. Indeed, microorganisms are known to play a major role in the degradation of organic compounds.

In this article we shall consider the extent to which chlorinated hydrocarbon pollutants can be degraded and thereby detoxified by microorganisms. We will first discuss the methods that are frequently used in the study of hydrocarbon biodegradation. The later sections will focus almost exclusively on the degradative activities of bacteria, since this group of microorganisms constitutes a major component of the soil and water microflora and since they have been the subject of most investigations of biodegradation. Comparable studies with fungi are rare, and the biodegradative potential of algae and protozoa remains virtually unstudied.

2. Methodological Approaches to Studying the Biodegradation of Pollutant Hydrocarbons

A prerequisite for examining the biodegradation of any compound is a reproducible, relatively sensitive and quantitative method for detection of the compound. The problems associated with the development of such analyses are familiar to chemists and, therefore, will not be described further.

Having selected a test substance whose degradation can be followed, the investigator has to find a suitable source of microorganisms capable of degrading the substance. For chlorinated hydrocarbons, the most promising sources are soil or water samples chronically polluted with these compounds. The samples are incubated in aqueous media containing varying concentrations of the selected chlori-

[*] Prof. Dr. F. Lingens, Dr. R. Müller
Institut für Mikrobiologie der Universität Hohenheim
Garbenstrasse 30, D-7000 Stuttgart 70 (FRG)

nated hydrocarbon. The incubations (often referred to as enrichments, since the investigator aims to enrich the sample with respect to specific degradative bacteria) are carried out under a wide range of conditions: for example, humidity, temperature, pH, trace element concentrations, and concentration of dissolved oxygen may be varied. Periodically, the concentration of the test substance, and possibly compounds derived from it, are monitored. If the test substance disappears, the investigator transfers a sample from the enrichment into fresh medium containing the test substance. By continuation of this procedure using either batch or continuous culture techniques, stable mixed populations of microorganisms, usually bacteria, can be obtained. Because it is usually simpler to work with pure cultures, the investigator will often aim to isolate single bacterial species capable of utilizing the test substrate as the sole source of carbon and energy. This may be done by plating out the mixed cultures on agar-based solid media in order to isolate single colonies (clonal populations) of bacteria.

Having isolated a single bacterial species, the investigator can attempt to identify the metabolic reactions that constitute the degradative pathway and to isolate the enzymes that catalyze these reactions. Ultimately, the degradative reactions may be carried out in vitro with purified enzymes, thereby allowing biotransformation of the test substance. Biotransformation, which is defined as the transformation of chemical substrates catalyzed by microorganisms, by cell-free extracts of microorganisms, or by isolated enzymes, can be carried out using a variety of techniques. For example, the test substance (the substrate) can be added to a growing bacterial culture so as to induce the synthesis of the enzymes catalyzing the desired reaction. Alternatively, biotransformations can be carried out using "resting cells," a technique in which the bacterial biomass is isolated from cultures growing under optimal conditions and then transferred into a special transformation medium containing the test substrate. An important variation of this technique is the immobilization of "resting cells" on an inert support. The advantage of using immobilized systems is that the biocatalyst is easily retained within a reaction vessel, facilitating continuous biotransformations. In some cases, undesirable interference from subsequent reactions as well as side reactions is best eliminated by the purification of the enzymes catalyzing the desired biotransformation and, where possible, their immobilization on inert supports.

In the following sections, the extent to which the methods described above have proved successful in studying biotransformations of the most important halogenated hydrocarbons will be described.

3. Halogenated Aliphatic Compounds

Halogenated aliphatic hydrocarbons are widely used as herbicides and solvents. In 1982, for example, more than 13 million tons of dichloromethane was produced throughout the world.[4] Some of these compounds are carcinogenic (e.g., vinyl chloride), whereas others (e.g., 1,2-dichloroethane) can be biologically or chemically converted into mutagenic products.[5,6] Repeatedly, contamination of ground and drinking water has resulted from careless handling of haloalkane-based solvents. Concern has also been voiced about the observation of chlorinated aliphatic hydrocarbons associated with chlorination of municipal water supplies.[7] Consequently, the biodegradation of these substances is of great interest. Two major groups of halogenated aliphatic compounds are of current importance: firstly, the haloalkanes used as intermediates in chemical syntheses and as solvents, and secondly, the haloalkanoic acids applied as disinfectants and herbicides.

3.1. Halogenated Alkanes

Brunner et al.[8] isolated a bacterium capable of utilizing dichloromethane as the sole source of carbon and energy, and *Stucki* et al.[9] have reported the isolation of a *Hyphomicrobium* species with the same degradative ability. The latter strain contains a glutathione-dependent dehalogenase, which was shown to catalyze the conversion of dichloromethane to formaldehyde. The disinfectant trichloronitromethane (chloropicrin) is another C_1 compound whose biodegradation has been studied:[10] this compound is converted, via a series of enzyme-catalyzed reactions, into nitromethane by a *Pseudomonas* species. Bacterial breakdown of carbon tetrachloride has also been demonstrated; chloroform and carbon dioxide were found as degradation products.[11]

Numerous C_2 haloalkanes have been reported to be subject to extensive biodegradation: e.g., 1,2-dichloroethane,[12,13] tetrachloroethylene, trichloroethylene, dichloroethylene, and vinyl chloride.[14] *Vogel* and *McCarthy*[14] have proposed a pathway for the degradation of tetrachloroethylene **1** by a mixed microbial culture grown under anaerobic conditions (Fig. 1). *Janssen* et al.[12] described the degradation of 1,2-dichloroethane **2** by a bacterium they classified as *Xanthobacter autotrophicus* strain GJ10. The first step in the catabolic sequence is the replacement of one halogen substituent by a hydroxyl group. The enzyme catalyzing this reaction has recently been purified.[15] The product, chloroethanol **3**, is oxidized, via the aldehyde **4**, to chloroacetate **5**, which undergoes hydrolytic removal of the second chlorine atom to give lactic acid **6** (Fig. 2). Interestingly, the two dehalogenation steps are catalyzed by two different enzymes.[12] *Jagnow* and coworkers[16,17] have described the biodegradation of the insecticide hexachlorocyclohexane (HCH, commercially available under the trade name Lindane) by obligate and facultative anaerobic bacteria. Although the complete degradative pathway remains to be elucidated, tetrachlorocyclohexane was identified as an intermediate.[17]

Long-chain haloaliphatic hydrocarbons have not assumed the same commercial importance as the substances discussed above; however, bacteria capable of dehalogenating and utilizing a number of such compounds (e.g., 1,5-dichloropentane, 1,6-dichlorohexane, 1,9-dichlorononane, 1,9-dibromononane, 1-chlorooctane, 1-chloro-, 1-bromo-, and 1-iodoheptane) have been isolated.[18]

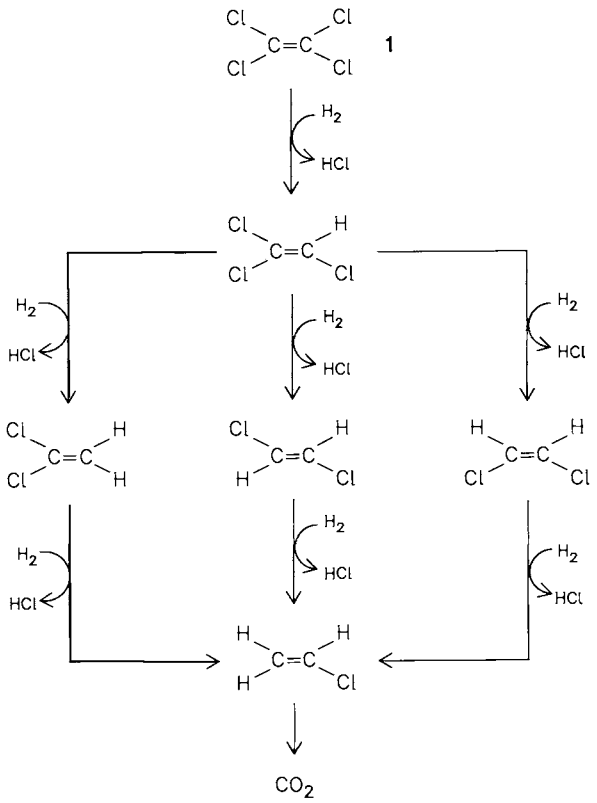


Fig. 1. The degradation of tetrachloroethylene **1** by a mixed microbial culture grown under methanogenic conditions.

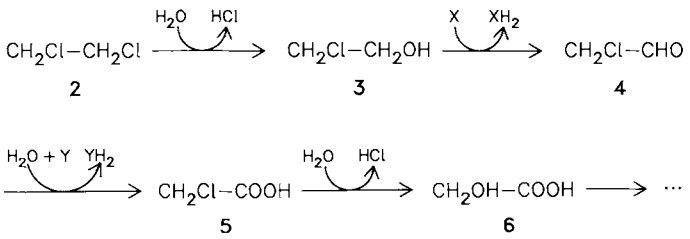


Fig. 2. The degradation of 1,2-dichloroethane **2** by *Xanthobacter autotrophicus* GJ10. The glyoxylic acid **6** so obtained is degraded by a known pathway.

3.2. Halogenated Alkanoic Acids

Chloroalkanoic acids, some of which are used as herbicides,[19] are toxic to a variety of organisms including mammals. As a group, the chloroalkanoic acids are relatively rapidly degraded by a variety of microorganisms. *Senior* et al. isolated several species from a mixed microbial culture that were capable of utilizing Dalapon (2,2-dichloropropionic acid) as the sole source of carbon and energy.[19] Several authors have reported the isolation of bacteria that can degrade chloroacetate,[21-23] fluoroacetate,[24,25] or chloropropionate[26] and their dichlorinated analogues. In all cases so far studied, the biodegradation is initiated by replacement of the halogen substituent of the α-substituted haloalkanoic acid with a hydroxyl group. Hydroxy acids are formed from monohalogenated acids and oxo acids from dihalogenated acids. Dehalogenating enzymes (dehalogenases) can be divided into two main groups: those that accept only halogenated acetic acids as substrates and those that can also dehalogenate longer chain substrates.[27] Both groups of dehalogenases accept only 2-substituted alkanoic acids as substrates. Optically active 2-haloalkanoic acids can react with either retention or inversion of configuration.[26] Some enzymes can only dehalogenate the L-isomer of the substrate, whereas others can transform both enantiomers. These different specificities can be exploited for the enzymatic synthesis of the two optically active forms of lactic acid from racemic 2-chloropropionic acid. The synthesis involves, first, the conversion of L-2-chloropropionate to D-lactate by the appropriate dehalogenase, followed by the separation of unconverted D-2-chloropropionate from the D-lactate and the conversion of the purified D-2-chloropropionate to L-lactate using an enzyme that can dehalogenate both isomers of the substrate.[28] Dehalogenases capable of converting D-2-chloropropionate exclusively into L-lactate, a reaction of commercial importance, have not yet been isolated.

4. Aromatic Hydrocarbons

4.1. Nonhalogenated Aromatic Hydrocarbons

The biodegradation of nonhalogenated aromatic compounds has long been intensively studied (for reviews see refs. [29-31]). The bacterial degradation of haloaromatic compounds involves the same basic principles as for the aerobic catabolism of corresponding unsubstituted compounds. These principles are exemplified below for the degradation of benzene by bacteria (Fig. 3). The first step is the formation of *cis*-3,5-cyclohexadiene-1,2-diol **7** by incorporation of both atoms of molecular oxygen into ben-

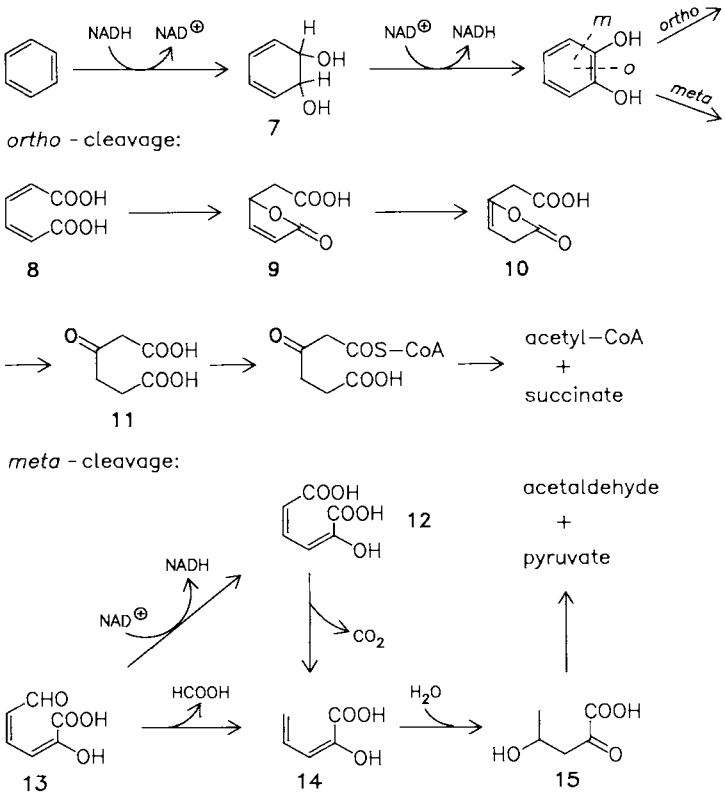


Fig. 3. The bacterial degradation of benzene.

zene. This reaction is catalyzed by a dioxygenase produced by benzene-degrading bacteria. The subsequent conversion of **7** to catechol is catalyzed by a dehydrogenase. At this stage a second molecule of oxygen is incorporated with cleavage of the aromatic ring. Two reaction pathways for aromatic ring cleavage of catechol are possible, each catalyzed by a distinct dioxygenase. Cleavage between the hydroxyl groups, called *ortho*-cleavage, produces *cis*,-*cis*-muconic acid **8**. Cleavage at a position adjacent to the two hydroxyl groups, called *meta*-cleavage, forms 2-hydroxymuconic semialdehyde **13**.

The first intermediate of the *ortho*-cleavage pathway, **8**, is converted by a cycloisomerase into muconolactone **9** which is further isomerized to form the enol lactone **10**. 2-Oxoadipic acid **11**, which is produced by hydrolase-catalyzed cleavage of the lactone **10**, is first esterified with coenzyme A and then cleaved into acetyl-CoA and succinate in an aldolase-catalyzed reaction.[32]

The product of the *meta*-cleavage pathway, **13**, can react further by either of two alternative routes. Dehydrogenase-catalyzed oxidation of **13** affords 2-hydroxymuconic acid **12**, which is then decarboxylated to 2-hydroxy-2,4-pentadienoic acid **14**. Hydrolase-catalyzed elimination of formic acid from **13**, on the other hand, results in direct conversion to **14**. Compound **14** is then converted into 4-hydroxy-2-oxovalerate by hydratase-catalyzed addition of water, and the product is cleaved by an aldolase to form pyruvate and acetaldehyde (Fig. 3).[31] Several enzymes involved in the catabolism of variously substituted aromatic hydrocarbons have been purified and characterized.[29,33-37]

4.2. Halogenated Aromatic Compounds

4.2.1. Polychlorinated Phenols

Polychlorinated phenols, in particular pentachlorophenol, are extensively used as fungicides, herbicides, disinfectants, and wood preservatives. Each year hundreds of thousands of tons are produced (wood preservatives constitute 80% of this production) and much of this enters the environment.[38] Bioaccumulation, a major problem associated with polychlorophenol pollution, has been highlighted by a study of the lake regions of Finland where these compounds were shown to be concentrated through food chains to high levels in fish.[39] Pentachlorophenol has been shown to be generally toxic[40] and may cause chloracne, irritation of the respiratory tract, and, in some cases, liver damage. Unequivocal association between exposure to pentachlorophenol and these symptoms is difficult to establish because technical-grade pentachlorophenol is contaminated with other chlorinated phenols and chlorinated dibenzo[1,4]dioxins, some of which are known to produce identical symptoms at low doses. New production methods are available for reducing the level of dioxin contamination in pentachlorophenol by about a hundredfold, but attempts to market this product have failed as a result of higher production costs.[38]

Anaerobic[41,42] and aerobic degradation[41,43-45] of pentachlorophenol by mixed microbial cultures has been reported. *Guthrie* et al.,[42] in a study of the anaerobic biodegradation of pentachlorophenol, found that the compound was undetectable ($< 5\ \mu g/L$) only ten days after its application to acclimated soil samples. Similar experiments were carried out by *Murthy* et al. with soil samples and radioactively labeled pentachlorophenol.[41] They found that CO_2 formation was severely reduced under anaerobic conditions but identified 2,3,5,6- and 2,3,4,5-tetrachlorophenol, 2,3,6-trichlorophenol, and pentachloroanisole as degradation products. In addition to these products, *Ide* et al.[46] identified 2,3,4,6-tetrachlorophenol, 2,4,5-trichlorophenol, 3,4- and 3,5-dichlorophenol, and 3-chlorophenol in acidic hexane extracts of soil samples taken from rice fields treated with pentachlorophenol and incubated for 30 days with the compound. These results strongly indicated that sequential reductive dechlorination reactions can be carried out by microorganisms degrading pentachlorophenol under anaerobic conditions.

Watanabe[47] and *Suzuki*[48] have both reported the isolation of a *Pseudomonas* species capable of utilizing pentachlorophenol as the sole source of carbon and energy. *Stanlake* and *Finn*[49] isolated a gram-positive *Arthrobacter* species with the same ability. In neither case was it possible to elucidate the complete pathways for the degradation of pentachlorophenol. However, *Suzuki*[48] and *Rott* et al.[50] identified tetrachlorocatechol and tetrachlorohydroquinone as aerobic biodegradation products, neither of which was a product of anaerobic degradation. In addition, *Rott* et al.[50] isolated tetrachlororesorcinol and corresponding derivatives in which either one or both hydroxyl groups were methylated or acetylated. Collectively, these results indicate that aerobic biodegradation of pentachlorophenol proceeds by replacement of a chlorine substituent by a hydroxyl group, although the reaction mechanism remains unclear. Both oxygenolytic and hydrolytic mechanisms are possible for the cleavage of the carbon–chlorine bond, but so far no enzymes have been isolated. The further steps in the aerobic degradation of pentachlorophenol also remain to be elucidated.

An interesting application of studies of pentachlorophenol biodegradation has been described by *Edgehill* and *Finn*,[51] who applied an inoculum of pentachlorophenol-utilizing bacteria, grown in a fermentor, to contaminated soil at a concentration of 10^6 cells (ca. 1 mg bacteria) per gram of soil (dry weight). The half-life of pentachlorophenol was thereby reduced from two weeks to less than one day. This and other studies strongly suggest that bacterial treatments could provide rapid, cheap, and effective methods for the decontamination of polluted soils.

4.2.2. Polychlorinated Biphenyls

Polychlorinated biphenyls (PCBs), which exhibit high chemical and thermal stabilities, have been widely used as insulating liquids for transformers, as greases for vacuum pumps and turbines, and as coolants. Moreover, they have found application in the production of wrapping paper, carbon paper, inks, paints, tires, and many other products. The commercial production of PCBs began in 1929 and today these compounds can be detected throughout the en-

vironment. Since PCBs are strongly hydrophobic, they are subject to bioaccummulation in the fatty tissue of humans and animals. For example, a variety of PCBs have been detected in fish, mussels, and birds living in and around the Rhine river.[1] Awareness of the environmental impact of PCBs has led to their replacement in industry by alternative, "safer" compounds, and to the relinquishment of PCB production in the Federal Republic of Germany.[52] Chloracne, skin pigmentation, hair damage, defective vision, fatigue, and liver damage are symptoms associated with acute exposure of mammals to PCBs.[53] Further studies on the biodegradation of PCBs are justified by the observation that most of the world's total production of PCBs still contaminates the environment.

Commercial formulations of polychlorinated biphenyls are made up of almost random mixtures of all 209 possible isomers. The degradation of both commercially available mixtures[54-59] and defined compounds[60-70] has been studied. Only the latter studies, however, can provide information on specific degradative reactions. Nonetheless, the former studies are of practical importance, especially with respect to the degradation of PCBs by mixed and pure microbial cultures. The most extensive studies of the biodegradability of specific chlorinated biphenyls have been carried out by *Furukawa* et al.,[65,70] who examined the degradation of 36 pure isomers, substituted with between one and five chlorine atoms, by an *Alcaligenes* species and an *Acinetobacter* species. Both the number and position of the chlorine atoms determined the extent of biodegradability. For example, the more highly substituted PCBs were metabolized less extensively than the mono- and dichlorinated biphenyls. Furthermore, the isomers bearing chlorine substituents on only one ring were more easily metabolized than those with substituents on both rings, and isomers doubly substituted in the *o*-positions (e.g., 2,2'- or 2,6-substitution) were generally recalcitrant to microbial degradation. Yellow *meta*-cleavage products were found to accumulate during the biodegradation of 2,4-dichlorobiphenyls,[70] whereas catabolism of other isomers (e.g., 4-chlorobiphenyl) led to the production of the correspondingly substituted chlorobenzoates.[65,67] A pathway for bacterial catabolism of PCBs is outlined in Figure 4. In agreement with this pathway, *Masse* et al.[64] identified 4-chlorobenzoate as a major product along with small amounts of other intermediates in the product mixture obtained by degradation of 4-chlorobiphenyl by an *Achromobacter* species. By adding a 4-chlorobenzoate-utilizing bacterium, *Pseudomonas* CBS3, a strain that was isolated and characterized in our laboratory, they observed that the mixed culture degraded not only the 4-chlorobenzoate but all other metabolites as well.[61]

An important general conclusion of investigations studying biodegradation of commercial PCB formulations is that the lower chlorinated isomers (one to three chlorine atoms) are rapidly degraded,[54,56,58] whereas those isomers substituted with between five and ten chlorine atoms are almost totally recalcitrant. *Kopecky*, however, has reported the isolation of bacteria capable of efficiently transforming Arochlor 1260, a commercial formulation containing highly substituted PCBs (five to nine chlorine atoms).[59] The involvement of plasmid DNA in the biodegradation of

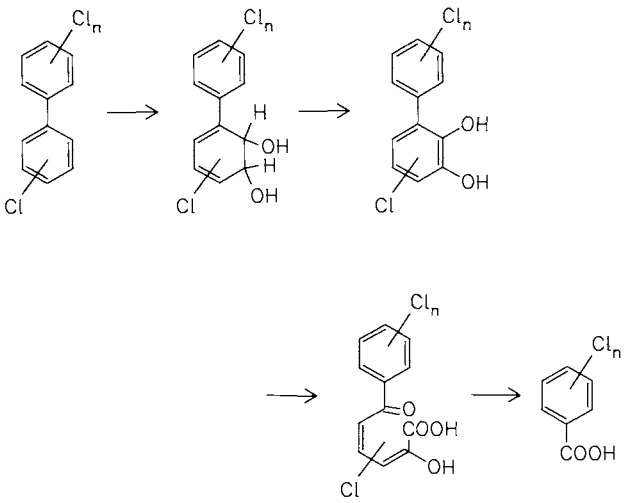


Fig. 4. The degradation of polychlorinated biphenyls by *Alcaligenes* sp. Y42 and *Acinetobacter* sp. P6. n = 1-5.

PCBs has been suggested by several investigators,[71,72] but the number of genes encoding the dehalogenating enzymes involved is unknown. In summary, polychlorinated biphenyls can be degraded by microorganisms, but the possibility remains that highly chlorinated isomers may be completely recalcitrant.

4.2.3. 1,1,1-Trichloro-2,2-bis(4-chlorophenyl)ethane (DDT)

Until recently, 1,1,1-trichloro-2,2-*bis*(4-chlorophenyl)ethane (DDT) was extensively used in the control of insect pests, especially in the fight against the spread of malaria. However, when DDT was found to be highly persistent in the environment (half-life more than 15 years)[3] and to undergo bioaccumulation through food chains, legislation banning its use was approved in North America and Western Europe.

Despite the persistence of DDT in the environment, it has been shown to be completely degraded by several different bacteria.[73,74] For example, *Golovleva* and *Skryabin*[74] reported the isolation of a *Pseudomonas* species that transformed DDT by "cometabolism."

The term cometabolism is used to describe the microbial transformation of a compound, in this case DDT, that does not serve as a source of carbon or energy. Alternative sources of carbon and energy, therefore, need to be supplied; in these experiments, lactic acid as carbon source and nitrate as electron acceptor were added to the medium. Phenylacetic acid, formed by bacterial cometabolism of DDT, was degraded by the producing organism aerobically (Fig. 5). Cometabolism of DDT by a *Hydrogenomonas* species to produce 4-chlorophenylacetic acid was reported by *Pfaender* et al.[73] These and other authors also showed that the product could be further degraded by a variety of microorganisms.[73,75] Yet, although DDT can be degraded by bacteria in the laboratory, it still persists in the biosphere. This paradox shows that the observation of extensive biodegradation of halogenated hydrocarbons by

bacteria in the laboratory does not guarantee that the corresponding degradative reactions occur to a significant extent in nature.

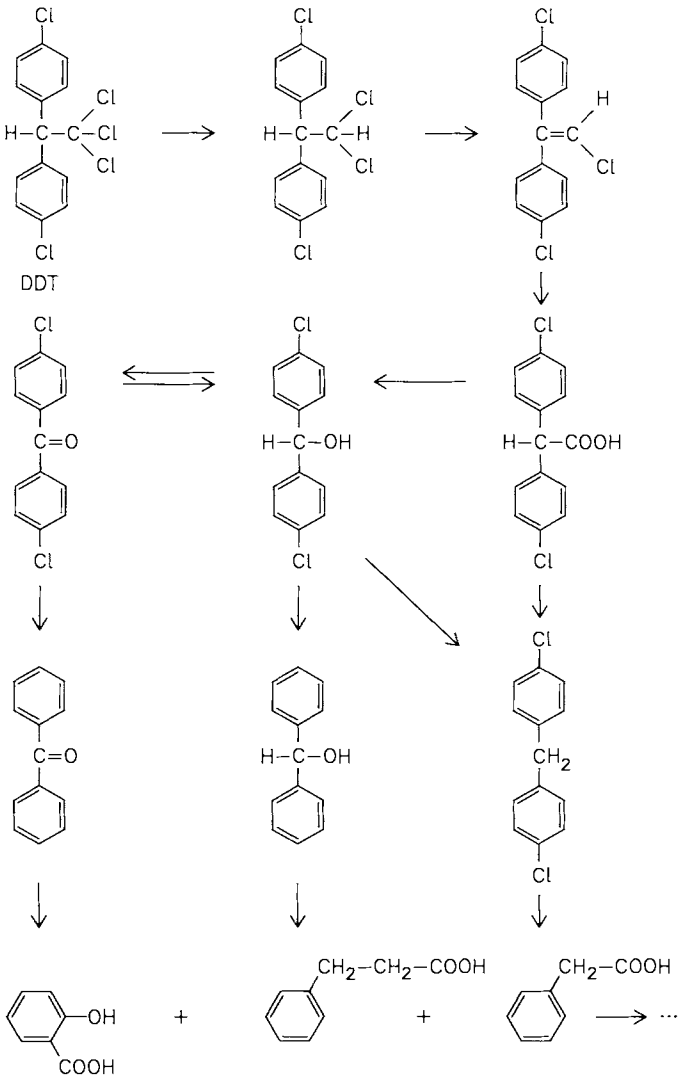


Fig. 5. The degradation of 1,1,1-trichloro-2,2-bis(4-chlorophenyl)ethane (DDT) by *Pseudomonas aeruginosa*.

4.2.4. *Chlorophenoxyalkanoic Acids*

The chlorophenoxyalkanoic acids constitute another economically important group of halogenated aromatic hydrocarbons. They are widely used as herbicides with hormone-like properties in the control of dicotyledonous weeds. The most important are 2,4-dichlorophenoxyacetic acid (2,4-D), its propionic acid and butyric acid homologues, 4-chloro-2-methylphenoxyacetic acid (MCPA), and 2,4,5-trichlorophenoxyacetic acid (2,4,5-T). The short half-life of 2,4-D in soils supports the idea that the herbicide is rapidly biodegraded. Further support comes from the ready isolation of microorganisms that utilize chlorophenoxyalkanoic acids as the sole source of carbon and energy or, at least, can cometabolize these herbicides. In all cases studied, aerobic biodegradation proceeds by removal of the aliphatic side chain with formation of the corresponding chlorinated phenol. Thus, formation of 2,4-dichlorophenol **16** from both 2,4-D and 4-(2,4-dichlorophenoxy)butyric acid, of 4-chloro-*o*-cresol from MCPA, and of 2,4,5-trichlorophenol from 2,4,5-T have been reported.[76,77] The subsequent degradative pathways differ in different microorganisms. For example, the biodegradation of 2,4,5-T by two bacterial species may involve the dehalogenase-catalyzed replacement of one chlorine substituent by a hydroxyl group, resulting in the formation of 3,5-dichlorocatechol.[78,79] The enzymes, however, have not been detected. Two pathways have been suggested for biodegradation of 2,4-dichlorophenol **16**: enzyme-catalyzed replacement of one chlorine substituent by a hydroxyl group gives 4-chlorocatechol,[76] and oxidation produces 3,5-dichlorocatechol.[77,80] Further degradation of 4-chloro- and 3,5-dichlorocatechol by one of these bacteria, a *Pseudomonas* species, involves dioxygenase-catalyzed cleavage of these intermediates between the hydroxyl groups to give the corresponding chloromuconic acids **17**.[77] By contrast, an *Achromobacter* species that cleaves chlorocatechols adjacent to the hydroxyl groups has been isolated (compare *ortho*- and *meta*-cleavage, Fig. 3).[81] Lactonization of **17** results in the removal of one chlorine substituent to form **18**, which is finally converted into 2-chloro-4-oxo-2-hexenedioic acid **19** (Fig. 6). Similar catabolic pathways[82]

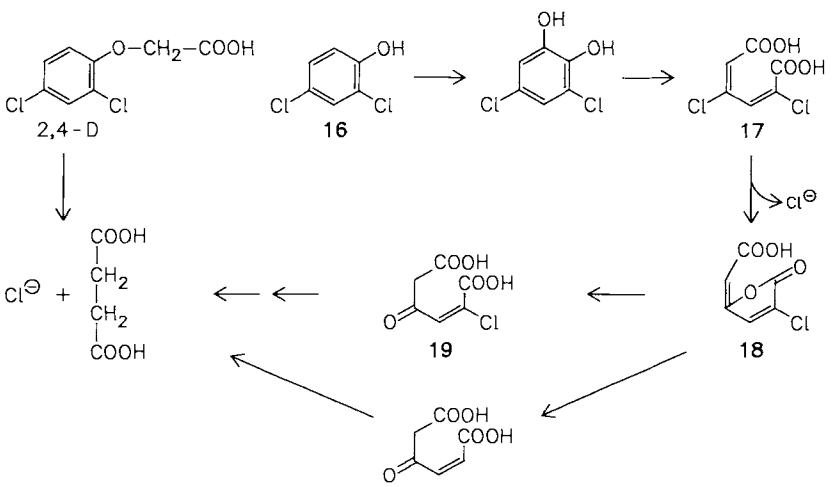


Fig. 6. The microbial degradation of 2,4-dichlorophenoxyacetic acid (2,4-D).

have been suggested for the degradation of the chloromuconic acids derived from 2,4-D and MCPA.[83-86]

4.2.5. Chlorobenzoic Acids

Chlorinated benzoic acids have been shown to be intermediates in the biodegradation of several chlorinated aromatic compounds; for example, 4-chlorobenzoic acid **20** is formed in the degradation of both PCBs[5,67] and the herbicide Bidisin.[87] These acids are relatively nontoxic and readily soluble in water. For these reasons, they are frequently used as model compounds for investigations of the mechanisms of biodegradation of chlorinated aromatic hydrocarbons.[88-91] Mixed microbial cultures, which have been studied by a number of groups, can, under aerobic conditions, degrade a wide range of chlorinated benzoic acids, including 2-, 3-, and 4-chlorobenzoic acid as well as 3,4-dichloro- and 2,4-dichlorobenzoic acid.[90] By contrast, under anaerobic conditions, only reductive dechlorination of *m*-substituted benzoic acids has been observed.[92-94] Cometabolism of chlorobenzoic acids in the presence of unsubstituted benzoic acids leads to the corresponding chlorocatechols in some pure cultures of bacteria.[95-98] These cultures were eventually poisoned, however, through accumulation of chlorocatechols, which could not be further catabolized and which polymerized to form toxic products. These results suggest that the enzymes involved in the conversion of unsubstituted benzoic acid to catechol can also transform some chlorobenzoic acids in an analogous manner. The critical step of these degradation reactions appears to be the ring cleavage. Conversion of 3-chlorocatechol to the corresponding acyl chloride and irreversible inhibition of a bacterial catechol 2,3-dioxygenase by the product (i.e., "suicide inactivation") has been reported by *Bartels* et al.[99] *Klecka* and *Gibson*,[100] who demonstrated reversible inhibition of the same enzyme in a different bacterium, suggested that the inhibition results from chelation of Fe(II), which is essential for the activity of the enzyme.

Several groups have isolated *Pseudomonas* species capable of utilizing 3-chlorobenzoate as the sole source of carbon and energy.[101-103] The *Pseudomonas* species described by *Johnston* et al.[101] degrades 3-chlorobenzoic acid via 3-hydroxybenzoic acid. This pathway indicates the involvement of an enzyme (not yet identified) that catalyzes the removal of the halogen substituent at an early stage of biodegradation. This enzyme allows the strain to avoid the problems associated with chlorocatechol degradation. *Dorn* et al.[102] and *Grishenkov* et al.,[103] on the other hand, found *Pseudomonas* species which convert 3-chlorobenzoic acid into 3- and 4-chlorocatechol, intermediates which are further catabolized via an *ortho*-cleavage pathway.

Kawasaki et al.[104] and *Knackmuss* and his co-workers[105-109] have studied the effects of various substituents upon enzymes catalyzing the individual reactions of the chlorobenzoate degradative pathway. In *Pseudomonas* sp. B13, for example, they detected two types of catechol 1,2-dioxygenase: one was mainly active in the ring cleavage of catechol and had low affinity for chlorinated catechols; the second enzyme could efficiently degrade chlorocatechols.[108] Furthermore, two cycloisomerases, catalyzing cyclization of the chloromuconic acids with cleavage of the chlorine substituent, were also isolated from strain B13. One was found to be specific for unsubstituted muconate, whereas the other was also capable of transforming chloromuconates.[109] These two enzymes, the dioxygenase and cycloisomerase, are responsible for the good growth of strain B13 on 3-chlorobenzoic acid.

From these studies, *Knackmuss* and his co-workers, using gene transfer techniques, were able to develop strategies that allowed *Pseudomonas* sp. B13 to degrade a wide range of halogenated aromatic compounds to the corresponding chlorocatechols. In this way, a gene encoding a broad-specificity benzoate 1,2-dioxygenase from *Pseudomonas* putida mt2, carried on the TOL plasmid, was transferred and expressed in strain B13. Since the TOL plasmid enzymes can also convert 4-chloro- and 3,5-dichlorobenzoic acids into the corresponding chlorocatechols, the hybrid strain B13 containing the plasmid was able to grow on these compounds as well. Genetic exchange between strain B13 and aniline-utilizing bacteria, containing plasmid-encoded enzymes that convert chloroanilines into chlorocatechols, allowed the construction of hybrid strains capable of degrading chloroaniline. Interestingly, in all of these genetically constructed hybrid strains production of plasmid-encoded enzymes catalyzing *meta*-ring cleavage was switched off by spontaneous mutations.[110,111] The prospects for constructing novel degradative pathways by means of genetic manipulation are interesting; however, it should be borne in mind that similar combinations can be obtained by developing continuous flow systems containing mixed cultures of the appropriate bacteria. Experience shows that genetic exchange can occur in these systems and, under appropriate selective conditions, can result in the formation of strains containing the desired degradative functions. Such strains are usually more stable than those produced by in vitro or in vivo genetic manipulations.

The biodegradation of 4-chlorobenzoic acid by pure cultures of bacteria has been described by American,[112] British,[113] Russian,[114] and German[115] groups. Work in our laboratory has resulted in the isolation of *Arthrobacter*, *Nocardia*, and *Pseudomonas* species capable of utilizing 4-chlorobenzoic acid as the sole source of carbon and energy.[115-117] In all of these bacterial strains, the first step of the catabolic pathway is replacement of the chlorine substituent by a hydroxyl group; the 4-hydroxybenzoic acid produced is converted into 3,4-dihydroxybenzoic acid **21** by oxygenase-catalyzed hydroxylation. Ring cleavage of this intermediate may be either of the *ortho*[117] or *meta*[116] type depending upon the bacterium. To date, enzymes catalyzing chlorine elimination from the aromatic ring have been identified in four different bacteria.[113,118,119] In vitro studies show that the enzymes catalyze the incorporation of ^{18}O-label, from $H_2{}^{18}O$, into the product of 4-chlorobenzoic acid dechlorination. They are, therefore, the only known examples of enzymes that have been unequivocally shown to catalyze direct substitution of the halogen on the aromatic ring by a hydrolytic mechanism.

The degradation of 2-chlorobenzoic acid by *Pseudomonas cepacia* also involves removal of the chlorine substituent in the first step,[122] but here the aromatic ring undergoes oxidation with elimination of CO_2. Catechol, which is

the first intermediate of this metabolic pathway, is further degraded by an *ortho*-cleavage pathway. An enzyme catalyzing the oxidative removal of the chlorine substituent from 4-chlorophenylacetic acid **22** has been isolated from *Pseudomonas* CBS3.[123] Expectations that this oxygenase, which converts 4-chlorophenylacetic acid into 3,4-dihydroxyphenylacetic acid, would be a nonspecific enzyme proved incorrect: only low activities were recorded in assays of the oxygenase with unsubstituted phenylacetic acid. Figure 7 outlines the catabolic pathways that have

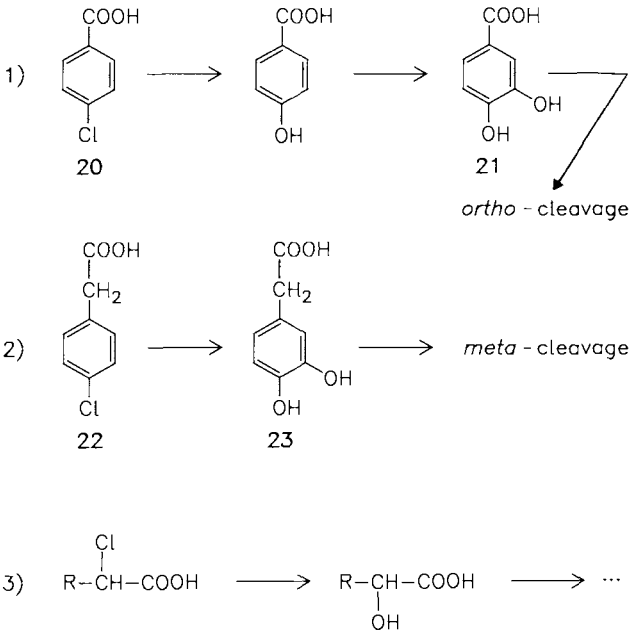


Fig. 7. Different dehalogenation mechanisms identified in *Pseudomonas* sp. CBS3. 1) Hydrolytic cleavage of the aromatic carbon-chlorine bond in the degradation of 4-chlorobenzoic acid **20**. 2) Cleavage of the aromatic carbon-chlorine bond and concomitant oxidation in the degradation of 4-chlorophenylacetic acid **22**. 3) Hydrolytic cleavage of the aliphatic carbon-halogen bond in the degradation of 2-haloalkanoic acids.

been shown to be responsible for the degradation of four kinds of halogenated aromatic compounds by *Pseudomonas* CBS3.

2-Fluorobenzoic acid can be degraded by a pathway entirely analogous to that described for 2-chlorobenzoic acid; oxygenase-catalyzed fluorine elimination produces catechol, which is then degraded by the β-oxoadipate pathway.[124-126] In contrast, degradation of 4-fluorobenzoic acid follows a pathway analogous to that described for the degradation of 3-chlorobenzoic acid by *Pseudomonas* sp. B13. Thus, 3- and 4-fluorocatechols are formed as intermediates, which, after *ortho*-cleavage to the corresponding fluoromuconates, may be defluorinated upon lactonization. Anaerobic degradation of 2-fluorobenzoic acid has recently been reported, although catabolic pathway intermediates and enzymes were not described.[128]

4.2.6. Polychlorinated Dibenzo[1,4]dioxins

Unlike the chlorinated hydrocarbons discussed so far, the polychlorinated dibenzo[1,4]dioxins have never been deliberately manufactured. Yet, they are dangerous environmental pollutants and have been detected even in the sediments of protected lakes situated in areas where no pollution should occur.[2] The question therefore arises as to the origin of dibenzodioxins. Polychlorinated dibenzodioxins are formed as side products during the manufacture of chlorinated phenols and biphenyls and are, for example, detectable in commercial wood preservatives that contain pentachlorophenol.[52] Another source of chlorinated dibenzodioxins is from the combustion of certain waste materials;[129] various isomers are, for example, formed during pyrolysis of chlorobenzenes, chlorophenols, and PCBs. Detection of chlorinated dibenzodioxins in biological samples sealed in 1933, well before the beginning of large-scale manufacture and use of chlorinated hydrocarbons, has led to the suggestion that the dibenzodioxins might have been produced by chlorination of domestic water supplies and by forest fires.[130] Analysis of sediment samples indicates that a rapid increase in the amount of chlorinated dibenzodioxins began in the 1940s and is likely to have been associated with commercial manufacturing of chlorinated hydrocarbons, which also began at about this time.

Public attention was focused on this group of compounds as a result of the disaster at Seveso,[52] where a reactor being used for production of 2,4,5-trichlorophenol exploded and showered the surrounding area with about 250 g of 2,3,7,8-tetrachloro[1,4]dibenzodioxin (TCDD), referred to erroneously as "dioxin" by the press. The extent of the damage at Seveso and the fears associated with the toxicity of TCDD prompted many detailed studies, both chemical and biological, of the compound and related isomers so that today it may be claimed that TCDD is one of the best studied chlorinated hydrocarbons.[131-136] TCDD is acutely toxic at low concentrations (< 1 μg per kg body weight), although carcinogenic effects associated with the compound probably result from induction of the enzymes involved in mammalian metabolism of xenobiotics. Thus, TCDD should be called a cocarcinogen.

What do microorganisms have to offer with regard to the biodegradation of this compound? Studies of microbial catabolism of TCDD and related compounds encounter two major obstacles from the outset: the compounds are almost insoluble in water and they adsorb strongly to surfaces. Consequently, quantitative analysis of chlorinated dibenzodioxins is complicated and the availability of the compounds as substrates for biodegradation is severely limited. Despite these problems, *Gibson* et al.[137,138] have shown that bacteria produce enzymes that catalyze the hydroxylation of TCDD at the 1-position, although it seems unlikely that these enzymes can be induced by the amounts of TCDD present in the biosphere. *Quensen* et al.[139] and *Philippi* et al.,[140] using media containing solvents to increase the solubility of TCDD, detected very low rates of degradation of ^{14}C-labeled TCDD by various bacteria. The products of biodegradation could only be detected by autoradiography after separation by thin layer chromatography. *Philippi* et al.[140] tentatively suggested that one of the polar metabolites produced during TCDD biodegradation was hydroxytetrachloro[1,4]dibenzodioxin, but further characterization of this product has not been forthcoming.

In summary, the notorious Seveso poison can, to some extent at least, be transformed by microorganisms. The concentrations of this compound in the environment, however, are too low and its water solubility and adsorptive properties are such that it probably would not induce the required enzymes in microorganisms. TCDD is, therefore, unlikely to be subject to extensive biodegradation. However, highly contaminated soils (such as those around Seveso) might be used to enrich for bacteria capable of detoxifying the compound if the TCDD can be solubilized so as to induce microbial degradative enzymes.

An alternative approach to the biodegradation of TCDD has been recently reported by *Bumpus* et al.,[141] who found that the enzymes involved in lignin degradation, excreted by fungi such as *Phanerochaete chrysosporium*, catalyze transformations of not only TCDD but also DDT, PCBs, and hexachlorocyclohexane. The fungus was incubated with the ^{14}C-labeled compounds, and, in all cases, $^{14}CO_2$ release was detected. The authors attributed this biodegradation to enzymes that produce carbon radicals capable of reacting nonspecifically with hydrocarbons in their vicinity. Applications of these studies to the control of environmental pollutants await further development.

5. Summary and Outlook

It has been the aim of this review to describe the range of degradative functions associated with microbial catabolism of halogenated hydrocarbons. Microorganisms capable of partially or completely degrading almost every pollutant known have been identified. However, the rates of degradation in the environment are often very slow and do not reflect the versatility of bacteria and fungi isolated in the laboratory. There might be several reasons for these conflicting observations. In some cases, the bacteria containing the appropriate enzymes might not be distributed widely enough. In others, natural conditions may not be optimal for biodegradation so that bacterial enzymes, although available, remain uninduced or inactive. Although the halogenated hydrocarbons discussed above are known to be degraded in the environment, the question remains, at what rate? Half-lives in aquatic and terrestrial environments of 15 years and more, as found for many halogenated compounds, are unacceptably high. What contribution to the solution of this problem might result from the isolation of microbes capable of degrading pollutant hydrocarbons and the elucidation of their degradative pathways?

The study of catabolic enzymes and biodegradative mechanisms in isolated microorganisms should reveal important pathways of biodegradation in the natural environment. Such pathways could be taken into consideration in the synthesis of new chemicals. Compounds that are liable to contaminate the environment (almost 100% of manufactured hydrocarbons) could be designed so as to combine efficacy with biodegradability. More direct applications may come from the use of isolated microorganisms or purifed enzymes for the decontamination of pollutant spillages. Such studies are currently being carried out in many countries, but the overall effectiveness of the approach is still in question. An example is the use of a bacterial inoculant to clean up pentachlorophenol contamination (Section 4.2.1). In some cases potential pollutants may be treated at the source before they enter the environment where dispersion creates problems. Thus, downstream waste treatments, either based upon domestic sewage plants or tailored for biodegradation of specific pollutant hydrocarbons, could be devised for detoxification of industrial effluents of known composition. Biological systems, comprising columns containing isolated bacteria and enzymes, are currently being used successfully for the degradation of dichloromethane and tetrachloroethylene. Mixed microbial cultures offer the best possibilities for efficient and robust treatments. In this respect, the results of laboratory-based studies with pure cultures growing in defined media under optimal conditions cannot immediately be applied to complex in situ and downstream treatments where considerations of fluctuating physico-chemical conditions and interactions between microorganisms may be as important as considerations of biodegradative mechanisms. Future research into these poorly understood aspects of biodegradation will be central to the development of treatment systems for toxic wastes.

Another exciting development of research into biodegradation of chlorinated hydrocarbons has been the biotechnological applications of novel enzymes as catalysts for commercial chemical syntheses. For example, dehalogenases are now being used for the production of optically active lactic acid from racemic 2-chloropropionic acid (Section 3.2). The synthesis of other optically active compounds is a future possibility.

Unfortunately, there are no obvious general biological solutions to the problems of environmental pollution by dispersed, low concentrations of halogenated hydrocarbons. We have little choice other than to continue to accept responsibility for controlling, at source or at production, the rate at which pollutants enter the environment. In the words of *Paracelsus von Hohenheim*, "prevention is better than cure."

The research described in this article that was carried out in the authors laboratory was supported by the Fonds der Chemischen Industrie.

Received: October 14, 1985;
revised: April 3, 1986 [A 589 IE]
German version: *Angew. Chem. 98* (1986) 778
Translated by Dr. *A. Weightman*, Cardiff (UK)

[1] J. H. Koeman, M. C. Ten Noever de Brauw, R. H. De Vos, *Nature (London) 221* (1969) 1126.
[2] J. M. Czuczwa, B. D. McVeety, R. A. Hites, *Science 226* (1984) 568.
[3] M. Alexander, *Biotechnol. Bioeng. 15* (1973) 611.
[4] T. Leisinger, *Experientia 39* (1983) 1183.
[5] J. McCann, V. Simmon, D. Streitwieser, B. N. Ames, *Proc. Natl. Acad. Sci. USA 72* (1975) 3190.
[6] C. Malaveille, H. Bartsch, A. M. Barbin, A. M. Camus, R. Montesano, A. Croisy, P. Jacquinon, *Biochem. Biophys. Res. Commun. 63* (1975) 363.
[7] T. A. Bellar, J. J. Lichtenberg, R. C. Kroner, *J. Am. Water Works Assoc. 66* (1974) 703.
[8] W. Brunner, D. Staub, T. Leisinger, *Appl. Environ. Microbiol. 40* (1980) 950.
[9] G. Stucki, R. Gälli, H.-R. Ebersold, T. Leisinger, *Arch. Microbiol. 130* (1981) 366.
[10] C. E. Castro, R. S. Wade, N. O. Belser, *J. Agric. Food Chem. 31* (1983) 1184.

[11] E. J. Bouwer, P. L. McCarthy, *Appl. Environ. Microbiol. 45* (1983) 1286.
[12] D. B. Janssen, A. Scheper, L. Dijkhuizen, B. Witholt, *Appl. Environ. Microbiol. 49* (1985) 673.
[13] G. Stucki, U. Krebser, T. Leisinger, *Experientia 39* (1983) 1271.
[14] T. M. Vogel, N. L. McCarthy, *Appl. Environ. Microbiol. 49* (1985) 1080.
[15] S. Keuning, D. B. Janssen, B. Witholt, *J. Bacteriol. 163* (1985) 635.
[16] K. Haider, G. Jagnow, *Arch. Microbiol. 104* (1975) 113.
[17] G. Jagnow, K. Haider, P.-C. Ellwardt, *Arch. Microbiol. 115* (1977) 285.
[18] T. Omori, M. Alexander, *Appl. Environ. Microbiol. 35* (1978) 512.
[19] E. Senior, A. T. Bull, J. H. Slater, *Nature (London) 263* (1976) 476.
[20] K. Motosugi, N. Esaki, K. Soda, *J. Bacteriol. 150* (1982) 522.
[21] J. H. Slater, D. Lovatt, A. J. Weightman, E. Senior, A. T. Bull, *J. Gen. Microbiol. 114* (1979) 125.
[22] A. J. Weightman, J. H. Slater, *J. Gen. Microbiol. 121* (1980) 187.
[23] P. Goldman, G. W. A. Milne, D. B. Keister, *J. Biol. Chem. 243* (1968) 428.
[24] H. Kawasaki, H. Yahara, K. Tonomura, *Agric. Biol. Chem. 48* (1984) 2627.
[25] K. G. Au, C. T. Walsh, *Bioorg. Chem. 12* (1984) 197.
[26] A. J. Weightman, A. L. Weightman, J. H. Slater, *J. Gen. Microbiol. 12* (1982) 1755.
[27] U. Klages, S. Krauss, F. Lingens, *Hoppe-Seyler's Z. Physiol. Chem. 364* (1983) 529.
[28] K. Motosugi, N. Esaki, K. Soda, *Biotechnol. Bioeng. 26* (1984) 805.
[29] R. Müller, F. Lingens in H. Sund, V. Ullrich (Eds.): *Biological Oxidations*, Springer, Berlin 1983, p. 278.
[30] F. Lingens, *Forum Mikrobiol. 5* (1979) 240.
[31] S. Dagley, *Adv. Microb. Physiol. 6* (1971) 1.
[32] R. Y. Stanier, L. N. Ornston, *Adv. Microb. Physiol. 9* (1973) 89.
[33] R. Müller, S. Haug, J. Eberspächer, F. Lingens, *Hoppe-Seyler's Z. Physiol. Chem. 358* (1977) 797.
[34] R. Müller, S. Schmitt, F. Lingens, *Eur. J. Biochem. 125* (1982) 579.
[35] S. Schmitt, R. Müller, W. Wegst, F. Lingens, *Hoppe-Seyler's Z. Physiol. Chem. 365* (1984) 143.
[36] K. Sauber, C. Fröhner, G. Rosenberg, J. Eberspächer, F. Lingens, *Eur. J. Biochem. 84* (1977) 89.
[37] J. Eberspächer, F. Lingens, *Hoppe-Seyler's Z. Physiol. Chem. 359* (1978) 1323.
[38] D. Dickson, *Nature (London) 283* (1980) 418.
[39] J. Paasivirta, J. Saerkkae, T. Leskijaervi, A. Roos, *Chemosphere 9* (1980) 441.
[40] R. J. Fiedler, G. S. Sorrie, C. M. Bishop, R. B. Jones, M. J. Van Den Heuvel, *Toxic. Rev. 5* (1982) 1.
[41] N. B. K. Murthy, D. D. Kaufman, G. F. Fries, *J. Environ. Sci. Health Part B 14* (1979) 1.
[42] M. A. Guthrie, E. J. Kirsch, R. F. Wukasch, C. P. L. Grady, Jr., *Water Res. 18* (1984) 451.
[43] I. Watanabe, *Soil Biol. Biochem. 9* (1977) 99.
[44] L. P. Moos, E. J. Kirsch, R. F. Wukasch, C. P. L. Grady, Jr., *Water Res. 17* (1983) 1575.
[45] R. Valo, J. Apajalahti, M. Salkinoja-Salonen, *Appl. Microbiol. Biotechnol. 21* (1985) 313.
[46] A. Ide, Y. Niki, F. Sakamoto, I. Watanabe, H. Watanabe, *Agric. Biol. Chem. 36* (1972) 1973.
[47] I. Watanabe, *Soil Sci. Plant. Nutr. (Tokyo) 19* (1973) 109.
[48] T. Suzuki, *J. Environ. Sci. Health Part B 12* (1977) 113.
[49] G. J. Stanlake, R. K. Finn, *Appl. Environ. Microbiol. 44* (1982) 1421.
[50] B. Rott, S. Nitz, F. Korte, *J. Agric. Food Chem. 27* (1979) 306.
[51] R. U. Edgehill, R. K. Finn, *Appl. Environ. Microbiol. 45* (1983) 1122.
[52] E. Heckel, *Chem.-Ing.-Tech. 56* (1984) A 390.
[53] D. Pal, J. B. Weber, *M. R. Overcash, Residue Rev. 74* (1980) 45.
[54] D. Liu, *Bull. Environ. Contam. Toxicol. 29* (1982) 200.
[55] R. R. Clark, E. S. K. Chian, R. A. Griffin, *Appl. Environ. Microbiol. 37* (1979) 680.
[56] D. Liu, *Bull. Environ. Contam. Toxicol. 27* (1981) 695.
[57] E. S. Tucker, V. W. Saeger, O. Hicks, *Bull. Environ. Contam. Toxicol. 14* (1975) 705.
[58] K. Furukawa, N. Tomizuka, A. Kamibayashi, *Appl. Environ. Microbiol. 46* (1983) 140.
[59] A. Kopecky in G. S. Omen, A. Hollaender (Eds.): *Genetic Control of Environmental Pollutants*, Plenum, New York 1984, p. 374.
[60] H.-L. Kong, G. S. Saylers, *Appl. Environ. Microbiol. 46* (1983) 666.
[61] M. Sylvestre, R. Masse, C. Ayotte, F. Messier, J. Fauteux, *Appl. Microbiol. Biotechnol. 21* (1985) 192.
[62] M. Sylvestre, R. Masse, F. Messier, J. Fauteux, J.-G. Bisaillon, R. Beaudet, *Appl. Environ. Microbiol. 44* (1982) 871.
[63] M. Sylvestre, *Appl. Environ. Microbiol. 39* (1980) 1223.
[64] R. Masse, F. Messier, L. Peloquin, C. Ayotte, M. Sylvestre, *Appl. Environ. Microbiol. 47* (1984) 947.
[65] K. Furukawa, N. Tomizuka, A. Kamibayashi, *Appl. Environ. Microbiol. 38* (1979) 301.
[66] K. Furukawa, K. Tonomura, A. Kamibayashi, *Agric. Biol. Chem. 43* (1979) 577.
[67] K. Ballschmiter, C. Unglert, H. J. Neu, *Chemosphere 1* (1977) 51.
[68] K. Furukawa, F. Matsumara, *J. Agric. Food Chem. 24* (1976) 251.
[69] M. Ahmed, D. D. Focht, *Can. J. Microbiol. 19* (1973) 47.
[70] K. Furukawa, K. Tonomura, A. Kamibayashi, *Appl. Environ. Microbiol. 35* (1978) 223.
[71] K. Furukawa, A. M. Chakrabarty, *Appl. Environ. Microbiol. 44* (1982) 619.
[72] G. S. Sayler, H.-L. Kong, M. S. Shields in G. S. Omen, A. Hollaender (Eds.): *Genetic Control of Environmental Pollutants*, Plenum, New York 1984, p. 117.
[73] F. K. Pfänder, M. Alexander, *J. Agric. Food Chem. 20* (1972) 842.
[74] L. A. Golovleva, G. K. Skryabin in T. Leisinger, A. M. Cook, R. Hütter, J. Nuesch (Eds.): *Microbial Degradation of Xenobiotic and Recalcitrant Compounds*, Academic Press, London 1981, p. 287.
[75] A. Markus, U. Klages, F. Lingens, *Hoppe-Seyler's Z. Physiol. Chem. 363* (1982) 431.
[76] I. C. MacRae, M. Alexander, A. D. Rovira, *J. Gen. Microbiol. 32* (1963) 69.
[77] W. C. Evans, B. S. W. Smith, H. N. Fernley, J. I. Davies, *Biochem. J. 12* (1971) 543.
[78] R. S. Horvath, *Bull. Environ. Contam. Toxicol. 5* (1970) 537.
[79] J. M. Suflita, J. Stout, J. M. Tiedje, *J. Agric. Food Chem. 32* (1984) 218.
[80] J.-M. Bollag, C. S. Helling, M. Alexander, *J. Agric. Food Chem. 16* (1968) 826.
[81] R. S. Horvath, *Biochem. J. 119* (1970) 871.
[82] J. M. Tiedje, J. M. Duxbury, M. Alexander, J. E. Dawson, *J. Agric. Food Chem. 17* (1969) 1021.
[83] T. I. Steenson, N. Walker, *J. Gen. Microbiol. 16* (1957) 146.
[84] J. K. Gaunt, W. C. Evans, *Biochem. J. 122* (1971) 533.
[85] Y. Gamar, J. K. Gaunt, *Biochem. J. 122* (1971) 527.
[86] J. K. Gaunt, W. C. Evans, *Biochem. J. 122* (1971) 519.
[87] H. Köcher, F. Lingens, W. Koch, *Weed Res. 16* (1976) 93.
[88] F. A. Lund, D. S. Rodriguez, *J. Gen. Appl. Microbiol. 30* (1984) 53.
[89] Y. N. Karasevich, G. M. Zaitsev, *Mikrobiologiya 53* (1984) 374.
[90] M. J. DiGeronimo, M. Nikaido, M. Alexander, *Appl. Environ. Microbiol. 37* (1979) 619.
[91] D. R. Shelton, J. M. Tiedje, *Appl. Environ. Microbiol. 48* (1984) 840.
[92] J. M. Suflita, J. A. Robinson, J. M. Tiedje, *Appl. Environ. Microbiol. 45* (1983) 1466.
[93] A. Horowitz, J. M. Suflita, J. M. Tiedje, *Appl. Environ. Microbiol. 45* (1983) 1459.
[94] J. M. Suflita, A. Horowitz, D. R. Shelton, J. M. Tiedje, *Science 218* (1982) 1115.
[95] J. R. Spokes, N. Walker, *Arch. Microbiol. 96* (1974) 125.
[96] W. Veerkamp, R. Pel, O. Hutzinger, *Chemosphere 12* (1983) 1337.
[97] H. D. Haller, R. K. Finn, *Eur. J. Appl. Microbiol. Biotechnol. 8* (1979) 191.
[98] R. S. Horvath, M. Alexander, *Appl. Microbiol. 20* (1970) 254.
[99] I. Bartels, H.-J. Knackmuss, W. Reineke, *Appl. Environ. Microbiol. 47* (1984) 500.
[100] G. M. Klecka, D. T. Gibson, *Appl. Environ. Microbiol. 41* (1981) 1159.
[101] H. W. Johnston, G. G. Briggs, M. Alexander, *Soil. Biol. Biochem. 4* (1972) 187.
[102] E. Dorn, M. Hellwig, W. Reineke, H.-J. Knackmuss, *Arch. Microbiol. 99* (1974) 61.
[103] V. G. Grishenkov, I. E. Fedechkina, B. P. Baskunov, L. A. Anisimova, A. M. Boronin, L. A. Golovleva, *Mikrobiologiya 52* (1983) 771.
[104] H. Kawasaki, M. Takao, A. Koiso, K. Tonomura, *Appl. Environ. Microbiol. 49* (1985) 1544.
[105] W. Reineke, H.-J. Knackmuss, *Biochim. Biophys. Acta 542* (1978) 412 and 424.
[106] H.-J. Knackmuss, W. Reineke, *Chemosphere 6* (1973) 225.
[107] E. Dorn, H.-J. Knackmuss, *Biochem. J. 174* (1978) 85.
[108] E. Dorn, H.-J. Knackmuss, *Biochem. J. 174* (1978) 73.
[109] E. Schmidt, H.-J. Knackmuss, *Biochem. J. 192* (1980) 339.
[110] W. Reineke, D. J. Jeenes, P. A. Williams, H.-J. Knackmuss, *J. Bacteriol. 150* (1982) 195.

[111] D. K. Chatterjee, A. M. Chakrabarty, *Mol. Gen. Genet. 188* (1982) 279.
[112] P. J. Chapman, *Abstr. Ann. Meet. Am. Soc. Microbiol. 75* (1975) 192.
[113] T. S. Marks, A. R. W. Smith, A. V. Quirk, *Appl. Environ. Microbiol. 48* (1984) 1020.
[114] G. M. Zaitsev, Y. N. Karasevich, *Mikrobiologiya 50* (1981) 35.
[115] S. Ruisinger, U. Klages, F. Lingens, *Arch. Microbiol. 110* (1976) 253.
[116] U. Klages, F. Lingens, *FEMS Microbiol. Lett. 6* (1979) 201.
[117] U. Klages, F. Lingens, *Zentralbl. Bakteriol. Parasitenkd. Infektionskr. Hyg. Abt. 1 Orig. C1* (1980) 215.
[118] R. Müller, T. P. Armbruster, F. Lingens, *13th Int. Congr. Biochem. Abstr. 1985*, 70.
[119] J. Thiele, R. Müller, F. Lingens, *Abstr. 20. Hauptvers. GDCh 1985*, 172.
[120] R. Müller, J. Thiele, U. Klages, F. Lingens, *Biochem. Biophys. Res. Commun. 124* (1984) 178.
[121] T. S. Marks, R. Wait, A. R. W. Smith, A. V. Quirk, *Biochem. Biophys. Res. Commun. 124* (1984) 669.
[122] G. M. Zaitsev, A. N. Karasevich, *Mikrobiologiya 53* (1984) 75.
[123] A. Markus, U. Klages, S. Krauss, F. Lingens, *J. Bacteriol. 160* (1984) 618; A. Markus, D. Krekel, F. Lingens, *J. Biol. Chem. 261* (1986), in press.
[124] K.-H. Engesser, E. Schmitt, H.-J. Knackmuss, *Appl. Environ. Microbiol. 39* (1980) 68.
[125] A. Schreiber, M. Hellwig, E. Dorn, W. Reineke, H.-J. Knackmuss, *Appl. Environ. Microbiol. 39* (1980) 58.
[126] G. W. A. Milne, P. Goldman, J. L. Holtzman, *J. Biol. Chem. 243* (1968) 5374.
[127] D. B. Harper, E. R. Blakely, *Can. J. Microbiol. 17* (1971) 1015.
[128] U. Schennen, K. Braun, H.-J. Knackmuss, *J. Bacteriol. 161* (1985) 321.
[129] J. W. A. Lustenhouwer, K. Olie, O. Hutzinger, *Chemosphere 9* (1980) 501.
[130] L. L. Lamparski, T. J. Nestrick, V. A. Stenger, *Chemosphere 13* (1984) 361.
[131] H.-J. Knackmuss, J. Hellwig, *Arch. Microbiol. 117* (1978) 1.
[132] H. Poiger, C. Schlatter, *Chemosphere 12* (1983) 453.
[133] H. Weber, H. Foiger, C. Schlatter, *Xenobiotica 12* (1982) 353.
[134] T. Sawahata, J. R. Olson, R. A. Neal, *Biochem. Biophys. Res. Commun. 105* (1982) 341.
[135] R. A. Neal, J. R. Olson, T. A. Gasiewicz, L. E. Geiger, *Drug. Metab. Rev. 13* (1982) 355.
[136] *Dioxin in der Umwelt, Chemie+Fortschritt, VCI Schriftenreihe Bd. 1*, Verband der Chemischen Industrie, Frankfurt 1985.
[137] G. M. Klecka, D. T. Gibson, *Appl. Environ. Microbiol. 39* (1980) 288.
[138] G. M. Klecka, D. T. Gibson, *Biochem. J. 180* (1979) 639.
[139] J. F. Quensen III, F. Matsumara, *Environ. Toxicol. Chem. 2* (1983) 261.
[140] M. Philippi, J. Schmid, H. K. Wipf, R. Hütter, *Experientia 38* (1982) 659.
[141] J. A. Bumpus, M. Tien, D. Wright, S. D. Aust, *Science 228* (1985) 1434.

Total Synthesis of Anthracyclinone

New Synthetic Methods (60)

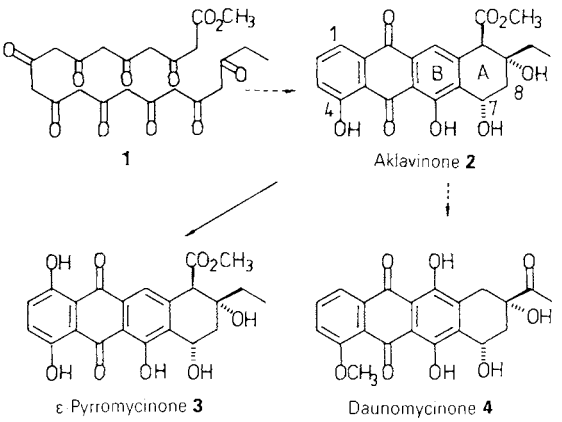
By Karsten Krohn*

Dedicated to Professor Albert Mondon on the occasion of his 70th birthday

The remarkable antitumor properties of anthracycline antibiotics have motivated synthetic chemists, and a large number of groups have been active recently in this field. Initially, there was very little hope for this class of substances due to their extreme toxicity. However, the dividing line between toxicity and desired pharmacological effect has broadened to such an extent, partly through microbiological methods (new strains, mutants) and partly through semisynthetic modifications, that today anthracyclines take number one place (over 20% of the market) in the chemotherapy of (human) cancer. The demands made on modern cytostatica are extremely high, as may be seen from the fact that of the more than 600000 drugs tested in animals, only about 40 are in clinical use. In the meantime, some anthracyclines obtained by total synthesis are also in clinical testing. In this review it will hopefully be demonstrated that all those concerned in the chemotherapeutic use of these substances have also contributed to the general progress made in the solution of regio- and stereochemical problems of linearly annelated ring systems.

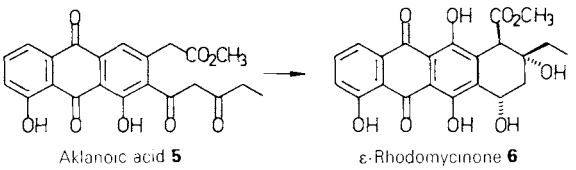
1. Structure and Nomenclature

Anthracyclinones are the aglycones of anthracyclines. The basic structure of the anthracyclinones has been elucidated by intensive investigations on the colored metabolites of *Streptomyces purpurascens* by *Brockmann* and his group.[1a] While the number of aglycones including other species of *Streptomyces*[1b,c] has increased only slightly, the number of the glycosidic anthracyclines, which contain up to eight sugar components, has in the meantime grown to over two hundred compounds.[2] The variety of structures encountered can be neatly underlined with a few examples of a biogenetic scheme (for further details compare reviews on the structure[1,2] and biological action of anthracyclinones[3]). The work of *Ollis* et al.[4a] on the biosynthesis of pyrromycinone[3] has shown that polyketides such as **1**, which consist of nine acetate units and one propionate unit, can be considered as precursors of anthracyclinones which are produced by *Streptomyces* species. Later works[4b-f] (review[4g]), including the labeling of precursors with ^{13}C, have presented further details of the biosynthetic pathway from aklavinone (**2**) to daunomycinone (**4**) (Scheme 1).



Scheme 1.

New findings have shown that aklavinone (**2**) (often in the form of its *O*-glycosides) is an early anthracyclinone precursor that is further transformed by certain *Streptomyces* species with hydroxylation of ring D into glycosides of ε-pyrromycinone (**3**) (*Actinosporangium sp.*[2f]) or with hydroxylation of ring B and oxidation of the side chain into daunomycinone (**4**) (*Streptomyces peucetius*[3c-f]). A particularly interesting variant is the incorporation of the tricyclic aklanoic acid **5** into ε-rhodomycinone **6** by certain mutants of *Streptomyces*.[4h] Although this finding—similarly as in the case of the tricyclic tetracycline precursors (pretetramides)[5]—must not necessarily correspond to the usual biosynthetic pathway, a number of new synthetic possibilities starting from tricyclic precursors are demonstrated (see, e.g., Section 4.1.1). Because of their different



position in the biogenesis and because of some chemical properties that influence the synthetic strategies, we have named anthracyclinones containing an ester group type B (e.g. **2**, **3**, **6**) and those without an ester group type A (e.g. **4**).[6] Otherwise, we follow the system proposed by *Brockmann*[1a] in the numbering and designation of the rings A–D because in this way both types A and B can be named uniformly. However, in many papers the systematic

[*] Prof. Dr. K. Krohn
Institut für Organische Chemie der Technischen Universität
Hagenring 30, D-3300 Braunschweig (FRG)

 © VCH Verlagsgesellschaft mbH, D-6940 Weinheim, 1986 0570-0833/86/0909-0790 $ 02.50/0

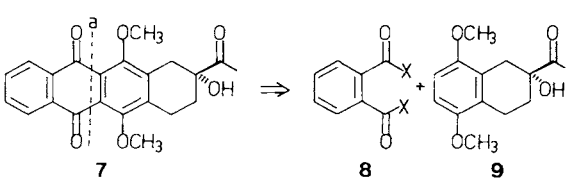
IUPAC nomenclature is used because the same numbering can be applied to natural as well as synthetic products (see for example[7, 8]). Furthermore, we also follow a ruling proposed by *Quinkert* et al.[9] for the designation of racemic mixtures and enantiomers so as to avoid confusion between optically pure products and racemic mixtures. For example, **4** represents the absolute configuration of daunomycinone, *ent*-**4** the enantiomer of **4** and *rac*-**4** racemic daunomycinone.

2. Total Syntheses

In the synthesis of anthracyclinones stereochemical problems of the hydroaromatic ring A with two, three, or four chiral centers have to be solved. Another equally exciting challenge is presented by the regiochemistry of the anthraquinone moiety. In the course of the synthesis, the relatively remote substituents of the rings A and D must occupy the correct positions (see Scheme 1). In a successful synthesis, both problems must be solved concomitantly, since a separation of isomeric tetracycles, which are often very sparingly soluble, can at best be achieved only on a very small scale. This additional difficulty, which often cannot be inferred from the synthetic schemes of a publication, is naturally solved with differing degrees of efficiency in subsequently reviewed methods. We follow a methodologically oriented earlier review by *Kelly*[10a] (for further reviews see [3e, 10]) with classification into cationic reactions (Friedel-Crafts reactions), Diels-Alder reactions, and anionic reactions (radical reactions have until now found no application in anthracyclinone synthesis).

2.1. Friedel-Crafts Reactions

The procedure shown in the retrosynthetic Scheme 2 is followed if a Friedel-Crafts reaction is used to construct the tetracylic anthraquinone skeleton via the usual method of anthraquinone synthesis.[11] It is well-conceived to choose the formation of the new bonds between rings B and C (disconnection "a" in **7**) to facilitate the Friedel-Crafts reaction by the donor-substituted, partially hydrogenated AB building block **9**. Basically, the acylation with the phthalic anhydride derivative **8** proceeds in two steps, whereby the first step deactivates the arene (the future ring B) for a second electrophilic attack; this holds, even if in practice one pot procedures (e.g. $AlCl_3$/NaCl melt[12]) are used. Consequently, vigorous reaction conditions can generally not be avoided.

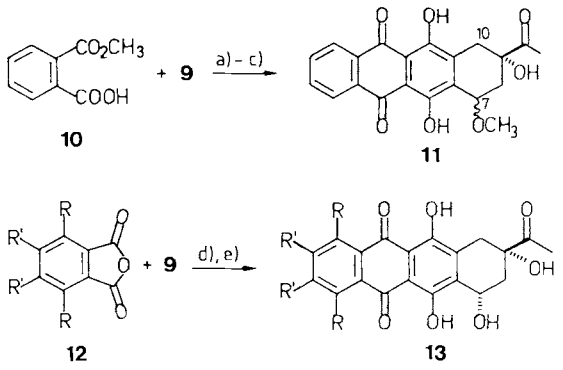


7 **8** **9**

Scheme 2.

In contrast to most other anthracyclinones with ethyl or methyl side chains, daunomycinone and its analogues possess an acetyl side chain, which gives the molecule a special stability. The carbonyl group makes the development of a positive partial charge on the neighboring tertiary carbon atom difficult, and, this in turn, hinders the acid-catalyzed dehydration that occurs easily with the other members of the anthracyclinone family.[1] Due to this particular stability, the first synthesis of 7-*O*-methyl-4-demethoxydaunomycinone (*rac*-**11**) by *Wong* et al.[13] was possible in which the phthalic acid half ester **10** (DC-building block) and *rac*-**9** (AB-building block) were combined to give *rac*-**11** in a stepwise Friedel-Crafts reaction (Scheme 3).

The Friedel-Crafts reaction with symmetrically substituted phthalic acid anhydrides **12a–12f** can also occur in a one pot procedure. 4-Demethoxydaunomycinone (*rac*-**13a**) is now manufactured on a large scale by Farmitalia, in addition to the other derivatives *rac*-**13b** to *rac*-**13f**[12] (Scheme 3).

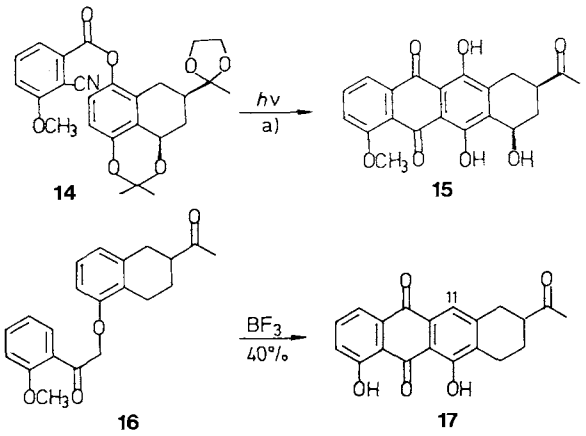


Scheme 3. a) 1) $(CF_3CO)_2O$; 2) HF. b) 1) $HOCH_2CH_2OH$, H^+; 2) *N*-bromosuccinimide (NBS); 3) CH_3OH. c) $AlCl_3$. d) NaCl/$AlCl_3$, 180°C, 2 min. e) Hydroxylation at C-7.—**a**, R = R′ = H; **b**, R = H, R′ = CH_3; **c**, R = H, R′ = Cl; **d**, R = CH_3, R′ = H; **e**, R = Cl, R′ = H; **f**, R + R′ = –CH=CH–CH=CH–.

The drastic conditions of the Friedel-Crafts reaction limit this method to daunomycinone-type anthracyclinones and do not allow the use of dihydroxylated AB building blocks. However, the introduction of a *cis*-hydroxy group at C-7 is of great importance, since the sugars that are essential for biological activity are bound at this position. Thus, the problem of hydroxylation at the benzylic position became evident at the very beginning of anthracyclinone synthesis. The decisive step that is still used today is the radical bromination of the benzylic position followed by solvolysis. *Wong* et al.[13] needed three steps to arrive at a mixture of the epimers *rac*-**11** starting from a 7-deoxy precursor. The reaction of daunomycinone precursors with silver trifluoroacetate likewise afforded a 5 : 2 mixture of epimers that could be equilibrated with trifluoroacetic acid to give a 6 : 1 ratio in favor of the natural 7,9-*cis*-configuration[14] (overall yield about 50%). In practice the scale of the reaction is limited by the low solubility of the hydroxylated tetracycles, both during the bromination in tetrachloromethane and also during the necessary chromatographic separation. Although the bromination of the more soluble 7-*O*-acetates leads stereoselectively to the *trans*-bromides (80–85%), a chromatographic separation of the solvolysis products (*cis* : *trans* = 41 : 20) cannot be circumvented.[15] A better *cis*-selectivity can be achieved via solvolysis with aqueous sodium hydroxide (43%).[16] Hy-

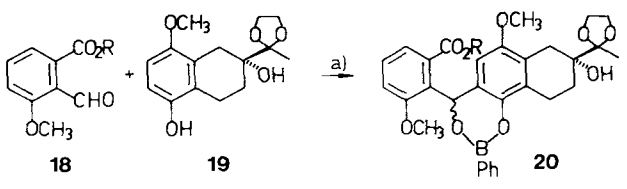
droxylation at C-7 seems to be a problematic reaction as long as the other position at C-10 is not blocked by a substituent such as a hydroxy or an ester group as in ε-rhodomycinone and all other type B anthracyclinones (see, e.g., Section 4.1.1).

A third limitation of Friedel-Crafts reactions is the lack of regioselectivity when using non-symmetrically substituted phthalic acid derivatives. Thus, an attempted regioselective synthesis of islandicin[17] failed due to Hayashi rearrangement as well as BF_3-catalyzed Fries rearrangement.[18] A chromatographic separation of regioisomers was also necessary in the first total synthesis of daunomycinone by *Wong* et al.[19] (cf. [20]), who closely followed the methods outlined in Scheme 3. However, a regioselectivity could be observed under the milder conditions of the photochemical Fries rearrangement of **14** to **15**[21] and with the BF_3 treatment of the precursor **16**, which led to an 11-deoxy compound **17**[22] (Scheme 4).



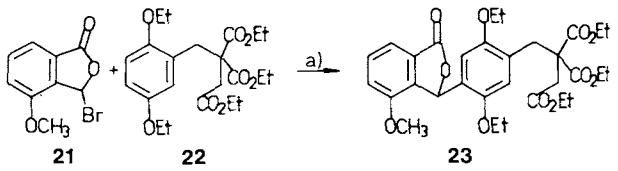
Scheme 4. a) Two further steps, 11%.

A regioselective coupling is also observed in the reaction of the aldehyde **18** with *rac*-**19** in the presence of phenylboronic acid to afford a mixture of diastereoisomers *rac*-**20**, which can be further transformed into *rac*-**4** in nine additional steps.[23] The preparative work necessary to achieve regioselectivity is largely shifted to the synthesis of the non-symmetrically substituted aromatic compounds **18** and **19** (Scheme 5). Obviously the phenylboronic acid prevents the usual rearrangements of the Friedel-Crafts acylation (cf. [24]).



Scheme 5. a) Phenylboronic acid, propionic acid, benzene, 20 h boiling.

A regioselective construction of the basic skeleton is also possible under the milder conditions of the Friedel-Crafts *alkylation* which was investigaged by *F. Johnson* et al.[25] The key step is the $SnCl_4$-catalyzed Friedel-Crafts alkylation of 3-bromo-4-methoxyphthalide (*rac*-**21**) in the *para*-position of the activating alkyl substituent in **22** to afford *rac*-**23**,[25a] which can be transformed into racemic daunomycinone (*rac*-**4**) in eleven additional steps[25b] (Scheme 6). This example clearly shows that the necessary regioselectivity in cationic cyclizations cannot be obtained without considerable synthetic effort!

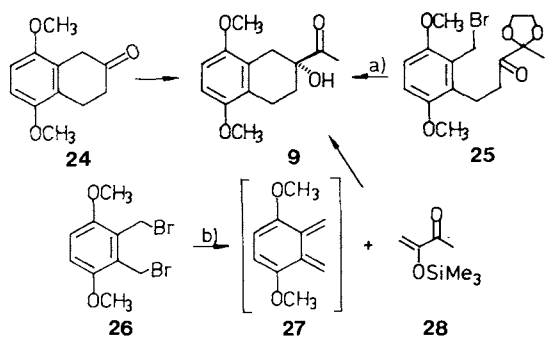


Scheme 6. a) $SnCl_4$, CH_2Cl_2, 25°C, 6 h.

A decisive criterion of modern total syntheses is the possibility of conducting reactions enantioselectively. Contradictory statements have been made in the literature concerning the racemization during conversion of the enantiomerically pure building block **9**. While *Arcamone* et al.[12] and *Rao* et al.[26] do not observe any racemization in the Friedel-Crafts reaction of **9** with phthalic acid anhydrides, *Terashima* et al.[27] and also *Russell* et al.[28] state that the same reaction is not free of racemization (70–81% *ee*). However, the coupling of the enantiomerically pure building blocks is possible with other methods. The synthesis of key intermediates, with emphasis on enantioselective methods, is therefore presented in this part of the review.

2.2. Synthesis of AB Building Blocks

Ready access to *rac*-**9** is possible by addition of organometallic compounds to β-tetralone **24**, which can be very easily obtained via Diels-Alder reaction of benzoquinone with 2-methoxy-[29] or 2-chloro-1,3-butadiene.[20] Ethynylmagnesium bromide,[20,30] 2-(trimethylsilyl)ethynylcerium(III) reagents,[31] lithiated 2-methyl-1,3-dithianes,[32] or methoxyvinyllithium[29] may serve as acetyl anion equivalents (Scheme 7). The key intermediate *rac*-**9** may also be obtained directly by Barbier reaction of **25**[33] or by Diels-Alder reaction of the intermediary *o*-quinodimethane **27** with 3-(trimethylsiloxy)-3-buten-2-one **28**.[34]



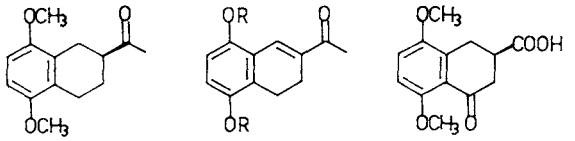
Scheme 7. a) Mg, 20°C, 6 h. b) 1) Zn, dimethylformamide (DMF) or $CrCl_2$; 2) HOAc, 45°C, 2 h.

The yields are especially high (85%) if **27** is generated from the dibromide **26** with chromium(II) chloride[35] (Scheme 7). The Barbier and Diels-Alder reactions can also be successfully applied to tetracycles (see Sections 3.1 and 4.1).

Frequently used building blocks are *rac*-**29**,[29,20,26,36-38] **30**,[26,27,39-42] R = $PhCH_2$, CH_3, and *rac*-**31**,[13,43,44] which can be obtained by cyclization of the corresponding open-chain precursors or their derivatives. The intermediates *rac*-**29** to *rac*-**31** can also be transformed into enantiomerically pure compounds by appropriate methods.

The missing tertiary hydroxy group in **29** or **31** can, as a result of activation by the neighboring center, be introduced via oxygenation of the corresponding enolate using the method of *Gardner* et al.[45] The reaction can be applied equally well to tetracyclic compounds (see Section 3.1). The replacement of one methoxy group in **30** by a selectively cleavable benzyloxy group is of great preparative value because it allows the synthesis of quinone monoacetals.[40,41]

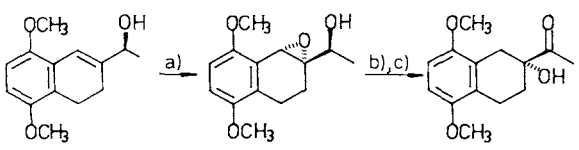
Special attention will be given here, however, to the preparation of enantiomerically pure AB building blocks. The classical methods of resolution of racemates may be employed for this purpose, which is especially easy with the brucine salt of an acid derived from **31**.[46] Precursors such as **9**, with acetyl side chains, can be resolved via diastereomeric Schiff bases obtained from (−)-1-phenylethylamine.[43,47]



29 **30** **31**

The Sharpless epoxidation can be employed for the kinetic resolution using the allyl alcohol **32** obtained from **30**.[48] The enantiomers of the racemic allyl alcohol **32** are epoxidized at different rates under the conditions defined by *Sharpless*. Unchanged *ent*-**32** remains in solution together with almost enantiomerically pure **33**. For the isolation of *ent*-**32**, the unstable epoxide **33** is reduced to a diol, which can be reoxidized with *Fetizon*s reagent[26] or dimethyl sulfoxide/sulfur trioxide[27] to the enantiomerically pure AB building block **9**. The "wrong" isomer *ent*-**32** can be recycled after inversion to **32** using the method of *Mitsunobu*[49] (Scheme 8).

Alternatively, **9** can be prepared via stereoselective reduction of *rac*-**9** with bakers' yeast *(Saccharomyces cerevisiae)* to diastereoisomeric diols followed by chromatographic separation and reoxidation to **9**.[50]

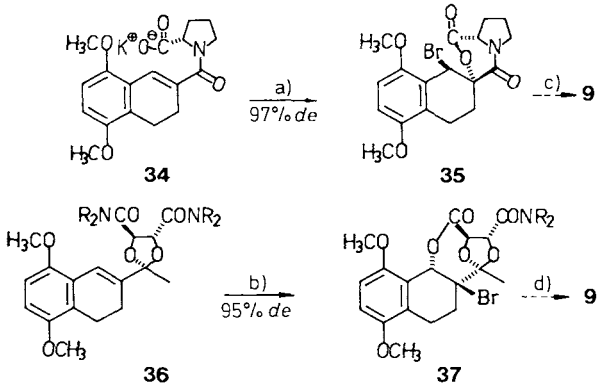


32 **33** **9**

Scheme 8. a) *t*BuOOH, $Ti(OiPr)_4$, (+)-diisopropyl tartrate, −55 °C. b) $LiAlH_4$. c) Ag_2CO_3 or dimethyl sulfoxide (DMSO), SO_3.

Asymmetric syntheses using chiral auxiliaries have been investigated by *Terashima*'s group. Particularly successful was the reduction of the prochiral α,β-unsaturated ketone **30** (R = CH_3) with $LiAlH_4$ in the presence of (−)-*N*-methylephedrine at −78 °C to give **32** (92% *ee*), followed by stereoselective Sharpless epoxidation (90% *de*) to **33**,[27] which can be transformed into **9** as shown in Scheme 8.

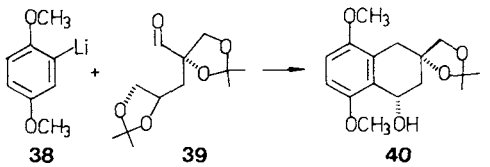
In another method, the decisive transfer of chirality to the tertiary center occurs during the bromolactonization of the proline derivative **34** to **35**[51] (cf. also [52]) or of the tartaric acid amide acetal **36** to **37**.[53a] In both cases the enantiomeric excess is greater than 95% (Scheme 9; for the extension of the latter method to tetracycles cf. [53b]).



34 **35** **36** **37**

Scheme 9. a) NBS. b) *N*-bromoacetamide. c) Four steps, 66%. d) Three steps, 47%.

Another method for the synthesis of enantiomerically pure products consists in the incorporation of derivatives from the chiral pool of natural products. *Florent* et al.[54] obtained the AB building block by addition of the aldehyde **39**, prepared in five steps from α-D-isosaccharinolactone,[55] to the aryllithium compound **38** (Scheme 10; for similar reactions leading to tetracycles, see [55]).

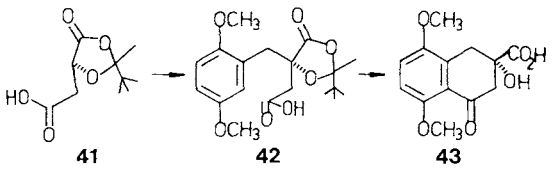


38 **39** **40**

Scheme 10.

In our group we were able to prepare the highly functionalized α-hydroxy acid **43** in only three steps incorporating L-malic acid.[56] The chiral information of L-malic acid is transferred to a non-racemizable tertiary center of the five-membered acetal **41**.[57] Stereoselective alkylation of **41** yields **42**, and this is followed by cyclization to **43** (Scheme 11).

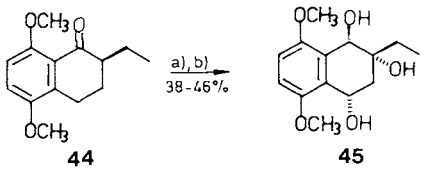
As already mentioned, the highly functionalized AB building blocks with benzylic hydroxy groups allow especially convergent anthracyclinone syntheses. Two hydroxy groups are introduced simultaneously during the oxygenation of the arene **44** at the positions activated by the car-



41 42 43

Scheme 11.

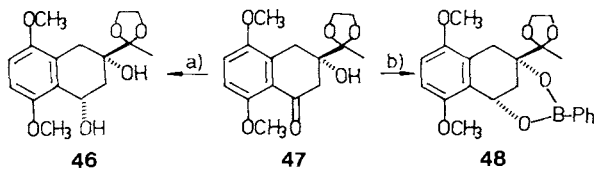
bonyl group. Reduction with $LiBH_4$ selectively affords the *trans*-1,2-diol **45** (8.6 : 1)[58] (Scheme 12; for further AB building blocks with *ethyl* side chains, see [59,60]).



44 45

Scheme 12. a) KO*t*Bu, $P(OEt)_3$, O_2. b) $LiBH_4$, toluene.

The reduction of the ketone **47** to the 1,3-*cis*-diol **46** with potassium selectride also proceeds with high stereoselectivity.[43] However, the much cheaper reducing agent $LiBH_4$ can be employed if the mixture of epimers is subsequently equilibrated with phenylboronic acid[44] (Scheme 13).

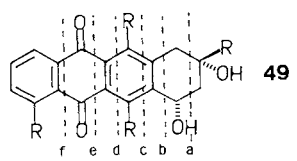


46 47 48

Scheme 13. a) K[*s*Bu$_3$BH] (potassium selectride). b) 1) $LiBH_4$; 2) phenylboronic acid, 18°C, 20 h.

3. Diels-Alder Reactions

[2+4]-Cycloadditions offer ideal possibilities for the construction of linearly annelated ring systems containing six-membered rings. It is thus not surprising that six of the eight possible ring couplings have been realized[3,10a] (disconnections "a–f" in **49**).



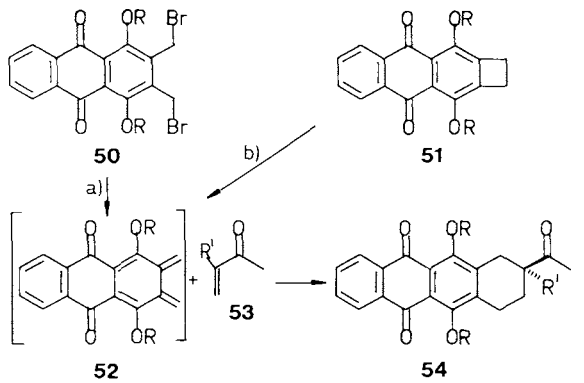
49

The specific conditions of the Diels-Alder reaction allow different degrees of control in the synthesis of various types of anthracyclinones. The control of the regiochemistry is, for example, less easy in compounds derived from rhodomycinone (1,4,5-trihydroxyanthraquinone) than in 11-deoxy compounds (aklavinone type). Problems of stereo- and enantio-control emerge, since the degree of functionalization of the building blocks varies considerably. However, elegant solutions to most problems have been found, making the use of Diels-Alder reactions an efficient method in anthracyclinone synthesis.

3.1. Construction of Ring A

The tricyclic DCB fragment can serve as a diene ("a" in **49**) as well as a dienophile ("b" in **49**) if ring A of the anthracyclinone is formed in a Diels-Alder reaction. *Cava* et al.[61,62] used the bis(bromomethyl)anthraquinones **50** for the generation of the tricyclic, highly-reactive intermediary *o*-quinodimethanes **52**, which are liberated on treatment of **50** with zinc[62] or sodium iodide.[61] The yield depends on the residue R; an optimum is attained in the reaction of methyl vinyl ketone **53**, R′ = H, with the methyl ether **50c** in the presence of zinc in dimethylformamide (DMF) or with the phenol **50a** in the presence of sodium iodide in dimethylacetamide (DMA) (69%).[34] More highly substituted dienes such as 1-acetylvinyl acetate **53**, R′ = OAc, or 3-(trimethylsiloxy)-3-buten-2-one **53**, R′ = $OSi(CH_3)_3$, can also be employed, but the yield of adduct *rac*-**54**, R′ = OH, is distinctly lower.[34,61]

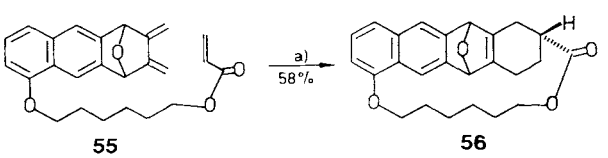
o-Quinodimethanes can also be generated thermolytically from the corresponding annelated cyclobutanes **51**, whereby the yields of *rac*-**54** are greatly improved[63] (Scheme 14).



50 51 52 53 54

Scheme 14. a) Zn, DMF or NaI, dimethylacetamide (DMA). b) 180–220 °C. **a**, R = H; **b**, R = Ac; **c**, R = CH_3; R′ = H, OAc, $OSi(CH_3)_3$, etc.

Attempts to conduct the reaction regioselectively with non-symmetrically substituted *o*-quinodimethanes have not been described in the literature. Interestingly, however, *P. Vogel* et al.[64] were successful in controlling the regioselectivity in the intramolecular Diels-Alder reaction of *rac*-**55** to give *rac*-**56**; diene and dienophile are linked by a spacer of appropriate chain length. This is reminiscent of the method described by *Breslow* for controlling the reaction in the case of steroids[65] (Scheme 15; cf. [66]).

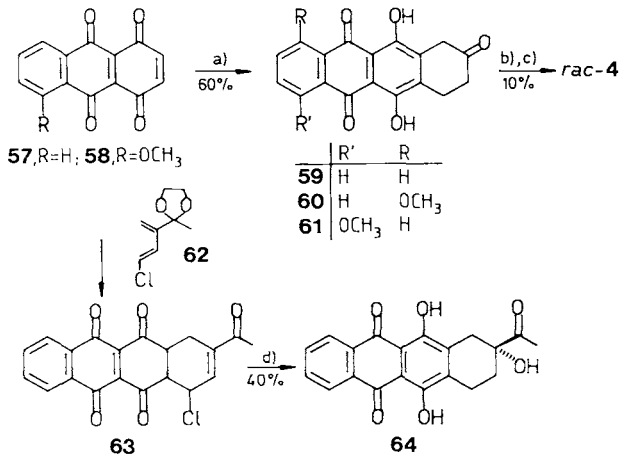


55 56

Scheme 15. a) 170 °C, 24 h, xylene.

A number of 1,4-anthraquinones are suitable as starting material if the DCB tricycle does not serve as diene but rather as dienophile ("b" in **49**). In the most simple case 1,4,9,10-anthradiquinones such as **57** can be used. These are obtained by oxidation of the corresponding 1,4-dihydroxy-9,10-anthraquinones with lead tetraacetate. Thus, depending on the diene employed in the reaction, precursors with (e.g. *rac*-**63**) or without an acetyl side chain (e.g. **59**) can be synthesized.

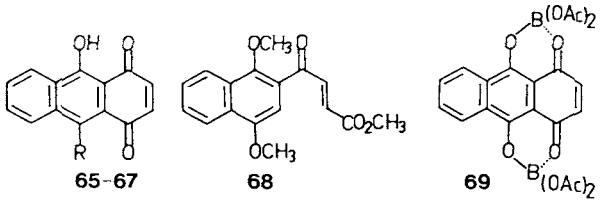
Many authors choose the route used by *Kende* et al.[14] in their pioneering total synthesis of racemic daunomycinone (*rac*-**4**). The key step in this synthesis is the addition of 1-methyleneallyl acetate to the anthradiquinone **58**. The reaction is not regioselective and yields a 1:1 mixture of primary adducts, which are hydrolyzed to **60/61** and separated by crystallization.[14] The further transformation into daunomycinone (*rac*-**4**) was completed by ethynylation, hydration and hydroxylation at C-7 (Scheme 16). The direct incorporation of a side chain was achieved by reaction of **57** with diene **62** to afford *rac*-**63**, followed by a five step transformation to *rac*-**64**[67] (Scheme 16).



Scheme 16. a) 1) 3 equiv. (1-methylenallyl) acetate ("2-acetoxy-1,3-butadiene"), 25°C, 4 d; 2) C_2H_5OH, 6N HCl, reflux, 6 h. b) 1) $BrMgC{\equiv}CH$; 2) dil. H_2SO_4/HgO, 70°C, 4 h. c) 1) Br_2, CCl_4, *hv*; 2) SiO_2/H_2O. d) Five steps.

However, the relatively short route via anthradiquinones has the disadvantage that many highly functionalized dienes add to the inner double bond of these bisdienophiles.[68,69]

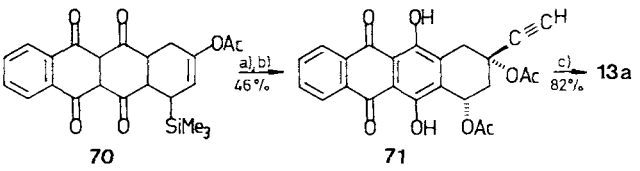
A conceptually interesting way to circumvent this problem is the Diels-Alder reaction of the 1,4-anthraquinones such as **65**,[70-72] **66**,[71] **67**[72] or the open-chain precursor **68**[73] with various dienes which must lead to linearly annelated products. The quinizarin boroacetate complex partly



65, R = Cl; 66, R = NH_2; 67, R = H

exists in the tautomeric form **69** and can also undergo Diels-Alder reactions.[74] However, the oxidation of the adducts proceeds under relatively drastic conditions and a synthesis of daunomycinone has not yet been realized in this way.

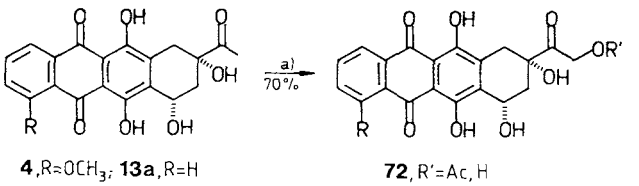
By contrast, the addition of *trans*-(1-methylene-3-trimethylsilylallyl) acetate to **57** affords the linearly annelated adduct *rac*-**70**. The decisive step in the further transformation of *rac*-**70** is the replacement of the trimethylsilyl group by an acetoxy group using fluoride and lead tetraacetate to yield *rac*-**71**[75] (Scheme 17).



Scheme 17. a) 1) H_2-Pd/$BaSO_4$; 2) CF_3COOH/H_2O; 3) $BrMgC{\equiv}CH$; 4) isopropenyl acetate, $H^{\oplus}$, 25°C, 16 h. b) 1) Oxidation and isomerization to the quinone; 2) 2 equiv. $Pb(OAc)_4$/HOAc, 18 h, $F^{\ominus}$; 3) $NaHSO_3$. c) HgO, $H^{\oplus}$, H_2O; $OH^{\ominus}$.

The use of the trimethylsilyl reagent, which enables the indirect introduction of the 7-hydroxy group, was later thoroughly investigated by *Bulman-Page* and *Ley*.[76] The authors also describe in detail the acetoxylation of the acetyl side chain of daunomycinone derivatives (e.g. *rac*-**13a**) to give the therapeutically even more important adriamycinone derivatives **72**, R = OCH_3, R' = Ac (Scheme 18).

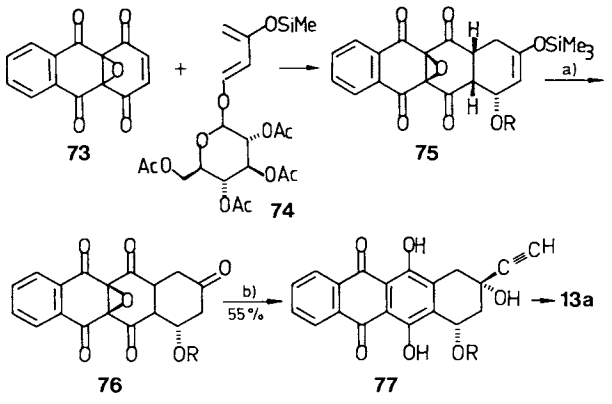
In addition to the usual bromination followed by solvolysis, the direct transformation can also be achieved with the new generally applicable hypervalent iodine reagent [bis(trifluoroacetoxy)iodo]benzene.[77]



Scheme 18. a) 1) Br_2, CCl_4; 2) NaOAc, 30-45 min boiling in acetone.

Exclusive addition of dienes to the terminal double bond is also achieved by the use of the anthraquinone monoepoxide **73**, which is readily accessible from anthradiquinone **57** by epoxidation with *m*-chloroperbenzoic acid (MCPBA). An enantioselective synthesis of 4-demethoxydaunomycinone was achieved by employing a chiral diene.[79] The crucial step of the transfer of chirality occurs during the addition of the diene **74** to the quinone **73**, which proceeds in favor of the desired adduct **75** (4:1 ratio). After hydrolysis of the crude product and recrystallization, the epoxy pentanone **76** is obtained in 45% overall yield. For further transformation, the precursor **77** is reduced with dithionite or zinc, followed by ethynylation and oxidation with lead tetraacetate. The enantiomerically pure 4-demethoxydaunomycinone **13a** is obtained after

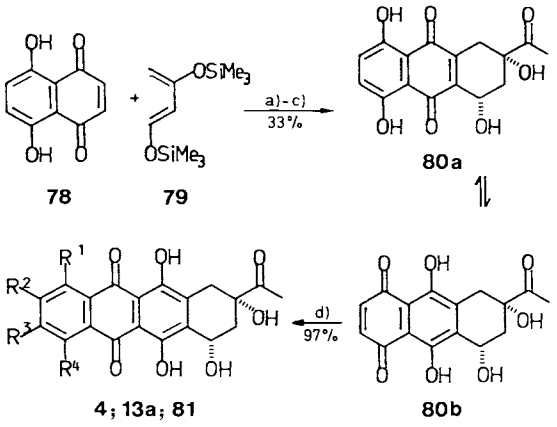
hydration and hydrolysis of **77**[79] (Scheme 19; for similar reactions with the epoxyquinone **73**, cf. [80,91]).



Scheme 19. a) Tetrahydrofuran (THF), 0.1 M HCl. b) 1) $Na_2S_2O_4$ or Zn/HOAc (71%); 2) 30 equiv. BrMgC≡CH, THF, 0°C, 30 min; 3) $Pb(OAc)_4$/HOAc (77%).

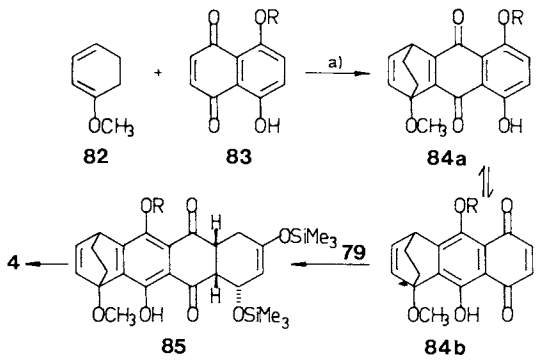
In our laboratories we have developed a method in which anthracyclinones are synthesized by two successive diene reactions with naphthazarin (**78**) (CB building block)[82] using bis(siloxy)butadiene **79**. Not only are both oxygen functions introduced simultaneously into ring A, but by variation of the second diene a large variety of substituents are easily introduced into ring D of daunomycinone. The synthetic strategy is based on the tautomerism of substituted naphthazarins such as **80a/80b** as described by *Fariña* and *Vega*.[83] The tautomeric form **80b** reacts with dienes to form linearly annelated ring systems. The flexibility of this synthetic principle is demonstrated by the variation of the open-chain and cyclic dienes used in the second Diels-Alder reaction: in addition to *rac*-**4** and *rac*-**13a**, four daunonomycinone derivatives not occurring naturally could also be prepared[82b] (Scheme 20).

Diels-Alder reactions with naphthazarin derivatives such as **80b** do not proceed regioselectively; however, they



Scheme 20. a) CH_2Cl_2, 5 h. b) $CH_2Cl_2/(C_2H_5)_2O/CH_3OH/0.2$ N HCl, 5°C, 6 h. c) 1) 30 equiv. BrMgC≡CH; 2) acetone, 7% H_2SO_4/HgO, 60°C, 5 min. d) 1) 1-Methoxy-1,3-butadiene, 40°C, 7 h; 2) 1% NaOH, $H^{\oplus}$ (transformation to **81** not given).—**4**, R^1-R^3 = H, R^4 = OCH_3; **13a**, R^1-R^4 = H; **81a**, **81b**, **81c**, R^1 and R^2 and R^3 = OCH_3, other R = H; **81d**, R^1 = R^4 = H, R^2 = R^3 = CH_3.

do so when converted into monoacylnaphthazarins. In order to exploit this selectivity in anthracyclinone synthesis it was necessary to find a suitable acyl group that undergoes acyl migration during the reaction from *rac*-**84a** to *rac*-**84b** and is later on readily removable. *Kelly* et al.[84] found that the *p*-nitrobenzoxycarbonyl group fulfills these conditions: The mononaphthazarin **83** reacts with the cyclic diene **82** to give *rac*-**84a**. The addition of the diene **79** to the tautomeric form *rac*-**84b** occurred regioselectively to give exclusively the expected adduct *rac*-**85**. The subsequent transformation to *rac*-**4** was achieved by a method similar to those described earlier[84] (Scheme 21).

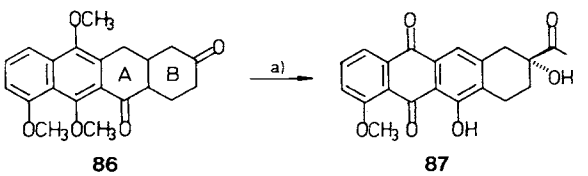


Scheme 21. a) 1) Without solvent, **82** : **83** = 2.5 : 1, 8 h; 2) THF, KH, PbO_2, 4°C, 12 h.—R = *p*-O_2N-C_6H_4-CH_2-O-CO.

The syntheses starting with naphthazarin require few steps and give excellent overall yields (29%,[82] 36%[84]), but the problems of enantioselectivity and *cis*-7,9-stereoselectivity are still to be solved. A possible solution to the latter problem is resort to the use of 1-*tert*-butoxy-3-trimethylsiloxy-1,3-butadiene.[81]

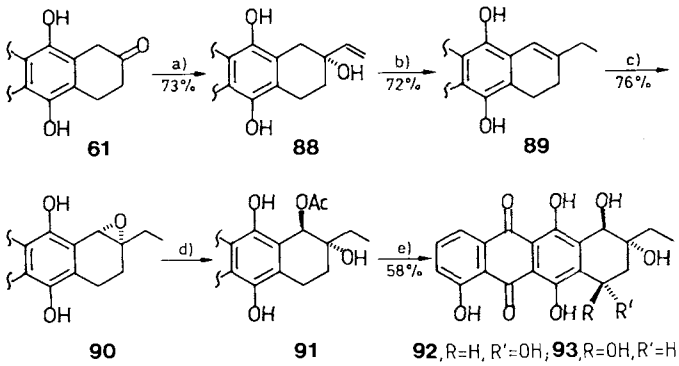
How general is the use of tetracyclic ketones of type **59**–**61** (Scheme 16) for the preparation of other anthracyclinone types (e.g. rhodomycinones) with alkyl or acetonyl side chains? The great tendency for enolization normally prevents the facile addition of organometallic reagents such as ethynylmagnesium bromide. Two solutions have been proposed: 1) prevention of aromatization using starting materials without aromatic ring B; 2) employment of organometallic compounds with less tendency to effect enolization. In the first approach *Sih* et al.[85] could prepare 7,11-dideoxydaunomycinone *rac*-**87** starting from **86** (Scheme 22).

Enolization occurred only slightly during the reaction of vinylmagnesium bromide with **61** to afford *rac*-**88**. Reduction with diimide and subsequent treatment with aluminum chloride effected both the cleavage of the C-4 methyl ether as well as the elimination of the tertiary hydroxy



Scheme 22. a) 1) BrMgC≡CH, THF, −20°C; 2) $Hg(OAc)_2$; 3) Ce^{4+}, Br_2; 4) $NaOCH_3/CH_3OH$.

group to give the olefin **89**. After epoxidation, opening of the resulting oxirane *rac*-**90** with sodium acetate afforded the *trans*-acetate *rac*-**91** with a *cis/trans* selectivity of 1:9. The subsequent hydroxylation at C-7 via homolytic bromination and exchange with silver acetate gave a 1:1 mixture of the 7,9-*cis*-diol *rac*-**92** (β-rhodomycinone) and the 7,9-*trans*-diol *rac*-**93** (α-rhodomycinone; Scheme 23).

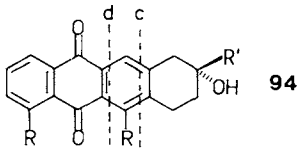


Scheme 23. a) $BrMgCH{=}CH_2$. b) HN=NH; 2) $AlCl_3$. c) *m*-Chloroperbenzoic acid (MCPBA). d) NaOAc/HOAc, 85°C. e) 1) Br_2, CCl_4, *hv*; 2) CF_3COOAg; 3) NaOH.

Little enolization is also observed in reactions with organomanganese compounds, which are generated in situ from alkenyl bromide, $MnCl_2$ and $LiAlH_4$. Thus, in the case of the allyl compounds, feudomycinone derivatives with acetonyl side chains are made available.[87]

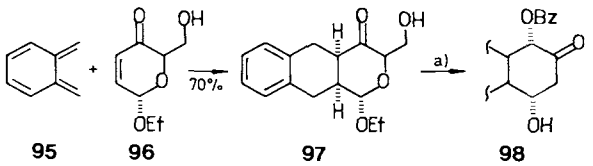
3.2. Formation of Ring B

The formation of new bonds in the construction of ring B can proceed via disconnection "c" (DC segment is the diene) or "d" (DC segment is the dienophile) in **94**.



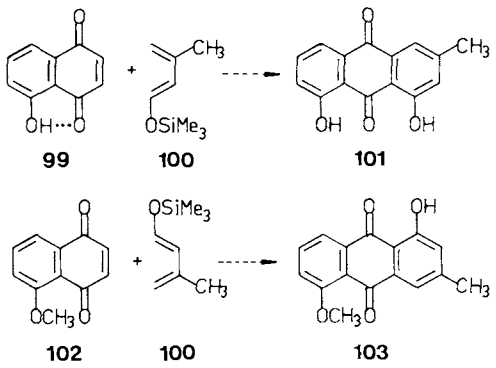
R = H, OH, OCH_3; R' = alkyl.

The disconnection "c" is only realized in a model reaction described by *Ferrier*[88] in which the tricycle **97** is formed by reaction of *o*-quinodimethane **95** with the pyranone **96**. The heterocycle **97** can subsequently be rearranged (Ferrier rearrangement[89]) to the carbocycle **98** in a six-step reaction sequence (Scheme 24). The potential importance of this method stems from the synthesis of enantiomerically pure anthracyclinones by addition of organometallic compounds to **98**.



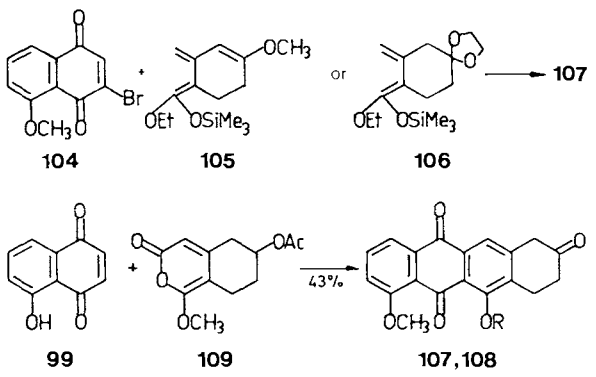
Scheme 24. a) 1) $NaBH_4$; 2) tosylation; 3) benzoylation; 4) NaI; 5) AgF, pyridine; 6) $Hg(OAc)_2$, acetone, H_2O. — Bz = PhCO.

Much more important is disconnection "d" in the synthesis of 11- and 6-deoxyanthracyclinones, using mainly derivatives of juglone as the DC-dienophile. The regioselectivity of Diels-Alder reactions with juglone derivatives has been thoroughly investigated experimentally[90-94] and is in good agreement with frontier orbital considerations.[95] The strong hydrogen bridge in juglone **99** is responsible for the extremely different orbital coefficients in the LUMO of the quinone, which consequently leads to the formation of **101** in the reaction of **99** with diene **100**. By contrast, the juglone methyl ether **102** yields the adduct **103** with inverse orientation of the methoxy group[91-93,96] (Scheme 25).



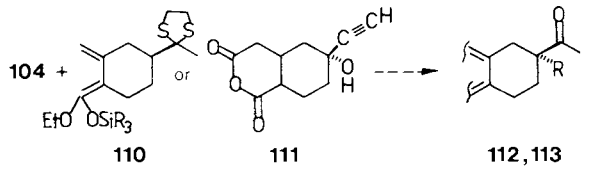
Scheme 25.

The reaction of the bromojuglone methyl ether **104** with the ketene acetals **105**[96] or **106**[97] to give the tetracycle **107** also proceeds with formation of ring B. In these cases the bromine atom directs the regioselectivity. The presence of the bromine atom simultaneously facilitates the aromatization of ring B with elimination of HBr and alcohol. An aromatization with CO_2 elimination follows the addition of juglone (**99**) to the bicyclic 6-alkoxypyranone **109** to afford **108**[98] (Scheme 26).



Scheme 26. **107**, R = H; **108**, $R = CH_3$.

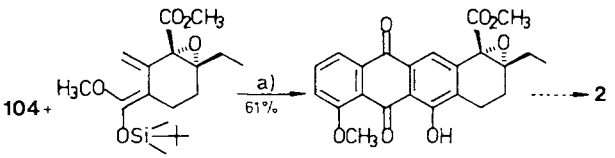
The attachment of side chains to the tetracyclic ketones of type **107** or **108** is difficult due to the great tendency for enolization.[99,100] Alternative pathways using the AB building block with side chain *rac*-**110**[96,99] or *rac*-**111**[101] in the reaction with bromojuglone **104** lead to the formation of *rac*-**112** or *rac*-**113** (Scheme 27).



110 111 112,113

Scheme 27. 112, R = H; 113, R = OR'.

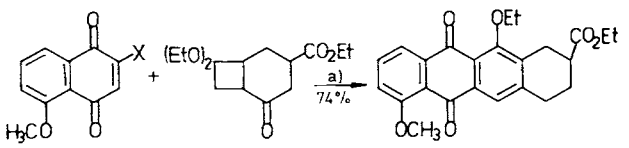
Rapoport et al.[102] were able to realize the use of the highly functionalized exocyclic diene **114**[102a] in a convergent synthesis of aklavinone via the intermediate *rac*-**115**[102] (cf. [97]). Carefully controlled reaction conditions (presence of triethylamine and molecular sieves to trap protons and methanol, respectively) were necessary in the Diels-Alder reaction so as to prevent aromatization of the primary adducts. Derivatives with a large variety of substituents in ring D are also available with the use of different naphthoquinones as dienophiles[102] (Scheme 28).



114 115

Scheme 28. a) 1) Benzene, 20 °C, 40 h, $N(C_2H_5)_3$, 4 Å molecular sieve; 2) nBu_4NF.

6-Deoxyanthracyclinones can also be obtained by this method by merely changing the position of the bromine atom in the juglone derivative. For example, the tetracyclic intermediate **118** is thus prepared by reaction of 2-bromo-*O*-methyljuglone **116** with the diene precursor **118**.[103] However, the intermediate **118** was in this case further transformed to daunomycinone (*rac*-**4**)[103] (Scheme 29; cf. [96]; for tandem Michael/Diels-Alder reactions or Claisen rearrangement/Diels-Alder reactions to 11-deoxyanthracyclinone precursors see [104, 105]).

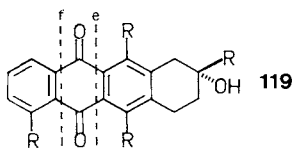


116 117 118

Scheme 29. a) 1) 185–190 °C, 1.5 h; 2) $NaOC_2H_5$, C_2H_5OH, O_2. – X = Br.

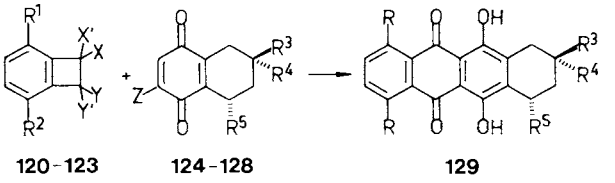
3.3. Formation of Ring C

Of the disconnections "e" and "f" in **119** only the first is of any importance because the AB building block can easily be incorporated in the form of tetrahydronaphthoquinones. However, following disconnection "e" only derivatives of rhodomycinones and no 6- or 11-deoxy compounds are available.

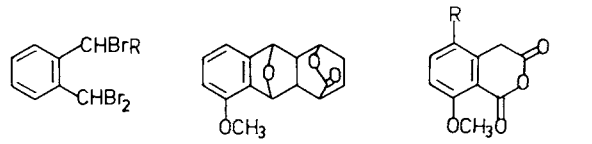


119

Intermediary *o*-quinodimethanes are also used as dienes. They can be generated thermolytically or photolytically from the cyclobutabenzenes **120–123**[60, 106–110] as shown in Scheme 30 (and also photolytically from *o*-methylbenzaldehydes[107]). Furthermore, the tri- or tetrabromides **130**[111, 112] or **131**[113] (generation of the *o*-quinodimethanes with NaI) can be used as precursors, as well as the isobenzofuran derivative **132**[30] or the homophthalic acid anhydrides **133**[114] or **134**[115] (treatment with strong bases). However, a general synthetic problem of this pathway is the subsequent oxidation of the 1,4-anthraquinone to derivatives of 1,4-dihydroxy-9,10-anthraquinone. An easy solution to the problem is only presented by the reaction of **123**[110] or **134**,[115] which directly yield 9,10-anthraquinones (Scheme 30).



120–123 124–128 129



130, R=H; **131**, R=Br **132** **133**, R=H; **134**, R=OAc

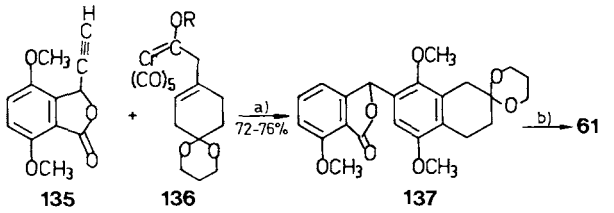
Scheme 30.

	R^1	R^2	X	X'	Y	Y'	Ref.
120	H	OMe	H	H	OH	H	[60, 106, 107]
121	OMe	OMe	H	H	–O–		[108]
122	H	H	OAc	H	OAc	H	[109]
123	H	OCH_2OMe	–O–		–O–		[110]

	R^3	R^4	R^5	Z	Ref.
124	$-O-(CH_2)_2-O-$		H	H	[106]
125	$-O-(CH_2)_2-O-$		H	Cl	[114]
126	Et	OH	OH	Cl	[60]
127	Ac	OH	H	H	[108]
128	Ac	–O–BPh–O–		H	[109]

The variety and different degree of functionality of AB quinones is shown in the examples **124–128**. Control of the regiochemistry is only possible with the corresponding chloro derivatives **125** and **126**. The quinones **124–128** can easily be prepared from the corresponding hydroquinone dimethyl ethers presented in Section 2.2; for instance, by oxidation with cerium(IV) reagents.[116] With chiral AB building blocks no racemization is observed under the conditions of the Diels-Alder reaction (Scheme 30).

A more unusual reaction is the addition of the Fischer carbene complex **136** to the acetylene *rac*-**135**. In this interesting reaction a molecule of CO is incorporated into ring B of *rac*-**137**[117] (for the mechanism see [117b]), which is then transformed (Scheme 31) in a further six steps to the known daunomycinone intermediate **61** (see Scheme 16).



Scheme 31. a) 1) THF, 45 °C, 12 h; 2) 2 equiv. $[Fe(dmf)_3Cl_2]FeCl_4$, THF. b) Six steps, 26–45%.

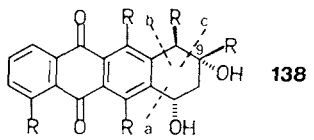
However, there are much shorter regioselective ways to **61** (see Section 4.1).

4. Anionic Reactions

The specific generation of anionic centers in one building block and acceptor centers in another enables selective bond formations and therefore an excellent control of regiochemistry. There are many possible methods for the first bond formation; however, Michael additions and the specific metalation of arenes certainly have priority. Although the coupling of the two building blocks is usually a two step process (the second step is often a Friedel-Crafts reaction) many condensations can in practice be conducted in a single reaction vessel.

4.1. Formation of Ring A

It is obvious that the tricyclic anthraquinones may be good starting materials for the synthesis of tetracyclic anthracyclinones. In many instances the syntheses starting from tricyclic precursors are much shorter and more efficient than the synthesis of AB fragments alone which must be coupled with further components to form tetracycles. The main reason for the success of this strategy stems from the fact that three excellent methods are available for the coupling of functionalized side chains to hydroxylated anthraquinones: 1) The Marschalk reaction; 2) nucleophilic additions to anthraquinones; and 3) the Claisen rearrangement.

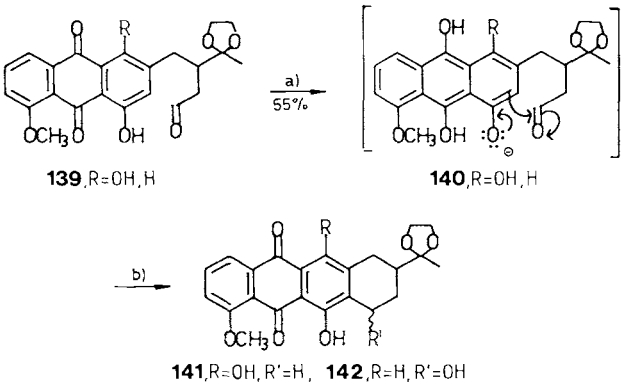


138

As shown in formula **138** the syntheses which proceed with formation of ring A can be divided into those which start from *mono*alkyl anthraquinones and those which require *di*alkylated anthraquinones. In the first case the ring of the arene is closed in the β-position ("a") or α-position ("b") to the tertiary center at C-9. In the second case, the formation of the bond leads, according to "c", via aldol reaction to anthracyclinones of type B or via Wittig reaction to anthracyclinones of type A.

4.1.1. Cyclization of Monoalkylanthraquinones

One of the earliest applications of the Marschalk reaction in anthracyclinone chemistry made use of disconnection "a" in **138**.[118] The strategy employed by *Sih* et al.[118] demonstrates the principles of this frequently used reaction. First the anthraquinone *rac*-**139** is reduced with dithionite in aqueous alkali to the hydroquinone *rac*-**140**, in which the electron density of the arene for an electrophilic attack of the aldehyde is considerably increased as compared to that in the anthraquinone *rac*-**139**. Thus, the reactive species *rac*-**140** is generated in a kind of "redox umpolung" from *rac*-**139**. Under the conditions originally employed by *Marschalk* (high temperatures) the benzylic hydroxy group that is formed during the addition is eliminated in an intramolecular redox process with regeneration of the anthraquinone,[119] as is shown by the cyclization to *rac*-**141** (Scheme 32). We have been able to demonstrate with many examples that the benzylic hydroxy group present in many anthracyclinones can easily be preserved by decreasing the reaction temperature.[120] This makes the Marschalk reaction an especially valuable tool in anthracyclinone chemistry. One example is the synthesis of 11-deoxydaunomycinone *rac*-**142** (R = H, R′ = OH) starting from aloe emodin, in which the benzylic hydroxy group is preserved during the cyclization of the aldehyde *rac*-**140** (R = H)[121] (Scheme 32).



139, R=OH, H **140**, R=OH, H

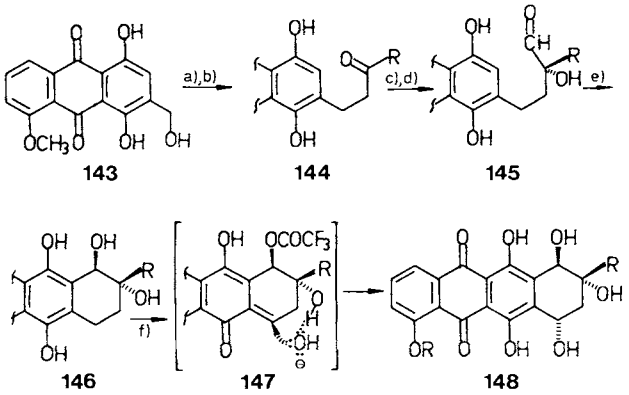
141, R=OH, R′=H, **142**, R=H, R′=OH

Scheme 32. a) NaOH, $Na_2S_2O_4$. b) O_2.

1,4-Dihydroxyanthraquinones not only react with aldehydes but also with other electrophiles such as α,β-unsaturated carbonyl compounds in a kind of Michael reaction[122, 123] (exceptions see [124a]), with halides[124b] and also intramolecularly with ketones.[120a, 125] A great advantage, moreover, is that with aldehydes (excepting formaldehyde) at low temperatures, directed *mono*alkylations can be achieved with 1,4-dihydroxyanthraquinones.[120] An intermolecular second alkylation is effected only under drastic conditions; however an *intra*molecular addition clearly occurs at −10 °C.[127] Aldehydes add *exclusively ortho* to the phenolic group, whereas halides also attack the *para* position.[124b] Esters do not react under the conditions of the Marschalk reaction; the products aromatize under more vigorous conditions.[118] According to *Whitlock* et al.,[128] a ring closure of esters can only be achieved by metalation of the arene.

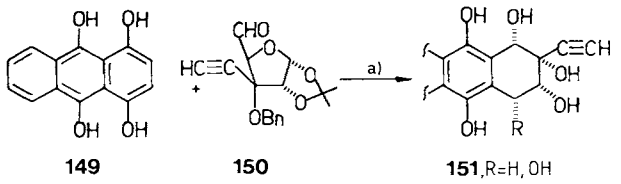
Excellent facilities to control stereo- and regiochemistry are also provided by disconnection "b" in **138** via α-hydroxyaldehydes such as *rac*-**145**. Starting from hydroxyme-

thylanthraquinone **143**, which is readily accessible from 1,4,5-trimethoxyanthraquinone[7] via selective cleavage of methyl ethers and Marschalk hydroxymethylation, it is possible to lengthen the side chain by standard methods to afford **144**. A further great advantage is that by reaction of **143** with 3-oxoesters, precursors with practically any side chain (e.g. CH_3, C_2H_5, C_3H_9) are available. The missing carbon atom can be introduced by reaction with acycl-anion equivalents. Lithiated 1,3-dithiane[129,130] and lithiated dichloromethane[7,127,131] have proven suitable for this purpose. The dichloromethane adducts are especially easily converted into the hydroxyaldehydes by treatment with aqueous alkali. Cyclization to the 9,10-diols **146** occurs in a one pot procedure after reduction with dithionite. The stereochemical outcome can largely be controlled by the choice of the reaction conditions: with non-chelating counter ions (e.g. Triton B), predominantly the *trans*-diols with the natural *trans* configuration are formed.[127] The synthesis is terminated by the hydroxylation at C-7. The benzylic hydroxy group is protected as trifluoroacetate prior to the usual bromination. The subsequent solvolysis with alkali yields almost exclusively the naturally configurated 7,9-*cis*-9,10-*trans* triols *rac*-**148**. The *cis*-selectivity is explained in terms of an elimination addition mechanism via an intermediate *o*-quinomethide *rac*-**147**, which is preferentially hydroxylated from the hydrophilic rear side.[132] Using this method, it was possible to prepare all the known natural rhodomycinones and feudomycinones of type A[7,127] (Scheme 33).



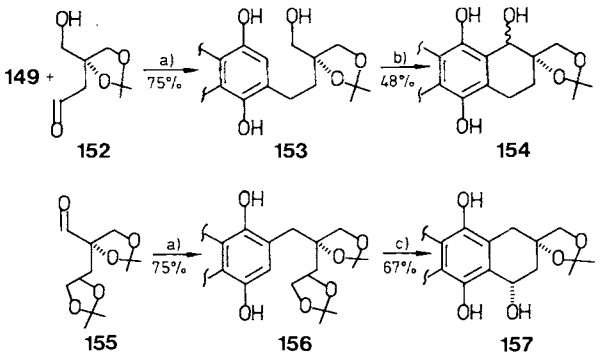
Scheme 33. a) SO_2Cl_2. b) 1) Alkylation with 3-oxo esters; 2) $OH^{\ominus}$; 3) $H^{\oplus}$; 4) $AlCl_3$ or BCl_3. c) Lithio-1,3-dithiane or dichlorolithiomethane, −100°C. d) NaOH, Triton B, CH_2Cl_2, 20°C. e) $Na_2S_2O_4$, −10°C, O_2, $H^{\oplus}$. f) 1) $(CF_3CO)_2O$; 2) Br_2, Azodiisobutyronitrile (AIBN) or *hv*; 3) $NaHCO_3$.

For the synthesis of enantiomerically pure natural products, the asymmetric synthesis of α-hydroxyaldehydes of type **148** with chiral auxiliaries is presently under investigation by our group. However, the Marschalk reaction also opens up ideal possibilities by incorporation of chiral derivatives from natural products, and both routes "a" and "b" (see **138**) are equally promising. Carbohydrates may be employed as natural products and *Shaw* et al.[133] have investigated the reaction of unbranched derivatives with leucoquinizarin **149**. The branched building block **150** was incorporated into the synthesis of the anthracyclinone **151** hydroxylated at C-8[133d] (Scheme 34).



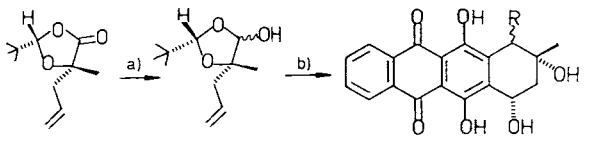
Scheme 34. a) Five steps. Bn = $PhCH_2$.

Both strategies "a" and "b" have been realized by *Monneret* et al.[55] The building blocks **152** and **155** were obtained in six steps from lactose. The first alkylation to **153** or **156** is carried out in boiling isopropanol with elimination of the benzylic hydroxy group (Lewis conditions[126]). Whereas cyclization of the aldehyde prepared from **153** under Marschalk conditions yields a 2:3 mixture of epimeric alcohols **154**, only the *cis*-diol **157** is obtained from **156** after partial cleavage of the terminal acetonide and cleavage of the diol to an aldehyde[55] (Scheme 35).



Scheme 35. a) 1) Isopropyl alcohol, Piperidinium acetate, 12 h boiling; 2) O_2. b) 1) DMSO, dicyclohexylcarbodiimide, pyridine, CF_3COOH; 2) $Na_2S_2O_4$, 0°C; 3) O_2. c) 1) 80% HOAc, 20°C, 1 h; 2) HIO_4; 3) $Na_2S_2O_4$, NaOH, −10°C; 4) O_2.

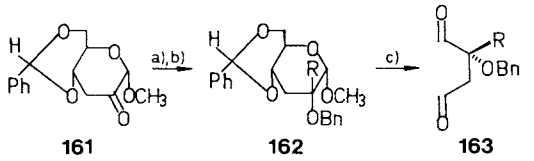
We in our group have been able to incorporate L-lactic acid into anthracyclinones **160** (R = H or OH) in a very short reaction sequence. The lactone **158** obtained by acetalation and alkylation[57] is easily reduced with diisobutylaluminum hydride to the relatively stable lactol **159**, which is transformed into **160** by a sequence of Marschalk reactions and ozonolysis[134] (Scheme 36).



Scheme 36. a) DIBAH, THF, −30°C. b) 1) **149**, NaOH; 2) O_3; 3) $Na_2S_2O_4$, NaOH.

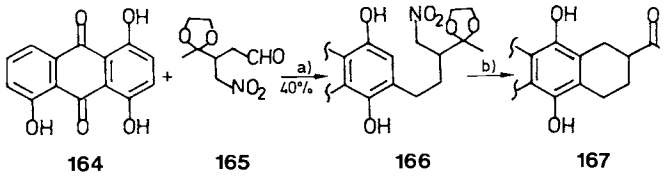
The incorporation of L-lactic acid is limited to the synthesis of anthracyclinones with methyl side chains. This restriction no longer exists when employing the 2-oxo-3-deoxy sugar **161** obtained from glucose, since a number of organometallic reagents can be added selectively to give **162** (R = ethyl, ethynyl). Benzylation, acetal cleavage and periodate cleavage affords the unstable dialdehydes **163**, which are added to leucoquinizarin **149** using the methods

outlined in Schemes 33–36[135] to give anthracyclinones (Scheme 37).



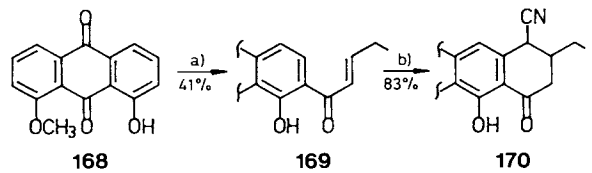
Scheme 37. a) BrMgR or LiR. b) Benzyl bromide, base. c) 1) HOAc, 60°C; 2) $NaIO_4$. — Bn = $PhCH_2$.

Anthracyclinone research has clearly shown that, in addition to electrophilic substitutions with hydroanthraquinones (Marschalk reaction), nucleophilic additions to anthraquinones are also possible. The additions are often surprisingly straightforward in *intra*molecular reactions. A combination of the Marschalk reaction with nucleophilic additions may be very advantageous, as has been shown by the work of *Sutherland* et al.[136] The nitroaldehyde *rac*-**165** is first added to the hydroquinone of **164** to give *rac*-**166**, which subsequently cyclizes with elimination of the nitro group[136] to give 7,9-dideoxycarminomycinone *rac*-**167** (Scheme 38). The C-3 selectivity (5 : 1) of the addition of *rac*-**165** to **164** under Lewis conditions is remarkable.[125, 126] The sequence of the reaction steps can also be reversed, whereupon nitroalkane building blocks add highly selectively at C-2.[136]



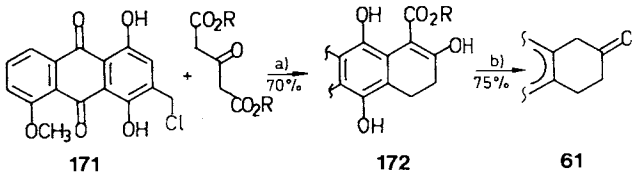
Scheme 38. a) Isopropyl alcohol, piperidinium acetate, 3 h boiling. b) 1) $NaOCH_3/CH_3OH$; 2) $H^{\oplus}$, H_2O, 10 h boiling.

Nucleophilic additions are a useful supplement to the Marschalk reaction insofar as the *ortho*-phenolic group is not a necessary prerequisite for the cyclization. This is demonstrated quite nicely in the synthesis of 11-deoxyaklavinone by *Cava* et al.[137] in which a kind of Michael addition of phenylthiomethyl cyanide to **169** is followed by ring closure to *rac*-**170** with elimination of phenyl sulfide[137] (Scheme 39).



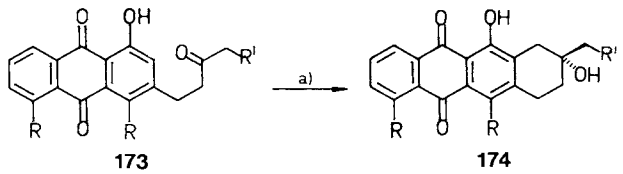
Scheme 39. a) Seven steps. b) $PhSCH_2CN$, $NaCH_2SOCH_3$/DMSO.

Unfortunately, the methods of *Sutherland* and *Cava* do not allow a direct introduction of an oxygen function at C-9. In our investigations we have paid special attention to this point. Thus, the daunomycinone precursor **61** (see Scheme 16) can be prepared regioselectively in only two steps from the tricycle **171**. The alkylation of acetonedicarboxylic ester leads under mild conditions via an open-chain intermediate directly to the tetracycle **172**, which is transformed into the ketone **61** by acid hydrolysis and decarboxylation[138] (Scheme 40).



Scheme 40. a) K_2CO_3, DMF. b) HOAc, H_2SO_4.

Another example is the addition of nitromethane to the 3-oxoalkylanthraquinone **173**, followed by cyclization with elimination of the nitro group to form the tetracycles *rac*-**174** (66–92% overall yield). A prerequisite is the presence of a phenolic hydroxy group at C-4[139] (Scheme 41). The alcohols *rac*-**174** can either be converted into feudomycinones by hydroxylation at C-7[127] or into β-rhodomycinones via elimination.[86]

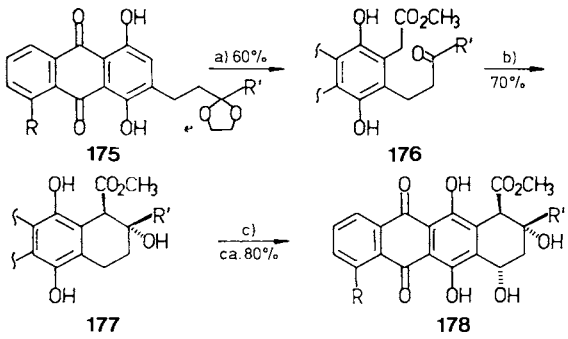


Scheme 41. a) CH_3NO_2, $C_2H_5O^-/C_2H_5OH$, 24 h boiling. R = H, OH, OCH_3; R' = H, CH_3.

4.1.2. *Cyclization of Dialkylanthraquinones*

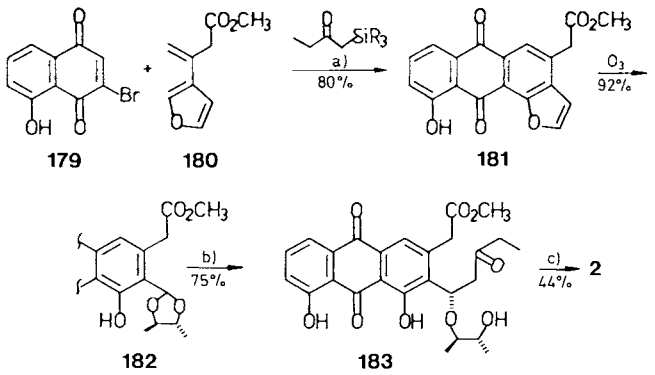
Anthracyclinone syntheses that start from bisalkylated anthraquinones are preparatively very profitable. Due to the specific substitution pattern of ring A, only the strategy based on disconnection "c" in **138** has so far been realized. One advantage of this pathway is the ready availability of the *ortho*-bisalkylated anthraquinones with differently substituted side chains. Two successive Marschalk reactions are ideal for the synthesis of the rhodomycinones with two *p*-hydroxy groups at C-6 and C-11, because a second, differently substituted side chain can only be introduced under more vigorous conditions. The procedure can be demonstrated with the synthesis of the ketoesters **176** which are made available from monosubstituted anthraquinones **175** via reaction with glyoxylic acid. In the subsequent treatment with base, the doubly activated benzylic position is deprotonated and the corresponding cyclic *p*-hydroxy esters are obtained almost quantitatively. The stereochemistry of the cyclization can easily be controlled: With lithium amides in aprotic medium, the *cis*-hydroxy esters are obtained exclusively, while treatment with Triton B in pyridine yields predominantly (at least 10 : 1) the 9,10-*trans*-anthracyclinones *rac*-**177** of natural configuration. The subsequent hydroxylation at C-7 is also highly selective and leads in good chemical yields almost exclusively to the 7,9-*cis*-diols *rac*-**178**[6, 140] (Scheme 42).

The two phenolic hydroxy groups at C-6 and C-11 are not available for the synthesis of aklavinone (**2**) or citromycinone (see, e.g., **194** and **205**), so another synthetic



Scheme 42. a) 1) $Na_2S_2O_4$, NaOH, OHC–COOH; 2) H^+; 3) CH_2N_2. b) Triton B, pyridine, 0°C, 10–20 min. c) 1) Br_2, CCl_4, *hv*; 2) $NaHCO_3$, H_2O.

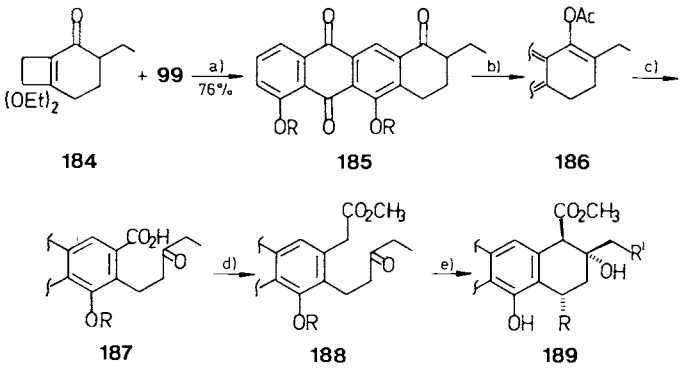
route has to be sought. The easiest approach is to generate the substitution pattern by Diels-Alder reaction, as demonstrated by the enantioselective synthesis of aklavinone by *Kishi* et al.[141] (Scheme 43). The Diels-Alder reaction of the bromojuglone **179** with the vinylfuran **180** affords the adduct **181**, which upon atmospheric oxidation and ozonolysis yields an ester aldehyde. The aldehyde group enables the introduction of a chiral auxiliary by acetalation with D-(−)-2,3-butanediol to give **182**. The decisive transfer of chirality is accompanied by chain elongation with 1-trimethylsilyl-2-butanone to give the keto alcohol **183** (selectivity 10:1 in favor of **183**). The cyclization with potassium carbonate in methanol yields 53% of a 7-*O*-methylaklavinone in addition to 43% of chromatographically separable *cis*-hydroxy esters. The intermediary ethers can be cleaved with trifluoroacetic acid to furnish the corresponding C-7 alcohols[141] (Scheme 43).



Scheme 43. a) Boiling in benzene, O_2, Hünig base. b) 2 equiv. CH_3CN, $SnCl_4$, −10°C, 5 h. c) 1) CH_3OH, K_2CO_3, 20°C, 2 h; 2) CF_3COOH, −78°C.

An enantioselective synthesis of 11-deoxydaunomycinone can be realized if the side chain of **183** contains an additional carbonyl group (initially masked as a methylene group).[142] The synthesis is completed by ozonolysis and decarboxylation (for further decarboxylations of type B anthracyclinones, see [143, 144]).

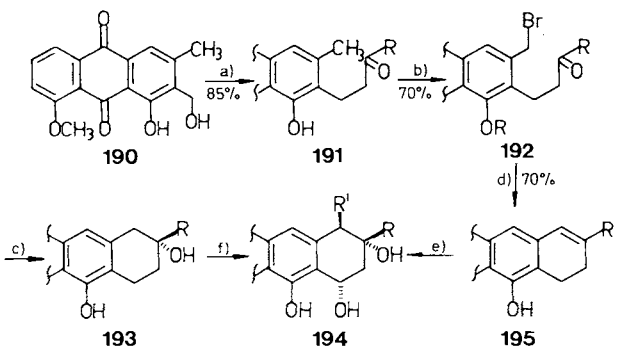
The advantage of the biogenetic type keto-ester cyclization is the generation of the acid-labile β-hydroxy ester under very mild conditions. It is therefore not surprising that seven of twelve published aklavinone or pyrromycinone syntheses follow this strategy, as was first resorted to in the synthesis of ε-rhodomycinones (see Scheme 42). However, the routes to the key intermediates are quite different. Most often an olefinic tetracyclic skeleton with ethyl side chain at C-9 is constructed by Diels-Alder reaction of juglone with diene precursors such as **184** (cf. Schemes 26–29), as may be seen in the synthesis of aklavinone by *Boeckman* et al.[145] (Scheme 44). The ozonolysis of **186** leads to a ketocarboxylic acid **187** lacking one carbon atom. Homologization of **187** via Arndt-Eistert reaction gives the keto ester **188**, subsequent cyclization and hydroxylation of which affords aklavinone (**2**),[145–147] pyrromycinone (**3**),[146] auramycinone (**189**)[147] (R′=CH_3) or 2-hydroxyaklavinone,[148] depending on the starting materials used (Scheme 44).



Scheme 44. a) 1) **184**:**99** = 4.4:1, 175–180°C; 2) methylation. b) Ac_2O, $HClO_4$. c) O_3. d) Arndt-Eistert homologization. e) Triton B, CH_3OH/CH_2Cl_2, −20°C; hydroxylation at C-7.

In our syntheses of aklavinone,[149] pyrromycinone and auramycinone[150] we have used the open-chain bromides **142**, which are accessible from the hydroxymethylanthraquinone **190** via the ketones **191**. Since a direct substitution of the bromide in **192** by carboxylate anion equivalents such as cyanide was not feasible (cf. [147]), we have also chosen the Arndt-Eistert reaction[149] or Grignardation at −78°C with highly reactive magnesium[151] to realize chain elongation.[150]

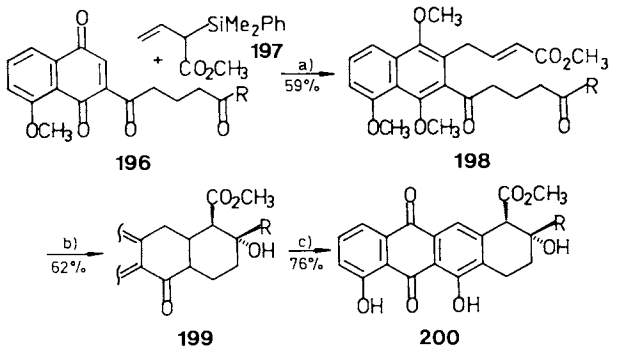
The reactive bromides **192** may also serve as starting materials for many 11-deoxyanthracyclinones of type A. They can be directly cyclized with magnesium to the alcohols *rac*-**193**[132] or by Wittig reaction, in excellent yields,



Scheme 45. a) Three steps see Scheme 44. b) 1) Pivaloyl chloride, dimethylaminopyridine (DMAP), pyridine; 2) NBS, CCl_4, *hv*. c) Activated Mg/THF. d) PPh_3, K_2CO_3, THF, [18]crown-6, 3 h boiling. e) 1) MCPBA; 2) NaOAc; 3) NaOH and finally hydroxylation. f) Hydroxylation.—R=CH_3, C_2H_5; R′=H, OH; R′+H-10=–O–.

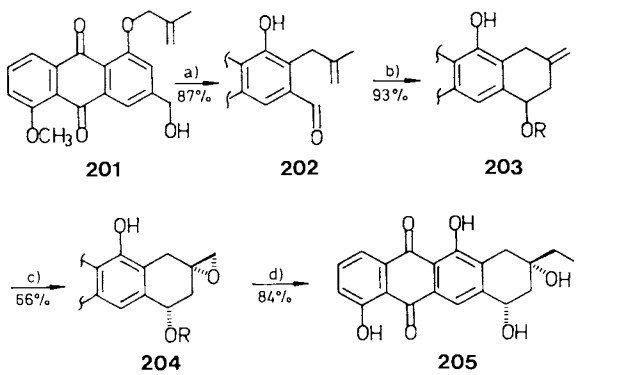
to the olefins **195**.[152] Starting from the olefins **195**, the citromycines *rac*-**194** (R′=H or OH)[132] or the 8-deoxyaranciamycinones *rac*-**194** (with oxo group at C-10)[152] are obtained by the methods of epoxidation, nucleophilic epoxide opening, and hydroxylation, as has already been mentioned (see Scheme 23 and Scheme 45; for the synthesis of 10-oxoanthracyclinones cf. [153, 154]). With lactamide complexes of oxodiperoxomolybdenum, an enantioselective epoxidation of olefins of type **195** with 73% *ee*[155] was possible.

Similarly as in *Muxfeldt*'s tetracycline synthesis, in the aklavinone synthesis described by *Maruyama* et al.[157] both rings A and B are built up in a sequential reaction ("Zipper reaction").[156] The bicyclic compound **198** which resembles the tricyclic ketoesters is obtained by Michael addition of the silyl ester **197** to the naphthoquinone **196**. Three stereoisomeric tetracyclic products in addition to a tricyclic ketone are formed upon base-catalyzed cyclization of **198**. By extensive optimization studies, the yield of the desired product *rac*-**199** could be increased to 62% using [2.2.2]cryptands (kryptofix). Oxidation to the quinone and aromatization of ring B affords 7-deoxyauramycinone (*rac*-**200**, R=CH_3), deoxyaklavinone *rac*-**200** (R=C_2H_5), and the 13-methyl compound *rac*-**200** (R=*i*Pr)[157] (Scheme 46).



Scheme 46. a) CH_2Cl_2, $SnCl_4$, −78 bis −20 °C, 2 h. b) 1) KH, Kryptofix 222/hexamethylphosphoric triamide (HMPT), THF, −78 to −50 °C, 3 h; 2) *t*$BuMe_2SiCl$, imidazole. c) 1) $Ce^{4\oplus}$; 2) $NaHSO_3$; 3) Br_2, AIBN, CCl_4; 4) $N(C_2H_5)_3$; 5) $AlCl_3$.

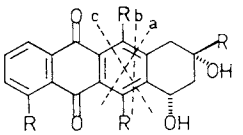
The synthesis of citromycinone by *Hauser* and *Mal*[158] also proceeds with formation of ring A. It is a beautiful example of the "reductive" Claisen rearrangement as introduced into anthracyclinone chemistry by *Rutledge* et al.[159] Thus, the reduced form of **201** rearranges to **202** at considerably lower temperatures than the quinoid form **201**. An interesting step is the $SnCl_4$-catalyzed cyclization of the unsaturated aldehyde **202** to the exocyclic olefin *rac*-**203**. The synthesis of γ-citromycinone (*rac*-**205**) is completed by epoxidation of *rac*-**203** to *rac*-**204**, opening of the oxirane with lithium dimethylcuprate, and ether cleavage[158] (Scheme 47).



Scheme 47. a) 1) $Na_2S_2O_4$, DMF, heating; 2) $BaMnO_4$, CH_2Cl_2. b) $SnCl_4$, CH_2Cl_2. c) Sharpless epoxidation. d) 1) 2 CuCN, 12 CH_3Li, THF, 0 °C; 2) $AlCl_3$.

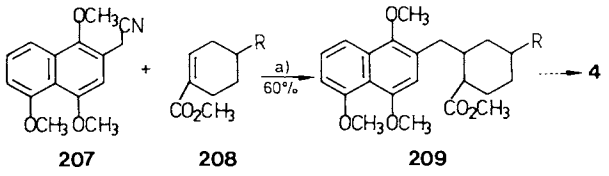
4.2. Formation of Ring B

Three of four possible pathways ("a", "b", and "c") are realized in the syntheses that proceed with construction of Ring B (see **206**). The anionic coupling of two unequal building blocks is also suitable for the synthesis of 6- and 11-deoxyanthracyclinones. The Michael addition and the nucleophilic addition of selectively lithiated arenes are most often employed.



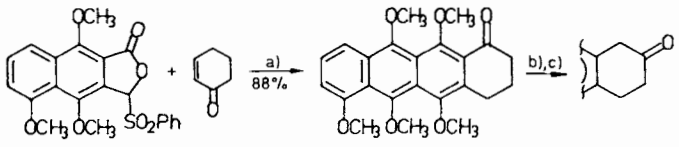
206

Parker et al.[160] as well as *Kende* et al.[161] make use of the Michael addition of the benzyl cyanide **207** to the cyclic α,β-unsaturated esters **208** for the regioselective synthesis of the precursors **209**. The further transformation to tetracycles is accomplished via an oxidative elimination of the cyano group and a Friedel-Crafts cyclization (Scheme 48).



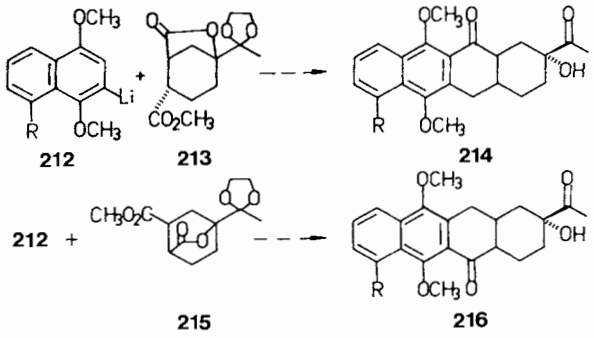
Scheme 48. a) Potassium enolate of **207**, −56 °C, 3 h.

The syntheses proceeding with formation of ring C following disconnection "b" in **206** have been systematically developed into a generally applicable synthetic method for linearly annelated ring systems, e.g. in the groups of *Hauser*,[162] *Kraus*,[163] *Staunton*,[164] *Swenton*,[43] and *Weinreb*.[165] The principle of the method is neatly demonstrated in the reaction of the tricyclic phenylsulfonylfuranone **210**.[166] A 1,4-dipole generated from **210** by deprotonation reacts sequentially with α,β-unsaturated carbonyl compounds such as cyclohexenone. A primary Michael reaction is followed by a nucleophilic addition of the intermediary enolate to the ester group to give the adduct **211**, which can be transformed into the daunomycinone precursor **61** by transposition of the carbonyl group from C-10 to C-9 as shown in Scheme 49.[166] Products with inverse substitution pattern can be obtained by regrouping the functional groups in the furanone **210**.[166] The reaction of bicyclic furanones with bicyclic enones leads to similar products[167] (Scheme 49).



Scheme 49. a) $LiNiPr_2$, THF, −78 °C, 30 min, then 0 °C. b) 1) $NaBH_4$; 2) $H^{\oplus}$. c) 1) $OsO_4/(C_2H_5)_3NO$; 2) $H^{\oplus}$, $HOCH_2CH_2OH$; 3) cerium ammonium nitrate; 4) AgO/HNO_3; 5) trifluoroacetic acid, HCl.

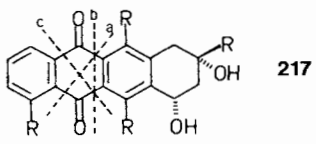
6-Deoxy-[168] as well as 11-deoxydaunomycinones[169] can be prepared in a very flexible manner by route "c" in **206**. Thus, *rac*-**214** can be prepared by coupling the lithiated naphthalene **212** with the ester lactone *rac*-**213**, while *rac*-**216** can obtained by reaction of **212** with *rac*-**215**.[170] It is remarkable that the ester group is attacked preferentially, thus controlling the regiochemistry of the adducts (Scheme 50). A disadvantage in the synthesis of 6-deoxy compounds is the low yield (26%) of the hydroxylation at C-7 due to the absence of the *peri* OH-group, which facilitates a twofold bromination of this position.[171] There is no such limitation when more highly functionalized AB building blocks are used (see Section 4.3).



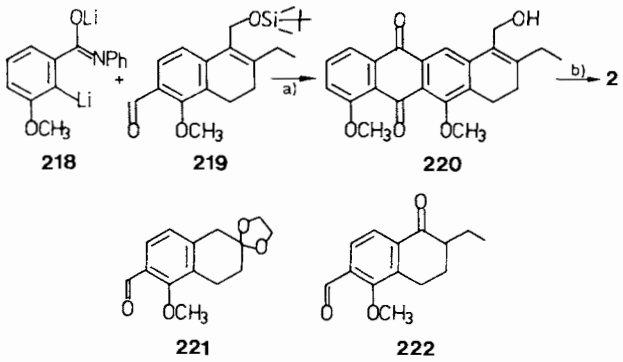
Scheme 50. R = H, OCH_3.

4.3. Formation of Ring C

The reactions proceeding with formation of ring B are very important because two equally large building blocks are coupled in a very convergent way, and ring D is introduced in the form of readily available benzene derivatives. Of four possible pathways, three ("a", "b", and "c") have been realized (see **217**).

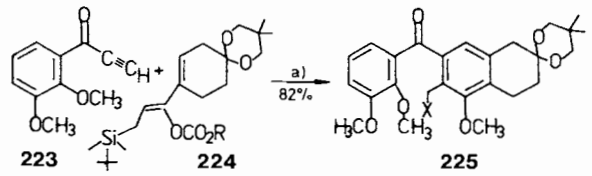


Disconnection "a" has been systematically investigated by *Kende* et al. for the synthesis of 11-deoxyanthracyclinones by coupling the lithiated benzamide **218** with the bicyclic aldehydes **221**,[100] *rac*-**222**[172] or **219**.[173] Especially elegant in the synthesis of aklavinone is the incorporation of the future ester group as hydroxymethyl group;[173] this enables the asymmetric epoxidation of the tetracyclic allyl alcohol by the method of *Sharpless*[48] (Scheme 51).



Scheme 51. a) *n*BuLi, tetramethylethylenediamine (TMEDA), four further steps. b) Sharpless epoxidation, Jones oxidation, esterification, five further steps.

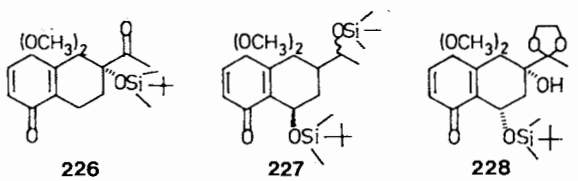
In a synthesis by *Vedejs* and *Nader*[174] the benzylic carbanion is not stabilized by a cyano group as in **207**, but by a silyl group. However, the replacement of the silyl group in **225** (X = SiR_3) by the cyano group (X = CN) is necessary in the nucleophilic cyclization step[176] via a kind of Hassall cyclization.[175] The adduct **225** (X = SiR_3) is accessible in a remarkably regioselective Diels-Alder reaction (11 : 1 in favor of the *meta* product) from the components **223** and **224**[176] (Scheme 52).



Scheme 52. a) 1) Toluene, 130 °C; 2) dichlorocyano-*p*-benzoquinone (DDQ), benzene, 50 °C. X = SiR_3 or CN.

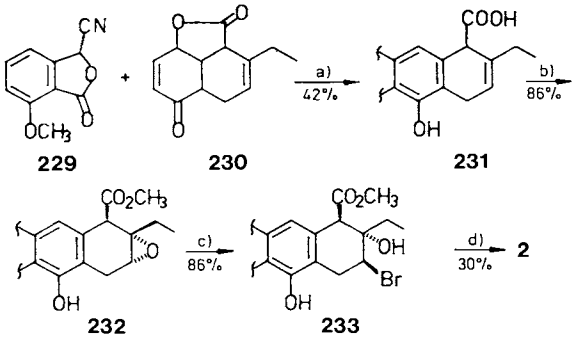
The disconnection "b" in **217** has, as already mentioned, claimed fundamental importance in the synthesis of linearly annelated ring systems. In addition to the phenylsulfonylisobenzofurans developed by *Hauser*'s group,[162] the analogous cyanides such as **229** first synthesized by *Kraus*[163] are also used (for the synthesis of derivatized isobenzofuranones with cyano groups see [177]). The common principle of all these reactions is the Michael reaction of the phthalide anion derived from **229** with α,β-unsaturated systems such as **226**,[178] *rac*-**227**,[179] **228**[43] or *rac*-**230**, followed by spontaneous cyclization to tetracyclic anthracyclinone precursors.

The quinone monoacetals are available from AB building blocks as mentioned in Section 2.2. The regioselectivity of the syntheses is determined by the efficient cleavage of the diacetals to the desired monoacetals. This cleavage in favor of the monoacetals was successfully performed in



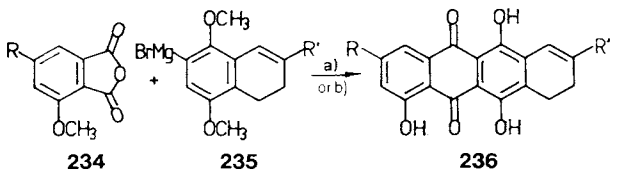
the ratios 87 : 13 and 9 : 2, respectively (cf. [180]) by *Swenton* et al.[43] and *Rodrigo* et al.[179] However, the cleavage is completely selective via the benzyl ethers **30** (R = OBn).[40,41,181]

The coupling of the phthalide **229** with the bicyclic Michael acceptor *rac*-**230** is the key step in the synthesis of aklavinone by *Li* et al.[182] For the hydroxylation in the tertiary position, the epoxide *rac*-**232** obtainable from *rac*-**231** is opened with hydrobromic acid and the bromine is removed reductively[182] (Scheme 53).



Scheme 53. a) 1) $LiNiPr_2$, THF/HMPT, + **230**, 20°C, 2 h; 2) O_2; 3) CH_2N_2. b) MCPBA. c) NaBr, TosOH, CH_3CN. d) Four steps.

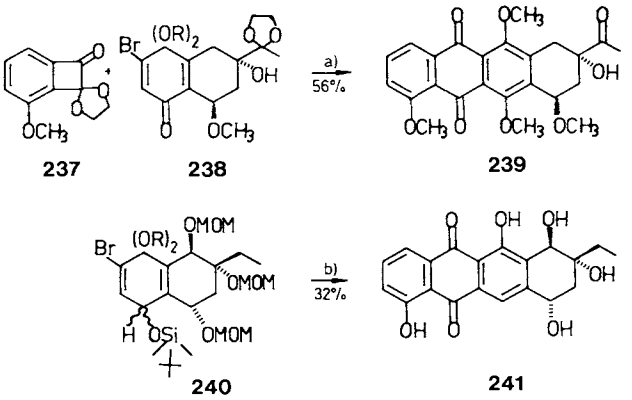
Daunomycinones as well as rhodomycinones can be prepared by the procedure of *Braun*.[59] The key step is the regioselective addition of the Grignard compound **235** (R′ = H or CH_3) to the phthalic acid anhydride **234** (R = H or OCH_3), which is followed by Friedel Crafts cyclization to **236**. The olefinic derivatives without side chains (R = H or OCH_3, R′ = H) are transformed into daunomycinones, those with ethyl side chains (**236**, R = H, R′ = C_2H_3) into rhodomycinones[59] (Scheme 54).



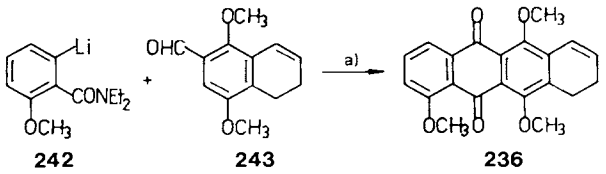
Scheme 54. a) For R = R′ = H: 1) THF/TMEDA; 2) HF; 3) $AlCl_3$, epoxidation and ring opening. b) For R = H or OCH_3, R′ = C_2H_5: 1) THF/TMEDA; 2) HF, MCPBA; 3) $H^{\oplus}$; 4) see Schemes 30-32.

Swenton et al. also allowed metalated AB-building blocks derived from *rac*-**238** and *rac*-**240** to react with the monoacetal **237** and obtained the daunomycinone derivative *rac*-**239**[183] and β-citromycinone *rac*-**241**, respectively.[184] The difficult problem of hydroxylation at C-7 is neatly solved by use of the highly functionalized AB building block *rac*-**240** (see Section 2.2) (Scheme 55; for a synthesis of citromycinone via α-hydroxyaldehydes see [185]).

Furukawa et al.[186] obtained the olefinic daunomycinone precursor **236** (R = H) via route "c" in **217**. In this pathway the lithiated aromatic compounds **242** are allowed to react with the aldehydes **243** (Scheme 56). The lithiation to **242** is selectively directed by the neighboring benzamide group to the *ortho* position. This reaction has also been exploited by other authors for the synthesis of anthracyclinone precursors.[42,187]



Scheme 55. a) *n*BuLi, b) *t*BuLi. R = CH_3, MOM = CH_2OCH_3.



Scheme 56. a) THF, −78 °C, then 2 h at 20 °C.

5. Outlook

The present synthetic task is not terminated with the synthesis of the anthracyclinones: The aglycones must be coupled with sugars such as daunosamine or rhodosamine to afford the biologically active glycosidic anthracyclines. An efficient synthesis of new anthracyclines that contain several sugar residues still remains an enormous challenge. Larger amounts of synthetic enantiomerically pure aglycones are needed, which cannot be prepared by the derivatization of natural products. Not only are aglycones with "unnatural" substitution patterns (e.g. 4-deoxy compounds) being intensively investigated but also their heteroanalogues.

We thank the Deutsche Forschungsgemeinschaft and the Fonds der Chemischen Industrie for financial support and BASF, Bayer and Hoechst AG for gifts of chemicals. Special thanks are due to Dr. W. Priyono for help with the literature search.

Received: November 18, 1985;
revised: April 28, 1986 [A 587 IE]
German version: *Angew. Chem. 98* (1986) 788

[1] a) Structure: H. Brockmann, *Fortschr. Chem. Org. Naturst. 21* (1963) 121; b) R. H. Thomson: *Naturally Occurring Quinones*, Academic Press, New York 1971, p. 536; c) J. Berdy, A. Aszalos, M. Bostian, K. L. McNitt: *Handbook of Antibiotic Compounds, Vol. 4*, CRC Press, Boca Raton, FL (USA) 1980, p. 81.

[2] Isolation of new structures: a) H. Brockmann, B. Scheffer, C. Stein, *Tetrahedron Lett. 1973*, 3699; b) H. Brockmann, H. Greve, *ibid. 1975*, 831; c) T. Oki, *J. Antibiot. 30* (1977) S-70; d) P. F. Wiley, R. B. Kelly, E. L. Caron, V. H. Wiley, J. H. Johnson, F. A. MacKellar, S. A. Mizsak, *J. Am. Chem. Soc. 99* (1977) 542; e) G. Cassinelli, G. Rivola, D. Ruggieri, F. Arcamone, A. Grein, S. Merli, G. Spalla, A. M. Casazza, A. DiMarco, G. Pratesi, *J. Antibiot. 35* (1982) 176; f) D. E. Nettleton, Jr., D. M. Balitz, T. W. Doyle, W. T. Bradner, D. L. Johnson, F. A. O'Herron, R. H. Schreiber, A. B. Coon, J. E. Moseley, R. W. Myllymaki, *J. Nat. Prod. 43* (1980) 242; *47* (1984) 698; g) T. Uchida, M. Imoto, T. Masuda, K. Imamura, Y. Hatori, T. Sawa, H. Nagunawa, M. Hamada, T. Takeuchi, H. Umezawa, *J. Antibiot. 36* (1984) 1083; h) A. Yoshimoto, Y. Matsuzawa, T. Ishikura, T. Sawa, T. Takeuchi, H. Umezawa, *ibid. 37* (1985) 920.

[3] Biological action: a) F. Arcamone, *Lloydia 40* (1977) 45; b) S. Penco, *Chim. Ind. (Milan) 65* (1983) 359; c) F. Arcamone: *Doxorubicin*, Aca-

demic Press, New York 1980; d) S. T. Crooke, S. D. Reich (Eds.): *Anthracyclines, Current Status and New Developments*, Academic Press, New York 1981; e) J. R. Brown, S. H. Imam, *Prog. Med. Chem. 21* (1984) 170; f) F. Arcamone, *Med. Res. Rev. 4* (1984) 153; g) B. R. J. Abdella, J. Fisher, *EHP, Environ. Health Perspect.* (1985); h) E. M. Acton, G. L. Tong, C. W. Mosher, R. L. Wolgemuth, *J. Med. Chem. 27* (1984) 638; i) G. Cassinelli, M. Ballabio, F. Arcamone, A. M. Casaza, A. Podesta, *J. Antibiot. 38* (1985) 856.

[4] Biogenesis: a) W. D. Ollis, I. O. Sutherland, R. C. Codner, J. J. Miller, G. A. Miller, *Proc. Chem. Soc. (London) 1960*, 347; b) M. L. Casey, R. C. Paulick, H. M. Whitlock, *J. Org. Chem. 43* (1978) 1627; c) P. F. Wiley, P. W. Elrod, V. P. Marshall, *ibid. 43* (1978) 3457; d) A. Yoshimoto, T. Oki, H. Umezawa, *J. Antibiot. 33* (1980) 1199; e) A. Yoshimoto, T. Oki, T. Takeuchi, H. Umezawa, *ibid. 33* (1980) 1158; f) A. Yoshimoto, Y. Matsuzawa, T. Oki, *J. Antibiot. 34* (1982) 951; g) C. R. Hutchinson, *Antibiotics 4* (1981) 1; *Chem. Abstr. 94* (1981) 188241x; h) C. Wagner, K. Eckardt, G. Schumann, W. Ihn, D. Tresselt, *J. Antibiot. 37* (1984) 691.

[5] T. M. Harris, C. M. Harris, K. B. Hindley, *Fortschr. Chem. Org. Naturst. 31* (1974) 217.

[6] K. Krohn, M. Radeloff, *Chem. Ber. 111* (1978) 3823.

[7] K. Krohn, B. Behnke, *Liebigs Ann. Chem. 1983*, 1818.

[8] T. R. Kelly, L. Ananthasubramanian, K. Borath, J. W. Gillard, R. N. Goerner, Jr., P. F. King, J. M. Lyding, W.-G. Tsang, J. Vaya, *Tetrahedron 40* (1984) 4569.

[9] G. Quinkert, H. Stark, *Angew. Chem. 95* (1983) 651; *Angew. Chem. Int. Ed. Engl. 22* (1983) 637.

[10] Synthesis: a) T. R. Kelly, *Annu. Rep. Med. Chem. 14* (1979) 288; b) W. A. Remers: *The Chemistry of the Antitumor Antibiotics, Vol. 1*, Wiley, New York 1979; c) T. Kametani, K. Fukumoto, *Med. Res. Rev. 1* (1980) 23; d) H. S. El Khadem (Ed.): *Anthracycline Antibiotics*, Academic Press, New York 1982; e) S. Terashima, *J. Synth. Org. Chem. Jpn. (Yuki Gosei Kagaku Kyokaishi) 40* (1982) 20; f) V. Sniekus, N. Altintas in J. ApSimon (Ed.): *The Total Synthesis of Natural Products, Vol. 8*, Wiley-Interscience, New York, in press; g) R. T. Kelly (Ed.): *Tetrahedron Symposium-in-Print No. 17: Recent Aspects of Anthracyclinone Chemistry, Tetrahedron 40* (1984) 4537–4793; h) M. J. Broadhurst, C. H. Hassall, G. J. Thomas, *Chem. Ind. (London) 1985*, 106.

[11] Review of anthraquinone chemistry: O. Bayer in *Houben-Weyl-Müller: Methoden der Organischen Chemie, Band VII/3c*, Thieme, Stuttgart 1979.

[12] F. Arcamone, L. Bernardi, B. Patelli, P. Giardino, A. Di Marco, A. M. Casazza, C. Soranzo, C. Pratesi, *Experientia 34* (1978) 1255.

[13] C. M. Wong, D. Popien, R. Schenk, J. Te Raa, *Can. J. Chem. 49* (1971) 2712.

[14] A. S. Kende, Y.-g. Tsay, J. E. Mills, *J. Am. Chem. Soc. 98* (1976) 1967.

[15] D. Dominguez, R. J. Ardeckey, M. P. Cava, *J. Am. Chem. Soc. 105* (1983) 1608.

[16] M. Suzuki, T. Matsumoto, R. Abe, Y. Kimura, S. Terashima, *Chem. Lett. 1985*, 57.

[17] R. D. Gleim, S. Trenbeath, F. Suzuki, C. J. Sih, *J. Chem. Soc. Chem. Commun. 1978*, 242.

[18] D. G. Miller, S. Trenbeath, C. J. Sih, *Tetrahedron Lett. 1976*, 1637.

[19] C. M. Wong, R. Schwenk, D. Popien, T.-L. Ho, *Can. J. Chem. 51* (1973) 466.

[20] R. J. Blade, P. Hodge, *J. Chem. Soc. Chem. Commun. 1979*, 85.

[21] A. S. Kende, J. L. Belletire, T. J. Bentley, E. Hume, J. Airey, *J. Am. Chem. Soc. 97* (1975) 4425.

[22] A. V. Rama Rao, A. R. Mehendale, K. Bal Reddy, *Tetrahedron Lett. 23* (1982) 2415.

[23] M. J. Broadhurst, C. H. Hassall, *J. Chem. Soc. Perkin Trans. 1 1982*, 2227.

[24] P. N. Confalone, G. Pizzolato, *J. Am. Chem. Soc. 103* (1981) 4251.

[25] a) K. S. Kim, E. Vanotti, A. Suarato, F. Johnson, *J. Am. Chem. Soc. 101* (1979) 2483; b) S. D. Kimball, K. S. Kim, D. K. Mohanty, E. Vanotti, F. Johnson, *Tetrahedron Lett. 23* (1982) 3871.

[26] A. V. Rama Rao, J. S. Yadev, K. Bal Reddy, A. R. Mehendale, *Tetrahedron 40* (1984) 4643.

[27] N. Tanno, S. Terashima, *Chem. Pharm. Bull. 31* (1983) 821.

[28] R. A. Russell, R. W. Irvine, A. S. Krauss, *Tetrahedron Lett. 25* (1984) 5817.

[29] J. R. Wiseman, N. I. French, R. K. Hallmark, K. G. Chiong, *Tetrahedron Lett. 1978*, 3765.

[30] A. S. Kende, D. D. Curran, Y.-g. Tsay, J. E. Mills, *Tetrahedron Lett. 1977*, 3537.

[31] M. Suzuki, Y. Kimura, S. Terashima, *Chem. Lett. 1984*, 1543.

[32] A. V. Rao, V. H. Deshpande, N. L. Laxma Reddy, *Tetrahedron Lett. 21* (1980) 2661.

[33] J. F. Honek, M. L. Mancini, B. Belleau, *Tetrahedron Lett. 24* (1983) 257.

[34] R. J. Ardecky, F. A. Kerdesky, M. P. Cava, *J. Org. Chem. 46* (1981) 1483.

[35] D. Stephan, A. Gorgues, A. Le Coq, *Tetrahedron Lett. 25* (1984) 5649.

[36] E. P. Kündig, V. Desobry, P. Simmons, *J. Am. Chem. Soc. 105* (1983) 6962.

[37] C. M. Wong, A.-Q. Mi, J. Ren, W. Haque, K. Marat, *Tetrahedron 40* (1984) 4789.

[38] A. V. Rama Rao, B. Chanda, H. B. Borate, *Tetrahedron 38* (1983) 3555.

[39] M. P. Reddy, G. S. Krishna Rao, *Tetrahedron Lett. 22* (1981) 3549.

[40] R. A. Russell, G. J. Collin, M. P. Crane, P. S. Gee, A. S. Krauss, R. N. Warrener, *Aust. J. Chem. 37* (1984) 1721.

[41] R. A. Russell, A. S. Krauss, R. W. Irvine, R. N. Warrener, *Aust. J. Chem. 38* (1985) 179.

[42] M. P. Sibi, N. Altintas, V. Snieckus, *Tetrahedron 40* (1984) 4593.

[43] J. S. Swenton, J. N. Freskos, G. W. Morrow, A. D. Sercel, *Tetrahedron 40* (1984) 4625, and references cited therein.

[44] M. J. Broadhurst, C. H. Hassall, G. J. Thomas, *J. Chem. Soc. Perkin Trans. 1 1982*, 2239.

[45] J. N. Gardner, F. E. Carbon, D. Gnoj, *J. Org. Chem. 33* (1968) 3294.

[46] M. J. Broadhurst, C. H. Hassall, G. J. Thomas, *J. Chem. Soc. Perkin Trans. 1 1982*, 2249.

[47] F. Arcamone, L. Bernardi, B. Patelli, A. Di Marco, DOS 2601795 (July 29, 1976); *Chem. Abstr. 85* (1976) 142918j.

[48] V. S. Martin, S. S. Woodard, T. Katsuki, Y. Yamada, M. Ikeda, K. B. Sharpless, *J. Am. Chem. Soc. 103* (1981) 6237.

[49] O. Mitsunobu, *Synthesis 1981*, 1.

[50] a) K. Tamoto, S. Terashima, *Tetrahedron Lett. 23* (1982) 3715; b) *Chem. Pharm. Bull. 32* (1984) 4328.

[51] S. Terashima, S. Jew, K. Koga, *Chem. Pharm. Bull. 27* (1979) 2351.

[52] R. A. Russell, P. S. Gee, R. W. Irvine, R. N. Warrener, *Aust. J. Chem. 37* (1984) 1709.

[53] a) M. Suzuki, Y. Kimura, S. Terashima, *Chem. Lett. 1985*, 367; b) *Tetrahedron Lett. 26* (1985) 6481.

[54] J.-C. Florent, A. Genot, C. Monneret, *Tetrahedron Lett. 26* (1985) 5295.

[55] a) F. Bennani, J.-C. Florent, M. Koch, C. Monneret, *Tetrahedron 40* (1984) 4669; b) A. Anne, F. Bennani, J.-C. Florent, J. Moiroux, C. Monneret, *Tetrahedron Lett. 26* (1985) 2641.

[56] K. Krohn, H. Rieger, unpublished.

[57] D. Seebach, R. Naef, G. Calderani, *Tetrahedron 40* (1984) 1313.

[58] C. E. Coburn, D. K. Anderson, J. S. Swenton, *J. Org. Chem. 48* (1983) 1455.

[59] M. Braun, *Tetrahedron 40* (1984) 3549, and references cited therein.

[60] J. R. Wiseman, G. F. Budde, M. P. Meyer, ACS-Meet. Philadelphia, August 1984.

[61] F. A. J. Kerdesky, R. J. Ardecky, W. V. Lakshmikantham, M. P. Cava, *J. Am. Chem. Soc. 103* (1981) 1992.

[62] R. J. Ardecky, D. Dominguez, M. P. Cava, *J. Org. Chem. 47* (1982) 409.

[63] T. Watabe, Y. Takahashi, M. Oda, *Tetrahedron Lett. 24* (1983) 5623.

[64] J. Tamirez, P. Vogel, *Angew. Chem. 96* (1984) 61; *Angew. Chem. Int. Ed. Engl. 23* (1984) 74.

[65] R. Breslow, R. J. Corcoran, B. B. Snider, R. J. Doll, P. L. Khanna, R. Kaleya, *J. Am. Chem. Soc. 99* (1977) 905.

[66] J. Tamirez, P. Vogel, *Tetrahedron 40* (1984) 4549, and references cited therein.

[67] T. R. Kelly, W.-G. Tsang, *Tetrahedron Lett. 1978*, 4457.

[68] W. W. Lee, A. P. Martinez, T. H. Smith, D. W. Henry, *J. Org. Chem. 41* (1976) 2296.

[69] R. P. Potman, F. J. van Kleef, H. W. Scheeren, *J. Org. Chem. 50* (1985) 1955.

[70] J. C. Carretero, J. C. Cuevas, A. Echavarren, F. Fariña, P. Prados, *J. Chem. Res. (S) 1984*, 6; *(M) 1984*, 147, and references cited therein.

[71] F. Fariña, M. T. Molina, M. C. Paredes, *Tetrahedron Lett. 26* (1985) 111.

[72] R. A. Russel, G. J. Collin, M. Sterns, R. N. Warrener, *Tetrahedron Lett. 1979*, 4229.

[73] A. V. Rama Rao, G. Venkatswamy, S. M. Javeed, V. H. Deshpande, B. R. Rao, *J. Org. Chem. 48* (1983) 1552.

[74] A. M. Birch, J. H. Mercer, *J. Chem. Soc. Chem. Commun. 1977*, 745.

[75] R. B. Garland, J. R. Palmer, J. A. Schulz, P. B. Sollman, R. Rappo, *Tetrahedron Lett. 1978*, 3669.

[76] P. C. Bulman-Page, S. V. Ley, *J. Chem. Soc. Perkin Trans. 1 1984*, 1847, and references cited therein.

[77] Y. Tamura, T. Yakura, J. Haruta, Y. Kita, *Tetrahedron Lett. 26* (1985) 3837.

[78] R. C. Gupta, D. A. Jackson, R. J. Stoodley, D. J. Williams, *J. Chem. Soc. Perkin Trans. 1 1985*, 525.

[79] R. C. Gupta, P. A. Harland, R. J. Stoodley, *Tetrahedron 40* (1984) 4657.

[80] P. N. Preston, T. Winwick, J. O. Morley, *J. Chem. Soc. Perkin Trans. 1 1985*, 39.

[81] R. P. Potman, N. J. M. L. Janssen, J. W. Scheeren, R. J. F. Nivard, *J. Org. Chem. 49* (1984) 3628.

[82] a) K. Krohn, K. Tolkiehn, *Chem. Ber. 112* (1979) 3453; b) *113* (1980) 2976.

[83] a) F. Fariña, J. C. Vega, *Tetrahedron Lett. 1972*, 1655; b) cf. review: S. Berger, A. Riecker in S. Patai (Ed.): *The Chemistry of Quinoid Compounds*, Wiley, New York 1974, p. 172.

[84] T. R. Kelly, J. Vaya, L. Ananthasubramanian, *J. Am. Chem. Soc. 102* (1980) 5983.
[85] J. Yadev, P. Corey, C.-T. Hsu, K. Perlman, C. J. Sih, *Tetrahedron Lett. 22* (1981) 811.
[86] A. S. Kende, Y.-G. Tsay, *J. Chem. Soc. Chem. Commun. 1977,* 140.
[87] T. Hiyama, M. Sawahata, Y. Kusano, *Chem. Lett. 1985,* 611.
[88] S. Chew, R. J. Ferrier, *J. Chem. Soc. Chem. Commun. 1984,* 911.
[89] R. J. Ferrier, *J. Chem. Soc. Perkin Trans. 1 1979,* 1455.
[90] a) H. H. Inhoffen, H. Muxfeldt, H. Schaefer, H. Kramer, *Croat. Chem. Acta 29* (1957) 329; b) H. Muxfeldt, *Angew. Chem. 74* (1962) 825; *Angew. Chem. Int. Ed. Engl. 1* (1962) 372.
[91] a) T. R. Kelly, J. W. Gillard, R. N. Goerner, *Tetrahedron Lett. 1976,* 3873; b) T. R. Kelly, N. D. Parekh, E. N. Trachtenberg, *J. Org. Chem. 47* (1982) 5009.
[92] a) R. K. Boeckman, Jr., T. R. Dolak, K. O. Culos, *J. Am. Chem. Soc. 100* (1978) 7098; b) *J. Org. Chem. 44* (1979) 4596.
[93] K. Krohn, *Tetrahedron Lett. 21* (1980) 3557.
[94] P. Brassard, J. Savard, *Tetrahedron Lett. 1979,* 4911.
[95] M. D. Rozeboom, I.-M. Tegmo-Larsson, K. N. Houk, *J. Org. Chem. 46* (1981) 2338.
[96] a) J. P. Gesson, J. C. Jacquesy, M. Mondon, *Tetrahedron Lett. 21* (1980) 3351; b) *Nouv. J. Chim. 7* (1983) 205.
[97] J. G. Bauman, R. B. Barber, R. D. Gless, H. Rapoport, *Tetrahedron Lett. 21* (1980) 4777.
[98] a) M. E. Jung, M. Node, R. W. Pfluger, M. A. Lyster, J. A. Lowe, *J. Org. Chem. 47* (1982) 1150; b) *Tetrahedron 40* (1984) 4751.
[99] J.-P. Gesson, M. Mondon, *J. Chem. Soc. Chem. Commun. 1982,* 421.
[100] A. S. Kende, S. Boettger, *J. Org. Chem. 46* (1980) 2799.
[101] Y. Tamura, M. Sasho, H. Ohe, S. Akai, Y. Kita, *Tetrahedron Lett. 26* (1985) 1549.
[102] a) J. G. Bauman, R. C. Hawley, H. Rapoport, *J. Org. Chem. 49* (1984) 3891; b) *50* (1985) 1569.
[103] R. K. Boeckman, Jr., S. H. Cheon, *J. Am. Chem. Soc. 105* (1983) 4112.
[104] Y. Naruta, M. Kashiwagi, Y. Nishigaichi, H. Uno, K. Maruyama, *Chem. Lett. 1983,* 1687.
[105] G. A. Kraus, B. S. Fulton, *J. Org. Chem. 50* (1985) 1782; b) *Tetrahedron 40* (1984) 4777.
[106] T. Kametani, M. Takeshita, H. Nemoto, F. Fukumoto, *Chem. Pharm. Bull. 26* (1978) 556.
[107] A. Amaro, M. C. Carreno, F. Fariña, *Tetrahedron Lett. 1979,* 3983.
[108] E. Broser, K. Krohn, P. Schiess, unpublished.
[109] M. J. Broadhurst, C. H. Hassall, G. J. Thomas, *Tetrahedron 40* (1984) 4649.
[110] M. E. Jung, J. A. Lowe, *J. Org. Chem. 42* (1977) 2371.
[111] F. Fariña, J. Primo, T. Torres, *Chem. Lett. 1980,* 77.
[112] J. R. Wiseman, J. J. Pendery, C. A. Otto, K. G. Chiong, *J. Org. Chem. 45* (1980) 516.
[113] J. R. Wiseman, N. I. French, R. K. Hallmark, K. G. Chiong, *Tetrahedron Lett. 1978,* 3765.
[114] Y. Tamura, M. Sasho, S. Akai, A. Wada, Y. Kita, *Tetrahedron 40* (1984) 4539, and references cited therein.
[115] Y. Tamura, M. Akai, H. Kishimoto, J.-i. Sekihachi, Y. Kita, *Tetrahedron Lett. 27* (1986) 195.
[116] Oxidation with Cerium (IV) cf. L. Syper, K. Kłoc, J. Młochowski, Z. Szulc, *Synthesis 1979,* 521.
[117] a) W. D. Wulff, P.-C. Tang, *J. Am. Chem. Soc. 106* (1984) 434; b) *Tetrahedron 41* (1985) 5813; c) K. H. Dötz, M. Popall, *ibid. 41* (1985) 5797.
[118] F. Suzuki, S. Trenbeath, R. D. Gleim, C. J. Sih, *J. Org. Chem. 43* (1978) 4159.
[119] a) C. Marschalk, F. Koenig, N. Ouroussoff, *Bull. Soc. Chim. Fr. 3* (1936) 1545; b) C. Marschalk, *ibid. 6* (1939) 655.
[120] a) K. Krohn, C. Hemme, *Liebigs Ann. Chem. 1979,* 19; b) *1979,* 35.
[121] K. Krohn, B. Sarstedt, *Angew. Chem. 95* (1983) 897; *Angew. Chem. Int. Ed. Engl. 22* (1983) 875; *Angew. Chem. Suppl. 1983,* 1267.
[122] G. Arsenault, A. D. Broadbent, P. Hutten-Czapski, *J. Chem. Soc. Chem. Commun. 1983,* 437.
[123] L. A. Mitscher, T.-S. Wu, I. Khanna, *Tetrahedron Lett. 24* (1983) 4809.
[124] a) K. Krohn, F. Miehe, *Liebigs Ann. Chem. 1985,* 1329; b) K. Krohn, W. Baltus, *ibid. 1982,* 1579.
[125] L. M. Harwood, L. C. Hodgkinson, J. K. Sutherland, P. Towers, *Can. J. Chem. 62* (1984) 1922.
[126] C. E. Lewis, *J. Org. Chem. 35* (1979) 2938.
[127] K. Krohn, W. Priyono, *Tetrahedron 40* (1984) 4609.
[128] R. J. Boatman, B. J. Whitlock, H. W. Sutherland, *J. Am. Chem. Soc. 99* (1977) 4822.
[129] B.-T. Gröbel, D. Seebach, *Synthesis 1977,* 357.
[130] a) K. Krohn, B. Behnke, *Liebigs Ann. Chem. 1979,* 2011; b) *Chem. Ber. 113* (1980) 2994.
[131] G. Köbrich, *Angew. Chem. 84* (1972) 557; *Angew. Chem. Int. Ed. Engl. 11* (1972) 473.
[132] K. Krohn, *Liebigs Ann. Chem. 1981,* 2285.
[133] a) D. J. Mincher, G. Shaw, E. De Clercq, *J. Chem. Soc. Perkin Trans. 1 1983,* 613; b) *1984,* 1279; c) S. Qureshi, G. Shaw, *ibid. 1984,* 1279; d) *1985,* 875; e) S. Qureshi, G. Shaw, G. E. Burgess, *ibid. 1985,* 1557.
[134] K. Krohn, U. Müller, unpublished.
[135] K. Krohn, E. Broser, H. Heins, unpublished.
[136] A. E. Ashcroft, D. T. Davies, J. K. Sutherland, *Tetrahedron 40* (1984) 4579.
[137] M. P. Cava, Z. Ahmed, N. Benfaremo, R. A. Murphy, Jr., G. J. O'Malley, *Tetrahedron 40* (1984) 4776.
[138] K. Krohn, W. Baltus, *Synthesis,* in press.
[139] K. Krohn, W. Priyono, *Angew. Chem. 98* (1986) 338; *Angew. Chem. Int. Ed. Engl. 25* (1986) 339.
[140] K. Krohn, W. Priyono, *Liebigs Ann. Chem.*, in press.
[141] J. M. McNamara, Y. Kishi, *Tetrahedron 40* (1984) 4685.
[142] H. Sekizaki, M. Jung, J. M. McNamara, Y. Kishi, *J. Am. Chem. Soc. 104* (1982) 7372.
[143] H. Tanaka, T. Yoshioka, Y. Shimauchi, Y. Matzuzawa, T. Oki, *J. Antibiot. 33* (1980) 1323.
[144] J. M. Essery, T. W. Doyle, *Can. J. Chem. 58* (1980) 1869.
[145] R. K. Boeckman, Jr., F.-W. Sum, *J. Am. Chem. Soc. 104* (1982) 4604.
[146] F. M. Hauser, D. Mal, *J. Am. Chem. Soc. 106* (1984) 1098.
[147] J. P. Gesson, J.-C. Jacquesy, B. Renoux, *Tetrahedron 40* (1984) 4743.
[148] H. Tanaka, T. Yoshioka, Y. Shimauchi, A. Yoshimoto, T. Ishikura, H. Naganawa, T. Takeuchi, H. Umezawa, *Tetrahedron Lett. 25* (1984) 3351.
[149] K. Krohn, *Liebigs Ann. Chem. 1983,* 2151.
[150] K. Krohn, M. Klimars, H. J. Köhle, E. Ebeling, *Tetrahedron 40* (1984) 3677.
[151] E. P. Kündig, C. Perret, *Helv. Chim. Acta 64* (1981) 2606.
[152] a) K. Krohn, E. Broser, *Liebigs Ann. Chem. 1982,* 1907; b) *J. Org. Chem. 49* (1984) 3766.
[153] J. P. Gesson, J.-C. Jacquesy, B. Renoux, *Tetrahedron Lett. 24* (1983) 2761.
[154] A. S. Kende, S. Johnson, *J. Org. Chem. 50* (1985) 727.
[155] E. Broser, K. Krohn, K. Hintzer, V. Schurig, *Tetrahedron Lett. 25* (1984) 2463.
[156] Review of tetracyclines: W. Dürkheimer, *Angew. Chem. 87* (1975) 751; *Angew. Chem. Int. Ed. Engl. 14* (1975) 721.
[157] a) K. Maruyama, H. Uno, Y. Naruta, *Chem. Lett. 1983,* 1767; b) *Tetrahedron 40* (1984) 4725.
[158] F. M. Hauser, D. Mal, *J. Am. Chem. Soc. 106* (1984) 1862.
[159] I. K. Boddy, P. J. Boniface, R. C. Cambie, P. A. Craw, Z.-D. Huang, D. S. Larsen, H. McDonald, P. S. Rutledge, P. D. Woodgate, *Aust. J. Chem. 37* (1984) 1511.
[160] a) K. H. Parker, J. L. Kallmerten, *J. Am. Chem. Soc. 102* (1980) 5881; b) K. A. Parker, E. A. Tallman, *Tetrahedron 40* (1984) 4781.
[161] A. S. Kende, J. Rizzi, J. Riemer, *Tetrahedron Lett. 1979,* 1201.
[162] a) F. M. Hauser, R. P. Ree, *J. Org. Chem. 43* (1978) 178; b) *44* (1979) 2596; c) *45* (1980) 3061.
[163] G. A. Kraus, H. Cho, S. Crowley, B. Roth, A. Sugimoto, S. Prugh, *J. Org. Chem. 48* (1983) 3439.
[164] F. J. Leeper, J. Staunton, *J. Chem. Soc. Perkin Trans. 1 1984,* 1053.
[165] J. H. Dodd, R. S. Garigipati, S. M. Weinreb, *J. Org. Chem. 47* (1982) 4045.
[166] F. M. Hauser, S. Prasanna, *J. Am. Chem. Soc. 103* (1981) 6378.
[167] F. M. Hauser, V. M. Baghdanov, *Tetrahedron 40* (1984) 4719, and references cited therein.
[168] F. Angelucci, F. Arcamone, G. Barchielli, A. Suarato, E. Vanotti, S. Penco, *J. Chem. Soc. Chem. Commun. 1984,* 530.
[169] S. Penco, F. Angelucci, B. Ballabio, G. Barchielli, A. Suarato, E. Vanotti, A. Vigevani, F. Arcamone, *Tetrahedron 40* (1984) 4677.
[170] F. Angelucci, G. Barchielli, G. A. Brussani, M. Gigli, B. Gioia, R. Hermann, A. Suarato, E. Vanotti, S. Penco, *Tetrahedron Lett. 26* (1985) 5693.
[171] B. Behnke, *Dissertation,* Universität Hamburg 1982.
[172] A. S. Kende, J. P. Rizzi, *Tetrahedron Lett. 22* (1981) 1779.
[173] A. S. Kende, J. P. Rizzi, *Tetrahedron 40* (1984) 4693.
[174] E. Vedejs, B. Nader, *J. Org. Chem. 47* (1982) 3193.
[175] M. J. Broadhurst, C. H. Hassall, G. J. Thomas, *J. Chem. Soc. Perkin Trans. 1 1977,* 2502.
[176] E. Vedejs, W. H. Miller, J. R. Pribish, *J. Org. Chem. 48* (1983) 3611.
[177] J. N. Freskos, G. W. Morrow, J. S. Swenton, *J. Org. Chem. 50* (1985) 805.
[178] R. A. Russell, A. S. Krauss, R. N. Warrener, R. W. Irvine, *Tetrahedron Lett. 25* (1984) 1517.
[179] B. A. Keay, R. Rodrigo, *Tetrahedron 40* (1984) 4597.
[180] C.-P. Chen, J. S. Swenton, *J. Org. Chem. 50* (1985) 4569.
[181] R. A. Russell, R. W. Irvine, R. N. Warrener, *Aust. J. Chem. 38* (1985) 189.
[182] T.-T. Li, Y. L. Wu, T. C. Walsgrove, *Tetrahedron 40* (1984) 4701.
[183] J. S. Swenton, D. K. Anderson, D. K. Jackson, L. Narasimhan, *J. Org. Chem. 46* (1981) 4825.
[184] J. S. Swenton, D. K. Anderson, C. E. Coburn, A. P. Haag, *Tetrahedron 40* (1984) 4633, and references cited therein.
[185] K. Krohn, B. Behnke, *Tetrahedron Lett. 23* (1982) 395.
[186] M. Watanabe, H. Maenosono, S. Furukawa, *Chem. Pharm. Bull. 31* (1983) 2662.
[187] I. Forbes, R. A. Pratt, R. A. Raphael, *Tetrahedron Lett. 1978,* 3965.

When submitting manuscripts, authors of articles intended for publication as "Communications" are requested to read the "Notice to Authors" reproduced in the January issue of the journal following the list of contents; upon request, a copy can be obtained from the editorial office.

Model Experiments on the Phytotoxicity of Halogenated Hydrocarbons

By *Gernot Grimmer* and *Werner Schmidt**

The proposals put forward thus far to explain the causes of the recent damage to forests are not totally satisfactory.[1] The forest damage that has occurred, to an increasing extent, during the last ten years in areas having clean air, especially at higher elevations with intense sunlight, has not been reproduced in the laboratory, either by exposure to SO_2 or by treatment with NO_x.[2] There is also considerable evidence that ozone is not a primary cause.[3] Besides microbes and insects, air-borne, anthropogenic photooxidants have been recently suggested as a source of the observed damage done to conifers, which is revealed by premature aging and loss of needles.[4]

Independently, *Frank*[5] and *Schenck*[6] recently suggested that halogenated hydrocarbons, upon exposure to light, might specifically damage the photosynthetic apparatus of conifers. In view of the large amounts of halogenated hydrocarbons produced annually (Table 1), their ubiquity, their persistence, and their good solubility in the cuticle layer of conifers, this hypothesis deserves closer scrutiny. *Frank* and *Frank*[5] were able to show, for example, that, upon treatment of a white pine with gaseous tri- and tetrachloroethylene and simultaneous irradiation with a high-pressure mercury lamp, the needles facing the light source turned yellow. In the extracts of such artificially aged needles, the amount of β-carotene and chlorophyll a had significantly decreased, as was the case for the extracts of "naturally" aged needles (HPLC). On the other hand, new products appeared, which were not found in the extracts of undamaged needles and which were not characterized further. They are possibly degradation products of these pigments. It is still unclear whether sunlight ($\lambda > 285$ nm) is able to activate halogenated hydrocarbons in vivo, since these compounds absorb at very short wavelengths ($\lambda_{max} \leq 230$ nm). We report here model experiments on β-carotene, which plays an important role as $^1O_2$ scavenger in all photosynthetically active organisms.[7]

Irradiation of a 1.6×10^{-5} M, air-saturated solution of β-carotene in cyclohexane with simulated sunlight[8] results in slow photodegradation (half-life $t_{1/2} \approx 540$ s) with loss of the conjugated double bond system (no absorption above 210 nm). This photodegradation is presumably the result of radical allyl oxidation with $^3O_2$ and ene reaction with $^1O_2$; it can be retarded by flushing the cuvettes with argon and degassing the solutions (four freeze-thaw cycles at 2×10^{-6} mbar) but not completely suppressed.[9]

Irradiation in the presence of a 150-fold molar excess of halogenated hydrocarbon, under the same conditions, leads, in the case of alkyl and aryl chlorides, to a significantly faster and, in the case of bromides and iodides, to a dramatically faster bleaching (Table 1). The chloroethylenes, which are important on account of the large amounts produced industrially and their good solubility, fall in the middle. This degradation can be inhibited neither by flushing with argon nor by degassing; even 1,4-diazabicyclo[2.2.2]octane, a good scavenger of $^1O_2$, has no significant effect. If the short-wavelength component of the light ($\lambda \leq 280$ nm) is eliminated by the use of normal glass instead of quartz cuvettes, then the bleaching is retarded ($t_{1/2} \approx 1600$ s) both in the absence and presence of a 150-fold excess of tetrachloroethylene. Moreover, selective irradiation in the long-wavelength absorption band ($\lambda_{max} = 454$ nm) of β-carotene in the absence and presence of tetrachloroethylene has no effect on the stability of the pigment.

Table 1. Half-lives, $t_{1/2}$, of the photodegradation [8] of β-carotene in cyclohexane (1.6×10^{-5} mol/L) in the presence of a 150-fold molar excess of halogenated hydrocarbons as well as the boiling points, long-wavelength absorption maxima in cyclohexane, distribution coefficients for olive oil/air [10], worldwide production [11], and tropospheric life-times, $\tau_{1/2}$ [12].

Halogenated hydrocarbon	$t_{1/2}$ [s]	B.p. [°C]	λ_{max} [nm]	Distrib. coeff.	Production [t/year]	$\tau_{1/2}$ [d]
$Br_3HC-CHBr_2$	3	237	227	—	—	—
$Cl_2C=CCl-CCl=CCl_2$	4	215	251	—	—	—
C_6H_5Br	7	156	271	—	—	22
BrH_2C-CH_2Br	8	132	214	—	—	64
C_6H_5I	9	188	ca. 280	—	—	17
CH_3I	12	42	257	—	—	—
$ClHC=CCl_2$	27	87	211	720	> 1000000	6
$Cl_2C=CCl_2$	30	121	211	1900	> 1000000	8
$H_2C=CCl_2$	40	32	207	—	[b]	—
CCl_4	49	77	ca. 207	360	1000000	—
C_2H_5Br	63	38	211	—	—	422
1,2,4-$C_6H_3Cl_3$	66	214	286	> 100000 [a]	—	32
n-C_3H_7Br	72	71	ca. 208	—	—	—
$Cl_2HC-CHCl_2$	85	147	212	13000	20000	—
H_3C-CCl_3	92	75	211	360	600000	788
C_6H_5Cl	104	132	271	3800	—	24
$CHCl_3$	169	61	ca. 205	400	300000	109
$ClF_2C-CFCl_2$	214	46	< 200	—	—	—
CH_2Cl_2	216	40	ca. 206	150	400000	120
ClH_2C-CH_2Cl	229	83	ca. 207	450	5000000 [b]	73

[a] Extrapolated on the basis of data for monochloro-, *o*-dichloro-, and *m*-dichlorobenzene. [b] Precursors in the production of polyvinyl chloride and its copolymers.

If the concentration of tetrachloroethylene is decreased, then the bleaching is retarded, but even for a molar ratio of tetrachloroethylene to β-carotene of 1 to 66, the bleaching takes place twice as fast as in the absence of tetrachloroethylene. These results are indicative of a radical chain reaction. The photochemical sensitivity of β-carotene toward anthropogenic halogenated hydrocarbons provides possible support for the validity of the Frank-Schenck hy-

[*] Dr. habil. W. Schmidt, Prof. Dr. G. Grimmer
Biochemisches Institut für Umweltcarcinogene
Sieker Landstrasse 19, D-2070 Ahrensburg (FRG)

 © VCH Verlagsgesellschaft mbH, D-6940 Weinheim, 1986 0570-0833/86/0909-0808 $ 02.50/0

pothesis.[5,6] The wavelength dependence of the quantum yields and the structures of the photoproducts remain to be elucidated.

Received: March 19, 1986;
revised: June 19, 1986 [Z 1706 IE]
German version: *Angew. Chem. 98* (1986) 807

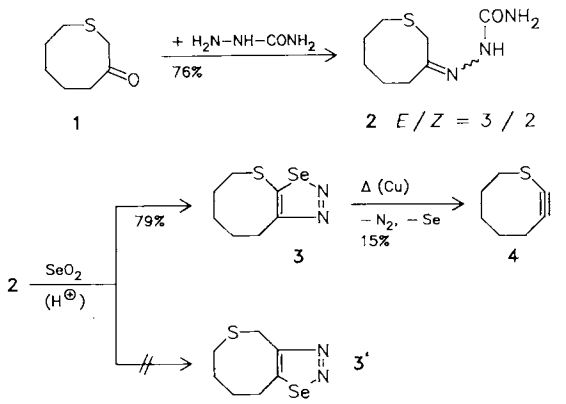
[1] "Classical" damage from industrial smoke has been known since the last century.
[2] N. Overrein, H. M. Seip, A. Tollan: *Acid precipitation—effects on forest and fish*, Fagrapport 19/80, Oslo 1981, p. 9; J. S. Amthor, *Environ. Pollut. 36A* (1984) 1; B. Prinz, G. H. M. Krause, H. Stratmann, *LIS-Report 28, Landesanstalt für Immissionsschutz des Landes Nordrhein-Westfalen, Essen 1982.*
[3] M. Ashmore, N. Bell, J. Rutter, *Ambio 14* (1985) 81.
[4] Seminar at the Kernforschungsanlage Jülich: The effect of atmospheric pollution on forests and forest soils, December 2–4, 1985.
[5] H. Frank, *Nachr. Chem. Tech. Lab. 32* (1984) 298; H. Frank, W. Frank, *Naturwissenschaften 72* (1985) 139; H. Frank, *Eur. Photochem. Assoc. Newsl. 1985*, No. 23/24, p. 7; H. Frank, W. Frank, *Nachr. Chem. Tech. Lab. 34* (1986) 15.
[6] G. O. Schenck, *VDI-Nachr. 39* (1985) No. 13, p. 11; *Eur. Photochem. Assoc. Newsl. 1985*, No. 23/24, p. 15; lecture at the annual meeting of the Fachgruppe Photochemie der GDCh, Siegen, November 20–22, 1985.
[7] M. Calvin, *Nature (London) 176* (1955) 1211; H. Claes, T. O. M. Nakayama, *Z. Naturforsch. B 14* (1959) 746; J. Feierabend, *Z. Naturforsch. C 39* (1984) 450; E. L. Schrott, *Pure Appl. Chem. 57* (1985) 729.
[8] 450-W xenon lamp (Osram, type XBO), filtered through a 60-mm thick layer of water to remove IR radiation, 10-mm quartz cuvette with 2.5-mL volume, distance from the xenon lamp 175 mm. According to the information supplied by the manufacturer, the lamp provides a small amount of UV-A, which is not present in sunlight (Dr. *F. Löchner*, Munich, private communication).
[9] In degassed solutions, an O_2-independent photodegradation pathway may also occur. It is also conceivable that traces of autooxidation products in the oxidation-sensitive β-carotene could lead to photochemically induced degradation via a radical chain reaction.
[10] A. Sato, T. Nakajima, *Arch. Envir. Health 34* (1979) 69.
[11] *IARC Monogr. Eval. Carcinog. Risk Chem. Man 20*, IARC, Lyon 1979; F. R. Atri: *Chlorierte Kohlenwasserstoffe in der Umwelt I*, Gustav-Fischer-Verlag, Stuttgart 1985; G. McConnel, D. M. Ferguson, C. R. Pearson, *Endeavour (dtsch. Ausgabe) 34* (1975) 13.
[12] Calculated from the measured rates of degradation by OH radicals: H. Güsten, L. Klasinc, D. Marić, *J. Atmos. Chem. 2* (1984) 83; H. Güsten, L. Klasinc, *Naturwissenschaften 73* (1986) 129.

1-Thia-2-cyclooctyne—A Strained Cycloalkyne with Polarized Triple Bond**

By *Herbert Meier,* Evaggelia Stavridou,* and *Christiane Storek*

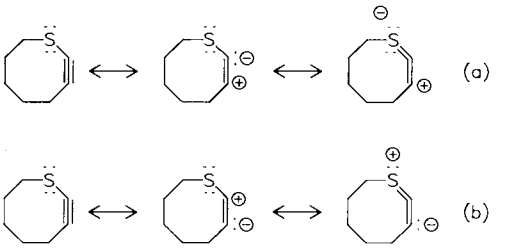
Dedicated to Professor Leopold Horner on the occasion of his 75th birthday

Very few representatives of strained heterocyclic alkynes have so far been reported in the literature.[1–3] We have now been able to synthesize the first molecule of this type, namely 1-thia-2-cyclooctyne **4**, whose triple bond is polarized by the heteroatom immediately adjacent to it. A preparative entry to **4** was accomplished by thermal fragmentation of the heterocycle **3**, which was obtained in good yields from the ketone **1**[4] via the semicarbazone **2**. Although the *E*-isomer dominates, the ring-closure reaction with selenous acid leads regioselectively to the 1,2,3-selenadiazole **3** (Scheme 1).



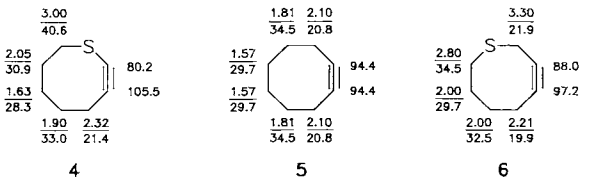
Scheme 1. Synthesis of **4**.

4, an oily liquid with a characteristic odor, is hardly less stable than cyclooctyne **5**. The crucial difference between **4** and **5** lies in the polarity of the triple bond. Aside from the −I effect of the sulfur atom, two mutual mesomeric effects are conceivable (Scheme 2).



Scheme 2. Possible mesomeric influence of the S atom in **4**.

The charge densities on the acetylenic C-atoms, which can be deduced from their ^{13}C-NMR shifts, confirm the above-mentioned mesomerism (a). The effect is strongly reversed in its direction to that in ynol ethers. The δ-values of C-2 and C-3 differ by ca. 25 ppm owing to the anisotropy and the polarization by the sulfur. The ^1H- and ^{13}C-NMR shifts of **4**, **5**, and the much more weakly polarized 1-thia-3-cyclooctyne **6**[5] compared to **4**, are given in Scheme 3.

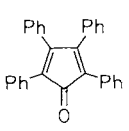


Scheme 3. Comparison of the ^1H- and ^{13}C-NMR shifts of the compounds **4**, **5**, and **6**.

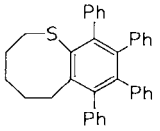
The polarity of the triple bond of **4** must confer remarkable chemical reactivity upon the molecule. Thus, on the one hand **4** undergoes reactions that are very common to other strained cycloalkynes, e.g. cycloaddition with tetracyclone **7** to give **8** (yield ca. 100% (80% for **3**→**8**), m.p. 234°C (decomp.)); on the other hand, however, it slowly adds water, even at room temperature. The regioselectivity

[*] Prof. Dr. H. Meier, Dipl.-Chem. E. Stavridou, Dipl.-Chem. C. Storek
Institut für Organische Chemie der Universität
J. J.-Becher-Weg 18-22, D-6500 Mainz (FRG)

[**] This work was supported by the Deutsche Forschungsgemeinschaft and the Fonds der Chemischen Industrie.

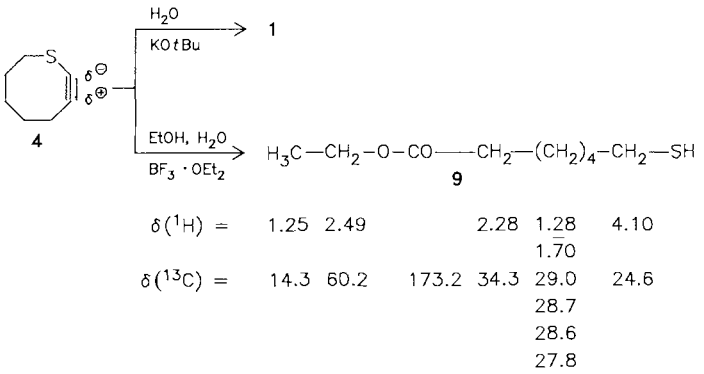


7



8

of the addition depends upon the pH (Scheme 4): In basic media C-3 is attacked nucleophilically, resulting in formation of **1**.[6] The direction of addition can be turned around by acid catalysis. However, the eight-membered ring thiolactone is not isolated, but the product of ring-opening, ethyl 7-mercaptoheptanoate **9**, in 40% yield. **9** reacts further in air to give the disulfide.[7]



Scheme 4. Addition of water to **4**.

The combined action of strain and polarization of the triple bond leads to **4** readily reacting both with electrophiles as well with nucleophiles. Thus, it not only differs significantly from other strained cycloalkynes, but also from open-chain alkynyl sulfanes containing a less reactive triple bond.[9]

Received: April 18, 1986;
supplemented: June 3, 1986 [Z 1737 IE]
German version: *Angew. Chem. 98* (1986) 838

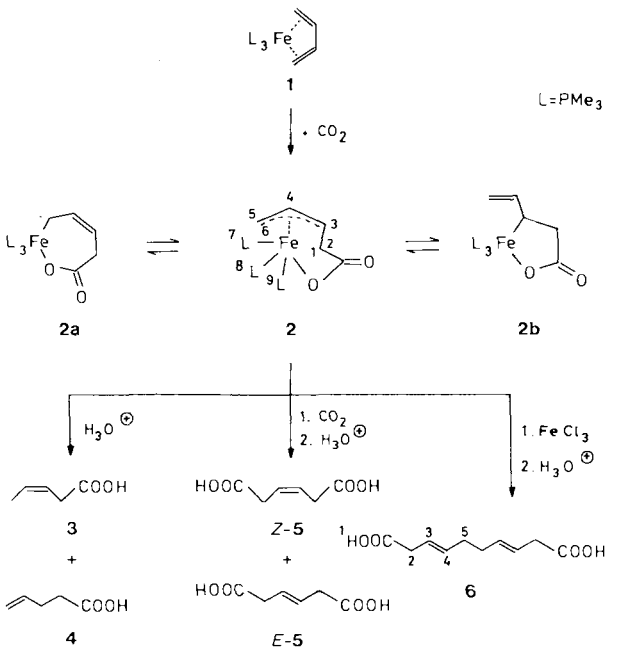
CAS Registry numbers:
1, 33131-80-5; (*E*)-**2**, 103794-89-4; (*Z*)-**2**, 103794-90-7; **3**, 103816-44-0; **4**, 103794-91-8; **7**, 479-33-4; **8**, 103794-92-9; 9, 1931-79-9.

[1] A. Krebs, J. Wilke, *Top. Curr. Chem. 109* (1983) 189, and references cited therein.
[2] M. Sakurai, Y. Nakadaira, A. Hosomi, Y. Eriyama, *J. Am. Chem. Soc. 105* (1983) 3359.
[3] E. Kloster-Jensen, G. A. Eliassen, *Angew. Chem. 97* (1985) 587; *Angew. Chem. Int. Ed. Engl. 24* (1985) 565.
[4] H. Ramane, R. Borsdorf, M. Mühlstädt, *J. Prakt. Chem. 312* (1971) 1058.
[5] Cf. H. Meier, H. Petersen, H. Kolshorn, *Chem. Ber. 113* (1980) 2398.
[6] This behavior is reminiscent of that of the nonisolable 2-cyclooctyn-1-one: P. E. Eaton, C. E. Stubbs, *J. Am. Chem. Soc. 89* (1967) 5722.
[7] If one compares the reactivity of **4** and **5**, then, aside from reactions which are possible only with **4**, and reactions which proceed analogously to **4** and **5**, also reactions with **4** can be expected that lead to quite different products than with **5**. For example, upon twofold reaction with 4-phenyl-1,2,4-triazolindone (molar ratio 1:2), **5** undergoes a twofold ene reaction [8], while **4** undergoes a double cycloaddition.
[8] C.-C. Cheng, F. D. Greene, J. F. Blount, *J. Org. Chem. 49* (1984) 2917.
[9] R. M. Wilson, D. N. Buchanan, *Method. Chim. 7* (1976) 652, and references cited therein.

CC Coupling of CO_2 and Butadiene on Iron(0) Complexes—A Novel Route to α,ω-Dicarboxylic Acids

By *Heinz Hoberg,* Klaus Jenni, Carl Krüger,* and *Eleonore Raabe*

Carbon dioxide is attracting increasing interest as a C_1 building block in preparative chemistry, particularly in synthetic methods involving its activation by transition metal complexes.[1] Stoichiometric (1 : 1) coupling reactions of CO_2 and systems containing multiple bonds have hitherto only been accomplished with Ni^0,[2a] W^0 and Mo^0 complexes.[2b] We have now also been able to induce such a CC coupling with Fe^0 complexes, whereby (η^4-butadiene)tris(trimethylphosphane)iron(0) **1**[3] has proven to be an especially suitable complex for this purpose.



Scheme 1. The (unsystematic) numbering in **2** and **6** serves only for assignment of the ^{1}H-NMR signals.

Treatment of a solution of **1** in tetrahydrofuran (THF) at 35°C with CO_2 (3 bar) leads to formation of the carboxylate complex **2** [diamagnetic, m.p. 110°C (decomp.)] in 75% yield.[4] Like most η^3-allyl-transition metal complexes **2** exhibits a dynamic behavior in solution, which manifests itself in the ^{1}H-NMR spectrum (25°C, [D$_6$]acetone) by very broad signals for the hydrogen atoms in the α-position to the carboxylate group. Whether this merely indicates a reorientation of the η^3-allyl moiety[5] or a dynamic equilibrium **2a** ⇌ **2** ⇌ **2b**, cannot be unequivocally decided from the available data. In contrast, at −80°C the compound is frozen-in in the η^3-allyl structure, and rotation of one of the three PMe_3 ligands is hindered. **2** also has the η^3-allyl

[*] Prof. Dr. H. Hoberg, Dipl.-Chem. K. Jenni, Prof. Dr. C. Krüger, [+] Dr. E. Raabe [+]
Max-Planck-Institut für Kohlenforschung
Kaiser-Wilhelm-Platz 1, D-4330 Mülheim a. d. Ruhr 1 (FRG)
[+] Crystal structure analysis.

structure in the crystalline state, as has been confirmed by an X-ray structure analysis on a single crystal (Fig. 1).[6]

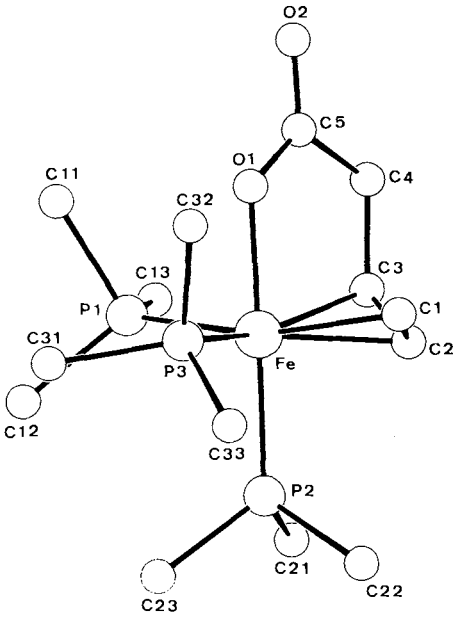


Fig. 1. Structure of **2** in the crystal. Selected bond lengths [Å] and angles [°]: Fe-C1 2.124(2), Fe-C2 2.050(2), Fe-C3 2.152(2); Fe-O1-C5 121.3(1), O1-C5-C4 115.5(2), C5-C4-C3 114.0(2), C4-C3-C2 123.3(2), C3-C2-C1 124.4(2).

The coordination at the Fe-atom can be described as trigonal-pyramidal: the atoms P1 and P3 as well as the center of the allyl group C1-C2-C3 occupy equatorial positions, while the O1 and P2 atoms occupy axial positions. The Fe-C distances in the η^3-bonded allyl unit are as usually found in such units. The carboxylate group is coordinated monodentate to the Fe atom; consequently, the C-O bond lengths are markedly different: 1.274(3) (C5-O1) as compared to 1.235(3) Å (C5-O2). The coordination of the chain at both ends leads to a geometrically enforced disposition, which manifests itself in the magnitude of the bond angles. That the axial bond Fe-P2 with a length of 2.213(1) Å is noticeably shorter than the two equatorial Fe-P bonds (2.249(1) and 2.236(1) Å, respectively) can be explained in terms of a *trans*-effect of the O-atom of the carboxylate group.

The reaction behavior of **2** in solution can only be explained in terms of the η^1-allyl structures **2a** and **2b**: acid hydrolysis in methanol (−30°C) affords the methyl esters of the two carboxylic acids **3** and **4** in the molar ratio 10:1,[7] from which it follows that the reactivity of **2a** is greater than that of **2b**. Consistent with this finding, **2** also reacts with CO_2 (90°C, 5 bar) with preferential insertion in the Fe-C σ-bond of **2a** and not in that of **2b**: after hydrolysis, only 1,4- and no 1,2-dicarboxylic acids were isolated.[8] The *Z*-isomer expected from **2a** is obtained as main product. The *E*-isomer is presumably formed by isomerization of *Z*-**5** (molar ratio *Z*-**5**/*E*-**5** = 27:1).

Completely unexpected was the nature of the product obtained upon reaction of **2** and $FeCl_3$ (molar ratio **2**/$FeCl_3$ = 1:2) in THF: acid hydrolysis of the reaction mixture furnished the symmetrical, linear α-ω-dicarboxylic acid **6** containing two isolated double bonds in 93% yield.[9] The formation of **6** can be explained in terms of an intermolecular CC coupling of the allyl ligands of two molecules of **2**. Once again, only the Fe-C σ-bond of **2a** reacts and not that of **2b**, since the latter reaction would have to lead to branched α-ω-dicarboxylic acids.

Received: April 25, 1986 [Z 1746 IE]
German version: *Angew. Chem. 98* (1986) 819

CAS Registry numbers:
1, 56315-41-4; **2**, 103677-24-5; **2a**, 103693-14-7; **2b**, 103693-15-8; **3** (methyl ester), 36781-66-5; **4** (methyl ester), 818-57-5; (*E*)-**5** (bis(methyl)ester), 25126-93-6; (*Z*)-**5** (bis(methyl)ester), 70354-00-6; **6**, 80557-04-6; CO_2, 124-38-9.

[1] T. Ito, A. Yamamoto in S. Inoue, N. Yamazaki (Eds.): *Organic and Bioorganic Chemistry of Carbon Dioxide*, Kodansha Ltd., Tokyo 1982.

[2] a) H. Hoberg, B. Apotecher, *J. Organomet. Chem. 270* (1984) C 15; H. Hoberg, D. Schaefer, B. W. Oster, *ibid. 266* (1984) 313; H. Hoberg, B. W. Oster, *ibid. 266* (1984) 321, and literature cited therein; D. Walther, E. Dinjus, H. Görls, J. Sieler, O. Lindqvist, L. Andersen, *ibid. 286* (1985) 103, and literature cited therein; b) R. Alvarez, E. Carmona, D. J. Cole-Hamilton, A. Galindo, E. Gutierrez-Puebla, A. Monge, M. L. Poveda, C. Ruiz, *J. Am. Chem. Soc. 107* (1985) 5529.

[3] a) T. V. Harris, J. W. Rathke, E. L. Muetterties, *J. Am. Chem. Soc. 100* (1978) 6966; b) S. S. Wreford, J. F. Whitney, *Inorg. Chem. 20* (1981) 3918.

[4] Procedure for **2**: A solution of **1** (6.75 g, 20 mmol) in THF (100 mL) was transferred to a 200-mL steel autoclave and treated with 1350 mL (60 mmol) of CO_2 at −78°C; the stirred mixture was heated to 35°C and kept at this temperature for 72 h. After cooling and removal of the sediment by filtration (0.45 g, discarded), two-thirds of the solvent was removed from the filtrate by distillation. An orange-red, microcrystalline solid precipitated from the concentrate. This was recovered by suction on a frit and dried. Yield 5.73 g (15 mmol, 75%); m.p. 110°C (decomp.); IR (KBr): ν = 1610 cm^{-1} (C=O); correct elemental analysis; ^{1}H-NMR [$(D_3C)_2CO$, δ = 2.04, −80°C, 400 MHz]: δ = 4.37 (q, 1H; H-4), 3.72 (q, 1H; H-3), 3.05 (t, 1H; H-5), 2.41 (dd, 1H; H-1), 1.65 (d, 1H; H-2), 0.66 (d, 1H; H-6), 1.48 (d, 9H; $(CH_3)_3$-7), 1.43 (d, 9H, $(CH_3)_3$-8), 0.88, 0.75, 0.74 (each d, 3H; $3CH_3$-9).

[5] A. N. Nesmeyanow, Yu. A. Ustynyuk, I. I. Kritskaya, G. A. Shchembelov, *J. Organomet. Chem. 14* (1968) 395.

[6] Crystal structure analysis of **2**: space group $P2_1/n$, Z = 4, ρ_{calc} = 1.28 g cm^{-3}; $\mu(Mo_{K\alpha})$ = 9.94 cm^{-1}; a = 8.661(2), b = 15.248(3), c = 15.223(1) Å; β = 98.069(7)°. Solution of structure by the Patterson method. 4349 independent reflections with $I > 2\sigma(I)$, R = 0.033, R_w = 0.043. Further details of the crystal structure investigation are available on request from the Fachinformationszentrum Energie, Physik, Mathematik GmbH, D-7514 Eggenstein-Leopoldshafen 2, on quoting the depository number CSD-51930, the names of the authors, and the full citation of the journal.

[7] Procedure for **3** and **4**: **2** (1.48 g, 3.88 mmol) was treated at −30°C with 5 mL of 6N methanolic HCl and the resulting solution, after 24 hours' stirring, was neutralized with $NaHCO_3$. The volatile components were then distilled off in a vacuum (2×10^{-4} bar). According to a GC analysis the distillate contained 314.0 mg (2.75 mmol; 70.8%) of the methyl ester of the acid **3** and 31.5 mg (0.28 mmol, 7.2%) of the methyl ester of the acid **4**. The products were unequivocally identified by combined GC-MS and comparison of the NMR spectral data with data given in the literature.

[8] Procedure for **5**: A solution of **2** (1.93 g, 5.05 mmol) in THF (80 mL) was treated at −78°C with 370 mL (15.2 mmol) of CO_2. The solution was transferred to a steel autoclave and stirred for 4 d at 90°C and 5 bar. The insoluble product was recovered by suction on a frit, dried, and worked-up as described for **3**, **4** in Ref. [7]. The quantitative GC analysis afforded the bis(methyl) esters of the acids *Z*-**5** (156.2 mg = 1.37 mmol; 27%) and *E*-**5** (1.37 mg = 0.05 mmol; 1%), which were identified as described in ref. [7] for **3**, **4**.

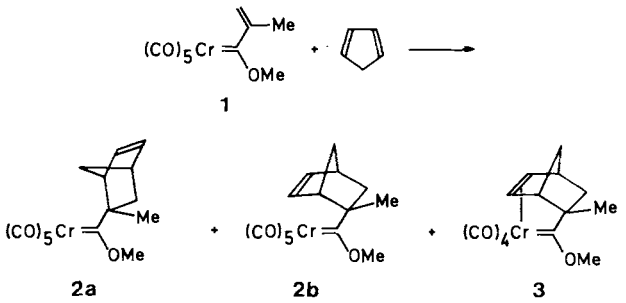
[9] Procedure for **6**: A solution of **2** (1.91 g, 5 mmol) in THF (150 mL) was treated at −78°C with 1.63 g (10 mmol) of $FeCl_3$ and the resulting mixture heated, with continuous stirring, to room temperature. After 24 h, the solvent was removed by distillation and the brown residue (3.36 g) remaining behind was hydrolyzed with ca. 5 mL of 2N H_2SO_4 in the presence of diethyl ether. The organic phase was dried over $MgSO_4$ and then purified by chromatography on silica gel 60 (toluene/diethyl ether 1:1). Yield of **6**: 461.3 mg (2.33 mmol; 93%). M.p. 52°C; correct elemental analysis; IR (KBr): ν = 1710 (C=O), 965 cm^{-1} (*E*-CH=CH); MS (CI, reactant gas NH_3): m/z 216 [$(M+NH_4^{\oplus})$, 100%]; ^{1}H-NMR ($CDCl_3$, 25°C, δ = 7.24, 200 MHz): δ = 8.62 (broad, 2H; H-1), 5.55 (m, 4H; H-3,4), 3.09 (dd, 4H, H-2), 2.12 (s, 4H; H-5).

Diels-Alder Reactions at Carbene Ligands: A Route to Olefin-Carbene Complexes**

By *Karl Heinz Dötz,* Werner Kuhn, Gerhard Müller, Brigitte Huber,* and *Helmut G. Alt*

Carbene complexes containing unsaturated carbene ligands have proved to be versatile synthetic building blocks.[2] In view of the isolobal relationship[3] between a pentacarbonylmetal fragment (M = Cr, Mo, W) and an oxygen atom, alkenyl(alkoxy)carbene complexes may be regarded as analogues of acrylic esters and thus as potential dienophiles in [4+2] cycloadditions.[1,4]

Pentacarbonyl[isopropenyl(methoxy)carbene]chromium **1** reacts with cyclopentadiene at room temperature to give the *endo/exo* cycloadduct **2a,b**. In the process, *the endo* compound **2b** already undergoes partial decarbonylation to form the olefin-carbene complex **3**.



The stereocontrol exerted by the $(CO)_5Cr$ fragment is revealed in the *endo/exo* ratio of (**2b** + **3**)/**2a** = 60/40. A similar ratio is observed for the isolobal methyl methacrylate in $AlCl_3$-catalyzed reactions;[5] however, the uncatalyzed reaction is known to satisfy poorly the Alder *endo* rule[6] and results therefore in a reversal of the product distribution.[7]

The olefin-carbene complex **3** belongs to a class of compounds that is important for the discussion of the mechanism of the olefin metathesis reaction.[8] To date only a few compounds containing other metals have been isolated;[9] **3** is the first example of a chromium compound. Complex **3** is preferentially formed in good yield by heating the mixture of isomers **2a,b** and can be separated from the unchanged *exo* isomer **2a** by column chromatography.

The structure of **3**[10] confirms the alkene coordination of the olefin-carbene ligand to the $Cr(CO)_4$ fragment, which is possible owing to the *endo* position of the carbene carbon atom C1 on the norbornene skeleton (Fig. 1). The alkene function is thereby bonded unsymmetrically to the metal; the Cr-C_{alkene} distances (2.286(3) and 2.366(3) Å[11]) are relatively long.[12] Both findings are a consequence of the rigidity of the norbornene skeleton and the short separation of the chromium-coordinated carbene and alkene functions by only two carbon atoms (C31, C36). The deviation from ideal octahedral symmetry at the central metal atom is due to the chelate structure. The Cr-C1 distance of 2.017(3) Å places **3** in the class of complexes with short Cr-$C_{carbene}$ bonds.[13]

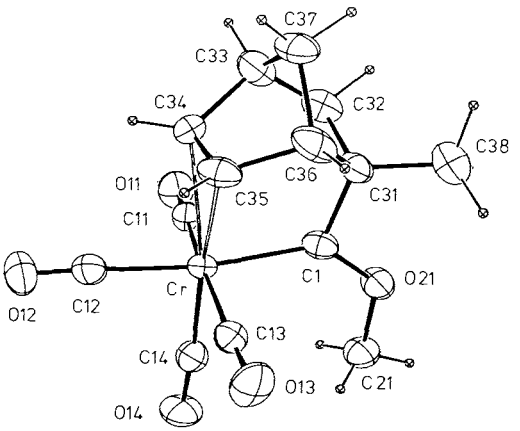


Fig. 1. Molecular structure of **3** in the crystal (ORTEP, thermal ellipsoids with 50% probability, H atoms with arbitrary radius). Selected bond distances [Å] and bond angles [°]: Cr-C1 2.017(3), Cr-C34 2.366(3), Cr-C35 2.286(3), Cr-C11 1.887(3), Cr-C12 1.902(3), Cr-C13 1.896(3), Cr-C14 1.842(3), C1-O21 1.312(4), C1-C31 1.523(4); C34-Cr-C1 86.1(1), C35-Cr-C1 79.2(1), C11-Cr-C1 91.4(1), C12-Cr-C1 168.8(1), C13-Cr-C1 85.4(1), C14-Cr-C1 102.8(1), Cr-C1-C31 118.0(2), Cr-C1-O21 134.0(2), C31-C1-O21 108.0(3).

Experimental Procedure

2a,b: A solution of **1** (0.68 g, 2.46 mmol) [14] in 10 mL of cyclopentadiene was allowed to warm slowly from −60 °C to room temperature. After 4.5 h, the solvent was removed and the residue was chromatographed at −30 °C on silica gel. The faster running orange-yellow band contained the mixture of isomers **2a,b** (0.57 g, 68%); the following fraction afforded **3** (0.13 g, 17%).—**2a,b**: IR (hexane): $\tilde{\nu}$(C=O) = 2061 m, 1983 w, 1960 s (sh), 1953 vs, 1938 s; MS: *m/z* 342 (M^+).—**2a**: ^{1}H-NMR (CD_3COCD_3): δ = 6.21 (m, 2H, =C*H*), 5.03 (s, 3H, OCH_3), 3.50 (m, 1H, C*H*), 2.82 (m, 3H, C*H*, CH_2), 1.42 (m, 2H, CH_2), 1.11 (s, 3H, CH_3); ^{13}C-NMR (CD_3COCD_3): δ = 371.7 ($C_{carbene}$), 224.2 (*trans*-CO), 217.6 (*cis*-CO), 140.9 (=CH), 135.1 (=CH), 73.1 (C_{quart}), 70.0 (OCH$_3$), 51.7 (CH), 50.3 (CH$_2$), 43.2 (CH), 42.4 (CH$_2$), 26.7 (CH$_3$).—**2b**: ^{1}H-NMR (CD_3COCD_3): δ = 6.02 (m, 2H, =C*H*), 4.96 (s, 3H, OCH_3), 2.97 (m, 4H, C*H*, CH_2), 1.44 (m, 2H, CH_2), 1.37 (s, 3H, CH_3); ^{13}C-NMR (CD_3COCD_3): δ = 373.5 ($C_{carbene}$), 224.3 (*trans*-CO), 217.3 (*cis*-CO), 137.2 (=CH), 136.8 (=CH), 74.3 (C_{quart}), 69.3 (OCH$_3$), 53.3 (CH), 47.2 (CH$_2$), 43.9 (CH), 43.2 (CH$_2$), 28.6 (CH$_3$).

3: A stream of N_2 was bubbled for 64 h through a solution of **2a,b** (0.48 g, 1.40 mmol) in 20 mL of *tert*-butyl methyl ether at 55 °C. After removal of the solvent, the residue was chromatographed at −30 °C with hexane on silica gel. Unchanged **2a** (0.22 g) was eluted initially, followed by a fraction that afforded orange-red crystals of **3** (0.21 g, 88%).—IR (hexane): $\tilde{\nu}$(C=O) = 2018 s, 1955 s, 1940 vs, 1905 s; MS: *m/z* 314 (M^+); ^{1}H-NMR (CD_3COCD_3): δ = 6.27 (m, 1H, =C*H*), 5.58 (m, 1H, =C*H*), 4.61 (s, 3H, OCH_3), 2.87 (m, 1H, C*H*), 2.55 (m, 2H, CH_2), 2.17 (m, 1H, C*H*), 1.41 (m, 2H, CH_2), 0.93 (s, 3H, CH_3); ^{13}C-NMR (CD_3COCD_3): δ = 363.6 ($C_{carbene}$), 238.0 and 226.9 (*trans*-CO), 226.2 and 224.4 (*cis*-CO), 102.4 (=CH), 95.2 (=CH), 69.5 (C_{quart}), 69.1 (OCH$_3$), 60.4 (CH$_2$), 53.6 (CH), 48.5 (CH$_2$), 42.2 (CH), 21.6 (CH$_3$).

Received: May 2, 1986 [Z 1755 IE]
German version: *Angew. Chem. 98* (1986) 826

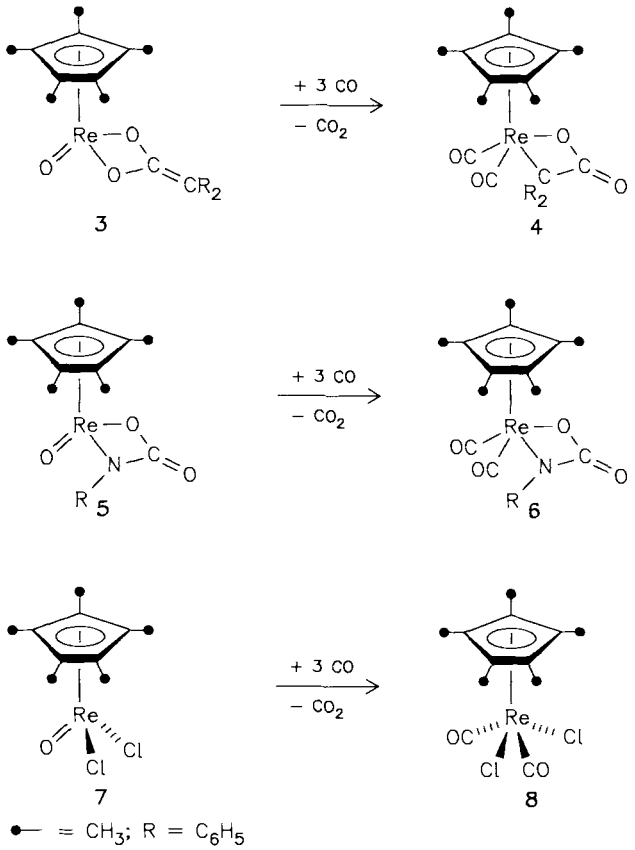
CAS Registry numbers:
1, 87965-61-5; **2a**, 103883-74-5; **2b**, 103958-04-9; **3**, 103904-00-3; cyclopentadiene, 542-92-7.

[*] Priv.-Doz. Dr. K. H. Dötz, Dr. W. Kuhn, Dr. G. Müller, B. Huber
Anorganisch-chemisches Institut der Technischen Universität München
Lichtenbergstrasse 4, D-8046 Garching (FRG)
Priv.-Doz. Dr. H. G. Alt
Laboratorium für Anorganische Chemie der Universität
Universitätsstrasse 30, D-8580 Bayreuth (FRG)

[**] Reactions of Complex Ligands, Part 26. This work was supported by the Deutsche Forschungsgemeinschaft and the Fonds der Chemischen Industrie. Part 25: [1].

[1] K. H. Dötz, W. Kuhn, *J. Organomet. Chem. 286* (1985) C23.
[2] Recent reviews: K. H. Dötz, *Angew. Chem. 96* (1984) 573; *Angew. Chem. Int. Ed. Engl. 23* (1984) 587; H. U. Reissig, *Nachr. Chem. Rech. Lab. 34* (1986) 22.
[3] Cf. F. G. A. Stone, *Angew. Chem. 96* (1984) 85; *Angew. Chem. Int. Ed. Engl. 23* (1984) 89.
[4] W. D. Wulff, D. C. Yang, *J. Am. Chem. Soc. 105* (1983) 6726; *106* (1984) 7565; W. D. Wulff, P.-C. Tang, K.-S. Chan, J. S. McCallum, D. C. Yang, S. R. Gilbertson, *Tetrahedron 41* (1985) 5813.
[5] T. Inukai, T. Kojima, *J. Org. Chem. 31* (1966) 2032.
[6] Review: H. Wollweber: *Diels-Alder-Reaktion*, Thieme, Stuttgart 1972.
[7] J. A. Berson, Z. Hamlet, W. A. Mueller, *J. Am. Chem. Soc. 84* (1962) 297.

[8] Recent review: K. J. Ivin: *Olefin Metathesis*, Academic Press, London 1983.
[9] M. J. McGeary, T. L. Tonker, J. L. Templeton, *Organometallics 4* (1985) 2102, and references cited therein.
[10] **3** is triclinic, space group $P\bar{1}$, $a=6.848(1)$, $b=8.412(1)$, $c=13.353(2)$ Å, $\alpha=92.74(1)$, $\beta=100.14(1)$, $\gamma=111.21(1)°$, $V=700.7$ Å^3, $\rho_{calcd}=1.489$ g cm^{-3} for $Z=2$ at $-40°C$, $F(000)=324$, $\mu(Mo_{K\alpha})=8.1$ cm^{-1}. 2468 independent reflections, 2232 "observed" with $I \geq 2.0\sigma(I)$, Lorentz and empirical absorption correction (ω scan, $\Delta\omega=1.4°$, $+h$, $\pm k$, $\pm l$, $(\sin\vartheta/\lambda)_{max}=0.595$, $Mo_{K\alpha}$, $\lambda=0.71069$ Å). Patterson methods, $R=0.042$, $R_w=0.056$, $w=[\sigma^2(F_0)+0.00013F^2]^{-1}$ for 181 refined parameters (anisotropic, H constant, $\Delta\rho_{fin}=+0.99/-0.28$ e/Å^3, SHELX 76). Further details of the crystal structure investigation may be obtained from the Fachinformationszentrum Energie, Physik, Mathematik GmbH, D-7514 Eggenstein-Leopoldshafen 2 (FRG), on quoting the depository number CSD 51952, the names of the authors, and the journal citation.
[11] Cf. Cr-C 2.168(8) and 2.185(6) Å in (η^2-maleic acid)(η^6-mesitylene)-$Cr(CO)_2$: Yu. T. Struchkov, V. G. Andrianov, V. N. Setkina, N. K. Baranetskaya, V. I. Losilkina, D. N. Kursanov, *J. Organomet. Chem. 182* (1979) 213. Also the Cr-C distances to the conjugated double bonds in η^6-bonded arenes are generally shorter: cf. B. Rees, P. Coppens, *Acta Crystallogr. B29* (1973) 2515.
[12] Only a few examples of monoalkene complexes of chromium have been reported earlier. In most of the examples known that have been characterized structurally, the coordinated double bond is part of a chelate ligand as in **3**; cf. R. Davis, L. A. P. Kane-Maguire in G. Wilkinson, F. G. A. Stone, E. W. Abel (Eds.): *Comprehensive Organometallic Chemistry, Vol. 3*, Pergamon Press, Oxford 1982, p. 953.
[13] U. Schubert in K. H. Dötz, H. Fischer, P. Hofmann, F. R. Kreissl, U. Schubert, K. Weiss: *Transition Metal Carbene Complexes*, Verlag Chemie, Weinheim 1983, p. 73ff; U. Schubert, *Coord. Chem. Rev. 55* (1984) 261.
[14] Synthesized analogously to the procedure in K. H. Dötz, W. Kuhn, K. Ackermann, *Z. Naturforsch. B38* (1983) 1351.



Reductive Carbonylation of High-Valent Oxorhenium Complexes—a New Route to Low-Valent Carbonylrhenium Compounds**

By *Wolfgang A. Herrmann,* Ulrich Küsthardt, Adolf Schäfer,* and *Eberhardt Herdtweck*

The Re^{VII} complex trioxo(η^5-pentamethylcyclopentadienyl)rhenium **1** has proved to be a versatile, key compound in organorhenium chemistry, because its oxo ligands can be both functionalized and exchanged.[1] If complexes having rhenium in intermediate oxidation states are specifically accessible by redox processes, these complexes would be of interest with respect to olefin metathesis, the best catalysts of which are oxidic molybdenum, tungsten, and rhenium species.[2] With this goal in mind, we have investigated the stepwise reduction of **1** in the presence of ligands that are capable of stabilizing both higher and lower oxidation states of the metal.

$[(\eta^5\text{-}C_5Me_5)ReO_3]$ **1** $\quad$ $[(\eta^5\text{-}C_5Me_5)ReO_2]_2$ **2**

Suitable precursors are the metallacycles **3** and **5**, which may be obtained in smooth two-step reactions from **1** and, respectively, diphenylketene and phenyl isocyanate via the binuclear complex **2**.[3,4] The Re^V complex **3** can be reduced under CO (50 bar) at room temperature in tetrahydrofuran (THF), with cleavage of the terminal oxo ligand, to give quantitatively the chiral Re^{III} derivative **4**.

The air- and heat-stable compound **4** (m.p. = 171 °C), like its precursor **3**, contains a four-membered metallacycle (Fig. 1); the 1,1-ethenediolato ligand, which was *O,O*-

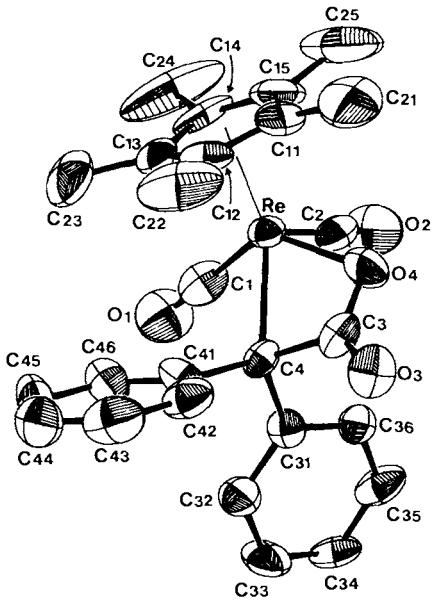


Fig. 1. Molecular structure of **4** in the crystal. Selected bond lengths [pm] and bond angles [°]: Re-C1 187.6(8), Re-C2 193.5(8), Re-C4 229.0(6), Re-O4 207.5(4), O4-C3 129.8(8), C3-C4 152.5(9), C3-O3 119.1(7), Re-C(11···15) 219–244; C4-Re-O4 62.4(2), Re-C4-C3 86.4(4), C4-C3-O4 106.6(6), Re-O4-C3 102.3(4), C1-Re-C4 80.9(3), C2-Re-O4 87.6(3), C1-Re-C2 79.4(3).—Further details of the crystal structure investigation may be obtained from the Fachinformationszentrum Energie, Physik, Mathematik GmbH, D-7514 Eggenstein-Leopoldshafen 2 (FRG), on quoting the depository number CSD-51877, the names of the authors, and the journal citation.

[*] Prof. Dr. W. A. Herrmann, U. Küsthardt, A. Schäfer, Dr. E. Herdtweck
Anorganisch-chemisches Institut der Technischen Universität München
Lichtenbergstrasse 4, D-8046 Garching (FRG)

[**] Multiple Bonds between Main-Group Elements and Transition Metals, Part 29. This work was supported by the Bundesministerium für Forschung und Technologie, the Deutsche Forschungsgemeinschaft, the Fonds der Chemischen Industrie, Hoechst AG, and the Hermann Schlosser-Stiftung der Degussa AG (fellowship for *U. K.*). Part 28: [4].

bonded in **3**, is *C,O*-bonded in **4**.[5] At first sight, the isomerization that occurs upon reductive carbonylation of **3** is surprising, because the sterically demanding phenyl substituents are thereby placed in closer proximity to the metal center and to the terminal ligands; however, it may be understood by taking into consideration the greater electron density on Re^{III}. The metal in **4** is coordinated in a (very distorted) square-pyramidal fashion; the metallacycle (sum of angles 358°) is only slightly bent along the C4···O4 vector (164.6°). Upon reduction of **3** to **4**, the mirror plane is lost.[6]

Under CO pressure, the Re^{V} complex **5** is also reduced. In this case, too, the deoxygenation gives exclusively the Re^{III} derivative **6**, but without isomerization of the *N,O*-imidocarboxylato ligand. The carbonylation of **7** under pressure leads stereoselectively to the *trans* isomer of the compound **8**, which until now was only accessible in admixture with the *cis* isomer.[7]

$$\mathbf{1} + [(\eta^5\text{-}C_5H_5)_2Ti(CO)_2] \longrightarrow$$

9

$$[(\mu\text{-}O)\{(\eta^5\text{-}C_5Me_5)Re(CO)_2\}_2] + [(\eta^5\text{-}C_5Me_5)Re(CO)_3]$$

10 **11**

Besides carbon monoxide, carbonyltitanium reagents are also suitable for the deoxygenating carbonylation of Re^{V} and Re^{VII} complexes of the class of compounds discussed here. Thus, reaction of **1** with **9** affords mainly the Re^{II} derivative **10** (>80%) along with a small amount of **11**.

Received: April 25, 1986;
supplemented: June 4, 1986 [Z 1745 IE]
German version: *Angew. Chem. 98* (1986) 818

[1] Reviews: W. A. Herrmann, *J. Organomet. Chem. 300* (1986) 111; W. A. Herrmann, E. Herdtweck, M. Flöel, J. Kulpe, U. Küsthardt, J. Okuda, *Polyhedron*, in press (1986).

[2] Reviews: N. Calderon, J. P. Lawrence, E. A. Ofstead, *Adv. Organomet. Chem. 17* (1979) 449; R. H. Grubbs, *Prog. Inorg. Chem. 24* (1978) 1; recent mechanistic studies: J. H. Wengrovius, R. R. Schrock, M. R. Churchill, J. R. Missert, W. J. Youngs, *J. Am. Chem. Soc. 102* (1980) 4515; C. J. Schaverien, J. C. Dewan, R. R. Schrock, *ibid. 108* (1986) 2771.

[3] W. A. Herrmann, R. Serrano, U. Küsthardt, M. L. Ziegler, E. Guggolz, T. Zahn, *Angew. Chem. 96* (1984) 498; *Angew. Chem. Int. Ed. Engl. 23* (1984) 515.

[4] U. Küsthardt, W. A. Herrmann, M. L. Ziegler, T. Zahn, B. Nuber, *J. Organomet. Chem.*, in press.

[5] *Experimental procedure:* A solution of 0.5 mmol of **3** or **5** in 20 mL of THF was allowed to stir under carbon monoxide (50 bar) at room temperature in a 100-mL steel autoclave. After removal of the solvent under vacuum, the residue (**4** or **6**) was recrystallized from THF/*n*-hexane (2:1 v/v).—**4**: Yield 98%; orange-red, air-stable crystals, m.p. = 171°C. IR (THF, cm^{-1}, $\tilde{\nu}_{CO}$): 2004 vs, 1926 vs, 1706 s; (KBr, cm^{-1}, $\tilde{\nu}_{CO}$): 1989 vs, 1909 vs, 1686 s. ^{1}H-NMR (270 MHz, $CDCl_3$, 28°C): $\delta CH_3 = 1.71$ (s, 15H), $\delta C_6H_5 = 7.3$-7.85 (m, 10H).—EI-MS (^{187}Re): *m/z* 588 (M^+, 35%), 544 ($M^+ - CO_2$, 25), 532 ($M^+ - 2CO$, 10), 488 ($[C_5Me_5ReCPh_2]^+$, 100).—**6**: Yield ca. 80%; red, air-stable crystals, m.p. = 152°C. IR (THF, cm^{-1}, $\tilde{\nu}_{CO}$): 2016 vs, 1932 vs, 1696 s; (KBr, cm^{-1}, $\tilde{\nu}_{CO}$): 2008 vs, 1924 vs, 1674 s.—^{1}H-NMR (270 MHz, $CDCl_3$, 27°C): $\delta CH_3 = 2.08$ (s, 15H), $\delta C_6H_5 = 6.89$-7.35 (m, 5H).—EI-MS (^{187}Re): *m/z* 513 (M^+, 20%), 469 ($M^+ - CO_2$, 20), 457 ($M^+ - 2CO$, 20), 441 ($[C_5Me_5Re(CO)NPh]^+$, 40), 413 ($[C_5Me_5ReNPh]^+$, 100).

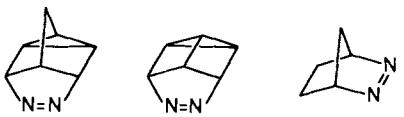
[6] **4**, bright red prisms, 0.21 × 0.11 × 0.14 mm^3; monoclinic, space group $P2_1/c$, $a = 880.0(2)$, $b = 1452.2(4)$, $c = 1808.3(5)$ pm, $\beta = 100.99(2)°$, $V = 2269 \times 10^6$ pm^3, $Z = 4$; $T = 22°C$; $\rho_{calcd} = 1.721$ g·cm^{-1}; $F(000) = 1152$; CAD4 (Enraf-Nonius), graphite monochromator, $\lambda = 0.7107$ Å ($Mo_{K\alpha}$), range of measurement: $1° \leq \theta \leq 20°$; $h(-8/8)$, $k(-13/13)$, $l(-17/17)$; 8364 measured reflections, of which 2154 were unobserved with $I < 1.0\sigma(I)$, 1795 unique reflections with $I > 1.0\sigma(I)$; structure solution with Patterson methods and direct methods; all non-hydrogen atoms were anisotropically refined, H atoms were calculated at ideal positions and included into the calculation of the structure factors. $R = \Sigma(||F_o| - |F_c||)^2 / \Sigma w|F_o|^2 = 0.027$; $R_w = [\Sigma w(|F_o| - |F_c|)^2 / \Sigma w|F_o|^2]^{1/2} = 0.031$.

[7] F. W. B. Einstein, A. H. Klahn-Oliva, D. Sutton, K. G. Tyers, *Organometallics 5* (1986) 53.

UV/VIS Laser Photochemistry: Intermediary Formation of Diazoalkanes versus Direct S_0,T_1 Transitions in the Photolysis of Azoalkanes**

By *Waldemar Adam,* Markus Dörr,* and *Peter Hössel*

Direct S_0,T_1 transitions[1] were reported some time ago to occur on irradiation of the azoalkanes **1**-**3**.[2] Thus, in the



1 **2** **3**

photolysis of **1**, besides traces of toluene and cycloheptatriene, norbornadiene **4** and quadricyclane **5** were observed as main products. The product composition was strongly dependent on the photolysis conditions (Table 1).

Table 1. Product composition obtained in the photolysis of azoalkane **1** to give norbornadiene **4**, quadricyclane **5**, 6-methylenebicyclo[3.1.0]hex-2-ene **6**, and toluene [a, b].



4 **5** **6**

No.	λ [nm]	Solvent	4	5	6	Toluene
1	350 [c]	pentane	53.4 (65)	37.7 (35)	7.8	1.1 (traces)
2	300 [c]	acetone	0.3 (5)	99.7 (95)	0.0	0.0
3	354 [d]	pentane	20.2	78.9	0.0	0.0
4	453 [e]	pentane	53.6 (10)	36.6 (90)	8.5	1.3
5	350 [c]	trifluoro-acetic acid	58.1	41.9	0.0	0.0

[a] The product composition was determined by means of capillary GC. GC conditions: OV 101, 50 m, column, injector, and detector temperatures of 150, 180, and 180°C, respectively, $p(N_2) = 0.5$ bar; products were calibrated against one another and were normalized to 100%. [b] Values in parentheses were taken from ref. [2]. [c] Irradiation in a Rayonet photoreactor; ca. 0.1 M pentane solutions were deaerated with nitrogen for 15 min; conversion ca. 100% for an irradiation time of ca. 30 min. [d] Laser photolysis at ca. 10 bar oxygen pressure; value in parentheses at ca. 100 bar. [e] Laser photolysis; average value of three runs (deviations ca. ±1.6%); conversion ca. 5% for an irradiation time of ca. 5 h.

Direct irradiation (singlet excitation) yielded mainly **4** (No. 1, values in parentheses), whereas acetone sensitization (triplet excitation) led almost exclusively to **5** (No. 2, values in parenthes). In view of the observation that in the direct photolysis with the 453-nm line of an argon ion laser the product composition corresponded to that of the triplet sensitization (No. 4, values in parentheses), the weak shoulder in the absorption spectrum of **1** (Fig. 1b) was assigned to the direct S_0,T_1 transition. However, our results (Tab. 1, Fig. 1) show that instead of the S_0,T_1 transition, the azoalkane **1** suffers photochemical cleavage to give the diazo compound **7**.

[*] Prof. Dr. W. Adam, Dipl.-Chem. M. Dörr, Dipl.-Chem. P. Hössel
Institut für Organische Chemie der Universität
Am Hubland, D-8700 Würzburg (FRG)

[**] This work was supported by the Deutsche Forschungsgemeinschaft and the Fonds der Chemischen Industrie (fellowships for *M. D.* and *P. H.*).

An aged pentane solution (exposed ca. 5 d to daylight) of **1** indeed exhibited a weak absorption at ca. 450 nm (Fig. 1b). However, this absorption completely disappeared, when freshly sublimed **1** (strict exclusion of light) was used (Fig. 1d). On the other hand, it could be augmented when the pentane solution of **1** was briefly (ca. 8 min) irradiated with the 354-nm line of the argon ion laser (Fig. 1a).

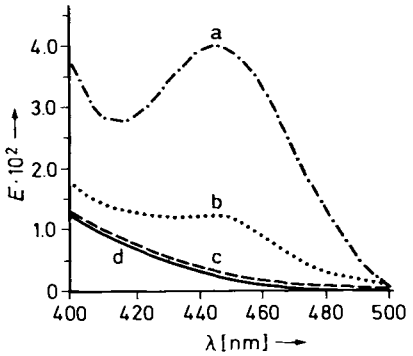
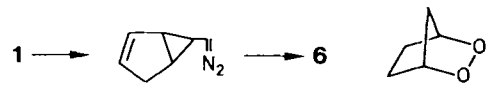


Fig. 1. Absorption spectra of the azoalkane **1** (all solutions ca. 0.1 M). a) **1** in pentane, after laser photolysis at $\lambda = 354$ nm for 8 min; b) **1** in pentane, after exposure to daylight for 5 d; c) **1** in trifluoroacetic acid, after exposure to daylight for 5 d; d) **1** in pentane, after sublimation under strict exclusion of light.

The IR spectrum exhibited a pronounced absorption at 2060 cm^{-1}, which is characteristic of diazo compounds. On addition of trifluoroacetic acid, the absorption at ca. 450 nm (Fig. 1c) disappeared. This absorption must be assigned to the diazo compound **7**, which was formed on direct photolysis of the azoalkane **1**.[3]



7 **8**

The photochemistry of **1** is also in agreement with this interpretation. Besides the already reported photoproducts (**4**, **5**, and toluene), a significant amount (ca. 8%) of 6-methylenebicyclo[3.1.0]hex-2-ene **6** was formed in the direct photolysis of **1** (Table 1, No. 1).[4] Analogous to other diazo compounds,[3] **7** extruded nitrogen under the photolysis conditions, leading to the bicyclic compound **6**, presumably via 1,2-hydrogen migration in the corresponding intermediary carbene.[5] Although an independent synthesis of **7** failed, it could be shown that the accumulated **7** led to increased amounts of **6** on subsequent photolysis (confirmed by capillary GC). Control experiments revealed that addition of trifluoroacetic acid led to formation of toluene via acid-catalyzed rearrangement of **6**. The direct photolysis of **1** in the presence of trifluoroacetic acid (No. 5) afforded only norbornadiene **4** and quadricyclane **5**. Apparently the diazo compound **7** was trapped, so that the formation of **6** and toluene was suppressed. That **7** was indeed produced by singlet excitation was supported by means of a triplet-sensitization experiment (No. 2). Besides traces of **4**, only **5** was produced.

The product composition obtained by laser photolysis at 453 nm (No. 4) proved that the 450-nm absorption must be ascribed to the diazo compound **7**. Within the limits of experimental error, the product composition was identical to that produced by direct photolysis at 350 nm (No. 1). In this context, the laser photolysis at 354 nm under oxygen pressure must be mentioned (No. 3). The product composition was unquestionably shifted toward that produced by triplet-sensitized photolysis (No. 2). Triplet oxygen catalyzes the $S_1 \rightarrow T_1$ spin inversion in the azoalkane **1**.[1]

Similarly, the reported experimental evidence[2] for direct S_0,T_1 transitions in the visible region (400–500 nm) of the azoalkanes **2** and **3** could not be confirmed. The laser photolysis of azoalkane **2** at 453 nm led to a product composition corresponding to that expected for singlet excitation. Mainly $(CH)_6$ products were formed and not 1,2-diazacyclooctatetraene, the product of the triplet sensitization. In the case of azoalkane **3**, the benzophenone-sensitized laser photolysis at 364 nm under oxygen pressure gave exclusively the endoperoxide **8**.[6] However, the laser photolysis of **3** at 453 nm under oxygen pressure (12 bar) did not afford even traces of **8**. Only bicyclo[2.1.0]pentane was detected. The absorption spectrum of an aged sample of **3** in pentane (0.75 M) exhibited a weak band at 410 nm. The long-wavelength spectrum ($\lambda > 400$ nm) of **3** in trifluoroacetic acid or of freshly sublimed **3** in pentane showed only the tail of the main absorption maximum at 349 nm.

On the basis of these results, we conclude that the weak absorption of aliphatic azo compounds in the visible region ($\lambda > 400$ nm) derives from impurities rather than direct S_0,T_1 transitions. In the case of azoalkane **1**, the impurity is the diazo compound **7**, produced via photochemical cycloreversion on n,π*-singlet excitation.[3] Experimental proof for direct S_0,T_1 transitions in azoalkanes is therefore still lacking.[1]

Received: May 6, 1986;
revised: June 27, 1986 [Z 1763 IE]
German version: *Angew. Chem. 98* (1986) 820

CAS Registry numbers:
1, 16104-45-3; **2**, 34122-54-8; **3**, 2721-32-6.

[1] P. S. Engel, *Chem. Rev. 80* (1980) 99.
[2] N. J. Turro, W. R. Cherry, M. J. Mirbach, M. F. Mirbach, V. Ramamurthy, *Mol. Photochem. 9* (1978) 111; N. J. Turro, W. R. Cherry, M. F. Mirbach, M. J. Mirbach, *J. Am. Chem. Soc. 99* (1977) 7388.
[3] W. Adam, W. D. Gillaspey, *Tetrahedron Lett. 24* (1983) 1699; W. Adam, M. Dörr, K. Hill, E.-M. Peters, K. Peters, H. G. von Schnering, *J. Org. Chem. 50* (1985) 587. W. Adam, W. D. Gillaspey, E.-M. Peters, K. Peters, R. J. Rosenthal, H. G. von Schnering, *ibid. 50* (1985) 580.
[4] Synthesis and characterization of all new compounds: W. Adam, M. Dörr, W. G. Gillaspey, A. Höhn, P. Hössel, T. Oppenländer, R. J. Rosenthal, H. Werner, to be submitted for publication.
[5] Rearrangement to the corresponding cyclobutene and fragmentation, as observed in the analogous dihydro derivative (W. Kirmse, K. H. Pook, *Chem. Ber. 98* (1965) 4022) or in cyclopropylidenemethylene itself (P. B. Shevlin, A. P. Wolf, *J. Am. Chem. Soc. 88* (1966) 4735), was not observed for the carbene derived from azoalkane **7**. We rationalize this in terms of the fact that **7** undergoes photochemical denitrogenation, whereas the above-mentioned examples entail thermal decomposition.
[6] W. Adam, K. Hannemann, R. M. Wilson, *J. Am. Chem. Soc. 108* (1986) 929.

Photoisomerization of Dihalomethanes**

By *Günther Maier** and *Hans Peter Reisenauer*

Dedicated to Professor Heinz A. Staab on the occasion of his 60th birthday

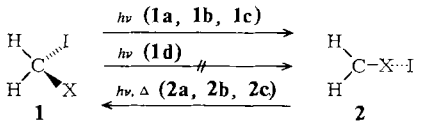
The first—flash photolytic—evidence of triplet[1a,b,d] and singlet methylene[1b,c] is to be found in the pioneering work

[*] Prof. Dr. G. Maier, Dr. H. P. Reisenauer
Institut für Organische Chemie der Universität
Heinrich-Buff-Ring 58, D-6300 Giessen (FRG)

[**] This work was supported by the Deutsche Forschungsgemeinschaft and the Fonds der Chemischen Industrie.

of *Herzberg*. Furthermore, triplet methylene has been isolated in a nobel-gas matrix and characterized by ESR[2] and IR spectroscopy.[3] No information is available, however, on the isolation of singlet methylene. This is not surprising, since the singlet molecule is 9.05 kcal/mol higher in energy than the triplet ground-state molecule.[4b]

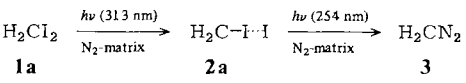
Is the failure to isolate $^1CH_2$ in matrix experiments perhaps due to the wrong choice of the precursor (diazomethane, diazirine)? In order to shed light on this matter, we have irradiated diiodomethane[5] in an argon or nitrogen matrix and observed a surprising result: when **1a** is irradiated in a matrix, a violet color is observed. However, this is only apparently an indication for the splitting off of iodine. We have now found that, upon irradiation, the dihalomethanes **1a**, **1b**, and **1c** undergo isomerization to form compounds of type **2**.



a, X = I; **b**, X = Br; **c**, X = Cl; **d**, X = F

Irradiation[6] of diiodomethane **1a** in argon at 12 K with 313-nm light leads within 1 to 3 min to a photoequilibrium between **1a** and a new species (ratio 70:30). This species exhibits a characteristic IR (see Table 1) and UV spectrum [$\lambda_{max}(\varepsilon)=370$ (≈ 10000), 545 nm (≈ 1300); see Fig. 2]. Upon irradiation with monochromatic light (366 or 545 nm), the matrix rapidly (< 1 min) loses its color, and both IR and UV spectroscopy reveal considerable—if not quantitative—re-formation of **1a**. This indicates that the compound formed upon irradiation of **1a** with light of wavelength 313 nm must be an isomer, which, on the basis of its spectra, can be assigned the structure **2a**.

If the irradiation of **1a** in a nitrogen matrix with wavelengths of 313 or 290 nm is not terminated after photoequilibrium has been attained, or if a low-pressure mercury lamp (254 nm) is used, then the new isomer **2a** reacts further photochemically. According to the IR spectra, diazomethane **3** is the main product (trapping of nitrogen by methylene[7]), along with the iodomethyl radical,[8] ethylene, and acetylene.



The photochemical interconversion **1a** $\rightleftharpoons$ **2a** can also be carried out in a polyethylene film, with the same results. In this way, it is possible to obtain a rough idea of the thermal stability of **2a**. Irradiation of the entrapped diiodomethane **1a** (313 nm, 13 K) leads once again to **2a** (IR: $\tilde{\nu}=3130.9$, 3005.8, 618.8 cm^{-1}; UV: $\lambda_{max}=560$, 385 nm). These absorptions vanish upon warming the film to about 100 K. In the process, partial re-formation of **1a** occurs, as revealed in the spectra.

The phenomena found for **1a** are also found for **1b** and **1c**. However, the isomerization of **1b** and **1c** to form **2b** and **2c**, respectively, upon irradiation of the matrix (313 nm), is slower. The photoequilibrium (ratio similar to **1a** : **2a**) is only attained after 40 min for **1b** and after 3 h for **1c**. The backward reaction can once again be induced by irradiation with light having the same wavelength as one of the UV maxima (see Fig. 2). The tendency to undergo a photochemical secondary reaction decreases in the series **1a**, **1b**, **1c**. In the case of **1b**, the IR bands of diazomethane **3** can be just barely perceived upon prolonged irradiation (5 h, 254 nm) in a nitrogen matrix. In the case of **1c**, trapping of nitrogen can no longer be observed. The thermal stability decreases markedly on going from **2a** to **2c**. The backward reaction **2c** → **1c** occurs already upon warming to 26–30 K. Finally, in accord with expectations based on the above results, fluoroiodomethane **1d**—despite its seemingly favorable absorption maximum at 255 nm ($\varepsilon=300$)—does not even afford traces of the photoisomer **2d** upon irradiation in a matrix at 12 K.

Only the IR spectra can be used to establish the structures of the new isomers. The bands of the educts **1** and the products **2** can be deduced by examining the difference spectra obtained from the irradiated and nonirradiated samples (forward reaction, Fig. 1) and from the

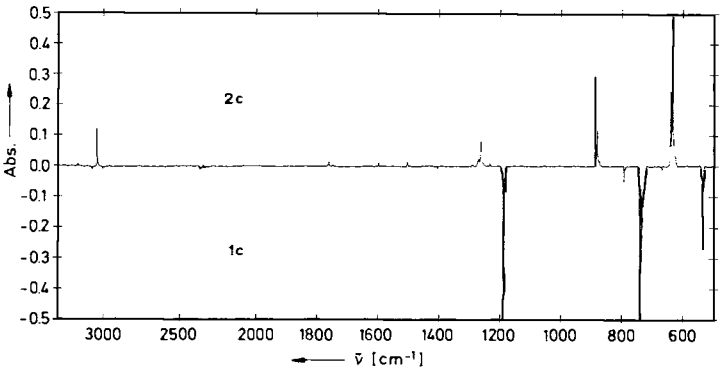


Fig. 1. Difference IR spectra (irradiated minus nonirradiated probe; Ar matrix, 12 K) of **2c** (upper) and **1c** (lower).

short-wavelength (313 nm) and long-wavelength irradiated samples (backward reaction). The spectra so obtained of the isomers **2** (Table 1) have the same appearance. Aside from the fact that the isomers must be more strongly polar than the educts (the bands of **2a–2c** are more intense), the following features are apparent: (1) A symmetric and an antisymmetric CH stretching vibration are observed for all species; these bands exhibit the expected shifts upon deuteration. A CH_2 group must therefore be present. (2) The most intense band is found for **2a**, **2b**, and **2c** at 610–640 cm^{-1}. The splitting is a result of matrix effects (annealing of the matrix changes the intensities within a group of bands). Upon deuteration, a strong shift is once again observed. Accordingly, this band may be assigned to a CH deformation vibration. The high intensity (in comparison with other examples) indicates a wagging vibration. (3) The question whether the methylene group also bears a halogen atom X can be answered by examination of the IR spectrum of **2c**. It shows a relatively intense double band at 886.2 and 879.4 cm^{-1} with the correct intensity ($^{35}Cl:^{37}Cl=3:1$) and frequency ratio, which only undergoes a small shift upon deuteration of the compound. These bands must therefore arise from the CCl stretching vibration.[9] (4) A band that could be assigned to an XI stretching vibration was not observed.

A normal coordinate analysis[10] for the pentaatomic molecule $H_2C{-}X\cdots I$ **2** and the pure cations $^{\oplus}CH_2{-}X$ with plausible geometries (C_{2v}, linear arrangement $C{-}X\cdots I$, shorter CX, longer XI separation), carried out on the basis of Table 1, affords good agreement between calculated

Table 1. IR spectra [Ar matrices, 12 K, [cm^{-1}] (E, rel. int.)] of the isomers **2a**, [D_2]**2a**, **2b**, **2c**, and [D_2]**2c**.

Assignment	**2a**	[D_2]**2a**	**2b**	**2c**	[D_2]**2c**
$\nu_{as}(CH_2,CD_2)$	3151.2 (0.01)	2377.6 (0.03)	3165.2 (0.02)	3168.8 (0.01)	2395.2 (0.03)
$\nu_s(CH_2,CD_2)$	3028.0 (0.03)	2213.0 (0.08)	3040.3 (0.04) [c] 3035.7 (0.08) 3030.9 (0.02)	3042.3 (0.24) [c] 3039.4 (0.13)	2228.2 (0.39) [c] 2226.5 (0.30)
$2\nu(CX)$				1760.5 (0.03) [d] 1747.2 (0.01)	1665.8 (0.04)
$\delta(CH_2,CD_2)$ [a]	1372.8 (0.05)	1040.7 (0.01) [c] 1032.7 (0.04)			1072.5 (0.16)
$\nu(CX) +$ $\omega(CH_2,CD_2)$	1291.3 (0.02)	1130.4 (0.02)		1510.3 (0.01) [c] 1503.5 (0.03)	1329.0 (0.02)
$2\omega(CH_2,CD_2)$	1231.8 (0.01) [c] 1210.6 (0.03)	968.3 (0.05) [c] 952.9 (0.08)	1260.8 (0.05) [c] 1247.3 (0.05)	1268.2 (0.06) [c] 1261.0 (0.17)	987.4 (0.26)
$\nu(CX)$	713.6 (0.04) [c] 704.6 (0.07)	645.3 (0.07)		886.2 (0.56) [d] 879.4 (0.23)	836.5 (0.96) [d] 829.5 (0.38)
$\omega(CH_2,CD_2)$ [b]	627.2 (0.20) [c] 622.7 (0.69) 618.3 (0.65) 616.2 (0.55) 611.1 (1.00) 606.8 (0.13)	498.0 (0.49) [c] 493.7 (0.21) 488.6 (1.00) 485.5 (0.25)	643.9 (0.07) [c] 640.5 (0.18) 638.1 (0.74) 630.6 (1.00) 629.2 (0.26)	639.0 (0.48) [c] 633.5 (1.00)	502.9 (0.48) [c] 498.8 (1.00)

[a] Scissoring-deformation vibration. [b] Out-of-plane (wagging) deformation vibration. [c] Splitting due to matrix effects. [d] Isotopic splitting ($^{35}Cl/^{37}Cl$).

and experimental spectra. Furthermore, a relatively large force constant (4.48 for the pentaatomic model, or 4.66 for the tetraatomic model) is found for the CCl bond in **2c**. This gives a bond order of about 1.2 according to the procedure of *Siebert*.[11] Correspondingly, a value of 1.4 is found for the CI bond in **2a**.

The UV/VIS spectra of **2a–2c** are also similar.[12] Characteristic is the systematic bathochromatic shift of both absorptions. The long-wavelength maxima (possibly charge-transfer transitions of the "iodide ion" to the "carbenium ion") are responsible for the intense color of the isomers **2** and also for the fact that the backward reaction already takes place upon exposure to daylight.

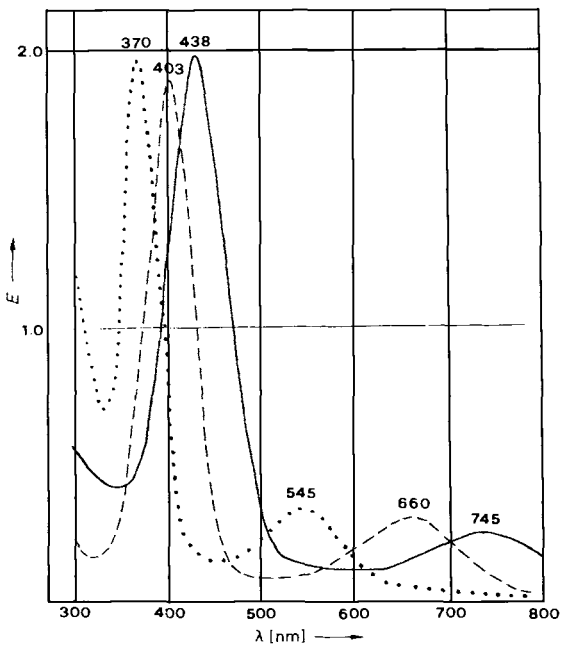
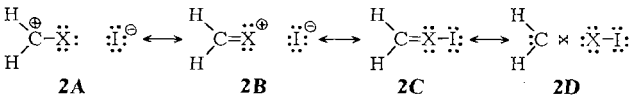


Fig. 2. UV spectra (N_2 matrices, 12 K) of the isomers **2a** [(——), 0.5 min irradiation, violet matrix], **2b** [(– – –), 10 min irradiation, green matrix], and **2c** [(· · · ·), 25 min, yellow matrix].

In summary, the photoexcitation of the dihalomethanes **1a–1c** leads to the isomers **2a–2c** (the weaker Cl bond is preferentially broken), which are best described as the contact ion pairs **2A** ↔ **2B**. Hypervalent resonances structures



such as **2C**[13,14] probably contribute less to the actual structure. It is evident, however, that the iodine must always exhibit, to a certain extent, bonding interactions with the heteroatom X. The resonance structure **2D**, corresponding to a carbene–halogen complex, is presumably even less important. A compound of this kind (having other bond lengths), however, may play a role in the transformation of **2a** into diazomethane **3**.

Received: May 28, 1986 [Z 1794 IE]
German version: *Angew. Chem. 98* (1986) 829

CAS Registry numbers:
1a, 75-11-6; **1b**, 74-95-3; **1c**, 75-09-2; **1d**, 75-10-5; **2A** (I), 103883-81-4; **2A** (Br), 103883-82-5; **2A** (Cl), 103883-83-6; H_2CN_2, 334-88-3; N_2, 7727-37-9.

[1] a) G. Herzberg, J. Shoosmith, *Nature (London) 183* (1959) 1801; b) G. Herzberg, *Proc. R. Soc. London Ser. A 262* (1961) 291; c) G. Herzberg, J. W. C. Johns, *ibid. A 295* (1966) 107; d) G. Herzberg, J. W. C. Johns, *J. Chem. Phys. 54* (1971) 2276.

[2] a) R. A. Bernheim, T. Adl, H. W. Bernard, A. Songco, P. S. Wang, R. Wang, L. S. Wood, P. S. Skell, *J. Chem. Phys. 64* (1976) 2747, and references cited therein; b) E. Wasserman, R. S. Hutton, *Acc. Chem. Res. 10* (1977) 27, and references cited therein; c) B. R. Bicknell, W. R. M. Graham, W. Weltner, *J. Chem. Phys. 64* (1976) 3319.

[3] a) Y.-P. Lee, G. C. Pimentel, *J. Chem. Phys. 75* (1981) 4241; b) C. B. Moore, G. C. Pimentel, *ibid. 41* (1964) 3504.—Under these conditions, $^3CH_2$ should be revealed by a band at 1115 cm^{-1}. According to [4a], the absorption for the bending vibration of $^3CH_2$ occurs at 957 cm^{-1} in the gas phase.

[4] a) T. J. Sears, P. R. Bunker, A. R. W. McKellar, *J. Chem. Phys. 75* (1981) 4731; b) A. R. W. McKellar, P. R. Bunker, T. J. Sears, K. M. Evenson, R. J. Saykally, S. R. Langhoff, *ibid. 79* (1983) 5251.

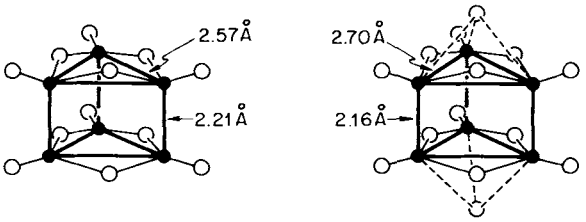
[5] Geminal diiodides as carbene sources: N. J. Pienta, P. J. Kropp, *J. Am. Chem. Soc. 100* (1978) 655; P. J. Kropp, *Acc. Chem. Res. 17* (1984) 131.

[6] Light sources: Osram HBO 200-W high-pressure mercury lamp equipped with Bausch & Lomb monochromator (halfwidth 10 nm); Gräntzel low-pressure mercury lamp (spiral lamp, 150 W). Cooling apparatus: Displex Closed Cycle Refrigeration System 202 (Air Products).
[7] The reaction of $^3CH_2$ with nitrogen upon irradiation of diazomethane **3** in a N_2 matrix was first suggested by *Pimentel* et al. [3b] on the basis of labeling experiments. The formation of **3** from **1a** via **2a** confirms the required type of reaction. This also explains why **3** and diazirine (which is converted into **3** before undergoing elimination of N_2 upon irradiation in a matrix) are very poor precursors for methylene in matrix isolation experiments. Under these conditions, **3** is apparently "photostable" for a long period of time because the N_2 formed is immediately trapped again by CH_2.
[8] D. W. Smith, L. Andrews, *J. Chem. Phys. 58* (1973) 5222.
[9] The position found by us differs considerably from that for the $^{\oplus}CH_2Cl$ cation (1040 cm^{-1}) derived from the PE spectra: L. Andrews, J. M. Dyke, N. Jonathan, N. Keddar, A. Morris, *J. Am. Chem. Soc. 106* (1984) 299.
[10] We thank Dr. *B. P. Winnewisser*, Universität Giessen, for this calculation.
[11] H. Siebert: *Anwendungen der Schwingungsspektroskopie in der Anorganischen Chemie*, Springer, Berlin 1966.
[12] Bands of the kind discussed here were observed previously in photolysis [G. P. Brown, J. P. Simons, *Trans. Faraday Soc. 65* (1969) 3245; H. Mohan, K. N. Rao, R. M. Fyer, *Radiat. Phys. Chem. 23* (1984) 505] and radiolysis of dihalomethanes [L. Andrews, F. T. Prochaska, B. S. Ault, *J. Am. Chem. Soc. 101* (1978) 9], but were assigned to other species.
[13] a) R. Weiss, H. Wolf, U. Schubert, T. Clark, *J. Am. Chem. Soc. 103* (1981) 6142; b) A. E. Reed, F. Weinhold, R. Weiss, J. Macheleid, *J. Phys. Chem. 89* (1985) 2688. c) Salt-like triiodocyclopropenylium iodide: R. Weiss, G.-E. Miess, A. Haller, W. Reinhardt, *Angew. Chem. 98* (1986) 102; *Angew. Chem. Int. Ed. Engl. 25* (1986) 103.
[14] Compare the radical cation of CCl_4: T. Drewello, T. Weiske, H. Schwarz, *Angew. Chem. 97* (1985) 855; *Angew. Chem. Int. Ed. Engl. 24* (1985) 869.

A Novel Electron Count and Metal–Metal Multiple Bonding in Trigonal Prismatic Clusters**

By *Ralph A. Wheeler* and *Roald Hoffmann**

Kryuchkov, Kuzina and *Spitsyn* recently synthesized two trigonal prismatic clusters, $[Tc_6Cl_{12}]^{2\ominus}$ **1** and $[Tc_6Cl_{14}]^{3\ominus}$ **2**, whose structures were determined by *Koz'min, Surazhskaya* and *Larina*. Both clusters have novel electron counts and unusually short metal–metal bonds.[1] **1** has 68 cluster electrons[2] (32 metal electrons), with Tc–Tc distances of 2.21 Å along the prism axis and 2.57 Å along triangular faces. **2** has two weakly μ_3-bound axial capping chloride ligands; if these are removed, $[Tc_6Cl_{12}]^{\ominus}$, with one electron less, is obtained. Relative to **1**, the short Tc–Tc distance in **2** is still shorter, and the longer one, in the triangles, still longer.



$[Tc_6Cl_{12}]^{2\ominus}$ $[Tc_6Cl_{14}]^{3\ominus}$

1 **2**

[*] Prof. Dr. R. Hoffmann, R. A. Wheeler
Department of Chemistry, Cornell University
Ithaca, NY 14853 (USA)

[**] This work was supported by the Cornell University Materials Science Center through grant number DMR 821722 from the National Science Foundation.

These clusters stand at the intersection of two strong currents of modern inorganic chemistry—metal–metal multiple bonding and cluster electron counting rules. The short prism dimensions indicate metal–metal multiple bonding,[3] and the cluster electron count is unique—compare, for example, octahedral $[Mo_6Cl_8]^{4\oplus}([Mo_6Cl_{14}]^{2\ominus}$, 24 cluster bonding electrons), $[Ta_6Cl_{12}]^{2\oplus}([Ta_6Cl_{18}]^{4\ominus}$, 16e), $[Zr_6I_{14}C]$(14e), $[Os_6(CO)_{18}]^{2\ominus}$(14e); and trigonal prismatic $[Rh_6C(CO)_{15}]^{2\ominus}$(18e).[4]

The Tc clusters thus have more electrons involved in metal–metal bonding than any other six-vertex clusters known. A detailed account of the bonding will be given elsewhere.[5] Here we focus on the metal–metal bonding, which is conveniently described by noting in the cluster the three Tc_2 units, each with well-defined σ, π, δ, δ*, π*, and σ* orbitals. Figure 1a shows the filled levels of **1**, labeled to indicate their bonding character within Tc_2 dimers.

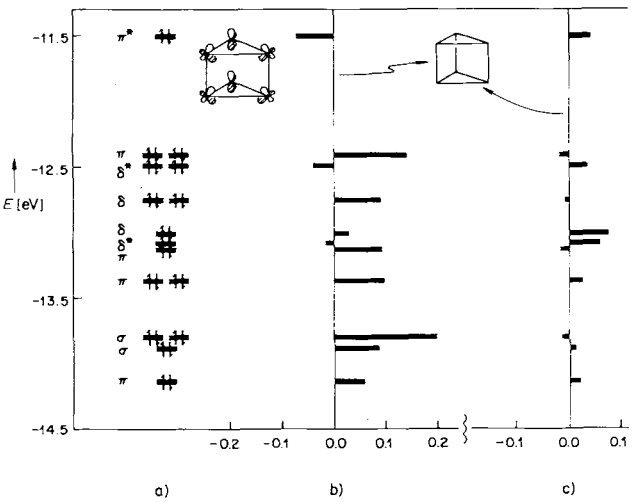


Fig. 1. a) Energy levels of the $[Tc_6Cl_{12}]^{2\ominus}$ cluster **1**. b) Orbital contributions to Tc–Tc overlap population within Tc–Tc dimers and (c) between them.

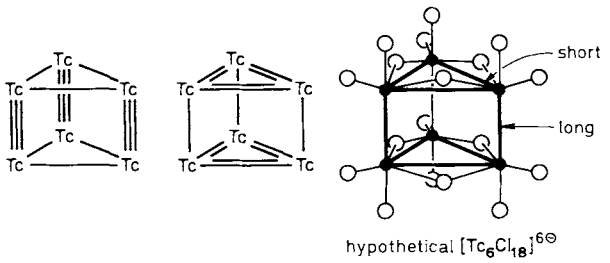
The lower 15 levels are three sets of σ, π_{xz}, π_{yz}, δ, and δ* orbitals. The HOMO of **1** (schematically drawn at the top of Figure 1a) has π* character within the Tc_2 units and π-bonding character between them. This description is consistent with electron-rich triple bonding ($\sigma^2\pi^4\delta^2\delta^{*2}$) within each Tc_2 unit, with two additional electrons in a π* orbital. Bonding between Tc_2 units is primarily through the HOMO of the cluster (π bonding between dimers) and localized δ and δ* orbitals (σ bonding between Tc_2 units).

The details of the bonding are neatly explored through examination of Figures 1b and 1c. The horizontal bars represent the contributions to the Tc–Tc overlap population of the corresponding levels in Figure 1a. Bonding within dimers (Fig. 1b) is much stronger than bonding between them (Fig. 1c). More levels are bonding in Figure 1b than in Figure 1c and their contributions to the overlap population are larger.

The observed bond-length changes on going from **1** to **2** (one-electron oxidation) are consistent with the composition of the HOMO. Figures 1b and 1c also show that the HOMO of $[Tc_6Cl_{12}]^{2\ominus}$ is net Tc–Tc antibonding, since its π* nature within Tc_2 units wins out over its bonding character between them.

In reply to the question, how many metal–metal bonding electrons are there in this cluster?, we would answer 30. As the syntheses of **1** and **2** show (and the calculations sup-

port), 32 and 31 electrons, respectively, are also satisfactory. We expect that 30-electron compounds in this system will also be synthesized.



3 **4** **5**

The 30 bonding electrons are in orbitals consistent with the localized description **3**. But since we know structures of the $[Re_3Cl_{12}]^{3\ominus}$ type,[3] an alternative trigonal prismatic valence structure of type **4** is possible, which is realizable perhaps as $[Tc_6Cl_{18}]^{6\ominus}$ **5**.

The interconversion of **3** and **4** is strongly (symmetry) forbidden. Will we ever see isomeric structures such as these?

Received: May 21, 1986;
supplemented: July 1, 1986 [Z 1786 IE]
German version: *Angew. Chem. 98* (1986) 828

CAS Registry numbers:
1, 101178-51-2; **2**, 103752-27-8.

[1] a) S. V. Kryuchov, A. F. Kuzina, V. I. Spitsyn, *Dokl. Adad. Nauk SSSR 266* (1982) 127; b) for relevant crystallographic details, see P. A. Koz'min, M. D. Surazhskaya, T. B. Larina, *Koord. Khim. 11* (1985) 1559. *Dokl. Akad. Nauk SSSR 271* (1983) 1157.

[2] We count edge-bridging chloride ligands as 4-electron donors and terminal ligands as 2-electron donors.

[3] F. A. Cotton, R. A. Walton: *Multiple Bonds Between Metal Atoms*, Wiley-Interscience, New York 1982.

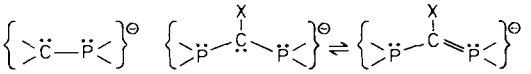
[4] D. M. P. Mingos, *Chem. Soc. Rev. 15* (1986) 31, and references cited therein; R. L. Johnston, D. M. P. Mingos, *Inorg. Chem. 25* (1986) 1661.

[5] R. A. Wheeler, R. Hoffmann, *J. Am. Chem. Soc.*, in press. Parameters for the extended Hückel calculations: Tc: $H_{ii}(5s) = -10.07$ eV, $H_{ii}(5p) = -5.40$, $H_{ii}(4d) = -12.82$ eV; Slater exponents $\zeta(5s) = 2.018$, $\zeta(5p) = 1.984$, $\zeta_1(4d) = 4.90$, $\zeta_2(4d) = 2.094$ with coefficients $C_1 = 0.5715$, $C_2 = 0.6012$. Cl: $H_{ii}(3s) = -30.0$, $H_{ii}(3p) = -15.0$ eV; Slater exponents $\zeta(3s) = \zeta(3p) = 2.033$. Geometrical parameters were taken from the crystal structure of **1** [1].

$[La\{(Ph_2P)_2CH\}_3]$— a Homoleptic Lanthanum Complex with π-Allyl-like Coordinated Diphosphinomethanide Ligands**

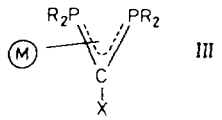
By *Hans H. Karsch,* Armin Appelt,* and *Gerhard Müller**

Investigations of the chemistry of carbon and of σ-bonded phosphorus have revealed an increasing number of parallels in unsaturated systems.[1] Also, for saturated systems, such parallels have been shown to be a valuable guide for structural comparison of molecules containing C–C and P–P bonds.[2] The reactivities of the two elements in molecules containing P–C bonds are expected to be similar when the two elements are isoelectronic, as, for example, in phosphinomethanides **I**. Indeed, in recent years a large number of ambident phosphinomethanides have been found in which carbon and phosphorus compete for electrophiles. Fine tuning of such systems may be effectively achieved by variation of the electrophile as well as of the number and kind of substituents on the carbanion.[3,4]



I **II**

With metals as electrophiles, coordination can occur in a variety of ways, including intermolecular interactions with formation of multinuclear complexes.[3,4] For di- and triphosphinomethanides **II** (X = H, $SiMe_3$, PMe_2), in particular, numerous coordination modes may be envisaged.[3,4] Already in the initial investigations,[5] the main question was whether diphosphinomethanides **II** (X = H) form π-type complexes **III** with fragments Ⓜ and thereby function as heteroallyl analogues. However, this type of coordination has not yet been unambiguously established. In comparing **II** with allyl ligands, it is important to realize that **II** (X = H) is a potential six-electron rather than a four-electron donor. A coordination of type **III** is opposed by the usually strong tendency of diphosphinomethanides to form M–P σ bonds in mononuclear complexes by coordinating both phosphorus atoms. Since lanthanoids and actinoids rarely form phosphane complexes,[6] a coordination of type **III** should be favored with these metals.



III

Indeed, by reaction of the potassium salt **1**[7] with $LaCl_3$, we have been able to prepare the lanthanum complex **2**[8] and to isolate it in pure form. Complex **2** is the first complex with π allyl-like η^3-coordinated diphosphinomethanide ligands.

$$LaCl_3 + 3\,K[(PPh_2)_2CH] \xrightarrow{THF} [La\{(PPh_2)_2CH\}_3]$$

1 **2**

The X-ray structure analysis of **2** · toluene[9] (Fig. 1) reveals that the La atom is trigonally planar coordinated by the diphosphinomethanide ligands. The midpoints of the PCP planes and the La atom lie in a plane (sum of angles at La: 360°, Fig. 1b). The distances between the central La atom and the coordinating atoms vary between 2.790(4) and 3.035(1) Å, the bonds to the C atoms being slightly *shorter* than those to the P atoms.[10] As a consequence of these nearly identical distances, the lines connecting the midpoints of the ligands with the La atom are not exactly perpendicular to the respective PCP planes, but form angles with their normals of 16.9, 6.5, and 17.0°. Of the possible conformations, which differ in the relative orientation of the ligands, **2** · toluene has that in which the ligands are arranged spokelike around the central atom.

The orientations of the phenyl substituents indicate that the lone pairs of electrons on the phosphorus atoms do not point optimally in the direction of the La atom. As is evident from Figure 1b, however, further rotation about the HC–P bonds, which would be required for a better posi-

[*] Priv.-Doz. Dr. H. H. Karsch, Dr. A. Appelt, Dr. G. Müller
Anorganisch-chemisches Institut der Technischen Universität München
Lichtenbergstrasse 4, D-8046 Garching (FRG)

[**] Complexes with Phosphinomethane and Phosphinomethanide Ligands, Part 10. – Part 9: H. H. Karsch, B. Milewski-Mahrla, J. O. Besenhard, P. K. Stauffert, P. Hofmann, T. A. Albright, *Inorg. Chem.*, in press.

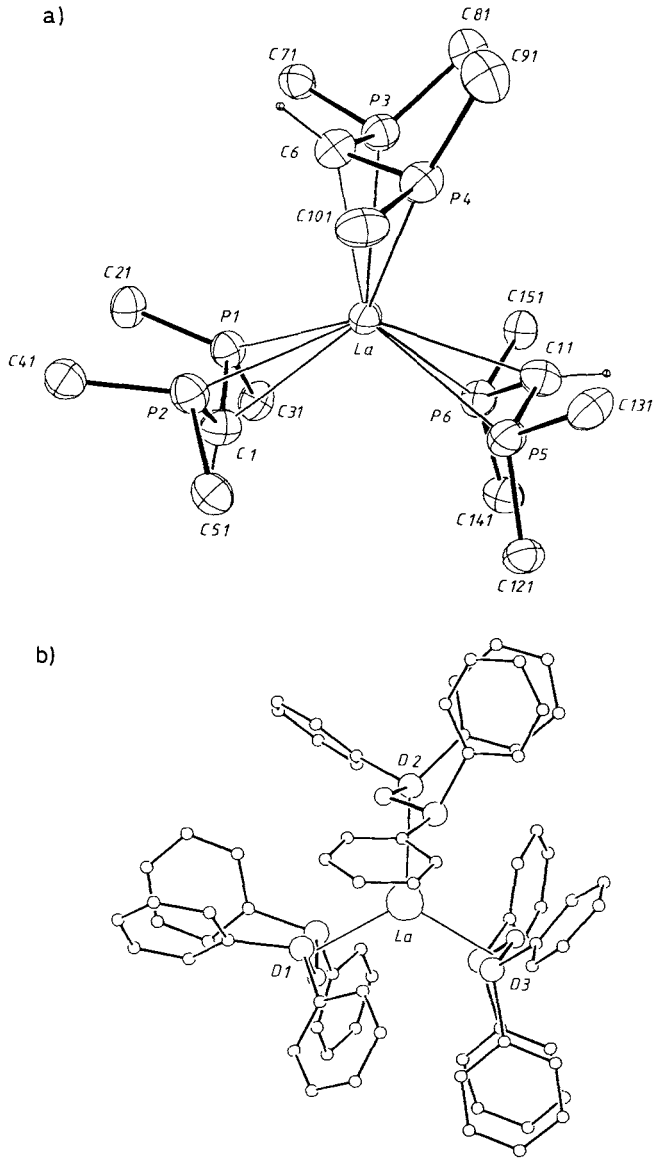
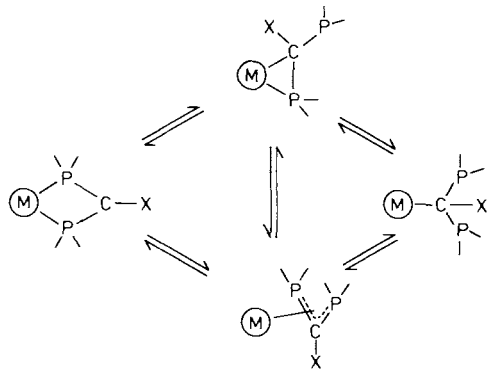


Fig. 1. a) Molecular structure of **2** (ORTEP), thermal ellipsoids at the 50% probability level, H atoms with arbitrary radii, only the *ipso*-C atoms of the phenyl rings are shown. Selected bond lengths [Å] and angles [°]: La-P1 2.955(1), La-P2 2.999(1), La-P3 2.965(1), La-P4 3.035(1), La-P5 2.940(1), La-P6 3.013(1), La-C1 2.890(5), La-C6 2.790(4), La-C11 2.908(5), C1-P1 1.771(5), C1-P2 1.768(5), C6-P3 1.778(5), C6-P4 1.764(5), C11-P5 1.769(5), C11-P6 1.780(5); P1-C1-P2 115.9(3), P3-C6-P4 111.2(3), P5-C11-P6 113.9(3). b) Conformation of the phenyl rings in **2** (ORTEP, atoms with arbitrary radii). D1, D2, and D3 are the midpoints of the PCP planes. The phenyl rings differ in their relative orientations with respect to the PCP planes ("axial", "equatorial"), the equatorial *ipso*-C atoms being 0.02–0.39 Å and the axial atoms 1.42–1.71 Å away from these planes. The respective C-P-C(phenyl) and La-P-C(phenyl) angles are significantly different. The La-arene distances are longer than 3.85 Å.

tioning of the electron pairs, would result in an increasingly close approach of the "axial" phenyl substituents.

The structure of **2** is in agreement with a more ionic character of the bonding, as is the case for organolanthanoid and -actinoid complexes.[11] The ^{31}P-NMR spectrum in benzene provides further support of this interpretation: the chemical shifts of the P atoms of the diphosphinomethanide in **1**[7] and **2** are nearly identical.

The coordination mode **III** found in **2** fills a gap in the coordination behavior of di- and triphosphinomethanides, which is important for a better understanding of the frequently observed fluxional behavior of these ligands in complexes with main-group and transition metals[3b,c,4a,b] (see Scheme 1).



Scheme 1.

Received: June 2, 1986;
revised: June 30, 1986 [Z 1799 IE]
German version: *Angew. Chem. 98* (1986) 832

CAS Registry numbers:
1, 103835-32-2; **2**, 103850-99-3; **2**·$C_6H_5CH_3$, 103851-00-9; $LaCl_3$, 10099-58-8.

[1] See H. H. Karsch, H.-U. Reisacher, B. Huber, G. Müller, W. Malisch, K. Jörg, *Angew. Chem. 98* (1986) 468; *Angew. Chem. Int. Ed. Engl. 25* (1986) 455.

[2] M. Baudler, *Angew. Chem. 94* (1982) 520; *Angew. Chem. Int. Ed. Engl. 21* (1982) 492.

[3] Compounds with electrophilic main-group elements: a) H. H. Karsch, L. Weber, D. Wewers, R. Boese, G. Müller, *Z. Naturforsch. B39* (1984) 1518, and references cited therein; b) H. H. Karsch, A. Appelt, G. Müller, *Organometallics*, in press, and references cited therein; c) H. H. Karsch, A. Appelt, J. Riede, G. Müller, *ibid.*, in press, and references cited therein.

[4] Compounds with electrophilic transition-metal centers: a) H. H. Karsch, *Chem. Ber. 117* (1984) 783, and references cited therein; b) H. H. Karsch, G. Müller, C. Krüger, *J. Organomet. Chem. 273* (1984) 195, and references cited therein.

[5] a) K. Issleib, H. P. Abicht, *J. Prakt. Chem. 312* (1970) 456; b) K. Issleib, H. P. Abicht, H. Winkelmann, *Z. Anorg. Allg. Chem. 388* (1972) 89.

[6] Only a few examples of phosphanelanthanoid complexes are known: a) H. Schumann, *Angew. Chem. 96* (1984) 475; *Angew. Chem. Int. Ed. Engl. 23* (1984) 474, and references cited therein; b) M. N. Bochkarev, G. S. Kalinina, L. N. Bochkarev, *Russ. Chem. Rev. Engl. Transl. 54* (1985) 802, and references cited therein.

[7] H. H. Karsch, A. Appelt, unpublished; ^{31}P-NMR (C_6D_6/THF): $\delta = -2.85$ (s).

[8] *Experimental procedure:* **1** (1.56 g, 3.70 mmol) in 40 mL of tetrahydrofuran (THF) was added to 303 mg (1.23 mmol) of $LaCl_3$. The suspension was stirred for 3 d at 25°C. The solution was then filtered and the solvent removed in vacuum. The residue was dissolved in 30 mL of toluene and the resulting solution was filtered once again. Upon slow concentration of the solution, yellow crystals formed. Together with the yellow solid isolated from the mother liquor, 1.36 g (86%) **2** was obtained; decomp. >150°C; ^{31}P-NMR (C_6D_6): $\delta = 0.84$ (s).

[9] Crystal structure data of **2**·$C_6H_5CH_3$: triclinic, space group $P\bar{1}$, $a = 12.368(2)$, $b = 13.749(1)$, $c = 21.748(2)$ Å, $\alpha = 89.26(1)$, $\beta = 95.24(1)$, $\gamma = 109.08(1)°$; $V = 3479.9$ Å^3; $\rho_{calcd} = 1.318$ g/cm^3 for $Z = 2$ at 22°C, $F(000) = 1420$, $\mu(Mo_{K\alpha}) = 7.9$ cm^{-1}; 10871 unique reflections, of which 8071 were observed with $I \geq 2.0\sigma(I)$, Lp, but no absorption correction [$(\theta - 2\theta)$ scan, $\Delta\omega = 0.9 + 0.35\tan\theta$, $(\sin\theta/\lambda)_{max} = 0.571$, $\pm$h, $\pm$k, +l, $Mo_{K\alpha}$, $\lambda = 0.71069$ Å, graphite monochromator, Enraf-Nonius CAD4]. Solution by Patterson methods (SHELXS-86), refinement by block-diagonal least-squares, $R = 0.035$, $R_w = 0.046$, $w = 1/\sigma^2(F_0)$ (anisotropic, H constant, 802 refined parameters, GBDL). $\Delta\rho_{max} = 0.52$ e/Å^3. Further details of the crystal structure investigation may be obtained from the Fachinformationszentrum Energie, Physik, Mathematik GmbH, D-7514 Eggenstein-Leopoldshafen 2 (FRG), on quoting the depository number CSD-51950, the names of the authors, and the journal citation.

[10] The positions of the (localized) methanide H atoms (Fig. 1a) indicate a pyramidal environment of the carbanionoid centers. Because no refinement was carried out for the H atoms, their positions are not very precise. Noteworthy, however, is the fact that all three H atoms point away from the La atom.

[11] K. N. Raymond, C. W. Eigenbrot, Jr., *Acc. Chem. Res. 13* (1980) 276.

 © VCH Verlagsgesellschaft mbH, D-6940 Weinheim, 1986 0570-0833/86/0909-0824 $ 02.50/0

$[Sb_3I_{10}^{\ominus}]_\infty$ — A Polymeric Anion with Transitions from Trigonal Pyramidal to Octahedral Coordination of Antimony(III)**

By *Siegfried Pohl,* Wolfgang Saak, Peter Mayer,* and *Alfred Schmidpeter**

The neutral and anionic halogen compounds of trivalent P, As and Sb include examples of three-, four-, five-, and sixfold coordination of the central atom, with the influence of the lone pair of electrons on the stereochemistry decreasing with increasing coordination number. The transitions between these coordination geometries are each characterized by a short bond and a long bond *trans* to each other.[1] In the anion $Sb_3I_{10}^{\ominus}$ these transitions can be observed within one and the same structure, since three forms of coordination of Sb[1] are present.

When a solution of tris(dimethylamino)cyclopropenylium iodide[2] and antimony triiodide (molar ratio 1:3) in acetonitrile was slowly evaporated to dryness, the complex $[C_3(NMe_2)_3]^{\oplus}Sb_3I_{10}^{\ominus}$ **1** crystallized (red prismatic crystals).[3] The compound was characterized by an X-ray structure analysis.[4] It contains a stoichiometrically and structurally novel anion.

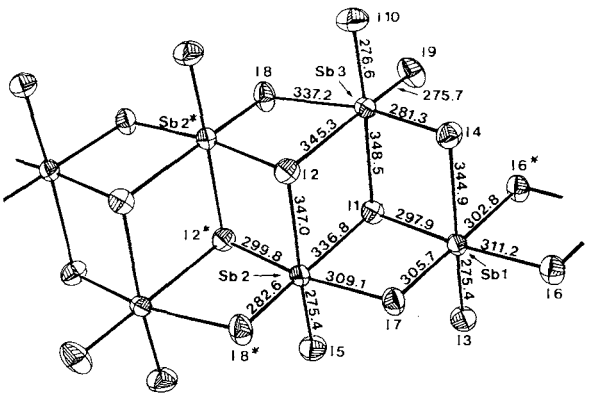


Fig. 1. Section from the structure of the polymeric anion $Sb_3I_{10}^{\ominus}$ in crystals of **1** (bond lengths in pm, vibration ellipsoids correspond to 50% probability).

The 18 independent Sb–I contacts (Fig. 1) lie in three clearly defined ranges: 275–282 (I), 298–311 (II) and 337–349 pm (III). If they are all considered as bond forming, then a distorted octahedral coordination results for all Sb atoms. The octahedra are linked edge-to-edge to give a polyanion whose structure can be regarded as a band-shaped section of the CdI_2 structure. However, adjacent bands are not bound together to form a layer structure analogous to CdI_2. The anionic bands and the planar cations are stacked alternately along the *b* axis.

The structure of the polymeric anion can plausibly develop if one consideres I6 (Fig. 1) as the original iodide, which now binds two SbI_3 molecules, and these in turn

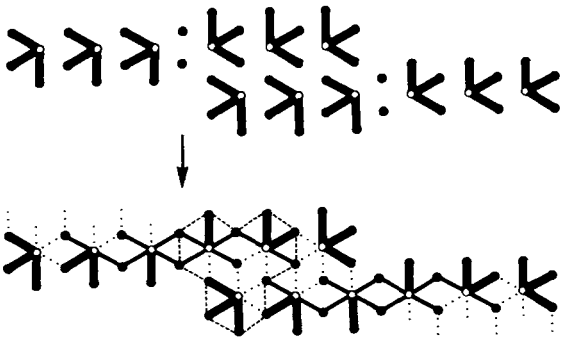


Fig. 2. Formation of four formula units of $Sb_3I_{10}^{\ominus}$ from I[⊖] and SbI_3; the distances in the ranges I, II and III are shown as thick lines, thin lines, and dotted lines, respectively (see text); the section corresponding to the 18 distances in Figure 1 is shown.

bind further SbI_3 molecules with decreasing strength (Fig. 2). If the bonding interactions are limited to Sb–I contacts in the ranges I and II, the reactivity of the lone pair will become manifest for each Sb atom: Sb1 is coordinated ψ-octahedrally, Sb2 almost ψ-trigonal pyramidally, and Sb3 ψ-tetrahedrally.

The larger the one of two *trans* contacts is, the smaller is the other (Fig. 1). This has indeed already been observed in the case of SbI_3[5] and the tetrameric tellurium(IV) halides[6] (further examples are given in refs. [1] and [7]), but the differences in these contacts in **1** vary remarkably, the consequence (or cause) of which is a divergence in the magnitude of the stereochemical effect of the non-bonding electron pairs at the three independent Sb atoms.

Received: January 27, 1986;
revised: July 1, 1986 [Z 1642 IE]
German version: *Angew. Chem. 98* (1986) 813

CAS Registry numbers:
1, 103817-68-1; SbI_3, 7790-44-5.

[1] A. F. Wells: *Structural Inorganic Chemistry*, 5th Edition, Clarendon Press, Oxford 1984; K. B. Dillon, A. W. G. Platt, A. Schmidpeter, F. Zwaschka, W. S. Sheldrick, *Z. Anorg. Allg. Chem. 488* (1982) 7; J. Kaup, W. S. Sheldrick, *Z. Naturforsch. B 39* (1984) 1252, 1257; A. Lipka, *Z. Kristallogr. 158* (1983) 88.

[2] R. Weiss, V. Jesch, unpublished; V. Jesch, *Diplomarbeit*, Erlangen 1981.

[3] M.p. 185°C (with charring); satisfactory C,H,N analysis.

[4] **1** crystallizes in the triclinic system, $P\bar{1}$, $a = 1084.4$, $b = 1102.1$, $c = 1575.3$ pm, $\alpha = 92.68$, $\beta = 104.65$, $\gamma = 108.0°$; 4180 observed reflections with $I > 1.96\sigma(I)$; 226 parameters, $R = 0.06$. Further details of the crystal structure investigation are available on request from the Fachinformationszentrum Energie, Physik, Mathematik GmbH, D-7514 Eggenstein-Leopoldshafen 2, on quoting the depository number CSD-52044, the names of the authors, and the full citation of the journal.

[5] H. Bräkken, *Z. Kristallogr. Kristallgeom. Kristallphys. Kristallchem. 74* (1930) 67; J. Trotter, T. Zobel, *ibid. 123* (1966) 67; S. Pohl, W. Saak, *Z. Kristallogr. 169* (1984) 177.

[6] B. Buss, B. Krebs, *Angew. Chem. 82* (1970) 446; *Angew. Chem. Int. Ed. Engl. 9* (1970) 463; *Inorg. Chem. 10* (1971) 2795; B. Krebs, V. Paulat, *Acta Crystallogr. Sect. B 32* (1976) 1470.

[7] H. Bürgi, *Angew. Chem. 87* (1975) 461; *Angew. Chem. Int. Ed. Engl. 14* (1975) 460.

[*] Prof. Dr. S. Pohl [+], W. Saak
Fakultät für Chemie der Universität
Universitätsstrasse, D-4800 Bielefeld 1 (FRG)
Prof. Dr. A. Schmidpeter, P. Mayer
Institut für Anorganische Chemie der Universität
Meiserstrasse 1, D-8000 München 1 (FRG)

[+] New address: Fachbereich Chemie der Universität
Carl-von-Ossietzky-Strasse, D-2900 Oldenburg (FRG)

[**] This work was motivated by Prof. *Robert Weiss*, Institut für Organische Chemie der Universität Erlangen-Nürnberg, with his studies on triaminocyclopropenylium salts [2]. We thank him for supplying us with a sample of $[C_3(NMe_2)_3]I$.

Oxygen Evolution by Water Oxidation Mediated by Heterogeneous Manganese Complexes

By *Ramasamy Ramaraj, Akira Kira,* and *Masao Kaneko**

Water oxidation is an important research topic, not only in connection with photosynthesis but also with regard to

[*] Prof. Dr. M. Kaneko, Dr. R. Ramaraj, Prof. Dr. A. Kira
Solar Energy Science Research Group
The Institute of Physical and Chemical Research
Wako, Saitama 351-01 (Japan)

the conversion of solar energy into chemically stored energy.[1-5] Manganese ions play an important role as oxidation centers in photosynthesis.[1,6-8] Although a number of manganese complexes have been proposed as model complexes for water oxidation, the evolution of oxygen has hitherto never been observed.[9-12] *Calvin* reported that the di-μ-oxo-bridged binuclear complex **1** was able to decompose water photolytically,[9] but the initial claims of his success with photolytic dioxygen evolution soon had to be withdrawn.[13] *Renger* has proposed a model for the water-splitting complex that is in better agreement with the reported experimental findings.[14] It postulates a binuclear manganese complex in which water ligands are finally oxidized to O_2 via the stage of a bridging peroxy ligand.

$[(bpy)_2Mn^{III}(\mu\text{-}O)_2Mn^{IV}(bpy)_2]^{3\oplus}$ **1**, bpy = 2,2′-bipyridyl

We have now found that the di-μ-oxo-bridged, binuclear manganese complex oxidizes water with the formation of visible oxygen bubbles when it is suspended in water as a heterogeneous catalyst in the presence of an oxidant such as Ce(IV) ion, although the same complex cannot oxidize water when used in homogeneous solution. The binuclear, cationic manganese complexes **1** and **2** have been prepared as the perchlorates[15] and characterized by UV-VIS and IR spectroscopy.

$[(phen)_2Mn^{III}(\mu\text{-}O)_2Mn^{IV}(phen)_2]^{3\oplus}$ **2**, phen = 1,10-phenanthroline

Cyclic voltammograms were recorded for the binuclear complexes **1** and **2** in aqueous solution using a three-electrode cell arrangement (basal plane pyrrolytic graphite (BPG) working electrode, platinum wire auxiliary electrode, and a saturated calomel reference electrode (SCE)). The cyclic voltammogram of **1** exhibits two electrochemically reversible redox reactions. At a scan rate of 50 mV s^{-1} the binuclear manganese complex **1** is found to undergo a reversible redox process at 1.14 V vs SCE. Another wave is located at 0.98 V vs SCE, presumably corresponding to the reduction of the $Mn^{III}Mn^{IV}$ complex to the $Mn^{III}Mn^{III}$ complex. The cyclic voltammogram of **2** exhibits two reversible redox processes at 1.23 V and 1.09 V vs SCE. The electrochemical properties of the complexes **1** and **2** have mainly been studied in acetonitrile as solvent,[15,16] and it has been reported that the anodic electrolysis of **1** and **2** in acetonitrile at 1.45 V vs SCE causes decomposition, while the color of the solution changes from green to reddish-brown. We have carried out the anodic electrolysis of the complexes **1** and **2** in water at 1.45 V SCE with continuous reversible scanning between the potentials 0.4 V and 1.5 V vs SCE. The anodic electrolysis and continuous repeated scanning of the potentials did not bring about any noticeable change in the voltammograms. Absorption spectra were recorded for the solutions obtained from the cyclic voltammetric experiments. The absorption measurements also showed that the complexes **1** and **2** are highly stable in water, in contrast to their instability in acetonitrile.

Water-oxidation experiments were carried out with the binuclear manganese complexes using $(NH_4)_2[(Ce(NO_3)_6]$ **3** as oxidizing agent. When the complex **1** or **2** was dissolved in water containing excess **3**, no evolution of gas was observed, and analysis of the gas phase confirmed that no oxygen was formed. A water mixture containing the perchlorate of **1** or **2**, partly dissolved and partly as solid suspension, was deaerated by bubbling argon gas through it for two hours. After the deaeration, an excess of **3** was added to the mixture. Gas bubbles began to form on the surface of the undissolved manganese compound already after 1 minute of mixing. The gas evolved in the reaction was analyzed gas-chromatographically using a 1.5-m column of molecular sieve 5Å and argon carrier. The gas was identified as oxygen from its retention time. The amount of oxygen evolved was calculated by subtracting the oxygen content of the residual air contained in the reaction vessel from the total oxygen observed. According to the mass spectrum the gas evolved contained 1.9% $H_2{}^{18}O$. The ratio $^{18}O^{16}O^{\oplus}/{}^{16}O_2^{\oplus}$ was found to be 2.16%, whereas a value of 0.3% was found for the oxygen from air. That the theoretical value of 3.87% was not reached could have been due to the residual air in the mass spectrometer during the measurement.

Table 1. Oxygen evolution mediated by binuclear manganese complexes under argon at 20°C. In each case, the yields were determined after 4 h [a].

Complex	Solvent	Yield of O_2 [μL] without stirring	with stirring
1·$(ClO_4)_3$	water	94	148
	0.1 N HNO_3	101	171
	0.1 N NaOH	113	144
2·$(ClO_4)_3$	water	26	32
	0.1 N HNO_3	29	39
	0.1 N NaOH	14	32

[a] 1.81×10^{-4} **1**·$(ClO_4)_3$ or **2**·$(ClO_4)_3$, 3.6×10^{-3} mol **3**, volume of solution 10 mL.

The amounts of oxygen evolved in four hours under different experimental conditions are listed in Table 1. The time-dependence of the evolution of oxygen measured by a Warburg apparatus is shown in Figure 1. Repeated experiments show that the results are reproducible. The observed data show that stirring of the reaction mixture leads to formation of more oxygen, and that the pH of the solution does not affect the water-oxidation process. This observation shows that the species oxidized is a water molecule rather than the $OH^{\ominus}$ ion. Ce^{IV} is consumed during the oxidation, so that the rate of oxygen evolution decreases with time (Fig. 1). The finding that **1** is a more efficient catalyst than **2** (Table 1) is consistent with the easier oxidizability of **1** inferred from the cyclovoltammetric data. Since the standard potential of Ce^{III}/Ce^{IV} is not distinctly more positive than that of the $Mn^{III}Mn^{IV}/Mn^{IV}Mn^{IV}$ couple a large excess of **3** is needed for the oxidation of **1** or **2**.

The redox potentials of the complexes **1** and **2** show that they can be used only as 1e-transfer agents for water-

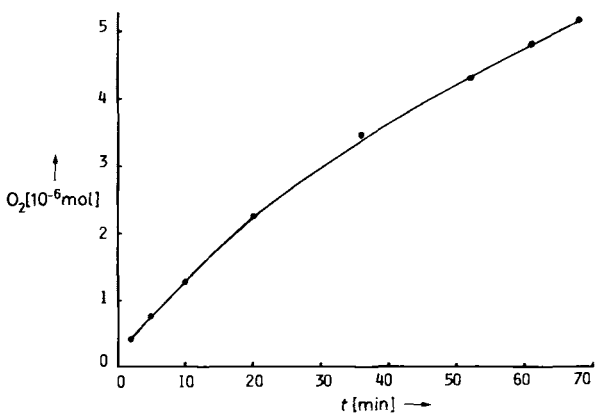


Fig. 1. Time-dependence of O_2-evolution at 25°C with stirring. 4.5×10^{-6} mol **1**·$(ClO_4)_3$, 1.82×10^{-4} mol **3**, 0.1 N HNO_3, volume of solution 1 mL.

 © VCH Verlagsgesellschaft mbH, D-6940 Weinheim, 1986 0570-0833/86/0909-0826 $ 02.50/0

oxidation. Since four electrons are required for the formation of an O_2-molecule, a water-oxidation can only be achieved if the 1e-processes can be efficiently coupled. This is obviously not the case in homogeneous phases, but is so in heterogeneous phases.

The heterogeneous water-oxidation system described here is of special interest with regard to the evolution of oxygen in photosynthesis. It has already been suggested[1,6-8] that the microheterogeneous environment around the manganese centers and the close proximity of the manganese atoms to one another are responsible for water-splitting in photosynthesis. This is supported by our finding that the complexes **1** and **2** are only catalytically active in the solid form. It is conceivable that four molecules of the binuclear manganese complex may be oxidized by four adjacent Ce^{IV} ions to produce a four-electron depletion center on the surface. This oxidizing center would then lead to the four-electron oxidation of two molecules of weakly bound water with subsequent evolution of oxygen.

Received: May 12, 1986;
supplemented: June 16, 1986 [Z 1767 IE]
German version: *Angew. Chem. 98* (1986) 824

CAS Registry numbers:
1, 47883-04-5; **2**, 58615-22-8; **3**, 16774-21-3; H_2O, 7732-18-5; O_2, 7782-44-7.

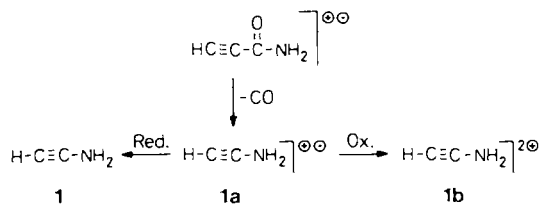
[1] M. Kaneko, Y. Yamada, *Adv. Polym. Sci. 55* (1984) 1.
[2] J. Kiwi, M. Grätzel, *Angew. Chem. 90* (1978) 900; *Angew. Chem. Int. Ed. Engl. 17* (1978) 860; *ibid. 91* (1979) 659 and *18* (1979) 624.
[3] J. A. Gilbert, D. S. Eggleston, W. R. Murphy, Jr., D. A. Geselowitz, S. W. Gersten, D. J. Hodgson, T. J. Meyer, *J. Am. Chem. Soc. 107* (1985) 3855.
[4] M. Kaneko, N. Takabayashi, A. Yamada, *Chem. Lett. 1982*, 1647.
[5] R. Ramaraj, A. Kira, M. Kaneko, *J. Chem. Soc. Faraday Trans. 1, 1986*, in press.
[6] L. G. Lawrence, D. T. Sawyer, *Coord. Chem. Rev. 27* (1978) 173.
[7] K. Sauer, *Acc. Chem. Res. 13* (1980) 249.
[8] Govindjee, T. Kambara, W. Coleman, *Photochem. Photobiol. 42* (1985) 187.
[9] M. Calvin, *Science 184* (1974) 375.
[10] D. T. Sawyer, M. E. Bodini, *J. Am. Chem. Soc. 97* (1975) 6588.
[11] G. Porter, *Proc. R. Soc. London Ser. A 362* (1978) 281.
[12] A. Harriman, *Coord. Chem. Rev. 28* (1979) 147.
[13] S. R. Cooper, M. Calvin, *Science 185* (1974) 376.
[14] G. Renger (Ed.): *Photosynthetic Water Oxidation*, Academic Press, London 1978, p. 229.
[15] S. R. Cooper, M. Calvin, *J. Am. Chem. Soc. 99* (1977) 6623.
[16] M. M. Morrison, D. T. Sawyer, *J. Am. Chem. Soc. 99* (1977) 257.

Aminoacetylene and Its Mono- and Dication—Identification of Potentially Interstellar Molecules**

By *Ben van Baar, Wolfram Koch, Carlito Lebrilla, Johan K. Terlouw, Thomas Weiske,* and *Helmut Schwarz**

Dedicated to Professor Ferdinand Bohlmann on the occasion of his 65th birthday

More than 20% of all identified organic molecules in interstellar space contain either an amino moiety or a CC triple bond.[1] The simplest molecule which contains both these structural units is aminoacetylene (ethynamine) **1**. It follows from ab initio calculations of the C_2H_3N hypersurface[2] that **1**, which so far has not been generated and characterized, should be a stable species, at least in the gas phase.[2c] Inspired by our recent successful preparation of the neutral molecule, radical cation and dication of hydroxyacetylene in the mass spectrometer,[3] we have now succeeded in generating **1** and its mono- and dications (**1a** and **1b**, respectively).



Scheme 1.

Decarbonylation of $HC{\equiv}CCONH_2^{\oplus\ominus}$ (produced by 70-eV electron impact ionization) yields a $C_2H_3B^{\oplus\ominus}$ ion, which, under the conditions of tandem mass spectrometry,[4] upon collision activation (CA)[5] displays a mass spectrum[6] which differs uniquely from the spectra of all other presently known isomeric $C_2H_3N^{\oplus\ominus}$ ions[7] (such as, for example, $H_2C{=}C{=}NH^{\oplus\ominus}$, $H_3CCN^{\oplus\ominus}$, $H_3CNC^{\oplus\ominus}$ or $H_2C{=}N{=}CH^{\oplus\ominus}$), inter alia, by a weak-intensity but, for the proposed structure **1a**, characteristic signal at *m/z* 16 ($NH_2^{\oplus}$) (Fig. 1). The corresponding collisional activation spectrum of the $C_2HD_2N^{\oplus\ominus}$ species produced by decarbonylation of $HC{\equiv}CCOND_2^{\oplus\ominus}$ shows the mass shift *m/z* 16→*m/z* 18 ($NH_2^{\oplus}\rightarrow ND_2^{\oplus}$). This is in agreement with our proposal that $HC{\equiv}CNH_2^{\oplus\ominus}$ (**1a**), like $HC{\equiv}COH^{\oplus\ominus}$,[3] is a stable ion which is prevented by sizeable barriers from undergoing unimolecular isomerizations. Neutralization of **1a** with Xe followed by reionization (*N*eutralization *R*eionization *M*ass *S*pectrometry, NRMS[8]) yields a CA spectrum which is *identical* with that of **1a**. It must therefore be concluded that neutralization of **1a** produces the long sought aminoacetylene **1**; isomerization to thermodynamically more stable C_2H_3N species does not occur. It should also be mentioned that under the conditions of charge stripping,[9] **1a** can be oxidized to a $C_2H_3N^{2\oplus}$ dication, which we assume (by way of analogy to $HC{\equiv}COH^{\oplus\ominus}\rightarrow HC{\equiv}COH^{2\oplus}$[3]) to be the aminoacetylene dication **1b**.

Ab initio MO calculations (Table 1) confirm and extend the interpretation of our observations on **1** and **1a**. Calculations of the ground state potential energy surface give the

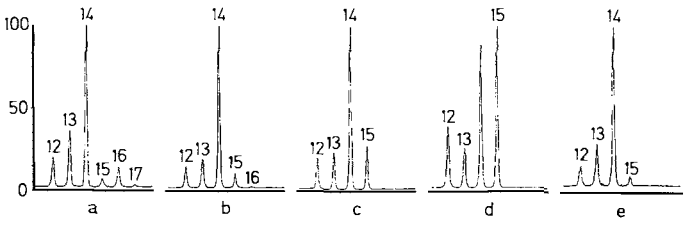


Fig. 1. Partial (*m/z* 12–*m/z* 17) CA mass spectra of $C_2H_3N^{\oplus\ominus}$ isomers. a) **1a** (generated from $HC{\equiv}COONH_2^{\oplus}$), b) $H_2C{=}C{=}NH^{\oplus\ominus}$ (from *n*-$C_3H_7CN^{\oplus\ominus}$), c) $H_3CCN^{\oplus\ominus}$, d) $H_3CNC^{\oplus\ominus}$, e) $H_2C{=}N{=}CH^{\oplus\ominus}$ (from *n*-$C_4H_9NC^{\oplus\ominus}$). The CA spectra were obtained with Vacuum Generators GmbH ZAB-3HF (TU Berlin) and ZAB-2F (Utrecht University) mass spectrometers.

[*] Prof. Dr. H. Schwarz, Dr. W. Koch, Dr. C. Lebrilla, Dr. T. Weiske
Institut für Organische Chemie der Technischen Universität
Strasse des 17. Juni 135, D-1000 Berlin 12
Dr. J. K. Terlouw, B. van Baar
Analytical Chemistry Laboratory, University of Utrecht
Croesestraat 77A, NL-3522 AD Utrecht (Netherlands)

[**] This work was supported by the Fonds der Chemischen Industrie, the Deutsche Forschungsgemeinschaft and the Freunde der Technischen Universität Berlin. *C. L.* thanks the Alexander von Humboldt-Foundation and *J. K. T.* the Deutscher Akademischer Austauschdienst (DAAD) for a stipend. *H. S.* acknowledges stimulative discussion with Professor *Albert Eschenmoser*, Zürich.

Table 1. Absolute (E_{tot} [Hartree]) and relative energies (E_{rel} [kcal/mol]) for neutral (**1**) and ionized (**1a**) aminoacetylene and for some isomers and dissociation products calculated at the 6-31G(d)//6-31G(d) [10] level of theory.

Species	E_{tot}	E_{rel}
$HC{\equiv}CNH_2$ [a] **1**	−131.84557	0.0
$H_2C{=}C{=}NH$ [a] **2**	−131.87126	−16.1
$C{\equiv}CNH_3$ **3**	−131.724450	75.9
$C{=}C(H)NH_2$ **4**	−131.775308	44.1
$HC{=}C(H)NH$ **5**	−130.982298 [b]	89.0
$HC{\equiv}CNH^{\oplus}$ + $H^{\odot}$ [c]	−131.741470	65.3
$HC{\equiv}C^{\odot}$ [a] + $NH_2^{\oplus}$ [d]	−131.707790	86.4
$^{\odot}C{\equiv}CNH_2$ + $H^{\odot}$	−131.194334	95.9
$HC{\equiv}CNH_2^{\oplus\odot}$ **1a**	−131.57314	0.0
$H_2C{=}C{=}NH^{\oplus\odot}$ **2a**	−131.60684	−21.1
$C{\equiv}CNH_3^{\oplus\odot}$ **3a**	−131.48947	52.5
$C{=}C(H)NH_2^{\oplus\odot}$ **4a**	−131.44186	82.3
$HC{=}C(H)NH^{\oplus\odot}$ **5a**	ca. −131.50 [e]	45.0
$HC{\equiv}CNH^{\oplus}$ + $H^{\odot}$	−131.38117	120.4
$HC{\equiv}C^{\odot}$ + $NH_2^{\oplus}(^3B_1)$ [f]	−131.35861	134.5
$C{\equiv}CNH_2^{\oplus}$ + $H^{\odot}$	−131.36608	129.8

[a] Taken from Ref. [2d]. [b] Calculated with a 3-21G//3-21G basis. c) $E_{tot}(H^{\odot}) = -0.49823$ Hartree. [d] $E_{tot}(NH_2^{\oplus}) = -55.55770$ Hartree. [e] Geometry optimization of **5a** demonstrated that this species does not correspond to a minimum of the potential hypersurface but rather rearranges to the azirine, $\overset{\frown}{CH{=}CHNH}^{\oplus\odot}$ (**6a**). The energy of **6a** was calculated to be −131.53174 Hartree. [f] $E_{tot}(NH_2^{\oplus}) = -55.20852$ Hartree [2d] and $E_{tot}(HCC^{\odot}) = -76.15009$ Hartree [2d].

following results: Isomerization of **1** to the ketenimine **2** (which is thermodynamically more stable by 16.1 kcal/mol) is computed at the 3-21G//3-21G level to involve a barrier of 155 kcal/mol; although this barrier may drop somewhat at a higher level of computation it will remain sufficiently high to prevent an isomerization **1** → **2**. Species **3–5** are thermodynamically quite unstable and thus isomerization of **1** to these can also be excluded. Similarly, we have calculated that the various dissociations of **1** which yield radicals as products will also be strongly endothermic. The MO calculations analogously confirm that the radical cation **1a** is also prevented by sizeable barriers from undergoing spontaneous isomerization or dissociation. Isomerization of **1a** to **3a–5a** is strongly endothermic (for that reason the barriers have not been computed), and, although isomerization to **2a** is exothermic (−21.1 kcal/mol), a spontaneous reaction is prevented by a barrier of ca. 90 kcal/mol. The dissociation of **1a** will also involve high energy barriers and it is therefore not surprising that **1a** and its neutral counterpart **1** are stable species in the gas phase. Finally, it is noted that theory predicts the vertical ionization of **1a** to the corresponding singlet dication **1b** to require an energy of 17.1 eV (MP3/6-31G(d)//6-31H(d)). For the generation of a triplet dication the calculated energy is 17.9 eV. Charge stripping[9] experiments yield a Q_{min} value for the ionization of **1a** to **1b** of 17.9 ± 0.1 eV.[11]

Received: May 30, 1986;
revised: June 30, 1986 [Z 1796 IE]
German version: *Angew. Chem. 98* (1986) 834

CAS Registry numbers:
1, 52324-04-6; **1a**, 103835-03-6; **1b**, 103835-04-7; **2a**, 81451-39-0; **3a**, 103835-06-9; **4**, 70277-79-1; **4a**, 103835-07-0; $HC{\equiv}CNH^{\odot}$, 73456-14-1; $^{\odot}C{\equiv}CNH_2$, 103835-05-8; $HC{\equiv}CNH^{\oplus}$, 103835-08-1; $HC{\equiv}C^{\odot}$, 2122-48-7; $C{\equiv}CNH_2^{\oplus}$, 85121-69-3.

[1] S. Green, *Annu. Rev. Phys. Chem. 32* (1981) 103.
[2] Selected references: a) T.-K. Ha, M. T. Nguyen, *J. Mol. Struct. (THEOCHEM) 87* (1982) 355; b) L. L. Lohr, Jr., M. Hanamana, K. Morokuma, *J. Am. Chem. Soc. 105* (1983) 5541; c) S. Saebø, L. Farnell, N. V. Riggs, L. Radom, *ibid. 106* (1984) 5047; d) R. A. Whiteside, M. J. Frisch, J. A. Pople: *The Carnegie-Mellon Quantum Chemistry Archive*, 3rd Edition, Pittsburgh, PA, USA 1983.
[3] B. van Baar, T. Weiske, J. K. Terlouw, H. Schwarz, *Angew. Chem. 98* (1986) 275; *Angew. Chem. Int. Ed. Engl. 25* (1986) 282.
[4] a) F. W. McLafferty (Ed.): *Tandem Mass Spectrometry*, Wiley Interscience, New York 1983; b) J. L. Holmes, *Org. Mass Spectrom. 20* (1985) 169.
[5] K. Levsen, H. Schwarz, *Mass Spectrom. Rev. 2* (1983) 77.
[6] The complete CA spectra and the NRMS spectra are not reproduced here, but they are available upon request.
[7] a) J. van Thuijl, J. J. van Houte, A. Maquestiau, R. Flammang, C. de Meyer, *Org. Mass Spectrom. 12* (1977) 196; b) E. K. Chess, R. L. Lapp, M. L. Gross, *ibid. 17* (1982) 475.
[8] Selected references: a) P. O. Danis, C. Wesdemiotis, F. W. McLafferty, *J. Am. Chem. Soc. 105* (1983) 7454; b) P. C. Burgers, J. L. Holmes, A. A. Mommers, J. K. Terlouw, *Chem. Phys. Lett. 102* (1983) 1; c) P. C. Burgers, J. L. Holmes, A. A. Mommers, J. E. Szulejko, J. K. Terlouw, *Org. Mass Spectrom. 19* (1984) 442; d) J. L. Holmes, A. A. Mommers, J. K. Terlouw, C. E. C. A. Hop, *Int. J. Mass Spectrom. Ion Processes 68* (1986) 249.
[9] Review: W. Koch, F. Maquin, D. Stahl, H. Schwarz, *Chimia 39* (1985) 376.
[10] P. C. Hariharan, J. A. Pople, *Theor. Chim. Acta 28* (1973) 213.
[11] **1** and **1a** have also been characterized recently by *Holmes* et al.: J. Buschek, J. L. Holmes, F. P. Lossing, *Org. Mass Spectrom.*, in press.

An Azimine-Triaziridine Transformation by Laser Photolysis**

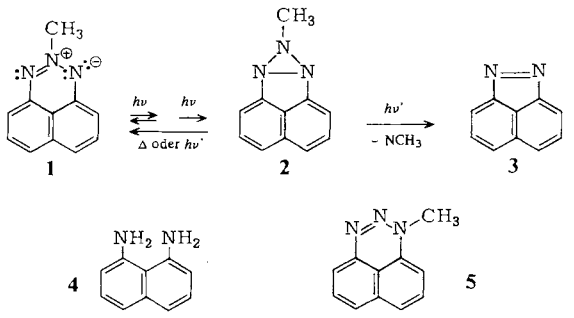
By *Gerd Kaupp** and *Jens A. Döhle*

Up to now, only triaziridines that are stabilized by carbonyl[1] or trifluoromethyl groups[2,3] could be prepared. We now report on the synthesis and characterization of the first triaziridine, **2**, not modified by electron abstraction or by incorporation of *all* three nitrogen atoms in a polycyclic framework.[4] As starting material we used the blue azimine **1**,[6] which is of interest as an inhibitor of the photooxidation of polymers and as a trapping reagent for the detection of free radicals[5] and whose absorption spectrum covers the whole UV/VIS region.[7] Furthermore, according to crystal structure investigations, **1** is planar.[8]

The azimine **1** can be regarded as a derivative of nitromethane. Like the latter it is usually described in terms of dipolar resonance formulas and referred to as a so-called "1,3-dipole". **1** proves to be photostable upon long wavelength (Hg high-pressure lamp TQ700/pyrex)[9] or short wavelength (Hg low-pressure lamp TNN15/quartz)[9] irradiation in ether (298 K) or in the crystal (303 K, 213 K). Even at high dilution ($< 10^{-2}$ and $< 2 \times 10^{-3}$ mol/L) in 2-methyltetrahydrofuran (MTHF) glass, **1** survives prolonged and intense irradiation at 77 K or 10 K (full exposure to a Philips HPK-125W lamp through pyrex (30 min) or a Hanau TNN 15 Hg-low-pressure lamp (90 min) at a distance of 5 cm)[9] without any signs of alteration (UV analysis). Apparently, the electrostatic promotion of ring closure, which is enforced by substitution in the case of unsymmetrical, polar azimines,[1,2] is lacking in the case of **1**. Only multiple excitation of **1** with the super performance of excimer laser pulses[9] at 10 K or 85 K led to successful results. The blue color and the UV absorptions of **1** almost completely disappear and the structured UV spectrum of **2** is obtained, whose principle absorption ($\lambda = 328.5$ nm) has the same intensity as that of **1** (at $\lambda = 383$ nm). At low extinctions (MTHF-glass: $E = 0.3$, soft-

[*] Prof. Dr. G. Kaupp, J. A. Döhle
Fachbereich Chemie—Organische Chemie I—der Universität
Postfach 2503, D-2900 Oldenburg (FRG)

[**] This work was supported by the Deutsche Forschungsgemeinschaft and the Fonds der Chemischen Industrie.



ened MTHF: $E = 0.15$) the reaction comes to a standstill. Since, according to molecular models, the conjugation between the α-n-electron pairs and the π-electron system is reduced by the formation of the three-membered ring, the UV absorptions of **2** have shorter wavelengths ($\Delta\lambda = 27$ nm) than those of the reference compound 1,8-diaminonaphthalene **4**.[7] Further support for the formation of **2** is provided by the quantitative re-formation of **1** within 10–15 min upon heating to 150 K and the lasting stability of **2** in non-degassed (liquid) MTHF at 110 K (unchanged absorption spectrum after 2 d). All these experiments are also reproducible after warming to room temperature.

In contrast to **4**, the triaziridine **2** exhibits neither fluorescence nor phosphorescence. Nor can fluorescent or phosphorescent byproducts be detected. Since fluorescence and phosphorescence measurements are very sensitive at low temperatures, **2** must be formed free of byproducts despite (selective) multiple excitation. That **2**, which contains the intact naphthalene ring, usually a very effective fluorophore, does not fluoresce, would indicate that the N–N bonds are cleaved in high quantum yields in the single quantum excitation of **2**. Indeed, on brief exposure of **2** to the low-pressure lamp at 10 K, 65% of **1** and at least six colorless, fluorescing byproducts are formed. According to an HPLC analysis including stopped-flow UV spectroscopic measurements,[7] the major byproduct is **3**.[10] The isomer **5**[6] is not formed.

The high thermal and photochemical lability of **2** and the necessity of pulsed (14 ns) megawatt irradiation explain the failure of earlier attempts to synthesize triaziridines.[1–4] Our data are consistent with the formation of **2** by multiple (presumably two-photon) excitation[11] of **1**. If photolabile **2** were to be formed in the non-selective single-photon excitation of **1**, the short-wave proportion of light would have to lead very efficiently to the byproducts of the photolysis of **2**. But the complete stability of **1** in the polychromatic excitation indicates that no triplets of **1** with lifetimes in the ms range (or above) occur as intermediates, for these would encounter further photons. The reaction **1** → **2** already takes place at low pulse frequencies (5–50 Hz), so it is safely established that the two-photon absorption takes place within the duration of the pulse of 14 ns. Hence, only the electronically excited singlet of **1** can occur as very short-lived intermediate, which because of the naphthalene ring, can absorb a second photon at 351 nm. The intermediate no longer appears to absorb at $\lambda = 548$ nm, for prolonged irradiation with a pulsed dye laser at this wavelength does not lead to any trace of reaction of **1**.

We conclude that **1** is promoted by two-photon excitation within 14 ns into an excited state in which it has real 1,3-dipolar character, and from which it cyclizes to **2**, just like the above cited polar azimines do after one-photon excitation.

The results suggest that attempts should be made to convert suitable nitro compounds and ozone into the still unknown[12] dioxaziridines and trioxirane (*cyclo*-O_3), respectively, by laser photolysis.

Experimental

2: A solution of **1** in a 0.2-mm quartz cuvette (extinction at 355.5 nm ca. 2) was cooled to 85 K, 77 K or 10 K (cell sealed with Viton O-rings; clamping in an aluminum cold head of a cryostat (LH RG 210) to an indium foil with window; insulator vacuum of a turbomolecular pump; electronically regulated electric counter-heating) and irradiated through the quartz window of the cryostat with the excimer laser EMG 102 (cf. [13]) at 351 nm (Xe/F_2, 1.2–0.5 W/cm² average performance, pulse frequency 5–50 Hz). With 24000–36000 pulses, conversions of 84% (10 K) and 90% (85 K), respectively, were achieved. Doubling of the number of pulses did not lead to any higher yields. UV and fluorescence measurements (from the surface at an angle of 30°) in the large sample compartments of the Perkin Elmer 551S and Perkin Elmer 650-40 (with quantum-corrected computation) spectrometers at these temperatures and after electrical heating.—A solution of $E_{548} = 0.8$ was employed for the irradiation with the dye laser (FL 2000, cf. [13]) at 10 K with $\lambda = 548$ nm (coumarin 6, 30 Hz, ca. 0.13 W/cm² average performance). After 108000 pulses a congruent VIS spectrum is recorded.

Photolysis of **2**: After its generation in MTHF at 10 K or 77 K, **2** is irradiated at these temperatures for 10 min with the TNN 15 or HPK 125/Pyrex lamp at a distance of 5 cm. Prolonged irradiation (45 min) does not lead to any further change. The samples show bright fluorescence.

Received: April 14, 1986;
revised: June 4, 1986 [Z 1731 IE]
German version: *Angew. Chem. 98* (1986) 814

CAS Registry numbers:
1, 40237-01-2; **2**, 103794-86-1; **3**, 209-15-4; **4**, 479-27-6.

[1] L. Hoesch, C. Leuenberger, H. Hilpert, A. S. Dreiding, *Helv. Chim. Acta 65* (1982) 2682; H. Hilpert, L. Hoesch, A. S. Dreiding, *ibid. 68* (1985) 1691.

[2] G. Kaupp, O. Dengler, K. Burger, S. Rottegger, *Angew. Chem. 97* (1985) 329; *Angew. Chem. Int. Ed. Engl. 24* (1985) 341.

[3] M. Klessinger, G. Kaupp, K. Burger, unpublished work.

[4] A hexacyclic all-*cis*-triaziridine has recently been reported: G. Fischer, H. Fritz, H. Prinzbach, *Tetrahedron Lett. 27* (1986) 1269. Whether in fact a triaziridine or a rapidly equilibrating azimine was involved remains unclear, since only ^{1}H- and ^{13}C-NMR data were given which fit for both structures. In any case, according to molecular models the triaziridine is more strained than the azimine.

[5] R. H. Whitfield, D. I. Davies, M. J. Perkins, *Chem. Ind. (London) 1980*, 418; R. H. Whitfield, D. I. Davies, *Polym. Photochem. 1* (1981) 261 (*Chem. Abstr. 95* (1981) 221067r); H. Beecken, P. Tavs, *Justus Liebigs Ann. Chem. 704* (1967) 172.

[6] M. J. Perkins, *J. Chem. Soc. 1964*, 3005; P. Tavs, H. Sieper, H. Beecken, *Justus Liebigs Ann. Chem. 704* (1967) 150.

[7] UV/VIS in MTHF: **1** (298 K): λ_{max} (log ε) = 231 (4.59), 235 (sh, 4.56), 251 (sh, 3.59), 286 (sh, 3.65), 300 (sh, 3.68), 315 (sh, 3.74), 329 (sh, 3.85), 344 (sh, 4.06), 351 (sh, 4.15), 355.5 (4.20), 363 (sh, 3.95), 367 (sh, 3.83), 375.5 (3.55), 383.5 (3.48), 450 (sh, 2.38), 485 (sh, 2.69), 524 (sh, 2.88), 555 (2.97), 598.5 (2.98), 653.5 (2.82), 720 nm (2.37); the progression of VIS absorption suggests a coupling of the transition to the dominating vibration in the IR spectrum with $\nu = 1370$ cm^{-1} (in analogy to nitro compounds it could be the symmetrical N-N-valence vibration).—**1** (10 K): λ_{max} (E_{rel}) = 253 (0.35), 280 (0.33), 310 (0.33), 327 (0.40), 335 (sh, 0.48), 340.5 (0.66), 343.5 (sh, 0.68), 345 (0.69), 350.5 (0.82), 357 (1.00), 363 (sh, 0.67), 367 (sh, 0.48), 375.5 (0.27), 383 (0.36, halfwidth 3.5 nm), 450 (sh), 483 (sh), 514, 548, 593, 647, 715 nm. **2** (10–85 K): λ_{max} (E_{rel}) = 289 (sh, 0.69), 295 (sh, 0.80), 301 (0.94), 309 (0.99), 313 (1.00), 321 (sh, 0.63), 325 (0.76), 328.5 nm (0.76); **3** (80% CH_3OH, resolution 4 nm): λ_{max} = 248, 280 (sh), 317 (sh), 330, 337 (sh), 345 (sh), 353 nm (sh). **4** (85 K): λ_{max} (E_{rel}) = 331 (sh, 0.85), 341.5 (0.97), 345 (sh, 0.92), 355.5 nm (1.00); fluorescence: **4** (cyclohexane, 298 K): λ_{max}^{corr} (Q_{rel}) = 354 (sh, 0.24), 360 (sh, 0.31), 383 (sh, 0.92), 392 (1.00), 428 (sh, 0.51), 452 nm (sh, 0.23); (MTHF, 13 K): λ_{max}^{corr} (Q_{rel}) = 375 (sh, 0.35), 381 (sh, 0.51), 396 (0.95), 413 (1.00), 424 (sh, 0.86), 450 nm (sh, 0.49); phosphorescence yield: 1.5% of the fluorescence yield; λ_{max}^{corr} = 520, 534, 550 (sh), 561, 567, 577 (sh), 592 nm (sh) (0/0-transition: cf. also G. N. Lewis, M. Kasha, *J. Am. Chem. Soc. 66* (1944) 2100).

[8] A. Gieren, V. Lamm, R. C. Haddon, M. L. Kaplan, M. J. Perkins, P. Flowerday, *Z. Naturforsch. B39* (1984) 975, and references cited therein.

[9] Lamp performances: TQ700/pyrex filter (arc length 12 cm): in the overall totally absorbed spectral region ca. 0.7, at 313 nm 0.078, at 365 nm 0.13 Einstein/h.—HPK 125W/pyrex filter (arc length 2.5 cm): at 313 nm 0.029, at 334 nm 0.004, at 365 nm 0.056 Einstein/h; at 313–365 nm 8.5 W; at a distance of 5 cm 0.11 W/cm^2.—TNN15 (arc length 2 × 16.5 cm): at 253.7 nm 50 mEinstein/h or 6 W; at a distance of 5 cm 12 mW/cm^2.—Excimer laser (351 nm): average power 13–5 mEinstein/h or 1.2–0.5 W/cm^2; peak pulse power 1.4–0.6 MW/cm^2; 7×10^{-8}–3×10^{-8} Einstein/pulse.

[10] H. Nakanishi, A. Yabe, K. Honda, *J. Chem. Soc. Chem. Commun. 1982*, 86.

[11] Review of nonlinear effects occurring in multiphoton excitations: U. S. Letokhov: *Nonlinear Laser Chemistry Multiple-Photon Excitation (Springer Series in Chemical Physics 22)*, Springer, Berlin 1983.

[12] Theoretical calculations of *cyclo*-NO_2, -$NO_2^{\ominus}$, -HNO_2: M. J. S. Dewar, H. S. Rzepa, *J. Am. Chem. Soc. 100* (1978) 784; C. F. Melius, J. S. Binkley, *ACS Symp. Ser. 249* (1984) 103 (*Chem. Abstr. 100* (1984) 21638h).

[13] G. Kaupp, E. Jostkleigrewe, *Angew. Chem. 94* (1982) 458; *Angew. Chem. Int. Ed. Engl. 21* (1982) 436; *Angew. Chem. Suppl. 1982*, 1089.

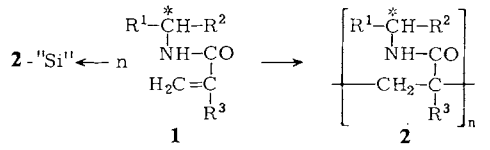
Enantiomeric Resolution by HPLC on Silica-Gel-Bound, Optically Active Polyamides**

By *Gottfried Blaschke,* Werner Bröker,* and *Werner Fraenkel*

Optically active polyacrylamides such as **2a**, with (*S*)-phenylalanine partial structures, and polymethacrylamides such as **2b** and **2c**, with (*S*)-1-phenylethyl and (*S*)-1-cyclohexylethyl moieties, respectively, have proved useful as adsorbents for direct chromatographic resolution of enantiomers.[1–6] These polymers, which are prepared by suspension polymerization in the presence of a cross-linking agent, swell in eluents to form gels and are therefore suitable for low-pressure liquid chromatography. However, they are not stable to pressure: at high pressure, they undergo compression and the rate of eluent flow decreases strongly. Further, the degree of swelling depends on the composition of the eluent. High-pressure liquid chromatography (HPLC) or gradient elution chromatography is therefore not possible.

These limitations can be circumvented by binding the optically active polyamides to silica gel; the separation properties are not thereby affected. To this end, commercially available silica gel that is substituted with diol groups (LiChrosorb® Diol) is esterified with methacrylic acid. The product is suspended in the solution of the monomeric acrylamide **1a**, without the addition of a cross-linking agent, and allowed to undergo radical polymerization to give **2a**-"Si." The acrylamide **1a** copolymerizes with the "methacryloyl silica gel" and is thereby bound covalently to the silica gel. Subsequently, the polyacrylamide that has not undergone copolymerization with the solid phase is solubilized in toluene and filtered off. The silica gel contains about 10 wt-% polyacrylamide. Likewise, copolymerization of the methacrylamides **1b** and **1c** with silica-gel-bound methacryloyl groups affords the polymethacrylamides **2b**-"Si" and **2c**-"Si," respectively.[7]

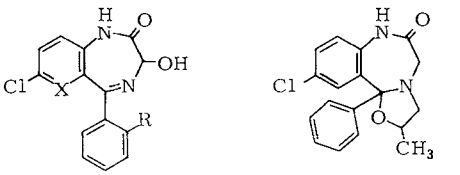
The silica-gel-bound adsorbents **2**-"Si" are suitable for direct enantiomeric resolution by HPLC.[8] Examples of chiral drugs that can be separated on the phenylalanine polymer **2a**-"Si" are the benzodiazepines oxazepam **3a**



1 **2**

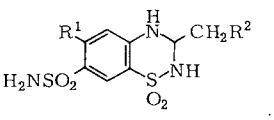
a: $R^1 = C_6H_5CH_2$, $R^2 = CO_2C_2H_5$, $R^3 = H$;
b: $R^1 = C_6H_5$, $R^2 = R^3 = CH_3$;
c: $R^1 = c\text{-}C_6H_{11}$, $R^2 = R^3 = CH_3$

and oxazolam **4** and the diuretic penflutizide **5a** (Fig. 1a). Oxazolam **4** has two centers of chirality and is therefore resolved into two pairs of enantiomers or a total of four peaks. The 1-phenylethyl polymer **2b**-"Si" allows the separation of *N*-demethylchlormezanone **6a** (Fig. 1b), the thalidomide derivative **7a**, and the diuretic cyclopenthiazide **5b**. The 1-cyclohexylethyl polymer **2c**-"Si" allows the separation of thalidomide **7b** (Fig. 1c), the benzodiazepine ketazolam **8**, and the anticoagulant acenocoumarol **9**. These racemates have already been separated by low-pressure liquid chromatography on cross-linked polyacrylamide gels, albeit at great expense of time and energy and often only very poorly. As in the case of the cross-linked polyacrylamide gels, the silica-gel-bound polyamides **2**-"Si" separate the racemates listed with different degrees of success.

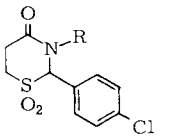


3a: X = CH, R = H
3b: X = N, R = Cl

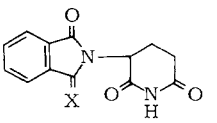
4



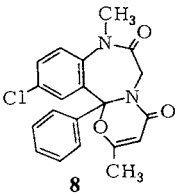
5a: $R^1 = CF_3$, $R^2 = n\text{-}C_4H_9$
5b: R^1 = Cl, $R^2 = c\text{-}C_5H_9$



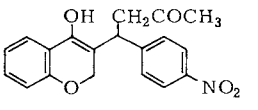
6a: R = H
6b: R = CH_3



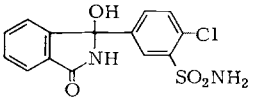
7a: X = H_2
7b: X = O



8



9



10

Reaction of an aminopropyl-substituted silica gel (LiChrosorb® NH_2) with acryloyl chloride followed by copolymerization with the monomeric acryl- and methacrylamides **1** also affords silica-gel-bound, optically active adsor-

[*] Prof. Dr. G. Blaschke, Apotheker W. Bröker, Apotheker W. Fraenkel
Institut für Pharmazeutische Chemie der Universität
Hittorfstrasse 58–62, D-4400 Münster (FRG)

[**] Chromatographic Separation of Enantiomers, Part 15. This work was supported by the Deutsche Forschungsgemeinschaft, the Bundesministerium für Jugend, Familie und Gesundheit, and the Fonds der Chemischen Industrie. Part 14: [1].

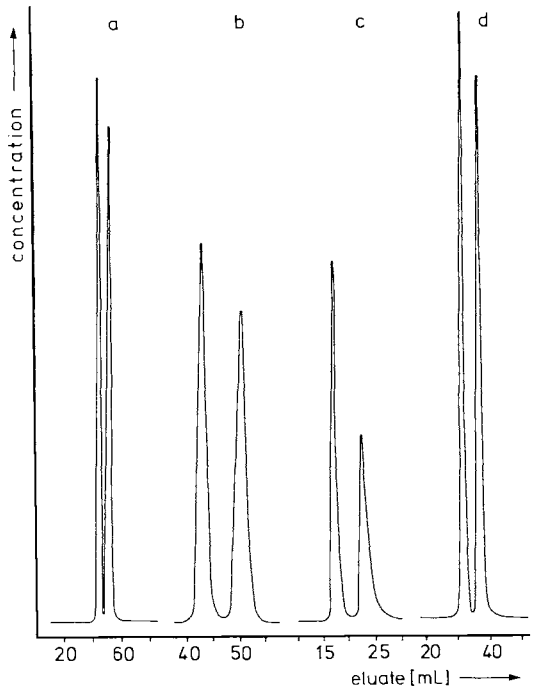


Fig. 1. Chromatography of a) penflutizide **5a** on **2a**-"Si"; b) *N*-demethylchlormezanone **6a** on **2b**-"Si"; c) thalidomide **7b** on **2c**-"Si"; d) chlorthalidone **10** (see text). Flow rate [mL/min], eluent composition (*n*-hexane/dioxane): a) 1.5, 53:47; b) 1.0, 65:35; c) 1.0, 75:25; d) 0.7, 55:45.

bents. However, apparently on account of nonspecific adsorption to the amide anchor groups that are additionally present, these preparations separate more poorly than do **2**-"Si."

If LiChrosorb® Diol is esterified with acetic acid instead of with methacrylic acid, then, as expected, no binding of the polyamide occurs upon polymerization of **1a** in the presence of this acetoxy-substituted silica gel. Similarly, polymerization of **1a** in the absence of a cross-linking agent affords a soluble polyamide that does not bind to LiChrosorb® Diol suspended in toluene solution upon heating. Surprisingly, however, polymerization of monomers such as **1a** in the presence of LiChrosorb® Diol or silica gel itself (LiChrosorb®) results, via an unknown mechanism, in anchoring of the polyamides (ca. 10 wt-%) to silica gel. Possibly, monomers and radical initiator are adsorbed by the silica gel. Upon heating, polymerization would then occur predominantly on the surface of the silica gel, whereby mechanical tangling of the growing polymer chain in the pores of the silica gel would result in anchoring. The polymer is not washed out by solvents such as *n*-hexane, toluene, dioxane, or 2-propanol.

The adsorbent[9] obtained by polymerization of **1a** in the presence of the diol phase is also suitable for direct resolution of enantiomers by HPLC. The studies carried out so far have shown that the separations obtained are at least as good as those with methacrylate-anchored polymerizates. For example, base-line separations have been achieved for the diuretic chlorthalidone **10** (Fig. 1d), the muscle relaxant chlormezanone **6b**, and the diazepine lopirazepam **3b**. The silica-gel-bound polyacryl- and polymethacrylamides of type **2**-"Si" described here exhibit unchanged separation ability even after repeated use.

Received: April 25, 1986 [Z 1744 IE]
German version: *Angew. Chem. 98* (1986) 808

CAS Registry numbers:
1a, 56598-30-2; **1b**, 56598-33-5; **1c**, 56636-18-1; **3a**, 35295-88-6; **3b**, 103794-96-3; **4**, 24143-17-7; **5a**, 96782-78-4; **5b**, 96782-85-3; **6a**, 102818-68-8; **6b**, 102818-65-5; **7a**, 103794-93-0; **7b**, 731-40-8; **8**, 103794-94-1; **9**, 103794-95-2; **10**, 74666-82-3; methacrylic anhydride, 760-93-0.

[1] G. Blaschke, J. Maibaum, *J. Chromatogr. 366* (1986) 331.
[2] G. Blaschke, *Angew. Chem. 92* (1980) 14; *Angew. Chem. Int. Ed. Engl. 19* (1980) 13.
[3] G. Blaschke, *J. Liq. Chromatogr. 9* (1986) 341.
[4] G. Blaschke, H. Markgraf, *Chem. Ber. 113* (1980) 2031.
[5] H. Kley, *Dissertation*, Universität Münster 1984.
[6] G. Blaschke, J. Maibaum, *J. Pharm. Sci. 74* (1985) 438.
[7] *Experimental procedure:* **2**-"Si": A suspension of diol phase (2.50 g, LiChrosorb® 5 μm, Merck, Darmstadt, C = 6.64%, H = 1.59%) in 20 mL of anhydrous dioxane was treated under a stream of nitrogen with a solution of methacrylic anhydride (1.50 g) in 10 mL of anhydrous dioxane and with diisopropylethylamine (0.80 g) in 30 mL of anhydrous dioxane. The resulting reaction mixture was stirred for 30 min at room temperature (RT), allowed to stand for 24 h at RT, filtered under suction through a G-4 glass-frit filtering crucible and finally washed with 100 mL of dioxane. After drying under high vacuum at RT, a snow-white product was obtained (C = 8.27%, H = 1.76%). A suspension consisting of 2.5 g of this silica-gel-bound methacrylate in 10 mL of anhydrous toluene was treated under N_2 with a solution of 7.5 g of **1a** in 20 mL of toluene and a solution of 22 mg of azobis(isobutyronitrile) in 10 mL of toluene, and the resulting reaction mixture was allowed to stir for 15 min at 80 °C. The polymerization was terminated by addition of a solution of 200 mg of 4-*tert*-butylcatechol in 10 mL of toluene. The product mixture was filtered through a G-4 glass-frit filtering crucible and then washed with toluene, dioxane, *n*-hexane, and 2-propanol. After drying in vacuum, ca. 3.0 g of **2a**-"Si" was obtained as a white powder, C = 21.35%, H = 3.1%, N = 1.16%. **2b**-"Si" and **2c**-"Si" were synthesized analogously from **1b** and **1c**, respectively. However, in these cases, the polymerization took 30 instead of 15 min.
[8] *Experimental procedure:* The adsorbents **2**-"Si," as suspensions in 30 mL of 2-propanol, were poured into steel columns (250 × 4.0 mm) under 450–500 bar pressure. In each case, 3–15 μg of the racemate in dioxane solution was chromatographed. The solvent flow was maintained at 0.5–2.0 mL/min, a pressure of 20–100 bar being required, depending on both the eluents and the flow rate. The products were detected with a photodetector at 254 nm.
[9] *Experimental procedure:* A suspension of 2.5 g of LiChrosorb® 100 Diol 5 μm, used without further modification, was heated under N_2 in a stirred solution of 7.5 g of **1a** and 22 mg of azobis(isobutyronitrile) in 40 mL of anhydrous toluene [10] at 80 °C. The reaction was terminated by addition of 200 mg of 4-*tert*-butylcatechol in 10 mL of toluene and the products were washed as described in [7]. Approximately 2.8 g of a white powder was obtained (C = 12.48%, H = 2.06%, N = 0.65%). FT-IR: $\tilde{\nu}$ = 1680 (amide), 1732 (ester) cm^{-1}. The silica gel contained approximately 10 wt-% polymerizate.
[10] Note added in proof (June 17, 1986): If the less polar cyclohexane is used instead of toluene as solvent, only 0.75 g of **1a** is required to obtain the same loading of polymerizate.

Bis(η^2-ethene)(η^6-toluene)iron**

By *Ulrich Zenneck** and *Walter Frank*

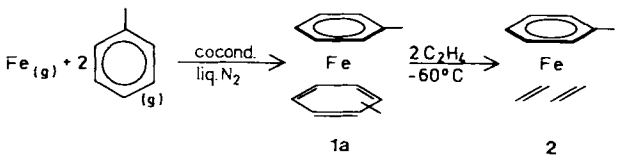
Preparative cocondensation reactions of iron atoms with arenes, carried out at liquid nitrogen temperatures, afford mainly the (η^6-arene)(η^4-arene)iron complexes **1**, which decompose above approximately −60 °C.[2,3] Trapping reactions with ligands have made it possible to synthesize numerous stable complexes of the type [(η^6-arene)FeL_n].[4] We

[*] Dr. U. Zenneck
Anorganisch-chemisches Institut der Universität
Im Neuenheimer Feld 270, D-6900 Heidelberg 1 (FRG)
Dr. W. Frank (crystal structure analysis)
Anorganische Chemie, Universität
D-6600 Saarbrücken (FRG)

[**] Reactive π Complexes of the Group VIII Transition Metals, Part 2. This work was supported by the Land Baden-Württemberg (Project No. 31-Complex Chemistry) and by BASF AG. Part 1: [1].

have now exploited the pronounced lability of one of the arene ligands of **1** to synthesize new, reactive arene-iron complexes, which, in contrast to **1**, are easier to handle. These complexes open up a convenient approach to the study of the organic chemistry of iron(0).

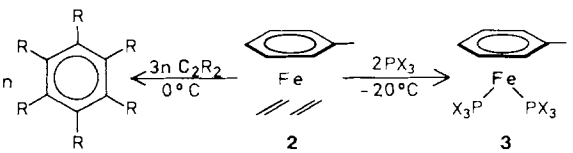
We report here the synthesis and characterization of bis(η^2-ethene)(η^6-toluene)iron **2**. We reported earlier the first evidence of complexes of this type.[1] Bis(toluene)iron **1a** is synthesized in situ and allowed to react at $-60\,^{\circ}C$ with ethylene;[5] the title compound **2** is obtained as a solution in toluene. After addition of *n*-pentane, the substance undergoes partial crystallization at $-78\,^{\circ}C$. The synthesis of **2** from iron takes only a few hours and affords a high yield of product (57%).



1a **2**

Complex **2** decomposes in solution above $-20\,^{\circ}C$ and its crystals burst at $0\,^{\circ}C$; greater stability is observed at $-78\,^{\circ}C$ under ethylene. The decomposition products are the ligands and metallic iron. Complex **2** has been characterized by ^{1}H-NMR spectroscopy and an X-ray structure analysis. The NMR spectra of **2** are difficult to obtain, because the complex decomposes to form metallic iron under vacuum and upon short contact with wall surfaces above $-20\,^{\circ}C$;[6] even traces of iron particles cause line-broadening of 100 Hz or greater. The ^{1}H-NMR spectrum of **2** suggests that it is very similar to cyclopentadienylbis(ethene)cobalt[7] but considerably more reactive. Both ethene ligands are rigidly bound on the NMR time scale at $-50\,^{\circ}C$.

In contrast to (η^6-arene)diolefin-iron complexes, the olefin ligands in **2** are readily exchanged. Complex **2** undergoes rapid reaction with phosphites, phosphanes, and diolefins to give often good yields of complexes of the type (η^6-toluene)FeL_2.[8] The known complex (η^6-toluene)$Fe[P(OCH_3)_3]_2$ **3**[4c] is formed quantitatively, so that this reaction is also suitable for the determination of yields of **2** in solution.



2 **3**

Complex **2** catalyzes the cyclotrimerization of alkynes such as 2-butyne or 3-hexyne above $0\,^{\circ}C$, 4–8 moles of hexaalkylbenzene being formed per mole of **2**.

Crystal structure analysis: Although the orange crystals of **2** are stable under ethylene at $-78\,^{\circ}C$, under nitrogen surface decomposition begins above $-50\,^{\circ}C$, resulting in the formation of thin layers of iron. The methods employed for the manipulation of the crystalline material must therefore take this sensitivity into consideration.[9, 10] The results of the X-ray structure analysis confirm the composition of the compound inferred from its reactions.

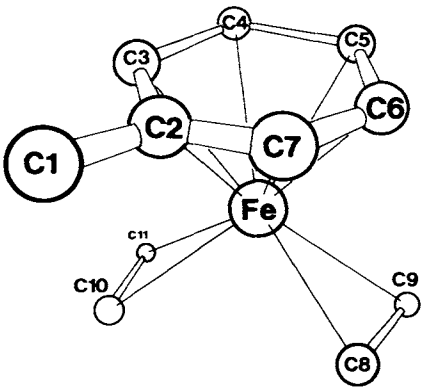


Fig. 1. Molecular structure of **2** in the crystal. Orthorhombic, space group $P2_12_12_1$, $a=811(2)$, $b=1038(2)$, $c=1148(2)$ pm at $T=-130\,^{\circ}C$, $Z=4$, $\mu(Cu_{K\alpha})=120.4\ cm^{-1}$, photometer data, 623 absorption-corrected unique reflections, 61 refined parameters, $R=0.087$. The solution of the structure could not be achieved by direct methods and the usual heavy-atom methods, but only after consideration of packing [13]. Selected distances [pm]: Fe-C2 215(2), Fe-C3 212(2), Fe-C4 211(2), Fe-C5 208(2), Fe-C6 211(2), Fe-C7 216(2), Fe-C8 207(2), Fe-C9 208(2), Fe-C10 202(2), Fe-C11 212(2), C1-C2 157(3), C-C(arene) 139(2) (averaged). Further details of the crystal structure investigation may be obtained from the Fachinformationszentrum Energie, Physik, Mathematik GmbH, D-7514 Eggenstein-Leopoldshafen 2 (FRG), on quoting the depository number CSD-51975, the names of the authors, and the journal citation.

The crystal lattice of **2** is made up of discrete molecules (point symmetry 1 (C_1) (compare Fig. 1). The deviation from the higher point symmetry *m* (C_s), which was found for (toluene)Fe(bpy)[4e], the only (η^6-arene)FeL_2 complex whose structure was investigated previously, is considerable. The methyl group of the toluene ligand is twisted by about 30° from the symmetrical position relative to the ethene ligands. These ligands are thus approximately parallel to the hypothetical lines joining C2 and C4 as well as C5 and C7. Examination of the Fe-C_{arene} distances (cf. caption to Fig. 1) clearly reveals, furthermore, that the aromatic ring is "placed crookedly" upon the iron atom. The angle between the best planes of the ethene and arene ligands is 4°. All the indicated deviations from the "symmetrical" molecular structure can be ascribed to packing effects on the basis of an analysis of the intermolecular distances. The bond lengths of **2** do not exhibit unusual values (mean values [pm] for **2**, $[(C_2H_4)_4Fe]^{2\ominus}$[11] and $[(C_2H_4)Fe(CO)_3(PPh_3)]$[12]: C-$C_{ethene}$: 141, 142, 140; Fe-$C_{ethene}$: 207, 207, 210; Fe-$C_{arene}$ **2**: 212, [(toluene)-Fe(bpy)][4e]: 209).

Received: January 31, 1986;
revised: May 27, 1986 [Z 1649 IE]
German version: *Angew. Chem. 98* (1986) 806

CAS Registry numbers:
1a, 103883-75-6; **2**, 100190-46-3.

[1] U. Zenneck, L. Suber, H. Pritzkow, W. Siebert, *Chem. Ber. 119* (1986) 971.
[2] P. L. Timms, *Chem. Commun. 1969*, 1033.
[3] S. F. Parker, C. H. F. Peden, *J. Organomet. Chem. 272* (1984) 411; G. A. Ozin, C. G. Francis, H. X. Huber, M. Andrews, L. Nazar, *J. Am. Chem. Soc. 103* (1981) 2453; P. D. Morand, C. G. Francis, *Organometallics 4* (1985) 1653.
[4] a) D. L. William-Smith, L. R. Wolf, P. S. Skell, *J. Am. Chem. Soc. 94* (1972) 4042; b) R. Middleton, J. R. Hull, S. R. Simpson, C. H. Tomlinson, P. L. Timms, *J. Chem. Soc. Dalton Trans. 1973*, 120; c) S. D. Ittel, C. A. Tolman, *J. Organomet. Chem. 172* (1979) C47; *Organometallics 1* (1982) 1432; d) L. K. Beard, Jr., M. P. Silvon, P. S. Skell, *J. Organomet. Chem. 209* (1981) 245; e) L. J. Radonovich, M. W. Eyring, T. J. Groshens, K. J. Klabunde, *J. Am. Chem. Soc. 104* (1982) 2816.

[5] *Experimental procedure:* **1a** was synthesized from iron (5.5 g, 98 mmol) and toluene (300 g) within 2 h by cocondensation at 10^{-2} Pa and −196 °C. Ethylene (140 g, 5 mmol) was added to the mixture by condensation. After the mixture had been stirred for 2 h at −80 to −40 °C and then filtered at −30 °C through Al_2O_3/5% H_2O, an orange solution of **2** was obtained. The yield of **2** was determined to be 11.4 g (55 mmol, 57%), based on Fe, by oxidative destruction of an aliquot (O_2, air or acid) and titration with Titriplex III. Addition of 300 mL of *n*-pentane to the solution of **2** resulted in the crystallization of approximately 1 g of the complex in the form of orange parallelepipeds at −78 °C.—^{1}H-NMR (300 MHz, [D$_8$]toluene, −50 °C): δ = 5.06 (br, 1H), 4.28 (br, 2H), 4.12 (br, 2H), 1.84 (s, 3H) (π-toluene); 1.91 ("d", $4H_{outside}$), 0.44 ("d", $4H_{inside}$), AA'BB', J_{AB} = 10.3 Hz (π-ethene).

[6] *Sample preparation:* A solution of **2** in [D$_8$]toluene was filtered through a small amount of Al_2O_3/5% H_2O at −50 °C into an NMR tube. The tube was then exposed to air for a short time until the solution adhering to the walls of the tube was oxidatively decomposed without noticeable oxidation of the solution itself. Afterwards, the sample was frozen and the tube sealed. Line widths of 5 Hz were attained if the sample was transferred sufficiently fast to the spectrometer.

[7] K. Jonas, E. Deffense, D. Habermann, *Angew. Chem. 95* (1983) 729; *Angew. Chem. Int. Ed. Engl. 22* (1983) 716; *Angew. Chem. Suppl. 1983*, 1005.

[8] U. Zenneck, H. Schäufele, A. Pfendert, unpublished results.

[9] M. Veith, H. Bärninghausen, *Acta Crystallogr. B 30* (1974) 1806.

[10] W. Frank, unpublished results.

[11] K. Jonas, L. Schieferstein, C. Krüger, Y.-H. Tsay, *Angew. Chem. 91* (1979) 590; *Angew. Chem. Int. Ed. Engl. 18* (1979) 550.

[12] E. Lindner, E. Schauss, W. Hiller, R. Faw, *Angew. Chem. 96* (1984) 727; *Angew. Chem. Int. Ed. Engl. 23* (1984) 711.

[13] A. J. Kitajgorodskij: *Organic Chemical Crystallography*, Consultants Bureau, New York 1959, p. 84–105.

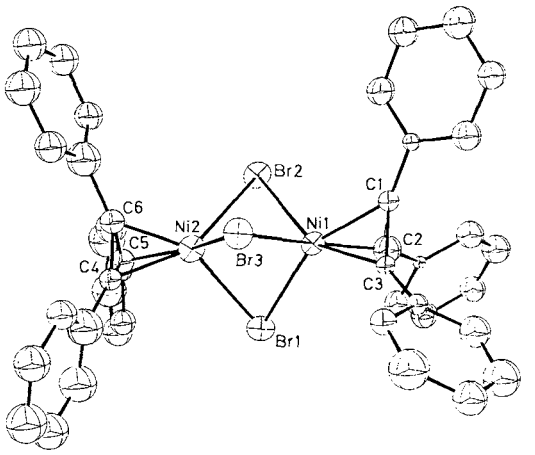


Fig. 1. ORTEP drawing (30% probability ellipsoids) of the complex anion of **1**. Selected bond distances [Å] and angles [°]: Ni-Br 2.486(8)–2.514(7), Ni1-Ni2 2.755(6), Ni-C 1.85(4)–1.98(4), Ni1-Cent1 1.72(4), Ni2-Cent2 1.75(4) (Cent1 and Cent2 are the points at the centers of the two cyclopropenyl ligands); Br1-Ni1-Br2 91.8(2), Br1-Ni1-Br3 92.1(2), Br2-Ni1-Br3 92.3(2), Br1-Ni1-Cent1 125(1), Br2-Ni1-Cent1 124(1), Br3-Ni1-Cent1 122(1), Br1-Ni2-Br2 92.6(2), Br1-Ni2-Br3 93.0(2), Br2-Ni2-Br3 93.4(2), Br1-Ni2-Cent2 122(1), Br2-Ni2-Cent2 125(1), Br3-Ni2-Cent2 122(1), Ni1-Br-Ni2 66.8(2)–67.1(2).

$[(C_3Ph_3)Ni(\mu\text{-}Br)_3Ni(C_3Ph_3)](C_3Ph_3)$— A Triple-Decker-like Complex with Triphenylcyclopropenyl as Ligand

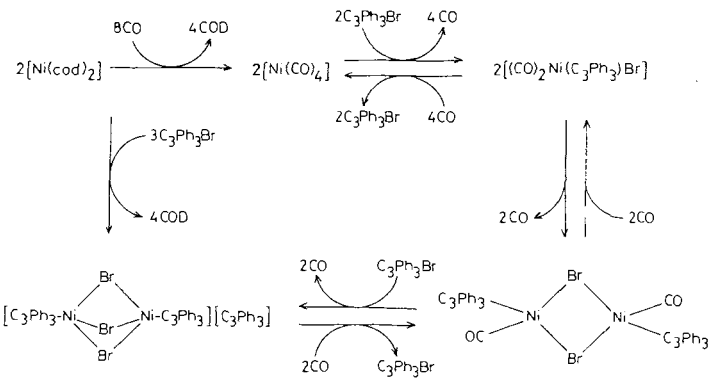
By *Franco Cecconi, Carlo A. Ghilardi, Stefano Midollini,* Simonetta Moneti,* and *Annabella Orlandini*

The cyclopropenylium system has recently attracted considerable interest in organometallic chemistry because it allows a variety of coordination types and reactions at transition-metal centers.[1] The cyclopropenyl complexes reported to date, however, contain strong donating ligands such as CO, C_5H_5, PR_3, and pyridine.[2] We now report the synthesis and the structural characterization of an organometallic compound containing triphenylcyclopropenyl as the only organic ligand.

In the course of repeated attempts to prepare the complex $[Ni_2(C_3Ph_3)_2Br_2]$, previously reported in a patent,[3] by the reaction of $[Ni(cod)_2]$ (COD = 1,5-cyclooctadiene) with C_3Ph_3Br in tetrahydrofuran (THF) solution, we succeeded in isolating deep-red crystals of a compound having the empirical formula $Ni_2(C_3Ph_3)_3Br_3$ **1**.[4] Complex **1** is only formed if the molar ratio between the reactants is $[Ni(cod)_2]/C_3Ph_3Br \geq 2/3$.[5] The X-ray structure determination[6] showed that **1** consists of $[(C_3Ph_3)Ni(\mu\text{-}Br)_3(C_3Ph_3)]^{\oplus}$ and $C_3Ph_3^{\oplus}$ ions (Fig. 1).

In the dimeric anion two eclipsed NiC_3Ph_3 fragments are linked together by three bridging Br atoms, which in turn are staggered with respect to the six C atoms of the η^3-coordinated cyclopropenyl ligands and lie on a plane that is parallel to those of the cyclopropenyl rings. The Ni atoms are thereby complexed in a double sandwich fashion between the cyclopropenyl rings and the three Br atoms. If the cyclopropenyl ring is considered to occupy one coordination site, then the Ni atoms are surrounded in a distorted tetrahedral fashion by three Br atoms and the cyclopropenyl ring, with angles around the nickel atoms of 91.8(2) to 125.4(10)°. The two Ni polyhedra are essentially similar, although corresponding bond distances and angles show some small deviations. The six Ni–Br bond distances range from 2.486(7) to 2.514(7) Å and are therefore essentially equivalent. The triphenylcyclopropenyl ion does not show any unusual features, displaying bond distances and angles in agreement with those reported for free $C_3Ph_3^{\oplus}$.[7]

Complex **1** is not air stable and is practically insoluble in THF, acetone and other polar organic solvents. It is slightly soluble in CH_2Cl_2, undergoing irreversible decomposition to yield a green solution.



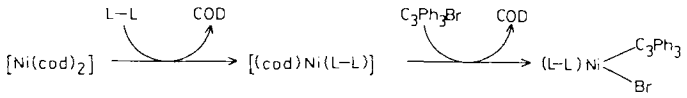
Scheme 1.

Complex **1** can also be prepared by reaction of $[(C_3Ph_3)Ni(CO)Br]_2$ with C_3Ph_3Br under a stream of N_2. This reaction can be reversed by bubbling CO through the

[*] Dr. S. Midollini, Dipl.-Chem. F. Cecconi, Dr. C. A. Ghilardi, Dr. S. Moneti, Dr. A. Orlandini
Istituto per la Studio della Stereochimica
ed Energetica dei Composti di Coordinatione, CNR
Via F. D. Guerrazzi 27, I-50132 Florence (Italy)

solution; if an excess of CO is used, $[Ni(CO)_4]$ is obtained as a final product. The interconversion in the nickel-cyclopropenyl-CO system, based on these results and those previously reported,[2a, e, 8, 9] are summarized in Scheme 1.

The addition of C_3Ph_3Br to [(cod)Ni(L-L)] complexes, which are easily prepared from $[Ni(cod)_2]$ and bidentate ligands, is a facile general method for the preparation of cyclopropenylnickel complexes. Two complexes have so far been synthesized in this way (Scheme 2).[10, 11]



Scheme 2. L-L = $Ph_2PCH_2CH_2PPh_2$ (DPPE), $Ph_2PCH_2CH_2CH_2PPh_2$ (DPPP).

Received: April 22, 1986;
revised: June 9, 1986 [Z 1740 IE]
German version: *Angew. Chem. 98* (1986) 815

CAS Registry numbers:
1, 103883-73-4; [(dppe)Ni(C_3Ph_3)Br], 103883-69-8; [(dppp)Ni(C_3Ph_3)Br], 103883-70-1; C_3Ph_3Br, 4919-51-1; $[Ni(cod)_2]$, 1295-35-8; [(dppe)Ni(cod)], 96055-24-2; [(dppp)Ni(cod)], 103883-71-2.

[1] E. D. Jemmis, R. Hoffmann, *J. Am. Chem. Soc. 102* (1980) 2570, and references cited therein.

[2] a) E. W. Gowling, S. F. A. Kettle, *Inorg. Chem. 3* (1964) 604; b) M. D. Rausch, R. M. Tuggle, D. L. Weaver, *J. Am. Chem. Soc. 92* (1970) 4981; c) R. M. Tuggle, D. L. Weaver, *Inorg. Chem. 10* (1971) 1504; d) M. Schneider, E. Weiss, *J. Organomet. Chem. 121* (1976) 345; e) R. B. King, S. Ikai, *Inorg. Chem. 18* (1979) 949; f) T. Chiang, R. C. Kerber, S. D. Kimball, J. W. Lauher, *ibid. 18* (1979) 1687; g) C. Mealli, S. Midollini, S. Moneti, L. Sacconi, *J. Organomet. Chem. 205* (1981) 273; h) C. Mealli, S. Midollini, S. Moneti, L. Sacconi, J. Silvestre, T. Albright, *J. Am. Chem. Soc. 104* (1982) 95; i) M. R. Churchill, J. C. Fettinger, L. G. McCullough, R. R. Schrock, *ibid. 106* (1984) 3356; j) R. Gompper, E. Bartmann, *Angew. Chem. 97* (1985) 207; *Angew. Chem. Int. Ed. Engl. 24* (1985) 209; k) R. P. Hughes, W. Klani, J. W. Reisch, A. Muller, *Organometallics 4* (1985) 1761, and references cited therein.

[3] G. Wilke (Studiengesellschaft Kohle m.b.H.), US-Pat. 3468921 (1969).

[4] *Experimental procedure:* C_3Ph_3Br (520 mg, 1.5 mmol) in 10 mL of MeOH was added to a solution of $[Ni(cod)_2]$ (275 mg, 1 mmol) in 20 mL of THF at 0°C. Red-brown crystals of **1** rapidly formed. Yield: 340 mg (60%). Correct elemental analyses.

[5] We were unable to isolate any identifiable compound when the reaction was performed with a molar ratio of 1:1.

[6] Monoclinic, space group Cc; $a = 26.616(15)$, $b = 15.330(9)$, $c = 16.205(10)$ Å, $\beta = 123.15(8)°$, $V = 5535.9$ Å^3, $Z = 4$, $\mu(Mo_{K\alpha}) = 28.6$ cm^{-1}, Philips PW 1100 automatic diffractometer, $\lambda(Mo_{K\alpha}) = 0.7107$ Å, $5° < 2\theta < 45°$, 2001 absorption-corrected reflections with $I > 3\sigma(I)$, Patterson and Fourier methods, full-matrix least-squares refinement, $R_w = 0.094$ and $R = 0.103$. The rather high values of the R factors may be attributed to the very poor quality of the crystals, because of which low-angle and low-intensity data were also collected. Further details are available on request from the Fachinformationszentrum Energie, Physik, Mathematik GmbH, D-7514 Eggenstein-Leopoldshafen 2 (FRG), on quoting the depository number CSD-51987, the names of the authors, and the full journal citation.

[7] M. Sundaralingam, L. H. Jensen, *J. Am. Chem. Soc. 88* (1966) 198.

[8] W. K. Olander, T. L. Brown, *J. Am. Chem. Soc. 94* (1972) 2139.

[9] C. A. Ghilardi, S. Midollini, A. Orlandini, *J. Organomet. Chem. 295* (1985) 377.

[10] *Experimental procedure:* A THF solution of [(L-L)Ni(cod)] (L-L = dppe, dppp), prepared by adding L-L (1 mmol) to a solution of $[Ni(cod)_2]$ (275 mg, 1 mmol) in THF (20 mL), was added at 0°C to a solution of C_3Ph_3Br (346 mg, 1 mmol) in 20 mL of EtOH; red crystals of [(L-L)Ni(η^3-C_3Ph_3)Br] rapidly formed.

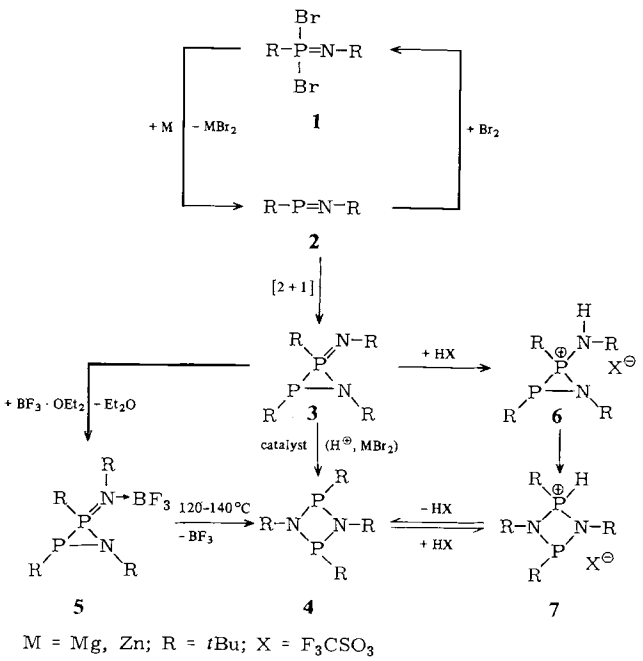
[11] Preliminary results of a X-ray analysis of [(dppp)Ni(C_3Ph_3)Br] showed that the triphenylcyclopropenyl ligand is η^3-coordinated: C. Mealli, S. Midollini, unpublished.

Acid-Catalyzed Isomerization of the [2 + 1]-Cyclodimer of an Iminophosphane to the Diazadiphosphetidine**

By *Edgar Niecke,* Dietrich Gudat,* and *Erhard Symalla*

The cleavage of hydrogen halide or halosilane from aminohalophosphanes leads to diazadiphosphetidines, whose versatile chemistry has recently been the subject of intensive studies.[1] For this reaction, both a two-step condensation via a *N*-phosphanylbis(amino)phosphane as well as a dimerization by [2 + 2]-cycloaddition of initially formed iminophosphane could be demonstrated experimentally. We have now found a novel entry to the diazadiphosphetidine system via the acid-catalyzed isomerization of the [2 + 1]-cycloadducts of iminophosphanes.[2]

The iminophosphorane **1** is readily accessible by oxidation of **2**[2] with bromine.[3] However, on attempting the reverse of its formation, namely the reductive dehalogenation of **1**,[4] we surprisingly obtained the isomeric tetra-*tert*-butyl-1,3,2,4-diazadiphosphetidine **4** instead of the [2 + 1]-cyclodimer **3**. When the reaction of **1** with an excess of zinc or magnesium powder in tetrahydrofuran (THF) at 40°C was investigated ^{31}P-NMR spectroscopically it was



M = Mg, Zn; R = *t*Bu; X = F_3CSO_3

found that the iminophosphane **2** initially formed not only dimerizes to give **3**, as expected, but also that the latter is not stable in the presence of the Lewis acid $MgBr_2$ (or $ZnBr_2$) and reacts further to give **4**.

A further indication of the action of Lewis acids as catalysts in the isomerization **3** → **4**, is afforded by the vacuum thermolysis (120–140°C, 0.1 torr) of the stable adduct **5**: likewise, the four-membered ring compound **4** was obtained by cleavage of BF_3. Moreover, the direct conversion

[*] Prof. Dr. E. Niecke, Dipl.-Chem. D. Gudat, Dipl.-Chem. E. Symalla
Fakultät für Chemie der Universität
Postfach 8640, D-4800 Bielefeld 1 (FRG)

[**] This work was supported by the Deutsche Forschungsgemeinschaft and the Fonds der Chemischen Industrie.

of **3** into **4** could be accomplished with a catalytic amount of $ZnBr_2$ (THF, 4 h at 45°C; **3** : $ZnBr_2$ = 1 : 0.05).

A much better insight into the mechanism of the isomerization is afforded by the reaction of **3** with trifluoromethanesulfonic acid. When this reaction is carried out in CH_2Cl_2 at −40°C, protonation of the imino nitrogen leads to formation of the phosphonium salt **6**, which can be isolated in pure form by immediate addition of *n*-hexane. In solution, **6** rearranges within a few days at room temperature via a 1,2 H-shift into the stable diazadiphosphetidinium ion **7**, which can be deprotonated with bases to **4**. Since the deprotonation of **7** is also possible with **3** as base—this leads to re-formation of the phosphonium salt **6**—here too only a catalytic amount of the acid suffices for the complete conversion of **3** into **4**. In all the reactions described, only one isomer of **4** is formed.

The composition and constitution of the compounds **1** and **4**–**7** have been confirmed by elemental analyses and NMR data.[5] The spectroscopic findings for **5** ($\delta(^{31}P) = 0.1$ (P^{III}), 11.1 (P^{V}), $J_{PP} = 189$ Hz, IR: absence of the characteristic intense bands for a P=N double bond[6]) are consistent with coordination of the Lewis acid to the exocyclic nitrogen atom. The coupling constant J_{HP} of the H atom bound directly to P in **7** is 520 Hz. The isomerization **6** → **7** is accompanied by a drastic decrease in J_{PP}, which together with the shift of both resonance signals to higher frequencies, is indicative of the formation of 1,3,2,4-diazadiphosphetidine (**6**: $\delta(^{31}P) = -20.9$ (P^{III}), 40.8 ($P^{\oplus}$); $^1J_{PP} = 197$ Hz; **7**: $\delta(^{31}P) = 210.2$ (P^{III}), 79.2 ($P^{\oplus}$); $^2J_{PP} = 18$ Hz). From the position of the ^{31}P-NMR signal (δ: 191.2), a *cis*-configuration is assumed for **4**.[7]

Experimental

1: A solution of bromine (4.00 g, 25 mmol) in heptane (30 mL) was added dropwise within 1 h to a stirred solution of **3** (4.00 g, 13 mmol) at 60°C. The mixture was cooled to room temperature, filtered, and the solvent removed under vacuum. Distillation of the residue furnished 4.90 g (61%) of **1** as a colorless liquid (b.p. 55–60°C, 0.1 torr).

4: An ice-cooled solution of **3** (1.59 g, 5 mmol) in CH_2Cl_2 (30 mL) was treated with a catalytic amount of F_3CSO_3H (75 mg, 0.5 mmol) and stirred for 72 h at 30°C. After removal of the solvent in vacuo, the residue was treated with 30 mL of hexane, the solution filtered, the filtrate evaporated to dryness, and the residue recrystallized from ether/acetonitrile (1 : 5). **4** (0.95 g, 60%) was obtained in the form of colorless needles (m.p. 66°C).

5: A stirred, ice-cooled solution of **3** (0.95 g, 3 mmol) in Et_2O (20 mL) was treated with a solution of $BF_3 \cdot OEt_2$ (0.425 g, 3 mmol) in Et_2O (2 mL). The mixture was warmed to room temperature, the solvent removed, and the residue dried in a high vacuum. **5** was obtained as a colorless solid (m.p. 64–68°C (decomp.)).

6 and **7**: A solution of **3** (1.59 g, 5 mmol) in CH_2Cl_2 (30 mL) was treated at −40°C with F_3CSO_3H (0.75 g, 5 mmol). Immediate addition of 30 mL of hexane led to precipitation of **6**. Subsequent filtration, repeated washing with hexane, and drying in vacuum furnished 1.28 g (55%) of **6** as a colorless solid (m.p. 101–103°C). For the synthesis of **7**, the reaction solution was warmed to room temperature, stirred for 4 d, treated with 30 mL of hexane, and then evaporated down to 40 mL. Recrystallization of the precipitate of **7** from a small amount of toluene/acetonitrile (1 : 1) furnished 1.05 g (45%) of **7** (m.p. 98–100°C).

Received: April 22, 1986 [Z 1741 IE]
German version: *Angew. Chem. 98* (1986) 817

CAS Registry numbers:
1, 103883-76-7; **3**, 79933-17-8; **4**, 103883-77-8; **5**, 103883-80-3; **6**, 103883-78-9; **7**, 103883-79-0.

[1] Recent reviews: O. J. Scherer, *Nachr. Chem. Tech. Lab. 28* (1980) 392; R. Keat, *Top. Curr. Chem. 102* (1982) 89.
[2] E. Niecke, R. Rüger, W. W. Schoeller, *Angew. Chem. 93* (1981) 1110; *Angew. Chem. Int. Ed. Engl. 20* (1981) 1034.
[3] E. Niecke, W. Bitter, *Chem. Ber. 109* (1976) 415.
[4] Cf. A. Schmidpeter, J. Luber, H. Tautz, *Angew. Chem. 89* (1977) 554; *Angew. Chem. Int. Ed. Engl. 16* (1977) 546.
[5] $^{31}P\{^1H\}$-NMR (32.2 MHz, $CDCl_3$, 28°C, external H_3PO_4) of **1**: $\delta = -44.4$; $^{13}C\{^1H\}$-NMR (20.0 MHz, $CDCl_3$, 28°C, internal TMS), the data in Hz are J_{PC} or $|J_{PC} + J_{P'C}|$ values: **1**: $\delta = 55.4$ (d, 21.5 Hz), 47.8 (d, 108.5 Hz), 32.1 (d, 20.3 Hz), 24.8 (s); **4**: $\delta = 52.6$ (t, 17.0 Hz), 34.5 (dd, 50.0 Hz), 29.6 (t, 8.4 Hz), 27.4 (m, 19.0 Hz); **5**: $\delta = 57.2$ (t, 9.3 Hz), 55.6 (d, 2.6 Hz), 42.6 (dd, 76.6 Hz), 35.0 (dd, 76.0 Hz), 32.1 (dd, 14.6 Hz), 30.1 (dd, 9.4 Hz), 29.5 (d, 1.6 Hz), 27.4 (dd, 25.7 Hz); **6** (−40°C): $\delta = 56.9$ (t, 9.2 Hz), 55.9 (d, 5.4 Hz), 40.1 (dd, 68.7 Hz), 35.0 (dd, 68.9 Hz), 31.0 (dd, 11.4 Hz), 30.2 (dd, 7.1 Hz), 27.9 (dd, 27.2 Hz), 27.6 (d, 0.6 Hz); **7**: $\delta = 55.8$ (dd, 12.2 Hz), 38.7 (dd, 57.7 Hz), 37.8 (d, 49.1 Hz), 30.7 (dd, 12.7 Hz), 25.2 (d, 1.0 Hz), 24.6 (d, 14.8 Hz); ^1H-NMR (300 MHz, $CDCl_3$, internal TMS, 28°C), the data in Hz are J_{HP} values: **1**: $\delta = 1.35$ (d, 1.9 Hz), 1.23 (d, 28 Hz; 9H); **4**: $\delta = 1.16$ (s; 18H), 1.07 (d, 12.4 Hz; 18H); **5**: $\delta = 1.48$ (d, 23.8 Hz; 9H), 1.39 (s; 9H), 1.37 (d, 1.0 Hz; 9H), 1.22 (d, 15.8 Hz; 9H); **6**: $\delta = 5.71$ (br. d, 6 Hz; 1H), 1.56 (d, 24.1 Hz; 9H), 1.41 (s; 9H), 1.37 (s; 9H), 1.25 (d, 14.8 Hz; 9H); **7**: $\delta = 8.87$ (d, 520 Hz; 1H), 1.48 (d, 20.8 Hz; 9H), 1.41 (s; 18H), 1.15 (d, 13.0 Hz; 9H).
[6] $\nu(P=N) = 1345$ (**1**), 1298 cm^{-1} (**3**) (both broad and strong).
[7] O. J. Scherer, G. Schnabl, *Angew. Chem. 88* (1976) 845; *Angew. Chem. Int. Ed. Engl. 15* (1976) 772.

Synthesis of Long-Chain Sugars by Iterative, Diastereoselective Homologation of 2,3-*O*-Isopropylidene-D-glyceraldehyde with 2-Trimethylsilylthiazole**

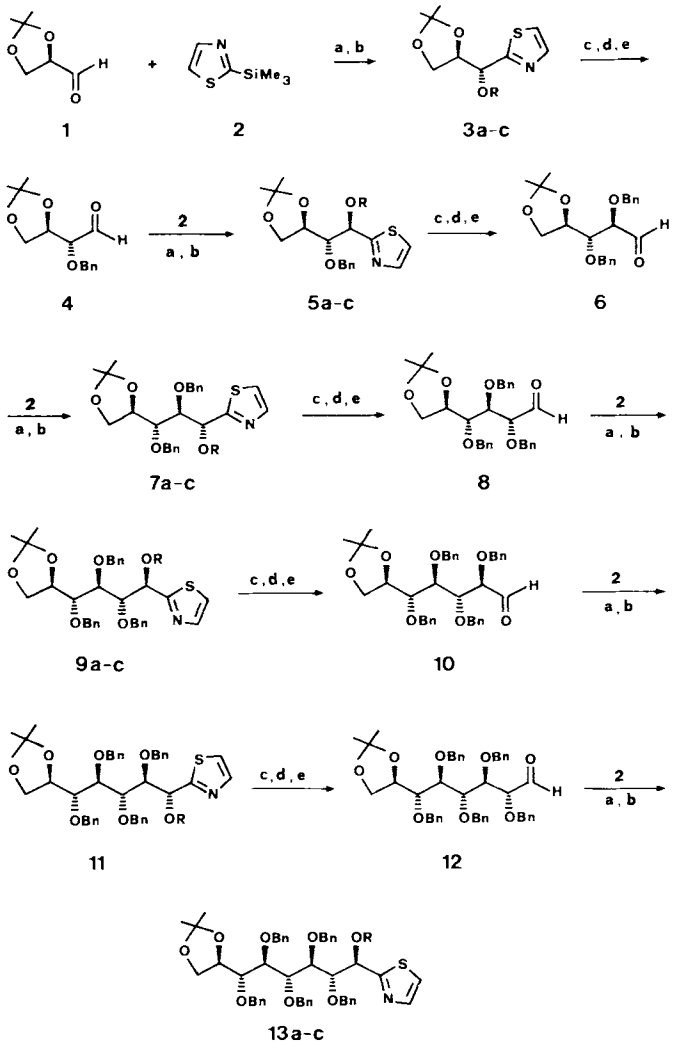
By *Alessandro Dondoni,** *Giancarlo Fantin, Marco Fogagnolo,* and *Alessandro Medici*

There is ever-growing interest in the use of carbohydrates as chiral precursors to complex natural products[1] and in their preparation from nonsugar compounds.[2] However, efficient iterative methods for the preparation of carbohydrates from short-chain precursors are rare.[2] We report here a new procedure for the iterative, diastereogenic homologation of 2,3-*O*-isopropylidene-D-glyceraldehyde **1**[3] to form D-aldoses with up to nine C atoms in the chain and an *anti* configuration of vicinal hydroxyl groups (Scheme 1). Each iteration is based on two key steps, both of which employ a 2-substituted thiazole: the diastereoselective addition of 2-trimethylsilylthiazole **2** to a chiral α-hydroxyaldehyde and the facile conversion of the thiazole ring into the formyl group. Earlier, we showed that these steps could be carried out once.[4] Here, we describe improved conditions and a synthesis that involves six cycles of repetition, thus demonstrating the potential of the methodology for the synthesis of long-chain sugars.

The one-carbon homologation of the protected D-glyceraldehyde **1** to give the D-erythrose **4** exemplifies both the principle and the details of the sequence.[5] Treatment of **1** with **2** followed by desilylation of the resulting adduct **3a** afforded the (*R,R*)-thiazole **3b** as a single diastereomer (Table 1).[6] Benzylation afforded **3c**, which was transformed by thiazole-formyl conversion into the aldose **4** in good overall yield (Table 1). This transformation was carried out by a slight modification of the literature procedure:[4] (1) *N*-methylation to give the thiazolium halide; (2) reduction to the thiazolidine; (3) hydrolysis to the alde-

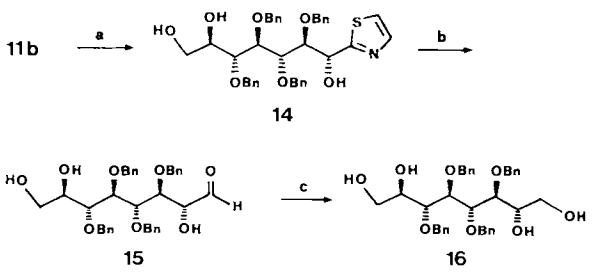
[*] Prof. Dr. A. Dondoni, Dr. G. Fantin, Dr. M. Fogagnolo, Dr. A. Medici
Dipartimento di Chimica, Laboratorio di Chimica Organica
Università di Ferrara
I-44100 Ferrara (Italy)

[**] This work was supported by the Ministero Pubblica Istruzione (Rome). We thank Prof. Dr. *S. Hanessian* (Montreal) and Prof. Dr. *V. Jäger* (Würzburg) for helpful discussions, and the High Field NMR Centre, CNR (Bologna), for recording the 300-MHz NMR spectra.



Scheme 1. Iterative homologation of **1**. **a**, R=$SiMe_3$; **b**, R=H; **c**, R=CH_2Ph. a) CH_2Cl_2, room temperature, then tetrahydrofuran (THF)/$F^{\ominus}$. b) NaH, $PhCH_2Br$, nBu_4NI, THF, room temperature. c) MeI, acetonitrile, reflux. d) $NaBH_4$, MeOH, −10°C. e) $HgCl_2$, acetonitrile/H_2O, room temperature.

hyde. The addition of **2** to the chiral aldehyde **1**, which takes place in good chemical yield and with a high degree of *anti*-diastereofacial selectivity, is the key step of the sequence, which could be repeated with equal efficiency five times (Scheme 1, Table 1).[7] In this way, the masked and protected pentoses **5** and **6** (D-riboses), the hexoses **7** and **8** (D-alloses), the heptoses **9** and **10**, the octoses **11** and **12**, and the nonose **13** were obtained. The synthesis of al-



Scheme 2. Conversion of **11b** into **16**. a) F_3CCO_2H (98%), 0°C. b) See c), d), and e) of Scheme 1. c) $NaBH_4$, MeOH, 0°C.

doses **9**–**13** having more than six C atoms is of especial relevance owing to the importance of long-chain sugars in natural products chemistry and the difficulty in preparing them by stereoselective methods from non-sugar precursors.[8,9]

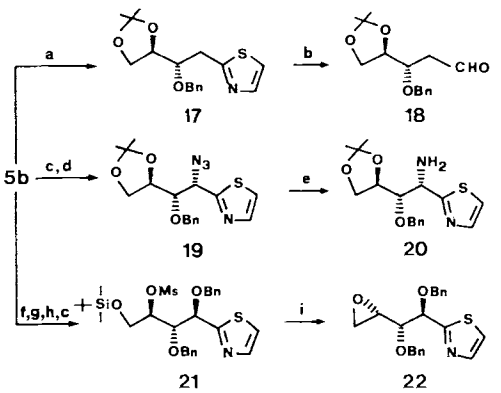
Evidence for the repeated *anti*-diastereoselectivity in the addition of **2** was provided by the X-ray structure determination of the D-ribose precursor **5b**[10] and the elaboration of **11b** into the partially protected *meso*-octitol **16** (Scheme 2).[11] By inference, the formation of the *anti*-adduct **13** was also assumed in the homologation of **12**.

Table 1. Homologation of chiral α-hydroxyaldehydes according to Scheme 1 [a].

Aldehyde →	Adduct → (yield [%])	Aldehyde (yield [%])	$[\alpha]_{20}^{D}$ [b] (conc. [g/100 mL])
1	**3b** (96)	**4** (60)	29.5 (1.70)
4	**5b** (90) [c]	**6** (89)	45.1 (1.20)
6	**7b** (92)	**8** (73)	38.7 (1.45)
8	**9b** (90)	**10** (85)	32.2 (1.13)
10	**11b** (83)	**12** (72)	28.5 (2.79)
12	**13b** (75) [d]		

[a] The diastereomeric purity was determined by ^{1}H-NMR (80 MHz in C_6D_6 or $CDCl_3$). [b] In $CHCl_3$. [c] Lower yields (70–75%) were occasionally obtained owing to the formation of another product, which was isolated as the *O*-benzyl derivative. [d] $[\alpha]_D^{20} = 17.3$ ($c = 0.99$, $CHCl_3$).

Selective elaborations of the above carbohydrate precursors can be carried out owing to the possibility of selectively protecting their hydroxyl groups, as exemplified for **5b** (Scheme 3). Reactions involving the hydroxyl group at C-2 are the Barton deoxygenation[12] to give **17**, which can be readily transformed into the protected 2-deoxy-D-ribose **18**,[13] and the azidodeoxygenation to give **19**,[14] a precur-



Scheme 3. Synthetic elaborations of the pentose precursor **5b**. a) Thiocarbonyldiimidazole, THF, reflux; nBu_3SnH, toluene, reflux. b) See c), d), and e) of Scheme 1. c) $MeSO_2Cl$(MsCl)/Et_3N, CH_2Cl_2, room temperature. d) NaN_3, dimethylformamide, 80°C. e) $LiAlH_4$, THF, room temperature. f) See b) of Scheme 1. g) See a) of Scheme 2. h) $Me_2(t\text{Bu})SiCl$/imidazole, CH_2Cl_2, room temperature. i) nBu_4NF, THF, room temperature.

sor of the masked amino sugar **20**. A third elaboration of **5b** exploits the hydroxyl groups at C-4 and C-5. In a five-step sequence, the 1,3-dioxolane ring of **5b** was stereospecifically converted, via the silyl ether **21**, into the L-lyxose **22**, with an epoxy group having the opposite configuration at C-4.[15]

In conclusion, this iterative one-carbon homologation of chiral α-hydroxyaldehydes with 2-trimethylsilylthiazole **2**[16] should have numerous synthetic applications, particularly for the synthesis of the less common L-sugars and of deoxysugars and amino sugars.[17]

Received: April 28, 1986;
supplemented: June 19, 1986 [Z 1748 IE]
German version: *Angew. Chem. 98* (1986) 822

CAS Registry numbers:
1, 15186-48-8; **2**, 79265-30-8; **3a**, 103795-09-1; **3b**, 103795-10-4; **3c**, 103795-11-5; **4**, 103795-12-6; **5a**, 103795-13-7; **5b**, 103795-14-8; **5c**, 103795-15-9; **6**, 103795-16-0; **7a**, 103795-17-1; **7b**, 103795-18-2; **7c**, 103795-19-3; **8**, 103795-20-6; **9a**, 103795-21-7; **9b**, 103795-22-8; **9c**, 103795-23-9; **10**, 103795-24-0; **11a**, 103795-25-1; **11b**, 103795-26-2; **11c**, 103795-27-3; **12**, 103795-28-4; **13a**, 103795-29-5; **13b**, 103795-30-8; **13c**, 103795-31-9; **14**, 103795-32-0; **15**, 103795-33-1; **16**, 103795-34-2; **17**, 103795-35-3; **18**, 103795-36-4; **19**, 103795-37-5; **20**, 103795-38-6; **21**, 103795-39-7; **22**, 103795-40-0.

[1] S. Hanessian: *Total Synthesis of Natural Products. The Chiron Approach*, Pergamon Press, Oxford 1983; B. Fraser-Reid, T. F. Tam, K. M. Sun in B. M. Trost, C. R. Hutchinson (Eds.): *Organic Synthesis, Today and Tomorrow*, Pergamon Press, Oxford 1981, p. 319; S. Hanessian, *Acc. Chem. Res. 12* (1979) 159; B. Fraser-Reid, *ibid. 8* (1975) 195; T. D. Inch, *Tetrahedron 40* (1984) 3161.

[2] Reviews: a) S. Y. Ko, A. W. M. Lee, S. Masamune, L. A. Reed III, K. B. Sharpless, F. J. Walker, *Science 220* (1983) 949; b) G. J. McGarvey, M. Kimura, T. Oh, J. M. Williams, *J. Carbohydr. Chem. 3* (1984) 125; c) recent articles: G. Fronza, C. Fuganti, P. Grasselli, S. Servi, *Tetrahedron Lett. 26* (1985) 4961; Y. Kita, Y. Yasuda, O. Tamura, F. Itoh, *ibid. 26* (1985) 5777; P. DeShong, J. M. Leginus, *ibid. 25* (1984) 5355; S. Hanessian, P. J. Murray, S. P. Sahoo, *ibid. 26* (1985) 5623, 5627, 5631; T. Mukaiyama, T. Yamada, K. Suzuki, *Chem. Lett. 1983*, 5; P. DeShong, C. M. Dicken, J. M. Leginus, R. R. White, *J. Am. Chem. Soc. 106* (1984) 5598; S. J. Danishefsky, W. H. Pearson, D. F. Harvey, C. J. Maring, J. P. Springer, *ibid. 107* (1985) 1256; S. J. Danishefsky, C. J. Maring, *ibid. 107* (1986) 1269; S. J. Danishefsky, M. Bednarski, *Tetrahedron Lett. 26* (1985) 3411; A. K. Forest, R. R. Schmidt, *ibid. 25* (1984) 1769; R. R. Schmidt, M. Maier, *ibid. 26* (1985) 2065; V. Jäger, I. Müller, *ibid. 26* (1985) 2997; A. P. Kozikowski, C.-S. Li, *J. Org. Chem. 50* (1985) 778; C. Papageorgiou, C. Benezra, *ibid. 50* (1985) 157; M. S. Manhas, V. R. Hegde, D. R. Wagle, A. K. Bose, *J. Chem. Soc. Perkin Trans. 1 1985*, 2045; S. Hanessian, J. Kloss, *Tetrahedron Lett. 26* (1985) 1261; F. Freeman, K. D. Robarge, *ibid. 26* (1985) 1943; T. M. Williams, H. S. Mosher, *ibid. 26* (1985) 6269.

[3] Review on the use of **1** in stereoselective synthesis: J. Jurczak, S. Pikul, T. Bauer, *Tetrahedron 42* (1986) 447.

[4] A. Dondoni, M. Fogagnolo, A. Medici, P. Pedrini, *Tetrahedron Lett. 26* (1985) 5477; A. Dondoni, *Lect. Heterocycl. Chem. 8* (1985) 13, and references cited therein.

[5] *General experimental procedure:* a) Addition reaction: A solution of the aldehyde (0.5 g) and 1.5 molar equivalents of **2** in anhydrous CH_2Cl_2 (20 mL) was stirred for 10 h at room temperature. The solvent was evaporated under reduced pressure and the residue was treated with 1.5 molar equivalents of nBu_4NF in 30 mL of tetrahydrofuran (THF). After 2 h, aqueous work-up of the solution and chromatography (silica gel, cyclohexane/ethyl acetate) furnished the desilylated adduct. A solution of the latter in 30 mL of THF was added to a suspension of NaH (1.2 molar equivalents) in 50 mL of THF. After 30 min at room temperature, 0.1 molar equivalents of nBu_4NI and 1.1 molar equivalents of $PhCH_2Br$ were added in that order. After 3 h, the usual work-up furnished the *O*-benzylated adduct in quantitative yield. b) Conversion of the thiazole ring into the formyl group: A solution of the *O*-benzylated adduct (1 g) and MeI (10 molar equivalents) in 20 mL of acetonitrile was heated under reflux until the adduct was totally consumed (as monitored by TLC). After distillation of the solvent and excess MeI under reduced pressure, the crude thiazolium iodide was dissolved in anhydrous MeOH and treated with 1.5 molar equivalents of $NaBH_4$ at −10°C. After 30 min, 2 mL of acetone was added; the solvent was then removed by distillation and the residue treated with a concentrated aqueous solution of NaCl. Extraction with ethyl acetate and distillation of the solvent furnished the crude thiazolidine, which was dissolved in 3 mL of acetonitrile and slowly added to a solution of $HgCl_2$ (1.2 molar equivalents) in 30 mL of acetonitrile/H_2O (4:1). The mixture was stirred for 30 min and then filtered. The filtrate was evaporated to dryness and the residue treated with water and extracted with CH_2Cl_2. Distillation of the solvent furnished the aldehyde essentially pure.

[6] In this as well as in the other sequences of Scheme 1, the product distribution in the crude reaction mixture and the diastereomeric purity of the chromatographically isolated adduct were determined by 80-MHz NMR. All products were identified on the basis of their mass and NMR (80- or 300-MHz) spectra as well as elemental analyses.

[7] Benzylation of the newly formed hydroxyl group affords 5–10% of the epimer.

[8] O. Achmatowicz in B. M. Trost, C. R. Hutchinson (Eds.): *Organic Synthesis, Today and Tomorrow*, Pergamon Press, Oxford 1981, p. 307.

[9] S. J. Danishefsky, E. Larson, J. P. Springer, *J. Am. Chem. Soc. 107* (1985) 1274; S. J. Danishefsky, W. H. Pearson, B. E. Segmuller, *ibid. 107* (1985) 1280; S. S. Danishefsky, M. Barbachyn, *ibid. 107* (1985) 7761; S. J. Danishefsky, C. J. Maring, *ibid. 107* (1985) 7762.

[10] The X-ray analysis and ^{1}H-NMR data reported in [4] refer to **5b** (R = H) rather than to **5a** (R = $SiMe_3$), as erroneously stated.

[11] **16**: 40% overall yield, optically inactive (c = 0.95, MeOH or $CHCl_3$); ^{1}H-NMR (300 MHz, $CDCl_3$): δ = 2.29 (br., 2H; 2OH), 3.27 (br., 2H; 2OH), 3.61 (m, 4H; 2 CH_2OH), 3.84 (s, 4H; 4 CH-OBn), 4.05 (s, 2H; 2 CH-OH), 4.57 (AB system, J = 11.4 Hz, 4H; 2 CHPh), 4.64 (AB system, J = 10.8 Hz, 4H; 2 CH_2Ph), 7.26 (s, 20H; 4 Ph); ^{13}C-NMR (20.115 MHz, C_6D_6): δ = 64.41 (t; CH_2OH), 72.56 (d; CH-O), 73.70 (d; CH-O), 74.01 (d; CH-O), 80.01 (t, CH_2Ph), 80.27 (t, CH_2Ph), 138.36 (s), 138.93 (s).

[12] D. H. R. Barton, W. B. Motherwell in B. M. Trost, C. R. Hutchison (Eds.): *Organic Synthesis, Today and Tomorrow*, Pergamon Press, Oxford 1981, p. 1.

[13] **18**: 45% overall yield, $[\alpha]_D^{20}$ = 4.5 (c = 2.75, $CHCl_3$); selected data: IR (film): ν = 1735 cm^{-1}; ^{1}H-NMR (80 MHz, $CDCl_3$): δ = 2.72 (dd, J = 0.22 Hz, 2H; CH_2CHO), 9.76 (t, J = 0.22 Hz, 1H; CHO). For syntheses of 2-deoxy-D-ribose from nonsugars see: T. Harada, T. Mukaiyama, *Chem. Lett. 1981*, 1109; M. Cherest, H. Felkin, N. Prudent, *Tetrahedron Lett. 1968*, 2119; Y. Kita, H. Yasuda, O. Tamura, F. Itoh, *ibid. 26* (1985) 5777.

[14] The inversion of configuration at C-2 was assigned on the basis of the reasonable assumption that the substitution occurs by an S_N2 mechanism. **19**: 60% overall yield, $[\alpha]_D^{20}$ = 39.7 (c = 1.75, $CHCl_3$); selected data: IR (film): ν = 2120 cm^{-1}; **20**: 82%; IR (film): ν = 3320, 3390 cm^{-1} (NH_2).

[15] **22**: 40% overall yield, $[\alpha]_D^{20}$ = 27.6 (c = 1.0, $CHCl_3$); ^{1}H-NMR (80 MHz, $CDCl_3$): δ = 2.33 (dd, J = 4.2 Hz, J = 4.8 Hz, 1H; 1H of CH_2-O), 2.66 (dd, J = 4.0 Hz, J = 4.2 Hz, 1H; 1H of CH_2-O), 3.17 (m (should be ddd with J = 4.0, 4.8, and 5.0 Hz) 1H, CH-O), 3.56 (dd, J = 5.0 Hz, J = 6.6 Hz, 1H; CH-OBn), 4.67 (AB system, J = 11.0 Hz, 2H; CH_2Ph), 4.68 (AB system, J = 12.0 Hz, 2H; CH_2Ph), 4.98 (d, J = 5.0 Hz, CH-OBn), 7.27 (m, 11H; Aryl-H), 7.78 (d, J = 3.2 Hz, 1H; 4-H of the thiazole ring).

[16] **2**, in virtue of its superior diastereofacial selectivity in the addition to chiral aldehydes, appears to be the reactant of choice with respect to other metalated heterocycles (see [4] and references cited therein).

[17] See [1, 2b] and S. Umezawa, *Adv. Carbohydr. Chem. Biochem. 30* (1974) 213; V. Jäger, I. Müller, R. Schohe, M. Frey, R. Ehrler, B. Häfele, D. Schröter, *Lect. in Heterocycl. Chem. 8* (1985) 79.

The Isolobal Analogy "d^6-$CpM(CO)_3^{\ominus}$ ⟷ $Cp^{\ominus}$"**

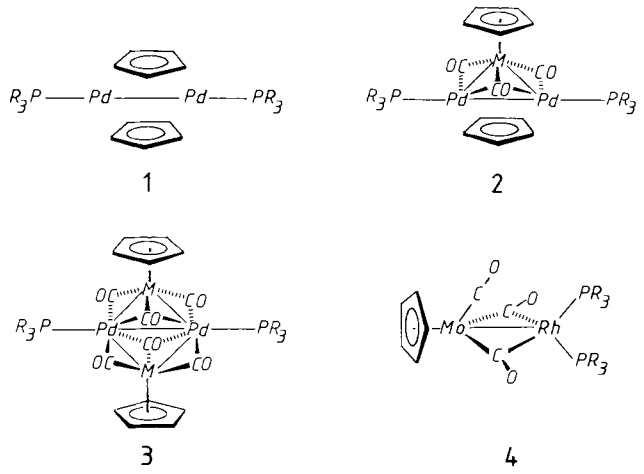
By *Peter Hofmann** and *Helmut R. Schmidt*

The isolobal concept[1] has proved to be a powerful principle in organometallic chemistry for the description of complex structures and the planning of synthetic strategies.[2] We show here an interesting isolobal analogy between the ubiquitous $C_5H_5^{\ominus}$ ($Cp^{\ominus}$) ligand and tricarbonyl(η^5-cyclopentadienyl)metalate ions $[(\eta^5\text{-}C_5H_5)M(CO)_3]^{\ominus}$ (M = Cr, Mo, W) having a d^6 configuration of the metal.

Recently, bimetallic sandwich compounds and clusters have been reported and structurally characterized in which $Cp^{\ominus}$ ligands and $CpM(CO)_3^{\ominus}$ fragments apparently can replace each other. Examples are **1**,[3] **2**,[4] and **3**.[5] A study of the electronic structure of **1** and its analogues has shown[6] that $Cp^{\ominus}$ functions only as a four-electron donor in these complexes, which apparently corresponds to M–Pd metal–metal interactions and μ_2- as well as μ_3-CO

[*] Prof. Dr. P. Hofmann, Dipl.-Chem. H. R. Schmidt
Anorganisch-chemisches Institut der Technischen Universität München
Lichtenbergstrasse 4, D-8046 Garching (FRG)

[**] This work was supported by the Deutsche Forschungsgemeinschaft and the Fonds der Chemischen Industrie.



bridges between the metals in clusters like **2** and **3**. The mononuclear groups $CpNi(CO)^{\oplus}$, $Ni(PR_3)_2^{\oplus}$, $Rh(PR_3)_2^{\oplus}$, and $Cu(PR_3)_2^{\oplus}$ are also known to function as binding partners toward $CpM(CO)_3^{\ominus}$ fragments,[7] displaying interactions between M and the second metal atom as well as between this metal atom and two carbonyl C atoms of the $CpM(CO)_3^{\ominus}$ fragment, as in **4**.[7c] Furthermore, a Pd_3Mo cluster was reported[8] recently, in which $CpMo(CO)_3^{\ominus}$ acts as a six-electron ligand. The isolobal relationship between $Cp^{\ominus}$ and d^6-$CpM(CO)_3^{\ominus}$ suggested[5b] by the existence of systems such as **2**, **3**, and **4**, and the general ability of such d^6 building blocks to replace $Cp^{\ominus}$ in a variety of bonding situations, is discussed in this communication.

Decisive for the electronic relationship to $Cp^{\ominus}$ are the highest occupied valence MOs of $CpM(CO)_3^{\ominus}$, $1a_1$ and 1e,[9] which display z^2, x^2-y^2, and xy character at the metal center ("pseudo-t_{2g} set")[1b] and contain π^* contributions from the three CO ligands mixed into these MOs in a bonding manner.

Figure 1, left, shows a qualitative drawing of these three MOs (for bent M–C–O units as in **2** or **3**); Figure 2, left, gives contour plots[10] of these orbitals in a plane below the three carbonyl C atoms, corresponding to those for the

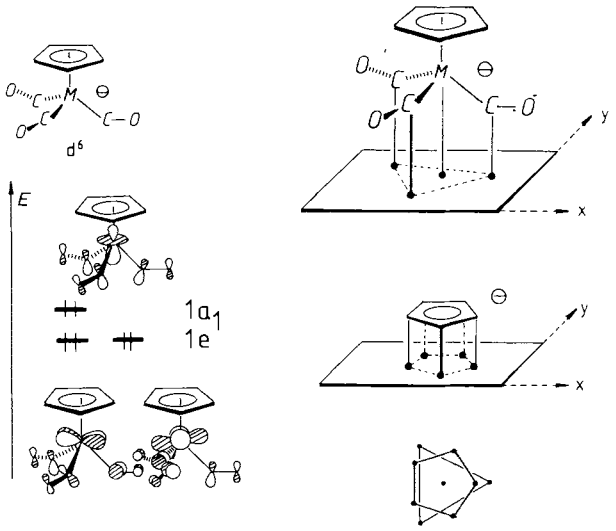


Fig. 1. Left: Qualitative depiction of the three highest occupied valence MOs of $CpMo(CO)_3^{\ominus}$ [10]; right (top to bottom): planes for plotting wave function contours for the MOs (see Fig. 2) of $CpMo(CO)_3^{\ominus}$ and of $Cp^{\ominus}$; comparison of the size of the Cp five-membered ring and the C_3 triangle of the carbonyl C atoms of $CpMo(CO)_3^{\ominus}$.

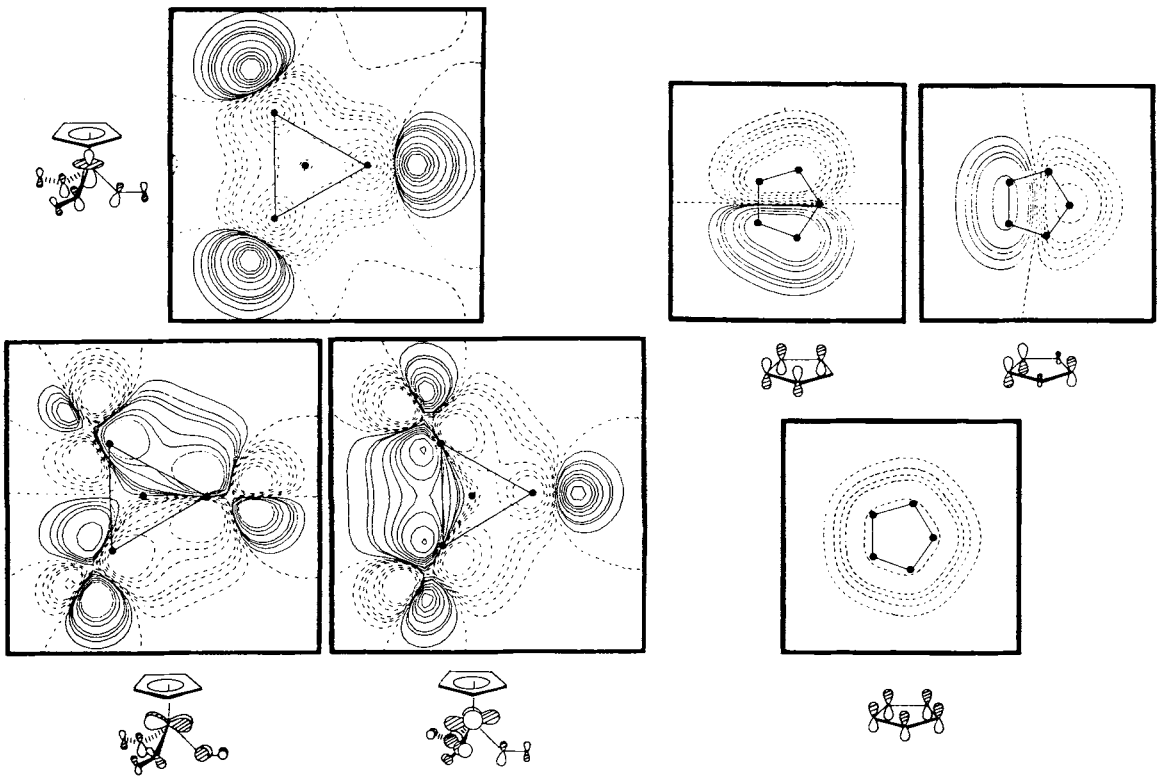


Fig. 2. Left: Representation of wave function contours for the three highest occupied valence MOs of $CpMo(CO)_3^{\ominus}$ [10] in a plane below the three carbonyl C atoms; right: corresponding representation for $Cp^{\ominus}$ (see Fig. 1).

three occupied π-MOs of $Cp^{\ominus}$ in Figure 2, right. The appearance and nodal properties of the three MOs for each of the two systems are very similar in the plane shown, that is, with respect to a potential binding partner in this position; moreover, the Cp five-membered ring and the C_3 triangle of the carbonyl C atoms have comparable dimensions (see Fig. 1, right).

Important is the fact that the areas of the wave functions of $CpM(CO)_3^{\ominus}$ that are available for bonding toward other fragments involve in each case the carbonyl C atoms *and* the metal center (in contrast to, for example, other "tripod" ligands[11]), so that overlap with a second metal fragment $M'L_n$ necessarily implies M–M′ interactions *as well*. Depending on the number and symmetry of the acceptor MOs[1] of a binding partner, $CpM(CO)_3^{\ominus}$ can formally provide two, four, or six electrons and, in analogy to η^1-, η^2-, ..., η^5-bonded Cp rings, can bind $M'L_n$ fragments more or less symmetrically to the carbonyl C atoms *and* M. As for the $Cp^{\ominus}$ rings in **1** and **2**, practically unhindered rotation of the $CpM(CO)_3^{\ominus}$ half-sandwich fragments in **2** and **3** is observed. Because the $1a_1$ and 1e MOs are nearly degenerate, the position of acceptor groups requiring less than six electrons (e.g., $Rh(PR_3)_2^{\oplus}$ or $Cu(PR_3)_2^{\oplus}$) can be adjusted quite flexibly. Of course, a direct bond to the metal atoms ("piano stool" structure) is preferred for pure σ-acceptors ($CH_3^{\oplus}$, $H^{\oplus}$). Interestingly, for $Cu(PR_3)_2^{\oplus}$ (d^{10}-ML_2) both structural alternatives are found.[7c] $M'L_n$ fragments with three acceptor MOs, such as $Mn(CO)_3^{\oplus}$, $CpFe^{\oplus}$, and $(\eta^6$-$C_6H_6)Mn^{\oplus}$, should bind $CpM(CO)_3^{\ominus}$ symmetrically and sandwichlike. *Härter* et al.[12] report the example of the complex composed of $(\eta^4$-$C_4H_4)Co^{\oplus}$ and $CpW(CO)_3^{\ominus}$.

It remains to be explored experimentally to what degree the isolobal analogy d^6-$CpM(CO)_3^{\ominus}$ ⟷ $Cp^{\ominus}$ discussed here, can be extended to analogous building blocks, such as the neutral species $(\eta^6$-$C_6H_6)Cr(CO)_3$ or $CpMn(CO)_3$ as binding partners of suitable, likewise neutral fragments. Undoubtedly, the redox compatability will also play a decisive role. The electronic structures specifically described[7b, 14] for $Ni(PR_3)_2^{\oplus}$ (one unpaired electron) and CpRh(CO) binding to d^6-fragments $CpW(CO)_3^{\ominus}$ and $(C_6H_6)Cr(CO)_3$ also emerge from the analogy d^6-$CpM(CO)_3^{\ominus}$ ⟷ $Cp^{\ominus}$. Its value—taking into account the known limitations[1, 2] of the isolobal principle and extending of alternative concepts—lies in the possibility of simply depicting electronic and structural relationships of complex molecules and of planning synthetic strategies.

Received: April 28, 1986 [Z 1751 IE]
German version: *Angew. Chem. 98* (1986) 810

CAS Registry numbers:
$Cp^{\ominus}$, 12127-83-2; $CpCr(CO)_3^{\ominus}$, 48121-47-7; $CpMo(CO)_3^{\ominus}$, 12126-18-0; $CpW(CO)_3^{\ominus}$, 12126-17-9.

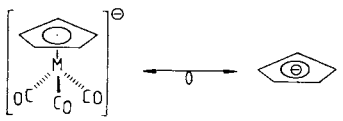
[1] a) R. Hoffmann, *Angew. Chem. 94* (1982) 725; *Angew. Chem. Int. Ed. Engl. 21* (1982) 711; b) T. A. Albright, J. K. Burdett, M. H. Whangbo: *Orbital Interactions in Chemistry*, Wiley, New York 1985.
[2] F. G. A. Stone, *Angew. Chem. 96* (1984) 85; *Angew. Chem. Int. Ed. Engl. 23* (1984) 85.
[3] H. Werner, *Adv. Organomet. Chem. 19* (1981) 155.
[4] H. Werner, H.-J. Kraus, P. Thometzek, *Chem. Ber. 115* (1982) 2914.
[5] a) R. Bender, P. Braunstein, J.-M. Jud, Y. Dusausoy, *Inorg. Chem. 22* (1983) 3394; b) analogous clusters are known with Pt in place of Pd: *ibid. 23* (1984) 4489.
[6] Presented at the Chemiedozententagung 1982, Kaiserslautern; P. Hofmann, R. Hoffmann, P. Dobosh, unpublished results, partly to be found in [3].
[7] a) $CpNi(CO)^{\ominus}$: T. Madach, H. Vahrenkamp, *Chem. Ber. 113* (1980) 2675; b) $Ni(PR_3)_2^{\ominus}$: L. Carlton, W. E. Lindsell, K. J. McCullough, P. N. Preston, *Organometallics 4* (1985) 1138; c) $Rh(PR_3)_2^{\oplus}$ and $Cu(PR_3)_2^{\oplus}$: L. Carlton, W. E. Lindsell, K. J. McCullough, P. N. Preston, *J. Chem. Soc. Dalton Trans. 1984*, 1693.
[8] P. Braunstein, J. Fischer, D. Matt, M. Pfeffer, *J. Am. Chem. Soc. 106* (1984) 410.
[9] $Cp^{\ominus}$ regarded as rotationally symmetric, pseudo-C_3, symmetry.
[10] $1a_1$ and 1e, obtained from EH-MO calculations, are shown for M = Mo.
[11] W. Kläui, M. Scotti, M. Valderrama, S. Rojas, G. M. Sheldrick, P. G. Jones, T. Schroeder, *Angew. Chem. 97* (1985) 697; *Angew. Chem. Int. Ed. Engl. 24* (1985) 638.
[12] P. Härter, H. Pfisterer, M. L. Ziegler, *Angew. Chem. 98* (1986) 812; *Angew. Chem. Int. Ed. Engl. 25* (1986) 839.
[13] a) The known $[(\eta^6$-$C_6H_6)_2Cr_2(\mu_2$-$CO)_3]$ can be regarded as an analogue of $[(\eta^6$-$C_6H_6)_2Cr]$: P. Klüfers, L. Knoll, C. Reiners, K. Reiss, *Chem. Ber. 118* (1985) 1852; b) $[(\eta^5$-$C_5Me_5)_2Fe_2(\mu_2$-$CO)_3]$, which has two unpaired electrons, corresponds to nickelocene: J. P. Blaha, B. E. Bursten, J. C. Dewan, R. B. Frankel, C. L. Randolph, B. A. Wilson, M. S. Wrighton, *J. Am. Chem. Soc. 107* (1985) 4561; c) heterodinuclear Mn–Cr and Mn–Fe systems are known (albeit without X-ray structure analyses): W. A. Herrmann, C. E. Barnes, R. Serrano, B. Koumbouris, *J. Organomet. Chem. 256* (1983) C30.
[14] R. D. Barr, T. B. Marder, A. G. Orpen, I. D. Williams, *J. Chem. Soc. Chem. Commun. 1984*, 112.

The Complex Ions $[C_5H_5M(CO)_3]^{\ominus}$ (M = Mo, W) as 6e-Ligands: Synthesis and Molecular Structure of $[(\eta^4$-$C_4Me_4)Co(\mu$-$CO)_3M(\eta^5$-$C_5H_5)]$ (M = Mo, W)**

By *Peter Härter,* Heike Pfisterer,* and *Manfred L. Ziegler*

The carbonyl metalates $[(\eta^5$-$C_5H_5)M(CO)_3]^{\ominus}$ of the chromium series display a wide range of bonding behavior toward acceptor molecules;[1, 2] they can coordinate directly through the metal without CO bridging, but they can also act as two-, four-, or six-electron ligands.[3–5]

On the basis of a theoretical analysis of this coordination behavior, *Hofmann* and *Schmidt* demonstrated the isolobal relationship of the organometallic fragment $[(\eta^5$-$C_5H_5)M(CO)_3]^{\ominus}$ with the cyclopentadienide ion $[C_5H_5]^{\ominus}$ in structurally related half-sandwich complexes.[6]



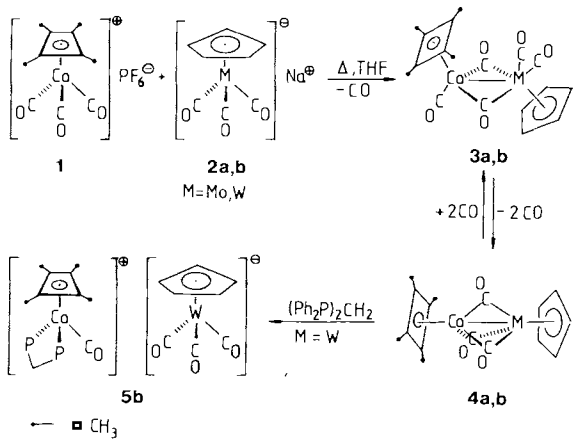
We have now found the first example of a symmetric coordination of $[(\eta^5$-$C_5H_5)M(CO)_3]^{\ominus}$ (M = Mo, W) in binuclear, sandwich-like complexes.

The cationic tetramethylcyclobutadiene complex **1**[7] reacts with the carbonyl metalates **2a**, **b** in tetrahydrofuran (THF) to give the new binuclear CoMo and CoW complexes **3a** and **3b**, which can be isolated in good yields by gentle column chromatography.[8] Upon heating, however,

[*] Dr. P. Härter
Anorganisch-chemisches Institut der Technischen Universität München
Lichtenbergstrasse 4, D-8046 Garching (FRG)
Dr. H. Pfisterer, Prof. Dr. M. L. Ziegler
Anorganisch-chemisches Institut der Universität
Im Neuenheimer Feld 270, D-6900 Heidelberg 1 (FRG)

[**] This work was supported by the Deutsche Forschungsgemeinschaft, the Fonds der Chemischen Industrie, and the Bundesministerium für Forschung und Technologie.

they are converted into the derivatives **4a** and **4b**, with loss of two carbonyl groups.



The initially formed complexes **3a** and **3b** exhibit the usual carbonyl bridging ligands (ν_{CO} = 1843 and 1856 cm^{-1}, respectively, in *n*-hexane), whereas the derivatives **4a** and **4b** were presumed to have carbonyl bridges with unusual coordination because of the positions of the CO bands at 1803 and 1805 cm^{-1}, respectively. Also striking were the strong high-field shifts of the methyl signals in the ^{1}H-NMR spectra (δ = 1.05 and 0.92, respectively, in C_6D_6) in comparison to the spectra of similar or even isoelectronic complexes such as **6**,[9] in which these signals

$[(\eta^4\text{-}C_4Me_4)Fe(\mu\text{-}CO)_3Mn(\eta^5\text{-}C_5Me_5)]$ **6** $[(\eta^4\text{-}C_4Me_4)Co(\eta^5\text{-}C_5H_5)]$ **7**

usually appear in the range δ = 1.5–2.1.[10] Only in the mononuclear sandwich complex **7**,[11] which has been known for a long time but is quite different at first glance, is the methyl signal of the four-membered-ring ligand found at δ = 1.22.

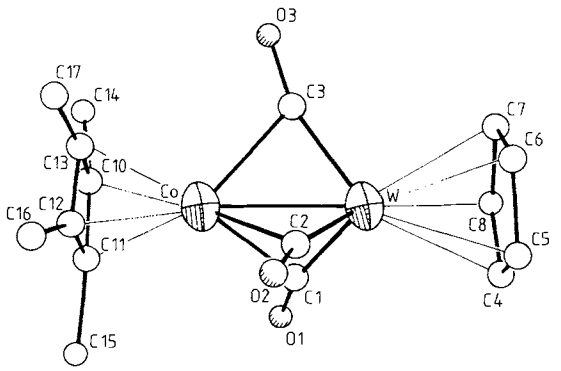


Fig. 1. Molecular structure of the CoW complex **4b** in the crystal (hydrogen atoms omitted). Monoclinic (from *n*-hexane/toluene, 98 + 2 vol.-%), space group C_{2h}^5-$P2_1/n$; a = 728.6(2), b = 2361.6(4), c = 1010.7(2) pm, β = 110.74(2)°, Z = 4; R_{aniso} = 0.071, R_w = 0.053. Selected bond lengths [pm] and angles [°]: W-Co 235.6(0), W-C1 196(3), W-C2 195(2), W-C3 188(3), Co-C1 219(3), Co-C2 215(4), Co-C3 204(2), C1-O1 115(3), C2-O2 121(3), C3-O3 121(4); W-C(1...3)-O(1...3) 162(2), Co-C(1...3)-O(1...3) 126(2), Co-W-C(1...3) 56.1–60.3, W-Co-C(1...3) 50.0–50.8, W-C1-CO 60(1), W-C2-Co 70(1), W-C3-Co 74(1).

In order to explain these observations, the crystal structure of **4b** was determined by X-ray diffraction analysis (Fig. 1).[12] The two ring ligands are parallel and form roughly a right angle with the CoW bond axis. The $(\eta^5\text{-}C_5H_5)W(CO)_3$ fragment has a slightly distorted trigonal-pyramidal structure and is held to the $(\eta^4\text{-}C_4Me_4)Co$ moiety through its carbonyl groups (interligand angle 94–97°); the metal atom of this moiety is thereby located in the center of a pyramidal structure. As a result of the metal binding of the $(\eta^5\text{-}C_5H_5)W(CO)_3$ partial structure, the W-C-O groups form an angle of ca. 162°. The M-CO distances also reflect the polar structure of the complex, the distances of the Co atom (the center of the acceptor portion), to C(1...3) are considerably larger than the W-C(1...3) distances. Similar differences have been observed in other polarized binuclear complexes.[13] Although the Co-W distance of only 235.6 pm can be correlated with a formal triple bond, it is more instructive, taking into consideration the isolobal analogy,[6] to view the new compounds discussed here as structural analogues of the sandwich complex **7**.

Preliminary investigations have shown that **4b** not only undergoes reversible CO addition to give **3b**, but also forms the ionic complex **5b** when it is allowed to react with chelating phosphanes such as methylenebis(diphenylphosphane).

Received: April 28, 1986;
revised: June 10, 1986 [Z 1750 IE]
German version: *Angew. Chem. 98* (1986) 812

CAS Registry numbers:
1, 86664-08-6; **2b**, 12107-36-7; **3a**, 103671-23-4; **3b**, 103693-13-6; **4a**, 103671-22-3; **4b**, 103671-19-8; **5b**, 103671-21-2; Co, 7440-48-4; Mo, 7439-98-7; W, 7440-33-7.

[1] M. Y. Darensbourg, *Prog. Inorg. Chem. 33* (1985) 221.
[2] C. P. Horwitz, D. F. Shriver, *Adv. Organomet. Chem. 23* (1984) 219.
[3] J. St. Denis, W. Butler, M. D. Glick, J. P. Oliver, *J. Am. Chem. Soc. 96* (1974) 5427.
[4] $[(\eta^5\text{-}C_5H_5)M(CO)_3]^\ominus$ as 4e donor: a) R. Bender, P. Braunstein, J. M. Jud, Y. Dusausoy, *Inorg. Chem. 23* (1984) 4489; b) H. Werner, H. J. Kraus, P. Thometzek, *Chem. Ber. 115* (1982) 2914; c) L. Carlton, W. E. Lindsell, K. J. McCullough, P. N. Preston, *J. Chem. Soc. Dalton Trans. 1984*, 1693.
[5] $[(\eta^5\text{-}C_5H_5)M(CO)_3]^\circ$ as 6e donor: P. Braunstein, J. Fischer, D. Matt, M. Pfeffer, *J. Am. Chem. Soc. 106* (1984) 410.
[6] P. Hofmann, H. R. Schmidt, *Angew. Chem. 98* (1986) 810; *Angew. Chem. Int. Ed. Engl. 25* (1986) 837.
[7] P. Härter, P. L. Pauson, S. S. Ullah, *J. Organomet. Chem. 247* (1983) C27.
[8] *Experimental procedure:* **1** (1.2 g, 3 mmol) and **2b** (1.14 g) were heated in 50 mL of THF for 3 h at reflux. After cooling of the solution, 2 g of silica gel was added to the mixture. The solution was evaporated to dryness and chromatographed (toluene/*n*-hexane 1 : 3) on silica gel (Merck 7734, activity II-III, column 60 × 1.4 cm, −15°C). After elution of a yellow band, which was discarded, **3b** eluted as a bright red band. The second product, **4b**, eluted as a brown band with toluene/*n*-hexane (1 : 1). After removal of the solvent, both products were purified by recrystallization: **3b** from toluene/*n*-hexane (1 : 2) at −35°C; 860 mg (51%); **4b** from toluene/*n*-hexane (1 : 1) at −35°C; 150 mg (10%). **3b** was converted into **4b**, with elimination of CO, by heating in refluxing toluene for 3 h; yield 80%.
[9] W. A. Herrmann, C. E. Barnes, R. Serrano, B. Koumbouris, *J. Organomet. Chem. 256* (1983) C30.
[10] A. Efraty, *Chem. Rev. 77* (1977) 691.
[11] R. Bruce, P. M. Maitlis, *Can. J. Chem. 45* (1967) 2017.
[12] Further details of the crystal structure investigation may be obtained from the Fachinformationszentrum Energie, Physik, Mathematik GmbH, D-7514 Eggenstein-Leopoldshafen 2 (FRG), on quoting the depository number CSD-52060, the names of the authors, and the journal citation.
[13] H. Werner, B. Klingert, R. Zolk, P. Thometzek, *J. Organomet. Chem. 266* (1984) 97, and references cited therein.

Stabilization of Carbenium Ions in Liquid Crystals**

By *Gerhard R. Bauer, Franz Dickert,** and *Albert Hammerschmidt*

Dedicated to Professor Walther Jaenicke on the occasion of his 65th birthday

Carbenium ions are usually prepared in non-nucleophilic solvents.[1-3] In order to establish whether ordered phases are also capable of stabilizing carbenium ions, it appeared especially advantageous to investigate the formation of the almost planar trityl ion $Ph_3C^{\oplus}$ from the tetrahedral Ph_3CX in nematic liquid crystals. The influence of ordered phases as solvents on chemical reactions is usually limited to viscosity effects.[4,5] Other phenomena are seldom observed.[6,7]

The dissociation equilibrium (a) of 4-methoxytriphenylmethyl trifluoroacetate **1** in a nematic phase (Licristal 1052 Merck = eutectic mixture of **4** and **5**) was investigated.

$$\underset{\mathbf{1}}{MeOC_6H_4{-}CPh_2{-}O_2CCF_3} \rightleftharpoons \underset{\mathbf{2}}{MeOC_6H_4{-}\overset{\oplus}{C}Ph_2} + \underset{\mathbf{3}}{F_3CCO_2^{\ominus}} \quad (a)$$

$$\underset{\mathbf{4}}{C_6H_{13}OC_6H_4CO_2{-}C_6H_4{-}C_5H_{11}} \qquad \underset{\mathbf{5}}{MeOC_6H_4CO_2{-}C_6H_4{-}C_5H_{11}}$$

The equilibrium (a) can be monitored by way of the characteristic absorption of the carbenium ion at 481 nm.[8] The measurements were carried out in cuvettes with a layer thickness of 10^{-3} cm. To ensure uniform orientation of the liquid crystals, and thus to avoid light-scattering, the surface of the glass was treated with Me_2SiCl_2. The liquid crystal is then homeotropically oriented, i.e. the longitudinal axes of the molecules in the mesophase are arranged perpendicular to the surface of the glass.[9-13] This can be ascertained by inspection under a polarizing microscope. On inspecting the textures, schlieren of strength $s = \pm 1$ but not $s = \pm 1/2$ are observed.[14,15] Moreover, with these glass plates, in contrast to those treated with diamond paste (orientation of the liquid crystal parallel to the glass surface[10]), no light-dark effect is observed on rotating the crossed nicol prisms.

The extinction of the solutions investigated is shown in Figure 1 as a function of the temperature. The sudden increase in the extinction for the phase transition isotropic→nematic is indicative of an increase in the concentration of carbenium ions. Hence, it can be concluded that, compared to the isotropic solution, the directed phase stabilizes carbenium ions. The same effect is also observed in the presence of trifluoroacetic acid, but the extinction is altogether greater.[3] Apparently, as shown schematically in Figure 2, the almost planar carbenium ion is preferably incorporated in the rod-shaped liquid crystal structure. The concentration of carbenium ions is increased by ca. 10% by the isotropic→nematic phase transition.

The position of the maximum absorption of the carbenium ion is identical in the isotropic and anisotropic

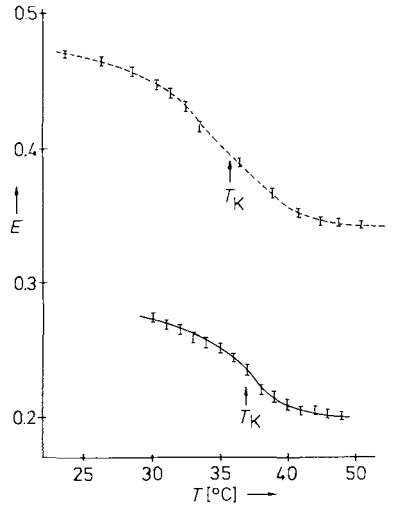


Fig. 1. Extinction of the 4-methoxytriphenylmethyl cation **2** (0.1 mol L^{-1}) in the nematic liquid crystals (——) and in presence of 10 mol-% F_3CCO_2H (----) as a function of temperature; corrected for residual scattering of the pure mesophase; T_K = clearing point for the nematic→isotropic transition.

phases, from which it can be concluded that the ion in both phases has the same electronic structure, particularly as regards twisting of the phenyl rings.[8] The free trifluoroacetate ion shows a typical, triplet-like structure in the ^{19}F-NMR spectra, because of the dipolar coupling in the nematic phase.

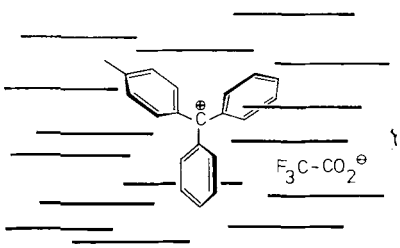


Fig. 2. Incorporation of the almost planar carbenium ion in the nematic liquid crystal (schematic).

The investigations showed that orientation phenomena favor ion formation even in hydrophobic media. Such effects could also be of interest for other directed phases such as micelles and membranes.

Received: April 30, 1986;
revised: June 16, 1986 [Z 1754 IE]
German version: *Angew. Chem. 98* (1986) 825

CAS Registry number:
MeO-*p*-$C_6H_4CPh_2O_2CCF_3$, 90173-59-4

[*] Prof. Dr. F. Dickert, Dipl.-Chem. G. R. Bauer, Dr. A. Hammerschmidt
Institut für Physikalische und Theoretische Chemie
der Universität Erlangen-Nürnberg
Egerlandstrasse 3, D-8520 Erlangen (FRG)

[**] This work was supported by the Deutsche Forschungsgemeinschaft and the Fonds der Chemischen Industrie. We thank Prof. Dr. *H. Hoffmann*, Institut für Physikalische Chemie der Universität Bayreuth, for the use of a polarizing microscope.

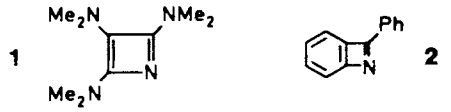
[1] G. A. Olah, J. A. Olah in G. A. Olah, P. von R. Schleyer (Eds.): *Carbonium Ions, Vol. II*, Wiley, New York 1970.
[2] H. Kessler, M. Feigel, *Acc. Chem. Res. 15* (1982) 2.
[3] F. L. Dickert, H. Fackler, *Angew. Chem. 94* (1982) 303; *Angew. Chem. Int. Ed. Engl. 21* (1982) 295.
[4] S. I. Torgova, E. I. Kovshev, V. V. Titov, *Zh. Org. Khim. 12* (1976) 1593.
[5] W. E. Bacon, G. H. Brown, *Mol. Cryst. Liq. Cryst. 12* (1971) 229.
[6] J. P. Otruba III, R. G. Weiss, *J. Org. Chem. 48* (1983) 3448.
[7] J. P. Otruba III, R. G. Weiss, *Mol. Cryst. Liq. Cryst. 80* (1982) 165.
[8] G. R. Bauer, *Dissertation*, Universität Erlangen-Nürnberg 1986.
[9] H. Kelker, R. Hatz: *Handbook of Liquid Cristals*, Verlag Chemie, Weinheim 1980.

[10] G. Meier, E. Sackmann, J. G. Grabmeier: *Applications of Liquid Crystals*, Springer, Berlin 1975.
[11] W. Greubel, H. Krüger, U. Wolff, DOS 2163606.
[12] F. J. Kahn, *Appl. Phys. Lett. 22* (1973) 386.
[13] E. Ruiz-Hitzky, J. M. Rojo, G. Lagaly, *Colloid Polym. Sci. 263* (1985) 1025.
[14] D. Demus, L. Richter: *Textures of Liquid Crystals*, Verlag Chemie, Weinheim 1978.
[15] J. Nehring, A. Saupe, *J. Chem. Soc. Faraday Trans. 2, 68* (1971) 1.

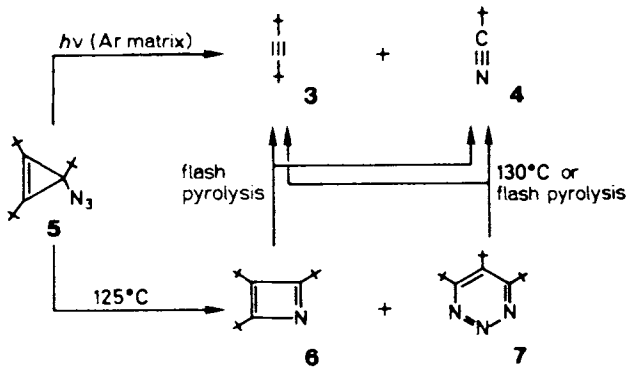
Tri-*tert*-butylazete—The First Kinetically Stabilized Azacyclobutadiene**

By *Uwe-Josef Vogelbacher, Manfred Regitz,** and *Richard Mynott*

Although a great deal has been published in the last few years about the chemistry of the cyclobutadienes,[1] our knowledge of the azetes (azacyclobutadienes) is still only scanty. Up to now only the two thermodynamically stabilized azetes **1**[2] and **2**[3] have been obtained, in admixture with other products, by flash pyrolysis of the corresponding triazines. All attempts to prepare electronically pure azetes have so far failed.



Thus, on low-temperature irradiation[4,5] or on flash pyrolysis[6] of 1,3-oxazin-6-ones, only nitriles and acetylenes, the formal decomposition products of the corresponding azetes, were obtained. The same holds for the thermal decomposition of Dewar-pyridazines[7] and for the photolysis of trimethylcyclopropenylazide.[8,9] Even the azide **5**, which has all the steric prerequisites for the generation of the kinetically stabilized azete **6**, afforded only N_2 and the fragments **3** and **4** under matrix conditions.[5,9] Despite these discouraging results, we have—based on experience gained in cyclobutadiene chemistry[10]—exploited the thermolysis of **5** as an entry to azete chemistry (Scheme 1).



Scheme 1.

When the azide **5**[11] was heated in the absence of solvent to 125°C and subsequently distilled under vacuum the azete **6** was obtained as the main product in the form of reddish-brown needles (m.p. 37°C) that are sensitive to oxidation. Chromatographic work-up of the residue from the distillation afforded the triazine **7**[11] (m.p. 130°C) as by-product. The "azete fragments" **3** and **4** could not be detected in the product by NMR spectroscopy, but they are formed quantitatively when **7** is photolytically ($\geq$280 nm) decomposed in pentane at 20°C. Since **6** is stable under these conditions, the formation of the fragments must start from tri-*tert*-butylcyclopropenylnitrene (presumably triplet). This explains why even matrix photolysis of **5**[5] fails to produce the target compound. The thermolysis **5**→**6** should therefore be interpreted as a synchronous reaction.

The azete **6** is characterized by its extreme thermal stability; no change was observed in its NMR spectra after several days in [D_8]toluene at 100°C. On the other hand, under flash pyrolysis conditions (700°C/5×10^{-6} mbar)—as in cyclobutadiene chemistry[12]—the cycloreversion **6**→**3**+**4** takes place (100%, 1:1). The same result is obtained upon thermolysis of the triazine **7** at 130°C or upon its flash pyrolysis.



The constitution of the azete **6** has been confirmed by elemental analysis, mass spectrometry, and NMR spectroscopy.[13] Only two *t*Bu signals in the intensity ratio 2:1 are observed in the ^{1}H-NMR spectrum at room temperature. Therefore, assuming that the ground-state is rectangular, it can be concluded that a rapid valence isomerization **6A**⇄**6B** is taking place. This has been proven by ^{13}C-NMR spectroscopy.[14] The resonance of C-3 at $\delta=134.4$ remains sharp in the temperature range from −110°C to +100°C. The other two ring carbon atoms, C-2 and C-4, however, give rise to one very broad signal at $\delta\approx181$ at room temperature; this signal becomes sharp at +100°C, while on cooling to −110°C it splits into two equally intense lines at $\delta=158.8$ and 203.7 (C-4 and C-2, respectively, in **6A**). The position of the latter line is comparable with that of the imino carbon atom of Dewar-pyridines.[15]

Experimental

6: 1.25 g (5 mmol) of **5** [11] was heated under argon for 90 min at 125°C (oil-bath temperature); the thermolysis product turned dark-brown (IR monitoring, disappearance of the azide absorption at 2090 cm^{-1}). Kugelrohr distillation at 60°C (oven temperature)/0.05 mbar afforded 0.61–0.72 g (55–65%) of a dark-brown oil, which immediately solidified; recrystallization from a small amount of pentane furnished reddish-brown needles of m.p. 37°C.

7: Obtained from the residue from the distillation by medium-pressure chromatography with petroleum ether (30–75°C)/ether (4:1). This afforded 40–60 mg (3–5%) of colorless crystals of m.p. 130°C (from pentane).

Received: June 6, 1986 [(1804 IE]
German version: *Angew. Chem. 98* (1986) 835

CAS Registry numbers:
5, 38409-72-2; **6**, 103794-87-2; **7**, 103794-88-3

[*] Prof. Dr. M. Regitz, Dipl.-Chem. U.-J. Vogelbacher
Fachbereich Chemie der Universität
Erwin-Schrödinger-Strasse, D-6750 Kaiserslautern (FRG)
Dr. R. Mynott
Max-Planck-Institut für Kohlenforschung
Kaiser-Wilhelm-Platz 1, D-4330 Mülheim an der Ruhr (FRG)

[**] Syntheses with Cyclobutadienes, Part 16. This work was supported by the Deutsche Forschungsgemeinschaft and the Fonds der Chemischen Industrie.—Part 15: H. Wingert, G. Maas, M. Regitz, *Tetrahedron*, in press.

[1] See, e.g., H. Kimling, A. Krebs, *Angew. Chem. 84* (1972) 952; *Angew. Chem. Int. Ed. Engl. 11* (1972) 932; S. Masamune, N. Nakamura, M. Suda, H. Ona, *J. Am. Chem. Soc. 95* (1973) 8481; G. Maier, S. Pfriem, U.

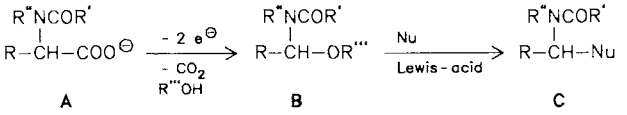
Schäfer, R. Matusch, *Angew. Chem. 90* (1978) 532; *Angew. Chem. Int. Ed. Engl. 17* (1978) 520.
[2] G. Seybold, U. Jersak, R. Gompper, *Angew. Chem. 85* (1973) 918; *Angew. Chem. Int. Ed. Engl. 12* (1973) 847.
[3] B. M. Adger, M. Keating, C. W. Rees, R. C. Storr, *J. Chem. Soc. Chem. Commun. 1973*, 19; B. M. Adger, C. W. Rees, R. C. Storr, *J. Chem. Soc. Perkin Trans. 1 1975*, 45.
[4] G. Maier, U. Schäfer, *Tetrahedron Lett. 1977*, 1053.
[5] G. Maier, U. Schäfer, *Liebigs Ann. Chem. 1980*, 798.
[6] T. O. Glasbey, P. W. Manley, R. C. Storr, *J. Chem. Res. (S) 1981*, 162.
[7] P. Eisenbarth, M. Regitz, *Chem. Ber. 117* (1984) 445.
[8] G. L. Closs, A. G. Harrison, *J. Org. Chem. 37* (1972) 1051.
[9] This suggests that the products of fragmentation are formed, at least in part, from cyclopropenylnitrenes; for an analogous reaction of cyclopropenylcarbenes see: P. Eisenbarth, M. Regitz, *Angew. Chem. 94* (1982) 935; *Angew. Chem. Int. Ed. Engl. 21* (1982) 913; *Angew. Chem. Suppl. 1982*, 2016.
[10] Synthesis of *tert*-butyl tri-*tert*-butylcyclobutadienecarboxylate by thermolysis of *tert*-butyl tri-*tert*-butylcyclopropenyldiazoacetate: H. Wingert, M. Regitz, *Chem. Ber. 119* (1986) 244.
[11] The isomerization is expressly ruled out in the literature: R. Curci, V. Luccini, G. Modena, P. J. Kocienski, J. Ciabattoni, *J. Org. Chem. 38* (1973) 3149.
[12] P. Eisenbarth, M. Regitz, *Chem. Ber. 115* (1982) 3796.
[13] **6**: IR (NaCl): 2960 (CH), 1569 cm^{-1} (C=N/C=C); MS (70 eV): *m/z* 221 ($M^{\oplus}$, 0.7%), 57 [$(H_3C)_3^{\oplus}$, 100]; ^{1}H-NMR (200 MHz, 40°C, $CDCl_3$): $\delta = 1.10$ (s, 9H, 3-*t*Bu), 1.15 (s, 18H, 2,4-*t*Bu); ^{13}C-NMR (75.5 MHz, [D_8]toluene, −110°C): $\delta = 203.7$ (s, 1C, C-2), 158.8 (s, 1C, C-4), 134.1 (s, 1C, C-3), 37.3, 34.9 [s, each 1C, 2,4-$C(CH_3)_3$], 30.5 [s, 1C, 3-$C(CH_3)_3$], 26.5 (br., 6C, C-methyl), 30.5 (3C, C-methyl); ^{13}C-NMR (50.3 MHz, [D_8]toluene, +100°C): $\delta = 180.9$ (s, 2C, C-2,4), 134.4 (s, 1C, C-3), 35.7 [s, 2C, 2,4-$C(CH_3)_3$], 30.4 [s, 1C, 3-$C(CH_3)_3$], 27.1 (6C, C-methyl), 30.9 (3C, C-methyl); UV (hexane): $\lambda = 320$ (broad, $\varepsilon = 145$).
[14] In the case of tri-*tert*-butylcyclobutadiene this has been achieved only by the isotopic-perturbation method described by Saunders: G. Meier, H. O. Kalinowski, K. Euler, *Angew. Chem. 94* (1982) 706; *Angew. Chem. Int. Ed. Engl. 21* (1982) 693.
[15] J. Fink, M. Regitz, *Bull. Soc. Chim. Fr. 1986*, 239.

Preparation of Chiral Building Blocks from Amino Acids and Peptides via Electrolytic Decarboxylation and $TiCl_4$-Induced Aminoalkylation**

By *Philippe Renaud* and *Dieter Seebach**

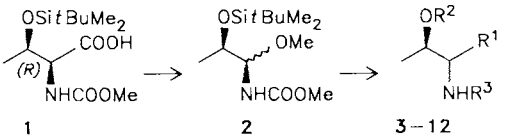
Dedicated to Professor Vladimir Prelog on the occasion of his 80th birthday

In the anodic oxidation of *N*-acylated amino acids **A** in protic media, *N,O*-acetal derivatives **B**[1] are formed. These can be used as electrophilic amidoalkylating[2] reagents[3,4] (Scheme 1). When the groups R, R′ and/or R″ are chiral there is the possibility of performing stereoselective nucleophilic substitutions to give compounds **C**. Until now, this was only performed in the case of cyclization reactions[4,5] and with cyclic[6] acetals,[7] which upon opening with nucleophiles underwent inversion of configuration at the acetal center.[8] We have now shown with appropriate amino acid derivatives which possess chiral substituents in all the three positions of **A** — R, R′, and R″ (Scheme 1)— that we are able to carry out diastereoselective substitutions and to prepare interesting, and in some cases novel, enantiomerically pure building blocks.



Scheme 1.

In the first case (R in **A** chiral) we chose the threonine derivative **1**,[9] which, by electrolysis in methanol, was converted into a 1:1 mixture of *N,O*-acetals **2** in 75% yield. This mixture was subsequently converted by reaction with nucleophilic reagents (see Table 1) into the amino alcohol derivatives **3**–**12** (Scheme 2), which included phosphonothreonine and phosphonoallothreonine esters **7**. The diastereoselectivity was between 55 and 85%; however, in some cases the major diastereoisomer could be isolated by recrystallization (see Table 1).



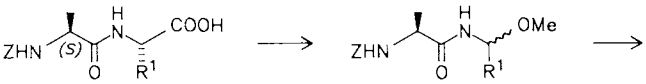
1 **2** **3**–**12**

a: (*R,R*); **b**: (*R,S*)

	R^2 = *t*BuMe$_2$Si R^1	R^3		R^2, R^3 = H R^1
3	CH_2–CH=CH_2	COOMe	**4**	CH_2–CH=CH_2
5	CN	COOMe		
6	$PO(OPh)_2$	COOMe	**7**	$PO(OH)_2$
8	$PO(OMe)_2$	COOMe		
9	Me	COMe	**10**	Me
11	C_6H_{13}	COC_6H_{13}	**12**	C_6H_{13}

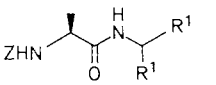
Scheme 2.

As examples for the second case (R′ in **A** chiral) we chose the N-protected dipeptides **13** and **14**, derived from the coupling of (*S*)-alanine with glycine and (*S*)-valine,[10] respectively, as our substrates. Electrolysis of the glycine derivative gave the acetal **15** in 95% yield. The anodic oxidation of the alanyl-valine dipeptide gave a mixture of two diastereoisomers **16** (95%, 1.2:1), the alkylation and phosphorylation of which gave the products **18** and **19** (see Scheme 3 and Table 1)[11]. Phosphonopeptides **17** (from



13: R^1 = H
14: R^1 = *i*Pr

15: R^1 = H
16: R^1 = *i*Pr



17: R^1 = H, R^2 = $PO(OPh)_2$
18: R^1 = *i*Pr, R^2 = CH_2–CH=CH_2
19: R^1 = *i*Pr, R^2 = $PO(OPh)_2$

Z = $PhCH_2OCO$; **a**: (*S,S*), **b**: (*S,R*)

Scheme 3.

15) and **19** are of particular interest because of their biological activity.[12]

Finally, in the third case (R″ in **A** chiral) we investigated the *cis* acetals **20** and **21** which were derived from serine methyl ester via treatment with isobutyraldehyde/methyl chloroformate and pivalaldehyde/methyl chloroformate, respectively, in accordance with an earlier published procedure[13]. These gave after electrolysis in acetic acid the acetoxy derivatives **22** and **23** (85% and 87% yield, 90% and >97% *ds*), respectively, both products arising from re-

[*] Prof. Dr. D. Seebach, Dipl.-Chem. P. Renaud
Laboratorium für Organische Chemie der
Eidgenössischen Technischen Hochschule
ETH-Zentrum, Universitätstrasse 16, CH-8092 Zürich (Switzerland)

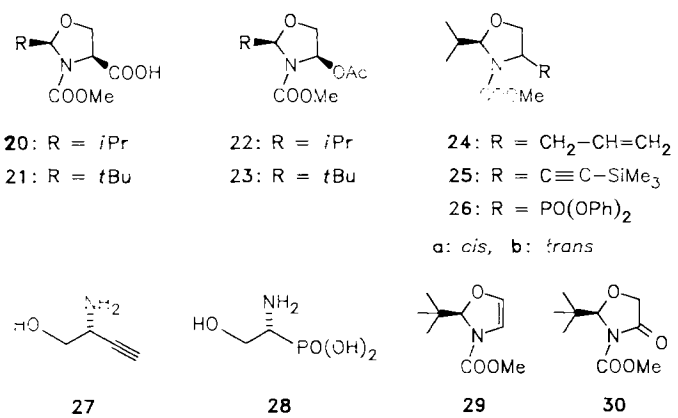
[**] Part of the projected Ph. D. thesis by *P. R.*, ETH Zürich.

Table 1. Yields and selectivities of the *N,O*-acetal reactions with nucleophiles. Concomitant with the substitution at the acetal center, the N-COOMe group was converted during the *Grignard* reaction into an *N*-acetyl- (**2** → **9** → **10**) and *N*-heptanoyl group (**2** → **11** → **12**), respectively. Products of hydrolysis are also given. For physical data see Table 2.—For details of the electrolysis technique see [16]; for general procedure see [8].

Educt	Reagent	Product	Yield [%]	**a** : **b** [a]	Product of hydrolysis	Method [b]	Yield [%]
2	CH_2=CH–CH_2–$SiMe_3$, $TiCl_4$	**3**	85	4 : 1	**4**,	A	80 [c]
2	Me_3SiCN, $TiCl_4$	**5**	93	2 : 1	L-threonine,	B [c]	
2	$P(OPh)_3$, $TiCl_4$	**6**	90	2 : 1 [c]	**7**,	B	92
2	$P(OMe)_3$, $TiCl_4$	**8**	90	1 : 1.2	**7**,	B	90
2	CH_3MgCl	**9**	70	1 : 4 [c]	**10**,	B	
2	$C_6H_{13}MgBr$	**11**	70	1 : 4	**12**,	B	
15	$P(OPh)_3$, $TiCl_4$	**17**	60	—			
16	CH_2=CH–CH_2–$SiMe_3$, $TiCl_4$	**18**	60	1.1 : 1 or 1 : 1.1 [c]			
16	$P(OPh)_3$, $TiCl_4$	**19**	60	1 : 1.4			
22	CH_2=CH–CH_2–$SiMe_3$,Cl_2Ti ($OiPr_2$)$_2$	**24**	80	4 : 1 [d]			
22	Me_3Si–C≡C–$SiMe_3$	**25**	80	9 : 1 [d]	**27**,	B	75
22	$P(OPh)_3$, $TiCl_4$	**26**	95	4 : 1 [d]	**28**,	B	80

[a] See schemes for specification. [b] Method A: KOH, NH_2NH_2, ethylene glycol; B: 6 N HCl. [c] Diastereomerically pure products were obtained by recrystallization. [d] Diastereomerically pure products were isolated after column chromatography.

tentive oxidative substitution. Only in the case of the isobutyraldehyde acetal **22** were we able to perform diastereoselective substitutions (80–90% *ds*), again principally with retention of configuration, thus giving us access to the allyl-, alkynyl- and diphenylphosphono derivatives **24–26** (Scheme 4 and Table 1). The configuration of **26** was proved by hydrolysis and subsequent correlation[14] with phosphoserine **28**; the configuration of **25** was determined



Scheme 4.

Table 2. Some characteristic physical data of the described compounds. For most of them, complete IR, ^{1}H- and ^{13}C-NMR, MS as well as $[\alpha]_D$ data and correct elemental analyses were obtained. All the $[\alpha]_D$ values were measured in $CHCl_3$ at $c = 1$. ^{31}P-NMR: δ values relative to $PO(OPh)_3$ (= 0).

4: as acetonide-hydrochloride, m.p. 129–130 °C
7a: ^{1}H-NMR (D_2O): 1.28 (d), 2.91 (dd), 3.96–4.09 (m), m.p. 234–236 °C
7b: ^{1}H-NMR (D_2O): 1.25 (d), 3.14 (dd), 4.12–4.24 (m), m.p. 220–221 °C
9b: m.p. 68.5–69.5 °C, $[\alpha]_D^{25} = -46.1°$
10b: ^{13}C-NMR ($CDCl_3$): 17.31, 17.67, 51.42, 70.38 (cf. [17])
12b: ^{13}C-NMR ($CDCl_3$): 14.06, 16.99, 22.65, 26.67, 29.53, 31.86, 32.91, 56.31, 69.67 (**12a**) (cf. [18])
17: m.p. 107.5–108.5 °C, $[\alpha]_D^{25} = -12.6°$
18: m.p. 99.5–101.0 °C
19: m.p. 113.5–114.5 °C, ^{31}P-NMR (DMSO): 21.06 (20.96 minor diastereomer)
20: m.p. 69.0–70.5 °C, $[\alpha]_D^{25} = -38.7°$
22: ^{1}H-NMR ($CDCl_3$): 2.06 (s), 3.73 (s), 5.03 (d), 6.47 (t)
23: $[\alpha]_D^{25} = +25.4°$, ^{13}C-NMR ($CDCl_3$): 97.78, 83.24, 72.70 [a]
24: $[\alpha]_D^{25} = +3.0°$, ^{13}C-NMR ($CDCl_3$): 94.38, 69.36, 56.73 [a]
25: $[\alpha]_D^{25} = +73.4°$, ^{13}C-NMR ($CDCl_3$): 94.53, 71.69, 48.54 [a]
26: $[\alpha]_D^{25} = -20.4°$, ^{31}P-NMR ($CDCl_3$): 12.60
29: b.p. (Kugelrohr): 120 °C/12 torr, $[\alpha]_D = +434°$
30: $[\alpha]_D^{25} = +121.7°$

[a] Signals of the three carbon atoms in the ring.

using NMR difference NOE measurements. The alkyne **25** can be hydrolyzed to the aminoalkynol **27**. Elimination of acetic acid from **23** gives access to the chiral glyoxal derivative **29**. In addition, alkaline hydrolysis of the acetates followed by oxidation (pyridinium dichromate) yields the chiral glycolic acid derivative **30**. Both of these compounds are starting materials for a large number of enantiomerically pure products.[15]

The fact that products of high diastereomeric purity are sometimes formed on starting from the diastereomeric mixture of *N,O*-acetals (cf. **2** → **3**) obtained by electrolysis indicates that an α-acylaminocarbocation is an intermediate.—Some characteristic physical data of the new compounds reported herein are given in Table 2.

Received: June 16, 1986 [Z 1820 IE]
German version: *Angew. Chem. 98* (1986) 836

[1] R. P. Linstead, B. R. Shepard, B. C. L. Weedon, *J. Chem. Soc. 1951*, 2854; T. Iwasaki, H. Horikawa, K. Matsumoto, M. Miyoshi, *J. Org. Chem. 44* (1979) 1552; *Bull. Chem. Soc. Jap. 52* (1979) 826; H. Hofer, M. Moest, *Justus Liebigs Ann. Chem. 323* (1902) 285.
[2] H. Hellmann, *Angew. Chem. 69* (1957) 463; H. E. Zaugg, *Synthesis 1984*, 85, 181, and references cited therein.
[3] T. Shono: *Electroorganic Chemistry as a New Tool in Organic Synthesis*, Springer, Berlin 1984.
[4] W. N. Speckamp, H. Hiemstra, *Tetrahedron 41* (1985) 4367.
[5] W. S. Johnson, C. A. Harbert, B. E. Ratcliffe, R. D. Stipanovic, *J. Am. Chem. Soc. 98* (1976) 6188.
[6] J. D. Elliott, J. Steele, W. S. Johnson, *Tetrahedron Lett. 26* (1985) 2535, and references cited therein.
[7] Exceptions: K. Irie, K. Aoe, T. Tanaka, S. Saito, *J. Chem. Soc. Chem. Commun. 1985*, 633; R. Imwinkelried, D. Seebach, *Angew. Chem. 97* (1985) 781; *Angew. Chem. Int. Ed. Engl. 24* (1985) 765; M. M. Campbell, N. I. Carruthers, *Tetrahedron 38* (1982) 2513.
[8] For a complete discussion see the review article: D. Seebach, R. Imwinkelried, T. Weber in R. Scheffold (Ed.): *Modern Synthetic Methods 1986, Vol. 4*. Springer, Berlin 1986, pp. 125–260.
[9] By methoxycarbonylation ($ClCOOCH_3$) and subsequent silylation ($tBuMe_2SiCl$) of L-threonine.
[10] Commercially available products were used directly.
[11] See the reductive decarboxylation of dipeptides: D. H. R. Barton, Y. Hervé, P. Potier, J. Thierry, *J. Chem. Soc. Chem. Commun. 1984*, 1298.
[12] J. W. Huber, W. F. Gilmore, L. W. Robertson, *J. Med. Chem. 18* (1975) 106; J. Rachon, *Chimia 37* (1983) 299, and references cited therein.
[13] D. Seebach, J. D. Aebi, *Tetrahedron Lett. 25* (1984) 2545.
[14] R. Huber, A. Knierzinger, J.-P. Obrecht, A. Vasella, *Helv. Chim. Acta 68* (1985) 1730.
[15] M. Gander-Coquoz, G. Stucky, ETH Zürich, unpublished results 1985/86.
[16] D. Seebach, P. Renaud, *Helv. Chim. Acta 68* (1985) 2342; P. Renaud, D. Seebach, *Synthesis 1986*, 424.
[17] H. J. Schneider, M. Lonsdorfer, *Org. Magn. Reson. 16* (1981) 133.
[18] M. Bessades, E. Abushanab, K. Antonal, *Tetrahedron Lett. 25* (1984) 5899.

Structures with Oligomeric Condensed Clusters in Indium Oxomolybdates

By *Arndt Simon,* Wilhelm Mertin, Hansjürgen Mattausch,* and *Reginald Gruehn*

In many cases the structures of metal-rich compounds of the transition metals are describable in terms of condensed clusters.[1] Thus, infinite chains of Mo_6-octahedra condensed via opposite edges are present in the structure of $NaMo_4O_6$, which are surrounded by O atoms, above all the free octahedral edges, in the same way as the known M_6X_{12} clusters.[2] Such Mo_4O_6 chains are found in a series of reduced oxomolybdates.[3]

The Mo_4O_6 chains can be interrupted by structural disorder in the crystal. $In_{11}Mo_{40}O_{62}$ is the first compound[4] where such structural "disorder" occurs at regular intervals with formation of defined fragments of the Mo_4O_6 chain. Discrete cluster anions with four or five condensed Mo_6-octahedra are arranged in layers, which are stacked in an alternating sequence (Fig. 1a). A single oligomeric cluster of five condensed octahedra is shown in Figure 1b. All (free) edges of the octahedra are bridged by O-atoms. The channels between the cluster anions are occupied by linear M–M bonded polycations (In_5^{7+} in the case of $(Mo_6)_4$-clusters and In_6^{8+} in the case of $(Mo_6)_5$-clusters). The layers seen in Figure 1a have the general composition $In_{n+1}Mo_{4n+2}O_{6n+4}$, where n indicates the number of Mo_6 octahedra in each cluster. The structure of $In_{11}Mo_{40}O_{62}$ is

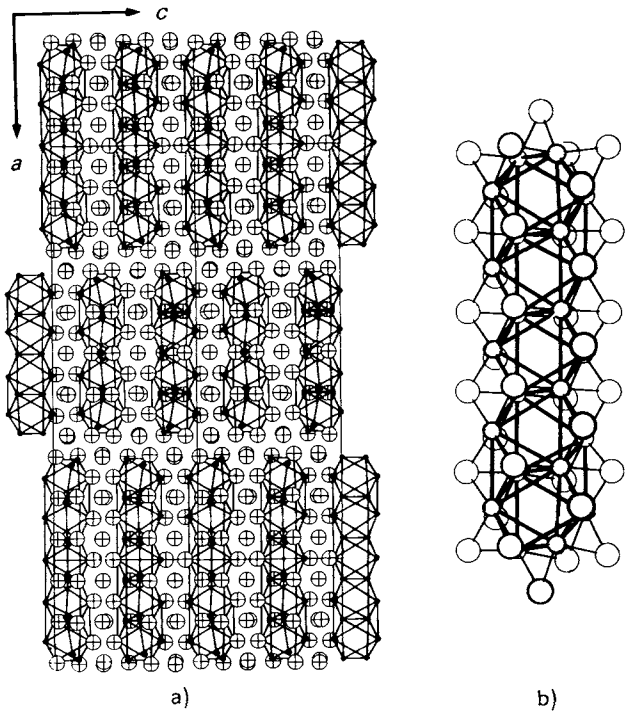


Fig. 1. a) Projection of the crystal structure of $In_{11}Mo_{40}O_{62}$ on (010). The oligomeric clusters containing four $(Mo_6)_4$ and five $(Mo_6)_5$ octahedra, respectively, are arranged in layers (small circles: Mo atoms; large circles with cross: O atoms). Between the clusters there are linear In_5^{7+} and In_6^{8+} ions (black circles), respectively. b) Oligomeric cluster with five edge-linked Mo_6 octahedra in $In_{11}Mo_{40}O_{62}$.

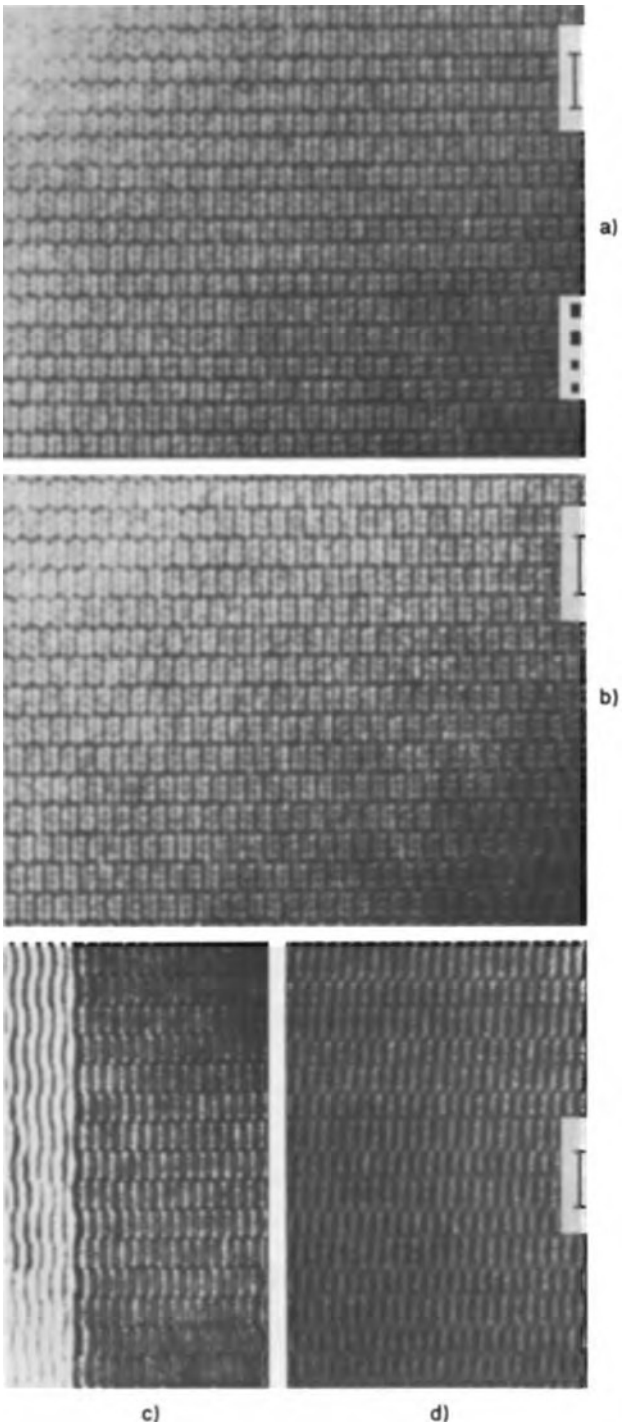


Fig. 2. Electron microscopic photographs of indium oxomolybdate with cluster layers of the general composition $In_{n+1}Mo_{4n+2}O_{6n+4}$. The lengths and orientations of the axes are indicated; cf. text (initial magnification 440000×, 120 kV; Philips EM 400 with HMG goniometer stage; LaB_6 electron source; computer simulations of the image contrast are presently under way. a) $In_{11}Mo_{40}O_{62}$ (h01); stacking disorders, which however do not lead to a change in composition, are shown by black rectangles (large, for two consecutive layers with $(Mo_6)_5$ clusters; small, with $(Mo_6)_4$ clusters. b, c) $In_3Mo_{11}O_{17}$: homogeneous sequences of layers with $(Mo_6)_5$ clusters viewed in two directions (*a* axis in the plane of the picture). d) $In_3Mo_{11}O_{17}$: modification with alternating sequences of $(Mo_6)_4$- and $(Mo_6)_6$-layers cluster (in the same direction as c).

[*] Prof. Dr. A. Simon, Dr. H. Mattausch
Max-Planck-Institut für Festkörperforschung
Heisenbergstrasse 1, D-7000 Stuttgart 80 (FRG)
Dr. W. Mertin, Prof. Dr. R. Gruehn
Institut für Anorganische und Analytische Chemie der Universität
Heinrich-Buff-Ring 58, D-6300 Giessen (FRG)

formed by intergrowth of $In_5Mo_{18}O_{28}$ and $In_6Mo_{22}O_{34}$ layers in the ratio 1 : 1.

The number of Mo–Mo bonding states can be estimated by suitable fragmentation of the oligomeric cluster into $Mo_6O_{12}+(n-1)Mo_4O_6$.[5,6] Accordingly, one expects, besides "homogeneous structures" (i.e. structures with a single type of layers), also structures with clusters of other lengths. A first confirmation of their existence was provided by high-resolution transmission electron microscopy.[7] Figure 2a shows the alternating sequence of cluster layers in an $In_{11}Mo_{40}O_{62}$ crystal fragment. The thicknesses of the layers are 1300 ($(Mo_6)_4$) and 1580 pm ($(Mo_6)_5$), respectively; the difference corresponds exactly to the mean length of an Mo_6-octahedron edge (280 pm), and the sum corresponds to the lattice constant, determined more accurately by X-ray diffraction ($a=2887.8$ pm), of $In_{11}Mo_{40}O_{62}$. Such alternating layer sequences occur in ordered regions of 10^5 pm. In Figure 2a a section is intentionally reproduced in which stacking disorder is recognizable. The variation in the composition of the crystal through two consecutive $In_5Mo_{18}O_{28}$ layers is compensated by two immediately adjacent $In_6Mo_{22}O_{34}$ layers. In the same sample, regions are found (Fig. 2b) that are exclusively made up of identical $In_6Mo_{22}O_{34}$ layers over distances of 10^5 pm. In the meantime, the respective new compound $In_3Mo_{11}O_{17}$ has been isolated as a homogeneous phase and has been characterized by X-ray crystallography ($a=3160.8$, $b=948.9$, $c=983.9$ pm).

Another crystal zone of the $In_3Mo_{11}O_{17}$ fragment is shown in Figure 2c. In Figure 2d, an alternate stacking of layers with $(Mo_6)_4$ and the new $(Mo_6)_6$ clusters can be seen, which, having regular sequences, likewise leads to the composition $In_3Mo_{11}O_{17}$ with the same translational period $a=3160$ pm.

Thus, there is every indication of a similar diversity of oligomeric clusters with edge-linked Mo_6 octahedra in the case of oxomolybdates, like that already known in the case of metal-rich chalcogenides with face-linked Mo_6-octahedra.[8] Furthermore, there is the possibility of determining the lengths of the polycations of main-group metals between the clusters via the lengths of the clusters.

Received: June 12, 1986 [Z 1814 IE]
German version: *Angew. Chem. 98* (1986) 831

CAS Registry numbers:
$In_{11}Mo_{40}O_{62}$, 103691-57-2; $In_3Mo_{11}O_{17}$, 103980-72-9.

[1] A. Simon, *Angew. Chem. 93* (1981) 23; *Angew. Chem. Int. Ed. Engl. 20* (1981) 1.
[2] C. C. Torrardi, R. E. McCarley, *J. Am. Chem. Soc. 101* (1979) 3963.
[3] R. E. McCarley, K.-H. Lii, P. A. Edwards, L. F. Brough, *J. Solid State Chem. 57* (1985) 17.
[4] H. Mattausch, A. Simon, E.-M. Peters, *Inorg. Chem.*, in press.
[5] A. Simon, H. Mattausch, E.-M. Peters, Z. Kristallogr. *174* (1986) 188.
[6] A. Simon in A. K. Cheetham, P. Day (Eds.): *Inorganic Solids*, Oxford University Press, in press.
[7] R. Gruehn, W. Mertin, *Angew. Chem. 92* (1980) 531; *Angew. Chem. Int. Ed. Engl. 19* (1980) 505.
[8] R. Chevrel, P. Gougeon, M. Potel, M. Sergent, *J. Solid State Chem. 57* (1985) 25.

BOOK REVIEWS

With Chemistry into the Third Millenium

Opportunities in Chemistry. Edited by: The Committee to Survey Opportunities in the Chemical Sciences, National Research Council. National Academy Press, Washington, D.C. 1985. vii, 344 pp., bound, $ 24.75.—ISBN 0-309-03633-X

This book, which has become known as the "Pimentel Report," is the outcome of a study endorsed by the US National Research Council. A 26-membered "Committee to Survey Opportunities in the Chemical Sciences" set up by the NRC has compiled, under the leadership of *George C. Pimentel* and with the cooperation of more than 350 experts, a report documenting quite convincingly "the critical role played by chemistry in raising the quality of life, meeting the needs of society, and contributing substantially to a nations economic strength".[*] The main aim of the study was to answer the following questions:

- What opportunities are there in chemistry?
- How can chemists most effectively deploy the possibilities of chemistry for the future economic well-being of the community?
- How can we make the general public and their representatives in government aware of the importance of chemistry in solving economic problems and in satisfying the needs of society?
- How can we best inform the politicians such that they meet the correct decisions when granting financial support of research programs?

The experts who participated in this study come from all areas of chemical research, from academic, industrial, and national research institutes. The report is not meant primarily for the chemist but rather is directed at the interested public and the scientific policy makers.

The areas of chemistry which could become increasingly important in the future are outlined and used as a basis for recommending a reassessment of priorities in research investment. Thus, it is expected that chemistry will play an increasingly decisive role in the development of new processes and new materials in, inter alia, power supply, nutrition, hygiene, biotechnology, environmental protection, and will help in maintaining the competitiveness of the American industry and in contributing to the national security of the USA.

[*] Cf. also C & EN, January 6, 1986, p. 2.

Of particular interest to the scientist is the account of the current state of chemical research and technology and the developments to be expected in the innovative areas of chemistry. These include, in particular, the following areas: chemical kinetics, theoretical chemistry, catalysis, synthesis, the chemical fundamentals of life, and analytical methods.

From their account of the current state of and possible fields of development in chemistry the authors derive, from the American viewpoint, a number of scientific, industrial, and political recommendations, many of which might also be relevant for other industrial nations, and not least for the Federal Republic of Germany. The state of competitiveness of US chemistry is carefully brought into relief and attention is drawn to what other industrial nations are doing; thus, for example, it is pointed out that the Max-Planck-Society in Mainz has founded a new Polymer Institute.

This excellent work is concomitantly a concise account of our present chemical knowledge and, as such, also an avowal to research and industrial progress: "Chemistry is a central science that responds to societal needs" (P. 19). The "Pimentel Report" provides a scientifically sound and critical argument for all, who, despite the prevailing scepticism in our society, have faith in the future of chemistry.

Jan Thesing [NB 758 IE]
Merck, Darmstadt (FRG)

The Chemistry of Natural Products. Edited by *R. H. Thomson*. The Blackie Publishing Group, Glasgow 1985. xii, 467 pp., bound, £ 46.00.—ISBN 0-412-00551-4

To produce a book about the progress made in the chemistry of natural products in the last ten years is by no means an easy task. The authors do not claim to have written a comprehensive work, but are concerned rather with giving an outline of progress in the main areas of the chemistry of natural products. As the foreword makes clear, the main emphasis in all the contributions is on structure, chemistry and synthesis, but each chapter also includes notes on biosynthesis. The book is divided into nine chapters.

Chapter 1 *(J. S. Brimacombe)* deals with the chemistry of carbohydrates. The applications of protecting groups are, of course, discussed in detail here. This is followed by a survey of the synthesis of sugars with antibiotic activity. The reader is also given a compilation of natural products syntheses which have employed sugars to transfer stereochemical information, and descriptions of some oligosaccharide syntheses. The chapter ends, with a survey of structure determination in polysaccharides.

In Chapter 2, *E. J. Thomas* describes syntheses of aliphatic natural products. Syntheses of fatty acids and their derivatives, of leukotrienes, marine natural products, pheromones, prostaglandins, polyether antibiotics, and macrolides are discussed in detail. The reactions described in the text are illustrated by detailed charts, thus ensuring that even very complex schemes are clearly presented. A feature deserving special mention is the inclusion of lists of review articles on each of the topics mentioned above, which should help the user to find further literature in a particular area.

In Chapter 3, *T. J. Simpson* has compiled information on syntheses of aromatic compounds. For biosyntheses the reader is referred to relevant books. Individual classes of compounds are briefly dealt with in turn, including coumarins, chromanes, cannabinoids, butenolides, lignans, flavonoids, naphthoquinones, ansamycins, and so on.

Chapter 4, by *J. R. Hanson*, is a survey of terpenoids. The terpenes are dealt with in order of increasing number of isoprene units, and the chapter concludes with a short section on carotenoids. Owing to the enormous number of compounds it is not possible to give complete details of all the syntheses and biosyntheses. Here too the reader is referred to review articles. An incidental point here is that the reactants given under Scheme 12 ought to be included in Scheme 14.

In Chapter 5, *B. A. Marples* gives a survey on steroids. A general introduction is followed by sections on rearrangements, biomimetic syntheses, polyene cyclizations, and more recent partial and total syntheses. Lack of sufficient space has prevented some aspects from being treated in detail, e.g. the synthesis of polyenes.

In Chapter 6 *(B. W. Bycroft* and *A. A. Higton)*, aminoacids, peptides and proteins are discussed. If in addition to their chemistry, the biochemical or biosynthetic aspects had also been covered, it would have exceeded the limits of such a chapter. The first section deals with various amino acids, with detailed descriptions of a small number of syntheses. In the sections on peptides and proteins too, the presentation is mainly concerned with structural aspects. Methods for sequence determination in peptides and proteins are touched on briefly. All the sections contain numerous references to biochemical studies.

The subject of Chapter 7, by *I. R. C. Bick*, is alkaloids, which have been classified according to their biogenetic origin. In this chapter the main emphasis is on synthesis, but numerous references to the biochemistry and biosynthesis of the compounds are included.

In Chapter 8, *J. B. Hobbs* covers recent developments in the area of nucleotide chemistry. The chapter begins with a section on nucleosides (synthesis, reactivity and alkylation), followed by a similarly organized section on nucleotides. Three sub-sections are devoted to chirality at the phosphorus atom. The final section of this chapter deals with syntheses of nucleic acids and techniques for sequence determination.

In Chapter 9, *A. H. Jackson* deals with porphyrins and related compounds. The emphasis is on synthetic methods, together with a few digressions into biosynthesis. Following a section on porphyrins, chlorophylls and their analogs are discussed. A comparatively large amount of space is given to syntheses of Vitamin B_{12} and related compounds. The chapter ends with sections on bile pigments and prodigiosins.

The book is a very successful cooperative effort by the various authors. It is not suitable as a beginner's introduction to the chemistry of natural products, since it assumes some specialist chemical knowledge, but because of the wealth of information which it contains on each group of substances it can be recommended for all research workers in the field, and for scientists who wish to keep up to date in these matters.

The book is very attractively produced, and contains remarkably few misprints in the text or errors in the diagrams. It is worth the price.

Werner Angst [NB 744 IE]
Laboratorium für Organische Chemie der
ETH Zürich (Switzerland)

Asymmetric Synthesis—The Current State of the Art

Asymmetric synthesis was considered as an academic curiosity until the 1950's, when a better understanding of reaction mechanisms and the development of conformational analysis revived interest in the field. During that period much attention was given to the interpretation and prediction of the steric course of reactions (Cram's rule, Prelog's rule, nomenclature, ...). In these investigations the absolute configurations of many compounds were determined. At the same time, many asymmetric reactions leading to optically active products were studied, but their preparative value remained low. The now classical book of *J. D. Morrison* and *H. S. Mosher* "Asymmetric Organic Reactions"[1] fully reviewed the field up to the 1970's. In this book there are only a few reports of asymmetric syntheses with *ee*'s higher than 90%. During 1970–1982 there was a tremendous increase in the number and efficiency of asymmetric syntheses. Many stoichiometric or catalytic reactions which lead to chiral products with *ee*'s higher than 90% became routine. Moreover, the progress of modern technology rendered the setting up of reliable methods (based on NMR, or HPLC) for the measurement of enantiomeric excesses possible. It was therefore very appropriate that *J. D. Morrison* decided upon a new venture; namely, to edit a series of five volumes devoted to the progress of asymmetric synthesis in the seventies and early eighties. The complete work,

Asymmetric Synthesis. Edited to *James D. Morrison*. Academic Press, Orlando, FL, 1983–1985.

Vol. 1, xiv, 201 pp., bound, \$ 32.00.–ISBN 0-12-507701-7.

Vol. 2, xiv, 278 pp., bound, \$ 45.00.–ISBN 0-12-507702-5.

Vol. 3, xiii, 578 pp., bound, \$ 84.50.–ISBN 0-12-507703-3.

Vol. 4, xii, 380 pp., bound, \$ 85.00.–ISBN 0-12-507704-1.

Vol. 5, xiv, 391 pp., bound, \$ 85.00.–ISBN 0-12-507705-X

which was written in collaboration with some 60 authors, who are also major contributors to various aspects connected with the art of asymmetric synthesis, was published between 1983 and late 1985.

Volume 1 begins with a short chapter written by *J. D. Morrison* on the various ways to obtain optically active compounds. This volume is indeed useful for everyone working on optically active compounds prepared either by resolution, asymmetric synthesis or arising from natural products. It is exclusively devoted to the purpose of measuring enantiomeric excess (*ee*) by direct or indirect methods and is not primarily concerned with the measurement of diastereomeric composition. The analytical methods which are described cover the whole spectrum of techniques with many useful indications for the practitioner. In Chapter 2, *G. G. Lyle* and *R. E. Lyle* present various aspects of polarimetry, including details of commercial apparatus. Determination of maximum specific rotations by competitive reactions is then dealt with in Chapter 3 *(A. R. Schoofs* and *J. P. Guetté)*. In Chapter 4, *K. K. Andersen, D. M. Gash,* and *J. D. Robertson* explain how isotope-dilution techniques can be used to measure *ee* values. Gas chromatographic methods are presented by *V. Schurig* in Chapter 5, while *W. H. Pirkle* and *J. Finn* discuss the separation of enantiomers by liquid chromatographic methods in Chapter 6. The volume concludes with three chapters on NMR spectroscopic methods for the analysis of enantiomers using chiral derivatives (*S. Yamagushi,* Chapter 7), chiral solvating agents (*G. R. Weisman,* Chapter 8), and chiral shift reagents (*R. R. Fraser,* Chapter 9).

Subsequent volumes cover various chemical reactions in which one or several asymmetric centers are created under the control of either external chirality centers (in a reagent or catalyst), or internal chirality centers (in the substrate). The diversity of situations emphasizes the difficulty of defining the exact meaning of "Asymmetric Synthesis", which is the title of this work. Some reactions are clearly oriented towards the creation of asymmetric centers and isolation of chiral products after removal of the chiral auxiliary material. These fit the classical definition of asymmetric synthesis (Enantioselective Synthesis of Chiral Compounds). Another group of transformations is also discussed in the work. In these the chiral centers preexisting in the substrate are not detached after the controlled formation of new elements of chirality. They are diastereoselective reactions which are often of prime importance to the achievement of the total synthesis of natural products. Most of the strategies may be applied to the resolved or racemic substrate, and then fit with the proposed extended definition of asymmetric synthesis.[1] A third group of reactions is directly connected with the use of the chiral pool as source of chiral synthons. Fairly complex chiral molecules can be synthesized by combining small chiral building blocks obtained from cheap natural products (sugars, amino acids, ...). This approach does not necessarily create new asymmetric centers, but involves chemical reactions with specific protecting groups and reactions compatible with the stability of some key stereocenters.

Volumes 2 and 3 have the common title "Stereodifferentiating Addition Reactions". This title, which is not redefined here for the benefit of the newcomer to the field, originates from the classification of the steric course of reactions as proposed by *Izumi* and *Tai*.[2]

Volume 2 begins with a chapter on asymmetric hydroboration by *H. C. Brown* and *P. K. Jadhav*. These authors review the synthesis of chiral compounds by hydroboration of alkenes and further transformations leading to asymmetric C–H, C–OH or C–C bond formation with *ee* values often close to 100%. *M. M. Midland* then presents the asymmetric reduction of carbonyl groups by chiral boranes or modified borohydrides. A survey by *E. R. Grandbois, S. I. Howard,* and *J. D. Morrison* on asymmetric reduction by modified lithium aluminum hydrides follows, some examples being of great preparative interest. Chapter 4 *(Y. Inouye, J. Oda,* and *N. Baba)* includes reductions with chiral dihydropyridines, which can be considered as biomimetic reactions. Chapter 5 *(E. L. Eliel)* covers the addition of chiral nucleophiles to chiral substrates, mostly as an application of the Cram rule. In Chapter 6, *G. Solladié* presents asymmetric syntheses based on the addition of chiral nucleophiles to aldehydes and ketones. The chiral nucleophiles are either organometallic compounds used in a chiral environment, anions of chiral sulfoxides, or chiral ester enolates. Conjugated addition to α,β-unsaturated carbonyl compounds is discussed by *K. Tomioka* and *K. Koga* in Chapter 7 (in those cases where the "chiral help" is either part of the unsaturated carbonyl compounds or of the nucleophile). The specific topic of 1,4-addition of organometallic compounds to alkenyl sulfoxides with the sulfur atom as chiral center is dealt with by *G. Posner* in Chapter 8. Volume 2 is concluded by a review of the alkylation of imine and enamine salts by *D. E. Bergbreiter* and *M. Newcomb*. These are good methods for the asymmetric α-alkylation of aldehydes and ketones.

In Volume 3, four chapters are devoted to the creation of asymmetric centers via enolate chemistry and related processes. In Chapter I, *D. A. Evans* covers the stereoselective alkylation reaction of chiral metal enolates. The various facets of asymmetric aldol reactions are discussed by *C. H. Heathcock* in Chapter 2. A review of asymmetric synthesis via chiral oxazolines is given in Chapter 3 by *K. A. Lutomski* and *A. I. Meyers*, while in Chapter 4 *D. E. Enders* discusses the α-alkylation of chiral hydrazones. Olefin cyclization processes (mostly electrophilic reactions) are dealt with by *P. A. Bartlett* in Chapter 5 (C-C bond formation) and Chapter 6 (carbon-heteroatom bond formation). These processes allow good control to be introduced into the relative stereochemistry of monocyclic and polycyclic systems. In Chapter 7, *L. A. Paquette* deals with asymmetric cycloaddition reactions, particular attention being paid to the Diels-Alder reaction. The last chapter of the volume is devoted to chirality transfer via sigmatropic rearrangements *(R. K. Hill)*, with special emphasis on the Claisen rearrangement.

Volume 4 comprises various topics: reference is made to the chiral carbon pool and also to the use of chiral compounds with asymmetric S, N, P, and Si centers. Chapter 1 (226 pages of the 380 pages) is written by *J. W. Scott* on the readily available chiral carbon fragments and their use in synthesis. A large comprehensive table is included which should prove especially useful to the chemist who is planning a synthetic strategy. Practical information such as the approximate price is given, and many total syntheses using synthons from the chiral carbon pool are presented in detail. There follow four short chapters on the chemistry of chiral compounds with heteroatoms as asymmetric centers (presentation of the compounds and their use in syntheses): Chapter 2 by *M. R. Barbachyn* and *C. R. Johnson* summarizes the routes to various types of chiral sulfur centers and their use in asymmetric synthesis; Chapter 3 *(D. Valentine Jr.)* discusses the methods used to prepare compounds containing a chiral phosphorus center. This is an important field because of the use of phosphanes as ligands in homogeneous catalysis; Chapter 4 *(F. A. Davis* and *R. H. Jenkins Jr.)* then deals with the synthesis and utilization of compounds with chiral nitrogen centers; the final Chapter, Chapter 5, is written by *C. A. Maryanoff* and *B. E. Maryanoff* on the synthesis and utilization of compounds with chiral silicon centers.

Volume 5, on Chiral Catalysis, appeared only a few months ago. It is mostly concerned with organometallic catalysis. Chapter 1 is a general presentation by *H. Kagan* of various types of chiral ligands which can be introduced into a complex. These ligands are classified as mono- or polydentate as well as according to the nature of the heteroatom (P, S, N, O, ...) and location of chirality. In Chapter 2, *J. Halpern* discusses the mechanism of asymmetric catalytic hydrogenation with rhodium complexes. Special importance is given to kinetic data, which allow the location of the origin of enantioselectivity in the catalytic cycle to be determined. The application of homogeneous catalyzed asymmetric hydrogenation is the topic of the next chapter written by *K. E. Koenig*. One application is the Monsanto process for the synthesis of (*S*)-dopa. Efficient asymmetric reductions of various types of functionalized olefins are listed, suggesting some applications. In Chapter 4, *I. Ojima* and *K. Hirai* review asymmetric hydrosilylation and hydrocarbonylation. Asymmetric hydrosilylation can at present give high *ee* values for the reduction of aromatic ketones but the enantioselectivity of hydrocarbonylation must be improved if it is to be used technically. Chapter 5 deals with asymmetric coupling reactions *(T. Hayashi* and *M. Kumada)*. Most of the reactions involve the coupling of Grignard reagents to vinylic halides or allylic alkylations in the presence of chiral organometallic catalysts. In Chapter 6, *S. Otsuka* and *K. Tani* present catalyzed asymmetric isomerization of functionalized olefins. The class of reactions which is detailed is the transformation of achiral allylamines into enamines bearing an asymmetric center in the γ-position with respect to nitrogen. The most effective catalyst is a rhodium/Binap complex; it has recently been used for the industrial synthesis of citronellal and menthol. The next two chapters are devoted to the most efficient and reliable asymmetric synthesis discovered in the past five years. The Sharpless reagent for asymmetric epoxidation of allylic alcohols is now widely used in syntheses, and hundreds of references in the recent literature show the usefulness of this reaction for the preparation of functionalized compounds in 95–98% *ee*. In Chapter 7, *B. E. Rossiter* describes the synthetic aspects and applications of asymmetric epoxidation by various methods, and the author gives details of the results obtained with asymmetric epoxidation by the Sharpless reagent. Applications in the total synthesis of natural products are listed. In Chapter 8, *M. G. Finn* and *K. B. Sharpless* discuss the mechanism of asymmetric epoxidation with titanium-tartrate catalysts. In this relatively long chapter (114 pages) structural information on various Ti-complexes (tartrate derivatives as well as kinetic data) is given. A mechanism is proposed, and the kinetic resolution of racemic allylic alcohols is also considered. Unpublished data on the results obtained with ligands other than diethyl tartrate are given in a table. No major improvements were noticed for these fifty ligands, so that the tartrates, which were the first to be tested, still remain the best choice. A useful (and still unpublished) procedure is described in detail by the authors, namely the possibility of the routine use of catalytic amounts of titanium-tartrate complexes in the presence of molecular sieves. This places the Sharpless epoxidation (which is patented) on the brink of industrial application. Two short chapters bring the final volume of the series to a close. In chapter 9, *J. B. Jones* discusses enzymes as chiral catalysts. This chapter includes an introduction to enzymes (classification, main reactions) followed by many examples of various types of asymmetric syntheses, and is a short but excellent presentation of an extremely important area. A few examples of kinetic resolution are also given. In Chapter 10, asymmetric heterogeneous catalytic hydrogenation is discussed by *K. Harada*. Most of the examples given concern either chiral ketoesters, imino esters or enaminoesters which are hydrogenated in the presence of a metal catalyst. Stereochemical models, based on the interaction with the surface are proposed.

In spite of the large number of authors and topics the complete work appears quite homogeneous in its presentation. Some of the material presented has already been reviewed but, nonetheless, it is very convenient for the practitioner or newcomer to find all the basic information concentrated in one work. Most of the contributions are well written and very informative, and include the most important literature references. There are only a few mistakes. The volumes on stereodifferentiating addition reactions deal with a field which is almost mature and can be considered as textbook material. By way of contrast, Volume 5, Chiral Catalysis, is not so satisfactory, since some areas are not covered, presumably due to lack of space. This is unfortunate because asymmetric catalysis is developing rapidly and is on the verge of industrial application.[3] The

work by *Izumi* and *Tai* on catalytic hydrogenation with metals modified by tartaric acid is neglected and could at least have been discussed in Chapter 10. It is a pity that no section is devoted to catalysis by chiral amines, amino acids or small peptides, despite spectacular results being obtained such as, e.g., the proline-catalyzed cyclization of triketones,[4,5] the alkaloid-catalyzed ketene addition,[6] and the asymmetric alkylation with a chiral phase-transfer catalyst.[7] Moreover, enzymatic reactions are presented in only thirty pages. As stated by the author, this chapter should serve more as an introduction than a comprehensive coverage of the topic because of lack of space. Despite these criticisms, however, the work as a whole is an invaluable tool for the chemist already engaged in the field, and should become a reference work for everybody working on the stereocontrolled synthesis of organic molecules. The stereochemical nature of the series is well evidenced by the names to whom the five volumes are dedicated: *H. S. Mosher, A. Horeau, D. Cram, S. Yamada,* and *V. Prelog.* Asymmetric syntheses and stereocontrolled processes abound in the current literature and are the topic of many international meetings and symposia. This collected work should greatly stimulate the advance of asymmetric synthesis. Perhaps in a few years time a new set of volumes will be needed in order to reassess the state of the art.

Henri B. Kagan [NB 759 IE]
Université de Paris-Sud, Orsay Cedex (France)

[1] J. D. Morrison, H. S. Mosher: *Asymmetric Organic Reactions*, Prentice Hall, Englewood Cliffs, NJ, USA 1971; reprint: American Chemical Society, Washington 1976.
[2] I. Izumi, A. Tai: *Stereo-differentiating Reactions*, Academic Press, New York 1977.
[3] B. Bosnich: *Asymmetric Catalysis (NATO ASI Series)*, Martinus Nijhoff, Dordrecht 1986.
[4] Z. G. Hajos, D. R. Parrish, *J. Org. Chem. 39* (1974) 1615.
[5] U. Eder, G. Sauer, R. Wiechert, *Angew. Chem. 83* (1971) 492; *Angew. Chem. Int. Ed. Engl. 10* (1971) 496.
[6] H. Wynberg, E. G. J. Staring, *J. Am. Chem. Soc. 104* (1982) 166.
[7] U. H. Dolling, P. Davis, E. J. J. Grabowski, *J. Am. Chem. Soc. 106* (1984) 446.

Air Pollution and Plants. By *C. Troyanowsky*. VCH Verlagsgesellschaft, Weinheim 1985. x, 298 pp., bound, DM 120.00.—ISBN 3-527-26310-1

This book contains the papers presented at the Second European Conference on Chemistry and the Environment, held in London in 1984 under the auspices of the Federation of European Chemical Societies and the German Chemical Society. They are concerned with the atmospheric chemistry of pollutants (processes involving the formation of photo-oxidants, and photo-degradation processes occurring at aerosol surfaces), the direct and indirect effects of pollutants on plants, trees, and the ground and water systems, and the relevant analytical methods and monitoring programs.

The papers reflect the wide variety of views that exist concerning the effects of atmospheric pollution on terrestrial ecosystems, and also a degree of confusion on the subject, notably with regard to cause-effect relationships. Many of the contributions are informative, but the book is by no means representative of all European research in this field. In particular, there is insufficient information on the basic chemistry involved, and the fact that shortcomings in our understanding of the processes are largely caused by a lack of adequate analytical methods to provide specific evidence for individual pollutants does not come out clearly enough. Some of the papers are only reported as abstracts which are not very meaningful by themselves. The contribution by *B. Ulrich* (Göttingen) concerning the direct and indirect effects of pollutants on forests, and the resulting changes to the ecosphere, is especially well-written and informative. *Ulrich* expresses the view that, although man cannot destroy nature itself, he can destroy the ecosystems on which it depends, and therefore pollution of the atmosphere needs to be eliminated as quickly as possible. An opposite view is given by *E. Weise* (Leverkusen), who asks for further clarification and for priorities to be decided, so as to avoid hasty and mistaken actions.

Werner Stumm [NB 766 IE]
Swiss Federal Institute for Water Resources
and Water Pollution Control,
Dübendorf (Switzerland)

Biological Oxidation of Nitrogen in Organic Molecules. Chemistry, Toxicology and Pharmacology. Edited by *J. W. Gorrod* and *L. A. Damani*. VCH Verlagsgesellschaft, Weinheim 1985. 445 pp., bound, DM 150.00.—ISBN 3-527-26299-7

Research into the metabolism of organic nitrogen compounds by *N*-oxidation began about 1920 with the isolation of *N*-acetylphenylhydroxylamine from the blood of cats which had been given acetanilide (Ellinger, *Hoppe-Seyler's Z. Physiol. Chem. 111* (1920) 86). Since then many nitrogen-containing xenobiotics have been studied, and in 1978 one of the editors of this book, *J. W. Gorrod,* reviewed progress up to then in this field of research. The present volume is concerned with the latest developments, some of which are extremely interesting, especially with regard to the biochemical pharmacology and toxicology of *N*-oxidations.

A short introductory chapter describes the possibilities of nitrogen oxidation in xenobiotics; the products consist essentially of hydroxylamines, hydroxamic acids, nitroso- and nitro-compounds, oximes, nitrones and *N*-oxides.

The rest of the book is divided into nine sections. The first describes the methods for analyzing *N*-oxidized compounds, especially those for arylhydroxylamines and tertiary amine oxides. Next, the flavin-containing monooxygenase ("Ziegler's enzyme") is discussed. A series of short chapters (about four or five pages each) then deal with pargyline, alicyclic amines, fomocaine, secondary aromatic amines, *N,N*-dimethylaniline, cimetidine, ranitidine and (*S*)-(−)-nicotine. The third section is concerned with oxidation and formation of aromatic amines, especially chemical carcinogens, and dietary control of the bacterial metabolism of the nitro group. The fourth section discusses the oxidation of amides and carbamates, especially of the known carcinogen 2-acetylaminofluorene. The next section deals with the *N*-oxidation of azaheteroaromatic compounds, and the following one with the oxidation of amidines, imines, triazenes, hydrazine and azo compounds.

The following two sections, on *N*-oxidations by prostaglandin-H-synthetase and by the peroxidase-H_2O_2 system, are highly topical and of particular biological interest ow-

ing to their close connection with the metabolism of polyunsaturated fatty acids and with the active hormones derived from these. The biological significance of these peroxidase-catalyzed reactions on model compounds is not yet known. In the final section dealing with toxicology, the interactions of the products of *N*-oxidation with nucleic acids, thiols, α-oxo-acids, hemoglobin, and fatty acids, and their mutagenic effects, are discussed.

On the whole, this collection of articles portrays very well the current state in this field of research. Most of the 47 contributions have been kept short, and give the essentials on their various topics. Readers interested in more detailed information will need to refer to the original papers listed, which may indeed have been the aim of the editors. In view of the flood of original papers that appear scattered through various specialized journals, this book is a good example of a manageable compilation of up-to-date information. The book should make it easier for chemists, toxicologists, pharmacologists and interested biochemists to quickly familiarize themselves with this expanding area of research.

Helmut Sies [NB 741 IE]
Institut für Physiologische Chemie
der Universität Düsseldorf (FRG)

Mass Spectral and GC Data of Drugs, Poisons and Their Metabolites. By *K. Pfleger, H. Maurer,* and *A. Weber.* VCH Verlagsgesellschaft, Weinheim 1985. **Part I: Introduction and Tables.** xxx, 208 pp., bound; **Part II: Mass Spectra and Indexes.** xii, 744 pp., bound, together DM 480.00.—ISBN 3-527-26303-9

The definitive identification of toxic substances by mass spectrometry has rapidly gained importance in recent years. *Karl Pfleger* is a pioneer of clinical toxicology who has used this work to pass on his experience to scientists in general.

These two volumes contain a wealth of clearly arranged GC and MS data which allow rapid identification of measured samples by comparison of spectra and data. Samples can be roughly classified by means of their retention indices, mass spectra are used for final identification. The line spectra are given in the form of computer print-outs and contain details of empirical and structural formulas, exact masses, retention indices and occurrence (urine, blood etc.). Reference spectra for purposes of identification are found primarily via the mass of the molecular ion. If the mass is not available the reference spectra can be located with the aid of the most intense peaks. Compounds are listed in an index so that a reference spectrum can also be found by looking up the name of the appropriate substance. The extensive tables are preceded by short sections on work-up, derivatization for GC analysis and artefacts that may appear in gas chromatographs.

Pfleger together with *Maurer* and *Weber* have created an extremely important work for practical purposes. It must however be mentioned that the book contains numerous errors: missing hydrogen atoms at the indole nitrogen (e.g. p. 200 and 201), missing double bonds in benzbromarone (p. 656) or a missing oxygen atom in the methylation of an alcoholic group (p. XXIV) are less serious but it is, however, very aggravating that computer print-outs that give incorrect masses due to incorrect calibration have been incorporated without any criticism. The key ion in the spectrum of stearic acid is, for instance, shifted from mass 60 to mass 61. The main ion of mass 56 shown in the spectrum of fatty acids is furthermore of minor intensity so that this compound would be difficult to identify. The main ion in the spectrum of bromopride (p. 599) is assigned a mass of 58 which is inconsistent with the structure of a diethylamino compound. As the molecular ion is missing and the other peaks cannot be correlated with the given structure, it seems likely that the spectrum shown belongs to another compound.

Despite this list of faults (which could be continued e.g. literature references are missing), this book written by *Pfleger* and co-workers is of great value for all toxicologists. Providing that it is read with an appropriate degree of criticism, it will be an important aid for helping to solve problems in all laboratories.

Gerhard Spiteller [NB 749 IE]
Lehrstuhl für Organische Chemie I
der Universität Bayreuth (FRG)

Molecular Semiconductors. Photoelectrical Properties and Solar Cells. By *J. Simon* and *J.-J. André.* Springer-Verlag, Berlin 1985. xiii, 288 pp., bound, DM 174.00.—ISBN 3-540-13754-8

An increasing amount of work has been published in recent years on organic, organometallic and polymeric compounds with unusual properties. The preparation of such materials and the study of their electrical, electrochemical, magnetic and optical properties has developed into one of the most attractive fields of research. In the next few years there will certainly be further important publications devoted to extending the range of these materials, and to understanding the phenomena of charge transport, charge interactions and charge storage at a molecular level. Because of the large number of publications in this field, the appearance of a monograph which critically reviews some aspects of materials of this kind is very welcome.

The first two chapters are concerned with the physical basis of charge transport in solids and of photoelectric phenomena. After first describing the behavior of inorganic solids, examples of various "molecular" crystals and polymers are discussed. On account of the wide variety of organic solids, this theoretical treatment is a useful starting point for understanding the processes concerned. These first two chapters will be of particular value to those who are just entering the field, because derivations have been avoided, and the understanding of the text is helped by the inclusion of many tables and figures.

In those classes of materials that are treated as "molecular" semiconductors, the authors have put the main emphasis on phthalocyanines and polyacetylenes. In each case the preparation and general physical properties of the materials are dealt with first, before describing the electrical and photovoltaic properties (including solar cell uses) which are chiefly of interest here. The sections on preparation and morphology are undoubtedly essential, in order to give the reader guidance in planning his own work. Studies of the properties of substances such as phthalocyanines in solution, e.g. their electronic spectra, photophysical properties, and redox behavior, could have been treated more briefly, as they do not really belong to the main subject of the book. It would have been better to increase the emphasis on solid state physical properties. In the chapter on the intrinsic conductivity of phthalocyanines, one would have liked to see a table of characteristic data on important in-

dividual phthalocyanines included. Under doped phthalocyanines, more detailed attention should have been given to the work of the Tübingen group led by *Hanack*. The description of the photochemical hole-burning technique for phthalocyanines, as an alternative method for storage at a molecular level, might also have been expanded. The topics covered in the chapter on polyacetylenes are appropriate to the objectives of the book, and are treated thoroughly.

The final chapter deals with other molecular semiconductors, but in most cases too briefly. Some of the latest "alternative" materials, such as polyphenylene sulfide, polyaniline and polythienylene, are regrettably not included at all. The reputation of the book could have been enhanced by looking at prospects for some of those molecular electronics developments (molecular conductors, storage devices, switches and transistors) which have been mentioned in several publications and at two conferences, but have not yet been achieved practically. The short chapter entitled "Conclusion" does not meet this need.

On the whole this book does fill a gap in the growing field of "alternative" materials. For scientists already working in the field the review is a useful addition to the literature, and it can also be recommended for those about to begin work in the area as a help in getting started.

Dieter Wöhrle, Andreas Jahn [NB 738 IE]
Institut für Organische und Makromolekulare Chemie
der Universität Bremen (FRG)

Photochemical Conversion and Stabilization of Polymers. By *V. Y. Shlyapintokh*. Hanser-Verlag. München 1984. xiv, 470 pp., Hardbound, DM 168.00.—ISBN 3-446-13670-3

The photochemical and photooxidation reactions of polymers, including their photostabilization, are presented in this book in a fundamental manner on the basis of primary physical processes, energy transport, chemical reaction mechanisms, and kinetics. All subjects are discussed in full detail; the emphasis given to a thorough treatment of photostabilization, including the more recent methods of stabilization with hindered amines, qualifies this book as a valuable addition to the monograph literature. Since all its chapters (except for Chapter 4) are written by the same author, which nowadays is rarely encountered in this field, the book exhibits homogeneity in styling, much to the profit of the reader.

Each chapter offers a self-contained treatment of its particular topic. Chapters 1–5 are devoted to photoinduced changes in polymers, Chapters 6–10 to photostabilization: 1—Photophysical processes; 2—Some characteristics of photochemical and dark reactions in polymer matrices; 3—Photooxidation of polypropylene; 4—Photoaging of aliphatic polyamides (by *L. M. Postrekov* and *A. L. Margolin*); 5—Singlet oxygen and the photooxidation of polymers; 6—Protective mechanisms of photostabilizers in model systems; 7—Physical mechanisms of inhibition of the phototransformation processes of polymers in solution; 8—Physical mechanisms of inhibition of the phototransformation processes in solid polymers; 9—Photostability of UV absorbers; 10—Protective action of some photostabilizers. By their length, Chapters 9 and 10 may be considered as the main part of the book; this means that stabilization phenomena are presented in sufficient detail to allow thorough interpretation.

The author with his research group at the Institute of Chemical Physics of the Soviet Academy of Sciences counts among today's most competent contributors to this field in the Soviet Union. His presentation is based throughout on experimental data, partly from his own laboratories, which are being presented and interpreted with great care. A detailed list of references at the end of each chapter provides access to the original literature up to approximately 1979.

This book is a valuable collection of knowledge on the fundamental scientific facts of photoinduced aging and photostabilization of polymers; nevertheless, its aim is not advice on practical application. Though, e.g., in the treatment of photostabilizers, the book concentrates interest upon practically employed stabilizer substances, it may not be considered as a guidebook, neither to the proper choice of stabilizer systems, nor to their applicational properties. Present argument going on with respect to the interpretation of certain results (especially as to the rôle of singlet oxygen in photooxidation) is reflected in the book. This is without doubt one of the useful features of the book, making the reader familiar with currently open questions. On the other hand, some topics, however thoroughly presented (like the Fries photorearrangement in UV absorbers), are of less actual interest today, while certain important aspects (like the controlled photodecomposition induced by additives) are omitted.

On the whole, this book has to be classified as a largely comprehensive and highly informative publication. It is virtually indispensable for those who are scientifically concerned with questions of stability and stabilization of polymers. Furthermore, it is highly recommended for all those chemists, physicists, and students who are interested in questions of reaction kinetics, photochemistry and photophysics. Finally, tribute may be made to the book's excellent appearance.

Joachim Voigt [NB 714 IE]
Hoechst AG, Frankfurt am Main (FRG)

Registered names, trademarks, etc. used in this journal, even without specific indication thereof, are not to be considered unprotected by law.

© VCH Verlagsgesellschaft mbH, D-6940 Weinheim, 1986. - Printed in the Federal Republic of Germany by Zechnersche Buchdruckerei, Speyer/Rhein.

All rights reserved (including those of translation into foreign languages). No part of this issue may be be reproduced in any form - by photoprint, microfilm, or any other means - nor transmitted or translated into a machine language without written permission from the publishers. Only single copies of contributions, or parts thereof, may be reproduced for personal use.

Valid for users in the USA: The appearance of the code at the bottom of the first page of an article in this journal (serial) indicates the copyright owner's consent that copies of the article may be made for personal or internal use, or for the personal or internal use of specific clients. This consent is given on the condition, however, that the copier pay the stated per-copy fee through the Copyright Clearance Center, Inc., for copying beyond that permitted by Sections 107 or 108 of the U.S. Copyright Law. This consent does not extend to other kinds of copying, such as copying for general distribution, for advertising or promotional purposes, for creating new collective works, or for resale. For copying from back volumes of this journal see 'Permissions to Photo-Copy: Publisher's Fee List' of the CCC.

Editorial office: Pappelallee 3, D-6940 Weinheim, Federal Republic of Germany, Telephone (06201) 602315, Telex 465516 vchwh d, Telefax (06201) 602328.

Editor: *P. Gölitz*.

Associate editors: *D. I. Loewus, A. Stimson*. **Editorial assistant:** *E. Schweikart*

Publishers: VCH Verlagsgesellschaft mbH. (Managing Directors: *Prof. Dr. Helmut Grünewald* and *Hans Dirk Köhler*), Pappelallee 3, D-6940 Weinheim, Federal Republic of Germany. Correspondence concerning advertisements should be addressed to VCH Verlagsgesellschaft mbH. (Advertising Manager *R. J. Roth*), Boschstr. 12, P.O. Box 1260/1280, D-6940 Weinheim, Federal Republic of Germany, Telephone Weinheim (06201) 602-0, Telex 465516 vchwh d, Telefax (06201) 602328.

ANGEWANDTE CHEMIE
International Edition in English
Volume 25 · Number 10
October 1986
Pages 853–946

Computer Graphics in the Study of Metal Cluster Compounds**

By Kim Henrick, Mary McPartlin,* and Jill Morris

Polynuclear carbonylmetal compounds provide convenient molecular analogues for the reactions occurring at metal surfaces during catalytic processes. Many properties of these cluster compounds are determined by the type and distribution of the ligands covering the metal polyhedral surface. Computer simulated space-filling models of these complicated molecules provide readily assimilated information about the arrangement of surface ligands, and in many cases lead to conclusions not readily deduced from other approaches.

1. Introduction

The importance of metal cluster compounds arises from the extra dimension to inorganic chemistry achieved by the presence of several metal atoms in one molecule. The challenge of these polynuclear systems lies not only in exploring their potential for reactions unknown for mononuclear compounds, but also in uncovering the range of possible polyhedral metal core geometries and the unusual bonding modes of the attached ligands. The present rapid expansion in transition metal cluster chemistry is a result of successful collaboration between the synthetic and crystallographic branches of chemistry. X-ray analysis is in most cases essential for complete characterization of a new cluster species, and has revealed discrete molecular structures with as many as 44 metal atoms.[1] The structural and chemical properties of these compounds are largely determined by the type and arrangement of the ligands on the cluster surface.[2,3] Such ligands also appear to play an important role in determining which of several alternative metal polyhedra is adopted by a particular cluster species with a given polyhedral electron count.[4,5] Examination of simulated 'space-filling' models using modern computer graphics techniques has proved a valuable tool in investigating these effects. Two types of surface ligand, apart from the carbonyl group, are particularly important and are being very widely studied. These are the single atom donors H and C (hydrido- and carbido-ligands, respectively), for which a wide variety of bonding modes has been observed.[6–9] Much of the current interest stems from a belief that formation of isolated H and C atoms on the surface of bulk metals is an important step in many catalytic processes.

2. Hydrido Cluster Derivatives

The interaction of hydrogen with transition metals plays a fundamental role in heterogeneous catalysis. Studies of the modes of bonding of H-atoms with polynuclear carbonyl-transition metal compounds are important in providing insight into reactions at bulk metal surfaces for which they are the nearest available molecular analogues. Location of hydrido ligands in transition metal compounds using X-ray analysis presents problems: the presence of metals of high atomic number makes direct location of the electron-deficient hydrogen atoms in a Fourier map very difficult. Even with the latest equipment and techniques there are very few examples in which the X-ray method has directly

[*] Dr. M. McPartlin, Dr. K. Henrick, Miss J. Morris
School of Chemistry, The Polytechnic of North London
London N7 8DB (UK)

[**] All the figures in this review were generated by computer and photographed directly from the screen. Color code: H (white), C (light blue), N (dark blue), O (red), I (green), all metals (yellow).

 © VCH Verlagsgesellschaft mbH, D-6940 Weinheim, 1986 0570-0833/86/1010-0853 $ 02.50/0

located hydrido-ligands in a large cluster, particularly of a third row transition metal.[9]

Neutron diffraction is ideal for H-atom detection but involves equipment which is not readily available, and an equally serious drawback is that relatively large crystals are required. Consequently the most widely used methods for polynuclear metal cluster compounds are indirect; the hydrogen bonding site is deduced from the effect of the repulsive interaction between the 'invisible' hydrogen atom and the surrounding carbonyl ligands. In most cases the extra information about the hydrogen ligand which might be obtained from neutron diffraction studies, such as accurate M–H bond lengths, would be of limited value even if suitable crystals were available, and would certainly not justify the extra expense and time required. We have found that computer graphics can provide a simple and unambiguous method of routinely deciding the hydrogen site from X-ray data.

2.1. Conventional Indirect Methods for the Location of Hydrido-Ligands

In earlier work we have made considerable use of the indirect methods of H-location originally pioneered by *Owston* et al.[10] for mononuclear species and by *Churchill* et al.[11] for cluster compounds. For example, the μ_3-position of the hydrido ligand in the $[HOs_6(CO)_{18}]^{\ominus}$ monoanion (threefold bridging via Os1, Os2, and Os3), was readily deduced by the characteristic 'pushing back' of the neighboring CO ligands together with a lengthening of the respective Os–Os bonds (Fig. 1a).[12] Very similar effects were previously observed by *Churchill* et al. round the μ_3-H ligand sites in the dihydride $[H_2Ru_6(CO)_{18}]$ (Fig. 1b), where the H-ligands bridge opposite faces of the Ru_6-octahedron (Fig. 1b).[11]

Later a more quantitative indirect location of hydrogen atoms, the 'potential energy' technique, was developed by *Orpen* and is very useful for symmetrically bonded H-ligands. For a large range of cluster geometries, H-coordinates calculated from data using this method agree well with those obtained from neutron diffraction data.[13]

The reliability of qualitative indirect methods is illustrated by the results of the X-ray structure analysis of the $[(Ph_3P)_2N]^{\ominus}$ salt of $[HRu_6(CO)_{18}]^{\ominus}$ (cf. Fig. 1c).[14] In contrast to the case of the analogous osmium monohydride $[HOs_6(CO)_{18}]^{\ominus}$ (Fig. 1a) and the corresponding ruthenium dihydride $[H_2Ru_6(CO)_{18}]$ (Fig. 1b), in $[HRu_6(CO)_{18}]^{\ominus}$ no bond lengthening and no 'pushing back' of the CO ligands was observed. The structure in fact looks almost identical to that of the dianion $[Os_6(CO)_{18}]^{2\ominus}$ (Fig. 1d),[12] with none of the disturbance of the CO ligands that would be expected from a surface H-ligand. From these results we concluded that this was the first example of an interstitial H-atom in a carbonyl cluster.[14] This assignment was later strongly contested,[15] mainly because the ^{1}H-NMR data appeared to be more consistent with the direct coordination of hydrogen to a carbonyl group to give a 'formyl-like' ligand. However, a subsequent neutron diffraction analysis of the $[Ph_4As]^{\ominus}$ salt established beyond doubt that the H-ligand is in the center of the Ru_6 octahedron,[16] and vindicated this indirect method of interstitial H-atom assignment. Clearly a more readily assimilated method of presenting the facts about hydrido-ligand steric requirements, deduced from X-ray analysis, would prevent such controversies.

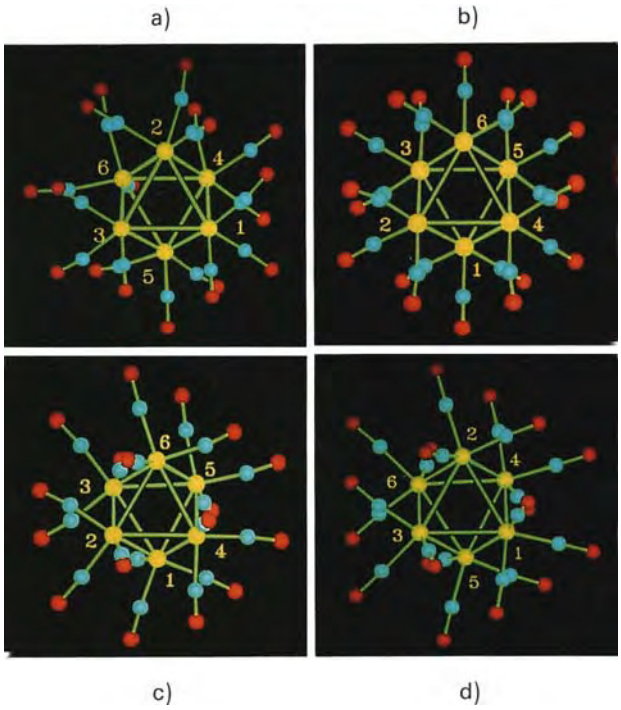


Fig. 1. A comparison of the carbonyl ligand distribution in hydrido and non-hydrido hexanuclear species, determined by X-ray structure analysis, illustrated using conventional computed 'ball-and-stick' models. a) $[HOs_6(CO)_{18}]^{\ominus}$, view onto μ_3-H site; b) $[H_2Ru_6(CO)_{18}]$, view onto one of the two μ_3-H sites; c) $[HRu_6(CO)_{18}]^{\ominus}$, with interstitial H; d) $[Os_6(CO)_{18}]^{2\ominus}$.

2.2. Hydrido-Ligand Location using Computer Graphics

Computer simulated space-filling models of the cluster molecules proved to be ideal for this purpose. We use a versatile program due to *Keller*,[17] which gives a computed model of the molecule, based on atomic coordinates established from X-ray analysis, with the atoms drawn as spheres of radius equal to the appropriate van der Waals value. In the original models the core metal atoms, which are not relevant to an examination of repulsion effects between ligands, partially obscured the surface atoms, and consequently it was difficult to deduce whether the ligands were in contact with each other. This effect arose from the relatively large size of the unnecessary metal van der Waals spheres and subsequent modification of the models by assigning covalent radii to these core atoms (Ru and Os 1.45 Å) allowed a clear view of the surface ligand contacts. Thus modified, the models proved a very valuable and powerful tool for the rapid location of hydrido-ligands in difficult cases.

The technique may first be demonstrated using well established clusters in which the H-site is undisputed. For example, in the space-filling model of the non-hydrido

dianion $[Os_6(CO)_{18}]^{2\ominus}$ (Fig. 2d) there is a symmetrical distribution of the carbonyl van der Waals spheres which are in tangential contact, efficiently covering the cluster surface and almost completely hiding the 'bonding' spheres of the core metal atoms.

In contrast, a similar view of the hydrido monoanion $[HOs_6(CO)_{18}]^{\ominus}$ onto the H-bridged face Os1, Os2, Os3 (Fig. 2a) shows a clear 'hole' in the carbonyl coverage through which the three Os atoms, bonded to the μ_3-H, can be readily seen. When this molecule is rotated in any direction from the bridged face a 'close-packed' array of CO ligands is obtained and the underlying metal atoms are completely obscured. The view of the dihydride $[H_2Ru_6(CO)_{18}]$ onto one of the H-bridged faces (Ru2, Ru4, Ru6, Fig. 2b) is similar to that of $[HOs(CO)_{18}]^{\ominus}$ but shows the three bridged Ru atoms through a more symmetrical 'hole' in the CO distribution. The models of these two hydrides demonstrate that the 'pushing back' of the CO ligands by the hydrido-ligand, and the resultant steric overcrowding, has produced a marked compression of the van der Waals spheres of the adjacent carbon atoms which are no longer in tangential contact as they were in $[Os_6(CO)_{18}]^{2\ominus}$. A contrast is evident in the structure of the analogous ruthenium monohydride $[HRu_6(CO)_{18}]^{\ominus}$ viewed down the C_3 axis onto the Ru2, Ru4, Ru6 face (Fig. 2c). The carbonyl ligands are once more in tangential contact with a distribution similar to that in the dianion $[Os_6(CO)_{18}]^{2\ominus}$ and from whatever direction this monohydride is viewed there is no sign of a 'hole' in the CO coverage and the 'bonding' spheres of the Ru atoms remain almost completely out of sight. Clearly the H-atom is not attached to the cluster surface. Had this type of model been used at the time of the original structure analysis of $[HRu_6(CO)_{18}]^{\ominus}$, the interstitial assignment of the H-atom at the center of the Ru_6 octahedron would probably have been undisputed.

The first application of the computer simulation technique to *location* of an H-ligand in a cluster, for which other methods had failed, was in the study of the neutral iodo-derivative $[HOs_8(CO)_{22}I]$. Indirect methods had allowed a ready assignment of the μ_2-H ligand site in the monoanion $[HOs_8(CO)_{22}]^{\ominus}$ from the ball-and-stick model shown in Figures 3a and 3b.[18, 19] The carbonyl ligands appear to be 'pushed back' from the Os7–Os8 bond, indicating that it is spanned by the H-ligand. In contrast the neutral compound, $[HOs_8(CO)_{22}I]$, obtained by reaction of the monoanion with iodine, has the complicated arrangement of core and surface atoms shown in Figure 3c, and this made it very difficult to apply the normal ligand displacement criteria in attempting to locate the H-ligand.[20]

Furthermore, no evidence could be obtained from the bond lengths nor from Orpen 'potential energy' calculations. In the dihydride $[H_2Os_7(CO)_{20}]$, characterized by *Holden* et al. (Fig. 3d), similar difficulties were experienced in locating the two hydrido-ligands.[21] Examination of computed space-filling models made the location of the H-ligands equally easy in all three cluster hydrides.

The computed Keller model of the monoanion $[HOs_8(CO)_{22}]^{\ominus}$ (Figs. 4a and 4b) shows only one 'hole' in the ligand coverage which is symmetrically located above the two atoms Os7 and Os8, where the μ_2-H site had earlier been deduced (Fig. 4b). Viewed from any other directions the carbonyl ligands are seen to be in close contact, com-

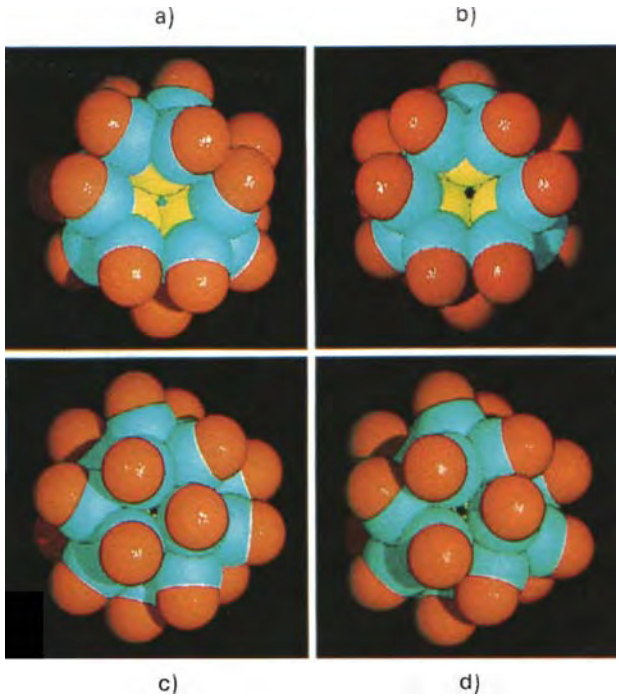


Fig. 2. The carbonyl ligand distribution of hydrido and non-hydrido cluster species (viewed as in Fig. 1) illustrated using computed 'space-filling' models. The van der Waals spheres of the carbonyl-C atoms (blue) are 'close-packed' except for clear gaps at the vacant H-atom sites where the underlying core of the metal 'covalent' spheres (yellow) is visible. a) $[HOs_6(CO)_{18}]^{\ominus}$ view onto the μ_3-H site; b) $[H_2Ru_6(CO)_{18}]$, view onto one of the two μ_3-H sites; c) $[HRu_6(CO)_{18}]^{\ominus}$, with interstitial H; d) $[Os_6(CO)_{18}]^{2\ominus}$.

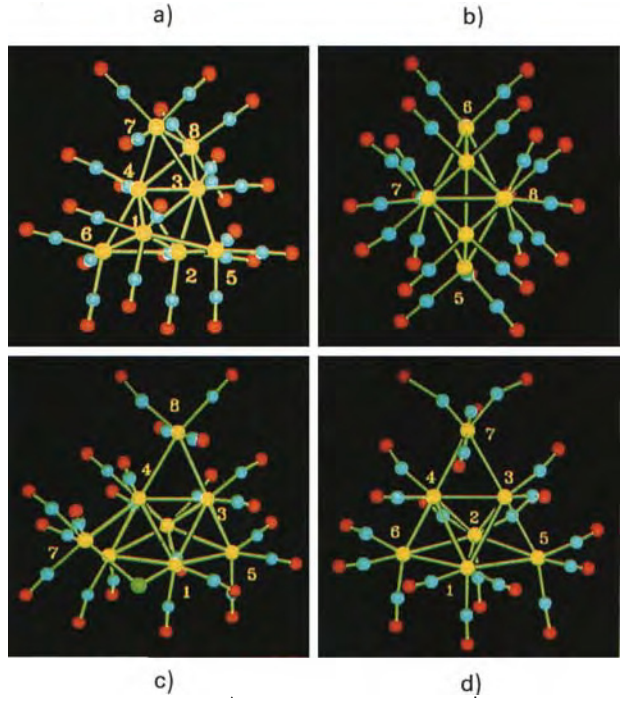


Fig. 3. Conventional computed 'ball-and-stick' models of some large hydridoosmium clusters, calculated using the atomic coordinates from X-ray structure analyses. a), b) $[HOs_8(CO)_{22}]^{\ominus}$, a general view and one onto the μ_2-H site, respectively; c) $[HOs_8(CO)_{22}I]$, view onto the μ_3-H site; d) $[H_2Os_7(CO)_{20}]$, view onto one of the two μ_3-H sites.

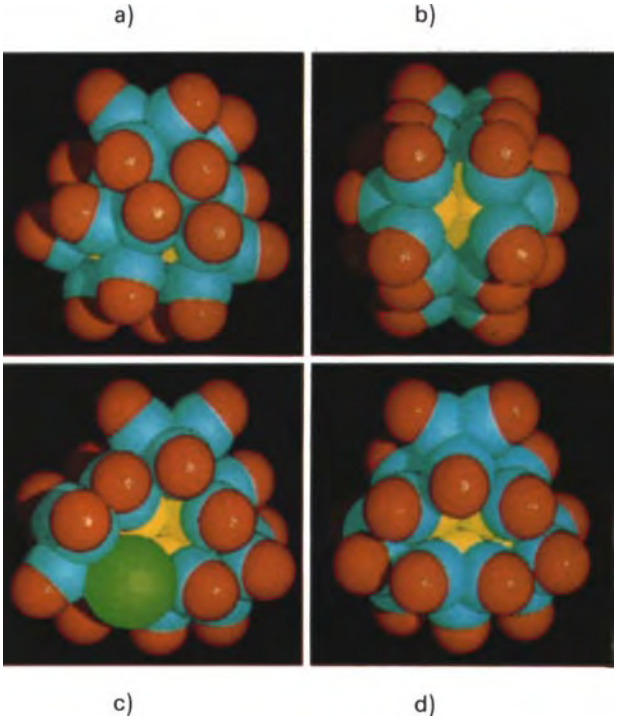


Fig. 4. The distribution of the non-hydrido surface ligands of the same large hydridoosmium clusters as in Fig. 3, illustrated using computed 'space-filling' models in which the ligand atoms (iodine: green) have been assigned van der Waals radii, but the underlying core osmium (yellow) atoms have been assigned covalent radii. a), b) $[HOs_8(CO)_{22}]^{\ominus}$, a general view and one onto the μ_2-H site, respectively; c) $[HOs_8(CO)_{22}I]$, view onto the μ_3-H site; d) $[H_2Os_7(CO)_{20}]$, view onto one of the two μ_3-H sites.

pletely obscuring the underlying osmium atoms of the core as shown, for example, in Figure 4a. The space-filling model of the neutral hydride $[HOs_8(CO)_{22}I]$ was equally unambiguous; there is only one gap in the surface ligand distribution (Fig. 4c).[19] Through this 'hole' in the carbonyl ligands the 'bonding' spheres of the three osmium atoms are visible, and it is apparent that the H-ligand is bridging these three atoms, Os1, Os3 and Os4. The areas of the three osmium atom spheres visible in this case are unequal, in contrast to the μ_3-bridged metal atoms in $[HOs_6(CO)_{18}]^{\ominus}$ and $[H_2Ru_6(CO)_{18}]$, so that it may be concluded that the H-ligand in $[HOs_8(CO)_{22}I]$ is not bonded symmetrically to the three osmium atoms. Very similar results were obtained from examination of the Keller model of the dihydride $[H_2Os_7(CO)_{20}]$. Here, two distinct 'holes' in the carbonyl distribution occur on opposite equivalent triangular faces of the cluster (Os1, Os3, Os4 and Os2, Os3, Os4). The view onto one of these H-bridged faces, Os2, Os3, Os4, is shown in Figure 4d. As in the case of the monohydride $[HOs_8(CO)_{22}I]$, an unusual asymmetric μ_3-H bonding mode is evident for both hydrogen atoms.

The asymmetry of the bridging modes observed in $[HOs_8(CO)_{22}I]$ and $[H_2Os_7(CO)_{20}]$, and the fact that the associated Os–Os bond lengths are not elongated but are in fact rather short in both structures, explains why the H-site could not be located readily by the normal qualitative indirect methods, nor by the Orpen 'potential energy' method which assumes symmetrical bonding of the H-ligands.

2.3. Computer-Generated 'Space-Filling' Models of Compounds with Directly Located Hydrido-Ligands

In the X-ray structure analysis[22] of the carbido(hydrido)nitrosyl cluster $[HRu_6C(CO)_{15}(NO)]$ (Fig. 5a) the hydrido-ligand was located directly, thus giving an opportunity to compare the results with those obtained with computer-generated space-filling models.

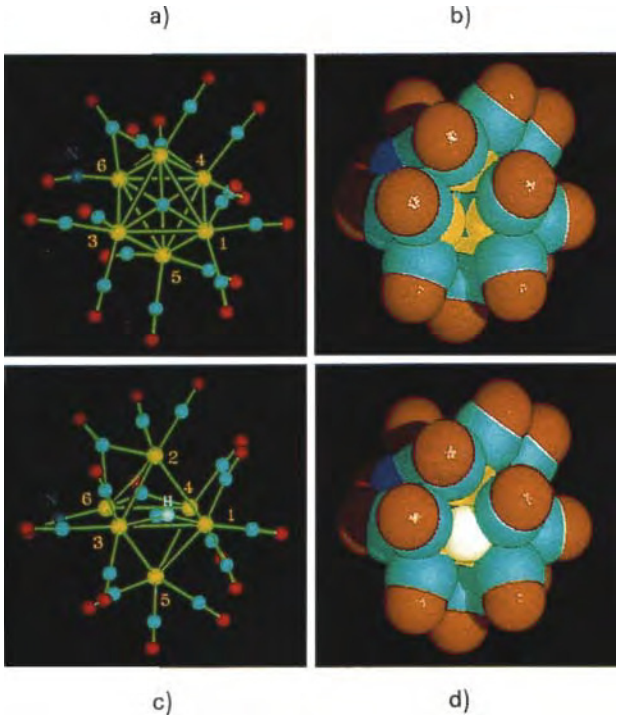


Fig. 5. A comparison of the ball-and-stick and space-filling models for illustrating surface ligand distribution using as example the structure of the carbido(hydrido)nitrosyl cluster $[HRu_6C(CO)_{18}(NO)]$, for which the H-atom was located directly from X-ray data. a) Ball-and-stick model computed without the H-atom; b) space-filling model with the metal atoms visible through the vacant H-site; c) ball-and-stick model including the H-atom; d) space-filling model, with the H-atom van der Waals sphere included (white).

Although the position of the H-ligand could not readily be deduced from the carbonyl distribution using conventional ball-and-stick diagrams, computed space-filling models of the molecule revealed only one gap in the close-packed surface ligands suitable to accommodate a hydrogen ligand (Fig. 5b). This 'hole', above the Ru1, Ru2, Ru3 face, was too asymmetric to be attributed to a μ_3-H atom and it was concluded that the H-ligand was in a μ_2-site bridging the Ru1–Ru3 bond but leaning over the face towards Ru2. After full refinement of the structure the highest peak in the final difference Fourier synthesis (ca. 1 e/Å^3) corresponded to the position of this μ_2-H atom, and the location is as predicted from the examination of the simulated model. Inclusion of the H-atom in the space-filling model (Fig. 5d) shows that the gap in the other surface ligands (Fig. 5b) exactly accomodates it. Figure 5c shows the hydrido-ligand at the observed site in the ball-and-stick model of the cluster.

2.4. Large Hydrido Clusters

As cluster size increases the ratio of surface area to number of metal atoms decreases so that interstitial ligands become important in preventing surface ligand overcrowding. Since the initial discovery of an interstitial H-ligand in a site of *octahedral* symmetry,[14] a number of polynuclear cluster compounds with ligands of this type have been characterized.[3,23] However, it was considered unlikely that H-atoms would be found in the smaller *tetrahedral* sites, except with metals of relatively large covalent radius.[9] Application of computer graphics to the study of some carbido(hydrido)decaosmium species, has indeed provided evidence for H-atoms in M_4 sites of this symmetry. For the dianion $[Os_{10}C(CO)_{24}]^{2\ominus}$, X-ray structure analysis (Fig. 6a) shows that the CO ligands are symmetrically arranged approximately perpendicular to the four flat surfaces of a giant tetrahedral osmium core;[24] this Os_{10}-cluster can, moreover, be regarded as a small fragment of a cubic close packed array of atoms, as is found in several metals.

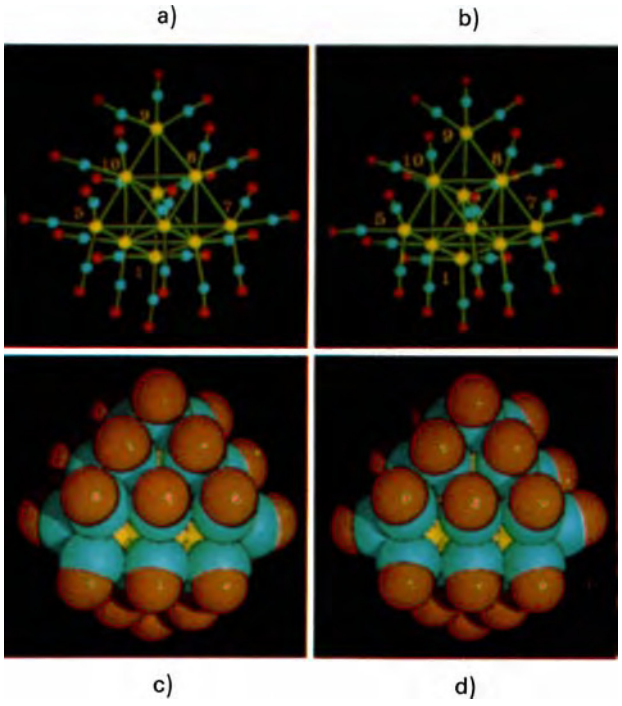


Fig. 6. Comparisons of the almost identical structures observed for the non-hydrido dianion $[Os_{10}C(CO)_{24}]^{2\ominus}$ and the hydrido monoanion $[HOs_{10}C(CO)_{24}]^{\ominus}$, which provide evidence that the H-ligand of the monoanion is not on the surface, but is the first example of an interstitial H-atom in a tetrahedral cavity of a cluster. a), c) Ball-and-stick and space-filling models, respectively, of $[Os_{10}C(CO)_{24}]^{2\ominus}$; b), d) ball-and-stick and space-filling models, respectively, of $[HOs_{10}C(CO)_{24}]^{\ominus}$.

The mono-hydrido derivative $[HOs_{10}C(CO)_{24}]^{\ominus}$ shows an almost identical ligand distribution to that of the dianion, with none of the characteristic displacement of the carbonyls expected if a surface H-ligand were present (Fig. 6b). This evidence together with a slight expansion of one of the capping Os_4 tetrahedra relative to the other three, led us to the conclusion that the H-atom in this cluster is in an interstitial tetrahedral site,[25] the only octahedral site being occupied by the carbido C-atom. The computed space-filling models of the dianion and the mono-hydride are shown for comparison in Figures 6c and 6d, respectively. The carbonyl atoms are 'close-packed' over each of the four 6-atom planar metal surfaces, with their van der Waals spheres in tangential contact. The carbonyls are eclipsed along all edges of both Os_{10}-tetrahedra in almost identical arrangements and remain in tangential contact. Overall, the two Keller models show a remarkable similarity and confirm the conclusion that there is no suitable site on the surface of $[HOs_{10}C(CO)_{24}]^{\ominus}$ to accomodate a hydrido-ligand. This was the first example of a hydrido-ligand in a tetrahedral site of a cluster compound, although this H-atom environment is well known in bulk metals. More recent evidence from X-ray structure analyses indicates that interstitial, tetrahedrally coordinated hydrido-ligands are also present in the non-carbido decaosmium species $[H_4Os_{10}(CO)_{24}]^{2\ominus}$,[26] where the absence of surface H-ligands is again indicated by the close contact of the surface ligands shown in computed space-filling models. It was very difficult to obtain crystals of these polynuclear hydrido-clusters suitable enough for X-ray analysis, and so far it has proven impossible to obtain the larger crystals needed for neutron diffraction studies. Consequently, the computer graphics method provides the best evidence to date for the presence of interstitial hydrogen atoms in these compounds.

3. Polynuclear Carbidometal Clusters

There is a great deal of interest in the chemistry of carbido(carbonyl)metal clusters, because it is widely believed that an important step in the Fischer-Tropsch hydrogenation of CO to produce hydrocarbons involves the formation of carbido species on the surface of the bulk metal catalyst.[6,7] Studies of the reactivity at the carbido-ligands in cluster compounds provide an insight into the reactions of similar atoms on bulk metal surfaces.

3.1. Clusters with μ_5-Carbido Ligands

The first carbido(carbonyl)transition metal cluster compound, $[Fe_5(\mu_5\text{-}C)(CO)_{15}]$ was reported in 1962,[27] and since then a large range of related compounds in which the carbido-C atom exhibits a number of different coordination geometries has been discovered. Many contain the carbido C-atom on the cluster surface in "semi-interstitial" sites. For example, in the series $[M_5C(CO)_{15}]$ (M = Fe, Ru, Os)[27,28,29,30] the C atom is 5-coordinate and lies slightly below the base of a square pyramidal M_5 arrangement as shown in Figures 7a and 7b for $[Os_5C(CO)_{15}]$.[29]

The reactions of the pentanuclear carbidoruthenium and -osmium species have been intensively studied by *Lewis, Johnson* et al.[7] They concluded that the dominant role of the semi-interstitial carbido ligand is to impart unusual stability to the metal framework. Although M–M bond cleavage takes place readily, reactions appear to be limited to those in which the M–C bonds are maintained throughout and any metal rearrangement occurs by swivelling

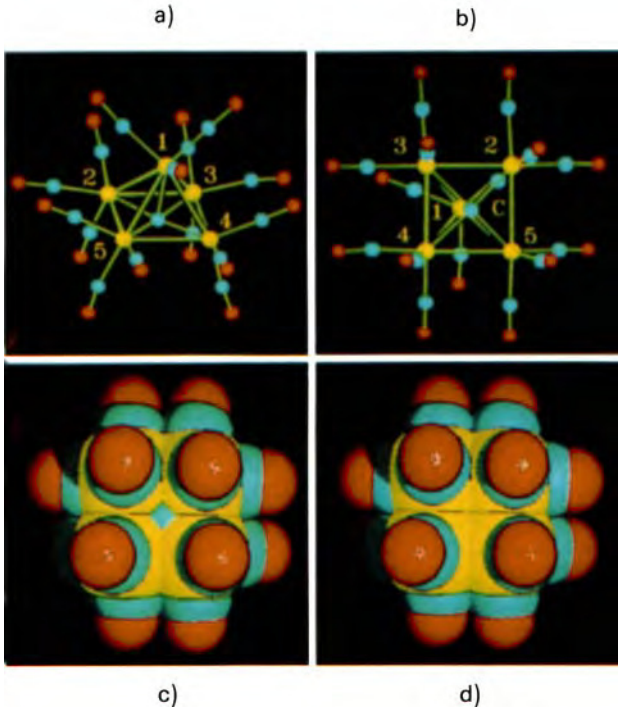


Fig. 7. Comparison of ball-and-stick models of the square-pyramidal structure of the carbido cluster $[Os_5(\mu_5\text{-}C)(CO)_{15}]$ (in which the carbido atom appears 'exposed') with space-filling models which show that in fact the 'bonding sphere' of the μ_5-C atom is completely covered by the van der Waals spheres of the four basal osmium atoms. a), b) Ball-and-stick models, viewed from the side and onto the square base, respectively; c), d) space-filling models, viewed onto the square base from below; the μ_5-carbido ligand is assigned a van der Waals sphere (small rectangle) and a covalent radius (not visible), respectively.

round the carbido-C atom. Significantly, they found no evidence of direct reaction at the μ_5-C atom.

Recent molecular orbital calculations indicate the involvement of the 'lone pair' electrons on the μ_5-C atom in the interaction with the basal metal atoms contributes to the lack of reactivity of the carbido ligand in $[Fe_5(\mu_5\text{-}C)(CO)_{15}]$.[31] Although non-bonded interactions of carbido substituents in clusters are thought to play a role in determining reaction pathways, and are currently being studied by interactive molecular graphics,[32] it has generally been accepted that unsubstituted C-atoms in pentanuclear cluster species are 'entirely exposed' and that there is no steric barrier to their reaction.[6,7,31] This assumption is proved wrong by computer simulated space-filling models of the $[M_5(\mu_5\text{-}C)(CO)_{15}]$ molecules which show that, although the surface ligands provide no steric barrier, the carbido-C atom is not as accessible as the usual ball-and-stick molecular models have indicated. For example the Keller model of $[Os_5(\mu_5\text{-}C)(CO)_{15}]$ (Fig. 7c), which is viewed onto the square-base shows that the van der Waals sphere of the carbido-C atom is almost completely 'swamped' by those of the four Os atoms. In considering the possibility of bond formation at the μ_5-C atom it is more appropriate to assign a covalent radius (0.77 Å) to it, as in Figure 7d. In this model the 'bonding' sphere of this atom cannot be seen because it is completely covered by the the van der Waals spheres of the metal atoms. Consequently, any reactant attempting a direct approach to within bonding distance of the carbido-C carbon atom would be repelled by the metal atoms. Clearly, in addition to the favorable bonding between the C-atom and the metal framework indicated by the MO calculations,[31] a kinetic contribution to the stability of this atom is important.[33] A group undergoing an initial bonding interaction with a metal atom would achieve a reaction pathway of lower energy, and it is significant that bond formation with the carbido atom has only been observed in the special case where a sixth metal adds to the four basal M atoms of $[M_5C(CO)_{15}]$ (M = Ru and Os) to form an octahedral cluster.[7]

3.2. Clusters with μ_4-Carbido Ligands

The first examples of four-coordinate carbido C-atoms were found in the tetranuclear species $[HFe_4(\mu_4\text{-}C)(CO)_{12}]^{\ominus}$,[34,35] and $[Fe(\mu_4\text{-}C)(CO)_{12}]^{2\ominus}$.[34,36] The 'butterfly' structure of the Fe_4 polyhedron in $[HFe_4(\mu_4\text{-}C)(CO)_{12}]^{\ominus}$ (Fig. 8a)[35] allows a more exposed site for the μ_4-C atom than any alternative μ_4-arrangement that may be envisaged, such as, for example, that of the distorted square planar $Re_4(\mu_4\text{-}C)$ core reported recently for $[Re_4(\mu_4\text{-}C)(CO)_{15}I]$.[37] Protonation of the μ_4-C in $[HFe_4(\mu_4\text{-}C)(CO)_{12}]^{\ominus}$ gives $[HFe_4(\eta^2\text{-}CH)(CO)_{12}]$ (Fig. 8b), and is the first example of such a reaction at a cluster carbido atom.[34]

This ready protonation has been attributed to the more accessible nature of the μ_4-bonding site in $[HFe_4(\mu_4\text{-}C)(CO)_{12}]^{\ominus}$ compared to that of the unreactive μ_5-C atom

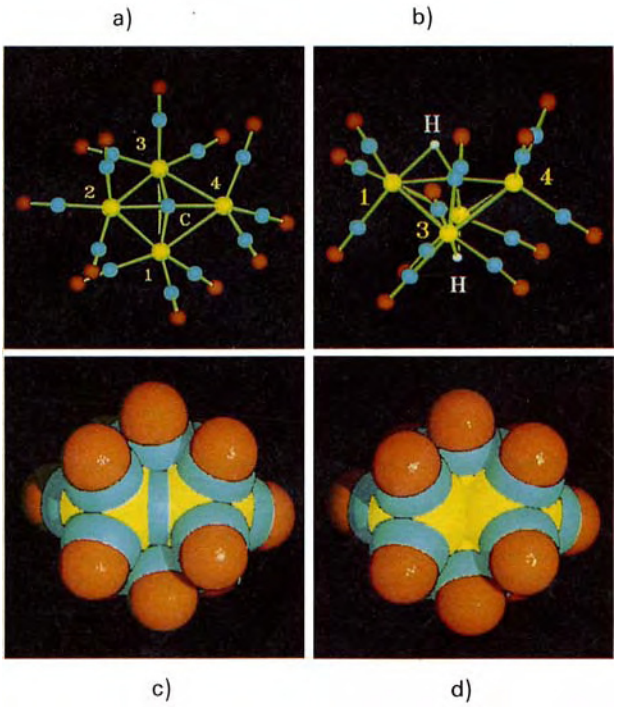


Fig. 8. Conventional ball-and-stick models showing the 'butterfly' structure of the carbido monoanion $[HFe_4(\mu_4\text{-}C)(CO)_{12}]^{\ominus}$ and that of the product of its protonation, $[HFe_4(\eta^2\text{-}CH)(CO)_{12}]$, together with space-filling models of the reactive monoanion showing that the μ_4-C atom is not exposed but engulfed by the van der Waals spheres of the 'wing tip' iron atoms. a), b) Ball-and-stick models of $[HFe_4(\mu_4\text{-}C)(CO)_{12}]^{\ominus}$ and $[HFe_4(\eta^2\text{-}CH)(CO)_{12}]$, respectively; c), d) space-filling models of $[HFe_4(\mu_4\text{-}C)(CO)_{12}]^{\ominus}$; the μ_4-carbido ligand is assigned a van der Waals sphere (visible as narrow strip) and a covalent radius (not visible), respectively.

in the widely studied $[M_5(\mu_5\text{-}C)(CO)_{15}]$ compounds. The computed space-filling models of the $[HFe_4(\mu_4\text{-}C)(CO)_{12}]^{\ominus}$ monoanion (Fig. 8c) show that even in this apparently very exposed site the carbido van der Waals sphere is only visible as a narrow strip between those of the adjacent 'wing-tip' metal atoms, Fe2 and Fe4. In Figure 8d, calculated with the more appropriate carbido covalent radius, the 'bonding' sphere of the μ_4-C atom has disappeared completely beneath the van der Waals spheres of the metal atoms.

The (CH) ligand formed by protonation of this C-atom forms an unusual type of η^2-μ_4-bridge with the H-atom bonded to both the C-atom and a wing-tip Fe atom (Fig. 8b).[38] In view of the repulsion by the wing-tip Fe atoms, experienced by any incoming group directly approaching the C-atom of $[HFe_4C(CO)_{12}]^{\ominus}$, we concluded that the attack by the proton involves initial bonding interaction with the iron atom;[33] the available coordination sites on the wing-tip iron atoms are directed towards the uncoordinated side of the C-atom so that sequential bonding of the proton, firstly to an iron atom and then to the C-atom is reasonable. Recent molecular orbital calculations also indicate that it is orbitals associated with the metal atoms that are most probably involved in the initial reaction, and that direct attack on the C-atom is unfavorable.[39] It therefore appears that, as in the case of the μ_5-C atom, there are both kinetic and thermodynamic factors contributing to the stability of μ_4-C atoms.

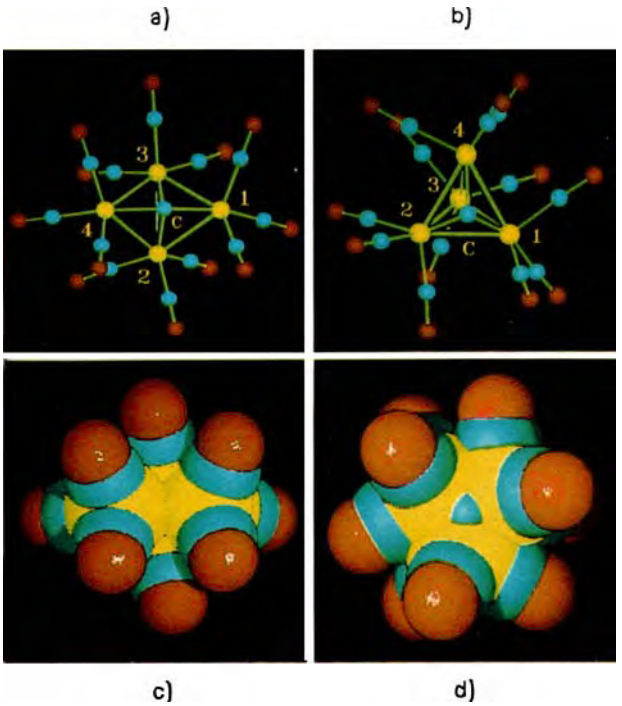


Fig. 9. A comparison of ball-and-stick and space-filling models for the observed 'butterfly' structure of $[Fe_4(\mu_4\text{-}C)(CO)_{12}]^{2\ominus}$ with those of an estimated tetrahedral structure for "$[Fe_4(\mu_3\text{-}C)(CO)_{12}]$", the proposed intermediate in the reaction of the dianion with hydrogen, demonstrating that in a μ_3-site the carbido atom would be exposed. a), b) Ball-and-stick models of $[Fe_4(\mu_4\text{-}C)(CO)_{12}]^{2\ominus}$ with a butterfly structure and "$[Fe_4(\mu_3\text{-}C)(CO)_{12}]$" with a tetrahedral structure; c), d) space-filling models of $[Fe_4(\mu_4\text{-}C)(CO)_{12}]^{2\ominus}$ and "$[Fe_4(\mu_3\text{-}C)(CO)_{12}]$" the carbido ligand is represented as a non-visible and visible covalent sphere, respectively.

3.3. The Effect of Rearrangement of the Metal Polyhedron

The only example of direct hydrogenation of a cluster carbido atom by molecular hydrogen has been observed under oxidizing conditions for the 'butterfly' cluster dianion $[Fe_4(\mu_4\text{-}C)(CO)_{12}]^{2\ominus}$ (Fig. 9a) and it is thought that the reaction proceeds via a neutral species "$[Fe_4C(CO)_{12}]$", generated by loss of two electrons from the dianion.[34] The proposed intermediate has only 60 valence electrons in the cluster; consequently, a tetrahedral arrangement can be assumed for the four iron atoms.[40] The resultant metal core rearrangement would force the carbido C-atom to adopt a μ_3-bonding mode on the tetrahedral "$[Fe_4C(CO)_{12}]$" intermediate, illustrated in Figure 9b as a ball-and-stick model computed from estimated atomic coordinates.

In the space-filling model of the hypothetical tetrahedral '$[Fe_4(\mu_3\text{-}C)(CO)_{12}]$' cluster (Fig. 9d), the 'bonding' sphere of the carbido-C atom, previously submerged in the 'butterfly' conformation (Fig. 9c), can now be seen quite clearly above the van der Waals spheres of the iron atoms. Approach of a reactant to within bonding distance of the μ_3-C atom could therefore occur without any repulsion by these metal atoms. On reaction with H_2 the electron count of "$[Fe_4(\mu_3\text{-}C)(CO)_{12}]$" would again increase by two, causing a return to a 'butterfly' structure in the derivative $[HFe_4(CH)(CO)_{12}]$ (cf. Fig. 8b). The computer models therefore demonstrate a possible kinetic advantage from initial cluster oxidation which, by producing a metal geometry rearrangement, forces the C-atom into an exposed μ_3-site and hence lowers the activation energy of the hydrogenation process.

Finally, it should be mentioned that the findings presented here about the different accessibility of μ_5-, μ_4-, and μ_3-carbido ligands using rigid models also apply, in principle, even when it is taken into account that real molecules perform vibrational movements.

3.4. The Extension to Bulk Metal Surfaces

The exposed μ_3-C bonding mode deduced for the C-atom of the intermediate in the protonation of $[HFe_4(\mu_4\text{-}C)(CO)_{12}]^{\ominus}$ (Figs. 9b and 9d) is closely similar to the probable bonding mode which may be envisaged for C-atoms on the 'close-packed' (111) surfaces of cubic close packed or (001) surfaces of hexagonal close packed bulk metals, so that it may be anticipated that isolated C-atoms on these surfaces will be highly reactive. Although some evidence of discrete molecular species with μ_3-C atoms has been reported,[41] the very high reactivity which would arise from their exposed position (Fig. 9b) may account for the fact that none has yet been characterized in the solid state. The metal-protected μ_5-carbido species which have so far proved unreactive in isolated clusters have the type of coordination that is most probable for C-atoms on (100) surfaces of cubic close packed arrays, and the μ_4-C bonding mode would occur along 'steps' between layers; carbon atoms attached in the μ_5- or μ_4-mode at such sites may in

part account for the tenacity with which contaminating C-atoms bind to metal surfaces.[31]

We wish to thank Professor H. Vahrenkamp of the University of Freiburg who first suggested to us the use of computer simulated 'space-filling' models in examining cluster compounds, and Dr. E. Keller for supplying us with a copy of his program and for valuable discussions. We also wish to thank the staff of the North London Computing Centre for encouragement and advice.

Received: August 29, 1985 [A 594 IE]
German version: *Angew. Chem. 98* (1986) 843

[1] A. Ceriotti, F. Demartin, G. Longoni, M. Manassero, M. Marchionna, G. Piva, M. Sansoni, *Angew. Chem. 97* (1985) 708; *Angew. Chem. Int. Ed. Engl. 24* (1985) 697.
[2] B. F. G. Johnson, J. Lewis, *Phil. Trans. R. Soc. London A 5* (1982) 308.
[3] P. Chini, *J. Organomet. Chem. 200* (1980) 37.
[4] R. E. Benfield, B. F. G. Johnson, *J. Chem. Soc. Dalton Trans. 1980,* 1743.
[5] M. McPartlin, D. M. P. Mingos, *Polyhedron 3* (1984) 1321.
[6] E. L. Muetterties, M. Tachikawa, *Prog. Inorg. Chem. 28* (1981) 203.
[7] B. F. G. Johnson, J. Lewis, W. J. H. Nelson, J. N. Nicholls, M. D. Vargas, *J. Organomet. Chem. 249* (1983) 252.
[8] S. Martinengo, D. Strumolo, P. Chini, V. G. Albano, D. Braga, *J. Chem. Soc. Dalton Trans. 1985,* 35.
[9] R. G. Teller, R. Bau, *Struct. Bonding (Berlin) 44* (1981) 1.
[10] P. G. Owston, J. M. Partridge, J. M. Rowe, *Acta Crystallogr. 13* (1960) 246.
[11] M. R. Churchill, J. Wormald, *J. Am. Chem. Soc. 93* (1971) 5670.
[12] M. McPartlin, C. R. Eady, B. F. G. Johnson, J. Lewis, *J. Chem. Soc. Chem. Commun. 1976,* 883.
[13] A. G. Orpen, *J. Chem. Soc. Dalton Trans. 1980,* 2509.
[14] C. R. Eady, B. F. G. Johnson, J. Lewis, M. C. Malatesta, P. Machin, M. McPartlin, *J. Chem. Soc. Chem. Commun. 1976,* 945.
[15] P. Chini, G. Longoni, S. Martinengo, A. Ceriotti, *Adv. Chem. Ser. 167* (1978) 1.
[16] P. F. Jackson, B. F. G. Johnson, J. Lewis, P. R. Raithby, M. McPartlin, W. J. H. Nelson, K. D. Rouse, J. Allibon, S. A. Mason, *J. Chem. Soc. Chem. Commun. 1980,* 295.
[17] Schakal-Program von *E. Keller,* Universität Freiburg 1980. Modified by the author of the program in 1982 for application to a high-resolution color graphic terminal. The following values for van der Waals radii are used: Os 2.35, Ru 2.35, Fe 2.15, C 1.60, O 1.40, H 1.20 Å.
[18] D. Braga, K. Henrick, B. F. G. Johnson, J. Lewis, M. McPartlin, W. J. H. Nelson, M. D. Vargas, *J. Chem. Soc. Chem. Commun. 1982,* 449.
[19] D. Braga, K. Henrick, B. F. G. Johnson, J. Lewis, M. McPartlin, W. J. H. Nelson, M. D. Vargas, *J. Chem. Soc. Dalton Trans. 1984,* 2151.
[20] D. Braga, J. Lewis, B. F. G. Johnson, M. McPartlin, W. J. H. Nelson, *J. Organomet. Chem. 249* (1983) C21.
[21] E. J. Ditzel, H. D. Holden, B. F. G. Johnson, J. Lewis, A. Sanders, M. J. Taylor, *J. Chem. Soc. Chem. Commun. 1982,* 1373.
[22] B. F. G. Johnson, J. Lewis, W. J. H. Nelson, J. Puga, M. McPartlin, A. Sironi, *J. Organomet. Chem. 253* (1983) C5.
[23] D. W. Hart, R. G. Teller, C.-Y. Wei, R. Bau, G. Longoni, S. Campanella, P. Chini, T. F. Koetzle, *Angew. Chem. 91* (1979) 86; *Angew. Chem. Int. Ed. Engl. 18* (1979) 80.
[24] P. F. Jackson, B. F. G. Johnson, J. Lewis, M. McPartlin, W. J. H. Nelson, *J. Chem. Soc. Chem. Commun. 1980,* 224; *J. Chem. Soc. Dalton Trans. 1982,* 2106.
[25] P. F. Jackson, B. F. G. Johnson, J. Lewis, M. McPartlin, W. J. H. Nelson, *J. Chem. Soc. Chem. Commun. 1982,* 49.
[26] D. Braga, J. Lewis, B. F. G. Johnson, M. McPartlin, W. J. H. Nelson, M. D. Vargas, *J. Chem. Soc. Chem. Commun. 1983,* 241.
[27] E. H. Braye, L. F. Dahl, W. Hubel, D. L. Wampler, *J. Am. Chem. Soc. 84* (1962) 4633.
[28] D. H. Farrar, P. F. Jackson, B. F. G. Johnson, J. Lewis, J. N. Nicholls, M. McPartlin, *J. Chem. Soc. Chem. Commun. 1981,* 415.
[29] P. F. Jackson, B. F. G. Johnson, J. Lewis, J. N. Nicholls, M. McPartlin, W. J. H. Nelson, *J. Chem. Soc. Chem. Commun. 1980,* 564.
[30] B. F. G. Johnson, J. Lewis, J. N. Nicholls, J. Puga, P. R. Raithby, M. J. Rosales, M. McPartlin, W. Clegg, *J. Chem. Soc. Dalton Trans. 1983,* 277.
[31] S. D. Wijeyesekera, R. Hoffmann, C. N. Wilker, *Organometallics 3* (1984) 962.
[32] J. M. Newsam, J. S. Bradley, *J. Chem. Soc. Chem. Commun. 1985,* 759.
[33] M. McPartlin, J. Morris: *Second International Conference on the Platinum Metals,* Edinburgh 1984.
[34] M. Tachikawa, E. L. Muetterties, *J. Am. Chem. Soc. 102* (1980) 4541.
[35] E. M. Holt, K. H. Whitmire, D. F. Shriver, *J. Organomet. Chem. 213* (1981) 125.
[36] R. F. Boehne, P. Coppens, *Acta Crystallogr. B 37* (1981) 1914.
[37] T. Beringhelli, G. Ciani, G. D'Alfonso, A. Sironi, M. Freni, *J. Chem. Soc. Chem. Commun. 1985,* 978.
[38] M. A. Beno, J. M. Williams, M. Tachikawa, E. L. Muetterties, *J. Am. Chem. Soc. 103* (1981) 1485.
[39] S. Harris, J. S. Bradley, *Organometallics 3* (1984) 1086.
[40] M. McPartlin, *Polyhedron 3* (1984) 1279, and reference cited therein.
[41] See, e.g., D. Seyferth, *Adv. Organomet. Chem. 14* (1976) 97.

High-Resolution Metal-NMR Spectroscopy of Organometallic Compounds

New Analytical Methods (30)

By Reinhard Benn* and Anna Rufińska

Great advances have been made in the past decade in the field of NMR spectroscopy. Apart from the development of completely new areas of application, such as in solid-state chemistry, in materials science, in physiological chemistry, and in medicine, with the introduction of new pulse spectroscopic methods and the application of high magnetic field strengths important progress has also been made in the traditional field of high-resolution NMR spectroscopy. Thus, among other things, the observation of metal resonances has been facilitated and new areas of application have been opened up in inorganic and organometallic chemistry. In this review, recent detection methods for spin-1/2 and quadrupolar metal nuclei are presented and discussed. The use of metal-NMR spectroscopy with respect to problems of a typical chemical nature, mainly from the field of organometallics, is demonstrated for a number of selected metal nuclei (^{25}Mg, ^{27}Al, ^{49}Ti, ^{57}Fe, ^{59}Co, ^{61}Ni, ^{91}Zr, ^{103}Rh, and ^{195}Pt). Relations found empirically between chemical shifts and coordination number, oxidation number, and electronic configuration of a metal bound in a complex are emphasized. Furthermore, cases in which the chemical shifts of metal nuclei can be interpreted in terms of the energy difference of frontier orbitals are presented. This aspect leads to the establishment of a relationship between chemical reactivity and NMR parameters for a series of related compounds.

1. Introduction

With the introduction of stable superconducting magnets and the development of new experimental techniques the last decade of NMR spectroscopy has seen the opening up of completely new areas of application, e.g. in the investigation of solids,[1] in physiological chemistry, and in medicine.[2] At the same time there has also been an active development in high-resolution Fourier transform NMR spectroscopy as it is used in chemistry for investigations of molecular properties. Consequently, a versatile repertoire of different techniques is available for structure determinations and reaction mechanism studies on molecules in solution. In this context the one- and two-dimensional pulse spectroscopic methods[3,4] warrant special mention. Initially, attention was focussed on ^{1}H and ^{13}C pulse NMR spectroscopy, later attempts were made to exploit improved sensitivity and greater signal dispersion for measurements on other magnetically active nuclei.[5] Naturally, these efforts concentrated first on those spin-1/2 nuclei which had already been investigated quite frequently, such as ^{31}P,[6] ^{15}N,[7] or ^{29}Si[8] as well as on some "friendly" quadrupolar nuclei such as ^{2}H,[9] ^{11}B,[10] and ^{17}O.[11] It was soon recognized that insensitive spin-1/2 metal nuclei like, e.g., ^{103}Rh which formerly were accessible only through special double resonance or pulse excitation techniques, could also be recorded directly within reasonable experimental times using the new high-field pulse NMR methods.[12]

Most metals, on the other hand, have a magnetically active isotope with a nuclear spin of quantum number $I > 1/2$. This can lead to resonances with large linewidths, thereby decreasing drastically the sensitivity. For such quadrupolar nuclei the new pulse techniques are only useful to a limited extent and the increase in sensitivity and signal selection available today results mainly from the more favorable Boltzmann distribution of the nuclear spins and the larger dispersion resulting from stronger magnetic fields.

It is mainly on the basis of these improved experimental conditions that the NMR spectroscopy of metal nuclei has been increasingly studied in recent years by several research groups.[5] In this review article it will be shown, primarily with organometallic compounds in solution as examples, how information on the structure, dynamics and chemical properties of metal complexes, which is difficult to obtain or not at all available from other sources, can be derived from the NMR spectroscopy of metal nuclei. Rather than a comprehensive and comparative review of all data already published, we present here a selection of typical results. Emphasis will be laid on such chemical aspects as coordination number, oxidation state, bonding situation and electronic configuration of the complexed metal. Although metal-NMR spectroscopy is only just beginning to assist solving problems regarding the chemical properties of complexes, we shall try to demonstrate these contributions and outline further lines of development.

We shall first give an introductory treatment of the various experimental aspects that originate from the magnetic properties of the metal isotopes. In two further sections we shall deal with the information that emerges from the NMR spectroscopy of metal nuclei. The primary source of such information is the chemical shift of the metal resonance, δ(M), while NMR parameters like relaxation times (T_1, T_2) and scalar spin-spin coupling constants involving metal nuclei, J(M,X), will be cited less frequently, although they are often extremely useful. As example of an

[*] Priv.-Doz. Dr. R. Benn, Dr. A. Rufińska
Max-Planck-Institut für Kohlenforschung
Kaiser-Wilhelm-Platz 1, D-4330 Mülheim a. d. Ruhr (FRG)

 © VCH Verlagsgesellschaft mbH, D-6940 Weinheim, 1986 0570-0833/86/1010-0861 $ 02.50/0

easily accessible spin-1/2 metal nuclei we shall discuss ^{195}Pt, while ^{103}Rh will serve to demonstrate the properties of the less sensitive spin-1/2 nuclei. From the quadrupolar nuclei of the main group elements of the Periodic Table, ^{27}Al and the ^{25}Mg serve as examples of a sensitive and an insensitive nucleus, respectively. As typical examples for the transition metals we have chosen ^{59}Co, ^{91}Zr, and ^{61}Ni.

2. Magnetic Properties of Metal Nuclei

The experimental requirements for NMR measurements as well as the suitability of a given isotope as NMR probe are primarily determined by the magnetic properties of the isotope. On the basis of the nuclear spin quantum number I, the magnetic isotopes can be divided into two classes: To the first one belong nuclei with $I = 1/2$, which usually yield sharp signals (in the case of small molecules the halfwidths $W_{1/2}$ lie between 1 and 10 Hz). The second class comprises nuclei with $I > 1/2$, which show considerably broadened lines with halfwidths of up to several kHz. This renders the observation of such resonances considerably more difficult.

2.1. Metal Nuclei with Spin Quantum Number 1/2

The sensitivity of a spin-1/2 nucleus depends upon its magnetogyric ratio γ, which determines the relative NMR sensitivity, and upon its natural isotopic abundance a (at constant magnetic field strength and constant temperature the intensity of the NMR signal is proportional to $a\gamma^3 I(I+1)$). Table 1 shows both properties for spin-1/2 metal nuclei. The absolute sensitivity or receptivity of a certain nucleus is the product of its relative sensitivity and its natural abundance. Since the signals in Fourier transform NMR spectroscopy[13] result from a summation of several free induction decays (FID), the repetition time for individual pulse experiments emerges as a further important factor which determines the total time of the experiment. A perturbation (for example, an excitation with a radio frequency pulse) changes the original z-magnetization, which is governed by the equilibrium Boltzmann distribution. The time necessary to re-establish the original equilibrium population is characterized by the longitudinal relaxation time T_1. It is proportional to the average lifetime of a spin in a certain energy state. The transport of spin population during the relaxation process to thermal equilibrium according to the Boltzmann theorem is achieved through interactions with fluctuating magnetic fields. These can originate from other magnetic moments present in the solution (the environment), the so-called lattice. However, since many of the magnetically active spin-1/2 metal nuclei only have a small magnetic moment, their interaction with the lattice is often very small and the relaxation times of such nuclei may become quite long. For instance, for silver ions in solution, T_1 of the silver isotope ^{109}Ag can be as large as 10^3 s.[14] This means that under conventional conditions the recording times for the measurement of insensitive spin-1/2 metal nuclei become prohibitively long. Therefore, besides the application of alternative experimental techniques, an estimate of the relaxation times and information about the mechanisms responsible for relaxation is of crucial importance for practical NMR measurements of insensitive spin-1/2 metal nuclei.

Table 1. Classification of spin-1/2 metal nuclei (except lanthanoids and actinoids) according to the magnitude of their elementary magnetic strength [a] and their natural isotopic abundance. Only the most favorable isotope of an element is listed.

Elementary magnetic strength	Natural abundance >90%	10-90%	<10%
strong		^{205}Tl	
medium		^{113}Cd, ^{195}Pt, ^{199}Hg, ^{207}Pb	^{119}Sn
weak	^{89}Y, ^{103}Rh	^{109}Ag, ^{183}W	^{57}Fe, ^{187}Os

[a] The elementary magnetic strength is defined here as the ration $\gamma(X)/\gamma(^1H)$ with $\gamma(^1H) = 26.7 \times 10^7$ rad T^{-1} s^{-1}. Isotopes of medium magnetic strength are those with $\gamma(X)/\gamma(^1H) = 0.9$ to 0.1 (see also ref. [5a]).

2.1.1. Longitudinal Relaxation Times of Spin-1/2 Metal Nuclei

Longitudinal relaxation times can be determined by various pulse techniques. For sharp signals that show no scalar coupling and that are distributed over a relatively narrow frequency range, relaxation time measurements present no problem and can be performed with high precision using the techniques known from ^{13}C-NMR spectroscopy.[13b,c] For nuclei that show scalar coupling to other magnetically active spin-1/2 nuclei, e.g. ^{195}Pt to ^{31}P in $[Pt(PMe_3)_4]$,[6a,15] difficulties may be encountered with T_1 measurements. Firstly, these are intrinsic, since relaxation in a coupled spin system (the spectrometers employed are often not equipped with the appropriate X nucleus decoupler for $X \neq {}^1H$) cannot be described in terms of a simple exponential behavior.[16] And secondly, they can arise from the experimental conditions employed. With the inversion-recovery method,[13b] for instance, it is difficult to invert all five lines of the ^{195}Pt spectrum of $[Pt(PMe_3)_4]$ completely by a single 180° pulse. This is because the lines are distributed over a frequency range of more than 15000 Hz (Fig. 1). The application of so-called composite pulses[17] can improve the inversion. With this technique the 180° pulse is replaced by a $90°_x\,180°_y\,90°_x$ sandwich pulse. Errors arising from imprecise adjustment of the pulse

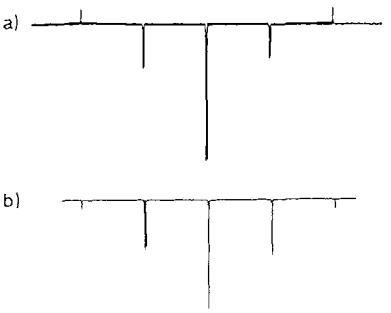


Fig. 1. Inversion of the ^{195}Pt quintet of $[Pt(PMe_3)_4]$ ($^1J(Pt,P) = 3835$ Hz) [15]: a) with a 180° pulse, and b) with a composite $90°_x\,180°_y\,90°_x$ pulse (duration of the 90° pulse 25 μs).

phases can be eliminated by additional phase cycling over all three directions in space.[18]

If spin-1/2 metal nuclei show scalar coupling to neighboring quadrupolar nuclei which have Zeeman states of only a short lifetime, fluctuating magnetic fields arise at the metal nucleus that contribute to its relaxation (scalar relaxation).[13c] This mechanism is, for example, observed for the relaxation of ^{195}Pt in platinum complexes with nitrogen ligands.[19] In the following we shall only rarely mention metal complexes with bonds between spin-1/2 metal nuclei and quadrupolar nuclei, and scalar relaxation as well as chemical exchange will not be considered further. Since only diamagnetic complexes are discussed, we shall also disregard relaxation through interactions with unpaired electrons, which can be very effective in solutions containing paramagnetic species. Brownian molecular motion together with dipole-dipole interactions (DD), spin rotation (SR) or chemical shift anisotropy (CSA)[13b] give rise to fluctuating magnetic fields which can contribute to relaxation of a spin-1/2 nucleus. The latter three of these mechanisms can be detected separately (see Table 2).

Table 2. Relaxation mechanisms of spin-1/2 metal nuclei in diamagnetic solutions (relaxation rate $R = 1/T_1$ under the following conditions: $\omega \cdot \tau_c < 1$, neglection of scalar couplings to quadrupolar nuclei and of chemical exchange, for details see Text) and quantities suitable for determining their contribution to the overall relaxation time.

Relaxation mechanisms	Detection
DD	experimental NOE faktor: $R_{DD}/R = \eta/\eta_{NOE}$
CSA	B_0 dependence: $R_{CSA} \sim B_0^2$
SR	temperature dependence: $\ln(R_{SR}) \sim -1/T$

Dipole-dipole relaxation results from the magnetic interaction of a spin-1/2 nucleus with neighboring magnetic dipoles. The strength of this interaction mainly depends upon the magnitude of the magnetic moments involved and upon the distance between them ($\sim r^{-6}$). The time dependence of the magnetic field at the position of the nucleus of interest follows from the fact that in solution all angles between the distance vector and the direction of the external magnetic field B_0 are possible. Dipole-dipole interaction is detected through the nuclear Overhauser effect.[20] For maximum NOE we have

$$\eta_{NOE} = 1 + \frac{\gamma_H}{2\gamma_X}$$

where η_{NOE} is the NOE enhancement factor (this holds if the correlation time for translations, τ_c, is small compared with the inverse Lamor frequency ω). From a comparison of the experimentally observed NOE enhancement factor η with the theoretical value η_{NOE} the contribution of dipole-dipole interaction to overall relaxation can be determined. While the maximum NOE factors for spin-1/2 metal nuclei are relatively large (Table 3), in practice frequently only small, or even no intensity increases due to proton NOE effects are observed at large magnetic fields (9.4 T) (see Fig. 2). Accordingly, other mechanisms contribute more effectively to the relaxation of spin-1/2 metal nuclei.

Table 3. Maximum signal enhancement factors η for nuclear Overhauser (NOE) and polarization transfer (PT) experiments (INEPT, DEPT), for pairs of protons and spin-1/2 metal nuclei.

X	^{13}C	^{57}Fe	^{103}Rh	^{109}Ag	^{183}W	^{187}Os	^{195}Pt
η_{NOE}	2.99	16.48	−16.89	−9.75	13.02	22.71	3.32
η_{PT}	3.98	30.95	31.77	21.50	24.04	43.42	4.65

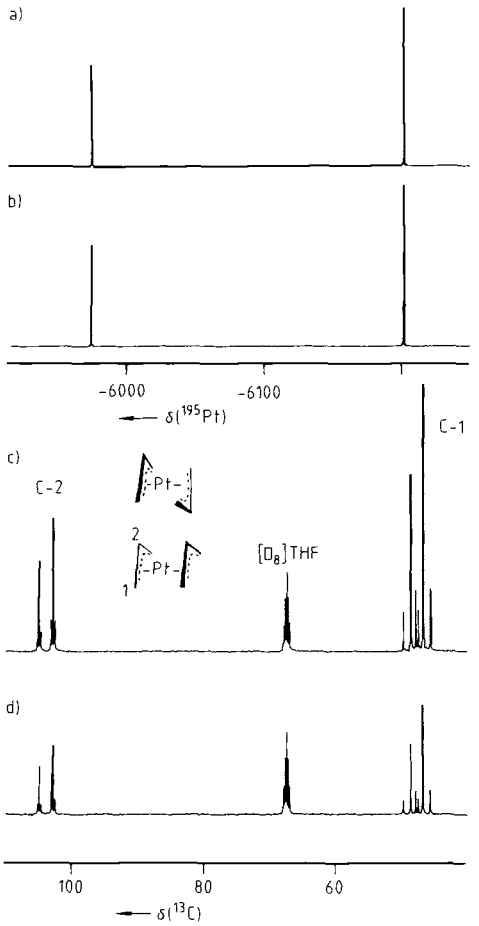


Fig. 2. Determination of the $^1H,^{195}Pt$- and $^1H,^{13}C$-NOE factors of *cis*- and *trans*-[Pt(η^3-allyl)$_2$] at 263 K and 9.4 T in the $^{195}Pt\{^1H\}$-NMR spectrum (a) with and (b) without ^1H irradiation; the $^1H,^{195}Pt$-NOE factor is zero. $^{13}C\{^1H\}$-NMR spectrum (c) with and (d) without ^1H irradiation. The $^1H,^{13}C$-NOE factor amounts to 2.3 for the central C-atoms and to 2.9 for the terminal C-atoms.

At high magnetic fields, and in particular for spin-1/2 metal nuclei with large chemical shift scales, relaxation is dominated by the CSA mechanism. The reason for this is that the nuclear shielding of metal isotopes depends on the relative orientation of the main molecular axis and the direction of the external magnetic field. Molecular motion creates a fluctuating magnetic field which induces transitions that restore thermal equilibrium for the population of nuclear spin states. This mechanism is characterized by the B_0^2-dependence of the relaxation rate. If the measurement of a relaxation time at different field strengths is not possible, then the contribution of this mechanism may, in favorable cases, be recognized by a comparison of T_1 (the longitudinal relaxation time) and T_2 (the transverse relaxation time). For CSA relaxation $T_1 = 7/6\,T_2$ holds[13b], while for the other mechanisms T_1 equals T_2, provided that $\omega\tau_c < 1$.

For certain complexes of Se,[21] Tl,[22] Pb,[23] Fe,[24] Hg,[25] Pt,[15,26,27] and Rh[28] it has been found that at high magnetic field strengths the CSA mechanism makes an important contribution to the relaxation of the spin-1/2 isotopes. For linear $[Pt(PR_3)_2]$ complexes, the ^{195}Pt relaxation rate depends upon B_0^2 for field strengths B_0 between 1.8 and 9.4 T, and extrapolation to $B_0 = 0$ yields a zero intercept (Fig. 3[15]). This demonstrates that ^{195}Pt relaxes exclusively

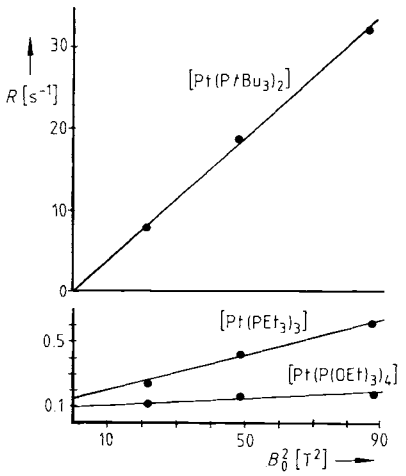


Fig. 3. B_0^2 dependence of the relaxation rate R of the ^{195}Pt nucleus in linear, trigonal, and tetrahedral (phosphane)platinum complexes at 310, 240, and 310 K, respectively. Spectra were measured at 9.4, 7.0, and 4.7 T (corresponding ^1H frequencies are 400, 300, and 200 MHz) [15].

by this mechanism in these compounds. In such complexes the chemical shift anisotropy, $\Delta\sigma$, can amount to several thousand ppm (e.g. $\Delta\sigma(^{199}Hg)$ in $HgR_2 = 5600$ ppm;[29] $\Delta\sigma(^{195}Pt)$ in $[PtL_2] = 11\,140$ ppm).[15]

Relaxation by the CSA mechanism has two important practical consequences: Firstly, information about bonding between the metal and the organic ligand may be lost if, as a consequence of fast relaxation of the spin-1/2 nuclei, the metal satellites in the ^1H- and ^{13}C-NMR spectra are severely broadened, thus precluding their detection.[25b] Secondly, as a positive consequence, especially for insensitive spin-1/2 metal nuclei like ^{103}Rh,[28] ^{57}Fe,[24] and presumably also for ^{183}W, the relaxation times are considerably shortened at high magnetic field strengths (see Table 4). This reduces significantly the time necessary for conventional experiments because fast accumulation of individual free induction decays becomes possible at 9.4 T. However, in unfavorable cases the signal of the metal nuclei can be severely broadened, so that the sensitivity gained due to the high magnetic field is lost.

In addition to the CSA mechanism, the SR mechanism in particular also contributes to relaxation of spin-1/2 metal nuclei in small isotropic molecules. In this case the electrons surrounding the nucleus give rise to fluctuating magnetic fields as a consequence of molecular rotation. A special feature of this mechanism, as opposed to the dipole-dipole and CSA mechanism, is that the relaxation times (for $\omega \cdot \tau_c < 1$) are shortened at elevated temperatures (Fig. 4).

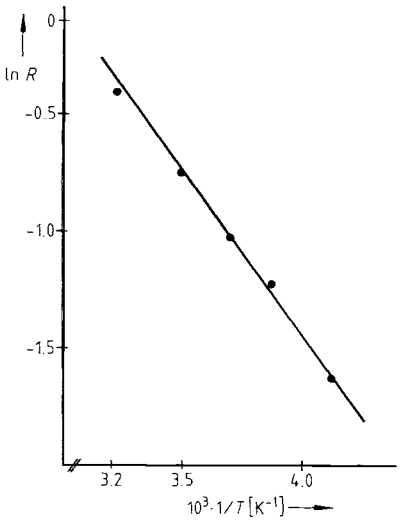
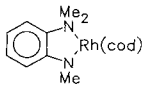
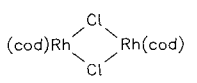


Fig. 4. Dependence of the natural logarithm of the relaxation rate R on the reciprocal of the temperature for $[Pt(PMe_3)_4]$ at 9.4 T [15].

To summarize, we can conclude that the most important relaxation mechanisms for spin-1/2 metal nuclei are spin rotation and chemical shift anisotropy. Their relative contributions depend on the one hand on molecular symmetry and on the other on the experimental conditions (magnetic field strength B_0, temperature, etc.). In the case of linear or anisotropic molecules, CSA is the dominant relaxation mechanism for spin-1/2 metal nuclei at high field strengths, whereas for metal nuclei in a tetrahedral, octahedral, or cubic environment at high temperatures, the SR mechanism is the most effective. It follows that in strong magnetic fields the relaxation times T_1 of insensitive spin-1/2 metal nuclei are shifted into a more favorable range enabling a faster detection of the metal resonances.

Table 4. Dependence of the ^{195}Pt- and ^{103}Rh-relaxation times and mechanisms on the geometry of the complexes. For the complexes listed, the ^1H-^{195}Pt- and ^1H-^{103}Rh-NOE factors are zero at 310 K (for $[Pt(PEt_3)_3]$ at 283 K) and 9.4 T, respectively. COD = cyclooctadiene.

Complex	$[Pt(PtBu_3)_2]$	$[Pt(PEt_3)_3]$	$[Pt(P(OEt)_3)_4]$			$[Rh(acac)_3]$
Complex geometry	linear	trigonal	tetrahedral	quasi square-planar		octahedral
T_1 at 9.4 T [s]	0.03	2.4	5.6	1.53	1.75	39
CSA [%]	100	ca. 50	10	96	80	10
SR [%]	0	ca. 50	90	4	20	90

2.1.2. *Methods for Improving the Signal Intensities*

Despite the shorter relaxation times in strong magnetic fields contributing to a reduction in the experimental time necessary to record NMR signals of spin-1/2 metal nuclei, in view of the low sensitivity of most of these nuclei further improvements for detection are still of interest. In this respect double resonance methods based on selective population transfer (SPT)[30,31] are of importance (Fig. 5). They have been used successfully before for the detection of a number of metal nuclei.[32] The intrinsic drawback of these methods is the fact that they rely on selective irradiation of a certain transition of a multiplet in the proton spectrum.

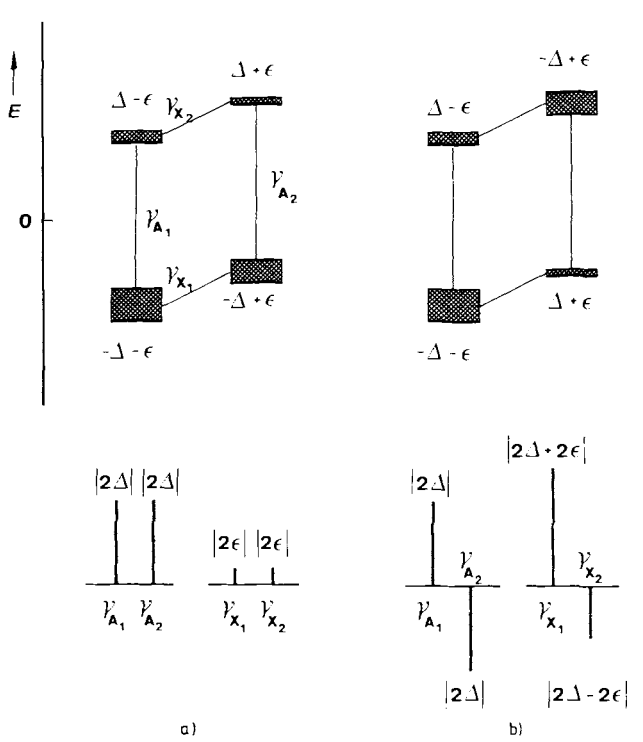


Fig. 5. Schematic representation of the SPT experiment [30] for sensitivity enhancement for a coupled AX spin system (e.g. A = ^{1}H, X = ^{103}Rh). Zeemann energies are $\pm\Delta = \pm\frac{1}{2}\hbar\gamma_A B_0$ for A and $\pm\varepsilon = \pm\frac{1}{2}\hbar\gamma_X B_0$ for X. In a) the relative signal intensities of the insensitive X-nucleus are proportional to ε, in b) to $\Delta \pm \varepsilon$.

In the case of complex and only partially resolved multiplets, as very often appear in the ^{1}H-NMR spectra of organometallic compounds, such a selectivity can seldom be achieved. This problem may be solved, however, by the use of the INEPT (*I*nsensitive *N*uclei *E*nhancement by *P*olarization *T*ransfer)[33] or the DEPT (*D*istortionless *E*nhancement by *P*olarization *T*ransfer)[34] sequence, since these polarization transfer methods allow all lines in the spectrum of the sensitive nucleus to be excited. Convincing applications of these techniques with ^{31}P as a source for polarization transfer have been presented by *Brevard* et al.[35] for the sensitivity enhancement of ^{57}Fe, ^{183}W, ^{109}Ag, and ^{103}Rh resonances in individual metal complexes. Protons can also be used for polarization transfer, as has been shown in the case of ^{109}Ag[36,37] and ^{103}Rh[37] nuclei. The success of such experiments is dependent mainly on the condition that the metal nucleus has a definite scalar coupling to neighboring protons and that these protons are not further coupled to other protons. Such simple cases are seldom encountered in organometallic compounds. For instance, in ^{103}Rh olefin complexes the metal-^{1}H coupling often amounts to only a few Hz[38] and therefore is smaller than the many vicinal inter-proton coupling constants. In such cases the use of the standard INEPT sequence may lead to difficulties and the expected gain in sensitivity is mostly not obtained.[39] If, however, only one multiplet of the ^{1}H-NMR spectrum that shows a metal-^{1}H coupling is inverted selectively, the experiment is known as the selective INEPT experiment (Fig. 6). This technique is of general

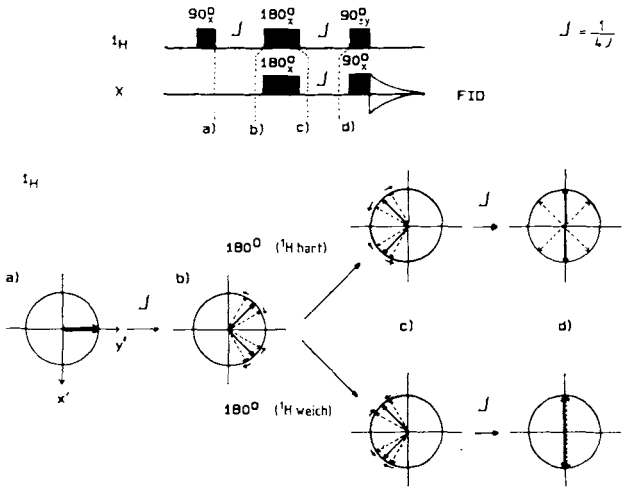


Fig. 6. Above: Pulse sequence of the INEPT experiment for a coupled AX spin system with hard and soft 180° proton pulse [28b]. Below: from the vector diagram in the rotating frame it is apparent that a non-selective (hard) 180° proton pulse does not lead to refocussing of the two proton magnetization vectors in the second time interval. In contrast, a selective (soft) 180° proton pulse only leads to a rotation around the x'-axis and does not interchange the precession frequencies. Consequently, the magnetization vectors which are further split due to coupling to other protons are refocussed at d). A complete polarization transfer is achieved through the 90°$_y$ pulse that follows.

applicability and allows considerable gain in sensitivity for the insensitive metal nucleus. It was first employed successfully in ^{15}N-,[40] ^{29}Si-,[41] and ^{13}C-NMR spectroscopy.[42,43] In particular, in the case of complexes which yield only one metal-NMR signal it is the method of choice, since polarization transfer from only *one* proton to the metal is already sufficient for sensitivity enhancement (Fig. 7).

For polarization transfer experiments a further gain in sensitivity results from the fact that the repetition rate of the pulse sequence is now governed by the relaxation time of the nucleus used as source of polarization transfer (^{1}H or ^{31}P) rather than by the T_1 value of the metal nucleus, which is usually longer. This aspect is of special importance for measurements made at low or intermediate magnetic field strengths.

Besides the improved possibility of recording metal resonances through direct detection by polarization transfer, the indirect detection of chemical shifts of spin-1/2 metal nuclei is of special importance. In their simplest form, indirect techniques are based on a heteronuclear spin-echo experiment designed for the detection of the sensitive nu-

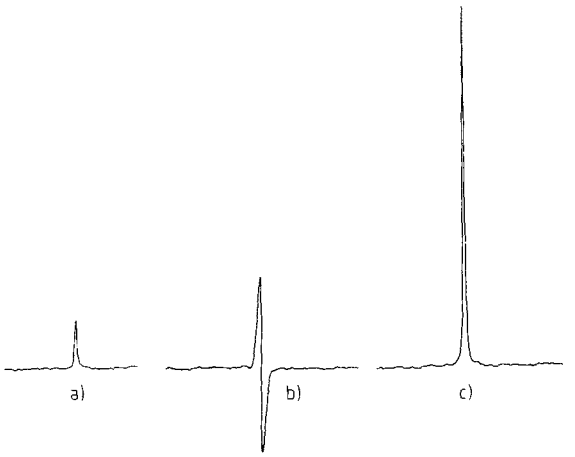


Fig. 7. Comparison of the intensity of the ^{103}Rh-NMR signal at $\delta = -6918$ in acetylacetonato(divinylcyclobutane)rhodium [Rh(acac)(dvcb)] for identical observation times [28b]. a) With proton-noise decoupling. b) In a selective INEPT experiment without proton decoupling. c) In a selective INEPT experiment followed by a refocussing period for the polarized transitions to a pure absorption signal and subsequent proton decoupling.

cleus. This technique was first reported for scalar coupled ^{199}Hg,^{1}H spin pairs.[44-46] The metal-NMR shifts are determined, with improved precision, by two-dimensional experiments (Fig. 8) in which the proton- and metal-NMR shifts are the two frequency axes and in which, in addition, the X,^{1}H coupling constants can also be determined. The important aspect of all these experiments is the detection of chemical shifts and scalar coupling constants of the insensitive spin-1/2 metal nucleus X with the sensitivity of the proton. Even for the two-dimensional version this amounts to an increase in signal intensity by several orders of magnitude.[47b, 48, 49, 137c]

The increased sensitivity achieved through faster relaxation at high field strengths and through application of various pulse techniques (INEPT, DEPT, selective polarization transfer, indirect one- and two-dimensional detection) have completely substituted the driven equilibrium (DEFT)[50] and Quadriga[51] techniques which had previously been used with success for this purpose.

2.2. Metal Nuclei with a Quadrupole Moment

There are many more magnetically active isotopes with $I > 1/2$ and thus with a quadrupole moment (Table 5) than there are with spin-1/2. Conclusions about the NMR sensitivity from a comparison of the individual data given in Table 5 are, however, less practical for quadrupolar nuclei than for spin-1/2 metal nuclei, since the linewidths of the

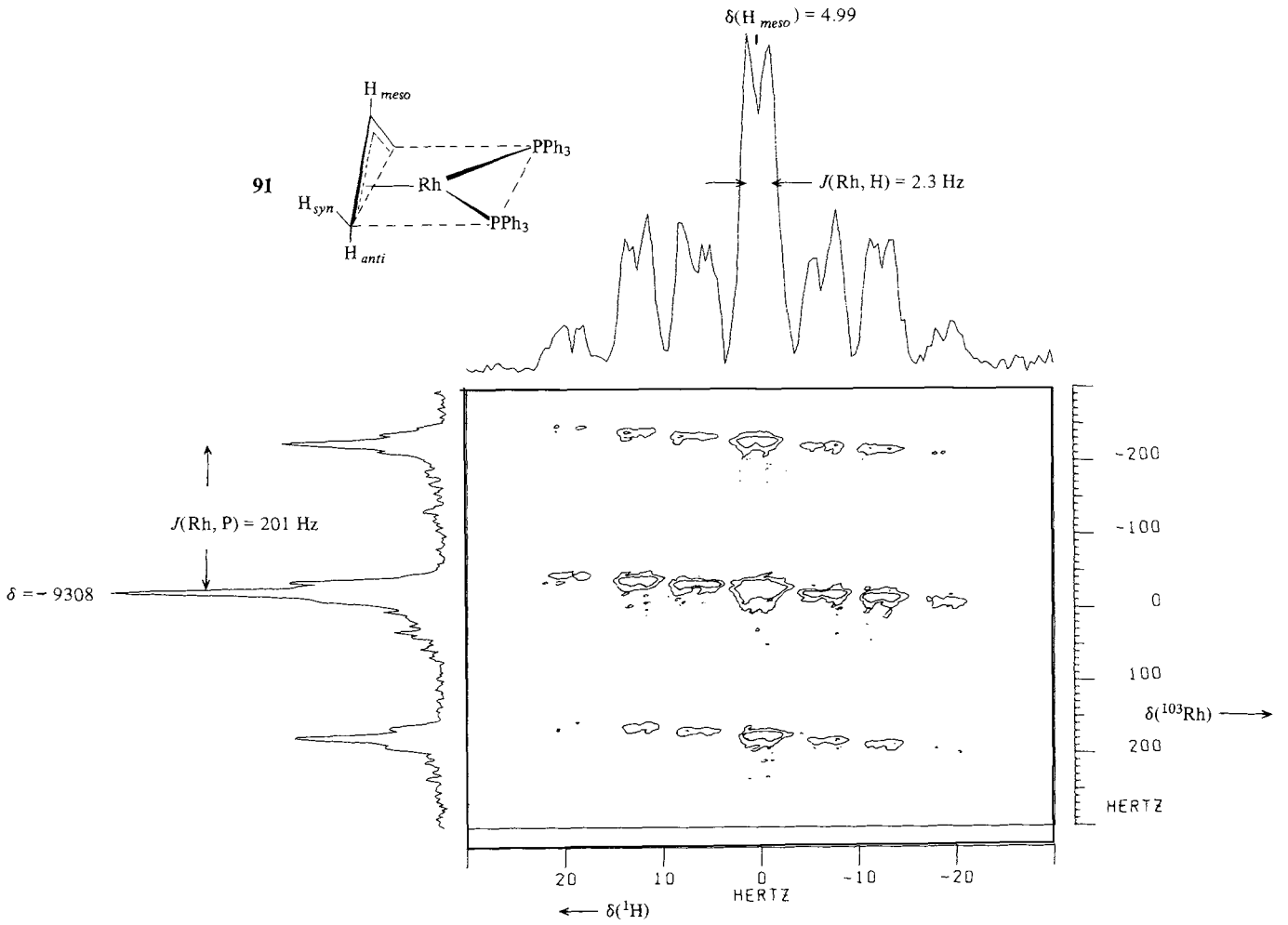


Fig. 8. Section from the two-dimensional ^{1}H{^{103}Rh}-NMR spectrum of [Rh(η^3-allyl)(PPh$_3$)$_2$] **91** in CD_2Cl_2 at $T = 310$ K (ca. 3% solution, 5 mm tube, WH 400). The F_2 dimension shows $\delta(^{1}H) = 4.99$, $J(H,H) = 7.0$ (*syn*), 12.4 (*anti*) and $J(Rh,H) = 2.3$ Hz of the meso protons (cf. horizontal protection). The F_1 dimension shows $J(H,H)$, $\delta(^{103}Rh) = -9308$ and $J(Rh,P) = 201$ Hz (cf. vertical projection) [47b].

Table 5. Classification of the quadrupolar metal nuclei of the main groups and subgroups of the Periodic Table (with the exception of the lanthanoids and actinoids) (see also Table 1). For each element only the nuclide with the highest absolute sensitivity is presented, neglecting the linewidth factor (including this factor, ^{99}Ru would be the more favorable isotope for NMR spectroscopy). Elements that possess a spin-1/2 isotope are also excluded. So far, resonances of ^{197}Au, ^{193}Ir, and ^{177}Hf have not been observed (see also ref. [5a]).

Elementary magnetic strength	Natural abundance >90%	10–90%	<10%
strong	^{7}Li		
medium	^{9}Be, ^{23}Na, ^{27}Al, ^{45}Sc, ^{51}V, ^{55}Mn, ^{59}Co, ^{75}As, ^{93}Nb, ^{115}In, ^{133}Cs, ^{181}Ta, ^{209}Bi	^{11}B, ^{63}Cu, ^{71}Ga, ^{87}Rb, ^{121}Sb, ^{137}Ba, ^{187}Re	
weak	^{39}K, (^{197}Au)	^{25}Mg, ^{91}Zr, ^{95}Mo, ^{101}Ru, ^{105}Pd, (^{177}Hf), (^{193}Ir), ^{189}Os	^{43}Ca, ^{49}Ti, ^{53}Cr, ^{61}Ni, ^{67}Zn, ^{73}Ge, ^{87}Sr

various isotopes can vary quite drastically (between several Hz and several kHz).

For a quadrupolar nucleus in a homogeneous magnetic field two energy terms have to be considered: the Zeemann energy and the energy resulting from interaction of the electrical quadrupole moment Q with electric field gradients q_{zz} that are due to the unsymmetrical charge distribution. For the NMR experiment (large B_0) the magnetic field determines the quantization, while the quadrupole interactions lead to further splitting of the Zeemann levels. In solution, the quadrupole interactions cause an uncertainty of the energy levels and this shortens the lifetime of the Zeemann states.[52]

Apart from its dependence upon the motion of the molecule, characterized in solution by the correlation time τ_c, the linewidth $W_{1/2}$ of a quadrupolar nucleus is also influenced by the magnitude of the spin quantum number I, by the electric quadrupole moment Q, and by the electric field gradient q_{zz}.

$$W_{1/2} = \frac{3}{10}\pi^2 Q^2 \frac{2I+3}{I^2(2I-1)} \frac{e^4}{\hbar^2} q_{zz}^2 \tau_c$$

For a certain nuclide, I and Q are already constant and they determine the linewidth factor $l = Q^2(2I+3)/[I^2(2I-1)]$ (Table 6).[5,52] In practice, this may however lead to a situation where a nuclide which is apparently less favorable for NMR detection because of its low natural isotopic abundance or relative NMR sensitivity is actually more readily detected because of its smaller linewidth. On the other hand, the dependence of the linewidth on q_{zz}^2 leads to very different linewidths for one and the same nuclide: relatively narrow signals are observed for nuclei in a cubic, tetrahedral, or octahedral environment or when τ_c is particularly small due to solvent effects[53] or high temperature.

Table 6. Linewidth factors l for quadrupolar nuclei and their dependence on I at constant Q. For the calculation of $W_{1/2}$, constant values for q_{zz} and τ_c have also been assumed.

I	1	3/2	2	5/2	3	7/2	4	9/2	5	11/2
l	5	1.33	0.58	0.32	0.2	0.16	0.098	0.074	0.058	0.046
$W_{1/2}$[Hz]	10	2.6	1.16	0.64	0.4	0.32	0.19	0.14	0.11	0.09

The broad lines frequently observed for quadrupolar nuclei lead to a number of difficulties in signal identification. The most important sources for errors are background signals and the phenomenon known as "acoustic ringing".[54] It is hardly possible to build a multinuclear probe head where the materials employed do not give rise to NMR signals of their own over the whole frequency range. Since these "probe head signals" are broad, they are especially misleading when trying to detect the resonances of quadrupolar nuclei (Fig. 9). It is therefore advisable (especially for insensitive nuclei and dilute solutions), to identify possible extraneous signals under identical experimental conditions with blank samples (i.e. the solvent only).

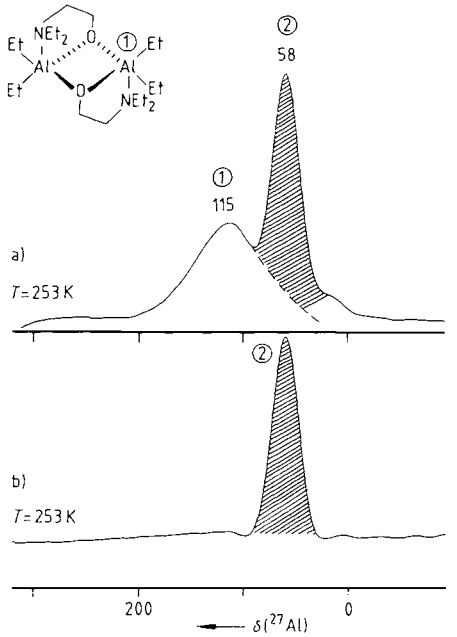


Fig. 9. Background signal (②) in the ^{27}Al-NMR spectrum of a multinuclear probe head. a) ^{27}Al-NMR spectrum of a 0.1 M solution of $[Et_2AlO(CH_2)_2NEt_2]_2$. b) Spectrum obtained with the test-tube filled with solvent only [95, 96a]. For resolution enhancement, the same Lorentz-Gauss transformation was used in both cases before Fourier transformation.

"Acoustic ringing" is caused by mechanical distortions that arise from Coulomb forces in the transmitter and receiver coils immediately after the high-power excitation pulse. In a static magnetic field these mechanical distortions give rise to high-frequency electromagnetic fields that cause broad signals, yielding spectra with "rolling base lines". Excitation pulses of reduced power or longer delays Δ between the end of the excitation pulse and the beginning of data acquisition can partly solve this problem.[55] Signals with linewidths larger than $1/\Delta$ are, however, suppressed by this technique and large phase errors arise over the entire spectrum. In the case of multiline spectra it is very difficult to correct the phase of all signals simultaneously. In a number of cases it is useful to nullify the first

points of the FID (Fig. 10); however, this method has the disadvantage that the signal intensity of fast relaxing quadrupolar nuclei is drastically reduced. Therefore, several pulse sequences[56] have been proposed to suppress error signals of the type discussed above. As a consequence of the proportionality between error signal intensity and pulse width, for application of the sequence $[(90°\text{-AQT})_3$ minus $(270°\text{-AQT})]_n$ (AQT = acquisition time) the error signals should be substracted and the sample signals added. Similar results are obtained on the basis of special sequences using spin-echo experiments.[57,58] The disadvantage of all these pulse techniques, however, is the fact that even with application of composite pulses it is not possible to produce perfect 90°, 180°, and 270° pulses over a spectral range of several 10 kHz.

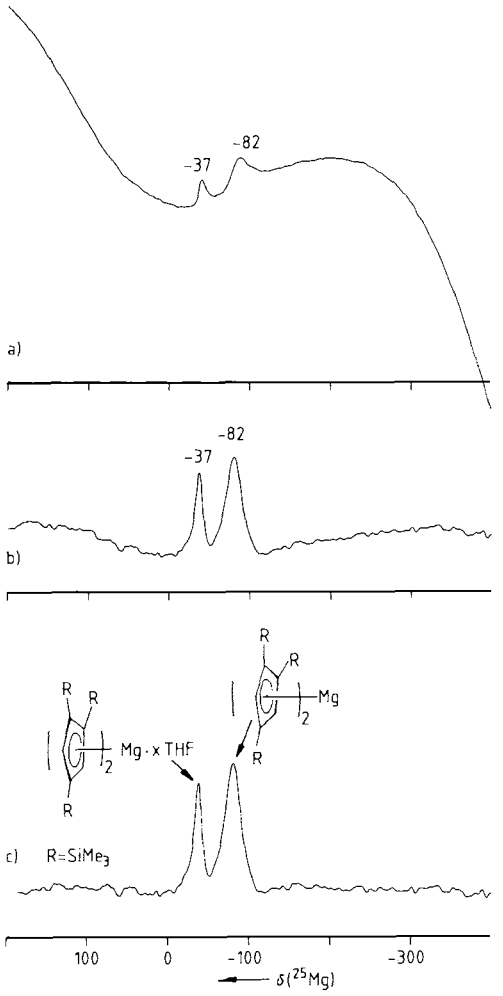


Fig. 10. ^{25}Mg-NMR spectrum of a solution of bis[1,2,4-tris(trimethylsilyl)cyclopentadienyl]magnesium in tetrahydrofuran (THF). a) Direct from the observed FID. b) After setting the intensity of the first six data points of the FID to zero. c) With additional baseline correction.

Pulse sequences aimed at sensitivity enhancement on the basis of polarization transfer experiments have also been proposed for the detection of quadrupolar nuclei.[59,60] Such enhancements have been realized in the case of ^{11}B,[61] ^{2}H,[62] ^{73}Ge[63] using ^{1}H and ^{11}B, respectively, as source for polarization transfer.[64] The short relaxation time of quadrupolar nuclei ($T_1 < 0.1$ s is not unusual for nuclei with $I > 1/2$) and the fact that the magnitude of the scalar spin-spin coupling constants is mostly unknown, however, severely limit the application of such experiments. For quadrupolar nuclei with linewidths of up to several 100 Hz the prospects of two-dimensional NMR experiments of the COSY- and NOESY-type[4] for the detection of connectivities or chemical exchange,[65] respectively, are somewhat more favorable, since they do not require a prior knowledge of J(X,X).

2.3. Metal-NMR Chemical Shifts

According to *Ramsey*,[66] chemical shifts are influenced by dia- and paramagnetic contributions to the shielding constant. In general it is assumed that for metal nuclei, where the chemical shift of even closely related complexes can easily vary by several 100 ppm, the paramagnetic contribution σ_{para} dominates.[67,68] It originates from the local anisotropic motion of the electrons surrounding the nucleus of interest. For related ligand fields, σ_{para} depends to a first (extremely rough) approximation on the average radius $\langle r \rangle$ of the valence orbital and the average electronic excitation energy ΔE:[69]

$$\delta \sim -\sigma_{para} \sim \frac{\langle r^{-3} \rangle}{\Delta E}$$

On this basis there emerges a relationship between NMR chemical shift and the effective nuclear charge of the metal atom, and the electronic energy states of the metal atom in a complex. This relationship will be used quite frequently in the following for a comparative interpretation of NMR shifts.

For practical reasons, because of the reactivity of many organometallic compounds, an internal reference often cannot be used. Calibration of δ-values is therefore frequently achieved by replacing the sample tube by a second tube that contains an appropriate reference, the signal of which is then measured under standard conditions ($\delta \equiv 0$) (Table 7).

All metal-NMR chemical shifts discussed in the following Tables are referred to the relevant standard listed in Table 7.[70] Since these shifts are strongly dependent on

Table 7. External standards for some metal nuclei. The Ξ-values hold for $T = 310$ K.

Nucleus	Compound	Solvent	Concentration	$W_{1/2}$ [Hz]	Ξ [MHz] (±10 Hz)
^{25}Mg	$MgSO_4 \cdot 7H_2O$	D_2O	0.18 mol/L	10	6.121636
^{27}Al	$[Al(acac)_3]$	$[D_6]$benzene	saturated	100	26.056908
^{49}Ti	$TiCl_4$	$[D_8]$toluene	80% (wt.)	4	5.639051[a]
^{57}Fe	$[Fe(CO)_5]$	neat			3.237792
^{59}Co	$K_3[Co(CN)_6]$	D_2O	saturated	100	23.727449
^{61}Ni	$[Ni(PMe_3)_4]$	$[D_8]$toluene	saturated	20	8.936408[b]
^{91}Zr	$[Cp_2ZrBr_2]$[c]	$[D_8]$THF/THF	0.25 mol/L	17	9.297303
^{103}Rh	$[Rh(acac)_3]$	$CDCl_3$	saturated	2	3.186447[d]
^{195}Pt	$H_2[PtCl_6] \cdot 6H_2O$	D_2O	0.50 mol/L	60	21.497151[e]

[a] The Ξ-value given in ref. [119] differs considerably from the value given here. [b] For $[Ni(CO)_4]$ $\Xi(^{61}Ni)$ is 8.936050 [173]. [c] Cp = cyclopentadienyl. [d] Considering the temperature coefficient of this standard (1.6 ppm/K), this value agrees well with the value given in ref. [144b]. [e] The value given in ref. [15] must be replaced by the present value.

concentration, temperature, and solvent, deviations in δ of several ppm for one and the same compound are not uncommon. Similar drawbacks hold for the Ξ-scale[71], which is, however, independent of the choice of a particular reference since all resonance frequencies measured are related to a magnetic field strength B_0 at which the protons of TMS resonate exactly at 100 MHz.

While it is clear from the foregoing discussion that experimental conditions and precision differ for the determination of chemical shifts of spin-1/2 and quadrupolar nuclei, the resulting information is, in principle, of the same type for both groups. In the following two sections we shall outline relations found experimentally between δ(M) and the coordination number, the formal oxidation state, and the average electronic excitation energy ΔE of organometallic complexes. In particular, we shall discuss the chemical shift ranges of the ^{27}Al and ^{25}Mg nuclei as well as those of the magnetically active metal isotopes of the fourth and eighth subgroups of the Periodic Table. With respect to the remaining metal nuclei, we shall refer to recent review articles[5,67,68] and a number of original papers: ^{6}Li, ^{7}Li, ^{23}Na, ^{39}K, ^{87}Rb, and ^{133}Cs;[72] ^{9}Be,[73] ^{43}Ca,[73a,74,75] ^{87}Sr,[73a] and ^{137}Ba;[73a] ^{45}Sc,[67,76] ^{89}Y,[67,77] and ^{139}La;[67] ^{51}V,[67,78] ^{93}Nb,[67] and ^{181}Ta;[67] ^{53}Cr,[67,80] ^{95}Mo,[67,79,80] and ^{183}W;[67,80] ^{55}Mn, ^{99}Tc, and ^{187}Re;[67] ^{63}Cu,[67,81] ^{109}Ag;[35b,36,67,82] ^{67}Zn,[67,83] ^{113}Cd,[67,84] and ^{199}Hg;[67] ^{11}B,[10] ^{71}Ga, ^{115}In,[85] and ^{205}Tl;[86] ^{29}Si,[8,87] ^{73}Ge,[63,87] ^{119}Sn,[87,88] and ^{207}Pb;[87] ^{75}As,[89] ^{121}Sb,[89] and ^{209}Bi.[90]

3. Organometallic Compounds of Main Group Metals

3.1. Relationship between ^{27}Al-NMR Shift and Coordination Number of Organoaluminum Compounds

In organoaluminum compounds[91] the metal can adopt different coordination numbers and undergo various types of bonding. In such compounds the ^{27}Al-NMR shifts correlate with the coordination number (CN) of the Al atom (Fig. 11[92]): The signals for organoaluminum compounds

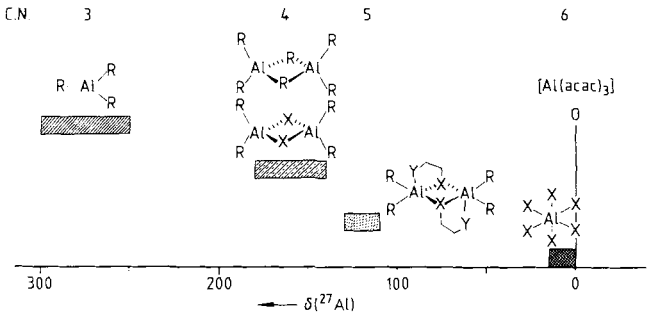


Fig. 11. Dependence of the ^{27}Al-NMR shifts on the coordination number of the Al-atom in organoaluminum compounds [92, 96].

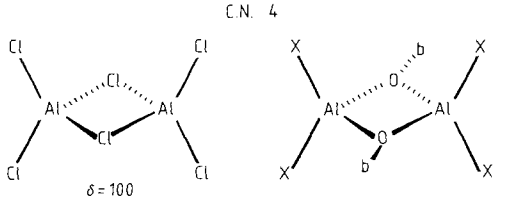
with CN = 3 resonate at the largest δ-values (250–300 ppm), while tetrahedrally coordinated aluminum atoms show $\delta(^{27}\text{Al})$ values of about 150 ppm. Apparently, these $\delta(^{27}\text{Al})$ values are more or less insensitive to the nature of the substituent in the multicenter bond, but are influenced quite strongly by substitution of the non-bridging alkyl groups by moieties with Cl, O, or N atoms (Table 8). Close to the region for tetrahedral organoaluminum complexes, the chemical shifts of aluminum compounds with fivefold coordinated aluminum atoms are found. Such organoaluminum compounds have so far been detected only rarely.[93] Apparently, this coordination number is preferred if bidentate ligands of a certain chain length (such as $O(CH_2)_2XR$, X = O, NR) are employed. In this way an optimal complexation of the second Lewis-base heteroatom can be achieved. The X-ray structure of the complexes **22**[92] and **26**[94] is known, and confirms the fivefold coordination of aluminum in the crystal. In the case of **25**, aside from the $\delta(^{27}\text{Al})$-value, the observation of diastereotopic α-CH_2 protons of the ethyl group in the low-temperature ^{1}H-NMR spectrum supports the existence of fivefold coordinated aluminum atoms. At elevated temperatures, these protons become enantiotopic due to the dissociation of the weaker Al donor bond. The ^{27}Al-NMR shift of the compounds, however, is temperature-independent between -40 and $+100$ °C, thus indicating that dissociation occurs only to a minor extent. The more readily soluble compound **24** yields a signal at $\delta(^{27}\text{Al}) = 123$,[95] which, due to its narrow linewidth, is easily identified even at -50 °C. As

Table 8. ^{27}Al-NMR parameters of **1–27**; measuring frequency: 104.2 MHz; external reference [Al(acac)$_3$] in [D$_6$]benzene (saturated); $T = 300$ K; 20–50% w/w solutions in [D$_8$]toluene; degree of association α, see ref. [91].

Compound	[a]	α	$\delta(^{27}\text{Al})$	$W_{1/2}$[Hz]	C.N.
$(i\text{Bu})_3\text{Al}$ **1**		1	276	6300	3
$(t\text{Bu})_3\text{Al}$ **2**		1	255	6100	3
$(i\text{Pr})_3\text{Al}$ **3**		1	256	5900	3
Me_3Al **4**	C	2	153	850	4
Et_3Al **5**	C	2	154	2550	4
$(cyclo\text{-}C_3H_5)_3Al$ **6**	C	2	143	2750	4
$(n\text{Pr})_3\text{Al}$ **7**	C	2	157	6300	4
$(n\text{Bu})_3\text{Al}$ **8**	C	2	152	7800	4
$(Me_3CCH_2CH_2)_3Al$ **9**	C	2	154	12000	4
Me_2AlH **10**	H	3	159	2500	4
Et_2AlH **11**	H	3	157	4500	4
$(i\text{Bu})_2\text{AlH}$ **12**	H	3	159	10000	4
Me_2AlCl **13**	Cl	2	180	2150	4
Et_2AlCl **14**	Cl	2	167	3300	4
$(t\text{Bu})_2\text{AlCl}$ **15**	Cl	2	170	4300	4
Et_2AlNEt_2 **16**	N	2	160	1220	4
Me_2AlOMe **17**	O	3	152	1400	4
Et_2AlOMe **18**	O	3	146	3400	4
Et_2AlOEt **19**	O	2	151	2450	4
$Et_2AlO(CH_2)_3Me$ **20**	O	2	152	7800	4
$Et_2AlO(CH_2)_3OEt$ **21**	O	2	150	7200	4
$[Me_2AlO(CH_2)_2OMe]$ **22**	O	2	121	1830	5
$[Et_2AlO(CH_2)_2OMe]$ **23**	O	2	121	5600	5
$[Et_2AlO(CH_2)_2OEt]$ **24**	O	2	126	6000	5
$[Et_2AlO(CH_2)_2NEt_2]$ **25**	O	2	112	7200	5
Et_2AlOCH_2–(N) **26**	O	2	106	5400	5
	O	2	105	4880	5 [b]
[Al(acac)$_3$] **27**		1	0	100	6

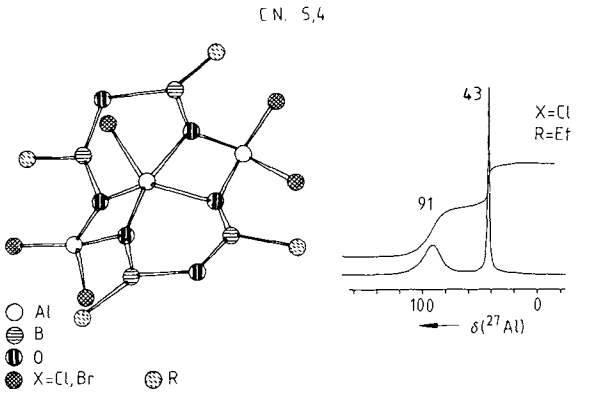
[a] Substituent at the multiple center bond. [b] With regard to **26** see also ref. [94, 95].

in the case of tetrahedral organoaluminum compounds, the variation of the non-bridging groups attached to aluminum leads to a considerable $\delta(^{27}Al)$ shift range for the complexes with fivefold coordinated Al atoms (Fig. 12).[97] Important here, however, is that there are still characteristic shift ranges for complexes with fourfold-, fivefold- and sixfold-coordinated aluminum atoms.



X	b	$\delta(^{27}Al)$	$W_{1/2}$[Hz]
Cl	BEt_2	90	960
Cl	$B(C_8H_{14})$[a]	91	700[b]
Br	BEt_2	88	1000
Br	$B(C_8H_{14})$[a]	88	600[b]
Cl	Et	98	230[c]

[a] 9-Borabicyclo[3.3.1]nonane. [b] At $T = 353$ K. [c] Trimer.



X	R	C.N. 4 $\delta(^{27}Al)$	C.N. 4 $W_{1/2}$[Hz]	C.N. 5 $\delta(^{27}Al)$	C.N. 5 $W_{1/2}$[Hz]
Cl	Me	90	1200	43	375
Cl	Et	91	1900	42	280
Cl	*n*Bu	97	≥5000	44	1400
Cl	Ph	92	≥5000	43	≥5000
Br	Et	90	1900	41	400

Fig. 12. ^{27}Al-NMR data of $[AlX_2(OBR_2)]_2$ [97] and $[AlX(OAlX_2)_2(OBR)_4]$ [97b] complexes and the 104.2-MHz ^{27}Al-NMR spectrum of $[AlCl(OAlCl_2)_2(OBEt)_4]$. The ^{27}Al-NMR signals of the four- and five-coordinated aluminum atoms, respectively, are clearly separated.

On the basis of their characteristic ^{27}Al-NMR parameters a number of structures proposed for organoaluminum compounds in the literature need reexamination (Fig. 13).[98–101]

The chemical shift region of aluminum atoms with coordination number 3, 4 and 5 is flanked at the high-field side by that of $\delta(^{27}Al)$ for octahedral aluminum compounds, as for instance aluminum tris-acetylacetonate $[Al(acac)_3]$. In accord with the coordination number 6 for Al, $\delta(^{27}Al)$ signals are found at lower frequencies and the lines have relatively small halfwidths. Associates that formally correspond to dialkoxy(alkyl)aluminum compounds have so far not been described in detail. They give signals in the region typical for four- and sixfold coordinated aluminum

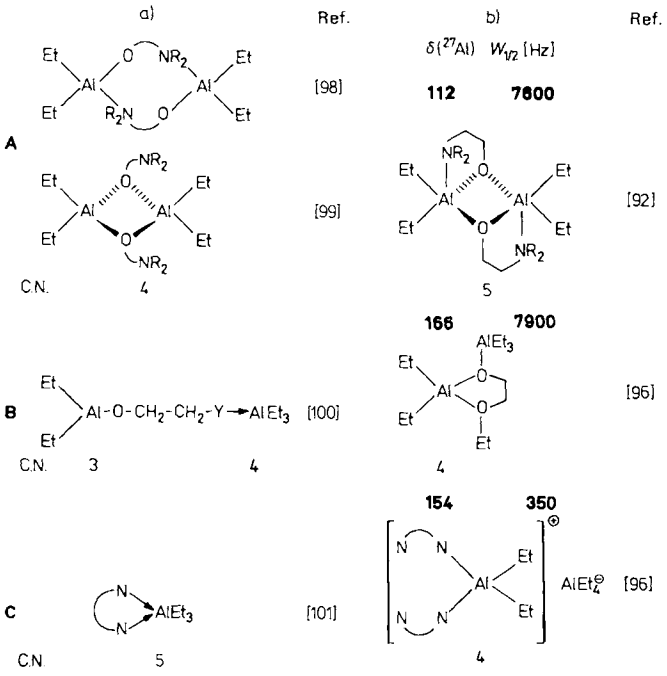


Fig. 13. Proposed structures for organoaluminum compounds. (a) From the literature (b) and on the basis of ^{27}Al-NMR data; **A** = $[Et_2Al(\widehat{O}NR_2)]$ ($\widehat{O}NR_2 = O(CH_2)_2NR_2$), **B** = $[Et_3Al(O(CH_2)_2Y)]\cdot AlEt_4$ (Y = OR, NR_2), **C** = $Et_3Al\cdot\widehat{N}\widehat{N}$ ($\widehat{N}\widehat{N}$ = 2,2'-bipyridyl).

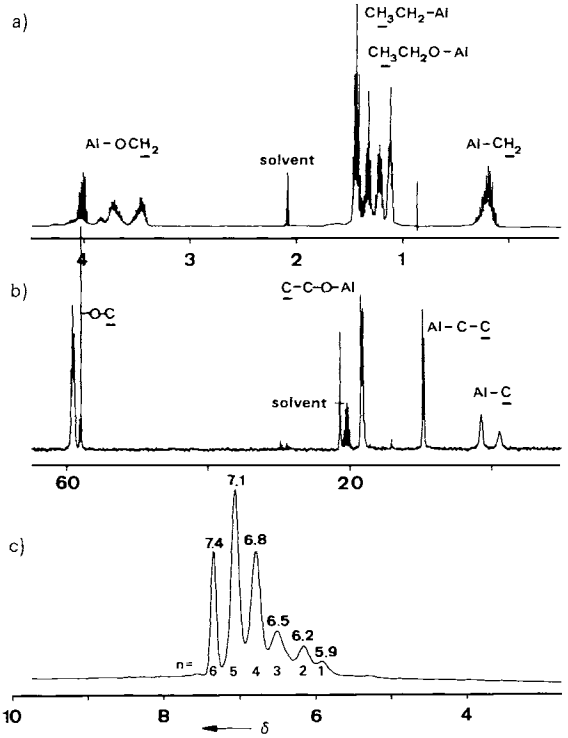


Fig. 14. ^1H-, $^{13}C\{^1H\}$-, and ^{27}Al-NMR spectra of dialkoxy(alkyl)aluminum compounds $[Et_nAl_4(OEt)_{12-n}]$ (n = 1,...6). (a) 400-MHz ^1H-NMR spectrum. (b) 100.6-MHz $^{13}C\{^1H\}$-NMR spectrum. (c) 104.2-MHz ^{27}Al-NMR spectrum in the region for octahedral coordinated aluminum.

atoms. For this reason and in agreement with mass spectroscopic results these compounds have been described as mixtures of $[R_nAl_4(OR)_{12-n}]$ (R = Et, n = 1...6) with a central, sixfold coordinated aluminum atom (Fig. 14),[92,96a] similarly to the tetrameric aluminum alkoxides.[102] Even though this structure proposal results from a combination of mass spectrometry and ^{27}Al-NMR spectroscopy, comparison of the non-resolved ^{1}H- and ^{13}C-NMR spectra with the ^{27}Al-NMR spectrum, which is well resolved in the region around 7 ppm, emphasizes immediately the practical importance of metal-NMR spectroscopy.

3.2. ^{25}Mg-NMR Spectroscopy for the Characterization of Organomagnesium Compounds

Organomagnesium compounds[103] play an important role in preparative organic chemistry. So far, ^{25}Mg-NMR investigations have concentrated on biological systems and inorganic complexes,[5] and only recently has the chemical shift range of organomagnesium compounds been determined.[104,105] In THF, the compounds R_2Mg, RMgX and MgX_2 (R = alkyl, aryl, X = halogen) are monomeric[106] over a wide range of concentrations and their $\delta(^{25}Mg)$ values lie between 0 and +100 ppm (Table 9).

The halfwidth of the ^{25}Mg-NMR signal of $MgBr_2$ in THF varies between 280 K (50 Hz) and 340 K (55 Hz) and reaches a minimum with 35 Hz at 330 K. This indicates a transition from a quasi octahedral[107] to a tetrahedral coordinated species as a consequence of the elimination of two THF molecules at higher temperatures.

From their characteristic signal positions at 310 K all three species present in the Schlenk equilibrium (Et_2Mg, EtMgBr and $MgBr_2$) can be detected.[104] One finds an average ^{25}Mg signal at $\delta = 54$, corresponding to an equilibrium shift in the direction of EtMgBr[106,108] at 340 K. Since the equilibrium constant for methylmagnesium bromide is larger than for ethylmagnesium bromide (K = 30 as compared to 5.1[108]), the first mixture of compounds already yields an average signal at $\delta = 67$ at T = 300 K.

The ^{25}Mg-NMR signals of bis(cyclopentadienyl)magnesium compounds appear outside of the range given above:[104,105] in unpolar solvents like toluene $\delta(^{25}Mg)$ values of about $\delta = -85$ have been measured for **32**, **34**, and **35** (Fig. 10).[109] The halfwidths of these resonances are unusually narrow (100–500 Hz), and have been interpreted in terms of a predominantly covalent bonding situation in η^5-Cp-Mg.[104,105] Here, ^{25}Mg-NMR spectroscopy provides a direct contribution to the controversal discussion of the bonding type in these systems (ionic or covalent).[110] For the elucidation of the bonding situation in allylmagnesium derivatives a number of complicated and subtle experiments and calculations have been performed:[111,112] The ^{25}Mg-NMR shift of **30**, with a value of $\delta = 70.4$, immediately demonstrates that the allyl groups are σ-bonded to magnesium.

The narrow linewidths of the ^{25}Mg-NMR signals of Cp-Mg derivatives also allow coordination compounds of Cp_2Mg with O-, N-, and P-containing Lewis-bases to be characterized with the help of ^{25}Mg-NMR spectroscopy.[104,105] In toluene, equilibria are established, from which, in some cases, defined complexes (1:1 adducts) could be isolated. For solutions of Cp_2Mg in different Lewis-bases a linear correlation between their ^{25}Mg-NMR shifts and ^{13}C-shifts of the corresponding Cp signals results (Fig. 15). The solutions of Cp_2Mg in anisole, diisopropyl ether and triethylamine show the same ^{25}Mg-NMR shifts as those of Cp_2Mg in toluene or cyclohexane (not shown). Complexation of Cp_2Mg by these Lewis-bases is therefore negligible. On the other hand, the ^{25}Mg-NMR shift of a solution of Cp_2Mg in PMe_3 is a direct proof for the coordination of phosphanes to organomagnesium com-

Table 9. ^{25}Mg-NMR parameters of magnesium compounds at 24.49 MHz and $T = 310$ K in THF [104, 105, 114]; external reference $MgSO_4 \cdot 7H_2O$ (0.18 mol/L); Cp* = Me_5C_5, TMEDA = tetramethylethylendediamine.

Compound	$\delta(^{25}Mg)$	$W_{1/2}$ [Hz]
R_2Mg		
Et_2Mg **28**	99.2	3200
$(nPr)_2Mg \cdot$TMEDA **29**	110.0	1700 [a]
$(C_4H_7)_2Mg$ [b] **30**	70.4	2000
$Ph_2Mg \cdot$Dioxan **31**	108.0	2800 [a]
Cp_2Mg [c] **32**	−85.4	105
$Cp_2Mg \cdot n$THF **33**	−33.8	90
Cp^*_2Mg [c] **34**	−78.3	350
Cp^*_2Mg **34**	−78.4	350
$^RCp_2Mg$ [c, d] **35**	−79.6	750
$^RCp_2Mg$ [d] **35**	−82.0	550
$^RCp_2Mg \cdot n$THF [d] **36**	−36.7	250
RMgR′		
CpMgEt **37**	−4.0	1500
$CpMg(C_4H_7)$ [b] **38**	−14.7	710
Cp*MgEt **39**	−10.0	1300
(Indenyl)MgEt **40**	26.6	900 [e]
^{R}CpMgMe·TMEDA [c, d] **41**	15.0	1100
$CpMg \cdot OEt_2$ **42**	−34.1	160
RMgBr		
MeMgBr **43**	67.8	1900
EtMgBr **44**	56.2	1100 [f]
(C_3H_5)MgBr [g] **45**	29.7	1000
CpMgBr **46**	−26.8	60
^{R}CpMgBr·TMEDA [c, d] **47**	−15.0	300
MgX_2		
$MgCl_2$ **48**	16.4	350
$MgBr_2$ **49**	14.1	36
$[Mg(acac)_2]$ **50**	6.3	650

[a] $T = 353$ K. [b] C_4H_7: $H_2C{=}CMeCH_2$. [c] In toluene/$[D_8]$toluene. [d] $^RCp = \eta^5$-1,2,4-$(SiMe_3)_3C_5H_2$. [e] $T = 343$ K. [f] $T = 340$ K. [g] $C_3H_5 = H_2C{=}CHCH_2$.

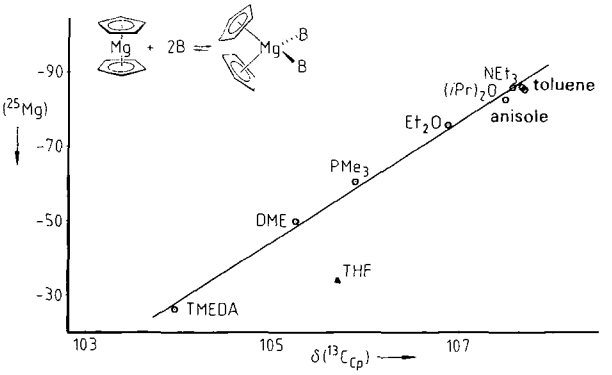


Fig. 15. Plot of the ^{25}Mg-NMR shifts of $[Cp_2MgB_2]$ complexes (solvents function as Lewis bases B) against the ^{13}C-NMR shifts of the Cp ligand in the given solvents [104, 105]. DME = 1,2-dimethoxyethane; TMEDA = tetramethylethylenediamine.

pounds. The ability of the Lewis-bases to coordinate increases in going from diethylether to tetramethylethylenediamine, a tendency which is reflected in a shift of the ^{25}Mg-NMR signal to higher δ values. The tetrahedral coordination of the metal atom has been confirmed in the case of the chiral 1,3-bis(dimethylamino)butane ligand by low-temperature ^{13}C-NMR spectroscopy (two Cp signals). The positions of the signals of Cp_2Mg in THF do not fit in the linear correlation of the ^{13}C- and ^{25}Mg-NMR data (Fig. 15). Hence, in agreement with chemical results, a coordination number five is proposed for Mg in THF through coordination of three THF molecules.[104, 105, 113] In substituted magnesocenes the ability of THF to coordinate to the metal is diminished: **35** exists in THF as a mixture of THF-free (**35**) and THF-complexed (**36**) compounds (see Fig. 10 and Table 9); in the case of **34** the ^{25}Mg-NMR shifts are nearly identical in THF and toluene, thus indicating negligible complexation by the solvent.

^{25}Mg-NMR spectroscopy is also useful for the detection and characterization of RMgR′ compounds (R = indenyl, cyclopentadienyl; R′ = alkyl, alkenyl, alkoxy) that are formed through comproportionation.[105] For instance, a 1:1 mixture of **32** ($\delta = -33.8$) and **30** ($\delta = 70.4$) in THF gives a ^{25}Mg-NMR signal at $\delta = -14.7$,[114a] which, through its deviation from the arithmetic mean of the chemical shifts of both individual components, immediately indicates the existence of a mixed compound **38**. This underlines the advantage of ^{25}Mg-NMR over the detection by ^{13}C-NMR spectroscopy.[114b]

4. Organometallic Compounds of Transition Metals

4.1. Metals of Group 4A

So far only very few NMR investigations have been carried out on the early transition metals. In the case of metals of group 4A there are presently only five publications dealing with titanium isotopes[115–119] and only three papers[120–122] on ^{91}Zr-NMR spectroscopy which focus upon chemical problems, while of the two magnetically active Hf isotopes no NMR investigations with any chemical relevance are known. As in the case of the MX_4 compounds (X = halogen) the metal resonances of $[Cp_2MX_2]$ complexes of Ti and Zr show an inverse halogen dependence[67] (Table 10). The reduced shielding of Ti in $TiBr_4$ as compared to $TiCl_4$ has been explained with the $1/\Delta E$ dependency of the paramagnetic shielding contribution.[115] The ^{49}Ti-NMR shifts of titanocene derivatives show an inverse correlation with Ti($2p_{3/2}$) bonding energies which were determined from photoelectron spectra.[117] A similar relationship was found upon comparison with the corresponding methyl-substituted titanocenes $[CpCp^*TiX_2]$ and $[Cp^*_2TiX_2]$. A considerable shift to higher frequencies has also been observed in the case of **62** (compared to **63**). These results show that a simple interpretation of metal resonances solely on the basis of charge density effects is not possible, but that the $1/\Delta E$ term of the paramagnetic shielding contribution can be of considerable importance.

For a further discussion of these relationships, a comparison of the $\delta(^{91}Zr)$ values in complexes of the type

Table 10. ^{49}Ti- and ^{91}Zr-NMR shifts and halfwidths of simple halometal compounds. For **51** and **52**, average electronic excitation energies ΔE of 34840 bzw. 28680 cm^{-1}, respectively, have been estimated [115]. $Cp^* = Me_5C_5$.

Compound	δ(M)	$W_{1/2}$ [Hz]	Lit.
$TiCl_4$ **51**	0	3	[116]
$TiBr_4$ **52**	482.9	3	[116]
TiI_4 **53**	1278.3	10	[116]
$[Cp_2TiF_2]$ **54**	−1036.5	10	[116]
$[Cp_2TiCl_2]$ **55**	− 771.6	30	[116]
$[Cp_2TiBr_2]$ **56**	− 668.3	30	[116]
$[Cp_2TiI_2]$ **57**	− 517.2	30	[116]
$[Cp^*_2TiF_2]$ **58**	− 823		[117]
$[Cp^*_2TiCl_2]$ **59**	− 443		[117]
$[Cp^*_2TiBr_2]$ **60**	− 293		[117]
$[(tBuC_5H_4)_2ZrCl_2]$ **61**	− 65	2400	[122b]
$[C^*_2ZrCl_2]$ **62**	82	90	[122b]
$[Cp_2ZrCl_2]$ **63**	− 113	250	[122a]
$[Cp_2ZrBr_2]$ **64**	0	15–20	[122a]
$[Cp_2ZrI_2]$ **65**	126	134	[120]

$[Cp_2ZrX_2]$ with those in $[Cp_2Zr(diene)]$ complexes[124, 125] is of interest (Table 11), since for both systems ΔE can be estimated with the help of MO diagrams.[126–129] In $[Cp_2Zr(butadiene)]$ complexes, the diene can be coordinated in the *s-cis*-η^4-conformation (**73**) or in the *s-trans*-η^4-conformation (**72**).[124] For a ca. 1:1 equilibrium mixture of **72** and **73**, however, only a broad unresolved ^{91}Zr-NMR signal is observed at $\delta = -384$ ($W_{1/2} = 3100$ Hz), even at higher temperatures (T = 353 K). The high shielding of the ^{91}Zr nucleus correlates with the relatively large HOMO-LUMO gap (approx. 2.3 eV[128]) in these com-

Table 11. ^{91}Zr-NMR shifts and halfwidths of organozirconium complexes at 37.12 MHz [122, 123]. $T = 310$ K, external standard: **64**; COT = η^8-cyclooctatetraene. Cp = η^5-cyclopentadienyl.

$(tBu)_4Zr$	66 [a]	799	20
(cot)Zr	67 [a]	148	220
(Cp)(Cp)Zr	68 [a]	90	1400
(Cp)(Cp)Zr	69 [a]	132	1400
(Cp)(Cp)Zr	70 [a]	142	2500
(Cp)(Cp)Zr	71 [b]	268	1000
Cp_2Zr	72 [c]	−384	3100
Cp_2Zr	73 [c]		
Cp_2Zr	74 [c]	−324	2200
Cp_2Zr	75 [c]	−257	1900

[a] In [D_8]toluene. [b] In THF + 10% [D_6]benzene. [c] In [D_6]benzene.

plexes (Fig. 16), so that the paramagnetic contributions to the shielding constant via the $1/\Delta E$ term are therefore comparatively small. For **63**, qualitatively the same MO diagram can be assumed as for **55**.[126, 129] Consequently, in the bent metallocenes the frontier orbitals $1a_1$, b_2 and $2a_1$ possess mainly metal character, while the b_1 and a_2 orbitals have considerable ligand character. For two residues σ-bonded to Zr the respective n+n and n−n orbital combinations are bonding and a_1 constitutes the LUMO of the complex. The HOMO-LUMO gap in these 16e compounds can be assumed to be smaller than in the 18e-diene complexes discussed above.[129] It is therefore plausible that the $1/\Delta E$ contributions to the paramagnetic shielding term for the $[Cp_2ZrL_2]$ complexes with L=σ-ligand are rather large (cf. **61–65** in Table 10 and **72–75** in Table 11).

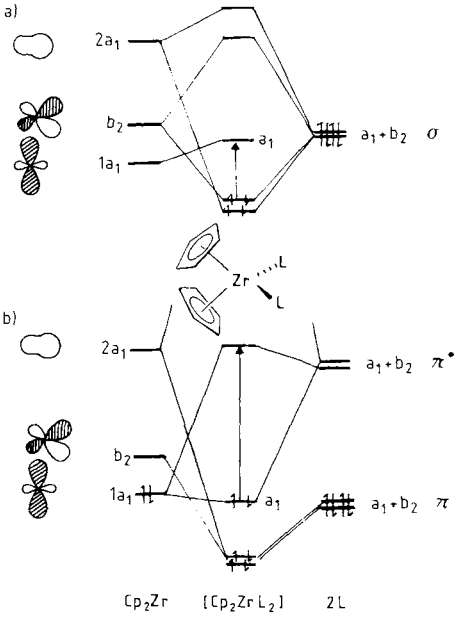


Fig. 16. Qualitative MO diagram for $[Cp_2ZrL_2]$ complexes [126]: (a) L=σ-ligand as halogen or alkyl and (b) L=olefin. For $[Cp_2Zr(\eta^4\text{-}C_4H_6)]$ a HOMO/LUMO gap of 2.3 eV was calculated [128]. For the σ-ligand, on the other hand, a smaller value can be assumed [129].

In the 16e complexes **67**[131] and **68**[130] $\delta(^{91}Zr)$ is about +100. As in the case of substitution at the η^5-Cp residue, methyl substitution at η^3-allyl and η^4-butadiene ligands leads to deshielding of the ^{91}Zr nucleus. Apparently these effects are additive: to a crude approximation the deshielding of Zr per methyl substituent amounts to 40 to 60 ppm. Similar effects are also observed upon methyl substitution in the 18e complexes of the $[Cp_2Zr(diene)]$ series.[122]

Since the shifts of Ti and Zr in organometallic compounds cover a large range and the signals are relatively narrow, high-field ^{49}Ti- or ^{91}Zr-NMR spectroscopy could be a valuable analytical method. The conversion of an 18e complex of the type $[Cp_2Zr(\eta^2\text{-}C_2H_4)_2]$ into a 16e metallacycle is symmetry-allowed,[126, 127] and on the basis of the different NMR shifts for Zr in both types of complexes the study of the relevant reactions with metal-NMR spectroscopy seems promising.

4.2. Metals of Group 8

4.2.1. The Elements of the Iron Group

The detection of magnetically active isotopes of the elements of the iron group (see Tables 1 and 5) is difficult, even with modern NMR techniques. However, the few ^{57}Fe-NMR investigations published so far[24, 35, 51c, 132–137] have clearly shown the potential of this spin-1/2 nucleus as a structural probe, inter alia, because it is important for chemical applications that in organo-iron $\delta(^{57}Fe)$ for Fe^{II} complexes is larger than for Fe^0 complexes (Fig. 17). This can be explained by the influence that electron density effects have upon the paramagnetic shielding contribution. In addition, the weaker shielding of the ^{57}Fe nucleus in ferrocene as compared to Fe^0 complexes might be caused by the $1/\Delta E$ term. A crude estimate for the ΔE term using the HOMO-LUMO gap shows that in $[Fe(\eta^4\text{-}C_4H_6)(CO)_3]$ it amounts to 2.9 eV[128] (extended Hückel MO calculations), while in $[Cp_2Fe]$ a value of 2.7 eV can be estimated from UV spectra.[138] As in the complexes $[Cp_2MX_2]$ (M=Ti, Zr), methyl substituents at the Cp-ring of the ferrocene cause a deshielding of the metal nucleus.[134] The great versatility of organoiron chemistry and the improved detection methods[137c] lead one to expect a broader application of ^{57}Fe-NMR spectroscopy in the near future. On the basis of the first measurements carried out on the ^{99}Ru quadrupolar nucleus[139–142] the same holds true for Ru complexes, since the halfwidths of these resonances are comparatively narrow even in unsymmetrical surroundings. In the case of the spin-1/2 nucleus ^{187}Os, apart from a paper dealing with the reference compound OsO_4,[143] only one publication concerning chemically relevant applications is known,[49] doubtlessly because of the low absolute NMR sensitivity of this nuclide. The quadrupolar nuclei ^{101}Ru and ^{189}Os seem to be less attractive from the point of view of chemical applications because of their insensitivity and the large halfwidths of their signals.[139]

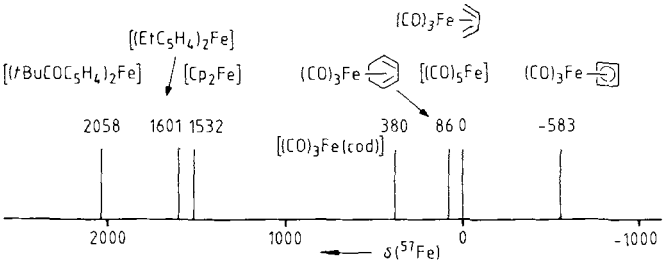


Fig. 17. ^{57}Fe-NMR shifts of organoiron compounds in which Fe has the formal oxidation state 2 or 0 [133, 134].

4.2.2. The Elements of the Cobalt Group

Of the magnetically active isotopes of the elements of the cobalt group, the ^{59}Co quadrupolar nucleus has been used since the advent of NMR spectroscopy for resolving various chemical problems.[5] Notwithstanding the natural abundance of 100% of the spin-1/2 nucleus ^{103}Rh, it is only because of the recent experimental techniques[47b, 144]

that this insensitive nucleus can be readily recorded.[144-147] In contrast, the magnetic properties of the two Ir isotopes exclude the general application of these nuclei in organometallic chemistry.

High-resolution metal-NMR spectra exist for diamagnetic Co- and Rh-complexes with the metals in the oxidation states +3, +1, 0, and −1 (Co).[133b, 148-152] The corresponding shift ranges cover more than 10000 ppm (Fig. 18).

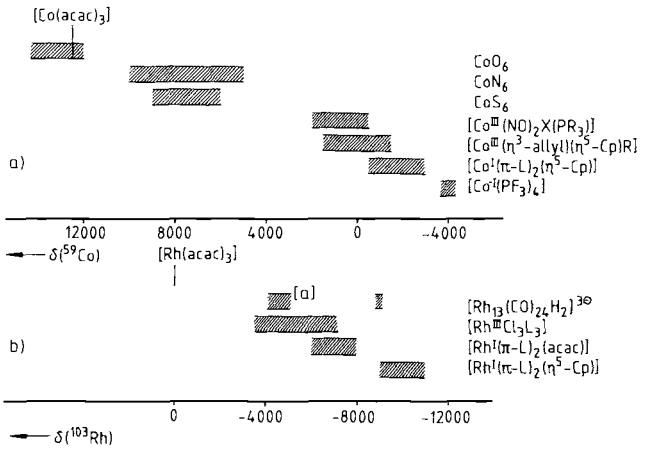
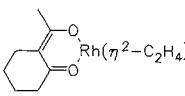
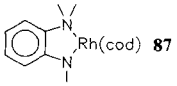
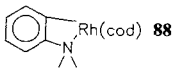
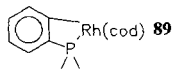


Fig. 18. M-NMR shifts of organometallic compounds [5a, 18, 148, 149]: a) M = ^{59}Co. CoO_6, CoN_6, and CoS_6 signify sixfold coordinated Co atoms via O, N, and S, respectively. b) M = ^{103}Rh. [a] Central Rh atom of the cluster.

It has been found empirically, that the shielding of the metal nucleus roughly correlates with the oxidation state of the metal atoms, even though individual subranges for the chemical shifts overlap. In octahedral Co^{III} complexes the shielding of the ^{59}Co nucleus increases in going from *O*- to *N*-, *S*-, *Se*-, *As*-, or *C*-bonded ligands.[5a] Here too, the shift ranges may in some cases overlap considerably. The chemical shifts of $[CpCo^{III}(\eta^3\text{-allyl})R]$ complexes lie within a range of ±1000 ppm around the standard $[Co(CN)_6]^{3\ominus}$.[148] Increasing donor properties of R lead to increased shielding of the ^{59}Co nucleus. Also extensive ^{59}Co-NMR investigations have been carried out on organocobalt(I) complexes with η^5-(Cp), η^3-(allyl), and η^2-bonded olefinic ligands as well as CO-ligands.[148-151] In addition, the ^{103}Rh-NMR shifts of many homologous Rh compounds[18b, 28b, 147] are known, thus permitting the question of which terms dominate the metal shifts to be discussed more broadly. Let us first compare only the ^{59}Co-NMR shifts of Co^I sandwich complexes with COD as one ligand and substituted cyclopentadienyl rings as second ligand.[148] Annelation of aromatic rings leads to a deshielding, while methyl substitution leads to a shielding, of a metal nucleus[148, 151] (if the cod ligand is replaced by two olefinic ligands, the changes for $\delta(^{59}Co)$ are similar). Such observations can be explained by charge density changes resulting from the −M and +I effects of the substituents. In $[(indenyl)Rh(\eta^2\text{-}C_2H_4)_2]$ the ^{103}Rh nucleus is more strongly deshielded by about 200 ppm than in $[CpRh(\eta^2\text{-}C_2H_4)_2]$.[153] Cyclopentadienylbis(π-L)cobalt complexes with substituted cyclopentadienyl ligands are powerful, homogeneous catalysts for the trimerization of alkynes and the cyclotrimerization of alkynes with nitriles to pyridine derivatives.[154] In the case of complexes with COD as π-ligand, a relationship between their activity and regioselectivity in catalysis and their ^{59}Co-NMR shifts has been established.[150]

As the ^{103}Rh-NMR shifts of rhodium(I) complexes[18b, 28b, 155] given in Table 12 show, the influence of the charge density on the paramagnetic shift term is here also decisive. Thus, the increasing donor properties of the ligands in the series COD, PPh_3, and *(cyclo*-$C_6H_{11})_2PCH_2CH_2P$(*cyclo*-$C_6H_{11})_2$ (DCPE) (**90**-**92**) effect an increased shielding of the ^{103}Rh nucleus.[18b]

Table 12. ^{103}Rh-NMR shifts of 16e organorhodium(I) complexes [18b] and $[Rh(\eta^3\text{-allyl})_3]$ [28b]; standard, see Table 7. dvcb = divinylcyclobutane, dcpe = (cyclo-$C_6H_{11})_2PCH_2CH_2P$(cyclo-$C_6H_{11})_2$.

Compound	$\delta(^{103}Rh)$	T [K]	Solvent
$[Rh(acac)(\eta^2\text{-}C_2H_4)_2]$ **76**	−7126	310	CD_2Cl_2
$[Rh(MeCOCHCOPh)(\eta^2\text{-}C_2H_4)_2]$ **77**	−7140	263	[D$_8$]THF
$[Rh(PhCOCHCOPh)(\eta^2\text{-}C_2H_4)_2]$ **78**	−7130	263	[D$_8$]THF
$[Rh(F_3CCOCHCOMe)(\eta^2\text{-}C_2H_4)_2]$ **79**	−7095	263	[D$_8$]toluene
$[Rh\{HC(COCF_3)_2\}(\eta^2\text{-}C_2H_4)_2]$ **80**	−7011	263	[D$_8$]toluene
 **81**	−7162	263	CD_2Cl_2
[Rh(acac)(dvcb)] **82**	−6918	310	CD_2Cl_2
$[Rh(acac)(PPh_3)_2]$ **83**	−7779	223	[D$_8$]THF
[Rh(acac)(*p*-chinon)] **84**	−6252	310	[D$_8$]THF
[Rh(acac)(cod)] **85**	−7014	310	[D$_6$]benzene
$[RhCl(cod)]_2$ **86**	−7205	310	[D$_6$]benzene
 **87**	−7445	310	[D$_8$]THF
 **88**	−7719	310	[D$_8$]THF
 **89**	−8278	310	[D$_8$]THF
$[Rh(cod)(\eta^3\text{-cyclooctenyl})]$ **90**	−8311	263	[D$_8$]toluene
$[Rh(\eta^3\text{-allyl})(PPh_3)_2]$ **91**	−9355	223	[D$_8$]THF
$[Rh(\eta^3\text{-allyl})(dcpe)]$ **92**	−9683	263	[D$_8$]THF
$[Rh(\eta^3\text{-allyl})_3]$ **93**	−8750	270	[D$_8$]toluene

Consistent with the strong influence of charge density on ^{59}Co- and ^{103}Rh-NMR shifts, the shifts known so far for Co^{III}, Rh^{III}, and Rh^I complexes show a normal dependence on halogen substitution. This property is in contrast to the expected decrease of ΔE with increasing atomic number of the halogen and the resulting increase of the paramagnetic shift term. The classical NMR spectroscopic investigations of octahedral Co^{III} complexes[69, 156] have shown, however, that the ^{59}Co-NMR shifts may also be dominated by the $1/\Delta E$ term of the paramagnetic shielding contribution. Such a relationship has also been demonstrated in the case of $[CpCo(\pi\text{-}L)_2]$ complexes (Fig. 19).[148] The parent compound of these Co^I complexes is $[CpCo(\eta^2\text{-}C_2H_4)_2]$,[157] from which further $CpCo^I$ derivatives are accessible by replacement of ethylene. In $[CpCo(C_2H_4)_2]$ the Co nucleus is strongly deshielded, in $[CpCo(CO)_2]$ strongly shielded. The shift difference of ca.

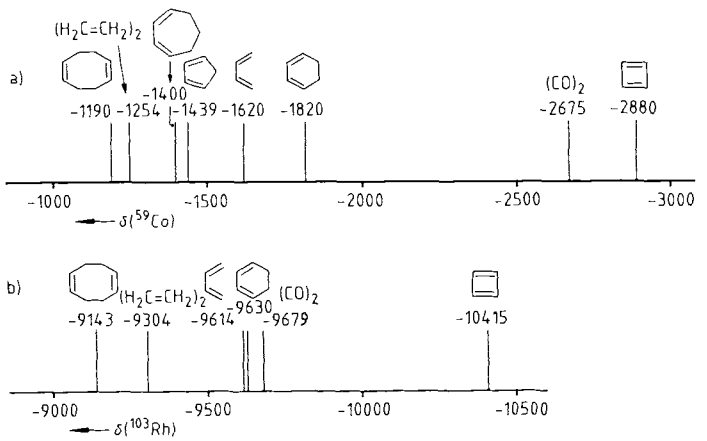


Fig. 19. Comparison of M-NMR shifts of $[CpM(\pi\text{-}L)_2]$ complexes: (a) M = ^{59}Co [148, 149]. (b) M = ^{103}Rh [18b, 149, 155]. The ^{59}Co-NMR shifts of the ^{59}Co-nucleus are referred to $[Co(CN)_6]^{3\ominus}$ as external standard, those of the ^{103}Rh nucleus to $[Rh(acac)_3]$ on the basis of the information given in [149]. The halfwidths of the ^{59}Co-NMR signals range from 7000 to 13000 Hz [148].

1500 ppm can be explained by the $1/\Delta E$ dependence of the paramagnetic shift contribution; ΔE was estimated[148] from quantitative EH-MO calculations (Fig. 20).[158] In these complexes the important interactions between the CpCo fragment and the other ligands are given by the combination of ligand orbitals ($\pi-\pi$, $\pi^*+\pi^*$, $n_{CO}-n_{CO}$, $\pi^*_{CO}+\pi^*_{CO}$) with the half-filled 2e-set of xz and xy CpCo-orbitals. In both cases the HOMO of the complexes, which is stabilized by back-donation, is of the type xz. The LUMO of the complexes is of the yz type and is destabilized by the antibonding combination with $n_{CO}-n_{CO}$ and $\pi-\pi$, respectively. As a consequence of better overlap between the donor orbitals n_{CO} (these are one-center orbitals of σ-type) the LUMO of the CO complex lies higher than that in the C_2H_4-complex. Since there is very little difference in the energies of the HOMOs of both complexes, the HOMO-LUMO gap in $[CpCo(C_2H_4)_2]$ is smaller by 0.31 eV than in $[CpCo(CO)_2]$. This result supports the conclusion that the ^{59}Co-NMR shifts in a series of CpCo complexes are influenced or even determined by the $1/\Delta E$ dependence of the paramagnetic shielding contribution. On the basis of the correlation between $\delta(^{59}Co)$ and $1/\Delta E$ which has been found by UV measurements on inorganic Co^{III} complexes,[69, 156] a decrease of ΔE by 2 cm^{-1} corresponds to a downfield shift of ca. 1 ppm. Consequently, the ^{59}Co upfield shift of 1448 ppm observed for $[CpCo(CO)_2]$ corresponds to a change in ΔE of 0.35 eV. This agrees surprisingly well with the calculated difference in ΔE of 0.31 eV.[148]

Since the ^{103}Rh-NMR shifts qualitatively show a trend similar to that of the ^{59}Co-NMR shifts of the analogous $(Cp)Co^{I}$ complexes (cf. Fig. 19), it may be assumed that

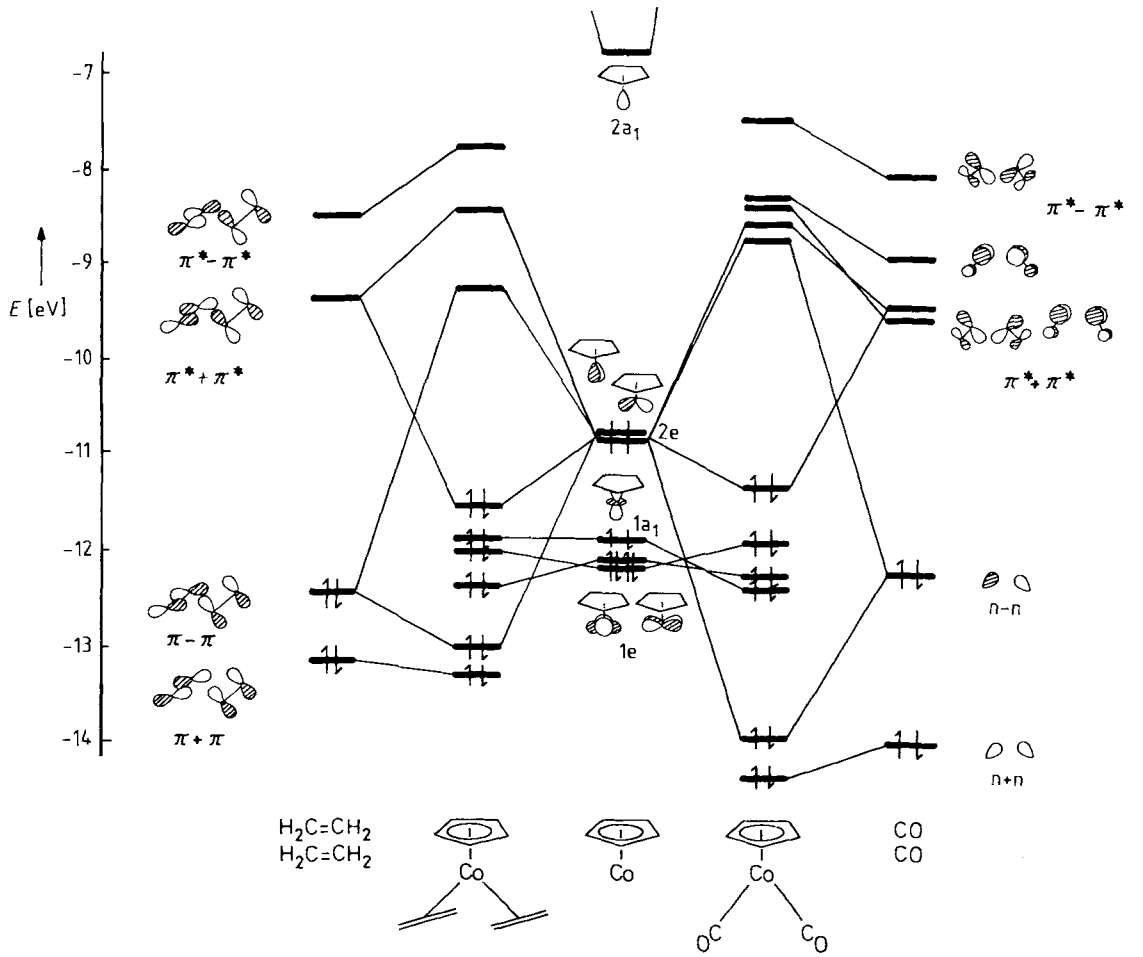


Fig. 20. Comparison of the EH-MO diagrams of $[CpCo(\eta^2\text{-}C_2H_4)_2]$ and $[CpCo(CO)_2]$ [148].

they are also affected by the $1/\Delta E$ term and the frontier orbitals of the complexes. Accordingly, the metal-NMR shifts reflect the strength of the interaction between CpM fragment and ligand, and therefore chemical shifts of a series of related complexes can serve as an indicator of complex properties. Indeed, for related Co-complexes the ^{59}Co-NMR shifts correlate with chemical properties.[148]

Of the isotopes of the elements of the nickel group, ^{195}Pt is the most attractive isotope for NMR investigations. As a consequence of its easy detectability a large number of ^{195}Pt-NMR data have already been reported in the literature.[5, 159, 160] The chemical shift range of the ^{195}Pt nucleus spans 16000 ppm;[5, 67, 159] that of the ^{195}Pt-NMR shifts of $[Pt^{IV}X_6]^{2\ominus}$ salts (X = F, Cl, I, Br) alone amounts to 13000 ppm.[67, 161] The dependence of the shifts on halogen substitution is quite normal. Anisotropic contributions to the paramagnetic shielding term may be considerably large. Depending on the geometry of the dissolved molecules, values between 1000 and 12000 ppm have been estimated for $\Delta\sigma = \sigma_{\parallel} - \sigma_{\perp}$.[15, 26, 27, 162]

So far, relatively little is known about $\delta(^{195}Pt)$ in Pt^0-compounds.[159, 160] Quantitative MO calculations and UV measurements on $[PtL_2(acetylene)]$ complexes showed that the $\delta(^{195}Pt)$ values in these compounds can be explained in terms of the $1/\Delta E$ dependence of the paramagnetic shielding term.[163] For phosphaneplatinum complexes $[Pt(PR_3)_n]$ (n = 2, 3, 4), of linear, trigonal and tetrahedral geometry, the order of the ^{195}Pt shifts ($\delta(Pt(PR_3)_2) < \delta(Pt(PR_3)_4) < \delta(Pt(PR_3)_3)$, see Table 13) has also been correlated with the $1/\Delta E$ term.[164] The average excitation energy ΔE has been estimated from qualitative MO diagrams and UV spectra.

Table 13. ^{195}Pt-NMR shifts of Pt^0 compounds and $[Pt(\eta^3\text{-allyl})_2]$ [15, 166]; dRpe = $R_2PCH_2CH_2PR_2$, standard, see Table 7.

Compound	$\delta(^{195}Pt)$	T [K]	Solvent
$[Pt(PiPr_3)_2]$ **94**	−6582	310	$[D_8]$toluene
$[Pt(PtBu_3)_2]$ **95**	−6471	310	$[D_8]$THF
$[Pt(P(cyclo\text{-}C_6H_{11})_3)_2]$**96**	−6501	310	$[D_8]$toluene
$[Pt(PEt_3)_3]$ **97**	−4517	310	$[D_8]$toluene
$[Pt(PPh_3)_4]$ **98**	−4583	193	$[D_8]$THF
$[Pt(PMe_3)_4]$ **99**	−4805	310	$[D_8]$toluene
$[Pt(cod)_2]$ **100**	−4625	263	$[D_8]$toluene
$(PPh_3)_2Pt$—⋈ **101**	−5102	240	$[D_8]$toluene
dRpe)Pt—‖ R = *t*Bu **102**	−5239	213	$[D_8]$toluene
‖ R = *cyclo*-C_6H_{11} **103**	−5230	213	$[D_8]$toluene
trans-$[Pt(\eta^3\text{-allyl})_2]$**104**	−6192	278	$[D_8]$THF
cis-$[Pt(\eta^3\text{-allyl})_2]$ **105**	−5963	278	$[D_8]$THF

As in the NMR spectroscopy of other spin-1/2 metal nuclei with large chemical shift ranges, important applications of ^{195}Pt-NMR spectroscopy in organometallic chemistry include the improved detection of isomers on the basis of the large signal dispersion of the ^{195}Pt resonances. Even a ^{195}Pt separation as small as 1 ppm is very often sufficient for exact integration. A particularly convincing example is the detection of optical isomers of square-planar Pt complexes with optically active ligands and prochiral π-bonded olefins.[159, 165] ^{195}Pt-NMR spectroscopy has also been used to elucidate the type of bonding between butadiene and a L_2Pt fragment[166] (see Fig. 21). This is of interest since butadiene can bind to transition metals in various ways.[167] Depending on the alkyl substituent R in the chelate-phosphane (dRpe), metallacyclopentene and $Pt(\eta^2$-diene) structures are found in the [Pt(dRpe)(butadiene)] complexes.[168] Their ^{195}Pt-NMR shifts are different by ca. 500 ppm.[166] This reflects the generally observed trend that for comparable ligands the ^{195}Pt-NMR signals of lower-valent Pt compounds resonate at lower frequencies. The shift ranges for complexes with Pt in different oxidation states are, however, not free of overlap.

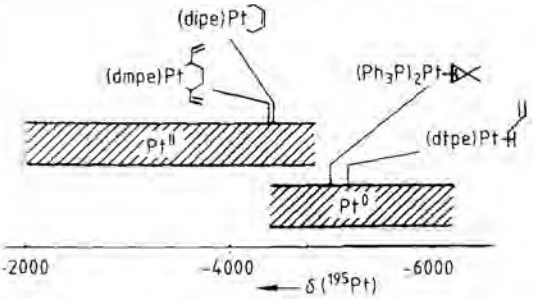


Fig. 21. ^{195}Pt-NMR shifts of bis(phosphane)platinum(0) and -platinum(II) complexes [166] relative to $[PtCl_6]^{2\ominus}$ as external standard. dmpe = $Me_2PCH_2CH_2PMe_2$; dipe = $iPr_2PCH_2CH_2PiPr_2$; dtpe = $tBu_2PCH_2CH_2PtBu_2$.

In the elucidation of the structures of clusters containing several chemically non-equivalent spin-1/2 metal nuclei, the NMR spectroscopy of metal nuclei is *a priori* superior to that of the traditionally measured nuclei. In the case of the compound $[Pt_9(CO)_{18}]^{2\ominus}$ it could be shown that quite different ^{195}Pt resonances are obtained for the inner and outer Pt cluster atoms.[169] The relatively high sensitivity of the ^{195}Pt nucleus and the comparatively large Pt-Pt spin-spin coupling constants should allow the connectivity of chemically nonequivalent cluster atoms to be determined with the aid of two-dimensional NMR techniques like COSY and INADEQUATE,[4] which have been used so successfully in the case of the ^{183}W isotope[170, 171] to determine the coupling pattern in Pt-clusters. These techniques should find widespread application.

In complete contrast, however, the low sensitivity and especially the large quadrupole moment of the ^{105}Pd nucleus leave little hope for its suitability for NMR investigations in the field of organopalladium complex chemistry. Similarily, the ^{61}Ni nucleus has unfavorable NMR properties and so far only two papers with chemically relevant ^{61}Ni-NMR data have been published.[172, 173] Organonickel complexes are, however, of great importance in preparative and mechanistic chemistry and in homogeneous catalysis.[174] The ^{61}Ni-NMR shifts already known[172, 173] and those determined by us[175] for complexes with tetrahedrally coordinated Ni span a range of ca. 2000 ppm (Fig. 22). These chemical shifts cannot be explained on the basis

of simple charge density arguments, since the shielding of the ^{61}Ni nucleus is strongest when ligands of high acceptor properties are coordinated. Ligands with good donor properties like COD, on the other hand, lead to a deshielding of ^{61}Ni. It is therefore reasonable to assume that the ^{61}Ni shift in tetrahedrally coordinated Ni complexes is determined by the frontier orbitals and in particular by the ΔE dependence of the paramagnetic shielding term (for MO calculations for these types of compounds cf. ref. [176]).

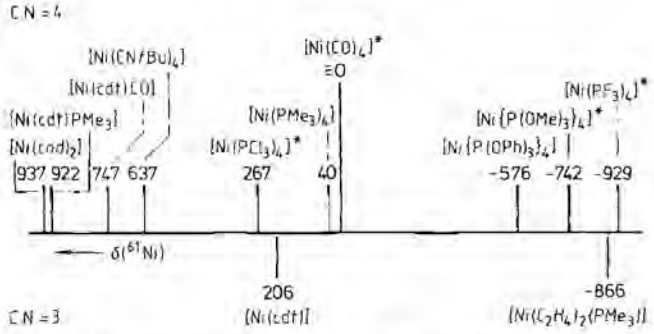


Fig. 22. ^{61}Ni-NMR chemical shifts of tetrahedral (upwards) and trigonal planar (downwards) Ni^0 complexes. The ^{61}Ni-data marked with (*) are from [173], the remaining data from [175]. cdt = all-*trans*-1,5,9-cyclododecatriene.

It would seem worth noting that for some $[NiL_4]$ complexes the strength of the Ni-L bond is reflected in an enhanced shielding of the ^{61}Ni nucleus. For example, $[Ni(PR_3)_4]$ complexes can be prepared from $[Ni(cod)_2]$ or $[Ni(CNtBu)_4]$ by ligand exchange, and the similarity of the ^{61}Ni-NMR shifts for $[Ni(CO)_4]$ and $[Ni(PMe_3)_4]$ are consistent with the finding that mixing of the complexes yields primarily the complexes $[Ni(CO)_n(PR_3)_{4-n}]$.[174] However, far more investigations will have to be carried out in order to establish a definite relationship between the ^{61}Ni-NMR shift and the strength of the Ni-L bond in NiL_4 complexes.

The ^{61}Ni-NMR shifts of the two trigonal-planar organonickel complexes known so far[175] differ by ca. 1000 ppm.

4.3. Metal-NMR shifts in Ally-Transition Metal Complexes

Most of the known pure allyl-transition metal complexes were synthesized more than 20 years ago[177] and since then have acquired great importance in preparative chemistry and in the catalytic transformation of olefins.[178] Even though the metal in $[M(allyl)_n]$ complexes formally has the oxidation number n, these compounds behave chemically very often like metal(0) complexes. The magnitude of the effective charge at the metal, for example in bis(η^3-allyl)nickel, has been the subject of numerous discussions and calculations;[179] a classification of such complexes according to their δ(M) shifts is therefore of great interest.

The following metal-NMR shifts in allyl complexes are already known: ^{195}Pt,[166] ^{59}Co,[148] and ^{103}Rh.[28b] An X-ray structure analysis of bis(η^3-allyl)platinum has shown that the allyl groups have a *trans*-arrangement in the crystal.[180] In solution, on the other hand, two isomers are observed, for which a *trans*- and a *cis*-arrangement of the allyl groups, respectively, is assumed.[181] The ^{195}Pt-NMR data support this assumption since the $\delta(^{195}Pt)$ values as well as the T_1 values for both isomers are considerably different.[166] The ^{195}Pt-NMR shifts of bis(η^3-allyl)platinum compounds fall in a range which, on the basis of data known sofar, is more typical for Pt^0-complexes (see Fig. 23). Application of the MO scheme for bis(η^3-allyl)nickel[176] to the homologous Pt-compound indicates almost a d^{10} configuration for the metal, so that the position of the ^{195}Pt-NMR shift in bis(η^3-allyl)platinum is not surprising.

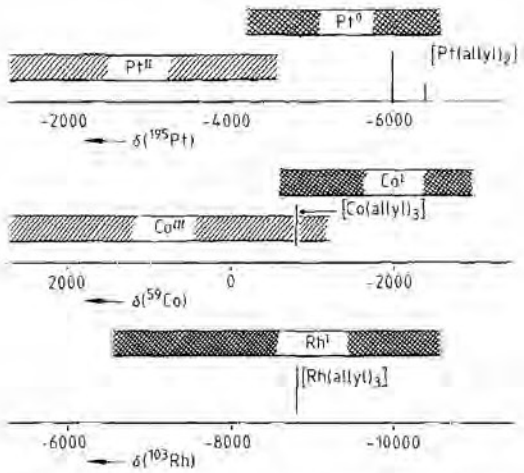


Fig. 23. M-NMR shifts in the allyl metal complexes *trans*-[Pt(η^1-allyl)$_2$], *cis*-[Pt(η^1-allyl)$_2$] [166], [Co(η^3-allyl)$_3$] [148] and [Rh(η^3-allyl)$_3$] [28b] (for reference compounds see Table 7). Characteristic ranges for the metal shifts of the respective organometallic compounds in different oxidation states are hatched.

Similar results are obtained for tris(η^3-allyl)cobalt and tris(η^3-allyl)rhodium, in which the metals are trigonal prismatic coordinated. Surprisingly, the halfwidths of the ^{59}Co-NMR signals of $[Co(\eta^3\text{-allyl})_3]$ and $[Co\{\eta^3\text{-}(H_2C{-}C(Me){=}CH_2)\}_3]$ are so small that the signals can be observed even at low temperatures.[148] (Relative to the nuclei in the respective $[CpM(\eta^4\text{-cod})]$ complexes (M = Rh, Co) those in the tris(allyl)metal complexes are strongly shielded, but the differences in the shifts are similar.) The metal shifts fall in a range which is more characteristic for the corresponding organometal(I) complexes. Qualitative MO considerations[176] show that the HOMO of $[M(\eta^3\text{-allyl})_3]$ is a pure ligand orbital, while the lower lying occupied orbitals still have considerable metal d-orbital character (Fig. 24). Therefore, the electronic configuration of Co and Rh, respectively, in the allyl complexes lies between d^6 and d^{10}, and the partial charges at the metal atoms are smaller than in normal M^{III} complexes. The stronger shielding ($\Delta\delta \approx 400$ ppm) of the ^{59}Co nucleus in $[Co\{\eta^3\text{-}(CH_2{-}C(Me){=}CH_2)\}_3]$, which has a structure (C_{3h} symmetry) similar to that of $[Co(\eta^3\text{-allyl})_3]$ but is thermally more stable than the latter, does not, however, fit into the qualitative picture described above.

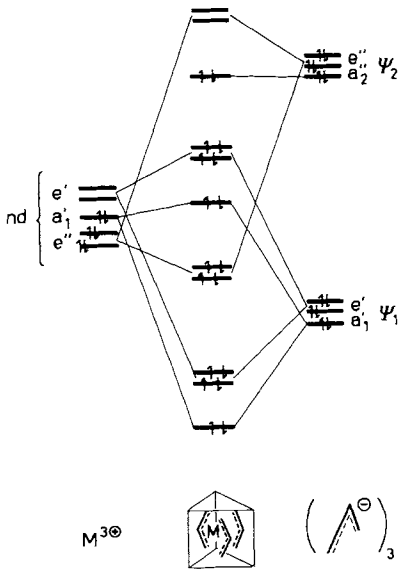


Fig. 24. Schematic MO diagram for $[M(\eta^3\text{-allyl})_3]$ complexes (M = Co, Rh) with trigonal prismatic coordination of the metal atom [176].

5. Conclusions

The examples discussed here show that NMR spectra of nearly all magnetically active metal nuclei can be obtained with reasonable effort. In particular, in the case of transition metals the chemical shift ranges are very often larger than 1000 ppm. Therefore, spin-1/2 metal nuclei and, within certain limits, also quadrupolar metal nuclei are very sensitive probes for investigating the chemistry of complexes. Since these nuclei are very often at or close to the center of the molecule of interest, the results obtained by high-resolution metal-NMR spectroscopy are mostly of a different nature from and complementary to the results obtained with nuclei at the periphery of the complex (as, e.g., ^1H and ^{13}C). Examples of where the NMR of metal nuclei is extremely useful are in investigations concerned with the coordination number, the oxidation state, the nature of the bonding and the electronic configuration of a metal atom in complexes.

Besides the possibility of determining the connectivity of magnetically active and chemically non-equivalent metals in polynuclear compounds and clusters, the relationship between the $\delta(M)$ values and the frontier orbitals of complexes deserves special attention, since this leads to a relationship between the chemical shift and the chemical properties of the complex.

Even if the examples discussed above can only partly demonstrate the present state of the art of the NMR spectroscopy of metal nuclei, it will be evident that the era of merely detecting NMR signals of metal nuclei is over, and that metal-NMR spectroscopy now constitutes a new, practical and useful method which will find application in many areas of inorganic and organometallic chemistry.

We are particularly indebted to the Director of the Max-Planck-Institut für Kohlenforschung, Prof. Dr. G. Wilke, for his generous support of our investigations. We are grateful to colleagues who have participated in joint projects (Prof. Dr. H. Lehmkuhl) or provided us with samples. R. B. thanks Dr. R.-D. Reinhardt for a number of investigations related to ^{195}Pt- and ^{103}Rh-NMR spectroscopy. R. B. gratefully acknowledges financial support by the Deutsche Forschungsgemeinschaft.

Received: September 4, 1985;
revised: January 28, 1986 [A 588 IE]
German version: *Angew. Chem. 98* (1986) 851

[1] a) R. E. Wasylishen, C. A. Fyfe, *Annu. Rep. NMR Spectrosc. 12* (1982) 1; b) C. S. Yannoni, *Acc. Chem. Res. 15* (1982) 201; c) J. R. Lyerla, C. S. Yannoni, C. A. Fyfe, *ibid. 15* (1982) 208; d) C. A. Fyfe, J. M. Thomas, J. Klinowski, G. C. Gobbi, *Angew. Chem. 95* (1983) 257; *Angew. Chem. Int. Ed. Engl. 22* (1983) 259; e) J. Klinowski, *Prog. Nucl. Magn. Reson. Spectrosc. 16* (1984) 193; f) W. S. Veeman, *ibid. 16* (1984) 237; g) G. Maciel, *Science (Washington DC) 226* (1984) 282; h) E. Oldfield, R. J. Kirkpatrik, *ibid. 227* (1985) 1537.

[2] a) R. E. Gordon, P. E. Hanly, D. Shaw, *Prog. Nucl. Magn. Reson. Spectrosc. 15* (1982) 1; b) R. A. Iles, A. N. Stevens, J. R. Griffiths, *ibid. 15* (1982) 49; c) P. Diehl, E. Fluck, R. Kosfeld, (Eds.): *NMR: Basic Principles and Progress, Vol. 19*, Springer, Berlin 1981; d) A. M. Gronenborn, K. Roth, *Chem. Unserer Zeit 16* (1982) 35; e) K. Roth: *NMR-Tomographie und -Spektroskopie in der Medizin*, Springer, Berlin 1984; f) P. Mansfield, P. G. Morris, *Adv. Magn. Reson. Suppl. 2* (1982) Academic Press, New York; g) S. L. Smith, *Anal. Chem. 57* (1985) 595; h) P. G. Morris: *NMR Imaging in Medicine and Biology*, University Press, Oxford 1984.

[3] The idea of two-dimensional NMR-Spectroscopy is due to *J. Jeener* (lecture given at the Ampère Int. Summer School, Basko Polje, Yugoslavia 1971) and its general importance was first recognized by *R. R. Ernst* (R. R. Ernst, *Chimia 29* (1975) 179; W. P. Aue, E. Bartholdi, R. R. Ernst, *J. Chem. Phys. 64* (1976) 2229). For an interesting review of the historical development see *Freeman* (R. Freeman, G. A. Morris, *Bull. Magn. Reson. 1* (1979) 5).

[4] For reviews on one- and two-dimensional pulse methods in high-resolution NMR spectroscopy see a) R. Benn, H. Günther, *Angew. Chem. 95* (1983) 381; *Angew. Chem. Int. Ed. Engl. 22* (1983) 350; b) C. J. Turner, *Prog. Nucl. Magn. Reson. Spectrosc. 16* (1984) 311; c) H. Günther, P. Schmitt, *Naturwissenschaften 71* (1984) 342; for reviews on 2D-NMR-spectroscopy: d) G. A. Morris in A. G. Marshall (Ed.): *Fourier, Hadamard and Hilbert Transformations in Chemistry*, Plenum, New York 1982; e) R. Freeman, *Proc. R. Soc. London Ser. A 373* (1980) 149; f) A. Bax: *Two-Dimensional Nuclear Magnetic Resonance in Liquids*, Reidel, Dordrecht 1982; g) *Top. Carbon-13 NMR Spectrosc. 4* (1984) 197; h) K. Nagayama, *Adv. Biophys. 14* (1981) 139; i) W. McFarlane, D. S. Rycroft, *Annu. Rep. NMR Spectrosc. 16* (1985) 293; j) G. A. Morris, *Magn. Reson. Chem. 24* (1986) 371.

[5] Recent reviews on multinuclar NMR-spectroscopy: a) R. K. Harris, B. E. Mann (Eds.): *NMR and the Periodic Table*, Academic Press, London 1978; b) C. Brevard, P. Granger: *Handbook of High Resolution Multinuclear NMR*, Wiley, New York 1981; c) J. B. Lambert, F. G. Riddell (Eds.): *The Multinuclear Approach to NMR Spectroscopy*, Reidel, Dordrecht 1983; d) P. Lazlo (Ed.): *NMR of Newly Accessible Nuclei, Vol. 1, 2*, Academic Press, New York 1983; e) B. E. Mann, *Spectrosc. Prop. Inorg. Organomet. Compd. 18* (1985) 1.

[6] a) P. S. Pregosin, R. W. Kunz (Eds.): *NMR: Basic Principles and Progress, Vol. 16*, Springer, Berlin 1979; b) D. G. Gorenstein, *Prog. Nucl. Magn. Reson. Spectrosc. 16* (1985), 1; c) A. Pidcock, ACS Symp. *Adv. Chem. Res. 196* (1982) 1.

[7] a) G. Levy, R. L. Lichter: *Nitrogen-15 NMR Spectroscopy*, Wiley, New York 1979; b) M. Witanowski, L. Stefaniak, G. A. Webb, *Annu. Rep. NMR Spectrosc. 11 B* (1981) 2; c) G. J. Martin, M. L. Martin, J.-P. Gouesnard, *NMR: Basic Princ. Prog. 18* (1981) 1; d) W. von Philipsborn, R. Müller, *Angew. Chem. 98* (1986) 381; *Angew. Chem. Int. Ed. Engl. 25* (1986) 383.

[8] a) T. A. Blinka, B. J. Helmer, R. West, *Adv. Organomet. Chem. 23* (1984) 193; b) E. A. Williams, *Annu. Rep. NMR Spectrosc. 15* (1983) 235.

[9] a) C. Brevard, J. P. Kintzinger in [5a] p. 107; b) I. C. P. Smith, H. H. Mantsch, *ACS Symp. Ser. 191* (1982) 97; c) I. C. P. Smith in [5d] *Vol. 2*, p. 1.

[10] a) L. J. Todd, A. R. Siedle, *Prog. Nucl. Magn. Reson. Spectrosc. 13* (1979) 87; b) A. R. Siedle, *Annu. Rep. NMR Spectrosc. 12* (1982) 177; c) B. Wrackmeyer, R. Köster (Eds) in: *Houben-Weyl, Methoden der Organischen Chemie*, Vol. XIII/3c, Thieme, Stuttgart 1984.

[11] a) J. P. Kintzinger, *NMR: Basic Princ. Prog. 17* (1981) 1; b) in [5d] *Vol. 2*, p. 79.

[12] D. S. Gill, O. A. Gansow, F. J. Bennis, K. C. Ott, *J. Magn. Reson. 35* (1979) 459.
[13] a) T. C. Farrar, E. D. Becker: *Pulse and Fourier Transform NMR*, Academic Press, New York 1971; b) D. Shaw: *Fourier Transform NMR Spectroscopy*, Elsevier, Amsterdam 1984; c) F. W. Wehrli, T. Wirthlin: *Interpretation of Carbon-13 NMR Spectra*, Heyden, London 1976; d) H. Günther: *NMR-Spectroscopy*, Wiley, New York 1980; e) A. Abragram: *The Principles of Nuclear Magnetism*, University Press, Oxford 1961, p. 309–312.
[14] J. Kronenbitter, U. Schweizer, A. Schwenk, *Z. Naturforsch. A 35* (1980) 319.
[15] R. Benn, H.-M. Büch, R.-D. Reinhardt, *Magn. Reson. Chem. 23* (1985) 559.
[16] R. L. Vold, R. R. Vold, *Prog. Nucl. Magn. Reson. Spectroscop. 12* (1978) 79.
[17] a) M. H. Levitt, R. Freeman, *J. Magn. Reson. 43* (1981) 65; b) M. H. Levitt, *J. Magn. Reson. 48* (1982) 234; c) R. Freeman, S. P. Kampsell, M. H. Levitt, *J. Magn. Reson. 38* (1980) 453.
[18] a) R. Benn, J. Klein, R.-D. Reinhardt, unpublished; b) R.-D. Reinhardt, *Dissertation*, Universität Bochum 1985.
[19] P. S. Pregosin, *Chimia 35* (1981) 43.
[20] J. H. Noggle, R. E. Schirmer: *The Nuclear Overhauser Effect*, Academic Press, New York 1971.
[21] T. C. Wong, T. T. Ang, F. S. Guziec Jr., Ch. A. Moustakis, *J. Magn. Reson. 57* (1984) 463.
[22] F. Brady, R. W. Mattheus, M. J. Forster, D. G. Gillies, *Inorg. Nucl. Chem. Lett. 17* (1981) 155.
[23] a) G. R. Hays, D. G. Gillies, L. P. Blaauw, A. D. H. Clague, *J. Magn. Reson. 45* (1981) 102; b) R. M. Hawk, R. R. Sharp, *J. Chem. Phys. 60* (1974) 1009.
[24] a) L. Baltzer, E. D. Becker, B. A. Averill, J. M. Hutchinson, A. O. Gansow, *J. Am. Chem. Soc. 106* (1984) 2444; b) T. Nozawa, M. Hatano, M. Sato, Y. Toida, E. Bartholdi, *Bull. Chem. Soc. Jpn. 56* (1983) 3837.
[25] a) D. G. Gillies, L. P. Blaauw, G. R. Hays, R. Huis, A. D. H. Clague, *J. Magn. Reson. 42* (1981) 420; b) R. Benn, H. Günther, A. Maerker, V. Menger, P. Schmitt, *Angew. Chem. 94* (1982) 314; *Angew. Chem. Int. Ed. Engl. 21* (1982) 295.
[26] J. Y. Lallemand, J. Soulie, J. C. Chottard, *J. Chem. Soc. Chem. Commun. 1980*, 436.
[27] J. J. Dechter, J. Kowalewski, *J. Magn. Res. 59* (1984) 146.
[28] a) M. Cocivera, G. Ferguson, R. E. Lenkinski, P. Szczecinski, *J. Magn. Reson. 46* (1982) 168; b) R. Benn, H. Brenneke, R.-D. Reinhardt, *Z. Naturforsch. B 40* (1985) 1763; c) R. Benn, R.-D. Reinhardt, *6. Magn. Reson. Diskussionstagung* (Berlin 1984) Abstr. P1; d) S. M. Socol, D. W. Meek, *Inorg. Chim. Acta 101* (1985) L45.
[29] a) J. D. Kennedy, W. McFarlane, *J. Chem. Soc. Faraday Trans. 2, 72* (1976) 1653; b) R. E. Wasylishen, R. E. Lenkinski, C. Rodger, *Can. J. Chem. 60* (1982) 2113.
[30] K. G. R. Pachler, P. L. Wessels, *J. Magn. Reson. 12* (1973) 337.
[31] Modified SPT-sequence for the suppression of unwanted signals: H. J. Jakobsen, P. J. Kanyha, W. S. Brey, *J. Magn. Reson. 54* (1983) 134.
[32] a) E. D. Baker, *J. Chem. Phys. 37* (1962) 911; b) T. H. Brown, P. J. Green, *J. Am. Chem. Soc. 92* (1970) 2359; c) H. C. E. McFarlane, W. McFarlane, D. S. Rycroft, *J. Chem. Soc. Dalton Trans. 1976*, 1616.
[33] G. A. Morris, R. Freeman, *J. Am. Chem. Soc. 101* (1979) 760.
[34] D. M. Doddrell, D. T. Pegg, M. R. Bendall, *J. Magn. Reson. 48* (1982) 323.
[35] a) C. Brevard, R. Schimpf, *J. Magn. Reson. 47* (1982) 528; b) S. J. Berners Price, C. Brevard, A. Pagelot, P. J. Sadler, *Inorg. Chem. 24* (1985) 4278.
[36] a) G. C. van Stein, G. van Koten, *J. Organomet. Chem. 226* (1982) C27; b) G. van Koten, A. F. M. J. van der Poeg, C. Brevard, *Inorg. Chem. 21* (1982) 2878; c) G. C. van Stein, G. van Koten, K. Vrieze, A. L. Spek, E. A. Klop, C. Brevard, *ibid. 24* (1985) 1367.
[37] C. Brevard, G. C. van Stein, G. van Koten, *J. Am. Chem. Soc. 103* (1981) 6746.
[38] a) R. Cramer, J. B. Kline, J. D. Roberts, *J. Am. Chem. Soc. 91* (1969) 2519; b) J. M. Brown, B. T. Golding, J. J. Stofko, *J. Chem. Soc. Perkin Trans. 2 1978*, 436; d) J. Powell, B. L. Shaw, *J. Chem. Soc. A 1968*, 583.
[39] An optimization of the INEPT and DEPT sequence for such problematic cases has been reported on by K. V. Schenker, W. von Philipsborn, *J. Magn. Reson. 61* (1985) 294.
[40] A. Bax, Ch.-H. Niu, D. Live, *J. Am. Chem. Soc. 106* (1984) 1150.
[41] J. Schraml, *J. Magn. Reson. 59* (1984) 515.
[42] A. Bax, *J. Magn. Reson. 57* (1984) 314.
[43] D. M. Doddrell, W. Brooks, J. Field, R. M. Lynden-Bell, *J. Magn. Reson. 59* (1984) 384.
[44] D. A. Vidusek, M. F. Roberts, G. Bodenhausen, *J. Am. Chem. Soc. 104* (1982) 5452.
[45] For the indirect observation of ^{183}W see: G. T. Andrews, I. J. Colquhoun, W. McFarlane, S. O. Grim, *J. Chem. Soc. Dalton Trans. 1982*, 2353; for ^{1}H{X}-Spin-Echo-Difference Spectroscopy see: J. S. Cohen, C.-W. Chen, A. Bax, *J. Magn. Reson. 59* (1984) 181; indirect ^{31}P{^{107}Ag, ^{1}H}-NMR spectra: I. J. Colquhoun, W. Mc Farlane, *T. Chem. Commun. 1980*, 145.
[46] The inverse INEPT sequence (R. Freeman, T. H. Mareci, G. A. Morris, *J. Magn. Reson. 42* (1981) 341; M. R. Bendall, D. T. Pegg, D. M. Doddrell, J. Field, *J. Am. Chem. Soc. 103* (1981) 934) and the inverse DEPT sequence (M. R. Bendall, D. T. Pegg, D. M. Doddrell, J. Field, *J. Magn. Reson. 51* (1983) 520), which were suggested in particular for the overlap-free presentation of proton multiplets can also be used for determining the shifts of insensitive X-nuclei.
[47] a) The first two-dimensional ^{1}H,X-shift correlations were performed with proton observation A. A. Maudsley, R. R. Ernst, *Chem. Phys. Lett. 50* (1977) 368; A. A. Maudsley, L. Müller, R. R. Ernst, *J. Magn. Reson. 28* (1977) 463; b) application of this method for the indirect measurement of the ^{103}Rh-resonance via two-dimensional, correlated ^{1}H,^{103}Rh-spectroscopy: R. Benn, unpublished; see also R. Benn, H. Brennecke, A. Rufińska, *J. Organomet. Chem.* (1986), in press [137c].
[48] If the insensitive X-nucleus has a low natural abundance (e.g. ^{13}C, ^{57}Fe), the indirect detection of its signal through the ^{1}H FID has to cope with the problem of the elimination of intensive ^{1}H-NMR signals of sites with magnetically inactive X-nuclei. The suppression of such signals using phase cycling is described by G. Bodenhausen, D. J. Ruben, *Chem. Phys. Lett. 69* (1980) 185; A. Bax, R. H. Griffey, B. L. Hawkins, *J. Magn. Reson. 55* (1983) 301 and, using presaturation through proton noise decoupling, by D. Neuhaus, J. Keeler, R. Freeman, *ibid. 61* (1985) 553.
[49] J. A. Cabeza, B. E. Mann, C. Brevard, P. M. Maitlis, *J. Chem. Soc. Chem. Commun. 1985*, 65.
[50] a) E. D. Becker, J. A. Foretti, T. C. Farrow, *J. Am. Chem. Soc. 91* (1969) 7784; b) J. S. Waugh, *J. Mol. Spectrosc. 35* (1970) 298.
[51] a) A. Schwenk, *Z. Phys. 213* (1968) 482; b) *Phys. Lett. A 31* (1970) 513; c) *J. Magn. Reson. 5* (1971) 376; d) *Prog. Nucl. Magn. Reson. Spectrosc. 17* (1985) 69.
[52] a) R. K. Harris: *Nuclear Magnetic Resonance Spectroscopy*, Pitman, London 1983; b) see also [13e], p. 313–315.
[53] J. M. Robert, R. E. Evilia, *J. Am. Chem. Soc. 107* (1985) 3733.
[54] E. Fukushima, S. B. W. Roeder, *J. Magn. Reson. 33* (1979) 199.
[55] C. H. A. Seiter, G. W. Feigenson, S. I. Chan, M.-C. Hsu, *J. Am. Chem. Soc. 94* (1972) 2535.
[56] a) C. Brevard in [5c] p. 22; b) G. A. Morris, M. J. Toohey, *J. Magn. Reson. 63* (1985) 629.
[57] D. Canet, J. Brondeau, J. P. Marchal, B. Robien-Lherbier, *Org. Magn. Reson. 20* (1982) 51.
[58] S. Patt, *J. Magn. Reson. 49* (1982) 161.
[59] D. T. Pegg, M. R. Bendall, *J. Magn. Reson. 55* (1983) 51.
[60] D. T. Pegg, M. R. Bendall, *J. Magn. Reson. 58* (1984) 14.
[61] D. P. Burum, *J. Magn. Reson. 59* (1984) 430.
[62] M. R. Bendall, D. T. Pegg, G. M. Tyburn, C. Brevard, *J. Magn. Reson. 55* (1983) 322.
[63] K. M. Mackay, P. J. Watkinson, A. L. Wilkins, *J. Chem. Soc. Dalton Trans. 1984*, 133.
[64] For the reverse experiment, namely polarization transfer from quadrupolar nuclei to Spin-1/2 nuclei see, for example, P. L. Rinaldi, N. J. Baldwin, *J. Am. Chem. Soc. 105* (1983) 7523; *J. Magn. Reson. 61* (1985) 165; N. Chandrakumar, *ibid. 60* (1984) 28.
[65] a) T. L. Venables, W. C. Hutton, R. N. Grimmes, *J. Am. Chem. Soc. 104* (1982) 4716; b) *ibid. 106* (1984) 29; c) R. Köster, G. Seidel, B. Wrackmeyer, *Angew. Chem. 96* (1984) 520; *Angew. Chem. Int. Ed. Engl. 23* (1984) 512; d) H. Günther, D. Moskau, R. Dujardin, A. Maerker, *Tetrahedron Lett. 27* (1986) 2251.
[66] N. F. Ramsey, *Phys. Rev. 78* (1950) 689.
[67] For a review of the NMR-spectroscopy of transition metals see: R. G. Kidd, *Annu. Rep. NMR Spectrosc. 10 A* (1980) 1; J. J. Dechter, *Prog. Inorg. Chem. 33* (1985) 393; see also [5].
[68] For a review on the NMR-spectroscopy of main group elements cf.: J. J. Dechter, *Prog. Inorg. Chem. 29* (1982) 285; see also [5].
[69] J. S. Griffith, L. E. Orgel, *Trans. Faraday Soc. 53* (1957) 601.
[70] With respect to the problems encountered here see [5b] p. 41 f.
[71] See [5a], p. 4–8; [5b] p. 43; W. McFarlane, *Proc. R. Soc. London Ser. A 306* (1968) 185; R. K. Harris, B. J. Kimber, *J. Magn. Reson. 17* (1975) 174; S. Brownstein, J. Bornais, *ibid. 38* (1980) 131.
[72] a) P. Laszlo in [5c] p. 261; b) C. Detellier in [5d] *Vol. 2*, p. 105; c) see also [68]; d) for ^{6}Li and ^{7}Li: G. Fraenkel, H. Hsu, B. M. Su in R. O. Bach (Ed.): *Lithium*, Wiley, New York 1985, p. 273; J. F. McGarrity, C. A. Ogle, Z. Birch, H. R. Loosli, *J. Am. Chem. Soc. 107* (1985) 1810.
[73] a) O. Lutz in [5c] p. 297; see also [68]; b) M. Jaber, G. Thomas-David, *Bull. Soc. Chim. Fr. 1985*, 644; c) D. F. Gaines, K. M. Coleson, D. F. Hillenbrand, *J. Magn. Reson. 44* (1981) 84.
[74] a) T. Drakenberg, S. Forsén in [5c] p. 309; b) K. J. Neurohr, T. Drakenberg, S. Forsén in [5d] *Vol. 2*, p. 231.
[75] S. Forsén, B. Lindman, *Annu. Rep. NMR Spectrosc. 11 A* (1981) 183.

[76] P. Bougeard, M. Mancini, B. G. Sayer, M. J. McGlinchey, *Inorg. Chem. 24* (1985) 93.

[77] W. J. Evans, J. H. Meadows, A. G. Kostka, G. L. Closs, *Organometallics 4* (1985) 324.

[78] D. Rehder, *Bull. Magn. Reson. 4* (1982) 33.

[79] a) B. P. Shehan, M. Kony, R. T. C. Brownlee, M. J. O'Connor, A. G. Wedd, *J. Magn. Reson. 63* (1985) 343; R. T. C. Brownlee, M. J. O'Connor, B. P. Shehan, A. G. Wedd, *ibid. 61* (1985) 516, and references cited therein; b) P. Granger in [5d] *Vol. 2*, p. 396.

[80] a) R. L. Keiter, D. G. Vander Velde, *J. Organomet. Chem. 258* (1983) C 34, and references cited therein; b) P. Granger in [5d] *Vol. 2*, p. 402; for ^{53}Cr, ^{95}Mo, ^{97}Mo and ^{183}W: M. Minelli, J. H. Enmark, R. T. C. Brownlee, M. J. O'Connor, A. G. Wedd, *Coord. Chem. Rev. 68* (1985) 169.

[81] a) D. Rehder, *Magn. Reson. Rev. 9* (1984) 125; b) G. Doyle, B. T. Heaton, E. Occhiello, *Organometallics 4* (1985) 1224.

[82] a) P. M. Henrichs in [5d] *Vol. 2*, p. 319; b) S. S. D. Brown, I. J. Colquhoun, W. McFarlane, M. Murray, I. D. Salter, V. Sik, *J. Chem. Soc. Chem. Commun. 1986*, 53.

[83] a) G. K. Kaarson, P. A. W. Dean, *Inorg. Chim. Acta 66* (1982) 157; b) D. Köhnlein, O. Lutz, P. Ruppert, *J. Magn. Reson. 57* (1984) 486.

[84] a) P. D. Ellis in [5c] p. 457; b) I. M. Armitage, Y. von Boulanger in [5d] Vol. 2, p. 337; c) D. H. Live, C. L. Kojiro, D. Cowburn, J. L. Markley, *J. Am. Chem. Soc. 107* (1985) 3043; d) M. H. Frey, G. Wagner, M. Vašák, O. W. Sorensen, D. Neuhaus, E. Wörgötter, J. H. R. Kogi, R. r. Ernst, K. Wüttrich, *J. Am. Chem. Soc. 107* (1985) 6847.

[85] R. G. Kidd in [5c] p. 329; see also [68].

[86] a) J. F. Hinton, *TrAC Trends Anal. Chem. Pers. Ed. 1* (1981/1982) 288; b) J. F. Hinton, K. R. Metz, R. W. Briggs, *Annu. Rep. NMR Spectrosc. 13* (1982) 211; c) J. F. Hinton, K. R. Metz in [5d] *Vol. 2*, p. 367.

[87] a) R. K. Harris in [5c] p. 343; b) see also [68]; c) B. Coleman in [5d] *Vol. 2*, p. 197.

[88] a) R. Hani, R. A. Geanangel, *Coord. Chem. Rev. 44* (1982) 229; b) M. Pereyre, J. P. Quintard, A. Rahm, *Pure Appl. Chem. 54* (1982) 29; c) B. Wrackmeyer, *Annu. Rep. NMR Spectrosc. 16* (1985) 73.

[89] R. G. Kidd in [5c] p. 379; see also [68].

[90] K. Morgan, B. G. Sayer, G. J. Schrobilgen, *J. Magn. Reson. 52* (1983) 139.

[91] See K. Ziegler, H. Lehmkuhl in: *Houben-Weyl-Müller: Methoden der Organischen Chemie, Band XIII/4*, Thieme, Stuttgart 1970.

[92] R. Benn, A. Rufińska, H. Lehmkuhl, E. Jansen, C. Krüger, *Angew. Chem. 95* (1983) 808; *Angew. Chem. Int. Ed. Engl. 22* (1983) 779.

[93] a) S. J. Rettig, A. Storr, B. S. Thomas, J. Trotter, *Acta Crystallogr. B 30* (1974) 666; b) R. A. Forder, K. Prout, *ibid. B 30* (1974) 2312; c) Y. Kai, N. Yasuoka, N. Kasai, M. Kakudo, *Bull. Chem. Soc. Jpn. 45* (1972) 3397.

[94] M. R. P. van Vliet, B. Buysingh, G. van Koten, K. Vrieze, B. Kojie-Prodic, A. L. Spek, *Organometallics 4* (1985) 1701; for the interpretation of NMR spectroscopic data see also [95].

[95] R. Benn, A. Rufińska, E. Janssen, H. Lehmkuhl, *Organometallics 5* (1986) 825.

[96] a) R. Benn, A. Rufińska, E. Janssen, H. Lehmkuhl, unpublished; b) For recent ^{27}Al-NMR data of organoaluminum compounds see also: H. H. Karsch, A. Appelt, F. H. Köhler, G. Müller, *Organometallics 4* (1985) 231; V. V. Gavrilenko, M. I. Vinnikova, V. A. Antonovich, L. I. Zakharkin, *Bull. Acad. Sci. USSR Div. Chem. Sci. (Engl. Transl.) 1982*, 2084.

[97] a) R. Köster in: *Houben-Weyl-Müller: Methoden der Organischen Chemie, Band XIII/3A*, Thieme, Stuttgart 1982, p. 602; b) R. Köster, J. Serwatowski, *XIV. Pol. GDR Colloq. Organomet. Chem.* (Stara Wieś, Poland 1984) Abstracts p. 13.

[98] H. Sato, R. Taro, H. Higashi, *Bull. Chem. Soc. Jpn. 42* (1969) 1588.

[99] a) E. G. Hoffmann, *Justus Liebigs Ann. Chem. 629* (1960) 104; b) O. T. Beachley, K. C. Racette, *Inorg. Chem. 15* (1976) 2110.

[100] T. Mole, E. A. Jeffery: *Organoaluminium Compounds*, Elsevier, Amsterdam 1972, p. 218.

[101] K. H. Thiele, *Z. Anorg. Allgem. Chem. 349* (1967) 33.

[102] a) D. C. Bradley, *Adv. Inorg. Chem. Radiochem. 15* (1972) 266; b) O. Kříž, B. Čásenský, A. Lyčka, J. Fusek, S. Heřmánek, *J. Magn. Reson. 60* (1984) 375.

[103] K. Nützel in: Houben-Weyl-Müller: Methoden der Organischen Chemie, Band XIII/2a, Thieme, Stuttgart 1973.

[104] R. Benn, H. Lehmkuhl, K. Mehler, A. Rufińska, *Angew. Chem. 96* (1984) 521; *Angew. Chem. Int. Ed. Engl. 23* (1984) 534.

[105] H. Lehmkuhl, K. Mehler, R. Benn, A. Rufińska, C. Krüger, *Chem. Ber. 119* (1986) 1054.

[106] E. C. Ashby, *Q. Rev. Chem. Soc. 21* (1967) 59.

[107] F. Schröder, L.-H. Spandau, *Naturwissenschaften 53* (1966) 360.

[108] D. F. Evans, G. V. Fazakerley, *J. Chem. Soc. A 1971*, 184.

[109] Synthesis of **35**, **41**, **47**: C.-P. Morley, P. Jutzi, unpublished.

[110] See also the references cited in [104] and [105].

[111] M. Schlosser, M. Stähle, *Angew. Chem. 92* (1980) 497; *Angew. Chem. Int. Ed. Engl. 19* (1980) 487.

[112] T. Clark, C. Rhode, P. von R. Schleyer, *Organometallics 2* (1983) 1344.

[113] Pentacoordinated organomagnesium compounds: a) M. Vallino, *J. Organomet. Chem. 20* (1969) 1; b) Y. Kai, N. Kanehisa, K. Miki, N. Kasai, K. Mashima, H. Yasuda, A. Nakamura, *Chem. Lett. 1982*, 1277; c) H. Lehmkuhl, K. Mehler, R. Benn, A. Rufińska, G. Schroth, C. Krüger, *Chem. Ber. 117* (1984) 389.

[114] a) R. Benn, H. Lehmkuhl, K. Mehler, A. Rufińska, *J. Organomet. Chem. 293* (1985) 1; b) e.g. Et_2Mg: $\delta(C_\alpha) = -2.12$, $\delta(C_\beta) = 14.26$ and Cp_2Mg: $\delta(Cp) = 105.80$ with EtMgCp: $\delta(C_\alpha) = -1.36$, $\delta(C_\beta) = 14.26$, $\delta(Cp) = 104.30$ (100.6 MHz, $T = 310$ K, [D$_8$]THF ($\delta_{C_\alpha} \equiv 67.40$)).

[115] R. G. Kidd, R. W. Matthews, H. G. Spinney, *J. Am. Chem. Soc. 94* (1972) 6686.

[116] N. Hao, B. G. Sayer, G. Dénès, D. G. Bickley, C. Detellier, M. J. McGlinchey, *J. Magn. Reson. 50* (1982) 50.

[117] P. G. Gassman, W. H. Campbell, D. W. Macomber, *Organometallics 3* (1984) 385.

[118] A. Dormond, M. Fauconet, J. C. Leblanc, C. Moise, *Polyhedron 3* (1984) 897.

[119] M. J. McGlinchey, D. G. Bickley, *Polyhedron 4* (1985) 1147.

[120] B. G. Sayer, N. Hao, G. Dénès, D. G. Bickley, M. J. McGlinchey, *Inorg. Chim. Acta 48* (1981) 53.

[121] B. G. Sayer, J. I. A. Thompson, N. Hao, T. Birchall, D. R. Eaton, M. J. McGlinchey, *Inorg. Chem. 20* (1981) 3748.

[122] a) R. Benn, A. Rufińska, *J. Organomet. Chem. 273* (1984) C 51; b) R. Benn, A. Rufińska, unpublished.

[123] P. Bougeard, J. J. McCullough, B. G. Sayer, M. J. McGlinchey, *Inorg. Chim. Acta 89* (1984) 133.

[124] Cf. a) C. Krüger, G. Müller, G. Erker, U. Dorf, K. Engel, *Organometallics 4* (1985) 215; b) G. Erker, C. Krüger, G. Müller, *Adv. Organomet. Chem. 24* (1985) 1.

[125] a) G. Erker, J. Wicher, K. Engel, F. Rosenfeldt, W. Dietrich, C. Krüger, *J. Am. Chem. Soc. 102* (1980) 6344; b) R. Benn, G. Schroth, *J. Organomet. Chem. 228* (1982) 71; c) H. Yasuda, Y. Kajihara, K. Mashima, K. Nagasuna, K. Lee, A. Nakamura, *Organometallics 1* (1982) 388.

[126] J. W. Lauher, R. Hoffmann, *J. Am. Chem. Soc. 98* (1976) 1729.

[127] T. A. Albright, *Tetrahedron 38* (1982) 1339.

[128] K. Tatsumi, H. Yasuda, A. Nakamura, *Isr. J. Chem. 23* (1983) 145.

[129] M. R. M. Bruce, A. Kenter, D. R. Tyler, *J. Am. Chem. Soc. 106* (1984) 639.

[130] G. Erker, K. Berg, R. Benn, G. Schroth, *Chem. Ber. 118* (1985) 1383.

[131] G. Wilke, *Fundam. Res. Homogeneous Catal. 3* (1979) 1.

[132] A. A. Koridze, P. V. Petrovskii, S. P. Gubin, E. I. Fedin, *J. Organomet. Chem. 93* (1975) C 26.

[133] a) T. Jenny, W. von Philipsborn, J. Kronenbitter, A. Schwenk, *J. Organomet. Chem. 205* (1981) 211; b) W. von Philipsborn, *Pure Appl. Chem. 58* (1986) 513.

[134] a) E. Haslinger, W. Robien, K. Schlögl, W. Weissensteiner, *J. Organomet. Chem. 218* (1981) C 11; b) E. Haslinger, K. Koci, W. Robien, K. Schlögl, *Monatsh. Chem. 114* (1983) 495.

[135] a) A. A. Koridze, N. M. Astakhava, P. V. Petrovskii, *Izv. Akad. Nauk SSSR Ser. Khim. 1982*, 956, 957.

[136] T. Nozawa, M. Sato, M. Hatano, N. Kobayashi, T. Osa, *Chem. Lett. 1983*, 1289.

[137] a) H. C. Lee, J. K. Gard, T. L. Brown, E. Oldfield, *J. Am. Chem. Soc. 107* (1985) 4087; b) L. Baltzer, E. D. Becker, R. G. Tschudin, O. A. Gansow, *J. Chem. Soc. Chem. Commun. 1985*, 1040; c) R. Benn, C. Brevard, *J. Am. Chem. Soc. 108* (1986), 5622.

[138] Y. S. Sohn, D. N. Hendrickson, H. B. Gray, *J. Am. Chem. Soc. 93* (1971) 3603.

[139] C. Brevard, P. Granger, *J. Chem. Phys. 75* (1981) 4175.

[140] R. W. Dykstra, A. M. Harrison, *J. Magn. Reson. 46* (1982) 338.

[141] C. Brevard, P. Granger, *Inorg. Chem. 22* (1983) 532.

[142] a) P. Bernhard, L. Helm, A. Ludi, A. E. Merbach, *J. Am. Chem. Soc. 107* (1985) 312; b) P. J. Steel, F. Lahousse, D. Lerner, C. Marzin, *Inorg. Chem. 22* (1983) 1488.

[143] W. Sahm, A. Schwenk, *Z. Naturforsch. A 29* (1974) 1763.

[144] For methodology see: a) [12, 28a, 28b, 35, 37, 47b]; b) K.-D. Grüninger, A. Schwenk, B. E. Mann, *J. Magn. Reson. 41* (1980) 354; B. E. Mann in [5d] *Vol. 2*, p. 301.

[145] Direct ^{103}Rh measurements of inorganic compounds: a) E. B. Boyar, S. D. Robinson, *Inorg. Chim. Acta 64* (1982) L193; b) B. E. Mann, C. M. Spencer, *ibid. 65* (1982) L 57; c) *ibid. 76* (1983) L65.

[146] ^{103}Rh.NMR measurements of clusters: a) O. A. Gansow, D. S. Gill, F. J. Bennis, J. R. Hutchison, J. L. Vidal, R. C. Schoening, *J. Am. Chem. Soc. 102* (1980) 2449; b) L. Garlaschelli, A. Fumagalli, S. Martinengo, B. T. Heaton, D. O. Smith, L. Strona, *J. Chem. Soc. Dalton Trans. 1982*, 2265; c) B. T. Heaton, R. D. Pergola, L. Strona, L. Garlaschelli, U. Satorelli, J. H. Sadler, *ibid. 1983*, 173; d) S. Aime, *Inorg. Chim. Acta 62* (1982) 51.

[147] ^{103}Rh-NMR measurements of organorhodium compounds:a) M. Cocivera, G. Ferguson, F. J. Lalor, P. Szczecinski, *Organometallics 1*

(1982) 1139; b) A. Salzer, T. Egolf, W. von Philipsborn, *Helv. Chim. Acta 65* (1982) 1145; c) M. Cocivera, A. J. McAlees, R. McCrindle, P. Szczecinski, *J. Organomet. Chem. 235* (1982) 97; d) R. Bonnaire, D. Davoust, N. Platzer, *Org. Magn. Reson. 22* (1984) 80; e) see also [18b, 28b, 149, 155].

[148] R. Benn, K. Cibura, P. Hofmann, K. Jonas, A. Rufińska, *Organometallics 4* (1985) 2214.

[149] T. Egolf, *Dissertation*, Universität Zürich 1983.

[150] a) H. Bönnemann, W. Brijoux, R. Brinkmann, W. Meures, R. Mynott, W. von Philipsborn, T. Egolf, *J. Organomet. Chem. 272* (1984) 231; b) H. Bönnemann, *Angew. Chem. 97* (1985) 264; *Angew. Chem. Int. Ed. Engl. 24* (1985) 248.

[151] ^{59}Co-NMR data of organocobalt complexes: R. Benn, R. Mynott, A. Rufińska, unpublished, see also [148, 150].

[152] P. Galow, A. Sebald, B. Wrackmeyer, *J. Organomet. Chem. 259* (1983) 253.

[153] These shift changes can also be explained by participation of 16-electron (η^3-allyl-bound indenyl structures); see X-ray data of [Co(η^4-cod)(η^5-indenyl)]: in H. Bönnemann, W. Brijoux, *Aspects on Homogeneous Catal. 5* (1984) 94.

[154] a) H. Yamazaki, N. Hagihara, *J. Organomet. Chem. 21* (1970) 431; b) *7* (1967) P22; c) K. P. C. Vollhardt, *Acc. Chem. Res. 10* (1977) 1; d) *Angew. Chem. 96* (1984) 525; *Angew. Chem. Int. Ed. Engl. 23* (1984) 539; e) references cited in [151, 153].

[155] E. Maurer, S. Rieker, M. Schollbach, A. Schwenk, T. Egolf, W. von Philipsborn, *Helv. Chim. Acta 65* (1982) 26.

[156] a) R. Freeman, G. R. Murray, R. E. Richards, *Proc. R. Soc. A 242* (1957) 455; b) R. L. Martin, A. H. White, *Nature (London) 223* (1969) 394; c) S. Fujiwara, F. Yajima, A. Yamasaki, *J. Magn. Reson. 1* (1969) 203; d) R. Bramley, M. Brosron, A. M. Sargeson, C. E. Schäffer, *J. Am. Chem. Soc. 107* (1985) 2780.

[157] K. Jonas, *Angew. Chem. 97* (1985) 292; *Angew. Chem. Int. Ed. Engl. 24* (1985) 295.

[158] a) R. Hoffmann, *J. Chem. Phys. 39* (1963) 1397; b) P. Hofman, M. Padmanabhan, *Organometallics 2* (1983) 1273.

[159] P. S. Pregosin, *Coord. Chem. Rev. 44* (1982) 247.

[160] For reviews on ^{195}Pt-NMR spectroscopy see: [5a] p. 249; [5c] p. 445f; [67]; P. S. Pregosin, *Ann. Rep. NMR Spectrosc. 17* (1986) 285.

[161] J. J. Pesek, W. R. Mason, *J. Magn. Reson. 25* (1977) 519.

[162] D. M. Doddrell, P. F. Barron, D. E. Clegg, C. Bowie, *J. Chem. Soc. Chem. Commun. 1982*, 575.

[163] Y. Koie, S. Shinode, Y. Saito, *J. Chem. Soc. Dalton Trans. 1981*, 1082.

[164] I. Georgii, B. E. Mann, B. F. Taylor, A. Musco, *Inorg. Chim. Acta 86* (1984) L81.

[165] P. S. Pregosin, S. N. Sze, P. Salvadori, R. Lazzaroni, *Helv. Chim. Acta 60* (1977) 2514.

[166] R. Benn, R.-D. Reinhardt, A. Rufińska, *J. Organomet. Chem. 282* (1985) 291.

[167] Cf. W. Mayer, G. Wilke, R. Benn, R. Goddard, C. Krüger, *Monatsh. Chem. 116* (1985) 879.

[168] For the corresponding Pd complexes see: P. W. Jolly, *Angew. Chem. 97* (1985) 279; *Angew. Chem. Int. Ed. Engl. 24* (1985) 283.

[169] C. Brown, B. T. Heaton, A. D. C. Towl, P. Chini, A. Fumagalli, G. Longoni, *J. Organomet. Chem. 181* (1979) 233.

[170] C. Brevard, R. Schimpf, G. Tourne, C. M. Tourne, *J. Am. Chem. Soc. 105* (1983) 7059.

[171] P. Domaille, *J. Am. Chem. Soc. 106* (1984) 7677.

[172] H. Schumann, H.-J. Kroth, *Z. Naturforsch. B 32* (1977) 768.

[173] N. Hao, M. J. McGlinchey, B. G. Sayer, G. J. Schrobilgen, *J. Magn. Reson. 46* (1982) 158.

[174] P. W. Jolly, G. Wilke: *The Organic Chemistry of Nickel, Vol. 1, 2*, Academic Press, New York 1974.

[175] R. Benn, A. Rufińska, to be published.

[176] a) N. Rösch, R. Hoffmann, *Inorg. Chem. 13* (1974) 2656; b) T. A. Albright, J. K. Burdett, M.-H. Whangbo: *Orbital Interactions in Chemistry*, Wiley, New York 1985.

[177] G. Wilke, B. Bogdanović, P. Hardt, P. Heimbach, W. Keim, M. Kröner, W. Oberkirch, K. Tanaka, E. Steinrücke, D. Walter, H. Zimmermann, *Angew. Chem. 78* (1966) 157; *Angew. Chem. Int. Ed. Engl. 5* (1966) 151.

[178] G. Wilke, *J. Organomet. Chem. 200* (1980) 157.

[179] a) See also [174] p. 329f; b) R. Goddard, C. Krüger, F. Mark, R. Stansfield, X.-S. Zhang, *Organometallics 4* (1985) 285; c) G. C. Hancock, N. M. Kostić, R. F. Fenske, *ibid. 2* (1983) 1089.

[180] C. Krüger, M. Rubach, unpublished.

[181] B. Henc, P. W. Jolly, R. Salz, G. Wilke, R. Benn, E. G. Hoffmann, R. Mynott, G. Schroth, K. Seevogel, J. C. Sekutowski, C. Krüger, *J. Organomet. Chem. 191* (1980) 425.

Geometric and Topological Thinking in Organic Chemistry

By Nicholas J. Turro*

The beginning student of organic chemistry is often bewildered by what appears to be an enormous maze of random structural variations and reactions that can be mastered only by tedious memorization. To the organic chemist, however, the same subject is often a beautifully ordered discipline of elegant simplicity. An important value of learning organic chemistry is the mastering of "organic thinking," an approach to intellectual processing whereby the "sameness" of many families of structures and reactions is revealed. This article offers the author's personal views of organic thinking and explores the intellectual and scientific foundations of organic chemistry and of the powerful methods that provide the field with a platform for making rapid conceptual and experimental advances. It is proposed that these methods involve a geometric and topological approach to scientific reasoning within the framework of scientific paradigms that guide experimental design and execution. The basis of this approach is considered in relation to day-to-day thinking, problem solving, and the psychological drive for intellectual closure. The power of the approach is illustrated by the analysis of several photochemical and chemiluminescent reactions.

1. Introduction—Intellectual Processing

1.1. Intellectual Processing, Problem Solving, and Closure

Normal day-to-day mental activity and learning involve a high degree of intellectual processing directed toward problem solving. Difficulties arise with the recognition of ambiguities that result from the existence of many possible solutions. These ambiguities and the recognition of potential deficiencies or conflicts associated with the selection of a single solution can give rise to anxiety and tension. On the other hand, the process of "closing out" a problem intellectually is a pleasant and reinforcing experience.

Figure 1 schematically depicts some relationships among the components involved in intellectual processing.[1,2] The phenomena (facts or events) in the world around us generate a set of beliefs. Intellectual processing involves preservation, rearrangement, or modification of these beliefs. Successful problem solving and concomitant closure reinforce beliefs and breed satisfaction. Failure to resolve problems breeds tension and conflict because of the implication that beliefs may be incomplete or incorrect. One may hypothesize that the dominant principle driving intellectual processes is a *Law of Intellectual Closure*:[2] intellectual processing is naturally driven toward as *closed* a mental state as circumstances permit. The origin of such a law could be traced to its survival value and the associated evolution of an appropriate genetic composition and constitution of the human brain.[3] The intellectual process of closure involves the goal of achieving a complete, stable, and self-consistent interpretation of a phenomenon or event. For example, an unfinished act tends to be mentally completed, an ambiguous object tends to be interpreted in terms of its familiar aspects, a word, an object, or a situation is perceived in a manner that allows achievement of a closed interpretation.

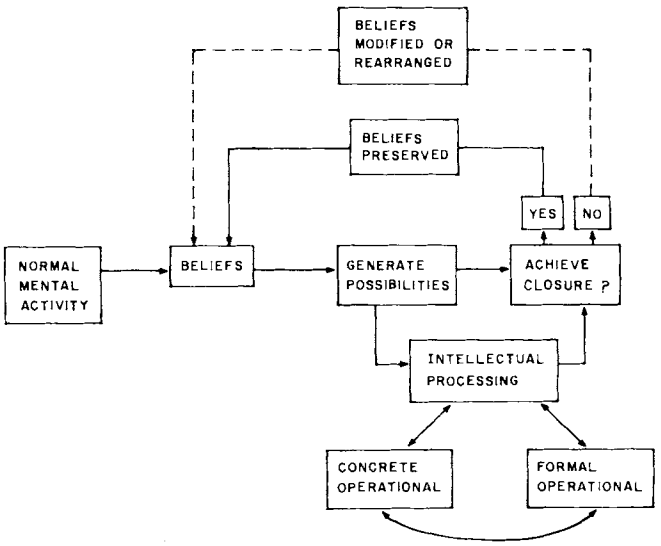


Fig. 1. A schematic representation of normal intellectual activity showing the interplay of beliefs, possibilities, closure, and intellectual processing (cf. Fig. 4).

Much of the learning experience consists of the process of resolving conflicts among related beliefs. Learning is facilitated and even made enjoyable by artificially creating intellectual conflicts that can be resolved to a high degree of closure. Students who learn to tolerate the tension that normally accompanies the process of resolving such intellectual conflicts often feel an excitement that is stimulating and rewarding in itself. Indeed, the development of an ability to tolerate tension during the activity of problem solving is important to the learning process. Intellectual processing that involves the achievement of problem definition and problem solution with a high degree of intellectual closure is naturally attractive and readily adopted. A

[*] Prof. N. J. Turro
Department of Chemistry, Columbia University
New York, NY 10027 (USA)

major aim of many motivational programs for learning is to promote the visibility of "living examples" of successful behavior or accomplishment and to suppress that of counterexamples.[2] This theme will reappear in the discussion of scientific paradigms (Section 3.3). Let us now consider two general and important classifications of intellectual processing that are employed in day-to-day thinking.

1.2. Concrete and Formal Operational Intellectual Processing

According to *Piaget*,[4] two distinct stages of intellectual development may be characterized, namely, *concrete operational* (typical of children from 6 to 12 years of age) and *formal operational* (typical of children from 11 to 16 years of age). In Figure 1, these stages may be viewed as alternative mechanisms for intellectual processing. During the concrete operational period, intellectual processing involving the logic of real (concrete) objects is mastered. This period is characterized by accepting concrete objects or events in the immediate present with little extrapolation to what hypothetically is possible in the future or was possible in the past. During the formal operational period, intellectual processing involving the generation and manipulation of possible combinations of objects and events is mastered. In this period, the mind becomes capable of extrapolating from objects and events in the immediate present to objects and events that are hypothetically possible.

At the concrete operational level, reality is accepted as it is found, perhaps without recognition that alternatives exist (for example, young children often may fail to acknowledge another's point of view because they do not consider the possibility that other points of view exist!). At the formal operational level, on the other hand, the recognition of competing possibilities often brings with it an ambiguity that may be psychologically unsettling. However, this uncomfortable feeling of ambiguity may be relieved and converted into a feeling of excitement by resorting to operations that solve problems effectively and thereby achieve intellectual closure. Let us now consider how geometry can assist thinking at either the concrete operational or formal operational levels.

1.3. The Role of Geometry in Intellectual Processing

Many of the beliefs that are employed in intellectual processing may be viewed as containing information, which, in turn, can be represented by concrete or abstract *forms*. According to *Thom*,[3a] there is a natural tendency of the mind to give the form or shape of an object some intrinsic meaning:

> ... our perceptual organs are genetically developed as to detect the living beings that play a large role, as prey or predators, in our survival and in the maintenance of our psychological equilibrium. It is clear that some forms have special value for us or are biologically important, for example, the shapes of foods, of animals, of tools. These forms are genetically imprinted into our understanding of space, and ... are narrowly and strictly adapted to them.

During the process of evolution of the brain, it is plausible that, since forms of information (beliefs) were generated from the stimuli provided by the environment in which we are embedded, the recognition of forms in terms of a three-dimensional (3-D) geometry had survival value and led to the development of perceptual receptors in the brain that are particularly suited to embrace and process 3-D geometric forms.[3] If so, facile recognition of 3-D geometric forms is genetically embedded into our ability to intellectualize and to understand space. It is easy to appreciate, therefore, how the use of geometry, with its powerful methods for processing geometric structures and its logical and internally consistent mathematical basis, both of which facilitate closure, can take on enormous importance as a vehicle for intellectual processing.

The notion that geometric thinking involves only 3-D forms, which correspond to figures in Euclidean geometry, is too restrictive, however. The geometric thinking that the author has in mind is much more "elastic" and general than that allowed by the rules of Euclidean geometry. An appreciation of what is meant by this elastic geometry may be obtained by considering some aspects of a branch of mathematics termed *topology*.[5]

2. Euclidean and Topological Geometry

2.1. Topology and Topological Geometry

Topology is a branch of mathematics concerned with the "sameness" of mathematical forms. Topology provides a basis for determining whether two mathematical forms are the same or not via a mapping procedure that attempts to place the topologically relevant properties of one form onto a second form.

Topology may be described as "rubber sheet" geometry.[6] This definition emphasizes the elasticity of the concepts of topology, which is concerned, in general, only with very fundamental geometric properties. Topological properties may be visualized as those geometric properties of a figure on a rubber sheet that are conserved upon twisting and stretching, such as the connectivity, the sequence, and the continuity of points. It is easy to visualize the continuous mapping of a figure on a rubber sheet onto the new image of the figure generated as a result of elastic twisting or stretching. No topological features of the figure are created or destroyed by the twisting or stretching process. However, tearing or joining parts of the original figure is not allowed, since this creates new topological properties and does not conserve the initial topological properties.

The model of the geometric figure on a rubber sheet provides the flavor of topological geometry, which emphasizes the possible rather than the concrete, an important feature of formal operational thinking. Euclidean geometry, on the other hand, emphasizes figures exactly as they are perceived, the essence of concrete operational thinking. Topological geometry considers geometric figures as they might be transformed by mapping procedures that conserve fundamental topological properties. To obtain a further appreciation for topological geometry, let us further compare

its essential features to the more familiar Euclidean geometry.

2.2. Comparison of Euclidean and Topological Geometry

Euclidean geometry is the study of certain properties of figures in space.[7] To a geometrician not all properties of a figure are of interest, only the geometric properties. What is a pertinent geometric property? In Euclidean geometry the key idea is that of *geometrically equivalent or congruent figures*. Two figures are called congruent if an intellectual transformation or mapping allows one figure to be "placed on the other" so that the two figures exactly coincide in all geometric properties. A geometric property of a figure is a property shared by every congruent figure.

Topological geometry also involves the study of certain properties of figures in space. Not all properties of a figure are of interest, only the topological properties. What is a pertinent topological property? In topology the key idea is that of *topologically equivalent or homeomorphic figures*. Two figures are called homeomorphic if an intellectual transformation or mapping allows one figure to be "placed on the other" so that the two figures exactly coincide in all topological properties. A topological property is one shared by every homeomorphic figure.

In Euclidean geometry, how do we "place one figure on another"? How can we move a figure? How can we conserve its geometric properties during the movement? The sameness or identity of geometric figures is established by transformations termed *isometries*. An isometry is an intellectual transformation that conserves the size and shape of a geometric figure. The three common isometries of Euclidean geometry are rotation, translation, and reflection. Shapes that are recognized to be the same by isometric transformations are termed *congruent*. In Euclidean geometry, we are allowed to move a figure only by applying motions that do not change the distance and angle relationships between any two points of the figure. Thus, the geometric properties of interest are those that are invariant during such motions. Euclidean geometric figures are characterized by rigidity owing to their characteristic metric (measurable) properties, such as the lengths and areas of sides and the angles between sides. A requirement of Euclidean figures is that motion of the figure in three-dimensional space cannot change its metric properties.

Euclidean figures may be similar but not identical, i.e., two figures may have the same shape but different sizes.

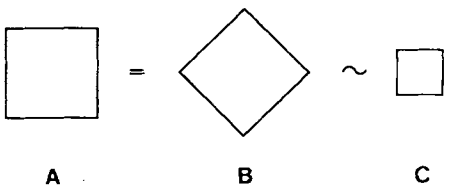


Fig. 2. Congruent (A and B) and similar (A and C, B and C) Euclidean geometric figures.

For example, **A** (Fig. 2) is a square whose sides are the same length as those of **B**. **A** and **B** are the same figure in Euclidean geometry, because they are congruent. **C** is a smaller square which is similar but not congruent to **A** and **B**.

Topological figures may be of different size and shape yet topologically equivalent (i.e., homeomorphic). For example, **D**, **E**, **F**, and **G** (Fig. 3) are all homeomorphic, because the points of any one figure may be continuously mapped onto those of the others by elastic motions that conserve sequence and connectivity. The differing size and shape of the figures is of no topological importance. Thus, **D**, **E**, **F**, and **G** are the same figures in topological geometry, because they are homeomorphic. Topological geometric figures are characterized by elasticity and complete lack of fixed metric properties such as lengths, areas, and angles. In terms of the rubber sheet analogy, elastic distortions of such figures do not change topological geometric properties such as the connectivity of points or the existence of an inside and an outside. Thus, in spite of the wide variation in appearance, **D**, **E**, **F**, and **G** are the same figures topologically in that they are closed simple curves, having an inside, an outside, and a boundary.

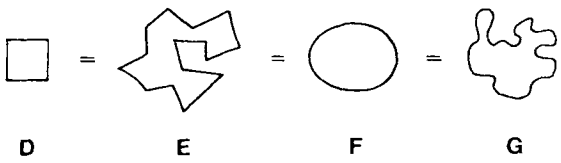


Fig. 3. Homeomorphic topological geometric figures.

The search for sameness in structural representations of objects is a crucial feature of geometric thinking. Given two structural representations of objects, how is it established whether the objects are identical or different? As may be inferred from the previous discussion, the terms identical and different need to be qualified. If we are interested in sameness in geometry, we must specify the level of sameness (topological or Euclidean, congruent or similar). In each case, however, the intellectual process of analyzing sameness can be viewed as a mapping procedure. In mathematics, the term *transformation* is used for such mapping. A mathematical transformation R→P (or its inverse R←P) may conserve certain topological properties or Euclidean properties. Sameness implies that the transformation (and its inverse) involves a one-to-one correspondence of the pertinent features of the structures. This observation is important because it implies, in turn, that if membership of a test structure within a topological family of homeomorphic structures can be established, then the test structure will share all the topological geometric features of the family.

The relationship of topological geometry and the elasticity of topological figures to formal operational thinking, that is, the extrapolation from the given to the possible, and the relationship of Euclidean geometry and the rigidity of Euclidean figures to concrete operational thinking are readily apparent.

3. The Scientific Method, Strong Inference, and Paradigms

3.1. The Scientific Method[*]

The scientific method is usually defined as an iterative inferential process involving the formulation of a hypothesis, followed by the devising of crucial experiments capable of a clean confirmation or rejection of the hypothesis and recycling as required by the outcome of the experiments. *Platt*[8] suggests that certain systematic methods of scientific thinking produce more rapid progress than others. He uses the term *strong inference* to describe a version of the scientific method that emphasizes the formal, explicit, and regular use of *alternative hypotheses and alternative crucial experiments*. The scientific method may be viewed as a specific form of intellectual processing.

Kuhn[9] takes the position that it is not the scientific method per se that leads to rapid progress, but rather the development of mature and effective *paradigms*, which are universally recognized scientific achievements that provide guidance to define scientific puzzles and to provide clues for their solution by a community of practitioners. Figure 4 is a transformation of the schematic description of normal mental activity (cf. Fig. 1) to that of normal science. In science, paradigms replace beliefs in the intellectual processing cycle. The role of geometric thinking in the scientific method is highlighted by replacing formal operational and concrete operational thinking with topological and Euclidean geometric thinking, respectively.

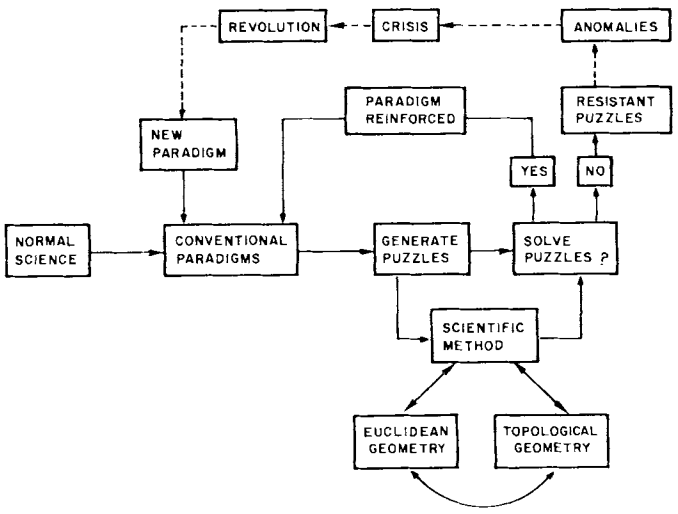


Fig. 4. A schematic representation of the activity of normal science showing the interplay of paradigms, puzzles, solutions, and the scientific method (cf. Fig. 1). Concrete and formal operational thinking "topologically map" onto Euclidean and topological geometry, respectively.

Thom[3] emphasizes the role of geometry in scientific analyses by suggesting that the human mind cannot be comfortable in a universe in which phenomena are governed by mathematic formulations that are coherent and quantitative but so abstract as to be impossible to visualize, that is, to interpret geometrically. The geometric interpretation allows the closure that drives intellectual processing. Furthermore, Euclidean geometry and topological geometry play an important role in structuring the thought processes involved in the scientific method.

The *Platt*[8] proposal of a strong inference methodology for solving puzzles scientifically raises two interesting questions: (1) Are there systematic and effective ways of generating alternative hypotheses and alternative crucial experiments?; (2) How does one best satisfy the Law of Closure in applying the strong inference approach (which inherently creates psychological tension by demanding the generation and consideration of possibilities and the resolution of the resulting conflicts)? We suggest that the use of paradigms and geometry can be effective in resolving these two issues.

3.2. Strong Inference

Some scientific fields appear to be capable of making more rapid advances than others. Clearly, development of instrumentation, funding, quality of practitioners, etc., all contribute to the speed of scientific advances in a field. *Platt*[8] suggests that an intellectual factor may also be important. He proposes that fields that systematically use and teach strong inference (the formal, regular, and explicit application of alternative hypotheses) are inherently better positioned for making rapid scientific advances.

The strong inference (scientific) method consists of the following steps: (1) creation of several alternative hypotheses; (2) devising of crucial experiments that exclude one or more of the hypotheses; (3) execution of experiments to allow "clean" exclusion of some hypotheses; (4) repetition of the cycle after refining the remaining hypotheses.

It is clear that observational knowledge must guide scientific ideas and that laboratory experiments must challenge and test the validity of the ideas. However, *Platt*[8] puts particular emphasis on the regular and explicit use of multiple hypotheses or possibilities. By embracing multiple hypotheses at the beginning of an inquiry, the scientist will exhibit less tendency to become attached to a single hypothesis (which may become a sort of intellectual offspring from the moment it is proposed as an original and satisfactory explanation of a phenomenon). The intellectual and experimental attempts to exclude hypotheses should provide an area of conflict, not between scientists, but between ideas. Excitement can be derived from the puzzles generated by alternative hypotheses. Which one will be right? Zeal and passion for experimental work surely can be derived from viewing the scientific method as requiring clever detective work in addition to experimental skill.

However, the question arises how scientists generate the formal schemata that guide them through the strong inference process without getting them bogged down in irrelevancies. The use of scientific paradigms provides such guidance.

[*] See also W. Wieland, *Angew. Chem. 93* (1981) 627; *Angew. Chem. Int. Ed. Engl. 20* (1981) 617.

3.3. Scientific Paradigms

The exact meaning of the term *paradigm*[9a] is a bit "fuzzy." A paradigm may be a constellation of beliefs, values, techniques, and methods that are shared universally by a community of practitioners. A paradigm may also be a smaller subset or a single element in such a constellation. In either case, the paradigms serve as models or examples that can replace explicit rules for generating and solving scientific puzzles. There is an implicit process of intellectual mapping of features of the paradigm onto the puzzle under analysis. Since topology is a branch of mathematics concerned with the identification of equivalences by mapping processes, we shall examine the possible interrelations of scientific paradigms and geometric methods, first considering the overall role of paradigms in scientific methodology.

According to *Kuhn*,[9a] paradigms provide a "mind set" for the execution of normal science. When scientific research is approached, questions of the following type arise commonly: How does one generate experiments to be performed? Of the many conceivable experiments that might be performed, how are priorities set? What aspects of a phenomenon are relevant for scientific examination? What questions may be legitimately asked and what techniques may be legitimately employed in seeking a scientific solution to a puzzle?

Effective paradigms, once established and accepted, provide a vehicle for the definition and solution of scientific puzzles. Successful paradigms prevent overt disagreements among practitioners concerning legitimate scientific problems and methods. As a result, practitioners spend little time involved in controversies over fundamentals. For example, a mature paradigm[9a] (1) generates an a priori ("intuitive") backdrop of expectations for the community by providing a common body of beliefs, (2) defines legitimate puzzles that may be addressed by the community of practitioners and legitimate methods for the solution of these puzzles, (3) guarantees that legitimate puzzles have solutions that are limited only by the cleverness and skill of the practitioner and the experimental technique used, and (4) allows the search for solutions to proceed rapidly, because irrelevancies and constant justification are avoided, since standards are universally accepted by practitioners.

The successful solution of a scientific puzzle within the protocol of the paradigm both demonstrates the skill of the practitioner and strengthens the authority of the paradigm. The iterative process of puzzle generation and puzzle solution also provides a high degree of closure to the intellectual processing involved in the scientific method and in this respect can be stimulating and fun for the successful practitioner.

Of course, the more powerful a paradigm becomes as the result of continuing successes, the deeper and more profound becomes its grip on scientific minds. Attempts to question an enshrined paradigm are typically dismissed out of hand. The scientist may become oblivious to even the existence of other possibilities. On the darker side, truly new paradigms are sometimes resisted because they challenge whole systems of scientific development which occurred over long periods of time and at great expenditure of energy and finances. A *scientific revolution*, as viewed by *Kuhn*,[9a] is the process of replacing an entrenched paradigm with a truly different one.

The course of a scientific revolution may be described by consideration of Figure 4. In normal science the conventional paradigms are employed to formulate legitimate puzzles which are solved by legitimate methods to reinforce the paradigm. However, according to *Kuhn*,[9b]

> ... sometimes a normal problem, one that ought to be solvable by known rules and procedures, resists the reiterated onslaught of the ablest members of the group within whose competence it falls ... when the profession can no longer evade anomolies that subvert the existing tradition of scientific practise—then begin the extraordinary investigations that lead the profession at last to a new set of commitments ...

Such resistant puzzles are typically viewed initially by practitioners as anomalies which will be resolved eventually within the framework of normal science. There is often an implicit suppression of such anomalies, because their existence reflects poorly on the operating paradigm. However, the accumulation of anomalies can lead to a vexation among practitioners because this raises doubts concerning the rules governing the prior practice of normal science and the scientific work already completed, that is, the occurrence of an anomaly implies that an error in the paradigm may have been propagated unknowingly at earlier times. If so, puzzles were solved incorrectly in the past. Eventually a crisis may develop among practitioners, who, in the face of paradigm collapse, are forced to seriously consider a tradition-shattering commitment to the new paradigm, that is, a scientific revolution is underway. Once a successful new paradigm has emerged, the practitioners are mercifully reinstated in the normal science loop (see Fig. 4). Candidates for new paradigms must resolve some outstanding and generally recognized puzzle that cannot be solved by the protocol of the existing paradigm. Furthermore, the new paradigm must preserve or replace the ability of the conventional paradigm to define and solve puzzles.

A true revolution (change of a paradigm) is much less common than an "articulation" of a paradigm (topologically speaking, an elastic distortion of the local rules within the global paradigm). Both, however, begin with the awareness of an anomaly that results from a disparity between paradigm-generated expectations and experimental or theoretical observations. This "opens" the paradigm and leads to a feeling of discomfort among the practitioners. Closure is sought and is only achieved when the paradigm has been replaced (rare) or the rules have been re-articulated (more common). The re-articulation of a paradigm often corresponds to merely a realization of some aspect of the conventional paradigm that had been previously ignored or overlooked.

It is important to note what organic chemists never do when confronted by a sudden and severe anomaly diagnostic of paradigm breakdown: they do not renounce the old paradigm out of hand. They almost always first con-

sider the anomaly to be the result of an artifact or to be interpretable in terms of a new articulation of the old paradigm. The old paradigm will survive until a viable alternative candidate is found. The decision to reject one paradigm is almost always coincident with the decision to accept another after comparison of both with the pertinent phenomena and with each other. Ad hoc modifications are usually a more preferable response than tossing out the conventional paradigm without a suitable replacement. Many of the paradigms of organic chemistry are retained, not because they are free of fault, or because they are infallible in their predictive ability, or because of their ineluctable logic. They are more often retained because they are useful for the understanding of observational knowledge at a qualitative level, because they are portable[10] and exploitable by practitioners, and because they provide the driving force for fast-developing experimental methodology.

The decision to employ a particular apparatus or a particular method to solve a chemical puzzle carries an assumption that certain chemical phenomena exist and can be investigated by means of the protocol set forth by the paradigm. Novelty and anomaly emerge against the backdrop of the expectation (intuition) provided by the paradigm. Since accepted paradigms are not readily surrendered, resistance guarantees that scientists will not be constantly distracted with irrelevancies and artifacts. So long as a paradigm continues to prove capable of identifying solvable problems, science moves fastest and penetrates most deeply through employment of the tools approved by the paradigm. In science as in industry, retooling is expensive and disruptive, and is reserved only for the special occasions that demand it.[9a]

It is the study of paradigms that prepares the student for admission to the scientific community. The practitioners share paradigms and are committed to the same rules and standards for scientific practice. By doing so, they can proceed rapidly in their research without having to start each time from first principles and to justify each basic concept that is used in an argument. Indeed, when we discuss research within a field, we usually assume that we are addressing colleagues who possess knowledge of a shared paradigm. The student is trained to attempt to "see" a new problem in the form of an old, solved problem and to replicate a solution by mapping the features of the "understood" problem onto the new problem. At the beginning of a scientific inquiry, the student is sometimes only vaguely aware of what he or she is expected to discover and may lack confidence in knowing what to look for. *Plato*[11] understood this dilemma when in the *Meno* he noted that if we know the solution to a puzzle there is no puzzle, but if we don't know the solution we do not know what we are looking for and can not expect to find anything. He concluded that problems are solved by remembering past incarnations. The protocol of scientific paradigms as a method of puzzle solving is somewhat akin to *Plato*'s reincarnations.

In organic chemistry there are numerous examples of revolutions in thinking that occurred as chemistry developed into a molecular science. First, the notion of composition (number and kinds of elements), then the notion of connectivity (the bonding between elements) and the concept of a three-dimensional representation (the stereochemical aspects of the array of bonded elements), and finally the concept of dynamic stereochemistry (the time-dependent conformational aspects of the array of bonded elements) were developed. At each of these stages in the development and refinements of the ideas of molecular structure a scientific revolution occurred because chemists changed entrenched paradigms which had previously determined the definition and solution of chemical puzzles.

4. The Relation of Euclidean and Topological Geometry to Chemical Structures

4.1. Mathematical Graphs, Forms, Figures, and Structures[*]

The scientific method often involves consideration of the information content of various mathematical objects. For the purposes of this article we wish to distinguish between mathematical graphs, forms, figures, and structures, which are used to model chemical objects. By a graph we shall mean a dimensionless but visualizable topological object that contains information concerning the components and connectivity relations of the chemical object to be modeled. By a form we shall mean an elastic topological geometric object that is embedded in Euclidean space. A figure shall mean a rigid Euclidean geometric object. We shall reserve the term structure for the mathematical object that models a chemical object (i.e., a molecule).

4.2. Transformation from Topological Objects to Euclidean Objects

We are all accustomed to analysis of concrete, readily visualized geometric figures embedded in Euclidean spaces of one, two, or three dimensions. We shall discuss briefly how objects in an abstract topological space can be transformed into objects in a concrete Euclidean space. In topology, sets (defined collections or families of objects) are employed for mathematical analysis. When relationships exist between members of the set, the objects of the set are said to constitute a topological space, T. How can one proceed from an abstract topological space to a concrete Euclidean space, R? In this section we suggest a pathway that uses topological structures, namely, graphs, as the bridge from T-space to R-space.

Topology involves the study of those properties of spaces that depend only on the "nearness" of the elements of the space and that are independent of geometric aspects such as distances and angles. A topological space,[6] $T(X, Y)$, is usually defined as a set, X, together with a family of subsets, Y, which satisfy certain conditions. Topological spaces have rich generality, but are completely abstract mathematical objects devoid of a visualizable geometric form. A finite topological space is said to have structure in the sets X and Y if there are some properties of the elements (members of the sets) that can be brought into

[*] See also I. Ugi, D. Marquarding, H. Klusacek, G. Gokel, P. Gillespie, *Angew. Chem. 82* (1970) 741; *Angew. Chem. Int. Ed. Engl. 9* (1970) 703.

correspondence. In order to "visualize" and eventually interpret a topological space geometrically, it is natural to speak of "points" rather than elements or members of the sets X and Y. The topological space can be visualized by imagining connections between the points of $T(X, Y)$. A *topological graph* is thereby produced. Among the most important fundamental properties of a topological space are neighborhood relations between points of the space. For an eventual chemical interpretation, it is natural to view the topological points in terms of atoms and the neighborhood relations in terms of chemical bonds. A finite topological space and its graph have the same number of components. A connected graph corresponds to a connected topological space.

A specific method of visualization, with powerful implications for chemistry, is to cast the topological space into the form of a connected graph, G, which is defined as an ordered pair, (V, E), where V is a set of points in a topological space and E defines the binary relations between the points. The points V are the vertices of the graph and the binary relations E are the edges connecting the vertices. The binary relations E can be viewed as the rules for a transformation that maps lines connecting elements of the abstract topological space $T(X, Y)$ to produce a visualizable graphical space, $G(V, E)$. Visualization is possible, for example, when the vertices are represented as small numbered circles and the connections are represented as lines. It is important to recognize that $G(V, E)$ is still a topological object, having no geometric parameters such as distances and angles. Chemists come into close contact with topological concepts when they use graphs to represent molecular structures. Indeed, in the usual mathematical sense, a graph, although it can be visualized, does not have dimensionality in the Euclidean sense.

As a concrete example of the conversion from a topological space to a connected graph let us consider the graph representing methane (Fig. 5). The members of the topological space $T(X, Y)$ represent carbon atoms and hydrogen atoms ($X = \{C, H\}$) and connections between carbon atoms and hydrogen atoms ($Y = \{C-H\}$). The degree of a vertex of a graph is the number of edges connected to the vertex. A connected graph of degree four is employed to represent the normal valence of carbon. In an abstract formulation of methane there are two different kinds of points in the topological space and one kind of connectivity relation. Embedding of the graph $G(V, E)$ into Euclidean space, R^n (R^1, R^2, and R^3 correspond to one-dimensional, two-dimensional, and three-dimensional spaces, respectively), produces an elastic object $R^n(V, E)$, which is a topological form having the flexible geometric properties of distance and angle.

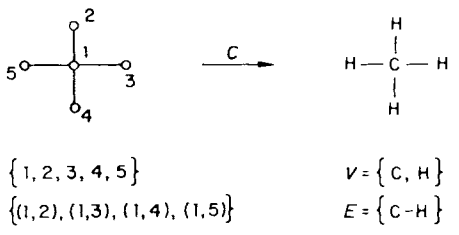


Fig. 5. A visualized connected graph (left) and a molecular graph (right) of methane. The molecular graph, which represents the molecular topology of methane, is produced by embedding the connected graph into the chemical paradigm for molecular structure, represented by the mapping process C. V is the set of points (left) or vertices (right); E is the set of binary relations between the points (left) or edges connecting the vertices (right).

In Figure 6, the visualized graph $G(V, E)$, which represents methane, is embedded in a dimensionless topological space to give a concrete Euclidean geometric figure. $R^3(V, E)$ represents any elastic distortion of the geometric form that conserves the constitutional properties of the figure. Application of a metric, M (corresponding to measurable distances and angles), to $R^n(V, E)$ produces a concrete object, $R^n(V, E, M)$, which is a rigid geometric figure that obeys the rules of ordinary Euclidean geometry.

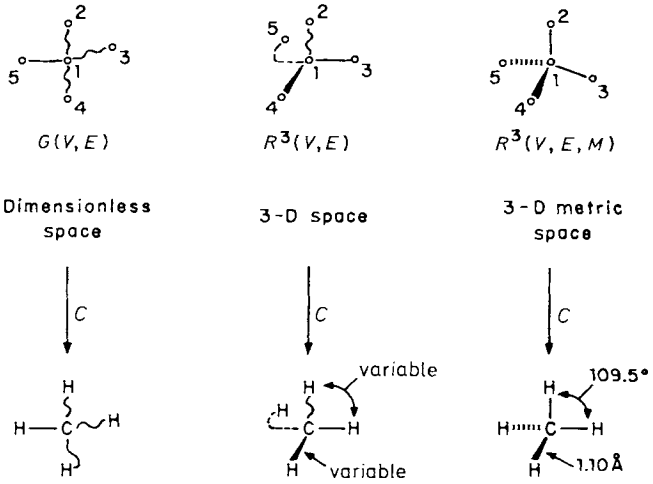


Fig. 6. Graphical topological, $G(V, E)$, topological geometric, $R^n(V, E)$, and Euclidean geometric, $R^3(V, E, M)$, representations of methane. The mathematical objects $G(V, E)$, $R^3(V, E)$, and $R^3(V, E, M)$ become models for the chemical object methane by embedding in the chemical paradigm, represented by the mapping process C. This produces a structural model at the graphical (left), topological (middle), or Euclidean (right) level of representation. V, points (vertices); E, lines (edges); M, metric (distances, angles).

4.3. Molecular Models

We have seen how mathematical objects may be used as models for molecular structures. The meaning of the term model, like that of the term paradigm, is a bit fuzzy. For the present purposes, a model is an alternative form of an object or concept, which is created with the expectation that it will provide some insight into the nature of the object or concept. The mind is a model builder par excellence as it seeks, with only fragmentary information, a closed interpretation of the surrounding world. To many organic chemists, models are the "pictures" on which imagination may be exercised and which enhance an intuitive understanding of the object or concept under consideration.

According to *Trindle*,[12a] in building a model we relinquish any claim to perfect truthfulness. Models are always different from the objects or concepts that are being represented. In science models are temporary aids, always subject to revision and usually destined for an intellectual junkyard. The best and most useful models have certain characteristic properties:[10] they are memorizable, port-

able, simple, self-consistent, elastic, and widely applicable. Models are particularly delightful when they produce surprises. Since it is now taken for granted that molecular objects in the real world can be faithfully represented by geometric objects, the wonderment of molecular models as representations of chemical reality is often no longer appreciated by the practitioner.

Up to this point we have considered purely mathematical (topological and geometric) objects, which can exist in intellectual processing but which do not require any relation to an ultimate reality. We now need a bridge from these objects to molecular structures, which are models[12] used to represent the reality of chemical systems. For our purposes we shall assume that the molecules we wish to model exist as real objects. *Mislow*[13] has provided a proper perspective for the approach we wish to embrace:

> The (geometric) figures which can be developed from molecules and which become their models are mathematical objects and intangible abstractions of the reality they are intended to represent ... Model and molecule are thus separate and distinct entities, one abstract, the other concrete ... By contrast, molecules and molecular ensemble exist entirely in the realm of observables.

The concepts of molecules and molecular structure, the so-called intellectual units of the chemist, are remarkably successful models of chemical reality. However, we should keep in mind the caution of *Hammond* et al.:[14]

> It is ... important to remember the fine distinction between ... models and physical reality. A good model can be so successful in ordering our thoughts and predicting the behavior of systems that we come to regard the model as real ... Trouble may arise when two scientists, using ... different models engage in a bitter conflict in which they try to prove, or disprove, the reality of their models ... We must remember that scientific thinking is really a branch of symbolic logic.

In Figure 7, the relationship of topological spaces, graphical forms, geometric forms, and geometric figures to molecular structure is shown schematically. A mapping process, C, which corresponds to the chemical paradigm, transforms mathematical objects such as spaces, forms, and figures into chemical objects such as molecular structures. We shall now discuss the nature of this mapping process.

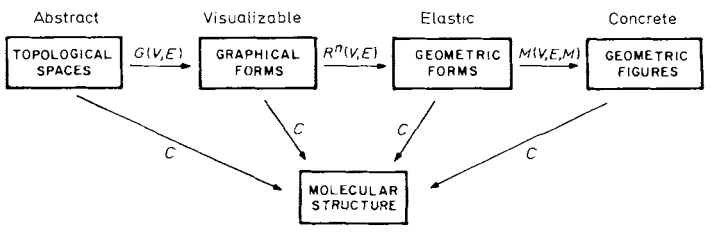


Fig. 7. A schematic representation of the interrelationship of topological spaces, graphical forms, geometric forms, and geometric figures. The embedding of any of these objects in conventional chemical paradigms produces a model of molecular structure. R^n, Euclidean space ($n = 1, 2, 3$). For other abbreviations, see Fig. 6 and text.

4.4. Transformation from Mathematical Objects to Chemical Objects

The transformation from mathematical objects (graphs, forms, figures) of topological geometry and Euclidean geometry may be viewed as the embedding of the mathematical objects into a chemical paradigm (see Fig. 7) to produce models for molecular structures. The paradigm provides the basis for the mapping process C that transforms mathematical objects into chemical objects. The historical pathway to modern chemical structure is related to that shown in Figure 7 except that Euclidean geometric figures (configurational stereochemistry) were accepted as the models for molecular structure before topological geometric forms (conformational stereochemistry).[15] The historical pathway is summarized in Figure 8 for cyclohexane as an example. Starting from the notion of composition (number and kinds of elements possessed by the chemical object), the notion of constitution[16] (bonding relations between elements) was introduced and visualization was achieved by creation of a molecular graph. The graph was then embedded in 3-D Euclidean space to produce a rigid configurational geometric model of the molecular structure of the chemical object.[17, 18] Finally, the molecular structure was allowed to be conformationally active by giving it an elasticity consistent with conventional chemical paradigms. The configurational level of representation may be viewed as corresponding to concrete operational thought and the conformational level of representation to formal operational thought.

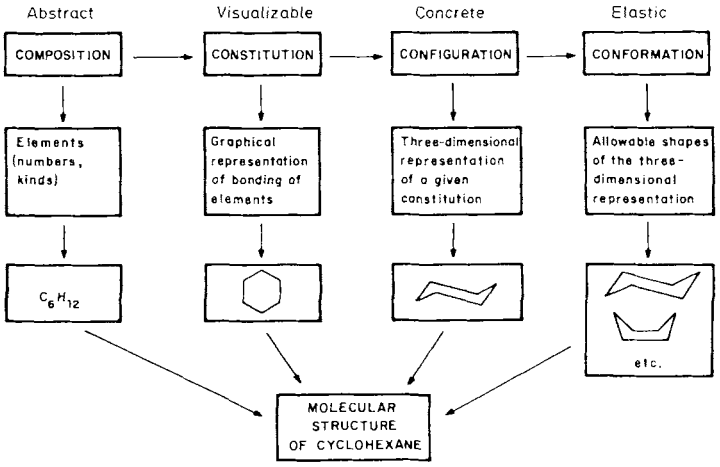


Fig. 8. The relationship between composition, constitution, configuration, and conformation in the mathematical and chemical sense. Molecular structure may be modeled at any of these levels. Cyclohexane is given as an example.

4.5. Molecular Graphs

Since chemists come into closest contact with topological ideas in the use of graphs to represent molecular struc-

tures, we now consider how graphs may be used to represent molecular topology and how these graphs are converted into geometric forms which model molecular structure.

The graphical method for representing molecules, which is nowadays taken for granted by organic chemists, represented a major intellectual breakthrough, since it provided a conceptual framework for further progress in organic chemistry. The informational content of a molecular graph and its ease of visualization are important reasons for its success among chemists. A special attraction of graphs is their power in handling combinational problems in chemistry. From a practical standpoint, the use of graphs and simple rules with pencil and paper, without need for lengthy calculation, allows representation and categorization of a large number of chemical systems. Let us analyze the basis for why graphs are so valuable in analyzing chemical systems and why these graphs appear to have such a broad and robust informational content.

In a molecular graph the vertices represent atoms (or groups of atoms considered as a unit) and the lines represent bonds. The points and the connections between points are topologically significant. The chemist would term the points the *composition* of the molecular graph, and the network of connections the *constitution* of the graph. To a topological chemist the composition and constitution of the graph are essentially global topological properties of the graph. The graph of a molecule may be viewed as an expression of the topological concept of special neighborhood relationships, which are chemically described by the valence of an atom (A). Only n atoms of the entire set of atoms in a molecule have a valency relationship with A, i.e., A has a valency of n. This topological notion of valency or bond order was the foundation of the first formulations of structural theory.[16] The actual arrangement of atoms in space, their bond lengths and bond angles, need not be specified. Indeed, at this level, bonded atoms may be drawn further apart than nonbonded atoms without reduction of the topological information, which is concerned only with the property of connectedness of atoms in the set with A.

Two graphs that have identical numbers of vertices connected in the same way are said to be *isomorphic*. The chemist recognizes two isomorphic molecular graphs as having identical composition and constitution. The type of line used to make the connection or the symbols used to represent the graph are not of topological significance.

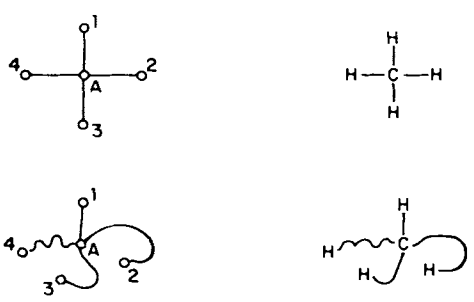


Fig. 9. Two isomorphic (mathematical) graphs of degree four (left) and two isomorphic molecular graphs representing methane (right).

Thus, a symmetrical, simple mathematical graph of degree four (see Section 4.2) is the same if it is written with a mixture of wiggly, straight, long and short lines (Fig. 9, left). The same holds true for the molecular graph of, for example, methane (Fig. 9, right). Because the points of the graph are abstract entities, the same molecular graph may represent many different molecules.

4.6. Stereochemistry in Euclidean and Topological Molecular Structures

Stereochemistry examines and categorizes relative spatial relationships between atoms and groups of atoms within a molecule and between different molecules.[15] From everyday experience, the chemist recognizes that, although the relative arrangements of atoms (configurations) and the relative shapes of networks of atoms (conformations) are of enormous importance, quantitative metric quantities such as bond lengths and bond angles may remain completely unspecified for many types of analyses. Within this framework, it is natural to employ an extension of topological ideas (which ignore metric relations) in stereochemical analysis.[19]

We have seen that graphs allow a topological representation of molecules in terms of the idealized entities that constitute geometry and that a molecular graph can be regarded as a representation of molecules in topological geometry. Examination of the stereochemical features of molecules requires the embedding of the molecular graph into Euclidean space, which produces geometric forms. This embedding is required because constraints, which are not fundamental to topology, are placed on the physical characteristics of molecular entities.

The step from geometric forms (topological) to geometric figures (Euclidean) involves the application of a metric. The introduction of distances and angles into *topological molecular structures* creates *geometric molecular structures*. The transition from topological to geometric structures is a profound one from the standpoint of intellectual processing; indeed, it is analogous to the distinction between formal operational and concrete operational thought! Thus, a geometric figure represents a concrete chemical object with fixed distances and angles, whereas a topological structure represents the chemical object only under the condition of conservation of topological properties. Finally, the labeling of the points of the geometric figure, which results in a fixed orientation of the figure, allows the representation of chemical objects such as enantiomers.[20]

The discovery of optical activity revealed a limitation of molecular graphs, which was overcome by introduction of the concept of configurational stereochemistry resulting from the arrangement of atoms in 3-D space. Optical isomerization could be understood in terms of the Euclidean 3-D geometry of n atoms connected to a central atom A. The key notion of the tetrahedral arrangement of valences about carbon is the same whether the configurational molecular figure representing the geometry is regular *(van't Hoff)*[17] or irregular *(Le Bel)*.[18] The neglect of metric relations, a fundamental feature of topological thinking, is apparent here. The bond lengths and bond angles of the te-

trahedral structure can vary over a wide range without changing the (nontopological) geometric property of configuration. Of course, in real systems a limit may be reached for which the configuration is not conserved (bond breaking, formation of an achiral structure, etc.).

In the light of scientific paradigms, the step from a graphical, abstract, hypothetical representation of real objects to the acceptance of atoms as real entities that may be modeled by molecular structures in 3-D space represented a scientific revolution because it profoundly changed the way the practitioners designed and interpreted chemical processes. The acceptance of the concept of stereochemistry met with the expected resistance of practitioners doing normal science under the guidance of entrenched paradigms. For example, *Kolbe*[21] castigated the new paradigm as a step backward:

> It is typical of the present time, when there is so little criticism and so much hatred of criticism, that two practically unknown chemists, one from a veterinary college, and the other from an agricultural institute, pass judgement on the loftiest problems of chemistry, those which will probably never be solved, particularly the question of the position of atoms in space, and they undertake to answer these problems with an impudence and assurance that absolutely astonish the true scientist.

Such a vitriolic attack on a paradigm that is now universally accepted brings to mind the skeptical but perceptive remark by *Planck*:[22]

> New scientific truth usually becomes accepted, not because opponents become convinced, but because opponents gradually die, and because the rising generation are familiar with the new truths at the outset.

4.7. Boundaries in Euclidean and Topological Molecular Structures

In mathematics a boundary implies a discontinuity, that is, the qualitative nature of a function changes as a "behavioral point" crosses from one side of the boundary to the other. In organic thinking, the notions of inside/outside and above/below are commonly used with reference to volumes or surfaces, respectively. For example, an organic molecule may be solubilized inside a micellar aggregate, outside the aggregate in the aqueous phase, or at the micellar/aqueous interface. A specific topological form that faithfully represents the inside/outside/boundary aspects of a micelle is a sphere. Of course, any geometric form that is homeomorphic with a sphere will also faithfully represent these topological aspects.

The wave functions of orbitals may or may not change sign when passing through a plane defined by certain nuclei of the molecule of interest, that is, the qualitative properties of the wave function either change or remain the same on passing through the plane. A specific topological form that faithfully represents the above/below/boundary aspects is a Euclidean plane. Of course, in topological terms, the plane is elastic and may be bent, twisted, and stretched without loss of the notion of above/below/boundary. The power and robustness of Hückel molecular orbital theory probably reflects its topological foundations and explains its remarkable ability to faithfully represent the qualitative features of molecules, even those with no apparent Euclidean geometric symmetry.[23]

5. The Use of Topological Thinking and Geometric Models to Examine Chemical Structures

5.1. Topological Thinking in Chemistry: A Qualitative but Precise Approach to the Scientific Method

Having given examples of geometric thinking and the use of topological concepts, we can suggest that there is a general procedure for structured intellectual processing that can be termed *topological thinking*. This method uses elastic mapping procedures for establishing the correspondence between a model, which can be expressed in topological form, and a phenomenon or observation. Geometric thinking emphasizes the concrete aspects of the model that relate to rigid forms and figures in space, whereas topological thinking emphasizes the elastic mapping process. Thus, the intellectual process by which a molecular structure is predicted to have a certain color or to be characterized by a certain NMR spectrum does not involve purely geometric components. The color or the spectrum can be related to a more general topological space in which the properties corresponding to color or the NMR spectrum can be defined.

Another way to view topological thinking is to consider it as an intellectual process that involves the pulling, stretching, and twisting of ideas in a search for sameness or correspondence in a manner reminiscent of the process involved in searching for homeomorphisms in topological geometry. Phenomena are imbued with properties that allow them to be converted into mathematical forms, which, in turn, can be mapped onto topological geometric forms.

Topological thinking is always qualitative, because, like topological geometry, it does not involve quantitative metric constraints. The term qualitative tends to have a pejorative connotation in the sciences. There is a tendency to assume that scientists are qualitative only when they are incapable of being quantitative; that is, qualitative is merely second best to quantitative. However, the history and incredible pace of progress in organic chemistry over the past two centuries is proof of the power of qualitative thinking in science. In most day-to-day organic research, what appears to be of greatest import is a qualitative result and not the precise value of a quantity; for example, is a rate slower or faster, is a yield higher or lower, does a structure contain a carbonyl or not. It is probable that the poor reputation of qualitative thinking is due to the naive and imprecise appearance of certain qualitative ideas. According to *Thom*,[3c] such need not be the case:

> (We can furnish) ... by a refinement of our geometric intuition ... our scientific investigations with a stock of ideas and procedures subtle enough to give satisfactory

> representations to ... phenomena ... we can now present qualitative results in a rigorous way, thanks to recent progress in topology ... for we know how to define a form and can determine whether two functions have or have not the same form or topological type.

Thom goes on to suggest that topological thinking is capable of releasing our intuition from the constraint of three-dimensional space and is capable of providing a more general, richer intuition for the examination of microscopic phenomena. Furthermore, topological thinking can be precise if only the topological aspects are considered in a geometric analysis. According to *Mislow*:[13]

> As chemists we often employ inexact terms such as fast/slow, strong/weak, concentrated/dilute, hot/cold, etc., yet we are confident that these words suffice to carry the desired message, unburdened by superfluous precision, within the context of the report.

Quantitative thinking, of course, plays a crucial role in the scientific method. However, quantitative, abstract mathematics may result in noncausal thinking that is mathematically precise, consistent, and rigorous, but chemically or physically irrelevant. *Thom*[3b] warns:

> The human mind would not be fully satisfied with a universe in which all phenomena are governed by a mathematical process that is completely coherent but totally abstract. Are we not then in wonderland? In the situation where man is deprived of all possibility of intellectualization, that is, of interpreting geometrically a given process, either he will seek to create, despite everything, through suitable interpretation, an intuitive justification of the process or he will sink into resigned incomprehension.

Perhaps *Platt*[8] best epitomizes the attitude of the topological thinker:

> Many—perhaps most—of the great issues of science are qualitative not quantitative, even in physics and chemistry. Equations and measurements are useful when and only when they are related to proof: but proof or disproof comes first and is in fact strongest when it is absolutely convincing without any quantitative measurement ... you can catch phenomena in a logical box or in a mathematical box. The logical box is coarse but strong. The mathematical box is fine-grained but flimsy. The mathematical box is a beautiful way of wrapping up a problem, but it will not hold the phenomena unless they have been caught first in a logical box.

In other words, a phenomenon should be mapped onto the correct topological form (logical box) before it is modeled in a quantitative fashion (mathematical box).

Topological thinking assumes that if the correct topological model for a phenomenon has been devised, then all of the topologically relevant aspects of the model can be "mapped onto" the phenomenon; that is, all the topological features of the model are enjoyed by the phenomena and vice versa. This potential relationship is extremely powerful when it exists because it automatically defines qualitative attributes that can be transferred from a given topological form to a wide range of chemical phenomena.

For example, the isoelectronic principle involves the mapping of the properties of a topological chemical structure having an array of valence electrons onto specific atoms. Thus, all atoms with octets of electrons "telescope down" to a single point in a topological space; the same is true for all atoms with sextets of valence electrons. In topological thinking, carbenes, nitrenes, oxygen atoms, etc., have the same qualitative chemical properties. This means that each reaction or physical property that is related to the topological aspects of a given chemical structure is shared qualitatively by every member or structure in the family. Other important examples of topological thinking in organic chemistry include the Hammond postulate,[24] the Woodward-Hoffmann rules,[25] and Salem diagrams.[26]

5.2. Tetrahedral Carbon: A Triumph of Topological Thinking

The first important step in the development of the structural theory of chemistry was probably the formulation of the concept of valency. This concept when mapped onto the concepts of graph theory naturally leads to the recognition of connectedness, the special chemical relationship that distinguishes the n atoms bound to an atom A from the rest of the set. The connectedness, in turn, is interpreted in terms of chemical bonds. Thus, at the earliest stages of development, the key concepts of bonding were topological and graphical.

Consider the following argument, based on the use of topological and geometric thinking, an experimental isomer count, and the assumption of the noninterconvertibility of isomers modeled by 3-D geometric figures. If the composition of methane is CH_4 and if it can be represented by a molecular graph and by a 3-D geometric figure, there are two distinct classes of possibilities (Fig. 10): either the vertices of the molecular graph are equivalent (class I) or they are not equivalent (class II). These two possibilities may be visualized with a molecular graph showing a C atom with four equivalent bonds to the H atoms, or by any other molecular graph with composition CH_4.

If I is the correct representation, then replacement of a single H atom by any equivalent atom will lead to one and only one isomer. If II is the correct representation, then replacement of a single H atom by any equivalent atom

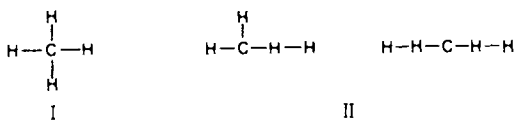


Fig. 10. Possible graphs for the representation of methane. Class I consists of a graph that shows four equivalent hydrogen atoms (and all isomorphous graphs) and class II consists of all other graphs of composition CH_4.

will lead, in principle, to two distinct isomers. Since all experimental examples have been consistent with I but would require an ad hoc explanation in each case to be consistent with II, strong inference suggests a molecular graph of CH_4 that has four equivalent H atoms and a C atom with a valency of four. By extrapolation, the valence of any member of the methane family is four. Any geometric figure that represents the molecular graph in 2-D or 3-D space and has four equivalent vertices and any molecular structure that has four equivalent H atoms bound to a C atom is consistent with the experimental finding that only one isomer is produced from methane by monosubstitution. In 2-D geometry the only such molecular graph places the H atoms at the corners of a square and the C atom at the center (square planar). In 3-D geometry the only such structures are a tetrahedron and a square pyramid. Thus, the experimental isomer count based on topological and geometric thinking reduces the choices to only three molecular structures (Fig. 11)!

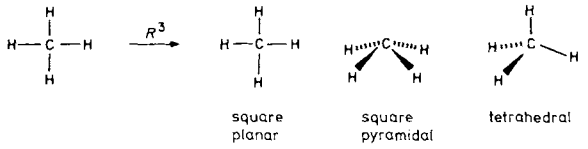


Fig. 11. Possible molecular structures produced by embedding the topological molecular graph for methane, deduced from the isomer count, into 3-D space (R^3). Three possible Euclidean molecular structures result.

By employing the isomer count criterion again (Fig. 12), the square-planar and square-pyramidal structures can be ruled out. Replacement of one H atom in a monosubstituted methane produces only one product, as expected for a tetrahedral structure. The square-planar and square-pyramidal structures, on the other hand, would have given two possible products (*cis* and *trans*).

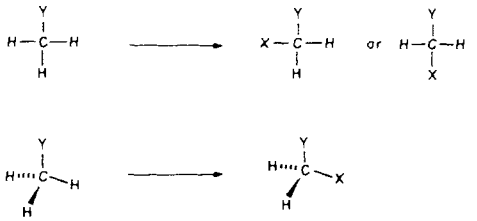


Fig. 12. Replacement of one H atom by a substituent X in square-planar or square-pyramidal (upper) and in tetrahedral (lower) monosubstituted methane, CH_3Y (see text).

The existence of enantiomers follows logically from the nonequivalence in 3-D space of mirror images of tetrahedral molecular figures having four different substituents. Moreover, these general conclusions are also valid for other molecular structures having a central atom of valence four.

A second example of topological thinking in organic chemistry is found in the use of the isomer count method to infer the structure of benzene (Fig. 13). If benzene has equivalent bonds, then only one type of 1,2-disubstituted benzene should exist; if benzene has alternating single bonds and double bonds, then two isomers of 1,2-disubstituted benzenes should exist. Since isomerism in 1,2-disubstituted benzenes has not been observed, it is inferred that the bonds in benzene are equivalent.

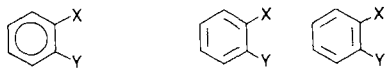


Fig. 13. Two representations of a 1,2-disubstituted benzene. Left: the bonds are equivalent (one possible structure). Right: alternating single and double bonds are present (two possible structures).

5.3. The Role of Time in Topological Thinking: Structural Stability and Chemical Reactivity

At the concrete operational level of thinking or the Euclidean geometric level of modeling, structures are rigid and do not change with time. At the formal operational level of thinking or the topological geometric level of modeling, structures are elastic and capable of changing with time. It is crucial to distinguish two types of time-dependent structural changes: those that conserve all topological properties and those that change the topological properties. For example, the former would correspond to the dynamic stereochemistry of a stable chemical structure and the latter to the dynamics of a chemical reaction.

Consider a structural model of a methane molecule. At any instant in time, a "snapshot" of the methane structure would not reveal a perfect tetrahedron, because vibrations will slightly change each bond length and bond angle (Fig. 14). Nevertheless, a chemist would not fail to recognize methane in any of its vibrational guises unless one of the C-H bonds becomes so long that it becomes unclear whether the observed structure corresponds to methane or to a methyl radical plus a hydrogen atom. The notion that methane, under "normal" conditions, can be modeled as a perfect tetrahedron derives from the premise that all experimental observations of methane correspond to a time-averaged structure and that the limiting time-averaged structure is a perfect tetrahedron. The time-averaged tetrahedral model is valid because, in a typical analysis, more than a trillion molecules are sampled.

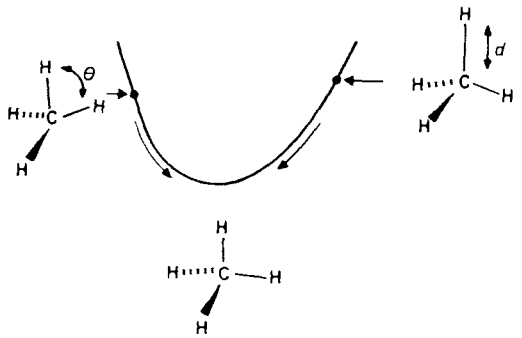


Fig. 14. Ideal tetrahedral representation of methane as an "attractor" structure for all homeomorphic representations of methane.

In topological terms the perfect tetrahedral structure represents an "attractor" structure toward which all other

topologically equivalent chemical structures tend. The chemical nature of methane does not change for sufficiently small deformations of its structure.

An experiment might be possible on a such short time scale, however, that most methane molecules would be "caught" in a nontetrahedral shape. Whatever the technical difficulties of such an experiment, it is topologically equivalent to an experiment for detecting cyclohexane conformers. Before fast methods of analysis were available, cyclohexane was considered as a single, static structure. Conformers were not detected because the time scale of the experiment was large relative to the time scale of the conformational change. With modern laser techniques, chemical structures may be examined on time scales of the order of 10^{-12} to 10^{-13} s. Many conformational systems in organic chemistry that are normally considered as being in dynamic equilibria are "static" on such a time scale.

6. The Use of Topological Thinking, Geometric Models, and Paradigms to Examine Chemical Reactivity

Are there archetypical graphs, topological forms, and geometric figures for modeling chemical reactivity? If we assume such models exist, we now have a recipe for anticipating their structure and the pathways for producing them; that is, we can map the pertinent aspects of the molecular graphs, molecular forms, and molecular figures used to model chemical structures onto reaction graphs, reaction forms, and reaction figures (i.e., a reaction network). It is natural to associate the points of the reaction network with the structures of reactants and products and the lines connecting the points with elementary reaction steps.

Topological thinking allows us to handle the multidimensionality of ground- and excited-state reactivity for a given structural transformation with a single reaction network generated by geometric procedures. Chemical paradigms guide the expression of specific geometric features of the reaction network.

6.1. Electronically Excited States and Diradicaloid Structures

Let us consider a chemical transformation of a reactant structure (R) to a product structure (P): R→P. The photochemist is concerned not only with the ground-state surface for this reaction but also with the excited-state surfaces associated with the same overall transformation. In constructing a reaction graph we need to establish the components (vertices) and connections (edges) of the graph. What are the components that correspond to the pertinent states of R and P? Using the highest occupied/lowest unoccupied (HO/LU) orbital paradigm for theoretical guidance,[27] there are four components or states, corresponding to the four possible electron occupancies of the HO and LU orbital of any R and P: S_0, S_1, S_2, and T_1 (Fig. 15). The energetic ordering of these states is invariably $S_0 < T_1 < S_1 < S_2$ for ordinary organic molecules.[28]

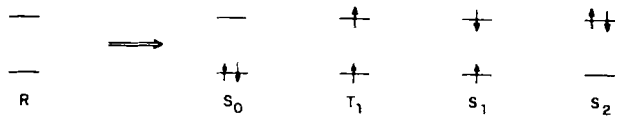


Fig. 15. The relationship between the HO and LU orbitals for a reactant structure R and its four lowest-lying electronic states: S_0, T_1, S_1, and S_2.

What are the connections between the components of R and P? If we can answer this question in a general way we will be able (as we are for molecular structures) to generate a visualizable reaction graph, which we can transform into a topological geometric form by embedding it in a Euclidean space, and which we can eventually transform into a Euclidean geometric figure with a metric, namely, the quantitative relationship of structure to energy. Before discussing examples of "reaction structures" (i.e., specific chemical reactions), we will discuss an important paradigm for the so-called "diradicaloid" structure that is commonly used for photoreactions.[26] This diradicaloid structure generally has four electronic states that are related to the S_0, S_1, S_2, and T_1 states of R and P. Importantly, we shall see that the diradicaloid structure is usually optimal for transformation from one energy surface to another, which occurs at the so-called "behavioral point" (corresponding to the change in atomic arrangement as R is transformed into P). Since getting from an excited-state surface to a ground-state surface is a critical aspect of all photochemical reactions, the diradicaloid geometry plays a crucial role in determining the possible "traffic patterns" at this behavioral point.

6.2. The Diradical/Zwitterion Paradigm

The important and extremely useful diradical/zwitterion (D/Z) paradigm for analyzing many photoreactions was proposed by *Salem*[26] as follows: If a molecular structure (having an even number of electrons) occurs along a reaction pathway for which the highest occupied orbital and the lowest unoccupied orbital are of comparable energy, the structure, termed a *diradicaloid or diradical/zwitterion structure*, will have four low-lying electronic states that will determine the chemical pathways leading to and from the structure. The diradical/zwitterion paradigm has the typical fuzziness of topological structures and qualitative organic thinking. The "composition" of the topology, namely, the set of four electronic states, is specified, but the energetic ordering of the states and the connectivity of the surfaces from R to P are not. We can proceed to the "constitutional" level of a reaction graph by assuming a common orbital situation for the reactant structure and then deriving the possibilities for the diradicaloid structure. By inspection, we can attempt to list the most probable state orderings of the diradicaloid structure and note the possible connections, thereby establishing the possible constitutional relationships between R and D/Z. We can then repeat the process to determine the connections between D/Z and P.

First, we consider a limiting situation in which the HO and LU orbitals have exactly the same energy at the D/Z structure (Fig. 16). Since composition is a topological property, we postulate that it must be conserved in an elementary, chemical step. Thus, there must be a one-to-one correlation between the number of electronic states for R and D/Z. What are the four lowest-lying states of the D/Z structure? How do they connect with the four lowest states of R?

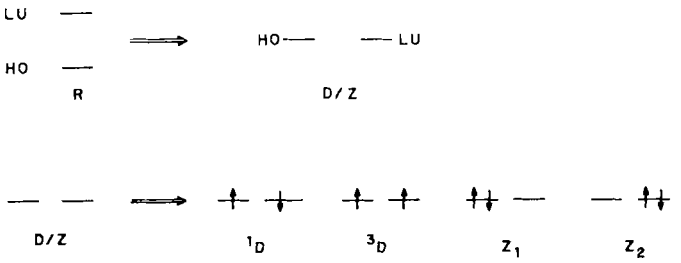


Fig. 16. The relationship between HO and LU orbitals and D/Z structures. Above: A chemical reaction results in transformation of the well-separated HO and LU orbitals of the starting structure R into a pair of orbitals of comparable energy for the diradicaloid structure D/Z. Below: The four electronic states (^1D, ^3D, Z_1, Z_2) of the D/Z structure.

In Figure 16, the states, (labeled ^1D, ^3D, Z_1, and Z_2) that are possible for the two electronic configurations of the D/Z structure, are shown. Let us now generate the possible connections that would constitute reaction graphs of a hydrocarbon system for which the state compositions are *only* S_0, T_1, S_1, and S_2 for R and ^1D, ^3D, Z_1, and Z_2 for D/Z. For hydrocarbons, the energy of the ^1D and ^3D states are expected to be similar, as are the energies of the Z_1 and Z_2 states.[29] The Z_1 and Z_2 states can be considered as a unit because of their similar energies and electronic and spin configurations. The ^1D and ^3D states, however, cannot be considered as a unit, because they have different spin configurations. In making connections between the states of R and D/Z, orbital occupancy and electron spin are used as descriptors at the topological level. In Figure 17, the transformation R→D/Z can be viewed as a reaction graph (termed a Salem diagram) for this structural change starting from any one of the four lowest-lying electronic states

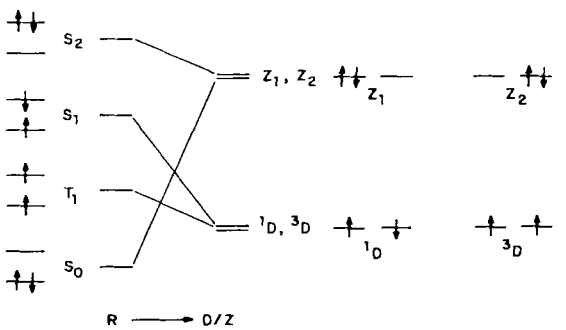


Fig. 17. Reaction graph for the transformation R→D/Z (see text).

of R. The topological arguments are independent of the detailed chemical structure of R or D/Z. The next critical questions are how to map the reaction graph of Figure 17 onto plausible experimental examples and how, for a given system, to generate crucial experiments to eliminate by strong inference all candidates that cannot be mapped onto the reaction graph.

6.3. Some Archetypical Reaction Graphs Involving D/Z Structure

As examples of topological thinking in the use of reaction graphs, we shall consider two families of reactions involving D/Z structures along the reaction pathways. One family is typified by the *cis-trans* isomerization of a carbon-carbon double bond and the other family by a hydrogen-abstraction reaction.

The twisting and breaking of a carbon-carbon π bond may be imagined to occur as follows:[27] as an ethylene molecule is twisted, it eventually arrives at a structure in which the two methylene groups are mutually perpendicular (Fig. 18). At this diradicaloid geometry the π bond is completely broken. The resulting 1,2-diradical can be described by four electronic D/Z states. Twisting about the

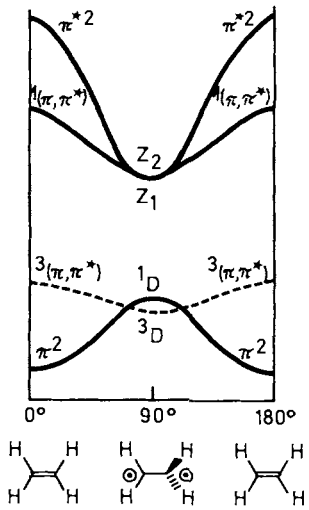
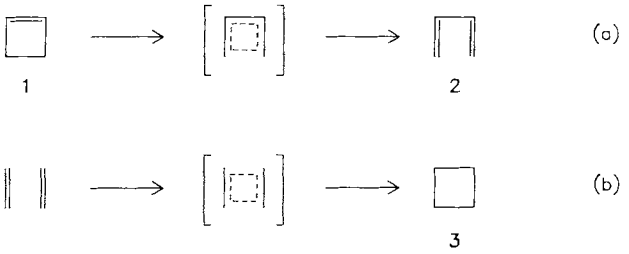


Fig. 18. State correlation diagram or reaction graph for the *cis-trans* isomerization of ethylene.

carbon-carbon bond of excited ethylene sharply relieves electron-electron repulsion, thereby lowering the energy of any ethylene state for which bonding is not important (because electronic excitation has already effectively broken the bond). As a result, the electronic energies of S_2, S_1, and T_1 drop rapidly as a function of the twist angle. At the same time, the electronic energy of S_0 increases as the molecule is twisted, because the π bond is being broken without any compensating bond formation. The breaking of a π bond by twisting is thus a prototype of a ground-state-forbidden concerted reaction, such as the disrotatory ring opening of cyclobutene **1** to give 1,3-butadiene **2** [Eq. (a)]

or the suprafacial-suprafacial [2+2] cycloaddition of two molecules of ethylene to give cyclobutane **3** [Eq. (b)].



(a)

(b)

The correlations $S_0 \rightarrow {}^1D$, $T_1 \rightarrow {}^3D$, $S_1 \rightarrow Z_1$, and $S_2 \rightarrow Z_2$ may be made on the basis of orbital-symmetry considerations.[26,27] The symmetry operation that brings the starting planar geometry into the twisted (diradicaloid) geometry is a rotation of one CH_2 group. The overall state symmetries must be definable in terms of this symmetry operation. Although the state correlation is best accomplished by use of group theory and point-group analysis, the following qualitative description indicates the basis of the correlation.

The wave function for the π^2 configuration (Fig. 18) at the planar geometry is essentially covalent in character, that is, there is very little ionic character to planar, ground-state ethylene; in terms of the p orbitals on the two carbon atoms, p_1 and p_2, the π^2 wave function has the form $p_1(\uparrow)p_2(\downarrow)$. This means that at all times there is only one p electron near each carbon atom, and the two electrons have paired spins. For the $^3(\pi,\pi^*)$ configuration at the planar geometry there can never be two electrons on one carbon in the same p orbital since the electrons have parallel spins (violation of the Pauli principle). The triplet (T_1) state is purely covalent and has no ionic character; its wave function has the form $p_1(\uparrow)p_2(\uparrow)$.

The wave functions for $^1(\pi,\pi^*)$ and π^{*2} must differ from that for π^2, because these two states are much higher in energy. They are best described by zwitterionic wave functions.[26,27]

The twisting of a π bond thus represents a prototype topological reaction surface. The state correlation diagram (Fig. 17) exhibits the following qualitative features:

1. The occurrence of minima in the S_2, S_1, and T_1 surfaces near the D/Z structure.
2. A maximum in the S_0 surface near the D/Z structure.
3. The close approach of the S_0 and T_1 surfaces near the D/Z structure.

The important topological features of these surfaces are the existence of four surfaces, their energetic ordering, and their electronic character. The closeness of approach of the ^1D and ^3D surfaces and of the Z_1 and Z_2 surfaces is not topologically significant but is geometrically significant, as shown for the examples discussed below.

6.4. Application of Prototype Surfaces to Experimental Examples

If they are to be useful, prototype reaction surfaces should be "topologically adjustable," that is, mappable onto different but related experimental examples. We shall start by considering the prototype surfaces for π-bond twisting, since we have just shown that the topological form of this surface may be viewed[26,27] as being equivalent to all thermally forbidden concerted ground-state reactions! This means that the twisting and breaking of the π bond of ethylene can be topologically mapped onto any 4n-electron concerted electrocyclic reaction or cycloaddition reaction.[25]

The mapping procedure can be simplified by invoking Kasha's rule,[30] which states that in solution only the S_0, T_1, and S_1 states are involved in organic photoreactions. Kasha's rule allows us to ignore S_2 (or any higher singlet state) and to consider only correlations involving the S_0, T_1, and S_1 states and the corresponding states of the D/Z structure. The movement of a representative point along each of the three lowest-energy surfaces (S_0, T_1, and S_1) in the prototype diagram is shown in Figure 19. Movement of the representative point along the S_0 and T_1 surfaces is chemically interesting in the region of the diradicaloid structure. At and near this structure, the S_0 and T_1 surfaces "come close together," so that there is a high probability for "jumping" from the S_0 to the T_1 surface (Fig. 19, left) or from the T_1 surface to the S_0 surface (Fig. 19, middle). Since jumping from one surface to another implies a topological change (in this case, change in the electron spin of the system), such jumps can only occur if the "topology" of the total experimental system is conserved. Therefore, somewhere in the experimental system a corresponding and compensating spin change must occur. Thus, an $S_0 \rightarrow T_1$ or $T_1 \rightarrow S_0$ jump is possible when the surfaces get close, but is not probable unless certain selection rules are obeyed. Chemically, the pertinent selection rules state that either strong electron spin-electron orbit (spin-orbit) coupling or electron spin-nuclear spin (hyperfine) coupling is needed for efficient $S_0 \rightarrow T_1$ or $T_1 \rightarrow S_0$ jumps near the diradicaloid structure.[31]

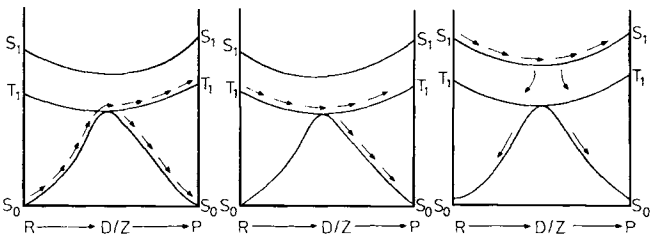


Fig. 19. Prototype reaction graph for a ground-state-forbidden concerted reaction showing various pathways for motions of a representative point along the reaction surfaces (see text).

The most important feature of the S_1 surface (Fig. 19, right) is the occurrence of a zwitterionic minimum near the D/Z structure; this minimum corresponds to the geometry at which $S_1 \rightarrow S_0$ transitions will occur. These transitions are spin allowed and can occur as rapidly as a means of "dumping" the electronic energy of the $S_1 \rightarrow S_0$ transition into vibrational or collision energy can be found. The position of the minimum is not a topological property of the system and may occur at the diradicaloid structure or at a

position corresponding to a structure "on either side" of the diradicaloid structure. Furthermore, other minima may occur owing to energetic features not explicitly considered.[32,33]

We have now developed a paradigm that can be used to generate experimental puzzles and to guide the search for solutions. To the extent that the paradigm is correct, only the experimentalist's ability to articulate the paradigm experimentally will determine whether the puzzle is solved. The paradigm has the following implications:

1. At diradicaloid geometries, $S_0 \rightarrow T_1$ and $T_1 \rightarrow S_0$ jumps are possible if an adequate mechanism for intersystem crossing is available and can operate. Since intersystem crossing can occur near the minimum of the T_1 surface, there is generally sufficient time for a spin-orbit or hyperfine interaction, which will promote the $T_1 \rightarrow S_0$ jump, to occur. A more remarkable possibility suggested by the paradigm (Fig. 19, left) is that an $S_0 \rightarrow T_1$ jump is possible, and, since this corresponds to a "chemiexcitation," it could result in chemiluminescence if phosphorescence can occur from T_1 of the product. The efficiency of the $S_0 \rightarrow T_1$ jump will depend on the efficiency of the spin change in the region of the diradicaloid structure.
2. An $S_1 \rightarrow S_0$ jump is possible from the minimum in the S_1 surface to the S_0 surface; the corresponding structure will reflect the nuclear geometry of the S_1 minimum. An intriguing possibility suggested by the paradigm is that the rapid removal of thermal energy will cause the representative point (Fig. 19) to "slide" rapidly toward the minimum on whichever side of the S_0 curve it lands.

We will now present experimental examples of photochemical and chemiluminescent reactions whose qualitative features can be readily interpreted in terms of "topological distortions" of the prototype energy surface.

6.4.1. The cis-trans Isomerization of Alkenes

An example of the archetypical reaction graph for a ground-state-forbidden reaction is shown in Figure 20, left, along with reaction graphs for the *cis-trans* isomerization of stilbene[34] (Fig. 20, middle) and 1-alkyl-2-anthrylethylenes[35] (Fig. 20, right). From experimental data the relative (and, in some cases, the absolute) positions of the S_0, S_1, and T_1 surfaces have been determined. The energy barrier indicated between the *trans*-stilbene structure and the D/Z structure on the S_1 and T_1 surfaces (Fig. 20, middle) is consistent with photochemical quenching data and temperature effects. There is no evidence for a barrier between the *cis*-stilbene structure and the D/Z structure on either the S_1 or T_1 surface. The representative behavioral points proceeding to *cis* and *trans* product starting from either *cis*- or *trans*-stilbene on either the S_1 or T_1 surface are consistent with the results of direct photoexcitation and triplet-sensitized excitation experiments.[34]

In the case of 1-alkyl-2-anthrylethylenes, e.g., *cis*- and *trans*-1-(2-anthryl)-3,3-dimethyl-1-butene,[35] the photoisomerizations are "one way" on both the S_1 and T_1 surfaces; that is, direct or triplet-photosensitized excitation of

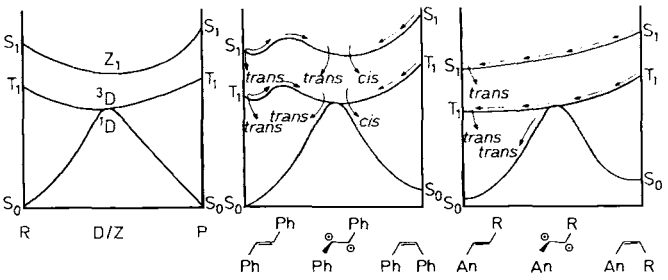


Fig. 20. Left: The prototype reaction graph of a ground-state-forbidden reaction. Middle: The "reaction structure" for *cis-trans* isomerization of stilbene. Right: The "reaction structure" for *cis-trans* isomerization of 1-alkyl-2-anthrylethylenes. An = anthryl. See text for discussion.

cis- or *trans*-1-alkyl-2-anthrylethylene results only in formation of *trans* product. This result is rationalized by postulating the lack of an effective attractor minimum at the D/Z structure on the S_1 or T_1 surface.

6.4.2. The Interconversion of Norbornadiene and Quadricyclane

The interconversion of norbornadiene (N) and quadricyclane (Q) is an example of a thermally forbidden concerted [2+2] cycloaddition reaction.[25,36] Accordingly, the prototype energy-surface diagram for thermally forbidden concerted reactions (cf. Fig. 20, left) can be used again as a paradigm to examine N and Q on the S_0, T_1, and S_1 surfaces.

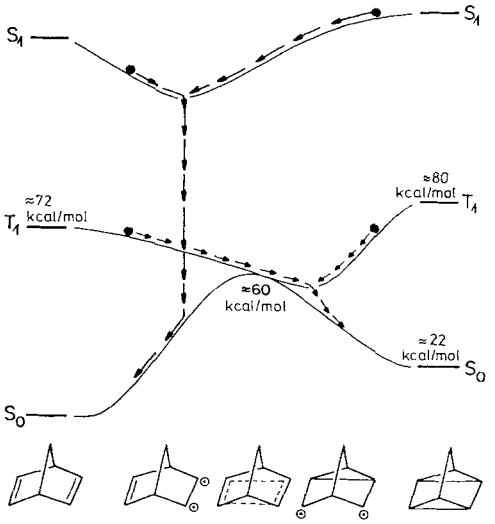


Fig. 21. Reaction graph for the norbornadiene to quadricyclane isomerization. See text for discussion. ● = representative point.

Mapping of prototype reaction graph for a thermally forbidden concerted reaction onto the N and Q systems produces the reaction graph shown in Figure 21. The prototype paradigm allows arguments to be made concerning the position of the minimum on the S_1 and on the T_1 surface relative to the ground-state maximum. Since the S_1 surface is expected to have zwitterionic character near the diradicaloid structure, a charge-separated zwitterionic

structure is expected. Of the two zwitterionic structures conceivably formed via approach from N or from Q, the one having a 1,2 arrangement of positive and negative charges, N_Z, is expected to be more stable than the one having a 1,3 arrangement, Q_Z, on account of simple Coulombic factors (Fig. 22, top). The structure corresponding to the S_1 minimum should therefore resemble the 1,2 charge-separated species N_Z; that is, the minimum on the S_1 surface should occur on the N side of the ground-state maximum.

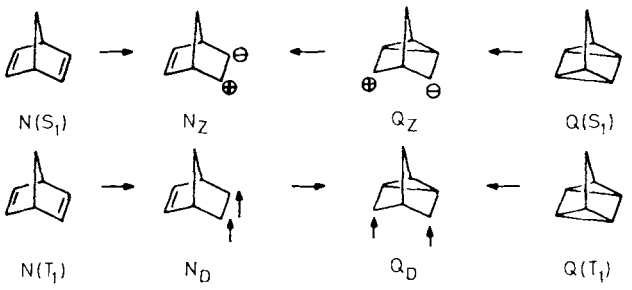


Fig. 22. Relationships of norbornadiene and quadricyclane structures to zwitterion species (top) and diradical species (bottom). See text for discussion.

A similar line of reasoning for the T_1 surface suggests that the species with a 1,3 separation of parallel spins, Q_D, should be more stable than that with a 1,2 separation, N_D (Fig. 22, bottom). The structure corresponding to the minimum on the T_1 surface should resemble the 1,3 diradical Q_D; that is, the minimum on the T_1 surface should occur on the Q side of the ground-state maximum.

Even though the above line of reasoning is qualitative, the paradigm leads to experimentally verifiable predictions; for example, either N or Q is the major product depending on the surface on which the representative point finds itself. Anytime a representative point is placed on the S_1 surface, N is the expected product, since the minimum on S_1 carries the point, via internal conversion, to S_0 on the N side. Anytime a representative point is placed on the T_1 surface, Q is the expected product, since the minimum on T_1, corresponding to Q_D, carries the point, via intersystem crossing, to S_0 on the Q side.

The paradigm has thus produced a framework to generate experimental puzzles and to articulate experimental solutions. How can the point be placed on the S_1 or T_1 surfaces? Experimentally the point can in principle be placed on the S_1 surface by direct photoexcitation of N or by direct photoexcitation of a precursor such as the azo compounds **4** and **5** (Fig. 23). The paradigm, if correct, predicts that, irrespective of precursor structure, the major product from the S_1 surface will be N and the major product from the T_1 surface will be Q. Thus, eight predictions can be made, each of which has been confirmed experimentally![37]

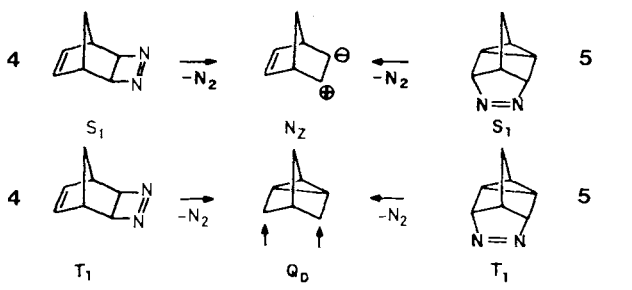


Fig. 23. Azo precursors **4** and **5** for N_Z (S_1 surface) and Q_D (T_1 surface). Top: On the S_1 surface both N and Q structures collapse to a zwitterionic structure, N_Z. Bottom: On the T_1 surface both N and Q structures collapse to a diradical structure, Q_D.

6.4.3. *The Chemiluminescent Electrocyclic Rearrangement of Dewar Benzene to Triplet Benzene*

The rearrangement of Dewar benzene to benzene may be viewed as a forbidden ground-state disrotatory electrocyclic reaction.[38] The prototype energy-surface diagram for thermally concerted reactions (Fig. 19) can therefore be used as a paradigm to examine the chemistry of Dewar benzene in its S_0, T_1, and S_1 states.

Initially, the prototype energy-surface diagram must be modified to accomodate any experimental data available for the Dewar benzene-benzene system. For example,[38] Dewar benzene is approximately 60 kcal/mol (ΔH_0) less stable than benzene, and the activation enthalpy, $\Delta H^{\neq}$, for the rearrangement of Dewar benzene to benzene is about 30 kcal/mol. The state energies for S_0, T_1, and S_1 for Dewar benzene and benzene are used to construct the energy-surface correlation diagram shown in Figure 24. The paradigm shows that three reactions are energetically conceivable: (1) the thermal production of triplet benzene; (2) the adiabatic conversion of triplet Dewar benzene to triplet benzene; (3) the adiabatic conversion of excited singlet Dewar benzene to excited singlet benzene.

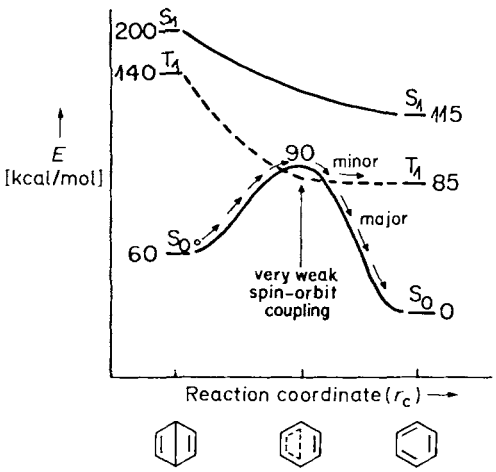


Fig. 24. Energy-surface correlation diagram ("reaction structure") for the Dewar benzene to benzene transformation.

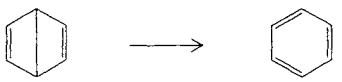
Experimentally, chemiluminescence is observed upon thermolysis of Dewar benzene and triplet benzene is produced, albeit in very low yield.[38] The reason for the low yield is readily explained by the paradigm in one of two ways: (1) The diradicaloid structure does not allow sufficiently strong spin-orbit coupling (which is expected to be

the only spin-flipping mechanism capable of causing an $S_0 \rightarrow T_1$ jump); (2) the time spent by the representative point in the region of the diradicaloid structure is too small to allow spin-orbit coupling to develop. Of course, a third possibility is that the paradigm is quantitatively incorrect with respect to the energetics; that is, the simplified two-dimensional representation may be misleading with respect to the energy of the diradicaloid structure.

The paradigm has thus created puzzles for the experimentalist: Is it the near absence of spin-orbit coupling, the too short time scale, or the energy that causes the low yield of triplet benzene? Can one devise a convincing test?

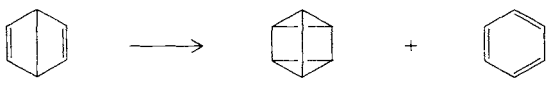
It is well established that certain "heavy atoms" such as halogens enhance spin-orbit coupling.[28] Thus, a specific test of the puzzle is to study the thermolysis of a Dewar benzene having a heavy-atom substituent. The paradigm suggests that thermolysis of a halogenated Dewar benzene should produce higher yields of triplet benzene if the near absence of spin-orbit coupling is the major factor in determining the yield of triplets. Experimentally, the thermolysis of 1,4-dichloro Dewar benzene produced a yield of triplets that was five times higher than that produced from Dewar benzene itself.[38]

The triplet state of Dewar benzene may be produced by triplet sensitization of Dewar benzene.[39] According to the paradigm (Fig. 24), an efficient adiabatic reaction along the T_1 surface is highly probable for the same reason that the $S_0 \rightarrow T_1$ jump is inefficient (i.e., the absence of an efficient spin-flipping mechanism). Experimentally, this prediction has been confirmed; triplet Dewar benzene **6**(T_1) produces triplet benzene **7**(T_1) [Eq. (c)].[39]



(c)

The paradigm further suggests that an adiabatic reaction along the S_1 surface is possible because S_1 of benzene is lower than S_1 of Dewar benzene and because the S_1 surface is separated from the S_0 surface all along the reaction coordinate. Experimentally, no evidence has been found for this adiabatic reaction. Instead, prismane **8** and ground-state benzene **7**(S_0) were produced by excitation of Dewar benzene **6** to the S_1 excited state [Eq. (d)].[38] This corresponds to a different process that is in competition with and evidently faster than the process leading to excited singlet benzene.

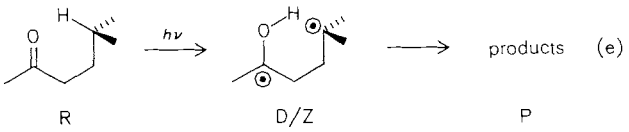


(d)

This paradigm has nothing to say directly about the formation of prismane **8**. The paradigm does, however, provide a possible explanation for the formation of ground-state benzene, since an attractor minimum on the S_1 surface is suggested as a possibility in the prototype surface (Fig. 19). Should the representative point be "captured" by this minimum, and if the minimum occurs on the benzene side of the ground-state maximum, internal conversion would lead to benzene.

6.4.4. *Reactions of n,π* Excited States*

The reactions of the n,π* excited states of carbonyl compounds are among the best understood of all photochemical processes. The n,π* state has topological features relative to a symmetry plane that allow the generation of topological reaction graphs that are applicable to a wide range of photoreactions.



(e)

A prototype reaction is intramolecular hydrogen abstraction by an excited carbonyl compound (Norrish type II photoreaction) [Eq. (e)]. The primary photochemical product is a diradicaloid structure, so that the overall transformation corresponds to an R→D/Z structural transformation. Application of the topological reaction graph for such transformations (Fig. 17) gives Figure 25. Starting from the $S_1(n,\pi^*)$ state there is an adiabatic connection to ^1D and starting from the $T_1(n,\pi^*)$ state there is an adiabatic connection to ^3D. Thus, both reactions are *topologically allowed* in the sense that the direct connections $S_1 \rightarrow {}^1D$ and $T_1 \rightarrow {}^3D$ exist.

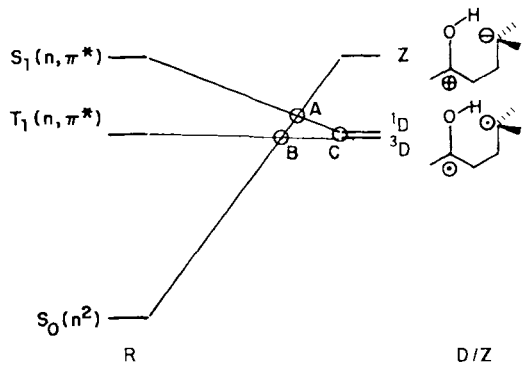


Fig. 25. Prototype reaction graph for the intramolecular hydrogen abstraction of photoexcited ketones. For A, B, and C, see text.

Since these arguments are topological, moreover, they are independent of the specific molecular structure we have selected to exemplify the reaction graph (i.e., S_0, T_1, S_1, ^1D, ^3D, and Z are merely symbols given to the abstract topological points!). Therefore, any conclusions derived for the specific example may be mapped onto all examples of H-atom abstractions from n,π* excited states of carbonyl compounds or n,π* states of compounds containing other functional groups. Furthermore, the reaction graph applies to any reaction that is topologically equivalent to (or homeomorphic with) hydrogen abstraction, that is, any

reaction involving low-lying $S_1(n,\pi^*)$ or $T_1(n,\pi^*)$ excited states in which the n orbital draws electron density from a substrate. Important examples are additions to alkenes, electron abstraction from amines, and the formation of exciplexes.[28]

Among the chemically interesting aspects of the reaction graph (Fig. 25) is the occurrence of three regions, A, B, and C, where different states have similar energies for the same structure. In these regions a transition from one state to the other is only expected to be favorable if a mechanism is available and if selection rules are obeyed. For example, the region A corresponds to structures for which the $S_1 \rightarrow {}^1D$ surface and $S_0 \rightarrow Z$ surface have comparable energies. This region is analogous to a traffic intersection. If a representative point moves down the $S_1 \rightarrow {}^1D$ surface relatively slowly, it may be driven by thermal collisions in one of three directions when it arrives in region A: toward Z, toward S_0, or toward ^1D. Since Z is higher in energy, this pathway is least likely. Thus, the plausible topological pathways are $S_1 \rightarrow A \rightarrow S_0$ and $S_1 \rightarrow A \rightarrow {}^1D$ (Fig. 26). In fact,

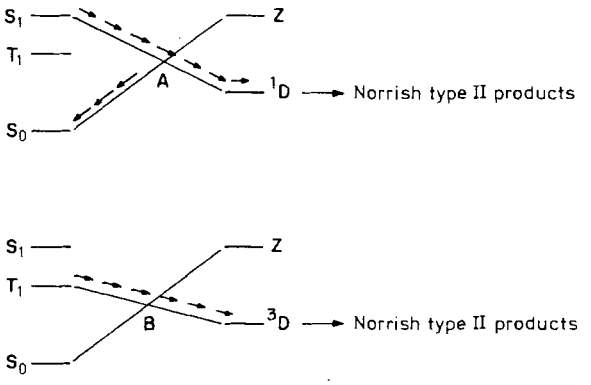
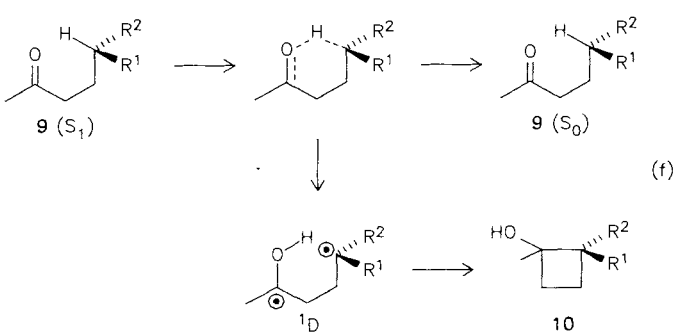


Fig. 26. Possible reaction pathways along the reaction graph for intramolecular hydrogen abstraction of photoexcited ketones.

experimental evidence in favor of the occurrence of both $S_1 \rightarrow A \rightarrow S_0$ and $S_1 \rightarrow A \rightarrow {}^1D$ pathways is available from the observation that an optically active ketone in the S_1 excited state, **9**(S_1), undergoes Norrish type II reaction both to form an optically active cyclobutanol **10** and to regenerate the starting structure **9**(S_0) without loss of optical activity [Eq. (f)].[40]

The situation is different for region B (Fig. 25), because the $S_0 \rightarrow Z$ surface is close to the $T_1 \rightarrow {}^3D$ surface and the surfaces differ in their spin characteristics. Transition from



(f)

one state to the other in region B requires a mechanism for intersystem crossing. In general, the rates of intersystem crossing in diradicals are relatively slow compared with motion (vibrational relaxation) along a surface. Nonetheless, the possibility of a jump from T_1 to S_0 is suggested by the reaction graph. Experimentally, it appears that only the $T_1 \rightarrow {}^3D$ pathway is followed (Fig. 26), since the quantum yield for product formation from T_1 can approach unity, that is, each molecule in the T_1 state produces products derived from the ^3D state.[41]

Region C (Fig. 25) is of interest from the standpoint of topology, because at geometries near C the ^1D and ^3D states are nearly degenerate. This means that weak magnetic forces whose energies are of the order of the energy difference between ^1D and ^3D can induce intersystem crossing between these states. There is considerable evidence that intersystem crossing from ^3D to ^1D is the rate-limiting step in reactions of triplet diradicals.[42]

7. Geometry, Intuition, and Imagination

In conclusion, we consider the possible relationships between geometry, intuition, and imagination. Intuition may be defined as an instantaneous comprehension or apprehension of an object or an event in the past, present, or future. In the spirit of the themes put forth in this article, some intuitions might be defined in terms of the instantaneous comprehension of a geometry representing an object or an event. Imagination may be defined as the power of creating or inventing mental images of what is not actually present and of perceiving the resemblances between apparently different objects and events. We can therefore view imagination as the manipulation of geometries, for example, in topological mapping.

In organic chemistry the classic figures of Euclidean geometry have provided the driving force for enormous efforts in organic syntheses. Of particular note is the role of the Platonic solids such as the tetrahedron,[43] the cube,[44] and the dodecahedron.[45] The belief in the reality of chemical objects that can be represented by these geometric figures and the realization of the syntheses of materials whose chemical properties correspond precisely to those expected from conventional scientific paradigms represents, in the author's opinion, a spectacular achievement of the highest order of intellect and scientific skill. Perhaps the future will bring comparable accomplishments involving the use of topological figures, especially those whose geometric properties are not revealed by an intuition that is provided by Euclidean geometry alone: for example, knots and Möbius strips.[46]

From time to time chemists create ideas that are judged by the profession to be imaginative, intuitive, and novel. Whether the values discerned in these ideas by the community of practitioners are intellectual, aesthetic, or practical, there is a consensus that such ideas increase the rate at which progress can be made in the field. It has been suggested that imaginative and creative thinking are distinguished from ordinary everyday thinking by a willingness to accept vaguely defined statements and to structure them, by a persistent preoccupation with puzzles before

solutions are apparent, and by extensive intuitive knowledge of the relevant aspects of puzzles.[47] The ability to achieve sudden insights into situations by recognizing similarities between new puzzles and solved puzzles would appear to depend on the ability of the brain to recognize familiar patterns and clues for the mapping of these patterns onto new puzzles.

Polanyi[48] has proposed that great scientific discoveries are made by practitioners who believe in the attribution of reality to scientific concepts, and that there can be an a priori knowledge of such underlying realities. He terms this knowledge a vision:

> ... the vision of a hidden reality, which guides a scientist in his quest, is a dynamic force. At the end of the quest the vision is becalmed in the contemplation of the reality revealed by a discovery; but the vision is renewed and becomes dynamic again in other scientists and guides them to new discoveries.

Polanyi[48] further notes that the vision is driven by the strength of imagination guided by intuition, which is homeomorphic with the view that the strengths of creativity in intellectual processing are guided by geometry.

The author thanks the National Science Foundation and the Air Force Office of Scientific Research for their generous support of this investigation. The author is also tremendously indebted to numerous friends and colleagues who over the past decade have participated with him in delightful discussions of the geometric and topological approaches to intellectual processing in the chemical sciences. A special thanks goes to Professor Lionel Salem for providing, over many years, a stimulating and revealing tutorial on seeking sameness in the solution of chemical puzzles.

Received: October 14, 1985 [A 592 IE]
German version: *Angew. Chem. 98* (1986) 872

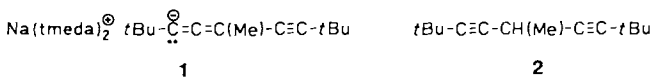
[1] H. Gardner: *Frames of Mind*, Basic Books, New York 1983.
[2] L. V. Rigby, *CHEMTECH 1* (1971) 348.
[3] a) R. Thom: *Structural Stability and Morphogenesis*, Benjamin, New York 1975, p. 11; b) *ibid.*, p. 5; c) *ibid.*, p. 6.
[4] J. Piaget, B. Inhelder *The Child's Conception of Space*, Routledge and Paul, New York 1956; J. Piaget, B. Inhelder, A. Szeminska: *The Child's Conception of Geometry*, Routledge and Paul, New York 1960; R. Good, E. K. Mellon, R. A. Kromhout, *J. Chem. Ed. 55* (1978) 688, and references cited therein.
[5] P. Alexandroff: *Elementary Concepts of Topology*, Dover, New York 1961.
[6] B. H. Arnold: *Intuitive Concepts in Elementary Topology*, Prentice-Hall, Englewood Cliffs, NJ 1962.
[7] D. Hilbert, S. Cohn-Vossen: *Geometry and the Imagination*, Chelsea Publishers, Chelsea, England 1952.
[8] J. R. Platt, *Science 146* (1964) 347.
[9] a) T. S. Kuhn: *The Structure of Scientific Revolutions*, University of Chicago Press, Chicago 1970; b) *ibid.*, p. 5.
[10] We thank Prof. *R. Hoffmann*, Cornell University, for a discussion and suggestions on these points.
[11] Plato: *Meno*.
[12] a) C. Trindle, *Croat. Chem. Acta 57* (1984) 1231; b) C. J. Suckling, K. E. Suckling, C. W. Suckling: *Chemistry Through Models*, Cambridge University Press, Cambridge, 1978.
[13] K. Mislow, *Isr. J. Chem. 15* (1976/77) 1.
[14] G. S. Hammond, J. Osteryoung, T. H. Crawford, H. B. Gray: *Models in Chemical Sciences*, Benjamin, New York 1971, p. 4.
[15] K. Mislow: *Introduction to Stereochemistry*, Benjamin, New York 1966; D. H. R. Barton, *Experientia 6* (1950) 316.
[16] A. M. Butlerov, *Z. Chem. Pharm. 1861*, 549; V. Prelog, *Chem. Br. 4* (1968) 382, and references cited therein.
[17] J. H. van't Hoff, *Chem. Weekbl. 1* (1904) 516.
[18] J. A. Le Bel, *Bull. Soc. Chim. Fr. 22* (1874) 337.
[19] V. I. Sokolov, *Russ. Chem. Rev. 42* (1973) 452.
[20] A. S. Dreiding, K. Wirth, *MATCH 1980*, 341.
[21] H. Kolbe, *J. Prakt. Chem. [2] 15* (1877) 473.
[22] M. Planck, *Naturwissenschaften 33* (1946) 230.
[23] K. Fukui, *Top. Curr. Chem. 15* (1970) 1; R. G. Pearson, *Symmetry Rules for Chemical Reactions*, Wiley, New York 1976.
[24] G. S. Hammond, *J. Am. Chem. Soc. 77* (1955) 334.
[25] R. B. Woodward, R. Hoffmann: *The Conservation of Orbital Symmetry*, Verlag Chemie/Academic Press, New York 1970; *Die Erhaltung der Orbitalsymmetrie*, Verlag Chemie, Weinheim 1970.
[26] L. Salem, *Pure Appl. Chem. 33* (1973) 317; *J. Am. Chem. Soc. 96* (1974) 3486.
[27] J. Michl, *Mol. Photochem. 4* (1972) 243, 257, 287.
[28] N. J. Turro: *Modern Molecular Photochemistry*, Benjamin/Cummings, Menlo Park, CA, USA 1978.
[29] W. G. Dauben, L. Salem, N. J. Turro, *Acc. Chem. Res. 8* (1975) 41.
[30] M. Kasha, *Discuss. Faraday Soc. 9* (1950) 14.
[31] L. Salem, C. Rowland, *Angew. Chem. 84* (1972) 86; *Angew. Chem. Int. Ed. Engl. 11* (1972) 92.
[32] B. Bigot, A. Devaquet, N. J. Turro, *J. Am. Chem. Soc. 103* (1981) 6.
[33] J. Michl, *Top. Curr. Chem. 46* (1974) 1.
[34] J. Saltiel, J. D'Agostino, E. D. Megarity, L. Mitts, K. Neuberger, M. Wrighton, O. C. Zabiriom, *Org. Photochem. 3* (1973) 1, and references cited therein.
[35] T. Arai, T. Karatsu, H. Sakuragi, K. Tokumaru, *Tetrahedron Lett. 24* (1983) 2873; T. Karatsu, T. Arai, H. Sakuragi, K. Tokumaru, *Chem. Phys. Lett. 115* (1985) 9.
[36] W. G. Dauben, R. L. Cargill, *Tetrahedron 15* (1961) 197; N. Ivanoff, F. Lahman, J. F. DeLouis, T. L. LeGouill, *J. Photochem. 2* (1973) 199; G. S. Hammond, N. J. Turro, A. Fischer, *J. Am. Chem. Soc. 83* (1961) 4674.
[37] N. J. Turro, W. R. Cherry, M. F. Mirbach, M. J. Mirbach, *J. Am. Chem. Soc. 99* (1977) 7388.
[38] P. Lechtken, R. C. D. Breslow, A. H. Schmidt, N. J. Turro, *J. Am. Chem. Soc. 95* (1973) 3025.
[39] N. J. Turro, V. Ramamurthy, T. J. Katz, *Nouv. J. Chim. 1* (1977) 363.
[40] N. C. Yang, S. P. Elliot, *J. Am. Chem. Soc. 91* (1969) 9550, 9551.
[41] N. J. Turro, V. Ramamurthy, *Mol. Photochem. 8* (1977) 239.
[42] J. C. Scaiano, *Tetrahedron 38* (1982) 819; P. J. Wagner, *Acc. Chem. Res. 16* (1983) 461; N. J. Turro, B. Kraeutler in W. T. Borden (Ed.): *Diradicals*, Wiley, New York 1982, p. 259.
[43] G. Maier, S. Pfriem, U. Schäfer, R. Matusch, *Angew. Chem. 90* (1978) 552; *Angew. Chem. Int. Ed. Engl. 17* (1978) 520.
[44] P. E. Eaton, T. W. Cole, *J. Am. Chem. Soc. 86* (1964) 3157.
[45] L. Paquette, R. J. Ternashy, D. W. Balogh, W. J. Taylor, *J. Am. Chem. Soc. 105* (1983) 544.
[46] D. M. Walba, *Tetrahedron 41* (1985) 3161.
[47] H. A. Simon, *Proc. Natl. Acad. Sci. USA 80* (1983) 4569.
[48] M. Polanyi, *Chem. Eng. News 44* (1966) No. 17, p. 85.

When submitting manuscripts, authors of articles intended for publication as "Communications" are requested to read the "Notice to Authors" reproduced in the January issue of the journal following the list of contents; upon request, a copy can be obtained from the editorial office.

The Structure of an Allenylsodium Derivative—Competition between Carbanion Resonance Delocalization and Gegenion Charge Localization**

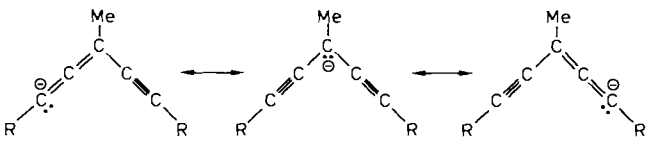
By *Christian Schade, Paul von Ragué Schleyer,* Maren Geissler,* and *Erwin Weiss**

Energies,[1] structures,[2] reactivities,[3] and reaction mechanisms[4] of the species often misleadingly designated "carbanions" may be influenced decisively by the alkali metal gegenions. A noteworthy example of the structural influence of such cations is provided by compound **1**, 3-[bis(tetramethylethylenediamine)sodium]-2,2,5,8,8-pentamethylnona-3,4-dien-6-yne,[5] the sodium salt of 2,2,5,8,8-pentamethyl-3,6-nonadiyne **2**. Concomitantly, compound **1** is the first allenylsodium derivative whose geometry has been determined by X-ray crystallography. The X-ray structures of two allenyllithium derivatives, one directly related to **1**, afford an interesting comparison.[8] Both of these are dimers, whereas **1** is a monomer.



1 **2**

Free carbanions (e.g. in the gas phase) may be stabilized by a group which delocalizes the negative charge. However, in the corresponding organometallic derivative in solution, the negative charge may be localized to a greater extent than in the free carbanion in order to maximize the electrostatic interaction with the alkali metal counterion. This principle[9] is demonstrated by the experimental results on **1**: a structure with a largely *localized* carbanion negative charge is favored over more *delocalized* alternatives.



3a, R=H; **3b**, R=Me; **3c**, R= *t*Bu

While qualitative theory (and MNDO calculations)[10] predict a resonance stabilized, symmetrical structure of the propargyl-type for the free carbanions, **3a** and **3b**, the crystal structure of **1** (Figure 1) shows the carbon skeleton to have an unsymmetrical allenyl anion topology. Hence, the resonance stabilization must have been reduced considerably. The sodium cation does not interact with the entire carbanion, as expected from the mesomeric formulations, but coordinates only with the end carbon, C_3. The bond lengths (Fig. 1) demonstrate **1** to be an allenyl derivative, with r(C3C4) = 124 pm and r(C4C5) = 138 pm. The ab initio bond lengths for allenylsodium, allenyllithium, and the allenyl anion are all about the same, 127 and 134 pm, and agree quite well with the experimental X-ray values not only for the sodium but also for both lithium derivatives (Table 1). In contrast, r(C5C6) = 144 pm and r(C6C7) = 119 pm in **1**; these bond lengths are close to those in propyne, 121 and 146 pm, as determined by microwave spectroscopy. The allene value is 131 pm.[11]

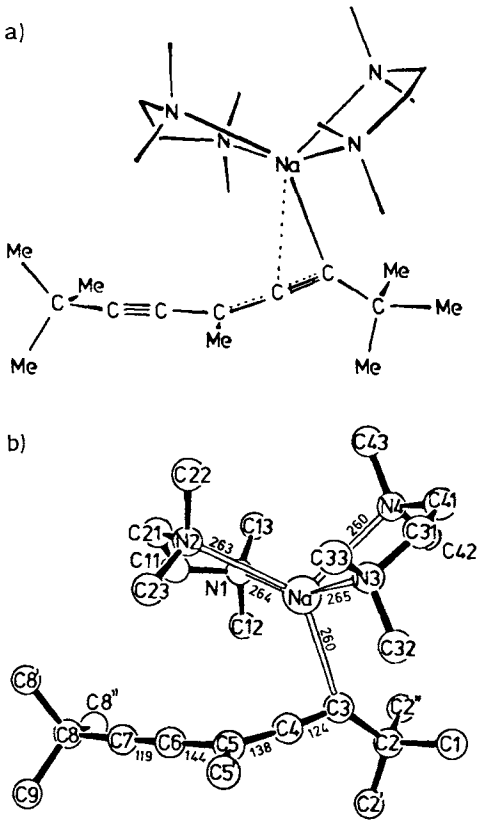


Fig. 1. Structure of **1** in the crystal. a) Schematic representation. b) SCHAKAL drawing with bond lengths [pm]. Monoclinic $P2_1/n$, a = 1005.3(4), b = 1943.8(4), c = 1620.1(4) pm, β = 99.78(3)°, ρ_{ber} = 0.9455 g cm^{-3}, Z = 4; $Mo_{K\alpha}$-radiation, structure determined with direct methods (SHELXS), refined until R = 0.090 (unweighted) with 1794 reflexes [$|F| > 4\sigma(F)$], measured until θ = 20°, H-positions isotropically refined. Important distances [pm] and angles [°]: Na-C3 259.5(9), Na-C4 280.3(9), Na-C5 345.2, Na-N (averaged) 264.6, C2-C3 152.5(14), C3-C4 124.4(14), C4-C5 137.9(14), C5-C5' 153.6(12), C5-C6 143.6(13), C6-C7 119.2(13), C7-C8 148.4(13); Na-C3-C4 86.2(6), C3-C4-C5 172.9(9), C1-C2-C3 129.0(8), C4-C5-C6 120.7(8), C4-C5-C5' 121.0(8), N1-Na-N2 71.2(3), N3-Na-N4 70.3(3). Further details of the crystal structure can be obtained from the Fachinformationszentrum Energie, Physik, Mathematik GmbH, D-7514 Eggenstein-Leopoldshafen 2 (FRG), on quoting the depository number CSD-52188, the names of the authors, and the journal citation.

[*] Prof. Dr. P. von R. Schleyer, Dipl.-Chem. C. Schade
Institut für Organische Chemie der Universität Erlangen-Nürnberg
Henkestr. 42, D-8520 Erlangen (FRG)
Prof. Dr. E. Weiss, Dipl.-Chem. M. Geissler
Institut für Anorganische und Angewandte Chemie der Universität
Martin-Luther-King-Platz 6, D-2000 Hamburg 13 (FRG)

[**] This work was supported by the Deutsche Forschungsgemeinschaft and the Fonds der Chemischen Industrie.

As the pentadiynyl anion system was too large for an examination at adequate ab initio levels, MNDO was employed for the free anions, **3a** and **3b**. However, symmetrical geometries were favored in both cases, and no allenic structures could be located on the MNDO-hypersurfaces. Instead, bending a terminal RCC angle in **3a** or **3b** by fixed increments (to approximate the allenyl geometry) led to a steady increase in energy. For example, at $\sphericalangle RCC = 129°$ (the experimental value for **1**), the energies of **3a** and **3b** are 14 and 19 kcal/mol, respectively above the equilibrium values. This result suggests that charge localization due to electrostatic interaction with the counterion competes successfully in **1** with resonance stabilization.

Table 1. Comparisons of the ab initio (6-31G* opt) and experimental (X-ray) geometries of allenyl anion moieties ($RC_\alpha=C_\beta=C_\gamma R'R'')^\ominus M^\oplus$.

Species	Bond lengths [pm]		Bond angles [°]		
	$C_\alpha C_\beta$	$C_\beta C_\gamma$	$C_\alpha C_\beta C_\gamma$	$RC_\alpha C_\beta$	$MC_\alpha C_\beta$
Calculations: R = R′ = R″ = H					
Anion (free) [12] [a, b]	127.6	134.6	175.7	118.5	—
M = Na [a]	127.6	134.0	167.0	122.7	75.8
M = Li [14e]	127.3	134.4	161.4	127.9	71.5
X-ray structure analysis: R = *t*Bu, R′ = CH_3, R″ = C*t*Bu					
M = Na (**1**) [a]	124.4(14)	137.9(14)	172.9(9)	129.0(9)	86.2(6)
M = Li, dimer [8]	128.1(2)	136.5(2)	165.6(1)	121.9(1)	73.3(1)
R = C*t*Bu, R′ = *t*Bu, R″ = H					
M = Li, dimer [8]	128.5(3)	132.5(3)	165.6(2)	126.4(2)	73.9(1)

[a] This work. [b] 6-31+G* opt.

While we believe this conclusion to be valid, another factor must be considered: the inherent preference of such anions for a more localized (bent, C_s) allenyl rather than a π-delocalized (linear, C_{2v}) propargyl structure. The latter geometry permits the charge to be distributed to a greater extent, but the former benefits from the sp^2-hybridization (more s-character) at the carbanion center. Thus, ab initio calculations show the vinyl anion to be strongly bent, with an inversion barrier of 27 kcal/mol; this value is reduced to 7 kcal/mol in the allenyl anion, due to the conjugation.[12] A gas phase photodetachment study indicates $C_3H_3^\ominus$ to have an allenyl rather than a propargyl anion structure.[13, 14]

In contrast, MNDO incorrectly finds the propargyl (C_{2v}) structure of $C_3H_3^\ominus$ to be the most stable; this systematic error must be taken into consideration in evaluating the MNDO results with **3a** and **3b**. However, the additional conjugation afforded by the acetylene substituent in **1** and **3** should favor the propargylic form and there probably is very little energy difference between C_{2v} and less symmetrical geometries for **3a** and **3b**. Counterion charge localization effects must contribute to the structures adopted by **1** and by the corresponding lithium derivative.[7]

Although sodium pentacoordination is found frequently in crystal structures,[2b] the presence of the two TMEDA ligands in **1** is noteworthy. These inhibit association; the analogous lithium compound, Li(thf)-**3c**, is a dimer.[8] The influence of these TMEDA ligands also is responsible for restricting the $Na^\oplus$ interaction to a single carbon[15] instead of allowing even the dihapto coordination in allenyl sodium. This is shown by the bond angles, NaC3C4 = 86° and C3C4C5 = 173° in **1**, compared with the calculated values of 76° and 167°, respectively, for the unsolvated species. In the latter, the sodium interacts with both end carbons of the allenyl anion system since C3 (C5 in **1**) also is negatively charged to some extent. Because of the competition due to the external complexation with two TMEDA ligands, this does not take place in **1**.

There is another consequence of the metal cation interaction: the bending of the allenyl CCC angle in **1** (173°) is closer to that calculated for the free allenyl anion (176°) than for allenylsodium (167°). Table 1 shows that these trends continue with allenyllithium. The CCC angle is 161° in the monomer, but is somewhat larger (166°) in both crystal structures. Dihapto lithium bonding (bridging) is favored in the monomer and in both crystals where the LiCC angles are all about 73°. The larger interaction energy of the smaller $Li^\oplus$ is responsible for the greater tendency towards bridging and the greater CCC deformation than in allenyl sodium. We are finding this difference in sodium-lithium behavior to be general.[16]

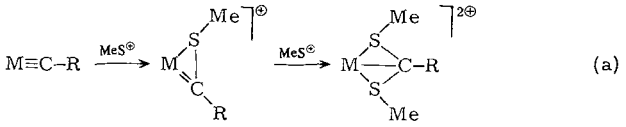
Received: May 5, 1986;
revised: July 21, 1986 [Z 1758 IE]
German version: *Angew. Chem. 98* (1986) 922

[1] P. von R. Schleyer, *Pure Appl. Chem. 55* (1983) 355; *ibid. 56* (1984) 151.
[2] a) Organolithium compounds: W. Setzer, P. von R. Schleyer, *Adv. Organomet. Chem. 24* (1985) 353; b) organometallic compounds of the higher alkali metals: C. Schade, P. von R. Schleyer, *ibid.*, in press.
[3] M. Schlosser: *Struktur und Reaktivität polarer Organometalle*, Springer, Heidelberg 1973; J. L. Wardell in G. Wilkinson, F. G. A. Stone, E. W. Abel (Eds.): *Comprehensive Organometallic Chemistry*, Vol. 1, Pergamon Press, Oxford 1982, p. 49.
[4] K. N. Houk, N. G. Rondan, P. v. R. Schleyer, E. Kaufmann, T. Clark, *J. Am. Chem. Soc. 107* (1985) 2821; E. Kaufmann, P. von R. Schleyer, K. N. Houk, Y.-D. Wu, *ibid. 107* (1985) 5560.
[5] To 2.5 g (13.2 mmol) of **2** [6] in 50 mL of dry hexane at −10°C, an equimolar quantity of the hexane-soluble *n*-butylsodium reagent with excess TMEDA [7] was added under argon. After 24 hours at −18°C, 4.6 g (10.8 mmol, 82%) of golden crystals form.
[6] W. Neugebauer, *Dissertation*, Universität Erlangen-Nürnberg 1983.
[7] C. Schade, W. Bauer, P. von R. Schleyer, *J. Organomet. Chem. 295* (1985) C 25.
[8] H. Dietrich, W. Neugebauer, P. von R. Schleyer, to be published. For details, see [1a], [2a], and [6].
[9] P. von R. Schleyer, J. Chandrasekhar, A. J. Kos, T. Clark, G. W. Spitznagel, *J. Chem. Soc. Chem. Commun. 1981*, 882; T. Clark, C. Rohde, P. von R. Schleyer, *Organometallics 2* (1983) 1344.
[10] M. J. S. Dewar, W. Thiel, *J. Am. Chem. Soc. 99* (1977) 4899, 4907; for the lithium parametrizations see W. Thiel, *QCPE 1983*, 438.
[11] J. H. Callaman, E. Hirota, K. Kuchitzu, W. J. Lafferty, A. G. Maki, C. S. Pote in K. H. Hellwege, A. M. Hellwege (Eds.): *Landolt-Börnstein Zahlenwerte und Funktionen aus Naturwissenschaften und Technik, Vol. 7 (Strukturdaten freier mehratomiger Molekeln)*, Springer, Berlin 1976.
[12] J. K. Wilmshurst, C. E. Dykstra, *J. Am. Chem. Soc. 102* (1980) 4668. Also see: J. Chandrasekhar, J. G. Andrade, P. von R. Schleyer, *ibid. 103* (1981) 5609.
[13] J. M. Oakes, G. B. Ellison, *J. Am. Chem. Soc. 105* (1983) 2969.
[14] a) Polar organometallic derivatives are known to favor allenyl over propargyl structures in solution, see J. Klein in S. Patai (Ed.): *The Chemistry of the Carbon-Carbon Triple Bond*, Part 1, Wiley, New York 1978, p. 386. This also is shown by ab initio calculations on allenyllithium: b) A. C. Hopkinson, M. H. Lien, K. Yates, P. G. Mezey, I. G. Csizmadia, *J. Phys. Chem. 67* (1977) 517; c) R. J. Bushby, A. S. Patterson, G. J. Ferbey, B. J. Duke, G. H. Whitham, *J. Chem. Soc. Perkin Trans. 2 1978*, 807; d) E. D. Jemmis, J. Chandrasekhar, P. von R. Schleyer, *J. Am. Chem. Soc. 101* (1979) 2848; e) P. von R. Schleyer, E. Kaufmann, G. W. Spitznagel, R. Janoschek, G. Winkelhofer, *Organometallics 5* (1986) 79.
[15] When quenched with D_2O or with Me_3SiCl, **1** reacts at C3.
[16] P. von R. Schleyer, T. Clark, A. J. Kos, G. W. Spitznagel, C. Rohde, D. Arad, K. N. Houk, N. G. Rondan, *J. Am. Chem. Soc. 106* (1984) 6973; J. Kaneti, P. von R. Schleyer, T. Clark, A. J. Kos, G. W. Spitznagel, J. G. Andrade, J. B. Moffatt, *ibid. 108* (1986) 1481.

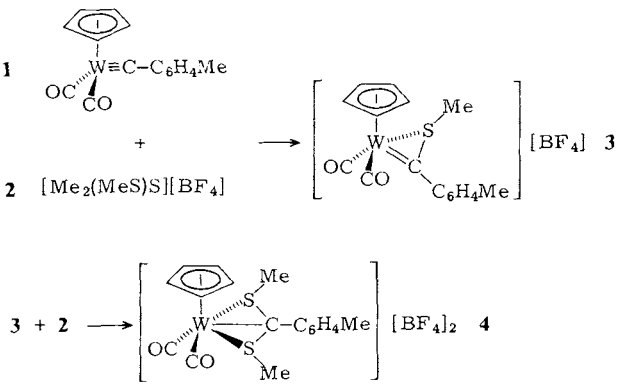
Stepwise Addition of $MeS^{\oplus}$ to a Metal–Carbon Triple Bond— A New Type of Reaction in the Chemistry of Carbyne Complexes**

By *Fritz R. Kreissl** and *Hans Keller*

Nucleophilic attack on the carbyne carbon atom predominates for carbyne transition-metal complexes;[1–4] only a few examples have been reported of electrophilic attack, which results in the formation of carbene,[5–8] acyl,[9] or binuclear alkyne complexes.[10] We have now found a novel reaction sequence (a), which is characterized by a twofold electrophilic attack on the C atom of a MC multiple bond.



Dicarbonyl(cyclopentadienyl)(4-methylphenylcarbyne)-tungsten **1**[11] reacts in a stepwise, easily observed manner with dimethyl(methylthio)sulfonium tetrafluoroborate **2** to give first the cationic η^2-thiocarbene complex **3** and then the dicationic dithiatungstabicyclo[1.1.0]butane complex **4**.[12] Complexes **3** and **4** are obtained as red and yellow solids, respectively, and are stable at room temperature. The field desorption mass spectrum of **3** exhibits a peak at *m/z* 456 ($[M+H]^{\oplus}$), that of **4** one at *m/z* 251 ($M^{2\oplus}$). In the IR spectra of **3** and **4**, recorded in solution, two very intense CO absorptions are present, the positions of which are shifted to higher wave numbers relative to those of **1** ($\tilde{\nu}_{CO}$: **3** 2052, 1995; **4** 2105, 2065 cm^{-1}). Their intensity ratio in the case of both **3** and **4** supports a *cis* arrangement of the two carbonyl ligands. The ^1H- and ^{13}C-NMR spectra[13] are in accord with the suggested structures. The position of the signal for the alkylidene C atom of **3** ($\delta = 233.1$) is in very good agreement with the shifts normally found for heteroatom-containing η^2-carbene complexes;[14] for acyclic thiocarbene complexes, however, chemical shifts are found in the region around $\delta = 330$.[15]



The addition of the $MeS^{\oplus}$ ion to **1** establishes the nucleophilic character of the carbyne C atom, as has been suggested by *Fenske* et al. for cyclopentadienyl-substituted transition-metal carbyne complexes[16] and has been demonstrated in a carbyne/acyl transformation.[9] These addition reactions can be compared very well with the protonation of a thiocarbyne complex described by *Angelici* et al.,[7] in which an η^2-thiocarbene complex is likewise formed. Until now, however, few reactions of either this η^2-thiocarbene tungsten complex or of an analogous osmium complex[17] have been described and no examples demonstrating the nucleophilic character of the carbene C atom were known. The addition of a $MeS^{\oplus}$ ion to the WC double bond present in **3** represents the first example of the electrophilic attack of a cation on a Fischer carbene complex.

Received: May 12, 1986;
revised: June 19, 1986 [Z 1768 IE]
German version: *Angew. Chem. 98* (1986) 924

CAS Registry numbers:
1, 60260-15-3; **2**, 5799-67-7; **3**, 104351-09-9; **4**, 104351-11-3.

[*] Priv.-Doz. Dr. F. R. Kreissl, Dipl.-Chem. H. Keller
Anorganisch-chemisches Institut der Technischen Universität München
Lichtenbergstrasse 4, D-8046 Garching (FRG)

[**] This work was supported by the Deutsche Forschungsgemeinschaft and the Fonds der Chemischen Industrie.

[1] F. R. Kreissl, *J. Organomet. Chem. 99* (1975) 305; F. R. Kreissl, W. Uedelhoven, G. Kreis, *Chem. Ber. 111* (1978) 3283.
[2] E. O. Fischer, P. Stückler, F. R. Kreissl, *J. Organomet. Chem. 129* (1977) 197.
[3] E. O. Fischer, W. Schambeck, *J. Organomet. Chem. 201* (1980) 311.
[4] F. R. Kreissl, P. Stückler, E. W. Meineke, *Chem. Ber. 110* (1977) 805.
[5] S. J. Holmes, D. N. Clark, H. W. Turner, R. R. Schrock, *J. Am. Chem. Soc. 104* (1982) 6322; S. J. Holmes, R. R. Schrock, *J. Am. Chem. Soc. 103* (1981) 4599; S. J. Holmes, R. R. Schrock, M. R. Churchill, H. J. Wasserman, *Organometallics 3* (1984) 476.
[6] G. R. Clark, K. Marsden, W. R. Roper, L. J. Wright, *J. Am. Chem. Soc. 102* (1980) 6570.
[7] H. P. Kim, S. Kim, R. A. Jacobson, R. J. Angelici, *Organometallics 3* (1984) 1124.
[8] F. R. Kreissl, W. J. Sieber, M. Wolfgruber, *J. Organomet. Chem. 270* (1984) C45.
[9] F. R. Kreissl, W. J. Sieber, M. Wolfgruber, J. Riede, *Angew. Chem. 96* (1984) 618; *Angew. Chem. Int. Ed. Engl. 23* (1984) 640.
[10] J. C. Jeffery, J. C. V. Laurie, I. Moore, F. G. A. Stone, *J. Organomet. Chem. 258* (1983) C37.
[11] E. O. Fischer, T. L. Lindner, F. R. Kreissl, *J. Organomet. Chem. 112* (1976) C27.
[12] *Experimental procedure*: **3**: **1** (0.36 g, 0.88 mmol) in 20 mL of acetonitrile was allowed to react at −30°C with a solution of **2** (0.15 g, 0.88 mmol) in 10 mL of acetonitrile (the solution turning from orange to red). After 1 h, unreacted **1** was extracted with 4 × 25 mL of pentane, the solvent was removed under high vacuum, and the red, oily residue was purified by repeated recrystallization from CH_2Cl_2/Et_2O/pentane. **3** (0.44 g, 95%) was obtained as an orange powder. **4**: **1** (0.66 g, 1.61 mmol) in 15 mL of acetonitrile was allowed to react with **2** (0.63 g, 3.23 mmol) in 10 mL of acetonitrile at −30°C (the solution turning yellow). Unreacted **1** was extracted once again with pentane. The acetonitrile was removed and traces of **3** were extracted from the residue with 4 × 25 mL of CH_2Cl_2. **4** was obtained as a yellow powder (1.05 g, 97%).
[13] ^1H-NMR (60 MHz, CD_3CN, CH_3CN signal ($\delta = 1.98$) as standard): **3**: $\delta = 7.73$ (m, 4H; C_6H_4), 6.16 (s, 5H; C_5H_5), 2.51 (s, 3H; SCH_3), 2.44 (s, 3H; CH_3); **4**: $\delta = 7.63$ (m, 4H; C_6H_4), 6.67 (s, 5H; C_5H_5), 2.61 (s, 6H; 2 SCH_3), 2.52 (s, 3H; CH_3). ^{13}C-NMR of **3** (90 MHz, CD_3CN, CD_3CN as standard ($\delta = 1.2$)): $\delta = 233.1$ (W=C), 209.9, 209.3 (W–CO), 145.0, 142.3, 133.9, 131.7 (C_6H_4), 96.0 (C_5H_5), 33.6 (SCH_3), 21.9 (CH_3). ^{13}C-NMR of **4** (270 MHz, CD_3NO, CD_3NO as standard ($\delta = 62.8$)): $\delta = 193.7$ (W–CO), 146.7, 137.0, 133.0, 121.8 (C_6H_4), 98.2 (C_5H_5), 27.9 (W–C), 25.9 (SCH_3), 21.6 (CH_3).
[14] F. R. Kreissl, M. Wolfgruber, W. J. Sieber, *J. Organomet. Chem. 270* (1984) C4.
[15] C. G. Kreiter, V. Formáček, *Angew. Chem. 84* (1972) 155; *Angew. Chem. Int. Ed. Engl. 11* (1972) 141.
[16] N. M. Kostic, R. F. Fenske, *J. Am. Chem. Soc. 103* (1981) 4677; *Organometallics 1* (1982) 489.
[17] G. R. Clark, T. J. Collins, K. Marsden, W. R. Roper, *J. Organomet. Chem. 259* (1983) 215.

Isothermal Magnetic Phase Transitions Controlled by Reversible Electron/Ion Transfer Reactions

By *Robert Schöllhorn** and *Andreas Payer*

One of the most intriguing aspects of the intercalation chemistry of electronically conducting host lattices is the possibility of reversibly modifying and controlling the physical properties of solid materials by chemical reactions at ambient temperature.[1] So far, interest has focused mainly on changes of electronic properties, superconductivity, optical properties and structural transitions with the reaction state. We report here on the control of *magnetic* phase transitions via reversible electron/ion transfer reactions at 300 K with copper selenospinels $Cu_{1+y}Cr_2Se_4$ as the model system. The process is correlated with the change in the stoichiometric index y; at a critical concentration y_c the *isothermal* transition takes place according to the scheme

$$\text{ferromagnetic state} \underset{y<y_c}{\overset{y>y_c}{\rightleftharpoons}} \text{paramagnetic state} \qquad (T=\text{const.})$$

Spinel type structures formally provide an excess of vacant tetrahedral and octahedral lattice sites for the potential uptake and bulk transport of additional cations. In a recent publication we have demonstrated that copper chalcogenospinels with appropriate electronic properties and mobile $Cu^{\oplus}$ ions are, in principle, able to undergo topotactic redox reactions.[2] Since the copper chromium selenospinel $CuCr_2Se_4$ exhibits metallic properties as well as ferromagnetic behavior at room temperature[3] we investigated the electrochemical behavior of this compound in aqueous and aprotic electrolyte solutions ($Cu^{\oplus}/CH_3CN$, $Cu^{2\oplus}/H_2O$). Copper ions were found to be mobile in $CuCr_2Se_4$ and a chemical diffusion coefficient $\tilde{D}(300\,K) = 5\times10^{-11}\ cm^2\ s^{-1}$ was measured. The selenospinel participates in reversible electron/ion transfer reactions according to Equations (a) and (b), which apply to the case of $Cu^{\oplus}$ and $Cu^{2\oplus}$ electrolytes, respectively.

$$Cu_1Cr_2Se_4 + \ ye^{\ominus} + yCu^{\oplus} \rightleftharpoons Cu_{1+y}Cr_2Se_4 \qquad (a)$$

$$Cu_1Cr_2Se_4 + 2ye^{\ominus} + yCu^{2\oplus} \rightleftharpoons Cu_{1+y}Cr_2Se_4 \qquad (b)$$

The potential/charge transfer diagram under dynamic conditions (galvanostatic mode) as well as equilibrium potentials for the cathodic reduction of $CuCr_2Se_4$ in aqueous $Cu^{2\oplus}$ electrolyte are given in Figure 1a. An almost continuous change in potential is observed until the potential of copper deposition where the solid state reaction has reached its endpoint. The integral charge transfer value thus obtained is $n(e^{\ominus}/CuCr_2Se_4)=2$. For aqueous electrolytes containing $Cu^{2\oplus}$ ions the formal correlation between n and the stoichiometric index y corresponds to $y=n/2$. This was confirmed by analytical data, which agree perfectly with this correlation, i.e. no measurable side reactions appear and the intercalation of copper proceeds quantitatively according to Equation (b). The X-ray data (Fig. 1b) similarly indicate a one phase system with a continuous change in lattice parameters for the range $0\leqq y\leqq 1$. The products retain cubic symmetry with $a=10.57$ Å for the terminal phase with $y=1$; the total change in volume of the unit cell amounts to 7.0%. On anodic oxidation of $Cu_2Cr_2Se_4$ the process is reversed and the starting material ($y=0$) is obtained again after a charge transfer of $n=2$; the same result is found on chemical oxidation, e.g. with I_2/CH_3CN leading to $CuCr_2Se_4$ and (soluble) CuI.

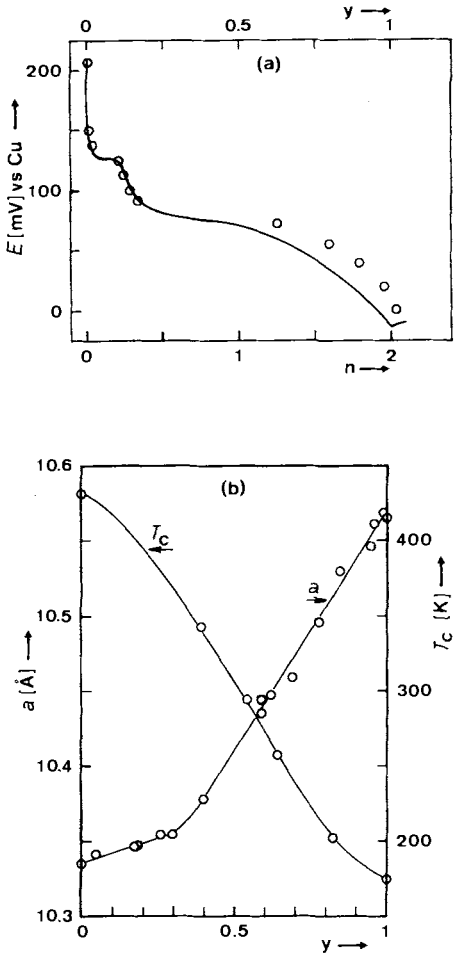


Fig. 1. a) Potential/charge transfer diagram for the galvanostatic cathodic reduction of $CuCr_2Se_4$ (pressed polycrystalline working electrodes, copper as counter electrode and as reference electrode) to $Cu_{1+y}Cr_2Se_4$ in aqueous electrolyte (0.5 M $CuSO_4$ + 0.5 M H_2SO_4); charge transfer $n(e^{\ominus}/CuCr_2Se_4)$; y = stoichiometric index; nominal current density = 1 A/m²; open circles refer to potentials measured under equilibrium conditions. b) Variation of cubic lattice constant *a* and Curie temperature T_c with the stoichiometry y of $Cu_{1+y}Cr_2Se_4$; the magnetic susceptibility was measured by means of a Faraday balance, T_c values were obtained from χ^{-1}/T plots. Results obtained for aqueous ($Cu^{2\oplus}/H_2O$) and aprotic ($Cu^{\oplus}/CH_3CN$) electrolytes are identical.

Figure 1b shows the change in Curie temperature T_c of the $Cu_{1+y}Cr_2Se_4$ phases as a function of composition in the range $0\leqq y\leqq 1$. With increasing copper content the critical temperature of the magnetic phase transition decreases significantly from 432 K ($y=0$) to 175 K ($y=1$). In the course of the *isothermal* electrochemical reaction at 300 K [Eq. (a), (b)] T_c is attained at a critical composition $y_c=0.52$ (Fig. 1b) which is correlated with a transition from the spin ordered ferromagnetic to the disordered paramagnetic state. The critical composition y_c is itself of course a function of the temperature at which the reaction proceeds. The chemical reaction is reversible and can thus be used to control the magnetic properties of the solid in

[*] Prof. Dr. R. Schöllhorn, Dipl.-Chem. A. Payer
Institut für Anorganische und Analytische Chemie
der Technischen Universität
Strasse des 17. Juni 135, D-1000 Berlin 12

dependence of the reaction state. Systems of this type are of potential interest for practical application; experiments with permanent magnets in contact with a spring loaded $Cu_{1+y}Cr_2Se_4$ working electrode demonstrated that, in principle, it is possible to construct a magnetic switch operated isothermally by the chemical process under discussion. Conversely, the latter arrangement represents a magnetic sensor device for the reaction state of the chemical system.

The characteristic difference in reactivity *direction* between $CuTi_2S_4$[2] and $CuCr_2Se_4$ can be discussed qualitatively in terms of the relative stability in chalcogenospinel lattices of the formal oxidation states of the transition metal ions involved. Since copper has the oxidation state +1 in chalcogenides,[4] the compounds can be described in an ionic model as mixed valence phases $Cu^{\oplus}(Ti^{3\oplus}Ti^{4\oplus})(S^{2\ominus})_4$ and $Cu^{\oplus}(Cr^{3\oplus}Cr^{4\oplus})(Se^{2\ominus})_4$. While $CuTi_2S_4$ can only be *oxidized* to Ti_2S_4, $CuCr_2Se_4$ can only be *reduced* to $Cu_2Cr_2Se_4$ under the conditions applied:

$$\left.\begin{matrix}Cu_{1-y}Ti_2S_4\\ Cu_{1+y}Cr_2S_4\end{matrix}\right\}\ 0\leqq y\leqq 1\ \left\{\begin{matrix}Ti^{3\oplus}/Ti^{4\oplus} \rightleftharpoons Ti^{4\oplus}/Ti^{4\oplus}+e^{\ominus}\\ Cr^{3\oplus}/Cr^{4\oplus}+e^{\ominus} \rightleftharpoons Cr^{3\oplus}/Cr^{3\oplus}\end{matrix}\right.$$

This can be explained reasonably well in terms of the lower stability of $Ti^{3\oplus}$ and the higher stability of $Cr^{3\oplus}$ in relation to the coexisting quadrivalent states in chalcogen ligand fields.

The magnetic ordering in copper chalcogenospinels $CuCr_2X_4$ has been interpreted in terms of Cr^{III}/Cr^{III} (superexchange) and Cr^{III}/Cr^{IV} interaction (double exchange).[5a, b] We attribute the significant decrease in T_c of $Cu_{1+y}Cr_2Se_4$ with increasing degree of conversion (y) to the higher strength of ferromagnetic coupling of Cr^{III}/Cr^{IV} as compared to Cr^{III}/Cr^{III}.[5c]

Extended studies of the related ferromagnetic chalcogenospinels $CuCr_2S_4$ and $CuCr_2Te_4$ revealed a behavior quite similar to that of the selenide. Current work is related to the investigation of the influence of $Li^{\oplus}$ intercalation in these phases because of the strong difference in bond ionicity Cu/X and Li/X; the possibility of $Li^{\oplus}$ insertion in spinel type oxides and chalcogenides has been demonstrated in recent publications.[2, 6, 7]

Received: May 12, 1986 [Z 1770 IE]
German version: *Angew. Chem. 98* (1986) 895

CAS Registry number:
$CuCr_2Se_4$, 12140-05-5.

[1] R. Schöllhorn, *Angew. Chem. 92* (1980) 1015; *Angew. Chem. Int. Ed. Engl. 19* (1980) 983; R. Schöllhorn in J. L. Atwood, J. E. D. Davies, D. D. MacNicol (Eds.): *Inclusion Compounds, Vol. 1*, Academic Press, New York 1984, p. 249; M. S. Whittingham, A. J. Jacobson: *Intercalation Chemistry*, Academic Press, New York 1982; F. A. Levy: *Intercalated Layered Materials*, Reidel, Dordrecht 1979.
[2] R. Schöllhorn, A. Payer, *Angew. Chem. 97* (1985) 57; *Angew. Chem. Int. Ed. Engl. 24* (1985) 67.
[3] T. Kanomata, H. Ido, *J. Phys. Soc. Jpn. 36* (1974) 1322.
[4] J. C. W. Folmer, F. Jellinek, *J. Less-Common Met. 76* (1980) 153.
[5] a) J. B. Goodenough, *J. Phys. Chem. Solids 30* (1969) 261; b) R. J. Bouchard, P. A. Russo, A. Wold, *Inorg. Chem. 4* (1965) 685; c) F. K. Lotgering, G. H. A. M. van der Steen, *Solid State Commun. 9* (1971) 1741.
[6] J. B. Goodenough, M. M. Thackeray, W. I. F. David, P. G. Bruce, *Rev. Chim. Minér. 21* (1984) 435.
[7] S. Sinha, D. W. Murphy, *Solid State Ionics 20* (1986) 81.

Tricyclo[5.3.0.0^{2,8}]deca-3,5-dien-9-one and a New Route to $C_{10}H_{10}$ Isomers**

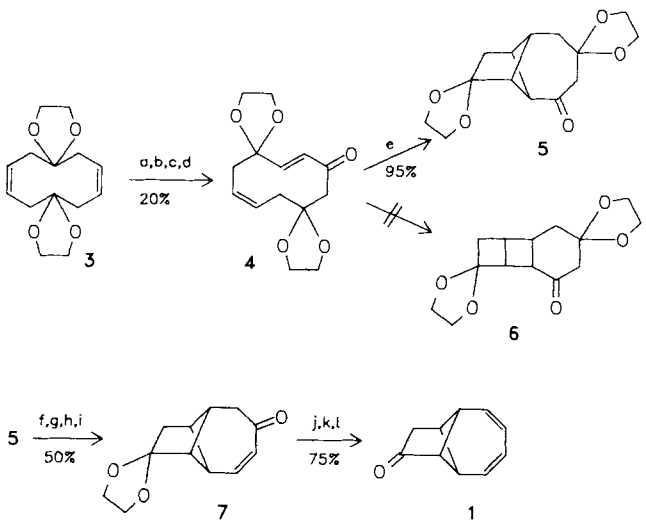
By *Rolf Gleiter,* Horst Zimmermann,* and *Wolfram Sander*

Tricyclo[5.3.0.0^{2,8}]deca-3,5-dien-9-one **1**, which is of interest as a precursor of tricyclo[5.3.0.0^{2,8}]deca-3,5,9-triene **2**, and its derivatives undergo unexpected rearrangements, which have allowed us to isolate several $C_{10}H_{10}$ isomers,



1 **2**

some of them previously unknown. Starting from 3,8-cyclodecadiene-1,6-dione bisethyleneacetal **3**, accessible in good yields from 1,4,5,8-tetrahydronaphthalene,[1] it is possible to synthesize the ketone **4** in three steps (oxidation with *m*-chloroperbenzoic acid (*m*-CPBA), reaction with PhSeSePh and then with H_2O_2 according to the Sharpless method,[2] and oxidation with CrO_3; Scheme 1). Irradiation of **4** affords only **5** (the other possible regioisomer, **6**, was not detected).

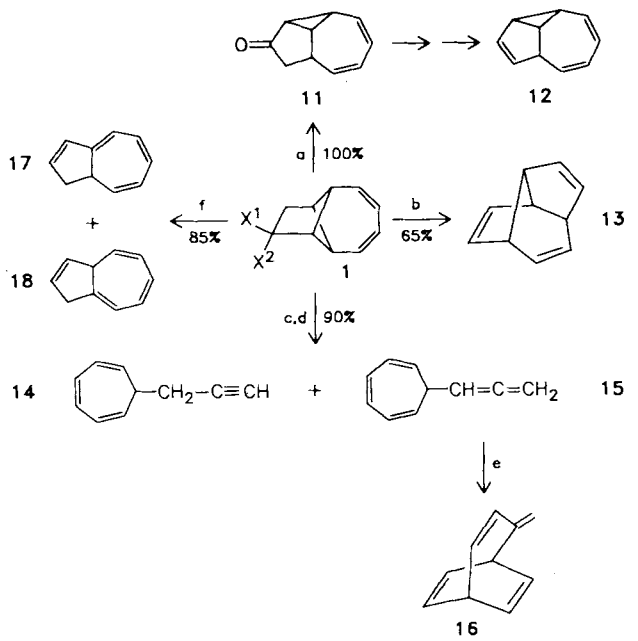


Scheme 1. Synthesis of **1**. a) *m*-CPBA, CH_2Cl_2. b) Ph_2Se_2, $NaBH_4$, *n*BuOH, 120°C, 24 h. c) H_2O_2, tetrahydrofuran (THF), 0°C, 20 h. d) CrO_3, pyridine. e) *hν*, H_3CCN, 0°C, 7 h. f) $NaBH_4$, EtOH. g) TsCl, pyridine. h) 1,5-Diazabicyclo[4.3.0]non-5-ene, H_3CCN, 70°C, 12 h. i) TsOH, H_2O/acetone. j) $LiAlH_4$, Et_2O. k) $(PhO)_3PCH_3I$, hexamethylphosphoric triamide, 80°C, 4 h. l) 1 N HCl, THF, 24 h.

The structure of the photoproduct was established from the ^{1}H-NMR spectrum and by comparison with the spectroscopic data for tricyclo[5.3.0.0^{2,8}]decane derivatives whose structures are known.[3] Reduction of the carbonyl group in **5** to the hydroxyl group, subsequent H_2O elimination, and acetal cleavage afford the ketone **7**, from which, in an analogous series of reactions, **1** is obtained.

[*] Prof. Dr. R. Gleiter, Dipl.-Chem. H. Zimmermann, Dr. W. Sander
Institut für Organische Chemie der Universität
Im Neuenheimer Feld 270, D-6900 Heidelberg (FRG)

[**] This work was supported by the Deutsche Forschungsgemeinschaft, the Fonds der Chemischen Industrie, and BASF AG. *W. S.* thanks the Studienstiftung des Deutschen Volkes for a fellowship. We thank Prof. *J. Dabrowski*, Dipl.-Chem. *M. Hauck*, and Dr. *P. Kunzelmann* for their help in recording and interpreting the NMR spectra.



Scheme 2. Reactions of **1** (X^1, X^2 = O; a), **8** (X^1, X^2 = N–NH–Ts; b), **9** (X^1, X^2 = N–NNa–Ts; c, d), and **10** (X_1 = H, X^2 = Me–SO_3; f). a) Al_2O_3. b) MeLi, Et_2O, 0°C. c) 125°C. d) *hv*, THF, 20°C. e) Preparative gas chromatography, Carbowax, 160°C. f) KO*t*Bu.

The rearrangements observed for **1** and its derivatives, such as the tosyl hydrazone **8** or the methanesulfonate **10**, are summarized in Scheme 2. Compound **1**, which is stable at room temperature, undergoes rearrangement within a few minutes in the presence of Al_2O_3 (neutral, activity I) to give quantitatively **11**,[4] from which the $C_{10}H_{10}$ isomer **12**[5] may be obtained. When **8** was allowed to react with excess MeLi in Et_2O at 0°C,[6] we obtained tricyclo[5.3.0.$0^{4,8}$]deca-2,5,9-triene **13**,[7] instead of the expected isomer **2**. The pyrolysis products obtained by heating **9** (sodium salt of **8**) without a solvent to 120°C were trapped at 10 K in an argon matrix on the window of an IR spectrometer; 7-(2-propynyl)-1,3,5-cycloheptatriene **14**[8] and 7-(1,2-propadienyl)-1,3,5-cycloheptatriene **15**, formed in a ratio of 2:1 (^{1}H-NMR spectrum), were detected. Compounds **14** and **15** were also obtained by irradiation of a solution of **9** in degassed THF at room temperature. Upon heating (GC), compound **15** undergoes rearrangement to give 2-methylenebicyclo[3.2.2]nona-3,6,8-triene **16**.[9]

The reaction of **10** with KO*t*Bu leads to the two unknown dihydroazulenes **17** and **18**, the structures of which were established from the spectroscopic data (Table 1) and from the observation that both compounds undergo oxidation with chloranil to give azulene. Two further isomeric dihydroazulenes were obtained in about 15% yield but could not be separated and identified.

Table 1. Spectroscopic data for the compounds **1**, **5**, **11**, **17**, and **18**. ^{1}H-NMR: 300 MHz, $CDCl_3$; ^{13}C-NMR: 75.46 MHz, $CDCl_3$.

1: IR (film): $\tilde{\nu}$ = 1755 cm^{-1}, ^{1}H-NMR: δ = 1.63 (s, 2H), 2.45 (s, 2H), 2.95–2.97 (d, 2H, J = 5.8 Hz), 6.11–6.22 (m, 4H); ^{13}C-NMR: δ = 23.9 (d), 43.0 (d), 45.8 (t), 52.1 (d), 126.8 (d), 132.5 (d), 212.4 (s); UV (H_3CCN): $\lambda_{max}(\varepsilon)$ = 275 nm (3870)

5: IR (KBr): $\tilde{\nu}$ = 1680 cm^{-1}; ^{1}H-NMR: δ = 2.03–2.12 (m, 2H), 2.33–2.42 (m, 3H), 2.73 (d, 1H, J = 7.5 Hz), 2.78 (d, 1H, J = 7.5 Hz), 2.84 (d, 1H, J = 5.75 Hz), 2.92 (d, 1H, J = 13.3 Hz), 2.98 (d, 1H, J = 13.3 Hz), 3.89–4.04 (m, 8H); ^{13}C-NMR: δ = 38.8 (t), 42.9 (d), 44.2 (t), 47.3 (d), 51.7 (t), 53.5 (d), 64.2 (d), 64.4 (t), 64.5 (t), 64.7 (t), 106.7 (s), 114.7 (s), 207.0 (s)

11: IR (film): $\tilde{\nu}$ = 1700 cm^{-1}; ^{1}H-NMR (500 MHz): δ = 1.80–1.83 (dd, 1H, J = 4.9, 10.3 Hz), 2.13–2.17 (m, 1H), 2.17–2.23 (dd, 1H, J = 19.2, 8.0 Hz), 2.45–2.53 (dd, 1H, J = 19.2, 10.6 Hz), 2.55–2.59 (ddd, 1H, J = 5.4, 6.4, 4.9 Hz), 3.24–3.32 (m, 1H), 5.80–5.84 (dd, 1H, J = 10.6, 5.6 Hz), 6.03–6.05 (ddd, 1H, J = 10.6, 5.6, 1.1 Hz), 6.17–6.27 (m, 2H); UV ($CDCl_3$): $\lambda_{max}(\varepsilon)$ = 258 nm (4200)

17: ^{1}H-NMR: δ = 2.54–2.61 (dd, 1H, J = 18.6, 9.3 Hz), 2.70–2.90 (m, 1H, J = 9.3 Hz), 3.12–3.27 (dd, 1H, J = 18.6, 9.3 Hz), 5.36–5.38 (dd, 1H, J = 9.7, 3.7 Hz), 6.01–6.09 (m, 2H), 6.19 (s, 2H), 6.23–6.25 (dd, 1H, J = 11.1, 6.2 Hz), 6.43–6.48 (dd, 1H, J = 11.1, 6.2 Hz); UV (*n*-hexane): λ_{max} = 318 nm

18: ^{1}H-NMR: δ = 3.06–3.10 (m, 1H), 3.30 (d, 2H, J = 4, 4 Hz), 5.00–5.04 (dd, 1H, J = 9.7, 4.4 Hz), 5.92–5.96 (m, 1H), 6.00–6.06 (m, 2H), 6.19–6.21 (br, 1H), 6.43–6.48 (dd, 1H, J = 11.5, 5.7 Hz), 6.52–6.58 (dd, 1H, J = 11.5, 5.7 Hz); UV (*n*-hexane): λ_{max} = 276 nm

Received: May 14, 1986;
revised: June 23, 1986 [Z 1774 IE]
German version: *Angew. Chem. 98* (1986) 893

CAS Registry numbers:
1, 104291-26-1; **3**, 53578-24-8; **4**, 104291-23-8; **5**, 104291-24-9; **7**, 104291-25-0; **8**, 104291-27-2; **9**, 104291-28-3; **10**, 104291-30-7; **11**, 15719-07-0; **13**, 16749-40-9; **14**, 14760-05-5; **15**, 104291-29-4; **16**, 38898-40-7; **17**, 104291-31-8; **18**, 104291-32-9.

[1] W. Hückel, H. Schlee, *Chem. Ber. 88* (1955) 346; C. A. Grob, P. W. Schiess, *Helv. Chim. Acta 43* (1960) 1546.
[2] K. B. Sharpless, R. F. Lauer, *J. Org. Chem. 39* (1974) 429, and references cited therein.
[3] R. Gleiter, W. Sander, H. Irngartinger, A. Lenz, *Tetrahedron Lett. 23* (1982) 2647.
[4] W. von E. Doering, B. M. Ferrier, E. T. Fossel, J. H. Hartenstein, M. Jones, Jr., G. Klumpp, R. M. Rubin, M. Saunders, *Tetrahedron 23* (1967) 3943.
[5] E. Vedejs, R. P. Steiner, *J. Chem. Soc. Chem. Commun. 1973*, 599.
[6] R. H. Shapiro, M. J. Heath, *J. Am. Chem. Soc. 89* (1967) 5735; R. H. Shapiro, *Org. React. 23* (1976) 405.
[7] M. Jones, Jr., *J. Am. Chem. Soc. 89* (1967) 4236; M. Jones, Jr., S. D. Reich, L. T. Scott, *ibid. 92* (1970) 3118.
[8] P. L. Pauson, G. H. Smith, J. H. Valentine, *J. Chem. Soc. C1967*, 1061.
[9] L. A. Paquette, M. J. Brodhurst, *J. Org. Chem. 38* (1973) 1893.

Synthesis and Structure of $[(C_5Me_5)_2M_2Se_5]$: Formation of a μ,η^2-Tetraselenide Ligand at the M–M Double Bond of $[(C_5Me_5)_2M_2(\mu\text{-}CO)_2]$ (M = Co, Rh)**

By *Henri Brunner, Walter Meier, Bernd Nuber, Joachim Wachter,** and *Manfred L. Ziegler*

A rational synthesis of chalcogen-rich cyclopentadienyl transition-metal complexes has been achieved by addition of elemental sulfur or selenium to the M–M triple bond of the complexes $[(C_5Me_5)_2M_2(CO)_4]$ (M = Cr, Mo, W).[1] Substitution of all the CO groups leads, via labile addition adducts,[2] to complexes having one- and two-atom chalcogen ligands displaying a variety of coordinations. Bridging ligands with more than two atoms are not formed in these reactions, however, even though they are well documented for sulfur (but not for selenium).[3] We report here the synthesis of a complex containing a tetraselenide ligand by stepwise addition of selenium to the M–M double bond of $[(C_5Me_5)_2M_2(\mu\text{-}CO)_2]$ (M = Co, Rh).

[*] Dr. J. Wachter, Prof. Dr. H. Brunner, W. Meier
Institut für Anorganische Chemie der Universität
Universitätsstrasse 31, D-8400 Regensburg (FRG)
Dr. B. Nuber, Prof. Dr. M. L. Ziegler
Anorganisch-chemisches Institut der Universität
Im Neuenheimer Feld 270, D-6900 Heidelberg (FRG)

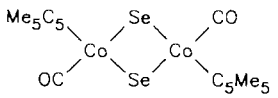
[**] Reactivity of the M–M Multiple Bond in Metal Carbonyl Derivatives, Part 12.—Part 11: I. Bernal, M. Draux, H. Brunner, B. Hoffmann, J. Wachter, *Organometallics 5* (1986) 655.

The reaction of the Co_2 and Rh_2 complexes **1** and **2**, respectively, with an excess of gray selenium in toluene (18 h, room temperature) affords, after chromatography on Al_2O_3, the carbonyl-free, diamagnetic complexes **3** (violet-brown) and **4** (dark green), respectively. Whereas the formation of **3** occurs surprisingly smoothly (80% yield), **4** (19% yield) is obtained along with two, as yet unidentified, likewise CO-free products. The ^{1}H-NMR spectra[4] of **3** and **4** support a symmetrical structure. Each of the ^{77}Se-NMR spectra[4] contains two groups of relatively broad signals having no fine structure (intensity ratio 3:2), the chemical shifts of which are strikingly similar to those of organic tetraselenides.[5] Less informative are the very weak IR absorptions between $\tilde{\nu}=300$ and 400 cm^{-1}, the region of M–Se–M and Se–Se vibrations.

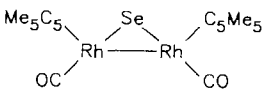
$[(C_5Me_5)_2M_2(CO)_2] \xrightarrow{Se_x} [(C_5Me_5)_2M_2Se_5]$

1, M = Co
2, M = Rh

3, M = Co
4, M = Rh



5



6

An X-ray structure analysis[6] revealed the presence of two types of selenide ligands in **4**: a $Se^{2\ominus}$ and a nearly planar $Se_4^{2\ominus}$ ligand are situated in the same plane (deviation ≤ 0.009 Å), which intersects the midpoint of the Rh–Rh axis and is perpendicular to it (Fig. 1). Owing to the eighteen-electron rule, the two ligands contribute eight electrons to the electron count of the two Rh atoms, which thereby achieve a nobel-gas configuration when the five electrons of the C_5Me_5 ligands are included, without the necessity of a metal–metal bond. The Se–Se distances in the $Se_4^{2\ominus}$ ligands are nearly identical and their average value (2.37 Å) is similar to those in trigonal selenium.[7] The relatively small Se1–Se4–Se5 angle (98.6(1)°) appears to be determined by the size of the ring. Se1, Se2, and Se3 form a nearly equilateral triangle with separations of about 3.101 Å, which are much less than the sums of the van der Waals radii of two Se atoms (3.80 Å). Interactions of this order of magnitude are sufficient, for example, to dimerize two $[W(CO)_5(\eta^2\text{-}Se_2)]^{\oplus}$ molecules to form a molecule with $Se_4^{2\ominus}$ bridges.[8] This tendency is further revealed, albeit less strongly, in the molecular lattice of **4**, in which neighboring molecules are linked together to form chains by means of intermolecular interactions ($d_{Se\text{-}Se}=3.50$ Å) between Se3 of one molecule and Se4/Se5 of another.

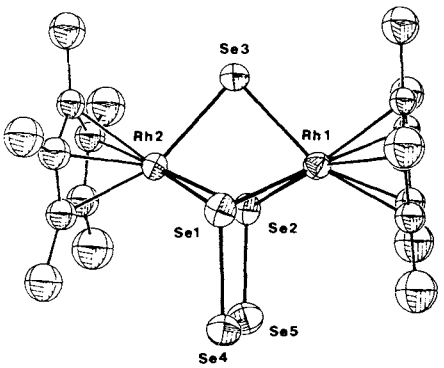


Fig. 1. Crystal structure of **4** (ORTEP plot). Selected bond lengths [Å] and bond angles [°]: Rh1-Se1 2.481(2), Rh1-Se2 2.460(2), Rh1-Se3 2.476(2), Rh2-Se1 2.479(2), Rh2-Se2 2.464(2), Rh2-Se3 2.473(2), Se1-Se4 2.373(2), Se2-Se5 2.370(2), Se4-Se5 2.368(2), Se1···Se2 3.115(2), Se1···Se3 3.102(2); Se1-Rh1-Se2 78.2(1), Rh1-Se1-Rh2 86.4(1), Rh1-Se2-Rh2 87.2, Rh1-Se3-Rh2 86.6(1), Rh1-Se1-Se4 105.2(1), Se1-Se4-Se5 98.6(1), Se2-Se5-Se4 99.5(1), Se2-Se1-Se3 60.3(0). Only one of the two independent, nearly identical molecules is shown.

These structural findings might explain the ready formation of the complexes **3** and **4**. The reaction of **1** with S_8 affords only a small yield of $[(C_5Me_5)_2Co_2S_4]$.[9] A Se analogue of the μ-η^1,η^2-S_2 ligand that characterizes this compound, namely, $[(triphos)_2Rh_2Se_4][PPh_4]_2$ (triphos = $H_3CC(CH_2PPh_2)_3$), is also known.[10] In the case of **3** and **4**, instead, a planar Se_4/Se ligand system is formed, which can be viewed alternatively as an η^3-Se_5 ligand. Comparable sulfur ligands are not planar.[11]

The stability of the polyselenide ligands in **3** and **4** is so pronounced that the dark brown diselenium adduct **5**,[4] obtained from **1** at 0°C, and the known monoselenium adduct **6**[12] undergo reaction at room temperature in toluene to afford mixtures from which **3** and **4**, respectively, may be isolated. Since **5** and **6** also undergo reaction with selenium in toluene to give **3** and **4** in appreciably better yields, the reactions **1**→**3** and **2**→**4** may be interpreted as occurring by stepwise addition of selenium to the M–M double bond with subsequent CO substitution.

Received: May 20, 1986;
revised: July 18, 1986 [Z 1784 IE]
German version: *Angew. Chem. 98* (1986) 907

[1] Sulfur-rich complexes of the general formula $Cp_2M_2S_x$ ($x \geq 4$) are discussed in J. Wachter, *J. Coord. Chem. B*, in press. Discussion of analogous reactions with oxygen are found in W. A. Herrmann, *J. Organomet. Chem. 300* (1986) 111.

[2] K. Endrich, *Dissertation*, Universität Heidelberg 1986.

[3] T. B. Rauchfuss, *Angew. Chem. 97* (1985) 745; *Angew. Chem. Int. Ed. Engl. 24* (1985) 742.

[4] ^{1}H-NMR (60 MHz, $CDCl_3$): $\delta=1.52$ (**3**), 1.66 (**4**), 1.78 (**5**). ^{77}Se-NMR (47.7 MHz, $CDCl_3$, standard: $SeMe_2$ ext.): **3**: $\delta=618.6$ (line width 64 Hz), 779.1 (110 Hz); **4**: $\delta=485.2$ (54 Hz), 783.1 (54 Hz); integral 3:2. IR (KBr): **5**: $\tilde{\nu}_{CO}=1988$ cm^{-1}. All compounds gave correct elemental analyses (C,H,Se) and were characterized by field-desorption mass spectroscopy.

[5] H. Eggert, D. Nielsen, L. Henriksen, *J. Am. Chem. Soc. 108* (1986) 1725.

[6] $P2_1/c$ C_{2h}^5, $a=20.513(7)$, $b=16.619(5)$, $c=15.315(3)$ Å, $\beta=107.48(2)°$, $V=4979.9$ Å^3, $Z=8$ (two independent molecules). Stoe Siemens diffractometer $Mo_{K\alpha}$ $2.5 \leq 2\theta \leq 60°$, 4805 measured reflections with $I>3\sigma(I)$, Patterson (Rh, Se) and Fourier methods, anisotropic refinement to $R_w=4.0$. Further details of the crystal structure investigation may be obtained from the Fachinformationszentrum Energie, Physik, Mathematik GmbH, D-7514 Eggenstein-Leopoldshafen 2 (FRG), on quoting the depository number CSD-51978, the names of the authors, and the journal citation.

[7] P. Cherin, P. Unger, *Inorg. Chem. 6* (1967) 1589.

[8] M. J. Collins, R. J. Gillespie, J. F. Sawyer, G. J. Schrobilgen, *Inorg. Chem. 25* (1986) 2053.

[9] H. Brunner, N. Janietz, W. Meier, G. Sergeson, J. Wachter, T. Zahn, M. L. Ziegler, *Angew. Chem. 97* (1985) 1056; *Angew. Chem. Int. Ed. Engl. 24* (1985) 1060.

[10] C. Bianchini, C. Mealli, A. Meli, M. Sabat, *J. Am. Chem. Soc. 107* (1985) 5317.

[11] G. Henkel, P. Betz, B. Krebs, *J. Chem. Soc. Chem. Commun. 1984*, 314; A. Müller, M. Römer, H. Bögge, E. Krickemeyer, D. Bergmann, *ibid. 1984*, 348.

[12] W. A. Herrmann, C. Bauer, J. Weichmann, *Chem. Ber. 117* (1984) 1271.

Carbonyl Olefinating Carbene-Tungsten Complexes and Their Suitability as Catalysts in Olefin-Metathesis**

By *Thomas Kauffmann,* Renate Abeln, Siegfried Welke,* and *Dorothea Wingbermühle*

Some readily accessible carbene-molybdenum complexes have proven to be suitable as reagents for carbonyl olefination. They are characterized by their high chemoselectivity (aldehyde-[2c] and grouping-selectivity[2d]) and low sensitivity towards hydroxy groups,[2b] but are so thermolabile that all attempts to isolate them have so far failed. In the hope of obtaining more stable complexes we allowed methyllithium to react with various tungsten halides and thus obtained complexes also suitable as reagents for carbonyl olefination.

A) Formation: Reaction of 2 molar equivalents of methyllithium with $WOCl_3(THF)_2$ or with $WOCl_4$ in tetrahydrofuran (THF) leads—in each case with cleavage of about one molar equivalent of methane—to formation of brown solutions with which acetophenone and cyclohexanone undergo methylenation in very good yield (Table 1); the reagent obtained from $WOCl_3(THF)_2$ is also suitable for aldehyde olefination (Table 1). The reagents most likely have the structures **1** and **2**, or structures derived therefrom (associates or LiCl-adducts).

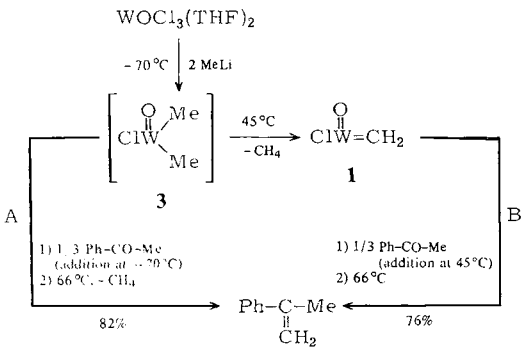
$$WOCl_3(THF)_2 + 2\,MeLi \xrightarrow[-0.9\,CH_4]{THF} ClW(O)=CH_2$$

1

$$WOCl_4 + 2\,MeLi \xrightarrow[-1.0\,CH_4]{THF} Cl_2W(O)=CH_2$$

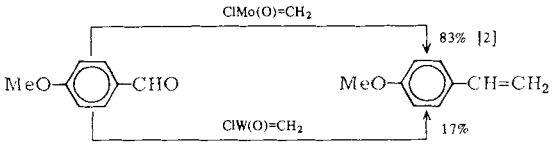
2

B) Comparison with carbonyl olefinating molybdenum complexes: The complexes **1** and **2**, to our knowledge the first carbonyl olefinating tungsten complexes, differ from the carbonyl methylenating molybdenum complexes[2], primarily in their greater activity towards ketones and in their greater thermal stability. Thus, it is possible in the case of carbonyl olefinations with $WOCl_3(THF)_2 + 2\,MeLi$ to prepare the carbene complex **1** first (heating to about 45 °C, *until evolution of methane subsides*) and thereafter to add the carbonyl component (Scheme 1, Method B), while in the case of carbonyl olefinations with the corresponding molybdenum compound the carbonyl compound must be added *before* the evolution of methane in order to ensure that the thermolabile molybdenum complex immediately has a reaction partner (Method A). In the carbonyl olefination with $WOCl_3(THF)_2 + 2\,MeLi$, Method A leads to yields of olefin that are equally as good as those obtained by Method B, and no methylation product is formed. Presumably, the dimethyl compound **3** is formed initially, and this cannot methylate the ketone employed in the reaction.



Scheme 1.

The tungsten complex **1**, which has been investigated in greater detail, is more reactive towards ketones than are carbene-molybdenum complexes. This, apparently, is the reason why **1** is less aldehyde-selective than the Mo-analogue in aldehyde/ketone competition experiments (cf. Table 1, Entry No. 7). A further difference appears to be less stability towards attack by water or ethanol: as can be seen from Entries No. 2 and 3, **1** is a much weaker carbonyl olefinating reagent in the presence of water and ethanol than in anhydrous THF. Scheme 2 shows that the complex $ClMo(O)=CH_2$ is significantly more effective in presence of water and ethanol than is **1**.



Scheme 2. Solvent THF/H_2O/EtOH (10:5:1); molar ratios, substrate : $ClMo(O)=CH_2$ = 1:2, substrate : **1** = 1:3.

Table 1. Carbonyl olefinations with carbene-tungsten complexes [a]. To obtain preparatively useful yields, a molar ratio of 3:1 of reagent and substrate was used in each experiment (in Entries No. 7 and No. 12, 3:1.1).

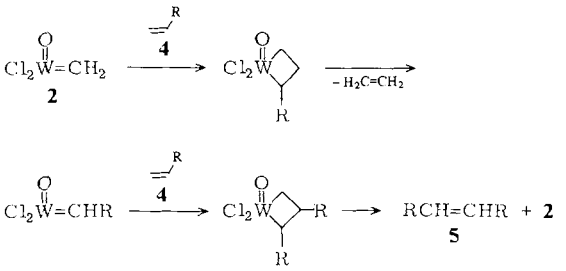
No.	Reagent	Substrate	Solvent	Olefin yield [%] [b]	Substrate recovered [%] [b]
1	**1**	Ph–CHO	THF	91	0
2	**1**	*p*-MeO–C_6H_4–CHO	THF	89	<3
3	**1**	*p*-MeO–C_6H_4–CHO	[c]	17	83
4	**1**	Ph–CO–Me	THF	82 (87)	11 (9)
5	**1**	cyclohexanone	THF	93	0
6	**1**	Ph–CO–Ph	THF	35	65
7	**1**	Ph–CHO + Ph–CO–Me	THF	90 (56) 27 (5)	0 (36) 65 (79)
8	**2**	Ph–CHO	THF	13	74
9	**2**	Ph–CO–Me	THF	77	17
10	**2**	Ph–CO–Me	cyclohexane	11 (6)	74 (81)
11	**2**	cyclohexanone	THF	96	0
12	**2**	Ph–CHO + Ph–CO–Me	THF	11 0 [d]	76 93

[a] The tungsten halide was treated at ca. −70 °C with 2 equivalents of MeLi. After 10 min, the carbonyl compound was added and the mixture heated to 66 °C (in Entry No. 10 to 80 °C) within 1.5 h. [b] Values in brackets apply for 20 °C. [c] THF : H_2O : EtOH = 10:5:1; for THF-dissolution of the reagent the carbonyl compound was added to a water/ethanol mixture. [d] The aldehyde apparently blocks the reagent.

C) Suitability as catalysts for olefin-metathesis: Since carbene-tungsten complexes have long been known to be suitable reagents for *olefin metathesis*,[3] we decided to check whether our *carbonyl olefinating* complexes are also suitable for this purpose; that is, whether they are suitable for both olefin metathesis as well as carbonyl olefination. In the presence of a tenfold excess of 1-hexadecene **4**, the reagent with the hypothetical structure **2** is converted into 15-triacontene **5** and ethylene (in cyclohexane/THF (9:1) at 80 °C, yield referred to **4**: 45% after 4 h; in THF-free cyclohexane, 20% after 14 h). It can be concluded, therefore, that the reaction proceeds as formulated in scheme 3.[4]

[*] Prof. Dr. T. Kauffmann, R. Abeln, Dipl.-Chem. S. Welke, D. Wingbermühle
Organisch-chemisches Institut der Universität
Orléans-Ring 23, D-4400 Münster (FRG)

[**] Transition Metal-Activated Organic Compounds, Part 21. This work was supported by the Deutsche Forschungsgemeinschaft and the Fonds der Chemischen Industrie.—Part 20: [1].



Scheme 3. R = n-$C_{13}H_{29}$.

The metathesis of **4** by **2** is almost completely suppressed in pure THF as solvent (ca. 2% **5**). Hence, we assume that a THF-solvate envelope around the Lewis acid **2** prevents access of the weakly basic olefin **4** to the central atom of **2**. In contrast, carbonyl compounds like acetophenone or benzaldehyde in THF can reach the central atom of **2**. This accessibility for carbonyl groups and the barrier to olefin groups makes it possible to carry out carbonyl olefinations without any interfering olefin metathesis, if THF is used as solvent.

No olefin metathesis could by achieved with the reagent **1**. Conversely, all attempts to carry out carbonyl olefinations with tungsten-containing compounds of well-defined structure known to catalyze olefin-metathesis[3] met without success.

Received: June 12, 1986;
revised: July 16, 1986 [Z 1812 IE]
German version: *Angew. Chem. 98* (1986) 927

[1] T. Kauffmann, C. Pahde, A. Tannert, D. Wingbermühle, *Tetrahedron Lett. 26* (1985) 4063.

[2] a) T. Kauffmann, B. Ennen, J. Sander, R. Wieschollek, *Angew. Chem. 95* (1983) 237; *Angew. Chem. Int. Ed. Engl. 22* (1983) 244; *Angew. Chem. Suppl. 1983*, 222; b) T. Kauffmann, P. Fiegenbaum, R. Wieschollek, *Angew. Chem. 96* (1984) 500; *Angew. Chem. Int. Ed. Engl. 23* (1984) 531; c) T. Kauffmann, G. Kieper, *ibid. 96* (1984) 502 and *23* (1984) 532; d) T. Kauffmann, T. Möller, H. Rennefeld, S. Welke, R. Wieschollek, *ibid. 97* (1985) 351 and *24* (1985) 348; e) note added in proof: A. Aguero, J. Kress, J. A. Osborn, *J. Chem. Soc. Chem. Commun. 1986*, 531 have recently described carbonyl olefinating reactions with complexes of the type $X_2Y_2W{=}CR^1R^2$.

[3] Cf., e.g., the review by N. Calderon, J. P. Lawrence, E. A. Ofstead, *Adv. Organomet. Chem. 17* (1979) 449; R. H. Grubbs in G. W. Wilkinson, F. G. A. Stone, E. W. Abel (Eds.): *Comprehensive Organometallic Chemistry, Vol. 8*, Pergamon Press, Oxford 1982, p. 499.

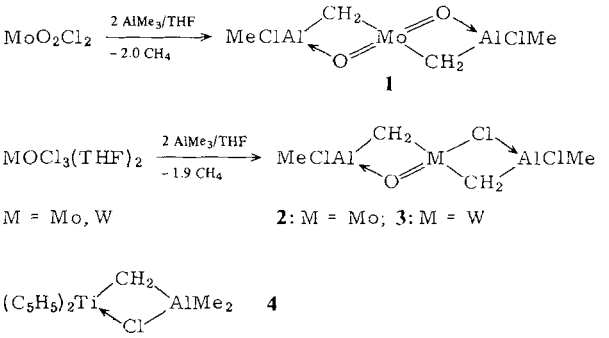
[4] E. L. Muetterties and E. Band (*J. Am. Chem. Soc. 102* (1980) 6572) found that a compound suitable as catalyst for olefin metathesis is formed in the thermal decomposition of $Cl_3OWMe{\cdot}OEt_2$ in benzene; they presumed that the compound had the structure **2**. Phosphane complexes of **2**, which proved to be weakly active catalysts for olefin metathesis, were isolated by R. Schrock. S. Rocklage, J. Wengrovius, G. Ruprecht, and J. Fellmann (*J. Mol. Catal. 8* (1980) 73).

Carbonyl Olefinating Aluminum-Molybdenum Complexes and an Analogous Tungsten Complex**

By *Thomas Kauffmann, Manfred Enk, Wilfried Kaschube, Euripides Toliopoulos,* and *Dorothea Wingbermühle**

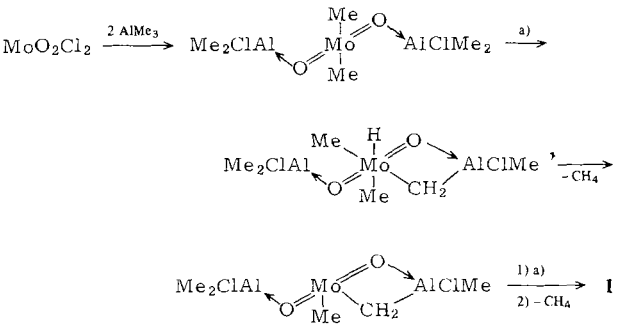
We have already reported on carbonyl olefinating molybdenum complexes that are formed on reaction of methyllithium with molybdenum halides via elimination of *one molar equivalent* of methane.[2] Since highly-active carbonyl olefinating reagents containing transition-metal atoms (Ti,[3a] Zr[3b]) and an aluminum atom are already known, our interest now turned to the possibility of preparing carbonyl olefinating aluminum-molybdenum complexes.

We found that reaction of two molar equivalents each of trimethylaluminum with MoO_2Cl_2 and with $MoOCl_3(THF)_2$ in tetrahydrofuran (THF) leads, via cleavage of *two molar equivalents* of methane, to the formation of complexes which in the course of a carbonyl olefination transfer about 1.5 CH_2 units per Mo atom to benzaldehyde present in excess (Table 1, Entries No. 1 and 6). We assume that bismethylene complexes are formed whose hypothetical structures **1** and **2** show similarities to the Tebbe reagent **4**.[3a] An analogous tungsten complex of hypothetical structure **3** was obtained from $WOCl_3(THF)_2$ (Scheme 1).



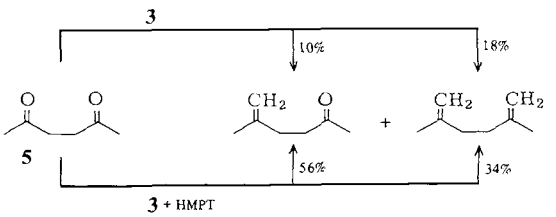
Scheme 1.

Our conception of the formation of **1** is outlined in Scheme 2; **2** and **3** could be formed analogously.



Scheme 2. a) denotes the cyclometalation step.

The carbonyl-olefinating activity of the Tebbe reagent **4** is enhanced by addition of base; this can be attributed to cleavage of the Al-CH_2 bond.[4] Analogous activations were observed in the case of **2** and **3** (Table 1, Entries 13 and 14; see also Schemes 3 and 4).

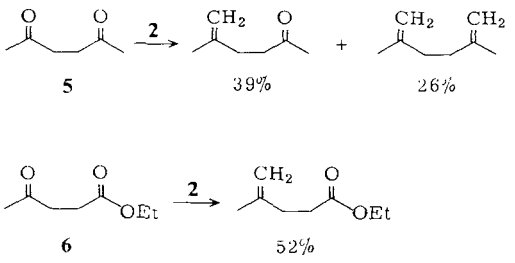


Scheme 3. Solvent: THF. Molar ratios: **5** : **3** = 1 : 1; **5** : **3** : HMPA = 1 : 1 : 2.

[*] Prof. Dr. T. Kauffmann, Dipl.-Chem. M. Enk, Dipl.-Chem. W. Kaschube, Dipl.-Chem. E. Toliopoulos, D. Wingbermühle
Organisch-chemisches Institut der Universität
Orléans-Ring 23, D-4400 Münster (FRG)

[**] Transition Metal-Activated Organic Compounds, Part 22. This work was supported by the Deutsche Forschungsgemeinschaft and the Fonds der Chemischen Industrie.—Part 21: [1].

Since the reagent **2** is practically inactive towards monoketones (Table 1, Entries 10 and 11), we attribute the surprisingly good olefination of dicarbonyl compounds according to Scheme 4 to the effectiveness of the second carbonyl group as activating base.



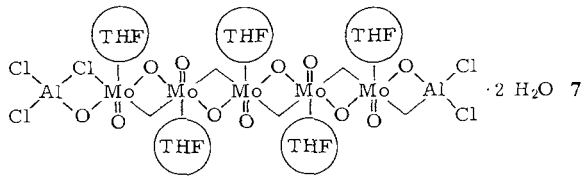
Scheme 4. Solvent: THF. Molar ratios: **5** : **2** = 1 : 1; **6** : **2** = 1 : 1.

Table 1. Examples of carbonyl olefinations [a].

No.	Reagent	Substrate	Reagent : Substrate	Olefin yield [%]	Substrate recovered [%]
1	**1**	Ph–CHO	1 : 1	98	—
2	**1**	Ph–CHO	1 : 2	75 [b]	3
3	**1**	*n*-C_6H_{13}–CHO	1 : 1	67	6
4	**1**	Ph–CO–Me	1 : 1	22	62
5	**1**	*n*Bu–CO–Me	1 : 1	14	46
6	**2**	Ph–CHO	1 : 1	62	—
7	**2**	Ph–CHO	1 : 2	76 [b]	3
8	**2**	[c]	1 : 1	60	—
9	**2**	[c]	1 : 2	50	22
10	**2**	Ph–CO–Me	1 : 1	<5	70
11	**2**	*n*Bu–CO–Me	1 : 1	<5	47
12	**3**	Ph–CO–Me	1 : 1	11	79
13	**3** + HMPA (1 : 1)	Ph–CO–Me	1 : 1	45	15
14	**3** + HMPA (1 : 2)	Ph–CO–Me	1 : 1	59	15

[a] In the experiments carried out in THF (Entries 1–11), the transition metal halide was allowed to react with 2 molar equivalents of $AlMe_3$ at −70 °C. After 2 h, the substrate was added and the solution heated to 20 °C within 14 h. In the case of the experiments carried out in *n*-hexane (Entries 12–14), $WOCl_3(THF)_2$ was allowed to react with 2 molar equivalents of $AlMe_3$. 1.4 molar equivalents of CH_4 were evolved. After 1 h, the substrate was added and the solution heated to 66 °C within 1 h. The addition of hexamethylphosphoric triamide (HMPA) immediately followed addition of the substrate. [b] 1.5 CH_2 groups were thus transferred per Mo-atom. [c] 2-Thiophenecarbaldehyde.

The hypothetical complexes **1** and **2** are thermolabile. Consequently, the products of carbonyl olefination are isolable in good yields only when the molybdenum halide is first allowed to react with trimethylaluminum at −70 °C before addition of the substrate at the same temperature, and the reaction mixture is then heated to 20 °C until evolution of CH_4 ceases. If the carbonyl compound is first added after evolution of gas ceases, then the yield of olefin is low. Apparently, the active carbonyl olefinating reagent initially formed undergoes decomposition when no carbonyl groups are available.[5] The decomposition has hitherto prevented the isolation of **1** and **2**, but enabled isolation of a primary product of the decomposition of **1**. This sparingly soluble, amorphous, air- and water-sensitive solid precipitates from the THF solution at 0 °C (stable only for a short time at this temperature) and can effect carbonyl olefination of benzaldehyde. According to elemental analysis, it would appear that one THF ligand is present per Mo atom, thus indicating a chain-like structure containing five $Mo(THF)O_2CH_2$ units. The Mo/Al ratio of 5 : 2 (i.e. large depletion of Al compared to **1**) suggests that the chain terminals are formed by $AlCl_2$ units, as tentatively formulated in **7**.—The moderate yield of olefin upon reaction of the yellow solid with benzaldehyde (31% per Mo atom of **7**) is understandable in view of the sparing solubility of this decomposition product.



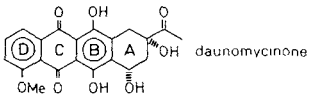
Received: June 12, 1986;
revised: July 16, 1986 [Z 1813 IE]
German version: *Angew. Chem. 98* (1986) 928

[1] T. Kauffmann, R. Abeln, S. Welke, D. Wingbermühle, *Angew. Chem. 98* (1986) 927; *Angew. Chem. Int. Ed. Engl. 25* (1986) No. 10.
[2] See [1], and references cited therein [2].
[3] a) F. N. Tebbe, G. W. Parshall, G. S. Reddy, *J. Am. Chem. Soc. 100* (1978) 3611; b) F. W. Hartner, Jr., J. Schwartz, S. M. Clift, *ibid. 105* (1983) 3270.
[4] Cf. K. A. Brown-Wensley, S. L. Buchwald, L. Cannizzo, L. Clawson, S. Ho, D. Meinhardt, J. R. Stille, D. Straus, R. H. Grubbs, *Pure Appl. Chem. 55* (1983) 1733.
[5] Similar studies with **3** have yet to be carried out.
[6] The values determined by atomic absorption spectrometry (Mo, Al) and combustion analysis (mean values of several measurements; oxygen value by difference) fit very well with the empirical formula $(C_{25}H_{54}Al_2Cl_5Mo_5O_{18})_n(1353.6)_n$ for **7**: calc. C 22.18, H 4.02, Al 3.99, Cl 13.10, Mo 35.44, O 21.27; found C 22.18, H 4.19, Al 3.97, Cl 13.15, Mo 35.84, O 21.57.

Carbene Complexes with Quinone Bisketal Functions**

By *Karl Heinz Dötz,* Michael Popall, Gerhard Müller,* and *Klaus Ackermann*

Carbene(carbonyl) transition-metal complexes are useful as synthetic building blocks for anthracyclinones.[1–4] For example, the rings B and C of the daunomycinone skeleton can be constructed by regiospecific annelation of arylcarbene complexes. In order to avoid the necessity of subsequent selective oxidation,[5] it would be useful to introduce the quinone ring C directly via the carbene complex. For this reason, we have investigated the synthesis and reactivity of carbene complexes having quinone bisketal functions.

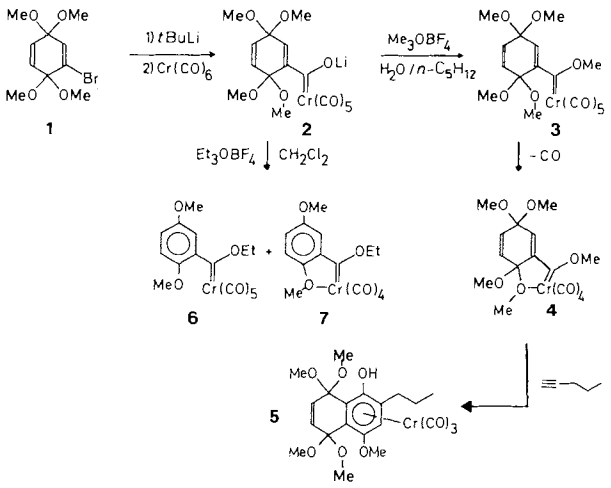


The lithiated quinone bisketals that are obtained from **1** and **8** by halogen–metal exchange undergo addition to hexacarbonylchromium and -tungsten at low temperatures with formation of the ocher-colored acylmetalates **2** and

[*] Priv.-Doz. Dr. K. H. Dötz, M. Popall, Dr. G. Müller, Dr. K. Ackermann
Anorganisch-chemisches Institut der Technischen Universität München
Lichtenbergstrasse 4, D-8046 Garching (FRG)

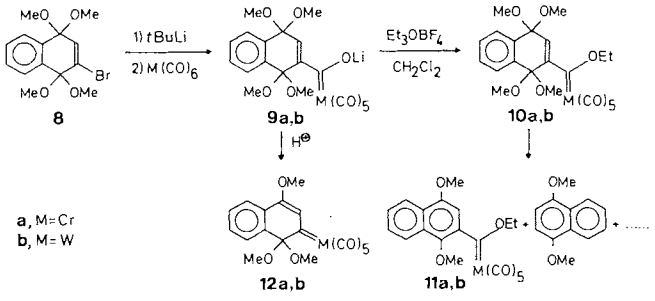
[**] Carbene Ligands as Anthracyclinone Synthons, Part 4. This work was supported by the Deutsche Forschungsgemeinschaft and the Fonds der Chemischen Industrie. Part 3: [3].

9a, **b**. Their conversion into the neutral carbene complexes is strongly dependent on the transition metal, the alkylating agent, and the reaction medium. Whereas **2** undergoes methylation with Me_3OBF_4 in pentane/water to give **3**, it reacts with Et_3OBF_4 in dichloromethane to give **6** (aromatization), which partially undergoes immediate decarbonylation to give **7**.[6]



The bisketal compound **3** also undergoes facile elimination of a CO ligand in the *cis* position. The chelate carbene complex thereby formed, **4**, was shown by X-ray structure analysis[7] to have a five-membered metallacycle with short Cr–C(carbene) and long Cr–O bonds (2.226(2) Å) (Fig. 1, above). The five-membered ring has an approximate envelope conformation, while the quinone bisketal six-membered ring, owing to the coordination of O31 to the Cr atom, is not exactly planar. The molecular geometry provides an explanation for the rapid exchange of the Cr-coordinated methoxy group with the geminal, free methoxy group in acetone solution at room temperature. An activation enthalpy of 9 kcal/mol can be estimated for this process from the coalescence temperature of $-73\,^{\circ}C$.[8] The facile opening of the chelate ring under mild conditions allows the coordination of an alkyne, which—as exemplified by 1-pentyne—is incorporated into the hydroquinone skeleton, the annelation of the carbene ligand occurring regiospecifically.

The alkylation of the 1,4-naphthoquinone bisketal derivatives **9a**, **b** with oxonium salts in dichloromethane leads ultimately to aromatic products.[9] In the case of tungsten, the bisketal carbene intermediate **10b**[10] may be detected, although it undergoes slow aromatization in solution to form **11b**. In contrast to the cyclohexadienyl system **2**, the acylmetalate **9a** is transformed by even traces of $H^{\oplus}$ into the golden dihydronaphthylidene complex **12a**. This unexpected fragmentation is presumed to occur via an initially formed hydroxycarbene complex.



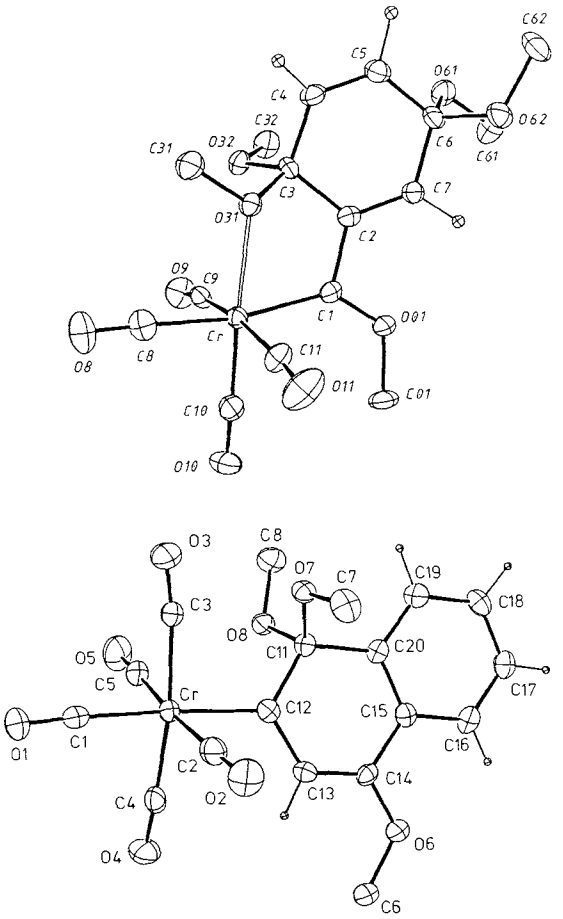


Fig. 1. Crystal structures of **4** (above) and **12a** (below) (ORTEP, thermal ellipsoids at the 50% probability level, H atoms with arbitrary radii, without methyl H atoms) [7]. Selected bond lengths [Å] and bond angles [°]: **4**: Cr-C1 1.978(3), Cr-C8 1.895(3), Cr-O31 2.226(2), Cr···O32 3.332(2), C1-O01 1.321(3), C1-C2 1.497(4), C2-C3 1.505(4), C3-C4 1.505(4), C4-C5 1.323(4), C5-C6 1.501(4), C6-C7 1.499(4), C2-C7 1.328(4), C3-O31 1.441(3), C3-O32 1.431(3); Cr-C1-C2 116.0(2), Cr-C1-O01 136.1(2), O01-C1-C2 108.0(2), C1-C2-C3 114.7(2), C2-C3-O31 103.6(2), C3-O31-Cr 109.6(1); torsion angle Cr-C1-C2-C3 −9.2, dihedral angle Cr, C1, C2, C3/Cr, O31, C3 44.3.— **12a**: Cr-C12 2.045(3), Cr-C1 1.897(4), C12-C13 1.410(4), C13-C14 1.376(4), C14-O6 1.333(4), C14-C15 1.460(4), C15-C20 1.403(4), C20-C11 1.532(4), C11-C12 1.541(4); Cr-C12-C13 121.4(2), Cr-C12-C11 122.8(2), C11-C12-C13 115.8(3).

In view of the absence of heteroatom substituents in α position at the carbene carbon atom, the thermal stability of **12a** is remarkable. It is due to conjugation of the carbene-metal and enol ether functions (vinylogous stabilization) as well as to the incorporation of the carbene carbon atom into a relatively rigid six-membered ring, as revealed by the molecular structure[7] (Fig. 1, below). The dihydronaphthylidene skeleton is nearly planar.

Experimental Procedure

2/9a, **b**: A solution of *tert*-butyllithium (30 mmol) in hexane was slowly added to a stirred solution of **1** or **8** (15 mmol) [11] in 60 mL of ether at $-75\,^{\circ}C$. The resulting orange suspension was stirred at this temperature for ca. 15 h and then added to a solution of $Cr(CO)_6$ or $W(CO)_6$ (15 mmol) in 150 mL of ether at $-60\,^{\circ}C$. The mixture was allowed to warm to room temperature over 4 h and the solvent then removed. After washing with pentane, the acylmetalate **2** or **9a**, **9b** was obtained.

3: **2** (5 mmol) was dissolved in 50 mL of ice water and a layer of 100 mL of pentane was added. After addition of Me_3OBF_4 (7.5 mmol), the mixture was extracted repeatedly with pentane and the extracts were dried over Na_2SO_4 and chromatographed on silica gel (Merck, type 60). Elution of the red, main zone with CH_2Cl_2 and recrystallization from ether/pentane afforded **3** in the form of light red needles (m.p. = 47 °C). Yield 58%. IR (pentane):

$\tilde{\nu}$(C=O) = 2064 (s), 1994 (s), 1955 (vs), 1942 cm^{-1} (vs). ^{1}H-NMR (CD_3COCD_3): δ = 6.07 (m, 3H; 3, 5, 6-H), 4.73 (s, 3H; carbene OCH_3), 3.33 (s, 6H; 1,1-OCH_3), 3.27 (s, 6H; 4,4-OCH_3). ^{13}C-NMR (CD_3COCD_3): δ = 355.5 ($C_{carbene}$), 225.4 (*trans*-CO), 216.1 (*cis*-CO), 153.5 (C-2), 130.7 (C-3), 126.1 (C-5,6), 96.4, 92.4 (C-1,4), 67.7 (carbene OCH_3); 48.8, 48.6 (1,1,4,4-OCH_3). MS: *m/z* 434 ($M^{\oplus}$).

4: **3** (5 mmol) was heated in 10 mL of *tert*-butyl methyl ether at reflux for 4 h. After recrystallization, **4** was obtained in the form of dark brown crystals (m.p. = 100°C). Nearly quantitative yield. IR (pentane): $\tilde{\nu}$(C=O) = 2019 (s), 1952 (s), 1938 (vs), 1865 cm^{-1} (vs). ^{1}H-NMR (CD_3COCD_3): δ = 6.34 (m, 3H; 3,5,6-H), 4.80 (s, 3H; carbene OCH_3), 3.36 (s, 6H; 1,1-OCH_3), 3.30 (s, 6H; 4,4-OCH_3). ^{13}C-NMR (CD_3COCD_3): δ = 341.5 ($C_{carbene}$), 233.1, 232.3 (*trans*-CO), 217.6, 216.9 (*cis*-CO), 145.1 (C-2); 133.8, 125.4, 119.6 (C-3,5,6), 100.0, 94.4 (C-1,4), 68.8 (carbene OCH_3), 56.5 (1,1-OCH_3), 50.3 (4,4-OCH_3). MS: *m/z* 408 ($M^{\oplus}$).

5: A solution of **4** (5 mmol) in 20 mL of *tert*-butyl methyl ether was heated to 55°C and, after addition of 5.5 mmol of 1-pentyne, allowed to stir for 0.5 h. **5** was precipitated by addition of pentane. IR (KBr): $\tilde{\nu}$(C=O) = 1938 (s), 1855 cm^{-1} (s). MS: *m/z* 474 ($M^{\oplus}$).

6/7: A solution of **2** (5 mmol) in 100 mL of CH_2Cl_2 was treated at 0°C with 7.5 mmol of Et_3OBF_4. After 1 h, the solvent was removed under high vacuum and the residue was dissolved in ether and quickly filtered over Al_2O_3 (neutral) at −20°C. Column chromatography on silica gel afforded **6** and **7** in a ratio of 10 : 1.

12a: A solution of **9a** (5 mmol) in 200 mL ether/water (1 : 1) was allowed to stir for 1 h at room temperature. After removal of the solvent (high vacuum), column chromatography on silica gel (Merck, type 60) with dichloromethane/pentane (2 : 1) followed by recrystallization from ether/pentane afforded **12a** in the form of golden crystalline platelets (m.p. = 100°C). Yield 56%. IR (pentane): $\tilde{\nu}$(C=O) = 2047 (s), 1988 (m), 1962 (vs), 1926 cm^{-1} (s). ^{1}H-NMR (CD_3COCD_3): δ = 8.91 (s, 1H; 3-H), 8.05 (m, 2H; 5,8-H), 7.62 (m, 2H; 6,7-H), 4.45 (s, 3H; 4-OCH_3), 2.78 (s, 6H; 1,1-OCH_3). MS: *m/z* 410 ($M^{\oplus}$).

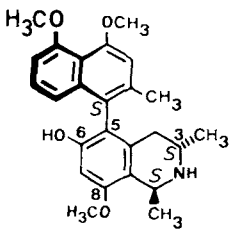
Received: May 21, 1986;
supplemented: June 25, 1986 [Z 1785 IE]
German version: *Angew. Chem. 98* (1986) 909

Regioselective and Atropoisomeric-Selective Aryl Coupling to Give Naphthyl Isoquinoline Alkaloids: The First Total Synthesis of (−)-Ancistrocladine**

By *Gerhard Bringmann,* Johannes R. Jansen,* and *Heinz-Peter Rink*

Dedicated to Professor Burchard Franck on the occasion of his 60th birthday

(−)-Ancistrocladine **1**[1] is regarded as "the most unusual of all the isoquinoline alkaloids"[2] on account of the methyl group at C-3 of a tetrahydroisoquinoline, the two oxygen functions at C-6 and C-8 in mutual *meta* positions, and the peculiar naphthalene substituent at C-5. For a thorough investigation of the biological activity of **1**, as well as for a reexamination of the insufficiently established structures of several related natural products,[3] the molecular skeleton of **1** — with the highly substituted biphenyl system that is configurationally stable to above 200°C — represents an attractive synthetic goal.



1

Neither **1** nor other *Ancistrocladus* alkaloids could so far be synthesized. We recently reported the first synthesis of a naphthyl isoquinoline alkaloid, the less sterically crowded and fully aromatic, albeit racemic, *Triphyophyllum* alkaloid *O*-methyltetradehydrotriphyophylline.[4]

We describe here the first, and, at the same time, asymmetric, synthesis of the main alkaloid (−)-ancistrocladine **1**. The required starting material for the synthesis of the optically active tetrahydroisoquinoline building block **5** is the arylpropanone **2a**,[5] which may be regarded as a simpler analogue of the assumed[6,7] biosynthetic diketo precursor **2b** (Scheme 1).

Reductive amination[8] of **2a** with (*S*)-1-phenylethylamine (*de* 92%) and subsequent hydrogenolysis selectively affords the desired,[9] enantiomerically pure,[10] primary amine **3** [84% yield, m.p. of the hydrochloride = 151.5°C, $[\alpha]_D^{20}$ = +14.8 (*c* = 1.0, MeOH)]. After Bischler-Napieralski cyclization to the (3*S*)-configurated dihydroisoquinoline **4** [76%, m.p. of the hydrobromide = 202°C, $[\alpha]_D^{20}$ = −141 (*c* = 1.0, MeOH], the heterocyclic molecular half, e.g., of the spasmolytically active ancistrocladidine,[3] also the second center of chirality (C-1) can stereoselectively be built up. Reduction of **4** with $LiAlH_4$ in the presence of $AlMe_3$[11] affords the (1*S*)-configurated tetrahydroisoquinoline **5** [85%, m.p. of the hydrobromide = 293°C, $[\alpha]_D^{20}$ = +7.6 (*c* = 1.0, MeOH)] with remarkably good stereoselectivity (*de* 92%).[12] A *trans* arrangement of the two secondary methyl

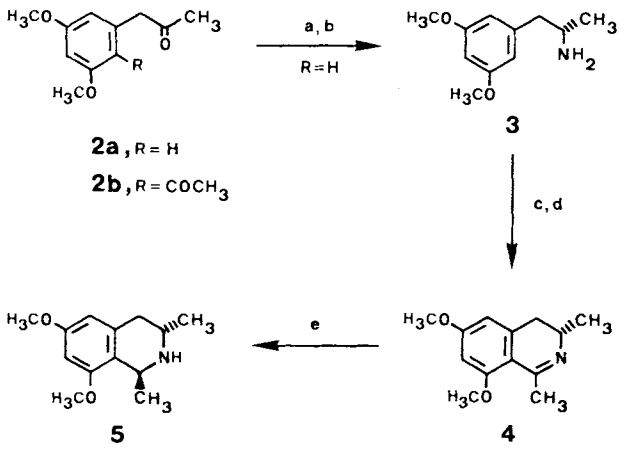
[1] Review: K. H. Dötz, *Angew. Chem. 96* (1984) 573; *Angew. Chem. Int. Ed. Engl. 23* (1984) 587.
[2] K. H. Dötz, M. Popall, *Tetrahedron 41* (1985) 5797.
[3] K. H. Dötz, M. Popall, *J. Organomet. Chem. 291* (1985) C 1.
[4] W. D. Wulff, P. C. Tang, *J. Am. Chem. Soc. 106* (1984) 434.
[5] Recent reviews: a) F. Arcamone: *Doxorubicin Anticancer Antibiotics*, Academic Press, New York 1981; b) H. S. El Khadem (Ed.): *Anthracycline Antibiotics*, Academic Press, New York 1982; c) K. Krohn, *Angew. Chem. 98* (1986) 788; *Angew. Chem. Int. Ed. Engl. 25* (1986) 790.
[6] Cf. K. H. Dötz, W. Sturm, M. Popall, J. Riede, *J. Organomet. Chem. 277* (1984) 267.
[7] Crystal structure data: **4**: orthorhombic, space group $P2_12_12_1$, a = 11.691(1), b = 11.970(1), c = 12.760(1) Å, V = 1785.7 Å^3, ρ_{calcd} = 1.511 g cm^{-3} for Z = 4 at −35°C, $F(000)$ = 840, $\mu(Mo_{K\alpha})$ = 6.7 cm^{-1}. 4631 measured reflections, of which 2758 were unique and 2645 "observed" with $I \geq 2.0\sigma(I)$ (ω scan, $\Delta\omega$ = 1.0°, $+h$, $\pm k$, $\pm l$, $(\sin\vartheta/\lambda)_{max}$ = 0.594, $Mo_{K\alpha}$, λ = 0.71069 Å, graphite monochromator, Syntex $P2_1$). Lp, but no absorption correction, Patterson methods R = 0.028, R_w = 0.032, $w = 1/\sigma^2(F_0)$ for 250 refined parameters (anisotropic, CH_3 as rigid groups, all other H atoms constant, $\Delta\rho_{fin}$(max/min) = 0.40/−0.37 e/Å^3, the refinement of the inverse set of coordinates gave R_w = 0.047, SHELX76). — **12a**: triclinic, space group $P\bar{1}$, a = 7.262(1), b = 11.151(2), c = 12.138(3) Å, α = 89.78(2), β = 104.50(2), γ = 112.48(1)°, V = 874.7 Å^3, ρ_{calcd} = 1.558 g cm^{-3}, Z = 2, T = −35°C, $F(000)$ = 420, $\mu(Mo_{K\alpha})$ = 6.8 cm^{-1}. 2740 measured, unique reflections, 2356 "observed" with $I \geq 2.0\sigma(I)$ ($+h$, $\pm k$, $\pm l$, $(\sin\vartheta/\lambda)_{max}$ = 0.572). Patterson methods, R = 0.040, R_w = 0.046 (244 refined parameters, anisotropic, H atoms constant, $\Delta\rho_{fin}$(max/min) = ±0.41 e/Å^3). Further details of the crystal structure investigations may be obtained from the Fachinformationszentrum Energie, Physik, Mathematik GmbH, D-7514 Eggenstein-Leopoldshafen 2 (FRG), on quoting the depository number CSD-51951, the names of the authors, and the journal citation.
[8] We thank Priv.-Doz. Dr. *H. G. Alt*, Bayreuth, and Dr. *P. Härter*, Munich, for recording the DNMR spectra.
[9] By the introduction of cyclic bisketal functions, the aromatization can be suppressed.
[10] **10b**: IR (pentane): $\tilde{\nu}$(C=O) = 2070 (w), 1952 (s, sh), 1945 cm^{-1} (vs). ^{1}H-NMR (CD_3COCD_3): δ = 7.56 (m, 4H; 5,6,7,8-H), 6.46 (s, 1H; 3-H), 5.14 (q, 2H; CH_2), 3.27 (s, 6H; 1,1-OCH_3), 3.12 (s, 6H; 4,4-OCH_3), 1.73 (t, 3H; CH_3).
[11] J. S. Swenton, P. W. Raynolds, *J. Am. Chem. Soc. 100* (1978) 6188.

[*] Priv.-Doz. Dr. G. Bringmann, Dipl.-Chem. J. R. Jansen, H.-P. Rink
Organisch-chemisches Institut der Universität
Orléansring 23, D-4400 Münster (FRG)

[**] Acetogenic Isoquinoline Alkaloids, Part 11. This work was supported by the Deutsche Forschungsgemeinschaft and the Fonds der Chemischen Industrie. — Part 10: [6].

groups, such as in **5**, is very common in the *Ancistrocladus* alkaloids,[3] but, up to now, could not be generated diastereoselectively.[4,6]

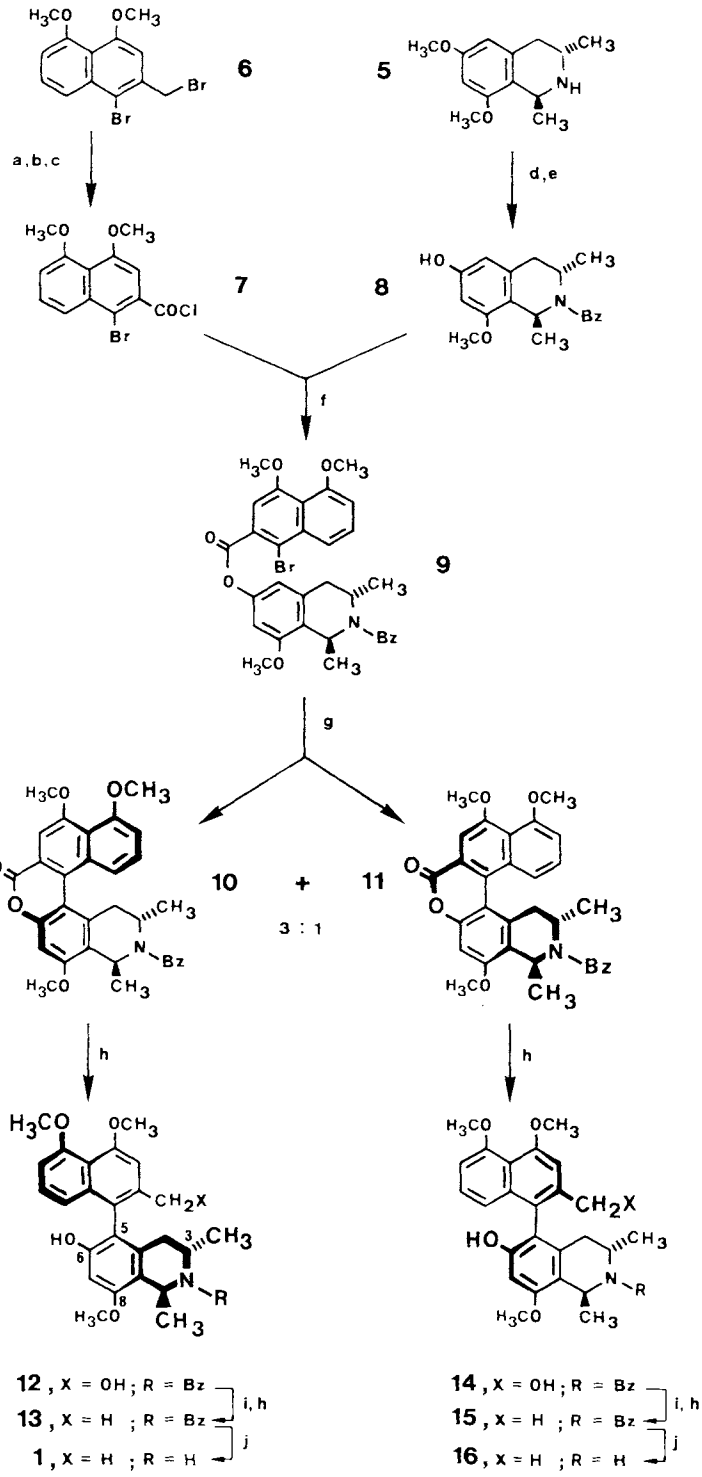
The subsequent procedure is summarized in Scheme 2. By *N*-benzylation and careful partial ether cleavage,[13] **5** can be converted regioselectively into **8** (65%). The coupling of the heterocyclic half of **1** thereby obtained with the naphthalene moiety—*inter*molecularly affording only very low yields—is performed *intra*molecularly, after the two coupling partners have been joined by an auxiliary bridge. Especially suitable for this purpose is an ester group, such as in **9**. The required difunctional naphthalene building block **7** is readily accessible (74%) from the dibromide **6**[4] and undergoes smooth esterification with the isoquinoline **8** to form **9** (86%).



Scheme 1. Stereoselective synthesis of the chiral isoquinoline building block **5**. a) (*S*)-1-Phenylethylamine, toluene, Δ; 5 bar H_2/Raney nickel W2, EtOH, 80 h. b) 5 bar H_2/10% Pd-C, MeOH, 120 h. c) H_3CCOCl, NEt_3, CH_2Cl_2. d) $POCl_3$, MeCN, reflux. e) $LiAlH_4/AlMe_3$, tetrahydrofuran (THF), −78°C→0°C, 3 h.

With the benzyl ether type auxiliary bridge, used by us earlier, the intramolecular aryl coupling, photochemically performed, occurred in maximum yields of only 15%—even in far simpler cases.[4] With **9**, under Pd^{II} catalysis, the coupling leads, in very satisfactory yields (49%) and with surprisingly high regioselectivity,[16] to the helicene-like atropoisomers **10** and **11**, which are difficult to separate. In this process, the diastereomer **10**, whose configuration corresponds to that of ancistrocladine, is preferentially formed. Reductive cleavage of the auxiliary bridge (95%) affords the atropoisomeric alcohols **12** and **14**, which, owing to the CH_2OH group on the naphthalene moiety, may be unusually easily separated in this state by chromatography (R_f of **12** = 0.26, R_f of **14** = 0.23; $CHCl_3$/MeOH = 100/7, silica gel). Mild deoxygenation and *N*-deblocking converts **12** into **1** [91%, m.p. = 261°C, $[\alpha]_D^{20}$ = −23 (*c* = 0.16, MeOH)], which is chromatographically and spectroscopically identical with authentic ancistrocladine.[17] The analogous transformation of the diastereomer **14**, via **15**, affords hamatine **16** [90%, m.p. = 250°C, $[\alpha]_D^{20}$ = +68 (*c* = 0.04, $CHCl_3$)],[17] the naturally occurring atropoisomer[18] of **1**. The atropoisomeric excess obtained in the aryl coupling of **9** is of the order of magnitude of that observed for these two alkaloids in the plants.

The presented first total synthesis of ancistrocladine **1** delivers the methodology for the stereocontrolled synthesis of further, related naphthyl isoquinoline alkaloids of



Scheme 2. Synthesis of ancistrocladine **1** and its natural atropoisomer hamatine **16**. a) Dimethyl sulfoxide (DMSO), $NaHCO_3$, 100°C. b) $NaClO_2$, resorcinol, dioxane/H_2O, NaOAc buffer (pH = 4.3). c) $(COCl)_2$, dimethylformamide (DMF; cat.), CH_2Cl_2. d) $PhCH_2Cl$ (BzCl), K_2CO_3, 1-propanol, reflux. e) 47% HBr, 70°C, 9 h. f) NEt_3, 4-*N*,*N*-dimethylaminopyridine, CH_2Cl_2. g) $Pd(PPh_3)_2Cl_2$, NaOAc, *N*,*N*-dimethylacetamide, 100°C [14]. h) $LiAlH_4$, THF. i) CCl_2Br–CCl_2Br [15]/polym. PPh_3, CH_2Cl_2. j) H_2/10% Pd–C, MeOH.

any absolute and relative configuration—for pharmacological investigations, but also for structural elucidations.

Received: May 20, 1986;
revised: August 1, 1986 [Z 1782/1783 IE]
German version: *Angew. Chem. 98* (1986) 917

[1] a) T. R. Govindachari, P. C. Parthasarathy, *Tetrahedron 27* (1971) 1013; b) T. R. Govindachari, K. Nagarajan, P. C. Parthasarathy, T. G. Rajagopalan, H. K. Desai, G. Kartha, S. Lai Chen, K. Nakanishi, *J. Chem. Soc. Perkin Trans. 1 1974*, 1413.

[2] M. Shamma: *The Isoquinoline Alkaloids*, Academic Press, New York 1972, p. 501.

[3] Reviews: a) T. R. Govindachari, P. C. Parthasarathy, *Heterocycles 7* (1977) 661; b) G. Bringmann (The Naphthyl Isoquinoline Alkaloids) in A. Brossi (Ed.): *The Alkaloids, Vol. 29*, Academic Press, New York, in press, p. 141; c) in: *35 Jahre Fonds der Chemischen Industrie, 1950–1985*, Verband der Chemischen Industrie, Frankfurt 1985, p. 151.

[4] G. Bringmann, J. R. Jansen, *Tetrahedron Lett. 25* (1984) 2537.

[5] For syntheses of arylpropanones, see a) S. Ahmad, W. B. Whalley, D. F. Jones, *J. Chem. Soc. C1971*, 3590; b) H. B. Hass, A. G. Susie, R. L. Heider, *J. Org. Chem. 15* (1950) 8.

[6] G. Bringmann, J. R. Jansen, *Heterocycles 24* (1986) 2407.

[7] G. Bringmann, *Liebigs Ann. Chem. 1985*, 2126.

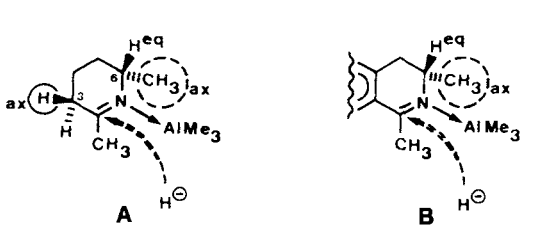
[8] a) F. Weinges, G. Graab, *Chem. Ztg. 94* (1970) 728; b) D. E. Nichols, C. F. Barfknecht, D. B. Rusterholz, *J. Med. Chem. 16* (1973) 480; c) G. Knupp, A. W. Frahm, *Arch. Pharm. (Weinheim, Ger.) 318* (1985) 535, and references cited therein.

[9] Not only **1** but, in fact, all naphthyl isoquinoline alkaloids whose structures have been elucidated unequivocally exhibit the (*S*) configuration at C-3 of the isoquinoline moiety. Cf. [3].

[10] Enantiomeric purity determined by ^{1}H-NMR spectroscopy of **3** as the amide of (*S*)-2-methoxy-2-trifluoromethylphenylacetic acid ≥93%, for an *ee* value of 94% for the phenylethylamine employed. For derivatization, see J. A. Dale, H. S. Mosher, *J. Am. Chem. Soc. 95* (1973) 512, and references cited therein.

[11] K. Maruoka, H. Yamamoto, *Angew. Chem. 97* (1985) 670; *Angew. Chem. Int. Ed. Engl. 24* (1985) 668, and references cited therein.

[12] Similarly high diastereomeric excess had previously been achieved in the reduction of tetrahydropyridines with $LiAlH_4/AlMe_3$ (see [11]). These results had been discussed in terms of the attack of "$H^{\ominus}$," occurring, on the one hand, as homosynplanar as possible to the axial CH_3 group on C-6 (dashed circle) and, on the other hand, as antiperiplanar as possible to the axial H atom on C-3 (circle) of the tetrahydropyridine ring, forced to adopt conformation **A** on account of the Al complexation. Since C-3 is no longer sp^3 hybridized in the dihydroisoquinoline system **B**, the latter effect is no longer present. As a result, such high diastereomeric excesses could not be expected. On the other hand, the results are stereochemically in agreement with the findings for iminium salts (and thus cationic systems). Cf. P. Deslongchamps: *Stereoelectronic Effects in Organic Chemistry*, Pergamon Press, Oxford 1983, Chap. 6.



[13] For selective ether cleavage in multiply methoxylated isoquinolines, see A. Brossi, S. Teitel, *Helv. Chim. Acta 53* (1970) 1779; R. W. Gray, A. S. Dreiding, *ibid. 63* (1980) 315.

[14] For similar coupling reactions involving appreciably simpler arenes, see D. E. Ames, A. Opalko, *Tetrahedron 40* (1984) 1919.

[15] G. Bringmann, S. Schneider, *Synthesis 1983*, 139.

[16] The likewise possible 7–1′ coupling, which is not observed in this case, would lead to the structural type of ancistrocladisine. Cf. [3].

[17] Authentic samples of **1** and **16** were isolated from *Ancistrocladus hamatus*. We thank Dr. *G. Reisch* and Prof. Dr. Dr. *J. Reisch*, Institut für Pharmazeutische Chemie der Universität Münster, and Prof. Dr. *A. A. L. Gunatilaka*, University of Peradeniya, Sri Lanka, for providing us with samples of the plants.

[18] T. R. Govindachari, P. C. Parthasarathy, T. G. Rajagopalan, H. K. Desai, K. S. Ramachandran, E. Lee, *Indian J. Chem. 13* (1975) 641.

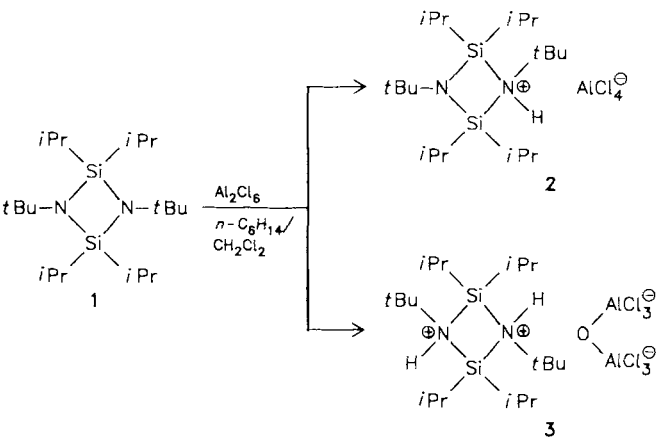
Cyclodisalazane Cations—Synthesis and Crystal Structure**

By *Ursula Kliebisch, Uwe Klingebiel,* Dietmar Stalke,* and *George M. Sheldrick*

The nitrogen atom in silicon-nitrogen compounds is almost always in a structurally planar environment, and rarely exhibits basic properties;[1,2] adducts—which frequently undergo further reaction and consequently cannot be isolated—are formed only with very strong Lewis acids. Protonated silazanes have, to our knowledge, never been detected so far.

Hitherto, there have been two major objectives on carrying out reactions of aluminum trihalides with silazanes: First, the synthesis of aluminum silazanes,[3-5] and second, the synthesis of compounds with threefold coordinated silicon.[6-8] The stabilization of silicon ylides by adduct formation with aluminum trihalides[8] motivated us into investigating reactions of cyclosilazanes with Al_2Cl_6.

When the cyclosilazane **1**[9] was heated in *n*-hexane/dichloromethane (10:3 v/v), a phase separation was observed upon cooling the mixture. Evaporation of the dichloromethane phase to dryness furnished the salts **2** and **3** as solids: monoprotonated **1** with $AlCl_4^{\ominus}$ as counter-



ion,[10] and diprotonated **1** with the novel dianion $^{\ominus}Cl_3Al-O-AlCl_3^{\ominus}$ as counterion.[11] Repeated crystallization from *n*-hexane/dichloromethane afforded crystals of **3** sufficiently suitable for an X-ray structure analysis. Apparently the formation of **3** involves participation of traces of water during the reaction and/or during the work-up of the reaction mixture.[12]

1 does not react with Al_2Cl_6 in the absence of dichloromethane, and can be recovered without decomposition; consequently, CH_2Cl_2 functions as a reactant. Degradation products of dichloromethane were not detected. The stability of salts such as **2** and **3** can be ascribed to kinetic stabilization by the large substituents.

It follows from the ^{29}Si-NMR spectra of **1** ($\delta = 7.44$),[9] **2** ($\delta = 30.05$) and **3** ($\delta = 30.84$) that the Si atoms in **2** and **3** are strongly deshielded. The ^{15}N-NMR resonances of **2** and **3** appear in the region characteristic for quaternary ammonium salts. The Si–N bonds in **1** (174.7 pm)[9] are

[*] Prof. Dr. U. Klingebiel, U. Kliebisch, D. Stalke, Prof. G. M. Sheldrick
Institut für Anorganische Chemie der Universität
Tammannstrasse 4, D-3400 Göttingen (FRG)

[**] This work was supported by the Deutsche Forschungsgemeinschaft and the Fonds der Chemischen Industrie.

significantly shorter than in **3** (179.2 pm), i.e. they are weakened due to the sp^3-hybridization of the nitrogen. The existence of the NH-protons was confirmed by ^{15}N- and ^1H-NMR spectroscopy. Each of the N-C bonds subtend an angle of 16.8° to the $(SiN)_2$ plane. This unusual configuration at the nitrogen is indicative of protonation.

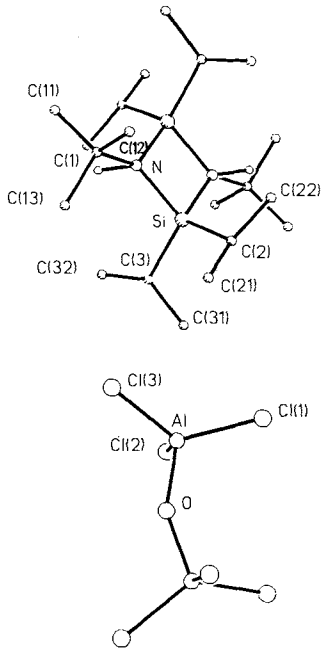


Fig. 1. Crystal structure of **3**. Stoe-Siemens AED diffractometer with graphite-monochromatized $Mo_{K\alpha}$ radiation ($\lambda = 71.069$ pm) at room temperature: size of crystal $0.46 \times 0.46 \times 0.77$ mm^3; 4652 reflections with $7° < 2\theta < 50°$, 1640 symmetry-independent with $F > 4\sigma(F)$. The structure was solved by direct methods. All atoms other than H were anisotropically refined. Geometrical placement of the nine H-atoms of the *tert*-butyl groups (C-H length: 96 pm, H-C-H bond angle 109.9°, U(H)-1.5 U_{eq}(C), U_{eq}(C) = 1/3 (trace of the orthogonal U_{ij} tensor)). The same holds true for the H atoms of the secondary-C-atoms of the isopropyl groups, but with $U(H) = 1.2\,U_{eq}(C)$. The H atoms on the nitrogen could not be unambiguously located, even by a high-angle refinement with subsequent difference Fourier synthesis. In the diagram they have been positioned according to their ideal geometry.—Space group $C2/c$, $Z = 4$, $a = 1482.5(2)$, $b = 1247.9(4)$, $c = 1866.7(3)$ pm, $\beta = 98.63(2)°$, $\mu(Mo_{K\alpha}) = 0.64$ mm^{-1}, $R = 0.055$, $R_w = 0.054$ ($w^{-1} = (\sigma^2(F) + 0.0002\,F^2)$). Further details of the crystal structure investigation are available on request from the Fachinformationszentrum Energie, Physik, Mathematik GmbH, D-7514 Eggenstein-Leopoldshafen 2 (FRG), on quoting the depository number CSD-52105, the names of the authors, and the full citation of the journal.

Experimental

A thick suspension of freshly sublimed Al_2Cl_6 (8 g, 0.03 mol) in *n*-hexane (100 mL) and CH_2Cl_2 (30 mL) was treated with 11.1 g (0.03 mmol) of **1** and the mixture heated for 2 h. Upon cooling, the mixture separated into two phases; the lower phase contained the aluminum salt. This phase was separated, covered with 10 mL of *n*-hexane, and cooled to −150°C. **3** crystallized out, while **2** was isolated as an amorphous powder after removal of the solvent. Yields: 7.3 g (45%) of **2** and 1 g (5%) of **3**.

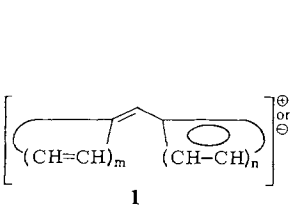
Received: May 26, 1986;
revised: July 11, 1986 [Z 1790 IE]
German version: *Angew. Chem. 98* (1986) 921

[1] E. A. V. Ebsworth in A. G. McDiarmid (Ed.): *The Bond to Carbon*, M. Dekker, New York 1968, p. 1.
[2] H. Bürger, *Angew. Chem. 85* (1973) 519; *Angew. Chem. Int. Ed. Engl. 12* (1973) 474.
[3] H. Schmidbaur, M. Schmidt, *Angew. Chem. 74* (1962) 327; *Angew. Chem. Int. Ed. Engl. 1* (1962) 327.
[4] U. Wannagat, T. Blumenthal, D. J. Brauer, H. Bürger, *J. Organomet. Chem. 249* (1983) 33.
[5] M. Veith, H. Lange, A. Belo, O. Recktenwald, *Chem. Ber. 118* (1985) 1600.
[6] A. H. Cowley, M. C. Cushner, P. E. Riley, *J. Am. Chem. Soc. 102* (1980) 624.
[7] W. Clegg, M. Haase, U. Klingebiel, J. Neemann, G. M. Sheldrick, *J. Organomet. Chem. 251* (1983) 281.
[8] W. Clegg, U. Klingebiel, J. Neemann, G. M. Sheldrick, *J. Organomet. Chem. 249* (1983) 47.
[9] W. Clegg, M. Haase, G. M. Sheldrick, N. Vater, *Acta Crystallogr. C40* (1984) 871; N. Vater, *Dissertation*, Universität Göttingen 1984.
[10] **2**: M.p. 120°C (decomp.); molecular mass osmometrically in $CHCl_3 = 553/2$; ^1H-NMR ($CDCl_3$, TMS int.): $\delta = 1.8$–1.2 (m, $CHMe_2$), 1.36 ($NCMe_3$), 1.53 ($NHCMe_3$), 3.58 (NH); ^{13}C-NMR ($CDCl_3$, TMS int.): $\delta = 16.34$ (SiC), 17.97, 18.18, 18.23, 18.81 ($SiCC_2$), 31.39 (NCC_3), 34.11 ($NHCC_3$), 51.50 (NC), 59.27 (NHC); ^{15}N-NMR ($CDCl_3$, $MeNO_2$ ext.): $\delta = -311.7$ ($NCMe_3$), −309.9 ($NHCMe_3$, $J_{NH} = 60$ Hz); ^{29}Si-NMR ($CDCl_3$, TMS int.): $\delta = 30.05$.
[11] **3**: ^{13}C-NMR ($CDCl_3$, TMS int.): $\delta = 33.46$ (NCC_3), 60.6 (NC); ^{15}N-NMR ($CDCl_3$, $MeNO_2$ ext.): $\delta = -296.8$ ($J_{NH} = 65$ Hz); ^{29}Si-NMR ($CDCl_3$, TMS int.): $\delta = 30.8$.
[12] D. Jentsch, P. G. Jones, E. Schwarzmann, G. M. Sheldrick, *Acta Crystallogr. C39* (1983) 1173; U. Thewalt, F. Stollmeier, *Angew. Chem. 94* (1982) 137; *Angew. Chem. Int. Ed. Engl. 21* (1982) 133; *Angew. Chem. Suppl. 1982*, 209.

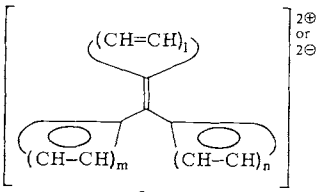
A Salt of the Dication Cycloheptatrienylidenemethyleneditropylium

By *Kiyoharu Mizumoto, Hideki Kawai, Keiji Okada,* and *Masaji Oda**

A number of ionic compounds having the bicyclic cross-conjugated structure **1** (m, n ≧ 1) have been synthesized as stable substances;[1–4] however, none of the tricyclic analogues **2** are known. These molecules would be of interest from both structural and physicochemical points of view. We wish to report the synthesis of cycloheptatrienylidenemethyleneditropylium **4**, a novel dication of type **2** (l = m = n = 3), which was isolated as the bis(tetrafluoroborate) salt, **4** · 2 $BF_4^\ominus$.



1
cation **3**, m = n = 3

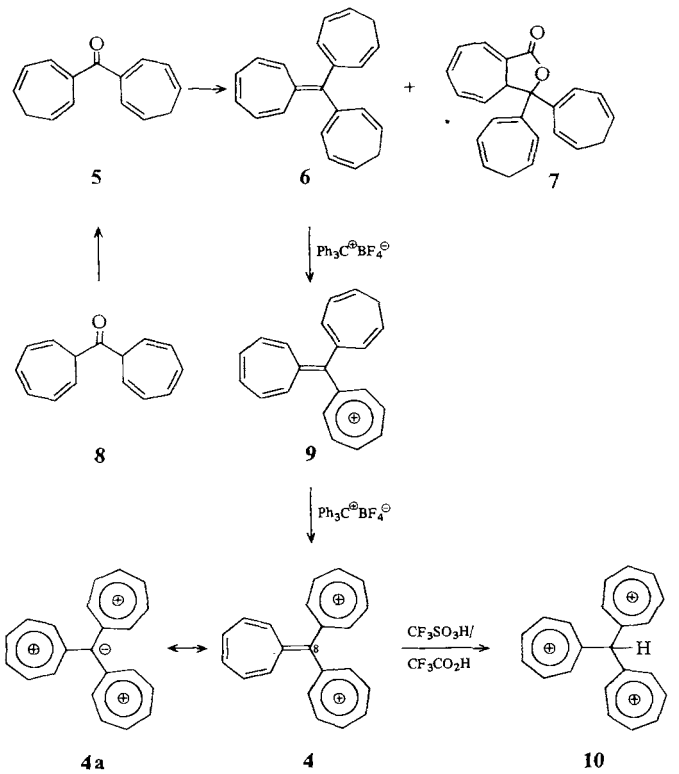


2
dication **4**, l = m = n = 3

Thermal sigmatropic [1, 5] hydrogen shift of the ketone **8**[5] (140°C, xylene, 6 h) gave di(1,3,6-cycloheptatrienyl) ketone **5** and 1,3,6-cycloheptatrienyl 2,4,6-cycloheptatrienyl ketone in 47 and 33% yield, respectively (Table 1).[6] As the key step for the construction of the carbon skeleton of **4**, the ketone **5** was transformed into the heptafulvalene **6** employing *Kitahara-Asao*'s heptafulvalene synthesis with 7-carbonylcycloheptatriene.[7] Thus, dropwise addition of 7-cycloheptatrienecarbonylchloride (1.7 equiv.) into a refluxing benzene solution of **5** and triethylamine (2.0 equiv.) under nitrogen atmosphere provided **6** in 5–10% yield as a red, acid- and air-sensitive oil, in addition to the lactone **7** (50–70% yield). Treatment of **6** with triphenylmethyl tetrafluoroborate (2.2 equiv.) in dry acetonitrile (room temperature, 1 d) gave the dication **4** as the salt

[*] Prof. Dr. M. Oda, Dipl.-Chem. K. Mizumoto, Dipl.-Chem. H. Kawai, Dr. K. Okada
Department of Chemistry, Faculty of Science, Osaka University
Toyonaka, Osaka 560 (Japan)

4·$2BF_4^{\ominus}$ (dark blue needles, m.p. = 245 °C (dec.)) in 60% yield. The hydride abstraction proceeded stepwise via the monocation **9** as monitored by thin layer chromatography (silica gel, acetone/trace of 42% HBF_4). Attempts to obtain **9** selectively using one equivalent of the reagent resulted, however, only in formation of a mixture with **4**.



5 **6** **7** **8** **9** **4a** **4** **10**

Table 1. Selected physical data for the compounds **4**–**7**, **9**, and **10**.

4: ^{1}H-NMR (100 MHz, CD_3CN): $\delta = 8.10$ (m, H-3,4), 8.55 (structured d, $J = 10$ Hz, H-2); ^{13}C-NMR (22.5 MHz, CD_3CN): $\delta = 133.2$ (s, C-8), 150.1, 150.3, 151.0 (each d, C-2–C-4 [8]), 168.5 (s, C-1)

5: ^{1}H-NMR ($CDCl_3$): $\delta = 2.36$ (t, $J = 7$ Hz, 4H), 5.49 (d, 9 Hz, 2H), 5.63 (dt, 9, 7 Hz, 2H), 6.28 (dd, 9, 6 Hz, 2H), 6.75 (d, 9 Hz, 2H), 7.15 (d, 6 Hz, 2H); IR (oil): $\tilde{\nu}_{C=O} = 1645$ cm^{-1}

6: ^{1}H-NMR ($CDCl_3$): $\delta = 2.29$ (t, $J = 7$ Hz, 4H), 5.2–5.6 (m, 6H), 5.75 (m, 2H), 5.9–6.3 (m, 6H), 6.51 (d, 6 Hz, 2H); UV (cyclohexane): $\lambda_{max} = 240$ nm ($\lg\varepsilon = 4.20$) sh, 270 (4.07) sh, 349 (3.93), tailing to 600 nm

7: m.p. = 89 °C; ^{1}H-NMR ($CDCl_3$): $\delta = 1.9$–2.6 (m, 4H), 3.05 (narrow m, 1H), 5.1–5.6 (m, 5H), 5.9–6.4 (m, 5H), 6.62 (d, $J = 6$ Hz, 1H), 6.78 (m, 2H), 6.94 (d, 6 Hz, 1H), 7.10 (structured d, 5 Hz, 1H); IR (KBr): $\tilde{\nu}_{C=O} = 1760$ cm^{-1}

9: ^{1}H-NMR (CD_3CN) (with a small amount of **4**): $\delta = 2.33$ (t, $J = 7$ Hz, 2H), 5.2, 6.4 (m, 4H), 6.60 (d, 6 Hz, 1H), 7.3 (m, 8H), 7.9 (m, 4H)

10: ^{1}H-NMR (CF_3SO_3H/CF_3CO_2H): $\delta = 7.92$ (s, 1H), 9.36 (m, 18H); ^{13}C-NMR (CF_3SO_3H/CF_3CO_2H): $\delta = 68.9$, 157.9, 159.2, 159.6, 166.4

The NMR spectra of **4** (Table 1), which showed little change down to −40 °C, are in accord with a C_3 symmetry of the molecule. The averaged chemical shifts of the ring protons and tertiary carbons ($\delta_{av} = 8.25$ and 150.5, respectively) lie between those of the bicyclic congener **3** ($\delta_{av} = 7.62$ and 141.4[4b]) and the tropylium ion ($\delta = 9.30$ and 155.4) in line with the number of charges per ring (**3**, 0.5; **4**, 0.66; tropylium ion, 1). Notably, the central carbon (C-8) is observed at the highest field in spite of being a quaternary carbon. This suggests some resonance contribution of the polar structure **4a**.[9] The absorption spectrum [$\lambda_{max}(CH_3CN) \approx 236$ nm ($\lg\varepsilon = 4.54$), 284 (4.15), 649 (4.39)] is redshifted by 53 nm in the visible region compared with that of **3**. The dication **4** gave two pK_{R^+} values (4.4 and 1.6), corresponding to the stepwise neutralization upon spectrophotometric measurements in 20% aqueous ethanol. These values are, however, considered to be somewhat smaller than the true values because **4** partially decomposed during the measurements. Cyclic voltammetry also showed two reduction potentials ($E = -0.36$ and -0.19 V vs. SCE, CH_3CN, $Bu_4N^{\oplus}ClO_4^{\ominus}$, 100 mV s^{-1}, 20 °C), which are ascribable to the two-stage reduction of the two tropylium groups to form a diradical. These pK_{R^+} values and reduction potentials lie between those of the tropylium ion (4.30[10] and −0.29 V, respectively) and **3** (7.49[4b] and −0.40 V, respectively). The poorer thermodynamic stability of **4** relative to **3** is perhaps associated with less coplanarity of **4** due to severer steric interactions among the three seven-membered rings.[11]

In agreement with the highest electron density shown in the ^{13}C-NMR spectrum, the dication **4** was protonated at the central carbon in CF_3SO_3H/CF_3CO_2H (1 : 1), though unchanged in CF_3CO_2H alone, to give the methylidynetritropylium ion **10**, which is the first trication in the methyltropylium series.[4b, 12]

Received: June 2, 1986;
revised: July 18, 1986 [Z 1800 IE]
German version: *Angew. Chem. 98* (1986) 930

CAS Registry numbers:
4·$2BF_4^{\ominus}$, 104422-35-7; **5**, 104422-30-2; **6**, 104422-32-4; **7**, 104438-49-5; **8**, 104422-29-9; **9**, 104422-33-5; **10**, 104422-36-8; (1,3,6-cycloheptatrienyl) (2,4,6-cycloheptatrienyl) ketone, 104422-31-3; 7-carbonylcycloheptatriene, 36374-18-2; tropylium tetrafluoroborate, 27081-10-3; nitromethane, 75-52-5; di(2,4,6-cycloheptatrienyl)nitromethane, 104422-37-9; di(2,4,6-cycloheptatrienyl)aminomethane, 104422-38-0.

[1] K. Komatsu, K. Masumoto, Y. Waki, K. Okamoto, *Bull. Chem. Soc. Jpn. 55* (1982) 2470.
[2] a) C. Jutz, H. Amschler, *Angew. Chem. 73* (1961) 806; b) A. Cassens, P. Eilbracht, A. Nazzal, W. Prossdorf, U. T. Mueller-Westerhoff, *J. Am. Chem. Soc. 103* (1981) 6367.
[3] M. Oda, K. Tamate, Y. Kitahara, *J. Chem. Soc. D 1971*, 347.
[4] a) T. Otomo, M. Oda, Y. Kitahara, *J. Chem. Soc. D 1971*, 114; b) Y. Kayama, M. Oda, Y. Kitahara, *Chem. Lett. 1973*, 1169; c) I. Fleming, *J. Chem. Soc. Perkin Trans. 1 1973*, 1019.
[5] Y. Kayama, M. Oda, Y. Kitahara, *Synth. Commun. 3* (1973) 53. An improved synthesis of **8** is achieved via di(2,4,6-cycloheptatrienyl)nitromethane, which is readily obtained by reaction of tropylium tetrafluoroborate with nitromethane (1 : 1, EtONa/EtOH, 77% yield), followed by reduction of the product with $LiAlH_4$ to the corresponding amine previously used as the precursor.
[6] Prolonged heating led to more complex mixtures due to further sigmatropic rearrangements.
[7] Y. Kitahara, *Pure & Appl. Chem. 44* (1975) 833, and references cited therein.
[8] Full assignment of these signals has not yet been achieved.
[9] HMO calculation also shows the highest electron density at C-8.
[10] K. Okamoto, K. Komatsu, O. Murai, O. Sakaguchi, Y. Matsui, *Bull. Chem. Soc. Jpn. 46* (1973) 1785.
[11] A dihedral angle of 31.5° between the seven-membered rings has been observed in the X-ray structure of **3**. C. Kabuto, M. Oda, Y. Kitahara, *Tetrahedron Lett. 1972*, 4851.
[12] K. Takeuchi, Y. Yokomichi, Y. Kubota, K. Okamoto, *Tetrahedron 36* (1980) 2939.

Poly-Onio-Substituted Quinones as Strong Electron Acceptors**

By *Robert Weiss,* Norbert J. Salomon, Georg E. Miess,* and *Reinhard Roth*

Because of their importance in natural products chemistry, biochemistry, pharmacy and the dyestuffs industry,

[*] Prof. Dr. R. Weiss, Dipl.-Chem. N. J. Salomon, Dipl.-Chem. G. E. Miess, Dipl.-Chem. R. Roth
Institut für Organische Chemie der Universität Erlangen-Nürnberg
Henkestrasse 42, D-8520 Erlangen (FRG)

[**] This work was supported by the Fonds der Chemischen Industrie.

quinones belong to one of the most thoroughly investigated classes of substances in organic chemistry. In organic synthesis, quinones have long played an outstanding role as oxidizing agents:[1] the synthesis of quinones having as positive a redox potential as possible has therefore always been of central interest,[2] 2,3-dichloro-5,6-dicyano-1,4-benzoquinone (DDQ) having thus far claimed special practical importance as one of the most powerful organic oxidizing agents.[3]

We now report the first synthesis of structurally novel poly-onio-substituted benzoquinones whose oxidative power clearly surpasses that of the known neutral systems. Reaction of trimethylsilyl trifluoromethanesulfonate (triflate) **1** with 4-dimethylaminopyridine **2** leads, in accord with equation (a), to formation of *N*-trimethylsilyl-4-dimethylaminopyridinium triflate in almost quantitative yield as thermally stable, colorless, hygroscopic crystals (for characteristic data see Table 1).[4]

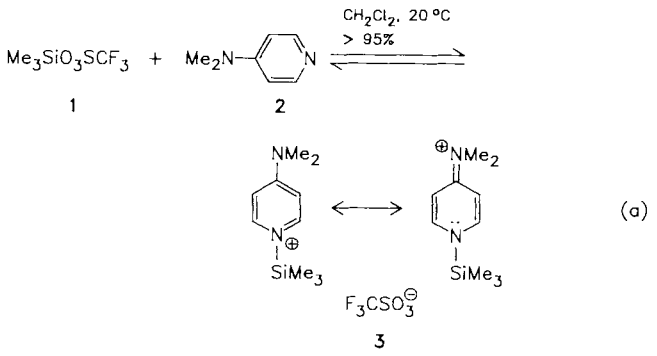
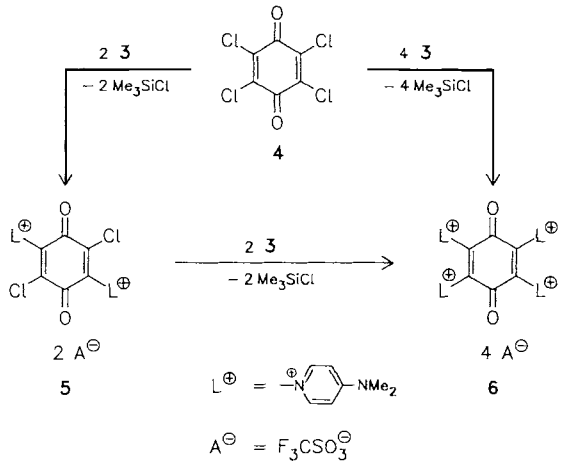


Table 1. Characteristic data of the cations in **3**, **5**, **6**, **7**, and **8** [a].

Cpd.	M.p. [°C]	λ_{max} [nm] (ε) [b]	IR (KBr) $\tilde{\nu}$ [cm^{-1}]	δ^1H (solvent)	$\delta^{13}C$ (solvent)
3	82 (decomp.)		1645 vs), 1575(s), 860(vs), 845(vs), 820(vs) [c]	0.63 (s, 9H), 3.27 (s, 6H), 7.48 (AA'BB', 4H) ($CDCl_3$)	
5	260 (decomp.)	435 (4293) [d]	1690(m), 1650(vs), 1580(s), 1410(m), 950(m), 820(m)	3.3 (s, 12H), 7.6 (AA'BB', 8H) (D_2SO_4)	40.6, 109.3, 136.9, 140.0, 141.5, 155.6, 172.5 (D_2SO_4)
6	305	450.9 (8791) [d]	1690(m), 1650(vs), 1590(s), 1410(m), 1315(m), 1115(vs), 820(m)	3.5 (s, 24H), 7.7 (AA'BB', 16H) (D_2SO_4)	43.2, 113.2, 137.8, 142.5, 158.2, 173.0 (D_2SO_4)
7	300 (decomp.)	397.5 (998.6) [e]	1650(vs), 1585(s), 1490(m), 1440(m), 820(m)	3.2 (s, 24H), 7.03 (AA'BB', 16H), 8.7 (b, 2H) (CD_3CN)	41.2, 109.7, 131.1, 142.9, 144.4, 157.9 (CD_3CN)
8	312 (decomp.)	393.4 (986.5) [e]	1650(vs), 1585(vs), 1485(s), 1455(s), 1440(s), 1405(s), 1095(s), 830(s), 630(vs)	0.83 (t, 6H), 3.29 (s, 24H), 3.53 (q, 4H), 7.75 (AA'BB', 16H) ([D_6]-DMSO)	15.0, 40.3, 72.2, 108.7, 133.8, 141.0, 147.3, 156.1 ([D_6]-DMSO)

[a] Correct elemental analyses for all salts. [b] Longest-wavelength absorption in the electron spectrum. [c] In nujol. [d] In CH_2Cl_2/CH_3CN. [e] In CH_3CN.

MNDO calculations show that the cation in **3** can, to a good approximation, be described as a silylated secondary amine.[5] Consistent with this description, **3** undergoes transamination reactions with numerous electrophilic organic halogen compounds, as are characteristic of silylamines.[5] Thus, on reaction of **3** with *p*-chloranil, **4**, in the molar ratio 2 : 1, the bispyridinio-substituted *p*-quinone **5** is obtained in quantitative yield as a vermilion crystalline powder (cf. Scheme 1 and data in Table 1). 2,5-Substitution is the rule in the case of nucleophilic difunctionalizations of *p*-chloranil, and will also be assumed here, although, according to the spectroscopic data, the equally possible 2,3-disubstitution pattern cannot be strictly ruled out. In no case, however, is the reaction product an isomeric mixture. Further reaction of **5** with 2 molar equivalents of **3** or direct reaction of **4** with 4 molar equivalents of **3** furnishes equally smoothly the dark red tetrakispyridinio-substituted quinone **6** in quantitative yield (cf. Scheme 1 and data in Table 1). In all cases the calculated amounts of Me_3SiCl could be detected in the mother liquor.



Scheme 1.

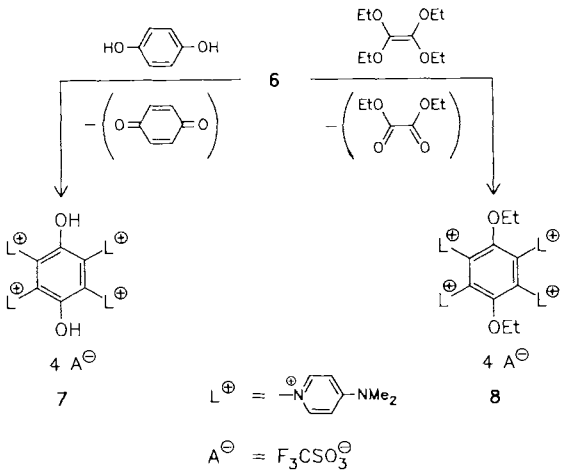
Mono-onio-substituted quinones have occasionally been postulated as strongly oxidizing, reactive intermediates, but in no case have they ever been isolated and convincingly characterized as such.[6] *Poly*-onio-substituted quinones have so far never been synthesized. Of central interest, aside from the reactivity of the new quinones **5** and **6**, is the influence of the pyridinio substituents on the redox potential. In Table 2 are listed, inter alia, the (reversible) redox potentials for the single and double reduction of salts **5** and **6**: It can be seen immediately that the dication in **5** is already a much stronger oxidizing agent than **4**. It ranks equal with DDQ, and even surpasses the latter when

Table 2. Reversible redox potentials of substituted 1,4-benzoquinones in CH_3CN.

Quinone	$E_{1/2}$ [V] 1st reduction step	2nd reduction step
1,4-Benzoquinone [a]	−0.51	−1.14
4 [b]	+0.089	−0.715
DDQ [a]	+0.51	−0.30
5 [b]	+0.49	−0.17
6 [b]	+0.73	+0.16

[a] M. E. Peover, *J. Chem. Soc. 1962*, 4540. [b] Cyclic voltammetry: Pt auxiliary and working electrodes; Ag/AgCl reference electrode: supporting electrolyte 0.1 N Et_4NBF_4.

the second reduction step is taken into consideration. On going to **6**, the redox potential increases even further. **6** exhibits the highest redox potential (+0.73 V) of all previously described quinone systems;[2] even the redox potential of the semiquinone form of **6** is comparable to that of **4**! As expected, **6** is easily reduced to tetrakispyridinio-substituted benzene derivatives—likewise a previously unknown class of substances. Thus, reaction with hydroquinone smoothly furnishes **7**, while reaction with tetraethoxyethylene affords the compound **8** by a previously undescribed reductive ethylation (cf. Scheme 2 and data in Table 1).



Scheme 2.

The finding that the redox potential is shifted by 1.24 V to more positive values on going from the parent *p*-benzoquinone to the salt **6** constitutes a very important facet of this investigation. This drastic effect could be attributed to an optimal electrostatic stabilization of the singly and doubly reduced forms of **6** by the four onio ligands. Undoubtedly, this finding will open up a new area of application in redox chemistry for **2**, which already finds frequent use in reactions catalyzed by Lewis bases.[7]

Reaction of **3** with *o*-chloranil instead of with **4** leads to the *o*-isomer of **6**; DDQ analogously affords a bis-onio-substituted product. In all cases, **2** can be replaced by *N*-methylimidazole; the substitution- and redox-chemistry of the new poly-onio-substituted quinones accessible in this way are presently under investigation.[8]

If the free *N*-bases are used instead of **3** or the analogous trimethylsilyl triflate adduct of *N*-methylimidazole in the reaction according to Scheme 2, then the stoichiometrically equivalent chlorides of the above triflates are obtained,[9] which, as a rule, can be converted with **1** into the triflates. As preliminary electrochemical measurements show,[8] the redox potential of the chlorides is distinctly less positive. Charge transfer interactions between the chloride ions and the electron-deficient quinone system might be responsible for this. The new oxidizing reagents presented here are especially attractive from the preparative point of view, in particular since they can be readily generated in situ; furthermore, in all three oxidation steps they are insoluble in the usual (aprotic) organic solvents, irrespective of the anion. Thus, they offer the same advantages in work-up procedures as immobilized (polymer-bound) reagents.[10]

Experimental procedures for 5 and 6

2,5-Bis[(4-dimethylamino)pyridinio]-3,6-dichloro-1,4-benzoquinone bis(trifluoromethanesulfonate) **5**: A solution of 4 mmol of **3** prepared in situ was added dropwise to a solution of **4** (0.492 g, 2 mmol) in anhydrous CH_2Cl_2 (25 mL). The mixture was stirred overnight at room temperature. The bright-red precipitate (**5**) that formed was filtered off, washed with CH_2Cl_2, and dried under vacuum (oil-pump). Yield: 96% of analytically pure **5**.

2,3,5,6-Tetrakis[(4-dimethylamino)pyridinio]-1,4-benzoquinone tetrakis(trifluoromethanesulfonate) **6**: A solution of **3** (4 mmol) in 25 mL of anhydrous CH_2Cl_2 prepared in situ was treated with 0.246 g (1 mmol) of solid **4**. A dark-red precipitate was immediately formed (**6**). The reaction mixture was stirred for 5 h and then worked up as described for **5**. Yield: 97% of analytically pure **6**. When using larger amounts of reagents it is advisable to heat the reaction mixture for a short while.

Received: June 6, 1986;
revised: July 16, 1986 [Z 1806 IE]
German version: *Angew. Chem. 98* (1986) 925

CAS Registry numbers:
1, 27607-77-8; **2**, 1122-58-3; **3**, 101300-49-6; **4**, 118-75-2; **5**, 104421-77-4; **6**, 104421-79-6; **7**, 104421-81-0; **8**, 104421-83-2; HO-*p*-C_6H_4OH, 123-31-9; $(EtO)_2C{=}C(OEt)_2$, 40923-93-1; *N*-methylimidazole, 616-47-7; *N*-methylimidazole (trimethylsilyltriflate adduct), 101300-51-0.

[1] H. D. Becker in S. Patai (Ed.): *The Chemistry of the Quinoid Compounds, Part 1*, Wiley, London 1974, p. 335ff.
[2] R. M. Scribner, *J. Org. Chem. 31* (1966) 3671.
[3] M. Fieser: *Reagents for Organic Synthesis*, Wiley, New York 1984, p. 166, and references cited therein.
[4] According to NMR spectroscopic investigations, adduct formation is also complete in solution: A. R. Bassindale, T. Stout, *Tetrahedron Lett. 26* (1985) 3403.
[5] R. Roth, *Diplomarbeit*, Universität Erlangen-Nürnberg 1985.
[6] Pyridinio-, sulphonio- and phosphonio-groups were used as onio ligands, cf. K. T. Finley in S. Patai (Ed.): *The Chemistry of the Quinoid Compounds, Part 2*, Wiley, London 1974, p. 877ff.
[7] G. Höfle, W. Steglich, H. Vorbrüggen, *Angew. Chem. 90* (1978) 602; *Angew. Chem. Int. Ed. Engl. 17* (1978) 569.
[8] R. Weiss, N. J. Salomon, unpublished.
[9] Regarding electronically related reactions of DMAP with electrophilic chloro compounds cf. a) A. R. Katritzky, B. Nowak-Wydra, O. Rubio, *Chem. Scr. 24* (1984) 7; b) J. Grünefeld, G. Zinner, *Chem. Ztg. 108* (1984) 112.
[10] A. S. Lindsey in S. Patai (Ed.): *The Chemistry of the Quinoid Compounds, Part 2*, Wiley, London 1974, p. 793ff.

Bis(pentamethylcyclopentadienyl)diphosphene—a Molecule with Fluxional Structure and Reactive P-C Bond**

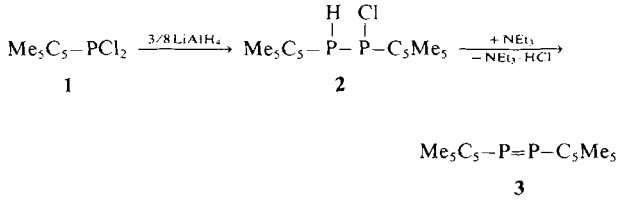
By *Peter Jutzi,* Udo Meyer, Bernt Krebs,* and *Mechthild Dartmann*

The σ-bonded pentamethylcyclopentadienyl (Cp*) ligand is, from our experience, of special interest for many reasons in the chemistry of the main-group elements: 1) the Cp* ligand enables the study of element-specific [1.5]-sigmatropic rearrangements;[1-3] 2) it is sterically demanding[4] and can thus kinetically stabilize reactive species; 3) element–Cp* bonds can be readily cleaved by nucleophilic or electrophilic agents, or even by reducing agents.[5] We now decided to test the potential of this ligand in the relatively new field of diphosphene chemistry.[6]

[*] Prof. Dr. P. Jutzi, Dipl.-Chem. U. Meyer
Fakultät für Chemie der Universität,
Anorganische Chemie
Universitätsstrasse, D-4800 Bielefeld 1 (FRG)
Prof. Dr. B. Krebs, M. Dartmann
Anorganisch-chemisches Institut der Universität
Corrensstrasse 36, D-4400 Münster (FRG)

[**] This work was supported by the Deutsche Forschungsgemeinschaft and by the Ministerium für Wissenschaft und Forschung des Landes Nordrhein-Westfalen.

We first obtained an indication of the existence of a bis(pentamethylcyclopentadienyl)diphosphene (**3**) that is stable under normal conditions during the reduction of Cp^*PBr_2.[7] At the time we were able to detect **3**, along with other products, in the reaction mixture by ^{31}P-NMR spectroscopy, but were unable to isolate it. In the meantime, however, we have succeeded in synthesizing **3** as an isolable compound via another route: Reduction of the dichlorophosphane **1** with $LiAlH_4$ furnished the chlorodiphosphane **2**,[8] which was dehydrohalogenated to **3** without prior isolation (Scheme 1).[9, 10]



Compound	4, 8	5, 9	6, 10	7, 11
R	$N(SiMe_3)tBu$	$N(SiMe_3)_2$	$CH(SiMe_3)_2$	$C(SiMe_3)_3$

Scheme 1. Synthesis and reactions of **3**.

3 was obtained in the form of air-sensitive, yellow crystals which can be stored without decomposition at -30 °C. The ^{31}P-NMR signal[10] lies in the region typical for diphosphenes. The crystal structure analysis carried out at -130 °C (Fig. 1)[11] confirms the presence of monohapto-bound cyclopentadienyl ligands. The P=P double bond has a length of 2.031(3) Å; the ligands are *trans*-oriented. The P–C single bonds are somewhat longer (1.893(7) and 1.883(7) Å, respectively) than in other diphosphenes (1.855–1.866 Å), but shorter than the P–C bond in Me_5C_5–P=C(SiMe$_3$)$_2$ (1.939 Å).[12] The P–P–C angles (103.4 and 103.9°, respectively) lie within the range of values typical for diphosphenes.[13]

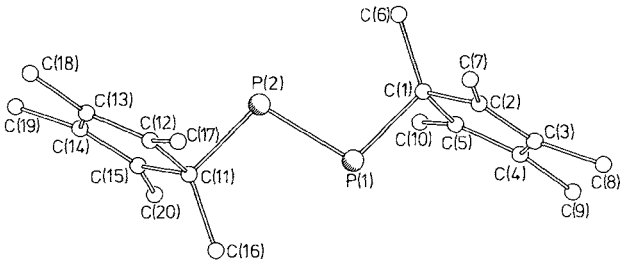


Fig. 1. Crystal structure of **3**.

The η^1-bonding of the Cp* ligand found in the crystal could not be detected in solution. Degenerate [1.5]-sigmatropic rearrangements at room temperature lead to a ^{1}H- and ^{13}C-NMR spectroscopic[10] equivalence, both of the ring carbon atoms as well as of the methyl groups. The ^{1}H- and ^{13}C-NMR signals exhibit the triplet structure to be expected because of coupling to P. We attribute the low activation energy for rearrangement (no change in the spectra down to -80 °C) to the stabilizing interaction of the Cp* ligands with the π^*-orbital of the (p-p)π bond in the η^2-transition state.[12, 14]

As anticipated, on grounds of the somewhat extended P–C bonds in **3**, the Cp* ligands can be readily substituted, e.g. stepwise by reaction with lithium-amides or -alkyls (Scheme 1). The unsymmetrical diphosphenes **4–7** are unequivocally characterized by the AX pattern in the ^{31}P-NMR spectra (Table 1). The diphosphenes **8–11** formed upon substitution of the second Cp* ligand and their ^{31}P-NMR data have already been reported in the literature.[6]

Table 1. ^{31}P-NMR data of the diphosphenes $R-P_A=P_B-C_5Me_5$ **4–7**. The spectra were recorded in solution with H_3PO_4 as external standard.

Compound	δP_A	δP_B	J_{PP}[Hz]
4	440.1	529.1	640
5	546.2	478.3	632
6	522.8	492.6	599
7	545.8	522.2	635

Summarizing, it has been established that the Cp* ligand kinetically stabilizes a P=P bond quite effectively, leads to a diphosphene with fluxional structure, and enables, for the first time, substitutions at a P=P bond.

Received: June 6, 1986;
revised: July 7, 1986 [Z 1805 IE]
German version: *Angew. Chem. 98* (1986) 894

[1] P. Jutzi, H. Saleske, *Chem. Ber. 117* (1984) 222.
[2] P. Jutzi, A. Seufert, *Chem. Ber. 112* (1979) 2481.
[3] P. Jutzi, H. Saleske, D. Bühl, H. Grohe, *J. Organomet. Chem. 252* (1983) 29.
[4] A. H. Cowley, E. A. V. Ebsworth, S. K. Mehrotra, D. W. H. Rankin, D. Walkinshaw, *J. Chem. Soc. Chem. Commun. 1982*, 1099.
[5] P. Jutzi, B. Hielscher, *Organometallics 5* (1986) 1201; P. Jutzi, B. Hampel, *ibid. 5* (1986) 730.
[6] A. H. Cowley, *Polyhedron 3* (1984) 389; C. Couret, J. Escudie, H. Ranaivonjatovo, J. Satgé, *Organometallics 5* (1986) 113.
[7] P. Jutzi, T. Wippermann, *J. Organomet. Chem. 287* (1985) C5.
[8] **2**: diastereomeric mixture 40:60; ^{31}P-NMR (123 MHz): $\delta = 150.0$ (d, $J_{PP} = 273$ Hz, PCl), -28.9 (dd, $J_{PP} = 273$ Hz, $^1J_{PH} = 257$ Hz); 150.4 (d, $J_{PP} = 233$ Hz, PCl), -53.8 (dd, $J_{PP} = 233$ Hz, $^1J_{PH} = 269$ Hz). Side product Me_5C_5–P(Cl)P(Cl)–C_5Me_5 (ca. 10%): ^{31}P-NMR (123 MHz): $\delta = 140.0$ (s), 131.5 (s).
[9] Similary as described by E. Niecke, R. Rüger, *Z. Naturforsch. B37* (1982) 1593; *Angew. Chem. 95* (1983) 154; *Angew. Chem. Int. Ed. Engl. 22* (1983) 155; E. Niecke, R. Rüger, M. Lysek, S. Pohl, W. Schoeller, *ibid. 95* (1983) 495 and *22* (1983) 486; *Angew. Chem. Suppl. 1983*, 639.
[10] *Procedure:* A solution of $LiAlH_4$ (1.97 g, 51.9 mmol) in Et_2O (25 mL) was added dropwise at 0 °C to a solution of **1** (32.8 g, 139 mmol) in petroleum ether (30/70, 270 mL). After 4 hours' stirring, the insoluble material was removed by filtration and the filtrate treated with triethylamine (100 mL, 725 mmol) and stirred for 5 d. After filtration and removal of all volatile components under vacuum, the residue was taken up in toluene. Crystallization at -30 °C afforded 5.42 g (23%) of **3** as yellow crystals (m.p. 120 °C, thermochromic behavior: bright yellow at -80 °C, reddish-orange at 100 °C). Correct elemental analysis. ^{31}P{^{1}H}-NMR (121 MHz, C_6D_6): $\delta = 504$ (s). ^{1}H-NMR (300 MHz, C_6D_6): $\delta = 1.80$ ("t", Me$_5$, $|^3J_{PH} + {}^4J_{PH}| = 1.2$ Hz). ^{13}C{^{1}H}-NMR (75.5 MHz, C_6D_6): $\delta = 123.9$ ("t", C$_5$, $|^1J_{PC} + {}^2J_{PC}| = 1.8$ Hz), 12.4 ("t", Me$_5$, $|^2J_{PC} + {}^3J_{PC}| = 3.1$ Hz). MS (70 eV): m/z 332 ($M^{\oplus}$, 6%), 197 ($M^{\oplus} - C_5Me_5$, 18%), 135 ($C_5Me_5^{\oplus}$, 100%). UV/VIS (pentane): λ(lgε): 236 (4.2), 275 (4.1), 407 nm (3.3).
[11] **3** crystallizes monoclinically; $P2_1/c$, $a = 8.297(5)$, $b = 17.883(10)$, $c = 13.562(7)$ Å, $\beta = 99.88(7)°$, $V = 1982.4$ Å^3, $\rho_{calc} = 1.11$ g cm^{-3}; solution of structure by direct methods (SHELXTL), $R = 0.087$ for 1977 independent reflections with $I > 2.5\sigma(I)$, Syntex-P2$_1$ diffractometer, $Mo_{K\alpha}$ radiation, graphite monochromator. Further details of the crystal structure investigation are available on request from the Fachinformationszentrum Energie, Physik, Mathematik GmbH, D-7514 Eggenstein-Leopoldshafen 2 (FRG), on quoting the depository number CSD-52104, the names of the authors, and the full citation of the journal.
[12] D. Gudat, E. Niecke, B. Krebs, M. Dartmann, *Chimia 39* (1985) 277.
[13] M. Yoshifuji, I. Shima, N. Inamoto, K. Hirotsu, T. Higuchi, *J. Am. Chem. Soc. 103* (1981) 4587; J. Escudie, C. Couret, H. Ranaivonjatovo,

J. Satge, *Phosphorus Sulfur 17* (1983) 221; A. H. Cowley, J. E. Kilduff, N. C. Norman, M. Pakulski, J. L. Atwood, W. E. Hunter, *J. Am. Chem. Soc. 105* (1983) 4845.

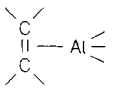
[14] Due to the isolobal behavior of the $-\bar{P}=$ and $-C(H)=$ fragments, a similar situation is found here as in the compound Me_5C_5-CHO: R. J. Bushby, D. W. Jones, *J. Chem. Soc. Chem. Commun. 1979*, 688.

Dimeric 1,4-Dichloro-2,3,5,6-tetramethyl-1,4-dialumina-2,5-cyclohexadiene, a Compound with Aluminum-Olefin π-Bonds**

By *Hansgeorg Schnöckel,* Manfred Leimkühler, Rainer Lotz,* and *Rainer Mattes*

π-Complexes of aluminum with olefins have long been regarded as intermediates in many reactions of organoaluminum compounds.[1] Results of IR and NMR spectroscopic investigations on alkenylaluminum compounds provided evidence of intramolecular interactions of the threefold coordinated aluminum with the C=C double bond.[2] We have now been able to prepare, for the first time, a compound containing the structural unit **I** and to characterize it by an X-ray structure analysis.

I



Treatment of the active species AlCl, generated at elevated temperature, with dimethylacetylene in a low-temperature reaction led, upon warming from -196 °C to room temperature, to formation of dimeric 1,4-dichloro-2,3,5,6-tetramethyl-1,4-dialumina-2,5-cyclohexadiene **1**.[3]

$$4\,AlCl + 4\,H_3CC{\equiv}CCH_3 \longrightarrow Al_4Cl_4C_{16}H_{24} \quad \mathbf{1}$$

In 1968, *Timms* prepared 1,4-dibora-2,5-cyclohexadienes under similar conditions by reaction of boron subhalides with alkynes.[4] The decomposition of **1** in solution and the NMR spectra obtained for such solutions indicate a complex dynamic behavior.

The elemental analysis of **1** (Al : Cl = 1 : 1), the detection of *cis*-2-butene as the sole product of hydrolysis, and the occurrence of a singlet in the ^{1}H-NMR spectrum at $\delta = 2.08$ (90 MHz, C_6D_6) afforded the first indications of the structure of **1**. Surprisingly, the extremely air- and moisture-sensitive compound **1** can be vaporized at ca. 140 °C, and its mass spectrum shows the expected molecular peak with the characteristic fine structure for four chlorine atoms. A compound related to the monomer of **1** is 1,4-diethyl-2,3,5,6-tetraphenyl-1,4-dialumina-2,5-cyclohexadiene·2THF **2** (THF = tetrahydrofuran).[5]

The investigation of the structure of **1** at -130 °C[6] gave the following result: Two nonplanar 1,4-dialuminacyclohexadiene moieties, twisted through 90° with respect to each other, are coupled via four aluminum-olefin π-bonds of type **I** to give the dimer **1** (Fig. 1). In contrast, **2** is monomeric; the Al atoms are coordinatively saturated by THF, and the Al_2C_4 ring is planar.[5]

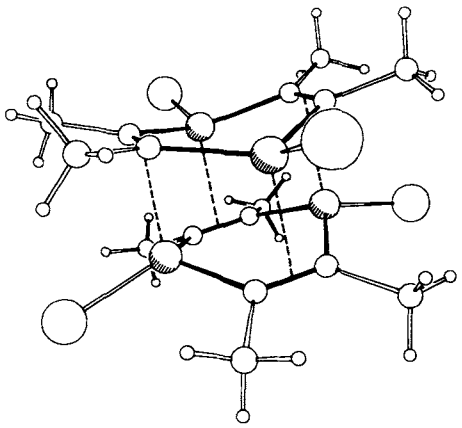


Fig. 1. Molecular structure of **1** in the crystal. Hatched, Al; large circles, Cl; dotted lines, Al-olefin π-bonds. Mean, selected distances [pm] and angles [°]: Al-Cl 210.9, Al-Al 300.5 and 337.0 (see text), Al-C (σ) 199.0, Al-C (π) 235.5, C=C 136.7; C-Al-C 115.1, C-Al-Cl 114.9, Al-C-CH_3 117.7 (standard deviations 0.1–0.3 pm). Further details of the crystal structure investigation are available on request from the Fachinformationszentrum Energie, Physik, Mathematik GmbH, D-7514 Eggenstein-Leopoldshafen 2 (FRG), on quoting the depository number CSD-52141, the names of the authors, and the full citation of the journal.

In **1**, the mean Al-C distance in the π-bonds is 235.4 pm, i.e. approximately 10% greater than the comparable distance in the Zeise salt $K[Pt(C_2H_4)Cl_3]$ (213.1 pm).[7] The average C=C distance in **1** is 136.7(3) pm (Zeise salt: 137.5(4) pm) and is thus longer than in an uncoordinated C=C bond. Other than in the Zeise salt, in which the C_2H_4 group is clearly no longer planar, the highly substituted double bonds of **1** are still almost planar. The interaction between the Al atoms and the C=C bonds is not optimal, since the Al,C=C vector deviates by 15.5° from the normal to the C=C group. The pyramidal coordination of the Al atoms by the Cl atom and the two C atoms clearly indicates presence of an aluminum-olefin π-bond.

The Al-Cl distance is 211 pm, and the length of the Al-C σ bonds is 199 pm (C-Al-C and C-Al-Cl: 114–116°). The distance between two Al atoms of different six-membered rings (ca. 300 pm) is relatively small. A closer proximity of two such atoms, which could lead to a shortening of the aluminum-olefin π bond, is therefore hindered. In contrast the distance between the Al atoms within the dialuminacyclohexadiene ring is 337 pm (in **2**, 347 pm); the transannular distance between the CC double bonds (334 pm) is of the same order of magnitude. The four Al atoms of **1** form a tetrahedron slightly compressed along the molecular axis.

Received: June 16, 1986;
revised: July 16, 1986 [Z 1821 IE]
German version: *Angew. Chem. 98* (1986) 929

[*] Priv.-Doz. Dr. H. Schnöckel, Dipl.-Chem. M. Leimkühler, Dipl.-Chem. R. Lotz, Prof. Dr. R. Mattes
Anorganisch-chemisches Institut der Universität
Corrensstrasse 36, D-4400 Münster (FRG)

[**] This work was supported by the Minister für Wissenschaft und Forschung des Landes Nordrhein-Westfalen and by the Fonds der Chemischen Industrie.

[1] J. J. Eisch in G. Wilkinson, F. G. A. Stone, E. W. Abel (Eds.): *Comprehensive Organometallic Chemistry, Vol. 1*, Pergamon Press, London 1982, p. 555.

[2] T. W. Dolzine, J. P. Oliver, *J. Am. Chem. Soc. 96* (1974) 1737; for π-alkynylaluminum compounds see, for example, G. D. Stucky, A. M. Mcpherson, W. E. Rhine, J. J. Eisch, J. L. Considine, *ibid. 96* (1974) 1941.

[3] Experimental procedure: Equimolar amounts (0.05 mol/h) of dimethylacetylene and AlCl were cocondensed onto a nitrogen-cooled surface

(≈ 4000 cm^2) for 2 h under vacuum conditions. During annealing to room temperature *n*-pentane was added. Colorless crystals of **1** separated from the yellow solution. Apparatus and technical details: H. Schnöckel, H. Kreienkamp, H. R. Lotz, unpublished.

[4] P. L. Timms, *J. Am. Chem. Soc. 90* (1968) 4585; *Adv. Inorg. Chem. Radiochem. 14* (1972) 118. In the meantime numerous reactions have been carried out with these boron compounds, which are exclusively monomeric, six-membered ring complexes; see for example W. Kaim, H. Bock, P. Hawker, P. L. Timms, *J. Chem. Soc. Chem. Commun. 1980*, 577; G. E. Herberich, B. Hessler, *Chem. Ber. 115* (1982) 3115.

[5] H. Hoberg, V. Gotor, A. Milchereit, C. Krüger, J. C. Sekutowski, *Angew. Chem. 89* (1977) 563; *Angew. Chem. Int. Ed. Engl. 16* (1977) 539.

[6] **1** crystallizes in the space group $P\bar{1}$, $a = 1078(2)$, $b = 1451(3)$, $c = 1560(3)$ pm, $\alpha = 97.9(1)$, $\beta = 109.4(1)$, $\gamma = 104.2(1)°$. Solution of structure by direct methods (SHELX). 8075 reflections with $F_0 > 6.0|F_0|$, $2\theta_{max} = 54°$; 497 parameters, CH_3 as rigid group; $R = 0.035$; $R_w = 0.038$. The unit cell contains two independent dimeric molecules. One is slightly distorted, the other has, to a good approximation, D_{2d} symmetry.

[7] R. A. Love, T. F. Koetzle, G. J. B. Williams, L. C. Andrews, R. Bau, *Inorg. Chem. 14* (1975) 2653.

Novel Modifications of Gold, Rhodium, and Ruthenium—M_{13} Clusters as Building Blocks of "Superclusters"**

By *Günter Schmid** and *Norbert Klein*

The unusual stability of transition-metal clusters with closed shells (so-called full-shell clusters) has already been demonstrated on a number of occasions.[1,2] They are compounds whose cluster skeleton is stabilized by a ligand shell. The question of the possibility of existence of closed shell clusters without protecting ligand peripheries, however, still remains unanswered. According to theoretical models by *Hoard* and *Pal*,[3,4] closed-shell clusters containing less than ca. 70 metal atoms should be incapable of existing; such aggregates form polytetrahedral structures. We have now succeeded, however, in converting ligand-stabilized M_{55} clusters into ligand-free M_{13} clusters and in identifying these as components of novel "superclusters".

Solutions of $[Au_{55}(PPh_3)_{12}Cl_6]$,[5] $[M_{55}\{P(tBu)_3\}_{12}Cl_{20}]$, M = Rh,[6] Ru,[7] and $[Pt_{55}\{As(tBu)_3\}_{12}Cl_{20}]$[7] in methylene chloride can be smoothly degraded on platinum electrodes at 20 V d.c. This type of degradation is not an electrolysis, since no discharging takes place. The compounds decompose upon contact with the cathode or anode, and the metals separate and are deposited on the platinum or are precipitated in the reaction vessel.[8] If contact of the clusters with the electrodes is prevented, e.g. by covering the methylene chloride solution with a layer of water, electrophoresis is observed, with the clusters migrating to the cathode. This process is reversible. The degradation of the M_{55} clusters gives, besides the metal, free phosphane and arsane and metal halide complexes that are soluble in CH_2Cl_2, in the case of gold $[(Ph_3P)_2AuCl]$, in the case of the other metals, complexes of unknown structure.

The cleavage of metal halide and phosphane (or arsane) leads to degradation of the whole external shell of 42 metal atoms of the M_{55}-cluster, thus leaving naked M_{13} cluster cores, which constitute the smallest conceivable closed-shell clusters. It may be assumed that they are not long-lived as isolated particles in solution, there being two routes open for their stabilization: a) degradation into small, e.g., tetrahedral particles, which, as predicted by model calculations could reassemble to form polytetrahedral structures, or b) the assemblage of M_{13} building blocks to give novel metal structures. It is found that the latter path is actually followed. If one imagines the M_{13} clusters in their simplest form as being spherically shaped, such clusters would try to adopt a cubic closest packed structure,which in the simplest case would be made up of thirteen M_{13} clusters. Even these $(M_{13})_{13}$ clusters could also aggregate in an organized way to form a second superstructure $[(M_{13})_{13}]_n$ consisting of closest packed $(M_{13})_{13}$ clusters.

This concept of novel metal modifications is confirmed by the Debye-Scherrer diffraction patterns ($Cu_{K\alpha}$, $\lambda = 1.5418$ Å) of the powders thus obtained. The metal atoms originating from the outer shell of the cluster upon degradation form "normal" metal (M_∞) which gives rise to the correspondingly well-known X-ray diffraction pattern. In addition, reflections are observed which are in very good agreement with the most important lattice planes to be expected for the superstructures illustrated below. Thus, for all metals, one finds three new lattice planes characterizing the superstructures which are integral multiples of the interplanar spacings of the metals. Rhodium, platinum, and gold crystallize in the cubic system, as do also the superstructures. Ruthenium, on the other hand, has a hexagonal structure; nevertheless, the reflections of the three superstructures observed even in the case of ruthenium are identical to those found with (the equally large) rhodium, i.e. ruthenium also forms $(Ru_{13})_{13}$ superclusters with cubic structure upon cluster degradation.

Table 1. *hkl* values, interplanar spacings *d* [Å] and 2θ-values of $(M_{13})_{13}$, $[(M_{13})_{13}]_n$ and, for comparison, M_∞-values.

M	$d(M_\infty)$	*hkl*	Occupation	$d(M_{13})_{13}$	$d[(M_{13})_{13}]_n$	2θ
Rh	1.902	200	$8 \times d(M_\infty) = 15.216$		15.3	5.8
	0.8725	331	$7 \times d(M_\infty) = 6.1075$	6.11 (d^2)		14.5
	1.0979	222	$3 \times d(M_\infty) = 3.2937$	3.24 (d^1)		27.5
Ru [a]					15.3	5.8
				6.11 (d^2)		14.5
				3.24 (d^1)		27.5
Au	2.039	200	$8 \times d(M_\infty) = 16.312$		16.8	5.3
	0.9358	331	$7 \times d(M_\infty) = 6.5551$	6.8(3) (d^2)		13.0(5)
	1.1774	222	$3 \times d(M_\infty) = 3.5322$	3.5(3) (d^1)		14.1(5)

[a] Ru_∞ crystallizes hexagonally; consequently, its structural data are not to be compared with those for $(Ru_{13})_{13}$.

In Table 1 the new 2θ-values and lattice planes are collected together with the corresponding values for the normal metals M_∞, where M = Rh, Ru, and Au. Figure 1 shows a model of the course of the lattice planes observed in the first superstructure $(M_{13})_{13}$, while Figure 2 shows a model of the second superstructure $[(M_{13})_{13}]_n$. All lattice planes necessary for characterization of the new metal structures are proven. That $[(M_{13})_{13}]_n$ is composed of closest packed $(M_{13})_{13}$ clusters is also confirmed by the occurrence of lattice planes with a separation of 15.3 and 16.8 Å, respectively. The magnitude of *n*, however, is still unknown.

[*] Prof. Dr. G. Schmid, Dipl.-Chem. N. Klein
Institut für Anorganische Chemie der Universität
Universitätsstrasse 5-7, D-4300 Essen 1 (FRG)

[**] Large Transitioh-Metal Clusters, Part 5. This work was supported by the Deutsche Forschungsgemeinschaft, the Fonds der Chemischen Industrie, and Degussa AG. We thank Dr. *R. Boese* for valuable discussions and Mrs. *G. Schmid* for help with the construction of the models. Thanks are also due to Dr. *H. Schweder* for the SEM photographs and to Mr. *W. Hüben* for the DMC measurements.—Part 4: [7].



Fig. 1. Model of a $(M_{13})_{13}$ cluster showing the interplanar spacings d^1 (3.24 Å for Rh/Ru and 3.5 Å for Au) and d^2 (6.11 Å for Rh/Ru and 6.8 Å for Au).

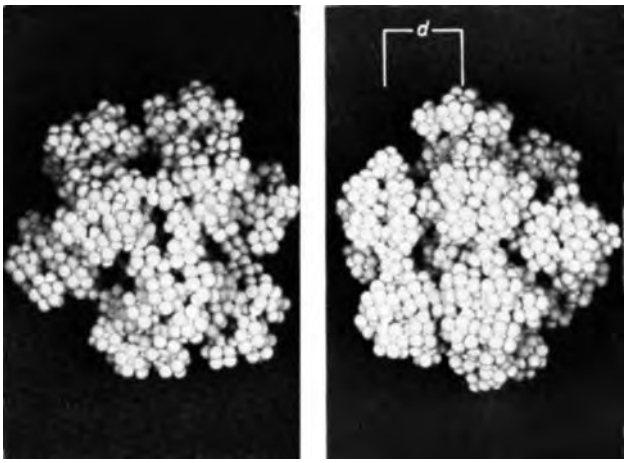


Fig. 2. Left: Model of a $[(M_{13})_{13}]_n$ cluster ($n = 13$) along a sixfold symmetry axis; right, model of a $[(M_{13})_{13}]_n$ cluster ($n = 13$), showing the interplanar spacing d (15.3 Å for Rh/Ru and 16.8 Å for Au).

Figure 3 shows a scanning electron (SEM) photomicrograph of $[(Ru_{13})_{13}]_n$ crystallites and Ru_∞, the latter of which appears amorphous. Platelet- and column-shaped crystallites of hexagonal morphology are indicated by arrows. The formation of hexagonal faces upon coupling of the $(M_{13})_{13}$ clusters as in Figure 2a is understandable. Crystallites of hexagonal morphology are also detectable by SEM in the case of gold and rhodium.

Preliminary DMC (differential microcalorimetry) measurements on $[(Au_{13})_{13}]_n$ show that phase-transitions take place irreversibly between 400 and 500°C, during which temperature range the superstructures are presumably destroyed. A great disadvantage regarding investigation of the physical properties of the new metal modifications is that they are formed in admixture with the normal metal.

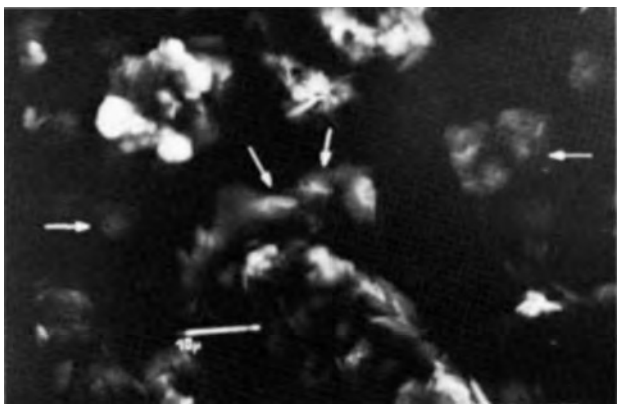


Fig. 3. SEM photograph of $[(Ru_{13})_{13}]_n$ crystallites mixed with Ru_∞. The arrows indicate particularly well formed six-membered ring faces.

Received: June 19, 1986;
supplemented: July 1986 [Z 1824 IE]
German version: *Angew. Chem. 98* (1986) 910

[1] G. Schmid, *Struct. Bonding (Berlin) 62* (1985) 51.
[2] M. N. Vorgaftik, V. P. Zagorodnikov, I. P. Stolyarow, I. I. Moiseev, V. A. Likholobov, D. I. Kochubey, A. L. Chuvilin, V. I. Zaikovsky, K. I. Zamaraev, G. I. Timofeeva, *J. Chem. Soc. Chem. Commun. 1985*, 937.
[3] M. R. Hoare, P. Pal, *J. Cryst. Growth 17* (1972) 77.
[4] M. R. Hoare, P. Pal, *Nature 236* (1972) 35.
[5] G. Schmid, R. Pfeil, R. Boese, F. Bandermann, S. Meyer, G. H. M. Calis, J. W. A. van der Velden, *Chem. Ber. 114* (1981) 3634.
[6] G. Schmid, U. Giebel, W. Huster, A. Schwenk, *Inorg. Chim. Acta 85* (1984) 97.
[7] G. Schmid, W. Huster, *Z. Naturforsch. B41* (1986) 1028.
[8] Elemental analysis of vacuum-dried precipitates show metal contents of between 95 and 99%. Preliminary DMC measurements indicate that traces of methylene chloride, water, or phosphanes are set free upon heating; these are apparently only loosely enclosed in the metal skeleton.

Heterometallic Dinuclear Complexes by Ethene Displacement with Grignard Compounds or Diorganomagnesium Compounds**

By *Klaus Jonas,** *Gerd Koepe,* and *Carl Krüger*

Cyclopentadienylbis(ethene)cobalt **1**,[1] a preparatively useful starting material which is a source of the synthetically versatile CpCo moiety,[1-4] reacts with phenyllithium with liberation of ethene to give the CpCo-complex salt **2** [Eq. (a)].[5,6] On the other hand, when **1** is treated with allyllithium, it reacts as one would expect of an ethene-cobalt(I) halide: the Cp ligand is smoothly replaced by an allyl group to form the lithium-cobalt compound **3a**. This ethene complex contains two π-allyl groups coordinated to cobalt and can be converted into the *N,N,N',N'*-tetramethylethylenediamine (TMEDA) complex **3b** [Eq. (b)].[2,5,6]

$$[CpCo(C_2H_4)_2] \xrightarrow[Et_2O,\ TMEDA]{LiC_6H_5,\ -C_2H_4} [Li(tmeda)_2][CpCo(C_2H_4)C_6H_5] \quad (a)$$

1 **2**

$$[CpCo(C_2H_4)_2] \xrightarrow[-LiCp,\ -C_2H_4]{2\,LiC_3H_5,\ Et_2O} Li[(C_3H_5)_2Co(C_2H_4)] \quad (b)$$

1 **3a**

$$\xrightarrow{TMEDA} [Li(tmeda)_2][(C_3H_5)_2Co(C_2H_4)]$$

3b

We have now found that the partial or complete removal of the ethene ligands in **1** can also be achieved with diorganomagnesium compounds [Eq. (c) and (d)], and that even Grignard compounds are reactive enough for this purpose [Eq. (e) and (f)]. A common feature of reactions (c)-(f) is that, unlike in reaction (b), the Cp group remains bonded to cobalt.[7] Reaction of **1** with $Mg(C_6H_5)_2$ in tetra-

[*] Prof. Dr. K. Jonas, Dipl.-Chem. G. Koepe, Prof. Dr. C. Krüger [+]
Max-Planck-Institut für Kohlenforschung
Kaiser-Wilhelm-Platz 1, D-4330 Mülheim a. d. Ruhr (FRG)
[+] Crystal structure analysis.

[**] We thank Priv.-Doz. Dr. *R. Benn* and Dr. *R. Mynott* for the NMR spectra.

hydrofuran (THF) leads to formation of **4** [Eq. (c)], while reaction of **1** with $Mg(C_3H_5)_2$ leads to the ethene-free MgCo dinuclear complex **5** [(Eq. (d)]. **5** contains two different allyl ligands, one of which is π-coordinated while the other is σ-coordinated to the magnesium and shows dynamic behavior.[6] Attempts to synthesize trinuclear complexes by coupling two CpCo moieties to $Mg(C_6H_5)_2$ or $Mg(C_3H_5)_2$ failed: for example, upon reaction of **1** with $Mg(C_6H_5)_2$ in the molar ratio 2:1, only one equivalent of ethene is liberated

$$\underset{\mathbf{1}}{[CpCo(C_2H_4)_2]} \xrightarrow[-C_2H_4]{Mg(C_6H_5)_2,\ THF} \underset{\mathbf{4}}{[CpCo(C_2H_4)(C_6H_5)Mg(C_6H_5)(thf)_2]} \quad (c)$$

$$\underset{\mathbf{1}}{[CpCo(C_2H_4)_2]} \xrightarrow[-2C_2H_4]{Mg(C_3H_5)_2,\ THF} \underset{\mathbf{5}}{[CpCo(\pi\text{-}C_3H_5)Mg(\sigma\text{-}C_3H_5)(thf)_2]} \quad (d)$$

Methyl- and phenylmagnesium bromide do not react with **1** in diethyl ether at room temperature; only when THF is added or used as solvent are the Grignard compounds reactive enough to displace ethene. After addition of TMEDA, the ethene-complexes **6** are formed [Eq. (e)]. Reaction of allylmagnesium bromide with **1** in THF leads to the ethene-free dinuclear complex **7** [Eq. (f)].

$$\underset{\mathbf{1}}{[CpCo(C_2H_4)_2]} \xrightarrow[-C_2H_4]{RMgBr,\ THF,\ TMEDA} \underset{\begin{array}{l}\mathbf{6a},\ R=CH_3\\ \mathbf{6b},\ R=C_6H_5\end{array}}{[CpCo(C_2H_4)RMgBr(tmeda)]} \quad (e)$$

$$\underset{\mathbf{1}}{[CpCo(C_2H_4)_2]} \xrightarrow[-2C_2H_4]{H_2C_3MgBr,\ THF} \underset{\mathbf{7}}{[CpCo(\eta^3\text{-}C_3H_5)MgBr(thf)_2]} \quad (f)$$

The composition of the new CoMg-complexes has been confirmed by elemental analyses. In addition, like **2**, **3b**, and **5**, the complexes **6b** and **7** have been investigated by NMR spectroscopy.[6] Characteristic for the complex **6b** is the pronounced upfield shift of the ^{13}C-NMR signals of the ethene ligand compared to the ethene signal of **1**.[1] In order to obtain more detailed information about the structure and bonding in these compounds, crystal structure analyses of **6b** and **7** were carried out.

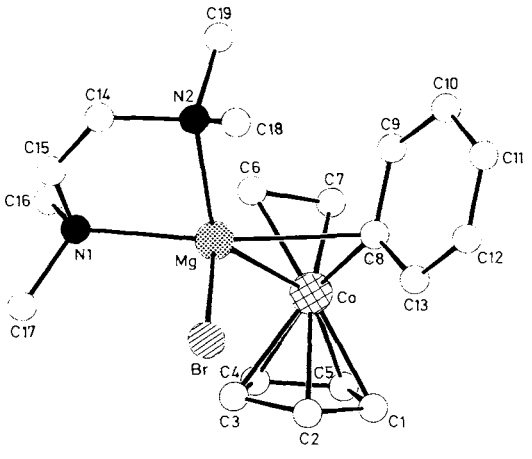


Fig. 1. Molecular structure of **6b** [8, 15].

A novel feature of the dinuclear complex **6b** is—apart from its formation upon reaction of a halogen-free transition-metal compound with a Grignard compound via liberation of ethene[9]—that it contains a TMEDA-modified, complete Grignard compound in the coordination sphere of a transition metal atom (Fig. 1). The central cobalt atom in **6b** is coordinated in an almost pseudo-tetrahedral fashion: ethene and the Cp ring each occupy a coordination site, while the other two coordination sites are occupied by magnesium and the carbanionic phenyl group. The phenyl group is σ-bonded to the cobalt atom and its ring plane is so oriented that, in addition to formation of a Co–Mg bond (2.565(3) Å), an ion pair interaction with the magnesium atom is also possible (Mg-C8 2.572(9) Å).[10] The presence of a Co–Mg bond is consistent with the finding that cobalt-containing 18e half-sandwich complexes such as $[CpCo(CO)_2]$ and $[CpCo(PMe_3)_2]$ have basic metal centers available and therefore can react with metal halides, for example $HgCl_2$, $ZnCl_2$, to give 1:1 adducts such as $[CpCo(CO)_2HgCl_2]$ and $[CpCo(PMe_3)_2HgCl_2]$ with metal-metal bonds.[12] Thus, **6b** can be regarded as a dinuclear complex which is formed by coupling of the singly negatively charged 18e anion $[Cp(C_2H_4)(C_6H_5)Co]^{\ominus}$ with the electrophilic $(tmeda)BrMg^{\oplus}$ ion (Lewis acid/Lewis base adduct with Co→Mg bond).

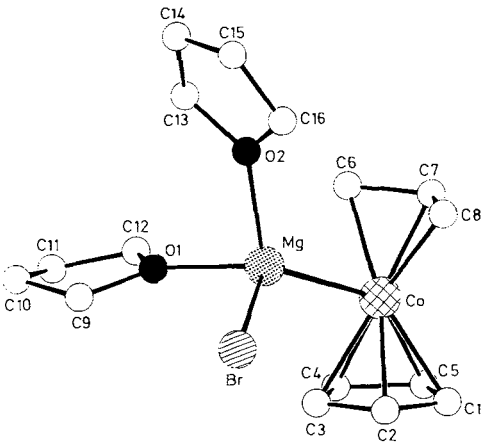


Fig. 2. Crystal structure of **7** [13, 15].

The distances between the Mg atom and terminal C atoms of the allyl group (Mg-C6 2.89(2) Å, Mg-C8 3.06(1) Å) in **7** (Fig. 2) are both significantly longer than the $Mg-C_{phenyl}$ distance in **6b**. Thus, in **7** there is no longer any bonding between the Mg atom and the allyl group introduced by the Grignard reagent; the C_3H_5-group is merely η^3-coordinated to the Co atom. As a result, the distance between the tetracoordinated Mg atom and the Co atom is shortened (2.480(4) Å).

$$L_nM + R{-}MgX \longrightarrow L_nM(R){-}MgX \quad (g)$$

There is no precedent for the insertion of ligand-transition metal fragments L_nM into the Mg–C bond of Grignard compounds [Eq. (g)] leading to stable heterometallic dinuclear complexes with RM–MgX moieties. The reactions of RMgX with $[Cp_2MoH_2]$ and with $[Cp_2WH_2]$ described by *Green* et al.[14] lead to cyclic hexanuclear complexes $[\{Cp_2MHMgR(\mu\text{-}Br_2)Mg(EtO)\}_2]$ (M = Mo, W), which likewise contain magnesium-transition metal bonds.

However, in these compounds the residues R are bound to the magnesium and not, as in **6b** and **7**, to the transition metal.

Received: May 15, 1986;
supplemented: July 2, 1986 [Z 1777 IE]
German version: *Angew. Chem. 98* (1986) 901.

[1] K. Jonas, E. Deffense, D. Habermann, *Angew. Chem. 95* (1983) 729; *Angew. Chem. Int. Ed. Engl. 22* (1983) 716; *Angew. Chem. Suppl. 1983*, 1005.

[2] K. Jonas, *Angew. Chem. 97* (1985) 292; *Angew. Chem. Int. Ed. Engl. 24* (1985) 295.

[3] R. Benn, K. Cibura, P. Hoffmann, K. Jonas, A. Rufinska, *Organometallics 4* (1985) 2214.

[4] Recent literature: W. Siebert, *Angew. Chem. 97* (1985) 924; *Angew. Chem. Int. Ed. Engl. 24* (1985) 943; R. Diercks, K. P. C. Vollhardt, *Angew. Chem. 98* (1986) 268; *Angew. Chem. Int. Ed. Engl. 25* (1986) 266; B. Eaton, J. M. O'Connor, K. P. C. Vollhardt, *Organometallics 5* (1986) 394. S. Gambarotta, S. Stella, C. Floriani, A. Chiesi-Villa, C. Guastini, *Angew. Chem. 98* (1986) 283; *Angew. Chem. Int. Ed. Engl. 25* (1986) 254.

[5] G. Koepe, *Diplomarbeit*, Universität Freiburg 1980.

[6] NMR data: **2**: ^{13}C-NMR (25.2 MHz, [D$_8$]toluene, −30°C): δ=82.9 (Cp), 25.1 (ethene), 55.7, 44.8 (tmeda 1), 58.3, 46.1 (tmeda 2), 141.4, 126.3, 119.6 (phenyl).—**3b**: ^{1}H-NMR (80 MHz, [D$_8$]THF, +35°C): δ=2.26 (ethene), 3.5 (br. s, *meso*-allyl), 1.25 (d, ^3J=6.5 Hz; *syn*-allyl), −0.45 (d, ^3J=9.5 Hz; *anti*-allyl).—**5**: ^{1}H-NMR (400 MHz, [D$_8$]THF, −115°C): δ=4.47 (s, 5H, Cp), 4.67 (dd, $^3J_{syn}$=4 Hz, $^3J_{anti}$=7 Hz; 1H, *meso*-allyl), 0.81 (d, *syn*, 2H); δ=−1.27 (d, *anti*, 2H); π-allyl group. δ=0.86 (d, ^3J=9 Hz, 2H; H$_\alpha$-σ-allyl), 6.22 (m, $^3J_{cis}$=10 Hz, $^3J_{trans}$=16 Hz, 1H; H$_\beta$-σ-allyl), 3.6, 3.97 (H$_\gamma$, 2H); dynamic σ-allyl group, equilibration of H$_\alpha$ and H$_\gamma$ with $\Delta G^{\neq}_{83°C}$=8.2 kcal/mol.—**6b**: ^{13}C-NMR (25.2 MHz, [D$_8$]THF, +40°C): δ=85.0 (d, Cp), 33.0 (t; ethene), 18.1 (t; ethene), 58.7 (t; tmeda), 46.5 (q; tmeda), 144.9, 125.9, 121.6 (phenyl).—**7**: ^{1}H-NMR (80 MHz, [D$_8$]toluene, +40°C): δ=4.74 (s, 5H; Cp), 5.39 (m, 1H; *meso*-allyl), 1.40 (2H; *syn*-allyl), −0.72 (d, ^3J=8 Hz, 2H; *anti*-allyl), 3.61, 1.24 (br. s; THF).

[7] Procedure for **4** and **5**: A solution of **1** in THF was treated at −78°C with Mg(C$_6$H$_5$)$_2$ or with Mg(C$_3$H$_5$)$_2$ (1:1); the reaction mixture was warmed to room temperature and finally recooled. **4** crystallized out at −30°C, **5** at −78°C.—**6** and **7**: **1** in THF was treated with (a) an equimolar amount of RMgX in Et$_2$O (R=CH$_3$, C$_6$H$_5$) or (b) with C$_3$H$_5$MgBr in THF at −78°C, respectively, and the reaction solution warmed to +20°C. After addition of TMEDA to (a) **6** crystallized out at −30°C, while on reducing the volume of (b) and addition of Et$_2$O 7 crystallized out at −30°C.—All cobalt-magnesium complexes were washed at 0°C with Et$_2$O and dried under oil-pump vacuum at 0°C.

[8] Crystal structure analysis of **6b**: Crystal size: 0.36, 0.36, 0.36 mm; space group $P2_1/n$, a=10.022(2), b=12.142(2), c=17.562(3) Å, β=101.26(1)°; Z=4, μ(Mo$_{K\alpha}$)=27.368 cm^{-1} (λ=0.71069 Å), 5072 reflections measured ($\pm h$, $+k$, $+l$), 1915 observed ($I>2\sigma(I)$), 225 refined parameters, R=0.0582, R_w=0.0519 ($w=1/\sigma^2(F_0)$), max. residual electron density 0.48 eÅ^{-3}, empirical absorption correction, max. 1.242, min. 0.655; see also [15].

[9] In contrast to this, the reaction of halogen-containing transition metal compounds with Grignard reagents is a classical type of reaction in which the halogen atoms on the transition metal are replaced by organic groups. Since MgX$_2$-salts are thus formed, these metathetical reactions lead to magnesium-free organo-transition metal compounds and not to compounds of type **6**, in which an entire Grignard compound is incorporated.

[10] The Mg-Fe distance in [CpFe(diphos)MgBr(thf)$_2$]·THF (diphos=1,2-bis(diphenylphosphino)ethane) is 2.593(7) Å: H. Felkin, P. J. Knowles, B. Meunier, A. Mitschler, L. Ricard, R. Weiss, *J. Chem. Soc. Chem. Commun. 1974*, 44.

[11] K. Jonas, C. Krüger, *Angew. Chem. 92* (1980) 513; *Angew. Chem. Int. Ed. Engl. 19* (1980) 520.

[12] H. Werner, *Angew. Chem. 95* (1983) 932; *Angew. Chem. Int. Ed. Engl. 22* (1983) 927, and references cited therein.

[13] Crystal structure analysis of **7**: crystal size 0.40, 0.11, 0.54 mm; space group $P\bar{1}$, a=7.552(1), b=11.003(2), c=11.805(2) Å, α=80.20(1), β=82.26(1), γ=76.46(1)°, V=935.18 Å^3; Z=2, μ(Mo$_{K\alpha}$)=30.65 cm^{-1} (λ=0.71069 Å), 4201 reflections measured ($\pm h$, $+k$, $+l$), 1919 observed ($I>2\sigma(I)$), 190 refined parameters, R=0.0797, R_w=0.106 ($w=1/\sigma^2(F_0)$), max. residual electron density 1.15 eÅ^{-3}, analytical absorption correction, max. 0.775, min. 0.536; see also [15].

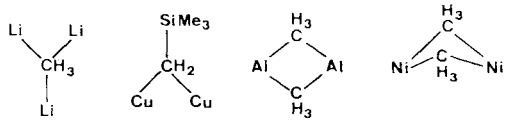
[14] M. L. H. Green, N.-T. Luong-thi, G. A. Moser, J. Packer, F. Pettit, D. M. Roe, *J. Chem. Soc. Dalton Trans. 1976*, 1988.

[15] Further details of the crystal structure investigations are available on request from the Fachinformationszentrum Energie, Physik, Mathematik GmbH, D-7514 Eggenstein-Leopoldshafen 2 (FRG), on quoting the depository number CSD-51933, the names of the authors, and the full citation of the journal.

First Dinuclear Complexes with Fourfold Alkyl-Bridging

By *Klaus Jonas,* Wolfgang Rüsseler, Carl Krüger,* and *Eleonore Raabe*

The bridging of metal atoms by alkyl or aryl groups via multicenter bonds is an important means of stabilizing electron-deficient organometallic compounds.[1] Methyllithium, for example, exists as a tetramer in the solid state,[2] with each of the four methyl groups bound to three lithium atoms (structure type **I**). [{Cu(CH$_2$SiMe$_3$)}$_4$][3] was the first example of an organometallic compound in which neighboring metal atoms are present as singly alkyl-bridged centers and in which each organo-ligand is attached to only two metal atoms (structure type **II**). Prototypes of dinuclear compounds with double alkyl-bridging are, in the case of main-group elements, hexamethyldialuminum, the structure of which has been investigated by several groups (structure type **IIIa**),[4] and in the case of transition metals, the nickel(II) complex [{(π-C$_3$H$_3$Me$_2$)NiCH$_3$}$_2$] (structure type **IIIb**).[5] We now report on the first dinuclear complexes whose metal atoms are coupled via more than two alkyl bridges.

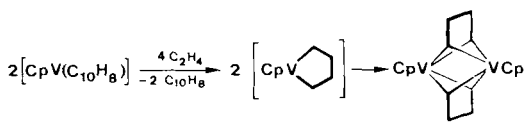


I **II** **IIIa** **IIIb**

For the synthesis of the new divanadium complex **3** we used the vanadium(I) complex **1**, which can be prepared according to reaction (a) by five-membered ring/six-membered ring exchange, and in which the naphthalene is markedly more loosely bound than the C$_6$H$_6$ ligand in the analogous benzene complex [CpV(C$_6$H$_6$)].[6, 7]

$$[Cp_2V] \xrightarrow[-KCp,\ -C_{10}H_8]{2\,K[C_{10}H_8]} K[CpV(C_{10}H_8)] \xrightarrow[-KCl,\ -1/2\,C_2H_4]{1/2\,Cl(CH_2)_2Cl} \underset{\mathbf{1}}{[CpV(C_{10}H_8)]} \quad (a)$$

We assume that the reaction of **1** with ethene (tetrahydrofuran (THF), 20°C, 15 bar), which leads to the dinuclear complex **3** in ca. 30% yield, proceeds via the metallacycle **2**. This coordinatively unsaturated 12e species stabilizes itself by dimerization. The four terminal methylene carbon atoms thereby take up bridging positions.



1 **2** **3**

The new divanadium complex **3** not only constitutes the first dinuclear complex with four pentacoordinated bridging carbon atoms, it also demonstrates that C$_4$H$_8$ ligands created by coupling of ethene molecules can function

[*] Prof. Dr. K. Jonas, Dipl.-Chem. W. Rüsseler, Prof. Dr. C. Krüger [+], Dr. E. Raabe [+]
Max-Planck-Institut für Kohlenforschung
Kaiser-Wilhelm-Platz 1, D-4330 Mülheim a. d. Ruhr (FRG)

[+] Crystal structure analyses.

 © VCH Verlagsgesellschaft mbH, D-6940 Weinheim, 1986 0570-0833/86/1010-0925 $ 02.50/0

as bridging ligands. In all other transition-metal complexes known to date which contain C_4H_8 ligands formed from ethene molecules, the butanediyl ligands are terminally bound,[8, 9] and in the hexanuclear complex $[Li_4Cr_2(C_4H_8)_4(thf)_4]$, obtainable from $CrCl_2$ and dilithiobutane, there is only double alkyl-bridging between each Li and a given Cr atom.[10]

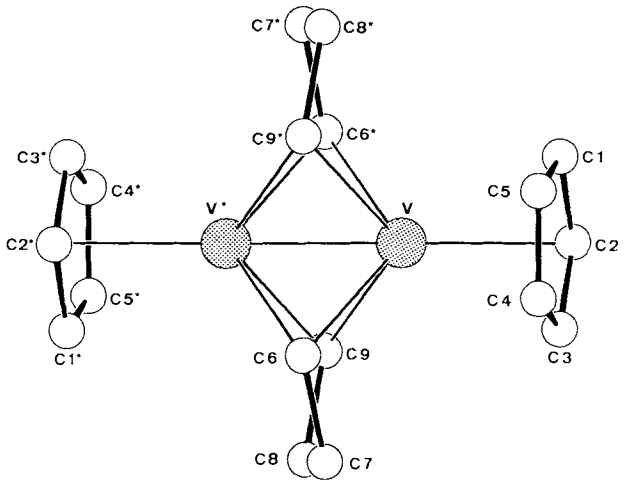


Fig. 1. Crystal structure of 3 [11].

In the dinuclear complex **3**, which has a center of inversion, the four methylene carbon atoms bridge the two vanadium atoms. At each of the two metal atoms there are two shorter and two longer V-C bonds: V-C6 2.211(2), V-C9* 2.202(2) Å; cf. V-C6* 2.299(2), V-C9 2.301(2) Å. The carbon chain C6-C7-C8-C9, in which the C-C distances fall in the expected range (mean value 1.53 Å), is slightly twisted (torsion angle 28.4°). The distances between the carbon atoms not coupled to each other (C6 and C9 2.618(3) Å and C6 and C9* 2.845(3) Å) are shorter than the sum of the van der Waals radii of two C atoms. The V-V distance of 2.315(1) Å is short and correspondingly the apical angles at the bridging carbon atoms (V-C6-V* 61.7(1)°, V-C9-V* 61.8(1)°), are unusually small even for three-center bonds. The cyclopentadienyl ring is oriented almost parallel to the plane through the four bridging carbon atoms (V-C mean value 2.347(3) Å).

Attempts to prepare the corresponding dinuclear compound with four bridging methyl groups have so far failed.[15] However, we discovered a reaction sequence which gives access to the structurally related dinuclear complex **8** with two pentamethylcyclopentadienyl (Cp*) ligands. For the synthesis of **8** we first prepared the chlorine-containing vanadium(II) complex **4** from vanadocene; **4** can also be prepared by degradation of the triple-decker sandwich complex $[(CpV)_2C_6H_6]$ with dichloroethane.[9] Reaction of **4** with LiCp* leads, in accordance with Equation (b), to formation of pentamethylvanadocene **5**, which can be converted in two steps into the new vanadium(III) complex **7** [Eq. (c)].

$$\underset{\mathbf{4}}{[CpVCl(thf)]} \xrightarrow[-LiCl,\ -THF]{LiCp^*} \underset{\mathbf{5}}{Cp^*CpV} \qquad (b)$$

$$\underset{\mathbf{5}}{[Cp^*CpV]} \xrightarrow[-1/2\,C_6H_{10}]{C_3H_5Br} \underset{\mathbf{6}}{[Cp^*CpVBr]} \xrightarrow[-LiBr]{LiCH_3} \underset{\mathbf{7}}{[Cp^*CpVCH_3]} \qquad (c)$$

As with many other transition metal compounds having Cp ligands,[9] the cyclopentadienyl ligand in **7** can be replaced by other organic residues by reaction with organolithium compounds. Upon reaction of **7** with $LiCH_3$ we obtained the divanadium complex **8** [Eq. (d)] in 70% yield, the composition of which was confirmed by elemental analysis and mass spectrometry [*m/z* 432 ($M^{\oplus}$, 68%)].

$$\underset{\mathbf{7}}{[Cp^*CpVCH_3]} \xrightarrow[-LiCp]{LiCH_3} 1/2\underset{\mathbf{8}}{[[Cp^*V(CH_3)_2]_2]} \qquad (d)$$

The crystal structure analysis of **8** revealed a constitution comparable with that of **3**; the disorder of the bridging carbon atoms, however, prevented an accurate determination of bond lengths and angles.

Experimental

1: A THF solution of naphthalenepotassium, prepared from 4.89 g (125.1 mmol) of potassium, 16.78 g (130.9 mmol) of naphthalene and 300 mL of THF at −15°C, was treated at −15°C with 11.41 g (63.0 mmol) of vanadocene. After two hours' stirring at 20°C, the reaction mixture was cooled to −78°C, allowed to stand for 8 h, and then filtered free of KCp. The filtrate was evaporated to dryness and the uncomplexed naphthalene was removed by sublimation at 20°C under high vacuum. The residue was dissolved in THF and the solution treated with 2.78 mL (34.7 mmol) of dichloroethane at 0°C. The mixture was evaporated to dryness, taken up in *n*-hexane, and filtered free of KCl. On cooling to −30°C, dark red crystals of **1** precipitated (yield 14.31 g, 93%). Correct elemental analysis. MS: *m/z* 244 ($M^{\oplus}$, 22%).

3: A solution of **1** (5.35 g, 21.9 mmol) in THF (300 mL) was treated with ethene in an autoclave at 20°C and 15 bar. The pressure was kept almost constant by repeated introduction of ethene under pressure. After 20 h the uptake of ethene noticeably slowed down, and, after 72 h, 229.6 mmol of 1-butene, 45.9 mmol of *trans*-2-butene, 193.9 mmol of 1-hexene, and 54.6 mmol of *trans*-2-hexene could be detected by mass spectroscopy and gas-chromatography. Evaporation of the contents of the autoclave to dryness and removal of the naphthalene by sublimation furnished a residue which was dissolved in hot toluene. Upon cooling the solution to −30°C, dark brown **3** crystallized out (yield 1.22 g, 33%). Correct elemental analysis. MS: *m/z* 344 ($M^{\oplus}$, 28%).

4: As in the case of **1**, naphthalenepotassium [19.11 g (149.1 mmol) of naphthalene, 5.71 g (146.0 mmol) of potassium] was first allowed to react in 300 mL THF with 13.02 g (71.9 mmol) of vanadocene and the mixture cooled to −78°C and filtered free of KCp. The filtrate was then allowed to warm to 20°C and treated with 2.88 mL (36.0 mmol) of dichloroethane. The resulting deep red solution was evaporated to dryness at 20°C. The residue was taken up in *n*-hexane and the solution filtered free of KCl. After treatment of the filtrate with 11.7 mL (143.9 mmol) of THF and 2.88 mL (36.0 mmol) of dichloroethane, violet crystals separated upon storage for 2 d at 20°C. These were washed with pentane and dried at 20°C under oil-pump vacuum (11.05 g, 69%). Correct elemental analysis.

Received: May 15, 1986 [Z 1778 IE]
German version: *Angew. Chem. 98* (1986) 902

[1] Review: J. Holton, M. F. Lappert, R. Pearce, P. I. W. Yarrow, *Chem. Rev. 83* (1983) 135.
[2] E. Weiss, E. A. C. Lucken, *J. Organometal. Chem. 2* (1964) 197.
[3] J. A. J. Jarvis, B. T. Kilbourn, R. Pearce, M. F. Lappert, *J. Chem. Soc. Chem. Commun. 1973*, 475.
[4] J. C. Huffman, W. E. Streib, *Chem. Commun. 1971*, 911, and references cited therein.
[5] B. Bogdanović, H. Bönnemann, G. Wilke, *Angew. Chem. 78* (1966) 591; *Angew. Chem. Int. Ed. Engl. 5* (1966) 582; C. Krüger, J. C. Sekutowski, H. Berke, R. Hoffmann, *Z. Naturforsch. B33* (1978) 1110.
[6] K. Jonas, W. Rüsseler, K. Angermund, C. Krüger, *Angew. Chem. 98* (1986) 904; *Angew. Chem. Int. Ed. Engl. 25* (1986) 927.
[7] It is already well known in the case of arenechromium(0) complexes that coordinated naphthalene can be much more easily displaced than complexed benzene: E. P. Kündig, C. Perret, S. Spichiger, *J. Organomet. Chem. 286* (1985) 183, and references cited therein. [CpV(naphthalene)] **1** and the corresponding Cp* complex, which we have prepared from **5** as starting compound analogously to the synthesis of **1** [12], are suitable sources of CpV and Cp*V fragments [12], respectively. In this respect they resemble the reactive half-sandwich complexes $[CpCo(C_2H_4)_2]$, [9, 13] $[IndCo(C_2H_4)_2]$, [9, 14] and [CpFe(cod)] [9] (Ind = η^5-indenyl, cod = 1,5-cyclooctadiene).

[8] a) S. J. McLain, C. D. Wood, R. R. Schrock, *J. Am. Chem. Soc. 101* (1979) 4558; b) M. R. Churchill, W. J. Youngs, *Inorg. Chem. 19* (1980) 3106; c) J. M. Manriguez, D. R. McAlister, R. D. Sanner, J. E. Bercaw, *J. Am. Chem. Soc. 100* (1978) 2716; d) G. Erker, K. Engel, U. Dorf, J. L. Atwood, W. E. Hunter, *Angew. Chem. 94* (1982) 915; *Angew. Chem. Int. Ed. Engl. 21* (1982) 913; *Angew. Chem. Suppl. 1982*, 1974.

[9] K. Jonas, *Angew. Chem. 97* (1985) 292; *Angew. Chem. Int. Ed. Engl. 24* (1985) 295, and references cited therein.

[10] J. Krausse, G. Schödl, *J. Organomet. Chem. 27* (1971) 59.

[11] Crystal structure analysis of **3**: space group $P2_1/n$, No. 14, $a = 6.8648(8)$, $b = 16.457(2)$, $c = 7.3057(7)$ Å, $\beta = 102.47(1)°$, $Z = 2$, $\rho_{calc} = 1.42\ g\,cm^{-3}$, $\mu(Mo_{K\alpha}) = 11.11\ cm^{-1}$; solution of structure by Patterson methods from 1577 independent reflections with $I > 2\sigma(I)$, $R = 0.034$, $R_w = 0.042$ ($w = 1/\sigma^2(F_0)$). Further details of the crystal structure investigation are available on request from the Fachinformationszentrum Energie, Physik, Mathematik GmbH, D-7514 Eggenstein-Leopoldshafen 2 (FRG), on quoting the depository number CSD-51934, the names of the authors, and the full citation of the journal.

[12] K. Jonas, W. Rüsseler, unpublished.

[13] K. Jonas, E. Deffense, D. Habermann, *Angew. Chem. 95* (1983) 729; *Angew. Chem. Int. Ed. Engl. 22* (1983) 716; *Angew. Chem. Suppl. 1983*, 1005.

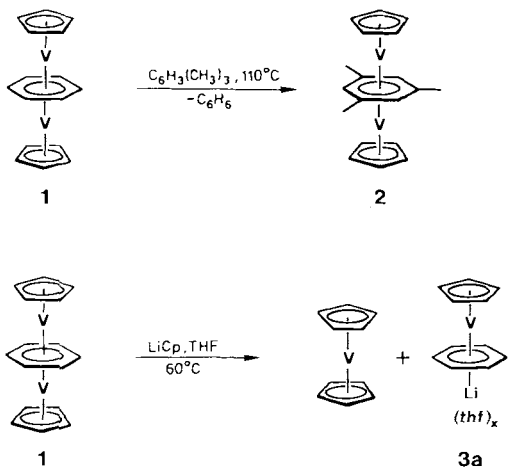
[14] R. Benn, K. Cibura, P. Hofmann, K. Jonas, A. Rufińska, *Organometallics 4* (1985) 2214.

[15] The mononuclear vanadium(III) complex $[CpV(Me)_2(PMe_3)_2]$ is already known: B. Hessen, J. H. Teuben, T. H. Lemmen, J. C. Huffmann, K. G. Caulton, *Organometallics 4* (1985) 946.

Benzene as Bridging Ligand in Main Group Metal-Transition Metal-Arene Complexes

By *Klaus Jonas,* Wolfgang Rüsseler, Klaus Angermund,* and *Carl Krüger*

μ-Benzene(dicyclopentadienyl)divanadium **1**,[1] the first triple-decker sandwich complex with benzene as "middle deck", can be converted into the mesitylene analogue **2** by heating in mesitylene.[1,2] By way of analogy we have now treated **1** with lithium cyclopentadienide (LiCp) in tetrahydrofuran (THF) with the aim of replacing the bridging benzene ligand by the isoelectronic cyclopentadienyl anion. It was found, however, that this reaction resulted in rupture of the triple-decker sandwich structure and formation of the lithium-vanadium complex **3a** and vanadocene. That is, the C_5H_5-ring of LiCp attaches to a CpV unit, while the Li atom coordinates to the arene ligand of $[CpV(C_6H_6)]$ **4**.



[*] Prof. Dr. K. Jonas, Dipl.-Chem. W. Rüsseler, Dipl.-Chem. K. Angermund [+], Prof. Dr. C. Krüger [+]
Max-Planck-Institut für Kohlenforschung
Kaiser-Wilhelm-Platz 1, D-4330 Mülheim a. d. Ruhr (FRG)
[+] Crystal structure analysis.

The novel lithium-vanadium complex **3a** is stable in toluene even at 100°C and is thus significantly more robust than the vanadium compounds that contain a second five-membered ring instead of the C_6H_6-ligand: $K[Cp_2V]$[2,3] and $K[(C_5Me_5)VCp]$.[2] The latter two complexes, which are obtained by reaction of the corresponding metallocenes with potassium and which are suitable starting compounds for the synthesis of half-sandwich complexes, are, like $M[Cp_2Co]$ (M = Li, K),[2,4] stable only at low temperatures.

Replacement of the THF ligands in **3a** by *N,N,N',N'*-tetramethylethylenediamine (TMEDA) affords crystalline $[(tmeda)Li(C_6H_6)VCp]$ **3b**. A novel feature of the structure of **3b** (Fig. 1) is that a transition metal atom and a main-group metal atom are bridged by a benzene molecule. The

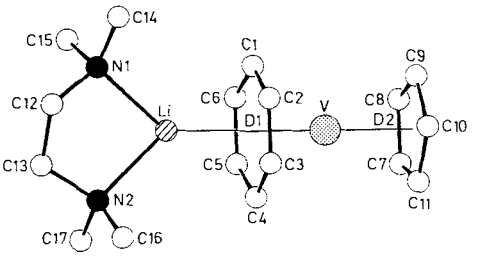
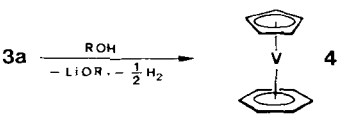


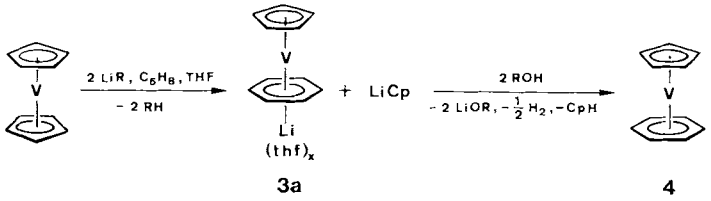
Fig. 1. Crystal structure of **3b** [5].

bridging ligand and the five-membered ring bound to the vanadium atom are parallel (angle between the least square planes through the carbon atoms C1–C6 (plane E1) and C7–C11 (plane E2): 1.1°); and are oriented almost perpendicularly to the line through the two metal atoms (angles between Li–V and E1 and E2: 89.0 and 88.6°, respectively). The benzene ligand is η^6-coordinated to both the lithium and the vanadium atom (angle between the normal of E1 and the line through the metal atom M and the center of the benzene ring: 1.4° for M = Li and 0.6° for M = V); the distances between the center of the benzene ring and the lithium and vanadium atoms are 1.938 Å and 1.590 Å, respectively. Taking into consideration the different ionic radii of lithium and potassium, it follows that the lithium-benzene distance in **3b** is ca. 0.5 Å shorter than the potassium-benzene distance in $[K(C_6H_6)Al(CH_3)_3NO_3]$.[6] The lithium atom is coordinated in a distorted pseudo-trigonal planar fashion, while the vanadium atom is sandwiched between the C_6H_6 ligand and the Cp ring (Cp-V-benzene angle: 179.3°). The V-Cp(center) distance (1.920 Å) is identical to that in **1**; the V-benzene (center) distance, on the other hand, is 0.11 Å shorter than that in the triple decker sandwich complex **1**.

The compounds **3a** and **3b** can be delithiated by alcoholysis. In both cases, this leads to evolution of H_2 and formation of the paramagnetic species benzene(cyclopentadienyl)vanadium **4**, which was thus prepared for the first time in pure form. In contrast, the reaction of $CpVCl_3$ with isopropylmagnesium bromide described by *Müller* and *Goll* furnished a product mixture, in which **4** was detected mass spectrometrically but could not be separated from $[Cp_2V]$ and $[(C_6H_6)_2]V$.[7]



The complex **4** can be prepared in pure form very much more easily and on a larger scale in a one-pot synthesis starting from vanadocene (Scheme 1).[8] Moreover, when methylcyclohexadiene is used in place of cyclohexadiene, the new vanadium complex cyclopentadienyl(toluene)vanadium is formed.



3a **4**

Scheme 1. One-pot synthesis of **4** from vanadocene (R = Me, Et, *n*Bu) [8].

That **4** reacts with lithium to give **3** is not surprising. Remarkable, however, is the reaction of **4** with magnesium: It leads in tetrahydrofuran to the novel trinuclear complex

$[(thf)_2Mg\{(C_6H_6)VCp\}_2]$

in which, analogous to the structure of **3b**, the benzene ligands probably form bridges between vanadium and magnesium.

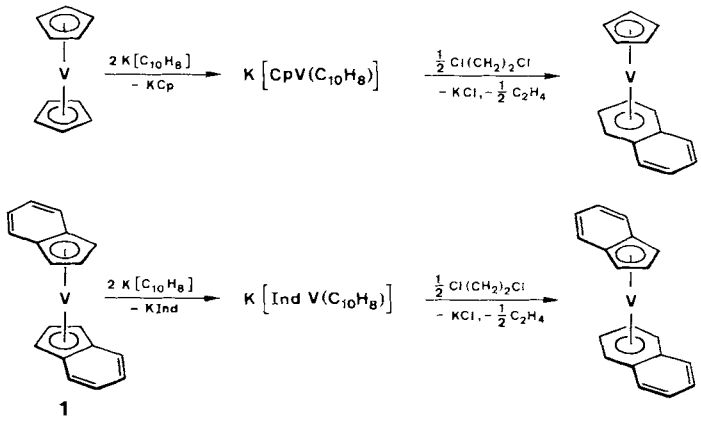
Received: May 15, 1986 [Z 1779 IE]
German version: *Angew. Chem. 98* (1986) 904

[1] A. W. Duff, K. Jonas, R. Goddard, H.-J. Kraus, C. Krüger, *J. Am. Chem. Soc. 105* (1983) 5497.
[2] K. Jonas, *Angew. Chem. 97* (1985) 292; *Angew. Chem. Int. Ed. Engl. 24* (1985) 295, and references cited therein.
[3] K. Jonas, V. Wiskamp, *Z. Naturforsch. B38* (1983) 1113.
[4] K. Jonas, C. Krüger, *Angew. Chem. 92* (1980) 513; *Angew. Chem. Int. Ed. Engl. 19* (1980) 520; K. Jonas, *Pure Appl. Chem. 56* (1984) 63.
[5] Crystal structure analyses of **3b**: Crystal dimensions: 0.14, 0.54, 0.32 mm, $P\bar{1}$ (No. 2); $a = 6.173(1)$, $b = 11.072(2)$, $c = 13.392(2)$ Å, $\alpha = 96.53(1)$, $\beta = 93.76(1)$, $\gamma = 99.21(1)°$, $Z = 2$; $\mu(Mo_{K\alpha}) = 5.3$ cm^{-1} ($\lambda = 0.71069$ Å), 4053 reflections measured ($\pm h$, $\pm k$, $+l$), 2322 observed ($I > 2\sigma(I)$), 190 refined parameters, $R = 0.054$, $R_w = 0.060$ ($w = 1/\sigma^2(F_0)$), maximum residual electron density 0.26 e Å^{-3}, no absorption correction, H atom positions calculated and not refined. Further details of the crystal structure investigation are available on request from the Fachinformationszentrum Energie, Physik, Mathematik GmbH, 7514 Eggenstein-Leopoldshafen 2 (FRG), on quoting the depository number CSD-51928, the names of the authors, and the full citation of the journal.
[6] J. L. Atwood, K. D. Crissinger, R. D. Rogers, *J. Organomet. Chem. 155* (1978) 1.
[7] W. Goll, J. Müller, *J. Organomet. Chem. 71* (1974) 257.
[8] Experimental procedure for **4**: A solution of vanadocene (13.18 g, 72.8 mmol) and 1,3-cyclohexadiene (10.4 mL, 109.2 mmol) in THF (200 mL) was treated with 69 mL of a 2.11 molar solution of *n*BuLi in hexane (145.6 mmol) at such a rate that the temperature of the solution increased to 50°C. After subsequent addition of 8.54 mL (145.5 mmol) of ethanol at 0°C and evaporation to dryness the resulting residue was sublimed under vacuum at 80–100°C. Dissolution of the sublimate in hot hexane furnished a solution from which the brown complex **4** crystallized at −30°C (yield 11.38 g, 81%). Correct elemental analysis. MS: *m/z* 194 ($M^{\oplus}$, 35%).
[9] Experimental procedure for **3b** (from **4**): A solution of **4** (2.42 g, 12.5 mmol) in THF (50 mL) was treated at 0°C with excess lithium sand. The mixture was stirred for 5 h and then filtered (to remove unchanged lithium). The filtrate was evaporated to dryness and the resulting residue treated, with vigorous stirring, with a mixture of Et_2O and TMEDA. Recrystallization of the solid product from Et_2O (36°C → −30°C) afforded 3.75 g (95%) of **3b** as red, needle-like crystals. Correct elemental analysis.

Synthesis of Diindenyldivanadium—a New Variant of the Reductive Degradation of Metallocenes and Related Compounds

By *Klaus Jonas,* Wolfgang Rüsseler, Carl Krüger,* and *Eleonore Raabe*

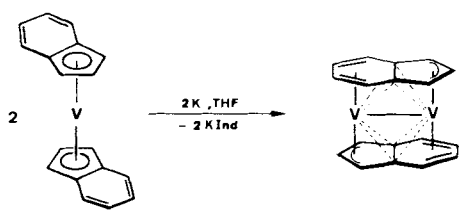
Partial or total degradation of metallocenes and related compounds with alkali metal in the presence of complexing agents such as olefins (reductive abstraction of five-membered ring ligands) produces reactive organometallic compounds with easily displaced ligands. Examples are ethene-transition metal complexes.[1–3] The ether soluble arene-alkali metal complexes such as naphthalenepotassium have also proven to be invaluable reducing agents. The arenes, which in these adducts act as alkali metal "carriers", can also become π-coordinated to the transition metal. Scheme 1 shows two such examples.[4,5]



1

Scheme 1. The double role of naphthalene in the synthesis of reactive vanadium complexes by reductive abstraction of five-membered ring ligands: alkali-metal carrier and π-bonded transition-metal ligand.

We have now found that alkali metal-reduction of diindenylvanadium **1** [$(Ind)_2V$], first prepared by us,[6] can be very easily converted into a diindenyldivanadium synthesis, in which reduction is carried out with potassium in tetrahydrofuran (THF) without addition of a complexing agent. By this simple trick one also uses the previously non-coordinated carbon atoms of the six-membered rings of two indenyl ligands to bind vanadium (Scheme 2 and Fig. 1). There is no other example of a dinuclear complex with one, let alone two, bridging indenyl ligands.



1 **2**

Scheme 2. Synthesis of diindenyldivanadium **2** [7].

[*] Prof. Dr. K. Jonas, Dipl.-Chem. W. Rüsseler, Prof. Dr. C. Krüger [+], Dr. E. Raabe [+]
Max-Planck-Institut für Kohlenforschung
Kaiser-Wilhelm-Platz 1, D-4330 Mülheim a. d. Ruhr (FRG)
[+] Crystal structure analysis.

In the paramagnetic dinuclear sandwich complex **2**, which has a center of inversion, the V-atoms (V-V* 2.351(1) Å) are each surrounded by a five-membered ring and six-membered ring. The bridging atoms C5 and C9 are located at an average distance of 2.274(6) Å from the central V atoms, a distance greater than all other V-C distances in the molecule. The same holds for the distances between C5/C9 and the neighboring C atoms. The C6-C7 (1.417(3) Å) and C7-C8 (1.411(2) Å) bonds in the five-membered ring are about 0.03 Å shorter than the other three C-C bonds, whereas a long-short-long sequence is observed for the C-C bond lengths between the C1-C4 atoms in the six-membered ring. The planar moiety C1-C4 ($V-C_{terminal}$ 2.166(2) Å, $V-C_{central}$ 2.236(2) and 2.239(2) Å, respectively) bound to vanadium like a diene forms an angle of 13.5° with the C1-C4-C5-C9 plane.

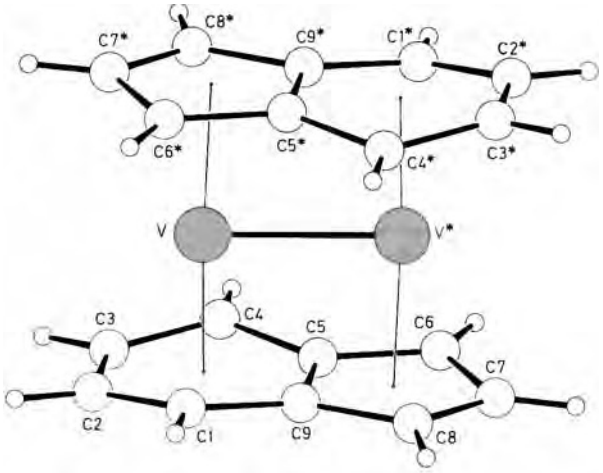


Fig. 1. Crystal structure of diindenyldianadium **2** [8]. Selected bond lengths [Å] and angles [°] (see text also): C1-C2 1.425(3), C2-C3 1.403(2), C3-C4 1.430(2), C5-C9 1.457(2); V-C6* 2.212(2), V-C7* 2.252(2), V-C8* 2.223(2).

Aside from **2**, there are only two other dinuclear complexes with two bridging ligands which are bicyclic annulated hydrocarbon systems. These compounds, which are formed in low yields (4% and 4–10%, respectively) upon reaction of $NiCl_2$ or $CoCl_2$ with dilithium pentalenide, have, on the basis of elemental analyses and ^{1}H-NMR and mass spectra, been characterized as $[(C_8H_6)_2Ni_2]$ and $[(C_8H_6)_2Co_2]$.[9, 10] *Katz* et al. have proposed a dinuclear sandwich structure for these two complexes, but such a structure has not, as yet, been confirmed by a crystal structure analysis.

Received: May 15, 1986;
revised: July 2, 1986 [Z 1780 IE]
German version: *Angew. Chem. 98* (1986) 905

[1] K. Jonas, *Angew. Chem. 97* (1985) 292; *Angew. Chem. Int. Ed. Engl. 24* (1985) 295, and references cited therein.
[2] R. Benn, K. Cibura, P. Hofmann, K. Jonas, A. Rufinska, *Organometallics 4* (1985) 2214.
[3] K. Cibura, *Dissertation*, Universität Bochum 1985.
[4] K. Jonas, W. Rüsseler, C. Krüger, E. Raabe, *Angew. Chem. 98* (1986) 902; *Angew. Chem. Int. Ed. Engl. 25* (1986) 925.
[5] K. Jonas, W. Rüsseler, unpublished.
[6] Experimental procedure for **1**: 20.31 g of the pale green product (43.1 mmol V, found 10.82% V), which was obtained by reaction of VCl_3 with zinc in THF [11], was added with stirring at 0°C to a solution of LiInd (prepared from indene and *n*BuLi in hexane) in THF (300 mL). After 15 hours' heating under reflux, the reaction mixture was evaporated to dryness and the residue sublimed under high vacuum at 120–140°C. Recrystallization of the sublimate from toluene/hexane furnished dark green crystals; these were washed and dried at 20°C under oil-pump vacuum (yield 10.34 g, 85%). Correct elemental analysis. MS: *m/z* 281 ($M^{\oplus}$, 100%). IR [cm^{-1}] (KBr): $\tilde{\nu}$(CH) = 3095 (w), 3074 (w), 3050 (m), 3008 (w); $\tilde{\nu}$(CC) = 1446 (m), 1326 (s), 1208 (m), 1149 (m); $\tilde{\nu}$(five-membered ring) = 1031 (s); π(CH) = 770 (vs), 730 (vs).
[7] Experimental procedure for **2**: to a stirred solution of **1** (17.48 g, 62.2 mmol) in THF (300 mL) at 0°C was added 2.41 g (61.6 mmol) of potassium pellets over a period of 3 h. After 10 hours' stirring at 20°C, the reaction mixture was evaporated to dryness and the residue taken up in boiling toluene. The hot solution was filtered free of insolubles. On cooling the filtrate to 20°C, dark purple crystals of **2** crystallized (4.74 g, 46%). Correct elemental analysis. MS: *m/z* 332 ($M^{\oplus}$, 100%). IR [cm^{-1}] (KBr): $\tilde{\nu}$(CH) = 3038 (m), 3049 (w), 3039 (w); $\tilde{\nu}$(CC) = 1457 (m), 1375 (m), 1294 (s), 1138 (m); $\tilde{\nu}$(five-membered ring) = 1030 (s); π(CH) = 736 (vs).
[8] Crystal structure analysis of **2**: space group $P2_1/n$, No. 14, $Z = 2$, $\rho_{calc} = 1.71$ g cm^{-3}, $\mu(Mo_{K\alpha}) = 13.86$ cm^{-1}, $a = 7.7537(9)$, $b = 8.1145(7)$, $c = 10.8774(6)$ Å, $\beta = 109.541(6)°$, solution of structure by Patterson methods. 1654 observed reflections with $I > 2\sigma(I)$, $R = 0.025$, $R_w = 0.034$ ($w = 1/\sigma^2(F_o)$). Further details of the crystal structure investigation are available on request from the Fachinformationszentrum Energie, Physik, Mathematik GmbH, D-7514 Eggenstein-Leopoldshafen 2 (FRG), on quoting the depository number CSD-51932, the names of the authors, and the full citation of the journal.
[9] T. J. Katz, N. Acton, *J. Am. Chem. Soc. 94* (1972) 3281; T. J. Katz, N. Acton, J. McGinnis, *ibid. 94* (1972) 6205.
[10] An article on di- and polynuclear sandwich complexes, in which almost exclusively hypothetical molecules are theoretically treated, appeared in 1985: J. K. Burdett, E. Cannadell, *Organometallics 4* (1985) 805.
[11] R. J. Bouma, J. H. Teuben, W. R. Beukema, R. L. Bansemer, J. C. Huffmann, K. G. Caulton, *Inorg. Chem. 23* (1984) 2715; F. A. Cotton, S. A. Duraj, W. J. Roth, *ibid. 23* (1984) 4113, and references cited therein.

Formal Insertion of the $HCO^{\oplus}$ Fragment into a Trinuclear Cluster Metal–Carbyne Bond: Synthesis, Structure and Reactivity of Cluster-bound Ethynol**

By *K. Peter C. Vollhardt** and *Matthias Wolfgruber*

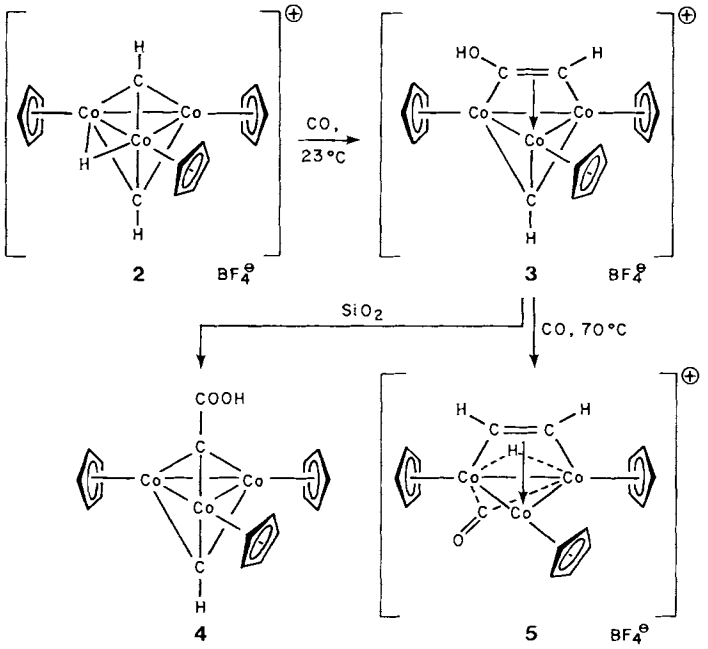
A recent report of the observation of ethynol (hydroxyacetylene) in the gas phase,[1] prompts us to disclose the isolation of this usually unstable molecule as a ligand to a trinuclear cobalt cluster. Its formation proceeds by the novel formal insertion of the hydroxymethylidyne cation HO-C:$^{\oplus}$ into a cobalt–methylidyne bond, the isoelectronic carbon version of the related reaction of $NO^{\oplus}$.[2]

Addition of $HBF_4 \cdot OEt_2$ to a slurry of the cluster **1**[3] in CH_2Cl_2 caused an immediate color change from red to bright green and complete dissolution. Addition of pentane precipitated the edge-protonated[4] cluster **2** (94%),[5] characterized by a single ^{13}C-NMR signal (CD_2Cl_2) at $\delta = 87.61$ (methylidyne C-signal not observed), and three ^{1}H-NMR signals (CD_2Cl_2, −90°C) at $\delta = -27.49$ (s, 1 H), 4.99 (s, 15 H), and 16.79 (s, 2 H). The single Cp resonance indicates either accidental isochronism or a fluxional process around the trinuclear core.[4]

[*] Prof. Dr. K. P. C. Vollhardt, Dr. M. Wolfgruber
Department of Chemistry, University of California
and the Materials and Molecular Research Division
Lawrence Berkeley Laboratory
Berkeley, CA 94720 (USA)

[**] This work was supported by the National Science Foundation (CHE 8504987). *K. P. C. V.* is a Miller Research Professor in Residence (1985–1986). *M. W.* was the recipient of a Deutscher Akademischer Austauschdienst Postdoctoral Fellowship (1984–1985). The X-ray structural analysis was carried out by Dr. *F. J. Hollander*, staff crystallographer.

$[(\mu_3\text{-}\eta^1\text{-}CH)_2(CpCo)_3]$ **1**, $Cp = \eta^5\text{-}C_5H_5$



$[(\mu_3\text{-}\eta^1\text{-}CCO_2CH_3)(\mu_3\text{-}\eta^1\text{-}CH)(CpCo)_3]$ **6**

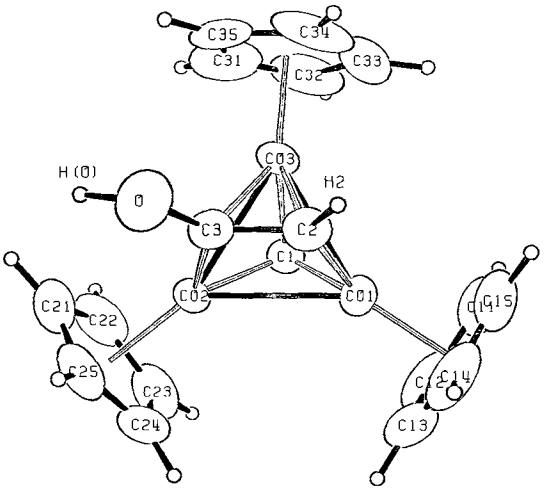


Fig. 1. ORTEP drawing of the crystal structure of the cation in **3**. Ellipsoids are scaled to represent the 50% probability surface. Hydrogen atoms are not refined and are represented by arbitrary spheres. H(O) and H2 are given in their positions as found on an electron density map. All other hydrogens are in idealized positions. Selected bond lengths [Å] and angles [°]: C2-C3 1.368(4), C2-H2 1.11, O-H(O) 1.02, Co1-C2 1.881(3), Co2-C3 1.886(3), Co3-C2 1.993(3), Co3-C3 2.036(3), Co1-Co2 2.501(1), Co1-Co3 2.392(1), Co2-Co3 2.435(1), Co1-C1 1.834(3), Co2-C1 1.830(3), Co3-C1 1.874(3), Co1-Cp1 1.695, Co2-Cp2 1.701, Co3-Cp3 1.677, Co1-C2-C3 108.1(2), Co1-C2-H2 131.2, C3-C2-H2 119.0, Co3-C3-C2 106.9(2), Co2-C3-O 128.1, C2-C3-O 123.6(3), C3-O-H(O) 107.8.

Remarkably, **1** is completely inert to CO at room temperature, whereas **2** is smoothly carbonylated (23 °C, 55 bar, CH_2Cl_2, 97%) to a new compound formulated as the ethynol complex **3**.[5] The composition of **3** is confirmed by elemental analysis. The ^{1}H-NMR spectrum ([D$_6$]acetone) exhibits signals at $\delta = 22.18$ (C–H of the intact methylydyne group), 11.16 (OH, assigned by deuterium exchange), 10.38 (C–H of the new ligand), and 5.10 (s, 15 H, Cp). Not unexpectedly,[2] the alkyne ligand is fluxional, leading to only a single peak for the Cp protons. The ^{13}C-NMR spectrum (CD_3NO_2) shows signals at $\delta = 197.52$ and 124.25 (ethynol C-atoms) and 87.69 (Cp); a methylidyne C-signal could not be observed. The IR spectrum (KBr) shows a broad peak at $\tilde{\nu} = 3380$ cm^{-1} and additional strong absorptions at $\tilde{\nu} = 1419$, 1266, 1070, 985, and 840 cm^{-1}. The mass spectrum contains characteristic fragments at m/z 426 ($M^{\oplus} - H$, 68%) and 398 ($M^{\oplus} - HCO$, 66%). Final structural confirmation of **3** was obtained by an X-ray structural analysis (Fig. 1).[6]

The alkynol ligand in **3** adopts a parallel[7] arrangement, and is bent and stretched as expected.[8] Its mechanism of formation by HOC$^{\oplus}$ coupling may be related to other acid-mediated methylidyne–CO couplings of interest as a fundamental step in hydrocarbon build-up by CO hydrogenation.[9] We have observed that this protonation-carbonylation sequence occurs also with other biscarbyne clusters of the type **1**.

On attempted chromatography (silica gel), **3** oxidized to the acid **4** in low yield,[10] synthesized independently from the cluster **6** (obtained by alkyne cleavage[3]) by hydrolysis (1. $HBF_4 \cdot OEt_2$, 2. H_2O; 94%). When **3** was treated with CO at 70 °C (CH_2Cl_2, 16 bar, 5 h, 73%) an unprecedented rearrangement to **5** occurred, involving apparent CO deinsertion and coupling of two methylidyne ligands! The IR spectrum of **5** (KBr) exhibits a strong peak at $\tilde{\nu} = 1845$ cm^{-1}, indicative of a bridging CO; the mass spectrum is identical to that of **3**, and the ^{1}H-NMR spectrum ([D$_6$]acetone) reveals the absence of the methylidyne signal and the presence of a peak at $\delta = 9.18$ (s, 2 H, ethyne H) in addition to two peaks at $\delta = 5.49$ (s, 10 H, 2 Cp) and 5.41 (s, 5 H, Cp). The hydride signal could not be detected. The ^{13}C-NMR spectrum (CD_3NO_2) shows absorptions at $\delta = 161.02$ (CO), 149.14 (ethyne), 91.48 and 87.52 (Cp). The elemental analysis and additional IR bands at 1000–1150 cm^{-1}[11] confirm the formulation of **5** as a $BF_4^{\ominus}$ salt. A related rhodium complex has been reported.[12] The transformation of **3** into **5** is analogous to the equally unprecedented base-induced NO-cleavage with CH/CH coupling of the related NO insertion products of **1**.[2]

Received: May 5, 1986;
revised: July 11, 1986 [Z 1759 IE]
German version: *Angew. Chem. 98* (1986) 919

CAS Registry numbers:
1, 74127-99-4; **2**, 104131-40-0; **3**, 104131-42-2; **4**, 104131-43-3; **5**, 104131-45-5; **6**, 104131-46-6; Co, 7440-48-4.

[1] a) B. van Baar, T. Weiske, J. K. Terlouw, H. Schwarz, *Angew. Chem. 98* (1986) 275; *Angew. Chem. Int. Ed. Engl. 25* (1986) 282; b) Complexed ethynol has been invoked as an intermediate: E. Boyar, A. J. Deeming, S. E. Kabir, *J. Chem. Soc. Chem. Commun. 1986*, 577.

[2] A. Goldhaber, K. P. C. Vollhardt, E. C. Walborsky, M. Wolfgruber, *J. Am. Chem. Soc. 108* (1986) 516.

[3] J. R. Fritch, K. P. C. Vollhardt, *Angew. Chem. 92* (1980) 570; *Angew. Chem. Int. Ed. Engl. 19* (1980) 559.

[4] D. E. Van Horn, K. P. C. Vollhardt, *J. Chem. Soc. Chem. Commun. 1982*, 203.

[5] All new compounds isolated were fully characterized.

[6] Monoclinic, $P2_1/n$, $a = 9.7371(6)$, $b = 12.0361(9)$, $c = 15.7240(17)$ Å, $\beta = 91.246(7)°$, $V = 1842.4(5)$ Å^3, $Z = 4$, $\rho_{calcd} = 1.85$ g cm^{-3}, $\mu_{calcd} = 27.1$ cm^{-1}, $Mo_{K\alpha}$ radiation (graphite monochromator); scan range: $3° \le 2\theta \le 45°$; reflections collected 2703; 2108 unique with $F_0 > 3\sigma(F^2)$, $R = 0.0329$, $R_w = 0.0532$. Further details of the crystal structure investigation are available on request from the Fachinformationszentrum Energie, Physik, Mathematik GmbH, D-7514 Eggenstein-Leopoldshafen 2 (FRG), on quoting the depository number CSD-51991, the names of the authors, and the full citation of the journal.

[7] A. D. Clauss, J. R. Shapley, C. N. Wilker, R. Hoffmann, *Organometallics 3* (1984) 619.
[8] See M. R. Churchill, J. C. Fettinger, J. B. Keister, R. F. See, J. W. Ziller, *Organometallics 4* (1985) 2112, and references cited therein. For a review see E. Sappa, A. Tiripicchio, P. Braunstein, *Coord. Chem. Rev. 65* (1985) 219.
[9] For selected recent work, see D. C. Brower, K. R. Birdwhistell, J. L. Templeton, *Organometallics 5* (1986) 94; J. Hriljac, D. F. Shriver, *ibid. 4* (1985) 2225; M. J. Sailor, D. F. Shriver, *ibid. 4* (1985) 1476; K. R. Birdwhistell, T. L. Tonker, J. L. Templeton, *J. Am. Chem. Soc. 107* (1985) 4474; S. J. Holmes, R. R. Schrock, M. R. Churchill, H. J. Wasserman, *Organometallics 3* (1984) 476; F. R. Kreissl, W. J. Sieber, M. Wolfgruber, J. Riede, *Angew. Chem. 96* (1984) 618; *Angew. Chem. Int. Ed. Engl. 23* (1984) 640; F. R. Kreissl, W. Sieber, M. Wolfgruber, *ibid. 95* (1983) 503 and *22* (1983) 493; *Angew. Chem. Suppl. 1983*, 631; M. R. Churchill, H. J. Wasserman, *Inorg. Chem. 22* (1983) 41.
[10] **4**: red powder; *m/z* 442 ($M^{\oplus}$, 39%), 189 (100); ^{1}H-NMR ($CDCl_3$): $\delta = 18.92$ (s, 1H), 10.00 (br. s, 1H), 4.55 (s, 15H); IR (KBr): $\tilde{\nu} = 3300$–2500 (br.), 1636, 1264, 808 cm^{-1}.
[11] K. Richter, E. O. Fischer, C. G. Kreiter, *J. Organomet. Chem. 122* (1976) 187.
[12] R. S. Dickson, C. Mok, G. Pain, *J. Organomet. Chem. 166* (1979) 385.

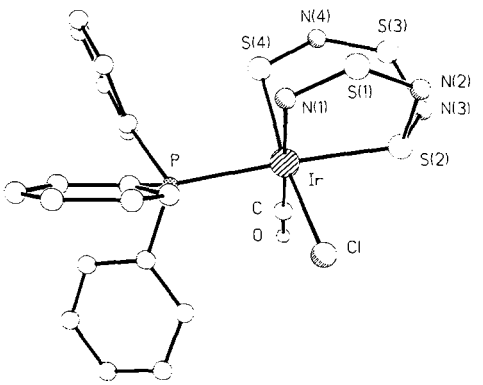


Fig. 1. Crystal structure of **2a** [4]. Selected bond lengths [pm] and angles [°]: Ir-N1 205.7(5), Ir-S2 239.1(3), Ir-S4 233.5(3), Ir-P 237.5(3), N1-S1 152.8(6), N2-S2 169.2(6), N3-S3 157.5(7), N4-S4 160.8(6), S1-N2 158.1(6), S2-N3 164.6(7), S3-N4 156.0(6), Ir-Cl 241.4(3), Ir-C 190.2(6), C-O 111.9(8); N1-Ir-S2 86.7(2), S2-Ir-S4 95.0(1), S2-Ir-Cl 79.6(1), N1-Ir-C 176.8(3), S4-Ir-C 94.3(2), N1-Ir-P 90.1(2), S4-Ir-P 89.9(1), C-Ir-P 89.8(2), N1-Ir-S4 82.4(2), N1-Ir-Cl 88.9(2), S4-Ir-Cl 170.0(1), S2-Ir-C 93.7(2), Cl-Ir-C 94.4(1), N2-S2-N3 103.4(3).

S_4N_4 as Tridentate Ligand in $[IrX(CO)(PPh_3)(S_4N_4)]$ Complexes**

By *Frank Edelmann, Herbert W. Roesky,* Claudia Spang, Mathias Noltemeyer,* and *George M. Sheldrick*

In all the adducts of S_4N_4 and transition metal halides described in the literature so far, S_4N_4 is coordinated to the metal atom via an electron lone pair on a nitrogen atom.[1] The Vaska complex $[IrX(CO)(PPh_3)_2]$ **1** reacts with S_4N_4 with elimination of triphenylphosphane to give $[IrX(CO)(PPh_3)(S_4N_4)]$ **2**. The chloro complex **2a** has already been mentioned in the literature,[2] but so far has not been satisfactorily characterized.

$$[IrX(CO)(PPh_3)_2] + S_4N_4 \longrightarrow [IrX(CO)(PPh_3)(S_4N_4)] + PPh_3$$
1 **2**

a, X = Cl; **b**, X = Br; **c**, X = I

The intense red complexes **2a–c** are stable towards air and hydrolysis. Their purity was checked by thin-layer chromatography (silica gel, benzene; **2**: $R_f = 0.8$).[3] The IR spectra of **2a–c** show a distinct shift of the $\tilde{\nu}$(CO) band of more than 100 cm^{-1} to higher frequency compared to that of the starting compounds (**1a** 1951, **2a** 2065, **1b** 1955, **2b** 2069, **1c** 1975, **2c** 2075 cm^{-1}). The increased bond order can be attributed to oxidative addition of S_4N_4 to the Ir atom. It leads to reduction of the electron density at the iridium, and consequently to a weakening of the d_π–p_π back-bonding to the carbonyl group. In the EI-mass spectra, lines for the molecule ions with relative intensities between three and eighteen percent were observed for all three complexes, thus underscoring the kinetic stability of **2a–c**.

Single crystals for an X-ray structure analysis[4] were obtained by the diffusion method from benzene/hexane. The crystals contain two molecules of benzene per molecule of **2a**. The distinguishing feature of the structure of **2a** (Fig. 1) is that the $[IrCl(CO)PPh_3]$ fragment is inserted into a sulfur–nitrogen bond (S4–N1) of S_4N_4 while S2 is coordinated to the iridium atom, thus resulting in formation of a bicyclo[4.3.0]-skeleton. Of the two sulfur atoms coordinating the Ir atom, one (S4) has a C.N. (coordination number) of 2, the other (S2) a C.N. of 3. The S-atom with the lower C.N. should have the higher electron density and, consequently, the shorter Ir–S distance; this is indeed found to be the case: Ir–S4 233.5(3), Ir–S2 239.1(3) ppm. However, it should also be noted that the Cl-atom is *trans* to S4 while the PPh_3 ligand is *trans* to S2, and that these influence the bond lengths differently. In $[(Me_3P)_3OsS_7]$ with similar phosphane ligands, however, the S-atom with C.N. 3 has a shorter Os–S bond than the two S-atoms with C.N. 2.[5]

Received: June 2, 1986;
supplemented: July 4, 1986 [Z 1798 IE]
German version: *Angew. Chem. 98* (1986) 908

[*] Prof. Dr. H. W. Roesky, Dr. F. Edelmann, Dipl.-Chem. C. Spang, Dr. M. Noltemeyer, Prof. G. M. Sheldrick
Institut für Anorganische Chemie der Universität
Tammannstrasse 4, D-3400 Göttingen (FRG)

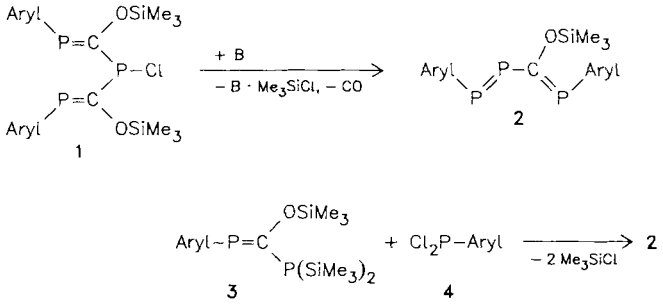
[**] This work was supported by the Deutsche Forschungsgemeinschaft and the Fonds der Chemischen Industrie.

[1] A. Gieren, C. Hahn, B. Dederer, H. W. Roesky, N. Amin, *Z. Anorg. Allg. Chem. 447* (1978) 179; U. Thewalt, B. Müller, *Z. Naturforsch. B37* (1982) 828; U. Thewalt, *Z. Anorg. Allg. Chem. 462* (1980) 221; U. Thewalt, *Angew. Chem. 88* (1976) 807; *Angew. Chem. Int. Ed. Engl. 15* (1976) 765; R. Christophersen, P. Klingelhöfer, U. Müller, K. Dehnicke, D. Rehder, *Z. Naturforsch. B40* (1985) 1631.
[2] B. J. McCormick, B. Anderson, *J. Inorg. Nucl. Chem. 32* (1970) 3414.
[3] Experimental procedure: **2a**: A solution of S_4N_4 (0.12 g, 0.65 mmol) and **1a** (0.5 g, 0.65 mmol) in benzene (50 mL) was stirred for 4 h at 50 °C. The solution turned from yellow to red-brown. It was filtered warm, and the filtrate treated with 10 mL of *n*-hexane and cooled within 0.5 h to 4 °C. Unchanged S_4N_4 that separated out was removed by filtration and the S_4N_4-free filtrate re-cooled to 4 °C. After a few hours, **2a** precipitated in the form of red crystals. Yield 0.2 g (40%), m.p. 186 °C. **2b** and **2c** can be prepared analogously. **2b**: yield 0.18 g (39%), decomposition at 190 °C. **2c**: yield 0.6 g (29%), decomposition at 192 °C.
[4] **2a** · $2C_6H_6$ crystallizes triclinically, $a = 1041.5(2)$, $b = 1249.3(2)$, $c = 1299.1(2)$ pm, $\alpha = 88.60(2)$, $\beta = 78.88(2)$, $\gamma = 86.12(2)°$, $Z = 2$, $\rho_{calc} = 1.723 \times 10^6$ g cm^{-3}, $\mu(Mo_{K\alpha})$ 4.42 mm^{-1}. Refined to $R(F) = 0.030$ for 2544 absorption-corrected data with $F > 3\sigma(F)$ with a riding model for the H atoms and the residual atoms anisotropic. Further details of the crystal structure investigation are available on request from the Fachinformationszentrum Energie, Physik, Mathematik GmbH, D-7514 Eggenstein-Leopoldshafen 2 (FRG), on quoting the depository number CSD-51977, the names of the authors, and the full citation of the journal.
[5] J. Gotzig, A. L. Rheingold, H. Werner, *Angew. Chem. 96* (1984) 813; *Angew. Chem. Int. Ed. Engl. 23* (1984) 814.

Synthesis of the First Triphosphabutadiene**

By *Rolf Appel,* Bärbel Niemann, Winfried Schuhn,* and *Falk Knoch*

Replacement of the carbon atoms of butadiene by dicoordinated phosphorus atoms has already been demonstrated on several occasions (mono- and diphosphabutadienes[1]). We now report the synthesis of the first 1,2,4-triphospha-1,3-butadiene, i.e. a compound in which a PP- and a PC-double bond are conjugated.



Aryl = 2,4,6-tri-*tert*-butylphenyl;
B = 1,8-diazabicyclo[5.4.0]undec-7-ene,
1,4-diazabicyclo[2.2.2]octane

We obtained the triphosphabutadiene **2** for the first time by reaction of the 3-chloro-substituted 1,3,5-triphospha-1,4-pentadiene **1**[2] with bases such as 1,8-diazabicyclo[5.4.0]undec-7-ene and 1,4-diazabicyclo[2.2.2]octane in toluene.[3] The reaction solution slowly changed color from yellow to red, with concomitant evolution of carbon monoxide and precipitation of the trimethylsilyl chloride adduct of the base. The red triphosphabutadiene **2** remained in solution, and, after removal of the solvent, could be isolated in crystalline form (m.p. 168 °C). It could also be prepared quite independently by condensation of the diphosphapropene **3**[4] and the dichlorophosphane **4**.[5,6]

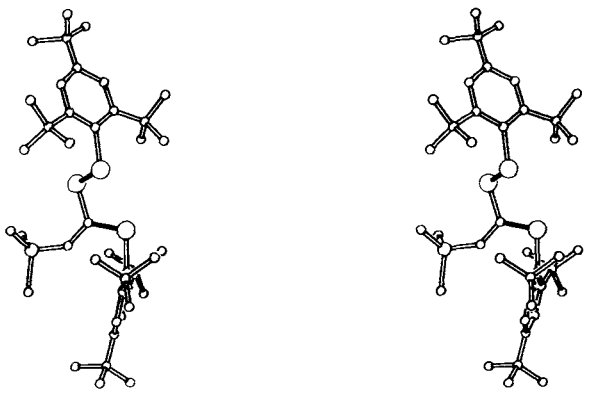


Fig. 1. Stereoview of the crystal structure of **2**.

[*] Prof. Dr. R. Appel, B. Niemann, W. Schuhn, Dr. F. Knoch
Anorganisch-Chemisches Institut der Universität
Gerhard-Domagk-Strasse, D-5300 Bonn 1 (FRG)

[**] Low Coordinate Phosphorus Compounds, Part 52. This work was supported by the Deutsche Forschungsgemeinschaft and the Minister für Wissenschaft und Forschung des Landes Nordrhein-Westfalen.—Part 51: R. Appel, C. Casser, F. Knoch, B. Niemann, *Chem. Ber. 119* (1986) 2609.

The constitution of **2** was confirmed by correct elemental analysis and by a molecular weight determination. According to the X-ray structure analysis,[7] the double bonds are arranged cisoid (Fig. 1). The ^{31}P-NMR spectrum shows the pattern expected for an ABX system with the AB part (PP double bond) shifted well downfield and an X part in the (PC)-double bond region.[8]

Received: June 27, 1986 [Z 1836 IE]
German version: *Angew. Chem. 98* (1986) 934

[1] a) R. Appel, H. Kunze, F. Knoch, *Chem. Ber. 117* (1984) 3151; b) R. Appel, V. Barth, F. Knoch, *ibid. 116* (1983) 938; c) R. Appel, U. Kündgen, F. Knoch, *ibid. 118* (1985) 1352; d) R. Appel, P. Fölling, W. Schuhn, F. Knoch, *Tetrahedron Lett. 27* (1986) 1661; e) G. Märkl, H. Seypka, *ibid. 27* (1986) 171.

[2] R. Appel, P. Fölling, B. Josten, H.-V. Wenzel, W. Schuhn, F. Knoch, unpublished.

[3] *Procedure:* 1,4-Diazabicyclo[2.2.2]octane (620 mg, 5.5 mmol) was added to a solution of **1** (4.11 g, 5 mmol) in toluene (25 mL) at room temperature and the mixture stirred for ca. 3 d (^{31}P-NMR control); the color of the solution changed from yellow to red. After removal of the solvent, the residue was dissolved in a small amount of warm dioxane/acetonitrile (1 : 1). Crystallization in a refrigerator (4 °C), yield 2.1 g (61%) of **2**.

[4] a) See [1d]; b) P. Fölling, *Diplomarbeit*, Universität Bonn 1984.

[5] M. Yoshifuji, I. Shima, N. Inamoto, *J. Am. Chem. Soc. 103* (1981) 4587; *104* (1982) 6167.

[6] *Procedure:* A mixture of **3** (2.8 g, 5 mmol) and **4** (1.7 g, 6 mmol) was stirred for several days at 50 °C under vacuum (5 torr). The oil that formed was taken up in dioxane (10 mL), whereupon **2** precipitated as a red powder. Further purification by recrystallization from hexane. Yield 1.0 g (30%); m.p. 168 °C.

[7] X-ray structure analysis of **2**: $a = 1042.4(3)$, $b = 1482.9(5)$, $c = 1584.1(5)$ pm, $\alpha = 65.50(3)$, $\beta = 85.59(2)$, $\gamma = 85.90(2)°$, $V = 2219.5(13) \times 10^6$ pm, $\rho = 1.02$ g/cm^3, $Z = 2$. Solution of structure by direct methods (SHELXTL), assymmetric data set with 9672 reflections, 3905 observed with $F > 6\sigma(F)$. $R = 0.071$, $R_w = 0.059$. Selected bond lengths [pm] and angles [°]: P=C 170, C–P 181, P=P 204, P···P 324; P=C–P 118, C–P=P 97, P=C–P=P (dihedral) 49. Both *p*-*t*Bu groups are disordered and were refined isotropically in two alternative positions. Further details of the crystal structure investigation are available on request from the Fachinformationszentrum Energie, Physik, Mathematik GmbH, D-7514 Eggenstein-Leopoldshafen 2 (FRG), on quoting the depository number CSD-51971, the names of the authors, and the full citation of the journal.

[8] Important NMR data: ^{31}P-NMR (32.2 MHz, external H_3PO_4, C_6D_6): ABX system with $\delta_A = 414.6$, $\delta_B = 394.3$, $\delta_X = 161.1$ ($J_{AB} = 510$, $J_{AX} = 113$, $J_{BX} = 60$ Hz). ^{1}H-NMR (90 MHz, C_6D_6): $\delta = -0.05$ (s, 9H; $SiMe_3$), 1.27 (s, 9H; *p*-*t*Bu), 1.31 (s, 9H; *p*-*t*Bu), 1.62 (s, 18H; *o*-*t*Bu), 1.68 (s, 18H; *o*-*t*Bu), 7.58 (m, 4H; Aryl-H). MS (870 mV, 200 °C): *m/z* (selection) 684 ($M^{\oplus}$, 2%), 627 ($M^{\oplus} - t$Bu, 20%), 571 ($M^{\oplus} - 2t$Bu, 17%), 481 ($M^{\oplus} - 2t$Bu – $OSiMe_3$, 15%), 307 (ArylPP$^{\oplus}$, 2%).

A Self-Replicating Hexadeoxynucleotide**

By *Günter von Kiedrowski**

Nonenzymatic, template-directed syntheses of oligonucleotides, first reported by *Naylor* and *Gilham* in 1966,[1] have been studied extensively by *Orgel* and colleagues[2] as an approach to model prebiotic condensation reactions using purine ribonucleoside 5′-phosphoimidazolides as activated monomers and oligomeric or polymeric ribo- and

[*] Dr. G. von Kiedrowski [+]
Chemical Evolution Laboratory, The Salk Institute
P.O. Box 85800, San Diego, CA 92138 (USA)

[+] Present address:
Institut für Organische Chemie der Universität
Tammannstrasse 2, D-3400 Göttingen (FRG)

[**] This work was supported by the National Aeronautics and Space Administration (NASA) and the Deutsche Forschungsgemeinschaft. The author wishes to thank Professor *L. E. Orgel* for support and many helpful suggestions during the course of this work, *A. Hill* for technical assistance, Dr. *N. Assa-Munt* for recording the NMR spectra, and Dr. *C. K. Biebricher* for help in performing dynamic simulations.

deoxyribonucleotides as templates. *Inoue* et al. have reported a case of transcriptive information transfer: starting from a mixture of guanosine 5′-, and cytidine 5′-phospho-2-methylimidazolides, and C-C-G-C-C as template; pG-G-C-G-G was formed in 18% yield.[3] This was the first demonstration that a template with defined sequence can catalyze the formation of its complementary (−)-strand under nonenzymatic conditions. However, a full round of replication in which the synthesized (−)-strand separates from its template to direct the synthesis of the original (+)-strand has not been observed in nonenzymatic experiments. Such a process is autocatalytic and has been proposed as the key step for the transition from chemical to biological evolution in many theories on the origin of life.[4–6]

We now report on the case of autocatalysis in a template-directed condensation of two trinucleotides leading to a hexameric template with palindromic sequence. The oligonucleotide constituents—synthesized using the phosphotriester method in solution[7]—are a trideoxyribonucleotide 3′-phosphate with its 5′-terminus protected as its methyl ether (d(MeC-C-Gp), **A**), a complementary trideoxyribonucleotide 3′-phosphate with its 3′-terminus protected with an *o*-chlorophenyl group (d(C-G-Gṗ), **B**), and a self-complementary hexameric template protected with a methyl group at its 5′-end and an *o*-chlorophenyl group at its 3′-end (d(MeC-C-G-C-G-Gṗ), **T**).[8] In accordance with the commonly used method for the chemical coupling of oligodeoxynucleotide 3′-phosphates,[9] water-soluble 1-(3-dimethylaminopropyl)-3-ethylcarbodiimide (CDI) was used to activate in situ the 3′-phosphate of **A** as its carbodiimide adduct $\overset{*}{\mathbf{A}}$.

detected: the template T and a 3′-3′-linked pyrophosphate **pp**, obtained from **A** through self-condensation:

$$\underset{\overset{*}{\mathbf{A}}}{\text{d(MeC-C-Gp)}} + \underset{\mathbf{B}}{\text{d(C-G-Gṗ)}} \longrightarrow \underset{\mathbf{T}}{\text{d(MeC-C-G-C-G-Gṗ)}}$$

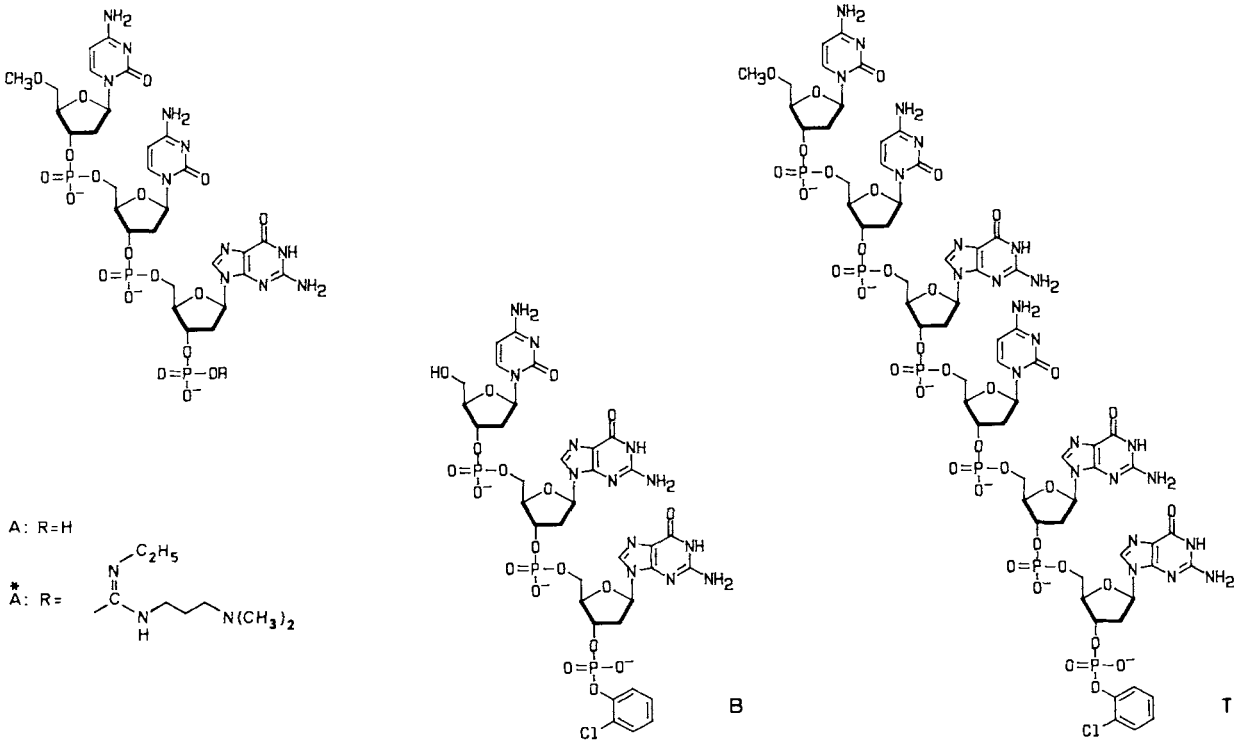
$$\underset{\overset{*}{\mathbf{A}}}{\text{d(MeC-C-Gp)}} + \underset{\mathbf{A}}{\text{d(MeC-C-Gp)}} \longrightarrow$$

$$\text{d(}^{5'}\text{MeC-C-G}^{3'}\text{pp}^{3'}\text{G-C-CMe}^{5'}\text{)}$$

pp

The same two reaction products were formed in experiments in which the 3′-phosphoimidazolide of **A** was used as activated material $\overset{*}{\mathbf{A}}$. An increase of temperature from 0 °C to 22 °C increases pyrophosphate formation and decreases template formation. Since an increase of temperature causes melting of double-stranded oligonucleotides, template formation should mainly proceed via double-stranded species, whereas pyrophosphate formation should predominantly proceed via single-stranded species.

In order to demonstrate autocatalysis in template production, reaction mixtures differing only in the initial concentration of template, c_o(**T**), were prepared. A 17-fold excess of CDI over **A** allowed repeated reactivation of **A**, since $\overset{*}{\mathbf{A}}$ is destroyed through hydrolysis. The trinucleotides **A** and **B** were introduced in at least 15-fold excess over **T** in order to determine the initial reaction order of template production with respect to template concentration. Figure 1, left, shows the time course of template production in the presence of differing values of c_o(**T**). An increase in c_o(**T**) clearly enhances the rate of production of **T**. Consequently, **T** acts as an autocatalyst for its forma-



The condensation reactions between $\overset{*}{\mathbf{A}}$ and **B** were performed in 1-μL capillaries at 0 °C and followed by HPLC.[2] In all experiments two reaction products were de-

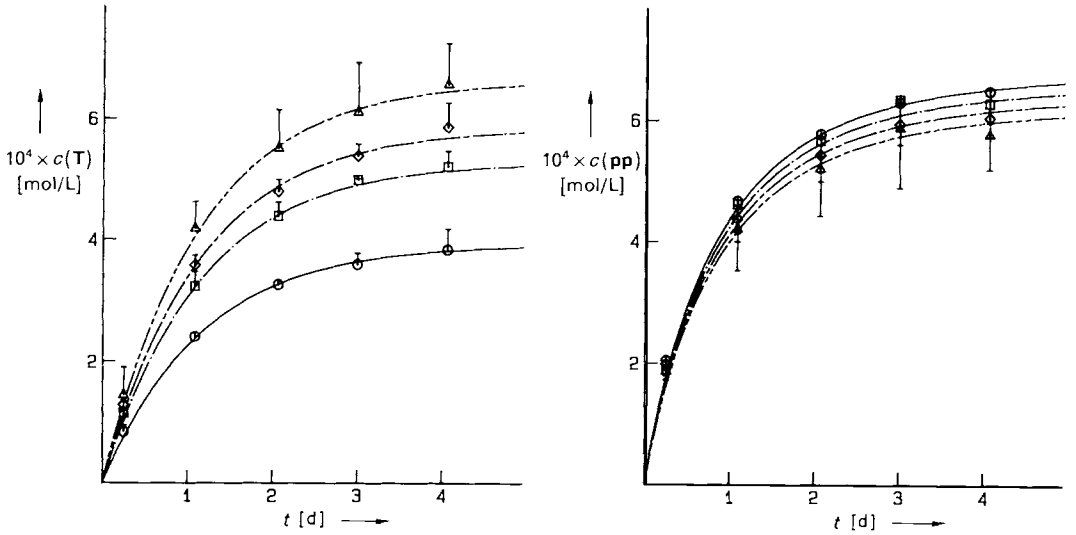


Fig. 1. Time course of template production (left) and pyrophosphate production (right) in reaction mixtures containing different initial concentrations of template. The points and error bars represent averaged concentrations and standard deviations, respectively, calculated from four series of experiments, each comprising four parallel experiments. Basic initial composition of reaction mixtures: 0.012 M **A**, 0.01 M **B**, 0.2 M CDI, 0.1 M 2-morpholinoethanesulfonic acid (pH 6.15), 0.05 M $MgCl_2$; initial template concentrations: ○ = 0 mM, □ = 0.2 mM, ◇ = 0.4 mM, △ = 0.8 mM. Each mixture (total volume: 10 μL) was prepared in a small test tube and then transferred into several 1 μL precision capillaries (Micro Caps). The capillaries were stored in a dessicator at 0°C and constant humidity for the reaction times given in the figure. HPLC samples were prepared by quenching the reaction mixtures with solutions of 10^{-3} M ethylenediamine-*N,N,N',N'*-tetraacetic acid at pH 11 (total volume, 4 mL; injection volume, 1 mL). Separations were performed on an RPC-5 column at pH 12 using a linear gradient of $NaClO_4$ (0–0.05 M, 50 min, flow rate: 1 mL/min) [2]. UV absorbance was monitored at 254 nm. Concentrations are calculated from peak integrals, no correction is made for hypochromicity.

tion. Under the same conditions, the rate of formation of the pyrophosphate **pp** (Fig. 1, right) is almost independent of $c_o(\mathbf{T})$. However, an increase in $c_o(\mathbf{T})$ slightly decreases the rate of formation of **pp**, simply because **T** and **pp** compete for the same activated species $\overset{*}{\mathbf{A}}$. As the combined yield of both products after four days is less than 12% (relative to **A**) in all experiments, the decreasing slope of the curves cannot be due to the consumption of the trinucleotides, but must be caused by the hydrolysis of the carbodiimide.

The initial rate of template formation, $[\mathrm{d}c(\mathbf{T})/\mathrm{d}t]_{\text{initial}}$, can be described using an empirical rate law which splits the rate of template formation, $[\mathrm{d}c(\mathbf{T})/\mathrm{d}t]_{\text{initial}}$, into a non-autocatalytic term (k_b) and an autocatalytic term comprising the constant k_a and the template concentration $c_o(\mathbf{T})$ with its reaction order p.

$$[\mathrm{d}c(\mathbf{T})/\mathrm{d}t]_{\text{initial}} = k_a c_o(\mathbf{T})^p + k_b$$

Using least-square approximation techniques, the constants k_a and k_b were calculated for varying reaction orders p from the initial rates of template formation. The best fit of parameters was obtained for p = .48. Assuming a reaction order of p = 1/2, approximation yields a set of parameters that fit the rates to only a slightly lesser extent: $k_a = 9.48 \times 10^{-8}\ \mathrm{M}^{1/2}\ \mathrm{s}^{-1}$, $k_b = 3.83 \times 10^{-9}\ \mathrm{M\ s}^{-1}$. As a consequence, the initial rate of template formation follows the square root of $c_o(\mathbf{T})$ as shown in Figure 2.

Autocatalysis in template production can be explained by the reaction mechanism shown in Figure 3, in which a mixed complex $\overset{*}{\mathbf{A}}:\mathbf{B}:\mathbf{T}$ is reversibly formed from the trimer compounds $\overset{*}{\mathbf{A}}$ and **B** and the template **T** through complementary base-pairing. Template-directed condensation in $\overset{*}{\mathbf{A}}:\mathbf{B}:\mathbf{T}$ yields a self-complementary duplex **T** : **T**. This duplex can dissociate to form two template molecules

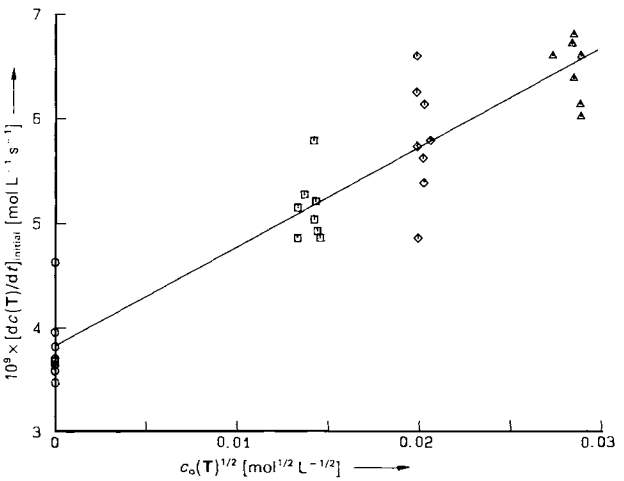


Fig. 2. Initial rate of template production, $[\mathrm{d}c(\mathbf{T})/\mathrm{d}t]_{\text{initial}}$, versus square root of initial template concentration, $c_o(\mathbf{T})^{1/2}$. Reaction conditions and analytical techniques as given in the legend of Figure 1. The initial rates shown are the slopes of template formation during the first 12-h period of linear evolution. The line drawn represents the solution of parameters k_a and k_b for a reaction order of p = 1/2, comprising all data-pairs given.

T, which again can undergo mixed complementary association with $\overset{*}{\mathbf{A}}$ and **B**, thus restarting the catalytic cycle. From thermodynamic and kinetic data for similar oligonucleotides[10] it can be concluded that, under the reaction conditions chosen, most template molecules should be present as **T** : **T**, a small fraction as $\overset{*}{\mathbf{A}}:\mathbf{B}:\mathbf{T}$, and only a very small fraction as single-stranded species **T**. Furthermore, since the rates of all reversible steps (in particular the dissociation rate of **T** : **T**) are supposed to be fast compared with the rate of phosphodiester formation, the olig-

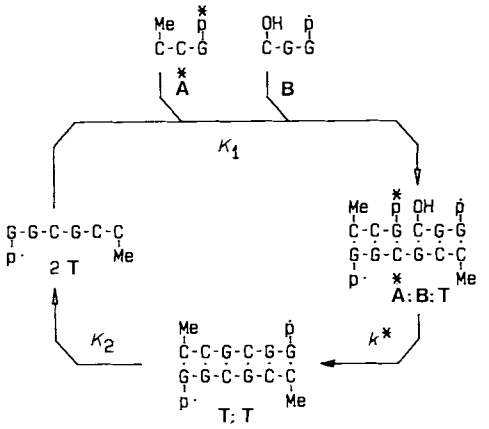


Fig. 3. Reaction mechanism of autocatalytic template production. Open arrows indicate reversible reactions, the closed arrow represents an irreversible reaction.

omers should be in equilibrium with respect to complex formation. Then, the equilibrium concentration of $\overset{*}{\mathbf{A}}:\mathbf{B}:\mathbf{T}$ can be expressed in terms of the equilibrium concentration of $\mathbf{T}:\mathbf{T}$. With

$$K_1=\frac{[\overset{*}{\mathbf{A}}:\mathbf{B}:\mathbf{T}]}{[\overset{*}{\mathbf{A}}][\mathbf{B}][\mathbf{T}]} \quad \text{and} \quad K_2=\frac{[\mathbf{T}:\mathbf{T}]}{[\mathbf{T}]^2}$$

the rate of template-directed condensation, which is first order in $\overset{*}{\mathbf{A}}:\mathbf{B}:\mathbf{T}$, is given by

$$\frac{d[\mathbf{T}:\mathbf{T}]}{dt}=k^*[\overset{*}{\mathbf{A}}:\mathbf{B}:\mathbf{T}]=k^*K_1K_2^{-1/2}[\overset{*}{\mathbf{A}}][\mathbf{B}][\mathbf{T}:\mathbf{T}]^{1/2}$$

Accordingly, the reaction order for $\mathbf{T}:\mathbf{T}$ formation in terms of $\mathbf{T}:\mathbf{T}$ is expected to be 1/2. Since the equilibrium concentration, $[\mathbf{T}:\mathbf{T}]$, is supposed to be only slightly different from half of the total template concentration $c(\mathbf{T})$, the equation gives an approximate solution for k_a in the autocatalytic term of the empirical rate law.

The rationale of this work is to demonstrate that, in fact, self-replication occurs without the help of any enzyme[11] in a *chemical* model system composed of simple oligonucleotides. Although the system chosen is not very efficient in terms of its autocatalytic rate, autocatalysis is clearly evident. Further experiments must show whether autocatalysis also occurs when using other oligonucleotides, and whether autocatalysis can be enhanced employing appropriate "environmental conditions" and "energy sources." If so, it can be expected that, under certain conditions, some interesting self-organization phenomena might show up, similar to natural selection processes in biological systems.[12]

Received: June 20, 1986;
revised: July 21, 1986 [Z 1825 IE]
German version: *Angew. Chem. 98* (1986) 932

[1] R. Naylor, P. T. Gilham, *Biochemistry 5* (1966) 2723.
[2] L. E. Orgel, R. Lohrmann, *Acc. Chem. Res. 7* (1974) 368; R. Lohrmann, L. E. Orgel, *J. Mol. Biol. 142* (1980) 555; T. Inoue, L. E. Orgel, *Science 219* (1983) 859; C. B. Chen, T. Inoue, L. E. Orgel, *J. Mol. Biol. 181* (1985) 271.
[3] T. Inoue, G. F. Joyce, K. Grzeskowiak, L. E. Orgel, J. M. Brown, C. B. Reese, *J. Mol. Biol. 178* (1984) 669.
[4] N. H. Horowitz, S. L. Miller, *Fortschr. Chem. Org. Naturst. 20* (1962) 423; S. L. Miller, L. E. Orgel: *The Origins of Life on the Earth*, Prentice Hall, Englewood Cliffs, NJ, USA 1974.
[5] M. Eigen, P. Schuster: *The Hypercycle*, Springer, Berlin 1979.
[6] H. Kuhn, J. Wasser, *Angew. Chem. 93* (1981) 495; *Angew. Chem. Int. Ed. Engl. 20* (1981) 500.
[7] W. A. Denny, W. Leupin, D. R. Kearns, *Helv. Chim. Acta 65* (1982) 2372, and references cited therein.
[8] Triethylammonium salts: ^{1}H-NMR (360 MHz, D_2O, 0.1 M NaCl, 0.1 M NaD_2PO_4/Na_2DPO_4, pD = 7.5): **A**: δ = 8.04 (s; 8-H, Gua), 7.65, 7.59 (d; 6-H, Cyt), 6.24, 6.16, 6.06 (t; 1'-H), 5.96, 5.91 (d; 5-H, Cyt), 3.36 (s; 5'-OCH_3); **B**: δ = 8.00, 7.81 (s; 8-H, Gua), 7.46 (d; 6-H, Cyt), 7.31, 6.98, 7.18, 7.22 (ABCD; *o*-chlorophenyl), 6.17, 6.01, 5.87 (t; 1'-H), 5.90 (d; 5-H, Cyt); **T**: δ = 7.98, 7.86, 7.86 (s; 8-H, Gua), 7.67, 7.58, 7.47 (d; 6-H, Cyt), 7.10–7.42 (m; *o*-chlorophenyl), 3.39 (s; 5'-OCH_3).
[9] Z. A. Shabarova, N. G. Dolinnaya, V. L. Drutsa, N. P. Melinkova, A. A. Purmal, *Nucleic Acid Res. 9* (1981) 5747; Z. A. Shabarova, M. G. Ivanovskaya, M. G. Isaguliants, *FEBS Lett. 154* (1983) 288.
[10] N. G. Dolinnaya, E. S. Gromova, *Usp. Khim. 52* (1983) 138; S. M. Freier, D. D. Albergo, D. H. Turner, *Biopolymers 22* (1983) 1107.
[11] Enzymatic replication of RNA in vitro has been studied extensively using Qβ-RNA/Qβ-replicase: see C. K. Biebricher, *Evol. Biol. 16* (1983) 1.
[12] According to *Eigen* and *Schuster*, systems composed of self-replicating molecules that compete for their constituents under the constraint of constant organization should show Darwinian selection behavior if the reaction order of autocatalysis is larger than zero and smaller than or equal to one [5], p. 12.

Asymmetric Elimination with High Induction: Synthesis of 1-Alkenylsulfoximides with Axial and Central Chirality**

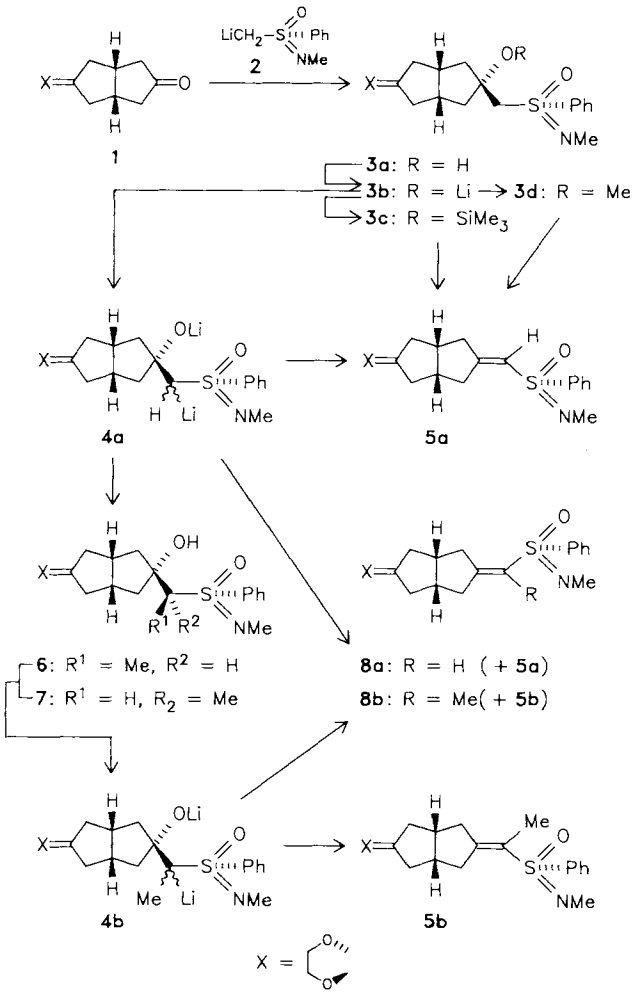
By *Irene Erdelmeier, Hans-Joachim Gais,** and *Hans J. Lindner*

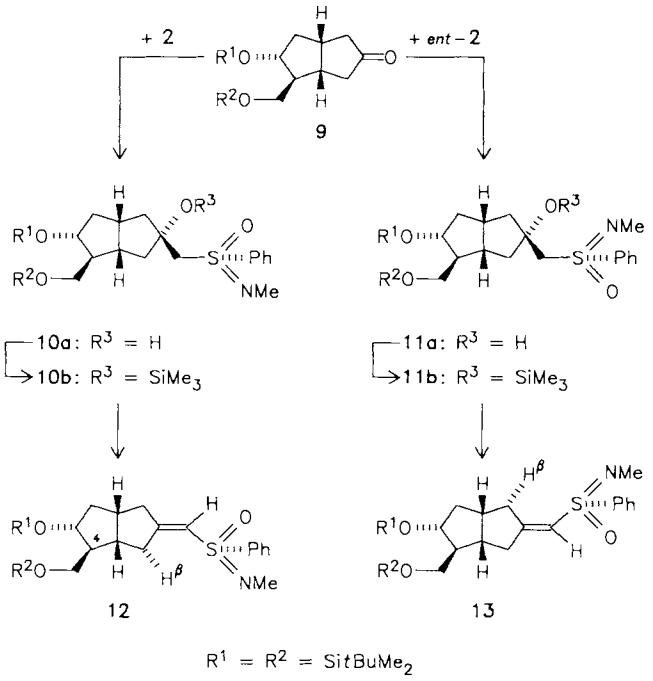
Asymmetric *eliminations* with high induction to give chiral alkenes are rarely observed;[1] the few known examples are characterized by removal of a chiral group with loss of chirality[1a,b] and/or transfer of chirality.[1c] We report here the synthesis of the axially chiral alkenylsulfoximides **5a**, **b** and **17** from the β-hydroxysulfoximides **3a**, **6/7**, and **15a**, respectively, which involves an asymmetric elimination that takes place with high diastereotopic differentiation and without loss of chirality. The stereoselective *carbonylolefination* of the ketone **9** to give either the (*Z*)- or the (*E*)-alkenylsulfoximide **12** or **13**, respectively, exemplifies the application of this reaction. Asymmetric carbonylolefinations with high and moderate selectivity to give axially chiral alkenes have been achieved previously by Horner–Emmons[2a] and Wittig reactions,[2b] respectively.

Selective *exo* addition [−78 °C, tetrahydrofuran (THF)] of the lithiosulfoximide **2**[3,4] to the ketone **1**[5] gave the β-hydroxysulfoximide **3a**[6a] in 96% yield and with ≥98% diastereoselectivity (*ds*). The surprisingly smooth silylation (−78 °C→25 °C, THF) of the lithium alkoxide **3b** with Me_3SiCl afforded the β-siloxysulfoximide **3c** in >95% yield. When this compound was treated with *n*-butyllithium (*n*BuLi) at −78 °C (molar ratio 1:1) in THF, asymmetric elimination of $LiOSiMe_3$ took place with high induction to give the (*S,aR*)-alkenylsulfoximide **5a**,[6b,7] which could be isolated in 91% yield and with ≥98% *ds*. From **1** and *rac*-**2**, *rac*-**5a** (90%) was also obtained with

[*] Prof. Dr. H.-J. Gais [+], Dipl.-Ing. I. Erdelmeier [+], Prof. Dr. H. J. Lindner
Institut für Organische Chemie und Biochemie der Technischen Hochschule
Petersenstrasse 22, D-6100 Darmstadt (FRG)
[+] Present address:
Institut für Organische Chemie und Biochemie der Universität
Albertstrasse 21, D-7800 Freiburg (FRG)

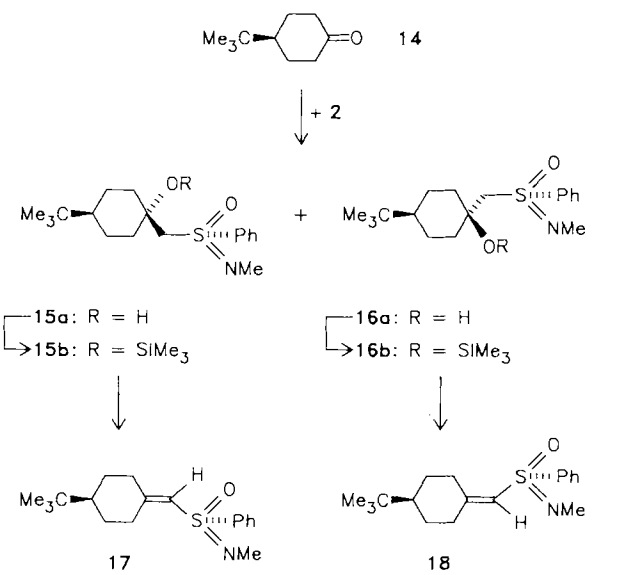
[**] This work was supported by the Fonds der Chemischen Industrie and by Schering AG, Berlin. *I. E.* thanks the Stiftung Stipendien-Fonds des Verbandes der Chemischen Industrie for a fellowship. We thank Prof. Dr. *H. Günther*, Siegen, for NOE data and Dr. *S. Braun* for the 2D ^{1}H-NMR spectra.





≥98% *ds*.[8] Interestingly, the extent and direction of the asymmetric induction observed in the elimination reaction of **3a** did not change when the dilithium compound **4a**, obtained by metalation of **3a** (2 *n*BuLi, −30°C, THF), was allowed to react with Me_3SiCl (−70°C); **5a** was isolated in 69% yield and with ≥98% *ds*. This was also true for the diastereomeric methyl derivatives **6**[6c] and **7**,[6d] which were obtained in 89% yield in a ratio of 3 : 1 by methylation (MeI, 0°C, THF, HMPA) of **4a**. The mixture of the two stereoisomers underwent metalation (2 *n*BuLi, 0°C, THF) to give the dilithium compound **4b** and subsequent reaction with Me_3SiCl (−30°C) to give the alkenylsulfoximide **5b**[6e] in 73% yield and with ≥98% *ds*. In contrast, we obtained mixtures of the diastereomers **5a/8a** (70%, 4 : 1) and **5b/8b** (75%, 1 : 1) when **4a** and **4b**, respectively, underwent titanation (−30°C, THF) with $Cl_2Ti(OiPr)_2$.

This asymmetric carbonylolefination also allowed us to selectively synthesize the (*Z*)- and (*E*)-alkenylsulfoximides **12** and **13**, respectively, which are potential precursors for the selective synthesis of the (5*E*) isomers of carbaprostacyclins,[9] from the ketone **9**.[10] Selective *exo* addition (−78°C, THF) of **2** to **9** to give the β-hydroxysulfoximide **10a**[6f] (93%, ≥98% *ds*), silylation (1 *n*BuLi, −78°C, THF; Me_3SiCl, −70°C→25°C) to give the β-siloxysulfoximide **10b**, and, finally, elimination (1 *n*BuLi, −78°C, THF) afforded the (*Z*)-alkenylsulfoximide **12**[6g,7] in 96% yield and with ≥98% *ds*. On the other hand, when *ent*-**2**[4] was added to **9** to give **11a**[6h] (93%, ≥98% *ds*) and this compound was then silylated to give **11b** and finally treated with *n*BuLi (−78°C, THF), the (*E*)-alkenylsulfoximide **13**[6i] was obtained, as expected, in 91% yield and likewise with ≥98% *ds*. Thus, the extent and direction of the asymmetric induction in the elimination reactions of **10b** and **11b** are independent of the chirality center in the 4-position and only determined by the choice of **2** or *ent*-**2** (reagent control). Unequivocal confirmation of the (*Z*) configuration of **12** (S(O)(NMe)Ph and R^2OCH_2 groups in *syn* positions) was achieved by NOE experiments and that of the (*E*) configuration of **13** (*anti* arrangement of the groups) on the basis of 2D ^{1}H-NMR spectra; in each case, the determination of configuration was based on the low-field shift of the resonance of H^β of the methylene group in the *syn* position, which is caused by the anisotropy effect of the sulfoximide functionality. Based on these results, the absolute configuration of the alkenylsulfoximides **5a** and **5b** was assigned.



Interesting differences in selectivity were found in the elimination reactions of the diastereomeric β-siloxysulfoximines **15b** and **16b**, which were obtained by addition[11a] of **2** to the ketone **14** to give the diastereomeric β-hydroxysulfoximines **15a** and **16a**[11b] followed by silylation. Whereas the elimination reaction of the *trans* diastereomer **15b** with *n*BuLi led to the (*S,aS*)-alkenylsulfoximide **17** (93%)[6j] with ≥98% *ds*, the elimination reaction of the *cis* diastereomer **16b** gave a mixture (94%) of the chromatographically separable (*S,aR*)- and (*S,aS*)-alkenylsulfoximides **18**[6k] and **17** in a ratio of 2.5 : 1.

The absolute configuration of **17** was determined by X-ray structure analysis,[12] in combination with the known (*S*) configuration of **2**,[13] to be (*S,aS*) (Fig. 1).

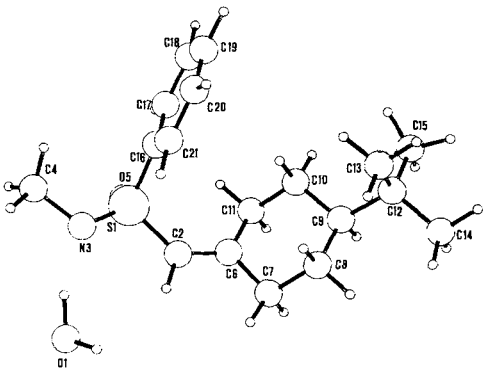
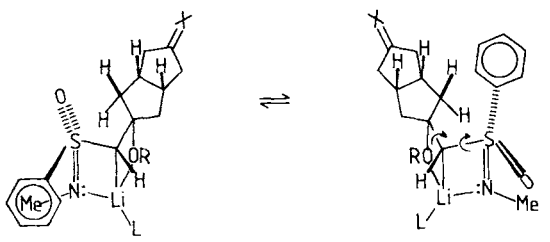


Fig. 1. Crystal structure of **17**·H_2O [12]. Selected bond lengths [Å] and bond angles [°]: S1-C2 1.741(7), S1-O5 1.427(5), S1-N3 1.534(5), S1-C16 1.804(5), C2-C6 1.353(8), C4-N3 1.504(8); C2-C6-C11 126.6(6), C2-C6-C7 119.4(7); N3-S1-C2-C6 −174(2), S1-C2-C6-C7 173(2), S1-C2-C6-C11 0(2).

We ascribe the similar directions and extents of asymmetric induction in the elimination reactions of **3**, **4**, **10**, and **15**—using **3c** and **4a** as examples and taking into consideration the crystal structure of **2** and the configurational stability of lithioalkylsulfoximides at the α-C atom[3]—to the following factors:

1. Initial metalation of **3c** to give the lithiosulfoximide **19** (Scheme 1), which is also presumably formed upon silylation of **4a** via *C/O* silyl migration[14] following *C*-silylation.

2. The establishment of a rapid equilibrium between the diastereomers **19A** and **19B**, even at low temperatures, on account of the low energy barrier for the configurational change at the anionic C atom in lithioalkylsulfoximides.[3]



Scheme 1. R = $SiMe_3$, X = $-OCH_2CH_2O-$, L = ligand.

3. The more rapid elimination of $LiOSiMe_3$ in **19A** than in **19B**, because the achievement of coplanarity of the p orbital on the anionic C atom and the siloxy group in **19B** is presumably more strongly hindered by the interaction between the phenyl and the *pro-R* methylene group than in the case of **19A** by the interaction between the O atom and the *pro-S* methylene group.[15]

Received: April 28, 1986;
revised: July 10, 1986 [Z 1749 IE]
German version: *Angew. Chem. 98* (1986) 912

CAS Registry numbers:
1, 51716-62-2; **2**, 34261-66-0; (*ent*)-**2**, 104264-21-3; (*rac*)-**2**, 80374-26-1; **3a**, 104264-16-6; **3b**, 104172-91-0; **3c**, 104172-92-1; **3d**, 104173-07-1; **4a**, 104172-94-3; **4b**, 104172-96-5; **5a**, 104172-93-2; (*rac*)-**5a**, 104264-17-7; **5b**, 104172-97-6; **6**, 104172-95-4; 7, 104264-18-8; **8a**, 104264-19-9; **8b**, 104264-20-2; **9**, 104172-98-7; **10a**, 104172-99-8; **10b**, 104196-36-3; **11a**, 104173-01-5; **11b**, 104173-02-6; **12**, 104173-00-4; **13**, 104173-03-7; **14**, 98-53-3; **15a**, 104264-22-4; **15b**, 104173-04-8; **16a**, 104264-23-5; **16b**, 104173-05-9; **17**, 104173-06-0; **17**·H_2O, 104264-25-7; **18**, 104264-24-6.

[1] a) G. Solladié, R. G. Zimmermann, R. Bartsch, H. M. Walborsky, *Synthesis 1985*, 662, and literature cited therein; G. Solladié, *Chem. Scr. 25* (1985) 149; b) S. I. Goldberg, M. S. Sahli, *J. Org. Chem. 32* (1967) 2059; c) A. C. Cope, C. F. Howell, A. Knowles, *J. Am. Chem. Soc. 84* (1962) 3190; d) see also S. I. Goldberg, *Sel. Org. Transform. 1* (1970) 363; J. D. Morrison, H. S. Mosher: *Asymmetric Organic Reactions*, Prentice-Hall, Englewood Cliffs, NJ (USA) 1976.

[2] a) S. Hanessian, D. Delorme, S. Beaudoin, Y. Leblanc, *J. Am. Chem. Soc. 106* (1984) 5754; S. Hanessian, *Chem. Scr. 25* (1985) 5; b) H. J. Bestmann, J. Lienert, *Angew. Chem. 81* (1969) 751; *Angew. Chem. Int. Ed. Engl. 8* (1969) 763; H. J. Bestmann, personal communication, Oct. 19, 1984.

[3] H.-J. Gais, I. Erdelmeier, H. J. Lindner, J. Vollhardt, *Angew. Chem. 98* (1986) 914; *Angew. Chem. Int. Ed. Engl. 25* (1986) 938.

[4] The (*S*)- and (*R*)-*S*-methyl-*S*-phenylsulfoximides required as starting materials for the preparation of **2** and *ent*-**2**, respectively, are readily available enantiomerically pure by resolution of the racemate with (+)- and (−)-10-camphorsulfonic acid (Aldrich): C. R. Johnson, C. W. Schroeck, *J. Am. Chem. Soc. 95* (1973) 7418. The *ee* values of the sulfoximides were determined by ^{1}H-NMR spectroscopy in the presence of 20 mol-% Eu(tfc)$_3$ in $CDCl_3$ on the basis of the resonances of the methyl groups ($\Delta\Delta\delta = 0.4$ ppm) and the *o*-H atoms of the phenyl groups.

[5] R. Lok, J. K. Coward, *J. Org. Chem. 39* (1974) 2377.

[6] a) M.p. = 132–133 °C, $[\alpha]_D^{20}$ +36.4 (*c* = 1.6, acetone); b) $[\alpha]_D^{20}$ −64.9 (*c* = 1.5, CH_2Cl_2); c) m.p. 142 °C, $[\alpha]_D^{20}$ +78.4 (*c* = 0.8, acetone); d) m.p. = 110 °C, $[\alpha]_D^{20}$ +45.3 (*c* = 0.5, acetone); e) $[\alpha]_D^{20}$ −85.6 (*c* = 0.5, CH_2Cl_2); f) m.p. = 65–66 °C, $[\alpha]_D^{20}$ +13.0 (*c* = 0.24, acetone); g) m.p. = 49–51 °C, $[\alpha]_D^{20}$ −79.0 (*c* = 0.63, acetone); h) m.p. = 67–68 °C, $[\alpha]_D^{20}$ −42.0 (*c* = 1.0, acetone); i) $[\alpha]_D^{20}$ +59.0 (*c* = 0.38, acetone); j) m.p. = 72 °C, $[\alpha]_D^{20}$ +46.0 (*c* = 0.5, acetone); k) $[\alpha]_D^{20}$ −99.0 (*c* = 0.25, acetone). All new compounds gave correct elemental analyses and fitting spectra (^{1}H- and ^{13}C-NMR, MS).

[7] Slow allyl isomerization of **5a** and **12** occurs for the substances both in pure form and on silica.

[8] The silyl group is not crucial for the high *ds* value, as revealed by the elimination reaction of β-methoxysulfoximide **3d** (73%), which was synthesized by methylation [MeI, hexamethylphosphoric triamide (HMPA), THF, 0 °C] of **3b**; after reaction of **3d** with *n*BuLi (−78 °C, THF), **5a** was isolated in 82% yield and with ≥98% *ds*.

[9] R. C. Nickolson, M. H. Town, H. Vorbrüggen, *Med. Res. Rev. 5* (1985) 1.

[10] **9**: $[\alpha]_D^{20}$ −27.5 (*c* = 0.50, acetone); synthesis by silylation (91%) of **9**, R^1 = H instead of $SiMe_2t$Bu. W. Skuballa, H. Vorbrüggen, *Angew. Chem. 93* (1981) 1080; *Angew. Chem. Int. Ed. Engl. 20* (1981) 1046. Asymmetric synthesis of **9**: H.-J. Gais, W. Ball, unpublished.

[11] a) C. R. Johnson, J. R. Zeller, *Tetrahedron 40* (1984) 1225; b) C. R. Johnson, C. W. Schroeck, J. R. Shanklin, *J. Am. Chem. Soc. 95* (1973) 7424.

[12] **17**·H_2O: orthorhombic, space group $P2_12_12$, *a* = 17.361(5), *b* = 17.244(5), *c* = 6.223(8) Å, *V* = 1863 Å^3, *Z* = 4, ρ_{calcd} = 1.107 g/cm^3; 4° ≤ θ ≤ 62.5° ($Cu_{K\alpha}$, λ = 154.18 pm, Weissenberg diffractometer), 1660 reflections, Lorentz and polarization correction, positions of the H atoms calculated for the ideal geometry, positions of the H atoms of the crystal water determined by difference Fourier synthesis, anisotropic refinement of the heavy atoms, *R* = 0.061 for 1533 unique structure factors $|F| > 3\sigma_F$. The sulfoximide molecules are linked along the *c* axis by hydrogen bonds to the crystal water. Surprisingly, hydrogen bonds are formed between the oxygen of the crystal water and N3 [N3···O1 2.888 Å], on the one hand and O5′ [O5′···O1 2.986 Å], on the other. Further details of the crystal structure investigation may be obtained from the Fachinformationszentrum Energie, Physik, Mathematik GmbH, D-7514 Eggenstein-Leopoldshafen 2 (FRG), on quoting the depository number CSD-52077, the names of the authors, and the journal citation.

[13] E. V. Johnson, C. R. Johnson, *J. Am. Chem. Soc. 93* (1971) 5308, and references cited therein.

[14] K. Yamamoto, Y. Tomo, S. Suzuki, *Tetrahedron Lett. 21* (1980) 2861.

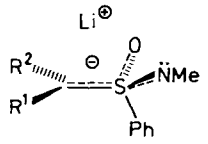
[15] The "inverse Peterson olefination" used for the synthesis of **5**, **12**, **13**, **17**, and **18** is particularly successful for readily enolizable carbonyl compounds. H.-J. Gais, I. Erdelmeier, unpublished; see also I. Erdelmeier, H.-J. Gais, *Tetrahedron Lett. 26* (1985) 4359.

 © VCH Verlagsgesellschaft mbH, D-6940 Weinheim, 1986 0570-0833/86/1010-0937 $ 02.50/0

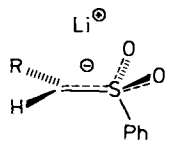
Lithium-Coordinated α-Sulfonimidoyl Carbanions: Crystal Study of [(*S*)-(*N*-Methyl-*S*-phenylsulfonimidoyl)methyllithium]$_4$ · 2(tmeda) and Configurative Stability of [(*N*-Methyl-*S*-phenylsulfonimidoyl)isopropyllithium]**

By *Hans-Joachim Gais,** *Irene Erdelmeier, Hans J. Lindner,* and *Jürgen Vollhardt*

Lithioalkylsulfoximides such as **1** have become firmly established as analogues of lithioalkylsulfones such as **2**, with an optically stable center of chirality at the S atom, in the arsenal of methods used in asymmetric synthesis.[1] In contrast to **2**,[2] almost no information is available on the structure of **1**.[2b,c] This fact, along with investigations on



1a, $R^1 = R^2 = H$
1b, $R^1 = R^2 = Me$



2a, R = H
2b, R = Ph
2c, R = CH=CH$_2$

the asymmetric induction in the elimination reactions of β-siloxylithioalkylsulfoximides,[3] prompted us to determine the crystal structure of [(*S*)-(*N*-methyl-*S*-phenylsulfonimidoyl)methyllithium]$_4$ · 2(tmeda) **3** (tmeda = tetramethylethylenediamine) and the configurative stability of **1b** at the α-C atom. Compound **3** was prepared by metalation of (*S*)-*N*,*S*-dimethyl-*S*-phenylsulfoximide with *n*-butyllithium (*n*BuLi) in TMEDA.[4] The single-crystal X-ray structure analysis of **3**[5] (Fig. 1) revealed a tetramer of **1a** with approximate C_2 symmetry and having two pairs each of differently coordinated lithium ions and (*S*)-(*N*-methyl-*S*-phenylsulfonimidoyl)methyl anions. The coordination of two lithium ions by TMEDA and two oxygen atoms of two anions [average Li···N 2.10(5) Å, Li···O1 1.90(5) Å] corresponds to that found for **2a** and **2b**.[2a] The two other lithium ions in close proximity to each other [Li···Li 2.78(5) Å] are each coordinated by three nitrogen atoms of the sulfoximide groups [average Li···N 2.09(5) Å] and—in contrast to **2a-c**[2a]—by one carbon atom of each of the methylene groups [average Li···C 2.49(5) Å]: S1, N11, Li3, and C71 as well as S3, N13, Li4, and C73 each form four-membered chelate rings. Each of the two other methylene carbon atoms, C72 and C74, has contact to the two central lithium ions Li3 and Li4 [average Li···C 3.24(4) Å]. The S-$C_{methylene}$ bonds [average 1.64(2) Å], like the bond in **2a**[2a] [1.608(3) Å], are significantly shorter than that in *S*-methylsulfoximides (average of nine compounds: 1.74 Å[7]), thus pointing to the double-bond character of this bond. The methylene carbon, the sulfur, the nitrogen, and the methyl carbon atoms lie nearly in the same plane [average of the C7-S-N1-C8 dihedral angles 177(6)°].

Information about the structure of **1** in solution—especially about the nature of the bond between the anionic C atom and the sulfonimidoyl group—was expected to be obtained from the determination of the energy barrier for diastereotopomerization[8] ($\Delta G^{\ddagger}_{top}$) of the methyl groups in **1b**. The diastereotopomerization is effected by rotation around the C-S bond for a planar configuration of the carbanionic center and by rotation and inversion for a pyramidal configuration.

The 75.5-MHz ^{13}C-NMR spectrum of [^{13}C-9, ^{13}C-10]-**1b** (degree of labeling 99%) in [D$_8$]THF[9] is temperature dependent.[10] At room temperature, an averaged signal at $\delta = 20.5$, which is due to the rapid exchange of the diastereotopic methyl groups, is found for **1b**. Coalescence is observed at −70 °C; at −103 °C, separated signals are found at $\delta = 19.4$ and 22.4. From the line separation of the signals of 220 Hz, $\Delta G^{\ddagger}_{top}$ was calculated to be 9.2 ± 0.2 kcal/mol for **1b** at the coalescence point. This reveals that the carbanions of **1** with $R^1 \neq R^2$ are not configurationally stable at the anionic C atom, even at low temperatures.[11]

Received: May 26, 1986;
revised: July 10, 1986 [Z 1789 IE]
German version: *Angew. Chem. 98* (1986) 914

CAS Registry numbers:
1a, 71098-63-0; **1b**, 104091-59-0; **3**, 104091-60-3.

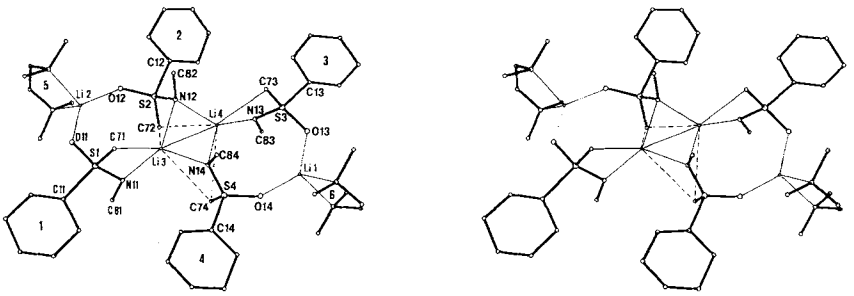


Fig. 1. Stereoview of the crystal structure of **3** (H atoms omitted). Selected distances [Å] and angles [°]: C11-S1 1.83(3), C12-S2 1.89(2), C13-S3 1.82(2), C14-S4 1.86(2), C71-S1 1.67(2), C72-S2 1.56(2), C73-S3 1.66(2), C74-S4 1.70(2), C71-Li3 2.53(5), C72-Li3 3.03(5), C72-Li4 3.24(5), C73-Li4 2.44(4), C74-Li3 3.34(5), C74-Li4 3.37(5), N11-Li3 2.01(4), N12-Li3 2.28(4), N12-Li4 2.06(5), N13-Li4 1.97(5), N14-Li3 2.05(4), N14-Li4 2.21(4), Li3-Li4 2.78(5); C71-S1-N11-C81 175(6), C72-S2-N12-C82 −180(6), C73-S3-N13-C83 173(6), C74-S4-N14-C84 180(6).

[*] Prof. Dr. H.-J. Gais [+], Dipl.-Ing. I. Erdelmeier [+], Prof. Dr. H. J. Lindner, Dipl.-Ing. J. Vollhardt [+]
Institut für Organische Chemie und Biochemie der Technischen Hochschule
Petersenstrasse 22, D-6100 Darmstadt (FRG)

[+] Present address:
Institut für Organische Chemie und Biochemie der Universität
Albertstrasse 21, D-7800 Freiburg (FRG)

[**] This work was supported by the Fonds der Chemischen Industrie and the Deutsche Forschungsgemeinschaft. *I. E.* thanks the Stiftung Stipendienfonds des Verbandes der Chemischen Industrie for a fellowship. We thank Dr. *S. Braun* for the NMR spectra.

[1] C. R. Johnson, J. R. Zeller, *Tetrahedron 40* (1984) 1225, and references cited therein; C. R. Johnson, *Aldrichim. Acta 18* (1985) 3, and references cited therein.

[2] a) Crystal structure analysis: H.-J. Gais, H. J. Lindner, J. Vollhardt, *Angew. Chem. 97* (1985) 865; *Angew. Chem. Int. Ed. Engl. 24* (1985) 859, and references cited therein (**2a**); G. Boche, M. Marsch, K. Harms, G. M. Sheldrick, *ibid. 97* (1985) 577 and *24* (1985) 573 (**2b**); H.-J. Gais, J. Vollhardt, H. J. Lindner, *ibid. 98* (1986) 916 and *25* (1986) 939 (**2c**); b) NMR investigations: G. Chassaing, A. Marquet, *Tetrahedron 34* (1978) 1399; c) C-H-acidity measurements: F. G. Bordwell, J. C. Branca, C. R. Johnson, N. R. Vanier, *J. Org. Chem. 45* (1980) 3884; d) reactions at the anionic C atom: J. N. Roitman, D. J. Cram, *J. Am. Chem. Soc. 93* (1971)

2225; E. J. Corey, T. H. Lowry, *Tetrahedron Lett. 1975*, 193; e) ab initio calculations: D. A. Bors, A. Streitwieser, Jr., *J. Am. Chem. Soc. 108* (1986) 1397; S. Wolfe, L. A. LaJohn, D. F. Weaver, *Tetrahedron Lett. 25* (1984) 2863.

[3] I. Erdelmeier, H.-J. Gais, H.-J. Lindner, *Angew. Chem. 98* (1986) 912; *Angew. Chem. Int. Ed. Engl. 25* (1986) 935.

[4] *Experimental procedure:* (*S*)-*N*,*S*-Dimethyl-*S*-phenylsulfoximide (240 mg, 1.42 mmol) was dissolved in 3 mL of anhydrous TMEDA and then treated with a solution of *n*BuLi (1.41 mmol) in *n*-hexane (0.9 mL) at 0°C. The resulting clear solution was concentrated to ca. 2 mL at room temperature and 10^{-3} torr. Precipitated **3** was redissolved by warming the solution to ca. 40°C. Upon cooling of the solution to room temperature, **3** crystallized out in the form of colorless rods or as rhombic platelets. The crystals were collected by filtration under N_2, washed with *n*-hexane, and dried (ca. 2 min at 25°C/10^{-3} torr).

[5] A single crystal was mounted in a glass capillary under argon. C_2, $a = 23.073(2)$, $b = 9.731(2)$, $c = 28.300(3)$ Å, $\beta = 119.88(6)°$, $V = 5509.3$ Å^3, $\rho_{calcd} = 1.125$ g·cm^{-3}, $\mu(Mo_{K\alpha}) = 1.7$ cm^{-1}, intensity measurement at room temperature, Siemens four-circle diffractometer, $Mo_{K\alpha}$ radiation, graphite monochromator, 4708 reflections ($1.5° \le \theta \le 22.5°$) measured, 2763 symmetry-independent reflections with $|F| \ge 4\sigma(F)$ [6], SHELX, direct methods, H atoms with the exception of those on C71, C72, C73, C74, and the methylene groups of the TMEDA molecules positioned on the basis of geometric arguments. 621 parameters, $R = 0.114$. Further details of the crystal structure investigation may be obtained from the Fachinformationszentrum Energie, Physik, Mathematik GmbH, D-7514 Eggenstein-Leopoldshafen 2 (FRG), on quoting the depository number CSD-52078, the names of the authors, and the journal citation.

[6] We thank Dr. *H. Paulus*, Institut für Physikalische Chemie, for this measurement.

[7] D. R. Band, T. A. Modro, L. R. Nassimbeni, J. Wieczorkowski, *Phosphorus Sulfur 22* (1985) 59; S. Neidle, D. Rogers, *J. Chem. Soc. B 1970*, 694; M. D. Cabezuelo, C. Foces-Foces, F. H. Cano, S. Garcia-Blanco, *Acta Crystallogr. B33* (1977) 3911.

[8] G. Binsch, E. L. Eliel, H. Kessler, *Angew. Chem. 83* (1971) 618; *Angew. Chem. Int. Ed. Engl. 10* (1971) 570.

[9] [$Me^{10}(Me^9)C^7$–S(O)(NMe^8)Ph^{1-6}]Li **1b**, 75.5-MHz ^{13}C-NMR data [[D_8]THF, 25°C, [D_8]THF ($\delta = 25.3$) int.] of **1b**. Values in curly brackets: 75.5-MHz ^{13}C-NMR data ($CDCl_3$, 25°C, TMS int.) of *N*-methyl-*S*-isopropyl-*S*-phenylsulfoximide. $\delta = 20.5$ (C-9, C-10) {15.6, 16.3}, 30.4 (C-8) {29.5}, 38.2 [$^1J(^{13}C,^{13}C) = 38.3$ Hz] (C-7) {55.7 [$^1J(^{13}C,^{13}C) = 34.8$ Hz}, 142.0 (C-1) {135.7}, 128.5, 127.8 (C-2, C-3, C-5, C-6) {129.3, 130.3}, 127.9 (C-4) {132.7}.

[10] Line-broadening but not coalescence was observed in the 300-MHz ^{1}H-NMR spectrum of **1a** and of **1b** in [D_8]THF down to −100°C.

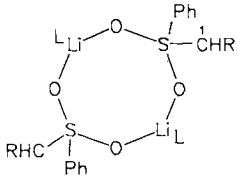
[11] The determination of the rate-limiting step in the topomerization of **1b** having a nonplanar configuration of the anionic C atom—rotation or inversion—is not possible on the basis of these results. However, on account of the reduced pyramidalization and the π delocalization of the carbanion, $\Delta G^{\neq}_{inv}$ should be smaller than $\Delta G^{\neq}_{rot}$ [2, 12].

[12] J. Kaneti, P. von R. Schleyer, T. Clark, A. J. Kos, G. W. Spitznagel, J. G. Andrade, J. B. Moffat, *J. Am. Chem. Soc. 108* (1986) 1481.

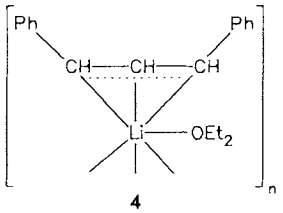
Solid-State and Solution Structure of α-(Phenylsulfonyl)allyllithium**

By *Hans-Joachim Gais,* Jürgen Vollhardt,* and *Hans J. Lindner*

Monometalated allylsulfones play an important role as reactive intermediates in organic synthesis,[1] for example, in the preparation of specifically functionalized diquinanes,[1b] in the synthesis of *di*lithiated (phenylsulfonyl)allyl compounds,[1b] and in asymmetric CC bond formation in the presence of chiral amines.[1c] In contrast, the question of their structure, which is not only important for the interpretation of stereochemical results, has not yet been answered; thus, no X-ray structure analyses or NMR investigations are available.[2]



1, R = H, L = tmeda
2, R = Ph, L = tmeda
3, R = CH=CH_2, L = diglyme



4

The crystal structures of two lithiated *alkyl*sulfones—[(phenylsulfonyl)methyllithium·(tmeda)]$_2$ **1**[3a] and [α-(phenylsulfonyl)benzyllithium·(tmeda)]$_2$ **2**[3b] (tmeda = tetramethylethylenediamine)—as well as of several allyllithium[4] compounds not containing sulfonyl groups, such as **4**,[4c] have been reported. Whereas the former display no C–Li contacts, but only O–Li contacts and short C–S bonds, η^3-complexation of the lithium ion and bond equalization in the anion is observed for the latter—with one exception.[4a]

Which type of bonding dominates for the α-(sulfonyl)allyllithium compounds, that with C–Li or that with O–Li contacts?

We report here on the crystal structure of [α-(phenylsulfonyl)allyllithium·(diglyme)]$_2$ **3** (diglyme = diethyleneglycol dimethyl ether), an allyllithium compound with an acceptor substituent that is important for synthesis,[5] and on the NMR investigations of the structure of α-(phenylsulfonyl)allyllithium **5a**[6] in solution.

Compound **3** was prepared by metalation of allylphenylsulfone with *n*-butyllithium (*n*BuLi) in diglyme.[7] The X-ray structure analysis of **3**[8] reveals dimers with a crystallographic center of inversion (Fig. 1), such as are also found in **1** and **2**, despite the change in the chelate ligand. The arrangement of the diglyme molecules results in a distorted trigonal-bipyramidal pentacoordination of the Li atoms by the O atoms; C-1 to C-3 of the allyl group bonded to the S atom lie *outside* the coordination sphere of Li. An interaction of the η^3-π-allyl type is not observed.

The anionic C-1 exhibits clear pyramidalization. H-1 and C-2 are displaced toward the phenyl ring, as revealed by the dihedral angle around the S1–C1 bond (Fig. 2). Similar results were found for the anionic C atom of **1** (Fig. 2)—although in that case more pronounced flattening was observed. The configuration corresponds to a nearly middle position between sp^3 and sp^2 hybridization.[9] However, one might have expected further flattening at C-1 in going from **1** to **3** on account of the additional conjugation of the sulfonyl carbanion with the double bond.[2,3b,10] The S1–C1 bond (1.668(8) Å) is longer than that in **1** and approximately the same length as that in **2**, but considerably shorter than in sulfones.[3] Together with the length of the bond between C-1 and C-2, that between C-2 and C-3, and the dihedral angle around the C1–C2 bond (Fig. 1), this indicates the presence of a conjugated π-electron system. Interestingly, the C1–C2–C3 angle is widened, as is the case in allyllithium compounds,[4] although, in contrast to such compounds, **3** exhibits no C–Li contacts.

[*] Prof. Dr. H.-J. Gais [+], Dipl.-Ing. J. Vollhardt [+], Prof. Dr. H. J. Lindner
Institut für Organische Chemie und Biochemie der Technischen Hochschule
Petersenstrasse 22, D-6100 Darmstadt (FRG)

[+] Present address:
Institut für Organische Chemie und Biochemie der Universität
Albertstrasse 21, D-7800 Freiburg (FRG)

[**] This work was supported by the Fonds der Chemischen Industrie. We thank Dr. *S. Braun* for the NMR spectra and Dr. *H. Paulus*, Institut für Physikalische Chemie, for the unit cell parameters.

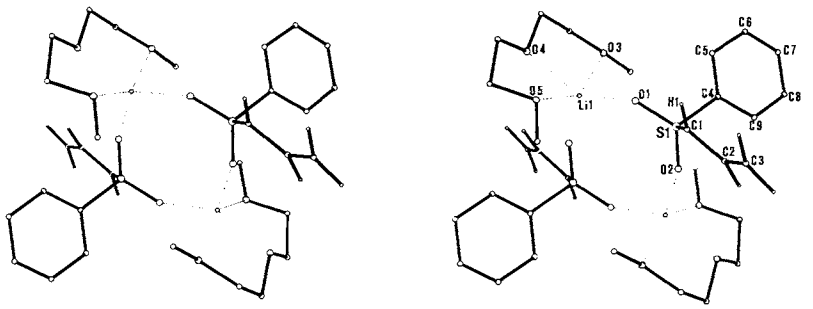


Fig. 1. Stereoview of the crystal structure of **3** (H atoms omitted with the exception of those on C-1 to C-3) [8]. Selected distances [Å] and angles [°]: S1-C1 1.668(5), S1-C4 1.791(5), S1-O1 1.451(4), S1-O2 1.426(4), C1-C2 1.445(9), C2-C3 1.352(9); C1-C2-C3 125.2(8); C4-S1-C1-H1 −78(3), C4-S1-C1-C2 76(1), O1-S1-C1-H1 36(3), O2-S1-C1-C2 −39(1), O1-S1-C1-C2 −171(1), S1-C1-C2-C3 −169(1).

The S-O bonds of **3**, like those of **1** and **2**, are no longer than those in sulfones.[3] In the crystal, a conformation of the sulfonyl carbanion is favored (Fig. 1 and 2) in which

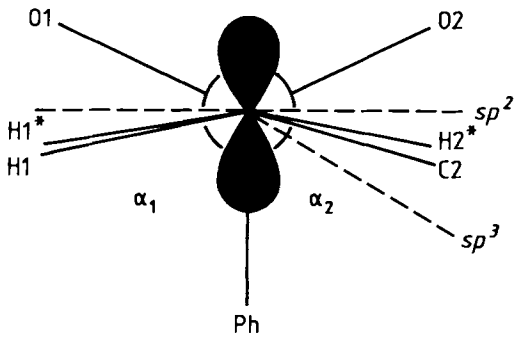
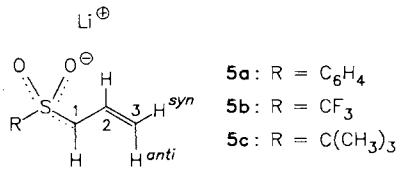


Fig. 2. Angles around the S-C1 bond in **1** (H1*, H2*) and **3** (H1, C2). O1, O2, and Ph apply to both compounds. **1**: $\alpha_1 = -81(3)°$, $\alpha_2 = 81(3)°$; **3**: $\alpha_1 = -78(3)°$, $\alpha_2 = 76(1)°$.

the lone pair of electrons at C-1, as in the case of **1**, is *gauche* to the two O atoms and periplanar to the S1-C4 bond.[9] Ab initio calculations carried out on (methylsulfonyl)methyllithium predict such a minimum energy conformation (n_C–σ^*_{SR} interaction).[11] Analogous conformations were also found for the isoelectronic sulfonamides in solution and in the crystal.[12]

Information on the structure of the title compound in solution is provided by the ^{13}C- and ^1H-NMR data (Table 1) (**3** ≡ [**5a** · diglyme]$_2$). The ^{13}C chemical shifts of **5a** and



5a: R = C_6H_4
5b: R = CF_3
5c: R = $C(CH_3)_3$

Table 1. ^{13}C and ^1H chemical shifts (δ values) and $^1J(^{13}C,^1H)$ and $J(^1H,^1H)$ couplings [Hz] (italics) for **5a** [a-c].

C-1	C-2	C-3	
61.6 (+0.9)	136.5 (+11.7)	86.1 (−38.5)	
163.2 (+24.9)	*144.6 (−17.2)*	*151.5 (−5.2), 155.4 (−4.5)*	
1-H	2-H	3-H_{syn}	3-H_{anti}
3.50 (−0.31)	6.25 (+0.50)	3.53 (−1.80)	3.87 (−1.28)
10.9	*10.5, 10.9, 16.6*	*10.5, 3.0*	*16.6, 3.0*

[a] Values in parentheses: changes in the chemical shifts [$\Delta\delta$(H,Li)] and couplings [ΔJ(H,Li)] upon replacement of H with Li in allylphenylsulfone. [b] 75.5-MHz ^{13}C-NMR spectra in [D_8]THF, 25°C, [D_8]THF (25.3 ppm) internal standard. [c] 300-MHz ^1H-NMR spectra in [D_8]THF, 25°C, [D_7H]THF (1.72 ppm) internal standard.

especially the pronounced high-field shift of the signal of C-3, which is caused by the higher electron density, indicate the presence of a conjugated π-electron system in solution as well. This conclusion is also supported by the ^1H chemical shifts. The apparent constancy in the position of the C-1 signal may be ascribed to two effects acting oppositely: a high-field shift owing to the higher charge density and a low-field shift owing to the partial $sp^3 \rightarrow sp^2$ rehybridization. The latter is further confirmed by the significant increase of ^1J(C,H) at C-1.[13] The ^1J(C,H) value of C-3 undergoes only minor change, in contrast to that of C-2, which significantly decreases. In analogy to the interpretation[14a,b] of this effect in the case of allyllithium compounds,[14] we ascribe the cause of the decrease of ^1J(C,H) at C-2 in the case of **5a** also to the widening of the angle at C-2. The ^1H-NMR data, particularly the ^3J(1-H,2-H) value of **5a**, show[6] that **5a** also exists in solution preferentially in the transoid conformation with respect to the C1-C2 bond.[15] ^1H-NMR investigations on **5a** in [D_{14}]diglyme at higher temperatures revealed that $\Delta G^{\neq}$ must be greater than 19.5 kcal/mol (130°C) for the "rotation" around the C2-C3 bond, since, up to 130°C, no line-broadening, pointing to exchange phenomena, was observed in the 300-MHz spectrum. The structure of **5a** can therefore be best described as a vinyl-substituted α-sulfonyl carbanion with a lithium counterion.

Received: May 12, 1986;
revised: July 10, 1986 [Z 1766 IE]
German version: *Angew. Chem. 98* (1986) 916

CAS Registry numbers:
3, 104131-47-7; **5a**, 77548-21-1; allylphenylsulfone 16212-05-8.

[1] a) B. M. Trost, N. R. Schmuff, *J. Am. Chem. Soc. 107* (1985) 396, and references cited therein; b) J. Vollhardt, H.-J. Gais, K. L. Lukas, *Angew. Chem. 97* (1985) 607; *Angew. Chem. Int. Ed. Engl. 24* (1985) 610; H.-J. Gais, W. Ball, unpublished results; c) T. Akiyama, M. Shimizu, T. Mukaiyama, *Chem. Lett. 1984*, 611.

[2] Chemical investigations on the structure of bicyclic (sulfonyl)allyllithium compounds: [1a].

[3] a) H.-J. Gais, H. J. Lindner, J. Vollhardt, *Angew. Chem. 97* (1985) 865; *Angew. Chem. Int. Ed. Engl. 24* (1985) 859; b) G. Boche, M. Marsch, K. Harms, G. M. Sheldrick, *ibid. 97* (1985) 577 and *24* (1985) 573: The configuration at C-1 of **2** has not yet been determined.

[4] a) H. Köster, E. Weiss, *Chem. Ber. 115* (1982) 3422; b) S. K. Arora, R. B. Bates, W. A. Beavers, R. S. Cutler, *J. Am. Chem. Soc. 97* (1975) 6271; c) G. Boche, H. Etzrodt, M. Marsch, W. Massa, G. Baum, H. Dietrich, W. Mahdi, *Angew. Chem. 98* (1986) 84; *Angew. Chem. Int. Ed. Engl. 25* (1986) 104; d) N. Hertkorn, F. H. Köhler, G. Müller, G. Reber, *ibid. 98* (1986) 462 and *25* (1986) 468; e) crystal structures of benzyllithium and related systems: W. N. Setzer, P. von R. Schleyer, *Adv. Organomet. Chem. 24* (1985) 354, and references cited therein.

[5] Further examples of such allyllithium derivatives LiC_3H_4X: X = CO−R, CN, $PO(R)_2$, SO−R, SO(NR)−R, etc.

[6] According to ^{13}C- and ^1H-NMR data, **5b** and **5c** have similar structures to that of **5a**; H.-J. Gais, J. Vollhardt, unpublished results.

[7] *Experimental procedure:* A solution of *n*BuLi (2.70 mmol) in *n*-hexane (1.7 mL) was added under N_2 to a solution of allylphenylsulfone (500 mg, 2.76 mmol) in 3.5 mL of anhydrous diglyme at 0°C. The solution immediately turned yellow-orange and **3** precipitated out as a yellow solid. *n*-Butane and *n*-hexane were removed at 25°C under vacuum. Upon warming of the solution to about 40°C, **3** dissolved completely. Upon cooling of the solution to 25°C, yellow rods or rhombic platelets formed within 20 min. These were filtered off under N_2, washed with diethyl ether, and dried (25°C, 10^{-2} torr).

[8] A single crystal of **3** was mounted in a glass capillary under argon. $P2_1/c$, $a=11.706(1)$, $b=9.898(5)$, $c=18.258(1)$ Å, $\beta=122.87(2)°$, $V=1776.8$ Å^3, $Z=4$, $\rho_{calcd}=1.209$ g·cm^{-3} (determined with a STOE Siemens four-circle diffractometer, $Mo_{K\alpha}$ radiation). Intensity measurements at room temperature with a STOE two-circle diffractometer, $Cu_{K\alpha}$ radiation, $\mu(Cu_{K\alpha})=16.7$ cm^{-1}, graphite monochromator, 3030 reflections with $(h0l\cdots h8l,\ 8°<2\theta<130°)$ measured, 2264 symmetry-independent reflections with $|F|>2\sigma(F)$, no absorption correction, SHELX, direct methods, H atoms on C1 to C3 from difference Fourier synthesis, all other H atoms positioned according to geometric arguments, H atoms refined isotropically, 277 variable, $R=0.082$. Maximal residual electron density +0.34, −0.73 e/Å^3 in the region of the S atom. Further details of the crystal structure investigation may be obtained from the Fachinformationszentrum Energie, Physik, Mathematik GmbH, D-7514 Eggenstein-Leopoldshafen 2 (FRG), on quoting the depository number CSD-52076, the names of the authors, and the journal citation.

[9] However, the position of the H atom on C-1 is not as precisely determined as that on C-2.

[10] See [3a] and the footnote [2] therein.

[11] D. A. Bors, A. Streitwieser, Jr., *J. Am. Chem. Soc. 108* (1986) 1397; S. Wolfe, *Stud. Org. Chem. (Amsterdam) 19* (1985) 133.

[12] T. Jordan, H. W. Smith, L. L. Lohr, W. N. Lipscomb, *J. Am. Chem. Soc. 85* (1963) 846; L. V. Vilkov, I. Y. Khargittai, *Dokl. Akad. Nauk SSSR 168* (1966) 1065; H. P. Klug, *Acta Crystallogr. B24* (1968) 792; W. B. Jennings, R. Spratt, *Chem. Commun. 1970*, 1418.

[13] G. Chassaing, A. Marquet, *Tetrahedron 34* (1978) 1399; R. Lett, G. Chassaing, *ibid. 34* (1978) 2705; G. Barbarella, P. Dembach, A. Garbesi, *Tetrahedron Lett. 21* (1980) 2109; T. Bottin-Strzalko, J. Corset, F. Froment, M. J. Pouet, J. Seyden-Penne, M.-P. Simonnin, *J. Org. Chem. 45* (1980) 1270; H. Schmidbaur, A. Schier, B. Milewski-Mahrla, *Chem. Ber. 115* (1982) 722.

[14] a) T. Clark, C. Rohde, P. von R. Schleyer, *Organometallics 2* (1983) 1344; b) H. Ahlbrecht, K. Zimmermann, G. Boche, G. Decher, *J. Organomet. Chem. 262* (1984) 1; c) M. Schlosser, M. Stähle, *Angew. Chem. 94* (1982) 142; *Angew. Chem. Int. Ed. Engl. 21* (1982) 145; *Angew. Chem. Suppl. 1982*, 198.

[15] See G. J. Heiszwolf, H. Kloosterziel, *Recl. Trav. Chim. Pays-Bas 86* (1967) 1345; V. R. Sandel, S. V. McKinley, H. H. Freedman, *J. Am. Chem. Soc. 90* (1968) 495; H. Kloosterziel, J. A. A. van Drunen, *Recl. Trav. Chim. Pays-Bas 89* (1970) 32; J. Klein, S. Brenner, *J. Am. Chem. Soc. 91* (1969) 3094.

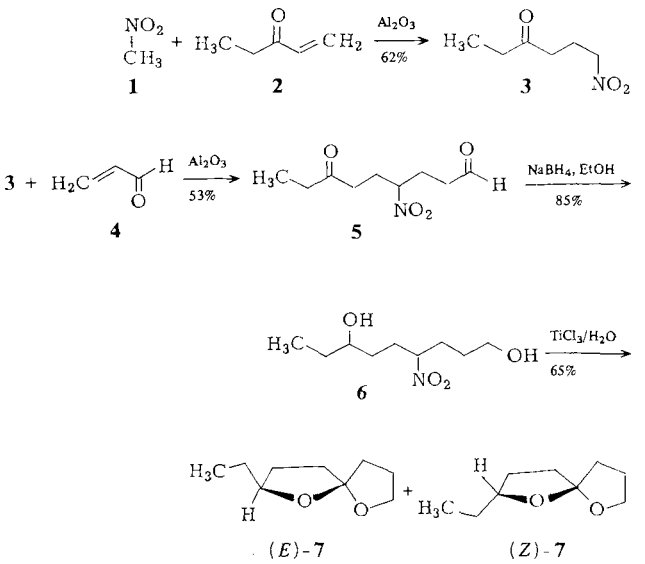
Nitromethane as d^1,d^1 Multiple Coupling Reagent for the Carbonyl Dianion Synthon. Practical Synthesis of Chalcogran**

By *Goffredo Rosini,* Roberto Ballini, Marino Petrini,* and *Emanuela Marotta*

One of the major objectives of modern organic synthesis is the broadening of techniques for assembling collections of carbon atoms and functional groups. In order to increase the arsenal of practical routes for the synthesis of complex molecules, we recently reported new applications of functionalized nitroalkanes as reagents corresponding to alkyl anion synthons.[1]

The spiroacetal moiety occurs in many biologically active, natural products, including insect pheromones;[2] consequently, new methods for their preparation are becoming increasingly important. Herein, we present a novel strategy for the synthesis of 1,6-dioxaspiro[4.4]nonane derivatives based on the utilization of nitromethane as a d^1,d^1 multiple coupling reagent[3] corresponding to a carbonyl dianion synthon. To test this concept, we chose 2-ethyl-1,6-dioxaspiro[4.4]nonane (chalcogran **7**), the main component in the aggregation pheromone of the bark beetle *Pityogenes chalcografus* (L.), also named "Kupferstecker." Since the identification of chalcogran by *Francke* et al.[4] in 1977, several syntheses of racemic[4,5] and optically active[6] **7** have been reported.

The starting point for our synthesis was the 1,4 addition of nitromethane **1** to 1-penten-3-one **2** (without solvent, in the presence of alumina,[7] 6 h at room temperature). which afforded **3**[8] (62%). The 1,4 addition of **3** to acrolein **4** under identical conditions gave **5**[8] (53%). On reduction with $NaBH_4$ in EtOH, **5** furnished 1,7-dihydroxy-4-nitrononane **6**, the open-chain chalcogran precursor. Finally, the transformation of the nitro group into a carbonyl group by reaction with an aqueous solution of $TiCl_3$[9] led, via spontaneous cyclization, to the desired chalcogran ((*E*)-**7**/(*Z*)-**7** = 39/61).[8]



All four steps of this procedure, including purifications, are simple and require cheap starting materials. Thus, for the synthesis of 1,6-dioxaspiro[4.4]nonane derivatives, the use of nitromethane as a d^1,d^1 multiple coupling reagent can be considered more convenient than the use of the most popular masked acyl anions (dithioacetals,[10] *O*-protected cyanohydrins,[11] and *N,N*-diethylaminoacetonitrile[12]).

Received: May 22, 1986;
revised: July 7, 1986 [Z 1787 IE]
German version: *Angew. Chem. 98* (1986) 935

[*] Prof. Dr. G. Rosini, Dr. E. Marotta
Istituto di Chimica Organica dell'Università
Viale Risorgimento n. 4, I-40136 Bologna (Italy)
Dr. R. Ballini, Dr. M. Petrini
Dipartimento di Scienze Chimiche dell'Università
Via S. Agostino n. 1, I-62032 Camerino (Italy)

[**] This work was supported by the Ministero della Pubblica Istruzione of Italy. *E. M.* thanks AGIP Petroli S.p.A. for a research studentship.

[1] G. Rosini, R. Ballini, P. Sorrenti, *Tetrahedron 39* (1983) 4127; G. Rosini, R. Ballini, M. Petrini, P. Sorrenti, *ibid. 40* (1984) 3809; G. Rosini, R. Ballini, M. Petrini, *Synthesis 1985*, 46, 269.

[2] W. Francke: *Les Médiateurs chimiques* (*Les Colloques d'INRA 7* (1982) 81).

[3] "Coupling reagent" according to D. Seebach, P. Knochel, *Helv. Chim. Acta 67* (1984) 261. The term "conjugative reagent" has also been used: E. Piers, V. Karunaratne, *J. Org. Chem. 48* (1983) 1774.

[4] W. Francke, V. Heemann, B. Gerken, J. A. A. Renwick, J. P. Vité, *Naturwissenschaften 64* (1977) 590.

[5] a) W. Francke, W. Reith, *Liebigs Ann. Chem. 1979*, 1; b) R. Jacobsen, R. J. Taylor, H. J. Williams, L. R. Smith, *J. Org. Chem. 47* (1982) 3140; c) O. A. Kozhich, G. M. Segal, I. V. Torgov, *Izv. Akad. Nauk SSSR Ser. Khim. 1982*, 325; d) A. M. Doherty, S. V. Ley, B. Lygo, D. J. Williams, *J. Chem. Soc. Perkin Trans. 1 1984*, 1371; e) R. E. Ireland, D. Häbich, *Tetrahedron Lett. 21* (1980) 1389.

[6] a) L. R. Smith, H. J. Williams, R. M. Silverstein, *Tetrahedron Lett. 1978*, 3231; b) K. Mori, M. Sasaki, S. Tamada, T. Suguro, S. Masuda, *Tetrahedron 35* (1979) 1601; c) E. Hungerbühler, R. Naef, D. Wasmuth, D. Seebach, H.-R. Loosli, A. Wehrli, *Helv. Chim. Acta 63* (1980) 1960; d) H. Redlich, W. Francke, *Angew. Chem. 92* (1980) 640; *Angew. Chem. Int. Ed. Engl. 19* (1980) 630; e) H. Redlich, *Liebigs Ann. Chem. 1982*, 708; f) D. Enders, W. Dahmen, E. Dederichs, P. Weuster, *Synth. Commun. 13* (1983) 1235.

[7] G. Rosini, E. Marotta, R. Ballini, M. Petrini, *Synthesis 1986*, 237.

[8] **3**: b.p. = 97°C/0.2 torr; IR (neat): $\tilde{\nu}$ = 1715, 1550 cm^{-1}; ^{1}H-NMR (90 MHz, $CDCl_3$): δ = 4.48 (t, 2H, J = 6.3 Hz), 2.72–1.88 (m, 6H), 1.08 (t, 3H, J = 7.2 Hz). Correct elemental analysis. **5**: obtained as an oil by chromatography on a SiO_2 column with EtOAc/*n*-hexane (2:8). IR (neat): $\tilde{\nu}$ = 1740, 1715, 1545 cm^{-1}; ^{1}H-NMR (90 MHz, $CDCl_4$): δ = 9.88 (s, 1H), 4.6 (m, 1H), 2.8–1.9 (m, 10H), 1.08 (t, 3H, J = 7.2 Hz). Correct elemental analysis. **7**: b.p. = 170–175°C (170–174°C [6b]). The spectral data are in agreement with the IR [6b], ^{1}H-NMR [6b], ^{13}C-NMR [6c], and mass spectral [4, 5a] data reported for authentic chalcogran. The diastereomeric composition of our chalcogran was determined by gas chromatography on a fused silica capillary column SE 45 at 65°C.

[9] J. E. McMurry, J. Melton, *J. Org. Chem. 38* (1973) 4367.

[10] D. Seebach, E. J. Corey, *J. Org. Chem. 40* (1975) 231.

[11] a) M. Hamana, T. Endo, S. Saeki, *Tetrahedron Lett. 1975*, 903; b) S. Hünig, G. Wehner, *Synthesis 1975*, 180.

[12] G. Stork, A. A. Ozorio, A. Y. W. Leong, *Tetrahedron Lett. 1978*, 5175.

BOOK REVIEWS

The ACS Style Guide. Edited by *J. S. Dodd*. American Chemical Society, Washington, DC, 1986. xviii, 264 pp., hardback, $ 29.95 (export), 24.95 (USA and Canada), ISBN 0-8412-0917-0; paperback, $ 17.95 (export), 14.95 (USA and Canada), ISBN 0-8412-0943-X

The contents and format of *The ACS Style Guide* fully justify the new title of a book whose predecessors, the first and second editions of the American Chemical Society's *Handbook for Authors*, have long been valuable resources in the preparation of manuscripts for chemistry journals. Indeed, a detailed comparison of the *Style Guide* with the earlier *Handbook* would serve little purpose, so numerous are the changes, additions, and improvements.

Of the seven chapters, three ("The Scientific Paper," "Grammar, Style, and Usage," and "Illustrations and Tables") deal with the scientific manuscript itself, one discusses "Copyright and Permissions," and three treat new subjects, namely, "Manuscript Submissions in Machine-Readable Form," "The Literature: Becoming Part of It and Using It," and "Making Effective Oral Presentations." The last two chapters, in particular, reveal that the title *Style Guide* is somewhat of an understatement. In keeping with this broader intent, discussions of ACS editorial procedures and of ACS books, journals, and services, as well as of Chemical Abstracts Service, are relegated to the appendixes, which further include ethical guidelines to publication of chemical research; element symbols, atomic numbers, and atomic weights; symbols for commonly used physical quantities; hints to the typist; and proofreaders' marks.

One (well-drawn) picture is worth a thousand words, especially in the verbose manuscripts often delivered to overworked editors. The clearly written, copiously illustrated chapter "Illustrations and Tables" should therefore be very useful to authors doing their own artwork. Much greater attention than in the earlier *Handbook* is given to the practical aspects of drawing formulas and figures. Further improvements are the longer lists of abbreviations and symbols and the more detailed discussions of punctuation and editorial style. Moreover, the layout of the book, from the comprehensive table of contents and the all-inclusive index to the clear listing of the specific recommendations and numerous examples, facilitates enormously the use of this book as a quick reference source.

Only the first chapter, "The Scientific Paper," leaves something to be desired. Less than two pages treat writing style in general. Although suggestions such as "avoid slang and jargon," "use strong verbs," and "be brief" are good, a few examples of the more common such pitfalls in scientific manuscripts might have been more helpful. This is especially true in view of the wealth of examples given in later chapters to illustrate much finer points, such as the use of italics and commas or the location of quotation marks (curiously, while standard American practice is to place them after periods and commas, ACS practice is the hybrid called "logical placement," which is virtually identical with German practice). Whereas a good in-house copy editor can take care of typefaces and punctuation, only the author can ensure the clear, crisp style so essential to good scientific writing.

The ACS Style Guide is a welcome addition to the reference library of both scientific authors and editors. In fact, *Angewandte Chemie International Edition in English* recommends the *Style Guide* in its Notice to Authors.

David I. Loewus [NB 760 IE]
Angewandte Chemie, Weinheim (FRG)

Biochemistry of Alkaloids. Edited by *K. Mothes, H. R. Schütte*, and *M. Luckner*. VCH Verlagsgesellschaft, Weinheim 1985. 496 pp., bound, DM 194.00.—ISBN 3-527-26079-X

Following the earlier monograph "Biosynthese der Alkaloide" (Editors: *K. Mothes, H. R. Schütte*, 1969), there is now an updated version available in English by the same authors. This volume both fills the information gap existing between 1969 and the present in this specialized field, and treats in detail nearly all the biochemical ramifications of this fascinating group of natural products. It includes 247 figures and more than 1200 structural formulas, and for the reader needing further details there are over 2300 literature references ranging from classical work on alkaloids to the most topical problems.

The monograph is divided into 19 chapters. The topics covered by the first nine of these include methods in biosynthetic research, the genetic aspects of alkaloid metabolism and its regulation, the classification of metabolic sequences, and the localization of alkaloids in living cells and its ecological significance.

Chapters 8 and 9 are concerned with the metabolism of those amino acids which are important as alkaloid precursors. These chapters also introduce the principles of biosynthesis of alkaloids, leading up to that part of the book which treats the various classes of alkaloids. The classification is along biogenetic lines, treating in turn the alkaloid groups derived from ornithine, lysine, nicotinic acid, phenylalanine and tyrosine, tryptophan, anthranilic acid and histidine, together with purine bases and alkaloids derived from isoprene.

The clearly written and well organized text takes the reader easily and directly through each topic, and the many biosynthetic reaction schemes provided are a valuable help. It would, however, have been desirable for teaching purposes to clearly indicate in the diagrams those biosynthetic pathways which are not yet proven. This would show at a glance the existing state of knowledge, and might inspire young investigators to check these hypotheses by experimental work.

The external appearance of the monograph is attractive, though the type quality leaves a little to be desired. While the text, apart from the appendix, contains only a few printing errors, there are some mistakes in the structural formulas, which one hopes will be corrected in a second edition.

This book gives an excellent and detailed survey of the biochemistry of alkaloids, and is as up to date as is practicable in representing the current state of research. It is a welcome addition to the literature on alkaloids, and is strongly recommended for natural products chemists, pharmacists and biologists. Nevertheless, its readership is likely to be limited to some extent by the relatively high price.

J. Stöckigt [NB 754 IE]
Pharmazeutische Biologie
der Universität München (FRG)

Industrielle Anorganische Chemie. By *W. Büchner, R. Schliebs, G. Winter,* and *K. H. Büchel.* Verlag Chemie, Weinheim 1984. xxiii, 645 pp., hardback, DM 108.00.—ISBN 3-527-25069-2

"Industrial Inorganic Chemistry" is a textbook as well as a reference work on inorganic products. The clear organization and the extensive index enable the book to be used quickly and conveniently and make it possible for the reader to obtain a survey over a diverse and important area of chemistry.

The main chapters are: inorganic basic products, mineral fertilizers, metals and their compounds, silicones, inorganic solid state materials and the cycling of nuclear fuel. These chapters are subdivided according to chemical criteria. For example, the chapter on inorganic basic products contains the sections: water, hydrogen, hydrogen peroxide and inorganic peroxides, nitrogen and nitrogen compounds, phosphorus and its compounds, sulfur and its compounds and halogens and halogen compounds. In each of these sections the following topics are dealt with: *distribution of raw materials, production processes, purification of products, economic significance and technical applications.* At the end of each section references give access to more detailed literature.

Production processes are described in close detail, discussing such aspects as the disposition of raw materials, energy consumption and ecological problems. Metallurgical processes, with a few exceptions, are not discussed. Particular attention is paid to economic aspects and to the application of products. These are illustrated by numerous tables, albeit containing data that is partly rather old.

In summary it can be said that this book covers a broad scope in a clear and concise way. The excellent realization of the book and the design with main and marginal columns justify the price of DM 108.00. It can therefore be recommended to students, teachers, chemists, and colleagues from related disciplines.

J. Köhler [NB 723 IE]
Max-Planck-Institut für Festkörperforschung,
Stuttgart (FRG)

Organomercury Compounds in Organic Synthesis. By *R. C. Larock.* Springer, Berlin 1985. xi, 423 pp., bound, DM 268.00.—ISBN 3-540-13749-1

In recent years organomercury compounds have, despite their toxicity, assumed increasing importance in organic synthesis, primarily because of their selectivity. The present monograph, written by an expert in this field, is a greatly extended version of an article in *Angewandte Chemie* (1978) and a 1982 "*Tetrahedron Report*". In addition to the preparation of organomercury compounds it deals with the substitution of the mercury atom by hydrogen or halogens, the synthesis of compounds containing heteroatoms, and with dimerization, alkylation, acylation, carbonylation, and addition to alkenes and alkynes. A newly added item is a particularly comprehensive chapter on carbene transfer reactions, a field in which much has occurred since the appearance twelve years ago of the "Houben-Weyl" work on organomercury compounds (Vol. XIII/2b).

Solvomercuration-demercuration reactions have been excluded, as these will be treated in a separate monograph by the same author. The advance notice of the latter book that is twice given in the preface would have been enough; the author did not really need to repeat the advertisement in twelve more places, including twice on p. 159, as his work advertises itself!

The book is truly a mine of information for all chemists engaged in preparative work, containing more than 2800 literature references, of which a considerable number are from the Russian-speaking world. Rather then merely listing the various reactions, their advantages and disadvantages compared with other methods of synthesis are thoroughly discussed. The book is also eminently suitable as a work of reference, especially on account of the twenty summary tables which are distributed through the text. Unfortunately an author index, which would also have been valuable in that respect, has not been included.

I could find very few typographical errors, although there are what I would describe rather as unattractive forms, e.g. the rendering of formulas for nitro compounds as NO_2-Ar instead of O_2N-Ar. The presentation is outstandingly good, and the printing really excellent com-

pared with that which nowadays we have come to expect with many books. This, together with the high-quality binding, is of course reflected in the price. Nevertheless, the book should not be missing from any departmental library, whether academic or in the chemical industry.

Adalbert Maercker [NB 763 IE]
Institut für Organische Chemie
der Universität Siegen (FRG)

Stereochemistry of Heterogeneous Metal Catalysis. By *M. Bartók*. John Wiley, Chichester 1985. xxiv, 632 pp., bound, £ 85.00.—ISBN 0-471-90553-4

How does an organic compound behave when on the surface of a heterogeneous catalyst, especially with regard to stereochemistry? What is the mechanism involved in the hydrogenation of an olefin, the dehydration of an alcohol, or the hydrogenolysis of an amine?

M. Bartók felt that it was timely to summarize the literature in this field in the form of a book. A first glance through the list of contents and introductory remarks was not very promising: few concise headings, a series of misprints, an unfortunate choice of symbols (asterisks which are distinguished only by a slight difference in size signify either an active center on the surface or a chiral atom), and a careless use of *E* and *Z* as synonymous with *cis* and *trans*, which is quite surprising in a book on stereochemistry. The contents are divided into twelve chapters, and are arranged according to compound types: alkanes, cycloalkanes, alkenes, alkynes, aromatics, alcohols, carbonyl compounds, and nitrogen compounds. The literature up to the end of 1982 is covered, with 2956 references. The book concludes with a 50-page author index and a 40-page subject index.

Each chapter is arranged according to the following scheme. First, all the available review articles are listed, then the possible adsorbed species are given and their structures shown. This is followed by results on isotope exchange and isomerization, then a description of the reactions of the individual classes of compounds, illustrated by numerous diagrams. The longest chapter (116 pp.) deals with hydrogenation of olefins, including also unsaturated steroids.

The contributions of the various co-authors (nine in all) have turned out very differently. The chapters on alkanes and cycloalkanes with which the book begins are not good. There are long passages in which the presentation of the material is in the style of "one cited paper = one sentence", which does not make for an easily readable text. The sequence of facts is often unrelated, thus confusing the reader. There are numerous instances like that on p. 40. Here it is first stated that a study of the hydrogenolysis of cyclopropane derivatives provides considerable information towards understanding the mechanism. However, after thirteen equations and five lines of text it is concluded that more data are needed before any general rule can be established regarding the stereochemistry of the hydrogenolysis of the cyclopropane ring.

The basic fault of this book is that the route from the formulation of the problem to the final result is not explained. An illustration of this is the treatment of isotope exchange in cyclopentane and cyclohexane (p. 26). Here the reader is presented with five different mechanisms: repeated second-point adsorption, exchange of two adjacent equatorial hydrogen atoms, a π-allyl mechanism, a rollover mechanism, and a "rock and roll" mechanism. He is also told that one author prefers this mechanism and rejects that, whereas another sees it differently, but the grounds on which they base their different views are not explained. This way of presentation not to demonstrate how the mechanisms shown were arrived at leaves one feeling very dissatisfied. This is not the way to hold a reader's attention.

After a weak beginning, there follow some chapters which are better written and well organized, e.g. those on carbonyl and nitrogen compounds. In some of them the topics are treated too briefly, e.g. in Chapter XI, where some aspects of enantioselective hydrogenation using heterogeneous catalysts are presented in a very sketchy way.

Those working in this field will buy the book for its comprehensive coverage of the literature, but anyone who is not so close to the topic will not find the book very pleasant to read.

Henri Brunner [NB 765 IE]
Institut für Anorganische Chemie
der Universität Regensburg (FRG)

The Industrial Uses of Tin Chemicals. By *S. J. Blunden, B. A. Cusack,* and *R. Hill*. The Royal Society of Chemistry, London 1985. ix, 337 pp., bound, £ 36.00.—ISBN 0-85186-927-0

For about thirty years the industrial uses of a wide range of organotin compounds have continued to grow in importance. Various tin compounds are very effective in applications such as the thermal and light stabilization of PVC, as catalysts in polyurethane and silicone manufacture, and as biocides used in agriculture, the timber industry, shipping, etc. Over 40000 tonnes of organotin compounds are used each year throughout the world.

The number of people in industry who are concerned with organotin compounds—chemists, engineers and technicians—also continues to grow, and there has long been a need for an informative handbook to help them. This book now fills that gap.

The book is divided into 15 chapters: 1. Introduction, 2. Industrial manufacture, 3. Toxicology, 4. Antifouling systems, 5. Agrochemicals, 6. Wood preservatives, 7. PVC stabilizers, 8. Catalysts, 9. Glass applications, 10. Fire retardants, 11. Pharmaceuticals, 12. Ceramics, 13. Reducing agents, 14. Miscellaneous uses, 15. Environmental aspects. Finally there is an index of manufacturers. Each chapter contains a separate list of literature references. Altogether 1224 such sources are mentioned, covering literature up to and including 1984.

A complete review of the literature would have been out of place in a handbook such as this. On the other hand, a selection of key publications on significant advances corresponding to the relative importance of each field needed to be described. A comparison of Chapters 6 and 7 shows that the book does not meet this need. The literature covered in Chapter 6 (wood preservatives, where organotin compounds take a share of under 3%) consists of 118 references, which is about 90% of the existing publications on this topic. By contrast, in Chapter 7 PVC stabilizers, where organotin compounds have a share of more than 60%, are given a mere 42 references, i.e. about 10% of the available literature, and of the 100 or so known patents in this field

only three are mentioned. The use of organotin stabilized PVC films in food packaging is mentioned only in passing, and there is no discussion of the numerous publications on this topic.

A bare mention of the applications in each of the specialized areas is not enough for someone working in the field; he also needs information about how organotin compounds can most effectively and safely be used. It is true that toxicological studies have revealed no carcinogenic or mutagenic effects, but the compounds used for technological purposes are certainly not harmless: some are quite toxic and affect the eyes, mucous membranes, and liver. It would certainly have been appropriate to include in the book an account of the precautions needed.

Use of these substances also calls for reliable methods of analysis. The book includes nothing on this subject apart from a list of references on Mössbauer spectroscopy.

Since there is still no really good handbook available for those who use organotin compounds, "The Industrial Uses of Tin Chemicals" is recommended despite its shortcomings.

Stephan Pawlenko [NB 752 IE]
Schering AG, Bergkamen (FRG)

The Chemistry of the Metal-Carbon Bond. Vol. 2: The Nature and Cleavage of Carbon-Metal Bonds. Vol. 3: Carbon-Carbon Bond Formation using Organometallic Compounds. Edited by *F. R. Hartley* and *S. Patai*. John Wiley, Chichester 1985. Vol. 2: xiii, 904 pp., bound, £ 155.00.—ISBN 0-471-90282-9; Vol. 3: xiv, 489 pp., bound, £ 98.00.—ISBN 0-471-90557-7

Following the publication in 1982 of Volume 1 of this series, Volumes 2 and 3, covering the topics named above, appeared almost simultaneously during last year. To come immediately to the point, both these volumes are a good deal more integrated than the initial volume, which seemed to have been put together without a clear guiding concept, and they are consequently more useful. It is regrettable that Volume 2 still does not contain a chapter on the important topic of photochemical cleavage reactions, and this ought to be remedied in a later volume. As no precise information is given about the scope of the series, one must for the time being wait to see which other subjects are planned.

Volume 2 starts with a not very detailed chapter on the electrochemical cleavage of metal-carbon bonds (24 pp., 99 references). In addition to M-C σ-bonds, this also includes bonds between metals and C_5H_5, C_6H_6, CO, CNR, carbenes and carbynes. Unfortunately the literature references for this very topical theme do not extend later than 1982, a shortcoming which also applies to most of the other contributions. Chapter 2 is quite extensive (124 pp., 591 references), dealing with heterolytic cleavage of bonds between carbon and main group metals, a topic which has been worked on intensively for several decades. This reviewer does not feel competent to give an authoritative verdict either on this chapter or the following one (66 pp., 276 references), devoted to homolytic cleavage of M-C bonds (but excluding metals of the 3rd-8th subgroups, the lanthanides and actinides). Both chapters lack any recent references; Chapter 2 contains none later than 1981. Chapters 4 and 5 deal with insertion reactions of metal-carbon compounds, first for main group metals (Chapter 4, 118 pp., 556 references), then for transition metals (Chapter 5, 60 pp., 280 references). The information given here is mainly of interest to organic chemists, and despite the large amount of material it is all clearly presented, partly in the form of tables. Chapter 5 and Chapter 6 (which covers the reactivity of organic transition metal compounds with nucleophiles) are notable exceptions as regards being up to date, as they contain many references to work published in 1982, and in places even 1983. Chapter 6 (112 pp., 464 references) is well worth reading; one senses from the start that this is the work of a very competent author *(L. S. Hegedus)*. Chapter 7 (45 pp., 206 references), which examines electrophilic attack on M-C σ-bonds, is short by comparison, and omits consideration of some important reactions, such as those of carbenium ions with alkyl and aryl metal complexes; no references later than 1981 are given. The next chapter (65 pp., 206 references), however, deserves praise, as it contains everything of importance on the subject of β-hydride elimination (and to some extent too on α- and γ-hydride elimination). At the present time there is certainly nothing better available on this topic. Chapter 9 (163 pp., 829 references), on the highly topical theme of oxidative addition and reductive elimination, would have received a similar commendation, were it not for the fact that 95% or more of the references are from before 1981. This is a great pity, especially since it would be difficult to find a more competent author than *J. K. Stille*. The final chapter (37 pp., 272 references) treats structure and bond formation in organometallic compounds of main group metals. It clearly ought to be in Volume 1, and appears rather isolated here; moreover, one would have wished for rather more information on this subject than the chapter contains.

The better overall impression made by Volume 2 compared with the first volume is also continued into Volume 3. Almost throughout the ten chapters, the authors have a high reputation gained by having themselves made important contributions in the fields about which they write here. Chapter 1 (C-C bond formation using organotin and organolead compounds) is fairly extensive (97 pp., 322 references), and is clearly aimed at synthetic organic chemists. The same also applies to Chapter 2 (42 pp., 489 references), which is concerned with the use of organozinc, organocadmium and organomercury compounds. In neither case is there any literature later than 1982, although here the limitation is less serious. However, so far as topicality is concerned, Chapter 3 (C-C bond formation using η^3-allyl complexes) steps into the breach; there are even references to papers from 1984, and the reports by *G. P. Chiusoli* and *J. Tsuji* (on π-allyl compounds of nickel and palladium) are a genuine pleasure to read. A great deal of work is now in progress in this area, and the synthetic potential of other η^3-allyl complexes (see e.g. the recent work of *Trost*) are still far from being exhausted. The following two chapters deal with topics which are also of industrial importance: oligomerization of olefins (Chapter 4, 52 pp., 114 references) and oligomerization of alkynes (Chapter 5, 35 pp., 116 references). As the literature covered in Chapter 4 (with one exception) ends with 1979, this means that in particular the recent publications from the Mülheim group (especially by *Heimbach*) have not been included. Chapter 6, which discusses the applications of transition metal carbonyls in organic synthesis, is very thoroughly organized but amazingly brief (38 pp., 186 references). Many of the topics here are merely touched on, and some, such as the use of metal carbonyl-carbene complexes in the synthesis of natural products, are missing completely. Chap-

ters 7 to 10 again treat important industrial topics: carbonylation of olefins and alcohols in Chapter 7 (24 pp., 155 references), olefin hydroformylation in Chapter 8 (28 pp., 112 references), Fischer-Tropsch syntheses in Chapter 9 (43 pp., 143 references), and olefin carbonylation in Chapter 10 (10 pp., 69 references). Leaving aside the fact that there is some overlapping on these topics, it must be remarked that in all of them the literature survey is more up to date. An overall view is provided for the reader with limited time available, which is as much as the writers set out to achieve.

In the review of the first volume the question was raised as to who could afford to buy this series. As the situation in our libraries has not improved since then, the recommendation with regard to buying remains as before that caution is advisable. For anyone who has the money and for whom a survey is sufficient, the books can be recommended, but anyone who wishes to familiarize himself with the current position in one of the fields dealt with must choose more recent publications.

Helmut Werner [NB 742 IE]
Institut für Anorganische Chemie
der Universität Würzburg (FRG)

The Structure of Volatile Sulphur Compounds. By *I. Hargittai*. D. Reidel Publishing Company, Dordrecht 1985. viii, 316 pp., bound, HFl 135.00.—ISBN 90-277-1395-2

This monograph, which has already appeared in Hungarian in 1981, deals with organic and inorganic sulfur compounds whose structures in the gas phase have been determined by microwave spectroscopy or electron diffraction. The extensive material which it contains is arranged according to the coordination number of the sulfur atom. In some cases the structures of analogous oxygen, selenium or tellurium compounds are also discussed, and the content of the book is therefore wider than the title suggests. The range of compounds treated extends from simple molecules such as H_2S, $PSCl_3$, $Se(GeH_3)_2$ and $(SF_5)_2O$, through the many organic thiocarbonyls, isothiocyanates, thiols, thioethers, sulfoxides, sulfones, and sulfur–nitrogen compounds, up to exotic examples such as the gaseous species of B_2S_3, TeO_2 and K_2SO_4, and the van der Waals molecule ArOCS. The main emphasis is on organic compounds, which occupy about 75% of the formula index. The results are clearly presented in 105 diagrams and 101 tables, and are critically analyzed in the associated text. The extensive formula index (8 1/2 two-column pages) and author index (12 1/2 two-column pages) facilitate rapid access, despite the great wealth of data, based on nearly 1000 literature references, which are listed alphabetically at the end of the text. In addition to the ordinary structural information, conformational problems such as intramolecular rotation are thoroughly discussed, and relationships between molecular geometry parameters or other bond properties (force constants or IR wave numbers) and those in related molecules are given. In particular sulfoxides, sulfones, and related four-coordinated (pseudo-tetrahedral) sulfur compounds are thoroughly discussed, on the basis of the VSEPR model.

In this book the author, who is well known for his many publications on electron diffraction research, has produced a useful work of reference containing information which would be difficult to obtain elsewhere. There is much interest in such information, as the sulfur compounds dealt with here are of great importance in many technical processes, in problems of environmental chemistry, and for innumerable chemical reactions that arise in research. It is, however, difficult to understand why the text was not thoroughly up-dated for the English edition. By far the greater part of the references are from the sixties and seventies, with only a few publications from 1980–1981 reviewed, and none of more recent years. Furthermore, only in a few cases is reference made to the many theoretical structural calculations that exist for the smaller molecules. One might also have wished to see the reported gas phase structures systematically compared with results from X-ray structure analyses on the same compounds, rather than only occasionally. The criticism that molecular structures in the solid phase are affected by intermolecular interactions is countered by the fact that the bond angles determined by electron diffraction are usually subject to appreciable errors, so that it is useful to compare the results with X-ray data.

Notwithstanding these critical comments, this monograph by *Hargittai* is a valuable addition to the previous most recent major survey on the structures of sulfur compounds by *P. Laur* in 1972. No library should therefore be without this book, which is good value for the price.

Ralf Steudel [NB 753 IE]
Technische Universität Berlin

Registered names, trademarks, etc. used in this journal, even without specific indication thereof, are not to be considered unprotected by law.

© VCH Verlagsgesellschaft mbH, D-6940 Weinheim, 1986. – Printed in the Federal Republic of Germany by Zechnersche Buchdruckerei, Speyer/Rhein.

All rights reserved (including those of translation into foreign languages). No part of this issue may be be reproduced in any form – by photoprint, microfilm, or any other means – nor transmitted or translated into a machine language without written permission from the publishers. Only single copies of contributions, or parts thereof, may be reproduced for personal use.

Valid for users in the USA: The appearance of the code at the bottom of the first page of an article in this journal (serial) indicates the copyright owner's consent that copies of the article may be made for personal or internal use, or for the personal or internal use of specific clients. This consent is given on the condition, however, that the copier pay the stated per-copy fee through the Copyright Clearance Center, Inc., for copying beyond that permitted by Sections 107 or 108 of the U.S. Copyright Law. This consent does not extend to other kinds of copying, such as copying for general distribution, for advertising or promotional purposes, for creating new collective works, or for resale. For copying from back volumes of this journal see 'Permissions to Photo-Copy: Publisher's Fee List' of the CCC.

Editorial office: Pappelallee 3, D-6940 Weinheim, Federal Republic of Germany, Telephone (06201) 602315, Telex 465516 vchwh d, Telefax (06201) 602328.

Editor: *P. Gölitz.*

Associate editors: *D. I. Loewus, A. Stimson.* **Editorial assistant:** *E. Schweikart*

Publishers: VCH Verlagsgesellschaft mbH. (Managing Directors: *Prof. Dr. Helmut Grünewald* and *Hans Dirk Köhler*), Pappelallee 3, D-6940 Weinheim, Federal Republic of Germany. Correspondence concerning advertisements should be addressed to VCH Verlagsgesellschaft mbH. (Advertising Manager *R. J. Roth*), Boschstr. 12, P.O. Box 1260/1280, D-6940 Weinheim, Federal Republic of Germany, Telephone Weinheim (06201) 602-0, Telex 465516 vchwh d, Telefax (06201) 602328.

ANGEWANDTE CHEMIE
International Edition in English
Volume 25 · Number 11
November 1986
Pages 947–1038

Selective Synthesis by Use of Lewis Acids in the Presence of Organocopper and Related Reagents

New Synthetic Methods (61)

By Yoshinori Yamamoto*

Organometallic compounds with pronounced nucleophilicity such as organocopper and organolithium compounds, and powerful electrophiles, such as BF_3 and $AlCl_3$, are generally thought to be incompatible under normal, homogeneous reaction conditions. As a matter of course, it is anticipated that the two species cannot coexist and undergo transmetalation reactions. To our surprise, however, RCu and BF_3 are compatible at low temperature. $RCu \cdot BF_3$ and related organocopper-Lewis acid reagents exhibit new and unique reactivities and selectivities: in conjugate additions, e.g., not only activation but also high regio-, stereo-, and chemo-selectivity as well as very high asymmetric induction is observed; allylic derivatives are alkylated regioselectively, and reaction towards carbonyl groups, imines, epoxides, aziridines, ethers, acetals, orthoformates, and pyridinium salts is in each case found to be selective. $RLi \cdot BF_3$ and related organolithium-Lewis acid reagents also exhibit noteworthy selectivities and reactivities. These complex reagents are utilized in the key steps of the total synthesis of many important natural products, such as certain terpenes, steroids, and alkaloids.

1. Introduction

Both in aldol reactions with silyl enol ethers[1] as well as in allylation reactions with allylsilanes[2] Lewis acids are added in order to increase the reactivity of the only weakly nucleophilic silyl reagents. That this succeeds was already established in 1973 and 1976, respectively. What then is to be expected when much harder nucleophiles, such as alkyllithiums and Grignard compounds, are treated with BF_3

$$RLi + TiCl_4 \longrightarrow RTiCl_3 + LiCl$$

$$RMgX + TiX_4 \longrightarrow RTiX_3 + MgX_2$$

Scheme 1.

[*] Prof. Dr. Yoshinori Yamamoto
Department of Chemistry, Faculty of Science
Tohoku University, Sendai 980 (Japan)

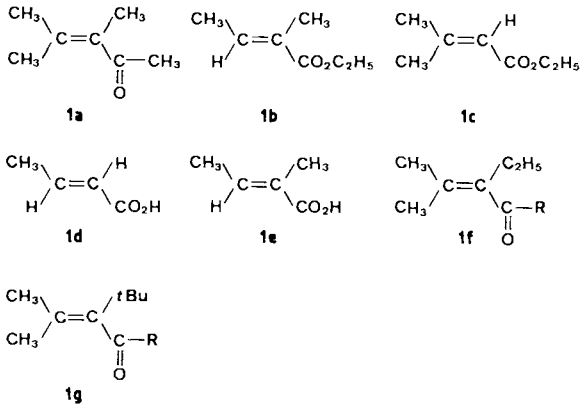
or $AlCl_3$? Foreseen is a rapid transmetalation. Indeed, organotitanium compounds, which have often been used in modern organic syntheses since 1980, can be prepared in this way (Scheme 1).[3]

In 1977 we found that the combination of $BF_3 \cdot OEt_2$ with organocopper compounds, which are harder than silyl enol ethers and allylsilanes but softer than organolithium and magnesium derivatives, yields a new complex reagent, $RCu \cdot BF_3$. To our surprise, RCu and BF_3 are compatible at low temperatures, and the two species are not so easily transmetalated as RLi·TiLn.[4] Since this discovery, $RCu \cdot BF_3$ and related organocopper-Lewis acid reagents have found frequent use in selective organic syntheses. More recently, organolithium-Lewis acid reagents have been developed which also exhibit unique reactivities and selectivities. In this review, the scope and limitation of these complex reagents will be summarized.

 © VCH Verlagsgesellschaft mbH, D-6940 Weinheim, 1986 0570-0833/86/1111-0947 $ 02.50/0

2. Activation in the 1,4-Addition to α,β-Unsaturated Carbonyl Compounds

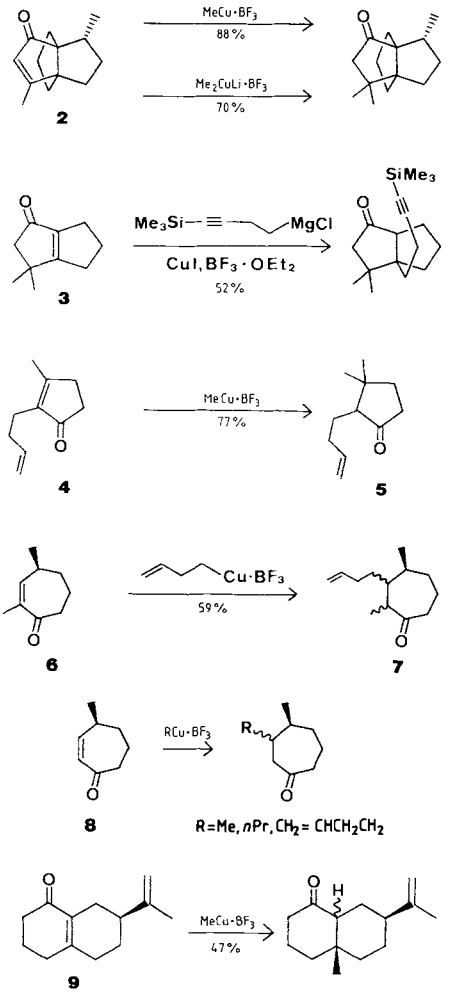
Although organocuprates (Gilman reagents) count among the most popular reagents for 1,4-additions (conjugate additions) there are still substrates with which they do not react as predicted. Thus, poor results are obtained with β,β-disubstituted acrylic ester derivatives, sterically highly crowded enones, and α,β-unsaturated carboxylic acids.[5] Organocopper-Lewis acid reagents have proven very useful for 1,4-additions to these previously "unreactive" substrates.[4,6] For example, $BuCu \cdot BF_3$ adds smoothly to **1a**–**1e**, whereas Bu_2CuLi does not. $MeCu \cdot BF_3$ is suitable for conjugate additions to the compounds **1f** and **1g** (Scheme 2).[7]



Scheme 2. **1f**, R = $CHEt_2$, *t*Bu; **1g**, R = Me, $CHEt_2$, *t*Bu, CMe_2*t*Bu, $CH(t\text{Bu})_2$.

In the total synthesis of modhephen, a 1,4-addition to **2** was carried out either with $MeCu \cdot BF_3$[8] or with $Me_2CuLi \cdot BF_3$.[9] No addition took place at all with Me_2CuLi alone. Similarly, a conjugate addition to **3** was achieved with the propargylcopper·BF_3 reagent,[10] while $MeCu \cdot BF_3$ was the reagent of choice for the transformation **4** → **5**, a step in the synthesis of (±)quadrone.[11] In the course of the total synthesis of (±)parthenin, a step involving the conversion of the enone **6** into **7** was essential. This could not be accomplished with the cuprate reagent, whereas the organocopper·BF_3 reagent furnished **7** in satisfactory yields.[12] Furthermore, upon reaction with **8**, $RCu \cdot BF_3$ exhibited higher diastereoselectivity than R_2CuLi,[12] and the 1,4-addition to **9**, which was not achievable with Me_2CuLi alone, could be realized with $MeCu \cdot BF_3$ (Scheme 3).[13]

The conversion of **10** into **11** with $RCu \cdot BF_3$ proceeded in good yield, while with R_2CuLi the yield was only 46% (R = 3-pentynyl).[14] Reaction of **12** with isopentyl$Cu \cdot BF_3$ afforded the conjugate adduct in good yield,[15] while reaction of the $RCu \cdot BF_3$ complex prepared from **13** with 2-cyclohexenone furnished the 1,4-adduct in good to excellent yields.[16] Conjugate addition to the sterically hindered cyclic enones **14**–**16** proceeded equally smoothly. The transformation of **17** to **18** required in the total synthesis of (+)hirsutene was accomplished by means of the reagent



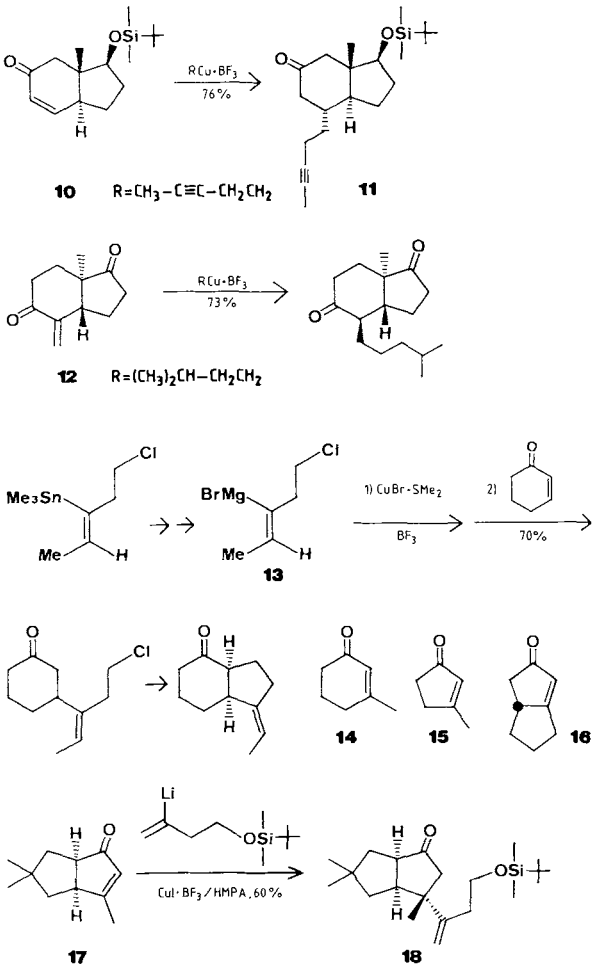
Scheme 3. Molecular ratio educt : reagent (from the top downwards): 1 : 5, 1 : 1.8; 1 : 2.8, 1 : 3, 1 : 2, no data, 1 : 3.

$RCu \cdot BF_3 \cdot HMPA$;[17] the addition took place exclusively from the α-side of **17** (Scheme 4).

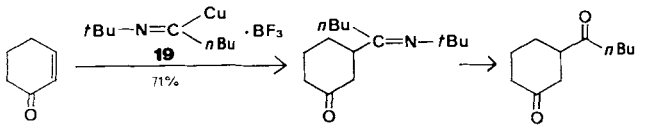
The 1,4-addition of copper-substituted Schiff bases to α,β-unsaturated enones could only be achieved by use of the corresponding BF_3-complex **19** (Scheme 5).[18] Other Lewis acids, such as $AlCl_3$, $TiCl_4$, $EtAlCl_2$, and Et_2AlCl, were also examined, but the results were very poor. The reagent **19** was prepared from the lithiated precursor and $CuI \cdot BF_3$; $CuBr \cdot SMe_2 \cdot BF_3$ and $CuI \cdot P(OMe)_3 \cdot BF_3$ likewise afforded good results. In the reaction according to Scheme 5, BF_3 presumably activates both the Schiff base **19** as well as the enone by coordination to the nitrogen atom.

The 1,4-addition of organocuprates such as $R_2Cu(CN)Li_2$ was also dramatically improved by $BF_3 \cdot OEt_2$.[19] Thus, the yield in the addition of **20** could be increased from 5 to 98% with BF_3, while **21** gave the conjugate adduct in >95% yield; without BF_3, however, no 1,4-adduct was obtained (Scheme 6). Other Lewis acids, such as $EtAlCl_2$, Et_2AlCl, $LiClO_4$, LiBr, $TiCl_4$, $SnCl_4$, $ZnCl_2$, $Ti(OR)_4$, $B(OR)_3$, and AlF_3, were ineffective.

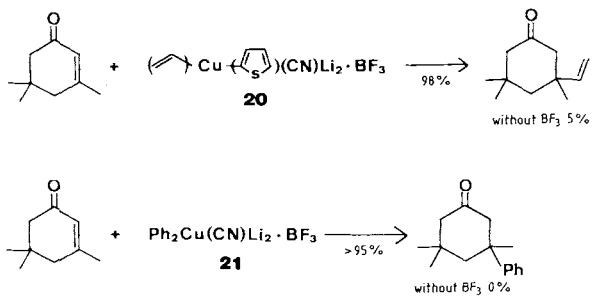
In the total synthesis of levuglandin E_2 (LG E_2), the conjugate addition of $R_2CuLi \cdot MgBr_2$ to **22** proceeded in ex-



Scheme 4. Molecular ratio educt : reagent (from the top downwards): 1 : 3.8, no data, 1 : 0.3, 1 : 1.4. HMPA = hexamethylphosphoric triamide.

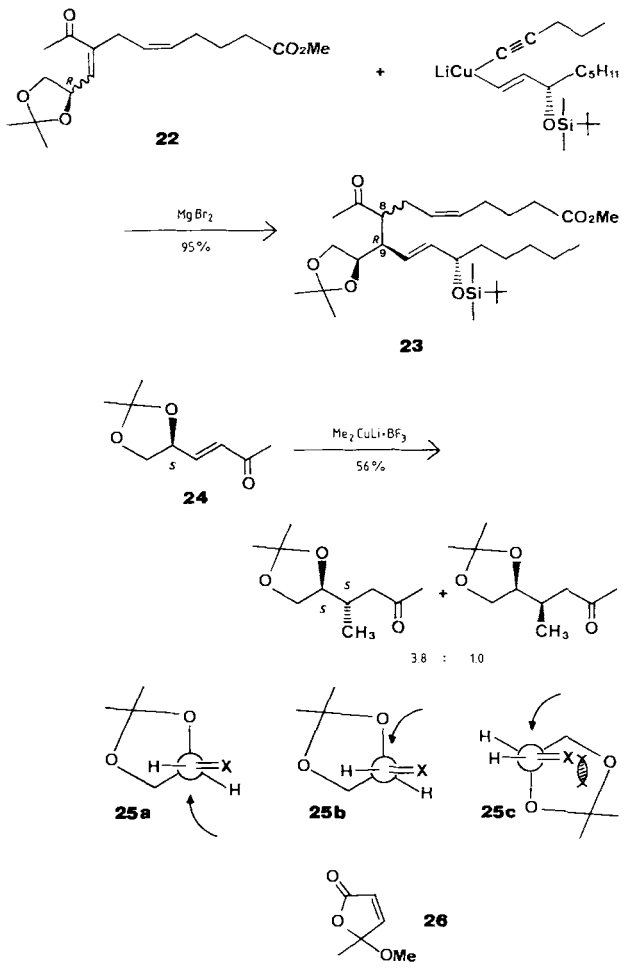


Scheme 5. Molecular ratio educt : **19** = 1 : 2.



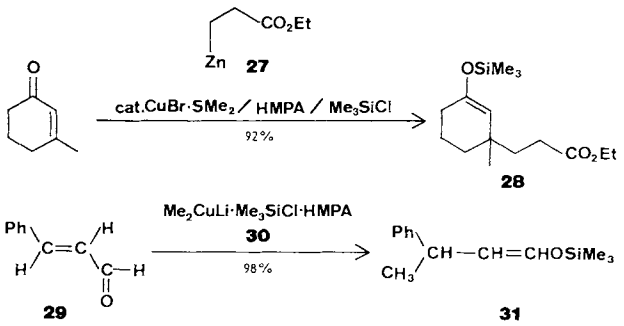
Scheme 6. Molecular ratio educt : reagent (from top downwards): 1 : 1.4, 1 : 1.

cellent yields, whereas without $MgBr_2$ the adduct **23** was not obtained.[20a] Although epimerization was observed at C-8 of **23**, an (*R*)-configuration [(*R,R*)-**23**] was selectively generated at C-9, thus indicating that very high acyclic stereoselection can be achieved in the 1,4-addition. Similarly, the conjugate addition of $Me_2CuLi \cdot BF_3$ to **24** afforded the (*S,S*)- and (*S,R*)-adducts in the ratio 3.8 : 1.[20b] Presumably, **25b** and **25c** are less stable than **25a** owing to steric hindrance, which leads to the (*S,S*)-isomer (Scheme 7). Although $R_2CuLi \cdot MgBr_2$ adds to **22** in a 1,4-manner, it does not react with **26**.[21] This is reasonable, since the reactivity of α,β-unsaturated ketones is generally greater than that of α,β-unsaturated esters in conjugate additions.



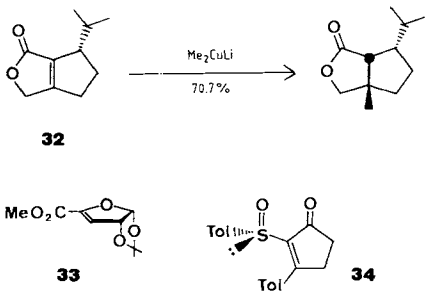
Scheme 7.

A 1,4-addition of the zinc-substituted ester **27** can be realized in the presence of catalytic amounts of CuBr and Me_3SiCl.[22] In the absence of Me_3SiCl, no such addition occurs. HMPA presumably plays an important role in the transmetalation state from **27** to the copper analogue. This reagent system demonstrates that the organocopper-Lewis acid method can even be carried out catalytically. $R_2CuLi \cdot Me_3SiCl$ can also be used for the 1,4-addition to enones.[23] The reaction of lithium diallylcuprate with 2-cyclohexenone, e.g., gave a 82 : 18 mixture of the 1,4- and 1,2-adducts, while the lithium diallylcuprate-trimethylsilyl chloride complex increased the ratio to >98 : <2. Reagents of this type have also proven effective in the case of α,β-unsaturated aldehydes. Thus, e.g., reaction of **29** with **30** afforded the 1,4-adduct **31** in 98% yield; with Me_2CuLi itself the yield of adduct was only 74% (Scheme 8).



Scheme 8.

There are, however, a few examples in which the organocopper-Lewis acid reagents do not work well. Although the addition of Me_2CuLi to **32** proceeded smoothly, use of $Me_2CuLi \cdot BF_3$ or $MeCu \cdot BF_3$ gave dark resinous materials.[24] 1,4-Addition to **33** did not occur with Me_2CuLi nor with $MeCu \cdot BF_3$,[25] and, although $Me_5Cu_3Li_2$ added smoothly to **34** in the sense of a Michael addition, $MeCu \cdot BF_3$ and $Me_2Cu(CN)Li_2$ proved ineffective (Scheme 9).[26]



Scheme 9. Molecular ratio **32** : reagent = 1 : 5.

3. Regio-, Stereo-, and Chemoselective 1,4-Addition

In the conjugate addition of $BuCu \cdot BF_3$ to the α,β,γ,δ-unsaturated ester **35** the 1,4-adduct was obtained, whereas with Bu_2CuLi the 1,6-adduct was formed;[4,6] a similar trend was observed in the case of α,β,γ,δ-unsaturated ketone **36**.[27] On the other hand, reaction of the corresponding acid **37** with $BuCu \cdot BF_3$ afforded almost exclusively the 1,6-adduct.[4,6] Reaction of $Me_2CuLi \cdot Me_3SiCl$ with **38** likewise gave the 1,6-adduct in excellent yield;[23] the same regioselectivity was found with Me_2CuLi itself (Table 1).

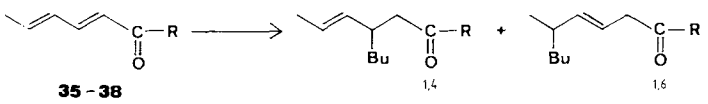
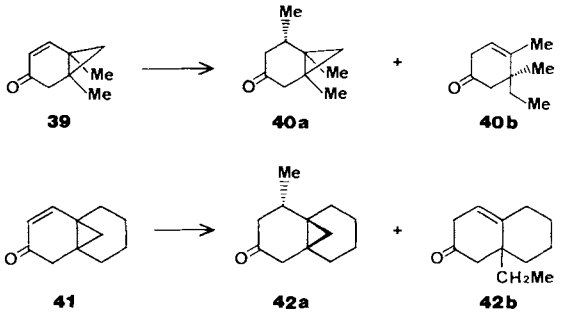


Table 1. Regioselectivity in the reaction of the diene derivatives **35**–**38**.

Educt	R	Reagent	Mol. ratio Educt : Reagent	Yield [%] 1,4 + 1,6	Yield [%] 1,4 : 1,6
35	OMe	$BuCu \cdot BF_3$	1 : 2	44	93 : 7
35	OMe	Bu_2CuLi	1 : 1	82	— 100
36	Me	$BuCu \cdot BF_3$		40	60 : 40
36	Me	Bu_2CuLi		60	— 100
37	OH	$BuCu \cdot BF_3$	1 : 3		14 : 86
38	Ph	$Me_2CuLi \cdot Me_3SiCl$			— 98[a]
38	Ph	Me_2CuLi			— 46[b]

[a] Me instead of Bu. [b] Me instead of Bu. A polar byproduct is also formed, presumably the dienol derivative, by 1,2-addition to **38** [27].

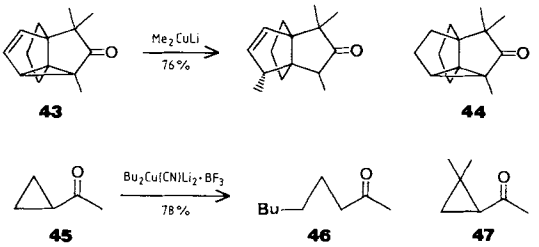
As *Ibuka* has already demonstrated, $RCu \cdot AlCl_3$ is a useful reagent for regio- and stereoselective 1,4-additions to β′-cyclopropyl-α,β-enones such as **39** and **41**.[28,29] Thus, $MeCu \cdot AlCl_3$ selectively produced the 1,4-adducts **40a** and **42a**, while Me_2CuLi afforded the 1,6-adducts **40b** and **42b** as major products. No ring-opening takes place with $RCu \cdot AlCl_3$, thus indicating that no electron transfer step participates in conjugate additions with RCu-Lewis acid reagents (Scheme 10).



	Yield	40a	: 40b
Me_2CuLi [30]		48	: 52
$MeCu \cdot AlCl_3$	72%	100	–
	Yield	42a	: 42b
Me_2CuLi [31]	90%	40	: 55
$MeCu \cdot AlCl_3$	75%	100	—

Scheme 10. Molecular ratio educt : reagent (from top downwards): 1 : 1, 1 : 5, no data, 1 : 5.

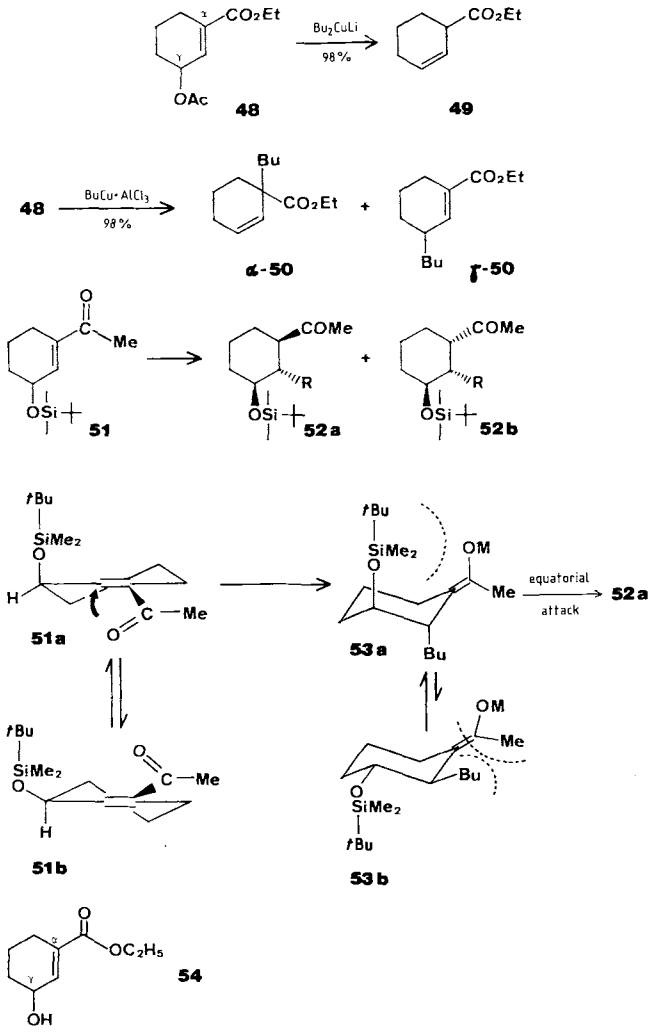
Cyclopropyl ketones, in which the cyclopropane ring is monoactivated by the carbonyl group, do not undergo homoconjugate addition (1,5-conjugate addition) with cuprate reagents, whereas diactivated cyclopropyl ketones do react with cuprates in this manner. For example, **44** was found to be completely resistant to 1,5-addition with Me_2CuLi and $Me_2CuLi \cdot BF_3$, while **43** diactivated with vinyl and carbonyl groups did undergo 1,5-addition.[32] The homoconjugate addition to monoactivated cyclopropanes was, however, realized with $Bu_2Cu(CN)Li_2 \cdot BF_3$.[33] The 1,5-adduct **46** was obtained from **45** in good yields; with $BuCu \cdot BF_3$, however, the 1,2-adduct was obtained as major product. Sterically bulky groups, such as *sec*- or *tert*-butyl, can be introduced in a similar way. In the case of **47**, the butyl group was regioselectively transferred to the less substituted carbon atom, indicating that the complexed reagent reacted in a concerted S_N2 manner (Scheme 11).



Scheme 11. Molecular ratio educt : reagent (from top downwards): 1 : 5, 1 : 3.

Both the γ-acetoxy-substituted α,β-unsaturated ester **48** as well as the related ketone **51** can, in principle, react in a 1,4-addition or allyl substitution. Exactly as in the case of the α,β-unsaturated ketone **22**, which readily undergoes 1,4-addition, and in the case of the α,β-unsaturated (cyclic) ester **26**, where this is not possible, one obtains with **51** a 1,4-addition, but with **48** a substitution at the allyl system. Whereas **48** was reduced with Bu_2CuLi to **49**, with $BuCu \cdot AlCl_3$ **α-50** and **γ-50** were obtained in the ratio 17:83.[34] The ratio increased to 3:97 on using $BuCu \cdot 5\,AlCl_3$. In the absence of $AlCl_3$, only the starting material was recovered. In the case of **51**, however, the conjugate addition took place.[35,37a] Although the reduced product, analogous to **49**, was again obtained as major product with R_2CuLi, reaction of the enone **51** with $RCu \cdot AlCl_3$ or $RCu \cdot BF_3$ gave the conjugate adducts **52a** and **52b**.[6]

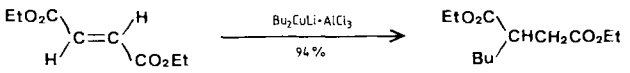
The preferential formation of **52a** can be explained as follows: Due to steric hindrance of the pseudoaxial siloxy group the butyl group of $BuCu \cdot AlCl_3$ or $BuCu \cdot BF_3$ attacks the planar enone system of **51a** from below, thus leading to **53a**. A similar attack in the case of **51b** is hindered by the bulky siloxy group. Although **53b** possesses two equatorial substituents, steric repulsion between the butyl group and the methyl substituent at the double bond of the enolate, which must occupy nearly the same plane, leads to preference of **53a**. Equatorial protonation then leads to **52a**, a reaction which was employed in the total synthesis of perhydrohistrionicotoxin.[36] As will be shown in Section 5, $BuCu \cdot BF_3$ can react with allylic alcohols to give predominantly the γ-substitution product.[38] Treatment of **54** with $BuCu \cdot BF_3$ in the molar ratio 1:4 afforded **α-50** (20%) and **γ-50** (55%).[6] Accordingly, the competition between conjugate addition and substitution in a single molecule leads, in the case of α,β-unsaturated ketones to 1,4-addition, and in the case of α,β-unsaturated esters to substitution (Scheme 12).



	Yield	52a	:	52b
$MeCu \cdot AlCl_3$	84%	90	:	10
Me_2CuLi	<7%	100		—
$BuCu \cdot AlCl_3$	87%	92	:	8
$BuCu \cdot BF_3$ [6]	75%	100		—

Scheme 12. Molecular ratio **48** : $BuCu \cdot AlCl_3 = 1:5$; **51** : $BuCu : BF_3 = 1:2$, in other reactions of **51** 1:1.

Reaction of electron deficient olefins, substituted with two carbonyl groups, with R_2CuLi leads to the reduced compound rather than to the conjugate adduct. The 1,4-addition to such olefins can, however, be accomplished with cuprate·Lewis acid reagents.[37b] Whereas reaction of diethyl fumarate with $Bu_2CuLi \cdot AlCl_3$ afforded the 1,4-adduct (Scheme 13), reaction of diethyl maleate gave

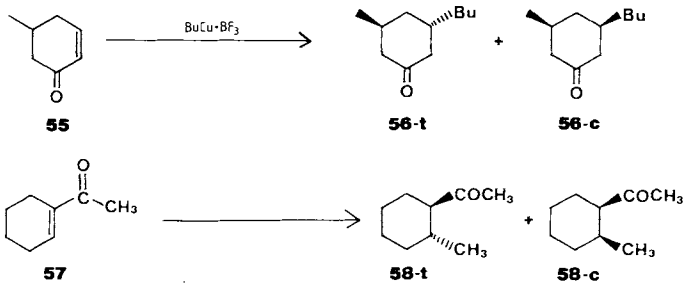


Scheme 13.

predominantly the reduction product under the same conditions. Reaction of triethyl ethylenetricarboxylate with $Me_2CuLi \cdot AlCl_3$ (or $Me_2CuLi \cdot BF_3$) furnished the conjugate adduct in 97% yield. As in the case of **39–42**, the Lewis acid complexes of organocopper compounds obviously do not react with α,β-unsaturated ketones and similar compounds via electron transfer. This is an advantage, since such an electron transfer often results in the reduction of substrates, and this can either be the main or side reaction.

The stereochemistry of the 1,4-addition with RCu-Lewis acid reagents was investigated for the compounds **8–10**, **17**, **22**, **24**, **32**, **39**, **41**, and **51**, as well as for some simpler and more general systems.[6] Treatment of **55** with $BuCu \cdot BF_3$ afforded a mixture of **56-t** and **56-c** in the ratio 90:10. With Bu_2CuLi, almost the same ratio was obtained. The preferred formation of **56-t** can be explained in terms of an antiparallel attack, as described in the case of **51a**. The *cis*-isomer **58-c** was formed as main product in the conjugate addition of **57**. The highest stereoselectivity was realized with $MeCu \cdot BF_3$. Also $MeCu \cdot BF_3 \cdot PBu_3$, a colorless compound that is soluble in ether and stable at 0°C,[6] has already been used with success for high asymmetric induction reactions (see Section 4)[39] (Scheme 14).

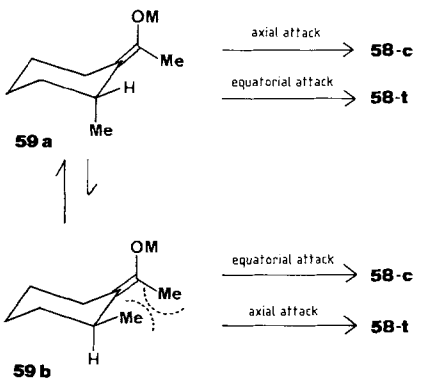
The *cis*-preference of **57** can be explained as follows: whereas an equatorial attack is more favorable in the case of **59b**, in the case of **59a** an axial attack occurs more readily than the equatorial attack owing to the steric bulkiness of the methyl group. **59b** is presumably less stable



	Yield	58-t : 58-c
$MeCu \cdot BF_3$	63%	14 : 86
Me_2CuLi	93%	31 : 69
$MeCu \cdot PBu_3$	55%	36 : 64
$MeCu \cdot BF_3 \cdot PBu_3$	39%	18 : 82

Scheme 14. Molecular ratio **57** : reagent, in all four examples 1 : 1.

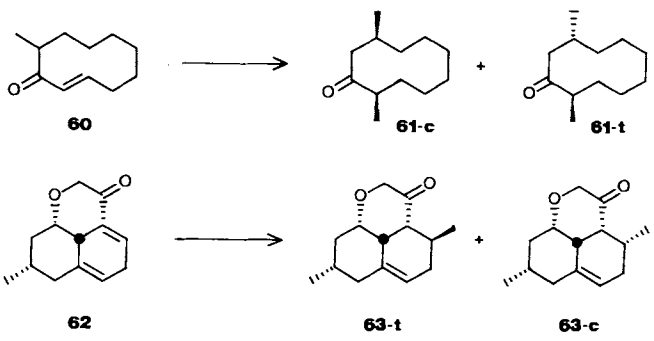
than **59a** owing to the same reasons given in the case of **53b**. That **57** exhibits *cis*-preference and **51** *trans*-preference could be explained in terms of the sterically very bulky silyl group, which must prevent the axial protonation of **53a** (Scheme 15).



Scheme 15.

The high stereoselectivity of organocopper-Lewis acid reagents is also observed in the reactions of macrocyclic enones.[40] Thus, the conjugate addition of $MeCu \cdot BF_3$ to **60** gave the compound **61-c** with a stereoselectivity of >99%. Me_2CuLi was not quite as effective. **8**[12] also reacts with higher diastereoselectivity (5 : 1) with $RCu \cdot BF_3$ than with R_2CuLi (4 : 1). In the total synthesis of mevinolin, a stereoselective conversion of **62** into **63-t** was necessary. Among several reagents examined, $MeCu \cdot BF_3$ showed the best stereoselectivity (Scheme 16).[41]

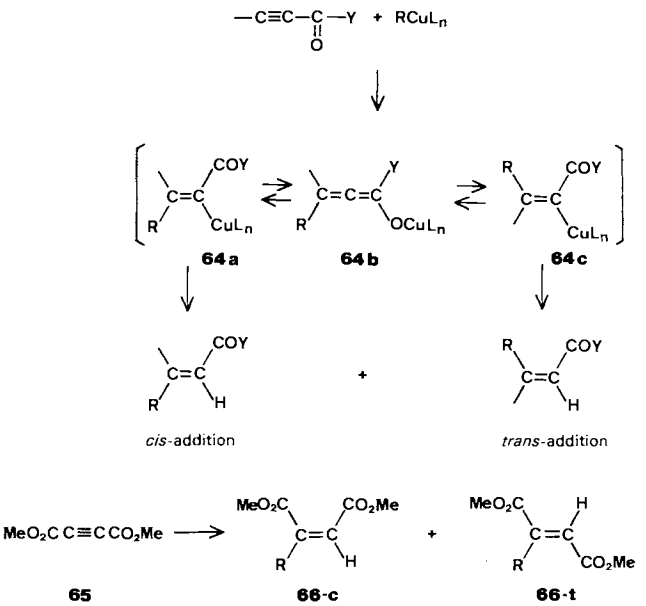
Since the conjugate addition to α,β-alkynones proceeds via the copper-substituted enolate **64**, the geometry of the products strongly depends on the temperature and duration of the reaction before quenching. Highly stereoselective *cis*-additions are achieved with reagents of the type $RCu \cdot BR'_3$.[42] Of the reagents examined for the conversion **65** into **66-c**, $BuCu \cdot BEt_3$ exhibited the highest stereoselectivity. Presumably, in this case, the intermediate **64a** initially formed via the organocopper compound is stabilized (Scheme 17).



	Yield	61-c : 61-t
Me_2CuLi	82%	94 : 6
$MeCu \cdot BF_3$	98%	>99 : <1

	Yield	63-t : 63-c
Me_2CuLi	77%	86 : 16
$Me_2Cu(CN)Li_2$	78%	80 : 20
$MeCu(CN)Li$	61%	67 : 33
$MeCu \cdot BF_3$	79%	>98 : <2

Scheme 16. Molecular ratio educt : reagent (from top downwards): 1 : 8, 1 : 5, no data for the next three examples, last example 1 : 3.



	Yield	66-c : 66-t
$BuCu \cdot BEt_3$	93%	>99 : <1
Bu_2CuLi	98%	60 : 40
$BuCu \cdot B(OMe)_3$	92%	91 : 9
$BuCu \cdot BF_3$	85%	87 : 13

Scheme 17.

4. Asymmetric Induction in 1,4-Additions

Very high asymmetric induction was achieved in the Michael addition to α,β-unsaturated esters by using $RCu \cdot BF_3$.[43] Thus, **67** reacts with $BuCu \cdot BF_3$ to give **68** in 99.5% *ee*. Presumably, the conformation of the enoate is fixed by the Lewis acid as indicated in **67**, and thus the R group is forced to attack from the direction depicted by an arrow. The enantiomer excess of 78% *ee* achieved by addi-

tion of $MeCu \cdot BF_3$ to **69** increased to 86.5% on using $MeCu \cdot BF_3 \cdot PBu_3$.[39] Me_2CuLi did not react with **70** at all, whereas reaction of $MeCu \cdot BF_3 \cdot PBu_3$ with **70** afforded the conjugate adduct in 94% *ee*. A very high asymmetric induction was similarly observed upon reaction of **74** with $RCu \cdot BF_3 \cdot PBu_3$.[44] Further examples are listed in Table 2.

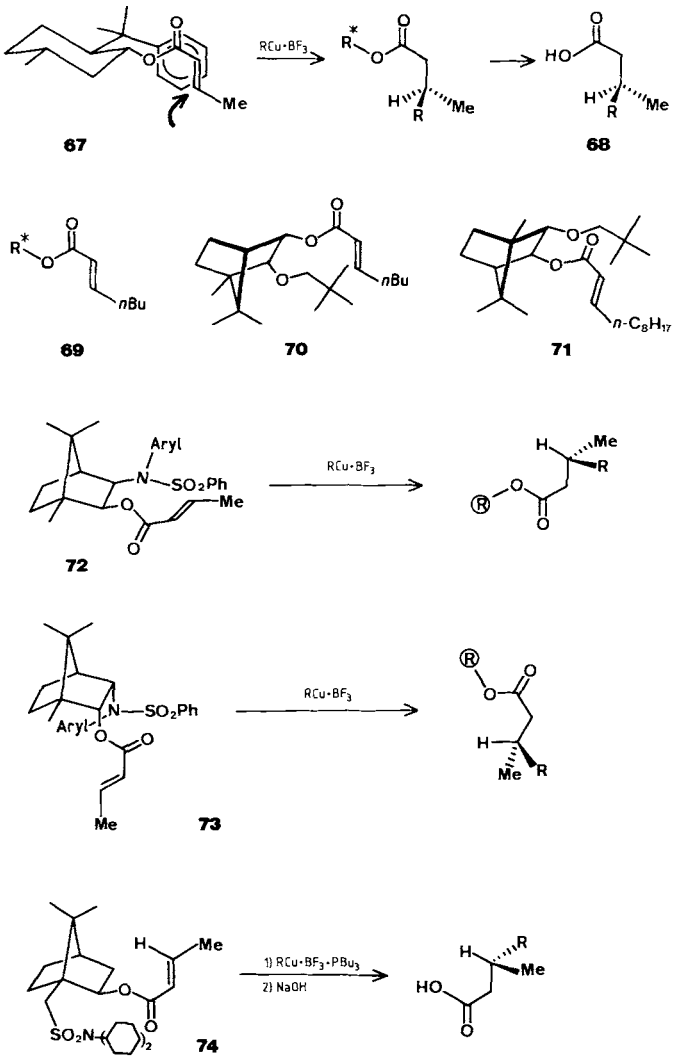
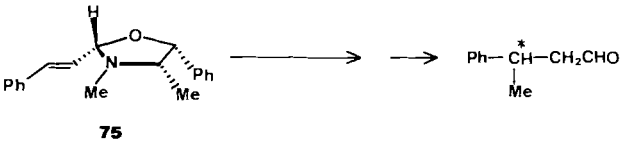


Table 2. Asymmetric induction in the reaction of the educts **67** and **69**–**73**. R*OH = 8-phenylmenthol; ®OH = sulfonamide-protected terpene alcohol.

Educt	Reagent	Mol. ratio Educt : Reagent	Yield [%]	*ee* [%] or Diastereomeric ratio	Ref.
67	$PhCu \cdot BF_3$	1 : 2	76	99.3	
67	$BuCu \cdot BF_3$	1 : 2	76	99.5	
69	$MeCu \cdot BF_3$			78	
69	$MeCu \cdot BF_3 \cdot PBu_3$			87	[39]
70	Me_2CuLi		—		
70	$MeCu \cdot BF_3 \cdot PBu_3$			94	
71	$MeCu \cdot BF_3 \cdot PBu_3$			98	
72	$EtCu \cdot BF_3$	1 : 5	90	>99 : <1	[45]
72	$iPrCu \cdot BF_3$	1 : 5	90	>99 : <1	[45]
72	$CH_2{=}CHCu \cdot BF_3$	1 : 5	94	>99 : <1	[45]
72	$PhCu \cdot BF_3$	1 : 5	97	>99 : <1	[45]
73	$EtCu \cdot BF_3$	1 : 5	84	>99 : <1	[45]
73	$iPrCu \cdot BF_3$	1 : 5	97	98 : 2	[45]
73	$CH_2{=}CHCu \cdot BF_3$	1 : 5	81	>99 : <1	[45]
73	$PhCu \cdot BF_3$	1 : 5	94	>99 : <1	[45]

A significant chiral induction was obtained upon addition of $Me_2CuLi \cdot BF_3$ to the chiral oxazolidine **75** in ether.[46] However, with hexane as solvent, high asymmetric induction was realized by use of Me_2CuLi itself. $MeCu \cdot BF_3$ in ether was ineffective (Scheme 18).

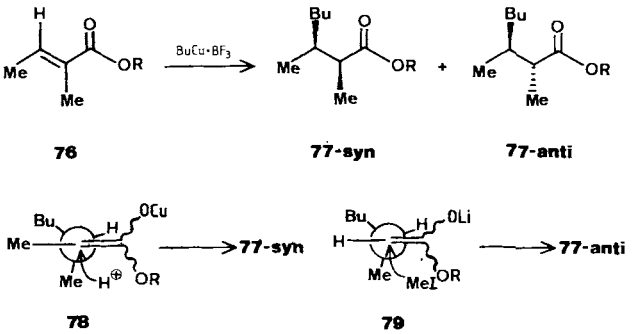


75

	Yield	*ee*
Me_2CuLi/THF	76%	10%
$Me_2CuLi \cdot BF_3$/Ether	88%	51%
Me_2CuLi/hexane	80%	80%
$MeCu \cdot BF_3$/ether	76%	9%

Scheme 18. THF = tetrahydrofuran.

Stereoselectivities in conjugate additions to α,β-unsaturated ketones and esters with chiral centers at their γ- or δ-positions have been investigated on **8**–**10**, **17**, **22**, **24**, **51**, **55**, and **60**. In addition, the stereochemistry of the protonation of enolates such as **53** and **59** obtained by conjugate addition have also been studied. Furthermore, the stereochemistry of the 1,4-addition of $RCu \cdot BF_3$ to the acyclic enoate **76** has also been studied;[47] reaction of **76** with $BuCu \cdot BF_3$ afforded **77** in good yields, though reaction with Bu_2CuLi gave poor results. The *syn*/*anti* ratio of **77** was ca. 7 : 3 regardless of the structure of R. The stereochemistry can be explained with the eclipsed model **78**: The protonation of the copper enolate occurs from the less hindered side, thus leading predominantly to **77-syn**. A similar eclipsed model can be applied to the methylation of the lithium enolate **79**; the methylation occurs from the less hindered side, leading to formation of **77-syn**/**anti** in the ratio 3 : 7 (Scheme 19).

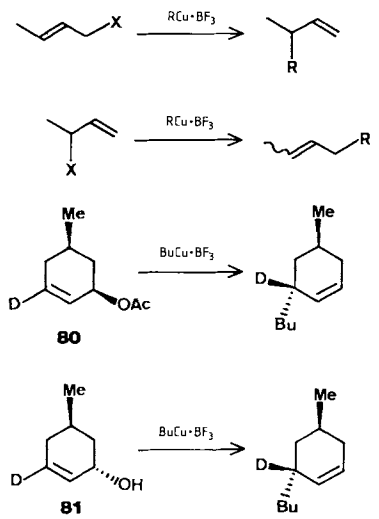


Scheme 19.

5. Regioselective Alkylation of Allylic Derivatives

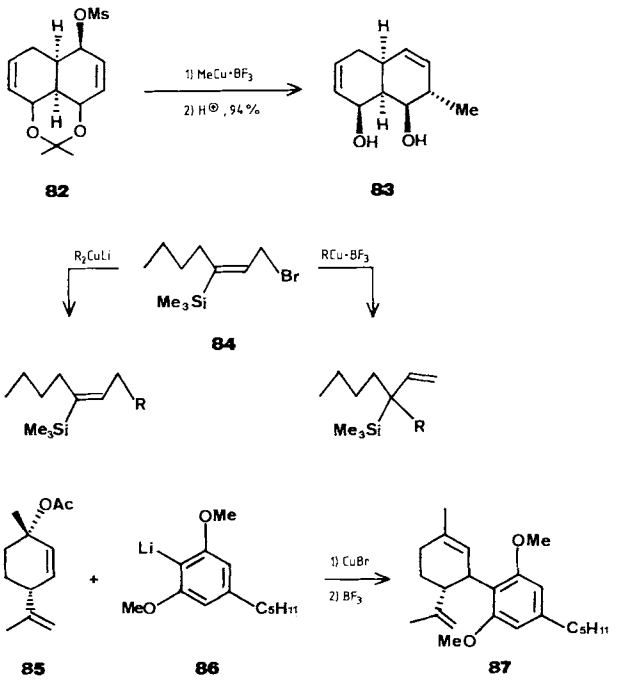
The γ-alkylation of allylic halides, alcohols, and their derivatives with $RCu \cdot BF_3$ is a highly regioselective process.[4,48] As expected the substitution reaction of **80** with $BuCu \cdot BF_3$ proceeds via an *anti*-S_N2' mechanism, while that of **81** proceeds via a *syn*-S_N2' mechanism. The surprising *syn*-S_N2' mechanism observed in the reaction of **81** is

presumably due to the coordination of $RCu \cdot BF_3$ to the OH group. Other organocopper reagents do not react with allylic alcohols (Scheme 20).



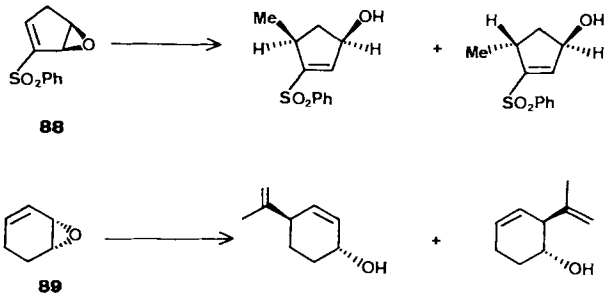
Scheme 20. X = halide, OH, OAc, etc.

Although treatment of **82** with Me_2CuLi gave the S_N2-type product, the *anti*-S_N2' reaction took place with $MeCu \cdot BF_3$ to give **83**.[49] Similarly, **84** reacts with $RCu \cdot BF_3$ via an S_N2' mechanism, but with R_2CuLi via an S_N2 mechanism.[50] In this case, the γ-substitution product was also obtained with RCu itself. The cuprate, $aryl_2CuLi$, derived from **86** did not react with **85**, whereas the complex $aryl_2CuLi \cdot BF_3$ did so, to give the *anti*-S_N2' product **87** in 78% yield, which was further transformed into tetrahydrocannabinol (Scheme 21).[51]



Scheme 21. Ms = methanesulfonyl.

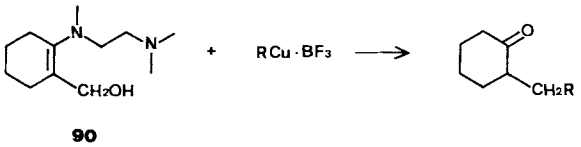
Reaction of the allylic epoxide **88** with $MeCu \cdot AlMe_3$ afforded the *anti*-S_N2' product, while reaction with $MeLi \cdot LiClO_4$ furnished the *syn*-S_N2' product.[52] Presumably the MeLi reagent coordinates to the epoxide oxygen, resulting in the *syn* attack; in contrast, such coordination is not observed in the case of $MeCu \cdot AlMe_3$ and **80**, **82**, or **85**. Treatment of **89** with $RCu \cdot BF_3$ again gave predominantly the *anti*-S_N2' product, along with the *anti*-S_N2 isomer; better regioselectivities were obtained with RCu(CN)Li than with $RCu \cdot BF_3$ (Scheme 22).[53]



	Yield			
$MeCu \cdot AlMe_3$	80%	<2	:	>98
$MeLi \cdot LiClO_4$	81%	95	:	5
	Yield			
$RCu \cdot BF_3$	26%	62	:	38
$RCu \cdot PBu_3$	23%	29	:	71
RCu(CN)Li	75%	75	:	25

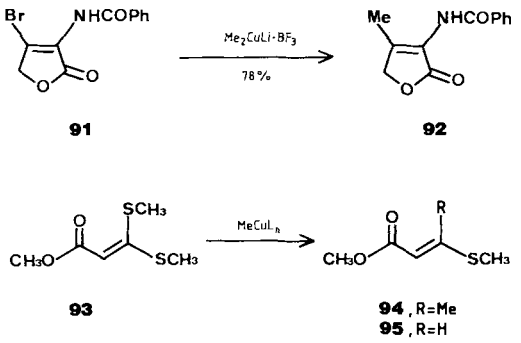
Scheme 22. R = isopropenyl.

Although RCu · Lewis acid reagents generally react γ-regioselectively with allylic derivatives, α-substitution is also observed, e.g., in the case of the γ-acetoxy-α,β-enoate **48**.[34,35] In this respect, the α-selectivity of the γ-hydroxy-α,β-enoate **54** is also interesting. Further, the α-substitution of the enamine alcohol **90** with $RCu \cdot BF_3$ has been reported recently;[54] the α-alkylated ketone was formed in good yields (Scheme 23).



Scheme 23. R = *n*Bu, 76% yield; R = *t*Bu, 54% yield.

Replacement of halogen at the β-position of α,β-unsaturated γ-lactones such as **91** proceeded quite smoothly with $Me_2CuLi \cdot BF_3$.[55] With Me_2CuLi, on the other hand, **92** could be obtained only in low yield (<30%), and with Me_3CuLi_2 or $MeLi \cdot BF_3$ it could not be obtained at all. Treatment of **93** with Me_2CuLi afforded **94** (16%) and **95** (61%); the amount of **94** could not be increased even on using $MeCu \cdot BF_3$.[56] It is anticipated that the yield may be improved by use of $Me_2CuLi \cdot BF_3$ (Scheme 24).



Scheme 24.

6. Selective Reactions with Carbonyl Compounds, Schiff Bases, Epoxides, Aziridines, Ethers, Acetals, Orthoformates, and Pyridinium Salts

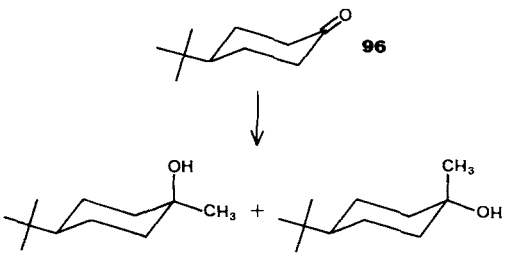
Very high chemoselectivity towards carbonyl groups can be realized with $RCu \cdot BF_3$ (Table 3).[6] Thus, propanal undergoes butylation almost exclusively in the presence of cyclohexanone.



Table 3. Chemoselectivity of some reagents towards carbonyl groups: reaction of a 1 : 1 propanal/cyclohexanone mixture.

Reagent	Molar ratio Educt : Reagent	Yield [%]	Propanal derivative : Cyclohexanone derivative
$BuCu \cdot BF_3$	1 : 2	95	95 : 5
$BuCu \cdot BF_3$	1 : 1	70	99 : 1
Bu_2CuLi	1 : 1	92	76 : 24
BuMgBr	1 : 1	91	88 : 12
BuLi	1 : 1	88	46 : 54

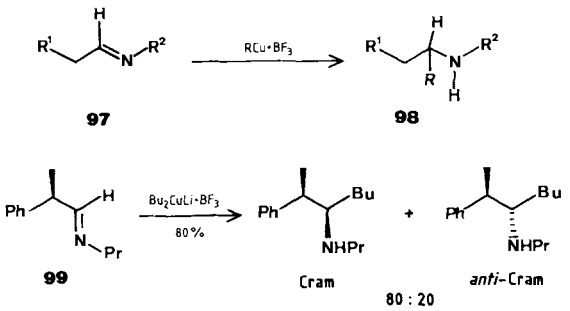
The stereoselectivity of the 1,2-addition was studied on the cyclic system **96**, but it was low in comparison to that observed in the reaction with MeLi or $MeLi \cdot AlEt_3$ (Scheme 25).



$MeCu \cdot BF_3$	68	:	32
MeLi	84	:	16
$MeLi \cdot AlEt_3$	87	:	13

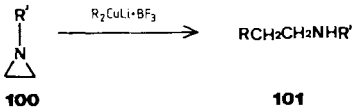
Scheme 25. Molecular ratio **96** : reagent (from top downwards): 1 : 3, 1 : 1, 1 : 1.

In general, the alkylation of Schiff bases with conventional organometallic compounds does not proceed smoothly; the reaction is often accompanied by α-deprotonation. However, **97** could be smoothly converted into **98** in high yields with $RCu \cdot BF_3$;[57] with RMgBr, RCu, or R_2CuLi, the desired product (**98**) was not obtained. $R_2CuLi \cdot BF_3$ was effective for the alkylation of sterically bulky Schiff bases, which do not react with $RCu \cdot BF_3$. The diastereofacial selectivity of the chiral Schiff base **99** was investigated by reaction with $Bu_2CuLi \cdot BF_3$; the ratio of Cram to *anti*-Cram compound (4 : 1)[58] was very close to that found in the butylation of the corresponding aldehyde (Scheme 26).



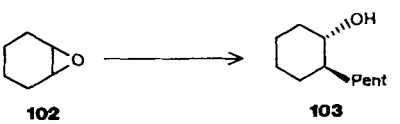
Scheme 26.

The alkylation of an ordinary aziridine with ring opening could not be accomplished with MeLi or RMgX. The alkylation of a strained tricyclic *N*-acylaziridine, however, was achieved with R_2CuLi in 15% yield. With $R_2CuLi \cdot BF_3$, the alkylation of **100** proceeded quite smoothly to give **101** in moderate to high yields (Scheme 27).[59]



Scheme 27. R = Me, Bu, Ph; R' = Me, Bu; yield 56–97%.

The stereoselective ring-opening alkylation of epoxides with $R_2CuLi \cdot BF_3$ takes place rapidly even at −78 °C.[60] For example, reaction of **102** with $R_2CuLi \cdot BF_3$ (R = pentyl) afforded **103** in 92% yield even at −78 °C, while the reaction with R_2CuLi or with $R_2Cu(CN)Li_2$ required higher temperatures and a prolonged reaction time (Scheme 28). $R_2Cu(CN)Li_2 \cdot BF_3$ was also found to be suitable for the stereoselective ring-opening alkylation of epoxides.[19] Unfortunately, however, **102** does not undergo such a ring opening reaction with $Me_3Si(PhS)CHCu \cdot BF_3$.[63]



			Yield
$R_2CuLi \cdot BF_3$	−78 °C, ether	10 min	92%
R_2CuLi	0 °C	2 h	97%
$R_2Cu(CN)Li_2$	−20 °C	2 h	95%

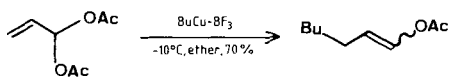
Scheme 28. R = *n*-pentyl. Molar ratio **102** : reagent (from top downwards): 1 : 1, 1 : 5, no data.

Whereas RCu and R_2CuLi are inert towards acetals, $RCu \cdot BF_3$ and $R_2CuLi \cdot BF_3$ react quite rapidly at low temperatures to give the monoalkylation product.[60] Ortho-

esters were likewise found to undergo monoalkylation at low temperatures. While reaction of the allyl acetate **104** with R_2CuLi furnished a mixture of S_N2- and S_N2'-type products, reaction with $RCu \cdot BF_3$ selectively afforded the S_N2' product (Scheme 29).[61]

$$MeCH(OEt)_2 + PhCu \cdot BF_3 \xrightarrow[30\ min,\ 89\%]{-30\,^\circ C,\ ether} PhMeCHOEt$$

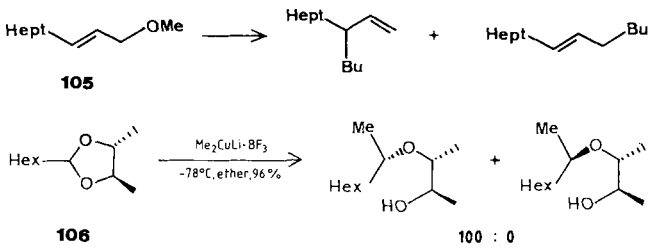
$$HC(OEt)_3 + n\text{-}C_7H_{15}Cu \cdot BF_3 \xrightarrow[20\ min,\ 88\%]{-20\,^\circ C,\ THF} n\text{-}C_7H_{15}CH(OEt)_2$$



104

Scheme 29.

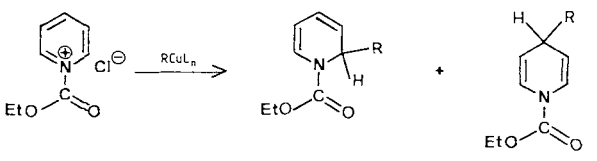
Reaction of the allylic ether **105** with $RCu \cdot BF_3$ proceeded predominantly via an S_N2' mechanism, while the substitution with $R_2CuLi \cdot BF_3$ furnished the S_N2 product.[61] Generally, the reaction of common allylic acetals with $RCu \cdot BF_3$ preferably leads to the S_N2' product, while reaction with $R_2CuLi \cdot BF_3$ preferentially affords the S_N2 product.[61] The chiral acetal **106** reacts with $R_2CuLi \cdot BF_3$ quite smoothly with 100% diastereoselectivity (Scheme 30).[62]



	Yield			
$BuCu \cdot BF_3$	82%	87	:	13
$Bu_2CuLi \cdot BF_3$	35%	2	:	98

Scheme 30. Molar ratio **105** : reagent (from top downwards): 1 : 2, 1 : 1.

Organometallic compounds, such as RLi, RMgX, and RCdX, add preferentially at the 2-position of pyridine derivatives. In contrast, organocuprates react predominantly at the 4-position to give 4-substituted pyridines. The highest regioselectivity was realized in the reaction of **107** with $RCu \cdot BF_3$.[64] The alkylation products (**108** and **109**) were not obtained at all upon reaction with BuLi, while reaction with $BuLi \cdot BBu_3$ furnished a mixture of **108** and **109** in acceptable yield (Scheme 31).



107 **108** **109**

	Yield			
$PhCu \cdot BF_3$	94%	1	:	99
Ph_2CuLi		10	:	90
$BuLi \cdot BBu_3$	58%	38	:	62

Scheme 31.

7. Organocopper-Lewis Acid Reagents: Past and Present

Only two organocopper-Lewis acid reagents, $RCu \cdot BF_3$ and $RCu \cdot BR'_3$, appeared in *Posner*'s book in 1980.[5] Since then, a number of new types of complex reagents have been developed (Table 4). For highly selective transformations, the organocopper- and related organometallic-Lewis acid complex reagents will become increasingly important. In fact, $RLi \cdot BF_3$ and lithium enolate $\cdot BF_3$ reagents have recently been developed, which have already proven to be very useful.

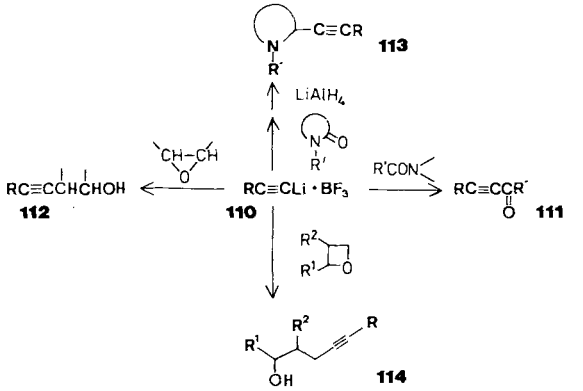
Table 4. Types of organocopper-Lewis acid reagents.

$RCu \cdot BF_3$,	$R_2CuLi \cdot BF_3$	$R_2Cu(CN)Li_2 \cdot BF_3$
$RCu \cdot BF_3 \cdot PBu_3$,	$RCu \cdot BF_3$(HMPA)	
$RCu \cdot BR'_3$		
$RCu \cdot AlCl_3$,	$R_2CuLi \cdot AlCl_3$,	$RCu \cdot AlR'_3$
$R_2CuLi \cdot MgX_2$,		
$R_2CuLi \cdot TiCl_4$		
$RCu \cdot Me_3SiCl$ [a],	$R_2CuLi \cdot Me_3SiCl$ (HMPA) [a]	

[a] Used as catalysts.

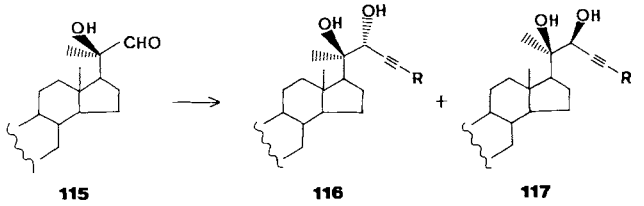
8. Organolithium $\cdot BF_3$ Reagents and Related Species

The complex reagents **110**, prepared in situ from lithium acetylides and BF_3 at $-78\,^\circ C$ in THF, react with tertiary amides at this temperature to give the corresponding alkynyl ketones **111** in high yields.[65] The formation of tertiary alcohols by further addition of the acetylide to the ketones was not observed. Oxiranes underwent ring-opening alkynylation under mild conditions to afford the alcohols **112** in high yields.[66] With other metal acetylides, the ring-opening reaction requires longer reaction times and/or higher temperatures and even then the yields are low. Alkynyl azacycloalkanes **113** were obtained in good yields by 1,2-addition of **110** to lactams followed by $LiAlH_4$ reduction of the adducts.[67] This transformation can not be achieved with the usual lithium or magnesium acetylides. Oxetanes react with **110** to give the compounds **114** in high yields.[68] Upon reaction with magnesium acetylides, considerable amounts of halohydrins were obtained as by-products; no reaction takes place with lithium acetylides (Scheme 32).



Scheme 32.

In the presence of catalytic amounts of trimethylgallium (0.08 equiv.) lithium acetylides react with epoxides to give **112** in good to excellent yields.[69] The addition of lithium acetylide to (20*R*)-20-hydroxypregnane-20-carbaldehyde **115** in the absence and in the presence of BF_3 gave predominantly **116** and **117**, respectively.[70] This finding provides a solution to the partial synthesis of either the ecdysone or the 22-epiecdysone side chain (Scheme 33). Formation of **116** can be explained in terms of a nucleophilic attack on the chelated substrate from the less hindered side (*Cram*'s cyclic model). In the presence of BF_3, the hydroxy group is presumably converted into an ate complex prior to nucleophilic addition. Consequently, the cyclic model is no longer applicable to the reaction of **110** with **115**; a non-cyclic mechanism (*Felkin*'s mechanism or *Cram*'s dipolar model) may be involved.



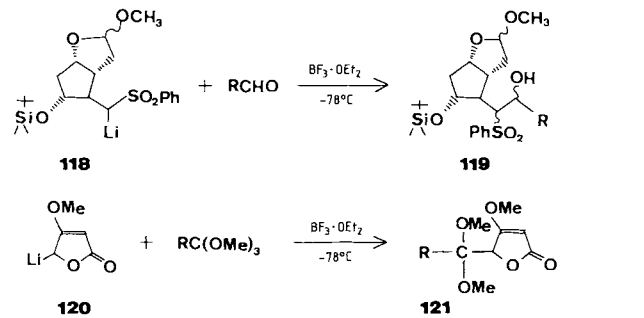
115 **116** **117**

	Yield			
RC≡CLi	91%	2.3	:	1
RC≡CMgBr	76%	6.9	:	1
110	40%	—		100

R = tetrahydropyranyl–O–CMe_2

Scheme 33.

Treatment of the lithiated sulphone **118** with aldehydes gave at best traces of the desired product **119**. Addition of $BF_3 \cdot OEt_2$ to **118** (1 : 1) prior to the addition of aldehydes resulted in formation of **119** in over 90% yield.[71] Similarly, the reaction of **120** with trimethyl orthoformate proceeded smoothly to give **121** in high yield; **121** was not obtained, however, when BF_3 was not present[72] (Scheme 34).

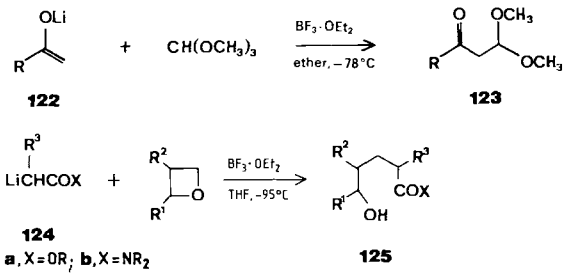


118 **119**

120 **121**

Scheme 34.

Reaction of the lithium enolate **122** with trimethyl orthoformate in the presence of BF_3 led to formation of the corresponding α-dimethoxymethyl ketone **123**.[73] The yield strongly depends on the manner and sequence of mixing of the reagents. BF_3 should be added in one portion to a solution of **122** and the orthoformate in ether. Prior mixing of **122** and BF_3 results in a drastic decrease in product yield. Oxetanes were allowed to react with compounds **124a** and **124b**, generated from esters and amides, respectively; in the presence of BF_3, the δ-hydroxyesters **125a** and amides **125b**, respectively, where formed in high yields (Scheme 35).[74]



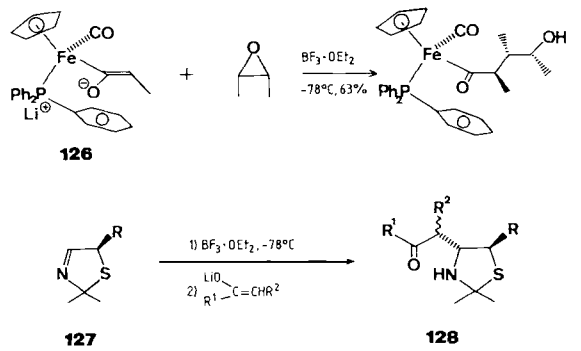
122 **123**

124
a, X = OR; **b**, X = NR_2

125

Scheme 35.

(*Z*)- and (*E*)-2-Butene oxides underwent S_N2 ring opening upon reaction with the lithium enolate **126** obtained from $[(\eta^5\text{-}C_5H_5)Fe(CO)(PPh_3)COCH_2CH_3]$ in the presence of $BF_3 \cdot OEt_2$.[75] Lithium enolates react with dihydrothiazolene **127** in the presence of $BF_3 \cdot OEt_2$ to give the 1,2-adducts **128** in good yields (Scheme 36).[76]



126

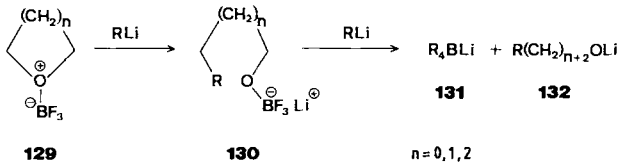
127 **128**

Scheme 36.

9. Mechanism of BF_3-Catalyzed Reactions of Organometallic Compounds

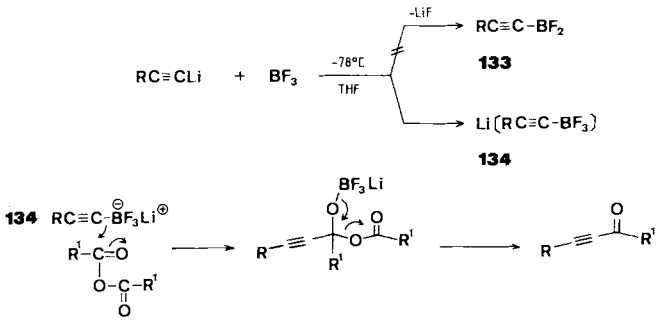
We have seen that combination of BF_3 with moderately basic main-group nucleophiles such as organocopper- and alkynyllithium compounds, lithium enolates, and stabilized lithium derivatives, leads to new reagents which exhibit synthetically useful selectivities and reactivities. However, the mechanisms according to which these new complex reagents react still remain unclear. With the aid of ^{11}B-NMR spectroscopy, *Ganem* et al. have recently established that RLi and $BF_3 \cdot OEt_2$ are reasonably stable together at low temperatures and react independently as potent nucleophile and strong Lewis acid, respectively.[77] In the reaction of RLi · BF_3 with epoxides and related electrophiles, coordination of the Lewis acid to give **129** takes place first and this is then followed by the nucleophilic addition of RLi to give the alkyltrifluoroborate **130**. The complex **130** undergoes attack by residual RLi much more rapidly than does $BF_3 \cdot OEt_2$; as a result tetraalkylborate **131** and lithium alkoxide **132** are formed. The intermediates **130** and **131** were detected by ^{11}B NMR spectros-

copy (Scheme 37). Substituted fluoroboranes such as RBF_2 or R_2BF would logically seem to be reactive intermediates; however, neither species convert epoxides into the corresponding alcohols, even in the presence of added LiF or $BF_3 \cdot OEt_2$.



Scheme 37.

Likewise with the aid of ^{11}B-NMR spectroscopy, *Brown* et al. have revealed that the real intermediate in the reaction of lithium acetylide with carboxylic acid anhydrides in the presence of $BF_3 \cdot OEt_2$ is not the alkynyldifluoroborane **133**, but the ate complex **134**.[78] Presumably the lithium alkynyltrifluoroborate **134** then reacts with anhydrides to give alkynyl ketones in very high yields (Scheme 38).



Scheme 38.

10. Conclusion

It is now clear from ^{11}B-NMR investigations that RLi and BF_3 can coexist at low temperatures, and that the coordination of BF_3 to heteroatoms (O, N, etc.) enhances the reactivity of nucleophiles (simple activation mechanism). As an alternative possibility, the ate complex like **134** may play a role in the BF_3-promoted reactions (ate-complex mechanism).

On the other hand, with regard to the $R_2CuLi \cdot Me_3SiCl$ reagent, *Corey* et al. state that the effect of the trimethylsilyl group is not due to prior complexation of Me_3SiCl with the carbonyl oxygen of the educt.[23] They suggest that the Cu^{III}–Si bond which would result from coupling is quite weak compared to the Si–Cl bond, making for a relatively low rate of replacement of chlorine by copper. Therefore, R_2CuLi and Me_3SiCl can presumably coexist in solution, but the activation of electrophiles as observed in the BF_3-promoted reactions is not expected since the coordination of Me_3SiCl is only very weak. Consequently, as a third possibility, the synergistic effect of substrate-Lewis acid-organometal complex should be considered (the synergistic mechanism or ternary-complex mechanism).[79]

From the synthetic point of view, the organometal-Lewis acid reagents are becoming increasingly important as a new synthetic tool; complex reagents other than organocopper-Lewis acid compounds should also be explored.[80] The types of complexes known so far are summarized in Table 5.

Table 5. Complex reagents formed by combination of nucleophiles and Lewis acids.

	Nucleophile		Lewis acid	Complex reagent
soft	$-C{=}C-O-Si$	hard	$TiCl_4$	[1]
↑	$-C{=}C-CH_2-Si$	↑	$TiCl_4$	[2]
	RCu		BF_3, $AlCl_3$ (solid)	$RCu \cdot BF_3$, $RCu \cdot AlCl_3$
	R_2CuLi			$R_2CuLi \cdot BF_3$, $R_2CuLi \cdot Me_3SiCl$
			BR'_3, AlR'_3	$RCu \cdot BR'_3$, $RCu \cdot AlR'_3$
	$-C{=}C-O-Li$		Me_3SiCl	$-C{=}C-O-Li \cdot BF_3$
	$-C{\equiv}C-Li$			$-C{\equiv}C-Li \cdot BF_3$
hard	RLi	soft		$RLi \cdot BF_3$

In the development of new complex reagents the following considerations can be used as a guideline: Combinations of soft nucleophiles and hard Lewis acids or of hard nucleophiles and soft Lewis acids seem to be compatible at low temperature, and to function as new complex reagents. Hard nucleophiles and hard Lewis acids readily undergo transmetalation reactions, even at low temperatures. Consequently, combinations along this line may produce a new complex reagent. Moreover, organometal-multidentate Lewis acid systems may exhibit interesting properties, since such Lewis acids could interact simultaneously with nucleophiles and with electrophiles.

Our work was supported primarily by the Ministry of Education (Japan). My thanks are due to my students for their intelligent questions and comments, especially H. Yatagai, S. Yamamoto, and Y. Ishihara. I would also like to thank Prof. T. Ibuka and Prof. R. W. Hoffmann for helpful discussions, and Mrs. T. Furuta and H. Azami for their help in the preparation of the manuscript.

Received: April 15, 1986 [A 597 IE]
German version: *Angew. Chem. 98* (1986) 945

[1] T. Mukaiyama, K. Narasaka, K. Banno, *Chem. Lett. 1973*, 1011; T. Mukaiyama, *Org. React. 28* (1982) 203.
[2] A. Hosomi, H. Sakurai, *Tetrahedron Lett. 1976*, 1295; H. Sakurai, *Pure Appl. Chem. 54* (1982) 1.
[3] a) M. T. Reetz, *Top. Curr. Chem. 106* (1982) 1; M. T. Reetz, J. Westermann, R. Steinbach, *Angew. Chem. 92* (1980) 931; *Angew. Chem. Int. Ed. Engl. 19* (1980) 900; b) D. Seebach, *Modern Synth. Method 3* (1983) 216; B. Weidmann, D. Seebach, *Helv. Chim. Acta 63* (1980) 2451.
[4] Y. Yamamoto, K. Maruyama, *J. Am. Chem. Soc. 100* (1978) 3240; *99* (1977) 8068.
[5] G. H. Posner: *An Introduction to Synthesis Using Organocopper Reagents*, Wiley, New York 1980; *Org. React. 19* (1972) 1; *22* (1975) 253.
[6] Y. Yamamoto, S. Yamamoto, H. Yatagai, Y. Ishihara, K. Maruyama, *J. Org. Chem. 47* (1982) 119.
[7] C. Lion, J. Dubois, I. Saumtally, *C. R. Acad. Sci. Ser. 2 298* (1984) 783.
[8] M. Karpf, A. S. Dreiding, *Tetrahedron Lett. 21* (1980) 4569; *Helv. Chim. Acta 64* (1981) 1123.
[9] A. B. Smith, III, P. J. Jerris, *J. Am. Chem. Soc. 103* (1981) 194; *J. Org. Chem. 47* (1982) 1845.
[10] H. Schostarez, L. A. Paquette, *J. Am. Chem. Soc. 103* (1981) 722; *Tetrahedron 37* (1981) 4431.

[11] A. S. Kende, B. Roth, P. J. Sanfilippo, T. J. Blacklock, *J. Am. Chem. Soc. 104* (1982) 5808.
[12] C. H. Heathcock, C. M. Tice, T. C. Germroth, *J. Am. Chem. Soc. 104* (1982) 6081.
[13] T. Cohen, M. Bhupathy, J. R. Matz, *J. Am. Chem. Soc. 105* (1983) 520. The diene was formed in 33% yield as byproduct by 1,2-addition/dehydration; with Me_2CuLi it was the main product.
[14] B. B. Snider, T. C. Kirk, *J. Am. Chem. Soc. 105* (1983) 2364.
[15] H. Nemoto, H. Kurobe, K. Fukumoto, T. Kametani, *Tetrahedron Lett. 25* (1984) 4669.
[16] E. Piers, A. V. Gavai, *Tetrahedron Lett. 27* (1986) 313; E. Piers, B. W. A. Yeung, *J. Org. Chem. 49* (1984) 4567.
[17] P. Magnus, D. Quagliato, *J. Org. Chem. 50* (1985) 1621.
[18] Y. Ito, H. Imai, T. Matuura, T. Saegusa, *Tetrahedron Lett. 25* (1984) 3091.
[19] B. H. Lipshutz, D. A. Parker, J. A. Kozlowski, S. L. Nguyen, *Tetrahedron Lett. 25* (1984) 5959.
[20] a) R. G. Salomon, *Acc. Chem. Res. 18* (1985) 294; R. G. Salomon, D. B. Miller, S. R. Raychaudhuri, K. Avasthi, K. Lal, B. S. Levison, *J. Am. Chem. Soc. 106* (1984) 8296; b) J. K. Cha, S. C. Lewis, *Tetrahedron Lett. 25* (1984) 5263.
[21] B. S. Levison, D. B. Miller, R. G. Salomon, *Tetrahedron Lett. 25* (1984) 4633.
[22] E. Nakamura, U. Kuwajima, *J. Am. Chem. Soc. 106* (1984) 3368.
[23] E. J. Corey, N. W. Boaz, *Tetrahedron Lett. 26* (1985) 6019.
[24] R. A. Roberts, V. Schüll, L. A. Paquette, *J. Org. Chem. 48* (1983) 2076.
[25] R. Bonjouklian, B. Ganem, *Carbohydr. Res. 76* (1979) 245.
[26] G. H. Posner, T. P. Kogan, M. Hulce, *Tetrahedron Lett. 25* (1984) 383.
[27] F. Barbot, A. K. Elban, P. Miginiac, *J. Organomet. Chem. 255* (1983) 1.
[28] T. Ibuka, E. Tabushi, *J. Chem. Soc. Chem. Commun. 1982*, 703.
[29] T. Ibuka, E. Tabushi, M. Yasuda, *Chem. Pharm. Bull. 31* (1983) 128.
[30] C. P. Casey, M. C. Cesa, *J. Am. Chem. Soc. 101* (1979) 4236.
[31] J. A. Marshall, R. A. Ruden, *J. Org. Chem. 37* (1972) 659.
[32] P. A. Wender, G. B. Dreyer, *J. Am. Chem. Soc. 104* (1982) 5805. These reactions were carried out in order to synthesize modhephen.
[33] C. Mioskowski, S. Manna, J. R. Falck, *Tetrahedron Lett. 24* (1983) 5521.
[34] T. Ibuka, H. Minakata, *Synth. Commun. 10* (1980) 119.
[35] T. Ibuka, H. Minaka, Y. Mitsui, K. Kinoshita, Y. Kawai, N. Kimura, *Tetrahedron Lett. 21* (1980) 4073.
[36] T. Ibuka, H. Minakata, Y. Mitsui, E. Tabushi, T. Taga, Y. Inubushi, *Chem. Lett. 1981*, 1409.
[37] a) T. Ibuka, H. Minakata, Y. Mitsui, K. Kinoshita, Y. Kawai, *J. Chem. Soc. Chem. Commun. 1980*, 1193; b) T. Ibuka, T. Aoyagi, K. Kitada, F. Yoneda, Y. Yamamoto, *J. Organomet. Chem. 287* (1985) C 18; T. Ibuka, T. Aoyagi, Y. Yamamoto, *Chem. Pharm. Bull. 34* (1986) 2417.
[38] Y. Yamamoto, K. Maruyama, *J. Organomet. Chem. 156* (1978) C 9.
[39] W. Oppolzer, R. Moretti, T. Godel, A. Meunier, H. Loher, *Tetrahedron Lett. 24* (1983) 4971.
[40] W. C. Still, I. Galynker, *Tetrahedron 37* (1981) 3981. For macrocyclic α,β-unsaturated esters, see W. C. Still, I. Galynker, *J. Am. Chem. Soc. 104* (1982) 1774.
[41] S. J. Hecker, C. H. Heathcock, *J. Org. Chem. 50* (1985) 5159.
[42] Y. Yamamoto, H. Yatagai, K. Maruyama, *J. Org. Chem. 44* (1979) 1744.
[43] W. Oppolzer, H. J. Löher, *Helv. Chim. Acta 64* (1981) 2808.
[44] W. Oppolzer, P. Dudfield, T. Stevenson, T. Godel, *Helv. Chim. Acta 68* (1985) 212.
[45] G. Helmchen, G. Wegner, *Tetrahedron Lett. 26* (1985) 6047.
[46] J. Berlan, Y. Besace, D. Prat, G. Pourcelot, *J. Organomet. Chem. 264* (1984) 399.
[47] Y. Yamamoto, K. Maruyama, *J. Chem. Soc. Chem. Commun. 1984*, 904.
[48] Y. Yamamoto, S. Yamamoto, H. Yatagai, K. Maruyama, *J. Am. Chem. Soc. 102* (1980) 2318.
[49] J. Kallmerten, *Tetrahedron Lett. 25* (1984) 2843.
[50] J. Kang, W. Cho, W. K. Lee, *J. Org. Chem. 49* (1984) 1838.
[51] R. W. Rickards, H. Rönneberg, *J. Org. Chem. 49* (1984) 572.
[52] J. C. Saddler, P. L. Fuchs, *J. Am. Chem. Soc. 103* (1981) 2112.
[53] T. Sato, Y. Gotoh, M. Watanabe, T. Fujisawa, *Chem. Lett. 1983*, 1533.
[54] G. Stork, C. S. Shiner, C.-W. Cheng, R. L. Polt, *J. Am. Chem. Soc. 108* (1986) 304.
[55] R. K. Olsen, W. J. Hennen, R. B. Wardle, *J. Org. Chem. 47* (1982) 4605.
[56] R. K. Dieter, L. A. Silks, *III*, J. R. Fishpaugh, M. E. Kastner, *J. Am. Chem. Soc. 107* (1985) 4679.
[57] M. Wada, Y. Sakurai, K. Akiba, *Tetrahedron Lett. 25* (1984) 1079.
[58] Y. Yamamoto, T. Komatsu, K. Maruyama, *J. Am. Chem. Soc. 106* (1984) 5031.
[59] M. J. Eis, B. Ganem, *Tetrahedron Lett. 26* (1985) 1153.
[60] A. Ghribi, A. Alexakis, J. F. Normant, *Tetrahedron Lett. 25* (1984) 3075.
[61] A. Ghribi, A. Alexakis, J. F. Normant, *Tetrahedron Lett. 25* (1984) 3079.
[62] A. Ghribi, A. Alexakis, J. F. Normant, *Tetrahedron Lett. 25* (1984) 3083. For $R_2CuLi \cdot TiCl_4$, see S. D. Lindell, J. D. Elliot, W. S. Johnson, *ibid. 25* (1984) 3947.
[63] T. Cohen, J. P. Sherbine, S. A. Mendelson, M. Myers, *Tetrahedron Lett. 26* (1985) 2965.
[64] K. Akiba, Y. Iseki, M. Wada, *Tetrahedron Lett. 23* (1982) 429.
[65] M. Yamaguchi, T. Waseda, I. Hirao, *Chem. Lett. 1983*, 35.
[66] M. Yamaguchi, I. Hirao, *Tetrahedron Lett. 24* (1983) 391.
[67] M. Yamaguchi, I. Hirao, *Tetrahedron Lett. 24* (1983) 1719.
[68] M. Yamaguchi, Y. Nobayashi, I. Hirao, *Tetrahedron Lett. 24* (1983) 5121.
[69] K. Utimoto, C. Lambert, Y. Fukuda, H. Shiragami, H. Nozaki, *Tetrahedron Lett. 25* (1984) 5423.
[70] E. K. Dolence, M. Adamczyk, D. S. Watt, G. B. Russell, D. H. S. Horn, *Tetrahedron Lett. 26* (1985) 1189.
[71] B. Achmatowicz, E. Baranowska, A. R. Daniewski, J. Pankowski, J. Wicha, *Tetrahedron Lett. 26* (1985) 5597.
[72] A. Pelter, R. Al-Bayati, *Tetrahedron Lett. 23* (1982) 5229.
[73] M. Suzuki, A. Yanagisawa, R. Noyori, *Tetrahedron Lett. 23* (1982) 3595.
[74] M. Yamaguchi, K. Shibato, I. Hirao, *Tetrahedron Lett. 25* (1984) 1159.
[75] S. G. Davies, P. Warner, *Tetrahedron Lett. 26* (1985) 4815.
[76] R. A. Volkmann, J. T. Davis, C. N. Meltz, *J. Am. Chem. Soc. 105* (1983) 5946; C. N. Meltz, R. A. Volkmann, *Tetrahedron Lett. 24* (1983) 4503, 4507.
[77] M. J. Eis, J. E. Wrobel, B. Ganem, *J. Am. Chem. Soc. 106* (1984) 3693.
[78] H. C. Brown, U. R. Racherla, S. M. Singh, *Tetrahedron Lett. 25* (1984) 2411.
[79] A similar concept has been proposed for organoaluminum reagents; K. Maruoka, H. Yamamoto, *Angew. Chem. 97* (1985) 670; *Angew. Chem. Int. Ed. Engl. 24* (1985) 668.
[80] That the combination of an organometallic compound and a Lewis acid is useful in synthesis had already been recognized by *Georg Wittig*; *Wittig*'s work on the system RLi·triphenylboron is mentioned in the following review article: W. Tochtermann, *Angew. Chem. 78* (1966) 369; *Angew. Chem. Int. Ed. Engl. 5* (1966) 351.

Hydroxide Ion Initiated Reactions Under Phase Transfer Catalysis Conditions: Mechanism and Implications

New Synthetic Methods (62)

By Mordecai Rabinovitz,* Yoram Cohen, and Marc Halpern

The development of Phase Transfer Catalysis (PTC) represents a major step forward in the employment of many organic reactions and renders them very convenient and useful processes. These reactions involve the application of nucleophiles in general, anions and bases in particular, in reactions carried out in a water-organic solvent system. They can be performed both in the laboratory and on an industrial scale. The ease of application of PTC processes is the main reason for their increasing utilization in industry. An outstanding achievement of this technique is the employment of aqueous bases in reactions which traditionally would otherwise require a strong base in a nonaqueous medium. The classical procedures that require severe anhydrous conditions, expensive solvents and dangerous bases such as metal hydrides and organometallic reagents are now replaced by aqueous solutions of, e.g., sodium or potassium hydroxides (PTC/OH processes). In contrast to the extensive synthetic applications of PTC/OH systems, the detailed mechanisms of these processes have been the subject of a great deal of controversy and various mechanisms have been suggested. However, it would seem that our knowledge concerning the mechanistic aspects of such reactions has now reached the stage where it can be used to advantage in synthesis planning. A better understanding of the various factors which influence the reaction would undoubtedly help to optimize PTC/OH processes such as to enable higher yields in shorter reaction times at lower temperatures. The importance of, inter alia, the catalyst will be pointed out and it is highly recommended that such catalysts be always available in the laboratory, for the range of organic reactions that they can efficiently, conveniently and safely catalyze is vast indeed.

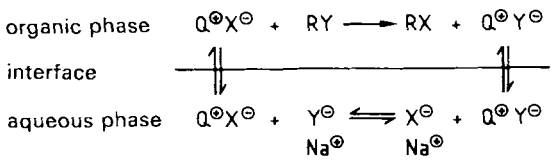
1. Introduction

Phase transfer catalysis (PTC)[1] enables reactions between anions or molecules soluble in one phase (usually aqueous) with organic substrates soluble in an organic phase. Typical examples are listed in Table 1.

Table 1. Selected applications of phase transfer catalysis with hydroxide ions (PTC/OH) or other ions (PTC/X).

PTC/OH	PTC/X
Alkylation (C-, N-, O-)	Halide exchange
Carbene addition	Esterification
Elimination	Other nucleophilic Substitution
Condensations	($CN^{\ominus}$, $RS^{\ominus}$, $N_3^{\ominus}$, $SCN^{\ominus}$, etc.)
(Wittig, Aldol, Darzens)	Oxidation
Michael addition	Reduction
Hydrolysis	Benzoin condensation
Deuterium exchange	Asymmetric induction
Isomerization	
Organometallic applications	

The key factor in such PTC systems is the catalyst. The most commonly used catalysts are quaternary ammonium and phosphonium ions ("quats"),[1] crown ethers,[2] cryptates,[3] and open chain polyethers.[4] The action of the catalyst may be illustrated as in the elegantly simple Scheme 1 proposed by *Starks*.[1] The quat-anion ion pair, $[Q^{\oplus}X^{\ominus}]$, possessing ionic character may be soluble in an aqueous phase. On the other hand, the alkyl chains of the quat lend the ion pair an organophilic nature and therefore may be soluble in an organic phase as well. The quat is said to "extract" the anion from the aqueous phase into the organic phase in the form of an ion pair, via an equilibrium process. The anion, once in the organic phase, may react with an organic substrate. The negatively charged leaving group $Y^{\ominus}$ pairs with the quat cation $Q^{\oplus}$ forming an ion pair, $[Q^{\oplus}Y^{\ominus}]$, which may again equilibrate between the two phases. If the aqueous phase is charged with an excess of the reacting anion, $X^{\ominus}$, for example, the quat may preferably associate with $X^{\ominus}$ and another cycle, initiated by the presence of $[Q^{\oplus}X^{\ominus}]$ may follow.



Scheme 1. The extraction mechanism [1].

The extraction mechanism and its modified form, in which the quat need not enter the aqueous phase but rather exchange $X^{\ominus}$ for $Y^{\ominus}$ at the interface,[5] has explained the behavior of hundreds of reactions with scores of participating anions.

[*] Prof. Dr. M. Rabinovitz, Y. Cohen, Dr. M. Halpern
Department of Organic Chemistry, Institute of Chemistry
Hebrew University of Jerusalem
Jerusalem 91904 (Israel)

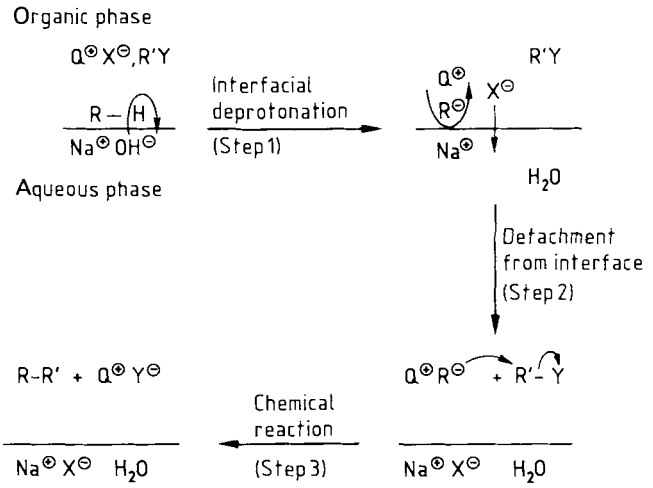
 © VCH Verlagsgesellschaft mbH, D-6940 Weinheim, 1986 0570-0833/86/1111-0960 $ 02.50/0

The concept of phase transfer catalysis is widely established in the literature and several excellent reviews[6–8] and monographs[9–11] have been published. Among the most outstanding achievements of PTC is the employment of aqueous sodium hydroxide as a base[12] in organic systems instead of the classical alkali metal alkoxides, amides and hydrides. However, it was realized quite early that the mechanism believed to operate for most PTC systems, i.e., the extraction mechanism (cf. Section 3) could not explain the behavior of those PTC systems involving the hydroxide ion. Therefore, another mechanism, namely the interfacial mechanism, was suggested (cf. Section 2). At present, PTC/OH systems operating via different mechanisms are known. In the present review, the characterization and implications of the mechanisms of hydroxide ion initiated reactions performed under phase transfer catalysis conditions ("PTC/OH systems") will be outlined. The favorable price and availability of the quaternary ammonium and phosphonium ions ("quats") renders them catalysts of choice, both in research as well as in industry. For this reason we chose to concentrate in this article on PTC/OH systems in which "quats", $Q^{\oplus}$, serve as catalysts. The two major PTC/OH mechanisms will be presented, together with supporting evidence drawn from the literature regarding their validity, and criteria for the determination of the mechanism valid for a particular reaction will be suggested. The implications of this knowledge will be discussed with the purpose of providing the synthetic organic chemist with a tool for evaluation and optimization of new potential applications of the PTC/OH method.

2. The Interfacial Mechanism

2.1. General

At first it was assumed that PTC/OH reactions proceed via a mechanism in which the hydroxide ion is extracted from aqueous NaOH into the organic phase.[13] Later, *Herriott* and *Picker* reported values for the distribution coefficients of various quaternary ammonium hydroxides between 2 M NaOH and benzene.[14] These values were determined by the HCl titration of the organic phase aliquots containing the quat and equilibrated with the aqueous NaOH. *Dehmlow* also employed this method for the determination of $[Q^{\oplus}OH^{\ominus}]$ concentrations in organic phases. However, *Brändström* warned that such determinations may be erroneous because of the possible presence of other contaminating bases in the medium (R_3HNX in R_4NX) resulting primarily from the catalyst's synthetic history or possible decomposition.[15] Reliable values for extraction constants of quaternary ammonium hydroxides, E_{QOH}, are thus hard to obtain, and, in benzene, cannot be precisely calculated even for lipophilic catalysts such as tetrapentyl or tetrahexylammonium hydroxide.[16] E_{QOH} for tetraheptylammonium hydroxide has been estimated to be 1.2 in benzene.[16] Tetrabutylammonium hydroxide (Bu_4NOH, TBA) is a quat frequently employed in PTC/OH reactions and does not exhibit a measurable ability to extract the hydroxide ion into benzene.[16] This would suggest that the classical catalyst for PTC/OH reactions, i.e. triethylbenzylammonium (TEBA), which is more hydrophilic than TBA, would extract hydroxide to an even lesser extent. Interestingly, TEBA induces enhanced reactivity in hundreds of PTC/OH reactions,[12] whereas nucleophilic substitutions performed in the presence of this catalyst proceed slowly if at all.[14] As these nucleophilic substitutions have been well characterized as extraction mechanism systems it was assumed that another mechanism must be involved in PTC/OH reactions with such hydrophilic catalysts as TEBA. Many other arguments were advanced against the hydroxide extraction mechanism, such as the complicated kinetics of PTC/OH reactions (compared to the simple pseudo-first or second order kinetics associated with the extraction mechanism) and the strong dependence of the reaction rate on stirring speed (compared to the independence of extraction systems on stirring speed). *Makosza* therefore proposed an alternative mechanism for PTC/OH systems called the "interfacial mechanism"[12] (see Scheme 2).



Scheme 2. The interfacial mechanism [12].

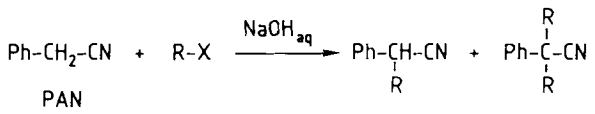
According to the interfacial mechanism a molecule of an organic substrate RH in the organic phase located near the interface, is deprotonated by the hydroxide ion, also located near the interface but within the aqueous phase (Step 1). An ion pair, $[Na^{\oplus}R^{\ominus}]$, is thus formed at the boundary and as such is insoluble in both phases. The anchored $[Na^{\oplus}R^{\ominus}]$ remains at the interface until the catalyst cation $Q^{\oplus}$ draws the organic anion deep into the bulk organic phase in the form of a new ion pair $[Q^{\oplus}R^{\ominus}]$. The quat's previous counteranion, $X^{\ominus}$, is simultaneously liberated into the aqueous phase (Step 2). Finally, $[Q^{\oplus}R^{\ominus}]$ reacts with a substrate R'Y to produce the product R-R' (Step 3) and the $[Q^{\oplus}Y^{\ominus}]$ thus formed may reenter a new catalytic cycle.

2.2. Evidence for the Interfacial Mechanism

Despite the relatively large number of reactions in which the interfacial mechanism is believed to be operative, only a few kinetic investigations have been carried out in this area. The reason for this may lie in the difficulty of per-

forming a comprehensive kinetic study due to the complexity of the kinetics of interfacial phenomena.

The importance of interfacial phenomena in the alkylation of phenylacetonitrile (PAN) was demonstrated by performing the reaction in the absence of catalyst (Scheme 3).[17] From the fact that the alkylation takes place, it may be concluded that the substrate is deprotonated at the phase boundary without the mediation of the catalyst.[17]



Scheme 3. Alkylation of phenylacetonitrile (PAN).

The resulting organic anion in this non-PTC system likewise reacts with the alkyl halide at the interface, as witnessed by the relative insolubility of $[Na^{\oplus}R^{\ominus}]$ in either phase (sodium ions are detected in the organic phase at a concentration of 5 ppm and PAN is detected in the aqueous phase at less than 2 ppm[17]). Under PTC/OH conditions, the deprotonation of PAN (Step 1, Scheme 2) was shown to be a fast equilibrium process. The absence of a kinetic isotope effect in the butylation of PAN in the presence of butyltriethylammonium bromide indicates that the acidic C-H bond is not ruptured during the rate determining step.[18a]

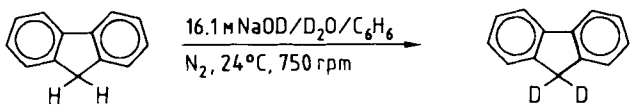


Figure 1 summarizes our results for the deuteration of fluorene. The results suggest that not only is Step 1 of the interfacial mechanism a fast equilibrium process, but also seems to constitute a necessary prerequisite for catalysis.[18a] This may be concluded from the observation that an induction period exists when the aqueous base is added last, but no induction period is observed when the catalyst is added last to a preequilibrated reaction mixture (Fig. 1).

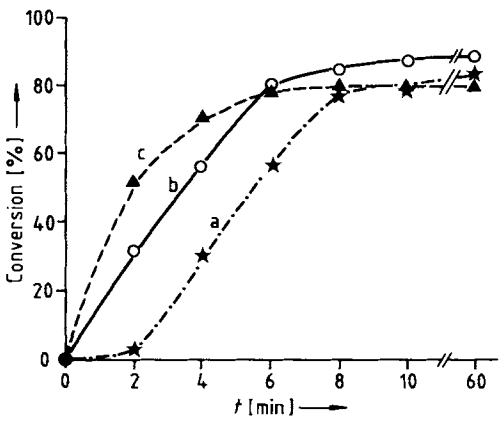


Fig. 1. Reaction profile of the deuteration of fluorene: a) $NaOD/D_2O$ added last; b) [TEBA] added after 20 minutes equilibration between organic and aqueous phase; c) as in (b) but for [TEBA] with $Br^{\ominus}$ instead of $Cl^{\ominus}$ as gegenion [18].

Indeed, it would seem that the role of the catalyst in this system (and probably in most PTC/OH systems) is to shift the equilibrium of fluorenyl anion formation at the interface to the right (Step 1, Scheme 2) by removing the organic anion into the organic phase (Step 2, Scheme 2). This would result in greatly increasing the quantity of fluorenyl anion in the overall system, and hence in increasing the rate of deuteration.

The dependence of the reaction rate on catalyst concentration was investigated for the ethylation of PAN.[19] A bilogarithmic plot of the reaction rate vs. the concentration of catalyst gave a straight line over a wide range of catalyst concentrations, but the slope was 0.6. This result suggests that the chemical reaction (Step 3, Scheme 2) is not the sole rate determining step. This is in contrast to simple nucleophilic substitutions in which the observed reaction rate is *linearly* dependent on catalyst concentration as found in the extraction mechanism (Section 3.2).[14,20-22] It was also found that, within a limited number of experiments (only three), the initial rate of reaction was linearly dependent upon both the PAN and the ethyl bromide concentrations. This may suggest that both the substrate and the alkylating agent participate in the rate determining step,[19] but it should be noted that only a very narrow range of molar ratios was investigated in this case.

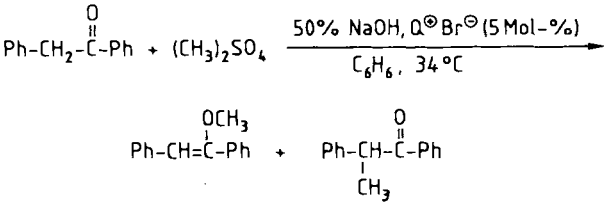
It has been reported that the rate of an interfacial reaction is proportional to the speed of stirring in the range of 600 up to 1700 rpm.[23] This criterium is a powerful one in detecting interfacial phenomena because it is easy to measure; one has only to repeat an experiment while varying the speed of stirring. Indeed, in the reaction of dihalocarbenes in the presence of haloform, 50% aqueous NaOH and TEBA as catalyst, stirring speeds of 750–800 rpm were needed[24] in order to obtain reproducible results. That the rate strongly depends on the speed of stirring is a clear indication of the validity of the interfacial mechanism in this case.[19] The rate of ethylation increases continuously even up to stirring speeds of 1950 rpm.

2.3. Effect of Catalyst Structure

The quaternary ammonium cations, "quats" ($Q^{\oplus}$), of the general class alkyltriethylammonium have been empirically found to induce maximum reactivity in PTC/OH systems.[12,24-27] Such small and frequently hydrophilic quats are known to be ineffective catalysts for most PTC reactions not involving the hydroxide ion.[14] Indeed, the enhanced reactivity observed for PTC/OH reactions in the presence of quats such as TEBA or methyltributylammonium encouraged the search for and acceptance of an alternate mechanism to the extraction mechanism.

The key role of the catalyst in the interfacial mechanism is believed to be detachment of the organic anion formed at the interface from its anchored position at the phase boundary by forming the ion pair $[Q^{\oplus}R^{\ominus}]$, which is subsequently drawn into the bulk organic phase. To do this the quat must successfully compete with the alkali metal cation for association with the organic ion. It has been suggested that as the alkyl chains of the quat decrease in length, the positive charge on the central nitrogen is more

electrostatically available (accessible) for interaction with the anion.[26] Thus, an ion pair consisting of an electrostatically available (accessible) quat and an organic ion will be of lower energy than a corresponding ion pair involving a quat having the positive charge buried deep within four long alkyl chains. Since the second and/or third step



(Scheme 2) of the interfacial mechanism is rate determining, the preferred interaction of the accessible quats with the organic anion promotes faster rates of reaction. Even when one of the four long alkyl chains of, e.g., tetraoctylammonium is replaced by one short alkyl group to produce, e.g., methyltrioctylammonium, a significant increase in the reactivity of the catalyzed system is observed (e.g., in the methylation of deoxybenzoin; see Fig. 2), testifying to

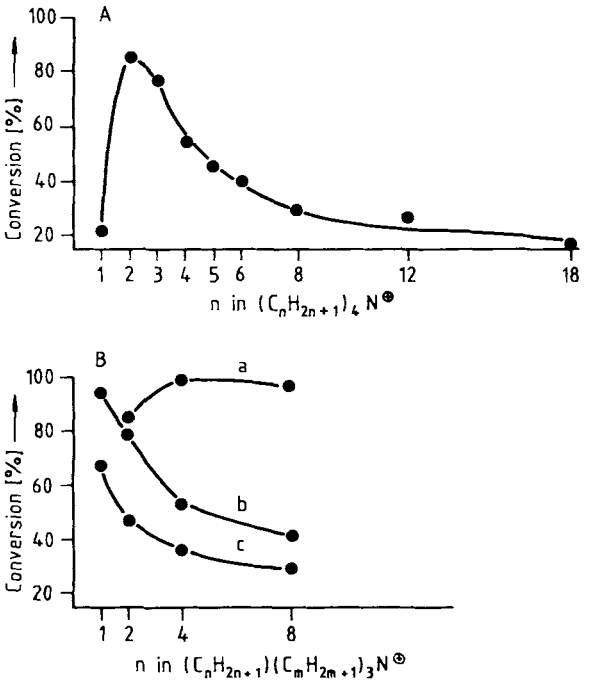
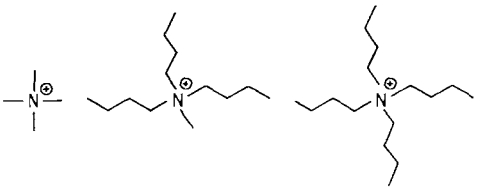


Fig. 2. Influence of quat structure on the reactivity of the alkylation of deoxybenzoin [26]. A) Conversions at 30 min for symmetrical quats of type $(C_nH_{2n+1})N^{\oplus}$; B) conversions at 30 min for nonsymmetrical quats of type $(C_nH_{2n+1})(C_mH_{2m+1})_3N^{\oplus}$, a) m = 2, b) m = 4, c) m = 8.

the importance of the accessibility of the positive charge of the central nitrogen. If the lengths of the alkyl chains are decreased to an extreme, e.g., tetramethylammonium, the ion pair $[Q^{\oplus}R^{\ominus}]$ will not be sufficiently organophilic to allow solubility of the ion pair in the organic phase. This will lead to a decreased rate of reaction similar to the case in which the non-catalyzed $[Na^{\oplus}R^{\ominus}]$ ion pair cannot enter the organic phase. Therefore, it may be concluded that the alkyltriethylammonium quats strike a near optimal balance between electrostatic availability (accessibility) of the positive charge and non-hydrophilicity. The structural demands of the optimal catalyst acting in an interfacial system are illustrated in Table 2.

Table 2. The structural demands of the quat in interfacial PTC/OH systems.



Catalyst			
Availability of positive charge	excellent	good	fair
Lipophilicity	very poor	moderate	good
Performance	poor	good	moderate

Enantioselective alkylations in the presence of chiral phase transfer catalysts have been reported showing some impressive results.[28-30] An enantiomeric excess of 92% has been achieved in the alkylation of an indanone derivative in the presence of benzylcinchoninium quats.[28] Consistent with the "three point interaction" theory for chiral recognition,[31] the planar indanone anion complexes with the chiral quat preferably on one side, on which two pi-complexation attractions and one hydrogen bonding provide a more stable ion pair. The correct stereopositioning of the hydroxy group is a necessary prerequisite for enantioselectivity. The presence of the hydroxy group in a related chiral phase transfer catalyst, benzylquininium, has been shown by comparing the asymmetric induction of reaction performed in the presence of this catalyst with the lack of asymmetric induction obtained in the presence of deoxybenzylquininium.[30] Thus, the effect of catalyst structure on the reactivity and selectivity of PTC/OH alkylations can be quite pronounced.

2.4. Effect of Water and Base Concentration

The role of water in interfacial PTC/OH systems is manifold, with two major effects particularly pronounced. First, the basicity of the hydroxide ion exhibited at the interface is strongly dependent on the aqueous base concentration.[19] As the concentration of base increases the extent of hydration of the hydroxide ion decreases and its basicity sharply increases. It has been estimated that the pK_a of water would be about 28 if the effect of hydrogen bonding of the surrounding hydration envelope could be isolated and removed.[32a] The proton affinity of the hydroxide ion at the interface is not totally uninfluenced by hydration, as water molecules are available for solvation from the nearby aqueous phase. The empirical upper limit found for substrate acidity in anionic reactions occurring via the interfacial mechanism lies at about $pK_a = 23$.[12] It is interesting to note that the following reaction (1) for NaOH[32b] happens to have an equilibrium constant of $K = 10^{-23}$:

$$2\,NaOH_{(s)} + H^{\oplus} \rightleftharpoons NaOH \cdot H_2O + Na^{\oplus} \qquad K = 10^{-23} \qquad (1)$$

This value hints at the upper limit of substrate acidity found, as it determines which substrates may form an ion pair, $[Na^{\oplus}R^{\ominus}]$, from thermodynamic considerations. Recently, a study on the efficiency of different bases for the alkylation of benzamide has been reported by *Dehmlow*.[33a] Although there is no clear-cut evidence for the reaction mechanism it seems reasonable that an interfacial process is operative as proposed by the authors.[33a] (The pK_a of benzamide is ≈ 20.[33b]) The main conclusion emerging from this publication is that the most effective base for carrying out dialkylation reactions is powdered KOH. It should be noted that for the above mentioned equilibrium for KOH the pK_a is about 31.[32b]

In the alkylation of PAN,[19] the effective kinetic order with respect to the hydroxide ion was found to be 5.3! This may be attributed to several factors, of which one is the strong dependence of the basicity of the hydroxide ion upon the extent of hydration. Undoubtedly, salting-out effects and other mass transfer effects are critical and result from the effect of water on the system.

The second factor is water of hydration, which can accompany organic anions as they are drawn from the interface into the organic phase,[34,35] just as inorganic anions carry with them hydration shells.[22] Hydration of organic anions in the organic phase may influence the reactivity and selectivity of alkylation reactions involving these anions.[34,35] The effect of water molecules on the reactivity of the fluorenyl anion has already been demonstrated.[35] Fluorene may be deuterated in the presence of TEBA, benzene, and 16.1 M NaOD at room temperature, but cannot be alkylated under the same conditions[18,35] (except in the presence of DMSO[36]). The fact that fluorene can be deuterated rapidly under these conditions suggests that the substrate is sufficiently acidic and that the interfacial deuteroxide ion is basic enough for interfacial deprotonation of the fluorene and that the catalyst is able to "detach" the organic anion from the interface. When fluorene is sugjected to the same alkylation conditions under which it is deuterated but substituting powdered NaOH for the base, alkylation proceeds in high yield.[35] The enhanced reactivity may be attributed to the decreased hydration shell of the fluorenyl anion in the system in which less water molecules are available, i.e. increased base concentration. Other alkylations have been credited with enhanced nucleophilicity due to decreased hydration.[36]

2.5. Effect of Anions

Many PTC/OH reactions are totally or partially suppressed by "catalyst poisoning".[13] This occurs in cases in which the deprotonated organic substrate[37] (when the interfacial mechanism is operative) or an extracted hydroxide ion[21,38] cannot compete successfully with a very lipophilic anion (e.g., iodide) for association with the quat in the organic phase. The lipophilic anion may have two sources: 1) as the counterion of the catalyst, or 2) as the leaving group eliminated from the substrate (for example in elimination reactions) or from an alkylating agent. In the second case, as the reaction progresses the concentration of the lipophilic anion increases. For this reason, one must carefully choose the leaving group liberated during the course of the reaction, i.e., one would prefer working with an alkyl chloride rather than an alkyl iodide, although the alkyl iodide is a better alkylating agent. The alkylation of PAN (which proceeds via the interfacial mechanism) was shown to be less sensitive to "catalyst poisoning" by two orders of magnitude relative to that expected theoretically if one assumes the extraction mechanism to be applicable in this case.[19] In general, it may be stated that in interfacial PTC/OH systems, the catalytic power of the quat is less hindered by the presence of lipophilic leaving groups than in the hydroxide extraction systems, since the organic anion $R^{\ominus}$ desired for reaction is inherently lipophilic in nature (much more than the hydroxide ion) and often competes successfully with other anions for association with the quat. Therefore, cases are known in which catalyst poisoning is not observed in the presence of the iodide anion.[39]

In the case of deuteration[18] it was shown that the initial rate of reaction was faster in the presence of bromide relative to chloride, as demonstrated in Figures 1b and 1c.[18a] This may have to do with the need to solubilize the hydrophilic TEBA in the organic phase in step 1 (Scheme 2).

3. The Extraction Mechanism

3.1. General

The extraction mechanism (Scheme 1) has been well characterized by several comprehensive kinetic studies of nucleophilic displacements involving many inorganic anions other than the hydroxide ion (halide ions, cyanide, azide, thiocyanate, etc.).[14,20,22] In the extraction of hydroxide the role of the catalyst is to carry the OH-anion into the depth of the organic phase where the reaction occurs. These systems are characterized by simple pseudo-first or second order kinetics, first order kinetics with respect to catalyst, increased reactivity in the presence of organophilic quats, independence of reaction rate on stirring speed (above ca. 300 rpm), strong dependence of the progress of the reaction upon the lipophilicity of the anions present, and the extent of hydration of the inorganic anion reacting in the organic phase.[5,14,20,22]

The hypothesis of an interfacial mechanism for PTC/OH systems by *Makosza*,[12] and the recognition, first by *Dehmlow* et al.[16] and then by others, that the extraction coefficients of $[Q^{\oplus}OH^{\ominus}]$ into organic solvents are very low, has aroused much skepticism regarding the possible validity of the extraction mechanism for such systems by the scientific community. But, despite the well documented low extractability of the hydroxide ion by quats, a growing number of reports have appeared in which synthetic achievements have been attributed to $OH^{\ominus}$ extraction.[38,40-42] Indeed, the kinetic and other parameters characteristic of the extraction mechanism have been identified as valid in several PTC/OH systems.

3.2. Evidence for the Hydroxide Extraction Mechanism

As mentioned earlier, the kinetics of the PTC/OH systems investigated have been found to be complicated and include fractional order dependency on catalyst concentration and non-simple general kinetic orders.[19,27] Much of the difficulty of deciphering the kinetics of these systems lies in their complexity, which includes the liberation of leaving groups and parallel and sequential reactions. Ideally, the optimum choice of a model reaction for kinetic characterization should be as simple a chemical system as possible. Systems such as isomerizations and deuterations alleviate the need to deal with added complicated equilibria due to constantly changing anionic compositions or additional competing reactions.

A comprehensive kinetic study of the isomerization of allylbenzene has been performed under PTC/OH conditions (see Scheme 4). The dependence of the reaction rate and induction periods on the substrate concentration, catalyst structure, catalyst concentration, speed of stirring, temperature, catalyst counterion and aqueous hydroxide ion concentration are consistent with a hydroxide ion extraction mechanism.[21]

$$\mathrm{Ph\text{-}CH_2\text{-}CH{=}CH_2} \xrightarrow[\text{toluene}\\ 75^\circ C,\ 850\ rpm]{Q^{\oplus}Br^{\ominus}\ (5\ Mol\text{-}\%)\\ NaOH_{aq}} \mathrm{Ph\text{-}CH{=}CH\text{-}CH_3}\ (trans/cis)$$

Scheme 4. Isomerization of allylbenzene [21].

The isomerization reaction constituted the first PTC/OH reaction to exhibit simple pseudo-first order kinetics with respect to substrate. Assuming the extraction mechanism to be applicable, one would expect the rate of reaction to be dependent on the concentration of substrate and the concentration of the quat-hydroxide ion pair in the organic phase since they both participate in the rate determining step (an energy of activation of ca. 17 kcal/mol was found indicative of chemical reaction control). Indeed, first order dependence with respect to both substrate and catalyst was observed (Fig. 3). The concentration of the quat-hydroxide ion pair is expected to be at a low steady state level and enters into the observed rate constant k_{obs}:[21]

$$\begin{aligned} rate &= k_{obs}[allylbenzene] \\ k_{obs} &= k_{chem}[Q^{\oplus}OH^{\ominus}]_{org} \end{aligned} \qquad (2)$$

Further evidence for the validity of the extraction mechanism is the independence of the rate of reaction on stirring speed above ca. 300 rpm (Fig. 4). Similar results have been obtained by *Starks* et al.[20] and others[13,22,43] and reflect kinetic control by the chemical reaction in which $[Q^{\oplus}X^{\ominus}]$ is at a steady state concentration. Below 300 rpm the requirement for sufficiently rapid mass transfer of the reacting anion is not met and diffusion controlled kinetics is observed. At these low stirring speeds the induction period of the isomerization which is observed, is stirring-speed dependent and is attributed to the need for attaining a steady state concentration of hydroxide in the organic phase.[21]

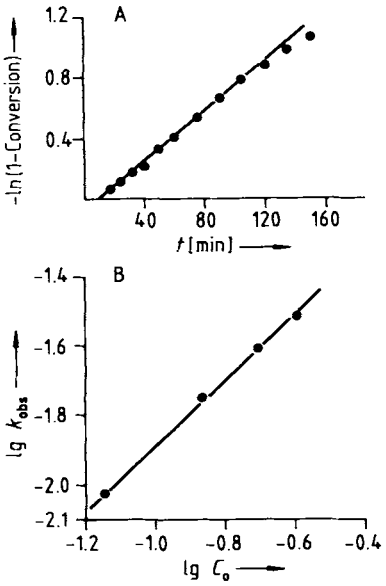


Fig. 3. A) Pseudo first order kinetics of the isomerization of allylbenzene under standard conditions [21] (cf. Scheme 4); B) determination of kinetic order with respect to the catalyst in the isomerization of allylbenzene (slope 0.97) [21]. C_0 = initial concentration of catalyst.

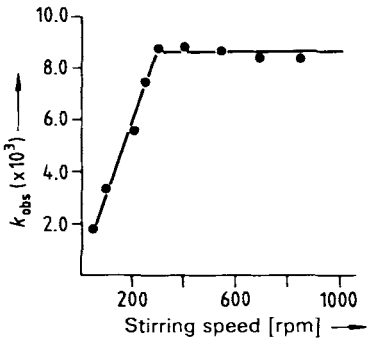


Fig. 4. Dependence of k_{obs} on stirring rate in the isomerization of allylbenzene [21] (cf. Scheme 4 and Table 3).

Other evidence in support of the extraction mechanism in this PTC/OH system lies in the dependence of the reaction rate on catalyst structure and the strong dependence of the reaction rate on the catalyst counterion (see Section 3.5). The behavior of this PTC/OH system with respect to the simple kinetics, catalyst structure and stirring-speed dependence is in direct contrast to the corresponding parameters which characterize the interfacial mechanism and is in direct correlation with the findings of the well documented extraction mechanism.[21]

3.3. Influence of Catalyst Structure

According to the extraction mechanism (Scheme 1) the main role of the catalyst is to extract the inorganic anion

into the organic phase. It has been shown that in S_N2-type reactions, the reaction rate increases as the organophilic character of the quat increases.[14,20,22] The extent of the extraction of the very hydrophilic hydroxide ion increases with the lipophilicity of the quat as demonstrated by *Dehmlow* et al.[16] In view of the above, it seems that the main structural demand of the quat in extractive systems is long alkyl chains. In the isomerization of allylbenzene a monotonic increase in the reaction rate was observed as the organophilicity of the symmetrical tetraalkylammonium quats increased (Fig. 5). The comparison of this observation with the effect of the catalyst structure in the interfacial mechanism (Fig. 2) is illustrative. This may be attributed to the increased solubility of the $Q^{\oplus}OH^{\ominus}$ ion pair in the non polar organic phase (e.g., tetrabutylammonium hydroxide may not be as soluble as tetraoctylammonium hydroxide in toluene). This would result in a greater observed rate constant since $[Q^{\oplus}OH^{\ominus}]_{org}$ enters into this term [see equation (2)]. Increasing the accessibility (electrostatic availability) and decreasing the organophilicity of a quat by replacing a long alkyl chain by a methyl group, e.g., by use of methyltrioctylammonium instead of tetraoctylammonium, results in a decrease in the rate of reaction. Again, this demonstrates the need for at least two PTC/OH mechanisms to be considered. Quats below a minimum organophilicity, such as tetrapropylammonium, are completely ineffective in this extractive system.[21]

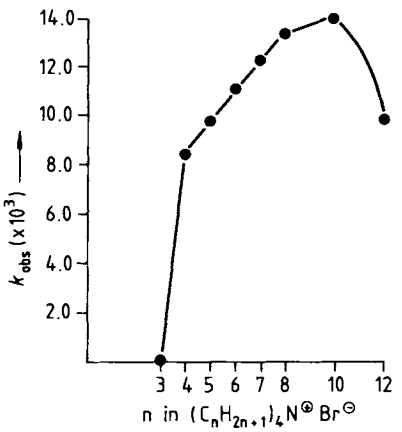
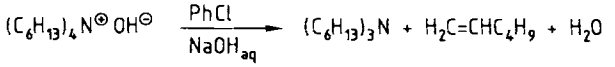


Fig. 5. Dependence of k_{obs} on quat structure in the isomerization of allylbenzene [21] (cf. Scheme 4 and Table 3).

3.4. Influence of Water and Base Concentration

Under liquid-liquid phase transfer catalysis conditions the anions transferred by the quats to the organic phase are solvated by a limited number of water molecules.[5,20,22,44] *Landini* et al. showed that the hydration number of the quat-anion ion pair depends largely on the nature of the anion.[5,20] The hydration number appears to be related to the size of the anion and its charge dispersion.[45] It has been suggested that hydration is one of the major factors that determines the nucleophilicity and reactivity orders of different inorganic anions in PTC systems. In anhydrous homogeneous solution the reaction rates are faster than in the two phase systems. It was possible to simulate these rate constants when the experiments were repeated in water-containing homogeneous systems.[22] The hydroxide ion is a small hard anion with barely any charge dispersion so one would expect it to be solvated to a great extent in water/organic solvent systems. At high NaOH concentrations only low concentrations of water molecules are available for concurrent transfer with the hydroxide ion into the organic phase. Varying extents of hydration of the hydroxide ion in the organic phase may significantly alter the basicity of the hydroxide ion. Indeed, the fact that allylbenzene ($pK_a = 34$[46]) may be deprotonated under PTC/OH conditions demonstrates the enhanced basicity of the extracted hydroxide relative to the interfacial hydroxide ion by a factor of at least eleven orders of magnitude. This assumption recently received strong support in a quantitative way in an elegant work published by *Landini* et al.[47] They examined the reactivity of $OH^{\ominus}$ as a function of its hydration sphere in the Hofmann elimination of tetrahexylammonium hydroxide in chlorobenzene (see Scheme 5). In the range of NaOH concentrations examined, the measured rate constants span up to four orders of magnitude. The basicity enhancements obtained by reducing the hydration sphere of the hydroxide ion from an average value of 11 to 3.5 molecules of water, is much more pronounced than those previously found in the dehydration of other anions.[48,49] This means that the basicity of the hydroxide ion may be dramatically increased when there are no water molecules available to solvate the hydroxide ion. In order words, we can say that we approach here the term "naked ion". The data presented by *Landini* and *Maia*[47] are comparable to those measured by *Bohme* et al.[50] on "real naked hydroxide ions" in the gas phase. The data confirm that gas phase reactivity can be approached by desolvating the anions in nonpolar organic solvents. This may explain, in part, the high sensitivity of the isomerization of allylbenzene[21] or H/D exchanges in weak CH-acids[51,52] to the NaOH concentration. In the case of the isomerization of allylbenzene, the effective kinetic order with respect to aqueous NaOH concentration was found to be 5.0. This result is similar to that obtained for the interfacial alkylation of PAN[19] and probably reflects similar phenomena (enhanced basicity, salting out, etc.), although it might be expected that enhanced basicity plays a special role in the deprotonation of very weak CH-acids.



Scheme 5. Hofmann elimination of tetrahexylammonium hydroxide [47].

3.5. Effect of Anions

The hydrophilicity of the hydroxide ion and the difficulty of its extraction into non polar organic solvents has been emphasized. It is a hard base and associates poorly

with the relatively soft quats, especially in the presence of other softer anions like bromide or iodide. It is therefore understandable that extractive PTC/OH reactions are subject to "catalyst poisoning" even more than the reactions which proceed via the interfacial mechanism. Such behavior has been demonstrated by the effect of counteranion on the rate of isomerization of allylbenzene. In the presence of a hundredfold excess of hydroxide over the catalyst counterion a change from $HSO_4^{\ominus}$ (effective ion: $SO_4^{2\ominus}$) to $Br^{\ominus}$ resulted in a fiftyfold decrease in the rate of reaction (Table 3). Despite the much greater solubility of tetrabutylammonium bromide in toluene, more hydroxide is

Table 3. Dependence of the rate constant k_{obs} on catalyst counterion in the isomerization of allylbenzene [21] (cf. Figs. 4 and 5) [a].

Catalyst	k_{obs} ($\times 10^3$)	Induction period [min]
$Bu_4N\ HSO_4$	114	<0.1
$Bu_4N\ Cl$	24	1.3
$Bu_4N\ Br$	2.4	10

[a] Reaction conditions: 1.42 M allylbenzene in toluene, 5 mol-% catalyst, 40% NaOH, 75 °C, 850 rpm.

extracted into the organic phase in the case of tetrabutylammonium hydrogensulfate. The order of lipophilicity $SO_4^{2\ominus} < Cl^{\ominus} < Br^{\ominus}$ also determines the ease of achieving the steady state concentration of $Q^{\oplus}OH^{\ominus}$ in the organic phase, as can be seen in a corresponding trend in the induction times.[21]

3.6. Examples of PTC/OH Extraction Systems

In Table 4 are shown some representative examples of synthetic applications that may proceed via a hydroxide ion extraction mechanism. The applications of PTC/OH under extractive conditions have been singled out since it

Table 4. Examples of reactions proceeding via a hydroxide ion extraction mechanism.

No.	Reaction	Conditions	Ref.
1	$R-CHBr-CHBr-R' \rightarrow R-C\equiv C-R' + 2HBr$	$Bu_4N^{\oplus}HSO_4^{\ominus}$ (300 mol-%), 50% NaOH, pentane, CH_2Cl_2, 20 °C	[38]
2	$R-C_6H_4OCH_2CH_2X \rightarrow R-C_6H_4OCH=CH_2 + HX$	$Bu_4N^{\oplus}HSO_4^{\ominus}$ (100 mol-%), 50% NaOH, benzene, 20 °C	[40]
3	As in reaction 1	$Octyl_4N^{\oplus}Br^{\ominus}$ (5 mol-%), solid KOH, petroleum ether, 80 °C	[41]
4	$ROOC-(CH_2)_n-COOR \rightarrow Na^{\oplus\ominus}OOC-(CH_2)_n-COO^{\ominus}Na^{\oplus}$	$Q^{\oplus}X^{\ominus}$ (1 mol-%), 50% NaOH, petroleum ether	[42]
5	Thiazole → 2-deuteriothiazole	$Bu_4N^{\oplus}HSO_4^{\ominus}$, NaOD/$D_2O$ (17 M)	[53]
6	$Ph-CH_2-CH_2-Br \rightarrow Ph-CH=CH_2 + HBr$	$Octyl_4N^{\oplus}Br^{\ominus}$ (5 mol-%), 50% NaOH, 75 °C, 750 rpm	[55, 56]
7	$p\text{-}Br-C_6H_4-CHCl-CH_3 \rightarrow p\text{-}Br-C_6H_4-CH=CH_2 + HCl$	$Q^{\oplus}X^{\ominus}$ (5 mol-%), solid or 50% NaOH, 75 °C, 1000 rpm	[35]

appears that general awareness to reactions proceeding via hydroxide ion extraction is not widespread.

One may identify the first three dehydrobromination[38,40,41] reactions as proceeding via a hydroxide ion extraction mechanism by examining the nature and the quantity of catalyst employed. In the first two cases the need for using stoichiometric amounts of catalyst[38,40] indicate that catalyst poisoning prevents extraction of hydroxide ion in the presence of catalytic amounts of quat. Indeed, when one mole-equivalent of tetrabutylammonium bromide was used in the dehydrobromination of 1,2-dibromo-1,2-diphenylethane (cf. No. 1 and 3) only monodehydrobromination occurred, affording α-bromostilbene[35] (the stereochemistry of the reaction under PTC/OH conditions indicates that the E2 elimination mechanism is valid in this case[35]). *Dehmlow* et al.[41] overcame the catalyst poisoning problem by employing a very organophilic quat, tetraoctylammonium.

The dependence of the reactivity of the hydrolysis of esters (No. 4) on the quat structure and the counteranion suggest the validity of the hydroxide extraction mechanism in this case.[42] In the case of the deuteration of thiazoles (No. 5), the authors suggest that the interfacial mechanism is operative.[53] But it would appear that the hydroxide ion extraction mechanism is the more valid assumption as the reaction follows first order kinetics with respect to substrate, the pK_a of the substrates are high (ca. 29, i.e. >23, the limiting pK_a for interfacial mechanism), and the hydrophilic catalysts seem to be less effective.[53,54]

The dehydrobromination of phenethyl bromide (No. 6) proceeds more rapidly in the presence of tetraoctylammonium bromide than in the presence of benzyltriethylammonium bromide.[55,56] But the zero order kinetics observed in the presence of the former catalyst and the low energy of activation (ca. 8 kcal/mol) possibly suggest a hydroxide ion extraction mechanism governed by diffusion control.[55]

In the dehydrohalogenation of a 1-phenethyl halide, chloride was chosen as the leaving group instead of bromide.[35] Despite the better capability of bromide as a leaving group, the chloride allows a greater extent of hydroxide extraction, and hence the reaction does not slow down as much as in the presence of bromide while the reaction progresses; indeed, chloride was in fact found to be the preferred choice.

We have employed the extraction mechanism to expand the scope of compounds which undergo H/D exchange under PTC/OH conditions (up to $pK_a = 37$).[58] The enhancement of the basicity of the hydroxide ion was achieved by using powdered NaOD, a lipophilic quat (TBA) with a very hydrophilic counter anion e.g. $HSO_4^{\ominus}$.[51,52]

4. PTC/OH Mechanisms: Determination and Implications

4.1. Determination of the Mechanism in PTC/OH Systems

The properties that characterize the main PTC/OH mechanisms are summarized in Table 5. With the aid of

this table it is easily understood how one may determine the mechanism of a given PTC/OH reaction, and choose reaction conditions for new potential applications of PTC/OH reactions. In all cases in which the interfacial mechanism is operative, the accessible quats are the most efficient catalysts;[24,26,27] a strong dependence of rate on stirring speed may be observed,[19,24,39] and the kinetics are not simple with respect to substrate[18,19,27] or catalyst.[19,27] In contrast, the three characteristics of the extraction mechanism are: organophilic quats are the more efficient catalysts;[14,20,21] independence of rate on stirring speed above a low value;[14,20–22,37] and, very simple kinetics with respect to substrate and catalyst (cf. Fig. 5).[14,20–22]

Table 5. Characteristics of PTC/OH mechanisms.

Characteristic	Extraction Mechanism Controlled by		Interfacial Mechanism
	Chemical Reaction	Diffusion	
Quat structure	Organophilicity	Organophilicity	Electrostatic availability
Stirring speed	Independent (above need for mass transfer)	Varying dependence	Strongly dependent
General kinetic order	Simple (pseudo-first or second order)	Zero order	Complicated (must determine v_0)
Kinetic order catalyst	First order	Fractional	Fractional
Counterion effect (sensitivity to poisoning)	Strongly dependent	Strongly dependent	Moderately dependent
Aqueous $OH^{\ominus}$ concentration	Very strongly dependent	Very strongly dependent	Very strongly dependent
Substrate acidity	$23 \leqslant pK_a \leqslant 37$ $pK_a < 16$	$23 \leqslant pK_a \leqslant 37$ $pK_a < 16$	$16 < pK_a < 23$
Energy of activation	> 10 kcal/mol	< 10 kcal/mol	> 10 kcal/mol

[a] Above a limiting value necessary for minimal mass transfer.

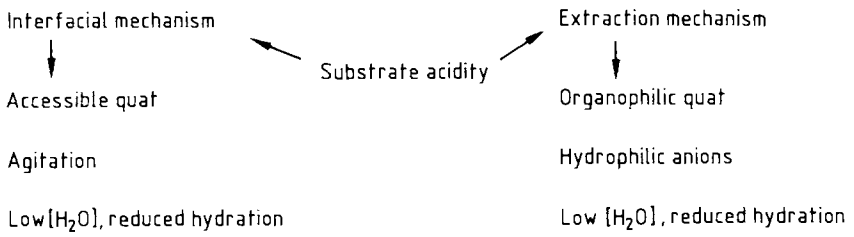
One may perform a simple experiment which allows for an educated guess in determining the valid PTC/OH mechanism of a given system. Two reaction vessels are set up next to one another under identical conditions, one containing an organophilic catalyst, such as tetraoctylammonium bromide or chloride, and the other containing an accessible (electrostatically available) catalyst, such as butyltriethylammonium bromide or chloride. If the organophilic catalyst induces the higher reactivity, then the extraction mechanism may be considered to be valid. One would expect to observe first order kinetics with respect to the substrate and the catalyst if the extraction mechanism is chemically controlled (not diffusion controlled). If the electrostatically accessible catalyst induces the higher reactivity, then the interfacial mechanism may be considered to be valid, and complicated kinetics are to be expected. An additional run at a significantly higher stirring speed would help differentiate between the two mechanisms, since the interfacial mechanism is strongly dependent on this parameter whereas the chemically controlled extraction mechanism is independent of the agitation efficiency (at least above a certain speed of stirring necessary for minimal extent of mass transfer). One may distinguish between the rare diffusion controlled mechanism and the other PTC/OH mechanisms by examining the kinetic order and energy of activation of the reaction. An energy of activation of above 10 kcal/mol suggests chemical control (etherification 14 kcal/mol,[37] alkylation 20 kcal/mol,[19] isomerization 17 kcal/mol[21]), whereas diffusion control exhibits an energy of activation under 10 kcal/mol (elimination 8 kcal/mol[55]).

4.2. Evaluation and Optimization of New Potential Applications of PTC/OH

In this section we would like to show how one can assess *a priori* whether or not a new potential application of PTC/OH is feasible, and, if so, how the reaction conditions can be optimized.

From Table 5 it may be concluded that it is possible to determine the mechanism of a given PTC/OH reaction with the aid of the first three criteria. But one additional critical parameter must be mentioned if an approach to the implementation of PTC/OH conditions is to be considered. This factor is the acidity of the substrate. It is possible to classify the substrates of PTC/OH reactions into four categories according to their pK_a values: a) $pK_a < 16$, b) $16 < pK_a < 23$, c) $23 < pK_a < 37$, d) $pK_a > 37$. In group (a) ($pK_a < 16$) the conjugate bases of the substrates are generally water soluble. In this case the deprotonation takes place in the aqueous phase and then the anion is extracted into the organic phase according to the extraction mechanism.[57] In group (b) ($16 < pK_a < 23$) we have two kinds of substrates: i) substrates that are water-soluble like alcohols; ii) substrates that are water-insoluble like PAN and fluorene. With water-soluble substrates, the extraction mechanism is usually operative. The $OR^{\ominus}$ anion formed in the aqueous phase is extracted into the organic phase and reacts with the electrophile. In contrast, if the pK_a of the substrate lies in the range between 16 and 23 and is not water soluble then it is likely that the substrate is acidic enough to be deprotonated by the hydroxide ion acting at the interface. An organic anion will then be produced which will subsequently react, and hydroxide ion extraction will be suppressed. If on the other hand, a stronger base is required to deprotonate the substrate ($23 < pK_a < 37$) then only the extracted hydroxide ion can be expected to be basic enough (due to its reduced hydration) to initiate the reaction (PTC/OH extractive mechanism is operative). If the pK_a of the substrate is greater than 37 it may be expected that the reaction will not succeed, judging by the data gathered hitherto; e.g., attempts to perform a deuterium exchange reaction of the benzylic protons of toluene have so far failed.[35]

Thus, we have experienced that the key to choosing initial reaction conditions for a PTC/OH reaction and deciding whether or not it is even worthwhile, is the acidity of the substrate (see Scheme 6). In our opinion, the acidity of the substrate should guide one to assessing which of the two PTC/OH mechanisms is likely to be valid for the PTC/OH reaction under consideration. Conversely, the synthetic implications of choosing one of the two mechanisms, result in totally opposite reaction characteristics.



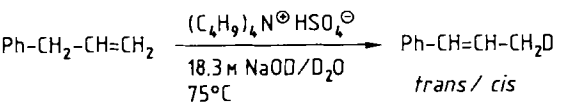
Scheme 6. Approach to evaluation and optimization of new potential applications of the PTC/OH method.

If the pK_a of the substrate is between 16 and 23 and the substrate is not water soluble, the interfacial mechanism may be anticipated to be valid. In this case, an accessible (electrostatically available) quat should be chosen, preferably with one methyl group or three ethyl groups and the remaining residues butyl to octyl groups. One need not be too concerned about the nature of the counteranion, though one should avoid very lipophilic anions (e.g., iodide) unless the substrate to be alkylated is very lipophilic. Accordingly, secondary substrates such as alkylating agents may possess leaving groups as lipophilic as bromide or even in some cases iodide, but again, it is better to avoid the accumulation of ions that might compete with the organic anion for association with the quat. For a reaction expected to proceed via the interfacial mechanism one should choose a method of agitation which is as practical or economically feasible as possible. High nucleophilicity of the organic anion may be achieved by reducing the water content of the system (high $OH^{\ominus}$ concentration). One must be aware, though, of the increased sensitivity of the accessible (electrostatically available) quats to $OH^{\ominus}$-induced decomposition, especially at higher than ambient temperatures.

If a stronger base is required to deprotonate the substrate ($23 < pK_a \leq 37$), the extraction mechanism may be assumed to be valid. In this case, one should choose an organophilic quat, such as tetraoctylammonium. One should take great care in choosing a catalyst with hydrophilic counterion (e.g., $HSO_4^{\ominus}$), since hydroxide ion extraction is hindered by all but a few anions. A high NaOH concentration (even powdered NaOH) should be chosen so as to increase the basicity of the hydroxide ion. The choice of a bulky quat, such as tetraoctylammonium, will also decrease its susceptibility to Hoffmann elimination or nucleophilic degradation by the hydroxide ion. One need not invest great effort in maximizing mixing between the two phases, as this will not induce any additional reactivity above a certain easily attainable rate.

It may be noted that Aliquat 336 is an inexpensive commercially available catalyst (in tank-car quantities), which is electrostatically available enough to efficiently catalyze interfacial type reactions, and organophilic enough to efficiently catalyze extraction type reactions. The chloride counterion does not hinder the $OH^{\ominus}$ ion extraction very much. The disadvantages of Aliquat 336 lie in its difficulty of separation from the reaction mixture, since it is always soluble in organic phases and usually the product must be distilled out (industry) or separated by chromatography (laboratory). Its high molecular weight also reduces its cost effectiveness. Recently, methyltributylammonium chloride has been introduced commercially, and could prove to be a very efficient catalyst for interfacial type reactions.

PTC/OH conditions are subject to limitations. It is currently believed that the maximum pK_a for applicable substrates is ca. 37 (benzothiophene has been deuterated[58]). This limit may be illustrated by the fact that allylbenzene will isomerize and monodeuterate in the terminal position in the presence of 18.3 M NaOD/D_2O and tetrabutylammonium hydrogensulfate at 75°C.[51] This implies that allylbenzene is acidic enough to deprotonate under these conditions, whereas β-methylstyrene is not (cf. Scheme 7).



Scheme 7. Isomerization and deuteration of allylbenzene [51].

Another limitation of PTC/OH reactions is the temperature range in which quats may be used. Most PTC/OH reactions cease to be efficient at temperatures of 75–90°C due to catalyst decomposition. A possible solution to this problem may be the use of polyethylene glycols[59] or crown ethers,[2b] all of which are more thermally stable than the quats. Moreover, it has recently been reported that pyridinium salts are stable at high temperature and can act as phase transfer catalysts in the case of nucleophilic substitutions with phenoxide and thiophenoxide ions.[73]

Choosing a solvent still seems to be a matter of trial and error. Methylene chloride and aromatic hydrocarbons have generally proved to be suitable solvents, but it should be noted that solvents not commonly used have been quite efficient in certain systems (e.g., methyl isobutyl ketone).[35] It has been suggested that chloroform be avoided in reactions in which concentrated NaOH is used because of the possibility of carbene generation. Even methylene chloride has its drawbacks; it has been known to generate formaldehyde[16] or act as an alkylating agent in PTC/OH systems.[60] Esters are usually not suitable as they are subject to hydrolysis.

5. Summary and Outlook

Although many novel applications of PTC have been published, the great value of the PTC method lies in the

vast range of basic and common everyday reactions that can be performed in high yields, simply, inexpensively and with simple work-up procedures. In particular, PTC/OH applications are especially attractive to the chemist, and these have been reviewed extensively.[6,7,9,11]

In conclusion, we believe that an understanding of the mode of action of such a widely employed synthetic technique as PTC/OH is of great importance, for it can contribute greatly to the development of synthetic processes. In this review we have presented many specific aspects of PTC/OH mechanisms and have then endeavored to bring the accumulated knowledge into general perspective. Two major mechanisms are accepted for PTC/OH systems, the interfacial mechanism and the extraction mechanism. We consider it imperative to be aware that the two mechanisms have opposite characteristics, for, as we have seen, the outcome of many PTC/OH reactions may totally succeed or totally fail, depending on the reactions conditions employed. This holds true, in particular, regarding the great potential that lies uncovered in performing PTC/OH reactions under extractive conditions. Now that the distinction between the two mechanisms has been made we anticipate that the reaction of CH-acids of very low acidity under PTC/OH conditions will form the subject of numerous studies in the next few years.

Although a complete understanding of PTC/OH mechanisms is still far from having been reached we do at least now have a working knowledge of such systems. A knowledge of the mode of action of these systems has provided the chemist with a preliminary tool with which to evaluate and optimize new potential applications of these systems. Currently, there is a great momentum in the publications and patents relating to the application of PTC/OH conditions. We believe that the added mechanistic understanding presented in this review will help promote new avenues of application of PTC/OH in organic synthesis.

Received: November 20, 1985;
revised: February 21, 1986 [A 596 IE]
German version: *Angew. Chem. 98* (1986) 958

[1] C. Starks, *J. Am. Chem. Soc. 93* (1971) 195.
[2] a) C. Pederson, *J. Am. Chem. Soc. 89* (1967) 2495; b) G. W. Gokel, H. D. Durst, *Synthesis 1976*, 168.
[3] B. Dietrich, J. Lehn, *Tetrahedron Lett. 1973*, 1225.
[4] J. Ugelstadt, P. Mork, B. Jensen, *Acta Chem. Scand. 17* (1963) 1455.
[5] D. Landini, A. Maia, F. Montanari, *J. Chem. Soc. Chem. Commun. 1977*, 112.
[6] E. Dehmlow, *Angew. Chem. 89* (1977) 521; *Angew. Chem. Int. Ed. Engl. 16* (1977) 493.
[7] E. Dehmlow, *Angew. Chem. 86* (1974) 187; *Angew. Chem. Int. Ed. Engl. 13* (1974) 170.
[8] G. Gokel, W. Weber, *J. Chem. Educ. 55* (1978) 350, 439.
[9] W. Weber, G. Gokel: *Phase Transfer Catalysis in Organic Synthesis*, Springer, Berlin 1977.
[10] C. Starks, C. Liotta: *Phase Transfer Catalysis: Principles and Techniques*, Academic Press, New York 1978.
[11] E. Dehmlow, S. Dehmlow: *Phase Transfer Catalysis*, 2nd Edition, Verlag Chemie, Weinheim 1983.
[12] M. Makosza, *Pure Appl. Chem. 43* (1975) 439.
[13] A. Herriott, D. Picker, *Tetrahedron Lett. 1972*, 4521.
[14] A. Herriott, D. Picker, *J. Am. Chem. Soc. 97* (1975) 2345.
[15] A. Brändström, *Adv. Phys. Org. Chem. 15* (1977) 267.
[16] E. Dehmlow, M. Slopianka, J. Heider, *Tetrahedron Lett. 1977*, 2361.
[17] M. Makosza, E. Bialecka, *Tetrahedron Lett. 1977*, 183.
[18] a) M. Halpern, Y. Cohen, Y. Sasson, M. Rabinovitz, *Nouv. J. Chim. 8* (1984) 443; b) E. V. Dehmlow, S. Barahona-Naranjo, *J. Chem. Res. Synop. 1982*, 186.
[19] R. Solaro, S. D'Antone, E. Chiellini, *J. Org. Chem. 45* (1980) 4179.
[20] C. Starks, R. Owens, *J. Am. Chem. Soc. 95* (1973) 3613.
[21] M. Halpern, Y. Sasson, M. Rabinovitz, *J. Org. Chem. 48* (1983) 1022.
[22] D. Landini, A. Maia, F. Montanari, *J. Am. Chem. Soc. 100* (1978) 2796.
[23] F. Menger, *J. Am. Chem. Soc. 92* (1970) 5965.
[24] E. Dehmlow, M. Lissel, *Tetrahedron Lett. 1976*, 1783.
[25] J. Dockx, *Synthesis 1973*, 441.
[26] M. Halpern, Y. Sasson, M. Rabinovitz, *Tetrahedron 38* (1982) 3183.
[27] M. Makosza, B. Serafinowa, *Rocz. Chem. 39* (1965) 1223.
[28] U. Dolling, P. Davis, E. Grabowski, *J. Am. Chem. Soc. 106* (1984) 446.
[29] J. Verbicky, E. O'Neil, *J. Org. Chem. 50* (1983) 1786.
[30] S. Collona, R. Annunziata, *Afinidad 38* (1981) 501; *Chem. Abstr. 97* (1982) 145091t.
[31] W. Pirkle, J. Finn in J. Morrison (Ed.): *Asymmetric Synthesis, Vol. 1*, Academic Press, New York 1983, p. 87-124.
[32] a) C. Ritchie, H. King, *J. Am. Chem. Soc. 90* (1968) 833; b) W. Jolly, *J. Chem. Educ. 44* (1967) 304.
[33] a) E. V. Dehmlow, B. Lipka, *J. Chem. Res. Synop. 1985*, 107; *J. Chem. Res. Miniprint 1985*, 1418; b) J. Hine, M. Hine, *J. Am. Chem. Soc. 74* (1952) 5266.
[34] M. Halpern, Y. Sasson, I. Willner, M. Rabinovitz, *Tetrahedron Lett. 1981*, 1719.
[35] M. Halpern, Ph. D. Thesis, Hebrew University of Jerusalem, 1983.
[36] M. Makosza, *Bull. Acad. Pol. Sci. Ser. Sci. Chim. 15* (1967) 165.
[37] H. Freedman, R. Dubois, *Tetrahedron Lett. 1975*, 3251.
[38] A. Gorgues, A. LeCoq, *Tetrahedron Lett. 1976*, 4723.
[39] A. Merz, *Angew. Chem. 85* (1973) 868; *Angew. Chem. Int. Ed. Engl. 12* (1973) 846.
[40] K. Mizuno, Y. Kimura, Y. Otsuji, *Synthesis 1979*, 688.
[41] E. Dehmlow, M. Lissel, *Tetrahedron 37* (1981) 1653.
[42] E. Dehmlow, S. Barahona-Naranjo, *J. Chem. Res. Synop. 1979*, 238.
[43] A. Brändström: *Preparative Ion Pair Extraction. An Introduction to Theory and Practice*, Apotekarsocieteten/Hassel Lakemedel, Stockholm 1974, pp. 139-140.
[44] F. Montanari, D. Landini, F. Rolla, *Top. Curr. Chem. 101* (1982) 147, and references cited therein.
[45] G. Illuminati in M. R. J. Dack (Ed.): *Chemistry, Vol. 8/2*, Wiley, New York 1976, Chapter 120.
[46] K. Bowden, R. Cook, *J. Chem. Soc. Perkin Trans. 2 1972*, 1407.
[47] D. Landini, A. Maia, *J. Chem. Soc. Chem. Commun. 1984*, 1041.
[48] D. Landini, A. Maia, G. Podda, *J. Org. Chem. 47* (1982) 2264.
[49] D. Landini, A. Maia, F. Montanari, *J. Am. Chem. Soc. 106* (1984) 2719.
[50] D. Bohme, G. Mackay, *J. Am. Chem. Soc. 103* (1981) 978.
[51] M. Halpern, D. Feldman, Y. Sasson, M. Rabinovitz, *Angew. Chem. 96* (1984) 79; *Angew. Chem. Int. Ed. Engl. 23* (1984) 54.
[52] D. Feldman, M. Halpern, M. Rabinovitz, *J. Org. Chem. 50* (1985) 1746.
[53] W. Spillane, P. Kavanaugh, F. Young, H. Dou, J. Metzger, *J. Chem. Soc. Perkin Trans. 1 1981*, 1763.
[54] See, for example: D. Brunelle, *J. Org. Chem. 49* (1984) 1309.
[55] M. Halpern, Y. Sasson, M. Rabinovitz, *J. Org. Chem. 49* (1984) 2011.
[56] M. Halpern, H. Sahalka, Y. Sasson, M. Rabinovitz, *J. Org. Chem.*, in press.
[57] C. Starks, *CHEMTECH 1980*, 110.
[58] D. Feldman, M. Rabinovitz, unpublished results.
[59] R. Neumann, Y. Sasson, *J. Org. Chem. 49* (1984) 1282.
[60] E. Dehmlow, J. Schmidt, *Tetrahedron Lett. 1976*, 95.

Charge Separation in Excited States of Decoupled Systems—TICT Compounds and Implications Regarding the Development of New Laser Dyes and the Primary Processes of Vision and Photosynthesis

By Wolfgang Rettig*

The understanding of the dual fluorescence of certain aromatic systems has greatly advanced in recent years. The accompanying large charge separation has been shown to be linked to a twisted (or small overlap) arrangement of the chromophores. Recent theoretical models are able to describe the excited-state twisting of both single bonds (TICT compounds) and double bonds (olefins) in a unified picture. These models can help to elucidate the photophysical behavior of many organic, inorganic, and biologically relevant compounds, and their application to laser dyes and fluorescent probes provides a route to new "tailor-made" fluorescent materials. Applied to the primary processes of vision and photosynthesis, these models can lead to a deeper understanding of basic photobiological processes.

1. Introduction

The separation of electrical charges is one of the processes upon which our existence depends and which is the basis for numerous present and possible future developments including organic conductors and superconductors as well as the production and storage of electricity. Most important, nearly all of earth's life forms use directly or indirectly the transformation of sunlight into chemical energy, which occurs via a charge-separation process.

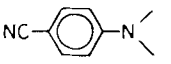
Since charge separation on a molecular level is often involved, the study of model systems displaying charge separation is essential to understand the mechanisms involved. An especially powerful tool is provided if such charge-separated systems luminesce, because internal and environmental influences affect this luminescence in a characteristic way, yielding detailed information on thermodynamic, kinetic, and other photophysical and even photochemical properties of such species.

Some simple bichromophoric organic molecules form luminescent species that display the characteristic features of charge separation and are therefore well-suited model systems. For the majority of these systems, the charge separation is most favorable in a twisted conformation, where the two moieties involved in charge transfer, the donor D and the acceptor A, are orbitally decoupled, i.e., nearly perpendicular in the case of two π systems. Initially, this led to the notion of "twisted intramolecular charge transfer" (TICT) states.[1–4] Later, it was realized that many TICT states are nonluminescent and are responsible for the rapid nonradiative decay of numerous important dyes leading to intramolecular fluorescence quenching. Their involvement in excited-state processes of biologically important compounds is just beginning to be understood.

This article first gives a brief survey of the development of the concept of TICT states and of our present knowledge of the broad variety of systems that form such states. The properties of TICT states are then discussed and some important implications connected with the formation of TICT states are outlined.

2. The Concept of TICT States—A Historical Overview

More than twenty years ago, a simple benzene derivative, *p-N,N*-dimethylaminobenzonitrile 1 was discovered to behave peculiarly in fluorescence spectroscopy. *Lippert*



1

et al.[5] showed that it emits a dual fluorescence (Fig. 1) consisting of two bands, one being that "normal" for closely related benzene derivatives, the other, at considerably lower energy, being an "anomalous" one. *Lippert* et al.[5] proposed a solvent-induced reversal of excited states. The anomalous band was assigned to fluorescence from the more polar ^1L_a-type state, which is preferentially stabilized by solvation. This led to the nomenclature still in use today: A band for the "anomalous" emission from the ^1L_a-type state, B band for the normal short-wavelength emission from the ^1L_b-type state. The emitting states, also called A* and B* states, could be in thermal equilibrium. The kinetics of this process are summarized in Scheme 1,[1–2] which contains the equilibration rate constants k_{BA} (forward reaction) and k_{AB} (backward reaction) as well as the rate constants for radiative decay (k_f^B and k_f^A) and nonradiative decay (k_o^B and k_o^A) to the ground state. The scheme is very similar to that for excimer formation,[7] with the difference that three temperature-dependent rate

[*] Priv.-Doz. Dr. W. Rettig
Iwan N. Stranski-Institut für Physikalische und Theoretische Chemie der Technischen Universität Berlin
Strasse des 17. Juni 112, D-1000 Berlin 12

 © VCH Verlagsgesellschaft mbH, D-6940 Weinheim, 1986 0570-0833/86/1111-0971 $ 02.50/0

constants (k_{BA}, k_{AB}, k_f^A) are needed to explain the experimental observations.[1,2,6,8-10]

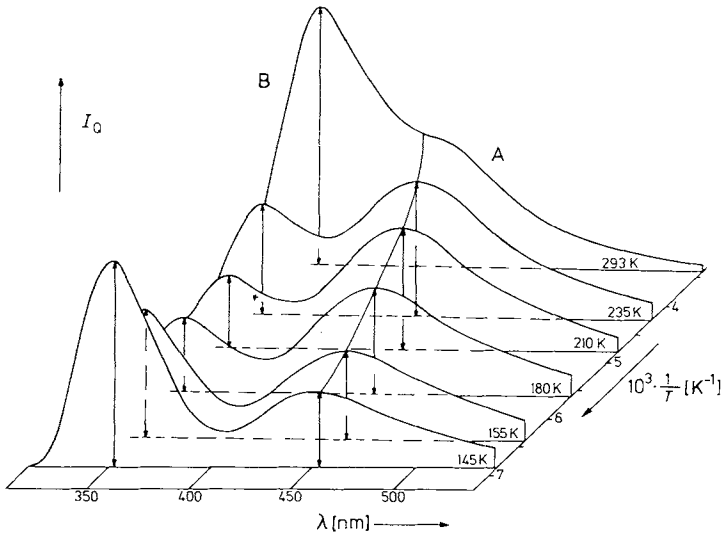
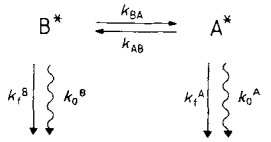


Fig. 1. Dual fluorescence of a 3×10^{-6} M solution of **1** in the medium polar, aprotic solvent *n*-butyl chloride as a function of temperature [6]. Both bands are independent of concentration and excitation wavelength over a large range. Upon increasing the solvent polarity, the longer-wavelength A band strongly shifts to the red and gains in relative intensity. The characteristic intensity minimum for the shorter-wavelength B band occurs at the temperature above which the excited B* and A* states reach a thermodynamic equilibrium B* $\rightleftharpoons$ A* during their nanosecond lifetime. Upon further increase of the temperature, this equilibrium is shifted toward B*, resulting in an increase of the total fluorescence quantum yield, because the deactivation of A*, unlike that of B*, occurs mainly via nonradiative processes. The slight increase of the quantum yield of the A fluorescence with temperature is due to the forbidden nature of this radiative process (hot fluorescence, see Fig. 10b). I_Q = number of quanta per nm and s.



Scheme 1.

As will be seen later, the above assignment to ^1L_a- and ^1L_b-type states is in fact true for **1** but breaks down for closely related compounds that emit a similar dual fluorescence. The excited-state reversal originally proposed by *Lippert* et al. is merely a manifestation of the underlying rules governing dual fluorescence of this type.

Rotkiewicz, Grellmann, and *Grabowski* were the first to suggest that these rules involved[11] a dynamic relaxation of **1** with internal twisting of the dimethylamino group, coupled with an electron transfer from the amino nitrogen to the far-away in-plane π_y^* orbital of the cyano group[11,12] or, in better agreement with later experiments, to the π_z^* orbital extending over the entire benzonitrile group.[1] Figure 2 shows schematically the two fluorescing species, the B* and the TICT state.

The suggestion of *Grabowski* et al. was at first mainly based on fluorescence polarization experiments in glycerol which showed that the two emission transition moments of **1** have the same polarization, along the axis connecting amino and cyano groups.[11] Thus, *Lippert*'s proposal of emitting ^1L_a- and ^1L_b-type states with perpendicular transition moments could not be true. For the same experiment in ethanol, however, the fluorescence polarization of the two bands is dissimilar, that of the B band being characteristic for a ^1L_b-type state with a transition moment perpendicular to the long molecular axis.[13] The B band in glycerol thus derives from a different state than in ethanol, namely from the ^1L_a-type state of the planar molecule, which is lower in energy than the ^1L_b-type one in this solvent. A similar case of solvent-induced level reversal in the nearly planar molecule has been found for a naphthalene analogue of **1**.[14-16] Level reversals of this type can also be induced by substituents. This is schematically shown in Figure 3.

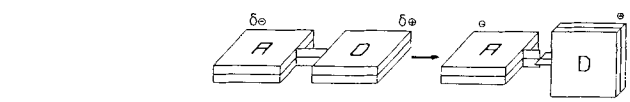


Fig. 2. Schematic representation of the change in geometrical arrangement of donor group D and acceptor group A upon going from the B* state to the TICT state. In the case of **1**, this transition involves (1) intramolecular rotation, (2) crossing of excited states and nonadiabatic coupling, (3) further charge transfer approaching a full electronic charge, and (4) relaxation of the polar solvent molecules around this increased dipole.

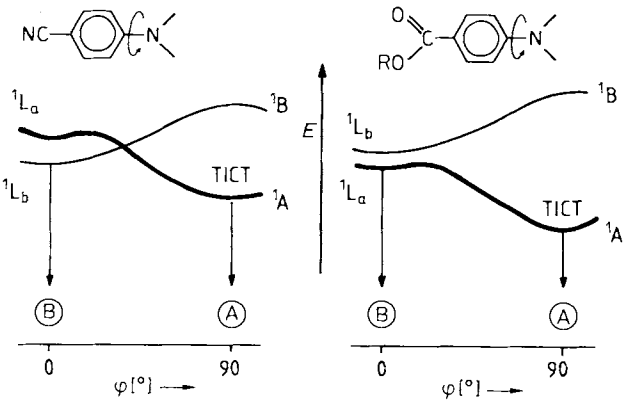
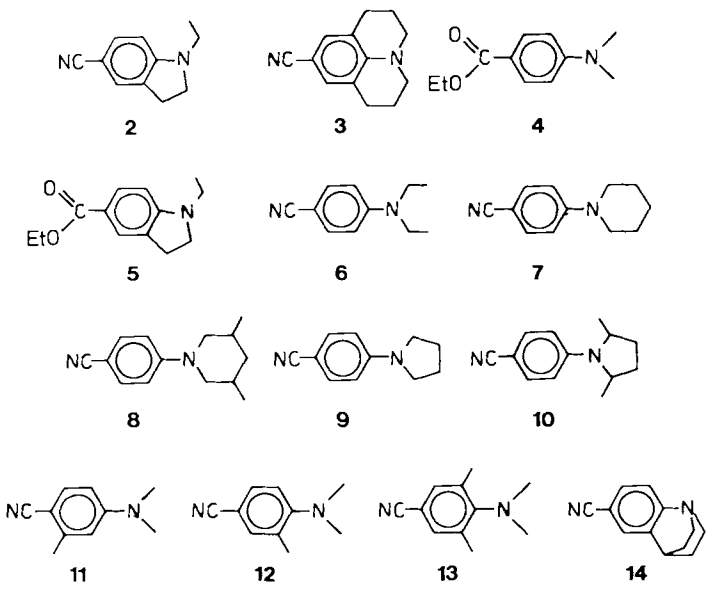


Fig. 3. *p*-Substituted dialkylanilines undergo substituent-induced level reversals for the excited states of the planar conformation. Upon going from the cyano to the alkoxycarbonyl derivatives, the ^1L_b-type state is shifted to higher energy, the ^1L_a-type state to lower energy compared with the nitriles [17]. Since both ^1L_a-type and TICT states are of symmetry species A (in the C_2 point group, which is valid for idealized nonpyramidal amino groups for any twist angle φ), they correlate without crossing (in the case of the alkoxycarbonyl derivatives) and with excited-state crossing (in the case of the cyano derivatives) [10, 15, 18]. As a result of the substituent-induced level reversal, the B fluorescence changes its nature. This can be followed by measurement of the fluorescence polarization and the rate constant for radiative decay [9, 10, 17]. Ⓐ = A band, Ⓑ = B band.

In a series of publications, *Grabowski, Rotkiewicz,* and co-workers presented convincing experimental proof for the twist hypothesis.[1-3,19,20] They synthesized model compounds for **1** where the dimethylamino group was rigidly held in the planar or perpendicular position, or where the planar arrangement of the dimethylamino group was increasingly hindered by *ortho* substituents in the benzene ring.[3] The bridged nitriles **2** and **3** as well as the ester **5** did not exhibit the A band in the fluorescence spectrum,[3,17,21] although they showed very similar absorption spectra. The fully perpendicular benzoquinuclidine **14**, on



the other hand, showed the A band but lacked the B band altogether.[19] Compounds with more flexible bridges were also synthesized by other groups.[22,23] These experiments clearly demonstrated that the possibility for reaching an orthogonal conformation of the dimethylamino group is a "sine qua non" for the occurrence of the A band.

In a different approach calling upon the dynamics of intramolecular twisting, the model compounds **7** and **8**[24] were found to exhibit similar electronic and steric properties, differing only in the size of the rotating volume. Figure 4 shows an example of such a "hydrodynamically" controlled dual fluorescence.

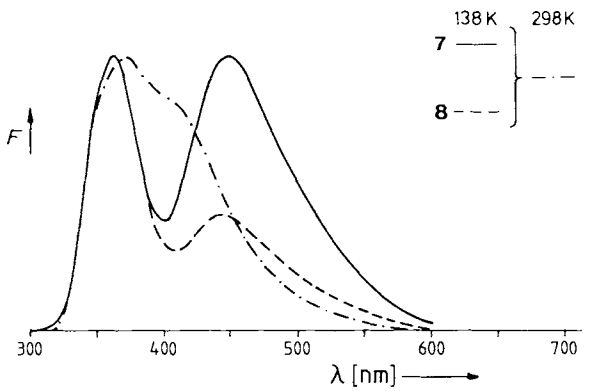


Fig. 4. Temperature dependence of the dual fluorescence of a pair of dynamically differing compounds, **7** and **8** (ca. 10^{-5} M in *n*-butyl chloride). At temperatures where the thermodynamic equilibrium $B^* \rightleftarrows A^*$ is established within the lifetime of the excited states, the dual fluorescences of **7** and **8** are identical. At low temperatures, however, the relative intensity of the TICT fluorescence of **8** is decreased considerably, which indicates slower formation of the TICT state A^* in **8** compared with **7** [24]. F = Fluorescence intensity in arbitrary units.

While these two approaches clearly show the necessity and the occurrence of intramolecular twisting in TICT formation, many factors are important in determining its actual rate. In a series of derivatives of **1** with different cyclic and open-chain alkyl substituents at the amino nitrogen (**6–10**), the rates (which differ by one order of magnitude) were shown to be governed by a complicated interplay of factors such as molecular flexibility, symmetry of the rotating moieties, the actual volume of solvent molecules displaced during rotation, and the mean ground-state twist angle (equal to the Franck-Condon twist angle, the starting angle for the relaxation in the excited state).[9,18,21,24]

The corresponding alkoxycarbonyl derivatives behave similarly.[18] However, the level crossing upon twisting, observed for **1**, is absent for the alkoxycarbonyl derivatives (Fig. 3), a fact that has profound effects on the potential hypersurfaces that ultimately govern all reaction dynamics. A qualitative drawing of these hypersurfaces is shown in Figure 5. Figure 6 displays the consequences for the dual fluorescence of these compounds.

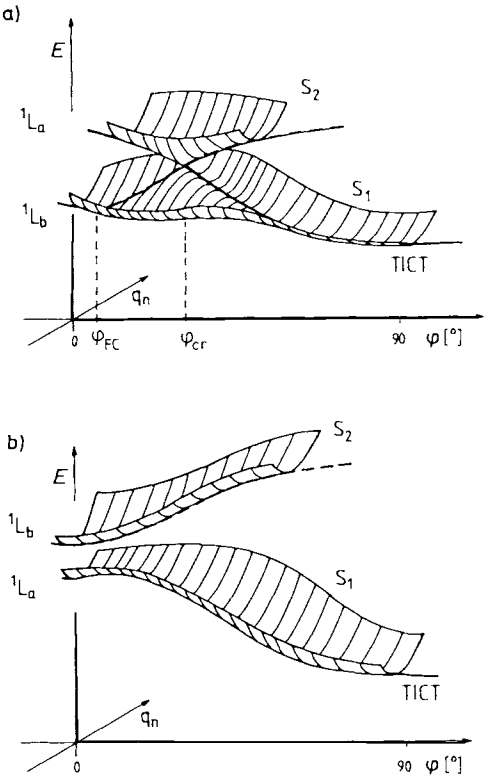


Fig. 5. Schematic representation of the potential hypersurfaces along the reaction coordinate toward the TICT state in *para*-substituted dialkylanilines [18]. a) In the cyano derivatives the crossing of ^1L_a- and ^1L_b-type states (cf. Fig. 3) causes a "conical intersection" at the critical twist angle ϕ_{cr} which necessitates the coupling with a non-totally symmetric vibration q_n or with solvent relaxation. b) For the alkoxycarbonyl derivatives, this coupling is not necessary; the reaction can proceed smoothly downhill (it is even possible that the indicated activation energy is not present). The experimental consequence is a readily observable TICT fluorescence even in nonpolar environments[9,18] and an increase of the rate constant k_{AB} for TICT formation by a factor of approximately 5 [18, 25]. A similar increase of k_{AB} should be expected for the CHO- and CRO-substituted anilines, but their weak fluorescence points to a complication by low-lying $n\pi^*$ states.

Recently, TICT emission in the gas phase was observed for **13**[26,27] and for an *N*-phenylpyrrole derivative (Fig. 7).[28] In each of these molecules, donor and acceptor are already strongly twisted in the ground state.

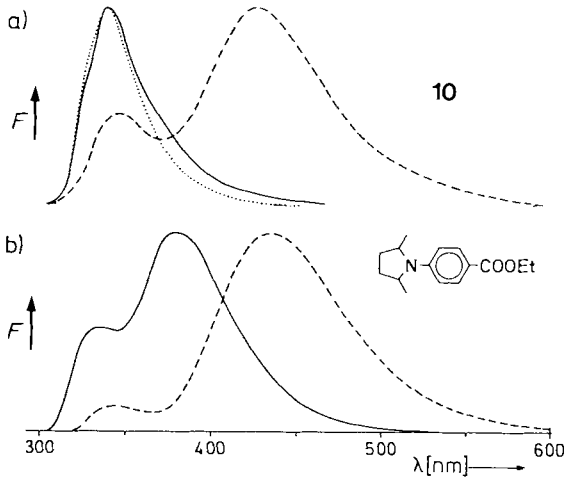


Fig. 6. Dual fluorescence spectra (a) of **10** and (b) of the corresponding alkoxycarbonyl derivative at room temperature [18] in *n*-hexane (——) and in *n*-butyl chloride (----). The TICT band for **10** in *n*-hexane is very weak (for comparison, the fluorescence spectrum of **1** in *n*-hexane is also shown, (·····)). The absence of the conical intersection, however, causes the TICT band to be the main fluorescence band for the corresponding alkoxycarbonyl derivative.

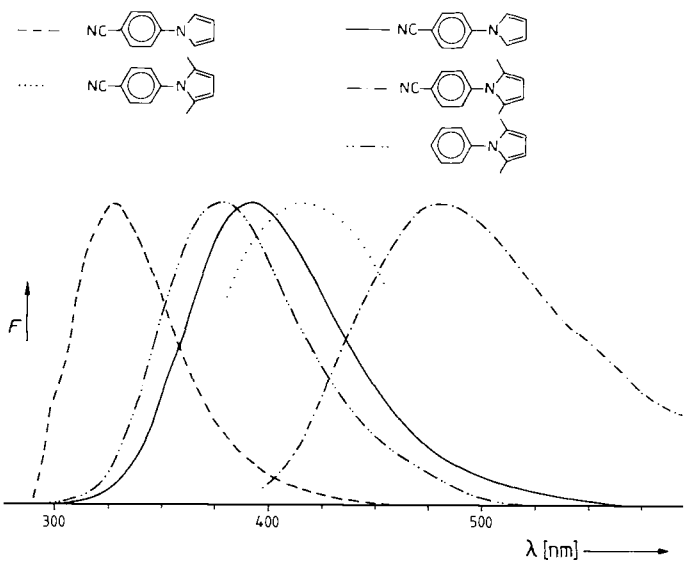


Fig. 7. TICT fluorescence bands of *N*-phenylpyrroles in *n*-butyl chloride (—, —·—, ··—··) and in *n*-hexane (----) at room temperature and in the gas phase at ca. 93 °C (···). The comparison of gas- and solution-phase spectra shows the stabilizing action of the solvent upon the fluorescent states. The concept of TICT states is not linked to the formation of specific solute-solvent interactions (ground-state complexes or exciplexes) and not even to the presence of a solvent at all. Increase of the acceptor strength (—·— versus ··—··) or of the donor capability (—·— versus ——) also lead to a lowering of the energy of the TICT state and a corresponding redshift of the emission (see Section 6).

3. Environmental Influences on TICT States

While it is perhaps most straightforward to learn more about the properties of TICT states by investigating them "naked" in the gas phase, most studies up to now have been done in solution, where the TICT molecule is surrounded by a swarm of more or less polar and polarizable solvent molecules, where specific solute-solvent interactions may play a role, and where the kinetics of formation may become strongly affected by cage effects (see Section 7 for the influence of free volume and microviscosity). In fact, because of these complications, the currently accepted notion of TICT states was slow to emerge.

In 1972, *Khalil, Hofeldt,* and *McGlynn*[29] repeated some of *Lippert*'s early experiments on **1** and found a third, longer wavelength emission band which they attributed to a ground-state dimer of **1**. The anomalous A band observed by *Lippert* et al. was assigned to an excimer, which was expected to form upon encounter of an excited molecule of **1** with a ground-state one.[29,30] Both the ground-state dimer and the excimer mechanisms would predict that the A band gains in relative importance if the concentration of **1** is increased. Although both mechanisms do actually take place for **1** and related molecules at high concentrations ($c \geq 10^{-4}$ mol/L),[31] or even for smaller ones at low temperatures,[32] *Mataga* et al.[33] showed that they are not the source of the anomalous A band. The ratio of fluorescence intensities of A to B, F_A/F_B, of a rigorously purified sample of **1** was independent of concentration over a range of more than two orders of magnitude. Moreover, the purified sample did not show the "dimer" emission reported by *Khalil* et al.[29] Thus, the latter was attributed to an impurity.

Kosower et al.[34] studied the effects of deuteration of the solvent on the ratio of the A to the B band in water and alcohols and concluded that the A band arises from a species protonated in the excited state. However, this mechanism could not explain the presence of the A band in rigorously dried aprotic solvents,[27,35] in saturated hydrocarbon solvents, or even in the gas phase. Although the deuterium effect has been observed by several other groups,[36,37] it does not necessitate a specific solute-solvent interaction for formation of the TICT state. For the deuterium effect to occur, it is sufficient that a competing kinetic process is isotope sensitive. A possibility for such a competing process is the photochemical reaction of excited **1** with an alcohol or water molecule to form a complex, which, in turn, decays to a thermally unstable ground-state product that rapidly reverts back to **1**. In fact, this possibility is supported by experimental data. Protic solvents strongly quench the total fluorescence yield of **1**, by a factor of about 10 for alcohols and even about 100 for water.[34] The quenching also takes place for the planar model compounds **2** and **5**.[17] Thus, it is not a feature specific for TICT states, but seems to be connected with the aromatic amine function. If substituent groups are absent altogether, as in TICT-forming biaryl systems, the quenching action of protic solvents is absent.[38,39]

Two additional ways in which the environment can affect the formation of a TICT state are outlined below. Both possibilities supplement but do not replace the twist mechanism and accompanying charge transfer accepted as the prerequisite for TICT-state formation.

Chandross[40] and later *Visser* and *Varma*[23,37,41] observed that the B band of **1** was strongly quenched as the amount of a polar solvent constituent in a mixture was increased. From a linear correlation of the F_A/F_B ratio with the concentration of polar solvent, the specific formation of a 1:1 exciplex of an excited molecule of **1** with one

polar solvent molecule was suggested.[23] This type of specific solute-solvent interaction may actually take place for certain solvents like alcohols[42-44] but is very unlikely to be a phenomenon generally linked with TICT emission on the following grounds: (1) There are some molecules that show TICT emission even in the gas phase. (2) The alkoxycarbonyl- and cyano-substituted dialkylanilines have fluorescence spectra in polar solvents that are similar,[18] and, moreover, the alkoxycarbonyl-substituted species show TICT emission even in aliphatic hydrocarbon solvents, where no specific interactions are possible (Fig. 6). (3) The fluorescence quenching of **1** by nitriles is of similar magnitude in high-viscosity paraffin as in low-viscosity hexane.[28] This suggests that the quenching phenomenon is not generally linked to diffusion kinetics, but that preferential ground-state solvation[45] (static quenching) plays an important role in mixed solvents. This is also suggested by the time-resolved measurements of alcohol/alkane mixtures.[42] (4) The redshift of the TICT fluorescence[5,46] (see also Fig. 9 in Section 5) is well correlated with solvent bulk-polarity properties for nearly all known molecules that exhibit TICT fluorescence, even though these species vastly differ in structure and electronic properties (see next section). A specific solvent interaction by overlapping electron clouds, however, should lead to stabilization energies that depend on properties other than the polarity of the interaction partners. Thus, the emission energy of exciplexes formed with ethers, chlorides, nitriles, ketones, or alcohols is not expected to correlate with solvent polarity. Some of the deviations from linearity of the solvatochromic plots (Fig. 9 in Section 5) are probably due to weak specific interactions of solute and solvent. (5) There are cases where true specific interaction has been observed and found not to correlate with polarity properties. One example is the quenching of TICT fluorescence by inorganic ions,[47] where the concept of hard and soft Lewis acids and bases is more important. Another example is the quenching of TICT fluorescence of **1** by interaction with trialkylamines.[48] A complex, $[^{\ominus}ArylMe_2N^{\oplus}:NR_3]$, is formed with a two-center three-electron bond; its rate of formation, however, is governed not by thermodynamic properties but by steric interactions.

Because of its strong response to environmental effects, **1** has been used as a fluorescence probe in micelles and in cyclodextrin inclusion complexes.[49]

4. TICT States and Dyes

The number of compounds able to form TICT states is rapidly increasing. Whereas the number of TICT-forming compounds known a few years ago filled one page,[4] a similar list (Fig. 8) is obtained today if one just takes one member of the various series of compounds that have been studied in this context. In the following, we will discuss very briefly some of the examples.

Of the three types of compound **15**–**17**,[1-3,5,6,8-10,23,24,50] **16** show the strongest TICT emission because the conical intersection is absent and because the $n\pi^*$ states are high in energy and do not lead to fast nonradiative decay. The dual fluorescence of **17**[31] is weaker on account of intramolecular quenching (nonradiative decay) by $n\pi^*$ states. Compared with **15**, compound **18**[14-16] contains a stronger acceptor group and **19**[46,51] a stronger donor group. Because of the increased donor capability of the pyrrole ring, even the parent compounds **20** and **21** show dual fluorescence.[46]

The carbazole group is also a good donor group, as seen from the TICT fluorescence of compounds **22**–**24**.[38,52,53] Therefore, one should expect the corresponding indole derivatives to behave similarly. In fact, recent experiments on **25** have shown that it exhibits a dual fluorescence. Other biologically relevant molecules like **26**[54] and **27**[55] also emit a dual fluorescence.

Very interesting examples are compounds that are nonpolar and highly symmetric in the ground state yet form a very polar TICT state upon excitation; examples include the biaryls **28**,[38,39,56-62] **29**,[63] **30**,[39] and **31**.[64] This symmetry breaking does not occur for all biaryls. The preconditions were first discussed by *Zachariasse*,[65] who correlated this property with the difference in oxidation and reduction potentials. In a more refined version (see also Section 6), this approach has been used to predict new TICT-forming members of the biaryl series.[39] Ionic biaryl derivatives like **32**[66] and possibly 9,9'-bisacridinium nitrate[67] show a similar dual fluorescence.

Diphenylmethane dyes like Michler's ketone **33** (X = O)[68,69] or Auramine O **33** (X = NH)[70] also exhibit multiple fluorescence. In the case of the sulfones **34**,[15,71] the TICT fluorescence is in fact strong, possibly due to p_π–d_π interaction at the sulfur atom.[71] In **33** and **34** and in **35**–**38**, the perpendicular TICT geometry is attained not by rotation around the N-aryl bond but by rotation around the S–C or C–C bond connecting the aniline moieties with the rest of the molecule. This has been concluded from the investigation of ring-bridged model compounds.[68,69,72-75]

For cationic triphenylmethane (TPM) dyes like Crystal Violet **35**·$Cl^{\ominus}$ or **35**·$ClO_4^{\ominus}$ as well as for the neutral fuchsone **36**, formation of the TICT state manifests itself by strong fluorescence quenching.[75] In this case, TICT states seem to be nonemissive, and have lifetimes of only a few picoseconds or less as judged from ground-state repopulation experiments.[76] If the system has two more π electrons, however, as is the case for neutral triphenylamines, long-lived emissive TICT states are possible (cf. results for **22**–**24**). The redshifted fluorescence of triphenylphosphane and its metal complexes[77] also seems to indicate the formation of TICT states.

If the energy of the TICT states is raised above that of the other "locally excited" (LE) states, TPM dyes fluoresce strongly. This is nicely shown for the Crystal Violet derivative **37**·$ClO_4^{\ominus}$, a xanthene dye that shows a fluorescence quantum yield of <0.01 in ethanol, owing to efficient formation of a weakly emissive or nonemissive TICT state by rotation around the C-anilino bond. Addition of a few drops of acid blocks the anilino lone pair by protonation and strongly reduces its donor capabilities. This results in an increase in the fluorescence quantum yield by more than two orders of magnitude.[70] Similar effects have been observed with the pyrenyl group as acceptor.[78] Such systems are potentially useful as fluorescent indicators.

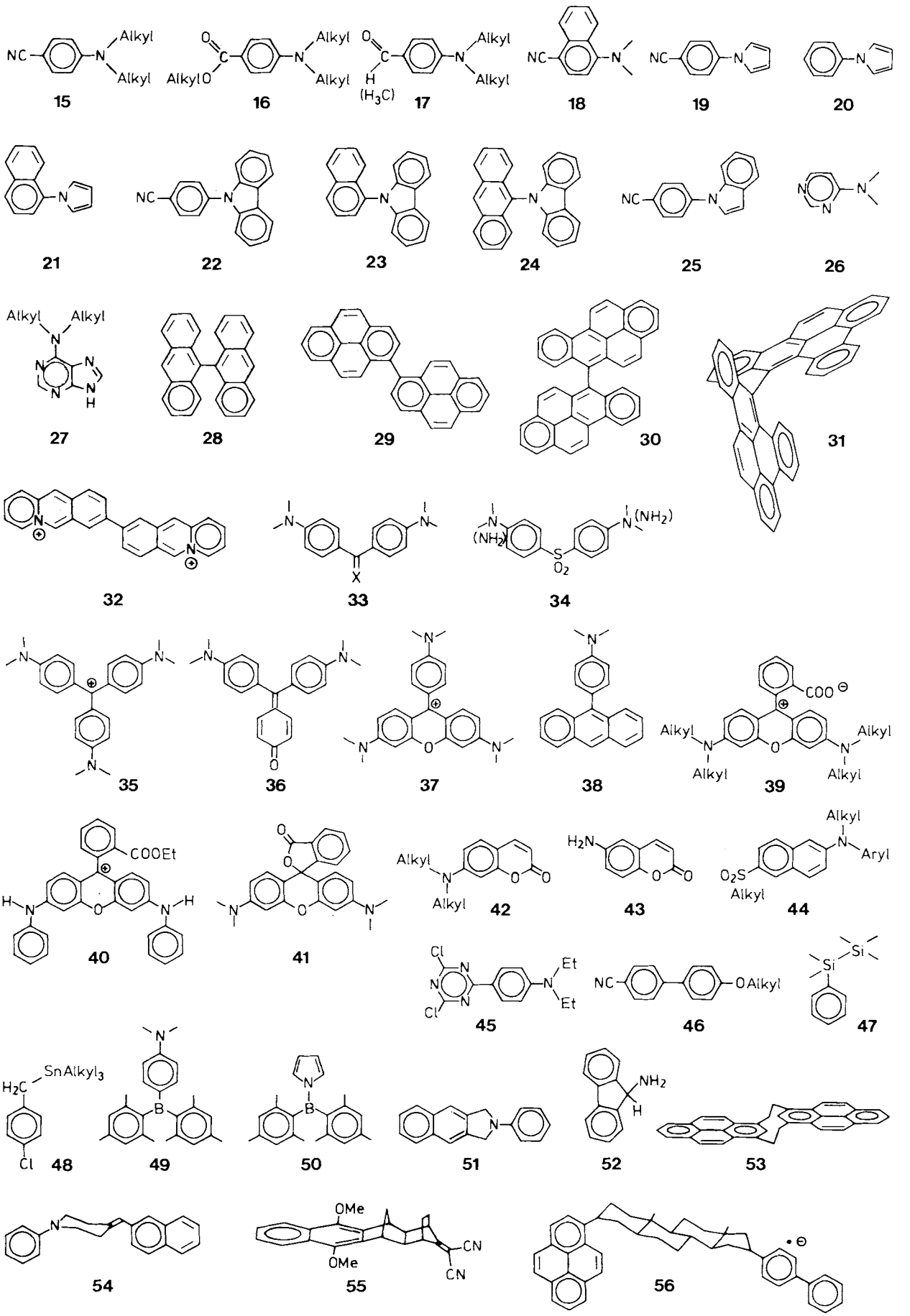


Fig. 8. A list of compounds known to form TICT states (or minimum overlap electron-transfer states). In many cases, one compound represents a large family of compounds with different substituents and/or substitution patterns. Since the notion of TICT states is spreading into organic as well as biochemistry, this list is expected to grow rapidly within the next few years.

Even for ordinary rhodamine dyes like **39**, in which the donor group is replaced by an acceptor group, TICT formation takes place, though only at higher temperatures and by rotation around the N-aryl bonds.[79] The rate of TICT formation is strongly increased by increasing the donor character of the amino groups, as in **40**·$Cl^{\ominus}$. Thus, Fast Acid Violet, a derivative of **40**·$Cl^{\ominus}$, has a strongly viscosity-dependent fluorescence lifetime in the subnanosecond range.[80]

In weakly polar solvents, compounds like **39** tend to exist in their lactone form **41**, a spiro compound with preformed TICT geometry. Emission spectra and lifetimes of these compounds do indeed indicate the population of a highly polar forbidden state.[81]

Also other laser dyes such as the coumarins **42** are strongly affected in their photophysical properties by a solvent-polarity-dependent decay toward a nonemissive TICT state.[82] In the case of **43**, this decay is so pronounced that even in saturated hydrocarbon solvents or in ethanol matrix at 77 K all excited molecules decay via the TICT state, which can be identified here by its weak emissive properties.[83]

Still another family of compounds is represented by **44**. These molecules have been used extensively as fluorescent probes in biology.[84] They decay like **40** by rotation of the anilino group around the N-naphthyl bond toward TICT states that are emissive in this case.[85]

Although biphenyl is predicted to possess only rather high-lying TICT states,[39] donor-acceptor-substituted biphenyls like **45**[86] and **46**[87] seem to decay via fluorescent TICT states. For sufficiently long alkyl chain lengths, the biphenyls **46** display liquid-crystalline behavior, and complicated phase transitions can be nicely probed by observing their unusual fluorescence properties.[88]

The range of TICT-forming compounds is not limited to pure organic chemistry. Some of the unusual fluorescence features observed in silicon or boron compounds, and even organometallic compounds, are in fact nothing else but a manifestation of TICT formation. Examples of such compounds are **47–50**. In **47**[89] and **48**,[90] a doubly occupied σ-orbital seems to act as the donor, because most of the unusual fluorescence is found when the Si-Si bond (a good donor[91]) is in the plane of the benzene ring, i.e., perpendicular to the benzene p_z orbitals. The boron compounds **49**[92] and **50**[93] are very similar to the triphenylmethane dyes (e.g., **35**·$Cl^{\ominus}$), but they are neutral, nonionic compounds.

Compounds **51**,[94] **52**,[95] **53**,[4,96] **54**,[97] and **55**[98] also undergo photoinduced charge separation, but no twisted bond is involved. Instead, a deeper principle is active here, which encompasses both TICT states and these molecules, that of "minimum overlap."[4,38,39] As discussed in Sections 8 and 9, flexible molecules spontaneously relax to a conformation with minimum interaction between LE and charge-transfer (CT) states (the "minimum overlap conformation"), which leads to full charge separation. If, however, one of the bridges is cut, say in **53**, and the sandwich-type conformation can easily be reached, the "maximum overlap rule" takes over, which describes the tendency for maximal LE-CT interaction.[99] Then, charge separation does not occur any more in symmetric systems.[38,100] The "minimum overlap rule" is probably also relevant for model systems (e.g., **56**) of photoinduced electron transfer over varying distances.[101]

As will be seen in Section 10, this notion of minimum overlap turns out to be a possible key for the understanding of the primary steps in photosynthetic charge separation. It probably also drives the very efficient *cis–trans* isomerization in the visual pigment rhodopsin (Section 9). Recent experiments indicate that TICT states may also be important in other fields of photobiology, for example in the photophysics of bilirubin.[102]

5. The Properties of TICT States

The most important feature of TICT states is their charge separation, which, neglecting σ–π interaction, amounts to transfer of exactly one electronic charge from donor to acceptor.[1–4] In more elaborate quantum chemical treatments,[20,103] the amount of charge transferred is still on the order of 0.8 of an electronic charge. This charge separation is detectable experimentally by measuring the dipole moment of the TICT state by means of the influence of an electrical field on the emission (*e*lectro*o*ptical *e*mission *m*easurements, EOEM).[27,35] Methods have even been developed which, in principle, allow the determination of the dipole moment of nonemissive TICT states (transient dielectric loss measurements).[41]

An experimentally much simpler approach is to measure either thermochromic shifts[104] or to probe the influence of the immense dielectric field set up by polar solvents. The emission bands in a series of such solvents are redshifted as polarity increases (Fig. 9a). A quantitative analysis of the spectra is shown in Figure 9b.

The dipole moment of the TICT state of **1** was determined to be about 12 D (40×10^{-30} Cm) by EOE measurements[27,35] and is compatible with the results of solvatochromic measurements if a so-called "harpooning mechanism"[28] is taken into account. This predicts that, upon charge separation, the molecule (and the cavity) should shrink in size, because the two oppositely charged molecular moieties attract each other. Quantum-chemical calculations on the CNDO/s level support this view.[55]

One of the main features of TICT states is their twisted geometry. It is interesting to ask, why, for planar molecules like **1** or **20**, a twisting to the perpendicular conformation should occur spontaneously in the excited stat. Quantum-mechanical calculations also predict this to occur (Fig. 10a). The answer can be given in terms of the valence bond model[109] (see Section 9) and leads to the "minimum overlap" rule.

Because the radiative transition TICT state → ground state (a back CT transition) involves two orbitals located on different π systems, perpendicular to each other on average, it is overlap forbidden (small transition probability) and thus expected to possess a small transition moment. A small TICT fluorescence quantum yield is therefore expected. However, by coupling to suitable vibrations, this transition can borrow intensity from higher-excited, more allowed states, which accounts for the many systems with

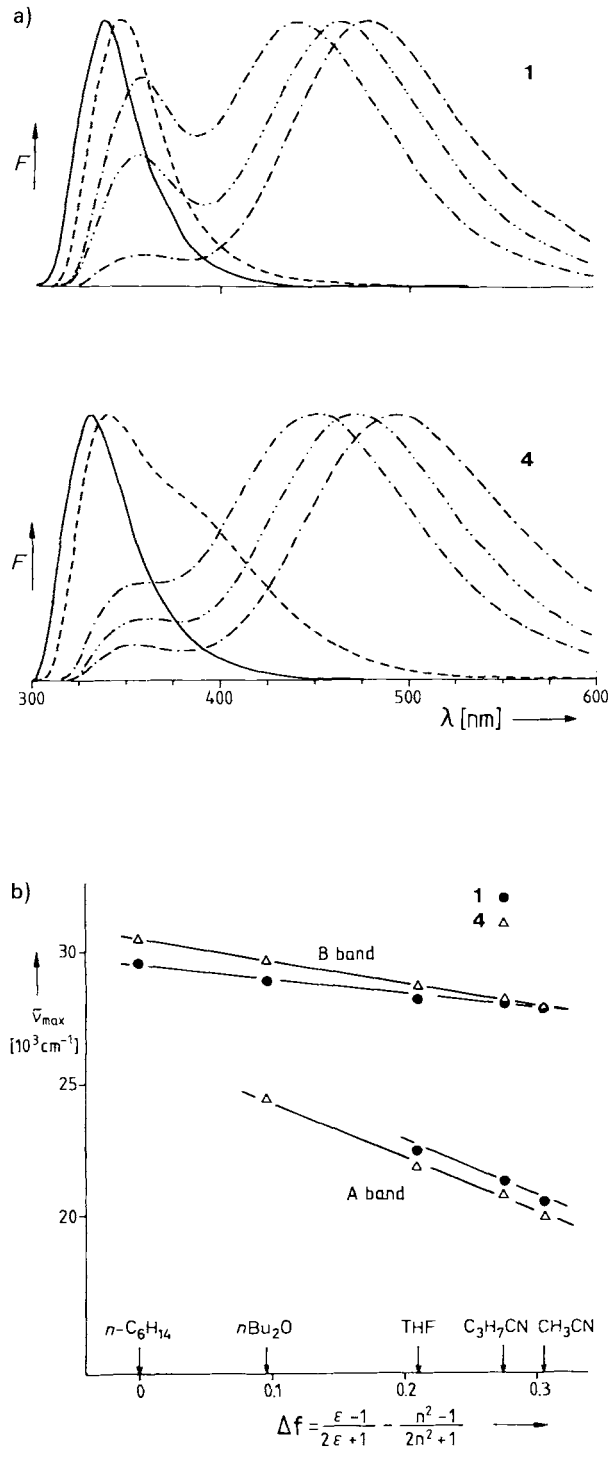


Fig. 9. a) Fluorescence spectra of **1** (upper) and **4** (lower) at room temperature in aprotic solvents of different polarity. The A band is strongly red-shifted and gains in relative intensity for increasing polarity. —— *n*-C_6H_{14}, --- nBu_2O, —·— tetrahydrofuran (THF), ··— C_3H_7CN, ·--· CH_3CN. b) Quantitative treatment by separation of the bands [9] and application of the solvatochromic equations derived by *Lippert* [105], *Mataga* [106], *Liptay* [107], or *Bilot* and *Kawski* [108]. The figure shows the fluorescence data derived from a) as a function of the solvent polarity parameter Δf [105], which depends on the dielectric constant ε and the refractive index n of the solvent. The point for THF is consistently slightly lower than the correlation line. This points to the existence of weak solvent-specific effects in addition to the strong bulk polarity ones. The B band of **4** is more strongly influenced than that of **1**, because B emission in **1** is from a ^1L_b-type state with a dipole moment smaller than that of the emissive ^1L_a-type state in **4**. The effect on the A bands is larger, but apparently similar for the two compounds. Precise relative TICT-state dipole moments may be determined if weak solvent-specific effects are excluded by using a series of homologous polar solvents, and if the variations in charge distribution and in molecular size and shape are taken into account [38, 39, 46].

appreciable TICT fluorescence quantum yields (**22–24**, **28**, **34**, **46**). Similar coupling effects may even lead to an unsymmetrical TICT equilibrium geometry in **12**.[43]

The fact that the rate constant for radiative decay of TICT states increases with temperature,[1,6,8,43,73] and that, therefore, a temperature-dependent fluorescence rate constant $k_f^{\wedge}(T)$ is required in Scheme 1, is in accordance with this picture of vibronic coupling. The major part of the observed TICT fluorescence is emitted from higher vibronic levels and is thus a "hot fluorescence" (Fig. 10b).

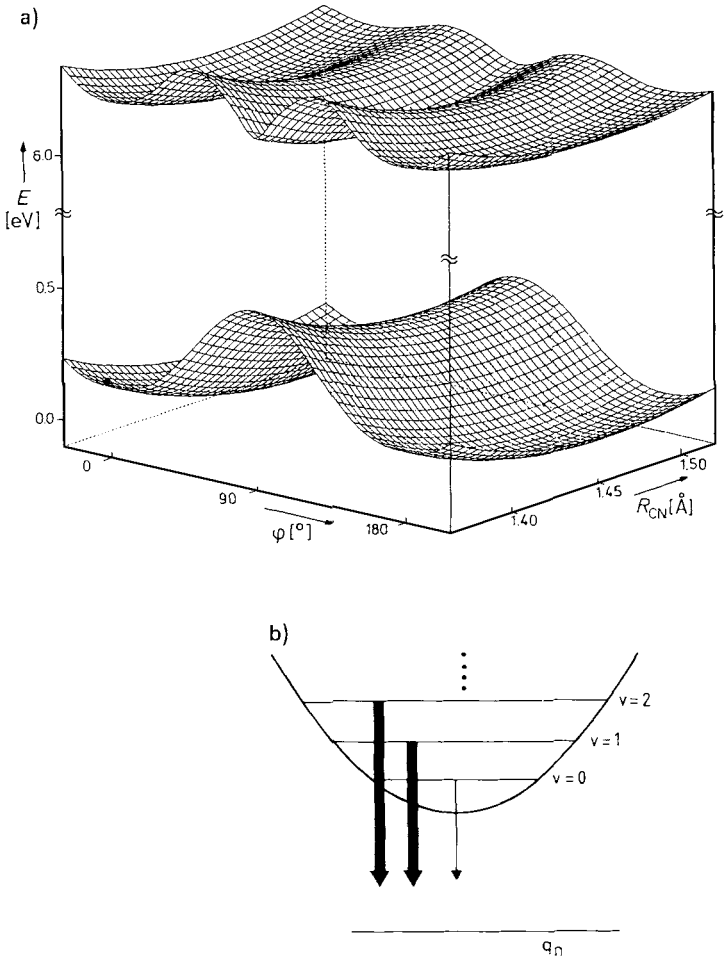


Fig. 10. a) Already a simple force field calculation for the ground and a higher excited state of **20** in the gas phase (S_5 at the planar geometry, i.e., $\phi = 0$, 180°) in the framework of the Pariser-Parr-Pople SCF-CI approximation predicts an energy minimum in the excited state at the twisted geometry ($\phi = 90°$, full charge separation), where the ground-state hypersurface possesses an energy maximum [51]. A polar environment will preferentially lower the excited-state minimum at 90° and may lead to the disappearance of the energy barrier between the conformations with $\phi = 0$ and $\phi = 90°$. b) Radiative decay from a TICT state with perpendicular conformation ($\phi = 90°$) is overlap forbidden (lowest vibrational level v = 0). For weak coupling, this level does not acquire much of the wave function of the upper allowed electronic state(s), quite different from the case for the higher-lying vibrational levels (v = 1, 2, ...) [1, 10, 17]. The TICT fluorescence therefore occurs mainly from molecules in excited vibrational states.

There are numerous similarities of TICT states to excimer or exciplex states. One of the main distinctions, however, is that excimers and exciplexes tend to follow the "maximum overlap rule," i.e., they assume sandwich-type structures if there are no geometric constraints.[99, 110–113]

Charge separation and symmetry breaking, however, are linked to a "minimum overlap" geometry (see Section 8). A more detailed discussion of the relation between exciplex, excimer, and TICT states can be found in a recent review by *Grabowski*.[114]

6. A Blueprint for Compounds with Energetically Low-Lying TICT States

Any bichromophoric system whose chromophores are linked by an essential single bond, like **15–50**, possesses, in the perpendicular conformation, several TICT states. Let us consider the simple case of dimethylaniline. The two most stable TICT states will be of different symmetries because they arise from the loss of an electron from the twisted amino group to one of the two lowest unoccupied benzene π^* orbitals. The energy of the lowest TICT state, however, is still unfavorable compared with that of the lowest excited state, LE1, of the planar conformation (Fig. 11b), and the twisting relaxation will not take place. If,

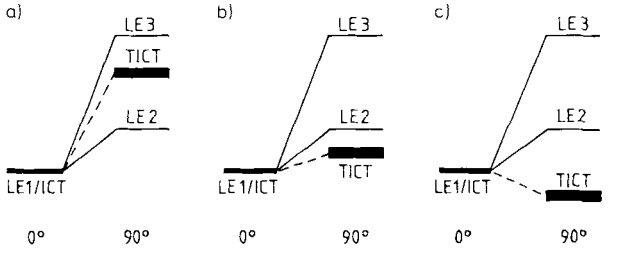


Fig. 11. Relative energy of the lowest TICT state in a twisted bichromophoric system. a) The TICT state is unfavorable with respect to the other states LE1, LE2 of both the perpendicular (90°) and the planar (0°) system. The term "locally excited" (LE) is somewhat misleading, because in a planar molecule like **1** the B* state (LE1) is delocalized over both acceptor and donor group and even contains quite substantial but never full intramolecular charge-transfer (ICT) character. In twisted **1**, however, the LE states are localized on the fragments, whereas the CT (TICT) states are still delocalized. b) The TICT state is unfavorable with respect to LE1, but favorable with respect to the LE states of the twisted conformation. c) The TICT state is lower in energy than the other excited states of both planar and perpendicular conformations.

however, the planar conformation cannot be reached because of steric hindrance, the lowest excited state is a TICT state. Benzoquinuclidine (**14** without the cyano group) actually shows such a TICT emission.[115] If the donor property of the dimethylamino group is weakened ($NMe_2 \rightarrow NH_2$), the situation in Figure 11a is expected, without TICT population even for rigidly perpendicular conformations. On the other hand, if the donor character is strengthened (e.g., the 2,5-dimethylpyrrolidino group in **10** is a better donor than the dimethylamino group in **1**[8]), and/or if the acceptor character is increased (*p*-cyano substituent), then the situation in Figure 11c arises, and the state LE1 can relax spontaneously to the lower-lying TICT state. This condition is given by Equation (a).

$$E(\mathrm{TICT}) - E(\mathrm{LE1}) < 0 \qquad \text{(a)}$$

The energy of the LE states can be determined by experiment. The energy of the TICT state can be approximated by Equation (b).[1,39,103]

$$E(\mathrm{TICT}) = IP(\mathrm{D}) - EA(\mathrm{A}) + C + \Delta E_{\mathrm{solv}} \qquad \text{(b)}$$

IP(D), the ionization potential of the donor moiety, and EA(A), the electron affinity of the acceptor, reflect the donor's capability to release an electron, and the acceptor's capability to bind it. Electron transfer results in the formation of a radical cation and a radical anion which attract each other, thereby stabilizing the system by the Coulomb energy C. Polar solvent molecules around the radical ion pair adjust to the increased electric field and stabilize the system by an amount ΔE_{solv}. A similar equation can be written in terms of oxidation and reduction potentials.[4]

Based on this equation, it is possible to rationalize the fluorescence behavior of biaryl compounds[65] and to predict new TICT-forming compounds.[39] Let us consider examples for each of the factors operating in Equation (b).

The first factor is the difference $IP(\mathrm{D}) - EA(\mathrm{A})$. Thus, for similar donors, the TICT state is lowered in energy with increasing acceptor strength. Examples are *N,N*-dimethylaniline and **1**, differently substituted TPM dyes like Crystal Violet **35**·$Cl^{\ominus}$ and Malachite Green (one NMe_2 group less than Crystal Violet),[75] or 7-dialkylamino coumarins **42**,[82] which are especially prone to form TICT states in polar solvents if they possess acceptor substituents on the coumarin skeleton. Examples for the variation of the donor capability are also found in the TPM series[75] and, particularly, for the phenylpyrrole derivatives (see **19**, **20**,[51] and Fig. 7), where the TICT emission is seen to follow the changes in the ionization potential of the donor group.

The Coulomb energy C can easily be calculated from the HOMO of the donor and the LUMO of the acceptor, as shown in Equation (c), where $c_{k,i}$ are the MO coefficients for atom i in the HOMO of the donor and $c_{l,j}$ those of atom j in the LUMO of the acceptor; e is the electronic charge and r_{ij} the internuclear distance.

$$C = -e^2 \sum_i \sum_j c_{k,i}^2 \cdot c_{l,j}^2 / r_{ij} \qquad \text{(c)}$$

C is an important factor in rationalizing and predicting which of a series of different isomers of the same D/A pair possesses the lowest-lying TICT state. Compare **1** with its *meta* isomer (Fig. 12a). The smaller absolute value for C for the *meta* isomer is one of the reasons why it does not show dual fluorescence. Similar arguments can be used for the behavior of naphthalene or coumarin as acceptor (Fig. 12b, c) or for different biaryl isomers (Fig. 12d).

ΔE_{solv} is given, in a simple form,[46,105] by Equation (d), where μ_T is the dipole moment of the TICT state, a the Onsager cavity radius, and ε the solvent dielectric constant.

$$\Delta E_{\mathrm{solv}} = -\mu_T^2 \cdot \frac{2}{a^3} \cdot \frac{\varepsilon - 1}{2\varepsilon + 1} \qquad \text{(d)}$$

There are cases where the condition in Equation (a) is met only above a certain threshold of the solvent polarity. Compound **1**, for example, shows a negligible amount of TICT fluorescence in nonpolar solvents;[18,116] this is also true for **34**[71] and **42**.[82,83] Polar solvents, however,

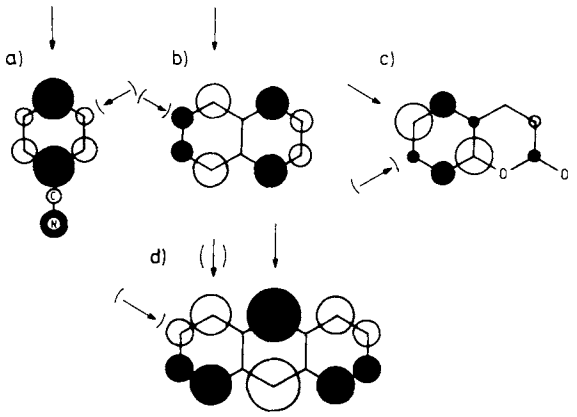


Fig. 12. LUMOs for some typical acceptor groups in TICT-forming compounds. The relative probability of finding the odd electron (negative charge) in the TICT state is given by the surface areas of the circles (square of the MO coefficients). The Coulomb stabilization C with an adjacent positive center is strongest if this center is next to an atom with a large MO coefficient (arrows) and less favorable for atoms with a smaller coefficient (arrow in brackets). a) Cyanophenyl: strongest stabilization is expected for the *para* isomer. b) Naphthyl: strongest stabilization for the α isomer; experimentally, **21** shows TICT fluorescence [46], whereas the corresponding β-naphthyl compound does not [55]. For better donors like carbazole, both α- and β-naphthyl derivatives show TICT fluorescence [53]. The behavior of isomeric coumarins [83] and of biaryl isomers [39] can also be rationalized in this way.

strongly enhance the TICT fluorescence. Such a change of the emitting state from ICT to TICT along a solvent polarity scale has been observed in several other cases. It usually shows up in a solvent polarity plot by a change in slope.[85]

ΔE_{solv} also depends on the size of the dipole moment of the TICT state, μ_T, which is mainly given by the distance between the center of gravity of negative and positive charge. For elongated systems such as anthracenes linked in the manner of **28** (in the 9-position), μ_T will be much smaller than if the linkage is in the 1- or 2-position; in the latter case, however, C is smaller (Fig. 12d); i.e., ΔE_{solv} and C can be compensating factors.[39]

Another interesting way for reaching TICT states is obviously not to lower E(TICT) but to raise E(LE) [Eq. (a)]. This is the case for sterically hindered dialkylanilines like **13** (twist ca. 60°) where the LE1/ICT state (Fig. 11) cannot be reached at the planar conformation and is thus raised in energy. This leads to the strong preference for TICT formation which even remains in the gas phase.[1,26,27]

For designing efficiently fluorescing systems, for example to obtain new laser dyes, it is important to control the formation of TICT states because these often act as intramolecular fluorescence quenchers. Two approaches are possible (Fig. 13). The first is to hinder the formation of the minimum overlap geometry, e.g., by bridging. Such "rigidized" systems are known to have substantially increased fluorescence quantum yields compared with their flexible counterparts.[17] The second way is to leave the system flexible but to increase the TICT energy relative to that of the LE1/ICT state. This second approach clearly invalidates an explanation of the decreased fluorescence quantum yield via a "loose bolt effect." In the case of infrared dyes, competing quenching processes without charge separation play an increasing role, too, because of the reduced S_0–S_1 energy gap.[79]

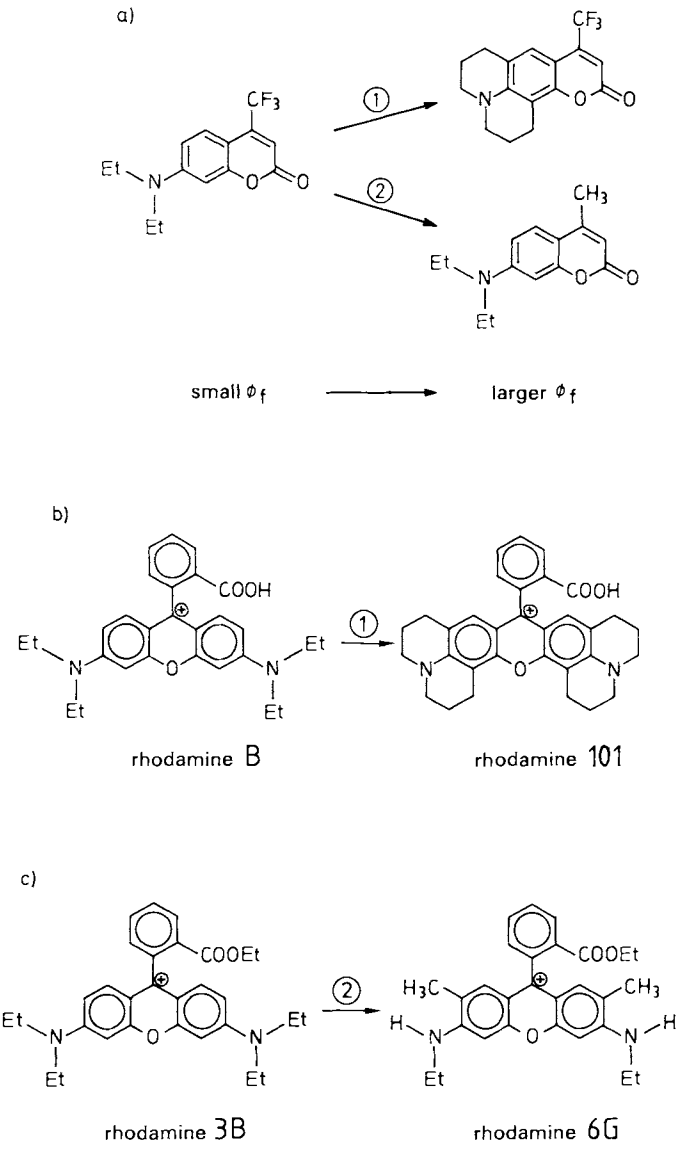


Fig. 13. a) The fluorescence quantum yield ϕ_f of certain coumarin dyes in polar solvents increases by a factor of nearly 10 if TICT formation is hindered by either "rigidizing" the system ① or raising the TICT energy ② (e.g., by reducing the acceptor strength) [82]. b, c) A similar approach explains the temperature dependence and reduced fluorescence quantum yield of flexible rhodamine dyes. The quenching effect disappears by a similar rigidization [117, 118] or by increasing the TICT energy (reduced donor strength of the amino groups [79]). In the case of rhodamines, also the phenyl substituent can act as a donor [75].

7. Kinetic Aspects of TICT Formation

Scheme 1 postulates the precursor-product relation of B* and A* states. This is experimentally supported by numerous nano- and picosecond studies on **1**,[12,25,42,119–124] which show that for the irreversible case (k_{AB} negligible) the A fluorescence builds up with a rise-time that is related to the decay time of the B fluorescence. Both solvent (viscosity, polarity) and solute parameters (structural: ground-state twist angle, rotating volumes, molecular shape and flexibility; electronic: state correlation, conical intersections) determine the rate k_{BA} for the formation of the TICT state.

In most cases, the temperature dependence of k_{BA} is weaker than that of the macroscopic solvent viscosity η [Eq. (e)].

$$k_{BA}^{-1} = C \cdot \eta^{x} \qquad 0.5 < x < 1 \qquad \text{(e)}$$

In the case of TPM dyes, the very well known Förster-Hoffmann model[125] gave $x = 2/3$. This value, however, does not even exactly hold for the case of the original study of relaxing TPM dyes in glycerol ($x = 0.8$[75]). In some cases, x depends on the type of solvent matrix (cross-linked versus *n*-alcohols),[126] in other cases (derivatives of **1**), on the size and shape of the rotating molecular moieties.[24] Microviscosity theory[127] can be used to describe these changes in x.[24, 128] The important points in this theory are, first, that the solvent environment is not a continuum but composed of discrete molecules which may even be larger than the solute itself and, second, that two types of diffusion exist: the diffusion that pushes away solvent molecules and the diffusion into holes between the solvent molecules (free volume). The free-volume effects become very important in polymers, where **1**, despite the very high macroscopic viscosity, shows a dual fluorescence in H-bonding[44] as well as in non-H-bonding matrices.[129] The small amino group in 6-aminocoumarin is even able to relax into the available free volume between the solvent molecules of a frozen ethanol matrix.[83]

The state crossing and conical intersection that occurs for **1** (Fig. 3 and 5) has very profound kinetic consequences. Figure 14 shows that the B decay (governed mainly by k_{BA}) is much slower for **1** than for the corresponding ester. The conical intersection (Fig. 5) seems to represent an "obstacle" on the lower surface. Its solvent dependence could explain the polarity-dependent activation energies as observed for **1**.[122]

Figure 14 also shows that the observed decays are non-exponential but can be described using a biexponential model. For the TPM dyes like **35**·$ClO_4^{\ominus}$, this has been known for some time.[130, 132] In **1**, the nonexponential decay is linked to a rise of the A fluorescence, which is *faster* than expected from the B decay.[25, 123]

A possible explanation is provided by the existence of broad rotational distribution functions in the ground state.[21, 25, 51, 130, 133] Projected onto the S_1 hypersurface by light absorption, these are transformed into broad relaxational distributions by the action of the coordinate-dependent driving force toward the TICT state (Fig. 15).[6, 18, 21] An alternative formalism uses a modified Smo-

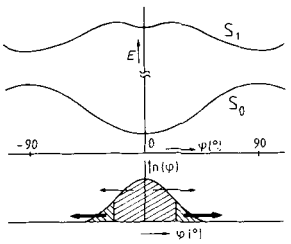


Fig. 15. Schematic potentials of ground and first excited states of a TICT-forming molecule with a planar ground-state geometry. By excitation, the broad angular distribution $n(\phi)$ is projected onto the S_1 hypersurface. Depending on its shape (the minimum at 0° may be actually present for **1** as shown, but in other cases the planar conformation may be a local maximum with regard to twisting), the different parts of the distribution are subject to different driving forces toward the TICT conformation (i.e., different slopes along the reaction coordinate). ● : large force; → : small force.

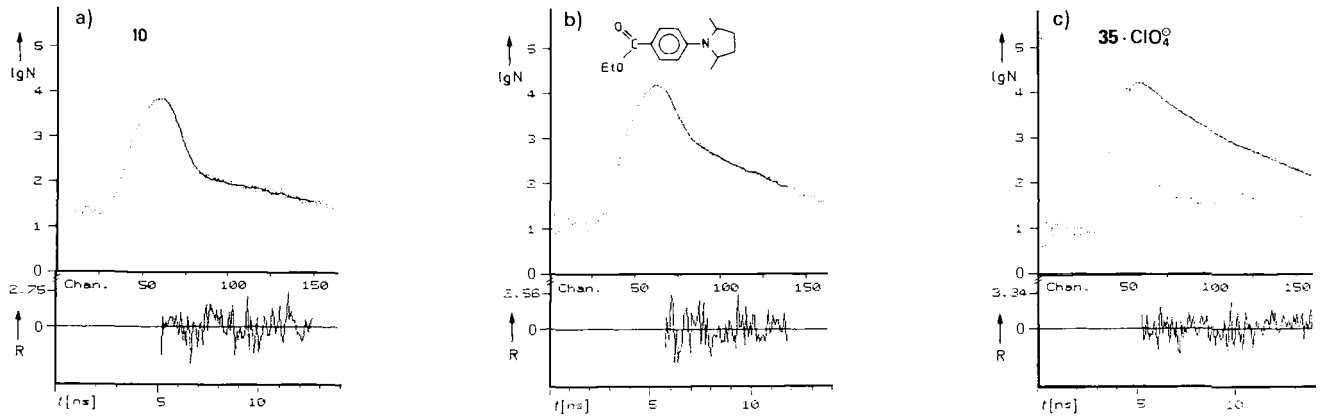


Fig. 14. Fluorescence decay curves of TICT-forming compounds. The excitation source was synchrotron radiation from the Berlin electron storage ring BESSY. (a, b) $\lambda_{ex} = 300 \pm 10$ nm. c) $\lambda_{ex} = 570 \pm 10$ nm) operated in the single bunch mode. Conventional single-photon counting equipment was used. a) **10** in *n*-butyl chloride at 234 K, b) the corresponding ester in the same solvent but at increased viscosity (at 152 K, just above the freezing point), both observed at 350 ± 10 nm. Both temperatures are in the range of irreversible kinetics ($k_{AB} \ll k_0^{\wedge} + k_f^{\wedge}$). The decays could be reasonably well fitted (——) by the iterative reconvolution method using a biexponential model. **10** and its ester are convenient kinetic model compounds for **1** and **4** because the irreversible temperature range extends up to room temperature [18] and because the decays are more easily monitored due to the reduced TICT formation rate (factor of about 4 [21]). The derived parameters are a) $\tau_1 = 0.21$, $\tau_2 = 3.6$ ns, $A_2/A_1 = 0.004$, b) $\tau_1 = 0.18$, $\tau_2 = 1.52$ ns, $A_2/A_1 = 0.02$. For these similar τ_1 times, the ester possesses a significantly increased weight of the second component [25]. For equal temperature (174 K) and viscosity, τ_1 for the ester is faster by a factor of 4.6. c) **35**·$ClO_4^{\ominus}$ in glycerol at 266 K, monitored at 620 ± 10 nm. The biexponential fit yields $\tau_1 = 0.59$, $\tau_2 = 1.67$ ns, $A_2/A_1 = 0.81$. The weight of τ_2 is considerably increased compared with a) and b). The prompt response function of the system (FWHM ≈ 800 ps) is also shown. R = deviation of the measured values from the average values. We consider these decays to be due to the combined effects of broad ground-state rotational distribution functions [25, 130] and of transient effects describable in a stochastic model [131] by means of time-dependent rate constants [123].

luchowski equation with sink terms[131] and leads to the time-dependent rate constants $k_{BA}(t)$.[123]

If the ground-state minimum is situated close to a conical intersection of excited states, then nonadiabatic effects will dominate the photo-physical properties,[134] and radiative and nonradiative decays of the excited states will be strongly coupled to nuclear motion. Such an example seems to be **13**[26] (Fig. 16). Depending on excitation wavelength, the relaxation is channeled toward different excited-state minima. Detailed picosecond kinetic investigations offer promise of shedding new light on nonadiabatic coupling phenomena.

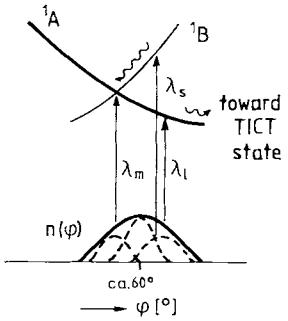


Fig. 16. Schematic excited-state potential surfaces for **13** as a function of twist angle [26]. At the point of crossing, a conical intersection, similar to that shown in Figure 5, occurs by vibronic coupling along a non-totally symmetric coordinate q_n (not shown). Steric hindrance by the two *ortho*-methyl groups shifts the ground-state minimum and the corresponding rotational distribution $n(\phi)$ below the crossing region. By varying the excitation wavelength, different parts of $n(\phi)$ can be excited. Upon excitation in the long wavelength tail (λ_l) of the absorption band, only the strongly redshifted TICT emission is observed, whereas exciting at shorter wavelengths (λ_m,λ_s) gradually results in the appearance of a second short-wavelength fluorescence band [26] probably derived from the relaxed ^1L_b state.

8. Symmetry Reduction and Charge Separation

Through coupling with nonsymmetric vibrational modes or with the environment, many symmetric molecules undergo a symmetry reduction. The most prominent example is the Jahn-Teller effect for coupling of degenerate states.[134] Other examples are nonadiabatic effects in cumulene radical cations, which lead to species twisted away from the symmetrical geometry by angles ranging from 25° (in $H_2C{=}CH_2^{\oplus\ominus}$) to 46° (in $H_2C{=}C{=}C{=}CH_2^{\oplus\ominus}$).[134] In 9,9′-bianthryl **28** and other symmetric biaryls, symmetry reduction is induced by a coupling with solvent fluctuations.[38,39] Symmetry reduction by the interaction of electronic and nuclear motion can occur only if the nonadiabatic coupling W exceeds a certain threshold (Fig. 17) given by Equation (f),[134,135] where E_2-E_1 is the energy difference between the unperturbed states, and f_n is the force constant of the coupling mode.

$$W^2 \geq 2f_n(E_2-E_1) \qquad \text{(f)}$$

In the highly symmetric **28**, the LE states (equal mixture of $\Psi(A^*-A)$ and $\Psi(A-A^*)$) and charge-resonance (CR) states (equal mixture of the CT wavefunctions $\Psi(A^{\oplus}-A^{\ominus})$ and $\Psi(A^{\ominus}-A^{\oplus})$) reflect this symmetry (dipole moment $\mu=0$). In CR states, which occur in symmetric excimers,[136] the coupling of the two CT wavefunctions with each other causes the symmetric equilibrium situation to be spontaneously restored every time external fluctuations disrupt the symmetry. To induce symmetry breaking, the coupling V_{CT} (equivalent to the right-hand side of Equation (f) has to be lowered below a certain threshold. The coupling occurs indirectly and is describable by the off-diagonal matrix elements $V_{CT}=\langle\Psi_{LE}|\hat{H}|\Psi_{CT}\rangle$ in a configuration-interaction treatment.[39] These matrix elements are strongly overlap dependent and vanish for the perpendicularly twisted conformation. At and close to this geometry, it is thus possible that the energy W_{solv} (interaction of CT wavefunctions with the fluctuating unsymmetrical solvent environment), which is equivalent to the left-hand side of Equation (f), exceeds that of V_{CT}. Then, spontaneous

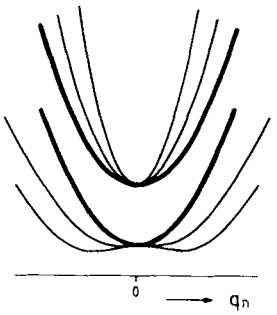


Fig. 17. Influence of a gradually growing vibronic interaction of two close-lying states (S_0 and S_1, or two excited states; bold lines) along a non-totally symmetric coordinate q_n. If the coupling W is below a certain threshold, both hypersurfaces change their shape, the higher one being steepened and the lower one flattened. The energy minimum, however, remains at the origin. Above this threshold, a double minimum develops for the lower state, and the energy minimum corresponds to an unsymmetric geometry (nonzero value of coordinate q_n). The upper state, however, retains its symmetric character [134, 135].

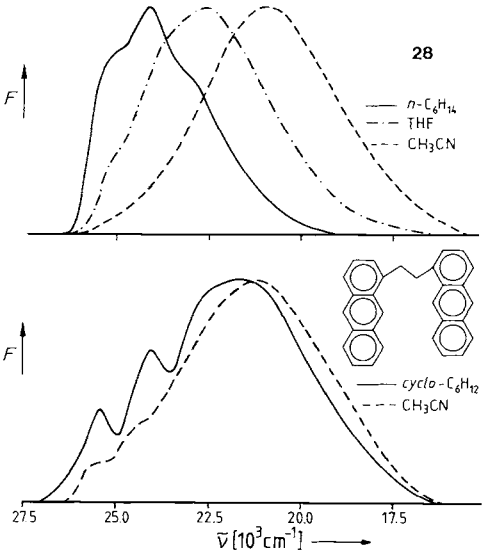


Fig. 18. The influence of polar solvents on the dual fluorescence spectra of **28** and 1,2-di(1-anthryl)ethane [100]. In both cases, the relative importance of the long-wavelength band increases with solvent polarity. Only for **28**, however, does it show a strong solvatochromic redshift indicative of an excited-state dipole moment (i.e., symmetry reduction). This is possible because the two CT wavefunctions are only very weakly coupled. In the case of 1,2-di(1-anthryl)ethane with sandwich-type overlap and strong coupling, the solvent fluctuation energies are not sufficient to induce the symmetry breaking, and a charge-resonance state with zero dipole moment is observed.

charge separation and symmetry reduction can occur, because the equal mixture of CT wavefunctions becomes unbalanced and is no longer restored. Figure 18 illustrates the effect of small and large overlap on the fluorescence spectra of **28** and 1,2-di(1-anthryl)ethane. The fact that **28**[61,137] and **30**[39] display TICT emission even in saturated hydrocarbons is evidence that even in these inert solvents non-negligible interaction energies W_{solv} are attained.

9. The Minimum Overlap Rule: A Bridge to Twisted Double Bonds

It was shown in the last section that for symmetry reduction to occur in symmetric biaryls, a perpendicular or minimum overlap-type conformation has to be adopted. A similar symmetry breaking can occur in olefins upon *cis–trans* isomerization. The phenomenon termed "sudden polarization" was discovered by quantum-mechanical calculations for pyramidalized ethylene, the simplest case.[138,139] Since then, the wide scope and applicability of this concept has been developed by very refined large-scale CI calculations.[109,140,141]

The calculations predict that substituted or pyramidalized ethylene, when electronically excited, spontaneously twists toward the perpendicular conformation, where the two charge-transfer or zwitterionic states $\Psi(C^{\oplus}-C^{\ominus})$ and $\Psi(C^{\ominus}-C^{\oplus})$ are very low lying. In contrast to the CT states of **28**, the subunits on either side of the twisted bond are closed-shell systems for ethylene. Nevertheless, the similarities are striking: Figure 19 compares the calculated excited-state dipole moment for **1** and ethylene. Charge separation and maximum dipole moment, as well as an energy minimum, occur in both cases at the perpendicular geometry.

Experimental evidence for the twisted state in olefins[143] is less well documented than for TICT states. In the case of the extensively studied stilbene, this state was termed a "phantom singlet" state.[144] It correlates with the S_4 state of *trans*-stilbene.[145] Its twisted geometry is experimentally established, but its dipolar nature awaits further experimental confirmation.

Recently, the characterization of MO wavefunctions by valence bond (VB)-like structures has greatly contributed to the rationalization of the "minimum overlap rule" for twisted single and double bonds.[109] Figure 20 shows the VB structures for two limiting cases, twisted ethylene and aminoborane. The states start to interact for twist angles different from 90°, causing a maximum in the ground state and a minimum in the excited state spaced by an energy separation ΔE (Fig. 21). For intermediate differences in

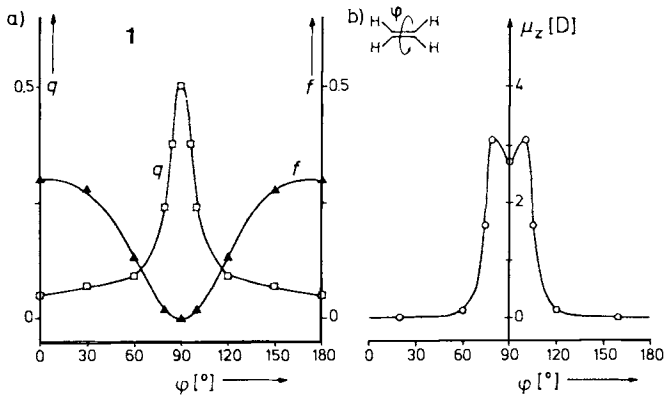


Fig. 19. Comparison of the calculated excited-state charge separation of **1** (CNDO/s-CI, 30 singly excited configurations) [15] and dipole moment of ethylene in the S_1 state for 10° pyramidalization (MRD-CI, ca. 8000 configurations) [139] as a function of twist angle. For ethylene, the calculations only lead to charge separation by introduction of a slight asymmetry (substitution or pyramidalization on one center). Such a symmetry breaking can also be brought about by a fluctuating solvent environment. Calculations on a variety of systems[140] indicate a less sudden nature of the "sudden polarization" than in the case of ethylene [142]. a) q = charge on the amino nitrogen atom; f = oscillator strength of the S_0–S_1 transition.

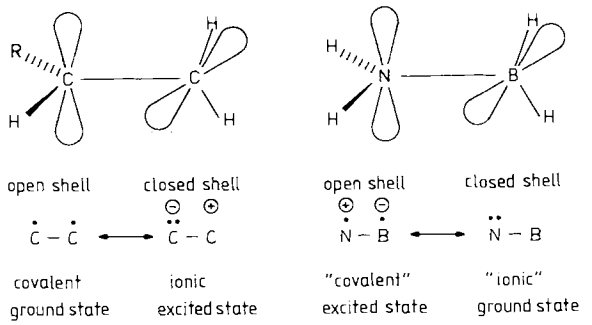


Fig. 20. The states of perpendicularly twisted substituted or pyramidalized ethylene (left) and of aminoborane (right) can be characterized approximately by VB-like structures [109]. The two states (covalent and ionic structures, open-shell and closed-shell character on the fragments) cannot interact for symmetry reasons. In substituted or pyramidalized ethylene, the ionic closed-shell state is the higher-energy one owing to charge separation. In aminoborane (different nuclear charges), the order is reversed. Charge separation occurs for the open-shell structure in this case.

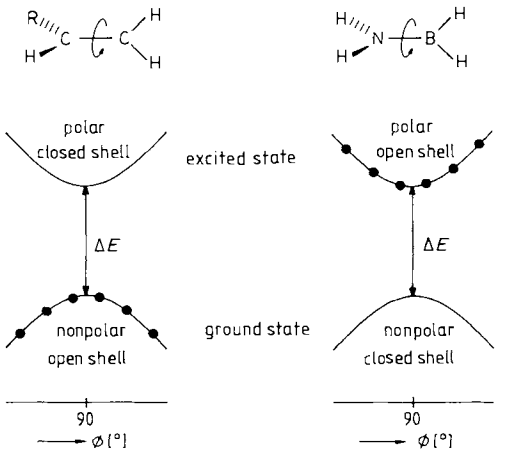


Fig. 21. Upon deviation from the perpendicular geometry, the states shown in Figure 20 start to interact and "repel" each other. An energetic maximum for the ground state and a minimum for the excited state results for the perpendicular geometry. The latter explains why compounds that undergo "sudden polarization" and compounds that form TICT states spontaneously twist toward 90° ("minimum overlap rule" [4]). The energy difference ΔE at the twisted geometry is given by the relative energy of the two VB-like structures. If ΔE is large, long-lived excited states are possible. If ΔE is very small, for cases intermediate between ethylene and aminoborane, nonadiabatic interactions are likely to lead to ultrafast nonradiative deactivation.

donor-acceptor strength, the potential surfaces are expected to get very close at a 90° twist and even to touch ($\Delta E = 0$)[109] (Fig. 22). Such borderline cases between TICT and "sudden polarization" behavior can lead to ultrafast nonradiative decay as observed for cyanine and TPM dyes.[76, 130, 132]

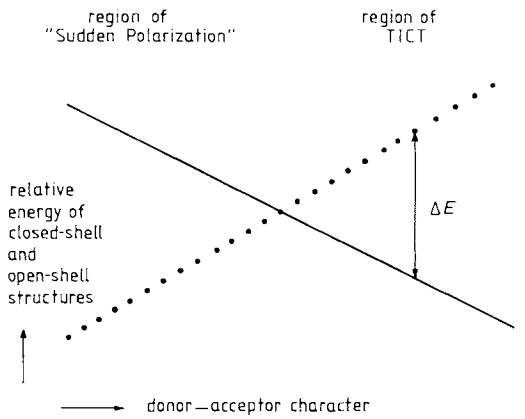


Fig. 22. If, for perpendicularly twisted compounds, the relative energy of the states characterizable by VB-like closed-shell and open-shell structures is changed continuously, these two states become isoenergetic. At this point, ground- and excited-state surfaces touch for 90° twist [109]. Compounds may be classified as belonging either to the region of "sudden polarization" with a closed-shell ionic excited state (left) or to the region of TICT states, where the ionic excited state is open-shell in nature (right).

The pigment of the visual process, the protonated Schiff base of retinal (Fig. 23), is probably also such a borderline case. Early calculations on "sudden polarization" in this

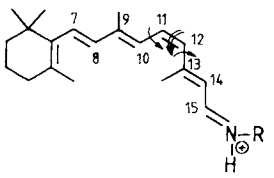


Fig. 23. In the protonated Schiff base of retinal (PRSB), the pigment of the visual process, light absorption leads to photoinduced *cis-trans* isomerization of the C11-C12 double bond. This occurs within a few picoseconds [146] or less [147], which seems impossible for large rotating parts. Concerted mechanisms involving the simultaneous twisting around several single and double bonds have therefore been developed ("bicycle-pedal" model [148] and "Hula-twist" model [149]). The extended polyene chain of PRSB possesses a strong acceptor ($=N^{\oplus}$) at one end, which leads to a behavior intermediate between "sudden polarization" and TICT states: small ΔE in the twisted geometry with charge separation, and large nonadiabatic effects.

polyene were connected with speculation whether the predicted charge separation is a key step in the primary process of vision.[150] Recent experiments,[147] as well as large scale CI calculations on model compounds,[109, 140] conclude that it is mainly the shape of the S_1 hypersurface (barrierless downhill transition from the planar to the perpendicular conformation) that drives the reaction toward the high-energy ground-state product in less than 1 picosecond (Fig. 24).

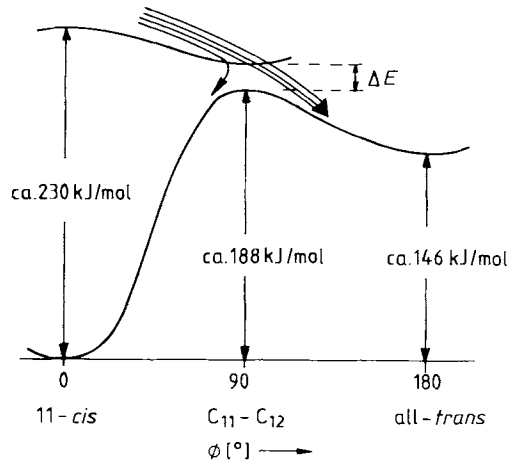


Fig. 24. Empirical ground- and excited-state potential energy surfaces for the primary step of the visual process (adapted from [147]). After initial excitation, an ultrafast, barrierless downhill transition toward the minimum at the perpendicular conformation occurs. There, the small ΔE leads to a strong coupling with the nuclear motions, so that the nonradiative transition to the ground state occurs preferentially in the "forward" direction [151], leading to highly efficient *cis-trans* conversion. The ground-state reaction is endothermic because the all-*trans* product has stored the energy needed for spatial separation of the $=N^{\oplus}$ end from its counterion [147, 152]. This energy is used to drive the ensuing chemical processes.

10. TICT States as Models for Photosynthetic Processes

The photosystems in green plants and photosynthetic bacteria store light energy by means of charge separation, which is subsequently used to drive chemical reactions (Fig. 25). Primary charge separation occurs in the so-called

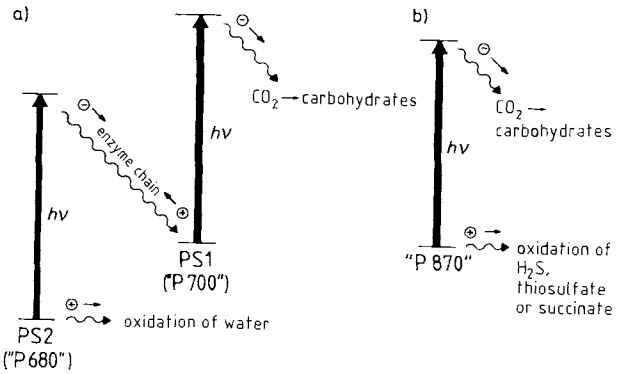


Fig. 25. a) In green plants, two quanta of light are used to pump an electron to a sufficiently high chemical potential so that CO_2 can be reduced and water oxidized (Z-Scheme [153, 154]). b) More simple photosynthetic bacteria possess only one photosystem, which resembles photosystem II (PS2) in green plants. They cannot oxidize water but need more easily oxidizable substrates like sulfides [154]. The secret of photosynthesis is connected with a problem of timing: The available energy stored by the charge-separation process has to be used chemically before the electron funnels back to the lower-energy level nonradiatively. Nature solved this problem by an electron-transfer chain.

reaction center (RC), and large progress has been made recently in elucidating its internal structure by an X-ray analysis of the RC of photosynthetic bacteria[155] (Fig. 26a). Before this, it was quite unclear whether the bacteriochlorophyll (BC) adjacent to the special pair (SP) was directly

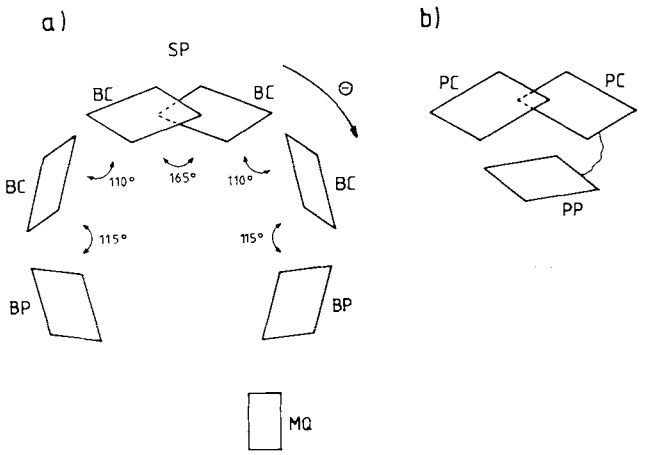


Fig. 26. a) Schematic drawing showing the spatial arrangement of chromophores of the electron-transfer chain in the reaction center of the photosynthetic bacteria *Rhodopseudomonas viridis*, according to an X-ray analysis [155]. The high degree of symmetry and the small-overlap arrangement between the chromophores is remarkable. From the antenna pigments (not shown), light energy is channeled to the "special pair" (SP), two nearly coplanar (deviation 15°) BC molecules overlapping with one of their pyrrole rings. There, the initial charge separation occurs. The electron is then transferred to a further BC molecule before it reaches a bacteriopheophytin (BP) (resembling in chemical structure the tetrapyrrole system of BC, but without a magnesium ion in its center). From there, transfer to menaquinone (MQ), the first stable intermediate species, occurs. b) Earlier photosynthetic model compounds [153] employed chromophores PC and PP, which are related to BC and BP, and used flexible linkages, which were not suitable to fix donor and acceptor in a small-overlap geometry.

involved in the electron-transport chain[156] or whether it played the role of "spectator chlorophyll."[154] Starting from SP, the chromophores are placed side by side in a two-ended symmetric chain, and not one on top of the other (Fig. 26b). They are rigidly held in this small overlap arrangement by proteins.

Several intriguing questions arise. (1) Why are the first members along the electron transport chain so similar chemically and electronically? (2) Why are the components of the RC disposed in a small overlap arrangement and not in a sandwich-type one? (3) Why is the back electron transfer to the ground state so remarkably slow[154]? (4) Why is the major part of the RC built up as an approximately symmetric double structure?

As the rate of both forward and backward electron transfer is slowed down with increasing charge separation distance,[154, 157] nature used several intermediate steps separating electron and hole further and further, until the deactivating processes become sufficiently slow (Fig. 27). A possible strategy for loosing as little energy per step as possible is shown in Figure 28. The smallest energy loss is obtained for nearly isoenergetic levels ($\Delta E \approx 0$), i.e., for electronically similar components, which answers question (1). But the small overlap arrangement (Fig. 28c) is by far superior both in the size of the actual energy loss and in the amount of charge transferred (question (2)). Moreover, a small overlap situation will automatically lead to a minimization of the back electron transfer rate for a given distance (question (3)).

The question remains why the RC is constructed in such a symmetrical manner. The primary charge separation in the SP is close to a symmetry-breaking process, resembling

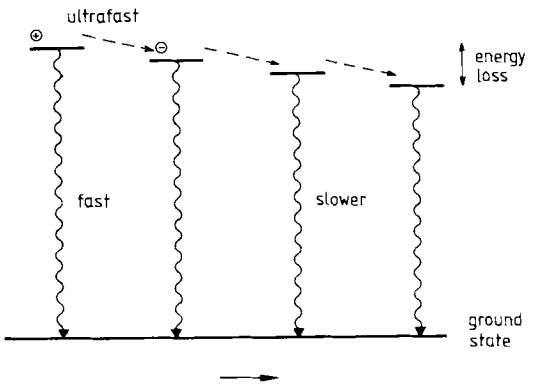


Fig. 27. The transfer of the electron along the chain has to be extremely rapid in order to prevent loss of quantum yield by the competing nonradiative decay to the ground state. As the separation between electron and hole increases, these decay processes slow down, and chemical reactions can compete with them. In order to retain enough chemically usable energy, the energy loss per single transfer step has to be kept to a minimum. A certain free-energy difference is, of course, necessary to drive the transfer. For simplicity, all the ground states have been drawn as a single level.

the situation in **28** (Section 8). Obviously, the perfectly symmetric situation is the best way for a minimal energy loss (compare Fig. 28c and d). In earlier evolutionary phases, the high symmetry of the RC seems to have included two MQ units.[155] Later, the two equivalent electron-transfer directions seem to have been given up in favor of the slightly biased system shown in Fig. 26a. It is conceivable that this biasing resulted in a considerable increase of the electron-transfer rates and thus efficiencies. A similar situation occurs in biased and nonbiased derivatives of BA,[38] which thus lend themselves to kinetic model studies.

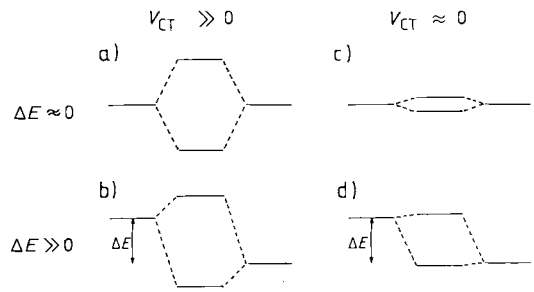


Fig. 28. Four types of interaction possible along the electron-transport chain. Left and right interacting levels, respectively, represent the situation before and after electron transfer, for infinitely separated chromophores; the center levels represent the energetic consequence of the interaction. a, b) In the large overlap case with strong interaction ($V_{CT} \gg 0$), the resulting wave functions always contain character from locally excited LE states; the CT character is thus "diluted" and never complete, especially in the case a of near degeneracy ($\Delta E \approx 0$). The resulting lower energy level is strongly stabilized (by an amount V_{CT} for case a, compared with the noninteracting levels). c, d) In the small overlap case ($V_{CT} \approx 0$), the charge separation is undiluted and complete, and the resulting lower energy level is not much stabilized, which is favorable for minimizing the energy loss per single transfer step.

11. Outlook

The notion of TICT states is just beginning to be understood as a basic mechanistic feature ("paradigm"[158]). As indicated in Section 4, the number of chemical species is rapidly growing in which unusual photophysical proper-

ties can be traced back to TICT states. The biological implications need to be explored more deeply, and the mechanistic concepts outlined may assist in the construction of more efficient model systems mimicking photosynthesis[159] and the development of new routes to artificial solar energy conversion.[160] These concepts are ready to be applied right now in the development of more efficient and versatile fluorescence and laser dyes and new fluorescent probes.

I wish to thank Prof. Z. R. Grabowski, Dr. K. Rotkiewicz, Prof. E. Lippert, Prof. J. Michl, Prof. M. W. Windsor, and Dr. D. F. Eaton for stimulating discussions. The organization of the "Workshop on the Nature of the so-called T.I.C.T. States" in June 1984 by Z. R. Grabowski and the physical chemistry group of the Polish Academy of Sciences, Warsaw, also gave a strong stimulus to this work. The skilful assistance of B. Burmeister, and Dr. H. Juds in synthesizing new TICT compounds, and of B. Dewald in the measurement of fluorescence spectra is gratefully acknowledged. Thanks are also due to the Deutsche Forschungsgemeinschaft and the Heisenberg Foundation, the Fonds der Chemischen Industrie, and the Bundesministerium für Forschung und Technologie for support of the work.

Received: October 30, 1985;
revised: February 3, 1986 [A 595 IE]
German version: *Angew. Chem. 98* (1986) 969

[1] Z. R. Grabowski, K. Rotkiewicz, A. Siemiarczuk, D. J. Cowley, W. Baumann, *Nouv. J. Chim. 3* (1979) 443.
[2] Z. R. Grabowski, K. Rotkiewicz, W. Rubaszewska, E. Kirkor-Kamińska, *Acta Phys. Pol. A 54* (1978) 767.
[3] Z. R. Grabowski, K. Rotkiewicz, A. Siemiarczuk, *J. Lumin. 18/19* (1979) 420.
[4] Z. R. Grabowski, J. Dobkowski, *Pure Appl. Chem. 55* (1983) 245.
[5] E. Lippert, W. Lüder, H. Boos, *Adv. Mol. Spectrosc. Proc. Int. Meet. 4th 1959* (1962) 443.
[6] W. Rettig, E. Lippert, *J. Mol. Struct. 61* (1980) 17.
[7] J. B. Birks: *Photophysics of Aromatic Molecules*, Wiley, London 1970.
[8] W. Rettig, *J. Lumin. 26* (1981) 21.
[9] G. Wermuth, W. Rettig, E. Lippert, *Ber. Bunsenges. Phys. Chem. 85* (1981) 64.
[10] W. Rettig, G. Wermuth, E. Lippert, *Ber. Bunsenges. Phys. Chem. 83* (1979) 692.
[11] K. Rotkiewicz, K. H. Grellmann, Z. R. Grabowski, *Chem. Phys. Lett. 19* (1973) 315; see also Erratum *ibid. 21* (1973) 212.
[12] K. Rotkiewicz, Z. R. Grabowski, A. Krówczyński, W. Kühnle, *J. Lumin. 12/13* (1976) 877.
[13] E. Lippert, W. Rettig, *J. Mol. Struct. 45* (1978) 373.
[14] A. A. Ayuk, W. Rettig, E. Lippert, *Ber. Bunsenges. Phys. Chem. 85* (1981) 553.
[15] E. Lippert, A. A. Ayuk, W. Rettig, G. Wermuth, *J. Photochem. 17* (1981) 237.
[16] A. A. Ayuk, *J. Mol. Struct. 84* (1982) 169.
[17] G. Wermuth, W. Rettig, *J. Phys. Chem. 88* (1984) 2729.
[18] W. Rettig, G. Wermuth, *J. Photochem. 28* (1985) 351.
[19] K. Rotkiewicz, W. Rubaszewska, *Chem. Phys. Lett. 70* (1980) 444.
[20] J. Lipiński, H. Chojnacki, Z. R. Grabowski, K. Rotkiewicz, *Chem. Phys. Lett. 70* (1980) 449.
[21] W. Rettig, R. Gleiter, *J. Phys. Chem. 89* (1985) 4676.
[22] E. A. Chandross, F. R. Wight, *VIth IUPAC Symp. Photochem.* (Aix-en-Provence, France 1976), Contributed Papers, p. 53.
[23] R. J. Visser, C. A. G. O. Varma, *J. Chem. Soc. Faraday Trans. 2 76* (1980) 453; R. J. Visser, C. A. G. O. Varma, J. Konijenberg, P. C. M. Weisenborn, *J. Mol. Struct. 114* (1984) 105; R. J. Visser, P. C. M. Weisenborn, C. A. G. O. Varma, *Chem. Phys. Lett. 113* (1985) 330.
[24] W. Rettig, *J. Phys. Chem. 86* (1982) 1970.
[25] W. Rettig, M. Vogel, E. Lippert, H. Otto, *Chem. Phys.*, in press; W. Rettig, E. Lippert, H. Otto, *Jahrb. Berl. Elektronenspeicherring Synchrotronstrahlung BESSY 1984*, 171.
[26] K. Rotkiewicz, W. Rubaszewska, *J. Lumin. 27* (1982) 221.
[27] H. Bischof, W. Baumann, N. Detzer, K. Rotkiewicz, *Chem. Phys. Lett. 116* (1985) 180.
[28] W. Rettig, *Eur. Photochem. Assoc. Newsl. 1984*, No. 21, p. 25 (conference report: Workshop on the Nature of the so-called T.I.C.T. States).
[29] O. S. Khalil, R. H. Hofeldt, S. P. McGlynn, *Chem. Phys. Lett. 17* (1972) 479; *J. Lumin. 6* (1973) 229; *Spectrosc. Lett. 6* (1973) 147.
[30] O. S. Khalil, *Chem. Phys. Lett. 35* (1975) 172.
[31] S. Dähne, W. Freyer, K. Teuchner, J. Dobkowski, Z. R. Grabowski, *J. Lumin. 22* (1980) 37; J. Dobkowski, E. Kirkor-Kamińska, J. Koput, A. Siemiarczuk, *J. Lumin. 27* (1982) 339.
[32] K. Rotkiewicz, W. Rubaszewska, *J. Lumin. 29* (1984) 329.
[33] N. Nakashima, N. Mataga, *Bull. Chem. Soc. Jpn. 46* (1973) 3016.
[34] E. M. Kosower, H. Dodiuk, *J. Am. Chem. Soc. 98* (1976) 924.
[35] W. Baumann, *Ber. Bunsenges. Phys. Chem. 80* (1976) 231; W. Baumann, H. Deckers, *ibid. 81* (1977) 786; H. Deckers, W. Baumann, *ibid. 81* (1977) 795; W. Baumann, H. Deckers, K.-D. Loosen, F. Petzke, *ibid. 81* (1977) 799; W. Baumann, *J. Mol. Struct. 47* (1978) 237; *Z. Naturforsch. A 36* (1981) 868; W. Baumann, H. Bischof, *J. Mol. Struct. 129* (1985) 125.
[36] K. H. Grellmann, K. Rotkiewicz, *Lumin. Cryst. Mol. Solutions Proc. Int. Conf. 1972* (1973) Abstract 345; K. Rotkiewicz, *2nd Pol. Lumin. Conf., Vol. A* (Institut of Physics, N. Copernicus University, Torun, Poland 1974), p. 123.
[37] R. J. Visser, C. A. G. O. Varma, J. Konijenberg, P. Bergwerf, *J. Chem. Soc. Faraday Trans. 2 79* (1983) 347.
[38] W. Rettig, M. Zander, *Ber. Bunsenges. Phys. Chem. 87* (1983) 1143.
[39] M. Zander, W. Rettig, *Chem. Phys. Lett. 110* (1984) 602.
[40] E. A. Chandross in M. Gordon, W. R. Ware (Eds.): *The Exciplex*, Academic Press, New York 1975, p. 187.
[41] R. J. Visser, P. C. M. Weisenborn, C. A. G. O. Varma, M. P. de Haas, J. M. Warman, *Chem. Phys. Lett. 104* (1984) 38.
[42] Y. Wang, M. McAuliffe, F. Novak, K. B. Eisenthal, *J. Phys. Chem. 85* (1981) 3736; Y. Wang, K. B. Eisenthal, *J. Chem. Phys. 77* (1982) 6076.
[43] *K. Rotkiewicz* recently reported that **12** forms specific ground-state complexes with protic solvents and that the transition moment of the TICT emission in nonpolar solvents is unusually high (*Spectrochim. Acta 42a* (1986) 575).
[44] C. Cazeau-Dubroca, A. Peirigua, S. Ait-Lyazidi, G. Nouchi, *Chem. Phys. Lett. 98* (1983) 511; C. Cazeau-Dubroca, A. Peirigua, S. Ait-Lyazidi, G. Nouchi, Ph. Cazeau, R. Lapouyade, *Chem. Phys. Lett. 124* (1986) 110; the unusual emission and photoconductivity properties of TICT molecules in polymers have been suggested to be useful in practical applications: C. Cazeau-Dubroca, A. Peirigua, P. Cazeau, Eur. Pat. 0 130 117, published January 2, 1985 (Bulletin 85/1).
[45] E. Butty, P. Suppan, *Polym. Photochem. 5* (1984) 171.
[46] W. Rettig, *J. Mol. Struct. 84* (1982) 303.
[47] R. Kolos, z. R. Grabowski, *J. Mol. Struct. 84* (1982) 251.
[48] Y. Wang, *Chem. Phys. Lett. 116* (1985) 286.
[49] O. S. Khalil, A. J. Sonnessa, *Mol. Photochem. 8* (1977) 399; G. S. Cox, P. J. Hauptmann, N. J. Turro, *Photochem. Photobiol. 39* (1984) 597.
[50] D. J. Cowley, P. J. Healy, *Proc. R. Ir. Acad. Sect. B 77* (1977) 397.
[51] W. Rettig, F. Marschner, *Nouv. J. Chim. 7* (1983) 425.
[52] W. Rettig, M. Zander, *Chem. Phys. Lett. 87* (1982) 229; *Z. Naturforsch. A 39* (1984) 41.
[53] M. Zander, *Z. Naturforsch. A 23* (1968) 950, *24* (1969) 254.
[54] J. Smagowicz, K. Berens, K. L. Wierzchowski in J. B. Birks (Ed.): *Biological Molecules in their Excited States*, Wiley, New York 1976, p. 24.
[55] W. Rettig, unpublished results.
[56] F. Schneider, E. Lippert, *Ber. Bunsenges. Phys. Chem. 72* (1968) 1155; *74* (1970) 624.
[57] H. Beens, A. Weller, *Chem. Phys. Lett. 3* (1969) 666.
[58] N. Nakashima, M. Murakawa, N. Mataga, *Bull. Chem. Soc. Jpn. 49* (1976) 854.
[59] E. M. Kosower, K. Tanizawa, *Chem. Phys. Lett. 16* (1972) 419; *26* (1974) 545.
[60] T. Kobayashi, S. Nagakura, M. Szwarc, *Chem. Phys. 39* (1979) 105.
[61] R. J. Visser, P. C. M. Weisenborn, P. J. M. van Kan, B. H. Huizer, C. A. G. O. Varma, J. M. Warman, M. P. de Haas, *J. Chem. Soc. Faraday Trans. 2 81* (1985) 689.
[62] K. Hara, T. Arase, J. Osugi, *J. Am. Chem. Soc. 106* (1984) 1968.
[63] K. Zachariasse (Göttingen), private communication 1983.
[64] R. Bunte, K. D. Gundermann, J. Leitich, O. E. Polanski, M. Zander, *Chem. Ber. 119* (1986) 1683.
[65] K. Zachariasse, *XIIIth Eur. Congr. Mol. Spectrosc.* (Wroclaw, Poland, September 1977).

[66] S. Helm, J. Bendig, D. Kreysig, J. Wilda, *Z. Chem. 20* (1980) 215; J. Bendig, S. Helm, D. Kreysig, J. Wilda, *Z. Phys. Chem. (Leipzig) 263* (1982) 577.

[67] M. Maeda: *Laser Dyes*, Academic Press, Orlando, FL 1984, p. 108–110.

[68] W. Rettig, Proceedings of the annual meeting, Fachgruppe Photochemie der GDCh, Tübingen 1983, p. 197; proceedings of the *Int. Symp. Mol. Lumin. and Photophy.*, Toruń 1986, p. 324.

[69] E. Kirkor-Kamińska, W. Liptay, F. Petzke, W. Rettig, H.-J. Schumann, unpublished results.

[70] M. Vogel, W. Rettig, unpublished results.

[71] W. Rettig, E. A. Chandross, *J. Am. Chem. Soc. 107* (1985) 5617.

[72] A. Siemiarczuk, Z. R. Grabowski, A. Krówczyński, M. Asher, M. Ottolenghi, *Chem. Phys. Lett. 51* (1977) 315.

[73] A. Siemiarczuk, J. Koput, A. Pohorille, *Z. Naturforsch. A 37* (1982) 598.

[74] W. Baumann, F. Petzke, K.-D. Loosen, *Z. Naturforsch. A 34* (1979) 1070; B. Schwager, W. Baumann, *12th Int. Conf. Photochem. (Tokio*, Japan, August 1985).

[75] M. Vogel, W. Rettig, *Ber. Bunsenges. Phys. Chem. 89* (1985) 962.

[76] The nonadiabatic transition from S_1 to S_0 in TPM dyes occurs in less than 1 ps: D. J. Erskine, A. J. Taylor, C. L. Tang, *J. Chem. Phys. 80* (1984) 5338.

[77] P. A. Grutsch, Ch. Kutal, *J. Am. Chem. Soc. 99* (1977) 6460; *101* (1979) 4228; D. P. Segers, M. K. DeArmond, P. A. Grutsch, Ch. Kutal, *Inorg. Chem. 23* (1984) 2874.

[78] S. Hagopian, L. A. Singer, *J. Am. Chem. Soc. 107* (1985) 1874.

[79] R. Sens, *Dissertation*, Siegen 1984.

[80] C. J. Tredwell, A. D. Osborne, *J. Chem. Soc. Faraday Trans. 2 76* (1980) 1627; A. D. Osborne, *ibid. 76* (1980) 1638; A. D. Osborne, A. C. Winkworth, *Chem. Phys. Lett. 85* (1982) 513.

[81] U. K. A. Klein, F. W. Hafner, *Chem. Phys. Lett. 43* (1976) 141.

[82] G. Jones II, W. R. Jackson, A. M. Halpern, *Chem. Phys. Lett. 72* (1980) 391; G. Jones II, W. R. Jackson, S. Kanoktanaporn, A. M. Halpern, *Opt. Commun. 33* (1980) 315; G. Jones II, W. R. Jackson, C. Choi, W. R. Bergmark, *J. Phys. Chem. 89* (1985) 294.

[83] W. Rettig, A. Klock, *Can. J. Chem. 63* (1985) 1649.

[84] W. O. McClure, G. M. Edelman, *Biochemistry 5* (1966) 1908.

[85] E. M. Kosower, H. Dodiuk, *Chem. Phys. Lett. 26* (1974) 545; *J. Am. Chem. Soc. 100* (1978) 4173; H. Dodiuk, E. M. Kosower, *J. Phys. Chem. 81* (1977) 50; E. M. Kosower, H. Dodiuk, H. Kanety, *J. Am. Chem. Soc. 100* (1978) 4179; D. Huppert, H. Kanety, E. M. Kosower, *Chem. Phys. Lett. 84* (1981) 48; E. M. Kosower, *Acc. Chem. Res. 15* (1982) 259; *J. Am. Chem. Soc. 107* (1985) 1114.

[86] D. J. Cowley, I. Pasha, *J. Chem. Soc. Perkin Trans. 2 1981*, 918.

[87] C. Cavid, D. Baeyens-Volant, *Mol. Cryst. Liq. Cryst. 59* (1980) 181.

[88] R. Subramanian, L. K. Patterson, H. Levanon, *Chem. Phys. Lett. 93* (1982) 578; N. Tamai, I. Yamazaki, H. Masuhara, N. Mataga, *ibid. 104* (1984) 485.

[89] H. Shizuka, Y. Sato, Y. Ueki, M. Ishikawa, M. Kumada, *J. Chem. Soc. Faraday Trans. 1 80* (1984) 341; H. Shizuka, K. Okazaki, M. Tanaka, M. Ishikawi, M. Sumitani, K. Yoshihara, *Chem. Phys. Lett. 113* (1985) 89.

[90] D. F. Eaton (Wilmington, DE, USA), private communication 1985.

[91] R. Gleiter, W. Schäfer, H. Sakurai, *J. Am. Chem. Soc. 107* (1985) 3046.

[92] J. C. Doty, B. Babb, P. J. Grisdale, M. Glogowski, J. L. R. Williams, *J. Organomet. Chem. 38* (1972) 229.

[93] D. Brittelli, Wilmington DE, private communication 1985.

[94] R. Haag, *Dissertation*, Basel 1980.

[95] B. S. Vogt, S. G. Schulman, *Chem. Phys. Lett. 89* (1982) 320.

[96] T. Hayashi, N. Mataga, T. Umomoto, Y. Sakata, S. Misumi, *J. Phys. Chem. 81* (1977) 424.

[97] G. F. Mes, B. de Jong, H. J. van Ramesdonk, J. W. Verhoeven, J. M. Warman, M. P. de Haas, L. E. W. Horsman-van den Dool, *J. Am. Chem. Soc. 106* (1984) 6524.

[98] N. S. Hush, M. N. Paddon-Row, E. Cotsaris, H. Oevering, J. W. Verhoeven, M. Heppener, *Chem. Phys. Lett. 117* (1985) 8.

[99] K. Zachariasse, W. Kühnle, *Z. Phys. Chem. (Wiesbaden) 101* (1976) 267; F. Hirayama, *J. Chem. Phys. 42* (1965) 3163.

[100] T. Hayashi, T. Suzuki, N. Mataga, Y. Sakata, S. Misumi, *J. Phys. Chem. 81* (1977) 420.

[101] J. R. Miller, L. T. Calcaterra, G. L. Closs, *J. Am. Chem. Soc. 106* (1984) 3047.

[102] S. E. Braslawski, M. Vogel, W. Rettig, unpublished results.

[103] W. Rettig, V. Bonačić-Koutecký, *Chem. Phys. Lett. 62* (1979) 115.

[104] P. Suppan, *J. Lumin. 33* (1985) 29.

[105] E. Lippert, *Z. Naturforsch. A 10* (1955) 541; *Z. Elektrochem. 61* (1957) 962.

[106] N. Mataga, Y. Kaifu, M. Koizumi, *Bull. Chem. Soc. Jpn. 29* (1956) 465.

[107] W. Liptay, *Z. Naturforsch. A 20* (1965) 1441.

[108] L. U. Bilot, A. Kawski, *Z. Naturforsch. A 17* (1962) 621.

[109] V. Bonačić-Koutecký, J. Köhler, J. Michl, *Chem. Phys. Lett. 104* (1984) 440; V. Bonačić-Koutecký, J. Michl, *J. Am. Chem. Soc. 107* (1985) 1765.

[110] M. Van der Auweraer, A. M. Swinnen, F. C. De Schryver, *J. Chem. Phys. 77* (1982) 4110; A. M. Swinnen, M. Van der Auweraer, F. C. De Schryver, C. Windels, R. Goedeweek, A. Vannerem, F. Meens, *Chem. Phys. Lett. 95* (1983) 467.

[111] F. C. De Schryver, J. Huybrechts, N. Boens, J. C. Dederan, M. Irie, K. Zachariasse in B. Pullmann, N. Goldblum (Ed.): *Excited States in Organic Chemistry and Biochemistry*, Reidel, Dordrecht, Holland 1977, p. 313.

[112] In face-to-face excimers, the stabilization is strongest if the π overlap is maximized, as can be seen in the case of the isomeric anthracenophanes [113].

[113] T. Hayashi, N. Mataga, Y. Sakata, S. Misumi, N. Morita, J. Tanaka, *J. Am. Chem. Soc. 98* (1976) 5910; for a recent review on excimers and exciplexes see N. Mataga, M. Ottolenghi in R. Foster (Ed.): *Molecular Association Including Molecular Complexes, Vol. 2*, Academic Press, London 1979.

[114] Z. R. Grabowski, *Chem. Rev.*, to be published.

[115] Z. R. Grabowski (Warsaw), private communication 1984.

[116] G. Wermuth, *Z. Naturforsch. A 38* (1983) 641.

[117] K. H. Drexhage in F. P. Schäfer (Ed.): *Dye Lasers*, Springer, New York 1977; *Top. Appl. Phys. 1* (1973) 144; R. Sens, K. H. Drexhage, *J. Lumin. 24/25* (1981) 709.

[118] T. Carstens, K. Kobs, *J. Phys. Chem. 84* (1980) 1871.

[119] N. Nakashima, H. Inoue, N. Mataga, Ch. Yamanaka, *Bull. Chem. Soc. Jpn. 46* (1973) 2288.

[120] W. S. Struve, P. M. Rentzepis, J. Jortner, *J. Chem. Phys. 59* (1973) 5014; W. S. Struve, P. M. Rentzepis, *ibid. 60* (1974) 1533; *Chem. Phys. Lett. 29* (1974) 23 (see also M. R. Topp, G. C. Orner, *Chem. Phys. Lett. 32* (1975) 407 for criticism); D. Huppert, S. D. Rand, P. M. Rentzepis, P. F. Barbara, W. S. Struve, Z. R. Grabowski, *J. Chem. Phys. 75* (1981) 5714.

[121] K. Rotkiewicz, Z. R. Grabowski, J. Jasny, *Chem. Phys. Lett. 34* (1975) 55.

[122] J. Hicks, M. Vandersall, Z. Babarogic, K. B. Eisenthal, *Chem. Phys. Lett. 116* (1985) 18.

[123] F. Heisel, J. A. Miehé, *Chem. Phys. Lett. 100* (1983) 183; *Chem. Phys. 98* (1985) 233; F. Heisel, J. A. Miehé, J. M. G. Martinho, *ibid. 98* (1985) 243.

[124] S. R. Meech, D. Phillips, *Chem. Phys. Lett. 116* (1985) 262.

[125] Th. Förster, G. Hoffmann, *Z. Phys. Chem. (Wiesbaden) 75* (1971) 63.

[126] R. Griebel, *Ber. Bunsenges. Phys. Chem. 84* (1980) 84.

[127] A. Spernol, K. Wirtz, *Z. Naturforsch. A 8* (1953) 522; A. Gierer, K. Wirtz, *ibid. 8* (1953) 532.

[128] A. H. Alwattar, M. D. Lumb, J. B. Birks in J. B. Birks (Ed.): *Organic Molecular Photophysics, Vol. 1*, Wiley, New York 1973, Chapter 8.

[129] K. A. Al-Hassan, W. Rettig, *Chem. Phys. Lett. 126* (1986) 273.

[130] C. A. Cremers, M. W. Windsor, *Chem. Phys. Lett. 71* (1980) 27.

[131] B. Bagchi, G. R. Fleming, D. W. Oxtoby, *J. Chem. Phys. 78* (1983) 7375.

[132] D. Magde, M. W. Windsor, *Chem. Phys. Lett. 24* (1974) 144; E. P. Ippen, C. V. Shank, A. Bergman, *ibid. 38* (1976) 611; M. D. Hirsch, H. Mahr, *ibid. 60* (1979) 299; J. M. Grzybowski, S. E. Sygamori, D. F. Williams, R. W. Yip, *ibid. 65* (1979) 456; G. S. Beddard, T. Doust, M. W. Windsor, *Springer Ser. Chem. Phys. 14* (1980) 167; V. Sundström, T. Gillbro, H. Bergström, *Chem. Phys. 73* (1982) 439; T. Doust, *Chem. Phys. Lett. 96* (1983) 522; R. Trebino, A. E. Siegman, *J. Chem. Phys. 79* (1983) 3621; V. Sundström, T. Gillbro, *ibid. 81* (1984) 3463; *Chem. Phys. Lett. 110* (1984) 303; D. Ben-Amotz, C. B. Harris, *ibid. 119* (1985) 305.

[133] W. Rettig, K. Rotkiewicz, W. Rubaszewska, *Spectrochim. Acta Part A 40* (1984) 241.

[134] H. Köppel, L. S. Cederbaum, W. Domcke, S. S. Shaik, *Angew. Chem. 95* (1983) 221; *Angew. Chem. Int. Ed. Engl. 22* (1983) 210; H. Köppel, W. Domcke, L. S. Cederbaum, *Adv. Chem. Phys. 57* (1984) 59, and references cited therein.

[135] R. M. Hochstrasser, C. A. Marzzacco in E. C. Lim (Ed.): *Molecular Luminescence*, Benjamin, New York 1969, p. 631.

[136] H. Beens, A. Weller in J. B. Birks (Ed.): *Organic Molecular Photophysics, Vol. 2*, Wiley, New York 1975.

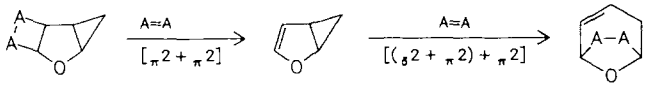
[137] A nonzero dipole moment for the emissive state of **28** in aliphatic hydrocarbons has also been found by EOE measurements: W. Baumann, E. Spohr, H. Bischof, *Int. Conf. Lumin.* (Madison, WI, USA 1984), paper FB6-1.
[138] V. Bonačić-Koutecký, P. Bruckmann, P. Hiberty, J. Koutecký, C. Leforestier, L. Salem, *Angew. Chem. 87* (1975) 599; *Angew. Chem. Int. Ed. Engl. 14* (1975) 575; V. Bonačić-Koutecký, *J. Am. Chem. Soc. 100* (1978) 396.
[139] R. J. Buenker, V. Bonačić-Koutecký, L. Pogliani, *J. Chem. Phys. 73* (1980) 1836.
[140] V. Bonačić-Koutecký, L. Pogliani, M. Persico, J. Koutecký, *Tetrahedron 38* (1982) 741; V. Bonačić-Koutecký, M. Persico, D. Döhnert, A. Sevin, *J. Am. Chem. Soc. 104* (1982) 6900; V. Bonačić-Koutecký, M. Persico, *ibid. 105* (1983) 3388.
[141] V. Bonačić-Koutecký, J. Michl, *Theor. Chim. Acta 68* (1985) 45; review: V. Bonačić-Koutecký, J. Koutecký, J. Michl, *Angew. Chem.*, in press.
[142] L. Pogliani, N. Niccolai, C. Rossi, *Chem. Phys. Lett. 108* (1984) 597.
[143] T. Tezuka, O. Kikuchi, K. N. Houk, M. N. Paddon-Row, C. M. Santiago, N. R. Rondan, J. C. Williams, Jr., R. W. Gandow, *J. Am. Chem. Soc. 103* (1981) 1367; R. F. Childs, T. DiClemente, E. F. Lund-Lucas, T. J. Richardson, C. V. Rogerson, *Can. J. Chem. 61* (1983) 856; O. Kikuchi, H. Yoshida, *Bull. Chem. Soc. Jpn. 58* (1985) 131; the kinetics of isomerization of *trans*-stilbene is different in polar and nonpolar solutions: V. Sundström, T. Gillbro, *Ber. Bunsenges. Phys. Chem. 89* (1985) 222.
[144] J. Saltiel, J. D'Agostino, E. D. Megarity, L. Metts, K. R. Neuberger, M. Wrighton, O. C. ZaFiriou, *Org. Photochem. 3* (1973) 1.
[145] G. Hohlneicher, B. Dick, *J. Photochem. 27* (1984) 215.
[146] M. C. Nuss, W. Zinth, W. Kaiser, E. Kölling, D. Oesterhelt, *Chem. Phys. Lett. 117* (1985) 1.
[147] A. G. Doukas, M. R. Junnarkar, R. R. Alfano, R. H. Callender, T. Kakitani, B. Honig, *Proc. Natl. Acad. Sci. USA 81* (1984) 4790.
[148] A. Warshel, *Nature (London) 260* (1976) 679.
[149] R. S. H. Liu, A. E. Asato, *Proc. Natl. Acad. Sci. USA 82* (1985) 259.
[150] L. Salem, *Science (Washington DC) 191* (1976) 822.
[151] R. M. Weiss, A. Warshel, *J. Am. Chem. Soc. 101* (1979) 6131.
[152] A. Warshel, N. Barboy, *J. Am. Chem. Soc. 104* (1982) 1469; F. Boucher, R. M. Leblanc, *Photochem. Photobiol. 41* (1985) 459.
[153] R. R. Alfano (Ed.): *Biological Events Probed by Ultrafast Laser Spectroscopy*, Academic Press, New York 1982, Chapter 1-5.
[154] M. W. Windsor, D. Holten, *Philos. Trans. R. Soc. London A 298* (1980) 335.
[155] J. Deisenhofer, O. Epp, K. Miki, R. Huber, H. Michel, *J. Mol. Biol. 180* (1984) 385; W. Zinth, E. W. Knapp, S. F. Fischer, W. Kaiser, J. Deisenhofer, H. Michel, *Chem. Phys. Lett. 119* (1985) 1; H. Michel, J. Deisenhofer, *Encycl. Plant Physiol. New Ser. Vol. 19* (1986) p. 371.
[156] V. A. Shuvalov, W. W. Parson, *Proc. Natl. Acad. Sci. USA 78* (1981) 957.
[157] J. R. Miller, J. V. Beitz, R. K. Huddleston, *J. Am. Chem. Soc. 106* (1984) 5057.
[158] N. J. Turro, *Angew. Chem. 98* (1986) 872; *Angew. Chem. Int. Ed. Engl. 25* (1986) 882.
[159] M. R. Wasielewski, M. P. Niemczyk, *J. Am. Chem. Soc. 106* (1984) 5043; A. D. Joran, B. A. Leland, G. G. Geller, J. J. Hopfield, P. B. Dervan, *ibid. 106* (1984) 6090; H. Heitele, M. E. Michel-Beyerle in M. E. Michel-Beyerle (Ed.): *Antennas and Reaction Centers of Photosynthetic Bacteria Structure, Interactions and Dynamics*, Springer, Berlin 1985, p. 250; N. Mataga, A. Keven, T. Okada, S. Nishitani, N. Kurata, Y. Sakata, S. Misumi, *J. Phys. Chem. 88* (1984) 5138; T. A. Moore, D. Gust, P. Mathis, J. C. Mialocq, C. Cachaty, R. V. Bensasson, E. J. Land, D. Doizi, P. A. Liddell, W. R. Lehmann, G. A. Nemeth, A. L. Moore, *Nature (London) 307* (1984) 630.
[160] J. K. Nagle, J. S. Bernstein, R. C. Young, T. J. Meyer, *Inorg. Chem. 20* (1981) 1760; K. S. Schanze, T. J. Meyer, *ibid. 24* (1985) 2121; **1** has also been used as a ligand in ruthenium complexes (K. S. Schanze (Berkeley, CA), private communication 1985).

When submitting manuscripts, authors of articles intended for publication as "Communications" are requested to read the "Notice to Authors" reproduced in the January issue of the journal following the list of contents; upon request, a copy can be obtained from the editorial office.

$[\pi^2+\pi^2]$ Cycloaddition of 4-Phenyl-4*H*-1,2,4-triazole-3,5-dione and Singlet Oxygen to Homofuran**

By *Waldemar Adam,* Axel Griesbeck, Frank-Gerrit Klärner,* and *Dietmar Schröer*

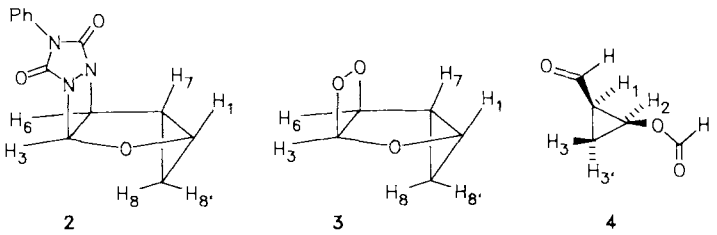
Homofuran **1** *can, in principle, undergo* $[\pi^2+\pi^2]$ *or* $[(\sigma^2+\pi^2)+\pi^2]$ cycloadditions with cyclophiles.[1] The latter possibility results in the opening of the central cyclopropane bond to give 8-oxabicyclo[3.2.1]oct-2-enes. In a broader sense, this cycloaddition mode is analogous to the well-known ene reaction.[2] For example, the reaction of **1** with typical dienophiles such as maleic anhydride or tetracyanoethylene (TCNE) affords quickly and in excellent yields the 8-oxabicyclo[3.2.1]octenes.



1

It was our goal, therefore, to prepare the diaza and dioxa bicyclic derivatives by using the established enophiles 4-phenyl-4*H*-1,2,4-triazole-3,5-dione (PTAD) and singlet oxygen, respectively. PTAD reacted already at -25 °C with **1** in solvents such as dichloromethane, chloroform, and Freon 11 to give quantitative yields of the $[\pi^2+\pi^2]$-cycloadduct **2**.[3] The ^{1}H-NMR data (Table 1) suggest that the cyclopropane and triazole rings are arranged *anti* to each other. For example, the missing coupling between 6-H and 7-H implies a dihedral angle of ca. 90°, as expected from Dreiding models.

Singlet oxygen, generated by photosensitization with tetraphenylporphine (TPP) or Rose Bengal (RB) also reacts with **1** to give the $[\pi^2+\pi^2]$ adduct, the dioxetane **3**. Compound **3** was formed independently of solvent polarity (chloroform, Freon 11, acetonitrile), and could be observed by means of ^{1}H-NMR spectroscopy. In most cases, *cis*-2-formyloxycyclopropanecarboxaldehyde **4**,[3,4] the decomposition product, could be isolated in high yields (up to 92%). However, when the photooxygenation was performed in a mixture of chloroform, Freon 11, and pyridine (2:1:0.1) at -30 °C, the solvent mixture removed by distillation at -20 °C/10^{-4} torr, and the residue allowed to warm up slowly at 10^{-4} torr, an 73:27 mixture of **3** and **4** could be distilled at ca. -5 °C. Comparison of the ^{1}H-NMR data of **3** (Table 1) with those of **2** clearly show formation of the *anti* product. The ^{13}C-NMR data of **3** are consistent with those of other known[5] tetrahydrofuran-annelated 1,2-dioxetanes; characteristic are the ^{13}C shifts of C-3 and C-6 (in order to facilitate comparison, structures **2** and **3** are not numbered systematically).



2 **3** **4**

Table 1. 400-MHz ^{1}H-NMR and 100-MHz ^{13}C-NMR data of the PTAD and the $^1O_2$ adducts **2** and **3**, respectively. *J* in Hz.

2, ^{1}H-NMR ($CD_3CN/(CD_3)_2CO$ 1:1, 50 °C): $\delta = 0.57$ (ddd, $^2J(8,8') = 7.2$, $^3J(8,7) = 5.3$, $^3J(8,1) = 1.7$, H-8), 0.98 (dddd, $^3J(8',7) = 11.0$, $^2J(8',8) = 7.2$, $^3J(8',1) = 5.3$, $^4J(8',6) = 0.6$, H-8' [a]), 2.20 (dt, $^3J(7,8') = 11.0$, $^3J(7,8) = 5.3$, $^3J(7,1) = 5.3$, H-7), 4.55 (td, $^3J(1,7) = 5.3$, $^3J(1,8') = 5.3$, $^3J(1,8) = 1.7$, H-1), 5.11 (dd, $^3J(6,3) = 4.5$, $^4J(6,8') = 0.6$, H-6), 5.83 (d, $^3J(3,6) = 4.5$, H-3). — ^{13}C-NMR ($CD_3CN/(CD_3)_2CO$ 1:1, 32 °C): $\delta = 12.03$ (t, C-8), 17.13 (d, C-7), 61.37 (d, C-1), 64.25 (d, C-6), 110.69 (d, C-3), 126.66 (d), 128.82 (d), 129.68 (d), 132.80 (s) (all phenyl C), 153.70 (s), 154.80 (s) (both carbonyl C)

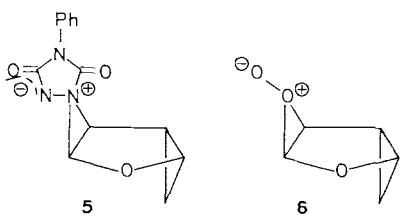
3, ^{1}H-NMR ($CDCl_3/CFCl_3$ 2:1, -50 °C): $\delta = 0.37$ (dd, $^2J(8,8') = 6.0$, $^3J(8,7) = 5.2$, H-8), 0.92 (ddd, $^3J(8',7) = 10.5$, $^2J(8',8) = 6.0$, $^3J(8',1) = 5.2$, H-8'), 2.16 (dt, $^3J(7,8') = 10.5$, $^3J(7,8) = 5.2$, $^3J(7,1) = 5.2$, H-7), 4.50 (br. m, H-1), 5.53 (d, $^3J(6,3) = 1.4$, H-6), 6.12 (d, $^3J(3,6) = 1.4$, H-3). — ^{13}C-NMR ($CDCl_3/CFCl_3$ 2:1, -50 °C): $\delta = 13.55$ (t, C-8), 20.82 (d, C-7), 60.32 (d, C-1), 88.83 (d, C-6), 109.02 (d, C-3)

[a] Confirmed by decoupling experiments.

Already at room temperature, solutions of **3** in toluene show a pronounced chemiluminescence. Determination of the dioxetane content by means of iodometry and application of known kinetic methods[6] afforded an activation energy of 19 ± 2 kcal/mol for the decomposition of the dioxetane. Thus, **3** belongs to the group of rather unstable dioxetanes.[7]

Homofuran **1** reacted only sluggishly with diethyl azodicarboxylate, dimethyl acetylenedicarboxylate, and (*E*)-1,2-bis(phenylsulfonyl)ethylene.[8] Even after one-day stirring of these dienophiles with **1** in dichloromethane, the starting materials could be reisolated. At 95 °C in benzene (ampoule), reaction with diethyl azodicarboxylate led to a low yield of the [2+2] adduct.

These results demonstrate that the quite reactive dienophiles PTAD and $^1O_2$ do not undergo the novel



5 **6**

[*] Prof. Dr. W. Adam, Dr. A. Griesbeck
Institut für Organische Chemie der Universität
Am Hubland, *D-8700 Würzburg (FRG)*
Prof. Dr. F.-G. Klärner, Dipl.-Chem. D. Schröer
Lehrstuhl für Organische Chemie I der Universität
Postfach 102148, D-4630 Bochum 1 (FRG)

[**] This work was supported by the Deutsche Forschungsgemeinschaft (Sonderforschungsbereich 172, "Molecular Mechanisms of Carcinogenic Transformations"), the Stiftung Volkswagenwerk and the Fonds der Chemischen Industrie.

$[(\sigma^2+\pi^2)+\pi^2]$ cycloaddition. While **1** reacts with maleic anhydride and TCNE presumably according to a classical, pericyclic mechanism,[1] reaction with PTAD or $^1O_2$ involves a $[\pi^2+\pi^2]$ cycloaddition, apparently via the dipolar intermediates **5** and **6**. These zwitterionic species appear to be sufficiently stable that exclusively $[\pi^2+\pi^2]$ adducts result. In contrast to the reaction of **1** with TCNE, for which increasing solvent polarity favors the $[\pi^2+\pi^2]$ mode over the $[(\sigma^2+\pi^2)+\pi^2]$ mode,[1] the reactions with PTAD and $^1O_2$ are not influenced by solvent polarity.

Received: April 24, 1986;
revised: July 28, 1986 [Z 1742 IE]
German version: *Angew. Chem. 98* (1986) 1006

CAS Registry numbers:
1, 6664-26-2; **2**, 104739-75-5; **3**, 104832-27-1; **4**, 104739-76-6; PTAD, 4233-33-4.

[1] R. Herges, I. Ugi, *Chem. Ber. 119* (1986) 829; the assignment of the ^{1}H-NMR spectrum of their product **3** formed from TCNE and **1** is questionable.
[2] H. M. R. Hoffmann, *Angew. Chem. 81* (1969) 597; *Angew. Chem. Int. Ed. Engl. 8* (1969) 556.
[3] Correct elemental analysis.
[4] **4** was isolated in 90% yield by short-path distillation at 46–50°C/0.1 torr as a pale yellow oil. ^{1}H-NMR (400 MHz, $CDCl_3$): $\delta=1.34$ (dt, $J=9.1$, 6.6, 6.6 Hz, H-3'), 1.59 (tdd, $J=6.8$, 6.6, 4.5, 0.6 Hz, H-3), 1.97 (dtd, $J=9.1$, 6.8, 6.8, 5.2 Hz, H-1), 4.39 (tdd, $J=6.8$, 6.6, 4.5, 0.5 Hz, H-2), 7.95 (br. s, OCHO), 9.08 (d, $J=5.2$ Hz, CH=O). ^{13}C-NMR (100 MHz, $CDCl_3$): $\delta=12.09$ (t); 27.53 (d); 53.43 (d); 160.41 (d); 196.75 (d). IR (film): $\tilde{\nu}=2960$, 1730, 1700, 1432, 1371, 1360, 1200, 1155, 998 cm^{-1}.
[5] W. Adam, A. Griesbeck, K. Gollnick, K. Knutzen-Mies, unpublished.
[6] W. Adam, K. Zinner in W. Adam, G. Cilento (Eds.): *Chemical and Biological Generation of Electronic Excited States*, Academic Press, New York 1982, Chapter 5.
[7] W. Adam, W. J. Baader, *J. Am. Chem. Soc. 107* (1985) 410.
[8] O. De Lucchi, V. Lucchini, L. Pasquato, G. Modena, *J. Org. Chem. 49* (1984) 596.

$[Cl_7Cu_5(ReS_4)]^{3\ominus}$, a Hexanuclear Complex Anion with Double Cubane-Like Structure

By *Achim Müller,* Erich Krickemeyer,* and *Hartmut Bögge*

Dedicated to Professor Oskar Glemser on the occasion of his 75th birthday

Although a large number of interesting coordination compounds containing thiometalates (such as $MoS_4^{2\ominus}$ and $WS_4^{2\ominus}$) are known,[1] no crystalline complexes containing the $ReS_4^{\ominus}$ ion, for which several crystalline salts have long been known,[2] have been reported. This is even more remarkable in that, owing to the strongly reducing $S^{2\ominus}$ ligands at the Re^{VII} center,[1] $ReS_4^{\ominus}$ should exhibit an interesting coordination chemistry. By reaction of $[NEt_4][ReS_4]$[3] with CuCl in CH_2Cl_2 in the presence of PPh_4Cl, we have now been able to obtain the diamagnetic, black Cu_5Re complex **1**, the first compound with a double cubane-like structure.[4] Compound **1** has been characterized by elemental analysis and by IR and UV/VIS spectroscopy,[5] as well as by a complete X-ray structure analysis.[6]

$[PPh_4]_2[NEt_4][Cl_7Cu_5(ReS_4)]$ **1**

[*] Prof. Dr. A. Müller, E. Krickemeyer, Dr. H. Bögge
Fakultät für Chemie der Universität
Postfach 8640, D-4800 Bielefeld 1 (FRG)

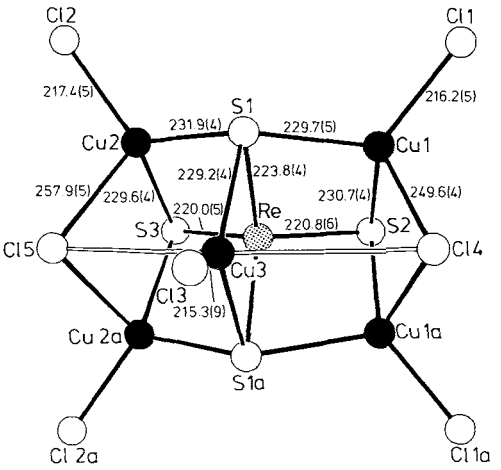


Fig. 1. Structure of the anion of **1** with bond lengths in pm. The atoms Re, S2, S3, Cu3, Cl3, Cl4, and Cl5 occupy a crystallographic mirror plane. Selected bond angles [°]: S-Re-S 106.4(2)–110.8(1), S-Cu-S 104.2(2)–105.8(2), S-Cu-Cl_{cube} 92.8(1)–100.0(2), S-Cu-$Cl_{term.}$ 119.4(2)–126.7(1), Cl-Cu-Cl 110.2(2), 110.4(2), Re-S-Cu 70.7(1)–72.2(1), Cu-S-Cu 84.4(2)–128.0(2), Cu-Cl-Cu 76.8(2)–79.5(2); further distances [pm]: Re-Cu1 263.8(2), Re-Cu2 263.7(2), Re-Cu3 266.8(4), Cu3···Cl4 331.8(6), Cu3···Cl5 293.9(6).

The anion of **1** is "rather symmetric" (Fig. 1); if the nonequivalence of the Cu3–Cl distances within the "double cubane" is ignored,[7,9] the anion has C_{2v} symmetry. Further notable features of the structure of the anion of **1** are the following: the arrangement of the six metal atoms, which form approximately a basal-plane-centered "rectangle pyramid"; the very short Re–Cu distances (263.7(2)–266.8(4) pm); the arrangement of fragments of a CuCl zigzag chain (a CuCl molecule and two Cu_2Cl_3 fragments); and, finally, the coordination number 4 for a sulfido ligand, which is relatively rare in inorganic complexes and enables the formation of the "double cubane." This coordination number has not been observed before for $MS_4^{2\ominus}$ (M = Mo, W) ligands.[1]

Received: May 30, 1986;
revised: July 16, 1986 [Z 1795 IE]
German version: *Angew. Chem. 98* (1986) 987

CAS Registry number:
1, 104350-75-6.

[1] A. Müller, E. Diemann, R. Jostes, H. Bögge, *Angew. Chem. 93* (1981) 957; *Angew. Chem. Int. Ed. Engl. 20* (1981) 934; A. Müller, *Polyhedron 5* (1986) 323; see also Y. Do, E. D. Simhon, R. H. Holm, *Inorg. Chem. 24* (1985) 4635.
[2] A. Müller, E. Diemann, V. V. K. Rao, *Chem. Ber. 103* (1970) 2961. The earlier reported $TlReS_4$ (W. Feit, *Z. Angew. Chem. 44* (1931) 65) is a mixture of Tl_2S and Re_2S_7 (A. Müller, B. Krebs, *Naturwissenschaften 53* (1966) 178).
[3] A. Müller, E. Krickemeyer, H. Bögge, M. Penk, D. Rehder, *Chimia 40* (1986) 50.
[4] *Experimental Procedure:* A mixture of $[NEt_4][ReS_4]$ (0.22 g, 0.5 mmol), anhydrous CuCl (1 g, 10.1 mmol), and PPh_4Cl (1 g, 2.7 mmol) in 100 mL of CH_2Cl_2 (p.a.) was allowed to stir under argon in a closed flask for 2.5 h. After filtration, 50 mL of *n*-pentane/diethyl ether (1:1) was added to the deep red-black filtrate and the resulting solution was kept in a closed flask under argon at 20°C. Within 2–3 d, black crystals of **1** precipitated out. They were filtered off, washed with H_2O, isopropyl alcohol, and diethyl ether, and dried in air. Yield: 0.18 g (21%). **1** is slightly soluble in polar organic solvents such as CH_3CN.
[5] IR spectrum (solid, Nujol mull): 451/442 (m, $\tilde{\nu}$(ReS)), 335 cm^{-1} (w, $\tilde{\nu}_{as}$(CuCl/S)); for the assignment, see A. Müller, W. Jaegermann, W. Hellmann, *J. Mol. Struct. 100* (1983) 559. Solid-state reflectance spectrum (cellulose mull): $\lambda=700$ (charge transfer $Cu^I \rightarrow Re^{VII}$), 480, 350 nm (charge transfer $S^{2-} \rightarrow Re^{VII}$).

[6] 1 forms monoclinic crystals ($P2_1/m$, $a=950.7(7)$, $b=2453.2(9)$, $c=1395.1(8)$ pm, $\beta=99.12(5)°$, $V=3212.7\cdot10^6$ pm^3, $Z=2$). An empirical absorption correction was applied. The structure was solved by heavy atom methods ($R=0.098$, $R_w=(\Sigma w(|F_0|-|F_c|)^2/\Sigma w|F_0|^2)^{1/2}=0.095$ ($1/w=\sigma^2(F_0)+0.0002F_0^2$) for 4802 unique reflections ($F_0>3.92\sigma(F_0)$); Syntex $P2_1$ diffractometer, $Mo_{K\alpha}$ radiation, graphite monochromator). Further details of the crystal structure investigation may be obtained from the Fachinformationszentrum Energie, Physik, Mathematik GmbH, D-7514 Eggenstein-Leopoldshafen 2 (FRG), on quoting the depository number CSD-51954, the names of the authors, and the journal citation.

[7] The Cu-Cl distance in the "more closed" [Cu_3ReS_3Cl] cube (cf. Fig. 1) is roughly comparable to the larger Cu-Cl distance (276.4(4) pm) in [(Cu_3MoS_3Cl)(PPh_3)$_3$S] [8] with cubane structure (compare the discussions in [8] and [9]).

[8] A. Müller, H. Bögge, U. Schimanski, *J. Chem. Soc. Chem. Commun. 1980*, 91.

[9] By use of a thiomolybdate synthon, it was possible to prepare, "by unit construction," specific cluster and cage structures: a complete cubane and cubes with one or two missing corners; the latter structural unit then represents "half" of another prismatic cage system [10].

[10] A. Müller, U. Schimanski, J. Schimanski, *Inorg. Chim. Acta 76* (1983) L245.

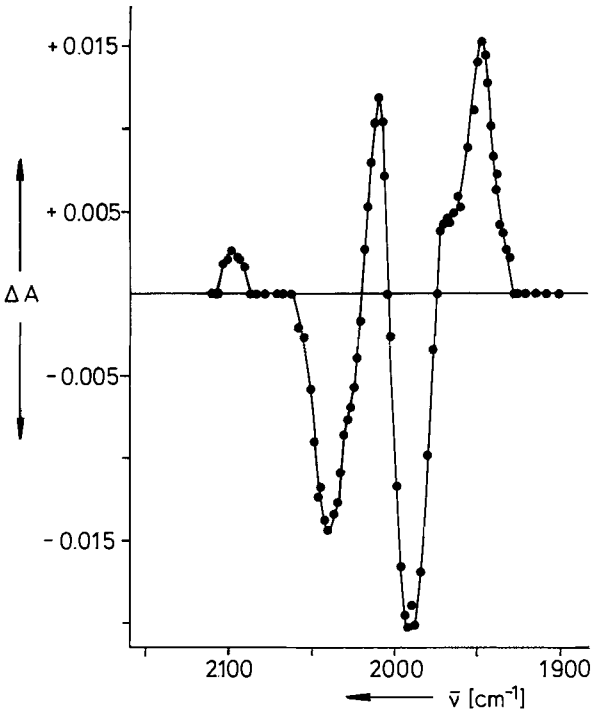


Figure 1. IR difference spectrum ca. 5 μs after flash excitation of $Os(CO)_5$ in CO-saturated C_6D_6. Positive bands correspond to $Os(CO)_4\cdot C_6D_6$, negative bands to photodepleted $Os(CO)_5$. The experimental setup for flash photolysis with fast IR detection has been described elsewhere [8, 9]. Instead of the previously used conventional flash lamps, an excimer laser (Lambda Physik EMG 200, operating on XeCl, $\lambda=308$ nm) was employed as the excitation source. For further details see text.

Flash Photolysis of $Os(CO)_5$ in Benzene Solution. Detection of $Os(CO)_4\cdot$benzene by Fast Time-Resolved IR Spectroscopy**

By *Stephen P. Church, Friedrich-Wilhelm Grevels,* Gong-Yu Kiel, William A. Kiel, Josef Takats,* and *Kurt Schaffner*

Although the photochemistry of $Fe(CO)_5$ has been extensively studied,[1] very little has been reported on the related photoreactions of $Os(CO)_5$.[2] Conversions to $Os_3(CO)_{12}$,[3] $Os_2(CO)_9$,[4] and $Os(CO)_4PPh_3$[5] are known. However, no mechanistic details have been published to date.

By means of fast time-resolved IR spectroscopy, we recently observed $Fe(CO)_4\cdot$benzene as an intermediate in the photochemistry of $Fe(CO)_5$ in benzene solution.[6,7] We now wish to report on the first experiments with the analogous osmium compound.

Flash photolysis of an 8×10^{-4} M solution of $Os(CO)_5$ in CO-saturated C_6D_6[10] yielded the transient difference spectrum shown in Figure 1, which exhibits four positive (2097, 2010, 1966 (sh), 1948 cm^{-1}) and two negative absorptions (2040, 1990 cm^{-1}) in the CO stretching vibrational region. The positive bands are different from those reported for $Os(CO)_4$ in a methane matrix[11] and are assigned to the species $Os(CO)_4\cdot C_6D_6$ formed through reaction (1).

$$Os(CO)_5 \xrightarrow[C_6D_6]{h\nu} Os(CO)_4\cdot C_6D_6 + CO \qquad (1)$$

The characteristic four-band pattern is in accordance with a C_{2v} structure of the $Os(CO)_4$ unit,[12] as has been proposed for the analogous $Fe(CO)_4\cdot C_6D_6$ complex.[6] The two negative absorptions, corresponding to photodepleted $Os(CO)_5$, occur in an intensity ratio of 1:1.4 as found in the IR spectrum of the pure compound, thus confirming that the absorptions of $Os(CO)_4\cdot C_6D_6$ are not overlapped by those of the starting material.

The transient $Os(CO)_4\cdot C_6D_6$ decays by first-order kinetics. The rate constant, k_{obs}, for the disappearance of $Os(CO)_4\cdot C_6D_6$ ([$Os(CO)_5$]$=8\times10^{-4}$ M; [CO]$=1.1\times10^{-2}$ M[13]) is 940 s^{-1}, i.e., two orders of magnitude faster than for $Fe(CO)_4\cdot C_6D_6$ under the same conditions.[6] $Os(CO)_5$ is regenerated concurrent with the decay of $Os(CO)_4\cdot C_6D_6$ and no other product is observed.[14] In a similar experiment, but with a CO concentration of only 10^{-3} M,[13] k_{obs} is markedly reduced to 150 s^{-1}. Furthermore, under these conditions the formation of $Os_2(CO)_9$ [$\tilde{\nu}$(CO)$=$2084 (s), 2042 (vs), 2032–2012 (unresolved), 1772 (m) cm^{-1}],[15] as a permanent product on the second time-scale, is also evident. Thus, the decay of $Os(CO)_4\cdot C_6D_6$ is CO-concentration dependent and the formation of $Os_2(CO)_9$ is favored at higher [$Os(CO)_5$]/[CO] ratios. Further, k_{obs} was shown to be inversely dependent on the C_6D_6 concentration in experiments performed in C_6D_6/cyclohexane mixtures. These observations are explained most simply in terms of reactions (2)–(4).

$$Os(CO)_4\cdot C_6D_6 \underset{k_2}{\overset{k_1}{\rightleftharpoons}} Os(CO)_4 + C_6D_6 \qquad (2)$$

$$Os(CO)_4 + CO \xrightarrow{k_3} Os(CO)_5 \qquad (3)$$

$$Os(CO)_4 + Os(CO)_5 \xrightarrow{k_4} Os_2(CO)_9 \qquad (4)$$

[*] Priv.-Doz. Dr. F.-W. Grevels, Dr. S. P. Church, Prof. Dr. K. Schaffner
Max-Planck-Institut für Strahlenchemie
Stiftstrasse 34-36, D-4330 Mülheim a. d. Ruhr (FRG)
Dr. G.-Y. Kiel, Dr. W. A. Kiel, Prof. Dr. J. Takats
Department of Chemistry, University of Alberta
Edmonton, Alberta T6G 2G2 (Canada)

[**] This work was supported by the Alexander von Humboldt Foundation through a stipend (to *S. P. C.*). We thank Dr. *H. Hermann* for his collaboration, Miss *K. Fuchs* for technical assistance, and Johnson Matthey & Mallory Ltd. for a generous loan of osmium tetroxide.

For $[CO]=10^{-3}$ M and $[Os(CO)_5]=8\times10^{-4}$ M, further depletion of the $Os(CO)_5$ band at 1990 cm^{-1} occurs concurrent with the decay of $Os(CO)_4\cdot C_6D_6$; thus, $k_4>k_3$. However, at $[CO]=1.1\times10^{-2}$ M and $[Os(CO)_5]=8\times10^{-4}$ M, reaction (4) does not compete with reaction (3). Thus, a reasonable estimate is $k_4/k_3\approx2$.

$Fe(CO)_4$·benzene reacts with CO two orders of magnitude slower than does $Os(CO)_4$·benzene. This sharply contrasts with the behavior of the pentacarbonylmetal·benzene compounds of the chromium group, where the complex of the heavier metal, $W(CO)_5$·benzene, reacts significantly slower than $Cr(CO)_5$·benzene.[8a] The opposite behavior of the iron and osmium species might be due to the triplet nature of $Fe(CO)_4$[16] or to the involvement of other intermediates.

Received: June 9, 1986 [Z 1807 IE]
German version: *Angew. Chem. 98* (1986) 993

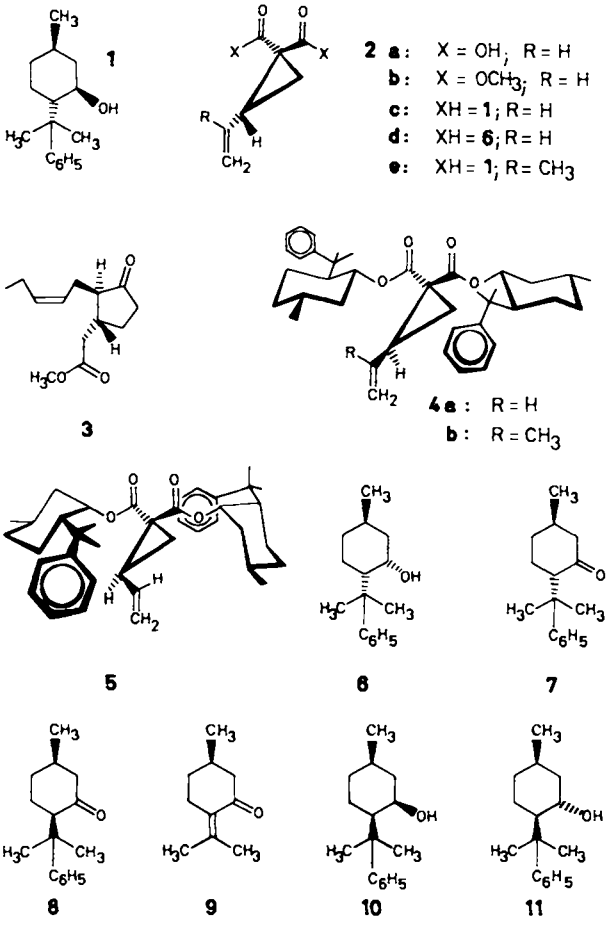
[1] a) E. Koerner von Gustorf, F.-W. Grevels, *Top. Curr. Chem. 13* (1969) 366; b) G. L. Geoffroy, M. S. Wrighton: *Organometallic Photochemistry*, Academic Press, New York 1979.
[2] For the synthesis of $Os(CO)_5$ see [3].
[3] F. Calderazzo, F. L'Eplattenier, *Inorg. Chem. 6* (1967) 1220; R. Rushman, G. N. van Buuren, M. Shiralian, R. K. Pomeroy, *Organometallics 2* (1983) 693.
[4] J. R. Moss, W. A. G. Graham, *J. Chem. Soc. Dalton Trans. 1977*, 95.
[5] F. L'Eplattenier, F. Calderazzo, *Inorg. Chem. 7* (1968) 1290.
[6] S. P. Church, F.-W. Grevels, H. Hermann, J. M. Kelly, W. E. Klotzbücher, K. Schaffner, *J. Chem. Soc. Chem. Commun. 1985*, 594.
[7] S. P. Church, F.-W. Grevels, H. Hermann, K. Schaffner, unpublished.
[8] a) H. Hermann, F.-W. Grevels, A. Henne, K. Schaffner, *J. Phys. Chem. 86* (1982) 5151.
[9] S. P. Church, F.-W. Grevels, H. Hermann, K. Schaffner, *Inorg. Chem. 23* (1984) 3830; *24* (1985) 418.
[10] C_6D_6 is much more transparent than C_6H_6 in the IR spectral region of interest.
[11] M. Poliakoff, J. J. Turner, *J. Chem. Soc. Dalton Trans. 1974*, 2276.
[12] Cf. the CO bands in the IR spectra of (η^2-olefin)$Os(CO)_4$ complexes; M. R. Burke, J. Takats, F.-W. Grevels, J. G. A. Reuvers, *J. Am. Chem. Soc. 105* (1983) 4092.
[13] CO concentrations are calculated from the CO pressure using literature data for C_6H_6: E. Wilhelm, R. Battino, *Chem. Rev. 73* (1973) 1.
[14] At all points of the spectrum shown in Figure 1, the same kinetic behavior was observed.
[15] $Os_2(CO)_9$ was previously identified in *n*-heptane solution as a product of the photolysis of $Os(CO)_5$ [4]. Unlike the familiar triply CO-bridged $Fe_2(CO)_9$, which is insoluble, $Os_2(CO)_9$ is singly bridged and soluble.
[16] M. Poliakoff, *Chem. Soc. Rev. 7* (1978) 527.

The Use of (+)-8-Phenylneomenthol in the Synthesis of Enantiomerically Pure (−)-Jasmonate Methyl Ester**

By *Gerhard Quinkert,* Hans-Günther Schmalz, Elmar M. Dzierzynski, Gerd Dürner,* and *Jan W. Bats*

Dedicated to Professor Vladimir Prelog on the occasion of his 80th birthday

(−)-8-Phenylmenthol **1**[1] has proved to be valuable as a chiral auxiliary reagent[3] for the synthesis of dimethyl (*R*)-(+)-2-vinyl-1,1-cyclopropanedicarboxylate **2b**,[4] a chiral building block for the synthesis of enantiomerically pure (+)-estrone[5] or (−)-norgestrel.[6] (+)-8-Phenylmenthol



ent-**1** would be a welcome chiral auxiliary reagent for the synthesis of enantiomerically pure (−)-jasmonate methyl ester **3**[7,8] via dimethyl (*S*)-(−)-2-vinyl-1,1-cyclopropanedicarboxylate *ent*-**2b**, but *ent*-**1** is difficult to prepare.[2b] Thus, up to now it has only been possible to obtain the chiral synthetic building block *ent*-**2b** via a detour by diastereomerization of **2c** to **4a**,[7,9] which is then converted into **3**.

As suggested by an analysis of the stereoelectronic requirements for cyclopropanation via an S_{cN} reaction,[10] (+)-8-phenylneomenthol **6** should act similarly to *ent*-**1**. Indeed, reaction of **6** (in the presence of imidazole and 4-(*N*,*N*-dimethylamino)pyridine in CH_2Cl_2) with malonyl dichloride gives the corresponding malonic diester (m.p. = 132 °C, $[\alpha]_{589}^{20}=+31.4°$; >80% yield), which, by reaction with (*E*)-1,4-dichloro-2-butene (analogously to the preparation of **2c** according to ref. [5]), affords the diastereomers **5** (in 57% yield based on the malonic diester) and **2d** in a ratio of 92:8.[11,12] The sterically congested three-membered ring compound **5**, which can be smoothly separated from **2d**, is converted into *ent*-**2b** by ester hydrolysis followed by treatment of the resulting dicarboxylic acid with diazomethane (analogously to the preparation of **2b** according to ref. [5]). This procedure considerably simplifies the synthesis of enantiomerically pure **3**.[7]

The new chiral auxiliary **6** can be conveniently and more easily prepared than the chiral auxiliary (+)-8-phenylisomenthol **11**[2a,3b] by reduction of a mixture of (−)-8-phenylmenthone **7** and (+)-8-phenylisomenthone **8** with $NaBH_4$, and, therefore, **6** may be prepared from (*R*)-(+)-pulegone **9**; overall yield of **6**: 47%, based on **9** (85%).

[*] Prof. Dr. G. Quinkert, Dr. H.-G. Schmalz, Dipl.-Chem. E. M. Dzierzynski, Dr. G. Dürner, Dr. J. W. Bats
Institut für Organische Chemie der Universität
Niederurseler Hang, D-6000 Frankfurt am Main 50 (FRG)

[**] This work was supported by the Deutsche Forschungsgemeinschaft (project Qu 15-20), by the Bundesministerium für Wirtschaft (project AIF No. 5811), by the Fonds der Chemischen Industrie, and by Hoechst AG.

Table 1. Values of the specific optical rotation in $CDCl_3$.

Compd	1	6	7	8	10	11
$[\alpha]_D^{20}$ [°]	−32.8	+36.1	−63.7	+89.4	−46.3	+16.0
c [g/100 mL]	1.00	0.75	0.72	1.42	0.61	0.76

Table 1 shows the values of the specific optical rotation for the menthone and menthol derivatives mentioned.[14]

Experimental Procedure

The crude product (68 g) obtained by copper-catalyzed addition of phenylmagnesium bromide to **9** (≈85%, Fluka) and equilibration of the resulting mixture of **7** and **8** with a solution of ethanolic potassium hydroxide (before, 54/46; after, 84/16) [2a] was dissolved in 450 mL of dry methanol and 5.65 g of $NaBH_4$ was added in portions to the vigorously agitated solution at −7°C. The mixture was then stirred for 4 h, returning to room temperature. After addition of 85 mL of 2N hydrochloric acid and 70 mL of saturated aqueous ammonium chloride solution followed by the usual workup, 68 g of oily product was obtained, which, according to HPLC analysis, consisted mainly of the stereoisomeric alcohols **6**, **10**, and **1** (68 : 19 : 13). Preparative HPLC (isohexane/ethyl acetate = 10 : 0.8, repeated once) and kugelrohr distillation (0.04 torr/160°C bath temperature) afforded 32 g of **6**. [$[\alpha]_\lambda^{20}$ = +36.1 (589), +37.5 (578), +42.1 (546), +71.0 (436), +107.5 (365 nm) (c = 0.75 g/100 mL in $CHCl_3$)].

Received: June 16, 1986;
revised: July 15, 1986 [Z 1819 IE]
German version: *Angew. Chem. 98* (1986) 1023

[1] **1**: [(1*R*,2*S*,5*R*)-5-Methyl-2-(1-methyl-1-phenylethyl)cyclohexanol] was prepared according to the outlines in [2] and purified by HPLC.

[2] a) E. J. Corey, H. E. Ensley, *J. Am. Chem. Soc. 97* (1975) 6908; b) H. E. Ensley, C. A. Parnell, E. J. Corey, *J. Org. Chem. 43* (1978) 1610.

[3] a) H. Kipphardt, D. Enders, *Kontakte (Darmstadt) 1985*, (2) 37; b) J. K. Whitesell, C.-L. Liu, C. M. Buchanan, H.-H. Chen, M. A. Minton, *J. Org. Chem. 51* (1986) 551.

[4] The *R* chirality was determined by single crystal X-ray structure analysis on the salt prepared from one equivalent each of the acid **2a** and (−)-brucine: $[C_{23}H_{27}N_2O_4]^{\oplus}[C_7H_7O_4]^{\ominus} \cdot 2H_2O$ complex, orthorhombic, space group $P2_12_12_1$; a = 7.9247(6), b = 12.455(1), c = 28.719(3) Å; V = 2834.6(8) Å^3; M_r = 586.64, Z = 4, ρ_{calcd} = 1.377 g/cm^3; Enraf-Nonius CAD4 diffractometer; $Cu_{K\alpha}$ radiation, quadrant to 2θ = 110°, 1851 unique reflections with $I > \sigma(I)$; structure determination by direct methods. $R(F)$ = 0.039, w$R(F)$ = 0.040; SDP program. Further details of the crystal structure investigation may be obtained from the Fachinformationszentrum Energie, Physik, Mathematik GmbH, D-7514 Eggenstein-Leopoldshafen 2 (FRG), on quoting the depository number CSD-51965, the names of the authors, and the journal citation.

[5] G. Quinkert, U. Schwartz, H. Stark, W.-D. Weber, F. Adam, H. Baier, G. Frank, G. Dürner, *Liebigs Ann. Chem. 1982*, 1999.

[6] H. Baier, G. Dürner, G. Quinkert, *Helv. Chim. Acta 68* (1985) 1054.

[7] G. Quinkert, F. Adam, G. Dürner, *Angew. Chem. 94* (1982) 866; *Angew. Chem. Int. Ed. Engl. 21* (1982) 856; *Angew. Chem. Suppl. 1982*, 1777.

[8] Concerning the 24 syntheses of **3**, *rac*-**3**, or **3**/*ent*-**3** ≠ **1** carried out so far, see *SYNFORM 1* (1983) 33; *3* (1985) 125.

[9] G. Quinkert in W. Bartmann, B. M. Trost (Eds.): *Selectivity–a Goal for Synthetic Efficiency*, Verlag Chemie, Weinheim 1984, p. 213.

[10] G. Quinkert, H. Stark, *Angew. Chem. 95* (1983) 651; *Angew. Chem. Int. Ed. Engl. 22* (1983) 637.

[11] According to HPLC, the diastereomeric mixture consists of **5** and **2d** in a ratio of 92 : 8. According to HPLC analysis (in the presence of $Eu(tfc)_3$ in $CDCl_3$ at room temperature) and the specific optical rotation in CCl_4, the mixture of enantiomeric dimethyl esters obtained therefrom consists of *ent*-**2b** and **2b** in a ratio of 11.8 : 1.

[12] The chirality transfer by means of cyclopropanation has so far proved useful in the preparation of the synthetic building blocks **2c** (and **4a** in a ratio of 98 : 2 [6]), **5** (and **2d** in a ratio of 92 : 8), and **2e** (and **4b** in a ratio of 84 : 16 [13]).

[13] G. Quinkert, H.-G. Schmalz, E. Walzer, S. Groß, G. Dürner, J. W. Bats, *Angew. Chem. 98* (1986) 732; *Angew. Chem. Int. Ed. Engl. 25* (1986) 732.

[14] All compounds reported herein were fully characterized by correct elemental analyses and complete spectroscopic data.

Crystal Structure of Cl_2O_6**

By *Klaus M. Tobias* and *Martin Jansen**

With the exception of iodine(v) oxide, the halogen oxides have positive enthalpies of formation. Despite (or because of?) the resulting instability (decomposition and disproportionation) this class of substances has been the subject of intensive investigation.[1] Nonetheless, there are still large gaps in our knowledge of the chemistry of such compounds. For instance, reliable data on the molecular structures are often lacking, so that systematic classification of these compounds and discussion of their bonding properties is not possible. To date, only the crystal structure of I_2O_5 has been determined.[2]

Of particular interest are halogen oxides with even-numbered oxidation states of the halogen atom, since these compounds have—at least for the monomer in each case—an odd total number of electrons. For the chlorine oxides, this is the case for ClO_3 (or Cl_2O_6) besides ClO_2. There is no uniform agreement as to the structure of Cl_2O_6. Depending on the state of aggregation and the method of detection, the following species have been proposed: a pyramidal monomer,[3] a symmetrical dimer which contains a Cl–Cl bond or is doubly μ-oxo-bridged,[4] an unsymmetrical dimer (mixed anhydride),[1a] and an ionic mixed-valent dimer ($ClO_2^+ClO_4^-$).[5] The ionic mixed-valent dimer formulation is supported, in particular, by the chemical action of Cl_2O_6 as a source of perchlorate groups, for example in the preparation of anhydrous perchlorates.[1a,6] We report here on the unambiguous structural characterization of Cl_2O_6 in the crystal.

Cl_2O_6[7] was prepared, according to a modified version of the classical procedure of *Bodenstein* et al.,[8] from ClO_2 and O_3. The yields can be significantly improved by combining the two gases by means of a Daniel's valve and by filling the reaction volume with Raschig rings, which results in good mixing of the two gases and a prolonging of the time the two compounds spend in the reaction zone. The crude product was purified by fractional condensation. The pure Cl_2O_6 so obtained is a crystalline, transparent red-brown solid. It reacts violently with water and with oxidizable substances, but can be stored safely at below −30°C. The crystallization was carried out by subliming pure Cl_2O_6 onto a cold finger (−2°C → −25°C), which results in the formation of coarse single crystals. For the X-ray structure analysis, the single crystals (m.p. = 3°C) were sealed under inert gas in Lindemann tubes.

The crystal structure analysis[9] shows unequivocally that Cl_2O_6 exists in the solid state as ionic chlorylperchlorate, $ClO_2^+ClO_4^-$. To a first approximation, the ions can be described as being "isolated." Their centers of gravity are arranged nearly as in the CsCl type of structure. The ClO_2^+ dipoles are oriented ferroelectrically. This polar arrangement is reflected in a similar orientation of the ClO_4 tetrahedra, one of the threefold axes being directed in each case toward [001] (compare Fig. 1).

Within the limits of error, the ClO_2^+ *ion has* C_{2v} symmetry (for structure data, see Fig. 1). Bond lengths and angles are in good agreement with those determined for ClO_2GeF_5;[10] compared with ClO_2 in the gaseous state (147.5(3) pm, 117.7(1.7)°), the Cl–O distance is considera-

[*] Prof. Dr. M. Jansen, Dipl.-Chem. K. M. Tobias
Institut für Anorganische Chemie der Universität
Callinstrasse 9, D-3000 Hannover 1 (FRG)

[**] This work was supported by the Fonds der Chemischen Industrie and the Deutsche Forschungsgemeinschaft.

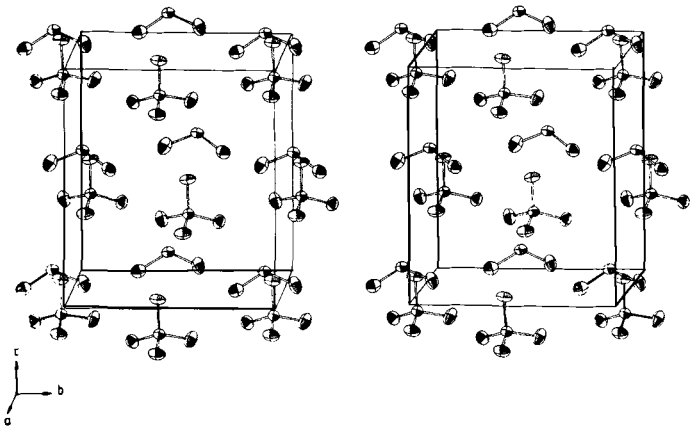


Fig. 1. Stereoview of the crystal structure of Cl_2O_6. Cl1 as well as O1 and O2 belong to ClO_2^+, Cl2 and O3-O6 to ClO_4^-. Selected bond lengths [pm] and bond angles [°]: Cl1-O1 140.6(2), Cl1-O2 141.0(2), Cl2-O3 146.7(2), Cl2-O4 143.0(2), Cl2-O5 145.7(3), Cl2-O6 141.7(3); O1-Cl1-O2 118.9(3), O-Cl2-O 108.0-110.8.

bly reduced. Since one electron is removed from an antibonding orbital in going from ClO_2 to ClO_2^+, a shortening of the Cl-O bond length would be expected, although not by this amount (Fig. 1). On the other hand, the widening of the bond angle relative to that in ClO_2—likewise expected[11]—is small (1.2°). The average of the bond lengths in the ClO_4^- ion (144.2 pm) is in agreement with expectations; however, the deviation of the individual values lies significantly above the experimental error. An association of cations and anions is suggested by the observation that precisely those oxygen atoms that have the smaller intermolecular distances to the chlorine atom in ClO_2^+ (250 and 251 pm) also have the (significantly) larger Cl-O distances in the ClO_4^- ion (146 and 145 pm). This certainly weak interaction cannot be viewed as a precursor for symmetrically μ-oxo-bridged dimers since each cation is linked with two anions (and vice versa) to form polymeric chains.

Since Cl_2O_6 undergoes sublimation, a transport as the ion pair $ClO_2^+ClO_4^-$ is unlikely, and a molecular monomeric or dimeric structure is therefore expected for gaseous Cl_2O_6. In fact, we found that a mixed anhydride of the chloric and perchloric acid is present in the gas phase.[12]

Received: June 26, 1986 [Z 1831 IE]
German version: *Angew. Chem. 98* (1986) 994

CAS Registry number:
Cl_2O_6, 104834-96-0.

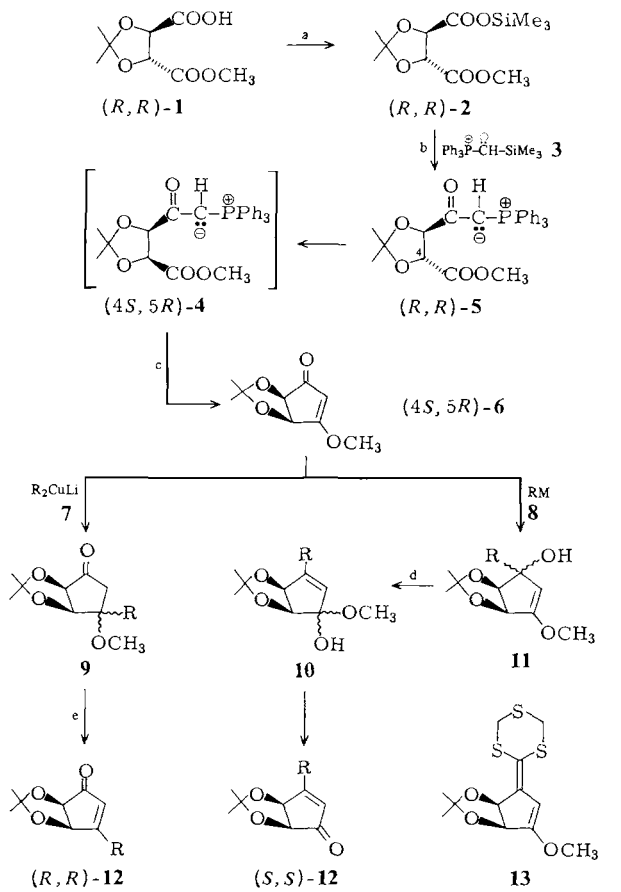
[1] a) M. Schmeisser, K. Brändle, *Adv. Inorg. Chem. Radiochem. 5* (1963) 41; b) O. H. Ellestad, T. Woldbaek, A. Kjekshus, P. Kleboe, K. Selte, *Acta Chem. Scand. A 35* (1981) 155; K. Selte, A. Kjekshus, *ibid. 22* (1968) 3309; J.-L. Pascal, A. C. Pavia, J. Potier, M. A. Potier, *C. R. Acad. Sci. 279* (1974) 43; J.-L. Pascal, A. C. Pavia, J. Potier, *ibid. 282* (1976) 53; J.-L. Pascal, J. Potier, *J. Chem. Soc. Chem. Commun. 1973*, 446; C. Campbell, J. P. M. Jones, J. J. Turner, *Chem. Commun. 1968*, 888; R. C. Loupec, J. Potier, *J. Chim. Phys. Phys.-Chim. Biol. 80* (1983) 449.
[2] K. Selte, A. Kjekshus, *Acta Chem. Scand. 24* (1970) 1912.
[3] C. F. Goodeve, F. A. Todd, *Nature (London) 132* (1933) 514.
[4] J.-L. Pascal, A. C. Pavia, J. Potier, J. M. Beny, B. Sombet, *Proc. Int. Conf. Raman Spectrosc. 6th, 2* (1978) 54.
[5] A. C. Pavia, J.-L. Pascal, A. Potier, *C. R. Acad. Sci. 272* (1971) 1495.
[6] J.-L. Pascal, J. Potier, C. S. Zhang, *J. Chem. Soc. Dalton Trans. 2 1985*, 297; *C. R. Acad. Sci. 298* (1984) 579.
[7] **Caution!** Cl_2O_6 reacts explosively with organic substances.
[8] M. Bodenstein, P. Harteck, E. Padlet, *Z. Anorg. Allg. Chem. 147* (1925) 233.
[9] *Cc*; $a = 556.3(2)$, $b = 861.3(3)$, $c = 978.5(3)$ pm, $\beta = 100.56(5)°$, $Z = 4$; Siemens AED2 four-circle diffractometer; $Mo_{K\alpha}$; data collected at −70°C, 666 unique structure factors, 661 with $F > 3\sigma(F)$; $R = 0.028$, $R_w = 0.025$. Further details of the crystal structure investigation may be obtained from the Fachinformationszentrum Energie, Physik, Mathematik GmbH, D-7514 Eggenstein-Leopoldshafen 2 (FRG), on quoting the depository number CSD-52047, the names of the authors, and the journal citation.
[10] T. E. Mallouk, B. Desbat, N. Bartlett, *Inorg. Chem. 23* (1984) 3160.
[11] A. D. Walsh, *J. Chem. Soc. 1953*, 2266.
[12] M. Jansen, K. M. Tobias, H. Willner, *Naturwissenschaften*, in press.

Optically Active Cyclopentanediol Synthetic Building Blocks from Tartaric Acid

By *Hans Jürgen Bestmann** and *Thomas Moenius*

Dedicated to Professor Vladimir Prelog on the occasion of his 80th birthday

Optically active hydroxylated cyclopentanes are of general interest as building blocks for the synthesis of cyclopentanoid natural products.[1] We report here a route to enantiomerically pure cyclopentanediol derivatives starting from tartaric acid (Scheme 1).



Scheme 1. a) 1. NaH, 2. $ClSiMe_3$, 95% yield of **2**, $[\alpha]_D$ −53.7° (THF, $c = 0.5$ g/100 mL), b.p. = 65°C/0.05 torr. b) Elimination of $Me_3SiOSiMe_3$, 56% yield of **5**, $[\alpha]_D$ −59.0° (methanol, $c = 0.5$ g/100 mL), m.p. = 121°C. c) 56% yield (based on **5**) of **6**, $[\alpha]_D$ +50.0° (methanol, $c = 0.5$ g/100 mL), m.p. = 91°C. d) $H^{\oplus}$. e) Na_2CO_3.

[*] Prof. Dr. H. J. Bestmann, Dr. T. Moenius
Institut für Organische Chemie der Universität Erlangen-Nürnberg
Henkestrasse 42, D-8520 Erlangen (FRG)

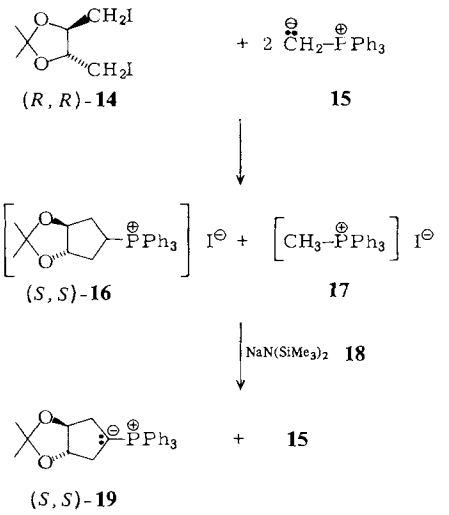
The known acetonide **1** of the monomethyl ester of (*R*,*R*)-(−)-tartaric acid[2] can be converted, via its sodium salt,[3] into the methyl trimethylsilyl ester **2**, which reacts in turn with the phosphorane **3** to give the acyl ylide **5**.[4] Heating of **5** for eight days in refluxing toluene leads to inversion at C4; the diastereomer **4** was detected by NMR spectroscopy. This diastereomerization is followed by an intramolecular Wittig reaction at the ester carbonyl group[5] to give the acetonide **6** of (4*S*,5*R*)-4,5-dihydroxy-2-cyclopentenone. The *cis* ring junction of the two five-membered rings in **6** could be shown by NOE ^{1}H-NMR experiments (identical interaction of a ketalic CH_3 group with both H atoms on C4 and C5). Further NMR investigations with optically active europium shift reagents show that, within the limits of error of this method, **6** is enantiomerically pure.[6] It is possible, in this way, to prepare **6** on a 5–10-g scale from inexpensive (*R*,*R*)-tartaric acid.—Starting from (*S*,*S*)-(+)-**1**, (4*R*,5*S*)-**6** may be prepared via (*S*,*S*)-**2** and (*S*,*S*)-**5**. The $[\alpha]_D$ values correspond to one another at each stage.

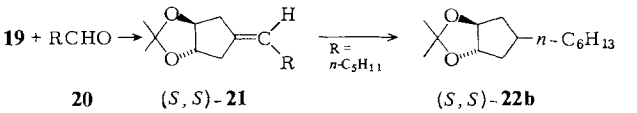
Compound **6** is a key synthetic intermediate. Regioselective 1,2 or 1,4 addition of organometallic compounds opens up the posssibility of obtaining the acetonide **12** enantioselectively from 3-alkyl-4,5-dihydroxy-2-cyclopentenones.

The reaction of **6** with strongly nucleophilic organometallic compounds **8** results in 1,2 addition to the carbonyl group to give compounds **11**. They are obtained as mixtures of diastereomers in which one component predominates; because of the lability of the compounds, it was not possible to make a definitive assignment of the main isomer. Proton catalysis results in the conversion of **11** into the compounds (*S*,*S*)-**12**, presumably via allyl rearrangement and the intermediacy of the nonisolable semiketal **10**.[7] The product was shown to be enantiomerically pure by NMR spectroscopy.[6] The results are presented in Table 1. Particularly noteworthy is the interesting change in $[\alpha]_D$ with increasing steric bulk of the group R. Proton-catalyzed elimination of water results in the formation of the ketene dithioacetal **13** from **11e** (Table 1).

Compound **6** undergoes 1,4 addition with the weakly nucleophilic lithium organocuprate **7**. Hydrolytic workup gives the compounds **9**, in which one diastereomer predominates. Base-catalyzed elimination of methanol leads once again to **12**. Since the allyl rearrangement does not occur in this case, one obtains the (*R*,*R*) enantiomer of **12**, whose optical purity was established by NMR spectroscopy.[6] The optical purity is also revealed in the $[\alpha]_D$ values of (*R*,*R*)-**12b** and (*R*,*R*)-**12d** (Table 1).

By selecting different nucleophilic organometallic compounds with the same R group—**7** or **8**—it is thus possible to synthesize selectively, via **6**, the optically pure enantiomers (*R*,*R*)- or (*S*,*S*)-**12** starting from inexpensive (*R*,*R*)-tartaric acid.





Scheme 2. (*S*,*S*)-**21a**, R = Ph, yield 38%, b.p. = 106 °C/0.05 torr (kugelrohr), $[\alpha]_D$ + 31.9° (methanol, *c* = 1.0 g/100 mL); (*S*,*S*)-**21b**, R = *n*-C_5H_{11}, yield 43%, b.p. = 80 °C/0.05 torr (kugelrohr), $[\alpha]_D$ + 113.8° (methanol, *c* = 1.5 g/100 mL); (*S*,*S*)-**22b**, yield 92%, b.p. = 75 °C/0.05 torr (kugelrohr).

Further, using the method described earlier by us,[8] we have carried out the reaction of the (*R*,*R*)-(−)-bisiodide **14**,[9] which is readily accessible from tartaric acid, with methylenetriphenylphosphorane **15** in a molar ratio of 1 : 2 (Scheme 2). This reaction resulted in the formation of a mixture of the phosphonium iodides (*S*,*S*)-**16**[10] and **17**, which are converted into the phosphonium ylides **19** and **15** by reaction with sodium bis(trimethylsilyl)amide **18**. Reaction of the mixture of **19** and **15** with the aldehydes **20** results in the formation, by Wittig reaction, of a mixture consisting of the cyclopentanediol derivatives **21**, with exocyclic double bond, and the unsaturated compounds (from **15**), which can be easily separated by distillation (Scheme 2). According to the ^{1}H-NMR spectra, only *one* diastereomer of **21** is present. On the basis of the optical activity of **21**, it is not possible to decide whether the two five-membered rings of **21** are *cis*- or *trans*-linked; the *trans* arrangement is demonstrated, however, by the formation of the hydrogenation product **22b** (Scheme 2). Compound **22b** is an optically active, diastereomerically pure acetal with $[\alpha]_D$ + 21.8° (methanol, *c* = 1.5 g/100 mL). For the *cis* arrangement, the hydrogenation product would have been achiral.

Table 1. Reaction of (4*S*,5*R*)-**6** to give (*S*,*S*)-**12** via **11** (above) and to give (*R*,*R*)-**12** via **9** (below).

	8		**11**			(*S*,*S*)-**12**	
	R	M	Yield [%]	B.p./0.05 torr [°C] [a]	Yield [%]	B.p./0.05 torr [°C] [a]	$[\alpha]_D$ [°] [b]
a	H	$AliBu_2$	90	49	62	50–55	−33.0
b	Me	Li	72	53–57	56	50–55	− 5.7
c	Et	MgBr	72	56–60	72	50–60	+ 8.0
d	*n*Bu	Li	78	57–62	78	55–60	+15.2
e	[c]	Li	75	[d]	[e]		
	7		**9**			(*R*,*R*)-**12**	
	R		Yield [%]	B.p./0.05 torr [°C] [a]	Yield [%]	B.p./0.05 torr [°] [a]	$[\alpha]_D$ [°] [b]
b	Me		75	55–60	64	50–55	+ 5.9
d	*n*Bu		72	60–65	68	65–70	−15.3

[a] Air temperature for the kugelrohr distillation. [b] In methanol, *c* = 0.5 g/100 mL. [c] 1,3,5-Trithia-2-cyclohexyl. [d] M.p. = 65–68 °C. [e] **11e** affords **13**, yellow crystals, yield 53%, m.p. = 107 °C (dec.), $[\alpha]_D$ + 285.1° (methanol, *c* = 0.5 g/100 mL).

Received: June 26, 1986;
revised: July 30, 1986 [Z 1832 IE]
German version: *Angew. Chem.* 98 (1986) 1007

CAS Registry numbers:
(*R*,*R*)-**1**, 67812-33-3; (*S*,*S*)-**1**, 67844-12-6; (*R*,*R*)-**2**, 104738-65-0; (*S*,*S*)-**2**, 104832-17-9; **3**, 3739-97-7; (4*S*,5*R*)-**4**, 104738-66-1; (*R*,*R*)-**5**, 104832-18-0; (*S*,*S*)-**5**, 104832-19-1; (4*R*,5*S*)-**6**, 104738-67-2; (4*S*,5*R*)-**6**, 104832-20-4; **9b**, 104738-68-3; **9d**, 104738-69-4; **11a**, 104738-70-7; **11b**, 104738-71-8; **11c**, 104738-72-9; **11d**, 104738-73-0; **11e**, 104738-74-1; (*S*,*S*)-**12a**, 104010-72-2; (*R*,*R*)-**12b**, 104738-75-2; (*S*,*S*)-**12b**, 104832-21-5; (*S*,*S*)-**12c**, 104738-76-3; (*R*,*R*)-**12d**, 104738-77-4; (*S*,*S*)-**12d**, 104832-22-6; **13**, 104738-78-5; (*R*,*R*)-**14**, 58342-57-7; **16**, 104738-79-6; **17**, 2065-66-9; (*S*,*S*)-**19**, 104738-80-9; (*S*,*S*)-**21**, 104738-81-0; (*S*,*S*)-**21a**, 104738-82-1; (*S*,*S*)-**22b**, 104738-83-2; $H_2C=PPh_3$, 3487-44-3; *n*-$C_5H_{11}CHO$, 66-25-1; PhCHO, 100-52-7.

[1] M. Harre, P. Raddatz, R. Valenta, E. Winterfeldt, *Angew. Chem. 94* (1982) 496; *Angew. Chem. Int. Ed. Engl. 21* (1982) 496; R. Noyori, M. Suzuki, *ibid. 96* (1984) 854 and *23* (1984) 847.
[2] J. A. Musich, H. Rapoport, *J. Am. Chem. Soc. 100* (1978) 4865.
[3] L. Hinsworth, Y. N. Kuo, *J. Organomet. Chem. 46* (1972) 73.
[4] H. J. Bestmann, R. Riemer, unpublished results.
[5] Cf. H. J. Bestmann, G. Schade, H. Lütke, T. Moenius, *Chem. Ber. 118* (1985) 2640.
[6] The ^{1}H-NMR experiments were carried out in $CDCl_3$ with tris[3-(2,2,2-trifluoro-1-hydroxyethylidene)-*d*-camphorato]europium as chiral shift reagent. There was no evidence for the presence of racemic components.
[7] M. Stiles, L. Longroy, *J. Org. Chem. 32* (1967) 1095.
[8] H. J. Bestmann, E. Kranz, *Chem. Ber. 102* (1969) 1802.
[9] J. M. Townsend, J. F. Blound, R. C. Sun, S. Zavoiski, D. Valentin, *J. Org. Chem. 85* (1980) 2995.
[10] The change in numbering results from the change in priority of the ligands at the chiral C atoms. A change in configuration has not occurred.

$NaNb_3O_5F$—A Niobium-Niobium Triple Bond with "Side-On" Coordination by Nb Atoms

By *Jürgen Köhler* and *Arndt Simon**

The halides and chalcogenides of transition metals in low oxidation states often contain metal-metal bonds occurring in isolated or condensed clusters.[1] The number of such cluster compounds is still small in the case of oxides and fluorides. A relatively large number are known for molybdenum (e.g., $LiZn_2Mo_3O_8$, $Ba_{1.14}Mo_8O_{16}$, $NaMo_4O_6$, $Ca_{5.45}Mo_{18}O_{32}$, $Sc_{0.5}Zn_{1.25}Mo_4O_8$,[2] $In_{11}Mo_{40}O_{62}$,[3a,b] $In_3Mo_{11}O_{17}$[3c]), but only a few examples have been observed for the neighboring elements ($Mg_3Nb_6O_{11}$,[4] La_2ReO_5,[5] $La_4Re_6O_{19}$,[6] $Nd_4Re_2O_{11}$,[7] $Mn_3Nb_6O_{11}$,[8] $BaRuO_3$[9]). In the alkali-metal oxoniobates $LiNbO_2$[10a] and $NaNbO_2$,[10b] short Nb-Nb distances are found within the NbO_2^- layers (isostructural with MoS_2), suggesting M-M bonds.[11]

The occurrence of discrete Nb_6X_{12} clusters in Nb_6F_{15}[12] and in $Mg_3Nb_6O_{11}$ has prompted the search for comparable compounds with niobium oxide fluorides. To date, only $ANbO_2F$ (A = Li, Na, K)[13] and the always oxygen-containing "NbF_3"[14] have been described.

By addition of NaF to the repeatedly studied system Na_2O-Nb-Nb_2O_5,[10b,15] it is possible, among other things, to vary the number of electrons available for the Nb-Nb bonds by means of the O/F ratio. In this way, a new oxide fluoride is obtained as a crystalline component of an always heterogeneous reaction product (see Experimental Procedure). The reaction aimed at the composition $NaNb_3O_5F$ has the highest yields. A pure oxide, $NaNb_3O_6$, cannot be synthesized, even in traces, despite wide variation of the experimental conditions.

A differentiation between O and F atoms is neither possible by crystal structure analysis[16] nor by MAPLE calculations[17] or bond length-bond strength considerations[18] on the basis of the positional parameters found. For simplicity, therefore, the formula "$NaNb_3X_6$" with X = O, F will be used in the discussion of the crystal structure (compare Table 1).

Table 1. Motifs of mutual adjunction [a] in $NaNb_3O_5F$ ($NaNb(1)Nb(2)_2X(1)X(2)X(3)_4$). C.N. = coordination number.

	X(1)	X(2)	4X(3)	C.N.
Na	2/2	2/2	4/1	8
Nb(1)	—	—	4/1	4 + Nb(1) (261.4 pm)
2 Nb(2)	1/2	1/2	4/2	6
C.N.	4	4	4	

[a] R. Hoppe, *Angew. Chem. 92* (1980) 106; *Angew. Chem. Int. Ed. Engl. 19* (1980) 110.

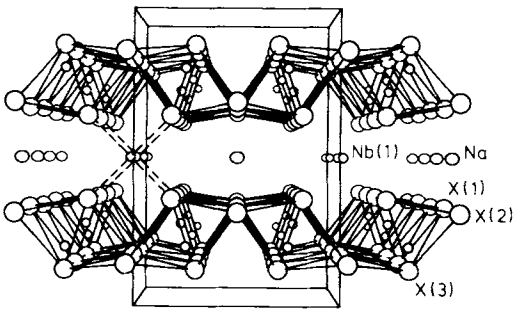


Fig. 1. $NaNb_3O_5F$, perspective drawing of the crystal structure along [001]. The layers formed from linked $Nb(2)X_6$ octahedra, as well as a $Nb(1)_2X_8$ arrangement, are graphically emphasized.

The structure (Fig. 1) contains chains of $Nb(2)X_6$ octahedra, which are *trans*-edge-linked via X(3) atoms and vertex-linked via X(1) and X(2) to form folded layers of composition $^2_\infty[NbX_{1/2}X_{1/2}X_{4/2}] = NbX_3$. Rows of Nb(1) and Na atoms are inserted between the layers. Whereas the Na atoms exhibit regular spacing, the distances between the Nb(1) atoms alternate along the chains leading to Nb-Nb pairs with the shortest distance known, $d_{Nb\text{-}Nb} = 261.4$ pm.

A $[Nb_2X_8]$ group (Fig. 2, left) is formed with the surrounding X(3) atoms. Such groups are found for molecular species, e.g., $[Re_2Cl_8]^{2-}$, as well as in the crystal structure of the ternary oxide $La_2ReO_5 = La_4O_2[Re_2O_8]$. Short Nb-Nb distances in Nb_2 pairs (though with intramolecular ligands) are known for $Cs_3Nb_2Cl_9$ (270 pm, double bond)[19] and $[Nb_2(CO)_2Cp_2(C_2R_2)]$ (R = CH_3CO_2) (273 pm, single bond).[20]

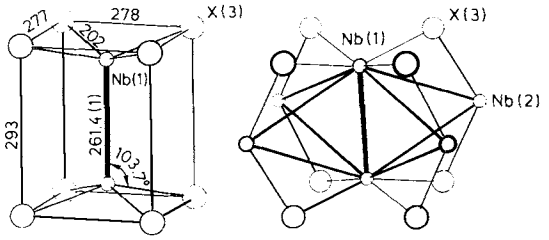


Fig. 2. Left: $[Nb_2X_8]$ subunit in $NaNb_3O_5F$. Interatomic distances are given in pm. Right: $[Nb_2Nb_4X_8]$ subunit in $NaNb_3O_5F$ with the $Nb(1)_2$ dumbbell [d(Nb(1)-Nb(1) = 261.4 pm] and the "side-on" bonded Nb(2) atoms [d(Nb(2)-Nb(1)) = 309 pm, d(Nb(2)-Nb(2)) = 327 pm and 456 pm].

[*] Prof. Dr. A. Simon, Dr. J. Köhler
Max-Planck-Institut für Festkörperforschung
Heisenbergstrasse 1, D-7000 Stuttgart 80 (FRG)

Comparative bond length-bond strength calculations[18] for NbO_2 and $NaNb_3O_5F$ show that the Nb(2) atoms are present in the +4 oxidation state. Thus, a formal charge of −12 is obtained for the $[Nb_2X_8]$ unit with Nb(1) in the oxidation state +2. In analogy to molecular species, e.g., $Mo_2(OR)_6$,[21] a $\sigma^2\pi^4$ triple bond comes into question for the Nb–Nb dumbbell.

However, Figure 2, right, indicates that each Nb_2 pair in the structure of $NaNb_3O_5F$ is "side-on" coordinated by four Nb^{4+} ions. The Nb^{4+} ions are displaced by about 15 pm from the centers of gravity of the (distorted) coordination octahedra in the direction of an edge X(3)–X(3) toward the Nb_2 dumbbell [d(Nb(1)–Nb(2))=309 pm, distance to the center of gravity of the dumbbell 281 pm)]. The d^1 ion Nb^{4+} apparently tends to engage in metal-metal bonding as observed in the structures of the tetrahalides NbX_4 (X=Cl, Br, I).[1a,22] For $NaNb_3O_5F$ these bonds can be regarded as two-electron three-center bonds between Nb^{4+} ($d_{x^2-y^2}$) and π orbitals of the Nb_2 dumbbell; other configurations are also conceivable. The diamagnetism found for $NaNb_3O_5F$ is in agreement with the assumption of a spin pairing of all ten valence electrons in the resulting [1.1.1.1]propellane-Nb_6 cluster, but is not a proof for this idea of bonding, since $NaNbO_2F$[13] also does not show the magnetism for a d^1 configuration.

It is remarkable that the arrangement $M_2M_4X_8$ (Fig. 2, right) is also found in the structure of Gd_2Cl_3,[23] although as part of an infinite chain. The electronic band structure calculated for the chain can also be interpreted in terms of the presence of $\sigma^2\pi^4$-bonded Gd_2 pairs, which form Gd–Gd bonds in the direction of the chain via their π systems.[24]

Experimental Procedure

Dried NaF (p.A Merck) was ground into a mass with Nb powder (LAB, Merck) and Nb_2O_5 (Merck, Patinal®) and placed in a corundum crucible. This was fused under argon in a quartz ampoule and annealed for 3 d at 800°C. In addition to NbO, NbO_2, and oxide fluorides (e.g., $NaNbO_2F$), black, metallic appearing, parallelepiped-shaped single crystals of $NaNb_3O_5F$ were formed. By repeated grinding, compression, and annealing of a tablet containing NaF, Nb, and Nb_2O_5 (molar ratio 1.2 : 1 : 1; each 1 d at 750°C), $NaNb_3O_5F$ in ca. 80% yield was obtained. Such a product, washed with hydrochloric acid, contained 5.6% F. This value exceeds the calculated one for $NaNb_3O_5F$ (4.7%) by only 0.9% and can be explained by the higher F content for the side products, e.g., $NaNbO_2F$ (11.4% F).

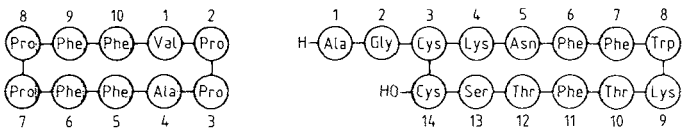
Received: June 27, 1986;
revised: August 21, 1986 [Z 1833 IE]
German version: *Angew. Chem. 98* (1986) 1011

[1] a) H. Schäfer, H. G. Schnering, *Angew. Chem. 76* (1964) 833; b) A. Simon, *ibid. 93* (1981) 23; *Angew. Chem. Int. Ed. Engl. 20* (1981) 1.
[2] R. E. McCarley, K.-H. Lii, P. A. Edwards, L. F. Brough, *J. Solid State Chem. 57* (1985) 17.
[3] a) A. Simon, H. Mattausch, E.-M. Peters, *Z. Kristallogr. 174* (1986) 188; b) H. Mattausch, A. Simon, E.-M. Peters, *Inorg. Chem. 25* (1986) 3428; c) A. Simon, M. Mertin, H. Mattausch, R. Gruehn, *Angew. Chem. 98* (1986) 831; *Angew. Chem. Int. Ed. Engl. 25* (1986) 845.
[4] B. O. Marinder, *Chem. Scr. 11* (1977) 97.
[5] K. Waltersson, *Acta Crystallogr. Sect. B 32* (1976) 1485.
[6] N. L. Morrow, L. Katz, *Acta Crystallogr. Sect. B 24* (1968) 1466.
[7] K.-A. Wilhelm, E. Lagervall, O. Muller, *Acta Chem. Scand. 24* (1970) 3406.
[8] R. E. McCarley, private communication, 1985.
[9] P. C. Donohue, L. Katz, R. Ward, *Inorg. Chem. 4* (1965) 306.
[10] a) G. Meyer, R. Hoppe, *J. Less-Common Met. 46* (1976) 55; b) *Z. Anorg. Allg. Chem. 424* (1976) 128.
[11] J. K. Burdett, T. Hughbanks, *Inorg. Chem. 24* (1985) 1741.
[12] H. Schäfer, H. G. Schnering, K.-J. Niehaus, H. G. Nieder-Vahrenholz, *J. Less-Common Met. 9* (1965) 95.
[13] W. Rüdorff, D. Krug, *Z. Anorg. Allg. Chem. 329* (1964) 211.
[14] O. Ruff, E. Schiller, *Z. Anorg. Chem. 72* (1911) 329; P. Ehrlich, F. Pfloger, G. Pietzka, *Z. Anorg. Allg. Chem. 282* (1955) 19.
[15] C. C. Addison, M. G. Barker, R. M. Lintonbon, R. J. Pulham, *Spec. Publ. Chem. Soc. 22* (1967) 460.
[16] Space group *Immm* (No. 71), a=649.7(1), b=1030.5(1), c=711.8 pm, Z=4, Syntex R3 diffractometer; $Mo_{K\alpha}$; 338 reflections, of which 322 had $|F_0| \geq 3\sigma|F_0|$, R(aniso)=0.0193, R(w)=0.0197; ρ_{calcd}=5.58 g/cm³. On account of the similarity of the lattice constants it may be concluded that the phase $Ca_{0.75}Nb_3O_6$ (orthorhombic, a=711.2, b=1028.9, c=656.1 pm), characterized by electron diffraction, is isotypic with $NaNb_3O_5F$ (S. J. Hibble, A. K. Cheetham: *IIIrd European Conference on Solid State Chemistry, Book of Abstracts, Vol. 1*, Regensburg 1986, p. 136). Further details of the crystal structure investigation may be obtained from the Fachinformationszentrum Energie, Physik, Mathematik GmbH, D-7514 Eggenstein-Leopoldshafen 2 (FRG), on quoting the depository number CSD-51994, the names of the authors, and the journal citation.
[17] R. Hoppe, *Angew. Chem. 82* (1970) 7; *Angew. Chem. Int. Ed. Engl. 9* (1970) 25.
[18] I. D. Brown in M. O'Keeffe, A. Navrotsky (Eds.): *Structure and Bonding in Crystals, Vol. II*, Academic Press, New York 1981.
[19] A. Broll, H. G. Schnering, H. Schäfer, *J. Less-Common Met. 22* (1970) 243.
[20] A. I. Gusev, N. I. Kirillova, Ya. T. Struchkov, *Zh. Strukt. Khim. 11* (1970) 62.
[21] F. A. Cotton, R. A. Walton: *Multiple Bonds Between Metal Atoms*, Wiley, New York 1982.
[22] L. F. Dahl, D. L. Wampler, *Acta Crystallogr. 15* (1962) 946; R. E. McCarley, B. A. Torp, *Inorg. Chem. 2* (1963) 540.
[23] J. E. Mee, J. D. Corbett, *Inorg. Chem. 4* (1965) 88.
[24] P. W. Bullett, *Inorg. Chem. 19* (1980) 1780.

Conformational Prerequisites for the in vitro Inhibition of Cholate Uptake in Hepatocytes by Cyclic Analogues of Antamanide and Somatostatin**

By *Horst Kessler,* Mechtild Klein, Arndt Müller, Klaus Wagner, Jan Willem Bats, Kornelia Ziegler,* and *Max Frimmer*

It is well known[1] that liver cells are protected by antamanide **1**[2] against poisons such as ethanol, dimethyl sulfoxide (DMSO), cysteamine, or phalloidin,[3] a toxin isolated from the mushroom *Amanita phalloides*. In recent years a similar cytoprotective effect has also been found for somatostatin **2**,[4] a naturally occurring peptide hormone.[5] Biochemical in vitro investigations of **1** and **2** as



antamanide **1** somatostatin **2**

well as of their derivatives have shown that the cause of this biological effect is the inhibition of a transport system.[6] This system is responsible for the transport of cholate from blood into the bile and also for the detoxification of the blood via the bile.[6] Searching for a common structural feature for the activity of antamanide and somatostatin, we found that cyclic peptides containing the modified

[*] Prof. Dr. H. Kessler, M. Klein, Dr. A. Müller, K. Wagner, J. W. Bats
Institut für Organische Chemie der Universität
Niederurseler Hang, D-6000 Frankfurt am Main 50 (FRG)
Dr. K. Ziegler, Prof. Dr. M. Frimmer
Institut für Pharmakologie und Toxikologie
Mehrzweckinstitut der Universität
Frankfurter Strasse, D-6300 Giessen (FRG)

[**] This work was supported by the Fonds der Chemischen Industrie and the Deutsche Forschungsgemeinschaft.

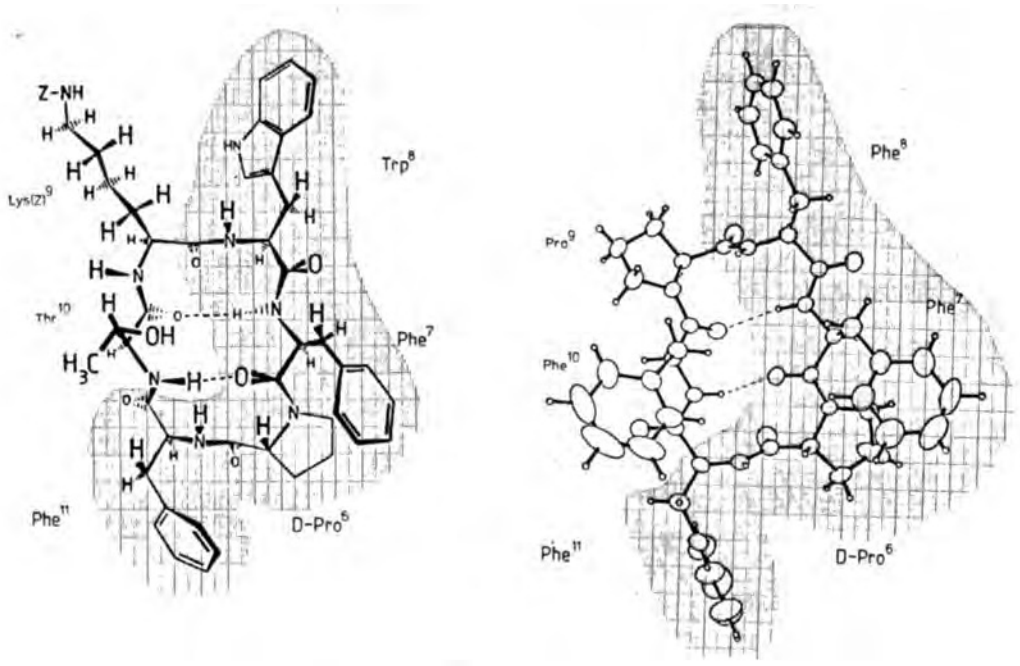


Fig. 1. Conformation of *cyclo*(-Phe-Thr-Lys(Z)-Trp-Phe-D-Pro-) **3** in DMSO (left) and *cyclo*(-Phe-Phe-Pro-Phe-Phe-D-Pro-) **5** in the crystal (right).

retro-sequence 6–11 of somatostatin[6] exhibit high cytoprotective activity. Figure 1 (left) shows the preferred conformation of the most effective peptide found so far

cyclo(-Phe-Thr-Lys(Z)-Trp-Phe-D-Pro-) **3**

(Z = benzyloxycarbonyl). The conformation was determined by means of 2D NMR methods[7] in DMSO solution.

The comparison of a number of cyclic peptides demonstrates that cytoprotective activity requires two adjacent aromatic amino acid residues. Activity is increased when an L-proline residue precedes this sequence or a D-proline residue follows (Table 1). Therefore, it was not surprising that cyclolinopeptide A **4**[8] (Table 1), which was isolated from linseed oil, also inhibits the uptake of cholate into hepatocytes. As far as we know, this is the first biological activity that has been found for this natural product.

Table 1. 50% Inhibition of cholate uptake in isolated hepatocytes by cyclopeptides [6].

No.	Peptide	Name	Concentration [μM]
2	H–Ala–Gly–Cys–Lys–Asn–**Phe→Phe→Trp** HO–Cys–Ser–Thr–Phe–Thr–Lys	Somatostatin	220
	Pro→Phe→D-Trp Phe–Thr–Lys	"Veberpeptide"	100
1	Phe–Pro–**Pro→Phe→Phe** Phe–Ala–Pro–Pro–Val	Antamanide	8
4	Val(Pro–**Pro→Phe→Phe**; Leu–Ile–Ile–Leu)	Cyclolinopeptide A	3
5	**D-Pro**–Phe–Phe **Phe**–**Phe**–Pro	"PFF"	3
3	**D-Pro**–Phe–Thr **Phe**–**Trp**–Lys(Z)	"008"	1.5

However, in addition to the sequence homology the spatial structure is also crucial for the biological effect.[9] To determine the conformational requirements *cyclo*(-Pro-Pro-Phe-Phe-Gly-) was synthesized. The conformation of this homologue of antamanide and cyclolinopeptide A was studied in solution.[10] The spatial arrangement of the backbone and the side chains of the two phenylalanine residues strongly differs from the conformations of the bioactive cyclopeptides mentioned above.[11,12] As expected, this cyclopentapeptide does not exhibit cytoprotective activity. In contrast, the crystal conformation of the sequence analogue of antamanide, *cyclo*(-Phe-Phe-Pro-Phe-Phe-D-Pro-) **5**,[13] agrees to a large extent with the conformation of **3** in solution (Fig. 1, right). Thus, in this peptide the constitutional and conformational requirements for biological activity are excellently fulfilled. Indeed, this compound strongly inhibits the uptake of cholate into hepatocytes (Table 1). Therefore, there is good reason to localize the hatched regions of the molecules **3** and **5**, shown in Figure 1, as that part of the peptide which is responsible for the biological activity. Computer-assisted molecular modeling will show whether other compounds affecting the cholate transport system will have the same spatial structure.

Received: June 27, 1986;
revised: July 10, 1986 [Z 1835 IE]
German version: *Angew. Chem. 98* (1986) 1030

[1] M. Frimmer, E. Petzinger, *Arzneim.-Forsch. 25* (1975) 1423.
[2] T. Wieland, G. Lüben, H. Ottenheym, J. Faesel, J. X. de Vries, W. Konz, A. Prox, J. Schmid, *Angew. Chem. 80* (1968) 209; *Angew. Chem. Int. Ed. Engl. 7* (1968) 204.
[3] T. Wieland, *Int. J. Pept. Protein Res. 22* (1983) 257.
[4] S. Raptis, J. Rosenthal, J. E. Gerich (Eds.): *Proc. 2nd Int. Symp. Somatostatin* (June 1-3, 1981, Athen (Greece)), Attempto Verlag, Tübingen 1984.
[5] S. Szabo, K. H. Usadel, *Experientia 38* (1982) 254.
[6] K. Ziegler, M. Frimmer, H. Kessler, I. Damm, V. Eiermann, S. Koll, J. Zarbock, *Biochim. Biophys. Acta 845* (1985) 86.
[7] H. Kessler, C. Griesinger, S. Koll, K. Wagner, unpublished results.
[8] H. P. Kaufmann, A. Tobschirbel, *Chem. Ber. 92* (1959) 2805; A. Prox, F. Weygand, *Peptides, Proc. 8th Eur. Pept. Symp.*, Noordwijle, Niederlande 1966, p. 158.

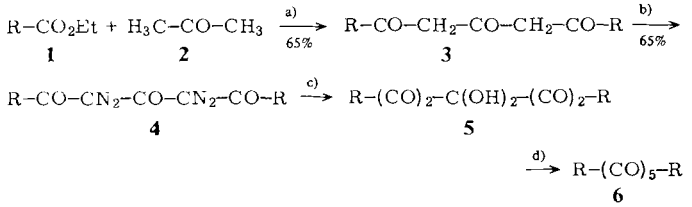
[9] H. Kessler, *Angew. Chem. 94* (1982) 509; *Angew. Chem. Int. Ed. Engl. 21* (1982) 512.
[10] H. Kessler, A. Müller, *Liebigs Ann. Chem.*, in press.
[11] A. Müller, *Dissertation*, Universität Frankfurt am Main 1986.
[12] M. Gehrke, *Diplomarbeit*, Universität Frankfurt am Main 1986.
[13] Crystal structure analysis of $5 \cdot 2CH_3OH \cdot H_2O$; triclinic, space group $P\bar{1}$; $a = 7.370(1)$, $b = 13.092(3)$, $c = 13.544(3)$ Å, $\alpha = 66.85(2)$, $\beta = 75.05(2)$, $\gamma = 76.07(2)°$; $V = 1146.6(3)$ Å^3; $Z = 1$, $\rho_{calcd} = 1.253$ g/cm^3; Enraf-Nonius CAD4 diffractometer; $Mo_{K\alpha}$ radiation, half-sphere up to $2\theta = 54°$, 4941 unique reflections with $I > \sigma(I)$; structure determination by direct methods; positions of hydrogens on the carbon framework calculated, all others determined from difference Fourier synthesis; structure refinement to $R(F) = 0.047$; SDP program. Further details of the crystal structure investigation may be obtained from the Fachinformationszentrum Energie, Physik, Mathematik GmbH, D-7514 Eggenstein-Leopoldshafen 2 (FRG), on quoting the depository number CSD-51982, the names of the authors, and the journal citation.

Vicinal Pentaketones**

By *Rolf Gleiter,* Gerhard Krennrich,* and *Michael Langer*

Dedicated to Professor Mordecai B. Rubin on the occasion of his 60th birthday

The kinetic stability decreases with increasing number of carbonyl groups in going from vicinal dicarbonyl to tricarbonyl to tetracarbonyl compounds. Vicinal tri- and tetraketones[1,2] react readily with water and rearrange in the presence of base, undergoing decarbonylation. Vicinal pentaketones have not yet been prepared. We report here on the synthesis (Scheme 1) and some properties of tBu(CO)$_5t$Bu **6a** and Ph(CO)$_5$Ph **6b**, the first vicinal pentaketones.



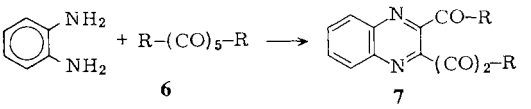
1 **2** **3** **4** **5** **6**

a, R = t-C$_4$H$_9$; **b**, R = C$_6$H$_5$

Scheme 1. a) NaH, monoglyme; b) p-CH$_3$–C$_6$H$_4$–SO$_2$N$_3$/Et$_3$N, CH$_3$CN; c) t-C$_4$H$_9$–OCl/HCOOH; d) P_2O_5, CHCl$_3$.

The readily available compounds 2,2,8,8-tetramethyl-3,5,7-nonanetrione **3a** and 1,5-diphenyl-1,3,5-pentanetrione **3b**[3] can be converted into the bisdiazo compounds **4a** and **4b**, respectively.[4] Reaction of these products with *tert*-butyl hypochlorite in formic acid[5] leads directly to the hydrates of the pentaketones **5a** and **5b**, respectively, which can be dehydrated to the deeply colored pentaketones **6a** and **6b**, respectively. Both pentaketones react smoothly with *o*-phenylenediamine to give the corresponding quinoxaline derivatives **7a** and **b**.

The most important spectroscopic data of **4**–**7** are given in Table 1. The electronic properties of the pentaketones fit in with their congeners having fewer CO groups. This is shown in Table 2 by comparison of the ionization energies of the lone pairs, the first reduction potentials, and the energies of the first bands of the UV/VIS spectra of the diphenylketones Ph(CO)$_x$Ph with x = 1–5. The first reduction potential decreases linearly with increasing x, while the first ionization energy and the energy of the first absorption band increase and level off to a final value.



6 **7**

a, R = t-C$_4$H$_9$; **b**, R = C$_6$H$_5$

Table 1. Spectroscopic data of **4**–**7** [6]. ^{1}H-NMR: 300 MHz, $CDCl_3$; ^{13}C-NMR: 75.46 MHz, $CDCl_3$; UV: CH_2Cl_2. DMSO = dimethyl sulfoxide.

4a: m.p. = 60–61 °C, yellow; IR (KBr): $\tilde{\nu} = 2105$, 1650 cm^{-1}; ^{1}H-NMR: $\delta = 1.28$; ^{13}C-NMR: $\delta = 195.9$ (s), 177.5 (s), 78.9 (s), 44.8 (s), 26.3 (q); UV: $\lambda_{max}(\varepsilon) = 381$ (186, sh), 290 (7900, sh), 238 nm (23600)

5a: m.p. = 64–65 °C, yellow; IR (KBr): $\tilde{\nu} = 3455$, 1725, 1700 cm^{-1}; ^{1}H-NMR: $d = 1.31$ (s, 18H), 4.76 (br. s, 2H); ^{13}C-NMR (DMSO): $\delta = 205.8$ (s), 187.8 (s), 93.6 (s), 42.3 (s), 25.7 (q); UV: $\lambda_{max}(\varepsilon) = 402$ nm (114)

5b: m.p. = 110–113 °C, yellow; IR (KBr): $\tilde{\nu} = 3460$, 1730, 1718, 1665 cm^{-1}; ^{1}H-NMR: $\delta = 5.0$ (2H, H/D, br.), 7.50–7.56 (4H, m), 7.67–7.73 (2H, m), 8.17–8.2 (4H, m); ^{13}C-NMR (DMSO): $\delta = 192.2$ (s), 191.5 (s), 135.6 (d), 132.4 (s), 130.1 (d), 129.5 (d), 95.5 (s); UV: $\lambda_{max}(\varepsilon) = 403$ (125), 284 nm (18900)

6a: IR (film): $\tilde{\nu} = 1734$, 1710, 1700 cm^{-1}; ^{13}C-NMR: $\delta = 204.9$ (s), 190.7 (s), 182.2 (s), 42.8 (s), 25.1 (q); UV: $\lambda_{max}(\varepsilon) = 559$ (96), 436 (101), 352 nm (sh, 196)

6b: ^{13}C-NMR: $\delta = 190.1$ (s), 188.4 (s), 182.4 (s), 136.0 (d), 131.3 (s), 130.7 (d), 129.2 (d); UV/VIS: $\lambda_{max}(\varepsilon) = 547$ (130), 437 nm (154)

7a: m.p. = 64–65 °C, yellow; IR (KBr): $\tilde{\nu} = 1710$, 1695, 1670 cm^{-1}; ^{1}H-NMR: $\delta = 1.41$ (s, 9H), 1.47 (s, 9H), 7.86–7.98 (m, 2H), 8.18–8.23 (m, 2H); UV: $\lambda_{max}(\varepsilon) = 425$ (100), 315 nm (7300)

7b: m.p. = 125–126 °C, yellow; IR (KBr): $\tilde{\nu} = 1710$, 1665, 1650 cm^{-1}; ^{1}H-NMR: $\delta = 7.45$–7.6 (m, 4H), 7.6–7.7 (m, 2H), 7.87–8.02 (m, 2H), 8.05–8.2 (m, 4H), 8.2–8.3 (m, 2H); UV: $\lambda_{max}(\varepsilon) = 402$ (sh, 124), 320 (sh, 9100), 261 nm (43600)

Table 2. Comparison between the ionization energies of the lone pairs, the first reduction potentials, and the energies of the first UV/VIS bands of the diphenyl ketones Ph(CO)$_x$Ph with x = 1–5.

Compound	$I_{v,j}$ [eV]					$E_1^{1/2}$ [V] [a]	λ_{max} [nm] (ε)
	n_1	n_2	n_3	n_4	n_5		
PhCOPh	9.4	—	—	—	—	< −2.0	337 (150) [2a]
Ph(CO)$_2$Ph	9.1	11.1	—	—	—	−1.25	380 (75) [2a]
Ph(CO)$_3$Ph	8.9	10.2	11.6	—	—	−0.88	450 (45) [2a]
Ph(CO)$_4$Ph	8.9	10.2	11.2	11.8	—	−0.52	515 (200) [2a]
Ph(CO)$_5$Ph	8.9	9.9	10.9	11.6	12.0	−0.27	547 (130)

[a] In CH_2Cl_2 with 0.1 M nBu$_4$N$^{\oplus}$PF$_6^{\ominus}$ under argon atmosphere, using a glassy-carbon electrode, Ag/AgCl in LiCl/ethanol as reference electrode, and Pt as counter electrode. Scan rate, 15 mV/s; Fe(Cp)$_2$[Fe(Cp)$_2$]$^{\oplus}$, +0.4 eV.

Received: July 2, 1986 [Z 1842 IE]
German version: *Angew. Chem. 98* (1986) 1019

CAS Registry numbers:
3a, 104779-75-1; **3b**, 1467-40-9; **4a**, 104779-76-2; **4b**, 22760-83-4; **5a**, 104779-77-3; **5b**, 104779-78-4; **6a**, 104779-79-5; **6b**, 104779-80-8; **7a**, 104779-81-9; **7b**, 104779-82-0; *o*-phenylenediamine, 95-54-5.

[*] Prof. Dr. R. Gleiter, Dipl.-Chem. G. Krennrich, Dipl.-Chem. M. Langer
Institut für Organische Chemie der Universität
Im Neuenheimer Feld 270, D-6900 Heidelberg (FRG)

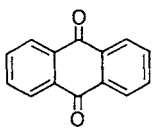
[**] This work was supported by the Deutsche Forschungsgemeinschaft, the Fonds der Chemischen Industrie, and BASF AG. We are grateful to Dr. *P. Kunzelmann, M. Rimmler,* and *G. Rissmann* for recording the spectra.

[1] M. B. Rubin, *Chem. Rev. 75* (1975) 177.
[2] a) L. Horner, F. Maurer, *Chem. Ber. 101* (1968) 1783; b) R. Gleiter, W. Dobler, *ibid. 118* (1985) 1917; c) R. Gleiter, G. Krennrich, *Angew. Chem. 98* (1986) 452; *Angew. Chem. Int. Ed. Engl. 25* (1986) 449.
[3] M. L. Miles, T. M. Harris, C. R. Hauser, *J. Org. Chem. 30* (1965) 1007.
[4] M. Regitz, H. J. Geelhaar, *Chem. Ber. 102* (1969) 1743.
[5] H. M. Teeter, E. W. Bell, *Org. Synth. 32* (1952) 20.
[6] For **4**, **5**, and **7**, correct elemental analyses have been obtained.

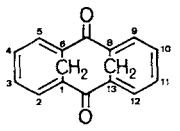
syn- and *anti*-Bishomoanthraquinone

By *Emanuel Vogel,* Stefan Böhm, Achim Hedwig, Bernd O. Hergarten, Johann Lex, Joachim Uschmann,* and *Rolf Gleiter**

Anthraquinone **1**, the parent substance of the anthraquinone dyes, is of great scientific and technical importance.[1] We therefore have undertaken the investigation of the bridged [14]annulenediones **2** and **3**, derived from the aromatic hydrocarbon *syn*-1,6:8,13-bismethano[14]annulene[2] and its olefinic *anti*-isomer,[3] respectively. In order to emphasize their structural relationship to **1**, these diones will henceforth be referred to as "bishomoanthraquinones."

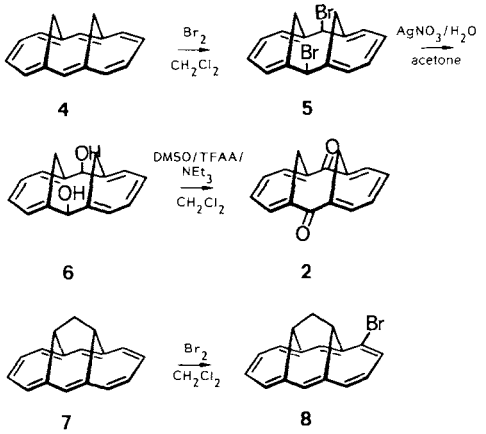


1



2 : *syn*-isomer
3 : *anti*-isomer

Our interest especially focused on the *syn*-isomer **2**, since this molecule, constituting a diketo derivative of a Hückel-aromatic hydrocarbon, might be endowed with quinonoid properties, as is found to be the case with the diones of some other [4n+2]annulenes.[4] The preparation of **3** was already reported in 1966,[5a] but apart from its reaction with zinc/acetic anhydride in pyridine leading to reductive acetylation,[5b] no further studies bearing on its redox behavior have been carried out. We now report on the synthesis of **2** and on the electrochemistry of **2** and **3**.



4 **5** **6** **2** **7** **8**

A possible route to the elusive *syn*-bishomoanthraquinone **2** was suggested by the surprising course, with regard to both regio- and stereoselectivity, of the bromination of **4** with elemental bromine in dichloromethane at room temperature. Whereas the very rigid 1,6:8,13-propanediylidene[14]annulene **7**,[6] which almost perfectly matches **4** in the conformation of the annulene ring, experiences attack of bromine (same conditions as above) at the 2-position with formation of the substitution product **8**,[7] the hydrocarbon **4** reacts with the halogen to give the 7,14-diadduct **5** having the bromine atoms *syn* with respect to the bridges [m.p. = 165–166 °C (dec.); colorless needles from ethyl acetate; yield 90%; see Table 1]. The NMR spectra of the dibromide did not allow us to distinguish unequivocally between **5** and its stereoisomer, in which the two bromine atoms are *trans* with respect to the bridges; therefore, an X-ray structure analysis[8] was performed in order to prove the presence of **5** beyond doubt (Fig. 1).

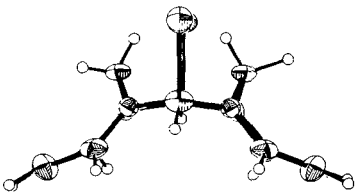


Fig. 1. Molecular structure of **5** in the crystal. Longitudinal profile of the molecule [8].

The findings on the bromination of **4** can be rationalized by an MO treatment, which shows that the chemical reactivity of **4** and **7**—like that of 1,6-methano[10]annulene[7b,9]—is influenced by π/σ interaction, leading to a rotation of the p_π atomic orbitals in the HOMO -1[10] as depicted in Figure 2. On the basis of the size of the orbital coefficients, electrophiles should attack the annulene ring at the sites adjacent to the bridges, addition to the outer positions (C-2, C-5, C-9, and C-12) being slightly preferred over addition to the central positions (C-7 and C-14). Sterically, *syn* addition (with respect to the bridges) should be favored, since the p_π orbitals of the HOMO -1, as a consequence of the rotation, are capable of overlapping with the vacant orbital of the electrophile more efficiently at the top side than at the bottom side of the molecule. The regioselective *syn* addition at the central positions observed with **4** becomes intelligible if one realizes that the rehybridization at C-7 and C-14 from sp^2 to sp^3 substantially reduces the nonbonding interaction between the internal bridge hydrogen atoms by causing folding of the C_{14} perimeter. Thus, the course of the bromination of **4**, which seems to be typical of the reactions of the hydrocarbon with electrophiles,[11] may be regarded as an unusual example of reaction control exerted by strain relief.

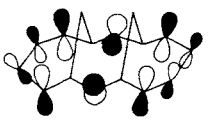


Fig. 2. Schematic representation, in the case of **4**, of the rotation of the p_π atomic orbitals in the HOMO -1 caused by π/σ interaction.

The dibromide **5**, which, contrary to expectation, is relatively stable thermally, exhibits no tendency to undergo elimination of HBr with formation of the 7-bromo derivative of **4**. As expected for an allylic halide, **5** is solvolytically very reactive, readily undergoing hydrolysis with silver nitrate in aqueous acetone (room temperature, 30 min) to give a sterically uniform symmetrical diol. Evidence that this diol possesses structure **6** [m.p. = 217–

[*] Prof. Dr. E. Vogel, S. Böhm, Dr. A. Hedwig, Dr. B. O. Hergarten, Dr. J. Lex
Institut für Organische Chemie der Universität
Greinstrasse 4, D-5000 Köln 41 (FRG)
Prof. Dr. R. Gleiter, Dr. J. Uschmann
Institut für Organische Chemie der Universität Heidelberg
Im Neuenheimer Feld 270, D-6900 Heidelberg (FRG)

Table 1. Selected spectral data of the compounds **2**, **3**, **5**, and **6**. ^{1}H-NMR spectra: 300 MHz, $CDCl_3$ [a]; ^{13}C-NMR spectra: 75.5 MHz, $CDCl_3$; IR spectra: KBr; UV/VIS spectra: dioxane.

2: ^{1}H-NMR: $\delta = 1.70$ and 5.27 (AX, 4H, H-15$_{exo}$,16$_{exo}$ and H-15$_{endo}$,16$_{endo}$, respectively, $J_{AX} = -14.4$ Hz), 6.76 and 6.85 (AA'BB', 8H, H-3,4,10,11 and H-2,5,9,12, respectively, $J_{2,3} = 6.11$, $J_{3,4} = 11.13$, $J_{2,4} = 0.23$, $J_{2,5} = 1.01$ Hz); ^{13}C-NMR: $\delta = 31.58$, 127.92, 131.02, 137.81, 191.54; MS (70 eV): *m/z* 236 ($M^{\oplus}$, 27%), 89 (100); IR: $\tilde{\nu} = 1650$ cm^{-1} (C=O); UV/VIS: $\lambda_{max} = 238$ nm ($\varepsilon = 20400$), 273 (27600), 303 (12300) sh, 371 (1100)

3: ^{1}H-NMR: $\delta = 1.65$ and 3.16 (AX, 4H, H-15$_{exo}$,16$_{exo}$ and H-15$_{endo}$,16$_{endo}$, respectively, $J_{AX} = -13.78$ Hz), 6.97 (degenerate AA'BB', 8H, H-2,3,4,5,9,10,11,12, $J_{2,3} = 5.98$, $J_{3,4} = 11.22$, $J_{2,4} = 0.44$, $J_{2,5} = 0.43$ Hz); ^{13}C-NMR: $\delta = 32.97$, 127.35, 132.20, 132.70, 200.15; MS (70 eV): *m/z* 236 ($M^{\oplus}$, 17%), 157 (100); IR: $\tilde{\nu} = 1657$ cm^{-1} (C=O); UV/VIS: $\lambda_{max} = 250$ nm ($\varepsilon = 26300$), 282 (9300), 362 (300) sh

5: ^{1}H-NMR: $\delta = 1.72$ and 4.66 (AX, 4H, $J_{AX} = -13.43$ Hz), 5.16 (s, 2H), 6.06 and 6.39 (AA'XX', 8H, *N* [b] = 6.0 Hz); ^{13}C-NMR: $\delta = 30.54$, 61.21, 121.35, 129.12, 140.44; MS (80 eV): *m/z* 366 ($M^{\oplus}$, 1.5%), 206 (100); IR: $\tilde{\nu} = 1610$ cm^{-1} (C=C); UV/VIS: $\lambda_{max} = 237$ nm ($\varepsilon = 23400$) sh, 253 (25700), 348 (980) sh

6: ^{1}H-NMR: $\delta = 1.54$ and 4.83 (AX, 4H, $J_{AX} = -12.80$ Hz), 2.13 (d, 2OH, $^3J = 1.7$ Hz), 4.63 (br. s, 2H), 5.88 and 6.32 (AA'XX', 8H, *N* [b] = 5.9 Hz); ^{13}C-NMR: $\delta = 27.12$, 78.46, 120.31, 128.33, 146.02; MS (80 eV): *m/z* 240 ($M^{\oplus}$, 48%), 91 (100); IR: $\tilde{\nu} = 3350$ cm^{-1} (O–H); UV/VIS: $\lambda_{max} = 234$ nm ($\varepsilon = 29400$), 255 (11850) sh, 315 (575) sh

[a] The coupling constants for **3** were measured in C_6D_6. [b] For nomenclature see: H. Günther, *Angew. Chem. 84* (1972) 907; *Angew. Chem. Int. Ed. Engl. 11* (1972) 861.

219°C; colorless rhombs (from ethyl acetate); yield 85%; see Table 1] was provided by an X-ray structure investigation.

The remarkable retention of configuration in the hydrolysis of **5** is most likely steric in origin, for a carbenium ion center at C-7 or C-14 is subject to shielding by the "cycloheptatriene wings" of the molecule in such a way as to leave no chance for the nucleophile to attack from the rear.[12]

In the last step of the synthesis, the oxidation of the sterically hindered diol **6** to **2**, the best results were achieved, as anticipated, when the reaction was carried out with the system dimethyl sulfoxide (DMSO)/trifluoroacetic anhydride (TFAA)/triethylamine[13] (in dichloromethane/DMSO; −78°C; 1 h). The dione **2**, isolated by chromatographic workup (silica gel; dichloromethane/ether 3:1) is a stable compound [m.p. = 198–199°C; yellow needles from dichloromethane/ether; yield 85%; see Table 1].

The ^{1}H-NMR spectrum of **2** (Table 1), consisting of an AA'BB' system for the vinylic protons and of an AX system for the bridge protons, exhibits chemical shifts and coupling constants indicative of an annulenedione (cycloheptatriene structural units). Apart from the observation that the internal bridge protons, owing to steric compression, resonate at unusually low field, this spectrum is in strikingly good agreement with that of the *anti*-isomer **3** (Table 1).

The electronic spectrum of **2** markedly differs from that of its colorless *anti*-isomer, but is similar to the spectrum of **1**, with which it has in common a band at relatively long wavelength, responsible for the yellow color of the compound.

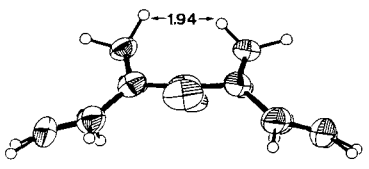


Fig. 3. Molecular structure of **2** in the crystal. Longitudinal profile of the molecule [14].

The molecular structures of **2** and **3**, as determined by X-ray investigations,[14] basically agree with those derived from an inspection of models. The CC bond lengths of the cycloheptatriene units of **2** and **3** strongly alternate, the degree of alternation being virtually the same in both compounds. That the steric repulsion of the internal bridge hydrogen atoms existing in **2**, (H,H distance 1.94 Å, compared to 1.78 Å in **4**) causes the C_{14} perimeter to be bent noticeably is revealed by the profile of the molecule given in Figure 3.[14]

On treatment with zinc/acetic anhydride in pyridine, the dione **2** undergoes reductive acetylation to give 7,14-diacetoxy-*syn*-1,6:8,13-bismethano[14]annulene [m.p. = 220°C (from dichloromethane/*n*-hexane); yield 76%], which, in contrast to its very reactive olefinic *anti*-isomer [m.p. = 135–136°C (from pentane/ether); yield 22%] is a stable aromatic compound.

The cyclovoltammetric investigation of **2** and **3** showed that both compounds undergo reduction by reversible one-electron transfers affording the corresponding semiquinone radical anions and dianions, respectively, as is typical of quinones.[15] The reduction potentials, including those of **1** and the reference compound *p*-benzoquinone, are listed in Table 2. As expected, **2**, which, in contrast to **3**, derives from an aromatic [14]annulene, is reduced to the radical anion and dianion more readily than **3**. In comparison with **1**, on the other hand, compound **2** is slightly less susceptible to radical anion formation; **2** and **1**, however, require about the same energy in order to be transformed into the corresponding dianions. Thus, **2** appears to be comparable to **1** with regard to quinonoid properties, yet noticeably differs in this respect from the planar [14]- and [18]annulenequinones (measured so far), which are more similar to *p*-benzoquinone in their reduction potentials ($E_1 + E_2$). This situation probably arises from steric factors, since the bent **2**, when reduced to the radical anion and dianion, will tend to flatten out, but can do so only at the expense of a sharp increase in the compression of the internal bridge hydrogen atoms.

Table 2. Comparison between the experimentally determined reduction potentials [a] and the orbital energies for the LUMO (ε_{LUMO}), calculated by the MINDO/3 method, the Coulomb integrals (J_{LUMO}), and the probability $A = \sum_{\mu} c_{\mu}^2$ of finding the electron at the CO groups.

Compound	E_1	E_2	$E_2 - E_1$	$E_1 + E_2$	ε_{LUMO} [eV]	J_{LUMO} [eV]	A [%]
p-benzoquinone	−0.23	−1.15	−0.92	−1.38	−1.03	6.23	51
1	−0.64	−1.39	−0.75	−2.03	−0.62	5.05	37
2	−0.78	−1.01	−0.23	−1.79	−0.48	4.56	13
3	−1.02	−1.27	−0.25	−2.29	−0.26	4.50	16

[a] Measurement conditions: dimethylformamide as solvent, glassy carbon electrode, Ag/AgCl reference electrode, Pt counter electrode, Bu_4NPF_6 as conducting salt. All values in V. Under the same conditions, the oxidation potential of ferrocene was determined to be $E^{1/2} = 0.705$ V. The values for the reduction potentials of the reference compounds *p*-benzoquinone and **1** and that of 1,4-naphthoquinone deviate by ca. 0.25 V from the values given in [4b], presumably owing to different measuring arrangements.

From Table 2 it follows that the E_1 values of **1**–**3** correlate with the energies for the LUMO calculated by the MINDO/3 method. The remarkably small difference between E_1 and E_2 observed with **2** and **3** is assumed to result mainly from a decreased Coulomb interaction of the electrons in the LUMO as compared with the case for **1**.[16]

This explanation not only ensues from the values of the Coulomb integrals in the LUMO, but also derives support from the finding that the probability density of the electron at the carbonyl groups becomes smaller as one goes from either **2** or **3** to **1**. The carbonyl groups of **2** and **3** are thus more involved in conjugation than those of **1**. An important reason for this is that the two bishomoanthraquinones are subject to π/σ interaction—a phenomenon especially pronounced in nonplanar π systems such as bridged annulenes.

Received: July 7, 1986 [Z 1848 IE]
German version: *Angew. Chem. 98* (1986) 1001

CAS Registry numbers:
2, 104713-91-9; **3**, 104713-92-0; **4**, 55821-04-0; **5**, 104642-05-9; **6**, 104642-06-0; 7,14-diacetoxy-*syn*-1,6:8,13-bismethano[14]annulene, 104642-07-1.

[1] a) O. Bayer in *Houben-Weyl-Müller: Methoden der Organischen Chemie, Bd. 7/3c*, Thieme, Stuttgart 1979; b) S. Patai (Ed.): *The Chemistry of the Quinonoid Compounds, Part 1/2*, Wiley, London 1974; c) the synthesis of *syn*- and *anti*-bishomoquinizarine, the 2,5-dihydroxy derivatives of **2** and **3**, respectively, will be reported in a forthcoming communication.

[2] a) E. Vogel, J. Sombroek, W. Wagemann, *Angew. Chem. 87* (1975) 591; *Angew. Chem. Int. Ed. Engl. 14* (1975) 564; b) X-ray structure analysis of **4**: R. Destro, T. Pilati, M. Simonetta, *Acta Crystallogr. B 33* (1977) 940; c) absorption spectra of **4**: H. J. Dewey, H. Deger, W. Frölich, B. Dick, K. A. Klingensmith, G. Hohlneicher, E. Vogel, J. Michl, *J. Am. Chem. Soc. 102* (1980) 6412.

[3] a) E. Vogel, U. Haberland, H. Günther, *Angew. Chem. 82* (1970) 510; *Angew. Chem. Int. Ed. Engl. 9* (1970) 513; b) the X-ray structure analysis of the 7-carboxylate methyl ester of *anti*-1,6:8,13-bismethano[14]annulene has been carried out: C. M. Gramaccioli, A. S. Mimun, A. Mugnoli, M. Simonetta, *J. Am. Chem. Soc. 95* (1973) 3149; M. Simonetta, *Pure Appl. Chem. 52* (1980) 1597.

[4] a) V. Boekelheide, J. B. Phillips, *J. Am. Chem. Soc. 89* (1967) 1695; V. Boekelheide, T. Miyasaka, *ibid. 89* (1967) 1709; b) R. Breslow, D. Murayama, R. Drury, F. Sondheimer, *ibid. 96* (1974) 249; c) M. Iyoda, Y. Onishi, M. Nakagawa, *Tetrahedron Lett. 22* (1981) 3645.

[5] a) E. Vogel, M. Biskup, A. Vogel, U. Haberland, J. Eimer, *Angew. Chem. 67* (1966) 642; *Angew. Chem. Int. Ed. Engl. 5* (1966) 603; b) E. Vogel, A. Vogel, unpublished results.

[6] a) E. Vogel, A. Vogel, H.-K. Kübbeler, W. Sturm, *Angew. Chem. 82* (1970) 512; *Angew. Chem. Int. Ed. Engl. 9* (1970) 514; b) X-ray structure analysis of **7**: A. Gavezotti, A. Mugnoli, M. Raimondi, M. Simonetta, *J. Chem. Soc. Perkin Trans. 2 1972*, 425.

[7] a) The formation of **8** probably occurs via an addition-elimination mechanism (detection of a labile adduct at low temperature): unpublished results with *A. Alscher* and *H. Wieland*; b) see also the investigations on the bromination of 1,6-methano[10]annulene: T. Scholl, J. Lex, E. Vogel, *Angew. Chem. 94* (1982) 924; *Angew. Chem. Int. Ed. Engl. 21* (1982) 920.

[8] **5**: tetragonal, space group $P4_2cm$, $a = 15.559(3)$, $c = 6.022(2)$ Å, $Z = 4$, 454 reflections, $R = 0.068$. Further details of the crystal structure investigation may be obtained from the Fachinformationszentrum Energie, Physik, Mathematik GmbH, D-7514 Eggenstein-Leopoldshafen 2 (FRG), on quoting the depository number CSD-52128, the names of the authors, and the journal citation.

[9] An MO model that explains the *syn* addition of bromine to 1,6-methano[10]annulene: R. Gleiter, M. C. Böhm, E. Vogel, *Angew. Chem. 94* (1982) 925; *Angew. Chem. Int. Ed. Engl. 21* (1982) 922.

[10] The HOMO that is ca. 0.2 eV higher in energy than the HOMO − 1 has large coefficients at the bridgehead positions.

[11] Exclusive *syn* addition at the 7,14 positions also occurs for chlorination with elemental chlorine and acetoxylation with lead tetraacetate.

[12] If norcaradiene valence tautomers are involved in the case of **5** (although no evidence of appreciable concentrations of such species exists), then the retention observed upon Br/OH exchange may be explained by a neighboring-group effect of the π system of the norcaradiene structural unit.

[13] a) K. E. Pfitzner, J. G. Moffat, *J. Am. Chem. Soc. 85* (1963) 3027; *ibid. 87* (1965) 5661; b) A. J. Mancuso, D. Swern, *Synthesis 1981*, 165.

[14] We will report later in more detail on the X-ray structure analyses of **2** and **3**, in connection with a study of their photoelectron spectra: R. Gleiter, E. Vogel, unpublished results.

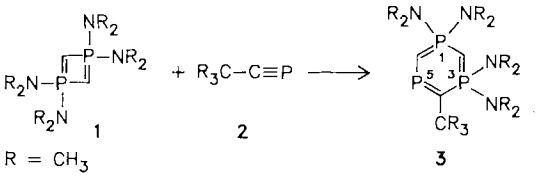
[15] We thank Prof. *S. Hünig* (Würzburg) for valuable suggestions on carrying out the electrochemical investigations.

[16] P. Čársky, S. Hünig, D. Scheutzow, R. Zahradnik, *Tetrahedron 25* (1968) 4781.

A $1\lambda^5,3\lambda^5,5\lambda^3$-Triphosphabenzene Derivative

By *Ekkehard Fluck,* Gerd Becker, Bernhard Neumüller, Robert Knebl, Gernot Heckmann,* and *Heinz Riffel*

Monophosphabenzene and a series of its derivatives were first described in the 1960s; later, diphosphabenzenes were also reported.[1] We report here the synthesis of the first 1,3,5-triphosphabenzene derivative. 1,1,3,3-Tetrakis(dimethylamino)-4-*tert*-butyl-$1\lambda^5,3\lambda^5,5\lambda^3$-triphosphabenzene **3** is the sole product formed upon reaction of 1,1,3,3-tetrakis(dimethylamino)-$1\lambda^5,3\lambda^5$-diphosphete **1**[2] with 2,2-dimethylpropylidynephosphane **2**.[3] The reaction can be regarded formally as an insertion. Mechanistically, it probably involves a cycloaddition, followed by spontaneous valence isomerization.[4]



Compound **3** forms air- and moisture-sensitive, pale yellow crystals, m.p. = 50–55 °C, which are soluble in benzene and *n*-pentane. In the $^{31}P\{^1H\}$-NMR spectrum (C_6D_6, standard 85% H_3PO_4) of **3**, the chemical shifts of the phosphorus atoms 1, 3, and 5 are $\delta = 57.5$, 59.0, and 295.5, respectively. In the $^{13}C\{^1H\}$-NMR spectrum (C_6D_6, standard TMS), the C atoms 6 and 4 exhibit the smallest chemical shifts ($\delta = 62.8$ and 100.8) so far recorded for phosphaalkenes. This is an indication of the significant ylide character of the C4–P5–C6 structural fragment. The ring structure of **3**, established by NMR triple resonance experiments, is in agreement with the results of an X-ray structure analysis (Fig. 1).[5]

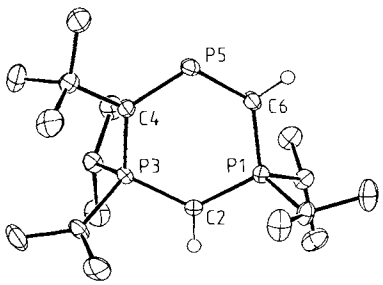


Fig. 1. ORTEP plot of the crystal structure of **3** (thermal ellipsoids at 50% probability). Bond lengths [pm] and angles [°]: P1-C2 168.8(2), C2-P3 169.7(2), P3-C4 175.8(2), C4-P5 170.9(2), P5-C6 170.0(2), C6-P1 171.5(2); P1C2P3 128.1(1), C2P3C4 111.9(1), P3C4P5 121.9(1), C4P5C6 113.7(1), P5C6P1 128.2(1), C6P1C2 109.4(1). The numbering of the atoms corresponds to the systematic name of **3**.

The six-membered ring is nearly planar and the distances between the ring atoms are nearly identical (170.2 ± 1.2 pm). An exception is the P3–C4 distance (175.8 pm). In the mass spectrum of **3**, the molecular-ion peak is very intense.

[*] Prof. Dr. E. Fluck
Gmelin-Institut für Anorganische Chemie der Max-Planck-Gesellschaft
Varrentrappstrasse 40/42, D-6000 Frankfurt am Main 90 (FRG)
Prof. Dr. G. Becker, Dipl.-Chem. B. Neumüller, Dipl.-Chem. R. Knebl, Dr. G. Heckmann, Dr. H. Riffel
Institut für Anorganische Chemie der Universität
Pfaffenwaldring 55, D-7000 Stuttgart 80 (FRG)

Experimental Procedure

All operations were carried out under argon. A solution of **1** [2] (2.07 g, 7.83 mmol) in 5 mL of dimethoxyethane was added dropwise over 20 min to a stirred solution of **2** [3] (1.06 g, 10.6 mmol) in 3 mL of dimethoxyethane at 0°C. The brown reaction mixture was allowed to warm slowly to room temperature and then stirred for 48 h. The solvent and excess **2** were removed under vacuum. The residual oil crystallized at −20°C and the solid was recrystallized three times from *n*-pentane. Yield of **3**: 1 g (35%).

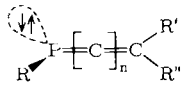
Received: July 15, 1986;
supplemented: August 13, 1986 [Z 1858 IE]
German version: *Angew. Chem. 98* (1986) 1018

[1] Cf., for example, G. Märkl, *Phosphorus Sulfur 3* (1977) 77; G. Märkl in *Houben-Weyl-Müller: Methoden der Organischen Chemie, 4. Aufl., Bd. E1*, Thieme, Stuttgart 1982, p. 72ff.
[2] J. Svara, E. Fluck, H. Riffel, *Z. Naturforsch. B40* (1985) 1258.
[3] G. Becker, G. Gresser, W. Uhl, *Z. Naturforsch. B36* (1981) 16.
[4] Cf. J. Fink, W. Rösch, U.-J. Vogelbacher, M. Regitz, *Angew. Chem. 98* (1986) 265; *Angew. Chem. Int. Ed. Engl. 25* (1986) 280.
[5] **3**: triclinic, space group $P\bar{1}$, $a=878.0(5)$, $b=971.2(5)$, $c=1279.2(6)$ pm; $\alpha=99.91(4)$, $\beta=91.33(4)$, $\gamma=104.68(4)°$; $Z=2$, $\rho_{calcd}=1.167$ g/cm^3. All atoms occupy the general positions of the space group. The structure was derived from 4754 unique reflections (of which 4071 were observed) by statistical methods and Fourier syntheses and refined to $R=0.038$. Further details of the crystal structure investigation may be obtained from the Fachinformationszentrum Energie, Physik, Mathematik GmbH, D-7514 Eggenstein-Leopoldshafen 2 (FRG), on quoting the depository number CSD-52046, the names of the authors, and the journal citation.

1-Phospha-1,2,3-butatrienes

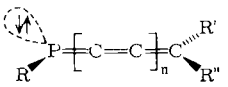
By *Gottfried Märkl,* Hans Sejpka, Stefan Dietl, Bernd Nuber,* and *Manfred L. Ziegler*

Whereas numerous open-chain, non-resonance-stabilized phosphaalkenes with kinetic or electronic stabilization have been prepared in recent years,[1] investigation of the phosphacumulenes began only recently with the synthesis of the phosphaallene **1a** by *Yoshifuji* et al.[2] and *Appel* et al.[3]



1, n = 1, 3, 5

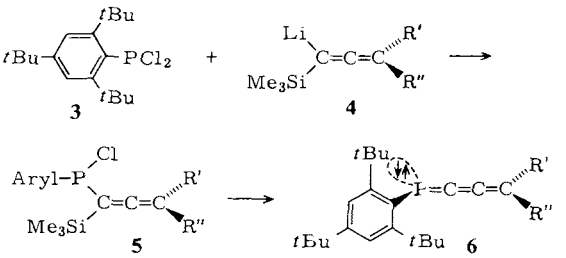
1a, n = 1, R = 2,4,6-tBu$_3$C$_6$H$_2$, R′ = R″ = Ph



2, n = 1, 2, 3

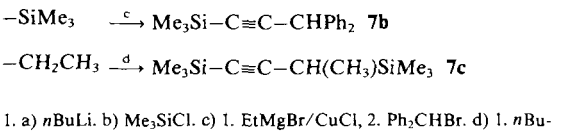
As in the case of the cumulenes, it is useful to divide the phosphacumulenes into the species **1** with an odd number of atoms in the polyene chain and the species **2** with an even number. If phosphorus is stable to inversion, the phosphacumulenes **1** with R′≠R″ are chiral; the formation of *E/Z* isomers is expected for the analogues **2** with R′≠R″.

We describe here the synthesis of the 1-phospha-1,2,3-butatrienes **6**, the first phosphacumulenes of type **2**, n = 1. Reaction of the monolithiated allenes **4** with the dichlorophosphane **3** results in the formation of the coupling product **5**, which undergoes elimination of trimethylchlorosilane, in a reaction analogous to the Peterson–Wittig reaction, to give the 1-phosphabutatrienes **6**.



a, R′ = R″ = SiMe$_3$; **b**, R′ = R″ = Ph;
c, R′ = Me(SiMe$_3$), R″ = SiMe$_3$(Me)
Aryl = 2,4,6-tBu$_3$C$_6$H$_2$

The monolithiated allenes **4** are obtained by metalation of the corresponding alkynes **7** with *n*BuLi in tetrahydrofuran (THF) (2 h at room temperature, 2–4 h at reflux). The synthesis of **7a** is carried out by modification of the procedure of *West* et al.;[4] **7b** and **7c** (see ref. [5]) were obtained for the first time according to Scheme 1.



Scheme 1. a) *n*BuLi. b) Me$_3$SiCl. c) 1. EtMgBr/CuCl, 2. Ph$_2$CHBr. d) 1. *n*BuLi, 2. Me$_3$SiCl.

The phosphabutatrienes **6** are pale yellow oils (**6a**, **6c**), which undergo crystallization upon prolonged standing in the cold, or form, for example, a yellow solid (**6b**), which, in turn, crystallizes from ethanol in the form of shining yellow leaflets.

The spectroscopic data for **6a–c** (Table 1) are in agreement with the structure given. The marked low-field shift of the ^{31}P-NMR signal of **6a**, R′ = R″ = SiMe$_3$ ($\delta=+343.3$) corresponds to the values observed for phosphaalkenes of type **8**.[6] The $\delta(^{31}P)$ value of **6b**, R′ = R″ = Ph (+156.7), lies closer to the value found for **9** (+233[7]). Comparison with the chemical shift of **1a**, R′ = R″ = Ph (+72[2]), indicates an alternation of the values of **2**, n = 0, 1 (corresponding to **8** and **9** and to **6**, respectively) compared with those of **1**, n = 1, which is probably caused by the different orbital geometries.

8 R–P=C(SiMe$_3$)$_2$ mesityl–P=CPh$_2$ **9**

In the ^{1}H-NMR spectra of **6**, the signals of the *E* and *Z* moieties R′ and R″ have different chemical shifts, the signals of the *E* substituents R′ having the larger low-field shift and the larger P/H coupling.[8] The ^{1}H-NMR spectrum of crude **6c** corresponds, as expected, to the presence of an *E/Z* mixture of isomers (≈10:1). *E*-**6c** and *Z*-**6c** may be cleanly separated by chromatography on silica gel with petroleum ether (40–60°C). In the ^{1}H-NMR spectrum

[*] Prof. Dr. G. Märkl, Dipl.-Chem. H. Sejpka, S. Dietl
Institut für Organische Chemie der Universität
Universitätsstrasse 31, D-8400 Regensburg (FRG)
Prof. Dr. M. L. Ziegler, Dr. B. Nuber
Anorganisch-chemisches Institut der Universität
Im Neuenheimer Feld 270, D-6900 Heidelberg (FRG)

of *E*-**6c** ($R' = SiMe_3$), the $SiMe_3$ signal has a larger low-field shift and P/C coupling than that of *Z*-**6c**. The CH_3 signal of *Z*-**6c** shows analogous behavior.

Table 1. Selected physical data for the compounds **6a-c** and **5b**. All NMR spectra in $CDCl_3$; δ values, J in Hz, ^{1}H-NMR at 250 MHz.

6a, yield 10%, pale yellow oil, which crystallizes slowly in the cold.—^{1}H-NMR: aryl: 7.41 (d, $^4J(PH) = 1.08$), *o*-*t*Bu: 1.45 (d, $^5J(PH) = 0.44$), *p*-*t*Bu: 1.32 (s), *E*-$SiMe_3$: 0.26 (d, $^6J(PH) = 0.97$), *Z*-$SiMe_3$: −0.13 (s).—^{31}P-NMR: 343.3.—^{13}C-NMR: P=C: 167.3 (d, $J = 73.9$), aryl: C1: 139.8 (d, $J = 68.3$), C2: 152.8 (s), C3: 122.1 (s), C4: 149.4 (s), P=C=*C*=: 106.5 (d, $J = 21.8$), P=C=*C*=C: 114.9 (d, $J = 10.6$), *o*-*t*Bu: 38.2 (s), 33.0 (d, $J = 6.0$), *p*-*t*Bu: 35.0 (s), 31.5 (s), *E*-$SiMe_3$: −1.06 (d, $J = 8.7$); *Z*-$SiMe_3$: −0.04.—MS (70 eV): $M^{\oplus\odot}$, 458 (20%); $[M - {}^{\odot}CH_3]^{\oplus}$, 443 (10%), $m^* = 428.3$; $[M - {}^{\odot}SiMe_3]^{\oplus}$, 385 (14%), $m^* = 323.6$; $[M - (SiMe_3)_2C{=}C{=}CH^{\odot}]^{\oplus}$, 275 (100%); $[275 - C_4H_8]^{\oplus\odot}$, 219 (14%), $m^* = 174.4$

6b, ^{1}H-NMR: Ph: 7.10-7.58 (m), aryl: 7.42 (d, $^4J(PH) = 1.33$), *o*-*t*Bu: 1.60 (d, $^5J(PH) = 1.06$), *p*-*t*Bu: 1.36 (s).—^{13}C-NMR (see Table 2): aryl: C1: 136.4 (d, $J = 59.3$), C2: 154.4 (s), C3: 121.8 (s), C4: 149.9 (s), phenyl: C1: 138.0 (d, $J = 21.6$), C2-C4: 127.7-129.5, *o*-*t*Bu: 38.2 (s), 33.8 (d, $J = 6.5$), *p*-*t*Bu: 35.0 (s), 31.4 (s).—MS (70 eV): $M^{\oplus\odot}$, 466 (46%); $[M - C_4H_8]^{\oplus\odot}$, 410 (27%); $m^* = 360.7$; $[M - {}^{\odot}C_4H_9]^{\oplus}$, 409 (29%); $[410 - C_4H_8]^{\oplus\odot}$, 354 (30%), $m^* = 305.6$; $[409 - C_4H_8]^{\oplus}$, 353 (15%); $[354 - C_4H_8]^{\oplus\odot}$, 298 (26%); $[353 - C_4H_8]^{\oplus}$, 297 (15%); $[M - Ph_2C{=}C{=}CH^{\odot}]^{\oplus}$, 275 (100%).—IR (KBr), $\tilde{\nu}$(C=C=C): broad signal at 1940 cm^{-1} (w); the IR spectrum is virtually identical with that of **1a** [2].—UV (*n*-hexane): $\lambda_{max} = 412$ nm ($\varepsilon = 20200$), 396 (19400), 305 (7000), 268 (19800), 238 (26700) [for comparison: λ_{max} (tetraphenylbutatriene) = 420 nm]

E-**6c**, yield 10%, colorless oil.—^{1}H-NMR: aryl: 7.37 (d, $^4J(PH) = 0.99$), CH_3: 1.59 (d, $^5J(PH) = 7.39$), $SiMe_3$: 0.21 (d, $^6J(PH) = 1.04$), *o*-*t*Bu: 1.43 (d, $^5J(PH) = 0.53$), *p*-*t*Bu: 1.31 (s).—^{31}P-NMR: 332.3.—^{13}C-NMR: P=*C*: 170.5 (d, $^1J(PC) = 71.8$), P=C=*C*=: 82.3 (d, $^2J(PC) = 23.1$), P=C=C=*C*: 108.2 (d, $^3J(PC) = 9.7$), CH_3: 5.11 (s), $SiMe_3$: −0.99 (d, $^5J(PC) = 8.5$).—MS (70 eV): $M^{\oplus\odot}$, 400 (22%); $[M - {}^{\odot}CH_3]^{\oplus}$, 385 (19%); $[M - C_4H_8]^{\oplus\odot}$, 344 (7%); $[M - {}^{\odot}C_4H_9]^{\oplus}$, 343 (5%); $[M - {}^{\odot}SiMe_3]^{\oplus}$, 327 (22%); $[M - Me_3Si(CH_3)C{=}C{=}C]^{\oplus\odot}$, 276 (21%); $[M - Me_3Si(CH_3)C{=}C{=}CH^{\odot}]^{\oplus}$, 275 (100%); $[276 - {}^{\odot}C_4H_9]^{\oplus}$, 219 (27%).—IR (film): $\tilde{\nu} = 2095$ cm^{-1} (vw)

Z-**6c**, yield ≈ 1%, colorless oil; ^{1}H-NMR: aryl: 7.41 (d, $^4J(PH) = 1.31$), CH_3: 2.16 (d, $^5J(PH) = 13.75$), $SiMe_3$: −0.15 (s), *o*-*t*Bu: 1.45 (d, $^5J(PH) = 2.02$), *p*-*t*Bu: 1.30 (s).—^{31}P-NMR: 288.6; the *E*/*Z*-^{31}P-NMR-shift difference of $\Delta\delta = 43.7$ ppm corresponds to the finding of *E*/*Z*-isomeric phosphaalkenes [6]

5b, yield 50%; m.p. = 139-140°C (light yellow crystals from EtOH).—IR: $\tilde{\nu}$(allene): 1885 cm^{-1} (s).—^{31}P-NMR: 73.3.—MS (70 eV): $M^{\oplus\odot}$, 574 (< 1%); $[M - Me_2SiCl]^{\oplus\odot}$, 481 (≈ 1%); $[M - Me_3SiCl]^{\oplus\odot}$, 466 (< 1%); $[Aryl{-}P{-}Cl]^{\oplus}$, 311 (3%); $[Ph_2C{=}C{=}CSiMe_3]^{\oplus}$, 263 (100%)

The alternation observed in the ^{31}P-NMR spectra is also revealed in the ^{13}C-NMR spectra (Table 2).

Table 2. Comparison of the ^{13}C-NMR data of the compounds **9**, **1a**, and **6b**.

	α		α β		α β γ		
	mesityl−P=CPh$_2$		Aryl−P=C=CPh$_2$		Aryl−P=C=C=CPh$_2$		
	9		**1a**		**6b**		
			α	β	α	β	γ
$\delta(^{13}C)$	193.7	237.6	128.3	164.8	138.1	178.8[a]
J [Hz]	45.5	26.6	6.4	35.9	5.7	25.1

[a]The reverse assignment of C_α and C_γ cannot be ruled out.

In the mass spectra of **6a-6c**, the parent peak is the ion *m*/*z* 275, formed by cleavage of the P=C bond with elimination of $[R^1R^2C{=}C{=}CH]^{\oplus\odot}$.

The X-ray structure analysis of **6b** confirms the assumed rodlike structure of the phosphabutatriene structural unit (Fig. 1).[9]

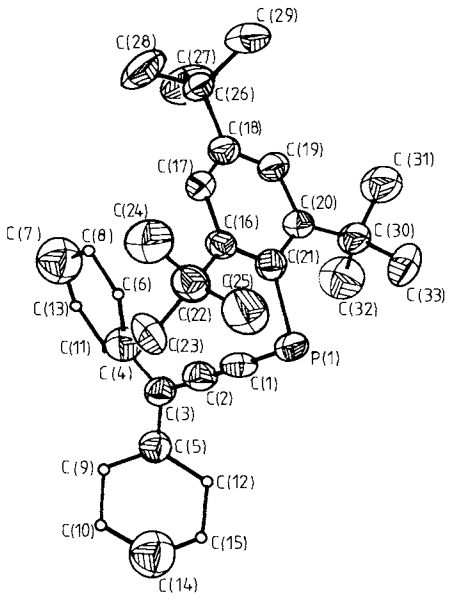


Fig. 1. Crystal structure of **6b** $P\bar{1}$, $Z = 2$, $a = 936.0(2)$, $b = 950.0(3)$, $c = 1840.0(7)$ pm, $\alpha = 80.91(3)$, $\beta = 85.59(2)$, $\gamma = 63.41(2)°$, $V = 1444.7 \times 10^6$ pm^3; 2074 of 5720 unique reflections, 313 parameters refined; $R_{aniso} = 0.068$, $R_w = 0.064$. Selected bond lengths [pm] and angles [°]: P1-C1 1.647(8), C1-C2 1.253(10), C2-C3 1.348(10), P1-C21 1.868(5), C3-C4 1.487(10), C3-C5 1.487(5), C21-P1-C1 98.4(3), P1-C1-C2 178.4(5), C1-C2-C3 178.3(6), C2-C3-C4 118.8(5), C2-C3-C5 121.9(6).

Experimental Procedure

4b: A solution of **7b** (3.97 g, 15.0 mmol) in 35 mL of dry THF was added slowly under inert gas to 15.0 mmol of *n*BuLi (1.6 N in *n*-hexane). The reaction mixture was then refluxed for 1 h.

6b: The dark red solution of **4b** was added to a solution of **3** (5.21 g, 15.0 mmol) in 45 mL of dry THF at −78°C. The reaction mixture was then allowed to warm over 4 h to room temperature and subsequently refluxed for 3 h [10]. After removal of the solvent, the residue was dissolved in petroleum ether (40-60°C) and filtered through silica gel to remove the salts. The clear yellow solution was chromatographed on oven-dried silica gel with petroleum ether/benzene (9/1). Recrystallization from dry ethanol afforded **6b** (3.15 g, 45%) as shining yellow crystals, m.p. = 156-158°C.

Received: July 16, 1986;
revised: August 5, 1986 [Z 1861 IE]
German version: *Angew. Chem. 98* (1986) 1020

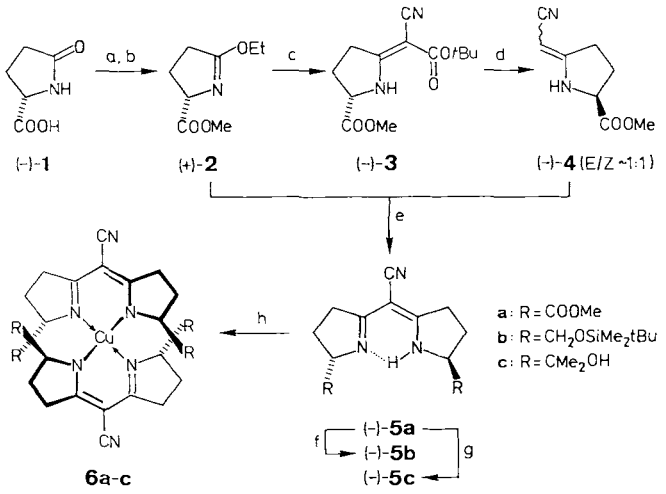
[1] See, e.g., review: R. Appel, F. Knoll, J. Ruppert, *Angew. Chem. 93* (1981) 771; *Angew. Chem. Int. Ed. Engl. 20* (1981) 731.
[2] M. Yoshifuji, K. Toyota, K. Shibayama, N. Inamoto, *Tetrahedron Lett. 25* (1984) 1809.
[3] R. Appel, P. Fölling, B. Josten, M. Siray, V. Winkhaus, F. Knoch, *Angew. Chem. 96* (1984) 620; *Angew. Chem. Int. Ed. Engl. 23* (1984) 619.
[4] R. West, P. A. Carney, I. C. Mineo, *J. Am. Chem. Soc. 87* (1965) 3788.
[5] R. West, P. C. Jones, *J. Am. Chem. Soc. 91* (1969) 6165.
[6] K. Issleib, H. Schmidt, C. Wirkner, *Z. Anorg. Allg. Chem. 473* (1981) 85; A. H. Cowley, J. E. Kilduff, M. Pakulski, C. A. Stewart, *J. Am. Chem. Soc. 105* (1983) 1656; D. Gudat, E. Niecke, B. Krebs, M. Dartmann, *Chimia 39* (1985) 277.
[7] T. C. Klebach, R. Lourens, F. Bickelhaupt, *J. Am. Chem. Soc. 100* (1978) 4886.
[8] G. Becker, O. Mundt, *Z. Anorg. Allg. Chem. 443* (1978) 53; K. Issleib, H. Schmidt, H. Meyer, *J. Organomet. Chem. 192* (1980) 33; G. Becker, W. Rössler, W. Uhl, *Z. Anorg. Allg. Chem. 473* (1981) 7; see also [1] and [6].
[9] The two phenyl rings on C3 are statistically distributed around the C5/C14- and C4/C7 axes. For clarity, only one position of the phenyl ring is drawn in each case. Further details of the crystal structure investigation may be obtained from the Fachinformationszentrum Energie, Physik, Mathematik GmbH, D-7514 Eggenstein-Leopoldshafen 2 (FRG), on quoting the depository number CSD-52018, the names of the authors, and the journal citation.
[10] If the reaction mixture **3** + **4b** is not heated to boiling, the chlorophosphane **5b** may be isolated in pure form.

Chiral Copper-Semicorrin Complexes as Enantioselective Catalysts for the Cyclopropanation of Olefins by Diazo Compounds**

By *Hugo Fritschi, Urs Leutenegger,* and *Andreas Pfaltz**

Metal-catalyzed reactions can be rendered enantioselective by complexation of the metal center with optically active ligands.[1] We report here the synthesis of enantiomerically pure, chiral ligands with structures of the semicorrin type **5**[2] and their use for enantioselective control of copper-catalyzed cyclopropanations of olefins by diazo compounds.

The synthesis is summarized in Scheme 1. Both halves of the C_2-symmetrical ligand skeleton are derived from pyroglutamic acid **1** and are joined by means of the iminoester-enamine condensation[3] method.[4] The overall yield of the crystalline, optically pure diester (−)-**5a**, based on L-pyroglutamic acid (−)-**1** is approximately 30%.



Scheme 1. a: MeOH, Dowex 50W X 8, reflux (yield >95%).—b: Et_3OBF_4, CH_2Cl_2, reflux (88% (+)-**2**).—c: 3 molar equiv. $NCCH_2CO_2tBu$, 100°C (81% (−)-**3**).—d: CF_3COOH, 23°C, 8 min; $NaHCO_3$, H_2O, 0°C (ca. 70% (−)-**4**).—e: 3 molar equiv. (+)-**2**, 3 molar equiv. CF_3COOH, 1,2-dichloroethane, 65°C (ca. 70% (−)-**5a**; m.p. 77°C, $[\alpha]_D = -140°$ ($CHCl_3$, $c = 2.2$, 23°C)). – f: $LiBH_4$, tetrahydrofuran (THF), 23°C; *t*$BuMe_2SiCl$, imidazole, dimethylformamide (DMF), 40°C (60% (−)-**5b**).—g: MeMgBr, Et_2O, 23°C (76% (−)-**5c**).—h: **6a**, **6b**: $Cu(OAc)_2$, MeOH, 23°C (91% **6a**, m.p. = 176°C; >95% **6b** (amorph.)); **6c**: $CuSO_4$, $NaHCO_3$, H_2O, CH_2Cl_2, 23°C (94% **6c**, m.p. = 196°C).

The semicorrins **5** possess several features that make them attractive candidates for enantioselective control of metal-catalyzed reactions. They are readily obtained in both enantiomeric forms from the commercially available starting materials (−)-**1** and (+)-**1** and form stable chelate complexes with a variety of metal ions (e.g., Cu^{II}, cf. Scheme 1).[5] Their structure is characterized by a rather rigid ligand skeleton and C_2 symmetry and may be modified in a variety of ways (cf. the derivatives **5b** and **5c**). In metal complexes, the two R substituents shield the metal center from two opposite directions and, therefore, are expected to have a pronounced effect on a reaction occurring in the coordination sphere.

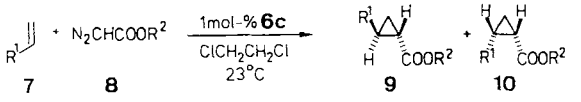


Table 1. Enantioselective cyclopropanation with the copper-semicorrin complex **6c** [a].

	R^1	R^2	Yields of **9** + **10** [%] [b]	Stereoselectivity **9** [% *ee*] [c]	**10** [% *ee*] [c]	**9** : **10**
a	Ph	Et	65	85	68	78 : 22
b	Ph	*t*Bu	60	93	92	84 : 16
c	Ph	*l*-menthyl	65–75	91	90	85 : 15
d	Ph	*d*-menthyl	60–70	97	95	82 : 18
e	$CH=CH_2$	*d*-menthyl	60	97	95	63 : 37
f	*n*-pentyl	*d*-menthyl	25–30	92	92	82 : 18

[a] The diazoester **8** was continuously injected over 10–16 h into a solution of **7** and 1 mol-% **6c** in 1,2-dichloroethane. The reaction was initiated by heating to reflux for a short time and then allowed to continue at 23°C. [b] After column chromatography: a–d, based on styrene; e, f, based on the diazo compound **8**. [c] Determined by gas chromatography after hydrolysis and reesterification with *d*- and *l*-menthol (reaction a–e) or with (*R*)- and (*S*)-2-octanol (reaction f). For **9** (R^1 = Ph, $CH=CH_2$) and **10** (R^1 = Ph), the values were confirmed by the optical rotation of the methyl ester [8]) and for **9** (R^1 = Ph, $R^2 = CH_3$) by ^{1}H-NMR spectroscopy with $Eu(tfc)_3$. In all cases, the products **9** and **10** have positive $[\alpha]_D$ values implying that the configuration at C1 is (*S*) [6–8].

As a possible application of the semicorrins **5**, we examined the metal-catalyzed cyclopropanation of olefins by diazo compounds. Chiral Cu^{II} and Co^{II} complexes have frequently been used as enantioselective catalysts for this type of reaction, some of them with considerable success.[6,7] We have found that the Cu^{II} complexes **6a**–**6c** efficiently catalyze the cyclopropanation of styrene with diazoacetates to give the diastereomeric 2-phenylcyclopropane carboxylates **9** and **10** in optically active form (cf. Table 1). The enantioselectivity and the reactivity of the catalysts increase in the order **6a** < **6b** < **6c** (for the reaction of **7** with **8** (R^1 = Ph, R^2 = Et) the temperature required and the *ee* of **9** were: with **6a**, ca. 60°C/23%; **6b**, 40°C/59%; **6c**, 23°C/85%). The selectivity of complex **6c** can be substantially improved by variation of the alkoxy group of the diazoacetate **8**. The optical yields of 95–97%, which we obtained with the *d*-menthyl ester, clearly exceed the selectivities previously observed in the cyclopropanation of styrene with other catalysts (81 and 78% *ee* for **9** and **10**, respectively, using Cu^{II}-salicylaldimine complexes (R^2 = menthyl);[6b] 88 and 81% *ee*, using Co^{II}-camphorquinone-dioximato complexes (R^2 = neopentyl)[7]). Butadiene and 1-heptene also react with high enantioselectivity. In the case of 1-heptene, however, the decreased reactivity of the double bond compared to styrene and butadiene results in lower chemical yields of cyclopropanes due to competing formation of other products such as menthyl fumarate and maleate. We are currently exploring the scope and limitations of the cyclopropanation catalysts **6**, as well as other applications of semicorrin ligands in enantioselective catalysis.

Received: July 21, 1986 [Z 1865 IE]
German version: *Angew. Chem.* 98 (1986) 1028

[*] Dr. A. Pfaltz, Dipl.-Chem. H. Fritschi,
Dipl.-Naturwiss. U. Leutenegger
Laboratorium für Organische Chemie der ETH
ETH-Zentrum, CH-8092 Zürich (Switzerland)

[**] This work was supported by the Schweizerischer Nationalfonds zur Förderung der wissenschaftlichen Forschung. We thank Prof. *A. Eschenmoser* for his support and *K. Siegmann* and *D. Müller* for their collaboration in the early stages of the investigation.

[1] a) H. B. Kagan ("Asymmetric Synthesis Using Organometallic Catalysts") in G. Wilkinson, F. G. A. Stone, E. W. Abel (Eds.): *Comprehensive*

Organometallic Chemistry, Vol. 8, Pergamon Press, Oxford 1982, p. 463; b) H. B. Kagan ("Chiral Ligands for Asymmetric Catalysis") in J. D. Morrison (Ed.): *Asymmetric Synthesis Vol. 5*, Academic Press, Orlando, FL, USA 1985, p. 1.

[2] The name "semicorrin" for bicyclic vinamidines of this type was first used by *R. V. Stevens* (cf. R. V. Stevens, L. E. DuPree, Jr., M. P. Wentland, *J. Chem. Soc. Chem. Commun. 1970*, 821).

[3] H. Bertele, H. Boos, J. D. Dunitz, F. Elsinger, A. Eschenmoser, I. Felner, H. P. Gribi, H. Gschwend, E. F. Meyer, M. Pesaro, R. Scheffold, *Angew. Chem. 76* (1964) 393; *Angew. Chem. Int. Ed. Engl. 3* (1964) 490.

[4] The cyanoenamine **4** was prepared earlier in connection with other work: A. Pfaltz, N. Bühler, R. Neier, K. Hirai, A. Eschenmoser, *Helv. Chim. Acta 60* (1977) 2653; N. Bühler: *Synthetische und mechanistische Studien zum Aufbau corrinoider Metallkomplexe durch lichtinduzierte A/D-Cycloisomerisierung, Dissertation ETH No. 5154*, Zurich 1973.

[5] Cf.: A. P. Johnson, P. Wehrli, R. Fletcher, A. Eschenmoser, *Angew. Chem. 80* (1968) 622; *Angew. Chem. Int. Ed. Engl. 7* (1968) 623; P. Wehrli, R. Neier, A. Eschenmoser, published in: P. Wehrli: *Versuche zur Synthese von Corrin-Komplexen, Dissertation ETH No. 4043*, Zurich 1967; R. Neier: *Über den Mechanismus der photochemischen A/D-Secocorrin→Corrin-Cycloisomerisierung, Dissertation ETH No. 6178*, Zurich 1978.

[6] a) H. Nozaki, H. Takaya, S. Moriuti, R. Noyori, *Tetrahedron 24* (1968) 3655; b) T. Aratani, Y. Yoneyoshi, T. Nagase, *Tetrahedron Lett. 1975*, 1707; *ibid. 1977*, 2599; *ibid. 23* (1982) 685; T. Aratani, *Pure Appl. Chem. 57* (1985) 1839; c) J. E. Baldwin, C. G. Carter, *J. Am. Chem. Soc. 104* (1982) 1362; d) S. A. Matlin, W. J. Lough, L. Chan, D. M. H. Abram, Z. Zhou, *J. Chem. Soc. Chem. Commun. 1984*, 1038; e) D. Holland, D. A. Laidler, D. J. Milner, *J. Mol. Catal. 11* (1981) 119; D. A. Laidler, D. J. Milner, *J. Organometal. Chem. 270* (1984) 121; f) H. Brunner, W. Miehling, *Monatsh. Chem. 115* (1984) 1237.

[7] A. Nakamura, A. Konishi, Y. Tatsuno, S. Otsuka, *J. Am. Chem. Soc. 100* (1978) 3443; A. Nakamura, *Pure Appl. Chem. 50* (1978) 37.

[8] P. E. Krieger, J. A. Landgrebe, *J. Org. Chem. 43* (1978) 4447; T. Schotten, W. Boland, L. Jaenicke, *Helv. Chim. Acta 68* (1985) 1186.

$[Ag(NCS)_2AsF_6]_n$—A Metal Complex with Dithiocyanogen as Ligand**

By *Herbert W. Roesky,* Jürgen Schimkowiak, Karen Meyer-Bäse,* and *Peter G. Jones*

Dedicated to Professor Oskar Glemser on the occasion of his 75th birthday

Söderbäck[1] reported the first synthesis of dithiocyanogen (dithiocarbonitrile), **1**, as long ago as 1919. The compound can be prepared quite simply from silver or lead thiocyanate and bromine. In the free state it polymerizes rapidly and irreversibly to a brick-red polythiocyanogen. Solutions of **1** in carbon tetrachloride are stable and are preparatively useful for the introduction of NCS groups into arenes or for addition to olefins.[2]

The thiocyanate ion, $NCS^{\ominus}$, is a good ligand, and numerous complexes are known in which $NCS^{\ominus}$ is bound via sulfur or nitrogen to a metal center.[3] We recently reported on the cycloaddition of hexafluoroacetone to **1** without cleavage of the S–S bond.[4] We have now succeeded, for the first time, in attaching **1** as ligand to a transition metal. This was achieved upon reaction of $AgAsF_6$ with **1** in liquid SO_2.

$$\underset{\mathbf{1}}{NCS{-}SCN} + AgAsF_6 \longrightarrow \frac{1}{n}\underset{\mathbf{2}}{[Ag(NCS)_2AsF_6]_n}$$

The title compound **2** is a white crystalline solid which decomposes with charring above 155 °C. The IR and Raman spectra indicate that **1** is coordinated to silver; the CN stretching vibration appears at 2196 cm^{-1}. In uncoordinated **1**, ν(CN) is observed at 2175 cm^{-1}.[5]

Crystals of **2** suitable for an X-ray structure analysis were obtained by recrystallization from liquid SO_2. The cation of **2** is a chain polymer (Fig. 1) with exactly linearly coordinated silver; the zig-zag chains display perpendicular dislocations at the S–S bonds.

The S-S distance (206.3(3) pm) lies in the usual range.[6] The upfield shift of the CN stretching vibration is consistent with the short N-C distance (111.6(9) pm). In accordance with the lower coordination number of the metal (2 as compared to 4), the Ag-N distance (211.7(6) pm) is significantly shorter than in polymeric $[Ag\{(CN)_2\}_2]^{\oplus}$ (239.9(6) pm)[7] and polymeric $[Ag\{S_n(CN)_2\}_2]^{\oplus}$ (227.4(11) for n = 3, 228.8(7) pm for n = 4).[6]

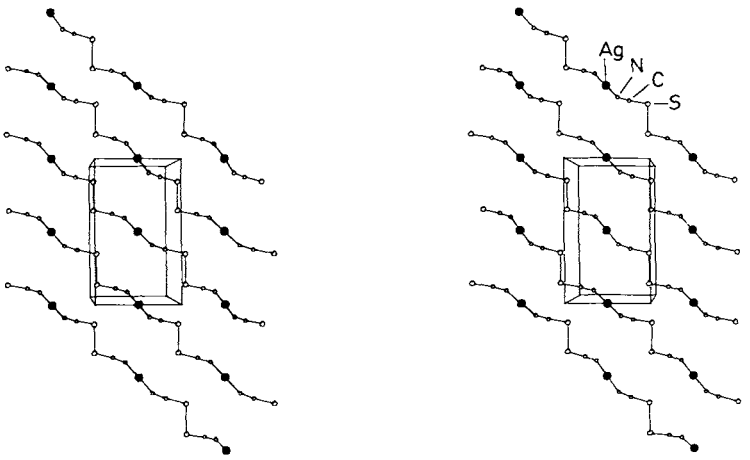


Fig. 1. Polymeric chains of $[Ag(SCN)_2]_n^{n\oplus}$ in **2**. View along y; the chains pass through the unit cell at $y = 0$ (shown here) and $y = \frac{1}{2}$ (omitted for clarity). Crystal data: orthorhombic, *Pbcn*, $a = 594.2(1)$, $b = 1608.0(4)$, $c = 1016(2)$ pm, $V = 0.9714$ nm^3, $Z = 4$ (monomers), $\rho_{calc} = 2.82$ g cm^{-3}, $Mo_{K\alpha}$ radiation, $\mu = 6.0$ mm^{-1}, $2\theta_{max}$ 50°, $R = 0.037$, $R_w = 0.039$ for 626 absorption- and extinction-corrected reflections with $F > 4\sigma(F)$. Ag lies on the symmetry center $\frac{1}{2}$,0,0 and As on the twofold axis 0,y,$\frac{1}{4}$. The anions (not shown) are disordered.—Bond lengths [pm] and angles [°]: Ag-N 211.7(6), N-C 111.6(9), C-S 170.8(7), S-S' 206.3(3); N-Ag-N' 180.0, Ag-N-C 154.4(6), N-C-S 174.6(6), C-S-S' 98.9(2). Further details of the crystal structure investigation are available on request from the Fachinformationszentrum Energie, Physik, Mathematik gmbH, D-7514 Eggenstein-Leopoldshafen 2 (FRG), on quoting the depository number CSD-51908, the names of the authors, and the full citation of the journal.

[*] Prof. Dr. H. W. Roesky, J. Schimkowiak, K. Meyer-Bäse, Prof. Dr. P. G. Jones
Institut für Anorganische Chemie der Universität
Tammannstrasse 4, D-3400 Göttingen (FRG)

[**] This work was supported by the Deutsche Forschungsgemeinschaft and the Fonds der Chemischen Industrie.

Experimental

1.93 g (6.5 mmol) of $AgAsF_6$ was added to 1.51 g (13 mmol) of **1** in a pressure vessel at −25 °C. After evacuation of the vessel, SO_2 (30 mL) was condensed into the reaction mixture at −80 °C. The mixture was allowed to warm to room temperature in the absence of light and then stirring was con-

tinued for 36 h. The clear bright yellow solution was filtered, and, after removal of solvent, the residue (**2**) was recrystallized from SO_2; yield 2.3 g (86%).

Received: March 10, 1986 [Z 1699 IE]
German version: *Angew. Chem. 98* (1986) 998

CAS Registry number:
2, 104693-65-4.

[1] E. Söderbäck, *Justus Liebigs Ann. Chem. 419* (1919) 217.
[2] R. G. R. Bacon, *Org. Sulfur Compds. 1* (1961) 316.
[3] A. M. Golub, H. Köhler: *Chemie der Pseudohalogenide*, Hüthig, Heidelberg 1979.
[4] H. W. Roesky, N. Homsy, M. Noltemeyer, G. M. Sheldrick, *Angew. Chem. 96* (1984) 1002; *Angew. Chem. Int. Ed. Engl. 23* (1984) 1000.
[5] C. E. Vanderzee, A. S. Quist, *Inorg. Chem. 5* (1966) 1238.
[6] H. W. Roesky, T. Gries, J. Schimkowiak, P. G. Jones, *Angew. Chem. 98* (1986) 93; *Angew. Chem. Int. Ed. Engl. 25* (1986) 84.
[7] H. W. Roesky, H. Hofmann, J. Schimkowiak, P. G. Jones, K. Meyer-Bäse, G. M. Sheldrick, *Angew. Chem. 97* (1985) 403; *Angew. Chem. Int. Ed. Engl. 24* (1985) 417.

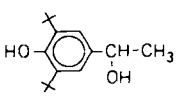
Recognition of Chirality by ENDOR Spectroscopy**

By *Hartmut B. Stegmann,* Helmut Wendel, Hoang Dao-Ba, Paul Schuler,* and *Klaus Scheffer*

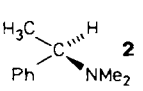
The unequivocal detection of enantiomeric compounds and the determination of their relative concentrations and absolute configurations have gained increasing importance in the last few years. Hitherto, polarimetry and (with the use of chiral auxiliaries) NMR spectroscopy as well as chromatographic methods were mainly employed for chiral recognition,[1] whereas the use of electron nuclear double resonance[2] (ENDOR) spectroscopy for solving such analytical problems has so far never been described. The great advantages of this technique are that very little sample material is required and the spectra thus obtained are virtually solvent-independent. Moreover, proton-containing matrices (solvent, chiral auxiliaries or other diamagnetic components) do not interfere with ENDOR investigations through self-absorption, and, other than in NMR spectroscopy, no signal multiplets occur, which, quite frequently might afford important information but sometimes make the analysis of ^{1}H-NMR spectra very difficult.

Numerous natural products such as ascorbic acid, noradrenalin, adrenalin, isoprenalin etc. contain an asymmetric C-atom with an OH-group as part of the structure. The semidiones[3] or semiquinones[4] formed by oxidation of these compounds could be investigated ESR spectroscopically using the spin-stabilization technique,[5] but it was found that, in most cases, pyridine had to be used as solvent owing to solubility problems. In order to carry out measurements in inert solvents and thus definitely decide whether an ENDOR spectroscopic recognition of enantiomers using chiral auxiliaries is possible, we synthesized racemic 2,6-di-*tert*-butyl-4-(1-hydroxyethyl)phenol **1**.[6]

Oxidation of **1** with lead dioxide in toluene furnished the corresponding, hitherto unknown, phenoxyl radical



1



2

[*] Prof. Dr. H. B. Stegmann, H. Wendel, Dipl.-Chem. H. Dao-Ba, P. Schuler, Prof. Dr. K. Scheffler
Institut für Organische Chemie der Universität
Auf der Morgenstelle 18, D-7400 Tübingen (FRG)

[**] This work was supported by the Deutsche Forschungsgemeinschaft and the Fonds der Chemischen Industrie.

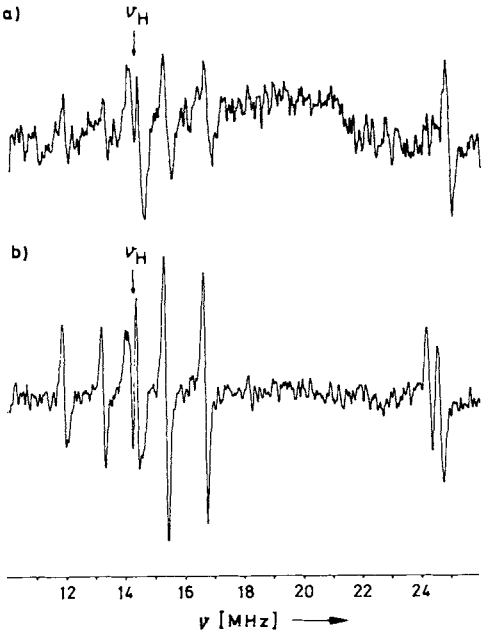


Fig. 1. ENDOR spectrum of **1**(−H) at 253 K. a) In toluene. b) In toluene after addition of **2**, molar ratio **2** : **1** = 9.2.

1(−H) which could be characterized by $a_{t\mathrm{Bu}} = 0.11$, $a_{3,5} = 1.75$, $a_{\mathrm{CH}} = 7.61$, and $a_{\mathrm{CH_3}} = 0.73$ G. Addition of (*R*)-(+)-*N*,*N*-dimethyl-1-phenylethylamine **2** did not alter the ESR spectrum, since the hyperfine structure is not fully resolved because of the small coupling to the protons of the *t*Bu groups. In the ENDOR spectrum (Fig. 1), on the other hand, the signal at ca. 25 MHz splits into two signals (intensity ratio about 1), which, on the basis of the ESR spectrum, we assign to the proton on the asymmetric C-atom. The corresponding low frequency absorption can hardly be detected according to the well known low signal-to-noise ratio at frequencies below 4 MHz. The distance between the two lines increases with increasing amine concentration, and at a molar ratio of **2** : **1** = 30 : 1 approaches a limiting value (Fig. 2). A similar behavior has already been observed in NMR investigations.[7]

A splitting of the remaining ENDOR signals was not observed. The linewidths merely increase with increasing amine concentration.

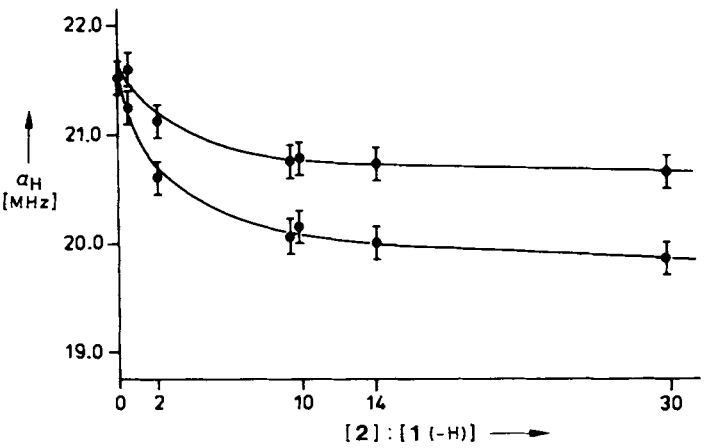


Fig. 2. Coupling of the proton at the asymmetric C-atom of **1**(−H) in both enantiomers as a function of the molar ratio **2** : **1**.

The intensity of the two lines at 25 MHz remained constant over the concentration range investigated, and, since the maximum line separation is ca. 0.4 MHz, that is the magnetic environment of the two protons is very similar, significantly different relaxation effects are highly improbable. For these reasons, differences in the solvation of the phenoxyl radicals can be ruled out as an explanation for the doublet at ca. 25 MHz. We therefore attribute the two signals to diastereomeric solvates.

The coupling of the proton at the asymmetric C-atom can be attributed to a hyperconjugation mechanism[8] corresponding to $a^{H}_{C-CH}=(B_0+B\langle\cos^2\Theta\rangle\rho C_\alpha)$. Whether B or the torsion angle Θ is responsible for the splitting will be explained by further systematic investigations of analogous systems. Since the couplings of the two ring protons $a_{3,5}$ remain constant no significant change in the spin density distribution can be expected during the formation of the diastereomers.

Received: May 30, 1986;
revised: July 14, 1986 [Z 1797 IE]
German version: *Angew. Chem. 98* (1986) 988

CAS Registry numbers:
1, 104438-67-7; **1** (−H), 104438-68-8; **2**, 19342-01-9.

[1] V. Schurig, *Kontakte 1985*, No. 1, p. 54.
[2] H. Kurreck, B. Kirste, W. Lubitz, *Angew. Chem. 96* (1984) 171; *Angew. Chem. Int. Ed. Engl. 23* (1984) 173.
[3] H. B. Stegmann, K. Scheffler, P. Schuler, *Angew. Chem. 90* (1978) 392; *Angew. Chem. Int. Ed. Engl. 17* (1978) 365.
[4] H. B. Stegmann, H. Dao-Ba, K. Stolze, K. Scheffler, *Fresenius Z. Anal. Chem. 322* (1985) 430.
[5] H. B. Stegmann, H. U. Bergler, K. Scheffler, *Angew. Chem. 93* (1981) 398; *Angew. Chem. Int. Ed. Engl. 20* (1981) 389.
[6] A. A. Volod'kin, V. V. Ershov, N. V. Portnykh, *Izv. Akad. Nauk SSSR Ser. Khim. 1967*, 409.
[7] W. H. Pirkle, D. J. Hoover, *Top. Stereochem. 13* (1982) 263; A. Mannschreck, *Nachr. Chem. Tech. 23* (1975) 295.
[8] K. Scheffler, H. B. Stegmann: *Elektronenspinresonanz*, Springer, Berlin 1970.

A Simple Route to Ruthenacycloalkanes**

By *Ekkehard Lindner,* Rolf-Michael Jansen*, and *Hermann August Mayer*

Metallacycloalkanes frequently occur as reactive intermediates in transition metal catalyzed organic syntheses such as olefin carbonylations, oligomerizations of olefins, or metathesis reactions.[1] In the past few years, such compounds have been described as model substances for numerous transition metals.[2] For lack of suitable synthetic methods, very few mononuclear carbonyl complexes of ruthenium containing metal-carbon σ bonds have been described in the literature.[3] By using the "nucleophilic elimination cycloaddition" method,[4] which has already been successful in the generation of tetracarbonylferracyclopentane,[5] we have now found a simple route to ruthenacycloalkanes.

$Na_2[Ru(CO)_4]$ reacts smoothly with the alkanediylbis(trifluoromethanesulfonates) $(YCH_2)_2$, $(YCH_2CH_2)_2$ and *cyclo*-$C_6H_{10}(CH_2Y)_2$ ($Y=CF_3SO_2O$) in dimethyl ether at −78°C to give the air-sensitive, thermolabile ruthenium compounds **1**–**3**, which are readily soluble in all the usual organic solvents.[6] Their composition and structures were established unequivocally from the IR, ^{1}H- and $^{13}C\{^1H\}$-NMR, and mass spectra (Table 1). **1** has already been detected before in solution by IR spectroscopy.[8] Due to the conformational mobility of **1**, only one signal each is observed for the two ethylene carbon atoms and for the four carbonyl carbon atoms; their position, as in the case of $[(\eta^2\text{-}C_2H_4)Fe(CO)_4]$,[5] is consistent with an ethylene complex rather than a ruthenacyclopropane.[9]

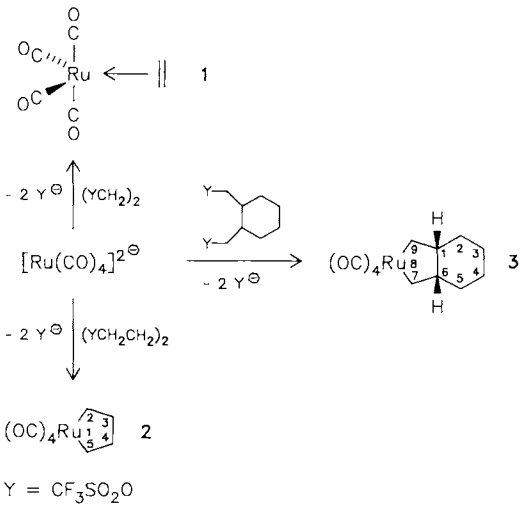


Table 1. Spectroscopic data and melting points of **1**–**3**.

Cpd.	IR ν(CO) [a]	^{1}H-NMR δ [b]	$^{13}C\{^1H\}$-NMR δ [b]	MS *m/z* [c]	M.p. [°C]
1	2107 (m)	2.16 (s)	25.15 (s)		−30 (decomp.)
	2025 (vs)		198.89 (s)		
	2000 (s)				
2	2119 (w)	1.58 (s)	11.63 (s, C2,5)	274	−20 (decomp.)
	2049 (s)		36.90 (s, C3,4)		
	2040 (vs)		189.70 (s, [d])		
	2023 (s)		197.28 (s, [e])		
3	2118 (s-m)	0.8–2.0 (m)	12.80 (s, C7,9)	326	− 3
	2048 (s)		23.34 (s, C3,4)		
	2039 (vs)		29.67 (s, C2,5)		
	2022 (s)		46.92 (s, C1,6)		
			189.39 (s, [d])		
			197.44 (s, [e])		
			198.47 (s, [e])		

[a] In *n*-hexane. [b] In $CDCl_3$, 80 and 20.115 MHz, δ values rel. $CDCl_3$, $T=233$ K. [c] ($M^{\oplus}$) referred to ^{104}Ru. [d] $Ru(CO)_2$ (*cis*). [e] $Ru(CO)_2$ (*trans*).

The appearance of four CO bands in the IR spectra of **2** and **3** is consistent with a pseudooctahedral coordination of the central atom. The ring skeleton of **2** and **3** gives rise to two and four signals, respectively, in the $^{13}C\{^1H\}$-NMR spectra. The carbonyl C-atoms absorb below $\delta=200$. The CO ligands oriented *cis* and *trans to each other* differ by virtue of the +I effect of the methylene groups. The signal appearing at lower field is *in each case* assigned to the *trans* CO groups in **2** and **3**. Due to their different environment the two carbonyl C-atoms oriented *trans to each other* in **3** give rise to two signals.

[*] Prof. Dr. E. Lindner, R.-M. Jansen, Dr. H. A. Mayer
Institut für Anorganische Chemie der Universität
Auf der Morgenstelle 18, D-7400 Tübingen 1 (FRG)

[**] Preparation and Properties of and Reactions with Metal-containing Heterocycles, Part 54. This work was supported by the Deutsche Forschungsgemeinschaft and the Fonds der Chemischen Industrie.—Part 53: E. Lindner, K. Auch, G. A. Weiss, W. Hiller, R. Fawzi, *Chem. Ber.*, in press.

When stored under carbon monoxide, the ruthenacyclopentane **2** decomposes only above 60 °C. At this temperature a (formal) insertion of CO[5] into a Ru–C bond with formation of cyclopentanone is observed,[10] the latter being formed from the non-isolable six-membered intermediate $[(OC)_4\overline{Ru}C(O)CH_2CH_2CH_2\overline{C}H_2]$ by reductive elimination. The same results upon reaction of **2** with PPh_3. In the absence of CO, **2** already decomposes at −20 °C with cleavage of 1,3-butadiene and *trans*- and *cis*-2-butene in the molar ratio 3:3:1. Prerequisite for the occurrence of butadiene is a twofold β-hydride transfer, which requires a free coordination site at the metal by elimination of CO. This explains the unusual stability of **2** in the presence of carbon monoxide. The elimination of *cis*- and *trans*-2-butene from **2** probably takes place via an allylic intermediate.[5]

Received: June 12, 1986 [Z 1811 IE]
German version: *Angew. Chem. 98* (1986) 1000

CAS Registry numbers:
1, 52621-15-5; **2**, 104739-34-6; **3**, 104739-35-7; $(CF_3SO_2OCH_2)_2$, 18928-34-2; $(CF_3SO_2OCH_2CH_2)_2$, 18934-34-4; *cyclo*-$C_6H_{10}(CH_2OSO_2CF_3)_2$, 100849-24-9; $Na_2[Ru(CO)_4]$, 57398-60-4.

[1] P. Binger, M. J. Doyl, R. Benn, *Chem. Ber. 116* (1983) 1; E. Weissberger, P. Laszlo, *Acc. Chem. Res. 9* (1976) 209; R. H. Grubbs, A. Miyashita, *Tetrahedron Lett. 22* (1981) 1255.
[2] E. Lindner, *Adv. Heterocycl. Chem. 39* (1986) 237.
[3] R. Kuwae, K. Kawakami, T. Tanaka, *Inorg. Chim. Acta 22* (1977) 39.
[4] E. Lindner, H.-J. Eberle, *Angew. Chem. 92* (1980) 70; *Angew. Chem. Int. Ed. Engl. 19* (1980) 73; E. Lindner, G. von Au, H.-J. Eberle, *Chem. Ber. 114* (1981) 810.
[5] E. Lindner, E. Schauss, W. Hiller, R. Fawzi, *Angew. Chem. 96* (1984) 727; *Angew. Chem. Int. Ed. Engl. 23* (1984) 711; *Chem. Ber. 118* (1985) 3915.
[6] Procedure: A solution of 3 mmol of $(CF_3SO_2OCH_2)_2$, $(CF_3SO_2OCH_2CH_2)_2$, or *cyclo*-$C_6H_{10}(CH_2OSO_2CF_3)_2$ [7], respectively, in dimethyl ether (100 mL) was added dropwise within 3 h at −78 °C to a suspension of $Na_2[Ru(CO)_4]$ (3 mmol) in dimethyl ether (50 mL). The mixture was stirred for 12 h at −78 °C, the solvent removed under vacuum at this temperature, and the residue dissolved in 100 mL of *n*-butane. Upon evaporation of the solution to dryness, the metallacycles (correct Ru values in atomic absorption spectral analyses) precipitated as colorless (**1**) or pale yellow (**2**, **3**) compounds. Recrystallization from *n*-butane at −78 °C; yields 50–60%.
[7] E. Lindner, E. Schauss, *Chem. Ber. 118* (1985) 4292.
[8] B. F. G. Johnson, J. Lewis, M. V. Twigg, *J. Organomet. Chem. 67* (1974) C75.
[9] M. L. Steigerwald, W. A. Goddard III, *J. Am. Chem. Soc. 107* (1985) 5027.
[10] F. W. Grevels, D. Schulz, E. Koerner von Gustorf, *Angew. Chem. 86* (1974) 558; *Angew. Chem. Int. Ed. Engl. 13* (1974) 534.

O_2-Generation by Oxidation of Water with Di- and Trinuclear Ruthenium Complexes as Homogeneous and Heterogeneous Catalysts

By *Ramasamy Ramaraj, Akira Kira,* and *Masao Kaneko**

Water-oxidation with generation of molecular oxygen was first realized only five years ago:[1] the strong one-electron oxidizing agent $Ru(bpy)_3^{3\oplus}$ (bpy = 2,2′-bipyridyl) is able to bring about the four-electron oxidation of water to oxygen on the surface of a suitable colloidal or powdered oxide catalyst such as RuO_2.[2] These catalysts are far from ideal, because the reaction is slow and there are many problems associated with their use in model systems. The main difficulty of constructing such models lies in the coupling of the one-electron oxidant with the four-electron formation of oxygen from water. We consider that the design of chemical models and the study of water-oxidation in non-biological systems are probably the best way of gaining an insight into the mechanism of the photosynthetic evolution of oxygen. It has already been shown[3,4] that dinuclear ruthenium complexes are capable of oxidizing water by a four-electron process without the addition of an external catalyst like RuO_2. However, the catalyst turnover number is not high and the total yield of oxygen obtainable from such systems remains low.[4] According to recent findings, not only homogeneous systems but also heterogeneous ones may be of importance.[5] We report here on the catalytic activity of oxo-bridged di- and trinuclear ruthenium complexes in the homogeneous and heterogeneous oxidation of water.

As trinuclear ruthenium complex we used commercially available ruthenium-red (Wako Chemicals); ruthenium-brown was prepared according to the procedure described in ref. [6] (with slight modification). The ruthenium-red cation is oxidized reversibly in acid solution to the ruthenium-brown cation.

$[(NH_3)_5Ru-O-Ru(NH_3)_4-O-Ru(NH_3)_5]Cl_6$
ruthenium red
abbreviation for the cation:
$Ru^{III}-O-Ru^{IV}-O-Ru^{III}$ or III, IV, III

$[(NH_3)_5Ru-O-Ru(NH_3)_4-O-Ru(NH_3)_5]Cl_7$
ruthenium brown
abbreviation for the cation:
$Ru^{IV}-O-Ru^{III}-O-Ru^{IV}$ or IV, III, IV

The dinuclear ruthenium complexes "Ru–Ru–H_2O" and "Ru–Ru–NO_2" were prepared and characterized according to previously reported procedures.[3,4]

$[(bpy)_2(H_2O)Ru-O-Ru(H_2O)(bpy)_2](PF_6)_4$
Ru–Ru–H_2O
abbreviation for the cation: $Ru^{III}-O-Ru^{III}$

$[(bpy)_2(NO_2)Ru-O-Ru(NO_2)(bpy)_2](PF_6)_2$
Ru–Ru–NO_2
abbreviation for the cation: $Ru^{III}-O-Ru^{III}$

The heterogeneous catalysts were prepared by mixing the di- or trinuclear ruthenium complex with commercially available kaolin (Nakarai Chemicals Ltd.) in deionized water and stirring the mixture until completion of adsorption (decolorization of the solution). The product was filtered, washed with deionized water, and dried in air. It has been reported[6,7] that the differences in the Mössbauer and electronic spectra of the cations of ruthenium red and ruthenium brown are consistent with the charge distribution indicated in Equation (1).

$$\underset{\text{Ru-red}}{Ru^{III}-O-Ru^{IV}-O-Ru^{III}} \underset{+e^{\ominus}}{\overset{-e^{\ominus}}{\rightleftharpoons}} \underset{\text{Ru-brown}}{Ru^{IV}-O-Ru^{III}-O-Ru^{IV}} \qquad (1)$$

The absorption spectra show that ruthenium-red undergoes thermal and photochemical decomposition in aqueous solution. In contrast, ruthenium-brown does not show

[*] Prof. Dr. M. Kaneko, Dr. R. Ramaraj, Prof. Dr. A. Kira
Solar Energy Science Research Group
The Institute of Physical and Chemical Research
Wako, Saitama, 351-01 (Japan)

any noticeable thermal or photochemical decomposition in acidic aqueous solution. The higher thermal and photochemical stability in the latter case may be due to a charge delocalization in the linearly oxo-bridged cations of ruthenium-brown.[8]

Cyclovoltammograms of the trinuclear ruthenium complexes were recorded in aqueous solution using a basal plane pyrrolytic graphite (BPG) working electrode and a saturated calomel electrode (SCE). The oxidation of water interferes in the higher potential region. However, a well defined cyclovoltammogram could be obtained in the same potential region by using a BPG electrode coated with poly(styrene sulfonate). The reversible one-electron reduction of ruthenium-brown [Eq. (1)] and the reduction of ruthenium-red have already been investigated.[6] In the present investigation, the cyclovoltammograms of ruthenium-red showed six reduction peaks which are reversible in the oxidative scan in the potential region -0.5 V to 1.4 V vs. SCE. The wave shapes indicate that five one-electron-transfer processes occur at potentials which are fairly close to each other. The redox process which occurs at -0.24 V closely resembles the reactions observed in the case of the monomeric ammine-ruthenium(III) complexes.[9] The cyclovoltammogram is consistent with a series of one-electron oxidations [Eq. (2)];

$$\begin{aligned}&\mathrm{III,III,III} \underset{-0.24\ \mathrm{V}}{\overset{-e^{\ominus}}{\rightleftharpoons}} \underbrace{\mathrm{III,IV,III}}_{\text{Ru-red}} \underset{0.72\ \mathrm{V}}{\overset{-e^{\ominus}}{\rightleftharpoons}} \underbrace{\mathrm{IV,III,IV}}_{\text{Ru-brown}} \underset{0.84\ \mathrm{V}}{\overset{-e^{\ominus}}{\rightleftharpoons}} \\ &\mathrm{IV,IV,IV} \underset{0.95\ \mathrm{V}}{\overset{-e^{\ominus}}{\rightleftharpoons}} \mathrm{IV,V,IV} \underset{1.08\ \mathrm{V}}{\overset{-e^{\ominus}}{\rightleftharpoons}} \mathrm{V,IV,V} \underset{1.16\ \mathrm{V}}{\overset{-e^{\ominus}}{\rightleftharpoons}} \mathrm{V,V,V}\end{aligned} \qquad (2)$$

From the cyclovoltammetric data it is evident that the trinuclear ruthenium complex exhibits multi-step reversible electron-transfer behavior and may be called an "electron sponge."

Oxygen evolution was investigated by adding excess ammonium ceric nitrate to a solution of the trinuclear ruthenium complex in a closed and degassed vessel. Gas bubbles were observed in the solution upon addition of excess cerium(IV) salt. The gas evolved was identified as oxygen by gas chromatography. When $H_2{}^{18}O$ was used, mass spectral analysis resolved the presence of $^{16}O_2$, $^{18}O^{16}O$ and $^{18}O_2$, respectively.

Table 1. Water oxidation by ammonium cerium(IV) nitrate in the presence of di- and trinuclear ruthenium catalysts in 1 h at 25°C under homogeneous and heterogeneous conditions (on Kaolin). Solution volume 5 mL. Molar ratio catalyst : cerium(IV) 1 : 400.

Catalyst		Homogeneous		Heterogeneous		Kaolin
		O_2	turnover	O_2	turnover	
	[mol]	[μL]	number	[μL]	number	[mg]
Ru-red	1×10^{-6}	1325	54.7	1022	42.2	300
Ru-brown	1×10^{-6}	1503	62.1	1084	44.8	300
Ru–Ru–H_2O	5×10^{-7}	88	7.3	55	4.5	250
Ru–Ru–NO_2	5×10^{-7}	30	2.5	18	1.5	250

The experimental results are summarized in Table 1, from which it is clear that the trinuclear ruthenium complexes are remarkably better catalysts for water-oxidation than are the dinuclear ruthenium complexes, both in homogeneous as well as heterogeneous phases. However, the trinuclear ruthenium complexes were found to undergo decomposition during the catalytic processes with a maximum turnover number of 62. Variation of the catalyst concentration in the homogeneous and heterogeneous phases had no influence on the catalytic activity. This finding suggests that a single molecule of the di- or trinuclear ruthenium complex is involved in the four-electron process of oxygen evolution. It has also been found that the addition of 0.1 M HNO_3 or 0.1 M NaOH does not affect the catalytic activity of the complexes. This shows that the oxidized species is a water molecule rather than a hydroxide ion. Ruthenium-red was converted into the stable ruthenium-brown in acidic solution. The anodic oxidation of ruthenium-red (+1.3 V vs. SCE) also led to the formation of ruthenium-brown; no formation of RuO_2 was observed.

The formation and stability of Ru^V in oxo-bridged dinuclear ruthenium complexes and its catalytic activity have been reported on just recently.[3,4,10] In the water oxidation experiment with ruthenium-red and Ce(IV) in the molar ratio 1 : 100, ruthenium-brown was observed spectrophotometrically at the end of the catalytic process. When, however, a molar ratio of 1 : 400 was used, the catalyst was found to undergo decomposition to a monomeric ruthenium complex at the end of the catalytic process. No formation of the black deposit characteristic of RuO_2 was observed.

From the observed data, it is concluded that the system ruthenium-red/ruthenium-brown catalyzes the water oxidation by Ce(IV). Ruthenium-red is converted into highly stable ruthenium-brown in acidic solutions as well as in the presence of anions such as $NO_3^{\ominus}$, $Cl^{\ominus}$ and $SO_4^{2\ominus}$; dinuclear ruthenium complexes, on the other hand, undergo decomposition to monomeric complexes.

$$\underbrace{\mathrm{Ru^{III}{-}O{-}Ru^{IV}{-}O{-}Ru^{III}}}_{\text{Ru-red}} + 5\ \mathrm{Ce^{IV}} \longrightarrow \mathrm{Ru^{V}{-}O{-}Ru^{V}{-}O{-}Ru^{V}} + 5\ \mathrm{Ce^{III}} \qquad (3)$$

$$\mathrm{Ru^{V}{-}O{-}Ru^{V}{-}O{-}Ru^{V}} + 2\ \mathrm{H_2O} \longrightarrow \mathrm{Ru^{V}(H_2O){-}O{-}Ru^{V}(H_2O){-}O{-}Ru^{V}} \xrightarrow{-4\ \mathrm{H^{\oplus}}} \qquad (4)$$

$$\mathrm{Ru^{III}}\begin{smallmatrix}\diagup\mathrm{O}\\ \mathrm{O{-}O}\diagdown\end{smallmatrix}\mathrm{Ru^{III}{-}O{-}Ru^{V}} \longrightarrow \underbrace{\mathrm{Ru^{IV}{-}O{-}Ru^{III}{-}O{-}Ru^{IV}}}_{\text{Ru-brown}} + \mathrm{O_2}$$

A trinuclear ruthenium complex in the oxidation state V,V,V [Eq. (2)] is formed upon addition of excess Ce(IV) to ruthenium-red [Eq. (3)]. Subsequent reaction with water yields oxygen and ruthenium-brown [Eq. (4)]. This ruthenium-brown is highly stable and catalyzes the oxidation of water in the presence of excess Ce(IV) in a cyclic process. In the case of dinuclear ruthenium complexes, the water-oxidation reaction is described by Equation (5).[4]

$$\mathrm{Ru^{V}{-}O{-}Ru^{V}} + 2\,\mathrm{H_2O} \longrightarrow \mathrm{Ru^{III}{-}O{-}Ru^{III}} + \mathrm{O_2} + 4\,\mathrm{H^{\oplus}} \qquad (5)$$

Earley and *Fealey*[6] studied the kinetics of the reduction of ruthenium-brown by hydroxide ion. They suggested that the attack of $OH^{\ominus}$ ion on the central ruthenium atom in ruthenium-brown would be the most probable step for which no symmetry restriction is to be anticipated, and that the reduction leads to the formation of ruthenium-red. According to *Endicott* and *Taube*[11] a spin-paired d^4 ion (Ru^{IV}) can accommodate seven groups in the coordination sphere; these authors assume that Ru^{III} also forms seven-

coordinate species as kinetic intermediates.[12] From these results we assume that two water molecules are involved in the formation of one molecule of oxygen. The first water molecule attacks the central Ru^V ion in the trinuclear ruthenium complex [Eq. (3)], the second one coordinates at one of the terminal Ru^V atoms. This intermediate may lead to the formation of an O–O bond between the two water molecules. This is followed by release of oxygen and the re-formation of ruthenium-brown. The formation of a peroxide intermediate and evolution of oxygen in the water-oxidation process with dinuclear ruthenium complexes has already been proposed by *Meyer* et al.[6] An analogous model for water-oxidation with manganese complexes in a heterogeneous environment could facilitate an understanding of the evolution of oxygen in photosynthesis.[13]

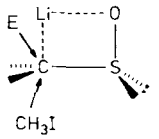
Received: July 8, 1986;
revised: September 15, 1986 [Z 1849 IE]
German version: *Angew. Chem. 98* (1986) 1012

[1] M. Grätzel (Ed.): *Energy Resources Through Photochemistry and Catalysis*, Academic Press, New York 1983; J. S. Connolly (Ed.): *Photochemical Conversion and Storage of Solar Energy*, Academic Press, New York 1981.
[2] K. Kiwi, M. Grätzel, *Angew. Chem. 90* (1978) 900; *Angew. Chem. Int. Ed. Engl. 17* (1978) 860; *ibid. 91* (1979) and *18* (1979) 624; J. M. Lehn, J. P. Sauvage, R. Ziessel, *Nouv. J. Chim. 3* (1979) 423; M. Kaneko, N. Awaya, A. Yamada, *Chem. Lett. 1982*, 619.
[3] J. A. Gilbert, D. S. Eggleston, W. R. Murphy, Jr., D. A. Geselowitz, S. W. Gersten, D. J. Hodgson, T. J. Meyer, *J. Am. Chem. Soc. 107* (1985) 3855.
[4] R. Ramaraj, A. Kira, M. Kaneko, *J. Chem. Soc. Faraday Trans. 1 82* (1986), in press.
[5] R. Ramaraj, A. Kira, M. Kaneko, *Angew. Chem. 98* (1986) 824; *Angew. Chem. Int. Ed. Engl. 25* (1986) 825.
[6] J. E. Earley, T. Fealey, *Inorg. Chem. 12* (1973) 323.
[7] J. M. Fletcher, B. F. Greenfield, C. J. Hardly, D. Scargill, J. L. Woodhead, *J. Chem. Soc. 1961*, 2000; C. A. Clausen, R. A. Prados, M. Good, *Inorg. Nucl. Chem. Lett. 7* (1971) 485.
[8] T. R. Weaver, T. J. Meyer, S. A. Adeyemi, G. M. Brown, R. P. Eckberg, W. E. Hatfield, E. C. Johnson, R. W. Murray, D. Unterker, *J. Am. Chem. Soc. 97* (1975) 3039.
[9] H. S. Lim, D. J. Barclay, F. C. Anson, *Inorg. Chem. 11* (1972) 1460.
[10] W. Kutner, J. A. Gilbert, A. Tomaszewski, T. J. Meyer, R. W. Murray, *J. Electroanal. Chem. 205* (1986) 185.
[11] J. F. Endicott, H. Taube, *Inorg. Chem. 4* (1965) 437.
[12] H. Scheidigger, J. Armor, H. Taube, *J. Am. Chem. Soc. 90* (1968) 5938.
[13] G. Renger (Ed.): *Photosynthetic Water Oxidation*, Academic Press, New York 1978, p. 229; Govindjee, T. Kambara, W. Coleman, *Photochem. Photobiol. 42* (1985) 187.

[α-(Phenylsulfinyl)-α-methylbenzyllithium-tetramethylethylenediamine]$_2$: Crystal Structure of an α-Sulfinyl "Carbanion"**

By *Michael Marsch, Werner Massa, Klaus Harms, Gerhard Baum,* and *Gernot Boche**

α-Sulfinyl "carbanions" $[R^1R^2\ddot{C}-\ddot{S}(O)R^3]^{\ominus}$ are important synthetic building blocks.[1] Thus, in reactions with electrophiles the chiral sulfoxide group determines the diastereofacial differentiation: oxygen-containing electrophiles E attack the anionic C-atom from the side of the S–O bond, whereas CH_3I approaches from the opposite side (Scheme 1).[2] On the basis of these, and other observations, an ion-pair structure (Scheme 1) was inferred for "α-lithiosulfoxides"[2b,e,f] and the diastereofacial differentiation was attributed to the attractive interaction of the electrophile E with $Li^{\oplus}$.



Scheme 1. Ion-pair structure model for α-sulfinylalkyllithium compounds [2b, e, f]. E = H_2O, D_2O, CO_2, RCHO, R_2CO, $(CH_3O)_3PO$.

We report here on the X-ray structure analysis of α-(phenylsulfinyl)-α-methylbenzyllithium-tetramethylethylenediamine **1a** (Fig. 1).[3] The diastereomer **1a** is formed from a ca. 1 : 1 mixture of the two diastereomeric α-methylbenzylphenyl sulfoxides **2** upon reaction with *n*-butyllithium in ether/TMEDA.[4]

$$\underset{\mathbf{2}}{PhCHMe-\ddot{S}(O)Ph} \xrightarrow[TMEDA/ether]{n\text{BuLi}} \underset{\mathbf{1a}}{[PhC\ddot{M}e-\ddot{S}(O)Ph]^{\ominus}Li^{\oplus}}$$

1a crystallizes as a dimer, with bonding occurring via a Li_2O_2 four-membered ring. Two further coordination sites on each $Li^{\oplus}$ are occupied by the TMEDA N-atoms. The

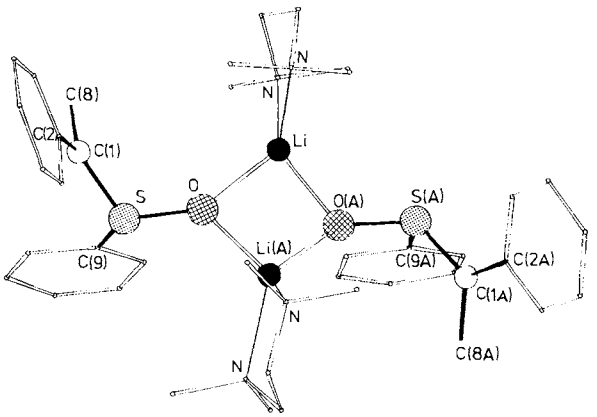


Fig. 1. Crystal structure of the dimer **1a** (H atoms omitted) at −65 °C. Space group $C2/c$, $a = 3855(2)$, $b = 1201.5(6)$, $c = 1813(1)$ pm, $\beta = 96.59(5)°$, $Z = 8$ (dimer). CAD4 (Enraf-Nonius) four-circle diffractometer, $Mo_{K\alpha}$ radiation, graphite monochromator, ω-scans, $\theta = 2$–$20°$. Because of the small crystals, with broad reflection profile ($\Delta\omega \approx 2°$)—larger crystals were always deformed—only 1865 of 4050 observed independent reflections measured; 317 parameters (only S, phenyl residues bound to S, and methyl C-atoms of TMEDA molecules with anisotropic temperature factors; H atoms placed at calculated sites). $R_w = 0.083$. The two crystallographically independent molecules are bound perpendicularly to the slightly folded Li_2O_2 four-membered ring via a pseudo C_2-axis to give the dimer.—Important bond lengths [pm] and angles [°] (mean values of both molecules): Li-O 192(2), Li-N 213(2), Li-Li(A) 265(4), S-O 158(1), S-C(1) 163(1), S-C(9) 181(1), C(1)-C(2) 144(2), C(1)-C(8) 154(2); O-Li-O 91(1), Li-O-Li 87(1), Li-O-S 148(1), Li(A)-O-S 123(1), O-S-C(1) 117(1), O-S-C(9) 101(1), C(1)-S-C(9) 104(1), S-C(1)-C(2) 120(1), S-C(1)-C(8) 119(1), C(2)-C(1)-C(8) 118(1). Further details of the crystal structure investigation are available on request from the Fachinformationszentrum Energie, Physik, Mathematik GmbH, D-7514 Eggenstein-Leopoldshafen 2 (FRG), on quoting the depository number CSD-52096, the names of the authors, and the full citation of the journal.

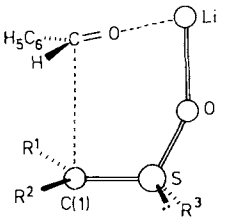
[*] Prof. Dr. G. Boche, M. Marsch, Priv.-Doz. Dr. W. Massa, G. Baum
Fachbereich Chemie der Universität
Hans-Meerwein-Strasse, D-3550 Marburg (FRG)
Dr. K. Harms
Institut für Anorganische Chemie der Universität
Tammannstrasse 4, D-3400 Göttingen (FRG)

[**] This work was supported by the Fonds der Chemischen Industrie and the Deutsche Forschungsgemeinschaft.

two phenyl rings on C(1) and S are *trans* oriented (dihedral angle C(2), C(1), S,C(9) = 152.1°). Since the protonation of **1a** in ether leads only to (*RR/SS*)-**2**[5] and the protonation of α-sulfinyl "carbanions" generally proceeds stereoselectively,[2] most likely only the one diastereomer **1a** found in the crystal is also present in solution.[6] The C(1)-S distance (163(1) pm) is distinctly smaller and the S-O distance (158(1) pm) somewhat larger than the corresponding distances in sulfoxides (dimethyl sulfoxide: 180 and 147 pm, respectively).[7] Such an alteration in bond lengths was also deduced from IR investigations on α-sulfinyl "carbanions".[2h] The torsion angle C(1),S,O,Li is 12(2)°. This means that the Li atom does not lie exactly in the C(1)-S-O plane. The C(1)-Li distance is exceptionally large (400(3) pm),[8] so C-Li bonding can be ruled out.[9]

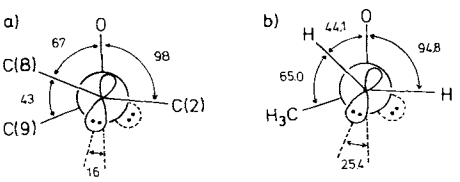
It follows from Scheme 2 that the observed diastereofacial differentiation in the addition of the electrophiles E to α-sulfinyl "carbanions" can be explained, as before, in terms of an attractive O-Li interaction.[2b,e,f] As far as the diastereoselectivity[1a] in the reaction of α-sulfinyl "carbanions" with, for instance, benzaldehyde is concerned, the one observed in the case of **1b** can also be rationalized on the basis of the structure of **1a** (Scheme 2): as in the case of **1a**, in **1b** and in the transition state of the reaction the larger substituents avoid sterically unfavorable interactions. It is equally understandable that **1c**, which is unsubstituted at the anionic C-atom, does not react diastereoselectively.[10d] That the products upon reaction of **1d**[10e] indicate the existence of more than one diastereomeric "anion" remains a mystery; possibly this can be attributed to the (experimentally confirmed[10e]) reversibility of the reaction.

The bonding situation at the anionic C(1) atom and that along the C(1)-S axis of **1a** deserve special attention.



Scheme 2. Model of the addition of α-sulfinyl "carbanions" (with the bonding situation at C(1), S, O, and Li as in **1a**) to benzaldehyde. **1a**: $R^1 = CH_3$, $R^2 = C_6H_5$, $R^3 = C_6H_5$; **1b**: $R^1 = H$, $R^2 =$ S-*p*-tolyl, $R^3 =$ *p*-tolyl [10a, b]; **1c**: $R^1 = H$, $R^2 = H$, $R^3 =$ *p*-tolyl [10d]; **1d**: R^1, $R^2 = H$, C_6H_5, $R^3 = C_6H_5$ [10e].

Thus, C(1) is not planar coordinated but rises out from the S-C(2)-C(8) plane by 12(1) pm, *away* from the S-O (and thus the O-Li) bond! ^{1}H- and ^{13}C-NMR investigations on α-sulfinyl "carbanions" in solution were not informative in this respect; accordingly C(1) could be planar, or "not quite" planar.[2f-h] Furthermore, the lone pair on C(1) is tilted by 16° away from the antiplanar conformation to the S-O bond, so that there is reduced repulsion between the two lone pairs (Scheme 3a). The crystal structure of **1a** is thus fully consistent with the results of theoretical investigations on $[CH_3\ddot{S}(O)\ddot{C}H_2]^{\ominus}$ (Scheme 3b).[11] That the benzylic C(1) atom of **1a** is flattened and that the rotation is less than in the case of $[CH_3\ddot{S}(O)\ddot{C}H_2]^{\ominus}$ is not surprising.[12]



Scheme 3. Angles [°]: a) at C(1) and S in **1a** (experimental, except for the positions of the lone pairs) and b) in $[CH_2\ddot{S}(O)\ddot{C}H_2]^{\ominus}$ (calculated) [11].

Received: June 20, 1986;
revised: July 31, 1986 [Z 1826 IE]
German version: *Angew. Chem. 98* (1986) 1004

[1] Reviews: a) G. Solladié in J. D. Morrison: *Asymmetric Synthesis, Vol. 2*, Academic Press, Orlando, FL, USA 1983, p. 157; b) G. H. Posner, *ibid.* p. 225; c) M. R. Barbachyn, C. R. Johnson, *ibid., Vol. 4*, p. 227; d) M. Venet, *Janssen Chimica Acta 3* (1985) No. 2, p. 18.

[2] Structure and diastereofacial differentiation: a) A. Rauk, E. Buncel, R. Y. Moir, S. Wolfe, *J. Am. Chem. Soc. 87* (1965) 5498; b) T. Durst, M. Molin, *Tetrahedron Lett. 1975*, 63, and references cited therein; c) R. R. Fraser, F. J. Schuber, Y. Y. Wigfield, *J. Am. Chem. Soc. 94* (1972) 8795; d) K. Nishihata, M. Nishio, *J. Chem. Soc. Perkin Trans. 2 1972*, 1730; *Tetrahedron Lett. 1976*, 1695; e) J. F. Biellmann, J. J. Vicens, *ibid. 1974*, 2915; *1978*, 467; f) G. Chassaing, R. Lett, A. Marquet, *ibid. 1978*, 471, and references cited therein; g) R. Lett, G. Chassaing, *Tetrahedron 34* (1978) 2705; h) G. Chassaing, A. Marquet, J. Corset, F. Froment, *J. Organomet. Chem. 232* (1982) 293, and references cited therein.

[3] The structure of $[C_6H_5\ddot{S}O)CH_2Li \cdot tmeda]_2$ is presently being investigated by *H.-J. Gais* et al., Freiburg; private communication, May 14, 1986.

[4] Procedure for **1a**: A solution of α-methylbenzyl(phenyl)sulfoxide **2** (100 mg, 0.43 mmol) (ca. 1 : 1 diastereomeric mixture) in diethyl ether (5 mL) was treated at room temperature with a solution of TMEDA (0.52 mmol) and *n*BuLi (0.52 mmol) in hexane. After 2 h the solution was evaporated down to ca. 1.5 mL. After 6-12 h, orange-red crystals could be recovered.

[5] Assignment of structure: K. Kobayashi, Y. Kodama, M. Nishio, T. Sugawara, H. Iwamura, *Bull. Chem. Soc. Jpn. 55* (1982) 3560.

[6] A free activation energy $\Delta G^{\neq}$ of about 13 kcal/mol is required for the exchange of both substituents on C(1) at −5°C [2h].

[7] a) M. A. Viswamitra, K. K. Kannan, *Nature (London) 209* (1966) 1016; b) R. Thomas, C. B. Shoemaker, K. Eriks, *Acta Crystallogr. 21* (1966) 12.

[8] In [1,3-diphenylallyllithium diethyl ether]$_n$ the largest Li-C distance is 252(3) pm: G. Boche, H. Etzrodt, M. Marsch, W. Massa, G. Baum, H. Dietrich, W. Mahdi, *Angew. Chem. 98* (1986) 84; *Angew. Chem. Int. Ed. Engl. 25* (1986) 104; in most cases, however, the Li-C bonds are significantly shorter; see W. Setzer, P. von R. Schleyer, *Adv. Organomet. Chem. 24* (1985) 353.

[9] From NMR investigations on fluorophenyl(sulfinyl)methyllithium (C. Najera, M. Yus, R. Hässig, D. Seebach, *Helv. Chim. Acta 67* (1984) 1100) it was deduced that $Li^{\oplus}$ possibly could only be bound to the O-atom and not to the C-atom.

[10] a) L. Colombo, C. Gennari, C. Scolastico, G. Guanti, E. Narisano, *J. Chem. Soc. Chem. Commun. 1979*, 591; b) *J. Chem. Soc. Perkin Trans. 1 1981*, 1278; c) see also D. G. Farnum, T. Veysoglu, A. M. Cardé, B. Duhl-Emswiler, T. A. Pancoast, T. J. Reitz, R. T. King, *Tetrahedron Lett. 1977*, 4009; d) G. I. Tsuchihashi, S. Iriuchijima, M. Ishibashi, *ibid. 1972*, 4605; e) C. A. Kingsbury, *J. Org. Chem. 37* (1972) 102.

[11] S. Wolfe, A. Stolow, L. A. La John, *Tetrahedron Lett. 24* (1983) 4071, and references cited therein; the distances calculated for S-$\ddot{C}H_2^{\ominus}$ and S-O are 1.672 and 1.524 Å, respectively. In $[H\ddot{S}(O)\ddot{C}H_2]^{\ominus}Li^{\oplus}$, however, the *H atoms* are bent away from the S-O bond (S. Wolfe, L. A. La John, D. W. Weaver, *ibid. 25* (1984) 2863). Such a result could be due to the extremely short C-Li distance (216 pm) determined in the 3-21G* calculations.

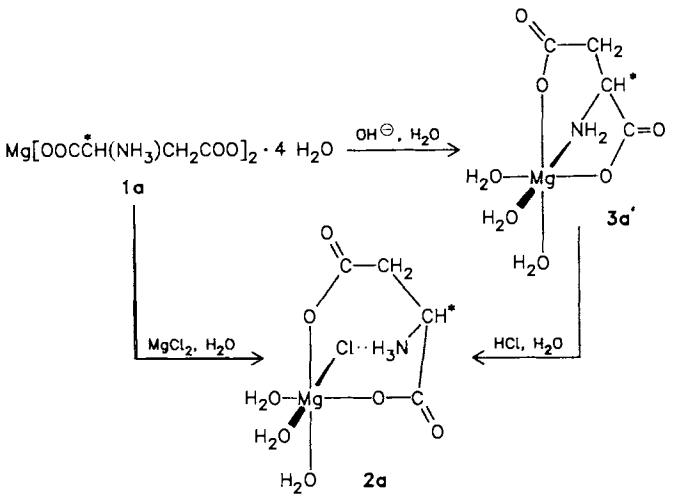
[12] All the more surprising is that the benzylic C(1)-atom, which does not undergo C-Li bonding, is not planar coordinated. In α-(phenylsulfonyl)benzyllithium (G. Boche, M. Marsch, G. M. Sheldrick, K. Harms, *Angew. Chem. 97* (1985) 577; *Angew. Chem. Int. Ed. Engl. 24* (1985) 573), α-cyanobenzyllithium (G. Boche, M. Marsch, K. Harms, *ibid. 98* (1986) 373 and *25* (1986) 373), and α-nitrobenzyllithium (G. Klebe, K. H. Böhn, M. Marsch, G. Boche, *ibid.*, in press) the benzylic C-atoms are planar coordinated. To study the possible influence of packing effects, crystals of an enantiomer of **1a** are required. Enantiomers and racemates usually crystallize in different space groups.

Elucidation of the Structure of Pharmacologically Active Magnesium L-Aspartate Complexes

By *Hubert Schmidbaur,* Gerhard Müller, Jürgen Riede, Gebhard Manninger,* and *Joachim Helbig*

Magnesium therapy has gained increasing importance in several quite diverse areas of medical application in recent years.[1,2] Of particular interest are the magnesium salts of L-aspartic acid and L-glutamic acid, which are the frequently preferred forms of magnesium in chemotherapeutical treatment.[3,4] There are good resons for assuming that the two aminodicarboxylic acids form weak complexes with magnesium[5,6] which are decisive for the transport of magnesium through membranes as well as across the blood-brain barrier. At the same time, however, the magnesium ion is not irreversibly complexed, but is apparently readily released again.[7]

Besides the salts **1a** and **1b**,[8] which are readily obtainable by neutralization of $Mg(OH)_2$, MgO or $MgCO_3$ with the free acids (but whose structures are still unknown), the magnesium halide aspartates and glutamates also play an important therapeutic role, for it follows from in vivo experiments that, e.g., optimal physiological activities are achieved with the composition Mg : Cl : Asp (Glu) = 1 : 1 : 1.[9] These salts are not usually formed completely from **1a**, **b** and the hydrochloric acid of the stomach. They are, however, readily prepared from magnesium halides and **1a**, **b**.[10] In the course of studies on the nature of the interaction between $(Mg^{2\oplus})_{aq}$ and aspartate or glutamate ions in solution and in the solid state, a magnesium aspartate trihydrate **3a**, which exists only in strongly basic aqueous medium, has been obtained for the first time in the crystalline state and has been structurally characterized.[11]



Mg[OOCCH(NH$_3$)CH$_2$CH$_2$COO]$_2$

1b

It follows from Figures 1 and 2 that the L-aspartate dianion in **3a** is facially bound to the metal atom as a tridentate ligand. Two further sites of attachment of the octahedral coordination sphere are saturated by water molecules, and the sixth by an oxygen atom of a carboxy group of a neighboring complex (O4*). The strands of **3a** thus formed run parallel to the crystallographic *a*-axis (Fig. 2) and are held together by a complicated system of hydrogen bonds in which the third water molecule of the crystalline *tri*hydrate also participates. During the process of dissolution, one water molecule presumably occupies the sixth coordination site of the decoupled complex molecules (Formula **3a'**). All aspartate ions have the L-configuration.

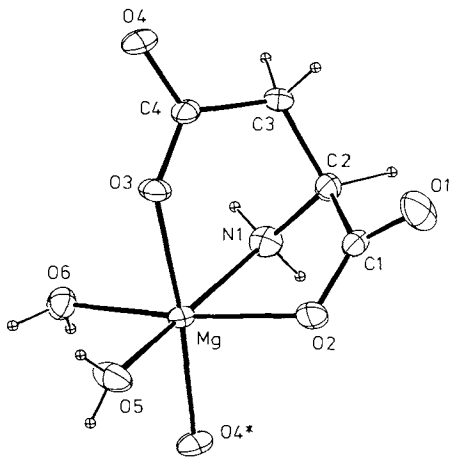


Fig. 1. Crystal structure of the complex **3a** (ORTEP, thermal ellipsoids 50%, H-atoms with arbitrary radius). O4* is the oxygen atom O4 of a neighboring molecule. All H atoms were located and refined; of the H atoms on O and N, only one on N does not participate in the three-dimensional hydrogen bonding network. Important bond lengths [Å] and angles [°]: Mg-O2 2.075(2), Mg-O3 2.066(2), Mg-O4* 1.999(2), Mg-O5 2.074(2), Mg-O6 2.090(2), Mg-N1 2.203(3); O3-Mg-O4* 174.1(1), O2-Mg-O3 90.0(1), O2-Mg-N1 77.2(1), O3-Mg-N1 84.4(1).

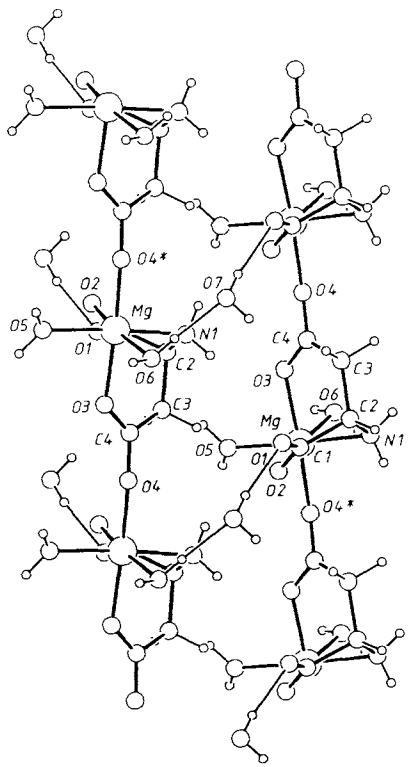


Fig. 2. Diagram of two strands of **3a** running parallel to the crystallographic *a*-axis of the crystal. The water molecule $H_2O(7)$ connects both strands through hydrogen bonds. There are further hydrogen bonds to other strands.

[*] Prof. Dr. H. Schmidbaur, Dr. G. Müller, J. Riede
Anorganisch-chemisches Institut der Technischen Universität München
Lichtenbergstrasse 4, D-8046 Garching (FRG)
Dr. G. Manninger, Dr. J. Helbig
Wissenschaftliche Abteilung der Verla-Pharm GmbH & Co. KG
D-8132 Tutzing (FRG)

3a reacts basic in water (pH = 9.85 at 20°C, saturated solution) and exhibits only slight electrical conductivity ($\chi_M = 2.55\ \Omega^{-1}\ cm^2$). On neutralization with HCl, the chloride aspartate is formed (pH = 7.13 at 20°C). The conductivity of this salt in water ($\chi_M = 5.35\ \Omega^{-1}\ cm^2$) remains well below the value expected for a 1:2 electrolyte. Hence, it can be concluded that dissociation of the chloride ion from the magnesium is far from complete. This finding corresponds very well with the physiological observations, according to which the solution with 1:1:1 stoichiometry is particularly active. An ionic association in the sense of Formula **2a** had already been deduced from earlier measurements with ion-sensitive electrodes.[12] Apparently, the ammonium group in **2a** formed by protonation of the amino group in **3a** promotes the coordination (electrostatically or via weak hydrogen bonding) and represses the dissociation of the chloride ion.

Table 1. ^{1}H- and ^{13}C-NMR data of the complexes **2a** and **3a'** (solvent D_2O/D_3COD [30:1], c = 5 wt-%, 30°C; chemical shifts relative to TMS ext. and $D_3{}^{13}COD$ (δ = 49.00); J values in Hz).

		2a	**3a'**
^{1}H-NMR	δCH_2	2.60	2.65
	δCH	3.74	3.58
	$^3J(H_2CCH)$	5.6	4.7
^{13}C-NMR	δCOO	182.74, 179.95	178.71, 175.52
	δCH_2	53.19	52.73
	δCH	40.56	37.30
	$^1J(CH_2)$	128.9	127.4
	$^1J(CH)$	141.7	144.5

As expected, the transition **2a** → **3a'** is also revealed in the ^{1}H- and ^{13}C-NMR spectra of the aqueous solutions by a noticeable shift of the signals and by changes in the coupling constants (Table 1). The deviations are greatest at the atoms adjacent to the amino/ammonium groups, so that a protonation at the nitrogen atom is assumed to take place also in solution.

All the above findings support the concept that complexes of type **2** exhibit carrier properties for magnesium ions that are decisive for pharmacological activity.

Received: June 30, 1986 [Z 1838]
German version: *Angew. Chem. 98* (1986) 1014

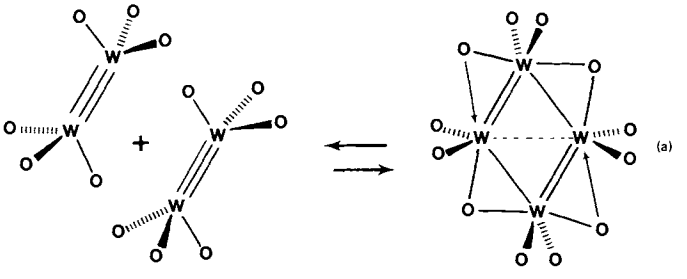
[1] H. G. Classen et al., *Magnesium Bull. 8* (1986) 127 (German edition); *8* (1986) 117 (English edition).
[2] H. G. Classen, *Magnesium 5* (1986) 105.
[3] H. Ippen: *Index Pharmacorum*, Thieme, Stuttgart 1968.
[4] Pharmazeutische Stoffliste, 4th Edit., Arzneibüro der Bundesvereinigung Deutsche Apothekerverbände, Frankfurt am Main 1984.
[5] $\lg K_\beta = 2.43$. R. F. Lumb, A. E. Martell, *J. Chem. Phys. 57* (1953) 690; L. G. Sillén, A. E. Martell, *Spec. Publ. Chem. Soc. 17* (1964).
[6] H. Sigel: *Metal Ions in Biological Systems, Vol. 9*, Dekker, New York 1979.
[7] G. L. Eichhorn (Ed.): *Inorganic Biochemistry, Vol. 1*, Elsevier, Amsterdam 1973, p. 121ff; H. C. Freeman, *Adv. Protein Chem. 22* (1967) 258.
[8] H. Tanner, P. Scherberich, DOS 2752287 (May 31, 1979).
[9] J. P. Pin, J. Bockaert, M. Recasesn, *FEBS Lett. 175* (1984) 31.
[10] F. Fischer, J. Helbig, E. Jaeger, E. Wünsch, DBP 2228101 (November 9, 1978).
[11] *Procedure:* A solution of 225 g of **1a** (as the tetrahydrate) in 250 mL of water was adjusted to pH = 10.6 with concentrated aqueous KOH. The solution was stirred for 1 h and then concentrated down at 40°C in vacuo to a volume of 250 mL. On allowing to stand, 60–65 g of colorless **3a** (40–45% yield) crystallized out. Subsequent washing of the crystals with water and acetone, followed by drying in vacuo at 80°C, furnished the analytically pure trihydrate. The product loses water at 147°C, but does not melt below 300°C.—*Crystallographic data:* $C_4H_5MgNO_4 \cdot 3H_2O$, $M_r = 209.4$, orthorhombic, $P2_12_12_1$, $a = 6.140(1)$, $b = 9.430(1)$, $c = 15.015(1)$ Å, $V = 869.4$ Å^3, $\rho_{calc} = 1.560$ g/cm^3 for $Z = 4$, 22°C, $\mu(Mo_{K\alpha}) = 2.0$ cm^{-1}, $F(000) = 440$. 4087 measured reflections, 1967 independent ($R_{int} = 0.02$) and 1849 "observed" with $I \geq 2\sigma(I)$ ($\theta - 2\theta$ scan, $\Delta\omega = 1.1 + 0.35\ \tan\theta$, $(\sin\theta/\lambda)_{max} = 0.648$, $\pm h$, $\pm k$, $+l$, $Mo_{K\alpha}$, $\lambda = 0.71069$ Å, Enraf-Nonius CAD4). Solution by Patterson methods and refinement of the correct enantiomorph (L-aspartate) to $R = 0.027$, $R_w = 0.041$, $w = 1/\sigma^2(F_0)$ (anisotropic, H-atoms isotropic, 162 parameters, $(\text{shift/error})_{max}$ 0.002, $\Delta\rho_{fin}(\text{max/min}) = 0.37/-0.50$ e/Å^3). $R_w = 0.042$ for inverse coordinate set. Further details of the crystal structure investigation are available on request from the Fachinformationszentrum Energie, Physik, Mathematik GmbH, D-7514 Eggenstein-Leopoldshafen 2 (FRG), on quoting the depository number CSD-52029, the names of the authors, and full citation of the journal.
[12] H. Schmidbaur, unpublished results.

The First Observation of the Equilibrium $2M{\equiv}M \rightleftarrows M_4$ (M = Transition Metal): Synthesis and Structure of Hexaisopropoxyditungsten and Its Dimer**

By *Malcolm H. Chisholm,* David L. Clark, Kirsten Folting,* and *John C. Huffman*

Only for certain elements of the first row are multiple bonds stable with respect to oligomerization at standard temperature and pressure; e.g., N≡N is stable with respect to N_x but P≡P will oligomerize to P_4 and then to P_x. Multiple bonds between metal atoms are stabilized with respect to clusters by ligand effects which may be steric or electrostatic or both.[1] Since our initial discovery of compounds of formula $[(RO)_3M{\equiv}M(OR)_3]$ for M = Mo[2] and W,[3] we have speculated about the dimerization of $[M{\equiv}M]^{6\oplus}$ units to give 12-electron M_4 clusters supported by alkoxide ligands. Although a variety of mixed halide-alkoxide Mo_4 12-electron clusters have been successfully characterized,[4–6] no compound of formula $[M_4(OR)_{12}]$ has been fully characterized because of either difficulties in obtaining crystals suitable for X-ray studies or the ease of oxidation of the $[M{\equiv}M]^{6\oplus}$ moiety.[7,8] An understanding of the factors facilitating the latter process allowed us to isolate a black crystalline compound of empirical formula $[W(OiPr)_3]$ (from elemental analysis), which appeared to be tetranuclear in benzene based on a cryoscopic molecular weight determination.[9] We now wish to report our characterization of $[W_2(OiPr)_6]$ **1** in equilibrium with its dimer, $[W_4(OiPr)_{12}]$ **2**. To our knowledge this is the first example of a reversible association of a dinuclear compound containing a multiple bond between metal atoms, though condensation reactions have been reported.[10,11]

$$2[W_2(OiPr)_6] \rightleftharpoons [W_4(OiPr)_{12}]$$
1 **2**



[*] Prof. Dr. M. H. Chisholm, Dr. D. L. Clark, K. Folting, Dr. J. C. Huffman
Department of Chemistry and Molecular Structure Center, Indiana University
Bloomington, IN 47405 (USA)

[**] We thank the National Science Foundation and the Wrubel Computing Center at Indiana University for support.

Addition of isopropyl alcohol (>6 equivalents) to a solution of $[W_2(OtBu)_6]$[3] in dimethoxyethane (DME) yields a brown solution from which dark crystals are obtained upon cooling. The latter were found by X-ray analysis to contain a 1:1 mixture of **1** and **2**.[12]

A view of the dinuclear species is shown in Figure 1, above, and provides the first structural characterization of an unligated $[W_2(OR)_6]$ compound. The W≡W bond distance (2.315(2) Å) is just slightly shorter than that found for the ligated compound $[W_2(OiPr)_6(py)_2]$ (2.332(1) Å).[3] The W-O bond distances (1.86-1.88 Å) are indicative of significant O-to-W π-donation.[13]

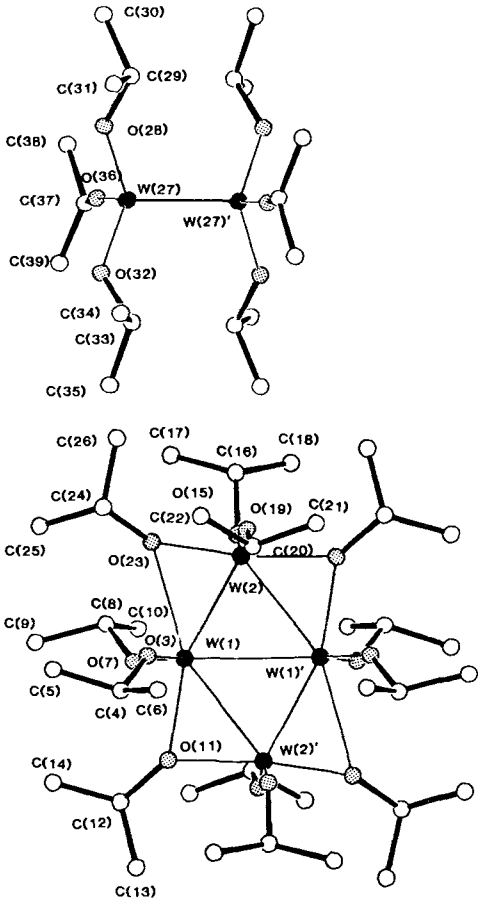


Fig. 1. Above: A ball- and-stick drawing of the centrosymmetric crystal structure of **1**. Bond distances [Å] and angles [°] (averaged where appropriate): W-W 2.315(2), W-O 1.87(1); W-W-O 106.7(7), O-W-O 112.1(9). Below: A ball-and-stick drawing of the centrosymmetric crystal structure of **2**. Bond distances [Å] and angles [°] (averaged where appropriate): W(1)-W(2) 2.502(1), W(1)-W(2)' 2.733(1), W(1)-W(1)' 2.807(2), W(1)-O(3) 1.91(1), W(1)-O(7) 1.89(1), W(1)-O(11) 2.18(1), W(1)-O(23) 2.59(3), W(2)-O(19) 1.99(1), W(2)-O(15) 1.89(2); W(2)-O(23) 1.87(2), W(2)-O(11)' 1.98(1), O(3)-W(1)-O(7) 122.9(6), O(11)-W(1)-O(23) 155.9(6), O(23)-W(2)-O(11)' 172(1), O(15)-W(2)-O(19) 150.2(7).

The W_4 cluster **2** (Fig. 1, below) consists of a rhombus of metal atoms having two short M-M distances (W(1)-W(2), W(1')-W(2') = 2.502(2) Å), and two longer distances, (W(1)-W(2'), W(2)-W(1') = 2.733(2) Å) with a short diagonal distance (W(1)-W(1') = 2.807(2) Å) still being worthy of mention with respect to M-M bonding interactions. There are four edge-bridging alkoxides whose oxygen atoms are contained in the W_4 plane; the remaining eight alkoxides are terminal, two per tungsten, with four lying above and four below the W_4 plane. The local WO_4 structural units may be viewed in terms of trigonal-bipyramidal fragments in which one equatorial OR group is missing. This site is directed toward the center of the cluster; the terminal and bridging alkoxide ligands make up the remaining equatorial and axial positions, respectively. It is possible to formulate the present distorted 12-electron W_4 rhombus as arising from a second-order Jahn-Teller distortion of a regular [W(1)-W(2) = W(1)-W(2)'] 10-electron $[W_4(OR)_{12}]^{2\oplus}$ cluster (compare 8- and 10-electron rhombs for $[W_4(OEt)_{16}]^{n\ominus}$, where n = 0 and 2).[14] Aside from the asymmetry within the W_4 unit, of particular note is the asymmetry in the $W_2(\mu\text{-}OR)$ moiety involving the short W-W distances: W(2)-O(23) = 1.87(2) Å, W(1)-O(23) = 2.59(4) Å.

Despite the fragility of the alkoxide bridges of **2** (noted above), the ^{1}H-NMR spectrum reveals a static structure on the NMR time-scale at 16 °C in [D$_8$]toluene. The CH resonances appear in a 2:2:1:1 ratio as expected based on consideration of the molecular structure found in the solid state. Upon heating the solution, the resonances assignable to **2** diminish as those associated with **1** increase, until at +65 °C only the latter are present. At this temperature the solution is pale yellow. Upon rapidly cooling to +16 °C, the resonances of **2** start to reappear only *slowly*, implying a significant energy barrier to dimerization of **1**.

Finally, it is worth mentioning that the pure compound **2**, as determined by ^{1}H-NMR spectroscopy, is obtained by crystallization from the reaction mixture of $[W_2(OtBu)_6]$ and *i*PrOH in hexane or toluene at 0 °C. The 1:1 mixture of **1** and **2** is obtained by crystallization from DME solutions. In hexane, toluene, or benzene at +65 °C only the dinuclear compound is present. Given the existence of a sizeable activation energy for the interconversion **1** ⇄ **2**, it should be possible under certain conditions to examine the separate reactivity of each species toward substrates of interest.

Received: August 26, 1986 [Z 1908 IE]
German version: *Angew. Chem. 98* (1986) 1021

CAS Registry numbers:
1, 71391-16-7; **2**, 104911-26-4; $W_2(OtBu)_6$, 57125-20-9; W, 7440-33-7.

[1] F. A. Cotton, R. A. Walton: *Multiple Bonds Between Metal Atoms*, Wiley, New York 1982.
[2] M. H. Chisholm, F. A. Cotton, C. A. Murillo, W. W. Reichert, *Inorg. Chem. 16* (1977) 1801.
[3] M. Akiyama, M. H. Chisholm, F. A. Cotton, M. W. Extine, D. A. Haitko, D. Little, P. E. Fanwick, *Inorg. Chem. 18* (1979) 2266.
[4] M. H. Chisholm, J. C. Huffman, R. L. Kelly, *J. Am. Chem. Soc. 101* (1979) 7100.
[5] M. H. Chisholm, R. J. Errington, K. Folting, J. C. Huffman, *J. Am. Chem. Soc. 104* (1982) 2025.
[6] M. H. Chisholm, D. L. Clark, J. C. Huffman, *Polyhedron 107* (1985) 1234.
[7] M. Akiyama, D. Little, M. H. Chisholm, D. A. Haitko, J. Leonelli, F. A. Cotton, M. W. Extine, *J. Am. Chem. Soc. 103* (1981) 779.
[8] M. H. Chisholm, J. C. Huffman, C. C. Kirkpatrick, J. Leonelli, *J. Am. Chem. Soc. 103* (1981) 6093.
[9] M. H. Chisholm, J. C. Huffman, C. A. Smith, *J. Am. Chem. Soc. 108* (1986) 222.
[10] R. N. McGinnis, T. R. Ryan, R. E. McCarley, *J. Am. Chem. Soc. 100* (1978) 7900.
[11] R. E. McCarley, T. R. Ryan, C. C. Torardi, *ACS Symp. Ser. 155* (1981) 44.
[12] Crystal data at −156 °C: space group $P\bar{1}$; $a = 12.277(3)$, $b = 12.890(3)$, $c = 12.118(3)$ Å, $\alpha = 94.60(1)$, $\beta = 81.86(1)$, $\gamma = 83.92(1)°$, $Z = 1$, $\rho_{calcd} = 1.915$ g cm^{-3}; 7316 measured reflections, 4935 unique reflections, 4042 with $F > 3\sigma(F)$. $R(F) = 0.0746$ and $R_w(F) = 0.0691$. The structure was determined by a combination of direct methods (MULTAN 78) and Fourier techniques. The asymmetric unit cell contains two halves of two different centrosymmetric tungsten complexes (**1** and **2**). Further details of the crystal structure investigation may be obtained from the Fachinformationszentrum Energie, Physik, Mathematik GmbH, D-7514 Eggenstein-Leopoldshafen 2 (FRG), on quoting the depository number CSD-52087, the names of the authors, and the journal citation.
[13] M. H. Chisholm, *Polyhedron 2* (1983) 681.
[14] F. A. Cotton, A. Fang, *J. Am. Chem. Soc. 104* (1982) 113.

Direct Measurement of the "Isokinetic Rate Constant" in Additions of Diarylcarbenium Ions to 2-Methyl-2-butene**

By *Reinhard Schneider* and *Herbert Mayr**

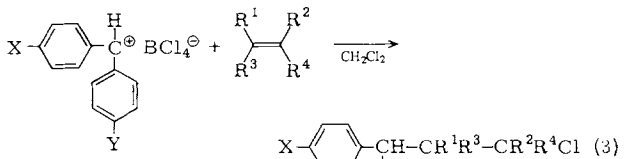
In a series of reactions where the temperature (T) and the structure of the reagents (σ) are the only variables, the rate constant k can be considered as a function of these parameters [Eq. (1)].

$$k=f(T,\sigma) \quad (1)$$

It is possible that k becomes independent of one of these parameters, if the second parameter adopts a certain value.[1-4] The rate constant k will be independent of the temperature, if the structure (σ) is so selected that the Arrhenius activation energy (E_a) equals zero. If an isokinetic relationship [Eq. (2)] exists, the rate constant k will be independent of structure at the isokinetic temperature $T_{iso}=\beta$, since the alteration $\delta\Delta H^{\neq}$, which is affected by the structural variation, is completely counterbalanced by the $T\delta\Delta S^{\neq}$ contribution.[5]

$$\delta\Delta H^{\neq}=\beta\cdot\delta\Delta S^{\neq} \quad (2)$$

If $k=f(T,\sigma)$ becomes independent of any one of the two variables, it will adopt the same value: k_{iso}, the isokinetic rate constant, the logarithm of which has been termed the isoparametric value[1] or the isokinetic point.[2b]



(3)

X	Y	
Me	Me	$Tol_2^{\oplus}CH$
OPh	H	$PopPh^{\oplus}CH$
H	OMe	$PhAn^{\oplus}CH$
Me	OMe	$TolAn^{\oplus}CH$
OMe	OMe	$An_2^{\oplus}CH$

We report here on a system which allows the direct measurement of k_{iso}.

Recently, we succeeded in determining the kinetics of the addition of diarylcarbenium ions to alkenes [Eq. (3)].[6] We found for the addition of *p*-substituted diarylcarbenium ions to 2-methyl-1-pentene that variation of the substituents affects only $\Delta H^{\neq}$, whereas $\Delta S^{\neq}$ remains constant within the limits of experimental error (-121 ± 4 J mol^{-1} K^{-1}). Table 1 shows a comparable situation for the addition of diarylcarbenium ions to 2-methyl-2-butene; variation of the substituents only influences $\Delta H^{\neq}$ while $\Delta S^{\neq}$ is almost unaffected.

As previously reported,[6] the log$k$ values of the additions of diarylcarbenium ions to alkenes are not linearly correlated with $\Sigma\sigma^{+}$. Steric effects inhibit the complete coplanarity of both aryl groups, and the individual torsional angles depend on the electron-releasing effects of both *p*-substituents with the consequence that the σ^{+} values are not additive. Figure 1b shows, however, that the reaction rates of the diarylcarbenium ions with 2-methyl-1-pentene (abscissa) and 2-methyl-2-butene (ordinate) are linked by a linear free enthalpy relationship (correlation coefficients 0.9995 to 0.99990).

Table 1. Activation parameters and rate constants for the addition of diarylcarbenium ions to 2-methyl-2-butene.

Carbenium ion	k_2 −70 °C [L mol^{-1} s^{-1}]	$\Delta H^{\neq}$ [kJ mol^{-1}]	$\Delta S^{\neq}$ [J K^{-1} mol^{-1}]	E_a [kJ mol^{-1}]	log$A$
$Tol_2^{\oplus}CH$	6.8×10^{4}	−1.6	−157	0.2	4.89
$PopPh^{\oplus}CH$	3.8×10^{3}	5.3	−147	7.1	5.42
$PhAn^{\oplus}CH$	2.5×10^{2}	7.5	−159	9.3	4.79
$TolAn^{\oplus}CH$	1.8×10^{1}	13.6	−151	15.5	5.24
$An_2^{\oplus}CH$ [a]	8.7×10^{-2}	22.0	−154	23.7	5.02

[a] Determinations in presence of $PhCH_2NEt_3^{\oplus}BCl_4^{\ominus}$; probably because of the reversibility of the addition step, the rate constants of this reaction increase when $BCl_4^{\ominus}$ salts are added.

Figure 1b corresponds to a Hammett plot, in which the log$k$ values of the reactions with 2-methyl-1-pentene at −70 °C are defined as the temperature-independent substituent constants σ. The slopes of the correlation lines correspond to the reaction constants ρ, which decrease with increasing temperature and become zero at the isokinetic temperature (extrapolated horizontal line).

The correlation lines intersect at the position of the ditolylcarbenium ion, the rate of addition of which is not influenced by variation of the temperature.[7] The ditolylcarbenium ion, therefore, corresponds to the critical value of σ,[1,2] also termed the isokinetic substituent,[3] which reacts with the isokinetic rate constant $k_{iso}=6.9\times10^{4}$ L mol^{-1}

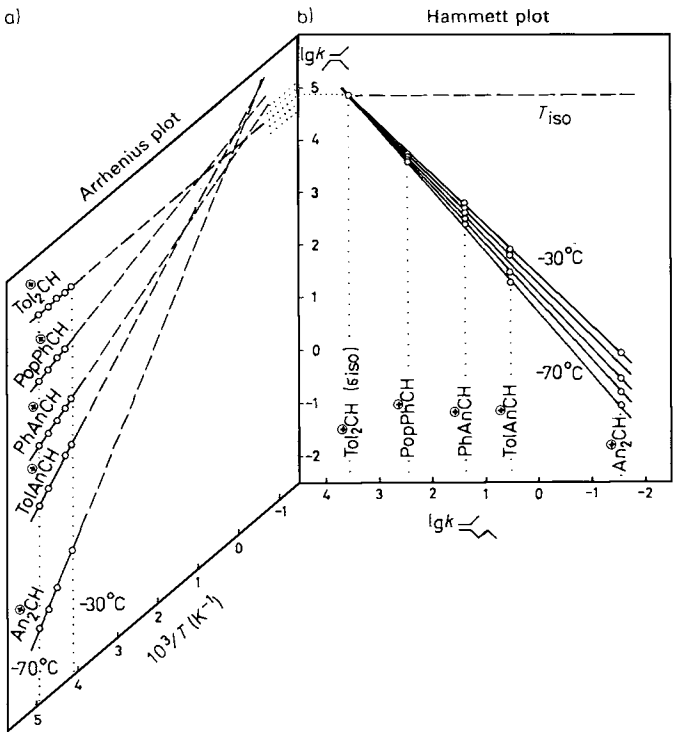


Fig. 1. Reactivity of the diarylmethyl cations towards 2-methyl-2-butene as a function a) of reciprocal temperature and b) of the reactivity towards 2-methyl-1-pentene at −70 °C (Ph = C_6H_5, Tol = *p*-CH_3–C_6H_4, An = *p*-CH_3O–C_6H_4, Pop = *p*-(C_6H_5O–C_6H_4).

[*] Prof. Dr. H. Mayr, Dipl.-Chem. R. Schneider
Institut für Chemie der Medizinischen Universität
Ratzeburger Allee 160, D-2400 Lübeck 1 (FRG)

[**] This work was supported by the Deutsche Forschungsgemeinschaft and the Fonds der Chemischen Industrie. We thank Ms. *U. Grabis* for experimental assistance.

$s^{-1} \pm 4\%$ at any temperature. As indicated in the Hammett plot, all cations of this series should react with this rate constant at the isokinetic temperature.

The same set of experimental data is plotted against the inverse temperature in Figure 1a[3] (Arrhenius plot). The slope of the lines ($=E_a$) decreases with increasing reactivity of the carbenium ions and adopts the value zero ($E_a=0$) for the ditolylcarbenium ion, the system with the isokinetic substituent.

As in the Hammett plot (Fig. 1b), it can be seen that the reactivity differences of the various carbenium ions decrease with increasing temperature. In the case of an ideal isokinetic relationship, all straight lines should intersect at one point (T_{iso}), at which the reactivity differences of the carbenium ions had vanished. A deviation from the ideal isokinetic relationship as well as the necessary extrapolation over a wide temperature range may be responsible for the fact that the points of intersection do not precisely coincide. It is evident, however, that the same order of magnitude of k_{iso}, which has been derived from the Hammett plot, is indicated by the points of intersection in Figure 1a.[3]

The ditolylcarbenium ion is the most reactive carbenium ion of this series which can be kinetically investigated with our present methods. The question arises, whether the linear free enthalpy relationships that have been described in this paper will also be valid beyond the isokinetic substituent, i.e., in the range of eventual negative activation energies.[8]

Received: July 10, 1986;
revised: September 1, 1986 [Z 1854 IE]
German version: *Angew. Chem. 98* (1986) 1033

CAS Registry numbers:
$Tol_2^{\oplus}CH \cdot BCl_4^{\ominus}$, 99796-97-1; $PopPh^{\oplus}CH \cdot BCl_4^{\ominus}$, 104910-82-9; $PhAn^{\oplus}CH \cdot BCl_4^{\ominus}$, 99796-96-0; $TolAn^{\oplus}CH \cdot BCl_4^{\ominus}$, 99796-95-9; $An_2^{\oplus}CH \cdot BCl_4^{\ominus}$, 99796-92-6; 2-methyl-1-pentene, 763-29-1; 2-methyl-2-butene, 513-35-9.

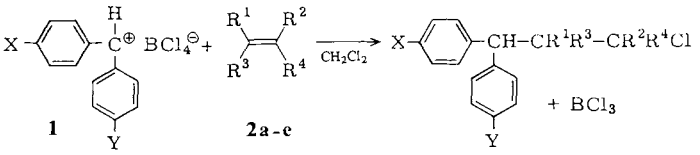
[1] V. A. Palm, B. I. Istomin, *Reakc. Sposobn. Org. Soedin. 6* (1969) 427.
[2] a) O. Exner, *Prog. Phys. Org. Chem. 10* (1973) 411; b) *Collect. Czech. Chem. Commun. 39* (1974) 515.
[3] a) R. Schmid, R. W. Soukup, V. N. Sapunov, W. Linert, *Z. Phys. Chem. (Frankfurt am Main) 126* (1981) 25; b) R. Schmid, V. N. Sapunov: *Non-Formal Kinetics*, Verlag Chemie, Weinheim 1982, p. 174f.
[4] W. Linert, *Aust. J. Chem. 39* (1986) 199.
[5] J. E. Leffler, *J. Org. Chem. 20* (1955) 1202.
[6] R. Schneider, U. Grabis, H. Mayr, *Angew. Chem. 98* (1986) 94; *Angew. Chem. Int. Ed. Engl. 25* (1986) 89.
[7] The temperature dependence of the addition rates has been investigated from $-70°C$ to $-30°C$, in some cases to $-20°C$.
[8] The question of negative $\Delta H^{\neq}$ values is discussed by: a) S. W. Benson: *Thermochemical Kinetics*, Wiley, New York 1976, p. 15ff; b) I. A. Leenson, G. B. Sergeev, *Russ. Chem. Rev. 53* (1984) 417.

Linear Reactivity-Selectivity Correlations in Additions of Diarylcarbenium Ions to Alkenes; a Rebuttal of the Reactivity-Selectivity Principle**

By *Herbert Mayr,** *Reinhard Schneider,* and *Ute Grabis*

The selectivity of a species, at one time frequently used for classifying the relative life times of reactive intermediates,[1] has repeatedly been disproven as a criterion for the determination of reactivity.[2-4] The intuitive rule that an increase of reactivity is related with a decrease of selectivity was demonstrated by *Ritchie* to be invalid for many cation-anion combinations. Numerous cations of different reactivity reveal identical selectivity towards pairs of n-nucleophiles.[2] For frontier orbital controlled reactions an increase of selectivity with increasing reactivity was reported.[3] The impression was created that different classes of reactions are related with a certain reactivity-selectivity pattern, which may reverse if the isoselective temperature[3] comes into the experimental range.

We report here on the additions of diarylcarbenium ions to various alkenes. For the first time we demonstrate the coexistence of constant, proportional and inversely proportional reactivity-selectivity behavior within a group of closely related reactions.



1 2a-e

In the preceding communication we reported the existence of a linear free enthalpy relationship between the additions of the diarylcarbenium ions **1** to 2-methyl-1-pentene **2a** and 2-methyl-2-butene **2b**.[5] Figure 1 shows that the corresponding additions to methylenecyclopentane **2c**, isoprene **2d** and styrene **2e** are also linearly correlated with $\log k(\mathbf{2a})$.

Figure 1 represents a linear reactivity-reactivity relationship. Since selectivity arises from two reactivities ($S=\log k_1/k_2=\log k_1-\log k_2$), the combination of two linear reactivity-reactivity relationships necessarily yields a

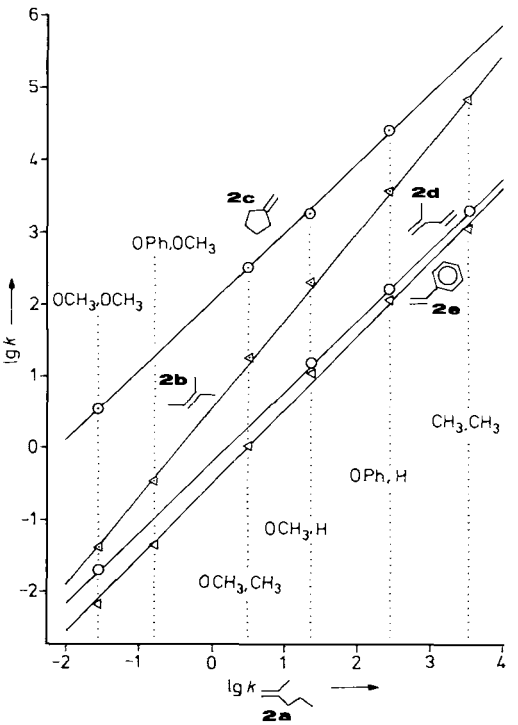


Fig. 1. Linear free enthalpy relationships between the rates of addition of a series of *p*-substituted diarylcarbenium ions **1** to alkenes **2** at $-70°C$ in CH_2Cl_2.

[*] Prof. Dr. H. Mayr, Dipl.-Chem. R. Schneider, U. Grabis
Institut für Chemie der Medizinischen Universität
Ratzeburger Allee 160, D-2400 Lübeck 1 (FRG)

[**] This work was supported by the Deutsche Forschungsgemeinschaft and the Fonds der Chemischen Industrie.

linear reactivity-selectivity relationship. Since the selectivity scale has to be spread out for the graphical display in Figure 2, minor deviations from the linear reactivity-reactivity relationships lead to noticeable deviations from the ideal linear reactivity-selectivity relationship.

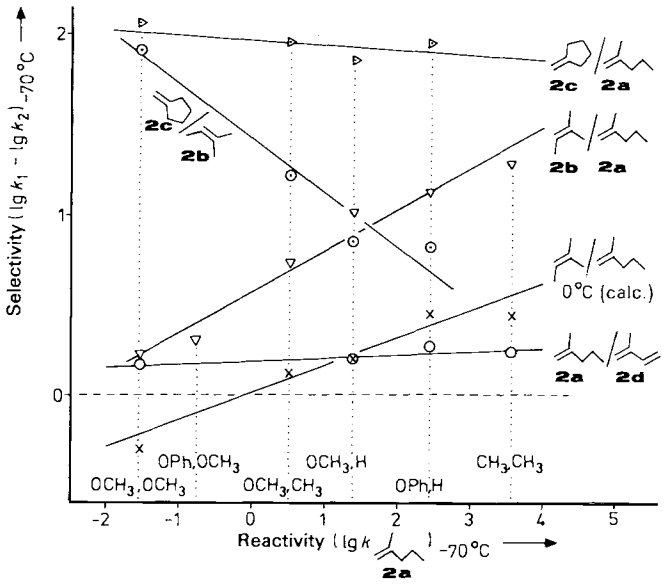


Fig. 2. Reactivity-selectivity relationships in the additions of *p*-substituted diarylcarbenium ions **1** to alkenes **2** at −70 °C in CH_2Cl_2.

Considering the pair **2c/2b**, one recognizes decreasing selectivity with increasing reactivity. The pairs **2c/2a** and **2a/2d** exhibit almost constant selectivity while the reactivity is varied, and the pair **2b/2a** shows even an increase of selectivity with increasing reactivity. If, finally, the pair **2b/2a** is considered at 0 °C, one finds the correlation line moving from bottom left towards the dashed zero selectivity level, i.e., in the range of low reactivity carbenium ions, the selectivity decreases with increasing reactivity[6] and is close to zero for the methoxyphenyl-tolyl compound. In the range of the more reactive carbenium ions, the selectivity increases with reactivity, but the relative reactivity of **2b** and **2a** is reversed compared with the left part of the correlation line.

Since it depends on the arbitrary selection of a pair of competing substrates whether constant, proportional or inversely proportional reactivity-selectivity behavior is encountered, we consider it to be impossible to derive reactivity sequences solely from competition experiments. Furthermore, our observation that all feasible types of linear reactivity-selectivity relationships are realized within a series of closely similar reactions indicates that a certain reactivity-selectivity behavior cannot be considered to be proof of a certain interaction mechanism.

The variety of reactivity-selectivity relationships in this system is due to the steeper correlation line of **2b** which is located *between* the almost parallel straight lines of the other alkenes (Fig. 1). Additional experiments should show whether the relation between ΔS^{+} and the slopes of Figure 1, as indicated by preliminary experiments, can be confirmed.

Received: July 10, 1986;
revised: September 1, 1986 [Z 1855 IE]
German version: *Angew. Chem. 98* (1986) 1034

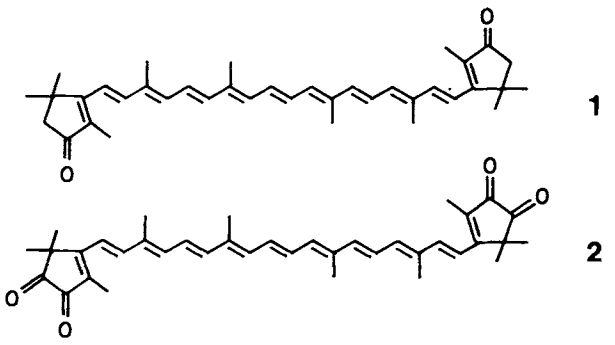
[1] R. Huisgen, *Angew. Chem. 82* (1970) 783; *Angew. Chem. Int. Ed. Engl. 9* (1970) 751.
[2] C. D. Ritchie, *Acc. Chem. Res. 5* (1972) 348.
[3] a) B. Giese, *Angew. Chem. 89* (1977) 162; *Angew. Chem. Int. Ed. Engl. 16* (1977) 125; b) *Acc. Chem. Res. 17* (1984) 438.
[4] a) A. Pross, *Adv. Phys. Org. Chem. 14* (1977) 69; b) C. D. Johnson, *Tetrahedron 36* (1980) 3461; c) Z. Rappoport, R. Ta-Shma, *J. Am. Chem. Soc. 105* (1983) 6082; d) E. M. Arnett, K. E. Molter, *Acc. Chem. Res. 18* (1985) 339.
[5] R. Schneider, H. Mayr, *Angew. Chem. 98* (1986) 1033; *Angew. Chem. Int. Ed. Engl. 25* (1986) 1016.
[6] Since the definition of *negative* selectivity is meaningless, we refer here to its absolute value.

Mini-Violerythrins: Why can C_{38}-Carotinoids be Blue?**

By *Matthias Kummer, Georg Martin,* and *Hans-Dieter Martin**

Dedicated to Professor Siegfried Hünig on the occasion of his 65th birthday

Most carotinoids are yellow to red.[1] A number of years ago, a blue carotinoid, violerythrin **2**, was obtained by alkaline hydrolysis of actinioerythrin, the red pigment of the sea anemone *Actinia equina*.[2,3] This drastic change in color in going from dinorcanthaxanthin **1** (λ_{max} = 487 nm)[4] to violerythrin **2** (λ_{max} = 580 nm) has thus far remained unexplained.



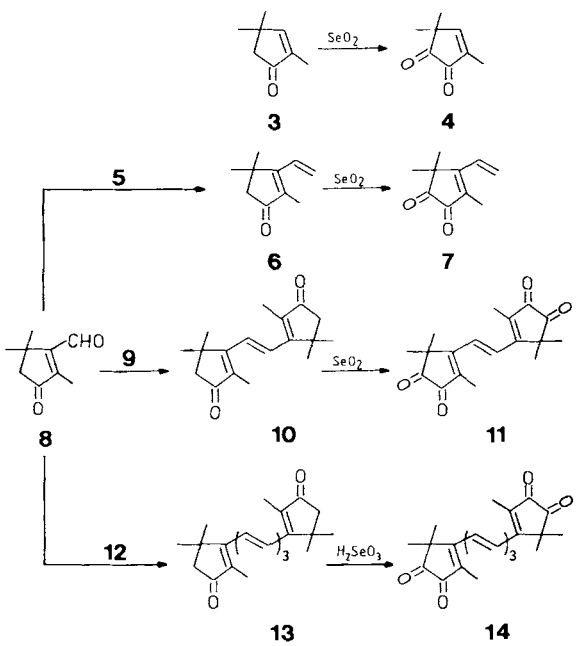
It has been pointed out that the terminal five-membered rings containing the dicarbonyl moieties are oriented approximately planar to the polyene chain and could thus contribute to this bathochromic shift.[5] Since we have already demonstrated with several examples that α-dicarbonyl chromophores can exhibit considerable lone-pair splitting (in a $n_+ + n'_+$ and a $n_+ - n'_+$ combination) over longer distances,[6,7] the question now arises as to whether the same applies in the case of the bis(α-dicarbonyl) chromophore of violerythrin **2**. The UV/VIS spectrum of **2** provides no information about the position of the $(n_+ + n'_+)\pi^*$ or $(n_+ - n'_+)\pi^*$ transition (the broad $\pi\pi^*$ absorption masks the likely region). Herein we report experiments and calculations which answer this question and, at

[*] Prof. Dr. H.-D. Martin, Dipl.-Chem. M. Kummer, Dipl.-Chem. G. Martin
Institut für Organische Chemie I der Universität
Universitätsstrasse 1, D-4000 Düsseldorf 1 (FRG)

[**] Small and Medium Sized Rings, Part 56. This work was supported by the Deutsche Forschungsgemeinschaft, the Fonds der chemischen Industrie, and the BASF AG.—Part 55: R. Braun, M. Kummer, H.-D. Martin, M. B. Rubin, *Angew. Chem. 97* (1985) 1054; *Angew. Chem. Int. Ed. Engl. 24* (1985) 1059.

the same time, shed light on the cause of the deepening in color in the transition from **1** to **2**.

Oxidation of trimethylcyclopentenone **3**[8] with selenium dioxide afforded the 1,2-diketone **4**[9] in 60–70% yield ($\lambda_{max}=486$ nm, $\varepsilon=19$). Wittig carbonyl olefination of the aldehyde **8**[4] with methylenetriphenylphosphorane **5** led to formation of the colorless vinyl derivative **6**, which was oxidized with selenium dioxide to the orange-colored diketone **7** [m.p. 98°C, $\lambda_{max}=496$ nm, $\varepsilon=28$; ^{1}H-NMR ($CDCl_3$/TMS): $\delta=1.37$ (s, 6H), 2.06 (s, 3H), 5.97 (d, 1H), 6.05 (d, 1H), 6.83 (dd, 1H)]. A Wittig-Horner reaction of the aldehyde **8** with the phosphonate **9**[4] ($NaNH_2$/tetrahydrofuran, −15°C) furnished the mini-dinorcanthaxanthin **10** in 40–45% yield as pale yellow scaly crystals [m.p. 162°C, $\lambda=355$ (sh), $\varepsilon=15300$, $\lambda_{max}=336$ nm, $\varepsilon=22600$, ^{1}H-NMR ($CDCl_3$/TMS): $\delta=1.38$ (s, 12H), 1.93 (s, 6H), 2.41 (s, 4H), 6.92 (s, 2H)]. Twofold oxidation with selenium dioxide afforded the deep-red mini-violerythrin **11** [m.p. 208°C; $\lambda_{max}=520$ nm, $\varepsilon=180$, $\lambda=406$ nm, $\varepsilon=22300$, $\lambda_{max}=383$ nm, $\varepsilon=27100$; ^{1}H-NMR ($CDCl_3$/TMS): $\delta=1.45$ (s, 12H), 2.13 (s, 6H), 7.30 (s, 2H)]. Lengthening of the polyene chain by two further double bonds was achieved by reaction of the aldehyde **8** with the bisphosphonate **12**.[10] The dione **13** obtained, a mini-dinorcanthaxanthin, is a brilliant orange-colored solid, whose absorption maximum lies at 412 nm, $\varepsilon=48700$ [^{1}H-NMR ($CDCl_3$/TMS): $\delta=1.32$ (s, 12H), 1.89 (s, 6H), 2.37 (s, 4H), 6.52–6.94 (m, 6H)].



5: $(C_6H_5)_3P{=}CH_2$ **9**: $CH_2P(O)(OC_2H_5)_2$

12: $(C_2H_5O)_2(O)P{-}CH_2{-}CH{=}CH{-}CH_2{-}P(O)(OC_2H_5)_2$

A remarkable bathochromic shift is observed upon oxidation of **13** with selenous acid, whereupon the intense red-violet mini-violerythrin **14** is obtained [m.p. 265–267°C (decomp.); $\lambda=546$ nm (sh), $\varepsilon=340$, $\lambda_{max}=465$ nm, $\varepsilon=78000$; ^{1}H-NMR ($CDCl_3$, TMS): $\delta=1.41$ (s, 12H), 2.21 (s, 6H), 6.68–7.37 (m, 6H)].

A comparison of the UV data of the model violerythrin compounds **4**, **7**, **11**, and **14** is very interesting.

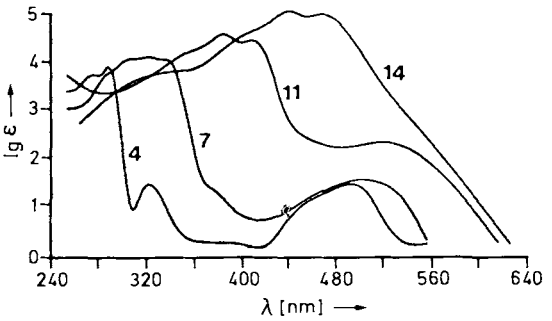


Fig. 1. UV/VIS spectra of the model violerythrin compounds **4**, **7**, **11**, and **14** (*in* $CHCl_3$).

The absorption spectra (Fig. 1) pose the following salient questions:

1. What gives rise to the bathochromic shift in the series of diones and tetrones **4** < **7** < **11** < **14**?
2. Why do the tetrones **11** and **14** absorb at longer wavelength than the precursors **10** and **13** (in analogy to **1** and **2**)?
3. Where are the $n_+\pi^*$ transitions to be located in those tetrones in which they are not recognizable under the broad $\pi\pi^*$ absorption.

To gain an insight into the energies of the occupied levels responsible for the observed electronic transitions, the He(I) photoelectron spectra of **4**, **7**, and **11** were measured. The MINDO/3[12] and HAM/3[13] calculations carried out with optimized MNDO[11] geometries, together with the ionization energies of other 1,2-diketones enable an unequivocal assignment. The splitting of the n-levels into an n_+- and n_--combination in **4** is $\Delta n=2.05$ eV, in good agreement with other data.[14] The additional conjugated double bond in **7** destabilizes the n_+-HOMO by 0.29 eV, whereas the π-SUBHOMO, however, is increased threefold (Fig. 2).

If the conjugated system is lengthened by a further violerythrin end group to give the tetrone **11**, the PE spectrum (Fig. 3) shows an almost constancy of the ionization energy for the HOMO compared to the ionization energies of the dione **7**. Whereas we have measured an n_+/n_+ splitting of ca. 1 eV in other tetrones,[6] in the case of mini-violerythrin **11** we obtained a value of ≤ 0.2 eV for Δn_+. It can be concluded, therefore, that there is no σ-orbital in the planar **11** to permit a clear discrimination of the two combinations $(n_+ + n'_+)$ and $(n_+ - n'_+)$. Aside from the HOMO/SUBHOMO energies, also the LUMO energies have to be taken into consideration for the drastic color change in the transition from the diones to the corresponding tetrones. The energy differences obtained by HAM/3 for $n_+\pi^*$ and $\pi\pi^*$ in the case of **4**, **7**, and **11** are: 2.31, 2.55, 1.66 eV and 3.34, 2.60, 2.05 eV, respectively. The strong bathochromic shift of both the $n_+\pi^*$ transition as well as the $\pi\pi^*$ transition of **11** is caused, in particular, by a drastic lowering of

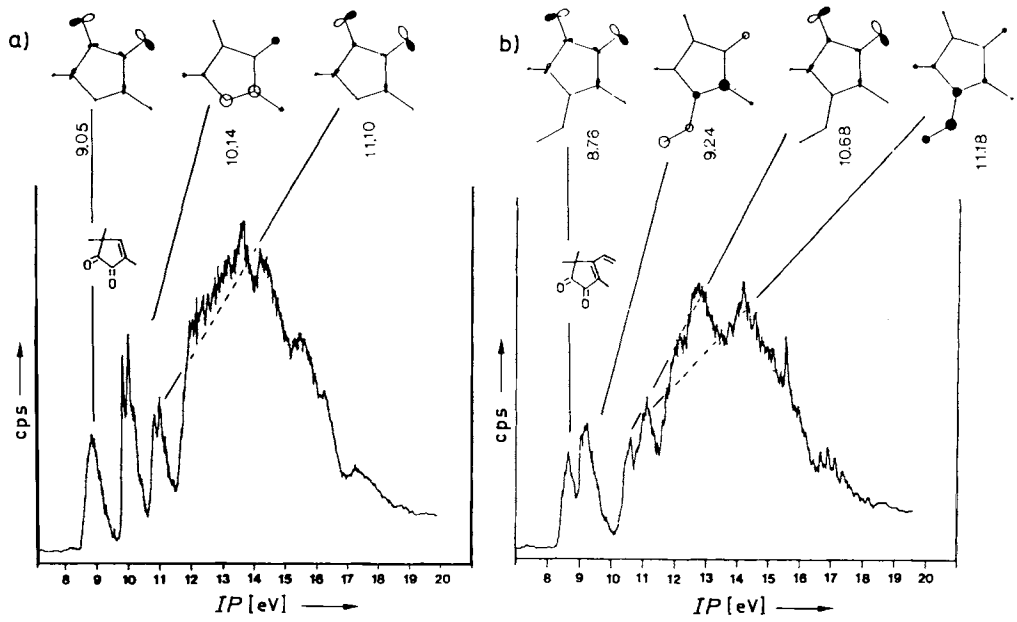


Fig. 2. He(I) photoelectron spectra and MO diagrams of the violerythrin end groups a) **4** and b) **7** (numerical values correspond to the maxima of the bands).

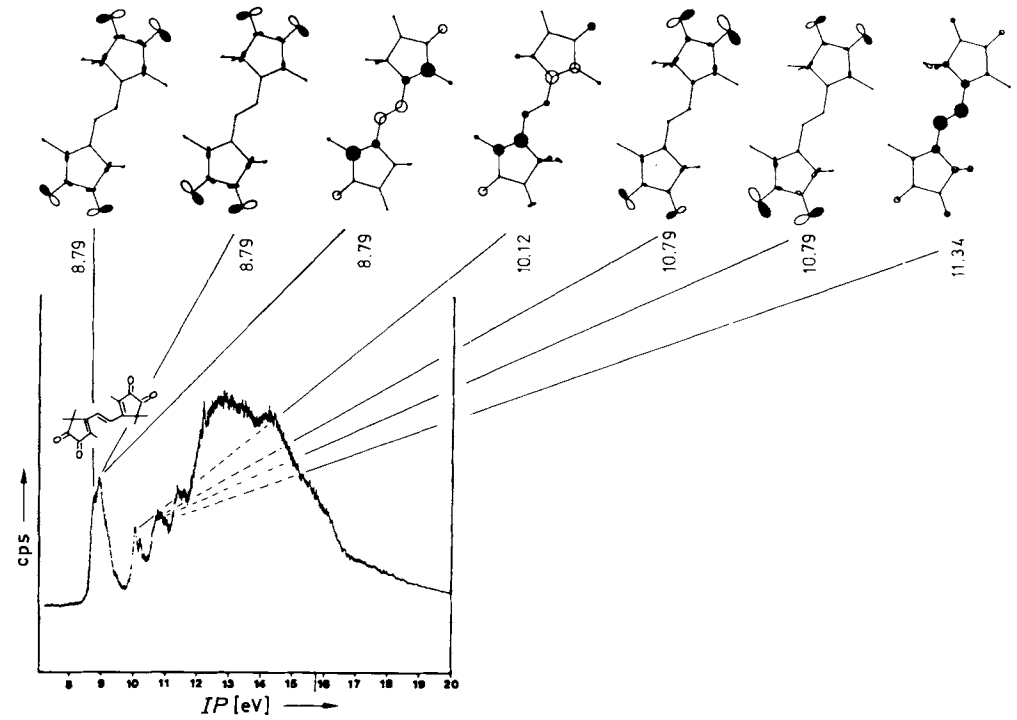


Fig. 3. He(I) photoelectron spectrum and MO diagram of mini-violerythrin **11** (numbers correspond to the maxima of bands).

the π^* LUMO level, besides a slight destabilization of the occupied n_+ level and, as a consequence, a substantial increase in the occupied π-level. A photoelectron spectrum of **14** could not be obtained. Calculations (MINDO/3, HAM/3), however, confirm the trend found in the case of **4**, **7**, and **11**.

Hence, the questions 1 and 2 can be answered as follows: The bathochromic shift in the series **4** < **7** < **11** < **14** is caused both by the increase of the occupied π level as well as by the lowering of the unoccupied π^* level, consistent with the lengthening of the π system. The dominant cause of the bathochromic shift upon oxidation of **10** to **11** and of **13** to **14** as well as of the red dinorcanthaxanthin **1** to the blue violerythrin **2**, however, can only be regarded as a lowering of the π^*-LUMO level.

Information about the $n_+\pi^*$ transition (question 3) can be deduced from Figure 1. Whereas the $n\pi^*$ transitions in the case of **4**, **7**, and **11** are well separated from the $\pi\pi^*$

transitions, the two $n_+\pi^*$ transitions of **14** are almost completely masked by the more intense and longer wavelength $\pi\pi^*$ transition, so that even in the case of **14** the more rapidly migrating $\pi\pi^*$ transitions have already caught up with the far less variable $n\pi^*$ transitions. As a result, a value of 580–600 nm can be extrapolated for the two $n_+\pi^*$ transitions in violerythrin **2**. Planar molecules with an *s-trans* conformation of the end groups to the ethene and hexatriene bridges were deduced on the basis of the calculations for **11** and **14**. The X-ray structure analysis of **11** confirms this geometry.[15] The torsion angles at the single bonds located between the double bonds are in each case 179.4°; hence, the end groups are coupled *s-trans* to the ethene bridge.

Received: June 9, 1986 [Z 1808 IE]
German version: *Angew. Chem. 98* (1986) 995

CAS Registry numbers:
3, 17190-21-5; **4**, 79699-69-7; **5**, 3487-44-3; **6**, 104642-15-1; **7**, 104642-16-2; **8**, 58626-49-6; **9**, 59534-37-1; **10**, 104642-17-3; **11**, 104642-18-4; **12**, 16626-80-5; **13**, 104642-19-5; **14**, 104642-20-8.

[1] J. C. Bauernfeind in J. C. Bauernfeind (Ed.): *Carotenoids as Colorants and Vitamin A Precursors*, Academic Press, New York 1981, p. 1.
[2] I. M. Heilbronn, H. Jackson, R. N. Jones, *Biochem. J. 29* (1935) 1384.
[3] S. Hertzberg, S. Liaaen-Jensen, C. R. Enzell, G. W. Francis, *Acta Chem. Scand. 23* (1969) 3290.
[4] F. Kienzle, R. M. Minder, *Helv. Chim. Acta 59* (1976) 439.
[5] S. Liaaen-Jensen, *Pure Appl. Chem. 20* (1969) 421.
[6] H.-D. Martin, B. Albert, H. J. Schiwek, *Tetrahedron Lett. 1979*, 2347.
[7] H.-D. Martin, B. Mayer, *Angew. Chem. 95* (1983) 281; *Angew. Chem. Int. Ed. Engl. 22* (1983) 283.
[8] H. J. E. Loewenthal, *Isr. J. Chem. 4* (1966) 31.
[9] **4** has already been synthesized via an alternative route: L. de Buyck, R. Verhe, N. de Kimpe, D. Courthyn, N. Schamp, *Bull. Soc. Chim. Belg. 90* (1981) 837.
[10] G. A. Lapitzki, S. M. Makin, E. K. Lyapina, A. S. Chebotarev, *Vysokomol. Soedin. Ser. B 11* (1969) 266; *Chem. Abstr. 71* (1969) 30750.
[11] M. J. S. Dewar, W. Thiel, *J. Am. Chem. Soc. 99* (1977) 4907.
[12] R. C. Bingham, M. J. S. Dewar, D. H. Lo, *J. Am. Chem. Soc. 97* (1975) 1285.
[13] L. Asbrink, C. Fridh, E. Lindholm, *Chem. Phys. Lett. 52* (1977) 69.
[14] D. Dougherty, P. Brint, S. P. McGlynn, *J. Am. Chem. Soc. 100* (1978) 5597.
[15] D. Mootz, B. Middelhauve, H.-D. Martin, M. Kummer, unpublished.

Unexpected "Two-Electron" Transfer in Cyclic Hydrazines—a Voltammetric Analysis**

By *Michael Dietrich, Jürgen Heinze,* Hans Fischer,* and *Franz A. Neugebauer**

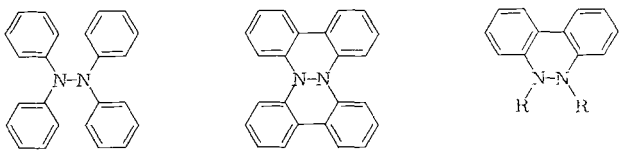
Dedicated to Professor Walther Jaenicke on the occasion of his 65th birthday

Of the primary oxidation products of aromatic hydrazines, only the radical cations have so far been described as stable particles;[1–3] the dications, on the other hand, have been found to be extremely reactive, and consequently an unequivocal characterization of their redox properties is still lacking.

[*] Priv.-Doz. Dr. J. Heinze, Dipl.-Chem. M. Dietrich
Institut für Physikalische Chemie der Universität
Albertstrasse 21, D-7800 Freiburg (FRG)
Prof. Dr. F. A. Neugebauer, H. Fischer
Max-Planck-Institut für medizinische Forschung,
Abt. Organische Chemie
Jahnstrasse 29, D-6900 Heidelberg (FRG)

[**] This work was supported by the Stiftung Volkswagenwerk and the Fonds der Chemischen Industrie.

In a cyclovoltammetric investigation of the series tetraphenylhydrazine **1**, benzo[*c*]benzo[3,4]cinnolino[1,2-*a*]cinnoline **2**, 5,6-dihydro-5,6-diphenylbenzo[*c*]cinnoline **3**, and 5,6-dihydro-5,6-dimethylbenzo[*c*]cinnoline **4** we have now succeeded for the first time to carry out the reversible oxidation of **1**–**4** in liquid SO_2 ($T < -10$ °C) up to the dications (Table 1). In the case of **2**, even the reversible formation of the trication was observed. SO_2, purified by a new technique developed by us, proved once again to be an excellent solvent for the generation and investigation of highly charged cations.[4]



1 **2** **3**, R = C_6H_5; **4**, R = CH_3

Table 1. Standard potentials of the compounds **1**–**4** [designated as X; cf. also reaction scheme (1)].

	E^0 ($X/X^{\oplus\odot}$) [V] [a]	E^0 ($X^{\oplus\odot}/X^{2\oplus}$) [V]	E^0 ($X^{2\oplus}/X^{3\oplus\odot}$) [V]
1	0.797	1.652	—
2	0.560	1.165	2.745
3	ee conf.: 0.240 [b] aa conf.: 0.990 [b]	0.840	—
4	ee conf.: 0.320 [b] aa conf.: 0.820 [b]	0.870	—

[a] The potentials were calibrated using an internal ferrocene standard and then referred to the standard Ag/AgCl reference electrode. [b] The standard potentials were determined by digital simulation.

Particularly suprising at first sight is the cyclovoltammogram of **3** at −50 °C (Fig. 1a): instead of the expected well separated oxidation steps for the formation of $\mathbf{3}^{\oplus\odot}$ and $\mathbf{3}^{2\oplus}$, the voltammogram shows only one, excessively large anodic wave, and in the reverse scan the rare trace crossing effect and a further wave shifted strongly cathodically.

Since **1** and **2** can be oxidized reversibly, a usual follow up reaction of $\mathbf{3}^{\oplus\odot}$ (e.g. addition or substitution) can be ruled out. Geometrical considerations based on the molecular model of **3** rather suggest that conformational trans-

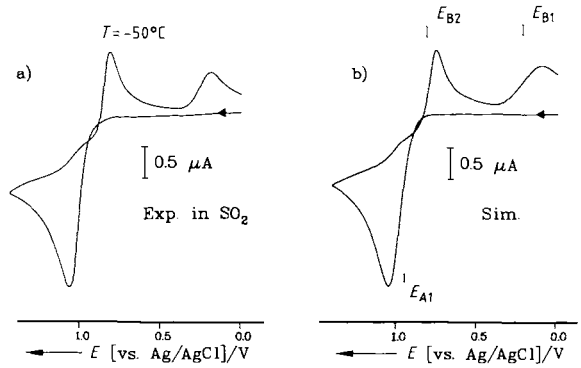
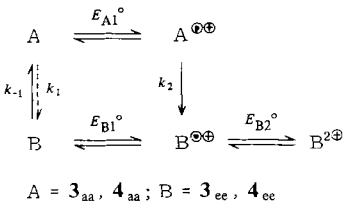


Fig. 1. Cyclovoltammogram of the oxidation of **3** ($c = 1 \times 10^{-3}$ M, $v = 100$ mV/s. a) Experimental voltammogram in SO_2 (working electrode Pt; 0.1 M Bu_4NPF_6). b) Simulated cyclovoltammogram (simulation data: $k^0(A/A^{\oplus\odot}) \cdot \sqrt{D} = 5.0 \times 10^{-6}$ cm^2 s$^{-3/2}$, $\alpha(A/A^{\oplus\odot}) = 0.39$, $k^0(B/B^{\oplus\odot}) \cdot \sqrt{D} = 3.1 \times 10^{-8}$ cm^2 s$^{-3/2}$, $\alpha(B/B^{\oplus\odot}) = 0.75$, $k^0(B^{\oplus\odot}/B^{2\oplus}) \cdot \sqrt{D} = 9.3 \times 10^{-6}$ cm^2 s$^{-3/2}$, $\alpha(B^{\oplus\odot}/B^{2\oplus}) = 0.35$, $k_1 \approx 0$, $k_{-1} = 100$ s^{-1}, $k_2 = 100$ s^{-1}).

formations take place after charge transfer. Due to steric factors, the two phenyl groups in uncharged **3** should be oriented axially to the predominantly sp^3-hybridized N-atoms (*aa* conformation).[5] Moreover, PE spectroscopic investigations on hydrazobenzenes closely related to **3** confirm that the antiperiplanar arrangement of the phenyl groups is, as a rule, preferred.[6] Oxidation to the radical cation $\mathbf{3}^{\oplus\ominus}$ leads, as shown by ESR investigations,[3] to a substantial planarization of the structural framework. The phenyl groups on the now sp^2-hybridized N-atoms are oriented equatorially (ee conformation) and acquire adequate space through an increase in the torsion angle about the N-C bond. *Nelsen* and *Evans* et al. have already been able to attribute the electrochemical behavior of cyclic aliphatic hydrazines to the existence of conformers.[7] Nevertheless, their findings and our results are not directly comparable.

We assume that **3** is oxidized to the dication in an ECE stepwise sequence,[8] whereby the C step leads to ee conformers. The conjugation between the two nitrogen centers is expanded to such an extent by planarization of the skeletal framework that the redox potential E^0_{B2} for the $\mathbf{3}^{\oplus\ominus}_{ee}/\mathbf{3}^{2\oplus}_{ee}$ pair lies on the negative side of E^0_{A1}. For this reason, only one wave is observed in the voltammetric experiment. In the reduction of the system, in the reverse scan, two well-separated reduction waves appear which lead from $\mathbf{3}^{2\oplus}_{ee}$ to the neutral $\mathbf{3}_{ee}$. The neutral species finally rearranges irreversibly again ($T=-50\,^\circ C$, $k_1\approx 0$, $k_{-1}\gg 0$) from the ee into the stable aa form (EEC).[8]

Thus, we have the simplified reaction scheme (1) (altogether eight conformers exist for the neutral species: two ee, two ae, and four ea forms[7]).



(1)

A = $\mathbf{3}_{aa}$, $\mathbf{4}_{aa}$; B = $\mathbf{3}_{ee}$, $\mathbf{4}_{ee}$

A formally analogous scheme has already been postulated by *Olsen* and *Evans* and by *Hammerich* and *Parker* for the reduction of bianthrone derivatives, whose radical anions likewise undergo conformational transformations.[9]

Two further results complete our interpretation. The distinctly visible trace crossing evidences a homogeneous disproportionation[10] of the type

$$B^{2\oplus} + A \longrightarrow B^{\oplus\ominus} + A^{\oplus\ominus} \qquad (2)$$

whereby the anodic current upon scan reversal results from the reoxidation of $B^{\oplus\ominus}$ to $B^{2\oplus}$ at the electrode surface. The digital simulation of the overall process including the disproportionation (Fig. 1b) excellently agrees with the experimental data. In principle, the experimental data at $-50\,^\circ C$ can also be simulated in terms of an E_iE_r mechanism[8] (i = irreversible, r = reversible) instead of the proposed ECE sequence. In this case, however, E^0_{A1} would have to be less than E^0_{B2}, and the transition $B^{\oplus\ominus}\rightarrow B$ at E^0_{B1} would be nonexistent. Measurements at $T>60\,^\circ C$ in benzonitrile, however, point to conformational transformations prior to charge transfer which, already in the neutral species, lead, even if only to a small extent, to the ee form and the ea forms ($k_1\gg 0$). In this case $\mathbf{3}^{\oplus\ominus}_{ee}$ is formed at the standard potential E^0_{B1}. The E_iE_r route can therefore be ruled out.

In a multisweep experiment in the range between $+0.6$ V and $+1.5$ V, an isopotential point (IPP) is observed at $+0.94$ V. The wave for the reversible redox pair $B^{\oplus\ominus}/B^{2\oplus}$ at $E^0_{B2}=0.840$ V continues growing at the same time as the wave for the formation of $A^{\oplus\ominus}$ at $E^0_{A1}=1.080$ V decreases. Isopotential points always occur when one electroactive species completely transforms into another electroactive species, i.e. in the present case axial $A^{\oplus\ominus}$ into equatorial $B^{\oplus\ominus}$.[11]

A reaction scheme very similar to that in the case of **3** is found for **4** at $-70\,^\circ C$ (Fig. 2). Due to less steric hindrance by the two methyl groups, E^0_{A1} remains less then E^0_{B2}, so there is no crossing effect. If the temperature is increased (Fig. 2), an anodic wave appears between $+0.3$ V and

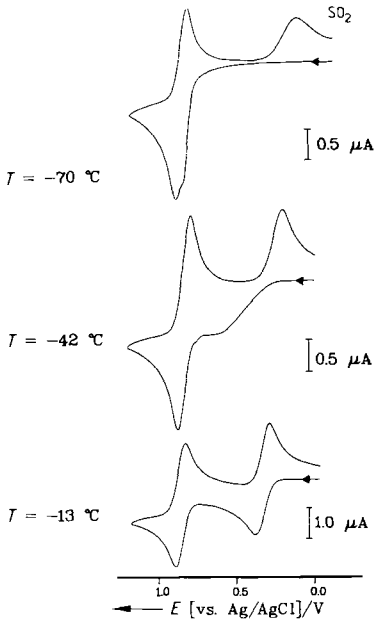


Fig. 2. Experimental cyclovoltammogram of the oxidation of **4** ($c=1\times 10^{-3}$ M, $v=100$ mV/s) in SO_2 at various temperatures (working electrode Pt; 0.1 M Bu_4NPF_6).

$+0.7$ V, and, at $-13\,^\circ C$, the normal form of a reversible peak-separated two-step oxidation is observed. **4** is transformed analogously to **3** from the aa or ea conformation into the ee conformation (CEE), but, because of the lower activation barrier at lower temperatures, before the electron transfer. Since there are eight conformations, the complete kinetic scheme is quite complex. NMR spectroscopic measurements over a very wide temperature range gave no indication of any change in conformation. It follows, therefore, that the thermodynamic equilibrium, consistent with the electrochemical findings, is on the side of the aa conformation. During the cyclovoltammetric experiment the ee conformer B is continually withdrawn from the equilibrium. Thus, this method allows an unequivocal detection of such thermodynamically less favored conform-

ers, provided that the rates of formation of B ($k_1 \gg 0$) are sufficiently high.

Received: June 12, 1986;
revised: July 11, 1986 [Z 1810 IE]
German version: *Angew. Chem. 98* (1986) 999

CAS Registry numbers:
$1^{\oplus\oplus}$, 34832-17-2; $2^{\oplus\oplus}$, 104419-46-7; $3^{\oplus\oplus}$, 104369-55-3; $4^{\oplus\oplus}$, 65938-53-6.

[1] G. Cauquis, M. Genies, *Tetrahedron Lett. 1971*, 3959; G. Cauquis, H. Delhomme, D. Serve, *ibid. 1971*, 4649; G. Cauquis, B. Chabaud, M. Genies, *Bull. Soc. Chim. Fr. 1973*, 3482; G. Cauquis, H. Delhomme, D. Serve, *Electrochim. Acta 20* (1975) 1019; U. Svanholm, V. D. Parker, *J. Am. Chem. Soc. 94* (1972) 5507.

[2] A. R. Forrester, J. M. Hay, R. H. Thomson: *Organic Chemistry of Stable Free Radicals*, Academic Press, London 1968, p. 123; R. M. Das, A. V. Patankar, B. Venkataraman, *Proc. Indian Acad. Sci. A 53* (1961) 273; F. A. Neugebauer, S. Bamberger, *Chem. Ber. 105* (1972) 2058; F. A. Neugebauer, H. Weger, *J. Phys. Chem. 82* (1978) 1152.

[3] F. A. Neugebauer, M. Bock, S. Kuhnhäuser, H. Kurreck, *Chem. Ber. 119* (1986) 980.

[4] M. Dietrich, J. Mortensen, J. Heinze, *Angew. Chem. 97* (1985) 502; *Angew. Chem. Int. Ed. Engl. 24* (1985) 508.

[5] This has been confirmed by an X-ray structure analysis; K. Krieger, unpublished.

[6] P. Rademacher, V.-M. Bass, M. Wildemann, H. Weger, *Chem. Ber. 110* (1977) 1939.

[7] S. F. Nelsen, L. Echegoyen, D. H. Evans, *J. Am. Chem. Soc. 97* (1975) 3530; S. F. Nelsen, L. Echegoyen, E. L. Clennan, D. H. Evans, D. A. Corrigan, *ibid. 99* (1977) 1130; S. F. Nelsen, E. L. Clennan, D. H. Evans, *ibid. 100* (1978) 4012; S. F. Nelsen, G. T. Cunkle, D. H. Evans, K. J. Haller, M. Kaftory, B. Kirste, H. Kurreck, T. Clark, *ibid. 107* (1985) 3829.

[8] J. Heinze, *Angew. Chem. 96* (1984) 823; *Angew. Chem. Int. Ed. Engl. 23* (1984) 831.

[9] B. H. Olsen, D. H. Evans, *J. Am. Chem. Soc. 103* (1981) 839; O. Hammerich, V. D. Parker, *Acta Chem. Scand. Ser. B 35* (1981) 395.

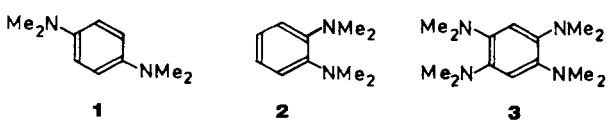
[10] C. Amatore, J. Pinson, J. M. Savéant, A. Thiebault, *J. Electroanal. Chem. 107* (1980) 59.

[11] J. G. Gaudiello, T. C. Wright, R. A. Jones, A. J. Bard, *J. Am. Chem. Soc. 107* (1985) 888.

1,2,4,5-Tetrakis(dimethylamino)benzene, a New Electron Donor with Unusual Properties**

By *Karin Elbl, Claus Krieger,* and *Heinz A. Staab**

Because of its distinct donor strength, 1,4-bis(dimethylamino)benzene **1** is one of the best investigated electron donors in organic chemistry. Its oxidation to "Wurster's Blue" salts has been known for more than 100 years.[2] 1,2-Bis(dimethylamino)benzene **2**, too, was described in the last century.[3] Therefore, it is all the more surprising that 1,2,4,5-tetrakis(dimethylamino)benzene **3**, which combines the structural elements of **1** and **2**, had not been synthesized so far, even though 1,2,4,5-tetraaminobenzene—also known for 100 years—is a readily accessible compound.[4] We were interested in **3** on account of its expected donor properties and, besides that, in connection with investigations of compounds with dimethylamino groups in close spatial proximity ("proton sponges").[5]



1 **2** **3**

[*] Prof. Dr. H. A. Staab, Dipl.-Chem. K. Elbl, C. Krieger
Abteilung Organische Chemie
Max-Planck-Institut für medizinische Forschung
Jahnstrasse 29, D-6900 Heidelberg (FRG)

[**] Electron Donor-Acceptor Compounds, Part 42—Part 41: [1].

Conventional methods[6] did not allow the permethylation of 1,2,4,5-tetraaminobenzene, which was achieved, however, by treatment of the tetrahydrochloride in acetonitrile with 36.5% aqueous formaldehyde solution in the presence of $Na[B(CN)H_3]$ under argon according to the method of *Borch* and *Hassid*.[7] Sublimation afforded analytically pure **3** in the form of colorless crystals (m.p. = 95 °C, 27% yield). In solution, compound **3** is oxidized readily by agents such as oxygen, bromine, or iodine, yielding green oxidation products.

The ^{1}H-NMR spectrum of **3** ($CDCl_3$, 360 MHz) shows, as expected, only two singlets at $\delta = 2.76$ (24 H) and 6.56 (2 H). The mass spectrum [*m/z* 250 (100%, $M^{\oplus}$), 235 (6), 220 (12), 125 (3, $M^{2\oplus}$)] is in agreement with the structure. IR absorptions [$\tilde{\nu}$ = 2980 (m), 2940 (m), 2820 (m), 2790 (m), 1510 (s) cm^{-1}; KBr] and UV spectra [λ_{max} ($\lg\varepsilon$) = 320 (3.68), 278 (3.85), 242 (4.32) nm; acetonitrile] also support the assigned structure.

Cyclovoltammetry indicates that **3** is a very strong electron donor. Under the conditions given in the caption to Figure 1, the first two oxidation steps are not separable and correspond to $E_{ox} = -0.266$ V. A third electron is removed, likewise reversibly, at $E = +1.266$ V. Under analogous conditions of measurement, the first oxidation potential of **1**, which corresponds to the radical-cation formation of Wurster's Blue, was measured to be $E_{ox} = -0.206$ V and the second oxidation potential was determined to be $E_{ox} = +0.378$ V.

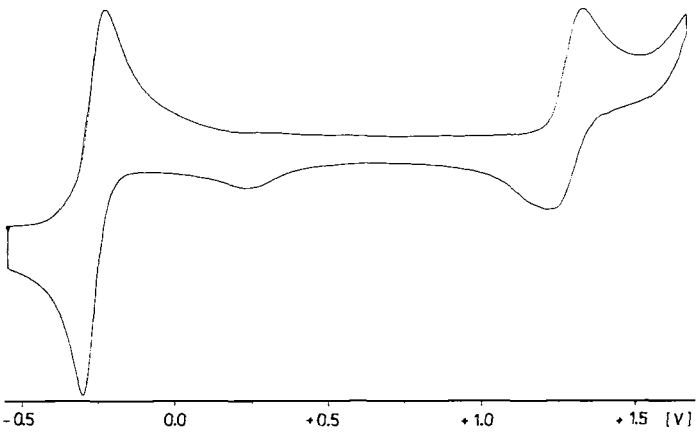
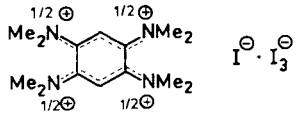


Fig. 1. Cyclovoltammogram of **3** [acetonitrile/0.1 M tetrabutylammonium perchlorate, "glassy carbon electrode" versus $Ag/Ag^{\oplus}$; ferrocene correction, $v = 220$ mV s^{-1}].

When **3** is treated with iodine in acetonitrile, lustrous black-violet crystals separate out of the dark green solution and can be recrystallized from acetonitrile: m.p. = 272 °C (development of iodine above 195 °C), elemental composition $C_{14}H_{26}N_4I_4$. This compound, in contrast to Wurster's Blue salts derived from **1**, is diamagnetic (ESR, acetonitrile). In the ^{1}H-NMR spectrum ([D_6]DMSO, 360 MHz), two singlets are observed, which with $\delta = 3.34$ (24 H) and 5.85 (2 H) show remarkable shifts compared to **3** ($\delta = 2.76$ and 6.56, respectively). The absorption spectrum in acetonitrile shows a long-wavelength absorption band at 573 nm ($\lg\varepsilon = 3.38$) along with additional bands at 368 and 290 nm ($\lg\varepsilon = 4.46$ and 4.74, respectively). All data are in accord with the structure of **4**, consisting of a dication of **3** with two mesomeric π-electron systems, which correspond to vinylogous amidinium units.[8]



4

An X-ray structure analysis confirmed that the product of the reaction of **3** with iodine is indeed **4**, in which the dication of **3** is present as the iodide-triiodide.[9] A remarkable feature of the bond lengths in the six-membered ring (Fig. 2a) is the fact that C(1)–C(1i) and C(1j)–C(1k) have nearly the lengths of single bonds. The remaining four C–C bond lengths are intermediate between standard single and double bond lengths.

In agreement with mesomeric systems of the polymethine type is the marked shortening of the C–N bonds compared with C–N single bonds. The side view (Fig. 2b) reveals that the two resonance-stabilized π-electron systems, each of which is roughly planar, are strongly tilted against each other so that the six-membered ring has a twist conformation. This conformation, which is made possible by the cancellation of the aromaticity of the six-membered ring, results in a largely strain-free structure.

In the crystal lattice of **4**, the organic dications are coordinated with iodide and triiodide as counterions. The lattice packing in the projection onto the *a*, *b* plane is shown in Figure 3. The iodide ions are hidden in the figure by the triiodide units lying in front of them on the *c* axis.

First results concerning the donor properties of **3** show that, because of the unique electronic structure of the dication, it is a strong *two*-electron donor, whose complexation with acceptors is of interest on account of a complex stoichiometry differing from that of **1** and other conventional donors. Thus, **3** forms a 1:2 complex (shining violet needles, m.p. = 213 °C, dec.) with tetracyanoquinodimethane

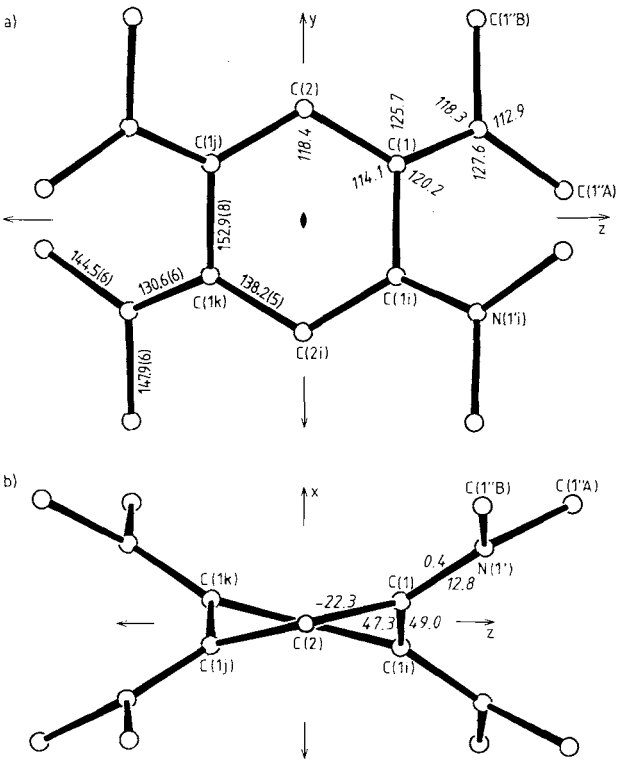


Fig. 2. Structure of the dication part of **4**; a) view from above; b) side view, with bond lengths [pm] and bond and twist angles (in italics) [°]. In parentheses: standard deviation in units of the last digit given.

(TCNQ) in acetonitrile. Conductivity measurements (single crystals, four-contact method) gave $\sigma \sim 10^{-1}$ $(\Omega\ \mathrm{cm})^{-1}$

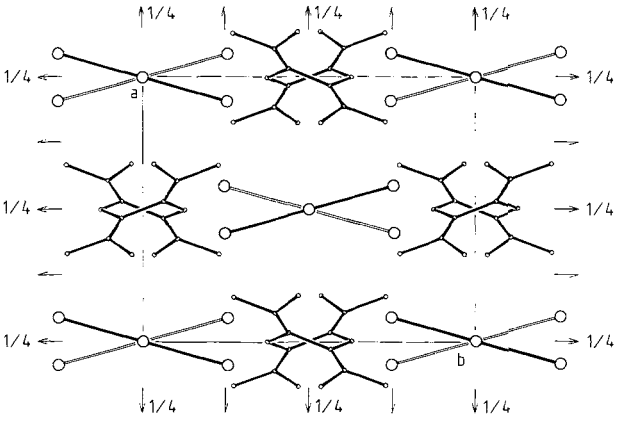
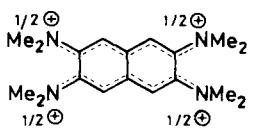


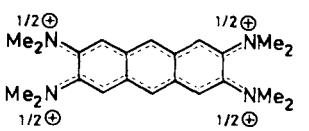
Fig. 3. Lattice packing of **4** in the projection onto the *a*,*b* plane.

for this complex; the temperature dependence of the conductivity showed that the behavior was that of a typical semiconductor.[10]

The dication **4**, derived from **3**, may be regarded as the first member of a series of vinylogous dications, to which **5** and **6** belong. The possibility of obtaining **5** and **6** from the corresponding, still unknown tetrakis(dimethylamino) derivatives of naphthalene and anthracene is currently the subject of investigation.



5



6

Received: June 30, 1986 [Z 1840 IE]
German version: *Angew. Chem. 98* (1986) 1024

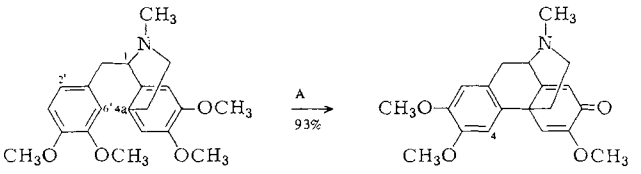
CAS Registry numbers:
3, 104779-70-6; **3**·2TCNQ, 104779-73-9; **3** (dication), 104779-71-7; **3** (trication), 104779-74-0; **4**, 104779-72-8; TCNQ, 1518-16-7; 1,2,4,5-tetraaminobenzene, 3204-61-3; 1,2,4,5-tetraaminobenzene tetrahydrochloride, 4506-66-5.

[1] H. Bauer, J. Briaire, H. A. Staab, *Tetrahedron Lett. 26* (1985) 6175.
[2] C. Wurster, *Ber. Dtsch. Chem. Ges. 12* (1879) 522, 2071; C. Wurster, E. Schobig, *ibid. 12* (1879) 1807; concerning the structure of radical-cation salts, see also R. Kuhn, H. Katz, *Z. Angew. Chem. 46* (1933) 478.
[3] O. Fischer, *Ber. Dtsch. Chem. Ges. 25* (1892) 2826.
[4] R. Nietzki, E. Hagenbach, *Ber. Dtsch. Chem. Ges. 20* (1887) 328; R. Nietzki, *ibid. 20* (1887) 2114; R. Nietzki, E. Müller, *ibid. 22* (1889) 440; P. Ruggli, R. Fischer, *Helv. Chim. Acta 28* (1945) 1270.
[5] T. Saupe, C. Krieger, H. A. Staab, *Angew. Chem. 98* (1986) 460; *Angew. Chem. Int. Ed. Engl. 25* (1986) 451; and references cited therein.
[6] S. Hünig, H. Quast, W. Brenninger, E. Frankenfeld, *Org. Synth. Coll. Vol. V* (1973) 1018; H. Quast, W. Risler, G. Döllscher, *Synthesis 1972*, 558.
[7] R. F. Borch, A. I. Hassid, *J. Org. Chem. 37* (1972) 1673.
[8] Cf. H. A. Staab: *Einführung in die theoretische organische Chemie*, 4th ed., Verlag Chemie, Weinheim 1964, p. 323, 639; S. Dähne, D. Leupold, *Angew. Chem. 78* (1966) 1029; *Angew. Chem. Int. Ed. Engl. 5* (1966) 984.
[9] Crystal structure of **4**: orthorhombic, space group *Ibam*; $a = 875.5(4)$, $b = 1109.8(5)$, $c = 2311.2(7)$ pm; $Z = 4$; $\rho_{calcd} = 2.242$ gcm^{-3}; 1456 measured, 1040 observed reflections with $I \geq 1.96\sigma(I)$; $R = 0.039$. Further details of the crystal structure investigation may be obtained from the Fachinformationszentrum Energie, Physik, Mathematik GmbH, D-7514 Eggenstein-Leopoldshafen 2 (FRG), on quoting the depository number CSD-51986, the names of the authors, and the journal citation.
[10] We thank Dr. *D. Schweitzer*, Heidelberg, for the conductivity measurements.

Total Synthesis of *rac*-Salutaridine and Sinoacutine ((−)-Salutaridine)— A New Route to the Morphine Skeleton**

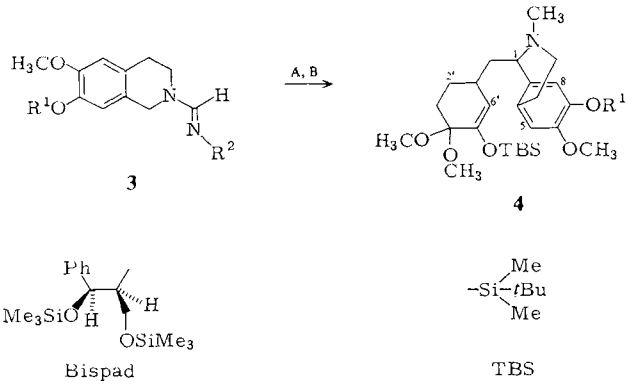
By *Wolfgang Ludwig* and *Hans J. Schäfer**

Despite its addicting side effects, morphine is of considerable importance as an analgesic.[1] It is isolated from *Papaver somniferum*; in addition, there exist several efficient total syntheses for the morphine skeleton involving various strategies.[2–6] Of these, the anodic coupling of the 1-benzyltetrahydroisoquinoline **1** is particularly attractive.[4] For steric and electronic reasons, however, morphinandienones of the flavinantine-type **2** are obtained, which, owing to the absence of the 4-hydroxy group, cannot be converted into morphine derivatives. Attempts to achieve the C6′-C4a coupling of **1** by blocking the C2′ position with halogen,[4a] nitro,[7] or *N*-acetylamino substituents,[7] however, have failed[8] (Scheme 1).



Scheme 1. A) 0.1 M $LiClO_4$, $CH_3CN/H_2O/NaHCO_3$ (99.5 : 0.5 : 2), electrolysis at Pt electrodes.

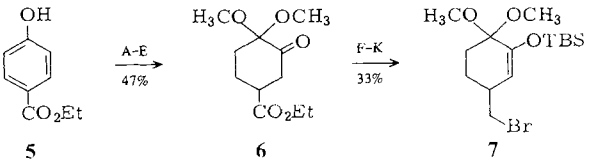
Prompted by work of *Evans* et al.,[9] we have now achieved the C6′ coupling by acid-catalyzed cyclization of **4**. Only C6′ is reactive in **4**, because the 1-benzyl moiety has been replaced by a tetrahydrobenzyl moiety.



a, R^1 = Me, R^2 = *t*Bu; **b**, R^1 = $PhCH_2$, R^2 = *t*Bu; **c**, R^1 = Me, R^2 = Bispad

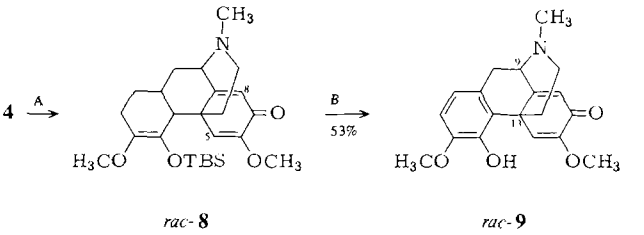
Scheme 2. A) 1. $LiNiPr_2$, −78 °C; 2. **7**, −78 °C; B) $NaBH_4$, MeOH. Yields: **4a**, 49% from **3a**, 44% from **3c**; **4b**, 53% from **3b**.

Compound **4** may be prepared in a convergent synthesis starting from **7** and C1-lithiated **3** (Scheme 2). The bromide **7** is obtained in 15% yield in 11 steps from ethyl *p*-hydroxybenzoate **5** via the ketoester **6** (Scheme 3). The formamidines **3a** and **3b** may be prepared in 61% and 27% yield, respectively, from β-(3,4-dimethoxyphenyl)ethylamine and vanillin, respectively (for **3c** see below).



Scheme 3. A) H_2, Raney Ni, 110 bar, EtOH, 160 °C; B) $Na_2Cr_2O_7$, H_2SO_4, ether/H_2O; C) $HC(OMe)_3$, MeOH, cat. TosOH; D) *m*-chloroperbenzoic acid, MeOH, 8–10 °C; E) $CrO_3 \cdot 2C_5H_5N$, CH_2Cl_2, 20 °C; F) $Me_3SiCH_2CO_2Et$, cat. $Bu_4N^{\oplus}F^{\ominus}$, tetrahydrofuran (THF), 20 °C; G) $LiAlH_4$, ether, 15 °C; H) hexamethyldisilazane, Me_3SiCl, *n*-hexane; I) 1. $LiNiPr_2$, *t*BuMe$_2$SiCl, THF, −78 °C; 2. H_2O, 0 °C; J) MesCl, Et_3N, ether; K) LiBr, acetone.

The cyclization of **4** to **8** was achieved by variation of the reaction parameters: Lewis acid ($SnCl_4$, $BF_3 \cdot Et_2O$, $AlCl_3$, $(CF_3CO)_2O/CF_3CO_2H$), equivalents of acid, temperature, reaction time, and leaving group R^1. The best combination is 1.5 equivalents of $SnCl_4$ at 20 °C, R^1 = $PhCH_2$ (= **4b**, yield 46% **8**) (Scheme 4); with R^1 = CH_3 (= **4a**), under otherwise identical conditions, only 27% of **8** is obtained. Compound **8** may be dehydrogenated in 53% yield to *rac*-salutaridine **9**, the spectroscopic data of which agree with those reported.[10]



rac-**8** *rac*-**9**

Scheme 4. A) $SnCl_4$, CH_2Cl_2, 20 °C; B) 2,3-dichloro-5,6-dicyano-*p*-benzoquinone in refluxing benzene.

Thus, *rac*-salutaridine **9** is available in an overall yield of 3% via a 15-step total synthesis; **9** may be converted via codeine[11a] into morphine.[11b]

The route described above also allows the enantioselective synthesis of sinoacutine ((−)-salutaridine).[12] According to the method of *Meyers* et al.,[13] it is possible to alkylate lithiated formamidines **3** with chiral auxiliary groups on the imine nitrogen to give (1*S*)-1-alkyltetrahydroisoquinolines with high enantioselectivity. We used this reaction for the formation of the (9*S*) and (13*R*) configuration in (−)-salutaridine. Reaction of 6,7-dimethoxy-1,2,3,4-tetrahydroisoquinoline with *N′*-bispad-*N*,*N*-dimethylformamidine gave **3c** (78%), which, like **3a**, was allowed to react with **7** to give, via **4c**, (−)-**9** in 6% yield (85.2% *ee*, see Table 1). Physical data for selected compounds are collected in Table 1.

[*] Prof. Dr. H. J. Schäfer, Dr. W. Ludwig
Organisch-chemisches Institut der Universität
Orléansring 23, D-4400 Münster (FRG)

[**] This work was supported by the Fonds der Chemischen Industrie.

Table 1. Selected physical data for the compounds **4b**, **7**, *rac*-**8**, and (−)-**9**.

4b: Colorless, decomposable oil; IR (film): $\tilde{\nu}$ = 1655 cm^{-1} (C=C, enol ether); ^{1}H-NMR ($CDCl_3$): δ = 0.15, 0.92 (2s, 15H, $-SiMe_2tBu$), 1.5–3.72 (m, 11H), 2.44 (s, 3H, NCH_3), 3.28, 3.81 (each s, 9H, OCH_3), 4.24, 4.65 (2m, 2H), 5.02 (s, 2H, CH_2Ph), 6.59, 6.60 (each s, 2H, 5-, 8-H), 7.2–7.5 (m, 5H, Ph); MS (70 eV): *m/z* 567 (1%, $M^{\oplus}$), 282 (100%)

7: Dark yellow oil; IR (film): $\tilde{\nu}$ = 3025 (vinyl. H), 1655 cm^{-1} (C=C, enol ether); ^{1}H-NMR ($CDCl_3$): δ = 0.15, 0.96 (each s, 15H, $SiMe_2tBu$), 2.2–2.45 (m, 4H, CH_2), 2.37 (m, 1H, CH), 3.24 (m, 2H, CH_2Br), 3.35 (s, 6H, OCH_3), 4.72 (d, 1H, vinyl. H); MS (70 eV): *m/z* 366 (0.5%, *M* + 1), 75 (100%)

rac-**8**: Yellow, viscous oil; UV (*n*-hexane): λ_{max} (lg ε) = 247 (4.2) nm; IR (film): $\tilde{\nu}$ = 1665 (C=O), 1655 cm^{-1} (enol ether); ^{1}H-NMR ($CDCl_3$): δ = 0.13, 0.92 (each s, 15H, $SiMe_2tBu$), 1.4–3.4 (m, 13H), 2.42 (s, 3H, NCH_3), 3.43, 3.52 (each s, 6H, OCH_3), 5.73 (s, 1H, 5-H), 6.24 (s, 1H, 8-H); MS (70 eV): *m/z* 445 (68%, $M^{\oplus}$)

(−)-**9**: M.p. = 197°C (ether); UV (methanol): λ_{max} (lg ε) = 276 (3.76), 240 (4.24) nm; IR (film): $\tilde{\nu}$ = 3555 (OH), 1670, 1645, 1622 cm^{-1} (cyclohexadienone); ^{1}H-NMR ($CDCl_3$) selected: δ = 2.44 (s, 3H, NCH_3), 3.75, 3.87 (each s, 6H, OCH_3), 6.31 (s, 1H, 8-H), 6.69 (d, *J* = 7.0 Hz, 1H, 1-H), 6.74 (d, *J* = 7.0 Hz, 1H, 2-H), 7.54 (s, 1H, 5-H); MS (70 eV): *m/z* 327 (100%, $M^{\oplus}$); $[\alpha]_D^{20}$ −98° (*c* = 0.55 g/100 mL CH_3OH), lit. [14]: $[\alpha]_D^{20}$ −115° (*c* = 0.55 g/100 mL CH_3OH) for optically pure (−)-**9**

Received: July 4, 1986;
revised: August 5, 1986 [Z 1844 IE]
German version: *Angew. Chem. 98* (1986) 1032

CAS Registry numbers:
3a, 81763-87-3; **3b**, 104779-65-9; **3c**, 104779-66-0; **4a**, 104779-63-7; **4b**, 104779-64-8; **5**, 120-47-8; **6**, 104779-68-2; **7**, 104779-67-1; (±)-**8**, 104779-69-3; (±)-**9**, 23979-21-7; (−)-**9**, 4090-18-0.

[1] G. Ehrhardt, H. Ruschig: *Arzneimittel, Vol. 1*, p. 316, Verlag Chemie, Weinheim 1968.
[2] a) R. Grewe, W. Friedrichsen, *Chem. Ber. 100* (1967) 1550; b) T. S. Lie, L. Maat, H. C. Beyerman, *Recl. Trav. Chim. Pays-Bas 98* (1979) 419 and earlier work; c) K. C. Rice, *J. Org. Chem. 45* (1980) 3135.
[3] a) D. H. R. Barton, D. S. Bhakuni, R. James, G. W. Kirby, *J. Chem. Soc. C 1967*, 128; b) M. A. Schwartz, I. S. Mami, *J. Am. Chem. Soc. 97* (1975) 1239; M. A. Schwartz, M. F. Zoda, *J. Org. Chem. 46* (1981) 4625; c) C. Szántay, G. Blaskó, M. Bárczai-Beke, P. Pechy, G. Dörnyei, *Tetrahedron Lett. 21* (1980) 3509.
[4] a) L. L. Miller, R. F. Stewart, J. P. Gillespie, V. Ramachandran, Y. H. So, R. F. Stermitz, *J. Org. Chem. 43* (1978) 1580 and earlier work; b) E. Kotani, S. Tobinata, *Tetrahedron Lett. 1973*, 4759; c) H. Klünenberg, C. Schäffer, H. J. Schäfer, *ibid. 23* (1982) 4581.
[5] D. A. Evans, C. H. Mitch, R. C. Thomas, D. M. Zimmerman, R. L. Robey, *J. Am. Chem. Soc. 102* (1980) 5955; D. A. Evans, C. H. Mitch, *Tetrahedron Lett. 23* (1982) 285.
[6] a) M. Chandler, P. J. Parsons, *J. Chem. Soc. Chem. Commun. 1984*, 322; b) A. G. Schultz, R. D. Lucci, J. J. Napier, H. Kinoshita, R. Ravichandran, P. Shannon, Y. K. Yee, *J. Org. Chem. 50* (1985) 217.
[7] H. Klünenberg, *Dissertation*, Universität Münster 1981.
[8] By suitable substitution of the 1-benzyl moiety with alkoxy groups it was possible to carry out the coupling to give morphine precursors. Thus, 2-hydroxy-3-deoxythebaine was obtained from 1-(3,5-dibenzyloxybenzyl)-6,7-dimethoxy-2-trifluoroacetyl-1,2,3,4-tetrahydroisoquinoline by means of anodic coupling in the key step: C. Schlegel, *Dissertation*, Universität Münster 1984.
[9] D. A. Evans, D. J. Hart, P. M. Koelsch, P. A. Cain, *Pure Appl. Chem. 51* (1979) 1285.
[10] a) D. M. S. Wheeler, T. H. Kinstle, K. L. Rinehart, Jr., *J. Am. Chem. Soc. 89* (1967) 4494; b) D. H. R. Barton, G. W. Kirby, W. Steglich, G. M. Thomas, A. R. Battersby, T. A. Dobson, H. Ramuz, *J. Chem. Soc. 1965*, 2423.
[11] a) J. D. White, G. Caravatti, T. B. Kline, E. Edstrom, K. C. Rice, A. Brossi, *Tetrahedron 39*, 2393 (1983); b) K. C. Rice, *J. Med. Chem. 20* (1977) 164.
[12] K. W. Bentley in R. H. F. Manske (Ed.): *The Alkaloids, Vol. 13*, Academic Press, New York 1971, p. 126.
[13] a) A. I. Meyers, M. Boes, D. A. Dickman, *Angew. Chem. 96* (1984) 448; *Angew. Chem. Int. Ed. Engl. 23* (1984) 458; b) A. I. Meyers, L. M. Fuentes, Y. Kubota, *Tetrahedron 40* (1984) 1361.
[14] T. Kametani, M. Ihara, K. Fukumoto, H. Yagi, *J. Chem. Soc. C 1969*, 2030.

Cope Rearrangement Induced by Medium-sized Ring Strain**

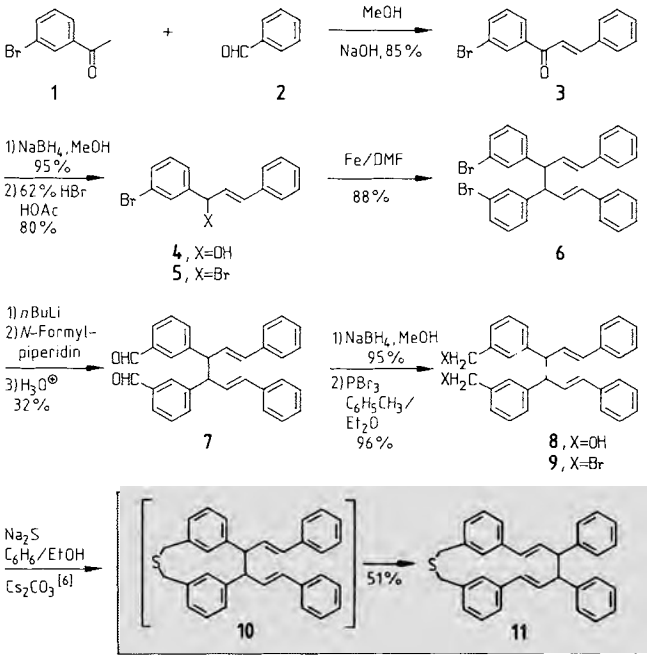
By *Norbert Eisen* and *Fritz Vögtle**

In the case of small-ring compounds, Cope rearrangements can be facilitated considerably by Baeyer ring strain.[1] We recently reported on degenerated rearrangements of Cope systems which are bridged on both sides by long chains.[2] Attempts to achieve strained hydrocarbons in this way met with difficulties. By bridging only one side of the biallyl system we have now succeeded in carrying out a shorter bracketing and thus, for the first time, also a Cope rearrangement in which the educt I is completely converted—with ring expansion—into the product II by virtue of the ring strain of a medium sized ring (Scheme 1).



Scheme 1. B = bridge.

Starting from the simple chalcone **3**, readily obtainable from the ketone **1** and benzaldehyde **2**, the open-chain, substituted tetraphenyl Cope system **9** was obtained via the intermediates **4**–**8**[3] (data for the substances, see Table 1). Tetraaryl-substituted biallyl compounds of this type first start to rearrange sigmatropically at temperatures higher than are necessary for the synthesis (< 85°C),[4] i.e. it can be assumed that **9** and not the Cope rearrangement



[*] Prof. Dr. F. Vögtle, Dipl.-Chem. N. Eisen
Institut für Organische Chemie und Biochemie der Universität
Gerhard-Domagk-Strasse 1, D-5300 Bonn 1 (FRG)

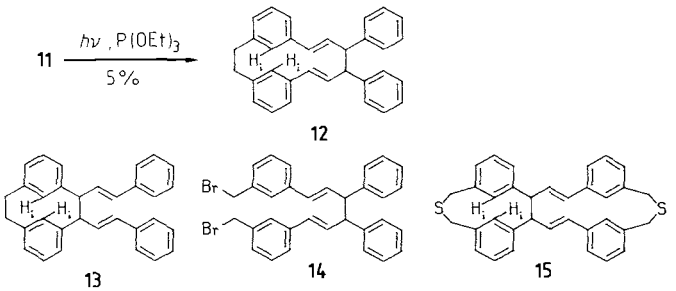
[**] This work was supported by the Deutsche Forschungsgemeinschaft. We thank Dr. *G. Eckhardt* and Mr. *C. Schmidt* for help with the spectroscopic studies.

product **14** is formed under the conditions chosen for the preparation of **9**. A comparison of the ^{1}H-NMR spectra (benzyl and vinyl protons) of **9** and otherwise substituted compounds prepared earlier[4a] show that **9** is formed as a mixture of the *meso*- and *d,l*-conformational isomers (ca. 1 : 1) (Table 1).

Cyclization of *meso-/d,l*-**9** with sodium sulfide in presence of cesium (Cs_2CO_3, in ethanol, benzene)[5] led to formation of the eleven-membered monosulfide **10**, which, however, could not be isolated; it isomerizes during work-up to give the 15-membered isomer **11**. This can be explained in terms of a ring strain-induced Cope rearrangement under the cyclization conditions (ca. 80 °C, 8 h).[6]

Desulfurization of **11** was achieved photochemically in triethyl phosphite as solvent (and thiophile),[7] albeit at higher temperatures than usual (60–80 °C). This afforded the 14-membered cyclic hydrocarbon **12**.

The constitution of **11** and **12** follow from the COSY-^{1}H-NMR spectra (Table 1). In the case of the sulfide **11** the H_i hydrogen atoms are not shifted upfield, whereas in the case of the [6.2]metacyclophane **12** they are found at somewhat higher field strength ($\delta = 5.7$). Signals are expected to be found at even higher field strength ($\delta = 4.6$) for the H_i atoms in the case of the constitutionally isomeric [2.2]metacyclophane **13**; in the case of the sulfide **10**, the signals for the H_i atoms should appear at $\delta \approx 5.3$, as indicated by a comparison with other cyclophane sulfides including the sulfide **15**.[8] These findings also suggest that a Cope rearrangement already takes place below 100 °C in the case of the sulfide **10**, and that **12** is formed by photochemical desulfurization of **11**.[9] Apparently, the comparatively low ring strain of an eleven-membered [3.2]metacyclophane already suffices in order to shift the equilibrium of the Cope rearrangement in favor of the larger, less strained 15-membered ring.



The configuration (*meso, d,l*) of the products of the Cope rearrangement cannot be derived with certainty from the ^{1}H-NMR spectra, since comparisons with known open-chain biallyl systems are difficult owing to the extremely different conformational possibilities. Molecular model considerations suggest that both diastereomers (*meso* and *d,l*) are possible with the size of the ring in **11**.

Thus, for the first time, it has been confirmed experimentally that a Cope rearrangement to the less strained product can be effected under mild conditions, not only by the ring strain of three- and four-membered rings ("small ring strain"), but also of medium sized rings. It now remains to explore the synthetic potential of this ring-expansion reaction (by four ring members). The possibility of 'fixing' conformations in the ground and transition state thus opens up new mechanistic aspects for sigmatropic reactions.

Table 1. Analytical data for the new compounds, all of which gave correct high-resolution mass spectra and C,H analyses.

Cpd.	M.p. [°C]	^{1}H-NMR (90 MHz, $CDCl_3$/TMS) [δ values]
3	92	7.26–7.2 (m, 9 aryl-H and 2 =CH)
4	oil	5.28 (d, J = 6 Hz, 1 −CH), 6.3 (dd, J = 16 and 6 Hz, 1 =CH), 6.66 (d, J = 16 Hz, 1 =CH), 7.08–8.1 (m, 9 aryl-H)
5	71	5.81 (d, J = 8 Hz, 1 −CH), 6.66 (m, 2 =CH), 7.17–7.68 (m, 9 aryl-H)
6	oil	3.82 (m, 2 −CH), 6.2, 6.41 (m, 4 =CH, *meso/d,l*-form), 6.93–7.53 (m, 18 aryl-H)
7	oil	3.95 (m, 2 −CH), 6.24, 6.5 (m, 4 =CH, *meso/d,l*-form), 7.05–7.88 (m, 18 aryl-H), 9.93, 10.0 (2 s, 2 CHO)
8	40	3.85 (m, 2 −CH), 4.33 (m, 2 CH_2OH, 4 H), 6.24, 6.44 (m, 4 =CH, *meso/d,l*-form), 6.88–7.42 (m, 18 aryl-H)
9	oil	3.84 (m, 2 −CH), 4.33 (m, 2 CH_2Br, 4 H), 6.22, 6.44 (m, 4 =CH, *meso/d,l*-form), 6.95–7.38 (m, 18 aryl-H)
11	48	3.55 (s, 4 H, CH_2–S–CH_2), 3.80 (m, 2 −CH), 6.44 (m, 4 =CH), 7.05–7.55 (m, 18 aryl-H)
12 [a]	170	2.33, 3.1 (AB, 4 H, CH_2–CH_2, J_{AB} = 9 Hz), 3.55 (dd, J = 9 and 3 Hz, 2 H), 5.7 (s, 2 H_i), 5.8 (m, 2 =CH), 6.05 (d, 2 =CH, J = 15 Hz), 6.84–7.26 (m, 18 aryl-H)
15 [b]	193	3.1 (m, 2 H, −CH), 3.48, 3.69 (AB, 4 H, J_{AB} = 14 Hz), 3.52, 3.88 (AB, 4 H, J_{AB} = 14 Hz), 5.35 (s, 2 H_i), 6.46 (m, 4 =CH), 7.05–7.44 (m, 16 Aryl-H)

[a] ^{1}H-NMR at 200 MHz. [b] ^{1}H-NMR at 400 MHz.

Received: July 7, 1986;
revised: July 21, 1986 [Z 1847 IE]
German version: *Angew. Chem. 98* (1986) 1029

CAS Registry numbers:
1, 2142-63-4; **2**, 100-52-7; **3**, 25023-37-4; **4**, 105065-87-0; **5**, 105065-88-1; *meso*-**6**, 105065-89-2; *rac*-**6**, 105066-00-0; *meso*-**7**, 105065-90-5; *rac*-**7**, 105066-01-1; *meso*-**8**, 105065-91-6; *rac*-**8**, 105066-02-2; *meso*-**9**, 105065-92-7; *rac*-**9**, 105065-93-8; **10**, 105065-95-0; **11**, 105065-94-9; **12**, 105065-96-1; **14**, 105065-99-4; **15**, 105065-98-3; 1,3,4,6-tetrakis(3-bromomethylphenyl)-1,5-hexadiene, 105065-97-2.

[1] Review: G. Maier: *Valenzisomerisierungen*, Verlag Chemie, Weinheim 1972. Cf. also: W. R. Roth, F.-G. Klärner, W. Grimme, H. G. Köser, R. Busch, B. Muskulus, R. Breuckmann, B. P. Scholz, H.-W. Lennartz, *Chem. Ber. 116* (1983) 2717, and references cited therein.

[2] F. Vögtle, N. Eisen, P. Mayenfels, F. Knoch, *Tetrahedron Lett. 27* (1986) 695.

[3] On the basis of earlier studies and the conditions used we can rule out allylic rearrangements of these compounds: D. Brombach, *Dissertation*, Universität Würzburg 1977; cf. [4c].

[4] a) F. Vögtle, E. Goldschmidt, *Chem. Ber. 109* (1976) 1; b) the activation parameters of tetraarylbiallyl compounds are: E_A = 127 kJ/mol, $\Delta G^{\neq}$ = 127 kJ/mol, $\Delta H^{\neq}$ = 124 kJ/mol, $\Delta S^{\neq}$ = −8.5 J/K mol. See c) D. Brombach, F. Vögtle, *Synthesis 1977*, 800.

[5] W. Kissener, F. Vögtle, *Angew. Chem. 97* (1985) 782; *Angew. Chem. Int. Ed. Engl. 24* (1985) 794.

[6] These conditions hold for the overall dilution principle reaction (**9** → **11**). Solutions of the bis(bromomethyl) compound **9** (2.00 mol) in benzene (250 mL) and $Na_2S \cdot 9\,H_2O$ in ethanol (250 mL) were added dropwise concurrently from separate dropping funnels within 8 h into 1.2 L of boiling benzene/ethanol (2.5 : 1) containing 1.00 mmol of Cs_2CO_3. The educt **9** reacts, according to our previous experience with similar reactions, within a few minutes to give the cyclic sulfide. Neither time nor temperature suffice for a Cope rearrangement of the open-chain educt **9** [4b]. The [3.2]phane **10** formed initially, however, has adequate time to undergo Cope rearrangement under the reaction conditions.

[7] K.-H. Duchêne, F. Vögtle, *Angew. Chem. 97* (1985) 867; *Angew. Chem. Int. Ed. Engl. 24* (1985) 885, and references cited therein.

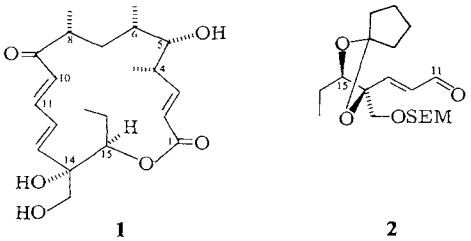
[8] The bis-sulfide **15** was obtained by reaction of the corresponding tetrakis(bromomethyl) compound with $Na_2S \cdot 9\,H_2O/CsCO_3$ in benzene/ethanol (2 : 1) in a dilution principle reaction, cf [2]. Yield: 36%, for data see Table 1.

[9] In the meantime, **12** has been obtained in 5% yield by direct phenyllithium cyclization from the bis(bromomethyl) compound **9** at 80 °C. This structural change **13** → **12** is explained by an intermediate Cope rearrangement.

Total Synthesis of Mycinolide V, the Aglycone of a Macrolide Antibiotic of the Mycinamycin Series**

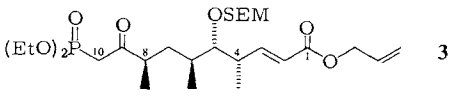
By *Klaus Ditrich, Tomas Bube, Rainer Stürmer,* and *Reinhard W. Hoffmann**

Of the mycinolides, a class of 16-membered macrolides,[1] only the simplest representative, the protomycinolide, has been synthesized so far.[2] Mycinolide V (**1**) is of interest insofar as it has a reversed configuration at the quaternary center C-14, compared to the majority of normal macrolide antibiotics. In the mycinolides the stereogenic centers are located in two separate regions of the molecule. Our synthesis of mycinolide V (**1**) takes this into account in that it involves coupling of the separately prepared enantiomerically-pure C-11–C-17 and C-1–C-10 building blocks **2** and **3**.



1

2



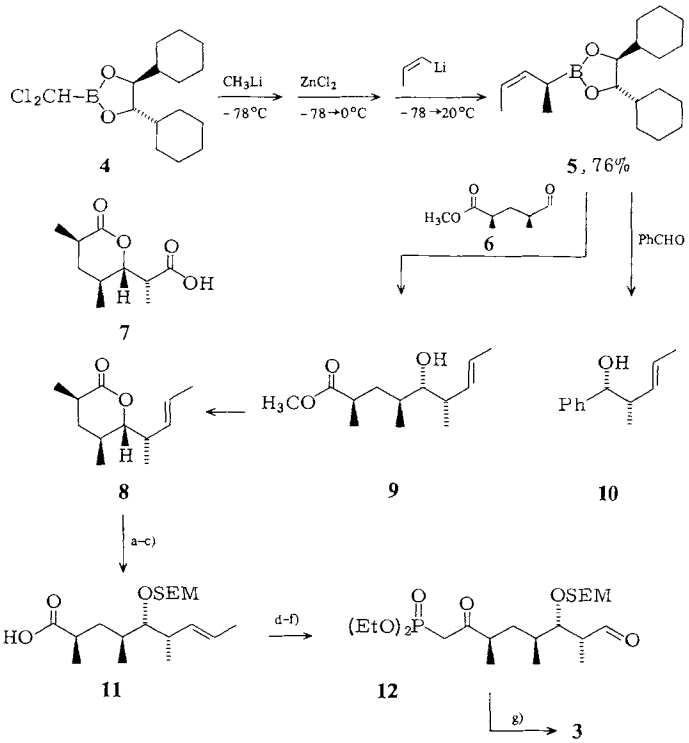
3

Table 1. Spectroscopic data of **1** and **2**.

1: ^{1}H-NMR ([D$_6$]acetone/D$_2$O, 400 MHz): δ = 0.80 (t, J = 7.4 Hz, 3H), 0.99 (d, J = 6.8 Hz, 3H), 1.01 (d, J = 6.7 Hz, 3H), 1.01–1.1 (m, 1H), 1.11 (d, J = 6.9 Hz, 3H), 1.37–1.46 (m, 1H), 1.54–1.63 (m, 1H), 1.68–1.78 (m, 2H), 2.40–2.46 (m, 1H), 2.48–2.56 (m, 1H), 3.19 (d, J = 9.6 Hz, 3H), 3.51 and 3.62 (AB system, J = 11.0 Hz, 2H), 4.92 (dd, J = 7.6 and 6.9 Hz, 1H), 5.88 (d, J = 15.5 Hz, 1H), 6.22 (d, J = 15.4 Hz, 1H), 6.47 (d, J = 15.1 Hz, 1H), 6.51 (dd, J = 15.5 and 10.2 Hz, 1H), 6.51 (dd, J = 15.4 and 11.1 Hz, 1H), 7.04 (dd, J = 15.1 and 11.1 Hz, 1H).—^{13}C-NMR ([D$_6$]acetone/D$_2$O, 100 MHz, internal standard: C$_3$D signal of the solvent at δ = 29.80): δ = 10.7, 17.6, 17.6, 19.6, 21.1, 32.1, 34.8, 41.0, 45.5, 65.6, 76.9, 78.4, 79.8, 121.8, 124.7, 130.8, 142.4, 144.8, 152.8, 167.3, 205.5

2: ^{1}H-NMR (CDCl$_3$, 400 MHz): δ = −0.01 (s, 9H), 0.90–0.94 (m, 2H), 1.03 (t, J = 7.4 Hz, 3H), 1.61–1.78 (m, 8H), 1.86–1.92 (m, 2H), 3.49 and 3.67 (AB system, J_{AB} = 9.8 Hz, 2H), 3.56–3.64 (m, 3H), 4.64 and 4.67 (AB system, J_{AB} = 6.8 Hz, 2H), 6.47 (dd, J = 15.6 and 7.0 Hz, 1H), 6.91 (d, J = 15.6 Hz, 1H), 9.59 (d, J = 7.0 Hz, 1H).—^{13}C-NMR (CDCl$_3$, 25 MHz): δ = −1.6, 11.3, 17.9, 21.4, 22.9, 23.7, 37.3, 37.4, 65.3, 68.6, 82.4, 84.3, 95.1, 118.3, 131.7, 155.4, 193.0

The synthesis of **3** (Scheme 1) concerns the construction of stereogenic centers in the region of C-4 and C-8. The partial structure of this segment of the molecule corresponds in its relative and absolute configuration to that of the Prelog-Djerassi lactone **7**. Numerous stereoselective syntheses have been described in recent years for this key building block in macrolide synthesis[3] which has set a standard for the degree of stereoselectivity that can be achieved. The present synthesis of mycinolide V (**1**) gave us the opportunity to establish the degree of stereoselectivity that can be achieved in the addition of chiral, α-substituted (*Z*)-crotylboronates to aldehydes. The boronate **5** required for this purpose was synthesized from **4** in a one-pot process using the method described by *Matteson* et al.[4] As chiral auxiliary we used 1,2-dicyclohexyl-1,2-ethanediol, which was obtained by hydrogenation (6–7 bar H_2, 5% Rh/Al_2O_3, CH_3OH, 60 °C) of enantiomerically pure hydrobenzoin.[5]



Scheme 1. a) 1 equiv. KOH, CH_3OH/H_2O, 12 h, 20 °C; b) 3 equiv. SEMCl, 4 equiv. ethyldiisopropylamine, CH_2Cl_2, 3 d, 20 °C; c) 25% aq. KOH, 6 h reflux; d) 1.2 equiv. $(CH_3)_2C{=}CCl[N(CH_3)_2]$, CH_2Cl_2, 3 h, 0 °C; e) 1.2 equiv. $(EtO)_2P(O)CH_2Li$, 1.2 equiv. CuI, tetrahydrofuran (THF), 12 h, 0→20 °C; f) 1. O_3, CH_2Cl_2, −78 °C; 2. Zn, AcOH, CH_2Cl_2, 2 h, 20 °C; g) 9 equiv. $(H_3CO)_2P(O)CH_2COOCH_2CH{=}CH_2$, 6 equiv. $KOC(CH_3)_3$, THF; reagent prepared at 0–20 °C (1 h), reaction at −78→20 °C, 12 h.

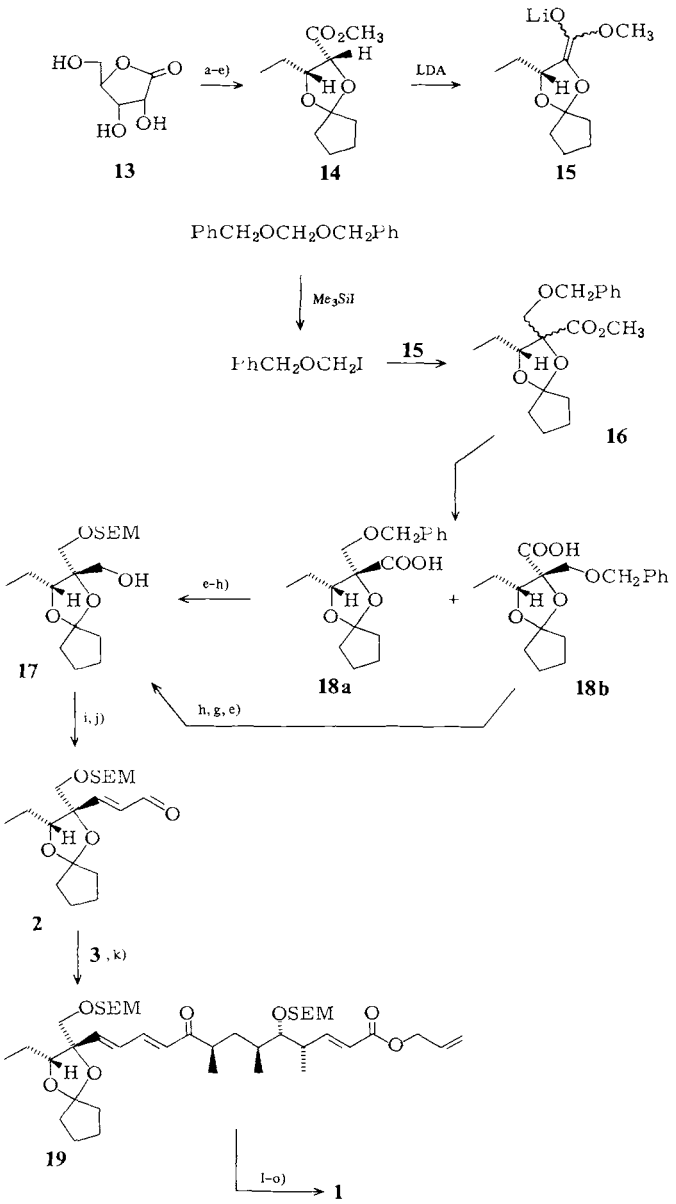
The diastereomeric purity of **5** could not be determined directly (^{13}C-NMR), but it was estimable from the extent of chirality transfer upon addition of **5** to benzaldehyde. This resulted in formation of the homoallyl alcohol **10** (68%) with an enantiomeric purity of 99.0% *ee*[6] (determined gas-chromatographically after derivatization with isopropyl isocyanate on a XE-60/*S*-valine/*S*-α-phenylethylamide column[7]). The absolute configuration of **5**—and thus indirectly that of **10**—followed from the reaction of the boronate **5** with the aldehyde **6**[8] (7 d, 20 °C). The hydroxy ester obtained thereby [in 85% yield and with a diastereoselectivity of >95% (^{1}H-NMR)] was converted into the lactone **8**, which was shown to have the same configuration as the Prelog-Djerassi lactone **7**. Assuming a cyclic transition state for the allylboronate-addition to aldehydes one can infer that the configuration of the new stereocenter in **5** is as shown, consistent with the results of *Matteson* et al.[4]

Thus, the stereogenic centers at C-4 to C-8 of the mycinolide skeleton have been constructed by coupling of the

[*] Prof. Dr. R. W. Hoffmann, Dipl.-Chem. K. Ditrich, T. Bube, R. Stürmer
Fachbereich Chemie der Universität
Hans-Meerwein-Strasse, D-3550 Marburg (FRG)

[**] This work was supported by the Deutsche Forschungsgemeinschaft and the Fonds der Chemischen Industrie.

boronate **5** with the aldehyde **6** to give the hydroxy ester **9**. In this reaction the use of a *chiral* boronate is decisive[9] for "reagent-control of selectivity".[10] For the subsequent conversion of the lactone **8** into the β-ketophosphonate **12** we followed the route used by *Yamaguchi* et al. in his synthesis of protomycinolide,[2] after the method originally developed by us[11] for this transformation proved unsuitable for production of the β-trimethylsilylethoxymethyl (SEM) derivatives. The carboxylic acid **11**, which was obtained in 78% yield after alkaline opening of the lactone, reaction with three equivalents of SEM-chloride, and alkaline hydrolysis of the SEM ester, was activated with an α-chloroenamine[12] and allowed to react with the cuprate of the methanephosphonate-anion to give the β-ketophosphonate.[13] This was followed by ozonolysis to give the aldehyde **12** (overall yield **8** → **12**: 40%). Finally, the building block **3** (cf. ref. [2]) was obtained in 84% yield by coupling of **12** with allyl phosphonoacetate. An intermolecular Horner-Emmons reaction was thereby realized with an external reagent on a substrate which is capable of undergoing by itself intra- or intermolecular Horner-Emmons reactions.



Scheme 2. a) 1,1-Dimethoxycyclopentane, cyclopentanone, $H^{\oplus}$, 12 h, 20°C; b) tosyl chloride, pyridine; c) 0.95 equiv. CH_3ONa, CH_3OH, cf. [14]; d) 3.2 equiv. Zn, 1.4 equiv. NaI, AcOH, NaOAc, 0→25°C [20]; e) 6–7 bar H_2, 5% Pd/C, AcOMe; f) CH_2N_2, ether; g) 3.5 equiv. SEMCl, 4.5 equiv. ethyldiisopropylamine, CH_2Cl_2, 12 h 20°C; h) 2.5 equiv. $LiAlH_4$, ether, 0→20°C, 4 h; i) oxalyl chloride, dimethyl sulfoxide (DMSO); j) 1 equiv. $Ph_3P{=}CH{-}CHO$, benzene, 5 d, 20°C; k) 0.95 equiv. $KOC(CH_3)_3$, THF, 1 h, 0→20°C; −78°C, **3**, →0°C, 12 h; l) $Pd(OAc)_2$, Ph_3P, 1.1 equiv. morpholine, THF, 12 h, 20°C; m) HCl, CH_3CN, 4 h, 20°C; n) 1 equiv. 2,4,6-trichlorobenzoyl chloride, 1.1 equiv. Et_3N, THF, then 6 equiv. DMAP, benzene, 80°C [17]; o) 8 equiv. $LiBF_4$, aqueous CH_3CN, 5 h, 72°C. — LDA = lithium diisopropylamide.

Starting material for the preparation of the highly functionalized C-11–C-17 fragment **2** (Scheme 2) was the ester **14**, which was obtained from D-ribonolactone **13** in five steps (37%) analogous to those described earlier by us.[14] For construction of the stereogenic center at C-14, the enolate **15** was alkylated with benzyloxymethyl iodide, prepared in situ. In the alkylation product **16**, obtained with a selectivity[15] of only 3:2, the benzyloxymethyl group has been incorporated *cis* to the ethyl residue on the dioxolane ring, as shown by the ^{13}C-NMR spectrum.[14] After hydrolysis to the carboxylic acid, the main isomer **18a** (41% referred to **14**) could be crystallized as the cyclohexylammonium salt. Concomitantly, the isomer **18b** could be isolated in 12% yield. During the conversion of **18a** into **17** (78%) the benzyl protecting group was replaced by the SEM protecting group. The subsequent elongation of the chain in **17** to give **2** was accomplished in two steps with a yield of 84%.

The coupling of the building block **2** with the C-1–C-10 fragment **3** furnished the complete molecular skeleton **19** of mycinolide V (**1**) in 88% yield. Cleavage of the allyl ester with $Pd(OAc)_2$ (85%)[16] and of the cyclopentylidene residue with HCl (44%) led to the desired dihydroxycarboxylic acid. This was activated with trichlorobenzoyl chloride[17] and macrocyclized with *N,N*-dimethylaminopyridine (DMAP) to the protected mycinolide V (46%). In the last step, the SEM groups were removed with $LiBF_4$[18] (72%). The melting point (267°C) rotation (+36°), solubility, and ^1H-NMR spectrum of the free mycinolide V (**1**) thus obtained were in complete agreement with data given in the literature.[19]

Received: July 23, 1986;
revised: August 25, 1986 [Z 1869/1870 IE]
German version: *Angew. Chem. 98* (1986) 1016

[1] K. Kinoshita, S. Satoi, M. Hayashi, K. Harada, M. Suzuki, K. Nakatsu, *J. Antibiotics 38* (1985) 525, and references cited therein.
[2] M. Honda, T. Katsuki, M. Yamaguchi, *Tetrahedron Lett. 25* (1984) 3857.
[3] See, e.g., I. Paterson, M. M. Mansuri, *Tetrahedron 41* (1985) 3569, especially p. 3575.
[4] K. M. Sadhu, D. S. Matteson, G. D. Hurst, J. M. Kurosky, *Organometallics 3* (1984) 804.
[5] F. Dietl, J. Haunschild, A. Merz, *Tetrahedron 41* (1985) 1193.
[6] The high asymmetric induction rests as good as exclusively on the transfer of chirality from the α-center of the boronate **5** and not on an induction from the chiral glycol moiety, for on addition of the crotylboronate corresponding to **5** to benzaldehyde the asymmetric induction was < 5% *ee*.
[7] W. A. König, W. Francke, I. Benecke, *J. Chromatogr. 239* (1982) 227.
[8] For the addition of other pentenylmetal compounds to **6** cf. Y. Yamamoto, K. Taniguchi, K. Maruyama, *J. Chem. Soc. Chem. Commun. 1985*, 1429; C. Santelli-Rouvier, *Tetrahedron Lett. 25* (1984) 4371.
[9] The selectivities achieved in the reaction of *rac*-**6** with *rac*-pentenylmetal compounds [8] cannot result on reaction of enantiomerically pure **6** with *rac*-pentenylmetal compounds. It should be pointed out that a *chiral* pentenylmetal reagent is necessary in order to achieve a high diastereoselectivity in the reaction of the enantiomerically pure aldehyde **6**.
[10] S. Masamune, W. Choy, J. S. Petersen, L. R. Sita, *Angew. Chem. 97* (1985) 1; *Angew. Chem. Int. Ed. Engl. 24* (1985) 1.
[11] K. Ditrich, R. W. Hoffmann, *Tetrahedron Lett. 26* (1985) 6325.

[12] T. Fujisawa, T. Mori, K. Higuchi, T. Sato, *Chem. Lett. 1983*, 1791.
[13] Cf. K. Hartke, O. Kunze, W. Hoederath, *Synthesis 1985*, 960.
[14] R. W. Hoffmann, W. Ladner, *Chem. Ber. 116* (1983) 1631.
[15] The low diastereoselectivity of the alkylation to **18a** is not serious, since the epimer **18b** could also be converted into the intermediate **17** (88%) in only three steps. An alkylation (57% yield) with >95% stereoselectivity is possible if a 3,3-dimethyl-2-butylidene group is used instead of a cyclopentylidene group in **15**.
[16] P. D. Jeffrey, S. W. McCombie, *J. Org. Chem. 47* (1982) 587.
[17] I. Inanaga, K. Hirata, H. Saeki, T. Katsuki, M. Yamaguchi, *Bull. Chem. Soc. Jpn. 52* (1979) 1989.
[18] B. H. Lipshutz, D. F. Harvey, *Synth. Commun. 12* (1982) 267.
[19] M. Hayashi, M. Ohno, K. Kinoshita, S. Satoi, M. Suzuki, K. Harada, *J. Antibiotics 34* (1981) 346.
[20] J. W. Cornforth, R. H. Cornforth, K. K. Mathew, *J. Chem. Soc. (London) 1959*, 112.

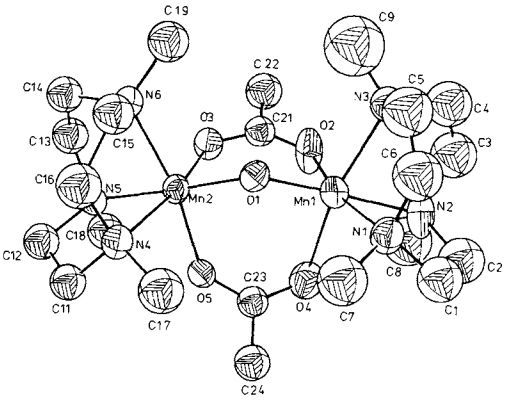
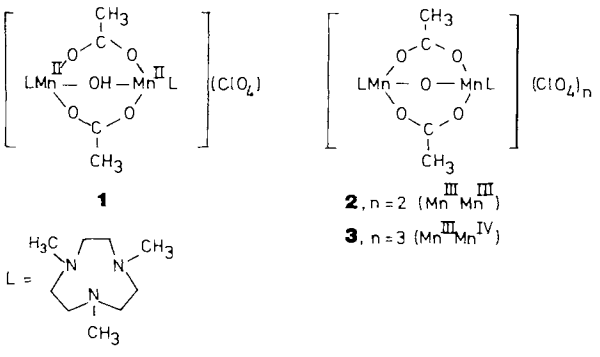


Fig. 1. Structure of the complex cation of **3** in the crystal. Important bond lengths [Å] and angles [°]: Mn1-O1 1.826(6), Mn1-O2 1.948(6), Mn1-O4 1.999(6), Mn1-N1 2.089(8), Mn1-N2 2.133(8), Mn1-N3 2.141(8), Mn2-O1 1.814(6), Mn2-O3 2.000(5), Mn2-O5 1.951(7), Mn2-N4 2.131(6), Mn2-N5 2.117(8), Mn2-N6 2.099(9), Mn1···Mn2 3.230(3); Mn2-O1-Mn1 125.1(3) [9].

Dinuclear Manganese(II,III,IV) Model Complexes for the Active Center of the Metalloprotein Photosystem II: Synthesis, Magnetism, and Crystal Structure of $[LMn^{III}(\mu\text{-}O)(\mu\text{-}CH_3CO_2)_2Mn^{IV}L][ClO_4]_3$ (L = *N,N',N''*-Trimethyl-1,4,7-triazacyclononane)

By *Karl Wieghardt,* Ursula Bossek, Jacques Bonvoisin, P. Beauvillain, Jean-Jacques Girerd, Bernhard Nuber, Johannes Weiss,* and *Jürgen Heinze*

Although it has long been known that manganese, as essential trace element in green plants and algae, participates in the active center of the membrane-bound metalloprotein photosystem II in the light-induced oxidation of water to oxygen, little is known about the structure of the active center.[1] It was concluded from EXAFS and ESR investigations that there are two (or four)[2d] manganese atoms per metalloprotein molecule with a Mn-Mn distance of about 2.7 Å, and that only N,O-donor atoms form the first coordination sphere. The oxidation state of these manganese centers is believed to vary between +II and +IV on going through the five Kok states ($S_0 \rightarrow S_4$).[3] The chemistry of dinuclear manganese complexes with manganese(II,III,IV) and O,N-donor ligands has been intensively studied for some time with the object of comparing the structural, magnetic, and spectroscopic properties of model complexes with those of the active center of the metalloprotein.[4] We report here on the synthesis of **1**,[5] a novel dinuclear Mn^{II} complex, and on its oxidation products, the Mn_2^{III} complex **2**,[6] the Mn^{III},Mn^{IV} mixed-valent complex **3**, and a Mn_2^{IV} complex.



In the cation **1**, two Mn^{II}-centers are coupled to each other via one μ-hydroxo and two symmetric μ-acetato bridges. The IR spectrum shows a sharp band at 3620 cm^{-1} ($\tilde{\nu}$(OH) stretching vibration). From the measurements of the molar susceptibility between 98 and 293 K a spin-exchange coupling constant J of -9 cm^{-1} was determined for the two high spin Mn^{II} centers ($H = -2JS_1 \cdot S_2$ with $S_1 = S_2 = 5/2$; $g = 2.0$; TUP = 0). This weak antiferromagnetic coupling resembles that observed for the isostructural iron(II) complex ($J = -14$ cm^{-1}).[7] The cyclovoltammogram of **1** in acetonitrile (0.1 M tetrabutylammonium (TBA) hexafluorophosphate) shows a reversible one-electron transition at 0.61 V versus the normal hydrogen electrode (NHE). The mixed-valent Mn^{II},Mn^{III} complex is formed, which, so far, has remained unisolable.

The Mn^{III},Mn^{III} complex **2** already described elsewhere by us could be converted *electrochemically* by a reversible one-electron oxidation into the mixed valent Mn^{III},Mn^{IV} complex **3** ($E_{1/2} = 0.585$ V (Fc^+/Fc, acetonitrile)). We have now been able to carry out this oxidation *chemically*, and to isolate the complex **3** in crystalline form.[8]

Figure 1 shows the structure of the mixed valent cation of **3**.[9] The complex cation contains no crystallographic symmetry elements. The Mn-O and Mn-N distances at both manganese centers are, within the limits of error, equal—other than in the case of $[(bpy)_4Mn^{III}Mn^{IV}(\mu\text{-}O)_2][ClO_4]_3 \cdot 3H_2O$, in which an Mn^{III}(d^4-high spin) ion and an Mn^{IV}(d^3) ion have significantly different Mn-O and Mn-N distances, i.e. in which localized valences are present.[10] However, owing to disorder of the perchlorate ions, the accuracy of the crystal structure analysis of **3** is not satisfactory enough for an unequivocal observation of delocalization of the valence of the manganese centers.

Figure 2 shows the electronic spectra of **2** and **3** in acetonitrile. Interestingly, in the case of **3** an additional intervalence band (not discernible in Fig. 2) appears at $\lambda = 1400$ ($\varepsilon = 100$ L mol^{-1} cm^{-1}). Measurements of the magnetic susceptibility on crystalline **3** between 5 and 300 K show a ground state $S = 1/2$ (Fig. 3). The data could be adjusted with an isotropic Heisenberg model, $H' = -JS_1 \cdot S_2$ ($S_1 = 4/$

[*] Prof. Dr. K. Wieghardt, U. Bossek
Lehrstuhl für Anorganische Chemie I der Universität
Postfach 102148, D-4630 Bochum-Querenburg (FRG)
Dr. J.-J. Girerd, J. Bonvoisin, P. Beauvillain
Laboratoire de Spectrochimie des Elements de Transition
Université de Paris-Sud
Batiment 420, F-91405 Orsay Cedex (France)
Prof. Dr. J. Weiss, Dr. B. Nuber
Anorganisch-chemisches Institut der Universität
Im Neuenheimer Feld 270, D-6900 Heidelberg (FRG)
Priv.-Doz. Dr. J. Heinze
Institut für Physikalische Chemie der Universität
Albertstrasse 21, D-7800 Freiburg (FRG)

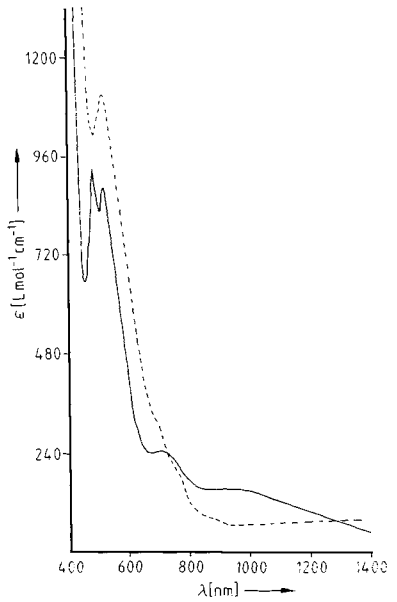


Fig. 2. Electronic spectrum of **2** (——) and **3** (----) in acetonitrile. In the case of **3**, a further broad band was observed at ca. 1400 nm ($\varepsilon = 100$ L mol^{-1} cm^{-1}).

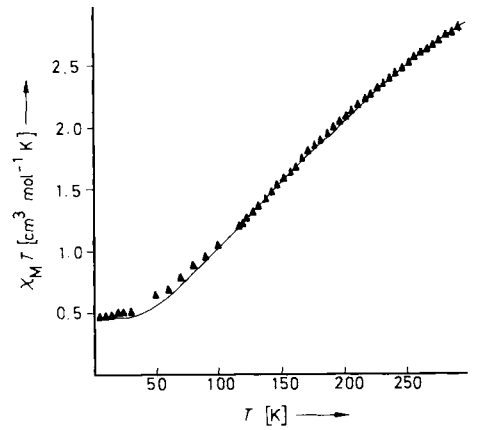


Fig. 3. Temperature dependence of the molar magnetic susceptibility of **3** (SQUID measurement) (▲: experimental data, —: calculated values).

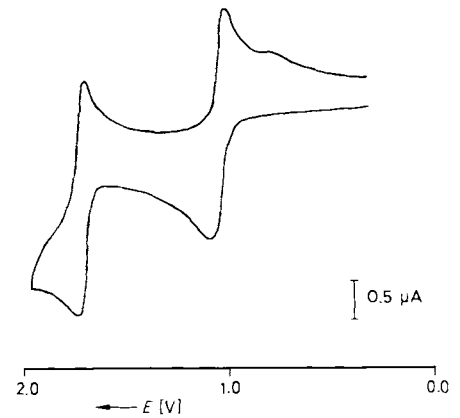


Fig. 4. Cyclovoltammogram of **2** (concentration ca. 10^{-4} mol/l) in liquid SO_2 (−40 °C, 0.1 M TBA-PF_6, $v = 50$ mV/s) vs. Ag/AgCl. Working electrode: Pt-button.

2; $S_2 = 3/2$) and $g = 2.2$ (TUP = 0). The spin-exchange coupling constant J is -80 cm^{-1}; i.e., the Mn^{III} (d^4-high spin) and Mn^{IV} centers in **3** are intramolecularly coupled antiferromagnetically. In **2**, on the other hand, the Mn^{III} centers are coupled ferromagnetically ($J = +18$ cm^{-1}).[6]

Finally, the oxidation of **3** to the Mn_2^{IV} complex was also accomplished electrochemically. Figure 4 shows the cyclovoltammogram of **2** in liquid SO_2 (0.1 M TBA-PF_6) at −40 °C. Two reversible one-electron transitions are observed at 1.25 and 1.92 V (NHE). The first transition corresponds to the reaction $\mathbf{2} \rightleftharpoons \mathbf{3}$, and the second to the oxidation of **3** to $[L_2Mn_2^{IV}(\mu\text{-}O)(\mu\text{-}CH_3CO_2)_2]^{4\oplus}$. This complex is stable only to a limited extent, even in liquid SO_2. From the two redox potentials, a comproportionation constant K of 7×10^8 can be calculated.

$$\mathbf{2} + [L_2Mn_2^{IV}(\mu\text{-}O)(\mu\text{-}CH_3CO_2)_2]^{4\oplus} \overset{K}{\rightleftharpoons} \mathbf{3} + \mathbf{3}$$

Thus, in the μ-oxo/(μ-hydroxo)-bis(μ-carboxylato)dimanganese system it is possible to vary the oxidation states of the manganese centers between +II and +IV by reversible one-electron transfers without destroying the coupling of the dinuclear complex.

The $[Mn^{III}(\mu\text{-}O)(\mu\text{-}CH_3CO_2)_2Mn^{III}]^{2\oplus}$ structural unit most likely occurs in the recently characterized manganese-containing metalloprotein of a pseudocatalase isolated from *Lactobacillus plantarum*; the electronic spectrum of this metalloprotein is remarkably similar to that of **3**.[11]

Received: June 23, 1986;
revised: September 3, 1986 [Z 1827 IE]
German version: *Angew. Chem. 98* (1986) 1026

CAS Registry numbers:
1, 104780-16-7; **2**, 97252-67-0; **3**, 104780-18-9; $[LMn^{II}(\mu\text{-}OH)(\mu\text{-}CH_3CO_2)_2Mn^{III}L]^{2\oplus}$, 104780-19-0; $[L_2Mn_2^{IV}(\mu\text{-}O)(\mu\text{-}CH_3CO_2)_2]^{4\oplus}$, 104780-20-3.

[1] a) B. Kok, B. Forbush, M. McGloin, *Photochem. Photobiol. 11* (1970) 457; b) T. Wydrzynski, K. Sauer, *Biochim. Biophys. Acta 589* (1980) 56; c) T. Livorness, T. D. Smith, *Struct. Bonding (Berlin) 48* (1982) 2; d) R. Radmer, G. Chemiae in J. Barber (Ed.): *Primary Processes of Photosynthesis*, Elsevier/North-Holland Biochemical Press, Amsterdam 1977, Chapter 8.

[2] a) J. A. Kirby, A. S. Robertson, J. P. Smith, A. C. Thompson, S. R. Cooper, M. P. Klein, *J. Am. Chem. Soc. 103* (1981) 5529; b) J. A. Kirby, D. B. Goodin, T. Wydrzynski, A. S. Robertson, M. P. Klein, *ibid. 103* (1981) 5537; c) D. B. Goodin, V. K. Yachandra, R. D. Britt, K. Sauer, M. P. Klein, *Biochim. Biophys. Acta 767* (1984) 209; d) G. C. Dismukes, K. Ferris, P. Watnick, *Photobiochem. Photobiophys. 3* (1982) 243; e) T. Kambara, Govindjee, *Proc. Natl. Acad. Sci. USA 82* (1985) 6119.

[3] a) A. N. Webber, L. Spencer, D. T. Sawyer, R. L. Heath, *FEBS Lett. 189* (1985) 258; b) G. C. Dismukes, Y. Siderer, *Proc. Natl. Acad. Sci. USA 78* (1981) 274.

[4] a) G. D. Lawrence, D. T. Sawyer, *Coord. Chem. Rev. 27* (1978) 173; b) W. M. Coleman, L. T. Taylor, *ibid. 32* (1980) 1.

[5] *Procedure*: **1**: A solution of 1 g of *N,N',N''*-trimethyl-1,4,7-triazacyclononane in 30 mL of anhydrous methanol was treated under argon with 0.5 g of $Mn(ClO_4)_2 \cdot 6H_2O$. After one hours' stirring at 20 °C, 0.25 g of sodium acetate was added, and the volume of the solution then reduced to 20 mL by passage of a stream of argon. On storage at 0 °C, transparent pale-blue, air-sensitive crystals of **1** precipitated out within 2–3 d (yield: ca. 0.7 g).

[6] K. Wieghardt, U. Bossek, D. Ventur, J. Weiss, *J. Chem. Soc. Chem. Commun. 1985*, 347.

[7] P. Chaudhuri, K. Wieghardt, B. Nuber, J. Weiss, *Angew. Chem. 97* (1985) 774; *Angew. Chem. Int. Ed. Engl. 24* (1985) 778.

[8] *Procedure*: **3**: A solution of 1 g of $\mathbf{2} \cdot H_2O$ [6] in 50 mL of 1 M HNO_3 was treated at 25 °C with 2 g of $Na_2S_2O_8$ and 5 g of $NaClO_4$. Small greenish-black crystals of **3** precipitated out; these were recrystallized from acetonitrile (yield ca. 0.8 g). **3** was also obtained from a solution of $\mathbf{2} \cdot H_2O$ in 1 M $HClO_4$ (in presence of atmospheric oxygen) after addition of $NaClO_4$. **1** and **3** gave correct elemental analyses (C, H, N, Mn, ClO_4).

[9] Monoclinic $C2/c$, $a = 34.875(10)$, $b = 10.616(4)$, $c = 21.416(8)$ Å, $\beta = 113.98(3)°$, $Z = 4$, 5454 observed, independent reflections, $R = 0.090$. Further details of the crystal structure investigations are available on request from the Fachinformationszentrum Energie, Physik, Mathematik GmbH, D-7514 Eggenstein-Leopoldshafen 2 (FRG), on quoting the depository number CSD-52021, the names of the authors, and the full citation of the journal.

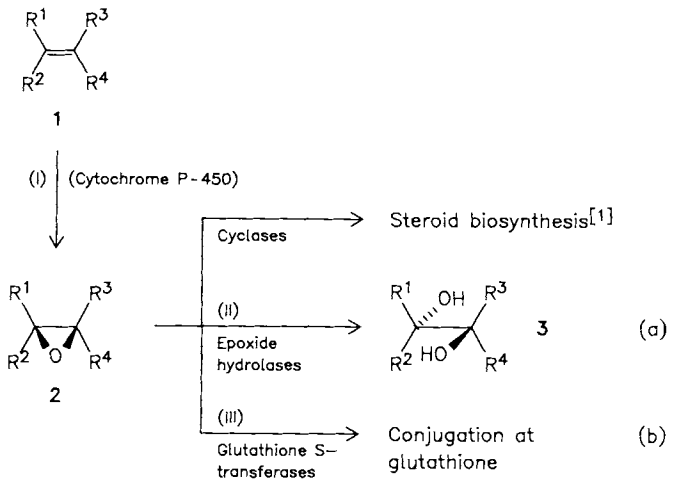
[10] a) P. M. Plaskin, R. C. Stoufer, M. Mathew, G. J. Palenik, *J. Am. Chem. Soc. 94* (1972) 2121; b) S. R. Cooper, G. C. Dismukes, M. P. Klein, M. Calvin, *ibid. 100* (1978) 7248.

[11] W. F. Beyer, Jr., I. Fridovich, *Biochemistry 24* (1985) 6460.

Complementary Epoxide Hydrolase- vs Glutathione S-Transferase-Catalyzed Kinetic Resolution of Simple Aliphatic Oxiranes—Complete Regio- and Enantioselective Hydrolysis of *cis*-2-Ethyl-3-methyloxirane**

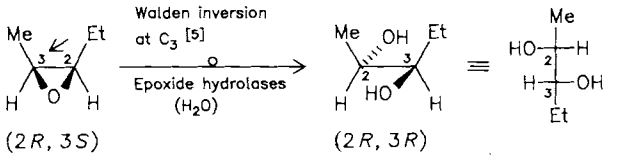
By *Dorothee Wistuba* and *Volker Schurig**

Inspired by the fascinating stereoselectivity observed in the biosynthesis of steroids (e.g. formation of enantiomerically pure lanosterol from achiral all-*trans*-squalene via 2,3-squalene oxide[1]) we have investigated the enantioselectivity of the biotransformation of simple xenobiotic oxiranes with microsomal and cytosolic rat liver enzymes.



In the reaction sequences (a) and (b) enantioselectivity can arise by epoxidation of an alkene possessing enantiotopic faces ("*prochiral* recognition", *product* enantioselectivity[2]) and/or by kinetic resolution of the intermediary oxirane **2** ("*chiral* recognition", *substrate* enantioselectivity[3]). For the formation of highly enantiomerically-enriched products ($ee > 99\%$) at least *one* step, (I), or (II) and (III), respectively, must be highly enantioselective. In the case of incomplete asymmetric induction the product and substrate enantioselectivities can either be mutually increased to high *ee* or compensated to lower *ee*. While the microsomal epoxidation of *cis*-2-pentene in step (I) shows no significant product enantioselectivity,[2] in the epoxide-hydrolase-catalyzed ring-opening (II) of *rac. cis*-2-ethyl-3-methyloxirane to give 2,3-pentanediol we found complete substrate regioselectivity *and* substrate enantioselectivity ($ee > 99\%$) within the precision of the measurement.[4]

Complexation gas chromatography, which enables time-dependent measurements in the nanogram range, was employed for the determination of the enantiomeric excess (*ee*) and the absolute configuration:[5] *cis*-2-ethyl-3-methyloxirane is separated into the antipodes on nickel(II) bis(3-heptafluorobutanoyl-(1*R*)-camphorate)[6a] (Fig. 1a); the (2*R*,3*S*)-enantiomer,[5] which was prepared free of racemization[6b] from *erythro*-(2*S*,3*R*)-2,3-pentanediol,[6c] is eluted as the first peak. The four configurationally isomeric 2,3-pentanediols can be separated on nickel(II) bis(3-heptafluorobutanoyl-(1*R*,2*S*)-4-pinanonate)[6d] (Fig. 1b). Both *threo*-(2*S*,3*S*)-2,3-pentanediol (prepared in nine steps from (2*R*,3*R*)-tartaric acid via (2*S*,3*S*)-isopropylidenethreitol by C_1 chain extension[6c]) as well as *erythro*-(2*S*,3*R*)-2,3-pentanediol (prepared in six steps from (2*S*,3*S*)-allothreonine via (2*S*,3*S*)-dihydroxybutyric acid by C_1 chain extension[6c]) are eluted as second peak of each enantiomeric pair (Fig. 1b). The stereochemistry of the epoxide-hydrolase-catalyzed ring-opening of *cis*-2-ethyl-3-methyloxirane follows from Figures 1a and 1c: only the (2*R*,3*S*)-configurated oxirane[5] is biotransformed, and exclusively *threo*-(2*R*,3*R*)-2,3-pentanediol is formed as metabolite by regioselective ring opening with Walden inversion at C-3.[5]



This result shows that substrate enantioselectivity, which has been demonstrated for sterically hindered bicyclic epoxides such as 3-*tert*-butyl-1,2-epoxycyclohexane,[7a] already occurs in the case of the smallest aliphatic *cis*-oxirane consisting of oppositely configurated carbon atoms. Since practically no product enantioselectivity is observed in step (I),[2] the enantiomer (2*S*,3*R*)-2-ethyl-3-methyloxirane being inactive towards epoxide-hydrolases must be detoxified via another pathway *(vide infra)* in the *in-vivo*-metabolization of *cis*-2-pentene.

In the case of *trans*-2-ethyl-3-methyloxirane, which is formed from *trans*-2-pentene without appreciable product enantioselectivity (I),[2] *no* complete substrate enantioselectivity is observed during the hydrolytic ring-opening (II): although the *trans*-(2*S*,3*S*) enantiomer, which has been chemically correlated with *threo*-(2*S*,3*S*)-pentanediol,[6c] is preferentially metabolized (significantly slower, however, than the *cis*-(2*R*,3*S*) isomer), the *trans*-(2*R*,3*R*) antipode (in contrast to the inactive *cis*-(2*S*,3*R*) isomer) is also a substrate, even if a poor one, for epoxide-hydrolases.[8] *erythro*-(2*R*,3*S*)-2,3-Pentanediol, whose enantiomeric composition is turn-over-dependent ($ee = 58\%$ after 2 h), is preferentially formed as metabolite of *rac. trans*-2-ethyl-3-methyloxirane.

A complementary behavior in regard to substrate diastereoselectivity (*cis-trans* geometry of the oxirane ring) and substrate enantioselectivity with epoxide-hydrolases appears during conjugation of the four configurationally isomeric 2-ethyl-3-methyloxiranes at glutathione (γ-(L)-glutamyl-(L)-cysteinyl-glycine) catalyzed by glutathione S-transferases (III). The rate of the catalytic ring-opening of the oxiranes decreases in the order:

Epoxide-hydrolases:
2*R*,3*S* (*cis*) ≫ [2*S*,3*S* (*trans*) > 2*R*,3*R* (*trans*)] ≫ 2*S*,3*R* (*cis*) (no reaction)

Conjugation at glutathione catalyzed by glutathione S-transferases (Fig. 2a):

2*R*,3*R* (*trans*) ≫ [2*S*,3*R* (*cis*) > 2*R*,3*S* (*cis*)] > 2*S*,3*S* (*trans*) (very slow)

[*] Prof. Dr. V. Schurig, Dr. D. Wistuba
Institut für Organische Chemie der Universität
Auf der Morgenstelle 18, D-7400 Tübingen (FRG)

[**] This work was supported by the Deutsche Forschungsgemeinschaft and the Fonds der Chemischen Industrie. Presented in part at the International Symposium on Activation of Dioxygen Species and Homogeneous Catalytic Oxidations, Galzignano (Padua, Italy), June 25, 1984. Extract from the Dissertation by *D. Wistuba*, Universität Tübingen 1986.

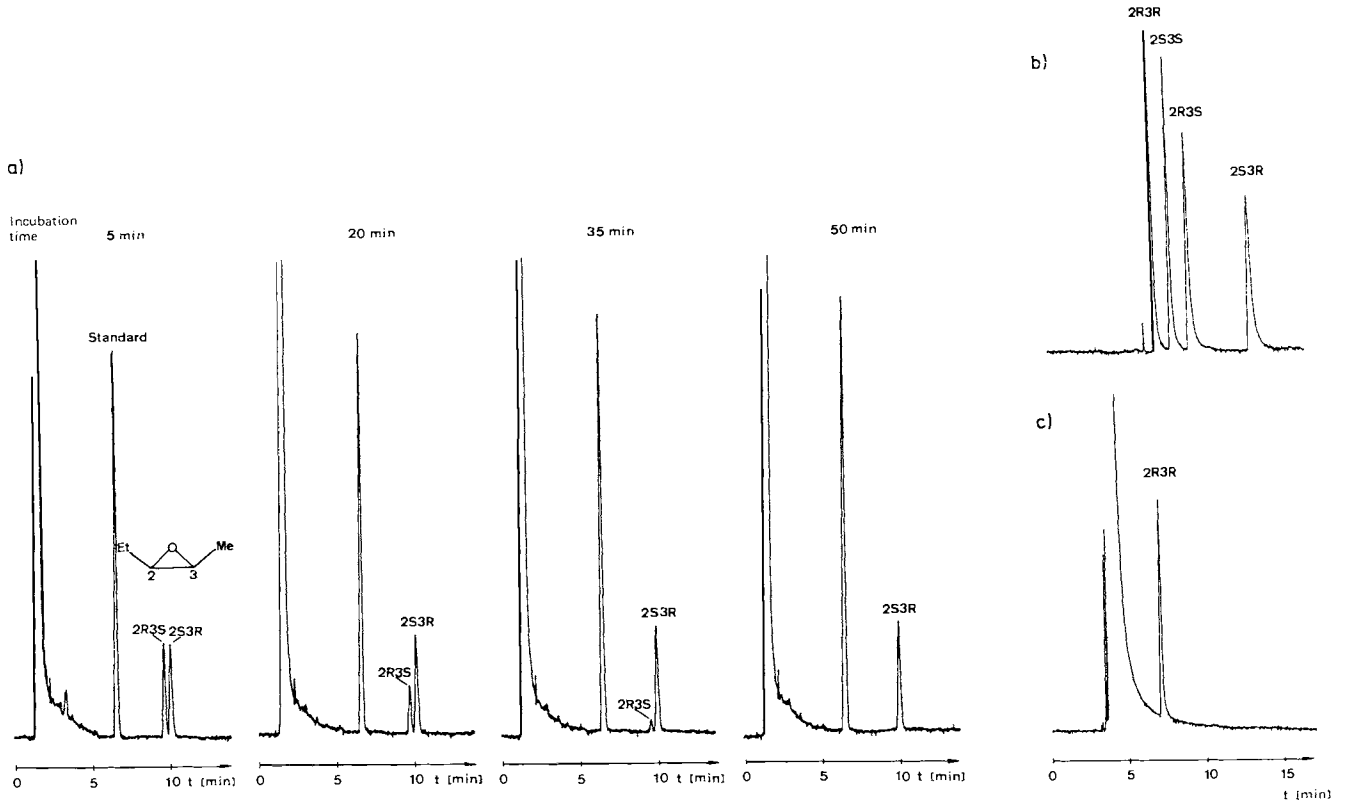


Fig. 1. a) Kinetic analysis of the enantiomeric composition of *rac. cis*-2-ethyl-3-methyloxirane during enzymatic hydrolysis by rat liver microsomes. Standard: 3-methyl-2-butanone (25 m × 0.25 mm glass capillary coated with 0.08 m nickel(II) bis(3-heptafluorobutanoyl-(1*R*)-camphorate) [6a] in OV 101, 80°C, 1.1 bar N_2). Incubation run (0.5 mL total volume): microsomes (1 mg protein/mL), 0.15 M phosphate buffer pH 7.4, *rac. cis*-2-ethyl-3-methyloxirane (4 mM), 37°C. Complexation gas-chromatographic head-space analysis of the oxirane. b) Quantitative complexation gas chromatographic separation of the four configurationally isomeric 2,3-pentanediols as acetonides [6d]. c) *threo*-(2*R*,3*R*)-2,3-pentanediol, formed in the enzymatic hydrolysis of *rac. cis*-2-ethyl-3-methyloxirane (36 m × 0.25 mm glass capillary coated with 0.075 m nickel(II) bis(3-heptafluorobutanoyl-(1*R*,2*S*)-4-pinanonate) in OV 101, 70°C, 1 bar N_2). Incubation run (cf. caption to Fig. 1a) (5 mL total volume): after cessation of reaction (−195°C) extracted six times with diethyl ether (0°C), concentrated, and diol converted into acetonide [6d].

Thus, the metabolites of the enzymatic epoxidation of *cis*/*trans*-2-pentene,[2] i.e. *cis*-(2*S*,3*R*)-2-ethyl-3-methyloxirane, which is completely inactive toward epoxide-hydrolases, is transformed by conjugation at glutathione, and *trans*-(2*S*,3*S*)-2-ethyl-3-methyloxirane, which is essentially inaccessible for conjugation, is a preferred substrate for epoxide-hydrolases.

The complementary chiral-recognition phenomena observed in the case of 2-ethyl-3-methyloxirane also occurs in a series of smaller, sterically less-demanding oxiranes. It follows from Table 1 that the *S*-configurated enantiomers are preferentially metabolized in the biotransformation of aliphatic oxiranes by epoxide-hydrolases while the *R* antipodes are preferentially metabolized by glutathione S-transferase-catalyzed conjugation at glutathione.

In the kinetic resolution of these substrates *in vitro* by glutathione S-transferase-catalyzed conjugation at glutathione we found a considerable substrate enantioselectivity that was dependent upon the degree of substitution and geometry of the oxirane (Fig. 2). Monoalkyl-substituted oxiranes **2** ($R^1=R^2=R^3=H$, $R^4=CH_3$, CH_2Cl, C_2H_5, $CH_2=CH_2$) of configuration *R* (*S* for the potential mutagen (chloromethyl)oxirane ≡ epichlorohydrin, cf. footnote [c] in Table 1) are conjugated significantly more rapidly than the antipodes at glutathione. Whereas (*R*)-ethyloxirane is completely conjugated after 30 minutes incubation time, the remaining (enantiomerically pure) *S* enantiomer was only consumed to the extent of 18%. 50% conversion is already observed after 5 min for the *R*-enantiomer of the cytotoxic 1,3-butadiene metabolite vinyloxirane,[9] and only after 25 min in the case of the *S* antipode (Fig. 2b). Dialkyl-substituted *trans*-oxiranes **2** ($R^2=R^3=H$, $R^1=R^4=CH_3$ and $R^1=CH_3$, $R^4=C_2H_5$) and trimethyloxirane **2** ($R^1=H$, $R^2=R^3=R^4=CH_3$) with *R* configuration are likewise conjugated more rapidly than

Table 1. Complementary *in vitro* substrate enantioselectivity of the biotransformation of racemic aliphatic oxiranes **2** during the hydrolysis to **3** catalyzed by epoxide-hydrolases and by the conjugation at glutathione catalyzed by glutathione S-transferases [a, b].

Oxirane **2**	Hydrolysis to **3** (epoxide-hydrolases)	Conjugation at glutathione (glutathione S-transferases)
Methyloxirane	*S* > *R*	*R* > *S*
(Chloromethyl)oxirane (epichlorohydrin)	*R* > *S* [c]	*S* > *R* [c]
Ethyloxirane	*S* > *R*	*R* ≫ *S*
Vinyloxirane	2*S*,3*S* > 2*R*,3*R*	2*R*,3*R* > 2*S*,3*S*
trans-2,3-Dimethyloxirane	2*S*,3*S* > 2*R*,3*R*	2*R*,3*R* ≫ 2*S*,3*S*
trans-2-Ethyl-3-methyloxirane	2*R*,3*S* ≫ 2*S*,3*R* (inactive)	2*S*,3*R* > 2*R*,3*S*
cis-2-Ethyl-3-methyloxirane	*S* ≫ *R*	*R* > *S*
Trimethyloxirane		

[a] Assignment of the absolute configuration of synthetic oxiranes of known chirality (K. Hintzer, Dissertation, Universität Tübingen 1983. Vinyloxirane: R. J. Crawford, S. B. Lutener, R. D. Cockroft, *Can. J. Chem. 54* (1976) 3364). [b] *S* > *R* means: the *S*-enantiomer reacts more rapidly than the *R*-antipode. [c] The chloro-substitution leads to a formal reversal of the descriptors *R* and *S*.

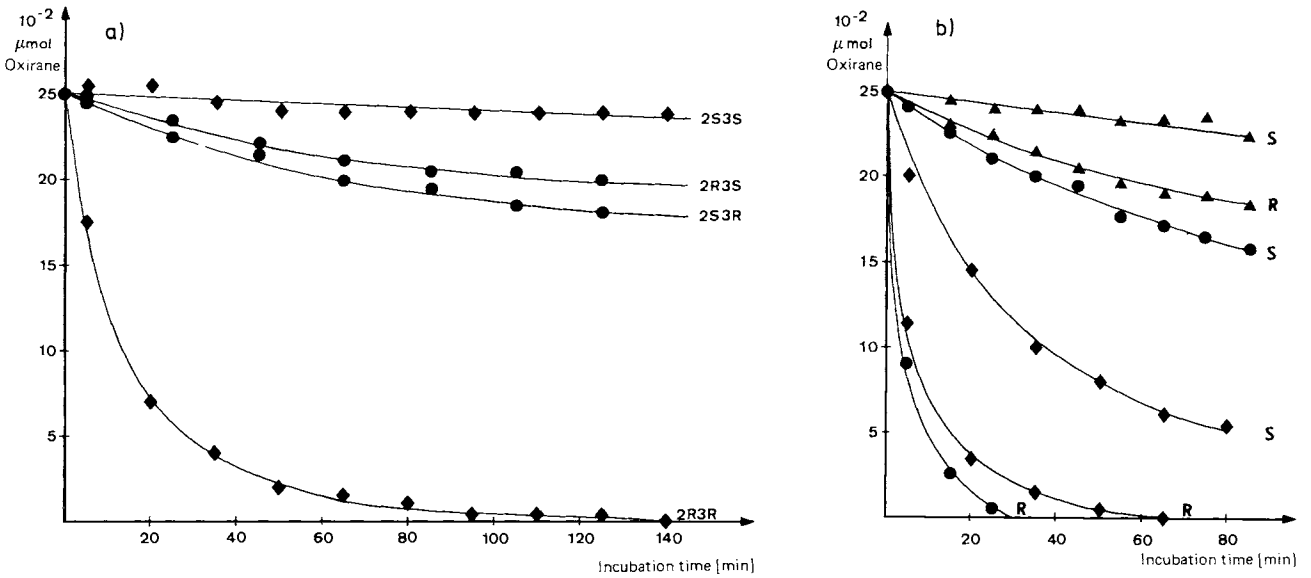


Fig. 2. Kinetic resolution by conjugation at glutathione catalyzed by glutathione S-transferases at 37°C. Incubation run (0.5 mL total volume): glutathione S-transferases (SIGMA, D-8024 Deisenhofen) (0.75 mg protein/mL; origin: rat); glutathione (SIGMA) (4 mM); 0.1 M phosphate buffer pH 6.5; oxirane (1 mM), (chloromethyl)oxirane (4 mM). Glutathione and glutathione S-transferases were pre-incubated in phosphate buffer for 5 min. Oxirane and standard (acetone or 3-methyl-2-butanone) were added as a solution in diethyl ether. The continuous determination of the oxirane enantiomers with respect to the standard was carried out by head-space analysis by means of complexation gas chromatography [2, 6a]. All incubations were repeated at least three times. a) *cis*- (●) and *trans*-2-Ethyl-3-methyloxirane (◆); b) ethyloxirane (●), vinyloxirane (◆) and trimethyloxirane (▲).

the *S* antipodes (50% conversion in 85 min in the case of *trans*-(2*R*,3*R*)-2,3-dimethyloxirane and 10 min in the case of *trans*-(2*R*,3*R*)-2-ethyl-3-methyloxirane, with less than 10% conversion in 20 min for (*R*)-trimethyloxirane and in 80 min for the *S*-antipode).

The occurrence of substrate enantioselectivity, arising from the chirality of the glutathione S-transferases and/or the configuration of the conjugation partner (L,L)-glutathione, has also been reported in the conjugation of phenyloxirane[10] and arene oxides.[11]

The chiral recognition phenomena found here for simple aliphatic oxiranes are of significance in the generalization of model concepts on the active center of the epoxide-hydrolases,[7b] for continuing mechanistic investigations on the conjugation at glutathione, and for the derivation of structure-activity relationships, which go beyond the uniform treatment of the antipodes in case of racemic substrates.[12] In conclusion, we have shown that the enzymatic kinetic resolution proves to be an efficient pathway for access to enantiomerically highly-enriched products of metabolization (*cf.* introductionary remarks).

Received: April 28, 1986;
supplemented: August 21, 1986 [Z 1752/1862 IE]
German version: *Angew. Chem. 98* (1986) 1008

[1] J. Rétey, J. A. Robinson: *Stereospecificity in Organic Chemistry and Enzymology*, Verlag Chemie, Weinheim 1982, p. 236.

[2] V. Schurig, D. Wistuba, *Angew. Chem. 96* (1984) 808; *Angew. Chem. Int. Ed. Engl. 23* (1984) 796.

[3] In the case of **2**, $R^1 = R^3 \neq R^2 = R^4$, product enantioselectivity can be effected by differentiation of enantiotopic groups of the achiral *meso*-substrate.

[4] High regioselectivity and insignificant enantioselectivity was found in the case of *cis*-2-methyl-3-pentyloxirane; R. P. Hanzlik, S. Heideman, D. Smith, *Biochem. Biophys. Res. Commun. 82* (1978) 310.

[5] The formal difference in the numbering of the C-atoms in the oxirane and epoxyalkane nomenclature should be noted (e.g. *cis*-(2*R*,3*S*)-2-ethyl-3-methyloxirane ≙ *cis*-(2*S*,3*R*)-2,3-epoxypentane).

[6] a)V. Schurig, W. Bürkle, *J. Am. Chem. Soc. 104* (1982) 7573; b) V. Schurig, B. Koppenhoefer, W. Bürkle, *J. Org. Chem. 45* (1980) 538, and references cited therein; c) K. Hintzer, *Dissertation*, Universität Tübingen 1983; d) V. Schurig, D. Wistuba, *Tetrahedron Lett. 25* (1984) 5633.

[7] a) G. Bellucci, G. Berti, R. Bianchini, P. Cetera, E. Mastrorilli, *J. Org. Chem. 47* (1982) 3105; b) G. Bellucci, G. Berti, M. Ferretti, E. Mastrorilli, L. Silvestri, *ibid. 50* (1985) 1471.

[8] In the case of *trans*-2,3-dimethyloxirane, the (2*S*,3*S*)-enantiomer is likewise hydrolyzed more rapidly than the (2*R*,3*R*)-antipode by epoxide hydrolases.

[9] H. M. Bolt, G. Schmiedel, J. G. Filser, H. P. Rolzhäuser, K. Lieser, D. Wistuba, V. Schurig, *J. Cancer Res. Clin. Oncol. 106* (1983) 112.

[10] T. Watabe, N. Ozawa, A. Hiratsuka, *Biochem. Pharmacol. 32* (1983) 777; cf. also T. Watabe, A. Hiratsuka, T. Tsurumori, *ibid. 33* (1984) 4051; *Biochem. Biophys. Res. Commun. 130* (1985) 65.

[11] O. Hernandez, M. Walker, R. H. Cox, G. L. Foureman, B. R. Smith, J. R. Bend, *Biochem. Biophys. Res. Commun. 96* (1980) 1494; C. Boehlert, R. N. Armstrong, *ibid. 121* (1984) 980.

[12] F. Oesch, N. Kaubisch, D. M. Jerina, J. W. Daly, *Biochemistry 10* (1971) 4858.

Surveys of Organometallic Chemistry

Until a few years ago it was not possible to find a comprehensive textbook on organometallic chemistry. This may at first seem surprising, but it is in fact quite understandable in view of the hectic pace of growth and expansions into new topics which has occurred in this field of chemistry during the past four decades. Those who had made significant contributions to the development of organometallic chemistry, and where thus the main potential authors, held back because each new publication on the current state of knowledge was likely to become outdated by the time the printing was finished and the book bound. Over the years, however, the principles have become progressively better defined; compound classes, reactivity patterns, structural characteristics and possible applications have emerged more clearly and are better understood. Thus, several books have just become available whose titles promise a more or less comprehensive treatment of organometallic chemistry:

Fundamental Transition Metal Organometallic Chemistry. By *C. M. Lukehart*. Brooks/Cole Publishing Company, Monterey, CA 1985. xiv, 447 pp., bound, $ 28.00.—ISBN 0-534-03801-8.

Metallo-organic Chemistry. By *A. J. Pearson*. John Wiley, Chichester 1985. xi, 398 pp., paperback, £ 9.95.—ISBN 0-471-90446-5.

Basic Organometallic Chemistry. By *I. Haiduc* and *J. J. Zuckerman*. Walter de Gruyter, Berlin 1985. xxviii, 376 pp., bound, DM 169.00.—ISBN 3-11-007184-3.

I found the book by *Haiduc* and *Zuckerman* the most useful, as it is generally well written from a teaching standpoint, and gives a not unduly detailed survey of the organometallic chemistry of the main and transition group elements. Although the treatment of laboratory techniques is unfortunately not completely up to date, the book makes a good impression in all other respects. It presents in a clear way the most important classes of compounds arranged under groups for the main-group elements, and for the transition metals according to the electron balance in the complexing ligands. For advanced chemistry students the section on "Organometallic compounds of non-transition elements" (pp. 45–222) will be of great benefit, as the information is presented free from inessentials and with the emphasis on basic principles throughout. However, I feel that an accompanying discussion article is needed as much for this topic as for the comprehensive chapters on "Organometallic compounds of transition metals" (pp. 223–376), as the importance of the various classes of compounds for present-day chemistry in universities and industry is seldom treated as thoroughly as it ought to be. This book is especially valuable for teaching purposes since, by means of clear structural diagrams, it enables one to easily grasp the essential facts. The price of the book is reasonable in view of its content.

On comparing the above book with that by *Lukehart*, it is evident at the first glance that this is a distinctly more specialized work. As the title indicates, only the transition metals are covered, though with a corresponding increase in depth and thoroughness since the two books contain similar numbers of pages. In the division of the book into topics *Lukehart* has reached a good compromise between important classes of compounds, principles of reactivity, and—especially valuable for the industrial chemist—the technical applications of modern organometallic chemistry. Classifications according to method of preparation, spectroscopy and structure are, of course, clearly and fully presented, and in many places further developed by comparison tables which contain a lot of information. The author's tendency towards detail sometimes interferes appreciably with the flow of the text, especially when quite unnecessary data are added below the chemical equations (e.g. on pp. 95, 97, 143, 145...). On the other hand *Lukehart* gives with each chapter a selection of literature references for studying the topics more thoroughly. The book is a useful monograph for the research chemist rather than a textbook, as the advanced chemistry student would find the large number of individual compounds and their properties too much to cope with. I would refer them instead to "Collman-Hegedus", which is much easier and comprehensible for students, although at present it is unfortunately out of print.[*] The book by *Lukehart* will be useful to doctoral and post-doctoral students and academic staff engaged in the organometallic field, especially when a quick survey of a specialized topic is wanted. The book is not lying before me on the desk, but I do have it in the bookshelf behind me.

I have not yet made so much of a start with the 400-page work by *A. J. Pearson*. Although the book contains much basic material on mechanisms and compound classes, I find it lacks the overall guiding themes which make a book valuable and worth reading. An incidental comment: the title of the book promises more than is contained in the text, as the main-group metals are not treated. Numerous references to original literature are given, but these have been covered more fully and effectively in other publications. I cannot recommend the purchase of this book to any of the groups of readers mentioned earlier.

Wolfgang A. Herrmann [NB 761 IE]
Anorganisch-chemisches Institut
der Technischen Universität München, Garching (FRG)

Boussingault. Chemist and Agriculturist. By *F. W. J. McCosh*. D. Reidel Publishing Co., Dordrecht 1984. xv, 280 pp., bound, Hfl. 140.00.—ISBN 90-277-1682-X

The French chemist and agronomist *Jean Baptiste Boussingault* (1802–1887) played a decisive role in determining the character of agricultural chemistry in the 19th century. A comprehensive biography in book form on his life and his scientific work has been lacking until now. The book under review fills this gap.

F. W. J. McCosh has compiled a very detailed account of the individual periods of *Boussingault*'s life, drawing upon all available source material. He thereby throws light on the manifold interrelations with political, social, and scientific communities.

[*] J. P. Collman, L. G. Hegedus: *Principles and Applications of Organo-transition Metal Chemistry*, University Science Books (Oxford University Press, Oxford 1982).

The focal point of the biography is *Boussingault*'s work as an agricultural chemist, above all his experimental activity at the Alsatian experimental farm Bechelbronn, where he carried out extensive laboratory and field experiments on mineral fertilization. *McCosh* has rightly given ample space to *Boussingault*'s experiments on the nitrogen requirements of plants. It was indeed *Boussingault* who in 1837 provided experimental evidence for the first time that leguminous plants can obtain the nitrogen that they need for growth from the air, even though this finding was acknowledged only fifty years later by the scientific community as a valid theory. 1986 is the 100th anniversary of *Hermann Hellriegel*'s disclosure of the basis for nitrogen binding in leguminous plants; in remembering this discovery, one must also think of *Boussingault*, the father of the idea of nitrogen fixation. Therefore *McCosh*'s biography appears at an opportune moment: it contains broad background information concerning the prehistory of *Hellriegel*'s discovery.

McCosh also gives proper attention to the significance of *Boussingault*'s major scientific work, his "Economie rurale" (first edition 1843/44) for the development of agricultural science. It thereby becomes clear that in this work, which was translated into several languages, *Boussingault* vigorously advocated the development of agricultural chemistry, soil science, and the science of plant cultivation into autonomous agricultural disciplines.

The reader is given an exhaustive survey of *Boussingault*'s many years of field studies in South America, his experiments on animal nutrition, his research work on photosynthesis, as well as his experiments in the field of metallurgy. This testifies to the versatility of this chemist, who in the brilliant period of French chemical theory did not rank among the theorists; on the contrary, he was at all times an advocate of applied chemistry.

The book's sources are conscientiously documented; numerous illustrations are included, as well as a bibliography of the scientific publications of *Boussingault* arranged by field. Many readers will perhaps generously overlook the infrequent misprints, which are noticeable above all in the German biographical and bibliographical references.

On the whole, this biography is a sound contribution, not only to the history of agricultural chemistry in the 19th century, but also to the general history of chemistry and science. It should not be absent from any private or public, specialized library.

Wolfgang Böhm [NB 733 IE]
Institut für Pflanzenbau und Pflanzenzüchtung
der Universität Göttingen (FRG)

Technology of Chemicals and Materials for Electronics. Edited by *E. R. Howells*. Ellis Horwood Ltd., Chichester 1984. 333 pp., bound, £ 39.50.—ISBN 0-85312-771-9

This book, published under the auspices of the Society of Chemical Industry (SCI), contains the papers presented at a joint symposium held in January 1984 by the SCI and the Institution of Electrical Engineers (IEE). The SCI has already occasionally concerned itself in the past with interdisciplinary areas where chemistry meets physics, biology or engineering. In the field discussed here the collaboration with the IEE has turned out to be particularly fruitful, as the electronics industry's need for chemicals and advanced materials is a topical theme, not only from a technical but also from an economic point of view. In Europe, where this meeting was held, the electronics industry faces a powerful challenge from the USA and the Far East, especially from Japan, but at the same time there is concentrated here a chemical industry which ranks as one of the most potent in world markets. Changes affecting the range of products supplied by the European chemical industry, and competition from oil-producing countries, have increased the importance of new markets such as the electronics industry, even though it appears that the quantities of materials needed annually are somewhat modest; these are mostly high quality specialty products of a sophisticated kind, whose prices are determined in a similar way to those of pharmaceutical products. Because materials for the electronics industry must meet very high specifications, a chemical industry that supplies them needs to have a very good infrastructure, so as to satisfy purity criteria, for example.

Although many aspects of the raw material requirements of the electronics industry have been discussed elsewhere, there has hitherto been no comprehensive treatment of this increasingly important field. The organizers of this symposium have provided here a clear and readable overview of the future materials needs of the modern electronics industry which, while it is by no means exhaustive, is useful and wide-ranging.

The first chapter looks at past trends and prospects for the future, mainly from an economic point of view, but also including readable accounts of some of the technical opportunities. The titles of the topics covered are as follows: Twenty-five years of molecular electronics (*D. H. Roberts*, General Electric); Advances in microelectronics via chemical and photoimaging innovations (*A. B. Cohen*, Du Pont); The anatomy of a discovery—biphenyl liquid crystals (*C. Hilsum*, General Electric); Electronic chemicals: a US view (*D. W. McCall*, AT & T Bell Laboratories); Future prospects of the Japanese electronics industry (*K. Odagawa*, Toshiba); New materials for electronics and electro-optics: some speculations and a peek into the future (*R. E. Schwerzel, R. L. Holman, G. P. Noel, V. E. Wood*, Battelle Memorial Institute); Trends in materials for modern electronic systems (*C. van de Stolpe*, Philips).

The second chapter is concerned with properties of materials, and consists of the following articles: The chemistry of polymer resists useful in microlithography (*A. Ledwith*, Pilkington Bros.); Molecular electronics using Langmuir-Blodgett films (*G. G. Roberts*, University of Durham); The influence of the electronics industry on the development of soft magnetic materials (*R. V. Major*, Telcon Metals); Gallium arsenide integrated circuit technology (*R. C. Eden*, GigaBit Logic); Growth technology of III-IV semiconductors for multilayer devices (*M. Razeghi*, Thomson-CSF); Ingegrated circuit packaging and lithography (*A. N. Broers*, IBM, New York); Materials cross-fertilization (*G. D. Pitt*, Standard Telecommunications Laboratories and University of Surrey); Electrochromic displays (*D. J. Barclay, D. H. Martin*, IBM, UK); The materials needs of optical communications (*M. J. Cardwell, R. C. Goodfellow*, Plessey Research).

An account of a panel discussion and a contribution by the editor give further insights in to the field, and some additional statistical data are included to round off the picture.

The appendix contains a list of the acronyms used, making the "computer Chinese" language a good deal more comprehensible. The list of the participants' addresses is a mine of information for all those who may want to ques-

tion the experts personally, or to send them advertising material.

The book fills a gap in a specialist area of growing importance. It is, moreover, highly recommended as bedtime reading for students seeking jobs, being an educational book on an otherwise neglected interdisciplinary field bordering on chemistry.

Joachim Bargon [NB 755 IE]
Institut für Physikalische Chemie
der Universität Bonn (FRG)

Oscillations and Traveling Waves in Chemical Systems. Edited by *J. R. Field* and *M. Burger*. John Wiley, Chichester 1985. xx, 682 pp., £ 98.30.—ISBN 0-471-89384-6

Chemical oscillations in time and space have been investigated extensively, especially in the last twenty years. The fascination with oscillating reactions following the discovery of the famous Belousov-Zhabotinsky reaction is reflected by the exponential growth in publications between 1965 and 1975. The study of chemical oscillators is also of interest from the standpoint of natural philosophy, namely in that the discussion of the significance of symmetry breaking and bifurcation in systems far from chemical equilibrium could affect the definition of time itself. There are still supposed to be skeptics who question the existence of chemical oscillations in a homogeneous system. They are in error! This book, written by several authors with strict organization by the editors, establishes unequivocally that chemical oscillations occur in inorganic reactions in a homogeneous system. This is also true for several biological systems, which are referred to only briefly, but which often motivated the study of the above reactions.

In general, chemical oscillations are possible only in thermodynamically open systems. The requirements for the occurrence of chemical oscillations are now adequately known and have been substantiated in a series of experimental systems. Chemical oscillators are non-linear oscillators. In addition to phenomena such as frequency-doubling, they show period-multiplication when "ideally" mixed. This may occur when the in-flow of reactants into a flow reactor is sinusoidally perturbed. Chaotic trajectories can also be produced; they are mentioned in this book, but are not dealt with further. In thin, liquid layers that are not stirred, spatial oscillations can appear in the form of chemical traveling waves and of standing waves. Here the coupling and interplay of the chemical reaction with diffusion or convection to form a spreading pattern prevail.

In the Introduction, *Zhabotinsky* reports on the interesting early history (1961–1969) and on the first mechanistic proposals for the Belousov-Zhabotinsky oscillations of a sulfuric acid solution of bromate, Ce^{III}/Ce^{IV}, and malonic acid, a reaction that also carries his name. The mathematically interested reader gets his money's worth, not only in the first chapter on the stability of steady states, on Hopf bifurcations, and on bilaterally coupled systems, but also throughout the entire book. The chapter on the inorganic Belousov-Zhabotinsky oscillator follows, in which the variations and subsystems are described in every detail. Except for chaotic movements, the well-known Field-Noyes "Oregonator" mechanism can account for almost all of the phenomena of the Belousov-Zhabotinsky reaction, such as bistability and traveling waves. It is given a comprehensive mathematical analysis in a separate chapter. Periodic gas-evolving and other chemical oscillators such as the Bray-Liebhafsky and the Briggs-Rauscher are discussed. The response of an oscillator to periodic perturbation is extremely varied. Mathematical methods of analysis are presented and also applied to non-isothermal oscillators. In this connection, the stability behavior of the system in the region of kinetic phase change is of great theoretical interest. The pattern formation produced by the crystallization of geological material, the propagation of reaction-diffusion fronts, or two- and three-dimensional periodic waves show a surprising abundance of forms. The chemical oscillations of carbon monoxide are treated in great detail in a further chapter. The last and somewhat curious chapter presents a statistical analysis and a "sociology" of the publications on chemical oscillations in the years from 1910 to 1981.

The references are very extensive and are carefully reported with titles. This book will surely be the standard work on inorganic chemical oscillations in the next years. Its purchase can be highly recommended, even though biological oscillators and chaos are not dealt with.

Friedemann Schneider [NB 735 IE]
Institut für Physikalische Chemie
der Universität Würzburg (FRG)

Über die Erhaltung der Kraft. Facsimile of the holograph text together with a commentated transcription. By *Hermann Helmholtz*. Physik-Verlag, Weinheim 1983. 124/67 pp., bound, DM 80.00.—ISBN 3-87664-071-7

The chemist *Döbereiner* who was appointed to the University of Jena at the instance of *Goethe* published a book in 1819 with the title "Anfangsgründe der Chemie und der Stöchiometrie". In § 5 of the introduction was the sentence "'Thorough study of chemistry begins, after mathematical and scientific preparation, with the study of the basic principles of chemistry in their most up-to-date form and then continues to the history of the same." The last portion of this sentence is applicable to all natural sciences. To know how scientific progress is made is extraordinarily instructive and useful for every representative of a science. Most important is to see on the basis of examples that science usually sprouts from the human endeavors of individual persons. This insight is excellently promoted by the publication of facsimile editions of manuscripts of great scientists. The publication reviewed here can be of great value to numerous scientists and particularly to physicists.

The essay by *Helmholtz* is particularly suited for the start of one's own involvement with the genesis of scientific ideas because the basic publication by *Julius Robert Mayer* the discoverer of the first main proposition appeared in *Liebig*'s "Annalen der Chemie" in 1842 and is relatively easy to include in a comparison. The reader will be able to establish that quite different avenues of thought can be of considerable importance for the achievement of new scientific insight.

As far as the technical representation of the present book is concerned it suffices to say that it consists of two part volumes; the first contains the facsimile of the holographic text and the second contains, after an introduction, the transcription and comments.

Hermann Hartmann (dec.) [NB 673 IE]
Institut für Physikalische Chemie
der Universität Frankfurt am Main (FRG)

Discarding the Double Bond Rule?

A sentence in the table of contents concerning the communication of *H. Hesse* and *U. Klingebiel (Angew. Chem. 98* (1986) 638; *Angew. Chem. Int. Ed. Engl. 25* (1986) 649) prompts me to make several comments. On page A-134 of the July issue there is the following statement:

> Once again we have found bulky substituents that enable the synthesis of a stable compound with a moiety that ... contradicts the double bond rule.[*]

First, I would like to point out that there is not only one "double bond rule," for a large number of authors in this country and elsewhere have considered this aspect of bonding in detail and have arrived at various conclusions. Thus, there are several double bond rules. The question therefore arises whether all such rules should be discarded, or, which rules are meant? Since I have spent considerable time thinking about this problem and, in fact, have published two articles in *Angewandte Chemie* dealing with the problem ("Mehrfachbindungen in der anorganischen Chemie," [Multiple Bonds in Inorganic Chemistry] *Angew. Chem. 69* (1957) 77 and "Force Constants and Bond Orders of Nitrogen Bonds," *Angew. Chem. 78* (1966) 565; *Angew. Chem. Int. Ed. Engl. 5* (1966) 567), I was disturbed by the above statement.

Secondly, my reflections on this matter started with earlier considerations of isosterism. The first prerequisite for a double bond is a deficiency of electrons. It then turned out that the higher the sum of the electronegativities of the two atoms involved in bonding, the higher the probability for formation of a double bond. As an approximate limit, I gave a value of 5.0 for the sum of electronegativities. A sum of 4.8 is obtained for the Si–N pair in question, a value that is not far from this limit. Further, it was found that larger values of the difference in electronegativities oppose the formation of double bonds. Thus, in the second article cited above, I suggested that, for the combinations of Si–N, higher bond orders would be probable.

Furthermore, in discussing multiple bonds, it is important to note that not only are single and double bonds possible, but also bond orders with all possible values between 1.0, 2.0, and 3.0. These bond orders can be derived from bond distances and force constants. None of these values is given in the communication of *Klingebiel* et al., so that it is not clear whether a pure double bond is involved. Because of the large difference in electronegativity, I would like to suggest that the bond order lies below 2.0.

Thirdly, I have to admit that, in formulating my rules, I would never have imagined that the superb experimental talent of chemists would allow them to so suppress the reactivity of double bonds with bulky ligands that they would become stable at conventional temperatures, and even tolerate higher temperatures, without undergoing polymerization. I am referring to "cemented double bonds," the reactivity of which is strongly hindered. The use of bulky ligands, for example, has allowed the synthesis of stable compounds having Si–Si (sum of electronegativities 3.6!) or P–P double bonds (sum 4.2). In a discussion concerning Si–Si double bonds, the author reported that polymerization is observed when even one of the four *tert*-butyl groups is replaced by an isopropyl group. The rules that I formulated can easily accomodate this result. It is only necessary to add that the rules apply only when small ligands are bonded to the atoms in question or when the reactivity is not hindered by bulky substituents.

Moreover, the same issue of *Angewandte Chemie* and *Angewandte Chemie International Edition in English* contains a communication by *Alexander Sax* and *Rudolf Janoschek* (p. 634 and p. 651, respectively) in which the authors report that, in the case of Si_6H_6, not the benzene structure (with "double bonds") but rather the prismane structure with single bonds is preferred, in full agreement with my ideas.

Prof. Dr. J. Goubeau
(Professor emeritus of the Universität Stuttgart)
Hallimaschweg 5
D-7000 Stuttgart 70 (FRG)

[*] This sentence is not from the author but rather from the editorial staff; it was merely intended, albeit somewhat overstated, to point out the large number of stable compounds with multiple bonds between elements of the higher periods that have been synthesized to date.

Registered names, trademarks, etc. used in this journal, even without specific indication thereof, are not to be considered unprotected by law.

© VCH Verlagsgesellschaft mbH, D-6940 Weinheim, 1986. – Printed in the Federal Republic of Germany by Zechnersche Buchdruckerei, Speyer/Rhein.

All rights reserved (including those of translation into foreign languages). No part of this issue may be be reproduced in any form – by photoprint, microfilm, or any other means – nor transmitted or translated into a machine language without written permission from the publishers. Only single copies of contributions, or parts thereof, may be reproduced for personal use.

Valid for users in the USA: The appearance of the code at the bottom of the first page of an article in this journal (serial) indicates the copyright owner's consent that copies of the article may be made for personal or internal use, or for the personal or internal use of specific clients. This consent is given on the condition, however, that the copier pay the stated per-copy fee through the Copyright Clearance Center, Inc., for copying beyond that permitted by Sections 107 or 108 of the U.S. Copyright Law. This consent does not extend to other kinds of copying, such as copying for general distribution, for advertising or promotional purposes, for creating new collective works, or for resale. For copying from back volumes of this journal see 'Permissions to Photo-Copy: Publisher's Fee List' of the CCC.

Editorial office: Pappelallee 3, D-6940 Weinheim, Federal Republic of Germany, Telephone (06201) 602315, Telex 465516 vchwh d, Telefax (06201) 602328.

Editor: *P. Gölitz.*

Associate editors: *D. I. Loewus, A. Stimson.* **Editorial assistant:** *E. Schweikart*

Publishers: VCH Verlagsgesellschaft mbH. (Managing Directors: *Prof. Dr. Helmut Grünewald* and *Hans Dirk Köhler*), Pappelallee 3, D-6940 Weinheim, Federal Republic of Germany. Correspondence concerning advertisements should be addressed to VCH Verlagsgesellschaft mbH. (Advertising Manager *R. J. Roth*), Boschstr. 12, P.O. Box 1260/1280, D-6940 Weinheim, Federal Republic of Germany. Telephone Weinheim (06201) 602-0, Telex 465516 vchwh d, Telefax (06201) 602328.

ANGEWANDTE CHEMIE
International Edition in English
Volume 25 · Number 12
December 1986
Pages 1039–1134

Preorganization—From Solvents to Spherands

By Donald J. Cram*

Dedicated to Professor Vladimir Prelog on the occasion of his 80th birthday

This article assesses the importance of molecular preorganization to the rapidly developing field of complexation involving designed synthetic organic compounds. Since its birth as a science, organic chemistry has drawn heavily on biological chemistry as a vast storehouse of evolutionary structures, reactions, and control mechanisms that serve as inspiration for designed organic-compound mimics. Biological systems, through highly structured complexation, accomplish complicated tasks. The receptor sites of enzymes, the genes, the antibodies, and ionophores possess high degrees of preorganization. In other words, their functional groups act cooperatively as binding or catalytic sites which are largely collected and oriented prior to complexation.—The strength of the organic chemist derives from his ability to design organic compounds, organic reactions, synthetic sequences, and test systems to evaluate hypotheses. The design of highly structured complexes and the discovery of the rules that govern their behavior are described here. Research in this field is particularly rewarding because scientific and aesthetic content merge and become visible in the structures of many of the complexes.

1. Introduction

1.1. Definitions

Complexes are defined as two or more compounds bound to one another in a definable structural relationship by forces such as hydrogen bonding, ion-pairing, metal-ion-to-ligand attractions, π-acid-to-π-base attractions, van der Waals attractions, and the entropic component of desolvation. Complexing partners are conveniently classified as *hosts* and *guests*. In complexes, the binding sites of hosts converge. *Hosts* are the synthetic counterparts of the receptor sites of enzymes, genes, antibodies of the immune system, or ionophores. *Guests* possess divergently arranged binding sites, and are the counterparts of substrates, inhibitors, cofactors, drugs, or antigens.[1]

1.2. Structuring of Complexes

Complexes are structured by contacts at multiple binding sites between host and guest. The binding energy at a single contact site is at most a few kilocalories per mole, much lower than that of a covalent bond. Contacts at several sites between hosts and guests depend on complementary placements of binding sites, making use of the self-evident principle of complementarity: "to complex, hosts must have binding sites which cooperatively contact and attract binding sites of guests without generating strong nonbonded repulsions."[2]

[*] Prof. D. J. Cram
Department of Chemistry and Biochemistry,
University of California at Los Angeles
Los Angeles, CA 90024 (USA)

 © VCH Verlagsgesellschaft mbH, D-6940 Weinheim, 1986 0570-0833/86/1212-1039 $ 02.50/0

1.3. Design of Complexes

The complexes discussed here were designed through extensive use of Corey-Pauling-Koltun (CPK) molecular models. These models were developed under the auspices of the U. S. National Institutes of Health, Education and Welfare, the National Science Foundation, and the American Society of Biological Chemists "for constructing macromolecules of biological interest." The models are based on crystal structures of biologically important compounds.[3] The crystal structures of over fifty complexes have been determined in our group alone.[4] We estimate that in about 95% of the crystal structures, the complexes turned out generally to have the structures anticipated based on CPK model building. Most of the complementary relationships between hosts and guests of our design could not have been anticipated without use of CPK models.

1.4. Solvent Effects

Binding forces between solvent and host, and solvent and guest, are frequently of the same type as those between host and guest. Thus, during complexation, solvent must be displaced from the binding sites needed to complete the complexation process. The solvation free energy is composed of an enthalpic term favoring solvent binding and an entropic term disfavoring solvent binding. Any net free-energy costs for this desolvation must be paid by decreasing the free energy of complexation. In effect, solvent competes with both host and guest for occupancy of the binding sites for each potential complexing partner. Host-guest complexes are formed in solution usually because of the *organization* of the binding sites of the host for complexation, and the lack thereof in the solvent.

1.5. Criteria of Structure

The criteria for host and complex organizations in the solid state are crystal structures. In solution, except for hosts rigidly preorganized for binding, conformational equilibria exist which complicate the structural picture, particularly since the relative populations of various conformations depend on the character of the solvent. Spectral techniques, particularly NMR, provide the most generally useful experimental criteria for solution structure. Correlations of binding free energies with structures of complexes, coupled with spectral data and expectations based on either CPK model building or molecular mechanical calculations,[5] are useful in assigning solution structures. Reasoning by analogy from crystal to solution structure is probably most sound when binding free energies are high, when solution spectra support the assignments, and when a series of related hosts and guests and their binding free energies are determined in the same medium under the same conditions.

Solution structures of complexes tend to be much more free of conformational equilibria than those of hosts, since the contacts between the binding sites of the complexing partners severely limit the movements of the parts of the complex with respect to one another. Complexes are frequently easier to purify and crystallize, and their ^{1}H-NMR spectra tend to be simpler than those of their hosts. Many hosts crystallize as solvates in which a solvent molecule is employed as a guest (inclusion complex), and (or) with other solvent molecules packed between hosts. Often, obtaining suitable crystals is a greater task than determining their crystal structures.

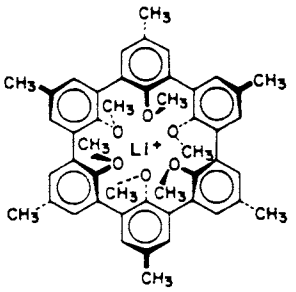
1.6. Types of Complexes

Of the many types of complexes designed and synthesized, we will treat here only those families that provide correlations between structures and binding free energies, or that illustrate hypotheses, principles, and generalizations. Section 2 is concerned with the types and family names of complexes formed between hosts and cationic guests such as alkali-metal, ammonium, and alkylammonium ions. Section 3 treats complementarity, and the number and character of binding sites of hosts. Structure-binding relationships with ammonium and alkylammonium ions as guests are considered in Section 4. Section 5 deals with the central theme of the effects of host preorganization on binding free energies and rates of complexation. Section 6 relates preorganization of hosts to specificity in complexation. The structures of compounds are found essentially only in the Figures, which also contain most of the literature references to their study.

2. Types and Family Names of Hosts and Their Complexes with Guest Cations

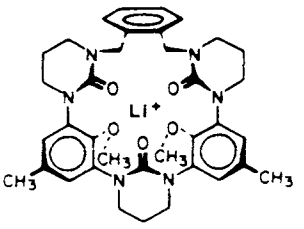
The most extensive studies of complexes involve the alkali-metal, ammonium, and alkylammonium picrates as guests. The hosts and complexes treated in this article contain as binding sites ether oxygens, tertiary amine or pyridine nitrogens, or cyclic urea oxygens. These sites are separated from one another by hydrocarbon spacers such as dimethylene, trimethylene, *ortho*- or *meta*-phenylene, or *ortho*- or *meta*-xylene (phenylenebis(methylene)) units.

Hosts that bind alkali-metal and ammonium cations divide into families named according to structural features that are illustrated in complexes of hosts **1**-**9** (Fig. 1). *Corands*,[6] hosts first studied by *Pedersen*,[7] are macrocyclic polyethers whose oxygens are separated by $(CH_2)_n$ groups or groups of the *ortho*-phenylene type. The host of complex **6** · K^+ is a derivative of [18]crown-6. *Cryptands* are macrobicyclic polyethers, designed and studied by *Lehn*,[8] which are characterized by their polycyclic structures and whose bridgeheads are composed of $N(CH_2)_3$ units. The host of complex **4** · K^+ is a [2.2.2]cryptand. *Spherands*, designed and studied by the author, are macrocyclic or macropolycyclic systems that contain enforced cavities fully organized for complexation during synthesis, rather than during the complexing act. The host of complex **1** · Li^+ is a prototypical spherand.[9] *Hemispherands*, exemplified by **5** and **9**, are hosts whose cavities are at least half preorganized for binding by the rigidity of the hydrocarbon support structure and the spatial requirements of the appended groups.[4] *Cryptaspherands* **3** and **8** blend the cavity-enforc-



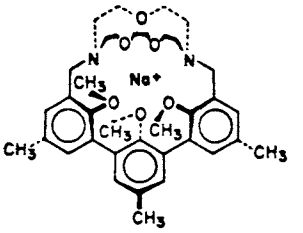
spheraplex [2]

$1 \cdot Li^+$ (>23)



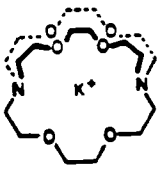
spheraplex [16]

$2 \cdot Li^+$ (18.3)



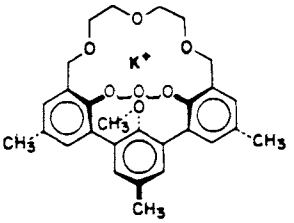
cryptaspheraplex [10,11]

$3 \cdot Na^+$ (21.0)



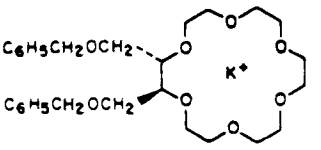
cryptaplex [11]

$4 \cdot K^+$ (18)



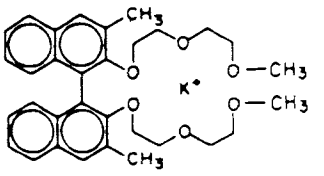
hemispheraplex [17]

$5 \cdot K^+$ (13.9)



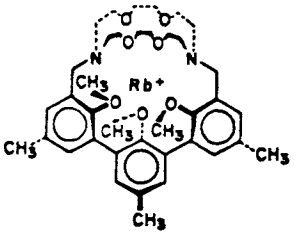
coraplex [18]

$6 \cdot K^+$ (11.4)



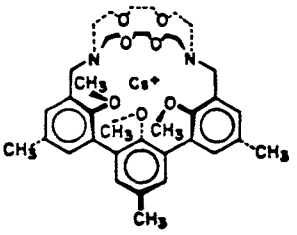
podaplex [18]

$7 \cdot K^+$ (5.9)



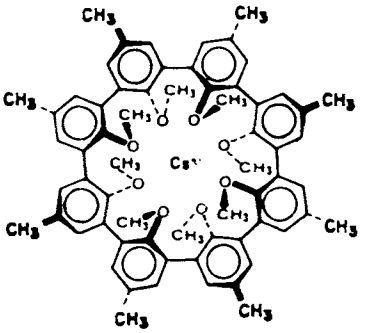
cryptaspheraplex [10,11]

$8 \cdot Rb^+$ (20.3)



cryptaspheraplex [10,11]

$8 \cdot Cs^+$ (21.7)



hemispheraplex [14]

$9 \cdot Cs^+$ (13.9)

Fig. 1. Structures of host-guest complexes, their family names, and binding free energies ($-\Delta G^0$ [kcal·mol^{-1}]) of their picrate salts at 25°C in $CDCl_3$ saturated with D_2O. These conditions will be referred to as "standard conditions."

ing features of three *para*-methylanisole groups with the multiple ligand-gathering features of the cryptands.[10,11] Figure 2 provides stereorepresentations of the crystal structures of **10** · Na^+, **3** · K^+, **8** · Na^+, **8** · K^+, and **8** · Cs^+ complexes. *Podands*, named by *Vögtle* and *Weber*,[6] who provided the first examples, are noncyclic arrays of binding sites, in some cases terminated by groups capable of complexing each other to stabilize the cyclic conformations of the free hosts. Host **7** is a podand containing a binaphthyl unit, which somewhat limits its conformations.[18] The crystal structures of many complexes of the kind listed in Figure 1 have been determined, e.g., those of **1** · Li^+, **3** · Na^+, **4** · K^+, **8** · Cs^+, and **9** · Cs^+.

The suffix *and*, appropriately borrowed from the word *ligand*, is common to these family names. The suffix *ate*, found in the crystallographic words *solvate* or *clathrate*, has been suggested for the family names of complexes,[6] e.g., cryptate.[15] Use of this suffix suffers two disadvantages. One is that most crystalline solvates or clathrates cannot survive dissolution because their structures are too dependent on lattice forces. The other is that the suffix *ate* has been generally used in chemical names to denote innumerable anions, such as acet*ate* or perchlor*ate*. All of the complexes of Figure 1, however, carry a positive charge.

Instead of *ate*, we suggest the use of the suffix *plex*, de-

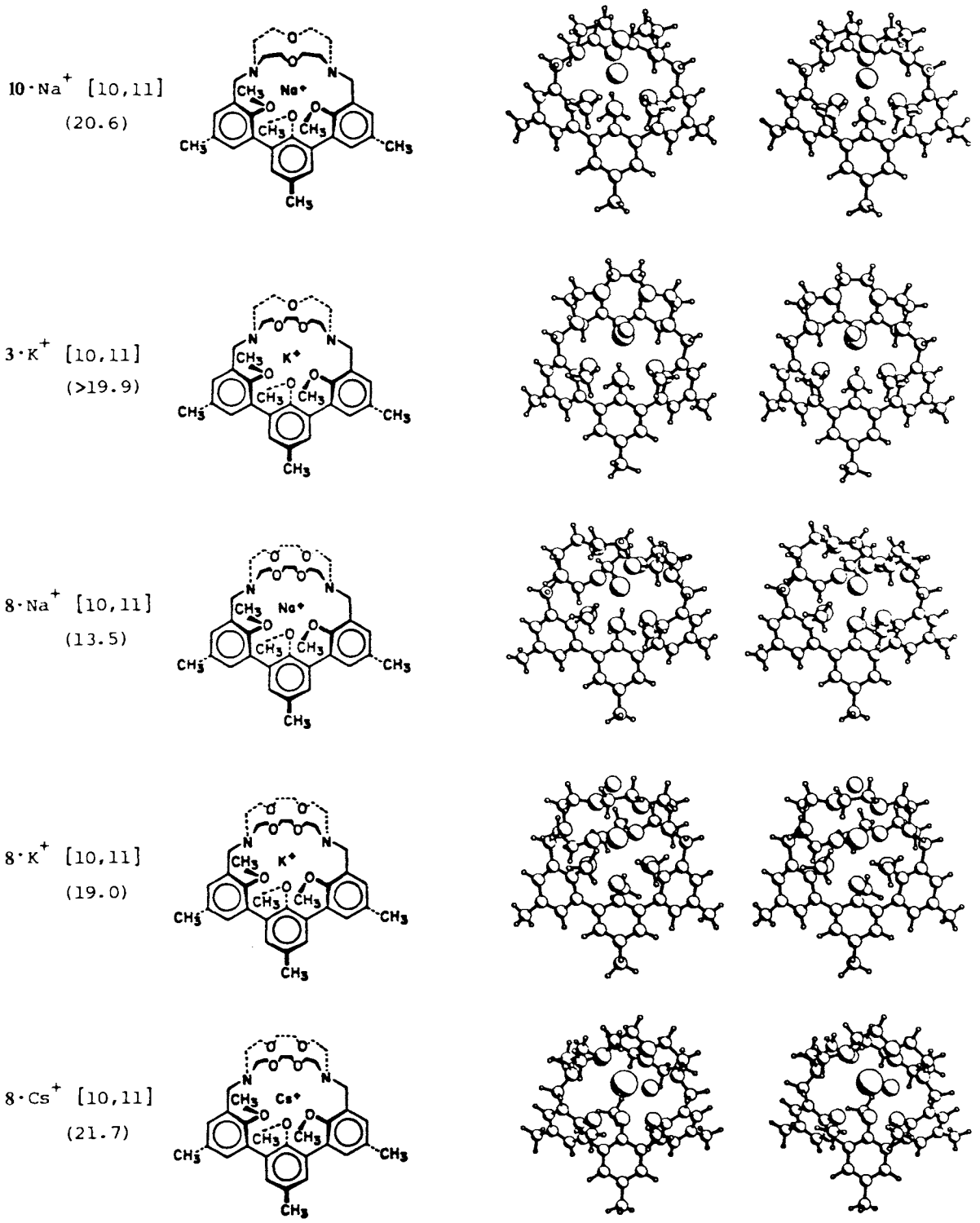
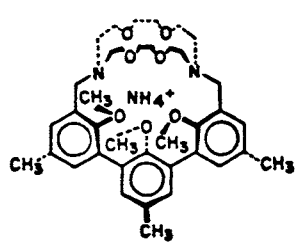
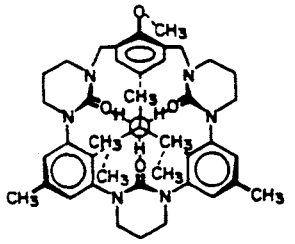


Fig. 2. Stereorepresentations of crystal structures of cryptaspheraplexes of alkali-metal ions, and binding free energies of their picrate salts ($-\Delta G^0$ [kcal·mol^{-1}]) under standard conditions. **3**·K^+, **8**·K^+, and **8**·Cs^+ also contain a water molecule.

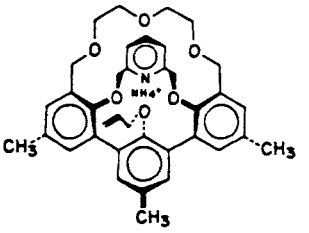
rived from the Latin word *plexus*, meaning an "interwoven arrangement of parts." The word *complex*, derived from the Latin word *complexus*, means a "weaving together of parts." The word complex is admirably suited as a class name for chemical entities such as those found in Figures 1 and 2, since the prefix *com* means "with or together." Transformation of the family names of the hosts to our suggested family names of their respective complexes provides the terms *spheraplex*, *cryptaplex*, *coraplex*, *podaplex*, *hemispheraplex*, and *cryptaspheraplex*, illustrated by **1**·Li^+, **4**·K^+, **6**·K^+, **7**·K^+, **5**·K^+, and **3**·Na^+, respectively, in Figure 1.



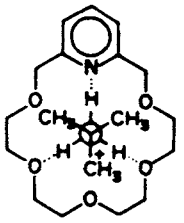
8·NH_4^+ [10,11]



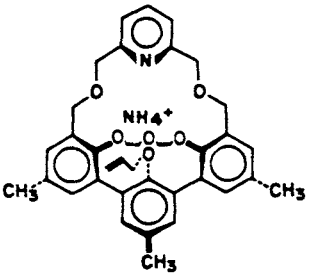
11·$(CH_3)_3CNH_3^+$ [19,20]



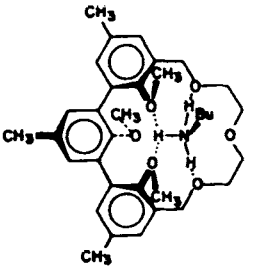
12·NH_4^+ [17]



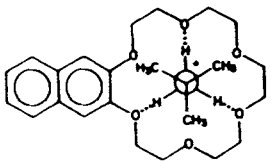
13·$(CH_3)_3CNH_3^+$ [4,21]

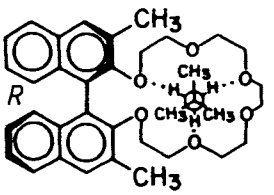


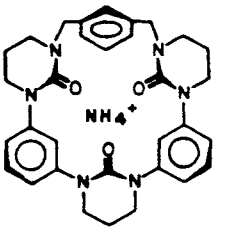
14·NH_4^+ [17]



15·$(CH_3)_3CNH_3^+$ [4,22]



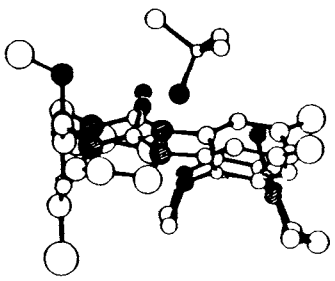




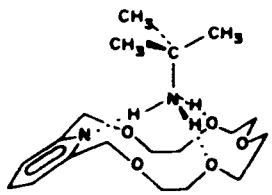
16·$(CH_3)_3CNH_3^+$ [4,18] **17**·$(CH_3)_3CNH_3^+$ [4,18] **18**·NH_4^+ [23]

Fig. 3. Structures of selected complexes with ammonium and *tert*-butylammonium ions (cf. Table 1). Bu in **15**·$(CH_3)_3CNH_3^+$ means *tert*-butyl. For the complexes with **11**, **13**, and **15**–**17**, the crystal structures of various salts have been elucidated.

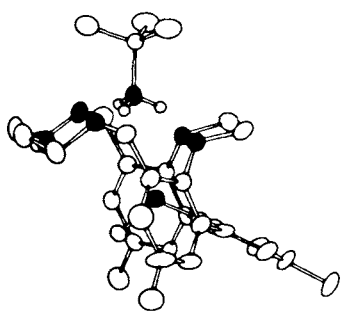
Many of the hosts that bind the alkali-metal cations also complex ammonium, methylammonium, and *tert*-butylammonium ions. Examples of the structures of some of the complexes of hosts **8** and **11**–**18** are listed in Figure 3. Those species for which crystal structures are known are indicated (for binding energies, see Table 1). In all of these crystal structures, the axis of the C–N bond of the guest is essentially perpendicular to the plane defined by the sites that form hydrogen bonds to the NH_3^+ group. The H–N–C–C dihedral angles are all 60°. The O···H–N or N···H–N bonds are nearly linear except for one of the hydrogen bonds in **15**·$(CH_3)_3CNH_3^+$, which is bifurcated.[4] In all of these structures, the $(CH_3)_3CNH_3^+$ guest perches on the electron-donating sites of the host to provide a tripod-type structure, as shown in Figure 4. The structures of the $CH_3NH_3^+$ complexes are probably similar.



11·$(CH_3)_3CNH_3^+$ [19]



13·$(CH_3)_3CNH_3^+$ [4]



15·$(CH_3)_3CNH_3^+$ [4]

Fig. 4. Side views of crystal structures of perching complexes.

3. Structure-Bonding Relationships Involving Alkali-Metal Cations

3.1. Complementarity

Binding free energies of hosts to their most complementary alkali-metal picrates are listed in Figure 1 below the

Table 1. Binding free energies ($-\Delta G^0$ [kcal·mol^{-1}]) of selected complexes as their picrate salts under standard conditions (cf. Fig. 3).

Guest \ Host	**8** [10, 11]	**11** [19, 20]	**12** [17]
NH_4^+	20.2	14.4	12.7
$CH_3NH_3^+$	—	14.4	11.9
$(CH_3)_3CNH_3^+$	—	13.2	11.7
Guest \ Host	**13** [4, 21]	**14** [17]	**15** [4, 22]
NH_4^+	10.5	9.2	9.9
$CH_3NH_3^+$	9.0	8.4	8.2
$(CH_3)_3CNH_3^+$	8.3	8.3	7.7
Guest \ Host	**16** [4, 18]	**17** [4, 18]	**18** [23]
NH_4^+	9.5	8.9	7.0
$CH_3NH_3^+$	7.5	6.9	7.4
$(CH_3)_3CNH_3^+$	6.9	6.4	8.6

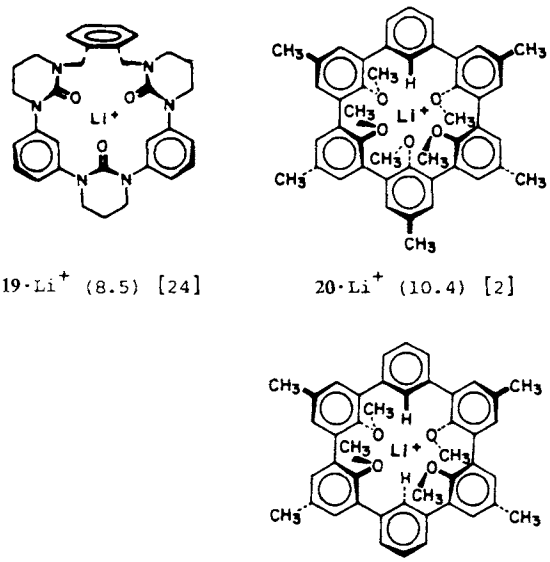


Fig. 5. Complexes of diminished spherands and the binding free energies ($-\Delta G^0$ [kcal·mol^{-1}]) of their picrate salts under standard conditions.

family names of the complexes. Notice that the $-\Delta G^0$ values range from a high of >23 kcal·mol^{-1} for spheraplex **1**·Li^+ to a low of 5.9 kcal·mol^{-1} for podaplex **7**·K^+. The structures of the complexes range from *capsular* (e.g., **1**·Li^+, **3**·Na^+, and **4**·K^+) to *nesting* (e.g., **2**·Li^+, **5**·K^+, and **6**·K^+) to *wrapping* (e.g., **7**·K^+). Values of at least 18 kcal·mol^{-1} of binding free energy have been realized for each of the alkali-metal ions by the appropriate design of the hosts. The $-\Delta G^0$ values provide a quantitative measure of the electronic and steric matching of the complexing partners, which is expressed by the term *complementarity*.

3.2. Number and Character of Binding Sites

The number of heteroatoms ligating the cations in the complexes of Figure 1 range from a high of nine for cryptaspheraplexes **8**·Rb^+ and **8**·Cs^+ to a low of five for spheraplex **2**·Li^+. Diminished spheraplex **19**·Li^+ in Figure 5 has a $-\Delta G^0$ value of 8.5 kcal·mol^{-1} and possesses only three host ligating sites, two less than **2**·Li^+ (Fig. 1), whose $-\Delta G^0$ value is 18.2 kcal·mol^{-1}. Spheraplex **1**·Li^+ with six ligating oxygens has a $-\Delta G^0$ value of >23 kcal·mol^{-1}; in comparison, **20**·Li^+, with five ligating oxygens, has a $-\Delta G^0$ value of 10.4 kcal·mol^{-1} and **21**·Li^+, with four ligating oxygens, a value of <6 kcal·mol^{-1}. These facts illustrate two important features of structure-binding correlation. First, in a series of hosts organized by a particular hydrocarbon framework, binding free energies decrease rapidly with a decrease in the number of ligating sites of the host. Second, the binding free energy is highly dependent on the electronic character of the ligating groups. Thus **19**·Li^+, with a $-\Delta G^0$ value of 8.5 kcal·mol^{-1} and only three binding sites, is much more stable than **21**·Li^+, whose four anisole oxygen binding sites provide a value of <6 kcal·mol^{-1}. The alternate placements of the three cyclic urea and the two anisole units to give five binding sites in the host **2** results in a $-\Delta G^0$ value of 18.2 kcal·mol^{-1} for **2**·Li^+, compared with the value of 10.4 kcal·mol^{-1} provided by the five anisole binding sites of **20**·Li^+. Clearly, the cyclic urea oxygen is a stronger ligating group than the anisole oxygen.[16]

Other interesting combinations of anisole and cyclic urea molecular units are illustrated by the crystal structures and binding free energies of the hemispheraplexes **22**·Na^+·H_2O, **22**·Cs^+·H_2O, **23**·Na^+·H_2O, and **11**·$(CH_3)_3CNH_3^+$. The structures suggested by CPK molecular model building and both face and side views of the crystal structures of these complexes are shown in Figure 6. For all four complexes, the general architectural features anticipated from CPK molecular model building were confirmed by the crystal structures. Notice the up-down-up arrangement of the alternate ligating oxygens as the eye passes clockwise around the face views of the macrocycles. The conformations of the bridging substituted *meta*-xylyl groups at "12 o'clock" are highly similar in the hosts of all four structures (see particularly the side views). As expected, **22**·Na^+·H_2O and **23**·Na^+·H_2O possess *nesting* structures, whereas **22**·Cs^+·H_2O and **11**·$(CH_3)_3CNH_3^+$ have *perching* structures, since the guests are too large to nest in the host.

The three metal-ion complexes in Figure 6 contain a molecule of water that ligates the metal ion from the side of the macroring opposite the methyl groups of the anisole units. The water molecules are held in place partially by hydrogen bonds to the bridging anisole oxygen in **22**·Na^+·H_2O and to the bridging aryl carboxylic carbonyl oxygen at "12 o'clock" in **23**·Na^+·H_2O. Surprisingly, these two oxygens do not directly ligate the nesting guests, although CPK models suggest that these contacts would put little strain on the support system. Other examples of a molecule of water ligating bound alkali-metal ions are found in the cryptaspheraplexes **8**·K^+ and **8**·Cs^+ in Figure 2. Water undoubtedly ligates the metal ions in solutions of $CDCl_3$ saturated with D_2O whenever the host structure in the complex provides an opening. The $-\Delta G^0$

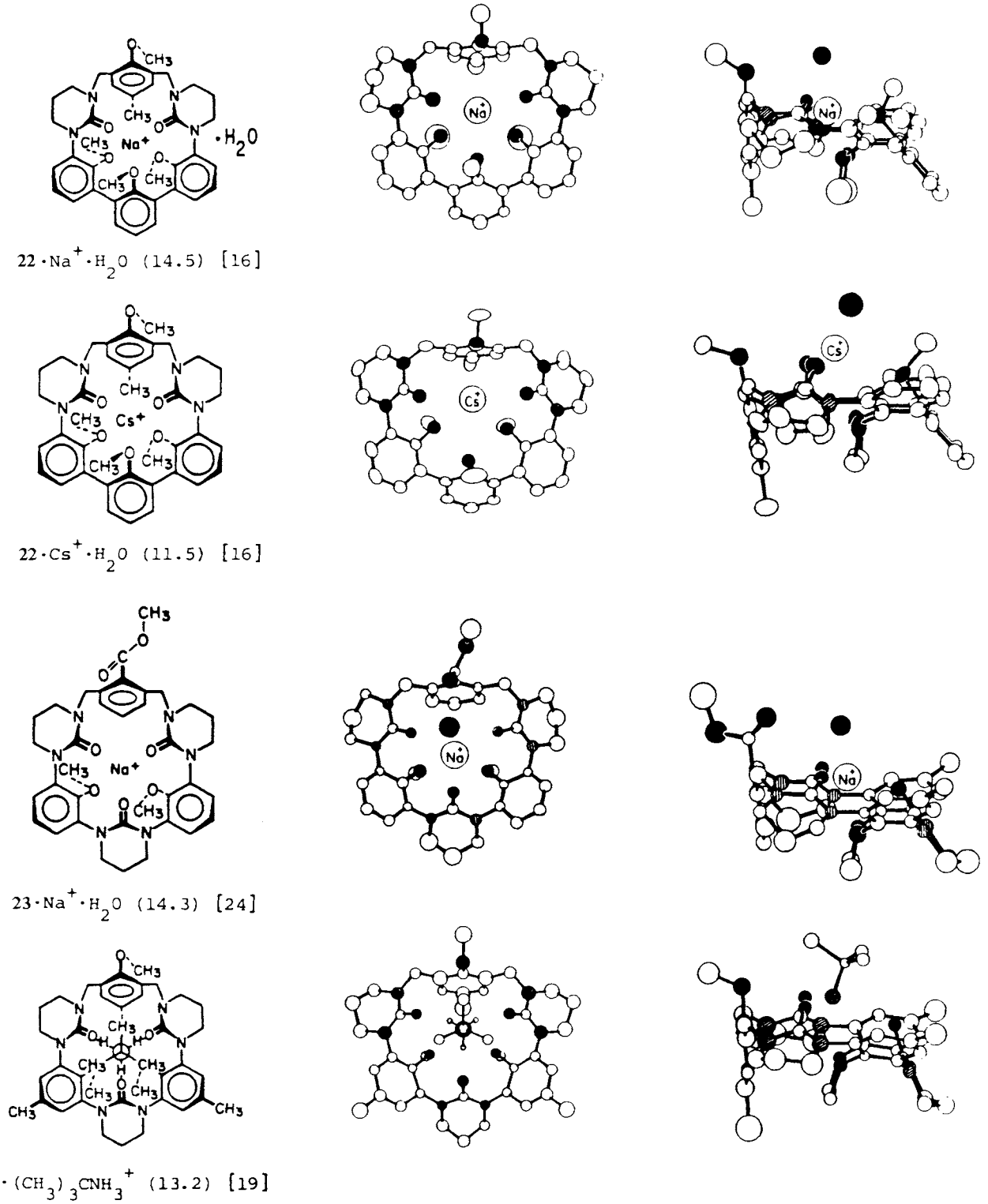


Fig. 6. Structural formulas of selected hemispheraplexes suggested by CPK models, face and side views of their crystal structures, and binding free energies ($-\Delta G^0$ [kcal·mol^{-1}], in parentheses) of their picrate salts under standard conditions.

values of the metal-ion complexes in Figure 6 are in the middle range (11.5 to 14.5 kcal·mol^{-1}), a fact discussed in Section 4.

The counting of the number of ligating sites used by a given host in binding a particular guest must be done cautiously. The problems are illustrated by the following comparisons. Host **8** complexing K^+ provides a $-\Delta G^0$ value of 19.0 kcal·mol^{-1}, and the crystal structure of **8**·K^+ in Figure 2 shows that all nine heteroatoms of the host ligate the K^+. Host **8** complexing Na^+, however, gives a $-\Delta G^0$ value of 13.5 kcal·mol^{-1}. Close scrutiny of the crystal structure of cryptaspheraplex **8**·Na^+ in Figure 2 indicates that although the orbitals of the unshared electron pairs of the heteroatoms are all pointing toward the Na^+ ion, only

five of the nine are actually within contact distance (those on the right of the drawing). The cavity is complementary to Na^+ in the sense that it is spherical, but its diameter is too large to match that of the Na^+ ion.

Somewhat different ligand-counting problems are encountered in spheraplexes **24** · Li^+ and **25** · Li^+, whose crystal structures are shown in Figure 7. Although host **24** contains six oxygens with inward-turned unshared electron pairs, the highly constrained *syn* bridges force the cavity to be somewhat elongated in one dimension so that the two methoxyl oxygens are more distant from each other than the pseudo-*para* pairs of oxygens found in the bridges. Thus, the Li^+ guest (effective diameter of 1.27 Å) is able to contact only five of the six oxygens in **24** · Li^+. A $-\Delta G^0$ value of 16.8 kcal·mol^{-1} results, considerably less than the $-\Delta G^0$ value of >23 kcal·mol^{-1} observed for **1** · Li^+ (Li^+ diameter of 1.48 Å). The $-\Delta G^0$ value for **24** · Na^+ is even lower at 13.3 kcal·mol^{-1}. The misshapen cavity is clearly visible in CPK models of **25**, modified by shaving the diameters of the four bridging oxygens, which violate one another's van der Waals volumes.

Host **25** contains eight oxygens with inward-turned electron pairs to provide a roughly spherical cavity. The crystal structure of **25** · Li^+ indicates that Li^+ (1.71 Å effective diameter) only contacts seven of the eight oxygens, the methoxyl oxygen at "6 o'clock" in the drawing being distant from the lithium ion. The $-\Delta G^0$ value for **25** · Li^+ is only 15.9 kcal·mol^{-1}, somewhat less than that for **24** · Li^+ with only five contacting ligands. As expected, the larger cavity diameter of **25** better matches the diameter of Na^+, so that **25** · Na^+ has a $-\Delta G^0$ value of 18.7 kcal·mol^{-1}, still somewhat less than the 19.2 kcal·mol^{-1} value for **1** · Na^+, whose host has only six available ligands.

We conclude from these results that the nearly perfect octahedral arrangement of the six oxygens in **1** more than compensates for the more rigid but somewhat misshapen oxygen cavity of eight oxygens in **25**. The nearly square-pyramidal arrangement of the five oxygens used by Li^+ in **24** · Li^+ provides slightly better binding than the seven more distant oxygens used in **25** · Li^+. These results further indicate that the effective diameter of Li^+ depends on the number of its ligands.[2, 12]

4. Structure-Binding Relationships Involving Ammonium and Alkylammonium Ions

4.1. Correlations of Binding Free Energies as Criteria of Structure

The structures and binding free energies for a variety of complexes of NH_4^+, $CH_3NH_3^+$, and $(CH_3)_3CNH_3^+$ are found in Figure 3 and Table 1. Of the many crystal structures known,[4] three are shown in Figure 4. Correlations of binding free energy with geometry for complexes of established crystal structure provide a basis for predicting structures of complexes from a combination of CPK molecular model examination and binding free energy measurements. For example, the highest $-\Delta G^0$ value we have measured (25 °C, $CDCl_3$ saturated with D_2O) for the binding of NH_4^+ picrate to a host is 20.2 kcal·mol^{-1} for **8** · NH_4^+ (Fig. 3). Complex **8** · Rb^+ has a $-\Delta G^0$ value of 20.3 kcal·mol^{-1} (Fig. 1), not far from that of **8** · K^+ (19.0 kcal·mol^{-1}) or **8** · Cs^+ (21.7 kcal·mol^{-1}) (Fig. 2). The crystal structures of **8** · K^+ and **8** · Cs^+ are both known to be *cap-*

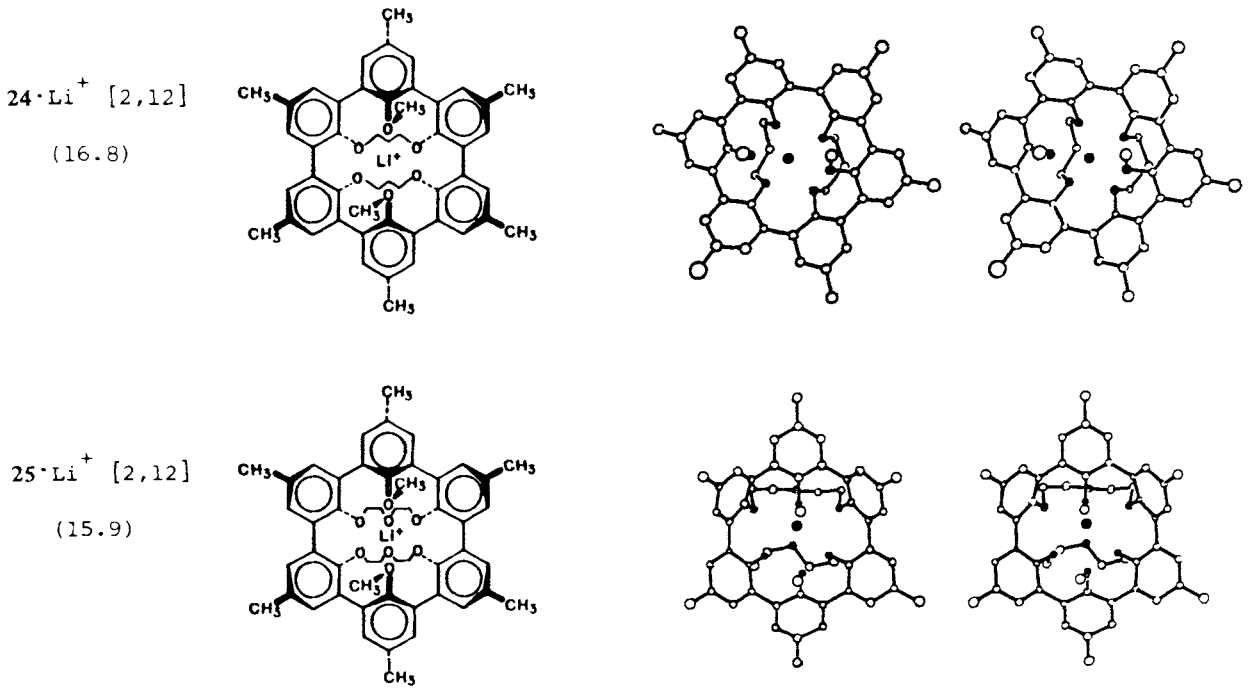


Fig. 7. Structural formulas of augmented spherands, stereodrawings of their crystal structures, and binding free energies ($-\Delta G^0$ [kcal·mol^{-1}], in parentheses) of their picrate salts under standard conditions. The stereodrawing of **24** · Li^+ is rotated by ca. 90° relative to its structural formula. The effective Li^+ diameter is 1.27 Å for **24** · Li^+ and 1.71 Å for **25** · Li^+.

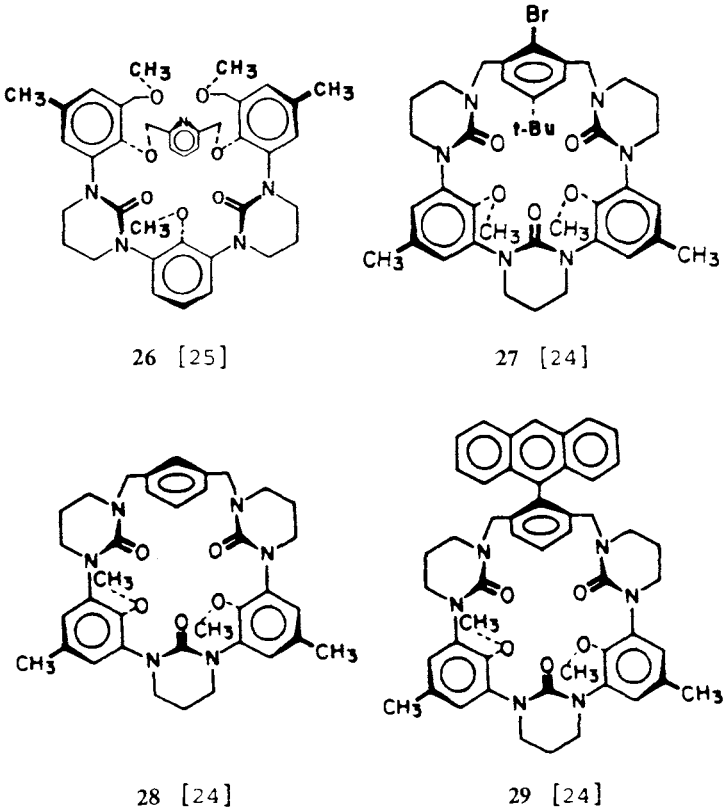
sular (Fig. 2), which strongly suggests **8** · Rb^+ to be capsular as well. The $-\Delta G^0$ values for the binding of NH_4^+ and Rb^+ picrates to a wide variety of hosts are within 1 kcal · mol^{-1} of one another. CPK molecular models indicate the potential cavity of **8** to be complementary to Rb^+ or NH_4^+ ions. We conclude that **8** · NH_4^+ is a capsular complex. Molecular models of **12** · NH_4^+ (Fig. 3) and **12** · Rb^+, with $-\Delta G^0$ values of 12.7 and 12.8 kcal · mol^{-1}, respectively, suggest that both probably have somewhat strained nesting structures. Models of **14** · NH_4^+ and **14** · Rb^+ ($-\Delta G^0$, 9.2 and 9.8 kcal · mol^{-1}, respectively),[17] and of **18** · NH_4^+ (Fig. 3) and **18** · Rb^+ ($-\Delta G^0$, 7.0 and 7.0 kcal · mol^{-1}, respectively) suggest that all four are perching.[23]

The patterns of $-\Delta G^0$ values (Table 1) for the complexes with NH_4^+, $CH_3NH_3^+$, and $(CH_3)_3CNH_3^+$ in Figure 3 suggest that most of them are of the perching-tripod variety, except for some of those discussed in Section 4.2. For hosts **11**–**17**, NH_4^+ is more strongly bound than $CH_3NH_3^+$, and $CH_3NH_3^+$ more strongly than $(CH_3)_3CNH_3^+$, the maximum differences of 2 kcal · mol^{-1} being between NH_4^+ and $CH_3NH_3^+$ complexes of **16** and **17** (Table 1). The low values of 6.9 and 6.4 kcal · mol^{-1} for the binding of $CH_3NH_3^+$ and $(CH_3)_3CNH_3^+$, respectively, to **17** are probably associated with steric encumbrance of the methyl groups of the guest by the methyl group of the host. In the crystal structure of **17** · $(CH_3)_3CNH_3^+$, the upward-thrusting methyl group of the host contacts the methyls of the guest at "7 and 12 o'clock" (see Fig. 3). The best plane of the macroring is folded away from the binaphthyl chiral barrier to accommodate the bulky guest perching on its top face.[4]

4.2. Di- and Tripodal Structures

In principle, guests such as RNH_3^+ can enter into tri-, di-, or monopodal binding with a host. Of these alternatives, tripodal binding provides a highly structured complex, dipodal binding a moderately structured complex, and monopodal binding a species with very little structure. The interesting question arises as to the relative $-\Delta G^0$ values for tripodal and dipodal binding. This question can be addressed in two ways. The first involves a comparison of $-\Delta G^0$ values for the binding of protonated primary amines to the hosts to form complexes having tripodal structures with the values for the binding of a protonated secondary amine, $(CH_2)_5NH_2^+$, to the same hosts to form complexes having dipodal structures (Fig. 8). The second requires a comparison of $-\Delta G^0$ values for NH_4^+, $CH_3NH_3^+$, and $(CH_3)_3CNH_3^+$ guests bound in a tripodal fashion by an unhindered host with the values obtained for a host whose CPK model suggests that, at least for $(CH_3)_3CNH_3^+$, only dipodal binding is sterically feasible. The relevant structures and $-\Delta G^0$ values are found in Figure 8 and Table 2, respectively.

The $-\Delta G^0$ values for **26** · $CH_3NH_3^+$ and **26** · $(CH_2)_5NH_2^+$ are 9.8 and 6.7 and those for **27** · $CH_3NH_3^+$ and **27** · $(CH_2)_5NH_2^+$ are 13.0 and 7.3 kcal · mol^{-1}, respectively. Thus, about a third of the total binding free energy is lost



26 [25] **27** [24]

28 [24] **29** [24]

Fig. 8. Structural formulas of selected hosts (cf. Table 2).

Table 2. Binding free energies ($-\Delta G^0$ [kcal · mol^{-1}]) of selected complexes as their picrate salts under standard conditions (cf. Fig. 8).

Guest \ Host	**26** [25]	**27** [24]	**28** [24]	**29** [24]
NH_4^+	9.5	13.8	13.9	10.3
$CH_3NH_3^+$	9.8	13.0	13.8	9.5
$(CH_3)_3CNH_3^+$	8.6	11.7	12.7	8.1
$(CH_2)_5NH_2^+$	6.7	7.3		

in passing from a tripodal to a dipodal structure. The $-\Delta G^0$ values for **28** · $CH_3NH_3^+$ and **29** · $CH_3NH_3^+$ are 13.8 and 9.5 kcal · mol^{-1}, and for **28** · $(CH_3)_3CNH_3^+$ and **29** · $(CH_3)_3CNH_3^+$ are 12.7 and 8.1 kcal · mol^{-1}, respectively. The results coupled with molecular model examination suggest the two complexes of **28** to be tripodal and those of **29** to be dipodal. The drop in $-\Delta G^0$ value of 3.6 kcal · mol^{-1} in passing from **28** · NH_4^+ to **29** · NH_4^+ is interpreted in terms of steric inhibition of solvation of the fourth and non-tripod-bound hydrogen in the tripodal structure of **29** · NH_4^+.

5. Effects of Preorganization of Hosts on Binding Free Energies and on Complexation-Decomplexation Rates

5.1. Families of Hosts Arranged According to Their Binding Powers

Families of compounds generally fall into the following order when arranged according to the $-\Delta G^0$ values with

which they bind their most complementary guests: spherands > cryptaspherands > cryptands > hemispherands > corands > podands > solvents. The structures and family names of twelve hosts are given in Figure 9. The $-\Delta G^0$ values are listed in Table 3. Spherand **1** shows peak binding with Li^+ ($-\Delta G^0 > 23$ kcal·mol^{-1}). Cryptaspherands show maximum $-\Delta G^0$ values for **10**·Na^+ (20.6), **3**·Na^+ (21.0), and **8**·Cs^+ (21.7 kcal·mol^{-1}). Cryptands provide maximal $-\Delta G^0$ values for **30**·Li^+ (16.6, probably the highest), **31**·Na^+ (17.7), and **4**·K^+ (18.0 kcal·mol^{-1}). Hemispherand binding power is strongest for **32**·Na^+ (12.2), **33**·Na^+ (13.5), and **34**·K^+ (11.6 kcal·mol^{-1}). Corand **6** peaks with **6**·K^+ (11.4 kcal·mol^{-1}). Podand **35** binds too poorly for its $-\Delta G^0$ values to be measured (< 6 kcal·mol^{-1} for all five ions), but it clearly binds better than *p*-methylanisole. In these particular hosts, the numbers of potential binding sites vary from a low of six for **1**, **30**, **32**, **33**, and **35** to a high of nine for **8**. Although the numbers of binding sites and their characters certainly influence the $-\Delta G^0$ values, as discussed in Section 3.2, a different factor appears to be overriding in providing the family order of binding power.

Table 3. Binding free energies ($-\Delta G^0$ [kcal·mol^{-1}]) of selected complexes as their picrate salts under standard conditions (cf. Fig. 9).

Guest \ Host	**1** [2]	**10** [10, 11]	**3** [10, 11]	**8** [10, 11]
Li^+	> 23	18.8	13.4	9.9
Na^+	19.2	20.6	21.0	13.5
K^+	≪ 6	15.0	> 19.9	19.0
Rb^+	—	13.3	20.4	20.3
Cs^+	—	10.4	16.4	21.7

Guest \ Host	**30** [11]	**31** [11]	**4** [11]	**32** [17]
Li^+	16.6	10.0	—	7.0
Na^+	—	17.7	14.4	12.2
K^+	—	15.3	18.0	11.9
Rb^+	—	12.7	16.8	10.4
Cs^+	—	—	10.3	9.0

Guest \ Host	**33** [26]	**34** [26]	**6** [18]	**35** [27]
Li^+	7.2	6.5	6.3	< 6
Na^+	13.5	7.1	8.4	< 6
K^+	10.7	11.6	11.4	< 6
Rb^+	8.4	11.4	9.9	< 6
Cs^+	7.1	10.8	8.5	< 6

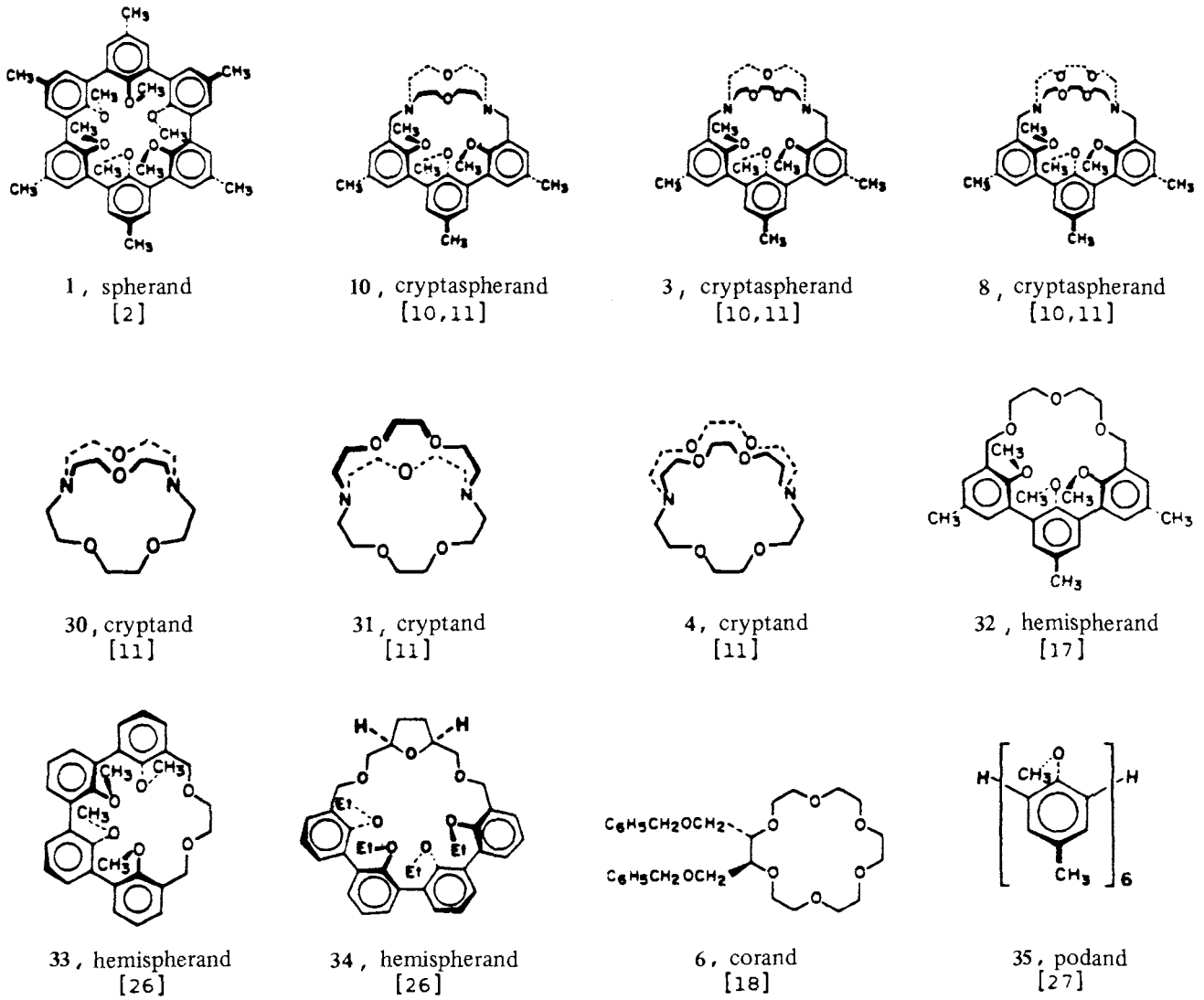


Fig. 9. Host structures and family names of alkali-metal picrate salt complexes (cf. Table 2).

5.2. Preorganization as a Central Determinant of Binding Power

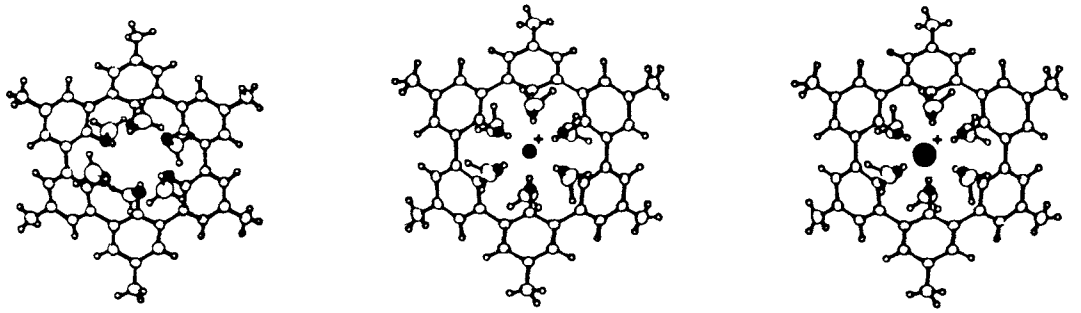
Crystal structures of **1**, **1**·Li^+, and **1**·Na^+ are shown in Figure 10. These three structures all resemble snowflakes and *possess the same conformation*. They differ mainly in the sense that **1** contains an empty cavity, which is filled in **1**·Li^+ and **1**·Na^+. Notice that the six oxygens of **1** are octahedrally arranged with the orbitals of their unshared electron pairs lining a roughly spherical hole whose diameter (1.62 Å) is between the diameters of Li^+ in **1**·Li^+ (1.48 Å) and of Na^+ in **1**·Na^+ (1.75 Å). The six oxygens are attached to six *equatorially* arranged *para*-tolyl groups and six *axially* arranged methyl groups. Thus, the oxygens are well buried within a hydrocarbon shell. The orbitals containing the unshared electron pairs of the oxygens are in a microenvironment whose dielectric properties are between those of a vacuum and those of a hydrocarbon. No solvent can approach the six oxygens, which remain unsolvated.[12]

Podand **35** differs constitutionally from spherand **1** only in the sense that **35** contains two hydrogen atoms in place of one aryl–aryl bond in macrocycle **1**.[27] The two hosts differ radically in their conformational structures. Spherand **1** possesses a single conformation ideally arranged for binding Li^+ and Na^+. Podand **35** can in principle exist in over 1000 conformations, only two of which bind Li^+ octahedrally. The free energy cost of organizing spherand **1** into a single conformation and of desolvating its six oxygens was paid for during its synthesis. Thus **1** is *preorganized* for binding. The free energy for conformationally organizing **35** into a binding conformation and desolvating its six oxygens must come from its complexation free energy. Thus **35** is not preorganized for binding, but is randomized to maximize the entropy of mixing of its conformers and to maximize the attractions between solvent and its molecular parts.[12]

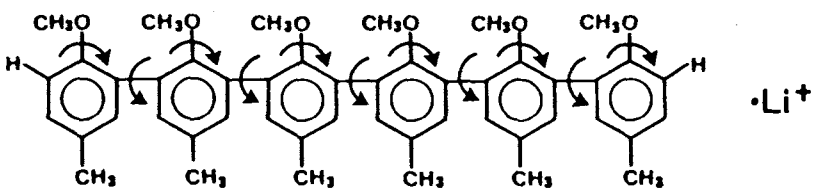
The difference in $-\Delta G^0$ values for the binding of Li^+ to spherand **1** and podand **35** is > 17 kcal·mol^{-1}. The difference in association constant values (K_a) is $> 10^{12}$ M^{-1}. The difference in $-\Delta G^0$ values for the binding of Na^+ to **1** and **35** is > 13 kcal·mol^{-1} (i.e., $K_a > 10^{10}$ M^{-1}). These differences are dramatically larger than any we have encountered associated with other effects on binding power toward alkali-metal ion guests. We conclude that *preorganization is a central determinant of binding power*. The principle of preorganization states that "the more highly hosts and guests are organized for binding and low solvation *prior* to their complexation, the more stable will be their complexes." Both enthalpic and entropic components are involved in preorganization, since solvation contains both components. Furthermore, binding conformations are sometimes enthalpically very rich. For example, the binding oxygens of bridged spherands **24** and **25** (Fig. 7) severely violate each other's van der Waals volumes, and the systems are very highly strained.[2, 12]

The structuring of host–guest complexes depends on cooperativity between many contacting sites which, because of their organization, are able to compete with solvent. As measured by its ability to form hydrogen bonds, the anisole group is an intrinsically poor ligand.[28] Thus it is hardly surprising that podand **35** is such a poor binding system.

In Figure 11, representations of crystal structures of a prototypical corand, a cryptand, and a spherand are compared. Notice that corand **36** and cryptand **4** fill their own



1 **1**·Li^+ (>23) **1**·Na^+ (19.2)



35·Li^+ (<6)

Fig. 10. Snowflake-like crystal structures of **1**, **1**·Li^+, and **1**·Na^+, and binding free energies ($-\Delta G^0$ [kcal·mol^{-1}], in parentheses) of their picrate salts for **1**·Li^+, **1**·Na^+, and **35**·Li^+ under standard conditions.

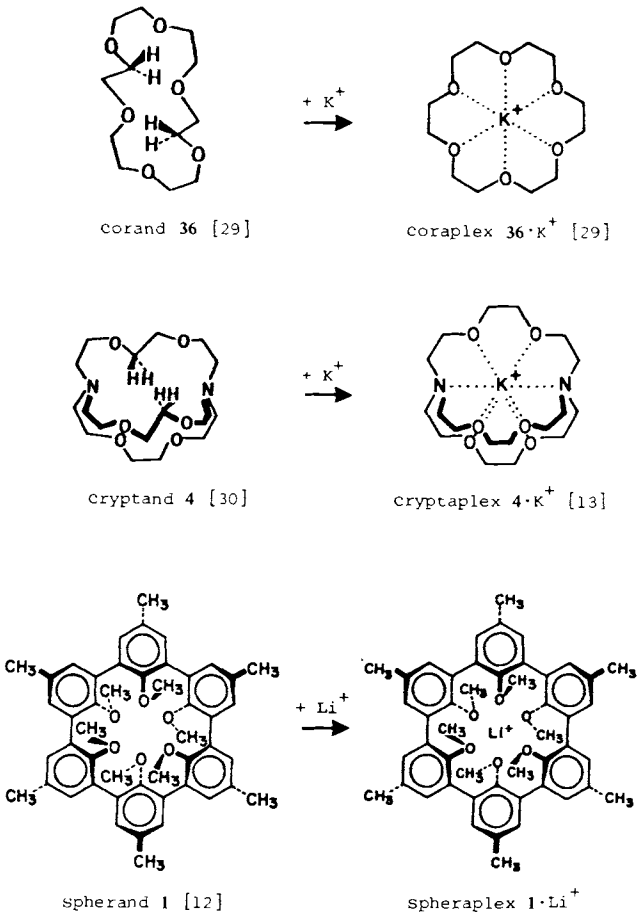


Fig. 11. Crystal structure comparisons of hosts and their complexes showing the relative states of preorganization of corands, cryptands, and spherands.

cavities with inward-turned methylene groups, which must be driven outward by the guest during complexation. In solution, the cavities are undoubtedly similarly unformed, either being filled with their own methylenes or with parts of solvent molecules, both of which must be displaced by a guest during complexation, and at some free energy cost. In contrast, spherand **1**, both in the crystalline state and in solution, is fully preorganized and its binding sites are nonsolvated. Crystal structures of cryptaspherands[10] and hemispherands[4] show that methylenes similarly fill their own potential cavities, but that their anisole parts are fully organized for complexation.[31]

When the families of hosts are arranged in decreasing order of their degrees of preorganization for binding, it is the same order observed when they are arranged in decreasing order of their $-\Delta G^0$ values. Thus spherands are completely preorganized. Cryptaspherands are largely preorganized by the anisoles and the conformational-solvation constraints of the bicyclic, cryptand part of the hosts. The bicyclic structure of the cryptands severely limits the number of their conformations and partially inhibits solvation of their binding sites. The anisole units of the hemispherands are self-organizing, whereas the corand portions are much more flexible, and their binding sites invite solvation. The corands are still more flexible in a conformational sense, and more of their binding sites are exposed to solvation than those of the hemispherands. Finally, the podands enjoy only the preorganization associated with the collection and potential spacing of their binding sites.

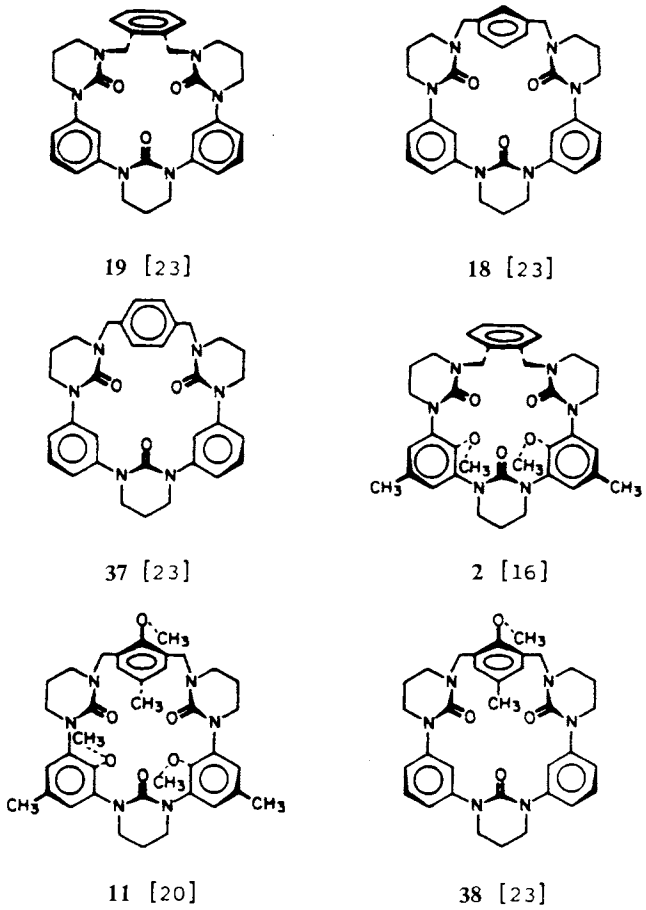


Fig. 12. Structures of selected hosts (cf. Table 4).

Table 4. Binding free energies ($-\Delta G^0$ [kcal·mol^{-1}]) of selected complexes as their picrate salts under standard conditions (cf. Fig. 12).

Guest \ Host	**19** [23]	**18** [23]	**37** [23]	**2** [16]	**11** [20]	**38** [23]
NH_4^+	7.0	7.0	8.0	11.8	14.4	8.4
$CH_3NH_3^+$	7.1	7.4	8.5	12.1	14.4	9.0
$(CH_3)_3CNH_3^+$	7.3	8.6	9.1	13.2	13.2	9.5

The power of preorganization is also evident in the binding of ammonium and alkylammonium guests by hosts. Comparisons of the structures and $-\Delta G^0$ values in Figure 12 and Table 4, respectively, indicate that hosts with anisole units separating their cyclic urea units are much stronger binders than the corresponding systems without the anisole units. For example, spherand **2** binds NH_4^+, $CH_3NH_3^+$, and $(CH_3)_3CNH_3^+$ with $-\Delta G^0$ values 5-6 kcal·mol^{-1} higher than those for **19**. Likewise, **11** binds the three ions with $-\Delta G^0$ values about 6 kcal·mol^{-1} higher than those for **18**. Even the one methoxyl and one methyl group attached to the bridging *meta*-xylyl unit in **38** enhance its binding by about 1 kcal·mol^{-1} over that of **18** without these substituents. All of the complexes in Figure

12 are probably held together by three NH···O=C hydrogen bonds as in the crystal structure of **11** · $(CH_3)_3CNH_3^+$ (Fig. 3). Thus the non-hydrogen-bonded oxygens account for about 40% of the free energy of binding for these hosts. We interpret this as being mainly due to the preorganizing effects that the space-occupying methoxyls exert on the cyclic ureas. The methoxyls not only organize the cyclic urea units for binding RNH_3^+ in a conformational sense, but they also partially shield them from solvation.

Comparisons of the $-\Delta G^0$ values for **19**, **18**, and **37**, on the one hand, and **2** and **11**, on the other, indicate that the larger the macrorings in this series, the stronger the binding. Model examination indicates that the NH_3^+ groups perch on orbitals deeper in the cavities of the larger macrorings, where microdielectric effects tend to stabilize charge. Interestingly, for **19**, **18**, and **37** (no anisole groups) the $-\Delta G^0$ values increase as the guest is changed from NH_4^+ to $CH_3NH_3^+$ to $(CH_3)_3CNH_3^+$. Molecular model examination of these complexes suggests that with $CH_3NH_3^+$ and $(CH_3)_3CNH_3^+$, the methyls contact the bridging xylene unit. These methyl protons are weakly acidic, and possibly form weak hydrogen bonds to the π systems of the bridging aryl group. The electrons of the bridging *para*-xylyl group of **37** · NH_4^+ can contact the fourth hydrogen of the NH_4^+ group in models, but those of the bridging units cannot without creating considerable strain in **19** · NH_4^+ and **18** · NH_4^+. This may account for the 1 kcal · mol^{-1} higher $-\Delta G^0$ value for **37** · NH_4^+ compared with **18** · NH_4^+ or **19** · NH_4^+.[16]

5.3. Preorganization and Rates of Complexation-Decomplexation

Equation (1) defines and relates the rate constants for complexation-decomplexation to the association constants (K_a) for complexation. The preorganized spherands **1**, **24**, and **25** (Fig. 13) complexed Li^+ and Na^+ picrates, at 25 °C in $CDCl_3$ saturated with D_2O, with rate constants (k_1 [M^{-1} s^{-1}]) that varied from $\approx 10^5$ for **1** · Li^+ to $\approx 10^6$ for **24** · Na^+ (Table 5). The decomplexation rate constants (k_{-1} [s^{-1}]) varied from $< 10^{-12}$ for **1** · Li^+ to $\approx 10^{-4}$ for **24** · Na^+. A plot of $\log K_a$ [M^{-1}] against $\log k_{-1}$ [s^{-1}] was

$$\text{Host} + M^+Pic^- \underset{k_{-1}}{\overset{k_1}{\rightleftharpoons}} \text{Host} \cdot M^+ \cdot Pic^- \qquad K_a = \frac{k_1}{k_{-1}} \tag{1}$$

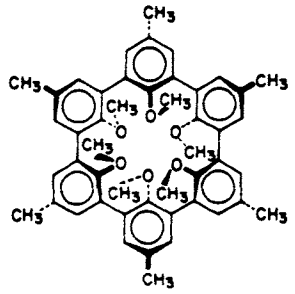
essentially linear for the six combinations of host and guest.[2] *Cox* et al. previously observed a linear correlation between $\log K_a$ and $\log k_{-1}$ for the binding of a variety of ions in several solvents to cryptands **31** and **4** (Fig. 9).[32] As with the spherands, the cryptands showed no correlation between k_1 and K_a. For the two cryptands **30** and **31** (Fig. 9), which are most complementary to Li^+ and Na^+, the k_1 values varied between 10^4 and 10^7 M^{-1} s^{-1} in a variety of solvents, most values lying in the same range as those mentioned above for the spherands.[32] The crystal structures of the spheraplexes and cryptaplexes show them to be capsular (Figs. 7, 10, and 11).

Values for k_1 and k_{-1} for the binding of K^+Pic^- to the hemispherands **39**–**41** under standard conditions are also given in Table 5. The k_1 values range from 10^7 to 10^9 M^{-1} s^{-1}, comparable to the range observed for the binding of K^+ to the least preorganized cryptand **4** (Fig. 9) in a variety of solvents at 25 °C. The k_{-1} values [s^{-1}] for release of K^+ from the three hemispherands varied only by a factor of 7, from 26 for **40** to 4 for **41**.[26] For binding of the relatively "soft" K^+ ion (compared with Na^+ and Li^+) to these partially preorganized and solvated hosts, the complexation rate constants play a larger role in determining K_a and $-\Delta G^0$ values than do the dissociation rate constants, in contrast to the results for spherands and cryptands. The hemispheraplexes of hosts **39**–**41** are undoubtedly nesting (CPK molecular model examination).

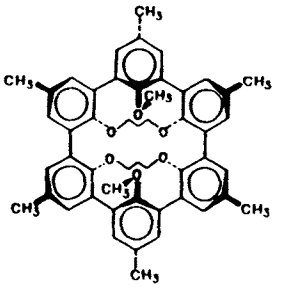
For the three hemispherands **11**, **38**, and **42**, the values of k_1 and k_{-1} for complexing and decomplexing of $(CH_3)_3CNH_3^+Pic^-$ are also listed in Table 5.[33] All three hosts undergo complexation with k_1 values [M^{-1} s^{-1}] of 10^{11} to 10^{12}, which indicates the reactions to be essentially diffusion controlled. Their decomplexation rate constants (k_1) vary from $\approx 10^3$ to $\approx 10^4$ s^{-1}. The hemispheraplexes of these hosts with $(CH_3)_3CNH_3^+$ have a perching structure (see crystal structure of **11** · $(CH_3)_3CNH_3^+$ in Fig. 4).

The three types of complexes referred to in Figure 13, when arranged in *decreasing* order of rate constant values for *either their formation or dissociation*, provide the same sequence: perching (**11**, **38**, **42**) > nesting (**39**–**41**) > capsular (**1**, **24**, **25**). These orders conform to expectations based on structure. The solvation shells of the cationic guests are least disturbed in forming a perching complex, more disturbed in forming a nesting complex, and the most disturbed in forming a capsular complex. Model examination of the transition states for Li^+ or Na^+ entering or leaving the preformed cavity of **1** indicates there is space available for only one ligand of the medium (H_2O or Pic^-) to contact the cation. Either cation is surrounded by a hydrocarbon sleeve of three methyl groups, capped at one end by the single ligand and at the other by the bulb of the preformed cavity. Thus it is hardly surprising that the rates of complexation and decomplexation for the spheraplexes are orders of magnitude slower than those for the hemispheraplexes. In the envisioned transition states for these complexation-decomplexation processes, both hosts and guests liberate or fix solvent at one binding site at a time, exchanging host-guest attractions for host-solvent and guest-solvent attractions, or the reverse. The transition states envisioned for complexation-decomplexation of the cryptaspheraplexes and the cryptaplexes are in between those for the spheraplexes and hemispheraplexes in their degrees of simultaneous stabilization by medium and by host-guest interactions. Those for the coraplexes and even more for the podaplexes should integrate stabilization by solvation with host-guest stabilization. Thus, *the more highly preorganized the host for complexation, the lower should be the rates for complexation and decomplexation.*

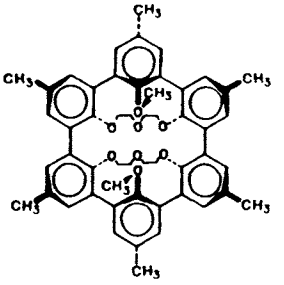
All of the complexation rates in homogeneous solutions are instantaneous on the human and ^{1}H-NMR time scales. The decomplexation rates of the hemispheraplexes and coraplexes are fast on the human and slow on the ^{1}H-NMR time scales. The decomplexation rates of the spheraplexes



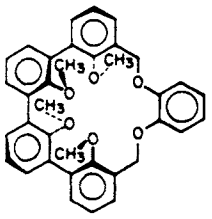
1 [2]



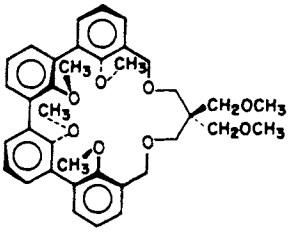
24 [2]



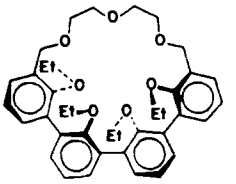
25 [2]



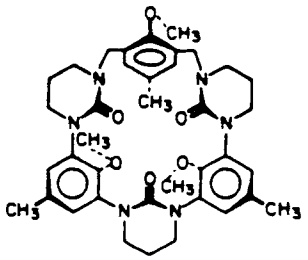
39 [26]



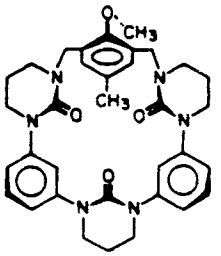
40 [26]



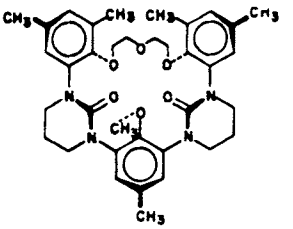
41 [26]



11 [33]



38 [33]



42 [33]

Fig. 13. Structures of selected hosts (cf. Table 5).

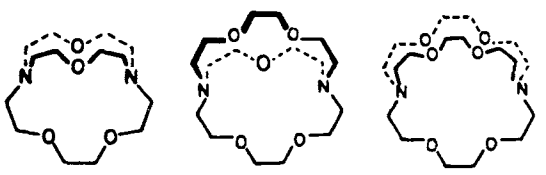
Table 5. Rate constants for the complexation (k_1) and decomplexation (k_{-1}) of selected picrate salts (Pic = picrate) under standard conditions (cf. Fig. 13).

		1 [2]	**24** [2]	**25** [2]
For LiPic:	k_1 [$M^{-1} \cdot s^{-1}$]	8×10^4	4×10^5	3×10^5
	k_{-1} [s^{-1}]	$< 10^{-12}$	2×10^{-7}	7×10^{-7}
For NaPic:	k_1 [$M^{-1} \cdot s^{-1}$]	4×10^5	1×10^6	9×10^4
	k_{-1} [s^{-1}]	3×10^{-9}	2×10^{-4}	2×10^{-9}
		39 [26]	**40** [26]	**41** [26]
For KPic:	k_1 [$M^{-1} s^{-1}$]	2×10^9	4×10^7	2×10^8
	k_{-1} [s^{-1}]	14	26	4
		11 [33]	**38** [33]	**42** [33]
For $(CH_3)_3CNH_3Pic$:	k_1 [$M^{-1} s^{-1}$]	3×10^{12}	4×10^{11}	3×10^{10}
	k_{-1} [s^{-1}]	7×10^2	4×10^4	2×10^3

and more stable cryptaspheraplexes are very slow on the human time scale at 25 °C.[11,12]

5.4. Preorganization and Solvation

The effects of changes in solvent on the $-\Delta G^0$ value for complexation have been the most thoroughly studied by *Cox* et al. with cryptand hosts and alkali-metal ion guests.[34] The solvents used were water, methanol, ethanol, acetonitrile, propylene carbonate, *N*-methylpropionamide, dimethylformamide, and dimethyl sulfoxide. The cryptaplexes are the most stable in the aprotic, least polar solvents, and are the least stable in aqueous and dipolar solvents. Examples of some of the highest values for $-\Delta G^0$ (kcal·mol^{-1}) are listed in Table 6 (see Fig. 14). A plot of the eight data points for $-\Delta G^0$ values in $CDCl_3$ saturated with D_2O against those in 95% CH_3OH–5% H_2O is roughly linear.[111] The $-\Delta G^0$ values in CH_3OH–H_2O are 5.2 ± 0.4 kcal·mol^{-1} lower than those in $CDCl_3$–D_2O. When the solvents are arranged in decreasing order of the observed $-\Delta G^0$ values, the sequence is $CDCl_3$–$D_2O \sim$ propylene-carbonate $\gg$ methanol $\sim$ methanol-water $>$ dimethyl sulfoxide $>$ water. The differences between $-\Delta G^0$ values in $CDCl_3$–D_2O and those in H_2O range from 6.4 to 11 kcal·mol^{-1}.[34] These large solvent effects on $-\Delta G^0$ indicate that solvent-host and solvent-guest attractions compete with host-guest interactions. Unfortunately, the $-\Delta G^0$ values for the binding of the alkali-metal ions to the spherands in solvents other than $CDCl_3$ saturated with water are not yet available. Since the binding sites of the spherands cannot be solvated for steric reasons, we expect solvent effects to be somewhat less important for this class of hosts than for the others.



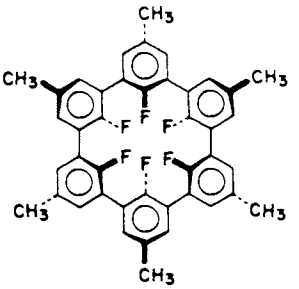
30 31 4

Fig. 14. Structures of selected cryptands (cf. Table 6).

Table 6. Binding free energies ($-\Delta G^0$ [kcal·mol^{-1}]) (cf. Fig. 14) for the binding of alkali-metal ions as their picrate salts by selected cryptands at 25 °C in the solvents given. Those in $CDCl_3$–D_2O are for $CDCl_3$ saturated with D_2O [11]; those in CH_3OH–H_2O are for 5% H_2O in CH_3OH [35]; those in the other media are taken from [34].

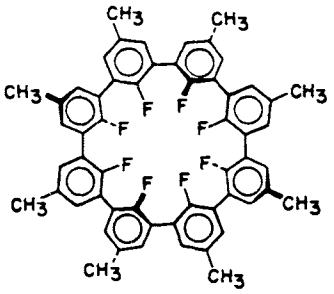
Complex \ Solvent	$CDCl_3$–D_2O	CH_3OH–H_2O	H_2O	CH_3OH	$(CH_3)_2SO$	PC [a]
30·Li^+	16.6	10.3	7.5	10.9	8.0	17.0
31·Li^+	10.0	5.7	3.4	7.3	3.8	13.1
31·Na^+	17.7	12.1	7.4	11.7	9.5	16.4
31·K^+	15.3	10.2	5.4	11.6	8.1	13.5
4·Na^+	14.4	9.8	5.4	10.9	7.3	14.4
4·K^+	18.0	13.3	7.5	14.2	9.7	15.3
4·Rb^+	16.8	11.5	5.8	12.2	8.0	12.3
4·Cs^+	10.3	4.8	2.0	6.0	1.9	5.7

[a] PC = propylene carbonate (1,3-dioxan-2-one).



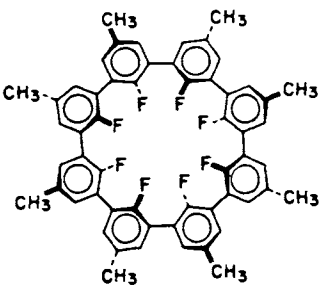
43 [36]

D_{3d} symmetry



44a [36]

D_{2d} symmetry



44b [36]

D_{4d} symmetry

Fig. 15. Fluorine analogues of spherands **1** and **9**.

5.5. Highly Preorganized Nonbinding Systems

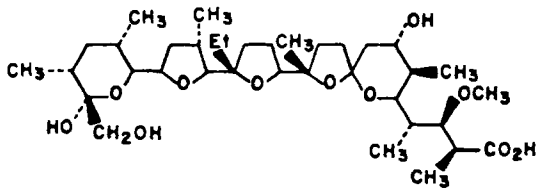
Spherand **1** is the strongest binder of Li^+ known, although its binding site is composed of the relatively weakly ligating anisole oxygens. The powerful binding of the ligand system is associated with its nearly perfect preorganization for binding. The question arises whether, by preorganization, the normally nonligating fluorobenzene might be made to ligate if six or eight of them are preorganized into a macroring analogously to **1** or **9** as in Figure 15. Accordingly, cavitands **43** and **44** were synthesized. Cavitand **43** is highly complementary in a geometric sense to Li^+, as is **44** to Cs^+. The crystal structure of **43** indicated it possessed the expected $\bar{3}$ (approximately D_{3d}) symmetry, with the fluorine atoms in an octahedral arrangement. The molecule has a roughly cylindrical cavity with a diameter of about 1.5 Å and a depth of ≈3.6 Å. However, the compound failed to complex Li^+.

The ^{1}H-NMR spectrum of **44** at −15 °C indicated the compound to have D_{2d} symmetry, consistent with structure **44a**, rather than **44b**, which possesses D_{4d} symmetry. At 97 °C, **44a** and **44b** are in equilibrium, giving rise to an average signal. The compound turned out to be a nonbinder of Cs^+. Thus, the intrinsic ability of the fluorines of aryl fluorides to ligate the alkali-metal ions appears to be too low to be brought on scale by preorganization.

The volume of the cavity of **44a** was estimated to be about 60% of that of **44b**. We postulate that minimizing the volume of such systems provides some of the driving force for the dominance of **44a** at low temperature.

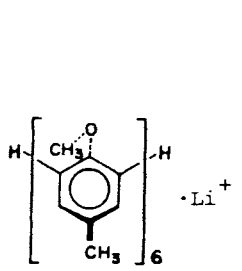
5.6. Partially Preorganized Podands

In a family of naturally occurring ionophores, rigid cyclic ether units are strung together in a chain terminated by hydrogen-bonding groups. When complexing, these chains wrap around the metal cations, their ends being held together by the hydrogen-bonded terminal functions. Monensin **45** is perhaps the most useful of these ionophores.

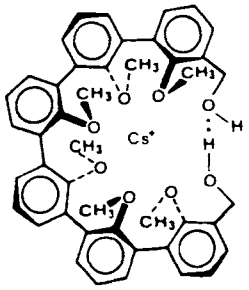


45

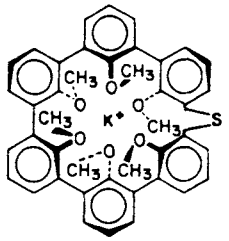
The question arises whether podands whose terminal groups can form hydrogen bonds to one another might preorganize themselves to form pseudomacrocycles having substantial binding potential. Although this possibility has not been systematically studied, the results of the few studies made thus far invite further investigation. In Figure 16 the structures of several podaplexes are shown, along with that of a hemispheraplex. The complex drawn in each case involves the alkali-metal ion that provides the maximum $-\Delta G^0$ value, which is listed in parentheses beneath each formula. A crystal structure of reference host **47** showed that the methyls of the two methoxyl groups flanking the sulfur are turned inward, effectively filling the cavity and reducing its preorganization for binding.



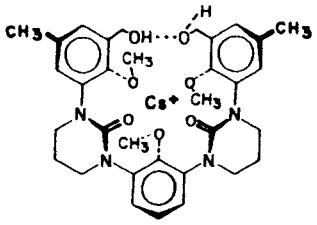
35·Li$^+$ (<6) [27]



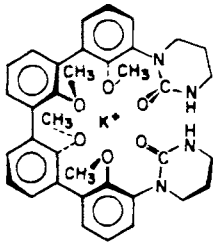
46·Cs$^+$ (9.1) [27]



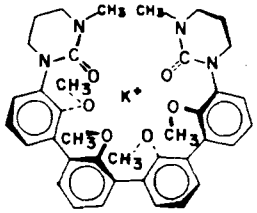
47·K$^+$ (10.1) [27]



48·Cs$^+$ (6.5) [25]



49·K$^+$ (8.3) [26]



50·K$^+$ (7.4) [26]

Fig. 16. The structures of podaplexes as pseudomacrocycles partially organized by hydrogen bonds between their terminal groups, along with the structures of model compounds. Their $-\Delta G^0$ values [kcal mol^{-1}] under standard conditions are listed in parentheses.

Podand **35** lacks terminal hydroxyl groups, and its $-\Delta G^0$ values for the alkali-metal ions were <6 kcal·mol^{-1} (Table 3). Podand **46** contains the same chain of six anisole groups but terminates in two CH_2OH groups. Molecular models indicate that these terminal groups can form hydrogen bonds to one another provided the methoxyl group possesses the alternate up-down conformational arrangement of **46**. Podand **46** binds Na^+, K^+, Rb^+, Cs^+, and NH_4^+ with $-\Delta G^0$ values that range from 6.2 to 9.1 kcal·mol^{-1}, the latter value being that of **46**·Cs^+. Model hemispherand **47** provides values for these same ions ranging from 7.3 to 10.1 kcal·mol^{-1}, the highest being that for **47**·K^+. We conclude that the CH_2OH groups terminating podand **46** substantially enhance the binding power of the system.[27] A less pronounced example of the same effect is observed with **48**, containing both anisole and cyclic urea units, whose $-\Delta G^0$ values for binding K^+, Rb^+, Cs^+, and NH_4^+ range from 5.8 to 6.5 kcal·mol^{-1}.[25]

Podand **49** is composed of four anisole units strung together and terminated at both ends with cyclic urea units each containing –CONH– moieties. The $-\Delta G^0$ values for the binding of the five alkali-metal ions and NH_4^+ to **49** range from 6.8 to 8.3 kcal·mol^{-1}. When the two NH groups are methylated as in **50**, these values drop to a range of 5.5–7.4 kcal·mol^{-1}. For both **49** and **50**, peak binding is reached with K^+. Thus, the hydrogen bonding possible with **49** but not with **50** is worth about 1 kcal·mol^{-1} in binding free energy.[26]

These meager results suggest that podands like their macrocyclic and bimacrocyclic counterparts are subject to design and are capable of providing substantial binding free energies. Central to such design is the limitation of the number of rotational degrees of freedom that must be frozen out during complexation. In other words, the principle of preorganization applies as well to podands as to other hosts.

6. Effect of Preorganization of Host on Specificity in Complexation

6.1. Specificity of Hosts in Binding Alkali-Metal Ions

This section is concerned with the connection between preorganization of hosts, their binding powers, and their selectivities (Fig. 17). The constants for distributing the five alkali-metal-ion picrate salts at 25 °C between D_2O and $CDCl_3$ differ from one another by factors of less than two for alkali-metal ions neighboring one another in the periodic table. The largest factor involving any of the five ions is only 3.8.[22] Thus, $K_a^A/K_a^{A'}$ ratios (K_a^A and $K_a^{A'}$ are association constants in $CDCl_3$ saturated with D_2O for complex formation involving alkali-metal ions A and A') provide a rough measure of ion selectivity in extraction, as well as in homogeneous media. The largest $K_a^A/K_a^{A'}$ values we have obtained for complexes at 25 °C in $CDCl_3$ saturated with water for neighboring alkali-metal ions are listed in Table 7. Interestingly, none of the hosts listed in Table 7 are either corands or podands.

Recall that when classes of hosts are arranged according to their states of preorganization for complexation, the sequence is spherands > cryptaspherands > cryptands > hemispherands > corands > podands. This same order is less rigidly followed when maximum ion selectivity is applied to the host classes, the sequence generally followed being spherands > cryptaspherands ~ cryptands > hemispherands > corands > podands. Thus the principle of preorganization is useful in designing both for selectivity and maximum binding power.

6.2. Effects of Small Structural Changes on Host Specificity

The question arises whether hosts can be designed which are strongly binding, but are indiscriminate in complexing a variety of guest cations. Hemispherand **11** exhibits $-\Delta G^0$ values in binding eight cations that range only from a low of 12.1 (for Li^+) to a high of 15.6 kcal·mol^{-1} (for K^+) (Fig. 18, Table 8). Furthermore, **11** binds $(CH_3)_3CNH_3^+$ ($-\Delta G^0 = 13.2$) almost as well as NH_4^+ ($-\Delta G^0 = 14.4$ kcal·mol^{-1}). Molecular model examination

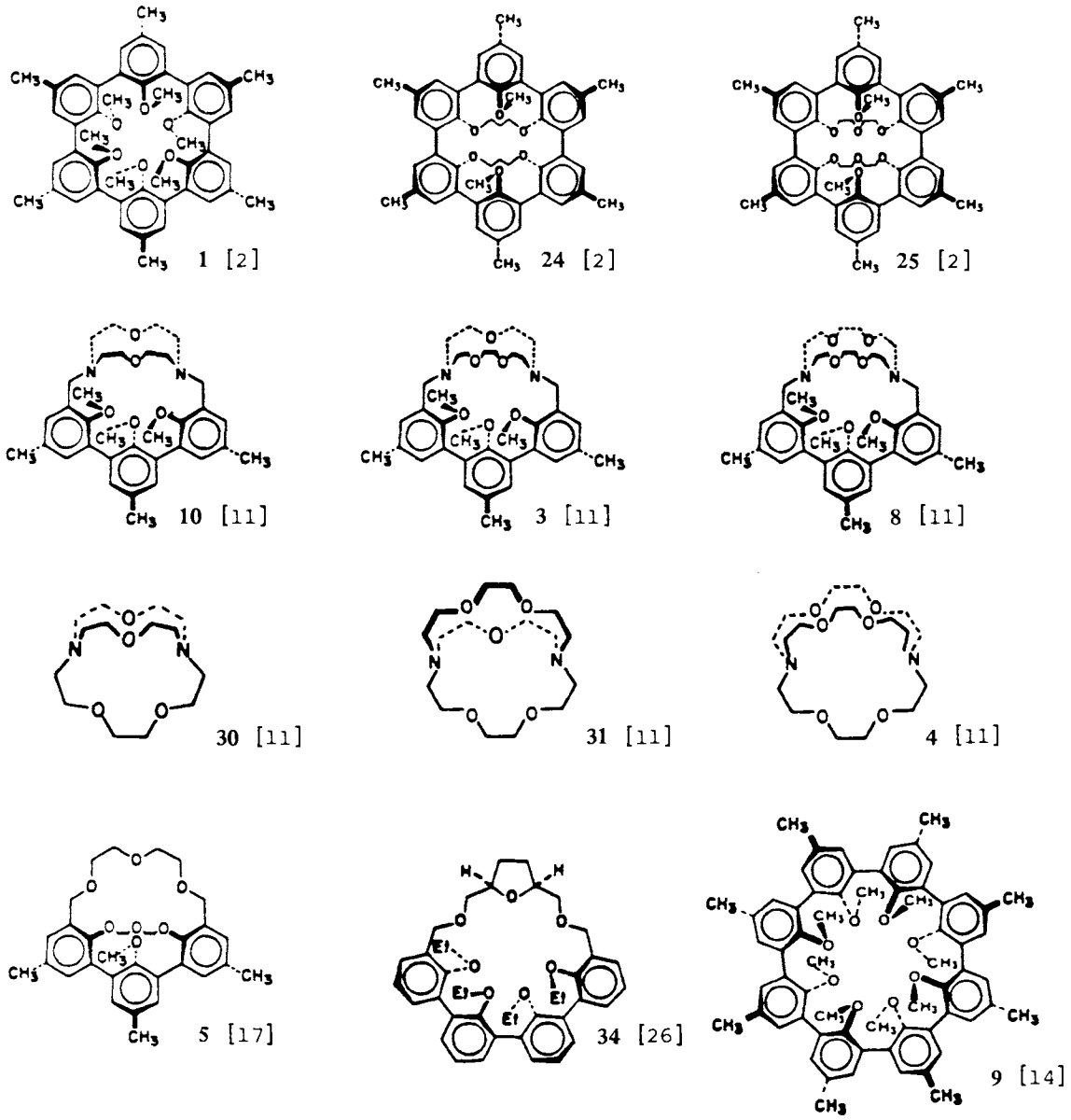


Fig. 17. Structures of selected hosts (cf. Table 7).

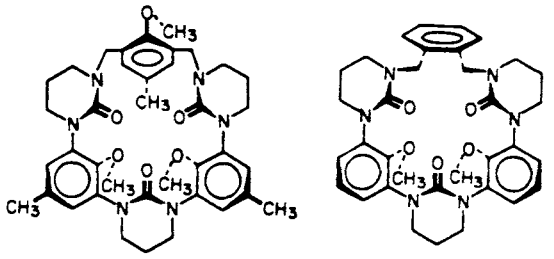
Table 7. Selectivity ($K_a^{\wedge}/K_a^{\wedge'}$) of selected hosts for pairs of alkali-metal picrates under standard conditions (cf. Fig. 17).

Host	**1**[2]		**24** [2]		**25** [2]	
Pair	Li^+/Na^+	Na^+/K^+	Li^+/Na^+	Na^+/K^+	Na^+/Li^+	Na^+/K^+
$K_a^{\wedge}/K_a^{\wedge'}$	>600	$>10^{10}$	360	$>10^5$	125	$>10^9$
Host	**10** [11]		**3** [11]		**8** [11]	
Pair	Na^+/K^+	Rb^+/Cs^+	Na^+/Li^+	Rb^+/Cs^+	Na^+/Li^+	K^+/Na^+
$K_a^{\wedge}/K_a^{\wedge'}$	13000	134	420000	900	440	11000
Host	**30** [11]		**31** [11]		**4** [11]	
Pair	Li^+/Na^+	Na^+/K^+	Na^+/Li^+	K^+/Rb^+	K^+/Na^+	Rb^+/Cs^+
$K_a^{\wedge}/K_a^{\wedge'}$	4800 [a]	260000 [a]	440000	81	440	58000
Host	**5** [17]		**34** [26]		**9** [14]	
Pair	Na^+/Li^+	K^+/Rb^+	K^+/Na^+	Rb^+/Cs^+	Rb^+/K^+	Cs^+/Rb^+
$K_a^{\wedge}/K_a^{\wedge'}$	9500	34	2000	5	14	370

[a] In propylene carbonate as solvent, which gives similar values to those in $CDCl_3$ [34].

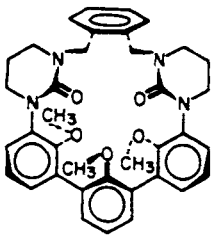
of **11** indicates the macroring is large enough (20-membered) to provide a high degree of conformational flexibility with respect to oxygen placement and cavity diameter. As the diameter of the guest decreases, the diameter of the cavity becomes complementary by the anisole and cyclic urea units decreasing their dihedral angles with respect to one another, which shrinks the distance between their attached oxygens.

Hosts **2** and **51** exhibit much higher structural recognition in their complexation. The $-\Delta G^0$ values of **2** range from 18.3 (for Li^+) to 11.4 kcal·mol^{-1} (for Rb^+). Those of **51** are 16.6 (for Li^+) and 7.8 kcal·mol^{-1} (for $(CH_3)_3CNH_3^+$). Macrocycles **2** and **51** are 19-membered, and must accommodate the structural requirements of the rigid *ortho*-xylyl unit. Both show high structural recognition favoring the smaller ions. Thus the K_a ratio for **2** · Li^+ vs. **2** · Na^+ is 290 and for **2** · Na^+ vs. **2** · K^+ it is 725. The K_a ratio for **51** · Na^+ vs. **51** · K^+ is 2300. Molecular models



11 [16]

2 [16]



51 [16]

Fig. 18. Structures of selected hosts (cf. Table 8).

Table 8. Binding free energies ($-\Delta G^0$ [kcal·mol^{-1}]) for similar hosts of varying states of preorganization under standard conditions. The cations were present as picrates (cf. Fig. 18).

Guest \ Host	11	2	51
Li^+	12.1	18.3	16.6
Na^+	15.4	16.3	15.4
K^+	15.6	12.4	10.8
Rb^+	14.2	11.4	9.4
Cs^+	13.1	11.8	10.5
NH_4^+	14.4	11.8	10.4
$CH_3NH_3^+$	14.4	12.1	9.7
$(CH_3)_3CNH_3^+$	13.2	13.2	7.8

of **2** and **51** are rigidly preorganized for binding with a much lower degree of conformational flexibility with regard to oxygen placement than host **11**. The average binding powers of **11** and **2** are about the same. In contrast to the five oxygens of **2**, host **11** has a sixth oxygen available for either direct ligation of the guest or for hydrogen bonding a water that ligates the guest. Thus **2** makes up in preorganization what it lacks in number of ligands, and in so doing gains in specificity.[16]

7. Summary and Outlook

This article summarizes and rationalizes the structure-complexation free-energy relationships involving oxygens or amine nitrogens ligating alkali-metal, ammonium, or alkylammonium ions. The host structures are rich in alkoxyaryl, cyclic urea, pyridyl, *ortho*- and *meta*-phenylene, *ortho*- and *meta*-xylene, dimethylene, and trimethylene units. The design of hosts and their complexes was accomplished through CPK molecular model examination, and many of their structures were confirmed through crystal structure, NMR spectra, and correlations between structure and free energies of complexation.

The hosts and their complexes were designed and their free energies of complexation were measured to test the principles of complementarity and preorganization. The structure-binding relationships that were obtained are interpreted in terms of these two principles. Application of these principles to host design has led to high structural recognition factors for most of the alkali-metal ions adjacent to one another in the periodic table. These factors range from a high of $>10^{10}$ for Na^+/K^+ to a low of 15 for K^+/Rb^+. The free energies of binding the alkali-metal ions vary from >23 to <6 kcal·mol^{-1}, depending on the degree of preorganization of the host.

The importance of Li^+, Na^+, and K^+ to biological processes, the susceptibility of Rb^+ and Cs^+ to neutron activation, and the possible use of $^6Li^+$ as a fusion fuel combine to generate increasing interest in hosts that differentially bind these ions. High selectivity factors for Li^+, Na^+, and K^+ are particularly important to analytical methods for measuring concentrations of these ions in serum and urine. The wide distribution of NaCl in the environment and its ability to harm circuit boards of computers and increase corrosion rates makes sensitive and simple methods for its detection important.

The opportunities for fruitful research in the host-guest complexation field are boundless. Preorganized hosts that complex specifically all of the ions of the periodic table remain to be synthesized and tested. The use in hosts of highly preorganized assemblies of cyano, isocyano, amido, oxo, ester, carboxy, nitro, sulfide, sulfoxide, sulfone, sulfimide, sulfodiimide, pyridine oxide, phosphane oxide, and heterocyclic groups invites systematic investigation. Uranium and gold remain to be extracted by practical methods from sea water. The actinoides and lanthanoides, as well as certain isotopes, even might be separated by complexation.

The complexation of organic guests further excites the imagination. Racemic amino acids and their ester salts have already been resolved into their enantiomers by extraction involving complex formation with chiral hosts.[37,38] A variety of other organic guests, e.g., carbohydrates and fats, remain to be complexed. Particularly challenging are the possibilities of designing and preparing hosts that catalyze organic reactions through complexation and preorganization.[39,40]

We warmly acknowledge the skill and scholarship of my co-workers who helped to develop this field. Support for the research on systems dominated by the binding of alkali-metal ions by anisole groups was generously provided by the Division of Basic Sciences of the Department of Energy, and on the cyclic urea systems by the National Science Foundation and the United States Public Health Service. We heartily thank Drs. K. N. Trueblood, C. B. Knobler, E. Maverick, and I. Goldberg for the many crystal structure determinations, and Mrs. June Hendrix for the artwork.

Received: June 19, 1986 [A 598 IE]
German version: *Angew. Chem. 98* (1986) 1041

[1] E. P. Kyba, R. C. Helgeson, K. Madan, G. W. Gokel, T. L. Tarnowski, S. S. Moore, D. J. Cram, *J. Am. Chem. Soc. 99* (1977) 2564.
[2] D. J. Cram, G. M. Lein, *J. Am. Chem. Soc. 107* (1985) 3657.

[3] W. L. Koltun, *Biopolymers 3* (1965) 665.
[4] D. J. Cram, K. N. Trueblood, *Top. Curr. Chem. 98* (1981) 43. Crystal structures reported after this paper are found in many of the literature references.
[5] For example, P. Kollman, G. Wipff, U. C. Singh, *J. Am. Chem. Soc. 107* (1985) 2212.
[6] E. Weber, F. Vögtle, *Top. Curr. Chem. 98* (1981) 3, suggested the term "coronands" as a family name for crown-shaped monocyclic polyethers. We have used the term "chorands," but now suggest adoption of a shortening of the Weber-Vögtle term "coronand" to the word "corand."
[7] C. J. Pedersen, *J. Am. Chem. Soc. 89* (1967) 2495, 7017.
[8] B. Dietrich, J. M. Lehn, J. P. Sauvage, *Tetrahedron Lett. 1969*, 2885.
[9] D. J. Cram, T. Kaneda, R. C. Helgeson, G. M. Lein, *J. Am. Chem. Soc. 101* (1979) 6752.
[10] D. J. Cram, S. P. Ho, C. B. Knobler, E. Maverick, K. N. Trueblood, *J. Am. Chem. Soc. 108* (1986) 2989.
[11] D. J. Cram, S. P. Ho, *J. Am. Chem. Soc. 108* (1986) 2998.
[12] D. J. Cram, T. Kaneda, R. C. Helgeson, S. B. Brown, C. B. Knobler, E. Maverick, K. N. Trueblood, *J. Am. Chem. Soc. 107* (1985) 3645.
[13] B. Metz, D. Moras, R. Weiss, *Acta Crystallogr. Sect. B 29* (1973) 1377.
[14] D. J. Cram, R. A. Carmack, K. N. Trueblood, C. B. Knobler, E. Maverick, unpublished results.
[15] J. M. Lehn, *Struct. Bonding (Berlin) 16* (1973) 1.
[16] D. J. Cram, I. B. Dicker, M. Lauer, C. B. Knobler, K. N. Trueblood, *J. Am. Chem. Soc. 106* (1984) 7150.
[17] G. M. Lein, D. J. Cram, *J. Am. Chem. Soc. 107* (1985) 448.
[18] R. C. Helgeson, G. R. Weisman, J. L. Toner, T. L. Tarnowski, Y. Chao, J. M. Mayer, D. J. Cram, *J. Am. Chem. Soc. 101* (1979) 4928.
[19] D. J. Cram, I. B. Dicker, C. B. Knobler, K. N. Trueblood, *J. Am. Chem. Soc. 104* (1982) 6828.
[20] D. J. Cram, H. E. Katz, I. B. Dicker, *J. Am. Chem. Soc. 106* (1984) 4987.
[21] M. Newcomb, J. M. Timko, D. M. Walba, D. J. Cram, *J. Am. Chem. Soc. 99* (1977) 6392.
[22] K. E. Koenig, G. M. Lein, P. Stückler, T. Kaneda, D. J. Cram, *J. Am. Chem. Soc. 101* (1979) 3553.
[23] R. J. M. Nolte, D. J. Cram, *J. Am. Chem. Soc. 106* (1984) 1416.
[24] K. D. Stewart, M. Miesch, C. B. Knobler, E. Maverick, D. J. Cram, in press.
[25] H. E. Katz, D. J. Cram, *J. Am. Chem. Soc. 106* (1984) 4977.
[26] S. P. Artz, D. J. Cram, *J. Am. Chem. Soc. 106* (1984) 2160.
[27] D. J. Cram, M. deGrandpre, C. B. Knobler, K. N. Trueblood, *J. Am. Chem. Soc. 106* (1984) 3286.
[28] a) J. Mitsky, L. Jaris, R. W. Taft, *J. Am. Chem. Soc. 94* (1972) 3442; b) H. W. Atkins, W. R. Gilkerson, *ibid. 95* (1973) 8551.
[29] J. D. Dunitz, M. Dobler, P. Seiler, R. P. Rhizackerly, *Acta Crystallogr. Sect. B 30* (1974) 2733 and following papers to p. 2750.
[30] R. Weiss, B. Metz, D. Moras, *Proc. Int. Conf. Coord. Chem. 13th 2* (1970) 85.
[31] Further examples are found with the crystal structures of **39** of Fig. 13 (D. J. Cram, C. B. Knobler, unpublished work), and **47** of Fig. *16* [27]. In the crystal structure of **47**, only the four inner anisole units—which are not bridged by sulfides—are preorganized for binding cations.
[32] B. G. Cox, J. Garcia-Rosas, H. Schneider, *J. Am. Chem. Soc. 103* (1981) 1054.
[33] T. Anthonsen, D. J. Cram, *J. Chem. Soc. Chem. Commun. 1983*, 1414.
[34] B. G. Cox, J. Garcia-Rosas, H. Schneider, *J. Am. Chem. Soc. 103* (1981) 1384.
[35] J.-M. Lehn, J. P. Sauvage, *J. Am. Chem. Soc. 97* (1975) 6700.
[36] D. J. Cram, S. B. Brown, T. Taguchi, M. Feigel, E. Maverick, K. N. Trueblood, *J. Am. Chem. Soc. 106* (1984) 695.
[37] S. S. Peacock, D. M. Walba, F. C. A. Gaeta, R. C. Helgeson, D. J. Cram, *J. Am. Chem. Soc. 102* (1980) 2043.
[38] D. S. Lingenfelter, R. C. Helgeson, D. J. Cram, *J. Am. Chem. Soc. 46* (1981) 393.
[39] D. J. Cram, *Science 217* (1982) 1177.
[40] D. J. Cram, P. Y.-S. Lam, S. P. Ho, *J. Am. Chem. Soc. 107* (1985) 839.

Biochemistry of Oxidative Stress

By Helmut Sies

As a normal attribute of aerobic life, structural damage to organic compounds of a wide variety (DNA, proteins, carbohydrates and lipids) may occur as a consequence of oxidative reactions. Oxidative damage inflicted by reactive oxygen species has been called "oxidative stress". Biological systems contain powerful enzymatic and nonenzymatic antioxidant systems, and oxidative stress denotes a shift in the prooxidant/antioxidant balance in favor of the former. Diverse biological processes such as inflammation, carcinogenesis, ageing, radiation damage and photobiological effects appear to involve reactive oxygen species. This field of research provides new perspectives in biochemical pharmacology, toxicology, radiation biochemistry as well as pathophysiology.

1. Introduction

This review article is concerned with oxidative damage in biological systems. First of all, the nature of the damage to organic compounds will be discussed. It will then be shown that, despite being variable in terms of the different kinds of compound afflicted, oxidative damage is ultimately exerted only by a small number of different reactive oxygen species. Finally, some new aspects of defense and repair in biological systems will be presented, i.e. antioxidants *sensu stricto* as well as in a more general sense.

One-electron reduction of oxygen was widely studied early this century (see *Warburg*[1] and *Battelli* and *Stern*[2]). *Michaelis*[3] pointed out that one-electron steps of oxygen reduction, leading to intermediate radical formation, may be of general importance in biological chemistry. These radical forms of oxygen are $O_2^{\ominus\cdot}$ and $O^{\ominus\cdot}$ and their protonated forms, $HO_2^{\cdot}$ and $HO^{\cdot}$. The perhydroxyl radical $HO_2^{\cdot}$ and the hydroxyl radical $HO^{\cdot}$ were recognized by *Haber* and *Weiss*[4] in their study on the iron salt-catalyzed decomposition of H_2O_2 as being important in chemical, photochemical and electrochemical processes. Biological research on the superoxide anion radical $O_2^{\ominus\cdot}$ received exceptional stimulus after the discovery of superoxide dismutase by *McCord* and *Fridovich*.[5]

Other reactive species of oxygen are of a nonradical nature. Hydrogen peroxide (H_2O_2) as the two-electron reduction state became important in the development of enzymology after the discovery of catalase Compound I by *Chance*.[6] Further, the electronically excited states of oxygen such as singlet molecular oxygen or excited carbonyls are also worthy of note. *Kautsky*[7] realized quite early on the potentially important role of a "metastable active oxygen species" (singlet oxygen), while *Schenck*[8a] and Gollnick[8b] made important fundamental contributions to the photochemistry of photooxygenation reactions. *Foote*[9] identified the role of singlet oxygen in photooxygenation.

In recent years, much interest has been focused on the biochemistry of oxygen activation and on the biological significance of the reactive oxygen species.[10–14] More recent developments can be found in Refs. [15–20].

[*] Prof. Dr. H. Sies
Institut für Physiologische Chemie I der Universität
Moorenstrasse 5, D-4000 Düsseldorf (FRG)

2. Oxidative Damage to Nucleic Acids

2.1. Causes and Effects

Oxidative damage to DNA can be initiated by ionizing radiation or photooxidation (UV light; visible light in the presence of photosensitizers), hydroperoxides, oxygen radicals or various other oxidizing agents. The nature of the damage is often complex. For example, a variety of radicals can be formed upon γ-irradiation of DNA, but only the radical **1** with a free electron on C-4 leads to strand breaks under anoxic conditions[21] (Fig. 1). In the presence of oxygen, the radical-mediated strand scission is more complex and proceeds via peroxy radicals of the bases and sugars. Base alteration has been studied most intensively with thymine and guanine. Thymine glycol **2** (Fig. 2) or 5-(hydroxymethyl)uracil are formed from thymine (cf. [23]). The base most readily lost upon γ-irradiation or photooxidation is guanine; some proposed reaction products are shown in Figure 3. Adenine and cytosine, on the other hand, appear to be more stable towards oxidation. Thymine dimers (Fig. 4) are also formed, and the chemical adducts upon reaction with epoxides, for example, usually involve guanine as shown for the adduct with aflatoxin epoxide (Fig. 5).

Strand scission by ionizing radiation is thought to be due to the hydroxyl radical (see [21, 22]). Likewise, the strand scission observed with superoxide is due to the hydroxyl radical formed from it.[26] However, in addition to this low-molecular weight molecule, other reactive species might be of interest; for example, the hydroperoxide of linoleic acid, 13-hydroperoxylinoleic acid, was found to cause the breakage of double-stranded DNA.[27] The breakage site was specific for guanine. The ultimate chemical agent interacting with the DNA, however, was not identified. Possibly a hydroxyl radical is generated from the hydroperoxide via homolytic scission, as has recently been found in the case of hydrogen peroxide.[28]

The damage to DNA (and possibly also to nucleoproteins) by ionizing radiation and by free radical oxidation also leads to chromosome damage. This is manifested by chromosome breaks and can be assayed by chromosome and chromatid aberrations. Chromosome breaks are particularly prevalent in diseases such as Bloom's syndrome,[29]

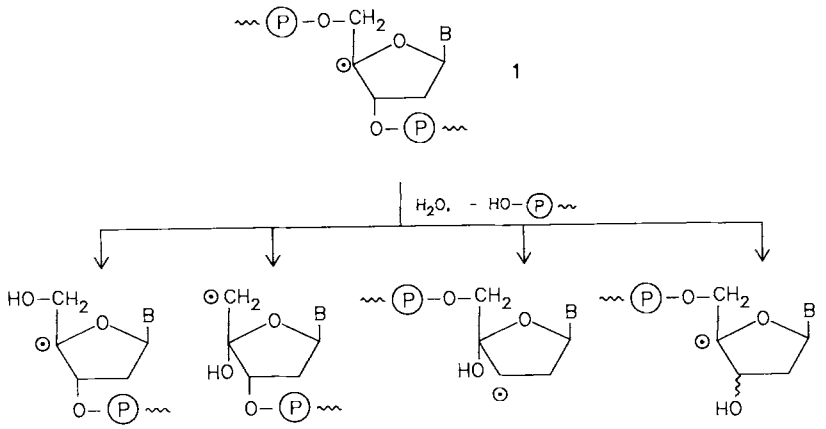


Fig. 1. Hydrolysis of the C-4'-radical **1** in DNA to yield strand breaks (anaerobic). The situation is more complex under aerobic conditions (modified after [21]).

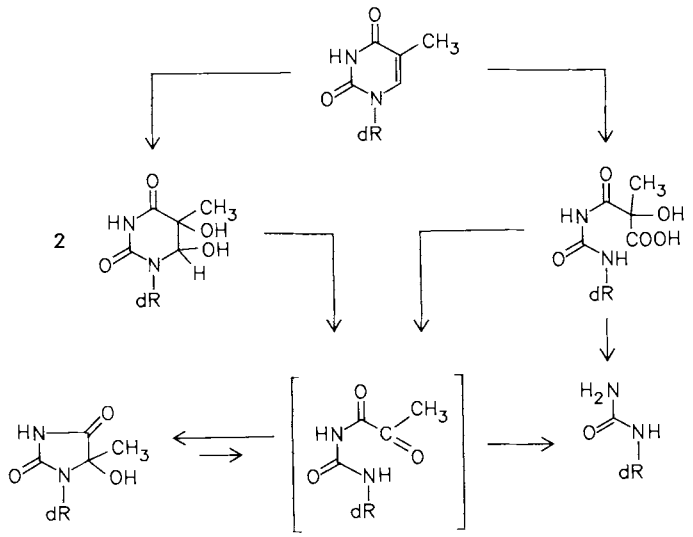


Fig. 2. Oxidative degradation of thymine residues in DNA. In addition to thymine glycol **2**, 5-hydroxymethyl uracil may also be formed (after [24]).

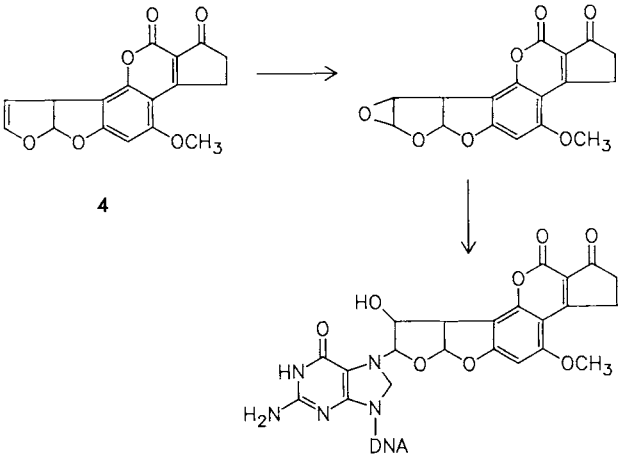


Fig. 5. Formation of the N-7 guanyl adduct of aflatoxin B_1 **4** from the 2,3-epoxide.

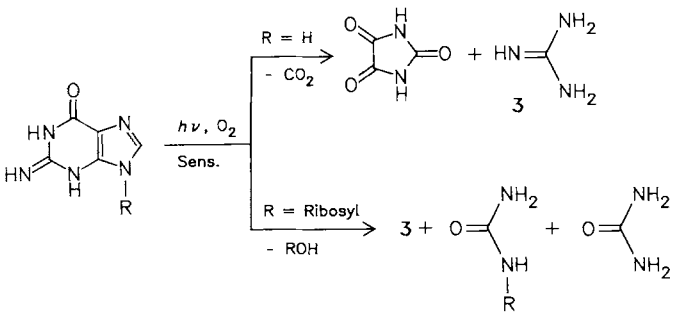


Fig. 3. Scheme for the oxidative degradation of guanine by photooxygenation. Sens. = sensitizer (after [25]).

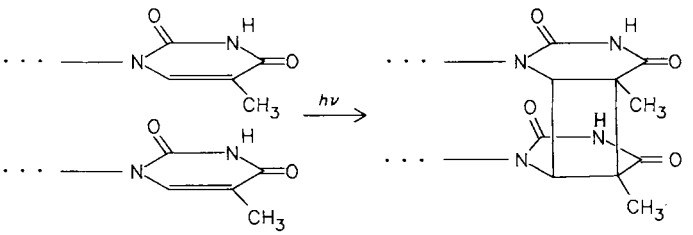


Fig. 4. Adjacent thymine residues in DNA can join upon irradiation to form a cyclobutylthymine dimer (sugar and phosphate residues omitted).

lupus erythematosus[30] or Fanconi's anemia.[31] Superoxide dismutase has an anticlastogenic (anti-chromosome-break) effect.[32] It is assumed that double-strand breaks of DNA are the initial lesion leading to chromosome breaks. The exact mechanism of chromosome breakage is not yet known.

2.2. Repair

Oxidized bases and strand breaks can be repaired enzymatically. It should be noted that oxidative damage is just one way of altering DNA; further routes of damage include errors in replication by recombination to produce mismatches, or by other ways of chemical alteration such as deamination. It has been estimated that the DNA of a mammalian cell probably loses 5000–10000 purine and 200–500 pyrimidine residues per 20 h generation time.[34] Nucleases involved in DNA repair have been shown to operate in several ways:[35,36] examples include nucleotide excision repair, base excision repair, recombinational repair, mismatch repair and error-prone repair. A given thymine glycol residue in DNA (cf. **2** in Fig. 2) may either be released as thymine glycol by a specific glycosylase, or it

may be released as thymidine glycol by an excision exonuclease (Fig. 6). These bases can be traced in the urine and have potential value for the screening of oxidative damage in man.[37] A similar pair of metabolites are 5-(hydroxymethyl)uracil and 5-(hydroxymethyl)-2′-deoxyuridine; a 5-hydroxymethyluracil glycosylase has recently been described.[38]

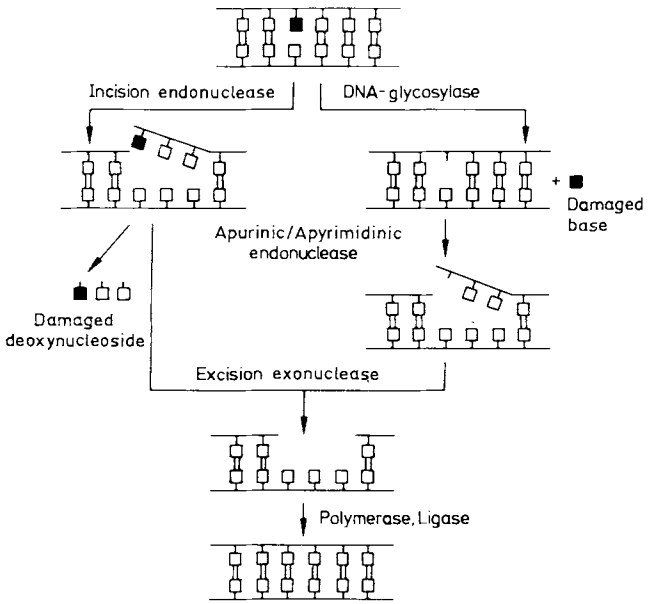


Fig. 6. Two pathways of excision repair. The left sequence is known as nucleotide excision repair, whereas the right sequence is base excision-repair (modified after [35]).

The intrastrand thymidine dimers that form as the predominant lesion in UV-irradiated DNA (Fig. 4) cannot only be repaired by the dimer-specific endonuclease, followed by DNA polymerase,[39] but also by a light-dependent repair reaction. This photoreactivation is catalyzed by a flavoenzyme.[40]

3. Oxidative Damage to Amino Acids and Proteins

The oxidation of amino acid side-chains in proteins has recently been recognized as being a potentially important signal in biological systems. The reversible oxidation-reduction of thiol groups is intimately linked to oxidative stress in a number of respects (see Sections 3.1, 3.4, and 3.5). Other types of oxidation of reactive groups are also reversible; for example, the oxidation of methionine to methionine sulfoxide and its enzymatic reduction back to methionine.[41] However, irreversible oxidative damage to amino acids may also occur; for instance, the ring cleavage in histidine or in tryptophan (see Fig. 7).

3.1. Methionine

Methionine can be oxidized by $HO^{\odot}$, $^1O_2$ or H_2O_2 to the sulfoxide and then further to the sulfone. This reaction sequence has now been established as an interesting metabolic signal.[42] Table 1 contains a list of enzymes in which a specific methionine residue has been shown to be oxidized. Oxidation to the sulfoxide can be associated with loss of function. A particularly striking example is that of α_1-antitrypsin. Oxidation of methionine-358 at the active site results in a dramatic decrease in inhibitory activity toward elastase.[43] This loss of control of elastase is thought to be responsible for the development of pulmonary emphysema.[44] Indeed, the development of emphysema can be limited by the intravenous injection of α_1-antitrypsin.[45] It is of interest to note that recently the problem of oxidative inactivation has been circumvented by producing an α_1-antitrypsin with valine at position 358 instead of methionine. This was achieved by site-directed mutagenesis and recombinant DNA techniques,[46] thus providing further evidence that critically targeted methionine oxidation

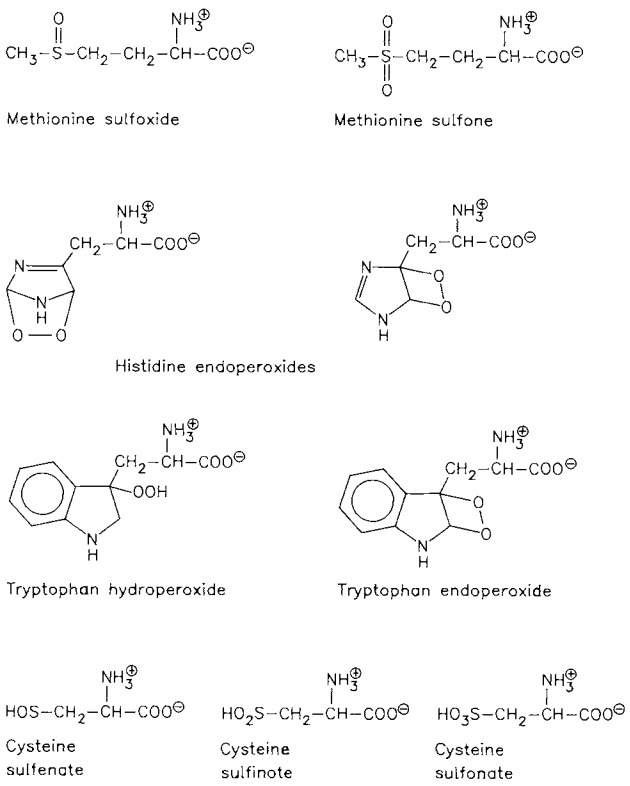


Fig. 7. End products or intermediates of the oxidative breakdown of some amino acids of biological interest.

Table 1. Some Proteins and peptides affected by oxidation.

Oxidized amino acid	Protein or peptide	Ref.
Methionine	Ribosomal protein L 12 (*E. coli*)	[42]
	Lysozyme	
	Pepsin	
	Ribonuclease	
	Phosphoglucomutase	
	α_1-Proteinase inhibitor	
	Calmodulin	
	ACTH (adrenocorticotropic hormone)	
	Chemotactic factors	
	fMet-Leu-Phe	
	Complement C5A	
	α_1-Antitrypsin	[43]
Histidine	Glutamine synthetase (*E. coli*)	[48, 49]

is biologically significant. The mechanism of inactivation of the human α_1-proteinase inhibitor by gas-phase cigarette smoke has been investigated (for mechanism, see Ref. [47]).

3.2. Histidine

Histidyl residues in proteins can play a role similar to that described for methionine. The selective loss of one histidine residue from sixteen per subunit leads to the inactivation of glutamine synthetase from *E. coli*.[48,49] Several other enzymes of interest in cellular metabolism were also found to be inactivated upon exposure to oxidizing conditions, as established, for example, in a mixed-functional system consisting of NADPH, cytochrome P-450 reductase, and cytochrome P-450.[49] It has been discussed that this "marking" of the protein by histidine oxidation may serve for its recognition by proteases, thus serving a function in protein turnover.

The products of histidine oxidation have not yet been completely identified. Loss of histidine is accompanied by the introduction of a carbonyl group, detectable as a stable dinitrophenylhydrazone.[48] Singlet oxygen can lead to the products shown in Figure 7.[50]

3.3. Tryptophan, Lysine and Tyrosine

These amino acids are also subject to oxidation at appreciable rates, but no detailed study of their oxidation in proteins seems to have been carried out as yet. Dityrosine and isodityrosine are oxidation products of tyrosine.

3.4. Proline

Proline in proteins may constitute a preferential target for the hydrolysis of peptide bonds, yielding new *N*-terminal glutamate residues in the fragments[51] (Fig. 8). Collagen was found to be particularly susceptible to oxidative attack.[52]

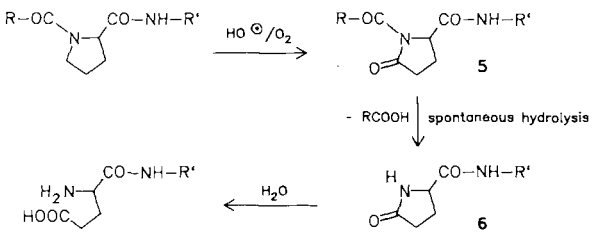


Fig. 8. Reaction scheme for cleavage of proteins at proline residues as proposed in [51]. In a first complex step initiated by hydroxyl radicals, hydrogen abstraction occurs and, in presence of O_2, leads to a 2-pyrrolidone intermediate **5** via an organic peroxy radical. This then undergoes hydrolysis at the peptide bond. The resulting pyroglutamate **6** may hydrolyze to a new *N*-terminal glutamate.

3.5. Cysteine

Although the formation of disulfide bonds as such cannot be considered as damage, because it is a reversible process, disulfide bridges in peptides and proteins may drastically alter biological functions. Alteration in the thiol/disulfide status, for example, has been found to lead to biological consequences,[53–57] including changes in enzyme properties (K_m or v_{max} effects) (see Table 2). Thus, the thiol redox status seems to serve as a metabolic signal. Intracellular proteins in general are predominantly present in the thiol form and have a low cysteine content (1.6%), whereas extracellular proteins (e.g. in blood plasma) are primarily disulfide proteins and have a high half-cystine content (4.1%).[58]

Table 2. Enzyme activities modified by thiol/disulfide exchange [55]. GSSG = disulfide of glutathione (GSH); cystamine = bis(2-aminoethyl) disulfide; DTNB = bis(3-carboxy-4-nitrophenyl) disulfide (dithionitrobenzoate).

Enzyme	Activation by
Glucose 6-phosphate dehydrogenase	GSSG
Collagenase (Leukocytes)	GSSG
Acid phosphatase (Spinach)	GSSG
Fructose 1,6-diphosphatase	Cystamine
δ-Aminolaevulinate synthetase	GSSG
Enzyme	**Inhibition by**
Pyruvate kinase	GSSG
Phosphorylase phosphatase	GSSG
Phosphofructokinase	GSSG
Glycogen synthase D	GSSG
HMG-CoA-reductase	GSSG
Adenylate cyclase (brain)	GSSG
Ribonucleotide reductase (*E. coli*)	GSSG
Hexokinase	Tetraethylcystamine
Tyrosine aminotransferase	Cystine
PDH kinase	DTNB
Fatty acid synthetase	DTNB
γ-Glutamylcysteine synthetase	Cystamine
Papain, trypsin	Dimethyl disulfide

Also of interest is the reversible formation of mixed disulfides between proteins and low-molecular weight thiols, in particular glutathione (GSH). ProtSSG have been observed in the soluble cytoplasm as well as in membranes.[54–57] The *S*-thiolation of proteins in heart cells treated with diamide and *tert*-butyl hydroperoxide showed distinct patterns, notably proteins with molecular masses of 23, 42 and 97 kD.[59] The levels of protein-glutathione mixed disulfides are low, for example, about 20–30 nmol/g of liver.[60,61] When the GSSG levels were increased, the concentration of mixed disulfides also increased,[60–62] possibly catalyzed by thiol transferases.[63]

There are also mixed disulfides of glutathione and coenzyme A (CoASSG). The fluctuations in their concentration can be metabolically significant; during oxidative challenge with *tert*-butyl hydroperoxide, the cellular free CoASH pool can be decreased to such an extent that coenzyme A-dependent processes are blocked:[64,65]

$$\text{CoASH} + \text{GSSG} \rightleftharpoons \text{CoASSG} + \text{GSH}.$$

In isolated mitochondria, respiration and ATP synthesis with CoA-dependent substrates such as pyruvate or 2-oxoglutarate are abolished, whereas there is little effect, for example, with β-hydroxybutyrate or succinate as substrate.[65]

Thiol groups may be further oxidized to alkylthio radicals and subsequently add oxygen:

$$RS^{\odot} + O_2 \longrightarrow RSO_2^{\odot}$$

Further rearrangements and oxidation steps lead to sulfenic, sulfinic, and, finally, sulfonic acids (cf. Fig. 7). The latter are stable enough to be detectable in assays of enzymatic oxidation; for example, glutathione sulfonate was detected in the enzymatic oxidation of glutathione by xanthine oxidase[66] and horseradish peroxidase.[67]

Alkylthio radicals have been detected by ESR methods in horseradish peroxidase-catalyzed reactions in vitro,[68,69] but no information is as yet available on the metabolic generation of these radicals in cells. Oxidation products of disulfides such as cystine *S*-monoxide or cystine *SS*-dioxide can also be formed, and they possibly occur in keratin fibers.[70]

3.6. Damage to Proteins by γ-Irradiation or Free Radical Attack

In radiation biochemistry, interest has recently focused on reactions of the hydroxyl radical ($HO^{\odot}$) and the peroxyl radical ($ROO^{\odot}$) with proteins (see [70b, 71]). Inactivation of yeast alcohol dehydrogenase and the protection of the enzyme by antioxidants[71] or the fragmentation of bovine serum albumin into peptides[72,73] are examples of studies in this area. As mentioned above, fragmentation via hydroxyl radicals is thought to occur preferentially at proline residues; reaction with a peroxyl radical leads to a 2-pyrrolidone intermediate, hydrolysis of which yields a new *N*-terminal glutamate residue[51] (cf. Fig. 8).

4. Oxidative Damage to Carbohydrates

As mentioned in Section 2, deoxyribose is prone to oxidative degradation. This property has even been exploited for the development of an assay of the formation of free-radicals. In the thiobarbiturate assay, deoxyribose yields a degradation product that is almost identical to the product obtained with malondialdehyde.[74]

Polysaccharides such as hyaluronic acid can be degraded by oxidative attack; superoxide dismutase was found to be capable of protecting hyaluronic acid against depolymerization in synovial fluid.[75,76] Proteoglycans may be subject to oxidative breakdown in a similar manner.[76]

5. Oxidative Damage to Lipids

5.1. Causes and Effects

Polyunsaturated fatty acids have become a central area of interest in the chemistry and biochemistry of oxidative reactions. These fatty acids, largely present in phospholipids of biological membranes, can be released into the pool of free fatty acids via the action of phospholipase A_2 before or after oxidative attack (Fig. 9). It is possible that oxidation before release from the phospholipid may serve as a marker for the phospholipase.

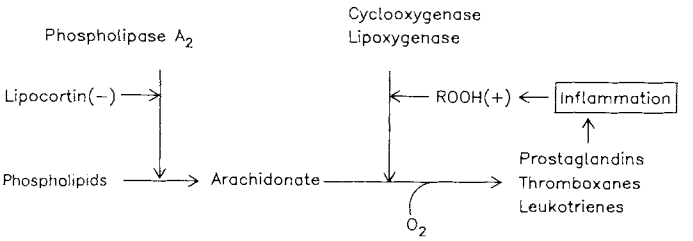


Fig. 9. Scheme of release of arachidonate from phospholipids and of eicosanoid formation. The inhibition of phospholipase A_2 by lipocortin, the inhibitory peptide inducible by glucocorticoids (see [77]) and the positive effect of organic hydroperoxides on cyclooxygenase [78] and lipoxygenase ("peroxide tone") are indicated.

The specific enzymatic oxidation of polyunsaturated fatty acids should not be considered as a damaging event, since it leads to a realm of extremely potent and biologically important signal compounds. The products of this specific oxidation are prostaglandins, thromboxane A_2, prostacyclin, and the leukotrienes (see [79]). Unspecific oxidation of polyunsaturated fatty acids is known as lipid peroxidation, a radical-mediated pathway (Fig. 10) leading to a number of stable degradation products (Table 3). The product pattern depends essentially on the nature of the initial fatty acid involved; for example, pentane is gener-

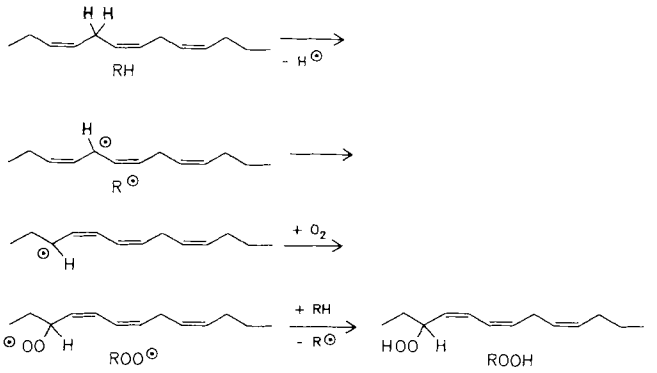


Fig. 10. Initial steps of lipid peroxidation, schematic for an unsaturated *n*-alkane (RH): H abstraction, diene conjugation, oxidation and reaction with RH (after [80]).

Table 3. Products of lipid peroxidation [81].

Chain cleavage and recurrent oxidation products:

Alkanes, alkenes, *n*-alkanals, 2-alkenals, 2,4-alkadienals, alkatrienals, hydroxyaldehydes, hydroperoxyaldehydes, 4-hydroxyalkenals, 4-hydroperoxyalkenals, malonaldehyde, dicarbonyl compounds, saturated and unsaturated ketones

Rearrangement and consecutive products:

Hydroxy acids, keto acids, ketohydroxy acids, epoxyhydroxy acids, dihydroxy acids, ketodihydroxy acids, trihydroxy acids

Further peroxidation products:

Cycloendoperoxides (prostaglandin G_2) and analogous compounds

Dimers and polymers

Dimers and polymers linked by –O–, –O–O–, –C–C– bridges

ated from an ω-6-polyunsaturated fatty acid, and ethane from an ω-3-polyunsaturated fatty acid. The chemistry of lipid peroxidation is complex, and will not be discussed here in detail (see Ref. [82]).

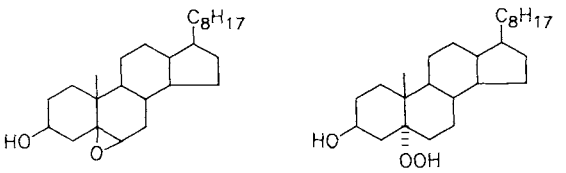


Fig. 11. Oxidation products of cholesterol: 5,6-epoxide and 5α-hydroperoxide.

The oxidation of cholesterol is of special biological interest, yielding a 5,6-epoxide and, in addition, the 5α-hydroperoxide (Fig. 11). This cholesterol epoxide occurs in high concentrations in human breast fluid[83] and has been identified as a directly acting mutagen.[84]

5.2. Atherogenesis

It has been suggested that lipid peroxidation is involved in the development of atherosclerotic lesions. It was found that modified forms of human low-density lipoprotein (LDL) cause an accumulation of large amounts of cholesterol esters in macrophages, e.g. after treatment of LDL with malonaldehyde.[85] 4-Hydroxynonenal is also capable of modifying LDL, and the concentrations required are one hundred to one thousand fold less than with malonaldehyde.[86] In addition to the enhanced accumulation of cholesterol esters, the binding of modified LDL to macrophages also leads to an increased release of a number of lysosomal enzymes.[87a] The molecular basis of modification of LDL by endothelial cells that leads to its enhanced uptake by macrophages remains to be defined.[87b]

6. Reactive Oxygen Species

The reactive oxygen species involved in biological systems are listed in Table 4. Most of them are free radicals; the term oxygen-free radicals is used more or less synonymously with reactive or aggressive oxygen species. However, it should be noted that ground state (triplet) molecular oxygen as a diradical is much less reactive than molecular oxygen in the excited state ($^1\Delta_gO_2$ abbrev. $^1O_2$). This singlet oxygen is diamagnetic and not of a radical nature.[88] Thus, non-radical excited states of molecular oxygen and of oxygen in organic compounds, e.g. in excited carbonyl compounds and dioxetanes,[89] as well as ozone fall into the category of reactive oxygen species of biological interest. The kinetic constants of the reactions of $HO_2^{\ominus}/O_2^{\ominus\ominus}$ with more than 300 organic and inorganic compounds in aqueous solution have recently been compiled.[90]

These reactive oxygen species are formed via several pathways, enzymatic and nonenzymatic. One-electron reduction, initially leading to the formation of the superoxide anion radical $O_2^{\ominus\ominus}$, is a major source (Table 5). Direct two-electron reduction generates hydrogen peroxide; an example for this is given by the fatty acyl-CoA oxidase in the peroxisome. The formation of the hydroxyl radical may occur directly through radiolysis of water, and also via the Fenton reaction:

$$Fe^{2\oplus} + H_2O_2 \longrightarrow Fe^{3\oplus} + OH^{\ominus} + OH^{\ominus}$$

The sources of the radical $O_2^{\ominus\ominus}$ produced via one-electron reduction of molecular dioxygen in the cell include the mitochondrial and microsomal respiratory chains as well as the bactericidal activity of leukocytes and macrophages. The physiological importance of the cellular

Table 4. Reactive oxygen species of interest in oxidative stress.

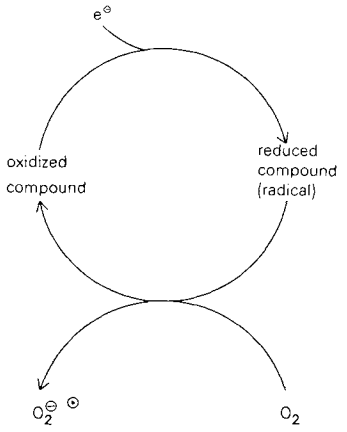
Species	Name	Remarks
$O_2^{\ominus\ominus}$	Superoxide or hyperoxide	One-electron reduction state, formed in many autoxidation reactions (e.g. flavoproteins; redox cycling)
$HO_2^{\ominus}$	Perhydroxyl	Protonated form of $O_2^{\ominus\ominus}$, more lipid-soluble
H_2O_2	Hydrogen peroxide	Two-electron reduction state, formed from $O_2^{\ominus\ominus}$ ($HO_2^{\ominus}$) by dismutation, or directly from O_2
$HO^{\ominus}$	Hydroxyl	Three-electron reduction state, formed by Fenton reaction, metal(iron)-catalyzed Haber-Weiss reaction; highly reactive
$RO^{\ominus}$	R–oxyl, e.g. alkoxyl	Oxygen-centered organic (e.g. lipid) radical
$ROO^{\ominus}$	R–dioxyl, e.g. alkoxydioxyl	Formally formed from organic (e.g. lipid) hydroperoxide, ROOH, by hydrogen abstraction
ROOH	R–hydroperoxide	Organic hydroperoxide (e.g. lipid-, thymine-OOH)
$^1\Delta_gO_2$ (also O_2^* or $^1O_2$)	Singlet molecular oxygen	First excited state, 22 kcal/mol above ground state (triplet) $^3O_2$; red (dimol) or infrared (monomol) photoemission
^{3}R′R″CO (also R′R″CO*)	Triplet carbonyl	Excited carbonyl compound, blue-green photoemission (e.g., formed via dioxetane as intermediate)

Table 5. Formation of the $O_2^{\ominus\ominus}$ radical in biological systems [176].

1. $O_2^{\ominus\ominus}$ formation by autoxidation (inclusive of "redox cycling")	Ref.
Hydroquinones (semiquinones)	[177]
Flavins	[177, 178]
Hemoglobin(s)	[179, 180]
Glutathione and other Thiols	[181, 182]
Catecholamines	[183]
Transition metal ions	[184, 185]
2. $O_2^{\ominus\ominus}$ formation by enzymes or enzyme complexes	
Flavin-dependent oxidations	[186, 187]
Photosynthetic oxygen reduction	[188]
Mitochondrial respiratory chain	[189]
Microsomal oxygenation	[190]
NADPH-dependent oxygen reduction by granulocytes and macrophages	[191–193]
3. Increased (enzymatic) $O_2^{\ominus\ominus}$ formation by xenobiotics	
Antimycin	[189]
Adriamycin	[194, 195]
Paraquat	[196, 197]
4. $O_2^{\ominus\ominus}$ formation by physical factors	
Ultraviolet light, Ultrasound, X-rays, γ-rays	

sources is difficult to assess in a general fashion; they could contribute to a large extent in maintaining the cellular steady state concentration of the $O_2^{\ominus\cdot}$ radical. Autoxidation reactions such as redox cycling (Fig. 12) are certainly also growing in importance for explaining the oxidative stress caused by several xenobiotics; these include compounds such as quinones, which are used in cancer chemotherapy.[91]

The steady-state *oxygen concentration* is of particular importance. At low O_2 partial pressure, in the area of hypoxia, there is an optimum for damage by lipid peroxidation, since reductive steps such as the transfer of electrons in redox cycling (Fig. 12) or the reduction of haloalkanes by cytochrome P-450 occur simultaneously with O_2-dependent steps of lipid peroxidation (Figs. 10 and 13).[91] For example, the optimum O_2 partial pressure was found to be 2 mm Hg for liver microsomal lipid peroxidation by CCl_4 or halothane ($CF_3CHBrCl$) using an oxystat system.[91b]



Reoctive oxygen species
H_2O_2, $OH^{\cdot}$, $ROO^{\cdot}$, $RO^{\cdot}$, $^1O_2$

Fig. 12. Scheme of redox cycling. The superoxide anion radical, $O_2^{\ominus\cdot}$, is generated under aerobic conditions, driven by electrons coming from NADPH as catalyzed by various reductases.

It is of interest to note that reactive oxygen intermediates often seem to be metabolized according to the principle of dismutation (Table 6). Not only the one-electron reduction state is eliminated in a disproportionation reaction, but also two-electron reduction products. Whereas the dismutation of $O_2^{\ominus\cdot}$ and of H_2O_2 by superoxide dismutase and catalase, respectively, yield ground-state triplet oxygen, the dismutation of prostaglandin G_2 or of organic hydroperoxides as products of lipid peroxidation affords singlet molecular oxygen.

Table 6. "Dismutation reactions" of oxygen metabolites; PG = prostaglandin.

Reaction	Enzyme
$2\,O_2^{\ominus\cdot} + 2\,H^{\oplus} \longrightarrow H_2O_2 + O_2$	Superoxide dismutase
$2\,H_2O_2 \longrightarrow 2\,H_2O + O_2$	Catalase
$2\,PG\,G_2 \longrightarrow 2\,PG\,H_2 + {}^1O_2$	PG hydroperoxidase
$2\,ROOH \longrightarrow 2\,ROH + {}^1O_2$	Cytochrome P-450
$2\,PhI{=}O \longrightarrow 2\,PhI + {}^1O_2$	Cytochrome P-450

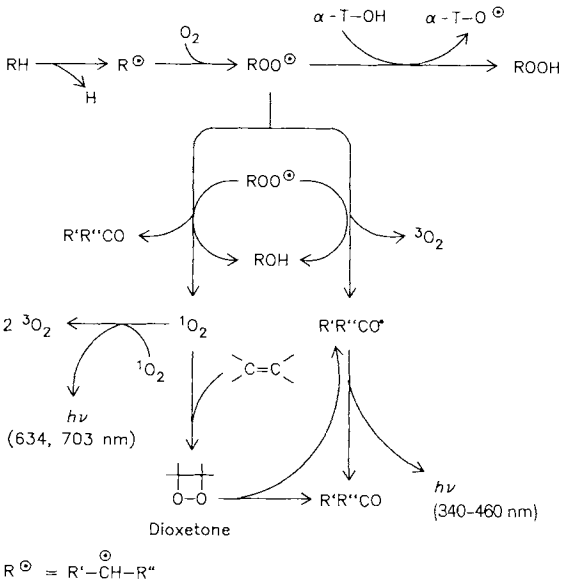


Fig. 13. Generation of excited oxygen (singlet oxygen; left-hand branch) or excited carbonyls R'R''CO* (triplet carbonyls; right-hand branch) from lipid peroxyl radicals, according to Russell's mechanism [92, 93]. α-T-OH signifies α-tocopherol (see Fig. 19).

Singlet oxygen is formed in biological systems (a) via photosensitization reactions, an appropriate sensitizer being electronically excited and then transferring energy to oxygen, and (b) via chemical excitation reactions. These latter pathways of singlet oxygen formation occur without activation by light, and are therefore also referred to as "photochemistry in the dark."[89]

In principle there are two pathways for the chemical excitation of oxygen. One proceeds via a radical-radical interaction[92,93] (Russell's mechanism) (see Fig. 13), the other via oxene transfer using heme iron (Fe^{3+}):[94]

$$(Fe^{3\oplus}) + ROOH \longrightarrow (Fe{=}O) + ROH$$

$$(Fe{=}O) + ROOH \longrightarrow (Fe^{3\oplus}) + ROH + {}^1O_2$$

$$2\,ROOH \longrightarrow 2\,ROH + {}^1O_2$$

Singlet oxygen may be of particular interest in biological systems, because it is capable of diffusing an appreciable distance in membranes. In stearate monolayers, the diffusion path for singlet oxygen for half-deactivation was estimated to be 115 Å (Fig. 14).[95] The formation of singlet oxygen in cellular systems has so far been demonstrated mainly by the detection of photoemission via the dimol reaction:

$${}^1O_2 + {}^1O_2 \longrightarrow 2\,{}^3O_2 + h\nu \quad (\lambda = 634\text{ nm}, 703\text{ nm}).$$

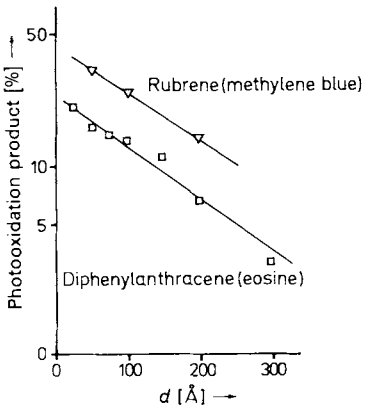


Fig. 14. Yield of photooxidation products in the reaction of rubrene and diphenylanthracene, respectively, in the presence of the sensitizers methylene blue and eosine. The photosensitizer was spaced by stearate monolayers of thickness d (after [95]).

Sensitive photon-counting equipment has made it possible to use this "low-level" chemiluminescence as an indicator of $^1O_2$ in intact cells and organs. The spectra as well as the enhancement of photoemission by diazabicyclooctane (DABCO) and the decrease of photoemission by azide indicate the occurrence of singlet oxygen in intact liver during the redox cycling of 2-methyl-1,4-naphthoquinone (menadione)[97] or 1,1'-dimethyl-4,4'-bipyridinium (paraquat).[98] Thus, singlet oxygen may be responsible for the toxic effects observed with these compounds. Menadione is mutagenic,[99] and singlet oxygen generated by microwave discharge has been shown to affect biologically active DNA, causing a loss of transforming activity in an assay system using the plasmid pBR 322.[100a] Similar results were obtained when $^1O_2$ was generated from a thermodissociable naphthalene endoperoxide.[100b]

In isolated enzymatic systems, the photoemission spectra resemble that of the H_2O_2/NaOCl reaction.[101] Two peaks near the 634-nm and 703-nm regions were observed with isolated ram seminal vesicle prostaglandin hydroperoxidase (cyclooxygenase)[94] (Fig. 15), or with cytochrome

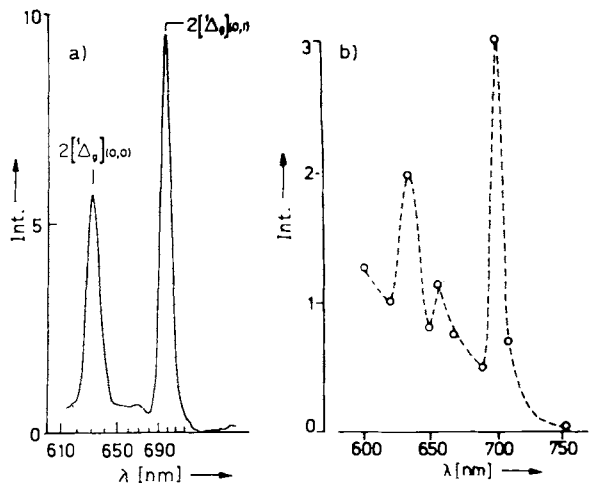


Fig. 15. Dimol emission spectrum of low-level chemiluminescence of singlet oxygen. Generation of $^1O_2$: a) in the hypochlorite-H_2O_2 reaction (after [101]); b) enzyme-catalyzed in the prostaglandin cyclooxygenase reaction (after [94]).

P-450 and iodosobenzene as substrate.[102] The monomol-photoemission of singlet oxygen occurs at $\lambda = 1270$ nm (in the IR). Recently, the lactoperoxidase reaction was shown to photoemit at $\lambda = 1270$ nm.[103]

7. Defense Against Oxidative Stress: Biochemical Antioxidants

The detoxication of reactive oxygen species is one of the prerequisites of aerobic life; the multiple lines of defense which have evolved form a veritable antioxidant defense system (Table 7). The repertoire to counteract the potentially hazardous reactions initiated by oxygen metabolites includes all levels of protection: prevention, interception, and repair. It comprises nonenzymatic scavengers and quenchers referred to under the term antioxidants in the more narrow sense, and also enzymatic systems.

Table 7. Anitoxidant defense in biological systems.

System	Remarks
Non-enzymatic	
α-Tocopherol (vitamin E)	Membrane-bound; receptors? Regeneration from chromanoxyl radical?
Ascorbic acid (vitamin C)	Water-soluble
Flavonoids	Plant antioxidants (rutin, quercetin, etc.)
Chemical antioxidants	Food additives, e.g. BHA (butylated hydroxyanisole), BHT (butylated hydroxytoluene) [a]
β-Carotene (vitamin A)	Singlet oxygen quencher
Uric acid	Singlet oxygen quencher, radical scavenger?
Plasma proteins	e.g., Coeruloplasmin
Enzymatic	
Superoxide dismutases	CuZn enzyme, Mn enzyme
GSH peroxidases	Selenoenzyme; non-Se enzyme; some GSH transferases, e.g., isoenzymes B and AA; cytosol and mitochondrial matrix
Catalase	Heme enzyme, predominantly in peroxisomal matrix
Ancillary enzymes	
NADPH-quinone oxidoreductase (DT-diaphorase)	Two-electron reduction, dicoumarol-sensitive
Epoxide hydrolase	
Conjugation enzymes	UDP-glucuronyl transferase Sulfotransferase GSH transferases
GSSG-reductase	
GSH synthesizing enzymes	
NADPH supply	Glucose 6-phosphate dehydrogenase 6-Phosphogluconate dehydrogenase Isocitrate dehydrogenases Malate enzyme Energy-linked transhydrogense
Transport systems	GSSG export Conjugate export
Semidehydroascorbate reductase	
Methionine sulfoxide reductase	
DNA repair enzymes	

[a] BHA = 2-*tert*-butyl-4-methoxyphenol; BTA = 2,6-di-*tert*-butyl-4-methylphenol (see **8** and **9** in Fig. 19).

7.1. Nonenzymatic Antioxidants

α-Tocopherol (vitamin E, cf. Fig. 19)[104] is the most important lipid-soluble antioxidant;[105] its unique function in

the membrane may be aided by the specific physicochemical interaction between the phytyl residue and the fatty acid residues of the polyunsaturated phospholipids in the membrane.[106] The proper insertion of the vitamin into the membrane increases its effectiveness by about 50-fold.[107]

Ascorbic acid (vitamin C), together with glutathione, is the important antioxidant in the aqueous phase. It can react with the vitamin E radical (chromanoxyl) and thus can regenerate tocopherol in the membrane. Further aspects of interest, e.g. in nutrition[109] (normal requirement: 12 mg of vitamin E and 75 mg of vitamin C per day[110]) cannot be discussed in detail here.

Further important antioxidants are listed in Table 7.

7.2. Enzymatic Antioxidants

The essential enzymes are the intensively studied *superoxide dismutases* and various hydroperoxidases such as *glutathione peroxidase, catalase,* and other hemoprotein peroxidases. They are characterized, in general, by high specific cellular content, by specific organ and subcellular localizations which often overlap in a complementary way, and by a specific form of metal involvement, especially of copper, manganese, iron (heme) and selenium, in the catalysis. These antioxidant systems have a wide distribution in nature, underscoring their importance for coping with the damaging effects of reactive oxygen metabolites in biological systems. Their distribution is crucial in target organ toxicity.[111] A comprehensive discussion of these central enzymes in antioxidant defense is beyond the scope of this article (see Refs. [13-20]). In the following, some more recent aspects of reactions involved more indirectly in antioxidant defense will be presented.

A novel protein which protects membranes from peroxidation and exhibits GSH peroxidase activity toward phosphatidylcholine hydroperoxides has been identified and characterized as a selenoenzyme.[112] Also new is a GSH-dependent heat-labile factor which inhibits lipid peroxidation in biological membranes.[113] Most recent findings indicate that this cytosolic protein is not one of the known GSH-dependent enzymes.[114a]

Some specific cell types may use extracellular GSH. The basolateral membrane of intestinal epithelial cells contains an $Na^{\oplus}$-dependent GSH uptake system, so that exogenous GSH protects these cells from oxidative injury.[114b] Most other cell types cannot utilize GSH as such, but have to synthesize their GSH intracellularly from the constituent amino acids.

It should be noted that a number of additional or ancillary systems are of crucial importance. For example, many of the radical or nonradical reactions in cells may lead to the oxidation of thiols to disulfides, i.e., the oxidation of glutathione (GSH) to form GSSG. Thus, the regenerative reaction of reduction to GSH as catalyzed by GSSG reductase can become pivotal in antioxidant defense. Naturally, the provision of reducing equivalents for this enzyme is also of importance. Thus, the NADPH regenerating systems (Table 7) are also of interest.

Diminution of the steady-state levels of reactive compounds capable of generating reactive oxygen species also results in a decreased expression of oxidative stress; in this respect, the two-electron reduction of quinones by NADPH:quinone oxidoreductase (DT diaphorase) and the subsequent conjugation reaction of the hydroquinone are part of the antioxidant defense.[97, 115]

Obviously, the export of reactive species in free or conjugated form also serves as a detoxication function, so that transport of conjugates as well as of GSSG from cells is of interest here. The binding of conjugates of glutathione to GSSG binding sites may have metabolic significance. It has been shown in kinetic and X-ray crystallographic studies that glutathione conjugates bind to the GSSG-binding site in the active center of GSSG reductase, causing inhibition of enzymatic activity[116] (Fig. 16). An increase in GSSG levels causes metabolic perturbations, including an inhibition of protein synthesis (see Ref. [53]).

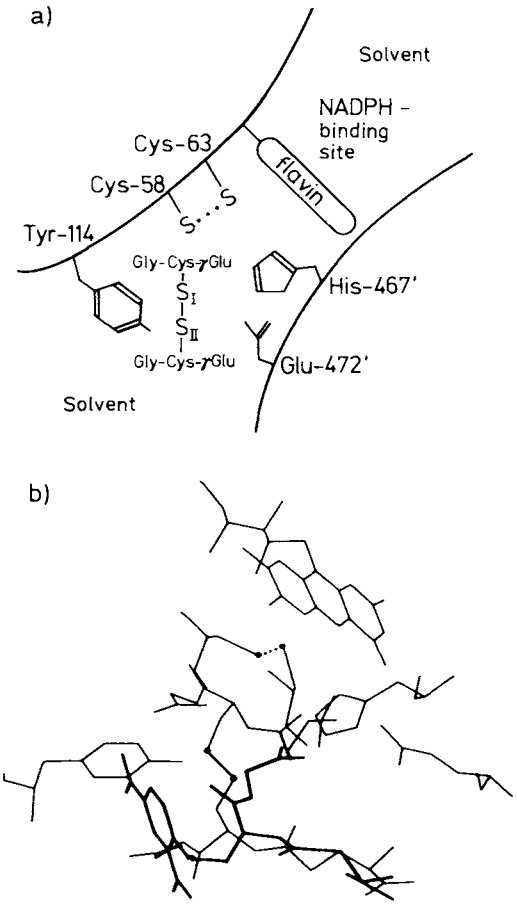


Fig. 16. a) GSSG binding site of glutathione reductase; b) the binding of *S*-(1,2-dinitrophenyl)glutathione (thick lines) at this site (after [116]).

The transport systems for GSSG and glutathione conjugates (thioethers) have been studied in some detail recently[117] (see Fig. 17). In liver, there is mutual competition of biliary export between these two types of glutathione derivatives,[118] indicating that the canalicular carrier system may accept both these substrates for transport. There appears to be a GSSG activatable ATPase in the hepatic plasma membrane.[119] Mutual competition for export of GSSG and GS-conjugates was also detected in the heart.[120] Using the creatine-kinase reaction as an indicator system, it was found that GSSG transport across the

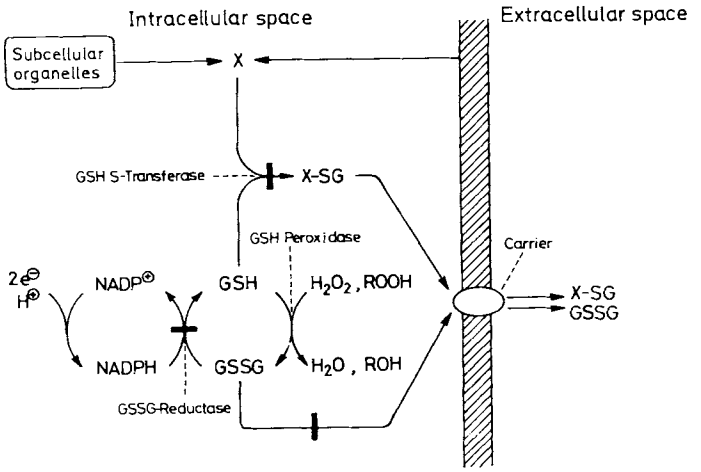


Fig. 17. Relations between GSH peroxidase and GSH transferase reactions. Glutathione disulfide (GSSG) and glutathione thioethers (X-SG) are exported from the cells, competing for transport. X-SGs inhibit GSSG reductase (after [120]).

cardiac plasma membrane was half-maximal at $(ATP/ADP)_{free}$ ratios of ≈ 10 in the intact perfused rat heart preparation.[121]

Interestingly, a prominent GSH transferase activity in the heart is isozyme 4-4, accepting 4-hydroxynonenal as a substrate[122] and, therefore, capable of detoxifying this biologically active product of lipid peroxidation.[123] Recently, another high-activity isozyme (8-8) was described.[122]

It should also be pointed out that some GSH transferase isozymes have the capacity to catalyze the GSH peroxidase reaction with organic hydroperoxides as substrate.[124] These non-selenium-dependent activities may become essential in states of selenium deficiency when the Se enzyme, GSH peroxidase, is very low in its cellular activity. However, since the GSH transferases do not accept H_2O_2 as substrate, there is no complete substitute for the selenoenzyme. This may explain why in Se-deficiency there can be overt clinical symptoms such as the cardiomyopathy known as Keshan disease.[125] This disease, which led to death in about one percent of the male population of school-age Chinese in the Keshan province, was found to be completely treatable by the oral application of 1 mg of sodium selenite per week.[125]

7.3. DNA Repair

Possibly the biologically most important line of defense for the organism consists in preserving the identity of the genetic material by repair after oxidative damage (cf. Fig. 6).[36] In addition, an equally important process for microorganisms is enzymatically controlled mutagenesis in order to ensure adaption to changing environmental conditions.

The repair system seems to be less sensitive to ionizing radiation than DNA. In yeast cells, the repair of single-strand breaks is dependent on the irradiation dose (up to high doses of 2400 Gy).[126] The repair enzymes are thus to be considered in a broad sense as a central component of the antioxidant enzymes for the cell.

7.4. Control of the Antioxidant Capacity

The level of antioxidant defense is regulated. For example, the induction of catalase and superoxide dismutase (SOD) in microorganisms such as *E. coli* or *S. typhimurium* during anaerobic shifts[127] or by treatment with H_2O_2[128] has been observed; there are also adaptation phenomena.[129-131] A double mutant of *E. coli* devoid of the two SOD activities was unable to grow on minimal glucose medium.[132] During adaptation of *S. typhimurium* to H_2O_2, 30 proteins are induced, and it was shown that nine of them are under positive control of a regulon for defense against oxidative stress, called oxyR.[133] The oxyR regulon controls a global response to a DNA damaging agent, in addition to three other global responses (the SOS response, adaptation to alkylating agents, and heat-shock). In cells in which the oxyR regulon is deleted, the rate of spontaneous mutagenesis is dramatically increased, and the level of mutagenesis is less than in the controls if the oxyR gene is overexpressed[134] (Table 8). Similarly, the *E. coli* mutants lacking SOD exhibit oxygen-dependent mutagenesis.[135]

While control of the patterns of antioxidant enzymes, and also the control of the levels of antioxidants such as vitamin E, are not well-characterized in mammalian cells, it appears that adaptation phenomena of this nature may also be important in eukaryotes. In this regard, the changes in the biochemical pattern exhibited in cells in hepatic nodules may be considered as adaptive. These nodules contain clones of hepatocytes in which a new state of liver differentiation is acquired, and this is considered as a physiological response to environmental perturbations,[136] like the oxyR response mentioned above. The changes observed in the nodules refer to some of the ancillary antioxidant enzymes mentioned in Table 7; these consist of increases in the cellular activities of some isozymes of glucuronyl transferases, glutathione transferases, γ-glutamyl transferase, epoxide hydrolase, and NADPH : quinone oxidoreductase. These enzymes are classified as belonging to the Phase II group of enzymes involved in xenobiotic transformation. Interestingly, the enzymes of Phase I, namely cytochromes P-450 and b_5, have drastically decreased cellular activities. It appears that these changes in gene expression are related to DNA methylation (cf. [137, 138]). In experiments to decrease DNA methylation at the cytosine residues by treatment of animals with the drug analog, 5-azacytidine, the content of cytochromes P-450 and b_5 was found to drop,[139] whereas the content of several isozymes of the glutathione transferases as well as of NADPH : quinone oxidoreductase in mouse liver was in-

Table 8. Spontaneous mutagenesis in relation to the presence of the OxyR regulon in *S. typhimurium* tester strains. Strains with His G428 containing plasmid pKM101 and the oxyR regulon ($oxyR^+$) or overexpressed (oxyR1) or deleted (oxyΔ2) in oxyR were assayed for spontaneous mutations in the His reversion assay (Ames test). For description of phenotype, zones of inhibition by H_2O_2 on the agar plates are also shown [134].

Strain	Description	Colonies per plate	Zone of inhibition [mm]
TA 4117	$oxyR^+$	33 ± 6	18.0
TA 4118	oxyR1	12 ± 4	12.5
TA 4119	oxyΔ2	1408 ± 160	33.5

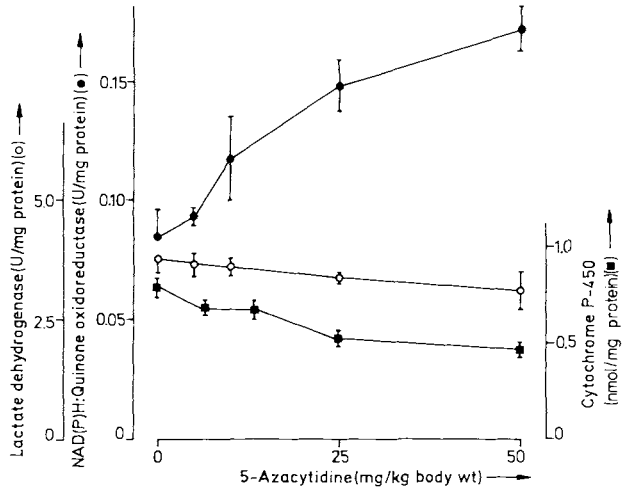


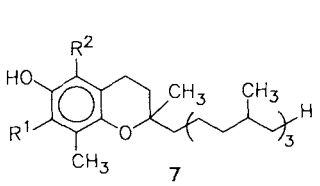
Fig. 18. Increase in NADPH : quinone oxidoreductase (DT-diaphorase) and decrease in cytochrome P-450 in mouse liver after injection of azacytidine for inhibition of DNA (cytosine-5) methyl transferase (after [140]).

creased[140] (Fig. 18). Recently, NADPH : quinone oxidoreductase was cloned and was described to be hypomethylated in persisting liver noduli.[141]

Thus, there are interesting relationships between the status of DNA methylation and the expression pattern for some enzymes of importance in defense against oxidative challenge (see also [142]).

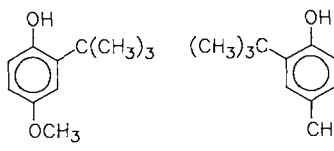
7.5. Synthetic Antioxidants

Numerous drugs serving as antioxidants have been synthesized and tested in biological environments, ranging from phenolic antioxidants added to foodstuffs to drugs used in medicine (Fig. 19). This subject cannot be treated here in detail. However, two selective aspects from our own research interest will be briefly mentioned.

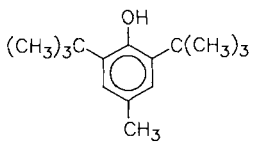


7

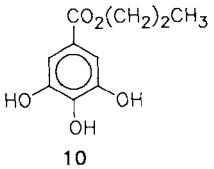
	R^1	R^2
α-T	CH_3	CH_3
β-T	H	CH_3
γ-T	CH_3	H
δ-T	H	H



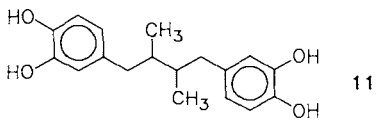
8



9



10



11

Fig. 19. Some antioxidant inhibitors of peroxidation reactions. 7: α- bis δ-tocopherol; 8: BHA = 2-*tert*-butyl-4-methoxyphenol; 9: BHT = 2,6-di-*tert*-butyl-4-methylphenol; 10: propyl gallate; 11: NDGA = nordihydroguaiaretic acid.

7.6. Ebselen, a Novel Organoselenium Compound

This synthetic organoselenium compound, 2-phenyl-1,2-benzoselenazol-3(2*H*)-one (ebselen), has been found to exhibit antioxidant capacity.[143] In an assay of lipid peroxidation using rat liver microsomes, the lag phase preceding the onset of ascorbate/ADP-Fe-induced lipid peroxidation is increased by the addition of ebselen, whereas the sulfur analog is inactive (Fig. 20); this pertains not only to the low-level chemiluminescence, but also to other parameters of lipid peroxidation like the evolution of ethane and *n*-pentane or the production of thiobarbiturate-reactive material.[94] In addition to this antioxidant activity, the compound acts catalytically in the GSH peroxidase reaction:[143, 144]

$$2GSH + ROOH \longrightarrow GSSG + ROH + H_2O$$

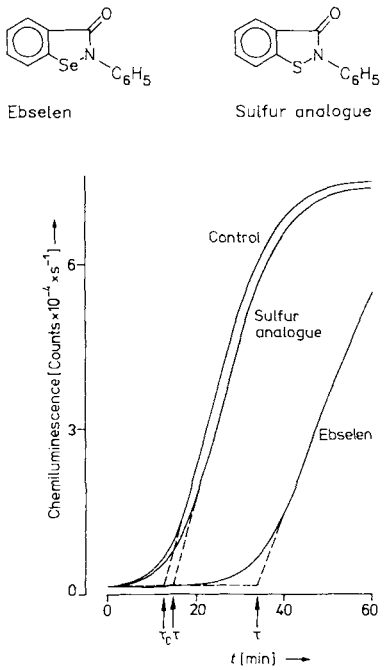


Fig. 20. Ebselen and its sulfur analog. The organoselenium compound exhibits antioxidant activity, shown by prolongation of lag phase in microsomal lipid peroxidation assay (after [143]).

This activity is thought to be responsible for the protection of isolated hepatocytes against oxidative challenge. Significant protection was afforded against ADP-Fe-induced cell damage in control cells, whereas cells previously rendered deficient in GSH were not protected by ebselen.[145a] The cytotoxicity of anticancer quinones in Ehrlich ascites cells was significantly decreased by ebselen.[145b] Recently, it was found that ebselen also exhibits an inhibiting activity in the lipoxygenase pathway.[146] Whether this can be explained by the removal of activatory hydroperoxide through the GSH peroxidase reaction (cf. Fig. 9), or by yet another site of action, is not clear.

Selenium displays a variety of biological effects (see [147]), a prominent one being its role as selenocysteine in the active center of GSH peroxidase.[148-150] It might be of interest to compare the mechanism of catalysis of the GSH peroxidase reaction identified for the enzyme with that of

ebselen. The role of selenium as an antioxidant[151] and as an anticarcinogen, as well as its potential as a carcinogen and as a cytotoxic agent, has been recently reviewed.[152a]

7.7. The Selenoenzyme GSH Peroxidase

This enzyme has recently been sequenced;[152b] its structure has been studied by X-ray crystallography.[152c] The gene from the mouse was cloned and it was found that the selenocysteine in the active site is encoded by the termination codon TGA.[152d] Likewise, this codon was found in formate dehydrogenase of *E. coli*.[152e]

7.8. Superoxide Dismutase as a Drug

The Cu,Zn-enzyme superoxide dismutase[5] has found a variety of applications as an antioxidant. In clinical medicine, the enzyme has been employed mainly in topical, e.g. intraarticular, applications, in the knee joint[153] and it was found to be active as an antiinflammatory agent. The enzyme has been cloned;[154] the recombinant human superoxide dismutase has been expressed in yeast.[155] The use of the human enzyme as obtained by gene-technological procedures may permit the systemic application and treatment of a variety of clinical conditions associated with oxidative stress. For example, there is evidence of free-radical involvement in ischemic myocardial[156] or intestinal injury or pancreatitis.[157] Recently, it was suggested that superoxide is involved in the breakdown of endothelium-derived vascular relaxing factor (EDRF).[158] However, this area of clinical research awaits further rigorous testing of the therapeutic benefits of oxygen radical scavengers.

8. Biology of Oxidative Stress: Some Aspects

The biological implications of oxidative stress have already been discussed at length (see, e.g., [13–20, 159]). It seems that almost all complex biological processes can be implicated with respect to reactive oxygen species and free radical involvement. Therefore, it seems that an in-depth treatment of such topics as the role of prooxidant states in *tumor promotion*[160] or in *spontaneous mutagenesis*[161] can only be referred to here. Similarly, the *ageing process*[162, 163] and the complex relations in *inflammatory states*[164] require a critical treatment from the biochemical standpoint. There is an intricate interorgan relationship in physiological and pathophysiological states; Figure 21 shows some of these for glutathione.

The biochemical events associated with radiation effects occur through free radicals (see Section 3.6). Recently, free radicals generated in brain, spleen and liver during γ-irradiation of mice (5 Gy) were detected by in vivo spin trapping.[165] Selenite and Vitamin E were found to inhibit radiogenic and chemically induced cell transformation in vitro[166] but, conversely, depletion of these antioxidants for six weeks had no effect on the radiation response in mice in vivo.[167] Radioprotectors and anticarcinogens should be viewed together.[168]

Biochemical-biological studies on oxidative stress have now reached a state where very careful and cautious use of

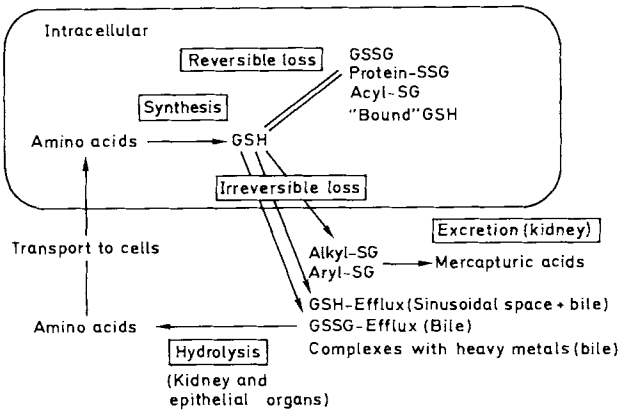


Fig. 21. Processes (chemical and translocation) that influence the intrahepatic and extrahepatic glutathione status (after [55]).

methods and concepts is called for. In this respect it should be mentioned that two volumes dealing with methods in this area of research have recently become available[169, 170] and should be consulted by workers interested in the biological effects of reactive oxygen species.

Finally, it should be pointed out that the term oxidative stress should not be interpreted solely in terms of a noxious challenge against which the organism must defend itself. As was recently pointed out,[171] numerous physiologically important chemical reactions occur in cells via reactive oxygen species and free radical reactions. These include the vital functions of macrophages[172] and neutrophils,[173] formate-pyruvate lyase,[174] ribonucleotide reductase necessary for deoxyribonucleotide production,[175a] and the vast area of selective oxidation of polyunsaturated fatty acids to produce the eicosanoids (see [79]) with far-reaching pathophysiological consequences, for example clinical states such as ischemia and shock.[175b]

The work carried out in the author's laboratory was supported by the Deutsche Forschungsgemeinschaft (Schwerpunktprogramm "Mechanismen toxischer Wirkungen von Fremdstoffen"), by the National Foundation for Cancer Research, Washington, by the Ministerium für Wissenschaft und Forschung des Landes Nordrhein-Westfalen, and by the Fonds der Chemischen Industrie. Thanks are due to numerous colleagues for valuable discussions, and to my co-workers in the laboratory whose contributions are cited in the text.

Received: April 7, 1986;
supplemented: August 25, 1986 [A 599 IE]
German version: *Angew. Chem. 98* (1986) 1061

[1] O. Warburg: *Über die katalytischen Wirkungen der lebendigen Substanz*, Springer, Berlin 1928.
[2] F. Battelli, L. Stern, *Ergebn. Physiol. 12* (1912) 96.
[3] L. Michaelis in D. E. Green (Ed.): *Currents in Biochemical Research*, Interscience, New York 1946, p. 207.
[4] F. Haber, J. Weiss, *Proc. R. Soc. London Ser. A 147* (1934) 332.
[5] J. McCord, I. Fridovich, *J. Biol. Chem. 244* (1969) 6049.
[6] B. Chance, *Acta Chem. Scand. 1* (1947) 236.
[7] H. Kautsky, H. de Bruijn, *Naturwissenschaften 19* (1931) 1043; H. Kautsky, H. de Bruijn, R. Neuwirth, W. Baumeister, *Ber. Dtsch. Chem. Ges. 66* (1933) 1588.
[8] a) G. O. Schenck, *Angew. Chem. 69* (1957) 579; b) K. Gollnick, *Adv. Photochemistry 8* (1968) 1.
[9] C. S. Foote, S. Wexler, *J. Am. Chem. Soc. 86* (1964) 3879, 3880.
[10] R. Gerschman, D. L. Gilbert, S. W. Nye, P. Dwyer, W. O. Fenn, *Science 119* (1954) 623.

[11] H. Sund, V. Ullrich (Eds.): *Biological Oxidations*, Springer, Berlin 1983.
[12] H. Sies, *Angew. Chem. 86* (1974) 789; *Angew. Chem. Int. Ed. Engl. 13* (1974) 706; H. D. Fahimi, H. Sies (Eds.): *Peroxisomes* in *Biology and Medicine*, Springer, Heidelberg 1987.
[13] B. Chance, H. Sies, A. Boveris, *Physiol. Rev. 59* (1979) 527.
[14] B. N. Ames, *Science 221* (1983) 1256.
[15] I. Fridovich, *Arch. Biochem. Biophys. 247* (1986) 1.
[16] M. A. Rodgers, E. L. Powers (Eds.): *Oxygen and Oxy-Radicals in Chemistry and Biology*, Academic Press, New York 1981.
[17] W. Bors, M. Saran, D. Tait (Eds.): *Oxygen Radicals in Chemistry and Biology*, de Gruyter, Berlin 1984.
[18] B. Halliwell, J. M. C. Gutteridge: *Free Radicals in Biology and Medicine*, Clarendon Press, Oxford 1985; *Arch. Biochem. Biophys. 246* (1986) 501.
[19] H. Sies (Ed.): *Oxidative Stress*, Academic Press, London 1985.
[20] a) H. A. O. Hill, *Phil. Trans. R. Soc. London Ser. B311* (1986) 451; b) G. Rotilio (Ed.): *Superoxide and Superoxide Dismutase in Chemistry, Biology and Medicine*, Elsevier, Amsterdam 1986.
[21] C. von Sonntag, U. Hagen, A. Schon-Bopp, D. Schulte-Frohlinde, *Adv. Radiat. Biol. 9* (1981) 109.
[22] D. Schulte-Frohlinde, C. von Sonntag in [19], p. 11.
[23] C. Decarroz, J. R. Wagner, J. E. Van Lier, C. Murali Krishna, P. Riesz, J. Cadet, *Int. J. Radiat. Biol. 50* (1986) 491.
[24] L. H. Breimer, T. Lindahl, *J. Biol. Chem. 259* (1984) 5543.
[25] J. S. Sussenbach, W. Berends, *Biochim. Biophys. Acta 76* (1963) 154; *Biochem. Biophys. Res. Commun. 16* (1964) 263; M. V. George, V. Bhat, *Chem. Rev. 79* (1979) 448; J. Cadet, C. Decarroz, S. Y. Wang, W. R. Midden, *Isr. J. Chem. 23* (1983) 420.
[26] S. A. Lesko, R. J. Lorentzen, P. O. T'so, *Biochemistry 19* (1980) 3023.
[27] S. Inouye, *FEBS Lett. 172* (1984) 231.
[28] A. C. Mello Filho, R. Meneghini, *Biochim. Biophys. Acta 781* (1984) 56.
[29] I. Emerit, P. Cerutti, *Proc. Natl. Acad. Sci. USA 78* (1981) 1868.
[30] I. Emerit, A. M. Michelson, *Proc. Natl. Acad. Sci. USA 78* (1981) 2537.
[31] H. Joenje, F. Arwert, A. W. Eriksson, H. de Koning, A. B. Oostra, *Nature (London) 290* (1981) 142.
[32] I. Emerit, A. M. Michelson, *Acta Physiol. Scand. Suppl. 492* (1980) 59.
[33] G. Obe, A. T. Natarajan, F. Palitti in A. T. Natarajan, G. Obe, H. Altmann (Eds.): *DNA Repair, Chromosome Alterations and Chromatin Structure*, Elsevier, Amsterdam 1982, p. 1.
[34] T. Lindahl, *Prog. Nucleic Acids Res. Mol. Biol. 22* (1979) 135.
[35] S. M. Linn in S. M. Linn, R. J. Roberts (Eds.): *Nucleases*, Cold Spring Harbor Laboratory, Cold Spring Harbor 1982, p. 59.
[36] E. C. Friedberg: *DNA Repair*, Freeman, New York 1985.
[37] R. Cathcart, E. Schwiers, R. L. Saul, B. N. Ames, *Proc. Natl. Acad. Sci. USA 81* (1984) 5633.
[38] M. C. Hollstein, P. Brooks, S. Linn, B. N. Ames, *Proc. Natl. Acad. Sci. USA 81* (1984) 4003.
[39] B. Demple, S. Linn, *Nature (London) 287* (1980) 203.
[40] R. Dulbecco, *J. Bacteriol. 59* (1950) 329; N. Iwatsuki, C. O. Joe, H. Werbin, *Biochemistry 19* (1980) 1172.
[41] W. R. Abrams, G. Weinbaum, L. Weissbach, H. Weissbach, N. Brot, *Proc. Natl. Acad. Sci. USA 78* (1981) 7483; H. Carp, A. Janoff, W. Abrams, G. Weinbaum, R. T. Drew, H. Weissbach, N. Brot, *Am. Rev. Respir. Dis. 127* (1983) 301; H. M. Morrison, D. Burnett, R. A. Stockley, *Biol. Chem. Hoppe-Seyler 367* (1986) 371.
[42] N. Brot, H. Weissbach, *Arch. Biochem. Biophys. 223* (1983) 271.
[43] K. Beatty, J. Bieth, J. Travis, *J. Biol. Chem. 255* (1980) 3931.
[44] S. Eriksson, *Acta Med. Scand. 175* (1964) 197.
[45] J. E. Gadek, R. G. Crystal, *Am. Rev. Resp. Dis. 127* (1983) *Suppl. 2*, 45.
[46] S. Rosenberg, P. J. Barr, R. C. Najarian, R. A. Hallewell, *Nature (London) 312* (1984) 77.
[47] W. A. Pryor, M. M. Dooley, D. F. Church, *Adv. Free Radicals Biol. Med. 2* (1986) 161.
[48] R. L. Levine, *J. Biol. Chem. 258* (1983) 11823.
[49] L. Fucci, C. N. Oliver, M. J. Coon, E. R. Stadtman, *Proc. Natl. Acad. Sci. USA 80* (1983) 1521.
[50] H. S. Ryang, C. S. Foote, *J. Am. Chem. Soc. 101* (1979) 6683.
[51] S. P. Wolff, A. Garner, R. T. Dean, *Trends Biochem. Sci. 11* (1986) 27.
[52] R. A. Greenwald, W. W. Moy, *Arthritis Rheum. 22* (1979) 251; J. C. Monboisse, P. Braquet, A. Randoux, J. P. Borel, *Biochem. Pharmacol. 32* (1983) 53.
[53] E. M. Kosower, N. S. Kosower, *Int. Rev. Cytol. 54* (1978) 109.
[54] R. Brigelius in [19], p. 243.
[55] E. Cadenas, R. Brigelius, T. P. M. Akerboom, H. Sies in [11], p. 288.
[56] H. F. Gilbert, *Methods Enzymol. 107* (1984) 330.
[57] D. M. Ziegler, *Annu. Rev. Biochem. 54* (1985) 305; H. Sies, R. Brigelius, P. Graf, *Adv. Enyzme Regulation 25* (1987), in press.
[58] R. C. Fahey, J. S. Hunt, G. C. Windham, *J. Mol. Evol. 10* (1977) 155.
[59] L. M. Grimm, M. W. Collison, R. A. Fisher, J. A. Thomas, *Biochim. Biophys. Acta 844* (1985) 50; M. W. Collison, D. Beidler, L. M. Grimm, J. A. Thomas, *ibid. 885* (1986) 58.
[60] R. Brigelius, C. Muckel, T. P. M. Akerboom, H. Sies, *Biochem. Pharmacol. 32* (1983) 2529.
[61] T. Higashi, M. Furukawa, K. Hikita, A. Naruse, N. Tateishi, Y. Sakamoto, *J. Biochem. (Tokyo) 98* (1985) 1661.
[62] P. L. Keeling, L. L. Smith, W. N. Aldridge, *Biochim. Biophys. Acta 716* (1982) 249.
[63] P. Askelof, K. Axelsson, S. Eriksson, B. Mannervik, *FEBS Lett. 38* (1974) 263.
[64] D. Crane, D. Häussinger, H. Sies, *Eur. J. Biochem. 127* (1982) 575.
[65] H. Sies, K. M. Moss, *Eur. J. Biochem. 84* (1978) 377.
[66] H. Wefers, H. Sies, *Eur. J. Biochem. 137* (1983) 29.
[67] H. Wefers, E. Riechmann, H. Sies, *J. Free Radicals Biol. Med. 1* (1985) 311.
[68] D. Ross, E. Albano, U. Nilsson, P. Moldeus, *Biochem. Biophys. Res. Commun. 125* (1984) 109.
[69] L. S. Harman, D. K. Carver, J. Schreiber, R. P. Mason, *J. Biol. Chem. 261* (1986) 1642.
[70] a) L. D. Setiawan, H. Baumann, D. Gribbin, *Surf. Interface Anal. 7* (1985) 88; b) M. Quintiliani, *Int. J. Radiat. Biol. 50* (1986), in press.
[71] R. L. Willson in [19], p. 41.
[72] H. Schüssler, K. Schilling, *Int. J. Radiat. Biol. 45* (1984) 267.
[73] S. P. Wolff, R. T. Dean, *Biochem. J. 234* (1986) 399.
[74] B. Halliwell, J. M. C. Gutteridge, *FEBS Lett. 128* (1981) 347.
[75] J. M. McCord, *Science 185* (1974) 529.
[76] R. A. Greenwald in W. H. Bannister, J. V. Bannister (Eds.): *Biological and Clinical Aspects of Superoxide and Superoxide Dismutase*, Elsevier, Amsterdam 1980, p. 160; S. F. Wong, B. Halliwell, R. Richmond, W. R. Skowroneck, *J. Inorg. Biochem. 14* (1981) 127; C. Kreisl, E. Lengfelder in A. M. Michelson, J. V. Bannister (Eds.): *Oxidative Damage and Related Enzymes*, Life Chemistry Reports, Harwood Publ., London 1984, p. 81.
[77] B. P. Wallner, R. J. Mattaliano, C. Hession, R. L. Cate, R. Tizard, L. K. Sinclair, C. Foeller, E. Pingchang Chow, J. L. Browning, K. L. Ramachandran, R. B. Pepinsky, *Nature (London) 320* (1986) 77.
[78] W. E. Lands, *J. Free Radicals Biol. Med. 1* (1985) 97.
[79] B. Samuelsson, *Angew. Chem. 95* (1983) 854; *Angew. Chem. Int. Ed. Engl. 22* (1983) 805.
[80] A. A. Barber, F. Bernheim, *Adv. Gerontol. Res. 2* (1967) 355.
[81] H. Esterbauer in D. C. H. McBrien, T. F. Slater (Eds.): *Free Radicals, Lipid Peroxidation and Cancer*, Academic Press, London 1982, p. 101.
[82] H. Kappus in [19], p. 273.
[83] N. L. Petrakis, L. D. Gruenke, J. C. Craig, *Cancer Res. 41* (1981) 2563.
[84] A. Sevanian, A. R. Peterson, *Proc. Natl. Acad. Sci. USA 81* (1984) 4198.
[85] M. A. Fogelman, I. Shechter, J. Seager, M. Hokom, J. S. Child, P. A. Edwards, *Proc. Natl. Acad. Sci. USA 77* (1980) 2214.
[86] G. Juergens, J. Lang, H. Esterbauer, *Biochim. Biophys. Acta 875* (1986) 103.
[87] a) H. P. Hartung, R. G. Kladetzky, M. Hennerici, *FEBS Lett. 186* (1985) 211; b) R. R. Montgomery, C. F. Nathan, Z. A. Cohn, *Proc. Natl. Acad. Sci. USA 83* (1986) 6631.
[88] H. H. Wasserman, W. A. Murray (Eds.): *Singlet Oxygen*, Academic Press, New York 1979.
[89] W. Adam, G. Cilento (Eds.): *Chemical and Biological Generation of Excited States*, Academic Press, New York 1982; *Angew. Chem. 95* (1983) 525; *Angew. Chem. Int. Ed. Engl. 22* (1983) 529.
[90] B. H. J. Bielski, E. E. Cabelli, R. L. Arudi, A. B. Ross, *J. Phys. Chem. Ref. Data 14* (1985) 1041.
[91] a) H. Kappus, H. Sies, *Experientia 37* (1981) 1233; b) H. de Groot, T. Noll, *Biochem. Biophys. Res. Comm. 119* (1984) 139; *Biochem. Pharmacol. 35* (1986) 15.
[92] G. A. Russell, *J. Am. Chem. Soc. 79* (1957) 3871.
[93] J. A. Howard, K. U. Ingold, *J. Am. Chem. Soc. 90* (1968) 1058.
[94] E. Cadenas, H. Sies, W. Nastainczyk, V. Ullrich, *Hoppe-Seyler's Z. Physiol. Chem. 364* (1983) 519.
[95] B. Schnuriger, J. Bourdon, *Photochem. Photobiol. 8* (1968) 361.
[96] A. Boveris, E. Cadenas, R. Reiter, M. Filipkowski, Y. Nakase, B. Chance, *Proc. Natl. Acad. Sci. USA 77* (1979) 347; E. Cadenas, H. Sies, *Methods Enzymol. 105* (1984) 221.
[97] H. Wefers, H. Sies, *Arch. Biochem. Biophys. 224* (1983) 568.
[98] E. Cadenas, R. Brigelius, H. Sies, *Biochem. Pharmacol. 32* (1983) 147.
[99] P. L. Chesis, D. E. Levin, M. T. Smith, L. Ernster, B. N. Ames, *Proc. Natl. Acad. Sci. USA 81* (1984) 1696.
[100] a) H. Wefers, D. Schulte-Frohlinde, H. Sies, FEBS Lett. (1986), in press; b) M. V. M. Lafleur, A. W. M. Nieuwint, J. M. Aubry, H. Kortbeek, F. Arwert, H. Joenje, *Free Radicals Res. Commun.* (1986), in press.
[101] A. U. Khan, M. Kasha, *J. Am. Chem. Soc. 92* (1970) 3293.
[102] E. Cadenas, H. Sies, H. Graf, V. Ullrich, *Eur. J. Biochem. 130* (1983) 117.
[103] J. R. Kanofsky, *J. Photochem. 25* (1984) 105.
[104] R. Porter, J. Whelan (Eds.): *Biology of Vitamin E, Ciba Found. Symp. 101*, Pitman, London 1983; L. J. Machlin in L. J. Machlin (Ed.): *Handbook of Vitamins*, Marcel Dekker, New York 1984, p. 100.
[105] G. W. Burton, A. Joyce, K. U. Ingold, *Arch. Biochem. Biophys. 221* (1983) 281.
[106] A. T. Diplock, J. A. Lucy, *FEBS Lett. 29* (1973) 205.
[107] E. Cadenas, M. Ginsberg, U. Rabe, H. Sies, *Biochem. J. 223* (1984) 755.

[108] A. L. Tappel, *Geriatrics 23* (1968) 97; J. E. Packer, T. F. Slater, R. L. Willson, *Nature (London) 278* (1979) 737.
[109] C. K. Chow, *Am. J. Clin. Nutr. 32* (1979) 1066.
[110] W. Wirth: *Nährwerttabelle*, Umschau Verlag, Frankfurt am Main 1984.
[111] T. Ishikawa, T. P. M. Akerboom, H. Sies in G. M. Cohen (Ed.): *Target Organ Toxicity, Vol 1*, CRC Press, Boca Raton 1986, p. 129.
[112] F. Ursini, M. Maiorino, M. Valente, L. Ferri, C. Gregolin, *Biochim. Biophys. Acta 710* (1982) 197; F. Ursini, M. Maiorino, C. Gregolin, *ibid. 839* (1985) 62.
[113] P. B. McCay, D. D. Gibson, K.-L. Fong, K. R. Hornbrook, *Biochim. Biophys. Acta 431* (1976) 459; R. F. Burk, M. J. Trumble, R. A. Lawrence, *ibid. 618* (1980) 35.
[114] D. D. Gibson, J. Hawrylko, P. B. McCay, *Lipids 20* (1985) 704; b) L. H. Lash, T. M. Hagen, D. P. Jones, *Proc. Natl. Acad. Sci. USA 83* (1986) 4641.
[115] a) C. Lind, P. Hochstein, L. Ernster, *Arch. Biochem. Biophys. 215* (1982) 178; b) H. Thor, M. T. Smith, P. Hartzell, G. Bellomo, S. A. Jewell, S. Orrenius, *J. Biol. Chem. 257* (1982) 12419.
[116] M. Bilzer, R. L. Krauth-Siegel, R. H. Schirmer, T. P. M. Akerboom, H. Sies, G. E. Schulz, *Eur. J. Biochem. 138* (1984) 373.
[117] H. Sies in Y. Sakamoto, T. Higashi, N. Tateishi (Eds.): *Glutathione: Storage, Transport and Turnover in Mammals*, Japan Scientific Societies Press, Tokyo 1983, p. 63; N. Kaplowitz, T. Yee Aw, M. Ookhtens, *Annu. Rev. Pharmacol. Toxicol. 25* (1985) 715; S. Bannai, N. Tateishi, *J. Membr. Biol. 89* (1986) 1.
[118] T. P. M. Akerboom, M. Bilzer, H. Sies, *FEBS Lett. 140* (1982) 73; *J. Biol. Chem. 259* (1984) 5838.
[119] P. Nicotera, M. Moore, G. Bellomo, F. Mirabelli, S. Orrenius, *J. Biol. Chem. 260* (1985) 1999.
[120] T. Ishikawa, H. Sies, *FEBS Lett. 169* (1984) 156; *J. Biol. Chem. 259* (1984) 3838.
[121] T. Ishikawa, M. Zimmer, H. Sies, *FEBS Lett. 200* (1986) 128.
[122] B. Mannervik, *Adv. Enzymol. 57* (1985) 357; H. Jensson, C. Guthenberg, P. Alin, B. Mannervik, *FEBS Lett. 203* (1986) 207.
[123] T. Ishikawa, H. Esterbauer, H. Sies, *J. Biol. Chem. 261* (1986) 1576.
[124] R. A. Lawrence, R. F. Burk, *Biochem. Biophys. Res. Commun. 71* (1976) 952; J. R. Prohaska, H. E. Ganther, *ibid. 76* (1977) 437.
[125] X. Chen, G. Yang, J. Chen, X. Chen, Z. Wen, K. Ge, *Biol. Trace Elem. Res. 2* (1980) 91.
[126] B. Ogorek, P. E. Bryant, *Mutat. Res. 146* (1985) 63.
[127] H. M. Hassan, I. Fridovich, *J. Biol. Chem. 252* (1977) 7667.
[128] G. J. Finn, S. Condon, *J. Bacteriol. 123* (1975) 570.
[129] B. Demple, J. Halbrook, *Nature (London) 304* (1983) 466.
[130] L. Winquist, U. Rannug, A. Rannug, C. Ramel, *Mutat. Res. 141* (1984) 145.
[131] R. M. Tyrrell, *Mutat. Res. 145* (1985) 129.
[132] A. Carlioz, D. Touati, *EMBO J. 5* (1986) 623.
[133] M. F. Christman, R. W. Morgan, F. S. Jacobson, B. N. Ames, *Cell 41* (1985) 753.
[134] H. Sies, M. F. Christman, G. Storz, B. N. Ames, unpublished (1986).
[135] S. B. Farr, R. D'Ari, D. Touati, private communication.
[136] E. Farber, *Biochim. Biophys. Acta 738* (1984) 171.
[137] W. Dörfler, *Angew. Chem. 96* (1984) 917; *Angew. Chem. Int. Ed. Engl. 23* (1984) 919; *Annu. Rev. Biochem. 52* (1983) 93.
[138] P. A. Jones, *Cancer Res. 46* (1986) 461.
[139] N. J. Gooderbaum, G. J. Mannering, *Cancer Res. 45* (1985) 1569.
[140] G. Wagner, H. Sies, unpublished (1986).
[141] J. B. Williams, A. Y. H. Lu, R. G. Cameron, C. B. Pickett, *J. Biol. Chem. 261* (1986) 5524.
[142] H. J. Prochaska, M. J. De Long, P. Talalay, *Proc. Natl. Acad. Sci. USA 82* (1985) 8232.
[143] A. Müller, E. Cadenas, P. Graf, H. Sies, *Biochem. Pharmacol. 33* (1984) 3235.
[144] A. Wendel, M. Fausel, H. Safayhi, G. Tiegs, R. Otter, *Biochem. Pharmacol. 33* (1984) 3241.
[145] a) A. Müller, H. Gabriel, H. Sies, *Biochem. Pharmacol. 34* (1985) 1185; b) J. H. Doroshow, *Proc. Natl. Acad. Sci. USA 83* (1986) 4514.
[146] H. Safayhi, G. Tiegs, A. Wendel, *Biochem. Pharmacol. 34* (1985) 2691.
[147] J. E. Spallholz, J. L. Martin, H. E. Ganther (Eds.): *Selenium in Biology and Medicine*, Avi Publ., Westport 1981.
[148] J. T. Rotruck, A. L. Pope, H. E. Ganther, A. B. Swanson, D. G. Hafeman, W. G. Hoekstra, *Science 179* (1973) 588; L. Flohé, W. A. Günzler, H. H. Schock, *FEBS Lett. 32* (1973) 132.
[149] J. W. Forstrom, J. J. Zakowsky, A. L. Tappel, *Biochemistry 17* (1978) 2639.
[150] A. Wendel, B. Kerner, K. Graupe, *Hoppe-Seyler's Z. Physiol. Chem. 359* (1978) 1035.
[151] L. Flohé, *Curr. Top. Cell. Res. 27* (1985) 473.
[152] a) L. N. Vernie, *Biochim. Biophys. Acta 738* (1984) 203; b) W. A. Günzler, G. J. Steffens, A. Grossmann, S.-M. A. King, F. Otting, A. Wendel, L. Flohé, *Hoppe Seyler's Z. Physiol. Chem. 365* (1984) 195; c) D. Epp, R. Ladenstein, A. Wendel, *Eur. J. Biochem. 133* (1983) 51; d) I. Chambers, J. Frampton, P. Goldfarb, N. Affara, W. McBain, P. R. Harrison, *EMBO J. 5* (1986) 1221; e) F. Zinoni, A. Birkmann, T. C. Stadtman, A. Böck, *Proc. Natl. Acad. Sci. USA 83* (1986) 4650.
[153] E. C. Huskisson, J. Scott, *Eur. J. Rheumatol. Inflammation 4* (1981) 212.
[154] L. Sherman, N. Defni, J. Lieman-Hurwitz, Y. Groner, *Proc. Natl. Acad. Sci. USA 80* (1983) 5465.
[155] R. A. Hallewell, F. R. Masiarz, R. C. Najarian, J. P. Puma, M. R. Quiroga, A. Randolph, R. Sanchez-Pescador, C. J. Scandella, B. Smith, K. S. Steimer, G. T. Mullenbach, *Nucleic Acids Res. 13* (1985) 2017.
[156] B. R. Lucchesi, K. M. Mullane, *Annu. Rev. Pharmacol. Toxicol. 26* (1986) 201.
[157] a) D. N. Granger, G. Rutili, J. M. McCord, *Gastroenterology 81* (1981) 22; b) H. Sanfay, M. G. Sarr, G. B. Bulkley, J. L. Cameron, *Acta Physiol. Scand. 126, Suppl. 548* (1986) 109.
[158] R. J. Gryglewski, R. M. J. Palmer, S. Moncada, *Nature (London) 320* (1986) 454.
[159] A. P. Autor (Ed.): *Pathology of Oxygen*, Academic Press, New York 1982; J. D. Balentine, *Pathology of Oxygen Toxicity*, Academic Press, New York 1982.
[160] P. A. Cerutti, *Science 227* (1985) 375.
[161] N. J. Sargentini, K. C. Smith, *Mutat. Res. 154* (1985) 1.
[162] R. J. Mehlhorn, G. Cole, *Adv. Free Radicals Biol. Med. 1* (1985) 165.
[163] R. S. Sohal, R. G. Allen, *Adv. Free Radicals Biol. Med. 2* (1986) 117.
[164] L. Flohé, R. Beckmann, H. Giertz, G. Loschen in [19], p. 403.
[165] E. K. Lai, C. Crossley, R. Sridhar, H. P. Misra, E. G. Janzen, P. B. McCay, *Arch. Biochem. Biophys. 244* (1986) 156.
[166] C. Borek, A. Ong, H. Mason, L. Donahue, J. E. Biaglow, *Proc. Natl. Acad. Sci. USA 83* (1986) 1490.
[167] G. Batist, A. Reynaud, A. G. Katki, E. L. Travis, M. C. Shoemaker, R. F. Greene, C. E. Myers, *Biochem. Pharmacol. 35* (1986) 601.
[168] O. F. Nygaard, M. Simic (Eds.): *Radioprotectors and Anticarcinogens*, Academic Press, New York 1983.
[169] L. Packer (Ed.): *Oxygen Radicals in Biological Systems, Methods Enzymol. 105*, Academic Press, New York 1984.
[170] R. A. Greenwald (Ed.): *Methods for Oxygen Radical Research*, CRC Press, Boca Raton 1985.
[171] R. J. P. Williams in [20a], p. 593.
[172] D. Evered, J. Nugent, M. O'Connor (Eds.): *Biochemistry of Macrophages*, Pitman, London 1986.
[173] M. N. Hamers, D. Roos in [19], p. 351; S. J. Weiss, G. J. Peppin, *Biochem. Pharmacol. 35* (1986) 3189.
[174] J. Knappe, F. A. Neugebauer, H. P. Blaschkowski, M. Gänzler, *Proc. Natl. Acad. Sci. USA 81* (1984) 1332.
[175] a) P. Reichard, A. Ehrenberg, *Science 221* (1983) 514; R. Eliasson, H. Jörnvall, P. Reichard, *Proc. Natl. Acad. Sci. USA 83* (1986) 2373; b) A. M. Lefer, *Biochem. Pharmacol. 35* (1986) 123; H. A. Ball, J. A. Cook, W. C. Wise, P. V. Halushka, *Intensive Care Medicine 12* (1986) 116.
[176] a) A. M. Michelson, J. M. McCord, I. Fridovich (Eds.): *Superoxide and Superoxide Dismutases*, Academic Press, London 1977; b) L. Flohé, G. Loschen, *Eur. J. Rheum. Inflammation 4* (1981) 183.
[177] H. P. Misra, I. Fridovich, *J. Biol. Chem. 247* (1972) 188.
[178] A. M. Michelson in [176a], p. 87.
[179] H. P. Misra, I. Fridovich, *J. Biol. Chem. 247* (1972) 6960.
[180] G. Rotilio, E. Fioretti, G. Falcioni, F. Brunori in [176a], p. 239.
[181] R. Zimmermann, L. Flohé, U. Weser, H.-J. Hartmann, *FEBS Lett. 29* (1973) 117.
[182] H. P. Misra, *J. Biol. Chem. 249* (1974) 2151.
[183] W. Bors, C. Michel, M. Saran, E. Lengfelder, *Biochim. Biophys. Acta 540* (1978) 162.
[184] J. Weiss, *Naturwissenschaften 23* (1935) 64.
[185] A. M. Michelson in [176a], p. 77.
[186] J. M. McCord, I. Fridovich, *J. Biol. Chem. 243* (1968) 5753.
[187] P. F. Knowles, J. F. Gibson, F. M. Pick, R. C. Bray, *Biochem. J. 111* (1969) 53.
[188] E. F. Elstner, A. Heupel, S. Vaklinova, *Z. Pflanzenphysiol. 62* (1970) 184.
[189] G. Loschen, A. Azzi, C. Richter, L. Flohé, *FEBS Lett. 42* (1974) 68.
[190] C. Richter, A. Azzi, U. Weser, A. Wendel in [176a], p. 375.
[191] B. M. Babior, R. S. Kipnes, J. T. Curnutte, *J. Clin. Invest. 52* (1973) 741.
[192] R. B. Johnston, B. B. Keele, H. P. Misra, J. E. Lehmeyer, L. S. Webb, R. L. Baehner, K. V. Rajagopalan, *J. Clin. Invest. 55* (1975) 1357.
[193] S. J. Klebanoff, H. Rosen, *Ciba Found. Symp. 65 (New Ser.)*, (1979) 263.
[194] W. S. Thayer, *Chem. Biol. Interact. 19* (1977) 265.
[195] N. R. Bachur, S. L. Gordon, M. V. Gee, *Cancer Res. 38* (1978) 1745.
[196] J. C. Gage, *Biochem. J. 109* (1968) 757.
[197] L. L. Smith, M. S. Rose, I. Wyatt, *Ciba Found. Symp. 65 (New Ser.)* (1979) 321.

Photochemistry of Transition-Metal Atoms: Reactions with Molecular Hydrogen and Methane in Low-Temperature Matrices

By Geoffrey A. Ozin,* John G. McCaffrey, and J. Mark Parnis

Reactions of metal atoms with molecular hydrogen and alkanes are prototypical of more complex systems involving metal-mediated reactions in solution, on supports, and on surfaces. The simplicity of metal-atom reactions makes them particularly attractive for fundamental experimental and theoretical studies. Following the first reports of H_2 and CH_4 activation by photoexcited metal atoms in cryogenic matrices, the behavior of a number of transition-metal atoms in their ground and selected electronically excited states has been examined with molecular hydrogen, methane, and ethane. A wealth of structural, electronic, reactivity, and selectivity information is emerging from these studies and it is now becoming possible to recognize the controlling factors at work in these fundamental chemical reactions. In this article, some experimental results for a number of metal-atom systems, in particular, those involving silver, copper, manganese, and iron atoms, are presented along with a discussion of the factors that are believed to be important in the understanding of the observed physical and chemical behavior.

1. Introduction

How can a metal atom have photochemistry? This is a question that a synthetic organometallic chemist might justifiably ask. One could respond by stating that it is expected that the chemical reactivity of a metal atomic species would be different for distinct electronic states of the metal atom. This general comment can be readily supported by thermodynamic and kinetic considerations. However, the exact nature of the resulting metal-atom reaction products cannot be so readily anticipated. In order to understand the types of photochemical processes initiated by the absorption of UV or visible light by isolated metal atoms entrapped at low temperatures with a co-reactant, it is necessary to use electronic, vibrational, and electron spin resonance spectroscopic studies of reaction intermediates and products.

The past decade has seen extensive development in the field of transition-metal vapor chemistry, although interest has been exclusively focused on the chemical reactivity of ground electronic state metal atoms in the condensed phase.[1] The analogous condensed-phase photochemistry of these systems has only recently been investigated.[2] On the other hand, extensive gas-phase photochemical studies have been performed on mercury and cadmium atoms since 1922, when *Cario* and *Franck*[3] discovered that photoexcited mercury atoms ($\lambda = 253.7$ nm) reacted with molecular hydrogen to produce free hydrogen atoms. A large body of data is available on the reactions of $^1P_1$ and $^3P_1$ mercury and cadmium atoms with hydrogen, methane, alkanes, and alkenes in the gas phase,[4,5] and results have recently been reviewed for similar reactions involving the analogous excited electronic states of magnesium and zinc atoms.[5]

Until recently, gas-phase investigations of electronically excited metal atoms have been limited to studies of relatively volatile metals, and hence only a small number of metal atomic species (alkali and alkaline-earth metals as well as metals of the zinc triad) have been studied in this way.[5] However, the advent of laser vaporization and molecular beam techniques has greatly extended the range of metals that are amenable to examination. Chemically interesting reactive intermediates such as RMH or HMH have not as yet been detected in the gas phase even by the highly sensitive laser-induced fluorescence technique, presumably because of their instability and transient nature and/or their low concentration.

In this paper the application of matrix isolation techniques to studies of certain classes of photochemical reactions of transition-metal atoms is described. Prior to our initial investigations in this field[6] there were apparently no studies of photochemical reactions of transition-metal atoms in low-temperature matrices.

It is now well-known that the matrix isolation spectroscopy (MIS) technique employs low-temperature solids as media for stabilizing relatively large quantities of reactive chemical species for long periods of time.[7] It is often the case that the interaction between the molecular guest species and the host matrix is sufficiently weak that electronic, vibrational, and ESR spectra differ insignificantly from what is predicted based on a simple model of a nonrotating but otherwise gaseous species with internal degrees of freedom (apart from rotation) equilibrated at the temperature of the matrix. Thus the low temperature of the matrix serves not only to stabilize the molecular species of interest but also to simplify its spectra. The number of chemical species for which MIS studies are possible is very large, being only limited by the requirement that the species itself, or a suitable photolytic precursor, be produced initially in a gaseous state. For the small quantities of material required in a MIS study (10^{-6} to 10^{-3} g) this presents no difficulty for all of the elements of the periodic table.

[*] Prof. G. A. Ozin, J. G. McCaffrey, J. M. Parnis
Department of Chemistry, University of Toronto
Toronto, Ontario M5S 1A1 (Canada)

 © VCH Verlagsgesellschaft mbH, D-6940 Weinheim, 1986 0570-0833/86/1212-1072 $ 02.50/0

Therefore, the MIS technique can be easily applied to a wide range of metal-atom photochemical studies, and considerable potential exists for systematic investigations of the reactivity of photoexcited transition-metal atoms.

A large number of reactions involving ground-state metal-atom reagents can be conducted in the range 4.2–40 K. In these cases small activation energy barriers (0–5 kcal mol^{-1}) can be surmounted by thermal assistance from metal-atom translational energies, matrix/ligand condensation energies, and metal-source radiation energies, which are in the range 3–5 kcal mol^{-1}. The major products formed in these reactive systems usually arise from low-activation-energy, simple orbital-mixing processes, such as the following:

$$Pt + CO \longrightarrow Pt(CO)_4$$ [8]

$$Ni + N_2 \longrightarrow Ni(N_2)_4$$ [9]

$$Rh + O_2 \longrightarrow Rh(O_2)_2$$ [10]

$$Cu + C_2H_4 \longrightarrow Cu(C_2H_4)_3$$ [11]

$$Cr + Mo \longrightarrow CrMo$$ [12]

At the same time a large number of "unreactive" metal/ligand systems exist, which yield matrix samples comprised only of isolated metal atoms coexisting with unreacted ligands.

In particular, reactions involving ground-state metal-atom-induced bond-cleavage processes do not usually proceed at 4.2–40 K.[13] An example is oxidative addition to a C–H bond:

$$M + RH \longrightarrow RMH$$

It is specifically this class of ligands, namely, those that are unreactive toward ground electronic state metal-atom reagents at 4.2–40 K, that this article addresses. The large body of photochemistry of matrix-isolated molecules has recently been reviewed[14] and will not be discussed here.

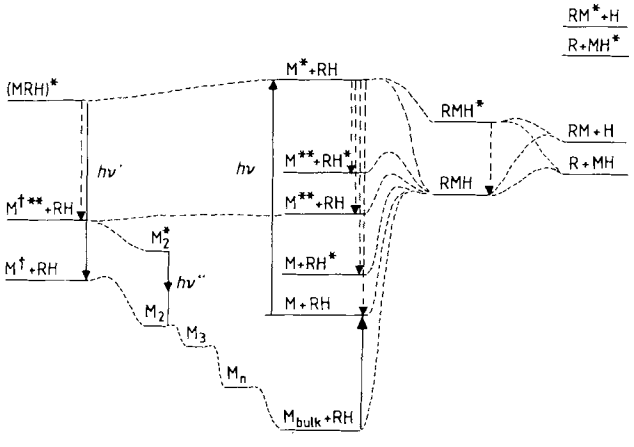


Fig. 1. A schematic view of condensed-phase energetics, dynamics, and reaction pathways of ground and excited electronic state metal atoms with alkanes and molecular hydrogen (R = H), $M^{\dagger}$ refers to a mobile metal atom; the asterisk denotes an electronically/vibrationally excited species; M_{bulk} is aggregate metal.

The basic physical and chemical mechanisms whereby fluorescence from the lowest M* and M** excited states of metal atoms is quenched by RH (R = H or CH_3) are shown in general terms in the energy-level scheme of Figure 1. The scheme shows that, in general, the reaction of the ground-state M with RH to give the insertion product RMH is sufficiently endothermic to not proceed at a measureable rate at 4.2–40 K. However, with respect to selected excited electronic states M* and M**, the situation can be quite different. Provided that there exist no insurmountable steric barriers, spin-selection restrictions, and/or orbital symmetry constraints, the reaction of M* or M** to yield RMH will likely be exothermic or at least thermoneutral, with either a negligible or a small activation barrier and hence will proceed at a measureable rate at 4.2–40 K. Whether RMH is directly formed in its electronic ground state or in an excited state (which may be unstable with respect to fragmentation) will depend intimately on the mechanism of chemical quenching of M* and M** as determined by the correlation of the electronic states of the metal atom plus reactant with those of the product.[15]

Another chemical quenching process of M* that can compete with the formation of the RMH insertion product involves vibrational relaxation of the matrix cage atoms or molecules around M* (Jahn–Teller effect, exciplex formation) followed by radiative and/or nonradiative decay to the ground-state M. The destabilization caused by producing a vibrationally excited ground-state "cage-complex" resulting from a Franck–Condon transition from the relaxed excited-state configuration can provide the driving force for photoinduced diffusion of ground-state M atoms and subsequent aggregation to M_2, M_3, M_4, etc. metal clusters (Fig. 1). Alternatively, M* can relax nonradiatively to a lower-energy electronically excited state M**. The energy thereby released into the matrix is thought to cause "local softening" of the surrounding cage resulting in photoinduced diffusion of M** (e.g., a long-lived mobile excited state) and reactive encounters with nearby ground-state M forming M_2, M_3, etc. metal clusters (Fig. 1). The metal-atom photoaggregation phenomenon (involving both ground-state and excited-state metal atoms) has been documented for Cu, Ag, Cr, Mo, and Rh atoms.[6]

Different behavior has been observed in recent studies of the quenching of electronically excited alkaline-earth metal atoms and atoms of the zinc triad (groups 2 and 12, respectively, of the periodic table) by alkanes or molecular hydrogen in the gas phase. These chemical quenching processes have a direct bearing on analogous processes involving electronically excited transition-metal atoms in low-temperature matrices. Three types of quenching processes have been identified in gas-phase studies based on the products observed:

(A) Photosensitization:

$$M^*RH \longrightarrow M + R^{\odot} + H^{\odot}$$

(B) Abstraction or insertion/fragmentation:

$$M^* + RH \longrightarrow MH + R^{\odot}$$

(C) Energy transfer:

$$M^* + RH(v=0) \longrightarrow M^{**} + RH(v=n)$$

Chemical quenching of the first $^1P_1$ excited states of certain group-2 and -12 metal atoms by H_2, CH_4, and alkanes is thought to occur by direct covalent chemical interaction between the excited metal atom and the quenching molecule.[4, 5, 16, 17] In this picture the reactions are envisaged as traversals of covalent potential energy surfaces, these surfaces correlating the separated reactants in their initial electronic states with the appropriate electronic states of the reactive complex and the final products. The reaction may or may not be adiabatic in the sense that the pathway may or may not involve a single potential energy surface exclusively.

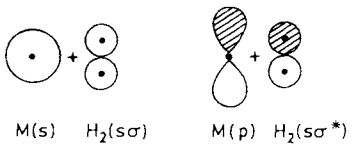


Fig. 2. Pictorial representation of the orbital interactions that are expected to be important in the quenching of excited P states of metal atoms by molecular hydrogen.

Callear et al.[4b] and *Breckenridge* et al.[16, 17] have considered reaction pathways including side-on attack on molecular hydrogen or on a C–H bond of an alkane molecule by the excited metal atom. The covalent chemical interactions that are expected to be important in the initial stages of such a reaction are illustrated in Figure 2 for excited electronic states derived from a ns^0np^1 or ns^1np^1 configuration. Here, the empty or singly occupied s and p metal atomic orbitals are available for bonding with the σ* antibonding molecular orbitals of H_2 or RH, respectively. Since the σ* orbital of H_2 or RH is unoccupied, the interaction with the singly occupied p orbital of the metal atom is believed to result in a transfer of charge from the metal atom to the antibonding orbital of H_2 or RH. At the same time the σ orbital of H_2 or RH is doubly occupied; therefore, it is expected that the M(s) + RH(σ) bonding interaction would lead to a transfer of electron density from the bonding molecular orbital of H_2 or RH to the metal atom. These metal-H_2 and metal-RH bonding interactions work in a synergistic sense and lead to a weakening of the H–H and R–H bonds, respectively. Considerations of this type may prove useful for deciphering the reactivity patterns of different electronic states of transition-metal atoms, in which the manifold of terms arising from a $(n-1)d^x ns^y np^z$ configuration is generally expected to be much more complex than the terms for s- and p-block metal atoms.

In what follows, selected physical and chemical aspects of the photochemistry of matrix-isolated transition-metal atoms, as well as of their reaction products, will be briefly illustrated by reference to some recent observations for electronically excited Mn, Fe, Cu, and Ag atoms with molecular hydrogen, methane, and ethane. For details of this work, the original literature references should be consulted.

2. Competing Photoinsertion and Photoaggregation Pathways in the Cu/CH_4, Cu/C_2H_6, Ag/CH_4, and Ag/C_2H_6 Systems

In all of the above systems, photoexcitation around 290–350 nm into the various components of the $^2P \leftarrow {}^2S$ atomic resonance transition of the entrapped Cu and Ag atoms causes rapid bleaching of the atomic absorption lines. Studies on the rate of loss of Cu atoms during photolysis in both CH_4[2c, 18] and C_2H_6[19] indicate that the quantum yield for chemical reaction does not vary with photolysis time and is essentially constant for CH_4, C_2H_6, CD_4, and CH_2D_2 matrices. For Cu/CH_4 and Cu/C_2H_6, no spectroscopic evidence for competing photoaggregation pathways to Cu_2, Cu_3, etc. clusters was obtained and no sign of Cu $^2D \rightarrow {}^2S$ fluorescence following $^2P \rightarrow {}^2D$ relaxation (easily observed in rare-gas matrices[20]) was apparent in CH_4 and C_2H_6 matrices. The UV/VIS spectroscopic and photochemical results, when taken in conjunction with IR, ESR, and isotope-labeling (^1H, ^2H, and ^{13}C) studies, serve to define the photochemical reaction of Cu atoms with CH_4 and C_2H_6 as one involving an initial insertion process to form RCuH followed by fragmentation to mainly R + CuH (see Section 3). With the Cu/CH_4 and Cu/C_2H_6 systems serving as control experiments, in that the excited-state Cu-atom reaction with the alkane can be considered to involve the direct reaction of the initially prepared ^2P state, we can now turn our attention to the corresponding Ag/CH_4 and Ag/C_2H_6 photochemical reactions.[21]

In the case of Ag/CH_4, using UV/VIS absorption and emission, IR, and ESR spectroscopy, one observes an insertion pathway to CH_3AgH with fragmentation of the intermediate to form $CH_3 + AgH$, but with an accompanying pathway to Ag_2 (Fig. 3). From UV/VIS spectroscopy, it is difficult to quantify the relative contribution of the photoinsertion and photodimerization pathways. However, the

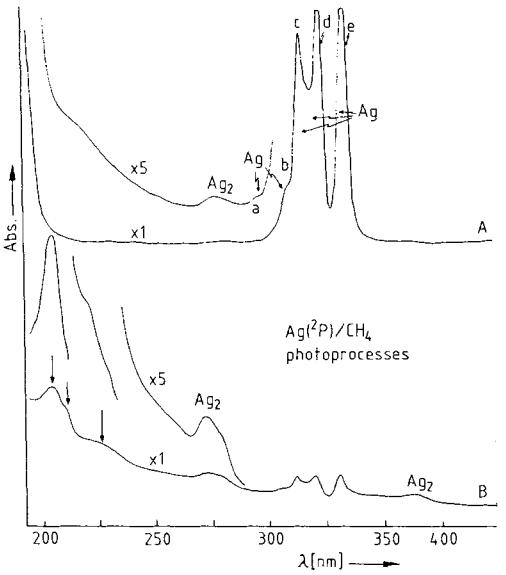


Fig. 3. UV/VIS spectrum illustrating competing 320-nm-induced photoinsertion and photodimerization matrix reactions of $Ag(^2P)/CH_4$ at 12 K. Absorptions due to Ag (maxima a–e) and Ag_2 are indicated; the arrows denote CH_3 and AgH absorptions. A) Spectrum before photoexcitation; B) spectrum following photoexcitation.

rate of Ag-atom loss observed for Ag/CH_4 was found to be roughly 60% as fast as that for Cu/CH_4 under similar photolysis conditions. The situation appears to be much the same for Ag/C_2H_6 matrices in terms of photodimerization yields, although the rate of Ag-atom loss with photolysis time diminished for excitation into all three major components of the $^2P \leftarrow {}^2S$ Ag atomic resonance absorption at 305, 320, and 347 nm, approaching the rate observed for Ag/Kr matrices (Fig. 4).

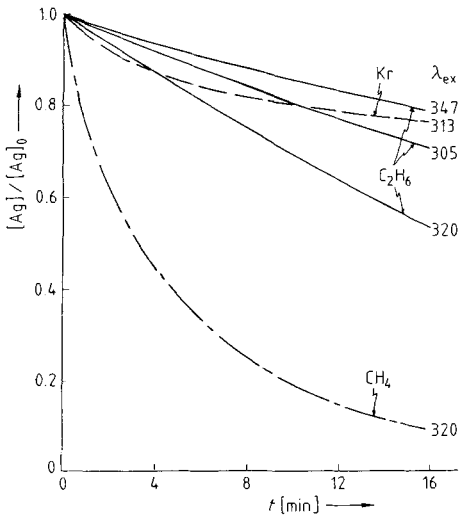


Fig. 4. Graphical representation of Ag(^{2}P) quenching behavior in Kr, CH_4, and C_2H_6 at 12 K. λ_{ex} = excitation wavelength. Identical concentration conditions were employed in these experiments.

In the following we attempt to provide a unified rationale for the above observations in terms of the ^{2}P- and ^{2}D-state energetics, dynamics, and cage structures for Cu and Ag atoms in CH_4 and C_2H_6 matrices.

2.1. Cage Structure of Cu and Ag Atoms in Solid CH_4

The p/T phase diagram of solid CH_4 has been well documented in the ranges 0–35 K and 0–5 kbar.[22] In this range, solid CH_4 exhibits the orientationally disordered phase I, the partially ordered phase II, and the ordered phases III and IV, which exist only under pressure. In phase II, which at low pressures exists between 10 and 20 K and is therefore pertinent to the present discussion, the carbon atoms are arranged in a face-centered cubic lattice with space group $Fm3c$. Three-quarters of the molecules are orientationally ordered with site symmetry D_{2d} and one-quarter are disordered with site symmetry O.

One can see that substitutional replacement of an ordered CH_4 molecule by a metal atom yields three kinds of nearest-neighbor $M \cdots CH_4$ interactions, two involving ordered CH_4 (face and apex aspects) molecules and one involving disordered CH_4 molecules. The latter may display face, edge, and apex aspects to the entrapped M atom. Alternatively, the $M \cdots CH_4$ interaction may freeze out the rotational disorder at the O sites and lock the CH_4 molecule in a preferred orientation with respect to the M atom. Substitutional replacement of a disordered CH_4 molecule by a M atom, on the other hand, results in just one kind of nearest neighbor $M \cdots CH_4$ interaction exhibiting a twofold edge aspect. Although differing in detail, similar considerations can be applied to the hexagonal close-packed lattice of solid C_2H_6, which exists in the range 10–20 K.

An examination of the $^2P \leftarrow {}^2S$ multiplet structure of Cu and Ag atoms in CH_4 and C_2H_6 matrices reveals five major components. From annealing studies,[18,21] this group of five observable lines can be divided into a group of three (major) and a group of two (minor), the origin of which can be traced to two different matrix trapping sites. It is proposed that Cu in CH_4 replaces a disordered CH_4 and thereby samples mainly edge aspects of the surrounding CH_4 molecules, whereas Ag in CH_4 replaces an ordered CH_4 and in doing so is able to sample face, edge, and apex aspects of the nearest-neighbor CH_4 molecules. Considerations of this type are thought to be important in discussions of the energetics, dynamics, and reactivity of metal atoms photoexcited in CH_4 and C_2H_6 matrices (see Sections 2.3 and 10).

2.2. C–H versus C–C Bond Insertion

In all cases one observes C–H bond-insertion pathways with fragmentation of the RMH intermediate to mainly R + MH.[2b,18,19] The disruption of RMH is more pronounced for C_2H_6 than CH_4 for both $^2P \leftarrow {}^2S$ Cu and Ag atoms. It is difficult to rationalize these results on the basis of C–C versus C–H bond energies or symmetry restrictions in C_2H_6 versus CH_4. One is obliged to consider a steric barrier for the attack of ^{2}P Cu or Ag atoms on the C–C bond of C_2H_6 (nonreactive site); such a barrier seems to be unimportant for the insertion into a C–H bond (reactive site). It is therefore to be expected that side-on attack of ^{2}P Cu atoms on the C–H bonds of CH_4 and C_2H_6 would involve similar $Cu(4s^0) + RH(\sigma)$ and $Cu(4p^1) + RH(\sigma^*)$ bonding interactions, which would lead to weakening of the C–H bonds in a comparable synergistic C–H bond activation process, resulting in essentially identical quantum yields, as observed experimentally through studies of rate of atom loss with photolysis time.

2.3. Photoinsertion versus Photodimerization

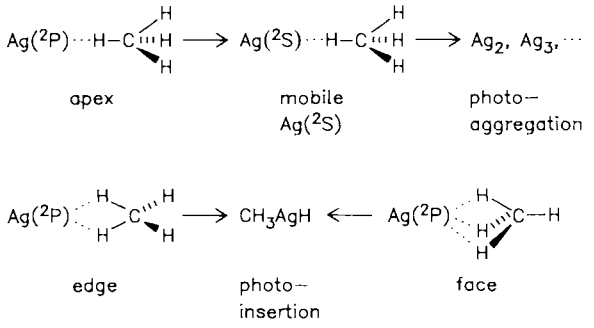
The observation of exclusive photoinsertion for ^{2}P Cu in CH_4 and C_2H_6 matrices yet competing photoinsertion/photodimerization pathways for ^{2}P Ag in CH_4 and C_2H_6 can be traced to differences in the cage geometries and relaxation dynamics for these metal atoms and matrices. In the case of Ag, it is the destabilization caused by formation of "ground state" Ag-atom-cage complexes in the relaxed ^{2}P excited-state configuration that provides the driving force for photoinduced diffusion of the Ag atoms.[6] In contrast, photoinduced diffusion of ^{2}P Cu atoms is promoted by $^2P \rightarrow {}^2D$ nonradiative transitions, allowing for reactive encounters of a long-lived ^{2}D Cu atom with nearby ground-state ^{2}S Cu atoms.[20,23] Thus, in the case of Cu, the ^{2}D state is intimately involved with both the photoinduced diffusion and dimerization mechanisms. Extending these ideas for ^{2}P Cu and Ag atoms in rare-gas

solids to the case of CH_4 and C_2H_6 matrices, one can propose the following:

(A) The ^2P state of the Cu and Ag atom is responsible for the insertion pathway for side-on approach to a C-H bond.

(B) In the case of Cu, the preferred cage geometry (major site replacing disordered CH_4, see Section 2.1) is such as to expose mainly C-H edge aspects of the CH_4 (or C_2H_6) molecule to the ^2P Cu atom, which inserts to form RCuH. The ^2D Cu state is never populated in this scheme and, therefore, the photodimerization route is completely quenched.

(C) In the case of Ag, the cage geometry is such that all face, edge, and apex aspects of the CH_4 (or C_2H_6) molecule are exposed (major site replacing ordered CH_4, see Section 2.1) to the ^2P Ag atom. Assuming that the apex approach represents a nonreactive encounter with respect to insertion, one can begin to appreciate how face and edge cage geometries can lead to photoinsertion, whereas apex geometries can lead to photodimerization (Scheme 1).



Scheme 1.

It remains to rationalize the more facile insertion of the ^2P Ag atom into the C-H bond of CH_4 compared with C_2H_6, remembering that the rates of the competing photodimerization appear to be about the same. A logical explanation stems from consideration of the number of reactive and nonreactive sites for Ag/CH_4 versus Ag/C_2H_6. For $Ag(^2P)/CH_4$ all face and edge encounters are productive for C-H bond insertion, whereas for $Ag(^2P)/C_2H_6$ only 25% of the face and 50% of the edge configurations can lead to C-H bond insertion, because of the proposed steric barrier to attack on the C-C bond. The less efficient C-H photoinsertion of $Ag(^2P)$ in C_2H_6 compared with CH_4 can be understood in this way although it is expected that other factors could also contribute to the overall scheme.

3. Fragmentation of CH_3CuH in the $Cu(^2P)/CH_4$ Matrix Reaction

Following $^2P \leftarrow {}^2S$ Cu-atom photolysis in 12-K CH_4 matrices, one observes by UV/VIS or ESR spectroscopy rapid depletion of the Cu-atom resonance lines with simultaneous formation of CH_3CuH, CH_3, CuH, CH_3Cu, and H.[18] Detailed kinetic and spectroscopic studies on the Cu/CH_4 system afford the following results: (1) the quantum yields for reaction in CH_4, CD_4, and CH_2D_2 are the same within experimental error. (2) The quantum yield does not vary with temperature between 12 and 25 K. (3) The $^2D \rightarrow {}^2S$ Cu-atom emission and Cu-atom photoaggregation processes seen in rare-gas matrices are completely quenched in solid CH_4. (4) As the photolysis proceeds, the concentration of CH_3CuH passes through a maximum and subsequently diminishes to zero (Fig. 5). At the same time, the concentration of $CH_3 + CuH$ and $CH_3Cu + H$ continue to increase and attain a constant value at very long photolysis times, the former pathway being favored over the latter by $>20:1$. (5) The measured [CuH]/[CuD] fragment ratio (IR absorbances corrected for the diatomic reduced masses) in the $Cu(^2P)/CH_2D_2$ reaction is unity within experimental error, implying that neither the formation nor fragmentation of CH_2DCuD compared with CHD_2CuH exhibits a measureable kinetic isotope effect. (6) Thermal annealing (12–40 K) of Cu/CH_4 matrices containing $CH_3 + CuH$ and $CH_3Cu + H$ leads to production of CH_3CuH, which itself decomposes above 40 K.

Of particular interest in the $Cu(^2P)/CH_4$ system is the mechanism of formation of fragments $CH_3 + CuH/$

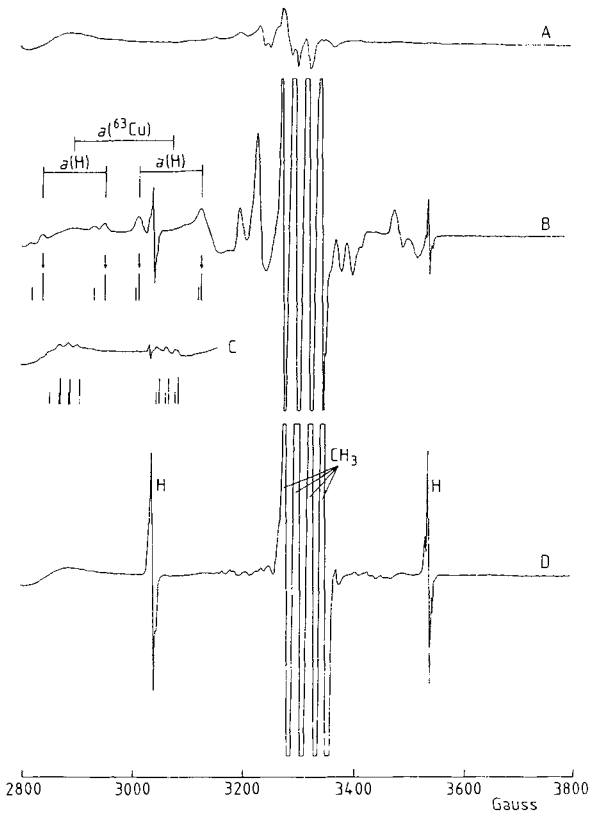


Fig. 5. ESR spectra showing changes caused by 320-nm photolysis of a Cu/CH_4 matrix ($\approx 1/10^4$) at 12 K. A) Freshly deposited matrix; B) after 2 min of 320-nm irradiation; D) after 15 min of 320-nm irradiation. The weak features near 3300 G in trace A are due to matrix impurities, mainly residual $Cu(O_2)$. Trace C shows a portion of the ESR spectrum of a Cu/CD_4 matrix ($\approx 1/10^4$) following 2 min of photolysis at 320 nm. The lines indicated by arrows in the upper stick spectrum show the positions of the lines in trace B that were used to measure the hyperfine splitting constants $a(^{63}Cu)$ and $a(H)$. The field positions of all other lines in the stick spectrum associated with ^{65}Cu hyperfine and H and D superhyperfine splitting represent calculated values using standard fitting procedures. The upper stick spectrum applies for CH_3CuH and should be compared with trace B, and the lower stick spectrum applies for CD_3CuD and should be compared with trace C. The microwave frequency was 9.280 GHz.

$CH_3Cu + H$. A broad UV/VIS absorption centered around 350 nm has been associated with CH_3CuH.[2c,18] Narrow-band excitation into this absorption causes rapid bleaching of all bands associated with CH_3CuH and concomitant production of CH_3, CuH, CH_3Cu, H, and Cu as seen by a combination of UV/VIS, vibrational, and ESR spectroscopy. Typical UV/VIS data for this photofragmentation are shown in Figure 6. Initial IR observations of the growth and decay characteristics of the intermediate and final products suggested that the reaction involves a two-step process in which the fragments $CH_3 + CuH$ and $CH_3Cu + H$ are formed exclusively from secondary photolysis of CH_3CuH. This is supported by the observation that final product distributions from 350-nm photolysis of CH_3CuH are similar to those obtained during 305–325-nm photolysis of Cu atoms, with the exception of regenerated Cu atoms in the former case.

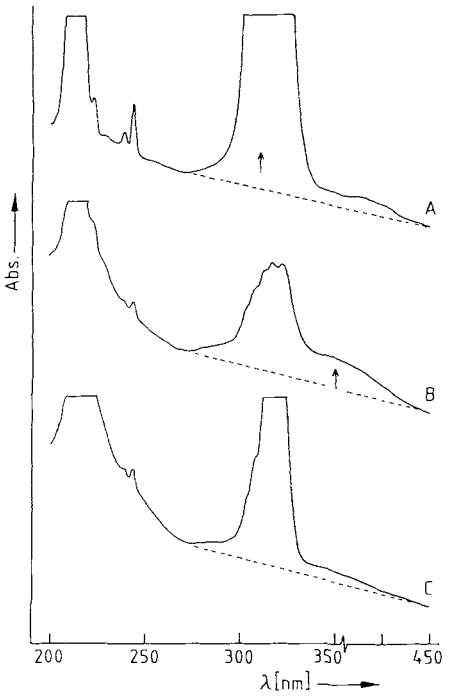


Fig. 6. UV/VIS spectrum of a Cu/CH_4 matrix: A) after deposition; B) following partial photolysis at 305 nm (60 min); C) following subsequent 350-nm photolysis (45 min).

A detailed study of the growth and decay behavior of the ESR signals due to Cu, CH_3, and CH_3CuH[28] has been done in order to establish the mechanistic routes by which the final products are formed. Theoretical growth and decay curves (Fig. 7) were generated by means of numerical integration of differential equations describing the routes for production and loss of these three species. The rate of change in the concentration of photochemically active species was related to the rate of photon absorption and the quantum efficiency for chemical reaction. From this analysis, it was clear that the growth of >90% of the final products is solely dependent upon the concentration of CH_3CuH, with only a small (<10%) amount that *may* be attributable to an abstraction or fragmentation process giving $CH_3 + CuH$ directly. Thus, it is established that the overall mechanism for the reaction of photoexcited ($^2P \leftarrow {}^2S$) Cu atoms in CH_4 is a two-step process involving the initial formation of CH_3CuH, which fragments photochemically to form all other products observed.

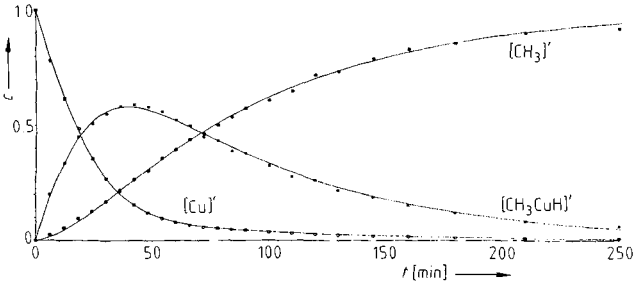


Fig. 7. Growth and decay behavior of Cu, CH_3CuH, and CH_3 during 305-nm photolysis. Points represent ESR experimental data and solid lines are the theoretically generated fit [18]. t = photolysis time.

To gain insight into the excited state(s) responsible for CH_3CuH fragmentation, SCF-Xα-SW MO calculations have been performed for linear CH_3CuH (Fig. 8).[24] Xα calculations show a low-lying $2a_1$ C–Cu–H σ-bonding level followed at higher energies by two near-degenerate and occupied levels designated 2e and 3e, corresponding to essentially pure $d_{x^2-y^2,xy}$ and $d_{xz,yz}$ Cu orbitals. Above these are two near-degenerate levels, designated $3a_1$ and $4a_1$, containing a single unpaired electron, thereby yielding a $^2A_1$ electronic ground state for CH_3CuH. The partial wave description of these $3a_1$ and $4a_1$ valence molecular orbitals is rather interesting. The $3a_1$ has mainly Cu and H σ-bonding character with a node between the Cu and C, while the $4a_1$ has mainly Cu and C σ-bonding character with a node between the Cu and H. These calculations indicate that 350-nm excitation of CH_3CuH probably involves the promotion of a σ-bonding electron from the $2a_1$ orbital to either one of the nearly degenerate $3a_1/4a_1$ pair of orbitals, which have σ*-antibonding character with respect to the Cu–C and Cu–H bonds, respectively (Fig. 8). If CH_3CuH in these $^2A_1$ excited electronic states has a linear geometry, then one can begin to understand why 305–325-nm photolysis of Cu atoms in CH_4 matrices leads not only to the production of CH_3CuH, but also to its destruction.

From the available data it is not immediately obvious whether the Cu atoms generated by photofragmentation of CH_3CuH arise by way of a concerted reductive-elimination pathway (as observed in the 420-nm photolysis of nonlinear CH_3FeH,[25] see Section 6) producing $Cu + CH_4$ or through complete photodissociation producing $Cu + CH_3 + H$.

An interesting perspective on the reactivity of atomic Cu toward CH_4 is afforded by a consideration of symmetry-based electronic-state correlations. A simple model for the $Cu + CH_4$ reaction considers the approach of the Cu atom in a C_{2v} side-on fashion to the CH_4 molecule, followed by insertion into a C–H bond, producing CH_3CuH initially with C_s symmetry. The $Cu \cdots CH_4$ bonding interactions that lead to a weakening of the C–H bond in a synergistic activation process have been described above. The symmetry species of the electronic states of the CH_3CuH mole-

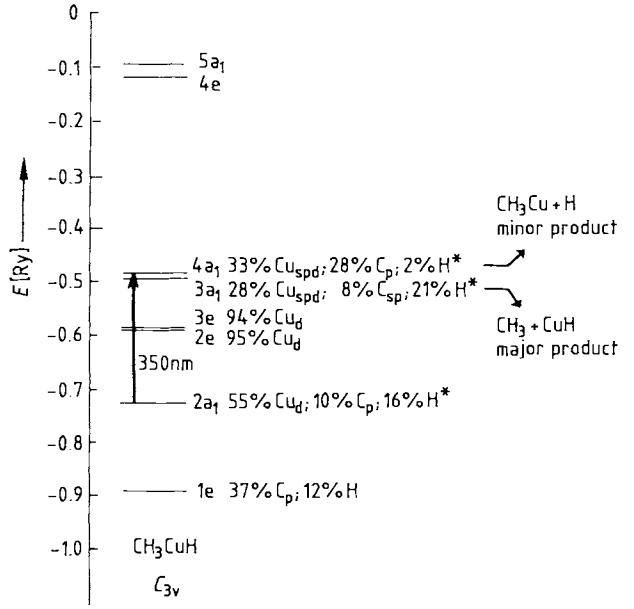


Fig. 8. Ground-state spin-restricted SCF-Xα-SW molecular orbital scheme for linear (C_{3v}) CH_3CuH: $\alpha_{Cu}=0.70697$, $\alpha_C=0.75928$, $\alpha_H=0.77725$, $r_{Cu-C}=1.94$ Å, $r_{Cu-H}=1.49$ Å, $r_{C-H}=1.12$ Å. The computed partial wave contributions to the various molecular orbitals are indicated in the energy-level diagram as well as the proposed 350-nm excitation responsible for secondary photolysis of CH_3CuH. The HOMO is the $4a_1$ orbital and contains a single unpaired electron, giving a $^2A_1$ ground electronic state to linear CH_3CuH.

cule that arise adiabatically from specified initial ^2S, ^2D, ^2P, and $^1A_1$ electronic states of Cu and CH_4, respectively, can be derived according to well-known correlation principles. In the same way a correlation may be made between CH_3CuH and CH_3+CuH and thus the electronic states of CH_3+CuH that arise adiabatically from the specified states of Cu and CH_4 may be ascertained. A correlation diagram of this type is shown in Figure 9. This diagram provides the basis for a qualitative discussion of the $Cu+CH_4$ photoinsertion step followed by dissociation of CH_3CuH to form the products CH_3+CuH. The ordering and relative energies of the electronic states shown for the $Cu+CH_4$ and CH_3+CuH positions of the correlation diagram were taken from UV/VIS spectroscopy data. It can be seen from the diagram that the reactants $Cu+CH_4$ in their ground electronic states correlate with the products CH_3+CuH in their ground electronic states. However, this reaction pathway is endothermic by about 38.5 kcal mol^{-1} and does not proceed from $Cu(^2S)+CH_4$ at 12 K. Reactions involving $Cu(^2D)$ or $Cu(^2P)$ and CH_4 in its ground electronic state lead to the products CH_3+CuH in combinations of ground and excited electronic states, designated $^2A_1+{}^1\Sigma^+$ in Figure 9. This combination of product states lies approximately 15 kcal mol^{-1} higher in energy than the highest-lying combination of reactant states $Cu(^2P)+CH_4(^1A_1)$ and thus all of the adiabatic reaction pathways considered in the diagram are endothermic by at least 15 kcal mol^{-1}. At the same time, the nonadiabatic reaction pathways leading from $Cu(^2D)+CH_4(^1A_1)$ and $Cu(^2P)+CH_4(^1A_1)$ to CH_3+CuH in their ground electronic states are nearly thermoneutral and exothermic, respectively. From the standpoint of energetics, therefore, and without regard for adiabaticity, the reaction is feasible at 12 K for either the directly excited ^2P state or the lower-lying ^2D state of $Cu(^2D_{3/2})$.

One can therefore deduce from these considerations that the initially formed excited state of CH_3CuH from $Cu(^2P)+CH_4(^1A_1)$ correlates adiabatically with CH_3+CuH excited states that are energetically inaccessible, but does not correlate directly with CH_3+CuH ground states because of avoided-crossing symmetry restrictions. Hence the reaction must proceed by way of a nonadiabatic transition corresponding to an electronic relaxation process of CH_3CuH in its initially formed excited state to its electronic ground state, as anticipated in the discussion above.

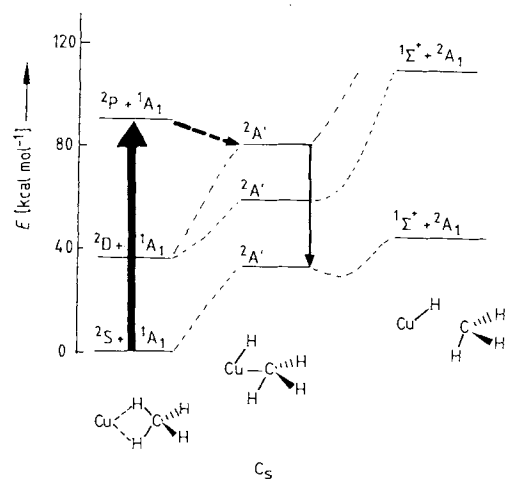


Fig. 9. Qualitative state correlation scheme for the reaction $Cu+CH_4 \rightarrow CH_3CuH \rightarrow CH_3+CuH$.

4. Thermal Reductive-Elimination: The CuH + H $\xrightarrow{h\nu}$ Cu + H_2 Matrix Reaction

The photochemical reaction of photoexcited Cu atoms ($\lambda=310$–320 nm) with H_2 in Kr and Xe matrices at 12 K shows some interesting differences from that observed for the similar Mn- and Fe-atom reactions.[26] This process exhibits pseudo-first-order photoinduced decay of Cu atoms and yields significant quantities of trapped CuH and H atoms as characterized by H_2, D_2, H_2/D_2, and HD isotopic substitution using IR and ESR spectroscopy.[27] The existence of a small ($k_H/k_D \approx 1.16$) kinetic isotope effect for the chemical quenching of photoexcited Cu atoms by H_2 and D_2 and the 2:1 [H]/[D] ratio observed for the reaction of photoexcited Cu atoms with HD are together indicative of the absence of a sizeable activation energy barrier. This is suggestive of a side-on attack[4] of the excited Cu atom on the H–H bond of H_2:

$$Cu + H_2 \xrightarrow[Kr,\ 12\,K]{h\nu} CuH + H$$

The end result of 310-nm $^2P \leftarrow {}^2S$ resonance excitation of Cu atoms in H_2/Kr ($\approx 1/10$) matrices at 12 K is thus an intimate mixture of immobilized CuH and H atoms, physically separated yet delicately poised to partake in a ther-

mal reaction which is the reverse of this photochemical step:

$$CuH + H \xrightarrow{\Delta} Cu + H_2$$

Such a reaction is of considerable theoretical interest since the ground state of, for example, NiH has been predicted to be unstable with respect to attack by H atoms, where the production of either NiH_2 or $Ni + H_2$ is dependent upon the geometry of approach of H to NiH.[28] In this study no activation energy barrier was found along the postulated reaction coordinates. Also, it is interesting to consider this process to be an analogue of the following, now classic gas-phase exchange reaction:

$$DH + H \longrightarrow D + H_2$$

Experimentally, one observes that careful annealing of matrices containing CuH + H at 18–20 K results in the regeneration of significant quantities of Cu atoms as observed by the monotonic reappearance of the $^2P \leftarrow {}^2S$ Cu atomic resonance absorption centered around 310 nm.[27b] A maximum of about 50% of the original Cu atoms can be regenerated using this thermal annealing technique, although the recovery rate is found to be very dependent on the choice of Cu/H_2/rare-gas concentrations, the type of matrix support, and the temperature at which CuH + H are photolytically generated. The inability to regenerate all of the original Cu atoms at 18–20 K can be traced to competitive H-atom recombination reactions forming H_2 and leaving behind unreacted CuH. This is thought to be most reasonable, since Cu-atom diffusion and agglomeration processes at 18–20 K in Kr/H_2 and Xe/H_2 matrices are found to be negligibly slow. The regeneration of Cu atoms follows a fairly well behaved second-order recombination rate law with respect to the reactants CuH + H and displays a kinetic isotope effect that is matrix dependent: $(k_H/k_D)_{Kr} \approx 3$, $(k_H/k_D)_{Xe} \approx 6$. The reaction rate appears to be diffusion controlled with a small but measureable activation energy barrier, with magnitude decreasing in the order Ar > Kr > Xe.

The regeneration of Cu atoms therefore appears to have its origin in the following thermal reaction:

$$CuH(^1\Sigma^+) + H(^2S) \xrightarrow[Kr\ or\ Xe]{18 \rightarrow 20\ K} Cu(^2S) + H_2(^1\Sigma_g)$$

This reaction can be considered to be the reverse of the photochemical reaction of $Cu(^2P)$ atoms with molecular $H_2(^1\Sigma_g^+)$.[27] In a series of careful IR and ESR experiments, no convincing evidence was obtained for a CuH_2 intermediate. It is therefore not possible to make any statement at this time as to whether the above reactions pass through an unstable copper dihydride species or proceed by way of an H-atom abstraction step. Nevertheless, it is quite clear that the activation energy for the production of $Cu + H_2$ from CuH + H has an upper limit of around 40 cal mol^{-1}, part or all of which might be associated with the barrier to thermal diffusion of H atoms in solid Kr or Xe at 18–20 K, and/or the rotational reorientation of CuH with respect to H to permit reaction.

Although the geometries, energy surfaces for different states, and atom–molecule state correlations for CuH_2, CuH + H, and $Cu + H_2$ have yet to be established and are not expected to be identical with those of the corresponding nickel–hydrogen system,[28] it is clear from the results of the present study that the reaction $CuH + H \rightarrow Cu + H_2$ proceeds with little or no barrier and is entirely downhill in energy.[27c]

5. Photoinsertion without Fragmentation: The $M + CH_4 \xrightarrow{h\nu} CH_3MH$ (M = Fe, Mn) Matrix Reaction

In this section the photochemical reaction of electronically excited Fe and Mn atoms with methane in a solid methane matrix will be described together since the behavior of the reaction in both metal-atom systems is similar. The UV/VIS spectra of Fe atoms and Mn atoms isolated in methane matrices of dilution ratios $1:10^4$ at 12 K can easily be correlated with their corresponding gas-phase spectra.[29,30] Photolysis at the 285-nm ($^6P, 3d^5 4s^1 4p^1 \leftarrow {}^6S, 3d^5 4s^2$) atomic resonance transition of Mn[26] and 300-nm ($^5P_3, 3d^6 4s^1 4p^1 \leftarrow {}^5D_4, 3d^6 4s^2$) atomic resonance transition of Fe[25] in neat methane matrices resulted in the bleaching of these absorptions in the UV/VIS spectrum and the growth of weak bands in the region of 300–339 nm and 420 nm (Fig. 10), respectively. IR experiments performed under similar metal/methane dilution ratios showed the growth of peaks upon photolysis at 285 nm and 300 nm for Mn/CH_4 and Fe/CH_4, respectively (for the frequencies of these peaks, see ref. [25, 26]). The Mn/CH_4 system is shown in Figure 11. With the exception of

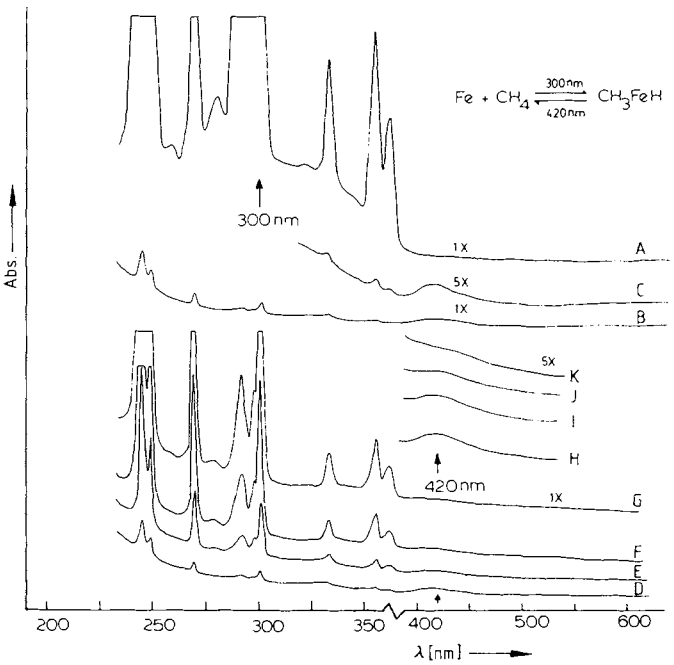


Fig. 10. UV/VIS spectra of Fe atoms isolated in solid CH_4 ($1/10^4$) at 12 K: A) after deposition; B) following 30 min of 300-nm photolysis; C) fivefold ordinate expansion of B in the 300–600-nm region; D)–G) samples similar to B after 0, 2, 7, and 12 min of 420-nm photolysis; H)–K) fivefold ordinate expansion of D–G in the 370–540-nm region [25].

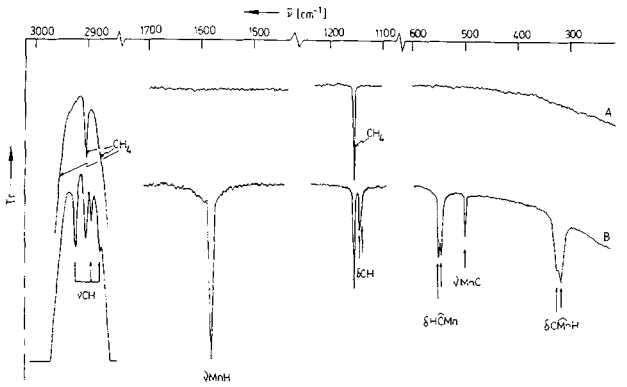


Fig. 11. IR spectrum of Mn/CH_4 (1/10⁴) at 12 K: A) following deposition, showing only CH_4 bands; B) following 120 min of photolysis at 285 nm, showing CH_3MnH product bands [32]. Tr = transmission; $\delta_{H\hat{C}Mn}$ and $\delta_{C\hat{M}nH}$ denote deformation modes.

the difference in frequencies of the bands for the Mn/CH_4 and Fe/CH_4 systems it is clear that the products resulting from the photolysis in both systems show distinct similarities. This is especially evident when it is noticed that the IR bands can be categorized as belonging to one of two types, namely, those arising from symmetrical stretching and bending modes (A_1) and those derived from doubly degenerate (E) modes for a linear C_{3v} molecule. From inspection of the spectra for both systems, it will be seen that the former modes appear as sharp singlets while the latter modes are split into doublets. This pattern of vibrational absorptions suggests that the product, CH_3MH, resulting from the atomic photolysis of Mn and Fe in neat methane matrices has a bent geometry.[25,26] No evidence is seen in the IR data to suggest that fragmentation of the intermediates CH_3MH (M = Mn or Fe) occurs during photolysis at the atomic resonance frequencies. This is in contrast to the Cu/CH_4 system where the fragmented products are observed. Such marked differences in behavior seem to arise from overlap of a dissociative molecular absorption of the product CH_3MH in the case of M = Cu with the atomic absorption, which is not present for the corresponding molecular absorption where M = Mn or Fe.

6. Photoreductive Elimination: The $CH_3MH \xrightarrow{h\nu} CH_4 + M$ (M = Mn, Fe) Matrix Reaction

As mentioned in Section 5 and as can be seen for iron in Figure 10, photolysis at the atomic resonance frequencies of Mn and Fe in solid methane results in the growth of weak absorptions in their UV/VIS spectra at 310 nm and 420 nm, respectively. Photolysis at the 420-nm absorption in the iron system resulted in the complete regeneration of the Fe-atom absorptions, while similar excitation at 310 nm in the Mn case resulted in the partial recovery of the original Mn atoms. In the IR spectrum the results of similar excitation at these optical frequencies resulted in a diminished intensity of the bands due to the insertion products CH_3MH. From this we can conclude that these weak optical bands correspond to absorptions into a dissociative molecular state of CH_3MH. It is particularly noteworthy that no evidence was seen in these IR studies or ESR experiments to suggest that any fragments such as $CH_3^{\odot}$, CH_3M, or $H^{\odot}$ were formed in the dissociation process. Thus it appears that dissociation of CH_3MH for M = Fe or Mn leads to the clean reverse of the atomic photolysis, i.e., the production of the metal atom and a methane molecule only. The nature of these excited states for CH_3MH are unknown but it seems reasonable to suggest that they have a large content of antibonding interaction between the metal atom and the hydrogen and carbon atoms. Detailed quantum mechanical calculations will be needed to provide suggestions as to the reasons for the difference in the photodissociation of the manganese and iron insertion products compared with that of the corresponding copper insertion intermediate.

7. Photoinsertion of Metal Atoms into Molecular Hydrogen: The $Fe + H_2 \xrightarrow{h\nu} FeH_2$ Matrix Reaction

The UV/VIS spectra of Fe atoms isolated in hydrogen/rare-gas (1/10) matrices can be readily correlated with those of Fe atoms in the gas phase.[29] The rate of loss of Fe atoms resulting from 307-nm ($^5P_3$, $3d^64s^14p^1 \leftarrow {}^5D_4$, $3d^64s^24p^0$) photolysis was found to exhibit a Beer–Lambert law dependence upon photon flux and to be roughly five times faster in H_2/Xe than in D_2/Xe matrices at 12 K.[30] Optical absorptions associated with photoproducts were observed to grow in at 400, 419, and 441 nm in H_2/Xe matrices (Fig. 12). The corresponding IR experiments led to the identification of an iron-hydrogen-containing species absorbing at 1636 and 323 cm^{-1} in H_2/Xe and at 1188 and 232 cm^{-1} in D_2/Xe matrices (Fig. 13). The analogous experiments in HD/Xe matrices show the respective stretching and deformational modes at 1665, 1198, and 280 cm^{-1}, which is the isotopic pattern expected for a FeHD insertion product rather than that of a molecular hydrogen complex, Fe(HD), thereby specifying the photochemical pathway leading to iron dihydride. The weak bands labeled a and a′ at 1660 cm^{-1} and 1204 cm^{-1} (Fig. 13), which are associated with FeH_2 and FeD_2, respectively, and which have slightly higher frequencies than the asymmetric νFeH_2 and νFeD_2 stretching modes, are *absent* in FeHD. They are therefore best ascribed to the symmetrical νFeH_2 and νFeD_2 stretching modes, rather than to a secondary matrix trapping site of iron dihydride, and hence provide evidence for a nonlinear geometry. On the other hand, the low-intensity shoulders denoted b and b′ (Fig. 13) do behave as multiple trapping sites of FeH_2 and FeD_2, respectively, and have been assigned accordingly. The ratio of the IR intensities of the stretching mode of FeH_2 is given in the bond dipole model by the following expression:

$$I_{B2}/I_{A1} = \tan^2\frac{\phi}{2}\,\frac{\left[m_{Fe} + 2m_H\sin^2\frac{\phi}{2}\right]}{\left[m_{Fe} + 2m_H\cos^2\frac{\phi}{2}\right]}$$

where ϕ is the apical angle. This yields a value of $\phi \approx 120°$ for FeH_2. The corresponding IR spectra recorded in Fe/

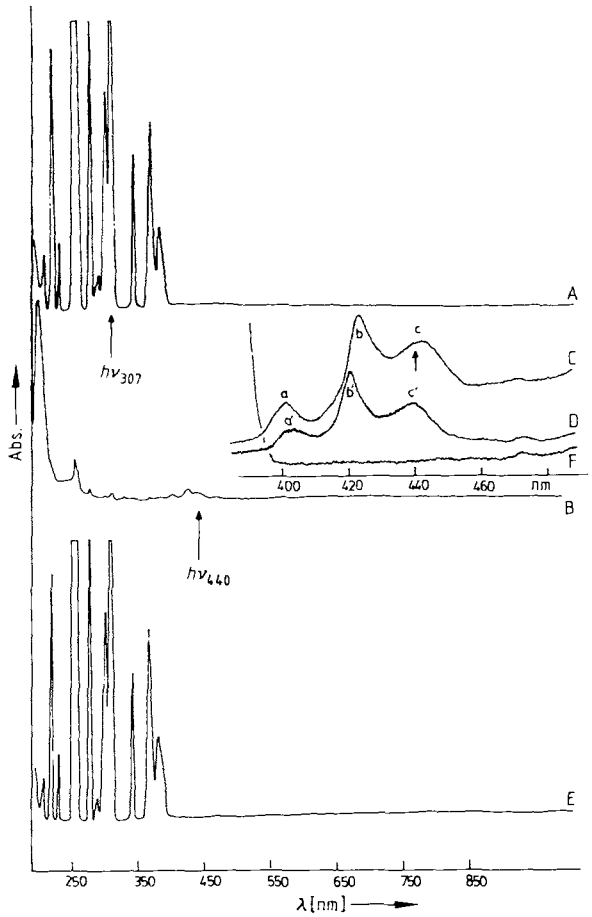


Fig. 12. Optical spectra of a $Fe/H_2/Xe$ ($\sim 1/10^3/10^4$) matrix at 12 K: A) freshly deposited; B) following 45 min of 307-nm atomic-Fe photolysis; C) scale expansion of 380–480-nm region of B; D) scale expansion of $Fe/D_2/Xe$ ($\approx 1/10^3/10^4$) analogue of C; E) the matrix sample shown in B following subsequent 15 min of 440-nm FeH_2 photolysis; F) scale expansion of the 380–480-nm region of E. The FeH_2 and FeD_2 product bands are denoted a, b, c and a', b', c', respectively [30].

$H_2/D_2/Xe$ mixed isotopic matrices display only those absorptions associated with FeH_2 and FeD_2 with no evidence for scrambling as seen by the absence of FeHD. In the $H_2/D_2/Xe$ matrices, FeH_2 is found to be formed preferentially over FeD_2 by a factor of 5.76 (IR absorbance measurements on the stretching modes, Fig. 13E). As expected, this parallels the approximately five times faster bleaching rate observed for 307-nm photoexcited Fe, reflecting the difference in the quenching cross section for this atom's excited state with H_2 and D_2 in Xe matrices (see Section 8). Note that for a pseudo-first-order competitive insertion reaction,

$$M^* + H_2 + D_2 \longrightarrow MH_2 + MD_2$$

the time dependence of the concentration of MH_2 and MD_2 photoproducts is given by the following expressions:

$$[MH_2] = \frac{k_H}{k_H + k_D}[M_0]\left(\exp\left[-\frac{1}{2}(k_H + k_D)t\right] - 1\right)$$

$$[MD_2] = \frac{k_D}{k_H + k_D}[M_0]\left(\exp\left[-\frac{1}{2}(k_H + k_D)t\right] - 1\right)$$

These lead directly to

$$k_H/k_D = [MH_2]/[MD_2]$$

These observations alert one to the existence of an activation energy barrier for the insertion step. Taking into account the low temperature at which the reaction was performed (zero point energy and possibly tunneling corrections), the observed k_H/k_D isotope ratio of around 5–6 for the $Fe^*/H_2(D_2)$ reaction translates into a k_H/k_D ratio of around 1.11–1.13 at ambient temperatures, which would indicate a small degree of H–H stretching in an "early"

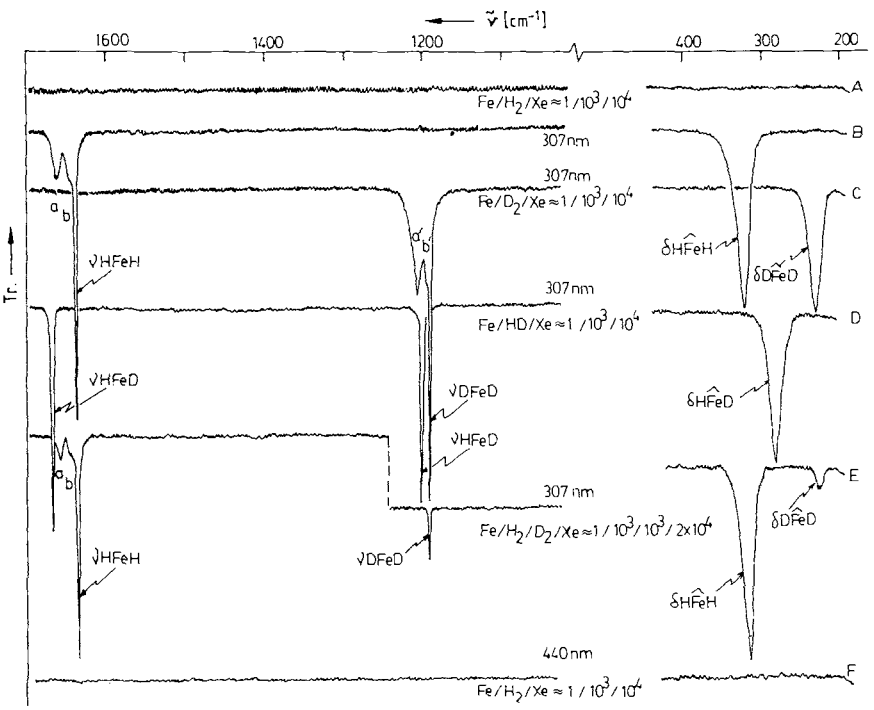


Fig. 13. IR spectra of a $Fe/H_2/Xe$ ($\sim 1/10^3/10^4$) matrix at 12 K: A) freshly deposited; B) following 120 min of 307-nm atomic-iron photolysis; C) as B for $Fe/D_2/Xe$ ($\approx 1/10^3/10^4$); D) as B for $Fe/HD/Xe \approx 1/10^3/10^4$; E) $Fe/H_2/D_2/Xe$ ($\approx 1/10^3/10^3/2\times10^4$); F) the matrix sample shown in B following subsequent 30 min of 440-nm FeH_2 photolysis. The stretching and bending deformation modes of FeH_2, FeD_2, and FeHD are indicated [30]. For a, a', b, b', see text.

transition state and probably a low activation barrier for insertion. These observations are in line with (1) theoretical studies of H_2 oxidative-addition to $[Pt(PH_3)_2]$, which have indicated around 0–18% stretching of the H–H bond in the transition state with a 2–16-kcal mol^{-1} activation energy barrier in a reactant-like transition state;[31] (2) experimental data for H_2 addition to a metal center in molecular ML_n complexes, which show a k_H/k_D isotope ratio of 1–2;[32] and (3) neutron diffraction data for the H–H bond length in the first example of a molecular hydrogen complex, $[W(CO)_3(PiPr_3)_2(\eta^2\text{-}H_2)]$, the H–H bond length being 0.84 Å compared with 0.74 Å for gaseous H_2.[33] Finally, no sign of FeH or FeH_x ($x \geq 3$) could be detected in the IR experiments,[30] nor H atoms in the analogous ESR experiments.

The accumulated spectroscopic and kinetic evidence therefore leans toward *concerted* insertion of a 307-nm photoexcited Fe atom into the hydrogen–hydrogen bond of H_2 to form FeH_2, having a nonlinear geometry, with no detectable participation of a molecular hydrogen complex,[34] nor indication of competing H-atom abstraction, secondary photolysis channels, or formation of higher iron hydrides, FeH_x ($x \geq 3$) (see Scheme 2). Similar, although not identical, effects have been discovered in the Mn/H_2/rare-gas system.[35]

8. Photoreductive Elimination: The $FeH_2 \xrightarrow{h\nu} Fe + H_2$ Matrix Reaction

In this section we will briefly consider the 440-nm photoreactivity of the FeH_2 insertion product generated cleanly and efficiently by 307-nm excitation of Fe atoms in the presence of H_2 in low-temperature matrices under rigorously mononuclear conditions.[30]

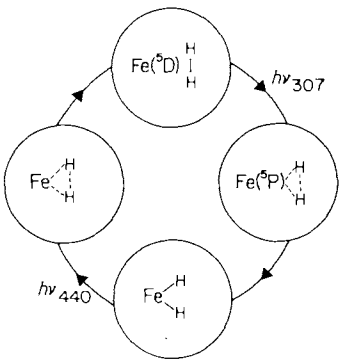
The UV/VIS and IR spectra both depict the monotonic bleaching of the FeH_2 absorptions with 440-nm irradiation time (Fig. 12, 13). Of particular note is the concurrent and rapid generation of atomic iron, clearly seen by the steady growth of the atomic resonance lines in the UV/VIS spectrum (Fig. 12E). During the photodissociation of FeH_2, neither IR nor ESR bands characteristic of FeH, H atoms, or FeH_x ($x \geq 3$) were ever observed. Furthermore, the 440-nm photobleaching of FeH_2 and FeD_2, with concomitant photoproduction of Fe atoms, was essentially quantitative (Fig. 12A, E), following a pseudo-first-order rate law and displaying no measureable kinetic isotope effect.

Collectively, the spectroscopic and kinetic evidence argues in favor of a *concerted reductive-elimination* of Fe atoms and H_2 from 440-nm photoexcited FeH_2 with no activation energy barrier, where FeH, H, $Fe(H_2)$, or FeH_x ($x \geq 3$) reaction intermediates, if involved, play only a minor role in the reaction since they remained below the detection limits of the analytical methods employed in this study. Again, the Mn/H_2/rare-gas system displays similar effects.[35]

It therefore seems likely that 440-nm photoexcitation of FeH_2 populates a low-lying electronic state having antibonding character between the iron–hydrogen bonds and bonding character with respect to the hydrogen–hydrogen bond. In a nonlinear configuration, this state is probably identical to or very closely resembles a three-center transition-state complex:



Such a complex could be responsible for the facile and concerted reductive-elimination of H_2 from FeH_2. This probably occurs in much the same way as that postulated to occur in the photoinduced reductive-elimination of H_2 from $[(\eta^5\text{-}C_5H_5)_2MoH_2]$, $[IrClH_2(PPh_3)_3]$, and $[IrH_3(PPh_3)_3]$ complexes.[36]



Scheme 2.

The photoinsertion of Fe atoms into H_2 leads to the first documented synthesis of FeH_2 and provides the first reported case of a "ligand-free," reversible, oxidative-addition, reductive-elimination reaction (Scheme 2).

$$M + H_2 \rightleftharpoons MH_2$$

This type of reaction is one of the most fundamental steps in homogeneous and heterogeneous catalysis involving molecular hydrogen.

9. SCF-Xα-SW MO Calculations for Nonlinear FeH_2: Relevance to the Photoreductive-Elimination Reaction

In order to gain a deeper understanding of the "ligand-free" photoreductive-elimination reaction, the electronic structure of some transition-metal dihydrides have been computed by the SCF-Xα-SW method. For illustrative purposes the MO energy level scheme for FeH_2 with an apical angle of 120° (IR intensity estimate) is shown in Figure 14.

It is significant that the optical spectra of FeH_2 show at least three low-energy absorptions around 400, 419, and 441 nm and that excitation into each of these leads to the clean and facile production of Fe atoms and H_2. Optical transitions that are computed to fall within this energy range are illustrated in Figure 14. One finds at best four possible transitions, calculated to occur at 396, 405, 414, and 509 nm. The latter two excitations involve promotion of FeH_2 σ-bonding electrons into essentially localized Fe 3d orbitals and are not expected to be effective in promoting reductive elimination to form Fe atoms and H_2. The

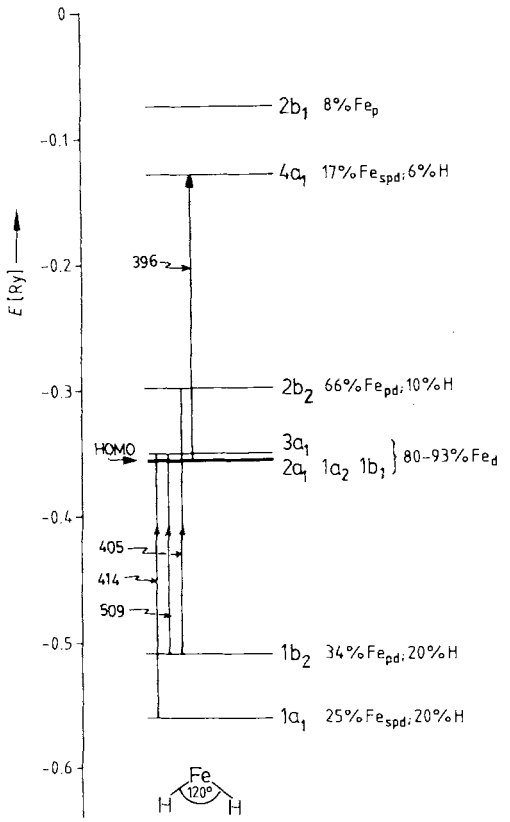


Fig. 14. Ground-state spin-restricted SCF-Xα-SW MO scheme for nonlinear (C_{2v}) FeH_2 ($\alpha_{Fe}=0.71151$; $\alpha_H=0.77725$; $r_{Fe\text{-}H}=1.77$ Å; H-Fe-H = 120°). The computed partial wave contributions to the various molecular orbitals are indicated in the energy-level diagram, as well as the proposed excitations in the 400–500-nm region thought to be responsible for the observed optical transitions in this range and the photoreductive-elimination pathway [26].

396-nm excitation involves promotion of Fe 3d localized electrons into a σ*-antibonding FeH_2 orbital and might be responsible for the Fe/H_2 elimination pathway. On the other hand, the 405-nm excitation takes a σ-bonding FeH_2 electron and places it in a σ*-antibonding orbital and could also be quite effective in promoting the observed photoreductive-elimination pathway. One or more of these excited states might turn out to closely resemble the three-center transition-state complex, proposed earlier to be responsible for the low activation energy and concerted reductive-elimination of Fe and H_2 from FeH_2. Further work is underway to explore this interesting result.

10. Factors Influencing the Reactivity of Electronically Excited Metal Atoms in Low-Temperature Matrices

It is worthwhile to briefly contemplate the factors that might affect the reactivity patterns of electronically excited metal atoms of the first transition series when co-isolated with different ligands in cryogenic matrices. As a first attempt at this, we will consider the photoinsertion reaction along a covalent chemical pathway in terms of what is currently known experimentally with respect to methane and molecular hydrogen.

For all of the cases studied so far, the initially prepared electronically excited metal atom (assuming this state to be reactive) was one of the following types:

$$3d^n4s^2 \longrightarrow 3d^n4s^14p^1;\ 3d^{n+1}4s^04p^1$$
$$3d^n4s^1 \longrightarrow 3d^n4s^04p^1$$

thereby presenting either an s^1p^1 or s^0p^1 orbital configuration to the CH_4 reactant.

The singly occupied 4s and 4p metal atomic orbitals are available for bonding with the σ-bonding and σ*-antibonding molecular orbitals of CH_4. Since the σ orbital of CH_4 is completely occupied, it is expected that the M*(3d/4s) + CH_4(σ) interaction would lead to a transfer of electron density from the $1t_2$ molecular orbital of CH_4 to the 3d/4s atomic orbitals of the excited metal atom. On the other hand, the σ* orbital of CH_4 is unoccupied and, thus, could result in a transfer of charge density from the singly occupied 4p atomic orbital of the excited metal atom to the $2a_1$ molecular orbital of CH_4. These combined interactions work in a "synergistic" sense and, overall, lead to a weakening of the C–H bond. Clearly the symmetry and energy matching of metal-atom valence orbitals in excited states with the ground-state σ($1t_2$) and σ*($2a_1$) orbitals of CH_4 are important factors in attempting to rationalize the reactivity patterns of excited metal atoms with CH_4. In the case of the first transition series, it has been observed that photoexcited[2a,21] Ti, V, Cr, and Ni atoms do not react with CH_4 at low temperatures whereas Mn, Fe, Co, Cu, and Zn atoms lead to CH_3MH insertion products.[2a,26] Similar reactivity patterns are also observed for reactions with H_2.[26] This series can be qualitatively understood in terms of the relative energies of the 3d, 4s, and 4p atomic orbitals of the excited metal atoms with respect to those of the $1t_2$ and $2a_1$ molecular orbitals of ground-state CH_4. Figure 15

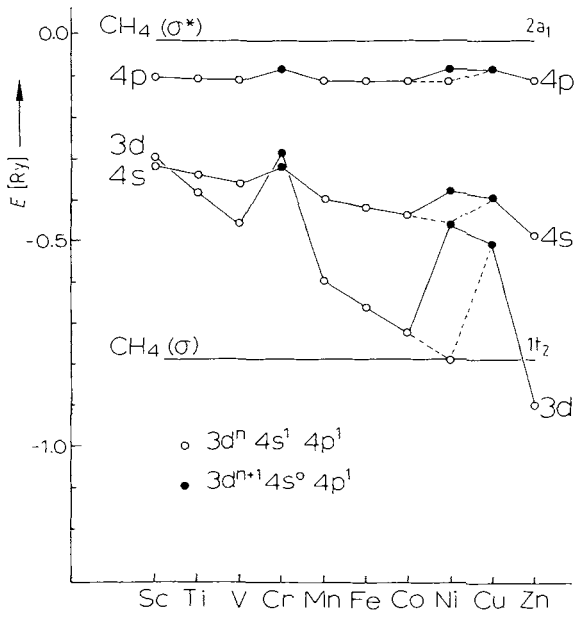


Fig. 15. SCF-Xα-SW spin-restricted orbital energies of CH_4 in its ground electronic state and the first-transition-series metal atoms in their low-lying excited states [26].

illustrates the variation of these energy levels across the first transition series, as determined by SCF-Xα-SW computations.[26] Except for Cr, Ni, and Cu, the energy levels were determined for $3d^n4s^14p^1$ excited-state configurations. For these three metals, however, a $3d^{n+1}4s^04p^1$ excited state configuration was considered, since this is the electronic configuration known to be populated for these metals. From Figure 15 it is clear that the nearly constant values of the 4p energy level for all the excited metal atoms, as well as its proximity to the energy value of the $2a_1$ level of CH_4, argue in favor of a similar $M^*(4p) \rightarrow CH_4(\sigma^*)$ interaction for the first-transition-series metal atoms. However, there is a dramatic difference among the metal atoms when one considers the $M^*(3d/4s)$-$CH_4(1t_2)$ energy separation. As one passes from Sc to Zn, the 3d and 4s orbitals are generally stabilized, becoming closer in energy to the $1t_2$ level of CH_4. Their interaction is thereby enhanced and, presumably, greater charge donation from CH_4 to M* is thereby promoted.

Both Cr and Cu have $3d^{n+1}4s^14p^0$ ground states in the gas and matrix phases. However, although Ni has a $3d^84s^24p^0$ ground-state configuration in the gas phase, recent studies[37] on its ground-state configuration in rare-gas matrices have shown that this changes to a $3d^94s^14p^0$ configuration. We have found this to be the case for CH_4 and H_2/rare-gas matrices as well. This has important consequences when one compares the $3d^84s^14p^1$ excited state of Ni (shown in dotted lines in Fig. 15) with the $3d^94s^04p^1$ excited-state configuration (solid lines in Fig. 15). In the former case, one would expect that the even closer proximity of the 3d and 4s levels of Ni* to the $1t_2$ level of CH_4 would result in the formation of reaction products, as observed for Mn, Fe, Co, Cu, and Zn. In the latter case, however, the dramatic *destabilization* of the 3d and 4s levels of the $3d^94s^04p^1$ excited state of Ni compared with the alternative excited-state $3d^84s^14p^1$ configuration, or with respect to Mn*, Fe*, and Co*, could result in anomalous behavior of Ni and might explain the lack of any observed reaction products when Ni is photoexcited in CH_4 matrices.[38]

The above discussion should only be regarded as a preliminary attempt to rationalize the reactivity patterns of electronically excited first-transition-series atoms with CH_4. Similar ideas seem to apply to the results so far obtained for H_2.[26] Clearly much more work needs to be done in this interesting area before one can fully appreciate the reactivity characteristics of selected metal-atom excited states with H_2 and CH_4 at low temperatures.

11. Conclusions and Outlook

The different kinds of photoprocesses accessible to metal atoms in selected excited states in the presence of hydrogen, methane, or ethane have been delineated and exemplified by experimental results. The photochemical and thermal behavior of reaction intermediates in these M/RH systems have also been considered, since they often play an important role in the scheme of events that correlate electronically excited metal-atom reagents with reaction products. Up to the present time these have included photooxidative-addition, photoaggregation, photoreductive-elimination and photofragmentation processes, most of which had not hitherto been observed with metal atoms in their ground electronic states.

In the case of methane and molecular hydrogen, this kind of metal-atom photochemistry has led to novel "ligand-free" CH_3MH and MH_2 insertion products as well as CH_3M and MH fragments. As a result of their inherent molecular simplicity, such species are ideally suited for detailed spectroscopic, photochemical, and structural investigations backed by quantum chemical calculations. This provides new opportunities for modeling CH_4 and H_2 chemisorption and desorption on metal surfaces and for probing CH_4 and H_2 oxidative-addition and reductive-elimination reactions in homogeneous catalysis in the absence of extraneous ligands.

Future studies are expected to focus attention on the photophysical and photochemical properties of transition-metal atoms and low-nuclearity metal clusters in selected excited states, as well as the reaction chemistry of RM_nH and M_nH_2 ($n = 1, 2, 3 \ldots$) with such ligands as N_2, CO, and C_2H_4, in an effort to secure ligand-free models of reactive intermediates in homogeneous and heterogeneous catalytic hydrogenations and alkylations of small molecules.

The generous financial assistance of the Natural Sciences and Engineering Research Council (NSERC) of Canada's Operating and Strategic Energy Programme is greatly appreciated. J. M. P. acknowledges NSERC for a graduate research scholarship.

Received: March 11, 1986;
revised: June 10, 1986 [A 600 IE]
German version: *Angew. Chem. 98* (1986) 1076

[1] G. A. Ozin, M. P. Andrews, L. F. Nazar, C. F. Francis, *Coord. Chem. Rev. 48* (1983) 203; G. A. Ozin, S. A. Mitchell, *Angew. Chem. 95* (1983) 706; *Angew. Chem. Int. Ed. Engl. 22* (1983) 674.

[2] a) W. E. Billups, J. L. Margrave, R. H. Hauge, *J. Am. Chem. Soc. 102* (1980) 7393; b) G. A. Ozin, D. F. McIntosh, S. A. Mitchell, J. Garcia-Prieto, *ibid. 103* (1981) 1574; c) G. A. Ozin, J. M. Parnis, S. A. Mitchell, J. Garcia-Prieto in H. Grünewald (Ed.): *Chemistry for the Future*, Pergamon Press, Oxford 1984, pp. 99–105.

[3] G. Cario, J. Franck, *Z. Phys. 11* (1922) 161.

[4] a) J. G. Calvert, J. N. Pitts: *Photochemistry*, Wiley, New York 1966, Chapter 2; b) A. B. Callear, J. C. McGurk, *J. Chem. Soc. Faraday Trans. 2 69* (1973) 97; c) W. H. Breckenridge, A. M. Renlund, *J. Phys. Chem. 82* (1978) 1474, 1484; *83* (1979) 303.

[5] W. H. Breckenridge in A. Fontijn, M. A. A. Clyne (Eds.): *Reactions of Small Transient Species*, Academic Press, London 1983, and references cited therein.

[6] a) H. Huber, G. A. Ozin, *Inorg. Chem. 17* (1978) 155; b) G. A. Ozin, *Symp. Faraday Soc. 14* (1980) 7; c) G. A. Ozin, S. A. Mitchell, *ACS Symp. Ser. 211* (1983) 303, and references cited therein..

[7] M. Moskovits, G. A. Ozin (Eds.): *Cryochemistry*, Wiley, New York 1976, and references cited therein.

[8] G. A. Ozin, E. P. Kundig, D. F. McIntosh, M. Moskovits, *J. Am. Chem. Soc. 95* (1973) 7234.

[9] G. A. Ozin, H. Huber, E. P. Kundig, M. Moskovits, *J. Am. Chem. Soc. 95* (1973) 332.

[10] G. A. Ozin, A. J. L. Hanlan, *Inorg. Chem. 16* (1977) 2848, 2857.

[11] G. A. Ozin, H. Huber, D. F. McIntosh, *Inorg. Chem. 16* (1977) 3070.

[12] G. A. Ozin, W. Klotzbucher, H. Kolari, J. G. Norman, Jr., *Inorg. Chem. 16* (1977) 2871.

[13] G. A. Ozin, W. Klotzbucher, S. A. Mitchell, *Inorg. Chem. 16* (1977) 3063; G. A. Ozin, H. Huber, P. McKenzie, S. A. Mitchell, *J. Am. Chem. Soc. 102* (1980) 1548.

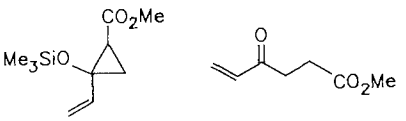
[14] R. N. Perutz, *Chem. Rev. 85* (1985) 77; *Ann. Rep. (RSC) 82* (1985) 157.
[15] R. J. Donovan, *Prog. React. Kinet. 10* (1979) 253.
[16] N. Adams, W. H. Breckenridge, J. Simons, *Chem. Phys. 56* (1981) 327.
[17] R. Blickensderfer, K. Jordon, N. Adams, W. H. Breckenridge, *J. Phys. Chem. 86* (1983) 1930.
[18] J. M. Parnis, S. A. Mitchell, J. Garcia-Prieto, G. A. Ozin, *J. Am. Chem. Soc. 107* (1985) 8169.
[19] G. A. Ozin, S. A. Mitchell, J. Garcia-Prieto, *Angew. Chem. 94* (1982) 218; *Angew. Chem. Int. Ed. Engl. 21* (1982) 211; *Angew. Chem. Suppl. 1982*, 369.
[20] G. A. Ozin, S. A. Mitchell, J. Garcia-Prieto, *J. Phys. Chem. 86* (1982) 473.
[21] G. A. Ozin, H. X. Huber, J. Garcia-Prieto, unpublished results.
[22] K. J. Lushington, *J. Chem. Phys. 76* (1982) 3843; F. D. Medina, *Chem. Phys. Lett. 85* (1982) 91; W. Press, *J. Chem. Phys. 56* (1972) 2597, and references cited therein.
[23] G. A. Ozin, S. A. Mitchell, J. Farrell, G. A. Kenney-Wallace, *J. Am. Chem. Soc. 102* (1980) 7702.
[24] G. A. Ozin, D. F. McIntosh, unpublished results.
[25] G. A. Ozin, J. G. McCaffrey, *J. Am. Chem. Soc. 104* (1982) 7351.
[26] G. A. Ozin, J. G. McCaffrey, D. F. McIntosh, *Pure Appl. Chem. 56* (1984) 111.
[27] a) G. A. Ozin, J. Garcia-Prieto, S. A. Mitchell, *Angew. Chem. 94* (1982) 380; *Angew. Chem. Int. Ed. Engl. 21* (1982) 380; *Angew. Chem. Suppl. 1982*, 785; b) G. A. Ozin, C. Gracie, *J. Phys. Chem. 88* (1984) 643; c) this has been confirmed by model potential CI-MO calculations, J. Garcia-Prieto, M. E. Ruiz, O. Novaro, *J. Am. Chem. Soc. 107* (1985) 5635, and references cited therein.
[28] M. R. A. Blomberg, P. E. M. Siegbahn, *J. Chem. Phys. 78* (1983) 5682, and references cited therein.
[29] C. Moore, *Natl. Bur. Stand. (US) Circ. 1949*, No. 467.
[30] G. A. Ozin, J. G. McCaffrey, *J. Phys. Chem. 88* (1984) 645.
[31] K. Kitura, S. Obara, K. Morokuma, *J. Am. Chem. Soc. 103* (1981) 2891; A. Sevin, *Nouv. J. Chim. 5* (1981) 233; J. O. Noell, P. J. Hay, *J. Am. Chem. Soc. 104* (1982) 4578; J. Low, W. A. Goddard, III, *ibid. 106* (1984) 8321.
[32] P. B. Chock, J. Halpern, *J. Am. Chem. Soc. 88* (1966) 3511; P. Zhou, A. A. Vitale, J. San Filippo, Jr., W. H. Saunders, Jr., *J. Am. Chem. Soc. 107* (1985) 8049, and references cited therein.
[33] G. J. Kubas, R. R. Ryan, B. I. Swanson, P. J. Vergamini, H. H. Wasserman, *J. Am. Chem. Soc. 106* (1984) 451.
[34] G. J. Kubas, R. R. Ryan, P. J. Vergamini, H. Wasserman, *ACS Meeting Seattle 1983*, paper 229 (Neutron Structure of $[W(CO)_3(PiPr_3)_2(\eta^2\text{-}H_2)]$).
[35] G. A. Ozin, J. G. McCaffrey, *J. Am. Chem. Soc. 106* (1984) 807.
[36] G. L. Geoffroy, R. J. Pierantozzi, *J. Am. Chem. Soc. 98* (1976) 8054; G. L. Geoffroy, M. G. Bradley, *Inorg. Chem. 17* (1978) 2410.
[37] B. Breithaupt, J. E. Hulse, D. M. Kolb, H. H. Rotermund, W. Schroeder, W. Schrittenlacher, *Chem. Phys. Lett. 95* (1983) 513.
[38] It is interesting to note that this maxtrix reaction was first attempted by G. A. Ozin, H. Huber, W. Trogler, D. Tyler and H. B. Gray at the Californian Institute of Technology (Caltech) in January 1977.

When submitting manuscripts, authors of articles intended for publication as "Communications" are requested to read the "Notice to Authors" reproduced in the January issue of the journal following the list of contents; upon request, a copy can be obtained from the editorial office.

Intramolecular Diels–Alder Reactions with Methyl 2-Trimethylsiloxy-2-vinylcyclopropanecarboxylates as Key Building Blocks**

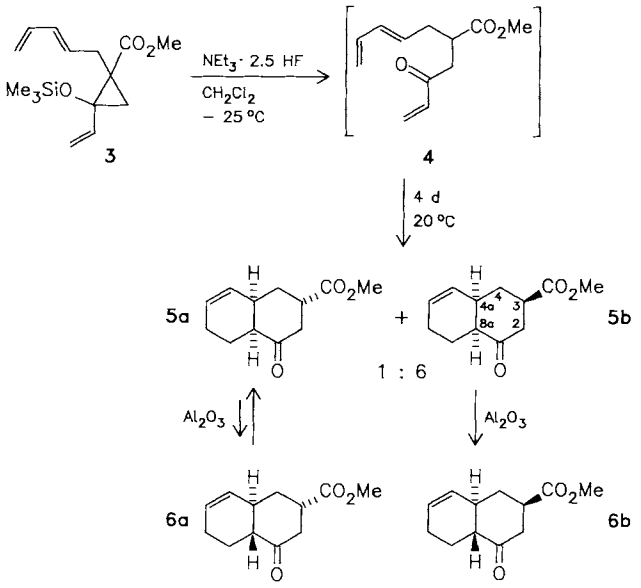
By *Ruth Zschiesche, Erich L. Grimm,* and *Hans-Ulrich Reissig**

Methyl 2-trimethylsiloxypropanecarboxylates with alkenyl substituents at C2 (e.g., **1**) can readily undergo reaction as masked vinyl ketones, resulting in C–C bond formation. We recently described efficient one-pot procedures for the ring-opening of **1** to give **2** and the subsequent Michael addition reactions of **2**.[1] The electron-poor C=C bond in **2** and in similar compounds should also undergo cycloaddition reactions.[2]



1 **2**

Of particular interest from a preparative and mechanistic standpoint is the intramolecular Diels–Alder reaction[3] starting from **3** (Scheme 1), which may be prepared in high yield (80%) by deprotonation of **1** followed by alkylation[4] with 5-bromo-1,3-pentadiene. Compound **3** is transformed by desilylation and subsequent ring-opening into the trienone **4**, which is ideally suited for a $[4\pi+2\pi]$ cycloaddition. The cycloaddition is complete after four days at room temperature. The crude product consists exclusively of the *cis*-octalone derivatives **5a** and **5b**, as shown by comparison of the NMR spectra with those of the separated isomers and by epimerization to give the *trans* compounds **6**. Pure **5b** (m.p. = 61–62.5 °C) can be isolated from the crude product in 47% yield by crystallization and **5a** can be obtained in 13% yield with a purity of > 90% (^{1}H-NMR) by chromatography (silica gel).



Scheme 1. Intramolecular Diels–Alder reaction of **4** to give **5a/5b** and isomerization providing **6a/6b**. For clarity, only one of the enantiomers of **5** and **6** is shown. All new isolated compounds (purified by recrystallization or kugelrohr distillation) gave appropriate spectra and correct elemental analyses.

When the crude product is chromatographed on alumina, however, the epimerized *trans*-octalone derivative **6b** is obtained in 57% yield as colorless crystals (m.p. = 90–92 °C). In this thermodynamically most stable isomer, all the substituents of the cyclohexanone portion are equatorial in the chair conformation. Compound **6b** is also formed upon treatment of pure **5b** with Al_2O_3, acids, or bases. However, the equilibrium between **5a** and **6a** lies on the side of **5a** (**5a** : **6a** = 2 : 1), since the methoxycarbonyl group in **6a** is arranged axially in a chair conformation. The relative configurations given in Scheme 1 are in accord with these equilibration experiments; moreover, they are supported by the comparison of the ^{13}C-NMR data[5] and are confirmed by selective proton decoupling experiments.[6]

As expected for trienones of type **4**,[3,7] the reaction proceeds via an *endo* transition state, which leads to the *cis*-linked bicyclic compounds **5**. The high selectivity with respect to the configuration at C3, however, is not obvious, since the folding of the chain joining the diene and the dienophile portions is crucial for the relative configuration of this center of chirality. Thus, the formation of the clearly preferred **5b** indicates a transition state **TS** with a boatlike conformation of this part of the molecule.

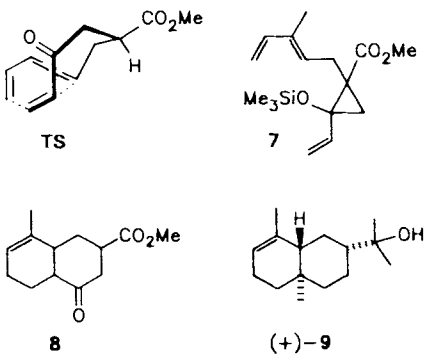
This short and efficient route to octalone derivatives is characterized by good stereocontrol and flexibility with respect to other substituents. For instance, the cyclopropane derivative **7** can be prepared in 90% yield by alkylation of **1** with 5-bromo-3-methyl-1,3-pentadiene; ring-opening of **7** results in rapid cycloaddition (compared with **4**) to give three diastereomers of 5-methyloctalone **8** in 79% yield. It has not yet been possible to separate these diastereomers (ratio of isomers corresponding to **5a**, **5b**, and **6b**, 3 : 6 : 1).

The synthetic route described here, involving intramolecular Diels–Alder reaction via **1**, should not only make

[*] Prof. Dr. H.-U. Reissig [+], Dipl.-Chem. R. Zschiesche, Dipl.-Chem. E. L. Grimm
Institut für Organische Chemie der Universität
Am Hubland, D-8700 Würzburg (FRG)

[+] Present address: Institut für Organische Chemie und Biochemie der Technischen Hochschule
Petersenstrasse 22, D-6100 Darmstadt (FRG)

[**] This work was supported by the Deutsche Forschungsgemeinschaft, the Fonds der Chemischen Industrie, and the Universitätsbund Würzburg. We thank Dipl.-Chem. *H. Bader* for some preliminary experiments. *H.-U. R.* thanks the Karl-Winnacker-Stiftung (Hoechst AG) for a fellowship.



possible the rapid and stereoselective preparation of terpenes such as α-eudesmol **9**,[8] but might also be suitable for the synthesis of more complex natural products of the compactin or mevinolin type.[9]

Received: July 21, 1986;
revised: September 16, 1986 [Z 1866 IE]
German version: *Angew. Chem. 98* (1986) 1104

CAS Registry numbers:
1, 90288-82-7; **3**, 105140-87-2; **5a**, 105140-88-3; **5b**, 105140-89-4; **6a**, 105140-90-7; **6b**, 105140-91-8; **7**, 105140-92-9; **8**, 105140-93-0; 5-bromo-3-methyl-1,3-pentadiene, 42162-66-3.

[1] E. L. Grimm, R. Zschiesche, H.-U. Reissig, *J. Org. Chem. 50* (1985) 5543. For isolation of **2**, see E. Kunkel, I. Reichelt, H.-U. Reissig, *Liebigs Ann. Chem. 1984*, 802.

[2] Thus, it is possible to prepare the plant constituent norbisabolide (4-methyl-4-(4-methyl-3-cyclohexenyl)-γ-butyrolactone; see, e.g., C. Gardrat, *Synth. Commun. 14* (1984) 1191, and references cited therein) from **2** with an overall yield of ca. 30%.

[3] Recent reviews: a) E. Ciganek, *Org. React. (NY) 32* (1984) 4; b) A. G. Fallis, *Can. J. Chem. 62* (1984) 183; c) D. F. Taber: *Intramolecular Diels-Alder and Alder Ene Reactions*, Springer, Berlin 1984.

[4] I. Reichelt, H.-U. Reissig, *Liebigs Ann. Chem. 1984*, 531.

[5] Especially characteristic are the chemical shifts of C2 (t), C3 (d), C4a (d) and C8a (d): **5a**: 42.8, 39.3, 35.6, 46.3; **5b**: 41.2, 40.2, 35.6, 48.6; **6b**: 42.8, 42.8, 40.8, 51.2.

[6] H.-U. Reissig, R. Zschiesche, unpublished results.

[7] For *endo* cycloaddition of the trienone corresponding to **4** but without a methoxycarbonyl group, see W. Oppolzer, R. L. Snowden, D. P. Simmons, *Helv. Chim. Acta 64* (1981) 2022; J. L. Gras, H. Bertrand, *Tetrahedron Lett. 1979*, 4549.

[8] For the synthesis of (±)-α-eudesmol, see M. A. Schwartz, A. M. Willbrand, *J. Org. Chem. 50* (1985) 1359, and references cited therein.

[9] S. J. Hecker, C. H. Heathcock, *J. Org. Chem. 50* (1985) 5159, and references cited therein.

Fast Ionic Conduction in LiI·4 Methanol: $[Li(CH_3OH)_4]^+I^-$

By *Werner Weppner, Wilfried Welzel, Rüdiger Kniep,* and *Albrecht Rabenau**

A detailed knowledge of ionic transport in solids is of fundamental importance not only for a complete understanding of the properties of materials at the microscopic level but also for the development of solid-state galvanic cells.[1] Special attention is paid to solid lithium ionic conductors, because of the low atomic weight of lithium and the high negative Gibbs free energies of formation of many lithium compounds in view of energy storage devices with high energy densities. So far, only Li_3N has been found to exhibit an exceptionally high conductivity at room temperature. The use of Li_3N, however, is limited by a low decomposition voltage.[2] Lithium cells employing solid ionic conductors have only been commercialized with thin-layer electrolytes, for example, in pacemaker batteries[2] using a charge-transfer complex, e.g., in the cell combination Li/LiI/1-butylpyridinium polyiodide.

In an attempt to find fast solid lithium ion conductors, we have investigated compounds of the system lithium halide-alcohol.[3] An indication of high ionic conductivity at room temperature was provided by the earlier described high ductility and the low melting points of a series of solid phases of these systems.[4,5] We report here on the phase diagram of the system LiI-CH_3OH and on the conductivity and crystal structure of the highest conducting phase, LiI·4CH_3OH.

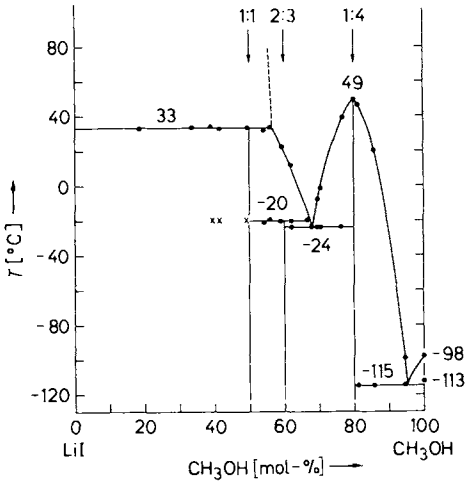


Fig. 1. Phase relationships in the system LiI-CH_3OH. See text and [6] for explanations.

Earlier studies had shown that lithium iodide reacts with methanol to form adducts having the molar ratios 1:1, 1:3, and 1:4.[4,5] Our determination of the phase equilibria along the section LiI-CH_3OH[6] (Fig. 1), carried out by differential thermoanalysis (DTA) and X-ray analysis, showed a quasi-binary section and confirmed the existence of the 1:1 (m.p. = 33 °C, incongruent) and 1:4 (m.p. = 49 °C, congruent) compounds. A compound having a 1:3 composition[5] was not observed; the investigations did, however, point to the existence of an additional (new) 2:3 phase (m.p. = −20 °C, incongruent).

Studies of the conductivity of polycrystalline samples of the compound LiI·4CH_3OH[7] (Fig. 2) gave a purely ionic conductance with the highest conductivity so far observed at room temperature (Fig. 3). The ionic conductivity has a value at room temperature of $2.7 \times 10^{-3}\ \Omega^{-1}\ cm^{-1}$ with an activation enthalpy of 0.36 eV. For quenched (glasslike) samples, conductivities were measured that were one to two orders of magnitude less. The experimental galvanic cells, prepared with lithium anodes and various cathodes (TiS_2, PbI_2, and MnO_2), gave the expected emf values. The emf corresponds to that of a lithium concentration cell. In contrast to methanol, LiI·4CH_3OH does not appear to react with lithium.

Single crystals of the hygroscopic 1:4 compound were grown from the melt in Lindemann capillaries;[8] the crys-

[*] Prof. Dr. A. Rabenau, Priv.-Doz. Dr. W. Weppner, Dipl.-Chem. W. Welzel [+], Prof. Dr. R. Kniep [+]
Max-Planck-Institut für Festkörperforschung
Heisenbergstrasse 1, D-7000 Stuttgart 80 (FRG)

[+] Permanent address:
Institut für Anorganische Chemie und Strukturchemie der Universität
Universitätsstrasse 1, D-4000 Düsseldorf (FRG)

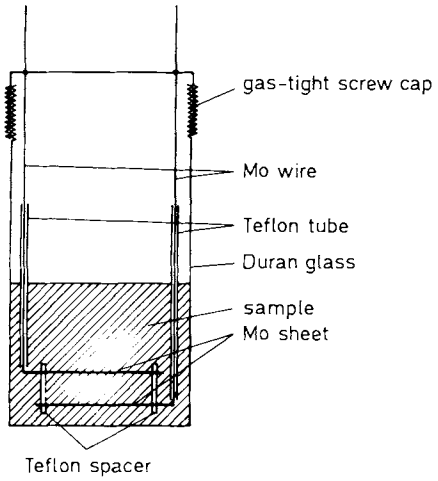


Fig. 2. Experimental setup for the conductivity measurement (cf. [7]).

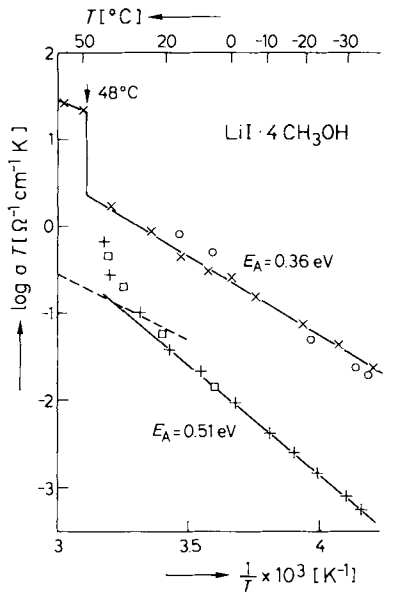


Fig. 3. Temperature dependence of the ionic conductivity of $LiI \cdot 4CH_3OH$ (cf. [7]). The product of the conductivity σ and the absolute temperature T is plotted logarithmically against the inverse of the absolute temperature (Arrhenius behavior). The values obtained for different samples are indicated by different symbols. The lower curve was obtained for quenched (glasslike) solids. For comparison, the conductivity of Li_3N (polycrystalline [2]) is shown. The arrow at the upper left points to the melting point.

tal structure[9] is shown in Figure 4. Lithium ions, are surrounded tetrahedrally by oxygen atoms of the methanol molecules with formation of the $[Li(CH_3OH)_4]^+$ units[10] (Li-O: 1.919(5) Å). The protons of the OH groups form hydrogen bonds with the iodide ions (O-H: 0.98(10) Å; H···I: 2.59(10) Å; angle O-H···I: 154(9)°). The arrangement of the anions and cations in this structure is similar to that of the zinc blende structure (corresponding unit cell shown by broken lines in Fig. 1; periodicity 13.301 Å); the c axis, however, is compressed by more than half (6.554 Å; direction of projection in Fig. 4). Compressed tetrahedral vacancies in the iodine matrix—alternately occupied and empty—therefore occur very closely one after the other in the [001] direction, thereby offering a preferred path for ion conductance in the crystal. The involvement of the protons of the OH groups in hydrogen bonds with the iodine

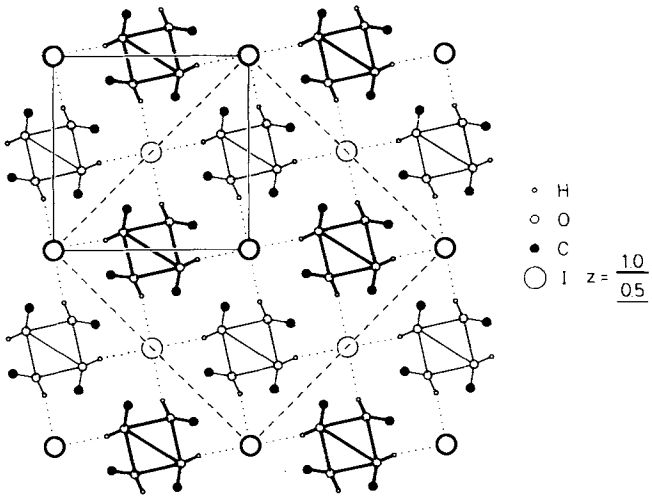


Fig. 4. Projection of the crystal structure of $Li(CH_3OH)_4I$ viewed along [001]. Centers of the $Li(CH_3OH)_4^+$ tetrahedra are in $z=0.75$ (thick) and $z=0.25$ (thin). The lithium ions in the centers of the tetrahedra are not shown. For further details, see text.

ions may explain the observation that the compound described here does not react with elemental lithium.

The results of the conductivity measurements and the crystal structure analysis are thus mutually consistent if one assumes that the ionic transport in the crystal is based on the mobility of the complex solvated cations $[Li(CH_3OH)_4]^+$.

Received: July 23, 1986 [Z 1871 IE]
German version: *Angew. Chem. 98* (1986) 1105

[1] W. Weppner, P. Hartwig, A. Rabenau, *J. Power Sources 6* (1981) 251.
[2] A. Rabenau, *Solid State Ionics 6* (1982) 277.
[3] B. Schoch, E. Hartmann, W. Weppner, *Solid State Ionics 18, 19* (1986) 529.
[4] F. Oschatz, *Dissertation*, Universität Jena 1926.
[5] W. E. S. Turner, C. C. Bisset, *J. Chem. Soc. 103* (1913) 1904.
[6] *Sample preparation and DTA measurements:* LiI (Cerac, 99%; dried at 250°C under vacuum) was added in known amounts to DTA ampoules made of Duran glass and having a thermocouple included internally. Methanol (Baker, >99.5%; distilled from magnesium) was then added with a calibrated syringe to ca. 80% capacity; sample volume ca. 1 cm^3. All operations were carried out under dried argon; the composition of the samples (see the data points in Fig. 1) was determined by re-weighing after sealing the ampoules. In order to achieve homogeneity the samples were melted and then quenched to liquid nitrogen temperature in a DTA apparatus (J. Oellers, *Diplomarbeit*, Universität Düsseldorf 1981). In order to achieve equilibrium the samples were heated repeatedly to the exothermic transition glassy→crystalline, until this effect was no longer observed. The rate of heating in the DTA measurements was 1.5°C/min (Ni/NiCr thermocouple; reference: aluminum oxide powder). The samples labeled with x in Fig. 1 could not be made completely homogeneous; the cause is presumably the marked incongruent melting behavior of the 1:1 phase.
[7] *For the conductivity measurements*, the compound was heated to melting in a sealed glass vessel equipped with plane-parallel molybdenum electrodes and then cooled (cf. Fig. 2). The electrodes (ca. 0.7 cm^2) were completely inserted, with appreciably larger separations from all surfaces than from each other. The molybdenum leads were electrically insulated by teflon tubings. Alternatively, samples consisting of compressed pellets were used. The conductivity was measured by impedance spectroscopy over a frequency range of 10 Hz-200 kHz using an HP 4192A low-frequency impedance analyzer. In the imaginary impedance plane, semicircles were obtained, which could be extrapolated to zero and were followed by a straight line forming an angle of about 45° with the axes. For the analysis, therefore, it was possible to use a simple De-

bye equivalent circuit. In order to check for ionic conductance, d.c. polarization measurements [11] were carried out in a potential range of 0 to 1 V.

[8] *For the growth of crystals*, $Li(CH_3OH)_4I$ was heated to melting in a Lindemann capillary (diameter 0.5 mm) by a perpendicularly applied stream of heated gas over a length of ca. 0.5 cm ($T_{max}=60°C$) and then cooled at 0.5°C/h.

[9] *Crystallographic data*: $Li(CH_3OH)_4I$; 517 (507) reflections (Syntex R3, $Mo_{K\alpha}$, room temperature; the authors thank Dr. *K. Peters* for the measurements on the single-crystal diffractometer). $R=0.030$; tetragonal, $I\bar{4}$; $a=9.405(5)$, $c=6.554(4)$ Å; $Z=2$. The proton of the OH group was located by a difference Fourier synthesis at $R=0.031$; the protons of the methyl groups could not be located. Further details of the crystal structure investigations may be obtained from the Fachinformationszentrum Energie, Physik, Mathematik GmbH, D-7514 Eggenstein-Leopoldshafen 2 (FRG), on quoting the depository number CSD-52181, the names of the authors, and the journal citation.

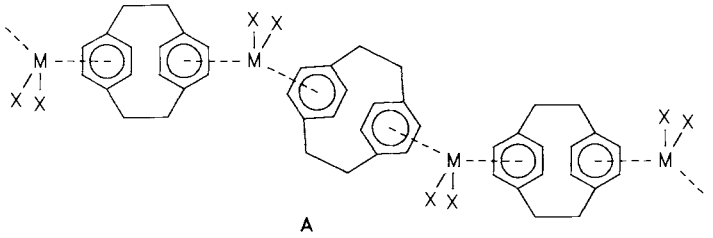
[10] For the stability of LiI-CH_3OH clusters in the gas phase, see T. P. Martin, T. Bergmann, *J. Phys. Chem.*, in press.

[11] C. Wagner, *Proc. Int. Comm. Electrochem. Thermodyn. Kinetics (CITCE)*, Lindau 1955, Butterworth, London 1957, p. 361.

Coordination-Polymeric Paracyclophane Complexes of Copper and Silver**

By *Hubert Schmidbaur*,* *Wolfgang Bublak*, *Brigitte Huber*, *Gabriele Reber*, and *Gerhard Müller*

Cyclophanes having short bridges between the benzene rings are highly strained molecules exhibiting strong repulsive interactions between the π systems.[1] In particular, for [2.2]paracyclophane this results in a strong deformation of the benzene rings and an increased donor effect of the external sides of the rings.[2] In cases with a deficiency or excess of electrons, the mutual interpenetration of the π systems leads to "spin communication," which is revealed by ESR spectroscopy or by magnetic anomalies.[3]



A

The number of transition metals[1,4] or appropriately configurated main-group metals ($d^{10}s^2$: Ga^I, Sn^{II}, Bi^{III}, etc.)[5] that form complexes with externally η^6-coordinated cyclophanes is increasing rapidly. With the coinage metals in the oxidation state +1 ($d^{10}s^0$ configuration), on the other hand, η^1- or η^2-coordinated arene complexes are expected to be formed for theoretical reasons.[6] In these complexes, the noncentric arrangement of the metal atoms should therefore dramatically affect the symmetry of the cyclophane moieties. In the presence of coordinating counterions, organometallic polymers similar to **A** might be formed, which, after partial oxidation (or reduction) should exhibit semiconducting or conducting properties.

With this goal in mind, we prepared the compounds $Cu[GaCl_4]$, $Ag[GaCl_4]$, and $Ag[GaBr_4]$ by reaction of CuCl, AgCl, and AgBr, respectively, with $GaCl_3$ or $GaBr_3$ in benzene, and then allowed them to react with equimolar amounts of [2.2]- and [3.3]paracyclophane in toluene. We thereby obtained nearly quantitative yields of the analytically pure, colorless crystalline products **1**–**4**, which have high melting or decomposition temperatures. The $AgClO_4$ complex **5** was prepared analogously.

	M.p. [°C]
1 $[Cu(GaCl_4)\cdot\{(p\text{-}C_6H_4CH_2CH_2)_2\}]$	230 (dec.)
2 $[Cu(GaCl_4)\cdot\{(p\text{-}C_6H_4CH_2CH_2CH_2)_2\}]$	225 (dec.)
3 $[Ag(GaCl_4)\cdot\{(p\text{-}C_6H_4CH_2CH_2)_2\}]$	223
4 $[Ag(GaBr_4)\cdot\{(p\text{-}C_6H_4CH_2CH_2)_2\}]$	185 (dec.)
5 $[Ag(ClO_4)\cdot\{(p\text{-}C_6H_4CH_2CH_2)_2\}]$	>300

Slow cooling of toluene solutions of **2** and **3** afforded transparent single crystals, whose structures could be determined by X-ray crystallography.[7] Both the copper complex **2** and the silver complex **3** are examples of organometallic coordination polymers. It was initially surprising to find that the metals differ in their hapticity: whereas Cu^I is η^2-bonded to each of the [3.3]paracyclophane units (Fig. 1a), Ag^I prefers η^2/η^3 coordination to the [2.2]paracyclophanes (Fig. 1b). Furthermore, the coordination sphere of the copper atom in **2** is saturated by a chelating $GaCl_4^{\ominus}$,

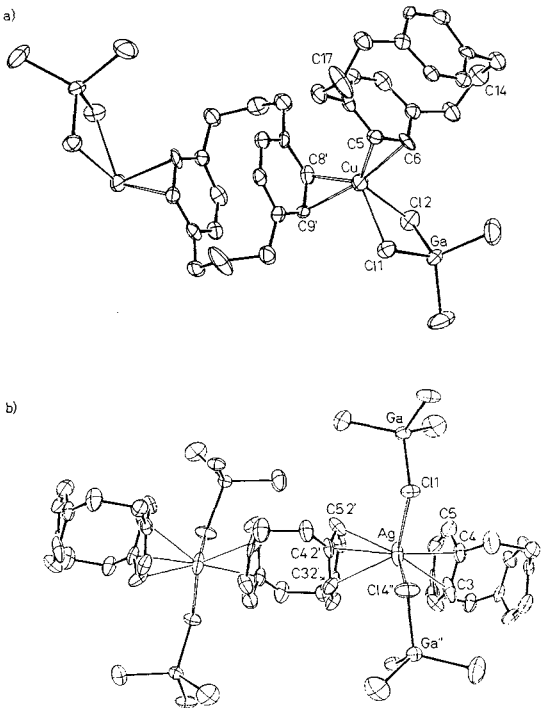


Fig. 1. Sections of the crystal structures of a) **2** and b) **3** (ORTEP, thermal ellipsoids at the 50% probability level, without H atoms; only one alternative for the disordered atoms C14/C17 in **2** is shown). The copper atom in **2** is, in each case, coordinated to the benzene ring through two nonbridging C atoms (η^2); in **3**, on the other hand, the silver atoms are also bonded to the bridgehead atoms (η^2/η^3). Important distances [Å]: **2**: Cu-C5 2.284(7), Cu-C6 2.139(7), Cu-C8' 2.230(7), Cu-C9' 2.163(7), Cu-Cl1 2.706(2), Cu-C12 2.718(2); **3**: Ag-C3 2.523(8), Ag-C4 2.434(7), Ag-C5 2.921(9), Ag-C32' 2.642(8), Ag-C42' 2.431(7), Ag-C52' 2.661(8), Ag-Cl1 2.719(2), Ag-Cl4'' 2.837(2).

[*] Prof. Dr. H. Schmidbaur, Dipl.-Chem. W. Bublak, Dipl.-Chem. B. Huber [+], Dipl.-Chem. G. Reber [+], Dr. G. Müller [+]
Anorganisch-chemisches Institut der Technischen Universität München
Lichtenbergstrasse 4, D-8046 Garching (FRG)

[+] X-ray structure analyses.

[**] This work was supported by the Fonds der Chemischen Industrie. We thank Professor *H. Hopf*, Braunschweig, and Priv.-Doz. Dr. *M. Haenel*, Mülheim, for the cyclophanes, *J. Riede* for the X-ray data collections, and *M. Barth*, *U. Graf*, and *B. Schuller* for the analyses.

whereas each silver atom in **3** is linked to two other silver atoms through two $GaCl_4^{\ominus}$ anions. Therefore, **2** forms screwlike chains; **3**, on the other hand, forms a layer structure that resembles somewhat the structure found for $Ga[GaCl_4]\cdot$[3.3]paracyclophane:[5c] in the latter, however, the Ga^I centers are twofold η^6-coordinated, as shown for **A**.

It remains an open question whether the different arene coordination of Cu^I and Ag^I in **2** and **3**, respectively, is due to the nature of the metal or to the difference in the cyclophane bridges.

It has often been observed that the coordination geometry of silver in its arene complexes is more variable than that of copper.[8] In certain cases, in fact, Ag^I is only η^1-bonded.[9] The considerable boat distortion of the benzene rings of the [2.2]cyclophane **3**, which is clearly visible in the structure (Fig. 1), necessarily leads to different donor properties, compared with those of **2**, in which the planarity of the benzene ring is better maintained.

The pure copper(I) compound **2** is electrically nonconducting; however, in air the compound turns slightly colored and becomes conducting. A partial oxidation to Cu^{II} can be assumed to have occurred, resulting in the formation of a mixed-valent organometallic polymer.[10] A detailed understanding of this phenomenon will only be possible if the properties of such polymers can be reliably controlled.

Experimental Procedure

$M[GaX_4]$: A solution of anhydrous $GaCl_3$ or $GaBr_3$ in benzene was treated with CuCl, AgCl, or AgBr (ca. 10% excess) and the resulting reaction mixture was refluxed for 10 h. Filtration of the hot solution and cooling of the filtrate resulted in the precipitation of the benzene complex $M[GaX_4]\cdot C_6H_6$, which, upon drying in a vacuum, was converted into the arene-free salt.

1–**4**: Solutions of $M[GaX_4]$ in toluene were treated with solutions containing equimolar amounts of cyclophane in toluene. The complexes **1**–**4** precipitated out at room temperature in the form of a colorless, microcrystalline, moisture- and air-sensitive powder in nearly quantitative yields. The products were washed with toluene and dried in a vacuum. By slow cooling (1°C/h) of the clear solutions from 100°C to room temperature, single crystals were obtained.

Received: July 24, 1986;
supplemented: August 19, 1986 [Z 1875 IE]
German version: *Angew. Chem. 98* (1986) 1108

[1] P. M. Keehn, S. M. Rosenfeld (Eds.): *Cyclophanes, Vol. I+II*, Academic Press, New York 1983.

[2] H. Hope, J. Bernstein, K. N. Trueblood, *Acta Crystallogr. Sect. B 28* (1972) 1733.

[3] E. Heilbronner, Z. Z. Yang, *Top. Curr. Chem. 115* (1984) 1; F. Gerson, *ibid. 115* (1984) 57.

[4] E. D. Laganis, R. G. Finke, V. Boekelheide, *Proc. Natl. Acad. Sci. USA 78* (1981) 2657; R. T. Swann, A. W. Hanson, V. Boekelheide, *J. Am. Chem. Soc. 108* (1986) 3324, and references cited therein.

[5] a) H. Schmidbaur, *Angew. Chem. 97* (1985) 893; *Angew. Chem. Int. Ed. Engl. 24* (1985) 893, and unpublished results 1986; b) H. Schmidbaur, W. Bublak, B. Huber, G. Müller, *Organometallics 5* (1986) 1647; c) *Helv. Chim. Acta 69* (1986) 1742.

[6] *Gmelin Handbook of Inorganic Chemistry, 8th ed., Silver* (*Part B 5*, Organosilver Compounds), Springer, Berlin 1975.

[7] **2**: monoclinic, $P2_1/c$, $a=12.087(2)$, $b=11.537(2)$, $c=13.848(1)$ Å, $\beta=93.00(1)°$, $V=1928.4$ Å^3, $\rho_{calcd}=1.761$ g cm^{-3}, $Z=4$; $F(000)=1024$, $\mu(Mo_{K\alpha})=30.6$ cm^{-1}; 3025 unique reflections, 2341 observed with $I\geq 2.0\sigma(I)$ (ω-scan, $\Delta\omega=0.8°$, $(\sin\theta/\lambda)_{max}=0.572$, hkl: +13, +13, ±15, $Mo_{K\alpha}$ radiation, $\lambda=0.71069$ Å, graphite monochromator, $T=-40$°C, Syntex $P2_1$); Lp and empirical absorption correction (relative transmission: 0.63–1.00). Solution by Patterson methods (SHELXS-86), $R=0.052$, $R_w=0.057$, $w=1/\sigma^2(F_0)$ (anisotropic, H constant, 235 parameters, SHELX-76). $\Delta\rho_{fin}=+0.63/-0.61$ eÅ^{-3}. **3**: orthorhombic, $P2_12_12_1$, $a=11.363(2)$, $b=11.767(2)$, $c=13.766(2)$ Å, $V=1840.6$ Å^3, $\rho_{calcd}=1.904$ g cm^{-3}, $Z=4$; $F(000)=1032$, $\mu(Mo_{K\alpha})=30.9$ cm^{-1}; 3233 unique reflections, 2687 observed (ω-scan, $\Delta\omega=0.9°$, $(\sin\theta/\lambda)_{max}=0.595$, hkl: +13, +13, +16 and Friedel reflections, $T=-35$°C). Lp and empirical absorption correction (relative transmission: 0.68–1.00). Patterson methods, $R=0.043$, $R_w=0.037$, $w=1/\sigma^2(F_0)$ (anisotropic, H constant, 199 parameters, $R_w=0.046$ for inverse set of coordinates). $\Delta\rho_{fin}=+1.67/-1.20$ eÅ^{-3} at Ag. Further details of the crystal structure investigations may be obtained from the Fachinformationszentrum Energie, Physik, Mathematik GmbH, D-7514 Eggenstein-Leopoldshafen 2 (FRG), on quoting the depository number CSD-52059, the names of the authors, and the journal citation.

[8] R. W. Turner, E. L. Amma, *J. Am. Chem. Soc. 85* (1963) 4046, *88* (1966) 1877.

[9] K. Shelly, D. C. Finster, Y. J. Lee, W. R. Scheidt, C. A. Reed, *J. Am. Chem. Soc. 107* (1985) 5955.

[10] We thank Dipl.-Chem. *M. Weis*, Garching, for the initial measurements.

Thermolytically Induced C–H Activation Using a 14-Electron Complex: Synthesis and Molecular Structure of $[IrHCl(C_6H_5)(PiPr_3)_2]$**

By *Helmut Werner,* Arthur Höhn,* and *Michael Dziallas*

The presently known methods of *inter*molecular C–H activation of aliphatic and aromatic hydrocarbons, which have been developed in the last few years, generally make use of a high-energy (i.e., very reactive and short-lived) metal–ligand fragment.[1] Such species are usually generated by photolysis (e.g., by loss of H_2 or CO from a stable precursor), by reaction of "hot" metal atoms with appropriate ligands in a matrix, or by reduction of metal–halogen compounds (mostly by using strong reducing agents). Examples of *thermolytic* reactions, according to Eq. (1), which take place at moderate temperatures and use *stable* metal complexes, $[ML_n]$, are rare.[2]

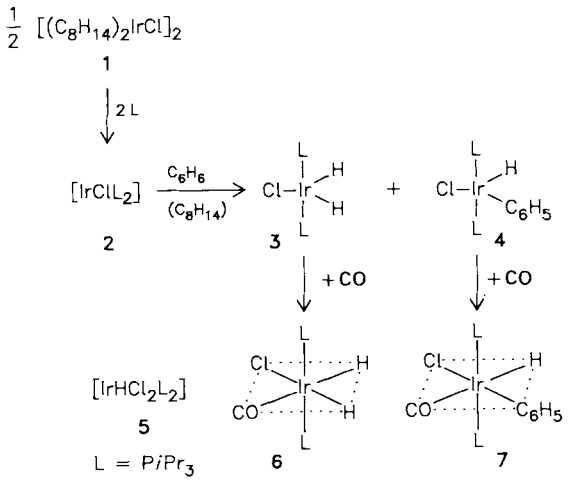
$$L_nM + R{-}H \longrightarrow L_nM\begin{matrix}R\\H\end{matrix} \qquad (1)$$

Recently, we showed[3] that the 14-electron species **2** formed in situ from **1** and triisopropylphosphane,[4] reacts at room temperature with H_2 and with HCl to form **3** and **5**, respectively. Under the same conditions, no reaction occurs with benzene. We have now found, however, that reaction does occur at higher temperatures. If a solution of **1** and $PiPr_3$ (molar ratio $\approx 1:4$) in benzene is heated to 80°C, a mixture of **3** and the hydrido(phenyl)iridium compound **4** in an approximate ratio of 1:2 is obtained (Scheme 1).[5a] The separation of the two products can be achieved by repeated crystallization, but is more conveniently performed by allowing the mixture of **3** and **4** to react with CO to produce the octahedral compounds **6** and **7**, which can easily be separated.[5b] Complex **6** has been previously prepared (although not isolated) from **8** and H_2 and studied with regard to its catalytic properties.[6] A compound analogous to **7** having the composition **9** (with, however, the hydride and CO ligands in *cis* positions) is also known but has been obtained via a completely different route, namely by oxidative addition of HBr to **10**.[7]

The problem of how **3** is formed from **1**, $PiPr_3$, and benzene has not been finally solved. Compound **4** is definitely

[*] Prof. Dr. H. Werner, Dipl.-Chem. A. Höhn, Dipl.-Chem. M. Dziallas
Institut für Anorganische Chemie der Universität
Am Hubland, D-8700 Würzburg (FRG)

[**] This work was supported by the Deutsche Forschungsgemeinschaft and the Fonds der Chemischen Industrie.



Scheme 1. C_8H_{14} = cyclooctene.

trans-[IrCl(CO)L_2] [IrHBr(C_6H_5)(CO)L_2]

8 **9**

trans-[Ir(C_6H_5)(CO)L_2] L = PEt_3

10

not a precursor of **3** since the hydrido(phenyl) complex **4** is quantitatively recovered after heating a benzene solution for several hours under reflux. Benzene is also not the source of the hydride ligands in **3**, because in C_6D_6 solution a mixture of **3** (not [IrD_2ClL_2]) and [IrDCl(C_6H_5)L_2] is produced, the latter being characterized by IR and mass spectra. We assume that cyclooctene formed in the reaction of **1** with $PiPr_3$ functions as the H_2-transfer reagent, which would be in agreement with very recent work by *Crabtree* et al.[8]

The spectroscopic data for **4**, **6**, and **7**[9] support the structural proposals for the complexes shown in Scheme 1. The most characteristic feature of the ^{1}H-NMR spectrum of **6** is the observation of *two* hydride signals in the high-field region that differ significantly in their chemical shift and thus reflect the differing *trans* influence of the Cl and CO ligands. A comparison of the NMR data of **6** and **7** led us to assume that in **7** the hydride ligand is in a *trans* position to CO.

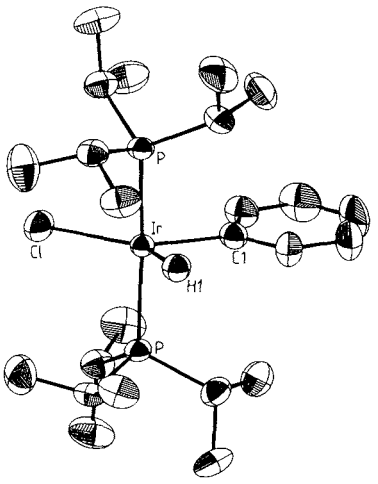
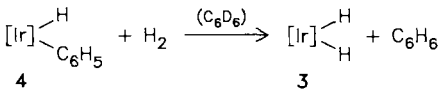


Fig. 1. Structure of **4** in the crystal. **4** has a mirror plane through Ir, Cl, and C1–C6. Selected bond distances [pm] and angles [°]: Ir-P 233.4(1), Ir-Cl 241.2(1), Ir-H1 144, Ir-C1 201.0(5); P-Ir-P 168.1(3), P-Ir-Cl 91.4(1), P-Ir-H1 85.5, P-Ir-C1 93.0(1), Cl-Ir-C1 136.1(1), Cl-Ir-H1 146.1, C1-Ir-H1 77.9.

The result of the X-ray structural analysis of **4** is shown in Figure 1.[10] The coordination sphere around the metal corresponds to a trigonal bipyramid with the phosphane ligands in axial positions. The P–Ir–P linkage is not completely linear (angle 168.1(3)°), presumably owing to steric hindrance between the isopropyl units and the phenyl group. The angles in the equatorial plane of the bipyramid differ significantly from 120°. Particularly noteworthy is the relatively small C1–Ir–H1 angle (77.9°), which possibly points to a still present (although weak) interaction between C1 and H1. This interaction may also explain the fact that in solution at room temperature there is no free rotation about the Ir–C1 bond as is proved by the appearance of *six* signals for the six phenyl carbon atoms in the ^{13}C-NMR spectrum.[9]



(2)

The hydrido(phenyl) complex **4** reacts with H_2 in C_6D_6 at room temperature in a few seconds to form **3** [Eq. (2)]. The rapid rate of this process is rationalized by supposing that one molecule of H_2 is oxidatively added to the coordinatively unsaturated metal center of the 16-electron complex **4** and the so-formed intermediate [$IrH_3(C_6H_5)ClL_2$] (a derivative of [IrH_5L_2][11]) preferentially eliminates C_6H_6 rather than H_2. It should be noted that the square-planar compounds *trans*-[IrR(CO)(PPh_3)$_2$] also react with H_2 by cleavage of the Ir–R bond and elimination of RH.[12]

Received: July 25, 1986;
revised: September 29, 1986 [Z 1877 IE]
German version: *Angew. Chem. 98* (1986) 1112

[1] For leading references see: A. H. Janowicz, R. A. Periana, J. M. Buchanan, C. A. Kovac, J. M. Stryker, M. J. Wax, R. G. Bergman, *Pure Appl. Chem. 56* (1984) 13; W. D. Jones, F. J. Feher, *J. Am. Chem. Soc. 106* (1984) 1650; M. L. H. Green, D. O'Hare, *Pure Appl. Chem. 57* (1985) 1897; J. Halpern, *Inorg. Chim. Acta 100* (1985) 41; R. H. Crabtree, *Chem. Rev. 85* (1985) 245; I. P. Rothwell, *Polyhedron 4* (1985) 77.

[2] For one recently published example see: P. J. Desrosiers, R. S. Shinomoto, T. C. Flood, *J. Am. Chem. Soc. 108* (1986) 1346.

[3] H. Werner, J. Wolf, A. Höhn, *J. Organomet. Chem. 287* (1985) 395.

[4] R. Meij, D. J. Stufkens, K. Vrieze, W. van Gerresheim, C. H. Stam, *J. Organomet. Chem. 164* (1979) 353.

[5] *Experimental procedure:* a) A stirred suspension of **1** (200 mg, 0.22 mmol) in 20 mL of benzene was treated at 25°C with $PiPr_3$ (160 mg, 1.00 mmol) and heated for 90 min under reflux. After removal of the solvent and repeated crystallization from pentane (25°C to −78°C), the less soluble compound **4** was obtained (orange-red crystals, m.p. = 112°C (dec.), yield 58%, correct elemental analysis), and from the mother liquor the better soluble compound **3** [3] (yield 29%).—b) CO was bubbled through a pentane solution of the mixture of **3** and **4** for a few seconds. A flaky bright-yellow precipitate was obtained which was filtered off, dried in vacuo, and washed with methanol (0°C). After concentrating the methanol solution and cooling to −78°C, yellow, moderately air-stable crystals of **6** were formed, m.p. = 185°C (dec.). On the frit, **7** remains as a pale yellow microcrystalline powder, m.p. = 187°C (dec.). Quantitative yield (correct elemental analysis).

[6] W. Strohmeier, F. J. Müller, *Z. Naturforsch. B24* (1969) 770; W. Strohmeier, R. Fleischmann, T. Onoda, *J. Organomet. Chem. 28* (1971) 281; W. Strohmeier, M. Lukacs, *ibid. 133* (1977) C47.

[7] a) L. Dahlenburg, R. Nast, *J. Organomet. Chem. 110* (1976) 395; b) U. Behrens, L. Dahlenburg, *ibid. 116* (1976) 103.

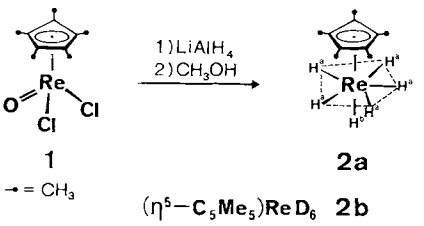
[8] R. H. Crabtree, C. P. Parnell, *Organometallics 4* (1985) 519; and references cited therein.

[9] **4**: $M_r = 626$ (MS); IR (KBr): $\tilde{\nu}$(IrH) = 2273, $\tilde{\nu}$(C=C) = 1568 cm^{-1}; ^{1}H-NMR (C_6D_6, 400 MHz): $\delta = 7.30$ and 6.83 (both m, C_6H_5), 2.53 (m, PC*H*), 1.19 (dvt, $J_{HH} = 7.1$, $N = 13.3$ Hz, PCHCH_3), 1.06 (dvt, $J_{HH} = 6.7$, $N = 13.3$ Hz, PCHCH_3) [2 signals due to diastereotopy], −32.23 (t, $J_{PH} = 12.5$ Hz, IrH); ^{31}P-NMR (C_6D_6, 90 MHz): $\delta = 28.84$ (s, d after selective decoupling of the non-hydridic protons); ^{13}C-NMR (C_6D_6, 400 MHz): $\delta = 19.56$ and 20.02 (s, PCH*C*H$_3$, 2 signals due to diastereotopy), 24.27 (vt, $N = 27.8$ Hz, P*C*H), 117.72 (s, ipso-C of C_6H_5), 121.08, 124.89, 128.85, 136.70, 147.17 (each s, 5C of C_6H_5; d in off-resonance).—**6**: $M_r = 578$ (MS); IR (KBr): $\tilde{\nu}$(IrH, *trans* to Cl) = 2205, $\tilde{\nu}$(IrH, *trans* to CO) = 2097, $\tilde{\nu}$(CO) = 1965 cm^{-1}; ^{1}H-NMR (C_6D_6, 60 MHz): $\delta = 3.37$ (m, PC*H*), 1.30 (dvt, $J_{HH} = 7.2$, $N = 14.0$ Hz, PCHCH_3), 1.25 (dvt, $J_{HH} = 7.0$, $N = 14.1$ Hz, PCHCH_3) [2 signals due to diastereotopy], −8.64 (dt, $J_{PH} = 17.5$, $J_{HH} = 5.5$ Hz, IrH *trans* to CO), −20.20 (dt, $J_{PH} = 13.2$, $J_{HH} = 5.5$ Hz, IrH *trans* to Cl); ^{31}P-NMR (C_6D_6, 90 MHz): $\delta = 32.91$ (s, t after selective decoupling of the non-hydridic protons).—**7**: $M_r = 654$ (MS); IR (KBr): ν(IrH) = 2140, ν(CO) = 1957 cm^{-1}; ^{1}H-NMR (C_6D_6, 400 MHz): $\delta = 7.74$ and 6.81 (both m, C_6H_5), 2.30 (m, PC*H*), 1.20 (dvt, $J_{HH} = 7.1$, $N = 14.0$ Hz, PCHCH_3), 1.14 (dvt, $J_{HH} = 7.0$, $N = 13.8$ Hz, PCHCH_3) [2 signals due to diastereotopy], −7.29 (t, $J_{PH} = 17.5$ Hz, IrH); ^{31}P-NMR (C_6D_6, 90 MHz): $\delta = 13.36$ (s, d after selective decoupling of the nonhydridic protons).

[10] Orthorhombic, space group *Pbnm*, $Z = 4$; $a = 974.0(2)$, $b = 1352.4(2)$, $c = 2078.9(3)$ pm, $V = 2738.5 \times 10^6$ pm^3; $\rho_{calcd} = 1.52$ g/cm^3; $5° \leq 2\theta \leq 51°$ ($Mo_{K\alpha}$, $\lambda = 71.069$ pm, ω-scan); 2619 independent reflections, Lorentz and polarization corrections, Patterson method (Syntex XTL), positions of hydrogen atoms partly determined from difference Fourier syntheses, partly calculated from ideal geometry, position of H1 not refined; $R_1 = 0.024$, $R_2 = 0.029$ for 2400 structure factors ($F_0 \geq 3.92\sigma(F_0)$). Further details of the crystal structure analysis are available on request from the Fachinformationszentrum Energie Physik Mathematik, D-7514 Eggenstein-Leopoldshafen 2 (FRG), on quoting the depository number CSD-52121, the names of the authors, and the journal citation.

[11] L. Garlaschelli, S. I. Khan, R. Bau, T. Koetzle, *J. Am. Chem. Soc. 107* (1985) 7212.

[12] L. Dahlenburg, F. Mirzaei, B. Pietsch, *Inorg. Chim. Acta 97* (1985) L5.



1 → = CH_3 **2a** $(\eta^5\text{-}C_5Me_5)ReD_6$ **2b**

If the methanolysis is not carried out carefully, then the dark red, binuclear hydrido complex $[(\eta^5\text{-}C_5Me_5)ReH_3]_2$[7] is formed as a side product. The hexadeuteride **2b** (deuterium content ≧97%, ^{1}H-NMR) can be obtained analogously by treatment of **1** with $LiAlD_4$ and CH_3OD. The simple composition of **2a** is supported by elemental analysis, vapor pressure osmometric molecular-weight determination, and FD mass spectrometry. The structure of a half-sandwich complex having a π-coordinated pentamethylcyclopentadienyl ligand is shown by IR and NMR spectroscopy. In the IR spectrum, in addition to the typical band pattern for the $(\pi\text{-}C_5Me_5)Re$ fragment, five relatively intense bands at 2018, 980, 822, 620, and 458 cm^{-1} are observed. In the deuterio derivative **2b**, these bands are shifted to 1453, 704, 600, 458, and 345 cm^{-1}, which supports their assignment as ReH stretching vibrational (2018 cm^{-1}) and bending vibrational modes. The frequencies correspond to those of other rhenium polyhydrides.[1,2] Whereas the $^{13}C\{^1H\}$-NMR spectrum at room temperature supports the η^5 coordination of the C_5Me_5 ligand to the formally heptavalent rhenium, the six hydride ligands are

Hexahydrido(pentamethylcyclopentadienyl)rhenium, $[(C_5Me_5)ReH_6]$**

By *Wolfgang A. Herrmann** and *Jun Okuda*

The rhenium complexes $K_2[ReH_9]$ and $[ReH_7(PR_3)_2]$ have played a major role[1,2] in the development of transition-metal polyhydride chemistry.[3] In recent years, complexes of the latter type, in particular, have become increasingly interesting, because they are capable of activating C-H bonds in saturated compounds[4] and because they can be formulated as $[ReH_5(\eta^2\text{-}H_2)(PR_3)_2]$ with η^2-coordinated molecular hydrogen.[5] Whereas the majority of the metal polyhydrides are stabilized by triorganophosphane ligands, the number of hydrido complexes stabilized by π-aromatic ancillary ligands (e.g., cyclopentadienyl derivatives) is limited to a few examples.[6] In the course of our investigations into the coordination chemistry of the $(C_5Me_5)Re$ fragment containing rhenium in higher oxidation states, we have now surprisingly been able to synthesize the new polyhydride $[(C_5Me_5)ReH_6]$ **2a**.

The title compound **2a** is prepared by treatment of the Re^V complex **1** in diethyl ether with $LiAlH_4$ followed by extremely careful methanolysis of the aluminopolyhydride formed as an intermediate. Complex **2a** forms colorless crystals, which are hardly air-sensitive, undergo sublimation quickly and without decomposition at ambient temperature in high vacuum, and are even readily soluble in nonpolar (!) hydrocarbons.

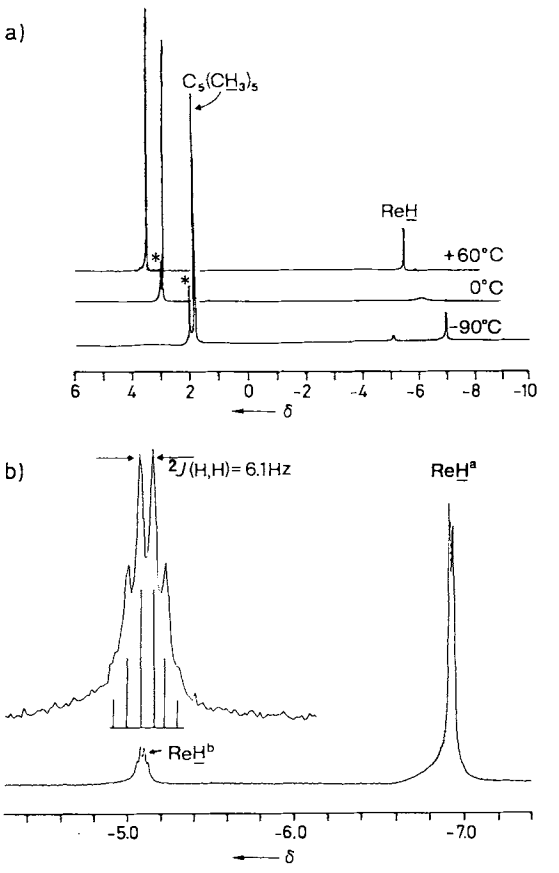


Fig. 1. a) ^{1}H-NMR spectra of the title compound **2a** at −90, 0, and 60°C (recorded in [D$_8$]toluene; 270 MHz, int. TMS); b) ReH region at −90°C, enlarged. The asterisks indicate signals due to solvent.

[*] Prof. Dr. W. A. Herrmann, Dr. J. Okuda
Anorganisch-chemisches Institut der Technischen Universität München
Lichtenbergstrasse 4, D-8046 Garching (FRG)

[**] This work was supported by the central research laboratory of Hoechst AG.

revealed as a sharp singlet besides the singlet for the CH_3 groups in the ^{1}H-NMR spectrum at 60°C.[9] We have also confirmed the number of hydride ligands by internal standardization with $[(C_5H_5)_2MoH_2]$.[8] Upon cooling of the probe, the high-field singlet undergoes significant line broadening. At −80°C, the low-temperature limit of the spectrum is reached, the practically unchanged singlet of the CH_3 groups being accompanied by a binominal sextet with a relative intensity of 1 ($\delta = -5.04$) and a doublet with a relative intensity of 5 ($\delta = -6.90$) (Fig. 1).[9]

These data show that the exchange of the six hydride ligands between two stereochemically independent positions is frozen at low temperature on the NMR time scale. If the C_5Me_5 ligand is placed at the corner of the coordination polyhedron, the coordination sphere around the rhenium atom can be regarded as a pentagonal bipyramid. On the other hand, the ring ligand can also be viewed as tridentate, and a polyhedron with nine edges can be used. In this case, the 3/3/3 coordination (tricapped trigonal prism) found in the $[ReH_9]^{2\ominus}$ ion is not preferred, but rather a 3/5/1 coordination derived from a monocapped square antiprism.

Since a pentagonal-bipyramidal structure with five hydrogen atoms in the equatorial plane has recently been found by neutron diffraction for the iridium hydride $[(PiPr_3)_2IrH_5]$,[10] we consider the above "classical" description of the coordination geometry of complex type **2** to be the most appropriate.

Experimental Procedure

A well-stirred suspension of **1** (200 mg, 0.49 mmol) in anhydrous diethyl ether (35 mL) was treated at −95°C with solid $LiAlH_4$ (190 mg, 5.0 mmol), added in portions. After 2 h, a nearly colorless mixture had formed and was allowed to warm slowly to 25°C. The mixture was cooled again to −95°C and methanol (1.0 mL, 24.8 mmol) in diethyl ether (10 mL) was added over 1 h, which resulted in violent evolution of gas. The reaction mixture was then stirred for 1 h at −95°C and allowed to warm to 25°C. After gas evolution had ceased, all volatiles were removed in vacuum, the white, powdery residue was extracted with 3 × 10 mL of toluene, and the extracts were filtered through a glass frit containing kieselguhr (dried by heating). After removal of the solvent from the yellowish filtrate in vacuum, the crude product was crystallized from a small amount of hexane at −30°C; colorless platelets, m.p. = 192°C (dec.), yield 120 mg (75%).—The derivative $[(\eta^5\text{-}C_5Me_4Et)ReH_6]$ (m.p. = 108°C, dec. above 170°C) was synthesized analogously.

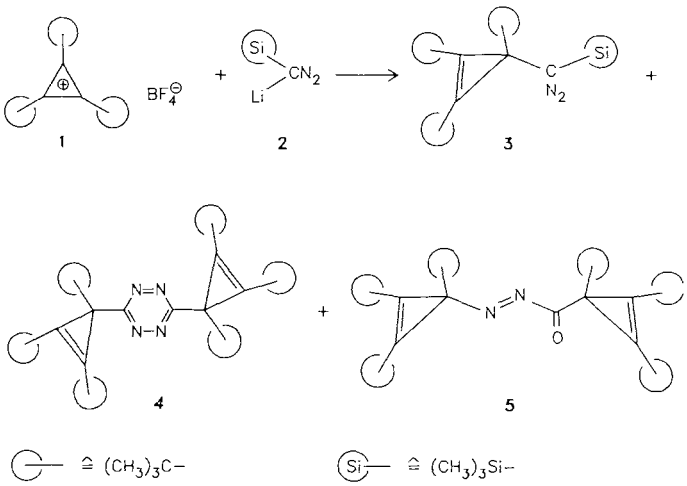
Received: August 6, 1986 [Z 1894 IE]
German version: *Angew. Chem. 98* (1986) 1109

[1] S. C. Abrahams, A. P. Ginsberg, K. Knox, *Inorg. Chem. 3* (1964) 558.
[2] J. Chatt, R. S. Coffey, *J. Chem. Soc. A 1969*, 1963.
[3] Recent reviews: A. P. Borisov, V. D. Makhaev, K. N. Semenenko, *Sov. J. Coord. Chem. 6* (1980) 549; D. S. Moore, S. D. Robinson, *Chem. Soc. Rev. 12* (1983) 415; G. G. Hlatky, R. H. Crabtree, *Coord. Chem. Rev. 65* (1985) 1.
[4] D. Baudry, M. Ephritikhine, H. Felkin, *J. Organomet. Chem. 224* (1982) 363.
[5] R. H. Crabtree, 191th National ACS Meeting, New York, April 1986; reported in *Chem. Eng. News 64* (1986) No. 18, p. 26.—Cf. R. H. Crabtree, D. G. Hamilton, *J. Am. Chem. Soc. 108* (1986) 3124; R. H. Crabtree, M. Lavin, L. Bonneviot, *ibid. 108* (1986) 4032.
[6] J. Okuda, R. C. Murray, J. C. Dewan, R. R. Schrock, *Organometallics*, in press; T. M. Gilbert, R. G. Bergman, *ibid. 2* (1984) 1458; *J. Am. Chem. Soc. 107* (1985) 3502; T. M. Gilbert, F. J. Hollander, R. G. Bergman, *ibid. 107* (1985) 3508.
[7] W. A. Herrmann, J. Okuda, E. Voss, unpublished results; cf. W. A. Herrmann, *J. Organomet. Chem. 300* (1986) 111.
[8] R. H. Crabtree, B. E. Segmuller, R. J. Uriarte, *Inorg. Chem. 24* (1985) 1949.
[9] Spectroscopic data of **2a**: ^{1}H-NMR (270 MHz, [D$_8$]toluene, 60°C): $\delta CH_3 = 2.00$ (s, 15H), $\delta ReH = -6.94$ (s, 6H).—^{1}H-NMR (270 MHz, [D$_8$]toluene, −80°C): $\delta CH_3 = 1.86$ (s, 15H), $\delta ReH^b = -5.04$ (sextet, 1H; $^2J(H,H) = 6.1$ Hz), $\delta ReH^a = -6.90$ (d, 5H, $^2J(H,H) = 6.1$ Hz).—$^{13}C\{^1H\}$-NMR (C_6D_6, 28°C): $\delta C_5Me_5 = 98.66$, $\delta CH_3 = 12.07$.—IR (KBr): $\tilde{\nu} = 2068$ m, 2018 sh, 2008 s [ν(ReH)]; 980 s, 837 (sh), 822 vs, 620 ms, 458 m [δ(ReH)]; further bands: 2985 mw, 2962 mw, 2915 m, 2850 w [$\nu(CH_3)$]; 1486 ms, 1454 mw, 1430 w, 1380 ms [$\delta(CH_3)$]; 1077 w, 1033 m, 397 w cm^{-1}.—FD-MS: m/z 328 ($M^{\oplus}$, ^{187}Re).—$M_r = 330$ (determined by vapor pressure osmometry in benzene).
[10] L. Garlaschelli, S. I. Khan, R. Bau, G. Longoni, T. F. Koetzle, *J. Am. Chem. Soc. 107* (1985) 7212.

Tandem Walk Rearrangement of a Protonated Dicyclopropenyl Ketone**

By *Günther Maier,* Ines Bauer, Dieter Born,* and *Hans-Otto Kalinowski*

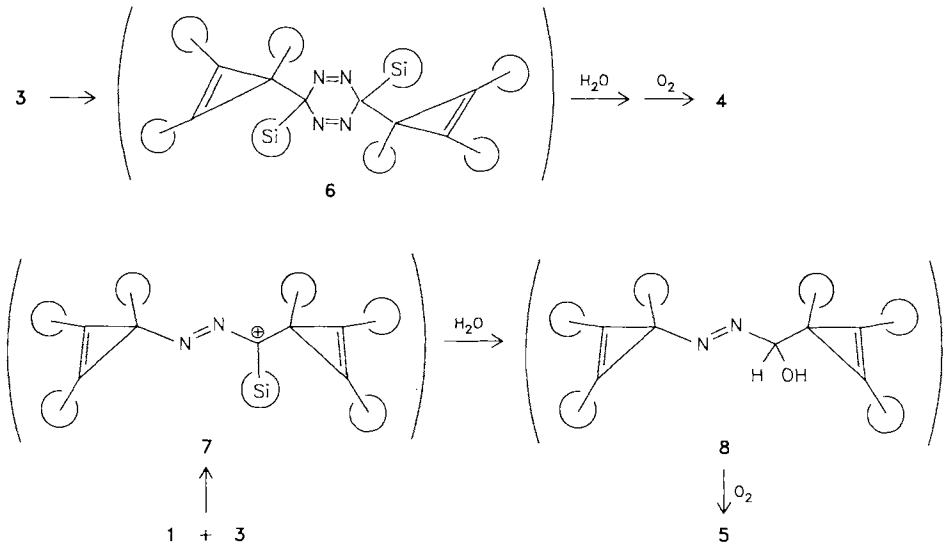
Tert-butyl tri-*tert*-butylcyclopropenyl ketone, upon protonation, undergoes a ring expansion to the corresponding hydroxyhomocyclopropenylium ion,[1] which, even at room temperature, undergoes a walk rearrangement.[2] The corresponding cyclopropenylcarbinyl cation represents the transition state of this process. If the *tert*-butyl group at the aliphatic C atom of the three-membered ring is not present in the starting ketone, the cyclopropenylcarbinyl system, initially formed upon treatment with acid, corresponds to an energy minimum and can therefore be observed directly.[3] How does a dicyclopropenyl ketone behave under similar conditions? To answer this question, we have synthesized bis(1,2,3-tri-*tert*-butyl-2-cyclopropenyl) ketone, which, to the best of our knowledge, is the first dicyclopropenyl ketone, and have investigated its behavior upon protonation by NMR spectroscopy.



The route to **13** is full of unique features: (a) **1** reacts with lithiated trimethylsilyldiazomethane **2** to give the cyclopropenyldiazomethane **3** (26%),[4] the tetrazine **4** (along with a small amount of the 1,4-dihydro derivative of **4**), and the acyl diimide **5**. The dimerization of **3**, leading ultimately to **4**, is unusual:[5] The initial product is probably the intermediate **6**, which undergoes hydrolysis followed by dehydrogenation by air to give the heteroarene **4**. The formation of **5** is still more surprising: The first step presumably involves attack of the terminal N atom of **3** on the cation **1**, resulting in the formation of **7**. Compound **7** un-

[*] Prof. Dr. G. Maier, Dr. I. Bauer, cand. chem. D. Born, Dr. H.-O. Kalinowski
Institut für Organische Chemie der Universität
Heinrich-Buff-Ring 58, D-6300 Giessen (FRG)

[**] Small Rings, Part 61. This work was supported by the Deutsche Forschungsgemeinschaft and the Fonds der Chemischen Industrie.—Part 60: [3].

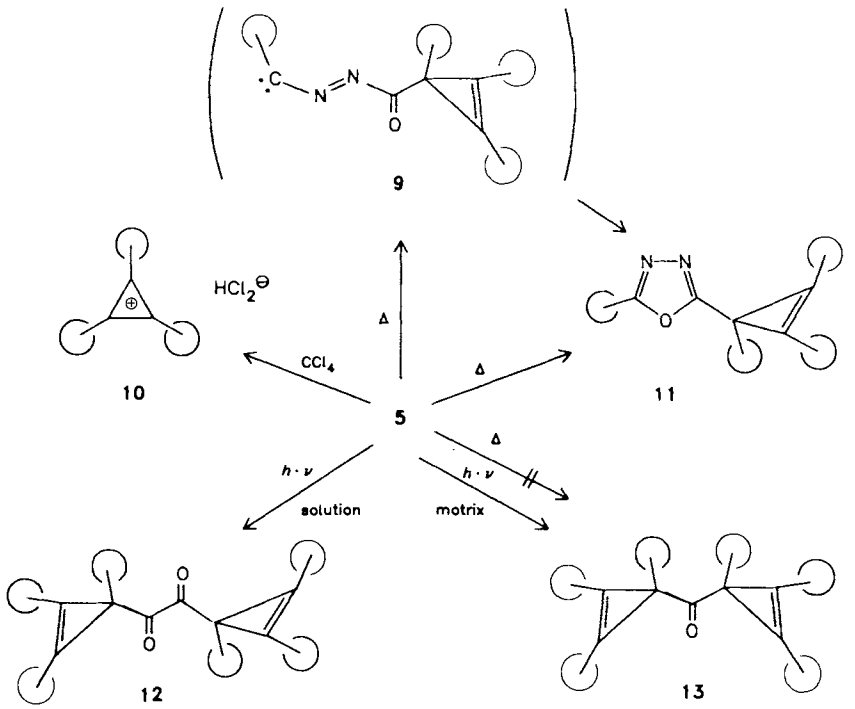


dergoes hydrolysis to give **8**, which, in turn, is oxidized by molecular oxygen to give the final product **5**.

(b) **5**, which is the potential precursor for **13**, also exhibits unusual behavior: Upon standing, a solution of **5** in tetrachloromethane forms beautiful crystals of the hydrogen dichloride **10**.[6] Heating of **5** does not result in elimination of nitrogen (and therefore formation of **13** does not occur), but rather in fragmentation to give di-*tert*-butylacetylene and the oxadiazole **11**. Thus, the cleavage begins on the C1–C2 bond of the cyclopropene ring adjacent to the nitrogen. Elimination of the alkyne affords carbene **9** (1,5 dipole), which, in turn, undergoes ring closure to give **11**.

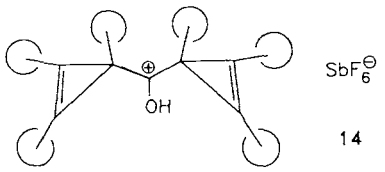
Compound **12** is formed by dimerization of the acyl radical, which is less hindered than the cyclopropenyl radical. Upon irradiation of **5** in an organic matrix at $-196\,^{\circ}C$, the acyl radical formed has no other choice than to combine with the cyclopropenyl radical formed in the same solvent cage. Indeed, under these conditions, the ketone **13** is obtained.

Protonation of **13** with hydrogen chloride followed by ion exchange with silver hexafluoroantimonate results in the formation of a stable salt having temperature-dependent NMR spectra (^1H, ^{13}C). The low-temperature spectra (Table 1) support structure **15**. Free rotation of the *tert*-butyl group on the aliphatic C atom of the three-mem-

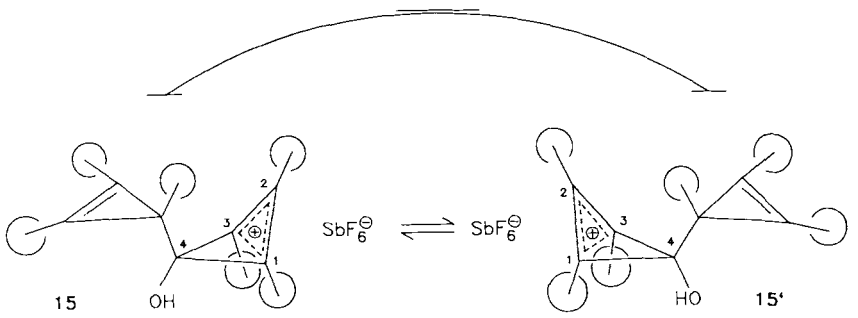


(c) The photochemical behavior of **5** is also unusual: Irradiation at room temperature (254 nm; benzene, cyclohexane, or tetrahydrofuran (THF)) results in gas evolution. However, instead of **13**, the α-diketone **12** is isolated.

bered ring is hindered, so that one observes two signals in the ratio of 2 : 1 for the methyl groups. If the changes in the ^1H-NMR spectra (100 MHz, CD_2Cl_2) are followed during warm-up of the sample, a first coalescence is observed at



14



15 15'

Table 1. Reaction conditions, yields, and NMR spectroscopic data for the compounds **4**, **5**, **10**–**13**, and **15**. NMR: δ values relative to TMS. RT = room temperature. All compounds gave correct elemental analyses.

Compound	Color, m.p. [°C]	Reaction conditions	Yield [%]	$\delta(^1H)$	$\delta(^{13}C)$
4	dark violet crystals	see Experimental Procedure	11	1.20 (s, 36H; *t*Bu), 1.16 (s, 18H; *t*Bu) [b]	171.2 (C=N), 123.0 (C=C), 44.2 (s; cyclopropene), 34.8 (s; *t*Bu), 31.6 (s; *t*Bu), 30.6 (q; *t*Bu), 30.1 (q; *t*Bu) [b]
5	orange-red crystals, 105	see Experimental Procedure	25	1.24 (s, 18H; *t*Bu), 1.16 (s, 18H; *t*Bu), 1.15 (s, 9H; *t*Bu), 0.95 (s, 9H; *t*Bu) [c]	199.4 (C=O), 125.0 (C=C), 119.9 (C=C), 74.9 (s; cyclopropene), 47.3 (s; cyclopropene), 34.8 (s; *t*Bu), 32.8 (s; *t*Bu), 31.1 (s; *t*Bu), 31.0 (s; *t*Bu), 30.8 (q; *t*Bu), 30.3 (q; *t*Bu), 30.1 (q; *t*Bu), 29.7 (q; *t*Bu) [c]
10	colorless crystals, 165–170	2 d, RT, CCl_4	46	8.66 (s, 1H; $HCl_2^\oplus$), 1.65 (s, 27H; *t*Bu) [c]	180.7 (ring), 35.5 (s; *t*Bu), 28.5 (q; *t*Bu) [b]
11	colorless crystals, 47	2 h, 130°C, neat	96	1.36 (s, 9H; *t*Bu), 1.24 (s, 18H; *t*Bu), 1.13 (s, 9H; *t*Bu) [c]	171.0 (C=N), 170.6 (C=N), 120.6 (C=C), 36.7 (s; cyclopropene), 33.8 (s; *t*Bu), 32.0 (s; *t*Bu), 31.1 (s; *t*Bu), 30.3 (q; *t*Bu), 29.3 (q; *t*Bu), 28.2 (q; *t*Bu) [c]
12	red crystals, 174	benzene, RT, 254 nm, 6 h, thin layer chromatographic separation	25	1.26 (s, 36H; *t*Bu), 1.02 (s, 18H; *t*Bu) [c]	205.7 (C=O), 120.9 (C=C), 50.0 (s; cyclopropene), 34.1 (s; *t*Bu), 31.5 (s; *t*Bu), 30.5 (q; *t*Bu), 30.4 (q; *t*Bu) [c]
13	colorless crystals, 94	Rigisolve [a], −196°C, 254 nm, 15 h	21	1.27 (s, 36H; *t*Bu), 0.95 (s, 18H; *t*Bu) [b]	216.5 (C=O), 126.0 (C=C), 56.3 (s; cyclopropene), 34.8 (s; *t*Bu), 31.9 (q; *t*Bu), 31.8 (s; *t*Bu), 31.4 (q; *t*Bu) [c]
15	yellow powder, 114 (dec.)	CH_2Cl_2, −15°C, 5 min HCl, evaporate, $AgSbF_6$ in THF, remove solvent again, digest residue with CH_2Cl_2	47	3.65 (s, 1H; OH), 1.56 (s, 9H; *t*Bu on C2), 1.47 (s, 18H; *t*Bu on C1/3), 1.30 (s, 18H; *t*Bu on C=C), 1.03 (s, 6H; $2CH_3$ of *t*Bu on cyclopropene), 0.58 (s, 3H; $1CH_3$ of *t*Bu on cyclopropene) [d]	183.5 (C2), 164.9 (C1/3), 128.3 (C=C), 94.8 (C4), 55.1 (s; cyclopropene), 37.7 (s; *t*Bu on C1/3), 35.7 (s; *t*Bu on C2), 34.4 (s; *t*Bu on cyclopropene), 31.3 (s; *t*Bu on C=C), 30.7 (q; 5*t*Bu), 30.0 (q; $2CH_3$ of *t*Bu on cyclopropene), 28.3 (q; $1CH_3$ of *t*Bu on cyclopropene) [e]

[a] 3,3-Dimethylbutane/*n*-pentane = 8/3 (Merck). [b] CD_2Cl_2. [c] $CDCl_3$. [d] CD_2Cl_2, −69.6°C. [e] CD_2Cl_2, −60°C.

−53.5°C ($\Delta\nu$ = 48 Hz, ΔG^+ = 44.7 kJ/mol) as a consequence of the faster rotation of the *tert*-butyl group, which gives rise to only one signal (δ = 0.94) at −24.3°C. Further warming results in a second coalescence at +18.7°C ($\Delta\nu$ = 10 Hz, ΔG^+ = 63.9 kJ/mol), due to the merging of the signals of the *tert*-butyl substituents on C2 and C1/3. This means that at this temperature the walk rearrangement in the homocyclopropenylium portion of **15** (C4 moves around the fragment C1/2/3[2]) is sufficiently rapid. Accordingly, the room-temperature spectrum of **15** shows only three broad signals for the *tert*-butyl groups at δ = 1.62, 1.53, and 1.04 in a ratio of 3:2:1. At +42.5°C ($C_2D_2Cl_4$; $\Delta\nu$ = 62 Hz, ΔG^+ = 64.4 kJ/mol), a third coalescence is observed. The three signals collapse to give only one signal. At +80°C,[7] only one relatively sharp signal at δ = 1.5 is observed for the *tert*-butyl groups. Apparently, the positive charge is now transferred to the other half of the molecule as well, with contraction of the four-membered and expansion of the three-membered ring in the sense of **15** ⇌ **15'**. Compound **15** undergoes a tandem walk rearrangement via the symmetric transition state **14**, in the course of which the C atom bearing the hydroxyl group migrates around six "equivalent" ring positions.

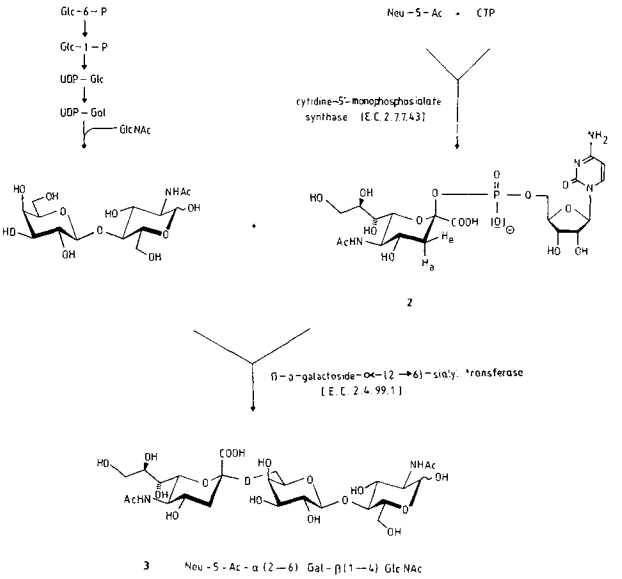
Experimental Procedure

4/5: A 1.64-molar solution of methyllithium in diethyl ether (16.2 mL) was added at −78°C to a solution of (trimethylsilyl)diazomethane (2.73 g, 24 mmol) in 250 mL of dry THF. The resulting colorless solution was then stirred for 1/2 h and subsequently treated at −78°C with **1** (7.02 g, 24 mmol), added in portions. After 4 h, the temperature was allowed to rise

slowly to −10°C and the reaction solution was poured under vigorous stirring into a mixture containing 600 mL of saturated sodium chloride solution and 300 mL of diethyl ether. In order to remove the THF, the organic phase was washed several times with water and then dried with sodium sulfate. After removal of the ether, the product mixture was separated on 400 g of neutral alumina (activity III) at −20°C with pentane/ether (100:1) as eluent. It was thereby possible to elute four fractions: diazo compound **3**[4], tetrazine **4**, acyl diimide **5**, and a small amount (4%) of the dihydro derivative of **4**.

Received: August 18, 1986;
supplemented: October 3, 1986 [Z 1905 IE]
German version: *Angew. Chem. 98* (1986) 1132

[1] G. Maier, R. Emrich, K.-D. Malsch, K.-A. Schneider, M. Nixdorf, H. Irngartinger, *Chem. Ber. 118* (1985) 2798.
[2] G. Maier, R. Emrich, H.-O. Kalinowski, *Angew. Chem. 97* (1985) 427; *Angew. Chem. Int. Ed. Engl. 24* (1985) 429.
[3] G. Maier, K. Euler, R. Emrich, *Tetrahedron Lett. 27* (1986) 3607.
[4] G. Maier, K. A. Reuter, L. Franz, H. P. Reisenauer, *Tetrahedron Lett. 26* (1985) 1845.
[5] It is known that ethyl diazoacetate undergoes a similar dimerization under basic conditions (review: R. Huisgen, *Angew. Chem. 67* (1955) 439). The same holds true for (diazomethyl)diphenylphosphane oxide (W. Disteldorf, M. Regitz, *Justus Liebigs Ann. Chem. 1976*, 225).
[6] Dr. *R. Boese* (Essen) is currently carrying out a detailed X-ray structure analysis of **10** in order to determine, in particular, the structure of the hydrogen dichloride anion.
[7] At this temperature, the irreversible decomposition of **15** is already complete after 30 min. For this reason, it was not possible with the apparatus at hand to confirm the results by parallel ^{13}C-NMR measurements.



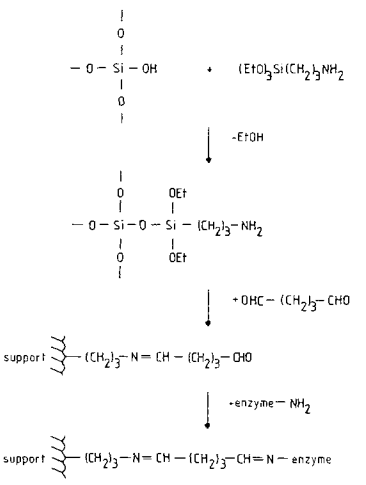
Scheme 1.

Synthesis of the Trisaccharide Neu-5-Ac-α(2→6)Gal-β(1→4)GlcNAc by the Use of Immobilized Enzymes**

By *Joachim Thiem** and *Wolfgang Treder*

The trisaccharide 5-acetamido-3,5-dideoxy-α-D-glycero-D-galacto-2-nonulopyranolonic acid-(2→6)-β-D-galactopyranosyl-(1→4)-2-acetamido-2-deoxy-D-glucopyranose [Neu-5-Ac-α(2→6)Gal-β(1→4)GlcNAc **3**] is frequently bound to the terminus of glycoproteins, e.g., in glycophorin A, a surface glycoprotein of erythrocytes. The trisaccharide—bound to a solid support—would be of particular interest as a receptor for proteins and as an immunoabsorbent. The multistep chemical synthesis[1] is very laborious and affords only low yields. An alternative is an enzymatic synthesis[2] involving the use of immobilized enzymes, which follows, on a preparative scale, the biosynthetic route. This is accomplished by transferring *N*-acetylneuraminic acid (Neu-5-Ac) via the nucleotide cytidine 5'-monophosphosialate **2** to *N*-acetyllactosamine **1** using sialyl transferase (Scheme 1).

1 is prepared by a modification of the enzymatic synthetic cycle introduced by *Wong* et al.[3] for the first time on a preparative scale, involving regeneration of cofactors. Glucose-6-phosphate (1.43 g, 4 mmol) is first converted, via glucose-1-phosphate and UDP-glucose, into UDP-galactose, which is then transferred to *N*-acetylglucosamine (0.88 g, 4 mmol) using galactosyl transferase. The six enzymes required for this purpose are immobilized on functionalized silica gel by means of glutardialdehyde according to the method of *Wheetall*[4] (Scheme 2).[5] This procedure is, in particular, less expensive than that usually employed involving the use of organic supports (yield of **1**: 405 mg, 30%).



Scheme 2.

2 is prepared from Neu-5-Ac (60 mg, 19.5 μmol) by enzyme-catalyzed reaction with cytidine triphosphate (CTP, 600 mg, 123 μmol).[6] For the first time, it was possible to use the enzyme required for this synthesis, cytidine-5'-monophosphosialate synthase (E.C. 2.7.7.43, 600 U) from bovine *Glandula submandibularis*, in the immobilized form shown in Scheme 2. This approach appreciably simplifies the workup of the reaction mixture. Instead of ion-exchange chromatography with gradient elution and subsequent gel filtration of the reaction mixture, **2** can be obtained in pure form simply by separation of the reaction mixture on Sephadex G-15 (yield of **2**: 87 mg, 72%).

Conversion to the trisaccharide **3** was achieved by incubation of **2** (60 mg, 0.1 mmol) with **1** (32 mg, 0.1 mmol) in the presence of the enzyme β-D-galactoside-α(2→6)sialyl transferase (E.C. 2.4.99.1, ca. 2.5 U) in excess, which can be isolated from colostrum by affinity chromatography with cytidine diphosphate-agarose.[7] The reaction solution with albumin and magnesium chloride was allowed to stand for 24 h at 37°C and pH = 6.5 and then worked up by

[*] Prof. Dr. J. Thiem, Dipl.-Chem. W. Treder
Organisch-Chemisches Institut der Universität
Orléans-Ring 23, D-4400 Münster (FRG)

[**] This work was supported by the Fonds der Chemischen Industrie.

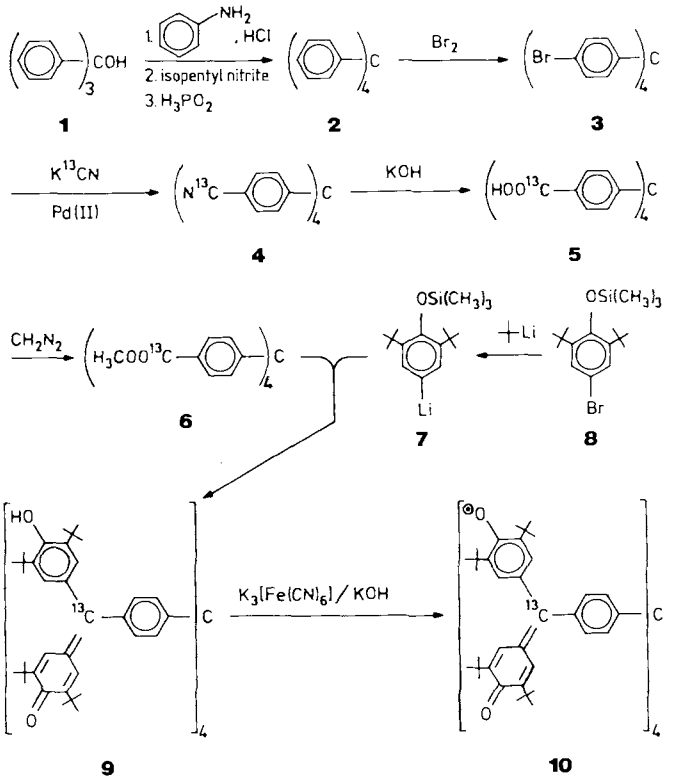
elution with 5 mM sodium phosphate buffer on a phosphate-containing Dowex 1-X2 column. The free trisaccharide **3**, whose interglycosidic linkages were confirmed by ^{1}H-NMR spectroscopy,[8] was thereby obtained directly on a 50-μmol scale (yield: 31 mg, 52%).

Received: June 30, 1986;
supplemented: September 2, 1986 [Z 1841 IE]
German version: *Angew. Chem. 98* (1986) 1100

CAS Registry numbers:
1, 32181-59-2; **2**, 3063-71-6; **3**, 78969-47-8; Neu-5-Ac, 131-48-6; CTP, 65-47-4; GlcNAc, 7512-17-6; UDP-Gal, 58-98-0; E.C. 2.4.99.1, 9075-81-4; E.C. 2.7.7.43, 9067-82-7.

[1] H. Paulsen, H. Tietz, *Carbohydr. Res. 125* (1984) 47; *Angew. Chem. 97* (1985) 118; *Angew. Chem. Int. Ed. Engl. 24* (1985) 128.
[2] G. M. Whitesides, C.-H. Wong, *Angew. Chem. 97* (1985) 617; *Angew. Chem. Int. Ed. Engl. 24* (1985) 617.
[3] C.-H. Wong, S. Haynie, G. M. Whitesides, *J. Org. Chem. 47* (1982) 5416.
[4] H. H. Wheetall, *Methods Enzymol. 44* (1976) 134.
[5] Galactosyl transferase [E.C. 2.4.1.22]: 2.5 U, 7.0 g support; UDP-galactose epimerase [E.C. 5.1.3.2]: 10 U, 3.0 g support; UDP-glucose pyrophosphorylase [E.C. 2.7.7.9]: 10 U, 1.0 g support; phosphoglucomutase [E.C. 2.7.5.1]: 50 U, 1.0 g carrier; inorganic pyrophosphatase [E.C. 3.6.1.1]: 100 U, 1.0 g carrier; pyruvate kinase [E.C. 2.7.1.40]: 100 U, 1.0 g carrier. In addition, phosphoenolpyruvate (0.87 g, 4.2 mmol) and uridine diphosphate (27.7 mg, 0.05 mmol) are required for cofactor regeneration.
[6] R. Schauer, M. Wember, C. Ferreira do Amaral, *Hoppe-Seyler's Z. Physiol. Chem. 353* (1972) 883.
[7] J. C. Paulson, J. E. Rearick, R. L. Hill, *J. Biol. Chem. 252* (1977) 2356.
[8] ^{1}H-NMR spectrum (300 MHz, D_2O): $\delta = 5.22$ (d, 1H, $J_{1,2} = 1.2$ Hz; 1-H-GlcNAc, β form), 4.48 (d, 1H, $J_{1,2} = 7.6$ Hz; 1-H-Gal), 1.71 (dd, 1H, $J_{3a,3c} = 13.3$, $J_{3a,4} = 11.8$ Hz; 3a-H-Neu-5-Ac), 2.68 (dd, 1H, $J_{3a,3e} = 13.3$, $J_{3e,4} = 4.7$ Hz; 3e-H-Neu-5-Ac), 2.03 (s, 3H; NAc of Neu-5-Ac), 2.05 (s, 3H; NAc of GlcNAc).

exhibit greater anisotropy of the hyperfine interaction, whereby their relaxation behavior is strongly influenced. Therefore, for an optimal ^{13}C-ENDOR effect, an even higher microwave and radiofrequency power is required.[1]



Scheme 1.

^{13}C-ENDOR Investigation of an Organic Tetraradical in the Quintet State; Synthesis of a Fourfold ^{13}C-Labeled Tetrakisgalvinol**

By *Michael Grimm, Burkhard Kirste,* and *Harry Kurreck**

Dedicated to Professor Georg Manecke on the occasion of his 70th birthday

Organic compounds carrying several unpaired electrons exhibit, in addition to Zeeman splitting and hyperfine interaction, magnetic peculiarities that are characterized as scalar exchange interaction and dipolar coupling of the unpaired electrons. If the exchange interaction is large compared with the hyperfine interaction ($|J| \gg |a|$), the number of EPR (electron paramagnetic resonance) hyperfine components increases, since the unpaired electrons are formally delocalized over the whole molecule and therefore couple with all magnetic nuclei. This leads to an increase in spectral line density, while the overall splitting is retained and the resolution of the EPR spectrum becomes poorer. The dipolar electron interaction generates additional relaxation processes, which lead to both a line broadening as well as to a reduction of the electron nuclear double resonance (ENDOR) effect. This results in a diminution of the resolution and requires higher microwave powers. Compared with protons, ^{13}C nuclei generally

Organic multispin systems with weak dipolar electron interaction have so far been investigated by ^{1}H-ENDOR spectroscopy up to a tetraradical in the quintet state and by ^{13}C-ENDOR spectroscopy[2] to a triradical in the quartet state.[3] We now report on the first ^{13}C-ENDOR investigation on the quintet state of a fourfold ^{13}C-labeled tetraradical with tetrahedral symmetry. The key compound for the selective generation of mono-, di-, tri-, and tetraradicals is the diamagnetic ^{13}C-tetrakisgalvinol **9**, which was obtained as follows (Scheme 1): First, tetraphenylmethane **2** was prepared by Friedel-Crafts alkylation,[4] diazotization, and deamination.[5] Stirring of powdered **2** in bromine led to **3**, which was converted into the ^{13}C-tetranitrile **4** with ^{13}C-potassium cyanide using palladium(II) acetate as catalyst.[6] Alkaline hydrolysis of **4** afforded the ^{13}C-tetracarboxylic acid **5**, which upon reaction with diazomethane furnished the ^{13}C-tetraester **6**. Modifying the previously published galvinol synthesis,[7] (2,6-di-*tert*-butyl-4-bromophenoxy)trimethylsilane **8** was converted with *tert*-butyllithium into (2,6-di-*tert*-butyl-4-lithiophenoxy)trimethylsilane **7**, which was subsequently treated with **6**. Addition of water and slow thawing led to a gentle, alkaline elimination of the trimethylsilyl groups with formation of the ^{13}C-tetrakisgalvinol **9**.

Figure 1 (left) shows the experimental EPR spectra of the mono- and tetraradicals that are accessible from **9** by oxidation with alkaline potassium hexacyanoferrate(III).[8]

[*] Prof. Dr. H. Kurreck, Dipl.-Chem. M. Grimm, Priv.-Doz. Dr. B. Kirste
Institut für Organische Chemie der Freien Universität
Takustrasse 3, D-1000 Berlin 33

[**] This work was supported by the Fonds der Chemischen Industrie and by the Deutsche Forschungsgemeinschaft.

The well-resolved EPR spectrum of the monoradical consists of a doublet of quintets (one ^{13}C-nucleus, four *m*-protons). The EPR spectrum of the tetraradical **10** shows a quintet splitting by four ^{13}C-nuclei, while the expected 17-fold splitting by 16 *m*-protons is not resolved.

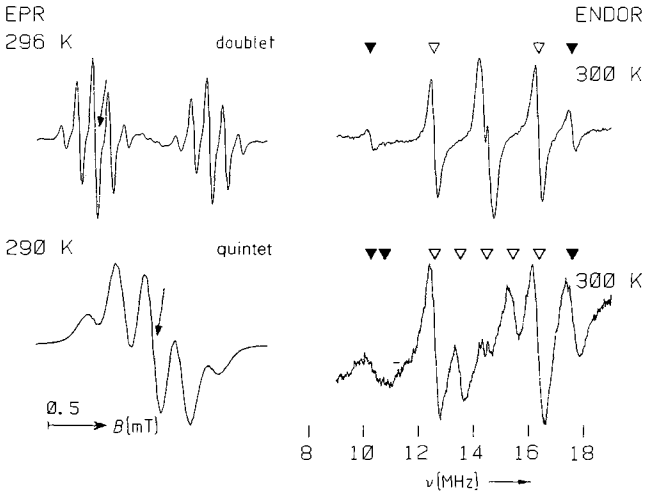


Fig. 1. EPR (left) and ENDOR spectra (right) of the monoradicals (top) and of the tetraradical (bottom) generated by selective oxidation of **9**. Also shown (left) are the field settings in the EPR spectra for recording the ENDOR spectra (arrows) and (right) the calculated ^1H-resonance frequencies (white triangles) and ^{13}C-resonance frequencies (black triangles).

In both cases, ENDOR spectra of the pure species (Fig. 1 right) can be obtained by appropriate positioning in the EPR spectra (arrows in Fig. 1 left). In Figure 1 (right), the ^1H-resonances (white triangles) and ^{13}C-resonances (black triangles) calculated on the basis of the ENDOR reson-

$$\nu_{ENDOR} = |\nu_n - M_S a^S| \qquad (a)$$

ance condition (Eq. (a); ν_n = free nuclear frequency, M_S = magnetic quantum number of the total electron spin, a^S = coupling constant for the electron spin quantum number S) are presented together with the experimental ENDOR spectrum. Whereas all the expected ^1H-ENDOR signals with the exception of those at the free proton frequency[2] can be observed in each case, only the ^{13}C-ENDOR line pairs belonging to $M_S = \pm S$ are clearly visible.[9] For experimental reasons, only the high frequency signal of the second ^{13}C-ENDOR line pair of the tetraradical ($M_S = \pm 1$) is accessible to the measurement. This signal, however, is broad or not present, which can be explained by the fact that the exchange interaction for the ^{13}C-tetraradical is of the order of magnitude of the ^{13}C-hyperfine interaction ($|J| \approx |a_C|$), whereas $|J| \gg |a_H|$ holds for the protons. The mixing of states due to the ^{13}C-hyperfine interaction should then strongly influence the relaxation behavior and the positions of the ^{13}C-ENDOR signals for $M_S \neq \pm S$.[10]

Procedure[11]

2: A mixture of **1** (52 g, 0.2 mol), aniline (28.5 mL, 0.3 mol), concentrated hydrochloric acid (90 mL), and glacial acetic acid (600 mL) was heated under reflux for 48 h; the intermediate product was isolated, dissolved in 1.5 L of ethanol and 100 mL of concentrated sulfuric acid, diazotized at −10°C with 60 mL of isopentyl nitrite, and, after 45 min, deaminated with 150 mL of 60% hypophosphorous acid under reflux; crude yield: 52.7 g (82.2%); after twofold recrystallization from 1,2-dichloroethane, 38.3 g of **2** (59.8%); m.p. 282–283°C.

3: 18 g (56.2 mmol) of powdered **2** was added to ca. 60 mL of pure bromine at room temperature; the mixture was stirred for 45 min and then diluted with ethanol in an ice-cooled vessel until no further crude product precipitated; the crude product was filtered off and washed with sodium bisulfite solution; crude yield 34.8 g (97.4%); after double recrystallization from chloroform/ethanol: 23.4 g of **3** (65.5%); m.p. 312.5–313°C.

4: A mixture of **3** (1.2 g, 1.89 mmol), ^{13}C-potassium cyanide (1 g, 15.13 mmol, 99 atom-% ^{13}C), potassium iodide (0.113 g, 0.68 mmol), palladium(II) acetate (0.026 g, 0.113 mmol), potassium hydroxide (0.21 mg, 3.8 μmol), and anhydrous hexamethylphosphoric triamide (12 mL) was heated under argon protective gas for 19 h at 85–95°C; the reaction solution was evaporated to dryness and the residue was taken up in methylene chloride and washed with water. Crude yield after removal of solvent: 0.83 g.

5: A mixture of **4** (0.8 g, 1.89 mmol), potassium hydroxide (1.88 g, 33.5 mmol), and ethylene glycol (20 mL) was heated under reflux for 18 h; after dilution with water, extraction with methylene chloride, and addition of diluted hydrochloric acid, **5** precipitated; crude yield after filtration by suction: 0.93 g.

6: **5** (0.93 g, 1.86 mmol) was esterified in an ethanol-methanol mixture at room temperature with diazomethane; crude yield: 1.2 g; purity determined by HPLC: 94.1%; a part of the sample was purified by HPLC (7 μm Polygosil 60 KN, 32 × 250 mm/methylene chloride + 0.25% 2-propanol); degree of labeling as expected within the accuracy of measurement (96% $^{13}C_4$, mass spectroscopy).

9: A solution of **7** (7.9 g, 22.11 mmol) in anhydrous tetrahydrofuran (100 mL) was cooled to −70°C under argon protective gas and treated within 45 min with a solution of *tert*-butyllithium (30.55 mL) in *n*-pentane (44.23 mmol); after 15 min a solution of **6** (0.4 g, 0.72 mmol) in anhydrous THF (20 mL) was added to the reaction solution; within 2.5 h the temperature was increased to −30°C. The solution was treated with a small amount of water and no longer subjected to cooling; it was then stirred for a further 12 h (cleavage of trimethylsilyl groups) and the organic phase separated, acidified with dilute hydrochloric acid, and washed with water; phenols (from **7**) were removed by flash chromatography[12] (silica gel 40–63 μm [Merck 9385], 80 × 80 mm/methylene chloride); yield: 1.47 g; purity determined by HPLC: 94.5%; a part was purified by HPLC (7 μm Polygosil 60 KN, 32 × 250 mm/methylene chloride).

Received: July 7, 1986;
revised: September 11, 1986 [Z 1845 IE]
German version: *Angew. Chem. 98* (1986) 1095

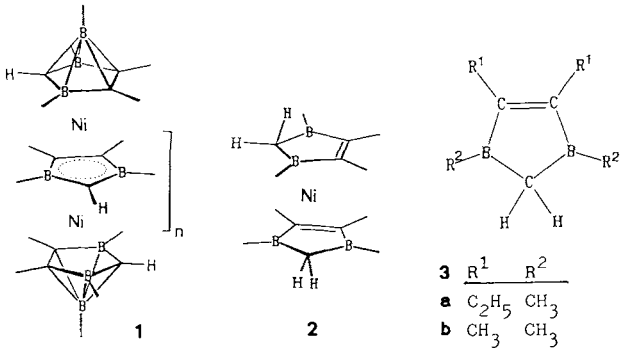
[1] H. Kurreck, B. Kirste, W. Lubitz, *Angew. Chem. 96* (1984) 171; *Angew. Chem. Int. Ed. Engl. 23* (1984) 173.
[2] B. Kirste, W. Harrer, H. Kurreck, *Angew. Chem. 93* (1981) 912; *Angew. Chem. Int. Ed. Engl. 20* (1981) 873.
[3] K. Schubert, B. Kirste, H. Kurreck, *Angew. Chem. 95* (1983) 149; *Angew. Chem. Int. Ed. Engl. 22* (1983) 150; *Angew. Chem. Suppl. 1983*, 128.
[4] F. Ullmann, A. Münzhuber, *Chem. Ber. 36* (1903) 404.
[5] N. Kornblum, *Org. React. 2* (1944) 262.
[6] K. Takagi, T. Okamoto, Y. Sakakibara, A. Ohno, S. Oka, N. Hayama, *Bull. Chem. Soc. Jpn. 48* (1975) 3298.
[7] W. Gierke, W. Harrer, H. Kurreck, J. Reusch, *Tetrahedron Lett. 1973*, 3681; W. Harrer, H. Kurreck, J. Reusch, W. Gierke, *Tetrahedron 31* (1975) 625.
[8] The EPR spectra of biradicals and triradicals, also accessible by oxidation, are however comparatively poorly resolved, inter alia, because of the unavoidable presence of other radical states due to redox equilibria. ENDOR spectra of the pure species can also be obtained in these cases by appropriate positioning in the EPR spectrum [9].
[9] Hyperfine coupling constants in toluene [MHz]: monoradical: $a^d_H = +3.78$, $a^d_C = -27.85$ (320 K); diradical: $a^1_H = +1.88$, $a^1_C = -13.92$ (310 K); triradical: $a^q_H = +1.25$, $a^q_H = -9.31$ (300 K); tetraradical: $a^q_H = +0.93$, $a^q_C = -6.97$ (300 K).
[10] B. Kirste, A. Krüger, H. Kurreck, *J. Am. Chem. Soc. 104* (1982) 3850.
[11] The melting points of the unlabeled compounds are: **4**: 311–312°C; **5**: >360°C; **6**: 211.5–212.5°C; **9**: >360°C; the proposed structures were confirmed by spectroscopic investigations and elemental analyses. The synthesis of **6** from **3** was carried out without purification of the intermediates; in the case of the unlabeled compounds corresponding to **4**, **5**, and **6**, the yields after purification were 96.5, 98.8, and 99.6%, respectively.
[12] W. C. Still, M. Kahn, A. Mitra, *J. Org. Chem. 43* (1978) 2923.

Bis(η^5-2,3,5-tricarbahexaboranyl)nickel, a Nickelocene Analogue**

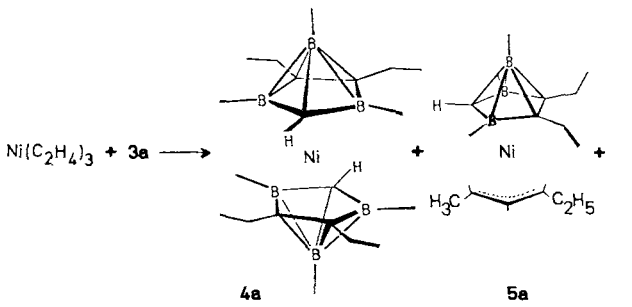
By *Joachim Zwecker, Hans Pritzkow, Ulrich Zenneck,* and *Walter Siebert**

The oligodecker complexes **1** (n = 1–8) with terminal 2,3,5-tricarbahexaboranyl ligands are formed in an as yet unclear way from the bis(2,3-dihydro-1,3,4,5-tetraalkyl-1,3-diborole)nickel sandwich compounds **2**.[1] Decisive for the carbaboranyl formation and the stacking reaction is the reactive axial CH-bond at the pentacoordinated C2 atom of the ligands **3a**, **b** in **2**.[2]

Bis(η^5-2,3,5-tricarbahexaboranyl)nickel **4**, the parent member of the class of compounds **1** (for n = 0), is not observed in the conversion of **2**.[3] We now report the synthesis and characterization of the paramagnetic complex **4a** as the first bis(tricarbahexaboranyl)metal complex analogous to the metallocenes.



Reaction of excess **3a** with tris(ethene)nickel[4a] (prepared from nickel/toluene cocondensate and ethene[4b]) at low temperature in toluene leads to the formation of crystalline **4a** in 12.5% yield. The tricarbahexaboranyl(allyl)nickel complex **5a**[5a] is formed at the same time and can be isolated by distillation. Since this 18e-complex is not converted into **4a** under the reaction conditions, **4a** must be formed from another precursor of the reaction of **3a** with $[Ni(C_2H_4)_3]$. We assume that the replacement of two ethene ligands in $[Ni(C_2H_4)_3]$ by **3a** leads to a labile 2,3-dihydro-1,3-diborolyl(ethene)hydridonickel complex.[5b] By uptake of a H_3CB group from **3a**, a reactive ethene(hydrido)-η^5-tricarbahexaboranylnickel complex may then form as educt of **4a**.



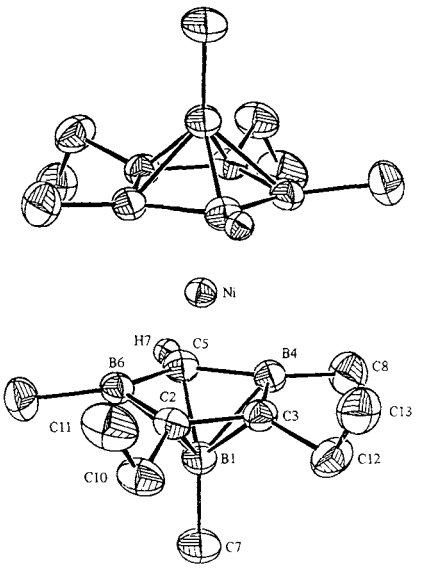


Fig. 1. Crystal structure of **4a**. Selected bond lengths [Å] (mean standard deviation 0.003 Å): Ni-B4(6) 2.198, 2.204; Ni-C2(3) 2.227, 2.240; Ni-C5 2.150; B1-B4(6) 1.802, 1.808; B1-C2(3) 1.711, 1.708; B1-C5 1.679; B4(6)-C3(2) 1.559, 1.551; B4(6)-C5 1.555, 1.566; C2-C3 1.484.

The structure proposed for **4a** is consistent with the analytical and mass spectrometric data and has been confirmed by an X-ray structure analysis (Fig. 1)[6]: In the crystal, the Ni atom is located at an inversion center; the molecule is therefore centrosymmetric. The structure of the carbaboranyl ligand does not differ from that in the triple decker **1**, n = 1.[1] The Ni-C and Ni-B distances are similar to those found for nickelocene[7] and the bis(dicarbollide)nickel dianion.[8] The distance of the nickel atom from the ring plane is 1.77 Å (maximum deviation of the ring atoms from the plane ±0.03 Å).

Both the cyclovoltammetrically determined electrochemical behavior of **4a** (Fig. 2a) and the ESR spectrum of the 19e-cation $4^{\oplus\ominus}$ (Fig. 2b) reveal the relationship between **4a** and nickelocene. Magnetic measurements on **4a** in the region of 120–300 K indicate Curie-Weiss behavior and give $\mu_{eff} = 3.06 \pm 0.2\,\mu_B$.[11] For nickelocene $\mu_{eff} = 2.89 \pm 0.15\,\mu_B$.[12] Thus, **4a** likewise occurs as triplet molecule. The results prove that the *nido*-2,3,5-tricarbahexaborate $C_3B_3R_5H^{\ominus}$ and the cyclopentadienide ion are isolobal.

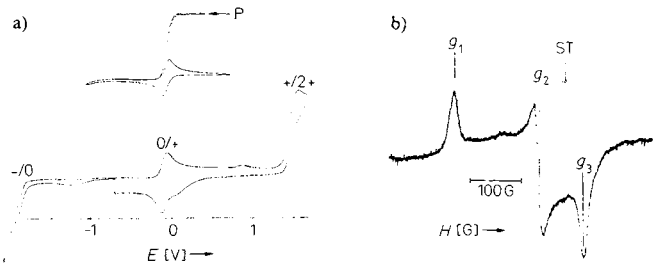


Fig. 2. a) Cyclovoltammogram of **4a** in $CH_2Cl_2/(C_4H_9)_4N^{\oplus}PF_6^{\ominus}$ at Pt wire electrodes vs. SCE; bottom: range +1.7 to −2.0 V, v = 200 mV/s; top: range +0.9 to −1.1 V, v = 200 mV/s; and P = polarogram at platinum rotating disc electrode (RDE): $E(0,+) = -0.11$ V (reversible), $E_p(+,2+) = 1.5$ V (irreversible), $E_p(-,0) = 2.0$ V (irreversible) [9]. b) X-band ESR spectrum of $\mathbf{4a}^{\oplus\ominus}$ (in closed ESR cell generated with $[(C_5H_5)_2Fe]BF_4$) in CH_2Cl_2 at $T = -160$ °C. Standard (ST): $Li^{\oplus}TCNQ^{\odot\ominus}$, $g_{ST} = 2.0025$. $g_1 \approx 2.14$, $g_2 = 2.03$, $g_3 = 1.98$; at room temperature $\langle g \rangle$ is not determinable [10].

[*] Prof. Dr. W. Siebert, Dr. J. Zwecker, Dr. H. Pritzkow, Dr. U. Zenneck
Anorganisch-chemisches Institut der Universität
Im Neuenheimer Feld 270, D-6900 Heidelberg 1 (FRG)

[**] η^5-Carbaboranylmetal Complexes, Part 2. This work was supported by the Deutsche Forschungsgemeinschaft, the Stiftung Volkswagenwerk, the Fonds der Chemischen Industrie, and BASF AG.—Part 1: [1].

Procedure

A solution of **3a** (0.9 g, 6.1 mmol) in toluene (40 mL) was treated at −50°C with 4 mL of a solution of tris(ethene)nickel in toluene (2.0 mmol $Ni(C_2H_4)_3$; titer determined by reaction with $P(OCH_3)_3$ and 1,5-cyclooctadiene). The stirred mixture was allowed to warm to room temperature in 30 min and the solvent was then removed under vacuum. At 45°C/10^{-2} torr, light green **4a** sublimed, which is colorless in thin layers (75 mg, 0.19 mmol, 12.5%). MS: m/z 403 ($M^{\oplus}$, 100%), correct isotopic distribution, hardly any fragmentation. Correct C,H analysis.

Received: July 22, 1986;
supplemented: September 1, 1986 [Z 1868 IE]
German version: *Angew. Chem. 98* (1986) 1129

[1] Th. Kuhlmann, H. Pritzkow, U. Zenneck, W. Siebert, *Angew. Chem. 96* (1984) 994; *Angew. Chem. Int. Ed. Engl. 23* (1984) 965.
[2] W. Siebert, *Angew. Chem. 97* (1985) 924; *Angew. Chem. Int. Ed. Engl. 24* (1985) 943.
[3] Th. Kuhlmann, *Dissertation*, Universität Heidelberg 1985.
[4] a) K. Fischer, K. Jonas, G. Wilke, *Angew. Chem. 85* (1973) 620; *Angew. Chem. Int. Ed. Engl. 12* (1973) 565; b) R. M. Atkins, R. Mackenzie, P. L. Timms, T. W. Turney, *J. Chem. Soc. Chem. Commun. 1975*, 764.
[5] a) W. Herter, *Dissertation*, Universität Heidelberg 1984. b) The reaction with $(C_5H_5)Co(C_2H_4)_2$ corresponding to the postulated oxidative addition of **3a** to the $(C_2H_4)Ni$ fragment leads to labile cyclopentadienyl(2,3-dihydro-1,3-diborolyl)hydridocobalt complexes: K. Stumpf, W. Siebert, R. Köster, G. Seidel, *Z. Naturforsch. B*, in press.
[6] **4a**: Space group $P2_1/n$, $a=9.074(1)$, $b=13.056(2)$, $c=10.166(2)$ Å, $\beta=95.23(1)°$, $V=1199.4$ Å^3, $Z=2$, $R=0.048$ for 2812 observed reflections (Stoe two-circle diffractometer, $Mo_{K\alpha}$ radiation). Further details of the crystal structure investigation are available on request from the Fachinformationszentrum Energie, Physik, Mathematik GmbH, D-7514 Eggenstein-Leopoldshafen 2 (FRG), on quoting the depository number CSD-52080, the names of the authors, and the full citation of the journal.
[7] P. Seiler, J. Dunitz, *Acta Crystallogr. Sect. B 36* (1980) 2255.
[9] R. M. Wing, *J. Am. Chem. Soc. 92* (1970) 1187.
[9] For data for nickelocene under comparable conditions see: J. L. Robbins, N. Edelstein, B. Spencer, J. C. Smart, *J. Am. Chem. Soc. 104* (1982) 1882.
[10] The ESR parameters of the two particles differ, mainly because of the Jahn-Teller activity of the nickelocene cation: M. V. Rajasekharan, R. Bucher, E. Deiss, L. Zoller, A. K. Salzer, E. Moser, J. Weber, J. H. Ammeter, *J. Am. Chem. Soc. 105* (1983) 7516.
[11] U. Zenneck, L. Vasquez, unpublished.
[12] H. P. Fritz, K.-E. Schwarzhans, *J. Organomet. Chem. 1* (1963/64) 208; P. Prins, J. D. van Voorst, C. J. Schinkel, *Chem. Phys. Lett. 1* (1967) 54.

Synthesis of a Fourfold Enlarged Porphyrin with an Extremely Large, Diamagnetic Ring-Current Effect**

By *Martin Gosmann* and *Burchard Franck**

Porphyrins have an aromatic π-electron system of the [18]annulene type.[1] Like the annulenes, they exhibit a diamagnetic ring current in the ^{1}H-NMR spectrum, which serves as a qualitative criterion for aromatic character.[2] By cyclotetramerization of the pyrrylpropenol **3a**, we have now achieved the first synthesis of a fourfold enlarged porphyrin, **7**, having a [26]annulene structure.

The deep red-violet compound **7** is characterized by the largest ring-current effect found so far for a cyclic conjugated π-electron system (Fig. 1). The shift difference ($\Delta\delta$) of the resonances for the inner ($\delta=-11.64$) and outer ring protons ($\delta=+13.67$) is 25.3 ppm! This shift difference is twice as large as that found for the [18]annulene **1** ($\Delta\delta=12.1$ ppm).[7] Because **7** combines marked annulene behavior with the porphyrin structure, we refer to it as "[26]porphyrin."[3]

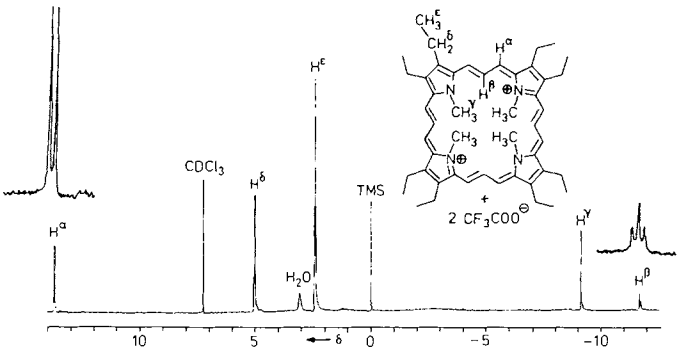
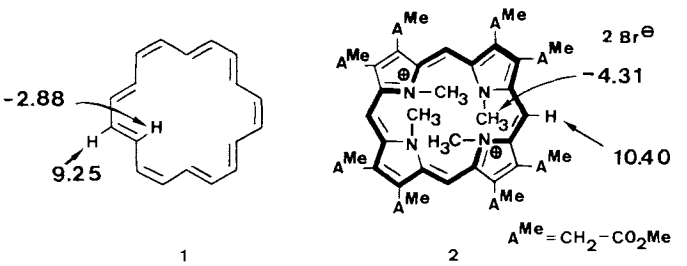


Fig. 1. 300-MHz ^{1}H-NMR spectrum of the [26]porphyrine **7b** in $CDCl_3$.

The motivation for the synthesis of **7** was the ring-current effect observed in the ^{1}H-NMR spectrum of the *N,N',N'',N'''*-tetramethylporphyrin **2**[4,5] (Scheme 1), which, despite the steric hindrance and nonplanar structure, exceeds that of the [18]annulene **1**. Since the steric hindrance in the ring center is reduced for the ring-enlarged [26]porphyrin **7**, an even larger ring-current effect was expected to be favored. On the other hand, according to several assumptions, a decrease in the ring-current effects was expected for larger annulenes.[6]



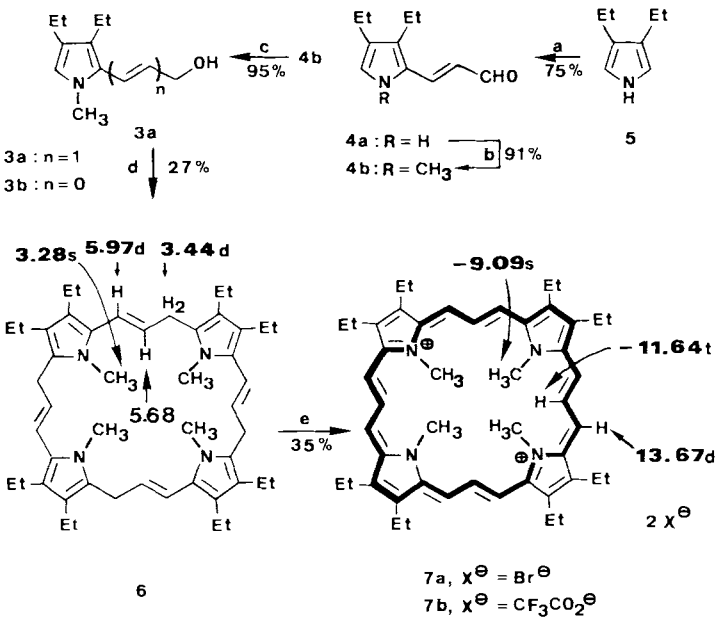
Scheme 1. ^{1}H-NMR signals (δ values) for inner and outer protons of the [18]annulene **1** (in $[D_8]$THF) [7] and of the *N,N',N'',N'''*-tetramethylporphyrine **2** (in CD_3CN) [5].

The *N*-methylpyrrylpropenol **3a** was selected as the key building block for the synthesis of the [26]porphyrin **7** (Scheme 2). It is known that 2-(aminomethyl)- and 2-(hydroxymethyl)pyrroles of type **3b** can be condensed, in analogy to the route of porphyrin biosynthesis, by acid-catalyzed cyclotetramerization to form porphyrinogens.[5,8] We were especially interested in whether the remarkable selectivity of this reaction (no oligomers, hardly any polymers) would also hold for the vinylogous compound **3a**.

For the synthesis of the very reactive compound **3a**, 3,4-diethylpyrrole **5**[9] was converted into **4a** by a vinylogous Vilsmeier formylation with 3-(dimethylamino)acrolein. Compound **4a** was *N*-methylated to **4b**, which, in turn, was reduced with $NaBH_4$ in situ to **3a**. Condensation of **3a** gave the colorless, non-cycloconjugated [26]porphyrinogen **6**[3] in 27% yield. Compound **6** was dehydrogenated with Br_2 to give the bisquaternary [26]porphyrin **7a**, chromatographically purified (silica gel, CH_3CN/trifluoroacetic

[*] Prof. Dr. B. Franck, Dipl.-Chem. M. Gosmann
Organisch-chemisches Institut der Universität
Orléansring 23, D-4400 Münster (FRG)

[**] This work was supported by the Deutsche Forschungsgemeinschaft and the Fonds der Chemischen Industrie.



Scheme 2. Synthesis of the [26]porphyrin **7** from 3,4-diethylpyrrole **5** [9]. For **6** and **7**, the ^{1}H-NMR data (δ, in $CDCl_3$) are included for comparison of the diamagnetic ring current. Reaction conditions: a) 3-(Dimethylamino)acrolein/$POCl_3$, CH_2Cl_2, −18°C, 90 min; **4a**: m.p. = 96°C; b) KOH, dimethyl sulfoxide, CH_3I, 20°C; **4b**: m.p. = 58°C; c) $NaBH_4$, methanol, 30 min; d) toluenesulfonic acid, acetic acid, 20°C, 30 min; **6**: m.p. = 250°C (dec.); e) Br_2/$CHCl_3$, 20°C.

acid = 250 : 1), and converted into the bis(trifluoroacetate) **7b** for elemental analysis.[11]

The remarkable ring-current effect of the [26]porphyrin **7** is presumably due to the flattening effect of the four pyrrole rings; the two cationic centers support this effect somewhat but are not decisive.[11] Thus, according to the ^{1}H-NMR criterion, **7b** contains a "superaromatic π-electron system." It demonstrates that the limits for aromatic behavior, so far expected to be reached with [26]annulenes, can be exceeded.

Apart from the ring-current effect of the [26]porphyrin **7**, its strong color intensity also deserves consideration. Thus, the molar extinction coefficient (ε) of its most intense absorption band at 547 nm (909600) is more than twice as large as that for the corresponding Soret band of porphyrins (maximally 400000). In the case of [26]porphyrin **7**, the visual effect of the color is increased still further by the fact that its most intense band lies in the middle of the visible range. In contrast, the Soret band of the porphyrins at 400 nm, compared with the longer-wavelength satellite maxima that are smaller by an order of magnitude, contributes little to the depth of color.

Received: July 24, 1986 [Z 1874 IE]
German version: *Angew. Chem. 98* (1986) 1107
Publication delayed at authors' request

CAS Registry numbers:
3a, 105140-95-2; **4a**, 105162-48-9; **4b**, 105140-94-1; **5**, 16200-52-5; **6**, 105140-96-3; **7a**, 105162-50-3; 3-(dimethylamino)acrolein, 972-63-9.

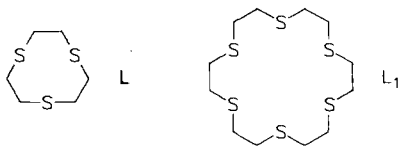
[1] The 18 π-electron system of the porphyrins can be viewed as a doubly bridged diaza[18]annulene or as a tetraaza[16]annulene dianion. The formulation as a dianion is in agreement with, among other characteristics, the spectroscopic properties of the metal complexes of the porphyrins: cf. H. Scheer, J. J. Katz in K. M. Smith (Ed.): *Porphyrins and Metalloporphyrins*, Elsevier, Amsterdam 1975; J. Griffiths: *Colour and Constitution of Organic Molecules*, Academic Press, London 1976.

[2] J. A. Elvidge, L. M. Jackson, *J. Chem. Soc. 1961*, 859; P. J. Garratt in D. H. R. Barton, W. D. Ollis (Eds.): *Comprehensive Organic Chemistry, Vol. 1*, Pergamon, Oxford 1979, p. 224.
[3] The term includes other enlarged porphyrins of this type, which we are currently studying [10]. In order to describe the structure more precisely, the number of C atoms between the pyrrole units can be included in the name; the skeleton of **7** would thus be a "[26]porphyrin-[3.3.3.3]."
[4] B. Franck, C. Wegner, *Angew. Chem. 87* (1975) 419; *Angew. Chem. Int. Ed. Engl. 14* (1975) 424.
[5] B. Franck, *Angew. Chem. 94* (1982) 327; *Angew. Chem. Int. Ed. Engl. 21* (1982) 343.
[6] M. J. S. Dewar, G. J. Gleicher, *J. Am. Chem. Soc. 87* (1965) 685; P. J. Garratt: *Aromaticity*, Wiley, New York 1986, pp. 51, 84ff.; S. Nakatsuji, S. Akiyama, M. Nakagawa, *Tetrahedron Lett. 1976*, 2623.
[7] J. M. Gilles, J. F. M. Oth, F. Sondheimer, E. P. Woo, *J. Chem. Soc. B 1971*, 2177.
[8] G. H. Cookson, C. Rimington, *Biochem. J. 57* (1954) 476.
[9] H. W. Withlock, R. Hanauer, *J. Org. Chem. 33* (1968) 2169.
[10] M. Gosmann, *Dissertation*, Universität Münster 1986.
[11] The new compounds **4a**, **4b**, **6**, and **7b** were completely characterized by elemental analysis and spectroscopic data. **7b**: MS (FD): *m/z* 697 (100%, $M-2CF_3CO_2^{\oplus}$), 695 (25%, $M-2CF_3CO_2H$); ^{1}H-NMR ($CDCl_3$) (see Fig. 1): $\delta = -11.64$ (t, $J = 13.7$ Hz, 4H), −9.09 (s, 12H), 2.43 (t, $J = 7.7$ Hz, 24H), 4.99 (q, $J = 7.7$ Hz, 16H), 13.67 (d, $J = 13.7$ Hz); UV/VIS ($CHCl_3$): λ_{max} (only band in the region 300–700 nm) = 547 nm ($\varepsilon = 909600$); $R_F = 0.20$ (CH_3CN/trifluoroacetic acid = 250 : 1).

Weak Pd···S Interactions in Palladium(II) Complexes with 1,4,7-Trithiacyclononane as Ligand**

By *Karl Wieghardt,* Heinz-Josef Küppers, Eleonore Raabe,* and *Carl Krüger*

The nine-membered rings of 1,4,7-triazacyclononane (tacn) and 1,4,7-trithiacyclononane (**L**) are especially suitable for occupying one or two faces in octahedral complexes of transition metals. The thermodynamic and kinetic stability of such complexes is very high (macrocyclic effect). It therefore appeared interesting to investigate the coordination behavior of these tridentate ligands toward metal centers, which, because of their electronic structure, prefer a square-planar coordination (e.g. Pd^{II},Pt^{II}). Thus we were able to show[1] that a square planar PtN_4 arrangement with two twofold coordinated macrocycles is indeed present in $[Pt(tacn)_2]Br_2 \cdot 2H_2O$.[2]



It is known that **L**[3] has *endo*-conformation, both in the solid state and in solution:[4] all three S-donors lie on the same side of the nine-membered ring, i.e. the conditions are ideal for the octahedral coordination of a metal center by two molecules of **L**. We report here on the complexation chemistry of **L** with Pd^{II} and on both the crystal struc-

[*] Prof. Dr. K. Wieghardt, Dipl.-Chem. H.-J. Küppers
Lehrstuhl für Anorganische Chemie I der Universität
Postfach 102148, D-4630 Bochum (FRG)
Dr. E. Raabe, Prof. Dr. C. Krüger
Max-Planck-Institut für Kohlenforschung
Postfach 101353, D-4330 Mülheim a. d. Ruhr 1 (FRG)

[**] This work was supported by the Fonds der Chemischen Industrie, the Deutsche Forschungsgemeinschaft, and Degussa AG (gifts of $K_2[PdCl_4]$).

ture and the electronic spectra of the complexes **1** (green), **2** (blue) and **3** (brown). *Schröder* et al.[5] recently detected two weak axial Pd···S interactions (Pd···S: 3.273(2) Å besides four normal, equatorial Pd–S bonds (Pd–S: 2.311(1) Å) in the yellow-brown complex $[PdL_1](BPh_4)_2$. The PdS_6 chromophore leads to a yellow-brown color, whereas **1** is green and **2** is blue.

$[PdL_2](PF_6)_2$ **1**

$[PdL_2](PF_6)_2 \cdot H_2O$ **2**

$[PdLBr_2]$ **3**

Pd^{II} acetate reacts with an excess of **L** in anhydrous methanol to give a clear, green solution, from which green crystals of **1** crystallize on addition of $NaPF_6$. In the presence of water, blue crystals of **2** precipitate out as well as the green crystals of **1**. The same products are also obtained from acetonitrile or acetone, whereupon a mixture of **1** and **2** or only **2** crystallizes out with increasing water content. **1** and **2** dissolve in water to give a blue solution. Addition of a solution of NaBr in methanol instead of $NaPF_6$ to the above reaction solution led to precipitation of orange-brown **3**. Measurements of the magnetic susceptibility between 100 and 300 K showed that **1**, **2** and **3** are diamagnetic.

Both **1** and **2** contain the cation $[PdL_2]^{2\oplus}$ and $PF_6^{\ominus}$ ions; in **2**, the asymmetric unit contains in addition one molecule of water of crystallization.[6] The structure of the $[PdL_2]^{2\oplus}$ ion in **1** and **2** is, within experimental error, the same (Fig. 1). In both structures it is located at a crystallographic inversion center. The central Pd atom is in a distorted octahedral environment: four short equatorial Pd–S bonds together with two weak axial Pd···S interactions. The axial Pd–S distances in $[PdL_1](BPh_4)_2$[5] are significantly longer than in **1** and **2**, while the four equatorial Pd–S bonds are comparable with those in **1** and **2**.[7] Paramagnetic complexes of Ni^{II} with NiS_6 polyhedra are octahedral.[8]

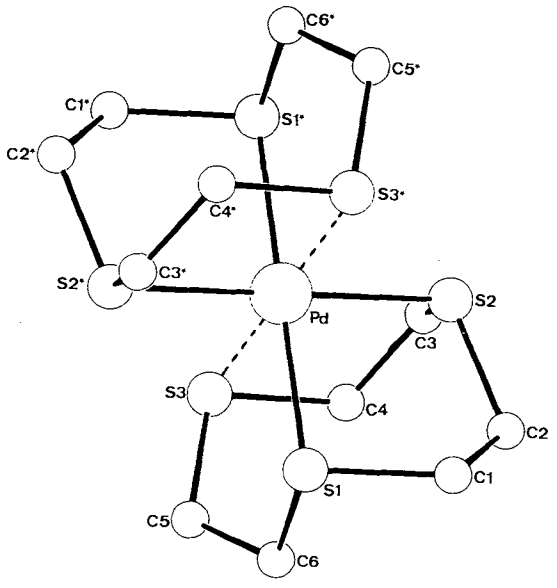


Fig. 1. Structure of the $[PdL_2]^{2\oplus}$ cation of **1** in the crystal. Important bond lengths [Å] and angles [°] (values for **2** in brackets): Pd-S1 2.333(2) [2.309(1)], Pd-S2 2.318(2) [2.314(1)], Pd-S3 2.957(2) [3.005(1)]; S1-Pd-S2 88.6(1) [89.2(1)], S1-Pd-S3 83.2(1) [83.9(1)], S2-Pd-S3 83.1(1) [82.5(1)]. In both structures the mean C–C bond length is 1.51(1) Å, the mean C–S bond length 1.82(1) Å.

The central Pd atom in **3** (Fig. 2) is surrounded by a distorted square-pyramidal array of two Br atoms and three S atoms. The Pd–S bond to the apical S atom is significantly longer than the bonds to the equatorial S atoms, each of which is oriented *trans* to a Br atom. Due to the *trans* influence of the Br atoms the equatorial Pd–S distance in **3** (2.66(3) Å) is 0.044 Å shorter than the corresponding distances in **1**, **2**, and $[PdL_1](BPh_4)_2$, whereas the Pd–Br distance is 0.02 Å longer than in $[PdBr_4]^{2\ominus}$.[9]

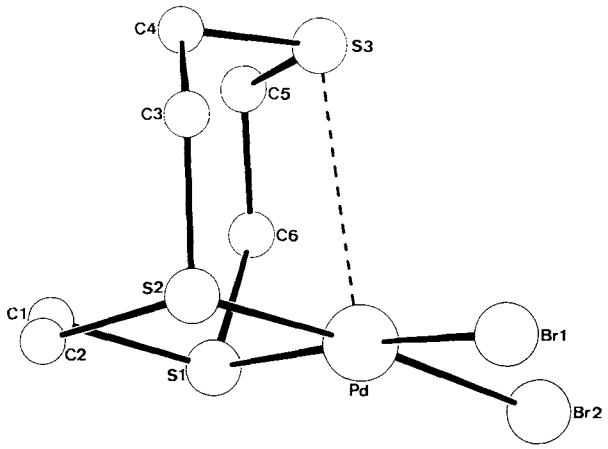


Fig. 2. Crystal structure of **3**. Important bond lengths [Å] and angles [°]: Pd-S1 2.275(2), Pd-S2 2.257(2), Pd-S3 3.125(1), Pd-Br1 2.456(1), Pd-Br2 2.468(1); S1-Pd-S2 89.3(1), S1-Pd-S3 78.7(1), S1-Pd-Br1 174.1(1), S1-Pd-Br2 89.3(1), S2-Pd-S3 81.7(1), S2-Pd-Br1 87.5(1), S2-Pd-Br2 175.5(1), S3-Pd-Br1 105.7(1), S3-Pd-Br2 102.2(1), Br1-Pd-Br2 93.4(1).

The reflection spectrum of **2** is identical with the spectra of **1** and **2** in water; an absorption maximum is observed at $\lambda = 620$ nm ($\varepsilon = 50$ L mol^{-1} cm^{-1}). In the reflection spectrum of **1**, this band is shifted to 575 nm. The change in color from blue (**2**) to green (**1**), however, is not due to this, but to the greatly enhanced intensity of the absorption between 400 and 470 nm (in **1**), which in **2** is additionally shifted to shorter wavelengths. The position of the metal-to-ligand charge-transfer bands is probably strongly dependent on the weak Pd···S interactions. In $[PdL_1](BPh_4)_2$, these are so weak that it can be assumed that only a square-planar PdS_4-coordination is present, whereas such a Pd···S interaction in **1** is relatively strong and in **2** only slightly weaker. Since the water of crystallization in **2** is not coordinated to the $[PdL_2]^{2\oplus}$ ions—weak hydrogen bonding with the $PF_6^{\ominus}$ ions cannot be ruled out—the different absorptions of **1** and **2** are attributed to different packing of the cations and anions.

Procedure

1, **2**: 0.1 g (0.45 mmol) of Pd^{II}-acetate was added at 20°C to a solution of **L** (0.18 g, 1.0 mmol) in anhydrous methanol (30 mL). Subsequent treatment of the green solution with $NaPF_6$ (1.0 g, 5.95 mmol) led to precipitation of **1** as green crystals. **1** dissolved in methanol/H_2O to give a blue solution, from which blue crystals of **2** [$\delta(CH_2)$ (80 MHz, D_2O) = 3.36 (s)] were obtained upon addition of $NaPF_6$. If a little water is present, **1** and **2** crystallize out together.

3: The above mentioned reaction solution was treated with a solution of NaBr (1.0 g, 9.72 mmol) in methanol (10 mL). Orange-brown crystals of **3** immediately separated out; these were recrystallized from acetonitrile.

All compounds gave correct elemental analyses (C, H, N, S (Br)).

Received: July 28, 1986;
revised: September 3, 1986 [Z 1880 IE]
German version: *Angew. Chem. 98* (1986) 1136

[1] K. Wieghardt, M. Köppen, W. Swiridoff, J. Weiss, *J. Chem. Soc. Dalton Trans. 1983*, 1869.
[2] The analogous Pd-complex is isostructural: A. McAuley, University of British Columbia (Canada), private communication.
[3] Prepared according to D. Sellmann, L. Zapf, *Angew. Chem. 96* (1984) 799; *Angew. Chem. Int. Ed. Engl. 23* (1984) 807.
[4] R. S. Glass, G. S. Wilson, W. N. Setzer, *J. Am. Chem. Soc. 102* (1980) 5068.
[5] A. J. Blake, R. O. Gould, A. J. Lavery, M. Schröder, *Angew. Chem. 98* (1986) 282; *Angew. Chem. Int. Ed. Engl. 25* (1986) 274.
[6] Crystal structure data: **1**: monoclinic, *C2/c* (No. 15), $a=17.91(2)$, $b=15.656(5)$, $c=11.512(5)$ Å, $\beta=126.03(5)°$, $V=2610.1$ Å^3, $Z=4$, $\rho_{calc}=1.925$ g cm^{-3}; $\mu=13.68$ cm^{-1}, 2968 independent reflections, 2321 with $I>2\sigma(I)$, $Mo_{K\alpha}$ radiation, 152 refined parameters, $R=0.053$, $R_w=0.067$.—**2**: monoclinic, $P2_1/c$ (No. 14), $a=10.521(2)$, $b=11.567(1)$, $c=11.552(1)$ Å, $\beta=112.246(8)°$, $V=1301.2$ Å^3, $Z=2$, $\rho_{calc}=1.98$ g cm^{-3}; $\mu=13.77$ cm^{-1}, 2925 independent reflections, 2422 with $I>2\sigma(I)$, $Mo_{K\alpha}$ radiation, 160 refined parameters, $R=0.032$, $R_w=0.042$.—**3**: orthorhombic, $P2_12_12_1$ (No. 19), $a=7.578(1)$, $b=12.281(3)$, $c=12.594(2)$ Å, $V=1171.1$ Å^3, $Z=4$, $\rho_{calc}=2.53$ g cm^{-3}; $\mu=87.79$ cm^{-1}, 2668 independent reflections, 2426 with $I>2\sigma(I)$, $Mo_{K\alpha}$ radiation, 110 refined parameters, $R=0.036$, $R_w=0.029$.—Empirical absorption corrections were carried out for **1**, **2**, and **3**. Further details of the crystal structure investigations are available on request from the Fachinformationszentrum Energie, Physik, Mathematik GmbH, D-7514 Eggenstein-Leopoldshafen 2 (FRG), on quoting the depository number CSD-52055, the names of the authors, and the full citation of the journal.
[7] A quasi-octahedral Pd^{II} complex with two weak Pd···S interactions (d(Pd-S) = 3.046(3) Å) has also been reported for [Pd{2-(2′-thienyl)pyridine}$_2$]Br$_2$: T. J. Giordano, W. M. Butter, P. G. Rasmussen, *Inorg. Chem. 17* (1978) 1917.
[8] a) W. N. Setzer, C. A. Ogle, G. S. Wilson, R. S. Glass, *Inorg. Chem. 22* (1983) 266; b) S. C. Rawle, J. A. R. Hartman, D. J. Watkin, S. R. Cooper, *J. Chem. Soc. Chem. Commun. 1986*, 1083.
[9] D. S. Martin, Jr., J. L. Bonte, R. M. Rush, R. A. Jacobson, *Acta Crystallogr. Sect. B 31* (1975) 2538.

2-Lithio-1-phenylpyrrole: X-Ray Structure Analysis and ^{6}Li-^{1}H 2D Heteronuclear Overhauser NMR Spectroscopy (2D HOESY)**

By *Walter Bauer, Gerhard Müller, Rafael Pi,* and *Paul von Ragué Schleyer**

Monolithiated organic compounds can often be converted further into synthetically useful dilithiated derivatives.[1] The first lithium substituent often determines the position of the second metalation.[2] Examples from our own work for such stereoselective second lithiation are 2,2′-dilithiobiphenyl,[3] 1,8-dilithionaphthalene,[4] and α,α′-dilithio-α,α′-diphenyl-*o*-xylene.[5] MNDO calculations indicate the presence of interactions between Li and the kinetically activated H atoms: the LUMO coefficients are largest at these atoms, and the corresponding C–H bond lengths are longest.[4] By means of the present example, 2-lithio-1-phenylpyrrole **1**,[6] we now show that the position of the second lithiation can also be predicted by X-ray and NMR analysis of the monolithiated precursor.

X-ray structure analysis[7] of **1** showed a dimer (**1**·TMEDA)$_2$ (TMEDA = *N,N,N′,N′*-tetramethylethylenediamine) with a central C2–Li–C2′–Li′ four-membered ring and crystallographic C_2 symmetry (Fig. 1), similar to that found for phenyllithium·TMEDA.[8] The two pyrrole rings are nearly orthogonal to the C_2Li_2 ring and *cis* to each another.[9] The angle between the pyrrole and phenyl rings is 26.1°. The C_2Li_2 four-membered ring is not planar (dihedral angle between the Li, Li′, C2 and the Li, Li′, C2′ planes 157.7°).

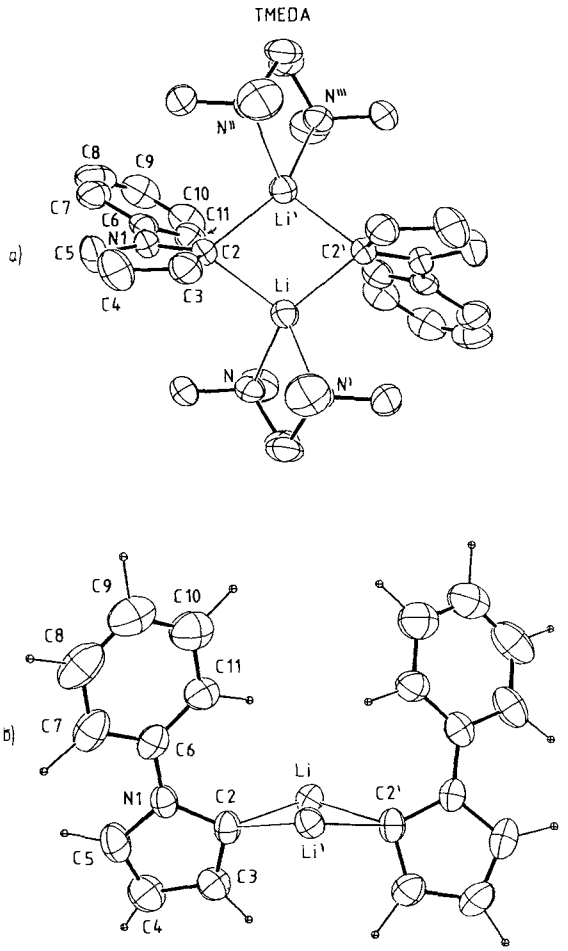


Fig. 1. Crystal structure of (**1**·TMEDA)$_2$ (ORTEP, thermal ellipsoids at the 50% probability level). a) View along the crystallographic C_2 axis (H atoms omitted). b) View when turned ca. 90° (TMEDA atoms omitted). Important distances [Å] and angles [°]: Li-Li′ 2.691(9), Li-C2 2.191(5), Li-C2′ 2.184(5), Li-N 2.304(5), Li-N′ 2.199(5), Li-H3 2.88(6), Li-H3′ 3.48(6), Li-H11 2.82(6), Li-H11′ 3.03(6); C2-Li-C2′ 101.4(3), Li-C2-Li′ 75.9(2). All other Li-H contacts are larger than 3.0 Å, the shortest of which are those to the Me groups (3.0–4.2 Å).

The position of the second metalation of **1** is expected to be indicated by a short distance between the lithium atom and the H atom that is thereby activated. As is clear from Figure 1, not only is the Li–H3 distance (average 3.2 Å) small, as expected, but also the Li–H11 distance (average 2.9 Å). MNDO calculations on **1**[10] are in good agreement with the crystal structure.

Through the use of a new NMR method, we have been able to find evidence *in solution* for the special activation of an H atom by a Li atom already present. Two-dimensional heteronuclear Overhauser NMR spectroscopy (2D HOESY) allows the spatial proximity of two heteronuclei, e.g., ^{13}C and ^{1}H, to be detected.[11] We have employed this pulse sequence for the first time to detect short ^{6}Li–^{1}H dis-

[*] Prof. Dr. P. von R. Schleyer, Dr. W. Bauer, Dr. R. Pi
Institut für Organische Chemie der Universität Erlangen-Nürnberg
Henkestrasse 42, D-8520 Erlangen (FRG)
Dr. G. Müller
Anorganisch-chemisches Institut der Technischen Universität München
Lichtenbergstrasse 4, D-8046 Garching (FRG)

[**] This work was supported by the Deutsche Forschungsgemeinschaft, the Fonds der Chemischen Industrie, and the Alexander-von-Humboldt Stiftung (*R. P.*).

tances in a molecule with *isotopes in their natural abundance*.[12, 13] Figure 2 shows the results on **1** of a ^{6}Li-^{1}H 2D HOESY experiment in [D$_8$]tetrahydrofuran ([D$_8$]THF).[14] Short Li-H separations (< ca. 3.5 Å) are indicated through cross peaks. The short Li-H11 distance already shown in the crystal structure and by MNDO calculations is also found in solution by this method. In agreement with the crystal structure, the cross peak between Li and H11 is more intense than that between Li and H3; this reflects the distances found experimentally. Also as expected from the crystal structure (Fig. 1), an additional cross peak was found between Li and the methyl hydrogens of the TMEDA ligand; the TMEDA methylene protons are further away. The assumption that the structure of **1** in the crystal is similar to that in solution is thus supported by the ^{6}Li-^{1}H 2D HOESY experiment.

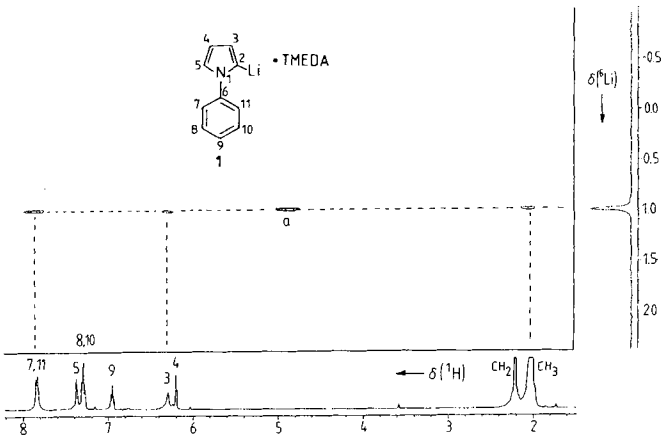


Fig. 2. ^{6}Li-^{1}H 2D HOESY spectrum of **1**·TMEDA in [D$_8$]THF, −70°C, natural abundance isotope distribution, contour plot; right: one-dimensional ^{6}Li-NMR spectrum; below: one-dimensional ^{1}H-NMR spectrum; mixing time [11] 1.5 s; a = axial cross peak at $f_1 = 0$.

As we have also found in numerous other instances, H atoms that are in proximity to the Li atom exhibit NMR signals with a significant shift to lower fields (Fig. 2). The ^{6}Li-^{1}H 2D HOESY method is thus demonstrated to be a new and useful method for the structural investigation of organolithium compounds in solution.

The introduction of a second Li atom takes place when **1** is treated with *n*BuLi. The product of this second metalation also can be obtained in crystalline form. In complete agreement with the expectation based on the evidence presented above, H11 undergoes substitution by Li.[15]

Experimental Procedure

1: *n*-Butyllithium in hexane (6.4 mmol) was added to a solution of *N*-phenylpyrrole (916 mg, 6.4 mmol) and TMEDA (1 mL, 6.6 mmol) in 25 mL of hexane under nitrogen. After 1 h at room temperature, the pale yellow solution was stored at −26°C for 2 days. The crystals formed were filtered, washed with hexane, and dried in vacuo.

Received: July 30, 1986;
revised: September 29, 1986 [Z 1881 IE]
German version: *Angew. Chem. 98* (1986) 1130

[1] J. L. Wardell in G. Wilkinson, F. G. A. Stone, E. W. Abel (Eds.): *Comprehensive Organometallic Chemistry, Vol. 1*, Pergamon Press, Oxford 1982, p. 43f.
[2] P. von R. Schleyer, *Pure Appl. Chem. 55* (1983) 355.
[3] U. Schubert, W. Neugebauer, P. von R. Schleyer, *J. Chem. Soc. Chem. Commun. 1982*, 1184; W. Neugebauer, A. J. Kos, P. von R. Schleyer, *J. Organomet. Chem. 228* (1982) 107.
[4] W. Neugebauer, T. Clark, P. von R. Schleyer, *Chem. Ber. 116* (1983) 3283.
[5] G. Boche, G. Decher, H. Etzrodt, H. Dietrich, W. Mahdi, A. J. Kos, P. von R. Schleyer, *J. Chem. Soc. Chem. Commun. 1984*, 1493.
[6] D. A. Shirley, B. H. Gross, P. A. Roussell, *J. Org. Chem. 20* (1954) 225; H. W. Gschwend, H. R. Rodriguez, *Org. React. (NY) 26* (1979) 1.
[7] (1-TMEDA)$_2$: monoclinic, $C2/c$, $a = 20.965(4)$, $b = 9.298(1)$, $c = 17.668(3)$ Å, $\beta = 107.37(1)°$, $V = 3287.0$ Å^3, $\rho_{calcd} = 1.072$ g cm^{-3} for $Z = 4$, $T = -40$°C, $F(000) = 1152$, $\mu(Mo_{K\alpha}) = 0.6$ cm^{-1}. 2523 measured reflections, of these 2290 independent and 1804 "observed" with $I \geq 1.0\sigma(I)$ (ω scan, $\Delta\omega = 1°$, $(\sin\theta/\lambda)_{max} = 0.550$, +h, +k, ±l, $Mo_{K\alpha}$, $\lambda = 0.71069$ Å, Syntex $P2_1$). Solution by direct methods which yielded all non-hydrogen atoms (including Li) (SHELX-86), H atoms by difference syntheses. $R = 0.069$, $R_w = 0.051$, $w = 1/\sigma^2(F_0)$ (anisotropic, H constant with $U_{iso} = 0.08$ Å^2, 181 parameters, SHELXS-76). $\Delta\rho_{max} = 0.46$ e/Å^3. Further details of the crystal structure investigation may be obtained from the Fachinformationszentrum Energie, Physik, Mathematik GmbH, D-7514 Eggenstein-Leopoldshafen 2 (FRG), on quoting the depository number CSD-52028, the names of the authors, and the journal citation.
[8] D. Thoennes, E. Weiss, *Chem. Ber. 111* (1978) 3157. Cf. review of organolithium compounds: W. Setzer, P. von R. Schleyer, *Adv. Organomet. Chem. 24* (1985) 353.
[9] The reason for the unexpected *syn* geometry, which is of lower symmetry than the *anti* geometry, might be the origin of (**1**·TMEDA)$_2$ from a dimer-tetramer equilibrium. (D. Seebach, R. Hässig, J. Gabriel, *Helv. Chim. Acta 66* (1983) 308; R. Amstutz, W. B. Schweizer, D. Seebach, J. D. Dunitz, *ibid. 64* (1981) 2617.) Thus, the crystal geometry of **1** would reflect a "bisected" Li tetrahedron.
[10] M. J. S. Dewar, W. Thiel, *J. Am. Chem. Soc. 99* (1977) 4899, 4907; lithium parametrization: W. Thiel, T. Clark, *QCPE Program*, No. 438.
[11] C. Yu, G. C. Levy, *J. Am. Chem. Soc. 106* (1984) 6533.
[12] The natural isotope abundance of ^{6}Li is 7.4%. Compared to ^{7}Li (92.6%), it has the advantage of a very small quadrupole moment and of large spin lattice relaxation times (T_1); this is a prerequisite for the application of the HOESY pulse sequence.
[13] NMR spectra were recorded on a JEOL JNM-GX400 spectrometer (^{1}H: 400 MHz). Spectral data on **1**·TMEDA ([D$_8$]THF, −70°C, $\delta_{TMS} = 0$, dissolved crystals): ^{1}H-NMR (α-H of [D$_7$H]THF as reference: $\delta = 3.58$; J [Hz]): 7.84 (d, 6.8, 2H; H7, 11), 7.37 (s, 1H; H5), 7.29 (dd, 6.8, 6.8, 2H; H8, 10), 6.95 (t, 6.8, 1H; H9), 6.29 (s, 1H; H3), 6.20 (s, 1H; H4), 2.20 (s, 4H; CH$_2$), 2.01 (s, 12H; CH$_3$); ^{13}C-NMR (α-C of [D$_8$]THF as reference: $\delta = 67.4$): 175.2 (C2), 148.1 (C6), 129.1 (C8, 10), 122.7 (C3), 122.1 (C9), 120.3 (C7, 11), 118.4 (C5), 111.2 (C4), 58.3 (CH$_2$), 46.3 (CH$_3$); ^{6}Li-NMR (1 M LiBr in THF/[D$_8$]THF as reference, −70°C, $\delta = 0$): 1.00 (s, $\Delta_{1/2} = 2$ Hz); ^{6}Li-^{1}H HOESY: sequence [11]: 90°(^{1}H)-t_1/2-180°(^{6}Li)-t_1/2-90°(^{1}H)-mixing time-90°(^{6}Li)-t_2/^{1}H-b.b.-decoupling-delay; 10-mm multinuclear probe, 5-mm sample tube; data matrix 128 (t_1) × 512 (t_2) points; 42 increments in t_1 with 32 pulses per increment; mixing time 1.5 s, delay 7.0 s; 90° pulse widths: ^{6}Li 33 μs, ^{1}H 87 μs. Exponential line broadening in t_2 ($BF = 0.8$ Hz), Lorentzian to Gaussian transformation in t_1 ($GF = 100$ Hz, $BF = -90$ Hz).
[14] Earlier observations of ^{6}Li{^{1}H} nuclear Overhauser effects: F. W. Wehrli, *Org. Magn. Reson. 11* (1978) 106.
[15] G. W. H. Cheeseman, S. G. Greenberg, *J. Organomet. Chem. 166* (1979) 139.

$(Me_4N)_3[Mo_4O_{12}F_3]\cdot 0.8H_2O$, A Salt with a Novel Fluorooxo Polyanion

By *Norbert Buchholz* and *Rainer Mattes**

A number of mono- and dinuclear as well as polymeric fluorooxo anions of molybdenum(VI) are known.[1] In the multinuclear anions, the coordination polyhedra are linked through common apexes or edges; the sole exception is the $[Mo_2O_6F_3]^{3\ominus}$ ion, for which two octahedra share a common face and the (formally) highly charged metal atoms are separated by 320.4 pm.[2] We have ascribed the stability of this anion and of the analogously structured $V_2O_4F_5^{3\ominus}$ and $V_2O_2F_7^{3\ominus}$ ions to the rigid crystal lattice of the $Cs_3[Fe_2F_9]$ type, in which the transition-metal atoms occupy octahedral voids in a close-packed lattice

[*] Prof. Dr. R. Mattes, Dipl.-Chem. N. Buchholz
Anorganisch-chemisches Institut der Universität
Corrensstrasse 36, D-4400 Münster (FRG)

made up of alkali-metal and oxygen or fluorine atoms.[2] Recently, the dimeric ions $V_2O_4F_5^{3\ominus}$ and $V_2O_2F_7^{3\ominus}$, having similarly short vanadium–vanadium distances (298 to 314 pm) were also obtained as the tetramethylammonium salts from nonaqueous solvents.[3] In contrast, the analogous reactions with molybdenum compounds did not lead to the compound $(Me_4N)_3[Mo_2O_6F_3]$ but rather to $(Me_4N)_3[Mo_4O_{12}F_3]\cdot 0.8\,H_2O$ **1**.

The anion of **1** is a novel fluorooxo polyanion (Fig. 1):[4] it has *mm* symmetry. Each molybdenum atom is surrounded in a distorted octahedral fashion by four oxygen and two fluorine atoms. Two coordination octahedra are joined through a common face, which contains one oxygen and two fluorine atoms, to form a double octahedron. Two double octahedra are joined through three apexes, which belong to two edges and are occupied by two oxygen atoms and one fluorine atom, to form a tetrameric anion. Thus, each of these oxygen atoms belongs to two molybdenum atoms and the fluorine atom to four molybdenum atoms. The linking of the octahedra in the anion of **1**, for which, to the best of our knowledge, no other examples are known, may also be described by the formula $[MoO_2O_{2/2}F_{1/2}F_{1/4}]_4^{3\ominus}$. The only fluorooxo polyanion reported thus far, $[Ta_4O_6F_{12}]^{4\ominus}$ has a Ta_4O_6 adamantane skeleton; all fluorine atoms are terminally bonded.[5]

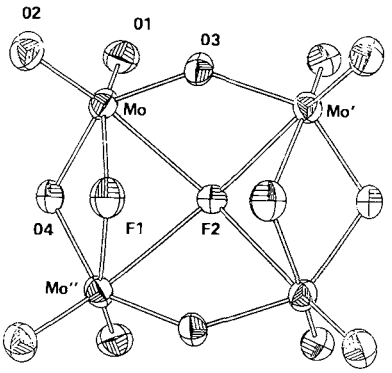


Fig. 1. Crystal structure of the anion of **1**. Selected bond lengths [pm] and angles [°]: Mo-O1 170.0(7), Mo-O2 169.3(7), Mo-O3 193.2(6), Mo-O4 192.3(6), Mo-F1 220.3(6), Mo-F2 244.6(6); O1-Mo-O2 104.3(1), Fe1-Mo-F2 69.4(1), Mo-O3-Mo' 109.5(1), and Mo-O4-Mo'' 122.9(1). Further details of the crystal structure investigation may be obtained from the Fachinformationszentrum Energie, Physik, Mathematik GmbH, D-7514 Eggenstein-Leopoldshafen 2 (FRG), on quoting the depository number CSD-52162, the names of the authors, and the journal citation.

The metal-ligand distances in **1**—like those in comparable fluorooxo anions[1]—vary according to the type of ligand bonding: the terminal Mo–O bonds are 169.3(7) and 170.0(7) pm, the bridging 192.3(6) and 193.2(6) pm. The distance of the two-coordinate fluorine atom from the molybdenum atom is 220.3(6) pm. The longest Mo–F bonds are those to the unusual four-coordinate fluorine atom (244.6(6) pm), which lies 80 pm outside of the plane of the four metal atoms.

The longer Mo–F bonds are, as expected, opposite the shorter terminal Mo–O bonds (e.g., Mo–F2 and Mo–O2). The Mo–Mo distance inside the double octahedron (315.2(2) pm) is even shorter than that in $Cs_3[Mo_2O_6F_3]$.[2] The molybdenum atoms, like those in all polymolybdates,[6] are displaced from the center of the polyhedra toward the terminal oxygen atoms. Accordingly, the O/F–Mo–O/F bond angles vary from 69 to 104°. As in the other polymeric fluorooxomolybdates(VI), oxygen prefers the terminal and fluorine the bridging positions.

In the IR and Raman spectra, the Mo–O stretching vibrations give rise to bands at 955 ($\tilde{\nu}_s$) and 915 ($\tilde{\nu}_{as}$) cm^{-1} (terminal oxygen atoms) and at 842, 798, 713, and 686 cm^{-1} (bridging oxygen atoms). The Mo–F stretching vibrations could not be assigned unequivocally. They are expected to occur below 550 cm^{-1}.

Compounds having the same kinds of structures and compositions that are found for the iso- and heteropolyoxometalates are not expected to be found, however, for polymeric fluorooxometalates, because the positive charge built up in the interior of the polyanions by the highly charged metal atoms is not sufficiently compensated by the fluorine atoms.

Experimental Procedure

A suspension of MoO_3 in *N,N*-dimethylformamide was heated to reflux with a 25% methanolic solution of nBu_4NOH (molar ratio 4:3), until a clear solution formed. A stoichiometric amount of HF was then added in the form of a 20% ethanolic solution and the reaction mixture was heated to reflux for 30 min. Methanol, ethanol, and the water formed were removed by distillation. **1** was precipitated by addition of Me_4NCl in ethanol. Single crystals were obtained by the diffusion procedure. Yield: 67%.

Received: July 9, 1986;
revised: August 15, 1986 [Z 1852 IE]
German version: *Angew. Chem. 98* (1986) 1101

[1] R. Mattes, H. Förster, *Z. Anorg. Allg. Chem. 494* (1982) 109.
[2] Cf. R. Mattes, K. Mennemann, H. Rieskamp, H. Jäckel, H.-J. Brockmeyer, *J. Less-Common Met. 76* (1980) 199, and references cited therein.
[3] N. Buchholz, M. Leimkühler, R. Mattes, *9th European Crystallographic Meeting* (Turin 1985), Abstracts, p. 134.
[4] **1** crystallizes in the space group *Cmcm*, $a=1040.9(3)$, $b=1501.2(7)$, $c=1854.0(7)$ pm, $Z=4$; Syntex-P2$_1$ diffractometer, 140 K, 1144 unique reflections with $F_0 \geq 3.92\sigma(F_0)$, 114 parameters, $R=0.051$, $R_w=0.048$. Four of the twelve $Me_4N^{\oplus}$ ions per unit cell are disordered on a mirror plane; the crystal water is also disordered (occupation factor 0.8(1)).
[5] J. Sala-Pala, J.-E. Guerchais, A. J. Edwards, *Angew. Chem. 94* (1982) 876; *Angew. Chem. Int. Ed. Engl. 21* (1982) 870.
[6] M. T. Pope: *Heteropoly and Isopoly Oxometalates*, Springer, Berlin 1983.

Preparation of Ultrathin Layers of Molecularly Controlled Architecture from Polymeric Phthalocyanines by the Langmuir-Blodgett-Technique**

By *Ernst Orthmann* and *Gerhard Wegner**

The Langmuir-Blodgett (LB) technique enables the preparation of layered structures consisting of a sequence of monolayers, each one exactly one molecule thick.[1] A compound of conventionally amphiphilic character is dissolved in an organic solvent and spread onto the water surface of a Langmuir trough. A surface film is formed which is compressed by the mobile barrier of the film balance so as to achieve a well defined, solid-analogous layer of single molecules. This layer is now transferred to a solid substrate by repeated dipping of the substrate into the trough at constant surface pressure. The number of immersions determines the number of layers transferred to the sub-

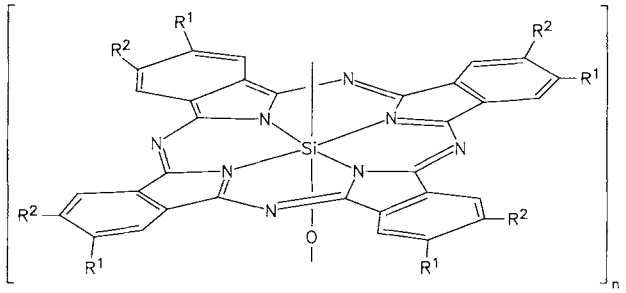
[*] Prof. Dr. G. Wegner, Dr. E. Orthmann
Max-Planck-Institut für Polymerforschung
Jakob-Welder-Weg 11, D-6500 Mainz (FRG)

[**] This work was supported by the Bundesministerium für Forschung und Technologie within the framework of the project "Ultrathin layers".

strate. Each single layer consists of domains which in total provide for a uniaxial texture of the layer system.[2] The size and orientation of the domains can be controlled only with difficulty. Thus, the orientation of the individual molecules or of the crystal axes of the domains with respect to an external reference system cannot be adjusted exactly. This constitutes one of the limiting factors for many of the potential applications of such systems as components in optical or electro-optical devices.[3]

We have now found a new class of compounds which allows for the preparation of homogeneous single layers on the substrate surface. The orientation of the molecules is uniquely fixed during transfer from the water surface to the substrate by the direction of immersion. The compounds concerned are unsymmetrically substituted polymeric phthalocyaninatosiloxanes, of which the tetramethoxy-tetraoctyloxy derivative **1** is the best example so far.

The polymer **1** is derived from the correspondingly substituted phthalocyaninatosilicon hydroxide **2** by $FeCl_3$-catalyzed condensation.[4] The monomer **2** is a mixture of the four positional isomers which are formed upon cyclization of 5-methoxy-6-octyloxy-1,3-isoindolediimine in the presence of $SiCl_4$ and subsequent hydrolysis to the dihydroxy compound.[4,5]



1, $R^1 = OCH_3$, $R^2 = OC_8H_{17}$

2, $(CH_3O)_4(C_8H_{17}O)_4$–phthalocyaninato–$Si(OH)_2$

Both monomer **2** as well as the polymer **1** (degree of polymerization $\bar{P}_w = 15$) are readily soluble in chloroform (solubility ca. 12 g L^{-1} at 20°C). **1** and **2** can be spread onto the water surface from such solutions. Figure 1 shows the force-area isotherms as measured by a Lauda-film balance.

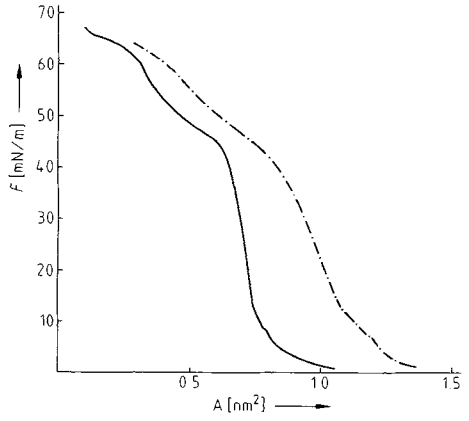


Fig. 1. Force-area isotherms of the monomer **2** (···) and of the polymer **1** (——) at 3°C.

The monomer **2** does not exhibit any sharp phase transition, whereas the polymer **1** gives rise to a solid-analogous phase with a characteristic area per repeat unit of 0.67 nm^2. This value corresponds to the cross-sectional area of the repeat unit as determined from X-ray and electron microscopic investigations of the multilayers. A distance of 0.34 nm is found for the chain repeat along the chain, and the average distance between adjacent chains and layers amounts to 1.96 nm.

Multilayers of the polymer can be built-up on hydrophobic substrates at constant pressure (usually 20 mN/m). Suitable substrates are, inter alia, glass with hydrophobic surface, polyethylene terephthalate films, or plates made of polytetrafluoroethylene, platinum or silicon. Transfer occurs to the same extent and proportional to the substrate area, both on immersion and on withdrawal of the substrate. Mixtures of **1** and **2** can be spread and transferred by the same technique.

The degree of orientation and the homogeneity of the layers can be examined with a polarizing microscope. When a glass plate covered with the polymer layers is viewed between crossed nicols the same birefringence and homogeneous extinction is observed over the whole area of a given preparation. Furthermore, the samples show dichroism. The absorption of a linearly polarized light beam impinging at right angles to the plane of the substrate depends on the angle between the plane of polarization and the direction of immersion, without any fluctuation over the whole surface of a sample of typically 2 cm^2 (Fig. 2a). The absorption increases linearly with the number of monolayers. The dichroic ratio is 2.7 at the maximum of the polymer absorption band (corrected for the self-absorption of the hydrophobic glass used as the substrate); this value is independent of the number of layers in a multilayer sample (cf. Fig. 2b). The dichroic ratio can be increased to 5.8 without changing the molecular orientation, which is uniquely determined by the direction of immersion, by annealing the freshly prepared multilayer sample at 140°C for 30 minutes. Intermediate values are obtained by variation of the annealing procedure. Once the

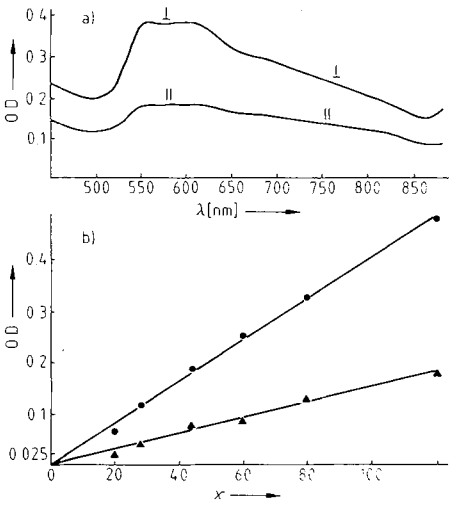


Fig. 2. a) UV/VIS absorption spectrum of the multilayer of polymer **1** (80 layers) on glass which had been pretreated with dichloromethylsilane (⊥) perpendicular to the plane of polarization, (∥) parallel to the direction of immersion of the substrate; -- self-absorption of the hydrophobicized glass. b) Optical density as a function of the number of layers (thickness of a single layer = 1.96 nm). (●) Perpendicular to the plane of polarization, (▲) parallel to the direction of immersion of the substrate.

dichroic ratio is fixed, either by annealing or by keeping the freshly prepared sample for two weeks at room temperature, it will stay constant, even if the sample is heated again (up to 260°C); thermal degradation of the sample will only occur above 280°C.

Multilayers transferred to platinum electrodes are electroactive. The polymer **1** showed its first reduction peak at -1.5 V and the first oxidation peak at $+0.25$ V vs. a Ag/AgCl reference electrode in a cyclovoltammetric experiment (acetonitrile, tetrabutylammonium perchlorate, 1 mmol).

The preparation of multilayers of unsubstituted or substituted phthalocyanines has been investigated by several authors.[6,7] However, in all cases the problem of formation of domains and of an ill-defined positioning of the ring plane with regard to the water surface was encountered. To the best of our knowledge, polymeric phthalocyanines have never been investigated by the LB-technique. Our results are very surprising for the following reasons:

1) the polymers investigated cannot be classified in the usual scheme as amphiphilic molecules;
2) the macrocycles are oriented with the molecular plane normal to the water surface, and normal to the plane of the substrate within the multilayer architecture. The latter is unambiguously derived from the force-area diagram and from the position of the diffraction peaks, which, together with the dichroic behavior, prove that the chain direction coincides with the direction of immersion;
3) the polymer exists at the water surface in a solid-analogous phase, which is mechanically deformable in the course of the transfer process, such that a unique orientation of all molecules results within the monolayer and domain formation can be suppressed; the dichroic ratio serves as the order parameter. Consequently, we assume that the polymer exists in a liquid crystalline state at the water surface and as monolayer at the substrate surface.[8] This is consistent with the observation that the molecular orientation can be improved by annealing subsequent to the preparation of the multilayer structure.

Received: July 31, 1986;
revised: September 9, 1986 [Z 1882 IE]
German version: *Angew. Chem. 98* (1986) 1114

[1] H. Kuhn, D. Möbius, *Angew. Chem. 83* (1971) 672; *Angew. Chem. Int. Ed. Engl. 10* (1971) 620; Special Issue on LB-films. *Thin Solid Films 66* (1980); Proc. First Int. Conf. on LB-Films. Durham 1982, *ibid. 99* (1983); Proc. Second Int. Conf. on LB-Films, Schenectady, NY 1985, *ibid. 134–136* (1985/86).

[2] G. Lieser, B. Tieke, G. Wegner, *Thin Solid Films 68* (1980) 77.

[3] M. Sugi, *J. Mol. Electronics 1* (1985) 3.

[4] a) E. Orthmann, G. Wegner, *Makromol. Chem. Rapid Commun. 7* (1986) 243; b) E. Orthmann, *Dissertation*, Universität Mainz 1986.

[5] The monomer **2** was obtained by double bromination of guajacol in the ring, etherification of the free hydroxy group according to Williamson, exchange of the bromine by nitrile groups, and transformation of the dinitrile into the isoindolediimine in the usual way. A detailed description of the synthesis is given in [4b].

[6] A. W. Snow, N. L. Jarvi, *J. Am. Chem. Soc. 106* (1984) 4706; J. R. Fryer, R. A. Hann, B. L. Eyres, *Nature (London) 313* (1985) 382; S. Baker, C. G. Roberts, M. C. Petty, M. V. Twigg, *Thin Solid Films 29* (1983) 71.

[7] D. W. Kalina, S. W. Crane, *Thin Solid Films 134* (1985) 109. These authors were able to produce a monolayer of octaalkoxy-substituted copper-phthalocyanines on the Langmuir trough; the macrocycles were reported to lay flat on the water surface initially, but are supposed to arrange like tiles on a roof in the course of the transfer to a solid substrate, where they form microstacks. These stacks show a preferential orientation similar to our results.

[8] We have so far been unable to obtain comparable results with polymers obtained from symmetrically substituted phthalocyanine monomers. We assume that the ability of the systems described here to be oriented relates to the fact that their structure cannot crystallize in a regular lattice.

A Simple Route to 2,3,11,12-Dibenzo-1,4,7,10,13,16-Hexathia-2,11-cyclooctadecadiene (Hexathiobenzo[18]crown-6)**

By *Dieter Sellmann** and *Peter Frank*

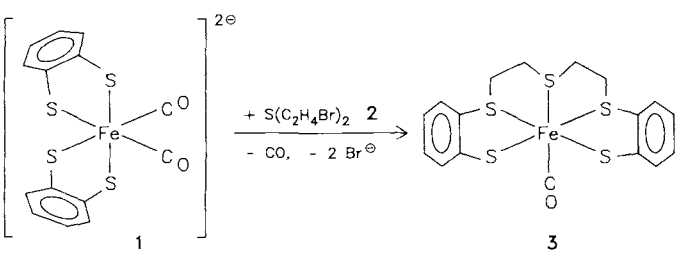
Cyclic polyethers are potentially strong ligands for many transition metals; consequently, they are important building blocks, inter alia, for model compounds of redox enzymes with sulfur-coordinated metal atoms at the active centers.[1]

However, a systematic study of the coordination chemistry of these ligands has been thwarted by the fact that in many cases they are accessible only with difficulty, if at all. The synthesis of such compounds by condensation reactions frequently affords, even according to the dilution or phase-transfer principle, only low yields of mixtures of products which require laborious separation.[2,3]

For 1,4,7-trithiacyclononane as example, it has recently been demonstrated how such compounds with suitable template centers can be obtained: reactions with 2,2'-thiodiethanethiol according to the dilution principle afford the desired product in only 0.04 to 4.4% yield,[3b] whereas reactions at $[Mo(CO)_3]$-centers afford up to 60% yield of the target compound.[4] Since template reactions are, in principle, catalytic reactions, it can be expected, in view of the course of the reaction and the substrate, that they are sensitively influenced by the properties of the metal template centers. We have now found that $[Fe^{II}CO]$ centers are exceptionally suitable for the synthesis of the novel ligand 2,3,11,12-dibenzo-1,4,7,10,13,16-hexathia-2,11-cyclooctadecadiene **5**; the compound **5** is the sulfur analogue of the well known cyclic polyether dibenzo[18]crown-6.

In the synthesis of the complex **3**,[5] the thiolate ligands of **1** are alkylated stepwise by **2** in tetrahydrofuran (THF) at room temperature. As has been observed with the corresponding ruthenium complexes, ligands such as those in **3** can be alkylated to polyethers under mild conditions only when substitution-labile (neutral) coligands are coordinated to the metal center. Replacement of these coligands by anions (from the alkylating agent) avoids formation of difficultly alkylatable complex cations.[6]

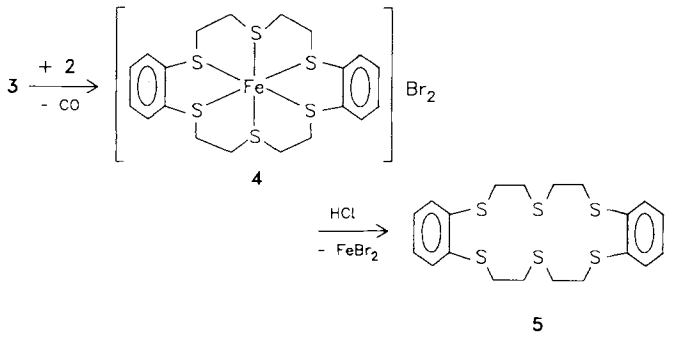
Since the CO ligand in **3** is inert to substitution at room temperature, we attempted to split it off under more drastic conditions (7 hours' reflux in THF) (**3** does not need to be isolated). A reddish-brown solid was obtained, an elemental analysis of which pointed to formation of the complex **4**. Hydrolysis of **4** with HCl afforded a yellowish solution, from which the title compound **5** could be isolated in 55% yield.



1 3

[*] Prof. Dr. D. Sellmann, Dipl.-Chem. P. Frank
Institut für Anorganische Chemie der Universität Erlangen-Nürnberg
Egerlandstrasse 1, D-8520 Erlangen (FRG)

[**] Transition Metal Complexes with Sulfur Ligands, Part 25. This work was supported by the Deutsche Forschungsgemeinschaft, the Fonds der Chemischen Industrie, and the Dr.-Otto-Röhm-Gedächtnisstiftung.— Part 24: D. Sellmann, J. Keller, H. P. Beck, W. Milius, *Z. Naturforsch.*, in press.



4

5

Procedure

5: A mixture of **3** (5.1 g, 11.17 mmol) and **2** (2.77 g, 11.17 mmol) was heated in 500 mL of boiling THF. This furnished a brown suspension, from which the solvent was completely removed. The reddish-brown residue was extracted with 2×50 mL Et_2O, taken up in 300 mL of THF, treated with 8 mL of conc. HCl, and heated to boiling for ca. 2 h until a yellow solution was obtained. Removal of the solvent furnished a yellow powder, which was washed with 2×25 mL of Et_2O and then dissolved in 200 mL of CH_2Cl_2. Extraction of the CH_2Cl_2 solution with 2×50 mL of H_2O, drying over Na_2SO_4, evaporation to a fifth of the original volume, and cooling, afforded a yellow solid. Recrystallization from 50 mL of CH_2Cl_2 at 30 °C → −30 °C yielded 2.85 g (55%) of analytically pure **5** in the form of colorless crystals; m.p. 161 °C; ^{1}H-NMR (270 MHz, CD_2Cl_2): $\delta(C_6H_4)=7.3$ (m, 4), 7.2 (m, 4); $\delta(CH_2)=3.1$ (m, 8), 2.7 (m, 8); MS (FD): m/z 456 ($M^{\oplus}$).

On using half the quantities of substrates mentioned above, yields of up to 75% could be obtained; the one-pot process with the educts $FeCl_2\cdot4H_2O$, $C_6H_4(SH)_2$, LiOH, CO and **2** afforded **5** in 45% yield.

Received: August 4, 1986;
supplemented: September 19, 1986 [Z 1890 IE]
German version: *Angew. Chem. 98* (1986) 1115

[1] a) K. Wieghardt, W. J. Küppers, J. Weiss, *Inorg. Chem. 24* (1985) 3067; b) P. W. R. Corfield, C. Ceccarelli, M. D. Glick, J. W.-Y. Moy, L. A. Ochroymowycz, D. B. Rorabacher, *J. Am. Chem. Soc. 107* (1985) 2399; c) A. J. Blake, R. O. Gould, A. J. Lavery, M. Schröder, *Angew. Chem. 98* (1986) 282; *Angew. Chem. Int. Ed. Engl. 25* (1986) 274, and references cited therein.

[2] Cf. also [1a, b] and C. Baldoli, P. DelButtero, S. Maiorana, A. Papagni, *J. Chem. Soc. Chem. Commun. 1985*, 1181; P. Singh, G. Arora, *Heterocycles 23* (1985) 2815; J. S. Bradshaw, J. Y. K. Hui, *J. Heterocycl. Chem. 11* (1974) 649. Special condensation reagents or ions, e.g. Cs_2CO_3 [3a] or benzyltrimethylammonium ions [3b], can in some cases drastically increase the yield; the separation problems, however, could not be circumvented.

[3] a) J. Buter, R. M. Kellogg, *J. Org. Chem. 46* (1981) 4481; b) W. N. Setzer, C. A. Ogle, G. S. Wilson, R. S. Glass, *Inorg. Chem. 22* (1983) 266.

[4] D. Sellmann, L. Zapf, *Angew. Chem. 96* (1984) 799; *Angew. Chem. Int. Ed. Engl. 23* (1984) 807.

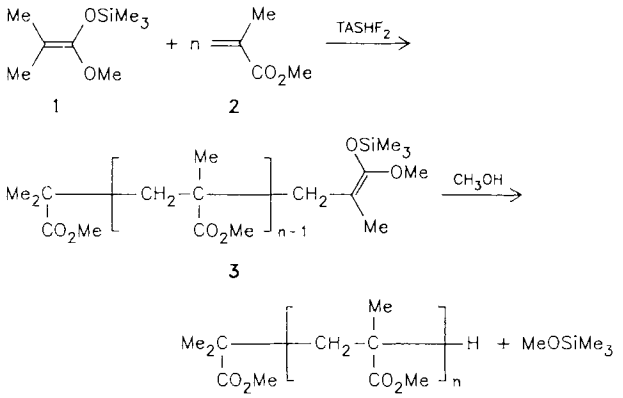
[5] D. Sellmann, U. Kleine-Kleffmann, *J. Organomet. Chem. 247* (1983) 307.

[6] Cf. also the systematic influence of the PR_3 ligands on the alkylation of $[Ru(PR_3)_2dttd]$ ($PR_3=PMe_3$, PPh_3; $dttd^{2\ominus}$ = 2,3,8,9-dibenzo-1,4,7,10-tetrathia-2,8-decadiene(2−)): D. Sellmann, M. Waeber, G. Huttner, L. Zsolnai, *Inorg. Chim. Acta 118* (1986) 49.

Group Transfer Polymerization of Acrylic Acid Esters with Alkylthio- or Arylthiosilanes as Initiators

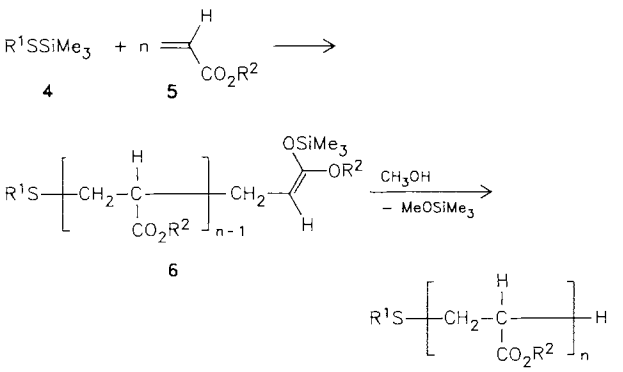
By *Manfred T. Reetz,* Ralph Ostarek, Karl-Erwin Piejko, Dieter Arlt,* and *Bruno Bömer*

The polymerization of methacrylic acid esters to living polymers with narrow molecular weight distribution at room temperature has only recently been made possible by group transfer polymerization.[1] This industrially promising process is initiated by a Michael addition, e.g., of the *O*-silylketene acetal **1**, to methyl methacrylate **2** in the presence of anionic catalysts. Examples of such catalysts are $(Me_2N)_3S^{\oplus}Me_3SiF_2^{\ominus}$ (TASF) and $(Me_2N)_3S^{\oplus}HF_2^{\ominus}$ ($TASHF_2$). Chain growth is achieved by repeated Michael additions in which the silyl group is transferred to the end of the chain. This leads to formation of the living polymer **3** with an *O*-silylketene acetal end group, which can be desilylated, e.g. by methanolysis.



In the case of acrylic acid esters, polymers with narrow molecular weight distribution are obtained only with electrophilic catalysts such as ZnI_2 (at room temperature) or diisobutylaluminum chloride (at −78 °C).[2] However, the ZnI_2-catalyzed polymerization of ethyl acrylate fails to provide a living polymer.[2,3]

We report here on the first use of alkylthio- and arylthiosilanes **4** as initiators for the group transfer polymerization of acrylic acid esters **5**.[4] In order to perform the polymerization, a mixture of initiator and catalyst in the proper solvent is treated with the monomer, the reaction temperature being kept constant by a thermostat. After quantitative conversion, the polymers **6** are desilylated by methanolysis. In the case of initiation with **4b** and **4d**, the trimethylsilyl protective group at the front of the chain is cleaved with CH_3OH/HCl.



The results listed in Table 1 show that the anionic catalyst $TASHF_2$ leads to polymers with relatively broad molecular weight distributions (No. 1, 2). In contrast, use of electrophilic catalysts affords polymers with narrow molecular weight distributions[5] (No. 3–8). The somewhat high molecular weights of the polymers prepared with **4c**

[*] Prof. Dr. M. T. Reetz, Dr. R. Ostarek
Fachbereich Chemie der Universität
Hans-Meerwein-Strasse, D-3550 Marburg (FRG)
Dr. K.-E. Piejko, Prof. Dr. D. Arlt, Dr. B. Bömer
Bayer AG, 5090 Leverkusen, Bayerwerk (FRG)

Table 1. Group transfer polymerization of acrylates **5** with alkylthio- or arylthiosilanes **4** as initiators. $TASHF_2 = (Me_2N)_3S^{\oplus}HF_2^{\ominus}$, THF = tetrahydrofuran.

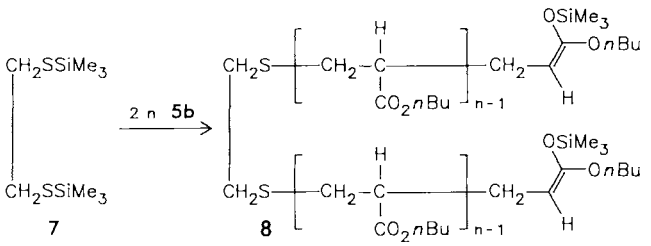
No.		R^1	Initiator (mmol)		R^2	Monomer [a] (mmol)	Catalyst (mmol)		Solvent [a]	t [h]	T [°C]	M_n(calc) [b] [kg·mol^{-1}]	M_n(obs) [c] hkg·mol^{-1}]	D [d]
1	**4a**	Me	(5.3)	**5b**	*n*Bu	(40)	$TASHF_2$	(0.1)	CH_3CN	1	22	1.0	1.5	1.44
2	**4b**	$CH_2CH_2OSiMe_3$	(3.0)	**5b**	*n*Bu	(30)	$TASHF_2$	(0.2)	THF	1	22	1.4	1.1	2.0
3	**4c**	Ph	(2.0)	**5b**	*n*Bu	(34)	ZnI_2	(0.4)	toluene	3	0	2.4	13 [e]	1.16 [e]
4	**4b**	$CH_2CH_2OSiMe_3$	(1.9)	**5b**	*n*Bu	(36)	$(i\text{Bu})_2AlCl$	(3.6)	CH_2Cl_2	2	−78	2.5	12	1.14
5	**4d**	$CH_2CO_2SiMe_3$	(2.1)	**5b**	*n*Bu	(36)	ZnI_2	(0.2)	toluene	3	0	2.3	3.0 [f]	— [f]
6	**4b**	$CH_2CH_2OSiMe_3$	(0.73)	**5a**	Me	(55)	ZnI_2	(0.2)	toluene	6	0	6.6	6.9	1.15
7	**4b**	$CH_2CH_2OSiMe_3$	(153)	**5b**	*n*Bu	(14800)	ZnI_2	(157)	toluene	24	0	12.5	14.2	1.08
8	**4b**	$CH_2CH_2OSiMe_3$	(0.76)	**5b**	*n*Bu	(36)	ZnI_2	(0.2)	toluene	4	22	6.1	8.6	1.10

[a] Concentration of the monomer ≈ 3 mol L^{-1}. [b] Calculated from monomer/initiator ratio. [c] Determined by gel permeation chromatography with universal calibration. [d] For the definition of polydispersity D see [5]. [e] Sample contained oligomers which were not taken into account in the calculation of the molecular weight distribution. [f] M_n from the sulfur content of the polymer, D not determined.

as initiator and diisobutylaluminum chloride as catalyst relative to the expected value (M_n(calc)) can be attributed to an incomplete initiation under the given conditions (No. 3 and 4, respectively). In combination with ZnI_2 as catalyst, however, the alkylthiosilanes **4a**, **4b**, and **4d** afford polyacrylates having molecular weights which correspond to the monomer/initiator ratio in the sense of a stoichiometric polymerization; the molecular weight distribution is also narrow (No. 5–7).

In the polymerization of **5b** with **4b** in the presence of ZnI_2 (22 °C), further monomer was added at room temperature three hours after termination of polymerization. This led to a continuation of the polymerization with quantitative formation of a polymer having a molecular weight distribution which is only slightly broadened ($D = 1.25$).

The polymers prepared with the functional initiators **4b** and **4d** have, after cleavage of the trimethylsilyl group, a hydroxy- and carboxy end group, respectively, which can be used for further reactions such as coupling reactions with other functionalized polymers.



The ethylenedi(thiosilane) **7** as initiator leads to a polymer **8** with two silylketene acetal end groups and narrow molecular weight distribution ($D = 1.07$; determined on the desilylated product; reaction with ZnI_2 as catalyst at 22 °C in toluene). In the case of the polymerization of the acrylate **5** (R^2 = 2-ethylhexyl) with **7**, anionic catalysts were also tested. $TASHF_2$ furnished only poor results, whereas $n\text{Bu}_4NF$ (THF/room temperature) afforded uniform polymers (e.g., $D = 1.07$; $M_n = 2.21$ kg mol^{-1}; M_n(calc) = 1.95 kg mol^{-1}).

In summary, alkylthiosilanes are excellent initiators for the polymerization of acrylates. In combination with ZnI_2 as catalyst, living polymers with narrow molecular weight distribution are obtained. The ready accessibility of functionalized initiators[6] enables the simple preparation of well defined functionalized polyacrylates which are suitable for the synthesis of block and graft polymers.

Received: August 11, 1986;
revised: October 1, 1986 [Z 1898 IE]
German version: *Angew. Chem. 98* (1986) 1116

[1] O. W. Webster, W. R. Hertler, D. Y. Sogah, W. B. Farnham, T. V. Rajan-Babu, *J. Am. Chem. Soc. 105* (1983) 5706; O. W. Webster, W. B. Farnham, D. Y. Sogah, Eur. Pat.-Anm. 0068887 (1983), Du Pont.
[2] W. R. Hertler, D. Y. Sogah, O. W. Webster, B. M. Trost, *Macromolecules 17* (1984) 1417.
[3] The authors [2] report that renewed addition of acrylate after termination of polymerization does *not* lead to a continuation of polymerization.
[4] M. T. Reetz, R. Ostarek, E. E. Piejko, DOS 3504168 (1986), Bayer AG.
[5] The molecular weight distribution can be characterized by the polydispersity D; $D = M_w/M_n$ (ratio of the weight average molecular weight to the number average molecular weight). With D values of ≤ 1.2 one speaks of narrow molecular weight distributions.
[6] See, e.g., W. P. Weber: *Silicon Reagents for Organic Synthesis*, Springer, Berlin 1983, Chapter 21.

Enantioselective Synthesis of α-Substituted Primary Amines by Nucleophilic Addition to Aldehyde-SAMP Hydrazones**

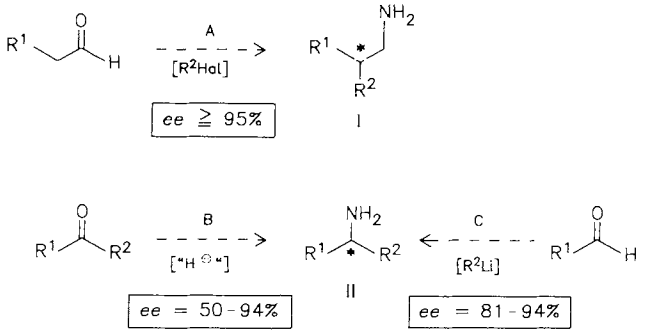
By *Dieter Enders,* Heinrich Schubert*, and *Christoph Nübling*

The SAMP/RAMP hydrazone method enables highly diastereoselective and enantioselective CC couplings at the α-position to the carbonyl group of ketones and aldehydes.[1] We recently reported on the extension of this method to the enantioselective synthesis of β-substituted primary amines I by α-alkylating, reductive amination of aldehydes (reaction A),[2] and on the reductive amination of unsymmetrical ketones to α-substituted primary amines II (Reaction B).[3] We have now succeeded in opening up a very flexible entry to the amines II via a CC coupling reaction (Reaction C). The new method is based on a nucleophilic addition to SAMP (or the enantiomeric RAMP) hydrazones of aldehydes (Scheme 1).

The aldehydes **1**, after conversion into the SAMP hydrazones (*S*)-**2**, are treated with organolithium compounds in ether or tetrahydrofuran (THF) at −78 °C. The reductive N–N cleavage of the hydrazines (*SR*)-**3** or (*SS*)-**3**, formed by selective diastereofacial addition at the CN double bond, with Raney nickel affords the α-substituted primary amines (*R*)- or (*S*)-**4** together with ((*S*)-**5**) in total yields of

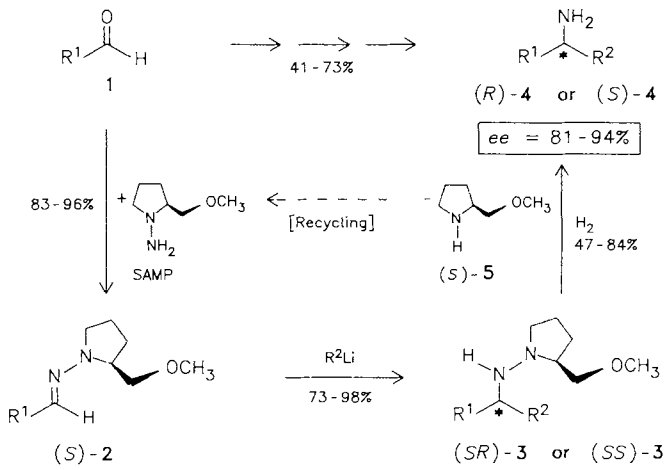
[*] Prof. Dr. D. Enders, Dr. H. Schubert [†], Dipl.-Chem. C. Nübling
Institut für Organische Chemie der Technischen Hochschule
Professor-Pirlet-Strasse 1, D-5100 Aachen (FRG)
[†] Present address: Henkel KG, Henkel-Strasse 67, D-4000 Düsseldorf (FRG).

[**] This work was supported by the Fonds der Chemischen Industrie, by the Minister für Wissenschaft und Forschung des Landes Nordrhein-Westfalen, and by BASF AG, Degussa AG, and Bayer AG. *C. N.* thanks the Stiftung Volkswagenwerk for a Kekulé Fellowship. We thank Prof. *W. A. König*, Hamburg, for valuable help with the GC *ee*-determination.



Scheme 1. A, B, C see text.

41–73% and enantiomeric excesses between 81 and 94% (Scheme 2, Table 1). The chiral auxiliary SAMP can be recovered from (*S*)-**5** as described in Refs. [1, 4].



Scheme 2. For experimental details see *Procedure*.

Table 1. Primary amines **4** prepared from the aldehydes R^1CHO **1** via the SAMP hydrazones (*S*)-**2** with orgaholithium compounds R^2Li. The amine (*S*)-**4a** was obtained with RAMP.

Product **4**	R^1	R^2	B.p. [°C/torr] [a]	Total yield [%]	$[\alpha]_D^{22}$ [°] (neat)	*ee* [%]
(*R*)-**4a**	C_6H_5	CH_3	80/20	47	+26.1	81
(*S*)-**4a**	C_6H_5	CH_3	87/25	48	−26.1	81
(*R*)-**4b**	t-C_4H_9	CH_3	55/95	41	− 4.5 [b]	81
(*S*)-**4c** [c]	c-C_6H_{11}	t-C_4H_9	39/0.4	64	−25.8	82
(*R*)-**4c** [c]	t-C_4H_9	c-C_6H_{11}	53/1	62	+27.4	90
(*R*)-**4d**	C_6H_5	n-C_4H_9	59/0.5	46	+14.1	85
(*S*)-**4d**	n-C_4H_9	C_6H_5	65/0.6	58	−13.9	83
(*S*)-**4e** [c]	i-C_3H_7	c-C_6H_{11}	39/0.6	63	+10.5	90
(*R*)-**4f**	i-C_3H_7	n-C_4H_9	76/40	57	+17.4 [d]	86
(*R*)-**4g** [e]	t-C_4H_9	n-C_4H_9	105/50 [f]	73	+31.9 [g]	93 [h]

[a] Data for short-path distillation. [b] $[\alpha]_D^{22} = 5.6°$ (neat) [9]. [c] The phenyl ring was hydrogenated during the N-N cleavage. [d] Measured in solution: $[\alpha]_D^{20}$ ($c = 3.3$, EtOH). [e] According to the GC retention time on a chiral stationary phase [6] **4g** has the (*S*)-configuration. [f] Oven temperature during Kugelrohr distillation. [g] Measured in solution: $[\alpha]_D^{22}$ ($c = 0.43$, benzene). [h] According to the ^{13}C-NMR spectrum **3g** is diastereomerically pure.

The *ee* values of the amines **4** were determined polarimetrically (**4b**), NMR spectroscopically by shift experiments with $Eu(hfc)_3$, and via the 3,3,3-trifluoro-2-methoxy-2-phenylpropionic acid (MPTA)-amides[5] (^1H, ^{13}C, ^{19}F), as well as by gas-chromatography on a chiral stationary phase after conversion into isopropylurea derivatives[6] [XE-60-C-valine-(*S*)-α-phenylethylamide]. The racemic amines *rac*-**4** required for comparison were synthesized analogously from the corresponding achiral *N,N*-dimethylhydrazones.[7]

Both enantiomers of the amines **4** can be obtained as desired by use of SAMP or RAMP [example (*R*)-**4a**/(*S*)-**4a** in Table 1] or by exchange of R^1 and R^2 in the synthetic building blocks [examples (*S*)-**4c**/(*R*)-**4c** and (*R*)-**4d**/(*S*)-**4d**]. The absolute configurations were determined polarimetrically (**4a**[8] and **4b**[9]) and via the CD spectra of the *N*-salicylidene derivatives.[10] They suggest a uniform relative topicity during mutual approach of the reactants.

All attempts to improve the diastereoselectivity by varying the chiral auxiliary have so far failed. Thus, only a slightly higher enantiomeric purity of 94% *ee* was found for (*R*)-**4g** on using the sterically more demanding (*S*)-1-amino-2-(1,1-dimethylmethoxymethyl)pyrrolidine.[11]

The new method of amination of aldehydes by nucleophilic addition to SAMP (or RAMP) hydrazones thus provides an enantioselective entry to both optical antipodes of α-substituted amines **4**.[12, 13]

Procedure

4: A solution of (*S*)-**2** (15 mmol) in a small amount of ether or THF was added at −78 °C under argon to a solution of R^2Li (30 mmol) in 50 mL ether or THF (in the case of hydrazones **2** without α-H atoms in R′, 15 mmol of R^2Li suffices). The reaction mixture was allowed to warm to room temperature within ca. 12 h and then poured into 50 mL of water, and extracted twice with 25 mL of ether. The combined extracts were dried over $MgSO_4$ and concentrated by evaporation. Subsequent short-path distillation afforded the air-sensitive hydrazines **3**. These were dissolved in 30–50 mL of methanol and hydrogenated in a Parr hydrogenation apparatus with freshly prepared alkaline Raney nickel [14]/H_2 (3.5–3.8 bar, 20–40 °C, 24 h). The catalyst was then removed by filtration over Celite and the filtrate evaporated to dryness. The residue was taken up in ether, refiltered, and treated with 1.5 equivalents of *p*-nitrobenzaldehyde. After 12 hours' stirring at room temperature, the resulting Schiff bases ($R_f \geq 0.9$) were separated from (*S*)-**5** (→recycling, $R_f \leq 0.2$) by column chromatography (SiO_2, ether/pentane). The solution was evaporated down (50 mL), treated with 3–4 N HCl, and stirred for 2 h. After removal of the aqueous phase, the solution was rendered alkaline with conc. KOH solution and re-extracted with ether. After drying over $MgSO_4$ the extract was evaporated down and distilled.

Received: September 8, 1986;
revised: October 7, 1986 [Z 1923 IE]
German version: *Angew. Chem. 98* (1986) 1118

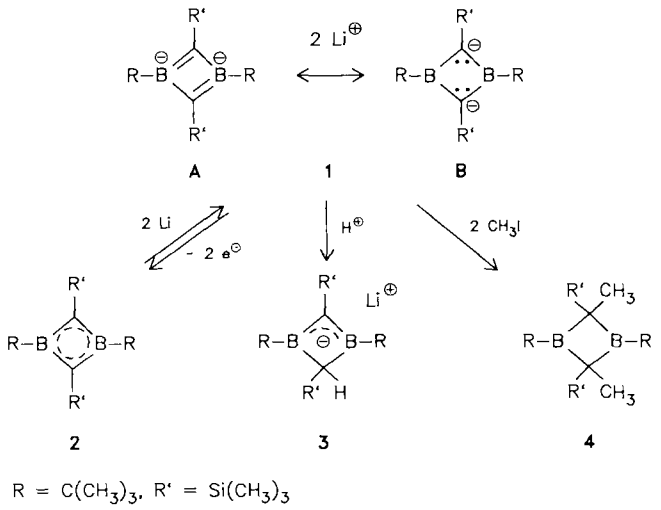
[1] a) D. Enders in J. D. Morrison (Ed.): *Asymmetric Synthesis, Vol. 3*, Academic Press, Orlando 1984, p. 275–339; b) D. Enders, H. Eichenauer, U. Baus, H. Schubert, K. A. M. Kremer, *Tetrahedron 40* (1984) 1345; c) D. Enders, K. Papadopoulos, B. E. M. Rendenbach, *Tetrahedron Lett. 27* (1986) 3491; D. Enders, B. E. M. Rendenbach, *Tetrahedron 42* (1986) 2235; D. Enders, P. Fey, H. Kipphardt, *Org. Synth. 65* (1987), in press.
[2] D. Enders, H. Schubert, *Angew. Chem. 96* (1984) 368; *Angew. Chem. Int. Ed. Engl. 23* (1984) 365.
[3] D. Enders in H. Nozaki (Ed.): *Current Trends in Organic Synthesis*, Pergamon Press, Oxford 1983, p. 151; D. Enders in W. Bartmann, B. M. Trost (Eds.): *Selectivity—a Goal for Synthetic Efficiency*, Verlag Chemie, Weinheim 1984, p. 65.
[4] D. Enders, P. Fey, H. Kipphardt, *Org. Prep. Proced. Int. 17* (1985) 1.
[5] J. A. Dale, H. S. Mosher, *J. Am. Chem. Soc. 95* (1973) 512.
[6] W. A. König, I. Benecke, S. Sievers, *J. Chromatogr. 238* (1982) 427.
[7] H. Schubert, *Dissertation*, Universität Bonn 1985.
[8] W. Leithe, *Ber. Dtsch. Chem. Ges. 65* (1932) 660.
[9] H. E. Smith, H. E. Ensley, *Can. J. Chem. 49* (1971) 2902.
[10] H. E. Smith, *Chem. Rev. 83* (1983) 359, and references cited therein.
[11] H. Kipphardt, *Dissertation*, Technische Hochschule Aachen 1986.
[12] Alternative methods are usually limited to aromatic aldehydes: a) G. Tsuchihashi, S. Iriuchijima, K. Maniva, *Tetrahedron Lett. 1973*, 3389; b) H. Takahashi, Y. Suzuki, *Chem. Pharm. Bull. 31* (1982) 4295, and references cited therein.
[13] All the new compounds gave correct elemental analyses and characteristic spectra (IR, ^1H-NMR, MS).
[14] *Organikum*, VEB Deutscher Verlag der Wissenschaften, Berlin 1977.

A 1,3-Diboratacyclobutadiene and Its Dimer, a Sandwich Compound with a Li_4 Layer**

By *Günter Schmidt, Gerhard Baum, Werner Massa,* and *Armin Berndt**

Dedicated to Professor Wilhelm Paul Neumann on the occasion of his 60th birthday

The 1,3-diboratacyclobutadiene (1,3-diboretanediide) **1** is formed, along with ca. 5% of products of unknown structure, upon reduction of the 1,3-dihydro-1,3-diborete **2**[1] with lithium powder in toluene. Compound **1** is isolated as the lithium salt, after a single recrystallization, in the form of pure yellow crystals. $[NiCl_2\{P(C_6H_5)_3\}_2]$ reoxidizes **1** to **2**. With bis(trimethylsilyl)amine in ethers, rapid monoprotonation of **1** occurs to give the 1,3-diboretanide **3**; with ethers, the reaction is slow. Compound **1** reacts with two equivalents of methyl iodide to give exclusively the—presumably *cis*-configurated—1,3-diboretane **4**.



R = $C(CH_3)_3$, R' = $Si(CH_3)_3$

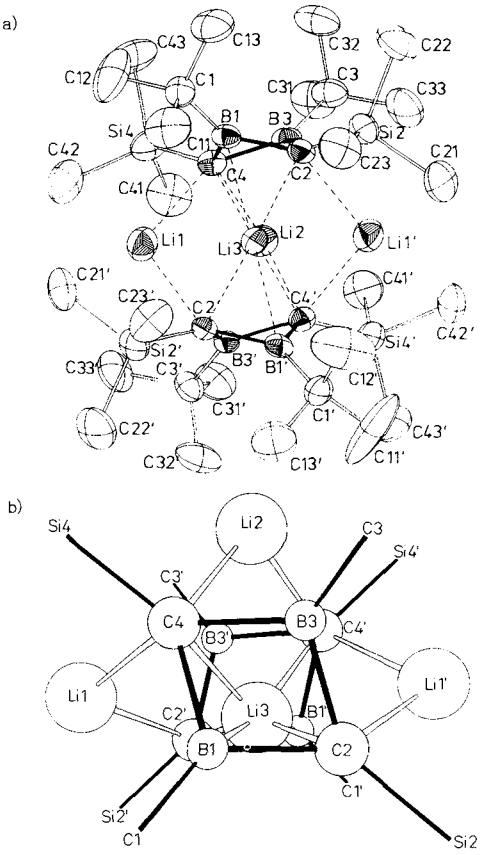


Fig. 1. ORTEP plot of the structure of dimeric **1** in the crystal (without H atoms). The ellipsoids of thermal vibration are at the 50% probability level. a) Projection roughly in the direction of the pseudo C_2 axis. b) Projection in the direction of the "sandwich axis." Arbitrary atomic radii, without methyl groups. Important distances [Å] and angles [°] averaged over both halves of the dimer: B1-C2 1.562(6), B1-C4 1.599(6), B3-C2 1.557(6), B3-C4 1.591(6) (average B-C(ring) 1.577), B1-C1 1.609(6), C2-Si2 1.832(4), B3-C3 1.619(6), C4-Si4 1.836(4), Li3-Li1 2.33(1), Li3-Li2 2.47(1), Li1-Li2 3.13(1); Li3-B1 2.237(8), Li3-C2 2.099(7), Li3-B3 2.454(8), Li3-C4 2.196(7), Li1-C4 2.346(8), Li1-C2' 2.276(8), Li2-C4 2.254(8); C2-B1-C4 101.3(3), B1-C2-B3 71.5(3), C2-B3-C4 101.9(3), B1-C4-B3 69.7(3) (average B-C-B 70.6, C-B-C 101.6).

The structures of the compounds **1**, **3**, and **4** were deduced from their ^1H-, ^{13}C-, and ^{11}B-NMR spectra[2] and from their pathway of formation; that of **1** was also derived from the reactions described and from an X-ray structure analysis. The strong shielding of the B atoms in **1** ($\delta(^{11}B) = 42$), compared with **4** ($\delta(^{11}B) = 81$) indicates considerable negative π charge at the boron atoms (1,3-diboratacyclobutadiene resonance structure **1A**). The ring C atoms in **1** ($\delta(^{13}C) = 93.5$) are shifted by 59 ppm to higher field in comparison with those of tetra-*tert*-butylcyclobutadiene ($\delta(^{13}C) = 152.7$);[4] this finding indicates considerable negative π charge at the ring carbon atoms (1,3-diboretanediide resonance structure **1B**).[5]

Compound **1** crystallizes as a dimer with a structure[6] that further expands the structural variety of organolithium compounds:[7] a layer of four Li atoms (greatest deviation from the common plane 0.013 Å) bridges two four-membered rings (Fig. 1). The separations of the Li atoms in the Li_4 layer are in part (Li3-Li1 2.33, Li3-Li2 2.47 Å) shorter than those found in the Li tetrahedra of tetrameric lithium compounds (average 2.56 Å[7]). The dimeric **1** possesses a pseudo C_2 axis in the Li_4 plane through Li2 and Li3. In the following discussion, therefore, average values of the geometric data for the two halfs of the dimer are given. The rings are arranged in an eclipsed fashion, a B atom lying above a C atom in each case; the lines drawn through the C2, C4 and C2', C4' atoms form an angle of 77° with each other. The separation of the centers of the four-membered rings is 3.84 Å. One Li atom (Li3) lies sandwiched between the rings, but—presumably owing to the unsymmetrical environment of the three Li neighbors—is displaced toward the Li-free side (angle formed between Li3 and the ring centers 155°). Apart from the two C atoms, therefore, only one of the two B atoms in each ring has a short distance from the Li atom (Li-C 2.09–2.20, Li3-B1 2.23, but Li3-B3 2.45 Å) (η^3 bond). Each of the remaining three Li atoms, which are situated in gaps between the bulky substituents, further bridges the rings from the outside through two C atoms (Li-C 2.25–2.38 Å). The atoms Li1 and Li1' have very short separations from methyl groups (Li1-C21 2.41, Li1-H212 2.19, Li1-H213 2.19 Å), which points to the existence of a metal-hydrogen interaction, as in the case for $LiB(CH_3)_4$ (Li-H 2.12 Å[8]).

[*] Prof. Dr. A. Berndt, G. Schmidt, G. Baum, Priv.-Doz. Dr. W. Massa
Fachbereich Chemie der Universität
Hans-Meerwein-Strasse, D-3550 Marburg (FRG)

[**] This work was supported by the Deutsche Forschungsgemeinschaft and the Fonds der Chemischen Industrie.

The rings themselves are strongly puckered: the puckering angle along C2C4 (C···C 2.45 Å) is 132°, so that the B atoms approach each other to within 1.82 Å, which is little more than the distance of a B-B single bond (1.71–1.75 Å[9]). In contrast, the 1,3-bis(dimethylamino)-2,4-di-*tert*-butyl-1,3-dihydro-1,3-diborete **2′**[10] (**2**, with R = $N(CH_3)_2$ and R′ = $C(CH_3)_3$) described by *Siebert* et al. is puckered along the B-B diagonal (2.16 Å), so that the C atoms come to within 1.81 Å of each other. The different puckering of **2′** and the dimeric **1** is reflected in the bond angles CBC and BCB, which are 101.6 and 70.6° on the average for the dimeric **1** and 74 and 92°, respectively, for **2′**. The B-C bonds within the four-membered rings are significantly longer for dimeric **1** (1.56–1.60 Å) than for **2′** (1.50 Å). This is presumably a consequence of the strong electrostatic repulsion within the doubly charged four-membered rings.[11] The bonds from the ring atoms to the substituents are in part considerably bent with respect to the partial planes of the rings (C-Si 25.2–34.4° with respect to the BCB plane, B-C 8.0–12.7° with respect to the CBC plane), so that substituents on opposite sides avoid each other. The twisting and puckering of the rings also reduces the steric hindrance between the large substituents. The especially strong bending of the C-Si bonds might be caused in part by steric interaction with the outer Li atoms as well as by the electronic influence of the Li atoms on the anionic C atoms.[12] Overall, a compact, nearly spherical shape of the dimeric **1** is found.

Experimental Procedure

1: **2** (2.27 g, 7.4 mmol) was stirred in 15 mL of toluene at room temperature with lithium powder (0.58 g, ca. 80 mmol) containing 2% sodium. After 15 h, the excess metal was separated from the solution using a G3 filter tube for inert gas handling and washed three times with 5 mL of toluene, and the yellow reaction solution was concentrated until it turned cloudy. The crystals that precipitated out after 15 h at −30°C were crystallized once from toluene. 1.78 g (75%) yellow crystals, m.p. = 190–195°C (dec.).

Received: September 2, 1986;
supplemented: September 18, 1986 [Z 1919 IE]
German version: *Angew. Chem. 98* (1986) 1123

[1] R. Wehrmann, Ch. Pues, H. Klusik, A. Berndt, *Angew. Chem. 96* (1984) 372; *Angew. Chem. Int. Ed. Engl. 23* (1984) 372.

[2] Spectra of **1** in C_6D_6, of **3** in [D_{10}]dimethoxyethane, of **4** in $CDCl_3$. ^{1}H-NMR: δ = 1.20 (s, 18H; *t*Bu), 0.33 (s, 18H; $SiMe_3$); ^{13}C-NMR: δ = 93.5 (br. s, 2C; BCB), 34.2 (q, 6C; *t*Bu), 23.0 (br. s, 2C; $BCMe_3$), 6.0 (q, 6C; $SiMe_3$); ^{11}B-NMR: δ = 42; ^{7}Li-NMR: δ = 0.67. **3**: Quantitative yield on the basis of ^{13}C-NMR spectroscopy; ^{1}H-NMR (C_6D_6): δ = 1.11 (s, 18H; *t*Bu), 0.85 (s, 1H; HCSi), 0.23 (s, 9H; $SiMe_3$), 0.04 (s, 9H; $SiMe_3$); ^{13}C-NMR (−40°C): δ = 129.8 (br. s, 1C; BCB), 33.2 (q, 6C; *t*Bu), 31.1 (br. d, 1C, ^1J(CH) = 114 Hz; BCH), 23.2 (br. s, 2C; $BCMe_3$), 6.1 (q, 3C; $SiMe_3$), 4.6 (q, 3C; $SiMe_3$); ^{11}B-NMR: δ = 40. **4**: Colorless crystals, m.p. = 143–145°C, crude yield 87%; ^{1}H-NMR: δ = 1.52 (s, 6H; CH_3), 1.04 (s, 18H; *t*Bu), 0.22 (s, 18H; $SiMe_3$); ^{13}C-NMR: δ = 50.6 (br. s, 2C; BCB), 27.9 (q, 6C; *t*Bu), 26.7 (br. s, 2C; $BCMe_3$), 17.9 (q, 2C; CH_3), 4.1 (q, 6C; $SiMe_3$); ^{11}B-NMR: δ = 81; for NMR data of comparable 1,3-diboretanes, see [3].

[3] R. Wehrmann, H. Klusik, A. Berndt, *Angew. Chem. 96* (1984) 810; *Angew. Chem. Int. Ed. Engl. 23* (1984) 826.

[4] G. Maier, S. Pfriem, U. Schäfer, R. Matusch, *Angew. Chem. 90* (1978) 552; *Angew. Chem. Int. Ed. Engl. 17* (1978) 520.

[5] Calculations (3-21G//3-21G) carried out on the unsubstituted 1,3-diboretanediide without counterions gave π charges of −0.425 at boron and −0.575 at carbon. The greater charge at carbon is due to its higher electronegativity (C, 2.5; B, 2.0); P. von R. Schleyer, private communication.

[6] Space group *Pccn*, Z = 8 dimers, a = 37.115(4), b = 12.268(1), c = 18.807(2) Å; 2995 unique reflections with $F > 3\sigma(F_o)$ measured on a four-circle diffractometer (CAD4, Enraf-Nonius) with $Mo_{K\alpha}$ radiation at −65°C; 397 parameters, H atoms refined with fixed isotropic temperature factors. R = 0.044. Further details of the crystal structure investigation may be obtained from the Fachinformationszentrum Energie, Physik, Mathematik GmbH, D-7514 Eggenstein-Leopoldshafen 2 (FRG), on quoting the depository number CSD-52182, the names of the authors, and the journal citation.

[7] W. N. Setzer, P. von R. Schleyer, *Adv. Organomet. Chem. 24* (1985) 353.

[8] W. E. Rhine, G. Stucky, S. W. Peterson, *J. Am. Chem. Soc. 97* (1975) 6401.

[9] M. Hildenbrand, H. Pritzkow, W. Siebert, *Angew. Chem. 97* (1985) 769; *Angew. Chem. Int. Ed. Engl. 24* (1985) 759.

[10] M. Hildenbrand, H. Pritzkow, U. Zenneck, W. Siebert, *Angew. Chem. 96* (1984) 371; *Angew. Chem. Int. Ed. Engl. 23* (1984) 371.

[11] T. Clark, D. Wilhelm, P. von R. Schleyer, *Tetrahedron Lett. 23* (1982) 3547, and references cited therein.

[12] Cf. the discussion for a dilithium benzocyclobutadienediide: G. Boche, H. Etzrodt, W. Massa, G. Baum, *Angew. Chem. 97* (1985) 858; *Angew. Chem. Int. Ed. Engl. 24* (1985) 863.

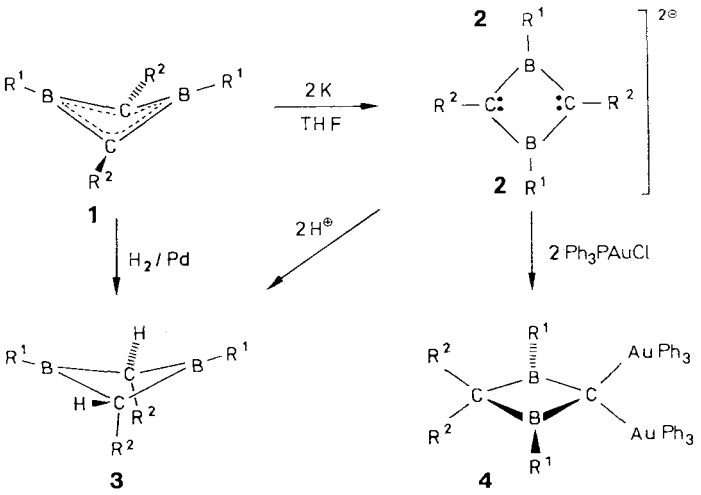
A Puckered and a Planar 1,3-Diboretane**

By *Pia Hornbach, Manfred Hildenbrand, Hans Pritzkow,* and *Walter Siebert**

1,3-Diboretanes were described earlier by *Berndt* et al.[1] We now report the first structurally confirmed 1,3-diboretanes (**3b** and **4b**).

The 1,3-dihydro-1,3-diboretes **1a**[2] and **1b** react with Na/K alloy in tetrahydrofuran (THF) to give the corresponding radical anions.[3] $\mathbf{1b}^{\ominus\ominus}$ ($a(^{11}B) = 8.6$, $a(^{29}Si) \approx 8.7$ G, $g = 2.0029$) undergoes further reduction to give the diamagnetic dianion **2b**, which can be isolated in the form of the powdery, reactive dipotassium salt having only two coordinated THF molecules (NMR spectra). This finding indicates good shielding of the potassium ions by the anion (cf. ref. [4]).

Protonation of **2b** with weakly acidic compounds ($HCCl_3$, $HN(SiMe_3)_2$) results in the formation of colorless 1,3-bis(diisopropylamino)-2,4-bis(trimethylsilyl)-1,3-diboretane **3b** (65% yield), which is also accessible by hydrogenation of **1b** using Pd/active carbon (85% yield). Reaction of **2b** with iodomethane affords **3b** with Me instead of H. According to the NMR spectrum, the B atoms of **3b** are deshielded by 12.1 ppm relative to those of **1b**. A high-



a, $R^1 = NMe_2$, $R^2 = t$Bu; **b**, $R^1 = N$*i*Pr_2, $R^2 = SiMe_3$

[*] Prof. Dr. W. Siebert, P. Hornbach, Dr. M. Hildenbrand, Dr. H. Pritzkow
Anorganisch-chemisches Institut der Universität
Im Neuenheimer Feld 270, D-6900 Heidelberg (FRG)

[**] This work was supported by the Deutsche Forschungsgemeinschaft, the Fonds der Chemischen Industrie, and BASF AG.

field shift from $\delta = 37$ to $\delta = 26$ is found for the C atoms in the ring. These data are in agreement with the loss of π-electron density in the ring.

The X-ray structure analysis (Fig. 1)[5a] shows that the puckering of the four-membered ring along C1C2 (32°) is significantly smaller than for **1a** (52°)[2] and **1b** (59°);[5b]

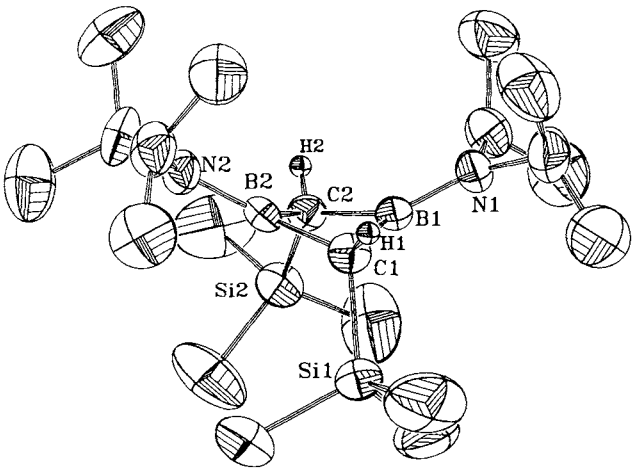


Fig. 1. ORTEP plot of the crystal structure of **3b** (thermal ellipsoids at 40% probability, methyl and *iso*-propyl H atoms omitted). Bond lengths [Å] and angles [°] (standard deviations 0.01 Å and 0.5°); calculated values for $C_2B_2H_6$ [6] in parentheses. BC 1.58–1.59 (1.587), BN 1.39, C(ring)Si 1.87; BCB 79.3 (78.6), CBC 96.8 (95.1); puckering angle 32.2 (36.2); for comparison **1b** (standard deviations 0.005 Å and 0.1°): BC 1.518 and 1.523, BN 1.388, C···C 1.805; BCB 89.0, CBC 72.8; puckering angle 59.

the value is in good agreement with that calculated for the 1,3-diboretane $C_2B_2H_6$ (36.2°).[6] The unsaturated ring (**1b**) and the saturated ring (**3b**) have different B–C distances (1.520 and 1.585 Å, respectively, (B–C) π bond in **1b**) and different angles (CBC = 72.8 and 96.8°, respectively). The structure of the four-membered ring in **3b** is similar to that in the dilithium-1,3-diboretanediide $[(Me_3C-B)_2(Me_3Si-C)_2]_2Li_4$,[4] in which the silyl groups are found in equatorial positions.

For further characterization, the dianion **2b** was allowed to react with Ph_3PAuCl. Brown and yellow crystals are formed which are not very air-sensitive but undergo decomposition upon sublimation. The brown crystals were identified as **4b**, which is formed by silyl group migration (cf. ref. [1]) and geminal substitution. According to an X-ray structure analysis (Fig. 2),[7] **4b** is surprisingly planar: The puckering of the four-membered ring along C1C2 is only 3°, presumably owing to the steric hindrance of the large substituents. Because of the different substituents on C1 and C2, the B–C distances are no longer the same: the B–C2 bonds are shorter than the B–C1 bonds.

The geometry of the Ph_3PAu substituents on C2 largely corresponds to that of other structures having geminal Ph_3PAu groups.[8] Only the Au–Au distance (2.98 Å) is larger, but still in accord with significant Au–Au interactions. Au1 and Au2 are not symmetrically arranged with respect to the four-membered ring; Au1 is closer to Si1. Thus, the silyl groups as well as P1 and P2 are no longer magnetically equivalent. A phenyl ring on P1 affects the methyl groups on Si1 via its anisotropy.

Our results confirm the structure calculated[6] for diboretanes. However, they also show that a planar structure is possible.

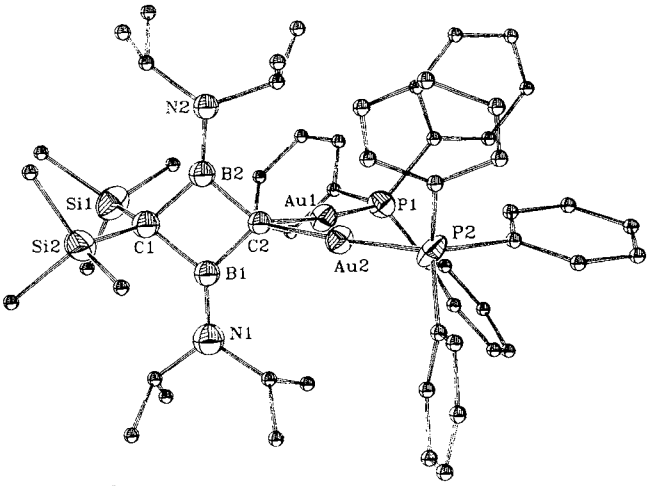


Fig. 2. ORTEP plot of the crystal structure of **4b** (thermal ellipsoids at 40% probability, phenyl, methyl, and *iso*-propyl C atoms with arbitrary radii). Bond lengths [Å] and angles [°] (standard deviations 0.03 Å and 1°): B1C2 1.53, B2C2 1.55, B1C1 1.62, B2C1 1.64; B1C1B2 81, B1C2B2 86, C1B1C2 97, C1B1C2 96; puckering angle 3.

Experimental Procedure

1b: $(Me_3Si)_2C=C(BCl_2)_2$ [3], obtained by addition of B_2Cl_4 to $Me_3Si-C\equiv C-SiMe_3$, was allowed to react with $HNiPr_2$ to give $(Me_3Si)_2C=C(BClNiPr_2)_2$. Its reaction, in turn, with Na/K alloy in THF or refluxing toluene (6–20 h), led, in analogy to the reaction of $(Me_3Si)_2C=C(BClt Bu)_2$ described in [1], to **1b**: 40% yield, b.p. = 120–130°C/0.01 torr, m.p. = 170°C (dec.). ^{1}H-NMR (300 MHz, $CDCl_3$): $\delta = 0.08$ (s, 18H; $SiCH_3$), 1.09, 1.12 (d, 12H each; $NCCH_3$), 3.44 (sept, 4H, $^3J(HH) = 6.6$ Hz; NCH); ^{11}B-NMR ($CDCl_3$): $\delta = 31.4$; ^{13}C-NMR ($CDCl_3$): $\delta = 1.20$ ($SiCH_3$), 23.13 ($NCCH_3$), 24.85 ($NCCH_3$), 37 (br.; CB), 49.47 ($NCCH_3$); MS: *m/z* 392 ($M^{\oplus}$, 93%), 319 ($[M-SiMe_3]^{\oplus}$, 47%).

2b: a) **1b** (392 mg, 1 mmol) was stirred with NaK_8 (74 mg, 0.2 mmol) in 10 mL of THF. After 15 h, the mixture was filtered, THF was removed, and the residue was washed with petroleum ether (PE). The white dipotassium salt of **2b** was dried in vacuum. Yield 16%. b) $(Me_3Si)_2C=C(BClNiPr_2)_2$ (4.62 g, 10 mmol) was treated with NaK_8 (1.48 g, 4.4 mmol) in THF. After 15–25 h, the reaction mixture was filtered, the THF was removed, and the residue was washed with PE and dried. Yield 65–80%. ^{1}H-NMR (90 MHz, C_6D_6): $\delta = 0.26$ (s, 18H; $SiCH_3$), 1.33 (d, 24H; $NCCH_3$), 3.11 (sept, 4H, $^3J(HH) = 6.5$ Hz; NCH); ^{11}B-NMR (C_6D_6): $\delta \approx 12$ (halfwidth ca. 1200 Hz); ^{13}C-NMR (C_6D_6): $\delta = 8.08$ (q; $SiCH_3$), 46.9 (br.; CB), 25.39 (q; $NCCH_3$), 67.88 (d; $NCCH_3$); ^{29}Si-NMR (C_6D_6): $\delta = -20.6$.

3b: **1b** (392 mg, 1 mmol) was stirred with Pd/active carbon (112 mg) in PE under H_2 for 2 d. After filtration of the reaction mixture, **3b** was sublimed at 100°C/0.01 torr. M.p. = 125°C. ^{1}H-NMR (300 MHz, $CDCl_3$): $\delta = 0.10$ (s, 18H; $SiCH_3$), 0.69 (s, 2H; BCH), 1.13 (d, 12H; $NCCH_3$), 1.14 (d, 12H; $NCCH_3$), 3.58 (sept, 4H, NCH); ^{11}B-NMR ($CDCl_3$): $\delta = 43.5$; ^{13}C-NMR ($CDCl_3$): $\delta = 3.93$ ($SiCH_3$), 23.46 ($NCCH_3$), 23.88 ($NCCH_3$), 26 (br.; CB), 47.94 ($NCCH_3$); ^{29}Si-NMR ($CDCl_3$): $\delta = 4.5$.

3b with Me instead of H: MeI (740 mg, 5.2 mmol) was added to **2b** (1.6 g, 2.6 mmol) in THF at −80°C. KI precipitated immediately. Sublimation at 125–130°C/0.01 torr afforded colorless crystals. M.p. = 118°C; yield: 494 mg (1.17 mmol, 45%). ^{1}H-NMR (90 MHz, C_6D_6): $\delta = 0.42$ (s, 18H; $SiCH_3$), 1.22 (s, 6H; $BCCH_3$), 1.37 (d, 24H, $^3J(HH) = 7$ Hz; $NCCH_3$), 4.18 (sept, 4H; NCH); ^{11}B-NMR (C_6D_6): $\delta = 48.7$; ^{13}C-NMR (C_6H_6): $\delta = 5.3$ (s; $SiCH_3$), 19.4 (s; $BCCH_3$), 26.3 (s; $NCCH_3$), 26.5 (s; $NCCH_3$), 49.9 (s; $NCCH_3$), 50.3 (s; $NCCH_3$); MS: *m/z* 422 ($M^{\oplus}$, 19%), 407 ($[M-Me]^{\oplus}$, 28%).

4b: **2b** (307 mg, 0.5 mmol) in 30 mL of THF was treated at −90°C with Ph_3PAuCl (494 mg, 1 mmol) in 10 mL of THF. The orange reaction solution turned dark red above −65°C. The THF was removed at room temperature; the residue was dissolved in PE, the resulting solution was filtered, and the combined filtrates were treated with toluene/pentane. Upon cooling, brown and slightly yellow crystals were formed. Yield: 230 mg **4b** (35%); m.p. = 154°C (dec.). (The constitution of the yellow crystals is not known). ^{1}H-NMR (300 MHz, C_6D_6): $\delta = 0.46$ (s, 9H; $SiCH_3$), 0.49 (s, 9H; $SiCH_3$), 1.26, 1.28, 1.52, 1.87 (d, 6H each, $^3J(HH) = 6.5$ Hz; $NCCH_3$), 3.59 (sept, 2H; NCH), 4.27 (sept, 2H; NCH); ^{11}B-NMR (C_6D_6): $\delta = 45.9$; ^{31}P-NMR (C_6D_6): $\delta = 37.8$, 41.2.

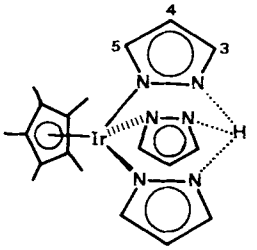
Received: September 2, 1986;
supplemented: September 25, 1986 [Z 1918 IE]
German version: *Angew. Chem.* 98 (1986) 1121

[1] R. Wehrmann, H. Klusik, A. Berndt, *Angew. Chem. 96* (1984) 810; *Angew. Chem. Int. Ed. Engl. 23* (1984) 826.
[2] M. Hildenbrand, H. Pritzkow, U. Zenneck, W. Siebert, *Angew. Chem. 96* (1984) 371; *Angew. Chem. Int. Ed. Engl. 23* (1984) 371.
[3] M. Hildenbrand, *Dissertation*, Universität Heidelberg 1986.
[4] G. Schmidt, G. Baum, W. Massa, A. Berndt, *Angew. Chem. 98* (1986) 1123; *Angew. Chem. Int. Ed. Engl. 25* (1986) 1111.
[5] a) **3b**: monoclinic, $P2_1/a$, $a=16.970(3)$, $b=9.169(2)$, $c=19.664(4)$ Å, $\beta=115.58(2)°$, $V=2759.8$ Å^3, $Z=4$. 2519 unique reflections observed with $I\geq 2\sigma(I)$; two-circle diffractometer, $Mo_{K\alpha}$ radiation, ω-scan, refinement of Si, N, C, B anisotropically, methyl groups as rigid groups, $R=0.076$, $R_w=0.063$ ($w=\sigma(F)^{-2}$). Further details of the crystal structure investigation may be obtained from the Fachinformationszentrum Energie, Physik, Mathematik GmbH, D-7514 Eggenstein-Leopoldshafen 2 (FRG), on quoting the depository number CSD-52130, the names of the authors, and the journal citation. b) **1b**: monoclinic, $C2/c$, $a=18.409(3)$, $b=9.287(2)$, $c=17.101(3)$ Å, $\beta=105.53(2)°$, $V=2817.0$ Å^3, $Z=4$. 1943 unique reflections observed with $I\geq\sigma(I)$; two-circle diffractometer, $Mo_{K\alpha}$ radiation, ω-scan, refinement of Si, N, C, B anisotropically, methyl groups as rigid groups, $R=0.065$, $R_w=0.059$. Further details of the crystal structure investigation may be obtained from the Fachinformationszentrum Energie, Physik, Mathematik GmbH, D-7514 Eggenstein-Leopoldshafen 2 (FRG), on quoting the depository number CSD-52130, the names of the authors, and the journal citation.
[6] K. Krogh-Jespersen, D. Cremer, J. D. Dill, J. A. Pople, P. von R. Schleyer, *J. Am. Chem. Soc. 103* (1981) 2589.
[7] **4b**: rhombic, $Pc2_1n$, $a=15.181(2)$, $b=16.497(2)$, $c=23.115(2)$ Å, $V=5789$ Å^3, $Z=4$. 4151 unique reflections observed with $I\geq\sigma(I)$; two-circle diffractometer, $Mo_{K\alpha}$ radiation, ω-scan, refinement of Au, P, Si anisotropically, N, C, B isotropically, phenyl rings as rigid groups, H atoms at calculated positions (methyl H atoms as rigid groups), $R=0.050$, $R_w=0.040$. Further details of the crystal structure investigation may be obtained from the Fachinformationszentrum Ehergie, Physik, Mathematik GmbH, D-7514 Eggenstein-Leopoldshafen 2 (FRG), on quoting the depository number CSD-52130, the names of the authors, and the journal citation.
[8] J. Vincente, M. T. Chicote, J. A. Cayuelas, J. Fernandez-Baeza, P. G. Jones, G. M. Sheldrick, P. Espinet, *J. Chem. Soc. Dalton Trans. 1985*, 1163; E. I. Smyslova, E. G. Perevalova, V. P. Dyadchenko, K. I. Grandberg, Yu. L. Slovokhotov, Yu. T. Struchkov, *J. Organomet. Chem. 215* (1981) 269.

Prototropism in (Pentamethylcyclopentadienyl)iridium Complexes with Pyrazole Ligands**

By *Daniel Carmona, Luis A. Oro,* M. Pilar Lamata, José Elguero,* María del Carmen Apreda, Concepción Foces-Foces,* and *Félix H. Cano**

There is an increasing interest in (pentamethylcyclopentadienyl)iridium complexes because of their ability to activate the C–H bonds of alkanes.[1] Most of this work has been carried out on trimethylphosphane derivatives.[1a,b] In contrast, few (pentamethylcyclopentadienyl)iridium complexes with nitrogen donor groups as ancillary ligands have been prepared.[2,3] We now describe the preparation and characterization of new mononuclear (pentamethylcyclopentadienyl)iridium(III) complexes with pyrazole ligands, some of them showing very unusual ^{1}H-NMR behavior in solution.

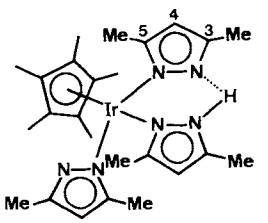


2 [(C$_5$Me$_5$)Ir(pz)$_2$(Hpz)] **2**

When [{(C$_5$Me$_5$)IrCl}$_2$(μ-Cl)$_2$] **1**[4] was allowed to react with pyrazole (Hpz) and KOH in methanol, complex **2** was obtained and identified on the basis of ^{1}H-NMR, IR, and analytical data.[5] In particular, the ^{1}H-NMR spectrum (200 MHz, $CDCl_3$, 293 K) shows, in addition to the C_5Me_5 signal at $\delta=1.50$, thrice the characteristic AMX system of *N*-substituted pyrazole ($\delta=6.14$ (H^4), 6.99 (H^5), 7.61 (H^3); $J(H^3H^4)=J(H^4H^5)=2.0$, $J(H^3H^5)=0.6$ Hz), and an N–H proton at $\delta=11.24$ (intensity ratio 15:9:1).[6] Thus the three pyrazole ligands are identical; although an *inter*molecular proton exchange cannot be completely ruled out, an *intra*molecular exchange should be more favorable because the pyrazole ligands should be capable of attaining any rotational conformation around the Ir–N bonds, and therefore a dynamic hydrogen bonding between the three pyrazoles is likely.

A "chelated proton" structure with only two pyrazole rings was proposed by *King* and *Bond*[7] for [(C$_5$H$_5$)Co(C$_n$F$_{2n+1}$)(pz)(Hpz)] (n = 1–3). In the case of **2**, our representation does not mean necessarily that there is a "bifurcated" hydrogen bond but most probably that three "chelated proton" structures are equilibrating fast on the NMR time scale.

The IR spectrum (Nujol mull) of complex **2** shows a medium and very broad $\tilde{\nu}$(NH) band (3200–2000 cm^{-1}) which suggests that, also in the solid state, a strong N–H···N association is present,[8] most probably between two pyrazole ligands from the same molecule.



3 [(C$_5$Me$_5$)Ir(dmpz)$_2$(Hdmpz)] **3**

When the reaction was carried out with 3,5-dimethylpyrazole (Hdmpz), the mononuclear yellow complex **3** was obtained according to spectroscopic and analytical data.[9] Its ^{1}H-NMR spectrum ($CDCl_3$, 200 MHz, 293 K) shows, along with the signal of the C_5Me_5 group at $\delta=1.45$, two classes of 3,5-dimethylpyrazole ligands in a 2:1 ratio. The two identical dmpz ligands share an N–H proton as shown by the relative deshielding of H^4 ($\delta=2.33$ (Me^3), 1.50 (Me^5), 5.72 (H^4), whereas the remaining pyrazole ligand is unprotonated ($\delta=2.22$ (Me^3), 0.42 (Me^5), 5.39 (H^4).[10] Two

[*] Prof. Dr. L. A. Oro, Dr. D. Carmona
Departamento de Química Inorgánica,
Instituto de Ciencia de Materiales de Aragón,
Universidad de Zaragoza—C.S.I.C.
E-50009 Zaragoza (Spain)
Dr. M. P. Lamata
Cátedra de Química I,
Escuela Universitaria de Ingenieros Técnicos Industriales
Corona de Aragón 35, E-50009 Zaragoza (Spain)
Prof. Dr. J. Elguero
Instituto de Química Médica, C.S.I.C.
Juan de la Cierva 3, E-28006 Madrid (Spain)
Prof. Dr. F. H. Cano, Dr. M. C. Apreda, Dr. C. Foces-Foces
Departamento de Rayos X, Instituto Rocasolano, C.S.I.C.
Serrano 119, E-28006 Madrid (Spain)

[**] This work was supported by C.A.I.C.Y.T. We thank Prof. *S. García-Blanco* for facilities.

features are noteworthy in this spectrum: (1) there is no prototropic exchange with the third ligand; (2) the signal of the Me^5 group is at a very low frequency in the third ligand.

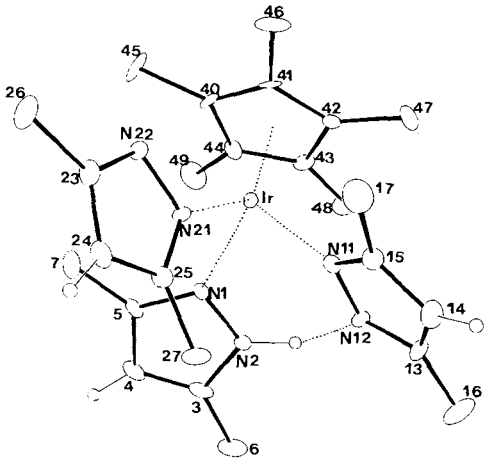
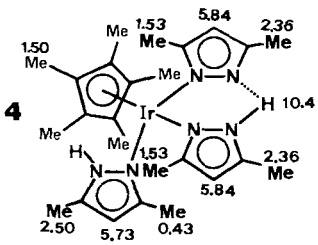


Fig. 1. ORTEP drawing of the crystal structure of complex **3**. Selected bond distances [Å] and angles [°]: Ir-C_5Me_5 1.800(7), Ir-N1 2.092(6), Ir-N11 2.078(6), Ir-N21 2.085(6), N2···N12 2.647(8); N1-Ir-C_5Me_5 125.3(3), N11-Ir-C_5Me_5 124.3(3), N21-Ir-C_5Me_5 131.9(4), N1-Ir-N11 89.2(2), N1-Ir-N21 84.8(2), N11-Ir-N21 87.8(2).

These observations prompted us to determine the X-ray structure of **3**.[11] Although the H atoms could not be located exactly, they are shown in Figure 1 for the sake of clarity. This structure explains both observations. (1) There is a short N2–N12 distance (2.647(8) Å) and the presence of an H atom between the two N atoms proves the existence of a strong hydrogen bond between the two ligands. The barrier for the proton transfer between N2 and N12 is certainly very low, and in solution, in accord with ^{1}H-NMR measurements, the proton exchange is fast. (2) The third ligand is in such a conformation that the nitrogen lone pair of N22 cannot participate in the prototropism and C27 lies just above one pyrazole ring, so that the Me^5 group is shielded by the ring current.



4 $[(C_5Me_5)Ir(dmpz)(Hdmpz)_2]$ **4**

Treatment of compound **3** in CH_2Cl_2/Me_2CO with an equimolar amount of aqueous HBF_4 afforded the yellow complex **4**.[12] The ^{1}H-NMR spectrum ($CDCl_3$, 293 K) of this complex clearly shows that the second proton is bonded to the nonchelated ligand, since its signals are the most affected. Consequently, a strong and sharp $\tilde{\nu}$(NH) band at 3410 cm^{-1} was observed in its IR spectrum (Nujol), along with the expected broad absorption in the 3200–2000 cm^{-1} region.[8]

Similarly, the addition of an equimolar amount of aqueous HBF_4 to complex **2** gives rise to the formation of $[(C_5Me_5)Ir(Hpz)_3](BF_4)_2$ **5**, which could also be prepared by the reaction of the solvated complex $[(C_5Me_5)Ir(Me_2CO)_3](BF_4)_2$ **6** with pyrazole.[13]

The strikingly different behavior of pyrazole and 3,5-dimethylpyrazole complexes is related to the steric hindrance of the 5-methyl group.[15] This substituent imparts to complex **3** a spatial structure in which a hydrogen bond links two ligands, while the third ligand does not participate in the prototropic exchange and remains, as expected, more basic when competing for a second proton.

Received: May 26, 1986;
revised: September 5, 1986 [Z 1791 IE]
German version: *Angew. Chem. 98* (1986) 1091

[1] a) A. J. Janowicz, R. G. Bergman, *J. Am. Chem. Soc. 105* (1983) 3929; b) M. J. Wax, J. M. Stryker, J. M. Buchanan, C. A. Kovac, R. G. Bergman, *ibid. 106* (1984) 1121; c) J. K. Hoyano, A. D. McMaster, W. A. G. Graham, *ibid. 105* (1983) 7190; d) recent review: R. H. Crabtree, *Chem. Rev. 85* (1985) 245.

[2] P. M. Maitlis, *Chem. Soc. Rev. 10* (1981) 1.

[3] L. A. Oro, D. Carmona, M. P. Puebla, M. P. Lamata, C. Foces-Foces, F. H. Cano, *Inorg. Chem. Acta 112* (1986) L11.

[4] J. W. Kang, K. Moseley, P. M. Maitlis, *J. Am. Chem. Soc. 91* (1969) 5970.

[5] *Experimental procedure:* **2**: To a suspension of **1** (100.0 mg, 0.125 mmol) in methanol (10 mL), pyrazole (51.3 mg, 0.753 mmol) and 5.84 mL of a methanolic solution of KOH (0.0852 M, 0.497 mmol) were added. Stirring (0.5 h), evaporation of the solvent, and recrystallization from CH_2Cl_2/*n*-hexane afforded yellow crystals of complex **2**; yield: 93.0 mg (70%); correct elemental analysis (C, H, N).

[6] The ^{13}C-NMR spectrum (75 MHz, $(CD_3)_2CO$, 293 K) of **2** is consistent with the proposed structure: δ=8.5 (^1J=128.5 Hz; C_5Me_5), 88.1 (^2J=2.8; C_5Me_5), 139.2 (^1J=183.9, ^2J=8.2, ^3J=5.4; C^3), 104.8 (^1J=172.9, ^2J=^2J=10.5; C^4), 136.6 (^1J=181.7, ^2J=^3J=6.9; C^5).

[7] R. B. King, A. Bond, *J. Am. Chem. Soc. 96* (1974) 1334.

[8] L. A. Oro, D. Carmona, M. P. Lamata, A. Tiripicchio, F. J. Lahoz, *J. Chem. Soc. Dalton Trans. 1986*, 5, and references cited therein.

[9] Complex **3** was prepared analogously to complex **2** [5], but using Hdmpz instead of Hpz. Yield: 70%; IR (Nujol): $\tilde{\nu}$=3200–2000 cm^{-1} (m, very broad; $\tilde{\nu}$(NH) [7]; correct elemental analysis (C, H, N).

[10] The ^{13}C-NMR spectrum (75 MHz, $(CD_3)_2CO$, 293 K) of compound **3** shows the following signals: δ=8.7 (C_5Me_5), 88.1 (C_5Me_5), 12.3 and 12.7 (Me^3 and Me^5), 149.9 (C^3), 106.0 (C^4), 144.4 (C^5) for the two Hdmpz ligands; 14.0 (Me^3), 11.1 (Me^5), 147.0 and 146.5 (C^3 and C^5) and 103.3 (C^4) for the third dmpz ligand.

[11] Crystal structure analysis of **3**: $P\bar{1}$, a=16.590(3), b=9.444(1), c=8.944(1) Å, α=100.97(1), β=75.95(1), γ=104.28(1)°, V=1034.7(3) Å^3, Z=2, R=0.044 for 4378 independent reflections with $I \geq 3\sigma(I)$ (Philips PW 1100 diffractometer, $Cu_{K\alpha}$). Further details of the crystal structure investigation may be obtained from the Fachinformationszentrum Energie, Physik, Mathematik GmbH, D-7514 Eggenstein-Leopoldshafen 2 (FRG), on quoting the depository number CSD-52145, the names of the authors, and the journal citation.

[12] *Experimental procedure:* **4**: A solution of **3** (150.0 mg, 0.244 mmol) in 10 mL of CH_2Cl_2/Me_2CO (4:1, v/v) and 48.6 µL of aqueous HBF_4 (wt.-% 35%, 0.244 mmol) was stirred for 0.5 h at room temperature. After concentration of the solution, addition of diethyl ether yields yellow crystals which were filtered off, washed with diethyl ether, and air dried. Yield: 144.1 mg (84%); correct elemental analysis (C, H, N).

[13] *Experimental procedures:* **5**: From **2**: Complex **5** was prepared analogously to complex **4** from **3** [12] but using a molar ratio HBF_4:**2** = 2:1. Yield: 74%. From **6** [14]: To a solution of **6** (prepared in situ by treating **1** (150.2 mg, 0.188 mmol) with $AgBF_4$ (147.1 mg, 0.755 mmol) in acetone (10 mL)), pyrazole (102.4 mg, 1.504 mmol) was added. The resulting solution was stirred for 1 h. Complex **5** was isolated by partial vacuum-evaporation and subsequent addition of diethyl ether. Yield: 213.0 mg (80%); ^{1}H-NMR (200 MHz, $(CD_3)_2CO$, 293 K, TMS ext.): δ=1.64 (C_5Me_5), 6.72 (H^4), 8.06, 8.18 (H^3, H^5), $J(H^3H^4)$=$J(H^4H^5)$=3 Hz and 12.37 (broad, NH); correct elemental analysis (C, H, N).

[14] C. White, S. J. Thompson, P. M. Maitlis, *J. Chem. Soc. Dalton Trans. 1977*, 1654.

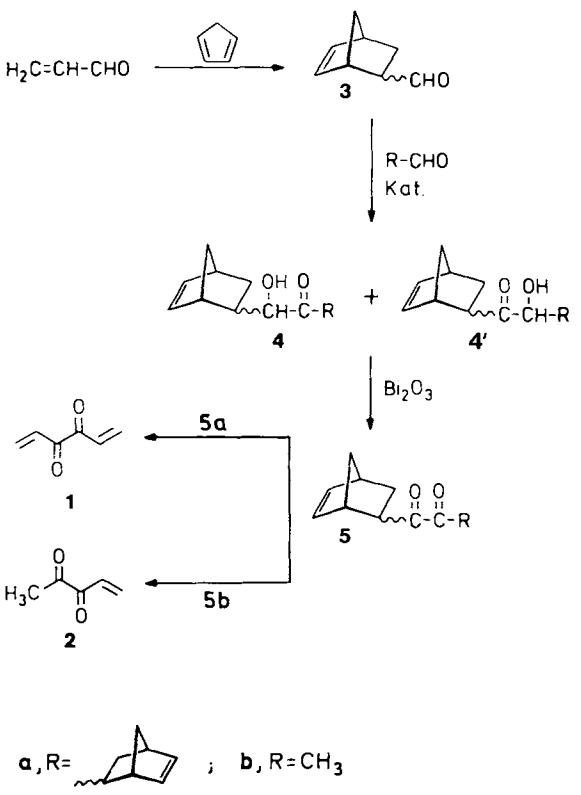
[15] Compare with the ^{1}H-NMR data of *ortho*- and *para*-methyl derivatives of $[(C_5Me_5)Rh(PMe_3)(C_6H_5)X]$; W. D. Jones, F. J. Feher, *Inorg. Chem. 23* (1984) 2376.

Divinylglyoxal and Methylvinylglyoxal**

By *Roland Kramme, Hans-Dieter Martin,* Bernhard Mayer,* and *Ralf Weimann*

Dedicated to Professor Edgar Heilbronner on the occasion of his 65th birthday

The spectroscopic and conformational properties of 1,2-diketones have been the subject of numerous studies in the past few years.[1,2] Interrelated with these properties are the colors of such simple organic chromophores. Open-chain, aliphatic 1,2-diketones with unsubstituted vinyl groups, however, were hitherto preparatively inaccessible. Only in the case of the alkylvinyl derivatives were the diketones obtainable, albeit in poor yields (2–10%).[3a] Methylvinylglyoxal (4-pentene-2,3-dione) **2** has been postulated as a significant component of the dione fraction formed in the tropospheric photooxidation of aromatic hydrocarbons.[3b] As we had already successfully prepared cyclobutenedione by gas-phase pyrolysis,[4] we resorted to the same method for the synthesis of divinylglyoxal (1,5-hexadiene-3,4-dione) **1** and methylvinylglyoxal (4-pentene-2,3-dione) **2**.



The dione **5** required for pyrolysis was synthesized essentially according to the method described by *Stetter* et al.[5] The bicyclic aldehyde **3** was obtained as an *endo/exo* mixture from cyclopentadiene and acrolein by Diels-Alder reaction. Subsequent reaction of **3** with aldehydes in the presence of thiazolium salt as catalyst afforded the acyloins **4** and **4'**, which could be oxidized with Bi_2O_3 in acetic acid solution to the 1,2-diketones **5**.[6] Gas-phase pyrolysis of **5a** and **5b** at 600°C/0.01 torr furnished **1** and **2** in yields of 81 and 89%, respectively.[7]

The compounds **1** and **2** are excellent dienophiles. With cyclopentadiene, for example, the *endo* products are formed highly stereoselectively at room temperature: **5a** > 98% as a diastereomeric mixture of the *meso* and D,L forms; **5b** ≈ 90%.[6]

The UV spectra of flexible 1,2-diketones usually show a maximum between 350 and 450 nm; further bathochromic shifts caused by various effects are observed.[4] As a result, all these compounds are colorless or bright yellow to orange. The position of the $n\pi^*$ maximum is influenced substantially by the torsion angle between the two carbonyl groups. This effect can be exploited for the conformational analysis of glyoxal derivatives, since a correlation of the wave number of the transition and the torsion angle has already been well documented for aliphatic 1,2-diketones.[2] From Figure 1 it can be seen that the measured absorption at ca. 23000 cm^{-1} for **1** and **2** corresponds to a CO-CO torsion angle of ca. 165°, which in turn corresponds to an almost antiperiplanar dicarbonyl unit-consistent with the yellow color of **1** and **2**.

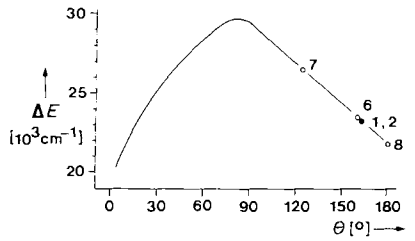


Fig. 1. Absorption maxima as a function of the torsion angle between the carbonyl groups: **1** and **2** ca. 165°, di-*tert*-butylglyoxal (2,2,5,5-tetramethyl-3,4-hexanedione) **7** 122° [2], dimethylglyoxal (biacetyl) **6** 160° [2], glyoxal **8** 180° [2]. (The left-hand side of the curve is ignored, since there is no synperiplanar arrangement in open-chain diones.)

Further insights into the electronic properties of **1** and **2** are provided by photoelectron spectroscopy (Fig. 2). The measured ionization energies are listed in Table 1 together with the energies assigned on the basis of MNDO,[8] MINDO/3[9] and HAM/3[10] model calculations, assuming the validity of Koopmans theorem.[11] A comparison with the data for known 1,2-diketones reveals that: the splitting between n_+ and n_- remains unaltered on going from biacetyl via **2** to **1** (n_+ and n_- are the n combinations formed by hyper- and homoconjugative interaction, respectively). The value of 1.9 eV for Δn lies in the middle of the usual range.[12] Noteworthy, is the intensity distribution in the PE spectrum of **1**: it is approximately 1 : 2 : 1. This would indicate that the ionization band at 10.78 eV is consistent with the theoretical predictions based on two π-ionization processes, which are not resolved in the spectrum. With respect to their ionization energy, the π orbitals of the two vinylglyoxals **1** and **2** are comparable with the π orbitals of acrolein. From the ionization energies I_j^m for **1** and **2** and the orbital energies of **1** calculated for two vinyl-CO torsion angles (0°, 51°) (Table 1), the following conclusion can be drawn: the vinyl group is comparable with a methyl group regarding its effect on the n_+ and n_- levels, and the n-ionization energies show no significant dependence on the vinyl-CO torsion angle.

[*] Prof. Dr. H.-D. Martin, Dipl.-Chem. R. Kramme, Dr. B. Mayer, Dipl.-Chem. R. Weimann
Institut für Organische Chemie I der Universität
Universitätsstrasse 1, D-4000 Düsseldorf (FRG)

[**] Small and Medium-Sized Rings Part 57. This work was supported by the Deutsche Forschungsgemeinschaft, the Fonds der Chemischen Industrie, and BASF AG.—Part 56: M. Kummer, G. Martin, H.-D. Martin, *Angew. Chem. 98* (1986) 995; *Angew. Chem. Int. Ed. Engl. 25* (1986) 1018.

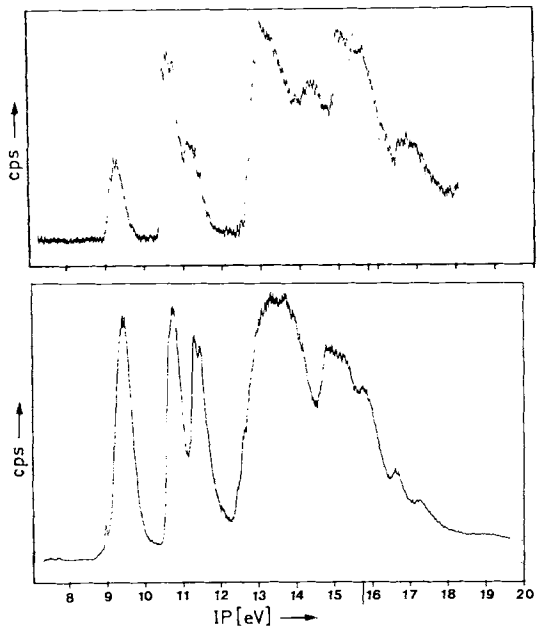


Fig. 2. He(1α)-photoelectron spectra of **1** (top) and **2** (bottom).

Table 1. Ionization energies I_j^m/eV (error ±0.03 eV) of **1** and **2**. Assignments according to MNDO, MINDO/3, and HAM/3. CO-CO torsion angle always 165°. A: Vinyl-CO torsion angle: A 0°, B optimized. Other parameters MNDO- and MINDO/3-optimized; HAM/3 calculations with MNDO-optimized parameters.

I_j^m		MNDO A	MNDO B	MINDO/3 A	MINDO/3 B	HAM/3 A	HAM/3 B [a]
1							
9.33	n_+	10.28	10.28	8.99	8.99	9.23	9.29
10.78	π	10.67	10.72	10.60	10.60	10.16	10.16
		10.68	10.73	10.63	10.63	10.19	10.28
11.25	n_-	12.47	12.48	11.30	11.30	11.13	11.29
2							
9.42	n_+	10.28	10.28	9.09	9.11	9.33	9.33
10.78	π	10.72	10.72	10.66	10.63	10.34	10.34
11.32	n_-	12.37	12.37	11.23	11.23	11.15	11.15

[a] In the case of **1**, vinyl-CO torsion angle 51°.

Experimental

5a and **5b** were pyrolized at 600°C and 0.01 to 0.02 torr in a gas-phase pyrolysis apparatus (small tube furnace fitted with quartz tube and directly coupled to four cooling traps). The cooling traps directly adjacent to the furnace, and in which the products were collected, were cooled to −78°C (1st trap) and −178°C (2nd trap), respectively. The storage vessel for **5** was heated to 110°C in the case of **5a**, and to 60°C in the case of **5b**. After ca. 2 h, there was no longer any starting compound **5** in the storage vessel; the first cooling trap contained the dione **1** (81%) or **2** (89%), the second trap cyclopentadiene.

Received: June 6, 1986 [Z 1809 IE]
German version: *Angew. Chem. 98* (1986) 1134

CAS Registry numbers:
1, 104910-78-3; **2**, 91238-45-8; **5a**, 74895-76-4; **5b**, 104910-80-7.

[1] R. Isaksson, T. Liljefors, *J. Chem. Soc. Perkin Trans. 2 1983*, 1351.
[2] P. L. Verheijdt, H. Cerfontain, *J. Chem. Soc. Perkin Trans. 2 1982*, 1541.
[3] a) S. L. T. Thuan, J. Wieman, *C. R. Hebd. Seances Acad. Sci. Ser. C 272* (1971) 233; b) P. B. Shepson, E. O. Edney, E. W. Corse, *J. Phys. Chem. 88* (1984) 4122.
[4] B. Albert, C. Heller, R. Iden, G. Martin, H.-D. Martin, B. Mayer, A. Oftring, *Isr. J. Chem. 25* (1985) 74.
[5] H. Stetter, R. Y. Ramsch, H. Kuhlmann, *Synthesis 1976*, 733; H. Stetter, G. Dämbkes, *ibid. 1977*, 403; *1980*, 309.
[6] *meso*- and D,L-form of bis(*endo*-bicyclo[2.2.1]hept-5-en-2-yl)ethanedione **5a**: ^{1}H-NMR (80 MHz, $CDCl_3$): δ = 1.38 (m; 7-H$_a$, 7-H$_b$, 3-H$_a$), 1.75 (m; 3-H$_b$), 2.90 (m; 4-H), 3.19 (m; 1-H), 3.65 (m; 2-H), 5.73 (m; 6-H), 6.20 (m; 5-H). 40:60 mixture of *endo*- and *exo*-1-(bicyclo[2.2.1]hept-5-en-2-yl)-1,2-propanedione **5b**: ^{1}H-NMR (80 MHz, $CDCl_3$): δ = 1.2–1.6 (m; *endo*: 3'-H$_n$, 7'-H$_a$, 7'-H$_b$; *exo*: 3'-H$_x$, 7'-H$_a$, 7'-H$_b$), 1.7–2.1 (m; *endo*: 3'-H$_x$; *exo*: 3'-H$_n$), 2.33 (s; *endo*: CH_3), 2.37 (s; *exo*: CH_3), 2.9–3.2 (m; *endo*: 4'-H; *exo*: 1'-H, 2'-H$_n$, 4'-H), 3.30 (bs; *endo*: 1'-H), 3.5–3.8 (dt; *endo*: 2'-H$_x$), 5.8 (dd; *endo*: 6'-H), 6.2–6.4 (m; *endo*: 5'-H; *exo*: 5'-H, 6'-H).
[7] **1** was hydrogenated (Pd/C) to the 3,4-hexanedione, which was identical with authentic material. **1**: ^{1}H-NMR (80 MHz, $CDCl_3$): δ = 6.0–7.2 (ABC-m; 6H, vinyl-H). ^{13}C-NMR ($CDCl_3$): δ = 130.1 (d; C-2, C-5), 133.0 (t; C-1, C-6), 189.0 (s; C-3, C-4). IR (film): $\tilde{\nu}$ = 1690 cm^{-1} (C=O). UV (acetonitrile): λ = 434 (ε = 19). — **2**: ^{1}H-NMR (80 MHz, $CDCl_3$): δ = 6.0–7.3 (ABC-m; 3H, vinyl-H), 2.47 (s; 3H, CH_3). ^{13}C-NMR ($CDCl_3$): δ = 24.2 (q; C-1), 128.7 (d; C-4), 133.1 (t; C-5), 186.8 (s; C-3), 197.9 (s; C-2). IR (film): $\tilde{\nu}$ = 1715 (C=O), 1690 (C=O) cm^{-1}. UV (acetonitrile): λ = 436 (ε = 20).
[8] M. J. S. Dewar, W. Thiel, *J. Am. Chem. Soc. 99* (1977) 4899, 4907.
[9] R. C. Bingham, M. J. S. Dewar, D. H. Lo, *J. Am. Chem. Soc. 97* (1975) 1285.
[10] L. Åsbrink, C. Fridh, E. Lindholm, *Chem. Phys. Lett. 52* (1977) 63, 69, 72.
[11] T. A. Koopmans, *Physika 1* (1933) 104.
[12] D. Dougherty, P. Brint, S. P. McGlynn, *J. Am. Chem. Soc. 100* (1978) 5597.

Asymmetric Photocycloadditions with Optically Pure, Spirocyclic Enones. Simple Synthesis of (+)- and (−)-Grandisol

By *Martin Demuth,* Albert Palomer, Heinz-Dieter Sluma, Ashesh K. Dey, Carl Krüger,* and *Yi-Hung Tsay*

Photochemical [2+2]-cycloadditions of enones and related chromophores to olefins have previously been the subject of numerous investigations from the standpoint of asymmetric induction.[1] In more recent studies of such cycloadditions based on a principle that has also been tested by us, enones[2] or compounds with enone-like photoreactive moieties[3] have been used which contain a chiral auxiliary group. After the cycloaddition the chiral auxiliary group is split off and can thus be recovered. The aim of our present investigation was to prepare an enone moiety in the simplest way from readily accessible materials and to couple it rigidly, i.e. spirocyclically, to the auxiliary material (novel principle of stereofacial differentiation) and to recover this under mild conditions after the cycloaddition (avoidance of isomerizations). The dioxacyclohexenones (−)-**2** and (−)-**3** have proven suitable for this strategy (Fig. 1).[4]

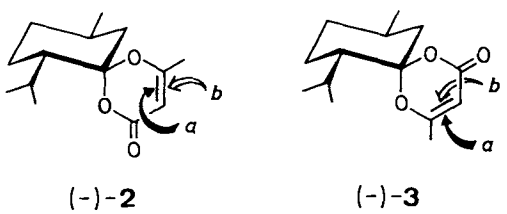
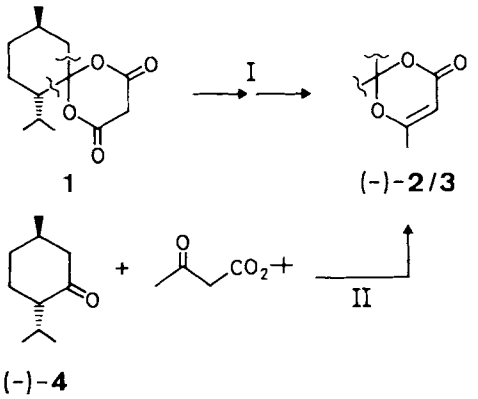


Fig. 1. Olefins add *a*-selectively to the dioxacyclohexenones (−)-**2** and (−)-**3**.

[*] Priv.-Doz. Dr. M. Demuth, Dipl.-Chem. A. Palomer, Dr. H.-D. Sluma, Dr. A. K. Dey
Max-Planck-Institut für Strahlenchemie
Stiftstrasse 34–36, D-4330 Mülheim a. d. Ruhr (FRG)
Prof. Dr. C. Krüger, Dr. Y.-H. Tsay (X-ray structure analysis)
Max-Planck-Institut für Kohlenforschung
Kaiser-Wilhelm-Platz 1, D-4330 Mülheim a. d. Ruhr (FRG)

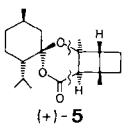
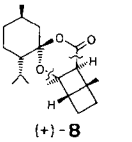
A mixture of (−)-**2** and (−)-**3** can be obtained via two routes: By rearrangement of the dioxacyclohexadione **1**[5] after acetylation (acetyl chloride, pyridine; analogously as in Ref. [6]) into a 1:1 mixture of (−)-**2** and (−)-**3** (diglyme, 120°C, analogously as in Ref. [7]) (Scheme 1, Route I; ca. 10% yield) or in *one step* by condensation of (−)-menthone, (−)-**4**, with *tert*-butyl acetoacetate in acetic anhydride in presence of sulfuric acid (Scheme 1, Route II; ca. 34% yield). The ratio in which the two isomers are formed can be varied: At −5°C, (−)-**2** and (−)-**3** are formed in the ratio 6:1, at 10°C in the ratio 1:1.



Scheme 1.

The products could be separated cleanly and easily by crystallization of (−)-**3** from *n*-hexane at −10°C and chromatography of the filtrate on silica gel [(−)-**2**]. The yields quoted for Routes I and II are the sum of the yields of pure (−)-**2** and (−)-**3**. The spectroscopic data are collected in Table 3.

Table 1. Photocycloadditions of the dioxacyclohexenones (−)-**2** and (−)-**3** with olefins [a]. The spectroscopic data of the products (+)-**5** and (+)-**8** are given in Table 3.

Expt.	Dioxacyclohexenone	Olefin	Photoproducts [b, c] [9] P′	P′
1	(−)-**2**		 (+)-**5**	
2	(−)-**2**			
3	(−)-**2**			
4	(−)-**3**		 (+)-**8**	

[a] Molar ratio dioxacyclohexenone:olefin = 1:4; $c((-)\text{-}2) = c((-)\text{-}3) \approx 0.2$ mol/L; experiments 1, 2, 4 in *n*-hexane, experiment 3 in acetonitrile. [b] Besides the regioisomers P and P′, small amounts of stereoisomers with complementary four-membered ring configurations are formed (cf. *a*:*b* values in Table 2). [c] Pure products after column-chromatographic separation.

The photocycloadditions of (−)-**2** and (−)-**3**[8] with the olefins listed in Table 1 (quartz vessel, medium-pressure mercury lamp) yielded products[9] which are *cis,anti,cis*-configurated at the new coupling sites (Table 2, experiments 1, 3, and 4).[10] The pronounced regioselectivity in additions with methylcyclobutene (experiments 1 and 4 at −78°C) decreases on using an acyclic olefin (experiment 2 at −78°C). The consistently high stereoselectivity (see *a*:*b* values in Table 2) lends support to the soundness of the spiro principle for stereofacial differentiation. Whereas a low reaction temperature is essential for a preparatively interesting stereoselectivity in the case of reactions 1, 2, and 4, considerable induction is already achieved at 5°C with

Table 2. Results of the reactions listed in Table 1.

Expt.	*T* [°C]	Yield [%] [a] P+P′	Regioselectivity P:P′	Stereoselectivity [b] *a*:*b*
1	−78	55 (70)	7:1	5:1
	+20	[c]	1:1	1:1
2	−78	33 (48)	3:1	8:1
	+20	[c]	1:1	2.5:1
3	−40	70 (82)	—	10:1
	+5	64 (81)	—	9:1
4	−78	56 (72)	7:1	5:1
	+20	[c]	1:1	1:1

[a] Purity of P and P′ > 96%; crude yields of all cycloadducts in brackets. [b] Corresponds to the facial selectivity (see Fig. 1); cf. also footnote [b] of Table 1. [c] Preparatively uninteresting yields.

Table 3. Spectroscopic data of the compounds (−)-**2**, (−)-**3**, (+)-**5**, and (+)-**8**. IR in $CHCl_3$; UV in *n*-hexane; ^{1}H-NMR: 400 MHz, $CDCl_3$; ^{13}C-NMR: 100.6 MHz, $CDCl_3$. The optical rotations were measured in $CHCl_3$ at 23°C (*c* [g/100 mL]) and converted to specific rotation values $[\alpha]_D$. All the compounds gave correct elemental analyses.

(−)-**2**: IR: $\tilde{\nu}$ = 1710, 1630, 1225, 1180, 1140, 1075 cm^{-1}; MS: *m/z* 238 ($M^{\oplus}$), 196, 154, 139, 112 (100%), 69, 55, 41; UV: $\lambda_{max}(\varepsilon)$ = 244 nm (5992); ^{1}H-NMR: δ = 5.12 (s, 1H), 2.56 (ddd, *J* = 2.5, 3.5, and 13.5 Hz, 1H), ca. 2.17 (d sept, *J* = 2.5 and 7 Hz, 1H), 1.94 (s, 3H), 1.42-1.80 (m, 6H), 0.97 (t, *J* = 13 Hz, 1H), 0.91 (d, *J* = 7 Hz, 3H), 0.87 (d, *J* = 7 Hz, 3H), 0.84 (d, *J* = 6 Hz, 3H); ^{13}C-NMR: δ = 168.65 (s), 161.04 (s), 109.75 (s), 93.12 (d), 49.39 (d), 40.98 (t), 34.08 (t), 28.58 (d), 25.55 (d), 23.19 (q), 22.22 (t), 21.58 (q), 20.07 (q), 18.48 (q); $[\alpha]_D$ = −27.4° (0.48)

(−)-**3**: single-crystal X-ray structure analysis (cf. Fig. 2); m.p. = 49-51°C; IR: $\tilde{\nu}$ = 1710, 1630, 1275, 1210, 1095, 1075 cm^{-1}; MS: cf. (−)-**2**; UV: $\lambda_{max}(\varepsilon)$ = 241 nm (5760); ^{1}H-NMR: δ = 5.16 (s, 1H), 2.57 (ddd, *J* = 1, 2, and 14 Hz, 1H), ca. 2.29 (d sept, *J* = 1 and 7 Hz, 1H), 1.95 (s, 3H), ca. 1.74 (dm, *J* = 13.2 Hz, 1H), ca. 1.65 (m, 1H), 1.44-1.56 (m, 4H), 1.05 (t, *J* = 13.2 Hz, 1H), 0.90 (d, *J* = 7 Hz, 3H), 0.85 (d, *J* = 7 Hz, 3H), 0.83 (d, *J* = 7 Hz, 3H); ^{13}C-NMR: δ = 168.01 (s), 161.5 (s), 109.44 (s), 93.69 (d), 49.19 (d), 40.52 (t), 33.87 (t), 29.65 (d), 25.0 (d), 23.08 (q), 21.78 (t), 21.54 (q), 20.02 (q), 18.11 (q); $[\alpha]_D$ = −22.5° (0.4)

(+)-**5**: single-crystal X-ray structure analysis; m.p. = 101-103°C; IR: $\tilde{\nu}$ = 1710, 1260, 915 cm^{-1}; MS: *m/z* 306 ($M^{\oplus}$), 239, 155, 124, 109 (100%), 84; ^{1}H-NMR: δ = 3.05 (s, 1H), ca. 2.41 (d sept, *J* = 2.5 and 7 Hz, 1H), 1.8-2.45 (m, 5H), 1.93 (ddd, *J* = 2.5, 6, and 13 Hz, 1H), 1.55 (s, 3H), 1.2-1.8 (m, 6H), 1.3 (t, *J* = 13 Hz, 1H), 1.15 (s, 3H), 0.91 (d, *J* = 7 Hz, 3H), 0.87 (d, *J* = 6.5 Hz, 3H), 0.85 (d, *J* = 7 Hz, 3H); ^{13}C-NMR: δ = 168.29 (s), 107.59 (s), 76.38 (s), 51.61 (d), 50.08 (d), 49.50 (t), 48.14 (d), 42.22 (s), 35.22 (t), 33.87 (t), 29.28 (d), 24.32 (d), 23.50 (q), 23.40 (q), 22.09 (q), 21.29 (q), 21.0 (t), 18.08 (q), 17.22 (t); $[\alpha]_D$ = +55.3° (1.2)

(+)-**8**: single-crystal X-ray structure analysis; m.p. = 98-100°C; IR: $\tilde{\nu}$ = 1715, 1320 cm^{-1}. MS: *m/z* 306 ($M^{\oplus}$), 239, 155, 124 (100%), 109, 84; ^{1}H-NMR: δ = 3.02 (s, 1H), 1.85-2.4 (m, 6H), 1.9 (ddd, *J* = 2.5, 6.5, and 12 Hz, 1H), 1.2-1.75 (m, 7H), 1.49 (s, 3H), 1.13 (s, 3H), 0.86 (d, *J* = 7.5 Hz, 3H), 0.85 (d, *J* = 6.5 Hz, 3H), 0.84 (d, *J* = 6.5 Hz, 3H); ^{13}C-NMR: δ = 168.69 (s), 109.07 (s), 77.0 (s), 51.34 (d), 51.26 (d), 48.11 (d), 46.76 (t), 42.26 (s), 35.20 (t), 34.20 (t), 29.84 (d), 25.01 (d), 23.54 (q), 22.44 (q), 22.07 (t), 21.30 (q), 21.23 (q), 18.38 (q), 17.29 (t); $[\alpha]_D$ = +18.9° (0.52)

cyclopentene. Since attack from the *a*-side is preferred to the same extent in the case of (−)-**2** and (−)-**3** (experiments 1 and 4) they are suitable educts for selective entry to complementary series of enantiomers without—as is otherwise usual—the chiral auxiliary having to be changed (see, e.g., [2]).

The preferred addition of the olefins to the *a*-side of the enones (−)-**2** and (−)-**3** rules out any effective shielding by the isopropyl group, and is apparently determined conformationally. We presume that the dioxacyclohexenone ring could adopt a twisted boat conformation in solution, an arrangement that exposes the *a*-side and which has been found X-ray crystallographically in crystalline (−)-**3** (Fig. 2).

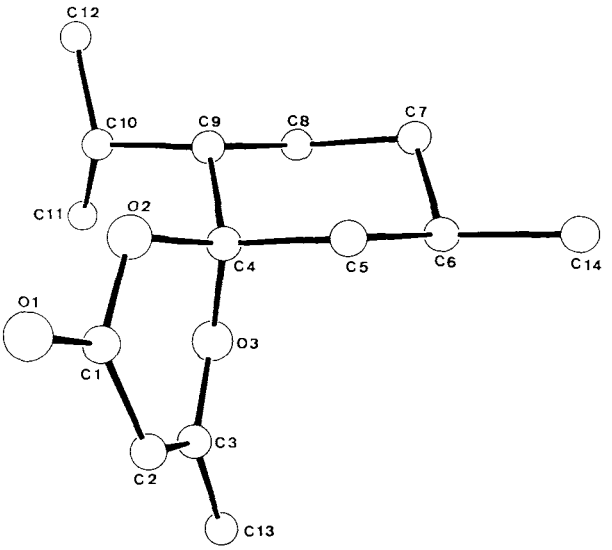
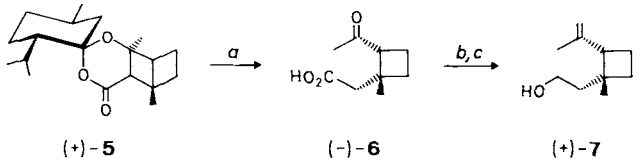


Fig. 2. Crystal structure of (−)-**3**. $a = 9.283(1)$, $b = 14.497(1)$, $c = 21.107(2)$ Å, $V = 2840.4$ Å^3, $\rho_{calc} = 1.11$ g cm^{-3}, $\mu = 0.72$ cm^{-1}, $Z = 8$, space group $P2_12_12_1$, 6640 reflections, 3976 observed ($I > 2\sigma(I)$), 307 refined parameters, $R = 0.056$, $R_w = 0.065$. Further details of the crystal structure investigation are available on request from the Fachinformationszentrum Energie, Physik, Mathematik GmbH, D-7514 Eggenstein-Leopoldshafen 2 (FRG), on quoting the depository number CSD-51953, the names of the authors, and the full citation of the journal.

The value of the method presented here has been confirmed by the first example of its application (Scheme 2). The major product of experiment 1, (+)-**5**, was smoothly hydrolyzed with formic acid to give (−)-**4** and (−)-**6**[11b] (80% yield after column chromatography) without epimerization occurring at the acetyl group.[2] (−)-**6** was converted into (+)-grandisol, (+)-**7**,[11-13] by a procedure already described in the literature.[13d] A specific rotation of $[\alpha]_D = +20°$ was calculated for (+)-**7** ($c = 0.3$ g/100 mL, *n*-hexane; corrected literature values: $[\alpha]_D = +18.5°$[11a] and $+19.6°$[11b]). Thus, it has been possible for the first time to synthesize the boll weevil (*Anthonomus grandis*) pheromone in optically pure form. At the same time, this five-step synthesis is the shortest sequence so far for the preparation of this highly active natural product,[14] the enantiomer of which, (−)-grandisol, can be obtained analogously from (+)-**8**.



Scheme 2. Shortest synthesis of (+)-grandisol, (+)-**7**, reported so far. a) HCOOH, H_2O/Me_2CO, 40 °C, 20 h. b) Me_3SiCH_2MgCl, tetrahydrofuran, reflux, $SOCl_2$, room temperature; analogously as in [13d]. c) $LiAlH_4$, Et_2O, room temperature; analogously as in [13d].

Received: June 13, 1986;
revised: September 1, 1986 [Z 1815 IE]
German version: *Angew. Chem. 98* (1986) 1093

[1] Review of photochemical [2+2]-cycloadditions: A. C. Weedon in W. M. Horspool (Ed.): *Synthetic Organic Photochemistry*, Plenum, New York 1984, p. 61.
[2] A. I. Meyers, S. A. Fleming, *J. Am. Chem. Soc. 108* (1986) 306.
[3] G. L. Lange, C. Decicco, S. L. Tan, G. Chamberlain, *Tetrahedron Lett. 26* (1985) 4707.
[4] a) M. Demuth, A. Palomer, unpublished; b) M. Demuth, *Pure Appl. Chem. 58* (1986) 1233.
[5] *Procedure*: **1**: Condensation of (−)-**4** and *tert*-butyl acetoacetate in acetic anhydride, catalytic amounts of sulfuric acid, room temperature, 24 h. The sole, previously described analogous condensation of (+)-camphor with α-methylmalonic acid required 200 days: A. Michael, N. Weiner, *J. Chem. Soc. 58* (1936) 680; B. Eistert, F. Geiss, *Chem. Ber. 94* (1961) 929.
[6] Y. Oikawa, K. Sugano, O. Yonemitsu, *J. Org. Chem. 43* (1978) 2087.
[7] M. Sato, H. Ogasawara, K. Oi, T. Kato, *Chem. Pharm. Bull. 31* (1983) 1896.
[8] D. Seebach, J. Zimmermann, *Helv. Chim. Acta 69* (1986) 1147; we thank Prof. *D. Seebach* (ETH Zürich) for sending his manuscript prior to publication.
[9] The analytical data for all the new products are consistent with the given structures; see also Table 3.
[10] Cf. also investigations with an achiral, monocyclic dioxacyclohexenone: a) S. W. Baldwin, J. M. Wilkinson, *J. Am. Chem. Soc. 102* (1980) 3634; b) S. W. Baldwin, G. F. Martin, D. S. Nunn, *J. Org. Chem. 50* (1985) 5720.
[11] Syntheses of (+)- and (−)-grandisol in optically enriched form: a) P. D. Hobbs, P. D. Magnus, *J. Am. Chem. Soc. 98* (1976) 4594; b) K. Mori, *Tetrahedron 34* (1978) 915; c) see also ref. [2].
[12] Structure: J. H. Tumlinson, R. C. Gueldner, D. D. Hardee, A. C. Thompson, P. A. Hedin, J. P. Minyard, *J. Org. Chem. 36* (1971) 2616.
[13] Syntheses of (±)-grandisol: a) K. Mori in J. ApSimon (Ed.): *The Total Synthesis of Natural Products, Vol. 4*, Wiley-Interscience, New York 1981; b) G. Quinkert, *Synform 1983*, 1; c) E. Negishi, L. D. Boordman, J. M. Tour, H. Sawada, C. L. Rand, *J. Am. Chem. Soc. 105* (1983) 6346; d) G. Rosini, E. Marotta, M. Petrini, R. Ballini, *Tetrahedron 41* (1985) 4633.
[14] For reference to a synthesis of (±)-grandisol based on the use of an achiral monocyclic dioxacyclohexenone see: S. W. Baldwin in A. Padwa (Ed.): *Organic Photochemistry, Vol. 5*, Dekker, New York 1981, p. 123.

Skeletal Rearrangements on Clusters: The Reaction of [(*t*BuP)Fe$_3$(CO)$_{10}$] with Diphenylacetylene**

By *Konrad Knoll, Gottfried Huttner,* Laszlo Zsolnai,* and *Olli Orama*

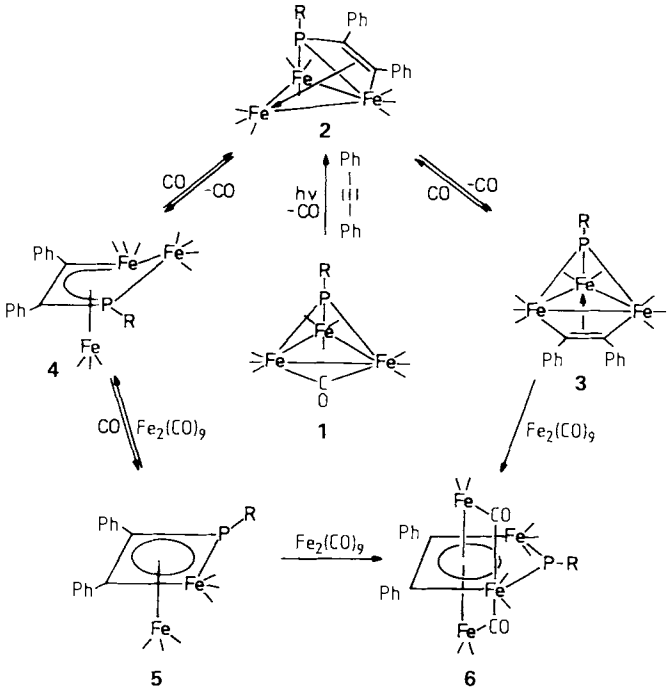
μ_3-RP groups have proved useful as building blocks for clusters. The metal atoms that they bridge are held together in the course of a reaction in such a way that the mechanism of reactions that involve cleavage of metal-metal bonds can be studied in detail.[1-3] This application of

[*] Prof. Dr. G. Huttner [+], Dipl.-Chem. K. Knoll, Dr. L. Zsolnai, Doz. Dr. O. Orama
Lehrstuhl für Synthetische Anorganische Chemie der Universität
Postfach 5560, D-7750 Konstanz (FRG)
[+] Present address:
Institut für Anorganische Chemie der Universität
Im Neuenheimer Feld 270, D-6900 Heidelberg (FRG)

[**] This work was supported by the Deutsche Forschungsgemeinschaft and the Fonds der Chemischen Industrie. *O. O.* thanks the Finnish Academy of Sciences for a fellowship.

μ_3-RP groups in cluster chemistry is based on the fact that the bonds to phosphorus are not affected by the reaction. However, we recently showed that, under some conditions, the phosphorus-metal bonds can indeed be attacked.[4-6]

We have now found the reaction of $[(\mu_3\text{-RP})Fe_3(CO)_{10}]$ with alkynes[5a] to be a system in which the enthalpies of the P-Fe, C-Fe, and P-C bonds are apparently so similar that a variety of skeletal rearrangements are possible. We report here on the photochemical reaction of the cluster **1**[2,7] with diphenylacetylene to give **2** and on the subsequent reactions of **2** involving skeletal rearrangement. Since **2** reacts to give **3** upon irradiation, reaction of **1** affords, in addition to 47% of **2**, 11% of **3** (Scheme 1).



Scheme 1. The terminal CO groups are indicated by lines. R = *t*Bu.

One of the P-Fe bonds of the starting cluster **1** is opened in **2**. The coordination site that thereby becomes free is involved in interaction with the π system of the alkyne, which bridges one of the two remaining P-Fe bonds. The lengths of the P-Fe bonds are normal (Fig. 1);[8] the distance between phosphorus and the iron atom not directly bonded to it is 272.8(3) pm. The P-C bond in the ring is significantly shorter than the bond to the *tert*-butyl group. The skeleton of **2** thus corresponds roughly to a trigonal prism, one of whose square faces has an additional diagonal bond (Fe2-Fe3) (Fig. 1).

2 undergoes both photochemical and thermal decarbonylation with accompanying skeletal rearrangement to give **3**. In **3**, the RP group functions again as a μ_3 ligand. The P-C bond to the alkyne fragment is broken, and the Ph_2C_2 fragment bridges an edge of the iron triangle. The coordination site that becomes free upon decarbonylation is involved in π interaction with the bridging alkyne (Fig. 2).

In a reversal of its photochemical formation, **3** reacts at 20°C under 1 bar of CO to give **2**. The reaction does not stop there, however, since, under these conditions, **2** adds CO to form **4**. Complex **4** reacts, in turn, to give the binuclear complex **5**,[11] one of the iron centers being carbonylated to $Fe(CO)_5$. Complex **5** is the stable end product of the reaction of **3** or **2** with CO. The intermediacy of **2** and **4** in the conversion of **3** to **5** is revealed, on the one hand,

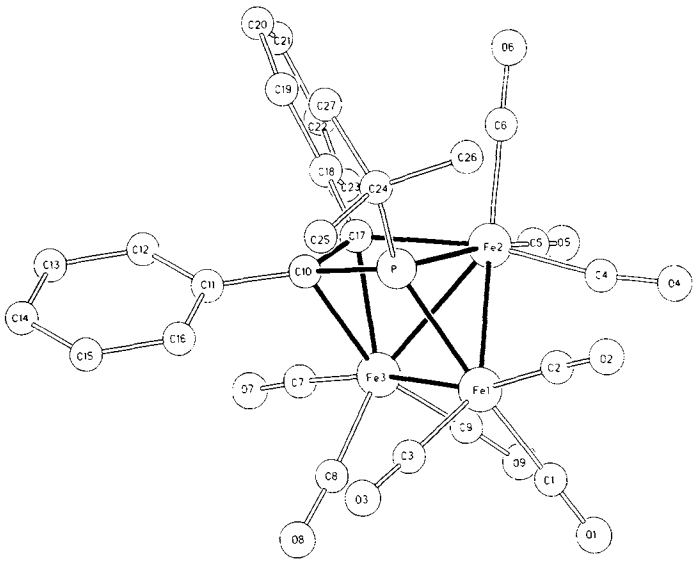


Fig. 1. Crystal structure of **2**. [8] Selected distances [pm]: Fe1-Fe2 267.5(3), Fe1-Fe3 267.4(3), Fe1-P 212.6(3), Fe2-Fe3 252.2(3), Fe2-P 222.8(3), Fe2-C17 203.3(8), Fe3-C17 201.5(7), Fe3-C10 212.2(7), C10-C17 142(1), C10-P 178.1(7), C24-P 185.5(7).

by the color change (**3**, red; **2**, green; **4**, red; **5**, yellow) and, on the other, by comparison of the IR spectra of the reaction solutions with those of authentic compounds of types **2** and **4**.[9]

Further evidence for the formation of **4** from **2** is the quantitative transformation of **3**, via the intermediate **2**, into a stable, structurally and analytically established sub-

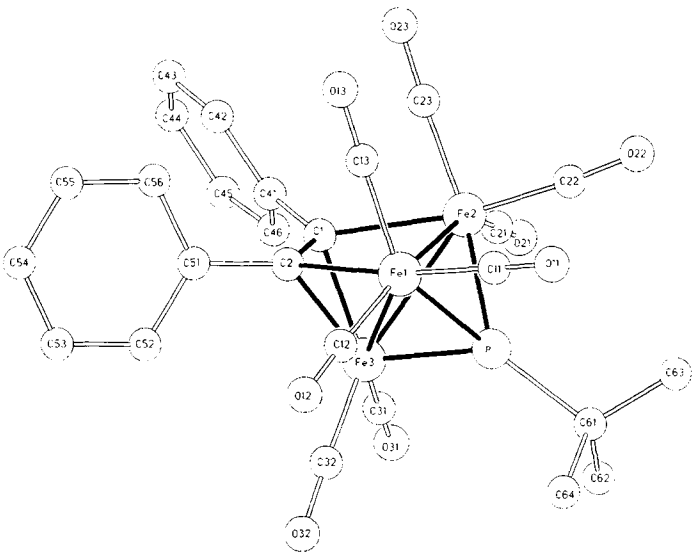


Fig. 2. Crystal structure of **3**. [8] Selected distances [pm]: Fe1-Fe2 260.5(3), Fe1-Fe3 255.4(3), Fe2-Fe3 257.7(3), Fe1-P 220.1(4), Fe2-P 218.9(4), Fe3-P 204.6(5), C61-P 184(1), Fe1-C2 213(1), Fe2-C1 216(1), Fe3-C1 196(1), Fe3-C2 197(1), C1-C2 136(2).

 © VCH Verlagsgesellschaft mbH, D-6940 Weinheim, 1986 0570-0833/86/1212-1120 $ 02.50/0 Angew. Chem. Int. Ed. Engl. 25 (1986) No. 12

stitution product of **4** when, instead of CO, trimethylphosphite is used as ligand. One trimethylphosphite ligand is bonded to each of the ring iron atoms in the resulting product of type **4**.[10]

Elimination of the $Fe(CO)_4$ group of **4** produces **5**, which contains a conjugated cyclic 4π system that is stabilized by the coordination to a $Fe(CO)_3$ group.[11]

Complex **5** reacts with an excess of $Fe_2(CO)_9$ at 25°C, undergoing formal insertion of an $Fe(CO)_4$ fragment into the ring P–Fe bond, to give **4** once again. Complex **4**, in turn, undergoes rapid decarbonylation to give **2**. At 60°C, **5**, as well as **3**, reacts with $Fe_2(CO)_9$ to give the triple-decker complex **6**.[10]

The closed sequence of reactions described here, in which the opening and formation of Fe–Fe, P–Fe, C–Fe, and P–C bonds occur alternately and sequentially, implies very similar enthalpies for these bonds. Overall, the observed pattern of reactions is strongly reminiscent of the chemistry of carboranes.[12]

Received: June 25, 1986;
supplemented: August 11, 1986 [Z 1829 IE]
German version: *Angew. Chem. 98* (1986) 1099

CAS Registry numbers:
1, 97913-15-0; **2**, 104779-83-1; **3**, 104779-84-2; **4**, 104779-85-3; **5**, 104779-86-4; **6**, 104779-87-5.

[1] G. Huttner, J. Schneider, H.-D. Müller, G. Mohr, J. von Seyerl, L. Wohlfahrt, *Angew. Chem. 91* (1979) 82; *Angew. Chem. Int. Ed. Engl. 18* (1979) 76; J. Schneider, G. Huttner, *Chem. Ber. 116* (1983) 917.

[2] K. Knoll, G. Huttner, L. Zsolnai, I. Jibril, M. Wasiucionek, *J. Organomet. Chem. 294* (1985) 91.

[3] J. Schneider, M. Minelli, G. Huttner, *J. Organomet. Chem. 294* (1985) 75.

[4] K. Knoll, G. Huttner, M. Wasiucionek, L. Zsolnai, *Angew. Chem. 96* (1984) 708; *Angew. Chem. Int. Ed. Engl. 23* (1984) 739; K. Knoll, G. Huttner, L. Zsolnai, O. Orama, M. Wasiucionek, *J. Organomet. Chem. 310* (1986) 225; cf. G. D. Williams, G. L. Geoffroy, R. R. Whittle, *J. Am. Chem. Soc. 107* (1985) 729.

[5] a) K. Knoll, O. Orama, G. Huttner, *Angew. Chem. 96* (1984) 989; *Angew. Chem. Int. Ed. Engl. 23* (1984) 976; K. Knoll, G. Huttner, L. Zsolnai, *J. Organomet. Chem. 312* (1986) C 57; b) cf. J. Lunness, S. A. MacLaughlin, N. J. Taylor, A. J. Carty, *Organometallics 4* (1985) 2066; T. Jaeger, H. Vahrenkamp, *Z. Naturforsch. B 41* (1986) 789; J. S. Field, R. J. Haines, E. Minshall, D. N. Smit, *J. Organomet. Chem. 310* (1986) C 69.

[6] K. Knoll, G. Huttner, L. Zsolnai, *J. Organomet. Chem. 307* (1986) 237.

[7] H. Lang, L. Zsolnai, G. Huttner, *J. Organomet. Chem. 282* (1985) 23.

[8] **2**: $C_{27}H_{19}Fe_3O_9P$, monoclinic, $P2_1/c$, $a=1416(1)$, $b=1107.2(8)$, $c=1710(1)$ pm, $\beta=97.50(8)°$, $Z=4$, $V=2658\times10^6$ pm^3, 2614 unique reflections ($I>2\sigma$), $R_1=0.048$, ω scan ($\Delta\omega=1°$, $2.0\le\dot{\omega}\le29.3°$ min^{-1}, $2°\le2\theta\le44°$), $T=198$ K. Structure solution: direct methods (SHELXTL).—**3**: $C_{26}H_{19}Fe_3O_8P$, monoclinic, $P2_1/c$, $a=827.4(5)$, $b=1619(1)$, $c=2019(1)$ pm, $\beta=111.15(5)°$, $Z=4$, $V=2521\times10^6$ pm^3, 2115 unique reflections ($I>2\sigma$), $R_1=0.067$, ω scan ($\Delta\omega=1°$, $1.6\le\dot{\omega}\le29.0°$ min^{-1}, $2°\le2\theta\le44°$), $T=233$ K. Structure solution: direct methods (SHELXTL). Further details of the crystal structure investigation may be obtained from the Fachinformationszentrum Energie, Physik, Mathematik GmbH, D-7514 Eggenstein-Leopoldshafen 2 (FRG), on quoting the depository number CSD-52085, the names of the authors, and the journal citation.

[9] **2**–**6**: IR (*n*-pentane); ^{1}H-NMR ($CDCl_3$, TMS int., 25°C); ^{31}P-NMR (toluene, 85% H_3PO_4 ext., 0°C).— **2**: IR: $\tilde{\nu}=2068$ s, 2027 vs, 2017 s, 2002 s, 1989 w, 1971 m, 1953 vw cm^{-1} (CO); ^{1}H-NMR: $\delta=1.43$ (d, 9H, J(PH) = 18.0 Hz), 7.10–7.48 (m, 10H); ^{31}P-NMR: $\delta=155.3$.—**3**: IR: $\tilde{\nu}=2066$ w, 2033 vs, 2012 s, 2003 m, 1990 vw, 1982 vw, 1957 w cm^{-1} (CO); ^{1}H-NMR: $\delta=2.18$ (d, 9H, J(PH) = 19.0 Hz), 7.05–7.29 (m, 10H); ^{31}P-NMR: $\delta=409.2$.—**4**: IR: $\tilde{\nu}=2087$ m, 2047 vs, 2044 sh, 2022 vs, 2014 s, 1992 w, 1978 w, 1965 vw, 1956 vw cm^{-1} (CO).—**5**: IR: $\tilde{\nu}=2065$ s, 2025 vs, 2024 sh, 1998 s, 1983 s, 1978 s, 1965 w cm^{-1} (CO); ^{1}H-NMR: $\delta=1.39$ (d, 9H, J(PH) = 19.0 Hz), 7.02–7.17 (m, 10H); ^{31}P-NMR: $\delta=129.7$.—**6**: IR: $\tilde{\nu}=2069$ w, 2050 vw, 2037 s, 2016 vw, 2012 sh, 2004 m, 1995 w, 1986 m, 1975 w, 1970 w, 1883 vw, 1943 m cm^{-1} (CO); ^{1}H-NMR: $\delta=1.09$ (d, 9H, J(PH) = 19.0 Hz), 6.28–6.39 (m, 4H), 6.77–6.94 (m, 6H); ^{31}P-NMR: $\delta=362.2$.

[10] K. Knoll, G. Huttner, unpublished results.

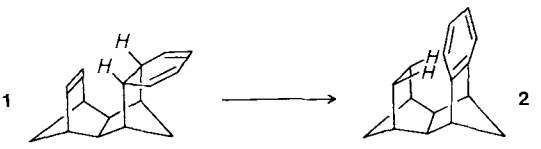
[11] H. Lang, L. Zsolnai, G. Huttner, *Chem. Ber. 118* (1985) 4426.

[12] Review: R. N. Grimes, *Adv. Inorg. Chem. Radiochem. 26* (1983) 55.

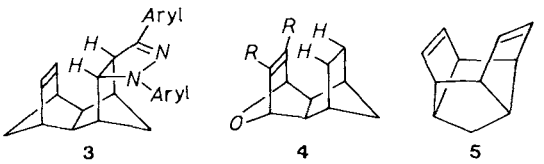
Dyotropic Hydrogen Migration in Pentacyclo[7.6.0.0^{2,13}.0^{3,8}.0^{10,14}]pentadeca-4,6,11-triene

By *Tahsin J. Chow** and *Mei-Fang Ding*

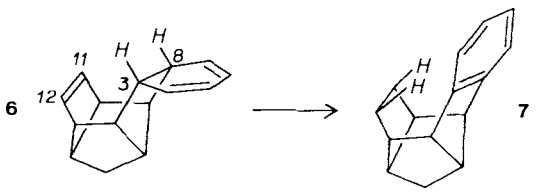
Nonbonding interactions between the two closely spaced ethylene bridges on an isodrin skeleton (cf. **11**) have been extensively analyzed. One of the most interesting phenomena is the dyotropic migration of two hydrogens from one bridge to the other.[1] Primary and secondary orbital effects of such transformations have been ana-



lyzed by *Reetz*.[2] Refluxing a toluene solution of **1** induces its smooth transformation to **2**. Two other derivatives, **3** (for example, Aryl = C_6H_5 or *p*-Me–C_6H_4)[3] and **4** (R = COOMe)[4], have also been shown to react in a similar fashion, and their thermodynamic parameters have been calculated. The energy of aromatization in **1** and **3** contributes part of the driving force, but the degree of orbital overlap between the *endo*-H atoms of the ethane bridge and the C atoms of the ethylene bridge also plays a determining role in these processes. The carbon-to-carbon dis-



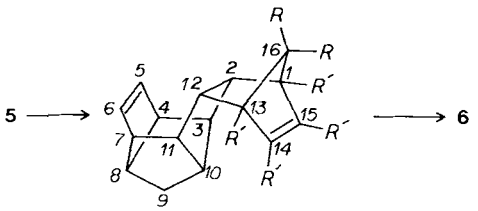
tance between the ethylene bridges of homohypostrophene, **5**,[5,6] is very close to that of isodrin,[7] but the two compounds have different directional angles between the π lobes and the C–H bonds of the opposite bridge.



A derivative of **5**, the title compound **6**, has now been prepared by us. Gas-phase flash pyrolysis of **6** at 400°C through a Vycor tube packed with glass beads was examined and shown to produce a high yield (ca. 70%) of **7**.[8] The presence of an aromatic ring in **7** was obvious since the ^{1}H-NMR spectrum showed a multiplet at $\delta=7.0$ (4H) and two upfield-shifted protons at $\delta=0.9$ for H-11 and H-12 due to a strong shielding effect from the proximately

[*] Prof. T. J. Chow
Institute of Chemistry, Academia Sinica
Nankang, Taipei (Taiwan)
and Chemistry Department, National Taiwan University
Taipei (Taiwan)
M.-F. Ding
Department of Chemistry, The Providence College
Taichung (Taiwan)

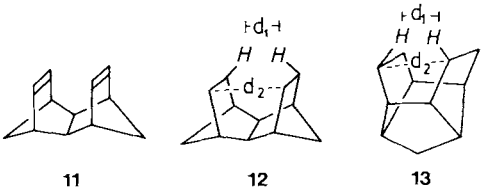
located aromatic ring. The reaction **6** → **7** is thus a rare example of an intramolecular dyotropic hydrogen migration between two nonconjugated ethylene moieties.



8, R=OMe; R'=Cl
9, R=OMe; R'=H
10, R,R=O; R'=H

Scheme 1.

The synthesis of **6**[8] is outlined in Scheme 1. Refluxing a xylene solution of **5** and 2,3,4,5-tetrachloro-1,1-dimethoxycyclopentadiene (molar ratio 1:1) for 24 h produced the [4+2] adduct **8**[8] in 50% yield. Dechlorination of **8** was effectively carried out in sodium/ethanol to give **9** in 60% yield. In the 200-MHz ^{1}H-NMR spectrum of **9**, H-2 and H-12 appear as a doublet of doublets at $\delta = 1.9$, which is 0.5 ppm more upfield than the signals of H-3 and H-11 ($\delta = 2.4$). The shift is believed to be due to the shielding caused by the ethylene bridge (C-5, C-6). Acidic hydrolysis of **9** (10% H_2SO_4, 20 °C, 2 h) gave **10**[8] quantitatively, which was then decarbonylated to form **6** by heating it in a sealed tube at 125 °C (2 h in CCl_4, quantitative yield). The triene **6** is a colorless solid (m.p. = 50–51 °C) with the vinylic protons appearing as three multiplets at $\delta = 5.5$, 5.7, and 6.1 (2H each).



11 **12** **13**

The distance between the two ethylene bridges of dechlorinated isodrin, **11**, is ca. 2.8 Å.[9] The corresponding distance for homohypostrophene, **5**, is also about 2.8 Å.[5] However, since the double bonds of **11** are nearly parallel to each other, the through-space interaction is maximized to produce a 1.26-eV energy gap between IP_1 (8.08 eV) and IP_2 (9.34 eV) in its photoelectron spectrum.[10] In **5**, the π lobes are not parallel but instead form an angle bending outward. The small difference between its IP_1 (8.6 eV) and IP_2 (8.8 eV) indicates a very weak interaction.[11] Moreover, a comparison based on the hydrogenated products **12** and **13** is also revealing. The ethane bridges of **12** and **13** are pushed apart by steric repulsions between the *endo* hydrogens but to different extents. The distance between the *endo* hydrogens (d_1) is 1.85 Å for **12**[12] and 2.14 Å for **13**.[6] However, the carbon-to-carbon distance (d_2) between the bridges increases by 0.4 Å to a value of 3.2 Å[12] in going from **11** to **12**, and by only 0.2 Å to a value of 3.0 Å in going from **5** to **13**.[6] These data clearly show that introduction of *endo* hydrogens induces a more severe distortion in **12** than in **13**. The same criterion can be equally applied to **1** and **6** (i.e., nonbonding interactions of **6** should be much weaker than those of **1**). The transannular strain of **1** has been calculated as ca. 0.3 eV;[13] thus, the corresponding value in **6** is expected to be much smaller. Nevertheless, our observation of double hydrogen migration suggests that orbital interactions across the bridges of **6** are still of significance.

Received: July 9, 1986;
revised: August 12, 1986 [Z 1951 IE]
German version: *Angew. Chem. 98* (1986) 1102

[1] a) K. Mackenzie, *J. Chem. Soc. 1965*, 4646; b) *ibid. C 1969*, 1784; c) C. H. M. Adams, K. Mackenzie, *ibid. C 1969*, 480.
[2] a) M. T. Reetz, *Tetrahedron 29* (1973) 2189; b) *Angew. Chem. 84* (1972) 161, 163; *Angew. Chem. Int. Ed. Engl. 11* (1972) 129, 130.
[3] K. Mackenzie, G. J. Proctor, D. J. Woodnutt, *Tetrahedron Lett. 25* (1984) 977.
[4] J.-P. Hagenbuch, B. Stampfli, P. Vogel, *J. Am. Chem. Soc. 103* (1981) 3934.
[5] W. Schmidt, B. T. Wilkins, *Tetrahedron 28* (1972) 5649.
[6] E. Osawa, *J. Am. Chem. Soc. 101* (1979) 5523.
[7] B. Alber, W. Berning, C. Burschka, S. Hünig, H.-D. Martin, F. Prokschy, *Chem. Ber. 114* (1981) 423.
[8] **6**: ^{1}H-NMR ($CDCl_3$): $\delta = 1.5$ (s, 2H), 2.0 (dd, $J = 4$ Hz, 9 Hz, 2H), 2.3 (m, 1H), 2.5 (m, 4H), 2.75 (m, 1H), 5.5, 5.7, 6.1 (3m, 2H each); MS (70 eV): *m/z* (rel. int.) 196 ($M^{\oplus}$, 19), 167 (43), 129 (100), 128 (48), 116 (91), 114 (52), 81 (24), 67 (24).—**7**: ^{1}H-NMR ($CDCl_3$): $\delta = 0.9$ (d, $J = 10$ Hz, 2H), 1.5 (dm, $J = 10$ Hz, 2H), 1.7 (s, 2H), 2.3 (m, 2H), 2.5 (m, 1H), 2.9 (dd, $J = 4$ Hz, 10 Hz, 2H), 3.1 (m, 1H), 7.0 (m, 4H); MS (70 eV): *m/z* (relat. int.) 196 ($M^{\oplus}$, 13), 155 (21), 154 (100), 153 (29), 152 (38), 129 (40), 116 (24), 115 (34), 114 (24), 77 (21).—**8**: ^{1}H-NMR (CCl_4): $\delta = 1.4$ (br. s, 2H), 2.1 (m, 1H), 2.2 and 2.5 (2m, 2H each), 2.6 (m, 1H), 2.75 (m, 2H), 3.5 and 3.55 (2s, 3H each), 6.1 (m, 2H); MS (70 eV): *m/z* 406 ($M^{\oplus}$ for Cl = 35), 371 ($M^{\oplus} - Cl$).—**9**: ^{1}H-NMR ($CDCl_3$): $\delta = 1.3$ (br. s, 2H), 1.9 (dd, $J = 2$ Hz, 9 Hz, 2H), 2.4 (dm, $J = 9$ Hz, 2H), 2.5 (m, 2H), 2.65 (m, 1H), 2.7 (m, 2H), 2.95 (m, 1H), 3.1 and 3.2 (2s, 3H each), 6.1 and 6.2 (2m, 2H each); MS (70 eV): *m/z* 270 ($M^{\oplus}$), 255 ($M^{\oplus} - CH_3$), 239 ($M^{\oplus} - OCH_3$), 223; correct elemental analysis.—**10**: ^{1}H-NMR ($CDCl_3$): $\delta = 1.3$ (br. s, 2H), 2.0–2.1 (m, 2H), 2.4 (m, 4H), 2.6 (m, 2H), 2.9 (m, 2H), 6.1 and 6.4 (2m, 2H each); IR ($CHCl_3$): $\tilde{\nu}$(C=O) = 1760 cm^{-1}; MS (70 eV): *m/z* (rel. int.) 196 ($M^{\oplus} - CO$, 40), 129 (100), 116 (80).
[9] O. Ermer, C.-D. Bödecker, H. Preut, *Angew. Chem. 96* (1984) 57; *Angew. Chem. Int. Ed. Engl. 23* (1984) 55.
[10] H.-D. Martin, R. Schwesinger, *Chem. Ber. 107* (1974) 3143.
[11] H.-D. Martin, S. Kagabu, R. Schwesinger, *Chem. Ber. 107* (1974) 3130.
[12] O. Ermer, *Angew. Chem. 89* (1977) 833; *Angew. Chem. Int. Ed. Engl. 16* (1977) 798.
[13] H. Prinzbach, G. Sedelmeier, H.-D. Martin, *Angew. Chem. 89* (1977) 111; *Angew. Chem. Int. Ed. Engl. 16* (1977) 103.

Large Molecular Cavities for Small Ions—Double Bridging of Three Bipyridine Units**

By *Smaragda Grammenudi* and *Fritz Vögtle**

We recently reported on a $Fe^{3\oplus}$-selective ligand of the siderophore-type, in which three pyrocatechol units are bridged symmetrically.[1] With the synthesis of the macrobicyclic ligand **10**, we have now been able to achieve for the first time an analogous bridging of three bipyridine units via two 1,3,5-substituted benzene rings as spacers. Compared to cryptands with two-membered chains between the donor centers and the coordinating bridgehead nitrogen atoms,[2] **10** has the great advantage that complexation and decomplexation are less sterically hindered because of the size of its cavity, which is of importance in chemical and biological applications.[3]

[*] Prof. Dr. F. Vögtle, Dipl.-Chem. S. Grammenudi
Institut für Organische Chemie und Biochemie der Universität
Gerhard-Domagk-Strasse 1, D-5300 Bonn 1 (FRG)

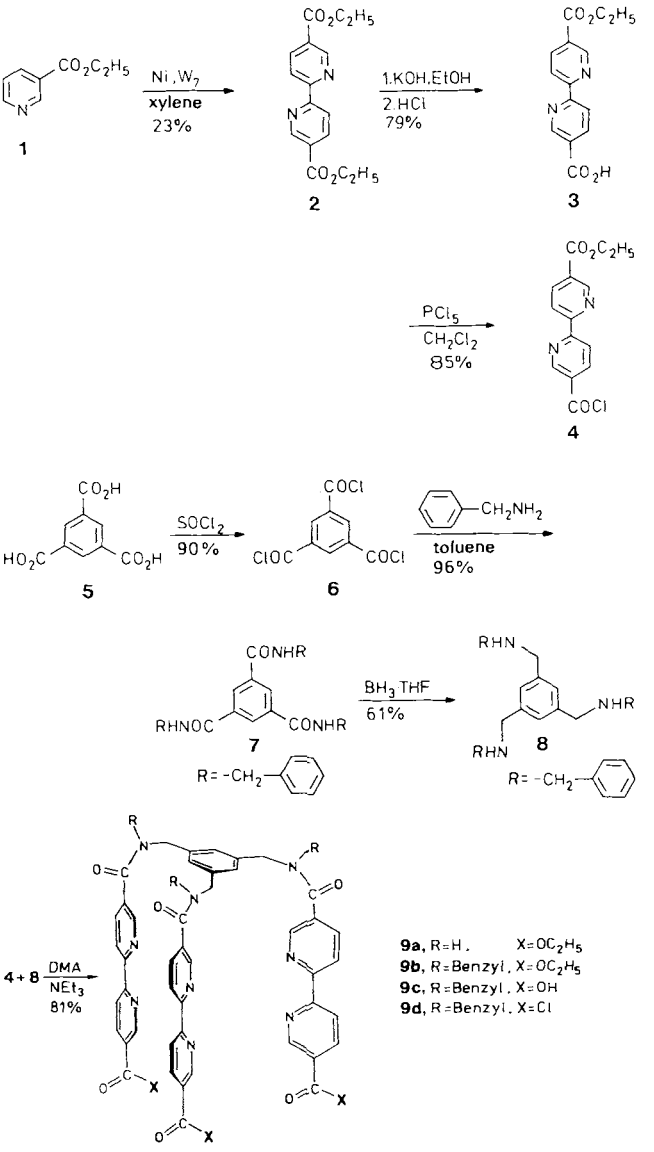
[**] Presented in part at the Fourth International Symposium on Inclusion Phenomena in Lancaster (England), July 20–25, 1986. This work was supported by the Deutsche Forschungsgemeinschaft. We thank Dipl.-Chem. *W. Calaminus*, Dipl.-Chem. *R. Thomessen* and *W. M. Müller* for assistance, and Frau Dr. *J. Peter*, Institut für Physiologische Chemie der Universität Bonn, for recording and evaluating the FAB mass spectra.

The synthesis of **10** starts from the nicotinate **1** and proceeds via the intermediates **2**–**9** shown in Scheme 1 (for data for the new compounds see Table 1). Since the *N*-unsubstituted intermediate **9a** presents solubility problems, the more readily soluble tribenzyl derivative **9b** was synthesized.[4] The decisive cyclization of **9d** and **8** to give the hexabenzyl-substituted ligand **10** was accomplished after numerous optimization experiments—other than usual[5]—in chlorobenzene/dimethylacetamide at room temperature under dilution principle conditions (yield 3%) (Scheme 2).[6]

The R_F value of the purified[6] ligand **10** (TLC plates Al_2O_3 neutral, $CHCl_3$/isopropyl alcohol/C_2H_5OH (100 : 1 : 0.6) is 0.43. Further data for **10** are listed in Table 1.

In the ^{1}H-NMR spectrum of **10** (400 MHz, [D_6]dimethyl sulfoxide) all the signals are broadened at room temperature. At 120°C, however, sharp absorptions appear: all benzyl CH_2-resonances centered at $\delta = 4.5$ overlap at 20°C, whereas at 120°C, two singlets are observed at $\delta = 4.51$ and 4.75. Because of hindered rotation about the amide bonds[7] the free ligand **10** shows limited free mobility, whose barrier ΔG^+ is approximately 60 kJ/mol assuming a coalescence temperature $T_c \approx 20$°C and a splitting of $\Delta\nu \approx 20$ Hz.

Although the 34-membered cavity[8] has to shrink drastically for the complexation of small metal ions, the macrobicyclic ligand **10**, which is strongly lipophilic because of the six benzyl residues, is an unusual complex ligand: the characteristic red color of the $Fe^{2\oplus}$-complex **12** is already observed during the cyclization reaction **9d** + **8**. Upon chromatographic separation, **10** always forms—other than in the case of the open-chain ligand **9b**—a red-violet zone at the upper rim of the column. Since the ligand **10** was not intentionally brought into contact with iron salts in these experiments, the formation of a complex had to be attributed to traces of iron in the reagents and/or parts of the apparatus. With $Fe^{3\oplus}$, $Co^{2\oplus}$, $Ni^{2\oplus}$, $Cu^{2\oplus}$ and $Cu^{\oplus}$, **10** forms only almost colorless solutions so that $Fe^{2\oplus}$ can be visually recognized even in the presence of these cations. Furthermore, the complex can be extracted with chloroform from aqueous alcoholic solution.

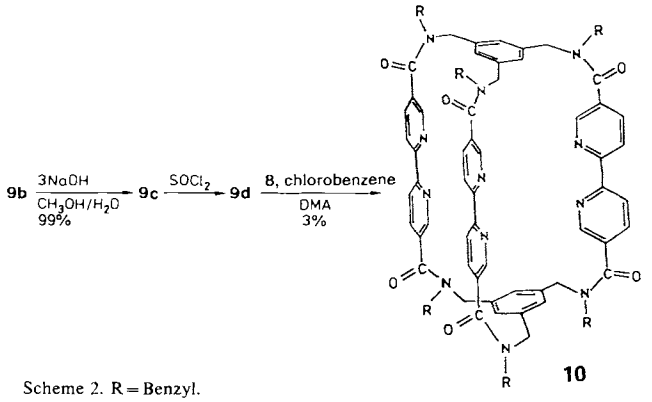


Scheme 1. W_7 = activity of Raney nickel used; DMA = dimethylacetamide.

Table 1. Data of the new compounds. All compounds except **8** gave correct elemental analyses. In the case of **8** the R_F value was determined: $R_F = 0.24$ (TLC aluminum foil Al_2O_3 neutral, CH_2Cl_2/CH_3OH 100 : 1). Because of its sensitivity towards hydrolysis, the triacid chloride **9d** was used as raw product.

Cpd.	Yield [%]	M.p. [°C] (solvent)	^{1}H-NMR (δ values)	High-resolution MS or $MH^{\oplus}$
2	23	148–149 (ethanol)	[a] 1.44 (t, CH_3), 4.48 (q, CH_2), 8.42–8.62 (dd, bipyridine-H), 9.31 (dd, –N=C–H)	calc. 300.3181 obs. 300.1112
3	79	268–270 (ethyl acetate)	[b] 1.37 (t, CH_3), 4.44 (q, CH_2), 8.51–8.66 (dd, bipyridine-H), 9.26 (2 dd, –N=C–H)	calc. 272.2639 obs. 272.0802
4	85	166–167 (benzene)	[a] 1.46 (t, CH_3), 4.5 (q, CH_2), 8.53–8.78 (dd, 2 d, bipyridine-H), 9.37–9.42 (2 dd, –N=C–H)	calc. 290.7092 obs. 290.0462
7	96	239–240 (ethanol)	[b] 4.51 (d, CH_2), 7.32 (m, aromat. H), 8.53 (s, aromat. H), 9.28 (t, NH)	calc. 477.5688 obs. 477.2055
8	61	*liquid*	[a] 1.58 (s, NH), 3.76 (s, CH_2), 7.3 (m, aromat. H)	calc. 435.6281 obs. 435.2668
9a	78	340 (dimethyl-acetamide)	[c] 1.53 (t, CH_3), 4.64 (q, CH_2), 4.77 (s, benzyl. H), 7.33 (s, aromat. H), 9 (m, bipyridine-H)	$MH^{\oplus}$: 928
9b	81	110 (ethyl acetate)	[d] 1.44 (t, CH_3), 4.37 (q, CH_2), 4.57 (s, CH_2), 7.03–7.27 (s, aromat. H), 7.96–8.47 (dd, bipyridine-H), 8.74–9.1 (2 dd, –N=C–H)	$MH^{\oplus}$: 1198
9c	99.5	180 (dec.)	[b] 4.64 (s, CH_2), 7.37 (s, aromat. H), 7.24–8.24 (m, bipyridine-H), 8.84—8.17 (2 s, –N=C–H)	$MH^{\oplus}$: 1114
10	3	319–320 ($CHCl_3$/CH_3OH 20 : 1)	[d] 4.51 (s, CH_2), 4.75 (s, CH_2), 6.91–7.31 (s, m, aromat. H), 7.57 (dd, bipyridine-H), 8.42 (d, –N=C–H), 8.58 (d, bipyridine-H)	FAB-MS: $MH^{\oplus}$: 1495

[a] $CDCl_3$, 90 MHz, 26°C. [b] [D_6]DMSO, 90 MHz, 26°C. [c] $CDCl_3$/trifluoroacetic acid, 90 MHz, 26°C. [d] [D_6]DMSO, 90 MHz, 120°C.



Scheme 2. R = Benzyl.

The absorption maximum of the red $Fe^{2\oplus}$-complex **12** of **10** in the visible region (in hexafluoroisopropyl alcohol/water 1 : 1) lies at $\lambda = 524$ nm, that of the violet open-chain complex **11** of **9b** at longer wavelength at $\lambda = 546$ nm. The intensity of the absorption of the $Fe^{2\oplus}$-complex **12** ($\varepsilon = 6426$) exceeds that of the complex **11** of the open-chain "tripod"[9] **9b** ($\varepsilon = 5748$) (Fig. 1).

UV/VIS spectra of freshly prepared mixtures of **10** and $Fe^{2\oplus}$ salt solutions [$(NH_4)_2Fe(SO_4)_2$] in water/hexafluoroisopropyl alcohol (1 : 1) recorded after various intervals of time show that formation of the $Fe^{2\oplus}$-complex in dilute solution is complete after ca. one hour at 20 °C. Titration of the ligands **9b** and **10** with $Fe^{2\oplus}$-solutions indicated 1 : 1 stoichiometry of the complex in each case.

It follows from competition experiments between the three ligands **10**, **9b**, and **2** (molar ratio 1 : 1 : 3) that **10** is capable of taking over the central ion ($Fe^{2\oplus}$) from the other ligands. The $Fe^{2\oplus}$-complex **12** of **10** cannot, however, be decomplexed, not even with ethylenediaminetetraacetic acid (disodium salt) or the bipyridine ester **2** in 1000-fold excess or with hydrochloric acid at pH = 1. In contrast, the $Fe^{2\oplus}$-complex of **2** is decolorized with excess EDTA.

The unusual stability of the oxidation state 2 in the $Fe^{2\oplus}$-complex **12** of **10** follows from the fact that 10^{-4} M solutions in dimethyl sulfoxide are not decolorized—by oxidation to $Fe^{3\oplus}$ or ligand removal—even after several days, whereas this already takes place in the case of the open-chain $Fe^{2\oplus}$-complex of **9b** after a few hours under analogous conditions, and much more rapidly so in the case of the $Fe^{2\oplus}$-complexes of the diester **2** and of unsubstituted bipyridine. The $Fe^{2\oplus}$-complex **12** survives drastic conditions, such as addition of aqueous H_2O_2, considerably longer than the above-mentioned comparison complex **9**.

It can be concluded from the high stability of the complex and the stabilization of the oxidation state that the $Fe^{2\oplus}$-ion is bound at the center of the cavity of **10**. Such a stability could not be explained in terms of an intermolecular bonding of $Fe^{2\oplus}$. As can be shown on the basis of molecular models, upon coordination of $Fe^{2\oplus}$ the ligand **10** assumes a helical conformation in which the bipyridine rings are inclined at almost 54° to the threefold molecular axis.

The intense red color of the $Fe^{2\oplus}$-complex can, in view of the negligible color reaction with $Fe^{3\oplus}$, be exploited for the sensitive photometric determination of $Fe^{2\oplus}$ in the presence of other ions. **10** (and **9**) can be useful for the complexation of ions of the noble metals Pd, Pt, Rh, etc.,[10] e.g. with respect to indirect electrochemical redox reactions[11] and photochemical cleavage of water. Similarly structured cation selective ligands with other spacer groups,[12] other donor units, and more than three bridges[13] can also be prepared via the route described here.

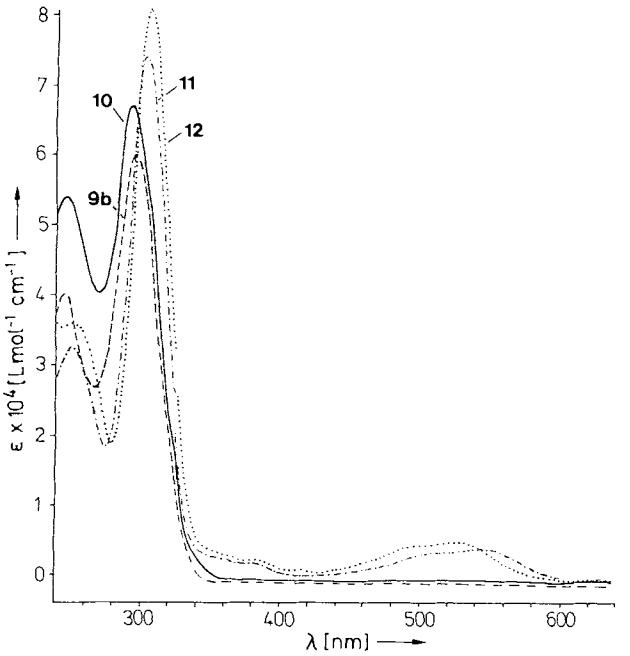
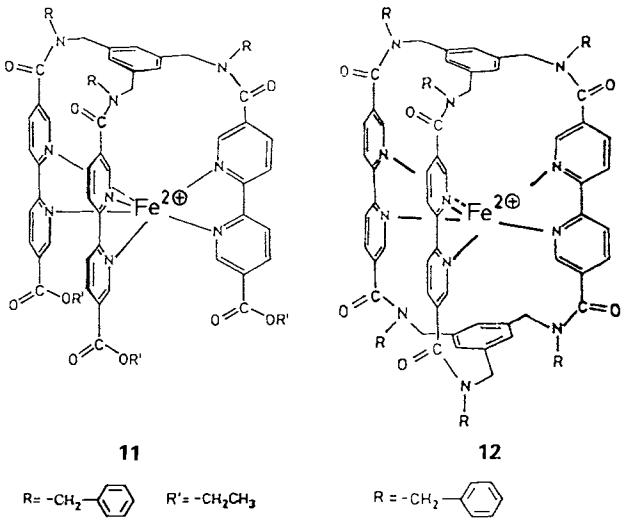


Fig. 1. UV/VIS spectra of the ligands **10** and **9b** (for comparison) and their $Fe^{2\oplus}$-complexes **12** and **11**, respectively [iron salt employed: $(NH_4)_2Fe(SO_4)_2 \cdot 6H_2O$] (in hexafluoroisopropyl alcohol/water 1 : 1).



Received: August 11, 1986 [Z 1899 IE]
German version: *Angew. Chem. 98* (1986) 1119

[1] W. Kiggen, F. Vögtle, *Angew. Chem. 96* (1984) 712; *Angew. Chem. Int. Ed. Engl. 23* (1984) 714; W. Kiggen, F. Vögtle, S. Franken, H. Puff, *Tetrahedron 42* (1986) 1859.
[2] Cf. J.-C. Rodriguez-Ubis, B. Alpha, D. Plancherel, J.-M. Lehn, *Helv. Chim. Acta 67* (1984) 2264.
[3] B. Tümmler, G. Maass, F. Vögtle, H. Sieger, U. Heimann, E. Weber, *J. Am. Chem. Soc. 101* (1979) 2588; B. Tümmler, G. Maass, E. Weber, W. Wehner, F. Vögtle, *ibid. 99* (1977) 4683.

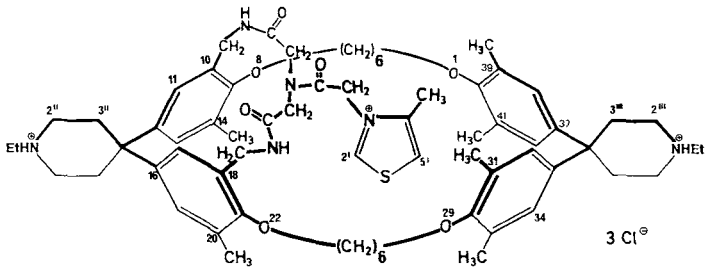
[4] This strategy had proven useful in a previous case: U. Werner, W. M. Müller, T. Merz, H.-W. Losensky, F. Vögtle, *J. Incl. Phenom. 4* (1986), in press.
[5] In this case the use of benzene as solvent, as was used previously [1], met without success.
[6] *Procedure:* **10**: Solutions of **9d** (5.00 g, 4.25 mmol) in chlorobenzene (200 mL) (dried over P_4O_{10}), dimethylacetamide (50 mL, 99% Janssen), and **8** (3.72 g, 8.55 mmol) in chlorobenzene (250 mL) were added concomitantly and dropwise under nitrogen within 12 h at room temperature to 1 L of chlorobenzene. A colorless flocculent precipitate formed; this was removed from the red solution by filtration, and then the solvent was removed from the filtrate by evaporation. After stirring of the residue with dichloromethane (with heating) and filtration, the dichloromethane solution was chromatographed on a silica gel column with chloroform/methanol (20:1). **10** crystallized from the eluent as the clathrate with $CHCl_3$ (1:2). The chloroform was completely removed at 100°C/0.05 torr (6.6 Pa) within a few days (see Table 1).
[7] E. Buhleier, W. Wehner, F. Vögtle, *Chem. Ber. 111* (1978) 559; cf. J. Sandström: *Dynamic NMR Spectroscopy*, Academic Press, New York 1982.
[8] Because of the stretched bipyridine unit and absence of intraannular substituents, the cavity is far larger than that in the previously described siderophore-like ligand (cf. [1]).
[9] F. Vögtle, E. Weber, *Angew. Chem. 91* (1979) 813; *Angew. Chem. Int. Ed. Engl. 18* (1979) 753.
[10] E. Steckhan, M. Franke, S. Grammenudi, F. Vögtle, unpublished electrochemical studies on the $Rh^{3\oplus}$-complex of **9b**.
[11] E. Steckhan, *Angew. Chem. 98* (1986) 681; *Angew. Chem. Int. Ed. Engl. 25* (1986) 693.
[12] T. Merz, H. Wirtz, F. Vögtle, *Angew. Chem. 98* (1986) 549; *Angew. Chem. Int. Ed. Engl. 25* (1986) 567; H. Schrage, J. Franke, F. Vögtle, E. Steckhan, *ibid. 98* (1986) 335 and *25* (1986) 336.
[13] W. Kissener, F. Vögtle, *Angew. Chem. 97* (1985) 782; *Angew. Chem. Int. Ed. Engl. 24* (1985) 794; B. Klieser, F. Vögtle, *ibid. 94* (1982) 632 and *21* (1982) 618; *Angew. Chem. Suppl. 1982*, 1392.

Synthesis of a Macrobicyclic Thiazolium-Host and Supramolecular Catalysis of the Benzoin Condensation**

By *Heinz-Dieter Lutter* and *François Diederich**

Dedicated to Professor Vladimir Prelog on the occasion of his 80th birthday

Thiamine pyrophosphate (TPP) participates as the essential cofactor in numerous enzymatic reactions involving formation and breaking of carbon–carbon bonds.[1] The catalytic action of TPP is mainly due to the thiazolium ring, and simple thiazolium salts catalyze many of the enzymatic transformations in the absence of the enzymes.[2]

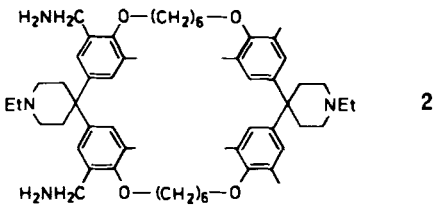


1

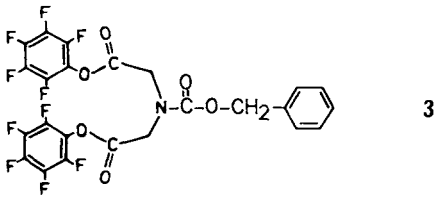
[*] Prof. Dr. F. Diederich
Department of Chemistry and Biochemistry
University of California, Los Angeles, CA 90024 (USA)
Dipl.-Chem. H.-D. Lutter
Max-Planck-Institut für medizinische Forschung,
Abteilung Organische Chemie
Jahnstrasse 29, D-6900 Heidelberg (FRG)

[**] This work was supported by the Deutsche Forschungsgemeinschaft.

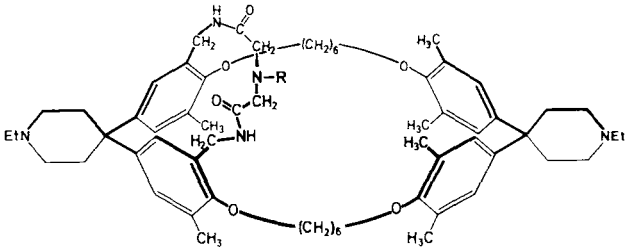
We report here for the first time on the preparation of a fully synthetic thiazolium-macrocycle (**1**) and its use as an efficient catalyst in the benzoin condensation.[3,4] Compound **1** was designed to provide in aqueous[5] and in organic solution[6] a binding cavity for the two benzaldehyde molecules that react to give benzoin. A thiazolium residue is connected by two side arms to the macrocyclic binding site of **1**. This double fixation atop the cavity was expected to limit the number of unproductive conformations of the catalytic residue and to prevent its competitive binding to the macrocyclic cavity. Favorable proximity and orientation of the reacting partners has been recognized as a major principle of enzymatic catalysis.[7] We therefore expected higher rates of benzoin formation in the presence of **1** than in the presence of thiazolium derivatives lacking the macrocyclic binding cavity.



2



3



4, R = -C(=O)-O-CH$_2$-C$_6$H$_5$
5, R = H
6, R = COCH$_2$Br

In the synthesis of macrobicycle **1**, the macrocyclic tetramine **2**[8,9] was cyclized in chloroform with the activated diester **3**[10] to give the macrobicycle **4**[9] in 50% yield. The *N*-protective group of **4** was removed catalytically [H_2/Pd on C (10%); 95%], and the secondary amino residue of **5**[9] was acetylated with α-bromoacetyl bromide in chloroform to give **6** (37%).[9] Reaction of **6** with excess 4-methylthiazole followed by ion exchange chromatography ($Cl^{\ominus}$) provided in 69% yield the target molecule **1**, which was analyzed as a dihydrate.[11] 1D- and 2D-(COSY) ^{1}H-NMR analysis of **1** shows that the bridge with the thiazolium residue takes several conformations as a consequence of the restricted rotation around the three amide linkages.[11] The contour plot of a 2D-NOESY ^{1}H-NMR experiment under

the same conditions indicates the location of the thiazolium ring on the cavity side in proximity to the tetramethyl-substituted diphenylmethane unit. Revealing connectivities are observed between 2′-*H*,5′-*H*, and 4′-CH_3 of the thiazolium ring and 31,35-CH_3, 32,34-*H*, and N–CH_2–CH_3 of the diphenylmethane unit.

We studied by ^{1}H-NMR (500 MHz) the catalysis of the benzoin condensation by **1** in [D_4]methanol in the presence of triethylamine as base (initial concentrations of: [**1**] = 20 mmol·L^{-1}, [PhCHO] = 400 mmol·L^{-1}, [NEt_3] = 60 mmol·L^{-1}; T = 323 K, under N_2). After 8 h, the signals of the benzaldehyde protons had almost completely disappeared and all new peaks could be assigned to benzoin. Chromatographic work-up of the reaction after 12 h afforded unchanged catalyst and analytically pure benzoin in 93% isolated yield. For kinetic analysis, we monitored the decrease in integrated intensity of the singlet for the aldehyde proton of benzaldehyde at $\delta = 9.97$ and the increase in integrated intensity of the isolated doublet at $\delta = 7.93$ for the two aromatic protons *ortho* to the carbonyl group of benzoin.[12] A plot of benzaldehyde disappearance and of benzoin formation versus time (Fig. 1) is best evaluated by assuming that the reaction is first order in benzaldehyde and the first order rate constant is calculated as $k = 2.0 \times 10^{-4}$ s^{-1}.[13] Under initial reaction conditions, **1** shows a turnover rate of 15 per hour.[13]

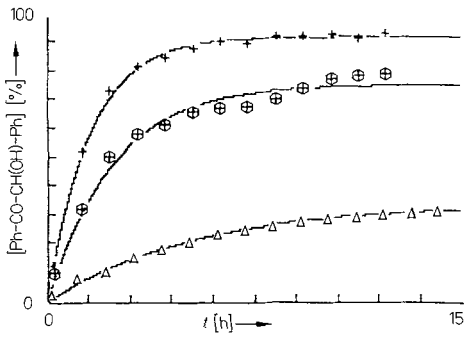
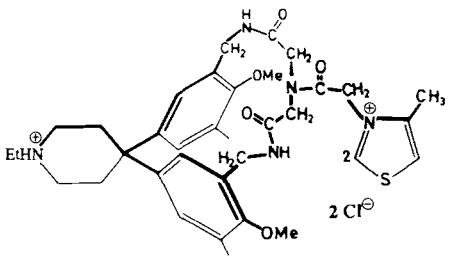


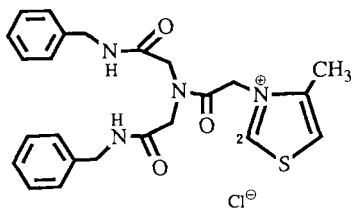
Fig. 1. Increase in benzoin concentration versus time followed by ^{1}H-NMR. [PhCHO]$_0$ = 400 mmol·L^{-1}, [NEt_3] = 60 mmol·L^{-1}, T = 323 K in [D_4]methanol. +: [**1**] = 20 mmol·L^{-1}, ⊕: [**7**] = 20 mmol·L^{-1}, Δ: [**8**] = 20 mmol·L^{-1}.

Using the above mentioned conditions, we compared the catalytic activity of **1** and of thiazolium derivatives lacking the macrocyclic binding site (Fig. 1): Reaction in the presence of macromonocycle **7**,[9] which was prepared following the procedures described above for **1**, led to a 74% isolated yield of benzoin after 12 h. We explain the considerable activity of **7** by the fact that this macromonocycle, according to examinations of CPK models, can provide a niche-binding site for benzaldehyde. The non-macrocyclic thiazolium-derivative **8**[9] gave only a 27% yield of benzoin after 12 h. Considerably smaller yields were also obtained in the presence of simple thiazolium salts like *N*-benzylthiazolium bromide, *N*-phenacylthiazolium bromide or thiamine (vitamin B_1). Macrobicycle **1** being a better catalyst than thiazolium derivatives without a macrobicyclic binding cavity demonstrates the importance of collecting and orienting the reacting partners by complexation prior to the catalytic event.

We have now started investigating in detail the mechanism of the benzoin condensation in the presence of **1**. From the dependence of the initial reaction rates on the aldehyde concentration we have obtained evidence for saturation kinetics. In dimethyl sulfoxide ([**1**] = 20 mmol·L^{-1}, [NEt_3] = 160 mmol·L^{-1}, and [$NHEt_3^{\oplus}Cl^{\ominus}$] = 100 mmol·L^{-1}) at 323 K the maximum rate of benzoin formation is observed at [benzaldehyde] ≈ 3.5 mol·L^{-1}.[14] We also observed that the molecular cavity binding site of **1** has a large effect on the rate of H/D-exchange at C-2′ of the thiazolium ring.[15] In a KCl/DCl buffer at pD = 1.84, T = 303 K, the rate of H/D-exchange observed by ^{1}H-NMR is $k_{obs} = 1.48 \times 10^{-3}$ s^{-1}.[16] Under the same conditions the rates of H/D-exchange at C-2 of the thiazolium rings in **7** ($k_{obs} = 4.88 \times 10^{-5}$ s^{-1}) and in **8**



7



8

($k_{obs} = 2.25 \times 10^{-5}$ s^{-1}) are considerably smaller. We tentatively explain the enhanced rate of H/D-exchange by a micropolarity effect of the cavity of **1** on the acidity of 2′-H of the thiazolium ring. The macrobicycle **1** also catalyzes the reverse reaction: With [**1**] = 20 mmol·L^{-1} and [Ph–CO–CH(OH)–Ph] = 800 mmol·L^{-1} in Me_2SO ([NEt_3] = 160 mmol·L^{-1} and [$NHEt_3^{\oplus}Cl^{\ominus}$] = 100 mmol·L^{-1}) at 323 K, we observed formation of benzaldehyde in 15% yield after 23 h. Under these conditions, the reaction starting with benzaldehyde leads to 50% yield of benzoin after 24 h.

In conclusion, **1** exhibits many features that are typical of the natural, TPP dependent enzymes and it is the most efficient molecular catalyst for the benzoin condensation known today. With **1**, we are currently investigating cross acetoin condensations[2e] between aromatic and alicyclic aldehydes with different affinity to the binding site as well as Stetter additions[17] of active aldehydes to complexed unsaturated carbonyls. The synthesis of molecular hosts with more enforced binding sites and with suitably located functional groups that provide intramolecular general acid-base catalysis as well as the preparation of chiral thiazolium-macrocycles for asymmetric acetoin condensations[2b, 3b] are now under way.

Received: August 29, 1986;
revised: September 29, 1986 [Z 1911 IE]
German version: *Angew. Chem.* 98 (1986) 1125

[1] a) L. Stryer, *Biochemistry*, Freeman, San Francisco 1981; b) C. Walsh, *Enzymatic Reaction Mechanisms*, Freeman, San Francisco 1979.

[2] a) R. Breslow, *J. Am. Chem. Soc. 80* (1958) 3719; b) J. C. Sheehan, T. Hara, *J. Org. Chem. 39* (1974) 1196; c) Y. Yano, Y. Tamura, W. Tagaki, *Bull. Chem. Soc. Jpn. 53* (1980) 740; d) T. Matsumoto, H. Yamamoto, S. Inoue, *J. Am. Chem. Soc. 106* (1984) 4829; e) T. Matsumoto, M. Ohishi, S. Inoue, *J. Org. Chem. 50* (1985) 603.

[3] For the benzoin condensation in thiazolium-micelles, see: a) W. Tagaki, H. Hara, *J. Chem. Soc. Chem. Commun. 1973*, 891; b) W. Tagaki, Y. Tamura, Y. Yano, *Bull. Chem. Soc. Jpn. 53* (1980) 478.

[4] For the benzoin condensation in the presence of thiazolium-cyclodextrin derivatives, see: D. Hilvert, R. Breslow, *Bioorg. Chem. 12* (1984) 206.

[5] a) F. Diederich, K. Dick, *J. Am. Chem. Soc. 106* (1984) 8024; b) F. Diederich, D. Griebel, *ibid.* (1984) 8037; c) F. Diederich, K. Dick, D. Griebel, *Chem. Ber. 118* (1985) 3588.

[6] a) F. Diederich, K. Dick, D. Griebel, *J. Am. Chem. Soc. 108* (1986) 2273; b) for the complexation between polar naphthalene derivatives and macrocyclic hosts in organic solvents, see: S. Ferguson, F. Diederich, *Angew. Chem. 98* (1986) 1127; *Angew. Chem. Int. Ed. Engl. 25* (1986) 1127.

[7] a) W. P. Jencks, *Adv. Enzymol. Relat. Areas Mol. Biol. 43* (1975) 219; b) T. C. Bruice, *Annu. Rev. Biochem. 45* (1976) 331; c) F. M. Menger, *Acc. Chem. Res. 18* (1985) 128.

[8] The preparation of the tetramine **2** follows the synthesis described for a similar macrocycle; see: G. Schürmann, F. Diederich, *Tetrahedron Lett. 27* (1986) 4249.

[9] Elemental analysis and spectroscopic data (IR, 500 MHz 1D- and 2D-COSY ^{1}H-NMR, EI-MS and FAB-MS) support the structures proposed for all new compounds.

[10] Diester **3** was prepared in 91% yield [9] from *N*-benzyloxycarbonyl-*N*-carboxymethylglycine and pentafluorophenol in the presence of dicyclohexylcarbodiimide.

[11] Compound **1**·2 H_2O: m.p. 265°C (dec.). FAB-MS (*m*-nitrobenzyl alcohol) for **1**: *m/z* 1139.8 (33.7%, $M^{\oplus}-3$Cl), 1138.8 (68.2%, $M^{\oplus}-H-3$Cl), 1137.8 (100%, $M^{\oplus}-2H-3$Cl), 1136.8 (15.8%, $M^{\oplus}-3H-3$Cl). IR (KBr): $\tilde{\nu}=1670$ cm^{-1} (C=O). ^{1}H-NMR (1D- and 2D-COSY, 500 MHz, [D_6]Me_2SO, 303 K): $\delta=1.15$–1.25 (m, 6H, $^{\oplus}NCH_2CH_3$), 1.45–1.60 (m, 8H, 4-, 5-, 25-, 26-*H*), 1.60–1.85 (m, 8H; 3-, 6-, 24-, 27-*H*), 2.11 (s, 6H; 14-, 20-CH_3), 2.16 (s, 12H; 31-, 35-, 39-, 41-CH_3), 2.31 (s, 3H; 4′-CH_3), 2.30–2.35 (m, 4H; 3″-5″-, 3‴-, 5‴-H_{ax}), 2.55–2.80 (m, 4H; 3″-, 5″-, 3‴-, 5‴-H_{eq}), 2.85–3.15 (m, 8H; $^{\oplus}NCH_2CH_3$, 2″-, 6″-, 2‴-, 6‴-H_{ax}), 3.40–3.50 (m, 4H; 2″-, 6″-, 2‴-, 6‴-H_{eq}), 3.55–3.75 (m, 8H; 2-, 7-, 23-, 28-*H*), 4.10–4.55 (m, 8H; CH_2NCH_2, aryl-CH_2NH), 5.30–6.15 (m, 2H; $CO-CH_2-N^{\oplus}$), 6.80–7.05 (m, 8H; 11-, 13-, 17-, 21-, 32-, 34-, 38-, 42-H), 7.98 (s, br, 1H; 5′-H), 8.68, 8.82, 9.26, 9.35 (4 "t", 2H; N–*H*), 10.12 (s, 1H; 2′-*H*). The spectrum of **1** at 303 K corresponds to a mixture of an unknown number of conformers since the rotations around the three amide bonds and the chair inversions of the two protonated spiro piperidinium rings [6a] with equatorially positioned *N*-ethyl groups are slow. In [D_6]Me_2SO at $T=418$ K (200 MHz) the rotations around the amide bonds and the chair inversions are fast on the NMR time scale and a considerably simpler spectrum corresponding to one homogeneous compound is obtained.

[12] The change in integrated intensity of the proton signals of substrate and product was followed relative to the intensity of the methyl signal of triethylamine as internal standard. A pulse width of 2 μs and a delay time of 3.6 s assured very reproducible integrations.

[13] The first-order rate constant was calculated using a computer program which fits the experimental data for the disappearance of the aldehyde proton according to the equation $y=a\cdot e^{-k\cdot t}+b$. A fit over all data points gives the empirical equation $y=14.83\cdot e^{-0.749\cdot t}+0.65$ and $k=0.75$ h^{-1}. No significant b-value is obtained, if only the four first data points are fitted. The experimental data could not be fitted according to an integrated second-order rate equation. The turnover rate is expressed as molecules of substrates (initial concentration) reacting per hour per molecule of catalyst; see H. R. Mahler, E. H. Cordes: *Biological Chemistry*, 2nd edit., Harper-Row, New York 1971, p. 277.

[14] A more detailed analysis will have to show whether the observed saturation kinetics corresponds to a 1:1 or to a 1:2 (catalyst: benzaldehyde) Michaelis-Menten complex.

[15] For the observation of a macrocyclic effect on H/D-exchange rates, see: F. Vögtle, W. M. Müller, *Angew. Chem. 96* (1984) 711; *Angew. Chem. Int. Ed. Engl. 23* (1984) 712; F. Vögtle, J. Franke, *ibid. 97* (1985) 224 and *24* (1985) 219.

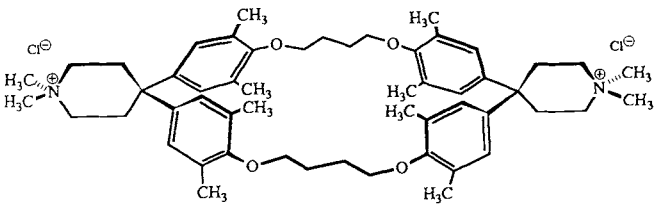
[16] For the determination of k_{obs} in the H/D-exchange of thiazolium derivatives, see: P. Haake, L. P. Bausher, W. B. Müller, *J. Am. Chem. Soc. 91* (1969) 1113.

[17] H. Stetter, *Angew. Chem. 88* (1976) 695; *Angew. Chem. Int. Ed. Engl. 15* (1976) 639.

Electron Donor-Acceptor Interactions in Host-Guest Complexes in Organic Solutions**

By *Stephen B. Ferguson* and *François Diederich**

The role of electron donor-acceptor (EDA) interactions in molecular complexation has attracted much interest over the past decades.[1] These weak intermolecular interactions may be a major driving force for specific complexation in biological systems.[2] Major components of the interaction energy in EDA complexes are defined as electrostatic interaction, polarization interaction, and charge-transfer interaction in addition to dispersion energy.[1a] In the growing field of host-guest chemistry, which mimics biological complexation, several researchers have discussed contributions of EDA interactions to the stability of complexes formed in solution and in the solid state.[3] We now report the first quantitative evidence for these interactions in designed host-guest complexes.



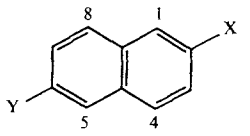
1

Our studies compare the strength of complexation between macrocycle **1**[4] as host and a series of sixteen 2,6-disubstituted naphthalene derivatives **2a**–**p** as guests. The binding cavity of **1** has high steric complementarity to all of these guests which have a similar size and shape but differ in their electronic properties. These guests can be divided into three categories: a) naphthalene derivatives with two donor substituents (e.g. CH_3-, CH_3O-, $HO-$, H_2N-; **2a**–**e**), b) naphthalene derivatives with two acceptor substituents (e.g. $-CN$, $-COOR$, $-NO_2$; **2l**–**p**), and c) naphthalene derivatives with one donor and one acceptor substituent (**2f**–**k**).

^{1}H-NMR complexation studies in [D_4]methanol ([host]$_0$ = [guest]$_0$ = 5.0 mmol·L^{-1}) indicate that all 2,6-disubstituted naphthalene guests form highly structured 1:1 complexes of similar geometry with **1**. Complexed guests prefer a pseudoaxial position in the cavity of **1**; Figure 1 shows the averaged geometry of the complexes as deduced from the NMR complexation shifts.[5] This geometry of the complexes allows for π-π interactions between the guest and the benzene rings of the host.[6] Due to the rapid equilibrium of complexation, ^{1}H-NMR titrations provided quantitative determination of the binding between **1** and **2a**–**p** in [D_4]methanol (500 MHz, $T=303$ K, methyl peak of the solvent taken as reference). Concentrations of host and guest were chosen to vary the percentage of complexation from about 10–80% (e.g. [**2p**] = 1.1 mmol·L^{-1}, [**1**] = 3.0 to 22 mmol·L^{-1}). The association

[*] Prof. Dr. F. Diederich, Stephen B. Ferguson
Department of Chemistry and Biochemistry
University of California
Los Angeles, California 90024 (USA)

[**] This work was supported in part by Merck Sharp & Dohme, Rahway, NJ; we thank Prof. *K. N. Houk* (Los Angeles) for valuable discussions.



2a-p

Table 1. Association constants (K_a, error: ±10%), free energies of complexation ($-\Delta G$), maximum observed ^{1}H-NMR upfield shifts ($\Delta\delta_{max.obs.}$) and calculated saturation upfield shifts ($\Delta\delta_{sat}$) for the complexes of host **1** and the 2,6-disubstituted naphthalene derivatives **2a-p** in [D$_4$]methanol, T=303 K.

	Guest Proton Evaluated	$\Delta\delta_{max.obs.}$ [ppm]	$\Delta\delta_{sat}$ [ppm]	K_a [L·mol^{-1}]	$-\Delta G$ [kcal·mol^{-1}]
Donor-donor guests:					
2a, X=Y=CH$_2$OH	1	0.48	1.80	20	1.80
2b, X=Y=OH	4	0.65	2.02	24	1.91
2c, X=Y=NH$_2$	1	0.57	1.51	33	2.11
2d, X=Y=OCH$_3$	1	0.75	1.57	47	2.32
2e, X=Y=CH$_3$	1	1.02	1.79	67	2.53
Donor-acceptor guests:					
2f, X=CH$_3$ Y=CHO	8	1.34	2.18	98	2.76
2g, X=NH$_2$ Y=NO$_2$	4	1.43	2.28	102	2.78
2h, X=OCH$_3$ Y=NO$_2$	8	1.53	2.23	109	2.82
2i, X=OCH$_3$ Y=CN	8	1.45	2.21	117	2.87
2j, X=OCH$_3$ Y=COOH	5	0.82	1.21	135	2.95
2k, X=OH Y=CN	8	1.65	2.24	157	3.04
Acceptor-acceptor guests:					
2l, X=Y=OAc	4	1.48	2.27	109	2.82
2m, X=Y=CO$_2$CH$_3$	4	1.87	2.36	188	3.15
2n, X=Y=CO$_2$H	4	1.90	2.33	210	3.22
2o, X=Y=NO$_2$	4	1.87	2.30	213	3.23
2p, X=Y=CN	1	2.11	2.47	277	3.39

constants of the 1:1 complexes were determined from the titration curves by using a computer-assisted non-linear curve-fitting procedure.[7] Table 1 gives the observed maximum complexation shift ($\Delta\delta_{max.obs.}$) of the guest proton whose signal can be best observed over the entire titration, the calculated complexation shift of this proton at saturation binding ($\Delta\delta_{sat}$), the association constants (K_a), and the free energies of complexation (ΔG).

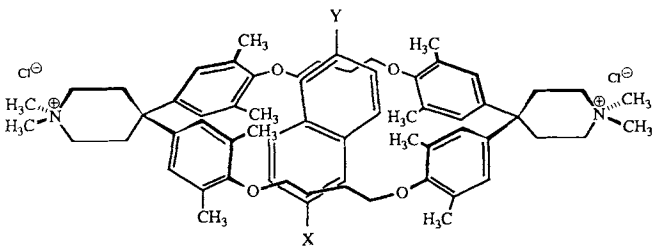


Fig. 1. Averaged geometry of complexes formed between host **1** and guests **2a-p**.

The K_a values in Table 1 show that electron-deficient (acceptor) guests (**2l-p**) form more stable complexes with host **1** than electron-rich (donor) guests (**2a-e**), while guests having one donor and one acceptor substituent (**2f-k**) demonstrate an intermediate stability of complexation. Differences in free energies of complexation can be as large as 1.59 kcal·mol^{-1}. We explain these differences by the major contribution of intermolecular EDA interactions to the stability of complexes. With its four trialkylsubstituted anisole units, compound **1** can be considered a donor host. Corresponding to the expectation that EDA interactions are a driving force for selective complexation, the acceptor guests (**2l-p**) form the most stable complexes with the donor-host **1**. Interestingly, these interactions also affect the geometry of complexes: the analysis of the complexation shifts of the protons of donor-acceptor substituted guests (**2f-k**) shows that in the averaged geometry of the complex the naphthalene moiety bearing the acceptor substituent is located more deeply in the cavity of **1** than the moiety with the donor-substituent. Further evidence that attractive interactions rather than entropically favorable desolvation represent the major driving force for selective complexation was provided by examining the temperature-dependence of the binding. For the **1**·**2p** complex in [D$_4$]methanol, the enthalpic and entropic contributions to the free energy of complexation ΔG are $\Delta H = -7.6$ kcal·mol^{-1} and $\Delta S_{303\,K} = -14.1$ cal·mol^{-1}·K^{-1}.

The conclusion that the differences in complexation, observed in [D$_4$]methanol, result from EDA interactions and not from special solvation effects of the polar protic solvent is clearly demonstrated by studies in [D$_6$]dimethyl sulfoxide. While considerably weaker binding of guests is observed in this solvent than in methanol, we find the same trends in complexation strength. Acceptor-acceptor guests form the strongest complexes with **1** while donor-acceptor and donor-donor guests form progressively weaker complexes. From the complexation shifts with [host]$_0$=20 mmol·L^{-1} and [guest]$_0$=5.0 mmol·L^{-1} and the saturation shifts obtained from methanol titrations, the association constants in dimethyl sulfoxide are estimated.[8,9] Examples of K_a values in [D$_6$]Me$_2$SO (T=303 K) are: for the **1**·**2d** complex $K_a \approx 1.6$ L·mol^{-1} ($-\Delta G \approx 0.28$ kcal·mol^{-1}), for the **1**·**2k** complex $K_a \approx 6.4$ L·mol^{-1}, and for the **1**·**2p** complex $K_a \approx 11.5$ L·mol^{-1} ($-\Delta G \approx 1.47$ kcal·mol^{-1}).

The electronic complementarity between host and guest is not as crucial for the strong complexation of substituted aromatic guests in aqueous solution. In D$_2$O/CD$_3$OD (60:40) with [host]$_0$=[guest]$_0$=5 mmol·L^{-1} (T=303 K), strong complexation between **1** and *all* naphthalene guests is evidenced by complexation shifts approaching the saturation shifts observed in [D$_4$]methanol.[10] In aqueous solution the entropically favored desolvation ("hydrophobic effect") rather than attractive EDA interactions provides the major driving force for complexation.[11]

In conclusion, our study demonstrates that electronic complementarity between host and guest is of special importance for the complexation of aromatic guests in organic solvents.[12] We were able to give quantitative evidence that electron donor-acceptor interactions can be a major driving force of complexation. The additional stabilization of donor host-acceptor guest complexes involves electrostatic and polarization interactions rather than charge-transfer (electron delocalization) interactions, since the complexes do not give any charge-transfer bands in the electronic absorption spectra.[13,14] We are currently preparing hosts with donor properties far superior to those of **1** as well as highly electron-deficient hosts. We expect to find significantly larger differences in the association constants of complexes formed by these new hosts and naphthalene guests with high and low electronic complementarity than we observed for the complexes of **1**.[15] It will be interesting to see if charge-transfer interactions can be observed in these complexes and if, as a consequence of par-

tial electron delocalization in the ground state, these complexes are more stabilized.

Received: August 29, 1986;
revised: September 29, 1986 [Z 1912 IE]
German version: *Angew. Chem. 98* (1986) 1127

[1] a) K. Morokuma, *Acc. Chem. Res. 10* (1977) 294. This review provides a comprehensive description of the component analysis to describe EDA interactions in complexes; b) M. W. Hanna, J. L. Lippert in R. Foster (Ed.): *Molecular Complexes*, Vol. 1, Elek Science, London 1973, pp. 1–48; c) H. A. Staab, C. P. Herz, C. Krieger, M. Rentea, *Chem. Ber. 116* (1983) 3813, and further references cited therein.

[2] For a discussion of EDA interactions in biological systems, see a) B. Pullman, A. Pullman, *Quantum Biochemistry*, Wiley Interscience, New York 1963; b) R. Foster, *Organic Charge-Transfer Complexes*, Academic Press, London 1969, Chapt. 12, pp. 335–373.

[3] a) D. J. Cram in J. B. Jones, C. J. Sih, D. Perlman (Eds.): *Applications of Biochemical Systems in Organic Chemistry*; A. Weissberger (Ed.): *Techniques in Chemistry*, Vol. 10, Part II, Wiley, New York 1976, pp. 815–873; b) H. M. Colquhoun, E. P. Goodings, J. N. Maud, J. F. Stoddart, J. B. Wolstenholme, D. J. Williams, *J. Chem. Soc. Perkin Trans. 2 1985*, 607; H. M. Colquhoun, S. M. Doughty, J. F. Stoddart, A. M. Z. Slawin, D. J. Williams, *ibid. 1986*, 253; c) J. Rebek, Jr., D. Nemeth, *J. Am. Chem. Soc. 107* (1985) 6738.

[4] F. Diederich, K. Dick, D. Griebel, *Chem. Ber. 118* (1985) 3588.

[5] For an extensive analysis of the ^{1}H-NMR complexation shifts of host and guest supporting a preferred time-averaged pseudoaxial inclusion of 2,6-disubstituted naphthalenes in cavities of hosts with two diphenylmethane units, see ref. [4] and F. Diederich, D. Griebel, *J. Am. Chem. Soc. 106* (1984) 8037; see also: K. Odashima, A. Itai, Y. Iitaka, Y. Arata, K. Koga, *Tetrahedron Lett. 21* (1980) 4347. The analysis of the ^{1}H-NMR complexation shifts indicates that in the complexes of the symmetrical guests, each ring of the naphthalene unit is located equally deep in the cavity; in the complexes of the donor-acceptor guests the naphthalene moiety bearing the acceptor substituent is, in the time average, enclosed more deeply in the cavity.

[6] The X-ray analysis of a benzene complex of a very similar host also supports the possibility of π-π interactions in the complexes of **1**: C. Krieger, F. Diederich, *Chem. Ber. 118* (1985) 3620.

[7] The function of $\Delta\delta_{obs}$ in terms of the initial host concentration is solved by a non-linear least squares curve fitting procedure to determine the two parameters $1/K_a$ and $\Delta\delta_{sat}$ for each titration. For a previously reported use of this method, see H. J. Schneider, K. Philippi, J. Pöhlmann, *Angew. Chem. 96* (1984) 907; *Angew. Chem. Int. Ed. Engl. 23* (1984) 908.

[8] The use of the saturation shifts obtained in [D$_4$]methanol for estimating the association constant of the same complex in [D$_6$]dimethyl sulfoxide is valid, since the geometries of complexes, according to ^{1}H-NMR, are almost identical in both solvents. For identical geometries of complexes, very similar complexation shifts at saturation binding can be assumed. For further discussions and support for this rapid method of estimating association constants of the same complex in various solvents, see: F. Diederich, K. Dick, D. Griebel, *J. Am. Chem. Soc. 108* (1986) 2273. From the detailed analysis provided in this paper, the error of the ΔG-values is estimated as ±10%.

[9] A series of nine complexes have been analyzed in [D$_6$]Me$_2$SO; the sequence of complexation strength is the same as in [D$_4$]methanol.

[10] Stoichiometric complexation in pure water could not be studied since the critical micelle concentration of **1** is too low (< 0.02 mmol·L^{-1}; [4]). The observation of near saturation binding of all guests in D$_2$O/CD$_3$OD (60/40) under our experimental conditions interferes with the estimations of association constants as described in ref. [8]. Therefore, differences in complexation strength in aqueous solutions due to EDA interactions can only be shown by further studies.

[11] These findings are in full agreement with previous studies in aqueous solution, see F. Diederich, K. Dick, *J. Am. Chem. Soc. 106* (1984) 8024.

[12] It is obvious that the steric complementarity between host and guest has to be optimal if weak attractive interactions that are extremely distance dependent are the major driving force of complexation. The importance of steric complementarity for complexation of neutral guests in organic solvents had been shown in a previous study with arenes of different size; see ref. [8].

[13] In the electronic spectrum of **1**·**2p** in methanol ([host]$_0$ = 5 mmol·L^{-1} and [guest]$_0$ = 1 mmol·L^{-1}), the bands of the complexed dinitrile at longest wavelength (λ_{max} = 328 and 342) that are not overlapped by bands of the host show small bathochromic shifts (2–4 nm), hypochromicity, and broadening indicating transannular interactions.

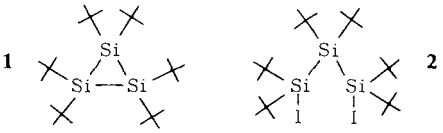
[14] Contributions to the observed binding differences from steric and polarization interactions of the various guest substituents with the host as well as contributions from the different solvation of the polar groups cannot be completely ruled out. To minimize these effects, we chose the 2,6-disubstituted naphthalenes as guests which locate the substituents more outside the cavity of **1**.

[15] In the meantime, we have prepared the *bis*(N-acetylpiperidine) derivative of a host very closely related to **1** with eight methoxy groups instead of eight methyl groups attached to the two diphenylmethane units. In preliminary studies, we observed almost complete absence of complexation of **2d** in [D$_4$]methanol, whereas considerable complexation occurs with **2p**; P. Inocencio, F. Diederich, unpublished results.

Hexa-*tert*-butyl-1,3-diiodotrisilane, a Molecule with Two Neighboring Very Long Si–Si Bonds**

By *Manfred Weidenbruch,* Bolko Blintjer, Karl Peters,* and *Hans Georg von Schnering**

About two years ago we reported the preparation of hexa-*tert*-butylcyclotrisilane (**1**), a molecule containing the longest intramolecular bond distances known at that time, namely d(Si–Si) = 251.1 pm, i.e. 16 pm longer than a normal Si–Si single bond (235 pm). This corresponds to a reduction of the Pauling bond order (PBO) to 0.54 and thus to a C–C bond length of 170 pm. Moreover, the stretching of the Si–C bonds to 198 pm (mean value in carbosilanes 188 pm) and the widening of all β(Si–C–C) bond angles at the central C atoms of the substituents impressively bear witness of the enormous intramolecular steric interactions in such a strained molecule.[1]



The remarkable stability of **1** has been attributed to optimal shielding of the Si–Si bonds by the closely packed substituents. Furthermore, the enforced conformation of the substituents on the three-membered Si$_3$ ring contributes quite significantly to a reduction in the repulsive interactions.[1] Namely, one can show, e.g., that the van der Waals contacts between Me-groups of neighboring C atoms in permethylated open-chain hydrocarbons are increased from 1.67 d in eclipsed conformations to 1.92 d in staggered conformations; in contrast, in hexamethylcyclopropane such contacts reach 2.00 d (d = C–C bond length).

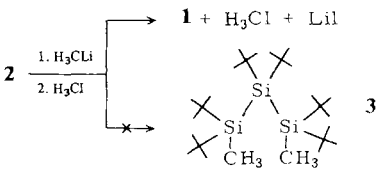
Opening of the cyclotrisilane ring of **1** should lead to formation of molecules with a staggered arrangement of the substituents, with bond angles β(Si–Si–Si) > 109.5° and, possibly, with even longer Si–Si bonds. With suitable reagents, such reactions take place in thermal equilibrium. They lead, on the one hand, to ring insertion,[2] and, on the other, also to open-chain trisilanes.[3] Of the latter, 1,1,2,2,3,3-hexa-*tert*-butyl-1,3-diiodotrisilane (**2**) is especially interesting because the steric influence of iodine is

[*] Prof. Dr. M. Weidenbruch, B. Flintjer
Fachbereich Chemie der Universität
Carl-von-Ossietzky-Strasse 9–11, D-2900 Oldenburg (FRG)
Prof. Dr. H. G. von Schnering, Dr. K. Peters
Max-Planck-Institut für Festkörperforschung
Heisenbergstrasse 1, D-7000 Stuttgart 80 (FRG)

[**] Silicon Bonds with Strong Intramolecular Steric Interactions, Part 25. This work was supported by the Deutsche Forschungsgemeinschaft and the Fonds der Chemischen Industrie. — Part 24: M. Weidenbruch, K.-L. Thom, *J. Organomet. Chem. 308* (1986) 177.

still considerable, even in presence of *tert*-butyl groups. **2** is formed as a colorless, crystalline product (m.p. 112°C) upon reaction of **1** with iodine.[3] The X-ray structure analysis confirms the above predictions (Fig. 1). Again the bond distances d(Si-Si) = 258.1 pm and 264.4 pm are drastically enlarged and correspond to Pauling bond orders[4] of 0.41 and 0.32, respectively. The β(Si-Si-Si) bond angle (115.8°) is widened considerably, despite the elongated Si-Si bonds. Here also, the Si-C bonds afford no compensation for the loss in bond strength; on the contrary, the stretching of the peripheral distances to $\bar{d}$(Si-C) = 198.9 pm and $\bar{d}$(Si-I) = 255.1 pm (instead of 188 and 246 pm, respectively) also indicate weakening of these bonds to PBO = 0.66 and 0.71, respectively. Finally, the strain also manifests itself in the increased bond angles $\bar{\beta}$(Si-C-C) = 112°.

The sum of the PBOs for the bonds to the Si atoms (nine in **1** and ten in **2**) are 5.70 and 6.11, respectively; i.e. the loss in bond order compared with Σ(PBO) = 9 and 10, respectively, increases from 3.30 to 3.89, thus indicating greater stability of the cyclic molecule **1**. An interesting observation in this respect is that the attempted formation of 1,1,2,2,3,3-hexa-*tert*-1,3-dimethyltrisilane **3** by dimetalation of **2** followed by methylation with iodomethane did not succeed, but led once again to the cyclic compound **1** [Eq. (a)]. Besides the presumably greater stability of **1**, the formation of crystalline LiI and volatile H_3CI is also important for the observed reaction.



(a)

In solution, both halves of the molecule **2** are equivalent, since the ^{1}H-NMR spectrum [δ = 1.38 (s, 36H) and 1.48 (s, 18H)] shows no splitting, even at −80°C. The remarkably large chemical shifts (downfield) in the ^{29}Si-NMR spectrum (79.47 MHz) are δ = 45.980 ppm for the two terminal Si atoms and δ = 32.945 ppm for the central Si atom.[5] In the crystal, the molecule **2** is unsymmetrical. The conformation and bond lengths in the two halves are different (Fig. 1 and Fig. 2); this could be due to the packing in the crystal. However, there are also arguments in favor of the observed deformations being an intrinsic property of **2**. Thus, we have found by a series of calculations that, on allowing for acceptable bond angles and stepwise rotation of the substituents, the spectrum of all non-bonding distances (van der Waals contacts) limits the allowed conformations considerably. In particular, it emerges that no twofold conformation with completely equivalent halves (C_2 axis) would lead to tolerable intramolecular distances, and, furthermore, that the observed deformations of the bond angles are necessary. According to these calculations it actually appears as though the observed conformation is at the same time the optimal one. However, one can only assume that unequal stretching of the two Si-Si bonds represents the optimal solution for internal strain.

In the meantime, *Wiberg* et al.[6] have described the synthesis of the thermally remarkably stable compound tBu$_3$SiSitBu$_3$, **4**, which exhibits an even larger intramolecular Si-Si bond distance (269.7 pm, PBO = 0.26[4]) than **1**. The stretching of the Si-C bonds and the angle deformations are similar to those observed in **1** and **2**. The d(Si-Si) bond lengths in **1**, **2**, and **4** are linearly correlated with n (the average number 2, 2.5, or 3 of bulkyl substituents per Si atom):

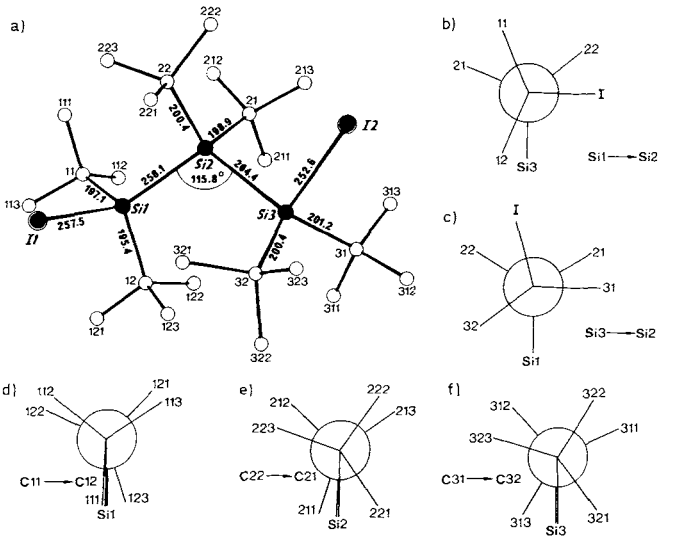


Fig. 1. a) Crystal structure of **2** (without H atoms) with bond distances in pm and the angle Si1-Si2-Si3. Standard deviations: σ(Si-I) = 0.1, σ(Si-Si) = 0.1, σ(Si-C) = 0.4 pm; σ(Si/Si/Si) = 0.1°. The numbers are the crystallographic denominations of the atoms. Si1, Si2, and Si3 each form the bridge atoms in the projections C11→C12, C22→C21, and C32→C31 (below), respectively. The compound crystallizes triclinically: $P\bar{1}$ (No. 2), a = 1094.2, b = 1827.8(5), c = 931.1(2) pm; α = 93.04(2), β = 111.39(2), γ = 99.88(2)°, Z = 2, ρ_{calc} = 1.360 g cm^{-3}, 6306 hkl with $F > 3\sigma(F)$, R = 0.030. Further details of the crystal structure investigation are available on request from the Fachinformationszentrum Energie, Physik, Mathematik GmbH, D-7514 Eggenstein-Leopoldshafen 2 (FRG), on quoting the depository number CSD-51754, the names of the authors, and the full citation of the journal. b) + c) Newman projections. d)-f) In these projections along the vector of two indirectly bound C atoms, in each case one Si atom is the center coupling the two C atoms.

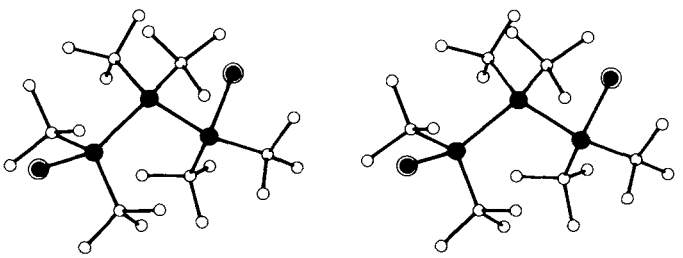


Fig. 2. Stereoview of **2** (Si = ●; I = ◉; C = ○; H atoms omitted). The orientation corresponds to that in Figure 1a.

$$d(\text{Si–Si}) = (18.6\,n + 214)\ \text{pm} \qquad \text{(b)}$$

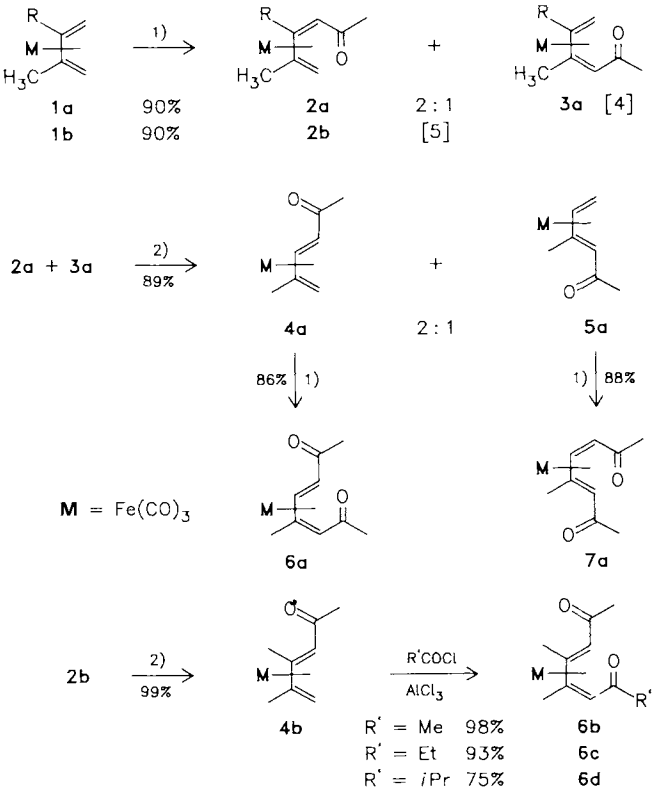
With n = 1.5 one obtains d = 245 pm, the mean value for the bond lengths in the *cis-cis*- and *cis-trans*-isomeric 1,2,3-tri-*tert*-butyl-1,2,3-trimesitylcyclotrisilanes.[7] This means that the steric influence of a mesityl group is about half as large as that of a *tert*-butyl group. The normal length of a single bond (235 pm) is expected with n ≤ 1.1, that is in a cyclotrisilane with six substituents, whose steric influence is half that of *tert*-butyl groups, or in a disilane with six substituents which have only a third of the influence of *tert*-butyl groups. That is, one could use the aforementioned relation (b) for the classification of the steric influence of substituents.

A further aspect emerges from a comparison of the Si–Si bonds in **1**, **2**, and **4**: if one assumes that the bonds of the Si_3 ring in **1** are arched, then the "analog calculation" with a model kit[8] using the Si–Si distance of 251 pm gives a value of 265 pm for the linear bond. This would then be the "normal" length of an Si–Si bond between two atoms with *tert*-butyl groups as substituents.

Received: January 16, 1986;
revised: September 1, 1986 [Z 1627 IE]
German version: *Angew. Chem. 98* (1986) 1090

CAS Registry numbers:
1, 89463-49-0; **2**, 105251-61-4.

[1] A. Schäfer, M. Weidenbruch, K. Peters, H. G. von Schnering, *Angew. Chem. 96* (1984) 311; *Angew. Chem. Int. Ed. Engl. 23* (1984) 302.
[2] M. Weidenbruch, A. Schäfer, *J. Organomet. Chem. 269* (1984) 201.
[3] Procedure: **2**: A solution of iodine in *n*-hexane was added dropwise at room temperature to a solution of **1** (2.00 g, 4.69 mmol) in *n*-hexane (30 mL) until the red-coloration no longer disappeared. After removal of the solvent by distillation and removal of the excess iodine under vacuum, subsequent recrystallization of the residue from isopropanol furnished 2.26 g (71%) of colorless crystals of **2**. MS (70 eV): *m/z* 623 ($M^{\oplus}-t$Bu, 4%), 539 ($M^{\oplus}-t$Bu$_2$Si, 39), 481 (53).
[4] Calculated according to the relationship $\log(PBO)=[d(1)-d(PBO)]/60$ with $d(1)$ = normal single bond distance (235 pm); cf. L. Pauling: *The Nature of the Chemical Bond*, Cornell Univ. Press, Ithaca 1973.
[5] A. G. Brook (Toronto), private communication.
[6] N. Wiberg, H. Schuster, A. Simon, K. Peters, *Angew. Chem. 98* (1986) 100; *Angew. Chem. Int. Ed. Engl. 25* (1986) 79.
[7] J. C. Dewan, S. Murakami, J. T. Snow, S. Collins, S. Masamune, *J. Chem. Soc. Chem. Commun. 1985*, 892.
[8] H. G. von Schnering, unpublished.



Scheme 1. 1) AcCl/$AlCl_3$. 2) 1. AcCl, 20°C, 0.5 h; 2. H_2O. **a**, R = H; **b**, R = Me.

2,4-Diene-1,6-diones and 2-Acyl-3-cyclopenten-1-ols by Double Friedel-Crafts Acylation of Tricarbonyl(diene)iron Complexes

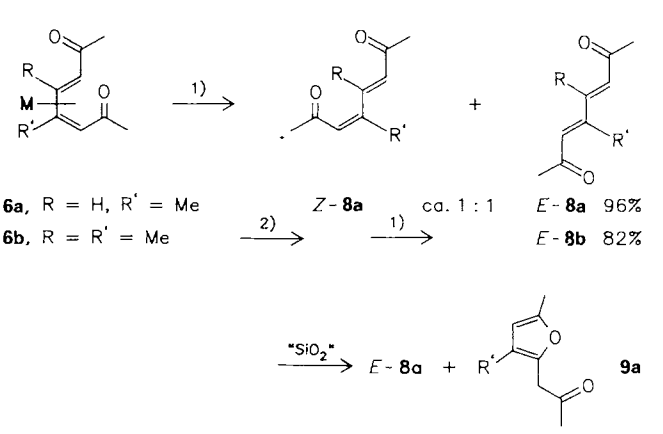
By *Michel Franck-Neumann,* Madjid Sedrati,* and *Mohamed Mokhi*

Dienes in tricarbonyl(diene)iron complexes (diene = unsubstituted, methyl- or aryl-substituted butadiene) are known to be acylated in the 1- or 4-position by Friedel-Crafts reagents.[1] The acyl residue is bonded *cis* to the diene moiety at the C-atom with the least number of substituents. A second acylation should not be possible, even after previous *cis-trans* isomerization.[1b,2]

As reported in a recent communication,[3] this does not apply in the case of the 2-triethylsilylbutadiene complex, which is successively acylated in the 4- *and* in the 1-position. This exception from the "rule" prompted us to reinvestigate the Friedel-Crafts acylation of dienone complexes. We found that exclusively carbon-substituted dienes such as isoprene **1a** or 2,3-dimethylbutadiene **1b** bound in complexes can also be acylated twice. The best yields are achieved at a molar ratio of *trans*-dienone complex/acyl chloride/aluminum chloride of 1/2/3 (Scheme 1).

For the *cis-trans*-isomerization, the diene complexes **2a** and **3a** as well as **2b** are dissolved in acetyl chloride; the solution is treated with ice-water and subsequently extracted with Et_2O.[6] The second acylation in dichloromethane at room temperature is a slow reaction, i.e. yields of 75–98% are achieved only after 20 h.[8] A terminal acyl substituent is thus not completely deactivating.

With few exceptions[9] the Friedel-Crafts acylation of tricarbonyl(diene)iron complexes has never been used for the synthesis of purely organic molecules, presumably since the methods for the cleavage of the dienone are not generally applicable. The usual cleavage methods proved unsuitable in particular in the case of the new dienedione complexes.[10] Finally, it was found possible to cleave the diketones by oxidation with H_2O_2 in methanolic NaOH[11] at −15°C (Scheme 2, Route 1).



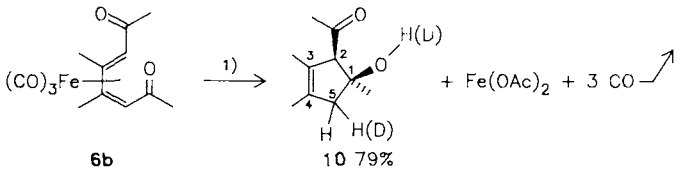
Scheme 2. 1) H_2O_2, NaOH, MeOH, −15°C, 0.5 h. 2) MeONa/MeOH, 20°C, 15 h.

Under these conditions the *cis-trans*-complexes **6** are partly converted into the *trans-trans*-isomers, so mixtures

[*] Dr. M. Franck-Neumann, Directeur de Recherche au CNRS,
Dr. M. Sedrati, Dr. M. Mokhi
Unité de Recherche Associée au CNRS n° 466,
Institut de Chimie de l'Université Louis Pasteur
1, rue Blaise Pascal, F-67008 Strasbourg (France)

of the dienediones *Z*-**8** and *E*-**8** are obtained. The isomer *Z*-**8a** is quantitatively cyclized to the furan derivative **9a** by chromatography on silica gel or, better, by slowly slurrying with silica gel. If the isomerization is carried out prior to the cleavage (Scheme 2, Route 2+1), only the dienediones *E*-**8** are obtained.

Another possible way of cleaving tricarbonyl(diene)iron complexes is by reductive photolysis in acetic acid.[12] Whereas β,γ-unsaturated ketones are obtained from dienone complexes, the photolysis of dienedione complexes leads stereospecifically[13] to *cis*-2-acyl-3-cyclopenten-1-ols (**6b** → **10**, Scheme 3).



6b **10** 79%

Scheme 3. 1) *hv*, AcOH(D), 15 °C [13].

Intermediates could not be detected. Upon irradiation in deuterated acetic acid and work-up with D_2O only a product deuterated at C5 is formed. This rules out formation of a β,γ-unsaturated 1,6-diketone as an intermediate.[14]

The double Friedel-Crafts acylation of tricarbonyl(diene)iron complexes with subsequent cleavage of the metal thus provides a new method for the direct synthesis of 2,4-diene-1,6-diones and 2-acyl-3-cyclopenten-1-ols.

Table 1. Spectroscopic data of the compounds **6b**, *E*-**8b**, and **10**. IR (CCl_4), ^{1}H-NMR (200 MHz, $CDCl_3$, TMS). All the compounds gave correct elemental analyses.

6b: $\tilde{\nu}$(C≡O) = 2060, 2005, 2000 cm^{-1}, $\tilde{\nu}$(C=O) = 1655, 1665 cm^{-1}; δ = 1.95 (1H, s), 2.17 (3H, s), 2.19 (3H, s), 2.20 (3H, s), 2.47 (3H, s), 3.22 (1H, s).

E-**8b**: $\tilde{\nu}$(C=O) = 1683 cm^{-1}, $\tilde{\nu}$(C=C) = 1602, 1588 cm^{-1}; δ = 2.23 (6H, d, J = 1.2 Hz), 2.28 (6H, s), 6.37 (2H, br. s); UV (CH_3CN): λ_{max} (ε) = 277 nm (18500)

10: $\tilde{\nu}$(OH) = 3200-3600 cm^{-1} (associated OH), no bands for free OH, $\tilde{\nu}$(C=O) ≈ 1700 cm^{-1}; δ = 1.44 (3H, s), 1.61 (3H, m), 1.66 (3H, m), 2.19 (3H, s), 2.36 (1H, br. d, J = 16 Hz), 2.46 (1H, s, exchange with D_2O), 2.62 (1H, br. d, J = 16 Hz), 3.33 (1H, br. s)

Procedure

6b: A suspension of anhydrous $AlCl_3$ (2.00 g, 15 mmol) in dichloromethane (10 mL) was treated dropwise at 0 °C, first with a solution of AcCl (0.78 g, 10 mmol) in dichloromethane (5 mL) and then with a solution of **4b** (1.32 g, 5 mmol) in dichloromethane (10 mL). The temperature of the stirred mixture was allowed to increase slowly to 20 °C, and stirring was then continued for a further 16 h. After dropwise addition of the reaction mixture to ice-water and extraction with ether, the organic phase was washed with aqueous $NaHCO_3$ and dried over $MgSO_4$. After removal of the solvent by evaporation, the residue was taken up in a little *n*-hexane, and the resulting solution filtered through a short silicagel column (*n*-hexane with 10% Et_2O): 1.50 g of **6b** (98%), yellow crystals, m.p. 71 °C.

E-**8b**: 1. Isomerization: A solution of **6b** (1.40 g, 4.6 mmol) in methanol (10 mL) was added to a solution of NaOMe (0.50 g (21.7 mmol) Na in methanol (15 mL)). After 15 h at 20 °C the mixture was diluted with water, extracted with ether, and, after removal of solvent, filtered over silica gel (*n*-hexane with 20% Et_2O): 1.29 g *trans-trans* complex (92%), m.p. 86 °C.—2. Cleavage of metal: A solution of 0.20 g (5 mmol) of NaOH in 0.2 mL water and 5 mL of methanol was added dropwise at −20 °C to a solution of 0.90 g (2.9 mmol) of the *trans-trans* complex and 1.50 mL of 30% H_2O_2 in 3 mL of methanol. After 0.5 h at 15 °C the mixture was treated with a saturated NH_4Cl solution and extracted with Et_2O. The extract was washed with water, dried over $MgSO_4$, and, after removal of solvent the residue was filtered over silica gel (*n*-hexane with 20% Et_2O): 0.44 g of *E*-**8b** (89%), pale yellow crystals, m.p. 78 °C.

10: A solution of **6b** (1.20 g, 3.9 mmol) in acetic acid (50 mL) was transferred to a Pyrex glass apparatus, flushed with argon, and then irradiated with a Philips HPK 125 mercury lamp until evolution of CO ceased (ca. 1 h). After dilution with 100 mL of water and neutralization with Na_2CO_3 powder, the mixture was extracted with Et_2O. The organic extracts were dried over $MgSO_4$; the solvent was removed by evaporation and the residue chromatographed on silica gel (*n*-hexane with 20% Et_2O): 0.52 g of **10** (79%), colorless liquid [13].

Received: July 18, 1986;
revised: September 19, 1986 [Z 1863 IE]
German version: *Angew. Chem. 98* (1986) 1138

[1] a) E. O. Greaves, C. R. Knox, P. L. Paulson, *J. Chem. Soc. Chem. Commun. 1969*, 1124; b) R. E. Graf, C. P. Lillya, *J. Organomet. Chem. 122* (1976) 377, and references cited therein.
[2] R. E. Graf, C. P. Lillya, *J. Organomet. Chem. 166* (1979) 53.
[3] M. Franck-Neumann, M. Sedrati, M. Mokhi, *Tetrahedron Lett. 27* (1986) 3861.
[4] R. E. Graf, C. P. Lillya, *J. Am. Chem. Soc. 94* (1972) 8282.
[5] A. N. Nesmeyanov, K. N. Anisimov, G. K. Magomedov, *Izv. Akad. Nauk SSSR Ser. Khim. 1970*, 959.
[6] The conditions for this isomerization of dienone complexes were found in the acetylation of tricarbonyl(2,3-dimethylbutadiene)iron (M. Franck-Neumann, D. Martina, F. Brion, unpublished); the method is not limited to acetylated complexes, however, and is at least comparable with other methods [1, 7]. The isomerization proceeds rapidly and without decomposition, such that the *trans*-dienone complexes are recovered almost quantitatively. Only when a chromatographic separation is necessary (**4a/5a**) is the yield somewhat lower. The separation of the *trans*-dienone complexes is much simpler than that of the original *cis*-dienone complexes.
[7] J. S. Frederiksen, R. E. Graf, D. G. Greshan, C. P. Lillya, *J. Am. Chem. Soc. 101* (1979) 3863.
[8] The parent compound (*trans*-1-acetylbutadiene)tricarbonyliron is converted to only about 60% even after this time, and *cis-trans*- and *trans-trans*-1,4-diacetylbutadiene complexes are formed besides the products of metal-cleavage.
[9] See, e.g. G. R. Knox, I. G. Thorn, *J. Chem. Soc. Chem. Commun. 1981*, 373.
[10] Cerium(IV) ammonium nitrate and trimethylamine oxide act as oxidizing agents, but only mixtures of complexes are formed—as also in the ligand-exchange experiments with phosphanes. With manganese dioxide in boiling benzene, and even with iron(III) chloride in boiling methanol, the complexes either remain unchanged or are isomerized to the *trans-trans* form only!
[11] M. Franck-Neumann, M. P. Heitz, D. Martina, *Tetrahedron Lett. 24* (1983) 1615.
[12] M. Franck-Neumann, D. Martina, F. Brion, *Angew. Chem. 90* (1978) 736; *Angew. Chem. Int. Ed. Engl. 17* (1978) 690.
[13] The *cis*-compounds **10** are solely obtained in ca. 80% yield by neutralization of the acetic acid with Na_2CO_3. With NaOH, the yield is increased considerably (95%), but partial epimerization is observed at the same time.
[14] Upon irradiation of 2-silyl-substituted dienedione complexes in acetic acid the corresponding β,γ-unsaturated diketone could be isolated as by-product. It is stable under the conditions of the photolysis and workup (M. Mokhi, *Dissertation*, Strasbourg 1985).

Valence Isomers of Compounds with Geminal Aryldiazene and Isocyanate Functions Stabilized by Protonation**

By *Hubert Gstach,* Patrick Seil, Joachim G. Schantl, Alfred Gieren, Thomas Hübner,* and *Jin Wu*

In some special cases an X-ray structure analysis of a molecule provides information that is useful not only

[*] Dr. H. Gstach, P. Seil, Prof. Dr. J. G. Schantl
Institut für Organische und Pharmazeutische Chemie der Universität Innrain 52a, A-6020 Innsbruck (Austria)
Prof. Dr. A. Gieren [+], Dr. T. Hübner, Dr. J. Wu
Max-Planck-Institut für Biochemie
Arbeitsgruppe für Chemische Kristallographie
Am Klopferspitz, D-8033 Martinsried (FRG)
[+] Present address:
Institut für Anorganische und Analytische Chemie der Universität Innrain 52a, A-6020 Innsbruck (Austria)

[**] This work was supported by the Sparkasse Innsbruck-Hall (Austria).

from the static point of view but also from the dynamic point of view.[1,2] 1-Aryl-2-(1-isocyanato-1-methylethyl)-diazenes **1a–d**[3] react with HBF_4 to give stable 1-aryl-4,5-dihydro-3,3-dimethyl-5-oxo-3*H*-1,2,4-triazolium tetrafluoroborates **2a–d** (Table 1). The structure of the compounds **2**, which corresponds to a protonated form of the non-isolable, highly reactive intermediates **3**, which are valence isomers of **1**, was confirmed by an X-ray structure analysis of **2a**.[4] **2a** can be described as an intermediate **3a** stabilized by protonation.

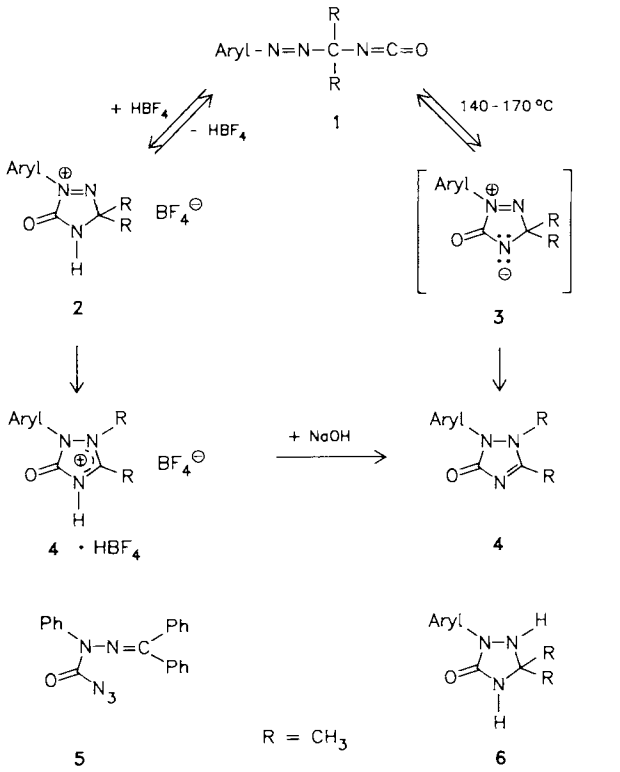


Table 1. 1-Aryl-4,5-dihydro-3,3-dimethyl-5-oxo-3*H*-1,2,4-triazolium tetrafluoroborates **2a–d**.

2	Aryl	Yield [%]	M.p. [°C]	IR [cm^{-1}] [a] ν(C=O)	UV/VIS [b] λ_{max}(log ε)
a	C_6H_5	96	146 (dec.)	1860	346 (3.97)
b	4-ClC_6H_4	86	130 (dec.)	1860	364 (3.98)
c	3-ClC_6H_4	45	125 (dec.)	1860	336 (3.87)
d	4-$CH_3OC_6H_4$	95	147–148	1850	423 (4.15)

[a] KBr pellet. [b] Acetonitrile.

The isocyanate function of **1**, revealed by IR spectra (ν(NCO) = 2200 cm^{-1}), is characterized by an unusual stability towards O- and C-nucleophiles. An interaction between the geminal aryldiazene function and the isocyanate function leading to **3** explains both the sluggish reactivity of the isocyanate group in addition reactions[5,6] as well as the enhanced electrophilicity of the diazene group.[7] Presumably **3** occurs as an intermediate in the thermolysis of the compounds **1**[8] and of *N*-aryl-*N*-azidocarbonylhydrazones such as **5**[9] to give 1,5-disubstituted 2-aryl-1,2-dihydro-1,2,4-triazol-3-ones **4**. It is also to be discussed as an intermediate in the synthesis of **1** by oxidation of **6**.[5,6]

In solution (e.g. in acetonitrile), the triazolium salts **2a–c** rearrange, slowly at room temperature but within a few minutes at 70 °C, with 1,2-shift of a methyl group to give the salts **4a–c** · HBF_4. The donor-substituted 4-methoxyphenyl derivative **2d**, on the other hand, is stable in solution at room temperature. The carbonyl function of **2** is not attacked by nucleophiles such as water or 2 N NaOH, but instead a deprotonation occurs, shifting the equilibrium from **2** to **1**.

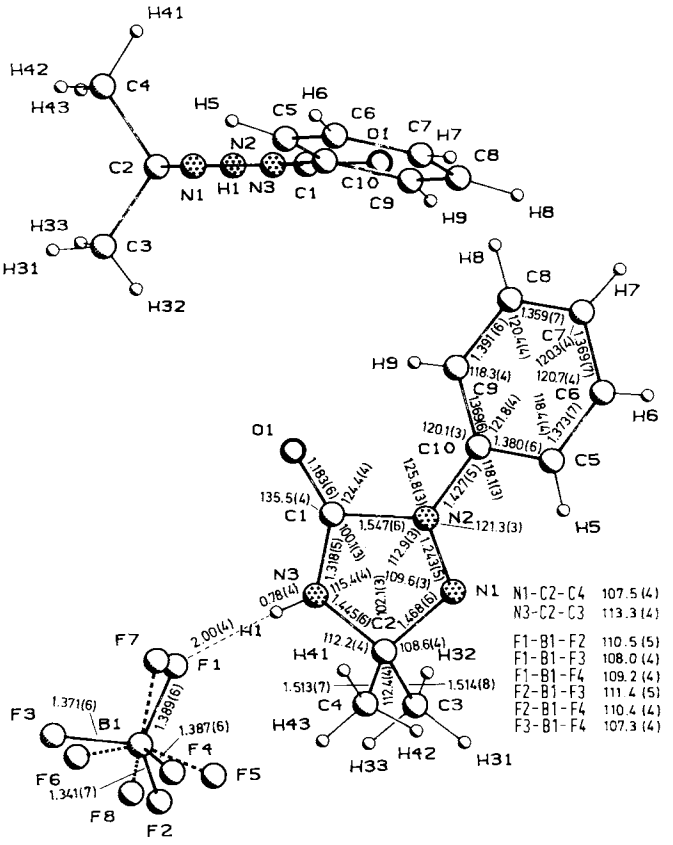


Fig. 1. Molecular structure of **2a** with two views of the cation. The $BF_4^{\ominus}$ ion is disordered. Bond lengths in Å, bond angles in degrees.

The cation of **2a** (Fig. 1) is almost planar. The planar five-membered ring and the phenyl substituent form an angle of only 17°. The molecular structure is characterized by an extremely long CN bond between the CO and the diazene group (C1–N2: 1.547(6) Å), which is 0.08 Å longer than the C2–N1 single bond, and an extremely short C=O bond (1.183(6) Å). This bonding geometry draws the molecule—consistent with the tendency shown by the bond angles at C1 of the isocyanate fragment to assume linearity—near to the transition state of the nucleophilic addition of a diazene nitrogen to the electrophilic carbon of a N-protonated isocyanate group. The geometry described is determined by intramolecular steric hindrance in the *all cis*-system O1 to H9, and possibly is one of the main reasons for the high reactivity of the compounds **2**. The extraordinarily high carbonyl frequency of **2a** at $\tilde{\nu}$ = 1860 cm^{-1} is readily explained by the extremely short C=O distance. This also holds for the finding that the C=O function is not a proton acceptor in the crystal but that instead a N–H···F bridge is present between cation and anion.

Procedure

1 mL of **1a–d** was dissolved in 75 mL of ether. The solution was cooled to 0 °C and, 10 mL of HBF_4 (50% w/w in water) were added dropwise with

stirring, during 5 min. The crystalline products were filtered off, washed twice with 40 mL of ether and dried (30°C/4×10^{-1} Pa); crystallization of **2c** necessitated cooling to −40°C. **2a**–**2d** gave correct elemental analyses.

^{1}H-NMR ([D$_6$]acetone, TMS): **2a**: $\delta = 1.90$ (s, 6H, CH_3), 4.50–6.50 (1H, NH), 7.37–8.10 (m, 5H, aromatic H).—**2b**: $\delta = 1.90$ (s, 6H, CH_3), 5.00–7.10 (1H, NH), 7.60–8.26 (AA'BB' system, 4H, aromatic H).—**2c**: $\delta = 2.03$ (s, 6H, CH_3), 5.10–7.10 (1H, NH), 7.60–8.39 (m, 4H, aromatic H).—**2d**: $\delta = 1.89$ (s, 6H, CH_3), 4.00 (s, 3H, OCH_3), 4.50–6.50 (1H, NH), 7.13–8.40 (AA'BB' system, 4H, aromatic H).

Received: July 25, 1986;
revised: September 8, 1986 [Z 1876 IE]
German version: *Angew. Chem. 98* (1986) 1111

CAS Registry numbers:
1a, 18440-33-0; **1b**, 28359-16-2; **1c**, 105122-05-2; **1d**, 105122-06-3; **2a**, 105122-08-5; **2b**, 105122-10-9; **2c**, 105122-12-1; **2d**, 105122-14-3.

[1] H. B. Bürgi, *Inorg. Chem. 12* (1973) 2321.
[2] H. B. Bürgi, J. D. Dunitz, E. Shefter, *Acta Crystallogr. B30* (1974) 1517.
[3] J. G. Schantl, P. Hebeisen, L. Minach, *Synthesis 1984*, 315.
[4] Crystallographic data: monoclinic $P2_1/n$, $a = 7.368(1)$, $b = 15.832(3)$, $c = 10.789(3)$ Å, $\beta = 92.86(2)°$; $V = 1257.0$ Å^3, $Z = 4$, $\rho_{calc} = 1.464$ g cm^{-3}, $\rho_{obs} = 1.45$ g cm^{-3}. CAD4, $Mo_{K\alpha}$, graphite monochromator, 1246 independent reflections ($I > 2\sigma(I)$), $0° < \theta < 25°$, $\omega/2\theta$-scan, direct methods, $R_w = 0.057$. Further details of the crystal structure investigation are available on request from the Fachinformationszentrum Energie, Physik, Mathematik GmbH, D-7514 Eggenstein-Leopoldshafen 2 (FRG), on quoting the depository number CSD-51862, the names of the authors, and the full citation of the journal.
[5] H. Schildknecht, G. Hatzmann, *Angew. Chem. 80* (1968) 287; *Angew. Chem. Int. Ed. Engl. 7* (1968) 293.
[6] J. G. Schantl, *Monatsh. Chem. 105* (1974) 427.
[7] J. G. Schantl, H. Gstach, *Monatsh. Chem. 116* (1985) 1051.
[8] H. Schildknecht, G. Hatzmann, *Angew. Chem. 81* (1969) 469; *Angew. Chem. Int. Ed. Engl. 8* (1969) 456.
[9] O. Tsuge, S. Kanemasa, *J. Org. Chem. 38* (1973) 2972.

BOOK REVIEWS

Synthetic Polymer Membranes. A Structural Perspective. 2nd edition. By *R. E. Kesting*. Wiley, Chichester 1985. xi, 348 pp., bound, £ 55.75.—ISBN 0-471-80717-6

This book provides an extensive survey of the application of synthetic membranes for separation processes in the chapters on *Membrane Separation Processes* (Chapter 2) and *Miscellaneous Uses of Membranes* (Chapter 3). The properties and solubility behavior of membrane specific polymers as well as the preparation and properties of various synthetic membranes are dealt with in chapters on *Membrane Polymers* (Chapter 4), *Polymer Solutions* (Chapter 5), *Dense Membranes* (Chapter 6), Phase Inversion Membranes (Chapter 7), *Other Porous Membranes* (Chapter 8), and *Liquid and Dynamically Formed Membranes* (Chapter 9). The final chapter 10 on *Biological Membranes* supplies a condensed overview of the structure and function of biological membranes.

The author is an internationally recognized expert in the field of synthetic membranes who has been concerned with the design and production of synthetic membranes for more than 20 years. His great experiences in this field are reflected, in particular, in Chapters 4, 6, and 7, which are really worth reading.

However, the vivid and interesting description of knowledge on synthetic membranes cannot obscure the fact that the treatment of the physico-chemical foundations of transport across membranes, of equilibria at solution/membrane interfaces, of the solubility of polymers, and of the water structure in membranes suffer from at least a one-sided view and from inaccuracies in some respects. Thus, the attempt at a purely kinetic explanation of the osmotic pressure fails (p. 24). A clear theoretical background is lacking with the presentation of electrochemical membrane processes. As a consequence of this, individual processes are treated independently without clearly elaborating the interrelations. As a result, an analytical relationship is given only for the diffusion potential whereas the streaming potential is discussed only qualitatively. Furthermore, a theoretical treatment of desalination is presented in the paragraph on hyperfiltration (pp. 64–78) which is essentially unaccepted till today. This biased presentation, which unfortunately extends throughout the whole book and also prevents a systematic classification of synthetic membranes according to their formation, results in a not really scientific and clear presentation of the membrane field.

Despite the shortcomings mentioned, the book is a valuable extension of the literature on membranes since the author is at least familiar with, and quotes, the published literature from the beginning of membrane research which was mainly published in German. Consequently it should be available in every library aiming at a reasonably complete coverage of the literature on membranes.

Wolfgang Pusch [NB 768 IE]
Max-Planck-Institut für Biophysik,
Frankfurt am Main (FRG)

Registered names, trademarks, etc. used in this journal, even without specific indication thereof, are not to be considered unprotected by law.

© VCH Verlagsgesellschaft mbH, D-6940 Weinheim, 1986. - Printed in the Federal Republic of Germany by Zechnersche Buchdruckerei, Speyer/Rhein.

All rights reserved (including those of translation into foreign languages). No part of this issue may be be reproduced in any form - by photoprint, microfilm, or any other means - nor transmitted or translated into a machine language without written permission from the publishers. Only single copies of contributions, or parts thereof, may be reproduced for personal use.

Valid for users in the USA: The appearance of the code at the bottom of the first page of an article in this journal (serial) indicates the copyright owner's consent that copies of the article may be made for personal or internal use, or for the personal or internal use of specific clients. This consent is given on the condition, however, that the copier pay the stated per-copy fee through the Copyright Clearance Center, Inc., for copying beyond that permitted by Sections 107 or 108 of the U.S. Copyright Law. This consent does not extend to other kinds of copying, such as copying for general distribution, for advertising or promotional purposes, for creating new collective works, or for resale. For copying from back volumes of this journal see 'Permissions to Photo-Copy: Publisher's Fee List' of the CCC.

Editorial office: Pappelallee 3, D-6940 Weinheim, Federal Republic of Germany, Telephone (06201) 602315, Telex 465516 vchwh d, Telefax (06201) 602328.

Editor: *P. Gölitz.*

Associate editors: *D. J. Loewus, A. Stimson.* **Editorial assistant:** *E. Schweikart*

Publishers: VCH Verlagsgesellschaft mbH. (Managing Directors: *Prof. Dr. Helmut Grünewald* and *Hans Dirk Köhler*), Pappelallee 3, D-6940 Weinheim, Federal Republic of Germany. Correspondence concerning advertisements should be addressed to VCH Verlagsgesellschaft mbH. (Advertising Manager *R. J. Roth*), Boschstr. 12, P.O. Box 1260/1280, D-6940 Weinheim, Federal Republic of Germany, Telephone Weinheim (06201) 602-0, Telex 465516 vchwh d, Telefax (06201) 602328.

AUTHOR INDEX [*Angew. Chem. Int. Ed. Engl. 25* (1986)]

The page numbers in square brackets refer to the German edition [*Angew. Chem. 98* (1986)] of Angewandte Chemie. In the case of book reviews the names of the authors are given; the corresponding GE-reference can be found in the Author Index of the German Edition.

ABELN, R. 909 [927]
Ackermann, K. 911 [909]
Adam, W. 101, 188, 269, 661, 818, 989 [85, 185, 279, 659, 820, 1006]
Adiwidjaja, G. 171 [162]
Agreda, T. C. 289 [278]
Ahlrichs, R. 82 [91]
Ahrendt, J. 746 [719]
Aika, K. 558 [556]
Akkerman, O. S. 639 [641]
Albiez, T. 479 [474]
Albone, E. S. 296
Albright, T. A. 581
Allmann, R. 183 [191]
Alt, H. G. 812 [826]
Amberger, E. 727, 729 [749, 751]
Anderson, D. G. 107 [97]
André, J.-J. 851
Anema, S. G. 759 [744]
Angermund, K. 364, 927 [356, 904]
Antberg, M. 260 [274]
Aped, P. 287 [289]
Appel, R. 567, 932 [570, 934]
Appelt, A. 823 [832]
Apreda, M. C. 1114 [1091]
Arenz, T. 559 [571]
Arlt, D. 1108 [1116]
Armstrong, J. C. 268 [270]
Arrhenius, G. 658 [654]
Ashe III, A. J. 571 [562]
Ashworth, T. V. 289 [278]
Aubry, A. 447 [449]
Aumüller, A. 740 [759]

BALLESTEROS, A. 181 [190]
Ballini, R. 941 [935]
Bankmann, M. 265 [287]
Barluenga, J. 181 [190]
Bartmann, E. 653 [629]
Bartok, M. 944
Bats, J. W. 732, 992, 997 [732, 1023, 1030]
Baudler, M. 471 [465]
Bauer, G. R. 841 [825]
Bauer, I. 1093 [1132]
Bauer, K. 582
Bauer, W. 1103 [1130]
Baum, G. 104, 1011, 1111 [84, 1004, 1123]
Beauvillain, P. 1030 [1026]
Beck, A. K. 98 [98]
Beck, J. 95 [106]
Beck, K. 187 [193]
Beck, W. 270, 734 [280, 739]
Becker, G. 1002 [1018]
Bender, D. 444 [446]
Benn, R. 78, 555, 646, 861 [80, 555, 628, 851]
Bergmeyer, H.-U. 291, 483
Bergmeyer, J. 291, 483
Bermel, W. 342 [352]
Berndt, A. 1111 [1123]
Bernhardt, W. 279, 479 [285, 474]
Berstermann, H.-M. 85 [99]
Bertsch, A. 377 [361]
Bertz, S. H. 760 [756]
Bestmann, H. J. 559, 994 [571, 1007]
Bhattacharya, A. 476 [442]
Bickelhaupt, R. 639 [641]
Binger, P. 644 [645]
Birnbach, S. 360 [354]
Blake, A. J. 107, 274 [97, 282]
Blaschke, G. 830 [808]
Blunden, S. J. 944
Boche, G. 104, 373, 562, 1011 [84, 373, 563, 1004]
Bock, H. 265 [287]
Bock, R. 294
Boese, R. 268, 469, 718, 755 [270, 463, 726, 737]
Bögge, H. 272, 273, 453, 990 [258, 259, 470, 987]
Böhm, M. C. 630 [646]
Böhm, S. 1000 [1001]
Böhnke, H. 90 [101]
Bömer, B. 1108 [1116]
Bonvoisin, J. 1030 [1026]
Borchert, H.-H. 293
Born, D. 1093 [1132]
Bosold, F. 562 [563]
Bossek, U. 1030 [1026]
Boudin, A. 473, 474 [472, 473]
Boussard, G. 447 [449]
Brand, M. 554 [565]
Brandsma, L. 465 [458]
Brauer, H. 764
Braunstein, P. 748 [721]
Brecht, A. 93 [105]
Bringmann, G. 177, 913 [167, 917]
Brode, S. 82 [91]
Bröker, W. 830 [808]
Brown, M. S. 583 [579]
Brückner, C. 556 [559]
Brunner, H. 371, 557, 907 [339, 551, 907]
Bube, T. 1028 [1016]
Bublak, W. 1089 [1108]
Büchel, K. H. 943
Buchholz, N. 1104 [1101]
Buchler, J. W. 286 [257]
Büchner, W. 943
Buckingham, J. 765
Bünning, P. 277 [264]
Burdett, J. K. 581
Burger, K. 85 [99]
Burger, M. 1037
Buscall, R. 766
Buschmann, J. 276 [254]
Butenschön, H. 719 [734]
CAIRNS-SMITH, A. G. 658 [654]
Campbell, F. T. 763
Cano, F. H. 1114 [1091]
Capponi, M. 344 [358]
Carmona, D. 1114 [1091]
Carneiro, T. M. G. 748 [721]
Castaldi, G. 259 [273]
Caulton, K. G. 262 [267]
Cavicchioli, S. 259 [273]
Cecconi, F. 833 [815]
Cerveau, G. 473, 474 [472, 473]
Chieh, C. 749 [718]
Chiesi-Villa, A. 254, 553 [283, 553]
Chisholm, M. H. 21, 446, 1014 [21, 448, 1021]
Chow, T. J. 1121 [1102]
Chucholowski, A. 655 [632]
Chuit, C. 473, 474 [472, 473]
Church, S. P. 991 [993]
Ciurli, S. 553 [553]
Clark, D. L. 1014 [1021]
Clark, R. J. H. 131 [131]
Clark, T. 169, 719 [164, 734]
Claude, P. G. J. M. 379
Cohen, M. P. 108 [109]
Cohen, Y. 960 [958]
Colquhoun, H. M. 487 [483]
Conroy, B. K. 446 [448]
Corner, T. 766
Corriu, R. J. P. 473, 474 [472, 473]
Cotton, F. A. 637 [652]
Cradock, S. 107 [97]
Craig, D. 165 [178]
Cram, D. J. 1039 [1041]
Cramer, R. E. 86 [95]
Csöregh, I. 746 [719]
Curda, J. 350 [369]
Curry, A. S. 485
Cusack, B. A. 944
Cutts, P. W. 577 [567]
Czisch, P. 364, 639 [356, 641]
Czugler, M. 746 [719]

DABBAGH, G. 760 [756]
Dahlenburg, L. 260 [274]
Damani, L. A. 850
Dance, I. G. 165 [178]
Dao-Ba, H. 1007 [988]
Dartmann, M. 919 [894]
Day, R. O. 457 [471]
de Boer, H. J. R. 639 [641]
de Meijere, A. 171, 335, 719 [162, 343, 734]
Demuth, M. 1117 [1093]
Derz, T. 650 [627]
Deschler, U. 236 [237]
Dey, A. K. 1117 [1093]
Dickert, F. 841 [825]
Diederich, F. 1125, 1127 [1125, 1127]

Diercks, R. 266, 268 [268, 270]
Dietl, S. 1003 [1020]
Dietrich, H. 104 [84]
Dietrich, M. 1021 [999]
Dines, T. J. 131 [131]
Ding, M.-F. 1121 [1102]
Dippel, J. 192 [187]
Ditrich, K. 1028 [1016]
Dodd, J. S. 942
Doering, W. von E. 108 [109]
Dogan, B. M. J. 108, 346 [109, 344]
Döhle, J. A. 828 [814]
Dolling, U.-H. 476 [442]
Dondoni, A. 835 [822]
Dörr, M. 818 [820]
Dötz, K. H. 812, 911 [826, 909]
Dresely, S. 189 [186]
Dubois, J. J. 379
Duchatsch, W. 720 [727]
Dürner, G. 732, 992 [732, 1023]
Dürr, H. 101, 572 [85, 565]
Dziallas, M. 1090 [1112]
Dzierzynski, E. M. 992 [1023]

EARNSHAW, A. 194
Ebsworth, E. A. V. 107 [97]
Eckert, H. 159 [168]
Eckroth, D. 194
Edelmann, F. 931 [908]
Egert, E. 192, 477 [187, 447]
Eggers, S. H. 656 [631]
Eisen, N. 1026 [1029]
Elbl, K. 1023 [1024]
Elguero, J. 1114 [1091]
Ellencweig, A. 286 [289]
Elliott, G. P. 190 [183]
Elliott, S. R. 31 [31]
Elsässer, K. 286 [257]
Elschenbroich, C. 571 [562]
Enders, D. 1109 [1118]
Enk, M. 910 [928]
Erdelmeier, I. 935, 938 [912, 914]
Erk, P. 740 [759]
Erker, G. 364, 463, 639 [356, 456, 641]
Ermer, O. 108 [109]
Escher, R. 277 [264]
Etzrodt, H. 104 [84]

FANTIN, G. 835 [822]
Fenske, D. 175, 338 [165, 357]
Ferguson, S. B. 1127 [1127]
Fiedler, J. 443 [444]
Field, J. R. 1037
Fink, J. 280 [265]
Fischer, G. 659
Fischer, Hans 374, 1021 [341, 999]
Fischer, Helmut 78, 744 [80, 753]
Fischer, J. 357 [347]
Fischer, R. D. 656, 738 [631, 748]
Fischer, Stefanie 630 [646]
Fischer, Stephan 85 [99]
Fitzi, R. 345 [363]
Flintjer, B. 1129 [1090]
Floriani, C. 254, 356, 553 [283, 376, 553]
Fluck, E. 1002 [1018]
Foces-Foces, C. 1114 [1091]
Fogagnolo, M. 835 [822]
Folting, K. 1014 [1021]
Fordham, R. J. 379
Fraenkel, W. 830 [808]
Franck, B. 1100 [1107]
Franck-Neumann, M. 1131 [1138]
Frank, P. 1107 [1115]
Frank, W. 831 [806]
Franke, E. 96 [83]
Franke, J. 336 [335]
Frauenrath, H. 274 [261]
Friedl, T. 465, 719 [458, 734]
Friedman, N. 284 [260]
Frim, R. 174 [160]
Frimmer, M. 997 [1030]
Fritschi, H. 1005 [1028]
Frolow, F. 650 [627]
Frömberg, W. 463 [456]
Fuchs, B. 287 [289]
Fuchs, H. 727, 729 [749, 751]
Fuchs, J. 569 [550]
Fujita, S. 751 [723]
Funhoff, D. J. H. 742 [757]

GABOR, B. 463 [456]
Gais, H.-J. 935, 938, 939 [912, 914, 916]
Gait, M. J. 296
Gambarotta, S. 254, 553 [283, 553]
Garbe, D. 582
Garbutt, R. 165 [178]
Geissler, M. 902 [922]
Gerbing, U. 78 [80]
Gerhartz, W. 763
Gerke, R. 578 [560]
Gerson, F. 335 [343]
Ghilardi, C. A. 833 [815]
Gieren, A. 1132 [1111]
Giese, B. 450 [459]
Ginsburg, D. 346 [344]
Giordano, C. 259 [273]
Girerd, J.-J. 1030 [1026]
Girreser, U. 167 [174]
Gleiter, R. 335, 449, 906, 999, 1000 [343, 452, 893, 1019, 1001]
Glück, C. 731 [735]
Goldstein, J. L. 583 [579]
Gondro, T. 650 [627]
Gorrod, J. W. 850
Gosmann, M. 1100 [1107]
Gotor, V. 181 [190]
Götzmann, W. 340 [359]
Goubeau, J. 1038 [944]
Gould, R. O. 274 [282]
Grabis, U. 89, 1017 [94, 1034]
Grabowski, E. J. J. 476 [442]
Grammenudi, S. 1122 [1119]
Grassl, M. 291, 483
Grau, U. 535 [530]
Graule, T. 167 [174]
Grayson, M. 194
Greenwood, N. N. 194
Grevels, F.-W. 991 [993]
Gries, T. 84 [93]
Griesbaum, K. 81 [108]
Griesbeck, A. 269, 989 [279, 1006]
Griesinger, C. 342 [352]
Grime, J. K. 482
Grimm, E. L. 1086 [1104]
Grimm, M. 1097 [1095]
Grimme, W. 377 [361]
Grimmer, G. 808 [807]
Gross, R. 363 [349]
Gross, S. 732 [732]
Gruehn, R. 845 [831]
Gstach, H. 1132 [1111]
Guastini, C. 254, 553 [283, 553]
Gudat, D. 834 [817]
Gull, R. 754 [755]
Günther, K. 278 [284]
Gut, I. 344 [358]
Güttes, D. 647 [635]

HAAS, W. 101 [85]
Habben, C. 741 [717]
Hachgenei, J. 175 [165]
Häfele, B. 87 [89]
Hafner, K. 466, 630, 632, 633 [477, 646, 648, 650]
Hahn, J. 471 [465]
Haiduc, I. 1035
Haimerl, A. 180 [179]
Haller, A. 103 [102]
Halpern, M. 960 [958]
Hammerschmidt, A. 841 [825]
Hanack, M. 184 [181]
Hanessian, S. 113
Hansen, A. 560 [552]
Hargittai, I. 946
Harms, K. 373, 1011 [373, 1004]
Harsch, G. 581
Härter, P. 839 [812]
Hartl, H. 185, 569 [189, 550]
Hartley, F. R. 945
Hartman, H. 658 [654]
Hartmann, C. 575 [573]
Hashimoto, S. 565 [569]
Hassner, A. 478 [479]
Hauptman, H. 603 [600]
Hauptreif, M. 192 [187]
Hay, R. W. 291
Heckmann, G. 1002 [1018]
Hedwig, A. 1000 [1001]
Heinze, J. 1021, 1030 [999, 1026]
Helbig, J. 1013 [1014]
Helmholtz, H. 1037
Hemminger, W. 482
Henrici-Olivé, G. 195
Henrick, K. 853 [843]
Herberich, G. E. 165, 642 [177, 637]
Herbst, R. 477 [447]
Herdtweck, E. 289, 563, 817 [278, 557, 818]
Hergarten, B. O. 1000 [1001]
Herrmann, G. 570 [568]
Herrmann, W. A. 56, 289, 563, 817, 1092 [57, 278, 557, 818, 1109]
Hertkorn, N. 468 [462]
Hesse, M. 649 [638]
Hessner, B. 165, 642 [177, 637]
Higashimura, H. 735 [740]
Hildenbrand, M. 1112 [1121]
Hill, R. 944
Himbert, G. 459 [443]
Hoberg, H. 810 [819]
Höck, N. 738 [748]
Hoffmann, R. 822 [828]
Hoffmann, R. W. 189, 1028 [186, 1016]
Hofmann, P. 837 [810]
Höhn, A. 737, 1090 [745, 1122]

Höhne, G. 482
Hojo, M. 735 [740]
Hol, W. G. J. 767 [765]
Holle, S. 555 [555]
Holmes, J. M. 457 [471]
Holmes, R. R. 457 [471]
Homma, J. Y. 293
Hönle, W. 352 [370]
Hopf, H. 174 [160]
Hoppe, D. 160 [171]
Hornbach, P. 1112 [1121]
Horspool, W. M. 381
Hössel, P. 818 [820]
Hostalek, M. 642 [637]
Howard, J. A. K. 165, 190 [177, 183]
Howells, E. R. 1036
Huber, B. 455, 812, 1089 [468, 826, 1108]
Huber, W. 443 [444]
Hübner, T. 1132 [1111]
Huch, V. 375 [367]
Hudlicky, M. 579
Huffman, J. C. 262, 446, 1014 [267, 448, 1021]
Huisgen, R. 297 [297]
Hünig, S. 187, 740 [193, 759]
Hupfeld, B. 754 [755]
Huttner, G. 1119 [1099]

IIZUKA, N. 751 [723]
Imwinkelried, R. 178 [182]
Ipaktschi, J. 354 [346]
Irngartinger, H. 340 [359]
Ise, N. 323 [323]

JÄGER, V. 87 [89]
Janoschek, R. 651 [634]
Jansen, J. R. 913 [917]
Jansen, M. 77, 993 [78, 994]
Jansen, R.-M. 1008 [1000]
Jasim, K. S. 749 [718]
Jenni, K. 810 [819]
Jolly, P. W. 555 [555]
Jonas, K. 923, 925, 927, 928 [901, 902, 904, 905]
Jones, P. G. 84, 371, 1005 [93, 339, 998]
Jones, R. 173 [176]
Jörg, K. 92, 455 [103, 468]
Jutzi, P. 164, 919 [163, 894]

KABE, Y. 173 [176]
Käfer, D. 375 [367]
Kaim, W. 363, 744 [349, 753]
Kaiser, F.-J. 183 [191]
Kakiuchi, K. 369 [364]
Kalinowski, H.-O. 1093 [1132]
Kammer, H.-W. 659
Kanegasaki, S. 293
Kaneko, M. 825, 1009 [824, 1012]
Kanne, D. 164 [163]
Karady, S. 476 [442]
Karcher, W. 379
Karle, J. 614 [611]
Karpf, M. 414 [413]
Karsch, H. H. 454, 455, 823 [467, 468, 832]
Kaschube, W. 910 [928]
Katti, K. V. 477 [447]
Kaub, J. 96 [83]
Kauermann, H. 557 [551]
Kauffmann, T. 909, 910 [927, 928]
Kaufmann, E. 169 [164]
Kaupp, G. 828 [814]
Kawai, H. 916 [930]
Keller, H. 904 [924]
Kessler, H. 342, 997 [352, 1030]
Kesting, R. E. 1134
Kiedrowski, G. von 932 [932]
Kiel, G.-Y. 991 [993]
Kiel, W. A. 991 [993]
Kieslich, K. 380
Kihn-Botulinski, M. 286 [257]
Kira, A. 825, 1009 [824, 1012]
Kirchmeyer, S. 171 [162]
Kirste, B. 1097 [1095]
Klärner, F.-G. 108, 346, 989 [109, 344, 1006]
Kläui, W. 97 [107]
Klebe, G. 740 [759]
Klein, M. 997 [1030]
Klein, N. 922 [910]
Kleinschmit, P. 236 [237]
Kliebisch, U. 915 [921]
Klingebiel, U. 649, 915 [638, 921]
Klusener, P. A. A. 465 [458]
Knaup, G. L. 633 [650]
Knebl, R. 1002 [1018]
Kniep, R. 525, 752, 1087 [520, 725, 1105]
Knoch, F. 932 [934]
Knoll, K. 1119 [1099]
Koch, W. 827 [834]
Köcher, M. 257 [262]
Koepe, G. 923 [901]
Köffer, D. P. J. 165 [177]
Köhler, F. H. 468 [462]
Köhler, J. 996 [1011]
Kohne, B. 650 [627]
Kolar, C. 342 [352]
Köll, P. 368 [362]
Kopf, J. 656 [631]
Kos, A. J. 169 [164]
Kosack, S. 459 [443]
Krämer, T. 160 [171]
Kramer, W. 731 [735]
Kramme, R. 1116 [1134]
Krebs, B. 919 [894]
Kreissl, F. R. 643, 904 [640, 924]
Krennrich, G. 449, 999 [452, 1019]
Krestel, M. 183 [191]
Krickemeyer, E. 272, 453, 990 [258, 470, 987]
Krieger, C. 374, 451, 1023 [341, 460, 1024]
Krimmer, H.-P. 630 [646]
Krohn, K. 339, 790 [338, 788]
Kroker, J. 571 [562]
Krüger, C. 164, 181, 364, 463, 639, 810, 923, 925, 927, 928, 1101, 1117 [163, 190, 356, 456, 641, 819, 901, 902, 904, 905, 1136, 1093]
Küfner, U. 89 [90]
Kuhlmann, T. 105 [87]
Kühn, V. 632 [648]
Kuhn, W. 812 [826]
Kull, J. 261 [276]
Kummer, M. 1018 [995]
Kunz, H. 170, 360 [170, 354]
Küppers, H.-J. 1101 [1136]
Kurreck, H. 1097 [1095]
Küsthardt, U. 817 [818]
Kuzaj, M. 85, 480 [99, 476]

LAITINEN, R. 99 [81]
Lamata, M. P. 1114 [1091]
Langer, M. 999 [1019]
Larock, R. C. 943
Lasowski, H.-J. 170 [170]
Laube, T. 349 [368]
Lauterbach, G. 354 [346]
Lavery, A. J. 274 [282]
Lebrilla, C. 827 [834]
Lehmkuhl, H. 646 [628]
Leibnitz, E. 580
Leimkühler, M. 921 [929]
Lemmen, T. H. 262 [267]
Lendvai, T. 719 [734]
Leutenegger, U. 1005 [1028]
Lex, J. 257, 720, 723, 1000 [262, 727, 729, 1001]
Lighthart, J. A. M. 379
Lindberg, T. 292
Lindner, E. 1008 [1000]
Lindner, H. J. 630, 633, 935, 938, 939 [646, 650, 912, 914, 916]
Lingens, F. 779 [778]
Lochschmidt, S. 253 [271]
Loerzer, T. 578 [560]
Lohray, B. B. 101, 188 [85, 185]
Lorenz, I.-P. 261 [276]
Lorey, H. 556 [559]
Lotz, R. 921 [929]
Luckner, M. 942
Lüderitz, O. 293
Ludwig, W. 1025 [1032]
Lüerssen, H. 85, 480 [99, 476]
Luger, P. 276 [254]
Lukehart, C. M. 1035
Lutter, H.-D. 1125 [1125]
Lüttke, W. 578 [560]

MACK, H. 184 [181]
Mackay, K. M. 759 [744]
Maercker, A. 167 [174]
Mahdi, W. 104 [84]
Maier, G. 819, 1093 [829, 1132]
Mak, T. C. W. 749 [718]
Malisch, W. 92, 455 [103, 468]
Malwitz, D. 762 [747]
Mann, B. E. 577 [567]
Manninger, G. 1013 [1014]
Marchant, N. S. 446 [448]
Marinder, B.-O. 431 [430]
Märkl, G. 264, 1003 [286, 1020]
Marotta, E. 941 [935]
Marraud, M. 447 [449]
Marsch, M. 104, 373, 1011 [84, 373, 1004]
Martens, J. 278 [284]
Martin, G. 1018 [995]
Martin, H.-D. 1018, 1116 [995, 1134]
Martin, T. P. 197 [197]
Masamune, S. 173 [176]
Mass, G. 459 [443]
Massa, W. 104, 571, 1011, 1111 [84, 562, 1004, 1123]
Mathey, F. 357 [347]
Matsumoto, K. 565 [569]

Matt, D. 748 [721]
Mattausch, H. 845 [831]
Mattes, R. 921, 1104 [929, 1101]
Maurer, H. 851
Mayer, B. 1116 [1134]
Mayer, H. A. 1008 [1000]
Mayer, P. 825 [813]
Mayr, H. 89, 1016, 1017 [94, 1033, 1034]
McCaffrey, J. G. 1072 [1076]
McCosh, F. W. J. 1035
McKenna, J. 577 [567]
McKenna, J. M. 577 [567]
McLeod, L. C. 759 [744]
McPartlin, M. 853 [843]
Medici, A. 835 [822]
Meier, H. 809 [838]
Meier, W. 907 [907]
Meine, G. 469 [463]
Meller, A. 741 [717]
Mercier, F. 357 [347]
Mertin, W. 845 [831]
Merz, A. 180 [179]
Merz, T. 567 [549]
Merzweiler, K. 338 [357]
Metzger, J. O. 80, 762 [79, 747]
Meyer, A. 92 [103]
Meyer, E. M. 356 [376]
Meyer, T. 353 [372]
Meyer, U. 919 [894]
Meyer-Bäse, K. 1005 [998]
Michels, M. 471 [465]
Michenfelder, M. 366 [337]
Midollini, S. 833 [815]
Miess, G.-E. 103, 917 [102, 925]
Milczarek, R. 644 [645]
Miller, S. L. 658 [654]
Mise, T. 190 [183]
Mizumoto, K. 916 [930]
Moenius, T. 994 [1007]
Mokhi, M. 1131 [1138]
Moneti, S. 833 [815]
Montforts, F.-P. 458 [451]
Moors, R. 567 [570]
Morris, J. 853 [843]
Morrison, J. D. 848
Mothes, K. 942
Mueller-Westerhoff, U. T. 702 [700]
Mukerji, I. 760 [756]
Müllen, K. 443, 444 [444, 446]
Müller, Achim 272, 273, 453, 990 [258, 259, 470, 987]
Müller, Arndt 997 [1030]
Müller, G. 454, 455, 468, 574, 643, 757, 812, 823, 911, 1013, 1089, 1103 [467, 468, 462, 572, 640, 742, 826, 832, 909, 1014, 1108, 1130]
Müller, H.-J. 734 [739]
Müller, Raffaello 383 [381]
Müller, Rudolf 779 [778]
Müllner, H. 535 [530]
Mulzer, J. 655 [632]
Münzmay, T. 572 [565]
Mura, P. 460 [453]
Murata, I. 635 [639]
Mynott, R. 367, 463, 555, 639, 644, 646, 842 [374, 456, 555, 641, 645, 628, 835]

NADER, F. W. 93 [105]
Nagel, U. 270, 734 [280, 739]
Nakamura, A. 86 [95]
Nehl, H. 646 [628]
Neidlein, R. 367, 640, 731 [374, 643, 735]
Nesper, R. 110, 350, 566 [111, 369, 558]
Neugebauer, F. A. 374, 1021 [341, 999]
Neumüller, B. 1002 [1018]
Nicholson, B. K. 759 [744]
Niecke, E. 834 [817]
Nieger, M. 192 [187]
Niemann, B. 932 [934]
Noltemeyer, M. 741, 931 [717, 908]
Nuber, B. 557, 907, 1003, 1030 [551, 907, 1020, 1026]
Nübling, C. 1109 [1118]
Nunn, C. M. 190 [183]

ODA, M. 916 [930]
Odaira, Y. 369 [364]
Oelting, M. 368 [362]
Okada, K. 916 [930]
Okahata, Y. 751 [723]
Oki, M. 658
Okuda, J. 1092 [1109]
Olah, G. A. 486
Olivé, S. 195
Ōmura, S. 580
Oppenländer, T. 661 [659]
Orama, O. 1119 [1099]
Orgel, L. E. 658 [654]
Orlandini, A. 833 [815]
Oro, L. A. 1114 [1091]
Oroschin, W. 738 [748]
Orthmann, E. 1105 [1114]
Osedo, H. 635 [639]
Ostarek, R. 1108 [1116]
Otani, S. 565 [569]
Ozin, G. A. 1072 [1076]

PAASHAUS, S. 752 [725]
Padwa, A. 112
Palamidis, E. 718 [726]
Palomer, A. 1117 [1093]
Panster, P. 236 [237]
Paolucci, G. 738 [748]
Papavassiliou, M. 99 [81]
Parnis, J. M. 1072 [1076]
Patai, S. 945
Patel, R. C. 381
Payer, A. 905 [895]
Pearson, A. J. 1035
Penk, M. 453 [470]
Peters, K. 79, 1129 [100, 1090]
Petrini, M. 941 [935]
Pfaltz, A. 1005 [1028]
Pfefferkorn, R. 763
Pfeifer, S. 293
Pfisterer, H. 839 [812]
Pfleger, K. 851
Philipps, T. 274 [261]
Philipsborn, W. von 383 [381]
Pi, R. 465, 1103 [458, 1130]
Pichl, R. 574 [572]
Piejko, K.-E. 1108 [1116]
Pieroth, M. 471 [465]
Pohl, S. 825 [813]
Poignée, V. 731 [735]
Polborn, K. 727, 729 [749, 751]
Pollok, T. 348 [365]
Popall, M. 911 [909]
Pople, J. A. 169 [164]
Praefcke, K. 650 [627]
Prakash, G. K. S. 486
Pritzkow, H. 1099, 1112 [1129, 1121]
Priyono, W. 339 [338]
Püttmann, W. 720 [727]

QUINKERT, G. 732, 992 [732, 1023]

RAABE, E. 810, 925, 928, 1101 [819, 902, 905, 1136]
Rabenau, A. 1087 [1105]
Rabinovitz, M. 174, 960 [160, 958]
Ramacher, L. 97 [107]
Ramaraj, R. 825, 1009 [824, 1012]
Ramirez, R. 353 [372]
Rankin, D. W. H. 107 [97]
Rao, C. N. R. 31, 753 [31, 736]
Raulfs, F.-W. 174 [160]
Reber, G. 468, 643, 1089 [462, 640, 1108]
Reed, R. 380, 764
Reetz, M. T. 1108 [1116]
Regitz, M. 280, 644, 842 [265, 645, 835]
Rehm, H.-J. 380, 764
Reich, W. 92 [103]
Rein, H. 294
Reinhardt, G. 377 [361]
Reinhardt, W. 103 [102]
Reisacher, H.-U. 454, 455 [467, 468]
Reisenauer, H. P. 819 [829]
Reissig, H.-U. 556, 1086 [559, 1104]
Reizig, K. 755 [737]
Renaud, P. 98, 843 [96, 836]
Rentzea, C. N. 652 [644]
Rétey, J. 366 [337]
Rettig, W. 971 [969]
Reye, C. 473, 474 [472, 473]
Richards, W. G. 484
Riede, J. 78, 744, 1013 [80, 753, 1014]
Riffel, H. 1002 [1018]
Rink, H.-P. 913 [917]
Roesky, H. W. 82, 84, 477, 931, 1005 [91, 93, 447, 908, 998]
Romão, C. C. 555 [555]
Rösch, W. 280, 644 [265, 645]
Rosini, G. 941 [935]
Roth, R. 917 [925]
Roth, S. 105 [87]
Rounsaville, J. F. 763
Rozen, S. 554 [565]
Rozière, J. 105 [87]
Ruckpaul, K. 294
Rudert, R. 276 [254]
Rufińska, A. 640, 861 [643, 851]
Rupp, J. 86 [95]
Rüsseler, W. 925, 927, 928 [902, 904, 905]
Ryan, K. M. 476 [442]

SAAK, W. 825 [813]
Sacher, W. 270 [280]

Saenger, W. 290
Saive, R. 165 [177]
Salomon, N. J. 917 [925]
Sander, W. 254, 906 [255, 893]
Sankar, G. 753 [736]
Saupe, T. 451 [460]
Sax, A. 651 [634]
Schade, C. 902 [922]
Schäfer, A. 817 [818]
Schäfer, H. J. 1025 [1032]
Schaffner, K. 991 [993]
Schantl, J. G. 1132 [1111]
Scharbert, B. 286 [257]
Scheffler, K. 1007 [988]
Scherer, O. J. 96, 363 [83, 349]
Schickedanz, M. 278 [284]
Schieb, T. 720, 723 [727, 729]
Schier, A. 757 [742]
Schimkowiak, J. 84, 1005 [93, 998]
Schleyer, P. von R. 169, 465, 902, 1103 [164, 458, 922, 1130]
Schliebs, R. 943
Schlund, R. 364 [356]
Schmalz, H.-G. 732, 992 [732, 1023]
Schmickler, H. 257, 720, 723 [262, 727, 729]
Schmid, G. 718, 922 [726, 910]
Schmidbauer, J. 371 [339]
Schmidbaur, H. 348, 574, 575, 757, 1013, 1089 [365, 572, 573, 742, 1014, 1108]
Schmidpeter, A. 253, 457, 825 [271, 471, 813]
Schmidt, G. 1111 [1123]
Schmidt, H. R. 837 [810]
Schmidt, K. 723 [729]
Schmidt, R. R. 89, 212, 725 [90, 213, 722]
Schmidt, W. 808 [807]
Schmitz, K. 453 [470]
Schneider, H.-J. 647 [635]
Schneider, R. 89, 1016, 1017 [94, 1033, 1034]
Schneider, S. 177 [167]
Schneider, U. 647 [635]
Schnering, C. von 279, 479 [285, 474]
Schnering, H. G. von 110, 350, 352, 353, 566, 1129 [111, 369, 370, 372, 558, 1090]
Schnöckel, H. 921 [929]
Schoenfeld, R. 378
Schöllhorn, R. 905 [895]
Schöllkopf, U. 192, 754 [187, 755]
Scholtissek, C. 47 [47]
Schommer, C. 572 [565]
Schöttle, T. 744 [753]
Schrage, H. 336 [335]
Schröder, M. 274 [282]
Schröer, D. 989 [1006]
Schröter, D. 87 [89]
Schubert, H. 1109 [1118]
Schubert, U. 92 [103]
Schuhn, W. 932 [934]
Schuler, P. 1007 [988]
Schultze, H. 656 [631]
Schulz, W. H. 723 [729]
Schulze, W. 185 [189]
Schumann, H. 718 [726]
Schurig, V. 1032 [1008]
Schuster, H. 79 [100]
Schütte, H. R. 942
Schütz, J. U. von 740 [759]
Schwabe, K. 659
Schwager, H. 367, 640 [374, 643]
Schwalb, J. 363 [349]
Schwarz, H. 282, 827 [275, 834]
Schwarz, M. 566 [558]
Schwotzer, W. 637 [652]
Scott, P. R. 484
Sedrati, M. 1131 [1138]
Seebach, D. 98, 178, 345, 843 [96, 182, 363, 836]
Segre, A. 460 [453]
Seidel, C. 159 [168]
Seil, P. 1132 [1111]
Seipke, G. 535 [530]
Seitz, F. 744 [753]
Seitz, G. 183 [191]
Sejpka, H. 264, 1003 [286, 1020]
Sekiguchi, Y. 86 [95]
Sellmann, D. 1107 [1115]
Seppelt, K. 185 [189]
Seseke, U. 477 [447]
Sheldrick, G. M. 371, 477, 741, 915, 931 [339, 447, 717, 921, 908]
Sheves, M. 284 [260]
Shiba, T. 293
Shlyapintokh, V. Y. 852
Shono, T. 380
Siebert, W. 105, 1099, 1112 [87, 1129, 1121]
Sies, H. 1058 [1061]
Simon, A. 79, 845, 996 [100, 831, 1011]
Simon, H. 462 [455]
Simon, J. 851
Simpson II, C.Q. 637 [652]
Sluma, H.-D. 1117 [1093]
Sommer, J. 486
Sommerlade, R. H. 562 [563]
Souhassou, M. 447 [449]
Spang, C. 931 [908]
Spencer, C. M. 577 [567]
Staab, E. 269 [279]
Staab, H. A. 451, 742, 1023 [460, 757, 1024]
Stageman, J. F. 766
Stalke, D. 915 [921]
Standke, B. 77 [78]
Stavridou, E. 809 [838]
Steckhan, E. 336, 693 [335, 681]
Stegmann, H. B. 1007 [988]
Stella, S. 254 [283]
Stern, M. 478 [479]
Steudel, R. 99 [81]
Stille, J. K. 508 [504]
Stöbbe, M. 171 [162]
Stoddart, J. F. 487 [483]
Stone, F. G. A. 190 [183]
Storek, C. 809 [838]
Stowasser, B. 466, 630 [477, 646]
Strähle, J. 95 [106]
Strauss, E.-M. 99 [81]
Struppe, G. 580
Stucky, G. 178 [182]
Stürmer, R. 1028 [1016]
Süss-Fink, G. 570 [568]
Symalla, E. 834 [817]

TAKATS, J. 991 [993]
Tamaru, Y. 735 [740]
Tartakovsky, E. 287 [289]
Tatsumi, K. 86 [95]
Terlouw, J. K. 282, 827 [275, 834]
Thanos, I. 462 [455]
Thiem, J. 1096 [1100]
Thomas, J. M. 31 [31]
Thomson, R. H. 847
Tiripicchio, A. 748 [721]
Tiripicchio-Camellini, M. 748 [721]
Tobe, Y. 369 [364]
Tobias, K. M. 993 [994]
Toliopoulos, E. 910 [928]
Tomás, M. 181 [190]
Torii, S. 484
Treder, W. 1096 [1100]
Trost, B. M. 1 [1]
Troyanowsky, C. 850
Tsay, Y.-H. 1117 [1093]
Turro, N. J. 882 [872]

UEDA, K. 369 [364]
Uggeri, F. 259 [273]
Unterberg, H. 444 [446]
Uschmann, J. 1000 [1001]

VAHRENKAMP, H. 279, 479 [285, 474]
van Baar, B. 282, 827 [275, 834]
van Eldik, R. 673 [671]
Veith, M. 375 [367]
Verkruijsse, H. D. 465 [458]
Vogel, E. 257, 346, 720, 723, 1000 [262, 344, 727, 729, 1001]
Vogelbacher, U.-J. 280, 842 [265, 835]
Vögtle, F. 336, 567, 1026, 1122 [335, 549, 1029, 1119]
Vollhardt, J. 938, 939 [914, 916]
Vollhardt, K. P. C. 266, 268, 929 [268, 270, 919]
Volpp, W. 81 [108]

WACHTER, J. 371, 557, 907 [339, 551, 907]
Wagner, K. 997 [1030]
Wald, D. 660
Wallis, J. M. 639, 757 [641, 742]
Walzer, E. 732 [732]
Wang, J. 485
Wayda, A. L. 760 [756]
Weber, A. 851
Weber, C. 563 [557]
Weber, D. 353 [372]
Weber, E. 746 [719]
Weber, L. 469, 755 [463, 737]
Wegner, G. 1105 [1114]
Weidenbruch, M. 1129 [1090]
Weider, R. 346 [344]
Weimann, R. 1116 [1134]
Weinstock, L. M. 476 [442]
Weiske, T. 282, 827 [275, 834]
Weiss, A. 112
Weiss, A. 162 [173]
Weiss, E. 902 [922]
Weiss, J. 1030 [1026]
Weiss, K. 359 [350]
Weiss, R. 103, 917 [102, 925]
Welch, A. J. 107 [97]
Welke, S. 909 [927]

Welzel, W. 1087 [1105]
Wenck, H. 335 [343]
Wendel, H. 1007 [988]
Wentrup, C. 295
Wentrup, C. 85, 480 [99, 476]
Weppner, W. 1087 [1105]
Werner, H. 737, 1090 [745, 1112]
Werner, H.-P. 740 [759]
Westphal, O. 293
Whangbo, M. H. 581
Wheeler, R. A. 822 [828]
Whittaker, J. M. 759 [744]
Wiberg, K. B. 312 [312]
Wiberg, N. 79 [100]
Wieghardt, K. 1030, 1101 [1026, 1136]
Wilke, G. 367, 640 [374, 643]
Willhalm, A. 457 [471]
Williams, D. J. 173, 487 [176, 483]
Wingbermühle, D. 909, 910 [927, 928]
Winter, G. 943
Wirtz, H. 567 [549]
Wirz, J. 344 [358]
Wistuba, D. 1032 [1008]
Witt, M. 477 [447]
Witte, H. 112
Witzel, T. 450 [459]
Wolf, J. 353 [372]
Wolff, B. 162 [173]
Wolfgruber, M. 929 [919]
Wolmershäuser, G. 363 [349]
Wu, J. 1132 [1111]
Wulff, G. 90, 560 [101, 552]
Wünsch, M. 571 [562]

YAMAMOTO, K. 635 [639]
Yamamoto, Y. 947 [945]
Yamamoto, Y. S. 763
Yamazaki, S. 635 [639]
Yoshida, Z. 735 [740]

ZAKI, C. 276 [254]
Zenneck, U. 831, 1099 [806, 1129]
Ziegler, K. 997 [1030]
Ziegler, M. L. 557, 839, 907, 1003 [551, 812, 907, 1020]
Zimmermann, G. 458 [451]
Zimmermann, H. 906 [893]
Zimmermann, H. W. 115 [115]
Zimmermann, M. 273 [259]
Zimmermann, P. 725 [722]
Zirzow, K.-H. 457 [471]
Zschiesche, R. 1086 [1104]
Zsolnai, L. 1119 [1099]
Zuckerman, J. J. 1035
Zuman, P. 381
Zwecker, J. 1099 [1129]

SUBJECT INDEX

(R) = Review Article (C) = Short Communication (B) = Book Review (L) = Correspondence

AB INITIO STUDY, 1,2-Dilithioethylene isomers and their mechanisms of interconversion: an ab initio study (C) 169

Acepentalene, Dihydroacepentalenediide, the dianion of acepentalene (C) 719

Acridine dyes, Physicochemical and cytochemical investigations on the binding of ethidium and acridine dyes to DNA and to organelles in living cells (R) 115

Activation, Thermolytically induced C-H activation using a 14-electron-complex: synthesis and molecular structure of $[IrHCl(C_6H_5)(PiPr_3)_2]$ (C) 1090

4-Acyl-5-aminoimidazoles, Rearrangement of 4*H*-1,2,4-triazolium salts to 4-acyl-5-aminoimidazoles (C) 652

1-Adamantyl cation, First crystal structure analysis of an aliphatic carbocation—stabilization of the 3,5,7-trimethyl-1-adamantyl cation by C-C hyperconjugation (C) 349

Addition, Intramolecular addition of 2-(trimethylsilyl)methyl-substituted allyl cations to double bonds—synthesis of bicyclo[3.3.0]octane derivatives (C) 354
Stepwise addition of $MeS^{\oplus}$ to a metal-carbon triple bond—a new type of reaction in the chemistry of carbyne complexes (C) 904
Vicinal dilithioalkenes by addition of lithium to simple cyclic and acyclic alkynes (C) 167

1,4-Addition, Selective synthesis by use of Lewis acids in the presence of organocopper and related reagents (R) 947

Agostic C-H→Mo bond, $[MoR(\eta^3\text{-}C_3H_5)_3]$, R = alkyl: alkylmolybdenum complexes with agostic C-H→Mo bond (C) 555

Alcohols, Preparation of optically active alcohols from 1,3-dioxan-4-ones. A practical version of the asymmetric synthesis with nucleophilic substitution at acetal centers (C) 178

Alkali metal hydride metalation reagents, Superactive alkali metal hydride metalation reagents: LiH, NaH, and KH (C) 465

Alkali metal silicides, Red, transparent alkali metal silicides with Si_4 tetrahedrons (C) 566

Alkaloids, Biochemistry of alkaloids (B) 942
The first evidence of endogenous pyridoxyl isoquinoline alkaloids in mammalian organisms (C) 177

Alkenylsulfoximides, Asymmetric elimination with high induction: synthesis of 1-alkenylsulfoximides with axial and central chirality (C) 935

Alkyl aryl ketones, Asymmetric bromination of enantiomerically pure acetals of alkyl aryl ketones (C) 259

Alkylation, The alkylation of epoxides with new organoyttrium and organolanthanoid reagents (C) 760

Alkyl azides, Synthesis of alkyl azides with a polymeric reagent (C) 478

Alkylmolybdenum complexes, $[MoR(\eta^3\text{-}C_3H_5)_3]$, R = alkyl: alkylmolybdenum complexes with agostic C-H→Mo bond (C) 555

Alkyl radicals, Metathesis of alkyl radicals and alkenes—a novel elementary reaction of alkyl radicals (C) 80

Alkyne ligand, Variable electron-donor ability of alkyne ligands—synthesis and structure of carbonyl(η^5-cyclopentadienyl)(η^2-1-diethylamino-1-propyne)(η^1-*p*-methylphenylketenyl)tungsten (C) 643

Allenylsodium derivative, The structure of an allenylsodium derivative—competition between carbanion resonance delocalization and gegenion charge localization (C) 902

Allyl cations, Intramolecular addition of 2-(trimethylsilyl)methyl-substituted allyl cations to double bonds—synthesis of bicyclo[3.3.0]octane derivatives (C) 354

Allylic hydroperoxides, A simple access to 2-epoxy alcohols: titanium(IV)-catalyzed oxygen transfer from allylic hydroperoxides (C) 269

Allyllithium compound, Crystal structure of the η^3-allyllithium compound [1,3-diphenylallyllithium·diethyl ether]$_n$ (C) 104

Allyl rearrangement, Optically active α-chloro-(*E*)-crotylboronate esters by allyl rearrangement (C) 189

Allylsulfones, Solid-state and solution structure of α-(phenylsulfonyl)allyllithium (C) 939

Aluminum-molybdenum complexes, Carbonyl olefinating aluminum-molybdenum complexes and an analogous tungsten complex (C) 910

Aluminum-olefin π-bonds, Dimeric 1,4-dichloro-2,3,5,6-tetramethyl-1,4-dialumina-2,5-cyclohexadiene, a compound with aluminum-olefin π-bonds (C) 921

Aluminum phosphates, Orthophosphates in the ternary system Al_2O_3-P_2O_5-H_2O (R) 525

Amination, *N*-Aryl-*O*-(diphenylphosphinoyl)hydroxylamines: electrophilic amination of amines to hydrazines; a model reaction for the carcinogenicity of aromatic amines (C) 562

Amines, Enantioselective synthesis of α-substituted primary amines by nucleophilic addition to aldehyde-SAMP hydrazones (C) 1109

Aminoacetylene and its mono- and dication—identification of potentially interstellar molecules (C) 827

Amino acid derivatives from *N*-(Arylmethylene)dehydroalanine methyl esters (C) 90

Amino acids, Simple synthesis of 1-amino-1-cyclopropanecarboxylic acids from *tert*-butyl isocyanoacetate and epoxides; synthesis of alkyl 5,6-dihydro-4*H*-1,3-oxazine-4-carboxylates (C) 754
Synthetic equivalent for aminocarboxycarbene; synthesis of 1-amino-1-cyclopropanecarboxylic acid methyl esters (C) 192

Amino acid synthesis, Enantiomer separation of (*R,S*)-2-(*tert*-butyl)-3-methyl-4-imidazolidinone, a chiral building block for amino acid synthesis (C) 345, 766

Aminocarboxycarbene, Synthetic equivalent for aminocarboxycarbene; synthesis of 1-amino-1-cyclopropanecarboxylic acid methyl esters (C) 192

1-Amino-1-cyclopropanecarboxylic acids, Simple synthesis of 1-amino-1-cyclopropanecarboxylic acids from *tert*-butyl isocyanoacetate and epoxides; synthesis of alkyl 5,6-dihydro-4*H*-1,3-oxazine-4-carboxylates (C) 754

1-Amino-1-cyclopropanecarboxylic acid methyl esters, Synthetic equivalent for aminocarboxycarbene; synthesis of 1-amino-1-cyclopropanecarboxylic acid methyl esters (C) 192

Aminolysis, Direct aminolysis of unactivated esters at high-pressure (C) 565

Ammonia synthesis, Heterogeneous catalysis of ammonia synthesis at room temperature and atmospheric pressure (C) 558

Amorphous solids, The chemistry of the noncrystalline state (R) 31

Analytical chemistry, Methoden der Analytischen Chemie. Eine Einführung. Band 2: Nachweis- und Bestimmungsmethoden, Teil 2 (B) 294

Analytical methods, High-pressure liquid chromatography (HPLC) of proteins (R) 535
High-resolution metal-NMR spectroscopy of organometallic compounds (R) 861
^{15}N-NMR spectroscopy—new methods and applications (R) 383
Resonance Raman spectroscopy and its application to inorganic chemistry (R) 131

Ancistrocladine, Regioselective and atroposelective aryl coupling to give naphthyl isoquinoline alkaloids: the first total synthesis of (−)-ancistrocladine (C) 913

Angiotensin converting enzyme, Synthesis of *N*-(1-carboxy-5-aminopentyl)dipeptides as inhibitors of angiotensin converting enzyme (C) 277

Anhydrohexitols, Carbohydrate-based liquid crystals: mesogenic 1-*O*-alkyl derivatives of 2,5-anhydrohexitols (C) 368

Anions, [2.2]Indenophane dianion: a novel double-layered dianion (C) 174

[14]Annulenes, Bridged [14]annulenes with a phenanthrene-perimeter: *anti*-1,6:7,12-bismethano[14]annulene (C) 723
Bridged [14]annulenes with a phenanthrene-perimeter: *syn*-1,6:7,12-bismethano[14]annulene (C) 720

Anomeric effect, Solvent polarity and the anomeric effect (C) 287

Antamanide, Conformational prerequisites for the in vitro inhibition of cholate uptake in hepatocytes by cyclic analogues of antamanide and somatostatin (C) 997

Anthracene electrophores, Synthesis and redox properties of compounds with several separated anthracene electrophores (C) 443

Anthracenes, Poly(anthrylenetrimethylene) and 9,10-bridged anthracenes by reductive alkylation (C) 444

Anthracyclinones, Simple synthesis of anthracyclinones by cyclization of an intermediate hydroxynitronate (C) 339
Total synthesis of anthracyclinones (R) 790

Antibiotics, Macrolide antibiotics. Chemistry, biology and practice (B) 580

Antimony(III) compounds, $[Sb_3I_{10}^{\ominus}]_\infty$—a polymeric anion with transitions from trigonal pyramidal to octahedral coordination of antimony(III) (C) 825

Arene C-H activation, Metal dependence of cyclometalation and arene C-H activation in the photolysis of *cis*-$H_2M[P(CH_2CH_2CH_2PMe_2)_3]$ (M = Fe, Ru) in benzene (C) 260

Arene complexes, Benzene as bridging ligand in main group metal-transition metal-arene complexes (C) 927
$[C_6H_3(CH_3)_3][BiCl_3]$ and $[C_6(CH_3)_6]$-$[BiCl_3]_2$, arene complexes of bismuth with

half-sandwich and "inverted" sandwich structures (C) 757

Flash photolysis of $Os(CO)_5$ in benzene solution. Detection of $Os(CO)_4$·benzene by fast time-resolved IR spectroscopy (C) 991

Arene-iron compounds, Bis(η^2-ethene)(η^6-toluene)iron (C) 831

Aromaticity, Bridged [14]annulenes with a phenanthrene-perimeter: *anti*-1,6:7,12-bismethano[14]annulene (C) 723

Bridged [14]annulenes with a phenanthrene-perimeter: *syn*-1,6:7,12-Bismethano[14]annulene (C) 720

9b-Methyl-9b*H*-benzo[*cd*]azulene—a novel antiaromatic 12π-electron system (C) 632

Novel synthesis of the angular [3]phenylene (terphenylene) by cobalt-catalyzed cyclization of bis(2-ethynylphenyl)ethyne: a molecule with an internal cyclohexatriene ring (C) 266

syn- and *anti*-Bishomoanthraquinone (C) 1000

Synthesis of a dicyclopenta[*a,e*]pentalene by [6+2]-cycloaddition of 1,3-di-*tert*-butyl-5-vinylidenecyclopentadiene and consecutive 8π-electrocyclic reaction (C) 466

Synthesis of a fourfold enlarged porphyrin with an extremely large, diamagnetic ring-current effect (C) 1100

Arsaalkenyl complex, Synthesis and structure of the first arsaalkenyl complex with FeAs single bond (C) 469

Arsabenzene ligand, Bis(η^6-arsabenzene)-chromium(0) (C) 571

Arsaethyne, 2-(2,4,6-Tri-*tert*-butylphenyl)-1-arsaethyne—the first compound containing an arsenic-carbon triple bond (C) 264

Arsenic-carbon triple bond, 2-(2,4,6-Tri-*tert*-butylphenyl)-1-arsaethyne—the first compound containing an arsenic-carbon triple bond (C) 264

Arsenic-cobalt-compounds, $[Co_4(\mu_3\text{-}As)_3(\mu_3,\eta^3\text{-}As_3)(PPh_3)_4]$, a product of the reaction of $[CoCl_2(PPh_3)_2]$ with $PhAs(SiMe_3)_2$ (C) 175

Arsenic-iron single bond, Synthesis and structure of the first arsaalkenyl complex with FeAs single bond (C) 469

Arsenic-niobium anions, $[NbAs_8]^{3-}$, a novel type of complex and an unexpected one-dimensional chain structure: $^1_\infty[Rb\{NbAs_8\}]^{2-}$ (C) 353

Arsenic-phosphorus compounds, Valence tautomerism of the heptaheteronortricycles $[P_{7-x}As_x]^{3-}$ (C) 352

Arsenic/sulfur system, Complex-induced fragmentation of As_4S_4: stabilization of an As_2S_3 ligand (C) 557

Arylchlorination, Pd^{II}-catalyzed regioselective arylchlorination and oxyarylation of unsaturated alcohols (C) 735

Asymmetric bromination of enantiomerically pure acetals of alkyl aryl ketones (C) 259

Asymmetric elimination with high induction: synthesis of 1-alkenylsulfoximides with axial and central chirality (C) 935

Asymmetric induction, Asymmetric photocycloadditions with optically pure, spirocyclic enones. Simple synthesis of (+)- and (−)-grandisol (C) 1117

Asymmetric molybdenum atom, $[Cp(CO)_2Mo\{NR^*[Rh(norbornadiene)]\text{-}CH(pyridyl)\}]$, a rhodium complex with an asymmetric molybdenum atom in the chelate skeleton (C) 371

Asymmetric synthesis (B) 848

Preparation of optically active alcohols from 1,3-dioxan-4-ones. A practical version of the asymmetric synthesis with nucleophilic substitution at acetal centers (C) 178

Attraction of similarly charged solutes, Ordering of ionic solutes in dilute solutions through attraction of similarly charged solutes—a change of paradigm in colloid and polymer chemistry (R) 323

1-Azabutadienes, A facile synthesis of a new class of eight-membered heterocycles from 1-azabutadienes (C) 181

Azacyclobutadiene, Tri-*tert*-butylazete—the first kinetically stabilized azacyclobutadiene (C) 842

Azete, Tri-*tert*-butylazete—the first kinetically stabilized azacyclobutadiene (C) 842

Azides, Synthesis of alkyl azides with a polymeric reagent (C) 478

Azimine-triaziridine transformation, An azimine-triaziridine transformation by laser photolysis (C) 828

Azirines, Nitrile ylides and azirines: gas-phase generation from 2,3-dihydro-1,4,2λ^5-oxazaphospholes and matrix isolation (C) 85

Azoalkanes, UV/VIS laser photochemistry: intermediary formation of diazoalkanes versus direct S_0,T_1 transitions in the photolysis of azoalkanes (C) 818

185-nm photochemistry of olefins, strained hydrocarbons, and azoalkanes in solution (R) 661

BACTERIAL ENDOTOXIN, Chemical, biological, and clinical aspects (B) 293

Bacteriorhodopsin pigments, Influence of external negative charges on the absorption maxima of symmetrical cyanines. A study with model compounds and artificial bacteriorhodopsin pigments (C) 284

Baeyer, Adolf von Baeyer's scientific achievements — a legacy (R) 297

Barium alkoxostannates(II), Strontium and barium alkoxostannates(II)—molecules with S_6 symmetry (C) 375

Benzene as bridging ligand in main group metal-transition metal-arene complexes (C) 927

Benzene oligomers, Diels-Alder adducts of benzene with arenes and their [4+2] cycloreversion (C) 377

Benzo[*cd*]azulene, 9b-Methyl-9b*H*-benzo[*cd*]-azulene—a novel antiaromatic 12π-electron system (C) 632

Benzo[*c*]benzo[3,4]cinnolino[1,2-*a*]cinnoline, a chiral hydrazine derivative (C) 374

Benzoin condensation, Synthesis of a macrobicyclic thiazolium-host and supramolecular catalysis of the benzoin condensation (C) 1125

Benzophenone *O*-oxide (C) 255

Benzotri(imidazole)—a new ring system derived from benzenehexamine (C) 650

(*Z*)-4-Benzylidene-2-methyl-5(4*H*)-oxazolone, $C_{phenyl}\text{-}H\cdots O$ and $C_{phenyl}\text{-}H\cdots N$ interactions: crystal structure of (*Z*)-4-benzylidene-2-methyl-5(4*H*)-oxazolone, an intermediate for dehydropeptide synthesis (C) 447

Benzyllithium compounds, [α-(Phenylsulfinyl)-α-methylbenzyllithium-tetramethylethylenediamine]$_2$: crystal structure of an α-sulfinyl "carbanion" (C) 1011

Bicyclo[3.2.1]octa-2,6-dienyllithium (C) 468

Bicyclo[3.3.0]octane derivatives, Intramolecular addition of 2-(trimethylsilyl)methyl-substituted allyl cations to double bonds—synthesis of bicyclo[3.3.0]octane derivatives (C) 354

Bilayers, Bilayer-immobilized films containing mesogenic azobenzene amphiphiles—electrically controllable permeability (C) 751

Bimetallic catalysts, Nature of Ni and Cu species in reduced bimetallic Ni-Cu/Al_2O_3 catalysts (C) 753

Bio-inorganic chemistry (B) 291

Biological oxidation of nitrogen in organic molecules. Chemistry, toxicology and pharmacology (B) 850

Biotechnology, A comprehensive treatise in 8 volumes (B) 764

A comprehensive treatise in 8 volumes. Vol. 6a: Biotransformations (B) 380

Biotransformation von Arzneimitteln. Band 4 (B) 293

Biphenyl ligand, $[(\eta^5\text{-}C_5Me_5)Co]_3C_{12}H_{10}]$—a complex of biphenyl with Kekulé structure (C) 646

Bis(η^6-arsabenzene)chromium(0) (C) 571

Bis(cyclopentadienyl)hafnacyclobutane, Reductive coupling of CO: formation of a 1:1 adduct of η^2-ketone- and enediolato-complex upon carbonylation of bis(cyclopentadienyl)hafnacyclobutane (C) 364

Bishomoanthraquinone, *syn*- and *anti*-Bishomoanthraquinone (C) 1000

Bishomoaromaticity, Bicyclo[3.2.1]octa-2,6-dienyllithium (C) 468

anti-1,6:7,12-Bismethano[14]annulene, Bridged [14]annulenes with a phenanthrene-perimeter: *anti*-1,6:7,12-bismethano[14]annulene (C) 723

syn-1,6:7,12-Bismethano[14]annulene, Bridged [14]annulenes with a phenanthrene-perimeter: *syn*-1,6:7,12-bismethano[14]annulene (C) 720

Bis(η-methylcyclopentadienyl)phenylethynylzirconium, Unusual bridging of the metal centers in dimeric bis(η-methylcyclopentadienyl)phenylethynylzirconium (C) 463

Bismuth compounds, $[C_6H_3(CH_3)_3][BiCl_3]$ and $[C_6(CH_3)_6][BiCl_3]_2$, arene complexes of bismuth with half-sandwich and "inverted" sandwich structures (C) 757

Bismuth-sulfur cluster, $[Bi_2^{III}S_{34}]^{4-}$, the hitherto sulfur-richest complex (C) 273

Bis(pentamethylcyclopentadienyl)diphosphene—a molecule with fluxional structure and reactive P–C bond (C) 919

Bisporphyrinates, Remarkable ease of ring oxidation in cerium(IV) bisporphyrinates with double-decker structure (C) 286

10,10′-Bi(trispiro[2.0.2.0.2.1]decylidene): a highly nucleophilic olefinic hydrocarbon (C) 335

Bond cleavage, Evidence for equilibria between μ-alkyne and alkylidyne complexes of tungsten alkoxides: $[W_2(OR)_6(\mu\text{-}C_2R_2')] \rightleftharpoons 2[(RO)_3W{\equiv}CR']$ (C) 446

Metal dependence of cyclometalation and arene C–H activation in the photolysis of *cis*-$H_2M[P(CH_2CH_2CH_2PMe_2)_3]$ (M = Fe, Ru) in benzene (C) 260

Bond length, Hexa-*tert*-butyldisilane—the molecule with the longest Si-Si bond (C) 79

Hexa-*tert*-butyl-1,3-diiodotrisilane, a molecule with two neighboring very long Si–Si bonds (C) 1129

π-Bonds, Dimeric 1,4-dichloro-2,3,5,6-tetramethyl-1,4-dialumina-2,5-cyclohexadiene, a compound with aluminum-olefin π-bonds (C) 921

Boranes, Reaction of phosphonium ylides with alkyldichloroboranes (C) 559

Boronate esters, Optically active α-chloro-(*E*)-crotylboronate esters by allyl rearrangement (C) 189

Boron heterocycles, A 1,2-diboratabenzene: lithium salt and transition metal complexes (C) 642

A 1,3-diboratacyclobutadiene and its dimer, a sandwich compound with a Li_4 layer (C) 1111

A puckered and a planar 1,3-diboretane (C) 1112

Polymeric (η^5,μ-2,3-dihydro-1,3-diborolyl)-nickel—the first polydecker sandwich compound (C) 105

Boron-nitrogen-sulfur compounds, Synthesis and molecular and crystal structure of a new tricyclic $B_3N_4S_2Si_2$ system (C) 741

Boussingault. Chemist and agriculturist (B) 1035

Bridging, Large molecular cavities for small ions—double bridging of three bipyridine units (C) 1122

Bridging ligands, Benzene as bridging li-

gand in main group metal–transition metal–arene complexes (C) 927
CF_2-bridged metal complexes (C) 185
Dimeric chloro[dicyclopentadienyl(dimethyl)silyl]ytterbium(III), a rare example of a complex involving metal-bridging instead of chelating $[Me_2Si(\eta^5\text{-}C_5H_4)_2]$ ligands (C) 738
Evidence for equilibria between μ-alkyne and alkylidyne complexes of tungsten alkoxides: $[W_2(OR)_6(\mu\text{-}C_2R'_2)] \rightleftharpoons 2[(RO)_3W{\equiv}CR']$ (C) 446
First dinuclear complexes with fourfold alkyl-bridging (C) 925
Unusual bridging of the metal centers in dimeric bis(η-methylcyclopentadienyl)phenylethynylzirconium (C) 463
Butterfly structure, $[(\eta^5\text{-}C_5H_5)_2Mo_2(CO)_4(PPh)_2]$, a diphosphene complex with a butterfly structure (C) 338
(*R,S*)-2-(*tert*-Butyl)-3-methyl-4-imidazolidinone, Enantiomer separation of (*R,S*)-2-(*tert*-butyl)-3-methyl-4-imidazolidinone, a chiral building block for amino acid synthesis (C) 345, 766

CADMIUM COMPOUNDS, The three-dimensionally non-molecular polyadamantanoid structure of $Cd(SPh)_2$ (C) 165
Cage structure, $[Pd_2S_{28}]^{4\ominus}$: a 30-membered cage containing an entrapped cation (C) 453
Calorimetry, Analytical solution calorimetry. Fundamentals and practice (B) 482
Carbanions, Bicyclo[3.2.1]octa-2,6-dienyllithium (C) 468
[(α-Cyanobenzyllithium·tetramethylethylenediamine)$_2$·benzene]: X-ray structure analysis of an α-nitrile "carbanion" (C) 373
Lithium-coordinated α-sulfonimidoyl carbanions: crystal study of [(*S*)-(*N*-methyl-*S*-phenylsulfonimidoyl)methyllithium]$_4$·2(tmeda) and configurative stability of [(*N*-methyl-*S*-phenylsulfonimidoyl)isopropyllithium] (C) 938
Solid-state and solution structure of α-(phenylsulfonyl)allyllithium (C) 939
The structure of an allenylsodium derivative—competition between carbanion resonance delocalization and gegenion charge localization (C) 902
Carbene complexes, Carbonyl olefinating aluminum-molybdenum complexes and an analogous tungsten complex (C) 910
Carbene complexes with quinone bisketal functions (C) 911
Carbenes, Diels-Alder reactions at carbene ligands: a route to olefin-carbene complexes (C) 812
ESR observation of thermally produced triplet nitrenes and photochemically produced triplet cycloheptatrienylidenes (C) 480
Carbene-tungsten complexes, Carbonyl olefinating carbene-tungsten complexes and their suitability as catalysts in olefin-metathesis (C) 909
Carbenium ions, Direct determination of rate constants for the addition of carbenium ions to alkenes (C) 89
Direct measurement of the "isokinetic rate constant" in additions of diarylcarbenium ions to 2-methyl-2-butene (C) 1016
Linear reactivity-selectivity correlations in additions of diarylcarbenium ions to alkenes; a rebuttal of the reactivity-selectivity principle (C) 1017
Stabilization of carbenium ions in liquid crystals (C) 841
Carbocations, First crystal structure analysis of an aliphatic carbocation—stabilization of the 3,5,7-trimethyl-1-adamantyl cation by C–C hyperconjugation (C) 349
Carbohydrate synthesis, 2-Substituted 1,3,2-dioxaboroles as synthetic equivalents for the glycolaldehyde anion (C) 560
Carbon-carbon bond formation, The palladium-catalyzed cross-coupling reactions of organotin reagents with organic electrophiles (R) 508
Carbon-carbon coupling, CC Coupling of CO_2 and butadiene on iron(0) complexes—a novel route to α,ω-dicarboxylic acids (C) 810
Carbon monoxide, The chemistry of the catalyzed hydrogenation of carbon monoxide (B) 195
Carbon monoxide reduction, Synthesis and structure of the Co_3Ti_2 complex$[\{\mu_3\text{-}[(C_5H_5)_2TiOC]\}_2\{(C_5H_5)_3Co_3\}]$: CO reduction by two different metal centers (C) 254
Carbon-nitrogen bond formation, Transition-metal clusters as catalysts of unconventional reactions: reductive C–N coupling of alkyl isocyanates (C) 570
Carbon suboxide, Wittig reaction with carbon suboxide: synthesis of dimethyl 1,5-diphenyl-1,2,3,4-pentatetraenedicarboxylate (C) 93
Carbonylation, Reductive coupling of CO: formation of a 1:1 adduct of η^2-ketone- and enediolato-complex upon carbonylation of bis(cyclopentadienyl)hafnacyclobutane (C) 364
Carbonyl dianion synthon, Nitromethane as d^1,d^1 multiple coupling reagent for the carbonyl dianion synthon. Practical synthesis of chalcogran (C) 941
Carbonyl olefination, Asymmetric elimination with high induction: synthesis of 1-alkenylsulfoximides with axial and central chirality (C) 935
Carbonyl olefinating aluminum-molybdenum complexes and an analogous tungsten complex (C) 910
Carbonyl olefinating carbene-tungsten complexes and their suitability as catalysts in olefin-metathesis (C) 909
Carbonyl oxides, Benzophenone *O*-oxide (C) 255
Thianthrene 5-oxide as mechanistic probe in oxygen transfer reactions: the nucleophilic character of carbonyl oxides (C) 101
N-(1-Carboxy-5-aminopentyl)dipeptides, Synthesis of *N*-(1-carboxy-5-aminopentyl)dipeptids as inhibitors of angiotensin converting enzyme (C) 277
Carbyne-complexes, The Schrock carbyne-complex $[Cl_3(dme)W{\equiv}CCMe_3]$, a highly reactive catalyst for the metathesis of alkenes (C) 359
Stepwise addition of $MeS^{\ominus}$ to a metal-carbon triple bond—a new type of reaction in the chemistry of carbyne complexes (C) 904
Carbyne-iridium complexes: evidence for an equilibrium between alkenylidene(hydrido) and carbyne isomers (C) 737
Carcinogenicity, *N*-Aryl-*O*-(diphenylphosphinoyl)hydroxylamines: electrophilic amination of amines to hydrazines; a model reaction for the carcinogenicity of aromatic amines (C) 562
Carotinoids, Mini-violerythrins: why can C_{38}-carotinoids be blue? (C) 1018
Catalysis, Heterogeneous catalysis of ammonia synthesis at room temperature and atmospheric pressure (C) 558
Synthesis of a macrobicyclic thiazolium-host and supramolecular catalysis of the benzoin condensation (C) 1125
Catalysts, Nature of Ni and Cu species in reduced bimetallic Ni–Cu/Al_2O_3 catalysts (C) 753
C–C bond formation, Synthesis of "*C*-disaccharides" by radical C–C bond formation (C) 450
C-Disaccharides, Synthesis of "*C*-disaccharides" by radical C–C bond formation (C) 450
Cerium(IV) bisporphyrinates, Remarkable ease of ring oxidation in cerium(IV) bisporphyrinates with double-decker structure (C) 286
C–H Activation, Thermolytically induced C–H activation using a 14-electron-complex: synthesis and molecular structure of $[IrHCl(C_6H_5)(PiPr_3)_2]$ (C) 1090
Chain elongation, Synthesis of long-chain sugars by iterative, diastereoselective homologation of 2,3-*O*-isopropylidene-D-glyceraldehyde with 2-trimethylsilylthiazole (C) 835
Chain reaction, Thermally induced redox reaction of carbonyl compounds and alcohols in a radical chain reaction: comproportionation to two hydroxyalkyl radicals (C) 762
Chain structure, $[NbAs_8]^{3-}$, a novel type of complex and an unexpected one-dimensional chain structure: $^1_\infty[Rb\{NbAs_8\}]^{2-}$ (C) 353
Chalcogran, Nitromethane as d^1,d^1 multiple coupling reagent for the carbonyl dianion synthon. Practical synthesis of chalcogran (C) 941
Chalcose, Synthesis of deoxyhexoses from divinylglycols—the synthesis of D- and L-chalcose (C) 89
Charge localization, The structure of an allenylsodium derivative—competition between carbanion resonance delocalization and gegenion charge localization (C) 902
Charge separation in excited states of decoupled systems—TICT compounds and implications regarding the development of new laser dyes and the primary processes of vision and photosynthesis (R) 971
Charge transfer, Unusual behavior of the stable paramagnetic dihydridoiridium(IV) complex $[Ir(H)_2(Cl)_2(iPr_3P)_2]$ in solution (C) 460
Charge-transfer interactions, A simple route to the intramolecular quinhydrone of [2.2]paracyclophanediene (C) 171
Electron donor-acceptor interactions in host-guest complexes in organic solutions (C) 1127
Chemical bonding, Kristallstruktur und chemische Bindung (B) 112
Chemical oscillations, Oscillations and traveling waves in chemical systems (B) 1037
Chemical technology, Kirk-Othmer concise encyclopedia of chemical technology (B) 194
Chiral building blocks, Preparation of chiral building blocks from amino acids and peptides via electrolytic decarboxylation and $TiCl_4$-induced aminoalkylation (C) 843
Chiral hydrazine derivative, Benzo[*c*]benzo[3,4]cinnolino[1,2-*a*]cinnoline, a chiral hydrazine derivative (C) 374
Chirality, Recognition of chirality by ENDOR spectroscopy (C) 1007
Chirality transfer, α-Deprotonation of an α-chiral 2-alkenylcarbamate with retention and lithium-titanium exchange with inversion—the homoaldol reaction with 1,3-chirality transfer (C) 160
Optically active α-chloro-(*E*)-crotylboronate esters by allyl rearrangement (C) 189
Chiron approach, Total synthesis of natural products: the "chiron" approach (B) 113
Chlorine oxides, Crystal structure of Cl_2O_6 (C) 993
Chlorins, Facile entry to geminally dialkylated chlorins (C) 458
Chloro-(*E*)-crotylboronate esters, Optically active α-chloro-(*E*)-crotylboronate esters by allyl rearrangement (C) 189
Chlorosilyl-*N,N*-dimethylamine, The structure of chlorosilyl-*N,N*-dimethylamine in the gaseous and solid phases (C) 107
Cholesterol homeostasis, A receptor-mediated pathway for cholesterol homeostasis (Nobel lecture) (R) 583
Choline, A macrobicyclic polyphenoxide as receptor analogue for choline and related ammonium compounds (C) 647

Chromatography, High-pressure liquid chromatography (HPLC) of proteins (R) 535
Clathrate structure, $Ge_{4.06}I$, an unexpected germanium subiodide—a tetragermaniodonium(III) iodide with clathrate structure $[Ge_{46-x}I_x]I_8$, $x = 8/3$ (C) 350
Cluster beam chemistry—from atoms to solids (R) 197
Clusters, A novel electron count and metal-metal multiple bonding in trigonal prismatic clusters (C) 822
$[Bi_2^{III}S_{34}]^{4-}$, the hitherto sulfur-richest complex (C) 273
$[Cl_7Cu_5(ReS_4)]^{3\ominus}$, a hexanuclear complex anion with double cubane-like structure (C) 990
Computer graphics in the study of metal cluster compounds (R) 853
$[Co_4(\mu_3\text{-}As)_3(\mu_3,\eta^3\text{-}As_3)(PPh_3)_4]$, a product of the reaction of $[CoCl_2(PPh_3)_2]$ with $PhAs(SiMe_3)_2$ (C) 175
Diastereoselective transformations on heterometal clusters (C) 479
Directed synthesis of rhenamolybdatetrahedranes: nucleophilic addition of pentacarbonylrhenate(1-) to alkyne ligands in cationic molybdenum complexes (C) 734
Formal insertion of the $HCO^{\oplus}$ fragment into a trinuclear cluster metal-carbyne bond: synthesis, structure and reactivity of cluster-bound ethynol (C) 929
Heteronuclear 'star clusters': $[Ni_2Pt_2W_4(\mu_3\text{-}CPh)_4(CO)_8(\eta\text{-}C_5H_5)_4]$ and $[Ni_2Pt_2W_4(\mu_2\text{-}CR)(\mu_3\text{-}CR)_3(CO)_8(\eta\text{-}C_5H_5)_4]$ (R = Ph or *p*-C_6H_4Me) (C) 190
Multiple bonds between transition metals and "bare" main group elements: links between inorganic solid state chemistry and organometallic chemistry (R) 56
$[Re_4^{IV}S_{22}]^{4-}$, a highly symmetrical metal-sulfur cluster with six S_3^{2-} ligands (C) 272
Reversible interconversion of C-C and C-N multiple bond systems on clusters (C) 279
Skeletal rearrangements on clusters: the reaction of $[(t\text{Bu}P)Fe_3(CO)_{10}]$ with diphenylacetylene (C) 1119
Structures with oligomeric condensed clusters in indium oxomolybdates (C) 845
Synthesis and structure of $[(Ph_3P)_3Ir(\mu_3\text{-}H)(\mu\text{-}H)_2Ag_2(OSO_2CF_3)(H_2O)](CF_3SO_3)$, a complex with a bent Ag-Ir-Ag chain (C) 748
Synthesis of $[Cu_3Os_3H_9(PMe_2Ph)_9]$, a bimetallic raft, by reductive elimination of alcohol or H_2 (C) 262
The $\sigma^2\pi^4$ triple bond between molybdenum and tungsten atoms: developing the chemistry of an inorganic functional group (R) 21
Cobalt-germanium triangles, Early members of a homologous series based on linked GeM_2 triangles, (M = Co, Fe): structures of $[Ge_2Co_4Fe_2(CO)_{21}]$ and $[Ge_3Co_8(CO)_{26}]$ (C) 759
Cobalt-magnesium compounds, Heterometallic dinuclear complexes by ethene displacement with Grignard compounds or diorganomagnesium compounds (C) 923
Cobalt-porphyrins, Reduced cobalt-*meso*-tetraphenylporphyrin complexes: synthesis and structure of $[Na(thf)_3]_2[Co(TPP)]$ (C) 553
Cobalt-titanium compounds, Synthesis and structure of the Co_3Ti_2 complex$[\{\mu_3\text{-}[(C_5H_5)_2TiOC]\}_2\{(C_5H_5)_3Co_3\}]$: CO reduction by two different metal centers (C) 254
Coenzyme A analogue, Methylmalonylcarba(dethia)-coenzyme A as substrate of the coenzyme B_{12}-dependent methylmalonyl-CoA mutase: enzymatic rearrangement of a β- to a γ-keto acid (C) 366
Colloid chemistry, Ordering of ionic solutes in dilute solutions through attraction of similarly charged solutes—a change of paradigm in colloid and polymer chemistry (R) 323
COLOC technique, The elucidation of the constitution of glycopeptides by the NMR spectroscopic COLOC technique (C) 342
Complexation, Preorganization—from solvents to spherands (R) 1039
Computer graphics in the study of metal cluster compounds (R) 853
Protein crystallography and computer graphics—toward rational drug design (R) 767
Conformation, Conformational prerequisites for the in vitro inhibition of cholate uptake in hepatocytes by cyclic analogues of antamanide and somatostatin (C) 997
Conjugation, Laticyclic 1,5-conjugation between parallel, neighboring azo-groups and phenyl groups (C) 187
Coordination, Crystal structure of the η^3-allyllithium compound [1,3-diphenylallyllithium · diethyl ether]$_n$ (C) 104
Dimeric 1,4-dichloro-2,3,5,6-tetramethyl-1,4-dialumina-2,5-cyclohexadiene, a compound with aluminum-olefin π-bonds (C) 921
$(Me_4N)_3[Mo_4O_{12}F_3]\cdot 0.8H_2O$, a salt with a novel fluorooxo polyanion (C) 1104
$NaNb_3O_5F$—a niobium-niobium triple bond with "side-on" coordination by Nb atoms (C) 996
$[NbAs_8]^{3-}$, a novel type of complex and an unexpected one-dimensional chain structure: $^1_\infty[Rb\{NbAs_8\}]^{2-}$ (C) 353
Novel octahedral Si and Ge complexes with a hexadentate diphenol ligand (C) 162
[α-(Phenylsulfinyl)-α-methylbenzyllithium-tetramethylethylenediamine]$_2$: crystal structure of an α-sulfinyl "carbanion" (C) 1011
Polymeric paracyclophane complexes of copper and silver (C) 1089
Reaction of Grignard reagents with dianionic hexacoordinated silicon complexes: organosilicon compounds from silica gel (C) 474
Reactivity of anionic pentacoordinated silicon complexes towards nucleophiles (C) 473
$[Sb_3I_{10}^{\ominus}]_\infty$—a polymeric anion with transitions from trigonal pyramidal to octahedral coordination of antimony(III) (C) 825
Second-sphere coordination—a novel rôle for molecular receptors (R) 487
Structures with oligomeric condensed clusters in indium oxomolybdates (C) 845
S_4N_4 as tridentate ligand in $[IrX(CO)(PPh_3)(S_4N_4)]$ complexes (C) 931
Trithiometaphosphate PS_3^-—an anion with phosphorus of coordination number 3 (C) 82
Coordination chemistry, Understanding reaction dynamics in coordination chemistry—application of high pressure techniques (R) 673
Coordination number, A 2-phosphonio-substituted 1-phospha-1-alkene: resonance between P^{III} alkene and P^{V} ylide (C) 454
2-Dewar phosphinines—a new class of compounds containing two-coordinate phosphorus (C) 280
$H_3C{-}{-}P{=}CH_2$: an ylide with two-coordinate phosphorus? (C) 265
Cope rearrangement induced by medium-sized ring strain (C) 1026
Copper iodides, $[Cu_{36}I_{56}]^{20\ominus}$—a novel polyanion in the compound $(pyH)_2[Cu_3I_5]$ (C) 569
Copper-osmium cluster, Synthesis of $[Cu_3Os_3H_9(PMe_2Ph)_9]$, a bimetallic raft, by reductive elimination of alcohol or H_2 (C) 262
Copper-semicorrin complexes, Chiral copper-semicorrin complexes as enantioselective catalysts for the cyclopropanation of olefins by diazo compounds (C) 1005
Coupling reactions, The palladium-catalyzed cross-coupling reactions of organotin reagents with organic electrophiles (R) 508
Transition-metal clusters as catalysts of unconventional reactions: reductive C-N coupling of alkyl isocyanates (C) 570
Coupling reagent, Nitromethane as d^1,d^1 multiple coupling reagent for the carbonyl dianion synthon. Practical synthesis of chalcogran (C) 941
Crown ethers, A simple route to 2,3,11,12-dibenzo-1,4,7,10,13,16-hexathia-2,11-cyclooctadiene (hexathiobenzo[18]crown-6) (C) 1107
Palladium(II) and platinum(II) complexes of 1,4,7,10,13,16-hexathiacyclooctadecane (C) 274
Cryptates, $[NbAs_8]^{3-}$, a novel type of complex and an unexpected one-dimensional chain structure: $^1_\infty[Rb\{NbAs_8\}]^{2-}$ (C) 353
Crystal structure, Kristallstruktur und chemische Bindung (B) 112
$[NbAs_8]^{3-}$, a novel type of complex and an unexpected one-dimensional chain structure: $^1_\infty[Rb\{NbAs_8\}]^{2-}$ (C) 353
Periodic potential surfaces in crystal structures (C) 110
The pentagonal column and the ReO_3-type structure (R) 431
Crystal structure determination, Direct methods and anomalous dispersion (Nobel lecture) (R) 603
Recovering phase information from intensity data (Nobel lecture) (R) 614
Cubane-like structure, $[Cl_7Cu_5(ReS_4)]^{3\ominus}$, a hexanuclear complex anion with double cubane-like structure (C) 990
Cumulenes, Structure determination of pentatetraenes—comparison of the structures of cumulenes (C) 340
Wittig reaction with carbon suboxide: synthesis of dimethyl 1,5-diphenyl-1,2,3,4-pentatetraenedicarboxylate (C) 93
Cyanine dyes, Influence of external negative charges on the absorption maxima of symmetrical cyanines. A study with model compounds and artificial bacteriorhodopsin pigments (C) 284
Cyanosulfanes, The polymeric silver complexes $[Ag\{S_n(CN)_2\}_2][AsF_6]$ (n = 3, 4): stable coordination compounds of dicyanotri- and dicyanotetrasulfanes (C) 84
Cycloaddition, [3 + 2] Cycloaddition approaches to five-membered rings via trimethylenemethane and its equivalents (R) 1
$[_\pi 2 + _\pi 2]$ Cycloaddition of 4-phenyl-4*H*-1,2,4-triazole-3,5-dione and singlet oxygen to homofuran (C) 989
[4 + 2] Cycloadditions with transition-metal-coordinated selenoaldehydes and selenoketones as heterodienophiles (C) 78
Organic reactions at high pressure: cycloaddition reactions of 11-methylene-1,6-methano[10]annulene (C) 346
Synthesis of a dicyclopenta[*a,e*]pentalene by [6 + 2]-cycloaddition of 1,3-di-*tert*-butyl-5-vinylidenecyclopentadiene and consecutive 8π-electrocyclic reaction (C) 466
Thioketone *S*-oxides by [2 + 2]-cycloaddition of ynamines to *N*-sulfinyltosylamide (C) 459
Tricyclo[5.3.0.$0^{2,8}$]deca-3,5-dien-9-one and a new route to $C_{10}H_{10}$ isomers (C) 906
1,3-Dipolar cycloaddition chemistry (B) 112
Cycloalkynes, 1-Thia-2-cyclooctyne—a strained cycloalkyne with polarized triple bond (C) 809
Cycloarene, Cyclo[*d.e.d.e.e.d.e.d.e.e.*]decakisbenzene, a new cycloarene (C) 742
Cyclo[*d.e.d.e.e.d.e.d.e.e.*]decakisbenzene, a new cycloarene (C) 742
Cyclodisilazane cations—synthesis and crystal structure (C) 915
Cyclohepta[*ef*]heptalene, Synthesis and dy-

namic properties of substituted cyclohepta[*ef*]heptalene (C) 633
Cycloheptatrienylidenemethyleneditropylium, A salt of the dication cycloheptatrienylidenemethyleneditropylium (C) 916
Cycloheptatrienylidenes, ESR observation of thermally produced triplet nitrenes and photochemically produced triplet cycloheptatrienylidenes (C) 480
Cyclohexatriene, Novel synthesis of the angular [3]phenylene (terphenylene) by cobalt-catalyzed cyclization of bis(2-ethynylphenyl)ethyne: a molecule with an internal cyclohexatriene ring (C) 266
Cyclohexatriene structure, $[\{(\eta^5\text{-}C_5Me_5)Co\}_3C_{12}H_{10}]$—*a complex of biphenyl with* Kekulé structure (C) 646
Cyclometalation, Metal dependence of cyclometalation and arene C-H activation in the photolysis of *cis*-$H_2M[P(CH_2CH_2CH_2PMe_2)_3]$ (M = Fe, Ru) in benzene (C) 260
Cyclopentane derivatives, Intramolecular addition of 2-(trimethylsilyl)methyl-substituted allyl cations to double bonds—synthesis of bicyclo[3.3.0]octane derivatives (C) 354
Cyclopentanediols, Optically active cyclopentanediol synthetic building blocks from tartaric acid (C) 994
Cyclophosphane oxides, P_6tBu_4O and P_7tBu_5O—the first polycyclophosphane oxides (C) 471
Cyclophosphanes, *cyclo*-P_5 as complex ligand—the phosphorus analogue of the cyclopentadienyl ligand (C) 363
New products from PCl_3, $P(NMe_2)_3$, and $AlCl_3$ (C) 253
Cyclopropabenzene, Nickelacyclobutabenzene compounds by oxidative addition of cyclopropabenzene to nickel(0) compounds (C) 640
Nickel-induced cyclotetramerization of cyclopropabenzene to 1,6:7,12:13,18:19,24-tetrakismethano[24]annulene (C) 367
Cyclopropanation, Chiral copper-semicorrin complexes as enantioselective catalysts for the cyclopropanation of olefins by diazo compounds (C) 1005
Cyclopropenylium salts, *cyclo*-C_3I_4—the first saltlike halocarbon (C) 103
Cycloreversion, Diels-Alder adducts of benzene with arenes and their [4 + 2] cycloreversion (C) 377
Cycloselanes, Selenium-rich chalcogen rings Se_5S, Se_5S_2, and Se_7 from titanocene pentaselenide (C) 99
Cyclosilanes, The tetrasilabicyclo[1.1.0]butane system: structure of 1,3-di-*tert*-butyl-2,2,4,4-tetrakis-(2,6-diethylphenyl)tetrasilabicyclo[1.1.0]butane (C) 173
Cyclotetradepsipeptide, Synthesis of the all-L-configurated cyclotetradepsipeptide *cyclo*[-L-Val-L-Lac-]$_2$ by the combined protection/activation method with the 2,4-bis(methylthio)phenoxycarbonyl group (C) 170
Cyclotetramerization, Nickel-induced cyclotetramerization of cyclopropabenzene to 1,6:7,12:13,18:19,24-tetrakismethano[24]-annulene (C) 367
Cytochrome P-450 (B) 294

DECAMETHYLSILICOCENE—synthesis and structure (C) 164
Dehydroalanine, Amino acid derivatives from *N*-(Arylmethylene)dehydroalanine methyl esters (C) 90
Dehydropeptide synthesis, $C_{phenyl}\text{-}H\cdots O$ and $C_{phenyl}\text{-}H\cdots N$ interactions: crystal structure of (*Z*)-4-benzylidene-2-methyl-5(4*H*)-oxazolone, an intermediate for dehydropeptide synthesis (C) 447
Dendralenes, A novel entry to dendralene systems (C) 578
Deoxyhexoses, Synthesis of deoxyhexoses from divinylglycols—the synthesis of D- and L-chalcose (C) 89
Depsipeptides, Synthesis of the all-L-configurated cyclotetradepsipeptide *cyclo*[-L-Val-L-Lac-]$_2$ by the combined protection/activation method with the 2,4-bis(methylthio)phenoxycarbonyl group (C) 170
2-Dewar phosphinines—a new class of compounds containing two-coordinate phosphorus (C) 280
Diastereoselective synthesis of functionalized tetrahydrofuran derivatives from γ-lactols (C) 556
Diastereoselective transformations on heterometal clusters (C) 479
Diazadiphosphetidine, Acid-catalyzed isomerization of the [2 + 1]-cyclodimer of an iminophosphane to the diazadiphosphetidine (C) 834
Diazenes, Valence isomers of compounds with geminal aryldiazene and isocyanate functions stabilized by protonation (C) 1132
Diazoalkanes, UV/VIS laser photochemistry: intermediary formation of diazoalkanes versus direct S_0,T_1 transitions in the photolysis of azoalkanes (C) 818
1,2-Diboratabenzene, A 1,2-diboratabenzene: lithium salt and transition metal complexes (C) 642
1,3-Diboratacyclobutadiene, A 1,3-diboratacyclobutadiene and its dimer, a sandwich compound with a Li_4 layer (C) 1111
1,3-Diboretanes, A puckered and a planar 1,3-diboretane (C) 1112
α,ω-Dicarboxylic acids, CC Coupling of CO_2 and butadiene on iron(0) complexes—a novel route to α,ω-dicarboxylic acids (C) 810
Dichlorine hexaoxide, Crystal structure of Cl_2O_6 (C) 993
Dicyclopenta[*a,e*]pentalene, Synthesis of a dicyclopenta[*a,e*]pentalene by [6 + 2]-cycloaddition of 1,3-di-*tert*-butyl-5-vinylidenecyclopentadiene and consecutive 8π-electrocyclic reaction (C) 466
Diels-Alder adducts of benzene with arenes and their [4 + 2] cycloreversion (C) 377
Diels-Alder reaction, Intramolecular Diels-Alder reactions with methyl 2-trimethylsiloxy-2-vinylcyclopropanecarboxylates as key building blocks (C) 1086
Mechanism of the thermal 1,3-cyclohexadiene dimerization: a non-concerted Diels-Alder reaction leading to the *exo*-[4 + 2] adduct and a novel [6 + 4]-ene reaction (C) 108
Diels-Alder reactions at carbene ligands: a route to olefin-carbene complexes (C) 812
Difluoromethylene bridge, CF_2-bridged metal complexes (C) 185
Dihalomethanes, Photoisomerization of dihalomethanes (C) 819
Dihydroacepentalenediide, the dianion of acepentalene (C) 719
Dihydroazulenes, Tricyclo[5.3.0.0^{2,8}]deca-3,5-dien-9-one and a new route to $C_{10}H_{10}$ isomers (C) 906
Diindenyldivanadium, Synthesis of diindenyldivanadium—a new variant of the reductive degradation of metallocenes and related compounds (C) 928
Diisopinocampheylborane, Secondary deuterium kinetic isotope effects in enantioselective hydroborations with (+)-diisopinocampheylborane (C) 577
Diketones, 2,4-Diene-1,6-diones and 2-acyl-3-cyclopenten-1-ols by double Friedel-Crafts acylation of tricarbonyl(diene)iron complexes (C) 1131
Dilithioalkenes, Vicinal dilithioalkenes by addition of lithium to simple cyclic and acyclic alkynes (C) 167
Dilithioethylene isomers, 1,2-Dilithioethylene isomers and their mechanisms of interconversion: an ab initio study (C) 169
Dimerization, The first observation of the equilibrium $2M \equiv M \rightleftarrows M_4$ (M = transition metal): synthesis and structure of hexaisopropoxyditungsten and its dimer (C) 1014
Dinuclear complexes, First dinuclear complexes with fourfold alkyl-bridging (C) 925
Heterometallic dinuclear complexes by ethene displacement with Grignard compounds or diorganomagnesium compounds (C) 923
Dioxaboroles, 2-Substituted 1,3,2-dioxaboroles as synthetic equivalents for the glycolaldehyde anion (C) 560
Dioxan-4-ones, Preparation of optically active alcohols from 1,3-dioxan-4-ones. A practical version of the asymmetric synthesis with nucleophilic substitution at acetal centers (C) 178
Dioxepins, Asymmetric double-bond isomerization of 4,7-dihydro- to 4,5-dihydro-1,3-dioxepins (C) 274
Dioxirane, Benzophenone *O*-oxide (C) 255
Diozonides, A stable diozonide of a conjugated diene by ozonolysis of 2,3,4,5-tetramethyl-2,4-hexadiene on polyethylene (C) 81
Dipeptides, Thin layer chromatographic separation of stereoisomeric dipeptides (C) 278
1,3-Diphosphacyclobutadienecobalt(I) complexes from phosphaalkynes (C) 644
1,3-Diphospha-4-metallabutadiene, Phosphorus analogues of unsaturated carbon compounds: an (*s-trans*)-1,3-diphospha-4-metallabutadiene and its (*s-cis*)-$Fe(CO)_3$ complex (C) 455
Diphosphathiophene, A stable 1,2,4-thiadiphosphole ("2,4-diphosphathiophene") (C) 567
Diphosphene complex, $[(\eta^5\text{-}C_5H_5)_2Mo_2(CO)_4(PPh)_2]$, a diphosphene complex with a butterfly structure (C) 338
Diphosphenes, Bis(pentamethylcyclopentadienyl)diphosphene—a molecule with fluxional structure and reactive P-C bond (C) 919
Transition metal-induced CO-insertion in the P=P bond of diphosphenes with formation of diphosphinomethanone derivatives (C) 755
Diphosphinomethanide ligands, $[La\{(Ph_2P)_2CH\}_3]$—a homoleptic lanthanum complex with π-allyl-like coordinated diphosphinomethanide ligands (C) 823
Diphosphinomethanone derivatives, Transition metal-induced CO-insertion in the P=P bond of diphosphenes with formation of diphosphinomethanone derivatives (C) 755
Dipolar cycloaddition, 1,3-Dipolar cycloaddition chemistry (B) 112
Disilane, Hexa-*tert*-butyldisilane—the molecule with the longest Si-Si bond (C) 79
Disorder, The chemistry of the noncrystalline state (R) 31
Disulfur dioxide, Complex stabilization of disulfur dioxide in the fragmentation of thiirane *S*-oxide on bis(triphenylphosphane)platinum(0) (C) 261
Dithiocyanogen, $[Ag(NCS)_2AsF_6]_n$—a metal complex with dithiocyanogen as ligand (C) 1006
Dititanacyclobutane, A polyfunctional dititanacyclobutane (C) 574
Divinylglyoxal and methylvinylglyoxal (C) 1116
DNA, Physicochemical and cytochemical investigations on the binding of ethidium and acridine dyes to DNA and to organelles in living cells (R) 115
Double-bond isomerization, Asymmetric double-bond isomerization of 4,7-dihydro- to 4,5-dihydro-1,3-dioxepins (C) 274
Double bond localization, $[\{(\eta^5\text{-}C_5Me_5)Co\}_3C_{12}H_{10}]$—a complex of biphenyl with Kekulé structure (C) 646
Synthesis and dynamic properties of substituted cyclohepta[*ef*]heptalene (C) 633

Double bond rule, Discarding the double bond rule? (L) 1038
Drug design, Protein crystallography and computer graphics—toward rational drug design (R) 767
Drugs, Biotransformation von Arzneimitteln. Band 4 (B) 293
Dyotropic hydrogen migration, An intramolecular dyotropic hydrogen migration in pentacyclo[7.6.0.0^{2,13}.0^{3,8}.0^{10,14}]pentadeca-4,6,11-triene (C) 1121

ELECTRICAL CONDUCTIVITY, A radical anion salt of 2,5-dimethyl-*N,N'*-dicyanoquinonediimine with extremely high electrical conductivity (C) 740
Electrochemistry, Ferrocene-modified polypyrrole films by electrochemical copolymerization (C) 180
Indirect electroorganic syntheses—a modern chapter of organic electrochemistry (R) 683
Unexpected "two-electron" transfer in cyclic hydrazines—a voltammetric analysis (C) 1021
Electron acceptors, Poly-onio-substituted quinones as strong electron acceptors (C) 917
Electron-donor ability, Variable electron-donor ability of alkyne ligands—synthesis and structure of carbonyl(η^5-cyclopentadienyl)(η^2-1-diethylamino-1-propyne)(η^1-*p*-methylphenylketenyl)tungsten (C) 643
Electron donor-acceptor interactions in host-guest complexes in organic solutions (C) 1127
Electron donor, 1,2,4,5-Tetrakis(dimethylamino)benzene, a new electron donor with unusual properties (C) 1023
Electronics, Technology of chemicals and materials for electronics (B) 1036
Electron/ion transfer reactions, Isothermal magnetic phase transitions controlled by reversible electron/ion transfer reactions (C) 905
Electron-transfer, Poly(anthrylenetrimethylene) and 9,10-bridged anthracenes by reductive alkylation (C) 444
Synthesis and redox properties of compounds with several separated anthracene electrophores (C) 443
Electroorganic chemistry as a new tool in organic synthesis (B) 380
Electroorganic syntheses, Part I: oxidations (B) 484
Electrophilic addition, Stereocontrolled synthesis of paraconates from β-lactones; stereochemistry of electrophilic additions to endocyclic paraconate-enolates (C) 655
Elementary reactions, Metathesis of alkyl radicals and alkenes—a novel elementary reaction of alkyl radicals (C) 80
Elements, Chemistry of the elements (B) 194
Enantiomerically pure C_2 units, Preparation of chiral building blocks from amino acids and peptides via electrolytic decarboxylation and $TiCl_4$-induced aminoalkylation (C) 843
Enantiomerically pure cyclopentanediols, Optically active cyclopentanediol synthetic building blocks from tartaric acid (C) 994
Enantiomeric resolution by HPLC on silica-gel-bound, optically active polyamides (C) 830
Thin layer chromatographic separation of stereoisomeric dipeptides (C) 278
Enantiomerization, Synthesis of *erythro*-D- and -L-4-pentenetriols. Selective epoxy allyl alcohol hydrolysis with retention or twofold inversion (enantiomerization) (C) 87
Enantiomer separation of (*R,S*)-2-(*tert*-butyl)-3-methyl-4-imidazolidinone, a chiral building block for amino acid synthesis (C) 345, 766
Enantioselective catalysts, Chiral copper-semicorrin complexes as enantioselective catalysts for the cyclopropanation of olefins by diazo compounds (C) 1005
[$Cp(CO)_2Mo$\{NR*[Rh(norbornadiene)]-CH(pyridyl)\}], a rhodium complex with an asymmetric molybdenum atom in the chelate skeleton (C) 371
Enantioselective hydroborations, Secondary deuterium kinetic isotope effects in enantioselective hydroborations with (+)-diisopinocampheylborane (C) 577
Enantioselective Robinson annelations via phase-transfer catalysis (C) 476
Enantioselective synthesis of α-substituted primary amines by nucleophilic addition to aldehyde-SAMP hydrazones (C) 1109
ENDOR spectroscopy, ^{13}C-ENDOR investigation of an organic tetraradical in the quintet state; synthesis of a fourfold ^{13}C-labeled tetrakisgalvinol (C) 1097
Recognition of chirality by ENDOR spectroscopy (C) 1007
Ene reaction, Mechanism of the thermal 1,3-cyclohexadiene dimerization: a non-concerted Diels-Alder reaction leading to the *exo*-[4+2] adduct and a novel [6+4]-ene reaction (C) 108
Enzymatic analysis, Methods of enzymatic analysis. Vol. 6. Metabolites 1: carbohydrates (B) 291
Methods of enzymatic analysis. Vol. 7. Metabolites 2: Tri- and dicarboxylic acids, purines, pyrimidines and derivatives, coenzymes, inorganic compounds (B) 483
Enzymatic hydrolysis, Complementary epoxide hydrolase- vs glutathione S-transferase-catalyzed kinetic resolution of simple aliphatic oxiranes—complete regio- and enantioselective hydrolysis of *cis*-2-ethyl-3-methyloxirane (C) 1032
Enzymatic rearrangement, Methylmalonyl-carba(dethia)-coenzyme A as substrate of the coenzyme B_{12}-dependent methylmalonyl-CoA mutase: enzymatic rearrangement of a β- to a γ-keto acid (C) 366
Enzymatic synthesis, Synthesis of the trisaccharide Neu-5-Ac-α(2→6)Gal-β(1→4)Glc-NAc by the use of immobilized enzymes (C) 1096
Enzyme inhibitors, Synthesis of *N*-(1-carboxy-5-aminopentyl)dipeptides as inhibitors of angiotensin converting enzyme (C) 277
Enzyme reagents, Stereospecific reductions with hydrogen gas, modified metal catalysts, methyl viologen and enzymes or microorganisms (C) 462
Epoxidation of olefins with elemental fluorine in water/acetonitrile mixtures (C) 554
Epoxides, Organometallic derivatives of epoxides (C) 653
The alkylation of epoxides with new organoyttrium and organolanthanoid reagents (C) 760
2-Epoxy alcohols, A simple access to 2-epoxy alcohols: titanium(IV)-catalyzed oxygen transfer from allylic hydroperoxides (C) 269
Equilibria, Evidence for equilibria between μ-alkyne and alkylidyne complexes of tungsten alkoxides: [$W_2(OR)_6(\mu\text{-}C_2R_2')$] ⇌ 2[$(RO)_3W{\equiv}CR'$] (C) 446
Ethanedithiolate complexes, [Et_4N][$M(SCH_2CH_2S)_3$] (M = Nb, Ta), homoleptic 1,2-ethanedithiolate complexes of niobium and tantalum (C) 86
Ethene displacement, Heterometallic dinuclear complexes by ethene displacement with Grignard compounds or diorganomagnesium compounds (C) 923
Ethidium dyes, Physicochemical and cytochemical investigations on the binding of ethidium and acridine dyes to DNA and to organelles in living cells (R) 115
Ethylene oxide —X-ray structure analysis (at 150 K) and ab initio calculations (C) 276
cis-2-Ethyl-3-methyloxirane, Complementary epoxide hydrolase- vs glutathione S-transferase-catalyzed kinetic resolution of simple aliphatic oxiranes—complete regio- and enantioselective hydrolysis of *cis*-2-ethyl-3-methyloxirane (C) 1032
Ethynol, Formal insertion of the $HCO^{\oplus}$ fragment into a trinuclear cluster metal-carbyne bond: synthesis, structure and reactivity of cluster-bound ethynol (C) 929
Evolution, Remarks on the review article "replication and evolution in inorganic systems" by *Armin Weiss* (C) 658

FERROCENE, Ferrocene-modified polypyrrole films by electrochemical copolymerization (C) 180
Ferrocenylmethyl(Fem) group, The ferrocenylmethyl(Fem) group as a highly lipophilic and chromophoric group for the masking of peptide bonds (C) 159
Fischer-Tropsch synthesis, The chemistry of the catalyzed hydrogenation of carbon monoxide (B) 195
Flash photolysis of $Os(CO)_5$ in benzene solution. Detection of $Os(CO)_4$-benzene by fast time-resolved IR spectroscopy (C) 991
Flavor materials, Common fragrance and flavor materials (B) 582
Fluorescence, Charge separation in excited states of decoupled systems—TICT compounds and implications regarding the development of new laser dyes and the primary processes of vision and photosynthesis (R) 971
Fluorine, Epoxidation of olefins with elemental fluorine in water/acetonitrile mixtures (C) 554
Fluoroorganic compounds, Di- and trifluoro-substituted dilithium compounds for organic syntheses (C) 98
Fluorooxo polyanion, $(Me_4N)_3[Mo_4O_{12}F_3]\cdot 0.8H_2O$, a salt with a novel fluorooxo polyanion (C) 1104
Fluxional structure, Bis(pentamethylcyclopentadienyl)diphosphene—a molecule with fluxional structure and reactive P-C bond (C) 919
Forest damage, Model experiments on the phytotoxicity of halogenated hydrocarbons (C) 808
Friedel-Crafts acylation, 2,4-Diene-1,6-diones and 2-acyl-3-cyclopenten-1-ols by double Friedel-Crafts acylation of tricarbonyl(diene)iron complexes (C) 1131
Full-shell clusters, Novel modifications of gold, rhodium, and ruthenium—M_{13} clusters as building blocks of "si perclusters" (C) 922
Fulvalene derivatives, Novel fulvalene derivatives of zirconium: a facile entry into organozirconium(III) chemistry (C) 289

GAS CHROMATOGRAPHY, Handbuch der Gaschromatographie (B) 580
Gas-phase flow thermolysis, Organic synthesis at high temperatures. Gas-phase flow thermolysis (R) 414
Germanium subiodide, $Ge_{4.06}I$, an unexpected germanium subiodide—a tetragermanioiodonium(III) iodide with clathrate structure $[Ge_{46-x}I_x]I_8$, x = 8/3 (C) 350
Glass, The chemistry of the noncrystalline state (R) 31
Glycolaldehyde anion, 2-Substituted 1,3,2-dioxaboroles as synthetic equivalents for the glycolaldehyde anion (C) 560
Glycopeptides, Synthesis of *O*-glycopeptides of the tumor-associated T_N- and T-antigen type and their binding to bovine serum albumin (C) 360

The elucidation of the constitution of glycopeptides by the NMR spectroscopic COLOC technique (C) 342

Glycosides, New methods for the synthesis of glycosides and oligosaccharides—are there alternatives to the Koenigs-Knorr method? (R) 212

Glycosphingolipids, Synthesis of glycosphingolipids and psychosines (C) 725

Gold-gold distances, Synthesis and structure of 1,3-Diphenyltriazenidogold(I), a tetrameric molecule with short gold-gold distances (C) 95

Gold(III) complexes, Methylene-bridged dinuclear gold(III) complexes with terminal and bridging ylide ligands (C) 575

Grandisol, Asymmetric photocycloadditions with optically pure, spirocyclic enones. Simple synthesis of (+)- and (−)-grandisol (C) 1117

Grignard reagents, Reaction of Grignard reagents with dianionic hexacoordinated silicon complexes: organosilicon compounds from silica gel (C) 474

Group theory, Gruppentheorie für Chemiker (B) 660

Group transfer polymerization of acrylic acid esters with alkylthio- or arylthiosilanes as initiators (C) 1108

HAFNIUM COMPOUNDS, Reductive coupling of CO: formation of a 1:1 adduct of η^2-ketone- and enediolato-complex upon carbonylation of bis(cyclopentadienyl)hafnacyclobutane (C) 364

Halogenated hydrocarbons, Microbial degradation of halogenated hydrocarbons: a biological solution to pollution problems? (R) 779

Model experiments on the phytotoxicity of halogenated hydrocarbons (C) 808

Hepatocytes, Conformational prerequisites for the in vitro inhibition of cholate uptake in hepatocytes by cyclic analogues of antamanide and somatostatin (C) 997

Heptaheteronortricycles, Valence tautomerism of the heptaheteronortricycles $[P_{7-x}As_x]^{3-}$ (C) 352

Heterocycles, A facile synthesis of a new class of eight-membered heterocycles from 1-azabutadienes (C) 181

Synthesis and molecular and crystal structure of a new tricyclic $B_3N_4S_2Si_2$ system (C) 741

Heterogeneous catalysts, O_2-Generation by oxidation of water with di- and trinuclear ruthenium complexes as homogeneous and heterogeneous catalysts (C) 1009

Oxygen evolution by water oxidation mediated by heterogeneous manganese complexes (C) 825

Heterometallic dinuclear complexes by ethene displacement with Grignard compounds or diorganomagnesium compounds (C) 923

Hexadeoxynucleotides, A self-replicating hexadeoxynucleotide (C) 932

Hexaethynylbenzene (C) 268

Hexahydrido(pentamethylcyclopentadienyl)rhenium, $[(C_5Me_5)ReH_6]$ (C) 1092

Hexaisopropoxyditungsten, The first observation of the equilibrium $2M{\equiv}M \rightleftarrows M_4$ (M = transition metal): synthesis and structure of hexaisopropoxyditungsten and its dimer (C) 1014

Hexasilabenzene, Si_6H_6: Is the aromatic structure the most stable one? (C) 651

Hexathiacyclooctadecane, Palladium(II) and platinum(II) complexes of 1,4,7,10,13,16-hexathiacyclooctadecane (C) 274

High-pressure liquid chromatography (HPLC) of proteins (R) 535

High-pressure reactions, Direct aminolysis of unactivated esters at high-pressure (C) 565

Organic reactions at high pressure: cycloaddition reactions of 11-methylene-1,6-methano[10]annulene (C) 346

High pressure techniques, Understanding reaction dynamics in coordination chemistry—application of high pressure techniques (R) 673

History of chemistry, Adolf von Baeyer's scientific achievements — a legacy (R) 297

History of science, Boussingault. Chemist and agriculturist (B) 1035

Über die Erhaltung der Kraft (B) 1037

2D HOESY, 2-Lithio-1-phenylpyrrole: X-ray structure analysis and ^6Li-^1H 2D heteronuclear Overhauser NMR spectroscopy (2D HOESY) (C) 1103

Homoaldol reaction, α-Deprotonation of an α-chiral 2-alkenylcarbamate with retention and lithium-titanium exchange with inversion—the homoaldol reaction with 1,3-chirality transfer (C) 160

Homofuran, $[_\pi 2 + _\pi 2]$ Cycloaddition of 4-phenyl-4*H*-1,2,4-triazole-3,5-dione and singlet oxygen to homofuran (C) 989

Homoleptic complexes, $[Et_4N][M(SCH_2CH_2S)_3]$ (M = Nb, Ta), homoleptic 1,2-ethanedithiolate complexes of niobium and tantalum (C) 86

Homologation, Synthesis of long-chain sugars by iterative, diastereoselective homologation of 2,3-*O*-isopropylidene-D-glyceraldehyde with 2-trimethylsilylthiazole (C) 835

Host-guest chemistry, Bicyclic host cavities derived from triphenylamine—guest selectivity and redox properties (C) 336

Electron donor-acceptor interactions in host-guest complexes *in organic solutions* (C) 1127

Large molecular cavities for small ions—double bridging of three bipyridine units (C) 1122

Preorganization—from solvents to spherands (R) 1039

Host molecules, Anionic host molecules with bicyclic carbon skeletons—synthesis and guest inclusion in aqueous solution (C) 567

HPLC, Enantiomeric resolution by HPLC on silica-gel-bound, optically active polyamides (C) 830

High-pressure liquid chromatography (HPLC) of proteins (R) 535

Hydrazines, *N*-Aryl-*O*-(diphenylphosphinoyl)hydroxylamines: electrophilic amination of amines to hydrazines; a model reaction for the carcinogenicity of aromatic amines (C) 562

Benzo[*c*]benzo[3,4]cinnolino[1,2-*a*]cinnoline, a chiral hydrazine derivative (C) 374

Unexpected "two-electron" transfer in cyclic hydrazines—a voltammetric analysis (C) 1021

Hydride reagents, Superactive alkali metal hydride metalation reagents: LiH, NaH, and KH (C) 465

Hydrides, Hexahydrido(pentamethylcyclopentadienyl)rhenium, $[(C_5Me_5)ReH_6]$ (C) 1092

Hydrido compounds, Unusual behavior of the stable paramagnetic dihydridoiridium(IV) complex $[Ir(H)_2(Cl)_2(iPr_3P)_2]$ in solution (C) 460

Hydrocarbon host lattices, Selective inclusion and separation of isomeric and homologous hydrocarbons by hydrocarbon host lattices (C) 746

Hydrogenation, The chemistry of the catalyzed hydrogenation of carbon monoxide (B) 195

Hydrogen bonds, C_{phenyl}-H···O and C_{phenyl}-H···N interactions: crystal structure of (*Z*)-4-benzylidene-2-methyl-5(4*H*)-oxazolone, an intermediate for dehydropeptide synthesis (C) 447

Hydrogen migration, An intramolecular dyotropic hydrogen migration in pentacyclo[7.6.0.0^{2,13}.0^{3,8}.0^{10,14}]pentadeca-4,6,11-triene (C) 1121

Hydroxyacetylene, generation and characterization of the neutral molecule, radical cation and dication in the gas phase (C) 282

Formal insertion of the $HCO^{\oplus}$ fragment into a trinuclear cluster metal-carbyne bond: synthesis, structure and reactivity of cluster-bound ethynol (C) 929

Hydroxylamines, *N*-Aryl-*O*-(diphenylphosphinoyl)hydroxylamines: electrophilic amination of amines to hydrazines; a model reaction for the carcinogenicity of aromatic amines (C) 562

Hyperconjugation, First crystal structure analysis of an aliphatic carbocation—stabilization of the 3,5,7-trimethyl-1-adamantyl cation by C-C hyperconjugation (C) 349

IMIDAZOLE, Benzotri(imidazole)—a new ring system derived from benzenehexamine (C) 650

Iminophosphane, Acid-catalyzed isomerization of the [2 + 1]-Cyclodimer of an iminophosphane to the diazadiphosphetidine (C) 834

Immobilized enzymes, Synthesis of the trisaccharide Neu-5-Ac-α(2→6)Gal-β(1→4)-*Glc*NAc by the use of immobilized enzymes (C) 1096

Inclusion compounds, Selective inclusion and separation of isomeric and homologous hydrocarbons by hydrocarbon host lattices (C) 746

Indacene, Synthesis and properties of 1,3,5,7-tetra-*tert*-butyl-*s*-indacene (C) 630

Indenophane dianion, [2.2]Indenophane dianion: a novel double-layered dianion (C) 174

Indium oxomolybdates, Structures with oligomeric condensed clusters in indium oxomolybdates (C) 845

Indolizines, Dihydropyrazolopyridine and bis(dihydroindolizine)—novel mono- and bifunctional photochromic systems (C) 572

Industrial chemistry, Industrielle Anorganische Chemie (B) 943

Ullmann's encyclopedia of industrial chemistry (B) 763

Influenza A viruses, Molecular biological background of the species and organ specificity of influenza A viruses (R) 47

Inorganic polymers, $[Ag(NCS)_2AsF_6]_n$—a metal complex with dithiocyanogen as ligand (C) 1006

$[Sb_3I_{10}^{\ominus}]_\infty$—a polymeric anion with transitions from trigonal pyramidal to octahedral coordination of antimony(III) (C) 825

Insecticides, Synthesis of bis(trifluoromethyl)-analogues of the pyrethroids (C) 184

Insertion, Transition metal-induced CO-insertion in the P=P bond of diphosphenes with formation of diphosphinomethanone derivatives (C) 755

Intellectual processing, Geometric and topological thinking in organic chemistry (R) 882

Ionic conduction, Fast ionic conduction in LiI·4methanol: $[Li(CH_3OH)_4]^+I^-$ (C) 1087

Iridium compounds, Prototropism in (pentamethylcyclopentadienyl)iridium complexes with pyrazole ligands (C) 1114

Thermolytically induced C-H activation using a 14-electron-complex: synthesis and molecular structure of $[IrHCl(C_6H_5)(PiPr_3)_2]$ (C) 1090

Unusual behavior of the stable paramagnetic dihydridoiridium(IV) complex $[Ir(H)_2(Cl)_2(iPr_3P)_2]$ in solution (C) 460

Iridium-silver compounds, Synthesis and structure of $[(Ph_3P)_3Ir(\mu_3\text{-}H)(\mu\text{-}H)_2Ag_2(OSO_2CF_3)(H_2O)](CF_3SO_3)$, a complex with a bent Ag-Ir-Ag chain (C) 748

Iron(0) compounds, Bis(η^2-ethene)(η^6-toluene)iron (C) 831
CC Coupling of CO_2 and butadiene on iron(0) complexes—a novel route to α,ω-dicarboxylic acids (C) 810
Isocyanates, Transition-metal clusters as catalysts of unconventional reactions: reductive C–N coupling of alkyl isocyanates (C) 570
Valence isomers of compounds with geminal aryldiazene and isocyanate functions stabilized by protonation (C) 1132
Isocyanide radical, An isocyanide radical as complex ligand (C) 744
Isokinetic rate constant, Direct measurement of the "isokinetic rate constant" in additions of diarylcarbenium ions to 2-methyl-2-butene (C) 1016
Isolobal concept, The complex ions $[C_5H_5M(CO)_3]^{\ominus}$ (M = Mo, W) as 6e-ligands: Synthesis and molecular structure of $[(\eta^4\text{-}C_4Me_4)Co(\mu\text{-}CO)_3M(\eta^5\text{-}C_5H_5)]$ (M = Mo, W) (C) 839
The isolobal analogy "d^6-$CpM(CO)_3^{\ominus}$ ⟷ $Cp^{\ominus}$" (C) 837
Isomerization, Acid-catalyzed isomerization of the [2+1]-Cyclodimer of an iminophosphane to the diazadiphosphetidine (C) 834
An azimine-triaziridine transformation by laser photolysis (C) 828
Asymmetric double-bond isomerization of 4,7-dihydro- to 4,5-dihydro-1,3-dioxepins (C) 274
Carbyne-iridium complexes: evidence for an equilibrium between alkenylidene(hydrido) and carbyne isomers (C) 737
Diastereoselective transformations on heterometal clusters (C) 479
Reversible interconversion of C–C and C–N multiple bond systems on clusters (C) 279
Isomorphism of tris(cyclopentadienyl)lutetium(III) and tris(cyclopentadienyl)scandium(III): an unexpected consequence of the lanthanoid contraction (C) 656
(*R*)-2-Isopropenylcyclopropane-1,1-dicarboxylic acid: absolute configuration and stereospecific ring expansion of its dimethyl ester (C) 732
Isotope effects, Secondary deuterium kinetic isotope effects in enantioselective hydroborations with (+)-diisopinocampheylborane (C) 577

KEKULENE, Cyclo[*d.e.d.e.e.d.e.d.e.e.*]decakisbenzene, a new cycloarene (C) 742
Ketenyl ligand, Variable electron-donor ability of alkyne ligands—synthesis and structure of carbonyl(η^5-cyclopentadienyl)(η^2-1-diethylamino-1-propyne)(η^1-*p*-methylphenylketenyl)tungsten (C) 643
Ketones, Synthesis of cyclic, vicinal tetraketones (C) 449
Kinetic isotope effects, Secondary deuterium kinetic isotope effects in enantioselective hydroborations with (+)-diisopinocampheylborane (C) 577
Kinetic resolution, Complementary epoxide hydrolase- vs glutathione S-transferase-catalyzed kinetic resolution of simple aliphatic oxiranes—complete regio- and enantioselective hydrolysis of *cis*-2-ethyl-3-methyloxirane (C) 1032
Kinetics, Direct determination of rate constants for the addition of carbenium ions to alkenes (C) 89
Direct measurement of the "isokinetic rate constant" in additions of diarylcarbenium ions to 2-methyl-2-butene (C) 1016
Linear reactivity-selectivity correlations in additions of diarylcarbenium ions to alkenes; a rebuttal of the reactivity-selectivity principle (C) 1017
Techniques in organic reaction kinetics (B) 381
The phenol ⇌ 2,4-cyclohexadienone equilibrium in aqueous solution (C) 344
Kirk-Othmer concise encyclopedia of chemical technology (B) 194
Koenigs-Knorr method, New methods for the synthesis of glycosides and oligosaccharides—are there alternatives to the Koenigs-Knorr method? (R) 212

γ-LACTOLS, Diastereoselective synthesis of functionalized tetrahydrofuran derivatives from γ-lactols (C) 556
Langmuir-Blodgett-technique, Preparation of ultrathin layers of molecularly controlled architecture from polymeric phthalocyanines by the Langmuir-Blodgett-technique (C) 1105
Lanthanoid contraction, Isomorphism of tris(cyclopentadienyl)lutetium(III) and tris(cyclopentadienyl)scandium(III): an unexpected consequence of the lanthanoid contraction (C) 656
Lanthanum compounds, $[La\{(Ph_2P)_2CH\}_3]$—a homoleptic lanthanum complex with π-allyl-like coordinated diphosphinomethanide ligands (C) 823
Laser dyes, Charge separation in excited states of decoupled systems—TICT compounds and implications regarding the development of new laser dyes and the primary processes of vision and photosynthesis (R) 971
Laser photochemistry, UV/VIS Laser photochemistry: intermediary formation of diazoalkanes versus direct S_0,T_1 transitions in the photolysis of azoalkanes (C) 818
Laser photolysis, An azimine-triaziridine transformation by laser photolysis (C) 828
Laticyclic 1,5-conjugation between parallel, neighboring azo-groups and phenyl groups (C) 187
Layer systems, Preparation of ultrathin layers of molecularly controlled architecture from polymeric phthalocyanines by the Langmuir-Blodgett-technique (C) 1105
Ligands, $[Ag(NCS)_2AsF_6]_n$—a metal complex with dithiocyanogen as ligand (C) 1006
An isocyanide radical as complex ligand (C) 744
$Me_3SiNPNSiMe_3^{\ominus}$, the monophosphorus analogue of a triazenido ligand (C) 96
$[\{(\eta^5\text{-}C_5Me_5)Co\}_3C_{12}H_{10}]$—a complex of biphenyl with Kekulé structure (C) 646
$[La\{(Ph_2P)_2CH\}_3]$—a homoleptic lanthanum complex with π-allyl-like coordinated diphosphinomethanide ligands (C) 823
$[(C_3Ph_3)Ni(\mu\text{-}Br)_3Ni(C_3Ph_3)](C_3Ph_3)$—a triple-decker-like complex with triphenylcyclopropenyl as ligand (C) 833
Complex-induced fragmentation of As_4S_4: stabilization of an As_2S_3 ligand (C) 557
Formal insertion of the $HCO^{\oplus}$ fragment into a trinuclear cluster metal-carbyne bond: synthesis, structure and reactivity of cluster-bound ethynol (C) 929
$[Et_4N][M(SCH_2CH_2S)_3]$ (M = Nb, Ta), homoleptic 1,2-ethanedithiolate complexes of niobium and tantalum (C) 86
cyclo-P_5 as complex ligand—the phosphorus analogue of the cyclopentadienyl ligand (C) 363
η^3-1-Phosphaallyliron complexes with additional $W(CO)_5$-coordination at the phosphorus—the 1-phosphaallyl ligand as 5e-donor (C) 357
Novel octahedral Si and Ge complexes with a hexadentate diphenol ligand (C) 162
Prototropism in (pentamethylcyclopentadienyl)iridium complexes with pyrazole ligands (C) 1114
S_4N_4 as tridentate ligand in $[IrX(CO)(PPh_3)(S_4N_4)]$ complexes (C) 931
The complex ions $[C_5H_5M(CO)_3]^{\ominus}$ (M = Mo, W) as 6e-ligands: Synthesis and molecular structure of $[(\eta^4\text{-}C_4Me_4)Co(\mu\text{-}CO)_3M(\eta^5\text{-}C_5H_5)]$ (M = Mo, W) (C) 839
The isolobal analogy "d^6-$CpM(CO)_3^{\ominus}$ ⟷ $Cp^{\ominus}$" (C) 837
Weak Pd···S interaction in palladium(II) complexes with 1,4,7-trithiacyclononane as ligand (C) 1101
Ligand-to-metal charge transfer, Unusual behavior of the stable paramagnetic dihydridoiridium(IV) complex $[Ir(H)_2(Cl)_2(iPr_3P)_2]$ in solution (C) 460
Liquid crystals, Bilayer-immobilized films containing mesogenic azobenzene amphiphiles—electrically controllable permeability (C) 751
Carbohydrate-based liquid crystals: mesogenic 1-*O*-alkyl derivatives of 2,5-anhydrohexitols (C) 368
Stabilization of carbenium ions in liquid crystals (C) 841
Lithioalkylsulfoximides, Lithium-coordinated α-sulfonimidoyl carbanions: crystal study of [(*S*)-(*N*-methyl-*S*-phenylsulfonimidoyl)methyllithium]$_4$·2(tmeda) and configurative stability of [(*N*-methyl-*S*-phenylsulfonimidoyl)isopropyllithium] (C) 938
2-Lithio-1-phenylpyrrole: X-ray structure analysis and ^6Li-^1H 2D heteronuclear Overhauser NMR spectroscopy (2D HOESY) (C) 1103
Lithium compounds, Vicinal dilithioalkenes by addition of lithium to simple cyclic and acyclic alkynes (C) 167
1,2-Dilithioethylene isomers and their mechanisms of interconversion: an ab initio study (C) 169
Lithium iodide, Fast ionic conduction in LiI·4methanol: $[Li(CH_3OH)_4]^+I^-$ (C) 1087
Lithium ketenimides, [(α-Cyanobenzyllithium·tetramethylethylenediamine)$_2$·benzene]: X-ray structure analysis of an α-nitrile "carbanion" (C) 373
Lithium-titanium exchange, α-Deprotonation of an α-chiral 2-alkenylcarbamate with retention and lithium-titanium exchange with inversion—the homoaldol reaction with 1,3-chirality transfer (C) 160
Living polymers, Group transfer polymerization of acrylic acid esters with alkylthio- or arylthiosilanes as initiators (C) 1108
Low-temperature matrices, Photochemistry of transition-metal atoms: reactions with molecular hydrogen and methane in low-temperature matrices (R) 1072
Lutetium-phosphane compounds, $[(Cp_2Lu\{\mu\text{-}PPh_2\}_2Li(tmeda)]\cdot 1/2\ C_6H_5CH_3$, the first organolanthanoid-phosphane compound to be characterized by X-ray structure analysis (C) 718

MACROBICYCLES, Large molecular cavities for small ions—double bridging of three bipyridine units (C) 1122
Macrobicyclic molecules, Anionic host molecules with bicyclic carbon skeletons—synthesis and guest inclusion in aqueous solution (C) 567
Synthesis of a macrobicyclic thiazolium-host and supramolecular catalysis of the benzoin condensation (C) 1125
Macrocycles, A macrobicyclic polyphenoxide as receptor analogue for choline and related ammonium compounds (C) 647
Bicyclic host cavities derived from triphenylamine—guest selectivity and redox properties (C) 336
Cope rearrangement induced by medium-sized ring strain (C) 1026
Electron donor-acceptor interactions in

host-guest complexes in organic solutions (C) 1127
(*Z*)-[6]Paracycloph-3-ene (C) 369
Porphycene—a novel porphin isomer (C) 257
Preorganization—from solvents to spherands (R) 1039
Macrolide antibiotics. Chemistry, biology and practice (B) 580
Total synthesis of mycinolide V, the aglycone of a macrolide antibiotic of the mycinamycin series (C) 1028
Magnesium L-aspartate complexes, Elucidation of the structure of pharmacologically active magnesium L-aspartate complexes (C) 1013
Magnesium therapy, Elucidation of the structure of pharmacologically active magnesium L-aspartate complexes (C) 1013
Magnetic phase transitions, Isothermal magnetic phase transitions controlled by reversible electron/ion transfer reactions (C) 905
Manganese(II) complexes, An α-functionalized organomanganese(II) derivative: a dinuclear manganese(II) complex with a σ-bonded α-thioalkyl ligand (C) 356
Manganese(II,III,IV) complexes, Dinuclear manganese(II,III,IV) model complexes for the active center of the metalloprotein photosystem II: synthesis, magnetism, and crystal structure of $[LMn^{III}(\mu\text{-}O)(\mu\text{-}CH_3CO_2)_2Mn^{IV}L][ClO_4]_3$ (L = *N,N',N''*-trimethyl-1,4,7-triazacyclononane) (C) 1030
Mangenese compounds, Oxygen evolution by water oxidation mediated by heterogeneous manganese complexes (C) 825
Mass spectrometry, Aminoacetylene and its mono- and dication—identification of potentially interstellar molecules (C) 827
Hydroxyacetylene: generation and characterization of the neutral molecule, radical cation and dication in the gas phase (C) 282
Mass spectral and GC data of drugs, poisons and their metabolites (B) 851
Materials science, 3-Chloropropyltrialkoxysilanes—key intermediates for the commercial production of organofunctionalized silanes and polysiloxane (R) 236
The chemistry of the noncrystalline state (R) 31
Membranes, Bilayer-immobilized films containing mesogenic azobenzene amphiphiles—electrically controllable permeability (C) 751
Synthetic polymer membranes. A structural perspective (B) 1134
Metabolites, The first evidence of endogenous pyridoxyl isoquinoline alkaloids in mammalian organisms (C) 177
Metal atoms, Photochemistry of transition-metal atoms: reactions with molecular hydrogen and methane in low-temperature matrices (R) 1072
Metal-carbon bond, The chemistry of the metal-carbon bond. Vol. 2: The nature and cleavage of carbon-metal bonds. Vol. 3: Carbon-carbon bond formation using organometallic compounds (B) 945
Metal-carbon triple bond, Stepwise addition of $MeS^{\oplus}$ to a metal-carbon triple bond—a new type of reaction in the chemistry of carbyne complexes (C) 904
Metallacycles, A simple route to ruthenacycloalkanes (C) 1008
Metallacyclobutanes, Metallacyclic four-membered ring systems: two independent routes to bis(cyclopentadienyl)titanacyclobutabenzene (C) 639
Metallaspiro compounds, Early members of a homologous series based on linked GeM_2 triangles, (M = Co, Fe): structures of $[Ge_2Co_4Fe_2(CO)_{21}]$ and $[Ge_3Co_8(CO)_{26}]$ (C) 759
Metal-ligand interactions, Weak Pd···S interaction in palladium(II) complexes with 1,4,7-trithiacyclononane as ligand (C) 1101
Metallocenophanes, [m.m]Metallocenophanes: synthesis, structure, and properties (R) 702
Metal-metal bond, The $\sigma^2\pi^4$ triple bond between molybdenum and tungsten atoms: developing the chemistry of an inorganic functional group (R) 21
Metal-metal bonds, Multiple bonds between transition metals and "bare" main group elements: links between inorganic solid state chemistry and organometallic chemistry (R) 56
Metal-metal double bond, Spontaneous intramolecular ring opening of the cyclopropyl group at a metal-metal double bond (C) 563
Synthesis and structure of $[(C_5Me_5)_2M_2Se_5]$: formation of a μ,η^2-tetraselenide ligand at the M-M double bond of $[(C_5Me_5)_2M_2(\mu\text{-}CO)_2]$ (M = Co, Rh) (C) 907
Metal-metal multiple bonding, A novel electron count and metal-metal multiple bonding in trigonal prismatic clusters (C) 822
Metal-metal triple bonds, The first observation of the equilibrium $2M{\equiv}M \rightleftarrows M_4$ (M = transition metal): synthesis and structure of hexaisopropoxyditungsten and its dimer (C) 1014
Metal-NMR-spectroscopy, High-resolution metal-NMR spectroscopy of organometallic compounds (R) 861
Metal-sulfur cluster, $[Re_4^{IV}S_{22}]^{4-}$, a highly symmetrical metal-sulfur cluster with six S_3^{2-} ligands (C) 272
Metaphosphate, Trithiometaphosphate PS_3^-—an anion with phosphorus of coordination number 3 (C) 82
Metathesis, Carbonyl olefinating carbene-tungsten complexes and their suitability as catalysts in olefin-metathesis (C) 909
Metathesis of alkyl radicals and alkenes—a novel elementary reaction of alkyl radicals (C) 80
The Schrock carbyne-complex $[Cl_3(dme)W{\equiv}CCMe_3]$, a highly reactive catalyst for the metathesis of alkenes (C) 359
Methylene, Photoisomerization of dihalomethanes (C) 819
11-Methylene-1,6-methano[10]annulene, Organic reactions at high pressure: cycloaddition reactions of 11-methylene-1,6-methano[10]annulene (C) 346
(−)-Methyl jasmonate, The use of (+)-8-phenylneomenthol in the synthesis of enantiomerically pure (−)-methyl jasmonate (C) 992
Methylvinylglyoxal, Divinylglyoxal and methylvinylglyoxal (C) 1116
Microcrystals, Cluster beam chemistry—from atoms to solids (R) 197
Mini-violerythrins: why can C_{38}-carotinoids be blue? (C) 1018
Mixed valence compounds, Dinuclear manganese(II,III,IV) model complexes for the active center of the metalloprotein photosystem II: synthesis, magnetism, and crystal structure of $[LMn^{III}(\mu\text{-}O)(\mu\text{-}CH_3CO_2)_2Mn^{IV}L][ClO_4]_3$ (L = *N,N',N''*-trimethyl-1,4,7-triazacyclononane) (C) 1030
Mixed valency gallium tellurohalides, E_3Te_3Hal, mixed valency tellurohalides of gallium and indium with one-dimensional structural units (C) 752
Molybdenum compounds, $(Me_4N)_3[Mo_4O_{12}F_3]\cdot 0.8H_2O$, a salt with a novel fluorooxo polyanion (C) 1104
Molybdenum-rhodium compound, $[Cp(CO)_2Mo\{NR^*[Rh(norbornadiene)]\text{-}CH(pyridyl)\}]$, a rhodium complex with an asymmetric molybdenum atom in the chelate skeleton (C) 371
Molybdenum-sulfur compounds, Synthesis and crystal structure of μ-thio-bis[tris(diethyldithiocarbamato)molybdenum(IV)-toluene 1:1, a compound containing a rare Mo-S-Mo core (C) 749
Morphine skeleton, Total synthesis of *rac*-salutaridine and sinoacutine ((−)-salutaridine)—a new route to the morphine skeleton (C) 1025
Multiple bonds between transition metals and "bare" main group elements: links between inorganic solid state chemistry and organometallic chemistry (R) 56
The $\sigma^2\pi^4$ triple bond between molybdenum and tungsten atoms: developing the chemistry of an inorganic functional group (R) 21
Mycinolide V, Total synthesis of mycinolide V, the aglycone of a macrolide antibiotic of the *mycinamycin* series (C) 1028
NAPROXEN, Asymmetric bromination of enantiomerically pure acetals of alkyl aryl ketones (C) 259
Natural compounds synthesis, Regioselective and atropoisomeric-selective aryl coupling to give naphthyl isoquinoline alkaloids: the first total synthesis of (−)-ancistrocladine (C) 913
Natural products, [3+2] Cycloaddition approaches to five-membered rings via trimethylenemethane and its equivalents (R) 1
The chemistry of natural products (B) 847
Total synthesis of natural products: the "chiron" approach (B) 113
Nickelacyclobutabenzene compounds by oxidative addition of cyclopropabenzene to nickel(0) compounds (C) 640
Nickelocene, Facile synthesis of pentaphenylnickelocene and other pentaphenylcyclopentadienylnickel and -cobalt complexes (C) 97
Nickelocene analogue, Bis(η^5-2,3,5-tricarbahexaboranyl)nickel, a nickelocene analogue (C) 1099
Niobium-niobium triple bond, $NaNb_3O_5F$—a niobium-niobium triple bond with "side-on" coordination by Nb atoms (C) 996
Nitrenes, ESR observation of thermally produced triplet nitrenes and photochemically produced triplet cycloheptatrienylidenes (C) 480
α-Nitrile "carbanion", [(α-Cyanobenzyllithium·tetramethylethylenediamine)$_2$·benzene]: X-ray structure analysis of an α-nitrile "carbanion" (C) 373
Nitrile ylides and azirines: gas-phase generation from 2,3-dihydro-1,4,2λ^5-oxazaphospholes and matrix isolation (C) 85
Nitrogen, Biological oxidation of nitrogen in organic molecules. Chemistry, toxicology and pharmacology (B) 850
Nitrogen fixation, Heterogeneous catalysis of ammonia synthesis at room temperature and atmospheric pressure (C) 558
Nitrogen-phosphorus ligands, $Me_3SiNPN\text{-}SiMe_3^{\ominus}$, the monophosphorus analogue of a triazenido ligand (C) 96
Nitrogen-silicon double bond, Diisopropyl(2,4,6-tri-*tert*-butylphenylimino)silane—a very stable, free silaimine (C) 649
Nitrogen-sulfur compounds, S_4N_4 as tridentate ligand in $[IrX(CO)(PPh_3)(S_4N_4)]$ complexes (C) 931
Nitromethane as d^1,d^1 multiple coupling reagent for the carbonyl dianion synthon. Practical synthesis of chalcogran (C) 941
NMR Spectroscopy, Applications of dynamic NMR spectroscopy to organic chemistry (B) 658
High-resolution metal-NMR spectroscopy of organometallic compounds (R) 861
The elucidation of the constitution of glycopeptides by the NMR spectroscopic *COLOC technique* (C) 342
2-Lithio-1-phenylpyrrole: X-ray structure

analysis and ^{6}Li-^{1}H 2D heteronuclear Overhauser NMR spectroscopy (2D HOESY) (C) 1103
^{15}N-NMR spectroscopy—new methods and applications (R) 383
Nobel lecture, A receptor-mediated pathway for cholesterol homeostasis (Nobel lecture) (R) 583
Direct methods and anomalous dispersion (Nobel lecture) (R) 603
Recovering phase information from intensity data (Nobel lecture) (R) 614
Nucleic acid structure, Principles of nucleic acid structure (B) 290
Nucleophilicity, 10,10'-Bi(trispiro[2.0.2.0.2.1]-decylidene): a highly nucleophilic olefinic hydrocarbon (C) 335

OLEFIN, 10,10'-Bi(trispiro[2.0.2.0.2.1]decylidene): a highly nucleophilic olefinic hydrocarbon (C) 335
Olefin-carbene complexes, Diels-Alder reactions at carbene ligands: a route to olefin-carbene complexes (C) 812
Olefin-iron compounds, Bis(η^2-ethene)(η^6-toluene)iron (C) 831
Oligonucleotides, A self-replicating hexadeoxynucleotide (C) 932
Oligonucleotide synthesis. A practical approach (B) 296
Oligosaccharides, New methods for the synthesis of glycosides and oligosaccharides—are there alternatives to the Koenigs-Knorr method? (R) 212
Opportunities in chemistry (B) 846
Orbital interactions, An intramolecular dyotropic hydrogen migration in pentacyclo[7.6.0.0^{2,13}.0^{3,8}.0^{10,14}]pentadeca-4,6,11-triene (C) 1121
Orbital interactions in chemistry (B) 581
Ordering of ionic solutes in dilute solutions through attraction of similarly charged solutes—a change of paradigm in colloid and polymer chemistry (R) 323
Organic chemistry, Geometric and topological thinking in organic chemistry (R) 882
Organic syntheses, Di- and trifluoro-substituted dilithium compounds for organic syntheses (C) 98
Strategies and tactics in organic synthesis (B) 292
Organocopper compounds, Selective synthesis by use of Lewis acids in the presence of organocopper and related reagents (R) 947
Organolanthanoid reagents, The alkylation of epoxides with new organoyttrium and organolanthanoid reagents (C) 760
Organomanganese(II) derivative, An α-functionalized organomanganese(II) derivative: a dinuclear manganese(II) complex with a σ-bonded α-thioalkyl ligand (C) 356
Organomercury compounds in organic synthesis (B) 943
Organometallic chemistry, Basic organometallic chemistry (B) 1035
Fundamental transition metal organometallic chemistry (B) 1035
Metallo-organic chemistry (B) 1035
Organometallic compounds, Dictionary of organometallic compounds (B) 765
Organometallic derivatives of epoxides (C) 653
Organotin reagents, The palladium-catalyzed cross-coupling reactions of organotin reagents with organic electrophiles (R) 508
Orthophosphates in the ternary system Al_2O_3-P_2O_5-H_2O (R) 525
Oxazolidines, Preparation of chiral building blocks from amino acids and peptides via electrolytic decarboxylation and $TiCl_4$-induced aminoalkylation (C) 843
Oxidation, Thianthrene 5-oxide as mechanistic probe in oxygen transfer reactions: substrate complexation in oxidations with transition metal peroxides (C) 188
Oxidative stress, Biochemistry of oxidative stress (R) 1058
Oxirane, Ethylene oxide—X-ray structure analysis (at 150 K) and ab initio calculations (C) 276
μ-Oxo complexes, Dinuclear manganese(II,III,IV) model complexes for the active center of the metalloprotein photosystem II: synthesis, magnetism, and crystal structure of $[LMn^{III}(\mu\text{-}O)(\mu\text{-}CH_3CO_2)_2Mn^{IV}L][ClO_4]_3$ (L = *N,N',N''*-trimethyl-1,4,7-triazacyclononane) (C) 1030
Oxygen, Biochemistry of oxidative stress (R) 1058
Oxygen transfer, A simple access to 2-epoxy alcohols: titanium(IV)-catalyzed oxygen transfer from allylic hydroperoxides (C) 269
Thianthrene 5-oxide as mechanistic probe in oxygen transfer reactions: substrate complexation in oxidations with transition metal peroxides (C) 188
Thianthrene 5-oxide as mechanistic probe in oxygen transfer reactions: the nucleophilic character of carbonyl oxides (C) 101
Ozonides, A stable diozonide of a conjugated diene by ozonolysis of 2,3,4,5-tetramethyl-2,4-hexadiene on polyethylene (C) 81
Ozonolysis, A stable diozonide of a conjugated diene by ozonolysis of 2,3,4,5-tetramethyl-2,4-hexadiene on polyethylene (C) 81
Benzophenone *O*-oxide (C) 255

PALLADIUM-SULFUR COMPOUNDS, $[Pd_2S_{28}]^{4\ominus}$: a 30-membered cage containing an entrapped cation (C) 453
Paraconates, Stereocontrolled synthesis of paraconates from β-lactones; stereochemistry of electrophilic additions to endocyclic paraconate-enolates (C) 655
Paracyclophane complexes, Coordination-polymeric paracyclophane complexes of copper and silver (C) 1089
Paracyclophanediene, A simple route to the intramolecular quinhydrone of [2.2]paracyclophanediene (C) 171
(*Z*)-[6]Paracycloph-3-ene (C) 369
Pentagonal column, The pentagonal column and the ReO_3-type structure (R) 431
Pentaketones, Vicinal pentaketones (C) 999
Pentaphenylnickelocene, Facile synthesis of pentaphenylnickelocene and other pentaphenylcyclopentadienylnickel and -cobalt complexes (C) 97
Pentatetraenedicarboxylate, Wittig reaction with carbon suboxide: synthesis of dimethyl 1,5-diphenyl-1,2,3,4-pentatetraenedicarboxylate (C) 93
Pentatetraenes, Structure determination of pentatetraenes—comparison of the structures of cumulenes (C) 340
Pentenetriols, Synthesis of *erythro*-D- and -L-4-pentenetriols. Selective epoxy allyl alcohol hydrolysis with retention or twofold inversion (enantiomerization) (C) 87
Peptide synthesis, The ferrocenylmethyl-(Fem) group as a highly lipophilic and chromophoric group for the masking of peptide bonds (C) 159
Periodic potential surfaces in crystal structures (C) 110
Phanes, A simple route to the intramolecular quinhydrone of [2.2]paracyclophanediene (C) 171
Coordination-polymeric paracyclophane complexes of copper and silver (C) 1089
[2.2]Indenophane dianion: a novel double-layered dianion (C) 174
Pharmacology, Physicochemical and cytochemical investigations on the binding of ethidium and acridine dyes to DNA and to organelles in living cells (R) 115
Phase-transfer catalysis, Enantioselective Robinson annelations via phase-transfer catalysis (C) 476
Hydroxide ion initiated reactions under phase transfer catalysis conditions: mechanism and implications (R) 960
Phenanthrene derivatives, 4,5-Bis(dimethylamino)phenanthrene and 4,5-bis(dimethylamino)-9,10-dihydrophenanthrene: syntheses and "proton sponge" properties (C) 451
Phenol ⇌ 2,4-cyclohexadienone, The phenol ⇌ 2,4-cyclohexadienone equilibrium in aqueous solution (C) 344
[3]Phenylene, Novel synthesis of the angular [3]phenylene (terphenylene) by cobalt-catalyzed cyclization of bis(2-ethynylphenyl)ethyne: a molecule with an internal cyclohexatriene ring (C) 266
(+)-8-Phenylneomenthol, The use of (+)-8-phenylneomenthol in the synthesis of enantiomerically pure (−)-methyl jasmonate (C) 992
α-(Phenylsulfonyl)allyllithium, Solid-state and solution structure of α-(phenylsulfonyl)allyllithium (C) 939
1-Phospha-1-alkenes, A 2-phosphonio-substituted 1-phospha-1-alkene: resonance between P^{III} alkene and P^{V} ylide (C) 454
Phosphorus analogues of unsaturated carbon compounds: an (*s-trans*)-1,3-diphospha-4-metallabutadiene and its (*s-cis*)-$Fe(CO)_3$ complex (C) 455
Phosphaalkenes, Dioxides of *C*-amino-substituted phosphaalkenes and phosphaallyl cations (C) 457
Phosphaalkynes, 1,3-Diphosphacyclobutadienecobalt(I) complexes from phosphaalkynes (C) 644
Phosphaallyl cations, Dioxides of *C*-amino-substituted phosphaalkenes and phosphaallyl cations (C) 457
η^3-1-Phosphaallyliron complexes with additional $W(CO)_5$-coordination at the phosphorus—the 1-phosphaallyl ligand as 5e-donor (C) 357
1-Phosphaallyl ligand, η^3-1-Phosphaallyliron complexes with additional $W(CO)_5$-coordination at the phosphorus—the 1-phosphaallyl ligand as 5e-donor (C) 357
Phosphabenzene derivative, A $1\lambda^5,3\lambda^5,5\lambda^3$-triphosphabenzene derivative (C) 1002
Phosphabutadiene, Synthesis of the first triphosphabutadiene (C) 932
1-Phospha-1,2,3-butatrienes (C) 1003
Phosphanes, New products from PCl_3, $P(NMe_2)_3$, and $AlCl_3$ (C) 253
2-Phosphapropene, $H_3C{-}P{=}CH_2$: an ylide with two-coordinate phosphorus? (C) 265
Phosphates, Orthophosphates in the ternary system Al_2O_3-P_2O_5-H_2O (R) 525
Phosphazene, A transition metal atom as building block of a cyclic phosphazene—synthesis and structure of $[Cl_3WN_3(PPh_2)_2]$ (C) 477
Phosphinines, 2-Dewar phosphinines—a new class of compounds containing two-coordinate phosphorus (C) 280
Phosphinoallenes, Tetrakis(diphenylphosphino)allene (C) 348
Phosphonium ylides, Reaction of phosphonium ylides with alkyldichloroboranes (C) 559
Phosphorus homocycles, *cyclo*-P_5 as complex ligand—the phosphorus analogue of the cyclopentadienyl ligand (C) 363
Phosphorus-tungsten double bond, Synthesis, structure, and addition reactions of $[Cp(CO)_2W{=}PR_2]$, R = *i*Pr, *t*Bu (C) 92
Photochemistry, Flash photolysis of $Os(CO)_5$ in benzene solution. Detection of $Os(CO)_4$·benzene by fast time-resolved IR spectroscopy (C) 991
Photochemistry of transition-metal atoms: reactions with molecular hydrogen and

methane in low-temperature matrices (R) 1072
Synthetic organic photochemistry (B) 381
185-nm photochemistry of olefins, strained hydrocarbons, and azoalkanes in solution (R) 661
Photochromic systems, Dihydropyrazolopyridine and bis(dihydroindolizine)—novel mono- and bifunctional photochromic systems (C) 572
Photocycloaddition, Asymmetric photocycloadditions with optically pure, spirocyclic enones. Simple synthesis of (+)- and (−)-grandisol (C) 1117
Photoisomerization of dihalomethanes (C) 819
Photolysis, UV/VIS Laser photochemistry: intermediary formation of diazoalkanes versus direct S_0,T_1 transitions in the photolysis of azoalkanes (C) 818
Photosynthesis, Remarkable ease of ring oxidation in cerium(IV) bisporphyrinates with double-decker structure (C) 286
Phthalocyanines, Preparation of ultrathin layers of molecularly controlled architecture from polymeric phthalocyanines by the Langmuir-Blodgett-technique (C) 1105
Physical chemistry, Vom Würfelspiel zum Naturgesetz. Simulation und Modelldenken in der Physikalischen Chemie (B) 581
Phytotoxicity, Model experiments on the phytotoxicity of halogenated hydrocarbons (C) 808
Polarity, Solvent polarity and the anomeric effect (C) 287
Pollution, Air pollution and plants (B) 850
Pollution problems, Microbial degradation of halogenated hydrocarbons: a biological solution to pollution problems? (R) 779
Polyadamantanoid structure, The three-dimensionally non-molecular polyadamantanoid structure of $Cd(SPh)_2$ (C) 165
Polyanions, $[Cu_{36}I_{56}]^{20\ominus}$—a novel polyanion in the compound $(pyH)_2[Cu_3I_5]$ (C) 569
Poly(anthrylenetrimethylene) and 9,10-bridged anthracenes by reductive alkylation (C) 444
Polycations, Poly-onio-substituted quinones as strong electron acceptors (C) 917
Polycyclic aromatic compounds, Spectral atlas of polycyclic aromatic compounds (B) 379
Polycyclophosphane oxides, P_6tBu_4O and P_7tBu_5O—the first polycyclophosphane oxides (C) 471
Polydecker sandwich compounds, Polymeric (η^5,μ-2,3-dihydro-1,3-diborolyl)-nickel—the first polydecker sandwich compound (C) 105
Polyenes, A novel entry to dendralene systems (C) 578
Polylithium compounds, 1,2-Dilithioethylene isomers and their mechanisms of interconversion: an ab initio study (C) 169
Polymer chemistry, Ordering of ionic solutes in dilute solutions through attraction of similarly charged solutes—a change of paradigm in colloid and polymer chemistry (R) 323
Polymerization, Group transfer polymerization of acrylic acid esters with alkylthio- or arylthiosilanes as initiators (C) 1108
Polymers, Photochemical conversion and stabilization of polymers (B) 852
Polyphenoxide, A macrobicyclic polyphenoxide as receptor analogue for choline and related ammonium compounds (C) 647
Polypyrrole films, Ferrocene-modified polypyrrole films by electrochemical copolymerization (C) 180
Polysiloxanes, 3-Chloropropyltrialkoxysilanes—key intermediates for the commercial production of organofunctionalized silanes and polysiloxanes (R) 236
Polysulfanes, The polymeric silver complexes $[Ag\{S_n(CN)_2\}_2][AsF_6]$ (n = 3, 4): stable coordination compounds of dicyano-tri- and dicyanotetrasulfanes (C) 84
Polysulfido complexes, $[Bi_2^{III}S_{34}]^{4-}$, the hitherto sulfur-richest complex (C) 273
$[Pd_2S_{28}]^{4\ominus}$: a 30-membered cage containing an entrapped cation (C) 453
Polythioethers, A simple route to 2,3,11,12-dibenzo-1,4,7,10,13,16-hexathia-2,11-cyclooctadiene (hexathiobenzo[18]crown-6) (C) 1107
Porphin isomer, Porphycene—a novel porphin isomer (C) 257
Porphycene—a novel porphin isomer (C) 257
Porphyrin analogue, Synthesis of a fourfold enlarged porphyrin with an extremely large, diamagnetic ring-current effect (C) 1100
Porphyrinates, Remarkable ease of ring oxidation in cerium(IV) bisporphyrinates with double-decker structure (C) 286
Porphyrins, Reduced cobalt-*meso*-tetraphenylporphyrin complexes: synthesis and structure of $[Na(thf)_3]_2[Co(TPP)]$ (C) 553
Potential surfaces, Periodic potential surfaces in crystal structures (C) 110
Preorganization—from solvents to spherands (R) 1039
Protecting groups, Synthesis of the all-L-configurated cyclotetradepsipeptide *cyclo* [-L-Val-L-Lac-]$_2$ by the combined protection/activation method with the 2,4-bis(methylthio)phenoxycarbonyl group (C) 170
The ferrocenylmethyl(Fem) group as a highly lipophilic and chromophoric group for the masking of peptide bonds (C) 159
Protein crystallography and computer graphics—toward rational drug design (R) 767
Proteins, High-pressure liquid chromatography (HPLC) of proteins (R) 535
Proton sponge, 4,5-Bis(dimethylamino)phenanthrene and 4,5-bis(dimethylamino)-9,10-dihydrophenanthrene: syntheses and "proton sponge" properties (C) 451
Prototropism in (pentamethylcyclopentadienyl)iridium complexes with pyrazole ligands (C) 1114
Psychosines, Synthesis of glycosphingolipids and psychosines (C) 725
Pyrazolopyridine, Dihydropyrazolopyridine and bis(dihydroindolizine)—novel mono- and bifunctional photochromic systems (C) 572
Pyrethroids, Synthesis of bis(trifluoromethyl)-analogues of the pyrethroids (C) 184
Pyridoxyl isoquinoline alkaloids, The first evidence of endogenous pyridoxyl isoquinoline alkaloids in mammalian organisms (C) 177

QUINHYDRONES, A simple route to the intramolecular quinhydrone of [2.2]paracyclophanediene (C) 171
Quinone bisketals, Carbene complexes with quinone bisketal functions (C) 911
Quinones, Poly-onio-substituted quinones as strong electron acceptors (C) 917
Quintet state, ^{13}C-ENDOR investigation of an organic tetraradical in the quintet state; synthesis of a fourfold ^{13}C-labeled tetrakisgalvinol (C) 1097

RADICAL ANION SALT, A radical anion salt of 2,5-dimethyl-*N*,*N*′-dicyanoquinonediimine with extremely high electrical conductivity (C) 740
Radical cation salts, ζ-$(ET)_2AuBr_2$, a new type of structure for the organic radical cation salts $(ET)_2AuX_2$ (C) 727
t-$(ET)_2Au(CN)_2$ and t-$(ET)_2AuBr_2$, organic radical cation salts with twist structure (C) 729
Radical chain reaction, Thermally induced redox reaction of carbonyl compounds and alcohols in a radical chain reaction: comproportionation to two hydroxyalkyl radicals (C) 762
Radical reaction, Synthesis of "*C*-disaccharides" by radical C–C bond formation (C) 450
Radicals, ^{13}C-ENDOR investigation of an organic tetraradical in the quintet state; synthesis of a fourfold ^{13}C-labeled tetrakisgalvinol (C) 1097
Raft structure, Synthesis of $[Cu_3Os_3H_9(PMe_2Ph)_9]$, a bimetallic raft, by reductive elimination of alcohol or H_2 (C) 262
Raman spectroscopy, Resonance Raman spectroscopy and its application to inorganic chemistry (R) 131
Rate constants, Direct determination of rate constants for the addition of carbenium ions to alkenes (C) 89
Reaction dynamics, Understanding reaction dynamics in coordination chemistry—application of high pressure techniques (R) 673
Reaction mechanism, Mechanism of the thermal 1,3-cyclohexadiene dimerization: a non-concerted Diels-Alder reaction leading to the *exo*-[4+2] adduct and a novel [6+4]-ene reaction (C) 108
Thianthrene 5-oxide as mechanistic probe in oxygen transfer reactions: substrate complexation in oxidations with transition metal peroxides (C) 188
Thianthrene 5-oxide as mechanistic probe in oxygen transfer reactions: the nucleophilic character of carbonyl oxides (C) 101
Reactive intermediates, Reactive molecules. The neutral reactive intermediates in organic chemistry (B) 295
Reactivity-selectivity correlations, Linear reactivity-selectivity correlations in additions of diarylcarbenium ions to alkenes; a rebuttal of the reactivity-selectivity principle (C) 1017
Rearrangements, Rearrangement of 4*H*-1,2,4-triazolium salts to 4-acyl-5-aminoimidazoles (C) 652
Skeletal rearrangements on clusters: the reaction of $[(tBuP)Fe_3(CO)_{10}]$ with diphenylacetylene (C) 1119
Tandem walk rearrangement of a protonated dicyclopropenyl ketone (C) 1093
Tricyclo[5.3.0.0^{2,8}]deca-3,5-dien-9-one and a new route to $C_{10}H_{10}$ isomers (C) 906
Receptor analogue, A macrobicyclic polyphenoxide as receptor analogue for choline and related ammonium compounds (C) 647
Receptors, Second-sphere coordination—a novel rôle for molecular receptors (R) 487
Redox agents, Indirect electroorganic syntheses—a modern chapter of organic electrochemistry (R) 683
Redox properties, Synthesis and redox properties of compounds with several separated anthracene electrophores (C) 443
Redox reaction, Thermally induced redox reaction of carbonyl compounds and alcohols in a radical chain reaction: comproportionation to two hydroxyalkyl radicals (C) 762
Reductions in organic chemistry (B) 579
Stereospecific reductions with hydrogen gas, modified metal catalysts, methyl viologen and enzymes or microorganisms (C) 462
Reductive carbonylation of high-valent oxorhenium complexes—a new route to low-valent carbonylrhenium compounds (C) 817
Reductive coupling of CO: formation of a 1:1 adduct of η^2-ketone- and enediolato-

complex upon carbonylation of bis(cyclopentadienyl)hafnacyclobutane (C) 364
Regioselective arylchlorination, Pd^{II}-catalyzed regioselective arylchlorination and oxyarylation of unsaturated alcohols (C) 735
Replication, A self-replicating hexadeoxynucleotide (C) 932
Resonance Raman spectroscopy and its application to inorganic chemistry (R) 131
Retinal, Influence of external negative charges on the absorption maxima of symmetrical cyanines. A study with model compounds and artificial bacteriorhodopsin pigments (C) 284
Reversible interconversion of C-C and C-N multiple bond systems on clusters (C) 279
Rhenamolybdatetrahedranes, Directed synthesis of rhenamolybdatetrahedranes: nucleophilic addition of pentacarbonylrhenate(1-) to alkyne ligands in cationic molybdenum complexes (C) 734
Rhenium compounds, Reductive carbonylation of high-valent oxorhenium complexes—a new route to low-valent carbonylrhenium compounds (C) 817
Rhenium hydrides, Hexahydrido(pentamethylcyclopentadienyl)rhenium, $[(C_5Me_5)ReH_6]$ (C) 1092
Rhenium-trioxide type structure, The pentagonal column and the ReO_3-type structure (R) 431
Ring expansion, (*R*)-2-Isopropenylcyclopropane-1,1-dicarboxylic acid: absolute configuration and stereospecific ring expansion of its dimethyl ester (C) 732
Ring opening, Spontaneous intramolecular ring opening of the cyclopropyl group at a metal-metal double bond (C) 563
Robinson annelations, Enantioselective Robinson annelations via phase-transfer catalysis (C) 476
Ruthenacycloalkanes, A simple route to ruthenacycloalkanes (C) 1008
Ruthenium compounds, O_2-Generation by oxidation of water with di- and trinuclear ruthenium complexes as homogeneous and heterogeneous catalysts (C) 1009

SALUTARIDINE, Total synthesis of *rac*-salutaridine and sinoacutine ((−)-salutaridine)—a new route to the morphine skeleton (C) 1025
SAMP Hydrazones, Enantioselective synthesis of α-substituted primary amines by nucleophilic addition to aldehyde-SAMP hydrazones (C) 1109
Sandwich anions, Synthesis of anionic triple-decker complexes having closed 30e valence shells by stacking of sandwich anions with $Cr(CO)_3$ fragments (C) 165
Sandwich complexes, Bis(η^5-2,3,5-tricarbahexaboranyl)nickel, a nickelocene analogue (C) 1099
$[C_6H_3(CH_3)_3][BiCl_3]$ and $[C_6(CH_3)_6][BiCl_3]_2$, arene complexes of bismuth with half-sandwich and "inverted" sandwich structures (C) 757
Polymeric (η^5,μ-2,3-dihydro-1,3-diborolyl)nickel—the first polydecker sandwich compound (C) 105
Synthesis of diindenyldivanadium—a new variant of the reductive degradation of metallocenes and related compounds (C) 928
Schrock carbyne-complex, The Schrock carbyne-complex $[Cl_3(dme)W{\equiv}CCMe_3]$, a highly reactive catalyst for the metathesis of alkenes (C) 359
Second-sphere coordination—a novel rôle for molecular receptors (R) 487
Selectivity, Bicyclic host cavities derived from triphenylamine—guest selectivity and redox properties (C) 336
Regioselective and atropoisomeric-selective aryl coupling to give naphthyl isoquinoline alkaloids: the first total synthesis of (−)-ancistrocladine (C) 913
Synthesis of deoxyhexoses from divinylglycols—the synthesis of D- and L-chalcose (C) 89
Synthesis of *erythro*-D- and -L-4-pentenetriols. Selective epoxy allyl alcohol hydrolysis with retention or twofold inversion (enantiomerization) (C) 87
Selenide ligand, Synthesis and structure of $[(C_5Me_5)_2M_2Se_5]$: formation of a μ,η^2-tetraselenide ligand at the M-M double bond of $[(C_5Me_5)_2M_2(\mu\text{-}CO)_2]$ (M = Co, Rh) (C) 907
Selenium-sulfur compounds, Selenium-rich chalcogen rings Se_5S, Se_5S_2, and Se_7 from titanocene pentaselenide (C) 99
Selenoaldehydes, [4+2] Cycloadditions with transition-metal-coordinated selenoaldehydes and selenoketones as heterodienophiles (C) 78
Selenocarbonyl ylides, Stable selenocarbonyl ylides (C) 183
Selenoketones, [4+2] Cycloadditions with transition-metal-coordinated selenoaldehydes and selenoketones as heterodienophiles (C) 78
Selenonium ions, Tris(pentacarbonylrhenium)-sulfonium, -selenonium, and -telluronium ions: synthesis and structure of $[\{(OC)_5Re\}_3E]^{\oplus}BF_4^{\ominus}$ (E = S, Se, Te) (C) 270
Self-replication, A self-replicating hexadeoxynucleotide (C) 932
Semiconductors, Molecular semiconductors. Photoelectrical properties and solar cells (B) 851
Semiochemistry, Mammalian semiochemistry. The investigation of chemical signals between mammals (B) 296
Signal agents, Mammalian semiochemistry. The investigation of chemical signals between mammals (B) 296
Silaaromaticity, Si_6H_6: Is the aromatic structure the most stable one? (C) 651
Silaimine, Diisopropyl(2,4,6-tri-*tert*-butylphenylimino)silane—a very stable, free silaimine (C) 649
Silanediyl, Decamethylsilicocene—synthesis and structure (C) 164
Silanes, The tetrasilabicyclo[1.1.0]butane system: structure of 1,3-di-*tert*-butyl-2,2,4,4-tetrakis-(2,6-diethylphenyl)tetrasilabicyclo[1.1.0]butane (C) 173
3-Chloropropyltrialkoxysilanes—key intermediates for the commercial production of organofunctionalized silanes and polysiloxanes (R) 236
Silica gel, Reaction of Grignard reagents with dianionic hexacoordinated silicon complexes: organosilicon compounds from silica gel (C) 474
Silicocene, Decamethylsilicocene—synthesis and structure (C) 164
Silicon complexes, Novel octahedral Si and Ge complexes with a hexadentate diphenol ligand (C) 162
Reaction of Grignard reagents with dianionic hexacoordinated silicon complexes: organosilicon compounds from silica gel (C) 474
Reactivity of anionic pentacoordinated silicon complexes towards nucleophiles (C) 473
Silicon compounds, Si_6H_6: Is the aromatic structure the most stable one? (C) 651
Silicon-silicon bonds, Hexa-*tert*-butyl-1,3-diiodotrisilane, a molecule with two neighboring very long Si-Si bonds (C) 1129
Hexa-*tert*-butyldisilane—the molecule with the longest Si-Si bond (C) 79
Silicon tetrahedrons, Red, transparent alkali metal silicides with Si_4 tetrahedrons (C) 566
Silver complexes, The polymeric silver complexes $[Ag\{S_n(CN)_2\}_2][AsF_6]$ (n = 3, 4): stable coordination compounds of dicyano-tri- and dicyanotetrasulfanes (C) 84
Silver oxide, Ag_3O_4, the first silver(II,III) oxide (C) 77
Silylamines, The structure of chlorosilyl-*N*,*N*-dimethylamine in the gaseous and solid phases (C) 107
Singlet oxygen, $[_\pi2+_\pi2]$ Cycloaddition of 4-phenyl-4*H*-1,2,4-triazole-3,5-dione and singlet oxygen to homofuran (C) 989
Sinoacutine, Total synthesis of *rac*-salutaridine and sinoacutine ((−)-salutaridine)—a new route to the morphine skeleton (C) 1025
Skeletal rearrangements on clusters: the reaction of $[(t\text{BuP})Fe_3(CO)_{10}]$ with diphenylacetylene (C) 1119
Solid state chemistry, Cluster beam chemistry—from atoms to solids (R) 197
Fast ionic conduction in LiI·4methanol: $[Li(CH_3OH)_4]^+I^-$ (C) 1087
Isothermal magnetic phase transitions controlled by reversible electron/ion transfer reactions (C) 905
Multiple bonds between transition metals and "bare" main group elements: links between inorganic solid state chemistry and organometallic chemistry (R) 56
Solution structure, Ordering of ionic solutes in dilute solutions through attraction of similarly charged solutes—a change of paradigm in colloid and polymer chemistry (R) 323
Solvent polarity and the anomeric effect (C) 287
Somatostatin, Conformational prerequisites for the in vitro inhibition of cholate uptake in hepatocytes by cyclic analogues of antamanide and somatostatin (C) 997
Spectral atlas of polycyclic aromatic compounds (B) 379
Spectroscopy, Structure and spectra of molecules (B) 484
Spherands, Preorganization—from solvents to spherands (R) 1039
Stacking, ζ-$(ET)_2AuBr_2$, a new type of structure for the organic radical cation salts $(ET)_2AuX_2$ (C) 727
E_3Te_3Hal, mixed valency tellurohalides of gallium and indium with one-dimensional structural units (C) 752
t-$(ET)_2Au(CN)_2$ and t-$(ET)_2AuBr_2$, organic radical cation salts with twist structure (C) 729
Star clusters, Heteronuclear 'star clusters': $[Ni_2Pt_2W_4(\mu_3\text{-}CPh)_4(CO)_8(\eta\text{-}C_5H_5)_4]$ and $[Ni_2Pt_2W_4(\mu_2\text{-}CR)(\mu_3\text{-}CR)_3(CO)_8(\eta\text{-}C_5H_5)_4]$ (R = Ph or *p*-C_6H_4Me) (C) 190
Stereochemistry of heterogeneous metal catalysis (B) 944
Stereocontrolled synthesis of paraconates from β-lactones; stereochemistry of electrophilic additions to endocyclic paraconate-enolates (C) 655
Stereospecific reductions with hydrogen gas, modified metal catalysts, methyl viologen and enzymes or microorganisms (C) 462
Stereospecific ring expansion, (*R*)-2-Isopropenylcyclopropane-1,1-dicarboxylic acid: absolute configuration and stereospecific ring expansion of its dimethyl ester (C) 732
Strain theory, Adolf von Baeyer's scientific achievements — a legacy (R) 297
The concept of strain in organic chemistry (R) 312
Stress, Biochemistry of oxidative stress (R) 1058
Stripping analysis. Principles, instrumentation, and applications (B) 485
Strontium alkoxostannates(II), Strontium and barium alkoxostannates(II)—molecules with S_6 symmetry (C) 375
Structural comparison, The structure of chlorosilyl-*N*,*N*-dimethylamine in the gaseous and solid phases (C) 107
Solid-state and solution structure of α-(phenylsulfonyl)allyllithium (C) 939
Style guide, The ACS style guide (B) 942
Style manual, The chemist's English (B) 378

Sugars, Synthesis of long-chain sugars by iterative, diastereoselective homologation of 2,3-*O*-isopropylidene-D-glyceraldehyde with 2-trimethylsilylthiazole (C) 835
α-Sulfinyl "carbanions", [α-(Phenylsulfinyl)-α-methylbenzyllithium-tetramethylethylenediamine]$_2$: crystal structure of an α-sulfinyl "carbanion" (C) 1011
Sulfones, Solid-state and solution structure of α-(phenylsulfonyl)allyllithium (C) 939
α-Sulfonimidoyl carbanions, Lithium-coordinated α-sulfonimidoyl carbanions: crystal study of [(*S*)-(*N*-methyl-*S*-phenylsulfonimidoyl)methyllithium]$_4$·2(tmeda) and configurative stability of [(*N*-methyl-*S*-phenylsulfonimidoyl)isopropyllithium] (C) 938
Sulfonium ions, Tris(pentacarbonylrhenium)-sulfonium, -selenonium, and -telluronium ions: synthesis and structure of $[\{(OC)_5Re\}_3E]^{\oplus}BF_4^{\ominus}$ (E = S, Se, Te) (C) 270
Sulfoximides, Asymmetric elimination with high induction: synthesis of 1-alkenylsulfoximides with axial and central chirality (C) 935
Lithium-coordinated α-sulfonimidoyl carbanions: crystal study of [(*S*)-(*N*-methyl-*S*-phenylsulfonimidoyl)methyllithium]$_4$·2(tmeda) and configurative stability of [(*N*-methyl-*S*-phenylsulfonimidoyl)isopropyllithium] (C) 938
Sulphur compounds, The structure of volatile sulphur compounds (B) 946
Superacids (B) 486
Superclusters, Novel modifications of gold, rhodium, and ruthenium—M_{13} clusters as building blocks of "superclusters" (C) 922
Superconduction, ζ-$(ET)_2AuBr_2$, a new type of structure for the organic radical cation salts $(ET)_2AuX_2$ (C) 727
Supramolecules, Second-sphere coordination—a novel rôle for molecular receptors (R) 487
Surface reactions, Reversible interconversion of C–C and C–N multiple bond systems on clusters (C) 279
Synthetic building blocks, Optically active cyclopentanediol synthetic building blocks from tartaric acid (C) 994
Synthetic methods, [3 + 2] Cycloaddition approaches to five-membered rings via trimethylenemethane and its equivalents (R) 1
Hydroxide ion initiated reactions under phase transfer catalysis conditions: mechanism and implications (R) 960
Indirect electroorganic syntheses—a modern chapter of organic electrochemistry (R) 683
New methods for the synthesis of glycosides and oligosaccharides—are there alternatives to the Koenigs-Knorr method? (R) 212
Organic synthesis at high temperatures. Gas-phase flow thermolysis (R) 414
Selective synthesis by use of Lewis acids in the presence of organocopper and related reagents (R) 947
The palladium-catalyzed cross-coupling reactions of organotin reagents with organic electrophiles (R) 508
Total synthesis of anthracyclinones (R) 790

TANDEM WALK RERANGEMENT of a protonated dicyclopropenyl ketone (C) 1093
T-antigen, Synthesis of *O*-glycopeptides of the tumor-associated T_N- and T-antigen type and their binding to bovine serum albumin (C) 360
Technetium cluster anions, A novel electron count and metal-metal multiple bonding in trigonal prismatic clusters (C) 822
Telluronium ions, Tris(pentacarbonylrhenium)-sulfonium, -selenonium, and -telluronium ions: synthesis and structure of $[\{(OC)_5Re\}_3E]^{\oplus}BF_4^{\ominus}$ (E = S, Se, Te) (C) 270
Terphenylene, Novel synthesis of the angular [3]phenylene (terphenylene) by cobalt-catalyzed cyclization of bis(2-ethynylphenyl)ethyne: a molecule with an internal cyclohexatriene ring (C) 266
Tetra-*tert*-butyl-*s*-indacene, Synthesis and properties of 1,3,5,7-tetra-*tert*-butyl-*s*-indacene (C) 630
Tetrahydrofuran derivatives, Diastereoselective synthesis of functionalized tetrahydrofuran derivatives from γ-lactols (C) 556
Tetraiodocyclopropene, *cyclo*-C_3I_4—the first saltlike halocarbon (C) 103
Tetraketones, Synthesis of cyclic, vicinal tetraketones (C) 449
Tetrakis(dimethylamino)benzene, 1,2,4,5-Tetrakis(dimethylamino)benzene, a new electron donor with unusual properties (C) 1023
Tetrakis(diphenylphosphino)allene (C) 348
Tetrakisgalvinol, ^{13}C-ENDOR investigation of an organic tetraradical in the quintet state; synthesis of a fourfold ^{13}C-labeled tetrakisgalvinol (C) 1097
Tetrakismethano[24]annulene, Nickel-induced cyclotetramerization of cyclopropabenzene to 1,6:7,12:13,18:19,24-tetrakismethano[24]annulene (C) 367
Tetraselenide ligand, Synthesis and structure of $[(C_5Me_5)_2M_2Se_5]$: formation of a μ,η^2-tetraselenide ligand at the M–M double bond of $[(C_5Me_5)_2M_2(\mu\text{-}CO)_2]$ (M = Co, Rh) (C) 907
Tetrasilabicyclo[1.1.0]butane system, The tetrasilabicyclo[1.1.0]butane system: structure of 1,3-di-*tert*-butyl-2,2,4,4-tetrakis(2,6-diethylphenyl)tetrasilabicyclo[1.1.0]-butane (C) 173
Thermodynamics, Thermodynamik irreversibler Prozesse. Eine Einführung (B) 659
Thermolysis, Organic synthesis at high temperatures. Gas-phase flow thermolysis (R) 414
Thiacyclooctadecane, Palladium(II) and platinum(II) complexes of 1,4,7,10,13,16-hexathiacyclooctadecane (C) 274
1-Thia-2-cyclooctyne —a strained cycloalkyne with polarized triple bond (C) 809
Thiadiphosphole, A stable 1,2,4-thiadiphosphole ("2,4-diphosphathiophene") (C) 567
Thianthrene 5-oxide as mechanistic probe in oxygen transfer reactions: substrate complexation in oxidations with transition metal peroxides (C) 188
The nucleophilic character of carbonyl oxides (C) 101
Thiazepine, A stable monocyclic 1,4-thiazepine: synthesis and characterization of 2,7-di-*tert*-butyl-5-methoxy-1,4-thiazepine (C) 635
Thiazolium compounds, Synthesis of a macrobicyclic thiazolium-host and supramolecular catalysis of the benzoin condensation (C) 1125
Thiepin, A stable monocyclic 1,4-thiazepine: synthesis and characterization of 2,7-di-*tert*-butyl-5-methoxy-1,4-thiazepine (C) 635
Thiirane *S*-oxide, Complex stabilization of disulfur dioxide in the fragmentation of thiirane *S*-oxide on bis(triphenylphosphane)platinum(0) (C) 261
Thin layer chromatography, Thin layer chromatographic separation of stereoisomeric dipeptides (C) 278
Thioethers, A simple route to 2,3,11,12-dibenzo-1,4,7,10,13,16-hexathia-2,11-cyclooctadiene (hexathiobenzo[18]crown-6) (C) 1107
Thioketone *S*-oxides by [2 + 2]-cycloaddition of ynamines to *N*-sulfinyltosylamide (C) 459
Thiometalates, $[Cl_7Cu_5(ReS_4)]^{3\ominus}$, a hexanuclear complex anion with double cubane-like structure (C) 990
TICT Compounds, Charge separation in excited states of decoupled systems—TICT compounds and implications regarding the development of new laser dyes and the primary processes of vision and photosynthesis (R) 971
Tin chemicals, The industrial uses of tin chemicals (B) 944
Titanium compounds, A polyfunctional dititanacyclobutane (C) 574
Metallacyclic four-membered ring systems: two independent routes to bis(cyclopentadienyl)titanacyclobutabenzene (C) 639
Topology, Geometric and topological thinking in organic chemistry (R) 882
Toxicology, Analytical methods in human toxicology (B) 485
Mass spectral and GC data of drugs, poisons and their metabolites (B) 851
Transition-metal clusters as catalysts of unconventional reactions: reductive C–N coupling of alkyl isocyanates (C) 570
Novel modifications of gold, rhodium, and ruthenium—M_{13} clusters as building blocks of "superclusters" (C) 922
Transition metal complexes, Second-sphere coordination—a novel rôle for molecular receptors (R) 487
Triafulvalene derivatives, Syntheses and spectroscopic properties of triafulvalene derivatives (C) 731
Triazadiphosphatungstacyclohexatriene, A transition metal atom as building block of a cyclic phosphazene—synthesis and structure of $[Cl_3WN_3(PPh_2)_2]$ (C) 477
Triazenido complexes, Synthesis and structure of 1,3-Diphenyltriazenidogold(I), a tetrameric molecule with short gold-gold distances (C) 95
Triaziridine, An azimine-triaziridine transformation by laser photolysis (C) 828
Triazolium ions, Valence isomers of compounds with geminal aryldiazene and isocyanate functions stabilized by protonation (C) 1132
Triazolium salts, Rearrangement of 4*H*-1,2,4-triazolium salts to 4-acyl-5-aminoimidazoles (C) 652
Tri-*tert*-butylazete —the first kinetically stabilized azacyclobutadiene (C) 842
Tricarbahexaboranyl ligand, Bis(η^5-2,3,5-tricarbahexaboranyl)nickel, a nickelocene analogue (C) 1099
Tricyclo[5.3.0.$0^{2,8}$]deca-3,5-dien-9-one and a new route to $C_{10}H_{10}$ isomers (C) 906
Trifluoromethyl group, Synthesis of bis(trifluoromethyl)-analogues of the pyrethroids (C) 184
Trimethylenemethane, [3 + 2] Cycloaddition approaches to five-membered rings via trimethylenemethane and its equivalents (R) 1
Triphenylcyclopropenyl ligand, $[(C_3Ph_3)Ni(\mu\text{-}Br)_3Ni(C_3Ph_3)](C_3Ph_3)$—a triple-decker-like complex with triphenylcyclopropenyl as ligand (C) 833
Triphosphabenzene derivative, A $1\lambda^5,3\lambda^5,5\lambda^3$-triphosphabenzene derivative (C) 1002
Triphosphabutadiene, Synthesis of the first triphosphabutadiene (C) 932
Triple bond, The $\sigma^2\pi^4$ triple bond between molybdenum and tungsten atoms: developing the chemistry of an inorganic functional group (R) 21
Triple-decker complexes, $[(C_3Ph_3)Ni(\mu\text{-}Br)_3Ni(C_3Ph_3)](C_3Ph_3)$—a triple-decker-like complex with triphenylcyclopropenyl as ligand (C) 833
Synthesis of anionic triple-decker complexes having closed 30e valence shells by stacking of sandwich anions with $Cr(CO)_3$ fragments (C) 165
Trisaccharides, Synthesis of the trisaccharide Neu-5-Ac-α(2→6)Gal-β(1→4)GlcNAc

by the use of immobilized enzymes (C) 1096
Trithiometaphosphate PS_3^-—an anion with phosphorus of coordination number 3 (C) 82
Tropylium salts, A salt of the dication cycloheptatrienylidenemethyleneditropylium (C) 916
Tumor cell membranes, Synthesis of *O*-glycopeptides of the tumor-associated T_N- and T-antigen type and their binding to bovine serum albumin (C) 360
Tungsten alkoxides, Evidence for equilibria between μ-alkyne and alkylidyne complexes of tungsten alkoxides: $[W_2(OR)_6(\mu\text{-}C_2R_2')] \rightleftharpoons 2[(RO)_3W{\equiv}CR']$ (C) 446
Tungsten compounds, The first observation of the equilibrium $2M{\equiv}M \rightleftarrows M_4$ (M = transition metal): synthesis and structure of hexaisopropoxyditungsten and its dimer (C) 1014
Twist structure, t-$(ET)_2Au(CN)_2$ and t-$(ET)_2AuBr_2$, organic radical cation salts with twist structure (C) 729
Two-electron transfer, Unexpected "two-electron" transfer in cyclic hydrazines—a voltammetric analysis (C) 1021

ULLMANN'S ENCYCLOPEDIA of industrial chemistry (B) 763
Uranium compounds, $[U_3(\mu^3\text{-}Cl)_2(\mu^2\text{-}Cl)_3(\mu^1,\eta^2\text{-}AlCl_4)_3(\eta^6\text{-}C_6Me_6)_3][AlCl_4]$—a trinuclear arene complex of U^{III} (C) 637

VALENCE ISOMERISM, Valence isomers of compounds with geminal aryldiazene and isocyanate functions stabilized by protonation (C) 1132
Valence tautomerism of the heptaheteronortricycles $[P_{7-x}As_x]^{3-}$ (C) 352
Vanadium compounds, Benzene as bridging ligand in main group metal–transition metal–arene complexes (C) 927
First dinuclear complexes with fourfold alkyl-bridging (C) 925
Synthesis of diindenyldivanadium—a new variant of the reductive degradation of metallocenes and related compounds (C) 928
Vibronic coupling (B) 659
Vicinal pentaketones (C) 999
Vinyl ketones, Divinylglyoxal and methylvinylglyoxal (C) 1116
Intramolecular Diels-Alder reactions with methyl 2-trimethylsiloxy-2-vinylcyclopropanecarboxylates as key building blocks (C) 1086
Violerythrins, Mini-violerythrins: why can C_{38}-carotinoids be blue? (C) 1018
Viruses, Molecular biological background of the species- and organ-specificity of influenza A viruses (R) 47
Vitamin B_{12}, Facile entry to geminally dialkylated chlorins (C) 458

WALK REARRANGEMENT, Tandem walk rearrangement of a protonated dicyclopropenyl ketone (C) 1093
Water oxidation, Oxygen evolution by water oxidation mediated by heterogeneous manganese complexes (C) 825
O_2-Generation by oxidation of water with di- and trinuclear ruthenium complexes as homogeneous and heterogeneous catalysts (C) 1009
Wittig reaction with carbon suboxide: synthesis of dimethyl 1,5-diphenyl-1,2,3,4-pentatetraenedicarboxylate (C) 93

YLIDES, $H_3C{-}P{=}CH_2$: an ylide with two-coordinate phosphorus? (C) 265
A 2-phosphonio-substituted 1-phospha-1-alkene: resonance between P^{III} alkene and P^{V} ylide (C) 454
A polyfunctional dititanacyclobutane (C) 574
Nitrile ylides and azirines: gas-phase generation from 2,3-dihydro-1,4,2λ^5-oxazaphospholes and matrix isolation (C) 85
Reaction of phosphonium ylides with alkyldichloroboranes (C) 559
Stable selenocarbonyl ylides (C) 183
Ylide ligands, Methylene-bridged dinuclear gold(III) complexes with terminal and bridging ylide ligands (C) 575
Ytterbium compounds, Dimeric chloro[dicyclopentadienyl(dimethyl)silyl]ytterbium (III), a rare example of a complex involving metal-bridging instead of chelating $[Me_2Si(\eta^5\text{-}C_5H_4)_2]$ ligands (C) 738

ZIRCONIUM COMPOUNDS, Unusual bridging of the metal centers in dimeric bis(η-methylcyclopentadienyl)phenylethynylzirconium (C) 463
Novel fulvalene derivatives of zirconium: a facile entry into organozirconium(III) chemistry (C) 289